Hells Canyon Complex CE-QUAL-W2 Water Quality Model Development and Calibration

Water Quality Research Group
Department of Civil and Environmental Engineering
Maseeh College of Engineering and Computer Science

January 2025

Portland State UNIVERSITY

Hells Canyon Complex CE-QUAL-W2 Water Quality Model Development and Calibration

by

Scott A. Wells, Bernadel Garstecki, Chris J. Berger, and Jesse Naymik

Water Quality Research Group
Department of Civil and Environmental Engineering
Maseeh College of Engineering and Computer Science
Portland State University
Portland, Oregon 97201-0751

Prepared for Idaho Power

January 2025

Contents

List of Figures iv
List of Tables xi
Introduction 1
CE-QUAL-W2 3
Model Bathymetry 4
Brownlee Reservoir 5
Oxbow Reservoir 16
Hells Canyon Reservoir 19
Meteorological Inputs 21
Brownlee Reservoir 21
Oxbow Reservoir 38
Hells Canyon Reservoir 48
Dam Outflows 52
Tributary Inflows 57
Temperature Inputs 62
Constituent Inputs 70
Sediment Diagenesis Inputs 100
Porosity 101
Particle Size 101
Bulk Density 102
POC, PON, and POP Ratios 102
Porewater Concentrations 102
Shading 102
Analysis of Light Extinction Data in Brownlee Reservoir to Determine Model Extinction Coefficients 107
Model Analyses 115
Sensitivity of Brownlee Reservoir to Channel Friction 115
Detention Time of Brownlee, Oxbow and Hells Canyon Reservoirs 119
Variation of Model Time Step 123
Flow and Water Level Calibration 124
Brownlee Reservoir 124

Oxbow Reservoir 126
Hells Canyon Reservoir 127
Temperature Calibration 128
Brownlee Reservoir 128
Oxbow Reservoir 131
Hells Canyon Reservoir 132
Water Quality Calibration 133
Brownlee Reservoir 137
Water Quality Model-Data Comparisons 137
Analysis of Model Fluxes 168
Sediment Nutrient Concentrations 173
Oxbow Reservoir 175
Water Quality Model-Data Comparisons 175
Analysis of Model Fluxes 191
Sediment Nutrient Concentrations 196
Hells Canyon Reservoir 198
Water Quality Model-Data Comparisons 198
Analysis of Model Fluxes 221
Sediment Nutrient Concentrations 226
Discussion of Model Calibration 228
Meteorological Data 228
Input Data 230
Water level 231
Temperature 231
Water Quality 231
Sediment Diagenesis 234
Summary and Conclusions 235
References 236
Appendix 238
A1. Algae Speciation 238
A2. Model Coefficients 238

A3. Brownlee Dam Spillway Gas Equation Updates 238
A4. Brownlee Reservoir Vertical Profiles 238
A5. Oxbow Reservoir Vertical Profiles 238
A6. Hells Canyon Reservoir Vertical Profiles 239
A7. Brownlee Reservoir USGS Continuous Temperature and Dissolved Oxygen in 2017 and 2018 239

List of Figures

Figure 1. The Hells Canyon Complex along the Snake River including Brownlee Reservoir, Oxbow Reservoir, and Hells Canyon Reservoir along the Idaho-Oregon border. 1
Figure 2. CE-QUAL-W2 model predictions for Lake Roosevelt, WA, for temperature as a function of depth and longitudinal distance in km from the Canadian border on July 31, 2000. 3
Figure 3. Brownlee Reservoir model grid segments, branches (BR), and water bodies (WB). 6
Figure 4. Mainstem branches of Brownlee Reservoir showing elevation along the channel bottom as a function of distance from RM 345.6. Branch 1 is in green; Branch 2 is in light blue; Branch 3 is in yellow, Branch 4 is in Orange, and Branch 5 is in darker blue. 7
Figure 5. Brownlee Dam inlet channel bathymetry and model segments. This is Branch 7 in the model and was composed of segments 236, 237 and 238 (next to the powerhouse intakes). 8
Figure 6. Upstream end of Brownlee River grid. Polygons and large numbers define model segments. Segment 2 begins at RM 345.6. The yellow dots are RM designations from Idaho Power. 8
Figure 7. Brownlee Reservoir model segments 2 through 22. 9
Figure 8. Brownlee Reservoir model segments 2 through 58. 9
Figure 9. Brownlee Reservoir model segments 56 through 107. 10
Figure 10. Brownlee Reservoir model segments 105 through 152. 11
Figure 11. Brownlee Reservoir model segments 153 through 238. The Powder arm branch (BR6) includes segments 205 through 233. Segments 236 to 238 are the outlet channel segments (BR7) that are barely visible near the dam. 12
Figure 12. Segments for the outlet channel (236-238) in Branch 7 are shown relative to the dam and the last segment in the mainstem (segment 202) in Branch 5. 12
Figure 13. Branch 5 side view for Brownlee Reservoir from model segment 86 to the dam at segment 202. Vertical layer spacing is 1 m, and longitudinal segment spacing is 500.06 m. The first figure shows elevations and distances in m and the second figure shows layers and segment numbers. 13
Figure 14. Branch 6 side view for Brownlee Reservoir (Powder River) from model segment 205 to the intersection with the Snake River mainstem at segment 233. Vertical layer spacing is 1 m, and longitudinal segment spacing is 503.05 m. The first figure shows elevations and distances in m and the second figure shows layers and segment numbers. 14
Figure 15. Volume-elevation curve for Brownlee Reservoir. 15
Figure 16. Oxbow Reservoir model segments. 17

Figure 17. Side view of model segments starting at 2 (on the right) and ending at segment 52 (on the left) for Oxbow Reservoir. 18
Figure 18. Volume-elevation curve for Oxbow Reservoir. 18
Figure 19. Hells Canyon model segments. 20
Figure 20. Hells Canyon Reservoir models segments near dam. All segments are a length of 350.83 m except segments 114 through 116, which are 228.7 m, 79 m, and 71 m to simulate the effects of an old coffer dam. The elevation of the crest between segment 114 and 115 is about 479 m. 20
Figure 21. Side view of model segments starting at 2 (on the right) and ending at segment 116 (on the left) for Hells Canyon Reservoir. 21
Figure 22. Volume-elevation curve for Hells Canyon Reservoir. 21
Figure 23. Locations of USGS wind speed measurement stations. 24
Figure 24. Locations of WRF-NAM meteorological predictions in Brownlee Reservoir. 25
Figure 25. Brownlee Reservoir model water bodies. One meteorological input file can be used per water body in the CE-QUAL-W2 model. 26
Figure 26. Wind speed measurement at Brownlee dam from IPC. The station is at an elevation of 2090 ft. 27
Figure 27. Air temperature inputs for water bodies 1 through 4 of the Brownlee Reservoir model. 28
Figure 28. Air temperature inputs for water body 5 of the Brownlee Reservoir model. 29
Figure 29. Dew point temperature inputs for water bodies 1 through 4 of the Brownlee Reservoir model. 30
Figure 30. Dew point temperature inputs for water body 5 of the Brownlee Reservoir model. 31
Figure 31. Wind speed inputs for water bodies 1 through 4 of the Brownlee Reservoir model. 32
Figure 32. Wind speed inputs for water body 5 of the Brownlee Reservoir model. 33
Figure 33. Polar wind diagrams of wind direction inputs for 2014-2018. The polar diagram for water bodies 1 through 4 of the Brownlee Reservoir model is shown on the left and on the right is the polar diagram for water body 5 of the Brownlee Reservoir model. 34
Figure 34. Solar radiation inputs for water bodies 1 through 4 of the Brownlee Reservoir model. 35
Figure 35. Solar radiation inputs for water body 5 of the Brownlee Reservoir model. 36
Figure 36. Cloud cover inputs for water bodies 1 through 4 of the Brownlee Reservoir model. 37
Figure 37. Cloud cover inputs for water body 5 of the Brownlee Reservoir model and for the Oxbow Reservoir and Hells Canyon Reservoir models. 38
Figure 38. Location of WRF-NAM meteorological predictions in Oxbow Reservoir. 40
Figure 39. Brownlee Reservoir and Hells Canyon reservoir air temperatures measured from 8/1/2012 – 11/5/2013. 41
Figure 40. Brownlee Reservoir and Hells Canyon reservoir relative humidity measured from 8/1/2012 – 11/5/2013. 42
Figure 41. Brownlee Reservoir and Hells Canyon reservoir wind speed measured from 8/1/2012 – 11/5/2013. 43
Figure 42. Air temperature inputs for the Oxbow Reservoir model. 45
Figure 43. Dew point temperature inputs for the Oxbow Reservoir model. 46
Figure 44. Wind speed inputs for the Oxbow Reservoir model. 47

Figure 45. Polar wind diagram of wind direction inputs for the Oxbow Reservoir model. 47
Figure 46. Location of WRF-NAM meteorological predictions in Hells Canyon Reservoir. 48
Figure 47. Air temperature inputs for the Hells Canyon Reservoir model. 49
Figure 48. Dew point temperature inputs for the Hells Canyon Reservoir model. 50
Figure 49. Wind speed inputs for the Hells Canyon Reservoir model. 51
Figure 50. Polar wind diagram of wind direction inputs for the Hells Canyon Reservoir model..... 51
Figure 51. Brownlee Dam outflow rates. 54
Figure 52. Oxbow Dam turbine, spill, and bypass flow rates..... 55
Figure 53. Hells Canyon Dam turbine and spill flow rates. 56
Figure 54. Flow rates of Brownlee Reservoir tributaries. 58
Figure 55. Wildhorse River flow rates into Oxbow Reservoir. 59
Figure 56. Pine Creek flow rates into Hells Canyon Reservoir. 60
Figure 57. Brownlee Reservoir inflow temperatures. Powder River temperatures were used for Daly Creek and the distributed tributary. 64
Figure 58. Powder River inflow temperatures. Powder River temperatures were estimated by calculating the flow-weighted average of Eagle Creek and Powder River (RM 22) data..... 65
Figure 59. Wildhorse River inflow temperatures to Oxbow Reservoir. 66
Figure 60. Plot of daily average Wildhorse River daily average temperatures versus Powder River daily average temperatures. A linear regression equation was used to estimate Wildhorse River temperatures within data gaps. 67
Figure 61. Pine Creek inflow temperatures to Hells Canyon Reservoir. 68
Figure 62. Plot of daily average Pine Creek daily average temperatures versus Powder River daily average temperatures. A linear regression equation was used to estimate Pine Creek temperatures within larger data gaps. 69
Figure 63. USGS TSS data with gaps filled using regression with IPC TSS data. 82
Figure 64. Brownlee Inflow USGS SPM (TSS) versus IPC TSS regression..... 83
Figure 65. IPC VSS data with gap filled using regression with USGS TSS data. 83
Figure 66. Brownlee Inflow USGS SPM (TSS) versus IPC VSS regression. 84
Figure 67. Fraction of total ISS split into ISS1 and ISS2 groups over the model simulation period. 84
Figure 68. USGS POC data with gaps filled using regression with IPC VSS data. 85
Figure 69. Brownlee Inflow USGS POC versus IPC VSS regression..... 85
Figure 70. Snake River, Powder River, and Burnt River chlorophyll a inputs. The purple line is where the Powder River and Snake River concentrations are the same. 86
Figure 71. Tributary chloride regressions for Burnt River, Eagle Creek, and Powder River. Tributary concentration versus Snake River inflow concentration (top) and tributary concentration versus tributary streamflow (bottom). The chosen regressions are highlighted in red. 87
Figure 72. Tributary TSS regressions for Burnt River, Eagle Creek, and Powder River. Tributary concentration versus Snake River inflow concentration (top) and tributary concentration versus tributary streamflow (bottom). The chosen regressions are highlighted in red. 87

Figure 73. Tributary sulfate regressions for Burnt River, Eagle Creek, and Powder River. Tributary concentration versus Snake River inflow concentration (top) and tributary concentration versus tributary streamflow (bottom). The chosen regressions are highlighted in red. 88
Figure 74. Tributary Fe(II) regressions for Burnt River, Eagle Creek, and Powder River. Tributary concentration versus Snake River inflow concentration (top) and tributary concentration versus tributary streamflow (bottom). The chosen regressions are highlighted in red. 89
Figure 75. Tributary Mn(II) regressions for Burnt River, Eagle Creek, and Powder River. Tributary concentration versus Snake River inflow concentration (top) and tributary concentration versus tributary streamflow (bottom). The chosen regressions are highlighted in red. 90
Figure 76. Tributary ortho-phosphate regressions for Burnt River, Eagle Creek, and Powder River. Tributary concentration versus Snake River inflow concentration (top) and tributary concentration versus tributary streamflow (bottom). The chosen regressions are highlighted in red. 91
Figure 77. Tributary nitrate regressions for Burnt River, Eagle Creek, and Powder River. Tributary concentration versus Snake River inflow concentration (top) and tributary concentration versus tributary streamflow (bottom). The chosen regressions are highlighted in red. 92
Figure 78. Tributary DOC regressions for Burnt River, Eagle Creek, and Powder River. Tributary concentration versus Snake River inflow concentration (top) and tributary concentration versus tributary streamflow (bottom). The chosen regressions are highlighted in red. 93
Figure 79. Tributary chlorophyll a regressions for Burnt River, Eagle Creek, and Powder River. Tributary concentration versus Snake River inflow concentration (top) and tributary concentration versus tributary streamflow (bottom). The chosen regressions are highlighted in red. 94
Figure 80. Constituent concentrations for sulfate, chloride, methane, ISS1, ISS2, and ortho-phosphate phosphorus. Daly Creek, Brownlee Reservoir distributed tributary, Pine Creek, and Wildhorse River are all set equal to flow weighted Powder River concentrations. Note that ISS3 is used only on the Snake inflow and is 11% of ISS2. Also, maximum ISS1 concentrations exceeded the axis limit 3 times especially for the Burnt River. 95
Figure 81. Constituent concentrations for ammonia nitrogen, nitrite-nitrate nitrogen, LDOM, RDOM, LPOM, and RPOM. Daly Creek, Brownlee Reservoir distributed tributary, Pine Creek, and Wildhorse River are all set equal to flow weighted Powder River concentrations. 96
Figure 82. Constituent concentrations for DO, total inorganic carbon, alkalinity, hydrogen sulfide, LDOM-P, and RDOM-P. Daly Creek, Brownlee Reservoir distributed tributary, Pine Creek, and Wildhorse River are all set equal to flow weighted Powder River concentrations. 97
Figure 83. Constituent concentrations for LPOM-P, RPOM-P, LDOM-N, RDOM-N, LPOM-N, and RPOM-N. Daly Creek, Brownlee Reservoir distributed tributary, Pine Creek, and Wildhorse River are all set equal to flow weighted Powder River concentrations. 98
Figure 84. Constituent concentrations for ISS3, zooplankton, Fe(II), FeOOH, Mn(II), and MnO2. Daly Creek, Brownlee Reservoir distributed tributary, Pine Creek, and Wildhorse River are all set equal to flow weighted Powder River concentrations. 99
Figure 85. Constituent concentrations for Algae1, Algae2, and Algae3. Daly Creek, Brownlee Reservoir distributed tributary, Pine Creek, and Wildhorse River are all set equal to flow weighted Powder River concentrations. 100

Figure 86. Topographic line segments around each segment center for Brownlee Reservoir to determine topographic shading angles for model segments 14, 76, 191, and 214. 104
Figure 87. Topographic line segments around each segment center for Oxbow Reservoir to determine topographic shading angles for segments 9, 38, and 52. 105
Figure 88. Topographic line segments around each segment center for Hells Canyon Reservoir to determine topographic shading angles for segments 59 and 101. 106
Figure 89. Light extinction computed from PAR with depth on 5/3/2016 at RM288. The constant in the exponential is the light extinction coefficient, in this case 0.6925 m^{-1}..... 108
Figure 90. Computed light extinction coefficients from PAR vs depth profiles from Idaho Power..... 109
Figure 91. Computed light extinction data and TSS measurements at RM 286 Brownlee Reservoir. 110
Figure 92. Correlation between TSS and light extinction coefficient at RM 286. 112
Figure 93. Correlation between TSS and light extinction coefficient at RM 300. 112
Figure 94. Correlation between TSS and light extinction coefficient at RM 310. 113
Figure 95. Correlation between TSS and light extinction coefficient at RM 318. 113
Figure 96. Correlation between TSS and light extinction coefficient using all the data between RM 286 and 318. 114
Figure 97. Water level variation in Brownlee Reservoir measured downstream of the confluence with the Powder River arm (always in the pool area) between 2014-2018. 115
Figure 98. Water surface elevations along the Brownlee model between RM 345.6 and 284.6 on Julian day 1348.2 (9/9/2017 at 4:48 am) and Julian day 1210.5 (4/24/2017 at 12 pm) using a Manning's friction factor of 0.035 an 0.045. 117
Figure 99 Water surface elevations and flow rates along the Brownlee model between RM 345.6 and 284.6 on Julian day 1348.2 (9/9/2017 at 4:48 am) and Julian day 1210.5 (4/24/2017 at 12 pm). 118
Figure 100. Brownlee Reservoir detention time as a function of elevation and flow rate assuming no short circuiting..... 120
Figure 101. Computed Brownlee Reservoir water age between 2014-2018. 121
Figure 102. Oxbow Reservoir as a function of flow rate and water surface elevation. 122
Figure 103. Hells Canyon Reservoir as a function of flow rate and water surface elevation. 123
Figure 104. Variation of model time step between 2014-2018 for the Brownlee Reservoir model using maximum time step of 60 s and a fraction of theoretical time step of 0.85. The average time step was about 24 s. 124
Figure 105. Water surface elevations in Brownlee Reservoir measured at segment 202 compared to model predictions between 2014-2018. 125
Figure 106. Water balance flows compared to inflows from January 1, 2014 through December 31, 2018. 126
Figure 107. Oxbow Reservoir model water level predictions compared with data. 127
Figure 108. Hells Canyon Reservoir model water level predictions compared with data. 128
Figure 109. Brownlee Dam model outflow temperatures compared to data. 130
Figure 110. Oxbow Dam model outflow temperatures compared to data. 131
Figure 111. Hells Canyon Dam model outflow temperatures compared to data. 133
Figure 112. Zooplankton profiles at river mile 286..... 137

Figure 113. Percent increase of dissolved oxygen of the Brownlee Reservoir turbines over the simulation period. 138
Figure 114. Brownlee Reservoir model outflow dissolved oxygen compared to data. 141
Figure 115. Brownlee Reservoir model outflow-weighted dissolved oxygen compared to data 142
Figure 116. Brownlee Reservoir model outflow chlorophyll a compared to data. 143
Figure 117. Brownlee Reservoir model outflow ammonia nitrogen compared to data. 144
Figure 118. Brownlee Reservoir model outflow nitrate nitrogen compared to data. 145
Figure 119. Brownlee Reservoir model outflow total Kjeldahl nitrogen compared to data. 146
Figure 120. Brownlee Reservoir model outflow particulate organic nitrogen compared to data. 147
Figure 121. Brownlee Reservoir model outflow orthophosphate compared to data. 148
Figure 122. Brownlee Reservoir model outflow total phosphorus compared to data. 149
Figure 123. Brownlee Reservoir model outflow total inorganic carbon compared to data. 150
Figure 124. Brownlee Reservoir model outflow dissolved organic carbon compared to data. 151
Figure 125. Brownlee Reservoir model outflow particulate organic carbon compared to data. 152
Figure 126. Brownlee Reservoir model outflow chloride compared to data. 153
Figure 127. Brownlee Reservoir model outflow sulfate compared to data. 154
Figure 128. Brownlee Reservoir model outflow hydrogen sulfide compared to data. 155
Figure 129. Brownlee Reservoir model outflow zooplankton compared to data. 156
Figure 130. Brownlee Reservoir model outflow FeII compared to data 157
Figure 131. Brownlee Reservoir model outflow FeOOH compared to data. 158
Figure 132. Brownlee Reservoir model outflow MnII compared to data. 159
Figure 133. Brownlee Reservoir model outflow MnO2 compared to data. 160
Figure 134. Brownlee Reservoir model outflow total suspended solids compared to data. 161
Figure 135. Brownlee Reservoir model outflow particulate organic carbon compared to volatile suspended solids data multiplied by 0.45 (assumed fraction of mg C to mg organic matter). 162
Figure 136. Brownlee Reservoir model outflow methane. In contrast note that Liu et al. (1996) reported in the anoxic hypolimnion of Lake Lugano concentrations of methane of 1 mg/L as C.] 163
Figure 137. Brownlee Reservoir model ammonia nitrogen in sediment compared to data. 164
Figure 138. Brownlee Reservoir model nitrate nitrogen in sediment and bottom of water column compared to data 165
Figure 139. Brownlee Reservoir model orthophosphate in sediment and bottom of water column compared to data 166
Figure 140. Brownlee Reservoir model DOC in bottom of water column compared to data. 167
Figure 141. Cumulative phosphorus mass in Brownlee Reservoir. TP in the waterbody, sediment and plants just shows the current amount of TP in each of those at different points in time. 169
Figure 142. Cumulative nitrogen mass in Brownlee Reservoir. TN in the waterbody, sediment and plants just shows the current amount of TN in each of those at different points in time. 170
Figure 143. Dissolved oxygen sources and sinks in Brownlee Reservoir. 171
Figure 144. Phosphorus sources and sinks in Brownlee Reservoir. 172
Figure 145. Nitrogen sources and sinks in Brownlee Reservoir 173
Figure 146. Labile POC, PON, POP at segments 25 and 201 in Brownlee Reservoir. 174

Figure 147. Refractory POC, PON, POP at segments 25 and 201 in Brownlee Reservoir. 174
Figure 148. Oxbow Reservoir model outflow dissolved oxygen compared to data. 176
Figure 149. Oxbow Reservoir model outflow nitrate nitrogen compared to data. 177
Figure 150. Oxbow Reservoir model outflow particulate organic nitrogen compared to data. 178
Figure 151. Oxbow Reservoir model outflow orthophosphate compared to data. 179
Figure 152. Oxbow Reservoir model outflow total inorganic carbon compared to data. 180
Figure 153. Oxbow Reservoir model outflow dissolved organic carbon compared to data. 181
Figure 154. Oxbow Reservoir model outflow particulate organic carbon compared to data. 182
Figure 155. Oxbow Reservoir model outflow chloride compared to data. 183
Figure 156. Oxbow Reservoir model outflow sulfate compared to data. 184
Figure 157. Oxbow Reservoir model outflow hydrogen sulfide compared to data. 185
Figure 158. Oxbow Reservoir model outflow zooplankton compared to data. 186
Figure 159. Oxbow Reservoir model outflow FeII compared to data. 187
Figure 160. Oxbow Reservoir model outflow FeOOH compared to data. 188
Figure 161. Oxbow Reservoir model outflow MnII compared to data. 189
Figure 162. Oxbow Reservoir model outflow MnO2 compared to data. 190
Figure 163. Oxbow Reservoir model outflow total suspended solids compared to data. 191
Figure 164. Cumulative phosphorus mass in Oxbow Reservoir. TP in the waterbody, sediment and plants shows the current amount of TP as a function of time. Inflow TP is Brownlee spill. Outflow TP is Oxbow bypass flow and spill. The Withdrawal TP (Oxbow powerhouse flows) is nearly identical to the Tributary TP (powerhouse inflow from Brownlee Reservoir and Wildhorse River) and falls on the same line. 192
Figure 165. Cumulative nitrogen mass in Oxbow Reservoir. TN in the waterbody, sediment, and plants show the current amount of TN as a function of time. Inflow TN is Brownlee spill. Outflow TN is Oxbow bypass flow and spill. The Withdrawal TN (Oxbow powerhouse flows) is nearly identical to the Tributary TN (powerhouse inflow from Brownlee Reservoir and Wildhorse River) and falls on the same line. 193
Figure 166. Dissolved oxygen sources and sinks in Oxbow Reservoir. 194
Figure 167. Phosphorus sources and sinks in Oxbow Reservoir. 195
Figure 168. Nitrogen sources and sinks in Oxbow Reservoir. 196
Figure 169. Labile POC, PON, POP at segments 12 and 51 in Oxbow Reservoir 197
Figure 170. Refractory POC, PON, POP at segments 12 and 51 in Oxbow Reservoir. 197
Figure 171. Hells Canyon Reservoir model outflow dissolved oxygen compared to data. 200
Figure 172. Hells Canyon Reservoir model outflow chlorophyll a compared to data. 201
Figure 173. Hells Canyon Reservoir model outflow ammonia nitrogen compared to data. 202
Figure 174. Hells Canyon Reservoir model outflow nitrate nitrogen compared to data. 203
Figure 175. Hells Canyon Reservoir model outflow total Kjeldahl nitrogen compared to data. 204
Figure 176. Hells Canyon Reservoir model outflow particulate organic nitrogen compared to data. 205
Figure 177. Hells Canyon Reservoir model outflow orthophosphate compared to data. 206
Figure 178. Hells Canyon Reservoir model outflow total phosphorus compared to data. 207
Figure 179. Hells Canyon Reservoir model outflow total inorganic carbon compared to data. 208
Figure 180. Hells Canyon Reservoir model outflow dissolved organic carbon compared to data. 209
Figure 181. Hells Canyon Reservoir model outflow particulate organic carbon compared to data. 210

Figure 182. Hells Canyon Reservoir model outflow chloride compared to data. 211
Figure 183. Hells Canyon Reservoir model outflow sulfate compared to data. 212
Figure 184. Hells Canyon Reservoir model outflow hydrogen sulfide compared to data. 213
Figure 185. Hells Canyon Reservoir model outflow FeII compared to data. 214
Figure 186. Hells Canyon Reservoir model outflow FeOOH compared to data. 215
Figure 187. Hells Canyon Reservoir model outflow MnII compared to data. 216
Figure 188. Hells Canyon Reservoir model outflow MnO2 compared to data. 217
Figure 189. Hells Canyon Reservoir model outflow total suspended solids compared to data. 218
Figure 190. Hells Canyon Reservoir model outflow particulate organic carbon compared to volatile suspended solids data multiplied by 0.45 (assumed fraction of mg C to mg organic matter). 219
Figure 191. Hells Canyon Reservoir model ammonia nitrogen in sediment compared to data 220
Figure 192. Hells Canyon Reservoir model nitrate nitrogen in sediment and bottom of water column compared to data 220
Figure 193. Hells Canyon Reservoir model orthophosphate in sediment and bottom of water column compared to data 220
Figure 194. Hells Canyon Reservoir model DOC in bottom of water column compared to data. 221
Figure 195. Cumulative phosphorus mass in Hells Canyon Reservoir. TP in the waterbody, sediment and plants just shows the current amount of TP in each of those at different points in time. 222
Figure 196. Cumulative nitrogen mass in Hells Canyon Reservoir. TN in the waterbody, sediment and plants just shows the current amount of TN in each of those at different points in time. 223
Figure 197. Dissolved oxygen sources and sinks in Hells Canyon Reservoir. 224
Figure 198. Phosphorus sources and sinks in Hells Canyon Reservoir. 225
Figure 199. Nitrogen sources and sinks in Hells Canyon Reservoir. 226
Figure 200. Labile POC, PON, POP at segments 15 and 115 in Hells Canyon Reservoir. 227
Figure 201. Refractory POC, PON, POP at segments 15 and 115 in Hells Canyon Reservoir. 227
Figure 202. Wind sheltering coefficient for Brownlee Reservoir between 2014-2018. 229
Figure 203. Wind sheltering coefficient for Hells Canyon Reservoir between 2014 and 2018. 230
Figure 204. Brownlee Reservoir model branch 5 volume of dissolved oxygen less than 1 mg/l compared to data. 233
Figure 205. Epiphyton concentrations at the upstream model segment adjacent to each dam. 234

List of Tables

Table 1. Brownlee Reservoir, Oxbow Reservoir, and Hells Canyon Reservoir model grid characteristics. .. 4
Table 2. Brownlee grid branch information. 15
Table 3. Available sources of measured data and model predictions for Brownlee Reservoir meteorological inputs. 22
Table 4. Time periods when USGS wind speed data were available for Brownlee Reservoir. 23
Table 5. Meteorological input files for Brownlee Reservoir. 38

Table 6. Meteorological adjustment factors for air temperature, relative humidity, and wind speed. 44
Table 7. Data sources for modeled outflows. 53
Table 8. Model outlet elevations for Brownlee, Oxbow, and Hells Canyon Reservoirs. 53
Table 9. Dam model outflows for Brownlee, Oxbow and Hells Canyon. 56
Table 10. Brownlee, Oxbow, and Hells Canyon Reservoir model inflows and tributaries. 60
Table 11. Data sources for modeled inflows. 62
Table 12. Temperature data sources for modeled inflows. 63
Table 13. Modeled HCC inflows. 71
Table 14. Development of modeled constituent concentrations in Snake River inflows to Brownlee Reservoir. 71
Table 15. Development of modeled constituent concentrations in the Burnt River and Powder River. Wildhorse River, Pine Creek, Daly Creek, and the distributed tributary concentrations were all set equal to flow weighted Powder River concentrations. 77
Table 16. Average values of shallow sediment parameters at various river miles for 2014-2018. 101
Table 17. Average values of shallow sediment pore water parameters at various river miles for 2016-2017. 101
Table 18. Average values of deep sediment parameters at various river miles for 2016. 101
Table 1. Example of the 757 profiles of PAR with depth collected by Idaho Power. This profile was taken on 5/3/2016 at RM 288. 107
Table 2. Summary of correlation coefficients for TSS and light extinction. 111
Table 19. Water level error statistics for Brownlee Reservoir. 125
Table 20. Water level error statistics for Oxbow Reservoir. 127
Table 21. Water level error statistics for Hells Canyon Reservoir. 128
Table 22. Temperature error statistics for Brownlee Reservoir vertical profiles. 128
Table 1. Error statistics for continuous temperature data measured by the USGS. 129
Table 23. Brownlee Dam outflow temperature error statistics. 131
Table 24. Oxbow Dam outflow temperature error statistics. 132
Table 25. Temperature error statistics for Hells Canyon Reservoir vertical profiles. 132
Table 26. Hells Canyon Dam outflow temperature error statistics. 133
Table 27. Data used for outflow and profile model comparisons. 134
Table 28. USGS data available for sediment and porewater model comparisons. Shaded rows indicate data used for comparisons. 135
Table 29. Comparisons of average historic and current Fe, Mn, Sulfide, and Methane concentrations. 136
Table 30. Water quality error statistics for Brownlee Reservoir outflow. 138
Table 31. Water quality error statistics for Brownlee Reservoir vertical profiles. 139
Table 35. Error statistics for continuous DO data measured by the USGS in Brownlee Reservoir in 2017 and 2018. 140
Table 32. Water quality error statistics for Brownlee Reservoir sediment and porewater comparisons. 141
Table 33. Water quality error statistics for Oxbow Reservoir outflow. 175
Table 34. Water quality error statistics for Oxbow Reservoir vertical profiles. 175

Table 35. Water quality error statistics for Hells Canyon Reservoir outflow. 198
Table 36. Water quality error statistics for Hells Canyon Reservoir vertical profiles. 198
Table 37. Water quality error statistics for Hells Canyon Reservoir sediment and porewater comparisons. 199

Introduction

Idaho Power Company is developing strategies for improving water quality in the Hells Canyon Complex (HCC) on the Snake River (see Figure 1). The HCC includes Brownlee, Oxbow, and Hells Canyon Reservoirs. The objective of this study was to develop a numerical model capable of simulating temperature, dissolved oxygen, organic matter, suspended solids, nutrient, algae, zooplankton, periphyton, Fe/Mn dynamics in the water, sediment, and biota of the HCC. This modeling tool would then be used to assess strategies for water quality improvement.



Figure 1. The Hells Canyon Complex along the Snake River including Brownlee Reservoir, Oxbow Reservoir, and Hells Canyon Reservoir along the Idaho-Oregon border.

This document describes the water quality and hydrodynamic model developed for the HCC Snake River system. A new Hg model has also been developed relies on the model documented in this report. The new Hg algorithm and model using CE-QUAL-W2 is documented in Wells et al. (2025).

Elements of this modeling study included the following:

- Modeling Brownlee Reservoir, Oxbow Reservoir, and Hells Canyon Reservoir over a 5-year period from 2014-2018.
- Updating reservoir computational grids for the three reservoirs based on recent bathymetric data.
- Constructing model input files for both boundary conditions and in-situ field data between 2014-2018.
- Calibrating the model for water level, temperature, organic matter (particulate and dissolved), nutrients, dissolved oxygen, Fe, Mn, S, algae, zooplankton, and periphyton
- Using the current version of the CE-QUAL-W2 model (Wells, 2024) which has been updated extensively since the last modeling study of the Hells Canyon complex.

The following topics are discussed in this report:

- CE-QUAL-W2 model background
- Model bathymetry development
- Meteorological input development
- Dam outflows
- Tributary input development
- Temperature input development
- Constituent input development
- Sediment diagenesis inputs
- Shading inputs
- Model sensitivity to grid friction
- Residence times in the Hells Canyon Complex
- Model internal time step variation
- Flow and water level model comparison to field data
- Temperature model comparison to field data
- Water quality predictions compared to field data
- Summary

CE-QUAL-W2

The model used for the project will be the public domain model, CE-QUAL-W2 (Wells, 2024). This model is a 2-dimensional (longitudinal-vertical) hydrodynamic and water quality model capable of predicting water surface, velocity, temperature, dissolved oxygen, algae, zooplankton, pH, alkalinity, phosphate, ammonia nitrogen, nitrite-nitrate nitrogen, total inorganic carbon (TIC), inorganic suspended solids, ferrous iron Fe(II), iron oxyhydroxide (FeOOH), Mn(II), manganese dioxide (MnO_2), multiple algae, zooplankton, periphyton, and macrophyte species, pH, alkalinity, multiple CBOD groups, multiple suspended solids groups, multiple generic constituents (such as tracer, bacteria, toxics), and multiple organic matter groups, both dissolved and particulate. The model is set up to predict these state variables at longitudinal segments and vertical layers (see Figure 2).

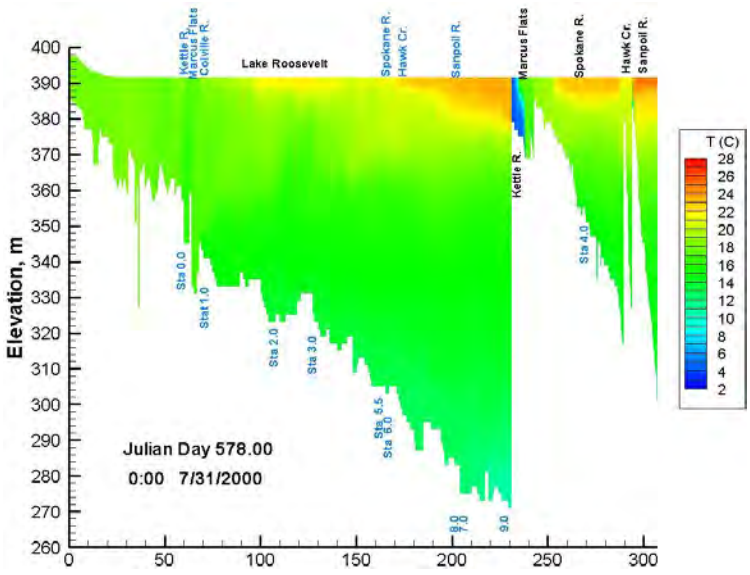


Figure 2. CE-QUAL-W2 model predictions for Lake Roosevelt, WA, for temperature as a function of depth and longitudinal distance in km from the Canadian border on July 31, 2000.

Typical model longitudinal resolution is between 100-1000 m; vertical resolution is usually between 0.5 m and 2 m. The model can also be used in quasi-3-D mode, where embayments are treated as separate model branches off the main stem of the reservoir. The user manual and documentation can be found at: http://www.cee.pdx.edu/w2. Since 2000, this model has been used extensively throughout the world in over 116 different countries. Model downloads average about 3-4 per day, and the W2 web site has on average 10-30 visitors per day.

Version 3.71 was released at the end of 2012 that included a new post-processor from DSI, and Version 3.72 was released in April 2015 with a new auto-port selection algorithm from the USGS. Version 4.1 included a full sediment diagenesis model with bubble formation, new state variables such as CH_4 and H_2S, variable alkalinity, and variable sediment pH and temperature. Version 4.2 included a feature for running multiple waterbodies in series much faster than earlier model versions. Version 4.2.2 included an updated atmospheric CO_2 computation procedure. Some of the updates in Version 4.5 include updated modules for sediment diagenesis, ability to use C instead of organic matter, ammonia volatilization, atmospheric deposition, cyanobacteria vertical migration and toxin production.

The CE-QUAL-W2 model is well suited for the HCC reservoirs for the following reasons: Brownlee Reservoir is a long-deep density stratified system with pronounced longitudinal and vertical gradients in temperature and water quality; Oxbow and Hells Canyon Reservoirs also have strong longitudinal and vertical gradients in temperature and water quality; the effect of organic sediments on water quality can be simulated using sediment diagenesis; the shading algorithm can be used to evaluate how topographic shade affects water temperature; and the hydraulic structure algorithms will be used for the hydraulic outlet structures at each of the HCC Dams.

Model Bathymetry

The HCC model grids were developed from bathymetry data provided by Idaho Power Company (IPC). The bathymetric maps provided by IPC were integrated into Surfer to delineate model segments and layers. The process for developing the model grid from bathymetric data is as follows:

1. Obtain x-y-z digital bathymetry and import into GIS.
2. Obtain Digital Elevation Maps (DEMS) for surrounding area around lake or reservoir to integrate with bathymetry data.
3. Decide on the model layout of waterbodies and branches.
4. Digitize the thalweg for each model branch.
5. Create model segment centers from the thalweg at a given longitudinal grid spacing.
6. Create polygons around each model segment.
7. Develop the volume-elevation curve for each segment and compute the width then for each layer.
8. Adjust small segment widths for model stability with a minimum segment width of 10 m.

Brownlee Reservoir, Oxbow Reservoir, and Hells Canyon Reservoir model grid characteristics are listed in Table 1.

Table 1. Brownlee Reservoir, Oxbow Reservoir, and Hells Canyon Reservoir model grid characteristics.

Parameter	Brownlee	Oxbow	Hells Canyon
# of segments	239 (193 active mainstem 29 active Powder arm, 3 active inlet channel)	53 (51 active)	117 (115 active)
# of layers	102	57	81
# of branches	7	1	1
# of water bodies	5	1	1
Vertical grid spacing, Δz	1 m	1 m	1 m
Δx, longitudinal segment spacing	500.06 m (mainstem) or 503.05 m (Powder River Arm) or 60.05 m (inlet channel)	356.79 m	350.83 m except last 3 segments at dam (228.7 m, 78.97 m, 71.25 m)

Parameter	Brownlee	Oxbow	Hells Canyon
Length of Mainstem Branch	96.5 km (60 miles)	18.196 km (11.3 miles)	39.643 km (24.6 miles)
Elevation of bottom of grid	541.5 m	505 m	441 m
Elevation of top of grid	641.5 m	560 m	520 m
Manning's friction factor, n	WB1: 0.044 WB2: 0.044 WB3: 0.043 WB4: 0.042 WB5: 0.02	0.025	0.025

Brownlee Reservoir

Brownlee Reservoir was divided into 5 water bodies and 7 branches (Figure 3). The mainstem includes 5 model branches (Figure 4) that allow for the reservoir to transition into upstream riverine segments as the pool elevation drops. The turbine inlet channel at Brownlee Dam (Branch 7) was modeled using 3 segments that were 60.05 m in length (Figure 5). Figure 6 shows the upstream end of the Brownlee Reservoir grid, which begins at River Mile (RM) 345.6. Model segments along the reservoir from RM 345.6 to RM 284.6 (at the dam) are shown in Figure 7 through Figure 11. More detail of the grid in the vicinity of the dam is shown in Figure 12. Side views of the grid longitudinally and vertically are shown in Figure 13 and Figure 14 for Branch 5 (mainstem pool) and Branch 6 (Powder River arm), respectively. This volume-elevation curve agreed exactly with the bathymetric data of Brownlee Reservoir from IPC because the segment widths varying with depth were determined by exactly matching the bathymetric data. The volume-elevation curve for Brownlee Reservoir for the model grid is shown in Figure 15. Table 2 shows information about the segments in each branch and their connectivity to other branches.

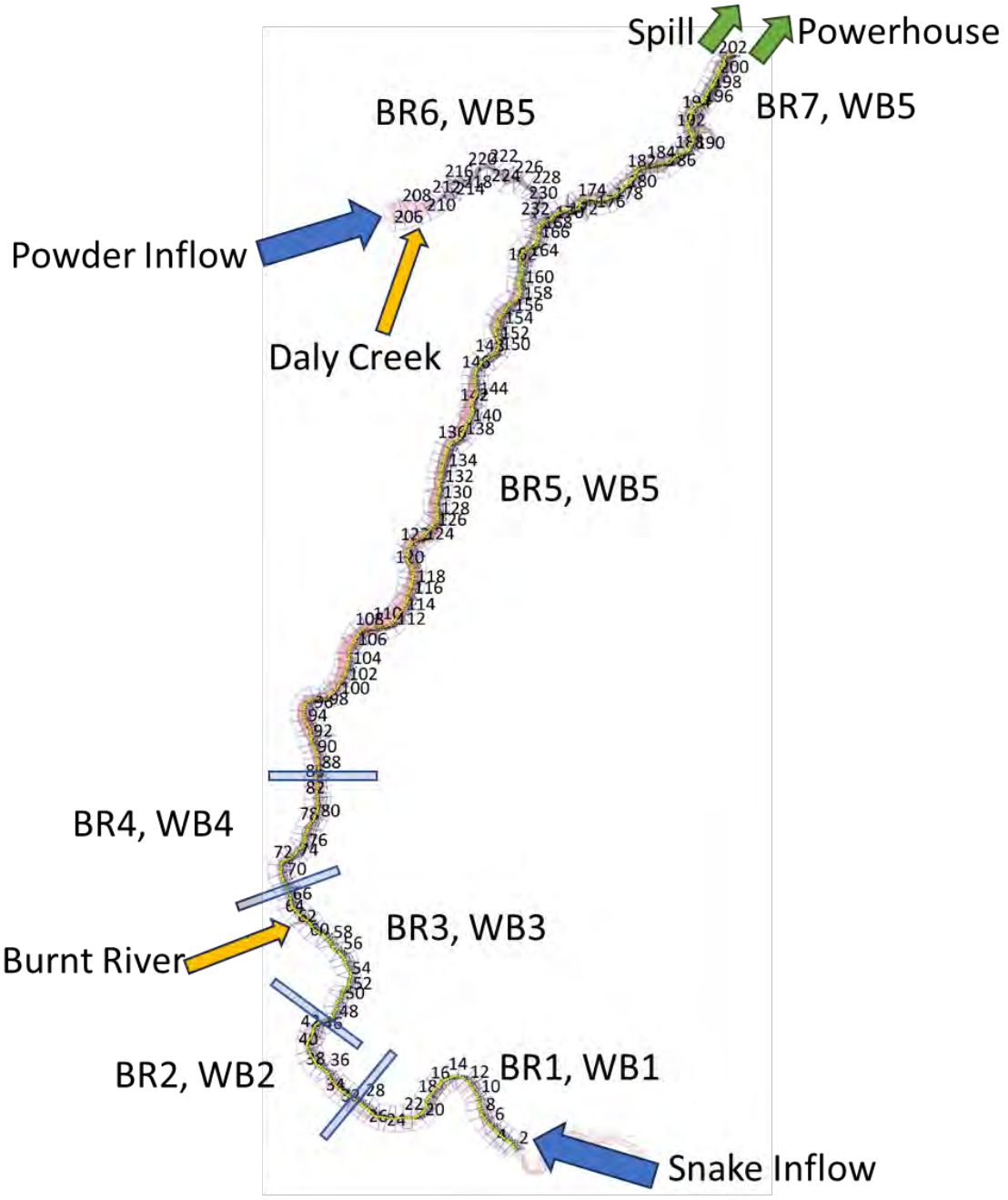


Figure 3. Brownlee Reservoir model grid segments, branches (BR), and water bodies (WB).

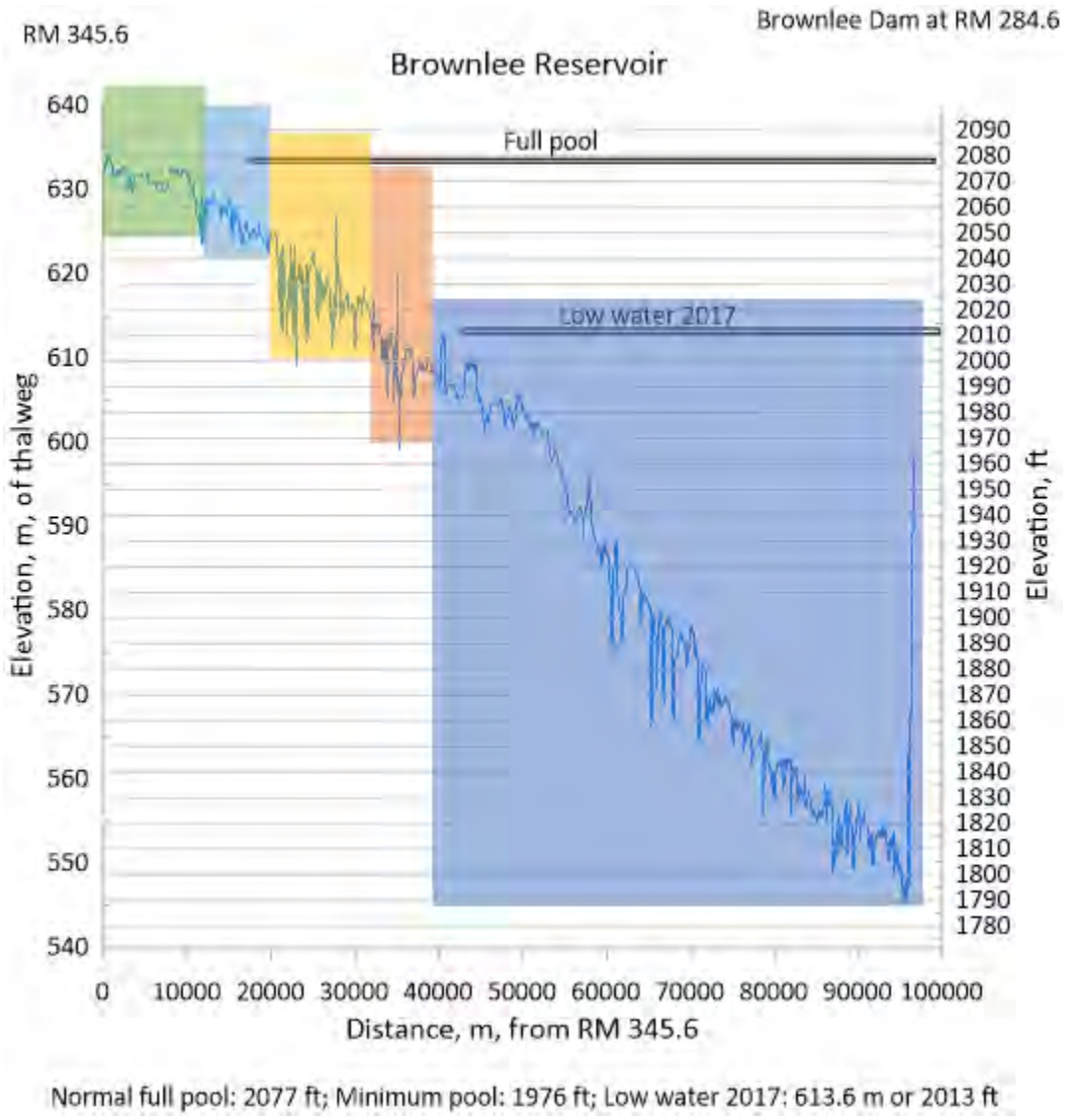


Figure 4. Mainstem branches of Brownlee Reservoir showing elevation along the channel bottom as a function of distance from RM 345.6. Branch 1 is in green; Branch 2 is in light blue; Branch 3 is in yellow, Branch 4 is in Orange, and Branch 5 is in darker blue.

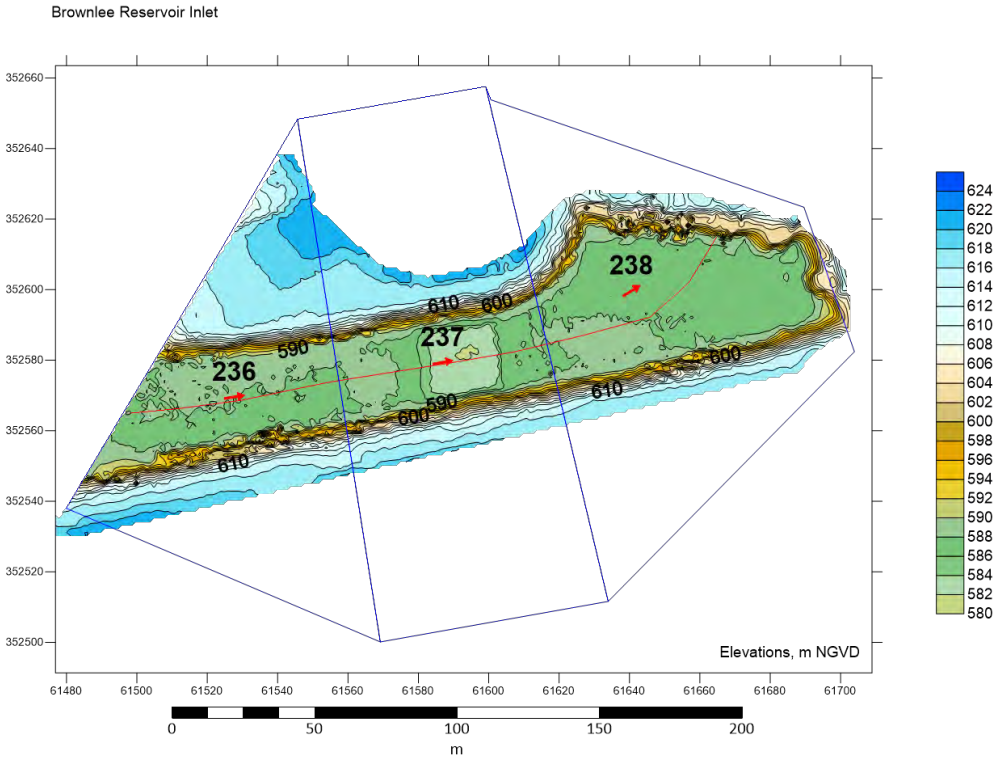


Figure 5. Brownlee Dam inlet channel bathymetry and model segments. This is Branch 7 in the model and was composed of segments 236, 237 and 238 (next to the powerhouse intakes).

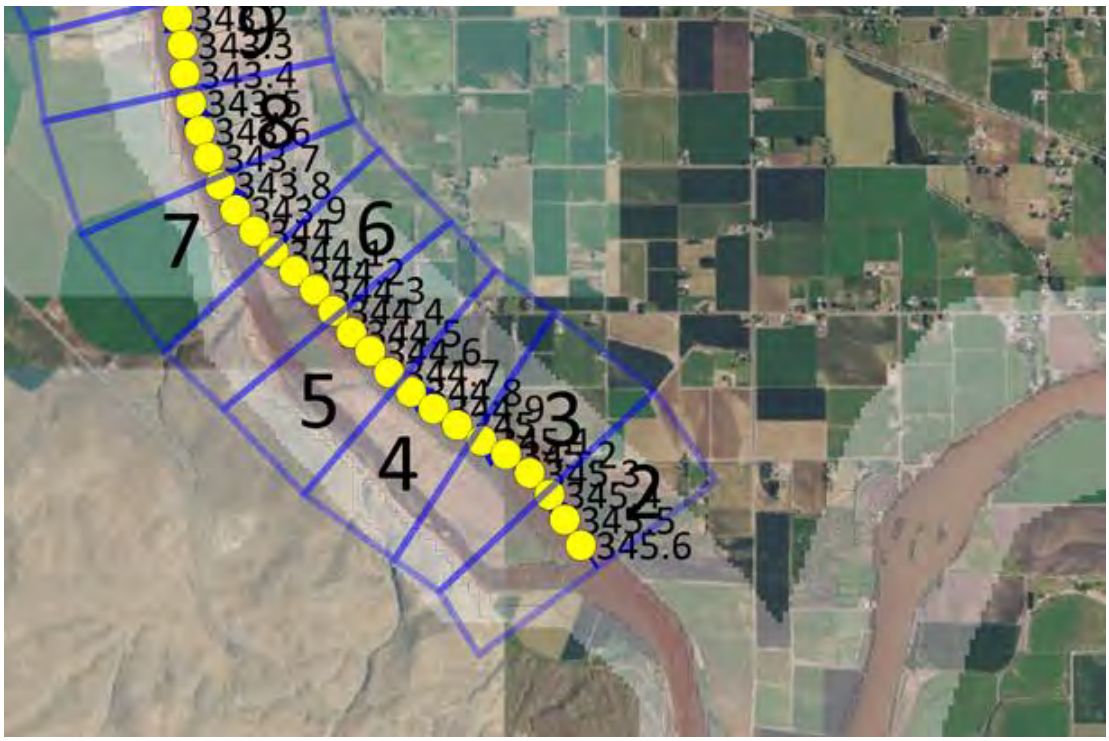


Figure 6. Upstream end of Brownlee River grid. Polygons and large numbers define model segments. Segment 2 begins at RM 345.6. The yellow dots are RM designations from Idaho Power.

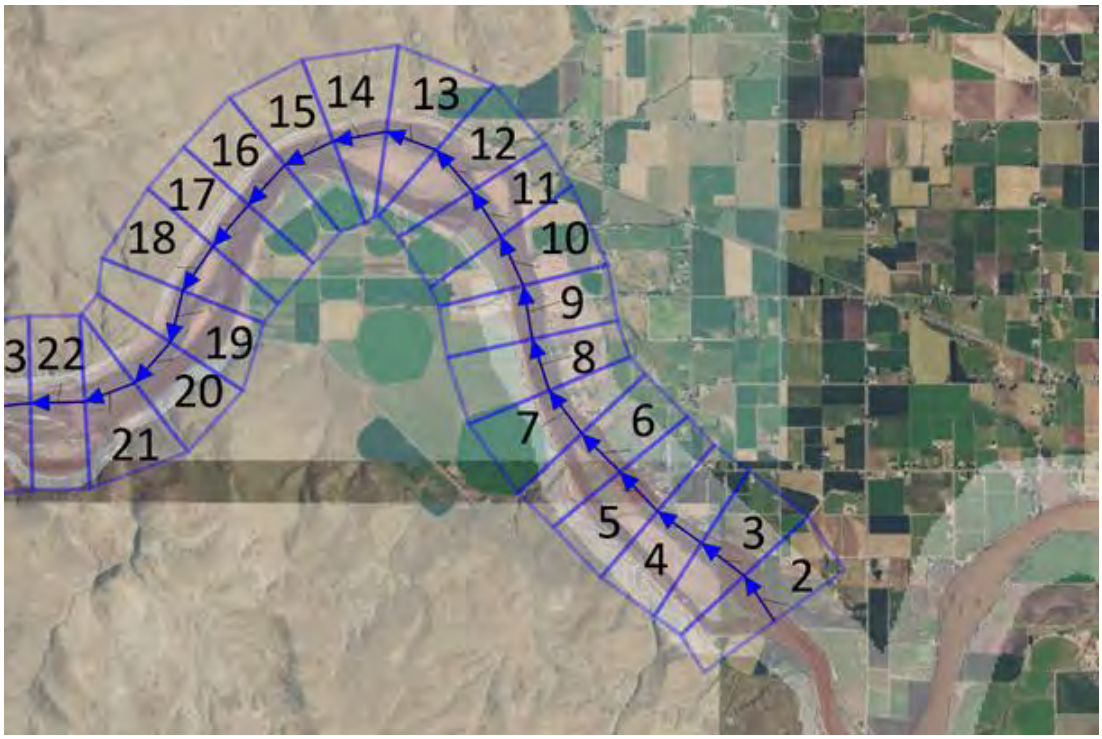
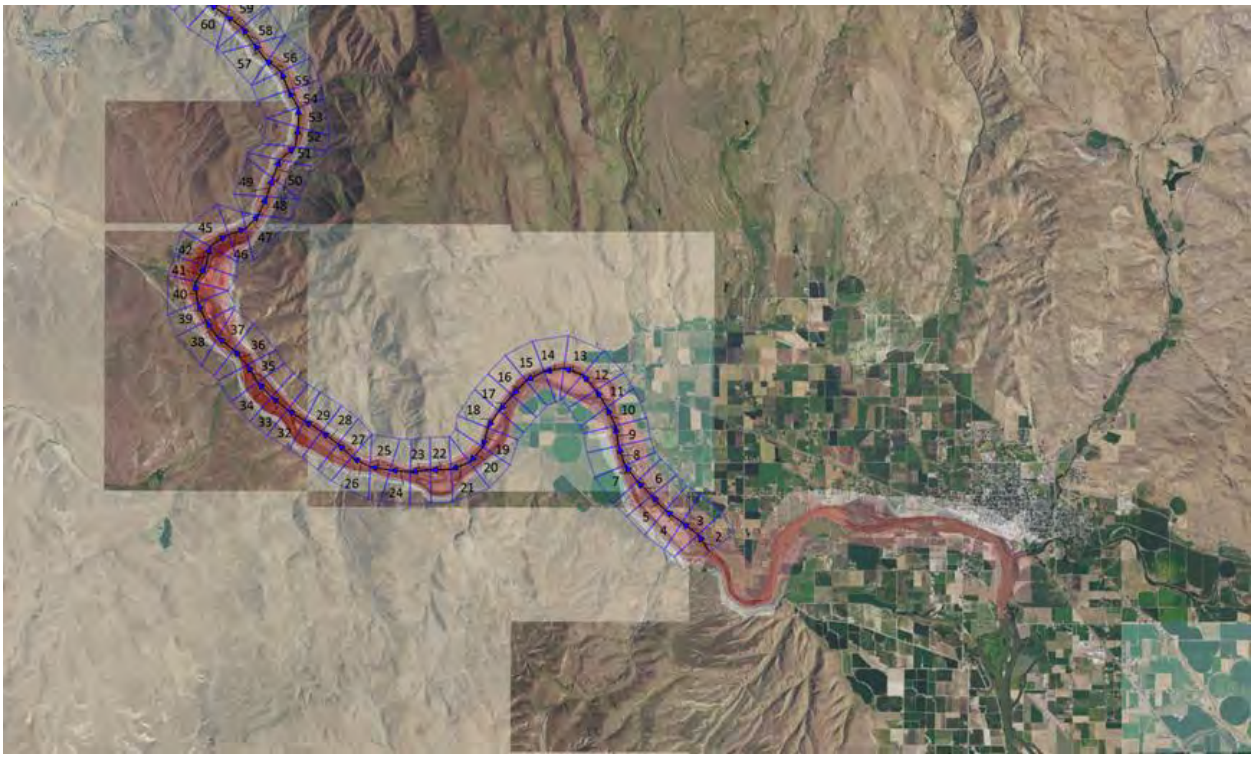


Figure 7. Brownlee Reservoir model segments 2 through 22.


Figure 8. Brownlee Reservoir model segments 2 through 58.

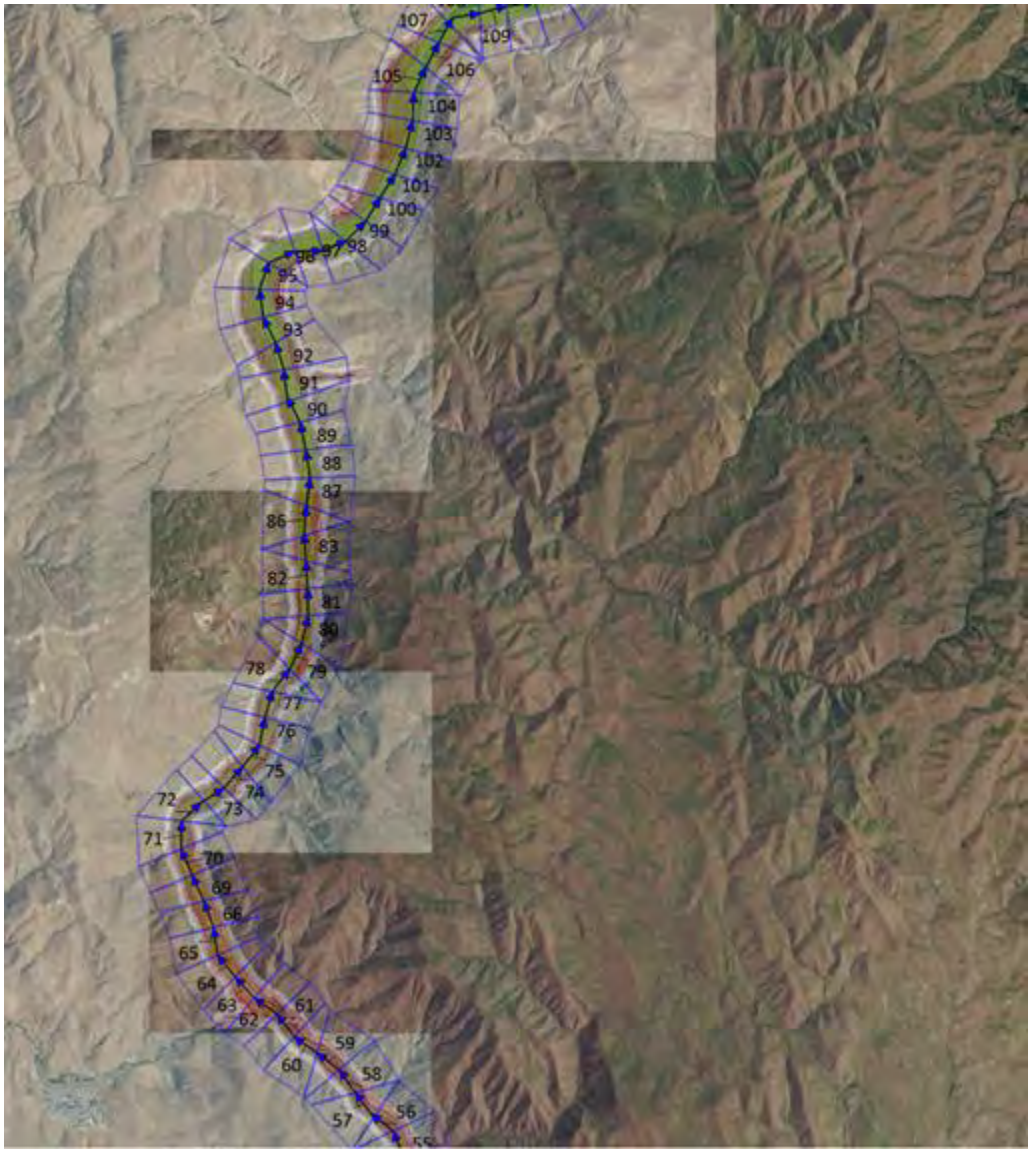


Figure 9. Brownlee Reservoir model segments 56 through 107.

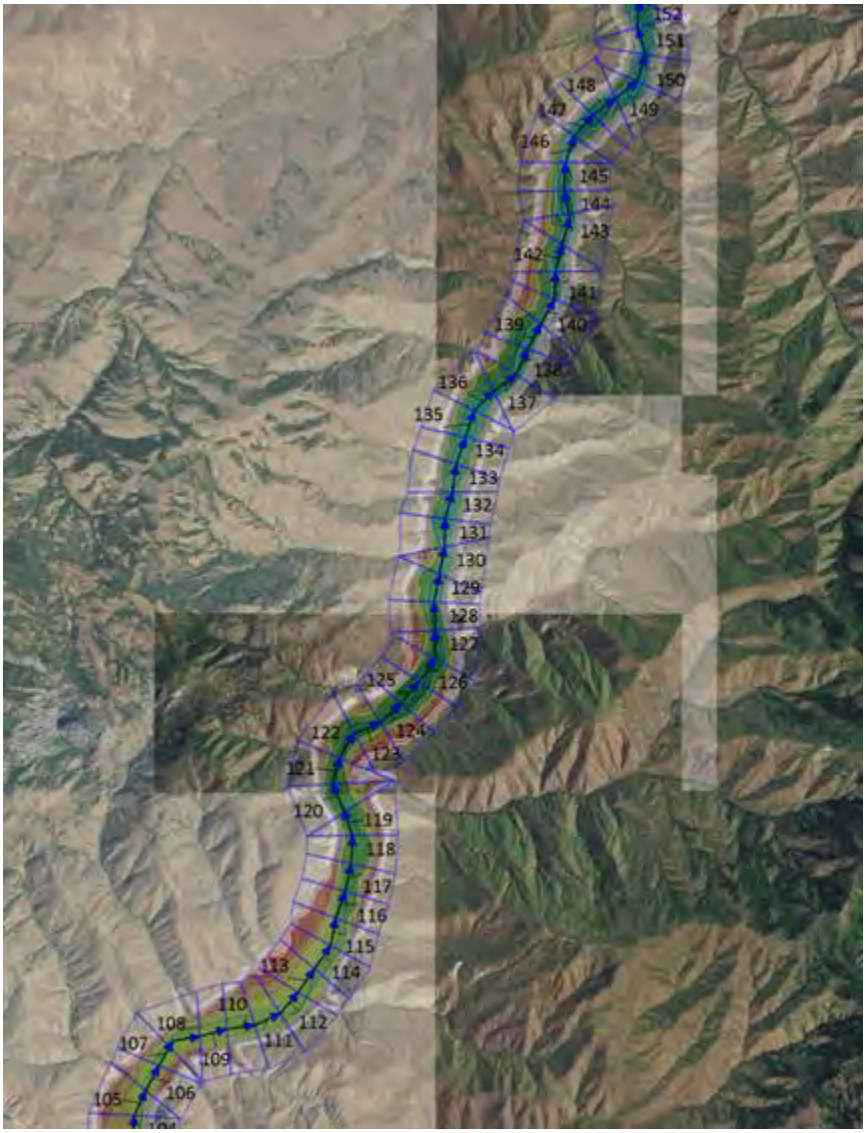


Figure 10. Brownlee Reservoir model segments 105 through 152.

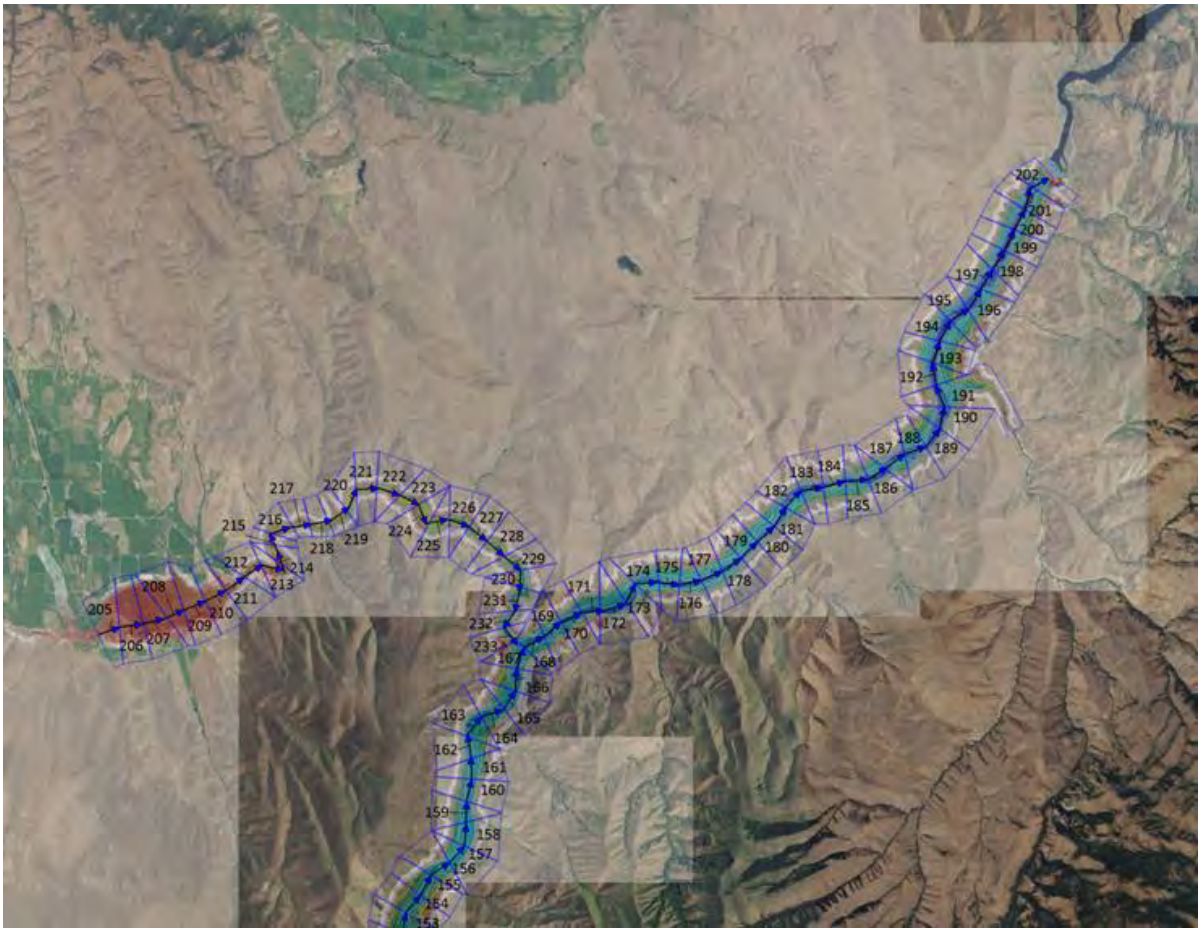


Figure 11. Brownlee Reservoir model segments 153 through 238. The Powder arm branch (BR6) includes segments 205 through 233. Segments 236 to 238 are the outlet channel segments (BR7) that are barely visible near the dam.

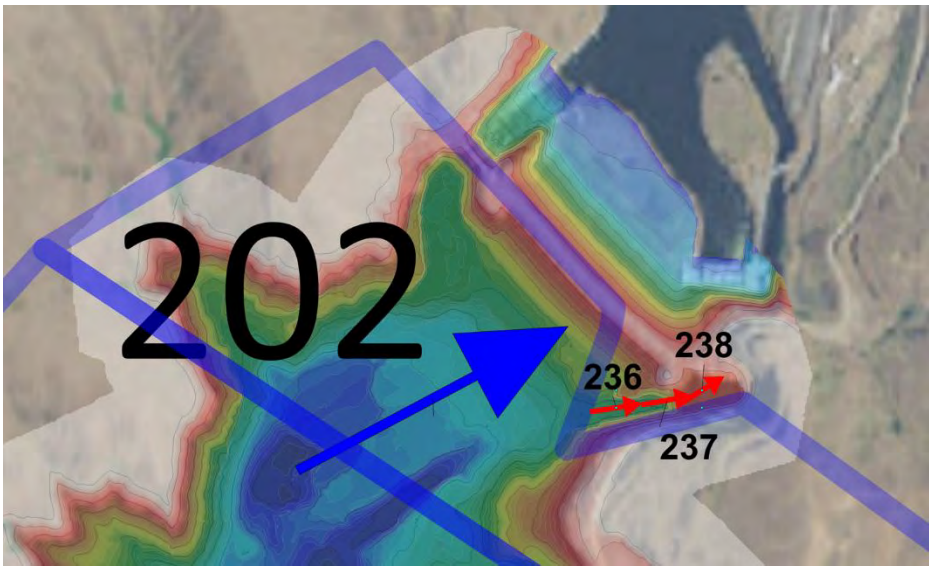


Figure 12. Segments for the outlet channel (236-238) in Branch 7 are shown relative to the dam and the last segment in the mainstem (segment 202) in Branch 5.

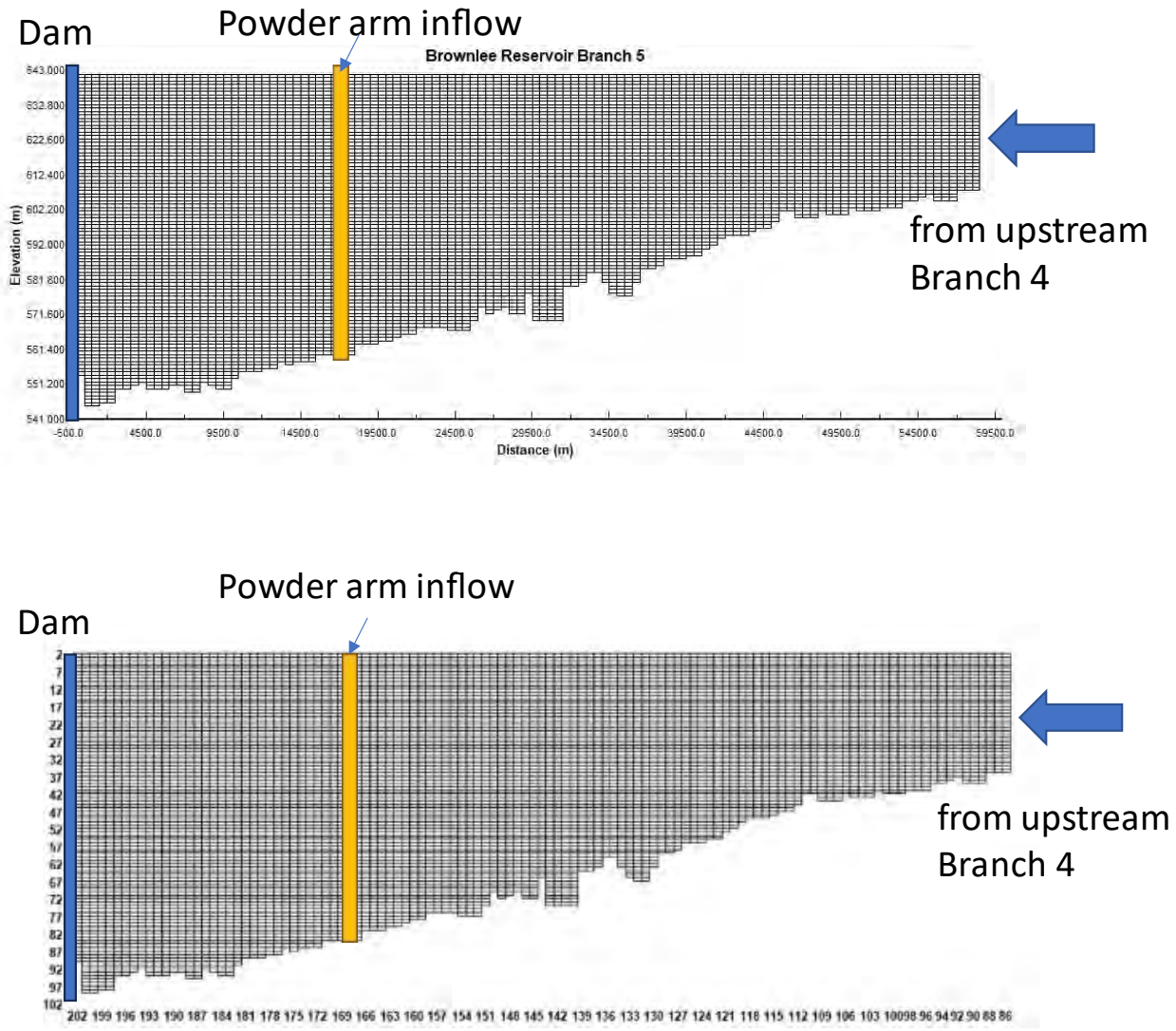


Figure 13. Branch 5 side view for Brownlee Reservoir from model segment 86 to the dam at segment 202. Vertical layer spacing is 1 m, and longitudinal segment spacing is 500.06 m. The first figure shows elevations and distances in m and the second figure shows layers and segment numbers.

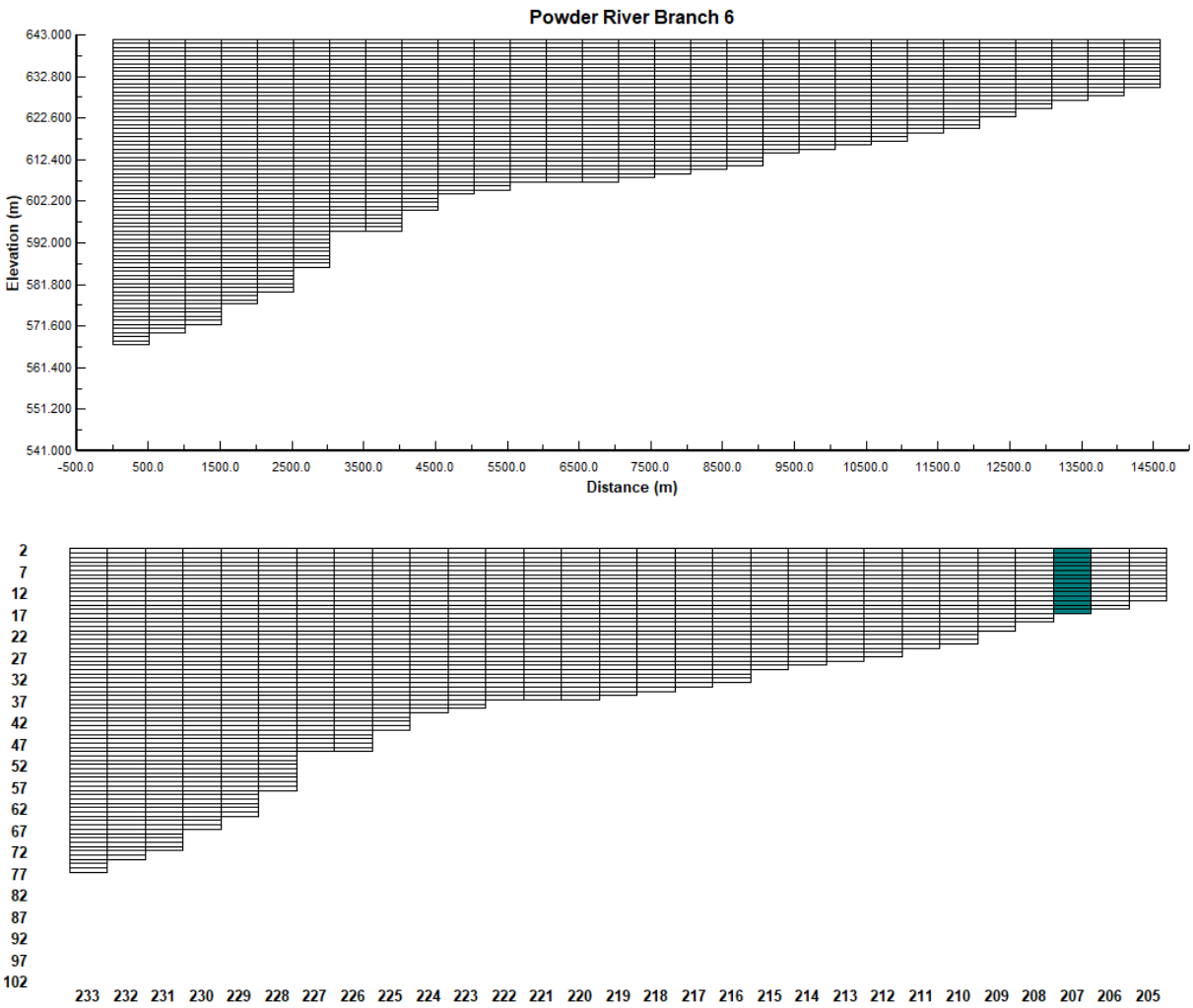


Figure 14. Branch 6 side view for Brownlee Reservoir (Powder River) from model segment 205 to the intersection with the Snake River mainstem at segment 233. Vertical layer spacing is 1 m, and longitudinal segment spacing is 503.05 m. The first figure shows elevations and distances in m and the second figure shows layers and segment numbers.

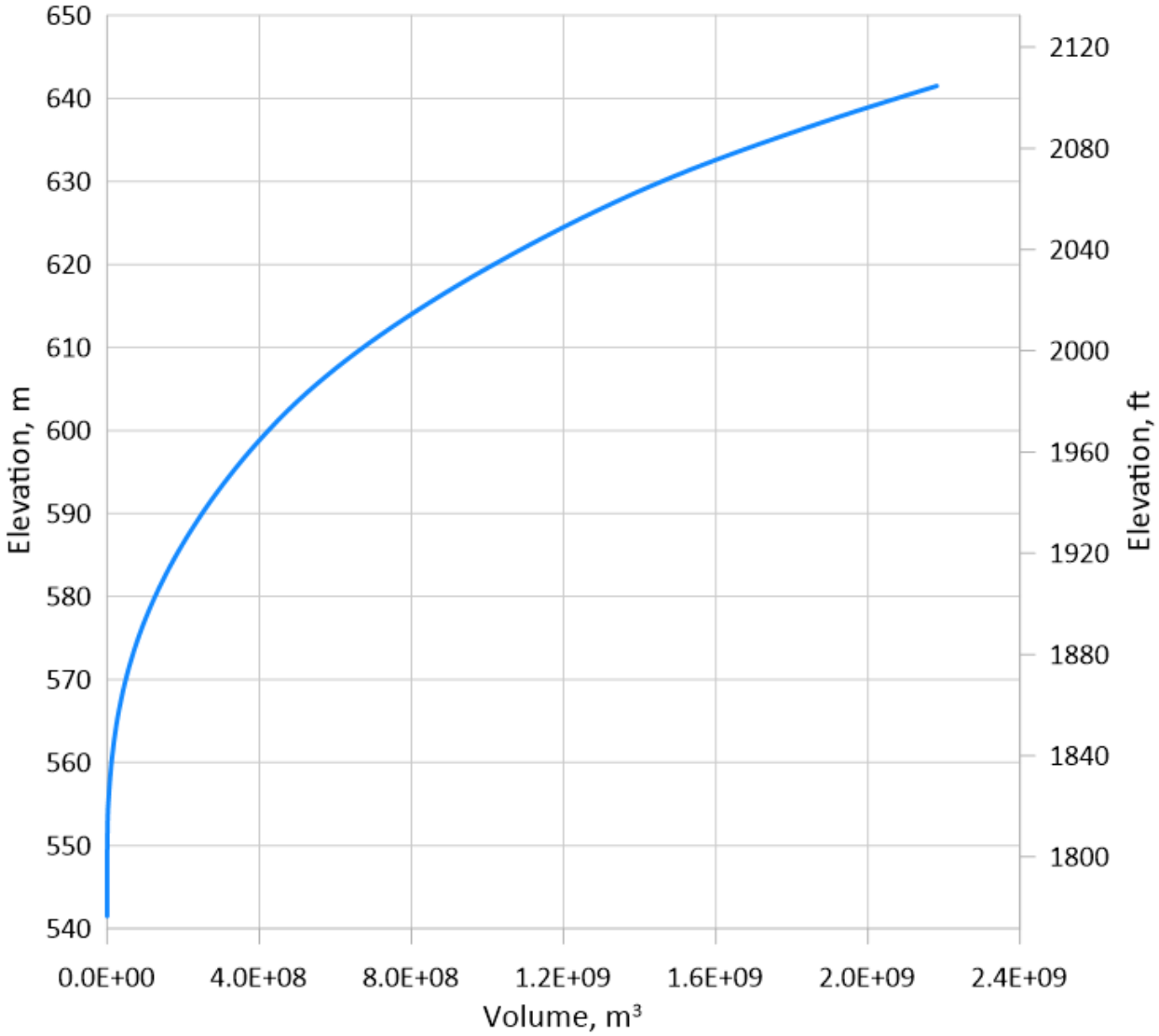


Figure 15. Volume-elevation curve for Brownlee Reservoir.

Table 2. Brownlee grid branch information.

Branch #	Segment lengths, m	Start segment	End segment	Downstream (DS) or upstream (US) segment connection	Distance of branch, km (miles)
1	500.06	2 (RM 345.6)	29	32 DS	14 (8.7)
2	500.06	32	42	45 DS	5.5 (3.4)
3	500.06	45	66	69 DS	11 (6.8)
4	500.06	69	83	86 DS	7.5 (4.7)
5	500.06	86	202 (RM 284.6, Dam)	-	58.5 (36.4)

Branch #	Segment lengths, m	Start segment	End segment	Downstream (DS) or upstream (US) segment connection	Distance of branch, km (miles)
6	503.05	205	233	167 DS	14.6 (9)
7	60.05	236	238	202 US	.2 (0.1)

Oxbow Reservoir

The Oxbow Reservoir model grid includes 51 active segments, with 1 water body and 1 branch (Figure 16). The segment start at segment 2 and end at segment 52 at the dam. Each segment has a length of 356.79 m. Figure 17 shows a side view of the grid showing the longitudinal segments and vertical layers of Oxbow Reservoir model cells. Figure 18 shows the volume-elevation curve for Oxbow Reservoir for the model grid.

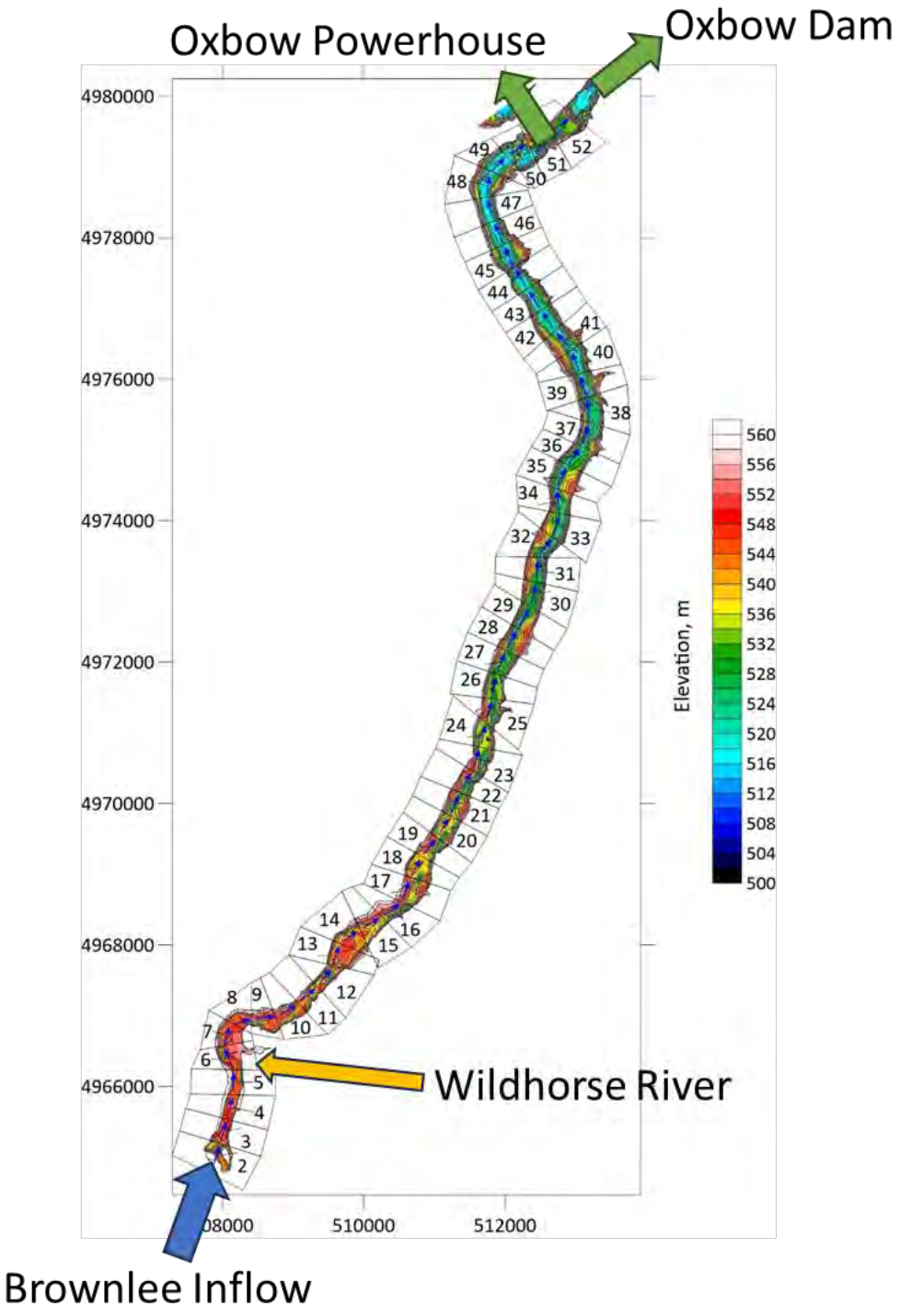


Figure 16. Oxbow Reservoir model segments.

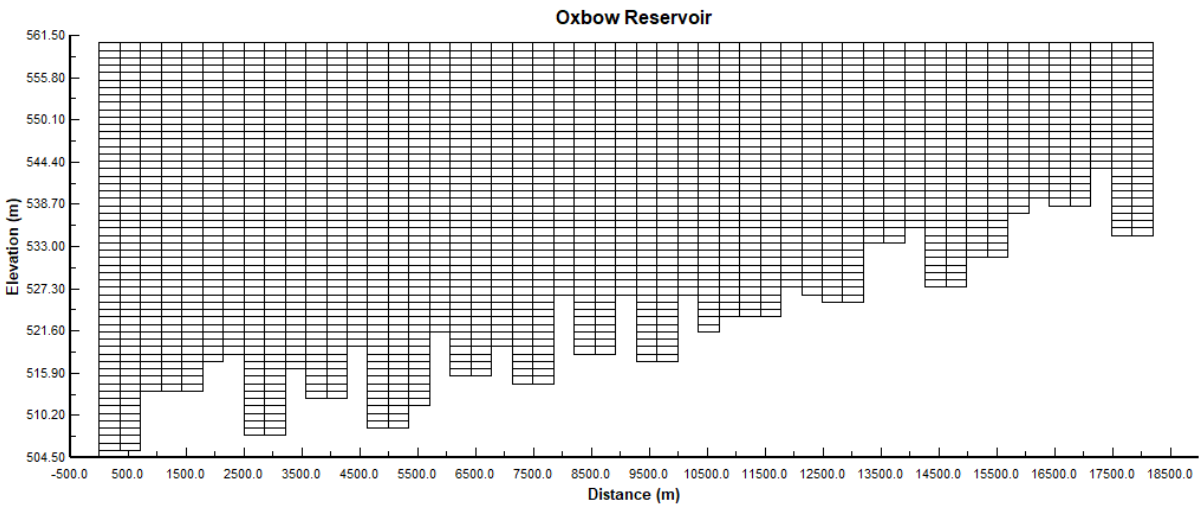


Figure 17. Side view of model segments starting at 2 (on the right) and ending at segment 52 (on the left) for Oxbow Reservoir.

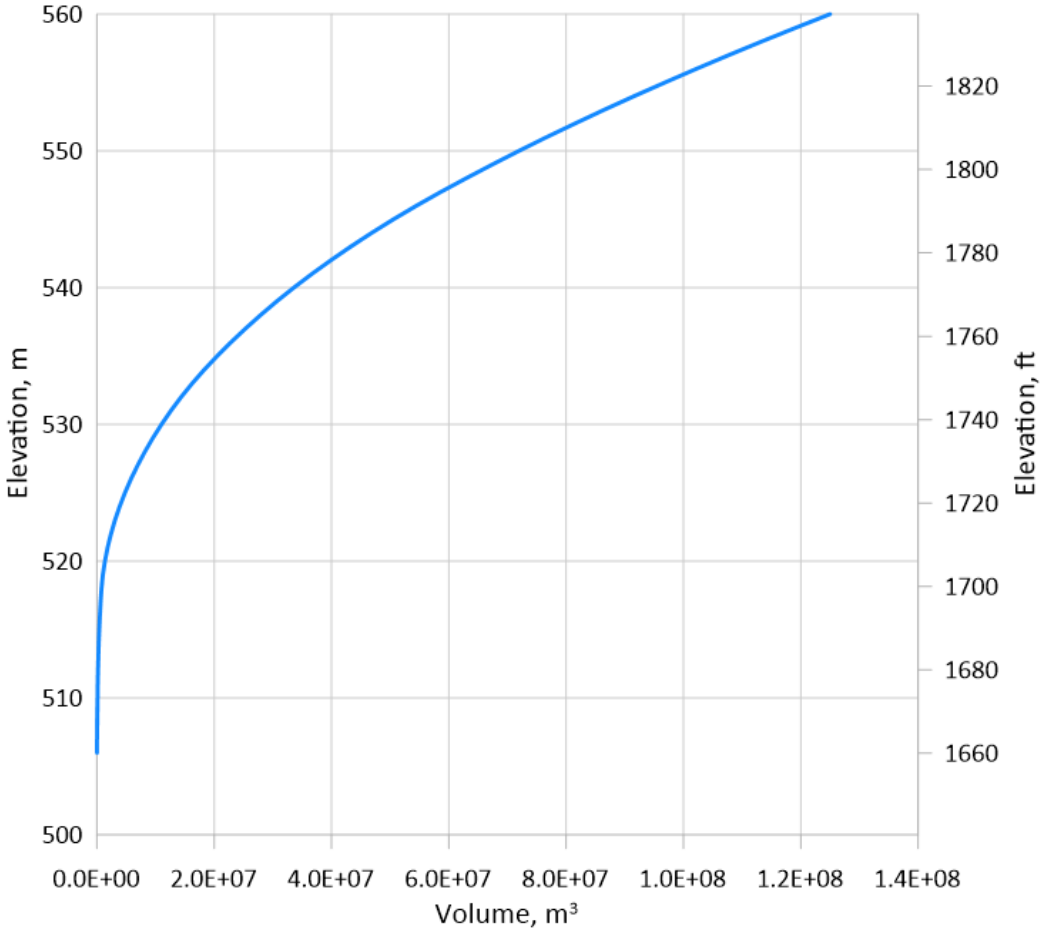


Figure 18. Volume-elevation curve for Oxbow Reservoir.

Hells Canyon Reservoir

Figure 19 shows the Hells Canyon Reservoir model segments from segment 2 to segment 116. The segments are 350.83 m long, except for 3 segments near the dam (segments 114, 115, and 116), which were 228.7 m, 79 m, and 71 m to account for the effects of an old coffer dam (Figure 20). A side-view of the model grid showing the longitudinal segments and vertical layers is shown in Figure 21. The volume-elevation curve for Hells Canyon Reservoir is shown in Figure 22.

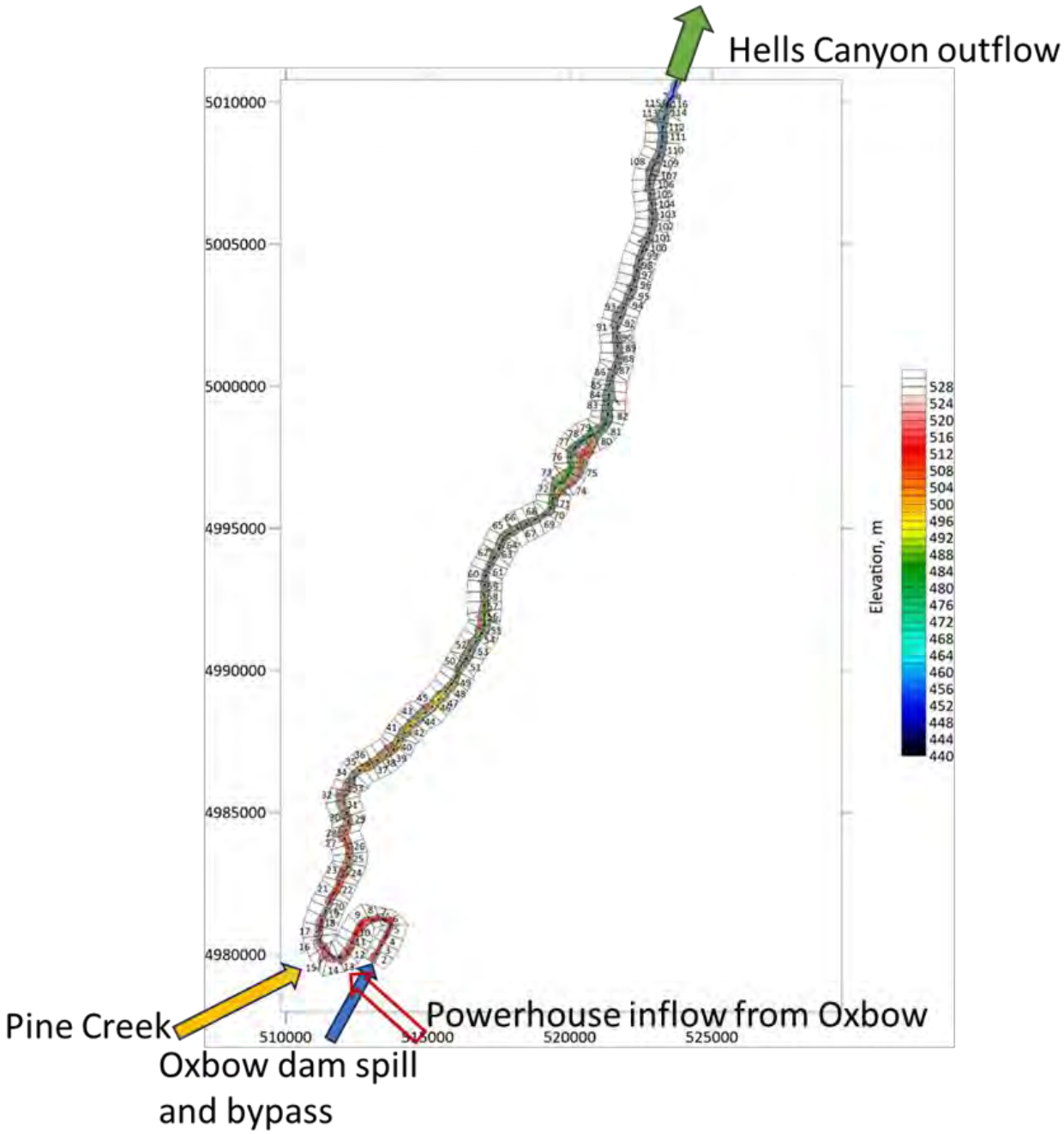


Figure 19. Hells Canyon model segments.

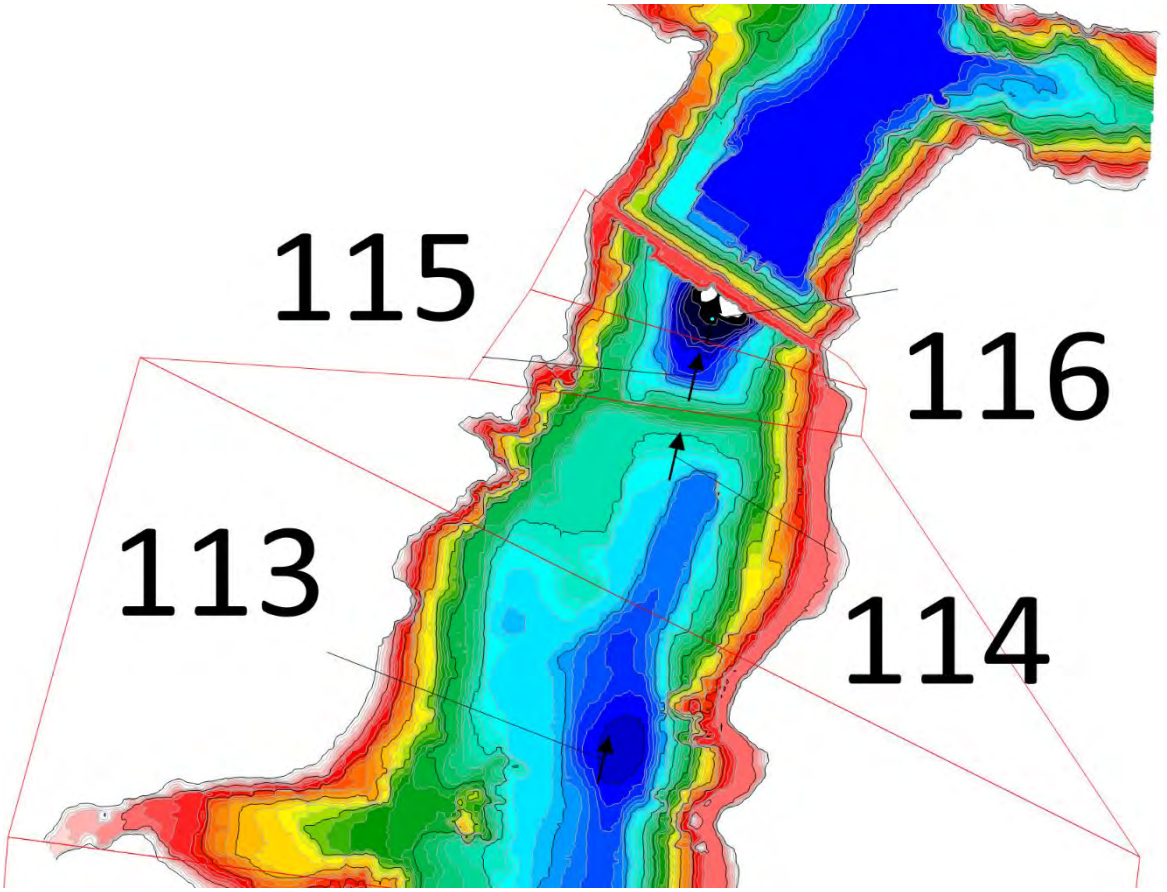


Figure 20. Hells Canyon Reservoir models segments near dam. All segments are a length of 350.83 m except segments 114 through 116, which are 228.7 m, 79 m, and 71 m to simulate the effects of an old coffer dam. The elevation of the crest between segment 114 and 115 is about 479 m.

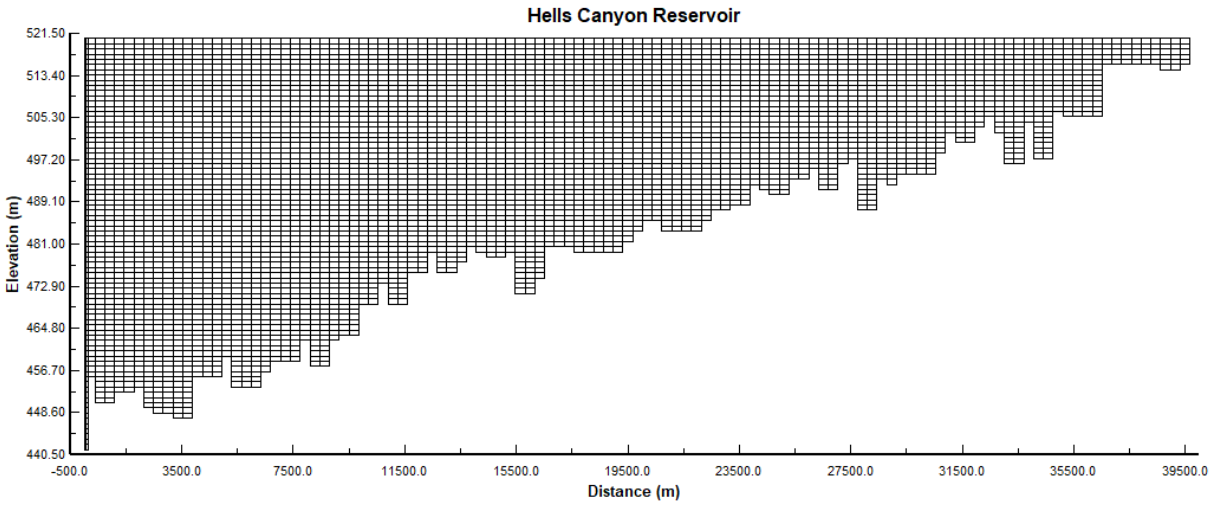


Figure 21. Side view of model segments starting at 2 (on the right) and ending at segment 116 (on the left) for Hells Canyon Reservoir.

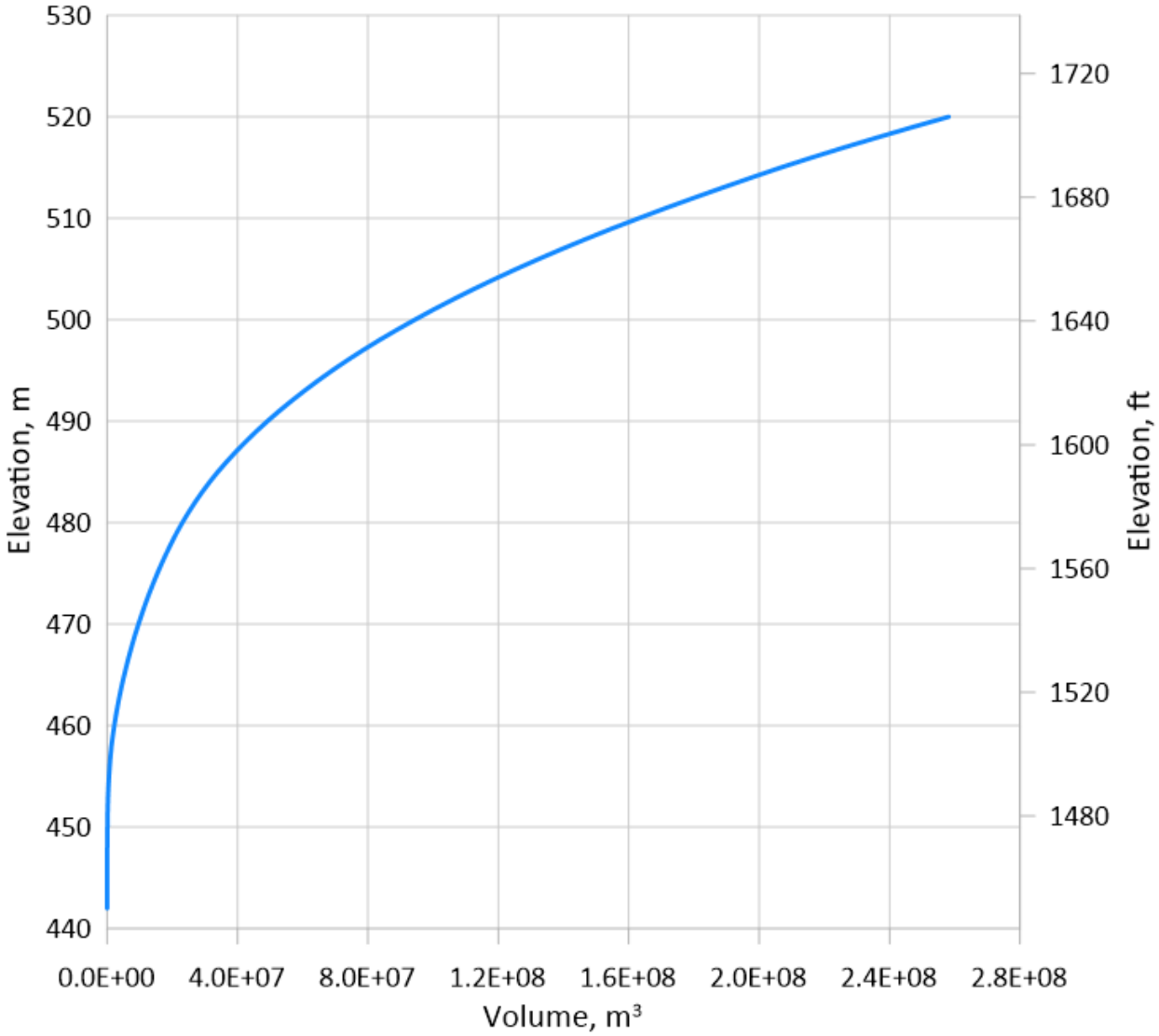


Figure 22. Volume-elevation curve for Hells Canyon Reservoir.

Meteorological Inputs

Brownlee Reservoir

Meteorological inputs for the Brownlee Reservoir model were developed from predictions of the WRF-NAM model (Fisher, 2021), USGS wind speed data collected on the surface of Brownlee Reservoir, and IPC meteorological data measured at Brownlee Dam. CE-QUAL-W2 requires air temperature, dew point temperature, wind speed, wind direction, solar radiation, and cloud cover. Cloud cover was back-calculated using short wave solar data. The available sources of measured data and model predictions for meteorological inputs are listed in Table 3.

USGS wind speed data were available for specific periods during 2017-2019 (Table 4). The locations of the USGS wind speed stations are shown in Figure 23.

The WRF-NAM model predictions of air temperature, relative humidity, wind speed, wind direction, solar radiation were available beginning on 5/11/2014 (Julian Day 131). The locations of the WRF-NAM predictions are shown in Figure 24. WRF-NAM solar radiation predictions were used in all meteorological inputs after 5/11/2014. Other WRF-NAM predictions were used for upper Brownlee Reservoir model water bodies and to fill in gaps of IPC Brownlee Dam meteorological data and USGS wind speed data. Before 5/11/2014, the Ontario Agrimet station measurements were used for solar radiation and dew point temperature inputs, while Brownlee Dam data were used for air temperature, wind speed, and wind direction.

The Brownlee Reservoir model is divided into 5 water bodies (Figure 25), and one meteorological input file can be specified per water body. Currently for the lower water body of Brownlee Reservoir (water body 5), IPC Brownlee Dam air temperature, wind speed, and wind direction data were used when available. The Brownlee meteorological station at the dam is shown in Figure 26. Gaps in air temperature, dew point temperature, wind speed, and wind direction, and solar radiation were filled using WRF-NAM RM 286 predictions.

For the water bodies 1 through 4 of the Brownlee model, WRF NAM predictions of air temperature, relative humidity, wind direction and wind speed were used after 5/11/2014 (as noted above, Ontario Agrimet data were applied before 5/11/2014). USGS wind speed data measured at RM 318 in 2018 were used when available.

Table 3. Available sources of measured data and model predictions for Brownlee Reservoir meteorological inputs.

Station Description	Type	Parameters	Source
Brownlee Dam	Measurements	air temperature, wind direction, wind speed	IPC
USGS RM 286	Measurements	wind speed	USGS
USGS RM 300	Measurements	wind speed	USGS
USGS RM 318	Measurements	wind speed	USGS
Snake River near river mile 286 above Brownlee Dam, ID	Model Predictions	air temperature, relative humidity, wind speed, wind direction, solar radiation	IPC
Snake River near river mile 300 above Brownlee Dam, ID	Model Predictions	air temperature, relative humidity, wind speed, wind direction, solar radiation	IPC
Snake River near river mile 310 above Brownlee Dam, ID	Model Predictions	air temperature, relative humidity, wind speed, wind direction, solar radiation	IPC

Station Description	Type	Parameters	Source
Snake River near river mile 318 above Brownlee Dam, ID	Model Predictions	air temperature, relative humidity, wind speed, wind direction, solar radiation	IPC
Ontario Agrimet (ONTO)	Measurements	air temperature, dew point temperature, wind speed, wind direction, solar radiation	USBR

Table 4. Time periods when USGS wind speed data were available for Brownlee Reservoir.

USGS Station	Year	Start Date	End Date
RM 286	2017	6/5/17	11/16/17
	2018	3/22/18	10/16/18
	2019	6/13/19	1/7/20
RM 300	2017	6/5/17	11/16/17
	2018	3/21/18	10/16/18
	2019	7/2/19	12/22/19
RM 318	2018	3/21/18	10/16/18
	2019	7/2/19	1/8/20

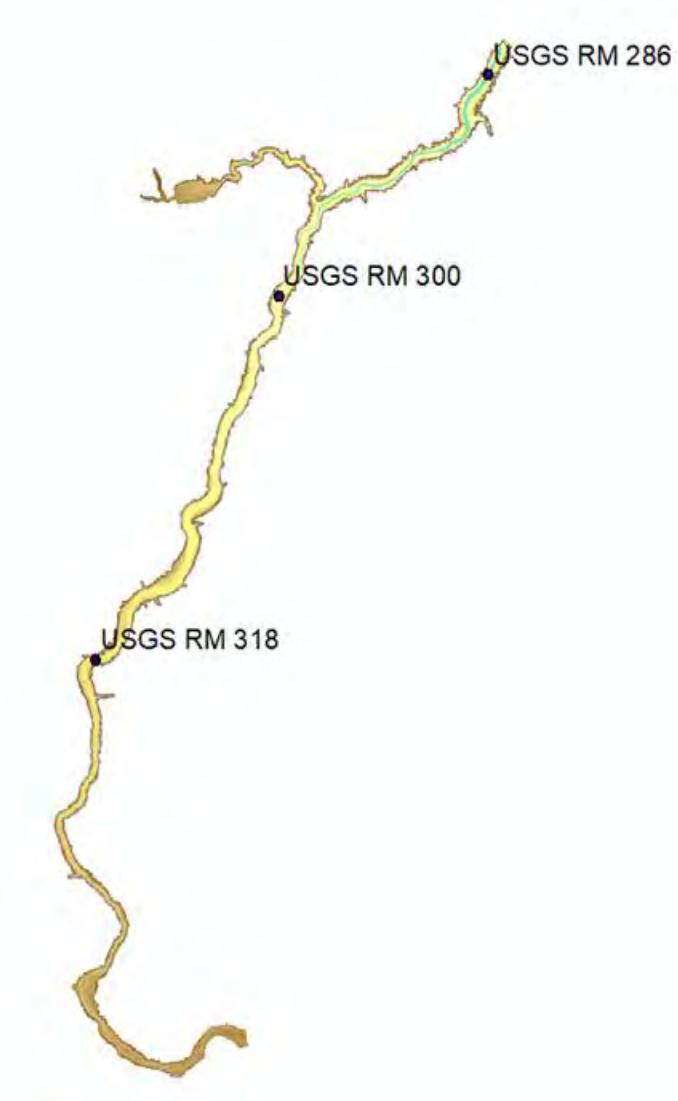


Figure 23. Locations of USGS wind speed measurement stations.

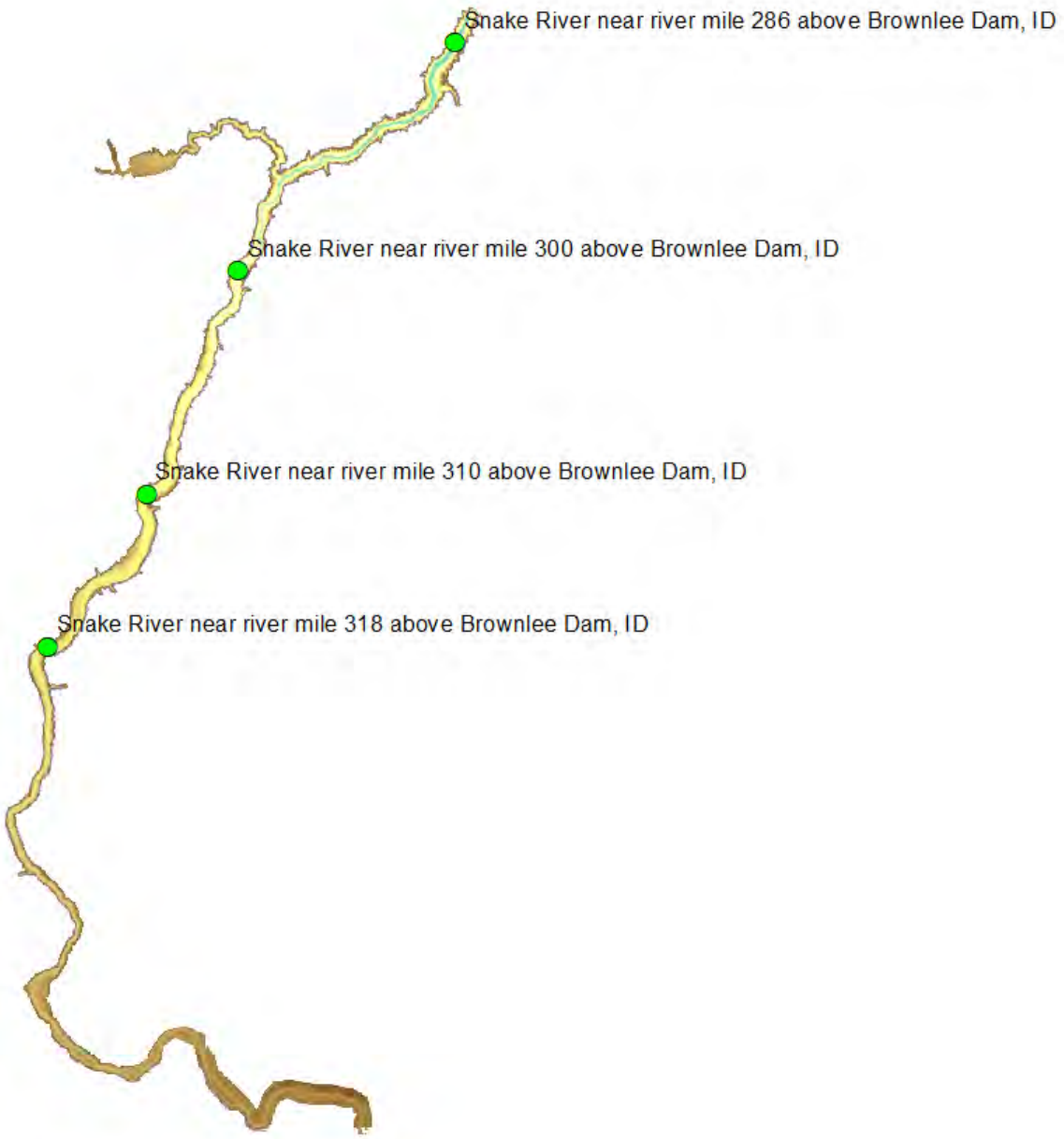


Figure 24. Locations of WRF-NAM meteorological predictions in Brownlee Reservoir.

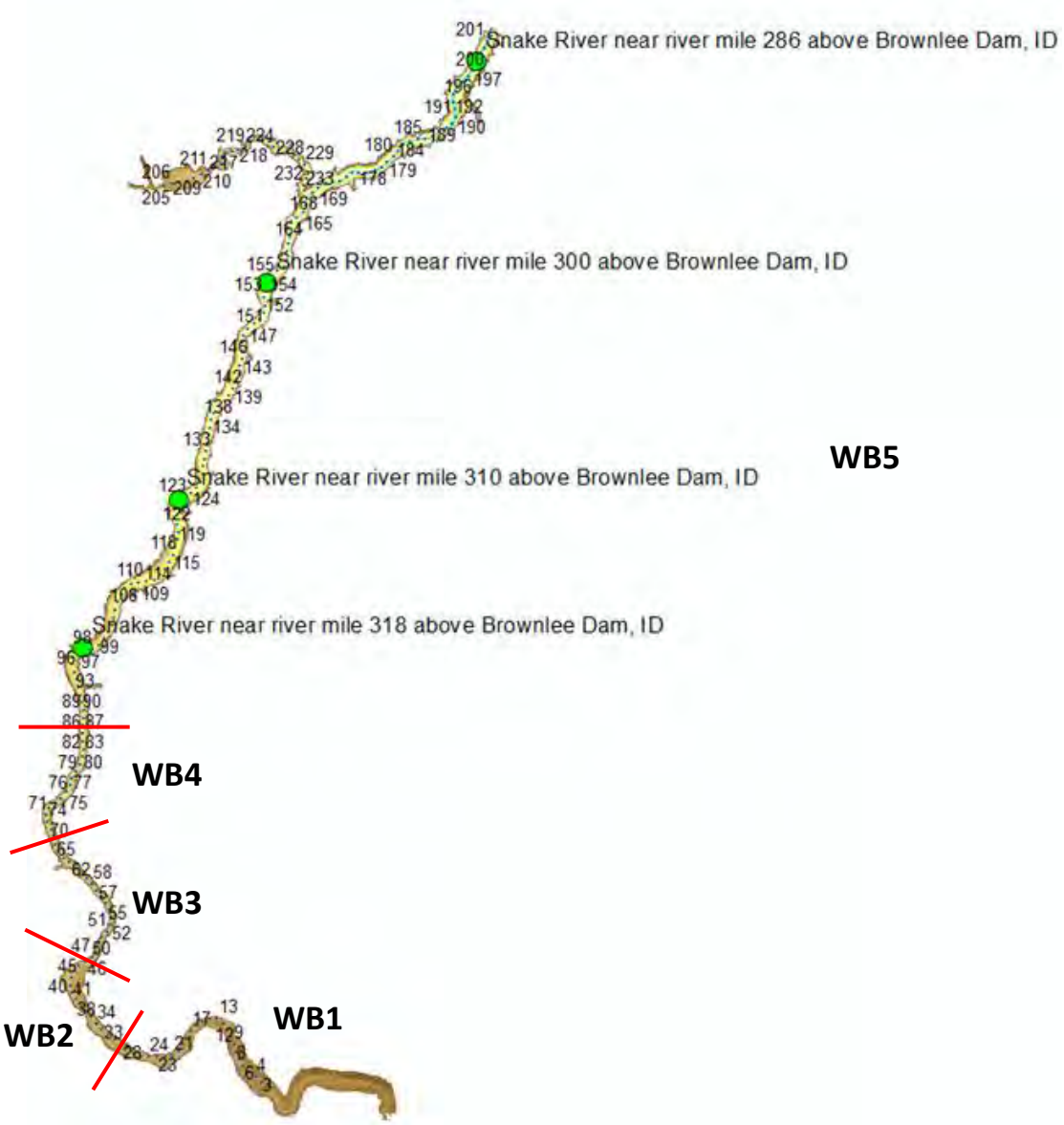


Figure 25. Brownlee Reservoir model water bodies. One meteorological input file can be used per water body in the CE-QUAL-W2 model.

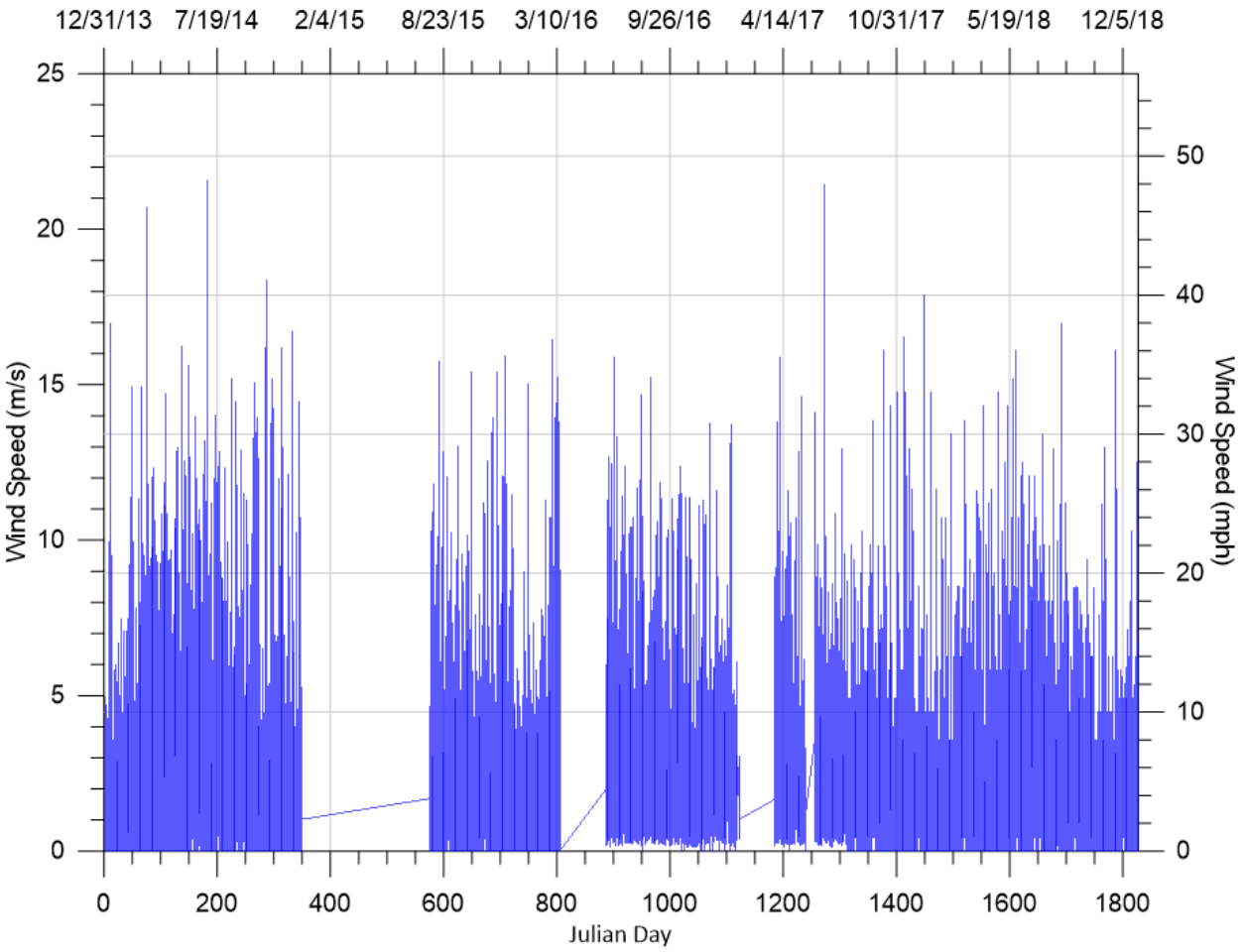


Figure 26. Wind speed measurement at Brownlee dam from IPC. The station is at an elevation of 2090 ft.

Air temperatures used for model inputs are shown in Figure 27 for waterbodies 1-4 and in Figure 28 for waterbody 5. Dew point tempreatures were calculated using WRF-NAM predictions of relativity humidity from (Singh, 1992):

$$\text{Dew Point Temperature} = (\text{RH}/100)^{1/8} \times (112 + 0.9T) - 112 + 0.1T$$

Where

T: Air temperature, C

RH: Relative Humidity, %

Figure 29 and Figure 30 show the modeled dew point temperatures for waterbodies 1-4 and waterbody 5, respectively.

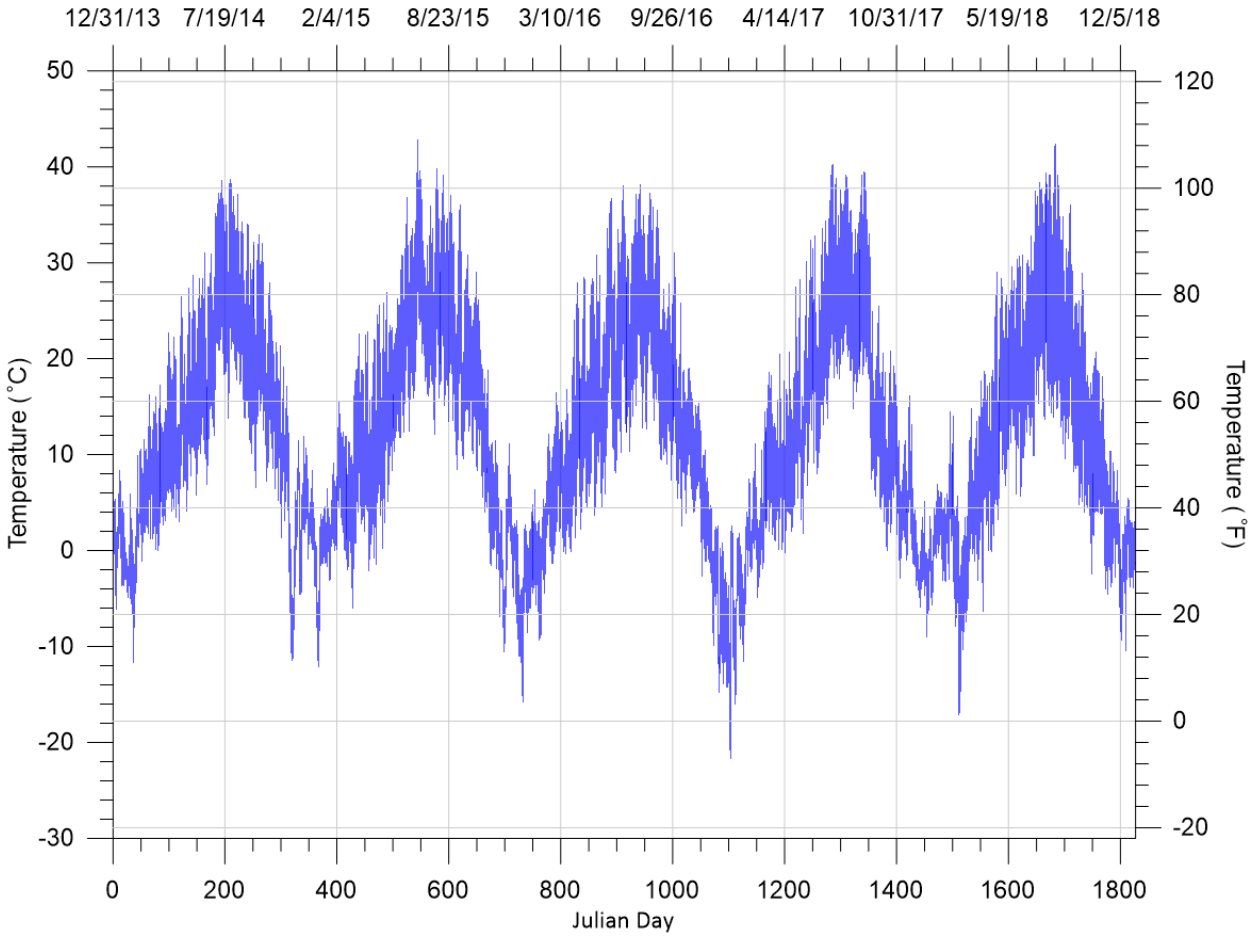


Figure 27. Air temperature inputs for water bodies 1 through 4 of the Brownlee Reservoir model.

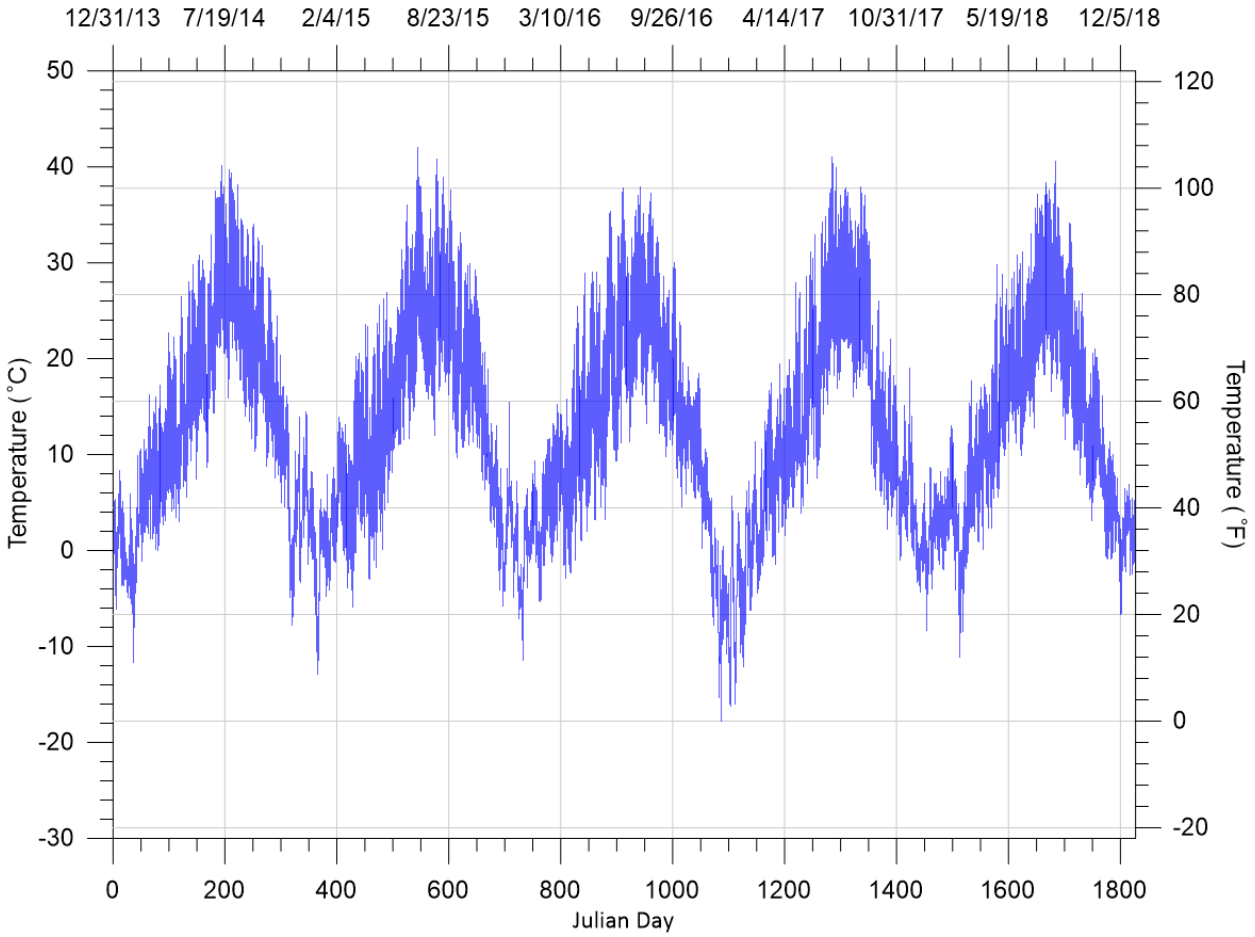


Figure 28. Air temperature inputs for water body 5 of the Brownlee Reservoir model.

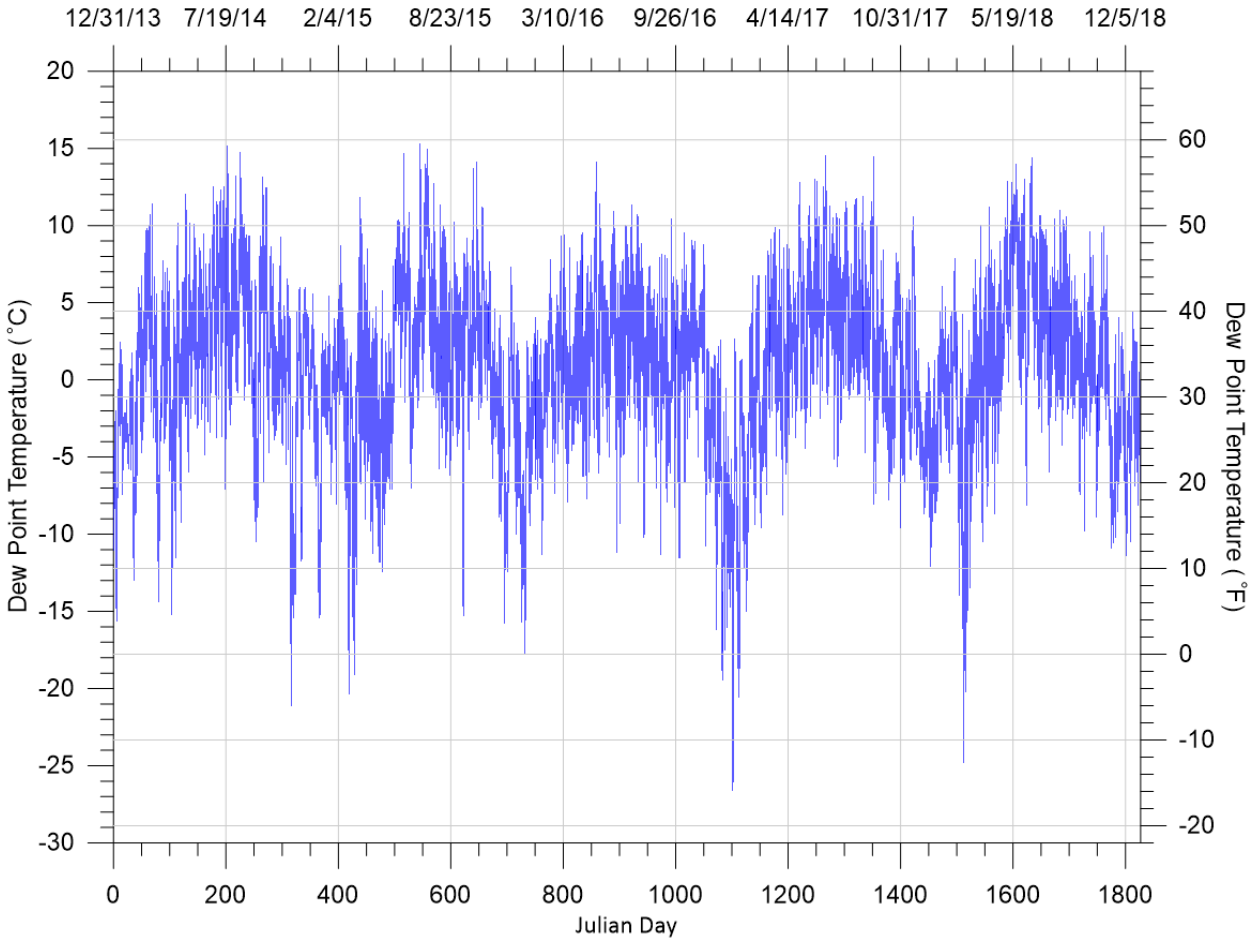


Figure 29. Dew point temperature inputs for water bodies 1 through 4 of the Brownlee Reservoir model.

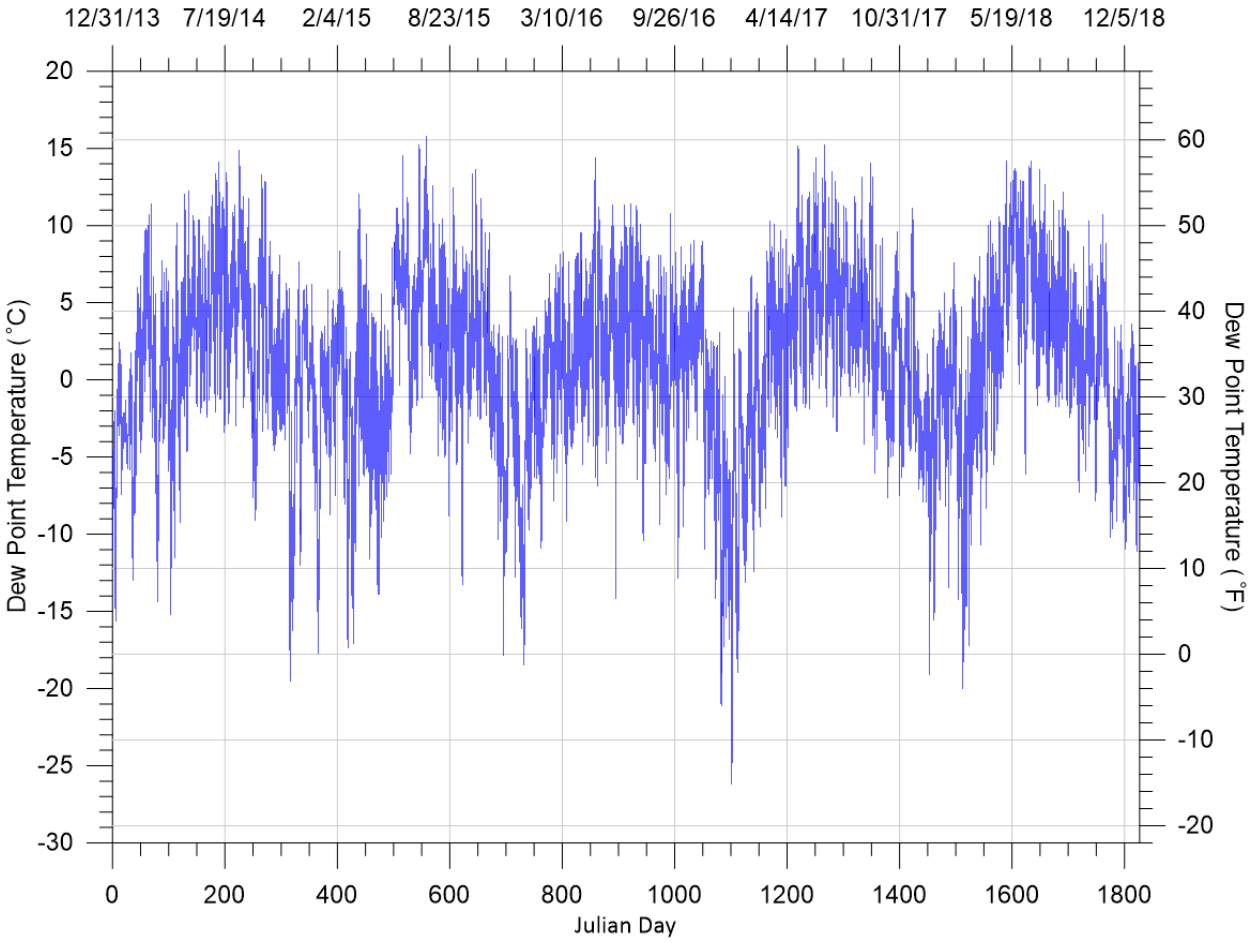


Figure 30. Dew point temperature inputs for water body 5 of the Brownlee Reservoir model.

Wind speed inputs are shown in Figure 31 and Figure 32, respectively. Rose diagrams illustrating wind direction at the two locations are shown in Figure 33.

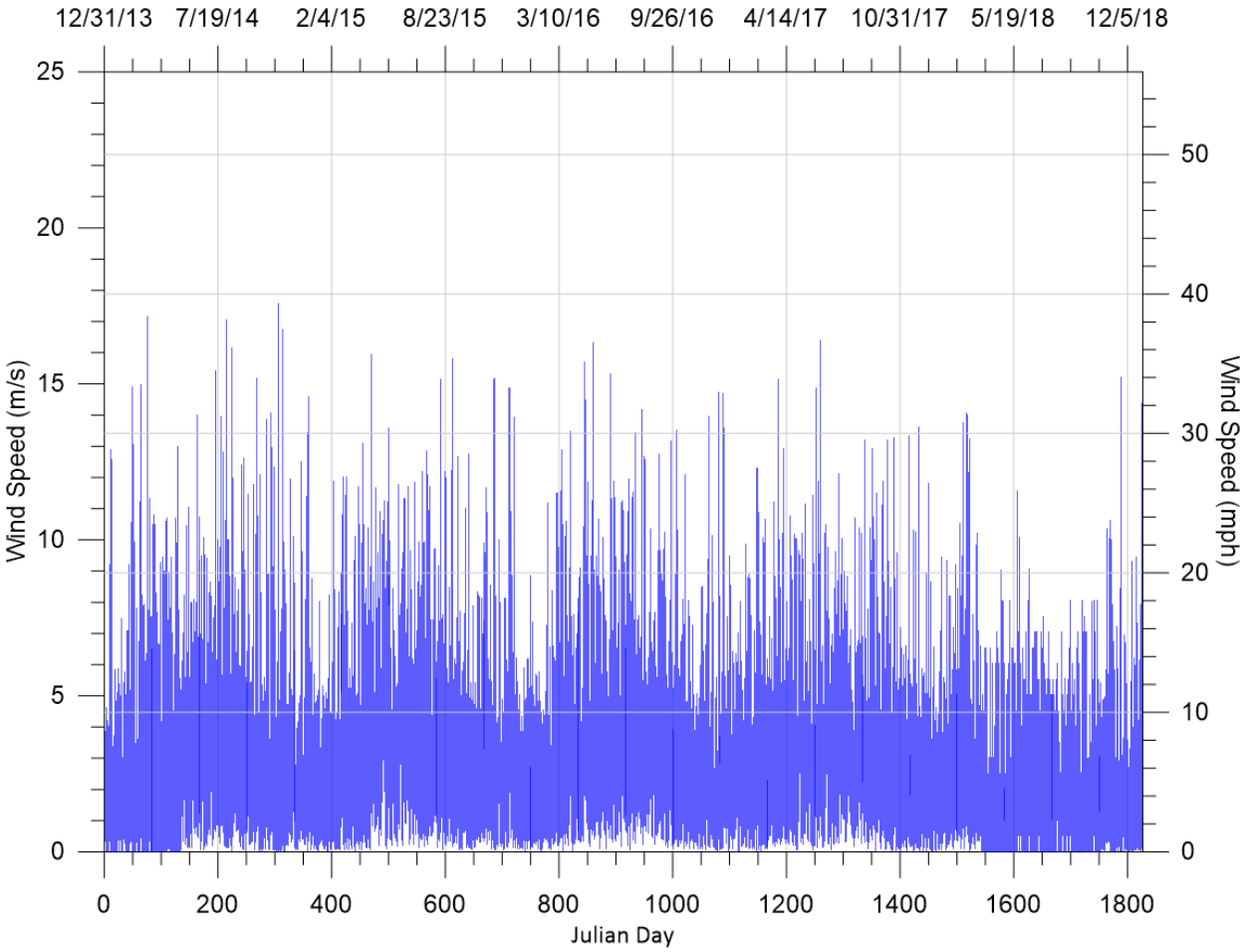


Figure 31. Wind speed inputs for water bodies 1 through 4 of the Brownlee Reservoir model.

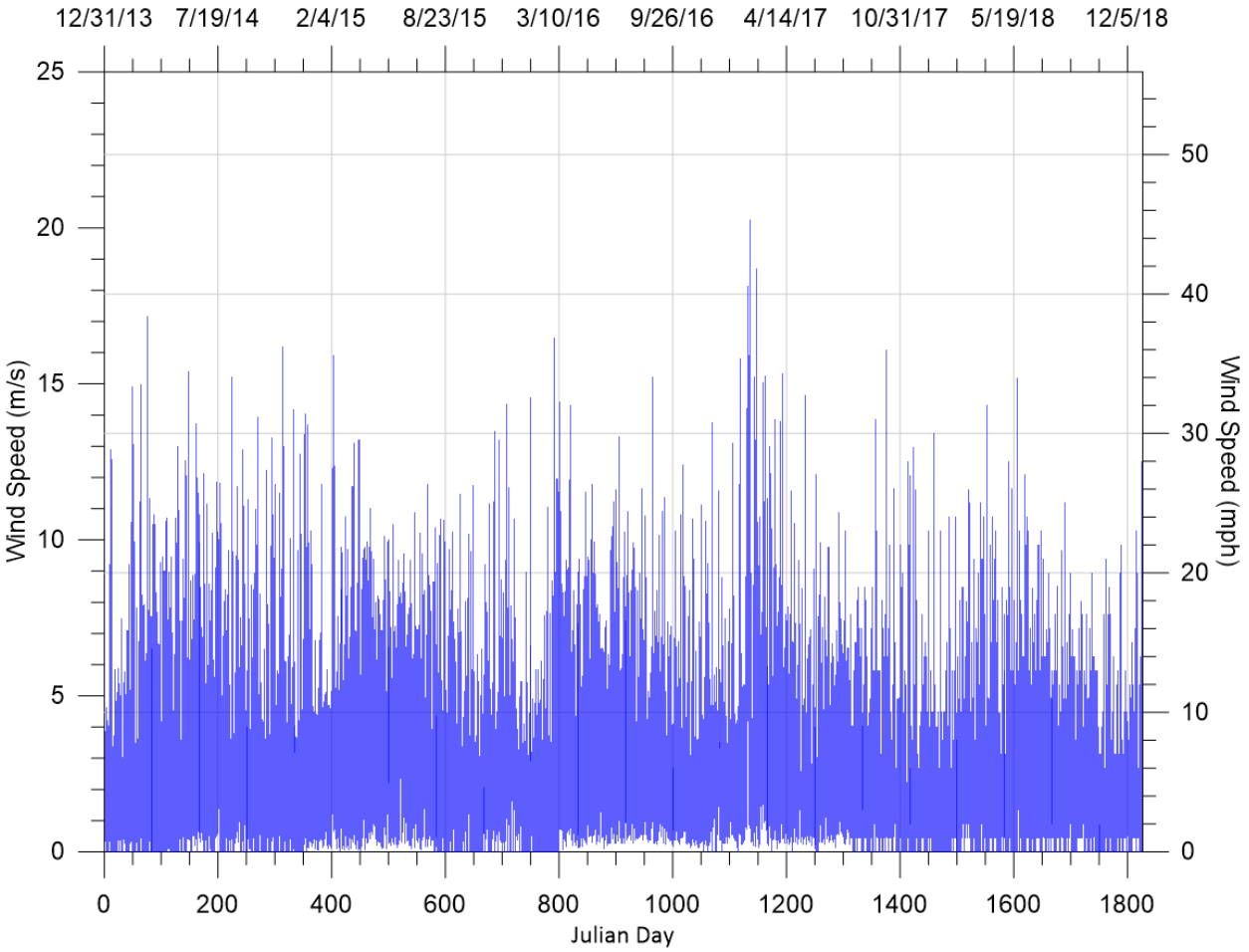


Figure 32. Wind speed inputs for water body 5 of the Brownlee Reservoir model.

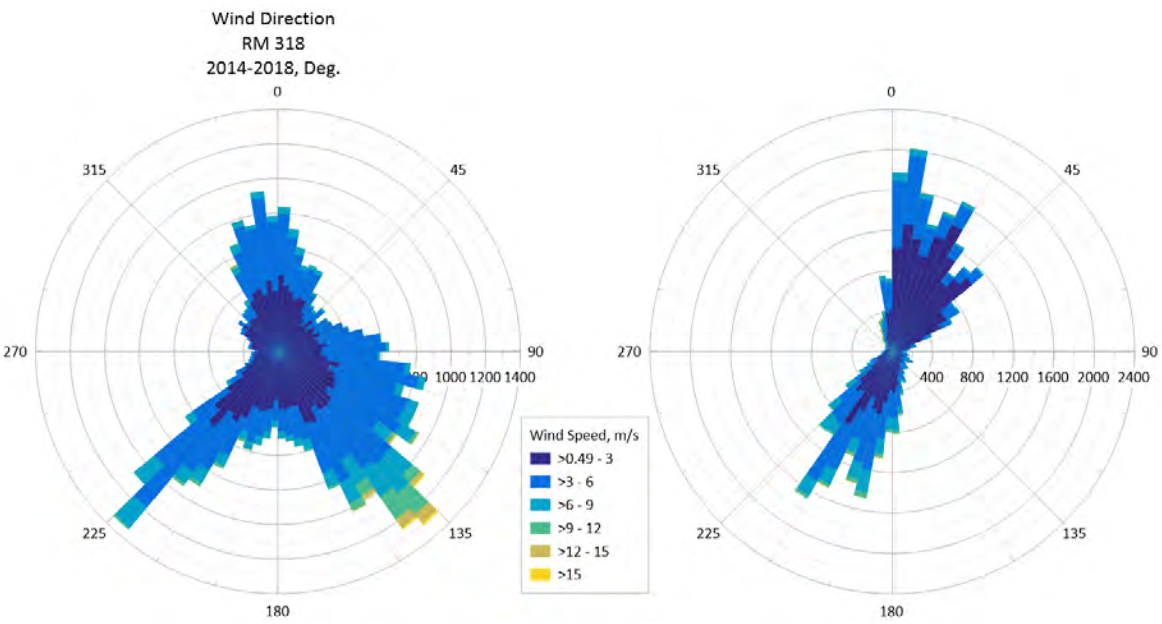


Figure 33. Polar wind diagrams of wind direction inputs for 2014-2018. The polar diagram for water bodies 1 through 4 of the Brownlee Reservoir model is shown on the left and on the right is the polar diagram for water body 5 of the Brownlee Reservoir model.

Short wave radiation inputs for the models were WRF-NAM predictions except for before 5/11/2014, when Ontario Agrimet station were used. Figure 34 plots solar radiation inputs for water bodies 1 through of the Brownlee Reservoir model, and Figure 35 shows solar radiation inputs for water body 5.

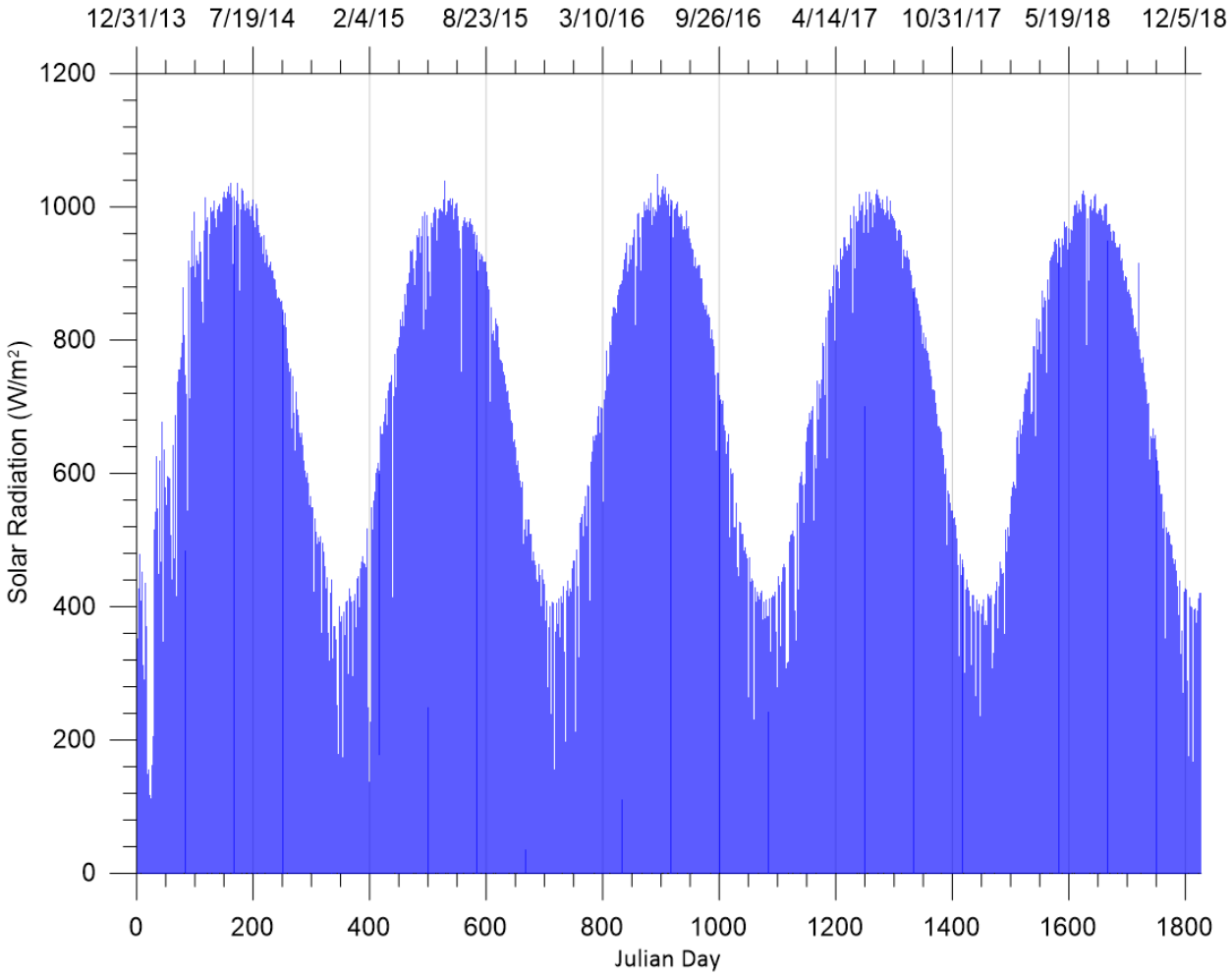


Figure 34. Solar radiation inputs for water bodies 1 through 4 of the Brownlee Reservoir model.

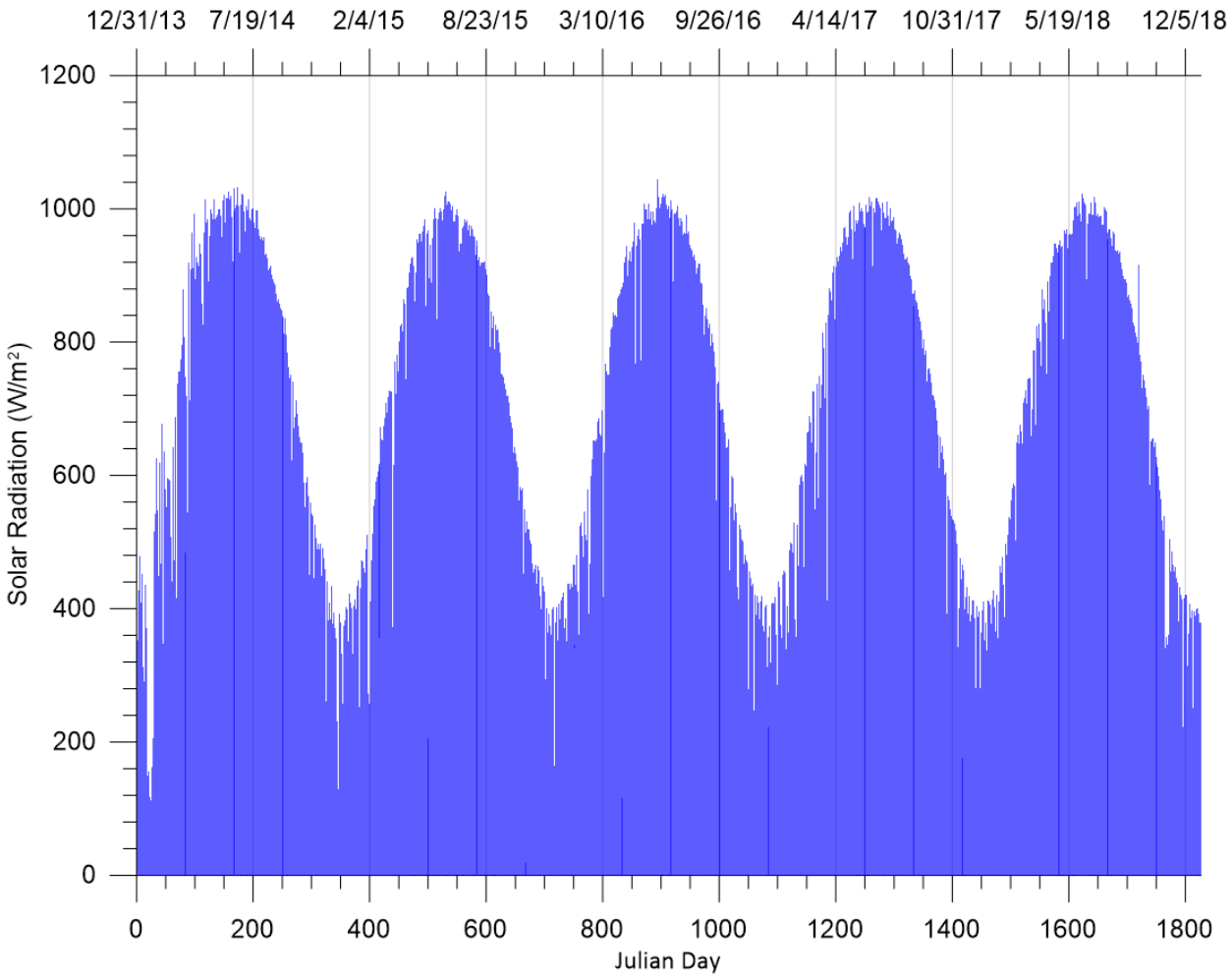


Figure 35. Solar radiation inputs for water body 5 of the Brownlee Reservoir model.

Modeled cloud cover inputs for all models were back calculated from WRF-NAM solar radiation predictions (Figure 36 and Figure 37). CE-QUAL-W2 uses cloud cover inputs and air temperature inputs to calculate long wave radiation. In the absence of measured cloud cover data, cloud cover inputs was back calculated (Wells, 2020). Theoretical clear sky solar radiation was calculated based on the geographic location of the meteorological station. The ratio between the measured value and the theoretical clear sky radiation is used to calculate cloud over a range of 0 (no clouds) to 10 (complete cloud cover):

$$C = \sqrt{\frac{1}{0.0065}\left(1 - \frac{\varphi_{measured}}{\varphi_{theoretical\,clear\,sky}}\right)}$$

where C: cloud cover in tenths

$\varphi_{measured}$: measured short-wave solar radiation

$\varphi_{theoretical\ clear\ sky}$: computed from theoretical formulae with no cloud cover

The file names of the meteorological time series (including air temperature, dew point temperature, wind speed and direction, cloud cover and short-wave solar radiation) used for Brownlee Reservoir are shown in Table 5.

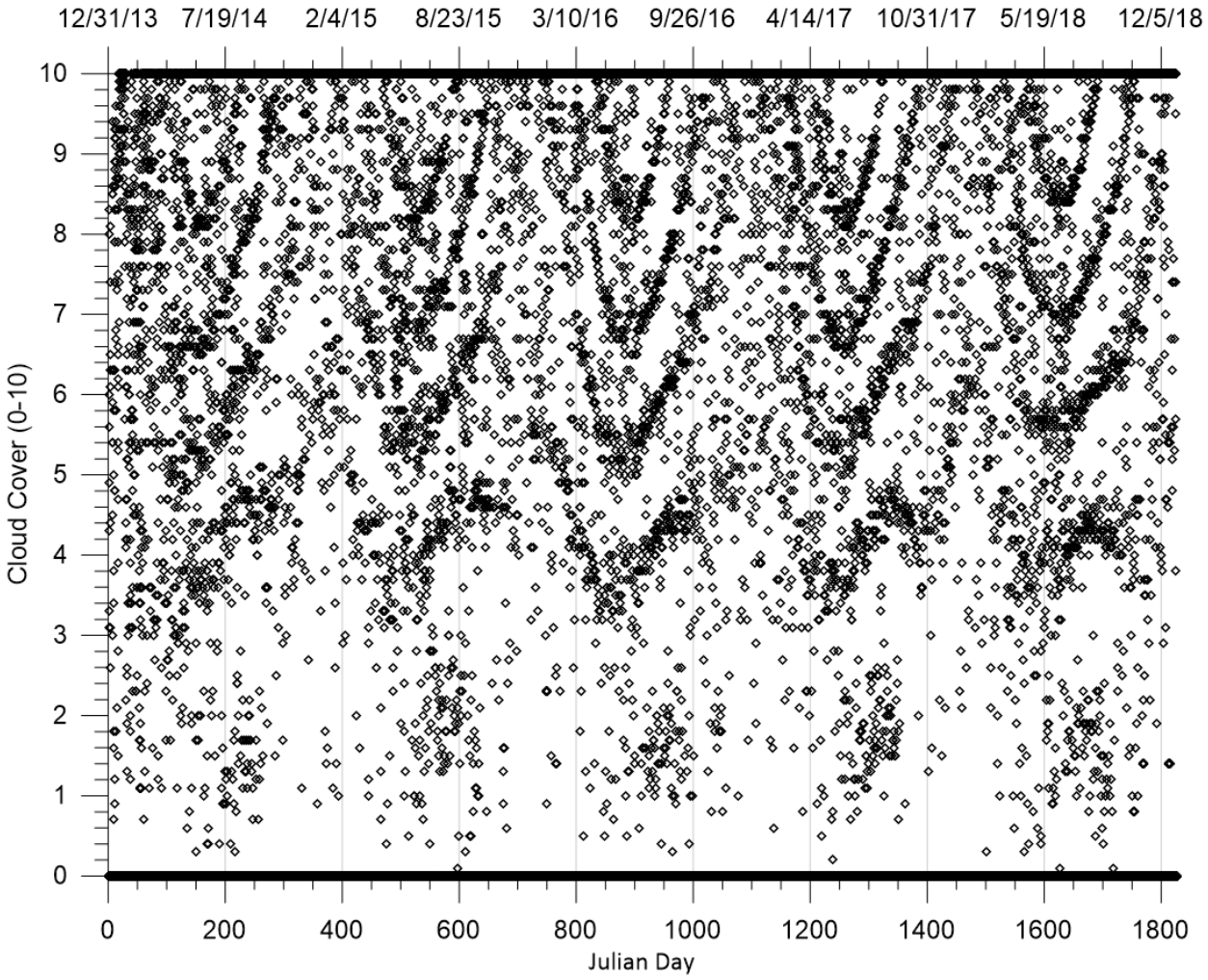


Figure 36. Cloud cover inputs for water bodies 1 through 4 of the Brownlee Reservoir model.

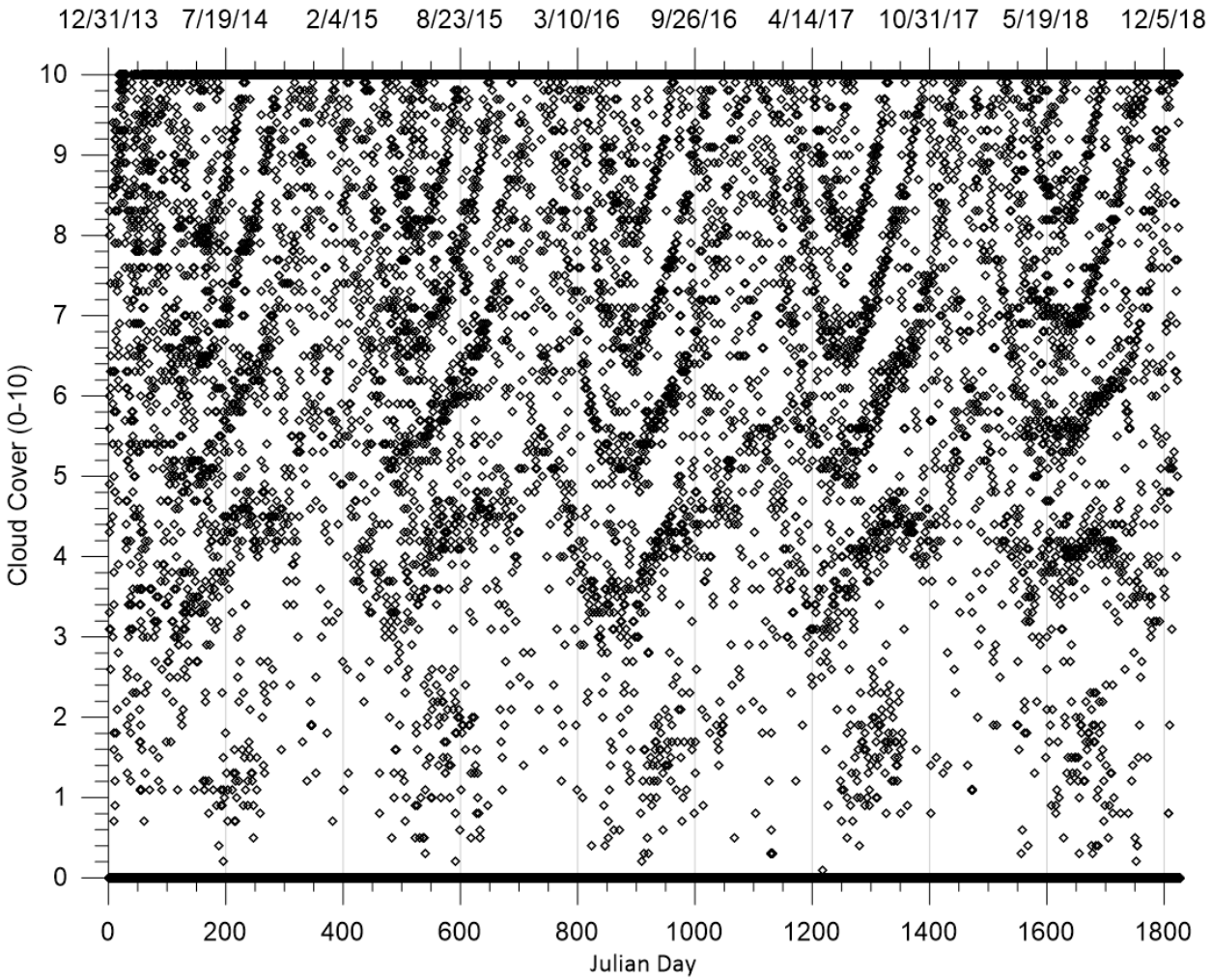


Figure 37. Cloud cover inputs for water body 5 of the Brownlee Reservoir model and for the Oxbow Reservoir and Hells Canyon Reservoir models.

Table 5. Meteorological input files for Brownlee Reservoir.

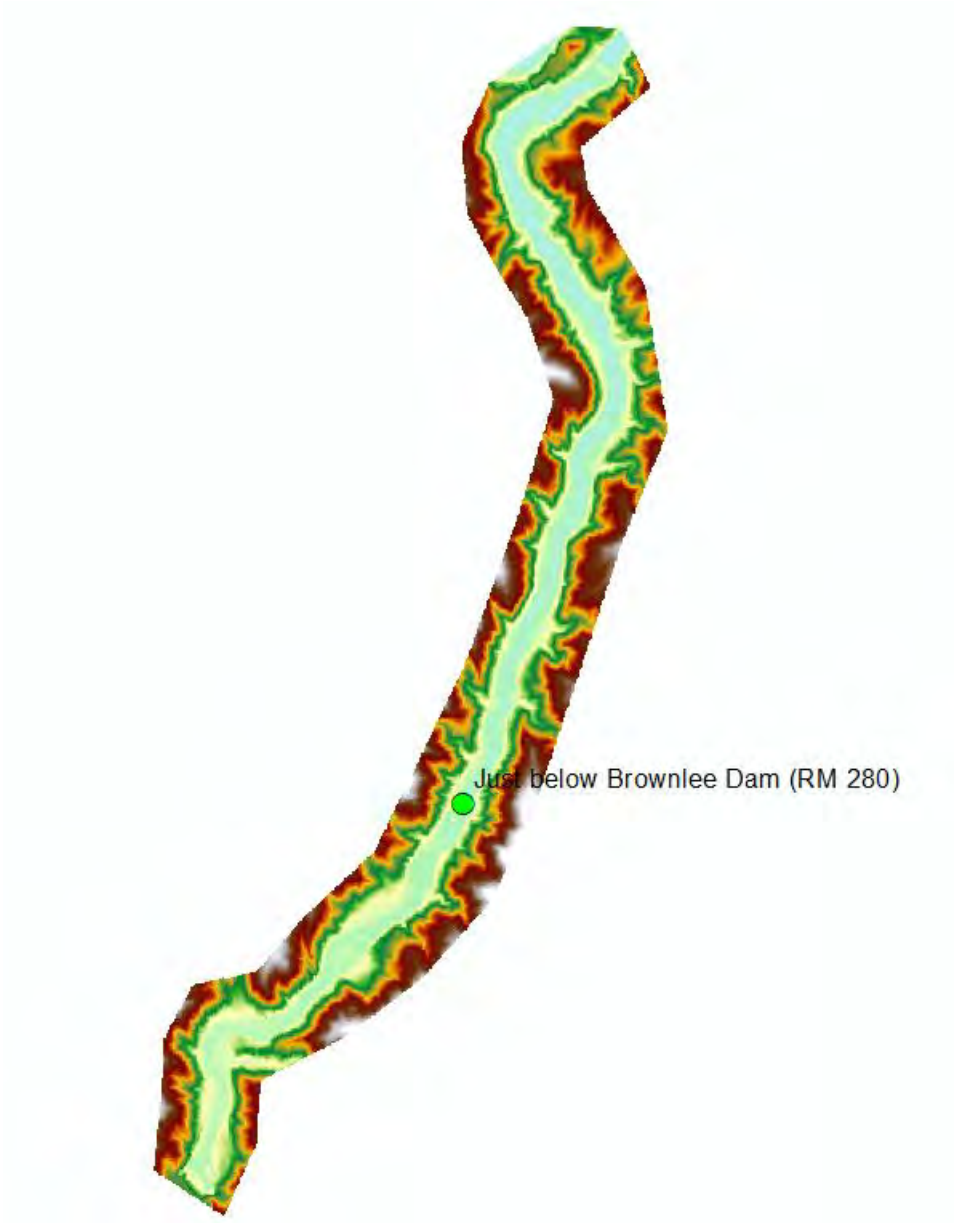
Water Body	Meteorological time series file name
1	met_Brownlee_wb1.csv
2	met_Brownlee_wb2.csv
3	met_Brownlee_wb3.csv
4	met_Brownlee_wb4.csv
5	met_Brownlee_wb5.csv

Oxbow Reservoir

WRF-NAM model predictions of air temperature, relative humidity, wind speed, wind direction, and solar radiation were available beginning on 5/11/2014 (Julian Day 131) for Oxbow Reservoir. The location of the WRF-NAM predictions (RM 280) is shown in Figure 24. However, the WRF-NAM model predicted lower air temperatures for Oxbow than for Brownlee even though it is at a lower elevation of approximately 120

m. IPC measured air temperature, relative humidity, and wind speed at Brownlee Reservoir and Hells Canyon Reservoir during the time period: 8/1/2012 – 11/5/2013, see Figure 39 through Figure 41. These data showed higher air temperatures at Hells Canyon Reservoir compared to Brownlee Reservoir. Due to these results, the WRF-NAM model was not used to create the Oxbow and Hells Canyon meteorological inputs, but instead the inputs from water body 5 of Brownlee Reservoir were adjusted to create the inputs for Oxbow and Hells Canyon reservoirs. Differences in average monthly values for air temperature, relative humidity, and wind speed were calculated between Brownlee and Hells Canyon reservoirs from the IPC data set to create monthly adjustment factors for Hells Canyon Reservoir. Only days with measurements for both Brownlee and Hells Canyon reservoirs were used to calculate averages. The Hells Canyon Reservoir adjustment factors were scaled by two thirds for Oxbow Reservoir since Oxbow Reservoir is approximately 80 meters below Brownlee Reservoir and Hells Canyon Reservoir is approximately 120 meters below Brownlee Reservoir. Table 6 shows the average monthly values and adjustment factors for Hells Canyon and Oxbow reservoirs for air temperature, relative humidity, and wind speed. Relative humidity was used to calculate dew point temperature using the same equation described for Brownlee Reservoir. A minimum relative humidity of five percent and a minimum wind velocity of zero m/s were applied to Oxbow and Hells Canyon reservoirs when converting the Brownlee Reservoir inputs. The same wind direction, cloud cover, and solar radiation inputs for water body 5 of Brownlee Reservoir were used for Oxbow and Hells Canyon reservoirs.

The file name of the meteorological input data for the Oxbow Reservoir model was *met_Oxbow_wb1.csv*.



5

Figure 38. Location of WRF-NAM meteorological predictions in Oxbow Reservoir.

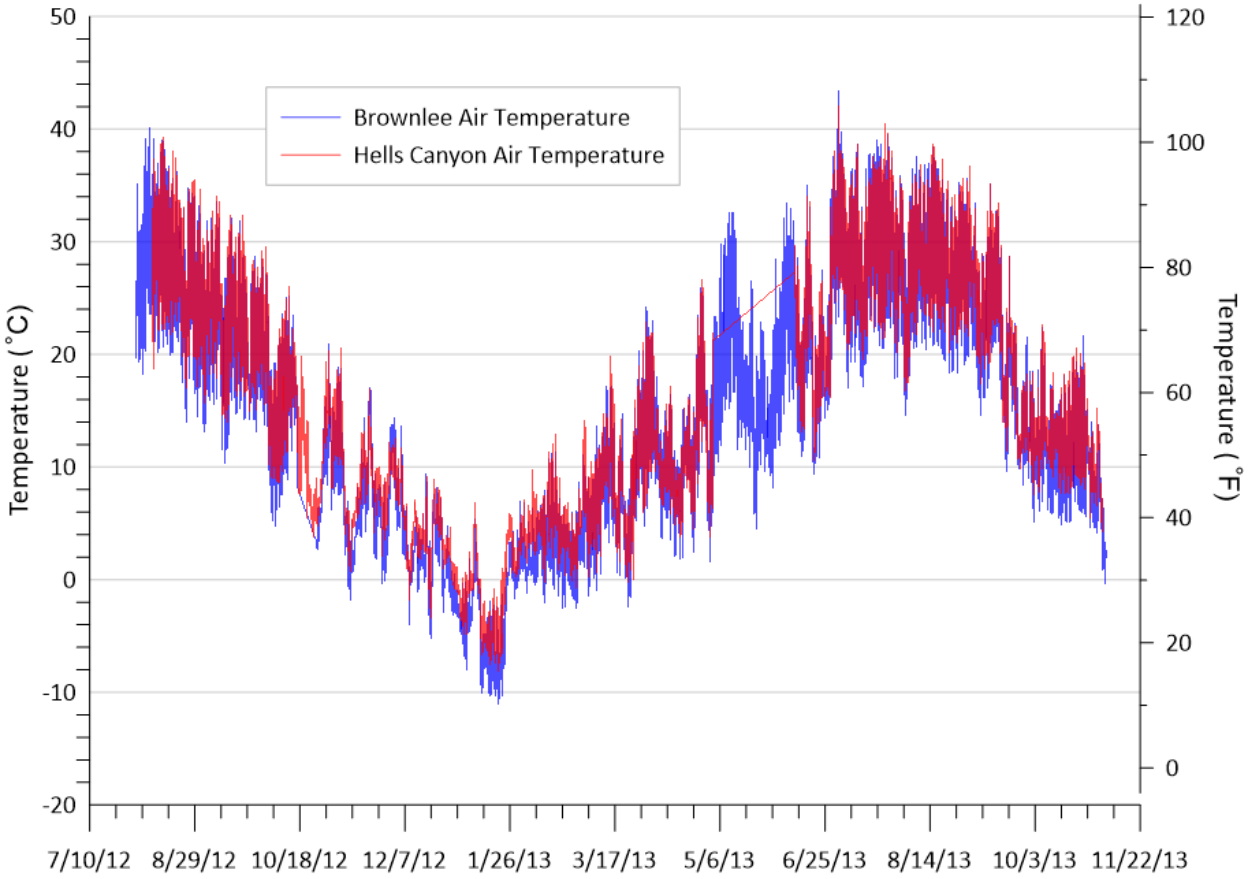


Figure 39. Brownlee Reservoir and Hells Canyon reservoir air temperatures measured from 8/1/2012 – 11/5/2013.

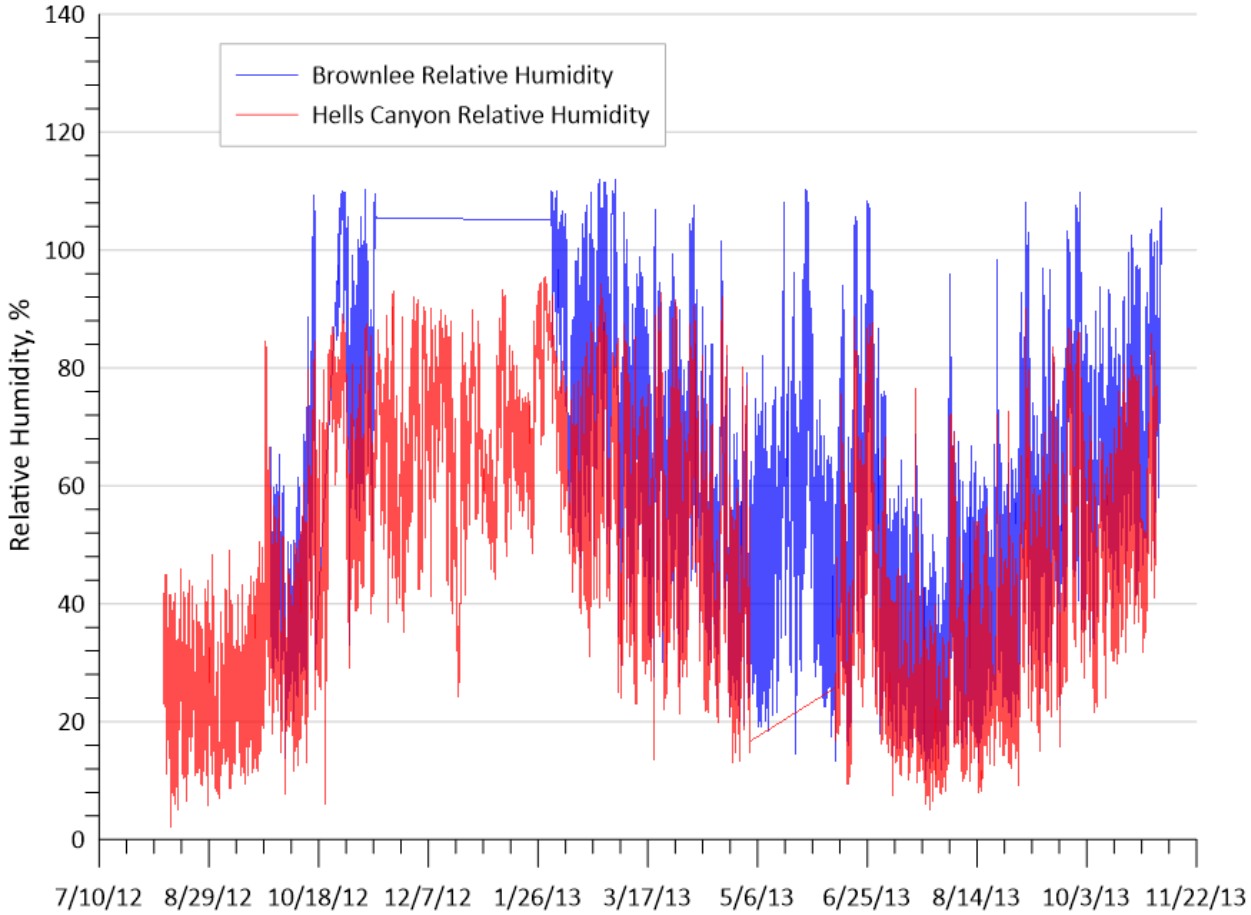


Figure 40. Brownlee Reservoir and Hells Canyon reservoir relative humidity measured from 8/1/2012 – 11/5/2013.

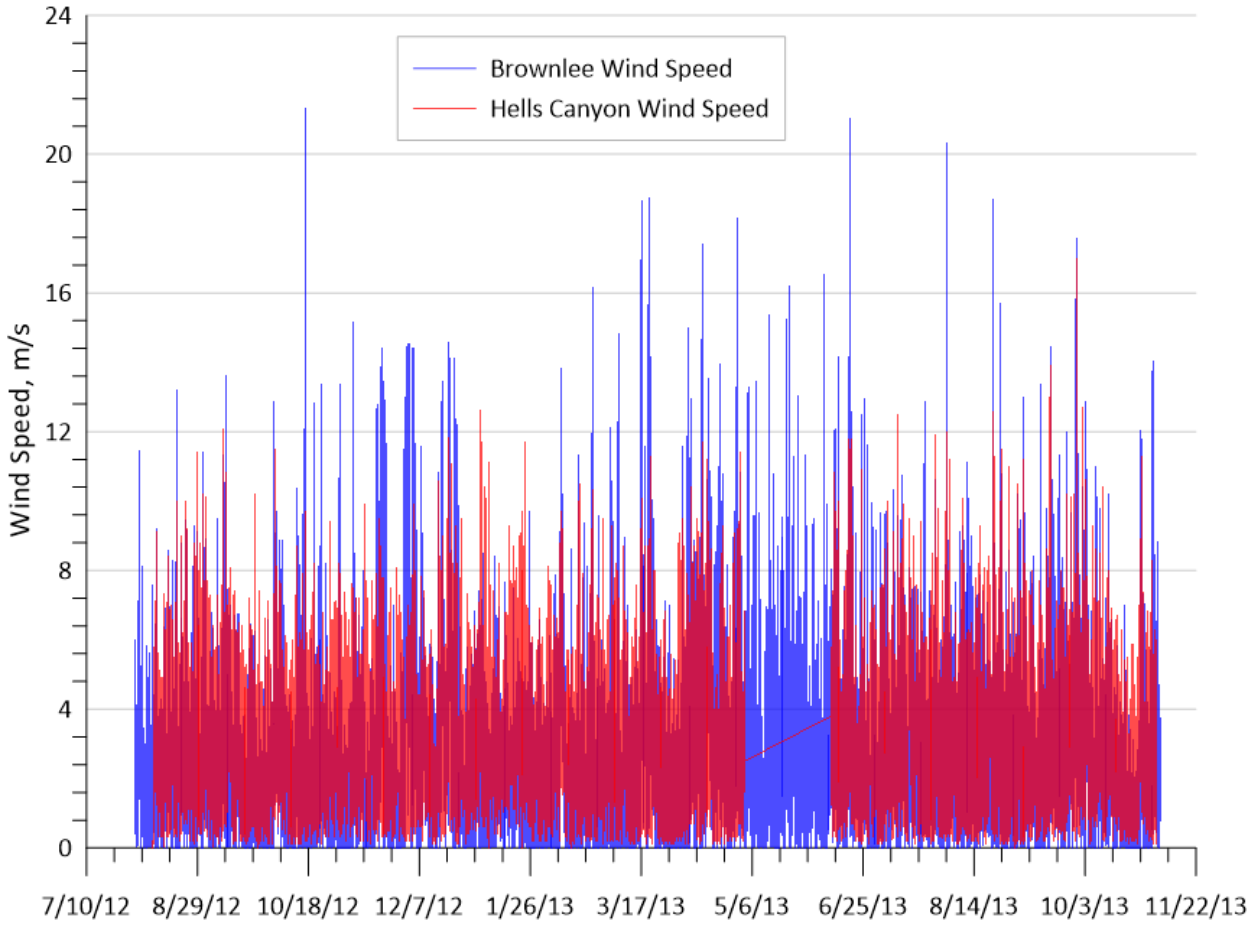


Figure 41. Brownlee Reservoir and Hells Canyon reservoir wind speed measured from 8/1/2012 – 11/5/2013.

Table 6. Meteorological adjustment factors for air temperature, relative humidity, and wind speed.

	Air Temperature, °C				Relative Humidity, %				Wind Speed, m/s			
	Average		Adjustment Factor		Average		Adjustment Factor		Average		Adjustment Factor	
Month	**BR**	**HC**	**BR-HC**	**BR-OX**	**BR**	**HC**	**BR-HC**	**BR-OX**	**BR**	**HC**	**BR-HC**	**BR-OX**
January	-3.3	-1.0	-2.4	-1.6	106	86	20	13	2.2	3.7	-1.5	-1.0
February	2.5	4.6	-2.2	-1.5	86	66	21	14	2.4	3.2	-0.8	-0.5
March	7.2	8.5	-1.3	-0.9	68	55	14	9	3.0	2.8	0.2	0.1
April	11.3	11.7	-0.4	-0.3	58	48	10	7	3.7	3.1	0.6	0.4
May	10.8	11.3	-0.5	-0.3	46	41	5	3	2.8	2.7	0.0	0.0
June	20.7	21.9	-1.3	-0.9	61	45	16	11	3.5	3.2	0.2	0.1
July	28.3	29.5	-1.2	-0.8	34	24	11	7	2.8	3.3	-0.5	-0.3
August	26.9	28.1	-1.3	-0.9	42	31	11	7	2.7	3.2	-0.5	-0.3
September	20.8	22.2	-1.4	-0.9	61	46	15	10	2.8	3.1	-0.4	-0.3
October	12.1	13.6	-1.4	-0.9	64	50	15	10	2.5	3.1	-0.6	-0.4
November	7.2	9.0	-1.8	-1.2	82	62	20	13	2.9	3.1	-0.2	-0.1
December	2.8	4.3	-1.5	-1.0	*		20	13	3.5	3.0	0.6	0.4

BR, Brownlee; OX, Oxbow; HC, Hells Canyon

* No data were available for relative humidity in December at Brownlee Reservoir so the average of November and January adjustment factors were used.

Air temperatures, dew point temperatures, and wind speeds used for model inputs for Oxbow Reservoir are shown in Figure 42 through Figure 44, respectively. A polar wind diagram of wind direction and wind speed is shown in Figure 45. Wind direction, cloud cover, and solar radiation are the same as water body 5 of Brownlee Reservoir.

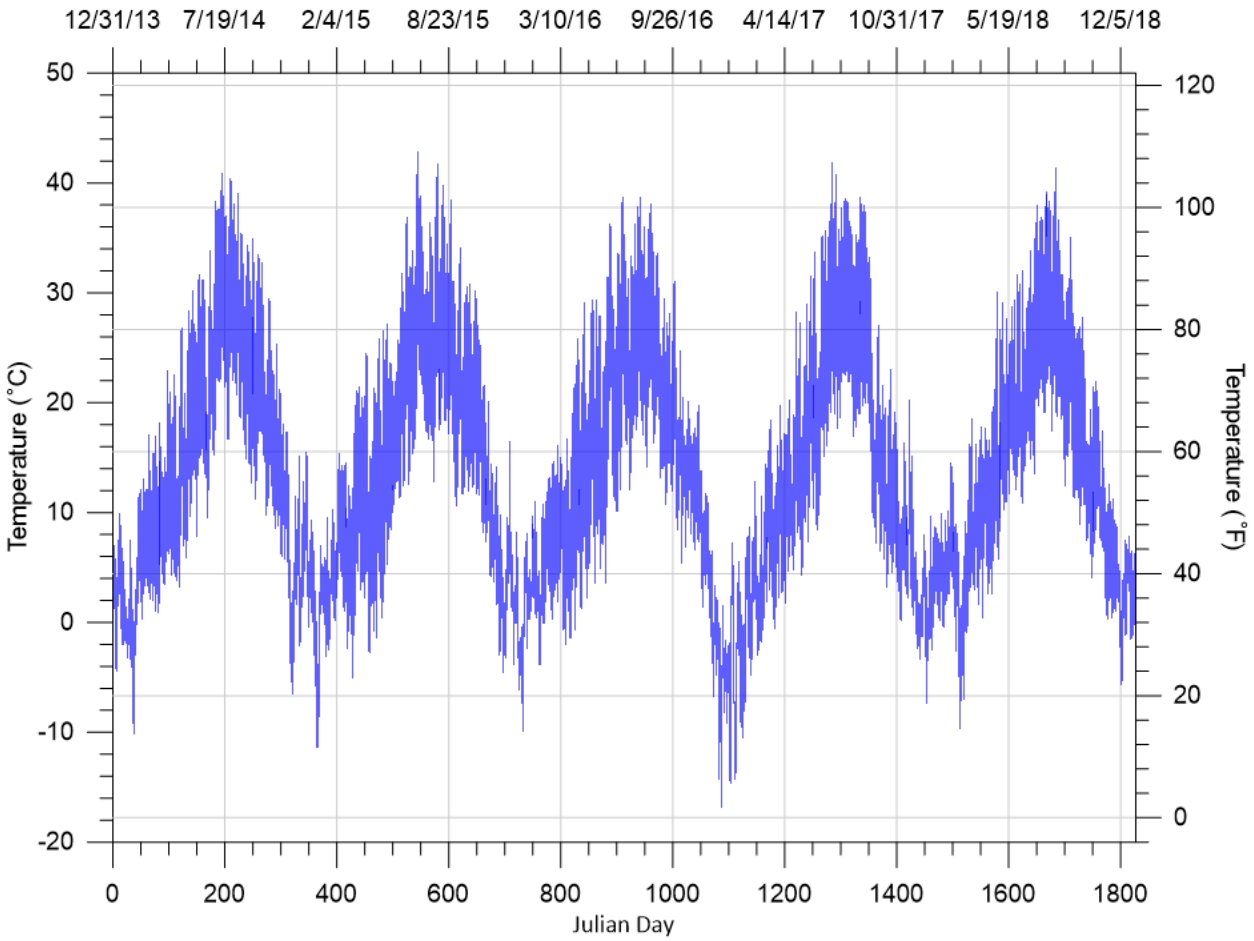


Figure 42. Air temperature inputs for the Oxbow Reservoir model.

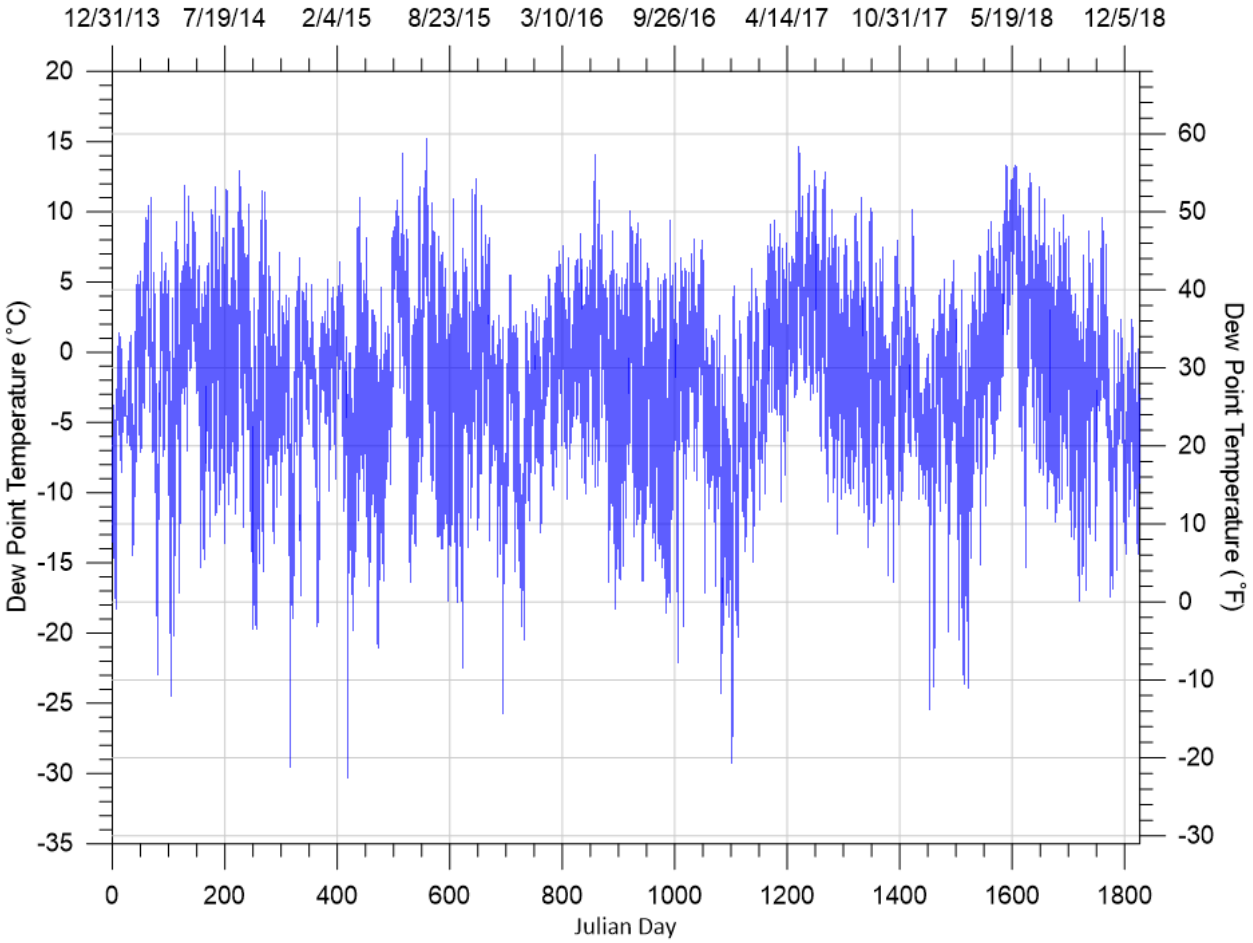


Figure 43. Dew point temperature inputs for the Oxbow Reservoir model.

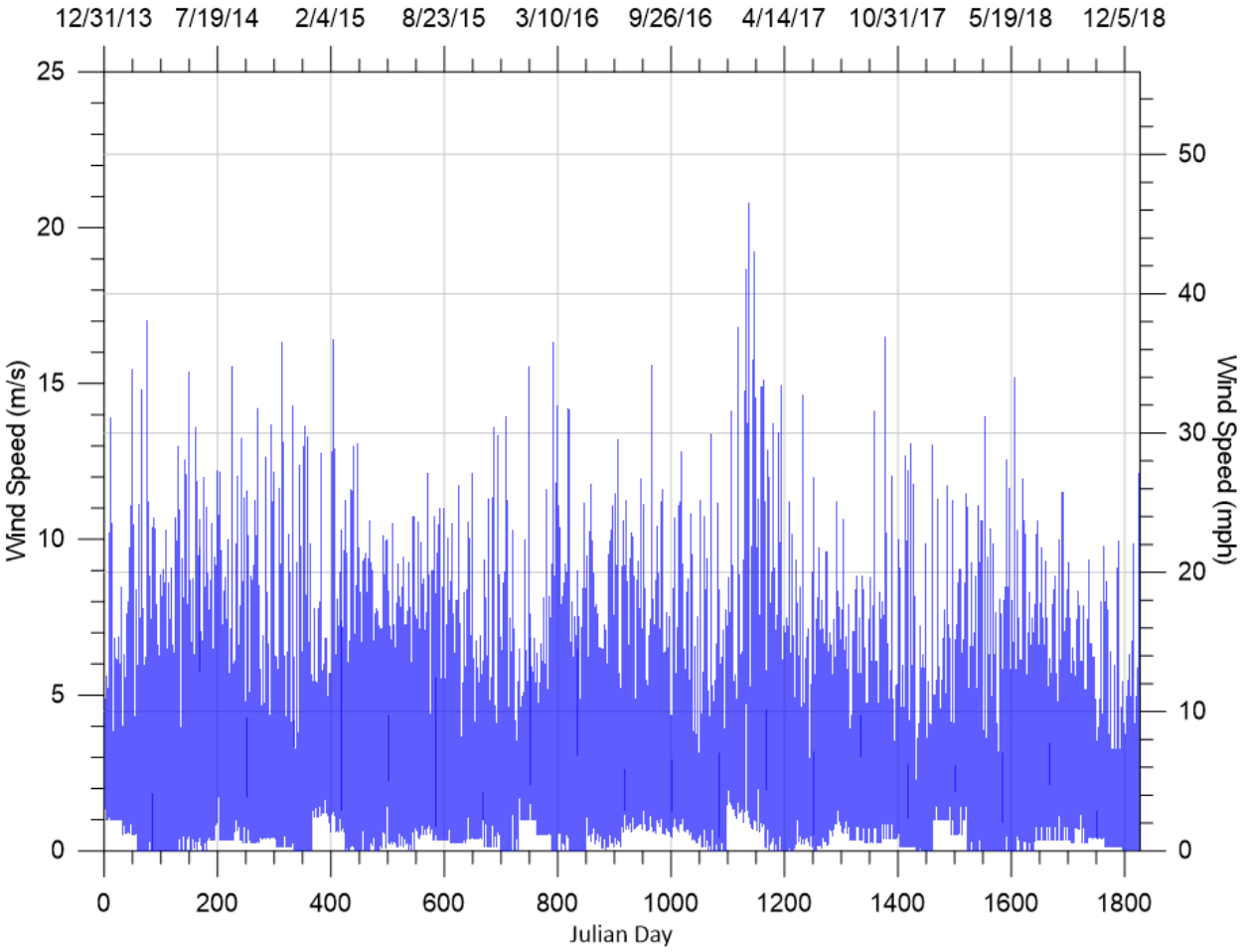


Figure 44. Wind speed inputs for the Oxbow Reservoir model.

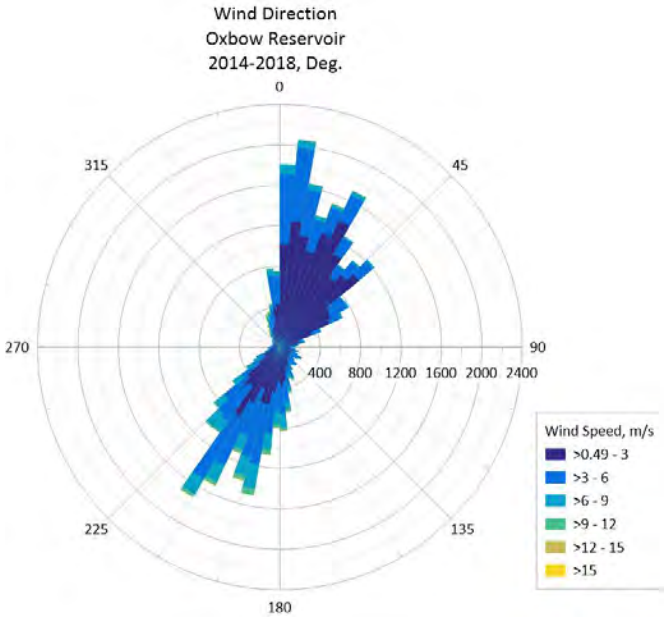


Figure 45. Polar wind diagram of wind direction inputs for the Oxbow Reservoir model.

Hells Canyon Reservoir

WRF-NAM predictions were available after 5/11/2014 for Hells Canyon Reservoir. The location within the reservoir of the WRF-NAM predictions (RM 248) is shown in Figure 46. As described for Oxbow Reservoir, the WRF-NAM model predictions were not applied. Instead, the meteorological inputs for water body 5 of Brownlee Reservoir were adjusted to create the inputs for Hells Canyon Reservoir.

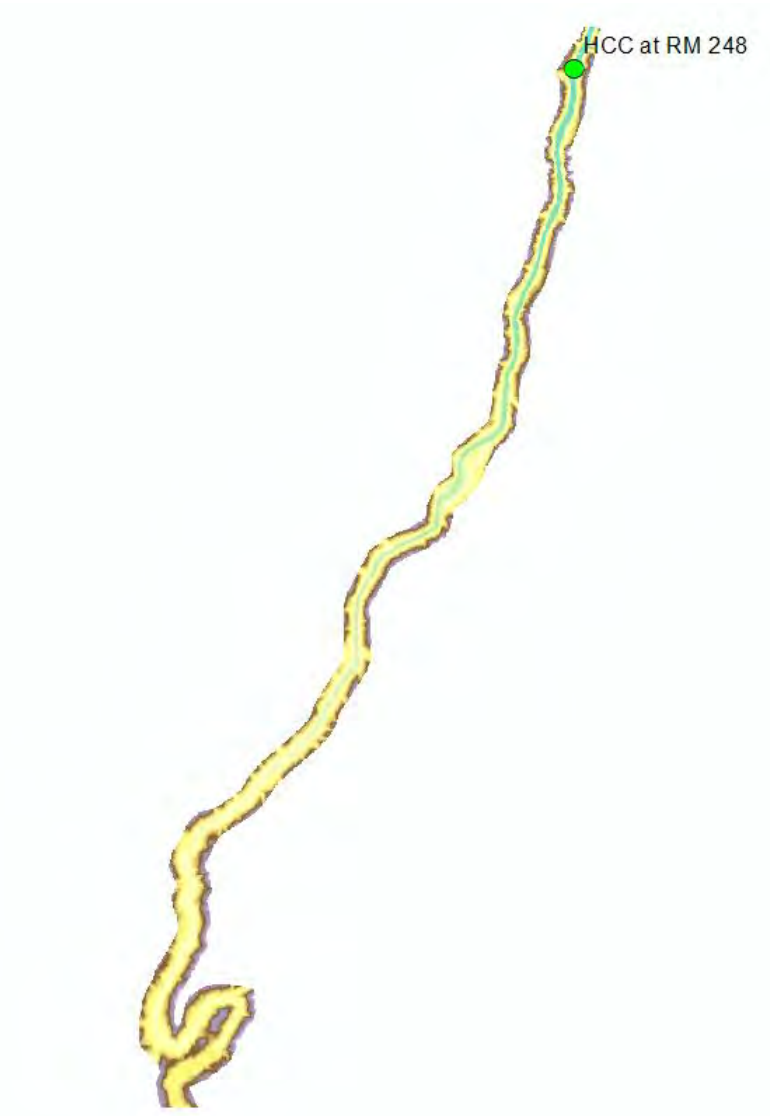


Figure 46. Location of WRF-NAM meteorological predictions in Hells Canyon Reservoir.

Air temperatures, dew point temperatures, and wind speeds used for model inputs for Hells Canyon Reservoir are shown in Figure 47 through Figure 49, respectively. A polar wind diagram of wind direction and wind speed is shown in Figure 50. Wind direction, cloud cover, and solar radiation are the same as water body 5 of Brownlee Reservoir. The file used for the Hells Canyon meteorological file was *met_HellsCanyon_wb1.csv*.

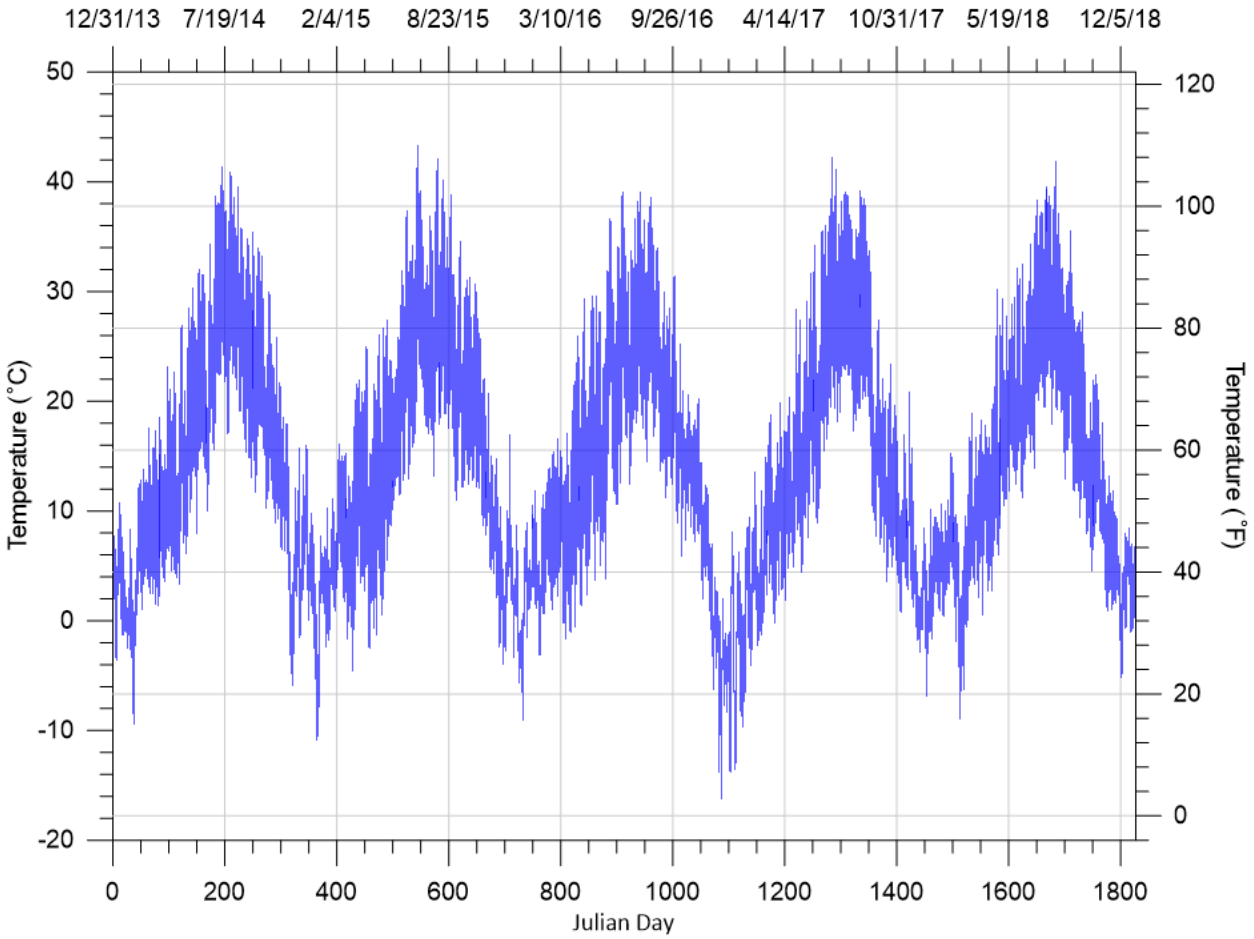


Figure 47. Air temperature inputs for the Hells Canyon Reservoir model.

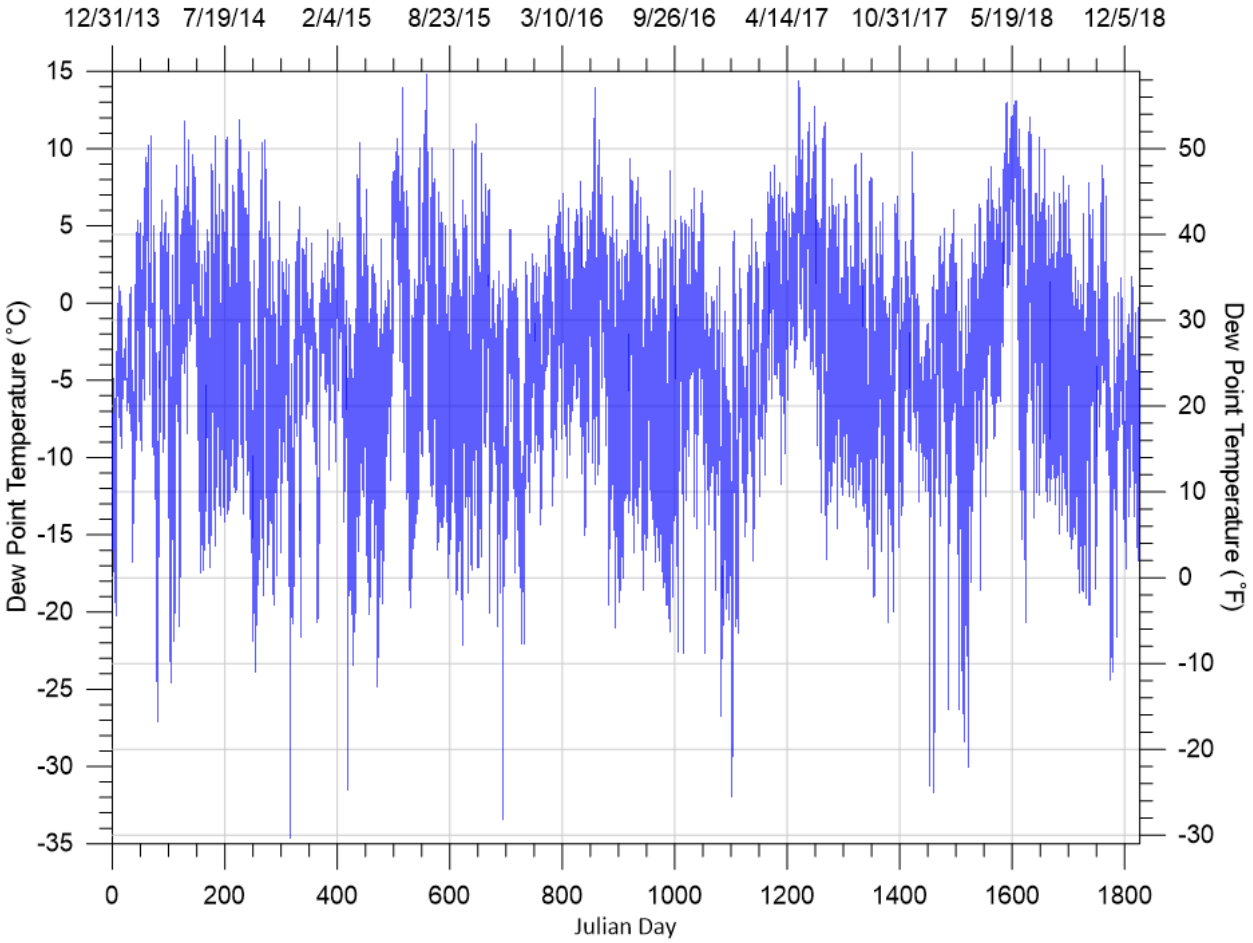


Figure 48. Dew point temperature inputs for the Hells Canyon Reservoir model.

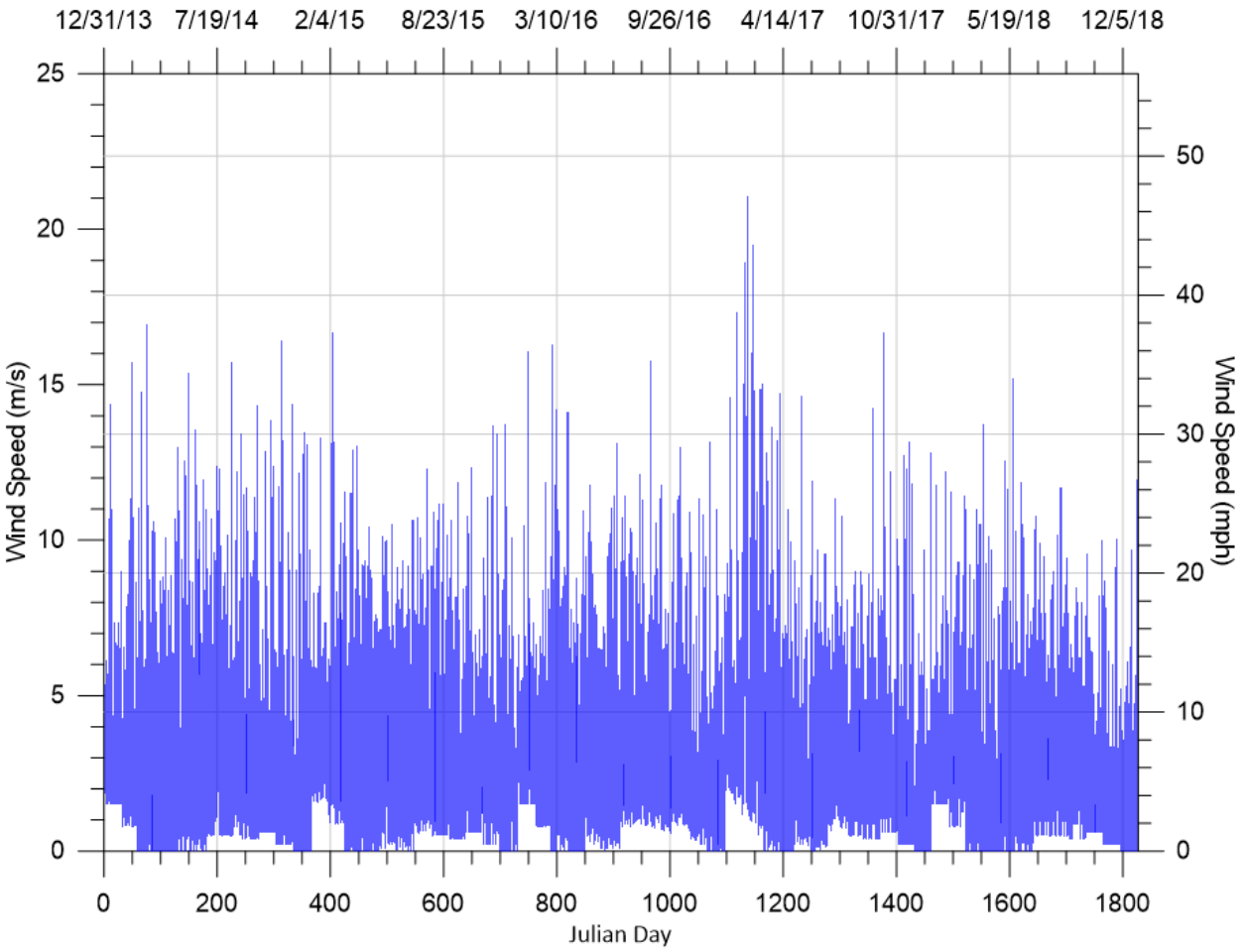


Figure 49. Wind speed inputs for the Hells Canyon Reservoir model.

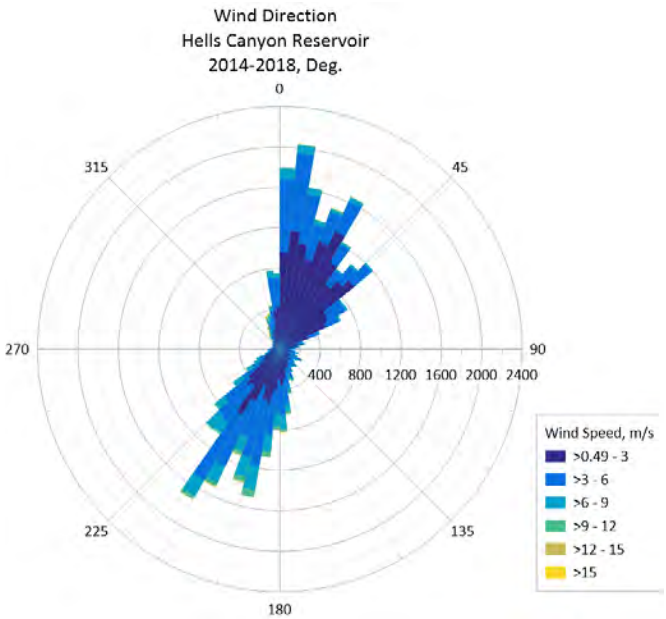


Figure 50. Polar wind diagram of wind direction inputs for the Hells Canyon Reservoir model.

Dam Outflows

For Brownlee Dam, spill flows and flows through every turbine were specified in the model (Figure 51). Oxbow Dam spill and bypass flows were specified in the model and the turbine flows were specified using dynamic weir elevations based on the observed elevations in the reservoir. A constant bypass flow of 100 cfs (2.832 m^3/s) was always released from Oxbow Reservoir. Due to the high frequency variations in water level of Oxbow and Hells Canyon, dynamic weir elevations (set to just below the measured water surface elevations at the dams) were used to calculate outflows rather than using measured outflows.

The dynamic weir requires a time series of elevations. If you give the dynamic weir the water surface elevations (or small adjustments below that water surface elevation), the model can mimic the actual water surface elevation at the dam. The model then computes using a weir equation of the form, $Q = \alpha \Delta h^{\beta}$, where the flow rate is a function of weir coefficients α and β and the height above the weir crest in m. So, the model dynamically computes the flow rate and comes close to matching the water surface elevation. This prevents having to add and subtract water to mimic the high frequency oscillations in the water surface.

By using a dynamic weir, a water balance was not required for these water bodies. Figure 52 shows Oxbow Dam model predicted turbine flows, spill flows, and bypass flows. Turbine flows (labeled as "Turbines – Data") calculated by subtracting measured bypass and spill flow rates from gage flows below the dam are also shown on Figure 52 as a relative comparison to the model predicted flows. Hells Canyon Dam spill flows were specified in the model, and turbine flows were specified using dynamic weir elevations based on the observed water surface elevations in the reservoir. Figure 53 shows Hells Canyon model predicted turbine flows and spill flows. Turbine flows (labeled as "Turbines – Data") calculated by subtracting spill flows from gage flows below the dam are also shown on Figure 53 as a relative comparison to the model predicted flows. Due to the high frequency variability of turbine flows out of Hells Canyon, a turbine baseflow of 200 m^3/s was included in the model as a structure outflow to smooth out the turbine outflow and better match the measured data. Data sources for flows and water surface elevations are listed in Table 7. The dyanmic weir elevations were set by subtracting 0.4 m and 0.15 m from the water surface elevations during model calibration for Oxbow and Hells Canyon, respectively. Outlet elevations for the reservoirs are listed in Table 8.

All spill flows, turbine flows, and bypass flows were modeled as gates in the model. The turbine baseflow at Hells Canyon was modeled as a structure. Gates were used to model the flows so that dissolved gas computations could be applied to the outflow. Further discussion of dissolved oxygen calibration at the dam outflows is described in the water quality calibration section of the report.

A summary of the model files used in the Brownlee, Oxbow, and Hells Canyon models are shown in Table 9.

Table 7. Data sources for modeled outflows.

Data	Reservoir	Frequency	Data Source
Turbines and Spill Flows	Brownlee	15-minute	IPC – 13289720 Snake River below Brownlee Dam (personal communication, 8/29/2019)
Spill Flows	Oxbow	15-minute	IPC – 13290030 Snake River below Oxbow Dam (personal communication, 12/3/2019)
Water Level	Oxbow	15-minute	IPC – 13289995 Oxbow Dam (personal communication, 1/17/2020)
Spill Flows	Hells Canyon	15-minute	IPC – 13290450 Snake River below Hells Canyon Dam (personal communication, 12/4/2019)
Water Level	Hells Canyon	15-minute	IPC – 13290445 Hells Canyon Dam (personal communication, 1/17/2020)

Table 8. Model outlet elevations for Brownlee, Oxbow, and Hells Canyon Reservoirs.

Reservoir	Outlet	Elevation (m)	Elevation (ft)
Brownlee	Turbine Units 1-5	593.8	1948.2
	Spill	625.5	2052.2
Oxbow	Turbines	533.4	1750.0
	Bypass	534.92	1755.0
	Spill	541.32	1776.0
Hells Canyon	Turbines	478.99	1571.5
	Turbine Baseflow	478.99	1571.5
	Spill	506.88	1663.0

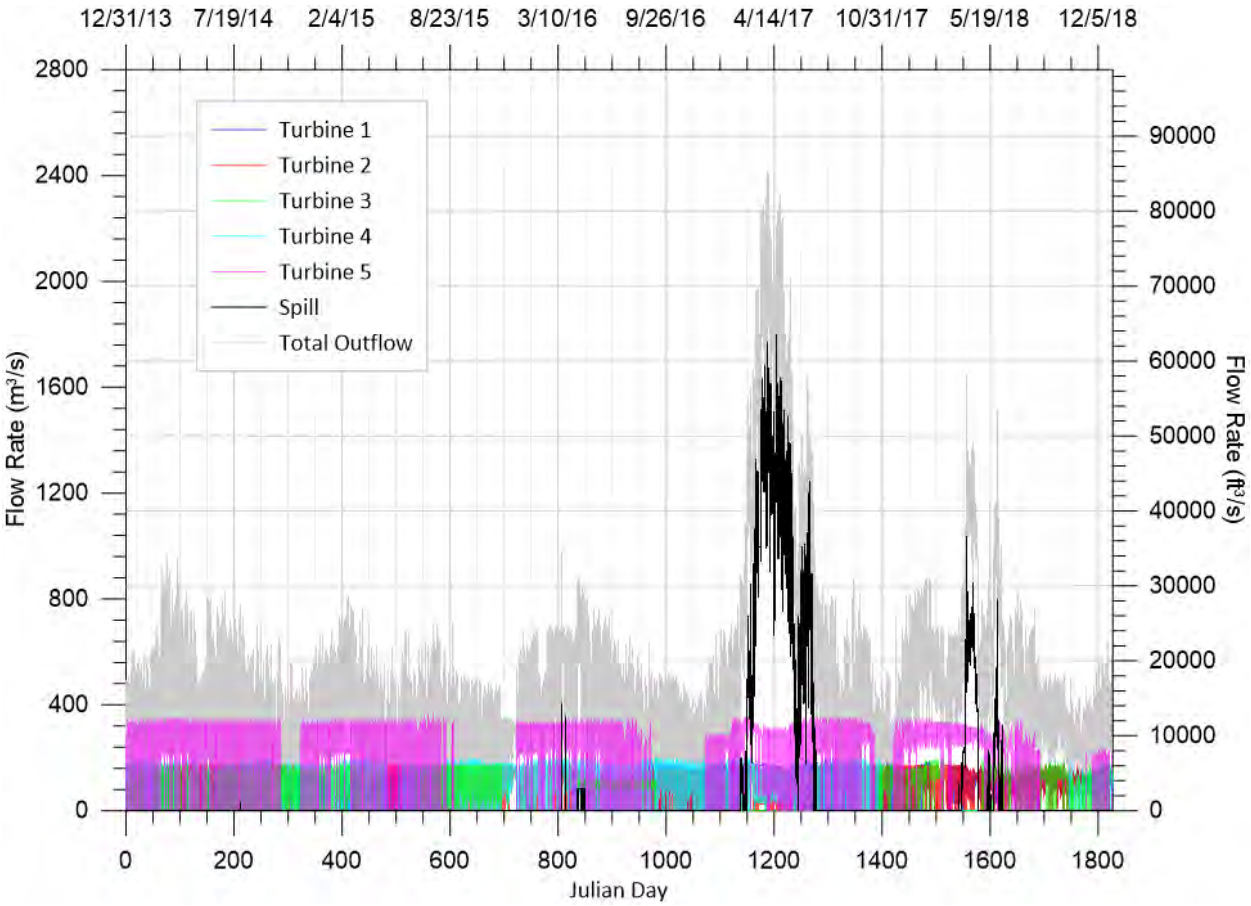


Figure 51. Brownlee Dam outflow rates.

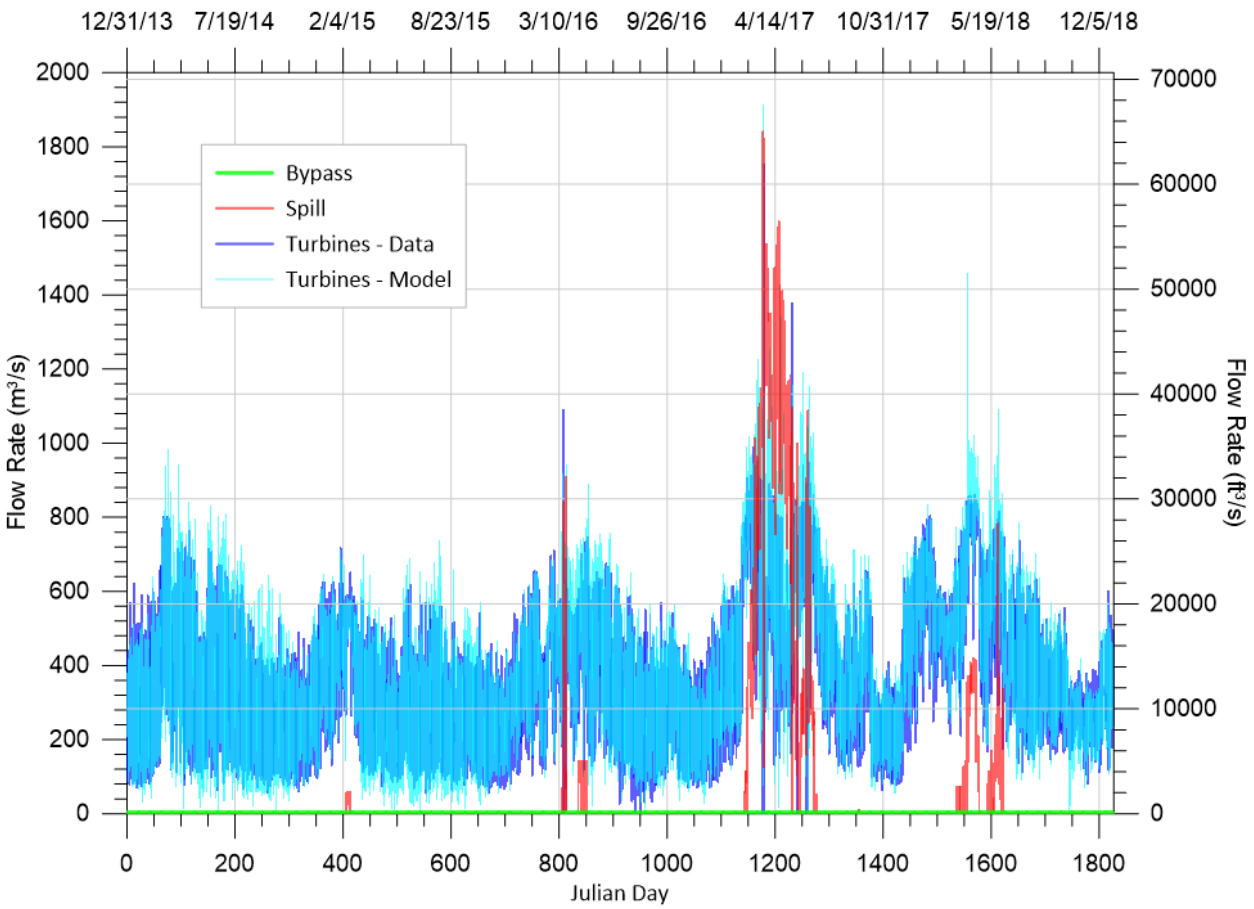


Figure 52. Oxbow Dam turbine, spill, and bypass flow rates.

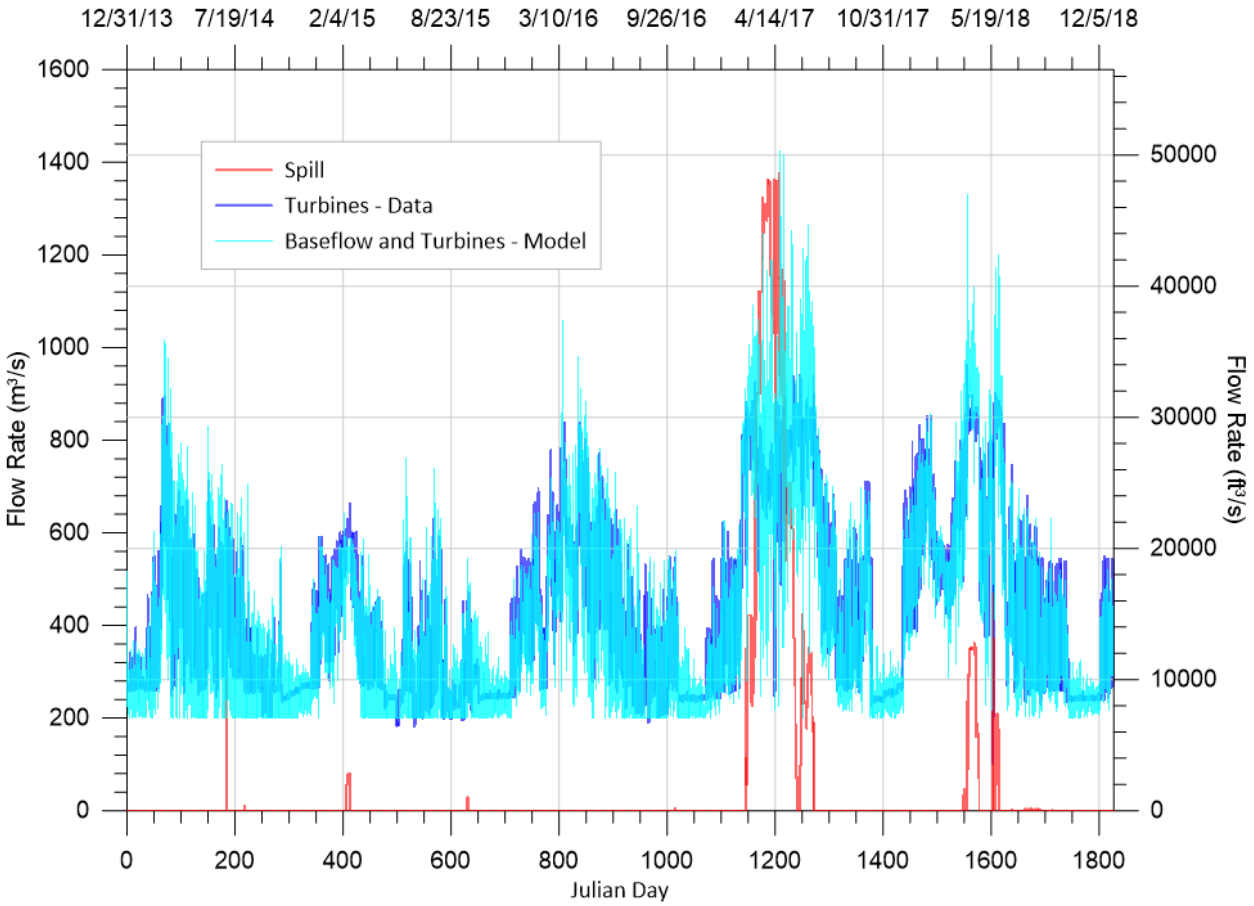


Figure 53. Hells Canyon Dam turbine and spill flow rates.

Table 9. Dam model outflows for Brownlee, Oxbow and Hells Canyon.

Name	Outflow Model Segment	Type of outflow	File name	Description
Brownlee Dam				
Spillway	202	Gate 1	qgate.csv	Spillway flow rate Column B, flow frequency every 15 min except 1 gap of 1 day (JD 1097)
Power House Unit 1	238	Gate 2	qgate.csv	Unit 1 turbine outflow Column C, flow frequency every 15 min except 1 gap of 1 day (JD 1097)
Unit 2	238	Gate 3	qgate.csv	Unit 2 turbine outflow Column D, flow frequency every 15 min except 1 gap of 1 day (JD 1097)
Unit 3	238	Gate 4	qgate.csv	Unit 3 turbine outflow Column E, flow frequency every 15 min except 1 gap of 1 day (JD 1097)

Name	Outflow Model Segment	Type of outflow	File name	Description
Unit 4	238	Gate 5	qgate.csv	Unit 4 turbine outflow Column F, flow frequency every 15 min except 1 gap of 1 day (JD 1097)
Unit 5	238	Gate 6	qgate.csv	Unit 5 turbine outflow Column G, flow frequency every 15 min except 1 gap of 1 day (JD 1097)
Oxbow Dam and Powerhouse				
Oxbow Spill	52	Gate 1	qgt_spill_bypass_ dynweir.csv	Oxbow fixed spill flow rate at a centerline elevation of 541.32 m
Bypass flow	52	Gate 2	qgt_spill_bypass_ dynweir.csv	Bypass flow at centerline elevation of 534.92 m, constant flow of 2.83 m^3/s.
Power House flow	50	Gate 3	qgt_spill_bypass_ dynweir.csv	Dynamic weir used to compute flow (rather than a water balance flow). Weir variable elevation from 584.2 to 549.7 m. This is the measured water level and a small correction to ensure water level matches field data.
Hells Canyon Dam				
Spillway	116	Gate 1	qgt_spill_dynweir.csv	Hells Canyon spillway flow at elevation 506.88 m
Hells Canyon dynamic flow above base flow	116	Gate 2	qgt_spill_dynweir.csv	Dynamic elevation weir (in lieu of water balance) with elevations (adjusted water surface elevations) ranging from 512.8 m to 514.4 m.
Hells Canyon base outflow (constant)	116	Structure 1	qot_br1_baseflow.csv	Structure outflow at centerline elevation of 478.99 m. This is a stable base flow of 200 m^3/s that is augmented by the dynamic weir. This prevents the dynamic weir from oscillating too much.

Tributary Inflows

Brownlee Reservoir tributary flow rates are shown in Figure 54. During water level calibration, a water balance file (distributed tributary) was created for Brownlee Reservoir to account for ungaged inflows and outflows and is described in the flow and water level calibration section. Powder River flow rates were estimated by summing Powder River flow rates measured at RM 22 with Eagle Creek data. Wildhorse

River and Pine Creek flow rates are shown in Figure 55 and Figure 56, respectively. Inflows to Brownlee, Oxbow, and Hells Canyon are summarized in Table 10.

Data sources for the tributary flows are listed in Table 11. Gaps were filled where possible in 15-minute flow data for the Snake River, Powder River, Eagle Creek, and Burnt River with daily averages. Daily average flows were applied at noon for the missing days.

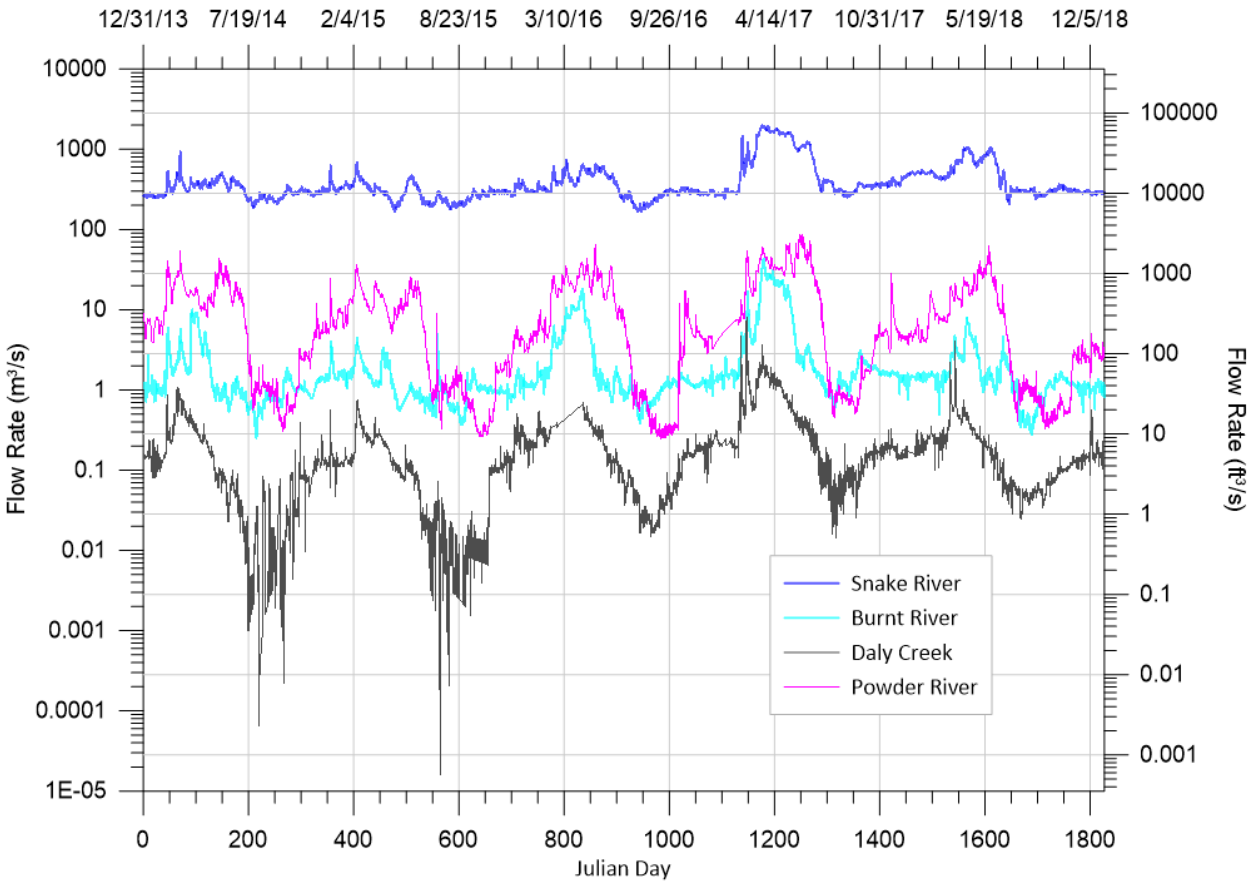


Figure 54. Flow rates of Brownlee Reservoir tributaries.

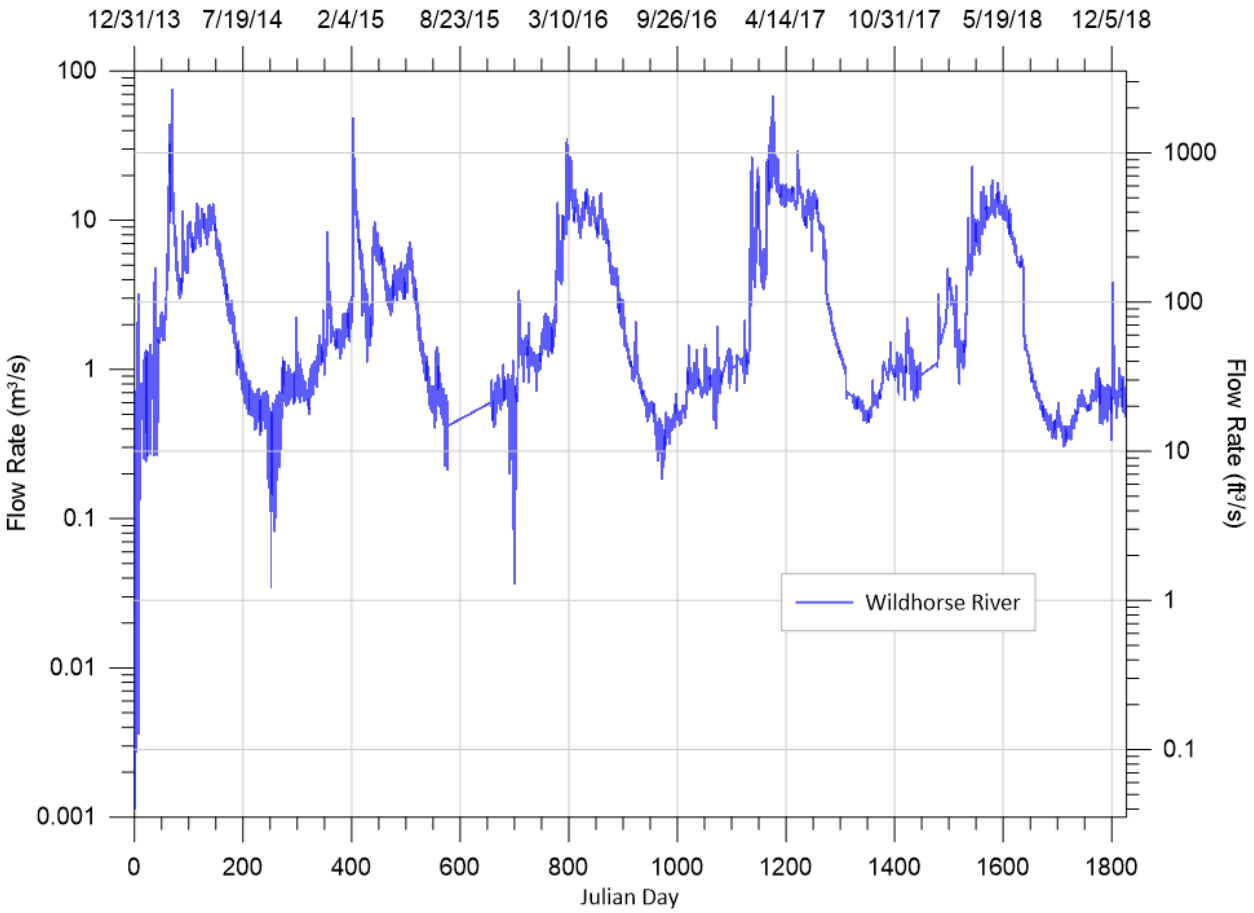


Figure 55. Wildhorse River flow rates into Oxbow Reservoir.

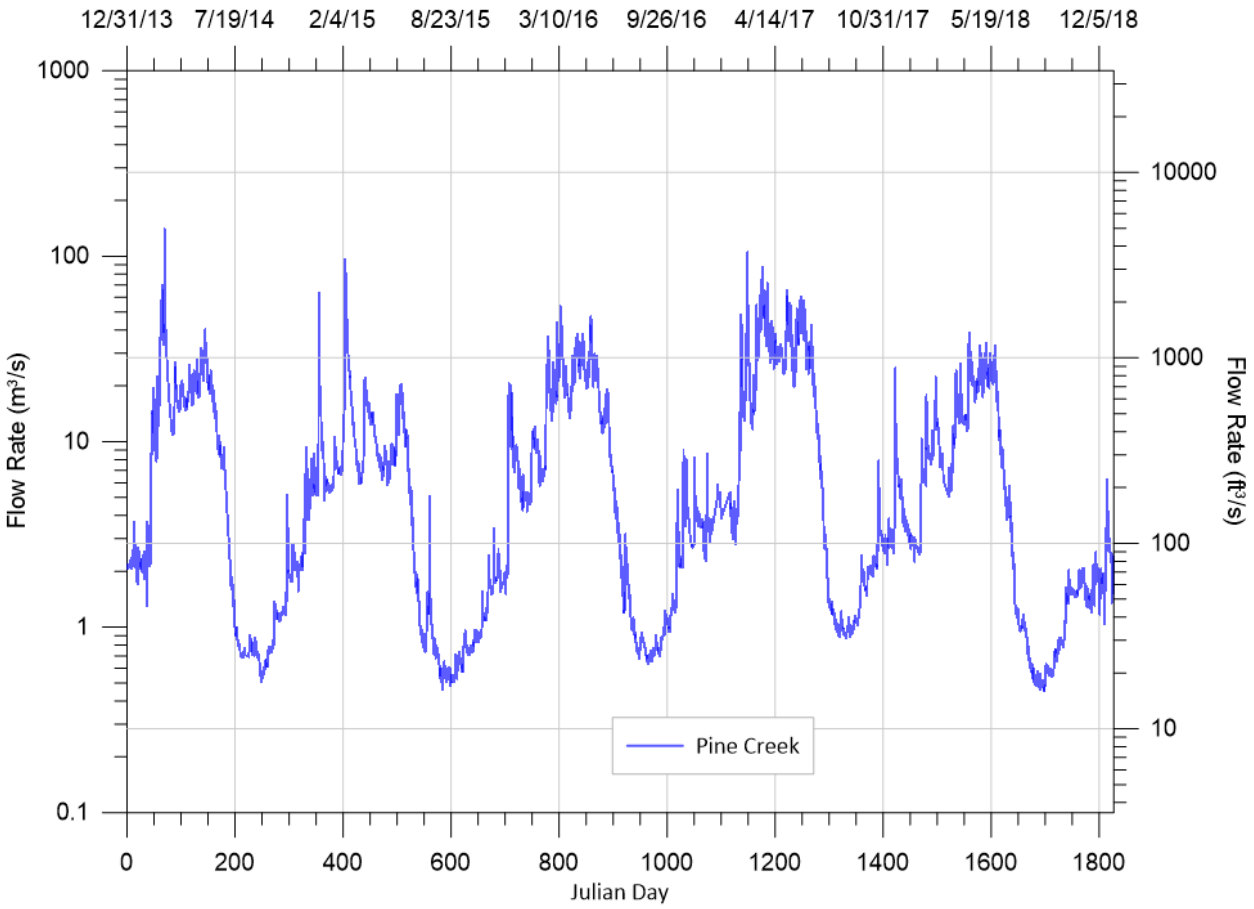


Figure 56. Pine Creek flow rates into Hells Canyon Reservoir.

Table 10. Brownlee, Oxbow, and Hells Canyon Reservoir model inflows and tributaries.

Name	Inflow Model Segment	Type of inflow	File names	Description
Brownlee Reservoir				
Snake River inflow	2	Branch inflow for branch 1 Snake River	qin_br1.csv tin_br1.csv cin_br1.csv	Snake River inflow for flow (q) (frequency every 15 min up to a day for data gaps), temperature (t), and concentration (c) [daily] from 1/1/2014 through 12/31/2018
Powder River inflow	205	Branch inflow for branch 6 Powder River	qin_br6_PowderR.csv tin_br6_PowderR.csv cin_br6_PowderR.csv	Includes Powder River near Richland (OWRD 13286700) and Eagle Creek at Richland (OWRD 13288300) flow measurements (frequency 0.1 day) from 1/1/2014-12/31/2018; temperatures are Flow weighted average of WTemp.Gage@Powder River_22_LB and

Name	Inflow Model Segment	Type of inflow	File names	Description
				WTemp.Gage@Eagle Creek_0.7_L data at a frequency usually of 0.1 days; concentrations are all daily
Burnt River	62	Tributary 1	qtr_tr1_BurntR.csv ttr_tr1_BurntR.csv ctr_tr1.csv	Burnt River inflow, flow frequency usually 15 mini but some gaps from 1-2 days and one gap of 18 days (JD 487-505.5); temperature gage at Burnt River with measurements usually every 15 min except 4 gaps from 5-90 days (the long gap is between JD 1240 and 1332 or 8/10/2010 but there is little inflow); concentrations are all daily
Daly Creek	207	Tributary 2	qtr_tr2_DalyCrk.csv ttr_tr2.csv ctr_tr2.csv	Daly Creek inflow at a frequency of 15 min (except for a couple data gaps of 1.6 days and 0.4 days); temperatures are the same as the Powder River; concentrations are all daily from Powder River
Water Balance	86-202	Distributed Tributary Branch 5	qwb_final_averaged.opt ttr_tr3.csv ctr_tr3.csv	This is a distributed tributary affecting Branch 5. The flow is from the water balance including positive and negative flows. The temperature and concentrations are from Powder River
Oxbow Reservoir				
Brownlee Spill inflow	2	Branch inflow	q_wdo_202.csv t_two_202.csv c_wdo_202.csv	Brownlee spill flow rate, temperature, and water quality computed from the Brownlee CE-QUAL-W2 model
Wildhorse River	6	Tributary 1	qtr_tr1_WildhorseR.csv ttr_tr1_WildhorseR.csv ctr_tr1_WildhorseR.csv	Flow rate at 15 min intervals with some data gaps of 2-80 days (80 day gap is between JD 557-657 during very low flow period); temperature at 15 min except a few gaps of 1 to 25 days; daily concentrations from Powder River
Brownlee turbine flow from Units 1-5	2	Tributary 2	q_wdo_238.csv t_wdo_238.csv c_wdo_238.csv	Brownlee turbine flow, temperature and water quality all combined
Hells Canyon Reservoir				
Oxbow inflow	2	Branch inflow	q_wdo_52.csv t_wdo_52.csv	Inflow from Oxbow spill and bypass flow into Hells Canyon

Name	Inflow Model Segment	Type of inflow	File names	Description
from spill and bypass flow			c_wdo_52.csv	
Oxbow inflow from power house	13	Tributary 1	q_wdo_50.csv t_wdo_50.csv c_wdo_50.csv	Flow, temperature, and water quality from Oxbow model for the Oxbow dynamic weir (power house flow)
Pine River	15	Tributary 2	qtr_tr2_Pine.csv ttr_tr2_Pine.csv ctr_tr2_Pine.csv	Flow, temperature, and water quality from Pine River inflow

Table 11. Data sources for modeled inflows.

Tributary	Reservoir	Frequency	Data Source
Snake River	Brownlee	15-minute	USGS – 13269000 Snake River at Weiser Idaho
Snake River	Brownlee	Daily average	USGS – 13269000 Snake River at Weiser Idaho
Burnt River	Brownlee	15-minute	IPC – 13275000 Burnt River at Huntington
Burnt River	Brownlee	Daily average	IPC – 13275000 Burnt River at Huntington
Powder River	Brownlee	15-minute	IPC – 13286700 Powder River near Richland
Powder River	Brownlee	Daily average	IPC – 13286700 Powder River near Richland
Eagle Creek	Brownlee	15-minute	IPC – 13288300 Eagle Creek at Richland
Eagle Creek	Brownlee	Daily average	IPC – 13288300 Eagle Creek at Richland
Daly Creek	Brownlee	15-minute	IPC – 13289030 Daly Creek below Diversion near Richland
Wildhorse River	Oxbow	15-minute	IPC – 13289960 Wildhorse River at Brownlee
Pine Creek	Hells Canyon	15-minute	IPC – 13290190 Pine Creek near Oxbow

IPC (Idaho Power Company, 2019-2022)

USGS (U.S. Geological Survey, 2019-2022)

Temperature Inputs

Inflow temperatures for the Hells Canyon Complex models included the Snake River temperatures at the upstream boundary condition of the Brownlee model and tributary temperatures. The file names of the temperature inputs are summarized in Table 10. Temperature data were available for the Snake River at RM 345.2, Burnt River, Powder River, Wildhorse River, Pine Creek and Eagle Creek.

Figure 57 shows Brownlee Reservoir inflow temperatures at the Snake River for the simulation period. Since the Powder River temperature station was located upstream of the Eagle Creek inflow, Powder River

temperatures were calculated using the flow-weighted temperature using Powder River temperature data (RM 22) and Eagle Creek temperature data (Figure 58). Flow weighted Powder River temperature data were used for Daly Creek inflows and the distributed tributary. Modeled Whitehorse inflow temperatures into Oxbow Reservoir are shown in Figure 59. Gaps in the Wildhorse data were filled using a linear regression equation between Wildhorse River temperatures and Powder River temperatures (Figure 59). Pine Creek temperatures are plotted in Figure 61. Gaps in the Pine Creek inflow temperatures were filled using a regression between Powder River and Pine Creek data (Figure 62).

Table 12. Temperature data sources for modeled inflows.

Tributary	Reservoir	Data Source
Snake River	Brownlee	IPC – WTemp.Logger@Snake River_345.2_LB
Burnt River	Brownlee	IPC – WTemp.Gage@Burnt River_2.5_RB
Powder River	Brownlee	IPC – WTemp.Gage@Powder River_22_LB and WTemp.Gage@Eagle Creek_0\.7_LB
Daly Creek	Brownlee	Used flow weighted Powder R. values
Wildhorse River	Oxbow	IPC – WTemp.Gage@Wildhorse_0.1_LB
Pine Creek	Hells Canyon	IPC – WTemp.Gage@Pine Creek_20.4_LB

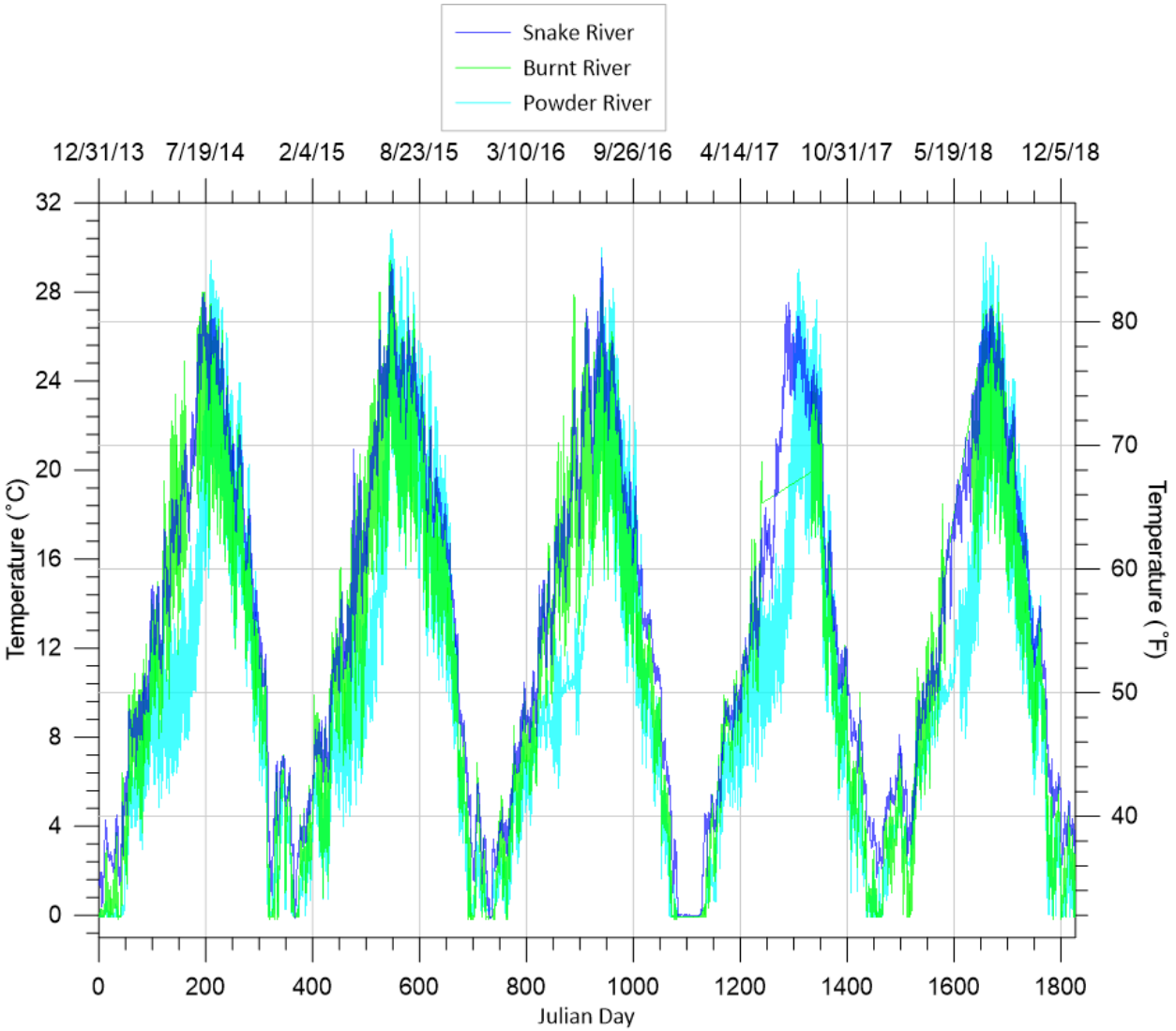


Figure 57. Brownlee Reservoir inflow temperatures. Powder River temperatures were used for Daly Creek and the distributed tributary.

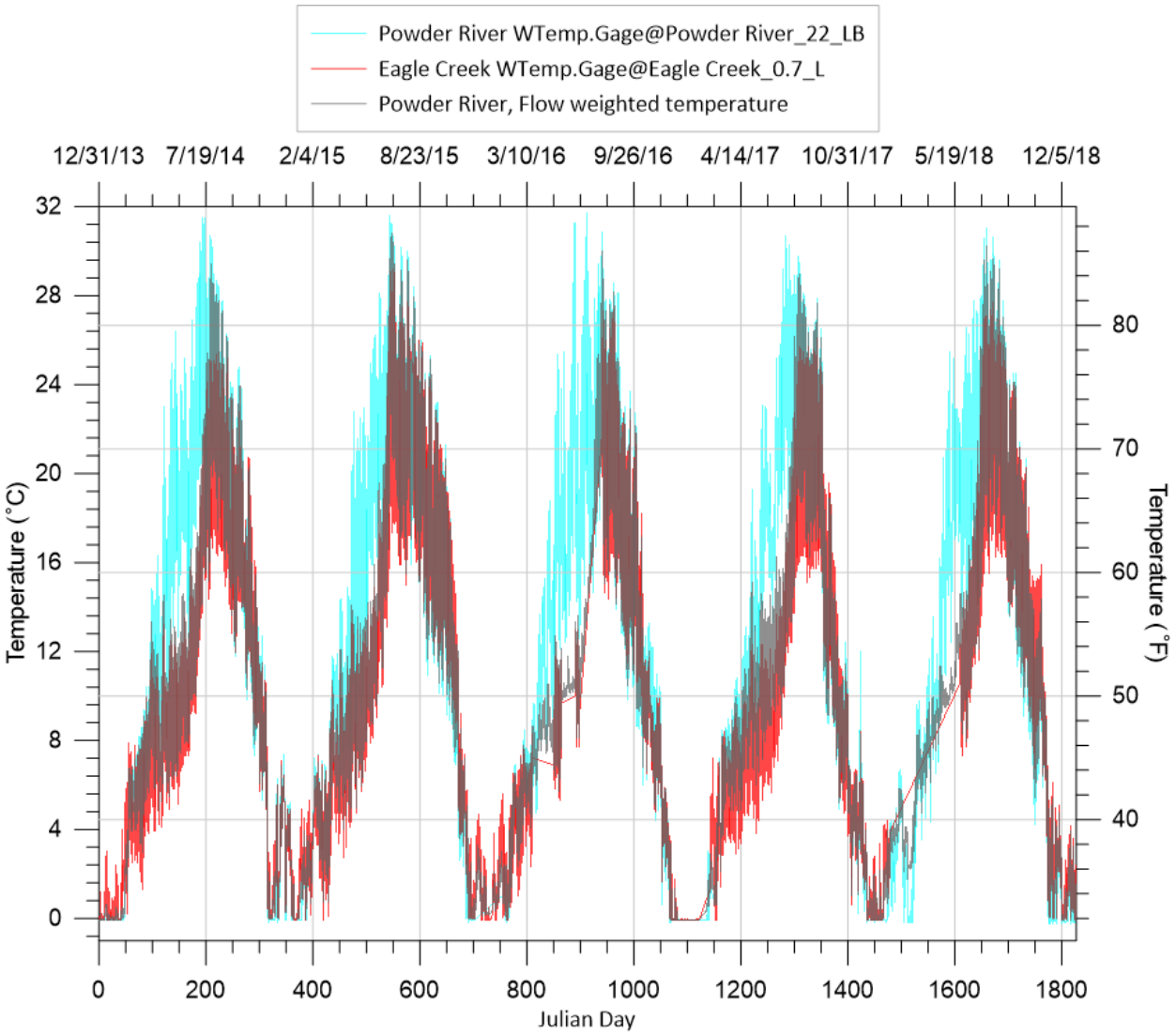


Figure 58. Powder River inflow temperatures. Powder River temperatures were estimated by calculating the flow-weighted average of Eagle Creek and Powder River (RM 22) data.

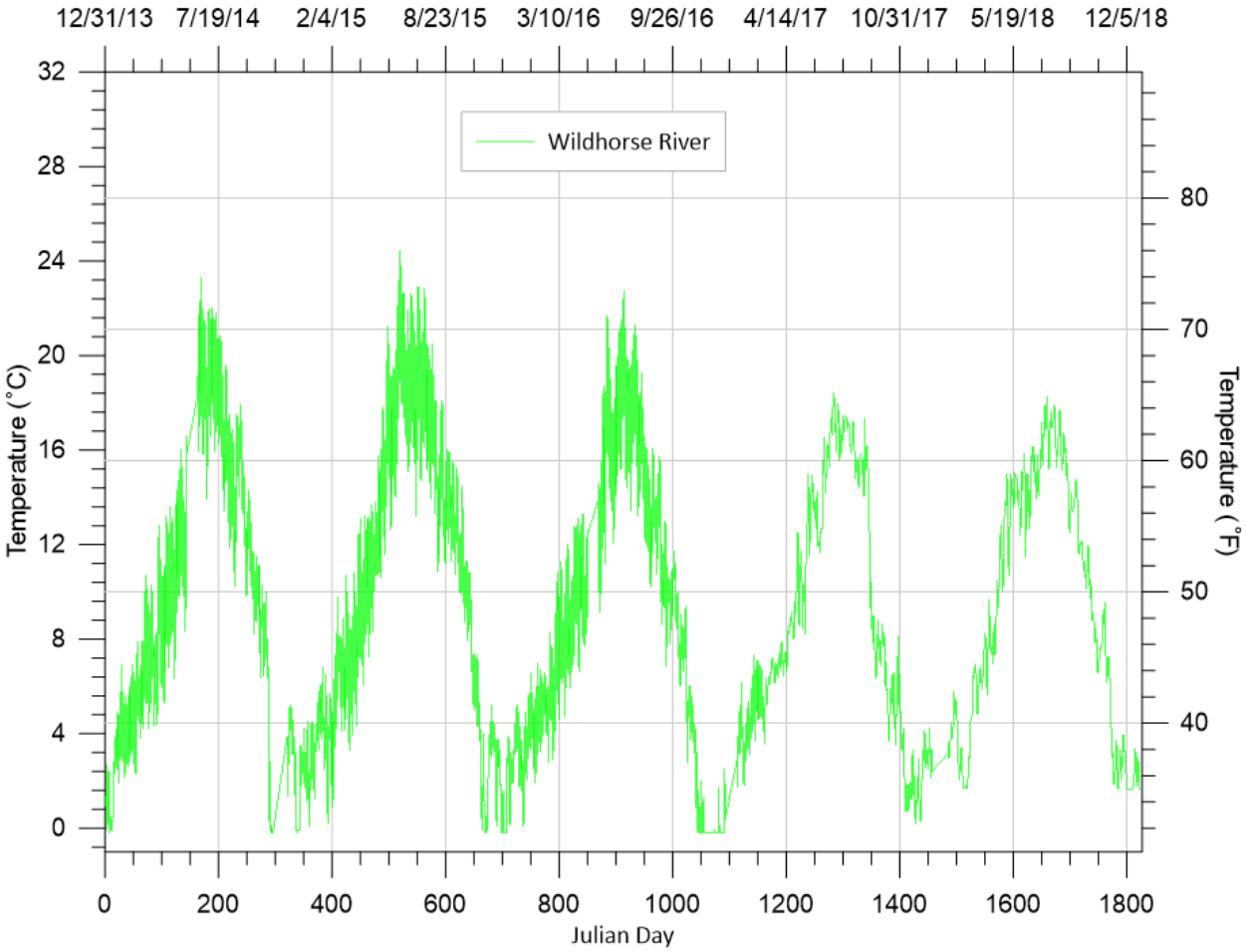


Figure 59. Wildhorse River inflow temperatures to Oxbow Reservoir.

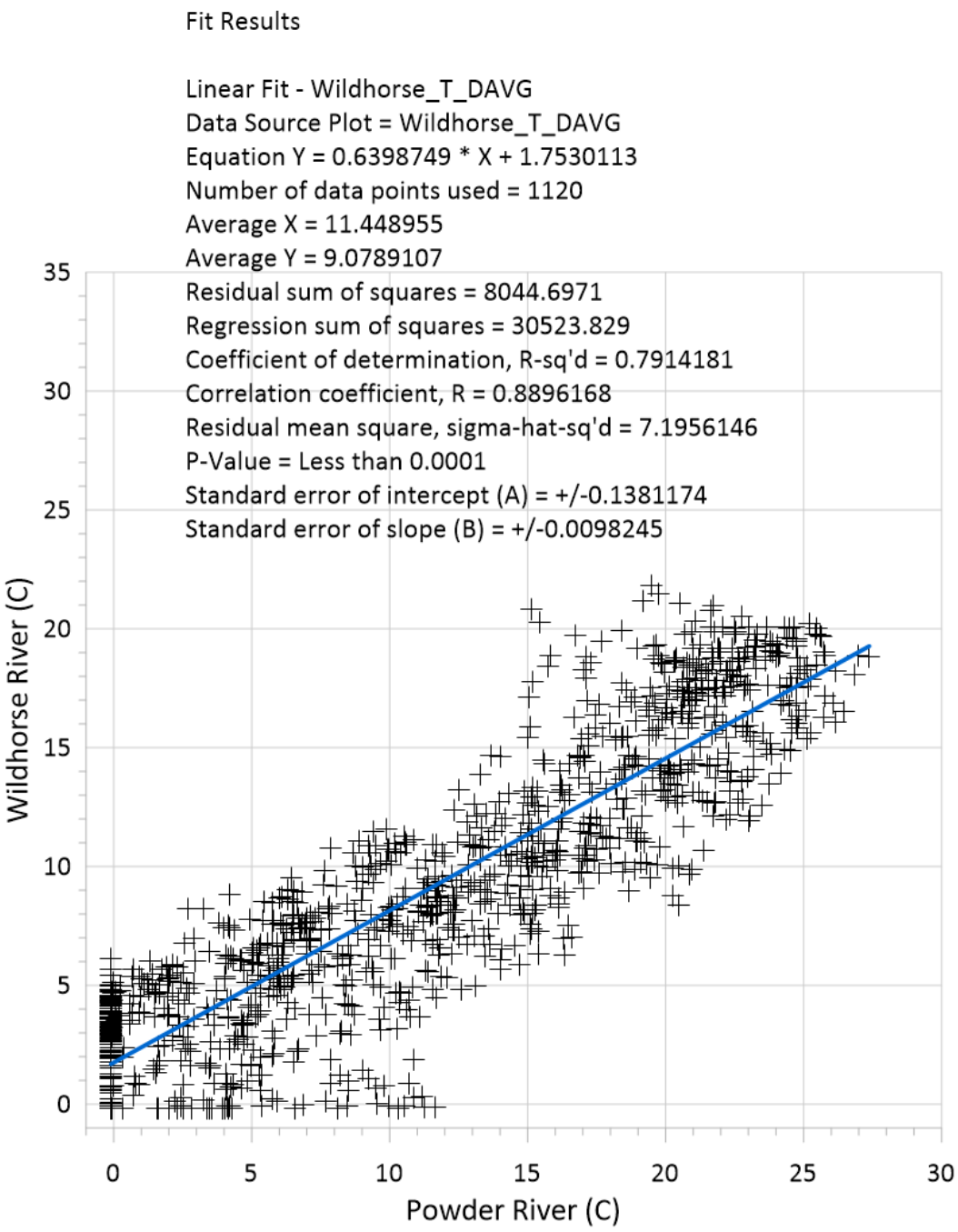


Figure 60. Plot of daily average Wildhorse River daily average temperatures versus Powder River daily average temperatures. A linear regression equation was used to estimate Wildhorse River temperatures within data gaps.

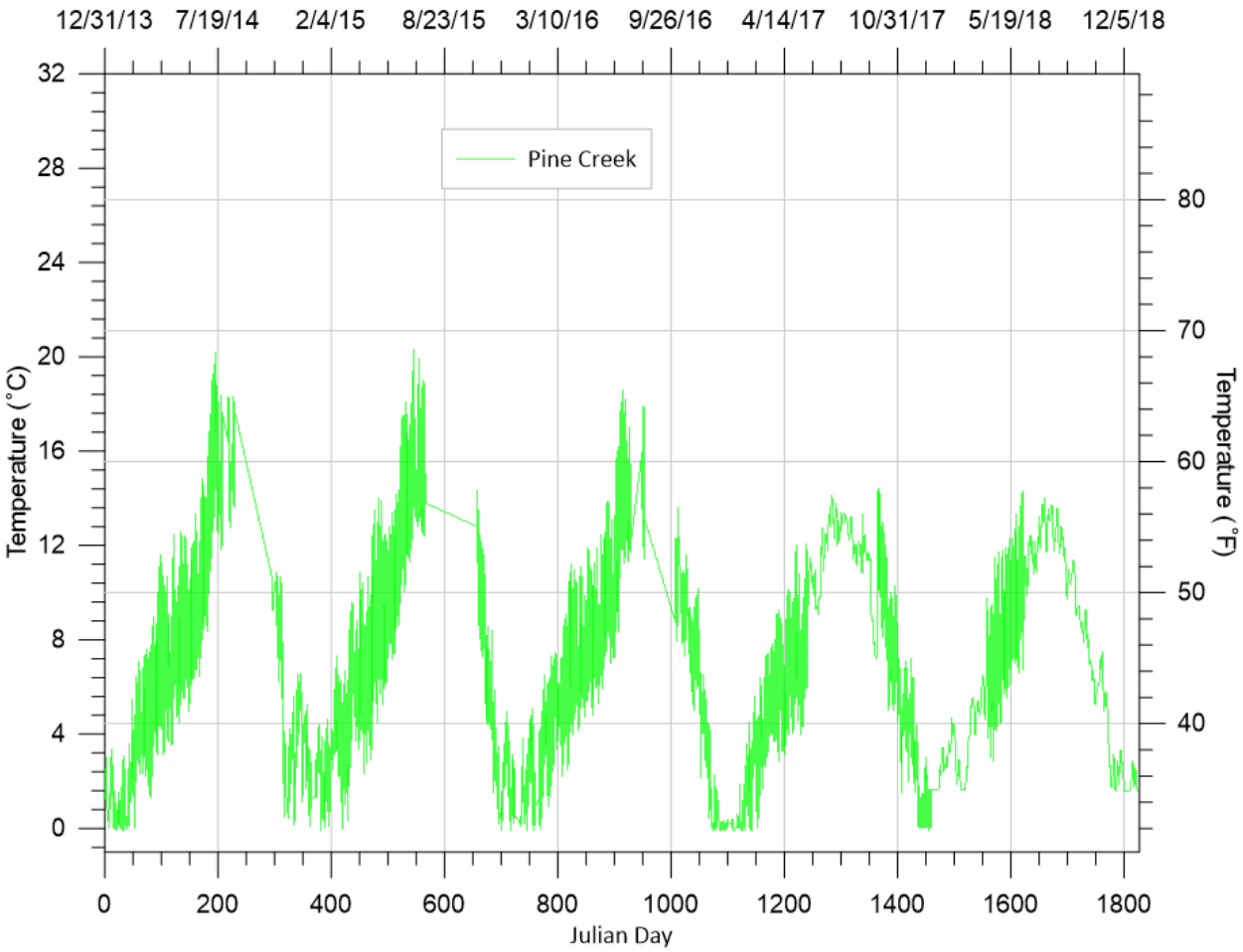


Figure 61. Pine Creek inflow temperatures to Hells Canyon Reservoir.

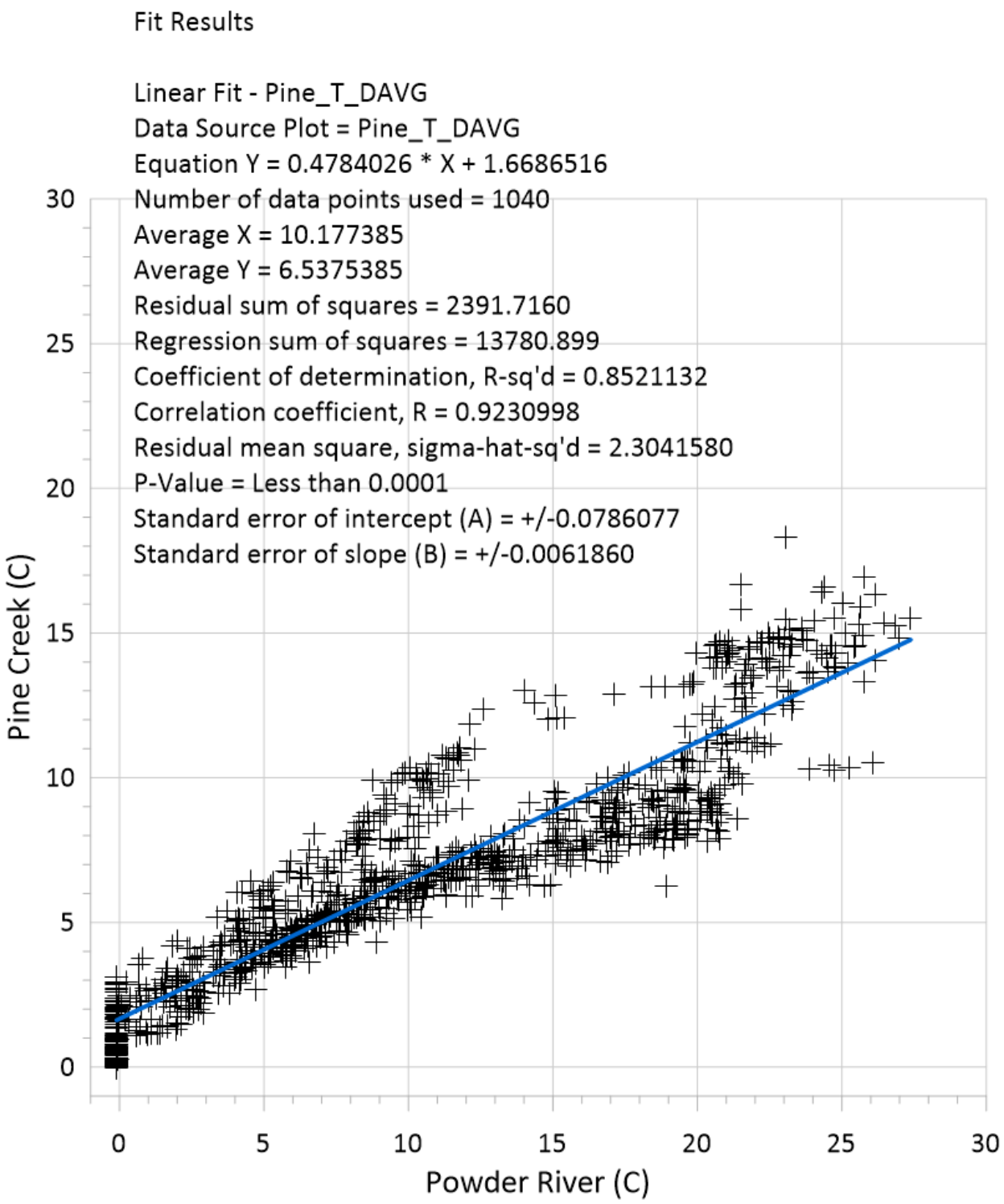


Figure 62. Plot of daily average Pine Creek daily average temperatures versus Powder River daily average temperatures. A linear regression equation was used to estimate Pine Creek temperatures within larger data gaps.

Constituent Inputs

Constituent concentrations for the Snake River inflow to Brownlee Reservoir were developed using IPC data and USGS (Poulin et al, 2022) data. Battelle data (included in the USGS data set) was only used for Hg inputs until July 2014. Data were collected from sampling stations located at RM 345.6. Data were not available for Powder River, Eagle Creek, or Burnt River during the simulation period, so input concentrations for these rivers were either set equal to Snake River inflow concentrations or regressions were developed to estimate certain parameters obtained by USGS and IPC. Regressions were created using either Snake River inflow concentrations of the same parameter or using tributary flows. The regressions that resulted in the best r-squared value were used for each site and for each parameter. Powder River input concentrations were calculated using a flow weighted average of Eagle Creek and Powder River concentrations near Richland, Oregon. Wildhorse River, Pine Creek, Daly Creek, and the distributed tributary concentrations were all set equal to flow weighted Powder River concentrations. For example, the overall contributions of Wildhorse and Pine are about 1% of the total inflow for PO_4-P. Daily average flows for Snake River, Powder River, Burnt River, and Eagle Creek were calculated from the 15-minute input flows to use in the regressions and flow weighting. Table 13 lists all the tributaries in each model and segment location. Table 14 lists each of each of the constituents and methods to create the constituent inflow timeseries for the Snake River. Table 15 lists each of the constituents and methods to create the constituent inflow timeseries for the Burnt River and Powder River. The file names of the concentration inputs are summarized in Table 10.

The following approach was used for processing data values for the input concentrations:

- USGS values with a "<" flag next to the reported value were halved when included in the inputs.
- IPC values with a "<" flag next to the reported value were halved when included in the inputs.
- Negative values and duplicates were removed.
- Any values of zero or "trace" were input as the minimum of (1) the lowest halved no detect ("<") value or (2) half of the lowest value observed (greater than zero).
- Negative depths were converted to positive and USGS depths of "SW" were converted to 0.3m. However, this didn't affect the input concentrations since depth was not used for generating inputs.
- All other values were included as the value listed, including values flagged as suspect or estimates or were filtered in the laboratory prior to analysis. USGS values that were flagged with "< RL, estimate based on lowest standard" were also left at the value listed.
- Gaps in data measurements were linearly interpolated except for when regressions or daily output from a loading model were used as described in the tables below.
- For linearly interpolated inputs, if multiple values were recorded on the same day, the average value was used for the input.
- Daily concentration output from loading models based on measured concentration, discharge, season, and time, were used to develop key input constituents. Kalman estimates from Weighted Regressions on Time Discharge and Season (WRTDS, Naymik et al. 2023, Hirsch 2019, Hirsch and De Cicco 2015) were used for nutrients, algae and TSS. Loadflex composite estimates (Appling et al. 2015, Aulenbach and Hooper 2006), which are similar to WRTDS Kalman estimates, were used for DOC (Yoder et al. 2024 *accepted*) and Hg inputs (Wells et al., 2025; Baldwin et al., 2022).

Table 13. Modeled HCC inflows.

Tributary	Model	Model Inflow Type, Number and Inflow Location
Snake River	Brownlee	Branch 1 Inflow, Segment 2
Powder River	Brownlee	Branch 6 Inflow, Segment 205
Burnt River	Brownlee	Tributary #1, Segment 62
Daly Creek	Brownlee	Tributary #2, Segment 207
Brownlee Water Balance Inflow	Brownlee	Branch 5 Distributed Tributary
Brownlee Dam Spill	Oxbow	Branch 1 Inflow, Segment 2
Wildhorse River	Oxbow	Tributary #1, Segment 6
Brownlee Turbines	Oxbow	Tributary #2, Segment 2
Oxbow Dam Spill and Bypass	Hells Canyon	Branch 1 Inflow, Segment 2
Oxbow Turbines	Hells Canyon	Tributary #1, Segment 13
Pine Creek	Hells Canyon	Tributary #2, Segment 15

Table 14. Development of modeled constituent concentrations in Snake River inflows to Brownlee Reservoir.

#	Constituent	ON or OFF in model	Comments
1	TDS, mg/L	OFF	
2	Tracer, mg/L	OFF	
3	Conductivity, uS/cm	OFF	
4	Chloride, mg/L	ON	USGS Data A minimum chloride of 0.001 mg/l was allowed in the inputs.
5	ISS1, mg/L	ON	Three ISS groups were simulated in the model (ISS1, ISS2, and ISS3). ISS1 was considered to consist of heavier particles with a faster settling rate of 5 m/day while ISS2 had a settling rate of 1 m/day. Total ISS concentrations (ISS1+ISS2+ISS3) were estimated using USGS total suspended solids (TSS) data with IPC volatile suspended solids (VSS) data: $$\Phi_{ISS} = \Phi_{TSS} - \Phi_{VSS}$$ A TSS timeseries was developed using USGS TSS data directly where available. USGS TSS data was preferred in this step because the TSS measurements are made directly from a filter where subsequent mercury measurements were made. For the large gaps in USGS TSS data, IPC TSS data (collected at the same time as mercury) were converted using a regression between paired IPC TSS and USGS TSS (Figure 64). $\Phi_{TSS} = (exp(0.58615 + 0.85003 * ln(\Phi_{TSS_IPC}))) * 1.092929)$

#	Constituent	ON or OFF in model	Comments
			Utilizing long-term IPC data the dataset extended back to 1995 and was used in the WRTDS model to estimate daily Kalman concentrations for TSS during the 2014-2018 model period following the analysis in Naymik et al (2023). A gap was then filled in the IPC VSS data (2/23/17 – 5/1/18, Figure 65) using a regression with USGS TSS data (Figure 66): $\Phi_{VSS} = (exp(-0.83480 + 0.72442 * ln(\Phi_{TSS}))) * 1.142356$ Then a VSS timeseries was then developed using VSS data directly where available. Utilizing long-term IPC data the dataset extended back to 1998 and was used in the WRTDS model to estimate daily Kalman concentrations for VSS during the 2014-2018 model period following the analysis in Naymik et al (2023). The fraction of total ISS in each of the three ISS groups varied over time and was determined through calibration to best match field data for TSS (see Figure 67 for the fraction of each group used over the simulation). A minimum value of 0.1 mg/l was allowed in the inflow for ISS.
6	ISS2, mg/L	ON	ISS2 was considered to consist of lighter particles with a slower settling rate. ISS2 was calculated as: $\Phi_{ISS2} = 0.89 * (ISS - \Phi_{ISS1})$
7	ISS3, mg/L	ON	ISS3 was considered to consist of lighter particles (considered 11% of the fraction) with a settling rate of . ISS3 was calculated as: $\Phi_{ISS3} = 0.11 * (ISS - \Phi_{ISS1})$
8	Age, days	ON	
9	Bacteria, col/100ml	OFF	
10	Dissolved Gas Pressure, atm	OFF	
11	N2 dissolved gas, mg/L	OFF	
12	H2S, dissolved gas, mg/L	ON	USGS data (labeled as filter-passing inorganic sulfide). Set to zero since only inflow data measurement was a no detect.
13	CH4 dissolved gas, mg/L	ON	Set to zero
14	SO4 dissolved, mg/L	ON	IPC and USGS Data linearly interpolated to daily A minimum SO4 of 0.001 mg/l was allowed in the inputs.
15	Reduced Fe(II), mg/L	ON	Assumed to be equal to USGS filtered Fe linearly interpolated to daily. A minimum Fe(II) of 0.0001 mg/l was allowed in the inputs.

#	Constituent	ON or OFF in model	Comments
16	Oxidized FeOOH, mg/L	ON	Assumed to be equal to USGS particulate Fe linearly interpolated to daily. Used ratio of average particulate Fe to average filtered Fe multiplied by the Fe(II) concentration to estimate FeOOH prior to start of particulate measurements in March 2017: $$\Phi_{FeOOH} = \frac{\Phi_{average\ particulate\ Fe}}{\Phi_{average\ filtered\ Fe}} * \Phi_{Fe(II)}$$
17	Reduced Mn(II), mg/L	ON	Assumed to be equal to USGS filtered Mn linearly interpolated to daily. A minimum Mn(II) of 0.0001 mg/l was allowed in the inputs.
18	Oxidized MnO2, mg/L	ON	Assumed to be equal to USGS particulate Mn linearly interpolated to daily. Used ratio of average particulate Mn to average filtered Mn multiplied by the Mn(II) concentration to estimate MnO2 prior to start of particulate measurements in March 2017: $$\Phi_{MnO2} = \frac{\Phi_{average\ particulate\ Mn}}{\Phi_{average\ filtered\ Mn}} * \Phi_{Mn(II)}$$
19	Ortho-phosphate, mg/L	ON	IPC Data. Daily WRTDS Kalman concentration estimates (Naymik et al. 2023).
20	Ammonium, mg/L	ON	IPC Data interpolated to daily.
21	Nitrate-Nitrite, mg/L	ON	IPC Data. Daily WRTDS Kalman concentration estimates (Naymik et al. 2023).
22	Dissolved silica, mg/L	OFF	
23	Particulate silica, mg/L	OFF	
24	Labile DOM, mg/L	ON	Estimated using USGS dissolved organic carbon (DOC) data and loadflex composite daily concentration estimates (Yoder et al 2024 *accepted)*: $$\Phi_{DOM} = \frac{\Phi_{DOC}}{orgc}$$ Φ_{DOM}= Dissolved organic matter concentration, mg/l Φ_{DOC}=Dissolved Organic Carbon, mg/l $orgc$=0.45, stoichiometric equivalent between organic matter and carbon Labile dissolved organic matter (LDOM) was then calculated with: $$LDOM = \Phi_{LDOM} = \alpha\Phi_{DOM}$$ α=Labile ratio of 10% (Harrison, 2005) The use of labile ratio of 10% was suggested by Harrison (2005).
25	Refractory DOM, mg/L	ON	Refractory dissolved organic matter (RDOM) calculated using

#	Constituent	ON or OFF in model	Comments
			$\Phi_{RDOM} = (1-\alpha)\Phi_{DOM}$
26	Labile POM, mg/L	ON	POC was estimated from the daily WRTDS Kalman VSS concentrations as (Figure 69): $POC = (exp(-0.9114 + 0.85045 * ln(VSS))) * 1.048809$ Particulate organic matter concentrations were then calculated from POC with: $\Phi_{POM} = \frac{\Phi_{POC}}{orgc} - \Phi_{algaeT} - \Phi_{zooT}$ Φ_{POM}= particulate organic matter concentration, mg/l Φ_{POC}=particulate organic carbon concentration, mg/l $orgc$=0.45, stoichiometric equivalent between organic matter and carbon Φ_{algaeT} = total algae concentration, mg/l Φ_{zooT} = total zooplankton concentration, mg/l Using a labile ratio of 28.5%, midpoint of the range between 12% and 45% suggested by Harrison (2005), labile particulate organic matter (LPOM) can be calculated from $LPOM = \Phi_{LPOM} = \beta\Phi_{POM}$ β=Labile ratio of 28.5% A minimum Φ_{POM} of 0.01 was allowed in the inputs.
27	Refractory POM, mg/L	ON	Refractory particulate organic matter (RPOM) calculated using $\Phi_{RPOM} = (1-\beta)\Phi_{POM}$
28	Algae1, mg/L	ON	See Appendix A1 for a summary of the phytoplankton speciation and biovolume data available. Algae concentrations were estimated using IPC chlorophyll *a* data, and daily WRTDS Kalman concentration estimates (Naymik et al. 2023) and biofractions for each algal group from the 2011 data set since this data set had similar values to the 2002 data set but was more recent. $\Phi_{algaeT} = \frac{\Phi_{chla}}{\frac{f_{alg1}}{achla1} + \frac{f_{alg2}}{achla2} + \frac{f_{alg3}}{achla3}}$ $\Phi_{algae1} = \Phi_{algaeT} \times f_{alg1}$ Where Φ_{algaT} = total algae concentration, mg/l Φ_{chla} = chlorophyll *a*, µg/l, IPC data f_{alg1} = 0.88, fraction of total algae that is algal group 1 f_{alg2} = 0.10, fraction of total algae that is algal group 2 f_{alg3} = 0.02, fraction of total algae that is algal group 3 $achla$ = chlorophyll a ratio of mg algae/µg chlorophyll *a* for each algal group

#	Constituent	ON or OFF in model	Comments
			$achla1$ = 0.05 $achla2$ = 0.02 $achla3$ = 0.02 A minimum chlorophyll a value of 0.001 mg/l was allowed in the inflows.
29	Algae2, mg/L	ON	$\Phi_{algae2} = \Phi_{algaeT} \times f_{alg2}$
30	Algae3, mg/L	ON	$\Phi_{algae3} = \Phi_{algaeT} \times f_{alg3}$
31	Dissolved oxygen, mg/L	ON	Bi-weekly IPC Data
32	Inorganic carbon, mg/L	ON	Assumed total inorganic carbon is equal to dissolved inorganic carbon (USGS DIC data).
33	Alkalinity, mg/L	ON	Calculated using temperature and IPC biweekly pH data and the carbonate-bicarbonate equilibrium reaction (Stumm and Morgan 1981). $\Phi_{Alkalinity} = function(\Phi_{TIC}, pH, Temperature)$ pH values of 10.21, 10.14, 10.34, 10.07, 9.84, 10.65, 10.48, 10.81, and 10.77 on 8/23/16, 10/6/16, 5/17/17, 7/13/17, 5/1/18, 8/22/18, 8/31/18, 9/19/18, and 9/24/18 were removed during calibration since these resulted in much higher pH than observed in Brownlee Reservoir.
34	Zooplankton, mg/L	ON	Set to constant 0.001 to seed the reservoir
35	LDOM P mg/L	ON	Dissolved organic matter phosphorus constituent concentrations were estimated from the daily WRTDS Kalman PO4-P concentrations and an estimate of the fraction of total dissolved phosphorus that is PO4-P based on a recent dataset from 2023 at the Snake River inflow to Brownlee (85%,.: $\Phi_{DOM-P} = (\Phi_{PO4-P}/0.85) - \Phi_{PO4-P}$ Φ_{DOM-P}=Dissolved organic matter phosphorus, mg/l Φ_{PO4-P}=ortho-phosphorus, mg/l, IPC data and USGS data The LDOM-P fraction of organic matter phosphorus Φ_{OM-P} was estimated using the relative fraction of labile dissolved organic matter to total dissolved organic matter: $\Phi_{LDOM-P} = \Phi_{DOM-P} \times \frac{\Phi_{LDOM}}{\Phi_{DOM}}$ Where $\Phi_{DOM} = \Phi_{LDOM} + \Phi_{RDOM}$
36	RDOM P, mg/L	ON	The RDOM-P fraction of dissolved organic matter phosphorus Φ_{DOM-P} was estimated using the relative fraction of refractory dissolved organic matter to total dissolved organic matter: $\Phi_{RDOM-P} = \Phi_{DOM-P} \times \frac{\Phi_{RDOM}}{\Phi_{DOM}}$

#	Constituent	ON or OFF in model	Comments
37	LPOM P, mg/L	ON	The particulate fraction of organic matter phosphorus Φ_{POM-P} was estimated using daily WRTDS Kalman concentration estimates of total phosphorus (TP) from IPC data (Naymik et al. 2023).: $$\Phi_{POM-P} = \Phi_{TP} - \Phi_{PO4-P} - \Phi_{DOM-P-}\Phi_{algaeT} \times algp - \Phi_{zooT} \times zoop$$ Φ_{POM-P}=Particulate organic matter phosphorus, mg/l Φ_{TP}=Total Phosphorus, mg/l, IPC data Φ_{PO4-P}=ortho-phosphorus, mg/l, IPC data and USGS data Φ_{DOM-P}=Dissolved organic matter phosphorus, mg/l $algp$=0.01, stoichiometric equivalent between algae and phosphorus $zoop$=0.005, stoichiometric equivalent between zooplankton and phosphorus A minimum of 0.0001 mg/L was allowed for Φ_{POM-P} The Labile fraction of Φ_{POM-P} was estimated using the relative fraction of labile particulate organic matter to total particulate organic matter $$\Phi_{LPOM-P} = \Phi_{POM-P} \times \frac{\Phi_{LPOM}}{\Phi_{POM}}$$
38	RPOM P, mg/L	ON	The RPOM-P fraction of organic matter phosphorus Φ_{OM-P} was estimated using the relative fraction of refractory particulate organic matter to total organic matter: $$\Phi_{RPOM-P} = \Phi_{OM-P} \times \frac{\Phi_{RPOM}}{\Phi_{POM}}$$
39	LDOM N, mg/L	ON	Organic matter nitrogen constituent concentrations were estimated from daily WRTDS Kalman concentration estimates of total nitrogen (TN) from IPC data (Naymik et al. 2023): $$\Phi_{OM-N} = \Phi_{TN} - \Phi_{NO3-N} - \Phi_{NH3-N} - \Phi_{algaeT} \times algn - \Phi_{zooT} \times zoon$$ Φ_{OM-N}=Organic matter nitrogen, mg/l Φ_{TN}=total nitrogen, mg/l, IPC data Φ_{NO3-N}=Nitrate nitrogen, mg/l, IPC data Φ_{NH3-N}=ammonia nitrogen, mg/l, IPC data $algn$=0.08, stoichiometric equivalent between algae and nitrogen *zoon*=0.08, stoichiometric equivalent between zooplankton and nitrogen

#	Constituent	ON or OFF in model	Comments
			The LDOM-N fraction of organic matter nitrogen Φ_{OM-N} was estimated using the relative fraction of labile dissolved organic matter to total organic matter: $$\Phi_{LDOM-N} = \Phi_{OM-N} \times \frac{\Phi_{LDOM}}{\Phi_{OM}}$$ Where $$\Phi_{OM} = \Phi_{LDOM} + \Phi_{RDOM} + \Phi_{LPOM} + \Phi_{RPOM}$$ A minimum Φ_{OM-N}/Φ_{OM} of 0.01 was allowed in the inputs.
40	RDOM N, mg/L	ON	The RDOM-N fraction of organic matter nitrogen Φ_{OM-N} was estimated using the relative fraction of refractory dissolved organic matter to total organic matter: $$\Phi_{RDOM-N} = \Phi_{OM-N} \times \frac{\Phi_{RDOM}}{\Phi_{OM}}$$
41	LPOM N, mg/L	ON	The LPOM-N fraction of organic matter nitrogen Φ_{OM-N} was estimated using the relative fraction of labile particulate organic matter to total organic matter: $$\Phi_{LPOM-N} = \Phi_{OM-N} \times \frac{\Phi_{LPOM}}{\Phi_{OM}}$$
42	RPOM N, mg/L	ON	The RPOM-N fraction of organic matter nitrogen Φ_{OM-N} was estimated using the relative fraction of refractory particulate organic matter to total organic matter: $$\Phi_{RPOM-N} = \Phi_{OM-N} \times \frac{\Phi_{RPOM}}{\Phi_{OM}}$$

Table 15. Development of modeled constituent concentrations in the Burnt River and Powder River. Wildhorse River, Pine Creek, Daly Creek, and the distributed tributary concentrations were all set equal to flow weighted Powder River concentrations.

#	Constituent	ON or OFF in model	Comments
1	TDS, mg/L	OFF	
2	Tracer, mg/L	OFF	
3	Conductivity, uS/cm	OFF	
4	Chloride, mg/L	ON	Burnt R., Powder R., and Eagle Cr. chloride concentrations during the simulation period were estimated using a regression with each tributary's flow data. Regressions were created using USGS chloride and flow data available after the simulation period (Figure 71). Burnt River Regression: $$\Phi Cl_{Burnt} = \exp\left(3.56 - 0.458\left(ln(Flow_{Burnt})\right)\right) * 1.02$$ Powder River Regression:

#	Constituent	ON or OFF in model	Comments
			$\Phi Cl_{Powder} = \exp\left(2.85 - 0.211\left(ln(Flow_{Powder})\right)\right) * 1.02$ Eagle Creek Regression: $\Phi Cl_{Eagle} = \exp\left(1.55 - 0.399\left(ln\left(Flow_{Eagle}\right)\right)\right) * 1.02$ A minimum chloride of 0.001 mg/l was allowed in the inputs.
5	ISS1, mg/L	ON	$\Phi_{ISS} = \Phi_{TSS} - \Phi_{LPOM} - \Phi_{RPOM} - \Phi_{algaeT} - \Phi_{zooT}$ Burnt R. and Eagle Cr. TSS concentrations during the simulation period were estimated using a regression with Snake River inflow USGS TSS data. Powder R. TSS concentrations were estimated using a regression with Powder R. flow data. Regressions were created using USGS TSS and flow data available after the simulation period (Figure 72). Burnt River Regression: $\Phi TSS_{Burnt} = \exp\left(-0.263 + 1.11\left(ln(\Phi TSS_{Snake})\right)\right) * 1.11$ Powder River Regression: $\Phi TSS_{Powder} = \exp\left(-1.65 + 0.723\left(ln(Flow_{Powder})\right)\right) * 1.11$ Eagle Creek Regression: $\Phi TSS_{Eagle} = \exp\left(0.0552 + 0.546\left(ln(\Phi TSS_{Snake})\right)\right) * 1.16$ Where ΦTSS_{Snake} is the final snake river TSS concentration after as described previously in Table 14. The same fractions that were used for the Snake River inputs were used to divide the total ISS into ISS1 and ISS2 for the tributaries. A minimum value of 0.1 mg/l was allowed in the inputs for ISS.
6	ISS2, mg/L	ON	The same fractions that were used for the Snake River inputs were used to divide the total ISS into ISS1 and ISS2 for the tributaries. There is no ISS3 for the tributaries.
7	Age, days	ON	
8	Bacteria, col/100ml	OFF	
9	Dissolved Gas Pressure, atm	OFF	
10	N2 dissolved gas, mg/L	OFF	
11	H2S, dissolved gas, mg/L	ON	Set to zero
12	CH4 dissolved gas, mg/L	ON	Set to zero

#	Constituent	ON or OFF in model	Comments
13	SO4 dissolved, mg/L	ON	Burnt R. and Powder R. SO4 concentrations during the simulation period were estimated using a regression with each tributary's flow data. Eagle Cr. SO4 concentrations were estimated using a regression with Snake River inflow USGS SO4 data. Regressions were created using USGS SO4 and flow data available after the simulation period (Figure 73). Burnt River Regression: $\Phi SO4_{Burnt} = \exp\left(5.50 - 0.347\left(ln(Flow_{Burnt})\right)\right) * 1.01$ Powder River Regression: $\Phi SO4_{Powder} = \exp\left(4.30 - 0.284\left(ln(Flow_{Powder})\right)\right) * 1.02$ Eagle Creek Regression: $\Phi SO4_{Eagle} = -4.96 + 0.214(\Phi SO4_{Snake})$ A minimum SO4 of 0.001 mg/l was allowed in the inputs.
14	Reduced FE(II), mg/L	ON	Burnt R., Powder R., and Eagle Cr. Fe(II) concentrations during the simulation period were estimated using a regression with each tributary's flow data. Regressions were created using USGS filtered Fe (units of µg/l) and flow data available after the simulation period (Figure 74). Burnt River Regression: $\Phi Fe(II)_{Burnt} = \left(\exp\left(-3.53 + 1.50\left(ln(Flow_{Burnt})\right)\right) * 1.83\right) /1000$ Powder River Regression: $\Phi Fe(II)_{Powder} = \left(\exp\left(0.410 + 0.608\left(ln(Flow_{Powder})\right)\right) * 1.11\right) /1000$ Eagle Creek Regression: $\Phi Fe(II)_{Eagle} = \left(\exp\left(2.31 + 0.00885\left(ln(Flow_{Eagle})\right)\right) * 1.07\right) /1000$ A minimum Fe(II) of 0.0001 mg/l was allowed in the inputs.
15	Oxidized FeOOH, mg/L	ON	Set to Snake River concentrations
16	Reduced Mn(II), mg/L	ON	Burnt R., Powder R., and Eagle Cr. Mn(II) concentrations during the simulation period were estimated using a regression with each tributary's flow data. Regressions were created using USGS filtered Mn (units of µg/l) and flow data available after the simulation period (Figure 75). Burnt River Regression:

#	Constituent	ON or OFF in model	Comments
			$\Phi Mn(II)_{Burnt} = \left(\exp\left(4.23 - 0.283\left(ln(Flow_{Burnt})\right)\right) * 1.28\right) /1000$ Powder River Regression: $\Phi Mn(II)_{Powder} = \left(\exp\left(-0.558 + 0.504\left(ln(Flow_{Powder})\right)\right) * 1.23\right) /1000$ Eagle Creek Regression: $\Phi Mn(II)_{Eagle} = \left(\exp\left(1.38 - 0.108\left(ln\left(Flow_{Eagle}\right)\right)\right) * 1.04\right) /1000$ A minimum Mn(II) of 0.0001 mg/l was allowed in the inputs.
17	Oxidized MnO2, mg/L	ON	Set to Snake River concentrations
18	Ortho-phosphate, mg/L	ON	Burnt R., Powder R., and Eagle Cr. PO4 concentrations during the simulation period were estimated using a regression with Snake River inflow USGS PO4 data. Regressions were created using USGS filter-passing phosphorus data (units of µg/l) available after the simulation period (Figure 76). Burnt River Regression: $\Phi PO4_{Burnt} = (41.7 + 1.89(\Phi PO4_{Snake}))/1000$ Powder River Regression: $\Phi PO4_{Powder} = (-8.14 + 3.67(\Phi PO4_{Snake}))/1000$ Eagle Creek Regression: $\Phi PO4_{Eagle} = (0.325 + 0.247(\Phi PO4_{Snake}))/1000$ A minimum PO4 of 0.0001 mg/l was allowed in the inputs.
19	Ammonium, mg/L	ON	Set to Snake River concentrations
20	Nitrate-Nitrite, mg/L	ON	Burnt R. and Powder R. nitrate concentrations during the simulation period were estimated using a regression with each tributary's flow data. Eagle Cr. nitrate concentrations were estimated using a regression with Snake River inflow USGS nitrate data. Regressions were created using USGS nitrate and flow data available after the simulation period (Figure 77). Burnt River Regression: $\Phi NO3_{Burnt} = \exp\left(-4.22 + 0.414\left(ln(Flow_{Burnt})\right)\right) * 1.11$ Powder River Regression: $\Phi NO3_{Powder} = \exp\left(-5.29 + 0.513\left(ln(Flow_{Powder})\right)\right) * 1.22$ Eagle Creek Regression:

#	Constituent	ON or OFF in model	Comments
			$\Phi NO3_{Eagle} = 0.0018 + 0.0256(\Phi NO3_{Snake})$ A minimum nitrate of 0.001 mg/l was allowed in the inputs.
21	Dissolved silica, mg/L	OFF	
22	Particulate silica, mg/L	OFF	
23	Labile DOM, mg/L	ON	Same method as Snake River. Burnt R., Powder R., and Eagle Cr. DOC concentrations during the simulation period were estimated using a regression with Snake River inflow USGS DOC data. Regressions were created using USGS DOC data available after the simulation period (Figure 78). Burnt River Regression: $\Phi DOC_{Burnt} = -0.815 + 2.35(\Phi DOC_{Snake})$ Powder River Regression: $\Phi DOC_{Powder} = -0.313 + 2.88(\Phi DOC_{Snake})$ Eagle Creek Regression: $\Phi DOC_{Eagle} = -0.723 + 0.895(\Phi DOC_{Snake})$ A minimum DOC of 0.0001 mg/l was allowed in the inputs.
24	Refractory DOM, mg/L	ON	Same method as Snake River.
25	Labile POM, mg/L	ON	Same method as Snake River. Using Snake River POC concentrations.
26	Refractory POM, mg/L	ON	Same method as Snake River.
27	Algae1, mg/L	ON	Same method as Snake River. Powder R. and Eagle Cr. chlorophyll a concentrations during the simulation period were estimated using a regression with each tributary's flow data. Burnt R. chlorophyll a concentrations were estimated using a regression with Snake River inflow IPC chlorophyll a data. Regressions were created using IPC chlorophyll a and USGS flow data available after the simulation period (Figure 79). During the higher flow months (January 1 – June 30), Powder River weighted chlorophyll a concentrations were set equal to Snake River inflow concentrations since using the regressions would lead to unrealistically high chlorophyll a values. A maximum value of 100 µg/l was allowed in the inflows for Powder River at all other times. Burnt River Regression: $\Phi Chla_{Burnt} = \exp\left(-0.331 + 0.856\left(ln(\Phi Chla_{Snake})\right)\right) * 1.09$ Powder River Regression: $\Phi Chla_{Powder} = \exp\left(-6.83 + 2.12\left(ln(Flow_{Powder})\right)\right) * 1.45$

#	Constituent	ON or OFF in model	Comments
			Eagle Creek Regression: $\Phi Chla_{Eagle} = \exp\left(3.39 - 0.739\left(ln\left(Flow_{Eagle}\right)\right)\right) * 1.07$ A minimum chlorophyll a value of 0.001 mg/l was allowed in the inflows. See Figure 70 for the chlorophyll a inputs for each tributary.
28	Algae2, mg/L	ON	Same method as Snake River.
29	Algae3, mg/L	ON	Same method as Snake River.
30	Dissolved oxygen, mg/L	ON	Set to Snake River concentrations
31	Inorganic carbon, mg/L	ON	Set to Snake River concentrations
32	Alkalinity, mg/L	ON	Same method as Snake River. Using tributary temperatures and Snake River IPC pH data.
33	Zooplankton, mg/L	ON	Set to constant 0.001 to seed the reservoir
34	LDOM P mg/L	ON	Same method as Snake River. Using Snake River total phosphorus concentrations and tributary ortho-phosphorus concentrations as calculated from regressions with USGS data.
35	RDOM P, mg/L	ON	Same method as Snake River.
36	LPOM P, mg/L	ON	Same method as Snake River.
37	RPOM P, mg/L	ON	Same method as Snake River.
38	LDOM N, mg/L	ON	Same method as Snake River. Using Snake River TKN and ammonia concentrations.
39	RDOM N, mg/L	ON	Same method as Snake River.
40	LPOM N, mg/L	ON	Same method as Snake River.
41	RPOM N, mg/L	ON	Same method as Snake River.

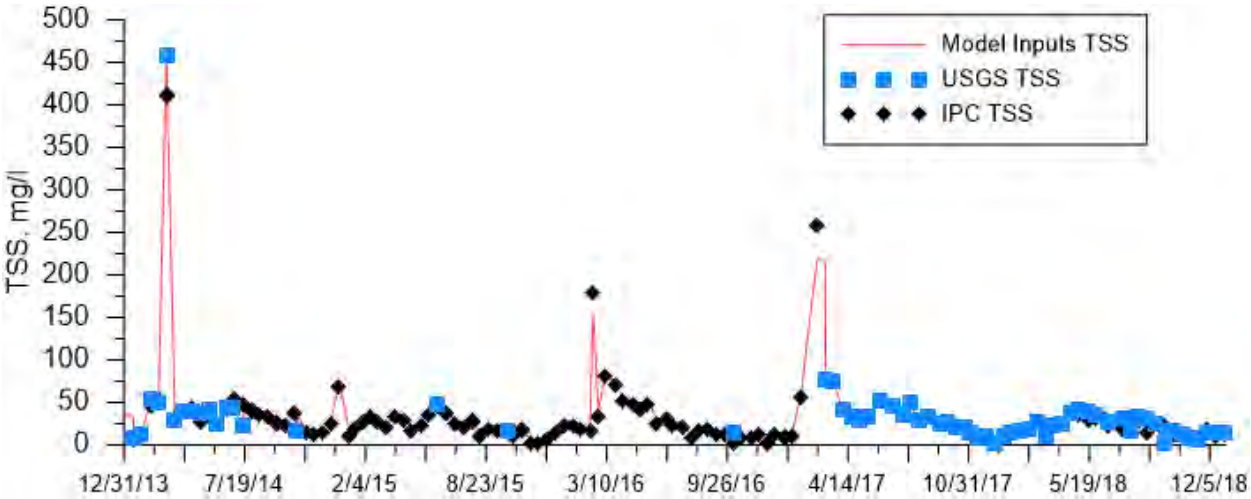


Figure 63. USGS TSS data with gaps filled using regression with IPC TSS data.

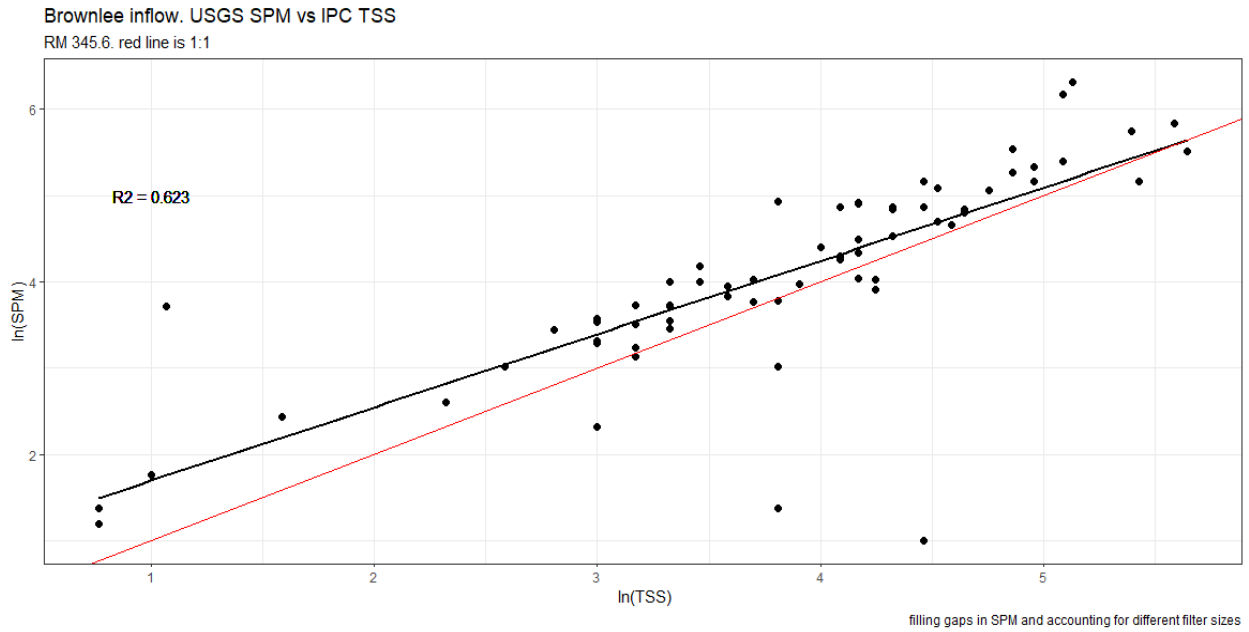


Figure 64. Brownlee Inflow USGS SPM (TSS) versus IPC TSS regression.

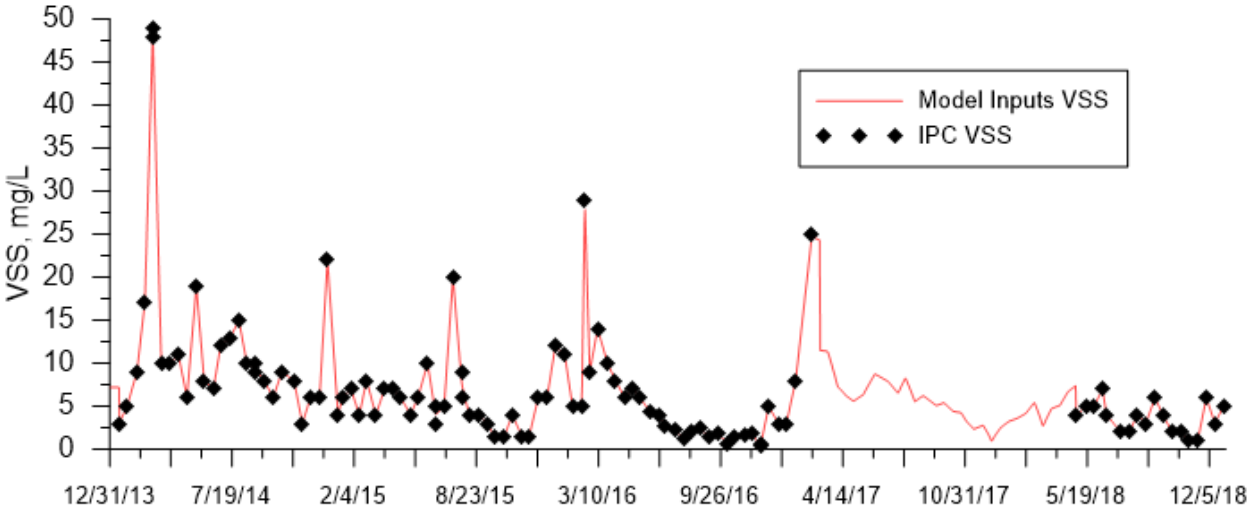


Figure 65. IPC VSS data with gap filled using regression with USGS TSS data.

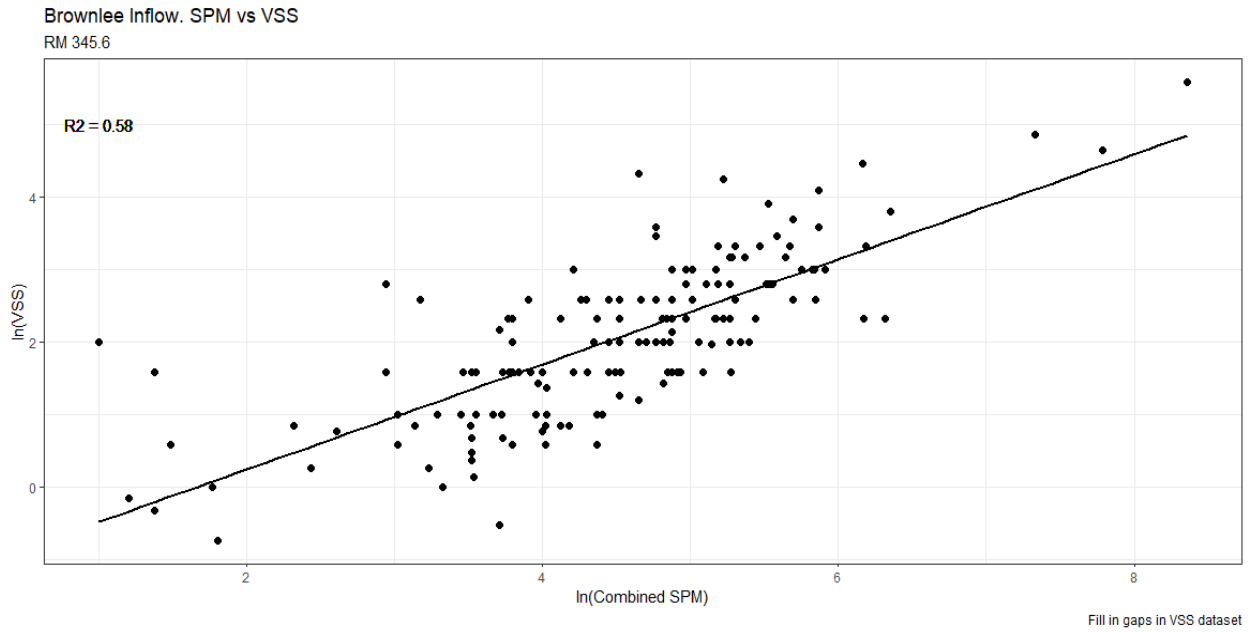


Figure 66. Brownlee Inflow USGS SPM (TSS) versus IPC VSS regression.

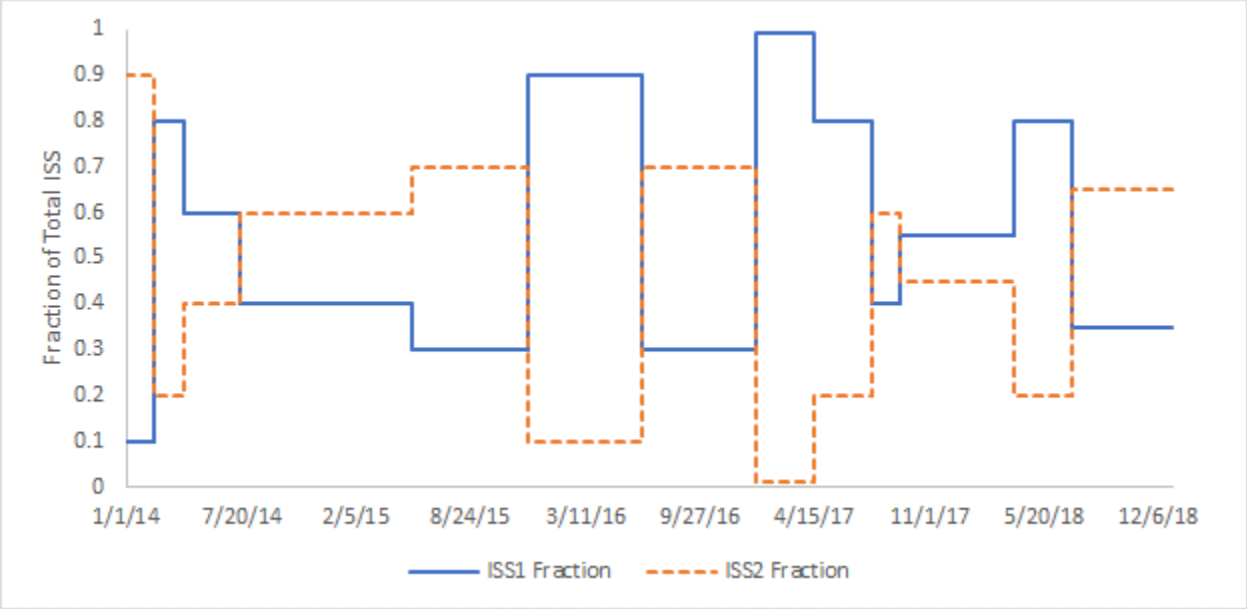


Figure 67. Fraction of total ISS split into ISS1 and ISS2 groups over the model simulation period.

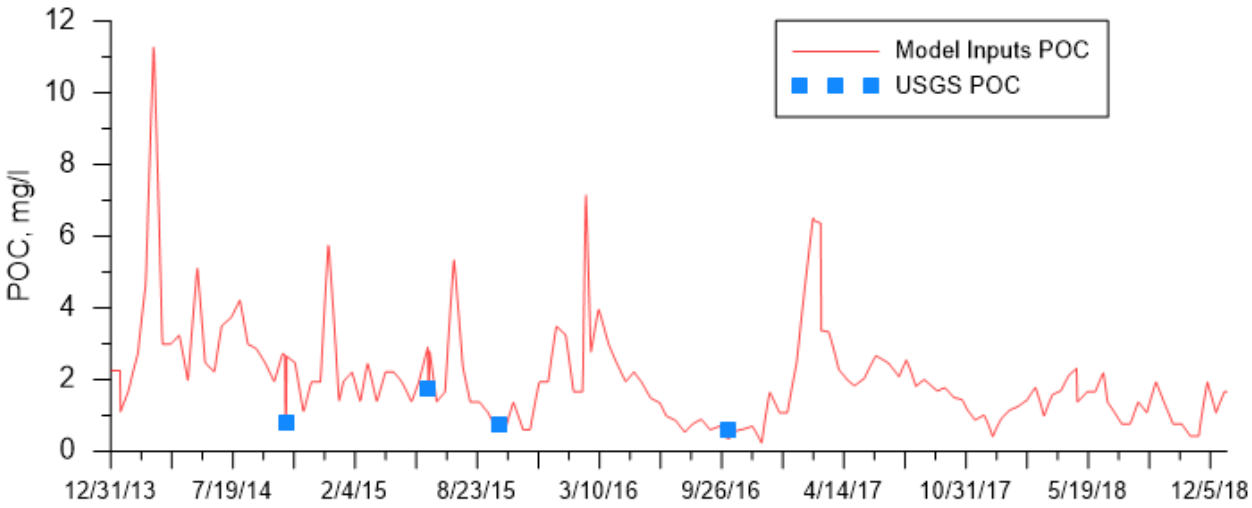


Figure 68. USGS POC data with gaps filled using regression with IPC VSS data.

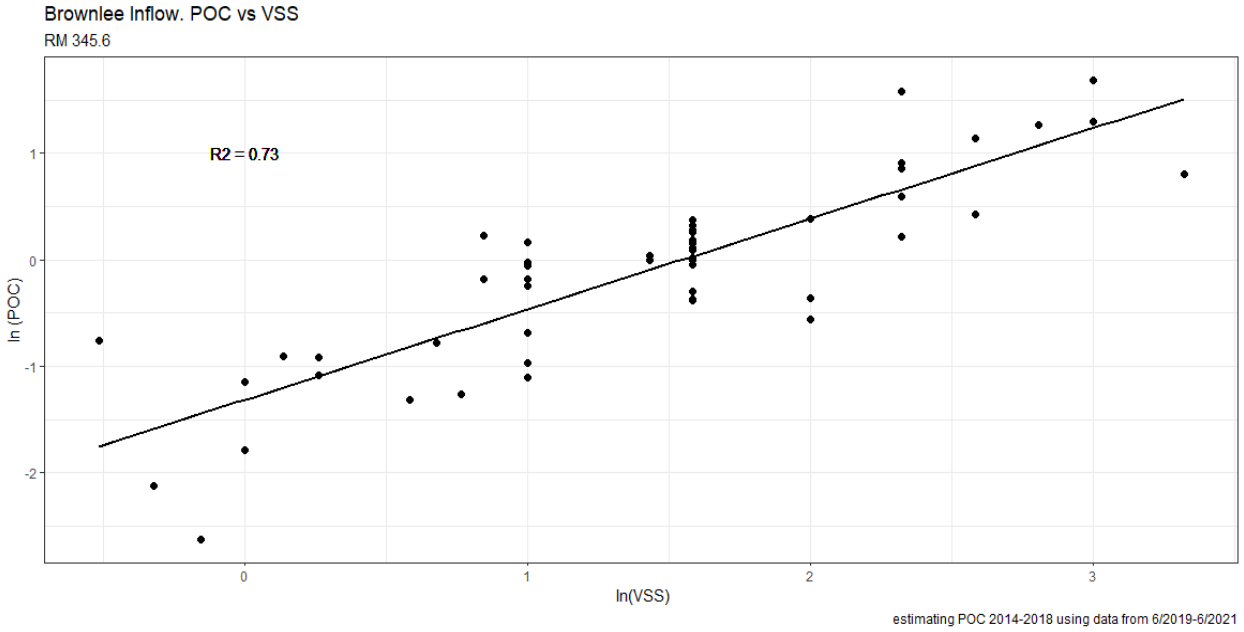


Figure 69. Brownlee Inflow USGS POC versus IPC VSS regression.

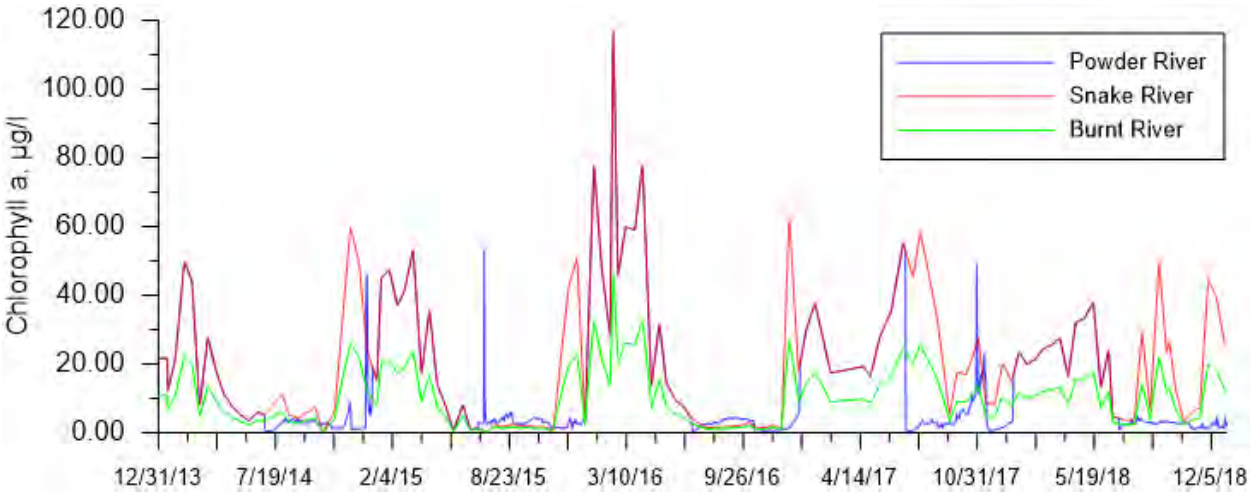


Figure 70. Snake River, Powder River, and Burnt River chlorophyll a inputs. The purple line is where the Powder River and Snake River concentrations are the same.

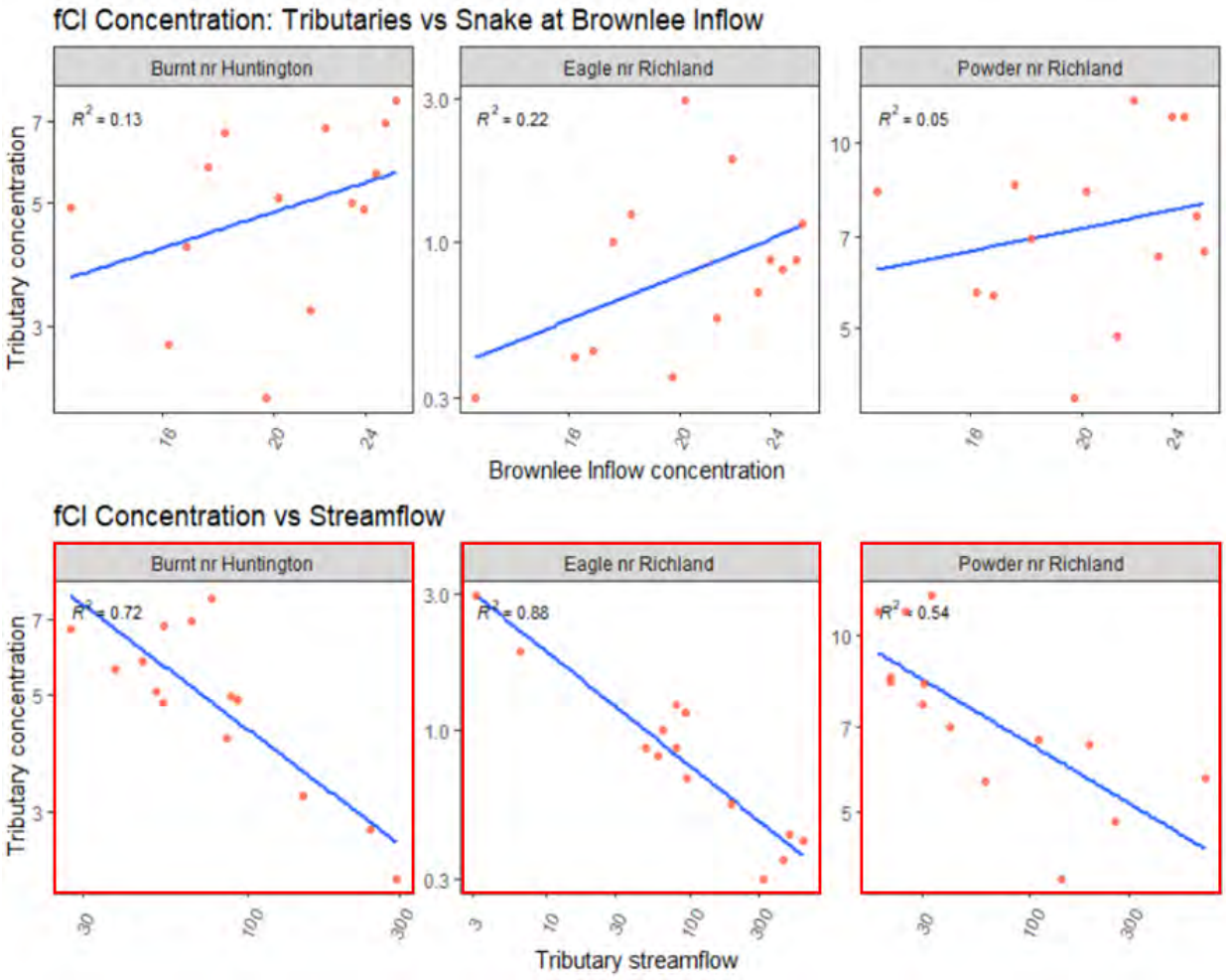


Figure 71. Tributary chloride regressions for Burnt River, Eagle Creek, and Powder River. Tributary concentration versus Snake River inflow concentration (top) and tributary concentration versus tributary streamflow (bottom). The chosen regressions are highlighted in red.

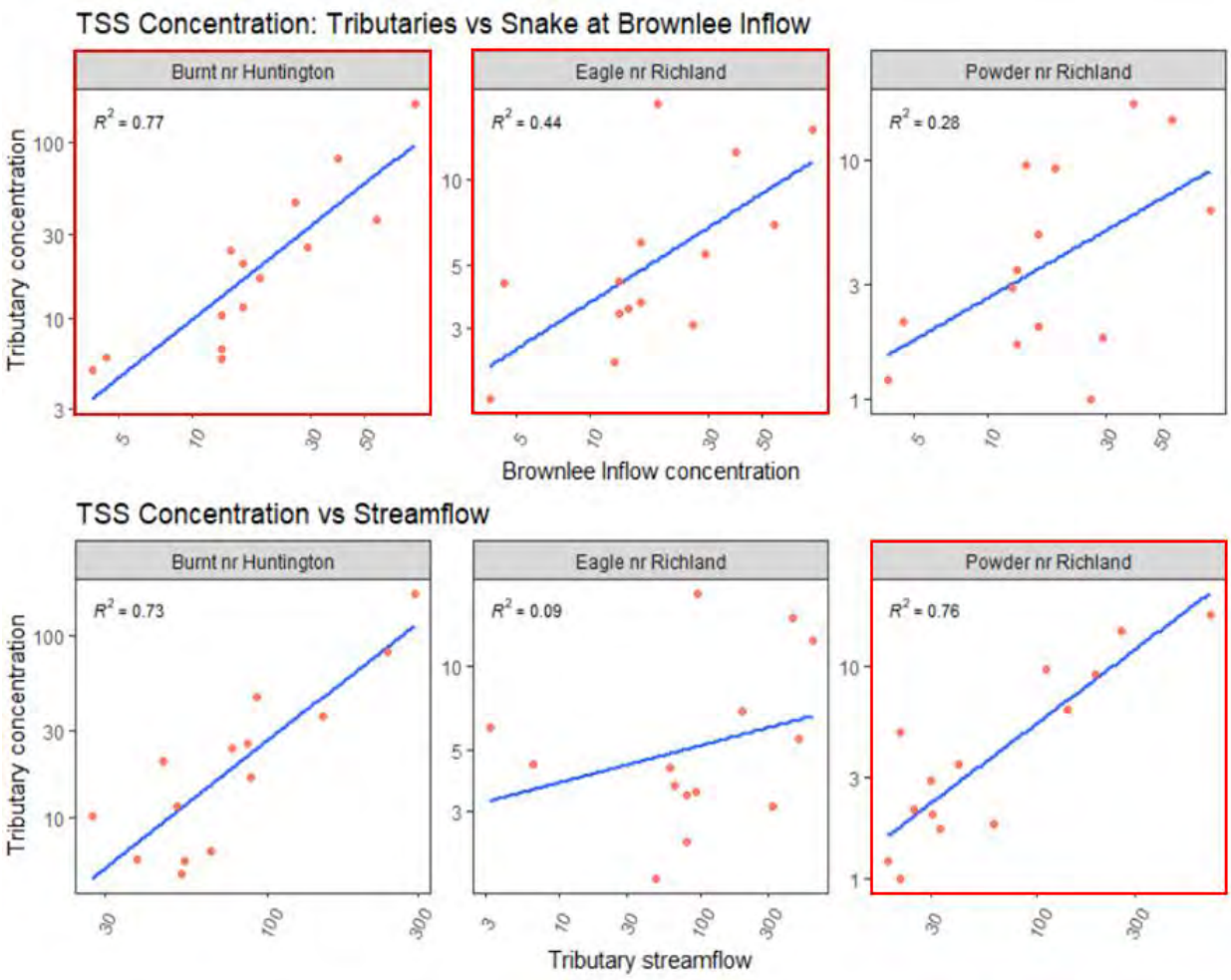


Figure 72. Tributary TSS regressions for Burnt River, Eagle Creek, and Powder River. Tributary concentration versus Snake River inflow concentration (top) and tributary concentration versus tributary streamflow (bottom). The chosen regressions are highlighted in red.

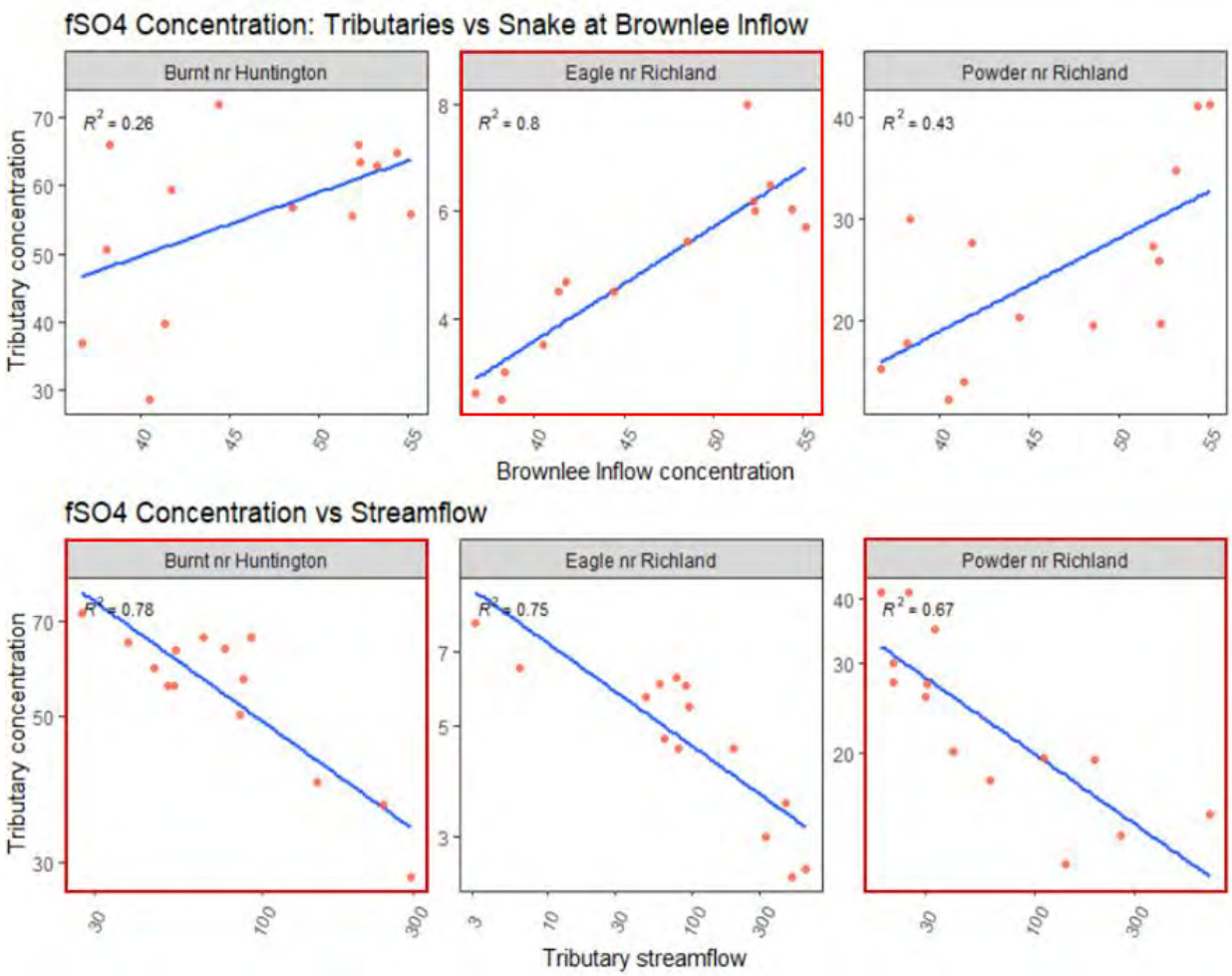


Figure 73. Tributary sulfate regressions for Burnt River, Eagle Creek, and Powder River. Tributary concentration versus Snake River inflow concentration (top) and tributary concentration versus tributary streamflow (bottom). The chosen regressions are highlighted in red.

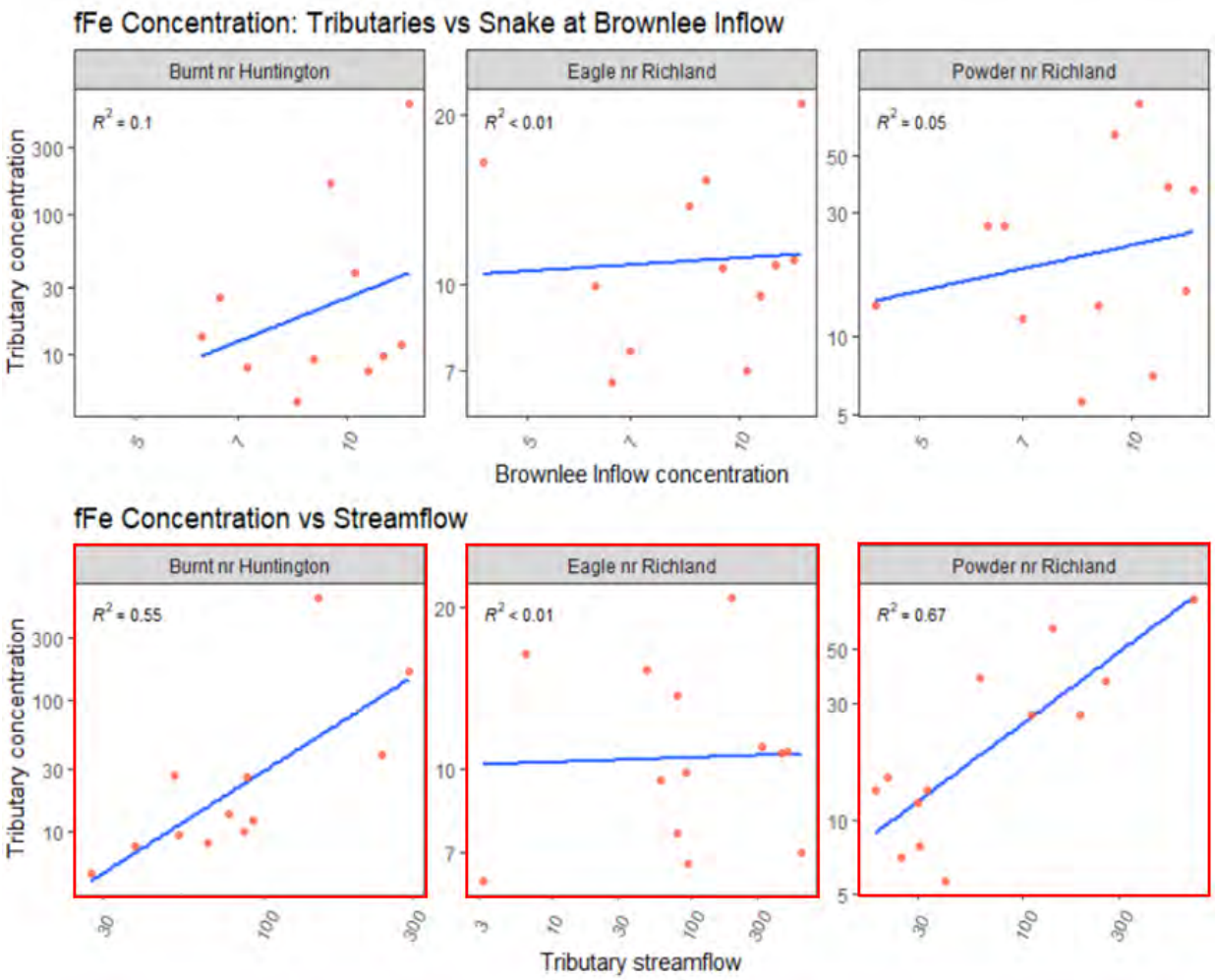


Figure 74. Tributary Fe(II) regressions for Burnt River, Eagle Creek, and Powder River. Tributary concentration versus Snake River inflow concentration (top) and tributary concentration versus tributary streamflow (bottom). The chosen regressions are highlighted in red.

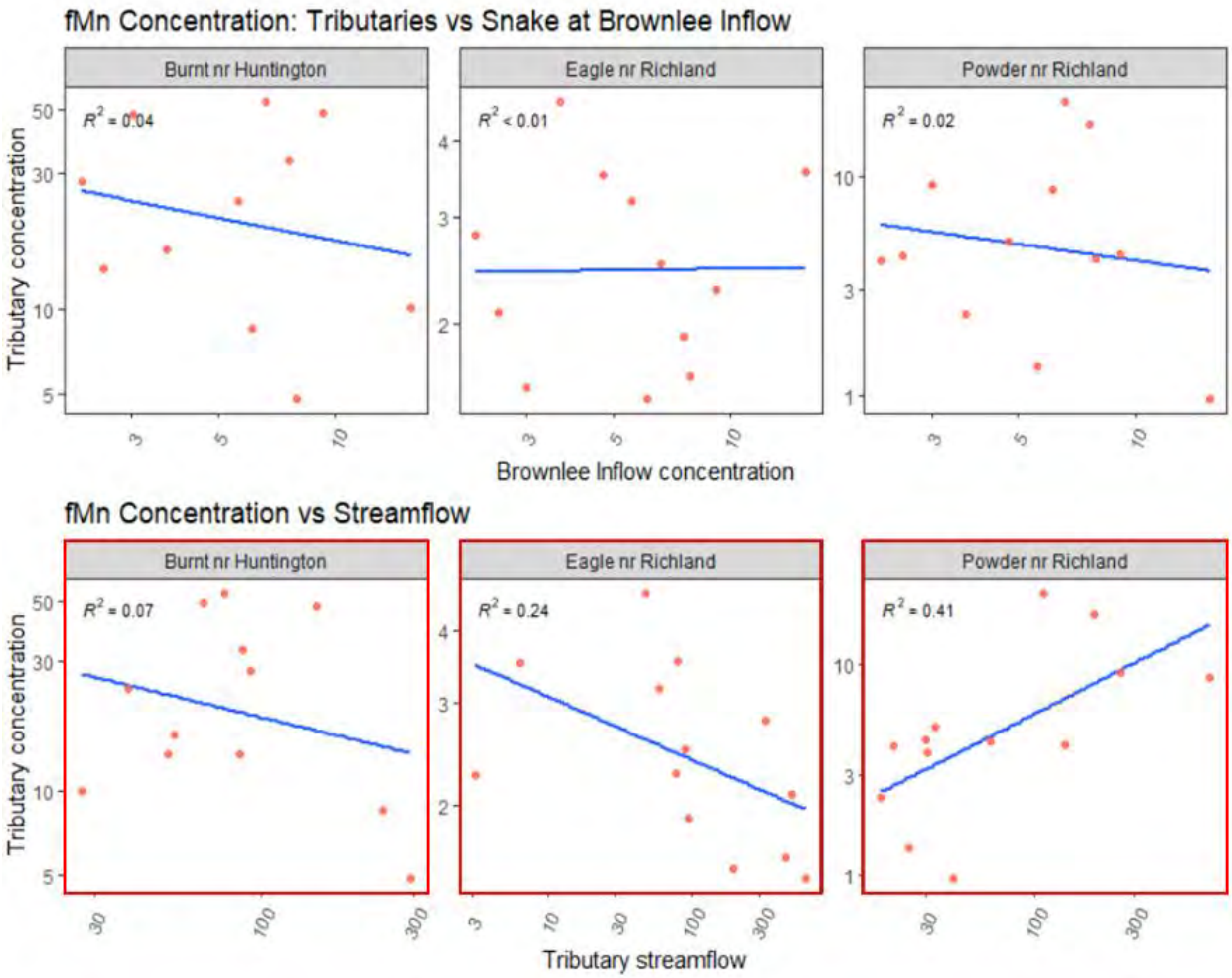


Figure 75. Tributary Mn(II) regressions for Burnt River, Eagle Creek, and Powder River. Tributary concentration versus Snake River inflow concentration (top) and tributary concentration versus tributary streamflow (bottom). The chosen regressions are highlighted in red.

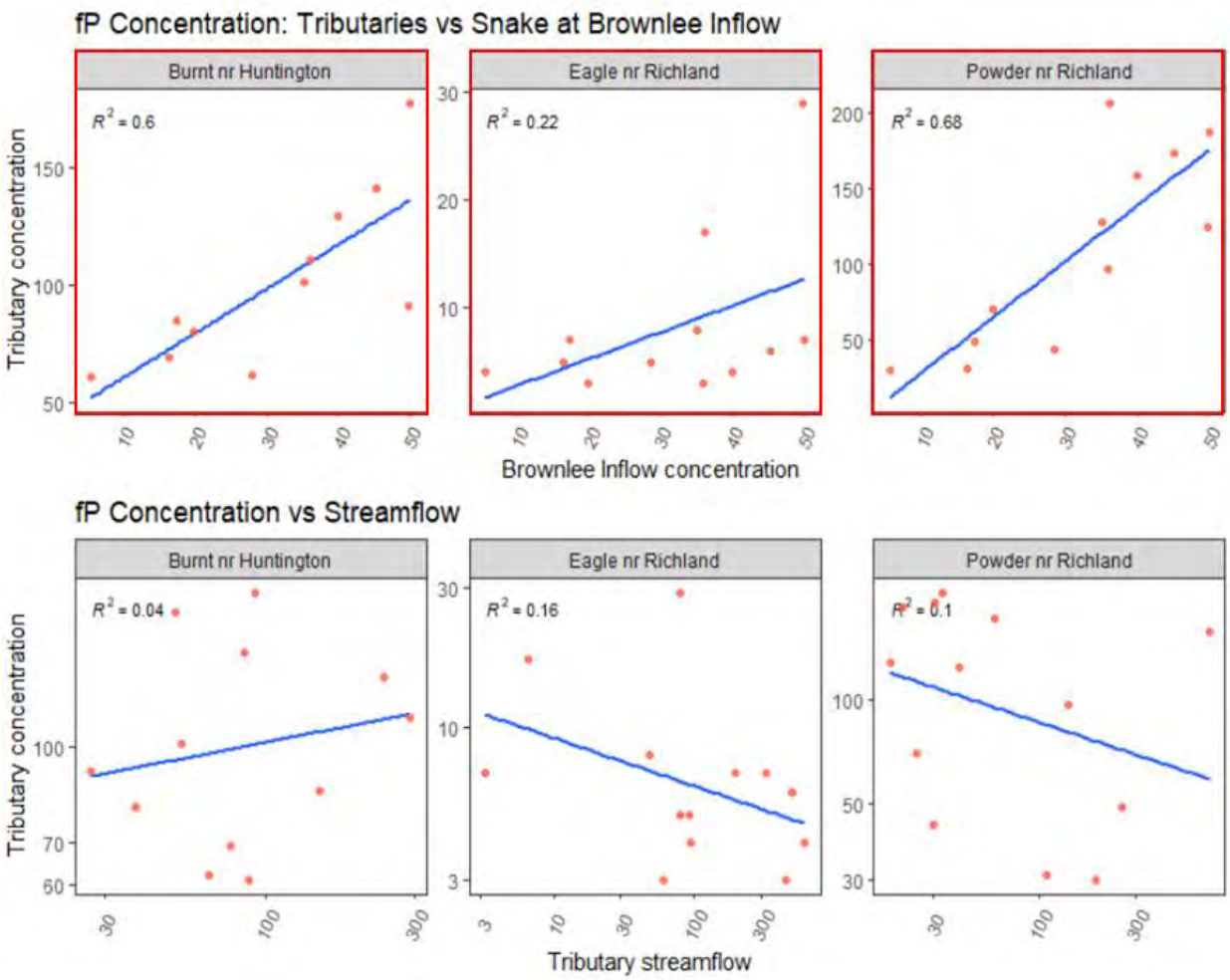


Figure 76. Tributary ortho-phosphate regressions for Burnt River, Eagle Creek, and Powder River. Tributary concentration versus Snake River inflow concentration (top) and tributary concentration versus tributary streamflow (bottom). The chosen regressions are highlighted in red.

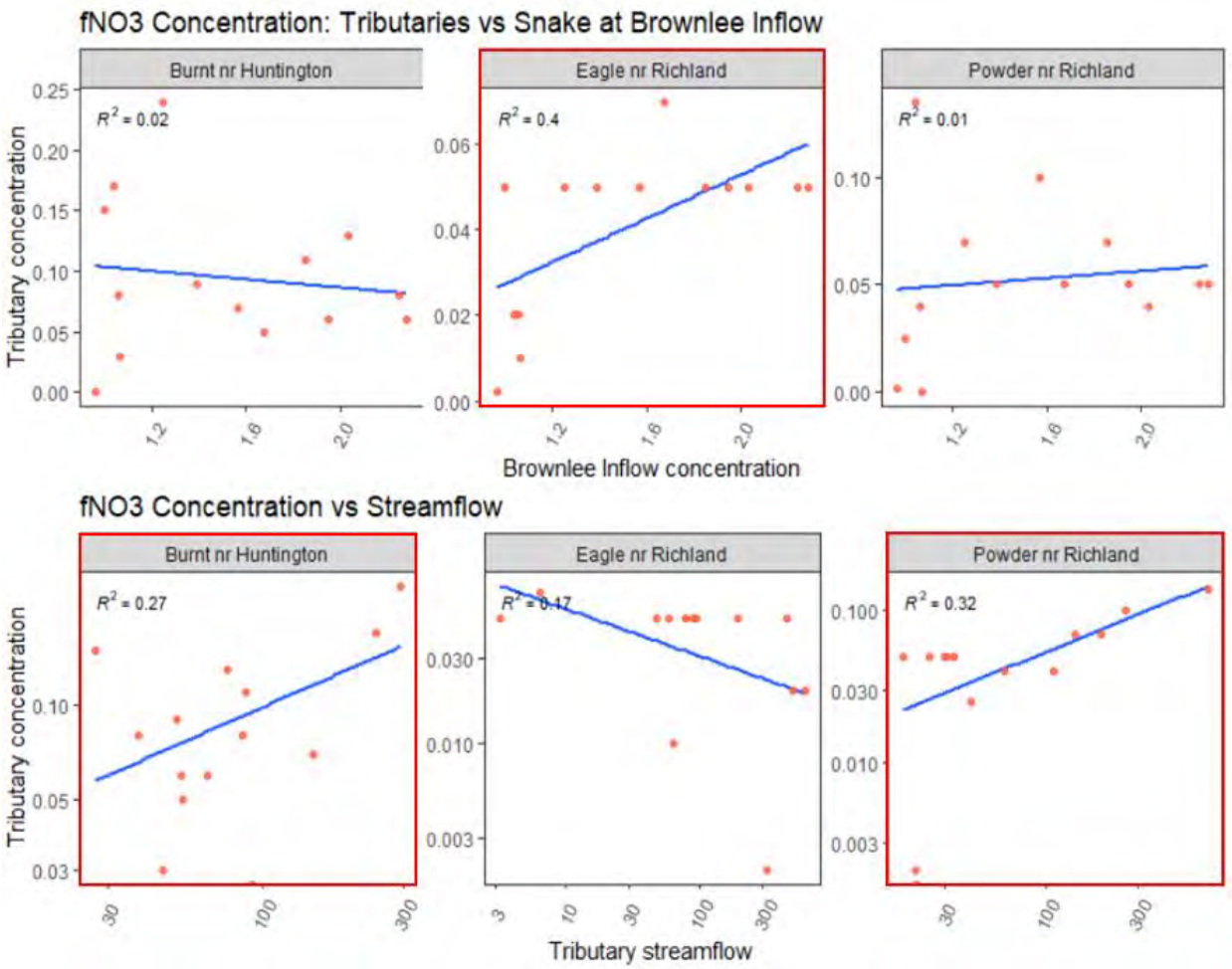


Figure 77. Tributary nitrate regressions for Burnt River, Eagle Creek, and Powder River. Tributary concentration versus Snake River inflow concentration (top) and tributary concentration versus tributary streamflow (bottom). The chosen regressions are highlighted in red.

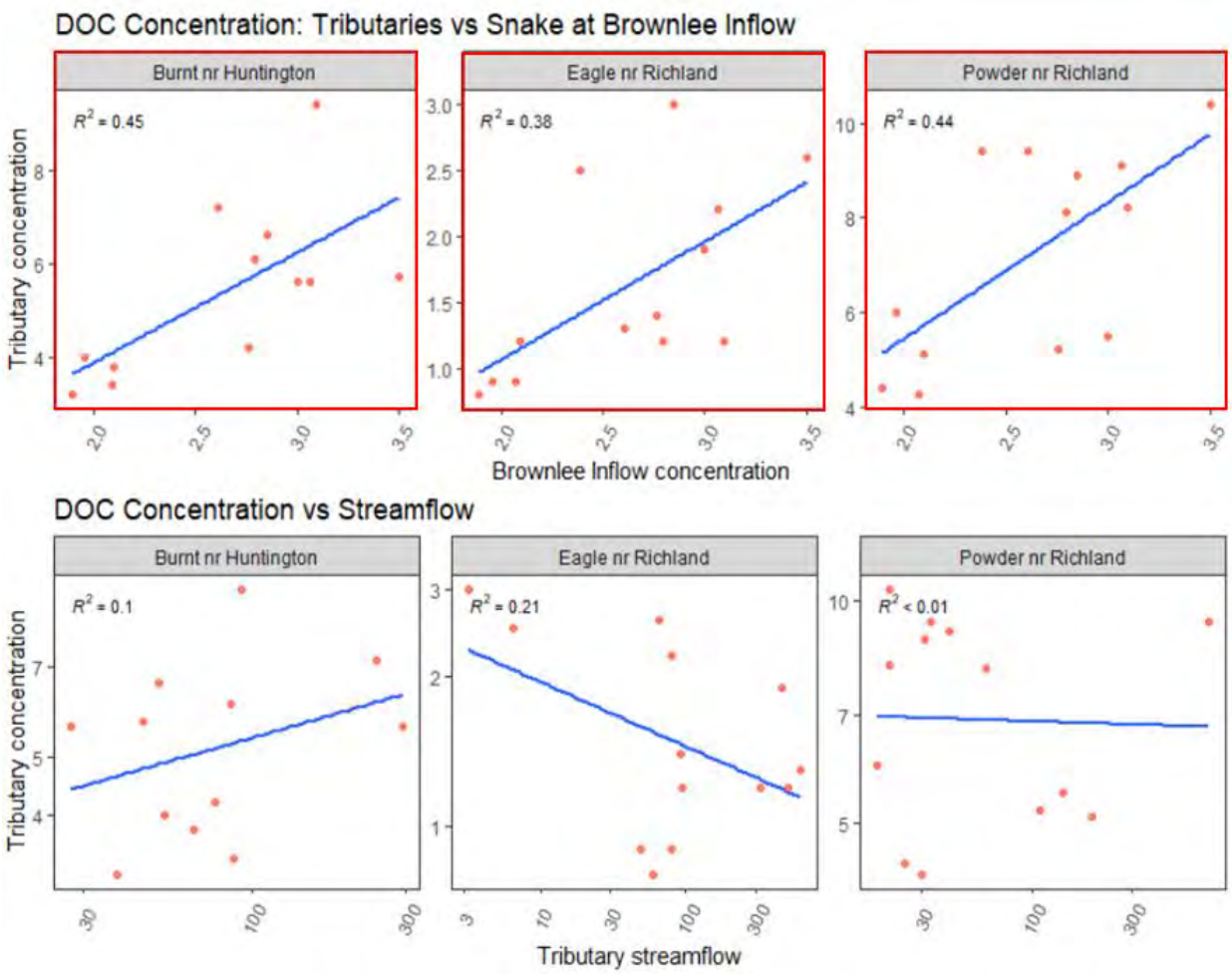


Figure 78. Tributary DOC regressions for Burnt River, Eagle Creek, and Powder River. Tributary concentration versus Snake River inflow concentration (top) and tributary concentration versus tributary streamflow (bottom). The chosen regressions are highlighted in red.

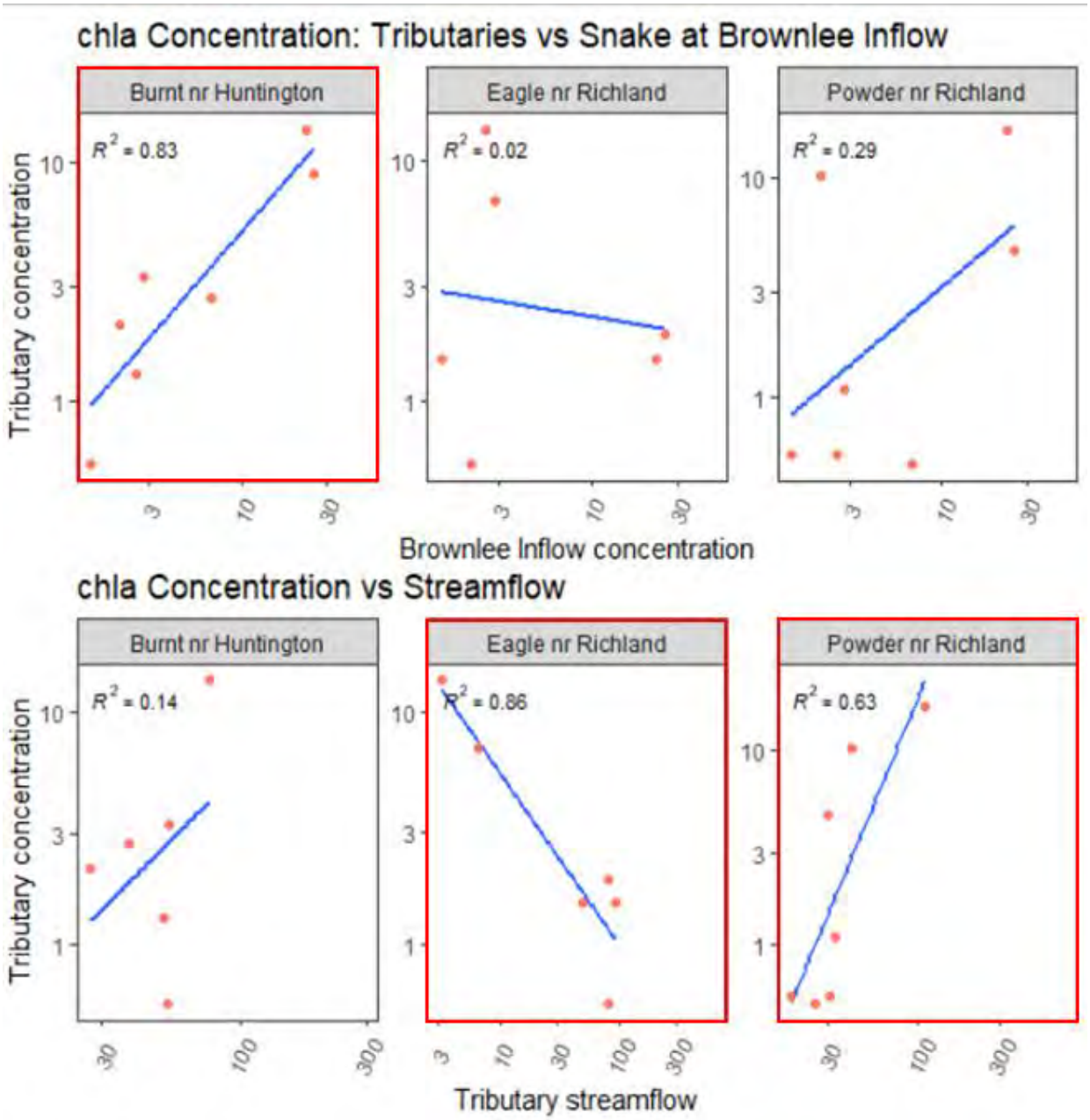


Figure 79. Tributary chlorophyll a regressions for Burnt River, Eagle Creek, and Powder River. Tributary concentration versus Snake River inflow concentration (top) and tributary concentration versus tributary streamflow (bottom). The chosen regressions are highlighted in red.

Constituent input concentrations for the Snake River inflow and tributaries are shown in Figure 80 through Figure 85.

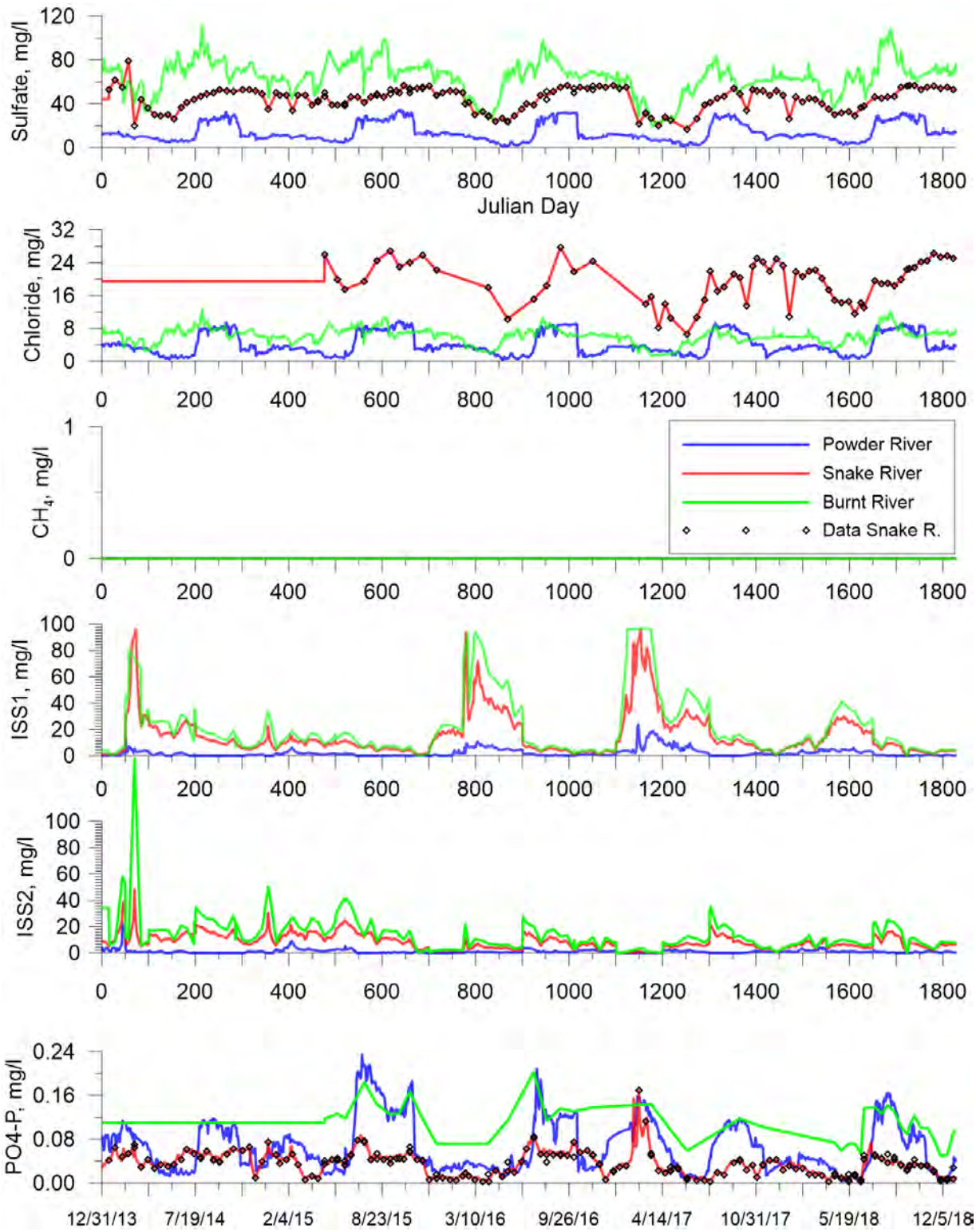


Figure 80. Constituent concentrations for sulfate, chloride, methane, ISS1, ISS2, and ortho-phosphate phosphorus. Daly Creek, Brownlee Reservoir distributed tributary, Pine Creek, and Wildhorse River are all set equal to flow weighted Powder River concentrations. Note that ISS3 is used only on the Snake inflow and is 11% of ISS2. Also, maximum ISS1 concentrations exceeded the axis limit 3 times especially for the Burnt River.

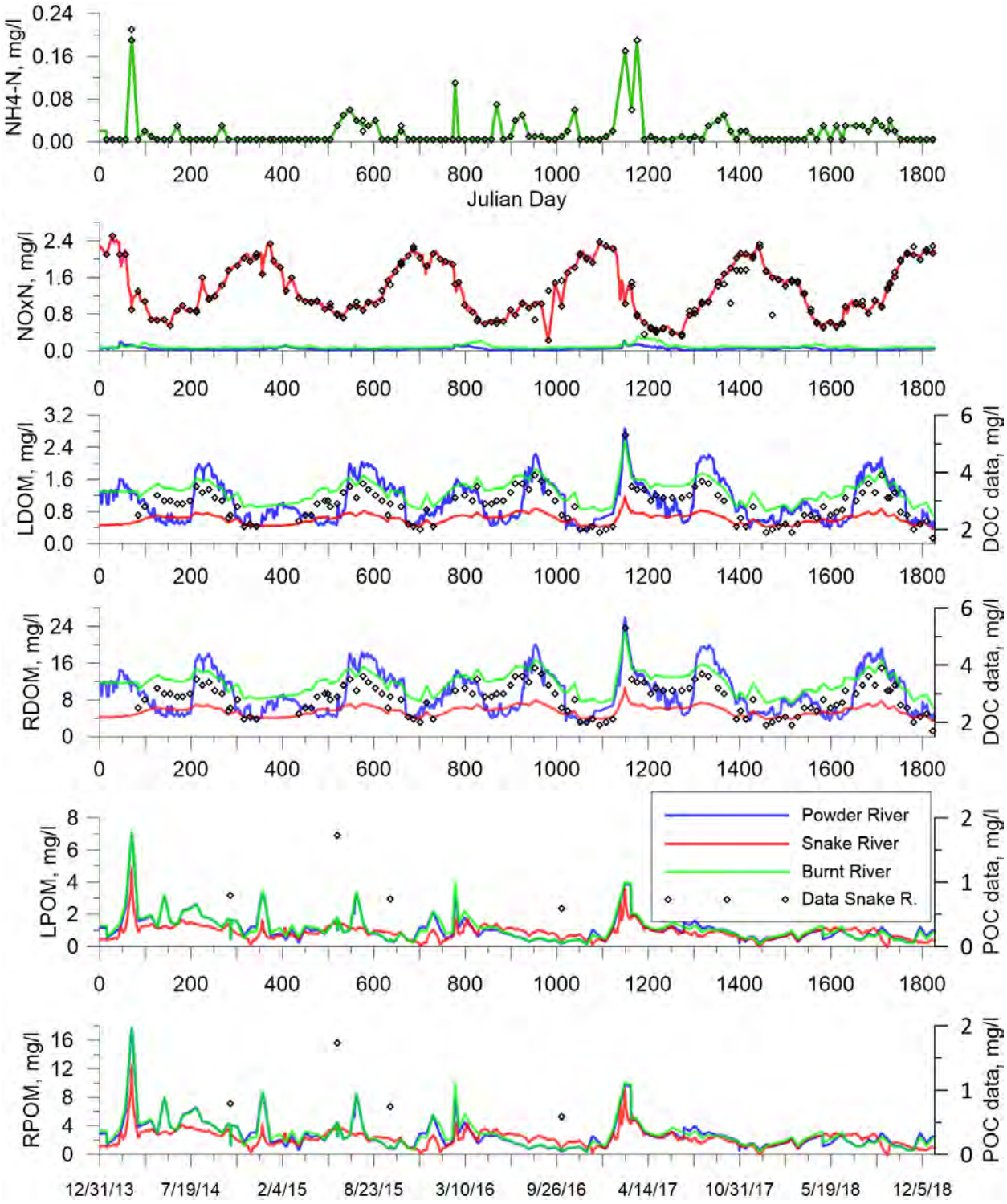


Figure 81. Constituent concentrations for ammonia nitrogen, nitrite-nitrate nitrogen, LDOM, RDOM, LPOM, and RPOM. Daly Creek, Brownlee Reservoir distributed tributary, Pine Creek, and Wildhorse River are all set equal to flow weighted Powder River concentrations.

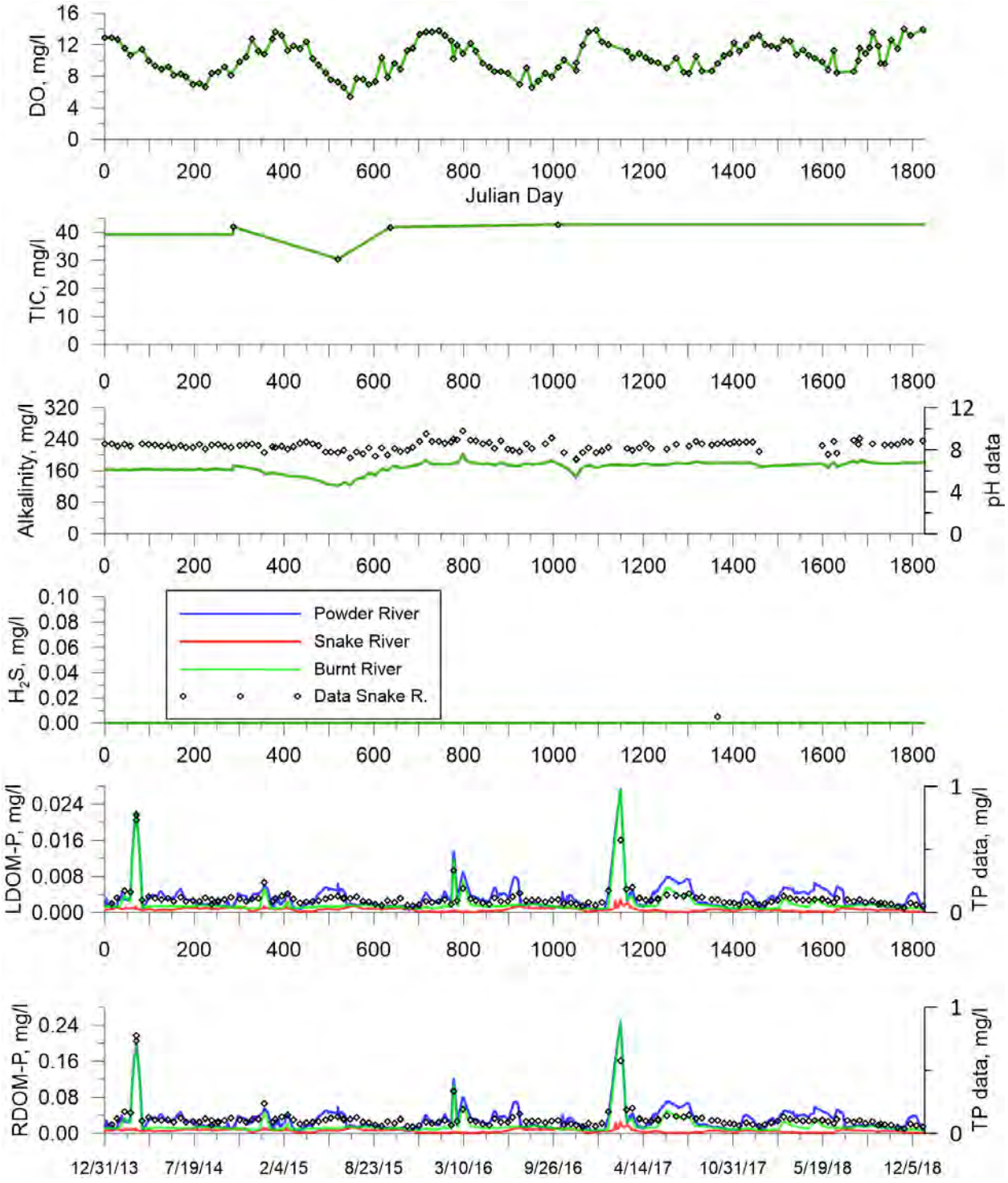


Figure 82. Constituent concentrations for DO, total inorganic carbon, alkalinity, hydrogen sulfide, LDOM-P, and RDOM-P. Daly Creek, Brownlee Reservoir distributed tributary, Pine Creek, and Wildhorse River are all set equal to flow weighted Powder River concentrations.

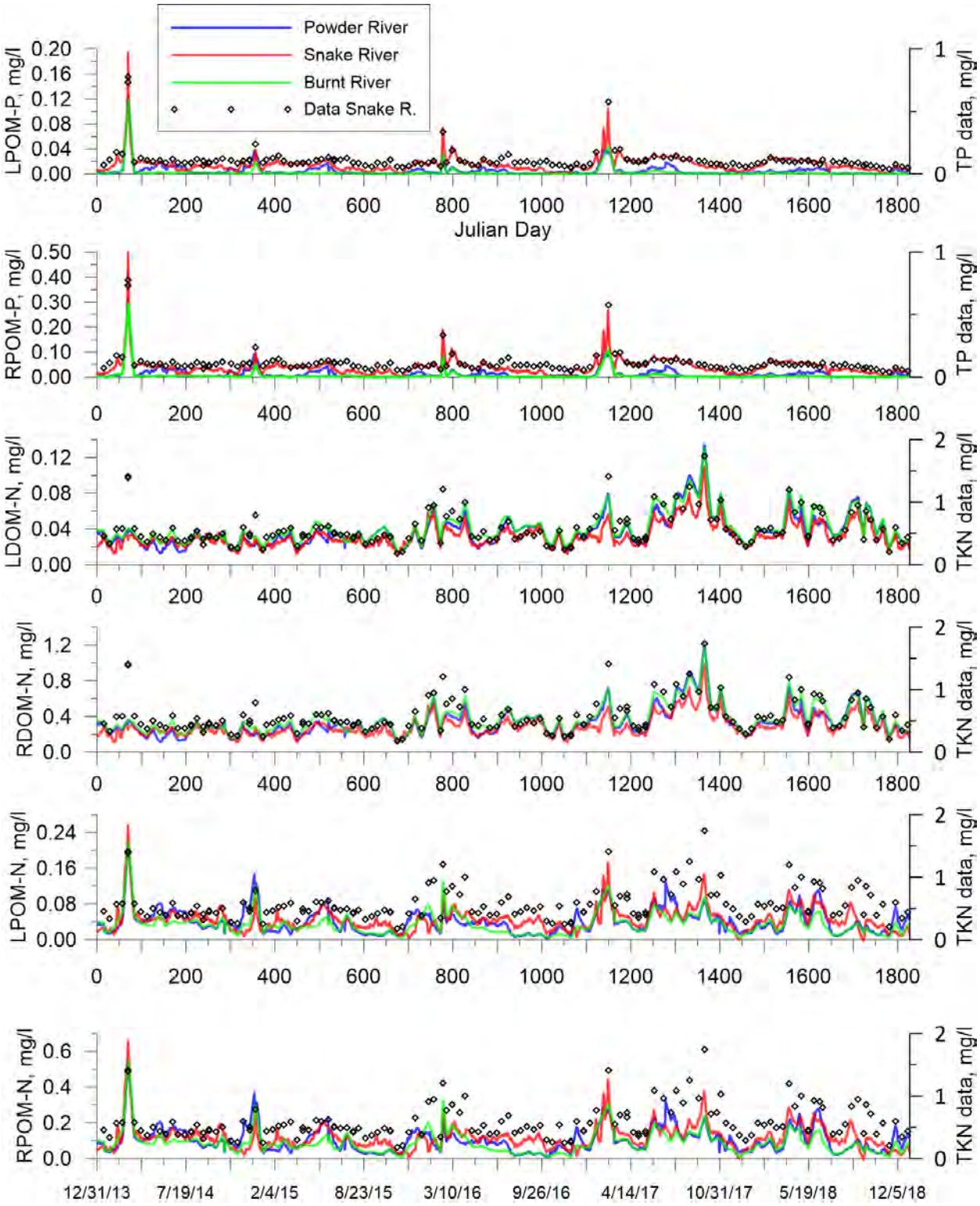


Figure 83. Constituent concentrations for LPOM-P, RPOM-P, LDOM-N, RDOM-N, LPOM-N, and RPOM-N. Daly Creek, Brownlee Reservoir distributed tributary, Pine Creek, and Wildhorse River are all set equal to flow weighted Powder River concentrations.

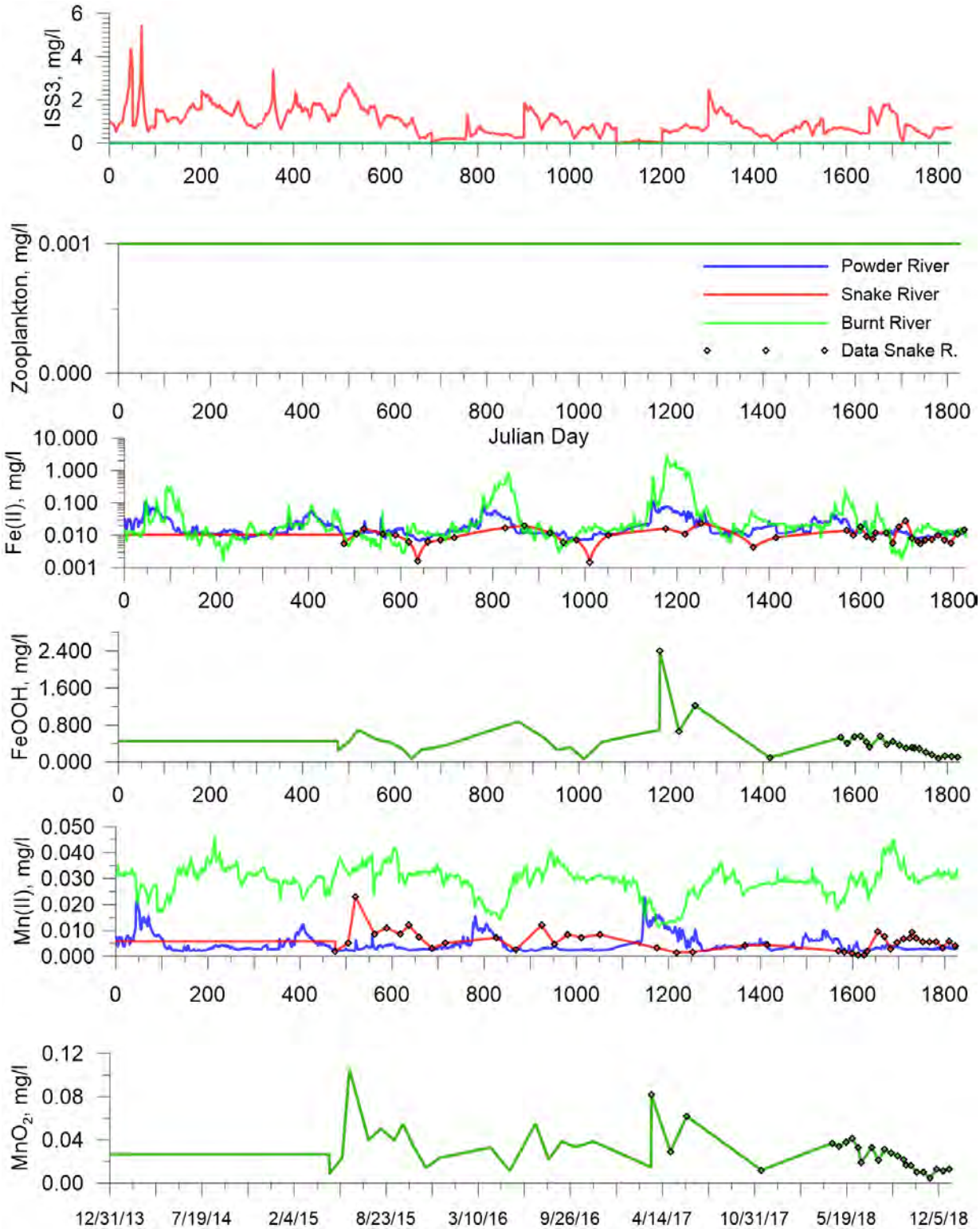


Figure 84. Constituent concentrations for ISS3, zooplankton, Fe(II), FeOOH, Mn(II), and MnO2. Daly Creek, Brownlee Reservoir distributed tributary, Pine Creek, and Wildhorse River are all set equal to flow weighted Powder River concentrations.

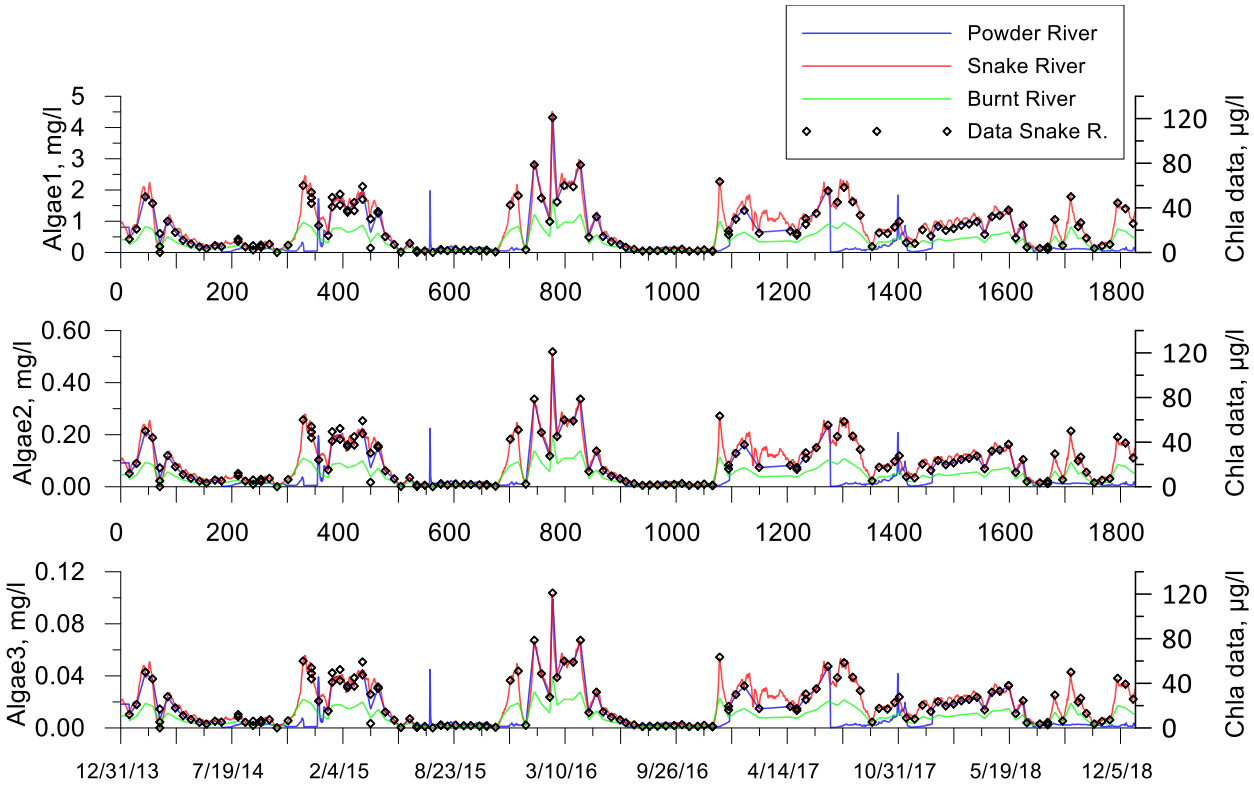


Figure 85. Constituent concentrations for Algae1, Algae2, and Algae3. Daly Creek, Brownlee Reservoir distributed tributary, Pine Creek, and Wildhorse River are all set equal to flow weighted Powder River concentrations.

Sediment Diagenesis Inputs

The CE-QUAL-W2 sediment diagenesis state variables include organic matter (labile, refractory and inert), P, N, inorganic C, alkalinity, oxidized forms of Fe and Mn, reduced forms of Fe and Mn, CH_4, H_2S, sulfate, and temperature. There are also options in the sediment diagenesis model for bubble formation and organic sediment resuspension.

The bubble formation model is computationally intensive and hence was not used. Assuming that most of the organic sediments settled in a region of Brownlee where there was little scour, this was not used at this time. Setting kinetic coefficients and initial conditions throughout the 3 reservoirs is challenging. Kinetic rates were chosen based on the User Manual recommendations and during the model calibration. We used a combination of measurements and initial conditions that did not vary significantly over the 5-year time period hoping that the conditions were in a semi-steady-state at the beginning of the simulation.

Sediment biogeochemical data published by USGS (Marvin-DiPasquale et al, 2020) was used to develop some of the sediment diagenesis parameters for the three reservoirs: porosity; particle size; bulk density;

particulate organic carbon (POC), particulate organic nitrogen (PON), and particulate organic phosphorus (POP) ratios; and porewater concentrations. Table 16 lists the average values of sediment parameters during the sampling period of 2014-2018 in shallow sediment (0-7 cm) samples for various river miles. Table 17 lists the average values of shallow sediment (0-5 cm) pore water parameters during the sampling period of 2016-2017 for various river miles. Table 18 shows average values of sediment parameters in October of 2016 in deep cores (0-1 m). River mile 248 and 252 correspond to Hells Canyon Reservoir, river mile 273 corresponds to Oxbow Reservoir, and river miles 286-318 correspond to Brownlee Reservoir.

Table 16. Average values of shallow sediment parameters at various river miles for 2014-2018.

Average	RM 248	RM 252	RM 273	RM 286	RM 300	RM 310	RM 318	Total Avg
Bulk Density (g/cm^3 wet sed)	1.06	1.06	1.03	1.01	1.04	1.05	1.13	1.05
Porosity (ml porewater/cm^3 wet sed)	0.87	0.86	0.87	0.90	0.91	0.88	0.85	0.88
Percent POC (%)	4.69	NA	NA	5.97	5.09	3.69	3.29	4.64
Percent PN (%)	0.59	NA	NA	0.85	0.74	0.55	0.44	0.65
Grain size wet sieve (% < 64 µm)	101.93	97.30	91.93	98.00	95.00	98.57	NA	97.17

Table 17. Average values of shallow sediment pore water parameters at various river miles for 2016-2017.

Average	RM 248	RM 286	RM 300	RM 310	RM 318	Total Avg
Ortho-P (mg P/l)	0.35	3.99	4.63	2.60	1.96	3.03
NH4 (mg N/l)	15.90	14.71	16.63	21.19	6.06	15.2
S(-II) (mg/L)	0.03	0.05	0.12	0.09	0.09	0.08
Fe (µg/l)	9949	8206	8998	10018	4064	8125
Mn (µg/l)	9050	14964	10357	7102	5861	9497
NO3 (mg N/l)	0.009	0.013	0.008	0.014	0.009	0.01
SO4 (mg/l)	1.96	2.51	1.67	5.81	4.86	3.46

Table 18. Average values of deep sediment parameters at various river miles for 2016.

Average	RM 286	RM 310	Total Avg
Particle Density (g/cm^3)	1.99	1.84	1.93
Sediment wet Density (g/cm^3)	1.11	1.12	1.12

Porosity

The average porosity varied between 0.85-0.91 ml/cm^3 across all three reservoirs for the shallow sediment samples. The average porosity of 0.88 ml/cm^3 was used for all reservoirs.

Particle Size

The average grain size varied between about 92-102% less than 64 µm across all three reservoirs with the total average of 97% less than 64 µm. 60 microns was chosen as the sediment particle size for all reservoirs.

Bulk Density

The average bulk density varied between 1.01-1.13 g/cm^3 across all three reservoirs. The total average bulk density of 1050 kg/m^3 was used for all reservoirs.

POC, PON, and POP Ratios

The ratio of average percent POC to average percent PN was about 7 for the shallow sediment samples. A ratio of 7 POC/PON was used for all reservoirs. A ratio of 8 was used for PON to POP concentrations assuming typical organic matter (OM) fractions of 0.08 (Nitrogen/OM) and 0.01 (Phosphorus/OM). The initial concentrations of POC, PON, and POP were adjusted during calibration (see Appendix A2 for the final values used in the model).

Porewater Concentrations

Initial porewater concentrations are required by the sediment diagenesis model input file for SO4, NH4, NO3, PO4, H2S, CH4, TIC, alkalinity, FeOOH, FeII, MnO2, and MnII. Data measurements for sulfide (S(-II)) were assumed to be equivalent to hydrogen sulfide (H2S). Default values for initial CH4, TIC, and alkalinity concentrations were chosen for the sediment diagenesis inputs: 0.092, 4.011, and 50 mg/l, respectively. Orthophosphate porewater concentrations varied between 0.35-4.63 mg P/l, ammonia concentrations varied between 6.06-21.19 mg N/l, sulfide concentrations varied between 0.03-0.12 mg/l, iron concentrations varied between 4064-10018 µg/l, manganese concentrations varied between 5861-14964 µg/l, nitrate concentrations varied between 0.008-0.014 mg N/l and sulfate concentrations varied between 1.67-5.81 mg/l. The total average concentration of each constituent (except for Fe and Mn) was used for the initial concentration of all three water bodies: 3.03 mg P/l for PO4, 15.2 mg N/l for NH4, 0.08 mg/l for H2S, 0.01 mg N/l for NO3, and 3.46 mg/l for SO4. During calibration, it was found that high initial concentrations of Fe and Mn in the sediment were required to match the field data. It was assumed that most of the Fe and Mn in the sediments would be of the reduced form. Initial concentrations of FeOOH and MnO2 were set to 0.5 mg/l, and initial concentrations of FeII and MnII were set to 100 mg/l and 500 mg/l, respectively.

Shading

Local topography around the HCC Reservoirs influences the amount of solar radiation reaching the water surface. The local topography around the reservoirs were developed using digital elevation maps (DEM). To characterize the influence of the topography, inclination angles were obtained every 20 degrees around each model segment center point. For each 20-degree increment around a model segment an array of elevation points and their distances from the center point were obtained from the DEM. The elevations and distances were then used to calculate the highest inclination angle relative to the center point. The distance away from each segment center point that should be analyzed to obtain the controlling inclination angle will vary depending on the terrain surrounding the river. The result of this analysis generated inclination angles, which control topographic shade for each of the 20-degree increments around a segment's center point.

The model uses all 18 topographic inclination angles. Based on the position of the sun the algorithm will interpolate between the two nearest inclination angles to get the most appropriate inclination angle.

Figure 86, Figure 87, and Figure 88 **Error! Reference source not found.** show topography angles for several model segments surrounding Brownlee, Oxbow, and Hells Canyon Reservoirs, respectively. These were computed for each model segment.

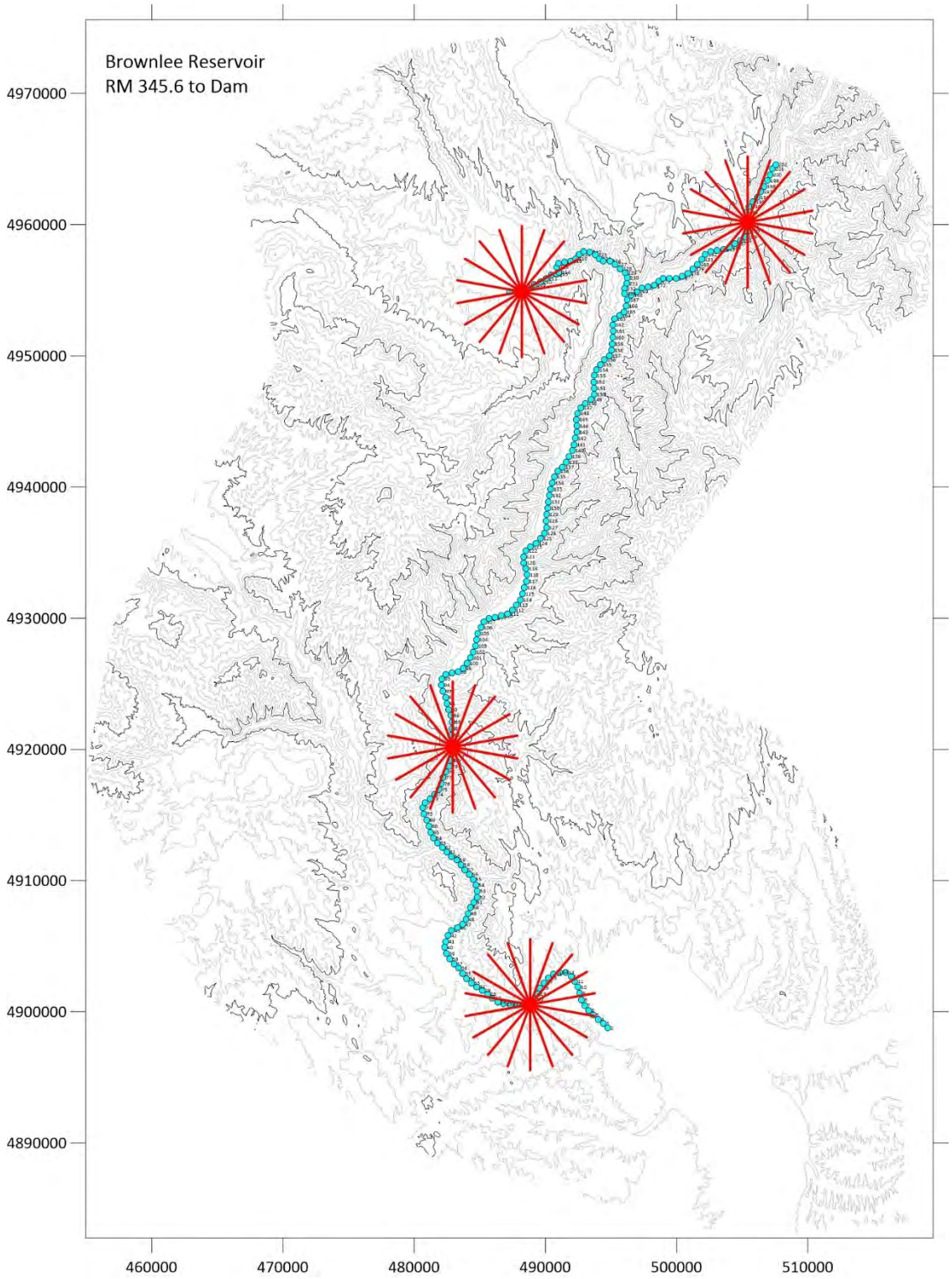


Figure 86. Topographic line segments around each segment center for Brownlee Reservoir to determine topographic shading angles for model segments 14, 76, 191, and 214.

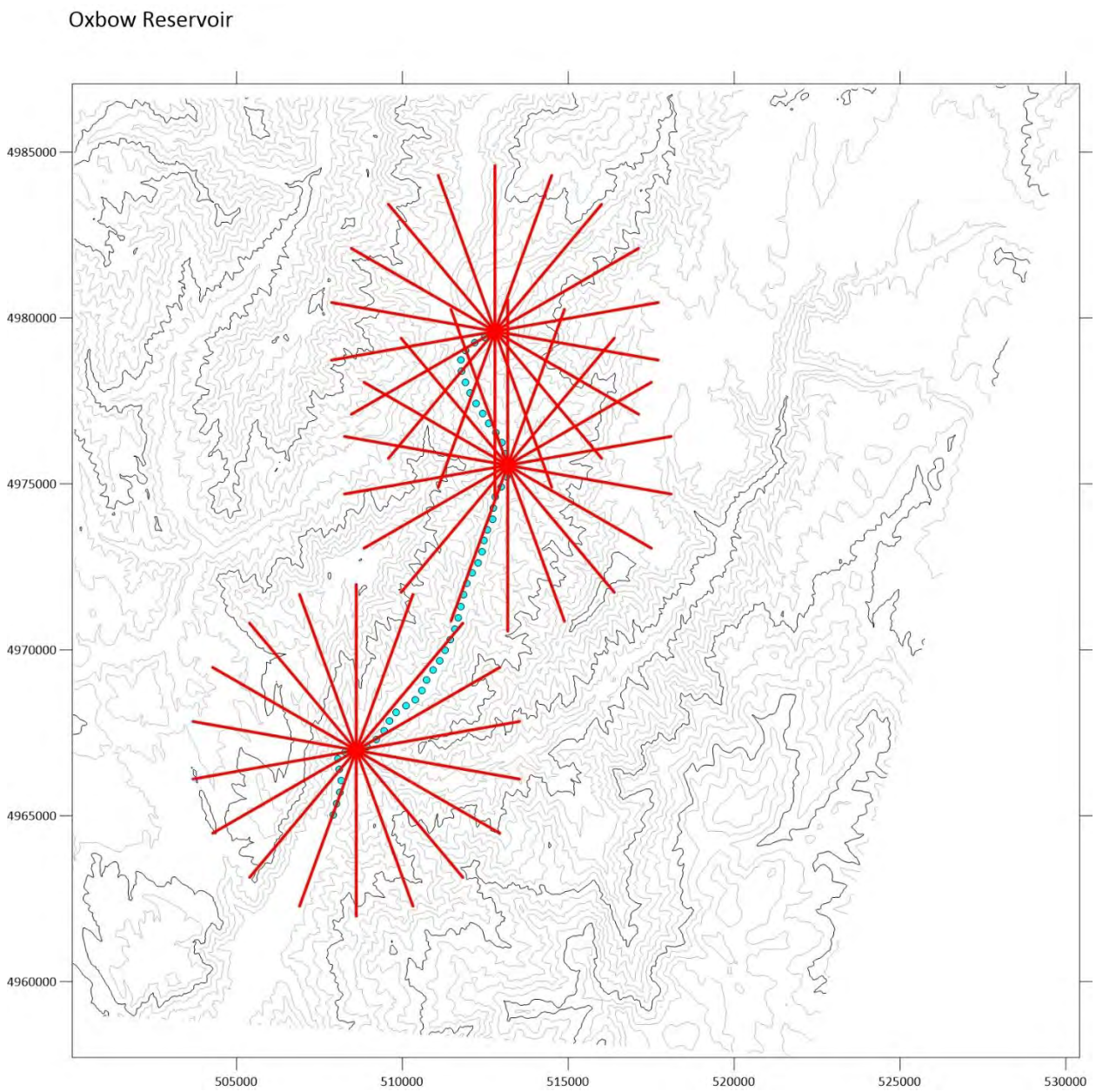


Figure 87. Topographic line segments around each segment center for Oxbow Reservoir to determine topographic shading angles for segments 9, 38, and 52.

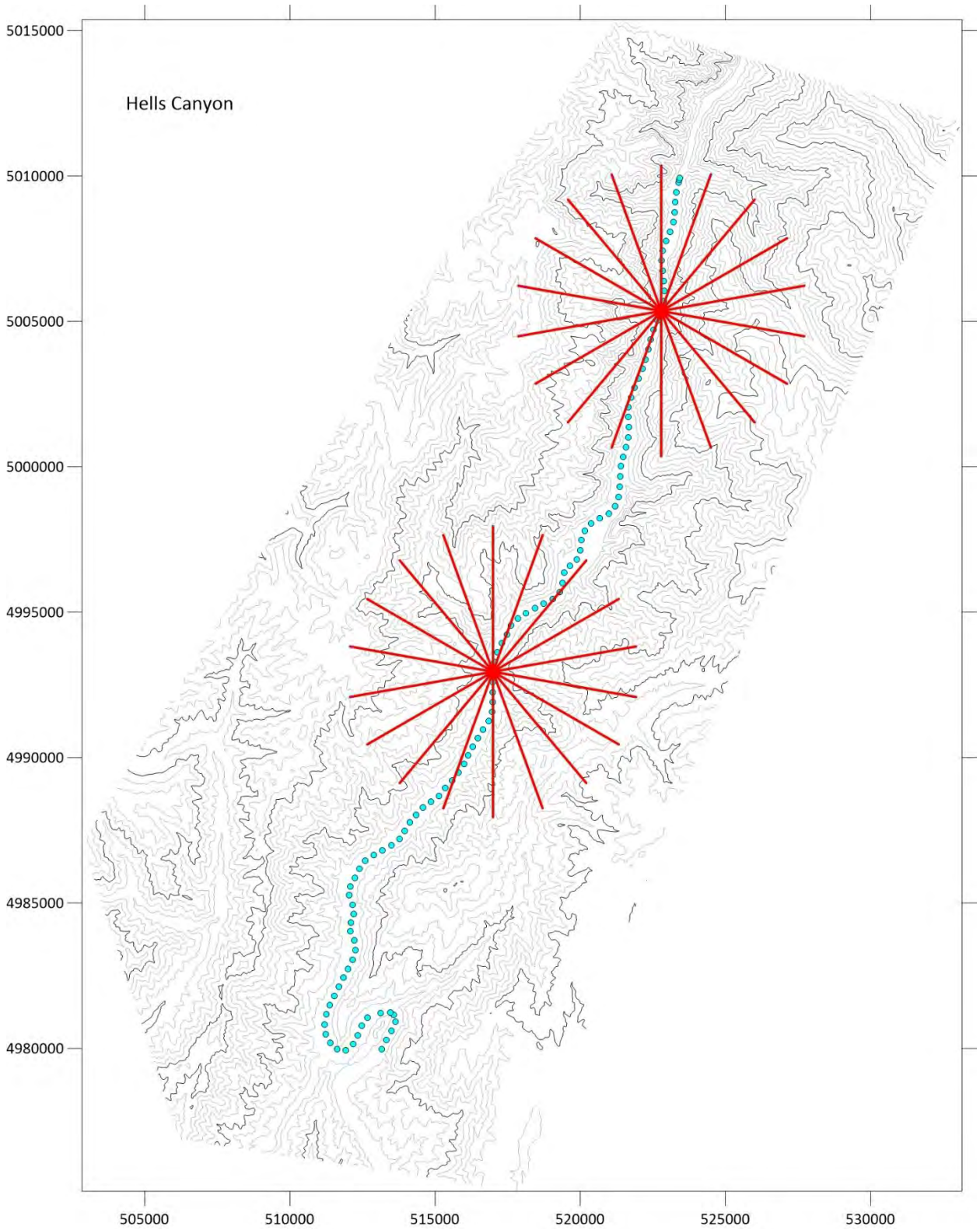


Figure 88. Topographic line segments around each segment center for Hells Canyon Reservoir to determine topographic shading angles for segments 59 and 101.

Analysis of Light Extinction Data in Brownlee Reservoir to Determine Model Extinction Coefficients

Idaho Power collected field data of PAR (photosynthetic active radiation) with depth during profile sampling in Brownlee Reservoir. Typical data are shown in Table 19.

Table 19. Example of the 757 profiles of PAR with depth collected by Idaho Power. This profile was taken on 5/3/2016 at RM 288.

5/3/2016	9:39 AM
PAR, µmol photons/m^2/sec	RM288 Depth, m
503.99	0.224
290.2	1.183
213.38	1.825
121.56	2.422
75.576	3.027
49.207	3.651
33.1	4.285
21.522	4.934
13.909	5.592
8.8413	6.263
5.657	6.933
3.6265	7.612
2.2844	8.285
1.4432	8.96
0.92041	9.634
0.56525	10.311
0.32032	10.991
0.14981	11.679
0.12852	12.376

These data were fit to an exponential curve in the region of decay of the light profile and curves like that shown in Figure 89 were constructed for each profile.

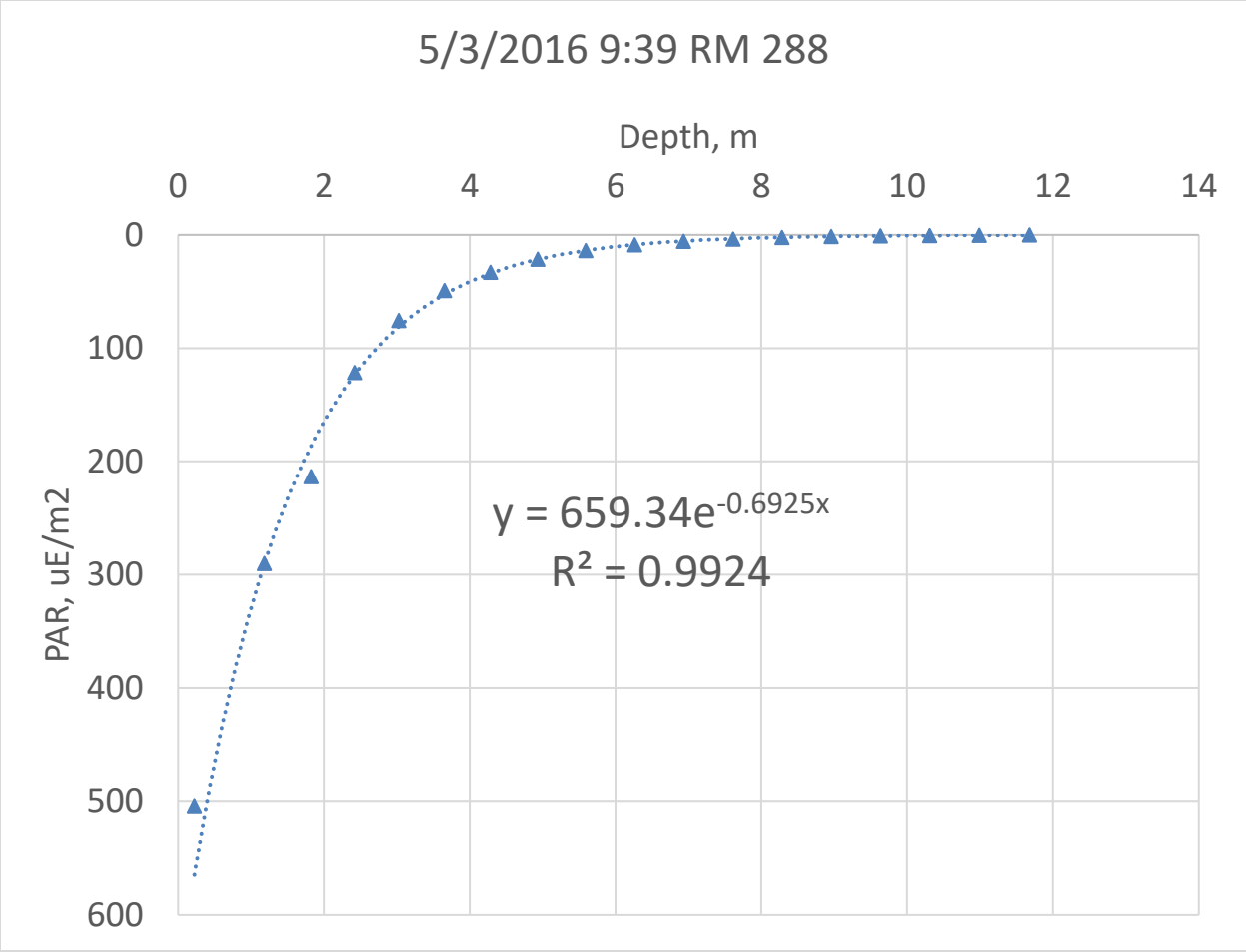


Figure 89. Light extinction computed from PAR with depth on 5/3/2016 at RM288. The constant in the exponential is the light extinction coefficient, in this case 0.6925 m^{-1}.

These computed values of light extinction are shown in Figure 90 as a function of RM and time. As evident from these data, the light extinction coefficient decreases as one moves down the reservoir as particles settle to the bottom.

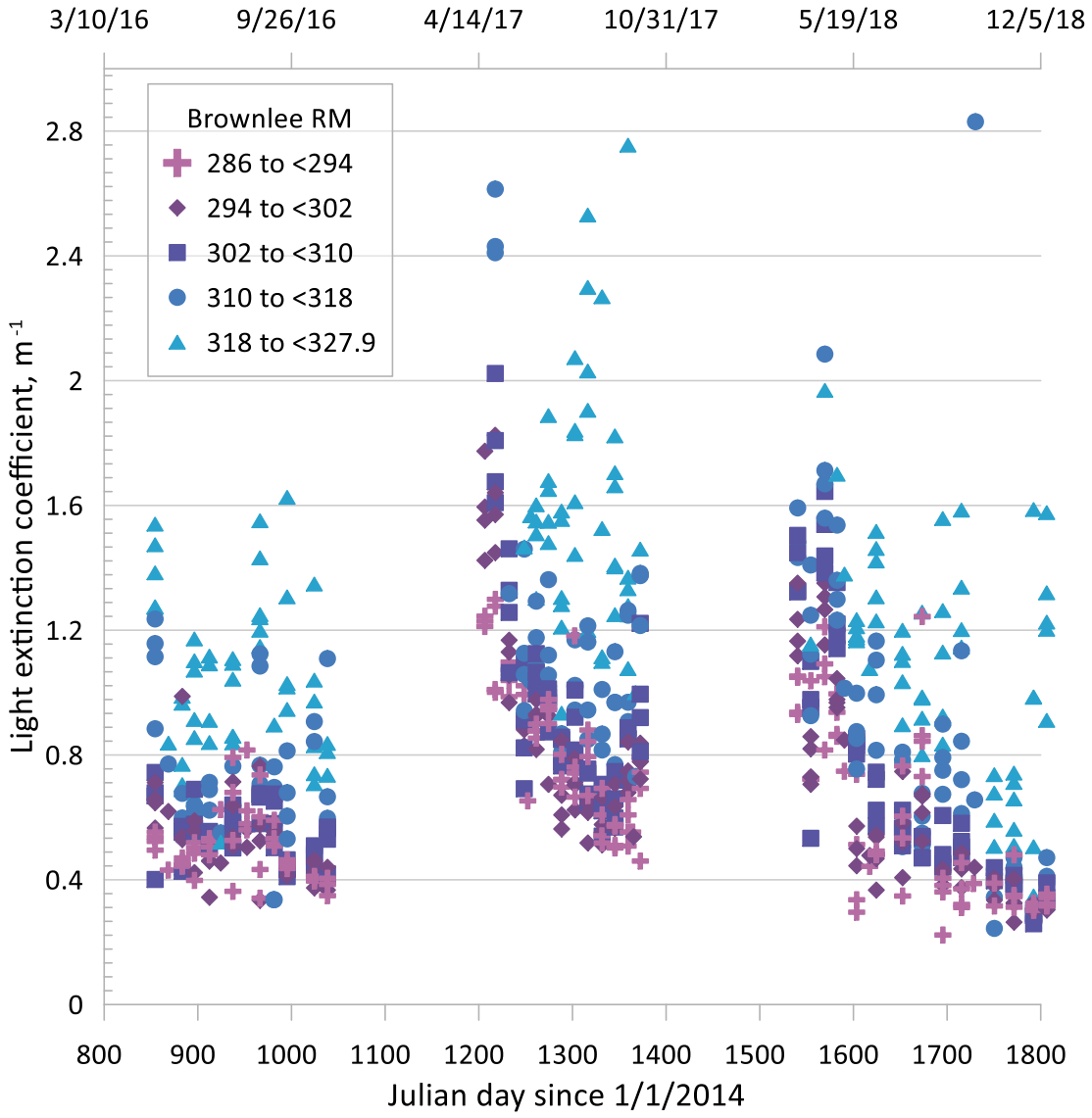


Figure 90. Computed light extinction coefficients from PAR vs depth profiles from Idaho Power.

USGS and Idaho Power also took total suspended solids (TSS) data at various depths often during the same day as the light extinction field data. Figure 91 shows an example where TSS and light extinction data were taken at RM 286. Hence, field data of TSS and computed light extinction were computed for several different locations on Brownlee Reservoir: RM 286, 300, 310, and 318. Figure 92, Figure 93, Figure 94, and Figure 95 show the computed correlation between TSS and light extinction at RM 286, 300, 310, and 318, respectively. Figure 96 shows the correlation using all the data at all River Miles.

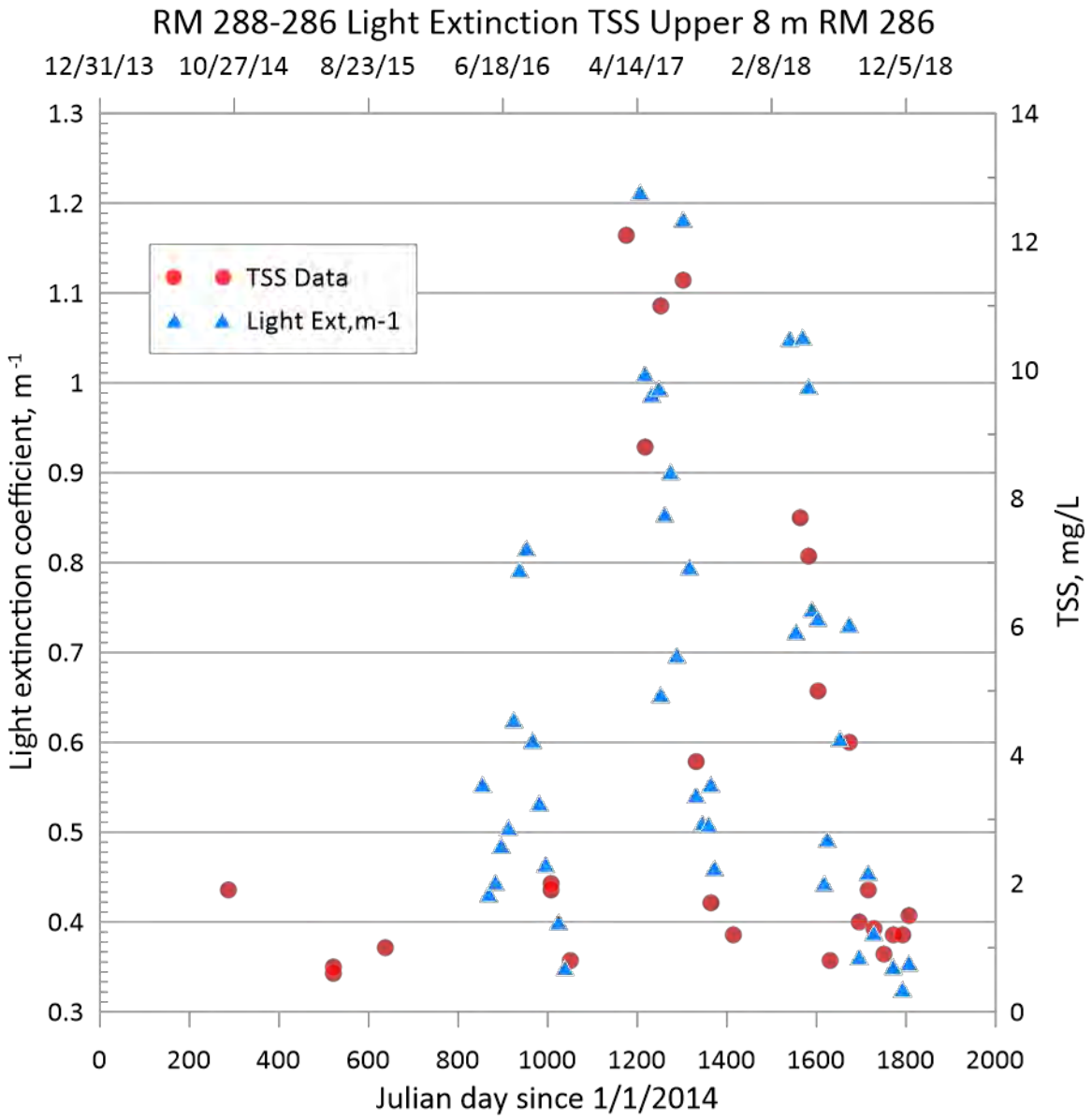


Figure 91. Computed light extinction data and TSS measurements at RM 286 Brownlee Reservoir.

In CE-QUAL-W2 extinction coefficients are used to calculate a net extinction coefficient, λ, which is determined from the following equation:

$$\lambda = \lambda_{H2O} + \lambda_{ISS} + \lambda_{POM} + \lambda_a + \lambda_{macro} + \lambda_{zoo}$$

where:

$\lambda_{ISS} = \varepsilon_{ISS} \sum_{\#ISS} \Phi_{ISS}$

ε_{ISS} = extinction parameter for inorganic suspended solids, $m^{-1}/(g\ m^{-3})$ - user supplied parameter

Φ_{ISS} = inorganic suspended solids concentration for each size fraction

$\lambda_{POM} = \varepsilon_{POM} \sum \Phi_{POM}$

ε_{POM} = extinction parameter for particulate organic matter, $m^{-1}/g\ m^{-3}$) - user supplied parameter

Φ_{POM} = particulate organic matter concentration = particulate labile + particulate refractory organic matter concentration

$\lambda_a = \sum \varepsilon_a \Phi_a$ algae extinction, m^{-1}

$\lambda_{zoo} = \sum \varepsilon_{zoo} \Phi_{zoo}$ zooplankton extinction, m^{-1}

$\lambda_{macro} = \sum \varepsilon_{macro} \Phi_{macro}$ macrophyte extinction, m^{-1}

ε_a = extinction coefficient for each algal group, $m^{-1}/g\ m^{-3}$) - user supplied parameter

Φ_a = algal concentration for each algal group, $g\ m^{-3}$

ε_{zoo} = extinction coefficient for each zooplankton group, $m^{-1}/g\ m^{-3}$) - user supplied parameter

Φ_{zoo} = zooplankton concentration for each zooplankton group, $g\ m^{-3}$

ε_{macro} = extinction coefficient for each macrophyte group, $m^{-1}/g\ m^{-3}$) - user supplied parameter

Φ_{macro} = macrophyte concentration for each macrophyte group, $g\ m^{-3}$

λ_{H2O} = extinction coefficient for water (for a wavelength of between 0.5 and 0.6μm, the absorption coefficient for *pure water* is about 0.1 m^{-1}).

Or it could be re-written as

$$\lambda = \lambda_{H2O} + \alpha TSS$$

Where α is a multiplier of all the TSS combined if each multiplier is the same for each component of TSS. From each of these correlations between TSS and light extinction, we obtain a correlation equation that gives us (1) the clear water light extinction coefficient (λ_{H2O}) and (2) the multiplier for light extinction of TSS (α). Hence, a summary of these correlations is shown in Table 20. Using data from all locations, then the model light extinction coefficients were λ_{H2O}=0.419 [1/m] and α=0.055 [1/(m mg/L)].

Table 20. Summary of correlation coefficients for TSS and light extinction.

Location (RM)	λ_{H2O}(1/m)	α (1/(m mg/L))
286	0.334	0.064
300	0.357	0.063
310	0.565	0.045
318	0.480	0.055
All locations	0.419	0.055

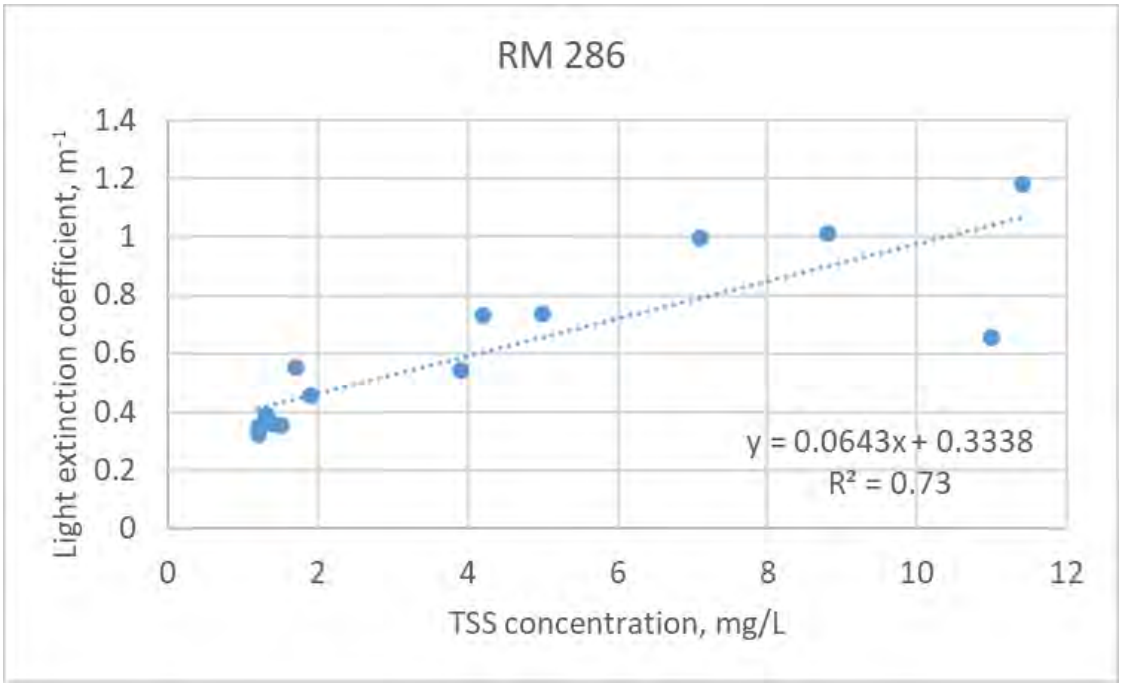


Figure 92. Correlation between TSS and light extinction coefficient at RM 286.

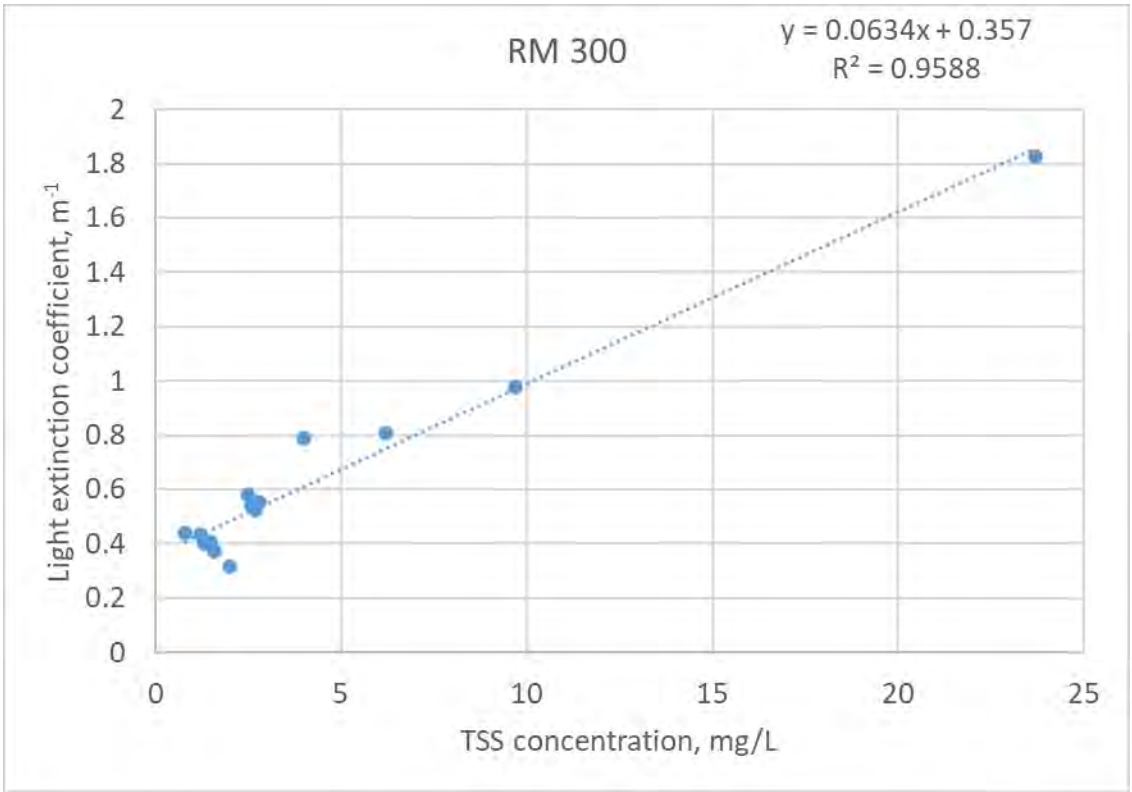


Figure 93. Correlation between TSS and light extinction coefficient at RM 300.

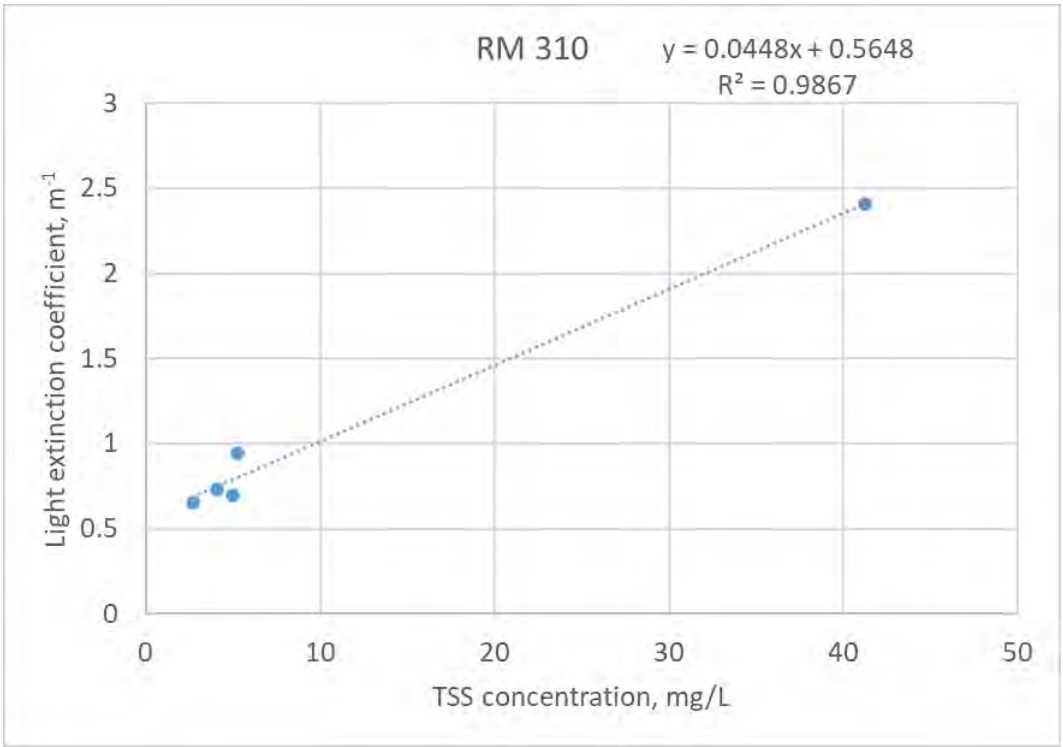


Figure 94. Correlation between TSS and light extinction coefficient at RM 310.

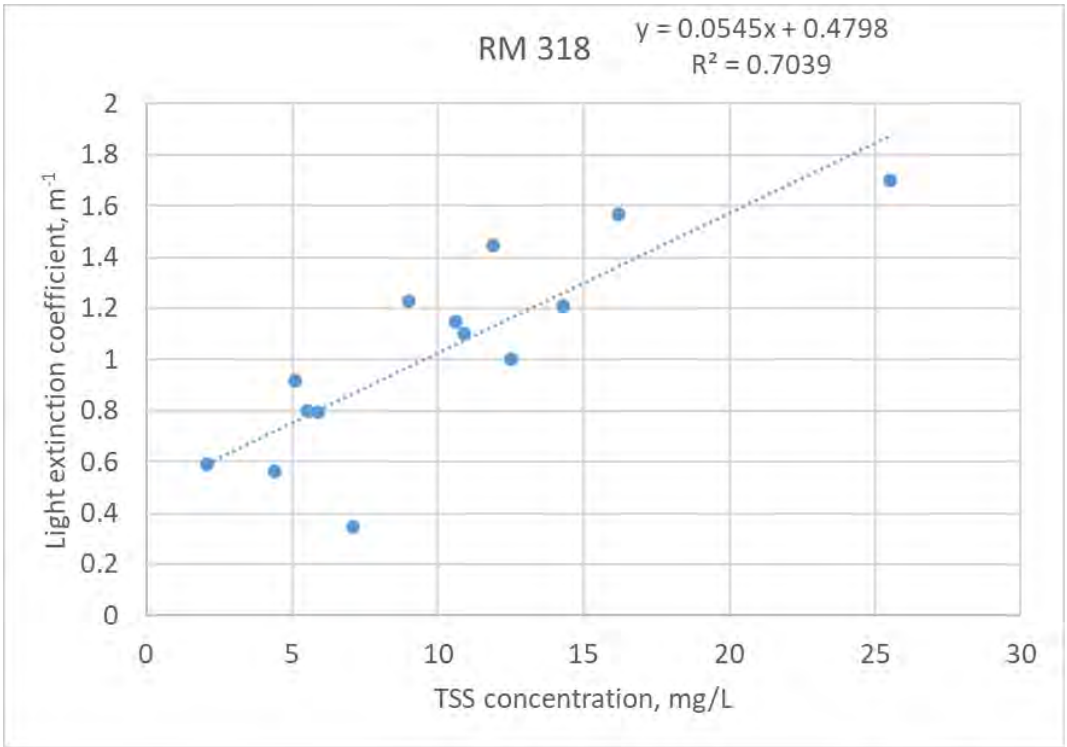


Figure 95. Correlation between TSS and light extinction coefficient at RM 318.

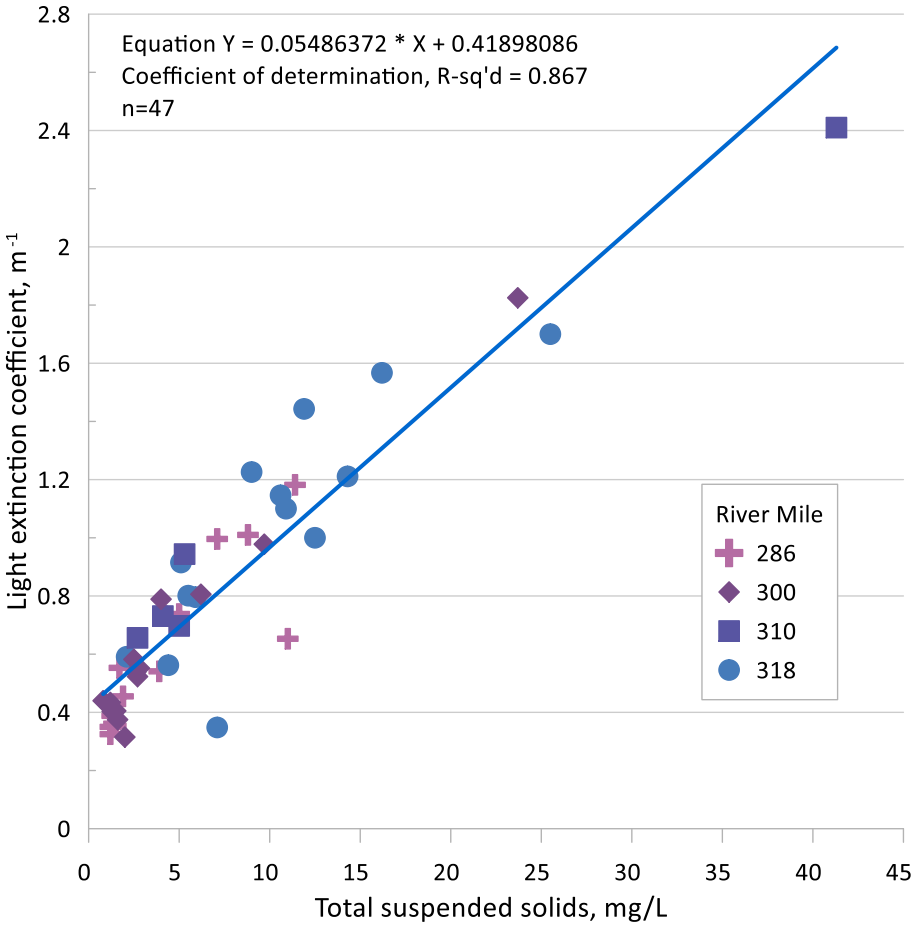


Figure 96. Correlation between TSS and light extinction coefficient using all the data between RM 286 and 318.

Model Analyses

Sensitivity of Brownlee Reservoir to Channel Friction

The CE-QUAL-W2 model is set up for wetting and drying of model segments as the water level changes over time. Since there were large variations in water level over the 5-year period (see Figure 97), a standard CE-QUAL-W2 model with one waterbody would have lost model segments from the upstream boundary as the pool retreated downstream (see Figure 4). To preserve the riverine section and allow that section to stratify as needed when water levels were high, the model grid was subdivided into multiple waterbodies that would not lose segments as the water level dropped. The upstream water bodies in Brownlee Reservoir allowed the system to transition from lacustrine to riverine as necessary by the change in pool and inflow.

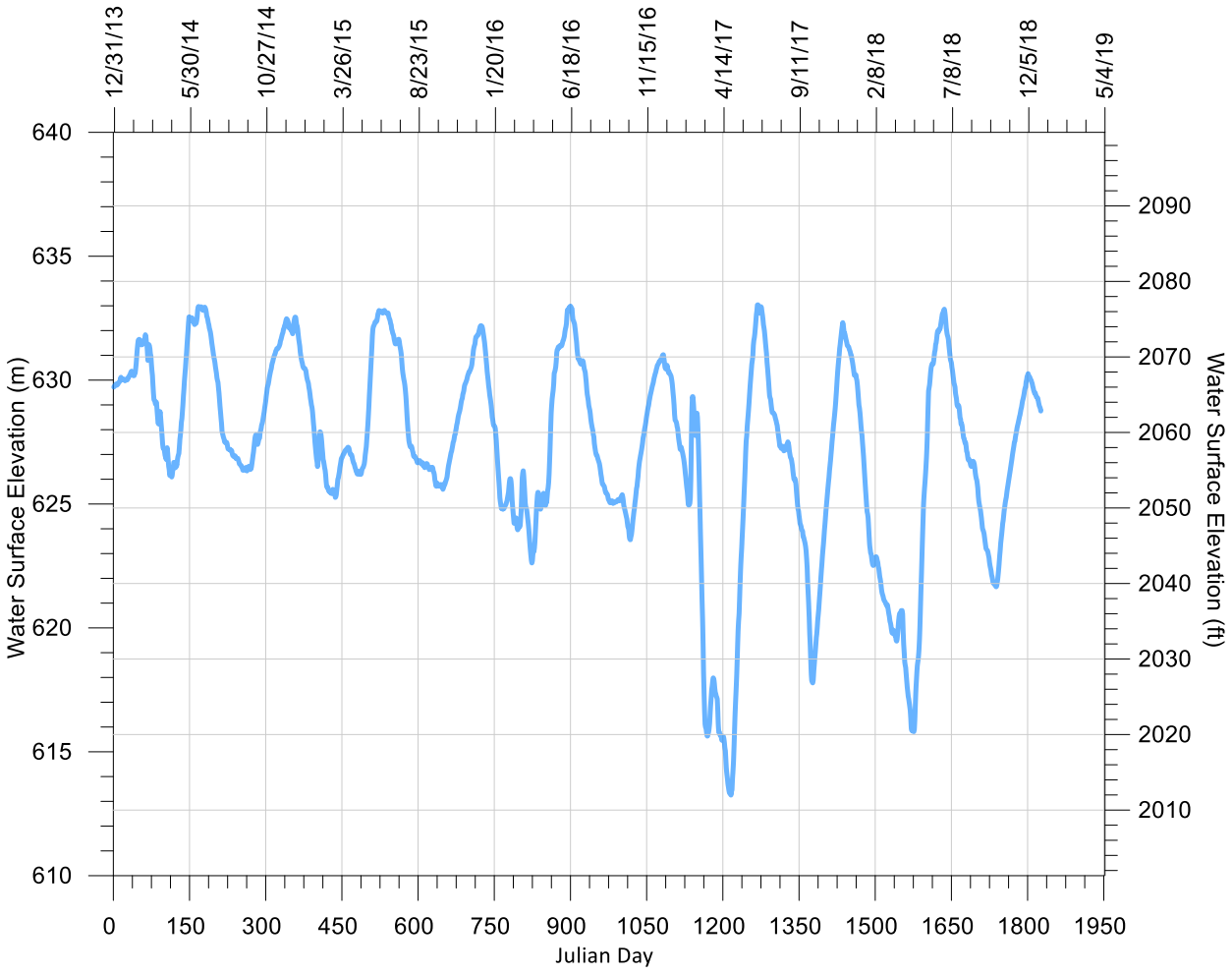


Figure 97. Water level variation in Brownlee Reservoir measured downstream of the confluence with the Powder River arm (always in the pool area) between 2014-2018.

It was relatively easy for the model grid to respond to changes in water level in 2014 through 2016. And since there were no water level elevation measurements in the riverine system when water levels were down, a question arose as to the sensitivity of the model to Manning's friction. The friction coefficients are usually not that important in a lake or reservoir with low velocities, but in the riverine sections velocities of 1 m/s were not uncommon. To illustrate how the multiple waterbodies and channel friction affected water levels from RM 345.6 to the dam at RM 284.6, Figure 98 shows the water level along the model grid for 2 different friction factors. The model with n=0.035 on Julian day 1348.2 (9/9/2017 at 4:48 am) was going unstable as evidenced by the water level instability around RM 330 (Model segment 40). Increased friction allowed the riverine sections to hold back more water (and deepen somewhat). This increased friction prevented the model from getting too shallow and becoming numerically unstable. This increased friction did somewhat lower the elevation in the pool area since water was being held back upstream. This is also the case for the water surface profile shown on Julian day 1210.5 (4/24/2017 at 12 pm). The model at both friction factors was stable at Julian day 1210.5 because even though the water level was low, there was a very high flow rate (see Figure 99).

Since there are approximate depth data from temperature profiles taken in the riverine section, we used those data to verify qualitatively the friction factors used in the riverine section of the model below RM 346.5. The model predicted depth to the bottom in the riverine sections showed reasonable water level agreement with the temperature profile data (see Temperature Calibration).

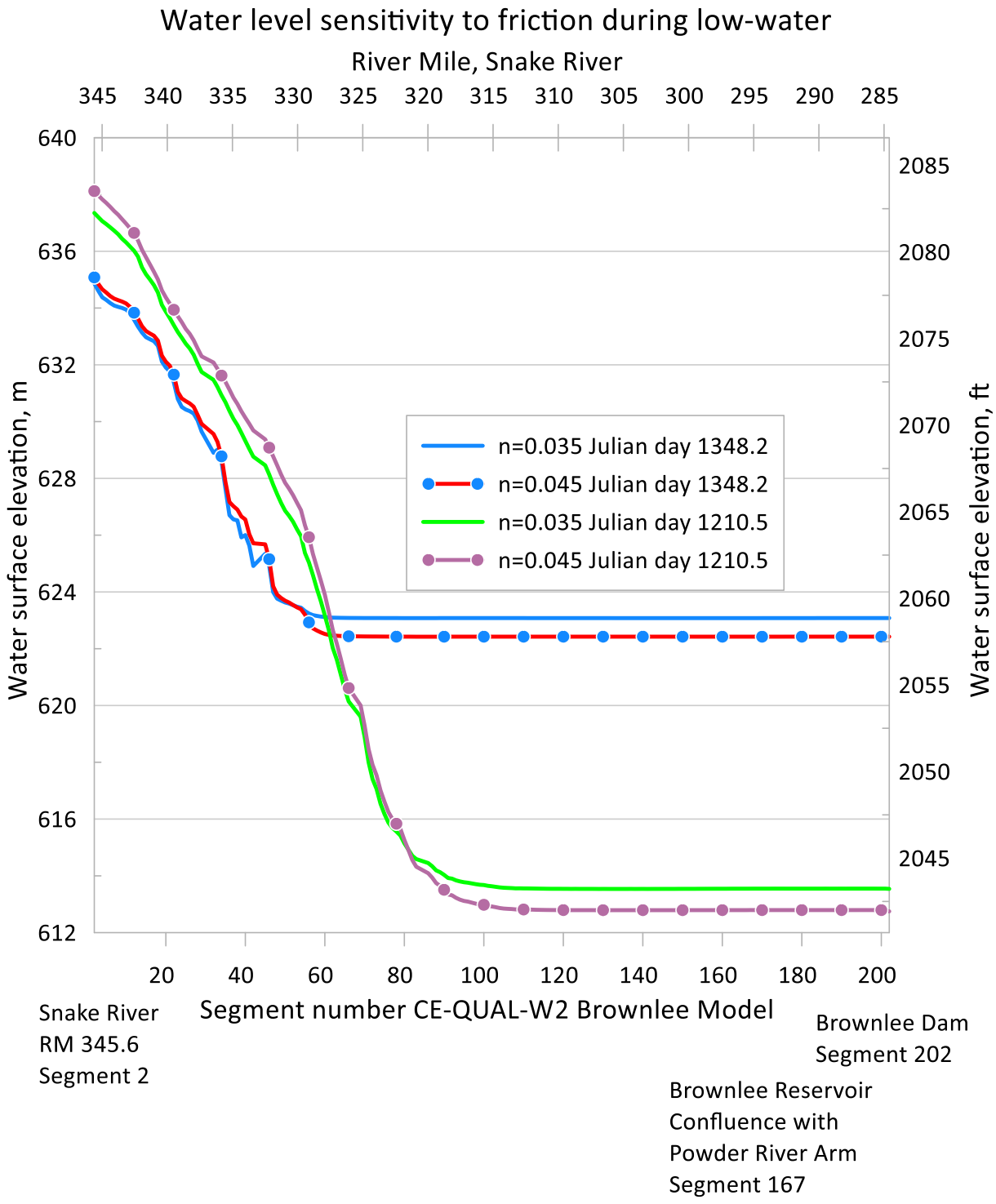


Figure 98. Water surface elevations along the Brownlee model between RM 345.6 and 284.6 on Julian day 1348.2 (9/9/2017 at 4:48 am) and Julian day 1210.5 (4/24/2017 at 12 pm) using a Manning's friction factor of 0.035 an 0.045.

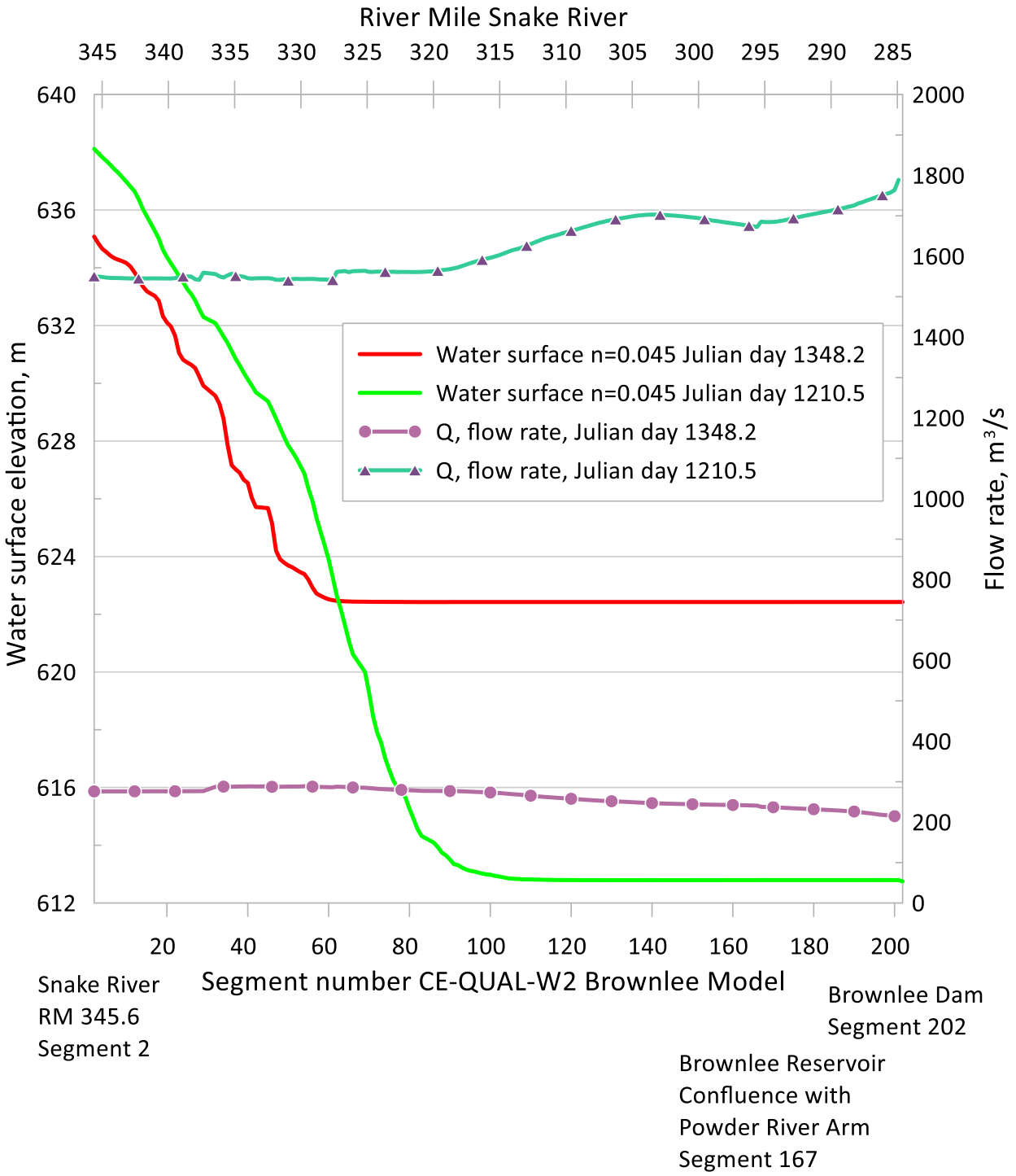


Figure 99 Water surface elevations and flow rates along the Brownlee model between RM 345.6 and 284.6 on Julian day 1348.2 (9/9/2017 at 4:48 am) and Julian day 1210.5 (4/24/2017 at 12 pm).

Detention Time of Brownlee, Oxbow and Hells Canyon Reservoirs

To understand how the reservoir detention times change with water level and flow, the detention time for each reservoir assuming no short circuiting was computed by dividing the volume of the reservoir at the specified elevation by the flow rate. This assumed no preferential flow paths through the reservoir, such as short circuiting caused by interflows.

Brownlee Reservoir detention time as a function of pool elevation and flow from the Snake River is shown in Figure 100. This does not account for the flow from the Powder River or other tributaries. At normal full pool (around 2075 ft or 632 m), the summer inflow varies from 7000-10,000 cfs (200-300 m^3/s) with a detention time of more than 65 days. Peak flows can reduce the travel time to less than 10 days. For the 2014-2018 period, the Brownlee model computes the age of water leaving the dam. All water entering the reservoir has an age of zero days. This computation accounts for stratification and short-circuiting. The age of water (detention time) computed from the Brownlee model between 2014-2018 is shown in Figure 101. This shows that once overturn occurs, the older water in the hypolimnion mixes with the rest of the reservoir volume and "older" water leaves the reservoir. Other than during overturn, typical detention times (or water age) are between 5 and 80 days.

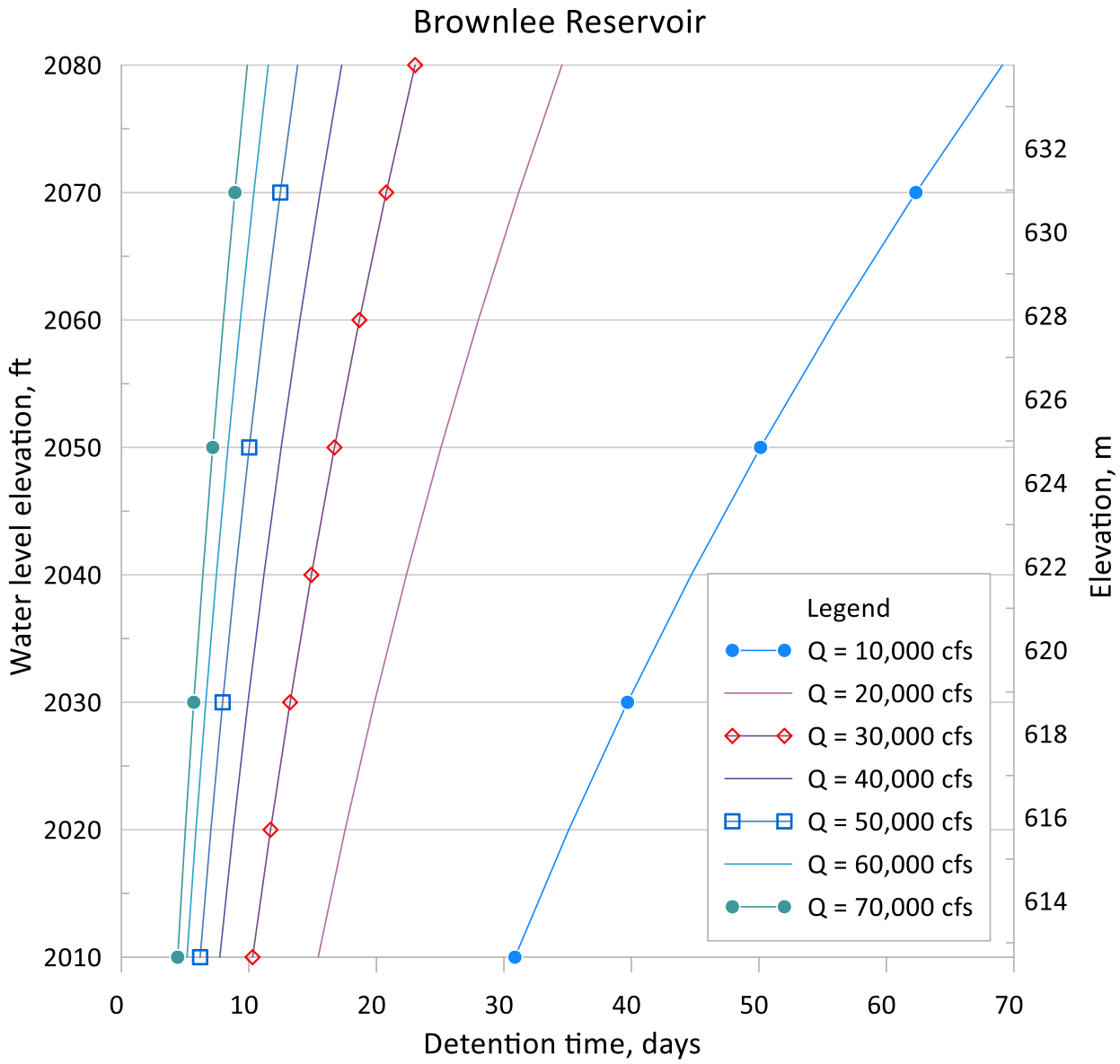


Figure 100. Brownlee Reservoir detention time as a function of elevation and flow rate assuming no short circuiting.

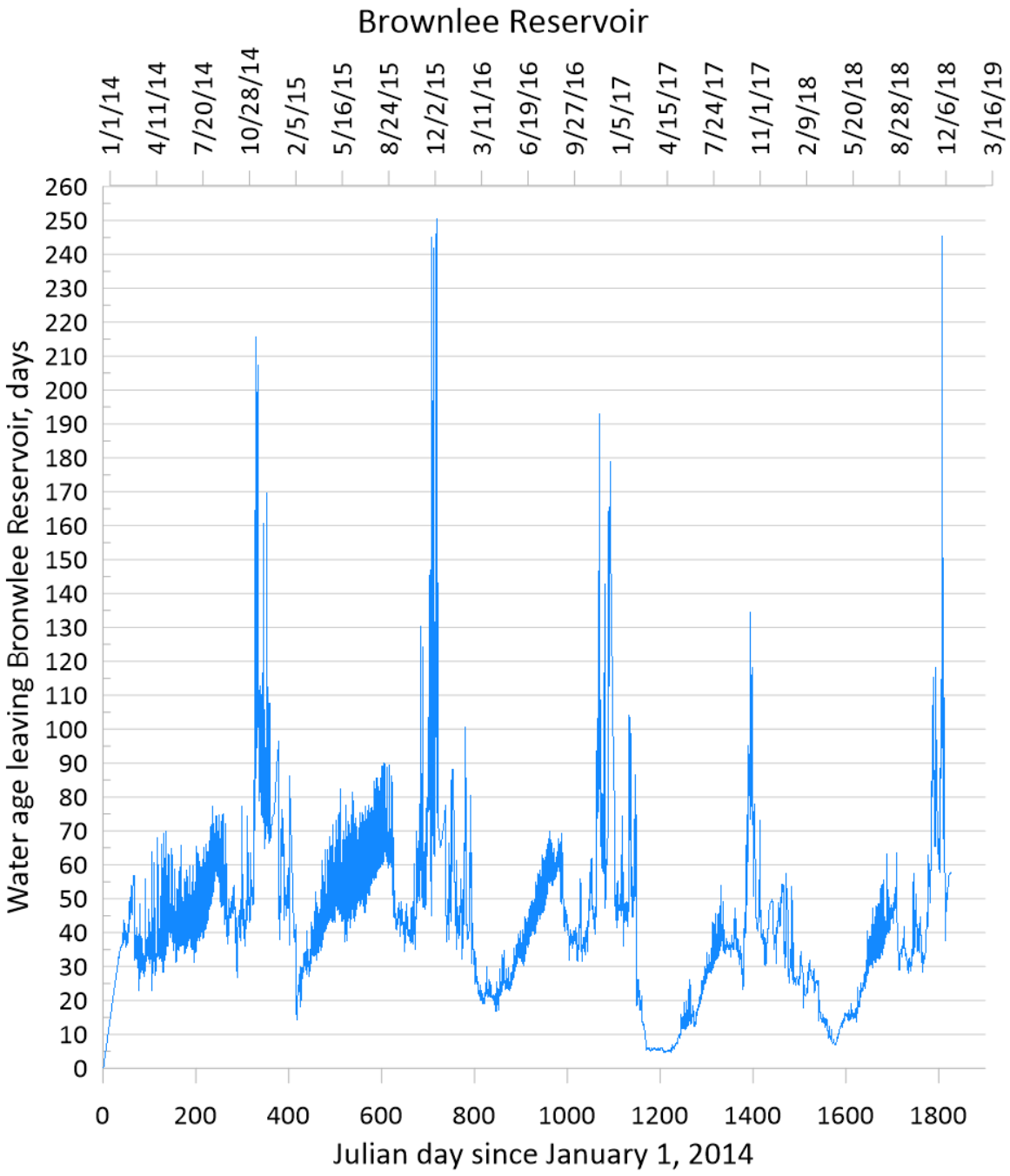


Figure 101. Computed Brownlee Reservoir water age between 2014-2018.

The detention time as a function of flow rate and water level fluctuation for Oxbow Reservoir is shown in Figure 102. The water level fluctuation is very small in Oxbow Reservoir usually only several feet per day. The residence times vary from low flows in the late summer and fall of 2-3 days to detention times less than 1 day during peak flows.

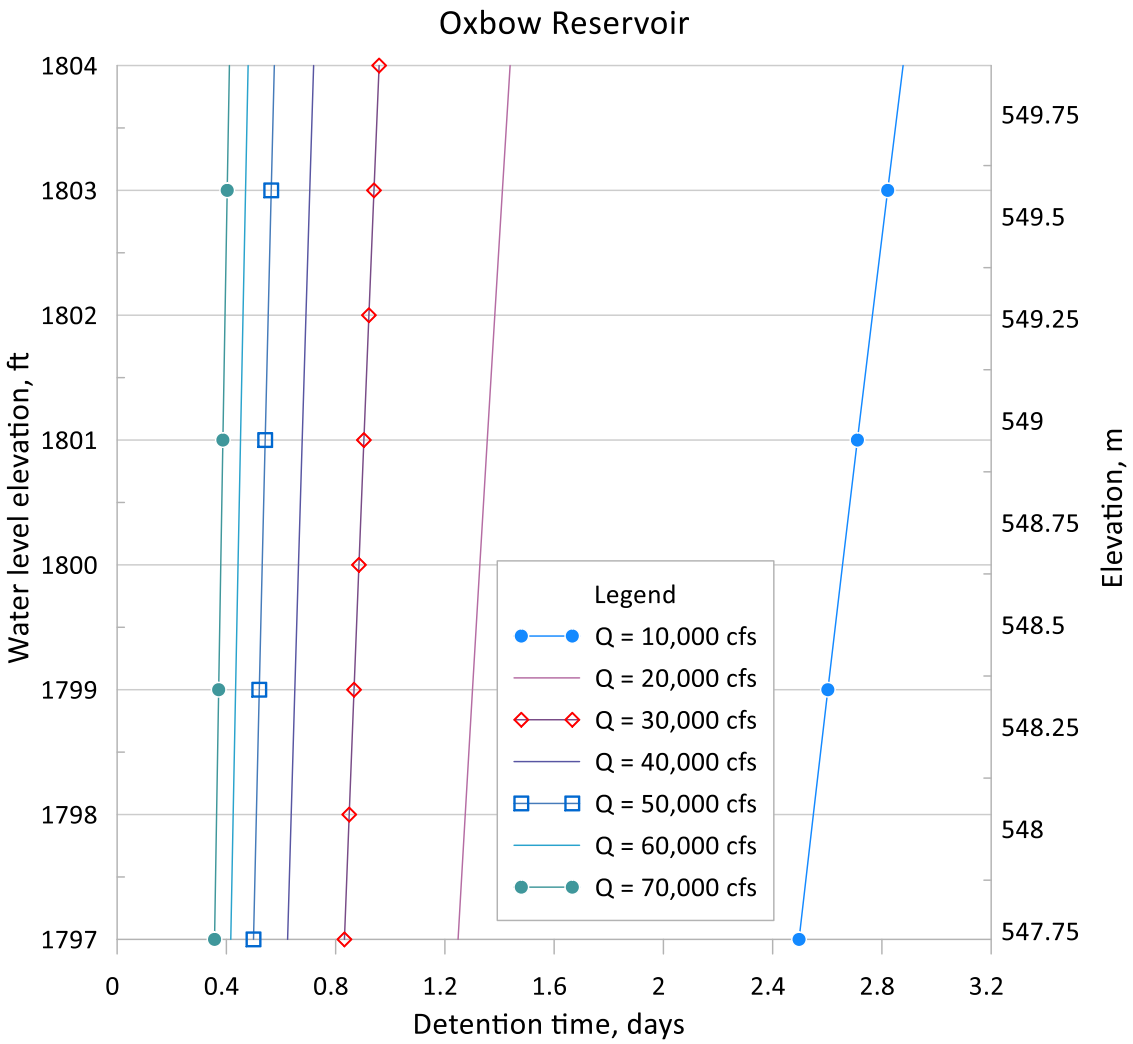


Figure 102. Oxbow Reservoir as a function of flow rate and water surface elevation.

The detention time as a function of flow rate and water level fluctuation for Hells Canyon Reservoir is shown in Figure 103. The water level fluctuation is very small in Hells Canyon Reservoir, like Oxbow Reservoir, usually only several feet per day. The residence times vary from low flows in the late summer and fall of 7-8 days to detention times less than 2 days during peak flows.

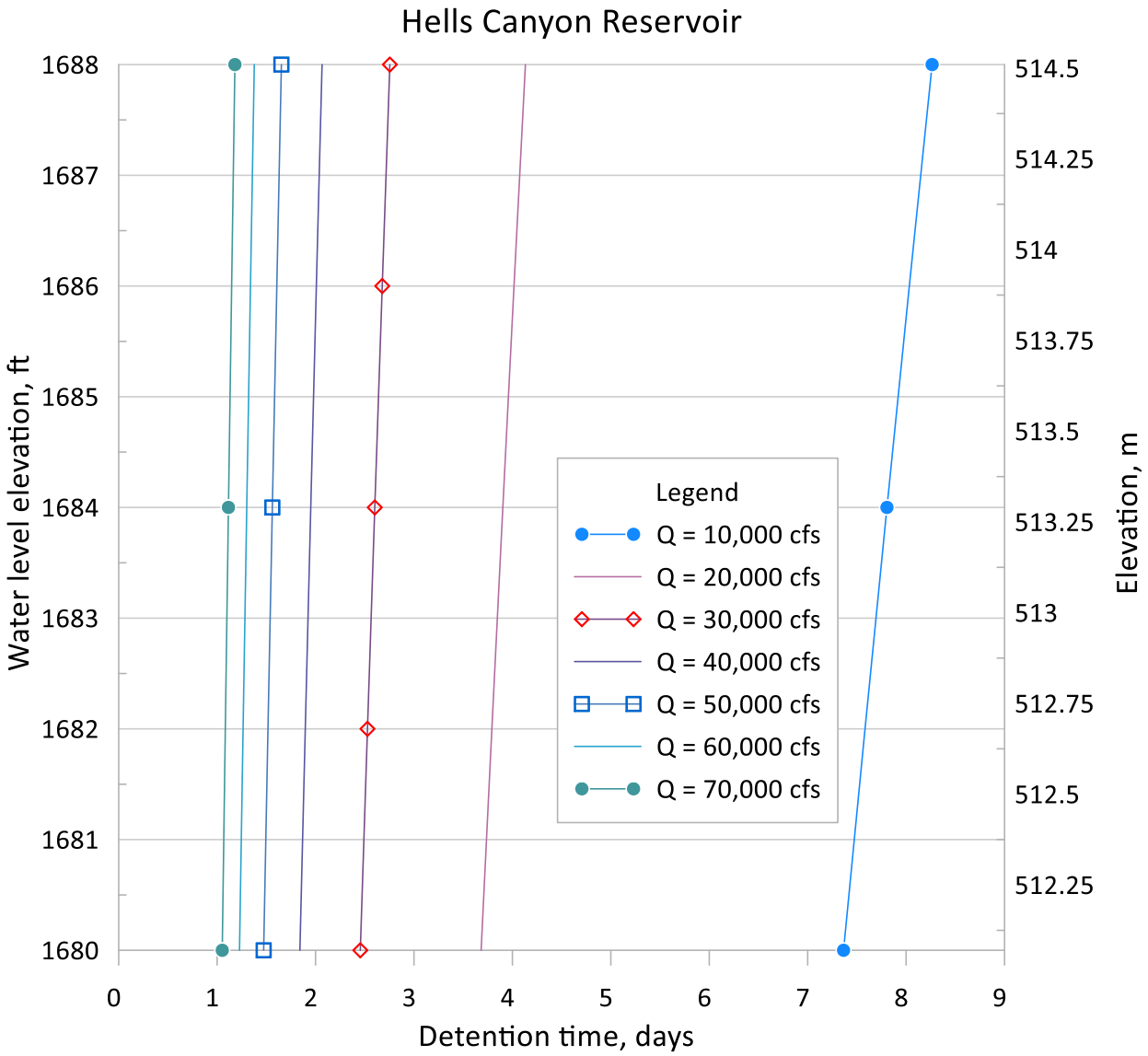


Figure 103. Hells Canyon Reservoir as a function of flow rate and water surface elevation.

Variation of Model Time Step

The CE-QUAL-W2 model uses auto variation of the maximum time step based on stability calculations. The model user can set the maximum time step and a fraction of the theoretical time step that the model will use. Using a maximum time step (DLTMAX) of 60 s and a fraction of theoretical (DLTF) of 0.85, the variation of the time step over the 5-year simulation period is shown in Figure 104 for Brownlee Reservoir, which takes the longest time to run. The variation in time step reflects changes in water level and flow in the system. As flow increases through the powerhouse or during high inflows from the Snake River, the time step for stability goes down. Often the critical location for the limiting time step is in the outlet channel which then controls the time step for the entire model. The time to complete the Brownlee model was about 5-6 hours for temperature only. Adding the water quality and Hg models a 5-year simulation of the 3 reservoirs was over 35 hours.

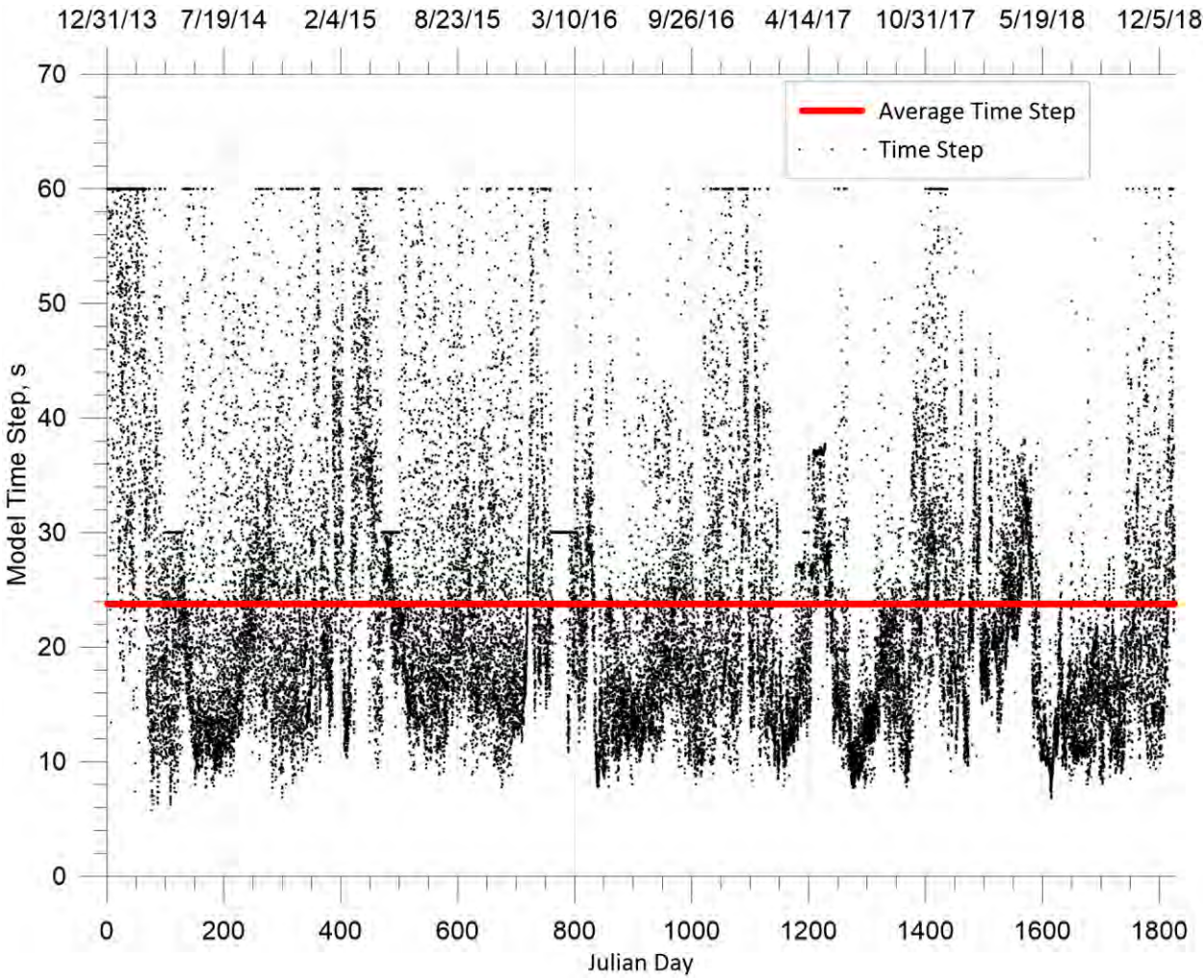


Figure 104. Variation of model time step between 2014-2018 for the Brownlee Reservoir model using maximum time step of 60 s and a fraction of theoretical time step of 0.85. The average time step was about 24 s.

Flow and Water Level Calibration

Brownlee Reservoir

A comparison of water levels predicted by the model (at segment 202) and measured water levels are shown in Figure 105. Error statistics of the water level predictions are listed in Table 21. In order to calibrate model water level predictions with data, a water balance flow was added to Branch 5 of Brownlee Reservoir that accounted for ungaged inflows, outflows and flow measurement error. These flows are added to the active surface layer of each segment in Branch 5.

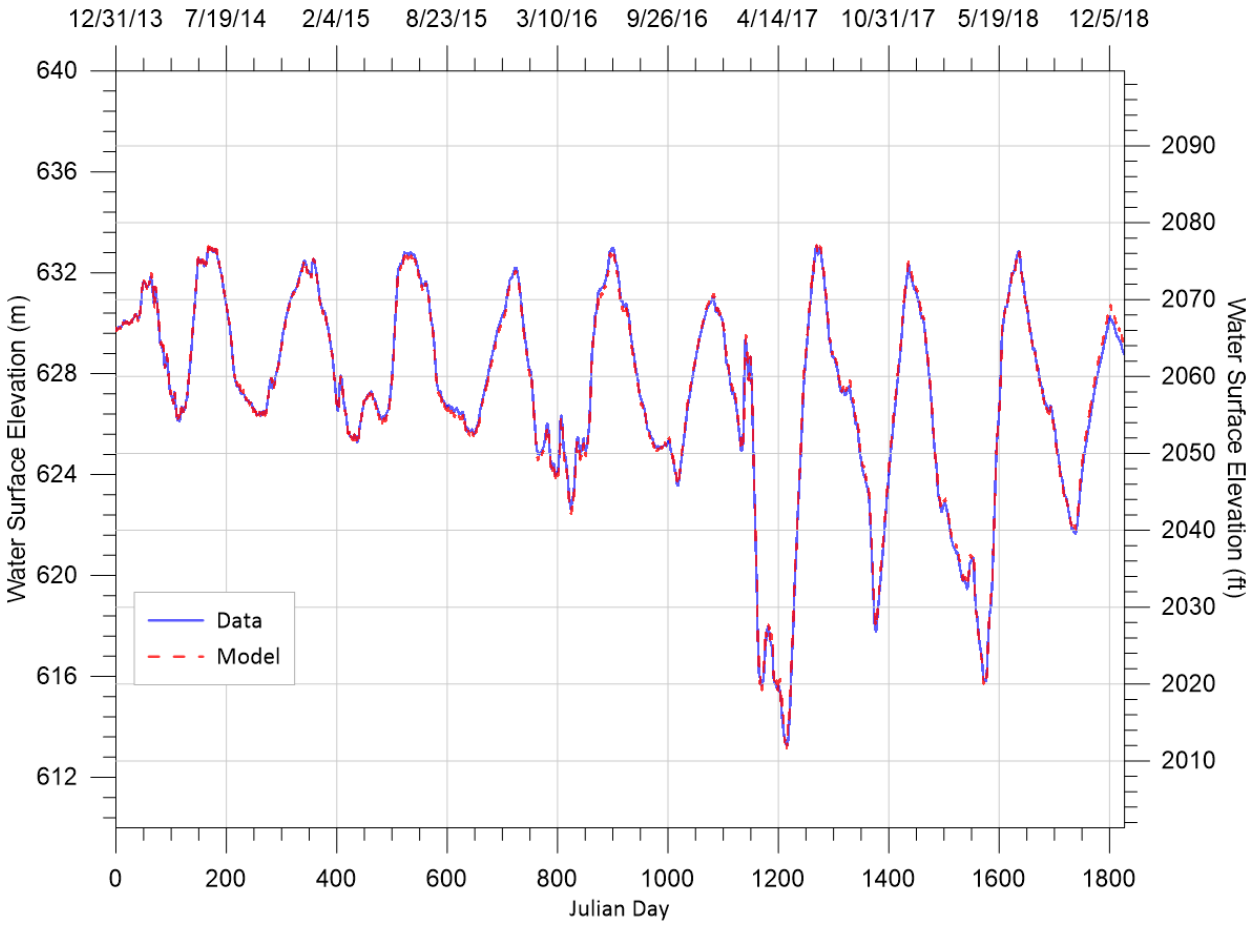


Figure 105. Water surface elevations in Brownlee Reservoir measured at segment 202 compared to model predictions between 2014-2018.

Table 21. Water level error statistics for Brownlee Reservoir.

# of data	Mean Error (m)	Mean Absolute Error (m)	Root Mean Square Error (m)
18252	0.02	0.15	0.18

The water balance flows were added to Branch 5 (the main pool of Brownlee Reservoir) to allow the model to match the water surface elevations as shown in Figure 105. These water balance flows averaged a positive 5 m^3/s over the 5 year-period indicating ungaged inflows along the drainage basin or flow measurement errors. Since gage flow can be often 5-10% in error, these flows represent what inflow or withdrawal is necessary to match the measured water level. A comparison of inflows at RM 345.6 and the water balance flows are shown in Figure 106.

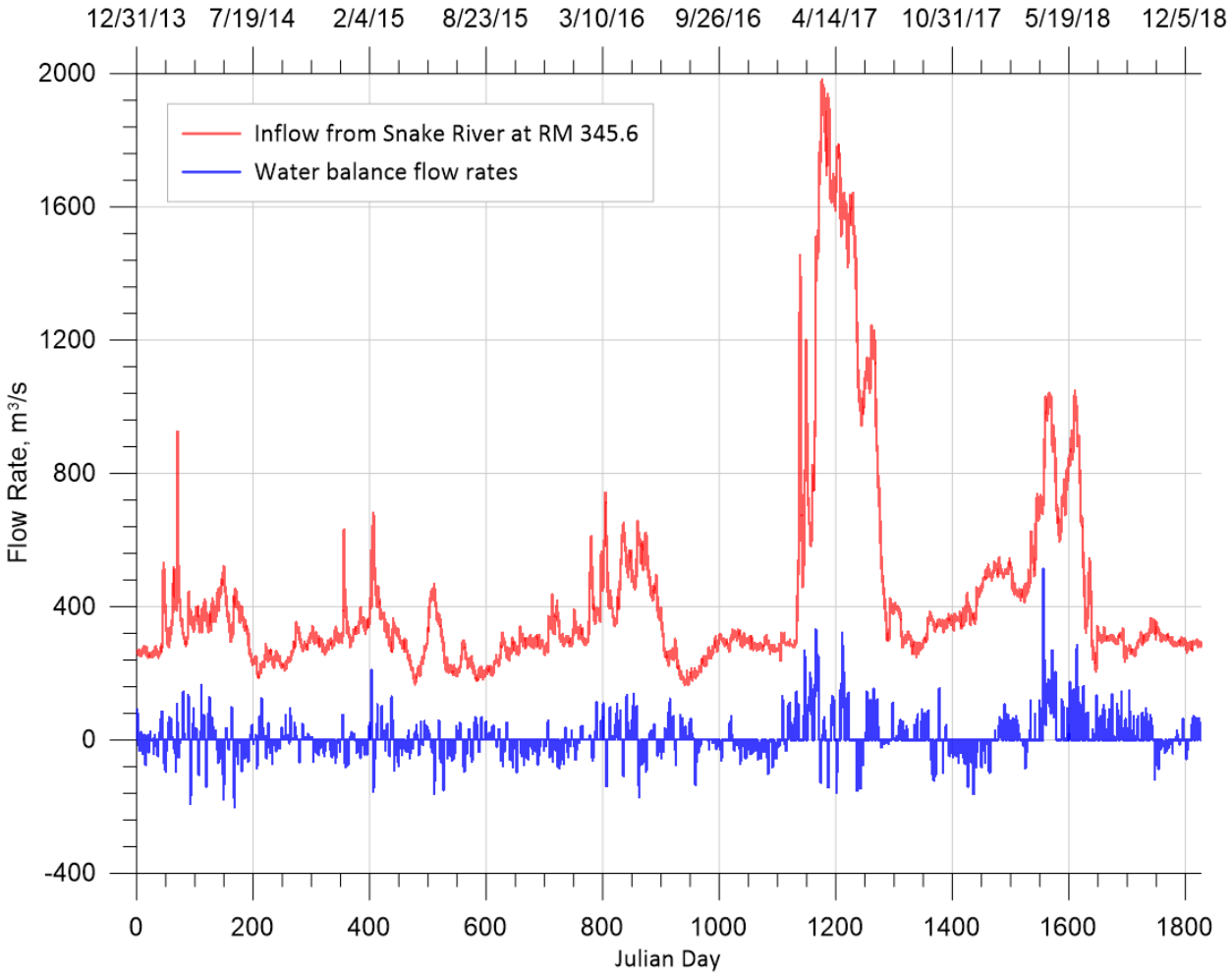


Figure 106. Water balance flows compared to inflows from January 1, 2014 through December 31, 2018.

Oxbow Reservoir

Oxbow Reservoir water level predictions are compared with data in Figure 107. Error statistics of the water level predictions are listed in Table 22.

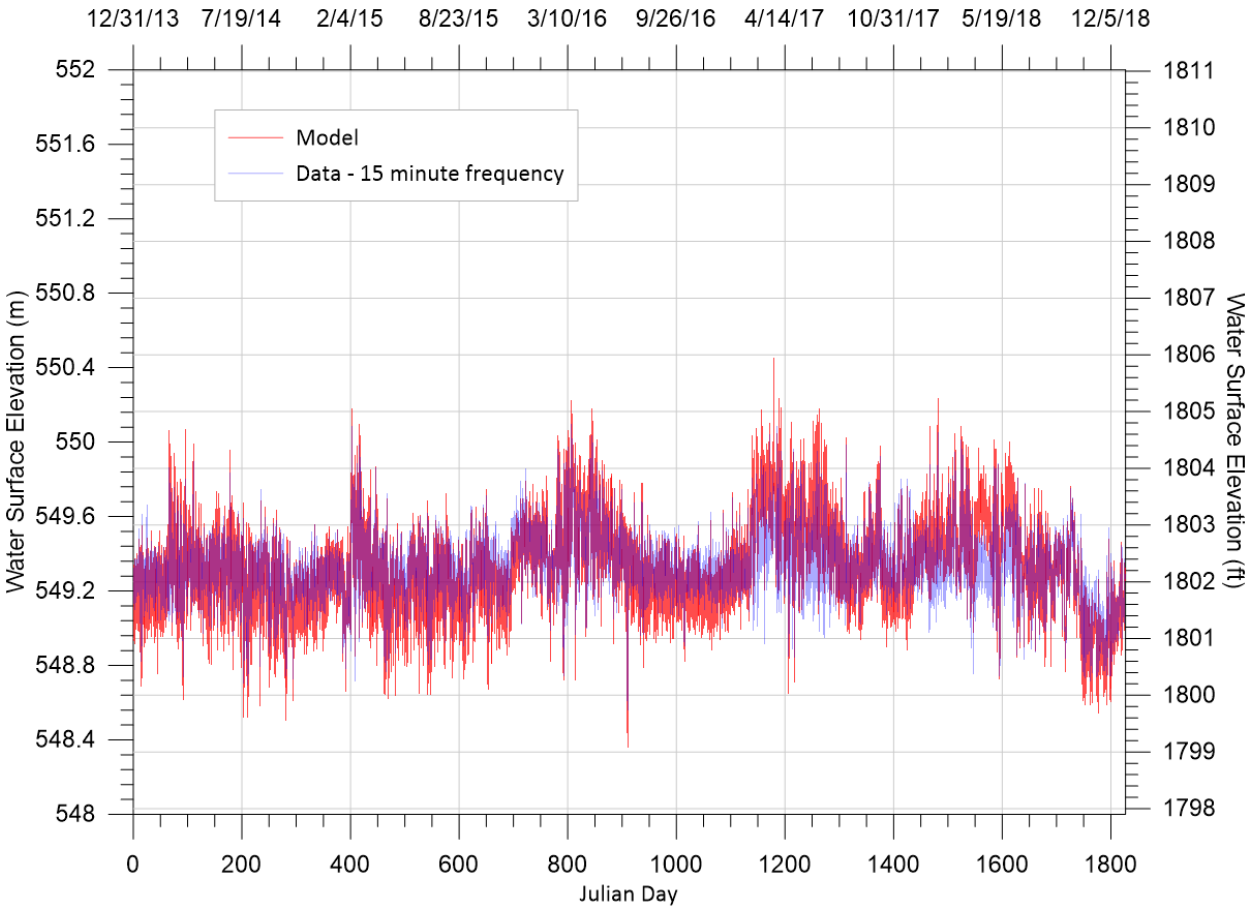


Figure 107. Oxbow Reservoir model water level predictions compared with data.

Table 22. Water level error statistics for Oxbow Reservoir.

# of data	Mean Error (m)	Mean Absolute Error (m)	Root Mean Square Error (m)
175181	-0.01	0.11	0.13

Hells Canyon Reservoir

Figure 108 compares the Hells Canyon Reservoir model predictions of water level with data. The error statistics of the water level predictions are listed in Table 23.

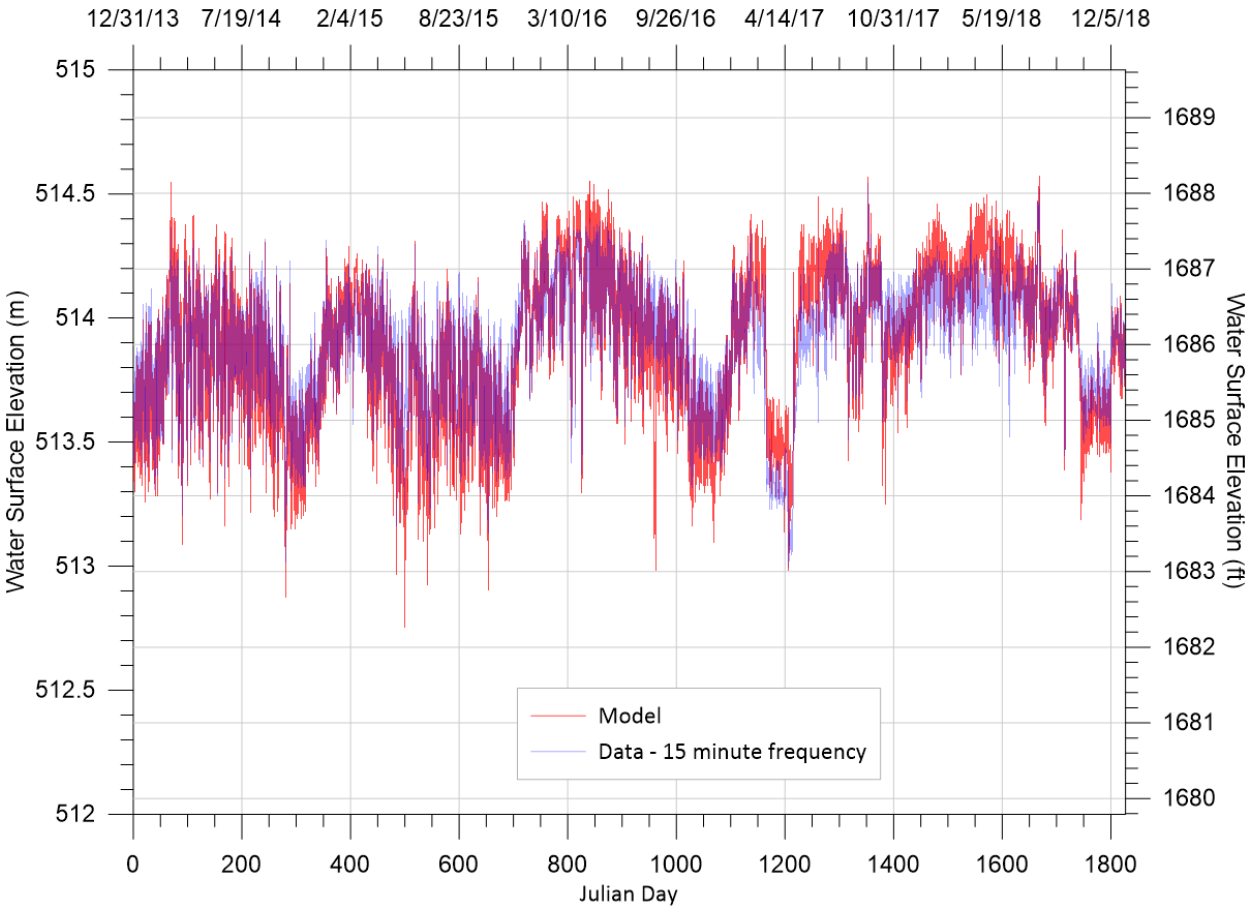


Figure 108. Hells Canyon Reservoir model water level predictions compared with data.

Table 23. Water level error statistics for Hells Canyon Reservoir.

# of data	Mean Error (m)	Mean Absolute Error (m)	Root Mean Square Error (m)
175198	-0.01	0.09	0.12

Temperature Calibration

Brownlee Reservoir

The Brownlee Reservoir model temperature predictions were compared with profiles measured within the reservoir and outflow temperatures measured immediately downstream. Error statistics of model predicted profile temperatures are provided in Table 24. Model predictions of vertical temperature profiles are compared with data in Appendix A4.

Table 24. Temperature error statistics for Brownlee Reservoir vertical profiles.

River Mile	Segment	# of Profiles	# of Data	ME (°C)	MAE (°C)	RMSE (°C)
327.8	62	32	719	-0.53	0.73	0.84

River Mile	Segment	# of Profiles	# of Data	ME (°C)	MAE (°C)	RMSE (°C)
326	69	43	1001	-0.36	0.67	0.80
324	76	47	1228	-0.43	0.73	0.86
322	82	47	1430	-0.62	0.88	1.01
320	91	47	1566	-0.56	0.81	0.96
318	97	62	2185	-0.37	0.71	0.84
316	103	53	2177	-0.33	0.74	0.87
314	109	55	2309	-0.26	0.66	0.79
312	116	55	2697	0.03	0.67	0.80
310	122	73	4041	0.25	0.77	0.97
308	128	59	3664	0.35	0.82	1.14
306	135	60	3813	0.37	0.82	1.15
304	141	59	4517	0.29	0.88	1.23
302	148	58	4216	0.39	0.87	1.21
300	154	74	6066	0.26	0.87	1.20
298	160	62	5366	0.24	0.88	1.19
296	166	64	5189	0.34	0.90	1.21
294	173	63	6060	0.23	0.91	1.24
292	179	61	5706	0.20	0.89	1.20
290	185	63	6399	0.13	0.88	1.19
288	192	64	6535	0.21	0.88	1.22
286	198	77	8858	0.15	0.85	1.18
Sum/Avg.		1278	85742	0.14	0.84	1.13

The USGS also measured continuous temperatures during several field surveys in Brownlee Reservoir in 2017 and 2018. These field data were taken at an interval of 10 min at various depths. The error statistics evaluating these data are shown in Table 25. Graphical comparisons of model predictions and field data are shown in Appendix 7.

Table 25. Error statistics for continuous temperature data measured by the USGS.

RM	Depth	Segment	Count	ME_Error	AME_Error	RMS_error
286	1	198	50351	0.764	0.818	1.012
286	3	198	29797	0.827	0.848	0.998
286	6	198	50259	0.747	0.794	0.961
286	10	198	29794	0.626	0.676	0.822
286	15	198	50290	0.387	0.482	0.604
286	21	198	29793	0.229	0.446	0.567
286	30	198	29795	0.274	0.899	1.286
300	1	154	50634	0.953	0.968	1.130
300	3	154	29949	0.841	0.853	0.970
300	6	154	50570	0.728	0.739	0.837
300	10	154	29948	0.610	0.632	0.736
300	15	154	50569	0.484	0.531	0.647

RM	Depth	Segment	Count	ME_Error	AME_Error	RMS_error
300	21	154	29947	0.306	0.450	0.557
300	30	154	29948	0.005	0.921	1.420
318	1	97	30017	0.005	0.539	0.717
318	3	97	30017	0.037	0.483	0.638
318	6	97	30018	0.037	0.367	0.484
318	10	97	30018	-0.072	0.345	0.483
Total/Average			661714	0.478	0.667	0.833

Figure 109 compares model predicted outflow temperatures with temperature data measured on the left and the right of the channel at the bridge located immediately downstream of Brownlee Dam. Model results from Oxbow Reservoir at segment 4 (closest model segment to the sampling location) were used to compare to field data. Error statistics of model predicted outflow temperatures are listed in Table 26.

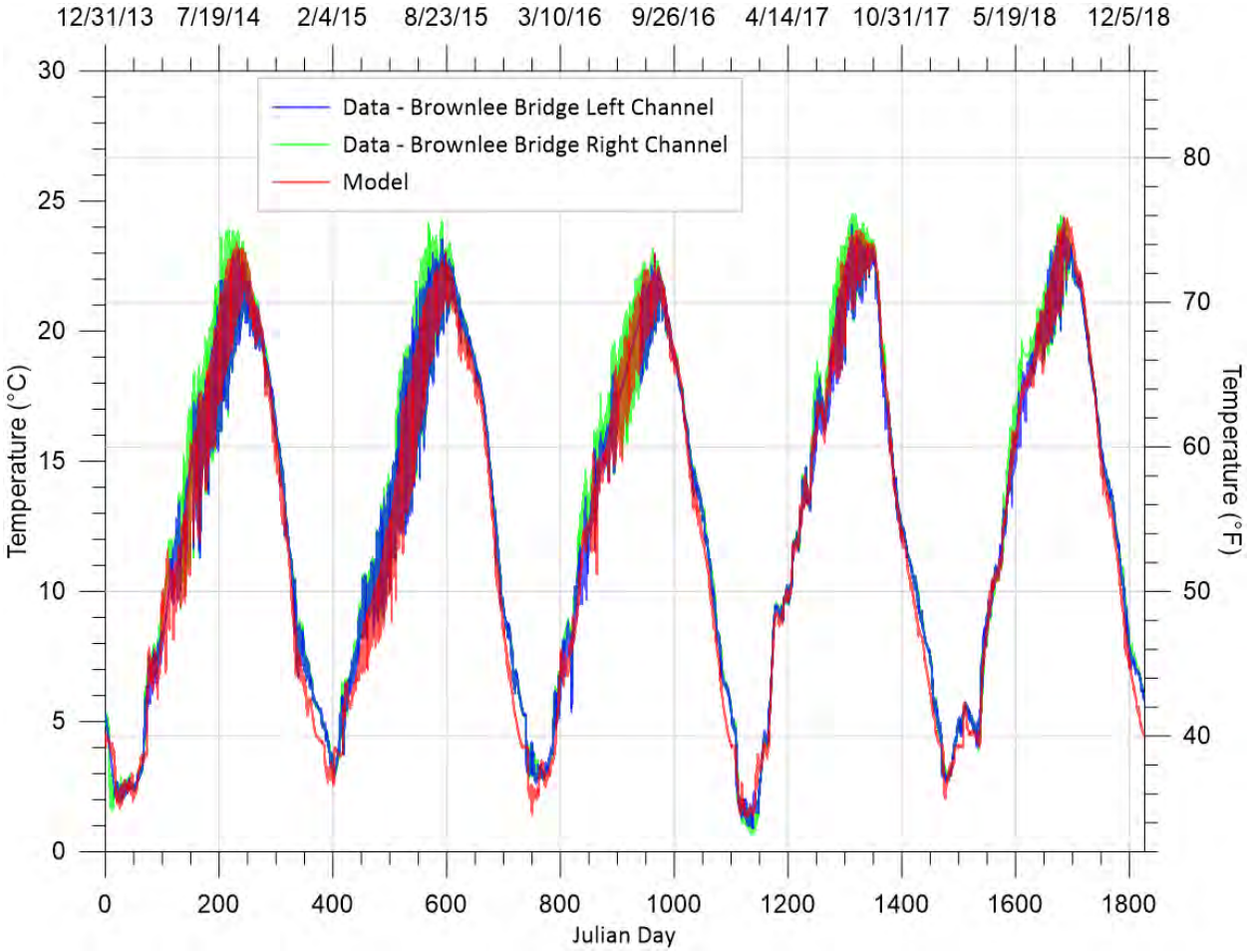


Figure 109. Brownlee Dam model outflow temperatures compared to data.

Table 26. Brownlee Dam outflow temperature error statistics.

Station	Model Average (°C)	# of data	Mean Error (°C)	Mean Absolute Error (°C)	Root Mean Square Error (°C)
Brownlee Outflow RM 283.9 Left Channel	12.57	256258	-0.29	0.58	0.73
Brownlee Outflow RM 283.9 Right Channel	12.57	265150	-0.47	0.66	0.84
Average	12.57	521408	-0.38	0.62	0.79

Oxbow Reservoir

Temperature data were available just downstream of the Oxbow Dam outflow. Model results from Hells Canyon Reservoir at segment 14 (closest model segment to the sampling location) were used to compare to field data. Model versus data comparisons are shown in Figure 110.

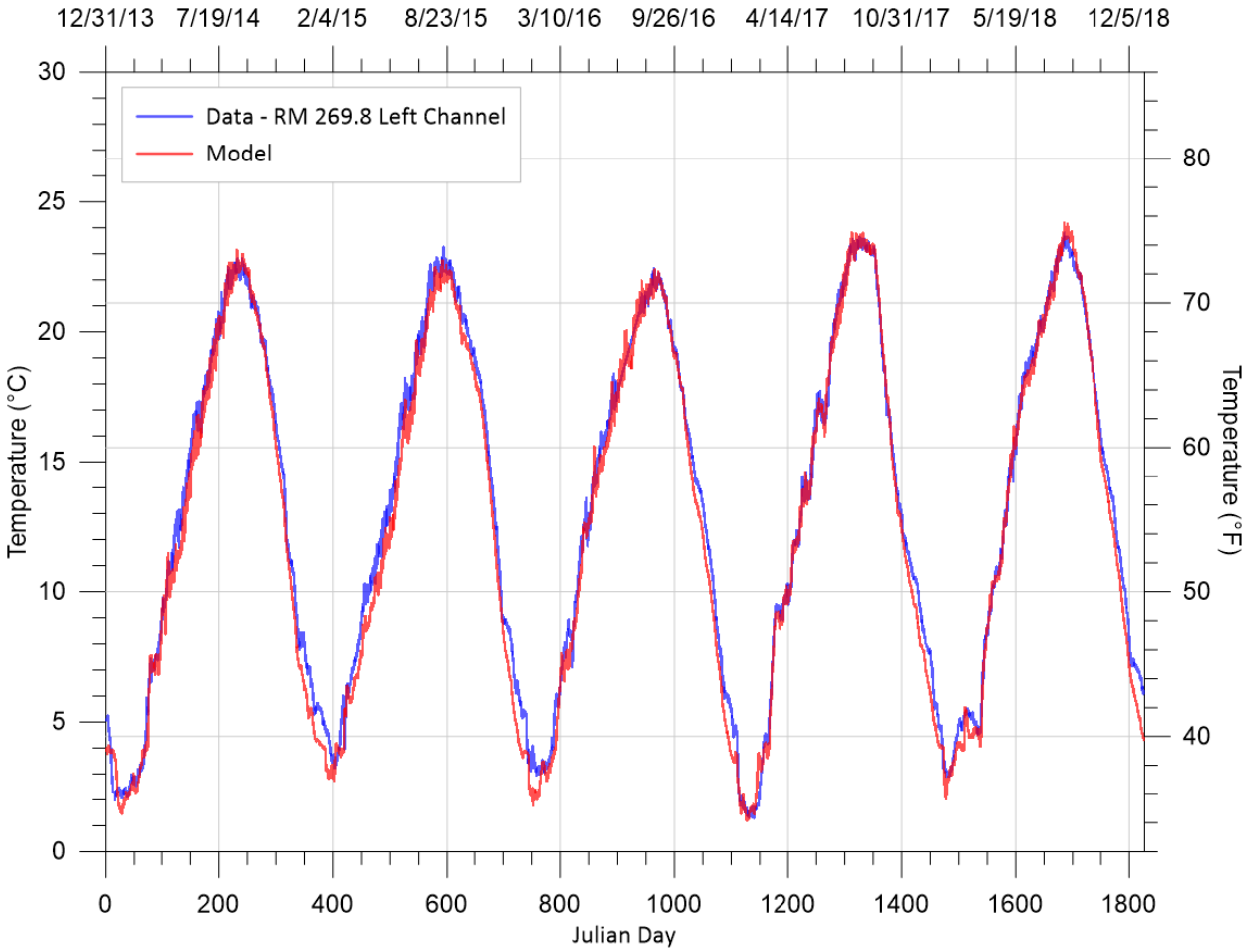


Figure 110. Oxbow Dam model outflow temperatures compared to data.

Table 27. Oxbow Dam outflow temperature error statistics.

Station	Model Average (°C)	# of data	Mean Error (°C)	Mean Absolute Error (°C)	Root Mean Square Error (°C)
Oxbow Outflow RM 269.8 Left Channel	12.71	254296	-0.50	0.62	0.77

Hells Canyon Reservoir

Vertical profile temperature data and outflow temperature data were available to calibrate the Hells Canyon Reservoir model. Table 28 lists error statistics for the Hells Canyon temperature profiles. Model versus data comparisons of the profiles are shown in Appendix A6. Dam outflow temperatures are compared with data in Figure 111. Since the outflow temperature was measured at the penstock intake for the turbines, only turbine (turbine + baseflow) temperatures were used for model comparisons. Most of the error occurred during the colder months.

Table 28. Temperature error statistics for Hells Canyon Reservoir vertical profiles.

River Mile	Segment	# of Profiles	# of Data	ME (°C)	MAE (°C)	RMSE (°C)
263.3	44	1	38	-0.29	0.40	0.43
259.7	60	1	62	-1.02	1.02	1.03
257.5	69	1	71	-0.48	0.59	0.68
255	81	1	60	-0.57	0.67	0.75
253	90	1	75	-0.75	0.91	1.09
252.3	93	8	691	-0.17	0.78	1.12
251.1	97	1	98	-0.23	0.78	0.92
249.5	106	1	98	-0.10	0.83	1.07
248.1	113	18	1738	0.08	0.85	1.08
247.9	114	2	178	-0.48	0.81	0.96
Sum/Avg.		35	3109	-0.10	0.82	1.05

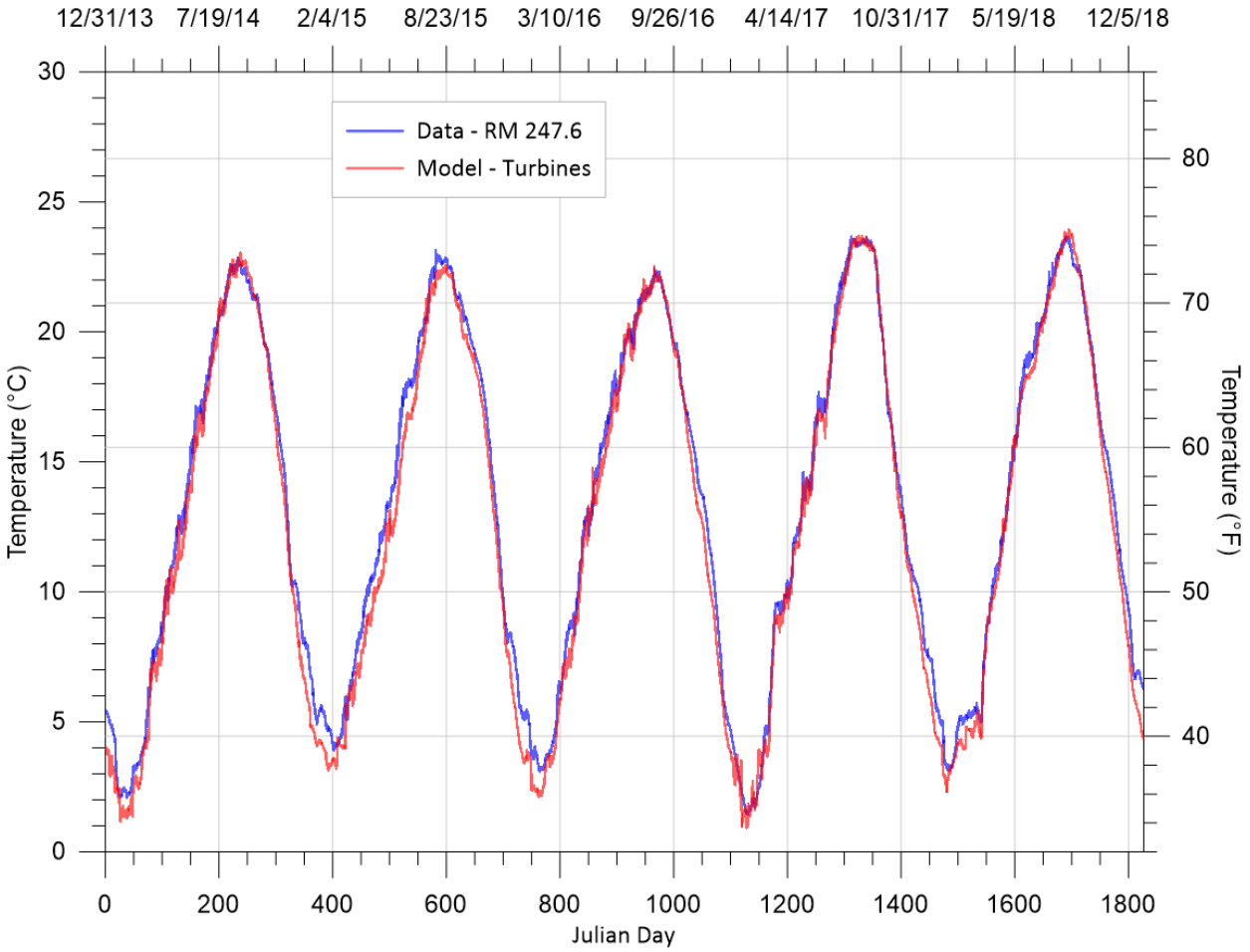


Figure 111. Hells Canyon Dam model outflow temperatures compared to data.

Table 29. Hells Canyon Dam outflow temperature error statistics.

Station	Model Average (°C)	# of data	Mean Error (°C)	Mean Absolute Error (°C)	Root Mean Square Error (°C)
Hells Canyon Outflow RM 247.6 PS1	12.77	251795	-0.57	0.64	0.80

Water Quality Calibration

Model results were compared to vertical profile data, outflow data, and sediment porewater data from IPC and USGS for the three reservoirs. Table 30 lists the locations with data used for outflow and profile model comparisons, and Table 31 lists the locations with USGS data used for sediment and porewater model comparisons. Brownlee Reservoir profile data were collected between (and including) river miles 327.8 to 286, Oxbow Reservoir profile data were collected at river mile 273, and Hells Canyon Reservoir profile data were collected between (and including) river miles 263.3 to 247.9. The following approach was used for processing data values for water quality comparisons:

- USGS values with a "<" flag next to the reported value were shown in figures as "no detects" at half the value listed and were omitted from statistics calculations.
- IPC values with a "<" flag next to the reported value were shown in figures as "no detects" at half the value listed in figures and omitted from statistics calculations.
- Negative values and duplicates were removed.
- Any values of zero or "trace" were shown on figures as the minimum of (1) the lowest halved no detect ("<") value or (2) half of the lowest value observed (greater than zero) and omitted from the statistics calculations.
- Negative depths were converted to positive and USGS depths of "SW" were converted to 0.3m. However, these only applied to inflow/outflow locations where flow was well-mixed and depth was not used for generating comparisons.
- All other values were included as the value listed, including values flagged as suspect or estimates or were filtered in the laboratory prior to analysis. USGS values that were flagged with "< RL, estimate based on lowest standard" were also left at the value listed.

Table 30. Data used for outflow and profile model comparisons.

Parameter	Source	BR Pr	BR Out RM 283.9	OX Pr	OX Out RM 269.9	HC Pr	HC Out RM 247.6	HC Out RM 246.9	Notes
Dissolved Oxygen	IPC	X	X	-	X	X	X	-	
pH	IPC	X	-	-	-	X	-	-	
Chlorophyll a	IPC	X	X	-	-	-	-	X	Outliers of 801 ug/l and 288 ug/l removed.
Ammonia	IPC	X	X	-	-	-	-	X	
Nitrate	IPC	X	X	-	-	-	-	X	
Nitrate	USGS	X	X	X	X	X	-	X	
Total Kjeldahl Nitrogen	IPC	X	X	-	-	-	-	X	
Particulate Organic Nitrogen	USGS	X	X	X	X	X	-	X	Using particulate nitrogen from data.
Orthophosphate	IPC	X	X	-	-	-	-	X	
Orthophosphate	USGS	X	X	X	X	X	-	X	Using filter-passing phosphorus from data.
Total Phosphorus	IPC	X	X	-	-	-	-	X	
Total Inorganic Carbon	USGS	X	X	X	X	X	-	X	Using dissolved inorganic carbon from data.
Dissolved Organic Carbon	USGS	X	X	X	X	X	-	X	Using "Boulder" DOC data
Particulate Organic Carbon	USGS	X	X	X	X	X	-	X	
Chloride	USGS	X	X	X	X	X	-	X	
Sulfate	IPC	X	X	-	-	-	-	X	
Sulfate	USGS	X	X	X	X	X	-	X	
H2S	USGS	X	X	-	X	X	-	X	Using filter-passing inorganic sulfide from data.

Parameter	Source	BR Pr	BR Out RM 283.9	OX Pr	OX Out RM 269.9	HC Pr	HC Out RM 247.6	HC Out RM 246.9	Notes
Zooplankton	IPC, USGS	X	X	X	X	X	-	-	Using plankton biomass from IPC data for outflow comparisons, and zooplankton biomass from USGS data for profile comparisons.
Fe(II)	USGS	X	X	X	X	X	-	X	Using filtered Fe from data. Outlier of 277 ng/l at RM 300 removed.
FeOOH	USGS	X	X	-	X	X	-	X	Using particulate Fe from data.
Mn(II)	USGS	X	X	X	X	X	-	X	Using filtered Mn from data.
MnO2	USGS	X	X	-	X	X	-	X	Using particulate Mn from data.
Total Suspended Solids	USGS	X	X	X	X	X	-	X	
Total Suspended Solids	IPC	X	X	-	-	-	-	X	
Volatile Suspended Solids	IPC	-	X	-	-	-	-	X	Model predictions of POC compared to VSS data x 0.45 as an estimate of POC from VSS.

Pr, Profile; Out, Outflow

Table 31. USGS data available for sediment and porewater model comparisons. Shaded rows indicate data used for comparisons.

Parameter	Source	BR RM 318	BR RM 314	BR RM 310	BR RM 305	BR RM 300	BR RM 286	OX RM 273	HC RM 252	HC RM 248/ 248.1	Notes
Dissolved Organic Carbon	2	X	-	X	-	X	X	-	-	X	
H2S	2	X	-	X	-	X	X	-	-	X	Using pore water sulfide from data.
Mn(II)	2	X	-	X	-	X	X	-	-	X	Using pore water manganese from data.
Fe(II)	2	X	-	X	-	X	X	-	-	X	Using pore water iron from data.
Orthophosphate	2	X	-	X	-	X	X	-	-	X	
Nitrate	2	X	-	X	-	X	X	-	-	X	
Sulfate	2	X	-	X	-	X	X	-	-	X	
Ammonia	2	X	-	X	-	X	X	-	-	X	
Chloride	4	X	X	X	X	X	X	-	-	X	
Dissolved Organic Carbon	4	X	X	X	X	X	X	-	-	X	
H2S	4	X	X	X	X	X	X	-	-	X	Using filter-passing inorganic sulfide from data.

Parameter	Source	BR RM 318	BR RM 314	BR RM 310	BR RM 305	BR RM 300	BR RM 286	OX RM 273	HC RM 252	HC RM 248/ 248.1	Notes
MnO2	4	X	X	X	X	X	X	-	-	X	Using particulate Mn from data.
Mn(II)	4	X	X	X	X	X	X	-	-	X	Using filtered Mn from data.
FeOOH	4	X	X	X	X	X	X	-	-	X	Using particulate Fe from data.
Fe(II)	4	X	X	X	X	X	X	-	-	X	Using filtered Fe from data.
Orthophosphate	4	X	X	X	X	X	X	-	-	X	Using filter-passing phosphorus from data.
Nitrate	4	X	X	X	X	X	X	-	-	X	
Sulfate	4	X	X	X	X	X	X	-	-	X	
Total Suspended Solids	4	X	X	X	X	X	X	-	-	X	

(1) Shallow bulk sediment, (2) Shallow sediment porewater, (3) Sediment deep cores, (4) Samples taken within approximately one meter above the sediments

While there were not any methane data available during the simulation period to compare to model results, methane data were measured by IPC from 2003 through 2007 for June through November (not all months had measurements every year) between river miles 286-330. In addition to methane data, dissolved iron, manganese, and sulfide were also measured by IPC during this time period. These three species were compared to the current USGS data to calculate percent differences between the species to estimate an approximate current average methane concentration in the reservoirs. All water column data (excluding the data sampled from overlying water of sediment cores) at all depths measured during the months of June through November for river miles 286-345.6 were included in the analysis. Values that were recorded as less than the minimum detect limit were also included as half of the minimum detect value. The average value of each species was calculated for the historic IPC data and current USGS data and is shown in Table 32.

Table 32. Comparisons of average historic and current Fe, Mn, Sulfide, and Methane concentrations.

	Average Dissolved Fe, mg/l	Average Dissolved Mn, mg/l	Average Sulfide, mg/l	Average Methane, mg/l
IPC	0.018	0.204	0.132	0.232
USGS	0.006	0.141	0.016	0.087*
% Difference	-69%	-31%	-88%	-63%*

*Methane percent difference was estimated using the average of the other three species, and the USGS concentration was back calculated from the average percent difference and IPC concentration.

Zooplankton data was measured throughout Brownlee, Oxbow, and Hells Canyon Reservoirs and comparisons to model data for reservoir outflows and profiles are shown in the following sections. One aspect of zooplankton that can be modeled is vertical migration within the water column over the course of a day. Profile data was measured over an approximate 24-hour period twice in 2015 at river mile 286 (Figure 112). The zooplankton biomass did not show any strong patterns of sinking or rising during the

day. The bulk of the biomass remained within the top 20 meters of the water column for all sample periods which indicated that vertical migration was likely not a significant aspect of the zooplankton population in the reservoirs. Therefore, zooplankton vertical migration was not included in this model.

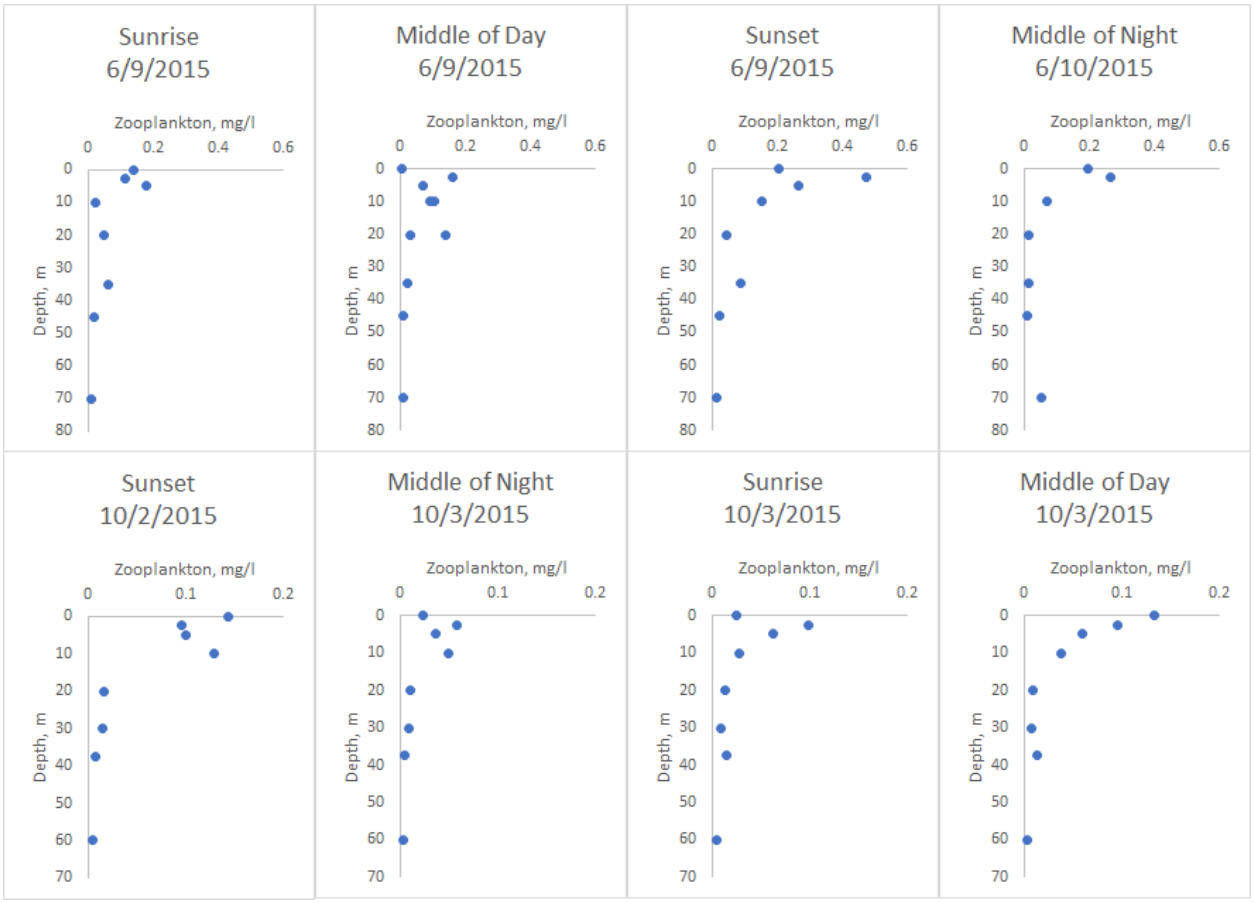


Figure 112. Zooplankton profiles at river mile 286.

Brownlee Reservoir

Water Quality Model-Data Comparisons

During calibration it was found that while the dissolved oxygen profiles at Brownlee Reservoir matched the field data well, the outflow dissolved oxygen was often too low compared to the field data. Vacuum breakers were used at the turbines to bring in air and help smooth the turbine operation. The vacuum breakers were likely increasing the DO of the discharge. To account for this in the model, outflow DO was increased by a variable fraction (10-50 percent) of the input dissolved oxygen into the turbines (Figure 113). Additionally, the spillway equation for dissolved gas was updated from the prior model developed using spill flow during the 2017 (high flow year) to better match the field data DO during spill events (Appendix A3).

Model results just downstream of Brownlee Dam (model segment 4 of Oxbow Reservoir at the water surface) were used for model-data outflow comparisons. Table 33 lists water quality error statistics for Brownlee Reservoir outflow. Table 34 lists water quality error statistics for Brownlee Reservoir vertical profiles (see Appendix A4 for vertical profile model-data comparison graphs).

The USGS recorded continuous dissolved oxygen in 2017 and 2018 in Brownlee Reservoir at several stations and at various depths. Model comparisons to these field data are summarized in Table 35 and are shown in Appendix A7. The very high surface concentrations (see Appendix A7) may not be accurate as a result of membrane fouling between field visits to the sites.

Table 36 lists water quality error statistics for Brownlee Reservoir sediment and porewater comparisons. Figure 114 through Figure 140 show the associated model-data outflow and sediment comparisons.

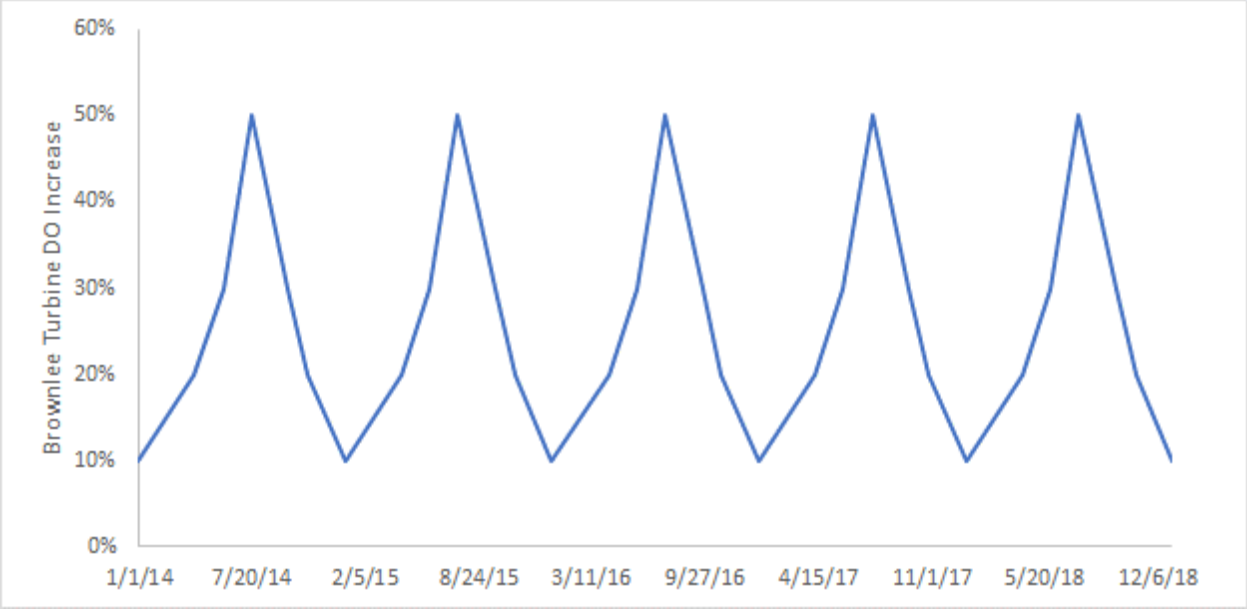


Figure 113. Percent increase of dissolved oxygen of the Brownlee Reservoir turbines over the simulation period.

Table 33. Water quality error statistics for Brownlee Reservoir outflow.

Parameter	Model Average	# of data	ME	MAE	RMSE	MAE/Model Average
DO - Left Channel (mg/l)	8.76	251474	-0.08	0.88	1.14	0.100
DO - Right Channel (mg/l)	8.76	258615	0.21	1.00	1.26	0.114
DO - LC and RC weighted (mg/l)	8.76	174672	0.03	0.88	1.12	0.100
Chlorophyll a (ug/l)	5.124	119	-1.991	4.930	8.052	0.962
Chloride (mg/l)	18.06	63	0.194	1.599	2.628	0.089
DOC (mg/l)	2.648	115	0.042	0.192	0.240	0.073
FeII (mg/l)	0.005	36	0.001	0.002	0.003	0.400

Parameter	Model Average	# of data	ME	MAE	RMSE	MAE/Model Average
FeOOH (mg/l)	0.076	24	0.038	0.060	0.106	0.789
MnII (mg/l)	0.004	40	0.001	0.007	0.020	1.750
MnO2 (mg/l)	0.039	24	0.013	0.022	0.035	0.564
Ammonia (mg/l)	0.043	85	-0.009	0.033	0.046	0.767
Nitrate (mg/l)	1.166	200	0.059	0.161	0.208	0.138
Ortho-phosphate (mg/l)	0.059	174	0.012	0.017	0.022	0.288
POC (mg/l)	0.594	4	-0.057	0.136	0.155	0.229
Sulfate (mg/l)	41.398	141	0.356	2.516	4.088	0.061
TKN (mg/l)	0.423	139	0.036	0.125	0.161	0.296
Total Phosphorus (mg/l)	0.086	137	0.018	0.020	0.025	0.233
TSS (mg/l)	2.589	122	-1.245	1.902	2.978	0.735
TIC (mg/l)	41.296	4	2.131	2.322	3.116	0.056
PON (mg/l)	0.076	4	-0.028	0.028	0.032	0.368
Zooplankton (mg/l)	0.105	13	0.083	0.146	0.222	1.390
POC (estimated from VSS data) (mg/l)	0.594	40	-0.358	0.773	1.039	1.301

Table 34. Water quality error statistics for Brownlee Reservoir vertical profiles.

Parameter	# of Profiles	# of Data	ME	MAE	RMSE
Chloride (mg/l)	118	515	0.578	1.788	2.088
H2S (mg/l)	3	4	-0.436	0.436	0.548
Sulfate (mg/l)	22	90	1.459	3.100	3.696
Fe(II) (mg/l)	118	967	0.002	0.005	0.006
FeOOH (mg/l)	71	281	-0.040	0.241	0.258
Mn(II) (mg/l)	118	508	-0.024	0.107	0.165
MnO2 (mg/l)	71	255	-0.004	0.023	0.029
Ortho-phosphate (mg/l)	142	1118	-0.007	0.033	0.043
Ammonia (mg/l)	133	427	0.000	0.127	0.163
Nitrate (mg/l)	142	1118	0.046	0.235	0.286
DO (mg/l)	1257	84242	0.187	1.000	1.332
TIC (mg/l)	13	88	1.427	3.077	3.619
Zooplankton (mg/l)	20	197	0.016	0.097	0.126
HgII (ng/L)	138	589	0.091	0.399	0.444
MeHg (ng/L)	143	604	-0.077	0.188	0.269
DOC (mg/l)	140	589	0.032	0.214	0.243
POC (mg/l)	13	80	0.167	0.350	0.402
PON (mg/l)	13	84	0.001	0.043	0.050
TKN (mg/l)	140	631	0.102	0.209	0.250
Total Phosphorus (mg/l)	140	634	0.000	0.039	0.049
Chlorophyll a (µg/l)	174	363	-1.300	10.032	11.133
TSS (mg/l)	136	568	-1.960	4.792	5.209
pH	1120	75812	-0.188	0.322	0.353

Table 35. Error statistics for continuous DO data measured by the USGS in Brownlee Reservoir in 2017 and 2018.

RM	Depth	Segment	Count	ME_Error	AME_Error	RMS_error
286	1	198	50351	-1.791	2.301	3.226
286	3	198	29797	-0.210	1.204	1.495
286	6	198	50259	-0.005	1.127	1.444
286	10	198	29794	0.195	0.879	1.111
286	15	198	50290	-0.097	1.211	1.700
286	21	198	29793	0.150	1.153	1.715
286	30	198	29795	1.104	1.496	2.346
300	1	154	50634	-0.696	1.502	2.096
300	3	154	29949	0.212	0.955	1.242
300	6	154	50570	0.642	1.137	1.542
300	10	154	29948	0.657	0.808	0.993
300	15	154	50569	0.811	0.967	1.326
300	21	154	29947	1.006	1.090	1.357
300	30	154	29948	1.240	1.394	2.099
318	1	97	30017	-0.264	1.325	1.872
318	3	97	30017	0.526	1.112	1.514
318	6	97	30018	0.837	1.100	1.435
318	10	97	30018	0.350	0.814	1.118
Total/Average			661714	0.176	1.231	1.691

Table 36. Water quality error statistics for Brownlee Reservoir sediment and porewater comparisons.

Parameter	Model Average	# of Data	ME	MAE	RMSE
PO4 - porewater (mg/l)	3.374	5	0.426	2.693	3.007
NO3 - porewater (mg/l)	0.052	12	0.028	0.032	0.044
NH4 - porewater (mg/l)	15.190	5	2.023	3.821	6.507
PO4 - bottom of water column (mg/l)	0.155	59	0.002	0.139	0.276
NO3 - bottom of water column (mg/l)	1.302	53	0.111	0.368	0.464
DOC - bottom of water column (mg/l)	2.502	61	-0.336	0.561	0.717

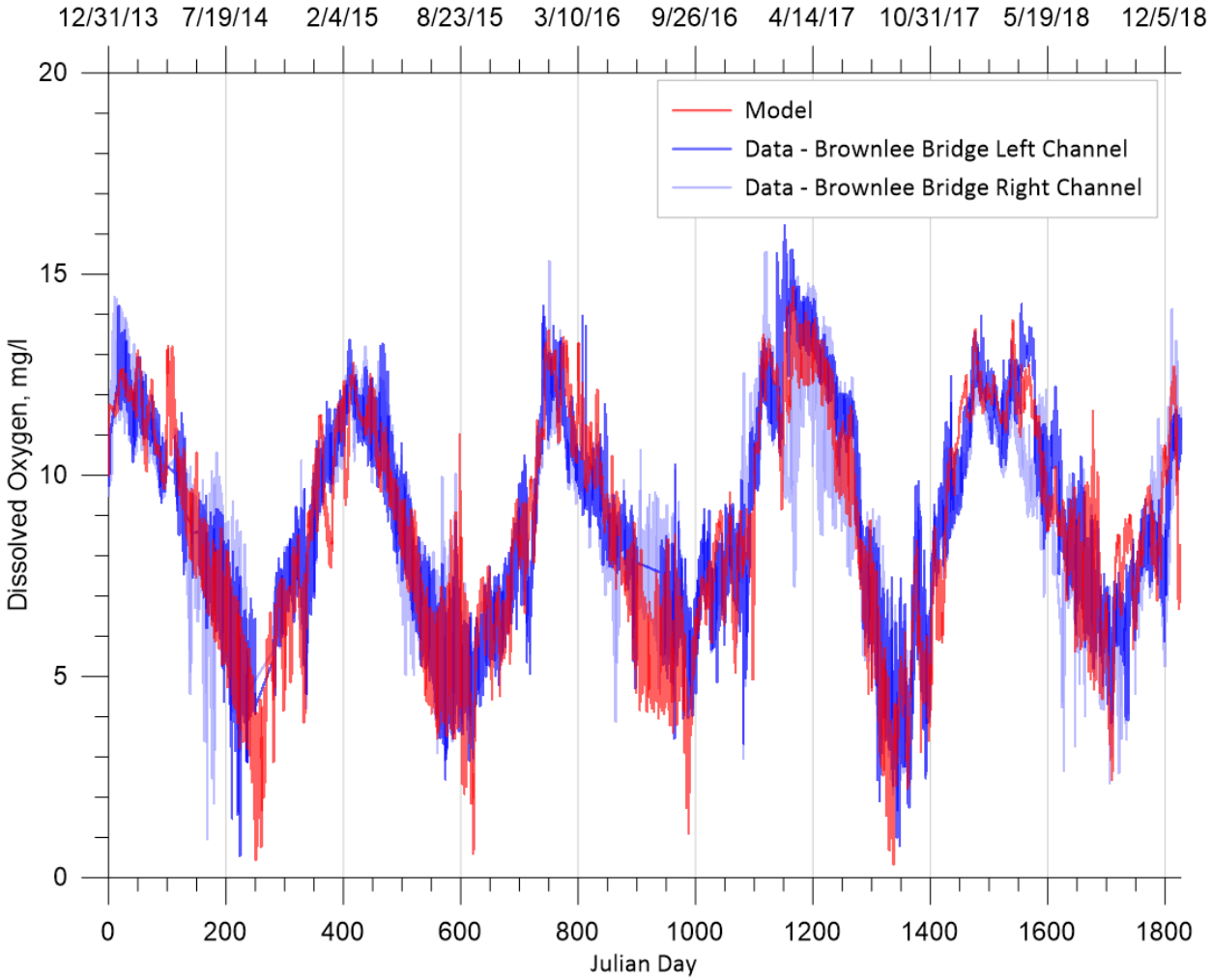
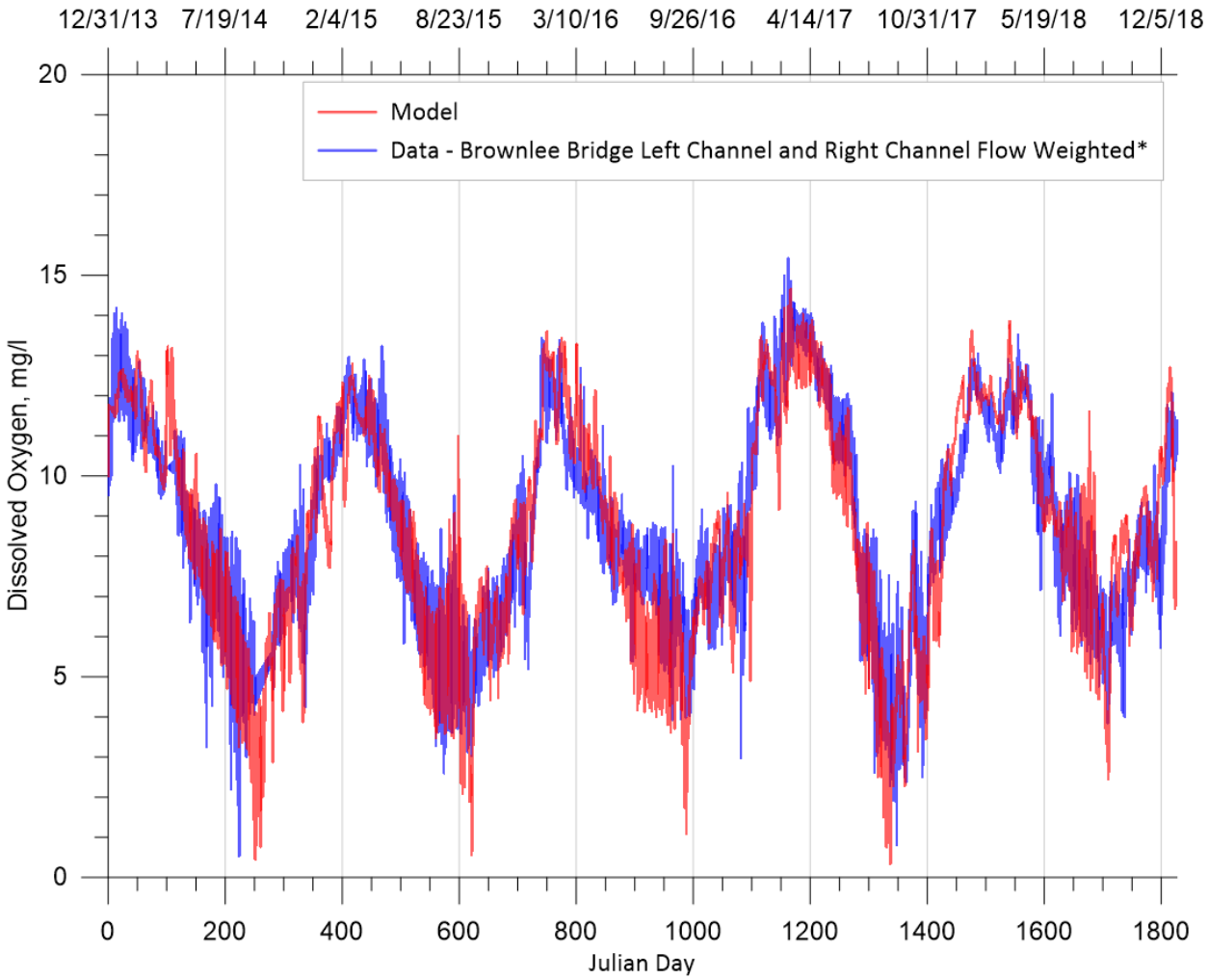


Figure 114. Brownlee Reservoir model outflow dissolved oxygen compared to data.



*Flow from turbines 1-4 and the spill were applied to the left channel DO and flow from turbine 5 was applied to the right channel DO. DO data was interpolated to flow data when sampling times did not match.

Figure 115. Brownlee Reservoir model outflow-weighted dissolved oxygen compared to data.

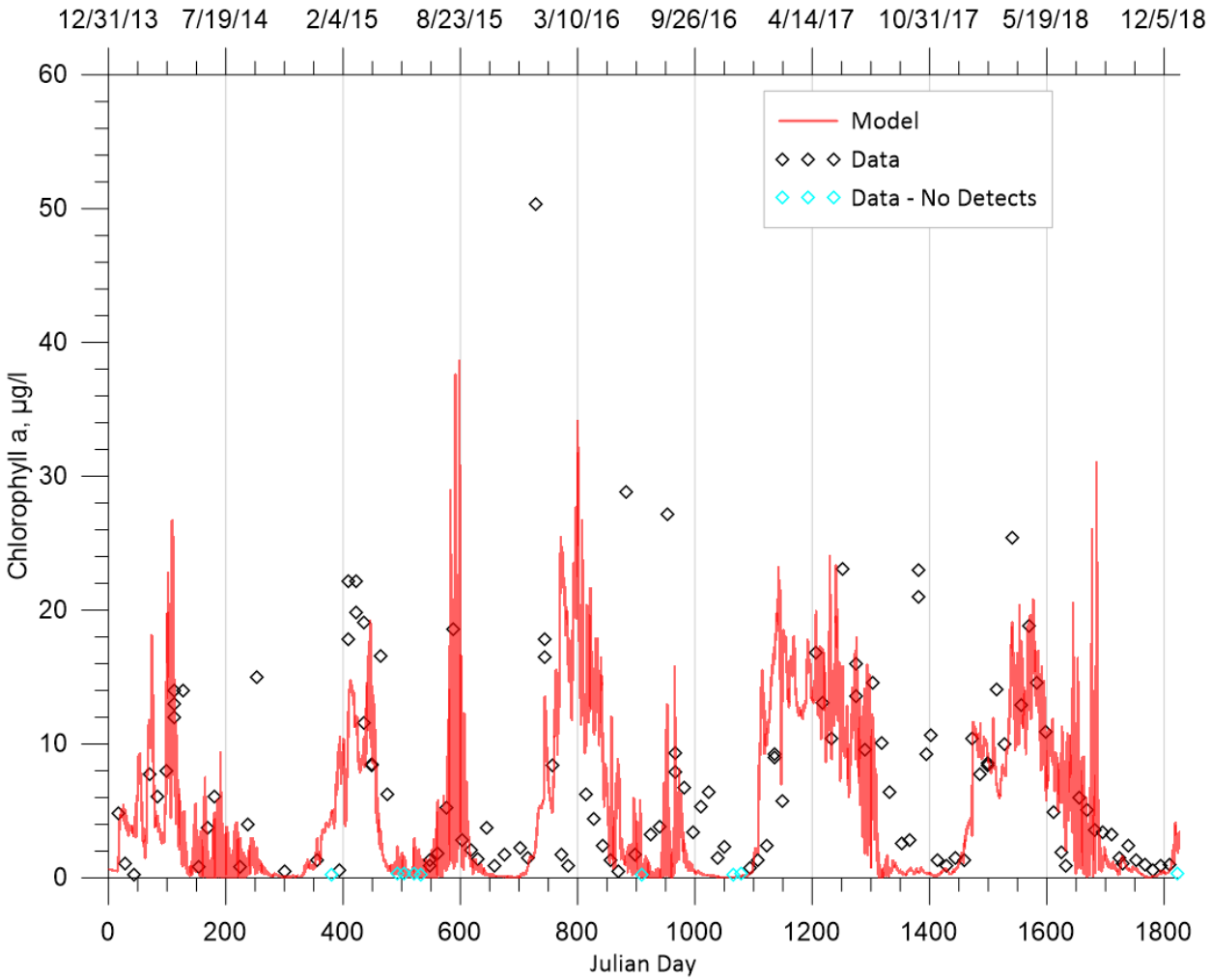


Figure 116. Brownlee Reservoir model outflow chlorophyll a compared to data.

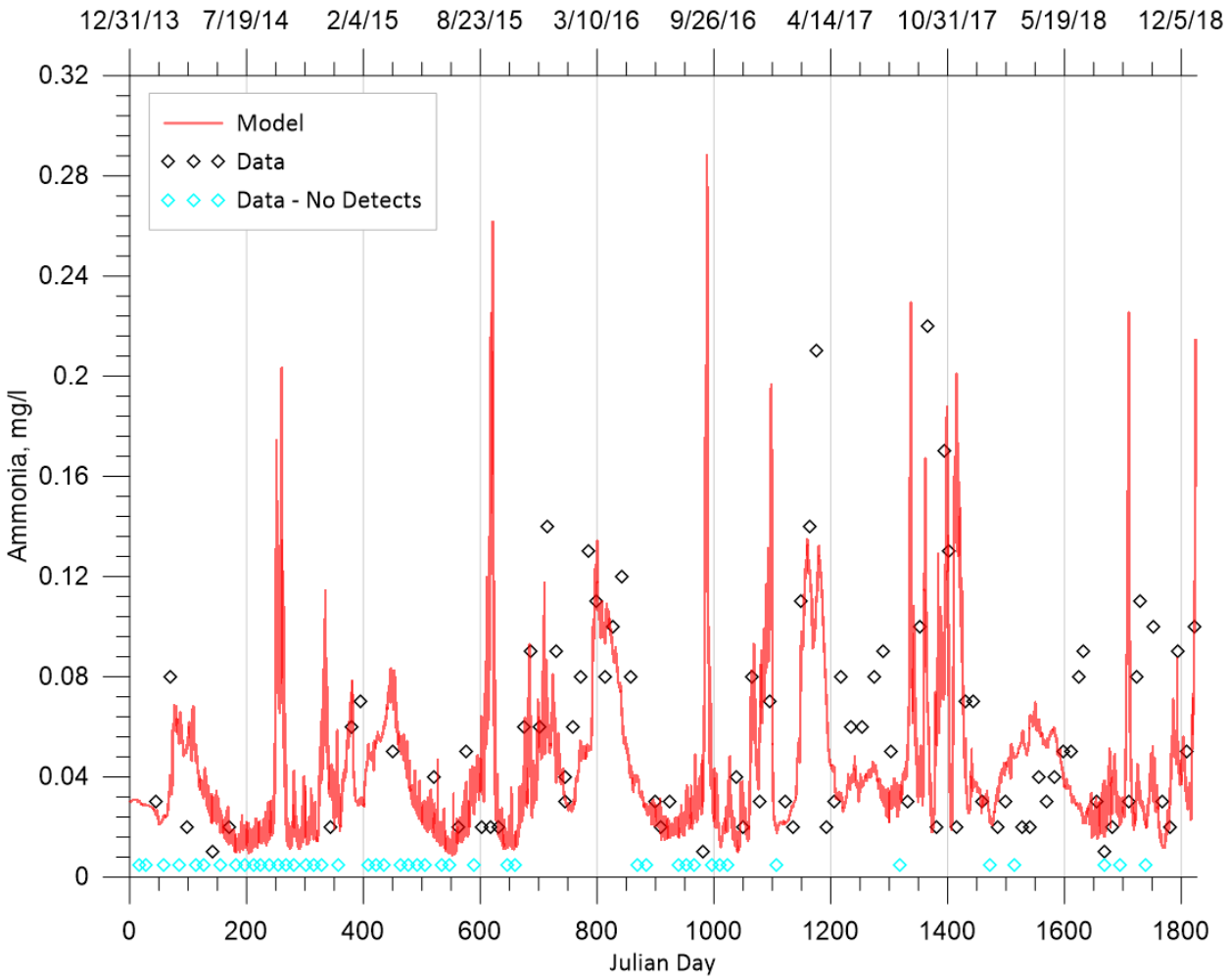


Figure 117. Brownlee Reservoir model outflow ammonia nitrogen compared to data.

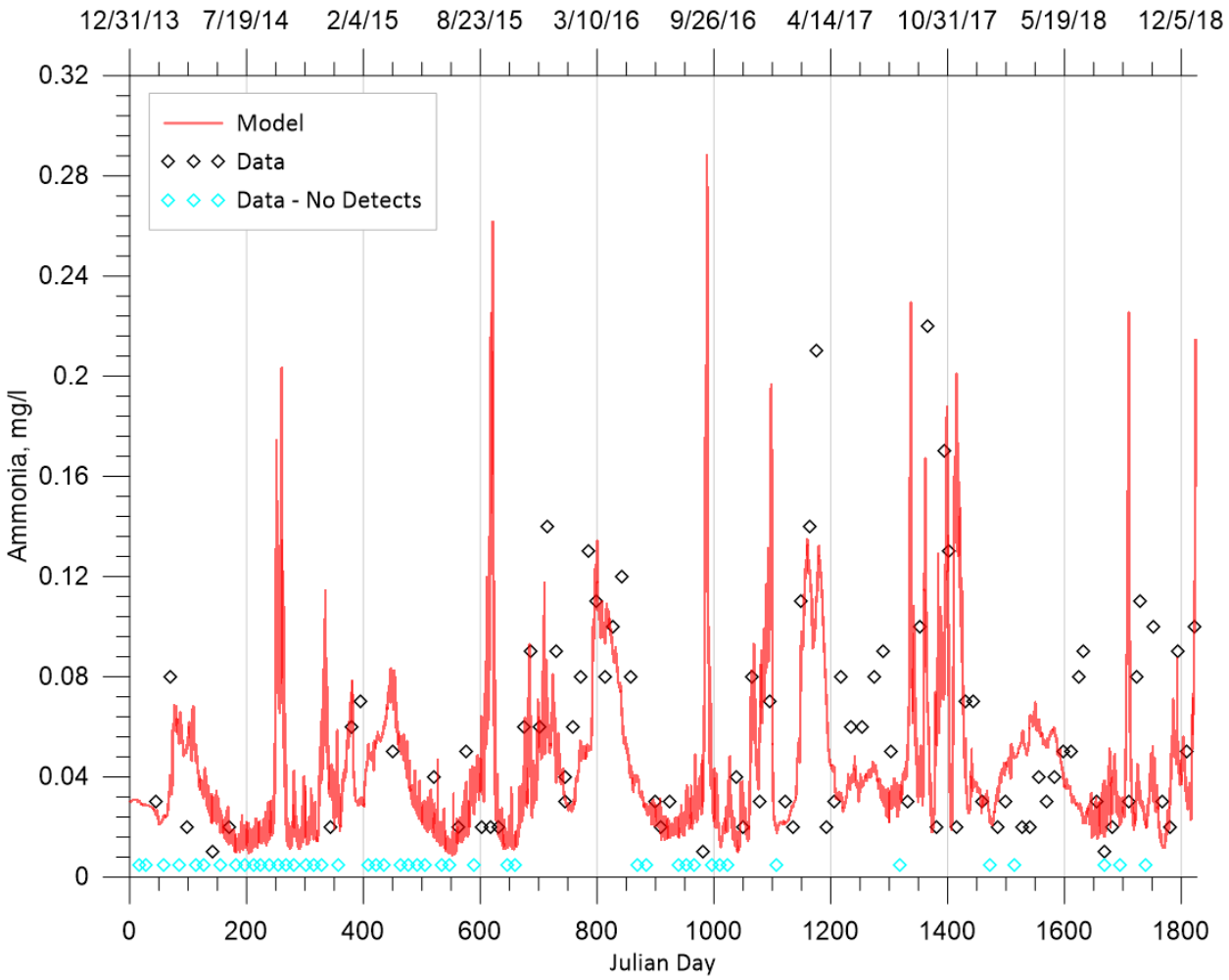


Figure 118. Brownlee Reservoir model outflow nitrate nitrogen compared to data.

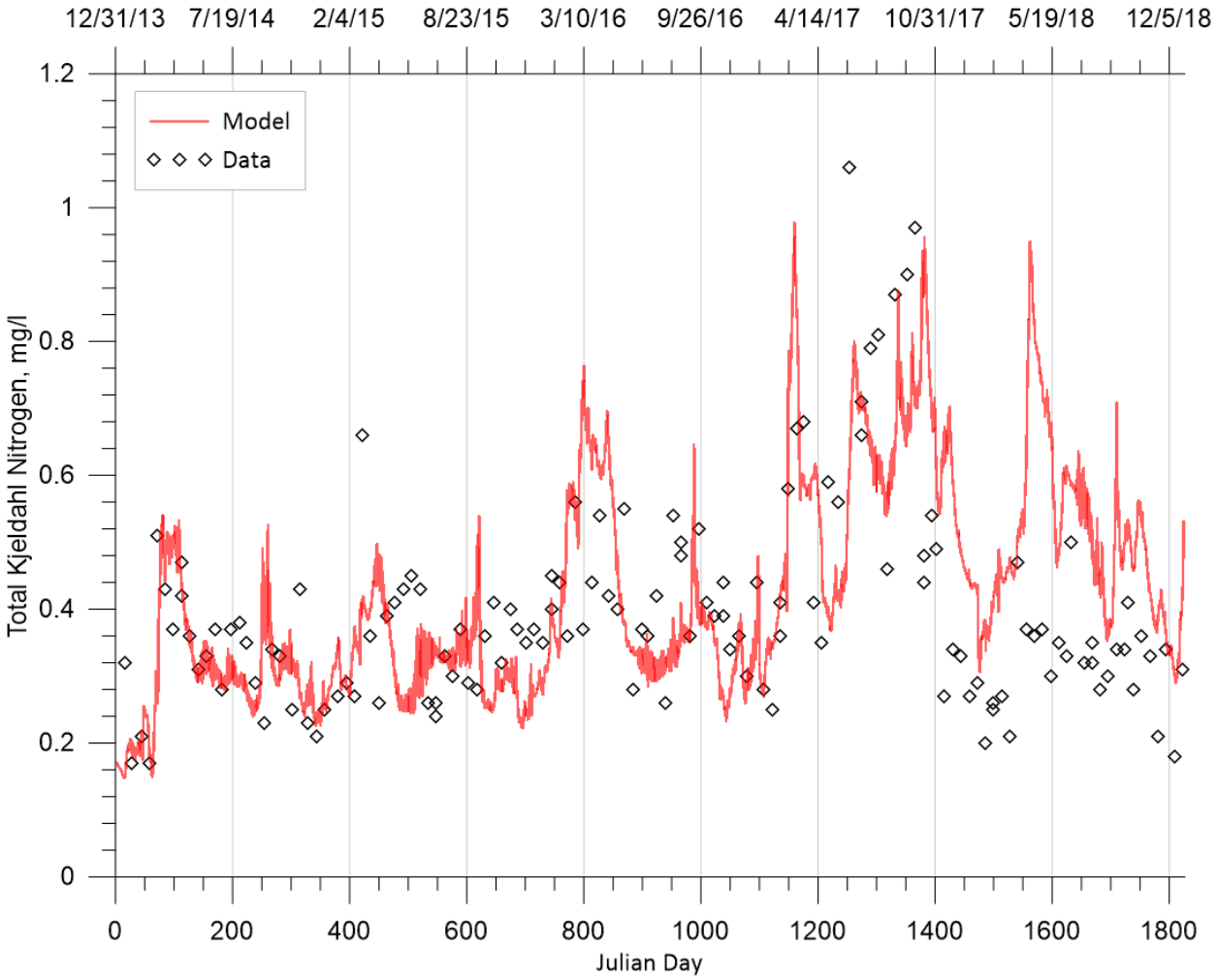


Figure 119. Brownlee Reservoir model outflow total Kjeldahl nitrogen compared to data.

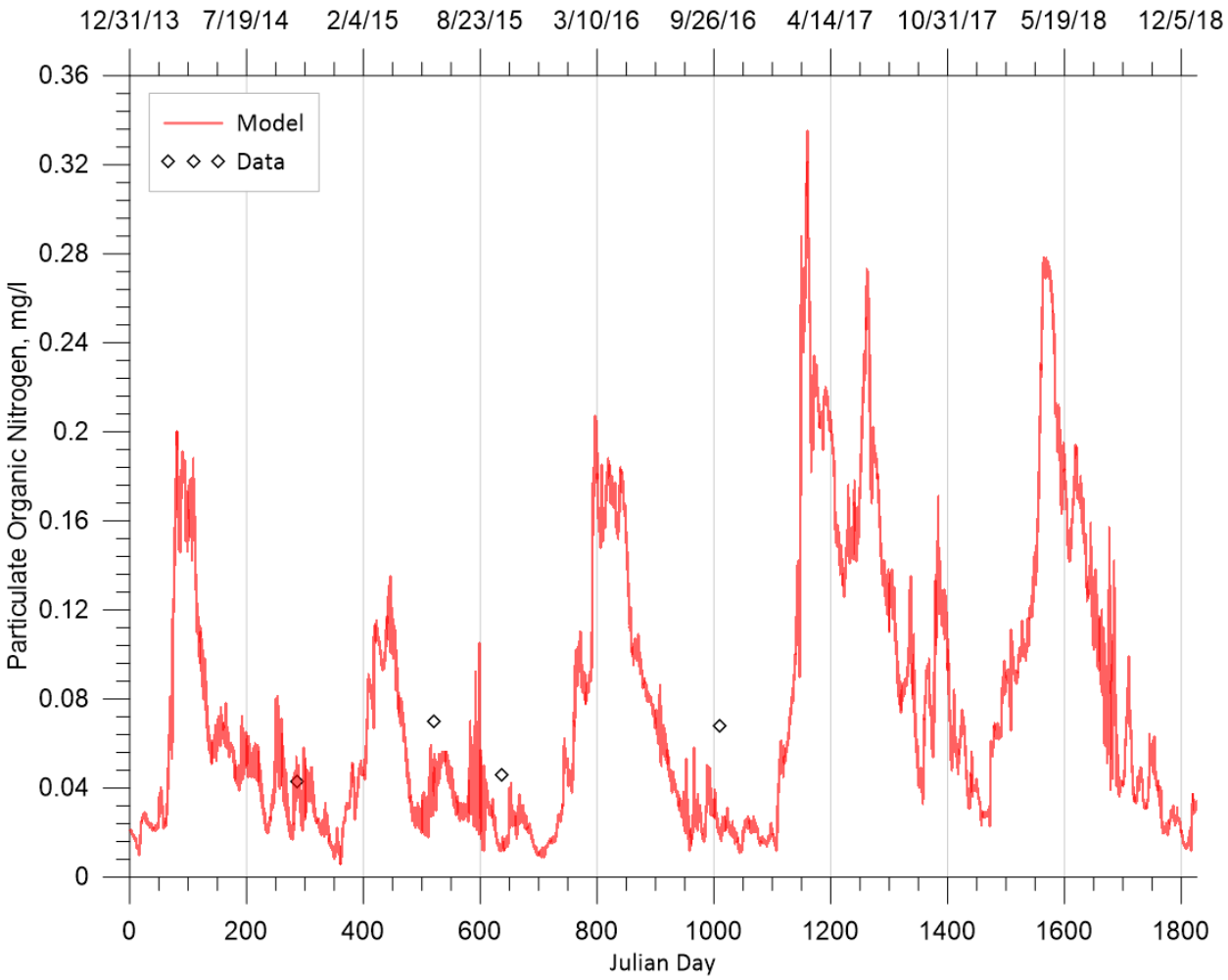


Figure 120. Brownlee Reservoir model outflow particulate organic nitrogen compared to data.

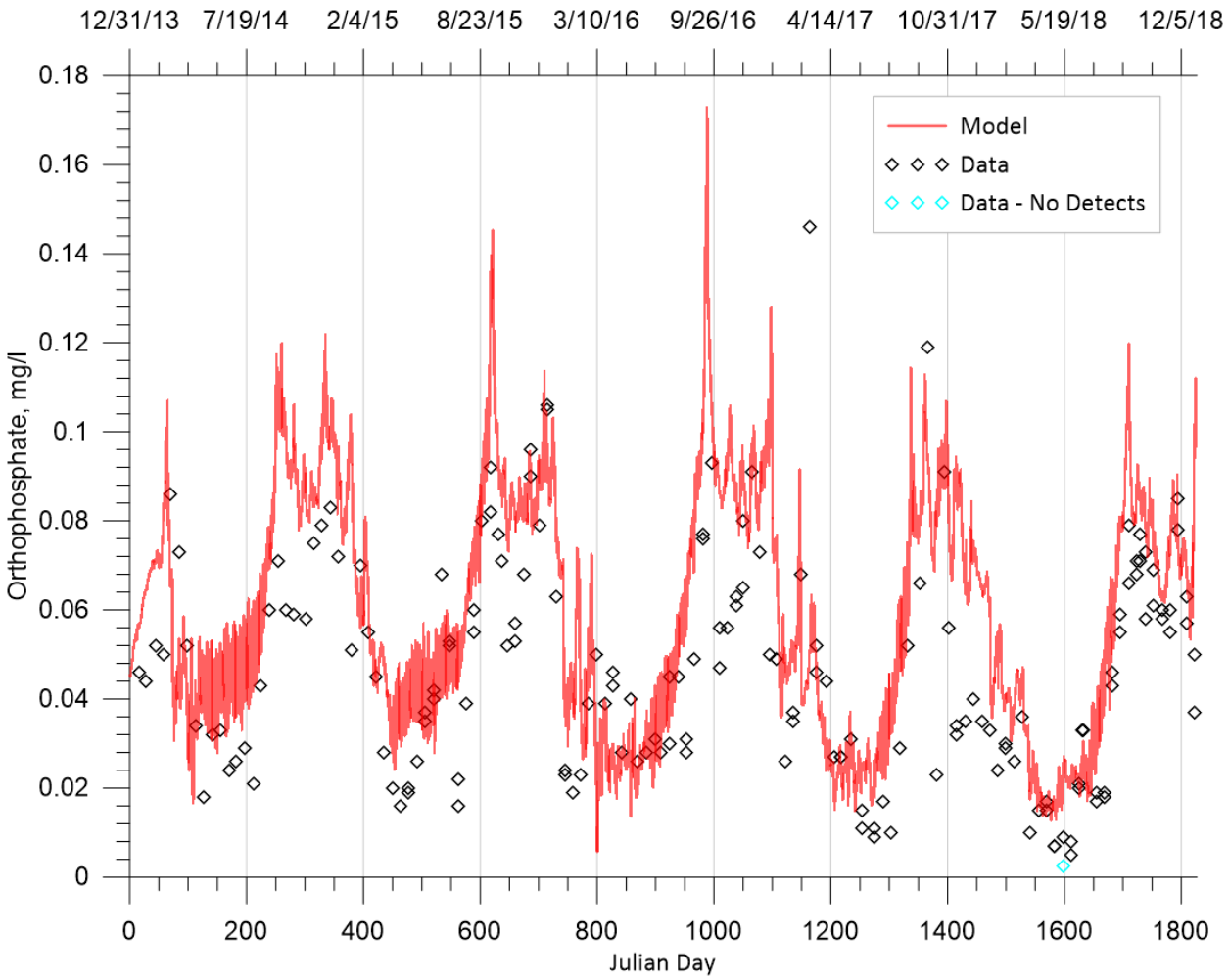


Figure 121. Brownlee Reservoir model outflow orthophosphate compared to data.

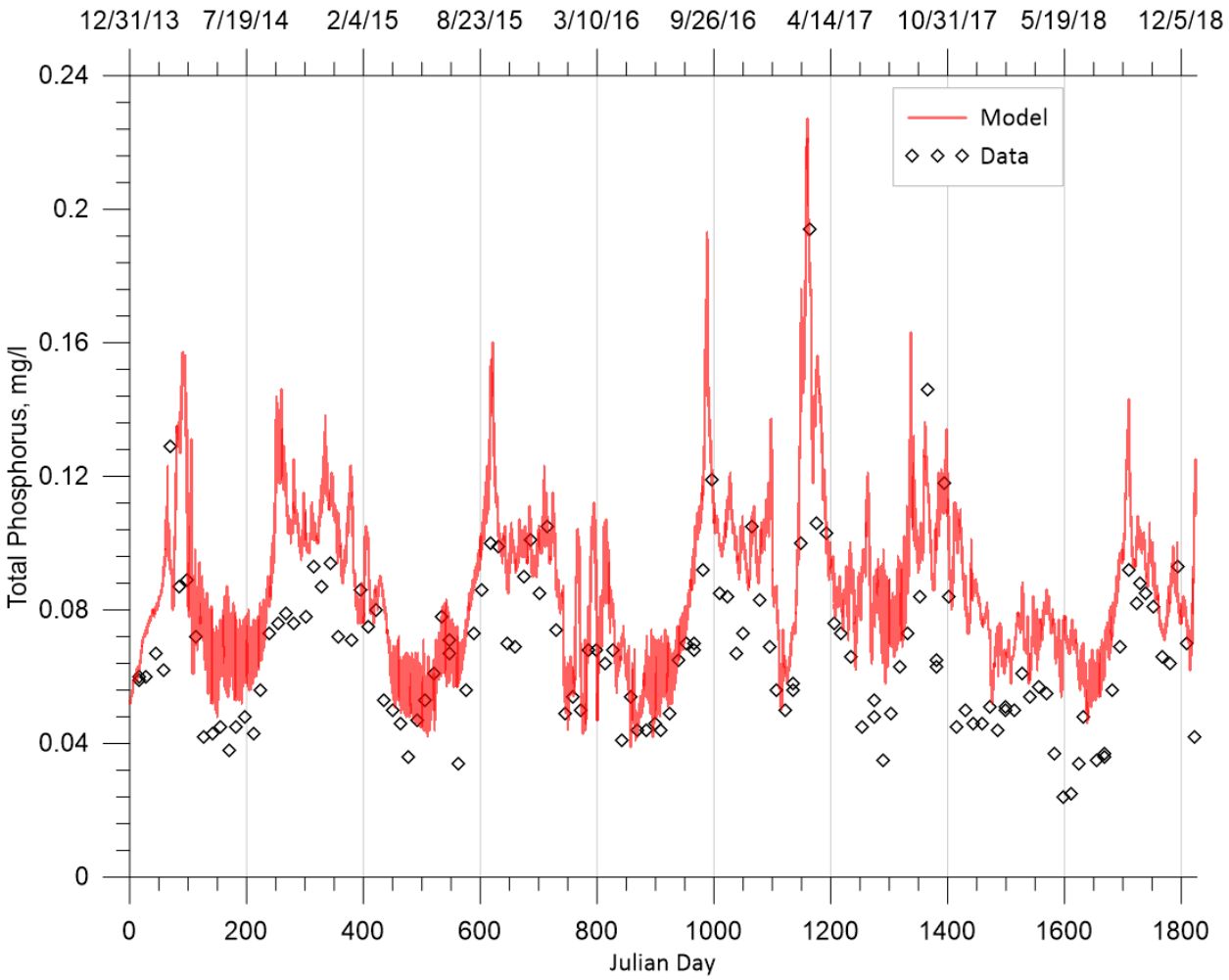


Figure 122. Brownlee Reservoir model outflow total phosphorus compared to data.

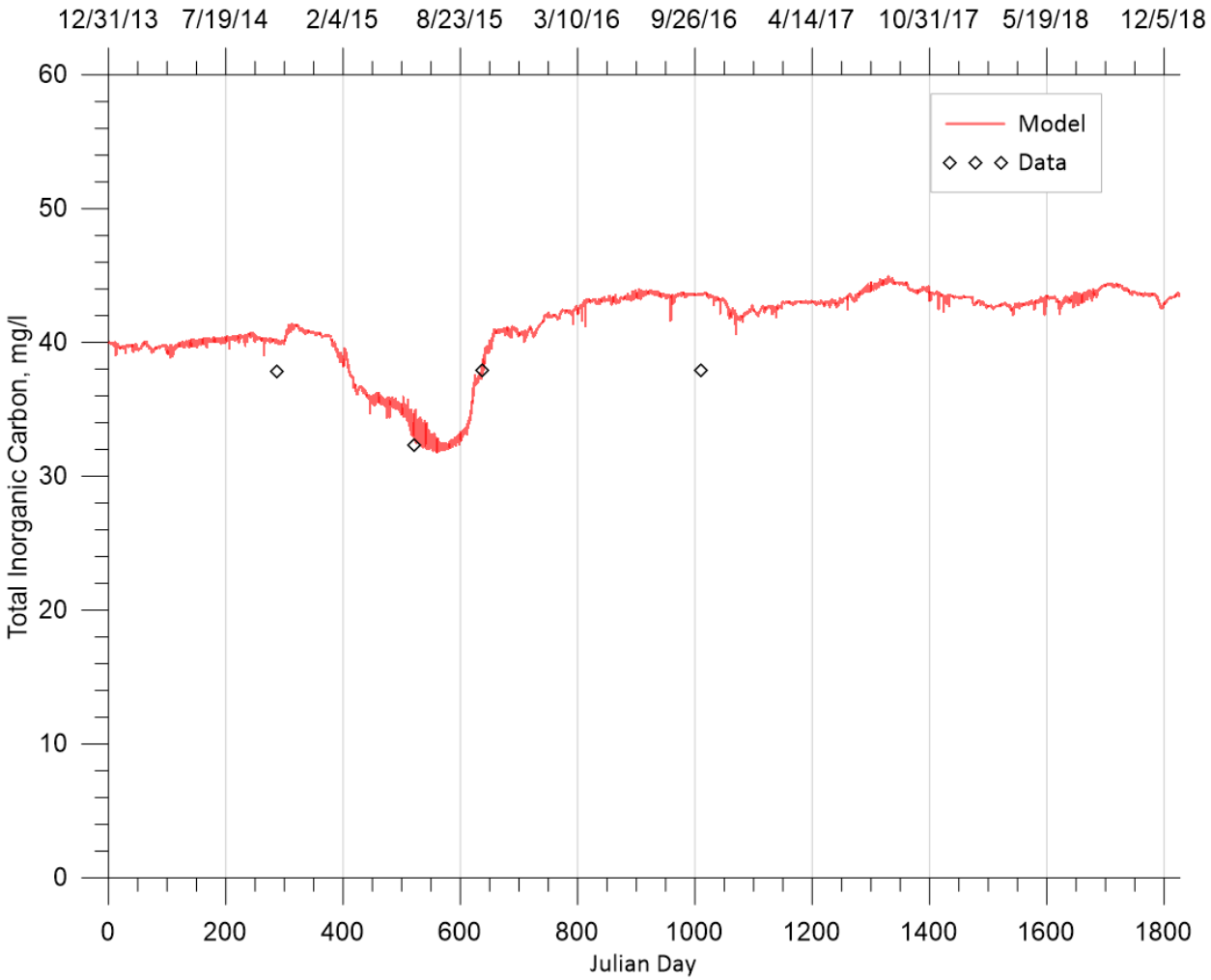


Figure 123. Brownlee Reservoir model outflow total inorganic carbon compared to data.

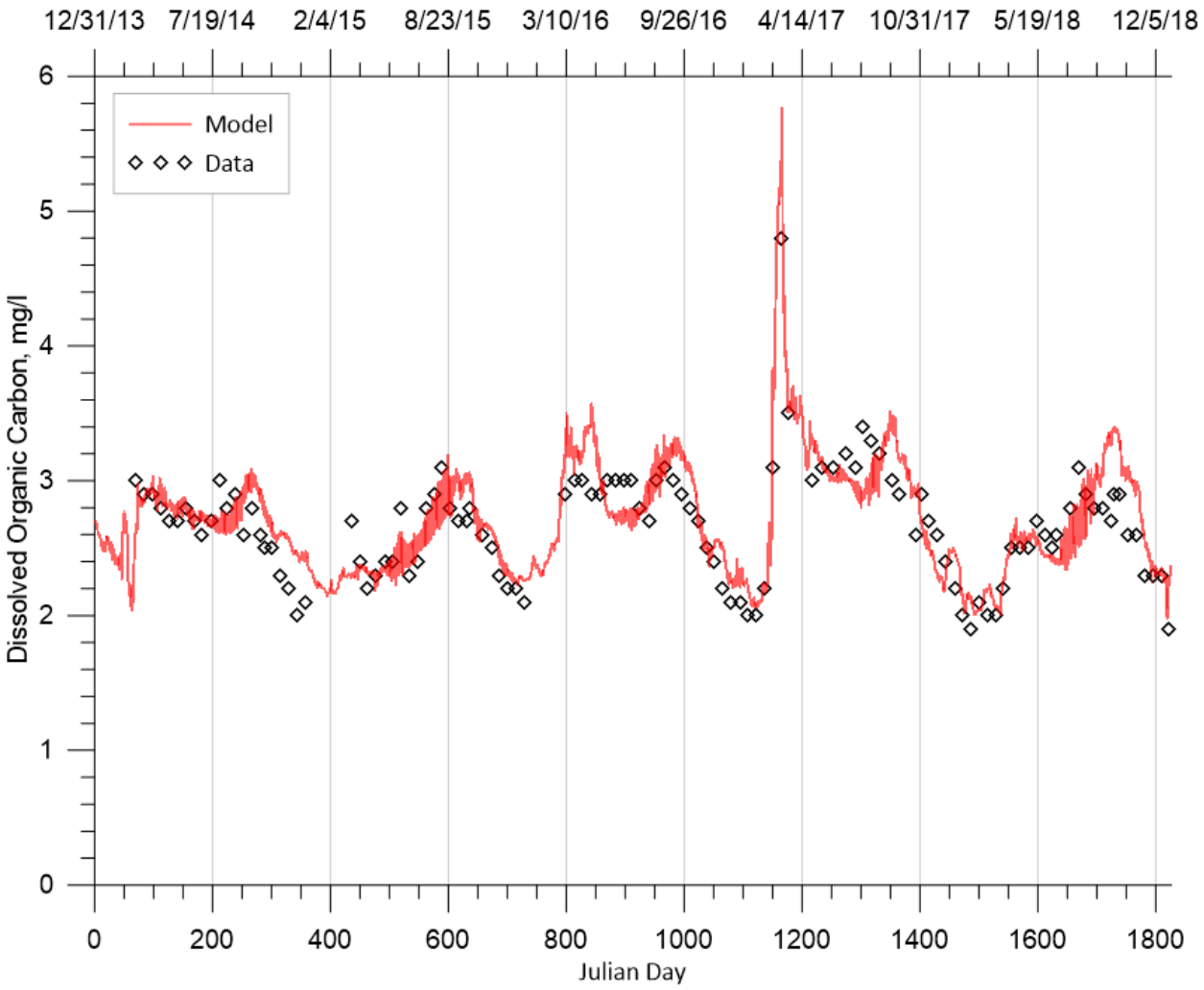


Figure 124. Brownlee Reservoir model outflow dissolved organic carbon compared to data.

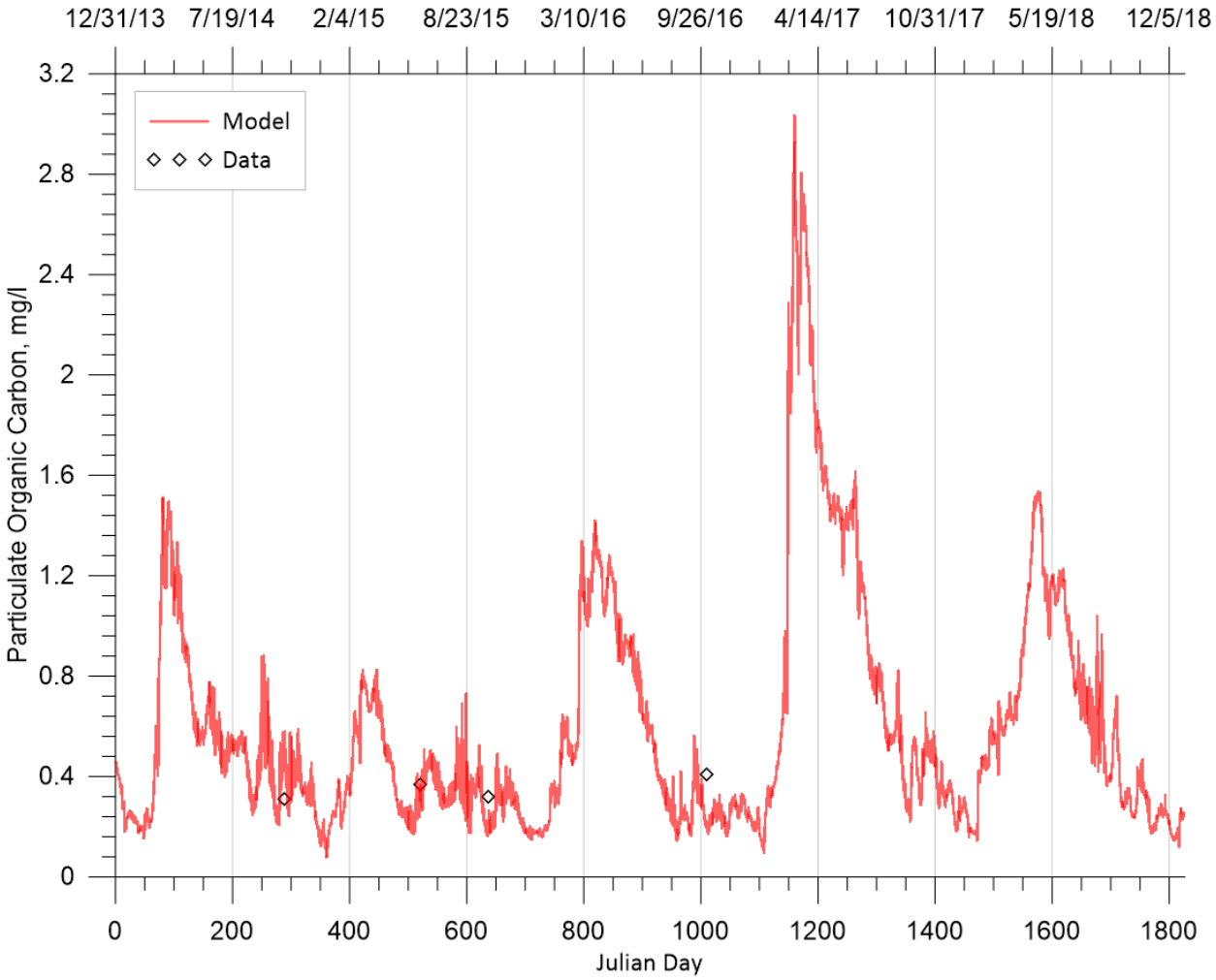


Figure 125. Brownlee Reservoir model outflow particulate organic carbon compared to data.

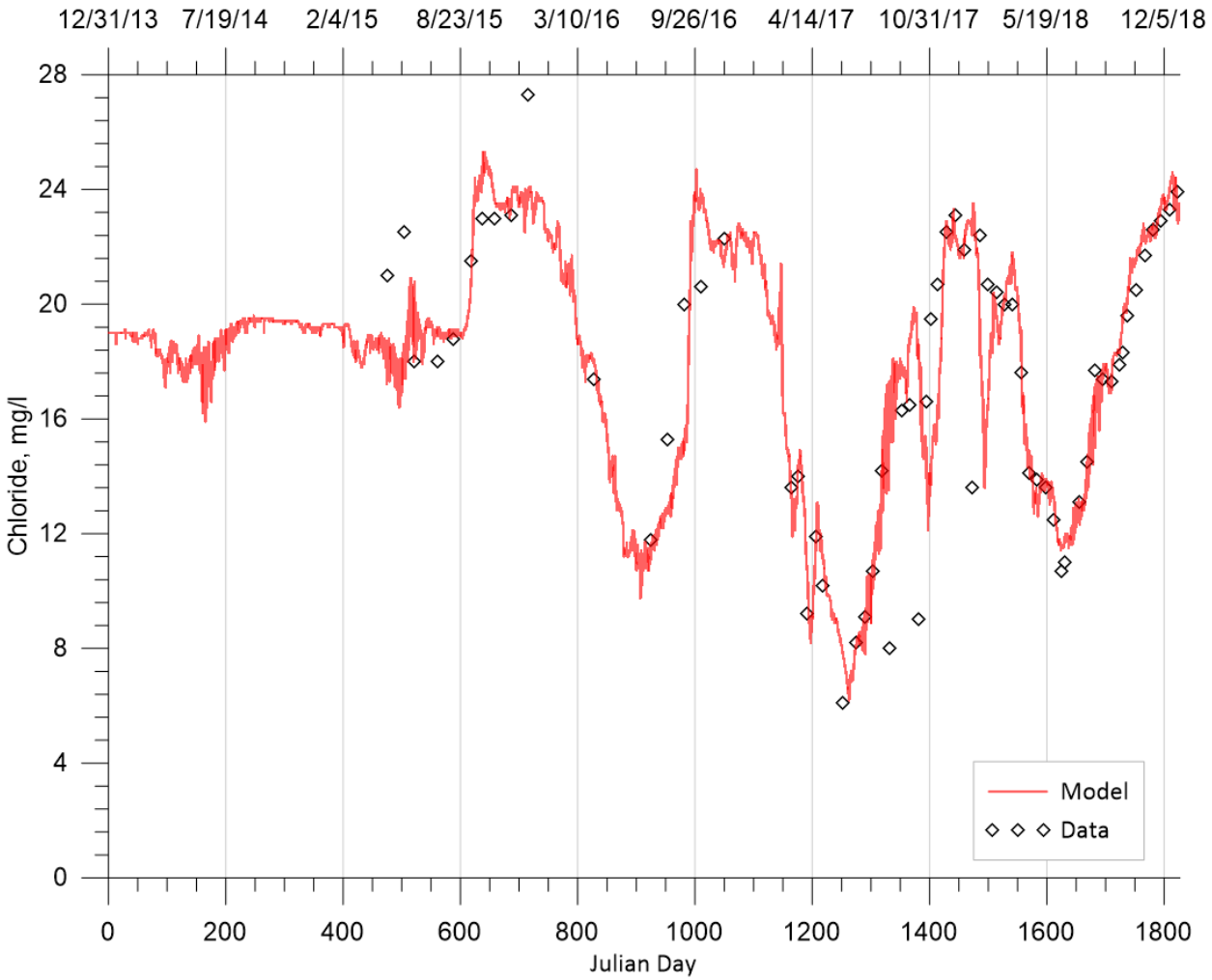


Figure 126. Brownlee Reservoir model outflow chloride compared to data.

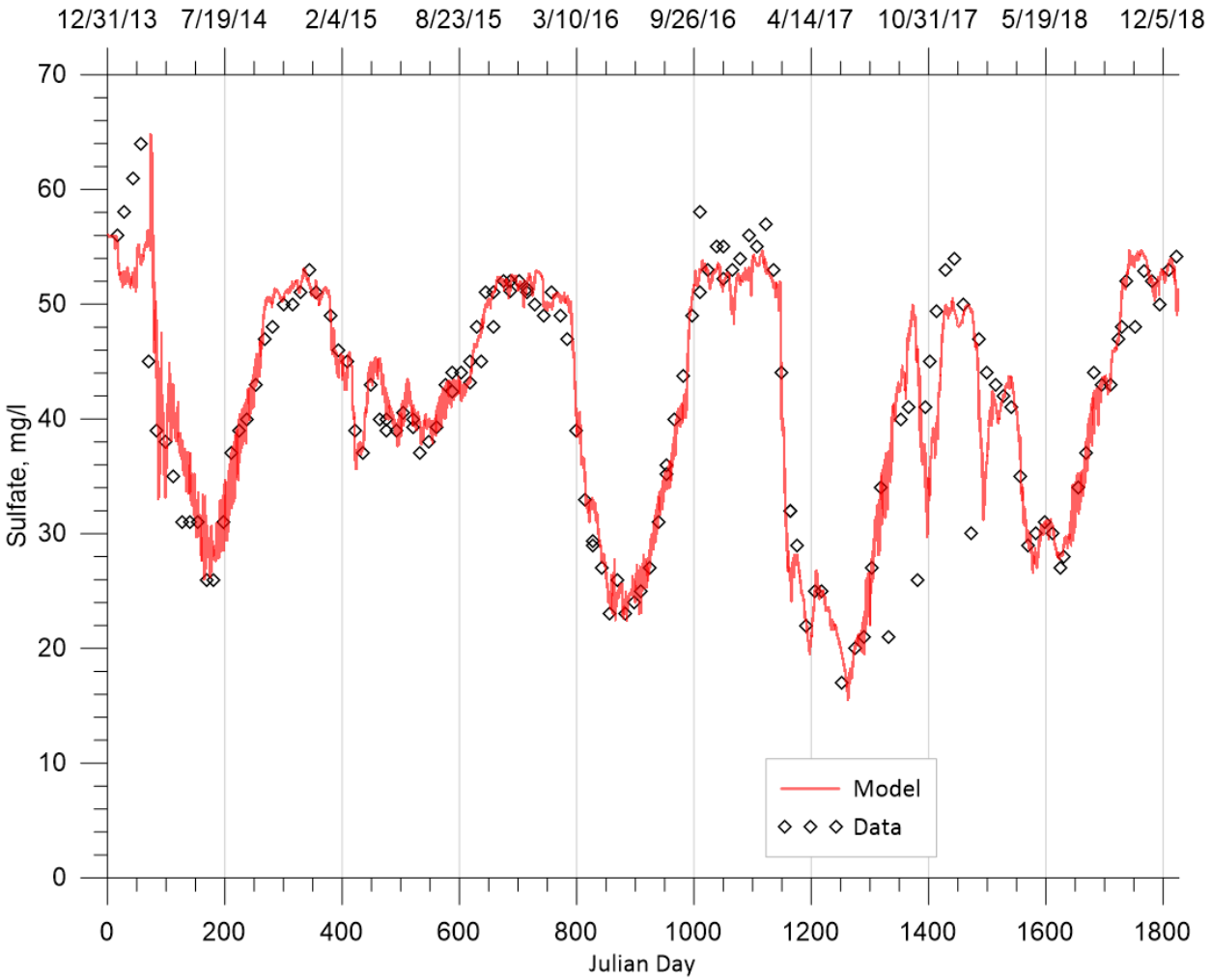


Figure 127. Brownlee Reservoir model outflow sulfate compared to data.

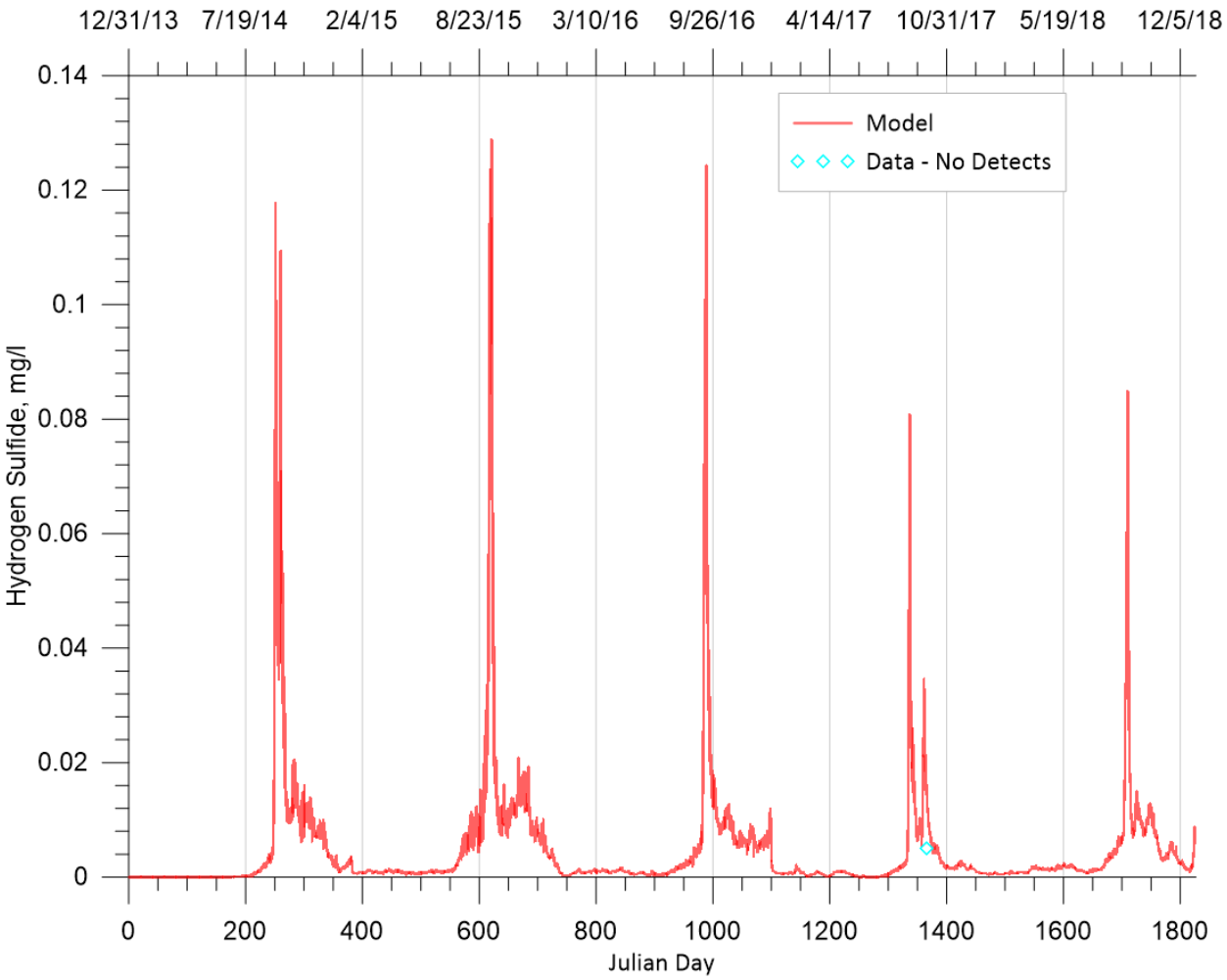


Figure 128. Brownlee Reservoir model outflow hydrogen sulfide compared to data.

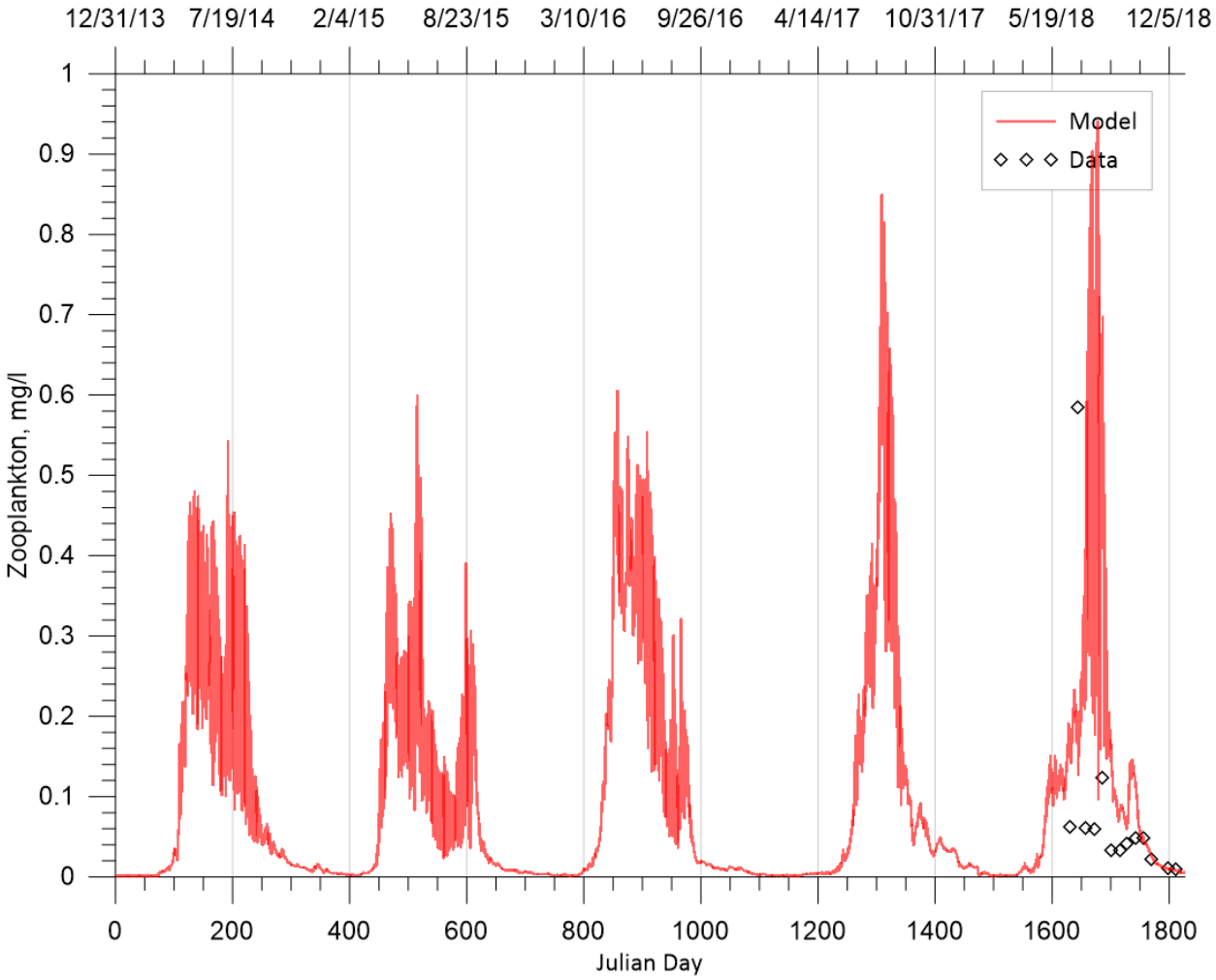


Figure 129. Brownlee Reservoir model outflow zooplankton compared to data.

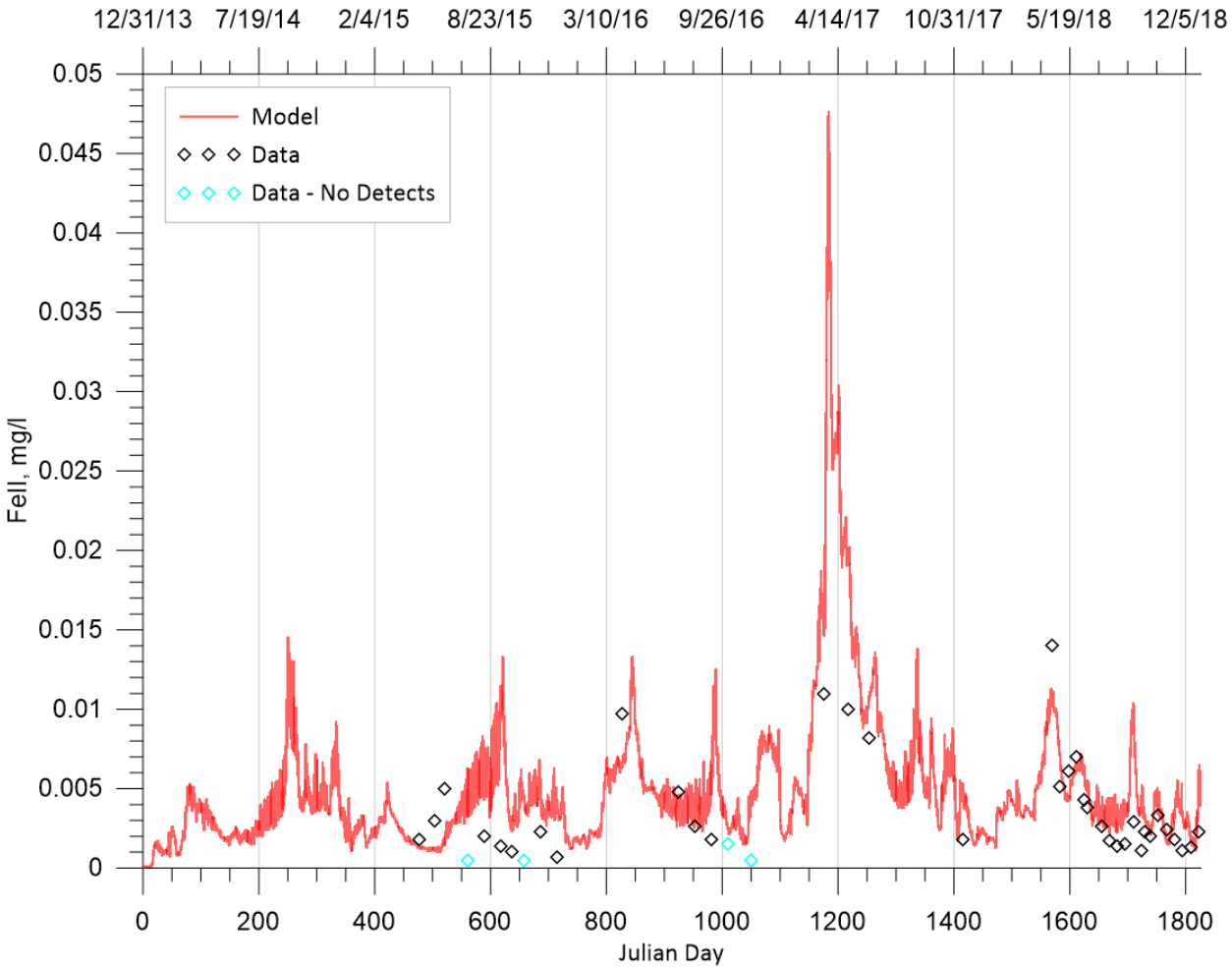


Figure 130. Brownlee Reservoir model outflow FeII compared to data.

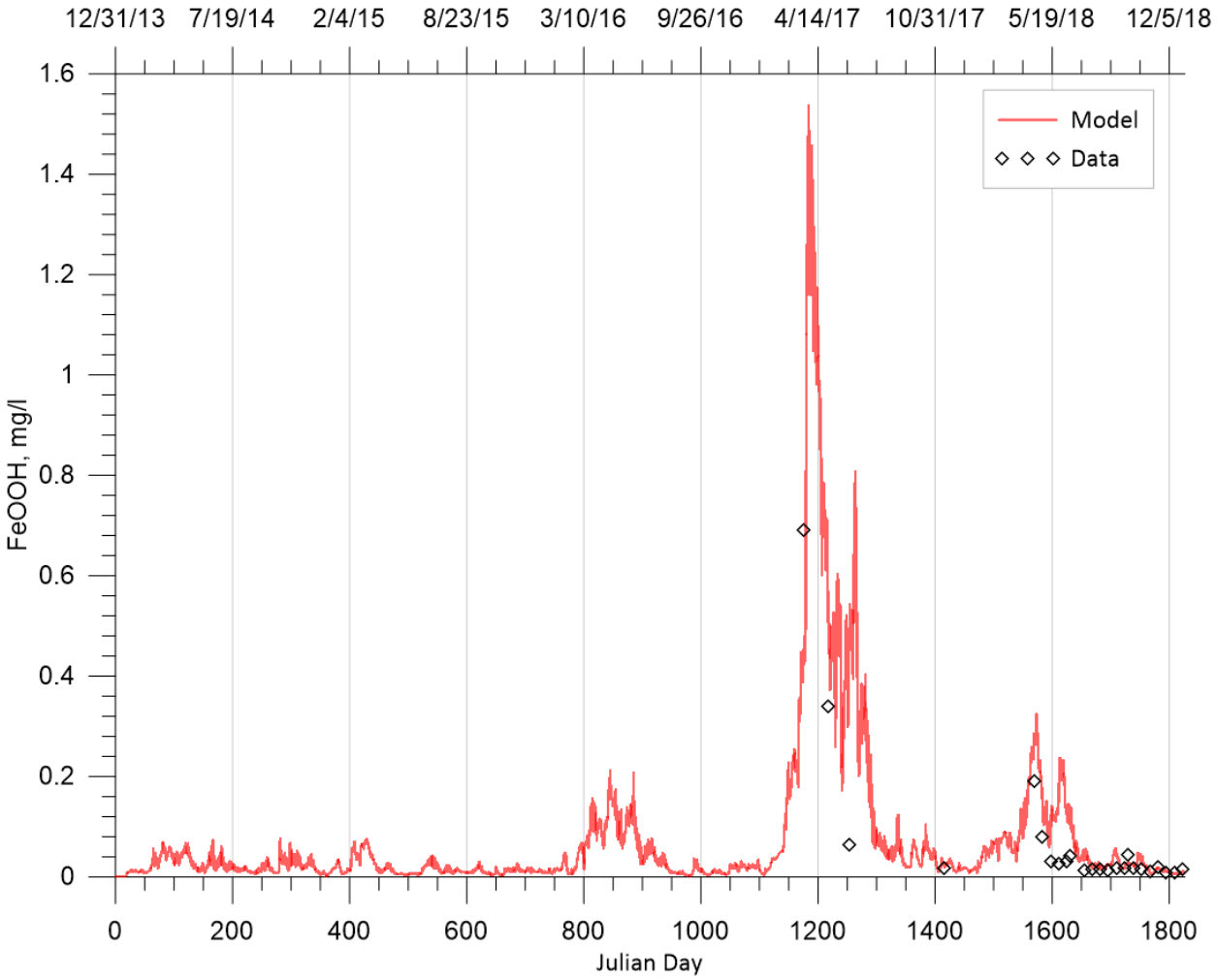


Figure 131. Brownlee Reservoir model outflow FeOOH compared to data.

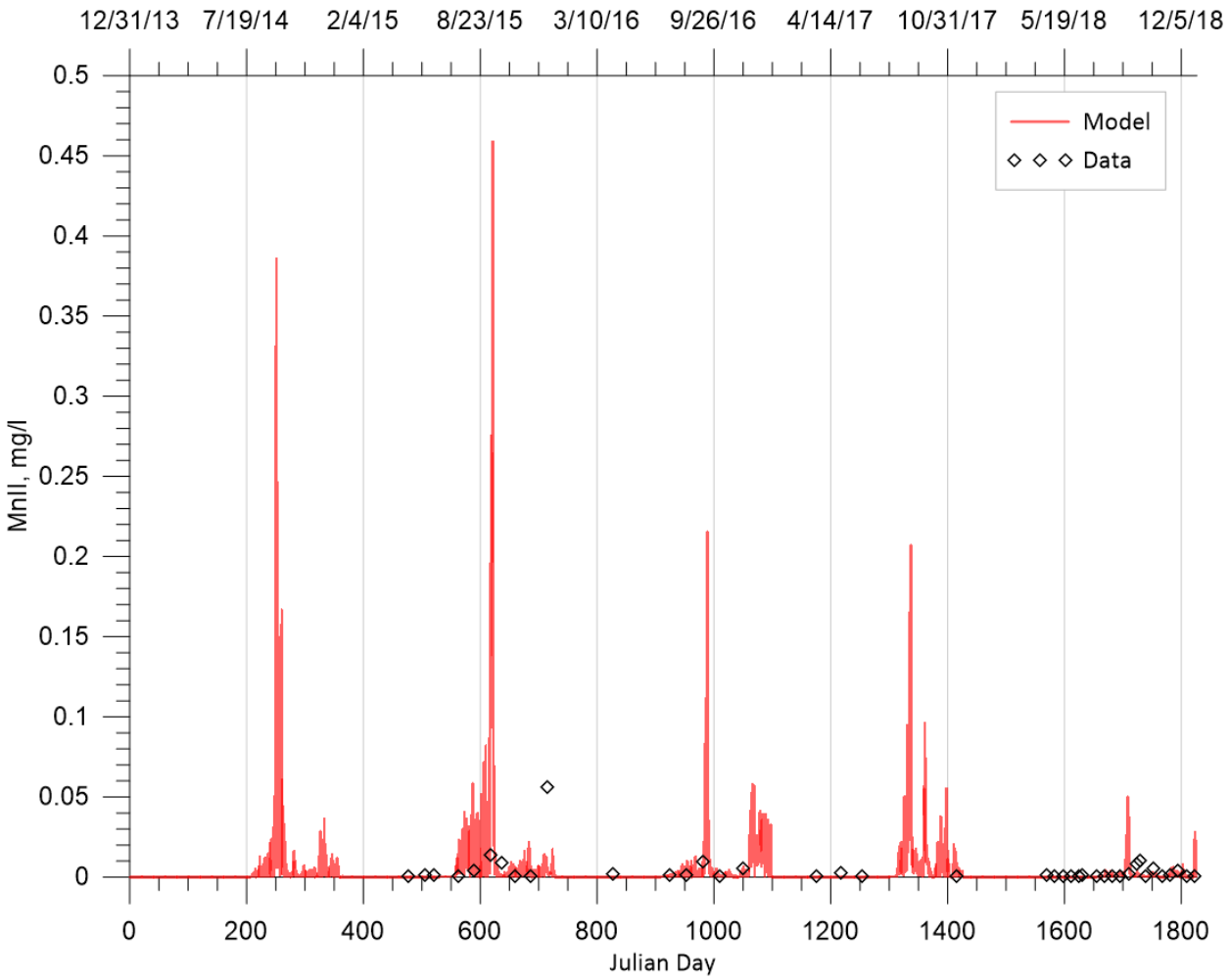


Figure 132. Brownlee Reservoir model outflow MnII compared to data.

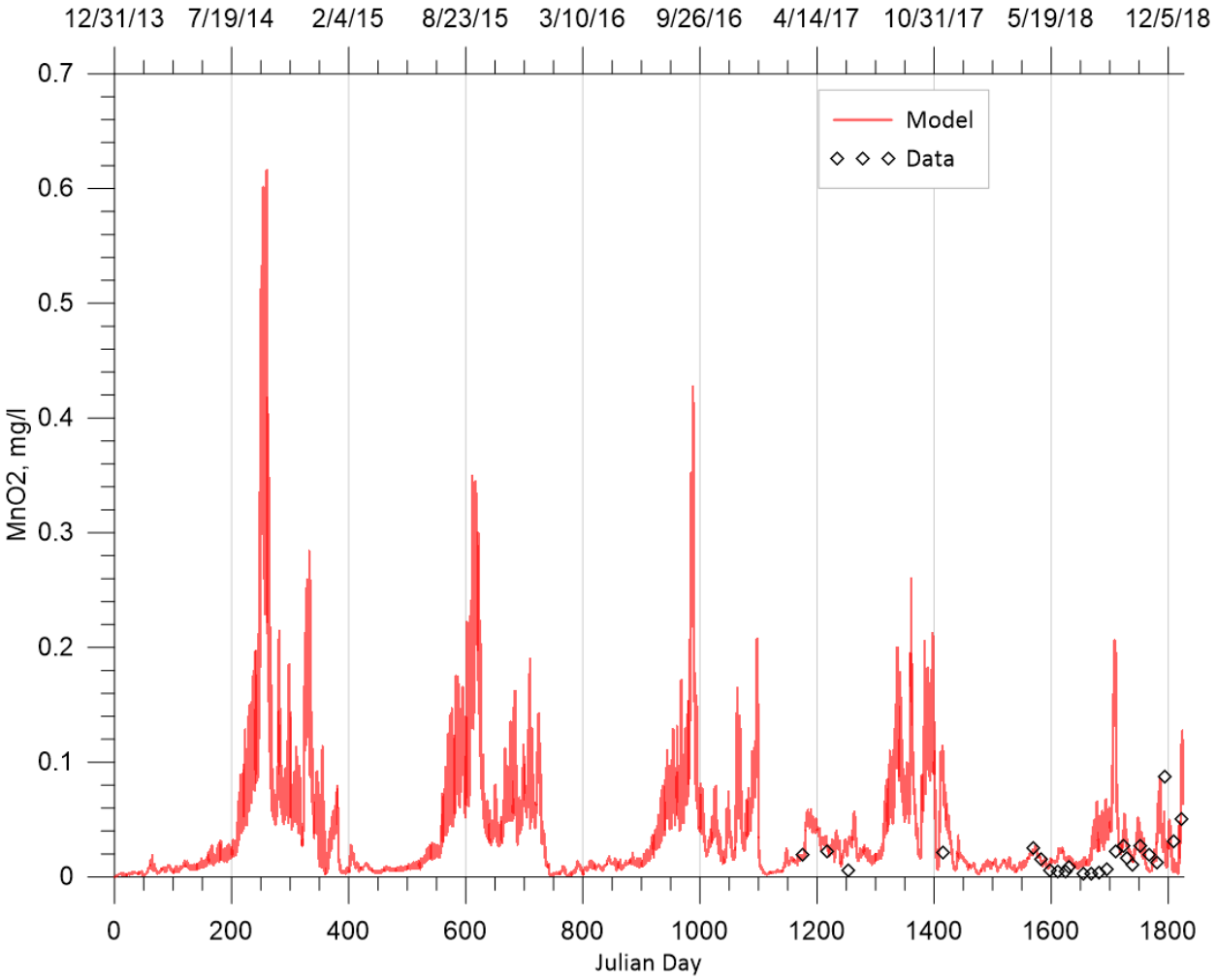


Figure 133. Brownlee Reservoir model outflow MnO2 compared to data.

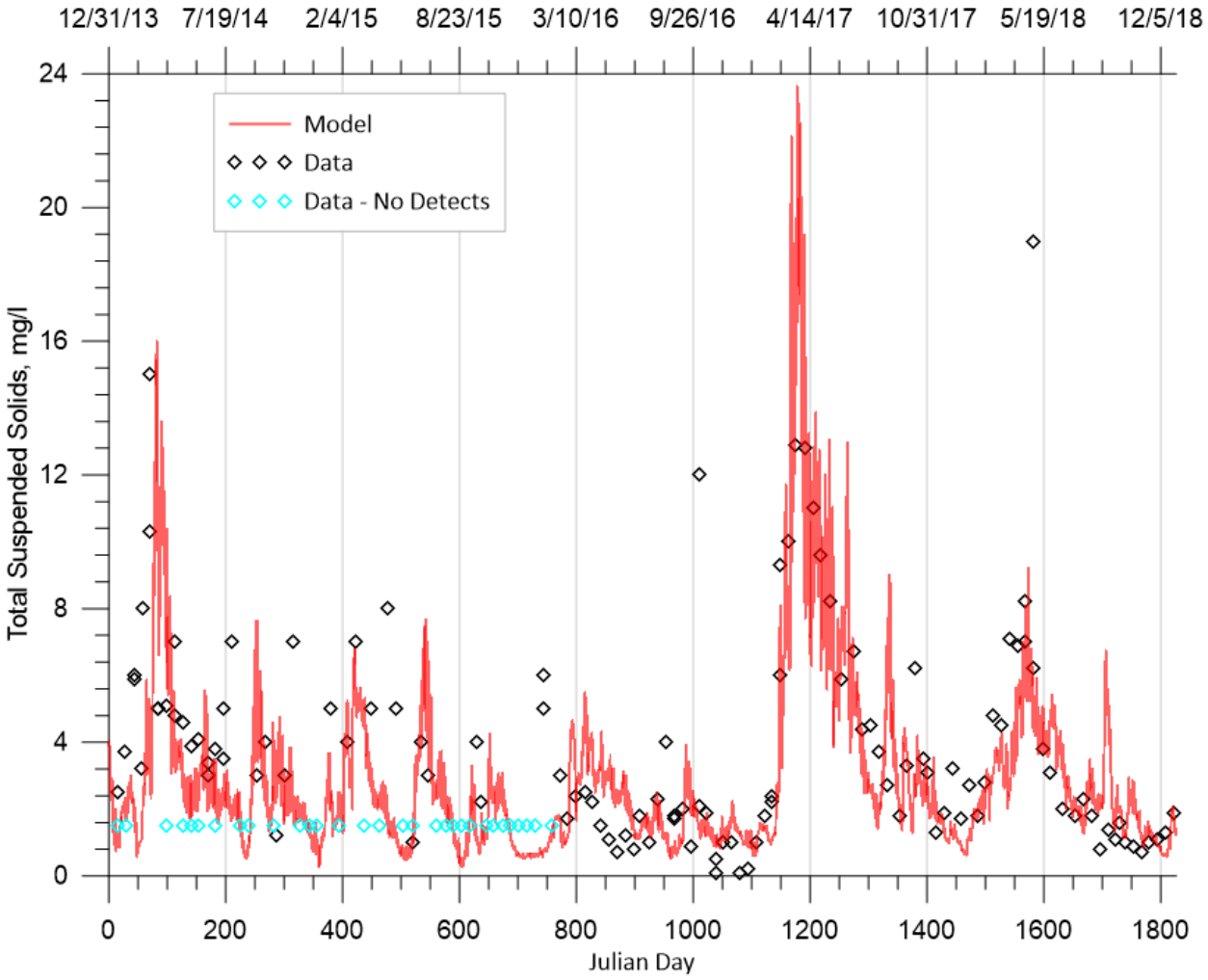


Figure 134. Brownlee Reservoir model outflow total suspended solids compared to data.

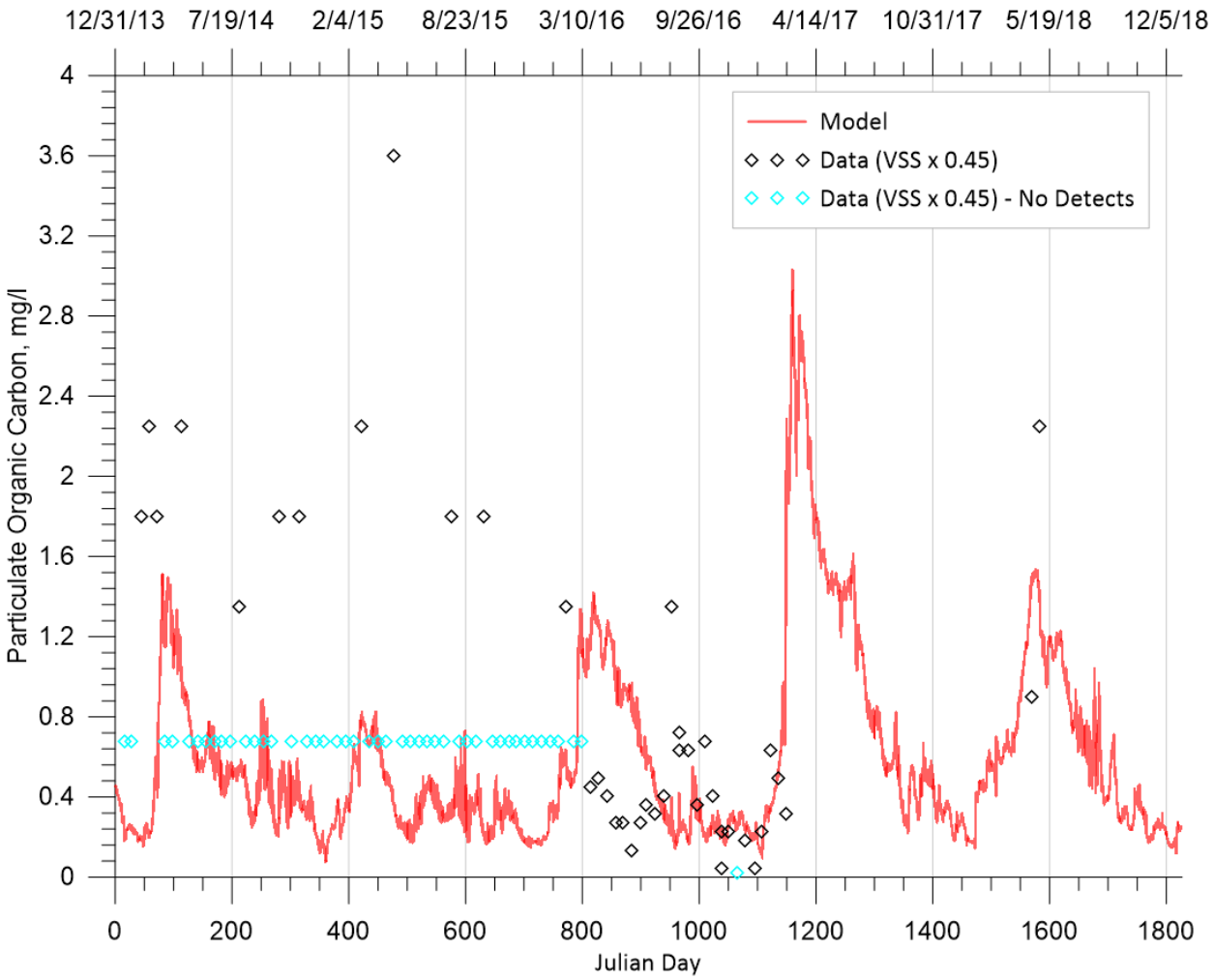


Figure 135. Brownlee Reservoir model outflow particulate organic carbon compared to volatile suspended solids data multiplied by 0.45 (assumed fraction of mg C to mg organic matter).

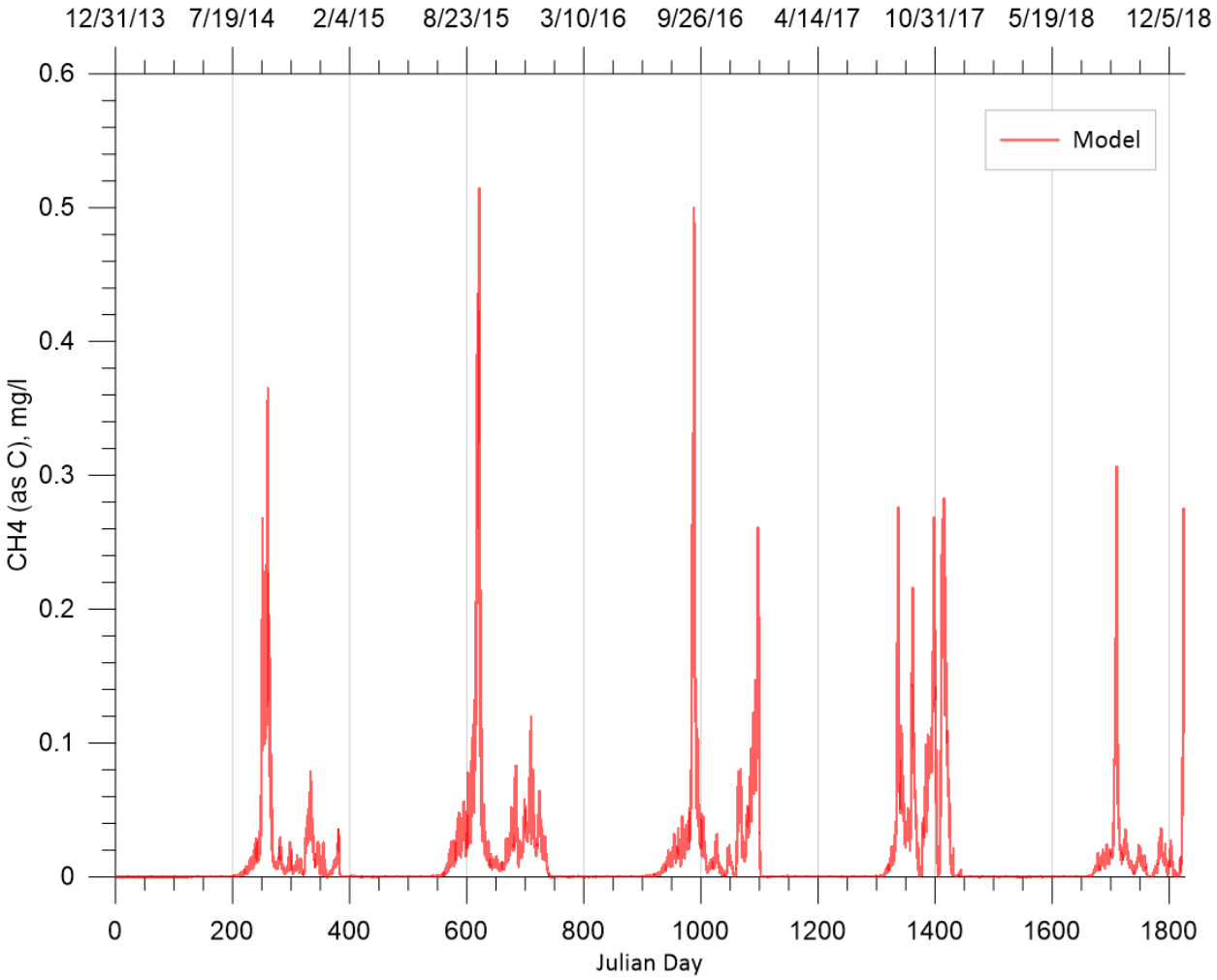


Figure 136. Brownlee Reservoir model outflow methane. In contrast note that Liu et al. (1996) reported in the anoxic hypolimnion of Lake Lugano concentrations of methane of 1 mg/L as C.]

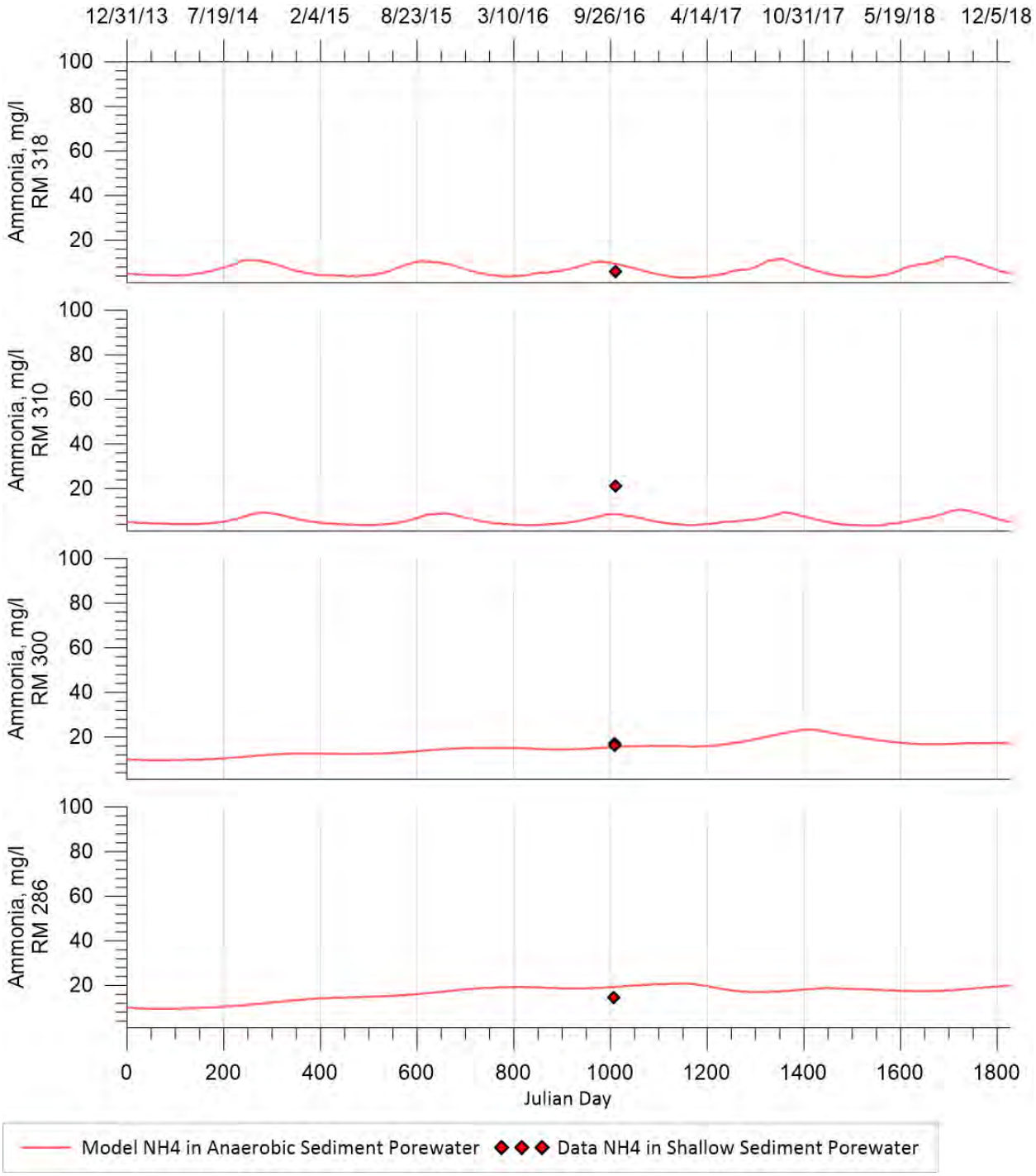


Figure 137. Brownlee Reservoir model ammonia nitrogen in sediment compared to data.

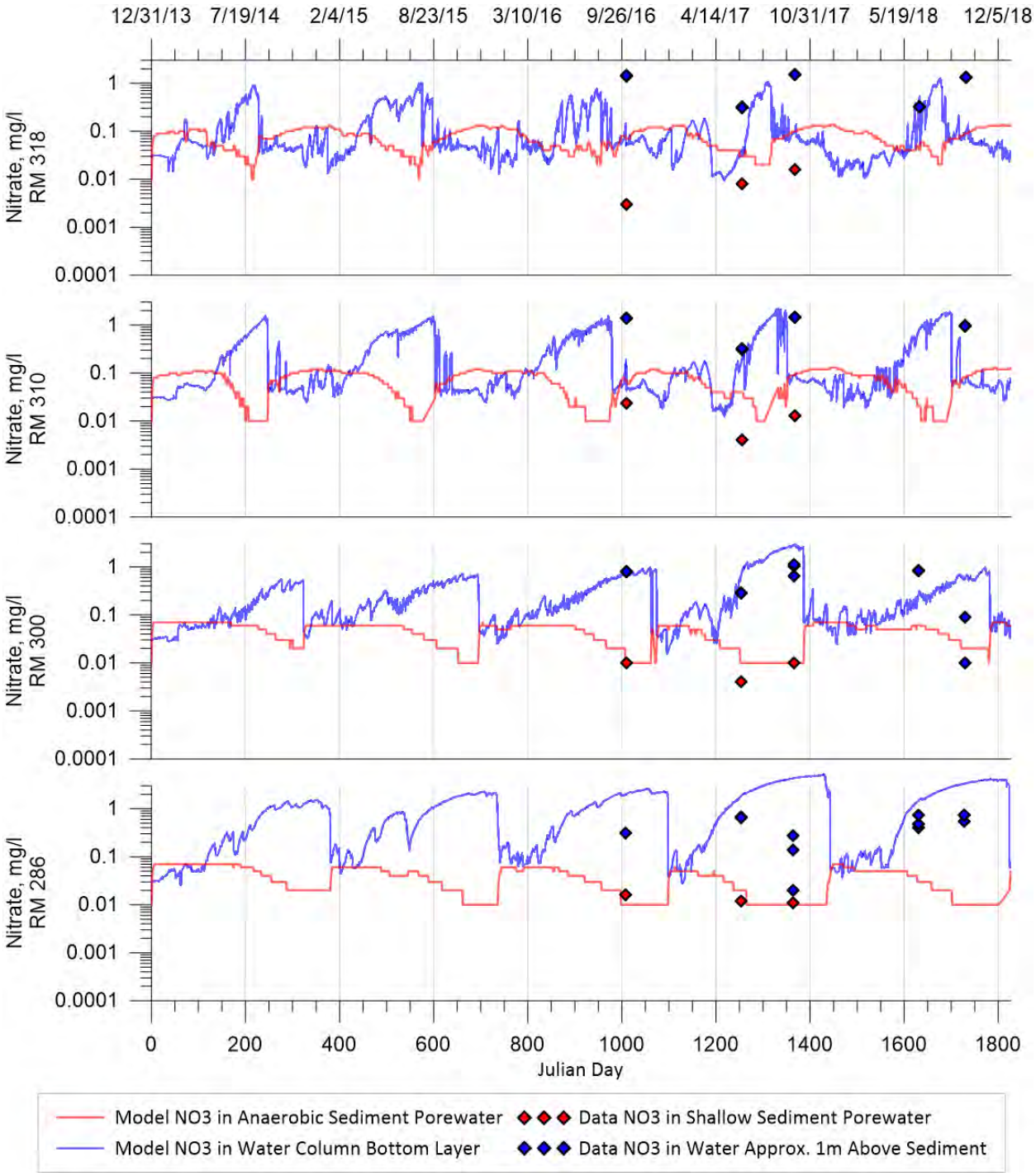


Figure 138. Brownlee Reservoir model nitrate nitrogen in sediment and bottom of water column compared to data.

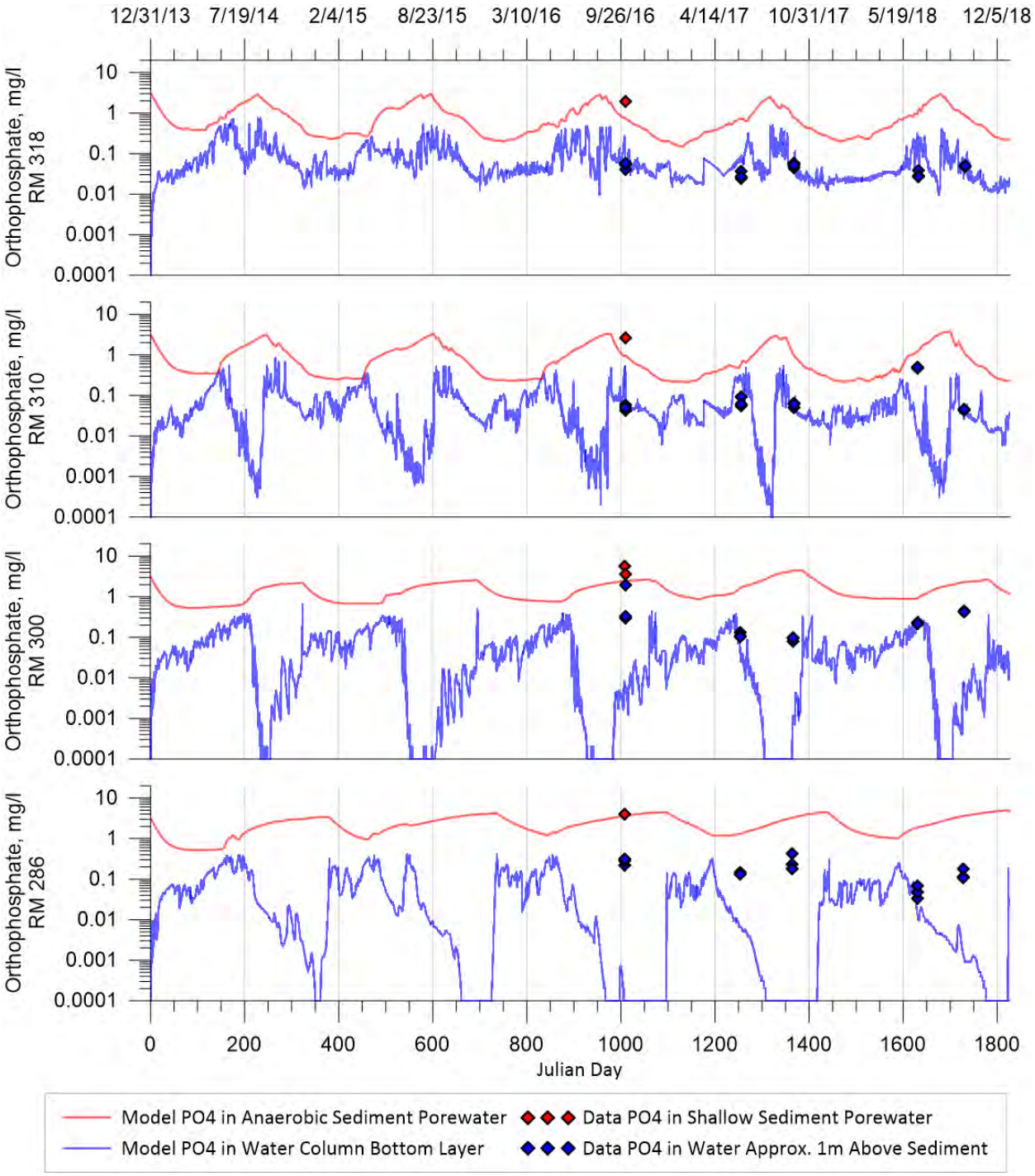


Figure 139. Brownlee Reservoir model orthophosphate in sediment and bottom of water column compared to data.

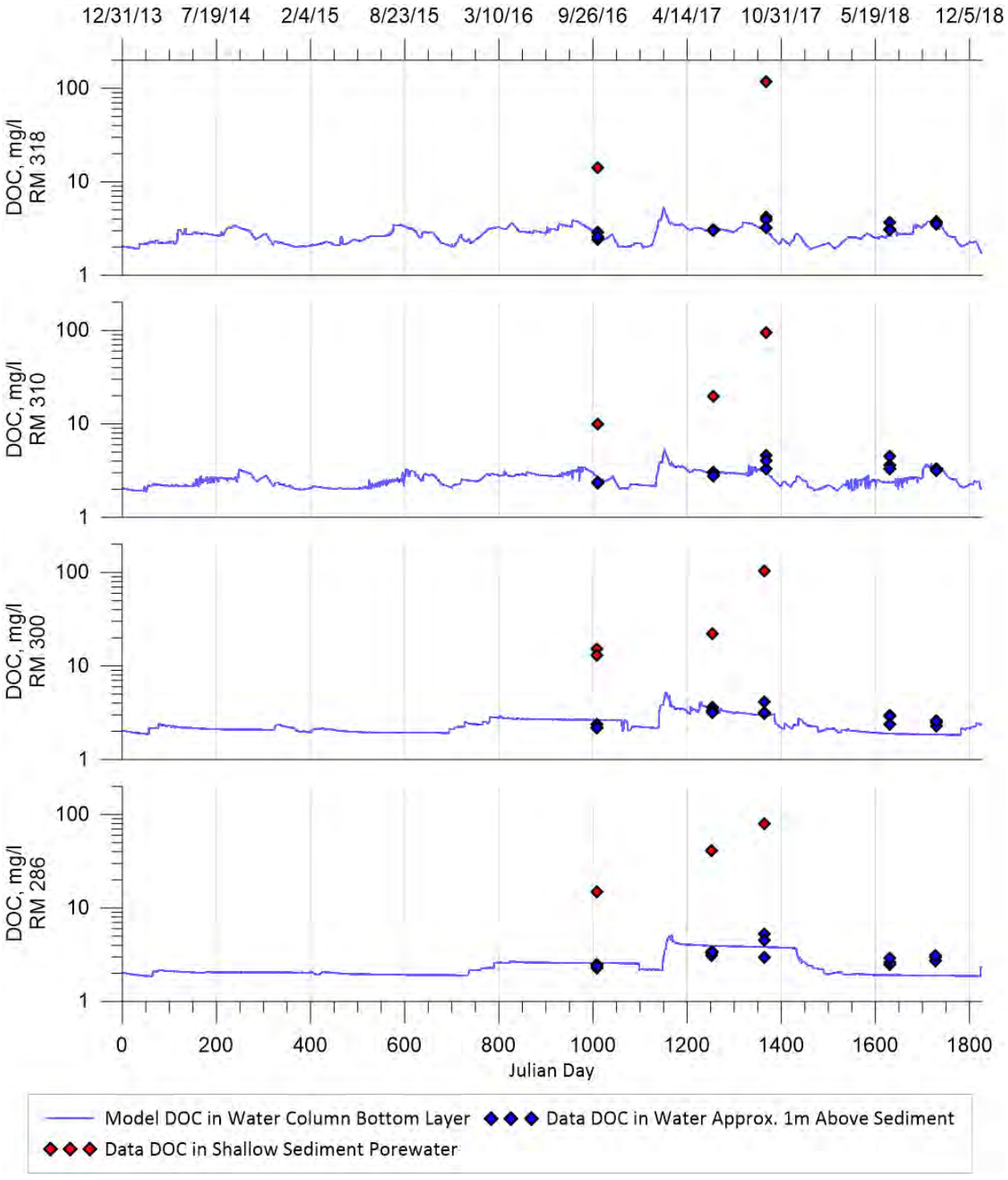


Figure 140. Brownlee Reservoir model DOC in bottom of water column compared to data.

Analysis of Model Fluxes

Phosphorus and nitrogen mass balances are shown in the following section. Sources and sinks of dissolved oxygen, phosphorus, and nitrogen are also plotted below. The fluxes predicted by the model show the importance of different source-sink terms in the water quality mass balances.

Phosphorus and nitrogen mass balances for Brownlee Reservoir (sum of all five water bodies) are shown in Figure 141 and Figure 142, respectively. For P, inflow and outflow are the largest fluxes, with inflow often exceeding outflow. The inflows include the Snake and Powder River together. This is similar for N, except that N inflow and outflow are usually of similar magnitude. P and N storage in the reservoir varies during the 5-year simulation period but is approximately steady. The sediment flux of P to the waterbody is several orders of magnitude less than the tributary P mass. NH_3 gas loss from Brownlee is predicted to be larger than the sediment flux of ammonia. Sources and sinks of dissolved oxygen, phosphorus, and nitrogen for WB5 of Brownlee Reservoir are shown in Figure 143 through Figure 145. Sources are shown as positive values and sinks are shown as negative values. The largest oxygen fluxes are algae production and respiration, reaeration and organic matter decay in the water column. The largest fluxes for P are also algae production, respiration, organic matter decay in the water column. Also in 2017, the settling loss of P was one of the largest flux terms. For N, besides the large fluxes associated with algae respiration and growth, nitrification and denitrification were significant fluxes during the period of simulation. On JDAY 1801 the net mass of P in Brownlee Reservoir was 2.73E06 kg (inflow TP + distributed tributary TP + tributary TP – Outflow TP), and the net mass of N was 4.97E06 kg (inflow TN + distributed tributary TN + tributary TN – Outflow TN). The positive values of P and N at the end of the simulation indicate that Brownlee Reservoir is a net sink of P and N since more mass came into the reservoir than left the reservoir.

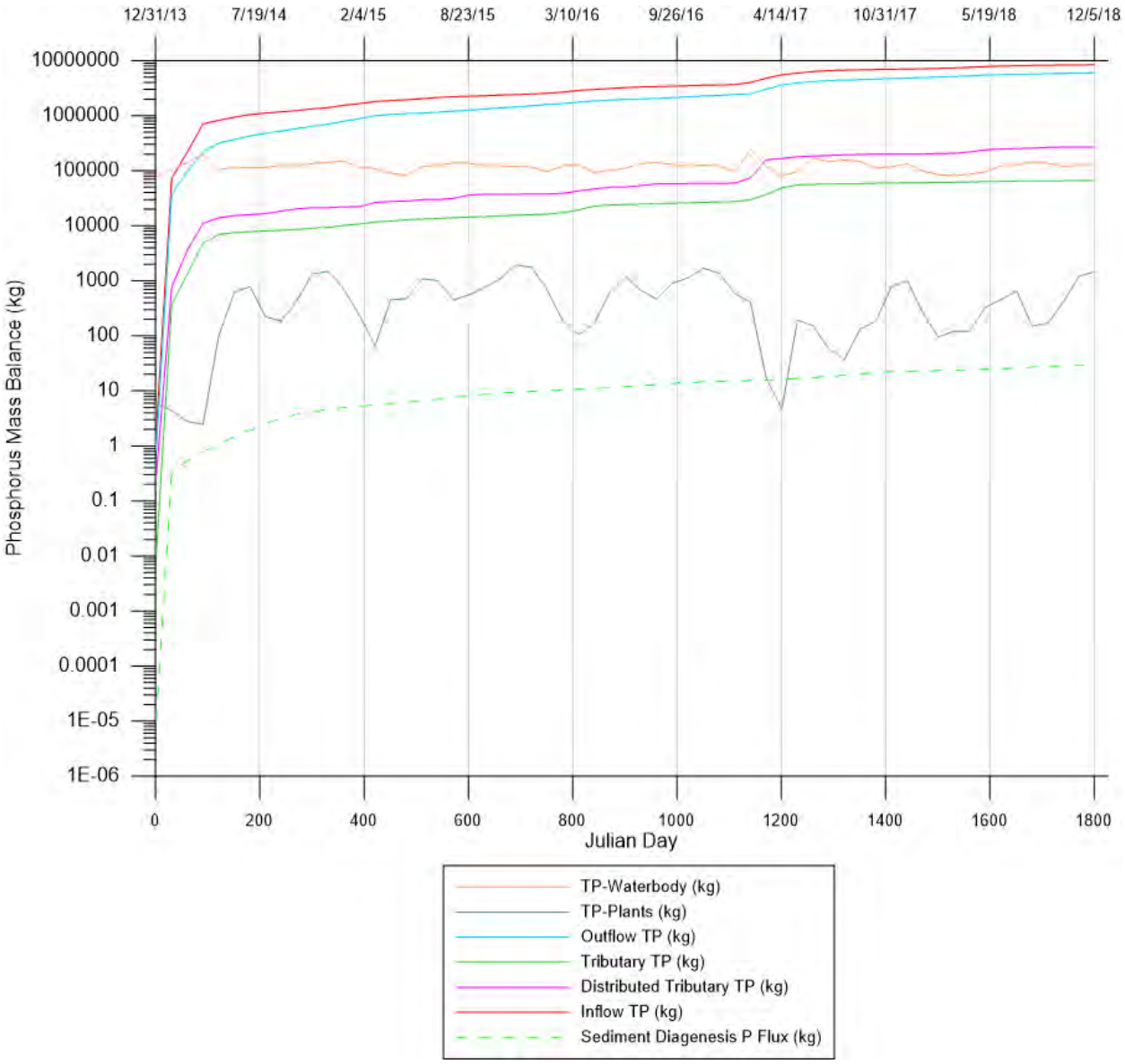


Figure 141. Cumulative phosphorus mass in Brownlee Reservoir. TP in the waterbody, sediment and plants just shows the current amount of TP in each of those at different points in time.

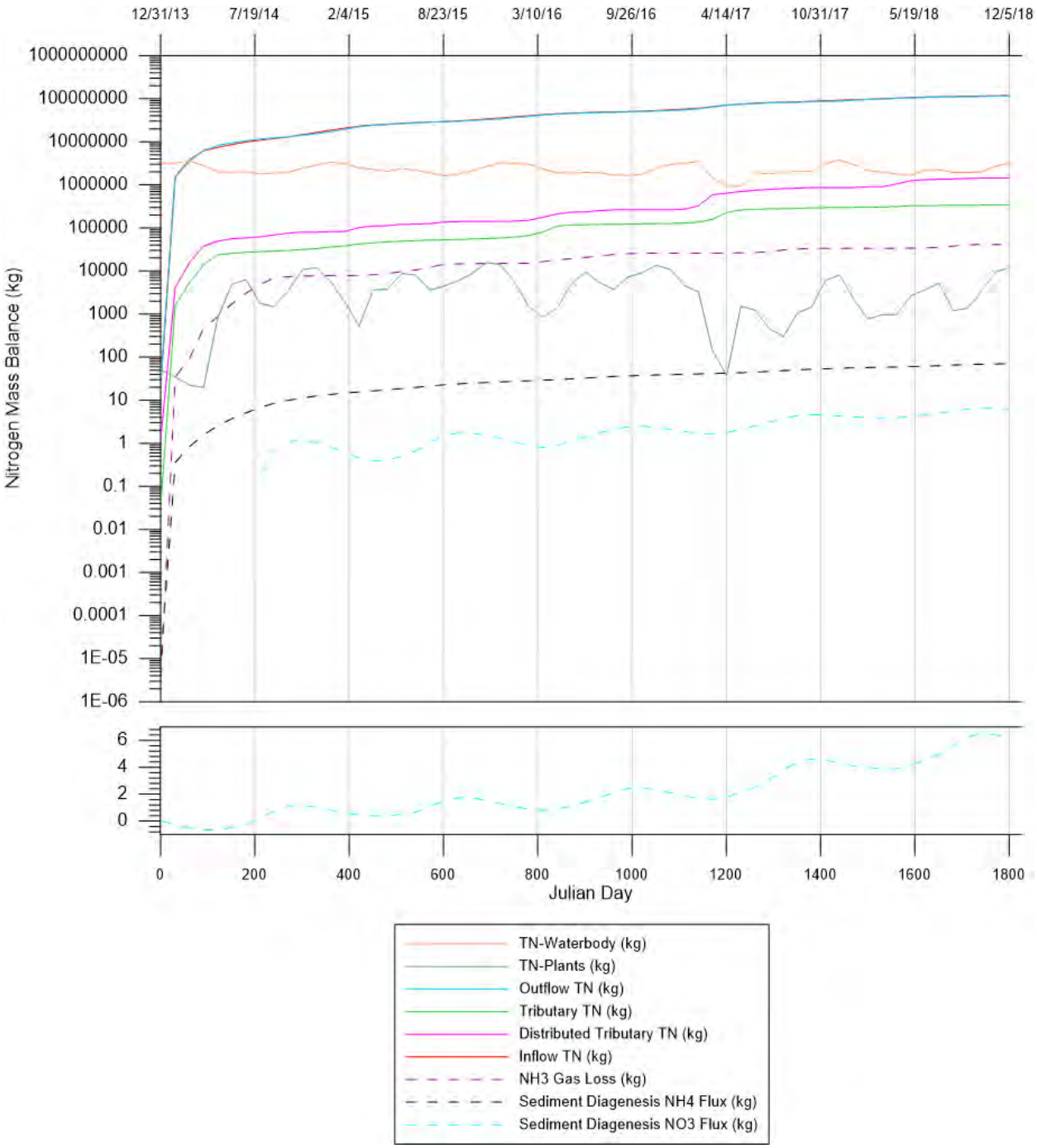


Figure 142. Cumulative nitrogen mass in Brownlee Reservoir. TN in the waterbody, sediment and plants just shows the current amount of TN in each of those at different points in time.

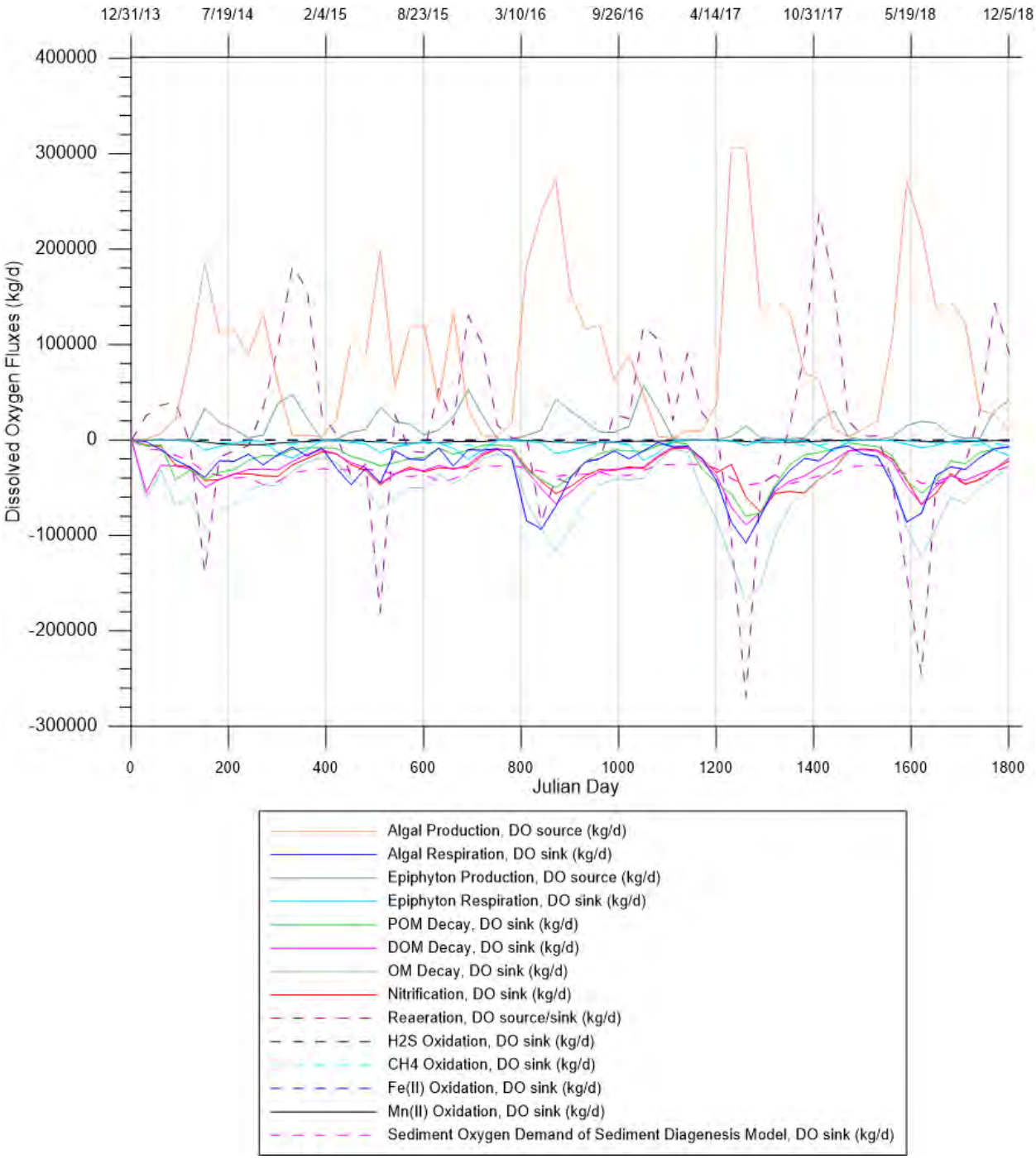


Figure 143. Dissolved oxygen sources and sinks in Brownlee Reservoir.

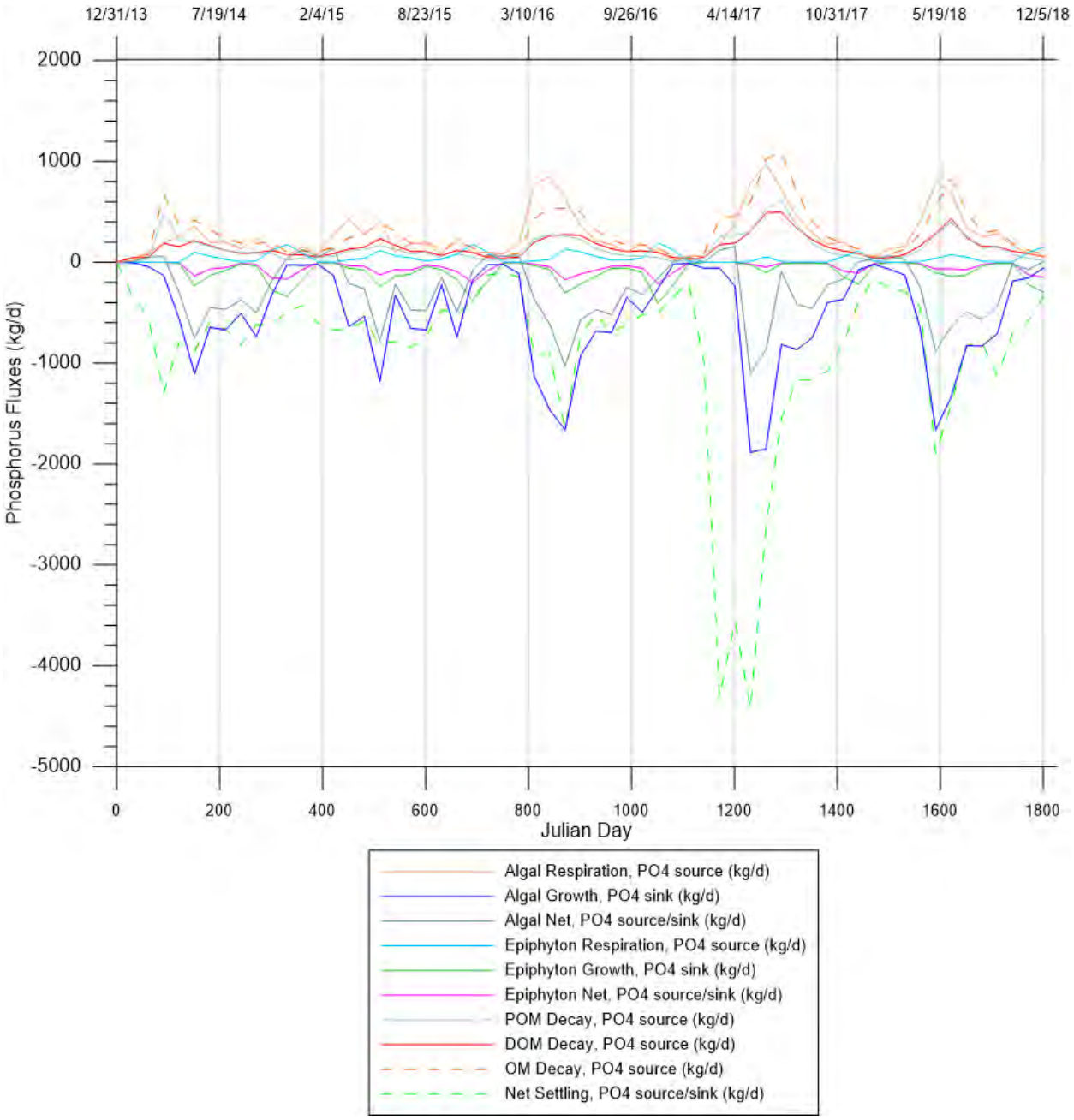


Figure 144. Phosphorus sources and sinks in Brownlee Reservoir.

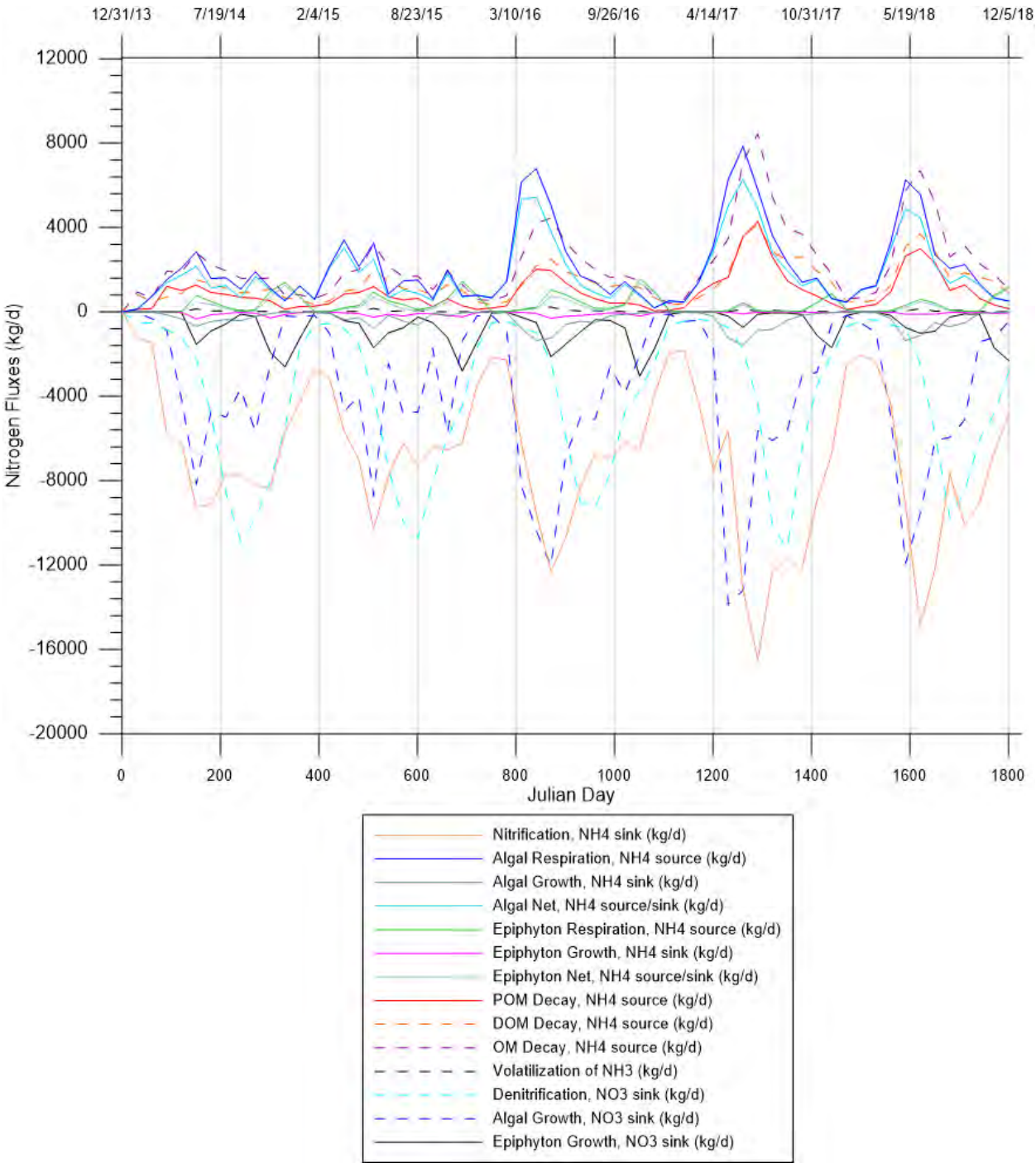


Figure 145. Nitrogen sources and sinks in Brownlee Reservoir.

Sediment Nutrient Concentrations

The sediment diagenesis model computes concentrations of particulate organic carbon, nitrogen, and phosphorus (POC, PON, and POP) in the sediments over time for each model segment. These concentrations are shown in Figure 146 and Figure 147 for select segments. Both labile and refractory pools are shown. These graphs show that the initial conditions for the sediments were approximately

maintained through the simulation period and did not take a long time to approach dynamic seasonal conditions.

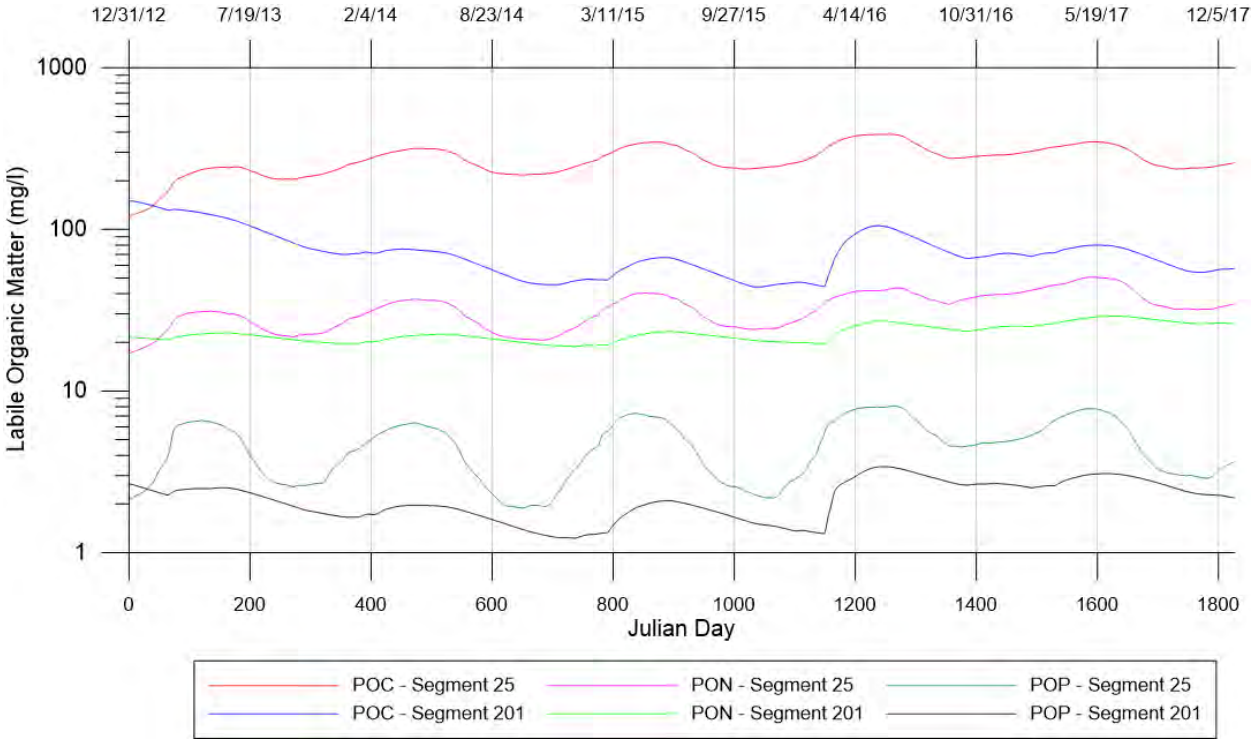


Figure 146. Labile POC, PON, POP at segments 25 and 201 in Brownlee Reservoir.

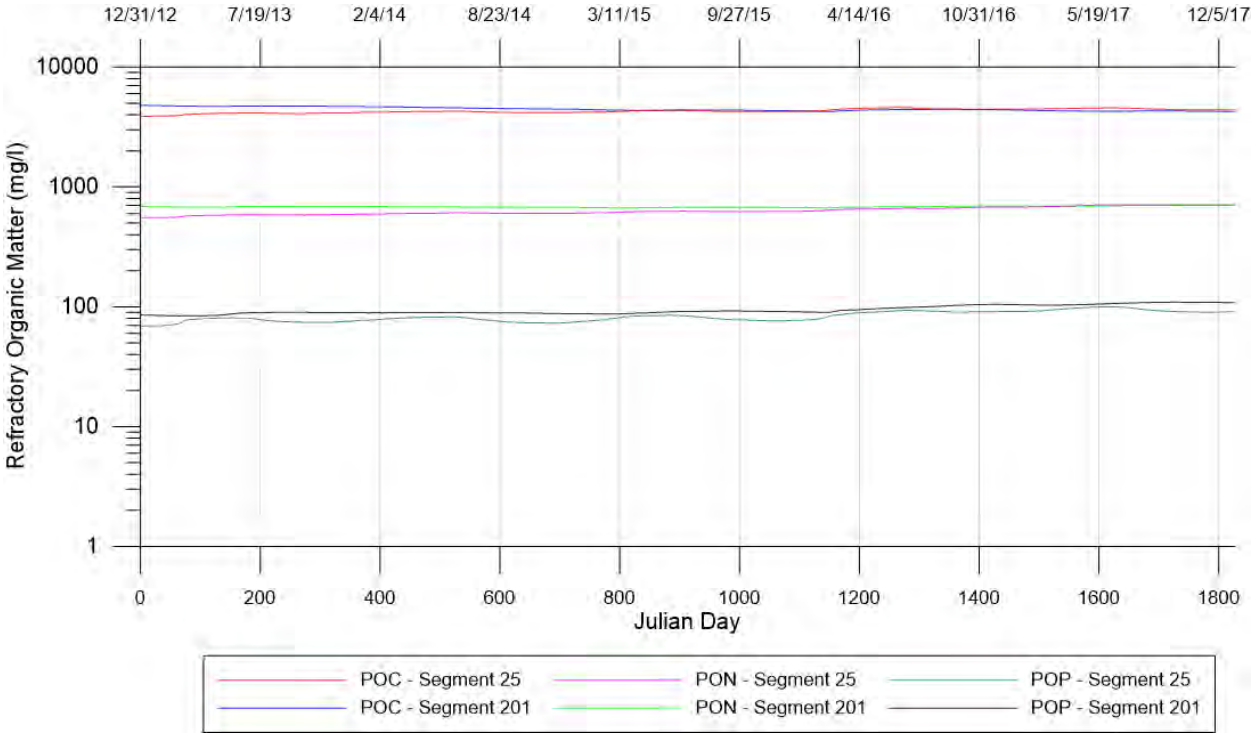


Figure 147. Refractory POC, PON, POP at segments 25 and 201 in Brownlee Reservoir.

Oxbow Reservoir

Water Quality Model-Data Comparisons

Model results just downstream of Oxbow Dam (model segment 14 of Hells Canyon Reservoir at the water surface) were used for model-data outflow comparisons. Table 37 lists water quality error statistics for Oxbow Reservoir outflow. Table 38 lists water quality error statistics for Oxbow Reservoir vertical profiles. Figure 148 through **Error! Reference source not found.** show the associated model-data outflow comparisons. Appendix A5 shows the associated model-data profile comparisons.

Table 37. Water quality error statistics for Oxbow Reservoir outflow.

Parameter	Model Average	# of data	ME	MAE	RMSE	MAE/Model Average
DO (mg/l)	9.306	246125	0.214	0.690	0.888	0.074
Chlorophyll a (ug/l)	4.68	0	N/A	N/A	N/A	N/A
Chloride (mg/l)	17.945	64	0.304	1.699	2.728	0.095
DOC (mg/l)	2.664	115	0.085	0.196	0.245	0.074
FeII (mg/l)	0.005	37	0.001	0.002	0.002	0.400
FeOOH (mg/l)	0.071	24	0.004	0.050	0.094	0.704
MnII (mg/l)	0.000	41	-0.001	0.001	0.001	N/A
MnO2 (mg/l)	0.033	24	0.014	0.017	0.036	0.515
Ammonia (mg/l)	0.039	0	N/A	N/A	N/A	N/A
Nitrate (mg/l)	1.150	64	0.059	0.139	0.195	0.121
Ortho-phosphate (mg/l)	0.059	42	0.012	0.015	0.019	0.254
POC (mg/l)	0.550	4	-0.058	0.151	0.199	0.275
Sulfate (mg/l)	41.181	64	0.861	2.702	5.292	0.066
TKN (mg/l)	0.412	0	N/A	N/A	N/A	N/A
Total Phosphorus (mg/l)	0.084	0	N/A	N/A	N/A	N/A
TSS (mg/l)	2.382	66	-1.311	1.731	2.858	0.727
TIC (mg/l)	41.071	4	1.344	1.930	3.013	0.047
H2S (mg/l)	0.002	0	N/A	N/A	N/A	N/A
PON (mg/l)	0.068	4	-0.026	0.026	0.037	0.382
Zooplankton (mg/l)	0.115	13	0.146	0.146	0.222	1.270
POC (estimated from VSS data) (mg/l)	0.550	0	N/A	N/A	N/A	N/A

Table 38. Water quality error statistics for Oxbow Reservoir vertical profiles.

Parameter	# of Profiles	# of Data	ME	MAE	RMSE
Chloride (mg/l)	3	14	1.803	1.803	1.832
Sulfate (mg/l)	3	14	1.443	1.630	2.486
Fe(II) (mg/l)	3	11	-0.001	0.002	0.002
Mn(II) (mg/l)	3	13	-0.128	0.128	0.236
Ortho-phosphate (mg/l)	3	14	-0.018	0.034	0.050

Parameter	# of Profiles	# of Data	ME	MAE	RMSE
Nitrate (mg/l)	3	14	-0.002	0.136	0.175
TIC (mg/l)	3	15	0.745	2.509	3.103
Zooplankton (mg/l)	2	13	0.137	0.143	0.150
DOC (mg/l)	4	17	0.162	0.194	0.239
POC (mg/l)	3	14	0.031	0.088	0.102
PON (mg/l)	3	14	-0.012	0.018	0.022
TSS (mg/l)	3	14	-0.337	0.756	1.059

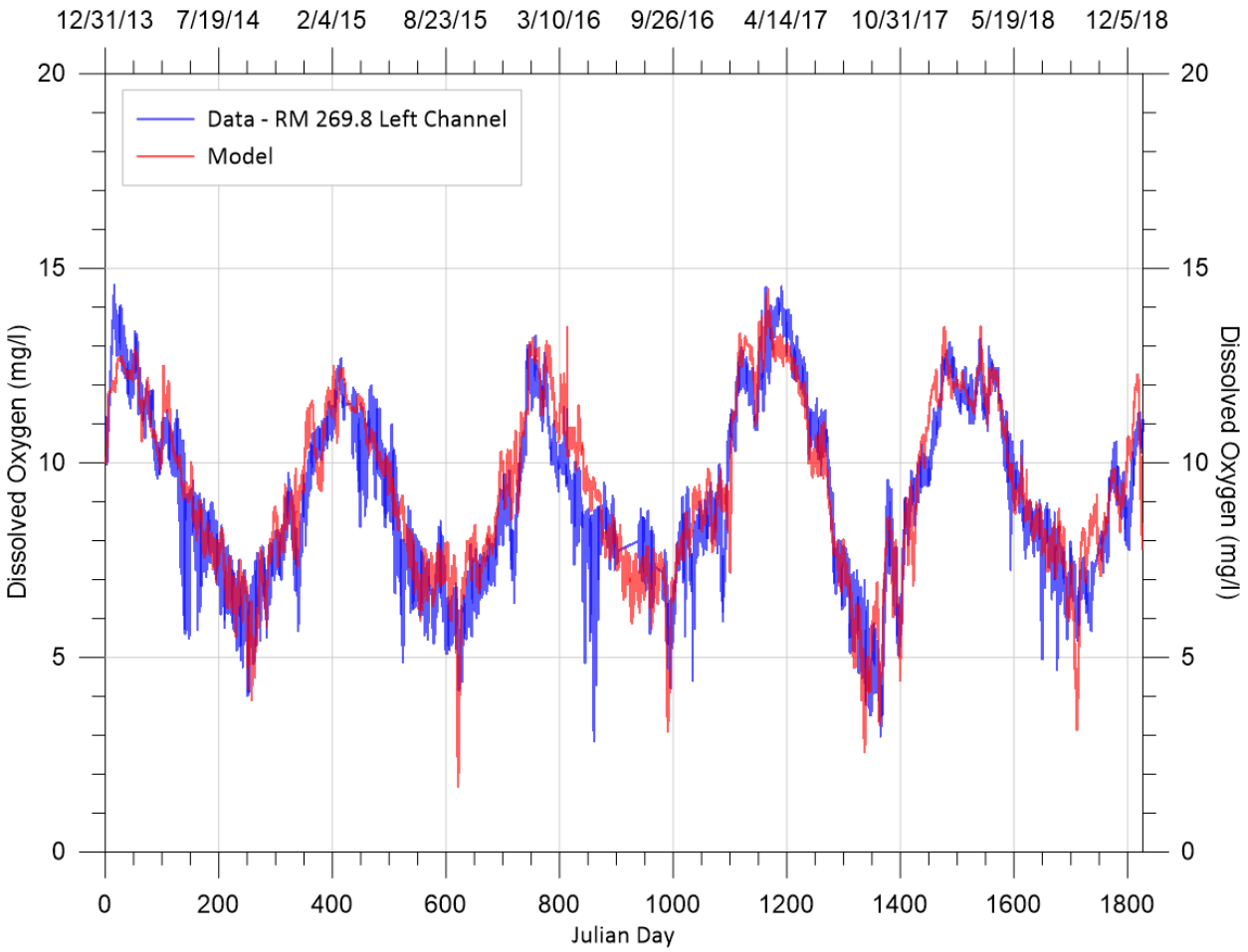


Figure 148. Oxbow Reservoir model outflow dissolved oxygen compared to data.

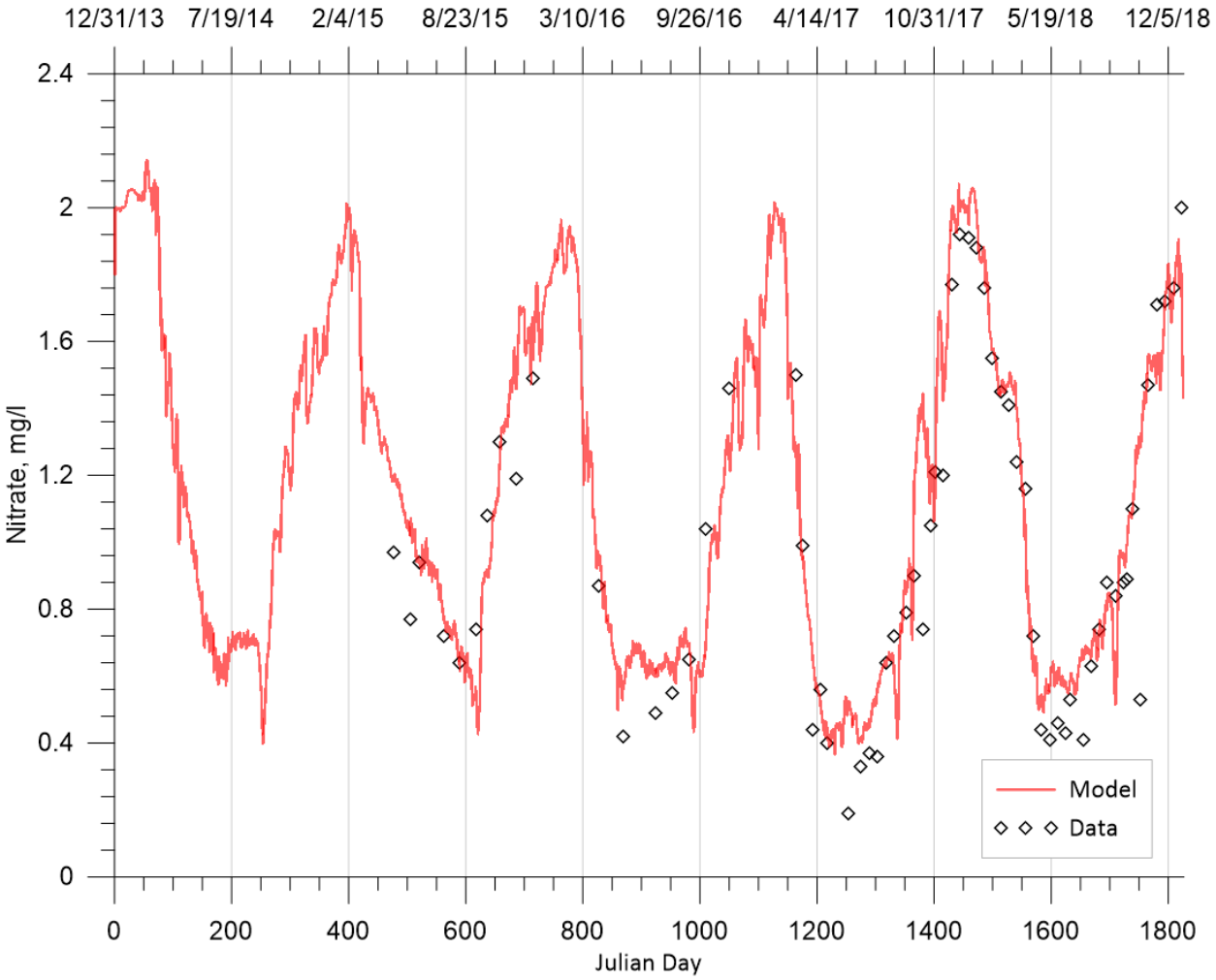


Figure 149. Oxbow Reservoir model outflow nitrate nitrogen compared to data.

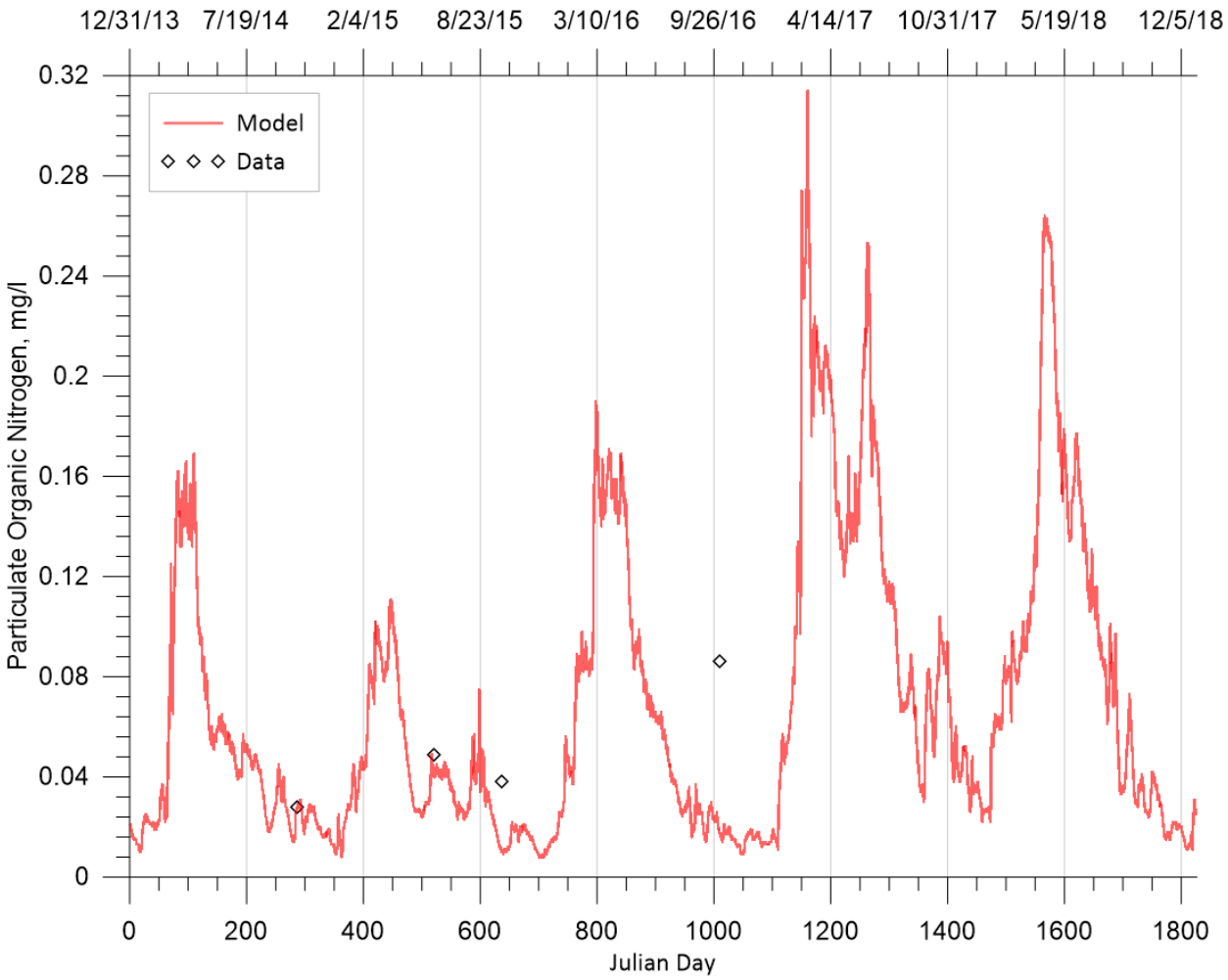


Figure 150. Oxbow Reservoir model outflow particulate organic nitrogen compared to data.

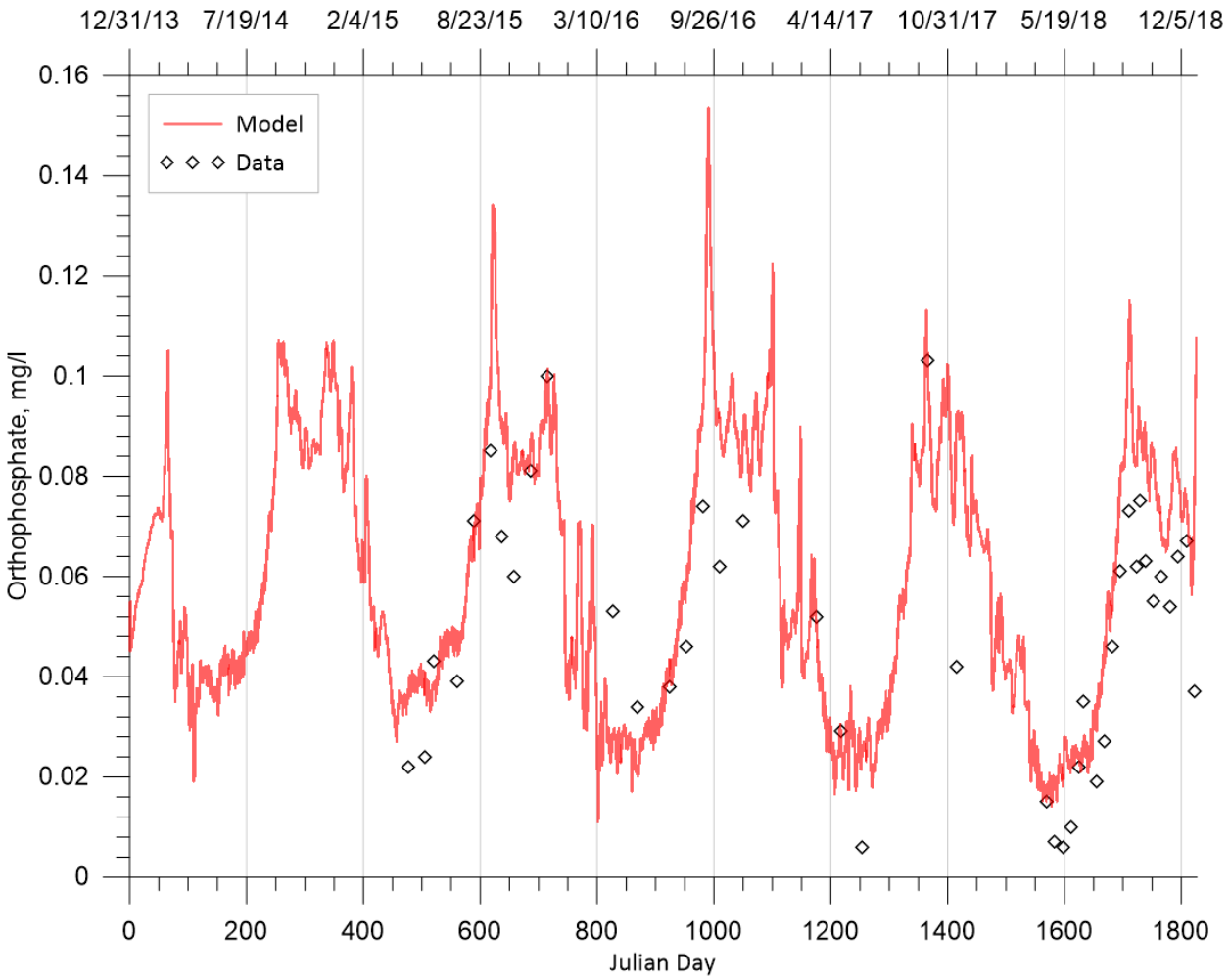


Figure 151. Oxbow Reservoir model outflow orthophosphate compared to data.

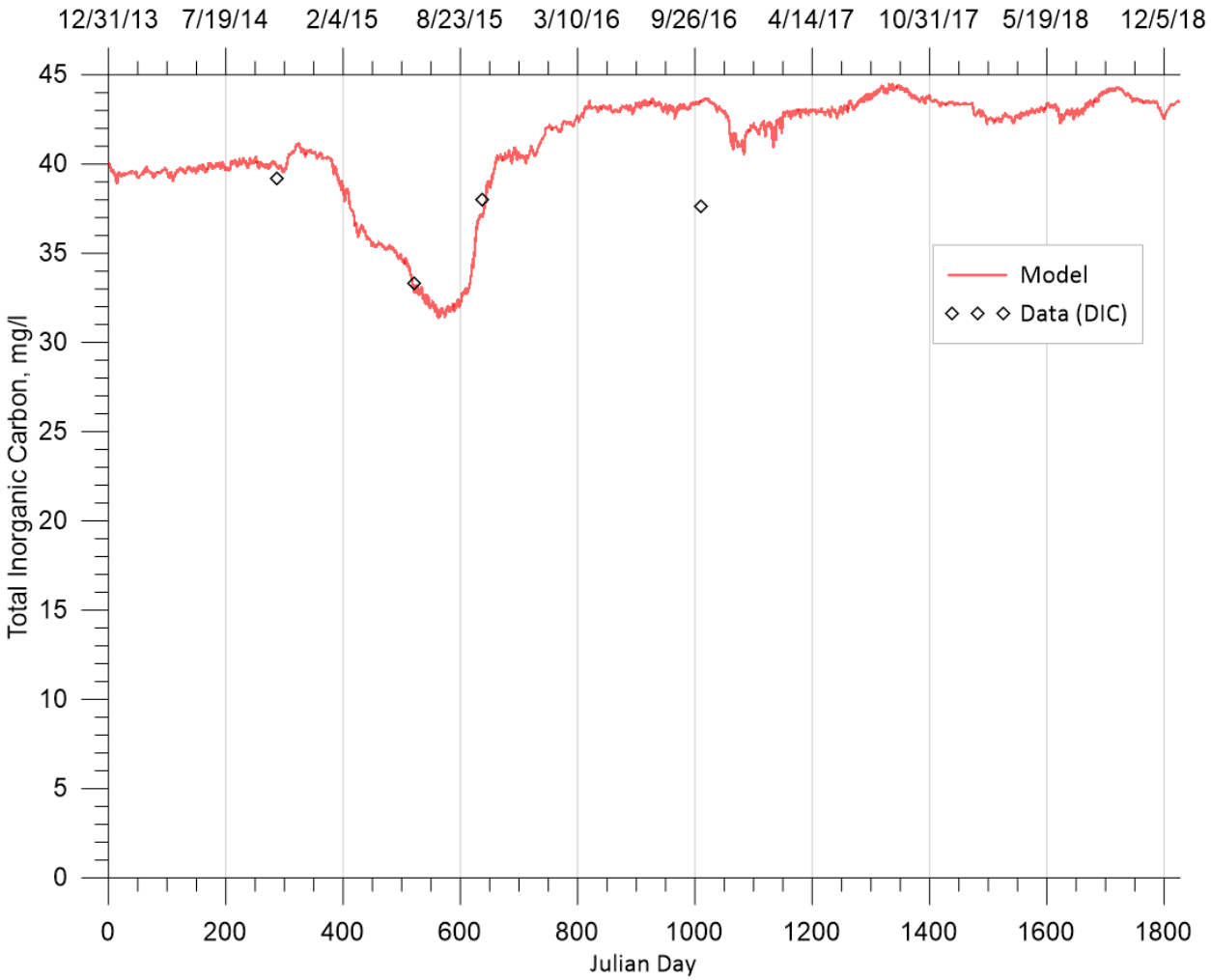


Figure 152. Oxbow Reservoir model outflow total inorganic carbon compared to data.

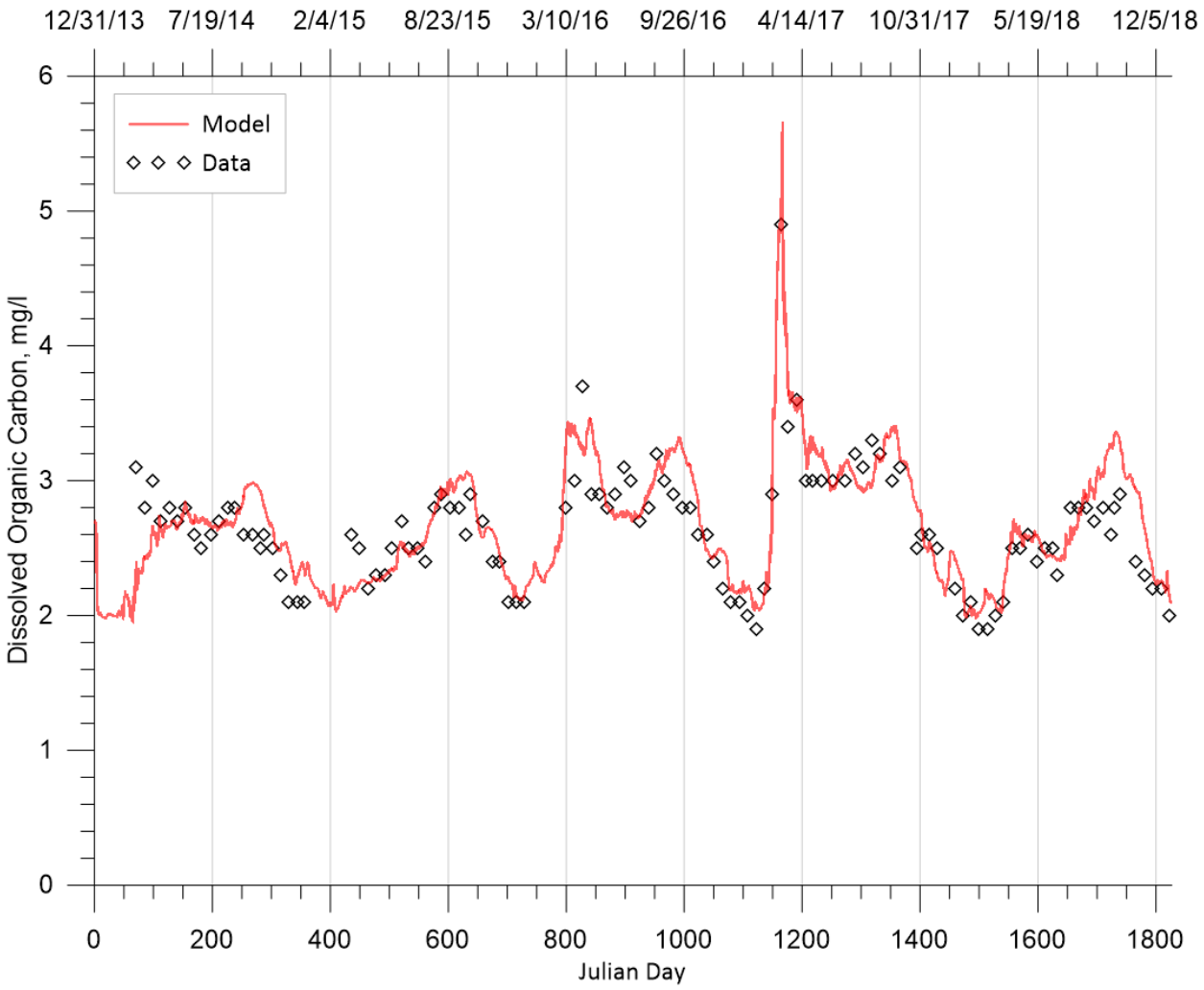


Figure 153. Oxbow Reservoir model outflow dissolved organic carbon compared to data.

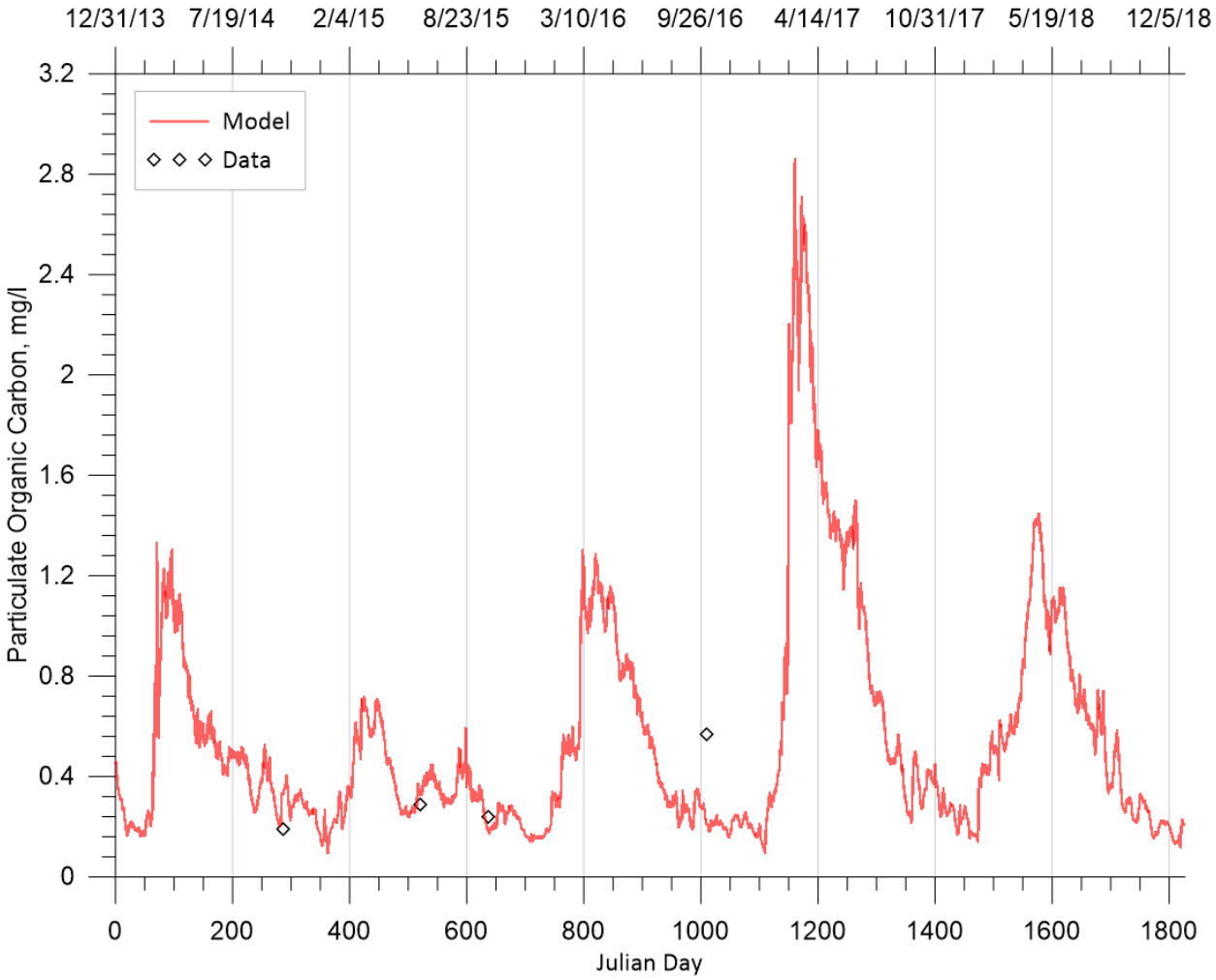


Figure 154. Oxbow Reservoir model outflow particulate organic carbon compared to data.

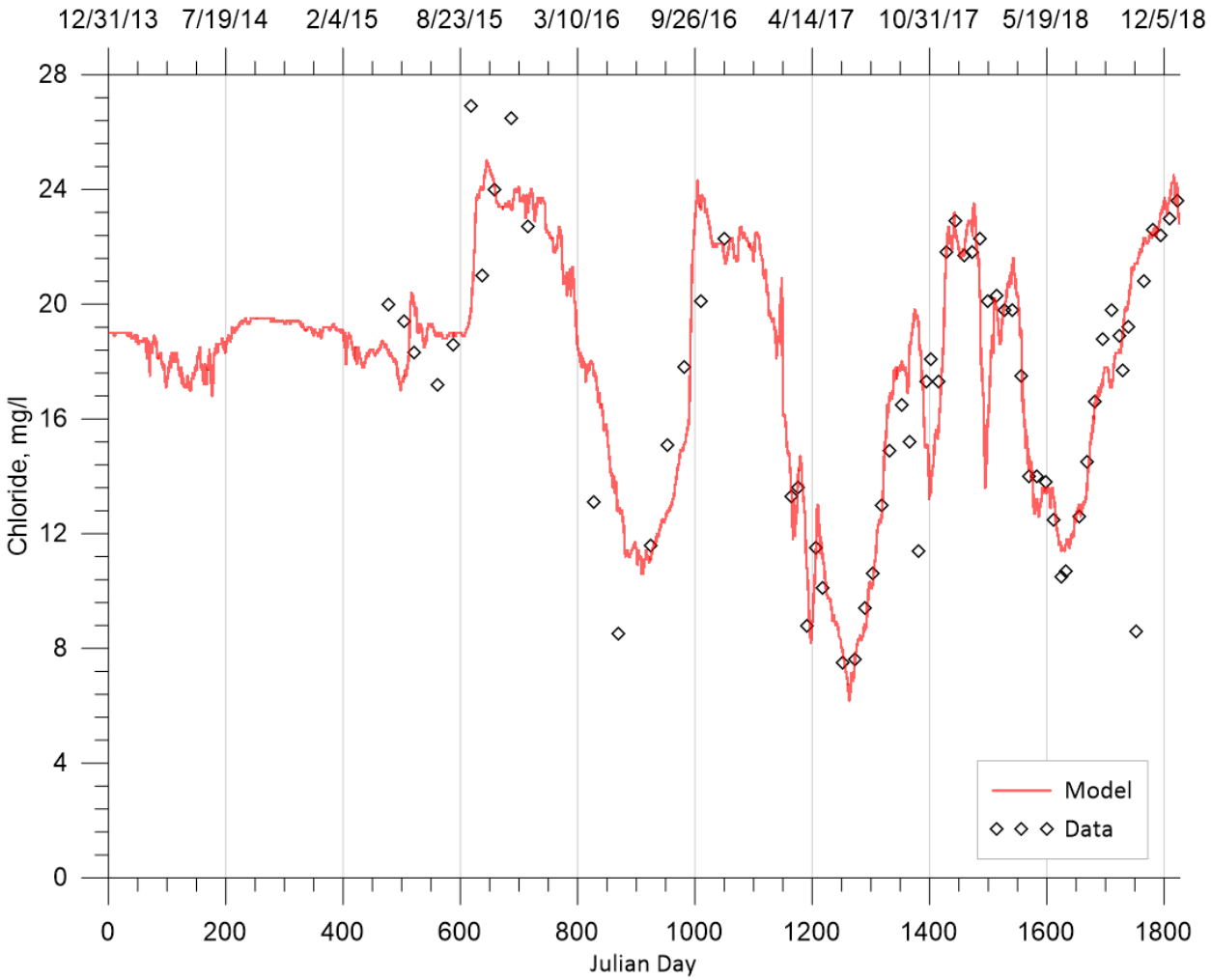


Figure 155. Oxbow Reservoir model outflow chloride compared to data.

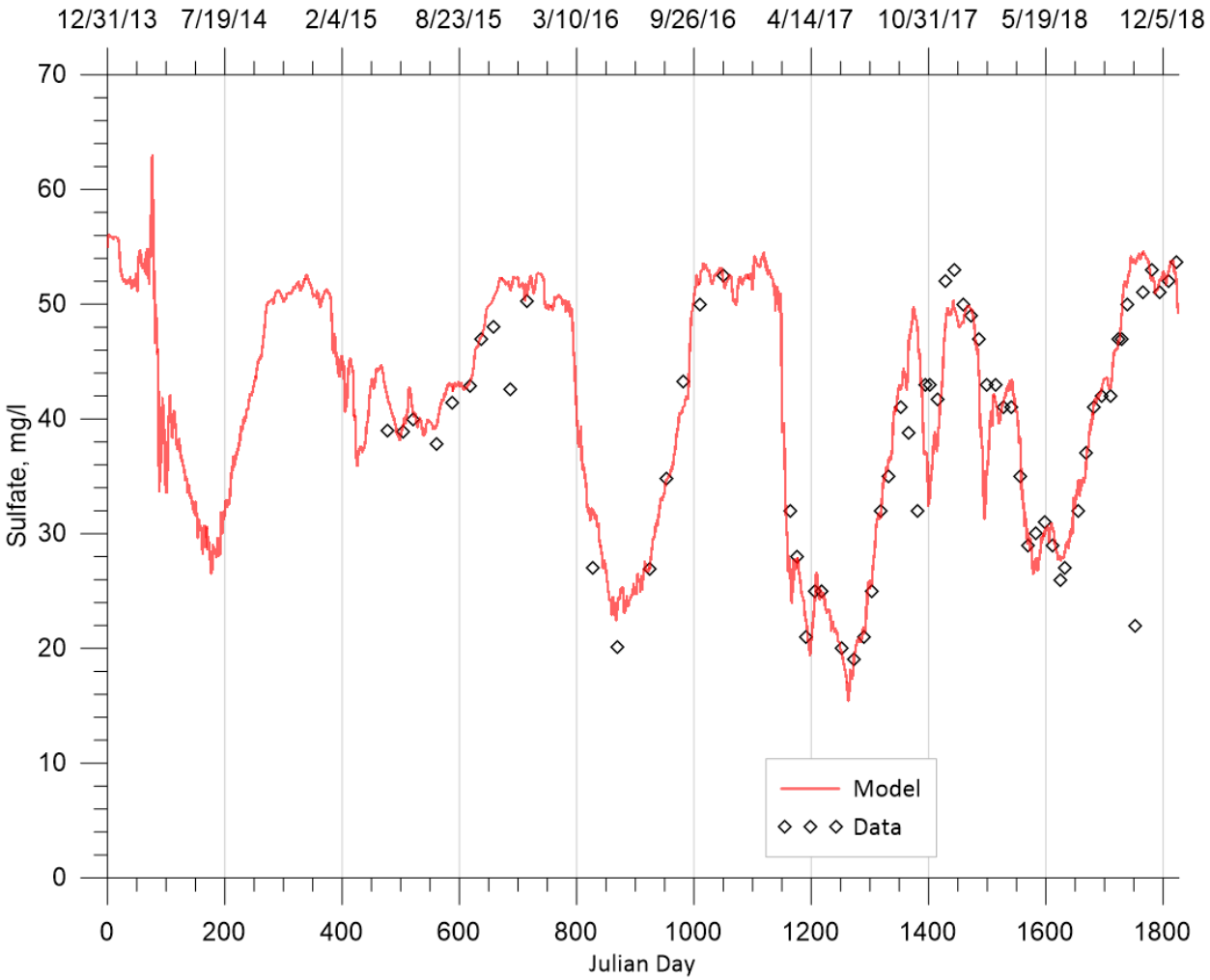


Figure 156. Oxbow Reservoir model outflow sulfate compared to data.

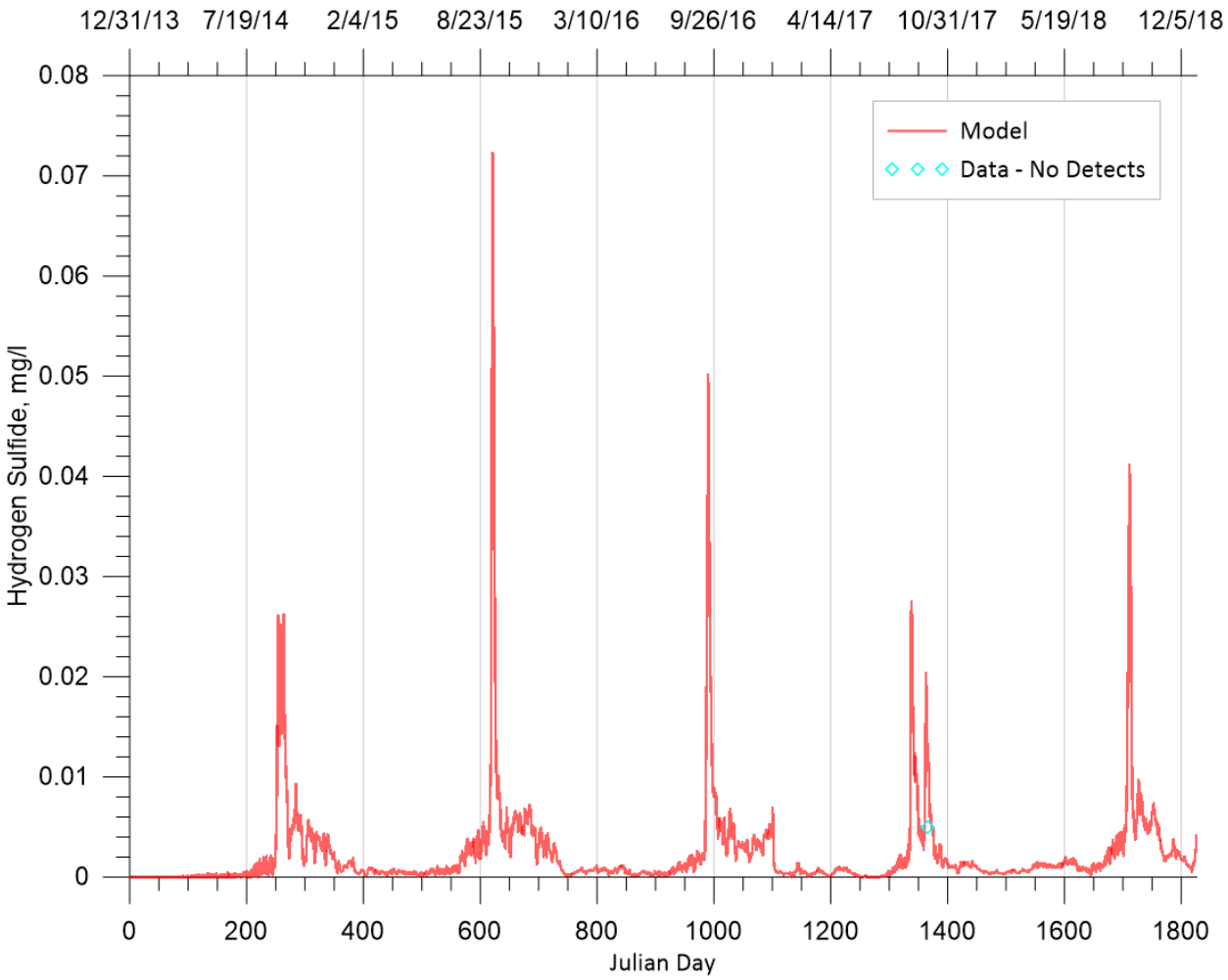


Figure 157. Oxbow Reservoir model outflow hydrogen sulfide compared to data.

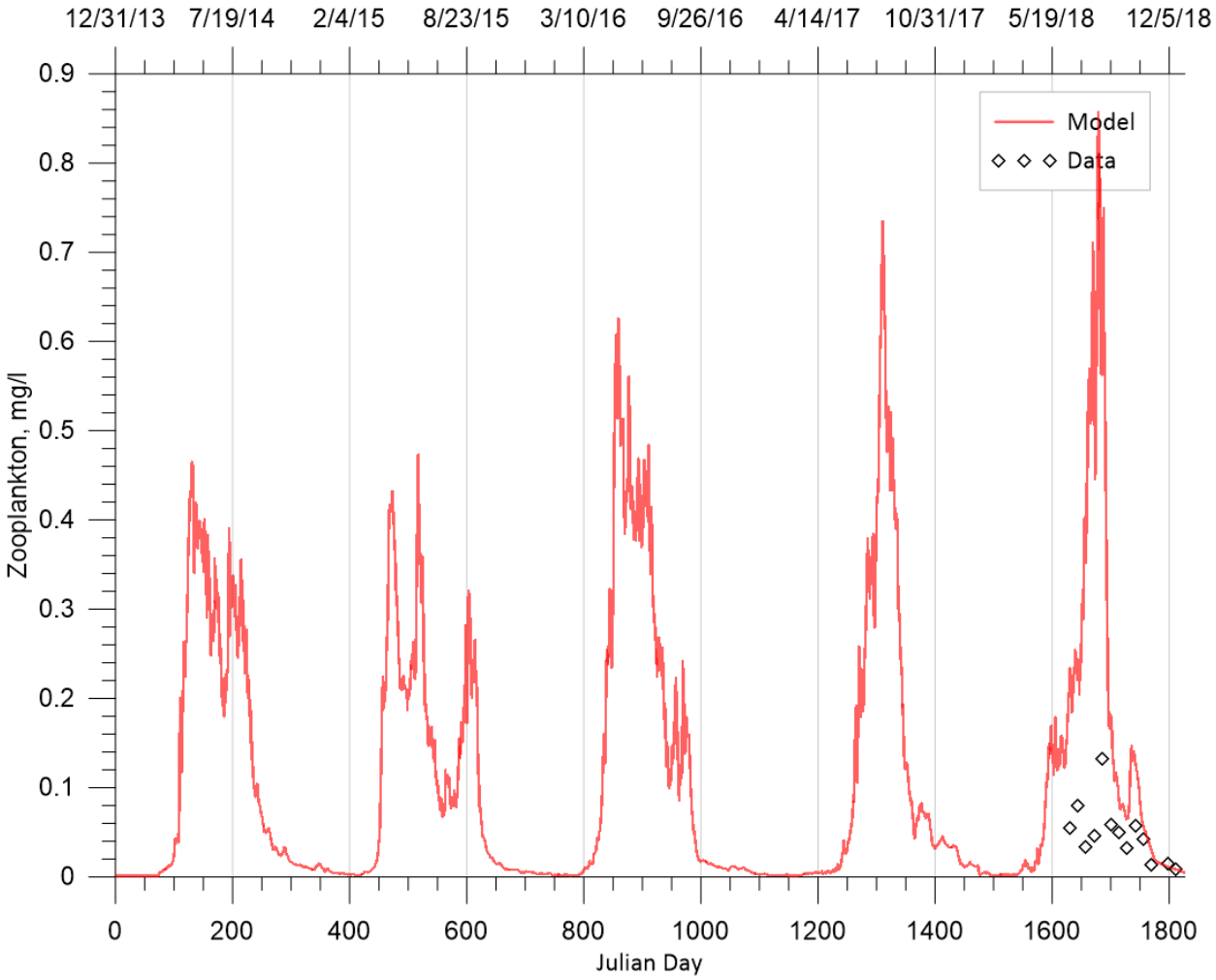


Figure 158. Oxbow Reservoir model outflow zooplankton compared to data.

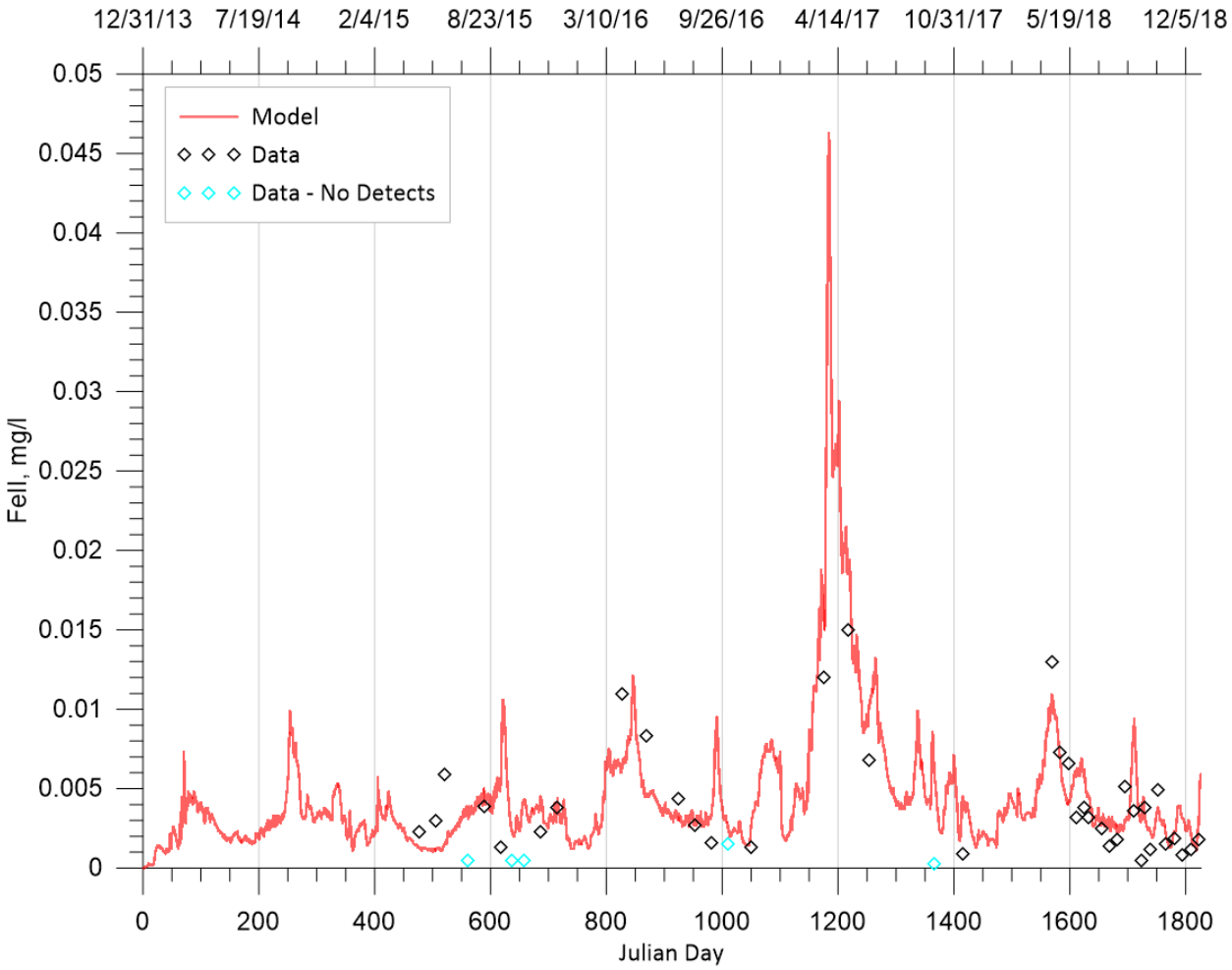


Figure 159. Oxbow Reservoir model outflow FeII compared to data.

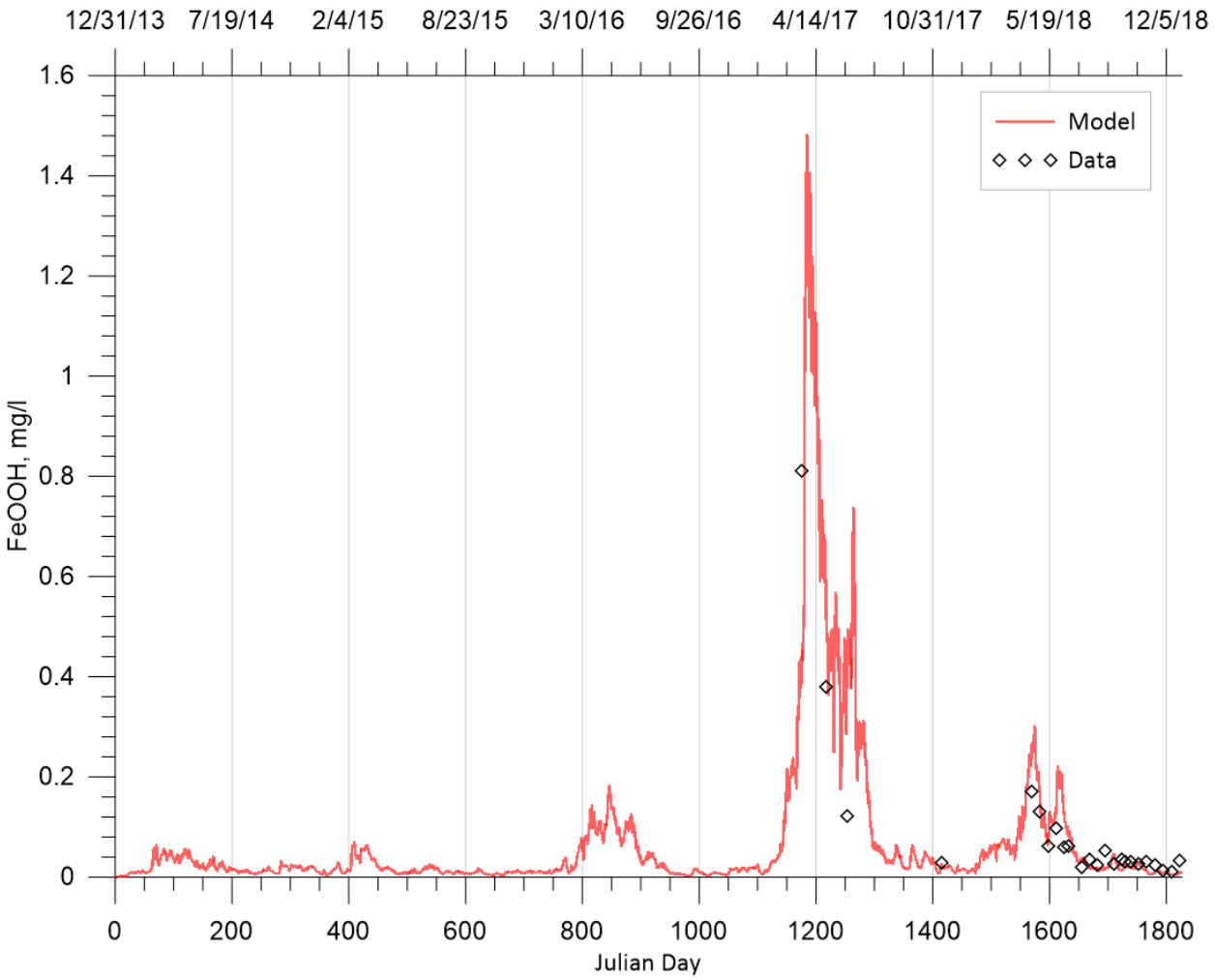


Figure 160. Oxbow Reservoir model outflow FeOOH compared to data.

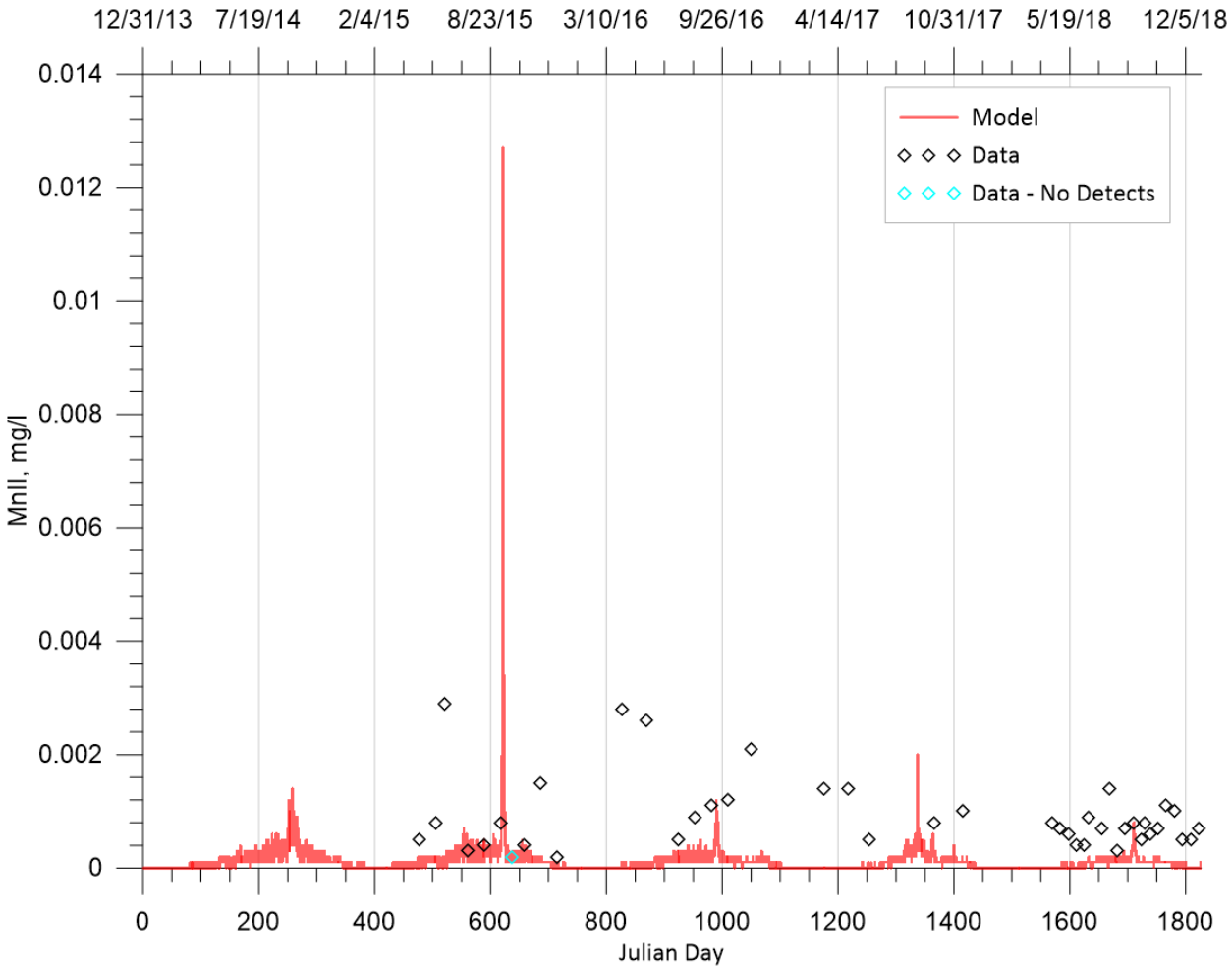


Figure 161. Oxbow Reservoir model outflow MnII compared to data.

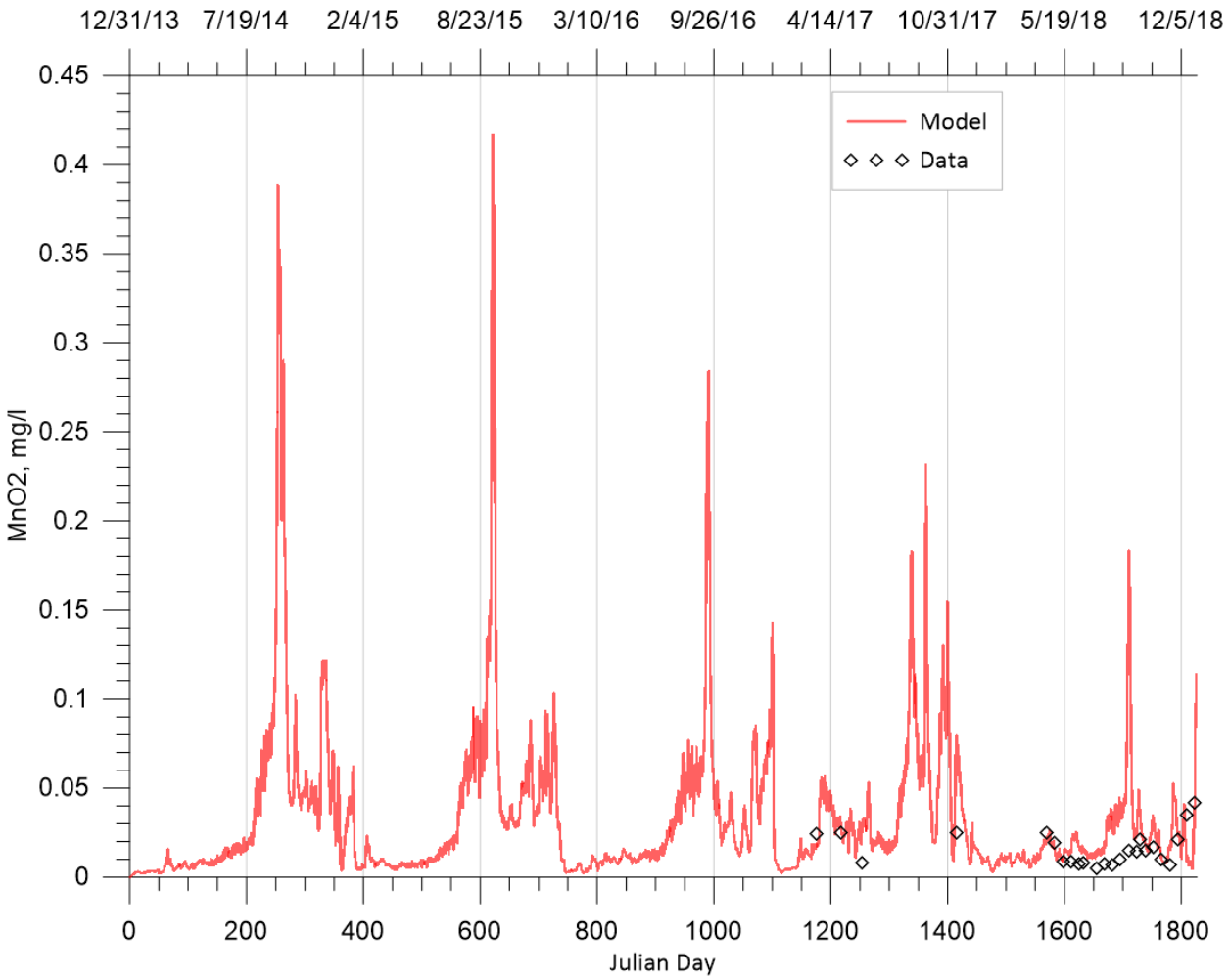


Figure 162. Oxbow Reservoir model outflow MnO2 compared to data.

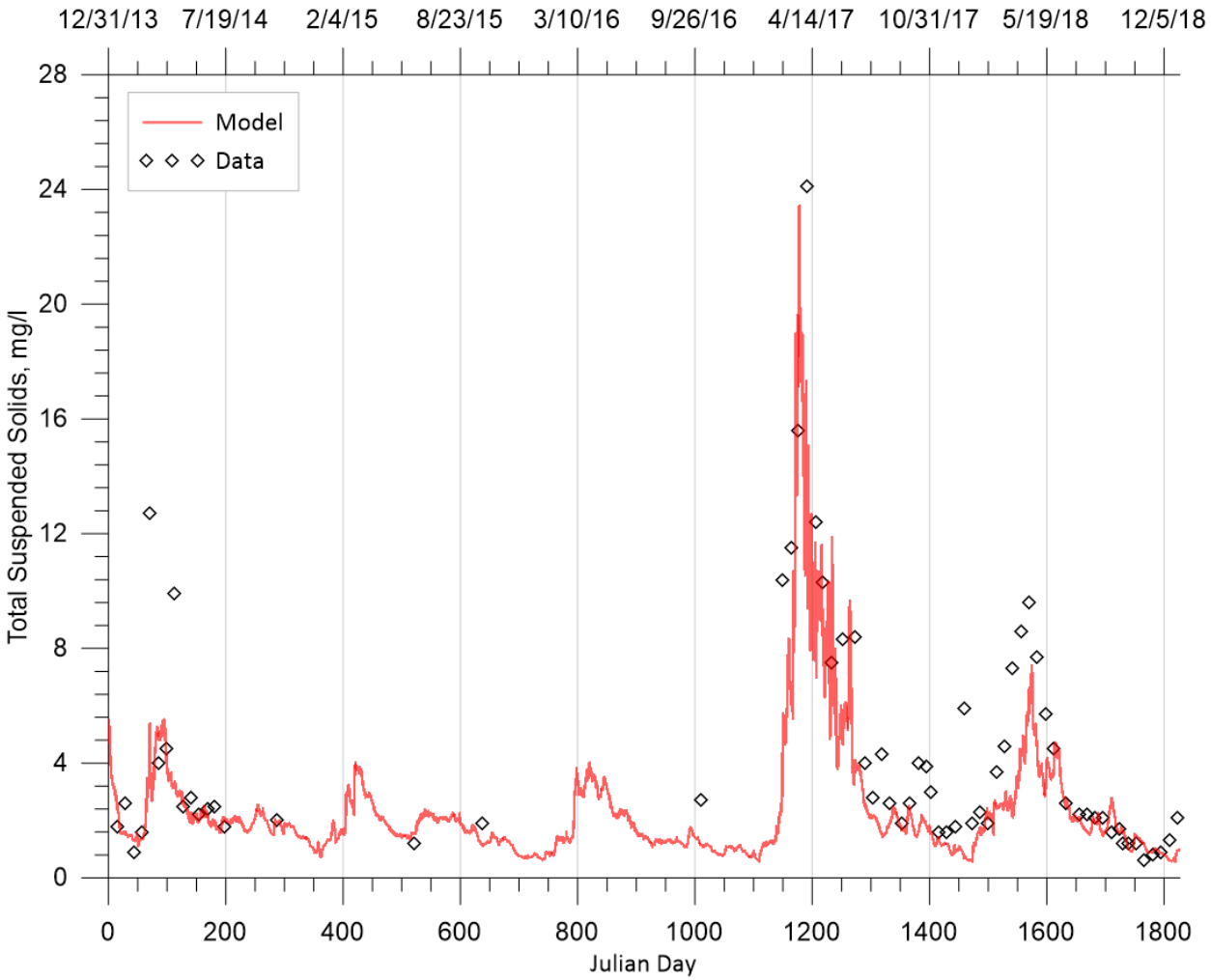


Figure 163. Oxbow Reservoir model outflow total suspended solids compared to data.

Analysis of Model Fluxes

Phosphorus and nitrogen mass balances are shown in the following section. Sources and sinks of dissolved oxygen, phosphorus, and nitrogen are also plotted below. The fluxes predicted by the model show the importance of different source-sink terms in the water quality mass balances.

Phosphorus and nitrogen mass balances for Oxbow Reservoir are shown in Figure 164 and Figure 165, respectively. Sources and sinks of dissolved oxygen, phosphorus, and nitrogen for Oxbow Reservoir are shown in Figure 166 through Figure 168. Sources are shown as positive values and sinks are shown as negative values. For Oxbow reaeration is the most important source/sink for dissolved oxygen. Reaeration is a sink when Oxbow is losing oxygen after large spill events and is a source when gaining oxygen during low-dissolved oxygen summer releases from Brownlee. Nitrogen and phosphorus inflows are largely

balanced by outflows. Algae and periphyton dynamics and organic matter decay are major source/sink terms for N and P. Nitrification is also an important process in Oxbow for N.

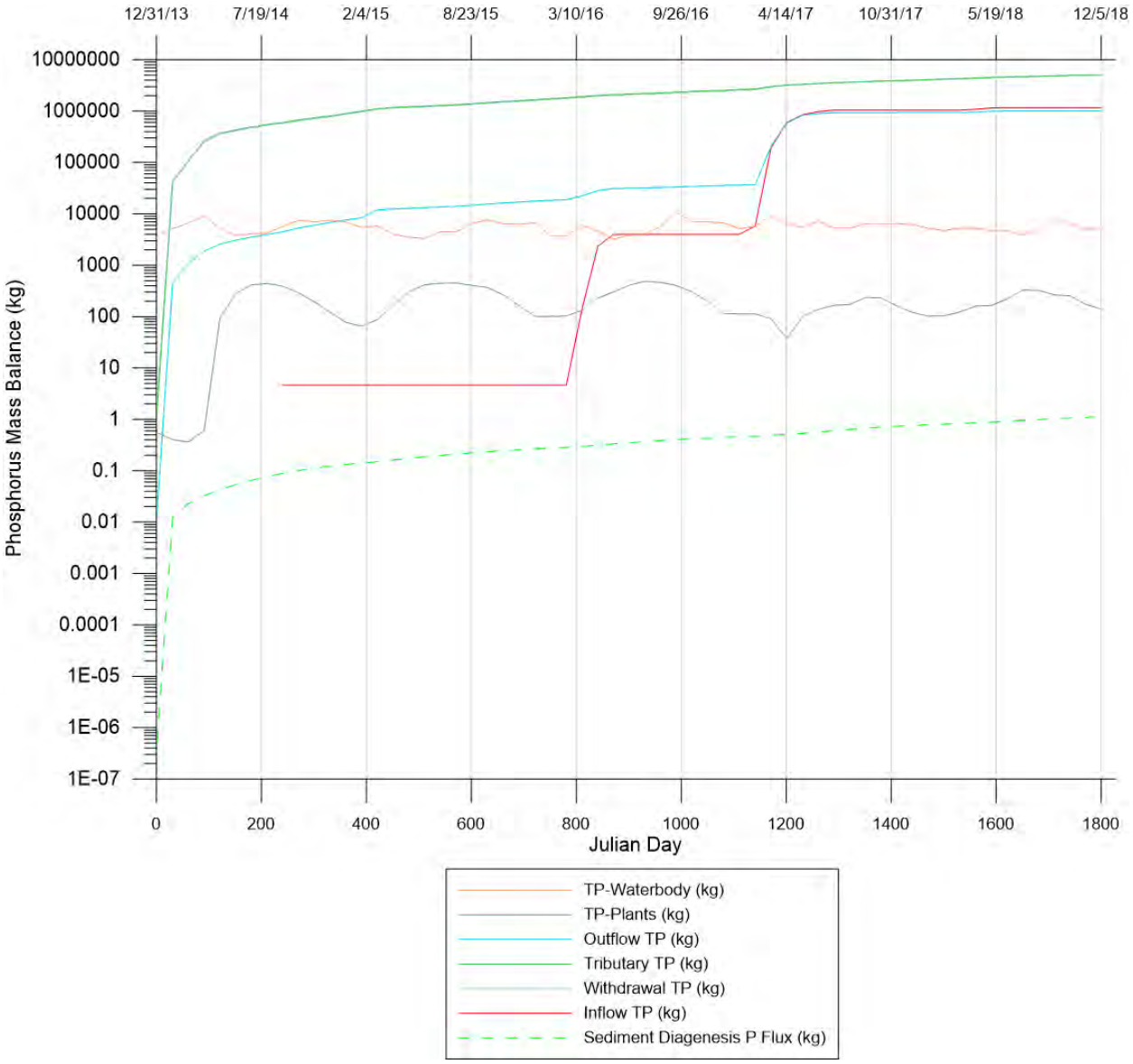


Figure 164. Cumulative phosphorus mass in Oxbow Reservoir. TP in the waterbody, sediment and plants shows the current amount of TP as a function of time. Inflow TP is Brownlee spill. Outflow TP is Oxbow bypass flow and spill. The Withdrawal TP (Oxbow powerhouse flows) is nearly identical to the Tributary TP (powerhouse inflow from Brownlee Reservoir and Wildhorse River) and falls on the same line.

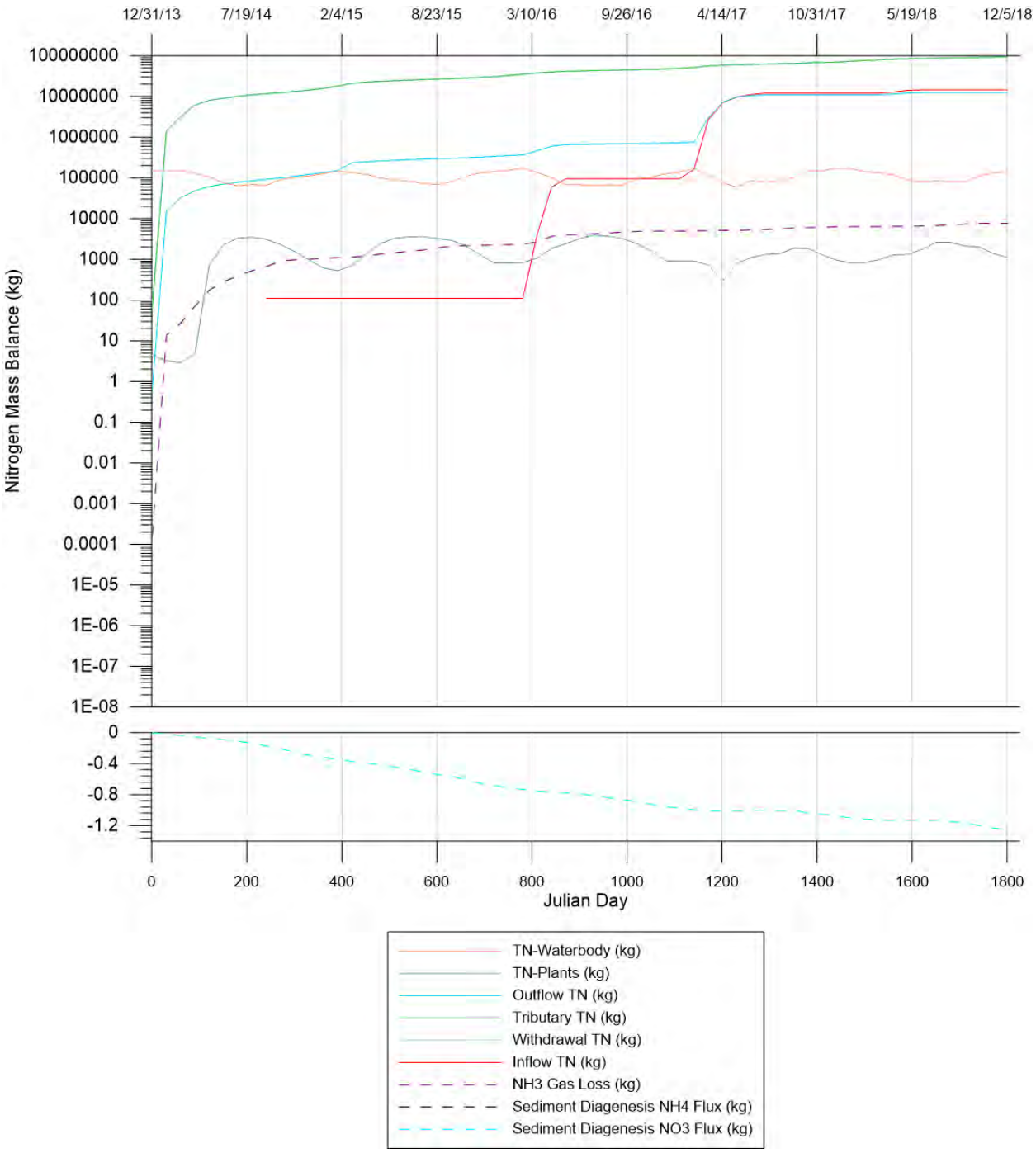


Figure 165. Cumulative nitrogen mass in Oxbow Reservoir. TN in the waterbody, sediment, and plants show the current amount of TN as a function of time. Inflow TN is Brownlee spill. Outflow TN is Oxbow bypass flow and spill. The Withdrawal TN (Oxbow powerhouse flows) is nearly identical to the Tributary TN (powerhouse inflow from Brownlee Reservoir and Wildhorse River) and falls on the same line.

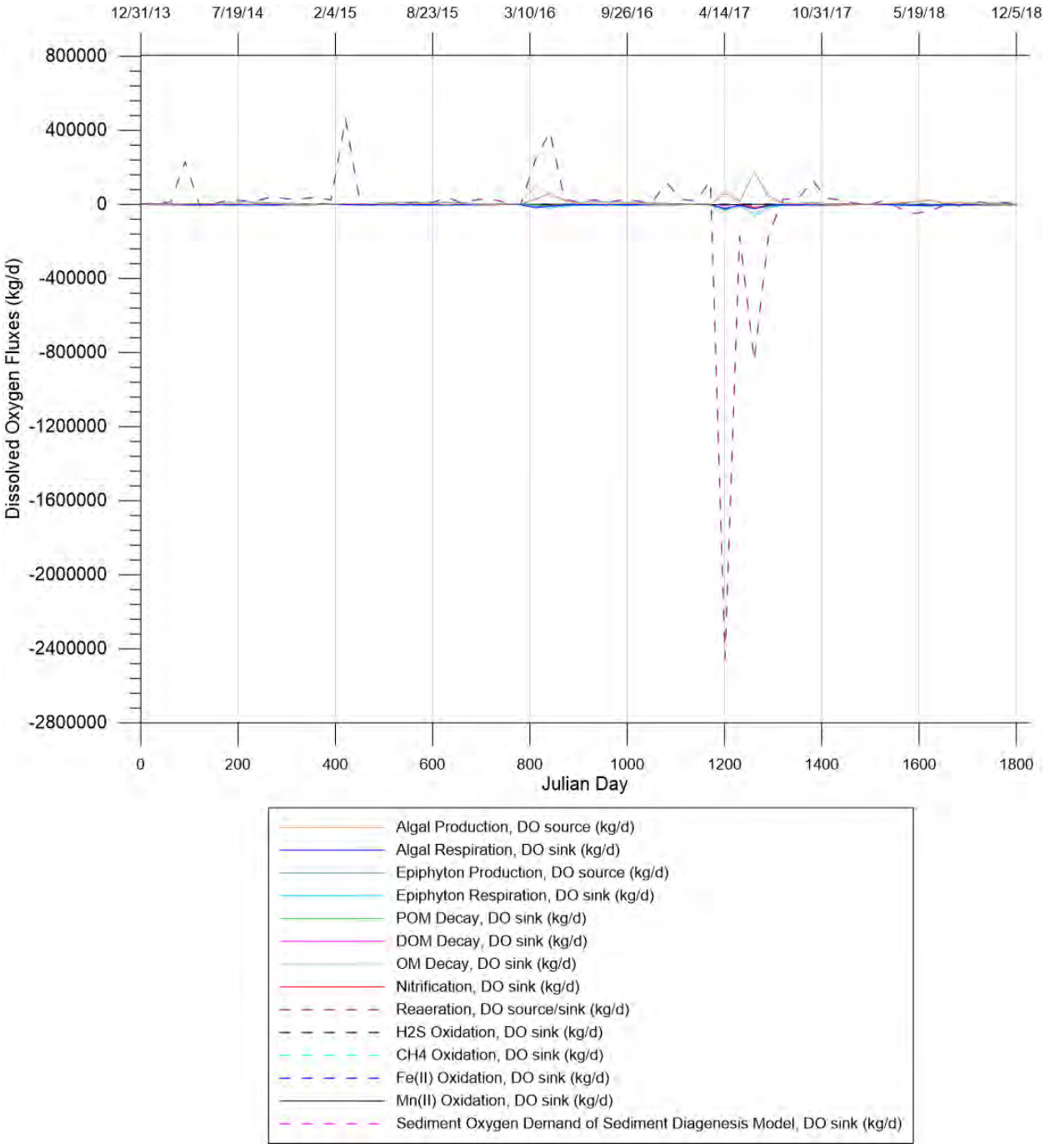


Figure 166. Dissolved oxygen sources and sinks in Oxbow Reservoir.

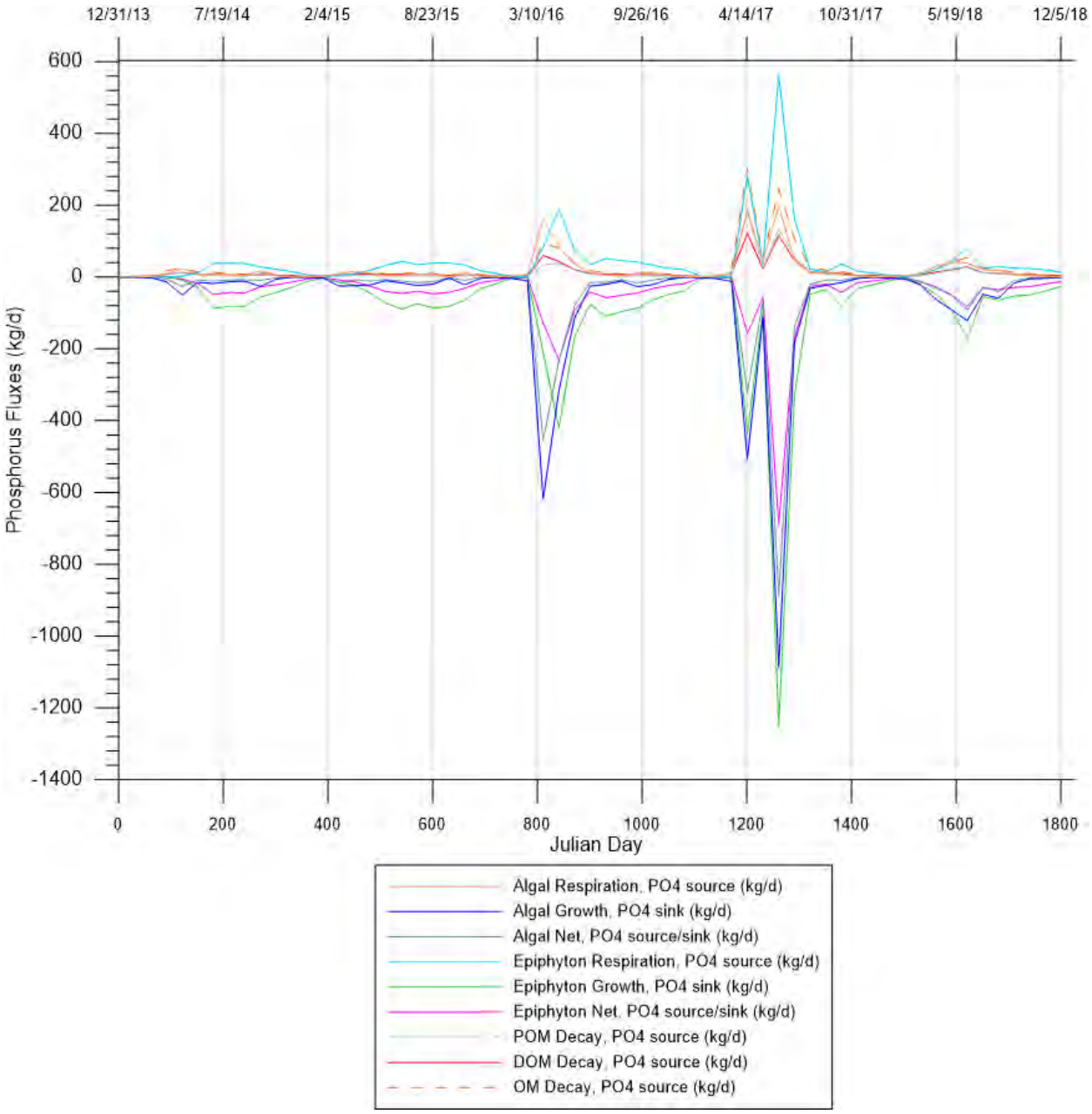


Figure 167. Phosphorus sources and sinks in Oxbow Reservoir.

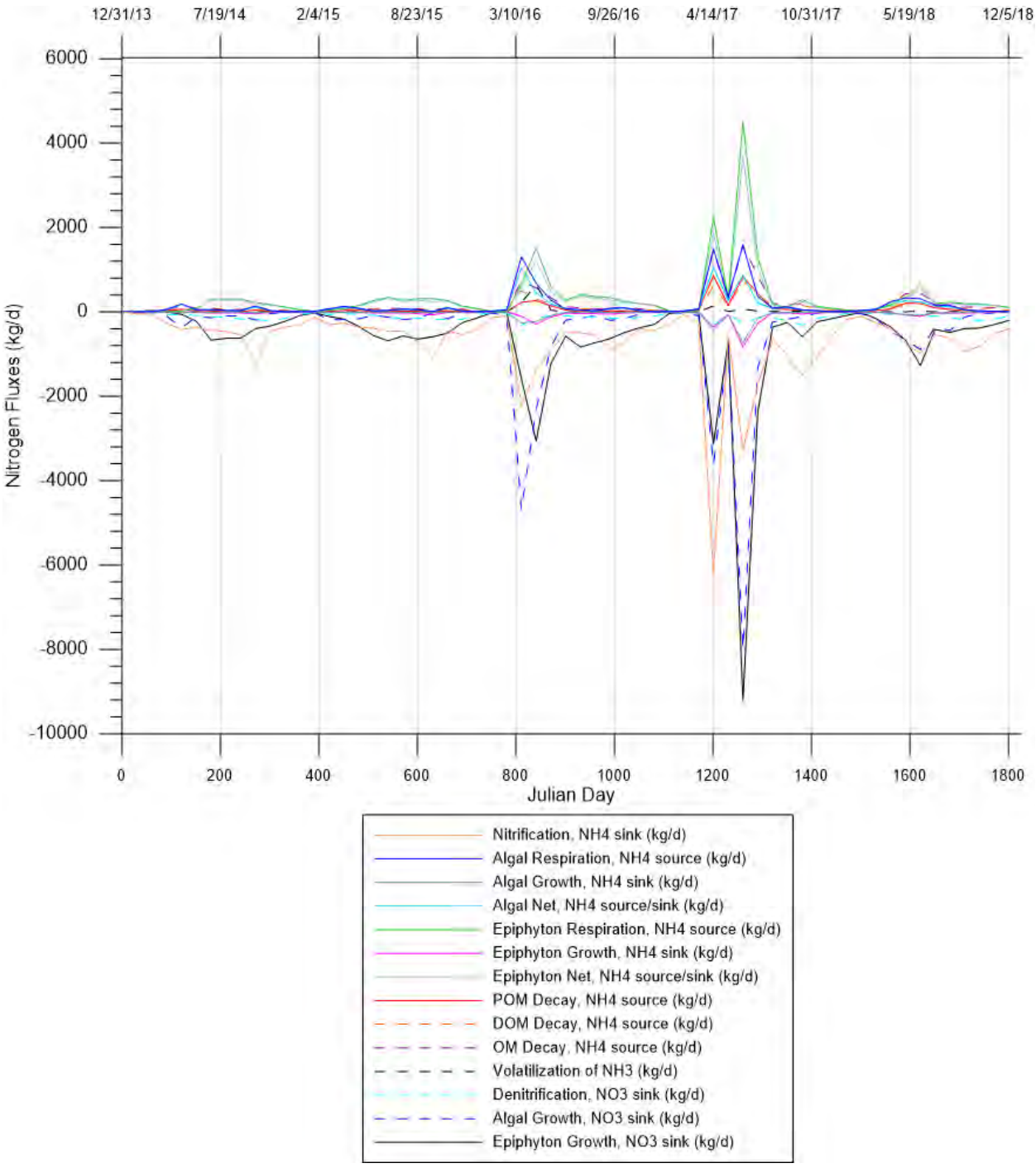


Figure 168. Nitrogen sources and sinks in Oxbow Reservoir.

Sediment Nutrient Concentrations

The sediment diagenesis model computes concentrations of particulate organic carbon, nitrogen, and phosphorus (POC, PON, and POP) in the sediments over time for each model segment. These concentrations are shown in Figure 169 and Figure 170 for select segments. Both labile and refractory pools are shown. Both the labile and refractory pools of particulate organic carbon, nitrogen, and

phosphorus fluctuate seasonally throughout the simulation period, but the fluctuation is relatively consistent between years.

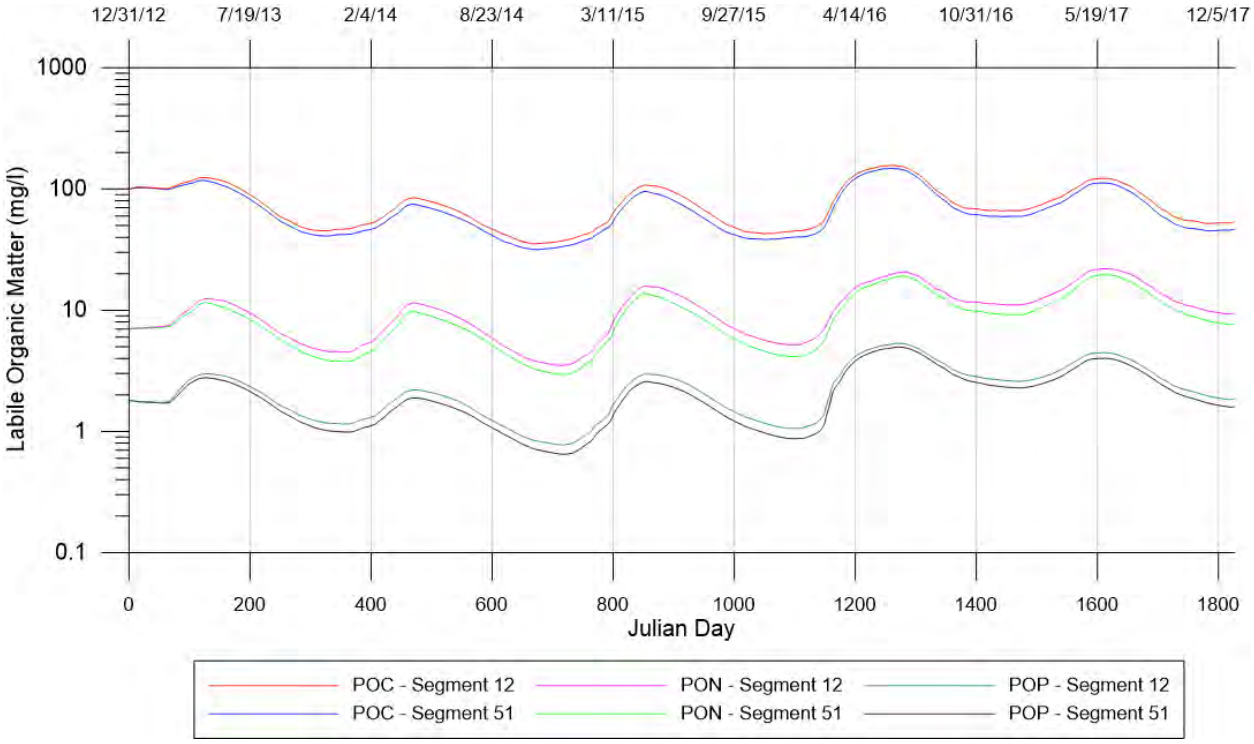


Figure 169. Labile POC, PON, POP at segments 12 and 51 in Oxbow Reservoir.

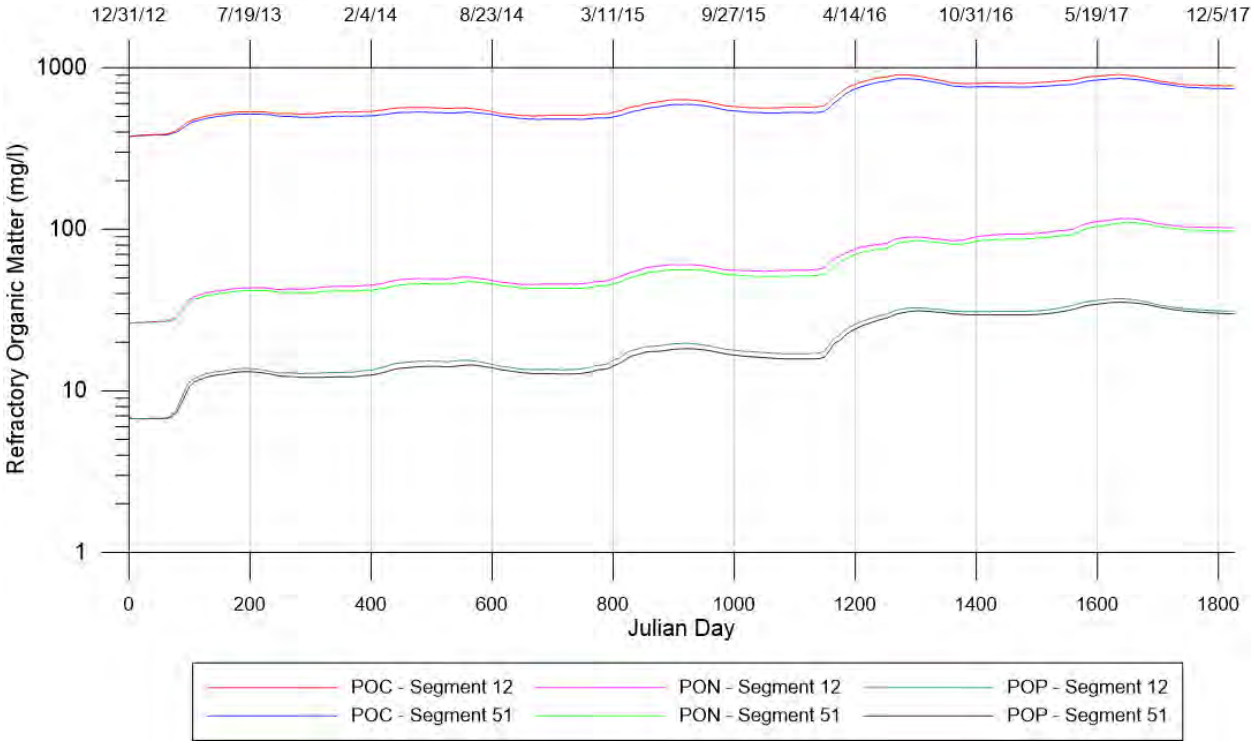


Figure 170. Refractory POC, PON, POP at segments 12 and 51 in Oxbow Reservoir.

Hells Canyon Reservoir

Water Quality Model-Data Comparisons

The outflow dissolved oxygen was measured at the penstock intake for the turbines, so only turbine (turbine and baseflow) dissolved oxygen were used for outflow model comparisons. All other data for Hells Canyon were measured at river mile 246.9 (about one mile downstream of the Hells Canyon dam), so the total combined dam outflow (turbine, baseflow, and spill) results were used for outflow comparisons to field data. Table 39 lists water quality error statistics for Hells Canyon Reservoir outflow. Table 40 lists water quality error statistics for Hells Canyon Reservoir vertical profiles. Table 41 lists water quality error statistics for Hells Canyon Reservoir sediment and porewater comparisons. Figure 171 through Figure 194 show the associated model-data outflow and sediment comparisons. Appendix A6 shows the associated model-data profile comparisons.

Table 39. Water quality error statistics for Hells Canyon Reservoir outflow.

Parameter	Model Average	# of data	ME	MAE	RMSE	MAE/Model Average
DO (mg/l)	9.062	247972	0.211	0.592	0.768	0.065
Chlorophyll a (ug/l)	3.407	119	-3.011	4.600	7.221	1.350
Chloride (mg/l)	17.595	63	0.172	1.628	2.563	0.093
DOC (mg/l)	2.675	111	0.101	0.206	0.262	0.077
FeII (mg/l)	0.004	38	0.000	0.002	0.003	0.500
FeOOH (mg/l)	0.066	24	-0.045	0.063	0.155	0.955
MnII (mg/l)	0.000	40	-0.002	0.002	0.003	N/A
MnO2 (mg/l)	0.033	24	0.008	0.016	0.019	0.485
Ammonia (mg/l)	0.037	89	-0.005	0.023	0.031	0.622
Nitrate (mg/l)	1.117	196	0.064	0.131	0.163	0.117
Ortho-phosphate (mg/l)	0.063	177	0.017	0.020	0.025	0.317
POC (mg/l)	0.461	4	-0.139	0.139	0.149	0.302
Sulfate (mg/l)	40.463	138	0.967	2.417	3.769	0.060
TKN (mg/l)	0.396	140	0.076	0.134	0.172	0.338
Total Phosphorus (mg/l)	0.086	142	0.021	0.023	0.026	0.267
TSS (mg/l)	2.036	111	-1.702	1.834	2.499	0.901
TIC (mg/l)	41.068	4	2.743	2.743	3.292	0.067
H2S (mg/l)	0.003	0	N/A	N/A	N/A	N/A
PON (mg/l)	0.056	4	-0.036	0.036	0.039	0.643
Zooplankton (mg/l)	0.120	0	N/A	N/A	N/A	N/A
POC (estimated from VSS data) (mg/l)	0.461	33	-0.388	0.607	0.946	1.317

Table 40. Water quality error statistics for Hells Canyon Reservoir vertical profiles.

Parameter	# of Profiles	# of Data	ME	MAE	RMSE
Chloride (mg/l)	33	161	0.190	1.456	1.640
H2S (mg/l)	2	6	-1.678	1.678	2.136
Sulfate (mg/l)	33	161	1.130	3.203	3.786
Fe(II) (mg/l)	33	136	-0.002	0.008	0.011
FeOOH (mg/l)	7	36	-0.052	0.178	0.190
Mn(II) (mg/l)	33	154	-0.209	0.302	0.478
MnO2 (mg/l)	6	31	0.015	0.037	0.051
Ortho-phosphate (mg/l)	33	159	-0.020	0.065	0.091
Ammonia (mg/l)	N/A	N/A	N/A	N/A	N/A
Nitrate (mg/l)	33	148	-0.009	0.197	0.231
DO (mg/l)	35	3103	0.381	0.854	1.154
TIC (mg/l)	7	48	2.237	4.714	5.186
Zooplankton (mg/l)	2	13	-0.096	0.124	0.174
DOC (mg/l)	37	179	-0.003	0.232	0.282
POC (mg/l)	7	44	-0.251	0.274	0.350
PON (mg/l)	7	44	-0.054	0.055	0.069
TKN (mg/l)	N/A	N/A	N/A	N/A	N/A
Total Phosphorus (mg/l)	N/A	N/A	N/A	N/A	N/A
Chlorophyll a (µg/l)	N/A	N/A	N/A	N/A	N/A
TSS (mg/l)	16	89	-2.403	2.538	2.892
pH	35	3109	-0.248	0.316	0.333
Dissolved HgII (ng/l)	38	181	0.017	0.168	0.200
Dissolved MeHg (ng/l)	38	178	-0.418	0.418	0.710

Table 41. Water quality error statistics for Hells Canyon Reservoir sediment and porewater comparisons.

Parameter	Model Average	# of Data	ME	MAE	RMSE
PO4 - porewater (mg/l)	3.172	1	2.110	2.110	2.110
NO3 - porewater (mg/l)	0.058	2	0.012	0.022	0.024
NH4 - porewater (mg/l)	12.873	1	-5.010	5.010	5.010
PO4 - bottom of water column (mg/l)	0.050	6	-0.028	0.136	0.145
NO3 - bottom of water column (mg/l)	0.574	6	0.859	0.859	1.089
DOC - bottom of water column (mg/l)	0.963	6	-2.246	2.246	2.278

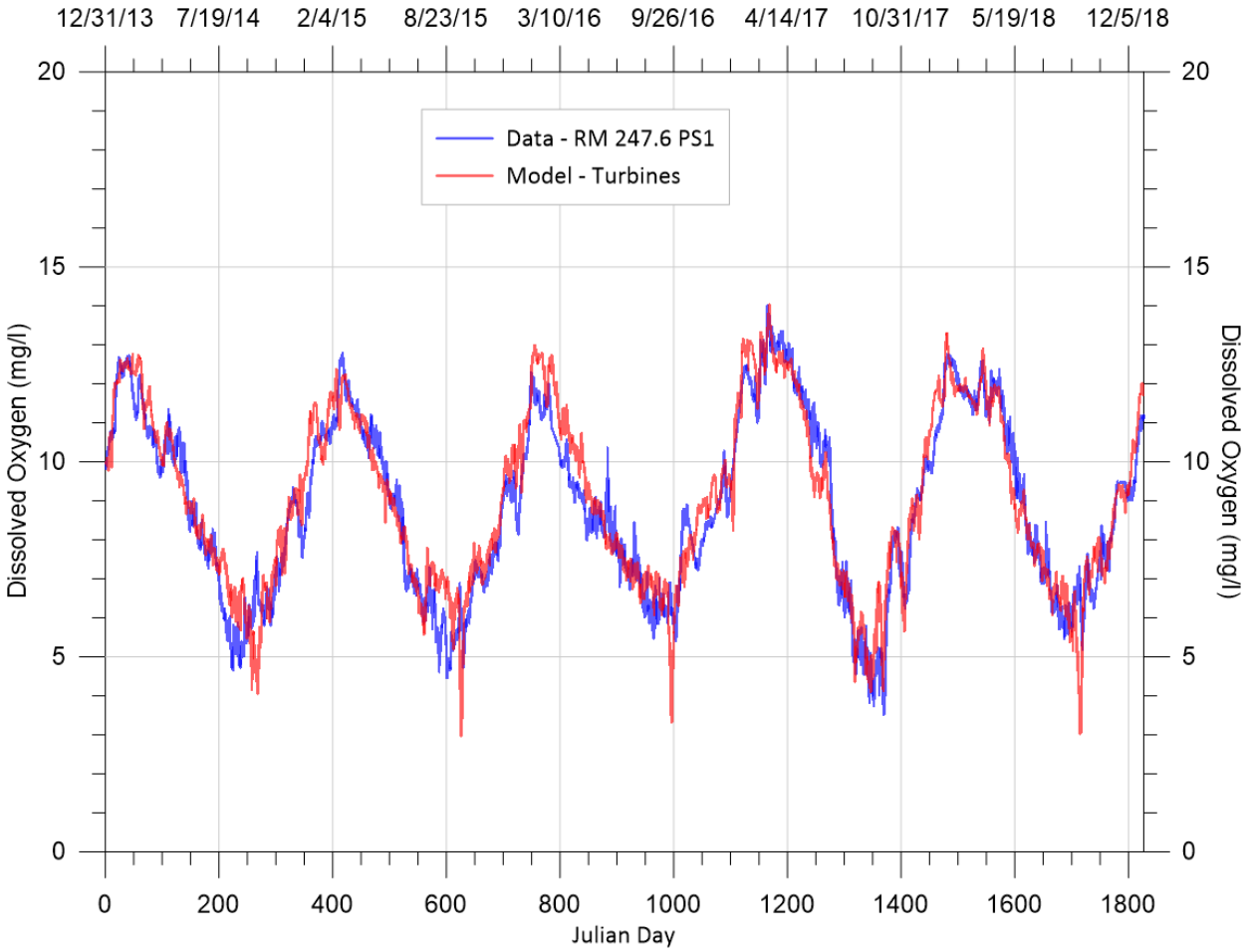


Figure 171. Hells Canyon Reservoir model outflow dissolved oxygen compared to data.

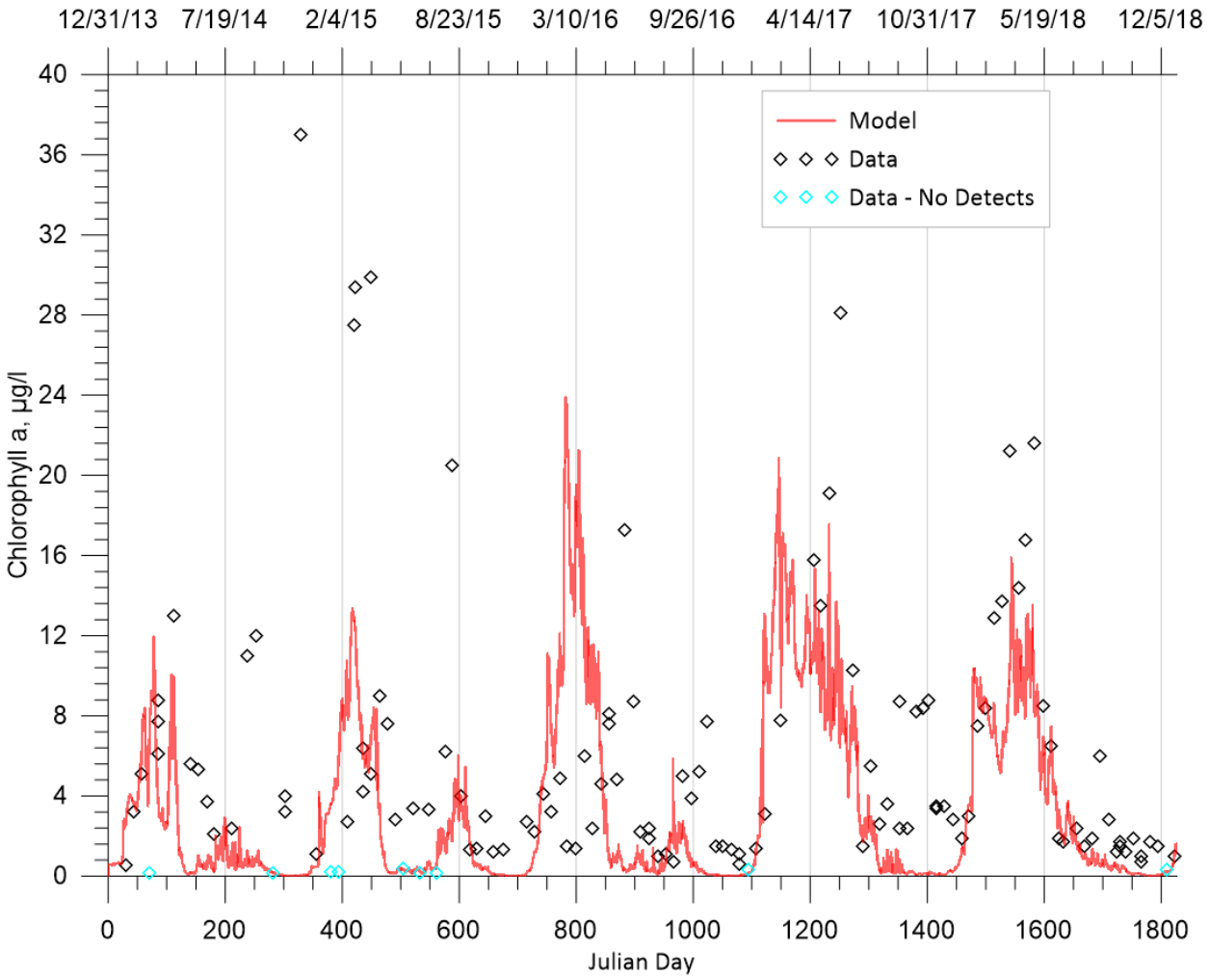


Figure 172. Hells Canyon Reservoir model outflow chlorophyll a compared to data.

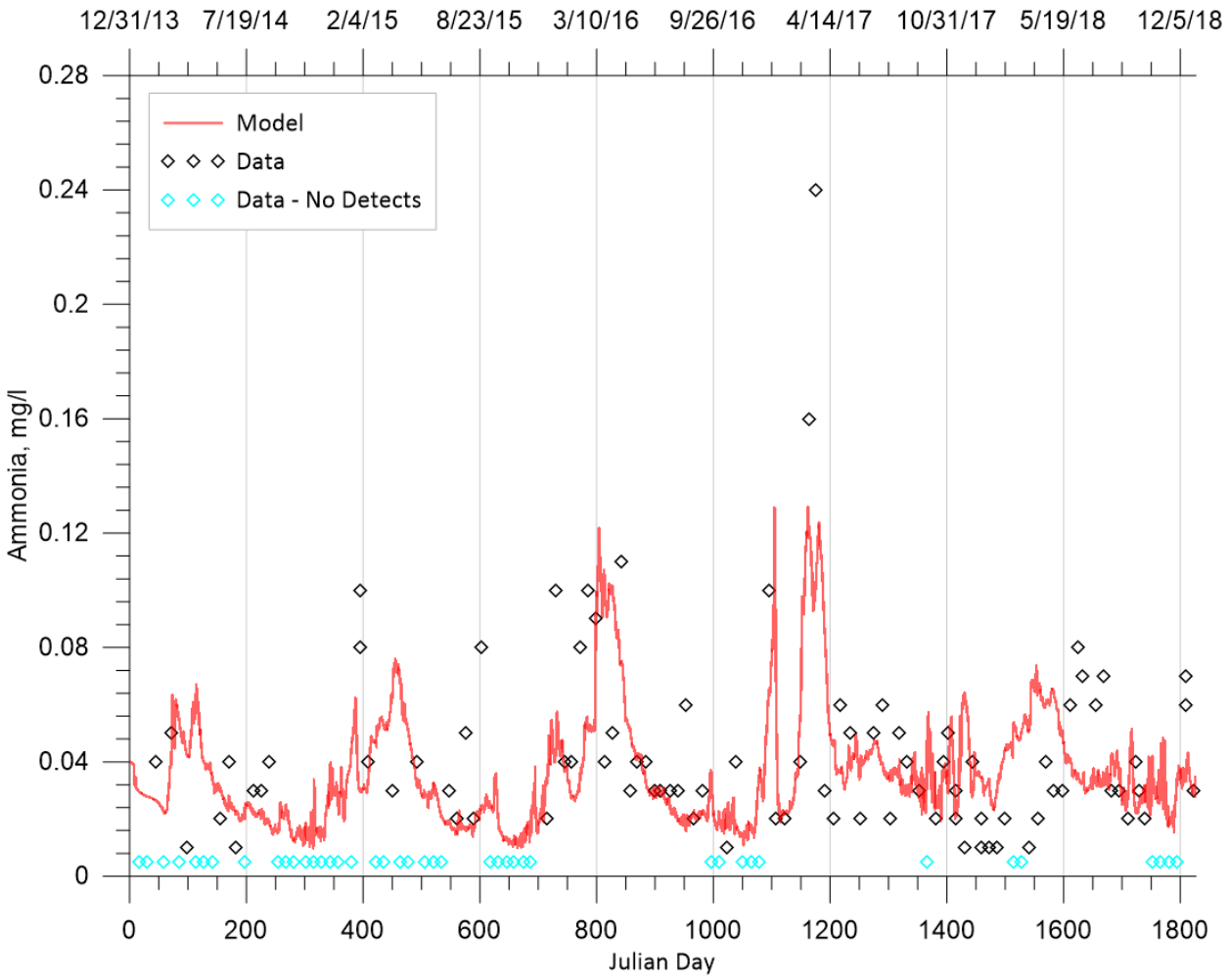


Figure 173. Hells Canyon Reservoir model outflow ammonia nitrogen compared to data.

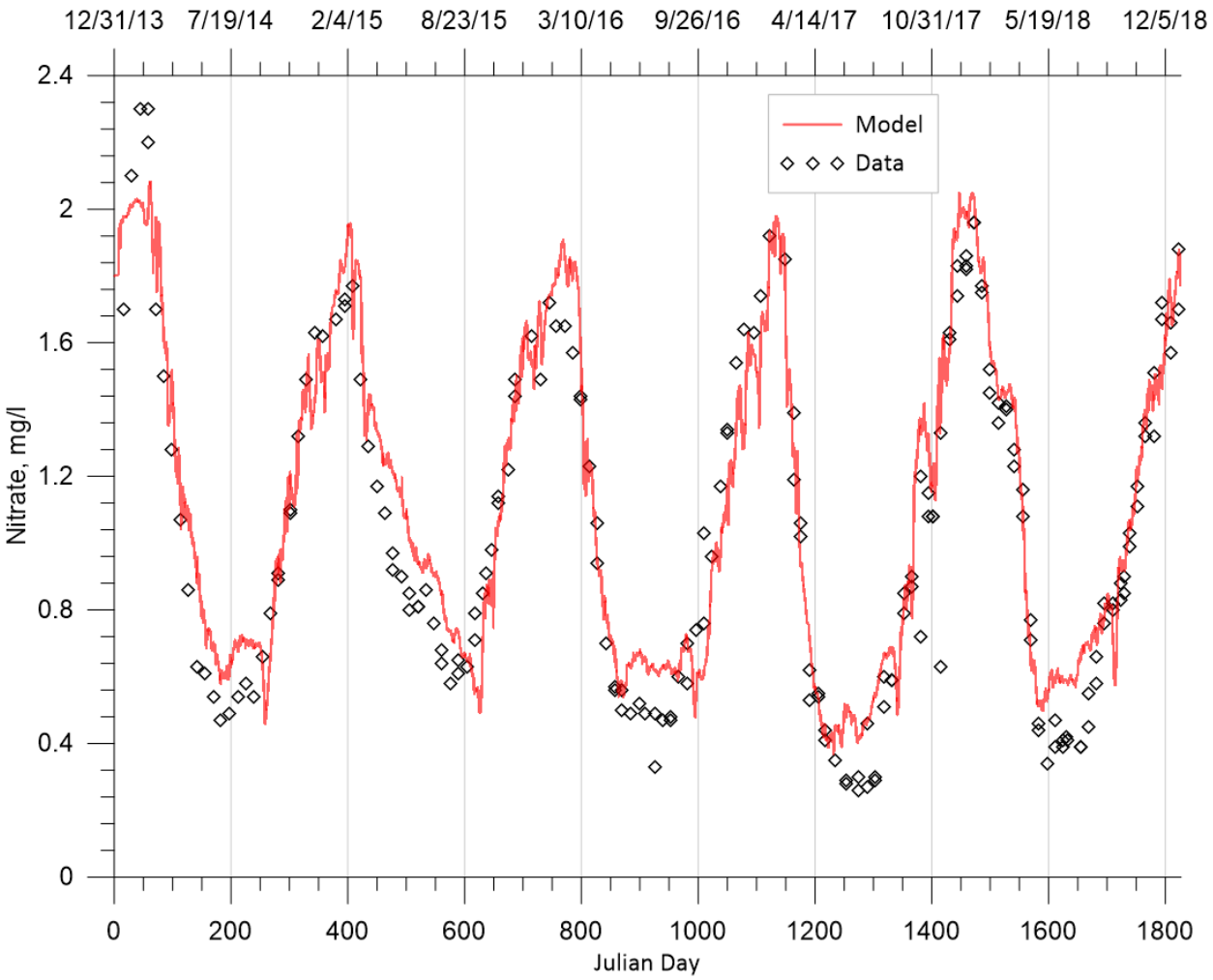


Figure 174. Hells Canyon Reservoir model outflow nitrate nitrogen compared to data.

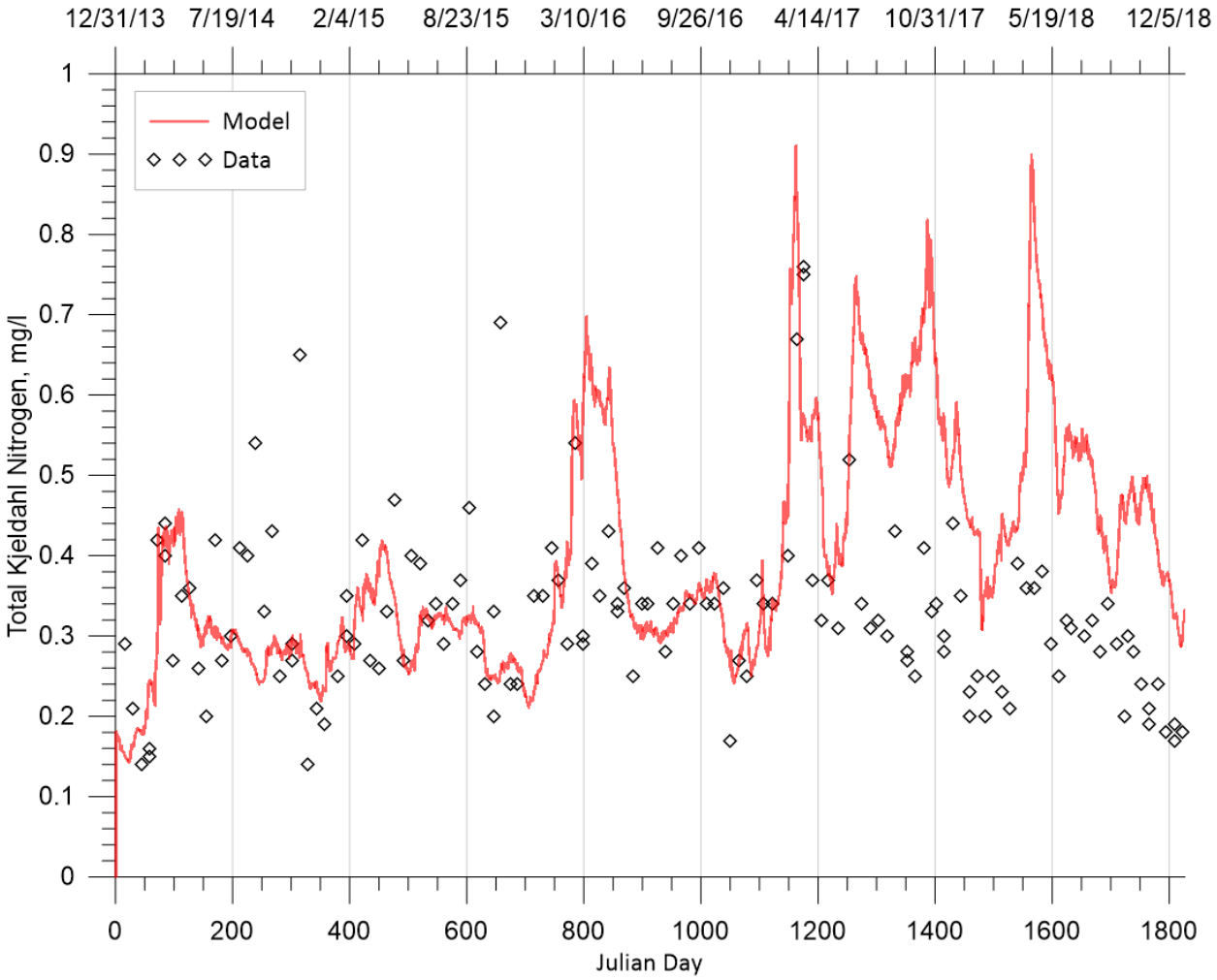


Figure 175. Hells Canyon Reservoir model outflow total Kjeldahl nitrogen compared to data.

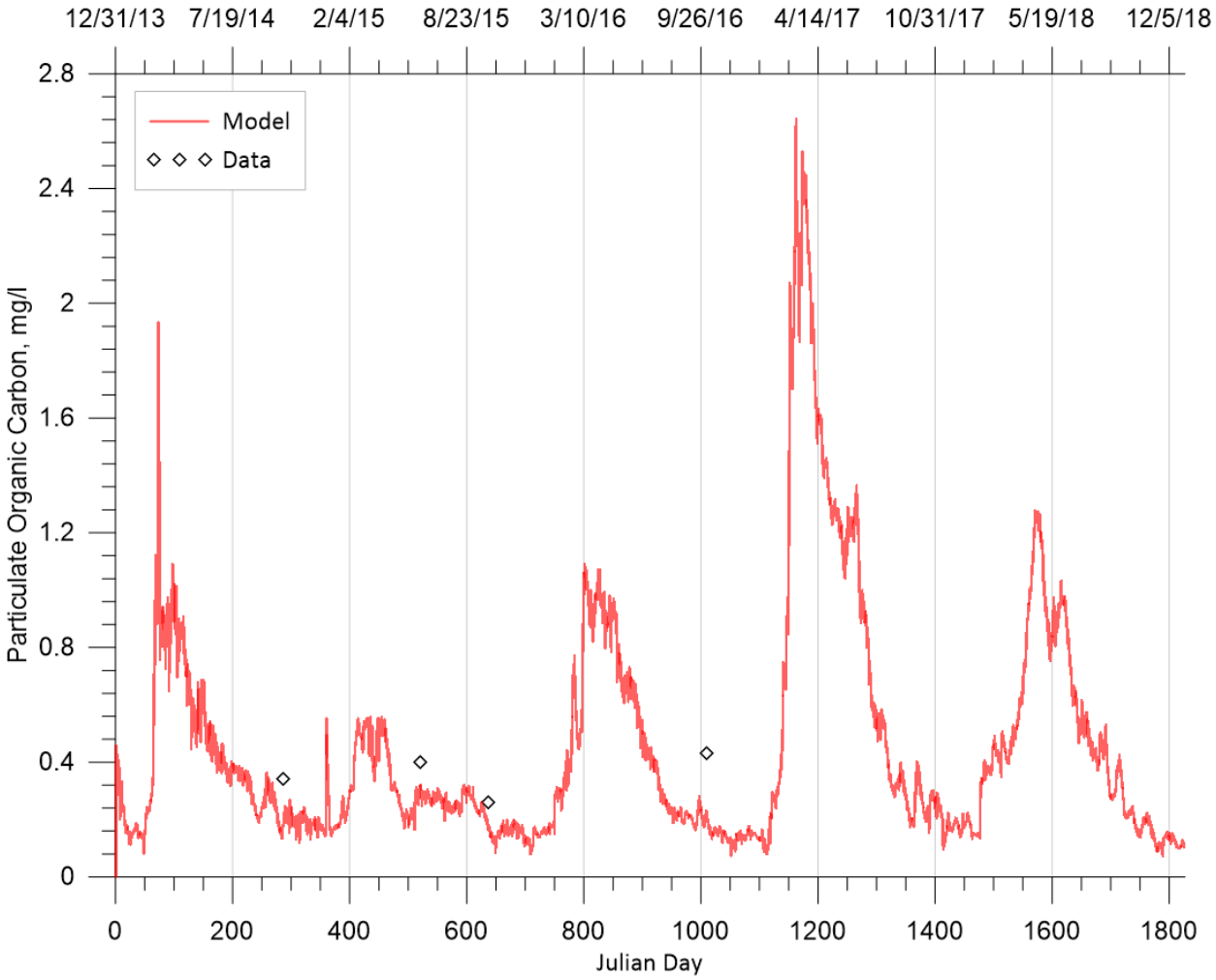


Figure 176. Hells Canyon Reservoir model outflow particulate organic nitrogen compared to data.

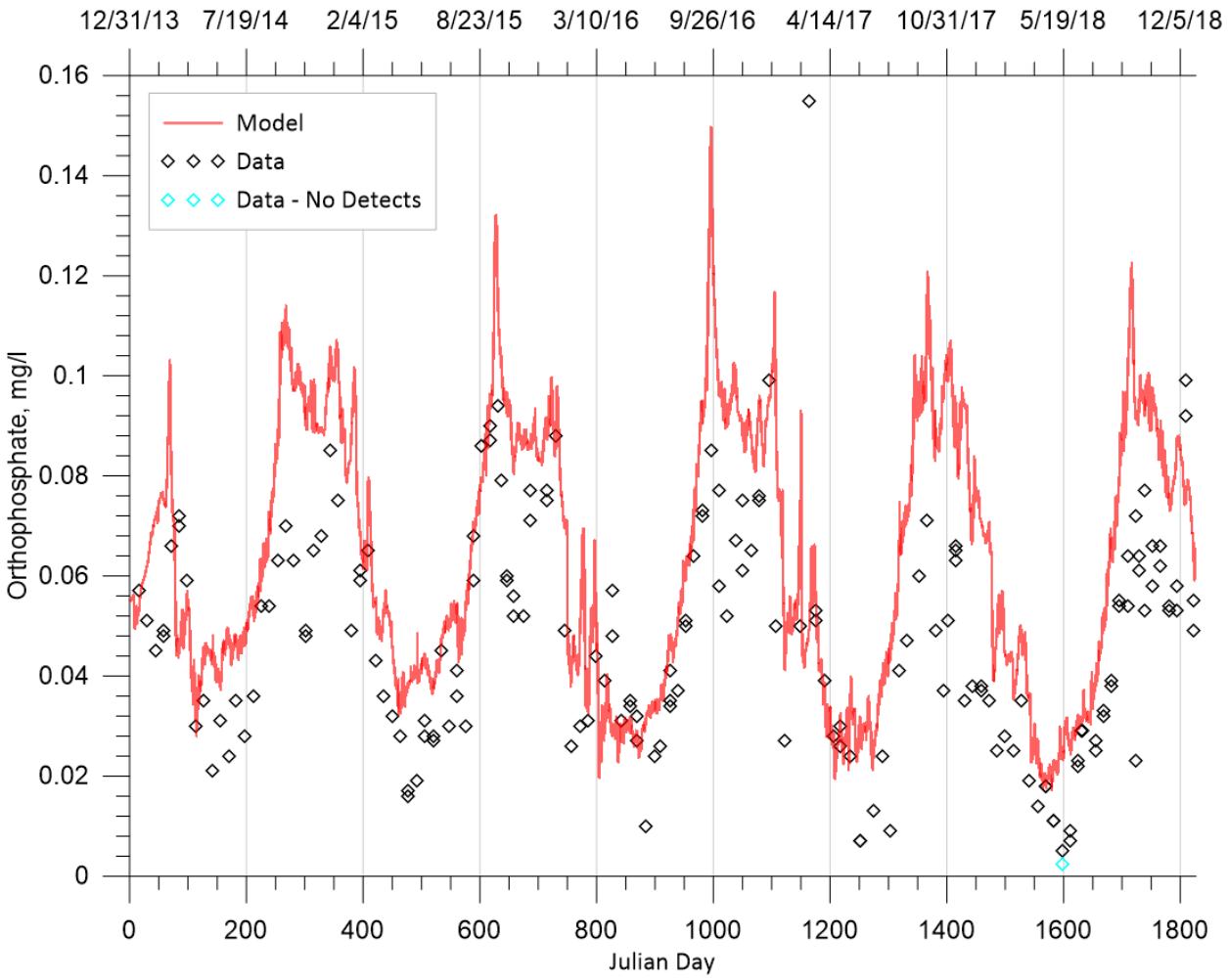


Figure 177. Hells Canyon Reservoir model outflow orthophosphate compared to data.

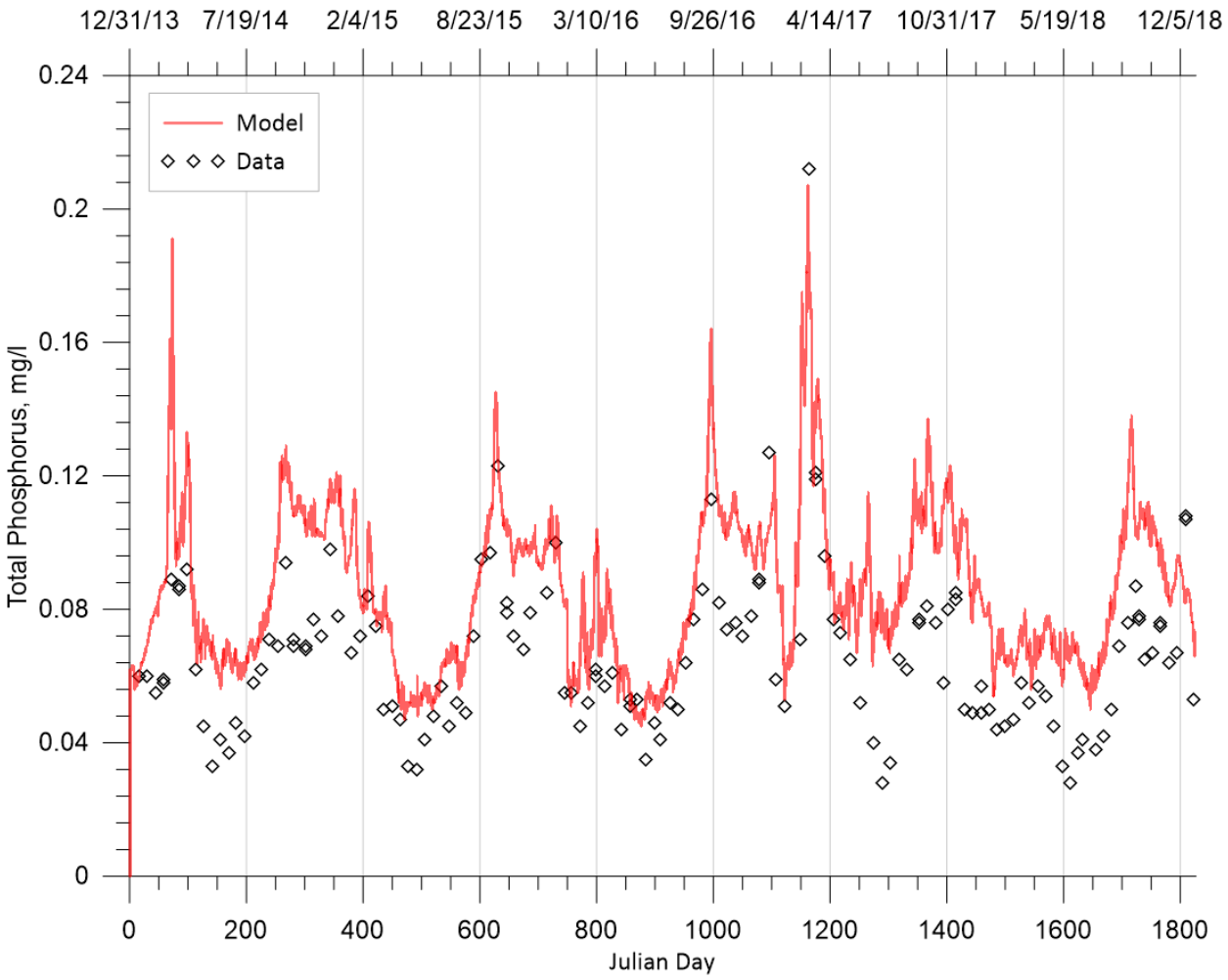


Figure 178. Hells Canyon Reservoir model outflow total phosphorus compared to data.

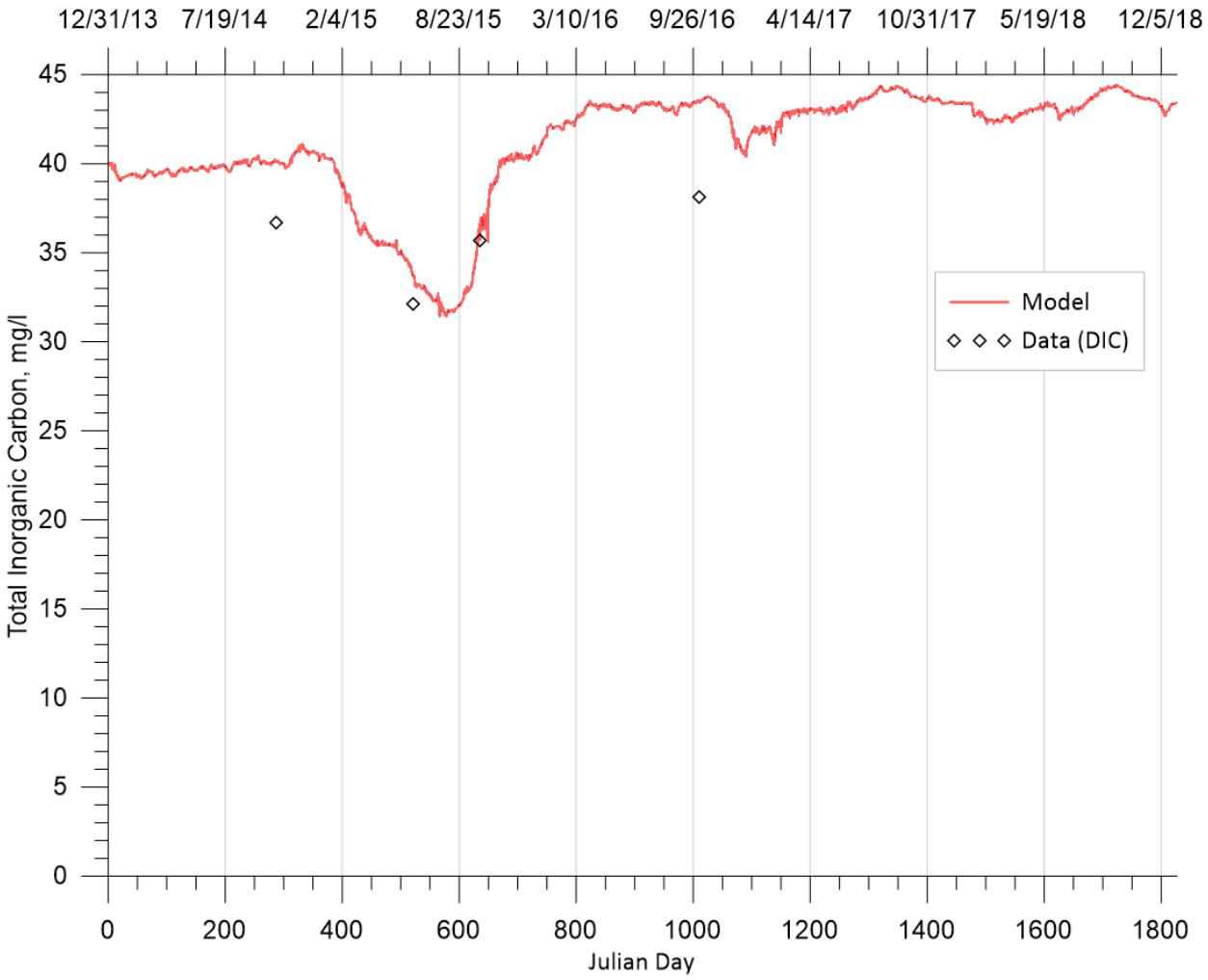


Figure 179. Hells Canyon Reservoir model outflow total inorganic carbon compared to data.

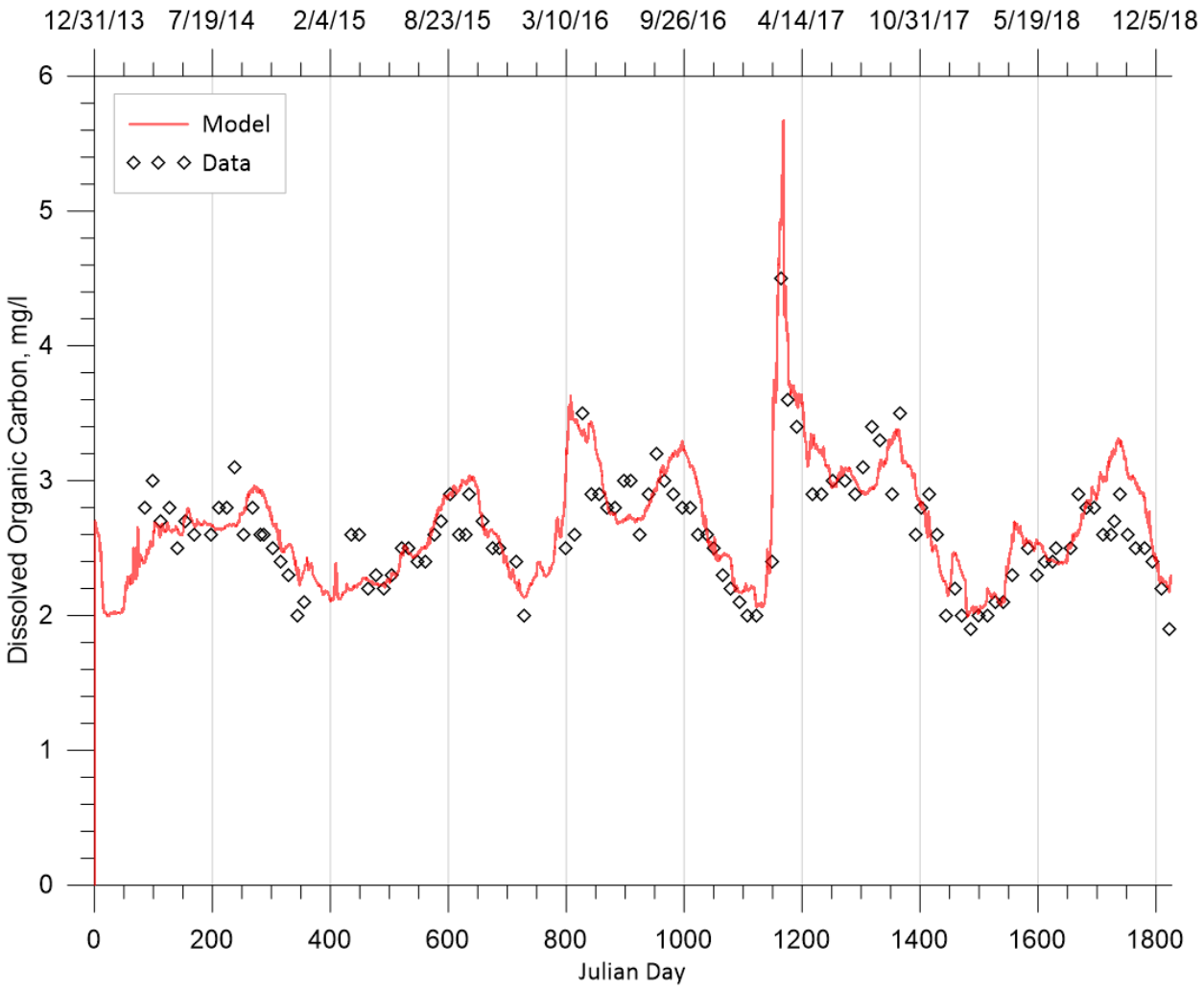


Figure 180. Hells Canyon Reservoir model outflow dissolved organic carbon compared to data.

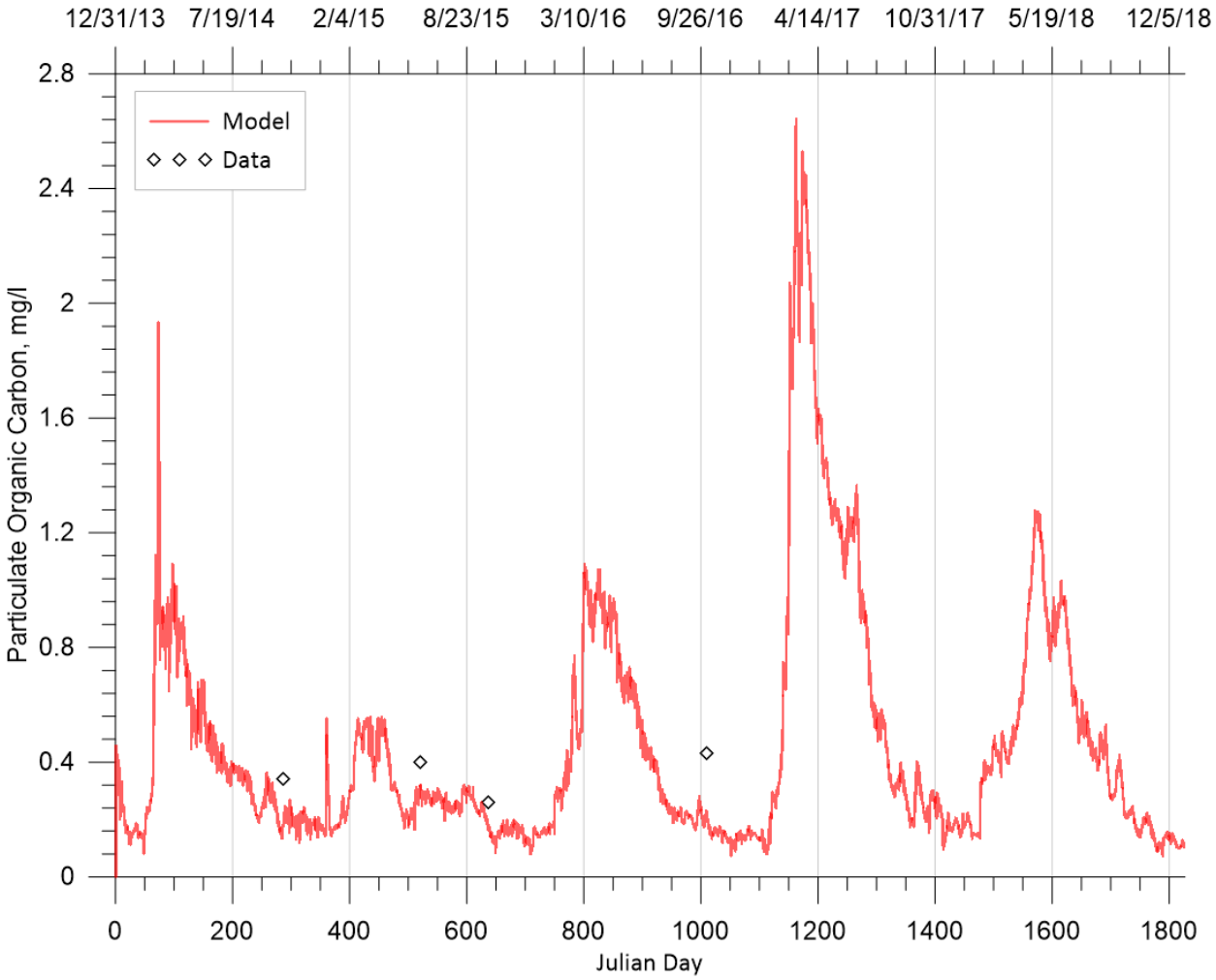


Figure 181. Hells Canyon Reservoir model outflow particulate organic carbon compared to data.

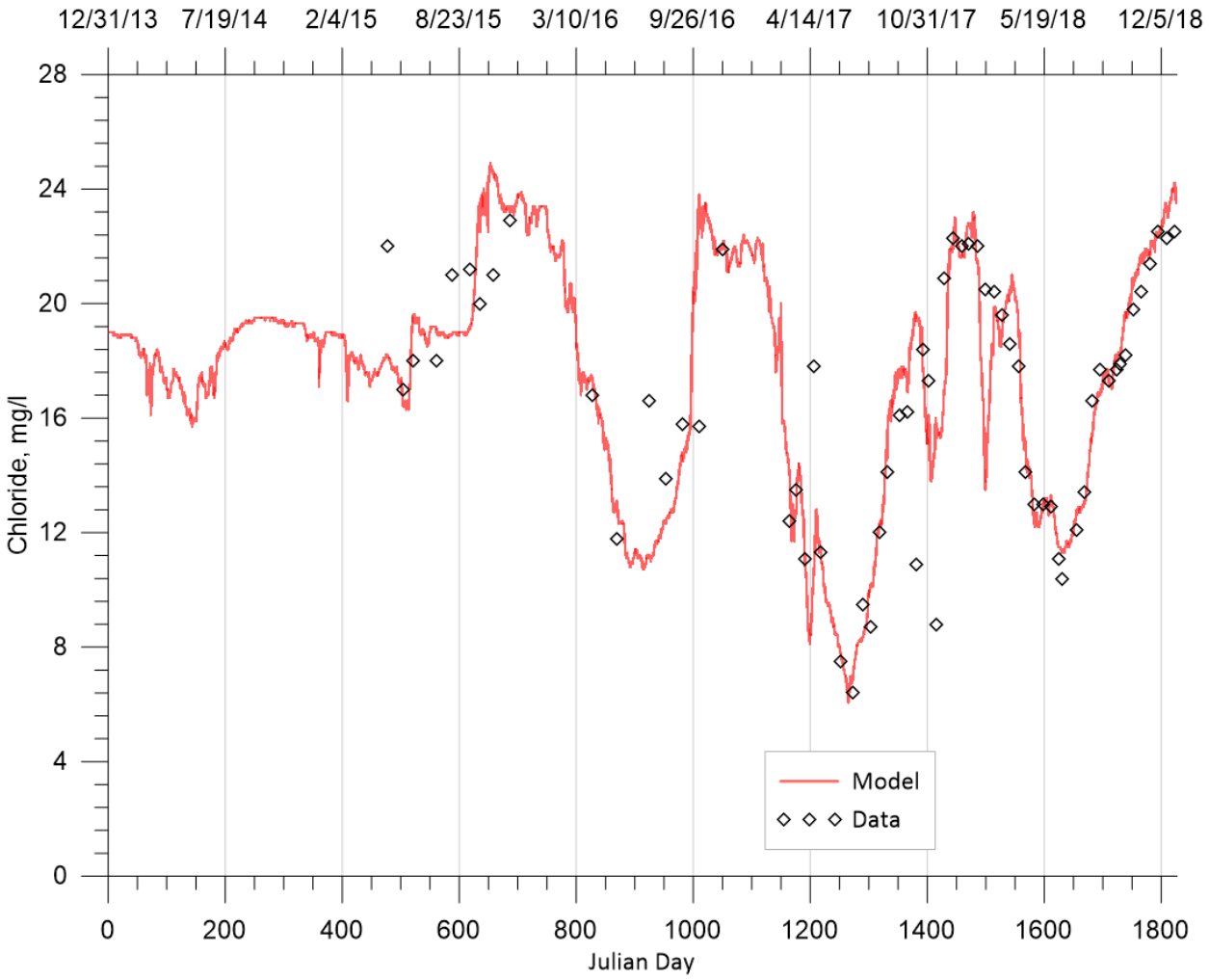


Figure 182. Hells Canyon Reservoir model outflow chloride compared to data.

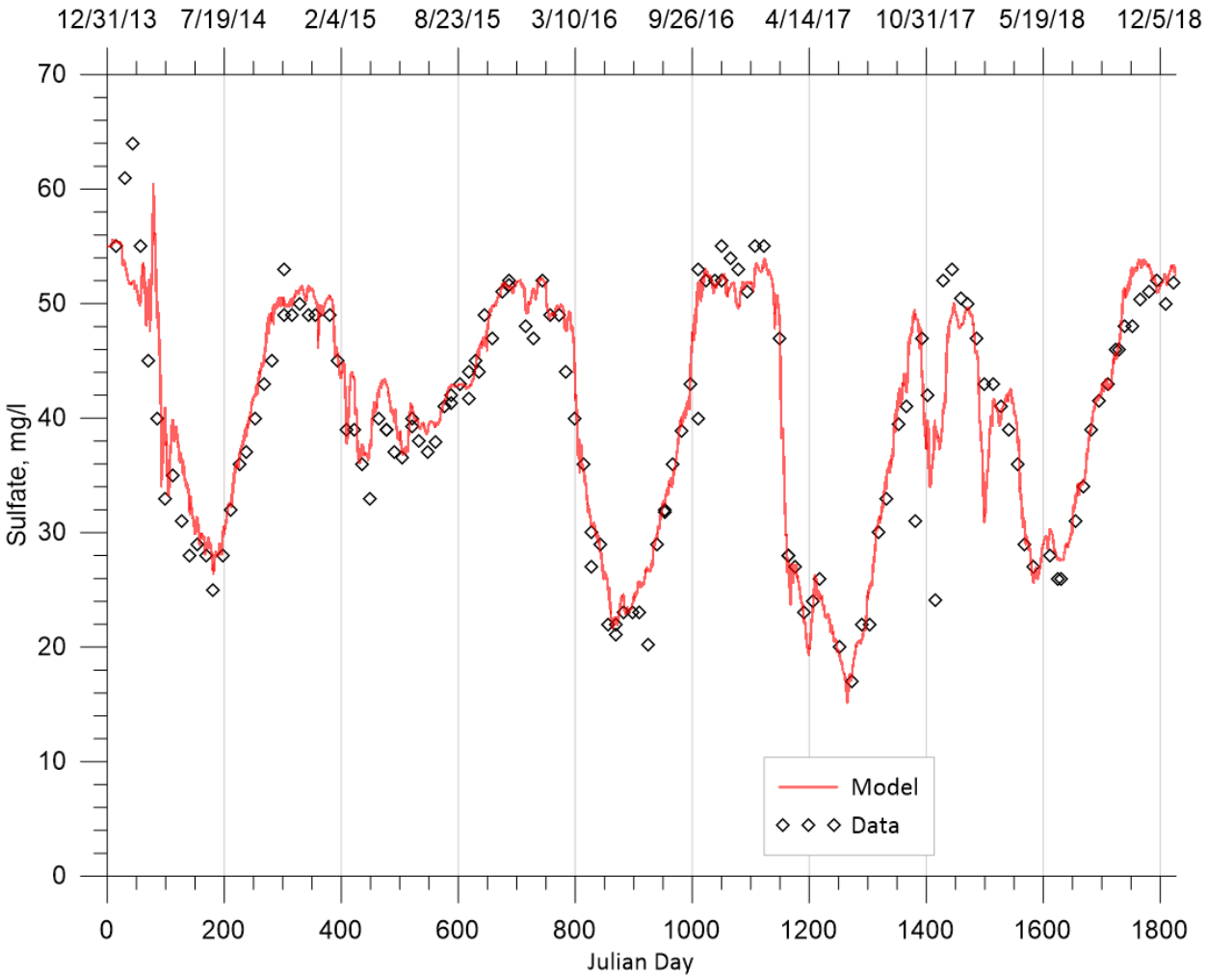


Figure 183. Hells Canyon Reservoir model outflow sulfate compared to data.

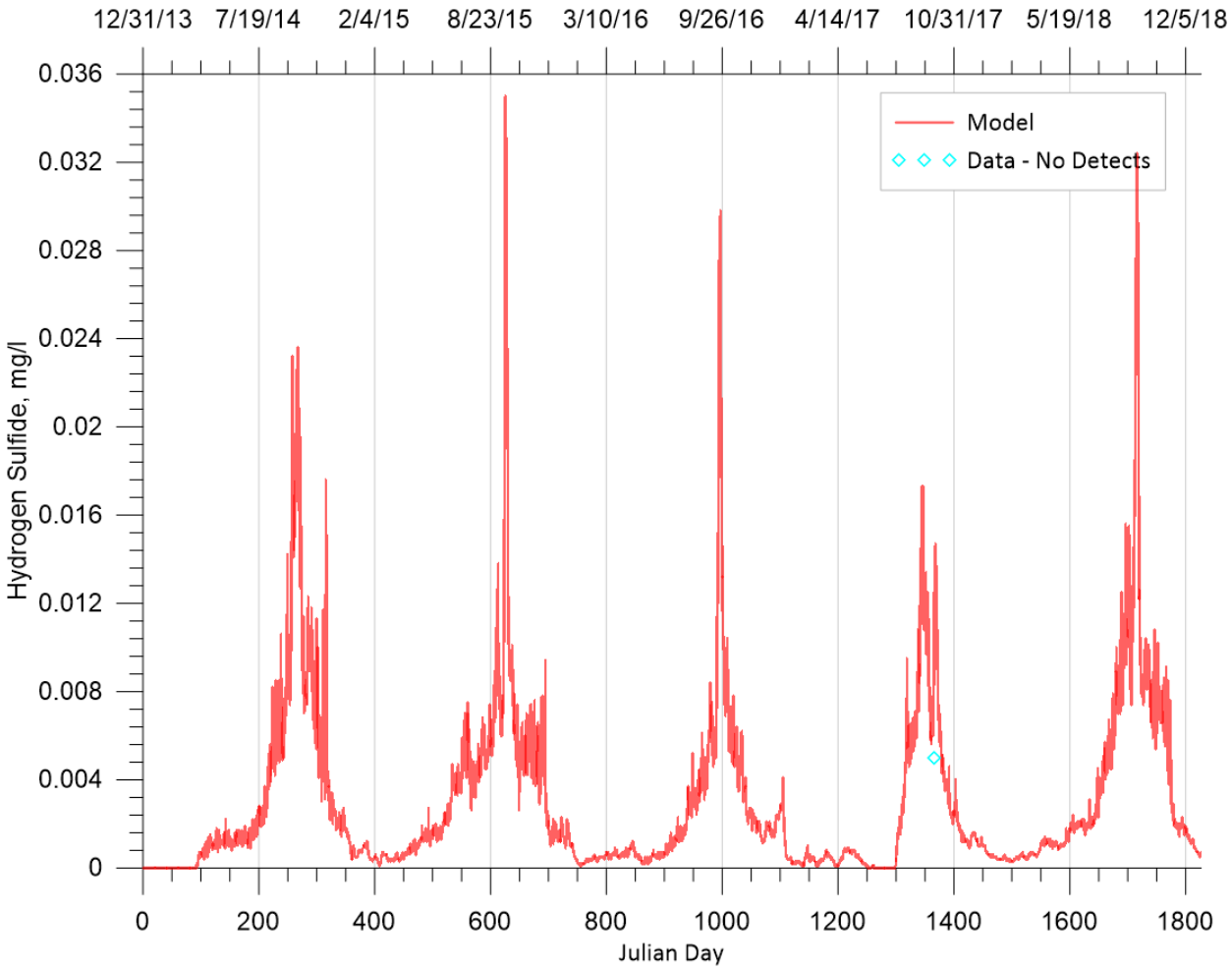


Figure 184. Hells Canyon Reservoir model outflow hydrogen sulfide compared to data.

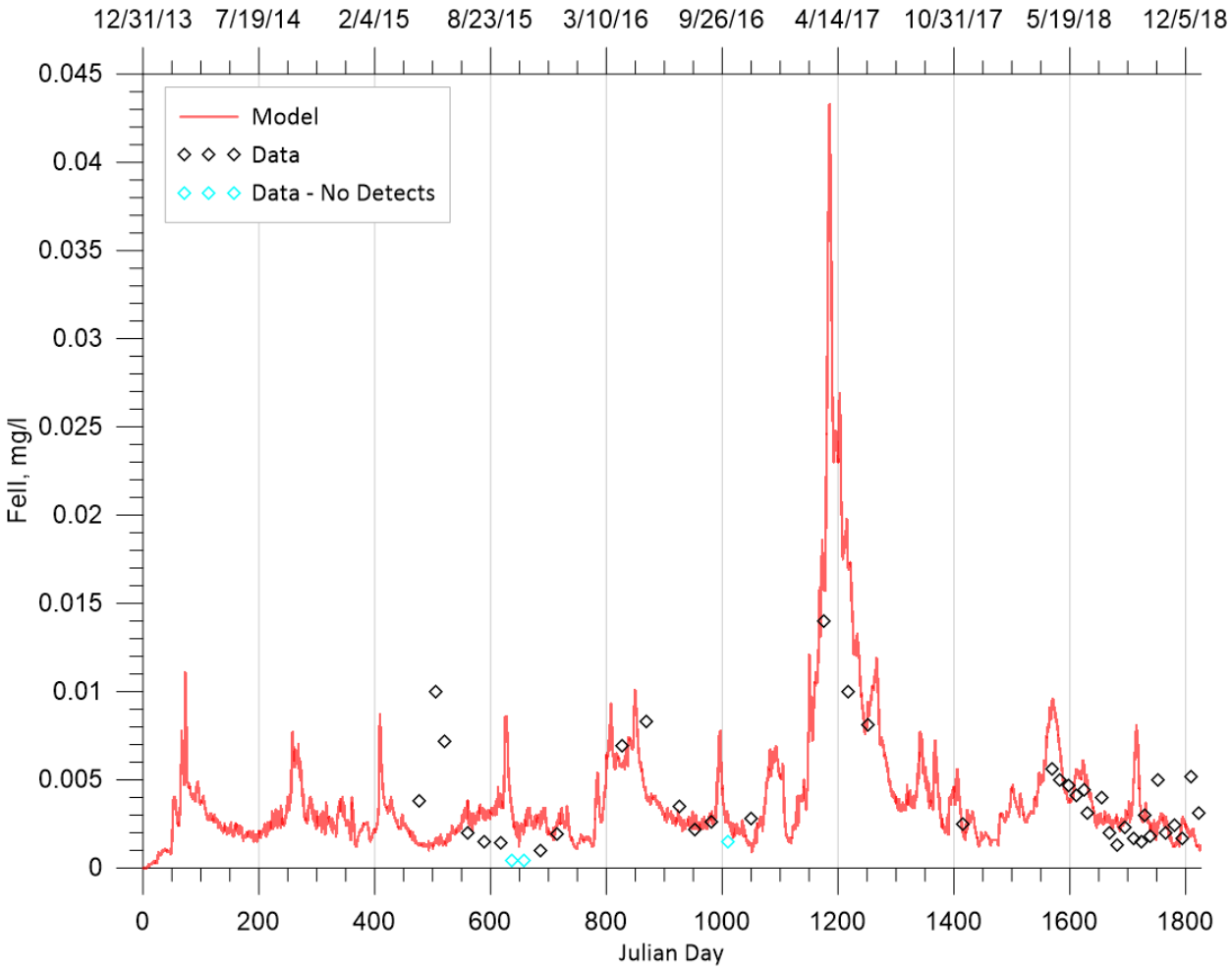


Figure 185. Hells Canyon Reservoir model outflow FeII compared to data.

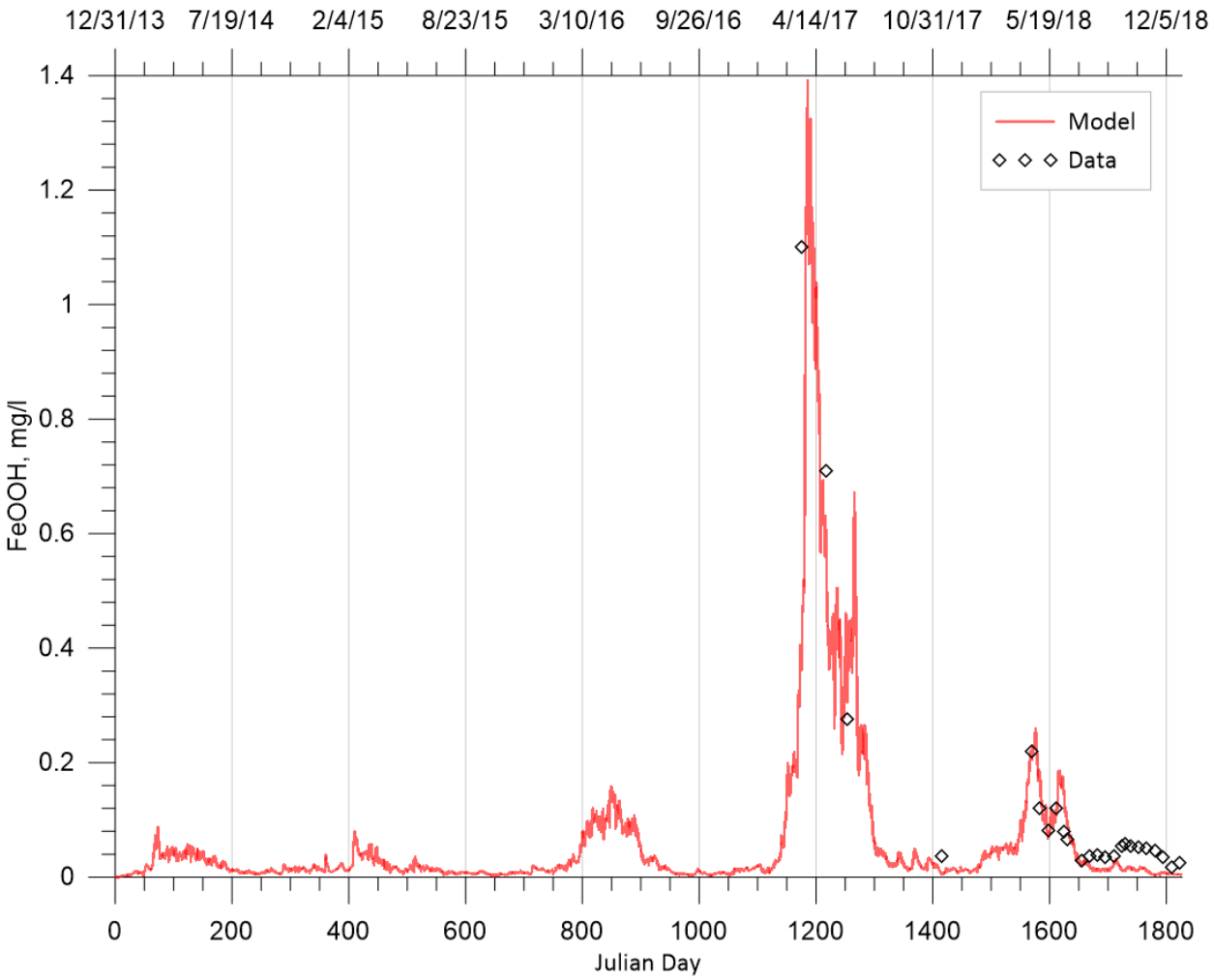


Figure 186. Hells Canyon Reservoir model outflow FeOOH compared to data.

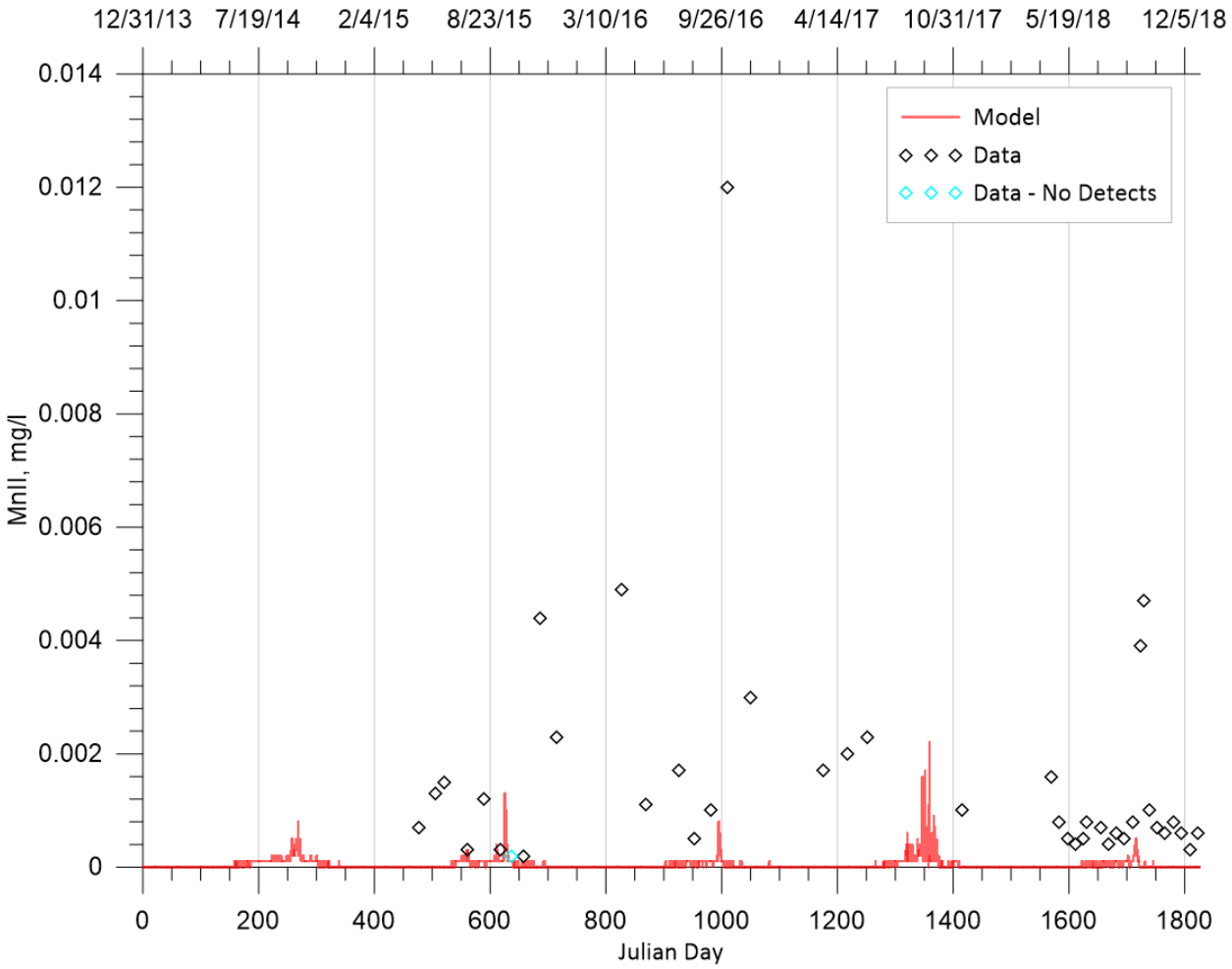


Figure 187. Hells Canyon Reservoir model outflow MnII compared to data.

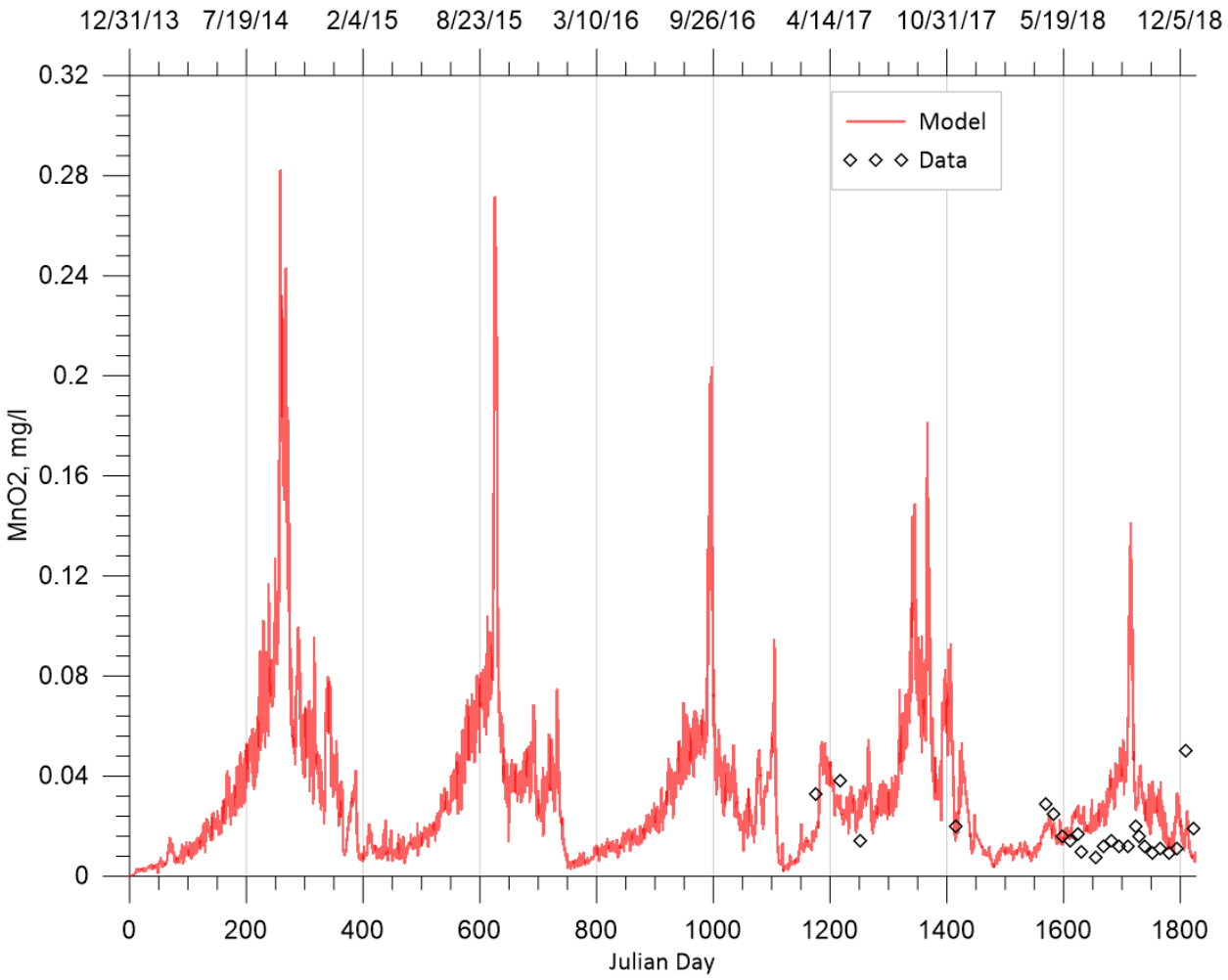


Figure 188. Hells Canyon Reservoir model outflow MnO2 compared to data.

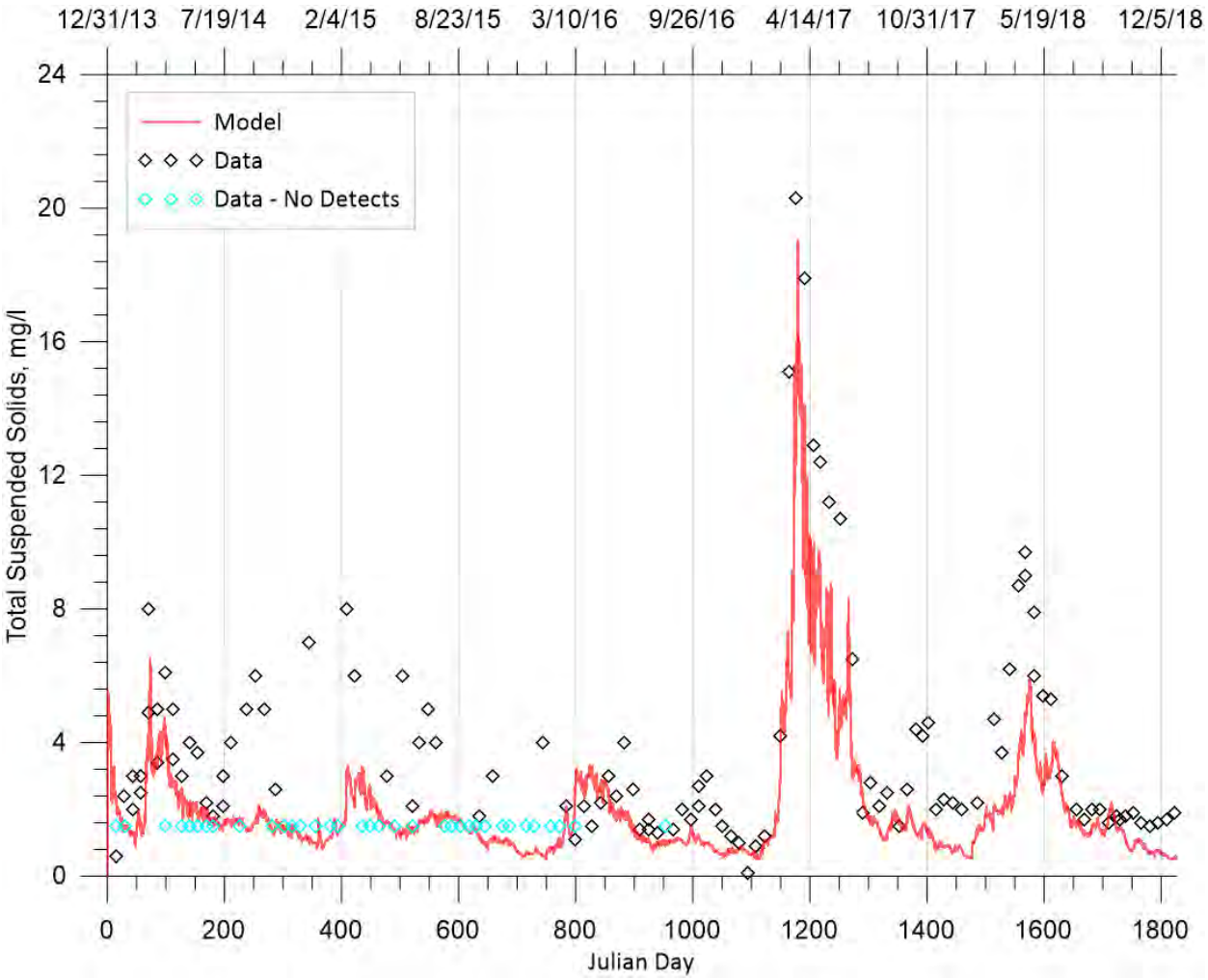


Figure 189. Hells Canyon Reservoir model outflow total suspended solids compared to data.

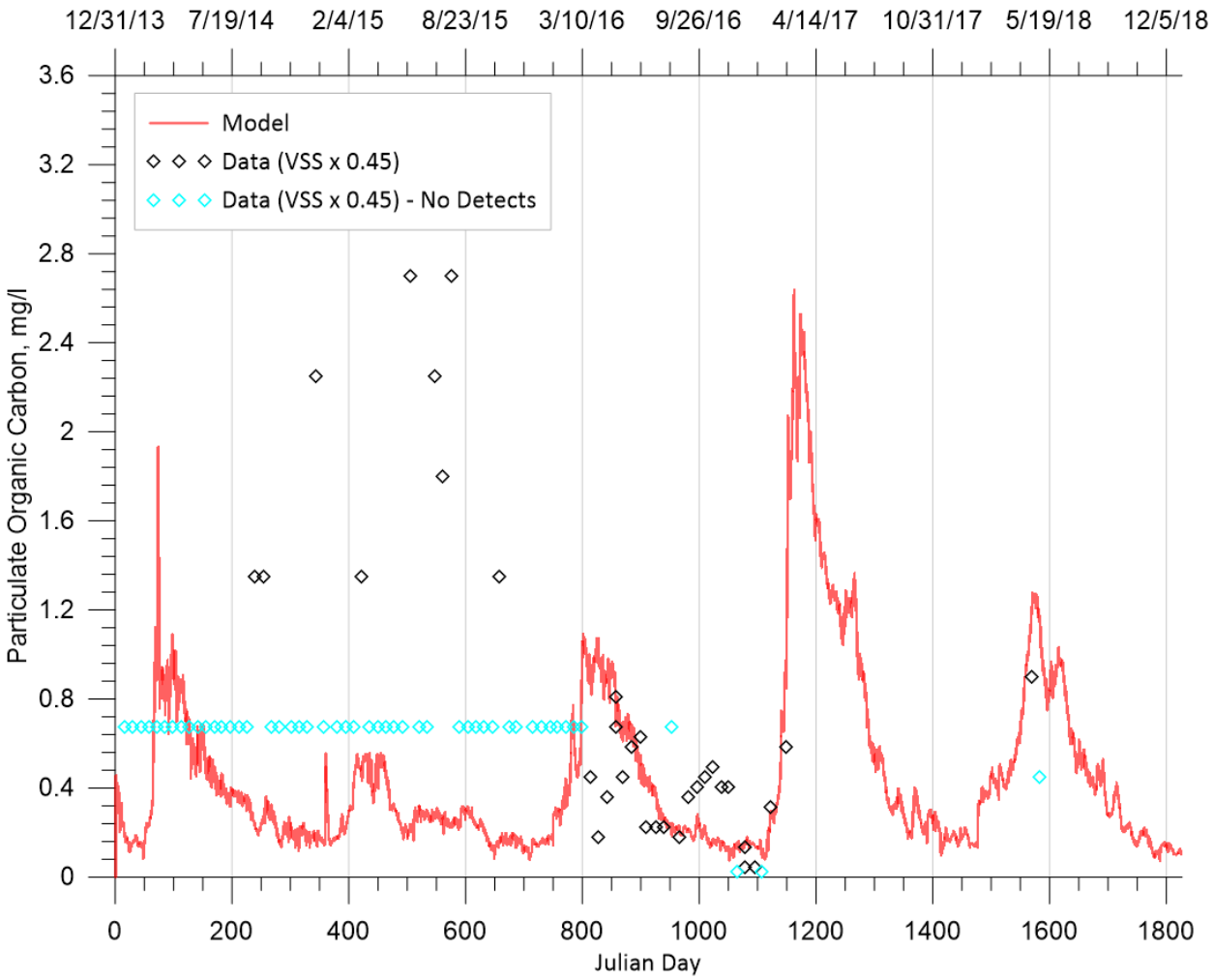


Figure 190. Hells Canyon Reservoir model outflow particulate organic carbon compared to volatile suspended solids data multiplied by 0.45 (assumed fraction of mg C to mg organic matter).

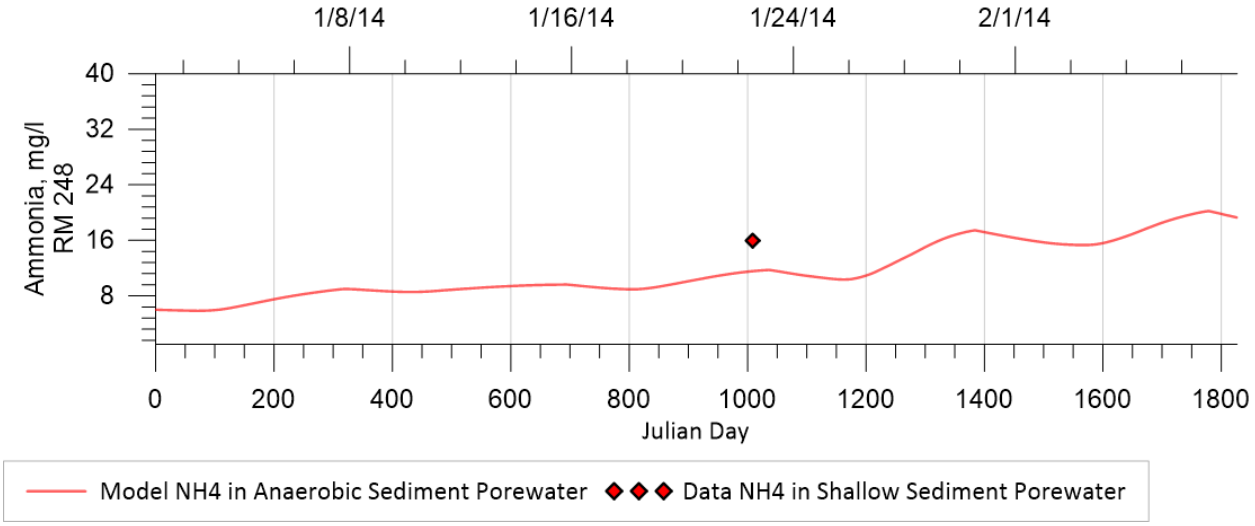


Figure 191. Hells Canyon Reservoir model ammonia nitrogen in sediment compared to data.

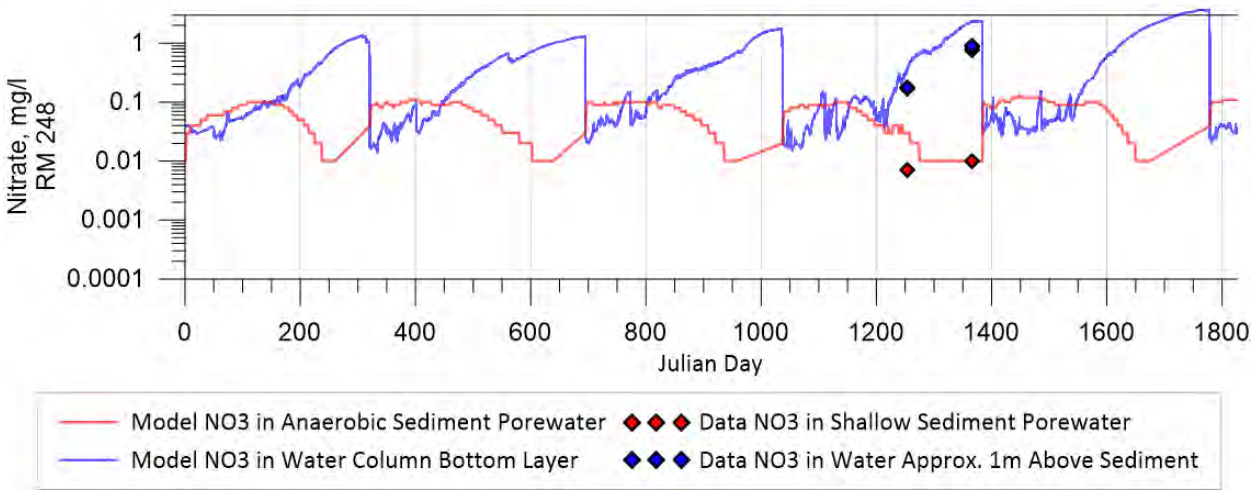


Figure 192. Hells Canyon Reservoir model nitrate nitrogen in sediment and bottom of water column compared to data.

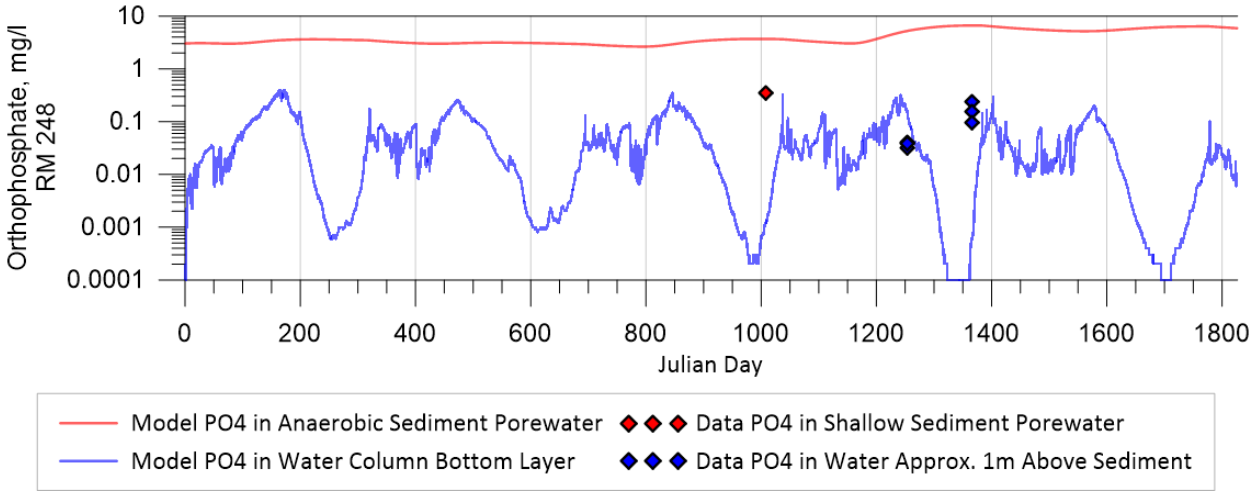


Figure 193. Hells Canyon Reservoir model orthophosphate in sediment and bottom of water column compared to data.

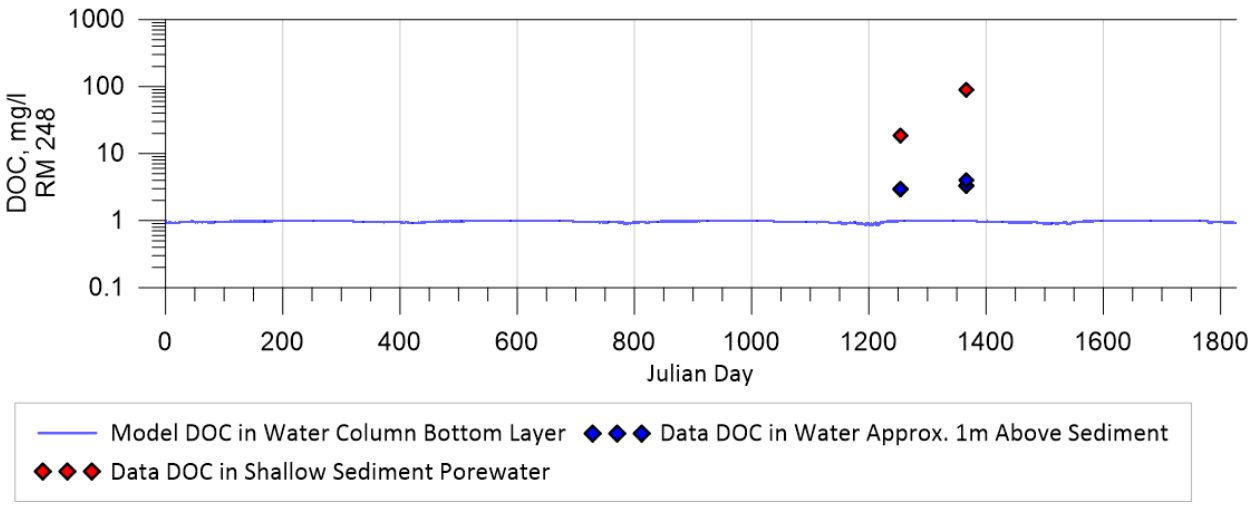


Figure 194. Hells Canyon Reservoir model DOC in bottom of water column compared to data.

Analysis of Model Fluxes

Phosphorus and nitrogen mass balances are shown in the following section. Sources and sinks of dissolved oxygen, phosphorus, and nitrogen are also plotted below. The fluxes predicted by the model show the importance of different source-sink terms in the water quality mass balances.

Phosphorus and nitrogen mass balances for Hells Canyon Reservoir are shown in Figure 195 and Figure 196, respectively. Sources and sinks of dissolved oxygen, phosphorus, and nitrogen for Hells Canyon Reservoir are shown in Figure 197 through Figure 199. Sources are shown as positive values and sinks are shown as negative values. On JDAY 1801 the net mass of P in Hells Canyon Reservoir was 2.63E06 kg (inflow TP + tributary TP – Outflow TP), and the net mass of N was 5.06E07 kg (inflow TN + tributary TN – Outflow TN). The positive values of P and N at the end of the simulation indicate that Hells Canyon Reservoir is a net sink of P and N since more mass came into the reservoir than left the reservoir. The main sources/sinks of oxygen are reaeration, algae and periphyton, and organic matter decay. For N and P, the main sources/sinks include algae and periphyton dynamics and organic matter decay. Also, nitrification is also important in the N balance for Hells Canyon.

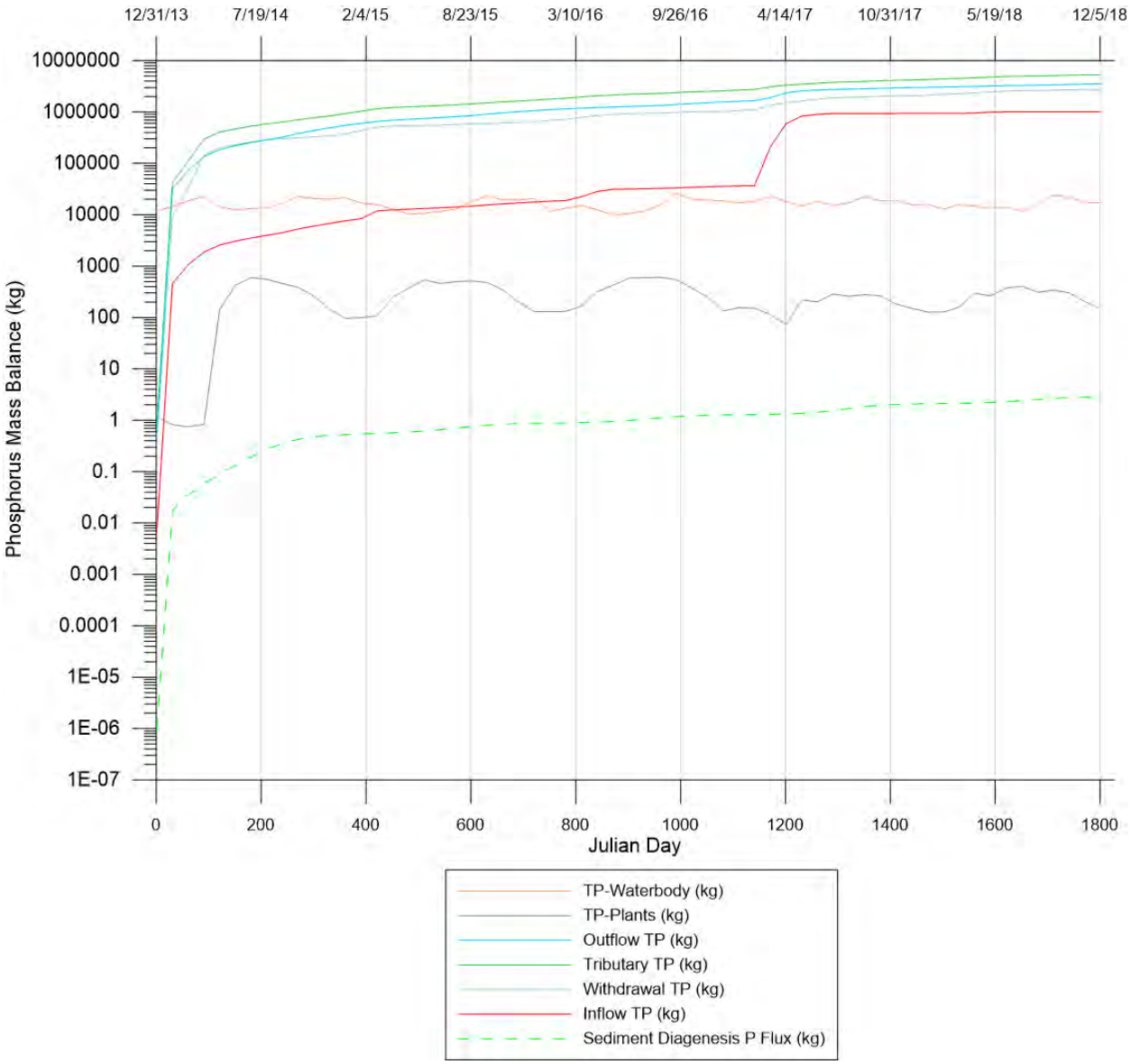


Figure 195. Cumulative phosphorus mass in Hells Canyon Reservoir. TP in the waterbody, sediment and plants just shows the current amount of TP in each of those at different points in time.

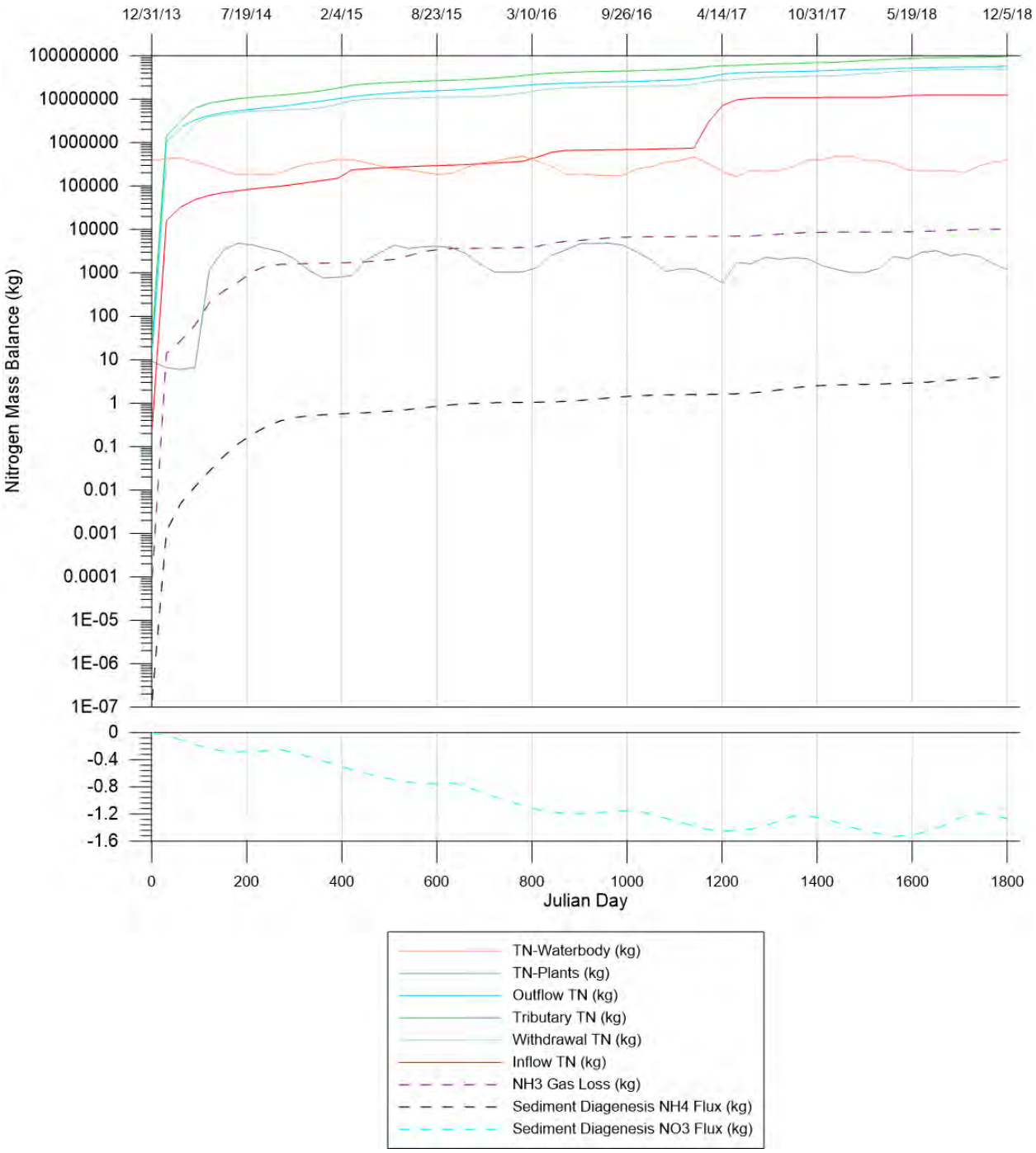


Figure 196. Cumulative nitrogen mass in Hells Canyon Reservoir. TN in the waterbody, sediment and plants just shows the current amount of TN in each of those at different points in time.

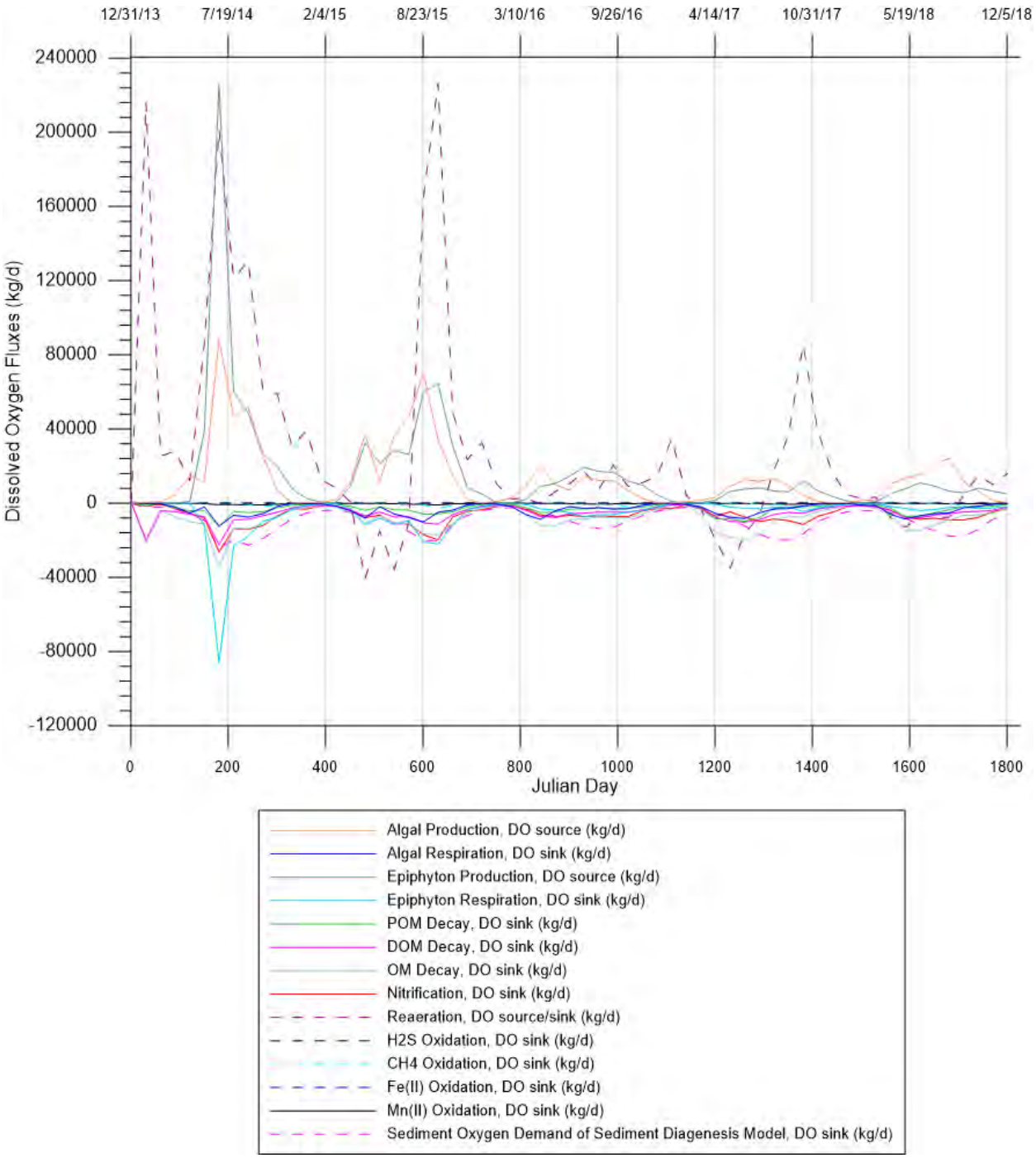


Figure 197. Dissolved oxygen sources and sinks in Hells Canyon Reservoir.

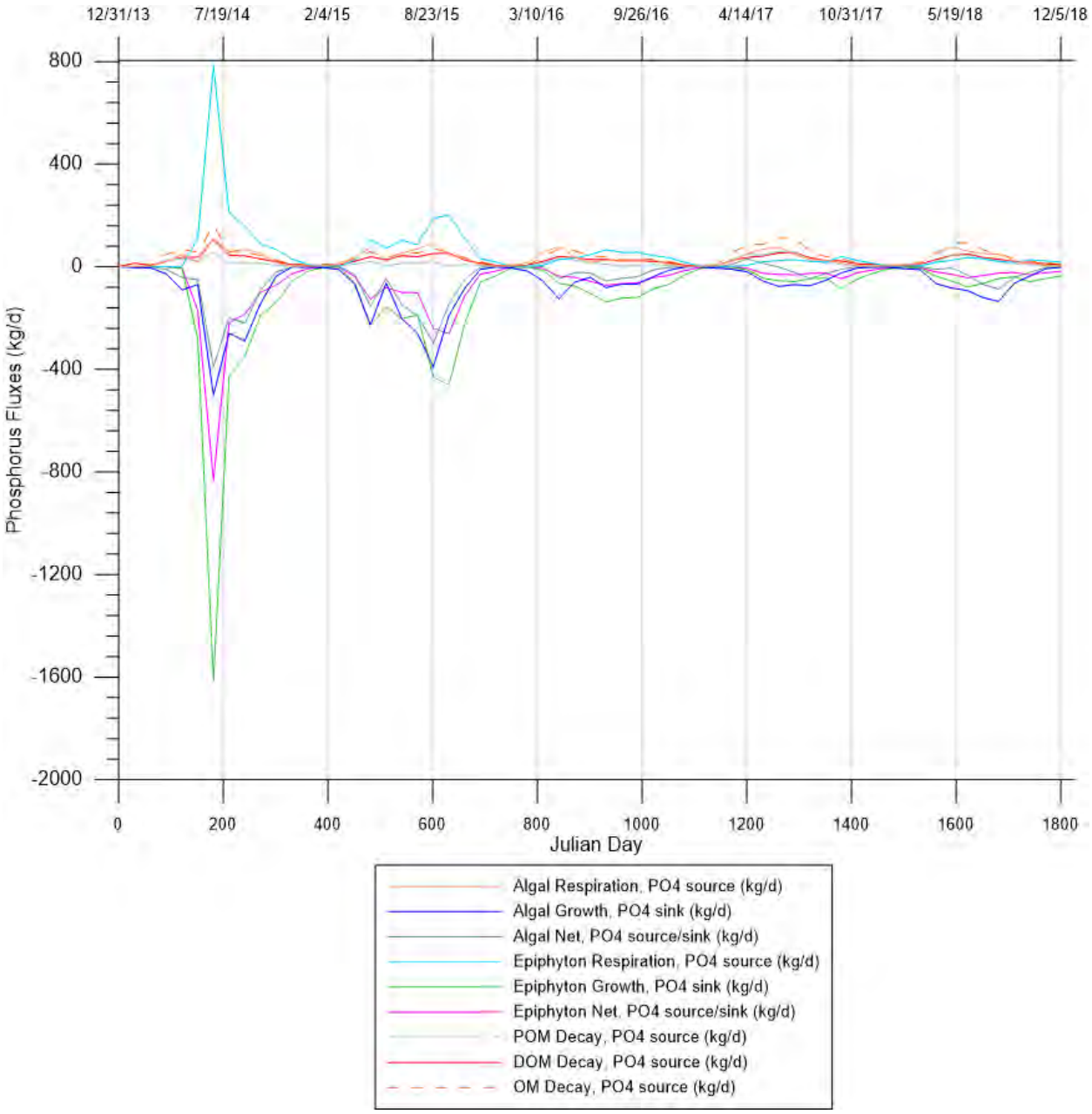


Figure 198. Phosphorus sources and sinks in Hells Canyon Reservoir.

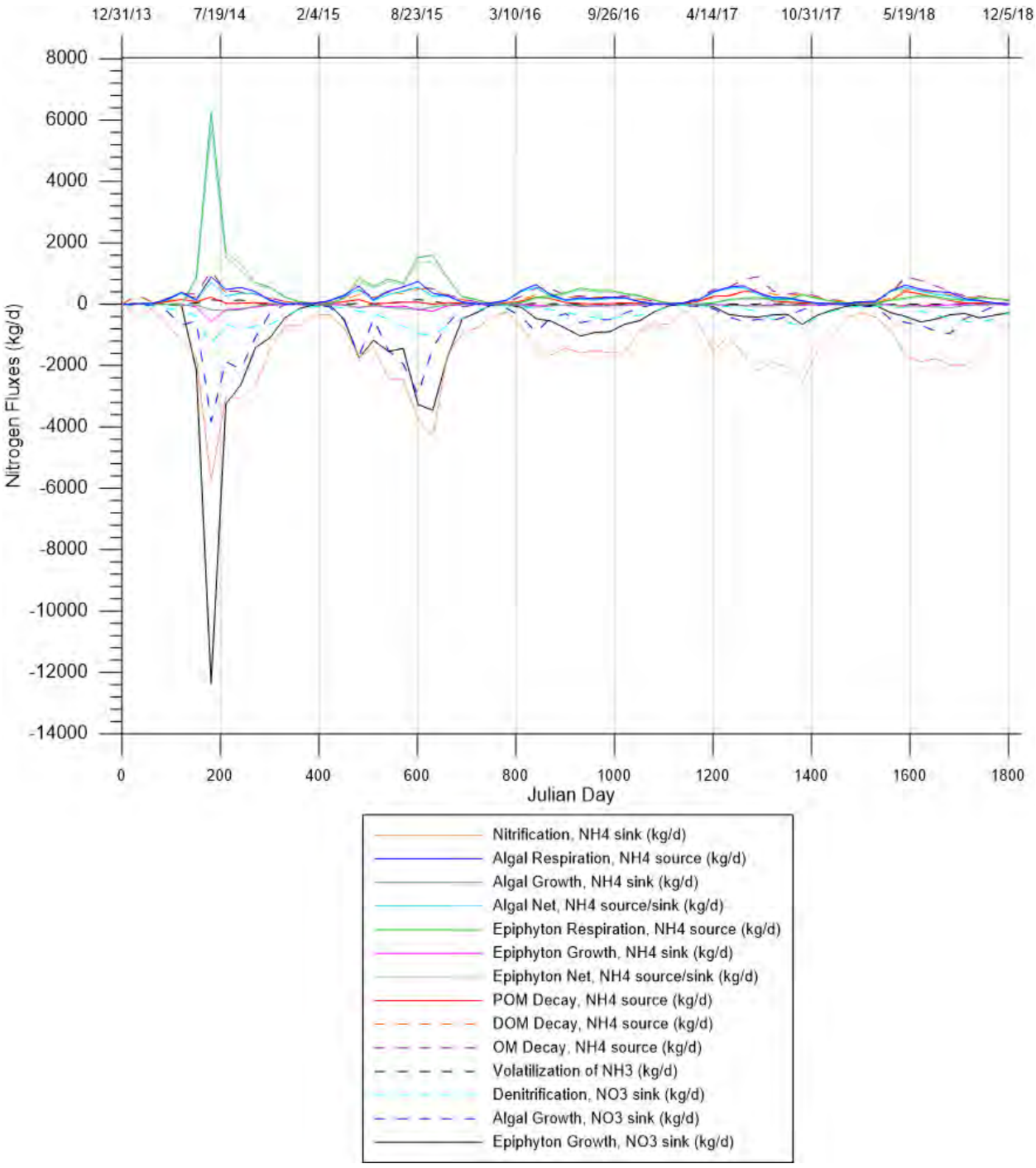


Figure 199. Nitrogen sources and sinks in Hells Canyon Reservoir.

Sediment Nutrient Concentrations

The sediment diagenesis model computes concentrations of particulate organic carbon, nitrogen, and phosphorus (POC, PON, and POP) in the sediments over time for each model segment. These concentrations are shown in Figure 200 and Figure 201 for select segments. Both labile and refractory pools are shown. Both the labile and refractory pools of particulate organic carbon, nitrogen, and

phosphorus fluctuate seasonally throughout the simulation period, but the fluctuation is relatively consistent between years.

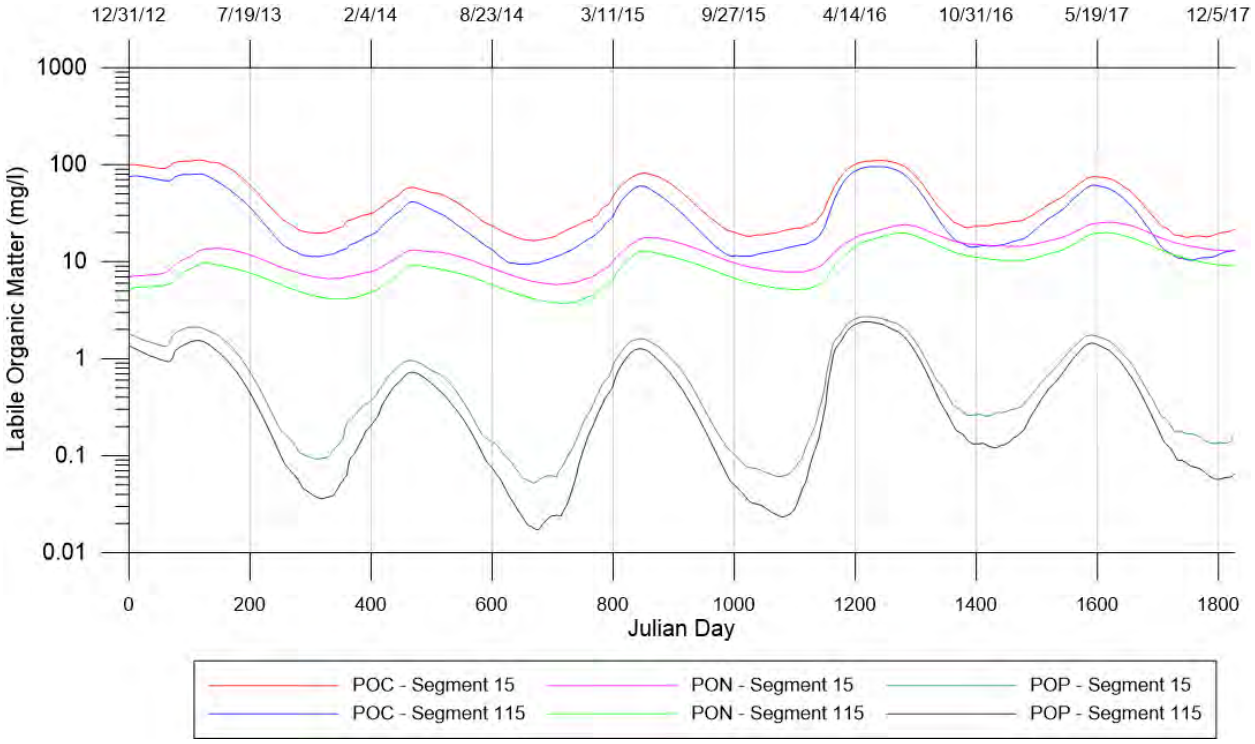


Figure 200. Labile POC, PON, POP at segments 15 and 115 in Hells Canyon Reservoir.

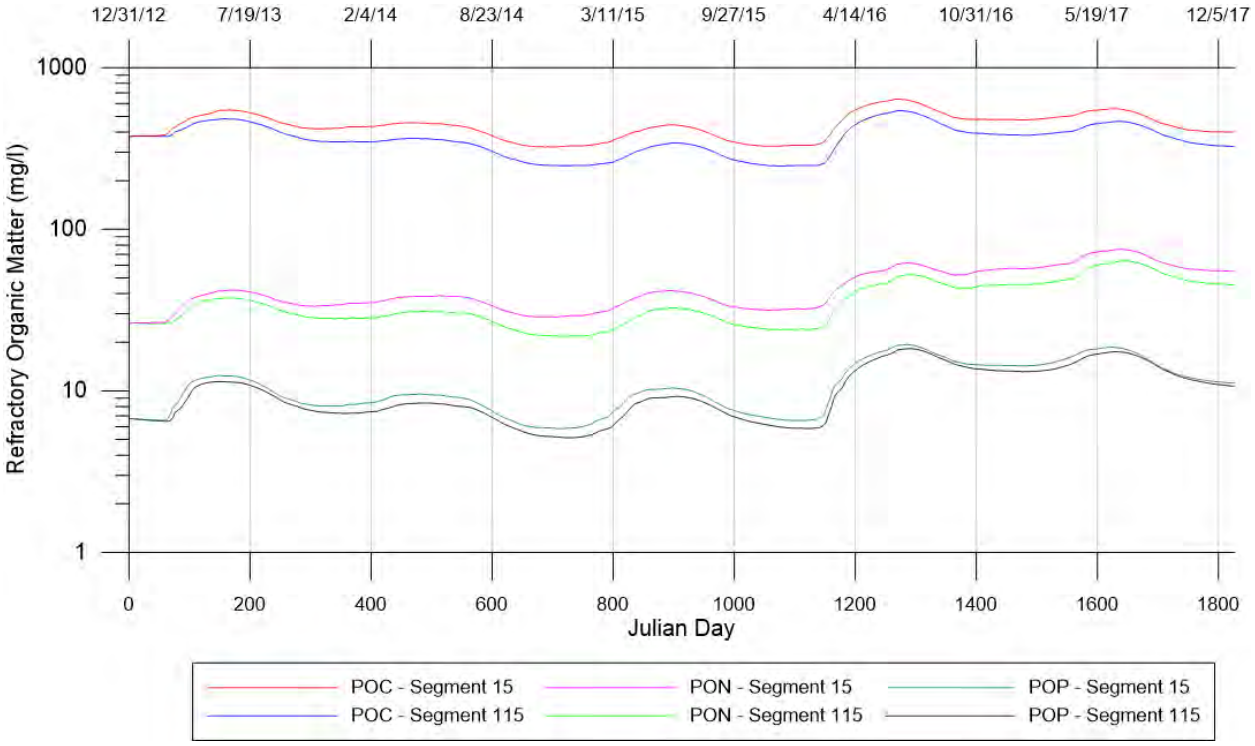


Figure 201. Refractory POC, PON, POP at segments 15 and 115 in Hells Canyon Reservoir.

Discussion of Model Calibration

Most of the temperature and water quality predictions were able to match field data and trends for each of the three reservoirs meeting criteria of absolute mean error for temperature of less than 1^{o}C and for dissolved oxygen of less than 1 mg/l. In the water quality statistics tables there is also a fraction of model absolute error over the mean of the field data. Donigian (2002) used a criterion where if this ratio is less than 0.15 it is “very good”, between 0.15-0.25 “good”, and between 0.25-0.35 “fair”. These are controversial and depend on many factors as to how well the model matches field data. In most cases a

An important aspect of evaluating the model is how well it is able to match trends and field data at the reservoir exit. The temperature and water quality in the reservoir outflow is not only based on in-reservoir processes but on the hydrodynamics of the outlet pulling water from various vertical layers. In the Brownlee Reservoir model, adding the outlet channel to the model grid greatly improved the model in predicting the vertical distribution of water leaving Brownlee even though it added a computational burden to the model because of the lower time step for numerical stability. However, there were certain constituents that proved to be more difficult to calibrate. The following sections describe in more detail some of the challenges in the model calibration and possible sources of error between model predictions and field data.

Meteorological Data

Meteorological data were determined from WRF-NAM model prediction and USGS and IPC data measured at Brownlee Dam. Brownlee Reservoir was divided into two regions for meteorological conditions: WB1-WB4, and WB5. Oxbow and Hells Canyon reservoirs both used meteorological data from WB5 of Brownlee Reservoir with adjustments applied to air temperature, dew point temperature, and wind speed based on measured values available before the simulation period. Since many of the meteorological inputs used were not measured directly, this could be a source of error in the model predictions.

The model was very sensitive to wind speed and direction affecting temperature stratification and other water quality processes. Besides the estimated wind used in the model, the model has a wind sheltering coefficient that adjusts the wind speed by segment and time. This is largely a calibration tool where the wind sheltering coefficient is a multiplier on the wind speed. The wind sheltering coefficient chosen for Brownlee reservoir is shown in Figure 202 and that for Hells Canyon is shown in Figure 203. Oxbow Reservoir had a wind sheltering coefficient of 2 for all time and segments.

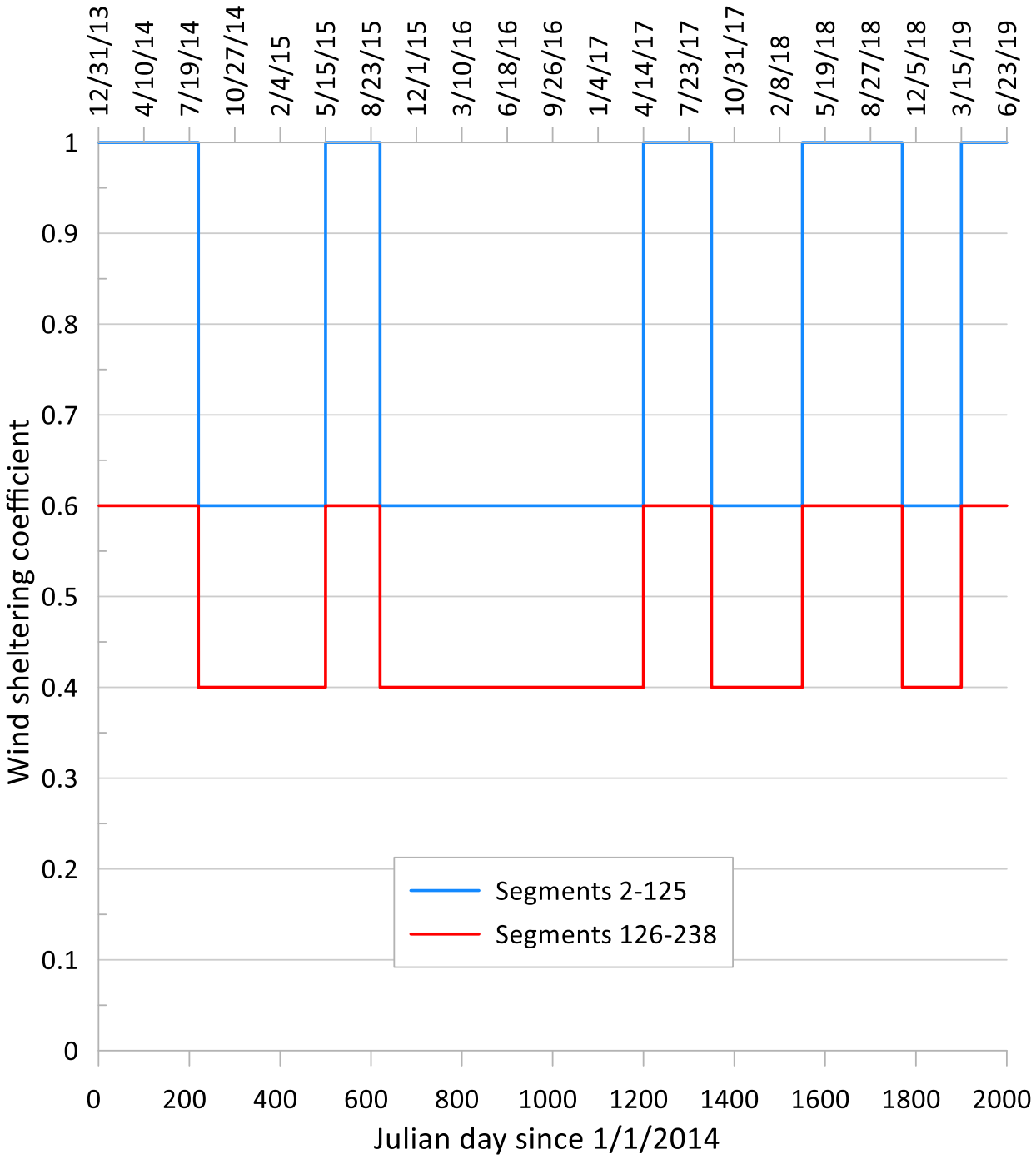


Figure 202. Wind sheltering coefficient for Brownlee Reservoir between 2014-2018.

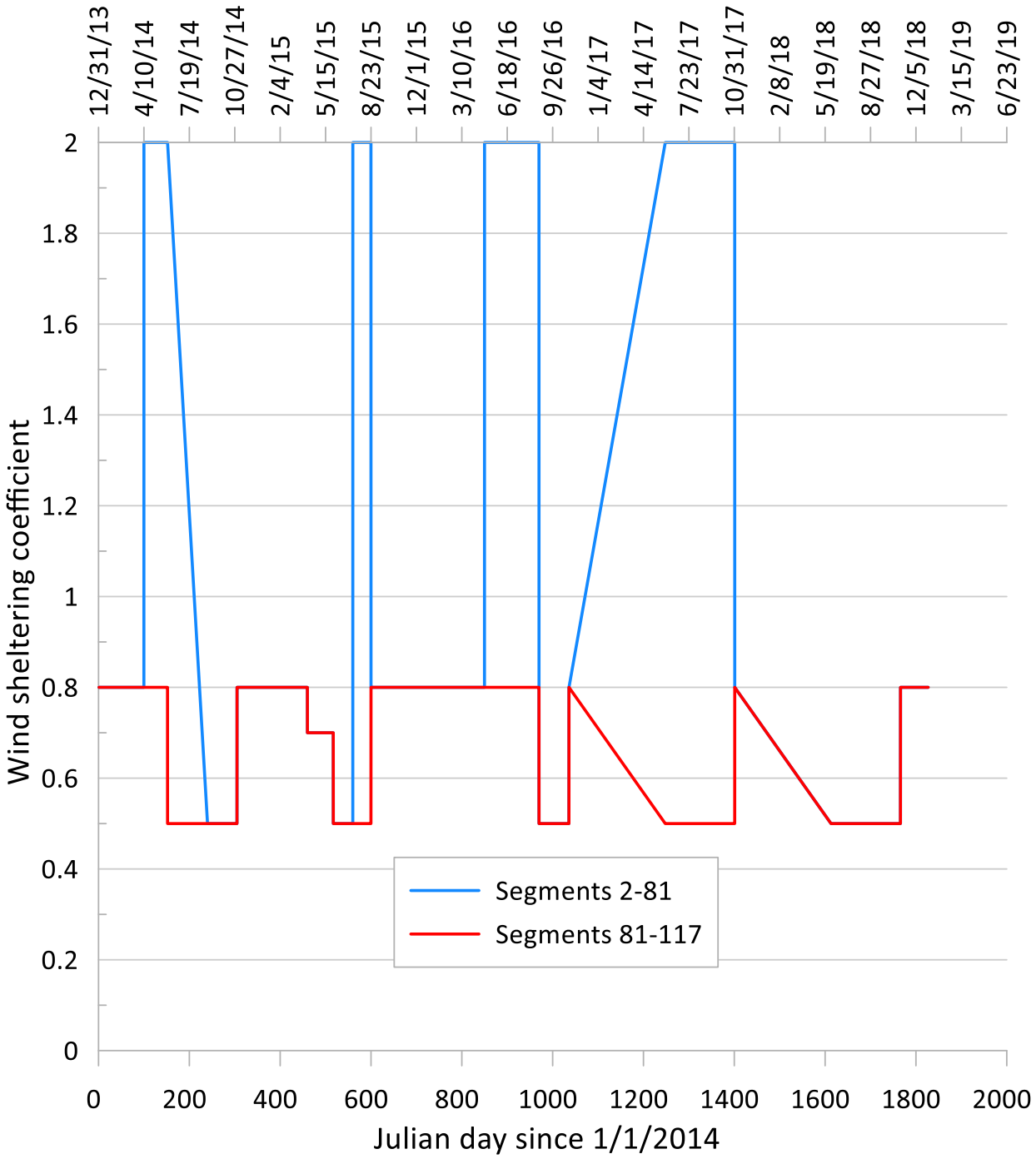


Figure 203. Wind sheltering coefficient for Hells Canyon Reservoir between 2014 and 2018.

Input Data

Data were used whenever available to create the input files for the three reservoirs. Where data did not exist, regressions or interpolation were used to fill gaps. Data were available to create most of the inputs for the Snake River, but regressions were required to create the concentration inputs for the tributaries. The regressions used for the constituent inputs varied in their correlation and r-squared values. While the

Snake River is the predominant contribution into the HCC system, there is likely some error associated with the use of regressions to estimate the tributary concentrations. Additionally, Powder River temperature inputs were used for Daly Creek and the distributed tributary, and Powder River constituent inputs were used for Wildhorse River, Pine Creek, Daly Creek, and the distributed tributary since no data were available to create regressions.

Water level

Water level was calibrated well for each reservoir with mean absolute errors around 0.1 m. Brownlee Reservoir used a water balance file that included inflows and outflows applied to the main waterbody 5. These flows were a result of ungauged inflows (especially during storm events) and errors in flow measurements. Oxbow and Hells Canyon used a dynamic weir to approximate water levels in their respective pools. Using a waterbalance flow would have been difficult in these systems since the water level varied at a high frequency.

Temperature

Temperature was also calibrated well for each reservoir with mean absolute errors of 0.84 °C for Brownlee Reservoir vertical profiles, 0.67 °C for Brownlee Reservoir continuous temperatures at various depths in 2017 and 2018 (over 660,000 measurements), 0.62 °C for Brownlee Reservoir outflow, 0.62 °C for Oxbow Reservoir outflow, 0.82 °C for Hells Canyon Reservoir vertical profiles and 0.64 °C for Hells Canyon Reservoir outflow. The calibration philosophy for the temperature profiles was to have simplified adjustment of wind in the different branches. We could have improved model-data error statistics by more aggressive adjustment of wind sheltering coefficients. Also, we decided to use field data derived light extinction coefficients (see Analysis of Light Extinction Data in Brownlee Reservoir to Determine Model Extinction Coefficients) rather than tuned light extinction coefficients which would also have improved the temperature calibration. This approach may have sacrificed slightly better error statistics but make the model easier to apply to management scenarios since the calibration was not overly tuned to the existing field data.

Water Quality

Two constituents that were difficult to calibrate were orthophosphate and total phosphorus. The profiles showed high levels of PO4 and TP near the bottom of the water column, but achieving high enough concentrations in the water column to match profiles often lead to overpredictions of the outflow concentrations. In order to best match both the outflow and profiles, Brownlee Reservoir used a value of 0.04 for the phosphorus partitioning coefficient (PARTP) while Oxbow and Hells Canyon reservoir used values of zero. This coefficient allowed some phosphorus to be taken out of the water column by sorption onto suspended solids and put into the sediments. PO4 and TP are still slightly overpredicted in the outflows (mean error of 0.012 for Brownlee PO4) and slightly underpredicted in the

profiles (mean error of -0.007 mg/l for Brownlee PO4), but the model matches the overall trend for both the profiles and outflow.

Iron and manganese were also difficult to calibrate, particularly the reduced form of manganese. It was possible to get close to matching the outflow concentrations by using low values of oxidation and reduction and high settling rates, but it was not possible to match the profiles for the reduced data using only the input concentrations. There were data values available to create the Snake River inputs for the Fe and Mn species, but regressions were used to create inputs for the tributaries. Measured inputs of MnII were around 0.01-0.04 mg/l but profiles had measured values around 1-2 mg/l for Brownlee Reservoir. Likewise, peak profile values of FeII were around 0.1-0.2, but FeII inputs rarely exceeded values of 0.1 mg/l. In order to best match both the profiles and outflow data, high initial concentrations of FeII and MnII (100 and 500 mg/l for FeII and MnII, respectively) were used in the sediments of the reservoirs with increased sediment sorption coefficients (50 and 5 m^3/g for FeII and MnII, respectively). Additionally, a high oxidation rate of Mn (0.3 m^3/day-g) was required for Brownlee and Oxbow reservoirs to lower the MnII concentration of Brownlee outflow after achieving higher profile concentrations. Since the Brownlee outflow concentrations are measured downstream of the dam in Oxbow Reservoir, the oxidation rate of the Oxbow Reservoir model was the contributing factor to lowering Brownlee MnII concentrations. However, a lower oxidation rate for Hells Canyon (0.1 m^3/day-g) was required to not completely deplete the outflow leaving Hells Canyon and Oxbow reservoirs (although the concentration is still low leaving Oxbow and Hells Canyon).

Calibrating dissolved oxygen was a main focus of this study. A few updates were made to the model code during the calibration process to better match field data for both outflows and profiles. Previously, when the model would encounter a density instability, a vertical diffusion coefficient (DZ) of 1000 m^2/s was used to instantaneously mix the model layers. The updated code uses a user specified multiplier on the value of DZ when an instability is detected. The multiplier for the three reservoirs is 100. There are periods of density instability in the model due to high suspended sediment concentration with warmer temperatures that would previously mix too quickly when the suspended solids settled out. The updated code allows for slower mixing during instabilities and subsequently improved the model profile comparisons to data. Another development to the model code that was added for this project was the ability to set the sediment temperature to an internally computed value or set equal to the overlying water temperature. It was observed in earlier model iterations that there was a significant amount of decay during the winter months that caused DO values to reach close to zero near the sediment in the deepest areas of Brownlee Reservoir. This older version of the model used an internally computed value of sediment temperature based on a supplied temperature value of the average year-round air temperature. In the deep areas, this value was likely too high which led to higher decay rates. The updated model uses the overlying water temperature as the sediment temperature which has much lower values in the winter and subsequently slower decay rates. Lastly, the outflow DO from Brownlee Reservoir was often too low, especially in the summer periods, even though profiles were slightly over predicting dissolved oxygen. It was determined from discussions with IPC that there was likely venting of the turbines that was supplying additional aeration to the outflow. To model this, a varying percent increase of DO was supplied to the turbines at Brownlee Reservoir (Figure 113). After making these

changes to the model, the dissolved oxygen was able to closely match both the observed outflow concentrations as well as the profiles. There are still some deviations in profile comparisons due to the high complexity of the system, but the model predicts the overall trend of DO during most of the simulation period. Figure 204 shows a comparison of the model predicted volume of DO less than 1 mg/l in branch 5 of Brownlee Reservoir compared to field data.

Periphyton concentrations at the upstream model segment adjacent to each dam are shown in Figure 205. With no field data for comparison, we are uncertain as to whether these results are valid.

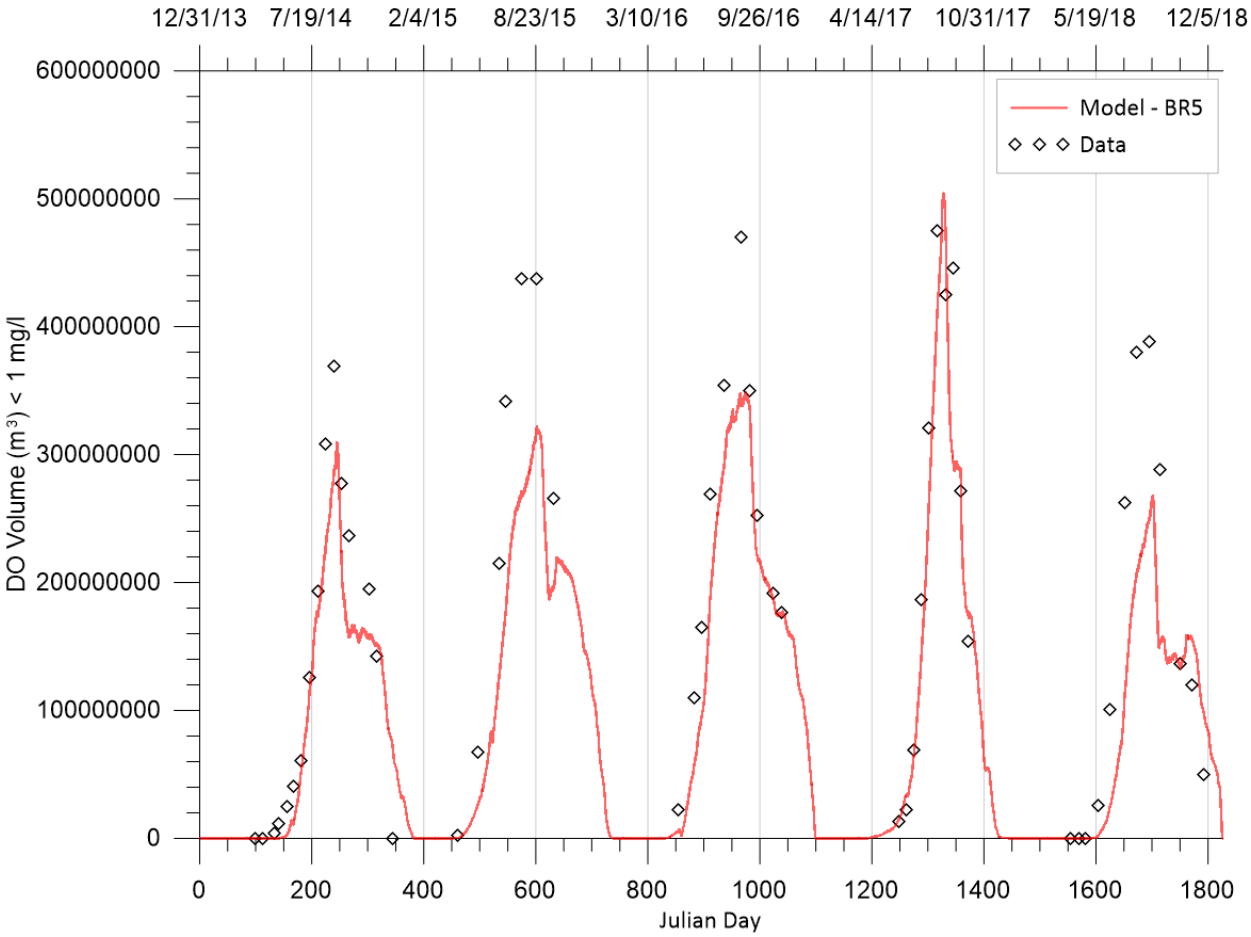


Figure 204. Brownlee Reservoir model branch 5 volume of dissolved oxygen less than 1 mg/l compared to data.

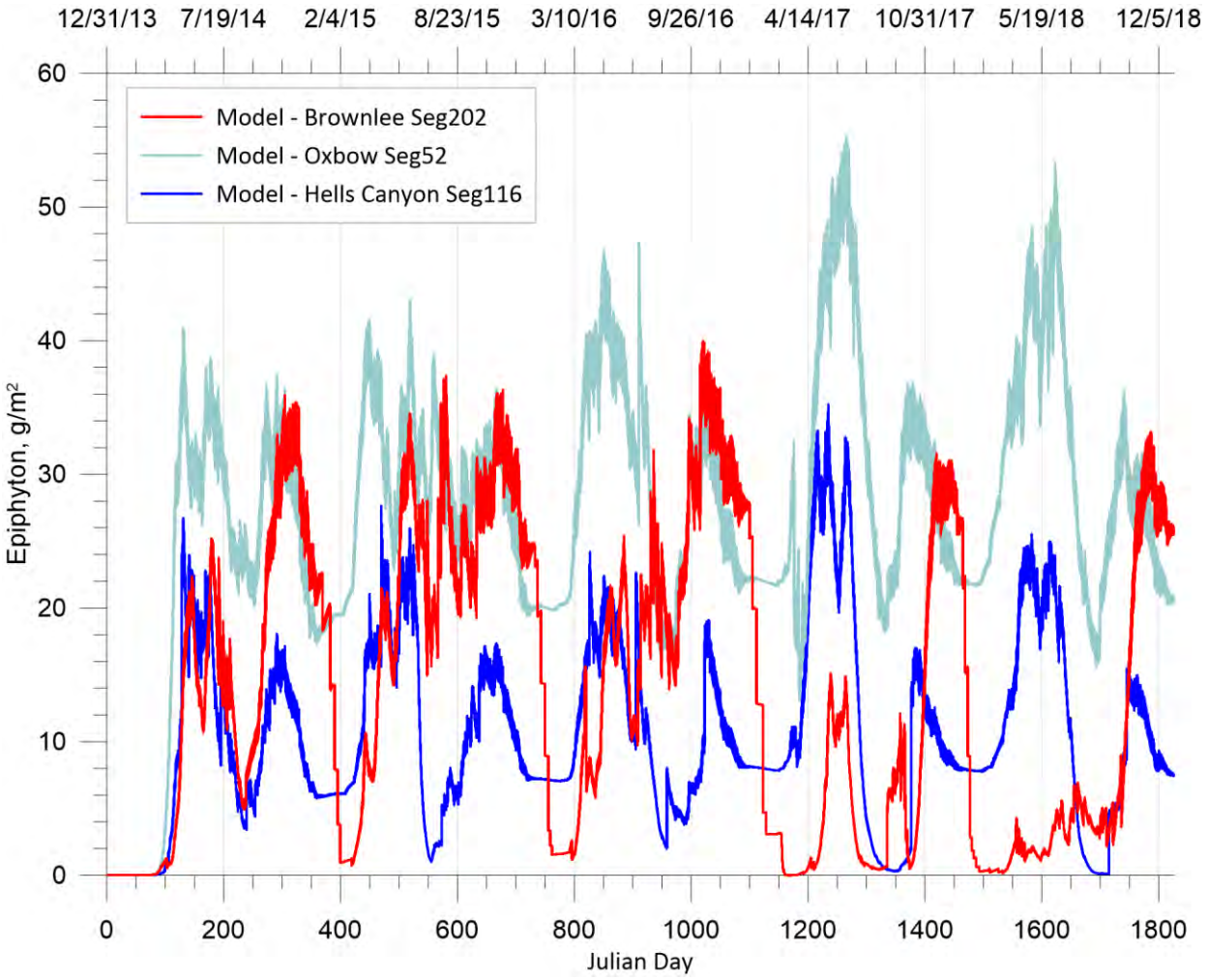


Figure 205. Epiphyton concentrations at the upstream model segment adjacent to each dam.

Sediment Diagenesis

One of the goals of the sediment diagenesis modeling was to (1) use limited field data to set initial conditions and (2) ensure that the sediment concentrations of C, P, and N varied in a natural fashion year -by-year. In other words, we did not want to set conditions so that we had a high concentration in the sediments that gradually declined from 2014-2018. One of the challenges of sediment diagenesis modeling is that we are assuming that the amount of particulate organic matter (POM) coming into the Snake River is correct. The sediment model is driven by particulate organic matter depositing into the sediment compartments. Missing a large POM source, like the detachment of aquatic plants/periphyton upstream, would cause the sediment diagenesis model to miss a source of POC, PON, and PON. In looking at the sediment nutrient concentrations in each reservoir, both the labile and refractory pools of particulate organic carbon, nitrogen, and phosphorus fluctuate seasonally throughout the simulation period, but the fluctuation is relatively consistent between years.

Summary and Conclusions

CE-QUAL-W2 Version 4.5 models were developed for Brownlee, Oxbow and Hells Canyon Reservoirs. The simulation period for the models was January 1, 2014 through December 31, 2018. This report outlined the development of the model computational grids (bathymetry), topographic shading for each model segment, as well as meteorological data, withdrawal data, and inflow data (flow rate, constituent, and temperature data). The model system of Brownlee, Oxbow, and Hells Canyon Reservoirs included 7 waterbodies and a total of 409 model segments. Segment lengths ranged from about 350 m (Oxbow and Hells Canyon) to 500 m (Brownlee). The vertical layers of 1 m in the models varied from 57 (Oxbow) to 102 (Brownlee).

The models were compared to temperature, water quality, and sediment field data taken by the USGS and Idaho Power. In most cases the graphical and statistical representation of the model compared to data showed good model agreement in temperature, dissolved oxygen, dissolved organic C, anoxia volume, and nutrients, as well as other variables. The model will be used to evaluate Hg conditions in the HCC complex.

In order to continue to improve the HCC system complex model the following areas could be explored further:

- Refine the meteorological data in different parts of Brownlee Reservoir. One analysis that could be performed is to use the WRF-NAM model meteorological data used in this study to compare to past times when meteorological buoys were used in different parts of the reservoir to understand the biases of the estimated meteorological data.
- Ensure that sampling on Brownlee, Oxbow and Hells Canyon is accompanied by wind speed and direction so that more understanding of meteorological data and how it varies longitudinally is determined.
- Consider using wind direction that is aligned along the axis of the reservoir (either up or down reservoir).
- Compare algae blooms on Brownlee Reservoir using Cyan (https://www.epa.gov/water-research/cyanobacteria-assessment-network-cyan) and other analyses to estimate location and duration of blooms. Use that information to correlate to bloom information from the model and improve the predictive capability of the model for chlorophyll a.
- Try to estimate the organic matter loading from inflows of vegetation from upstream of RM 345.6 either through satellite imagery or from tuned sampling of the inflow which may have been missed in this study.
- Consider improving the model grid for upstream branches in Brownlee Reservoir to allow for much lower pool elevations in the system than what was used during this study.
- As a comparison to earlier model studies, use the existing model framework to assess the calibration to field data in other years such as 1994, 1995, 2002 and other years since the input files are largely the same.
- Continue to assess the best method to allow entrainment of oxygen into the Brownlee turbines since they affect downstream oxygen levels.
- Examine periphyton densities in Brownlee, Oxbow and Hells Canyon to guide changes in epiphyton kinetic coefficients since there were no field data to compare to predictions.

- The current CE-QUAL-W2 code used in this report did not include in TSS output particulate Fe and Mn. A future version will include these. But for this study including Fe and Mn in the TSS computation was negligible since the average TSS over the 5 years was 2.6 mg/L while the average FeOOH was 0.076 mg/L and the average MnO_2 was 0.039 mg/L.

References

Appling, A. P., Leon, M.C., McDowell, W.H. 2015. Reducing Bias and Quantifying Uncertainty in Watershed Flux Estimates: The R Package Loadflex. Ecosphere, 6, pp 1-25.

Aulenback, B.T., Hooper, R.P. 2006. The Composite Method: An Improved Method for Stream-Water Solute Load Estimation. Hydrol. Processes. 20, pp. 3029-3047.

Baldwin, A.K., C.A. Eagles-Smith, J.J. Willacker, B.A. Poulin, D.P. Krabbenhoft, J. Naymik, M.T. Tate, D. Bates, N. Gastelecutto, C. Hoovestol, and C. Larsen. 2022. In-reservoir physical processes modulate aqueous and biological methylmercury export from a seasonally anoxic reservoir. Environ Sci Technol. 56(19):13751–13760. doi:10.1021/acs.est.2c03958.

Donigian, A. 2002. Watershed Model Calibration and Validation: The HSPF Experience, January 2002. Proceedings of the Water Environment Federation, 2002(8):44-73, DOI: 10.2175/193864702785071796

Fisher, J. 2021. WRF-NAM historic modeled weather data: Data derivation and precision. Idaho Power, Boise, ID.

Idaho Power Company. 2019-2022. Idaho Power River Flow and Reservoir Information. https://www.idahopower.com/community-recreation/recreation/water-information/stream-flow-data/. (accessed 2019-2022).

Harrison, J.R.H. 2005. Partitioning Snake River Organic Matter and Modeling Aerobic Oxidation in Brownlee Reservoir, Idaho. Ph. D. dissertation. College of Graduate Studies. University of Idaho. 245 p.

Hirsch RM. 2019. Making WRTDS_K flux estimates: U.S. Geological Survey Exploration and Graphics for RivEr Trends (EGRET); [cited 4 Nov 2020]. Available from http://usgsr.github.io/EGRET/articles/Making%20 WRTDS_K%20flux%20estimates.html.

Hirsch RM, De Cicco LA. 2015. User guide to Exploration and Graphics for RivEr Trends (EGRET) and dataRetrieval: R packages for hydrologic data (version 2.0, Feb 2015): U.S. Geological Survey Techniques and Methods 4-A10; 104 p.

Liu, R., Hofmann, A., Gülaçar, F., Favarger, P., Dominik, J. 1996. Methane concentration profiles in a lake with a permanently anoxic hypolimnion (Lake Lugano, Switzerland-Italy), Chemical Geology, Volume 133, Issues 1–4, 1996, Pages 201-209.

Marvin-DiPasquale, M., Agee, J.L., Kakouros, E., Kieu, L.H., Arias, M.R., Baesman, S.M., Poulin, B.A., Antweiler, R.C., Fuller, C.C., Tate, M.T., and Krabbenhoft, D.P. 2020, Biogeochemical Data for Mercury and other Constituents in Surface Sediment and Deep Cores from the Hells Canyon Reservoir Complex, Idaho and Oregon 2014-2018: U.S. Geological Survey data release, https://doi.org/10.5066/P9L4XCD0.

Naymik J., Larsen C.A., Myers R., Hoovestol C., Gastelecutto N., and Bates, D. 2023. Long-term trends in inflowing chlorophyll a and nutrients and their relation to dissolved oxygen in a large western reservoir, Lake and Reservoir Management, DOI: 10.1080/10402381.2022.2160395

Poulin, B. A.; Breitmeyer, S. E.; Krabbenhoft, D. P.; Tate, M. T.; DeWild, J. F.; Ogorek, J. M.; Babiarz, C. L.; Janssen, S. E.; Marvin-DiPasquale, M. C.; Agee, J. L.; Kakouros, E.; Kieu, L.; Arias, M.; Conaway, C.; Antweiler, R. C.; Baldwin, A. K.; Yoder, A.; Clark, G. M.; Aiken, G. R. 2022. Chemical Characterization of Water and Suspended Sediment of the Snake River and Hells Canyon Complex (Idaho, Oregon); U.S. Geological Survey Data Release. https://doi.org/10.5066/P9DT2B6J.

Singh, V. P. 1992. Elementary Hydrology. Prentice Hall.

U.S. Geological Survey. 2019-2022. National Water Information System: U.S. Geological Survey web interface. http://dx.doi.org/10.5066/F7P55KJN. (accessed 2019-2022).

Wells, S. A., Editor. 2024. CE-QUAL-W2: A two-dimensional, laterally averaged, hydrodynamic and water quality model, version 4.5, User Manual. Department of Civil and Environmental Engineering, Portland State University, Portland, OR.

Wells, S., Zhang, Z., and Garstecki, B. 2025. Hg Model Development in CE-QUAL-W2 for the Hells Canyon Complex. Department of Civil and Environmental Engineering, Portland State University, Portland, OR. Report prepared for Idaho Power, 77 pp.

Yoder, A.M., Baldwin, A., Marvin-DiPasquale, M., Poulin, B. A., Naymik, J., Krabbenhoft, D. P. 2024 *accepted*. Longitudinal and seasonal changes of organic matter sources through a semi-arid river-reservoir system. Journal of Geophysical Research – Biogeosciences.

Appendix

A1. Algae Speciation

See attached appendix for memo summarizing algae speciation in the Snake River and Hells Canyon Complex.

A2. Model Coefficients

See attached appendix for model coefficients and sediment diagenesis parameters.

A3. Brownlee Dam Spillway Gas Equation Updates

See attached appendix for memo summarizing the updates made to the gas equation for the Brownlee Dam Spillway.

A4. Brownlee Reservoir Vertical Profiles

See attached appendix for Brownlee Reservoir water quality profiles of:

1. Temperature
2. Dissolved Oxygen
3. pH
4. Chlorophyll a
5. Ammonia Nitrogen
6. Nitrate Nitrogen
7. Total Kjeldahl Nitrogen
8. Particulate Organic Nitrogen
9. Orthophosphate
10. Total Phosphorus
11. Total Inorganic Carbon
12. Dissolved Organic Carbon
13. Particulate Organic Carbon
14. Chloride
15. Sulfate
16. Hydrogen Sulfide
17. Zooplankton
18. Fe(II)
19. FeOOH
20. Mn(II)
21. MnO2
22. Total Suspended Solids

A5. Oxbow Reservoir Vertical Profiles

See attached appendix for Oxbow Reservoir water quality profiles of:

1. Nitrate Nitrogen
2. Particulate Organic Nitrogen
3. Orthophosphate
4. Total Inorganic Carbon

5. Dissolved Organic Carbon
6. Particulate Organic Carbon
7. Chloride
8. Sulfate
9. Zooplankton
10. Fe(II)
11. Mn(II)
12. Total Suspended Solids

A6. Hells Canyon Reservoir Vertical Profiles

See attached appendix for Hells Canyon Reservoir water quality profiles of:

1. Temperature
2. Dissolved Oxygen
3. pH
4. Nitrate Nitrogen
5. Particulate Organic Nitrogen
6. Orthophosphate
7. Total Inorganic Carbon
8. Dissolved Organic Carbon
9. Particulate Organic Carbon
10. Chloride
11. Sulfate
12. Hydrogen Sulfide
13. Zooplankton
14. Fe(II)
15. FeOOH
16. Mn(II)
17. MnO2
18. Total Suspended Solids

A7. Brownlee Reservoir USGS Continuous Temperature and Dissolved Oxygen in 2017 and 2018

See attached appendix for model-data comparisons of continuous temperature and dissolved oxygen in Brownlee Reservoir at several longitudinal stations and depths.

1. Temperature
2. Dissolved Oxygen

Appendix A1 Algae Speciation

HCC Phytoplankton Summary

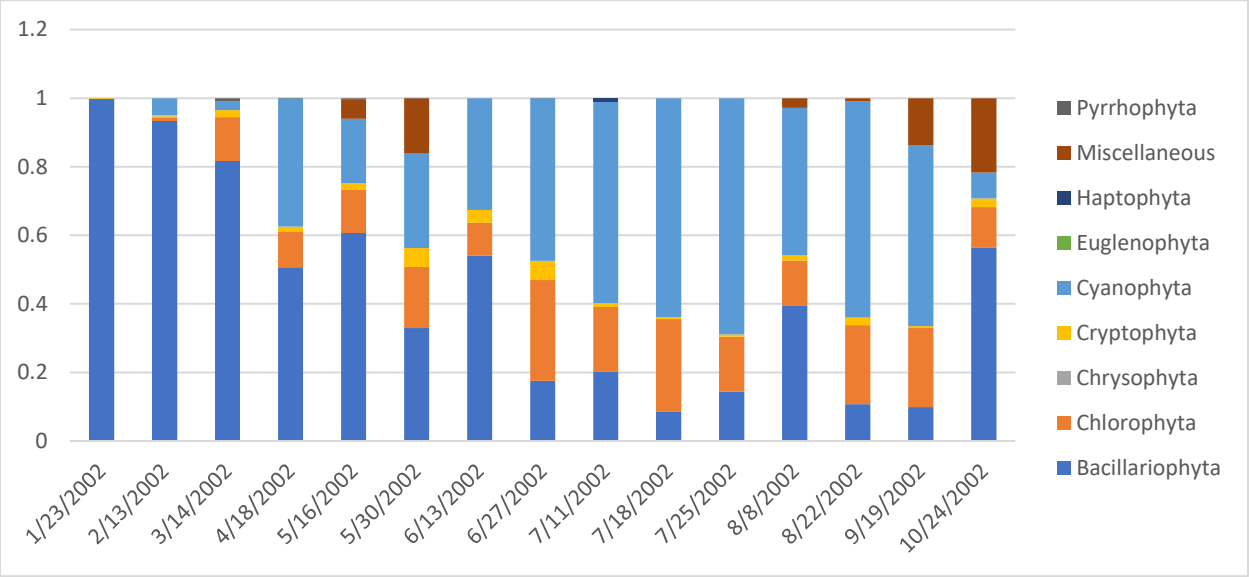
Portland State University

November 16, 2021

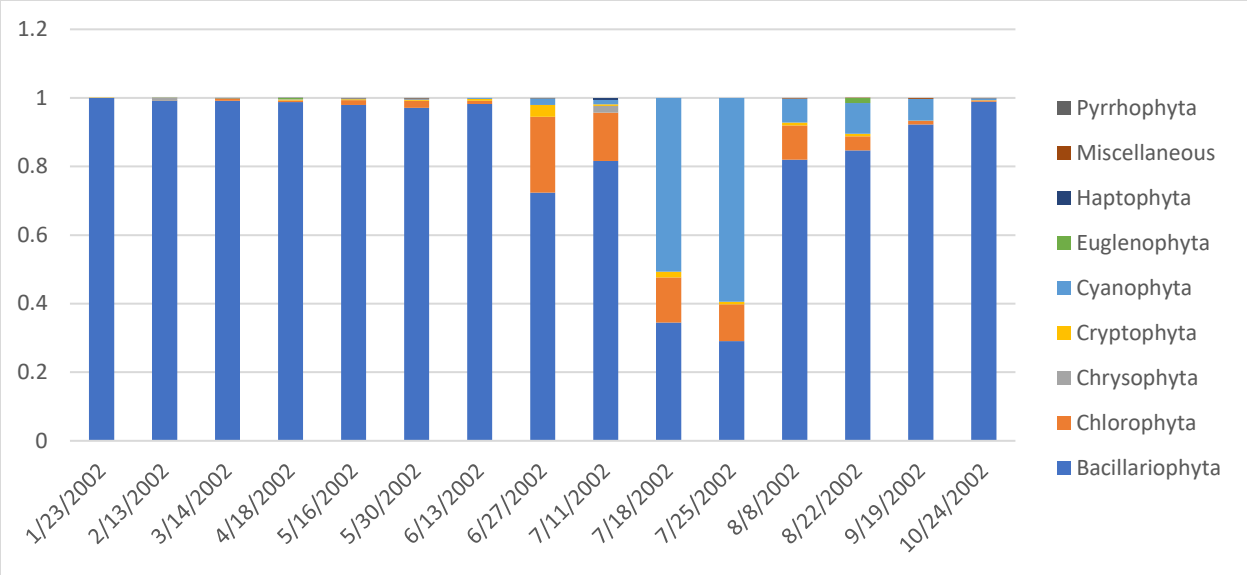
2002 Algal Species Raw Data

This data set included algal species data from Idaho Power Company (IPC) as relative abundance and biovolume measured at the inflow to the Brownlee model (RM 345.6) as well as data at sites 340, 385, 403, and 449.3. However, sites 385, 403, and 449.3 only had one sample date in January. Data from sites 340 and 345.6 are summarized below.

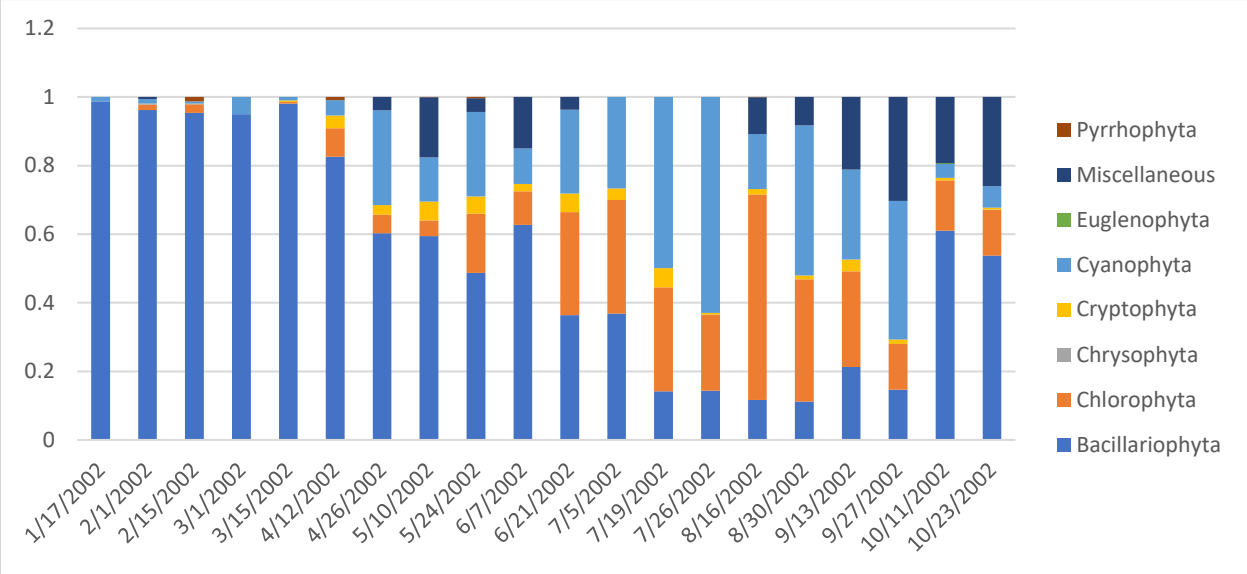
Relative Abundance at RM 340:



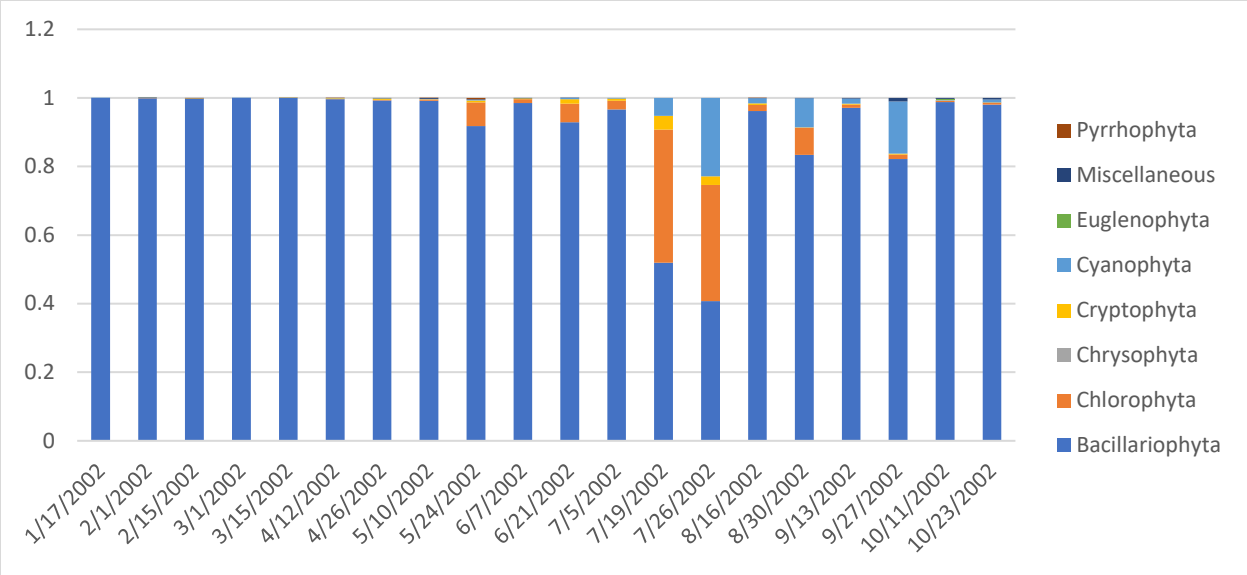
Biovolume at RM 340:



Relative Abundance at RM 345.6:



Biovolume at RM 345.6:



Algae group percentages using each recording technique (biovolume or relative abundance) were calculated using the following equation:

$$Algae\ Group\ Percent = \frac{Sum\ of\ percentages\ for\ all\ divisions\ in\ algae\ group}{20\ (number\ of\ sampling\ days)}$$

The three model algal groups were split up such that Algae1 included Bacillariophyta, Algae2 included all divisions not in Algae1 or Algae3, and Algae3 included Cyanophyta. Using the above calculation, Table 1 shows the percentages of each algae group from the two recording techniques for each site.

Table 1. Algae group delineation from 2002 algal species data.

RM 340		
Model Algae Groups	Relative Abundance	Biovolume
Algae1 (Diatoms)	43%	84%
Algae2 (Greens, others)	21%	6%
Algae3 (Cyanobacteria)	35%	9%
RM 345.6		
Model Algae Groups	Relative Abundance	Biovolume
Algae1 (Diatoms)	54%	91%
Algae2 (Greens, others)	27%	6%
Algae3 (Cyanobacteria)	19%	3%

2011 Data from Wood and Etheridge (USGS)

This data included algal abundance and biovolume data on the Snake River at Nyssa, Oregon presented in a report by Wood and Etheridge at the USGS (2011). The Nyssa site is about 30 miles upstream from the Brownlee model inflow site. Table 8 below was copied from the report summarizing the algae groups.

Table 8. Summary of sestonic algae taxonomic results from analyses of samples collected in the Boise River near Parma, Idaho; Snake River near Adrian, Oregon; and Snake River at Nyssa, Oregon; water year 2010.

[Abbreviations: EWI, Equal Width Increment; mL, milliliter; µg/L, micrograms per liter; µm³/mL, cubic micrometers per milliliter

Sample date	Chlorophyll-*a* from EWI sample (µg/L)	Uncorrected chlorophyll-*a* fluorescence (µg/L)	Relative percent difference	Algal Concentration (1,000cells/mL)	Biovolume (µm³/mL)	Abundance		Biovolume		Species richness
						Diatoms (percent)	Green algae (percent)	Diatoms (percent)	Green algae (percent)	
					Parma					
February	18.1	5.35	109	9.25	18,057	91.2	6.19	94.2	5.68	25
March	18.8	4.70	120	25.3	45,610	91.6	5.07	95.6	3.49	27
May	14.0	8.30	51.1	66.4	112,375	71.1	11.4	90.0	7.59	27
July	13.7	6.30	74.0	2,720	4,089,436	64.4	21.5	89.6	9.21	28
August	4.00	5.32	28.3	632	592,760	46.2	37.3	67.1	29.5	33
September	5.50	4.96	10.3	1,540	1,934,423	64.4	13.6	92.5	6.13	27
					Adrian					
March	95.7	47.4	67.5	27.3	17,018	97.2	1.90	98.2	1.72	14
May	25.3	10.2	85.1	64.6	102,662	87.0	7.74	88.8	10.7	25
July	1.30	1.10	17.1	768	801,498	54.2	24.4	75.7	19.6	34
September	2.30	3.49	41.1	634	1,158,625	62.0	21.8	94.7	4.01	36
					Nyssa					
February	16.5	7.48	75.3	9.61	19,352	93.7	3.76	95.0	4.88	22
March	89.2	21.8	121	28.7	22,873	97.4	0.59	98.9	0.06	19
May	24.4	11.4	72.7	64.4	80,279	79.5	9.94	88.7	8.65	39
July	2.3	2.47	7.02	1,492	1,775,430	74.1	9.52	70.8	26.1	31
September	5.1	2.93	54.0	1,142	1,399,485	43.3	30.6	86.7	11.0	27

Table 2 summarizes the algae data at the Nyssa site using the same calculation as mentioned previously:

$$Algae\ Group\ Percent = \frac{Sum\ of\ percentages\ for\ all\ divisions\ in\ algae\ group}{5\ (number\ of\ sampling\ months)}$$

Table 2. Algae groups from 2011 data.

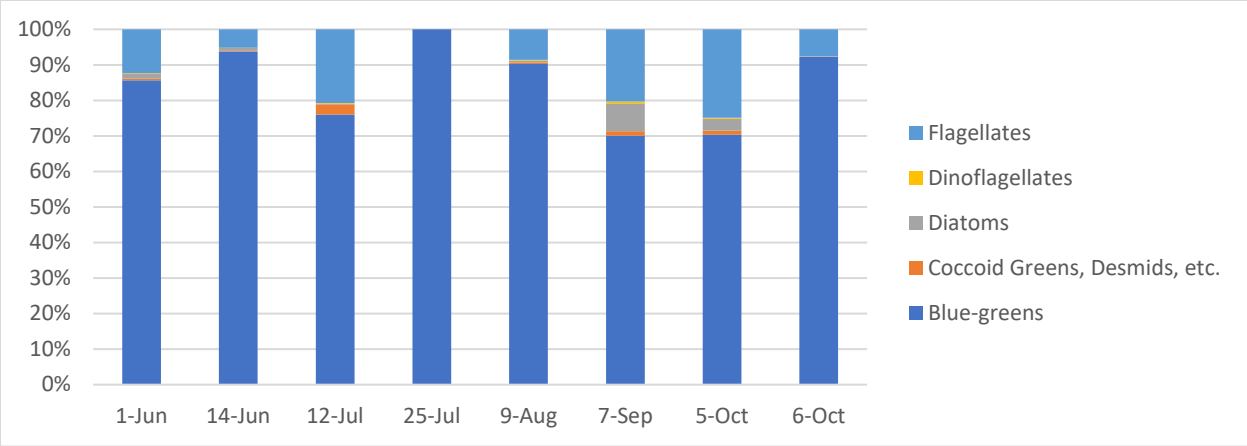
Algae Group	Relative Abundance	Biovolume
Diatoms	78%	88%
Greens	11%	10%
Remainder	11%	2%

These values were similar to the 2002 percentages for each group.

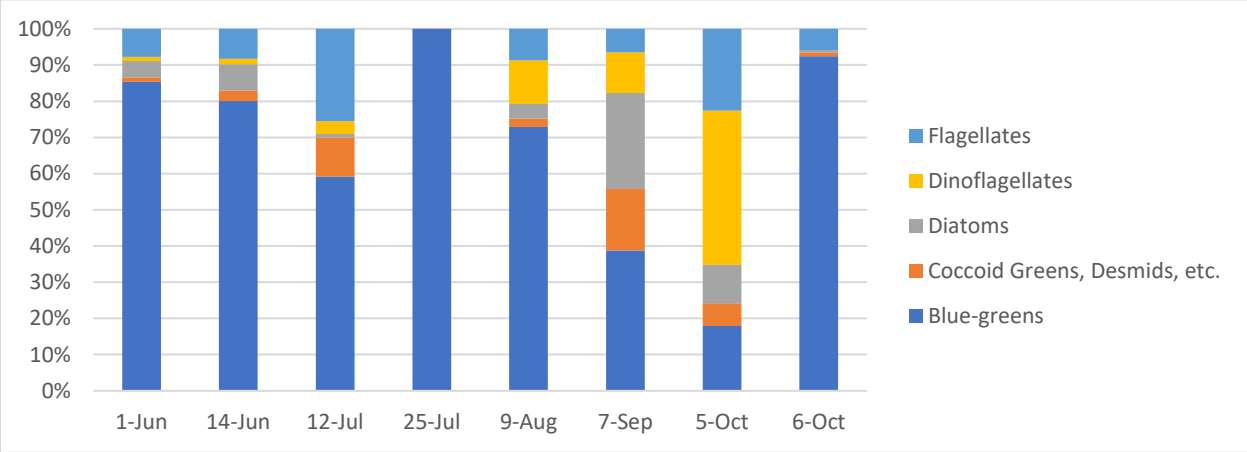
2016 Phytoplankton Raw Data

This data set included algae relative abundance and biovolume data from IPC for sample dates from 5/18/2016 to 10/13/2016 at sampling sites in all three reservoirs: Hells Canyon (RMs 248.1, 252), Oxbow (RM 273), and Brownlee (RMs 286, 292, 302, 318, 320). The relative abundance and biovolume data are summarized below for each reservoir.

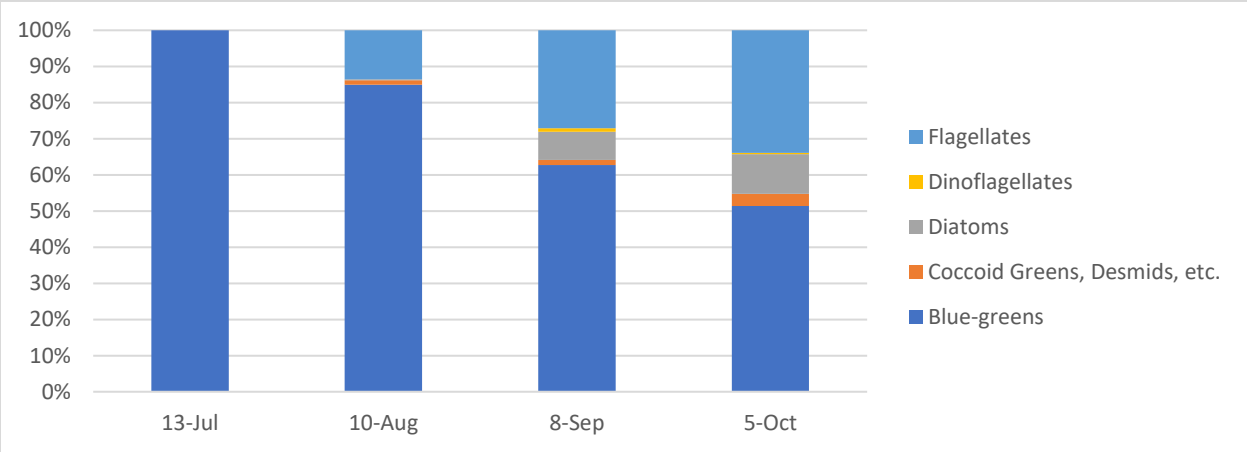
Brownlee Relative Abundance:



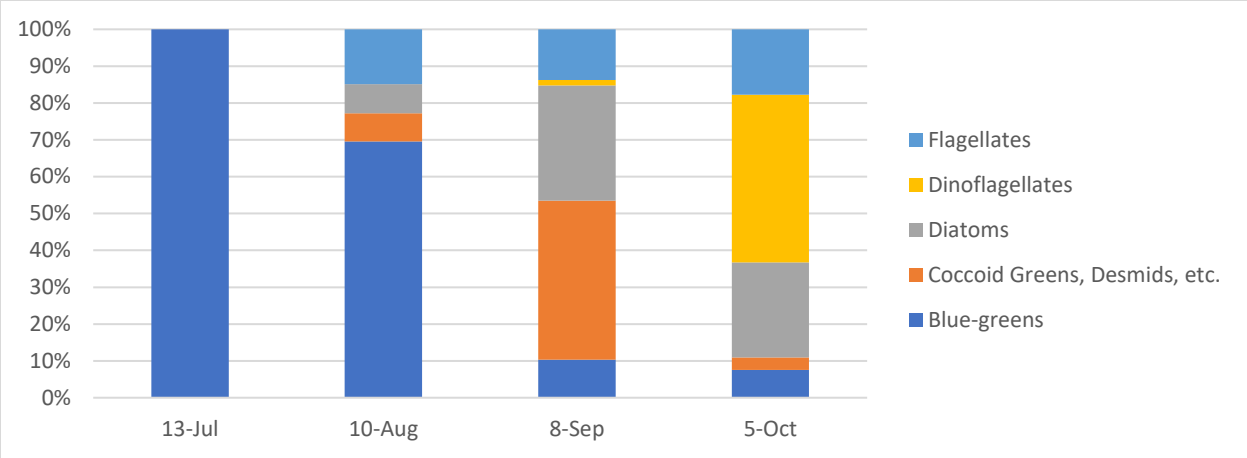
Brownlee Biovolume:



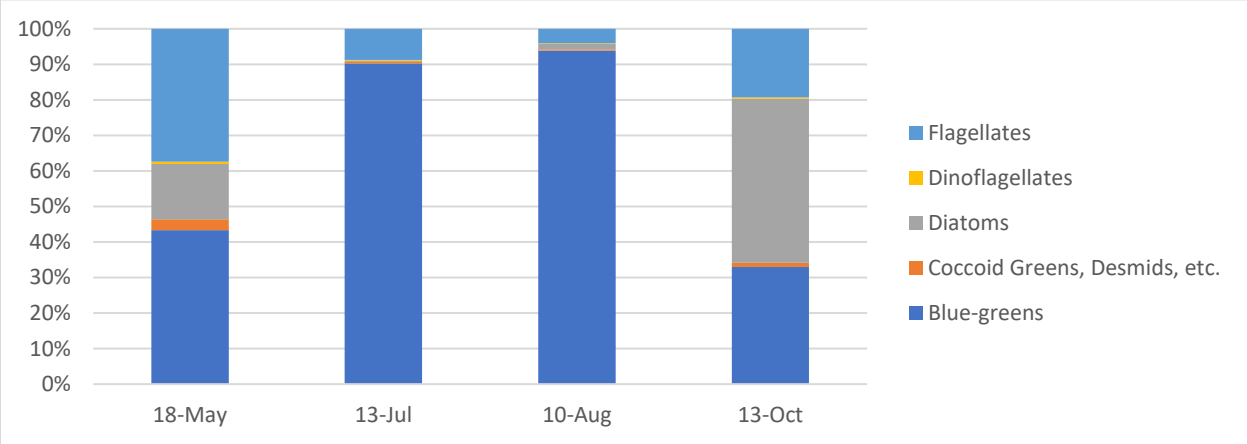
Oxbow Relative Abundance:



Oxbow Biovolume:



Hells Canyon Relative Abundance:



Hells Canyon Biovolume:

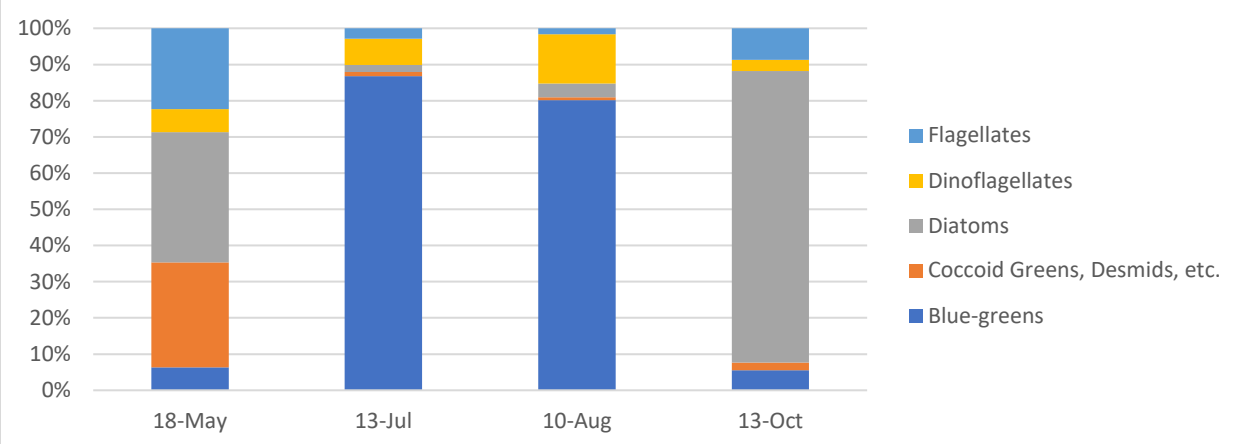


Table 3 shows the percentages of each algae group from the two organizational methods for each reservoir using the same calculation as mentioned previously:

$$Algae\ Group\ Percent = \frac{Sum\ of\ percentages\ for\ all\ divisions\ in\ algae\ group}{number\ of\ samples}$$

Table 3. Algae groups from 2016 data.

Brownlee		
Model Algae Groups	Relative Abundance	Biovolume
Algae1 (Diatoms)	2%	8%
Algae2 (Greens, others)	15%	27%
Algae3 (Cyanobacteria)	83%	65%
Oxbow		
Model Algae Groups	Relative Abundance	Biovolume
Algae1 (Diatoms)	5%	16%
Algae2 (Greens, others)	20%	37%
Algae3 (Cyanobacteria)	75%	47%
Hells Canyon		
Model Algae Groups	Relative Abundance	Biovolume
Algae1 (Diatoms)	16%	31%
Algae2 (Greens, others)	19%	25%
Algae3 (Cyanobacteria)	65%	45%

These percentages varied quite a bit from the 2002 and 2011 inflow river percentages. However, the 2002 and 2011 percentages included sampling dates earlier in the year which included a lot more diatoms and therefore weighted the overall percentages more towards diatoms.

References

Wood, M. S., and Etheridge, A., 2011, Water-quality conditions near the confluence of the Snake and Boise Rivers, Canyon County, Idaho. No. 2011-5217. U.S. Geological Survey. https://doi.org/10.3133/sir20115217

Appendix A2

Model Coefficients

Model coefficients used in the first order and sediment diagenesis models are shown below in Table 1.

Table 1. W2 Model Water Quality Parameters.

Variable	Description	Units	Typical values*	Calibration Values
Hydrodynamics and Longitudinal Transport				
AX	Longitudinal eddy viscosity (for momentum dispersion)	m^2/sec	1	BR: 0.5 OX: 1 HC: 1
DX	Longitudinal eddy diffusivity (for dispersion of heat and constituents)	m^2/sec	1	BR: 0.5 OX: 1 HC: 1
FI	Interfacial friction factor		0.01	All WBs: 0.01
Z0	Water surface roughness height for wind shear	m	0.001	All WBs: 0.001
AZC	Form of vertical turbulence closure algorithm		TKE	Brownlee: W2 Oxbow: TKE Hells Canyon: TKE
AZMAX	Maximum value for vertical eddy viscosity	$m^2\ s^{-1}$	1.0	All WBs: 1
Temperature				
H SLHTC	Heat computation method	-	TERM	All WBs: TERM
AFW	a coefficient in the wind speed formulation,	Wm^{-2} mm Hg^{-1}		BR: 8.8 OX: 9.2 HC: 9.2
BFW	b coefficient in the wind speed formulation,	Wm^{-2} mm Hg^{-1}		BR: 2.94 OX: 0.46 HC: 0.2
CFW	C coefficient in the wind speed formulation	-		All WBs: 1
WINDH	Wind height measurement above ground surface	m	2	All WBs: 2
SLICEC	Ice cover computation method	-	DETAIL	All WBs: DETAIL
ALBEDO	Ratio of reflection to incident radiation (albedo of ice)		0.25	All WBs: 0.25
HWI	Coefficient of water-ice heat exchange	$W\ m^{-2}\ {}^{o}C^{-1}$	10	All WBs: 10

Variable	Description	Units	Typical values*	Calibration Values
BETAI	Fraction of solar radiation absorbed in the ice surface		0.6	All WBs: 0.6
GAMMAI	Solar radiation extinction coefficient	m^{-1}	0.07	All WBs: 0.07
ICEMIN	Minimum ice thickness before ice formation is allowed	m	0.05	All WBs: 0.05
ICET2	Temperature above which ice formation is not allowed	^oC	3	All WBs: 3
CBHE	Coefficient of bottom heat exchange	Wm^2/sec	0.30	All WBs: 0.3
T2I	Initial water temperature	^oC		Brownlee: 2-4.5 OX: 4 HC: 4
TSED	Sediment (ground) temperature	^oC		Brownlee: 4-10 OX: 10 HC: 10
TSEDF	Fraction of heat lost to sediments that is added back to water column	-		All WBs: 1
WSC	Wind sheltering coefficient		0.5 – 3	BR: 0.4-1 OX: 2 HC: 0.5-2
BETA	Fraction of incident solar radiation absorbed at the water surface		0.45	All WBs: 0.45
Water Quality				
EXH20	Extinction for water	/m	0.25	Brownlee: 0.419 OX:0.25 HC:0.25
EXSS	Extinction due to inorganic suspended solids	m3/m/g	0.01-0.2	Brownlee: 0.055 OX:0.2 HC:0.2
EXOM	Extinction due to organic suspended solids	m3/m/g	0.1-0.2	Brownlee: 0.055 OX:0.2 HC:0.2
SSS	Suspended solids settling rate for suspended solids groups 1, 2	m/day	0.5-2	All WBs: 5, 1.9, 0.2
H2SQ10	Arhennius temperature rate multiplier	-		All WBs: 1.04
H2S1DK	1st-order decay rate	/day		All WBs: 0.1
CH4Q10	Arhennius temperature rate multiplier	-		All WBs: 1.04
CH41DK	1st-order decay rate	/day		All WBs: 0.5
KFE_OXID	Rate of Fe oxidation under oxic conditions	m3/day/g		All WBs: 0.0001
KFE_RED	Rate of iron reduction under anaerobic conditions	/day		All WBs: 0.001

Variable	Description	Units	Typical values*	Calibration Values
KFEOOH_HalfSat	Half-saturation constant for O2 for FeOOH reduction to Fe(II)	g/m3		All WBs: 0.2
FeSetVel	Settling velocity of Fe oxide	m/day		All WBs: 1.5
KMN_OXID	Oxidation rate of manganese	m3/day/g		All WBs: 0.3
KMN_RED	Rate of Mn reduction under anaerobic conditions	/day		All WBs: 1
KMNOH_HalfSat	Half-saturation constant of oxygen for manganese dioxide reduction	g/m3		All WBs: 0.2
MnSetVel	Settling velocity of Mn oxide	m/day		All WBs: 1.7
EXA	Extinction due to organic algal type 1, 2, 3	m3/m/g	0.1-0.2	Brownlee: 0.055 OX:0.15 HC:0.13
AG	Algal growth rate for algal type 1, 2, 3	/day	1-3	All WBs: 1.7,1.7,1.5
AM	Algal mortality rate for algal type 1, 2, 3	/day	0.04 -0.1	All WBs: 0.1
AE	Algal excretion rate for algal type 1, 2, 3	/day	0.04 -0.1	All WBs: 0.05, 0.055, 0.055
AR	Algal dark respiration rate for algal type 1, 2, 3	/day	0.04 -0.1	All WBs: 0.1
AS	Algal settling rate for algal type 1, 2, 3	/day	0.08 – 1.0	All WBs: 0.25, 0.1, -0.05
ASAT	Saturation intensity at maximum photosynthetic rate for algal type 1, 2, 3	W/m^2	10-170	All WBs: 60, 100, 100
APOM	Fraction of algal biomass lost by mortality to detritus for algal type 1, 2, 3		0.8	All WBs: 0.8
AT1	Lower temperature for algal growth for algal type 1, 2, 3	^oC		All WBs: 4
AT2	Lower temperature for maximum algal growth for algal type 1, 2, 3	^oC		All WBs: 10, 15, 22
AT3	Upper temperature for maximum algal growth for algal type 1, 2, 3	^oC		All WBs: 15, 25, 30
AT4	Upper temperature for algal growth for algal type 1, 2, 3	^oC		All WBs: 40
AK1	Fraction of algal growth rate at AT1 for algal type 1, 2, 3			All WBs: 0.3, 0.07, 0.07
AK2	Fraction of maximum algal growth rate at AT2 for algal type 1, 2, 3			All WBs: 0.98
AK3	Fraction of maximum algal growth rate at AT3 for algal type 1, 2, 3			All WBs: 0.98
AK4	Fraction of algal growth rate at AT4 for algal type 1, 2, 3			All WBs: 0.1

Variable	Description	Units	Typical values*	Calibration Values
ALGP	Stoichiometric equivalent between organic matter and phosphorus for algal type 1, 2, 3		0.005-0.02	All WBs: 0.01
ALGN	Stoichiometric equivalent between organic matter and nitrogen for algal type 1, 2, 3		0.08	All WBs: 0.08
ALGC	Stoichiometric equivalent between organic matter and carbon for algal type 1, 2, 3		0.45	All WBs: 0.45
ALGSI	Stoichiometric equivalent between organic matter and silica for algal type 1, 2, 3		0.18	All WBs: 0
ACHLA	Ratio between algal biomass and chlorophyll a for algal type 1, 2, 3	mg algae/ µg chl a	0.05	All WBs: 0.05, 0.02, 0.02
AHSP	Algal half-saturation constant for phosphorous for algal type 1, 2, 3	g/m^3	0.003	All WBs: 0.005, 0.005, 0.001
AHSN	Algal half-saturation constant for ammonia for algal type 1, 2, 3	g/m^3	0.014	All WBs: 0.014
AHSSI	Algal half-saturation constant for silica for algal type 1, 2, 3	g/m^3	0.0	All WBs: 0
ANEQN	Ammonium preference equation number for algal type 1, 2, 3			All WBs: 1
ANPR	Parameter for ANEQN equation number 2			N/A
EG	Maximum growth rate for epiphyton	/day	1-3	All WBs: 1.5
EM	Mortality rate for epiphyton	/day	0.04 -0.1	All WBs: 0.1
EE	Excretion rate for epiphyton	/day	0.04 -0.1	All WBs: 0.04
ER	Dark respiration rate for epiphyton	/day	0.04 -0.1	All WBs: 0.1
EB	Burial rate for epiphyton	/day		All WBs: 0.001
ESAT	Saturation intensity at maximum photosynthetic rate for epiphyton	W/m^2	10-170	All WBs: 85
EPOM	Fraction of biomass lost by mortality to detritus for epiphyton		0.8	All WBs: 0.8
ET1	Lower temperature for growth of epiphyton	^oC		All WBs: 4
ET2	Lower temperature for maximum growth of epiphyton	^oC		All WBs: 10
ET3	Upper temperature for maximum growth for epiphyton	^oC		All WBs: 20
ET4	Upper temperature for growth for epiphyton	^oC		All WBs: 30

Variable	Description	Units	Typical values*	Calibration Values
EK1	Fraction of growth rate at ET1 for epiphyton			All WBs: 0.1
EK2	Fraction of maximum algal growth rate at ET2 for epiphyton			All WBs: 0.99
EK3	Fraction of maximum growth rate at ET3 for epiphyton			All WBs: 0.99
EK4	Fraction of growth rate at ET4 for epiphyton			All WBs: 0.1
EP	Stoichiometric equivalent between organic matter and phosphorus for epiphyton		0.005-0.02	All WBs: 0.01
EN	Stoichiometric equivalent between organic matter and nitrogen for epiphyton		0.08	All WBs: 0.08
EC	Stoichiometric equivalent between organic matter and carbon for epiphyton		0.45	All WBs: 0.45
ESI	Stoichiometric equivalent between organic matter and silica for epiphyton		0.18	All WBs: 0
ECHLA	Ratio between epiphyton biomass and chlorophyll a		0.05	All WBs: 0.1
EHS	Biomass limitation factor	g/m^2		All WBs: 35
EHSP	Epiphyton half-saturation constant for phosphorous	g/m^3	0.003	All WBs: 0.005
EHSN	Epiphyton half-saturation constant for ammonia	g/m^3	0.014	All WBs: 0.014
EHSSI	Epiphyton half-saturation constant for silica	g/m^3		All WBs: 0
ENEQN	Epiphyton ammonium preference equation number			All WBs: 1
ENPR	Epiphyton half-saturation constant for ammonium preference if ENEQN=2	mg/l	0.001	N/A
EXZ1	Extinction due to zooplankton	m3/m/g	0.2	All WBs: 0.2
ZG	Maximum growth rate for zooplankton	/day	1.0	All WBs: 1
ZM	Mortality rate for zooplankton	/day	0.1	All WBs: 0.1
ZR	Dark respiration rate for zooplankton	/day	0.1	All WBs: 0.1
ZEFF	Zooplankton assimilation efficiency or the proportion of food assimilated to food consumed		0.5	All WBs: 0.5
PREFP	Preference factor of zooplankton for detritus or LPOM		0.5	All WBs: 0.5

Variable	Description	Units	Typical values*	Calibration Values
ZOOMIN	Threshold food concentration at which zooplankton feeding begins	g/m^3	0.01	All WBs: 0.001
ZS2P	Zooplankton half-saturation constant for food ingestion	g/m^3	0.3	All WBs: 0.3
ZS	Zooplankton settling velocity	m/day	0.0	All WBs: 0
ZT1	Lower temperature for growth of Zooplankton	^oC		All WBs: 4
ZT2	Lower temperature for maximum growth of Zooplankton	^oC		All WBs: 10
ZT3	Upper temperature for maximum growth for Zooplankton	^oC		All WBs: 25
ZT4	Upper temperature for growth for Zooplankton	^oC		All WBs: 30
ZK1	Fraction of growth rate at ZT1 for Zooplankton			All WBs: 0.07
ZK2	Fraction of maximum algal growth rate at ZT2 for Zooplankton			All WBs: 0.85
ZK3	Fraction of maximum growth rate at ZT3 for Zooplankton			All WBs: 0.98
ZK4	Fraction of growth rate at ZT4 for Zooplankton			All WBs: 0.1
ZP	Stoichiometric equivalent between organic matter and phosphorus for Zooplankton		0.005	All WBs: 0.005
ZN	Stoichiometric equivalent between organic matter and nitrogen for Zooplankton		0.08	All WBs: 0.08
ZC	Stoichiometric equivalent between organic matter and carbon for Zooplankton		0.45	All WBs: 0.5
PREFA-A1	Preference factor of zooplankton for algal type 1			All WBs: 0.5
PREFA-A2	Preference factor of zooplankton for algal type 2			All WBs: 0.3
PREFA-A2	Preference factor of zooplankton for algal type 3			All WBs: 0.1
PREFZ	Preference factor of zooplankton for zooplankton			All WBs: 0
LDOMDK	Labile DOM decay rate	/day	0.06 - 0.12	Brownlee: 0.08 OX: 0.1 HC:0.1

Variable	Description	Units	Typical values*	Calibration Values
RDOMDK	Maximum refractory decay rate	/day	0.001	Brownlee: 0.0015 OX:0.001 HC:0.001
LRDDK	Labile to refractory DOM decay rate	/day	0.001	All WBs: 0.01
LPOMDK	Labile Detritus decay rate	/day	0.06 - 0.12	All WBs: 0.08
RPOMDK	Refractory Detritus decay rate	/day	0.001	Brownlee: 0.0015 OX:0.001 HC:0.001
LRPDK	Labile to refractory POM decay rate	/day	0.001	All WBs: 0.01
POMS	Detritus settling rate	m/day	0.2 – 1.0	All WBs: 1.2
ORGP	Stoichiometric equivalent between organic matter and phosphorus		0.005	All WBs: 0.001
ORGN	Stoichiometric equivalent between organic matter and nitrogen		0.08	All WBs: 0.02
ORGC	Stoichiometric equivalent between organic matter and carbon		0.45	All WBs: 0.45
ORGSI	Stoichiometric equivalent between organic matter and silica		0.18	All WBs: 0.18
OMT1	Lower temperature for organic matter decay	^{o}C	4	All WBs: 4
OMT2	Lower temperature for maximum organic matter decay	^{o}C	30	All WBs: 30
OMK1	Fraction of organic matter decay rate at OMT1		0.1	Brownlee: 0.25 OX:0.15 HC:0.15
OMK2	Fraction of organic matter decay rate at OMT2		0.99	All WBs: 0.99
PARTP	Phosphorous partitioning coefficient for suspended solids		0	BR: 0.04 OX: 0 HC: 0
NH4DK	Ammonia decay rate (nitrification rate)	/day	0.01-0.3	Brownlee: 0.4 OX:0.4 HC:0.3
NH4T1	Lower temperature for ammonia decay	^{o}C	5	All WBs: 4
NH4T2	Lower temperature for maximum ammonia decay	^{o}C	20	All WBs: 30
NH4K1	Fraction of nitrification rate at NH4T1		0.1	All WBs: 0.1
NH4K2	Fraction of nitrification rate at NH4T2		0.99	All WBs: 0.99

Variable	Description	Units	Typical values*	Calibration Values
KGH2O	Constant used in calculation of ammonia gas transfer coefficient		168	All WBs: 168
NO3DK	Nitrate decay rate (denitrification rate)	/day	0.03-0.15	All WBs: 0.12
NO3S	Nitrate loss velocity to the sediments because of sediment denitrification	m/day	0.001	All WBs: 0
FNO3SED	Fraction of NO_3-N diffused into the sediments that becomes part of organic N in the sediments			All WBs: 0.37
NO3T1	Lower temperature for nitrate decay	^oC	5	All WBs: 4
NO3T2	Lower temperature for maximum nitrate decay	^oC	25	All WBs: 30
NO3K1	Fraction of denitrification rate at NO3T1		0.1	All WBs: 0.1
NO3K2	Fraction of denitrification rate at NO3T2		0.99	All WBs: 0.99
O2NH4	Oxygen stoichiometric equivalent for ammonia decay		4.57	All WBs: 4.57
O2OM	Oxygen stoichiometric equivalent for organic matter decay		1.4	All WBs: 1.4
O2AR	Oxygen stoichiometric equivalent for dark respiration algal type 1, 2, 3		1.1	All WBs: 1.1
O2ER	Oxygen stoichiometric equivalent for epiphyton dark respiration		1.1	All WBs: 1.1
O2ZR	Oxygen stoichiometric equivalent for zooplankton dark respiration		1.1	All WBs: 1.1
O2AG	Oxygen stoichiometric equivalent for algal growth algal type 1, 2, 3		1.4	All WBs: 1.6, 1.8, 1.8
O2EG	Oxygen stoichiometric equivalent for epiphyton growth		1.4	All WBs: 1.4
O2LIM	Dissolved oxygen concentration at which anaerobic processes begin	g/m^3	0.05	All WBs: 0.2
AANOX	Ratio of anoxic to oxic carbon decomposition rate			All WBs: 0.1
REARC	Type of waterbody, RIVER, LAKE, or ESTUARY			All WBs: LAKE
EQN#	Reaeration equation number			All WBs: 6
DGPO2	Fraction of oxygen transfer that is total gas transfer at the air-water interface			All WBs: 1
MINKL	Minimum gas transfer coefficient	m/d (lakes), /day (river)		BR: 0.6 OX: 1.2 HC: 1.2
* Wells (2022)				

Sediment Diagenesis Coefficients

The sediment diagenesis coefficients for each water body are shown below.

Brownlee Reservoir

$ W2_diagenesis input file					
$ All lines at top of file starting with $ are comments and disregarded by the model					
$ 08/29/2020 Additional inputs are required if a group switch is ON					
$ SW/Bernadel					
"Global Switch for all sediment diagenesis features"	.TRUE.				
"Include FFT layer (Fine Fluids Tailing - for Pit Lakes)"	.FALSE.				
"FFT layer number of periods"	5				
"FFT layer start times"	1	65	125	200	300
"FFT layer end times"	50	100	175	250	400
"Initial tailings concentration in FFT (gm/m3)"	360000				
"Sediment settling velocity of FFT to MFT (m/d)"	0				
"Move FFT layer during consolidation"	.FALSE.				
"Include bed consolidation"	.FALSE.				
"Fraction of layer thickness at which water layer is added"	1				
"Number of bed consolidation regions"	1				
"Starting segment for regions"	1				
"Ending segment for regions"	239				
"Data type for bed consolidation for each region (0: Constant, 1: Time varying)"	1				
"Bed consolidation rate (m/d)"	0.027397				
"Bed consolidation data file"	Regn.npt				
"Write bed elevation snapshot output"	.FALSE.				
"Write bed porosity snapshot output"	.FALSE.				
"Include sediment diagenesis simulation"	.TRUE.				
"Initial bed thickness in meters"	0.4				
"Initial sediment bed porosity"	0.88				
"Sediment bed particle size in microns"	60				
"Sediment type (1: Cohesive, 2: Non-cohesive)"	2				
"Sediment bulk density (kg/m3)"	1050				
"Sediment particle settling velocity (m/d)"	5				
"Include sediment resuspension and deposition processes"	.FALSE.				
"Include bubble release"	.FALSE.				
"Gas diffusion coefficient in sediment in m/s"	1.0d-9				
"Calibration parameter R1 in m"	0.0014				
"Young's modulus E in N/m2"	1.4d+9				
"Critical stress intensity factor for sediments K1c in N/m^3/2"	300				
"Bubbles release scale"	0.02				

"Fraction of critical pressure at which cracks close"	0.2				
"Switch to limit bubble size"	.TRUE.				
"Maximum bubble radius in mm"	80				
"Switch to use slow release of bubbles"	.TRUE.				
"Bubbles release fraction (sediments)"	0.005				
"Bubbles accumulation fraction"	0.1				
"Number of bubbles release array"	2000				
"Bubbles release fraction (atmosphere)"	0.001				
"Bubbles-water gas exchange rate (1/s)"	1.0d-7				
"Apply additional turbulence due to bubbles release"	.FALSE.				
"Turbulence scaling factor for bubbles release"	0.001				
"Include POM resuspension"	.FALSE.				
"Critical shear stress for POM resuspension dynes/cm^2"	0.001				
"Critical Shields parameter for POM"	10				
"Use Cao method to estimate critical Shields parameter (rather than using input value)"	.FALSE.				
"POM specific gravity"	1.5				
"POM particle diameter m"	0.0001				
"Include modeling of alkalinity/pH in sediments"	.TRUE.				
"Include modeling of Iron (FeOOH and Fe(II)) in sediments"	.TRUE.				
"Include modeling of Manganese (Mn(II) and MnO2) in sediments"	.TRUE.				
"Number of regions for different initial sediment concentrations"	4				
	Region1	Region 2	Region3	Region4	Region5
"Starting segment for regions"	2	70	129	167	
"Ending segment for regions"	69	128	166	239	
"Initial sediment temperature oC"	5	5	5	5	
"Initial sediment pH (only used if include modeling dynamic pH)"	6.8	6.8	6.8	6.8	
"Initial POC (total) concentration mgC/L"	4000	5500	5000	5000	
"Initial PON (total) concentration mgN/L"	570	785	714	714	
"Initial POP (total) concentration mgP/L"	71	98	89	89	
"Initial SO4 concentration mgS/L"	3.46	3.46	3.46	3.46	
"Initial dissolved NH4 concentration mgN/L"	5	5	10	10	
"Initial dissolved NO3 concentration mgN/L"	0.01	0.01	0.01	0.01	
"Initial total PO4 concentration mgP/L"	3.03	3.03	3.03	3.03	
"Initial dissolved H2S concentration mgS/L"	0.08	0.08	0.08	0.08	
"Initial CH4 concentration mgC/L"	0.092	0.092	0.092	0.092	

"Initial TIC concentration mgC/L"	4.011	4.011	4.011	4.011	
"Initial Alkalinity concentration for each region mg/l as CaCO3"	50	50	50	50	
"Initial Ferrous Iron concentration for each region mgFe/l"	100	100	100	100	
"Initial Iron Oxyhydroxide concentration for each region mgFe/l,"	0.5	0.5	0.5	0.5	
"Initial Mn(II) concentration for each region mgMn/l,"	500	500	500	500	
"Initial manganese dioxide concentration for each region mgMn/l,"	0.5	0.5	0.5	0.5	
"Number of regions for different diagenesis related rates"	4				
	Region1	Region 2	Region3	Region4	Region5
"Starting segment for regions"	2	70	129	167	
"Ending segment for regions"	69	128	166	239	
"Fraction of labile POC"	-0.03	0.03	0.03	0.03	
"Fraction of refractory POC"	0.97	0.96	0.96	0.96	
"Fraction of labile PON"	0.03	0.03	0.03	0.03	
"Fraction of refractory PON"	0.97	0.96	0.96	0.96	
"Fraction of labile POP"	0.03	0.03	0.03	0.03	
"Fraction of refractory POP"	0.97	0.96	0.96	0.96	
"Pore water diffusion coefficient m2/d"	0.0011	0.0011	0.00006	0.00006	
"Particle mixing velocity between aerobic and anaerobic layers m2/d"	0.00006	0.00006	0.000006	0.000006	
"Burial velocity m/d"	0.00001	0.000001	0.000001	0.000001	
"Reference POC G1 concentration for bioturbation mg-C/g Calculation of final benthic particle mixing velocity Equation 13.6 in DoToro (2001)"	0.01	0.01	0.01	0.01	
"CH4 production calculation method (0: Analytical 1: Numerical)"	1	1	1	1	
"DO threshold for aerobic layer oxidation rates mgO2/L"	2	2	2	2	
"Nitrification rate in aerobic layer at DO below threshold m/d"	0.3	0.3	0.3	0.3	
"Nitrification rate in aerobic layer at DO above threshold m/d"	0.6	0.6	0.6	0.6	
"Denitrification rate in aerobic layer at DO below threshold m/d"	0.1	0.1	0.1	0.1	
"Denitrification rate in aerobic layer at DO above threshold m/d"	0.1	0.1	0.1	0.1	
"Denitrification rate in anerobic layer m/d"	0.1	0.1	0.1	0.1	
"CH4 oxidation rate in aerobic layer m/d"	1.5	1.5	1.5	1.5	
"Half-saturation oxygen constant for CH4 oxidation mg-O2/L"	0	0	0	0	
"Nitrification half-saturation constant for NH4 in aerobic layer mgN/L"	0.4	0.4	0.4	0.4	

"Nitrification half-saturation constant for O2 in aerobic layer mgO2/L"	0.37	0.37	0.37	0.37	
"Temperature coefficient for pore water diffusion between layers"	1.11	1.11	1.11	1.11	
"Temperature coefficient for particle mixing diffusion coefficient"	1	1	1	1	
"Temperature coefficient for nitrification"	1.11	1.11	1.11	1.11	
"Temperature coefficient for denitrification"	1.11	1.11	1.11	1.11	
"Temperature coefficient for methane oxidation"	1.11	1.11	1.11	1.11	
"SO4 concentration above which sulfide over methane is produced mgS/L"	20	20	20	20	
"H2S oxidation rate in aerobic layer m/d"	0.2	0.2	0.2	0.2	
"Temperature coefficient for H2S oxidation"	1.11	1.11	1.11	1.11	
"H2S oxidation normalization constant for O2 mgO2/L"	4	4	4	4	
"Diagenesis rate for labile POC (G1) 1/d"	0.005	0.005	0.018	0.018	
"Diagenesis rate for refractory POC (G2) 1/d"	0.0005	0.0005	0.00015	0.00015	
"Diagenesis rate for inert/slow refractory POC (G3) 1/d"	0.000001	0.000001	0.0000001	0.0000001	
"Diagenesis rate for labile PON (G1) 1/d"	0.0051	0.0051	0.0051	0.0051	
"Diagenesis rate for refractory PON (G2) 1/d"	0.00026	0.00026	0.0007	0.0007	
"Diagenesis rate for inert/slow refractory PON (G3) 1/d"	0.000001	0.000001	0.0000001	0.0000001	
"Diagenesis rate for labile POP (G1) 1/d"	0.01	0.01	0.015	0.015	
"Diagenesis rate for refractory POP (G2) 1/d"	0.001	0.001	0.00015	0.00015	
"Diagenesis rate for inert/slow refractory POP (G3) 1/d"	0.000001	0.000001	0.0000001	0.0000001	
"Temperature coefficient for labile POC"	1.11	1.11	1.11	1.11	
"Temperature coefficient for refractory POC"	1.11	1.11	1.11	1.11	
"Temperature coefficient for inert/slow refractory POC"	1.11	1.11	1.11	1.11	
"Temperature coefficient for labile PON"	1.11	1.11	1.11	1.11	
"Temperature coefficient for refractory PON"	1.11	1.11	1.11	1.11	

"Temperature coefficient for inert/slow refractory PON"	1.11	1.11	1.11	1.11	
"Temperature coefficient for labile POP"	1.11	1.11	1.11	1.11	
"Temperature coefficient for refractory POP"	1.11	1.11	1.11	1.11	
"Temperature coefficient for inert/slow refractory POP"	1.11	1.11	1.11	1.11	
"PO4 sorption coefficient in anaerobic layer m^3/kg"	0.05	0.05	0.05	0.05	
"Incremental PO4 partition coefficient"	0.02	0.02	0.02	0.02	
"Critical oxygen concentration for incremental sorption mg-O2/L"	0.01	2	2	2	
"NH4 sorption coefficient in aerobic layer m^3/kg"	0	0	0	0	
"NH4 sorption coefficient in anaerobic layer m^3/kg"	0.001	0.001	0.001	0.001	
"H2S sorption coefficient in aerobic layer m^3/kg"	0	0	0	0	
"H2S sorption coefficient in anaerobic layer m^3/kg"	0	0	0	0	
"Algorithm for POM resuspension (0: Wind induced resuspension, 1: Bottom scour resuspension) Only used if Include POM resuspension is .TRUE."	1	1	1	1	
"Fe(II) sorption coefficient in aerobic layer m^3/g"	50	50	50	50	
"Fe(II) sorption coefficient in anaerobic layer m^3/g"	50	50	50	50	
"Mn(II) sorption coefficient in aerobic layer m^3/g"	5	5	5	5	
"Mn(II) sorption coefficient in anaerobic layer m^3/g"	5	5	5	5	
"Write sediment fluxes"	.TRUE.				
"Frequency of output days"	1				
"Sediment Temperature Computations=1 (internal calcs or =2 neighboring water)"	2				
"Subdirectory for Sediment Diagenesis Output (no quotes needed if no spaces in name)"					

Oxbow

$ W2_diagenesis input file Oxbow						
$ All lines at top of file starting with $ are comments and disregarded by the model						
$ 08/29/2020 Additional inputs are required if a group switch is ON						
$ Zhong Zhang						
"Global Switch for all sediment diagenesis features"	.TRUE.					
"Include FFT layer (Fine Fluids Tailing - for Pit Lakes)"	.FALSE.					
"FFT layer number of periods"	5					
"FFT layer start times"	1	65	125	200	300	
"FFT layer end times"	50	100	175	250	400	

"Initial tailings concentration in FFT (gm/m3)"	360000
"Sediment settling velocity of FFT to MFT (m/d)"	0
"Move FFT layer during consolidation"	.FALSE.
"Include bed consolidation"	.FALSE.
"Fraction of layer thickness at which water layer is added"	1
"Number of bed consolidation regions"	1
"Starting segment for regions"	1
"Ending segment for regions"	53
"Data type for bed consolidation for each region (0: Constant, 1: Time varying)"	1
"Bed consolidation rate (m/d)"	0.027397
"Bed consolidation data file"	Regn.npt
"Write bed elevation snapshot output"	.FALSE.
"Write bed porosity snapshot output"	.FALSE.
"Include sediment diagenesis simulation"	.TRUE.
"Initial bed thickness in meters"	0.4
"Initial sediment bed porosity"	0.88
"Sediment bed particle size in microns"	60
"Sediment type (1: Cohesive, 2: Non-cohesive)"	2
"Sediment bulk density (kg/m3)"	1050
"Sediment particle settling velocity (m/d)"	5
"Include sediment resuspension and deposition processes"	.FALSE.
"Include bubble release"	.FALSE.
"Gas diffusion coefficient in sediment in m/s"	1.0d-9
"Calibration parameter R1 in m"	0.0014
"Young's modulus E in N/m2"	1.4d+9
"Critical stress intensity factor for sediments K1c in N/m^3/2"	300
"Bubbles release scale"	0.02
"Fraction of critical pressure at which cracks close"	0.2
"Switch to limit bubble size"	.TRUE.
"Maximum bubble radius in mm"	80
"Switch to use slow release of bubbles"	.TRUE.
"Bubbles release fraction (sediments)"	0.005
"Bubbles accumulation fraction"	0.1
"Number of bubbles release array"	2000
"Bubbles release fraction (atmosphere)"	0.001
"Bubbles-water gas exchange rate (1/s)"	1.0d-7
"Apply additional turbulence due to bubbles release"	.FALSE.
"Turbulence scaling factor for bubbles release"	0.001
"Include POM resuspension"	.FALSE.

"Critical shear stress for POM resuspension dynes/cm^2"	0.001					
"Critical Shields parameter for POM"	10					
"Use Cao method to estimate critical Shields parameter (rather than using input value)"	.FALSE.					
"POM specific gravity"	1.5					
"POM particle diameter m"	0.0001					
"Include modeling of alkalinity/pH in sediments"	.TRUE.					
"Include modeling of Iron (FeOOH and Fe(II)) in sediments"	.TRUE.					
"Include modeling of Manganese (Mn(II) and MnO2) in sediments"	.TRUE.					
"Number of regions for different initial sediment concentrations"	1					
	Region1	Region 2	Region 3	Region 4	Region 5	
"Starting segment for regions"	2					
"Ending segment for regions"	53					
"Initial sediment temperature oC"	10					
"Initial sediment pH (only used if include modeling dynamic pH)"	6.5					
"Initial POC (total) concentration mgC/L"	500					
"Initial PON (total) concentration mgN/L"	35					
"Initial POP (total) concentration mgP/L"	9					
"Initial SO4 concentration mgS/L"	3.46					
"Initial dissolved NH4 concentration mgN/L"	6					
"Initial dissolved NO3 concentration mgN/L"	0.01					
"Initial total PO4 concentration mgP/L"	3.03					
"Initial dissolved H2S concentration mgS/L"	0.08					
"Initial CH4 concentration mgC/L"	0.092					
"Initial TIC concentration mgC/L"	4.011					
"Initial Alkalinity concentration for each region mg/l as CaCO3"	50					
"Initial Ferrous Iron concentration for each region mgFe/l"	100					
"Initial Iron Oxyhydroxide concentration for each region mgFe/l,"	0.5					
"Initial Mn(II) concentration for each region mgMn/l,"	500					
"Initial manganese dioxide concentration for each region mgMn/l,"	0.5					
"Number of regions for different diagenesis related rates"	1					
	Region1	Region 2	Region 3	Region 4	Region 5	

"Starting segment for regions"	2					
"Ending segment for regions"	53					
"Fraction of labile POC"	-0.2					
"Fraction of refractory POC"	0.75					
"Fraction of labile PON"	0.2					
"Fraction of refractory PON"	0.75					
"Fraction of labile POP"	0.2					
"Fraction of refractory POP"	0.75					
"Pore water diffusion coefficient m2/d"	0.0001					
"Particle mixing velocity between aerobic and anaerobic layers m2/d"	0.00006					
"Burial velocity m/d"	0.00001					
"Reference POC G1 concentration for bioturbation mg-C/g Calculation of final benthic particle mixing velocity Equation 13.6 in DoToro (2001)"	0.01					
"CH4 production calculation method (0: Analytical 1: Numerical)"	1					
"DO threshold for aerobic layer oxidation rates mgO2/L"	2					
"Nitrification rate in aerobic layer at DO below threshold m/d"	0.3					
"Nitrification rate in aerobic layer at DO above threshold m/d"	0.6					
"Denitrification rate in aerobic layer at DO below threshold m/d"	0.1					
"Denitrification rate in aerobic layer at DO above threshold m/d"	0.1					
"Denitrification rate in anerobic layer m/d"	0.1					
"CH4 oxidation rate in aerobic layer m/d"	1.5					
"Half-saturation oxygen constant for CH4 oxidation mg-O2/L"	0					
"Nitrification half-saturation constant for NH4 in aerobic layer mgN/L"	0.4					
"Nitrification half-saturation constant for O2 in aerobic layer mgO2/L"	0.37					
"Temperature coefficient for pore water diffusion between layers"	1.08					
"Temperature coefficient for particle mixing diffusion coefficient"	1					
"Temperature coefficient for nitrification"	1.123					
"Temperature coefficient for denitrification"	1.08					
"Temperature coefficient for methane oxidation"	1.079					
"SO4 concentration above which sulfide over methane is produced mgS/L"	20					
"H2S oxidation rate in aerobic layer m/d"	0.2					
"Temperature coefficient for H2S oxidation"	1.079					

"H2S oxidation normalization constant for O2 mgO2/L"	4
"Diagenesis rate for labile POC (G1) 1/d"	0.009
"Diagenesis rate for refractory POC (G2) 1/d"	0.002
"Diagenesis rate for inert/slow refractory POC (G3) 1/d"	0.000001
"Diagenesis rate for labile PON (G1) 1/d"	0.007
"Diagenesis rate for refractory PON (G2) 1/d"	0.0018
"Diagenesis rate for inert/slow refractory PON (G3) 1/d"	0.000001
"Diagenesis rate for labile POP (G1) 1/d"	0.007
"Diagenesis rate for refractory POP (G2) 1/d"	0.0018
"Diagenesis rate for inert/slow refractory POP (G3) 1/d"	0.000001
"Temperature coefficient for labile POC"	1.08
"Temperature coefficient for refractory POC"	1.1
"Temperature coefficient for inert/slow refractory POC"	1
"Temperature coefficient for labile PON"	1.08
"Temperature coefficient for refractory PON"	1.1
"Temperature coefficient for inert/slow refractory PON"	1
"Temperature coefficient for labile POP"	1.08
"Temperature coefficient for refractory POP"	1.1
"Temperature coefficient for inert/slow refractory POP"	1
"PO4 sorption coefficient in anaerobic layer m^3/kg"	0.001
"Incremental PO4 partition coefficient"	0
"Critical oxygen concentration for incremental sorption mg-O2/L"	0.01
"NH4 sorption coefficient in aerobic layer m^3/kg"	0
"NH4 sorption coefficient in anaerobic layer m^3/kg"	0.001
"H2S sorption coefficient in aerobic layer m^3/kg"	0
"H2S sorption coefficient in anaerobic layer m^3/kg"	0
"Algorithm for POM resuspension (0: Wind induced resuspension, 1: Bottom scour resuspension) Only used if Include POM resuspension is .TRUE."	1
"Fe(II) sorption coefficient in aerobic layer m^3/g"	50
"Fe(II) sorption coefficient in anaerobic layer m^3/g"	50
"Mn(II) sorption coefficient in aerobic layer m^3/g"	5
"Mn(II) sorption coefficient in anaerobic layer m^3/g"	5
"Write sediment fluxes"	.TRUE.
"Frequency of output days"	1
"Sediment Temperature Computations=1 (internal calcs or =2 neighboring water)"	2

Hells Canyon

$ W2_diagenesis input file		

$ All lines at top of file starting with $ are comments and disregarded by the model		
$ 08/29/2020 Additional inputs are required if a group switch is ON		
$ Zhong Zhang		
"Global Switch for all sediment diagenesis features"	.TRUE.	
"Include FFT layer (Fine Fluids Tailing - for Pit Lakes)"	.FALSE.	
"FFT layer number of periods"	5	
"FFT layer start times"	1	65
"FFT layer end times"	50	100
"Initial tailings concentration in FFT (gm/m3)"	360000	
"Sediment settling velocity of FFT to MFT (m/d)"	0	
"Move FFT layer during consolidation"	.FALSE.	
"Include bed consolidation"	.FALSE.	
"Fraction of layer thickness at which water layer is added"	1	
"Number of bed consolidation regions"	1	
"Starting segment for regions"	1	
"Ending segment for regions"	117	
"Data type for bed consolidation for each region (0: Constant, 1: Time varying)"	1	
"Bed consolidation rate (m/d)"	0.027397	
"Bed consolidation data file"	Regn.npt	
"Write bed elevation snapshot output"	.FALSE.	
"Write bed porosity snapshot output"	.FALSE.	
"Include sediment diagenesis simulation"	.TRUE.	
"Initial bed thickness in meters"	0.4	
"Initial sediment bed porosity"	0.88	
"Sediment bed particle size in microns"	60	
"Sediment type (1: Cohesive, 2: Non-cohesive)"	2	
"Sediment bulk density (kg/m3)"	1050	
"Sediment particle settling velocity (m/d)"	5	
"Include sediment resuspension and deposition processes"	.FALSE.	
"Include bubble release"	.FALSE.	
"Gas diffusion coefficient in sediment in m/s"	1.0d-9	
"Calibration parameter R1 in m"	0.0014	
"Young's modulus E in N/m2"	1.4d+9	
"Critical stress intensity factor for sediments K1c in N/m^3/2"	300	
"Bubbles release scale"	0.02	
"Fraction of critical pressure at which cracks close"	0.2	
"Switch to limit bubble size"	.TRUE.	
"Maximum bubble radius in mm"	80	
"Switch to use slow release of bubbles"	.TRUE.	
"Bubbles release fraction (sediments)"	0.005	

"Bubbles accumulation fraction"	0.1	
"Number of bubbles release array"	2000	
"Bubbles release fraction (atmosphere)"	0.001	
"Bubbles-water gas exchange rate (1/s)"	1.0d-7	
"Apply additional turbulence due to bubbles release"	.FALSE.	
"Turbulence scaling factor for bubbles release"	0.001	
"Include POM resuspension"	.FALSE.	
"Critical shear stress for POM resuspension dynes/cm^2"	0.001	
"Critical Shields parameter for POM"	10	
"Use Cao method to estimate critical Shields parameter (rather than using input value)"	.FALSE.	
"POM specific gravity"	1.5	
"POM particle diameter m"	0.0001	
"Include modeling of alkalinity/pH in sediments"	.TRUE.	
"Include modeling of Iron (FeOOH and Fe(II)) in sediments"	.TRUE.	
"Include modeling of Manganese (Mn(II) and MnO2) in sediments"	.TRUE.	
"Number of regions for different initial sediment concentrations"	1	
	Region1	Region2
"Starting segment for regions"	2	
"Ending segment for regions"	117	
"Initial sediment temperature oC"	10	
"Initial sediment pH (only used if include modeling dynamic pH)"	6.5	
"Initial POC (total) concentration mgC/L"	500	
"Initial PON (total) concentration mgN/L"	35	
"Initial POP (total) concentration mgP/L"	9	
"Initial SO4 concentration mgS/L"	3.46	
"Initial dissolved NH4 concentration mgN/L"	6	
"Initial dissolved NO3 concentration mgN/L"	0.01	
"Initial total PO4 concentration mgP/L"	3.03	
"Initial dissolved H2S concentration mgS/L"	0.08	
"Initial CH4 concentration mgC/L"	0.092	
"Initial TIC concentration mgC/L"	4.011	
"Initial Alkalinity concentration for each region mg/l as CaCO3"	50	
"Initial Ferrous Iron concentration for each region mgFe/l"	100	
"Initial Iron Oxyhydroxide concentration for each region mgFe/l,"	0.5	
"Initial Mn(II) concentration for each region mgMn/l,"	500	
"Initial manganese dioxide concentration for each region mgMn/l,"	0.5	

"Number of regions for different diagenesis related rates"	2	
	Region1	Region2
"Starting segment for regions"	2	87
"Ending segment for regions"	86	117
"Fraction of labile POC"	-0.2	0.15
"Fraction of refractory POC"	0.75	0.75
"Fraction of labile PON"	0.2	0.15
"Fraction of refractory PON"	0.75	0.75
"Fraction of labile POP"	0.2	0.15
"Fraction of refractory POP"	0.75	0.75
"Pore water diffusion coefficient m2/d"	0.0015	0.0015
"Particle mixing velocity between aerobic and anaerobic layers m2/d"	0.00006	0.00006
"Burial velocity m/d"	0.00001	0.00001
"Reference POC G1 concentration for bioturbation mg-C/g Calculation of final benthic particle mixing velocity Equation 13.6 in DoToro (2001)"	0.01	0.01
"CH4 production calculation method (0: Analytical 1: Numerical)"	1	1
"DO threshold for aerobic layer oxidation rates mgO2/L"	2	2
"Nitrification rate in aerobic layer at DO below threshold m/d"	0.3	0.3
"Nitrification rate in aerobic layer at DO above threshold m/d"	0.3	0.3
"Denitrification rate in aerobic layer at DO below threshold m/d"	0.1	0.1
"Denitrification rate in aerobic layer at DO above threshold m/d"	0.1	0.1
"Denitrification rate in anerobic layer m/d"	0.1	0.1
"CH4 oxidation rate in aerobic layer m/d"	1.5	1.5
"Half-saturation oxygen constant for CH4 oxidation mg-O2/L"	0	0
"Nitrification half-saturation constant for NH4 in aerobic layer mgN/L"	0.728	0.728
"Nitrification half-saturation constant for O2 in aerobic layer mgO2/L"	0.37	0.37
"Temperature coefficient for pore water diffusion between layers"	1.08	1.08
"Temperature coefficient for particle mixing diffusion coefficient"	1	1
"Temperature coefficient for nitrification"	1.123	1.123
"Temperature coefficient for denitrification"	1.08	1.08
"Temperature coefficient for methane oxidation"	1.079	1.079
"SO4 concentration above which sulfide over methane is produced mgS/L"	20	20
"H2S oxidation rate in aerobic layer m/d"	0.2	0.2
"Temperature coefficient for H2S oxidation"	1.079	1.079

"H2S oxidation normalization constant for O2 mgO2/L"	4	4
"Diagenesis rate for labile POC (G1) 1/d"	0.017	0.018
"Diagenesis rate for refractory POC (G2) 1/d"	0.0036	0.004
"Diagenesis rate for inert/slow refractory POC (G3) 1/d"	0.000001	0.000001
"Diagenesis rate for labile PON (G1) 1/d"	0.005	0.005
"Diagenesis rate for refractory PON (G2) 1/d"	0.0034	0.0038
"Diagenesis rate for inert/slow refractory PON (G3) 1/d"	0.000001	0.000001
"Diagenesis rate for labile POP (G1) 1/d"	0.025	0.027
"Diagenesis rate for refractory POP (G2) 1/d"	0.0045	0.0045
"Diagenesis rate for inert/slow refractory POP (G3) 1/d"	0.000001	0.000001
"Temperature coefficient for labile POC"	1.08	1.08
"Temperature coefficient for refractory POC"	1.1	1.1
"Temperature coefficient for inert/slow refractory POC"	1	1
"Temperature coefficient for labile PON"	1.08	1.08
"Temperature coefficient for refractory PON"	1.1	1.1
"Temperature coefficient for inert/slow refractory PON"	1	1
"Temperature coefficient for labile POP"	1.08	1.08
"Temperature coefficient for refractory POP"	1.1	1.1
"Temperature coefficient for inert/slow refractory POP"	1	1
"PO4 sorption coefficient in anaerobic layer m^3/kg"	0.0001	0.0001
"Incremental PO4 partition coefficient"	0	0
"Critical oxygen concentration for incremental sorption mg-O2/L"	0.01	0.01
"NH4 sorption coefficient in aerobic layer m^3/kg"	0	0
"NH4 sorption coefficient in anaerobic layer m^3/kg"	0	0
"H2S sorption coefficient in aerobic layer m^3/kg"	0	0
"H2S sorption coefficient in anaerobic layer m^3/kg"	0	0
"Algorithm for POM resuspension (0: Wind induced resuspension, 1: Bottom scour resuspension) Only used if Include POM resuspension is .TRUE."	1	1
"Fe(II) sorption coefficient in aerobic layer m^3/g"	50	50
"Fe(II) sorption coefficient in anaerobic layer m^3/g"	50	50
"Mn(II) sorption coefficient in aerobic layer m^3/g"	5	5
"Mn(II) sorption coefficient in anaerobic layer m^3/g"	5	5
"Write sediment fluxes"	.TRUE.	
"Frequency of output days"	1	
"Sediment Temperature Computations=1 (internal calcs or =2 neighboring water)"	2	

A3. Brownlee Dam Spillway Gas Equation Updates

The equation simulating total dissolved gas (TDG) in the Brownlee Dam Spillway has been updated using data from the high flow year of 2017. The spill equation for TDG is a bounded exponential with the following form:

$$\%TDG = a + be^{cQ}$$

where
Q=Total Spill, kcfs
a, b, c=empirical coefficients

In the equation that was formerly applied in the Brownlee model, the empirical coefficients had the values a=122.1, b=-48.3, and c=-0.039. Modeled dissolved oxygen predictions using the former equation are compared with data measured downstream of the dam at Brownlee Bridge in Figure 1. Data were measured at two locations, corresponding to the left and right abutments.

Predictions using an updated equation where the empirical coefficient a=140 is shown in Figure 2. DO prediction of only the spill and the combined spill plus turbines are compared with data. The DO concentrations of turbine flows may change in the future as the Brownlee model is updated.

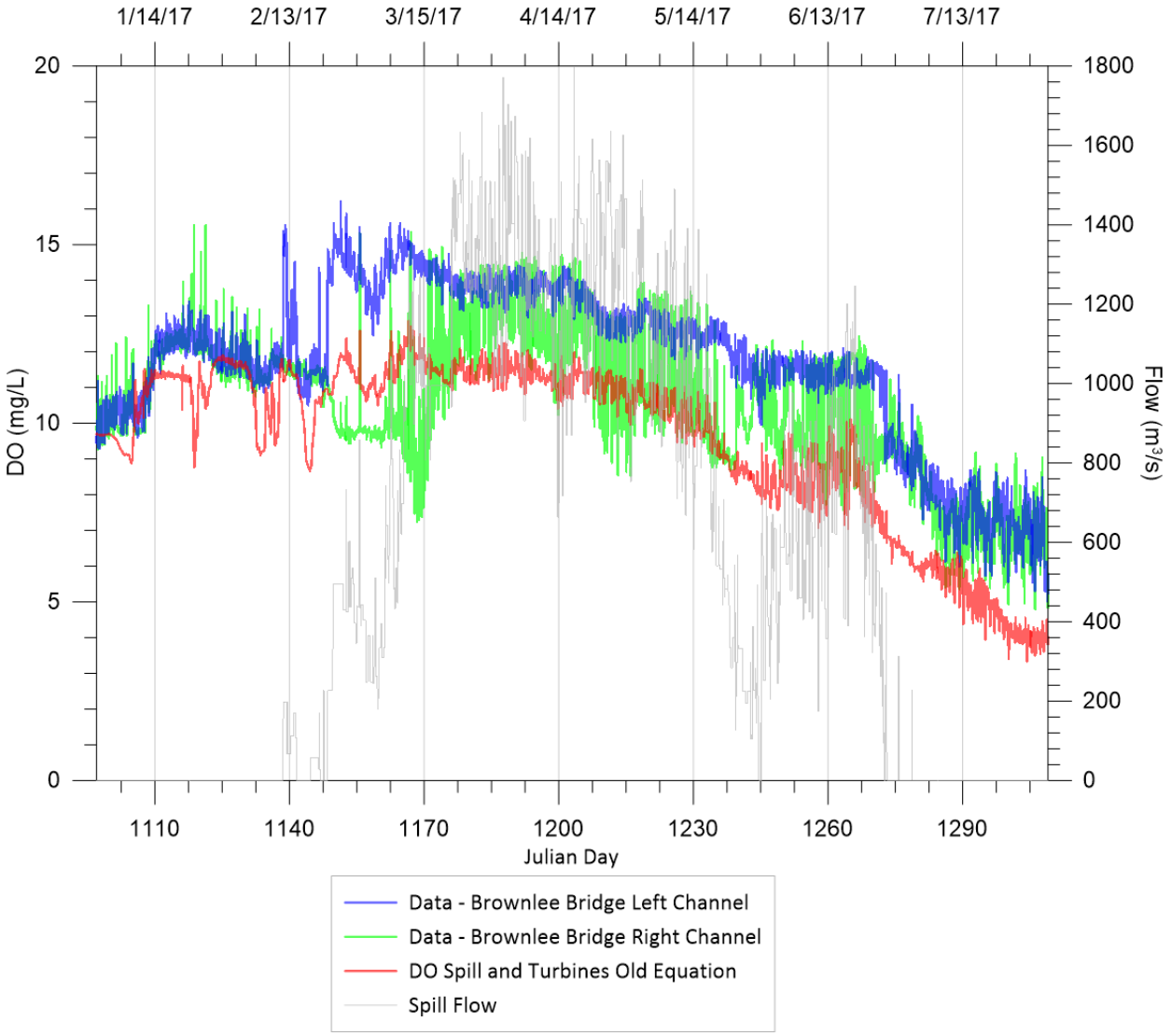


Figure 1. Brownlee Dam outflow DO predictions using old TDG equation.

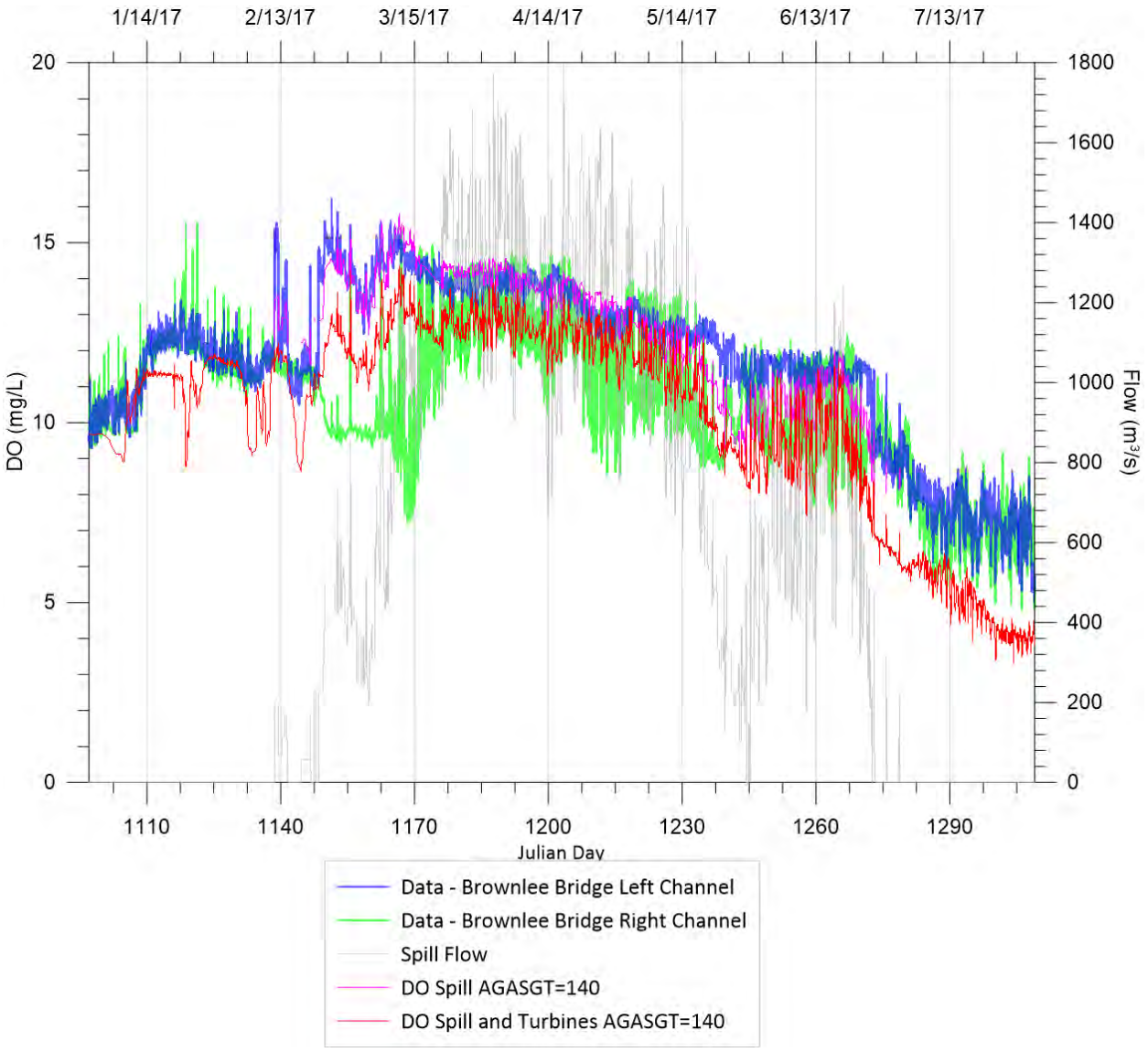


Figure 2. Brownlee Dam outflow prediction using updated equation with the empirical coefficient *a*=140. DO predictions for the spillway and the combined spillway and turbines are plotted.

Appendix A4 Brownlee Reservoir Vertical Profiles

Chloride

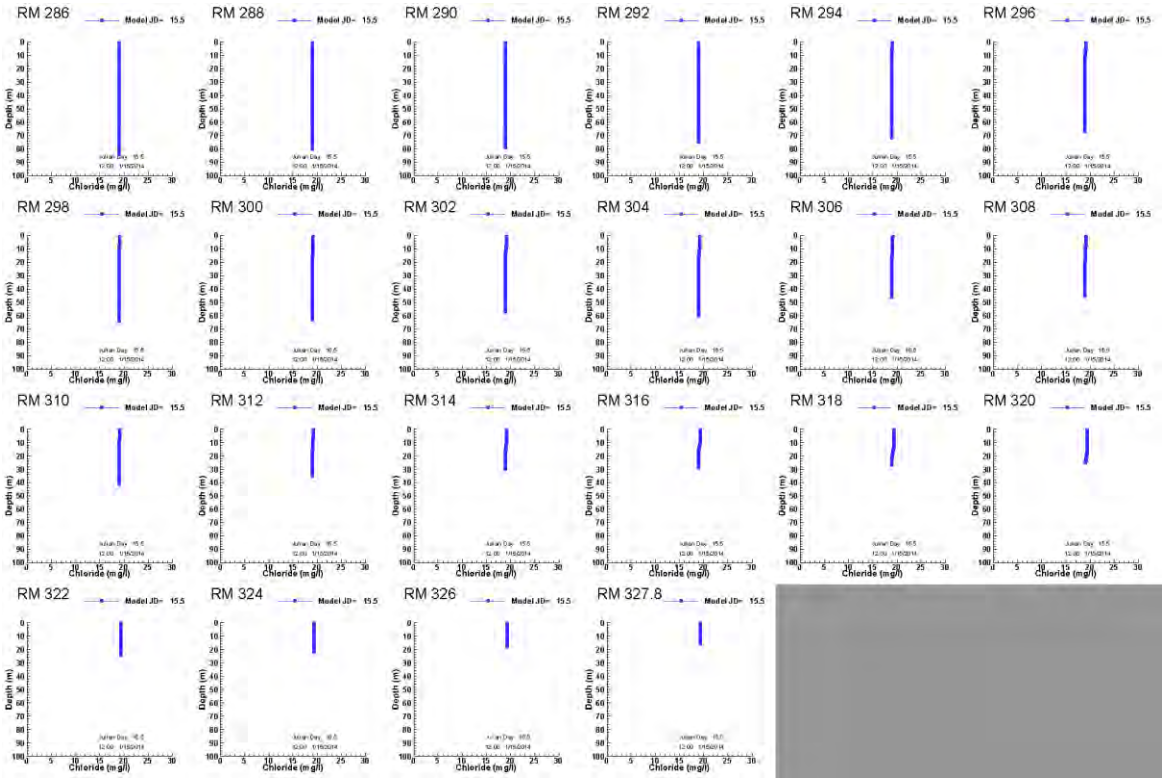


Figure 1. Vertical profiles of chloride compared with data for 1/15/2014.

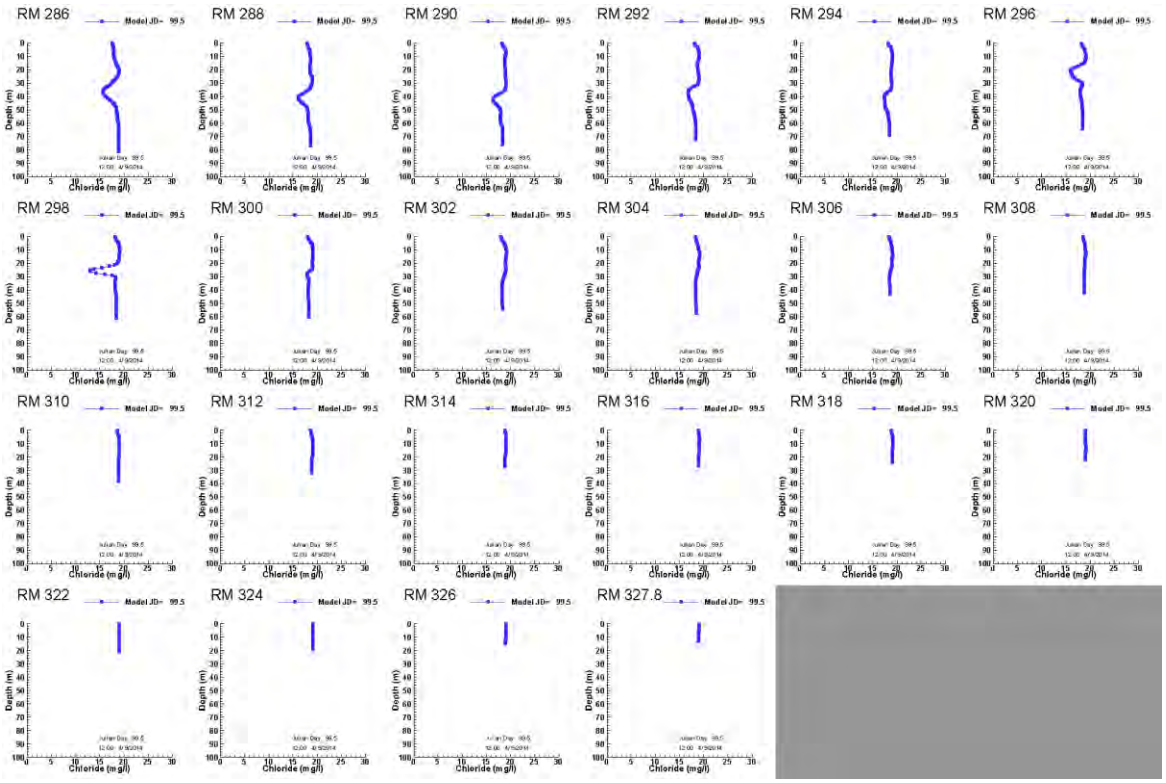


Figure 2. Vertical profiles of chloride compared with data for 4/ 9/2014.

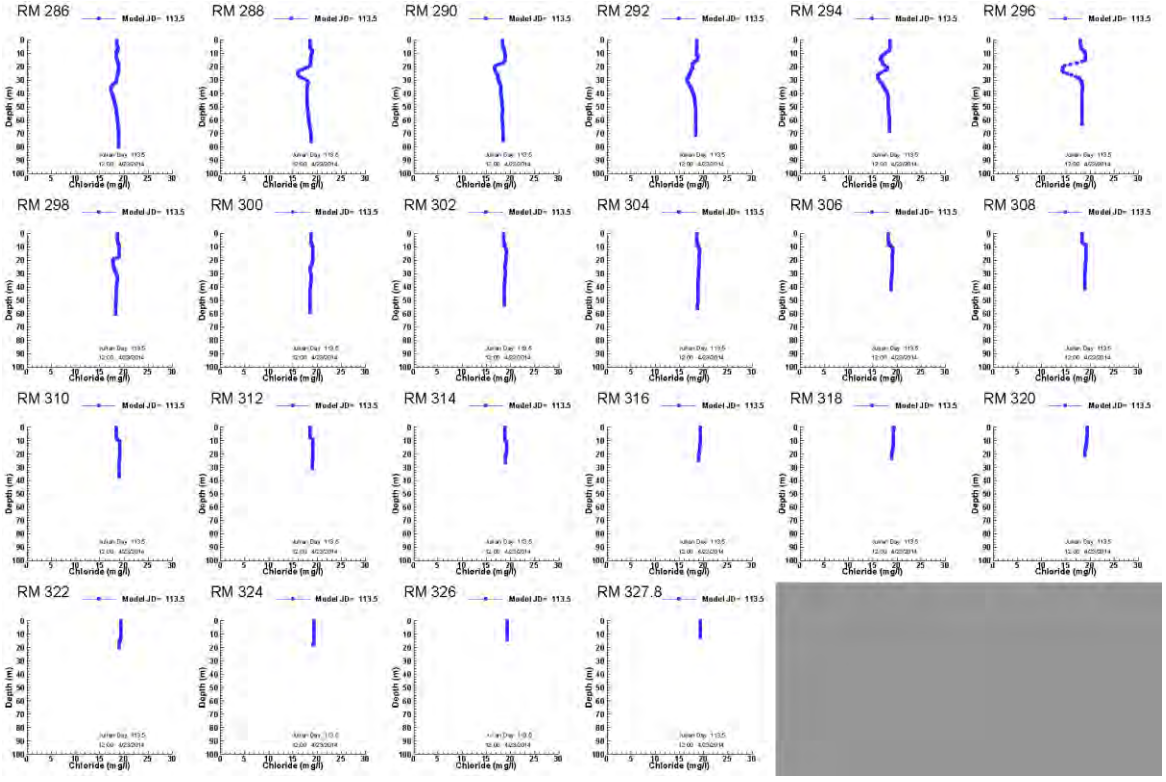


Figure 3. Vertical profiles of chloride compared with data for 4/23/2014.

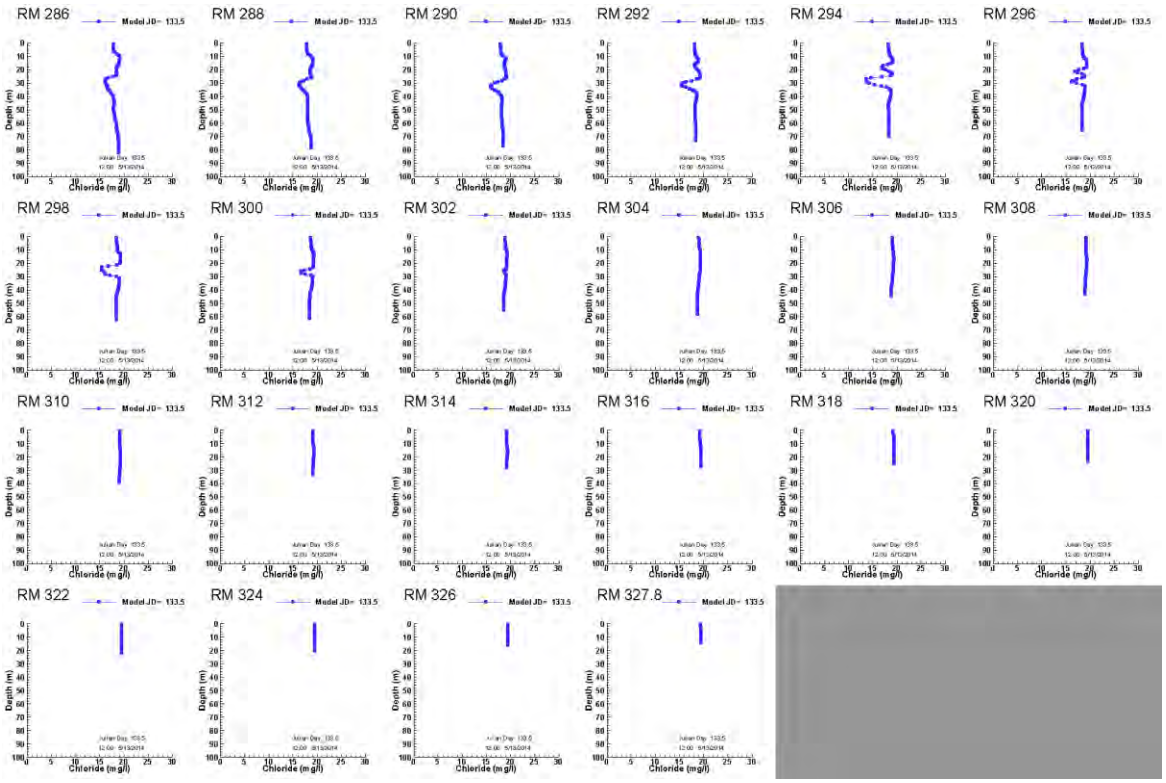


Figure 4. Vertical profiles of chloride compared with data for 5/13/2014.

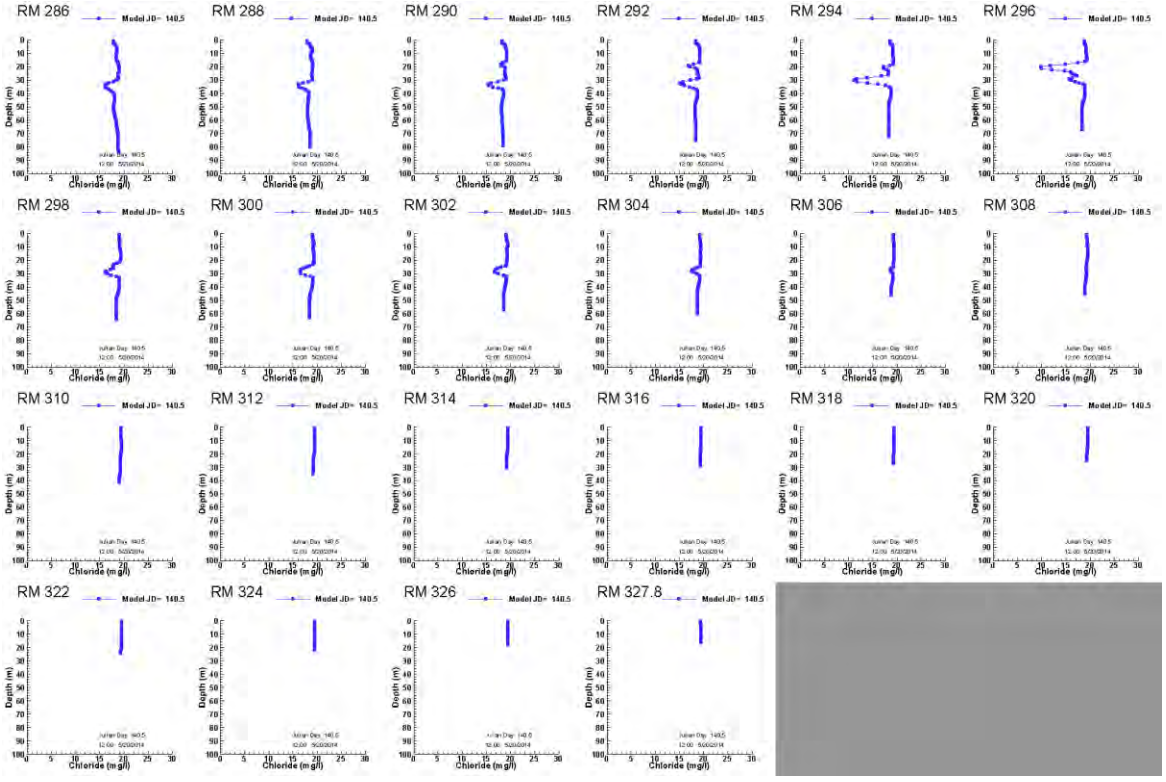


Figure 5. Vertical profiles of chloride compared with data for 5/20/2014.

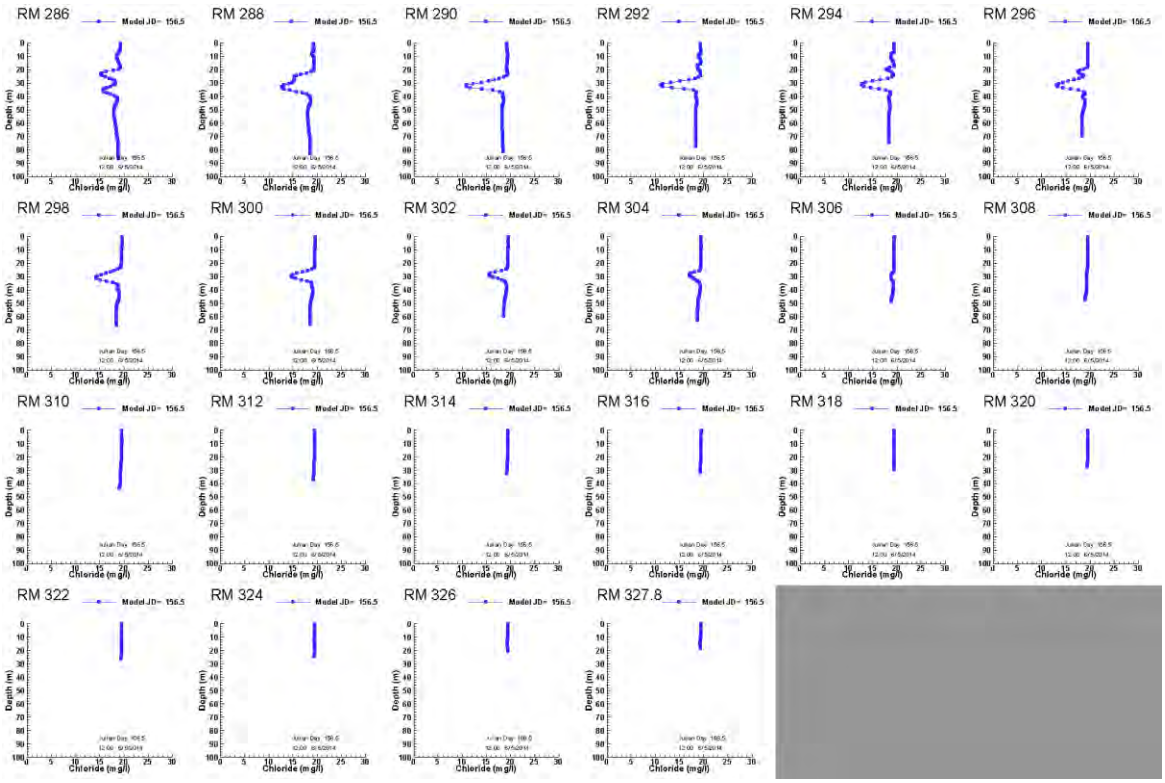


Figure 6. Vertical profiles of chloride compared with data for 6/ 5/2014.

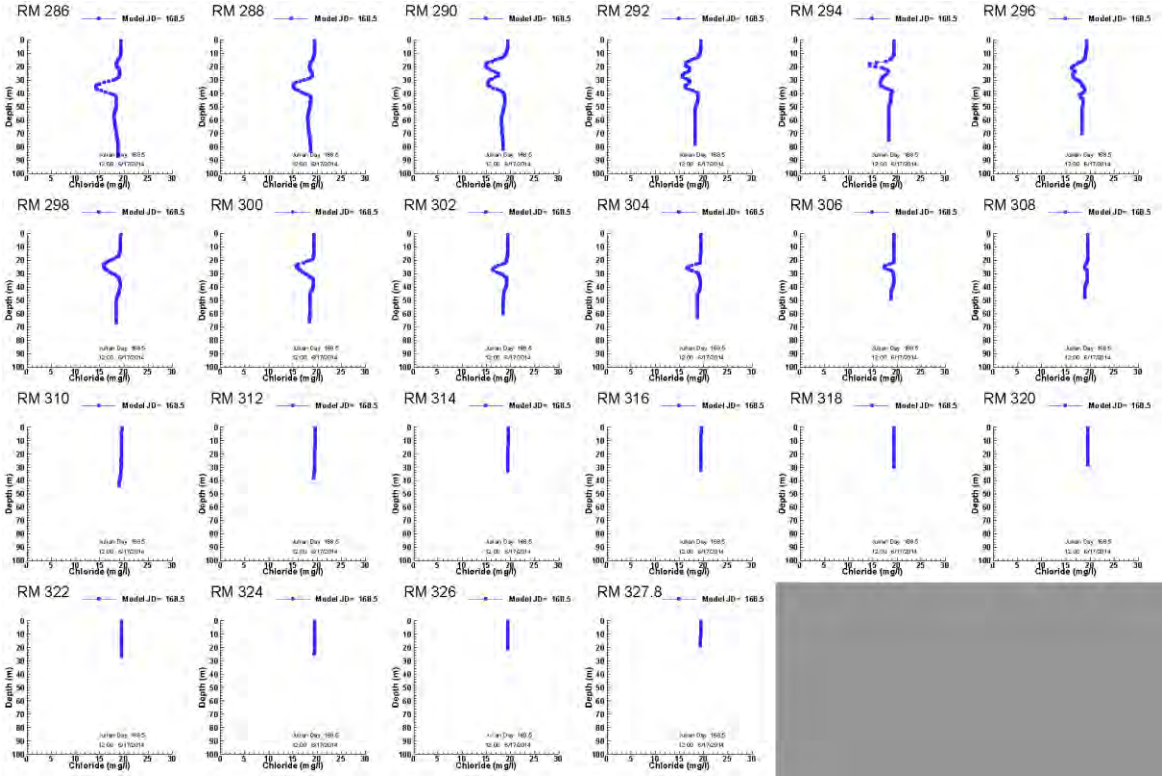


Figure 7. Vertical profiles of chloride compared with data for 6/17/2014.

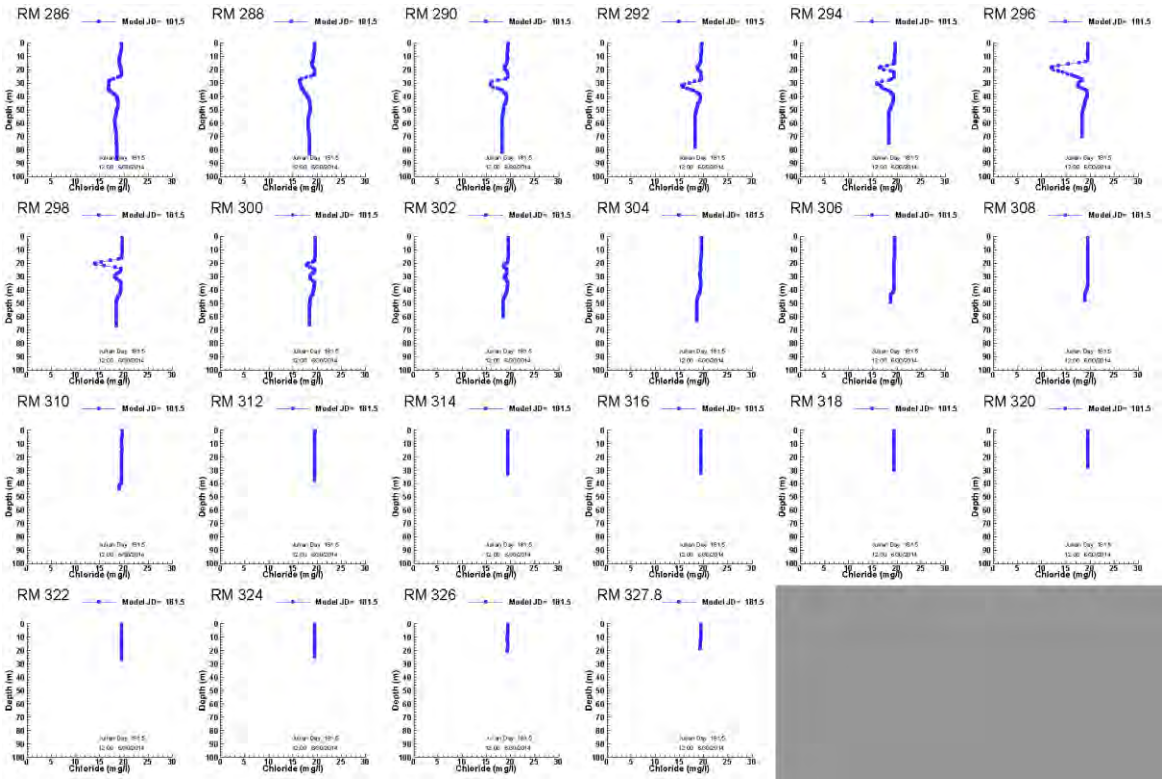


Figure 8. Vertical profiles of chloride compared with data for 6/30/2014.

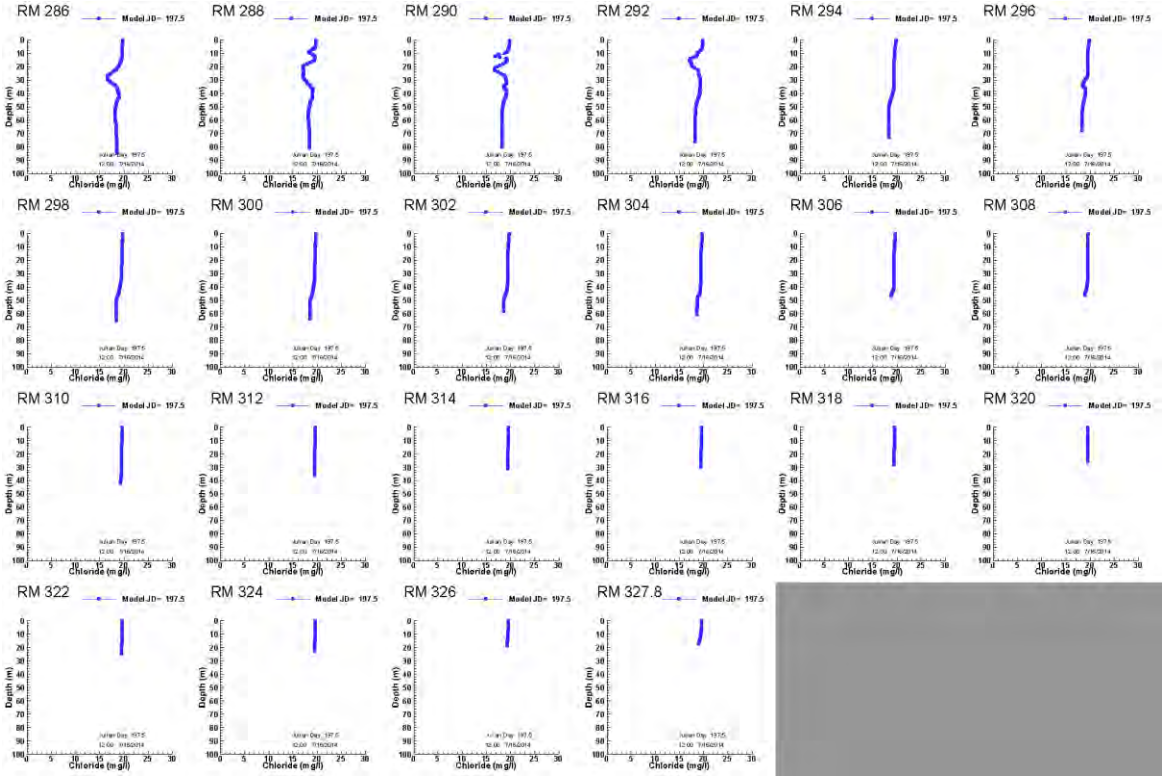


Figure 9. Vertical profiles of chloride compared with data for 7/16/2014.

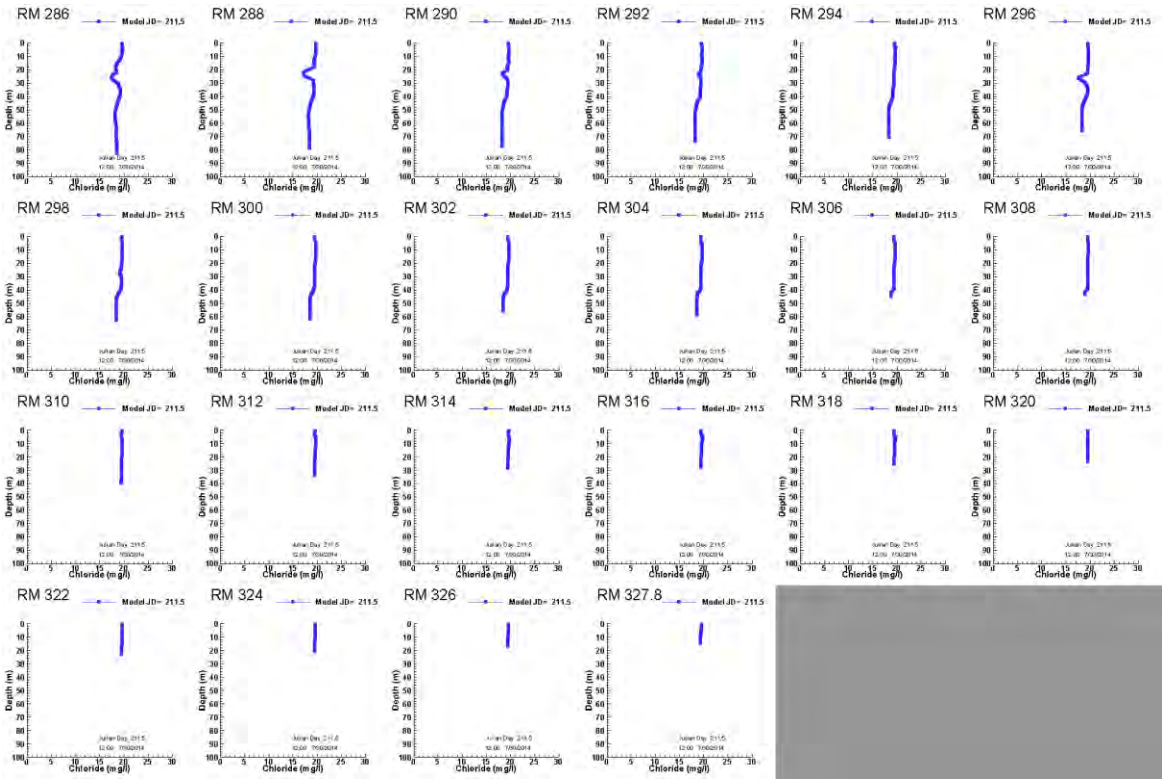


Figure 10. Vertical profiles of chloride compared with data for 7/30/2014.

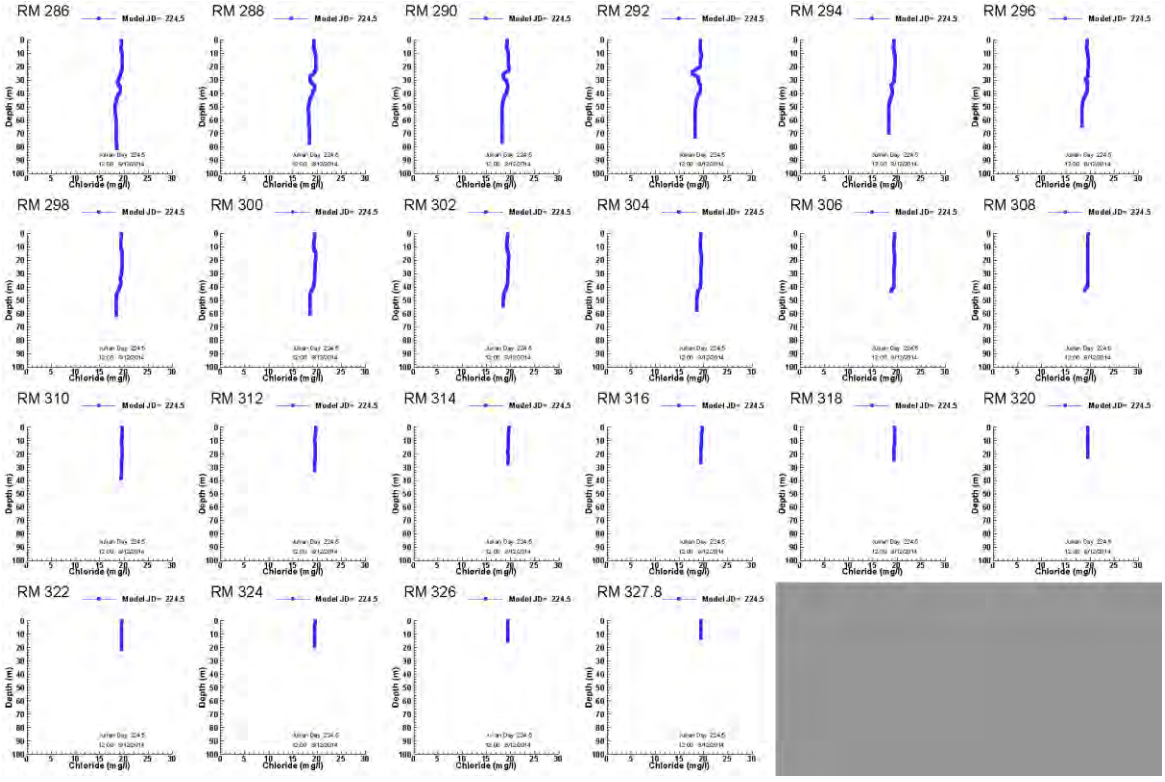


Figure 11. Vertical profiles of chloride compared with data for 8/12/2014.

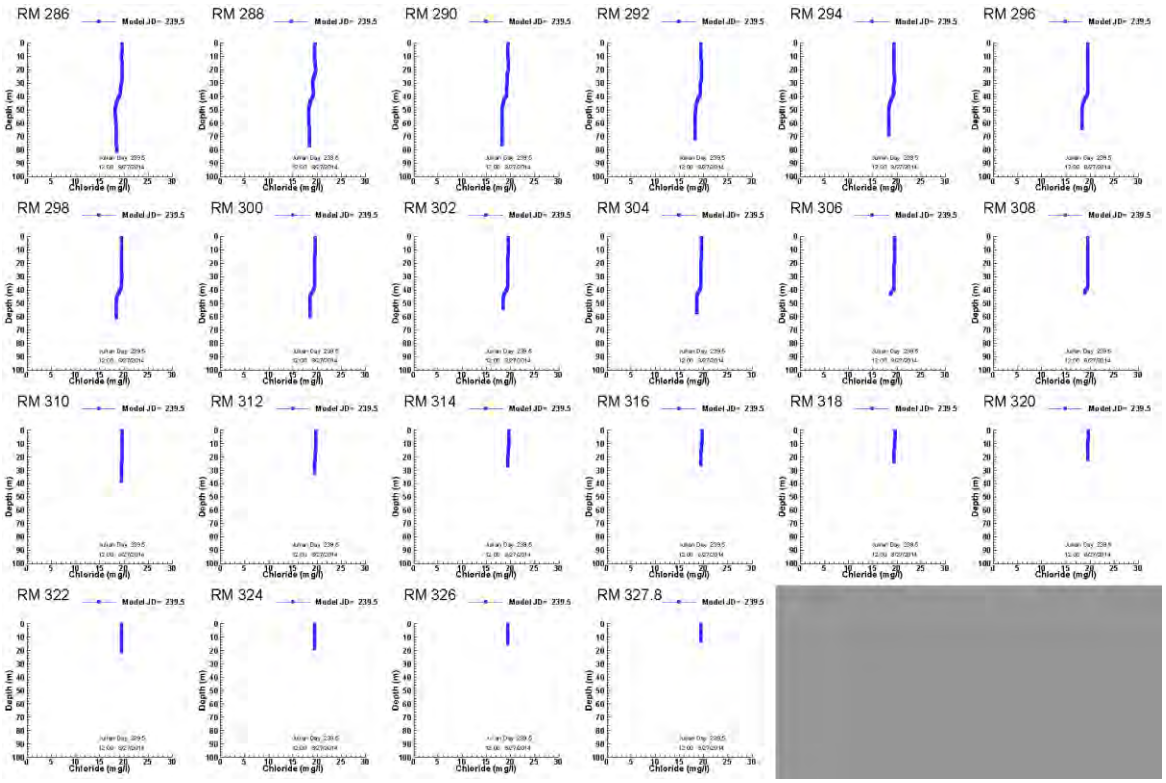


Figure 12. Vertical profiles of chloride compared with data for 8/27/2014.

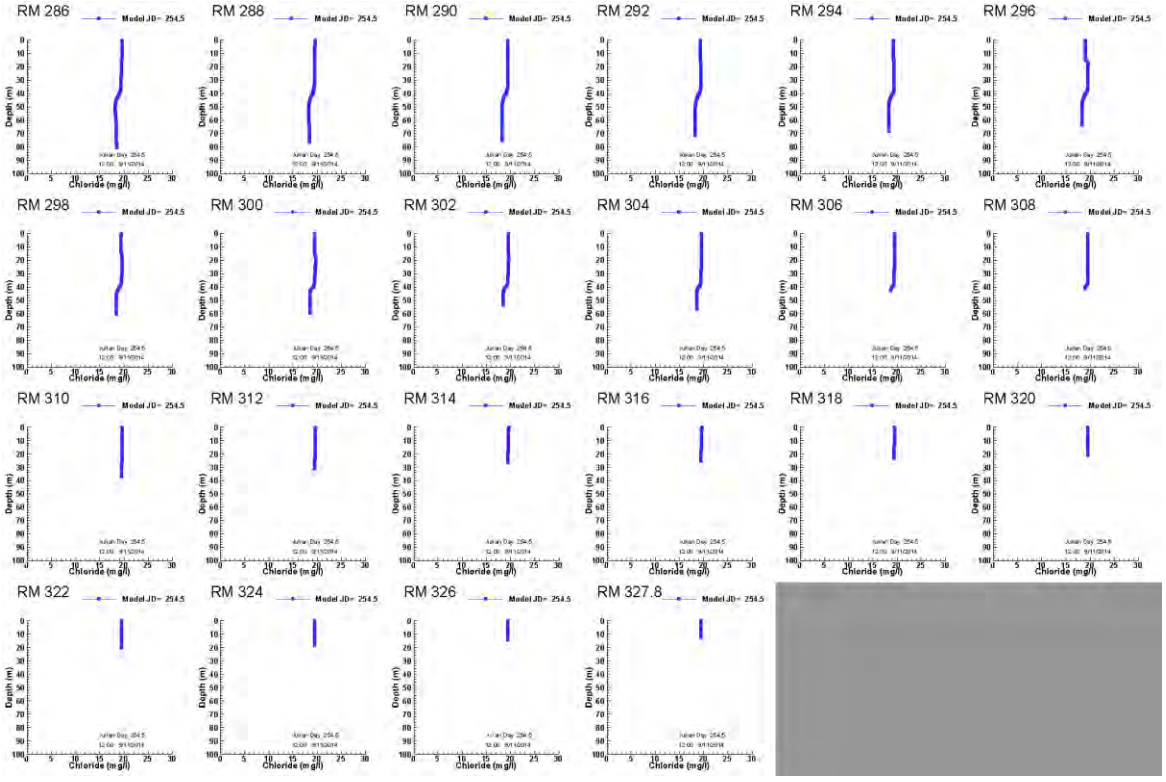


Figure 13. Vertical profiles of chloride compared with data for 9/11/2014.

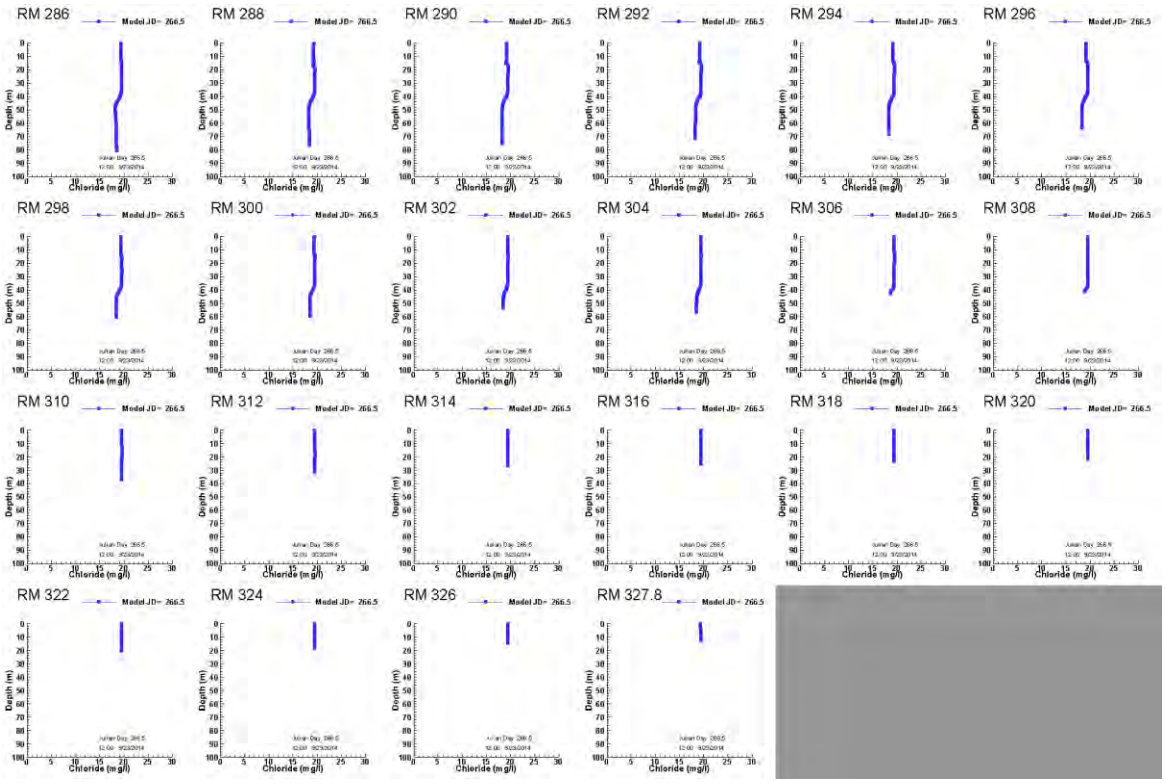


Figure 14. Vertical profiles of chloride compared with data for 9/23/2014.

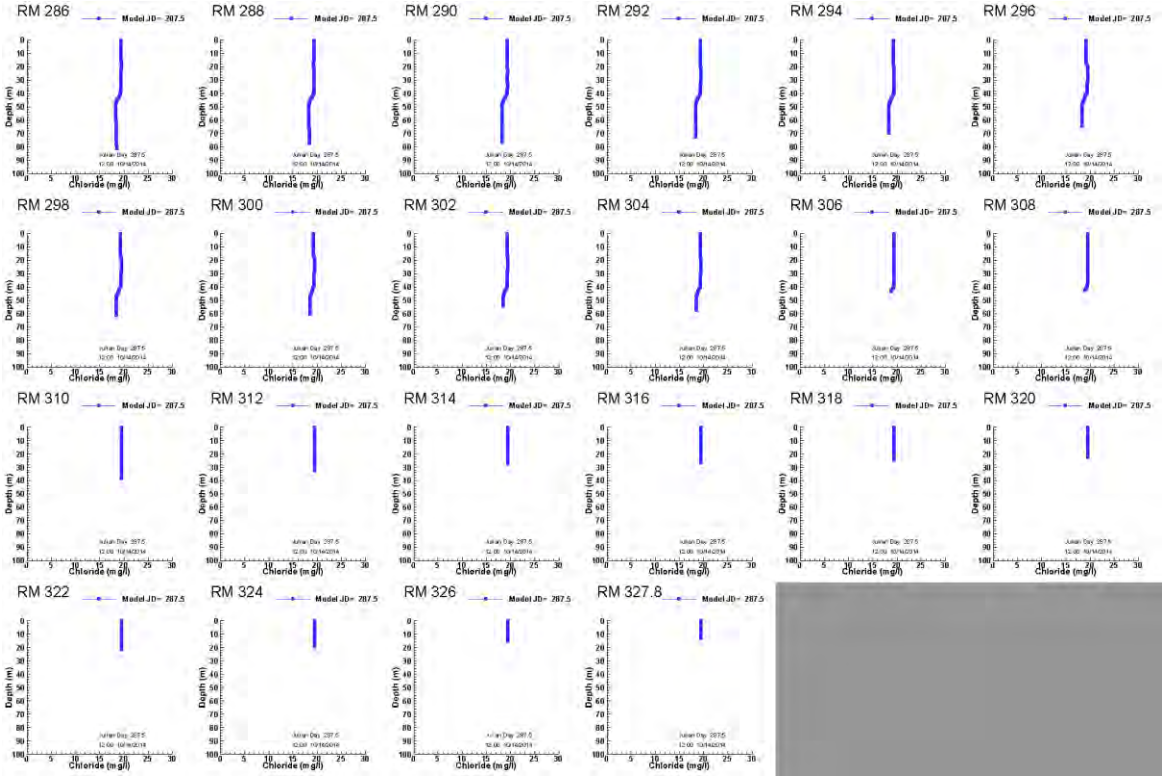


Figure 15. Vertical profiles of chloride compared with data for 10/14/2014.

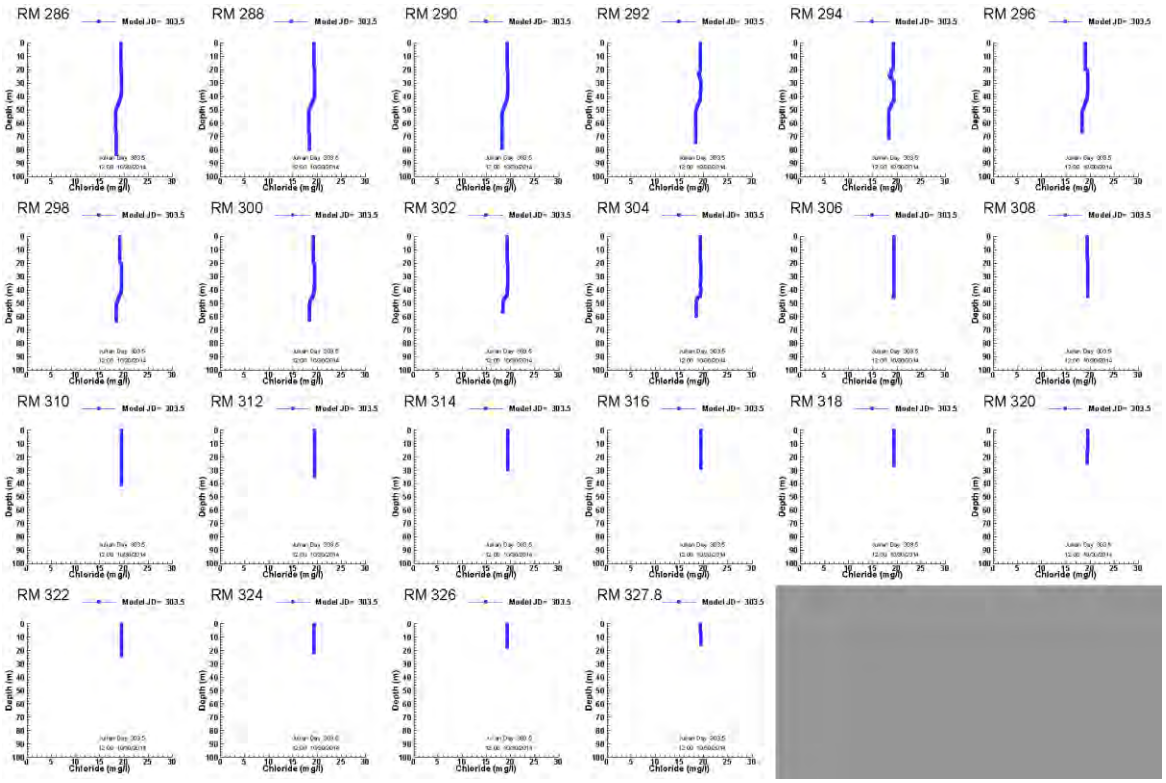


Figure 16. Vertical profiles of chloride compared with data for 10/30/2014.

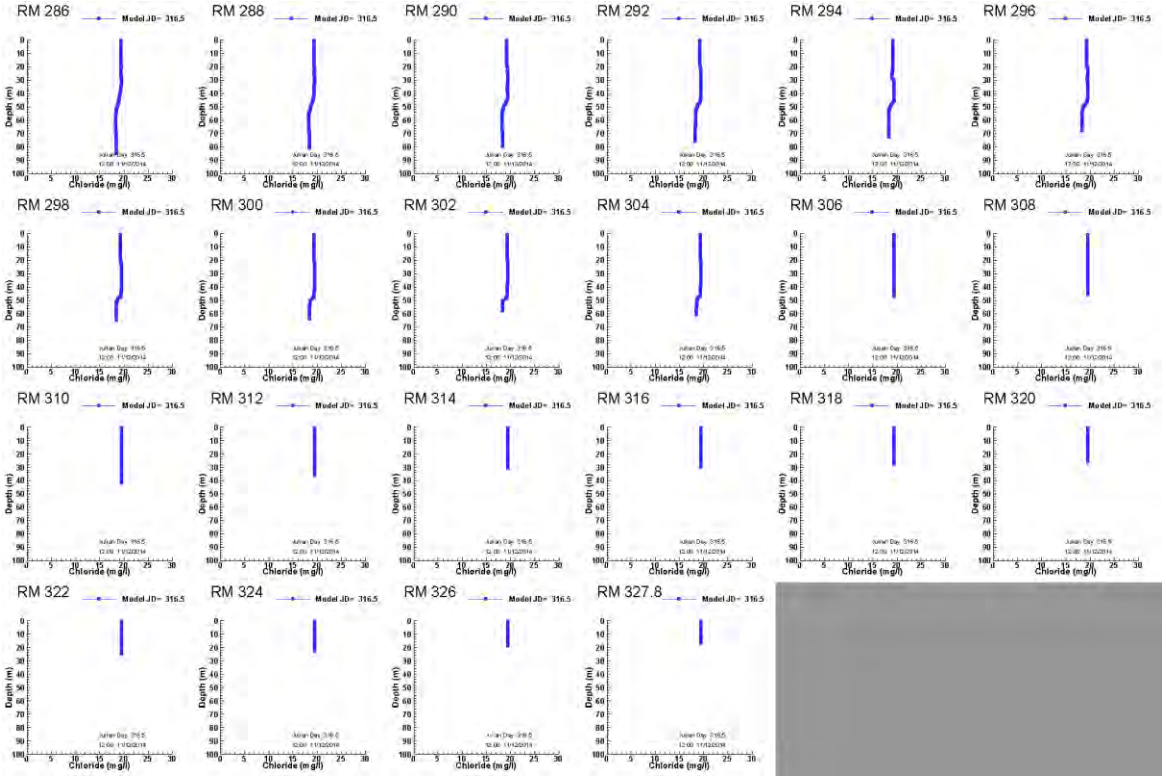


Figure 17. Vertical profiles of chloride compared with data for 11/12/2014.

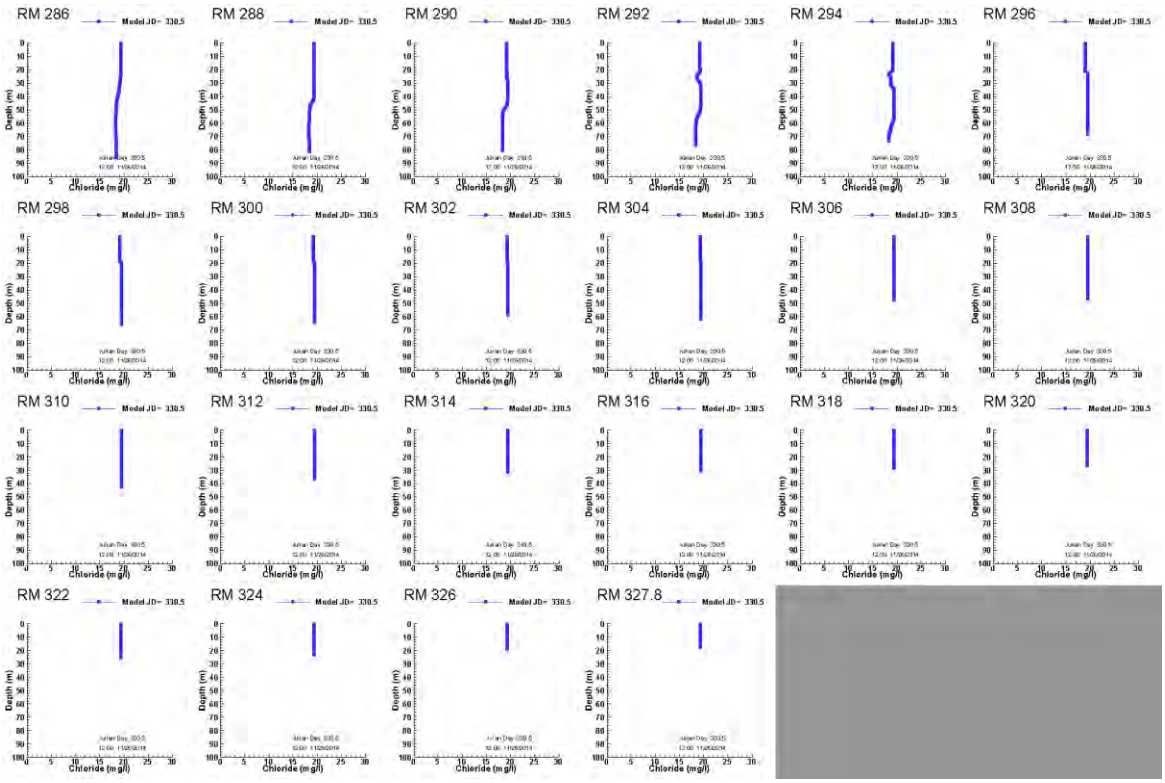


Figure 18. Vertical profiles of chloride compared with data for 11/26/2014.

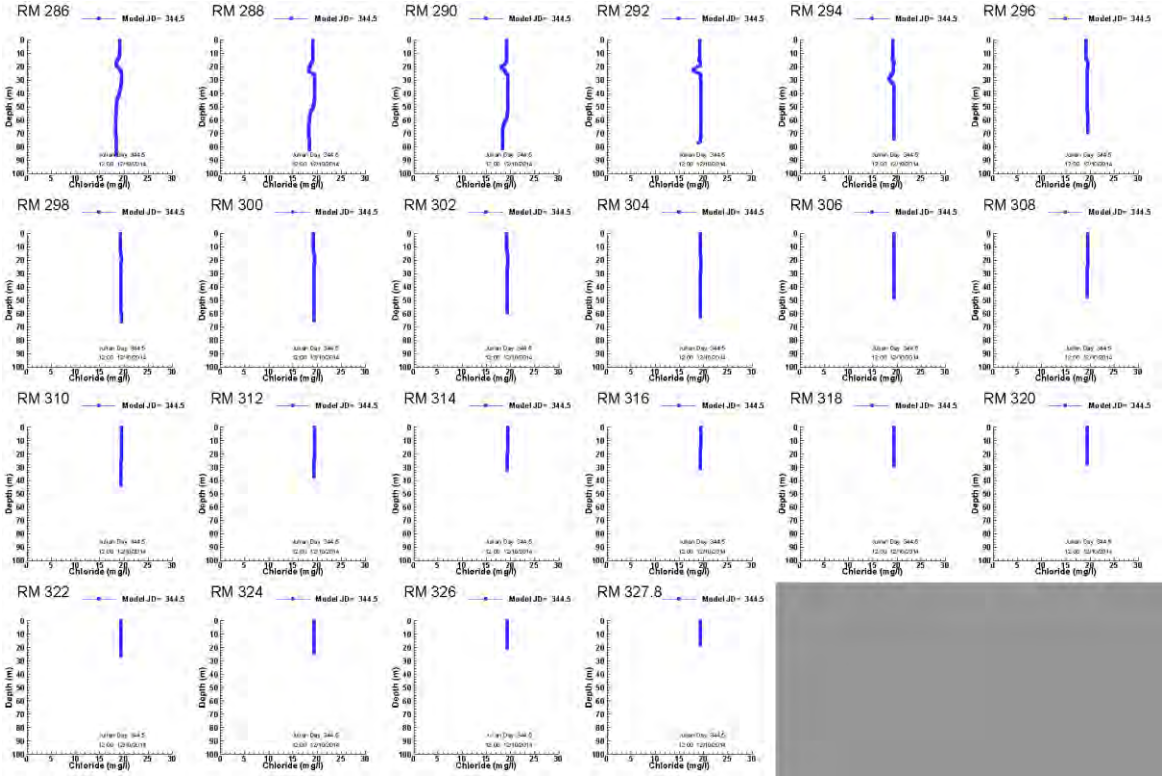


Figure 19. Vertical profiles of chloride compared with data for 12/10/2014.

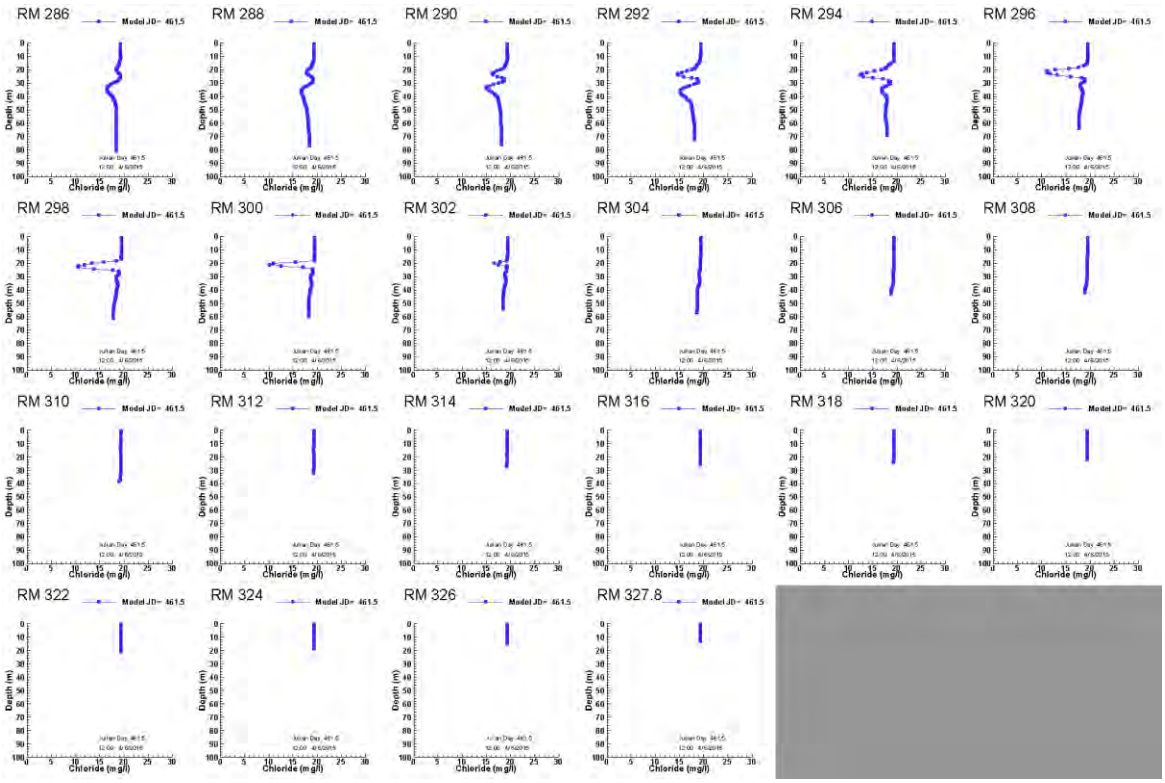


Figure 20. Vertical profiles of chloride compared with data for 4/ 6/2015.

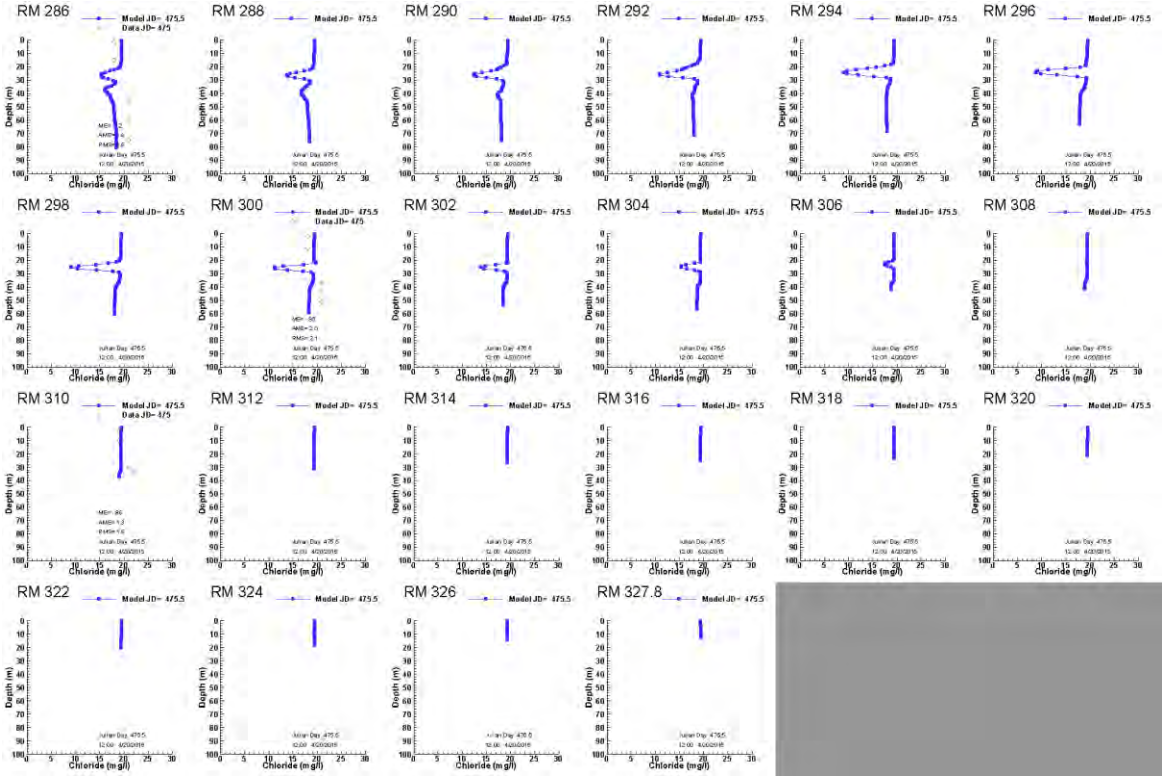


Figure 21. Vertical profiles of chloride compared with data for 4/20/2015.

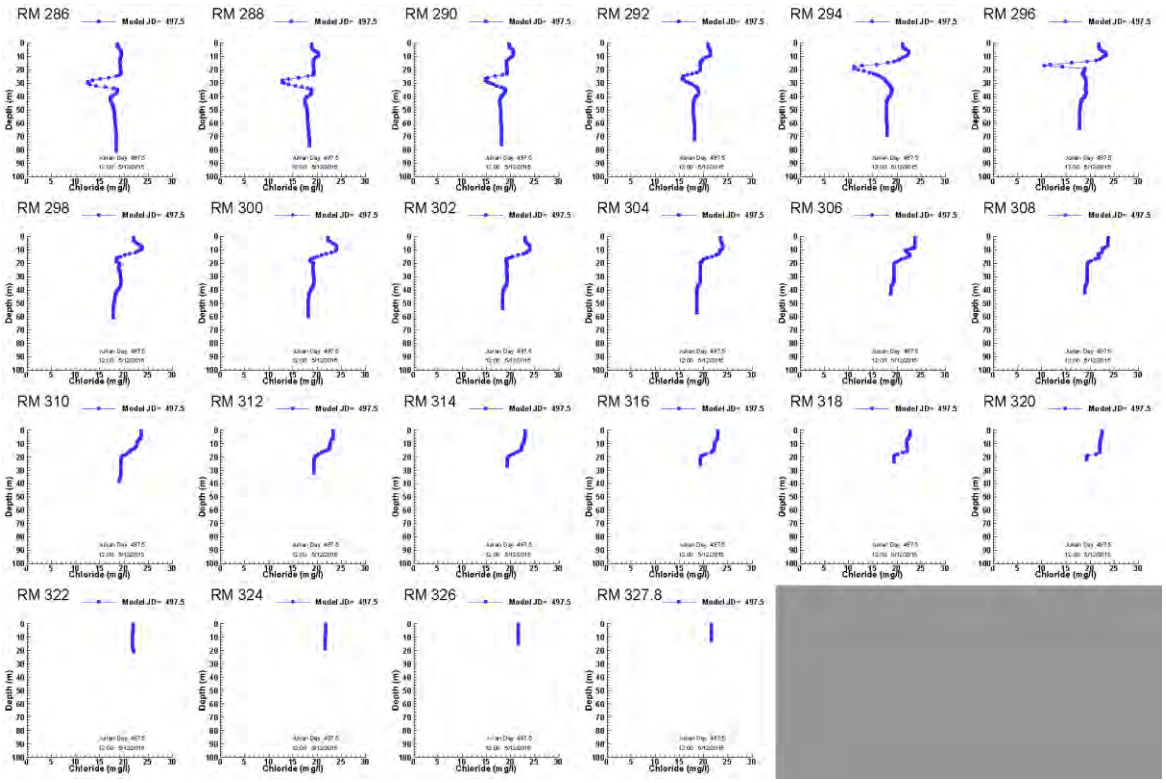


Figure 22. Vertical profiles of chloride compared with data for 5/12/2015.

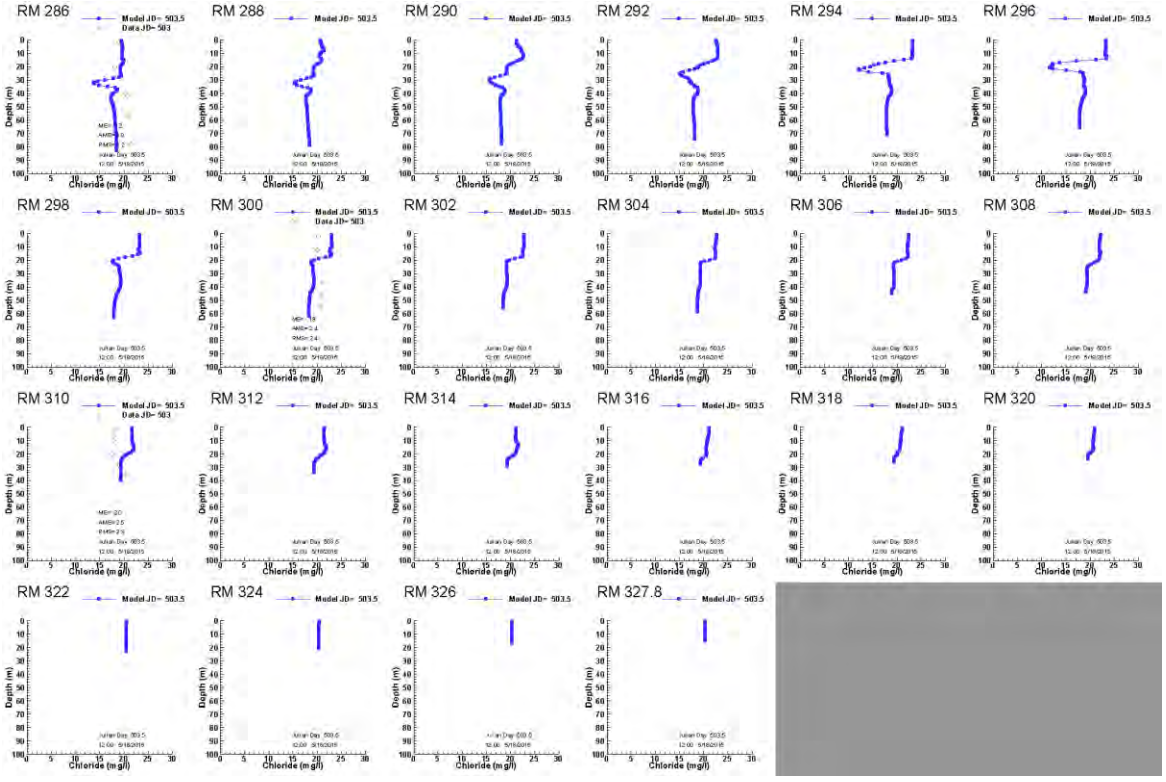


Figure 23. Vertical profiles of chloride compared with data for 5/18/2015.

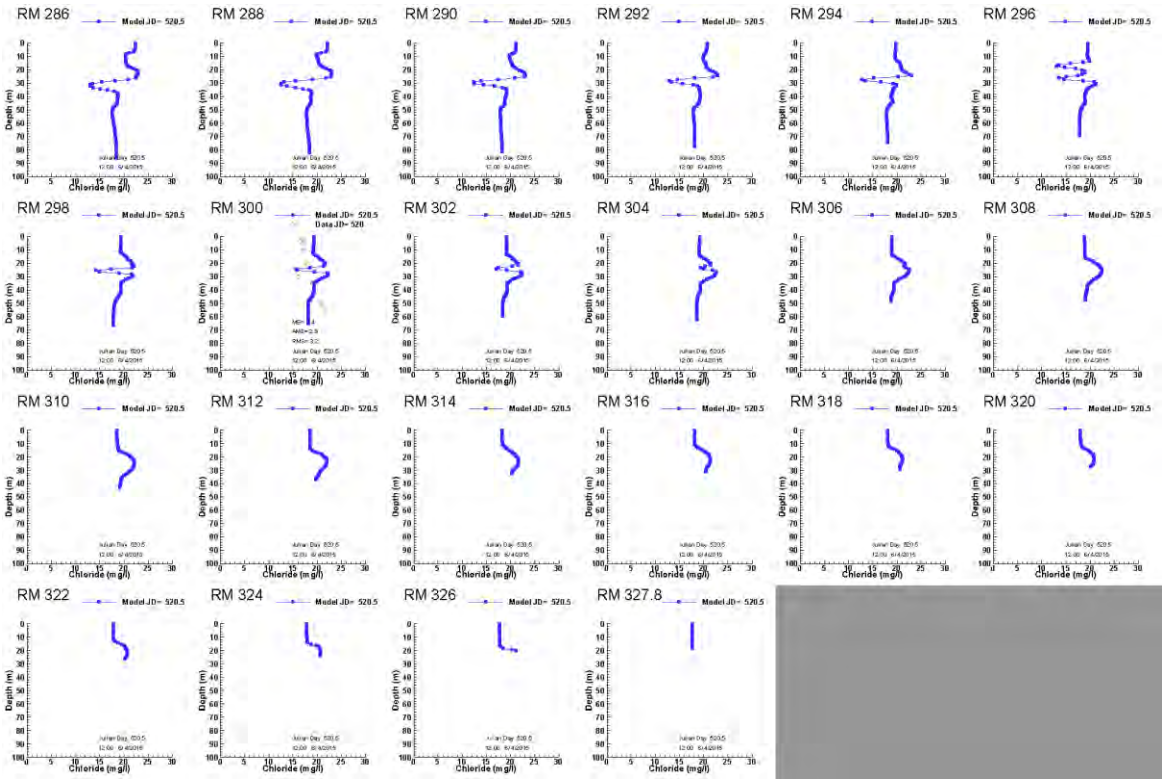


Figure 24. Vertical profiles of chloride compared with data for 6/ 4/2015.

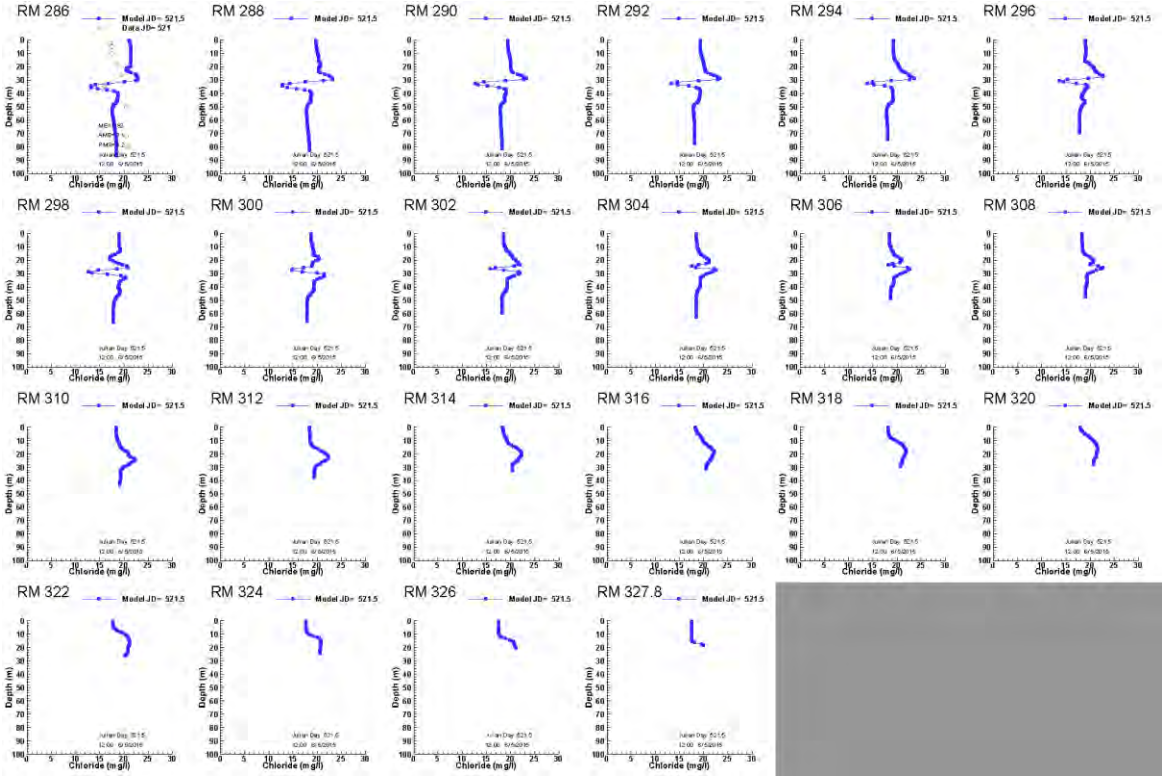


Figure 25. Vertical profiles of chloride compared with data for 6/ 5/2015.

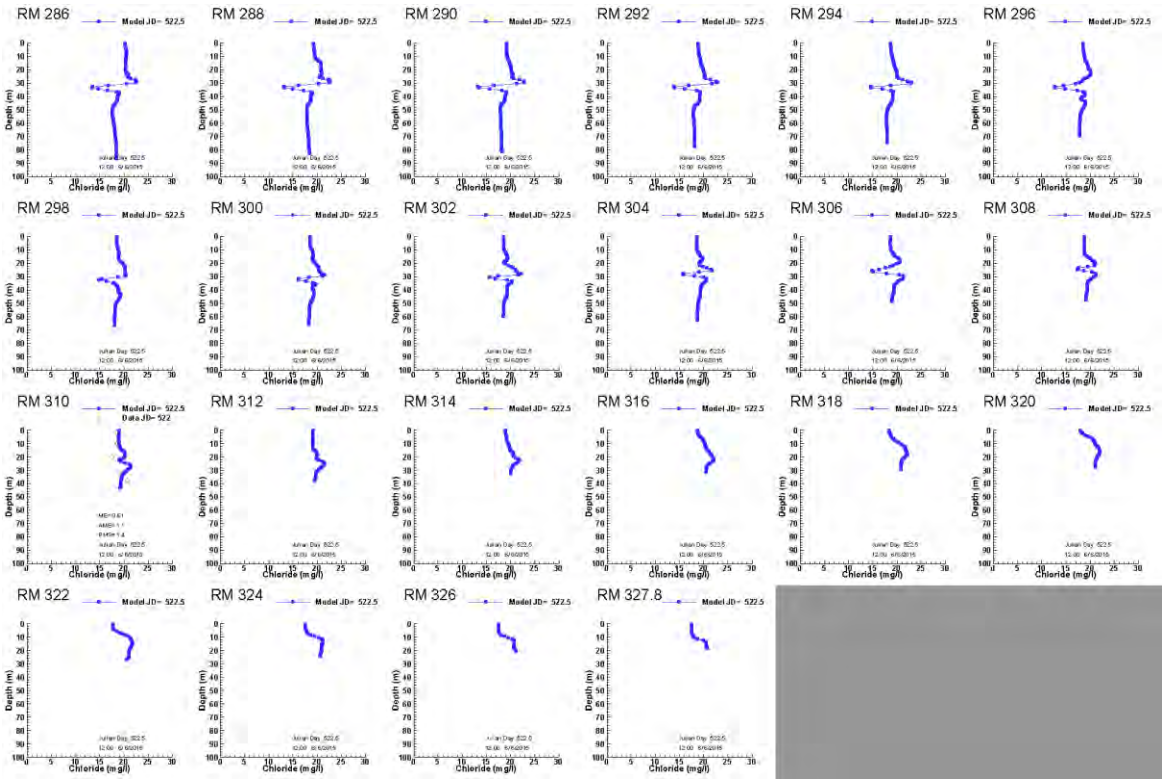


Figure 26. Vertical profiles of chloride compared with data for 6/ 6/2015.

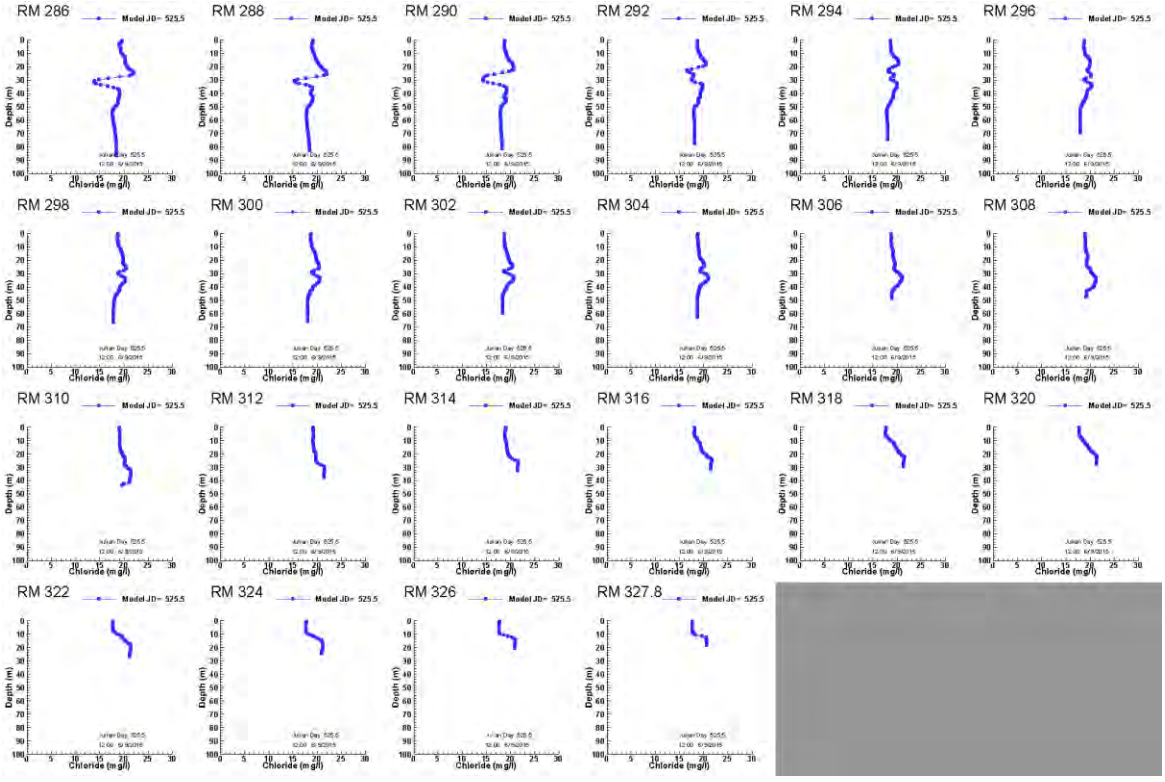


Figure 27. Vertical profiles of chloride compared with data for 6/ 9/2015.

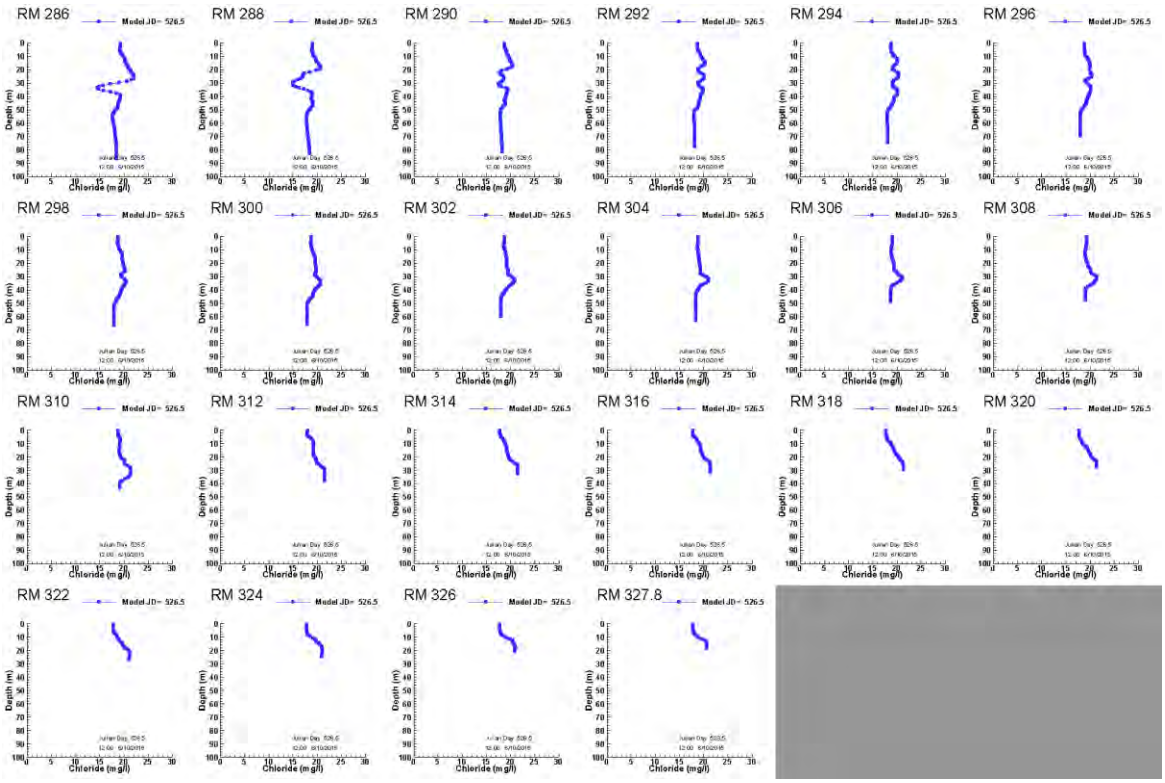


Figure 28. Vertical profiles of chloride compared with data for 6/10/2015.

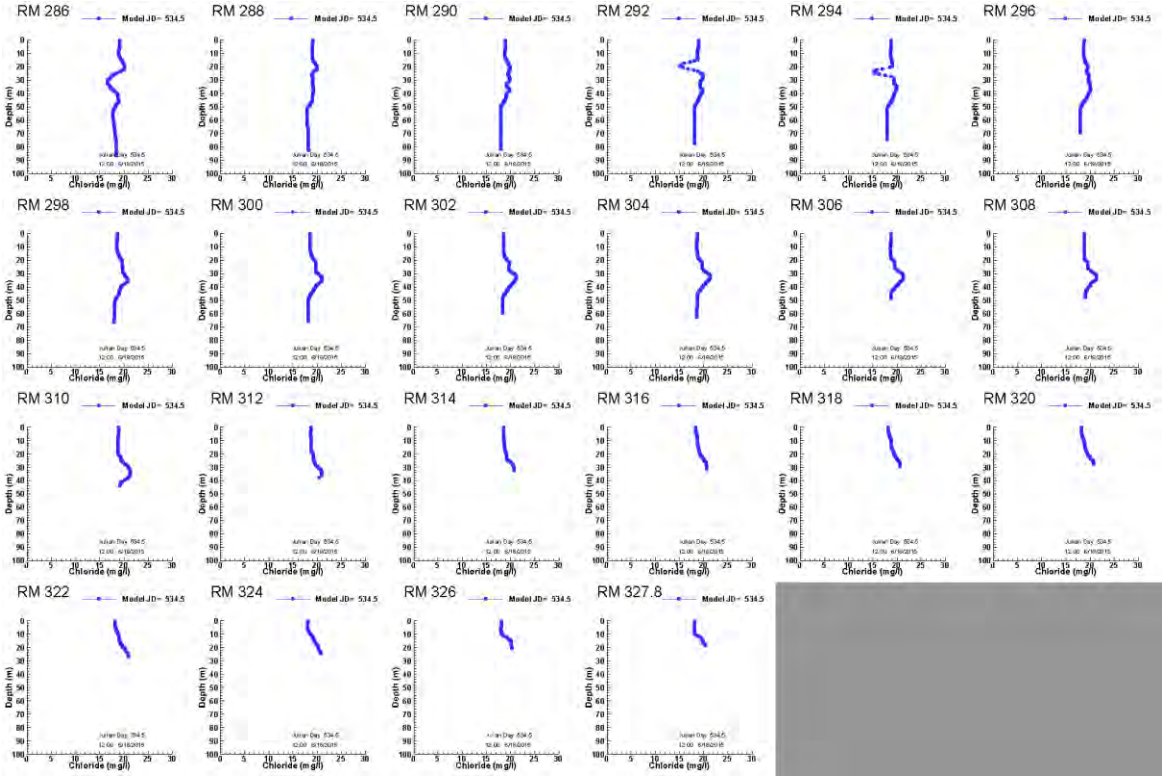


Figure 29. Vertical profiles of chloride compared with data for 6/18/2015.

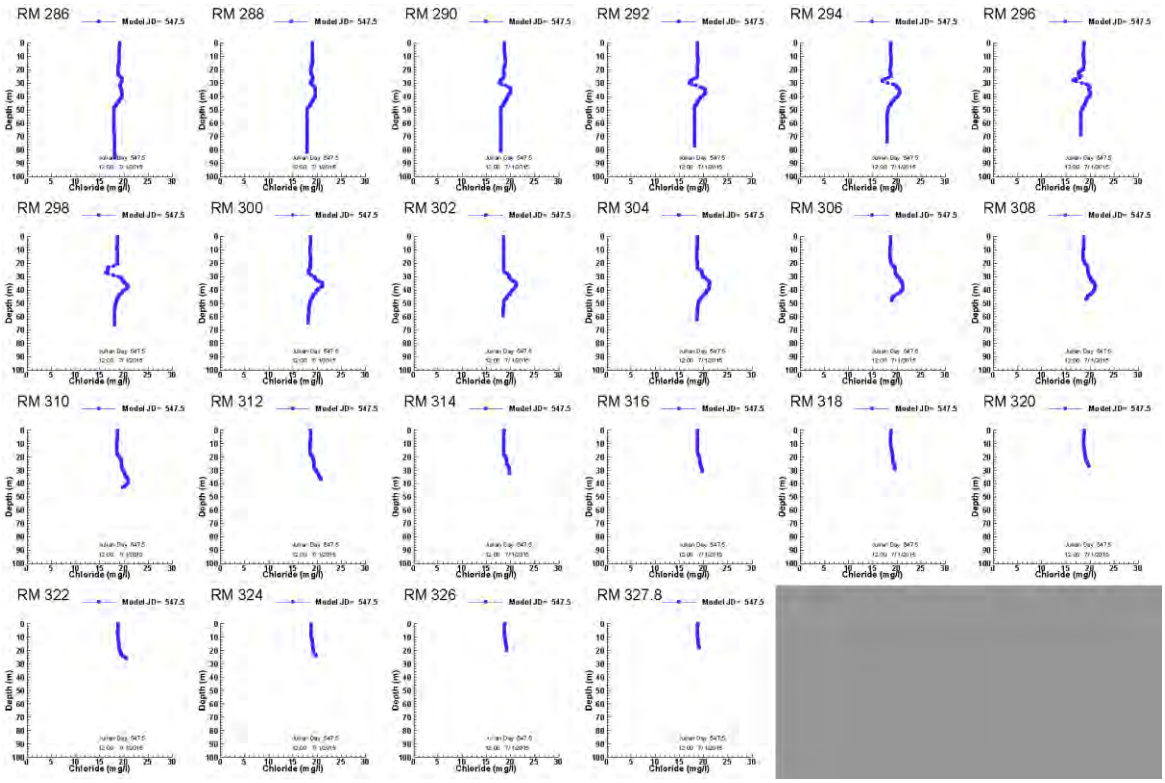


Figure 30. Vertical profiles of chloride compared with data for 7/ 1/2015.

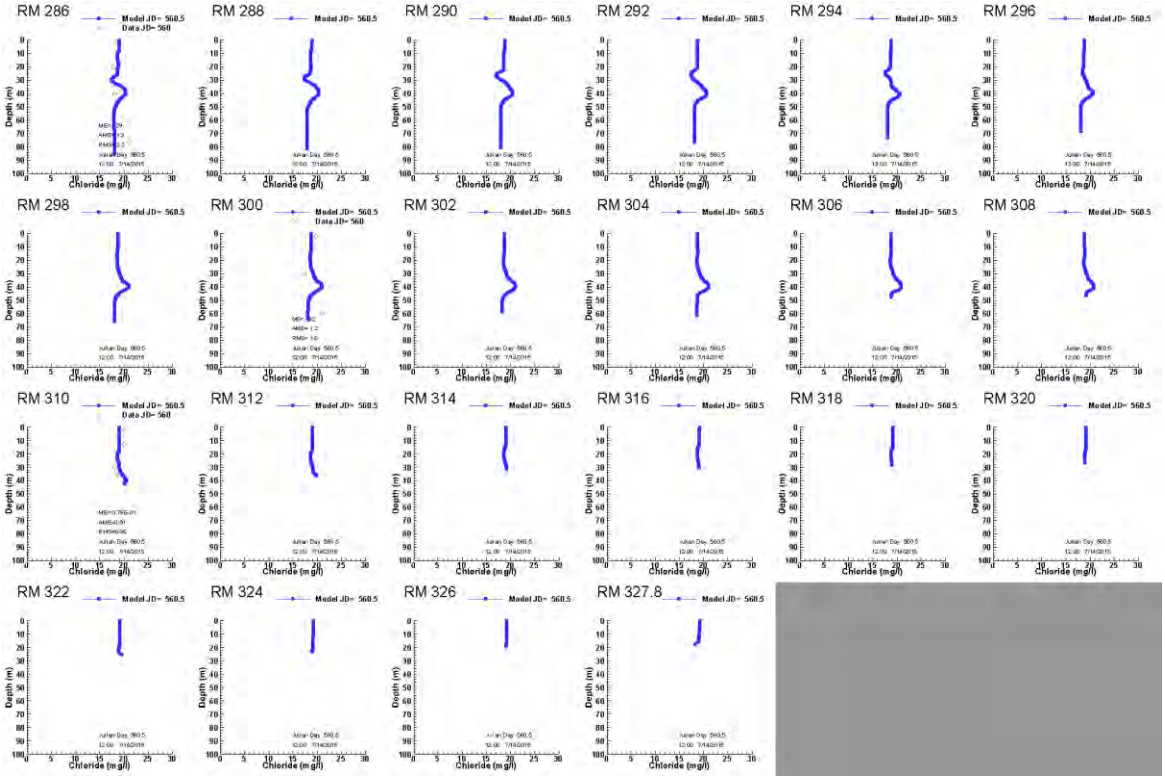


Figure 31. Vertical profiles of chloride compared with data for 7/14/2015.

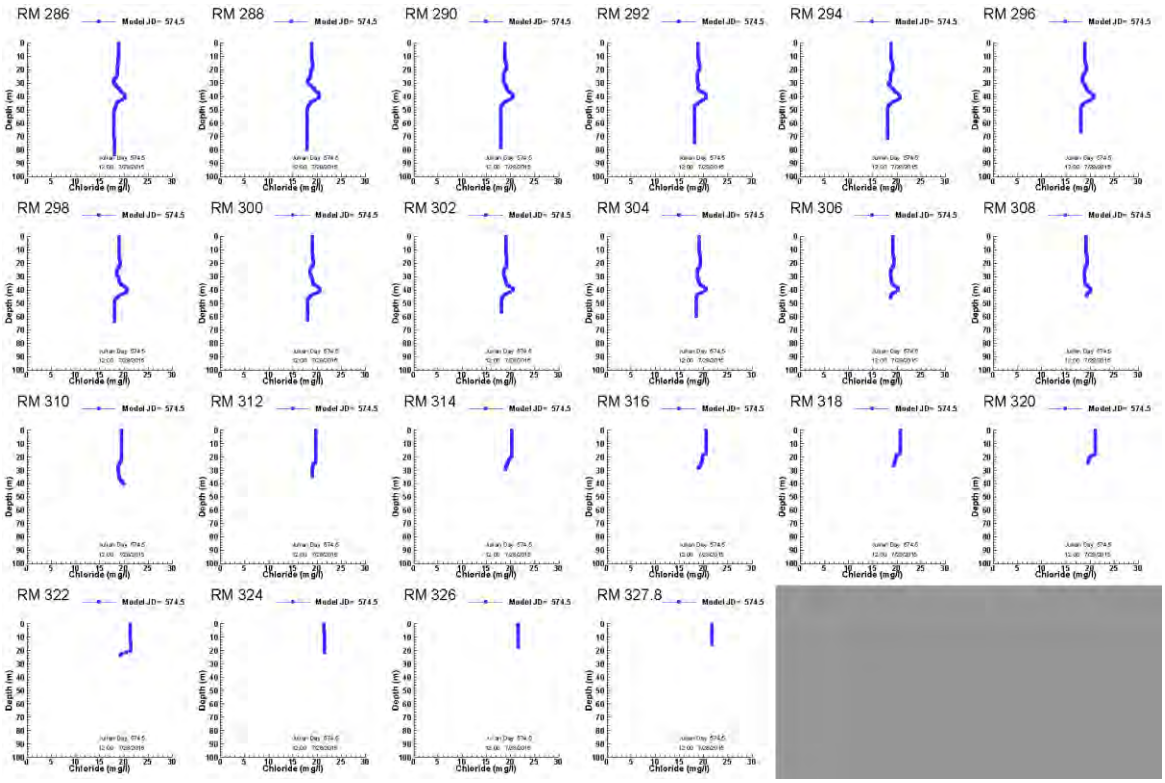


Figure 32. Vertical profiles of chloride compared with data for 7/28/2015.

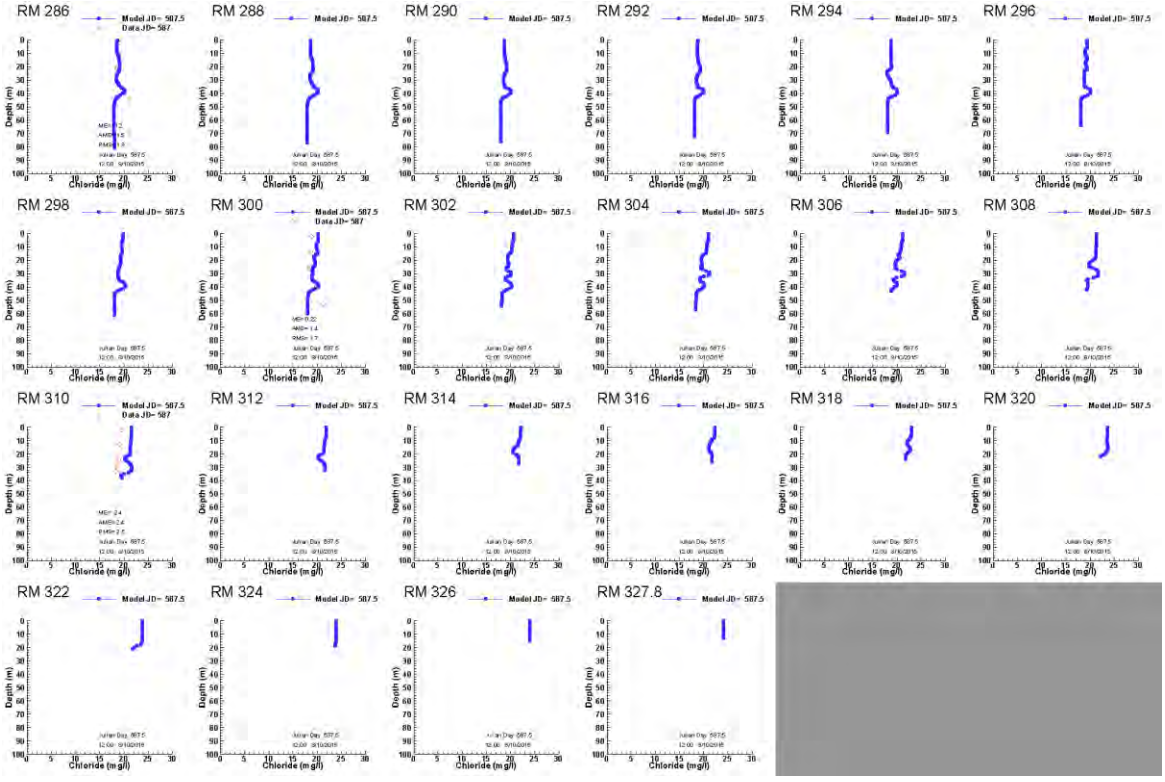


Figure 33. Vertical profiles of chloride compared with data for 8/10/2015.

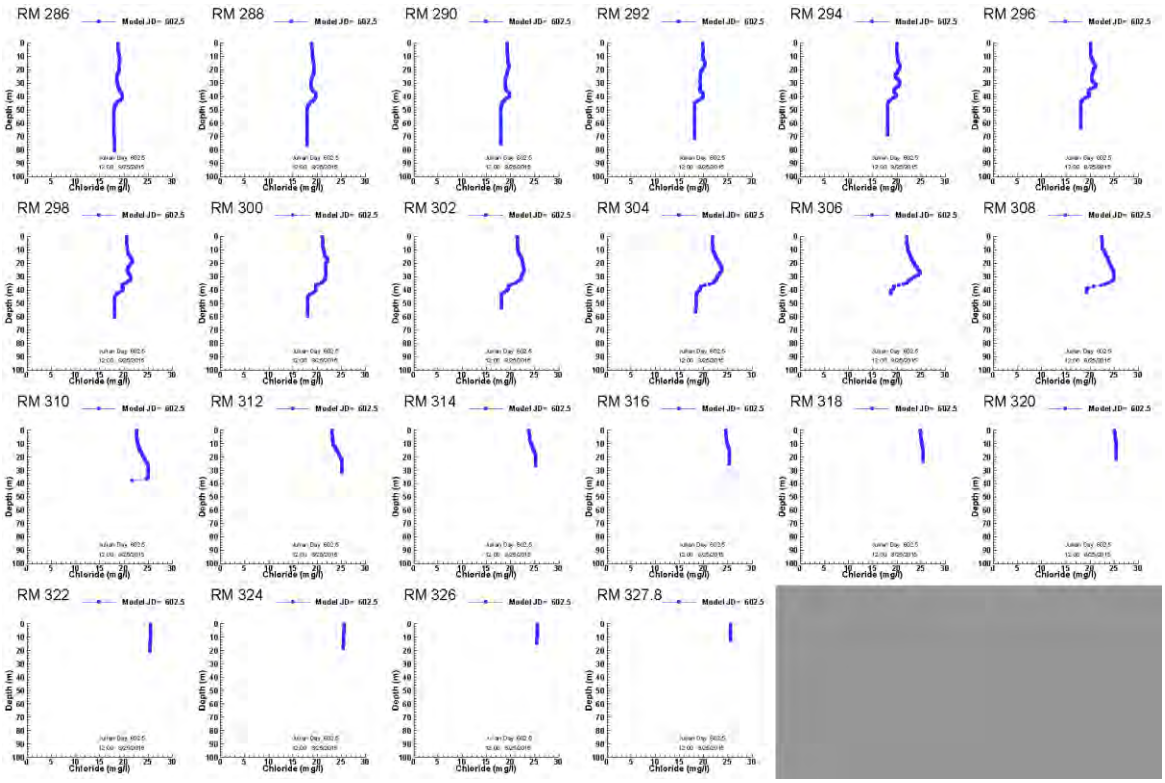


Figure 34. Vertical profiles of chloride compared with data for 8/25/2015.

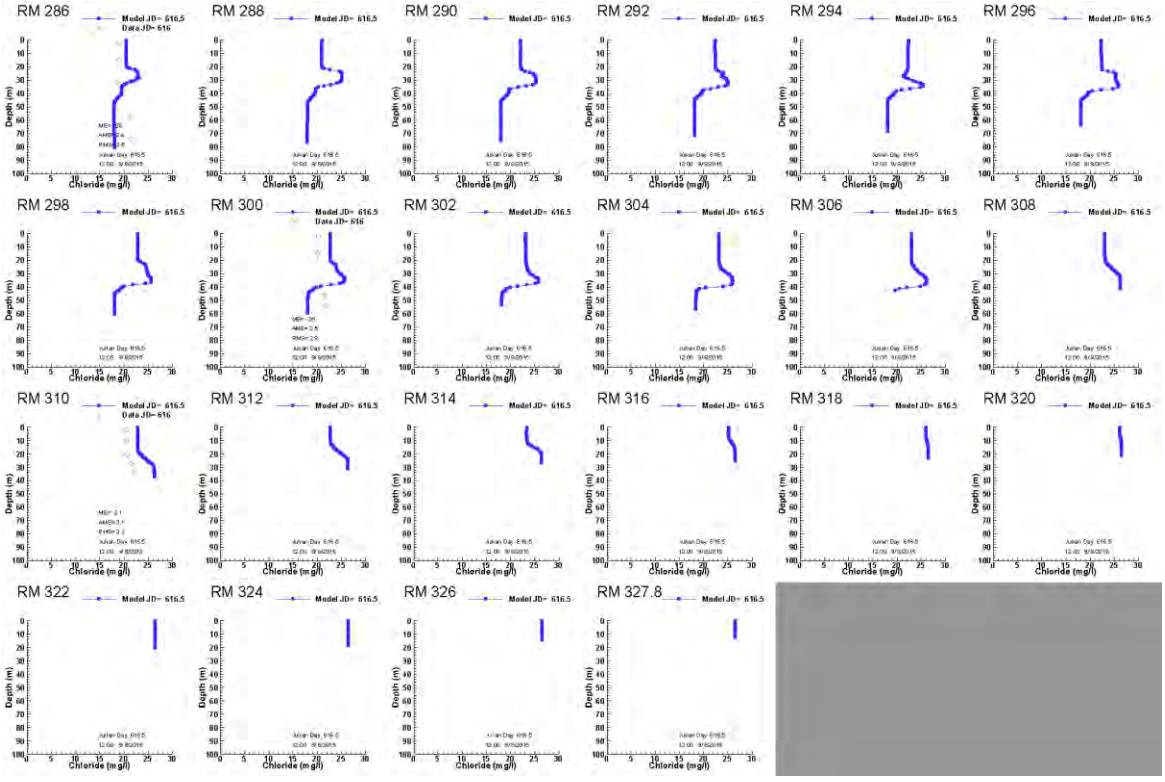


Figure 35. Vertical profiles of chloride compared with data for 9/ 8/2015.

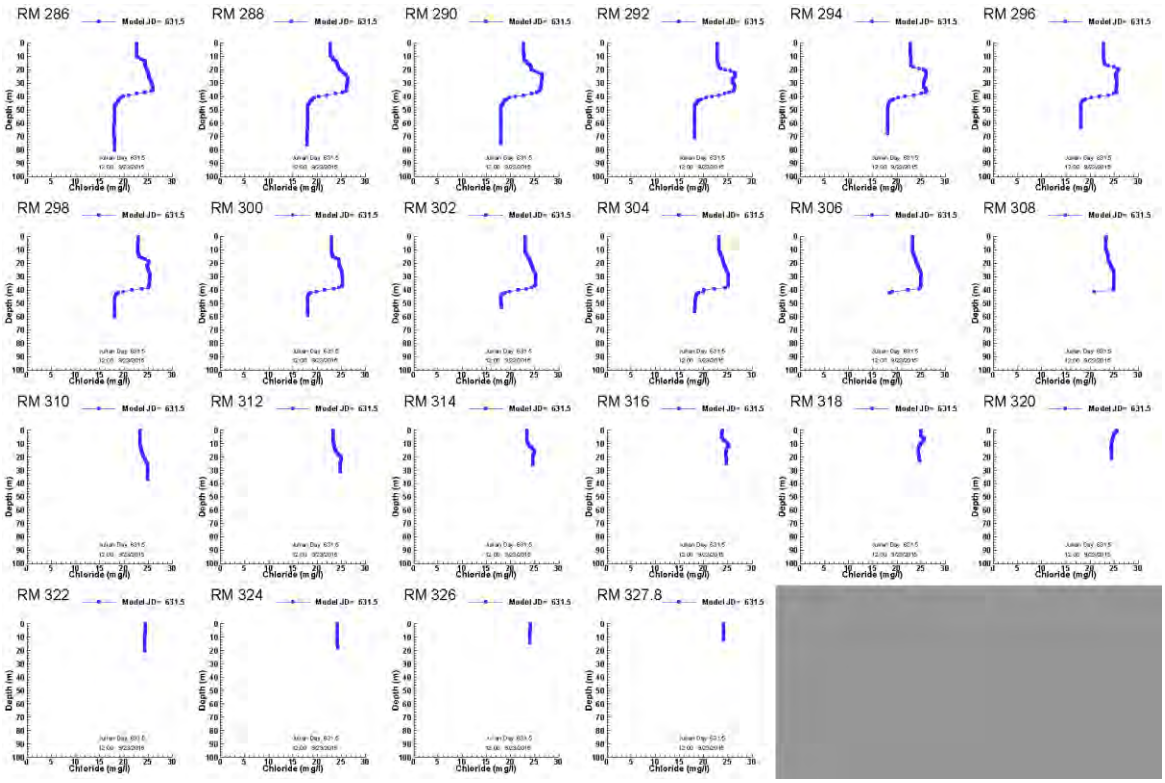


Figure 36. Vertical profiles of chloride compared with data for 9/23/2015.

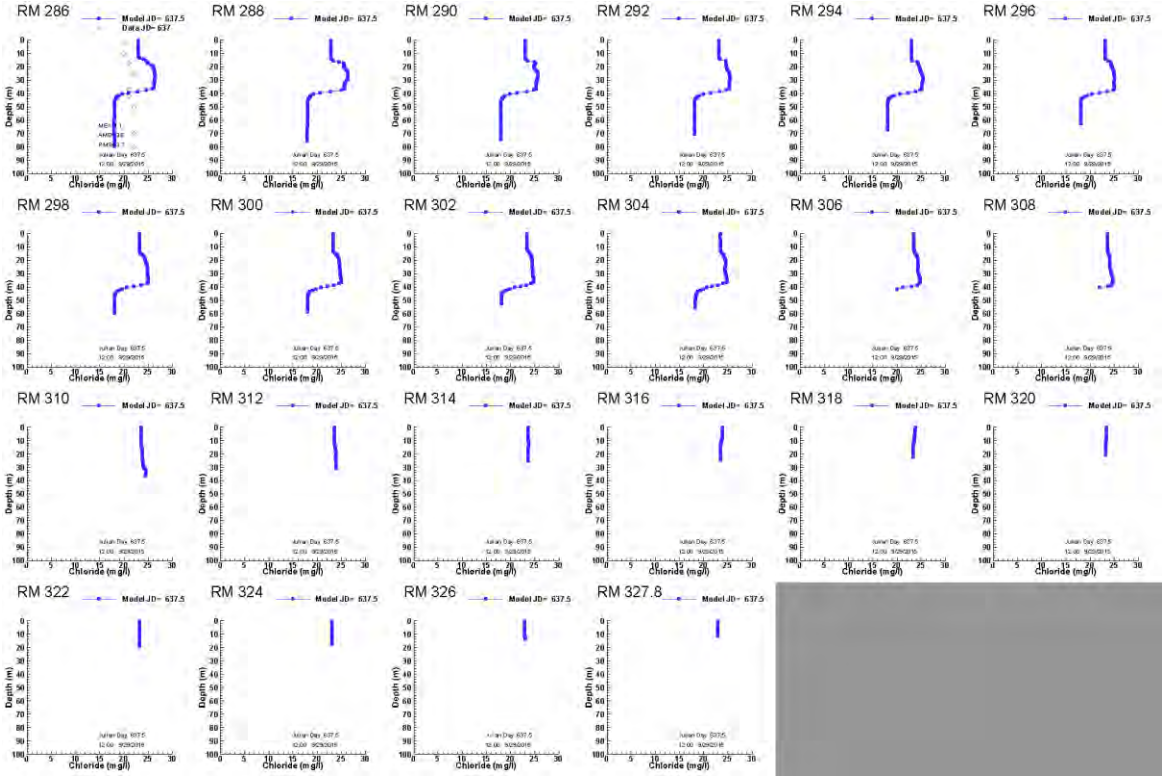


Figure 37. Vertical profiles of chloride compared with data for 9/29/2015.

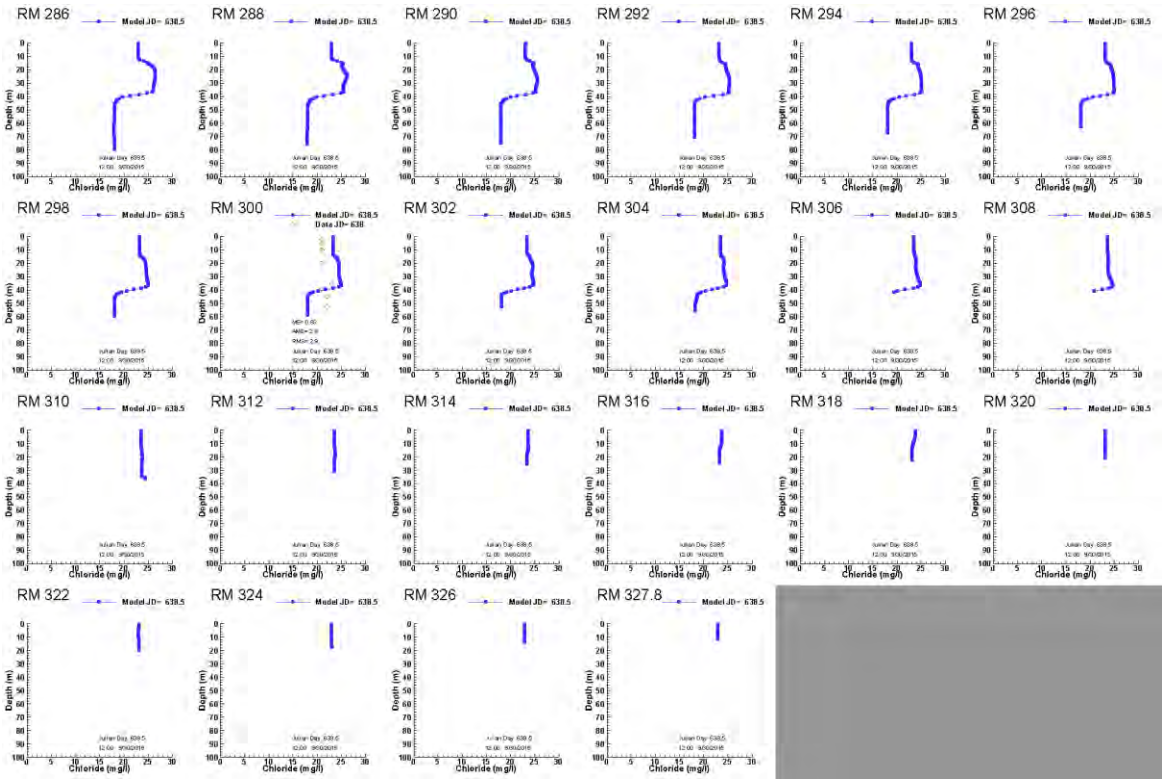


Figure 38. Vertical profiles of chloride compared with data for 9/30/2015.

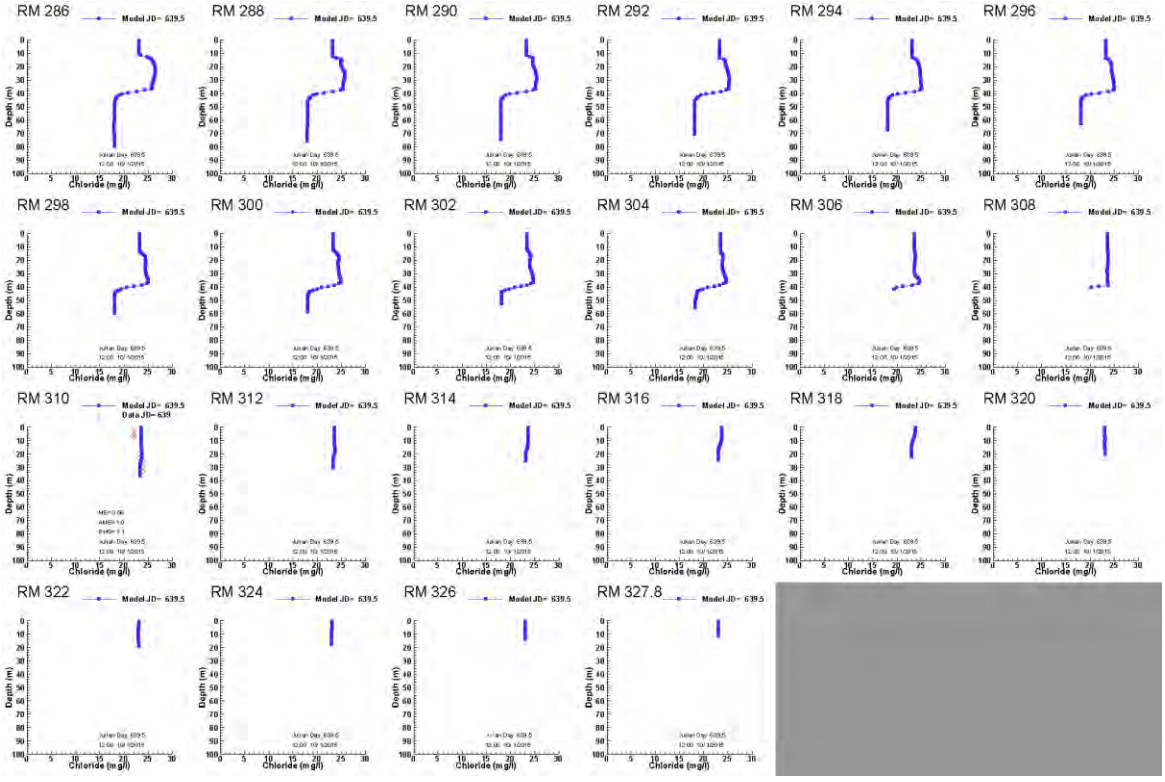


Figure 39. Vertical profiles of chloride compared with data for 10/ 1/2015.

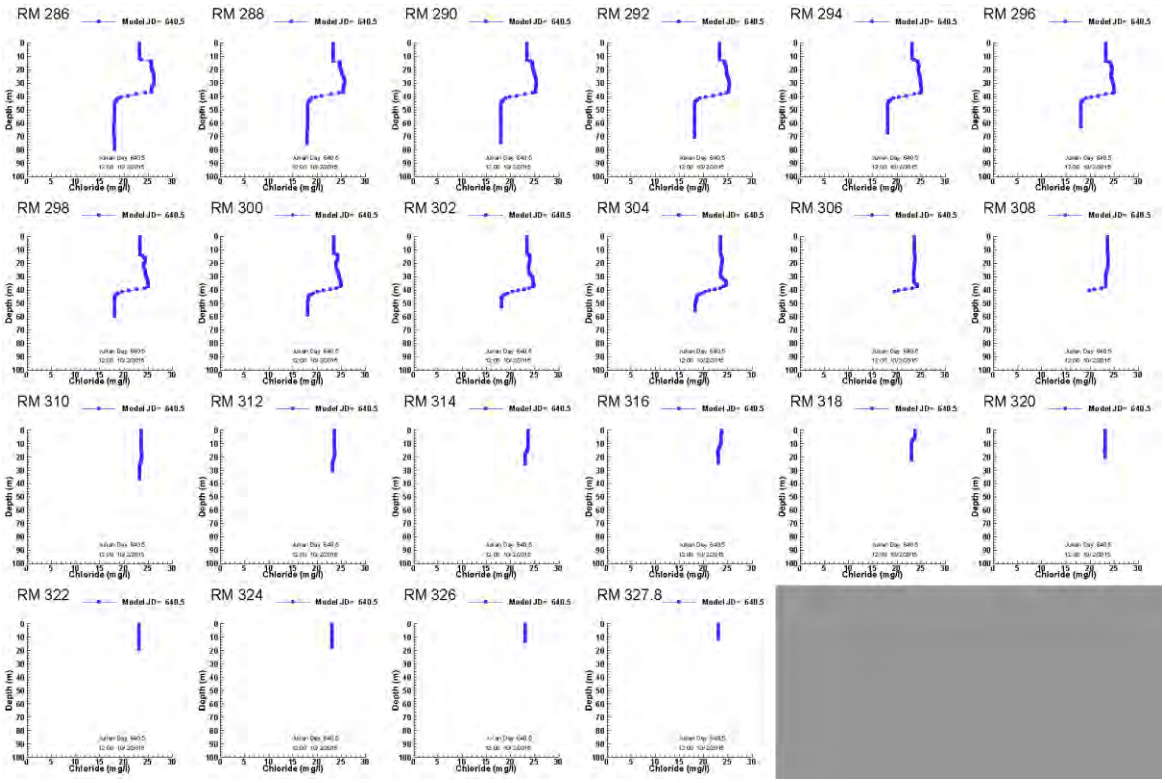


Figure 40. Vertical profiles of chloride compared with data for 10/ 2/2015.

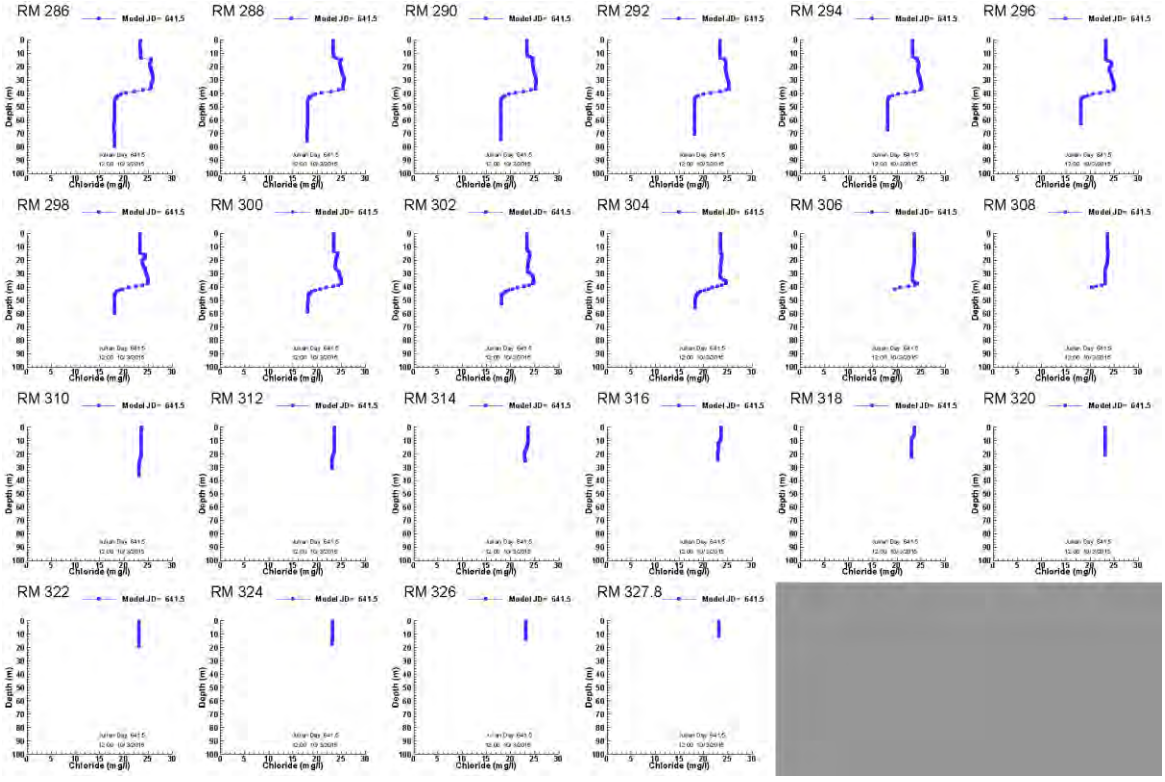


Figure 41. Vertical profiles of chloride compared with data for 10/ 3/2015.

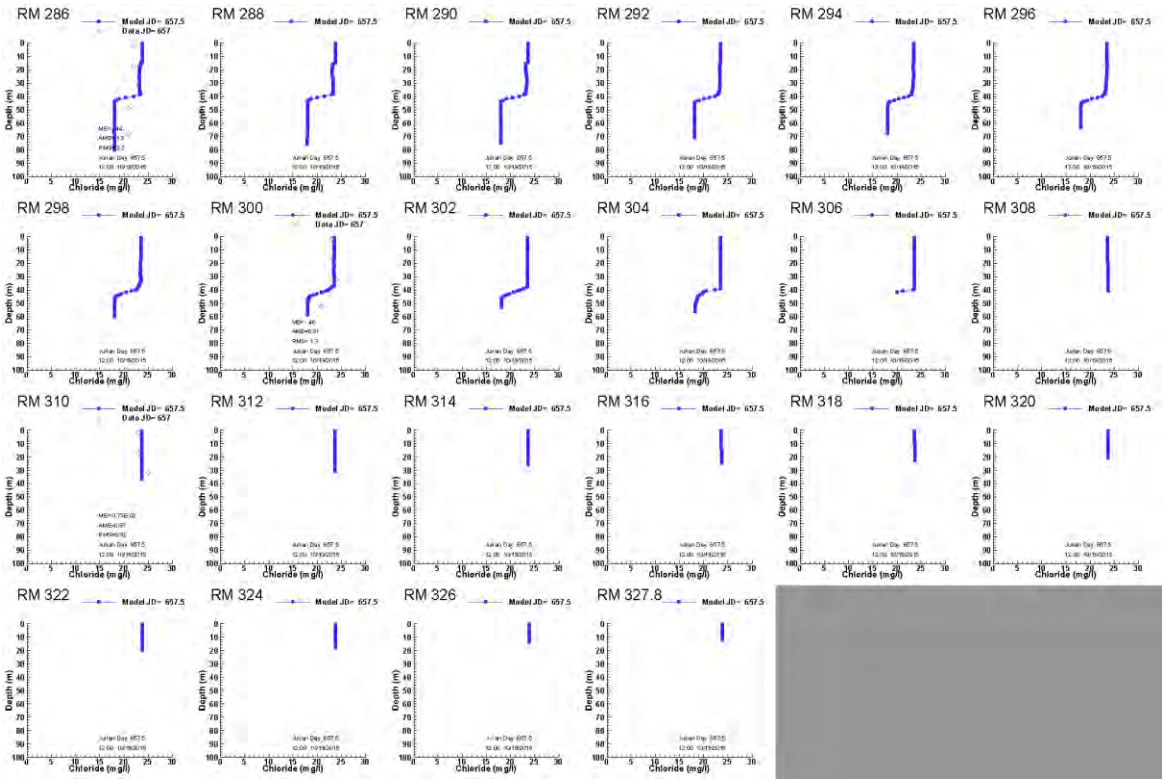


Figure 42. Vertical profiles of chloride compared with data for 10/19/2015.

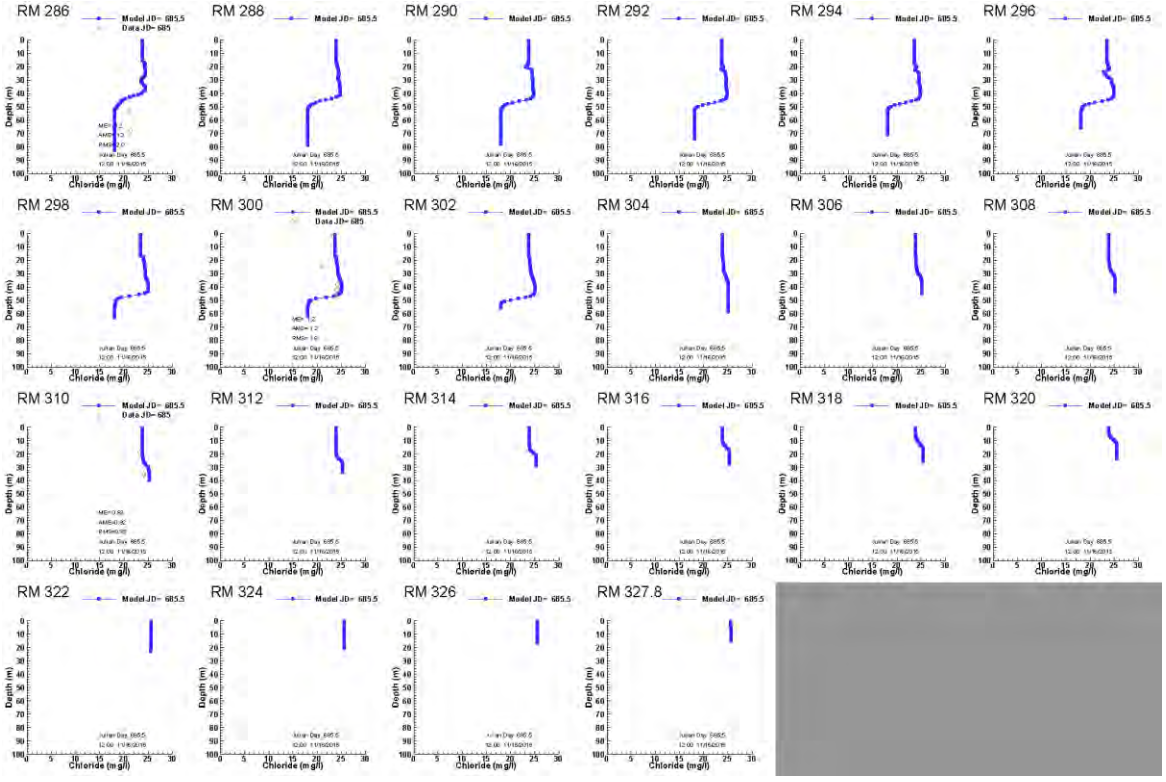


Figure 43. Vertical profiles of chloride compared with data for 11/16/2015.

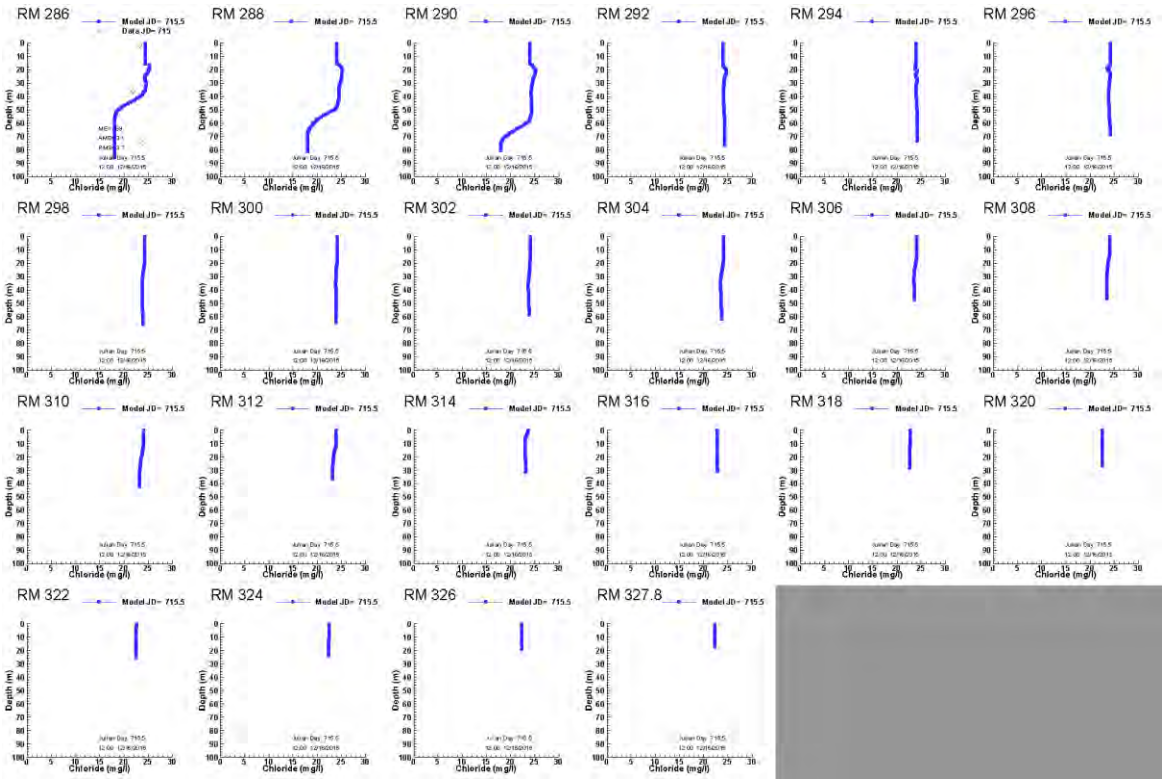


Figure 44. Vertical profiles of chloride compared with data for 12/16/2015.

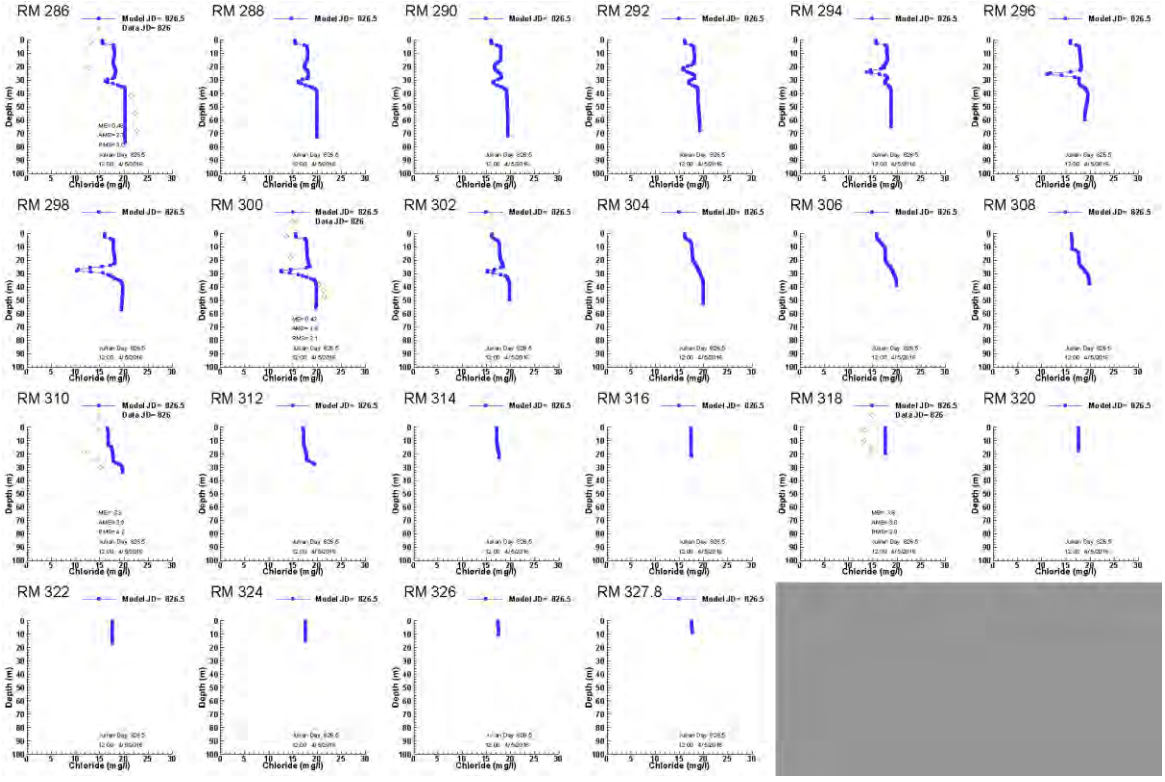


Figure 45. Vertical profiles of chloride compared with data for 4/ 5/2016.

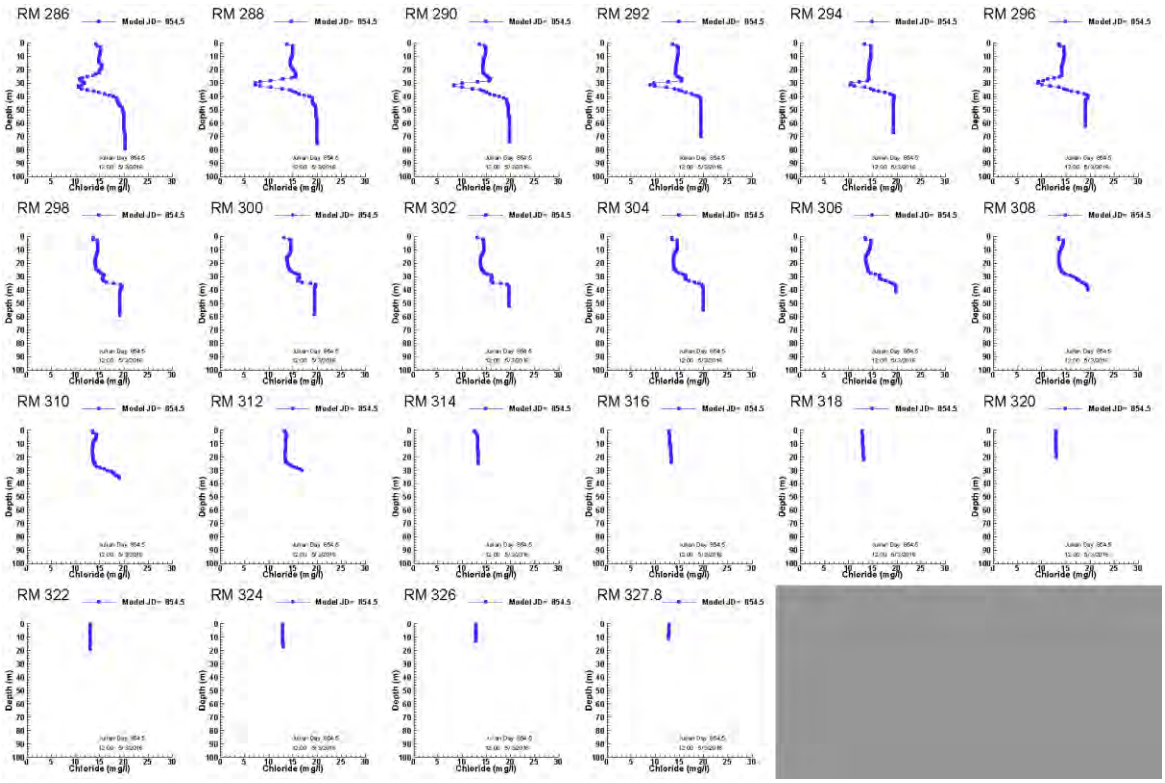


Figure 46. Vertical profiles of chloride compared with data for 5/ 3/2016.

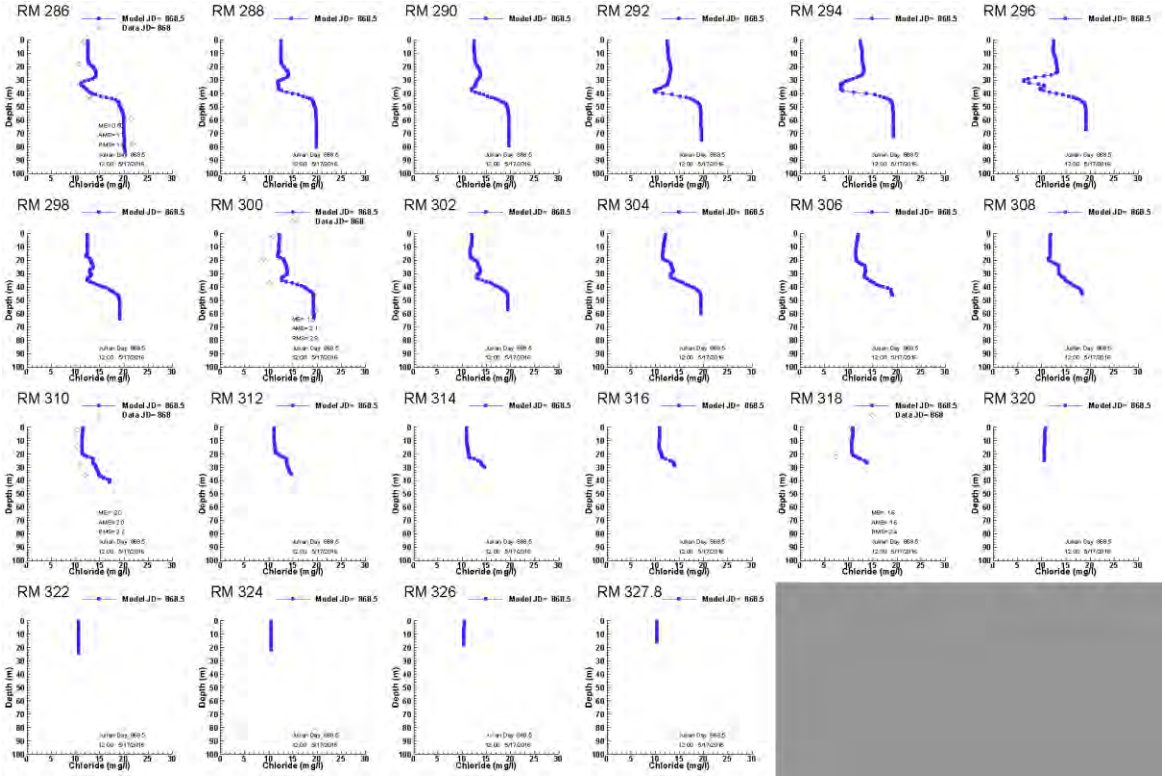


Figure 47. Vertical profiles of chloride compared with data for 5/17/2016.

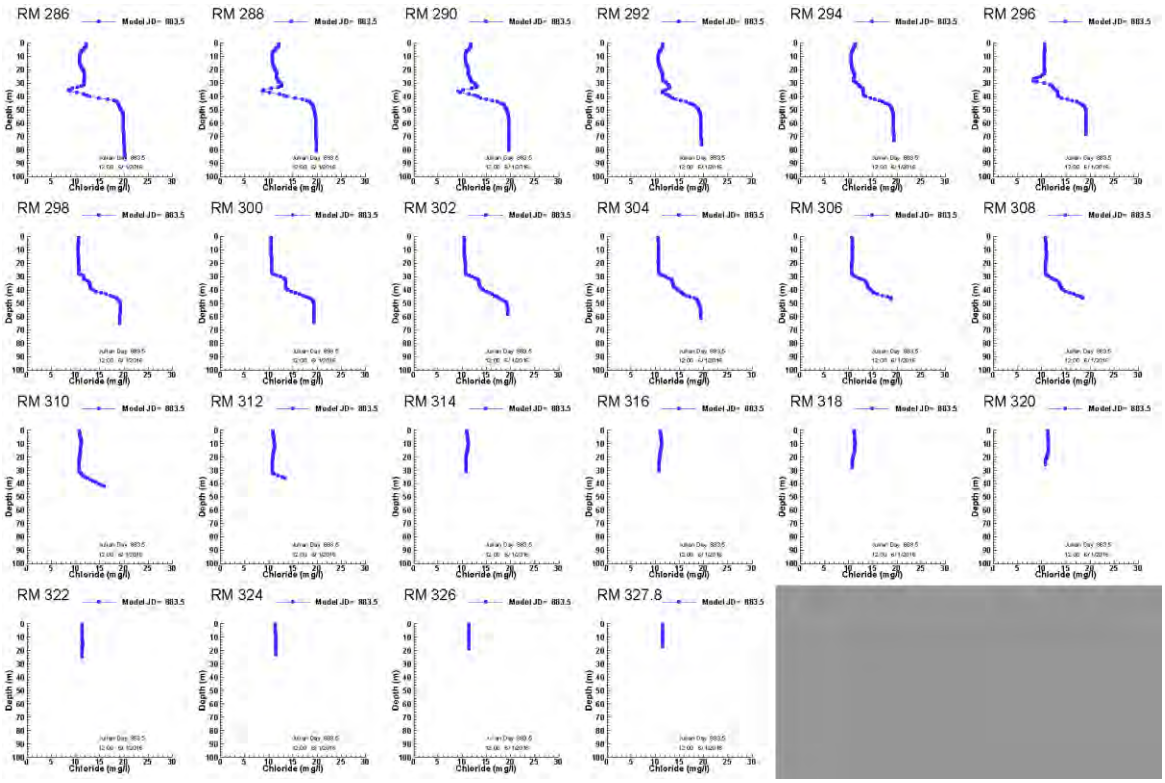


Figure 48. Vertical profiles of chloride compared with data for 6/ 1/2016.

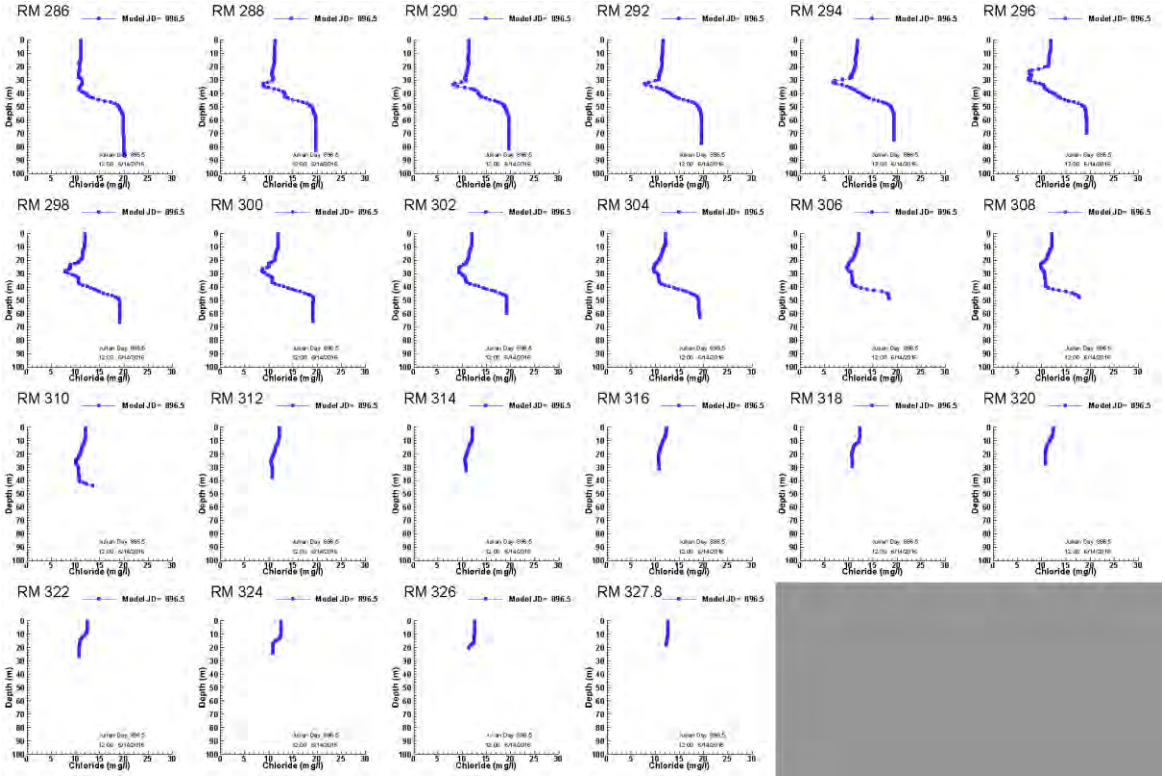


Figure 49. Vertical profiles of chloride compared with data for 6/14/2016.

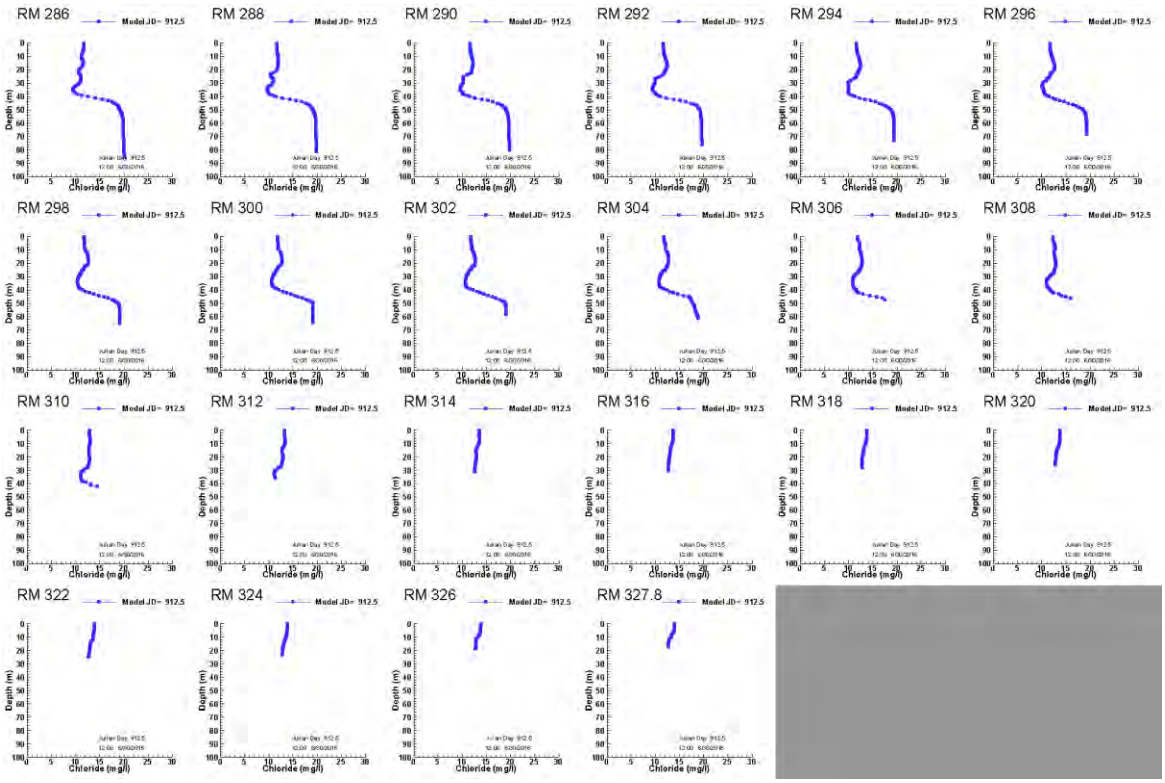


Figure 50. Vertical profiles of chloride compared with data for 6/30/2016.

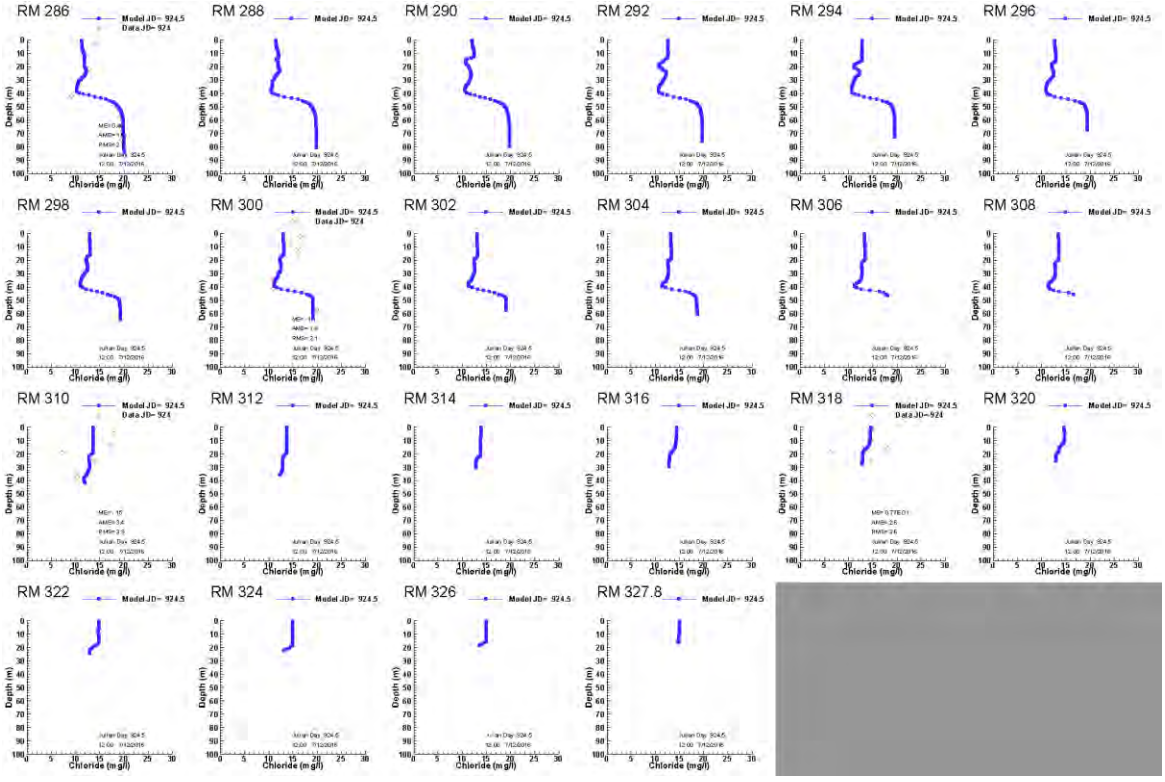


Figure 51. Vertical profiles of chloride compared with data for 7/12/2016.

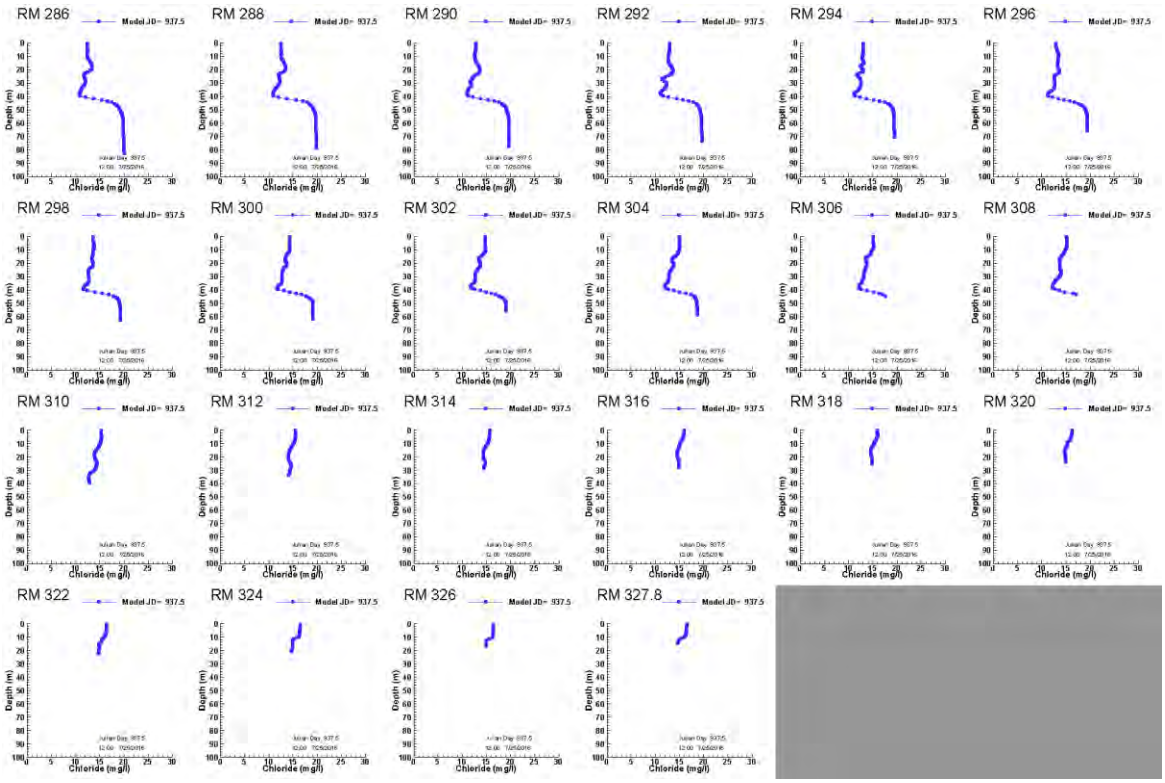


Figure 52. Vertical profiles of chloride compared with data for 7/25/2016.

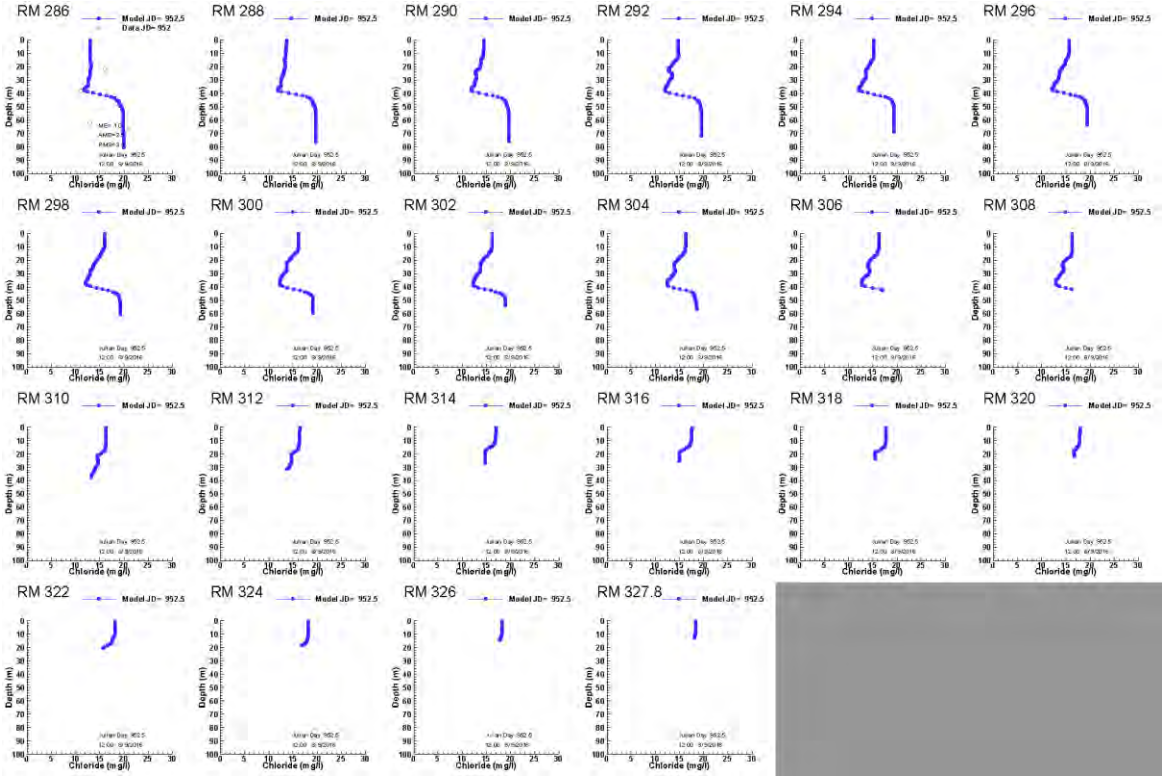


Figure 53. Vertical profiles of chloride compared with data for 8/ 9/2016.

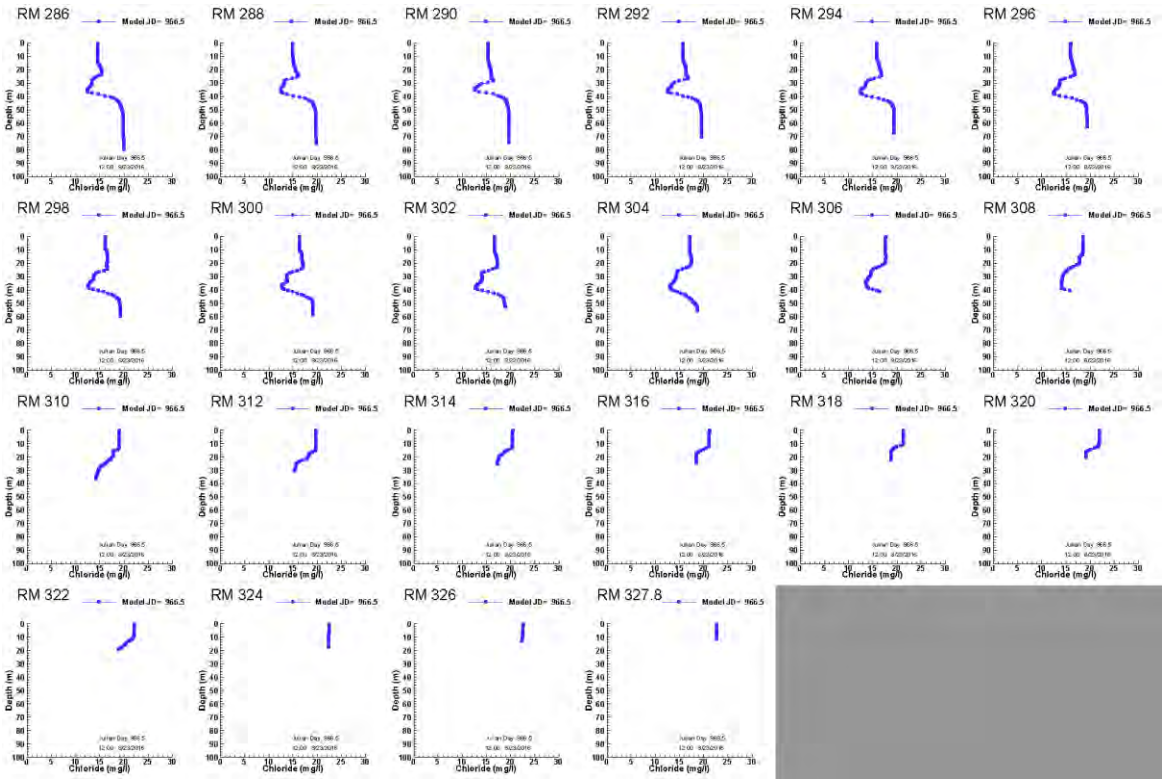


Figure 54. Vertical profiles of chloride compared with data for 8/23/2016.

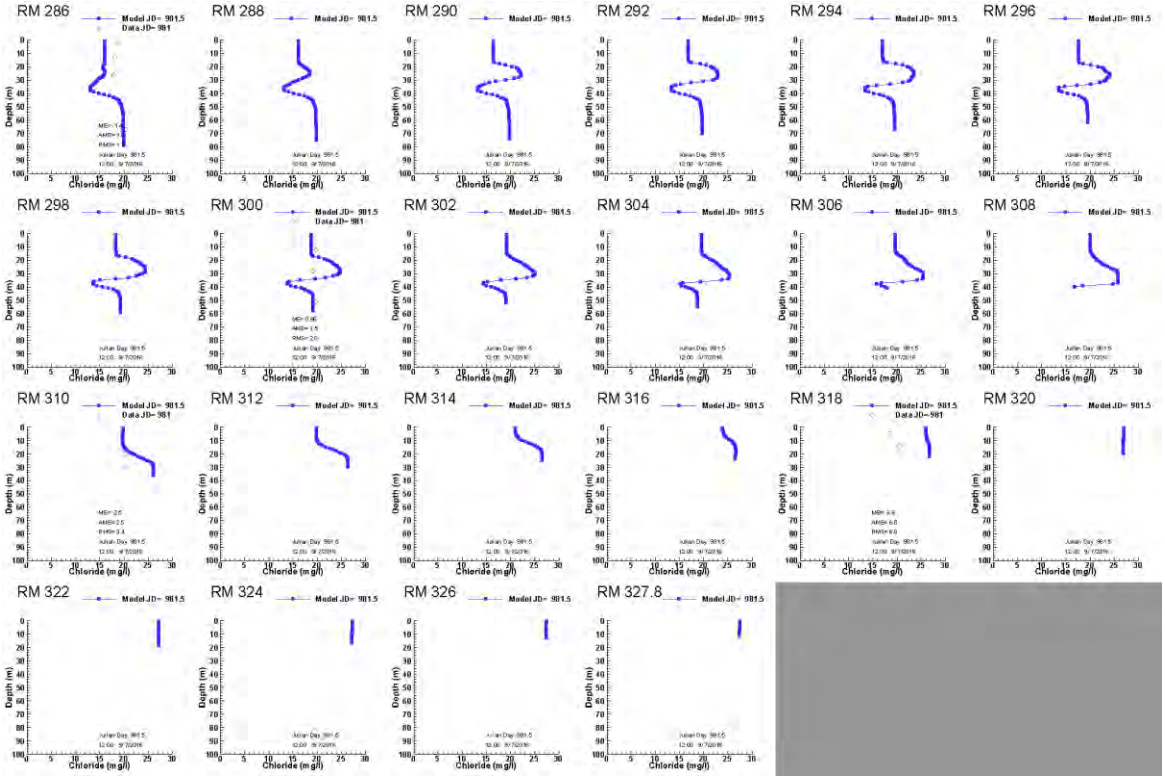


Figure 55. Vertical profiles of chloride compared with data for 9/ 7/2016.

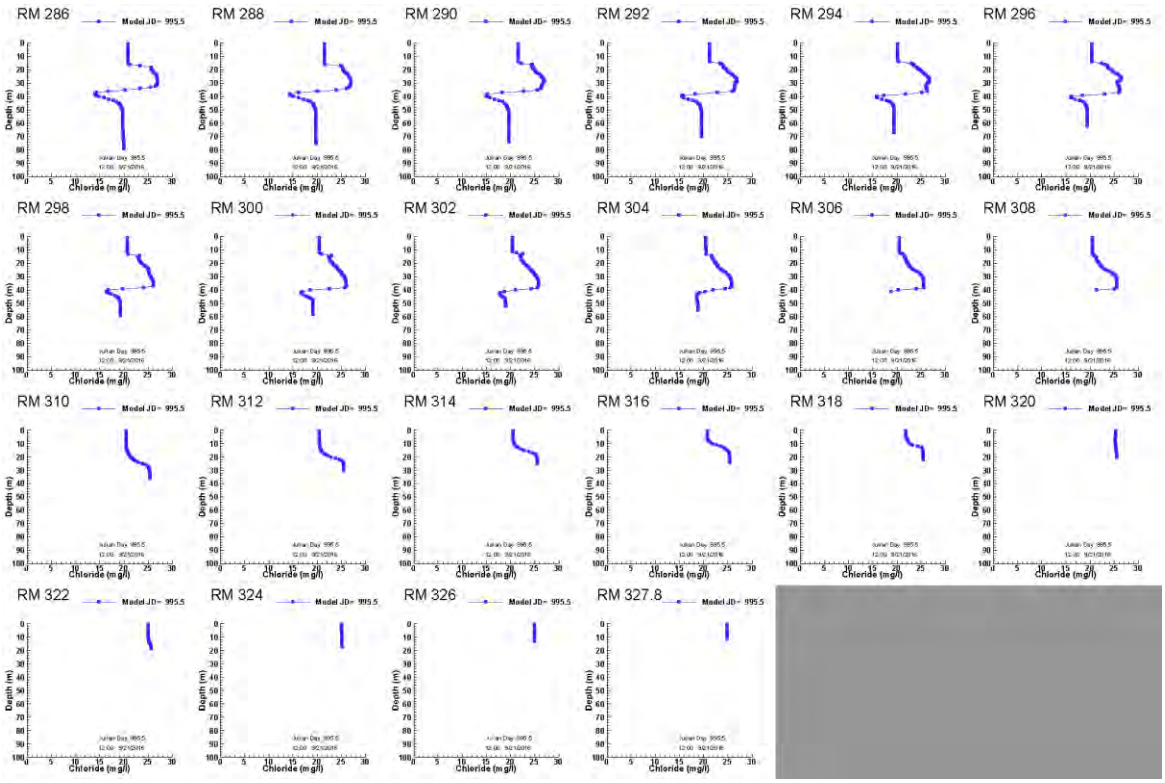


Figure 56. Vertical profiles of chloride compared with data for 9/21/2016.

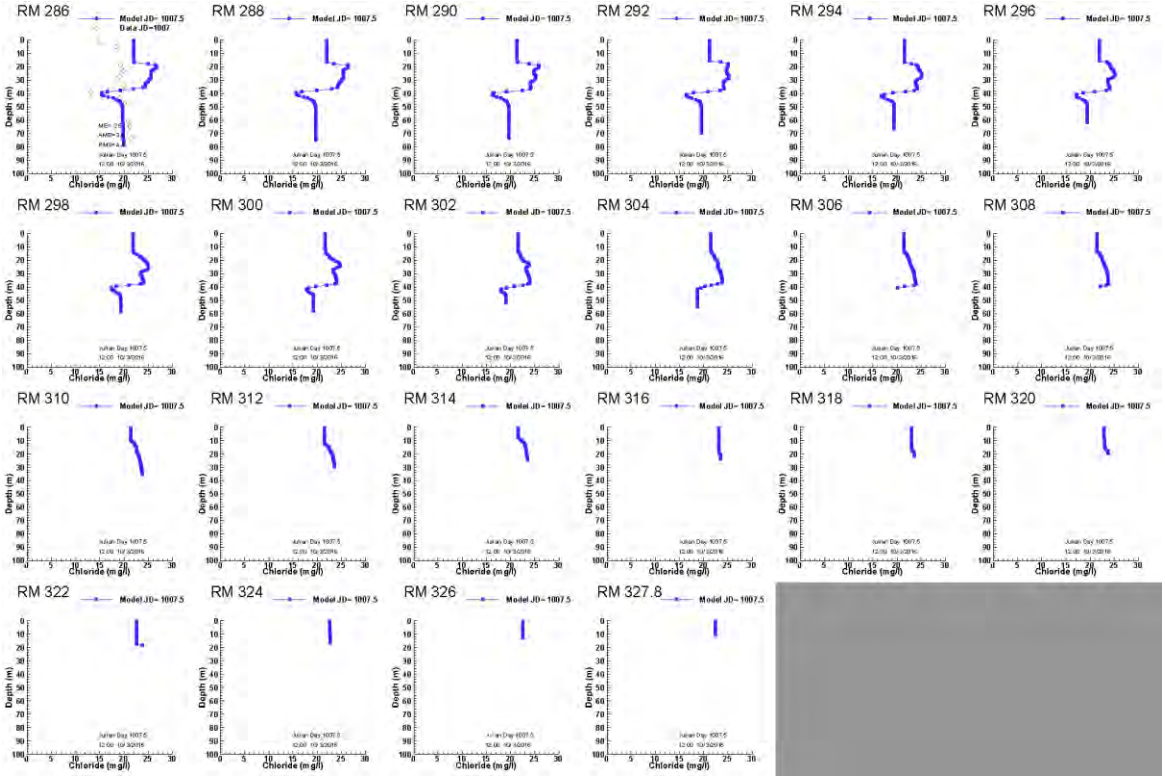


Figure 57. Vertical profiles of chloride compared with data for 10/ 3/2016.

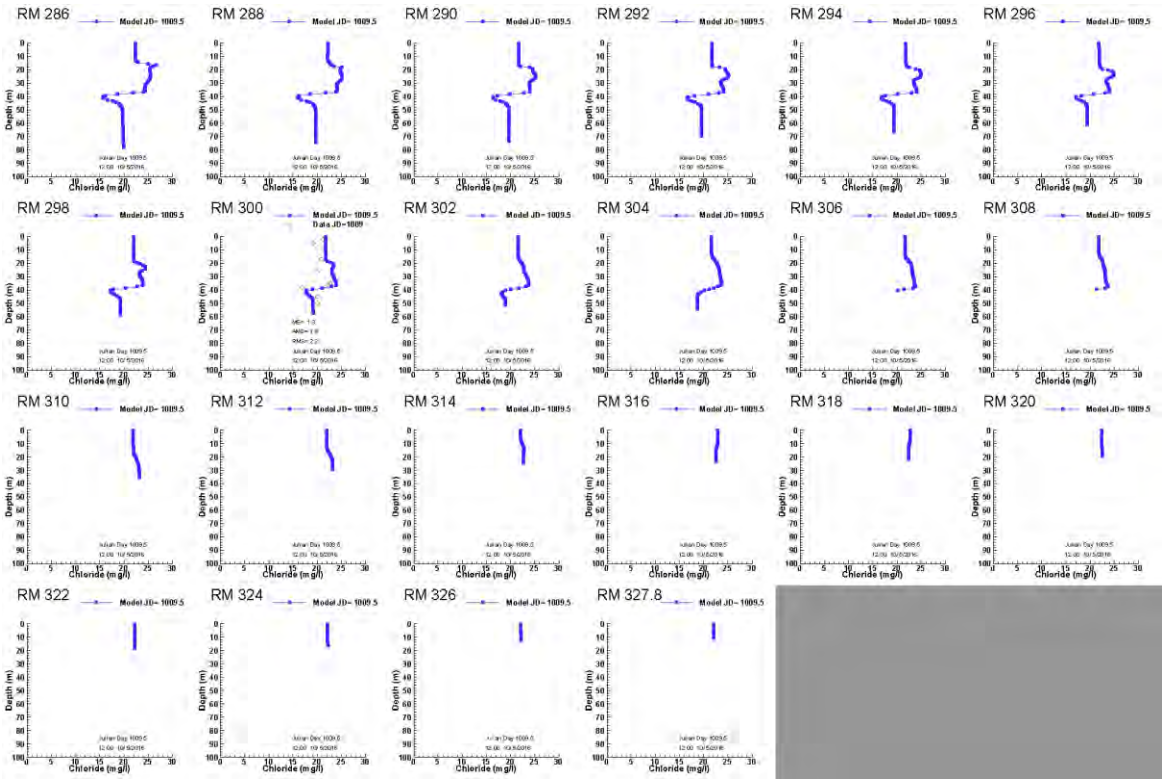


Figure 58. Vertical profiles of chloride compared with data for 10/ 5/2016.

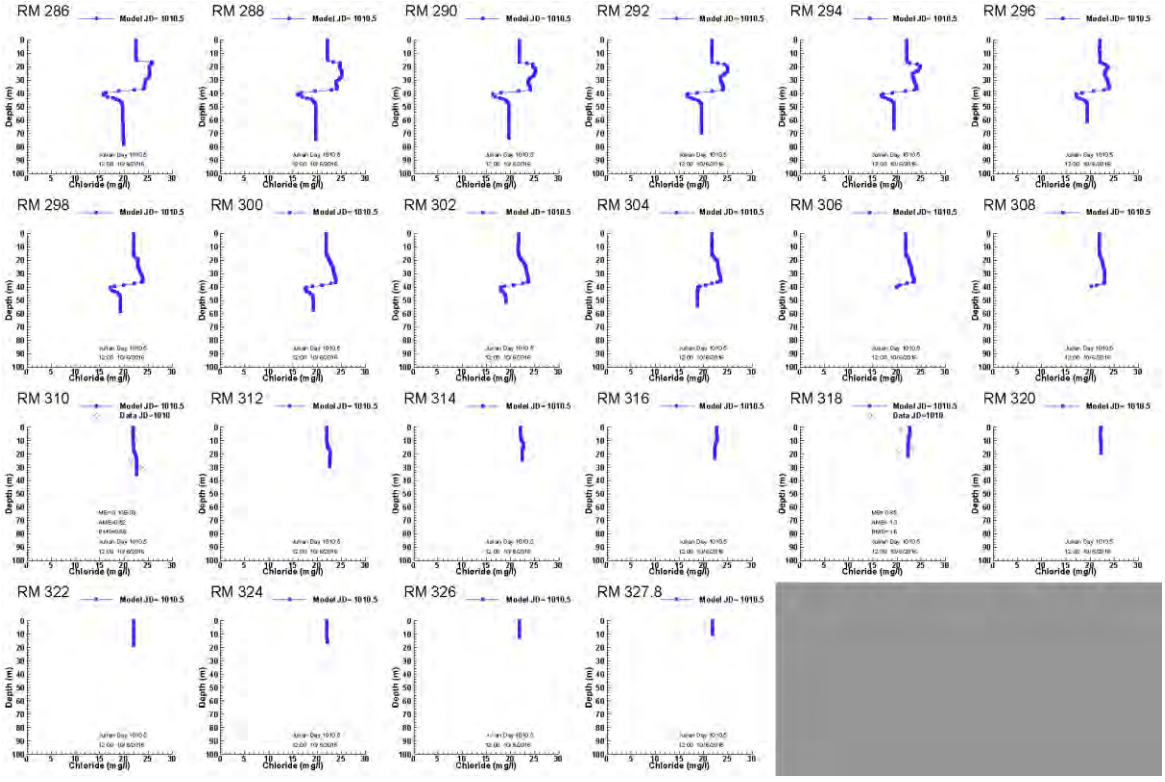


Figure 59. Vertical profiles of chloride compared with data for 10/ 6/2016.

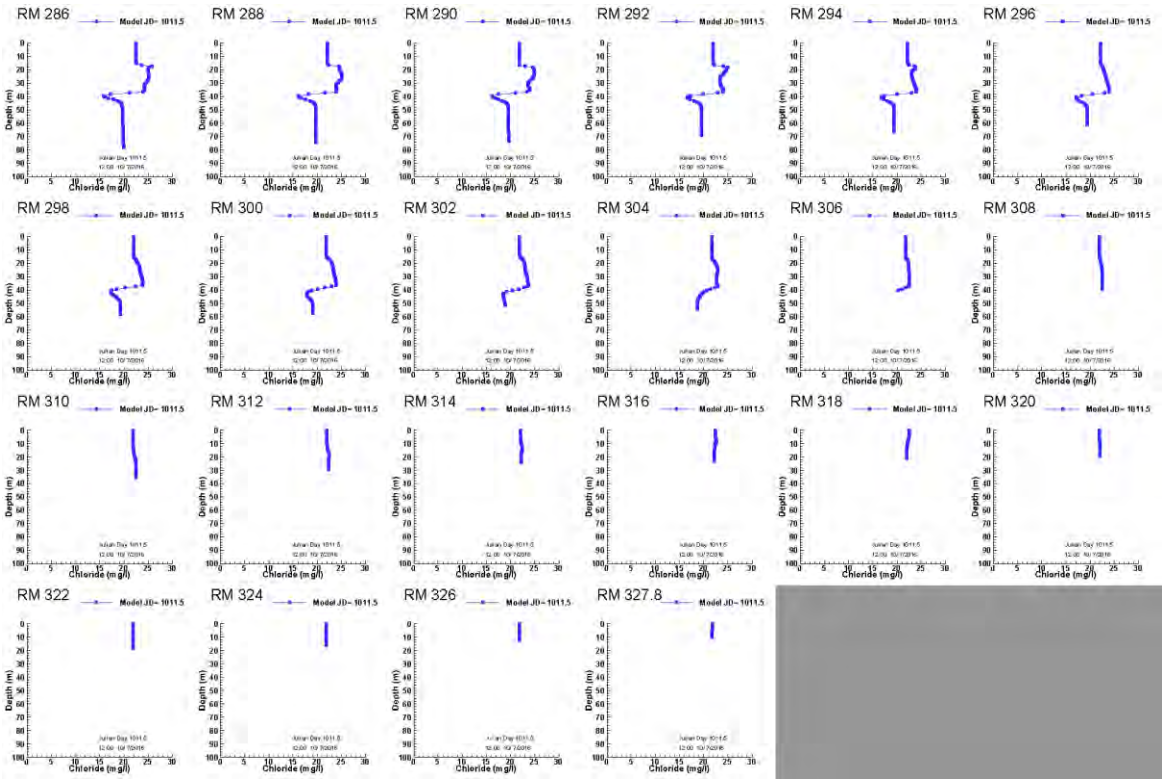


Figure 60. Vertical profiles of chloride compared with data for 10/ 7/2016.

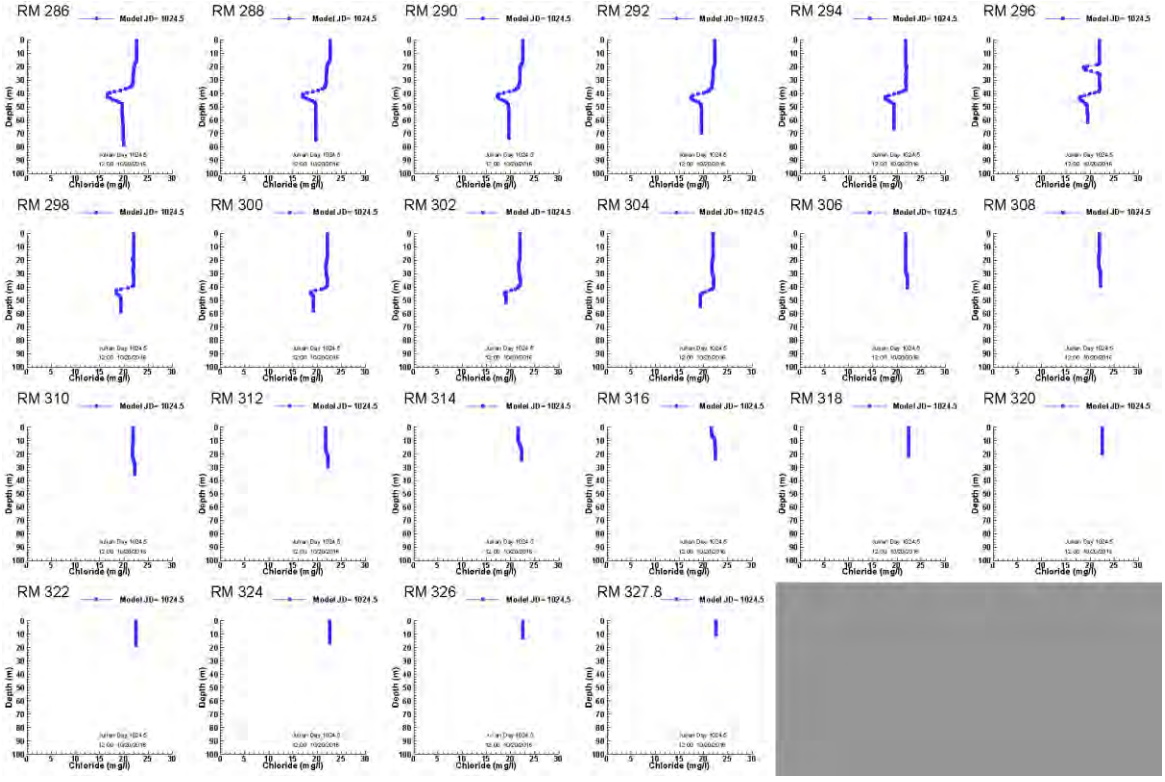


Figure 61. Vertical profiles of chloride compared with data for 10/20/2016.

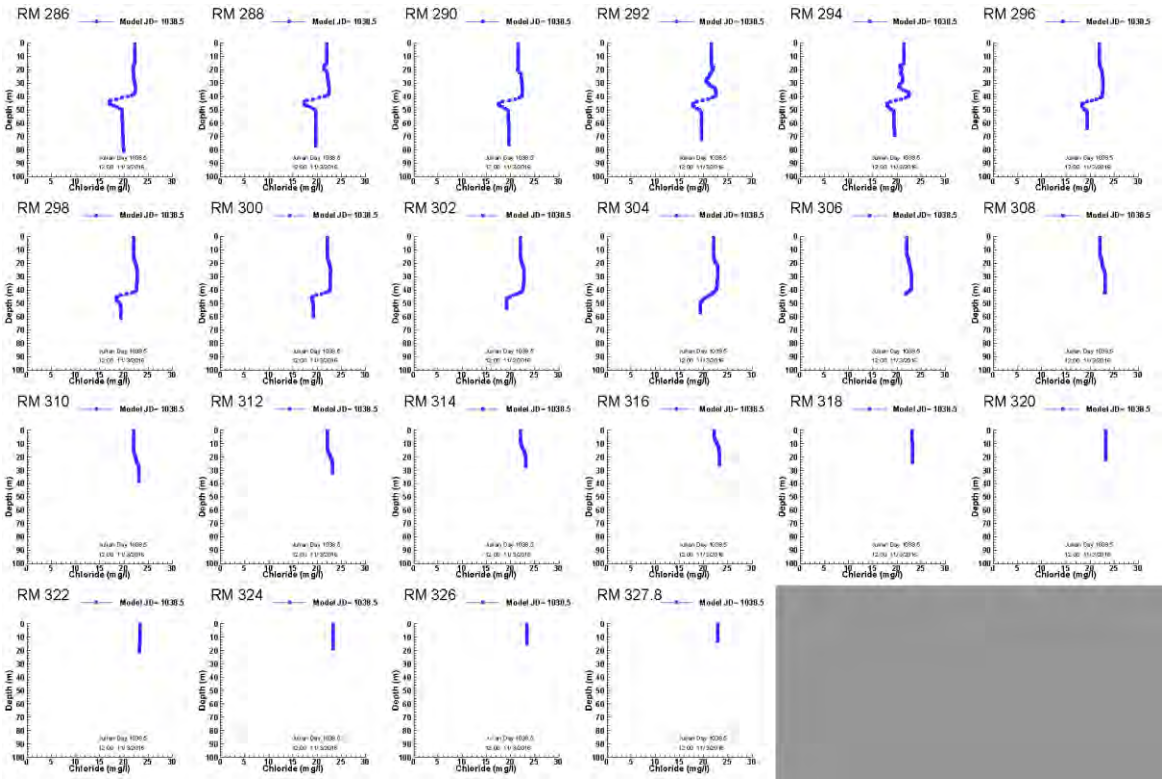


Figure 62. Vertical profiles of chloride compared with data for 11/ 3/2016.

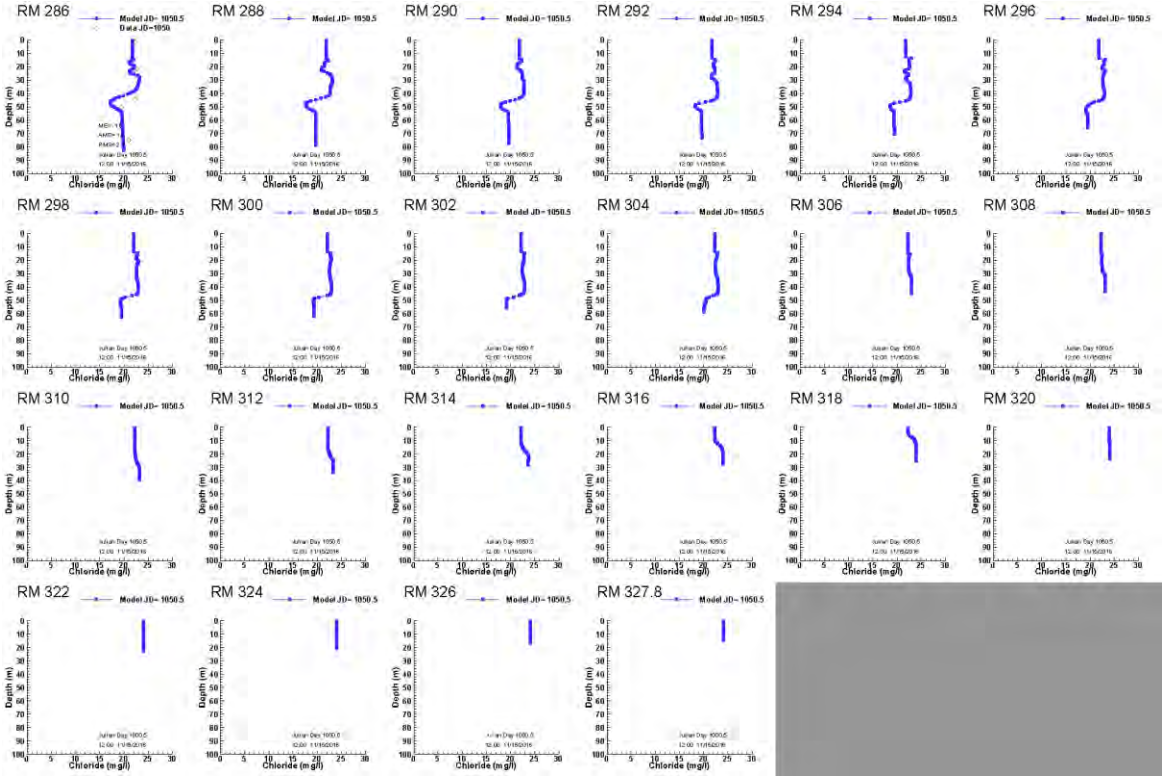


Figure 63. Vertical profiles of chloride compared with data for 11/15/2016.

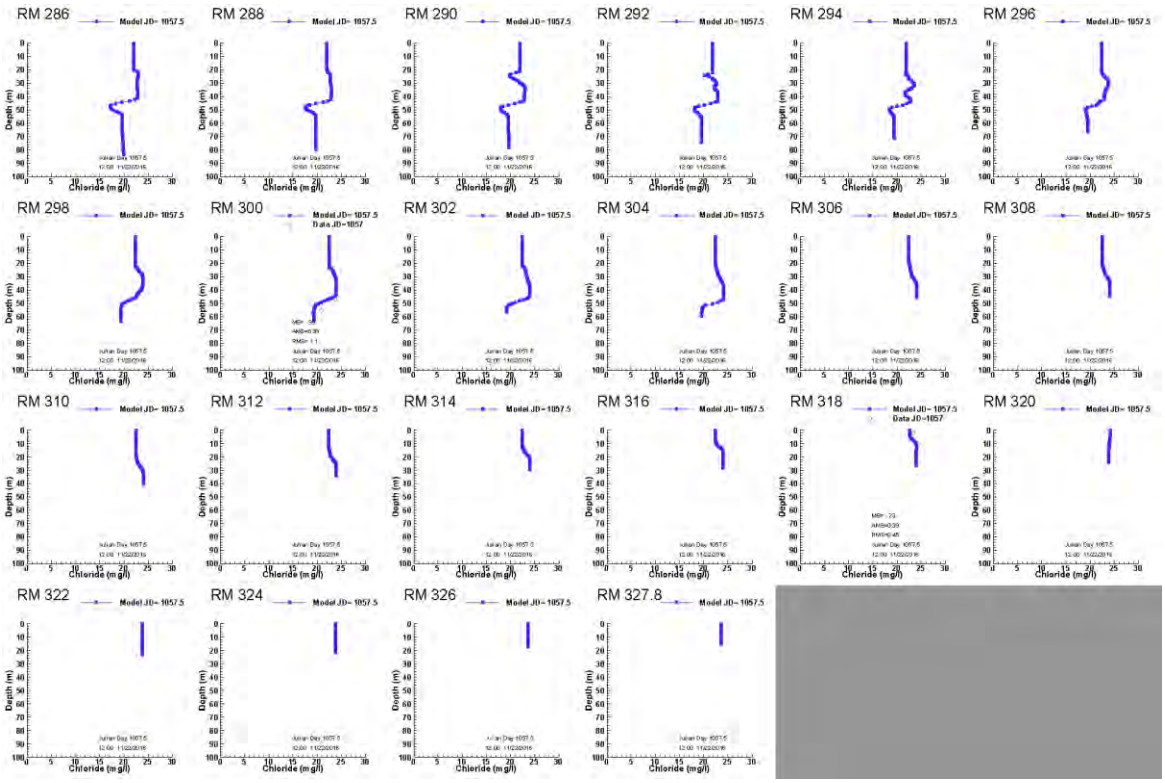


Figure 64. Vertical profiles of chloride compared with data for 11/22/2016.

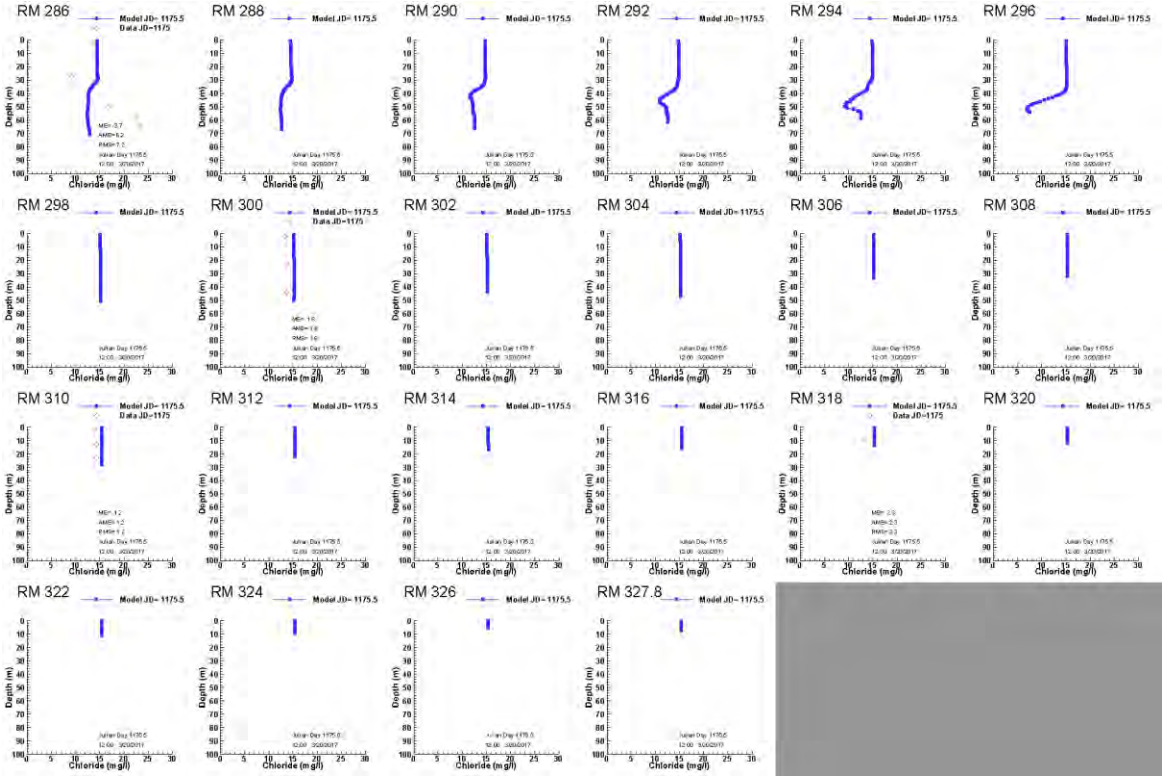


Figure 65. Vertical profiles of chloride compared with data for 3/20/2017.

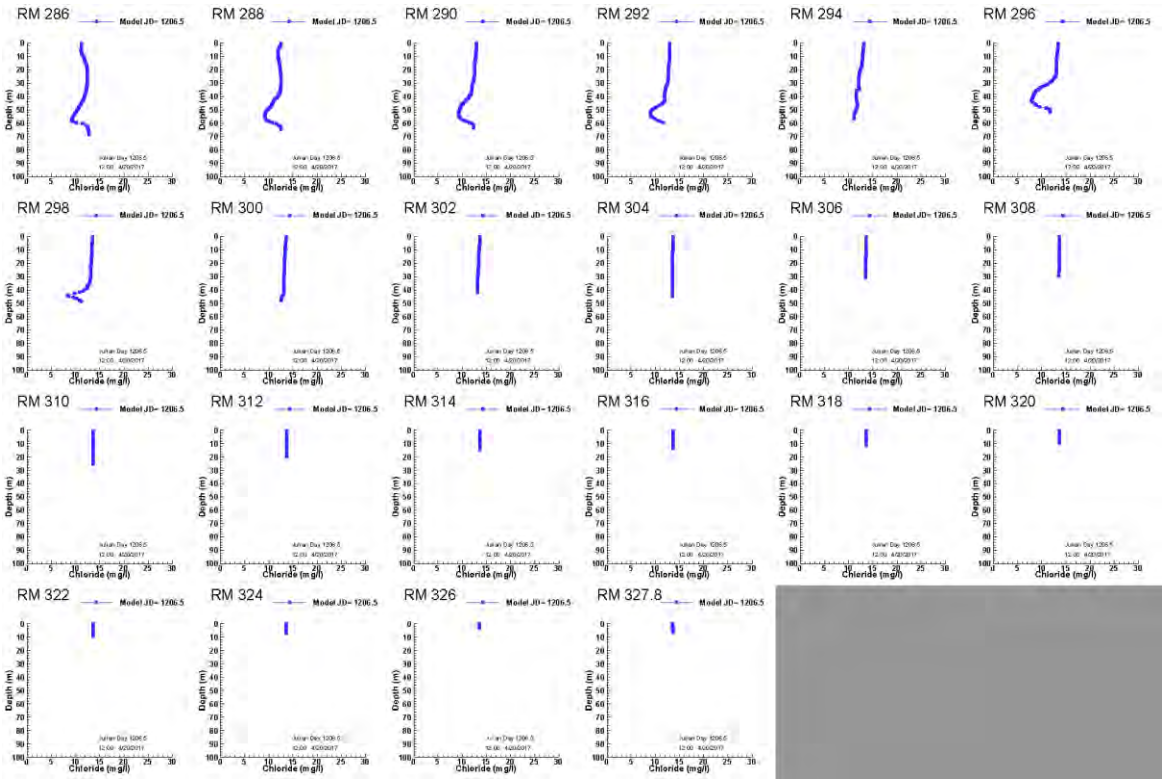


Figure 66. Vertical profiles of chloride compared with data for 4/20/2017.

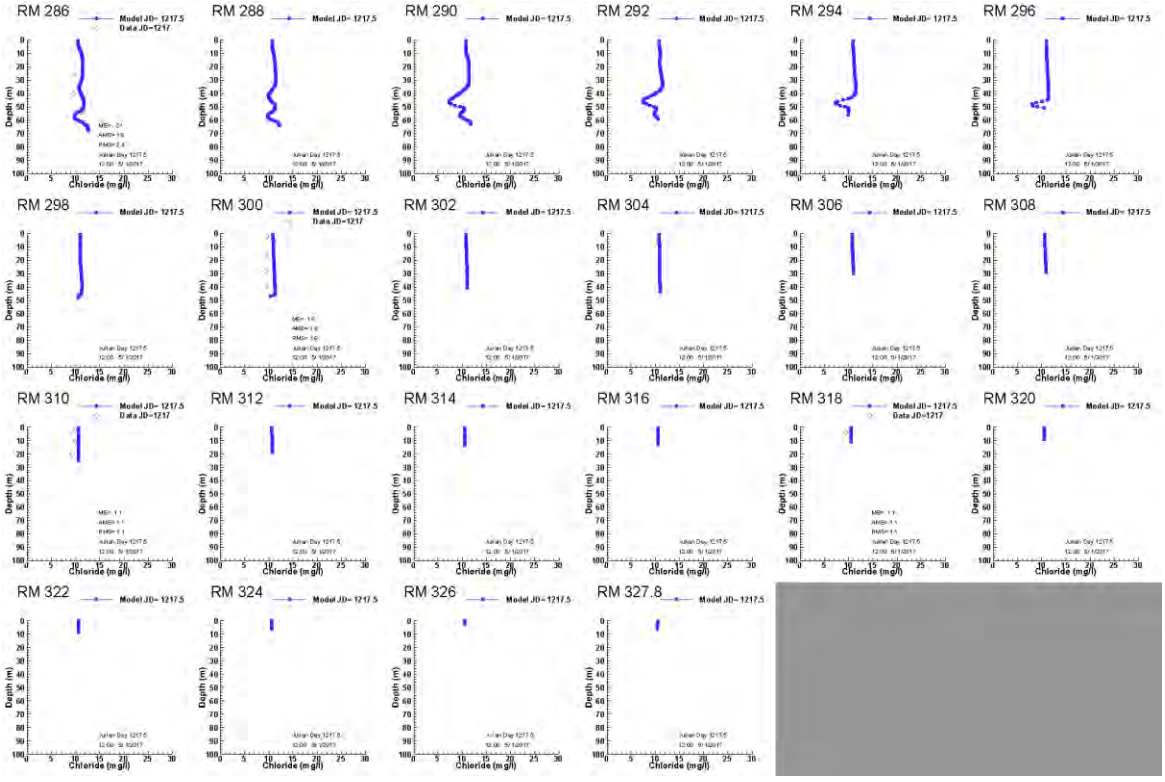


Figure 67. Vertical profiles of chloride compared with data for 5/ 1/2017.

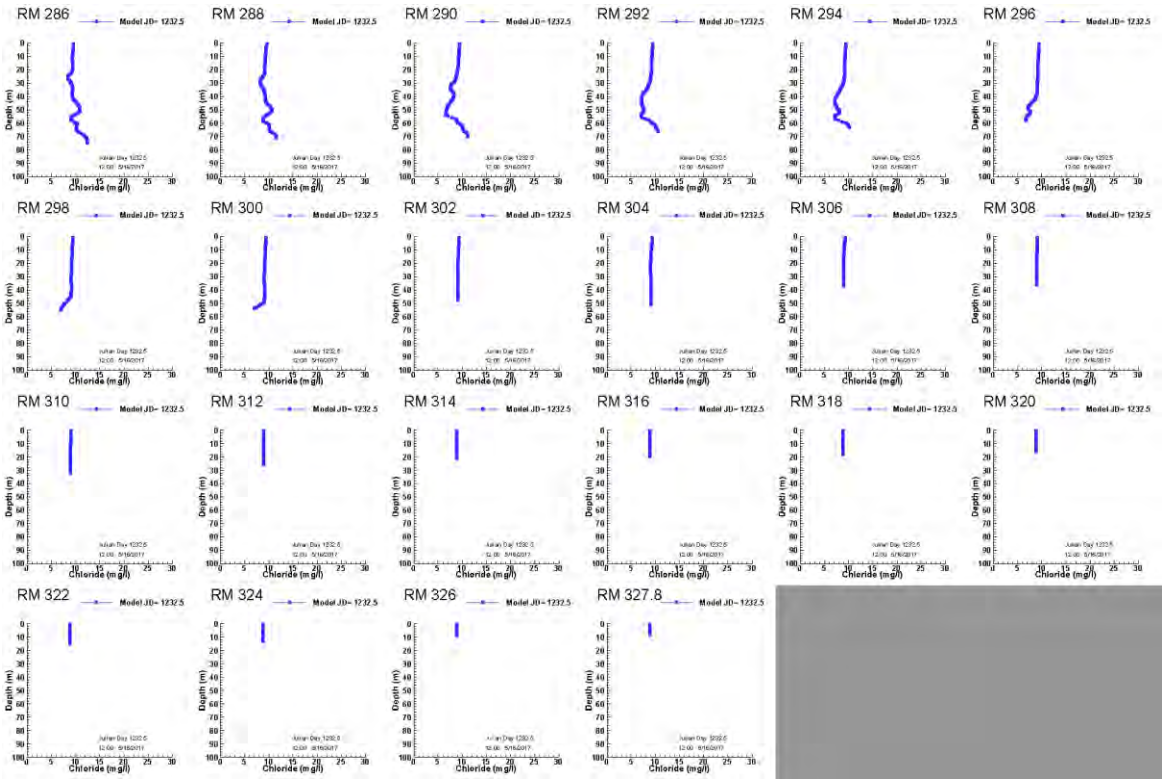


Figure 68. Vertical profiles of chloride compared with data for 5/16/2017.

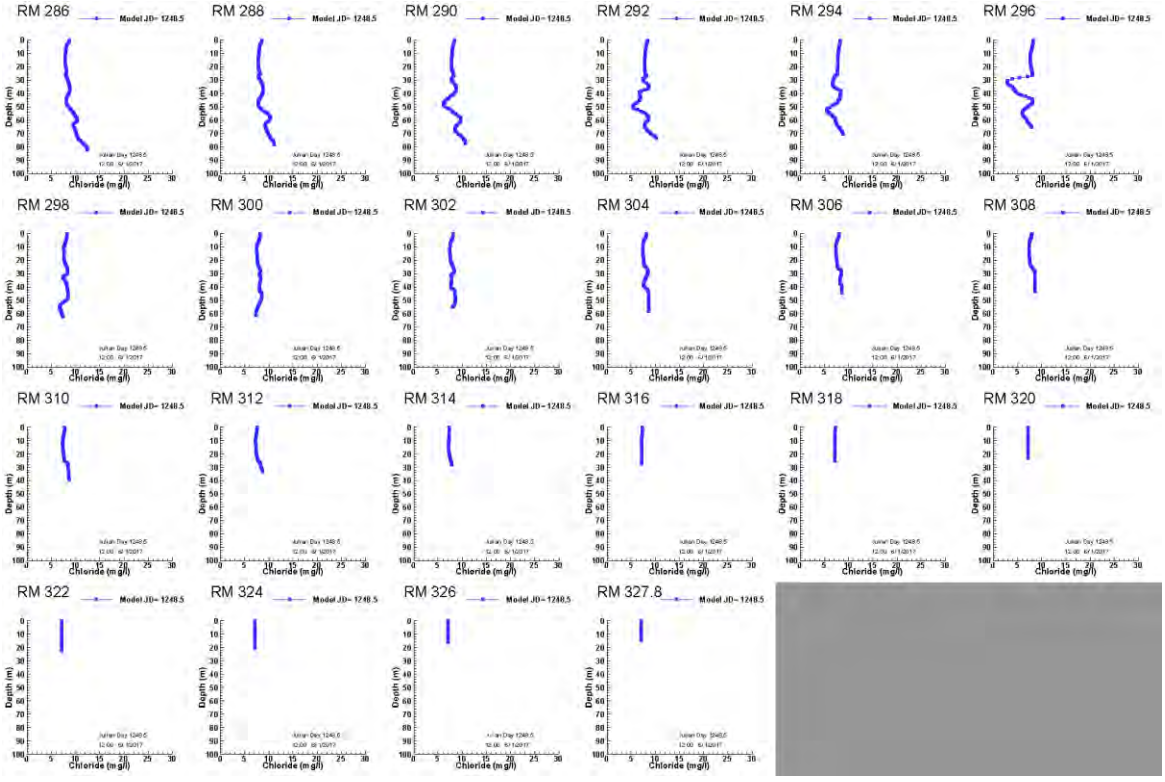


Figure 69. Vertical profiles of chloride compared with data for 6/ 1/2017.

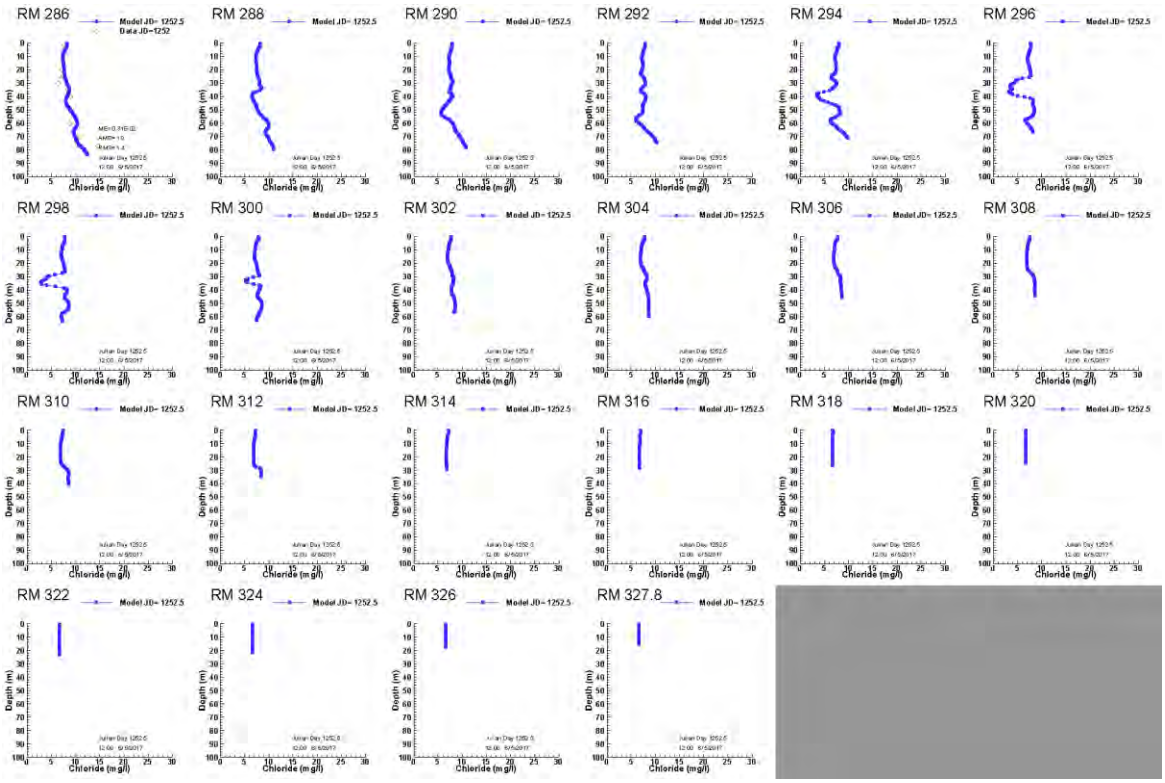


Figure 70. Vertical profiles of chloride compared with data for 6/ 5/2017.

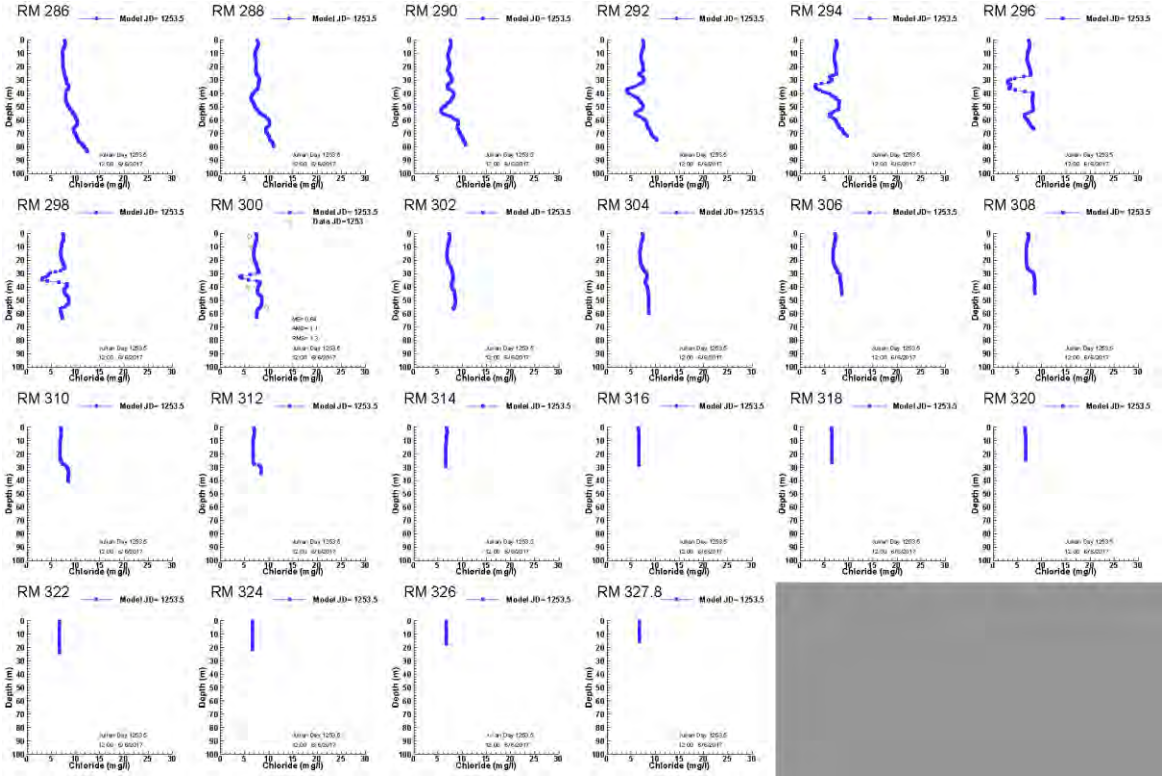


Figure 71. Vertical profiles of chloride compared with data for 6/ 6/2017.

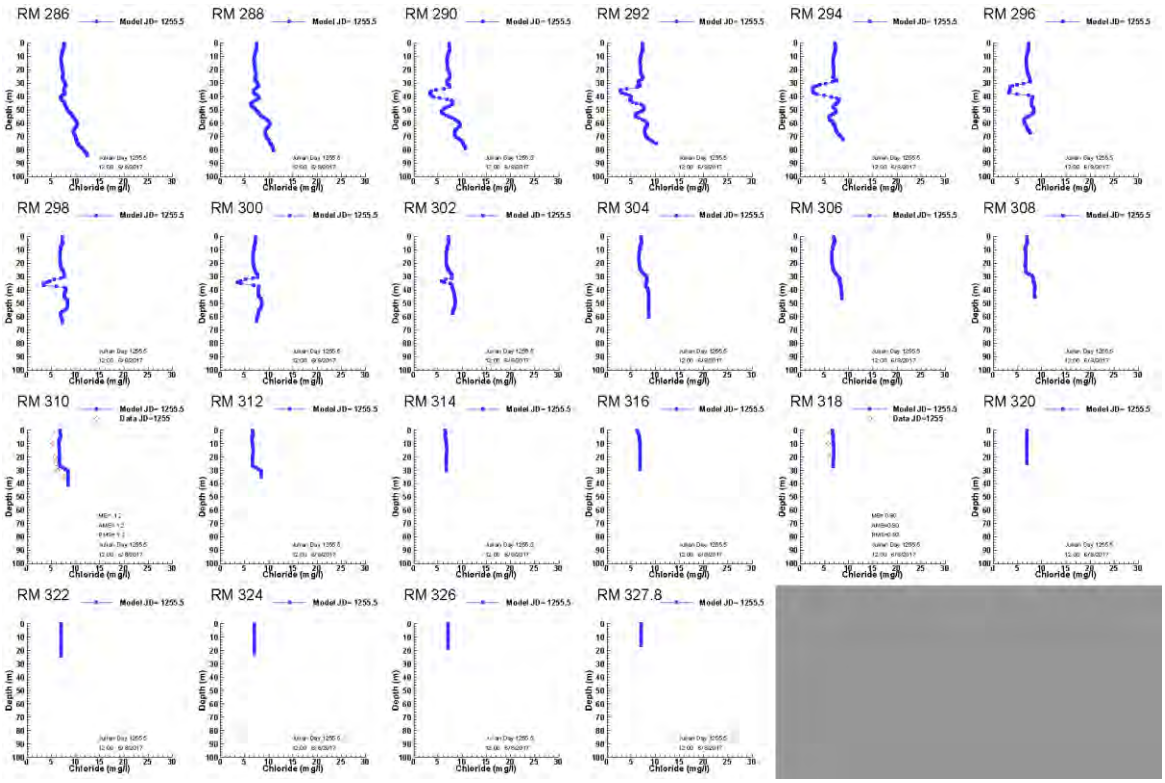


Figure 72. Vertical profiles of chloride compared with data for 6/ 8/2017.

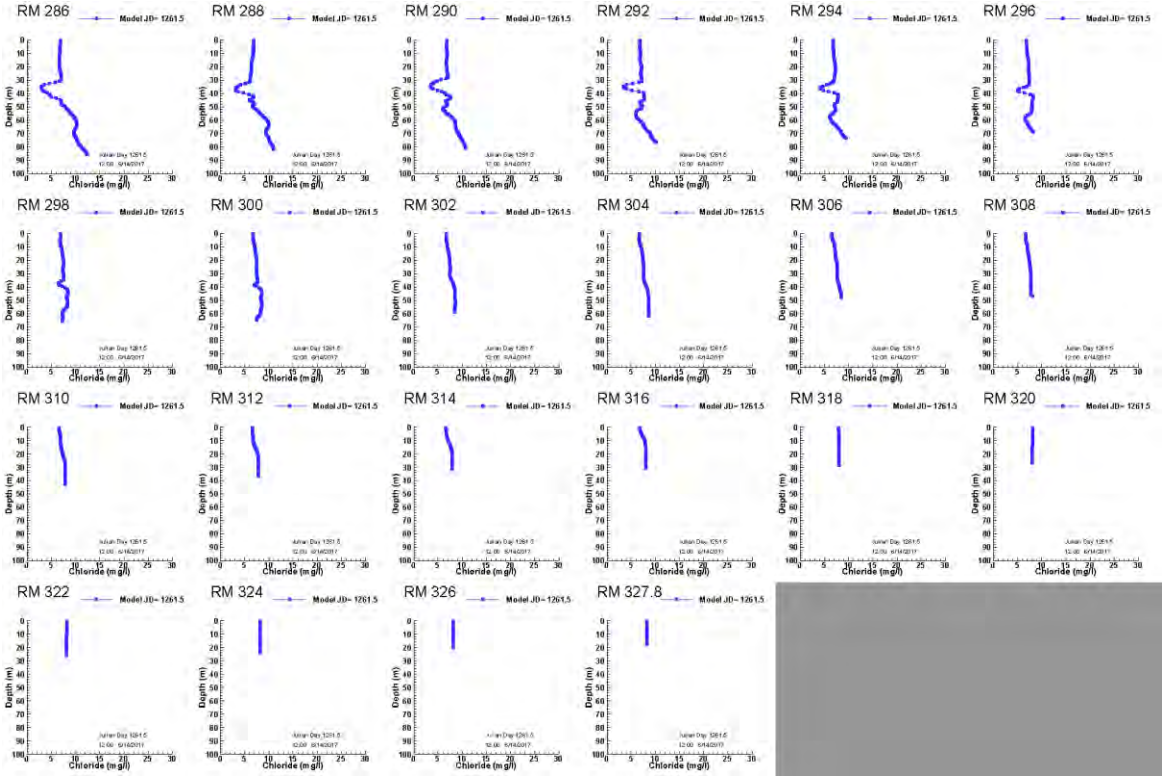


Figure 73. Vertical profiles of chloride compared with data for 6/14/2017.

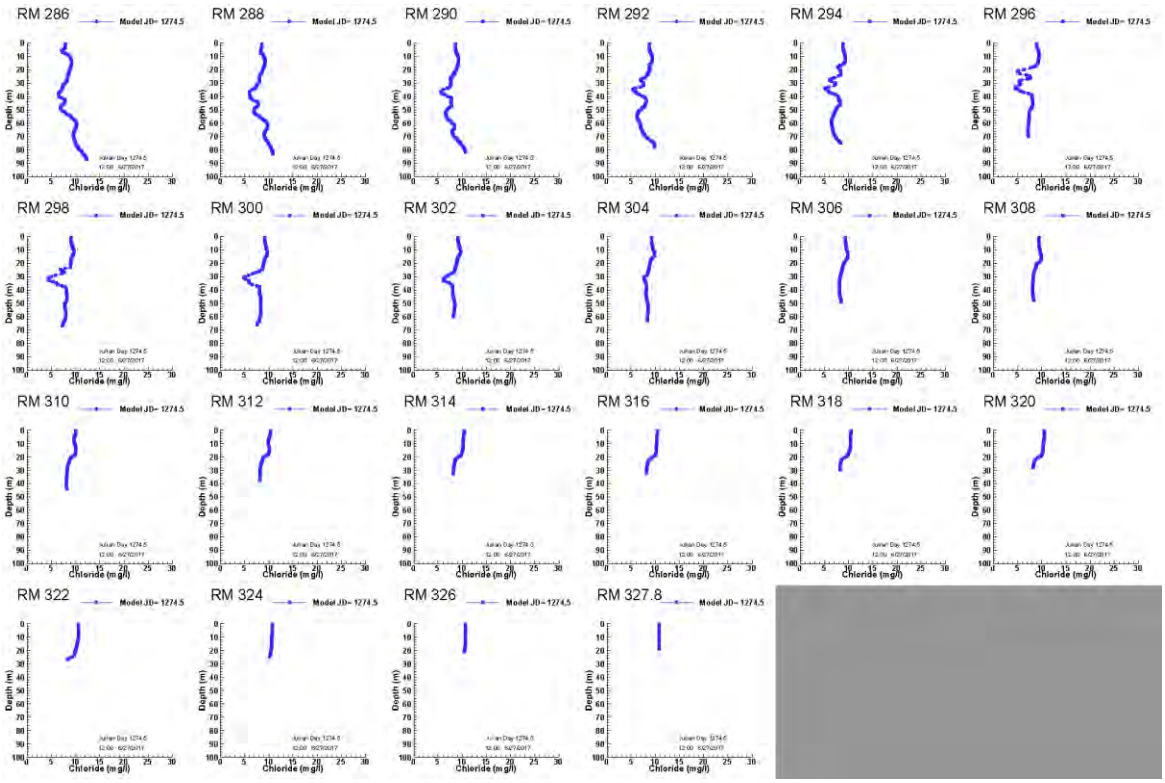


Figure 74. Vertical profiles of chloride compared with data for 6/27/2017.

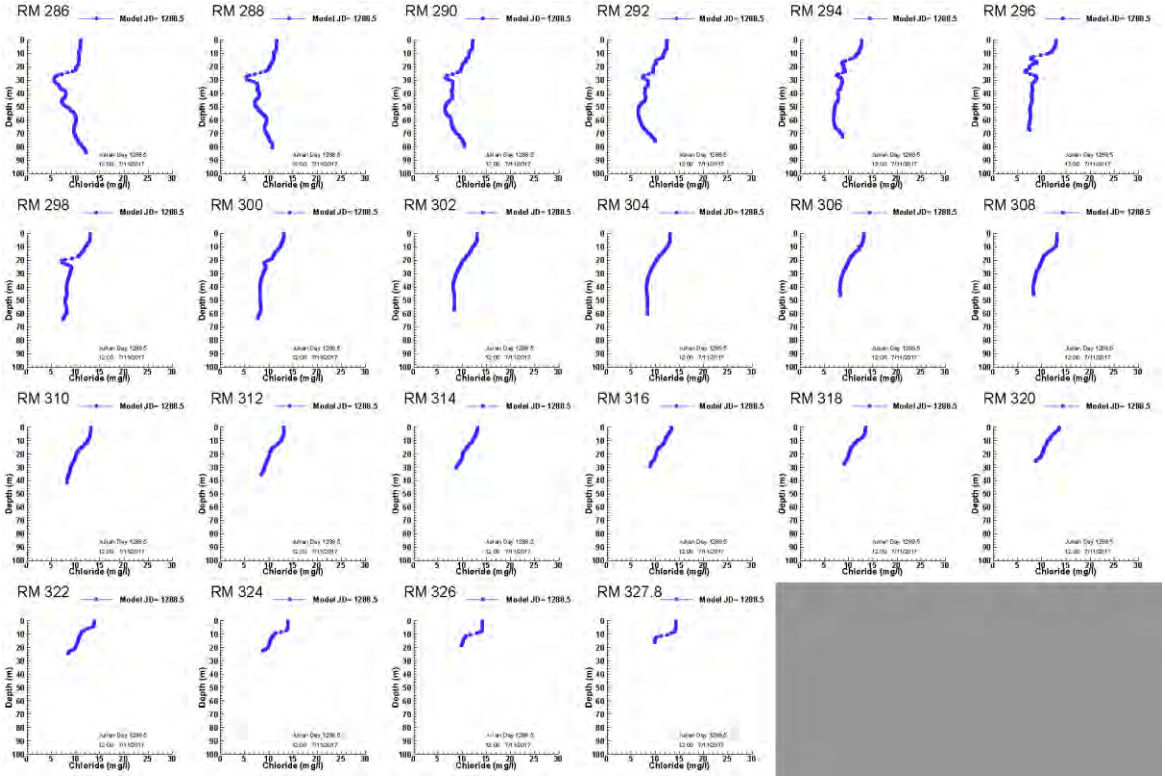


Figure 75. Vertical profiles of chloride compared with data for 7/11/2017.

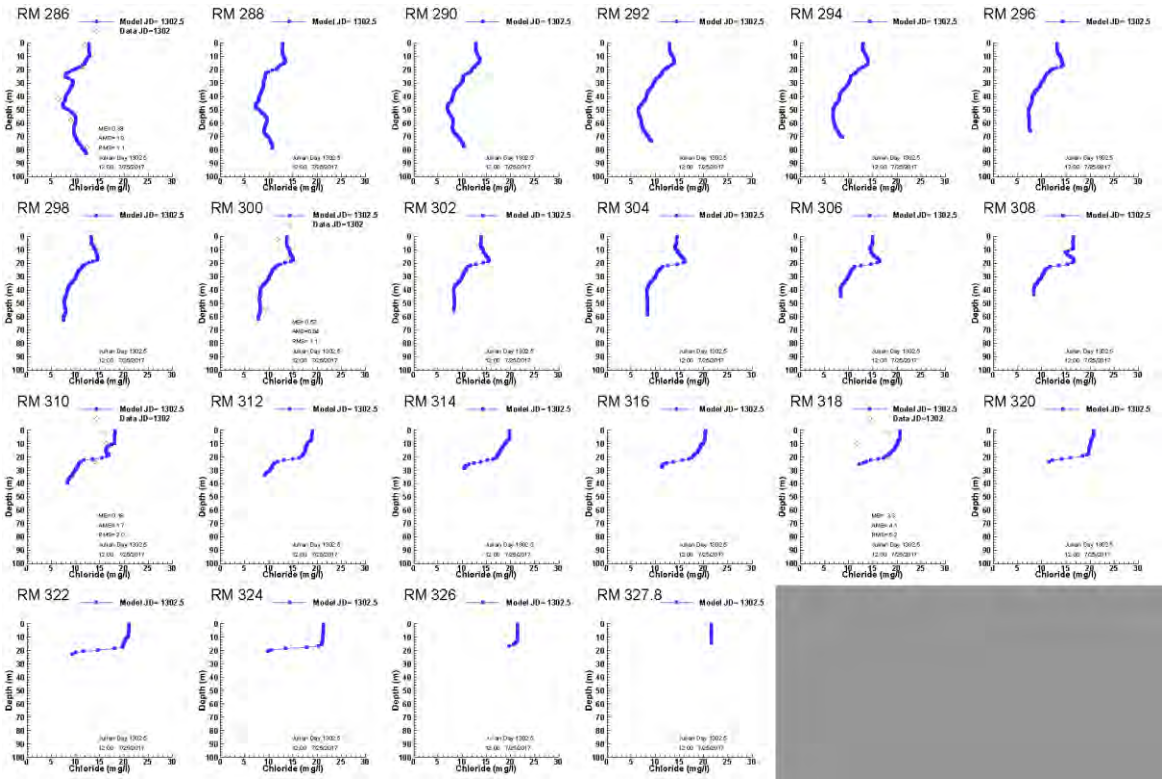


Figure 76. Vertical profiles of chloride compared with data for 7/25/2017.

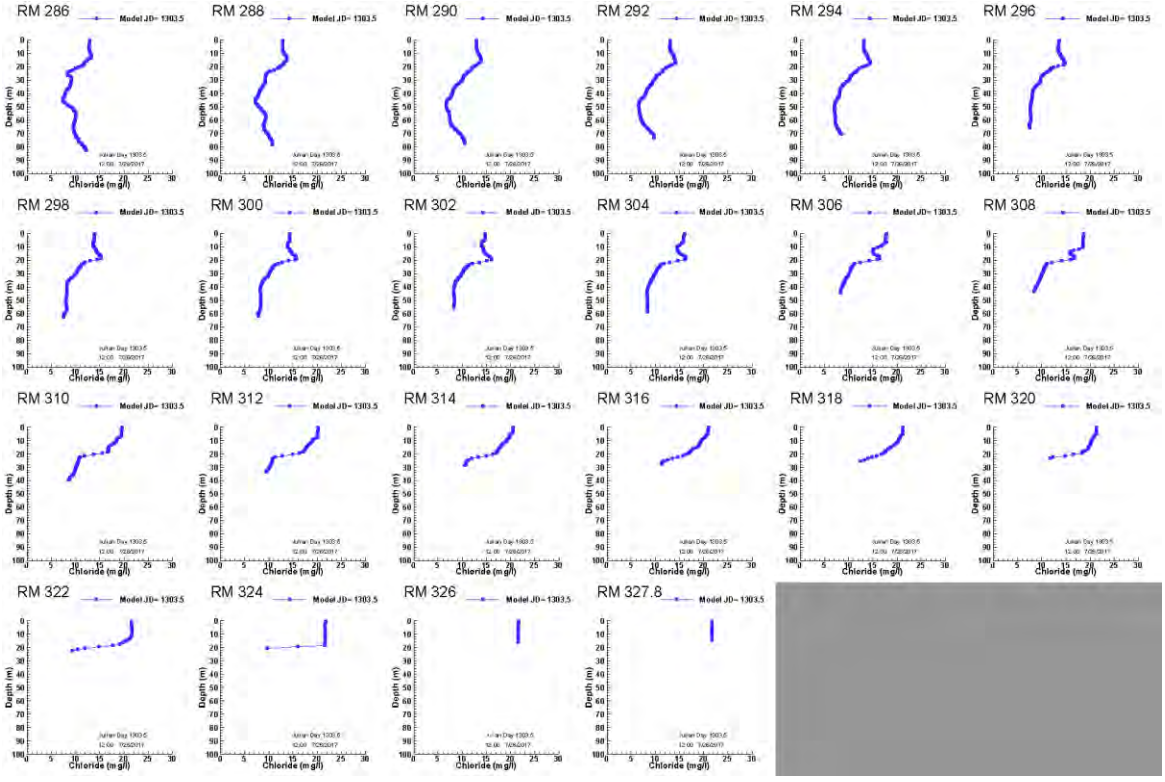


Figure 77. Vertical profiles of chloride compared with data for 7/26/2017.

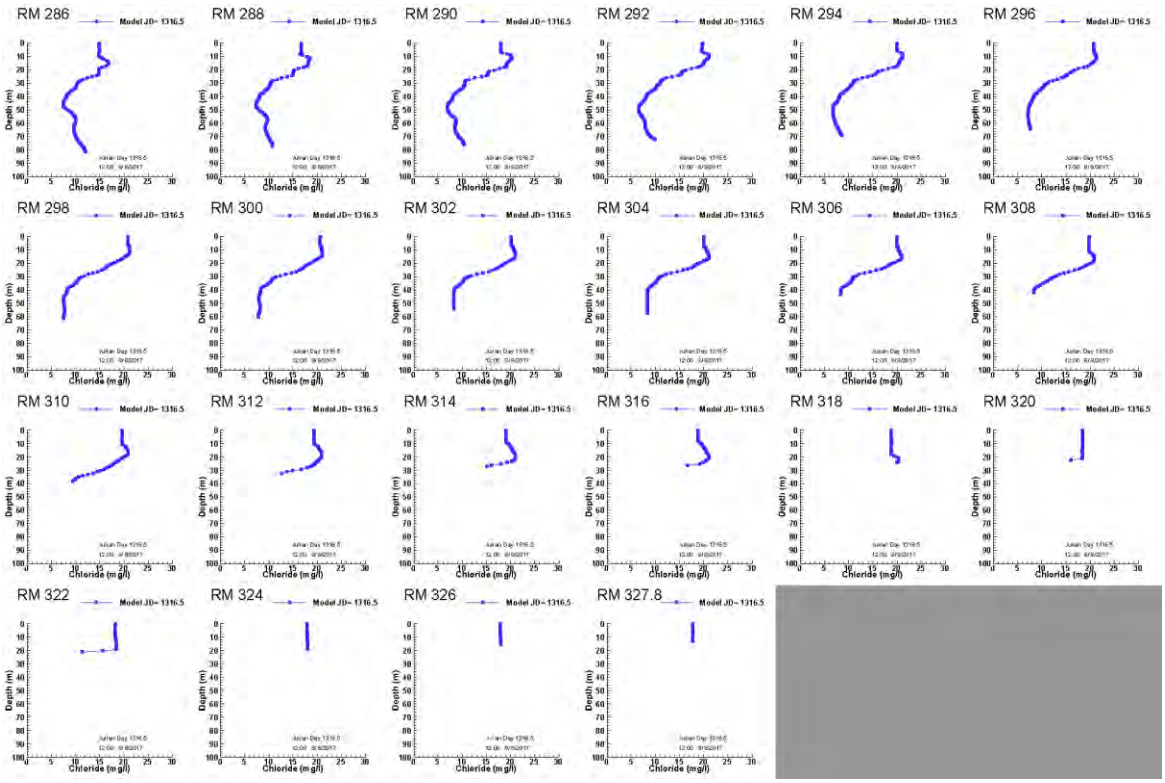


Figure 78. Vertical profiles of chloride compared with data for 8/ 8/2017.

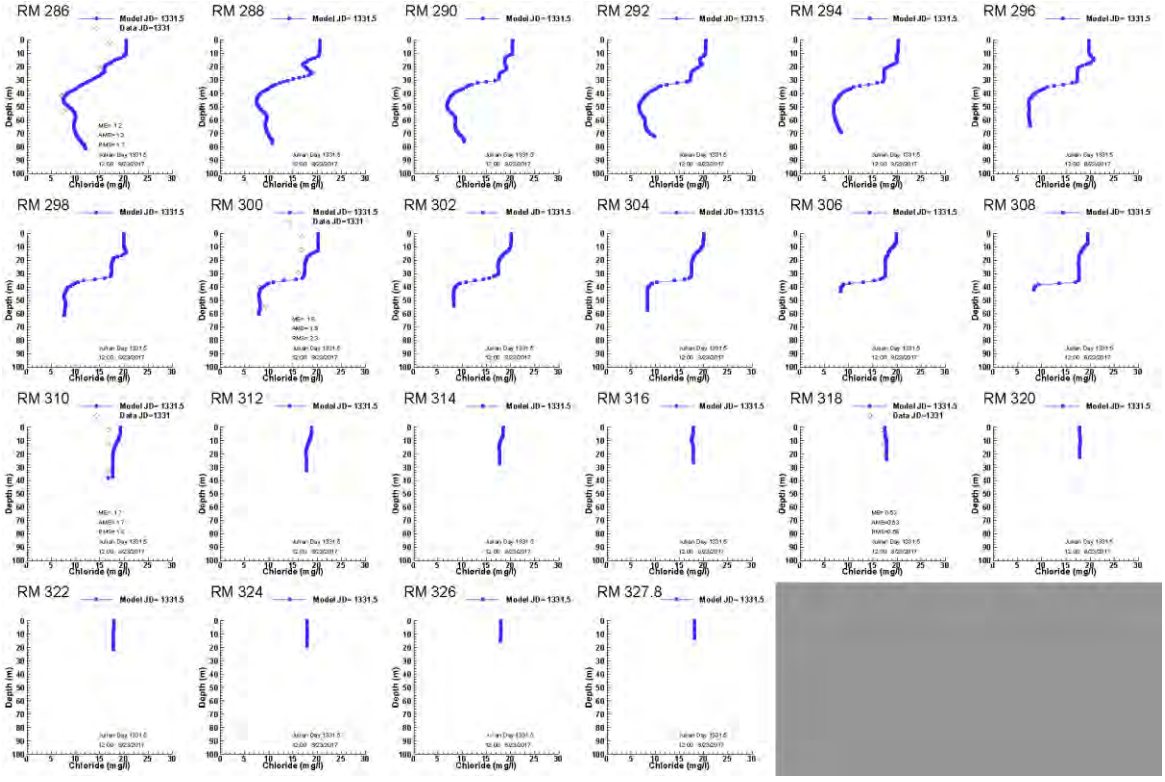


Figure 79. Vertical profiles of chloride compared with data for 8/23/2017.

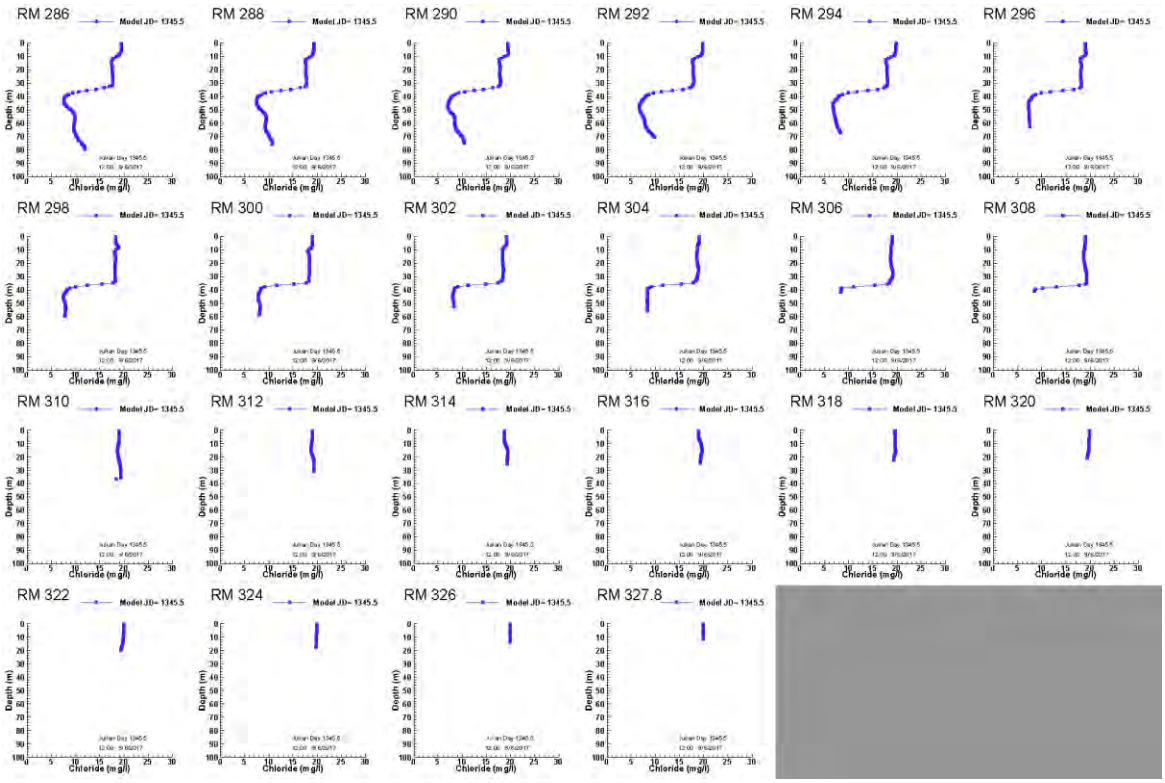


Figure 80. Vertical profiles of chloride compared with data for 9/ 6/2017.

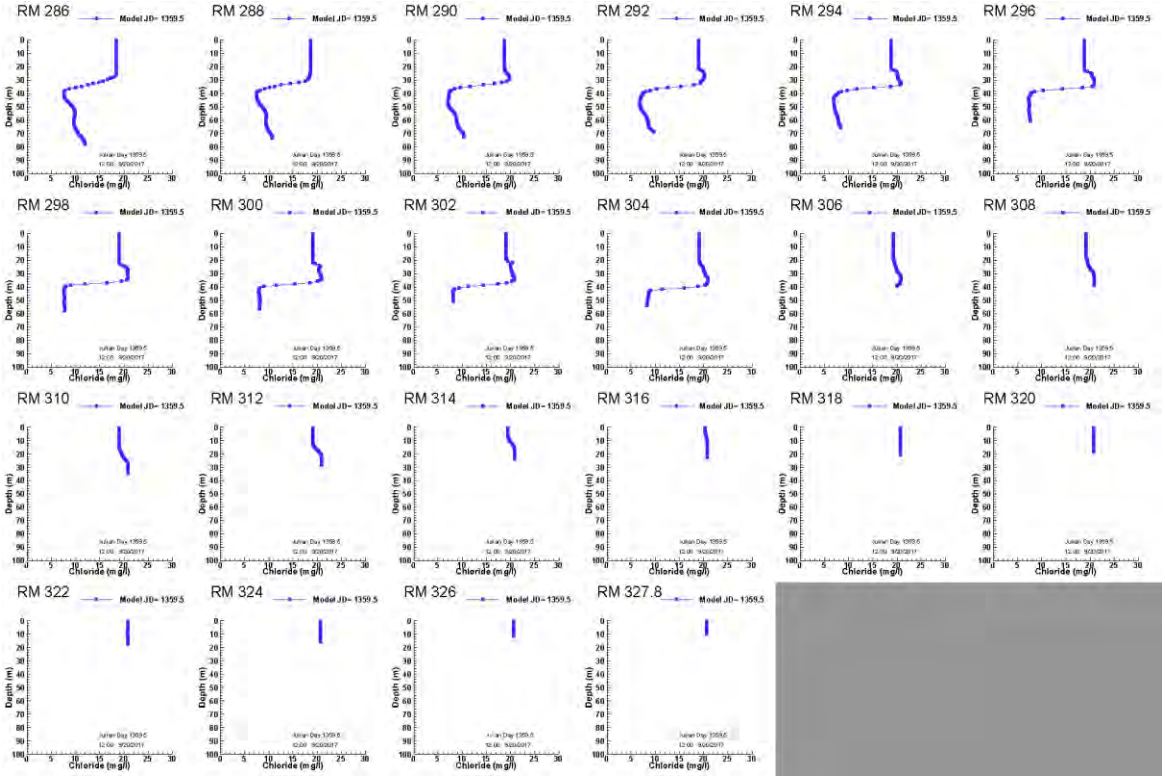


Figure 81. Vertical profiles of chloride compared with data for 9/20/2017.

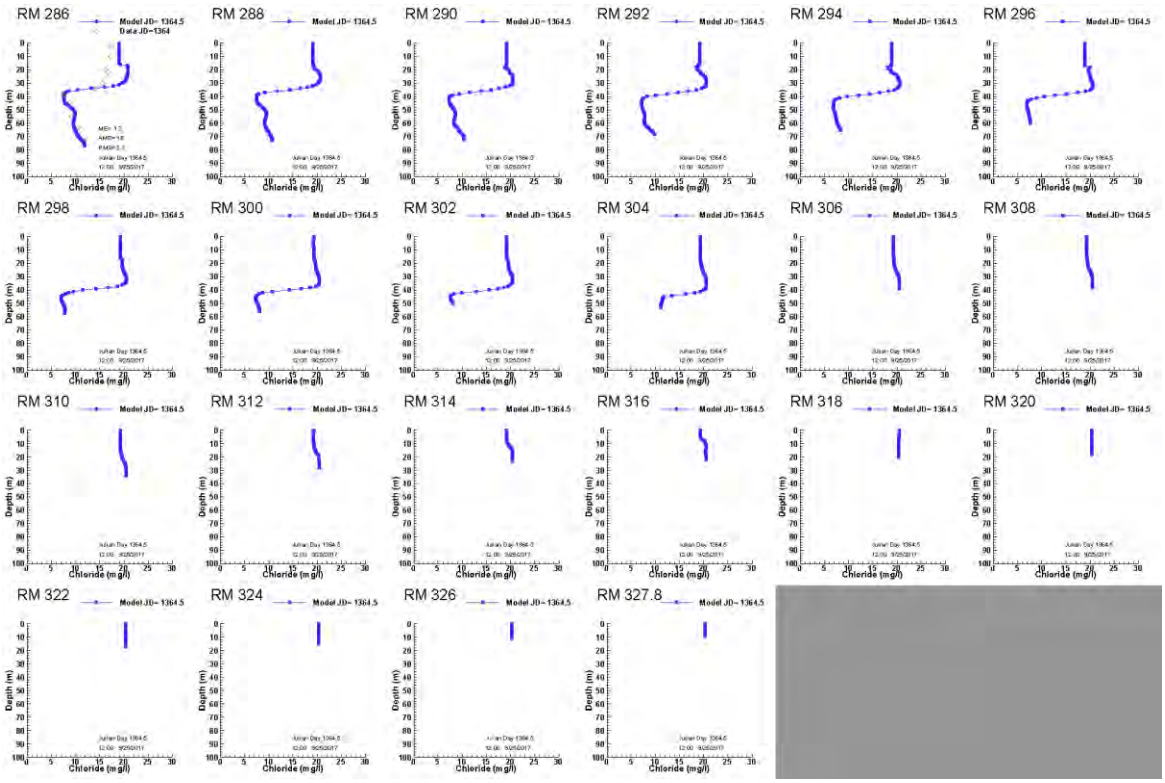


Figure 82. Vertical profiles of chloride compared with data for 9/25/2017.

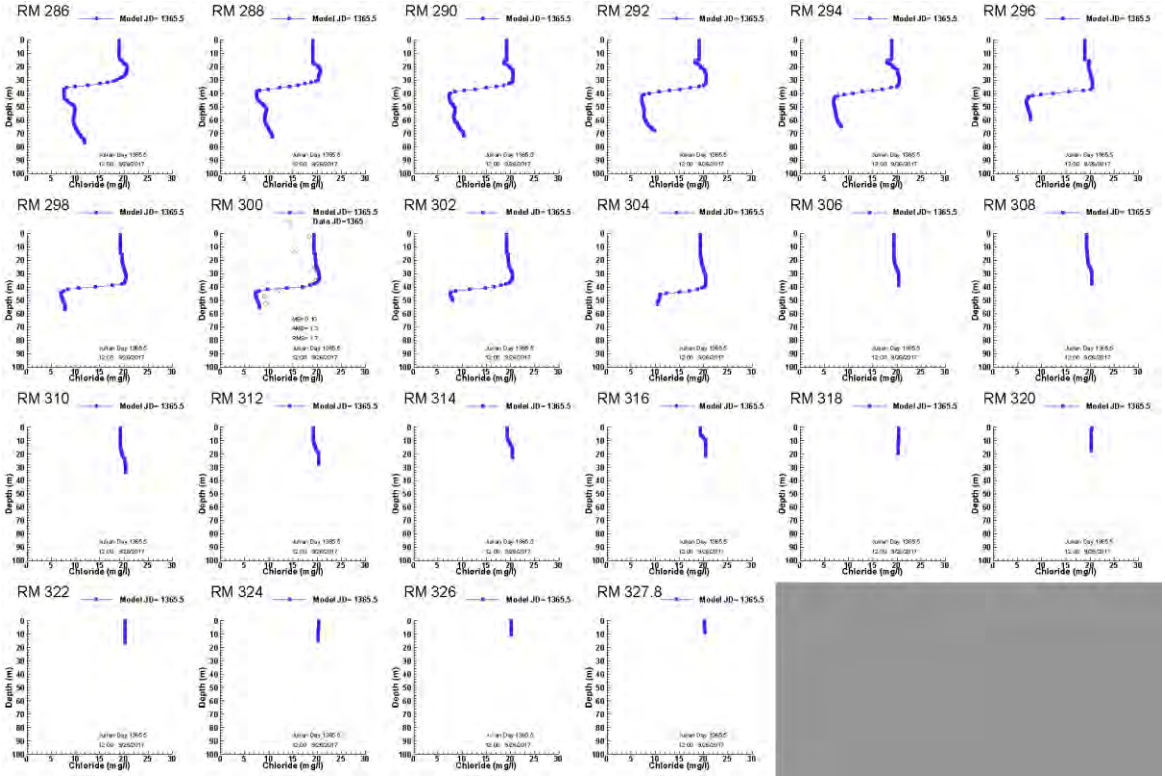


Figure 83. Vertical profiles of chloride compared with data for 9/26/2017.

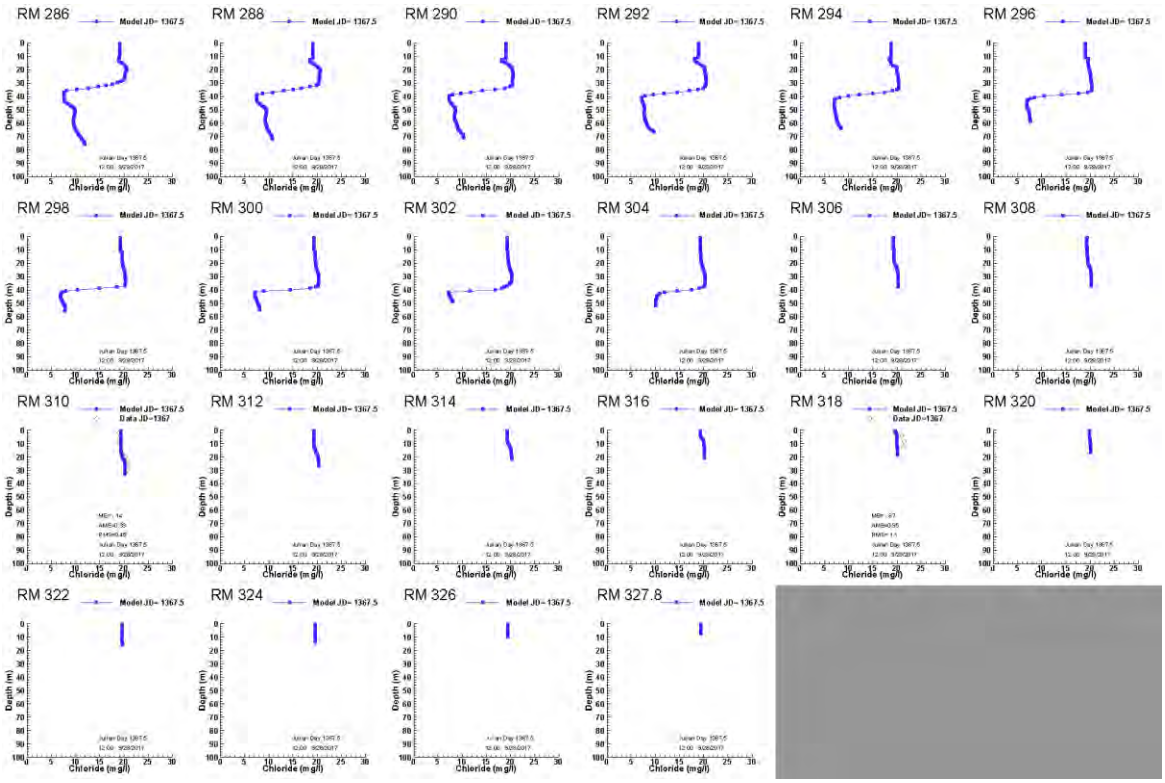


Figure 84. Vertical profiles of chloride compared with data for 9/28/2017.

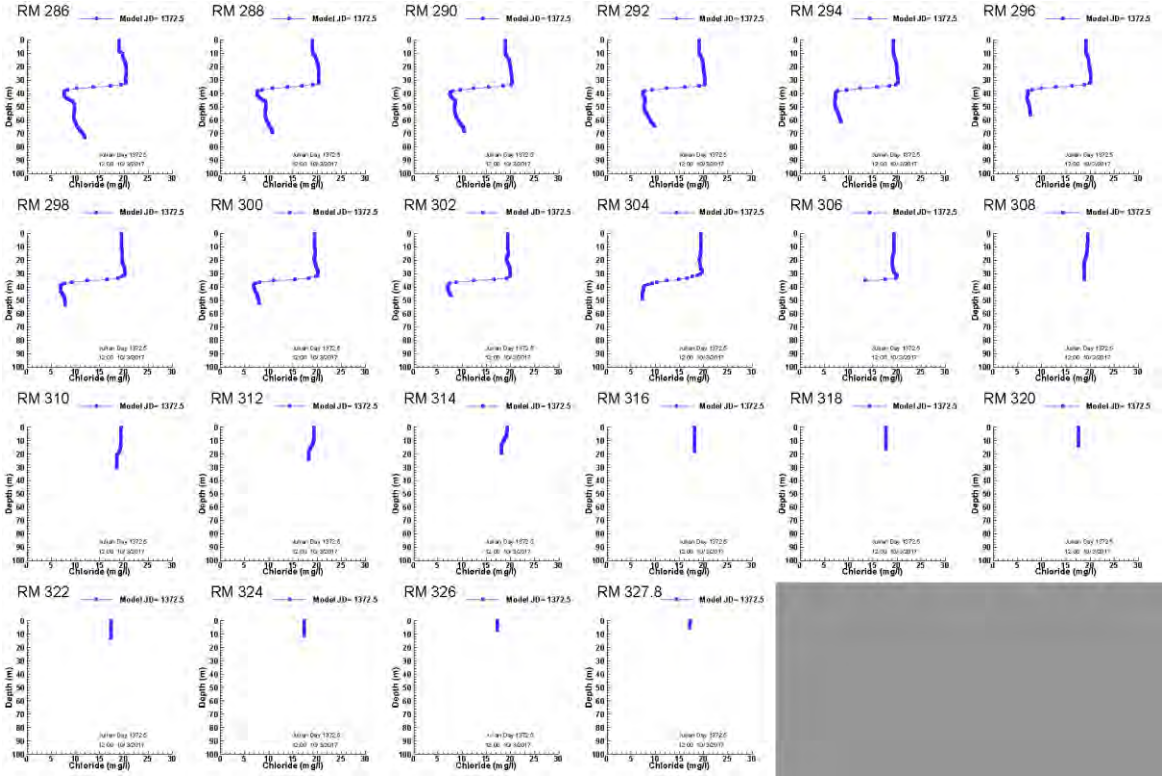


Figure 85. Vertical profiles of chloride compared with data for 10/ 3/2017.

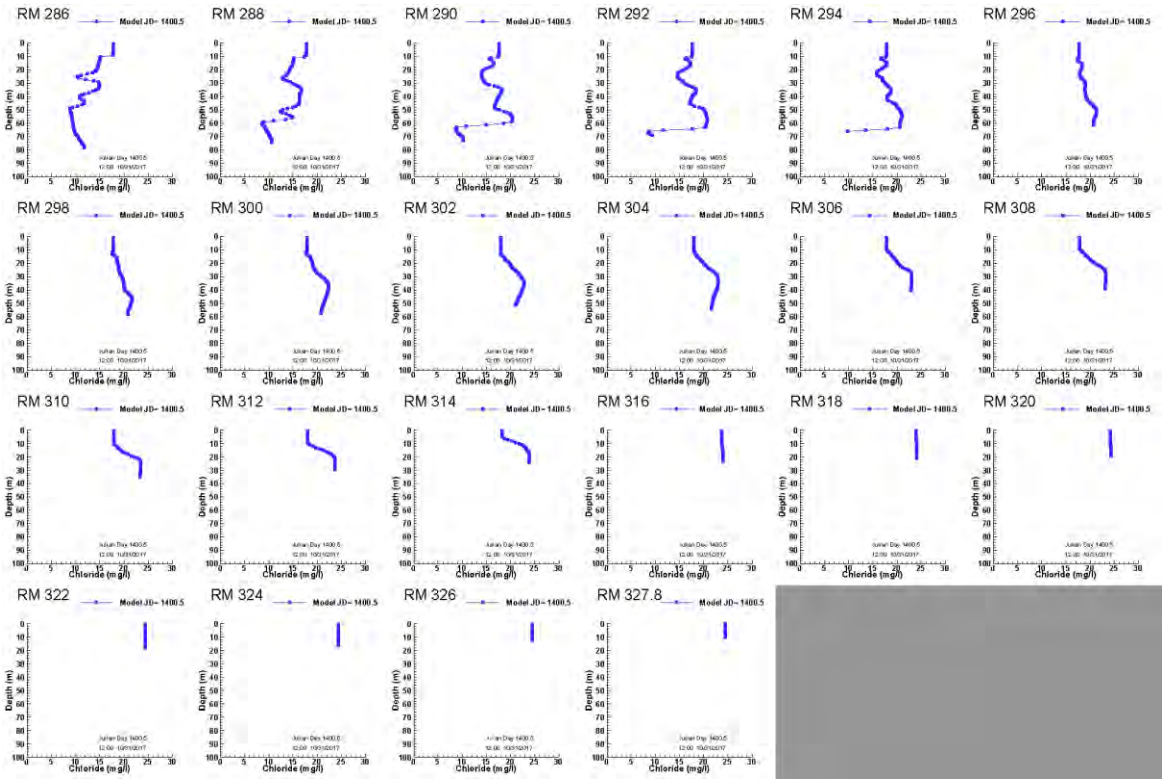


Figure 86. Vertical profiles of chloride compared with data for 10/31/2017.

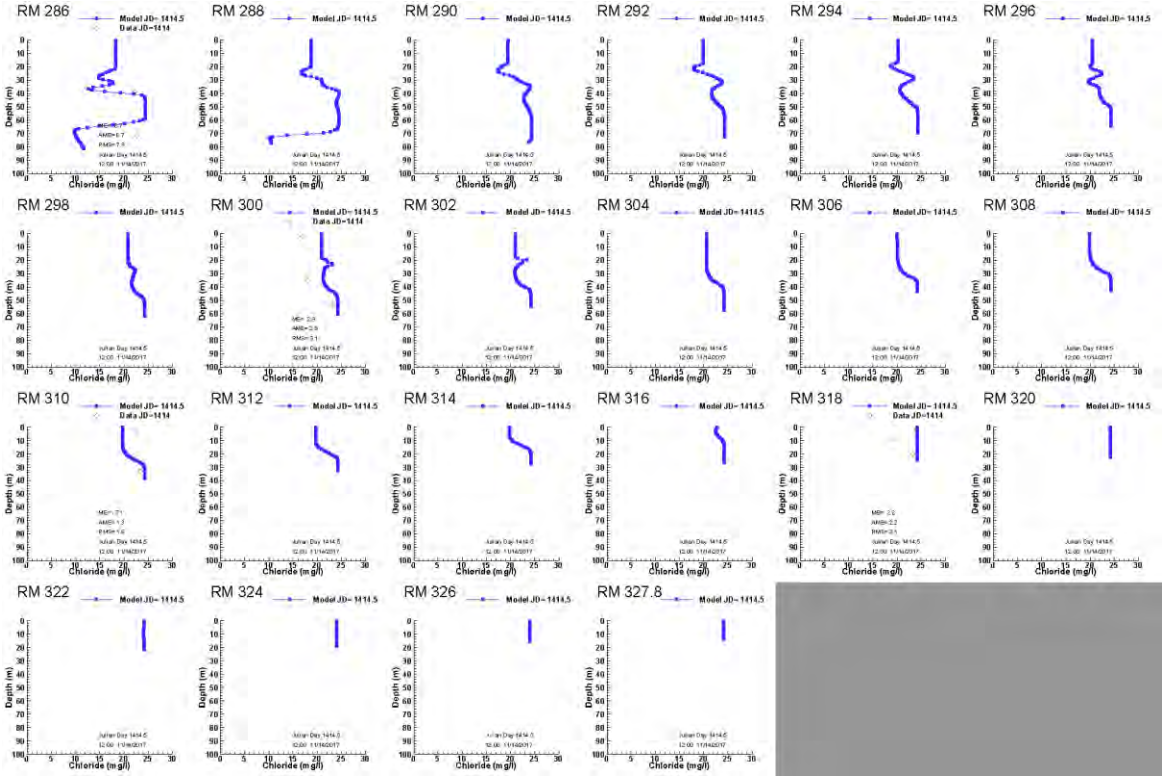


Figure 87. Vertical profiles of chloride compared with data for 11/14/2017.

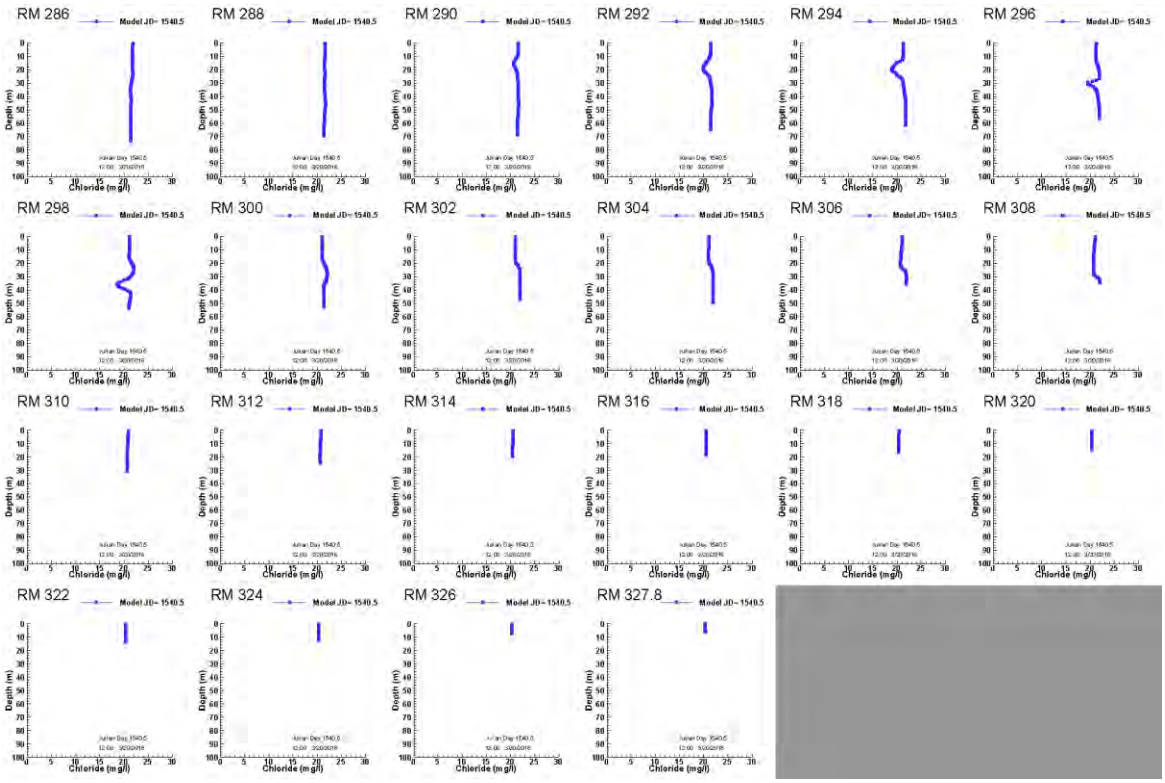


Figure 88. Vertical profiles of chloride compared with data for 3/20/2018.

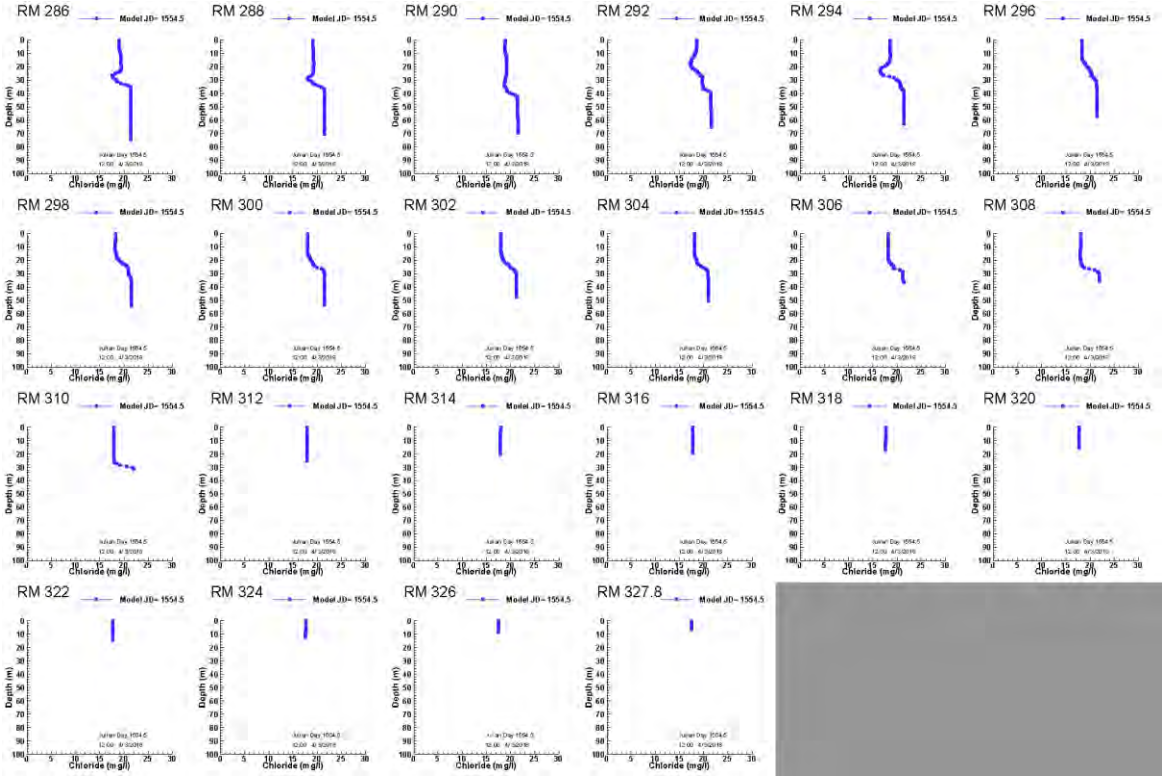


Figure 89. Vertical profiles of chloride compared with data for 4/ 3/2018.

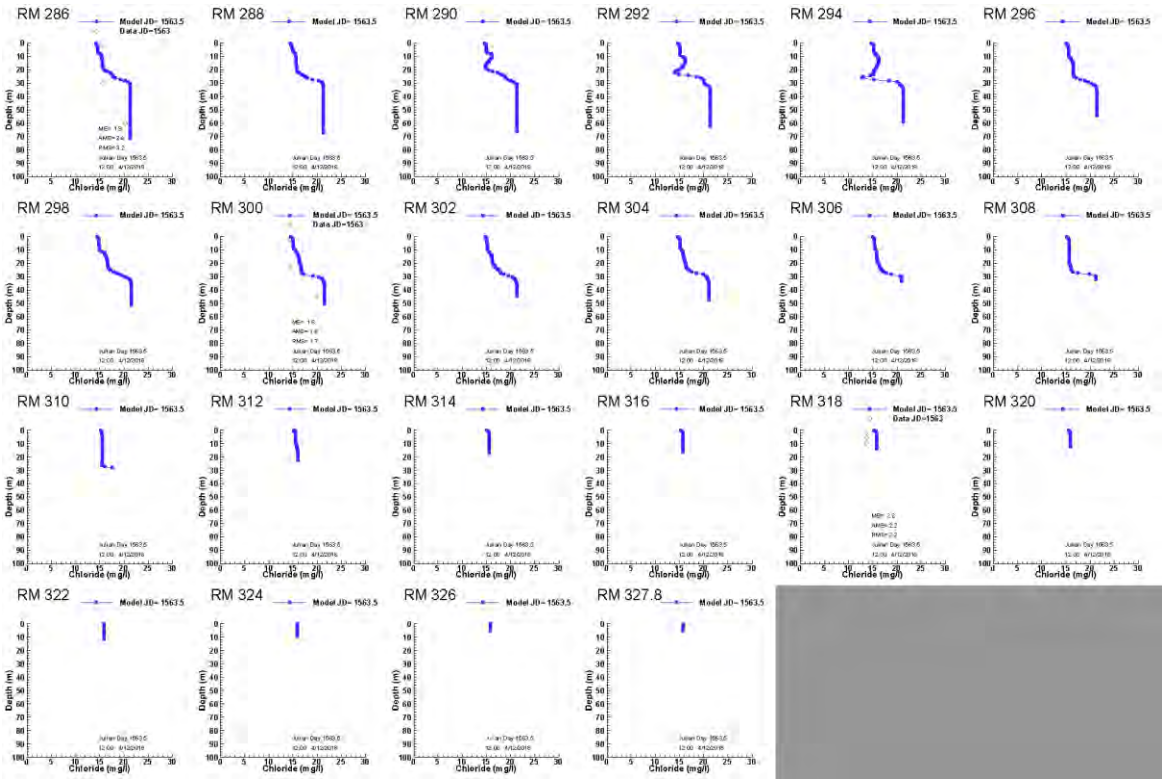


Figure 90. Vertical profiles of chloride compared with data for 4/12/2018.

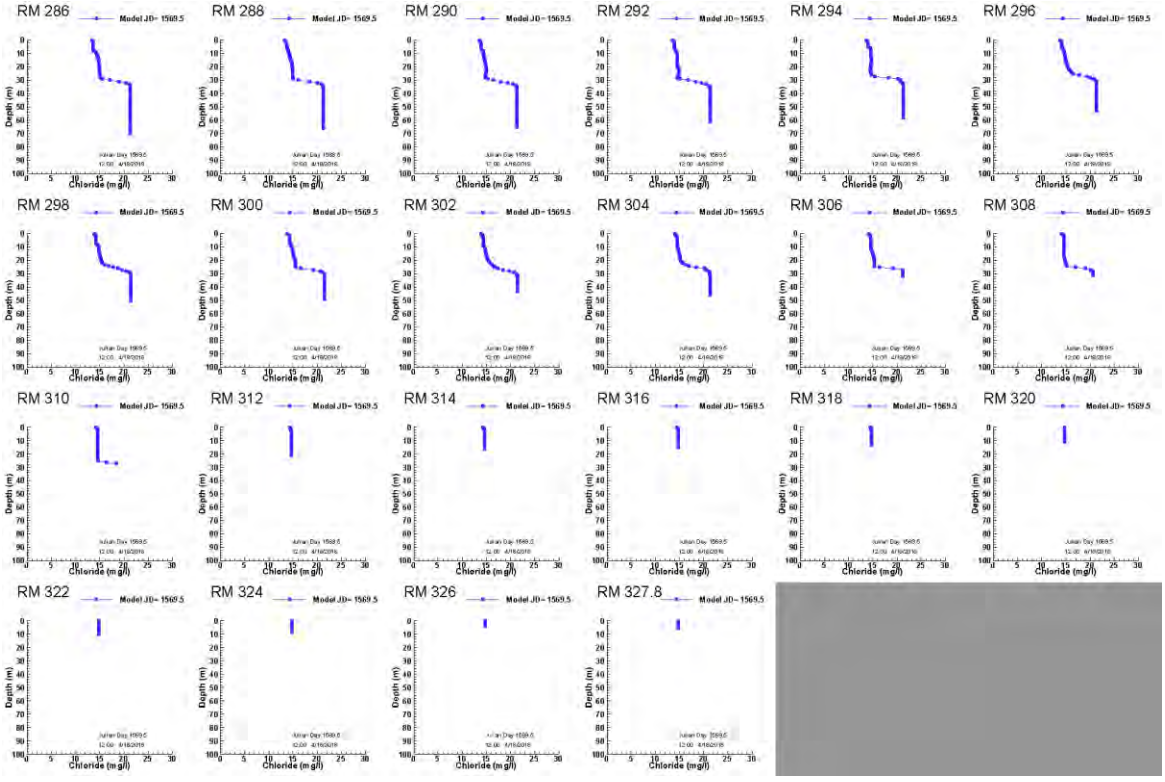


Figure 91. Vertical profiles of chloride compared with data for 4/18/2018.

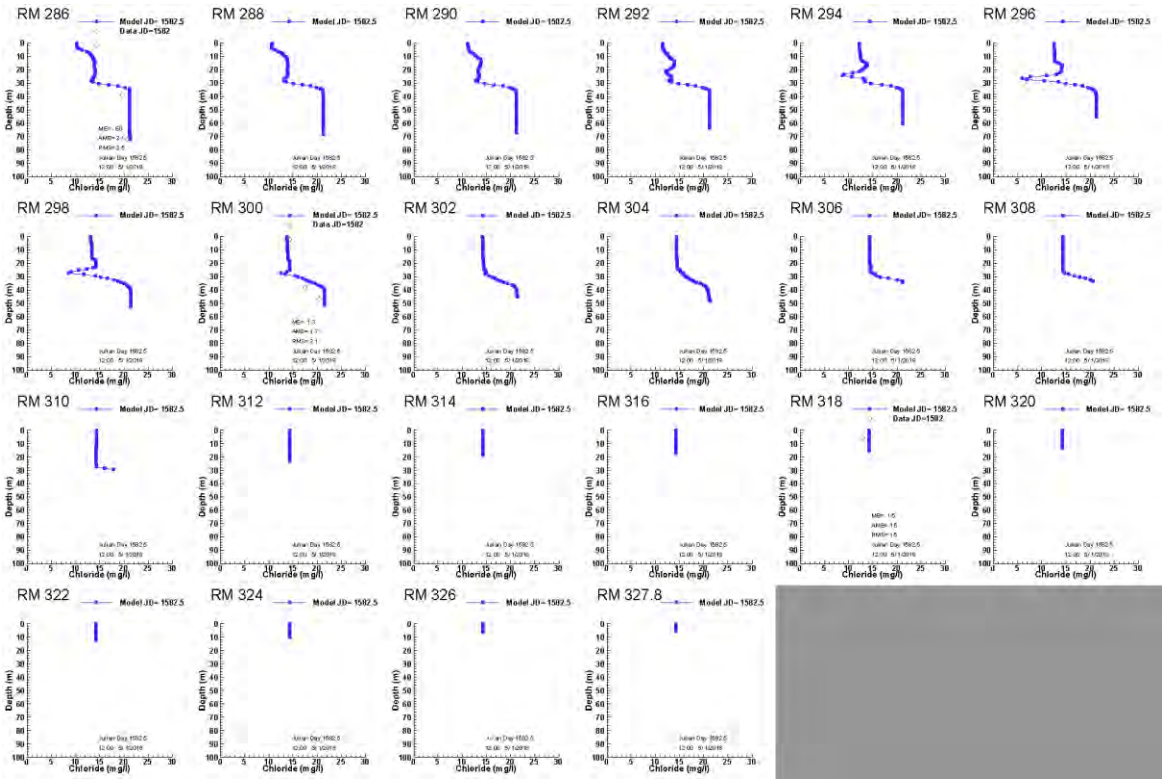


Figure 92. Vertical profiles of chloride compared with data for 5/ 1/2018.

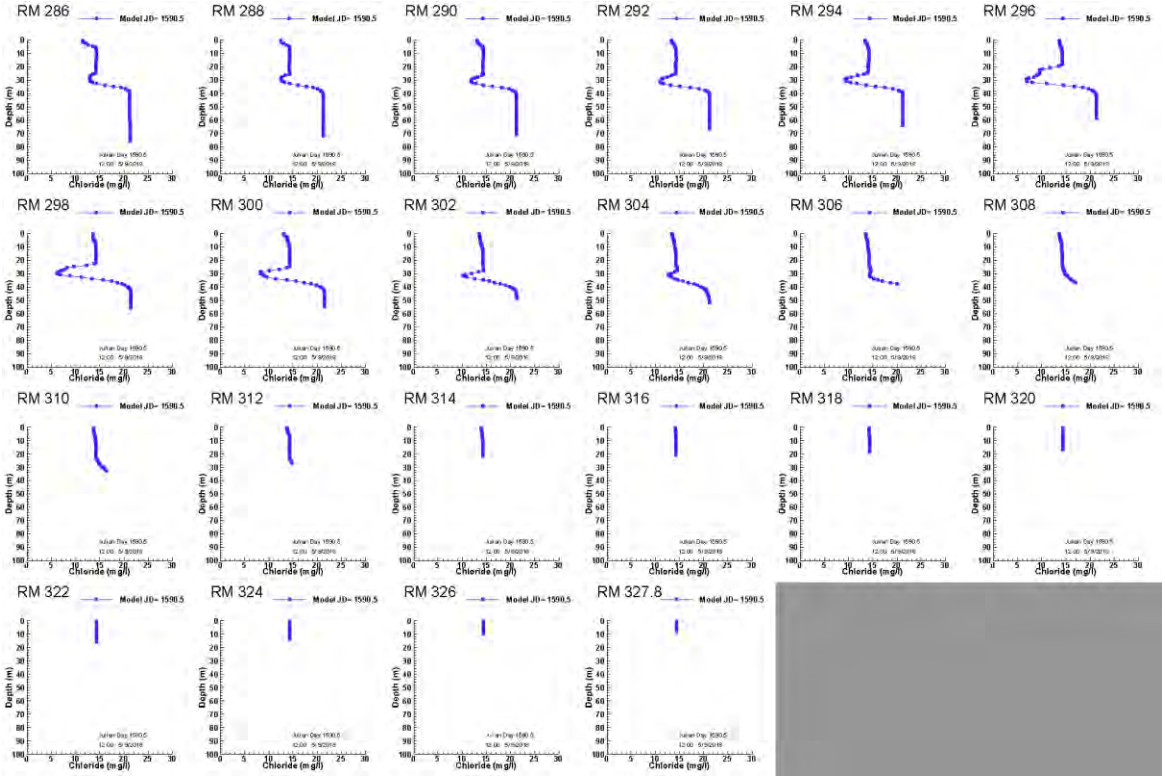


Figure 93. Vertical profiles of chloride compared with data for 5/ 9/2018.

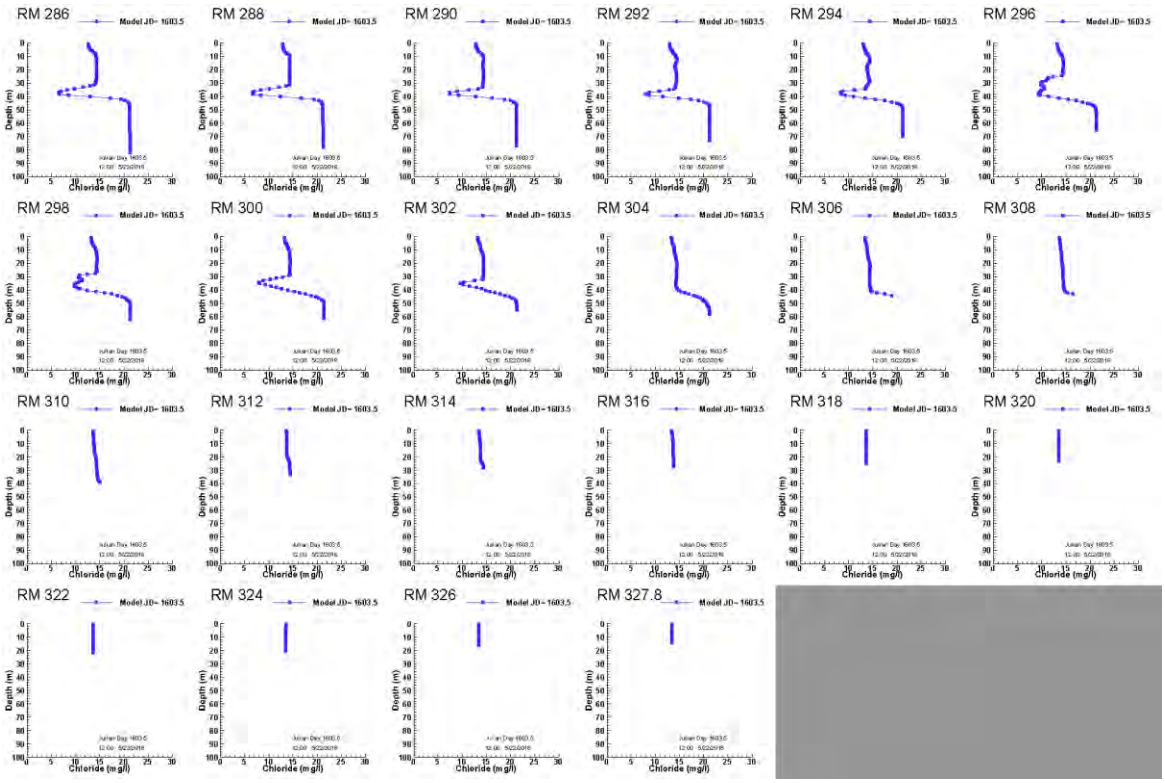


Figure 94. Vertical profiles of chloride compared with data for 5/22/2018.

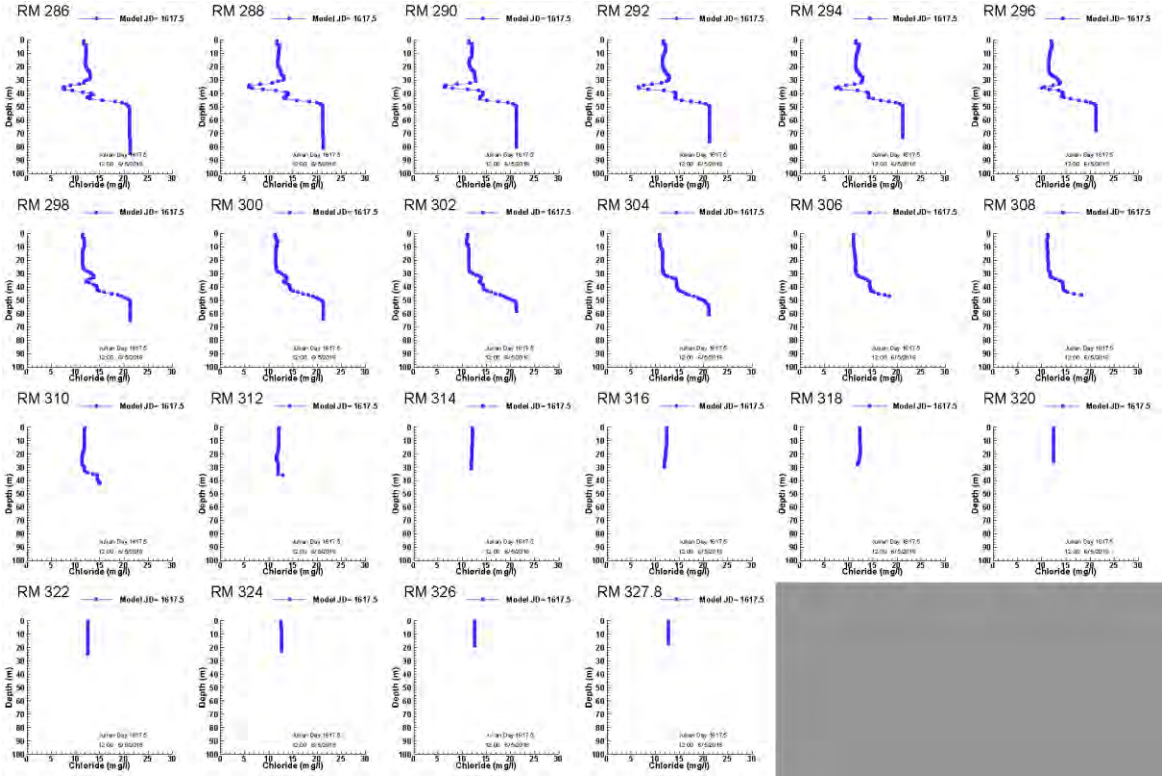


Figure 95. Vertical profiles of chloride compared with data for 6/ 5/2018.

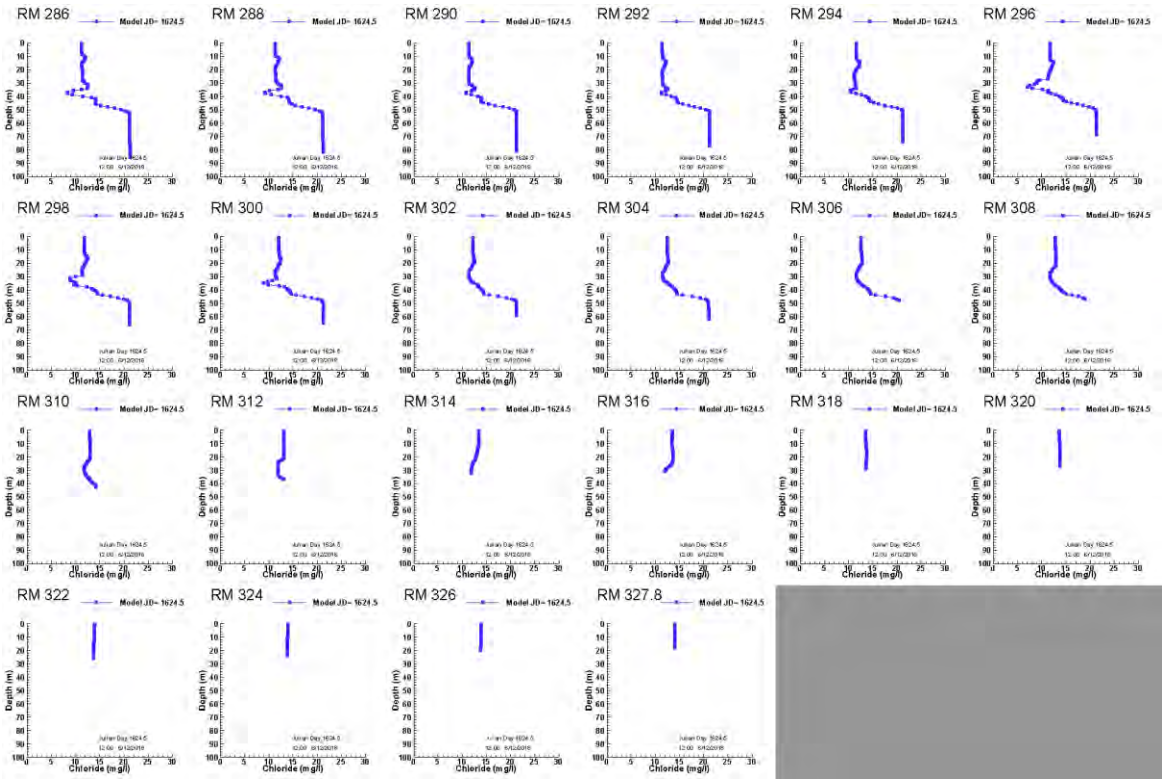


Figure 96. Vertical profiles of chloride compared with data for 6/12/2018.

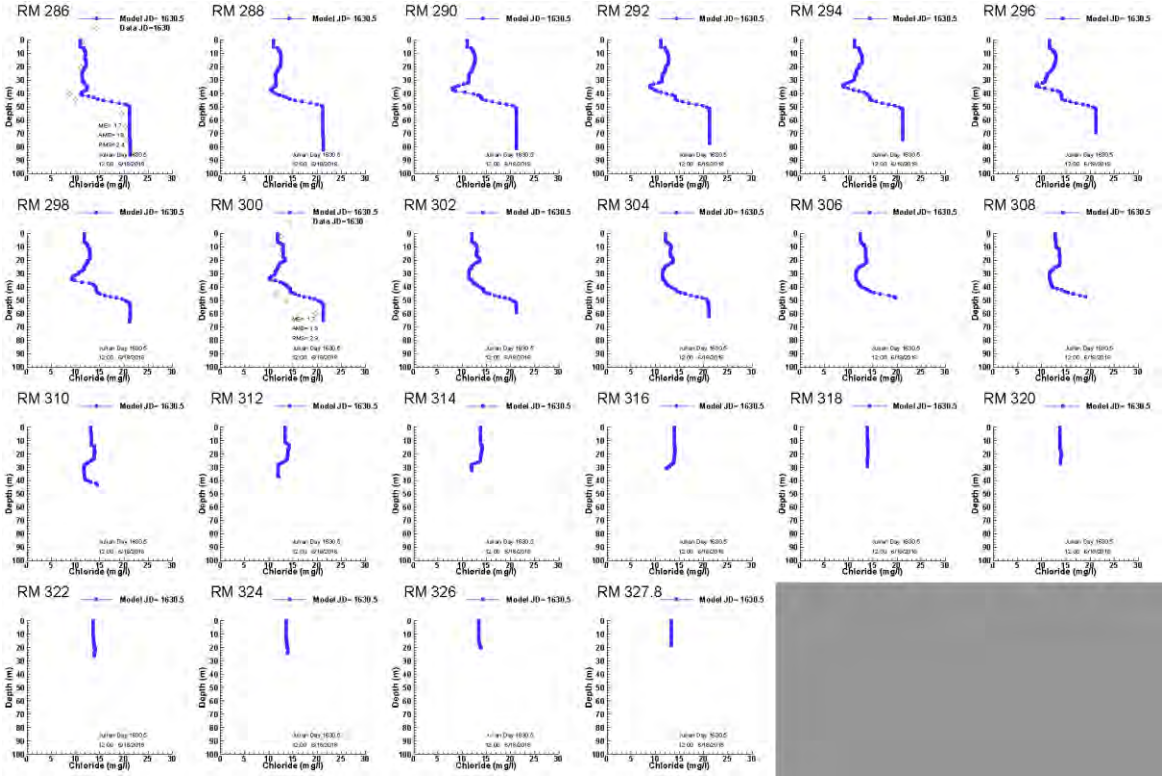


Figure 97. Vertical profiles of chloride compared with data for 6/18/2018.

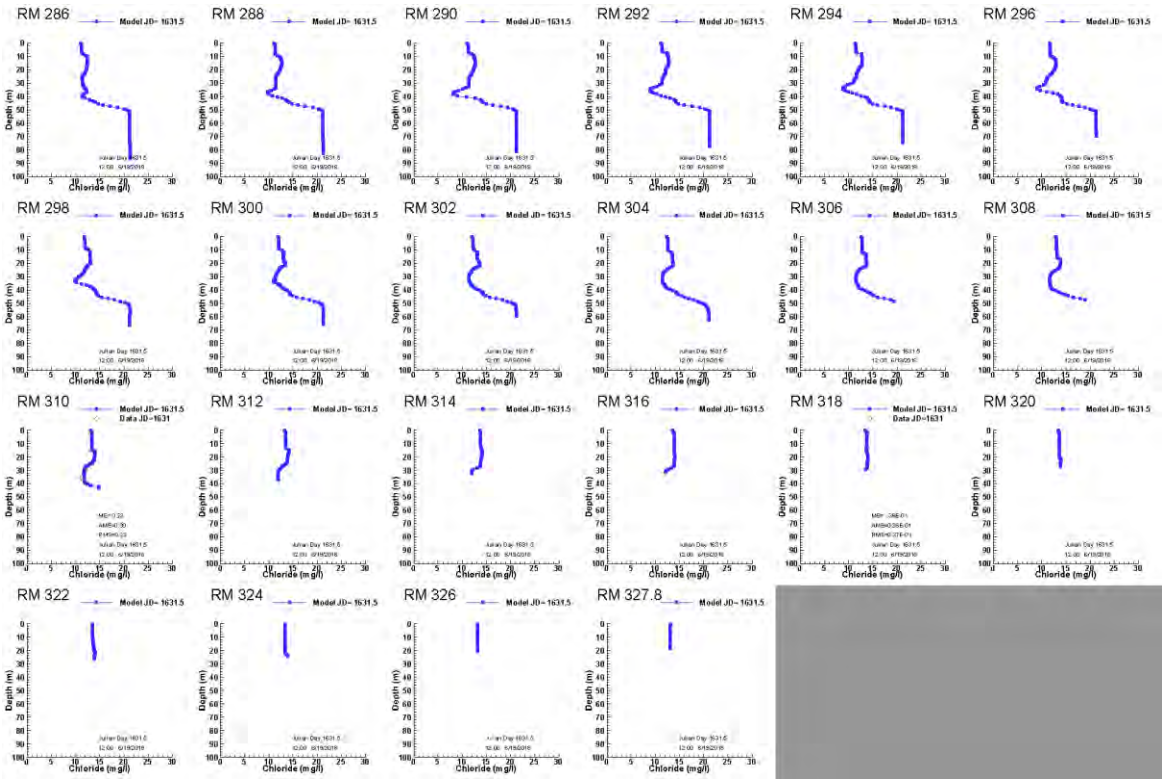


Figure 98. Vertical profiles of chloride compared with data for 6/19/2018.

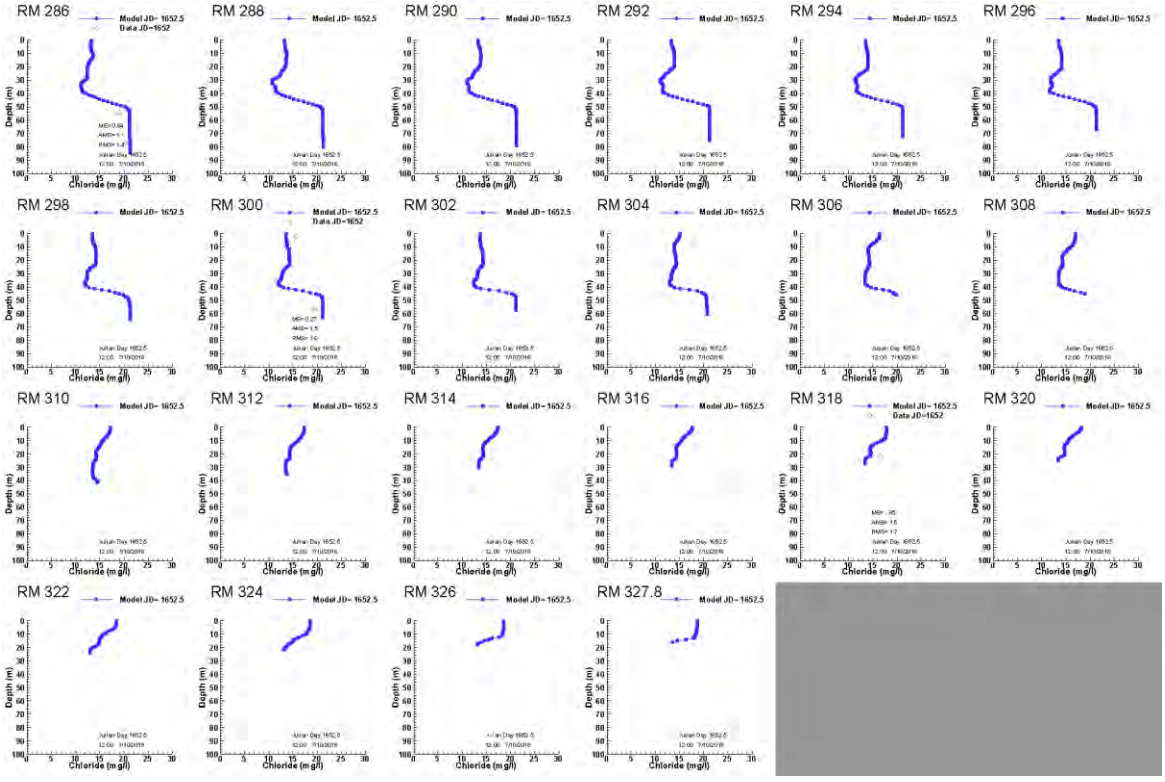


Figure 99. Vertical profiles of chloride compared with data for 7/10/2018.

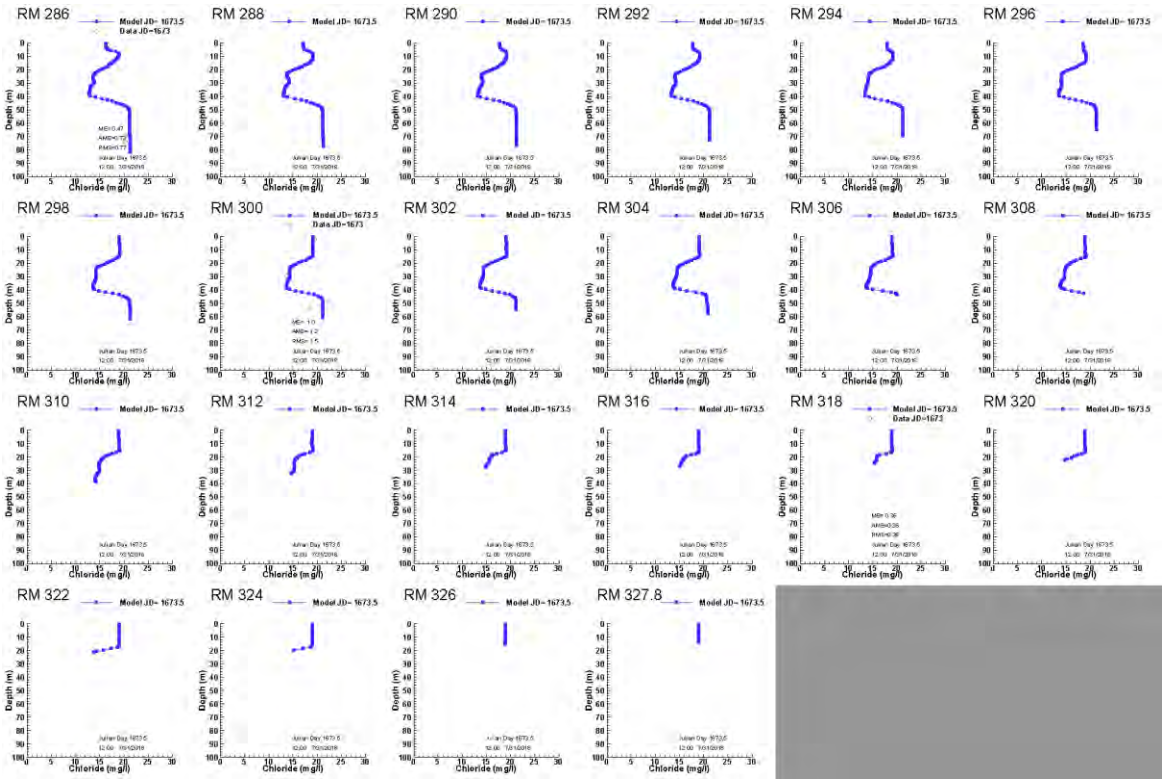


Figure 100. Vertical profiles of chloride compared with data for 7/31/2018.

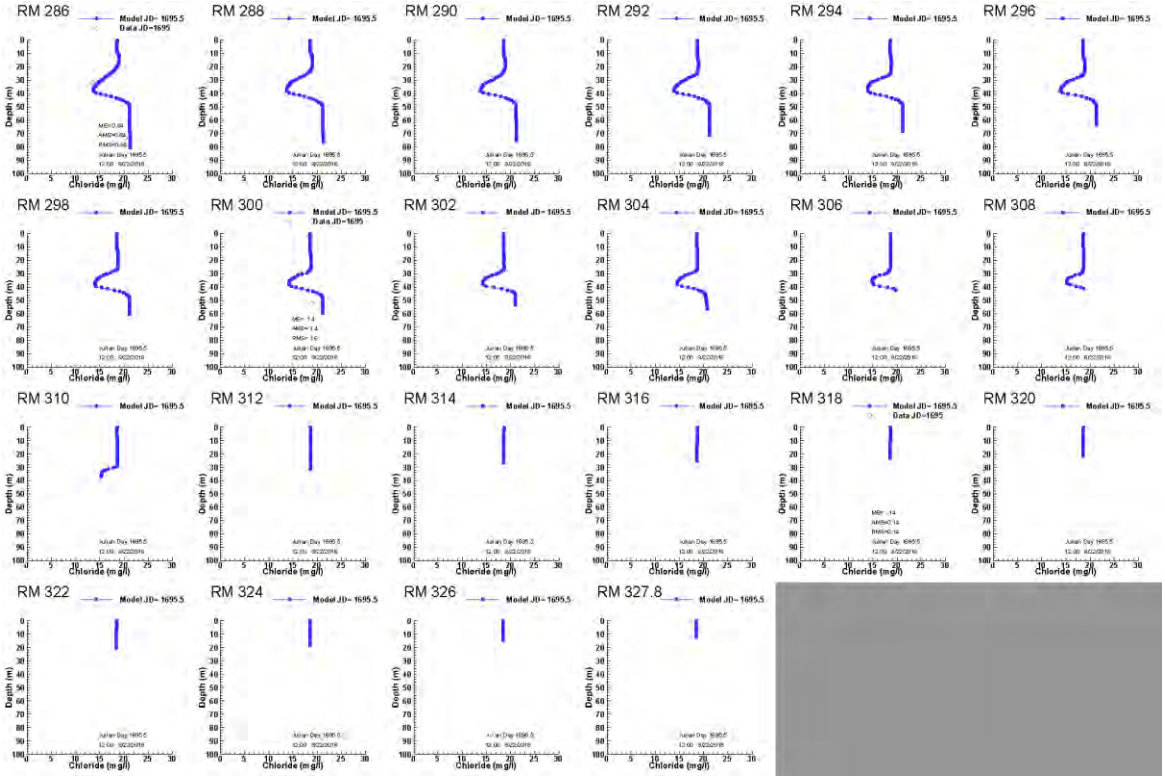


Figure 101. Vertical profiles of chloride compared with data for 8/22/2018.

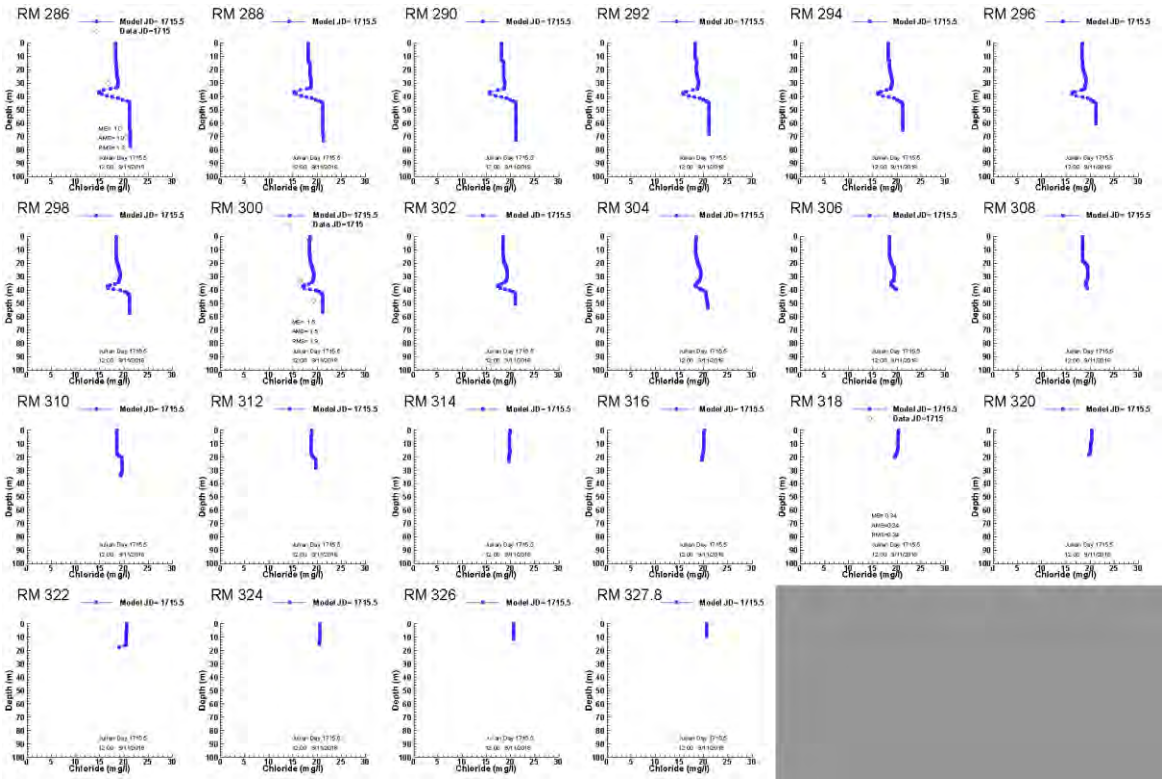


Figure 102. Vertical profiles of chloride compared with data for 9/11/2018.

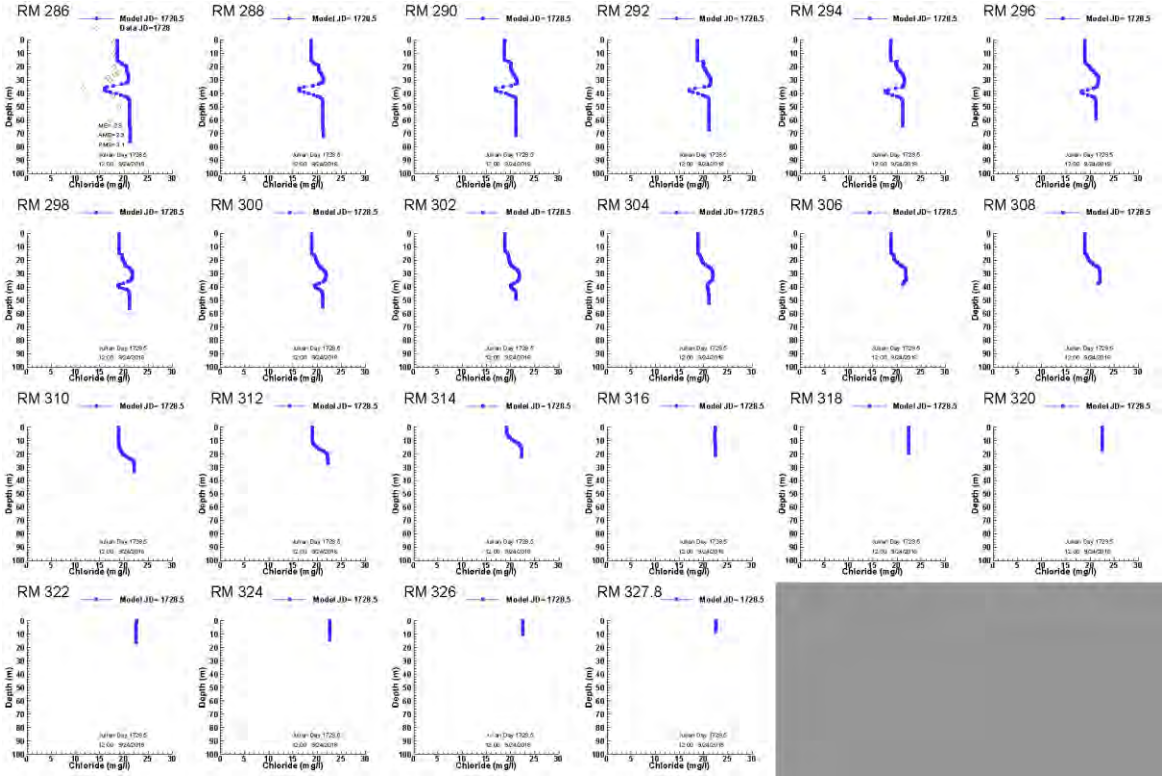


Figure 103. Vertical profiles of chloride compared with data for 9/24/2018.

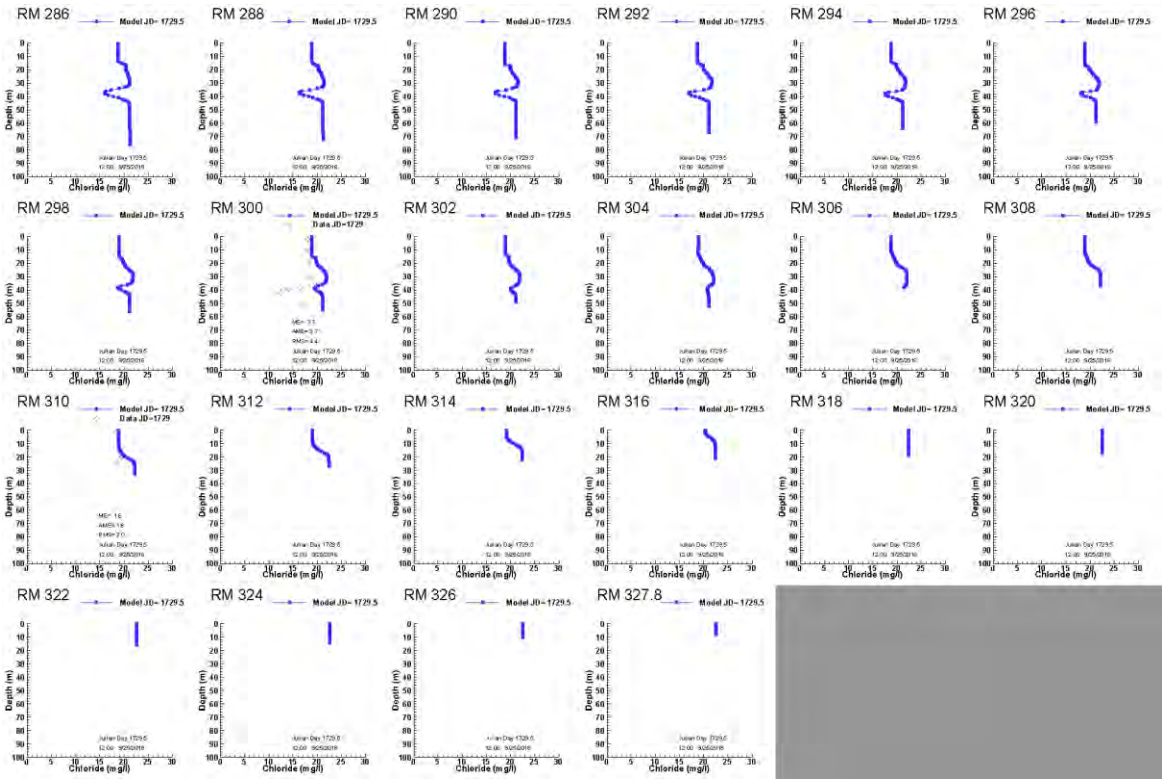


Figure 104. Vertical profiles of chloride compared with data for 9/25/2018.

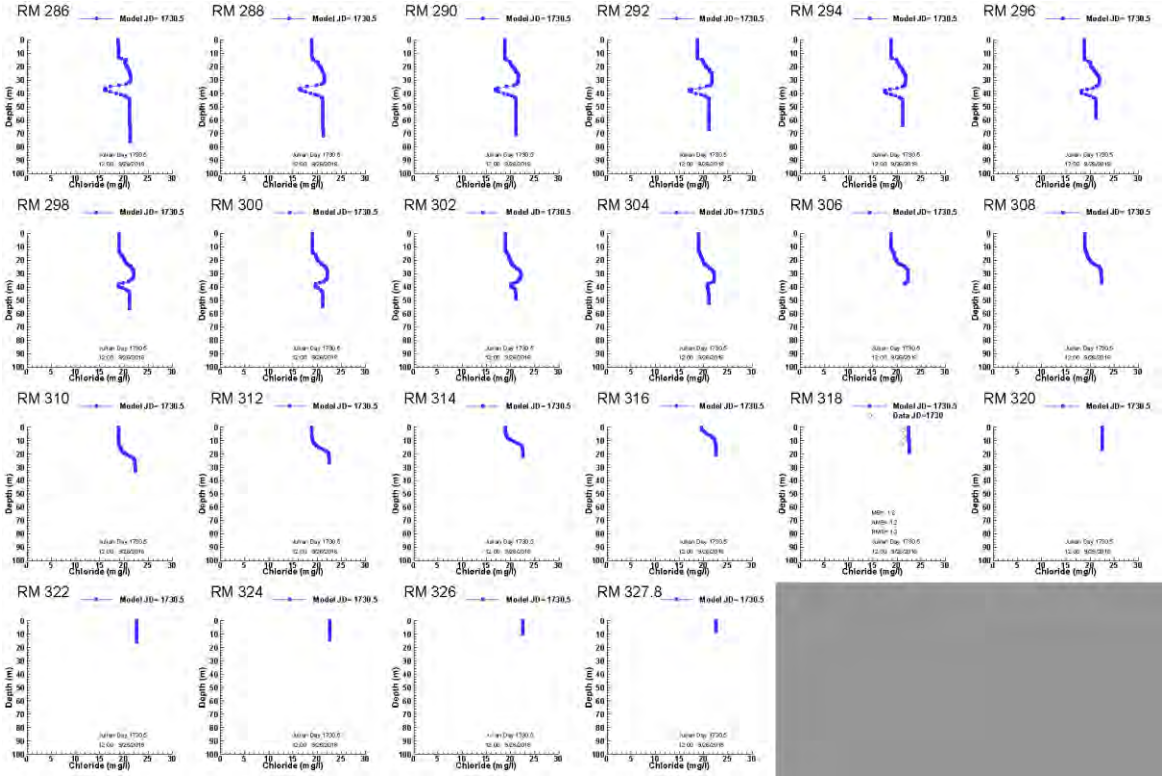


Figure 105. Vertical profiles of chloride compared with data for 9/26/2018.

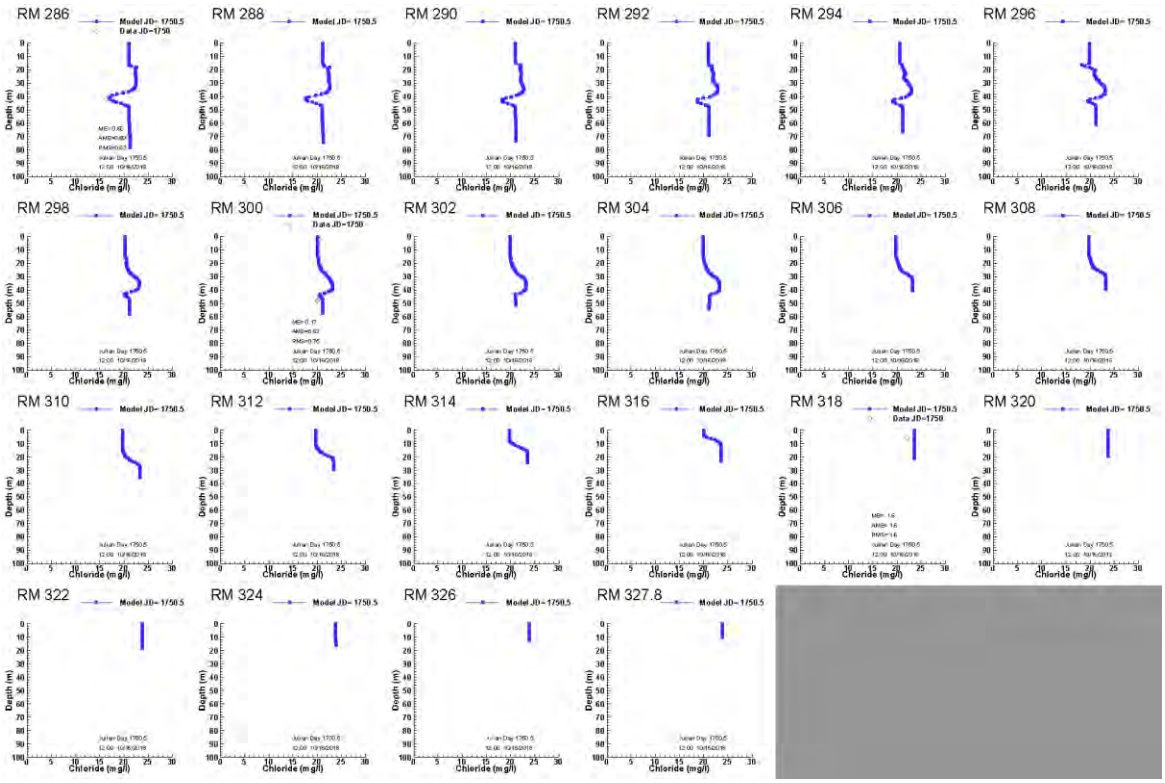


Figure 106. Vertical profiles of chloride compared with data for 10/16/2018.

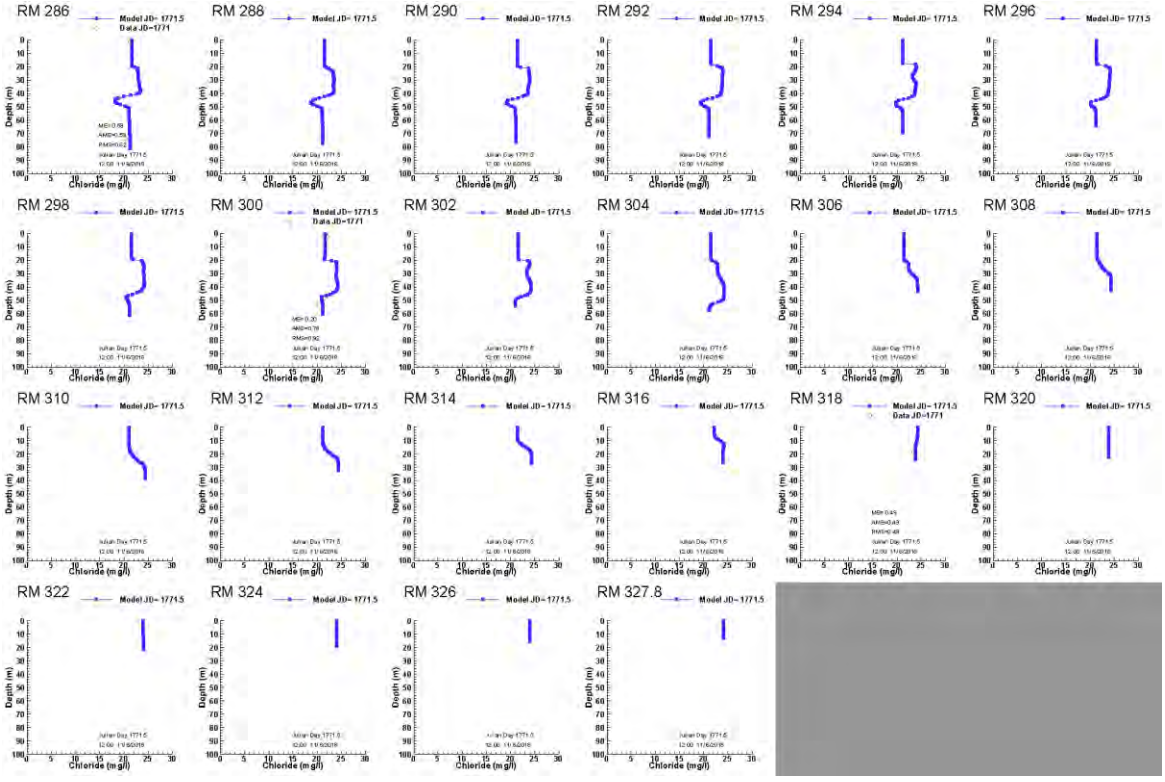


Figure 107. Vertical profiles of chloride compared with data for 11/ 6/2018.

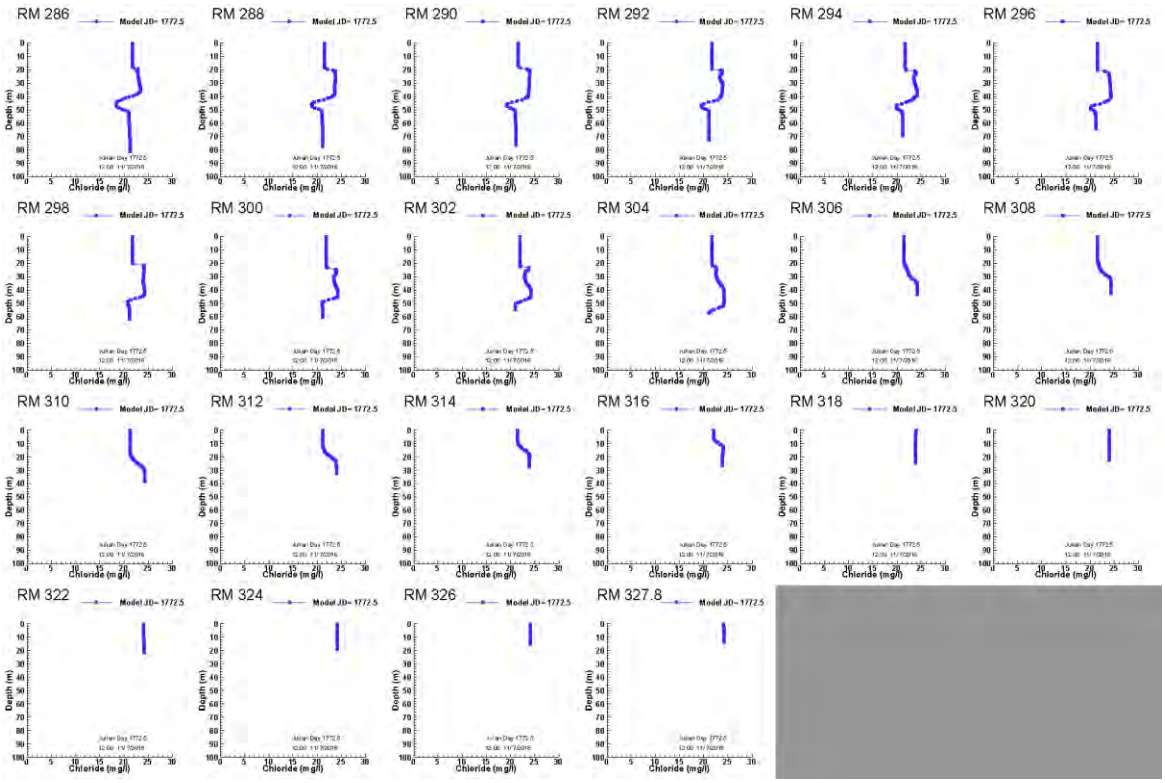


Figure 108. Vertical profiles of chloride compared with data for 11/ 7/2018.

Hydrogen Sulfide

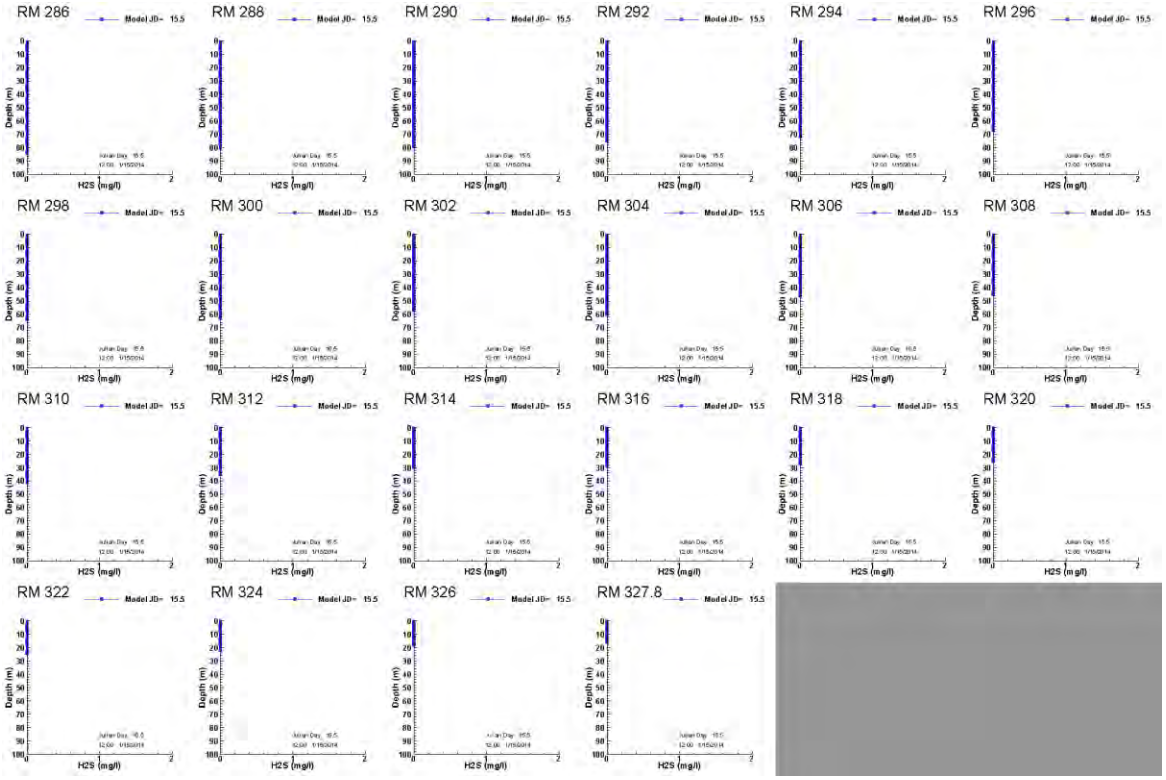


Figure 109. Vertical profiles of hydrogen sulfide compared with data for 1/15/2014.

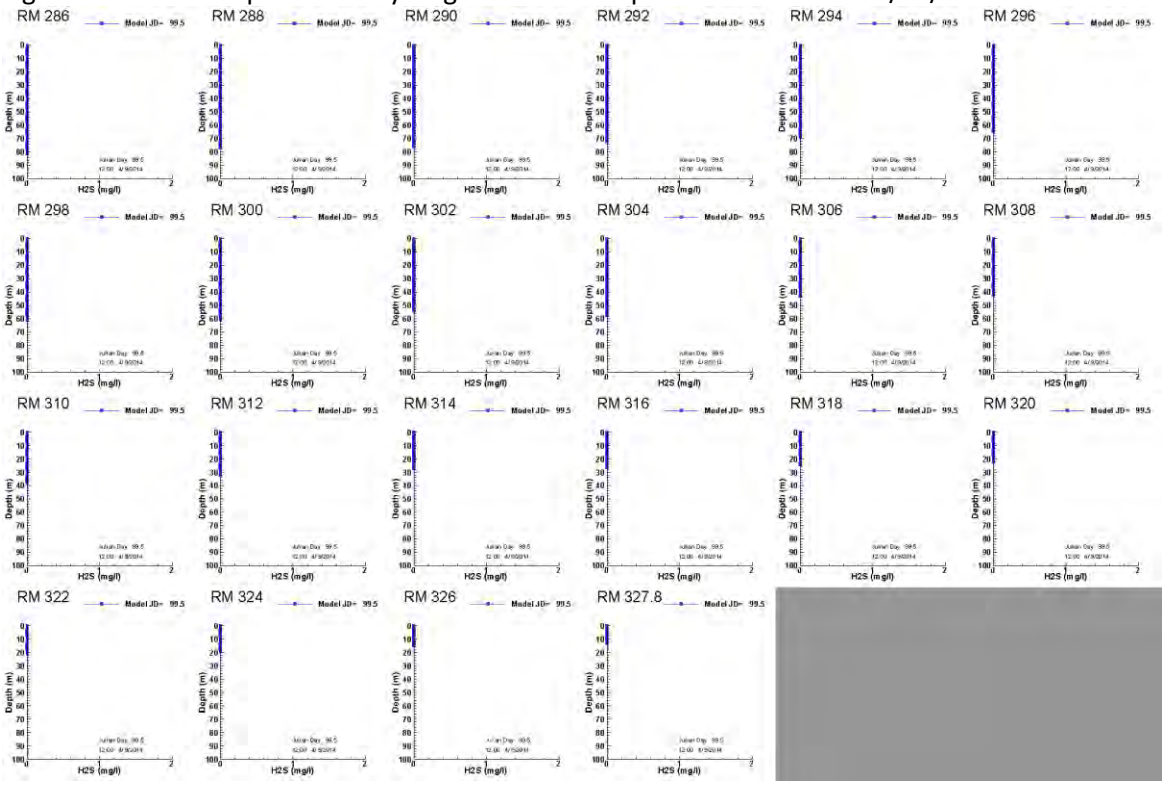


Figure 110. Vertical profiles of hydrogen sulfide compared with data for 4/ 9/2014.

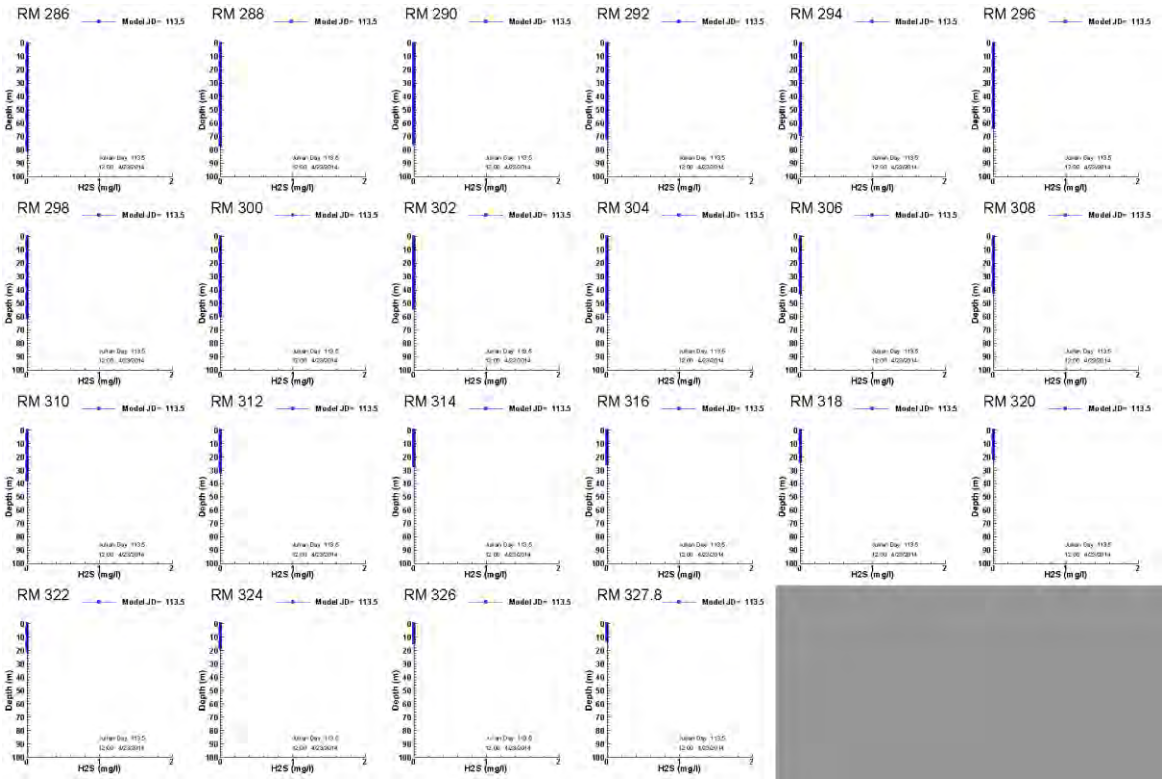


Figure 111. Vertical profiles of hydrogen sulfide compared with data for 4/23/2014.

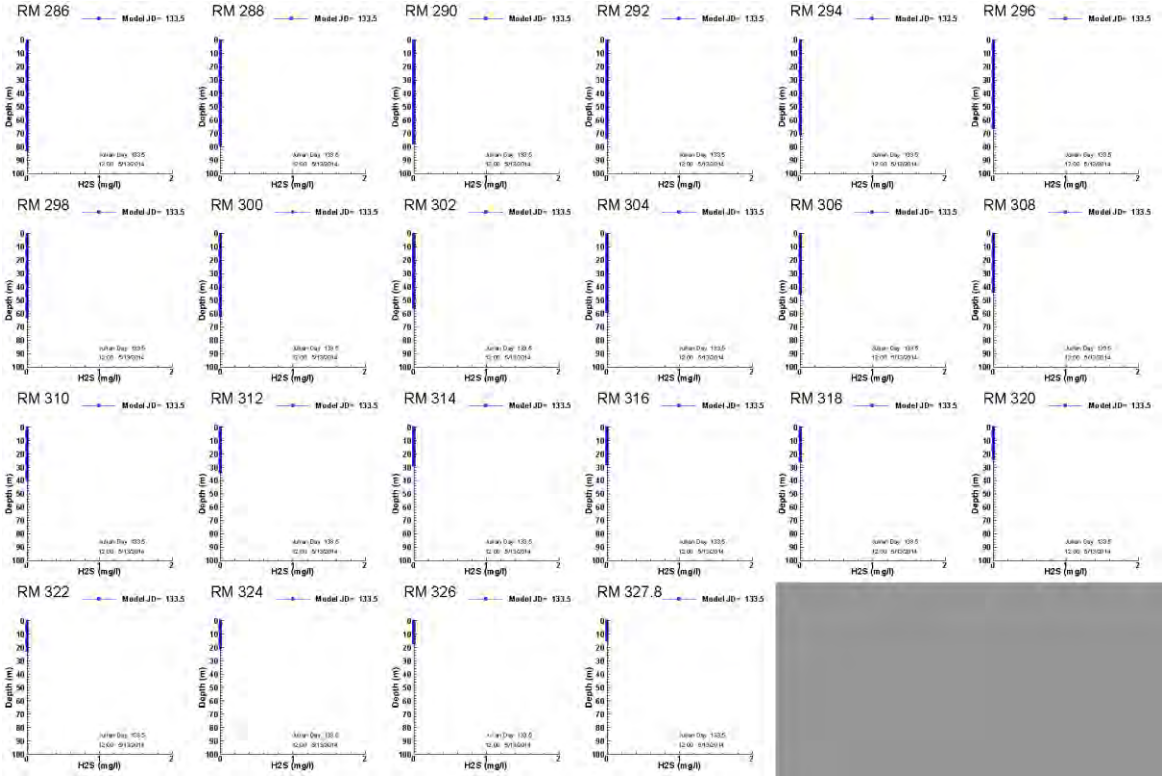


Figure 112. Vertical profiles of hydrogen sulfide compared with data for 5/13/2014.

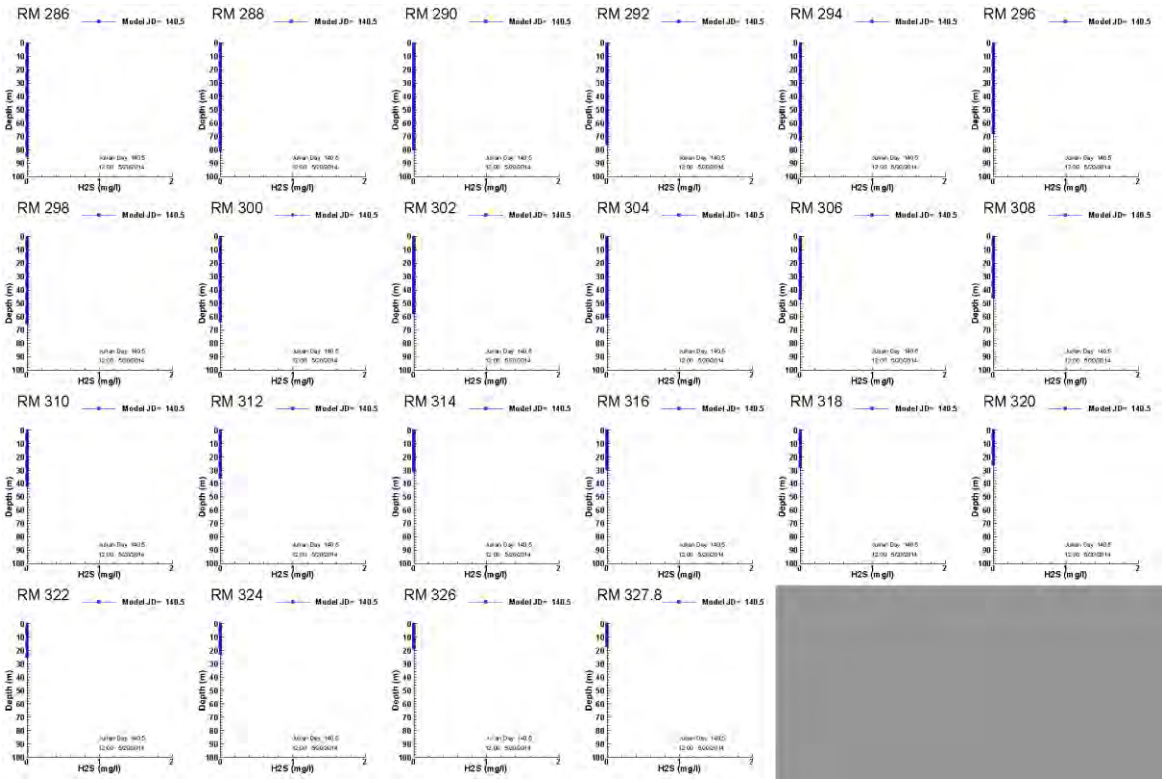


Figure 113. Vertical profiles of hydrogen sulfide compared with data for 5/20/2014.

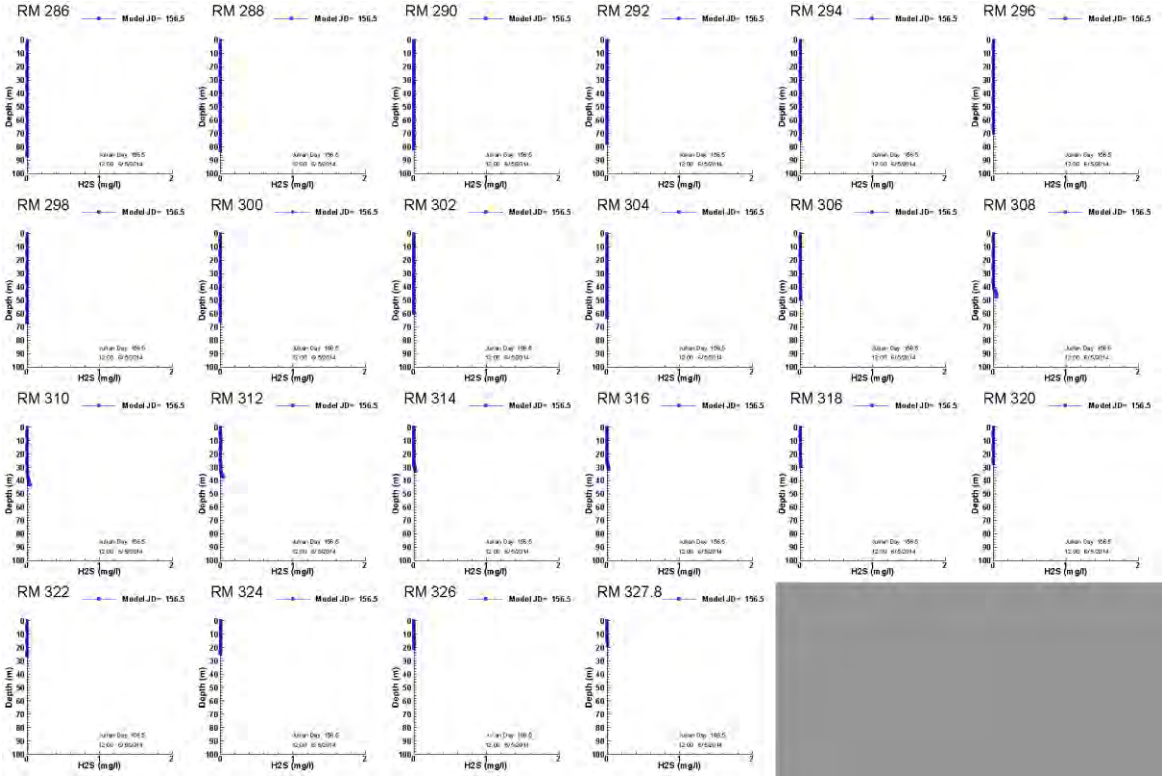


Figure 114. Vertical profiles of hydrogen sulfide compared with data for 6/ 5/2014.

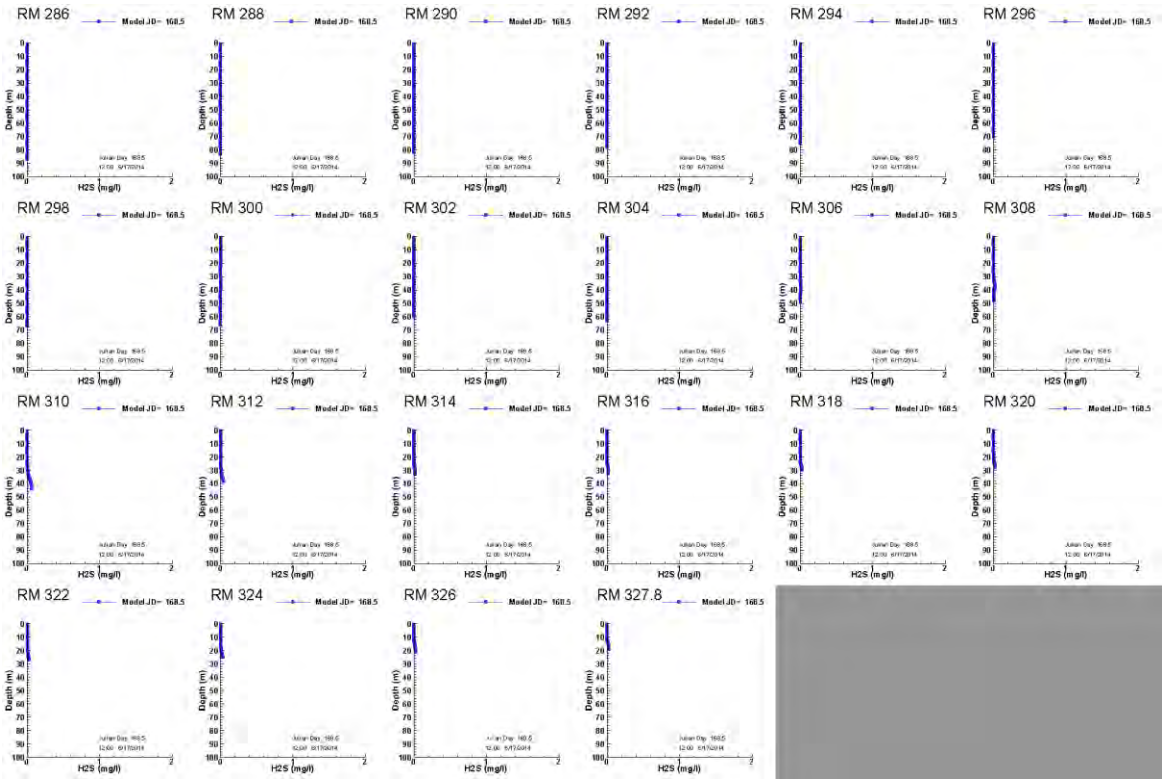


Figure 115. Vertical profiles of hydrogen sulfide compared with data for 6/17/2014.

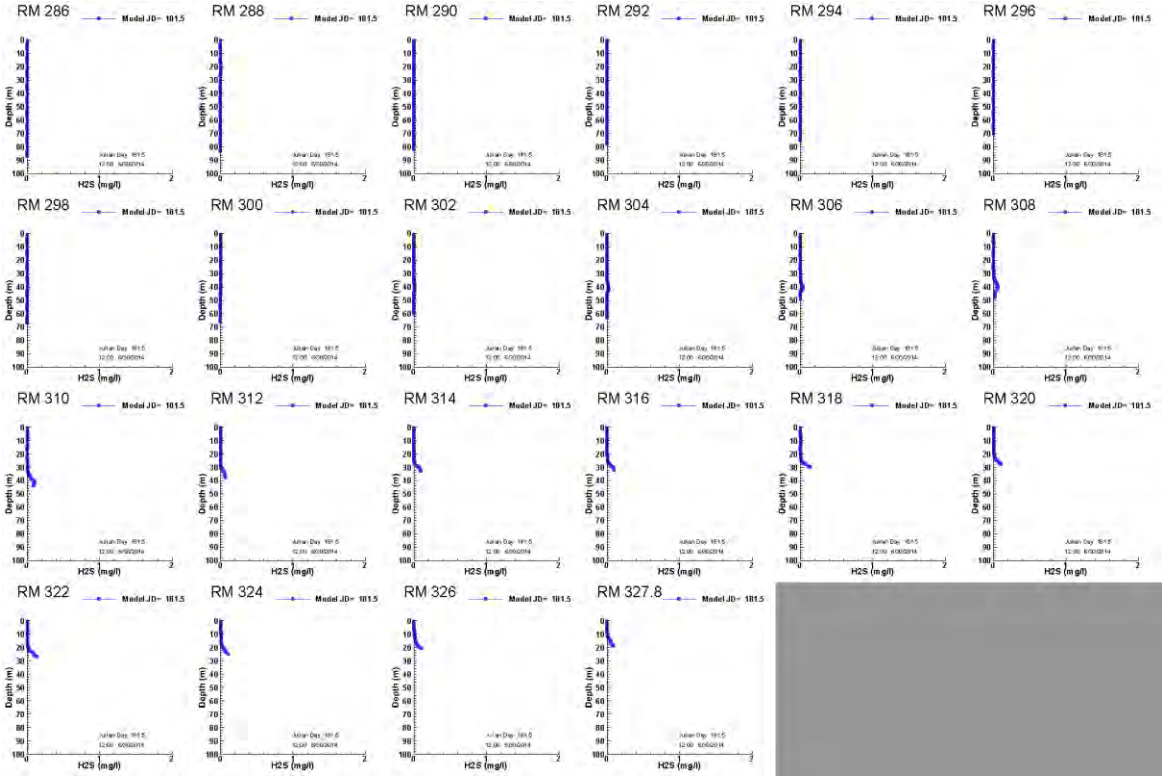


Figure 116. Vertical profiles of hydrogen sulfide compared with data for 6/30/2014.

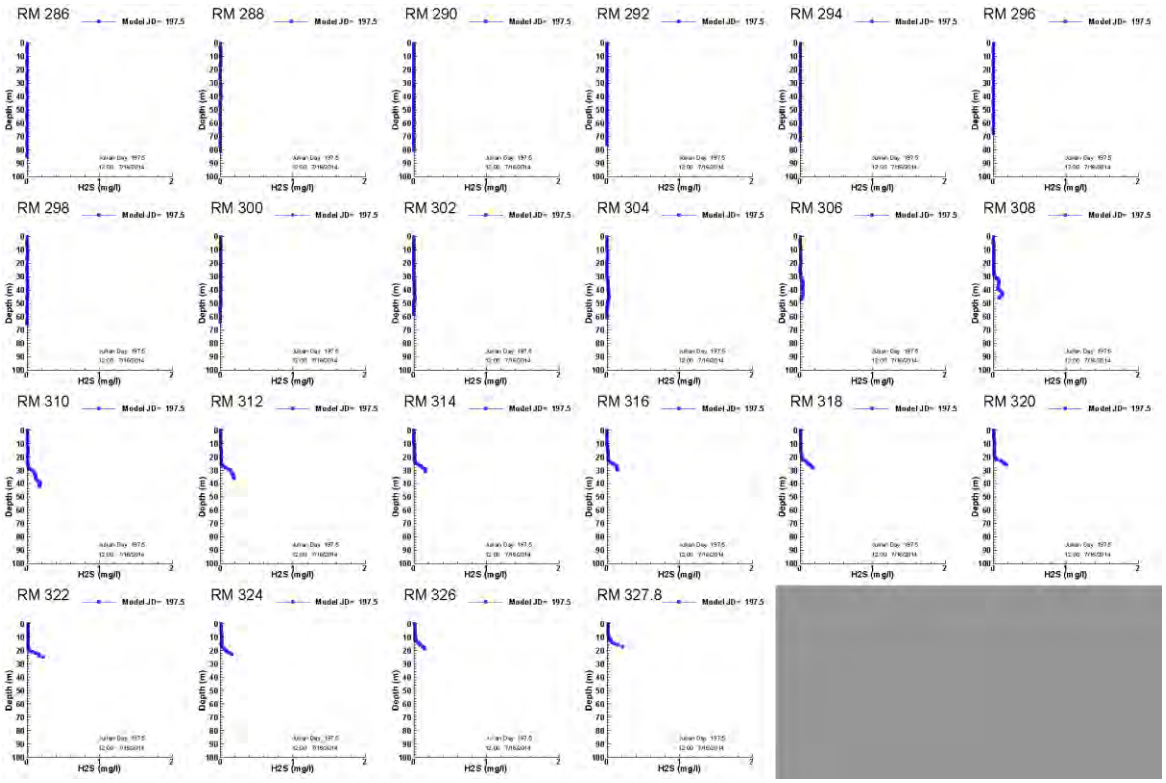


Figure 117. Vertical profiles of hydrogen sulfide compared with data for 7/16/2014.

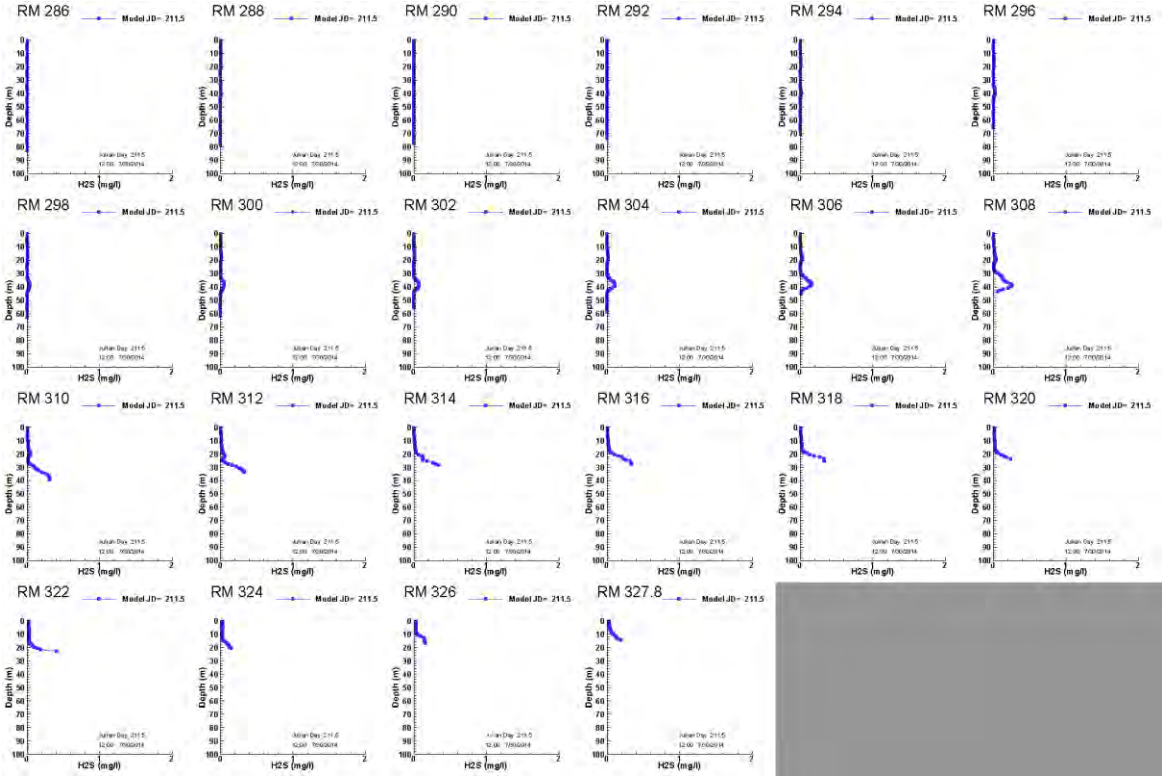


Figure 118. Vertical profiles of hydrogen sulfide compared with data for 7/30/2014.

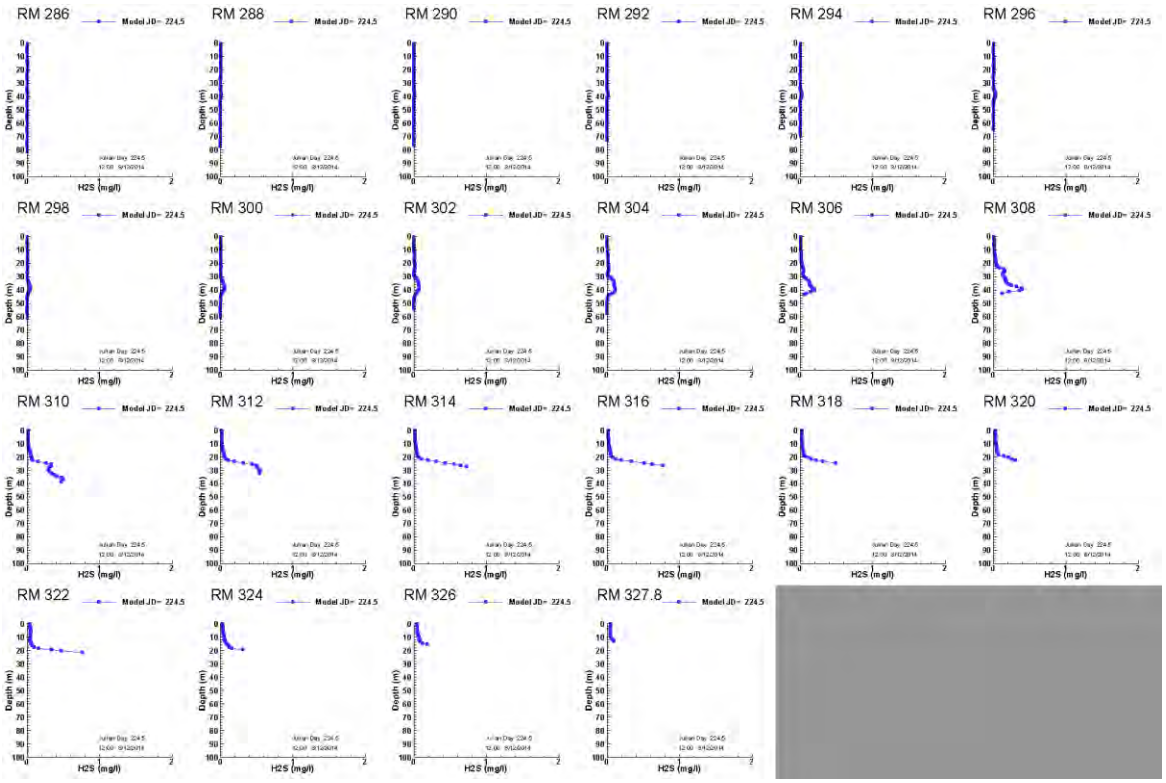


Figure 119. Vertical profiles of hydrogen sulfide compared with data for 8/12/2014.

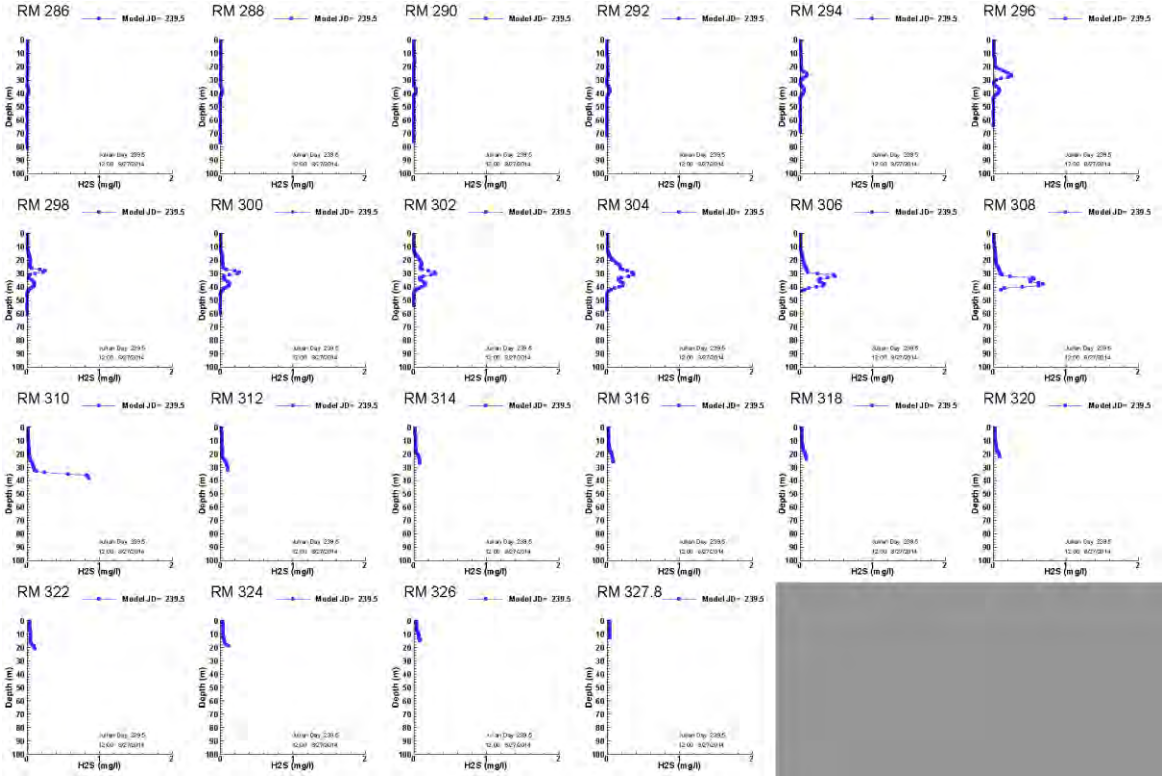


Figure 120. Vertical profiles of hydrogen sulfide compared with data for 8/27/2014.

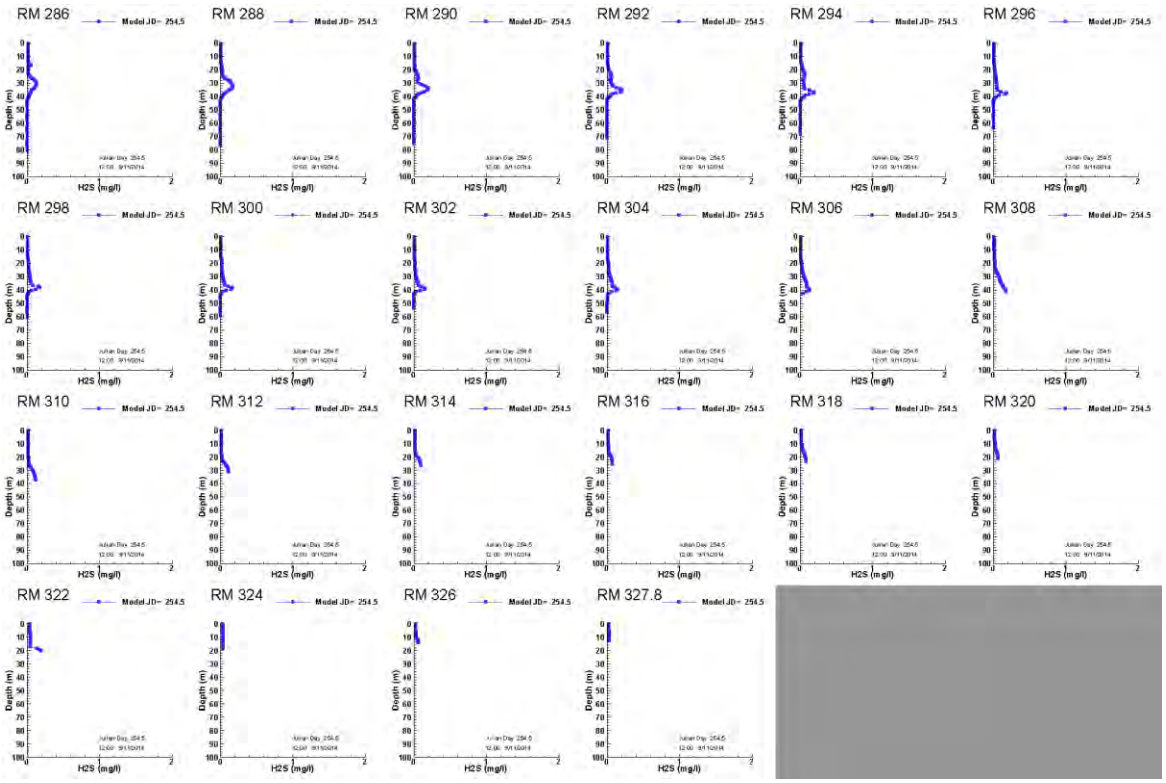


Figure 121. Vertical profiles of hydrogen sulfide compared with data for 9/11/2014.

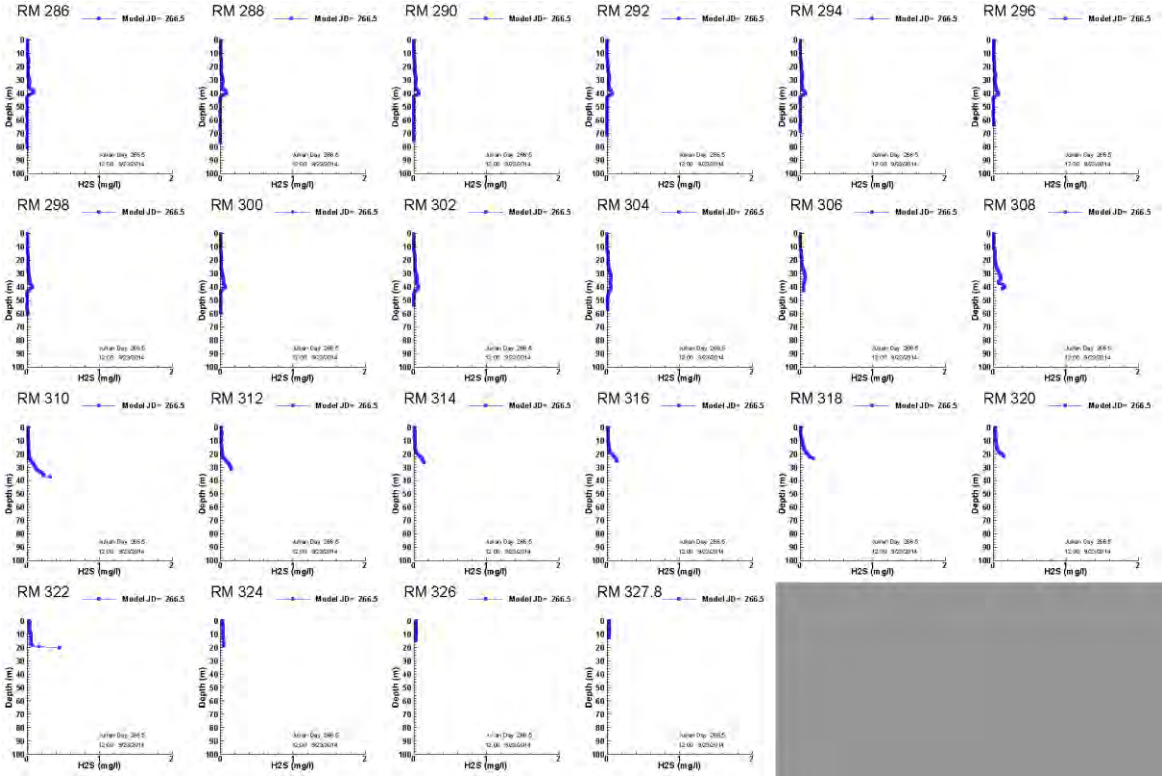


Figure 122. Vertical profiles of hydrogen sulfide compared with data for 9/23/2014.

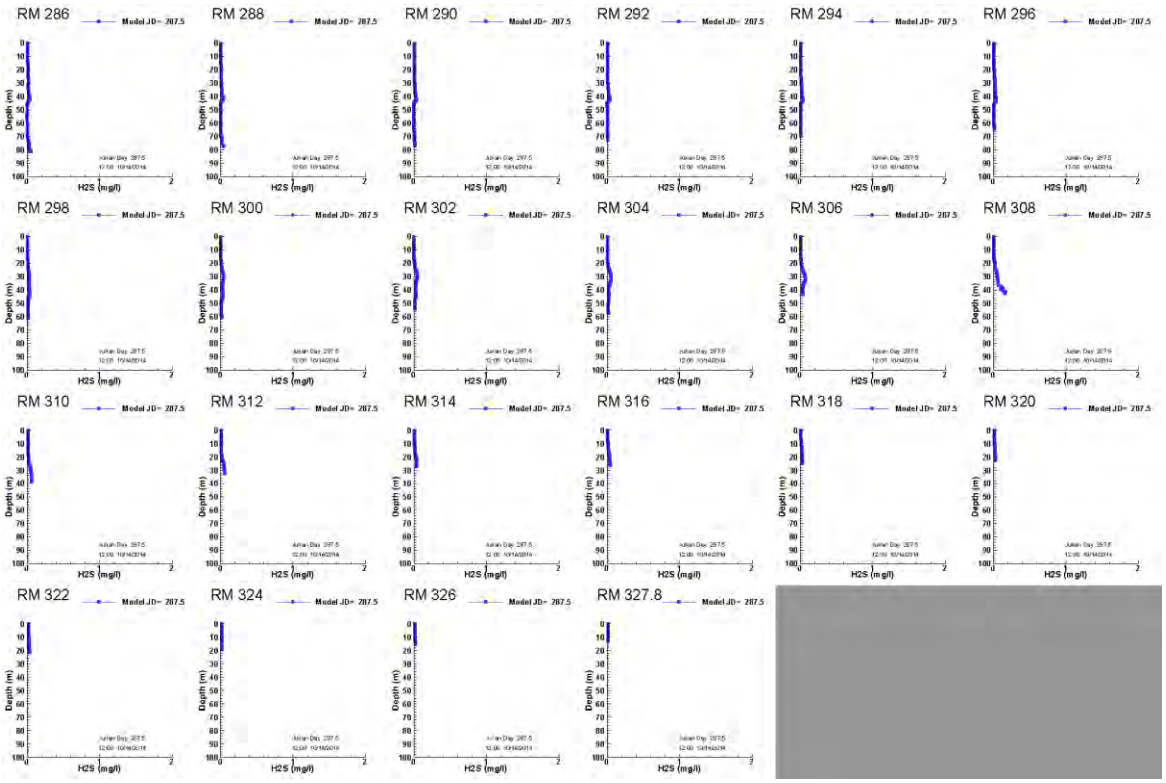


Figure 123. Vertical profiles of hydrogen sulfide compared with data for 10/14/2014.

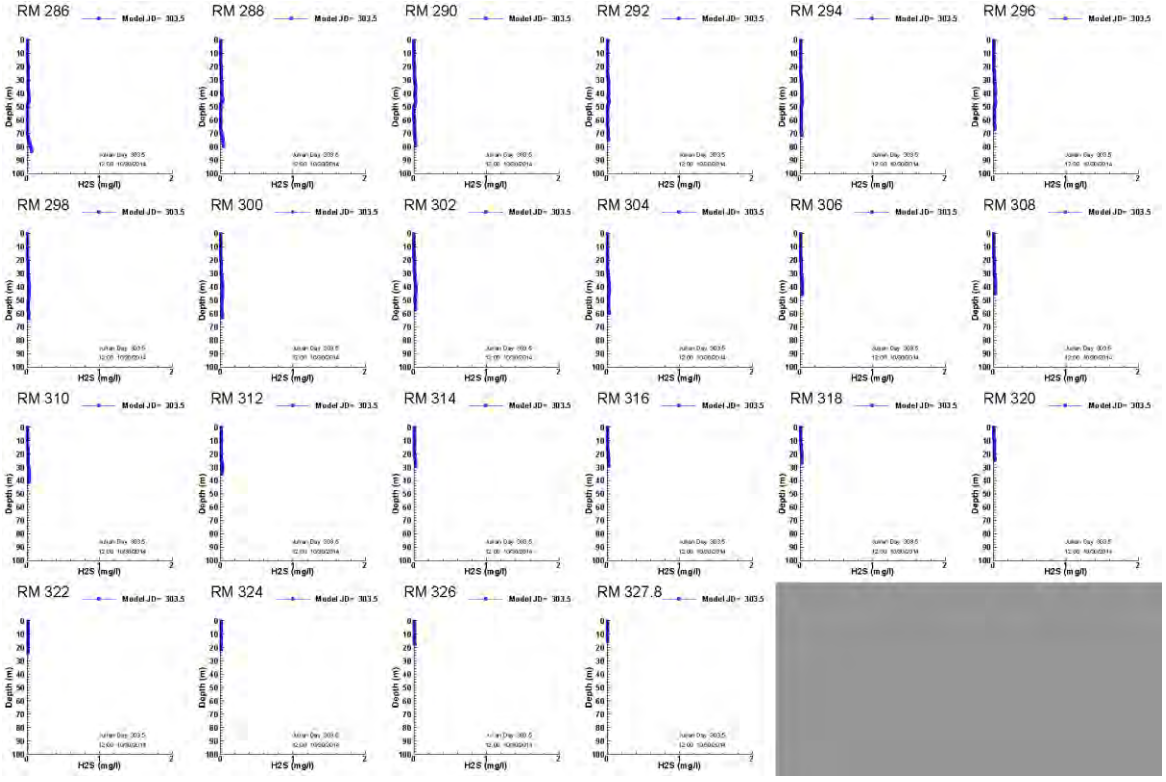


Figure 124. Vertical profiles of hydrogen sulfide compared with data for 10/30/2014.

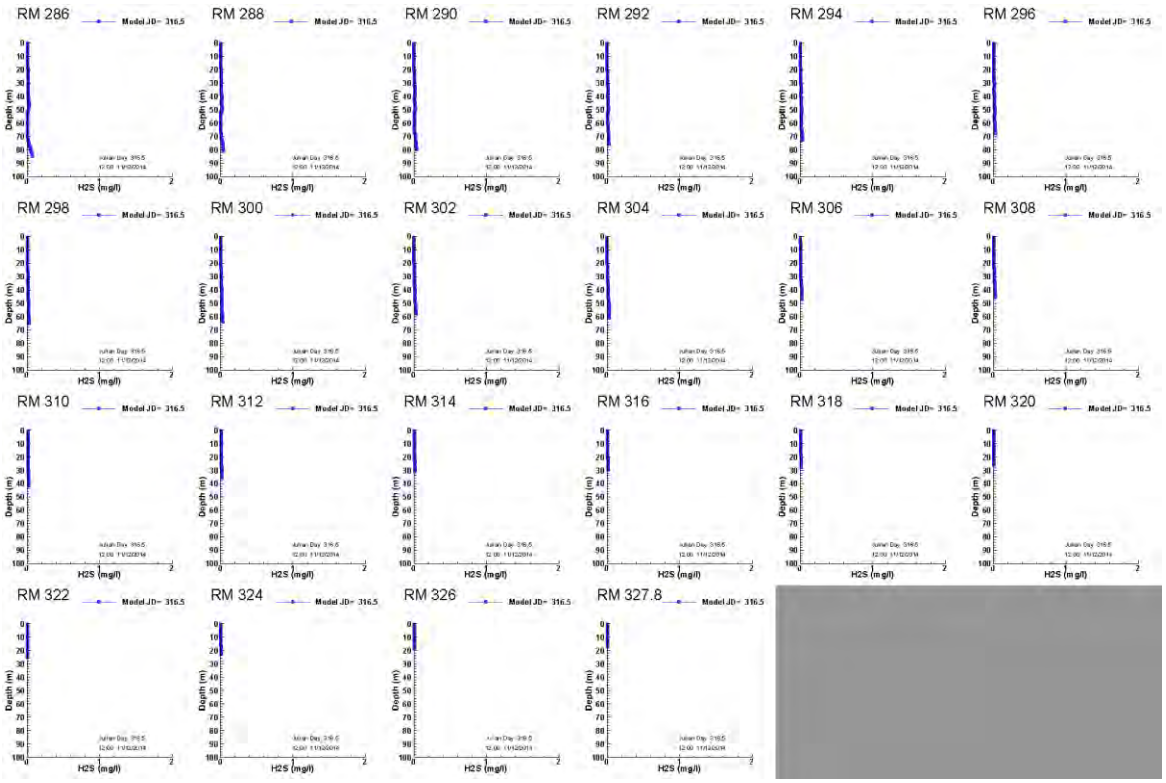


Figure 125. Vertical profiles of hydrogen sulfide compared with data for 11/12/2014.

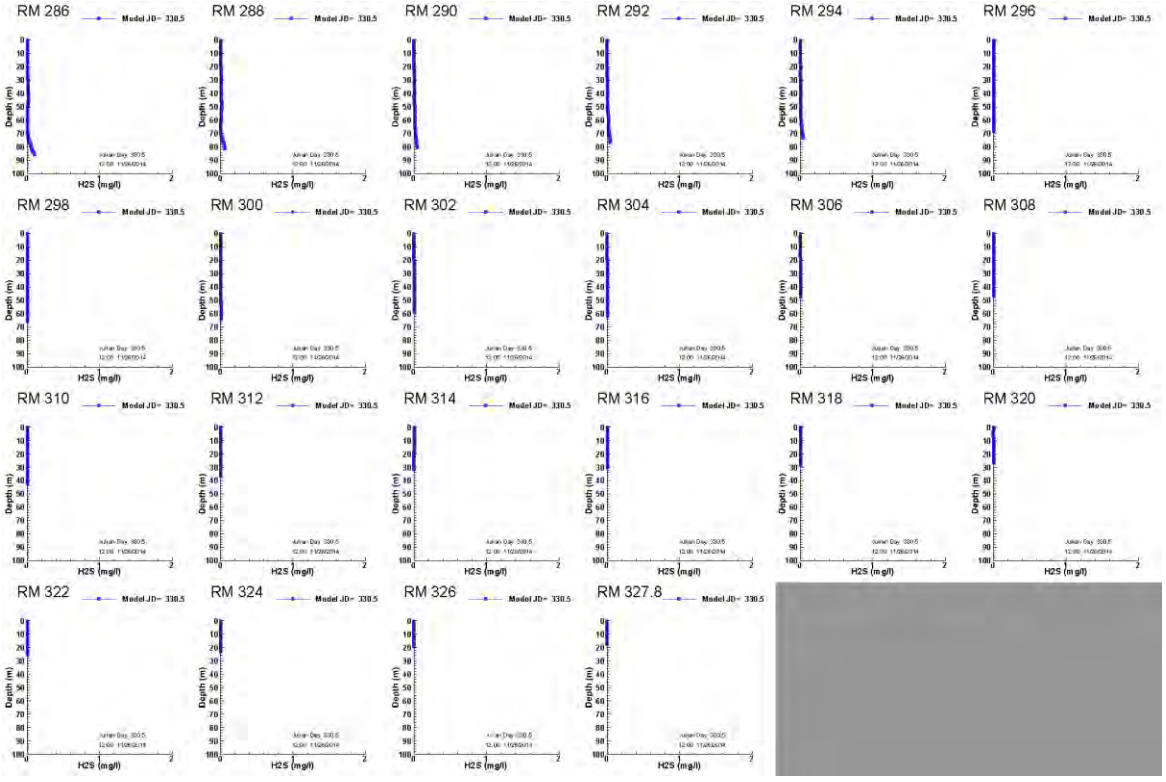


Figure 126. Vertical profiles of hydrogen sulfide compared with data for 11/26/2014.

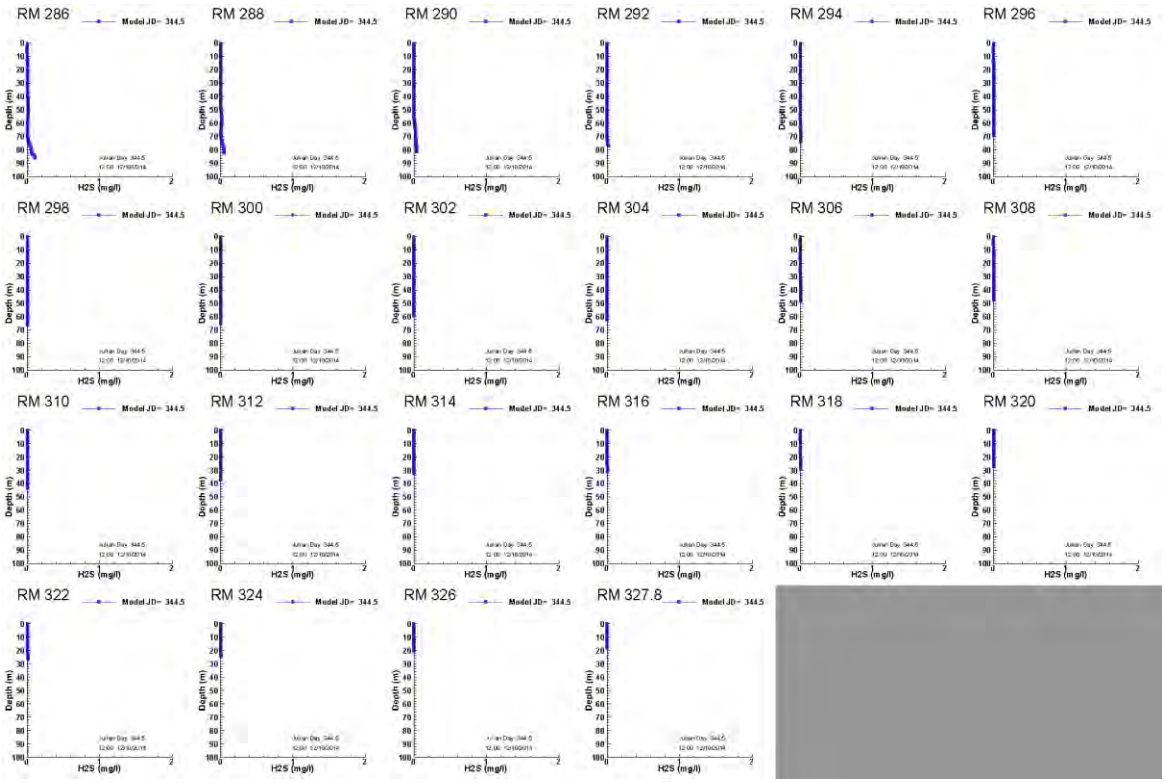


Figure 127. Vertical profiles of hydrogen sulfide compared with data for 12/10/2014.

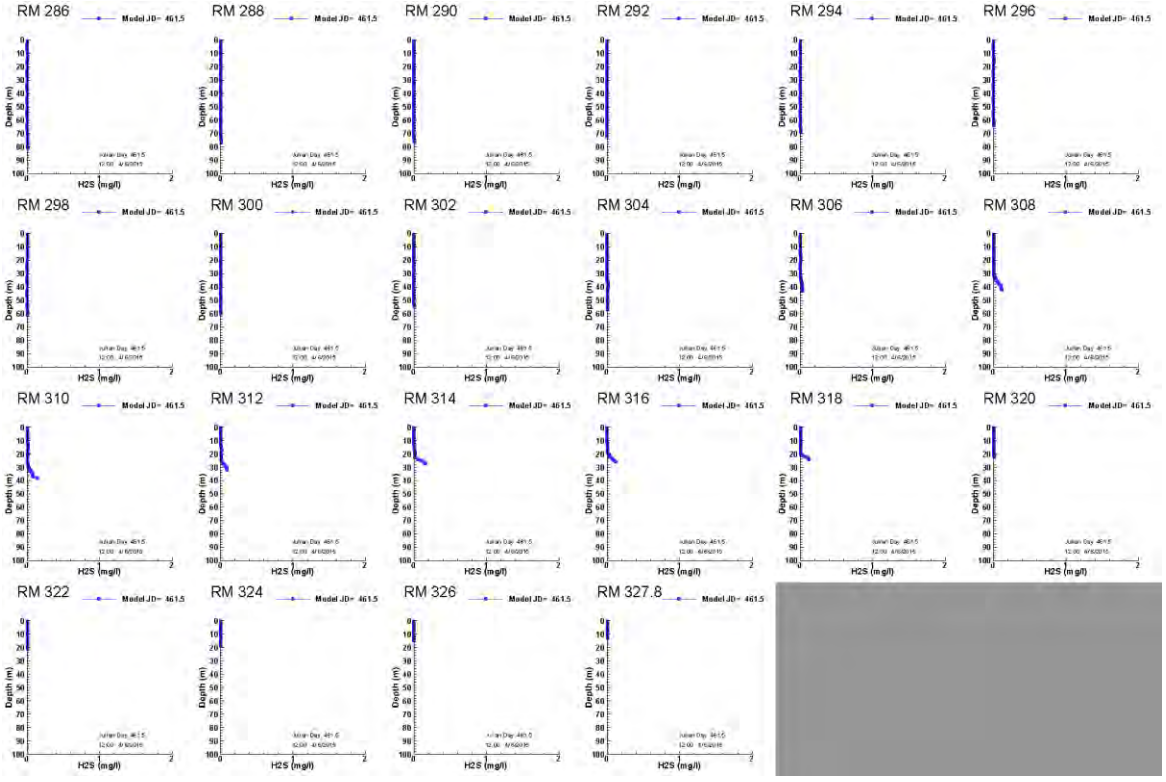


Figure 128. Vertical profiles of hydrogen sulfide compared with data for 4/ 6/2015.

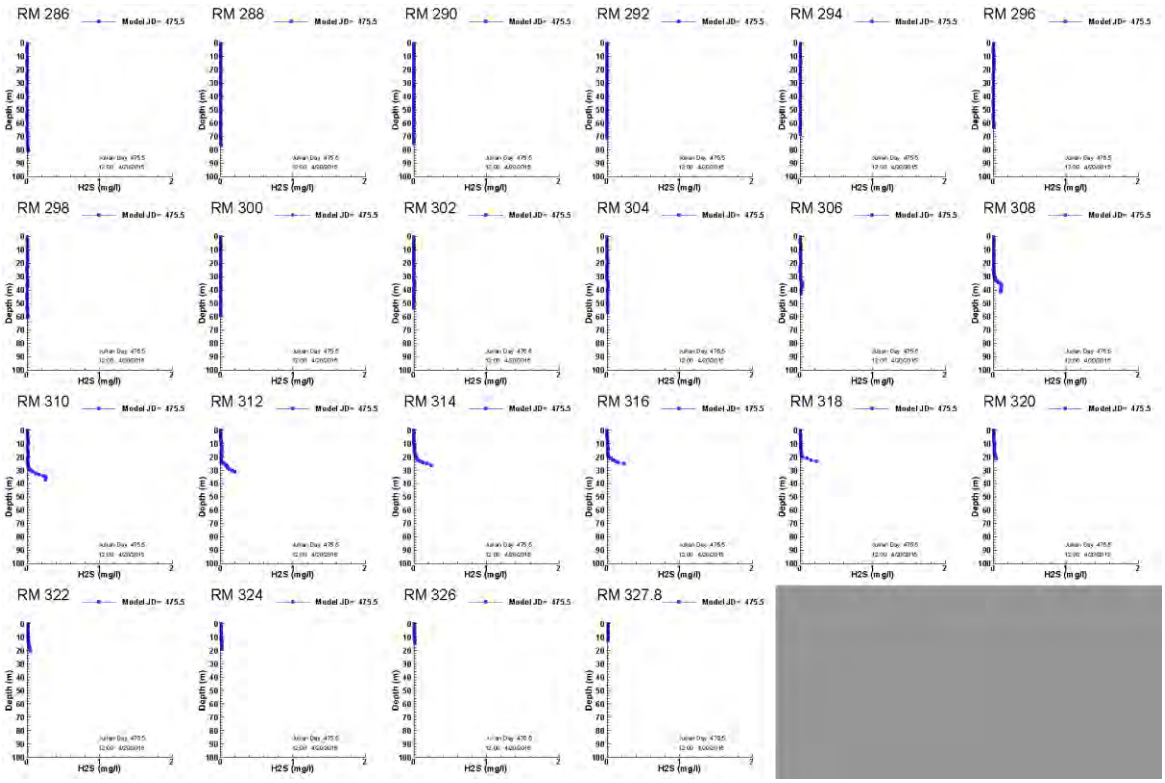


Figure 129. Vertical profiles of hydrogen sulfide compared with data for 4/20/2015.

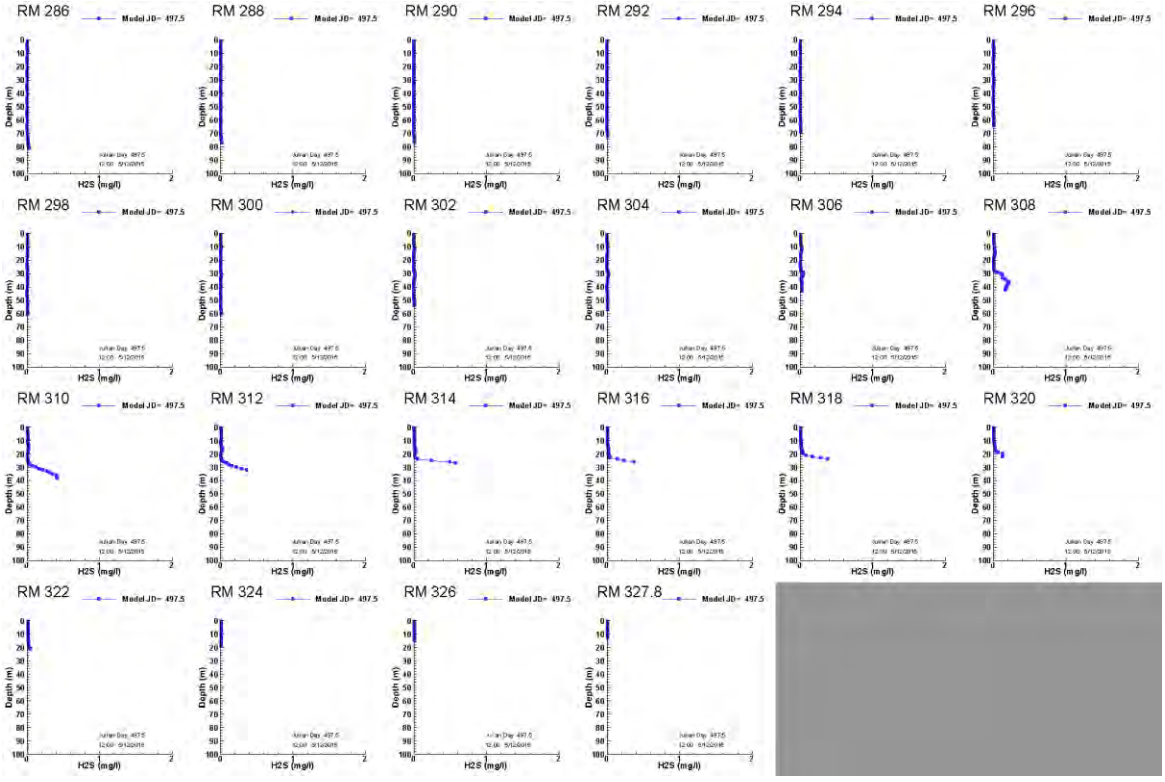


Figure 130. Vertical profiles of hydrogen sulfide compared with data for 5/12/2015.

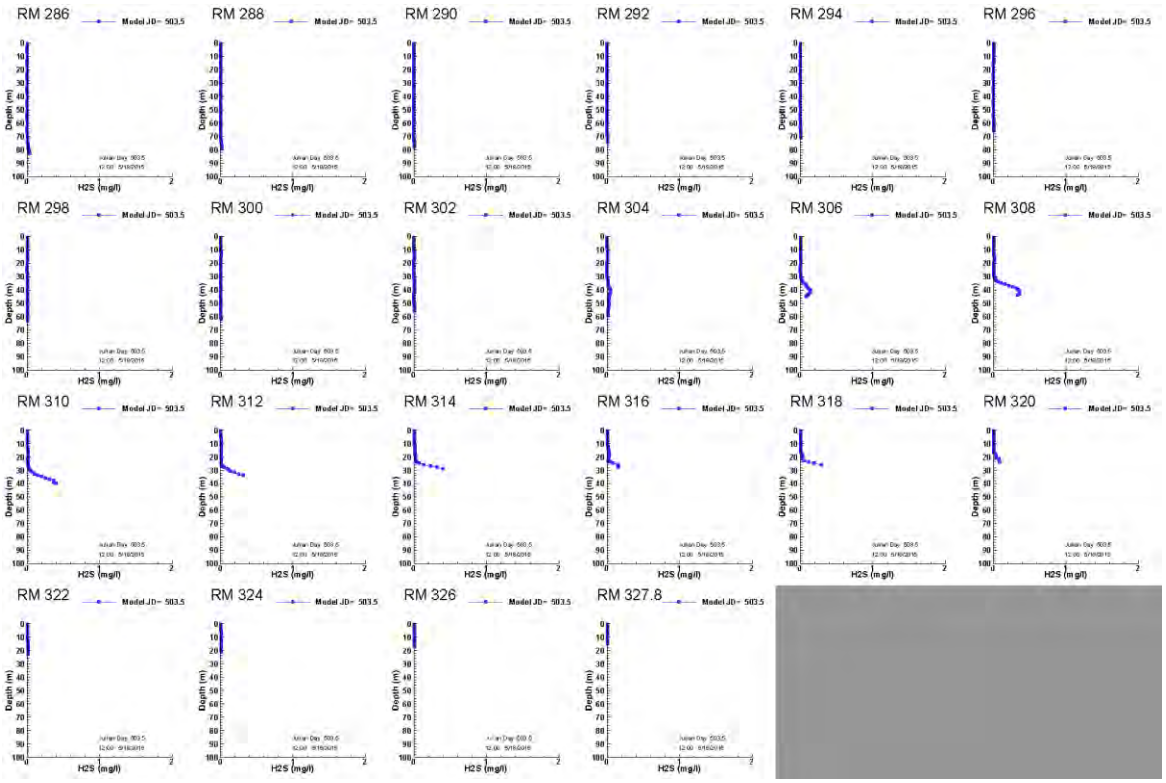


Figure 131. Vertical profiles of hydrogen sulfide compared with data for 5/18/2015.

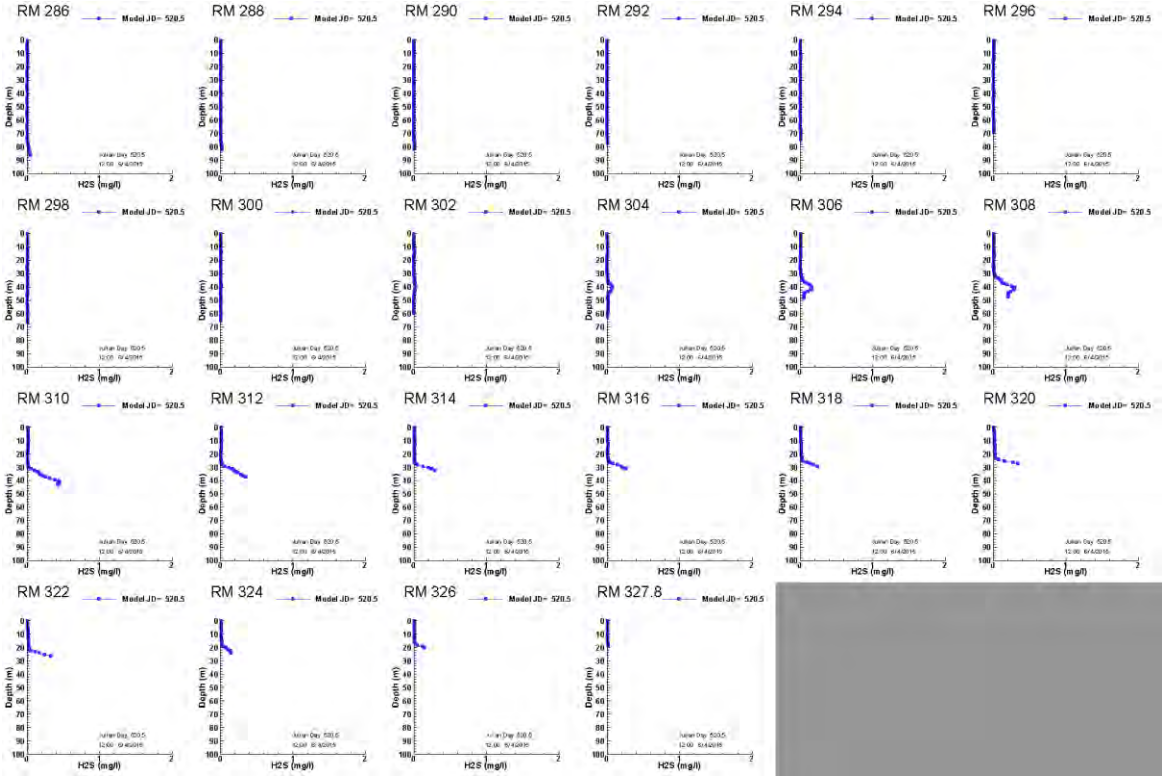


Figure 132. Vertical profiles of hydrogen sulfide compared with data for 6/ 4/2015.

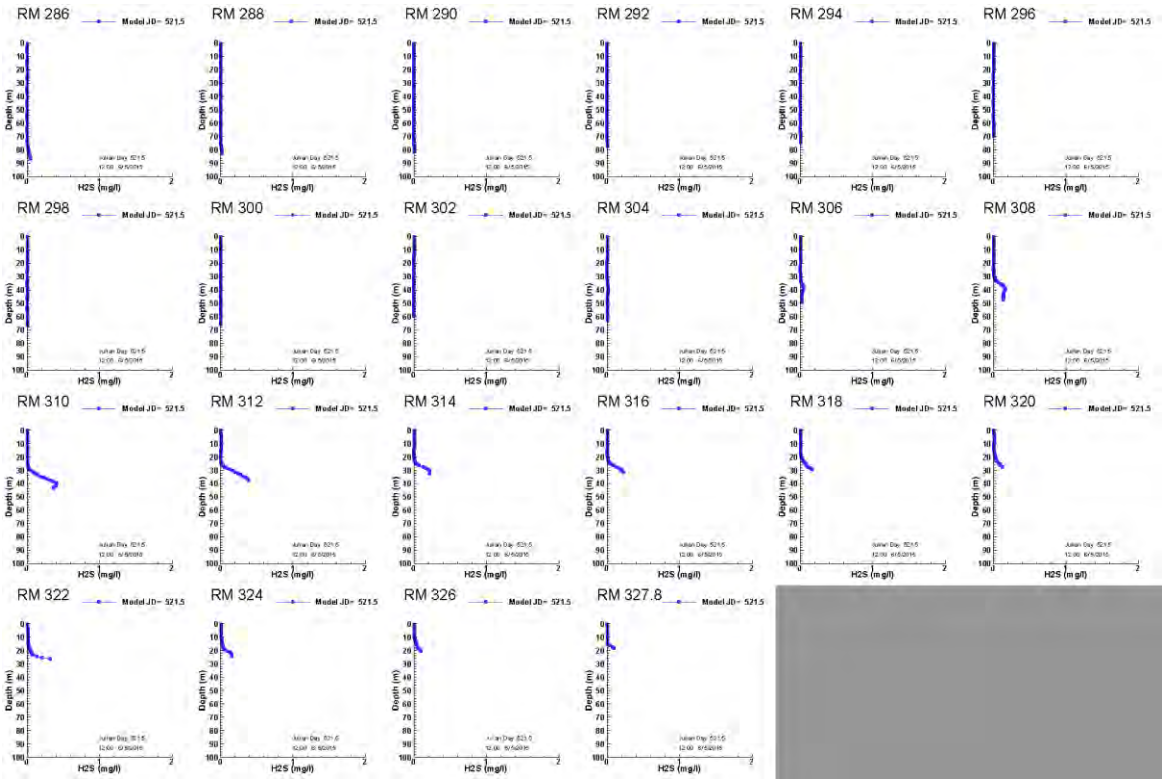


Figure 133. Vertical profiles of hydrogen sulfide compared with data for 6/ 5/2015.

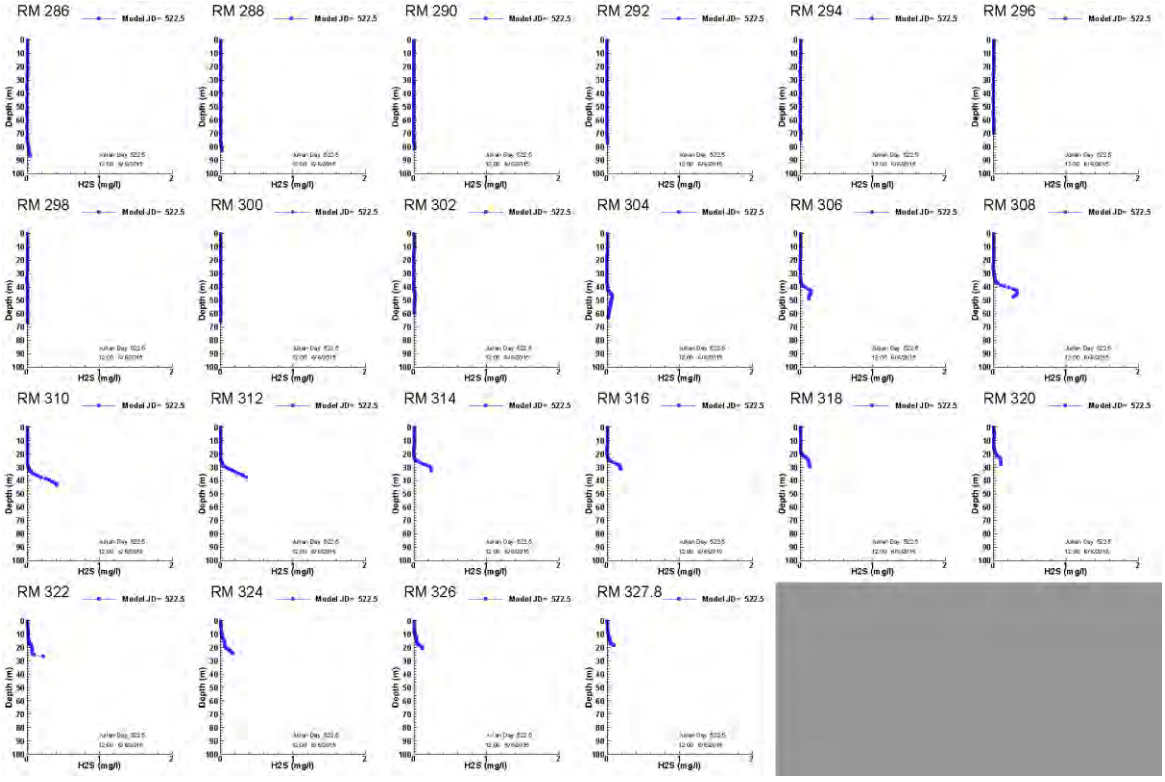


Figure 134. Vertical profiles of hydrogen sulfide compared with data for 6/ 6/2015.

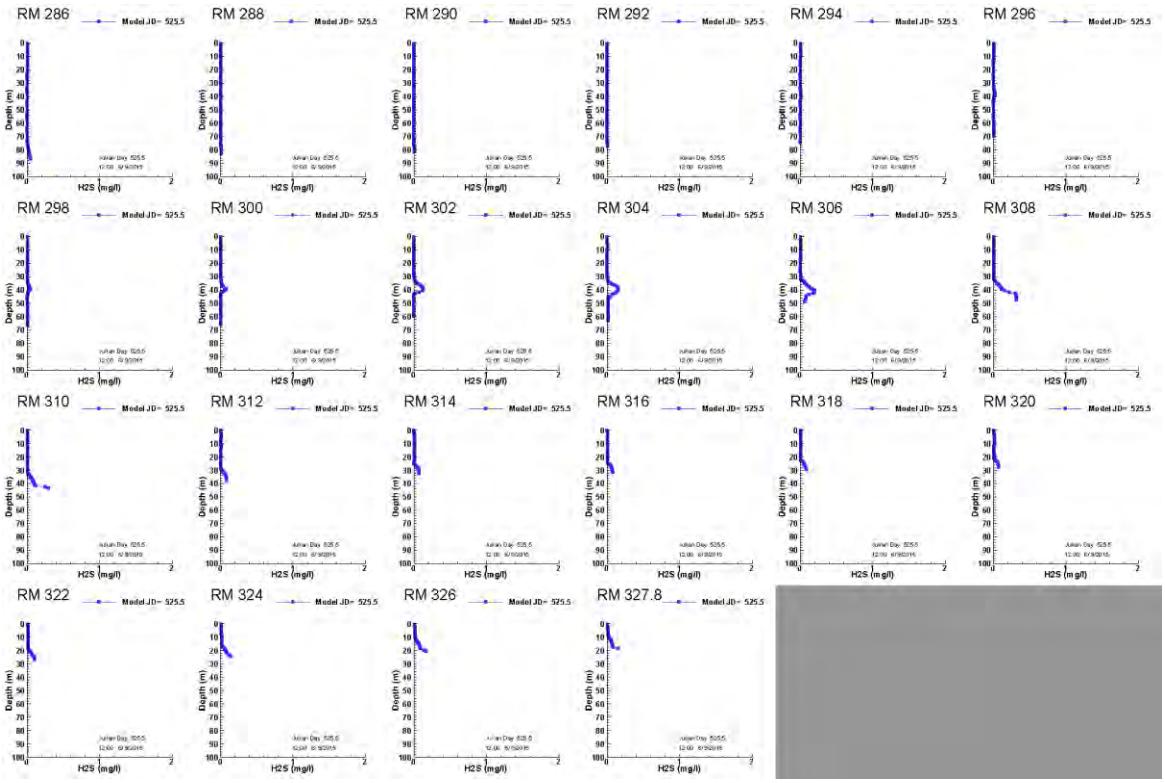


Figure 135. Vertical profiles of hydrogen sulfide compared with data for 6/ 9/2015.

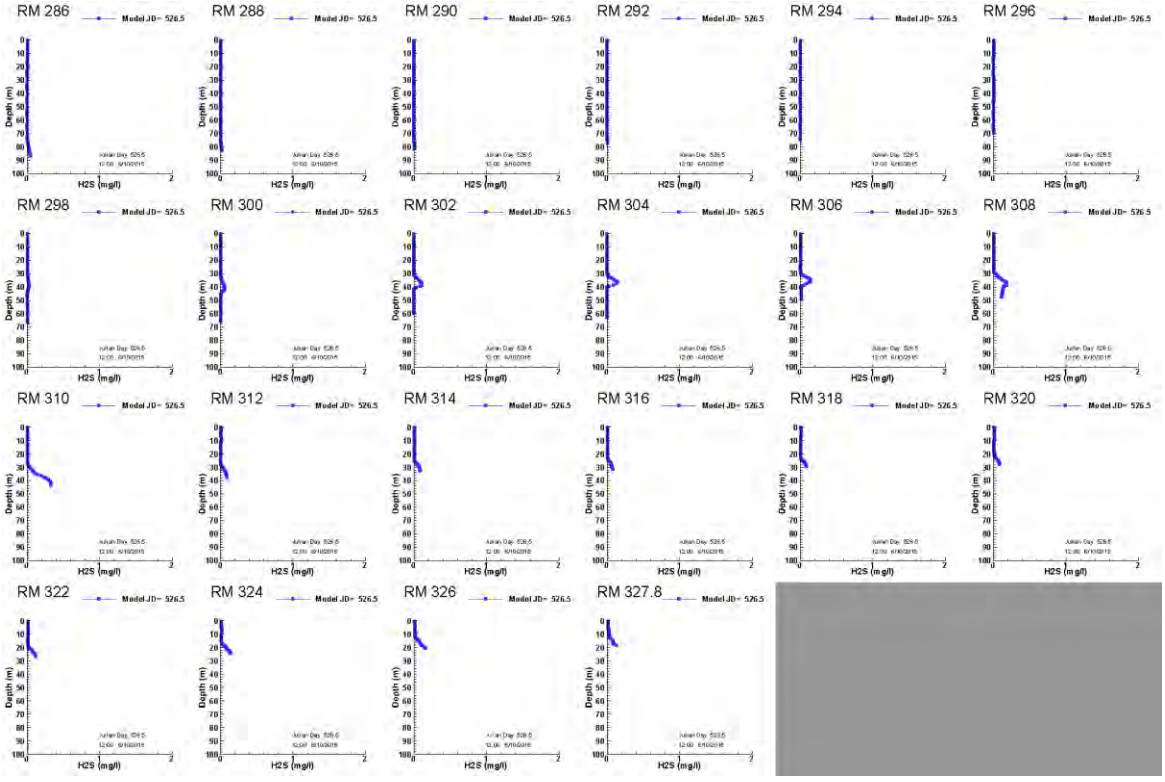


Figure 136. Vertical profiles of hydrogen sulfide compared with data for 6/10/2015.

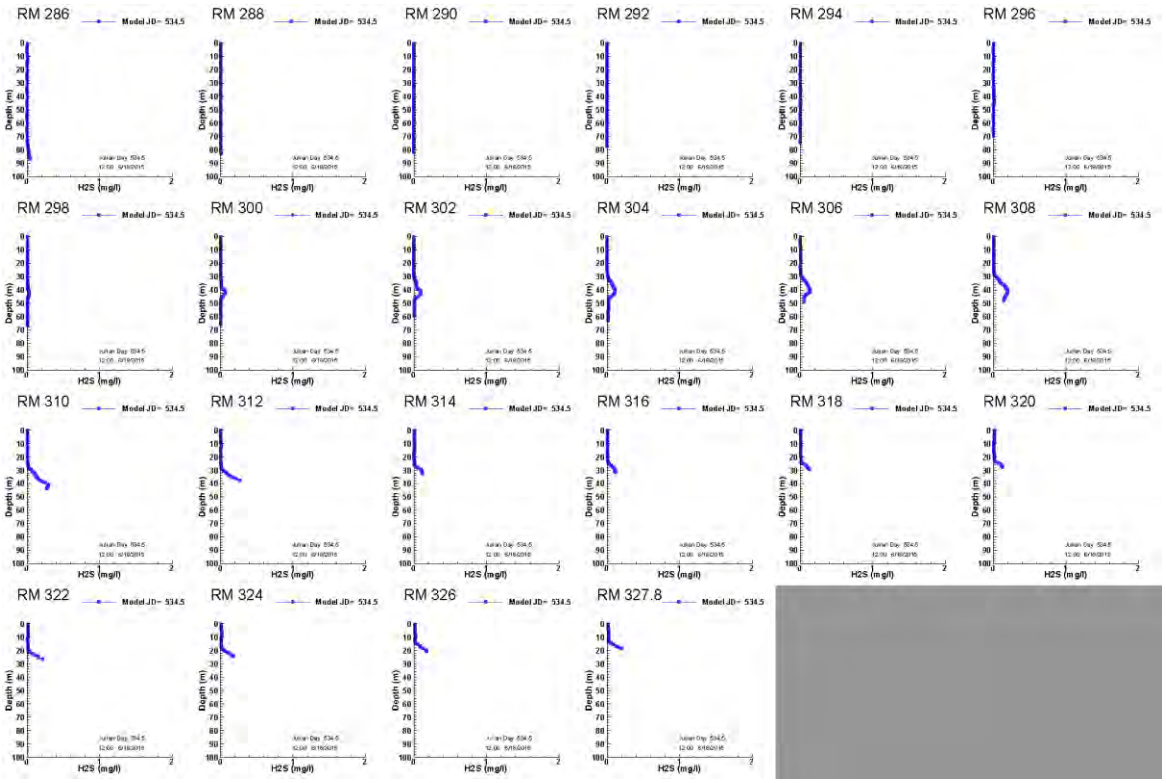


Figure 137. Vertical profiles of hydrogen sulfide compared with data for 6/18/2015.

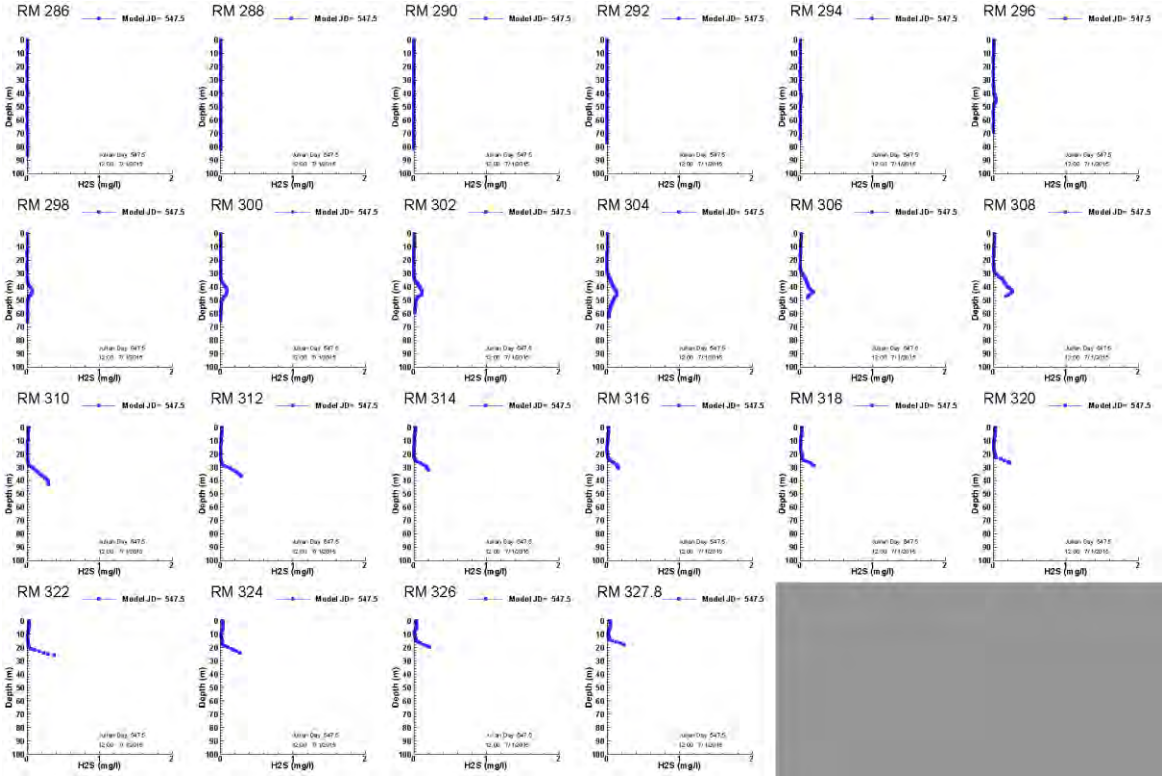


Figure 138. Vertical profiles of hydrogen sulfide compared with data for 7/ 1/2015.

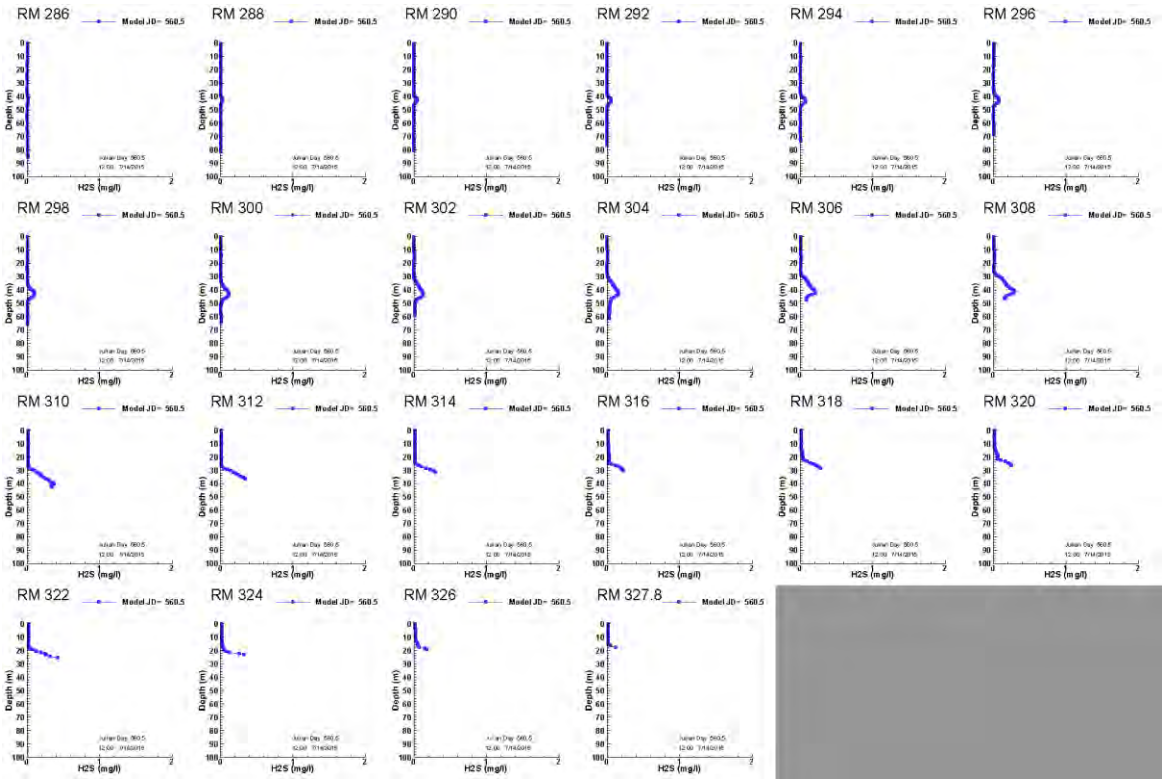


Figure 139. Vertical profiles of hydrogen sulfide compared with data for 7/14/2015.

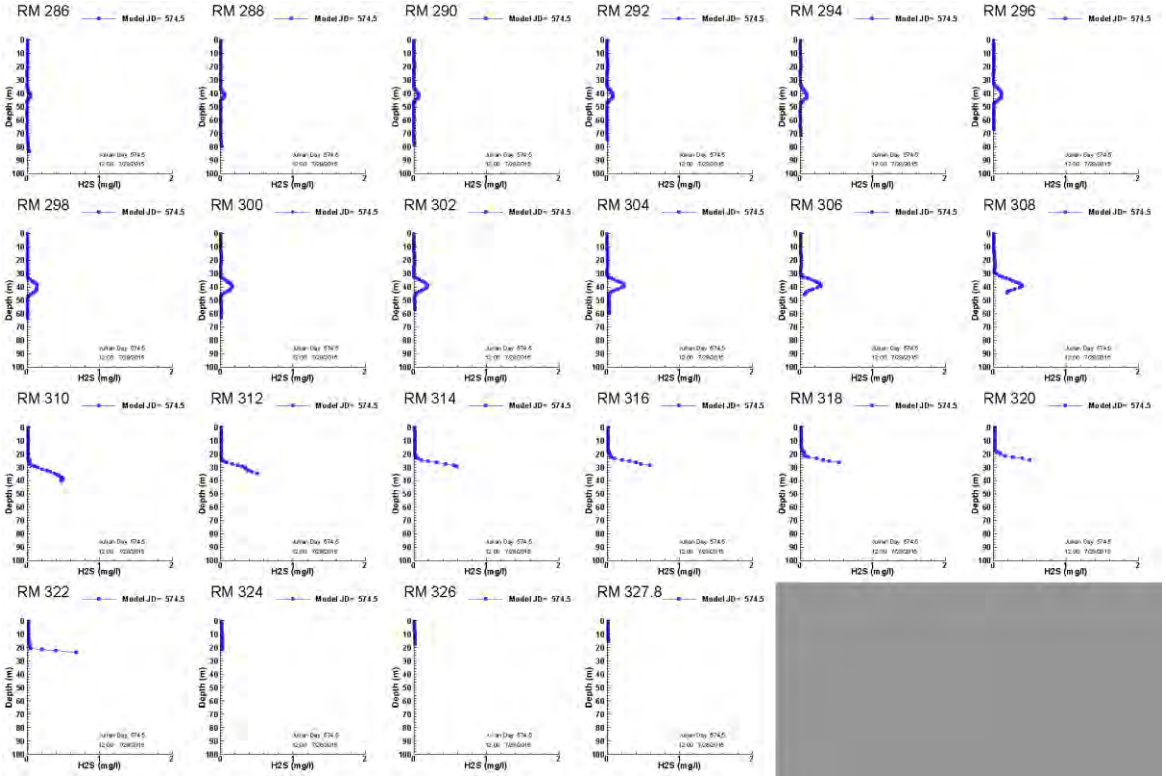


Figure 140. Vertical profiles of hydrogen sulfide compared with data for 7/28/2015.

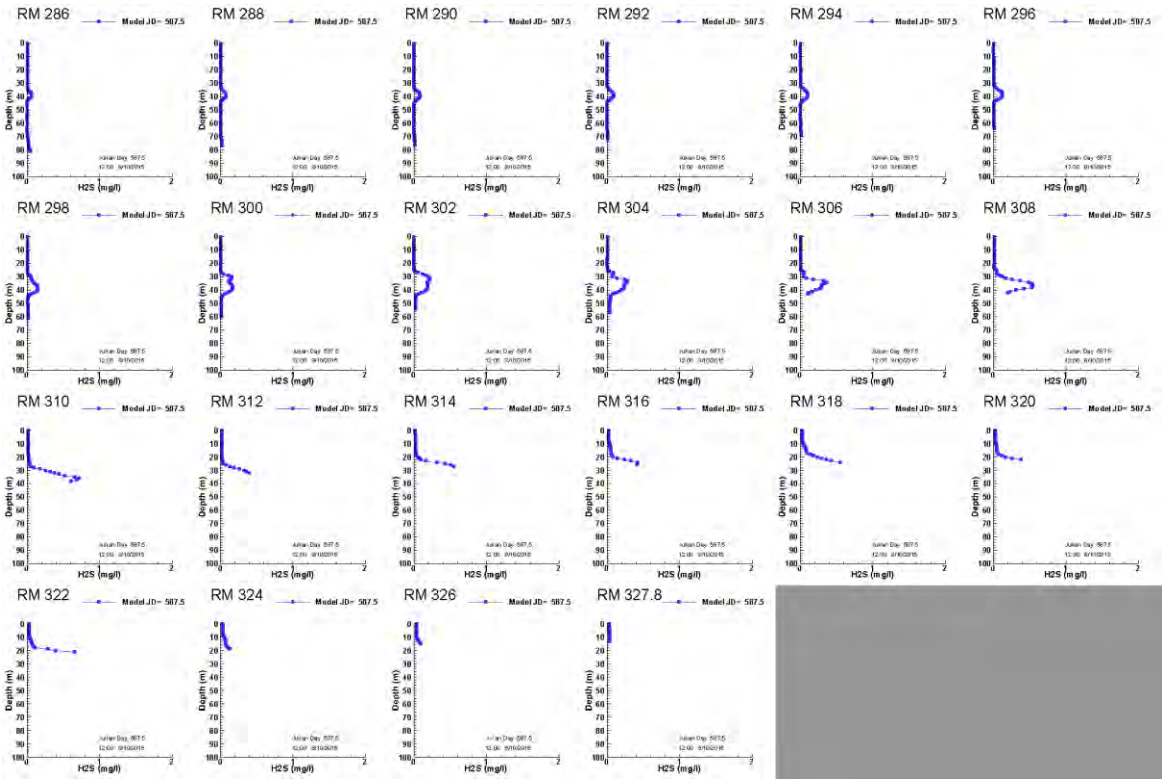


Figure 141. Vertical profiles of hydrogen sulfide compared with data for 8/10/2015.

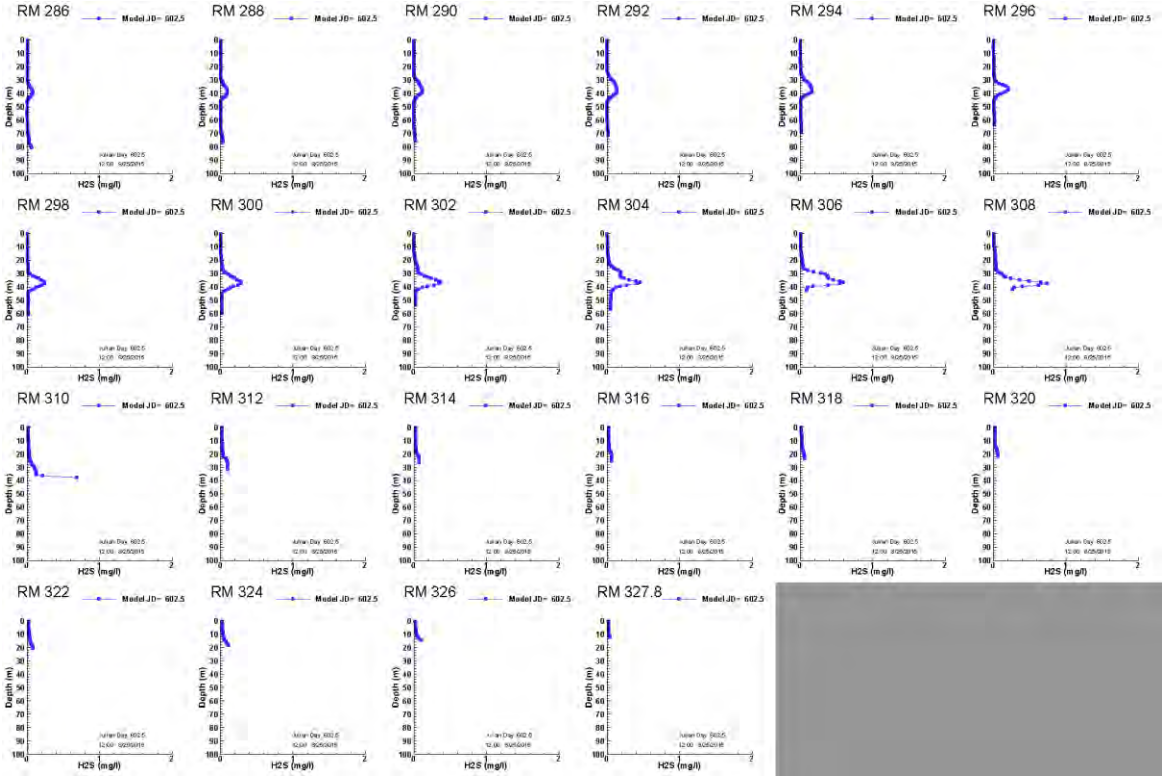


Figure 142. Vertical profiles of hydrogen sulfide compared with data for 8/25/2015.

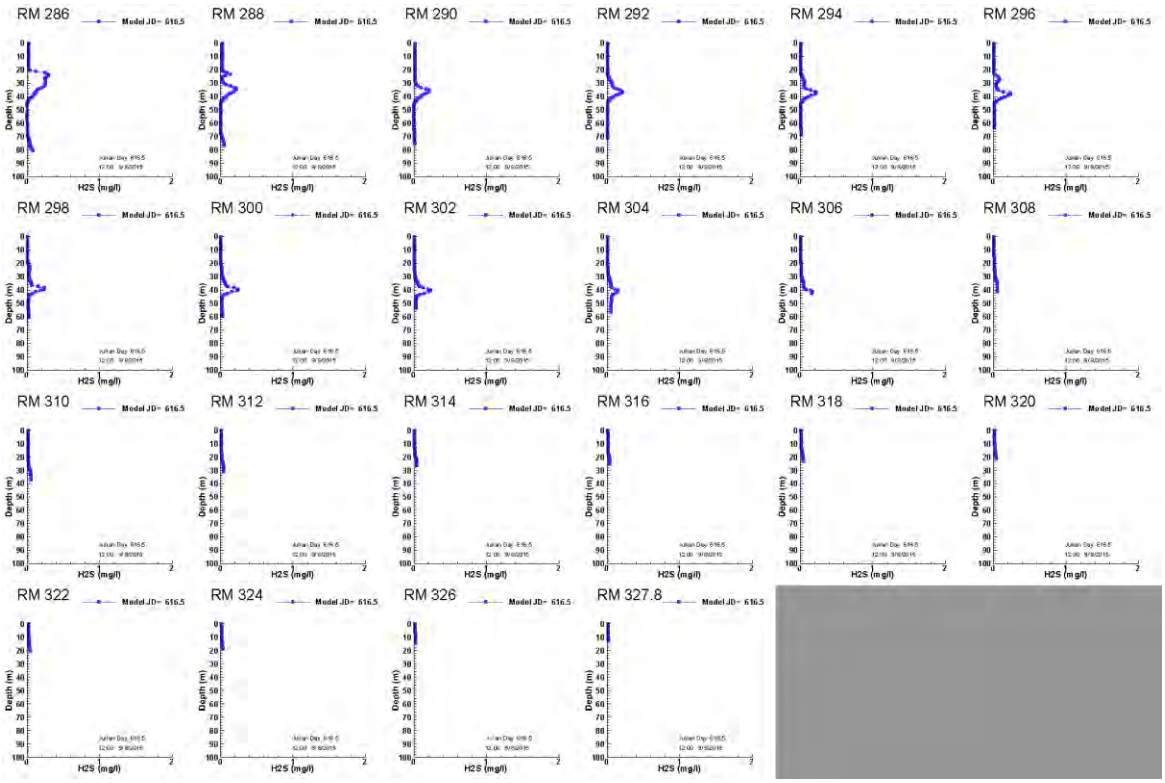


Figure 143. Vertical profiles of hydrogen sulfide compared with data for 9/ 8/2015.

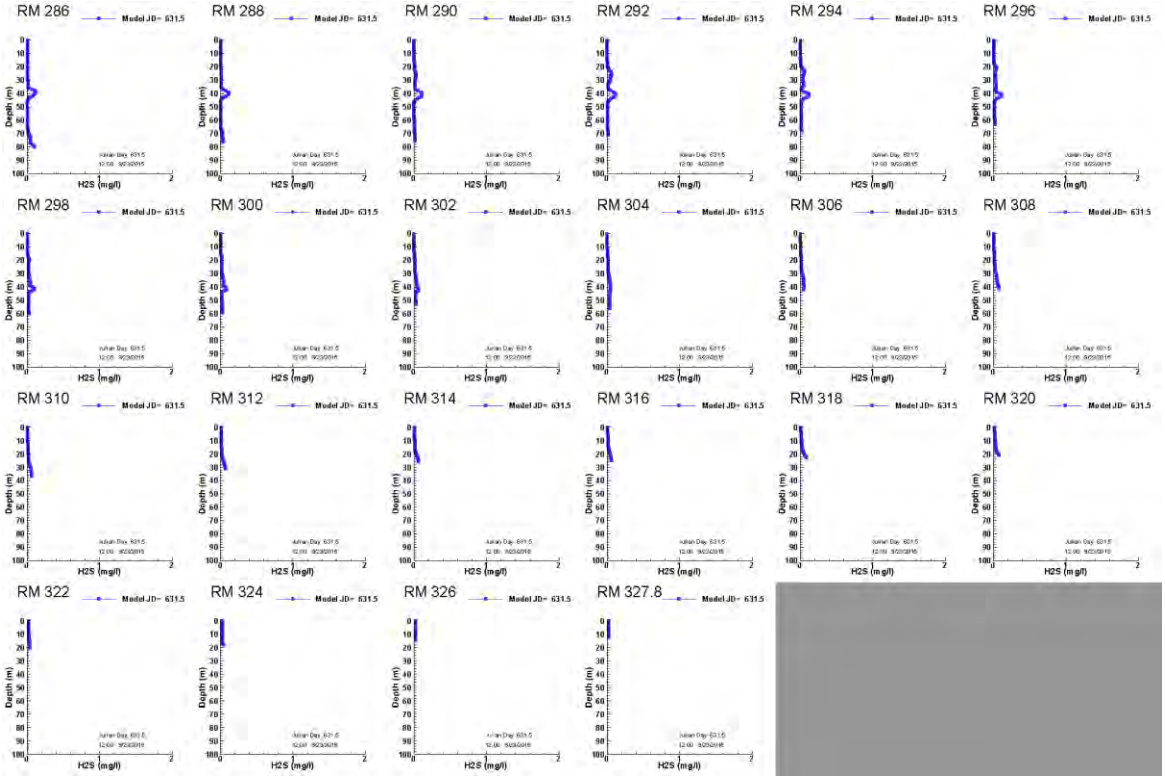


Figure 144. Vertical profiles of hydrogen sulfide compared with data for 9/23/2015.

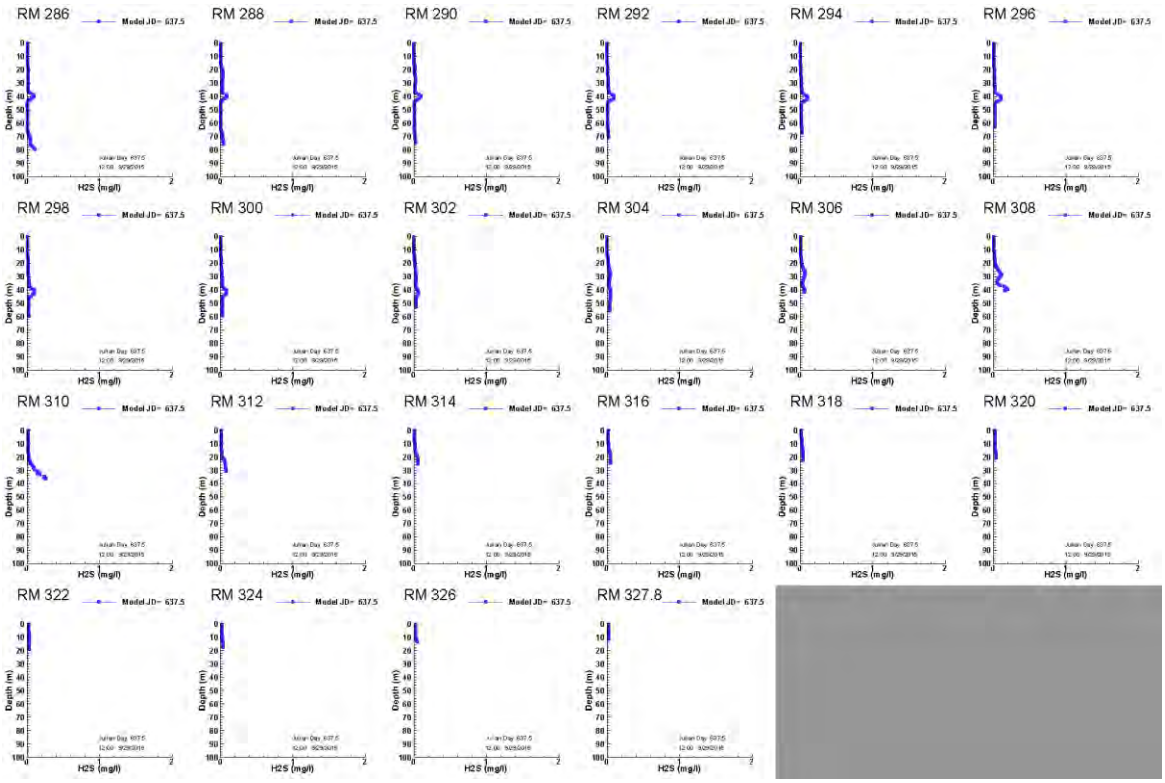


Figure 145. Vertical profiles of hydrogen sulfide compared with data for 9/29/2015.

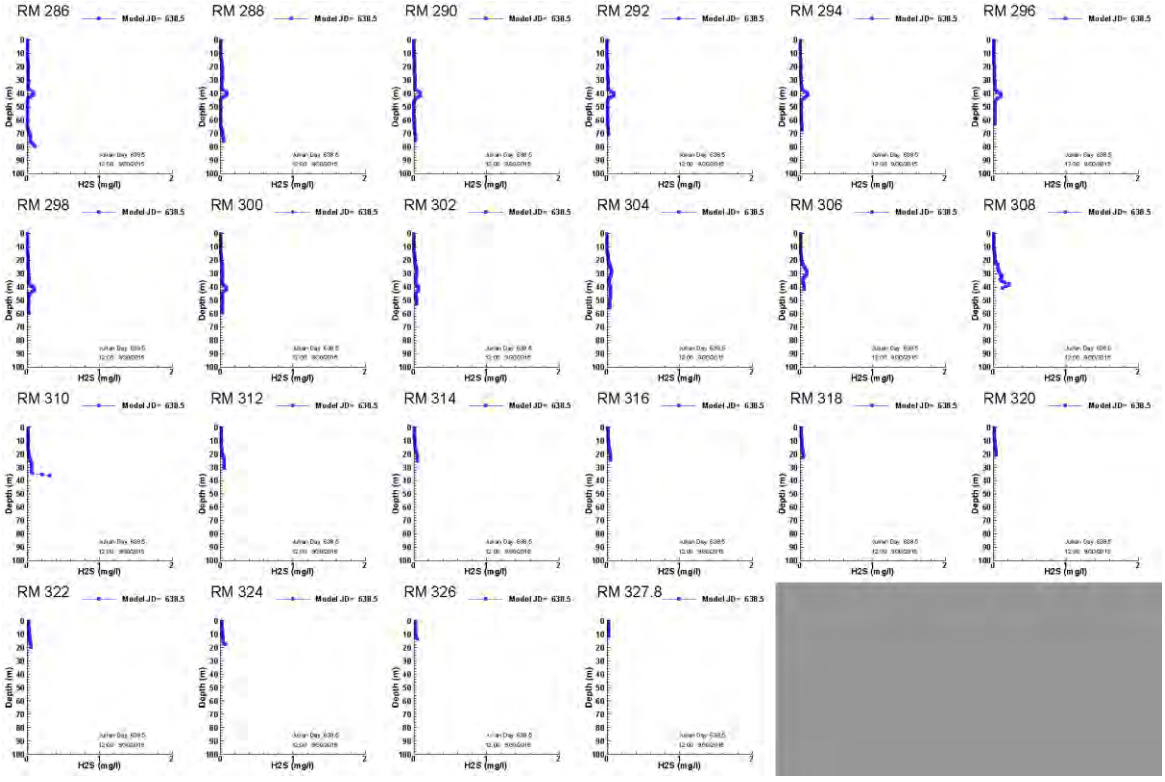


Figure 146. Vertical profiles of hydrogen sulfide compared with data for 9/30/2015.

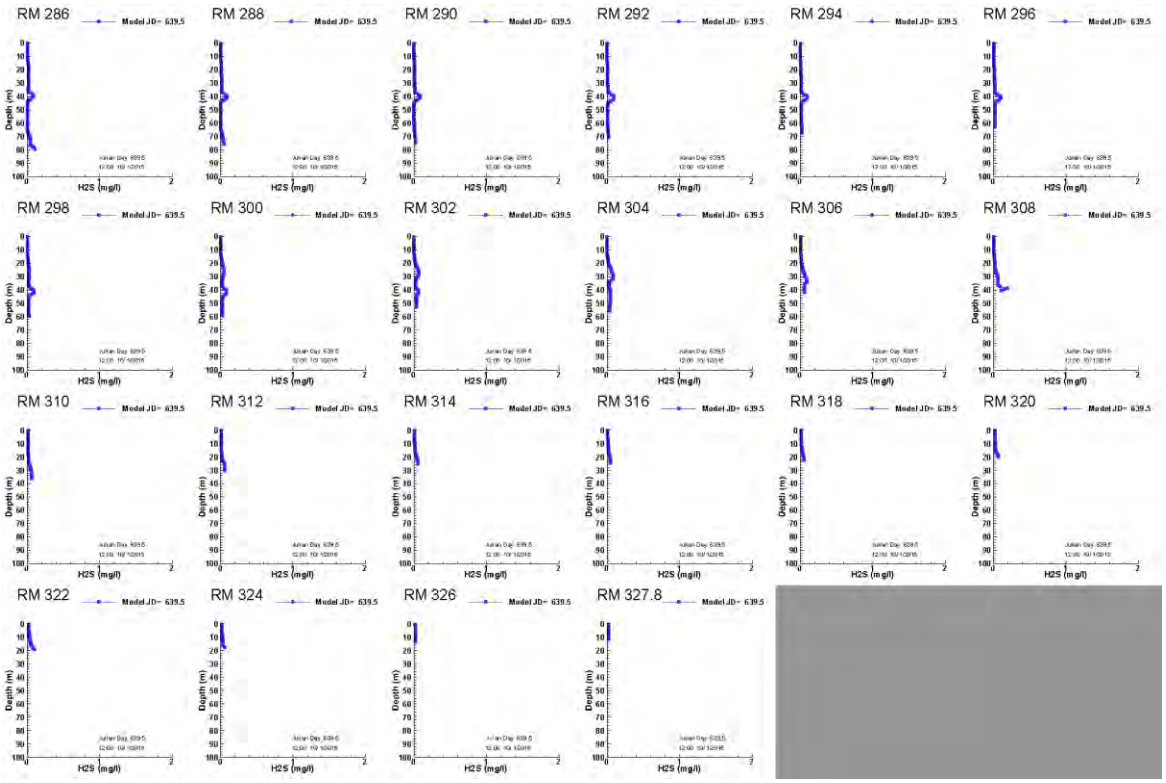


Figure 147. Vertical profiles of hydrogen sulfide compared with data for 10/ 1/2015.

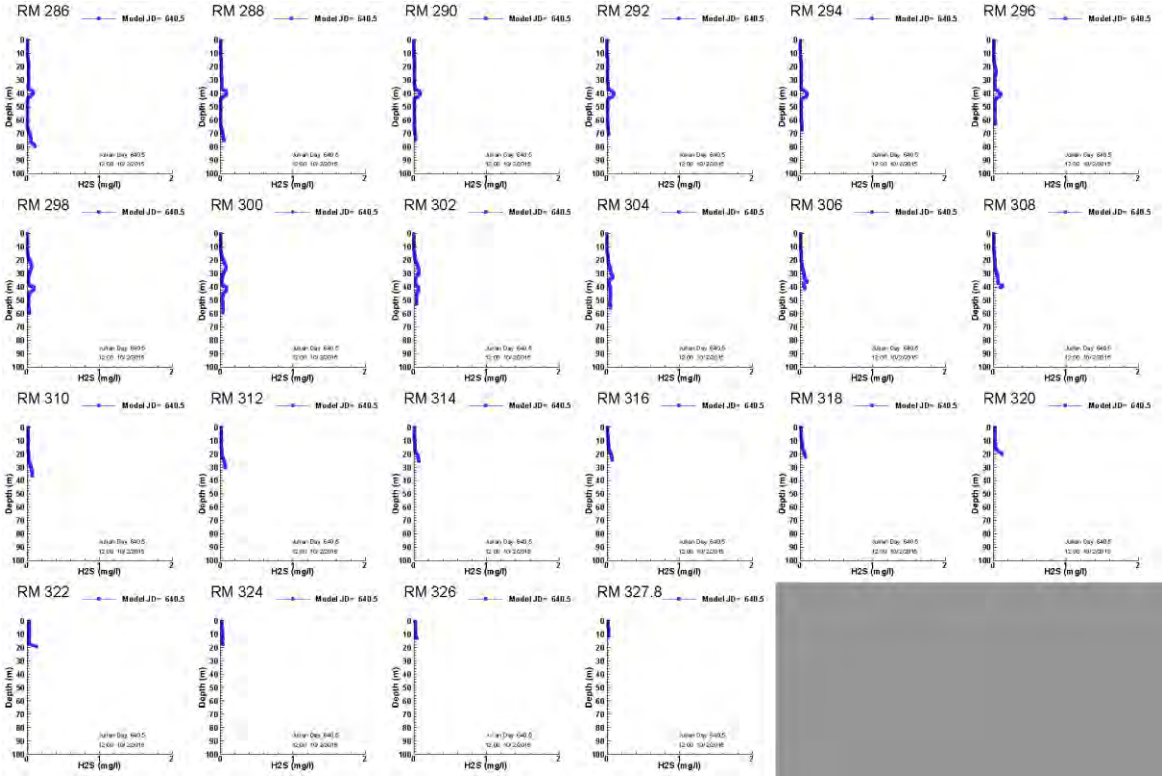


Figure 148. Vertical profiles of hydrogen sulfide compared with data for 10/ 2/2015.

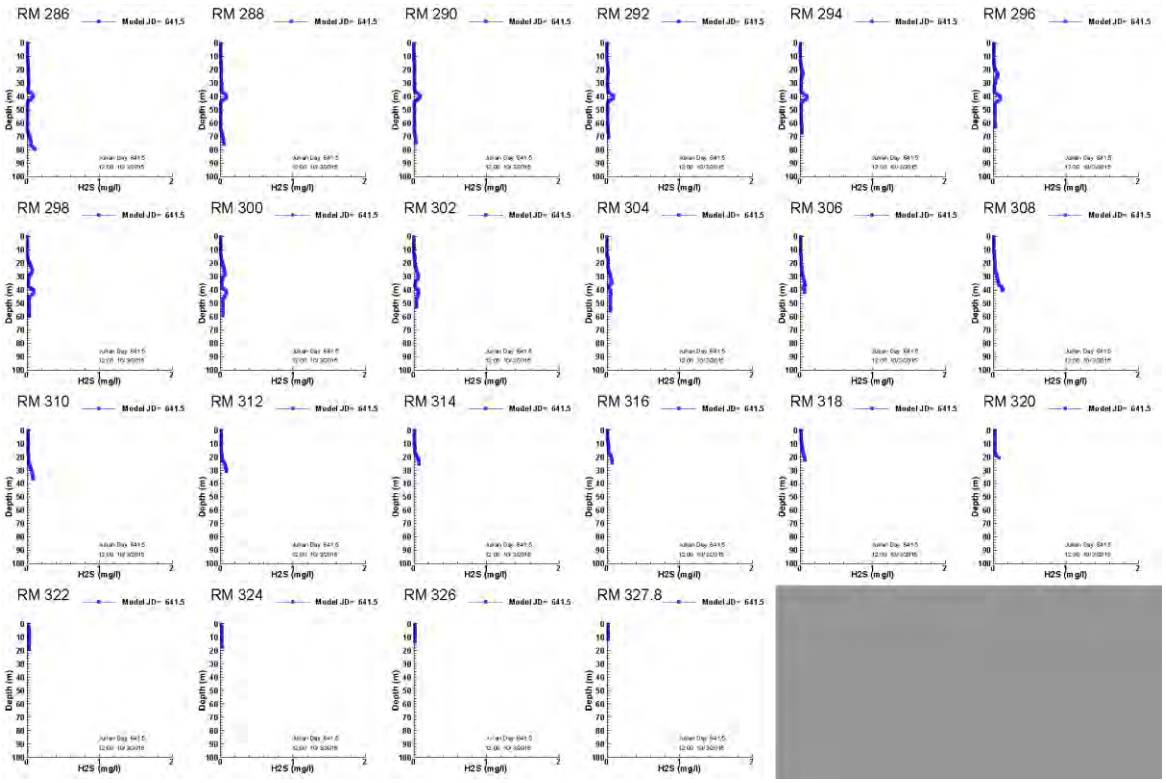


Figure 149. Vertical profiles of hydrogen sulfide compared with data for 10/ 3/2015.

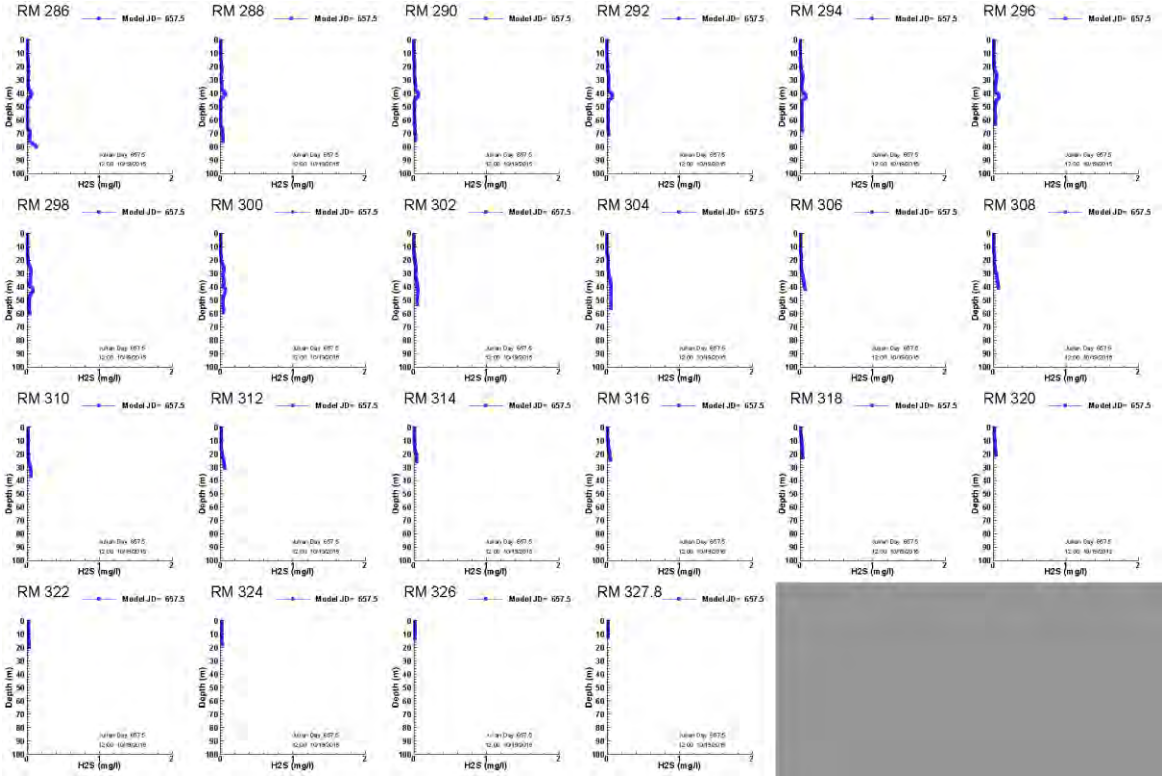


Figure 150. Vertical profiles of hydrogen sulfide compared with data for 10/19/2015.

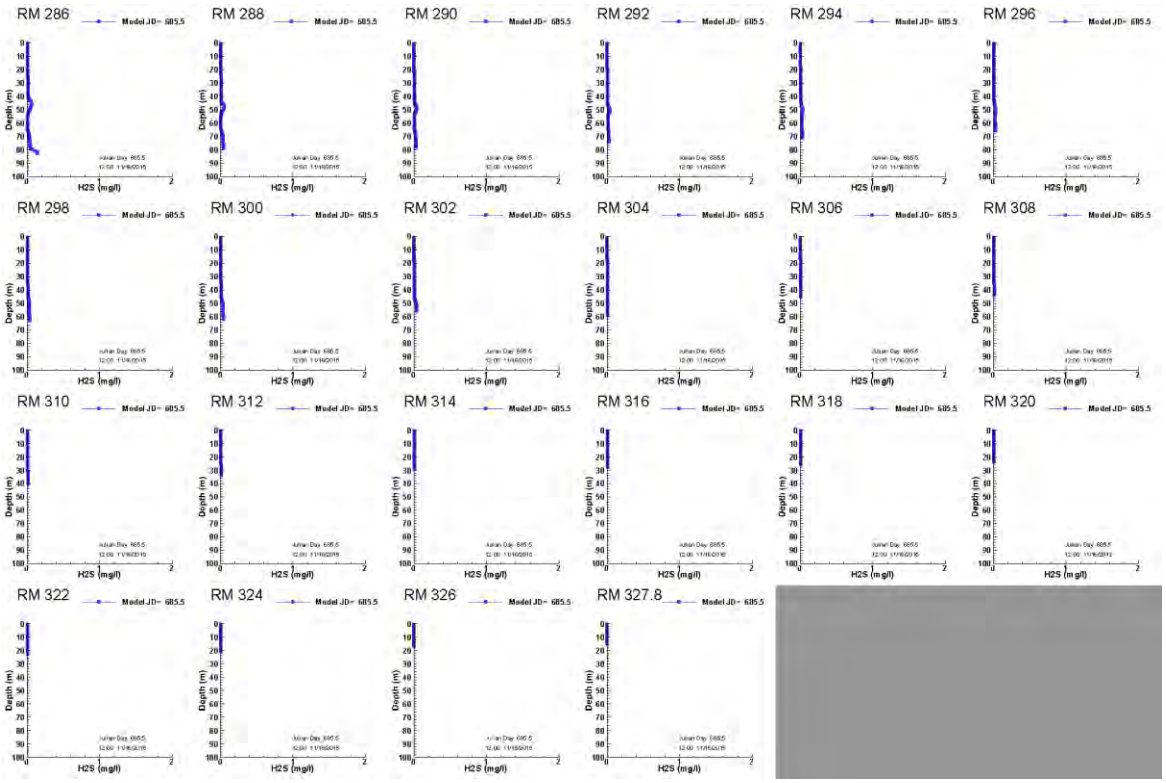


Figure 151. Vertical profiles of hydrogen sulfide compared with data for 11/16/2015.

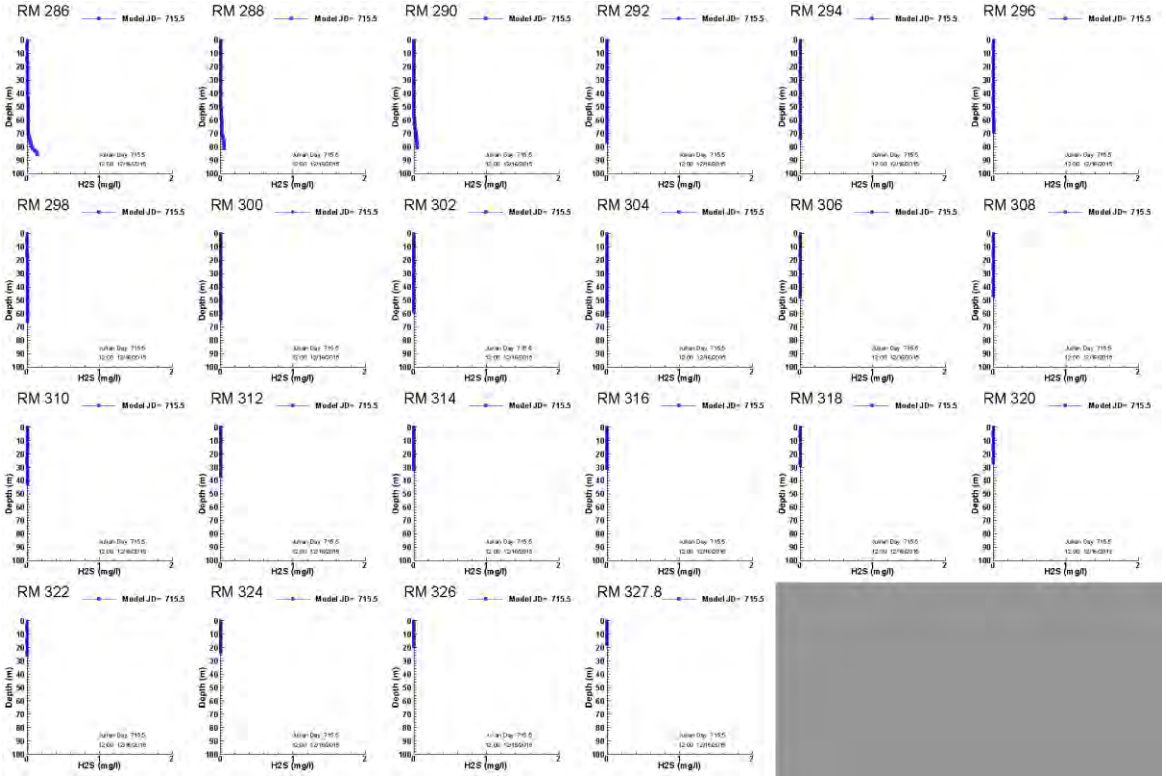


Figure 152. Vertical profiles of hydrogen sulfide compared with data for 12/16/2015.

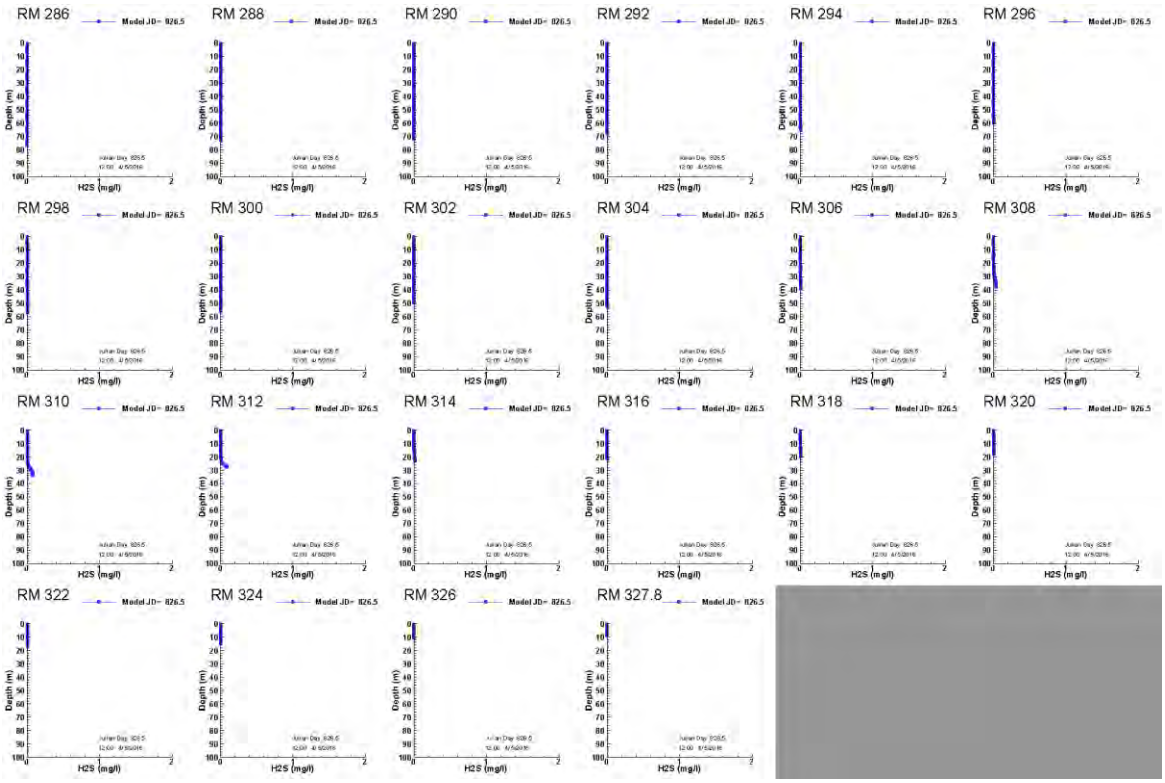


Figure 153. Vertical profiles of hydrogen sulfide compared with data for 4/ 5/2016.

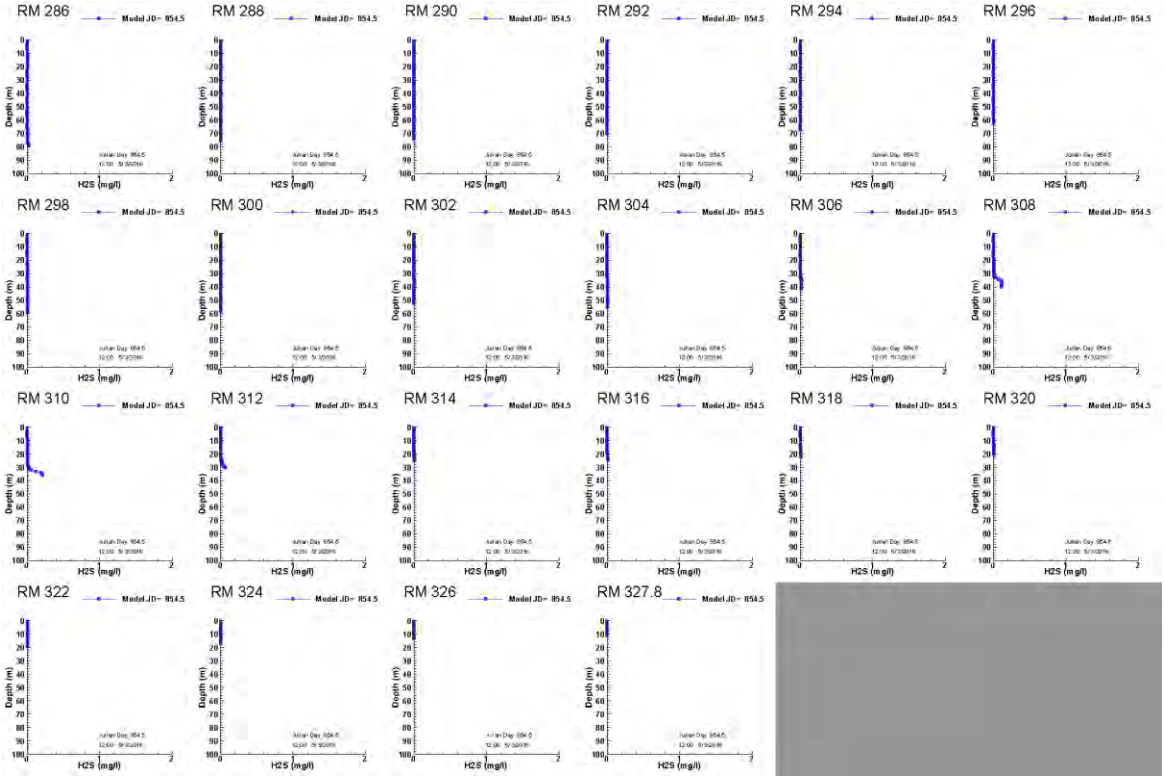


Figure 154. Vertical profiles of hydrogen sulfide compared with data for 5/ 3/2016.

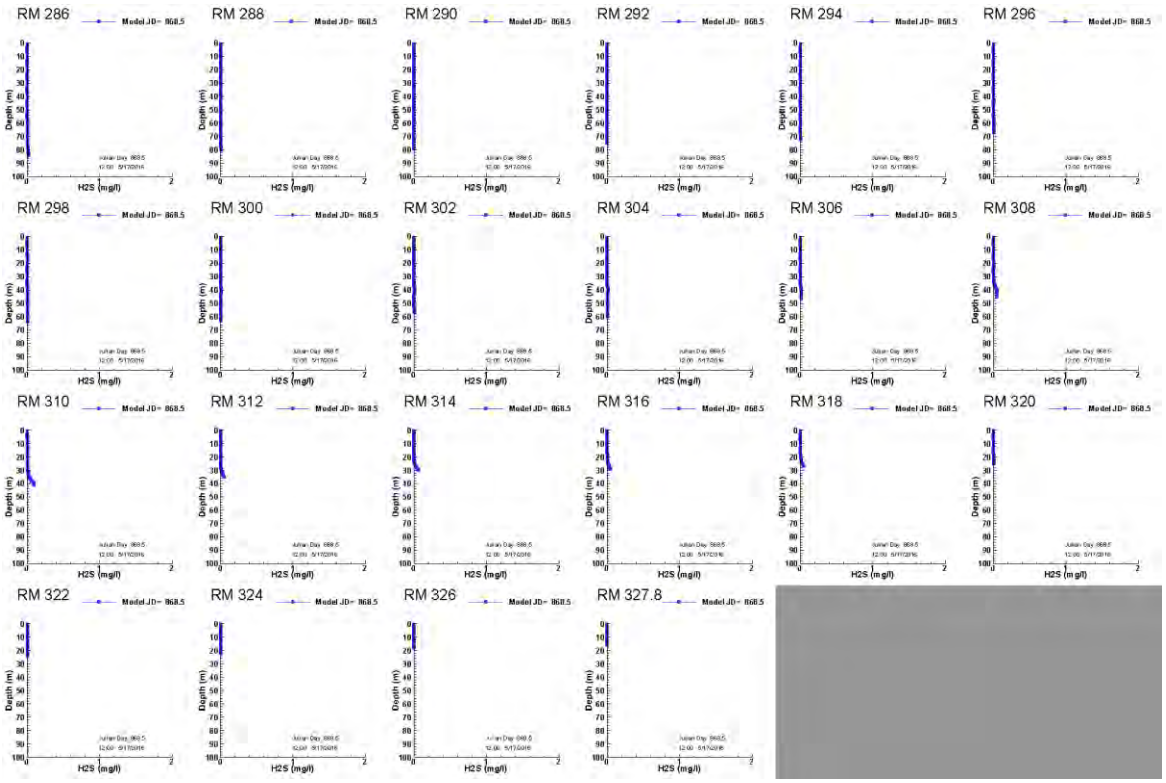


Figure 155. Vertical profiles of hydrogen sulfide compared with data for 5/17/2016.

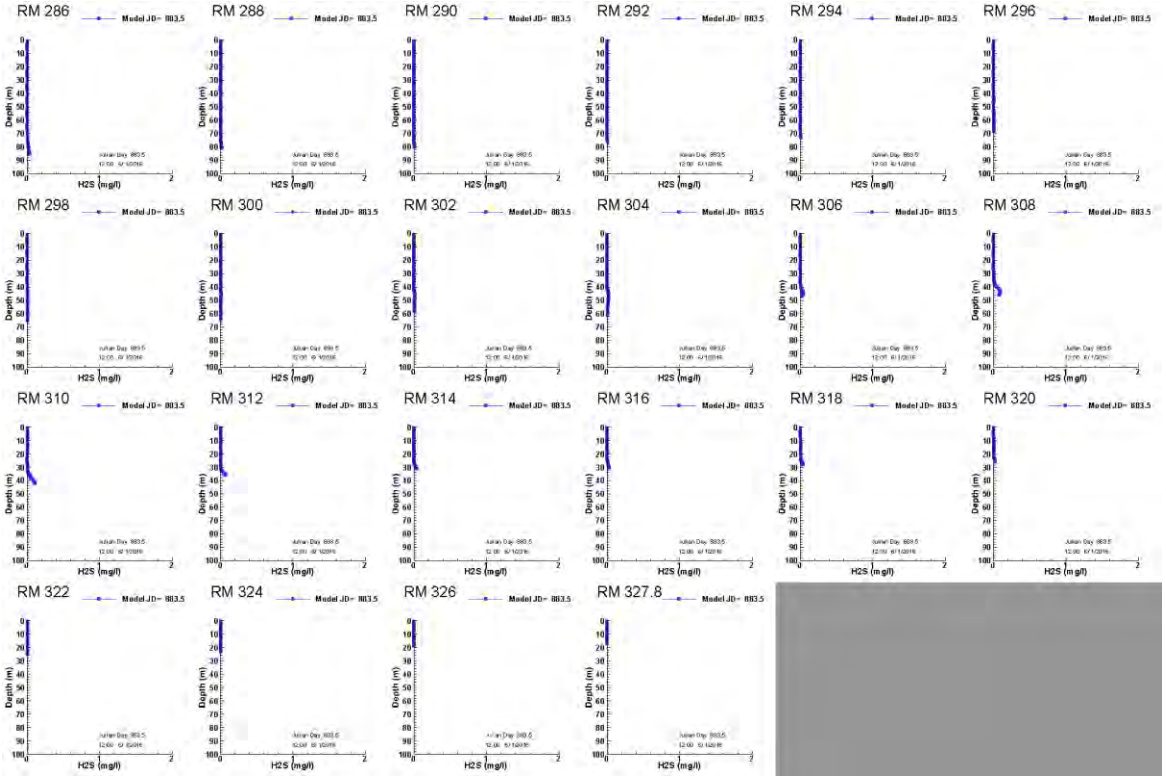


Figure 156. Vertical profiles of hydrogen sulfide compared with data for 6/ 1/2016.

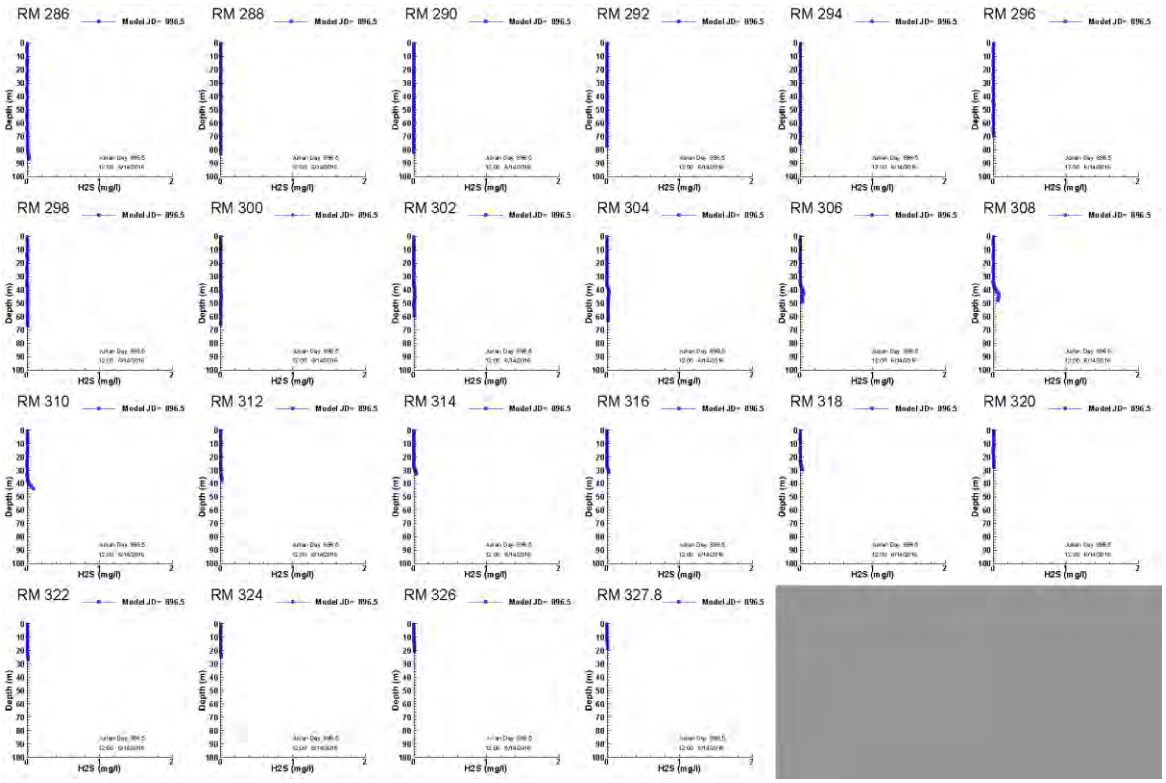


Figure 157. Vertical profiles of hydrogen sulfide compared with data for 6/14/2016.

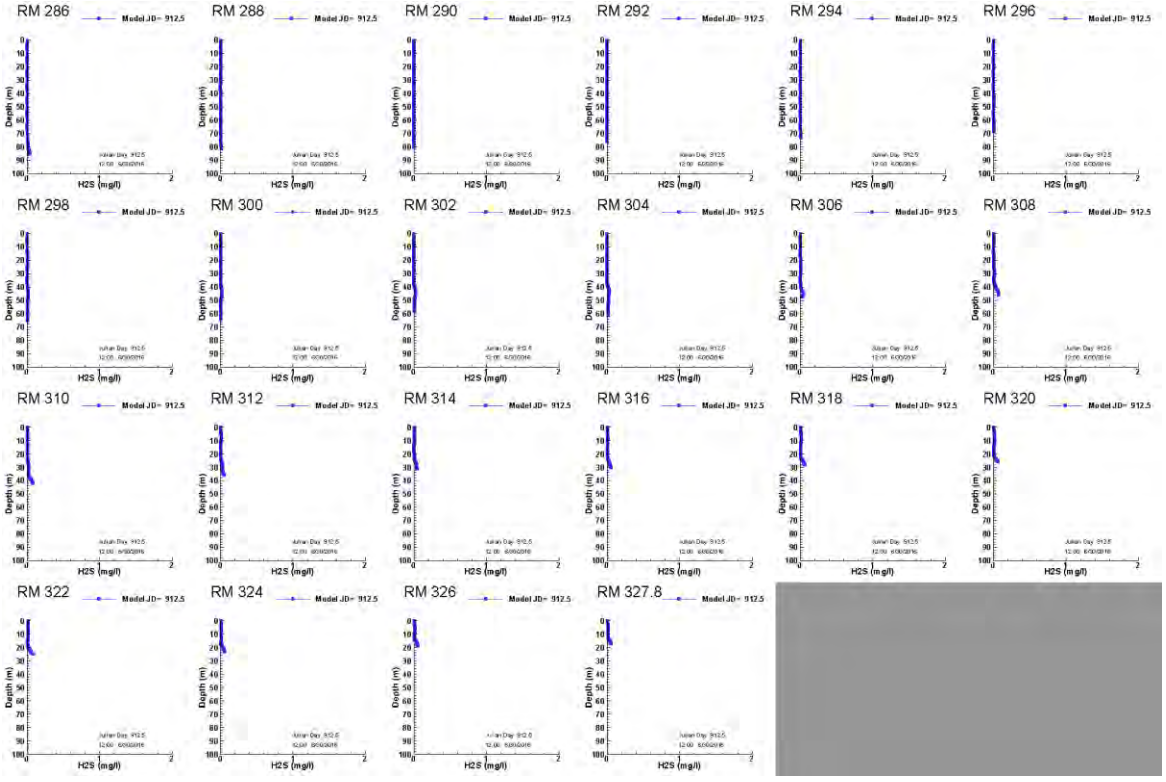


Figure 158. Vertical profiles of hydrogen sulfide compared with data for 6/30/2016.

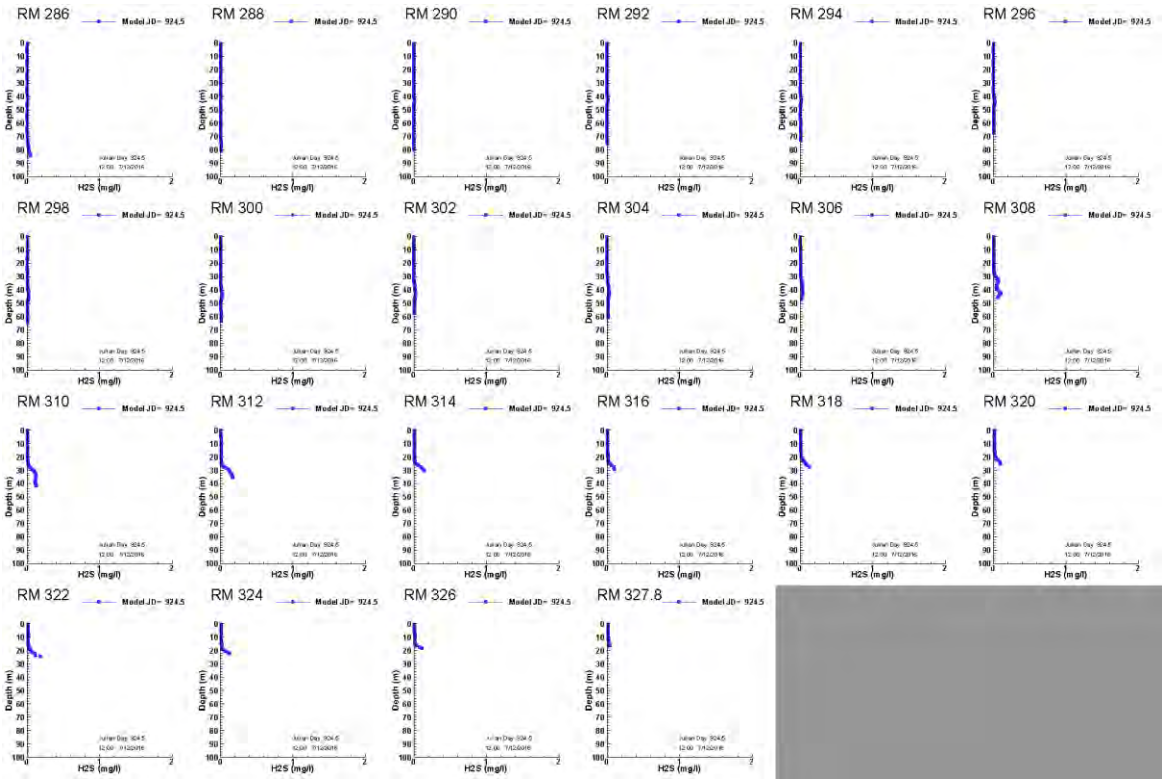


Figure 159. Vertical profiles of hydrogen sulfide compared with data for 7/12/2016.

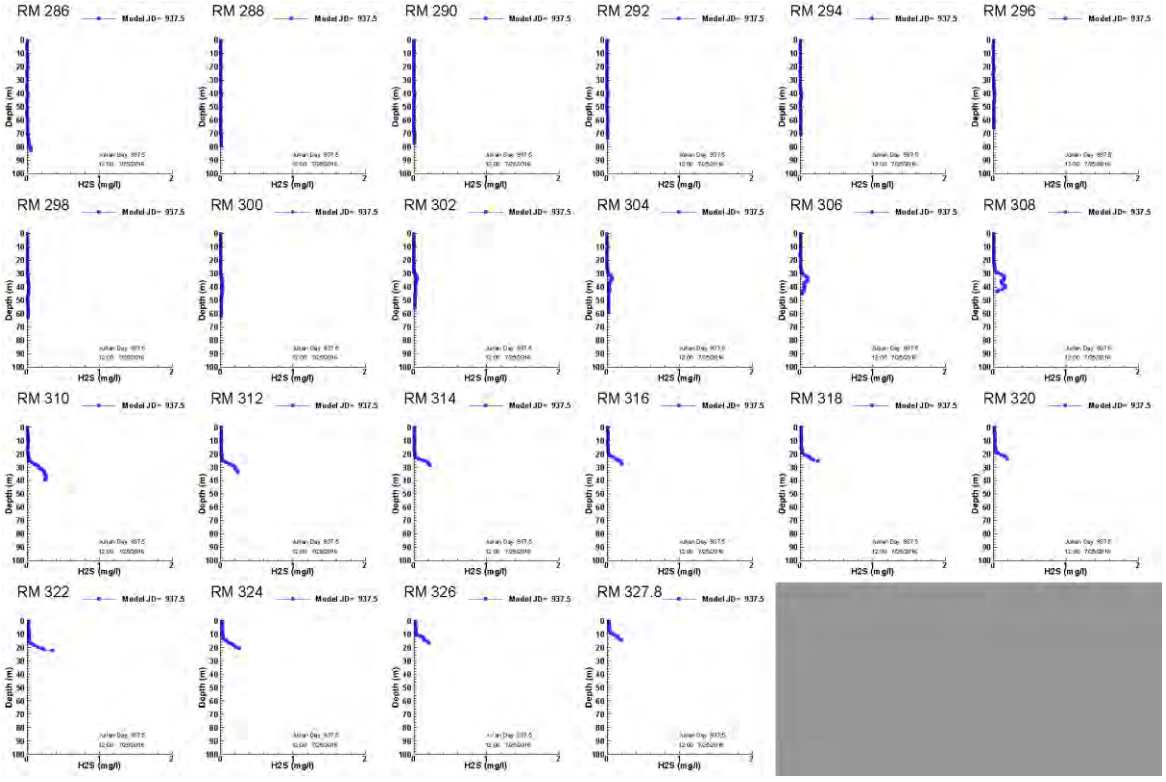


Figure 160. Vertical profiles of hydrogen sulfide compared with data for 7/25/2016.

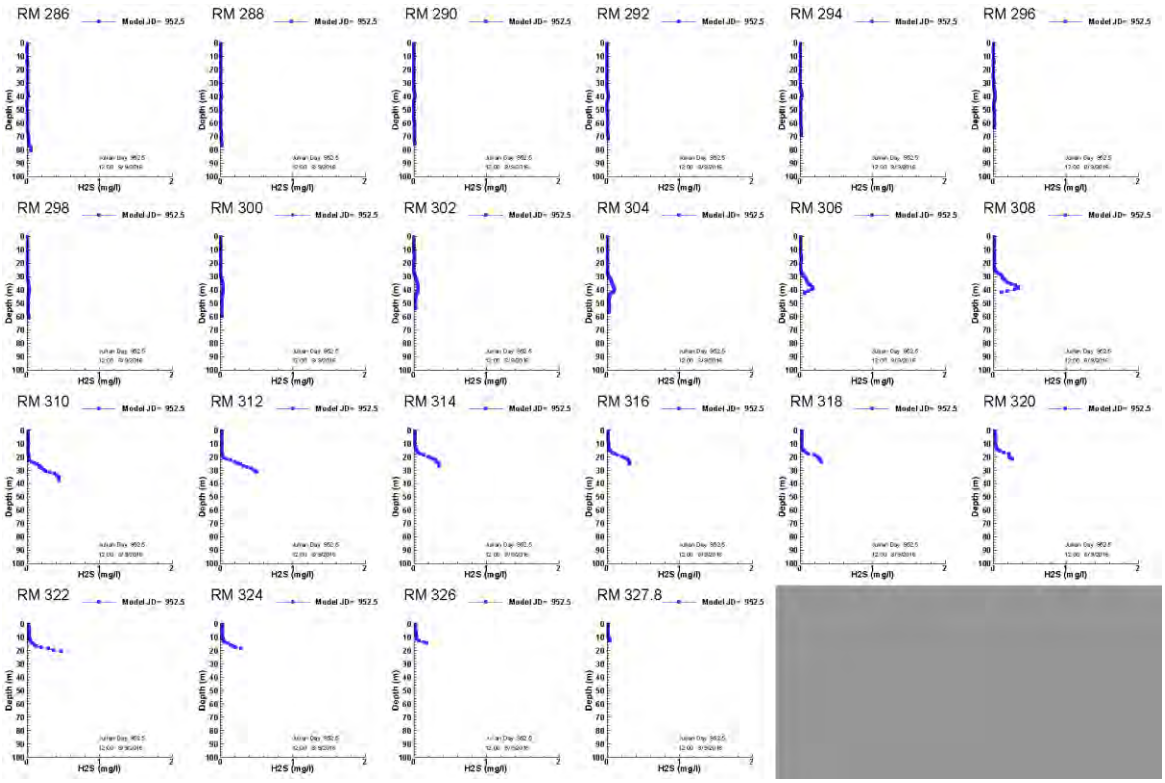


Figure 161. Vertical profiles of hydrogen sulfide compared with data for 8/ 9/2016.

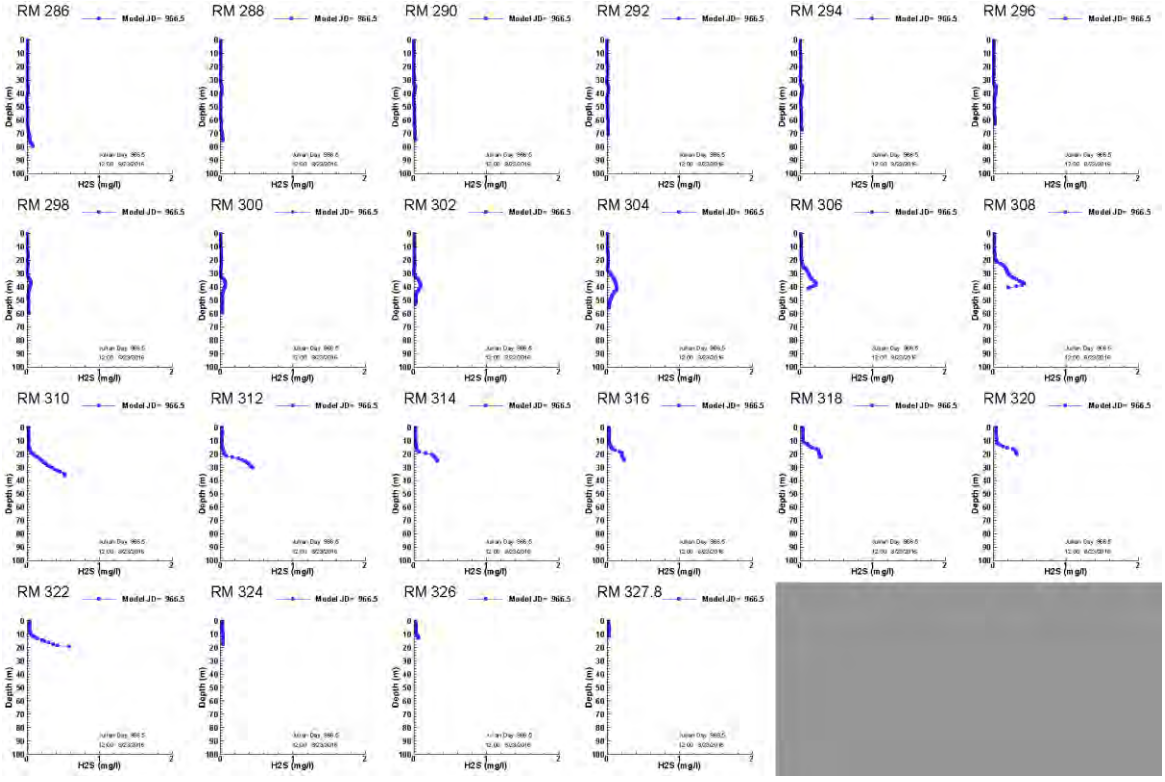


Figure 162. Vertical profiles of hydrogen sulfide compared with data for 8/23/2016.

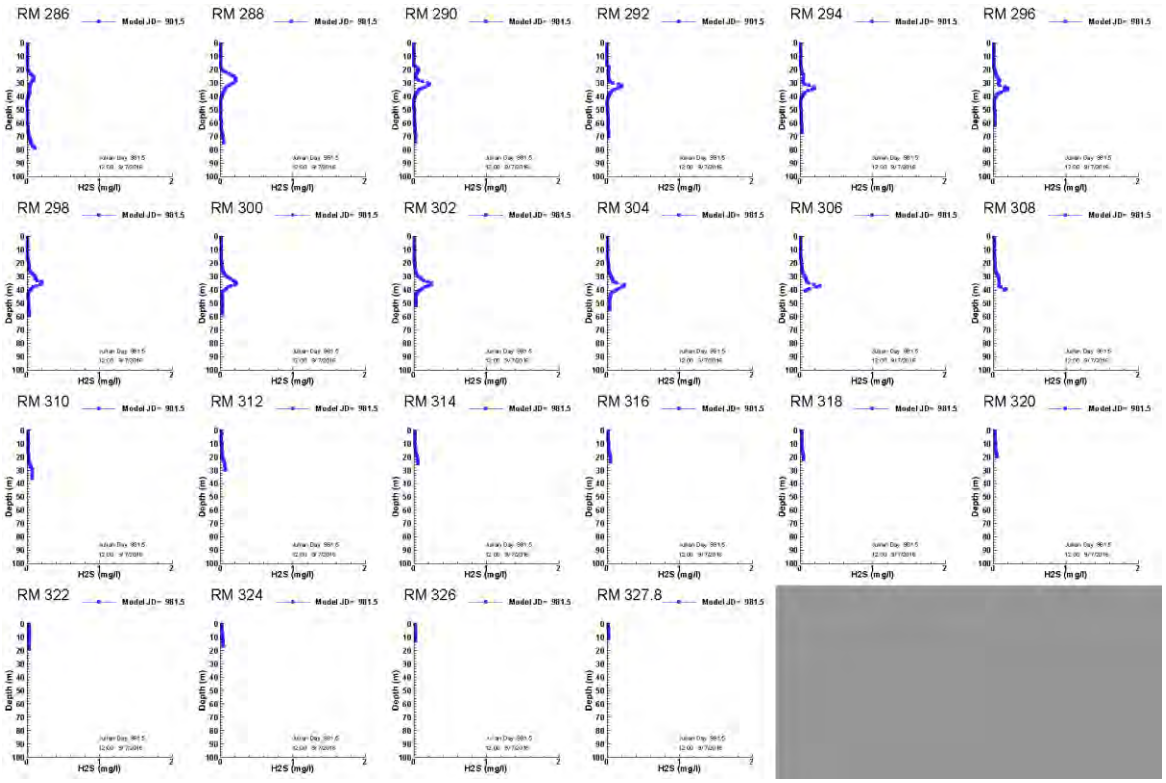


Figure 163. Vertical profiles of hydrogen sulfide compared with data for 9/ 7/2016.

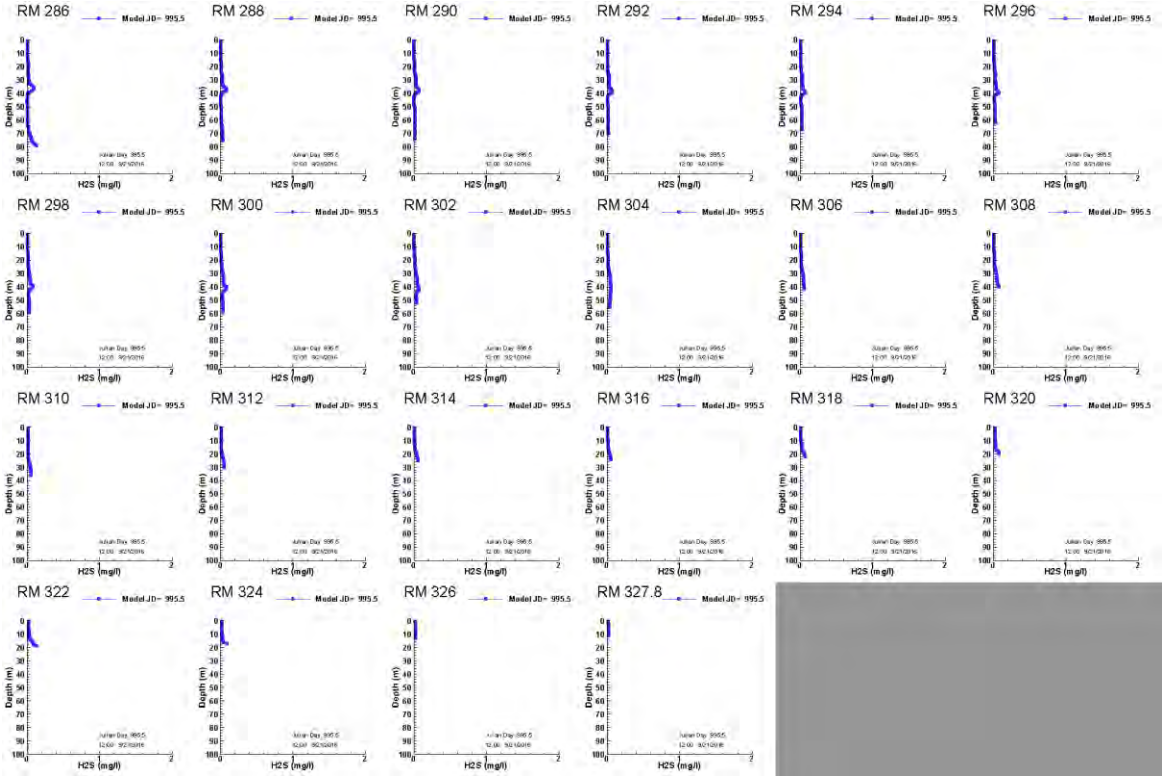


Figure 164. Vertical profiles of hydrogen sulfide compared with data for 9/21/2016.

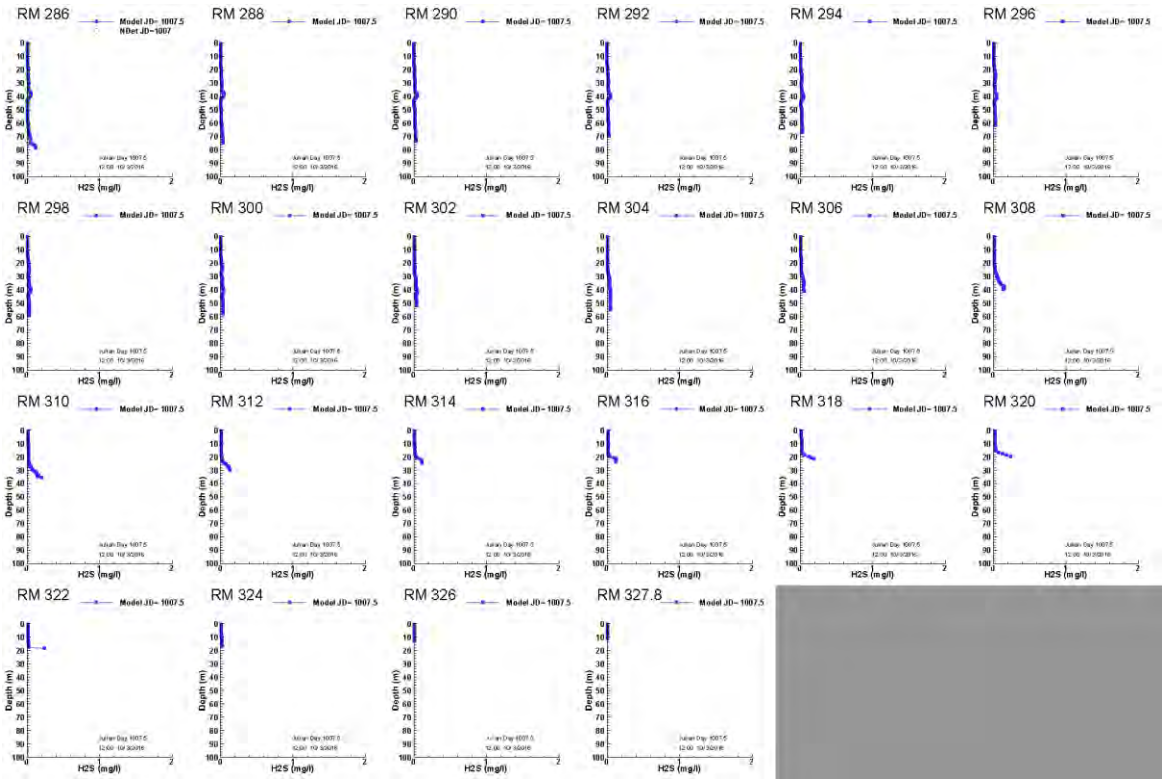


Figure 165. Vertical profiles of hydrogen sulfide compared with data for 10/ 3/2016.

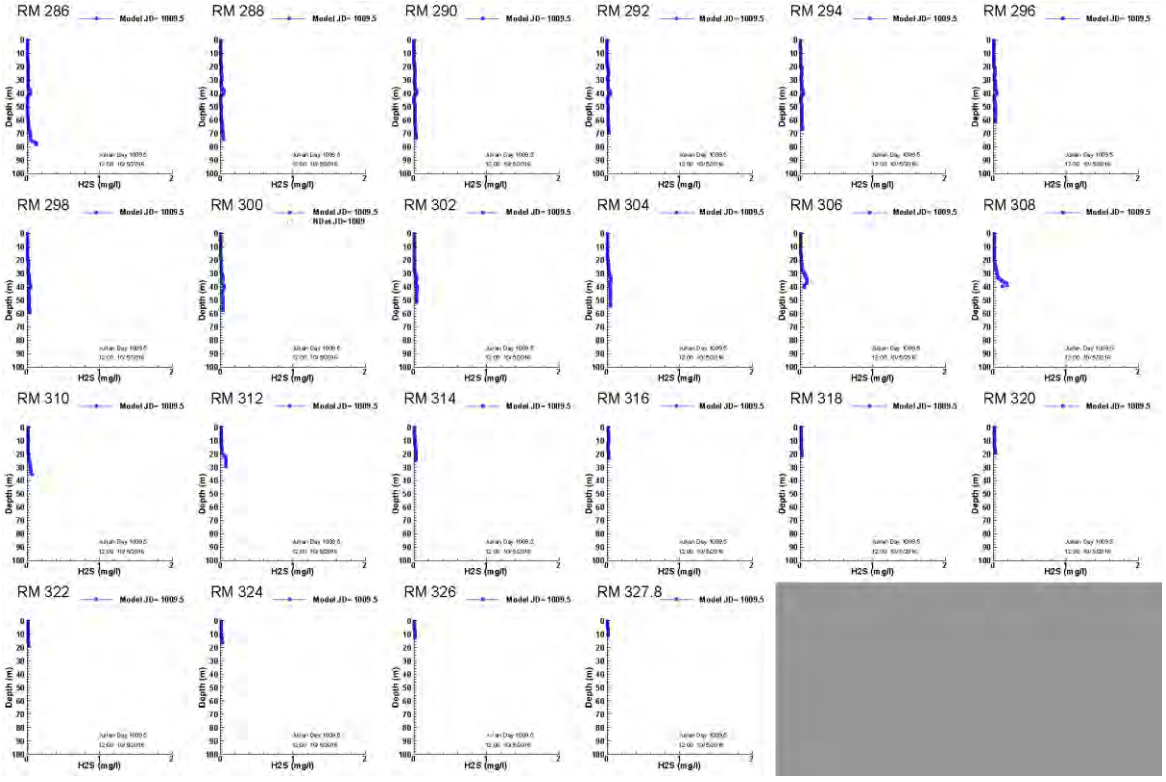


Figure 166. Vertical profiles of hydrogen sulfide compared with data for 10/ 5/2016.

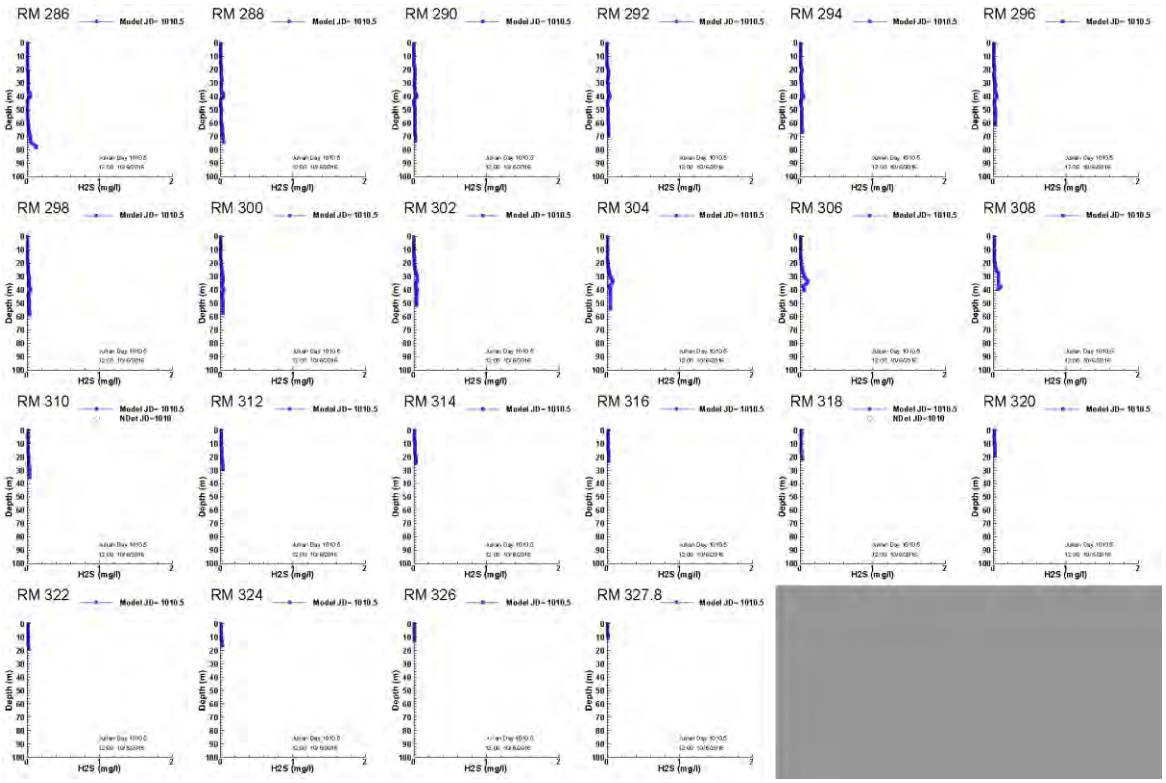


Figure 167. Vertical profiles of hydrogen sulfide compared with data for 10/ 6/2016.

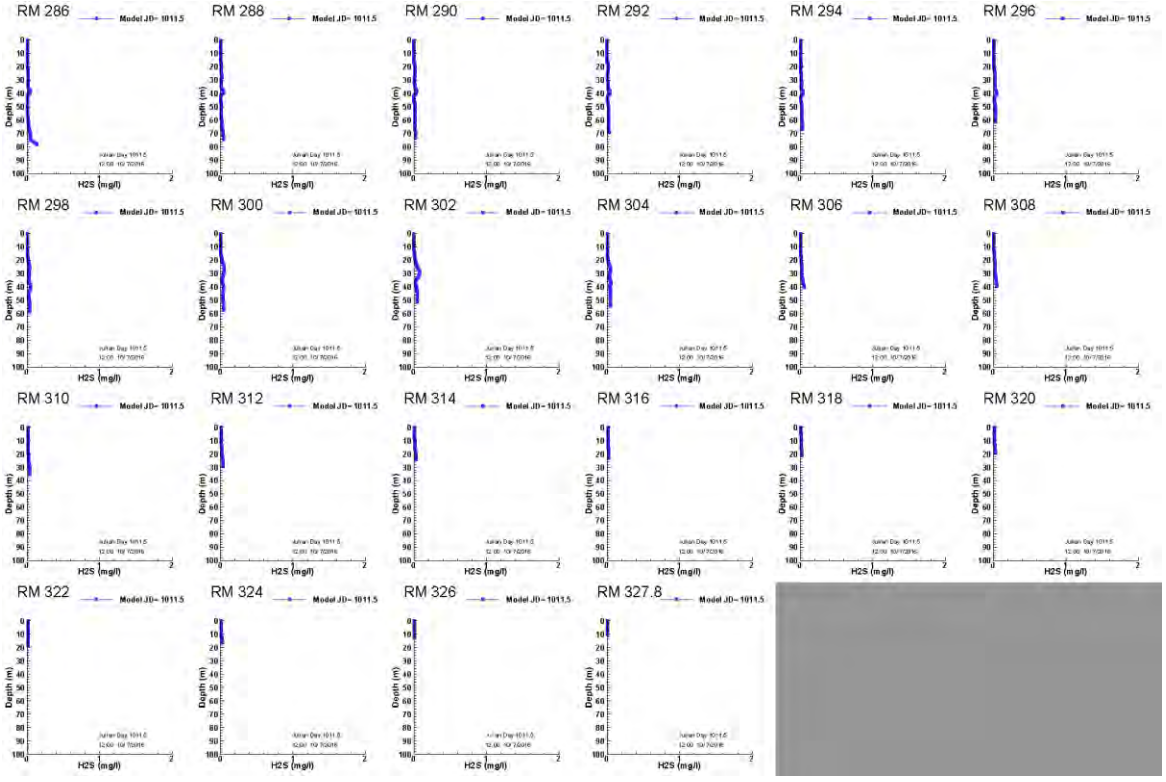


Figure 168. Vertical profiles of hydrogen sulfide compared with data for 10/ 7/2016.

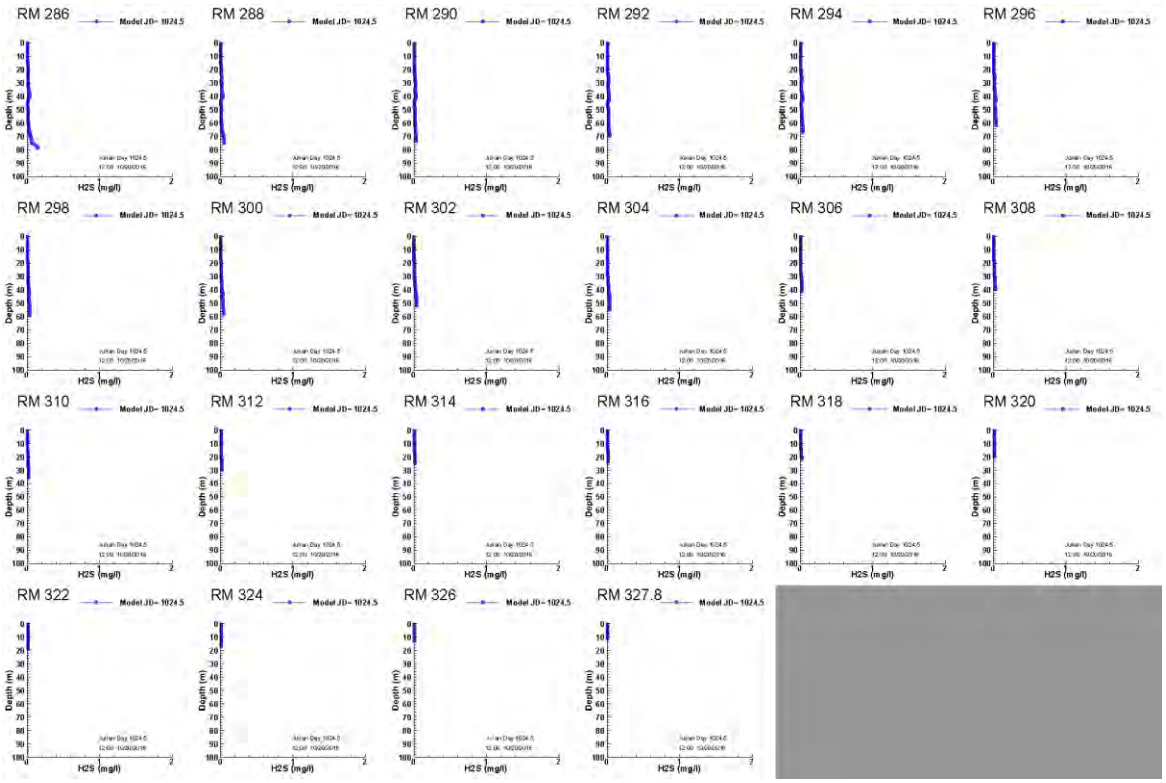


Figure 169. Vertical profiles of hydrogen sulfide compared with data for 10/20/2016.

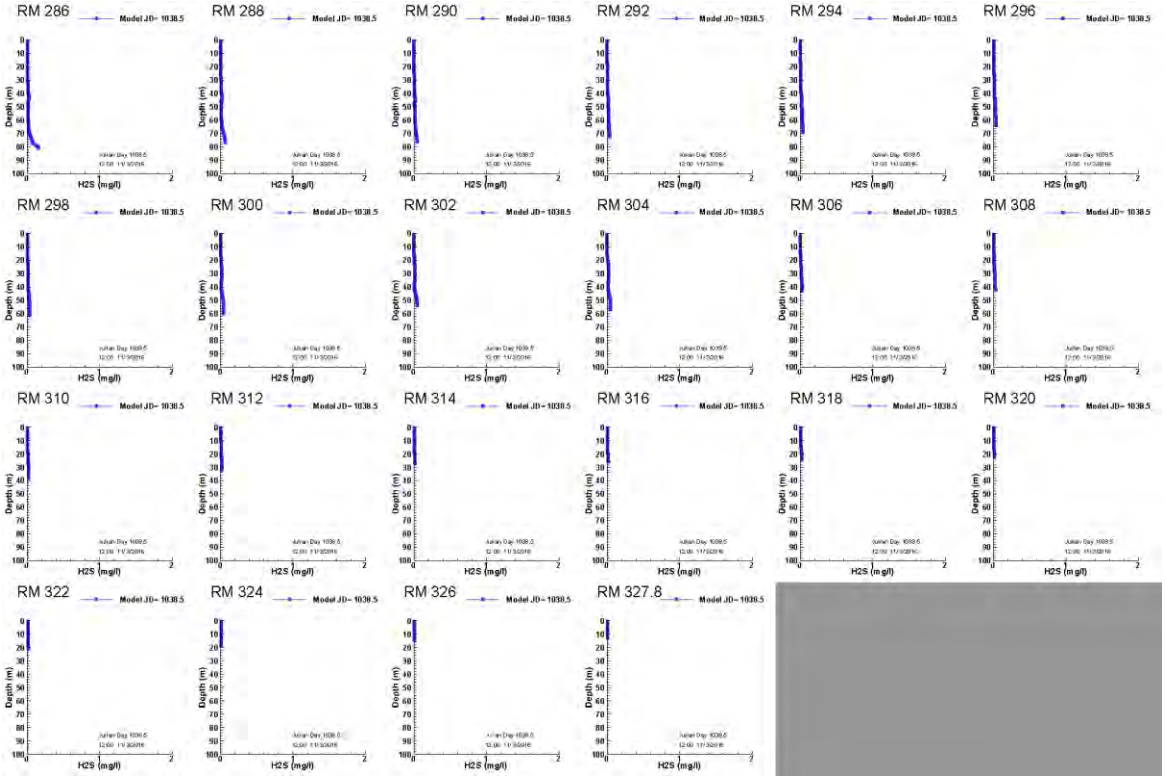


Figure 170. Vertical profiles of hydrogen sulfide compared with data for 11/ 3/2016.

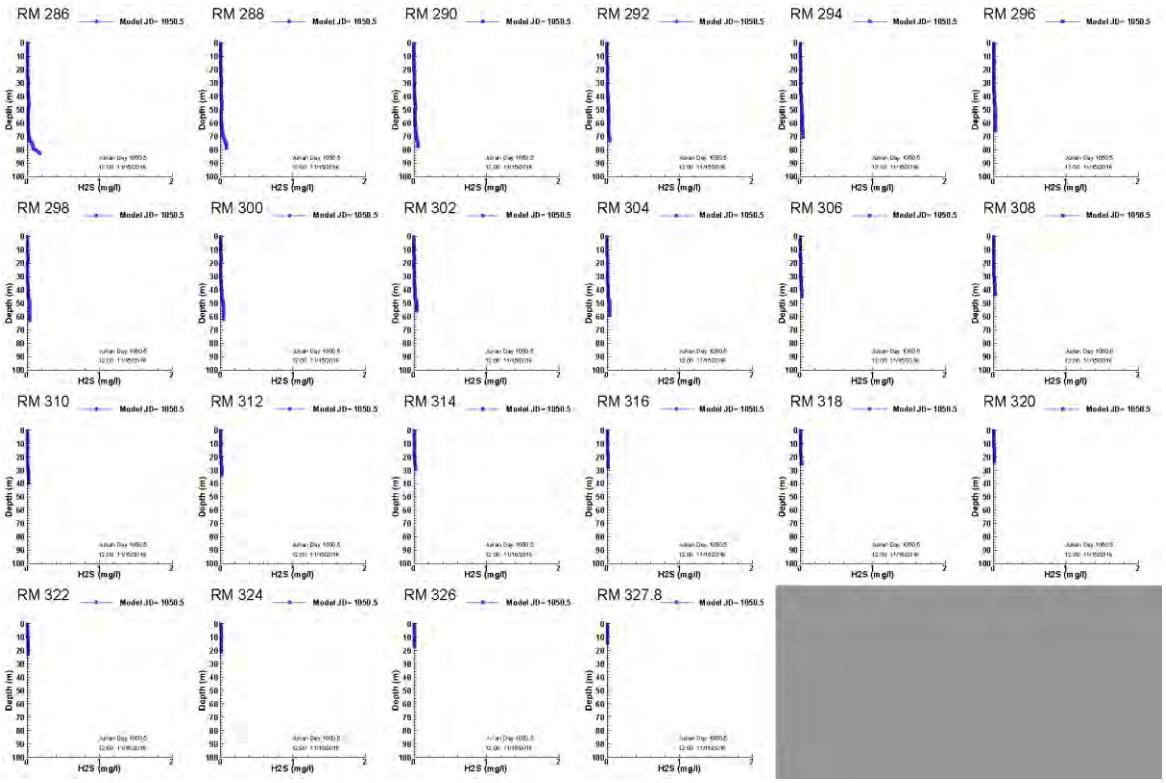


Figure 171. Vertical profiles of hydrogen sulfide compared with data for 11/15/2016.

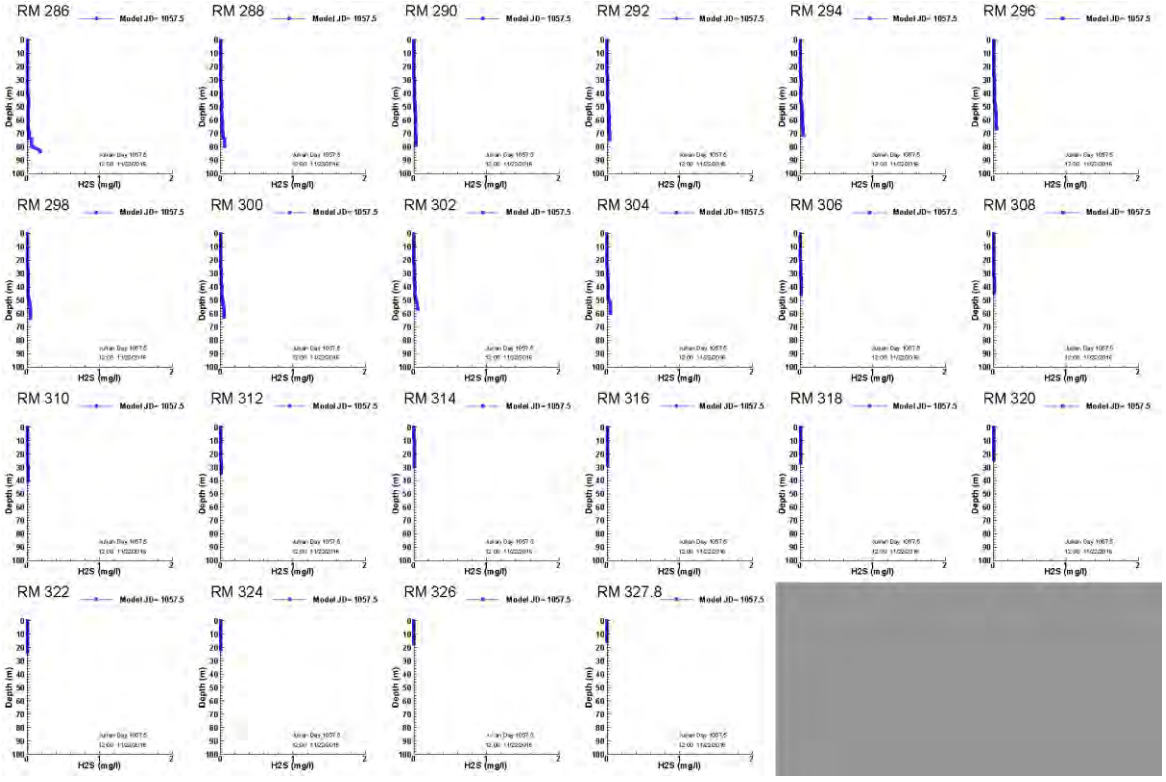


Figure 172. Vertical profiles of hydrogen sulfide compared with data for 11/22/2016.

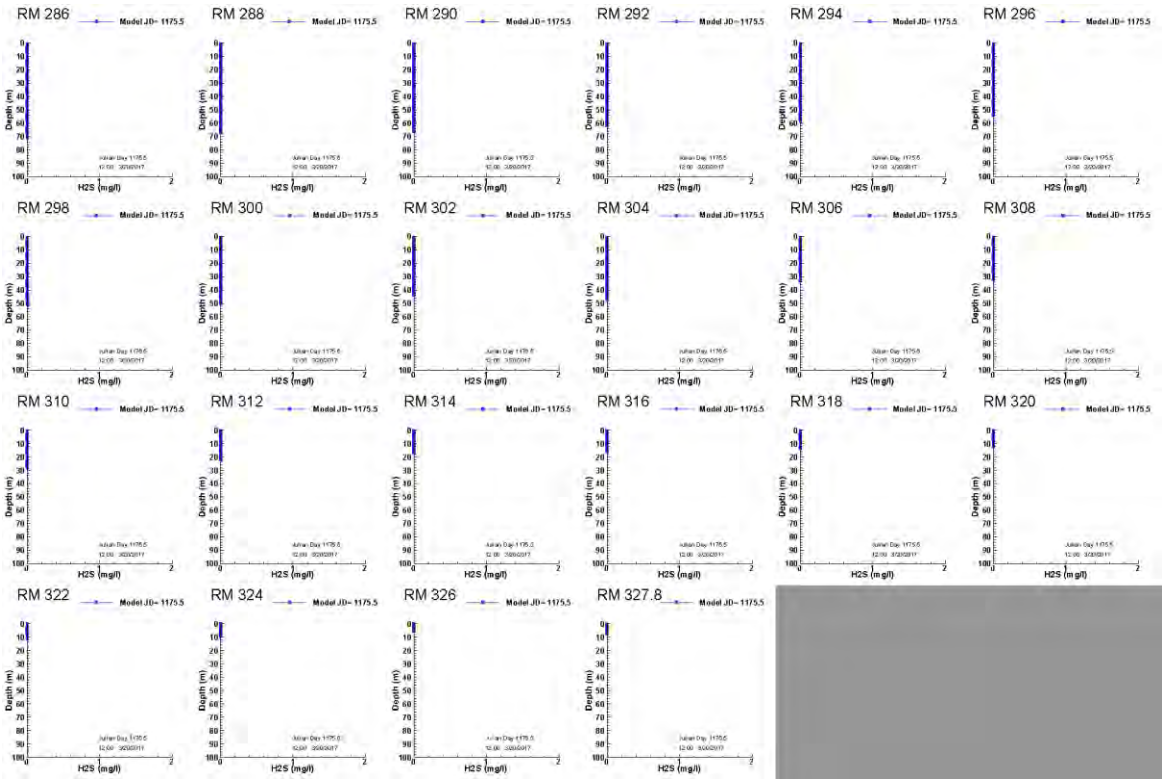


Figure 173. Vertical profiles of hydrogen sulfide compared with data for 3/20/2017.

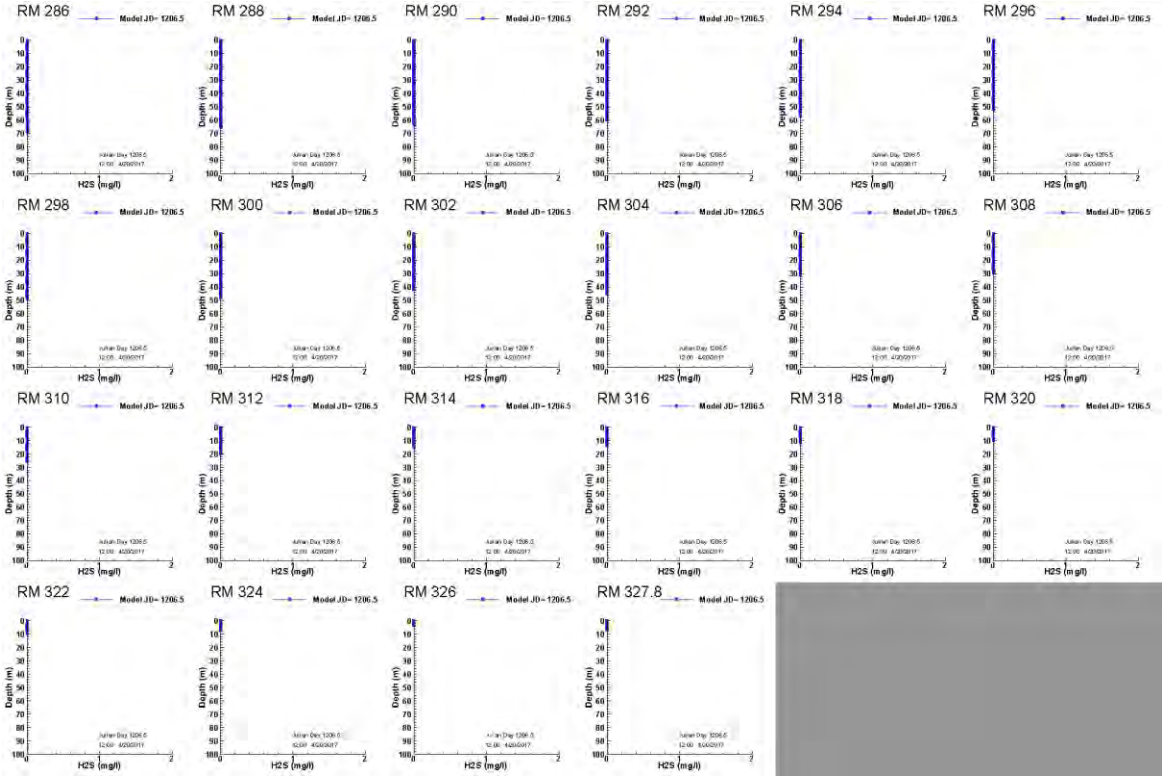


Figure 174. Vertical profiles of hydrogen sulfide compared with data for 4/20/2017.

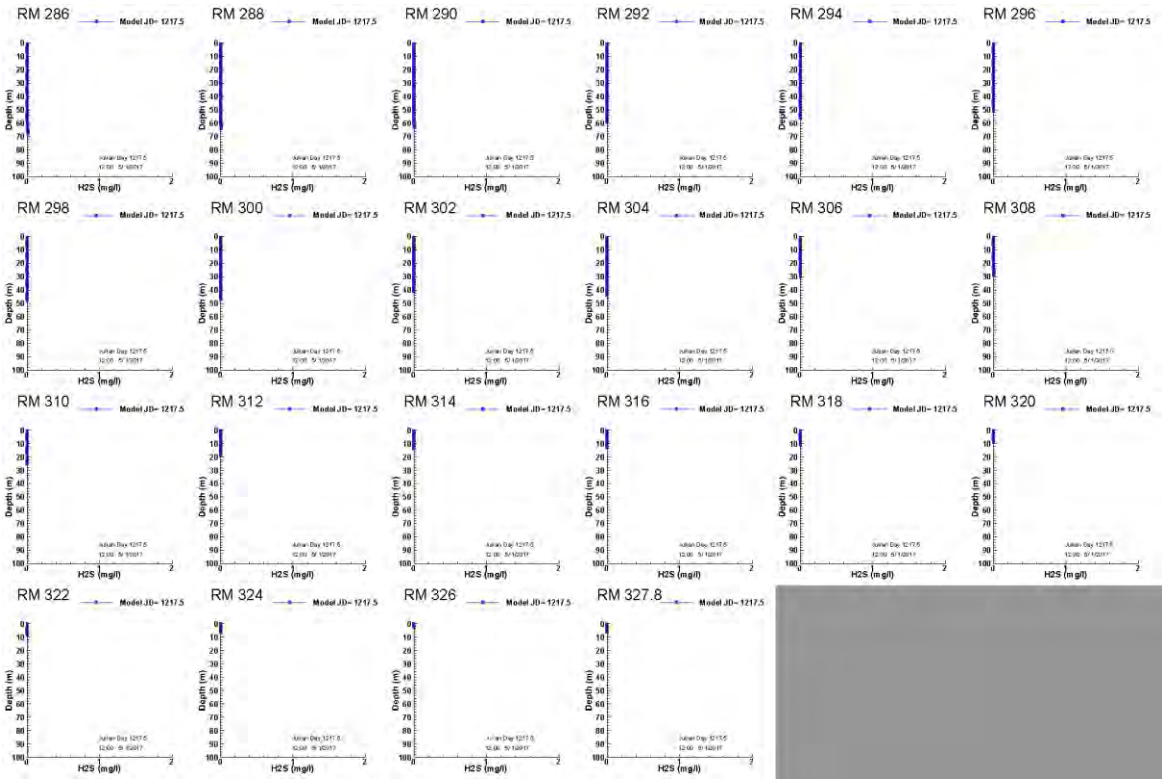


Figure 175. Vertical profiles of hydrogen sulfide compared with data for 5/ 1/2017.

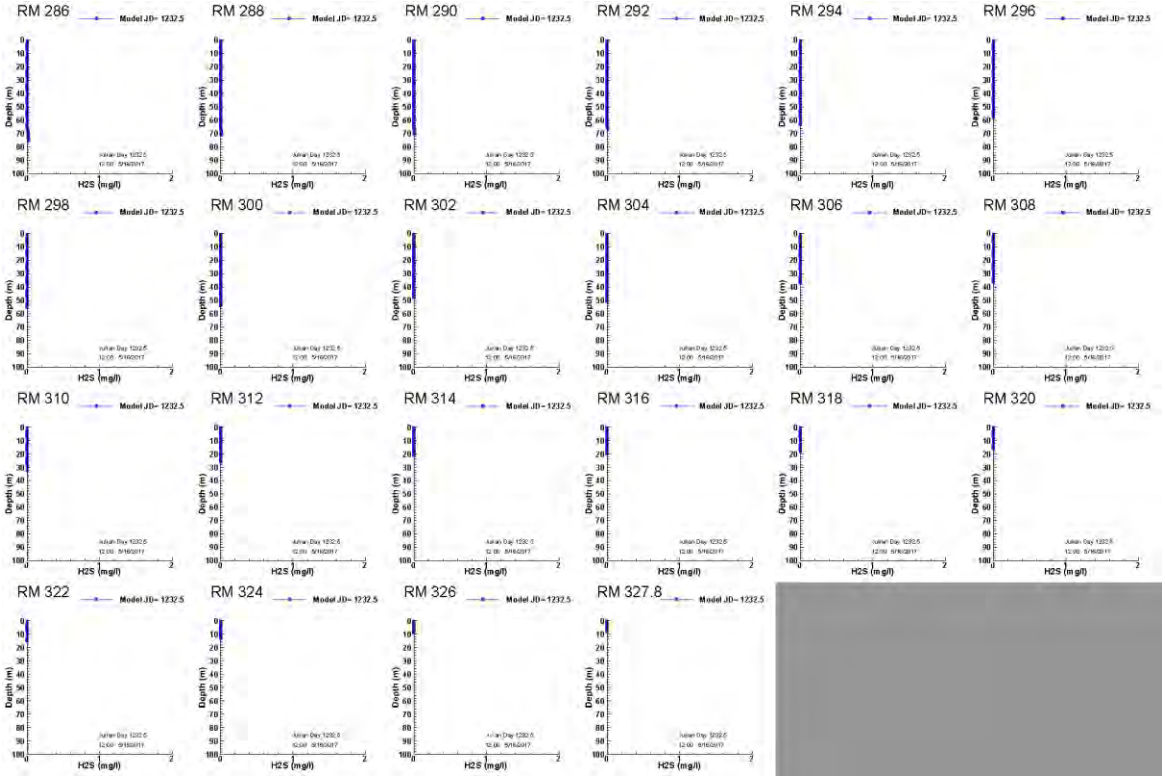


Figure 176. Vertical profiles of hydrogen sulfide compared with data for 5/16/2017.

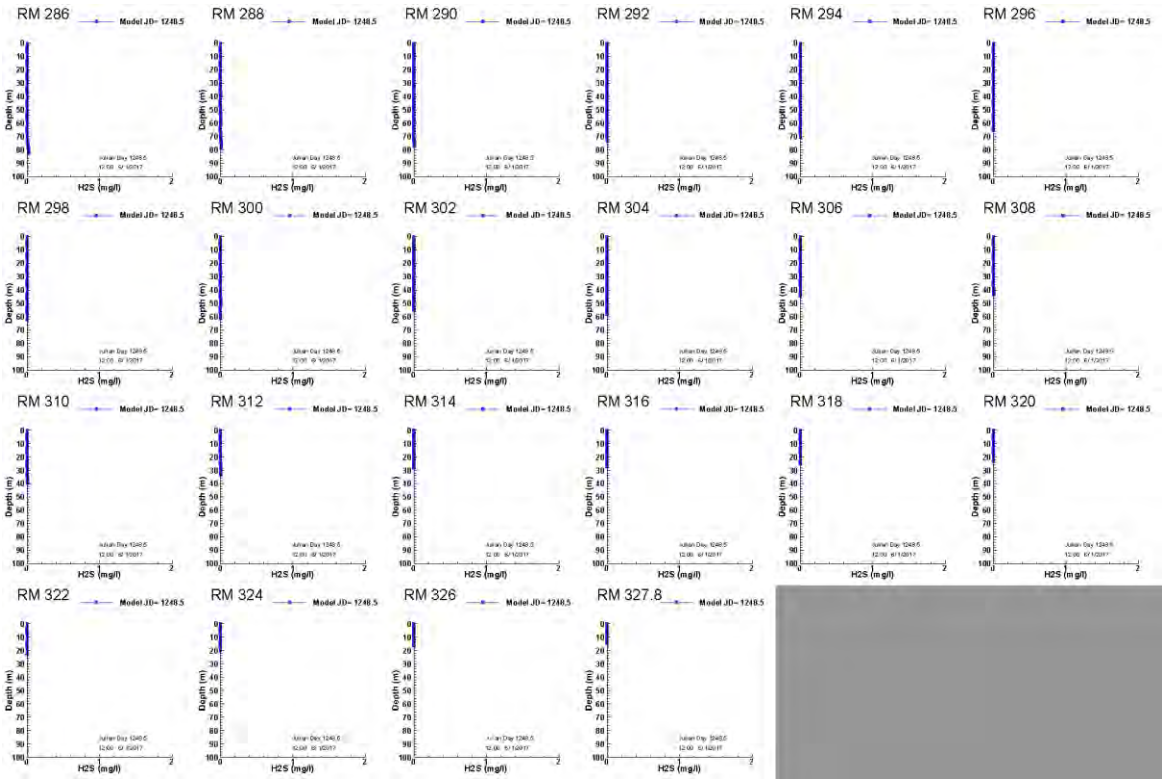


Figure 177. Vertical profiles of hydrogen sulfide compared with data for 6/ 1/2017.

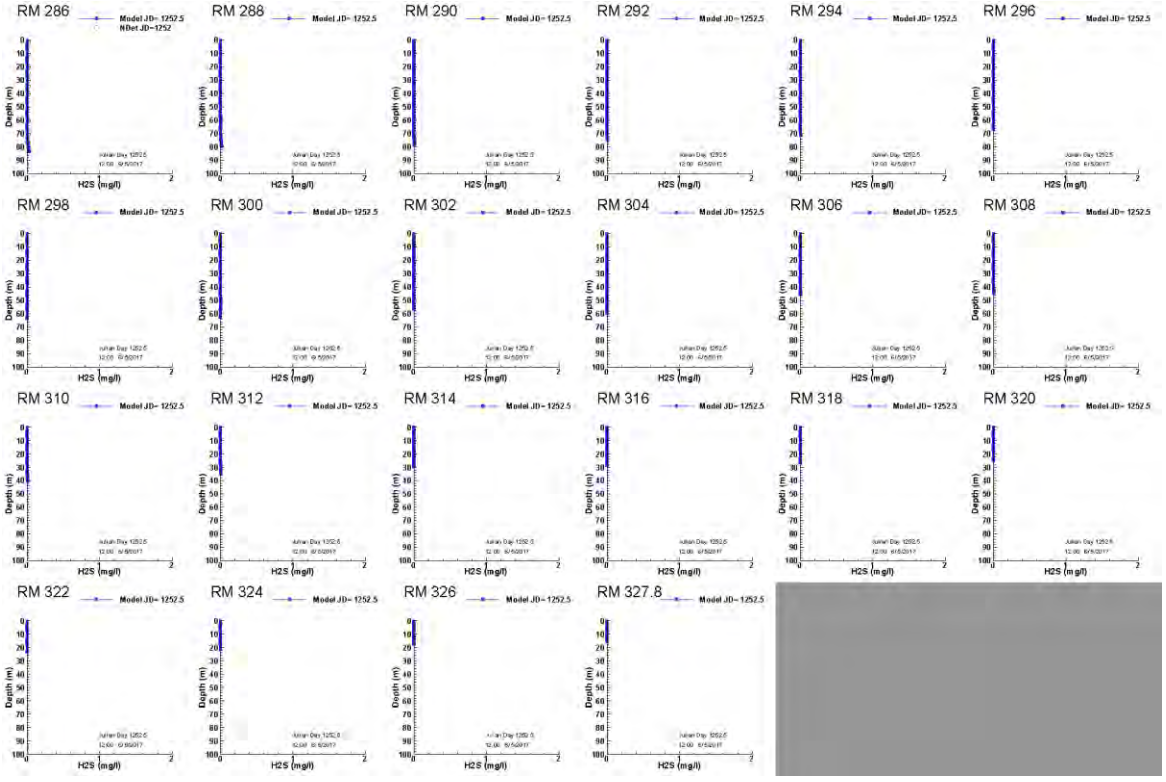


Figure 178. Vertical profiles of hydrogen sulfide compared with data for 6/ 5/2017.

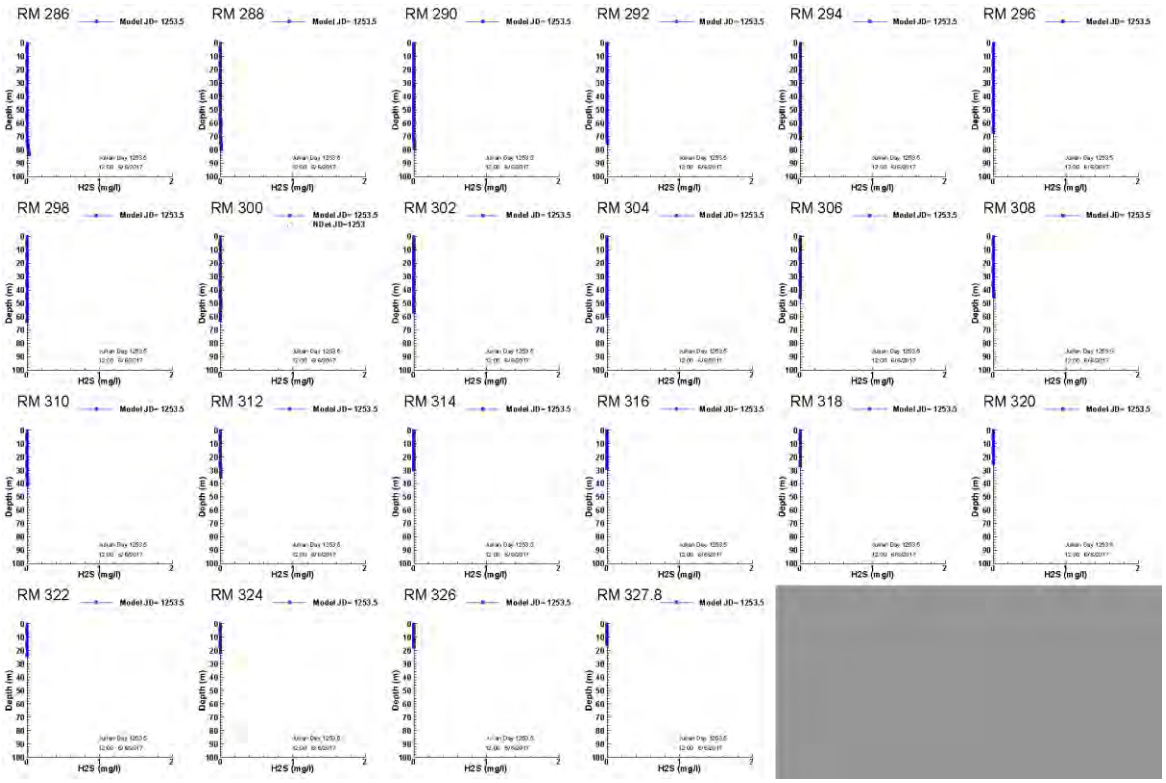


Figure 179. Vertical profiles of hydrogen sulfide compared with data for 6/ 6/2017.

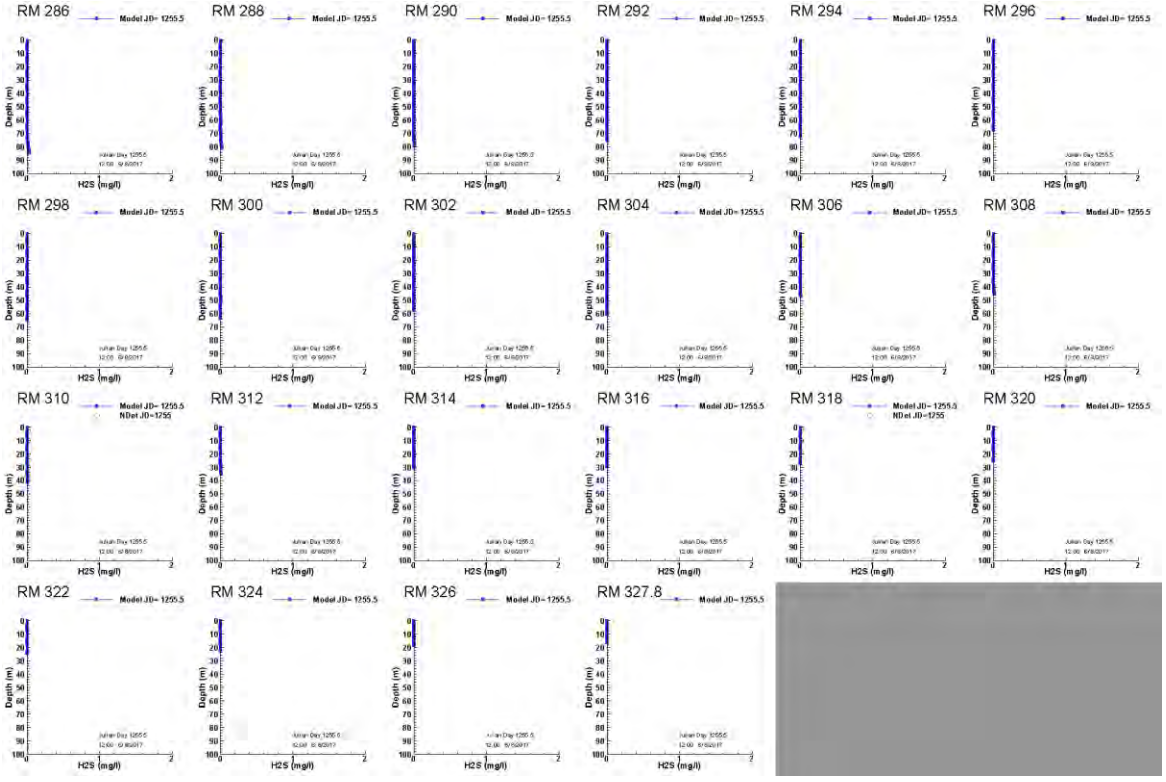


Figure 180. Vertical profiles of hydrogen sulfide compared with data for 6/ 8/2017.

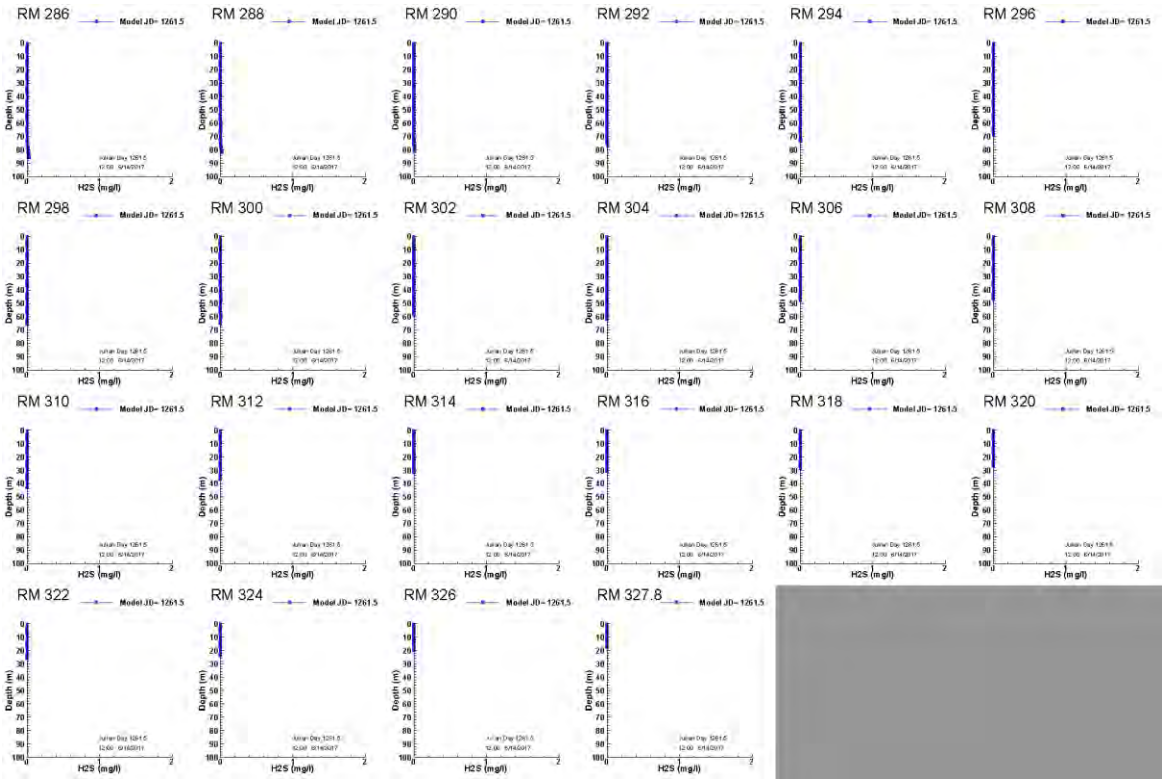


Figure 181. Vertical profiles of hydrogen sulfide compared with data for 6/14/2017.

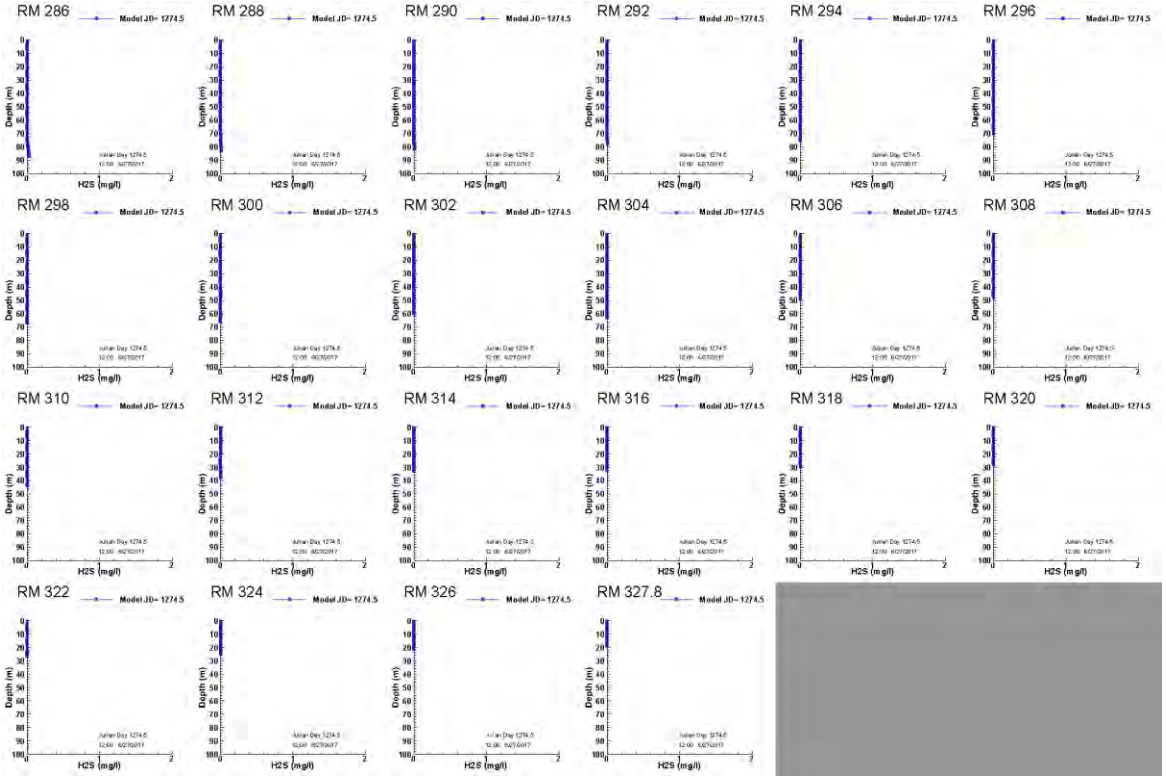


Figure 182. Vertical profiles of hydrogen sulfide compared with data for 6/27/2017.

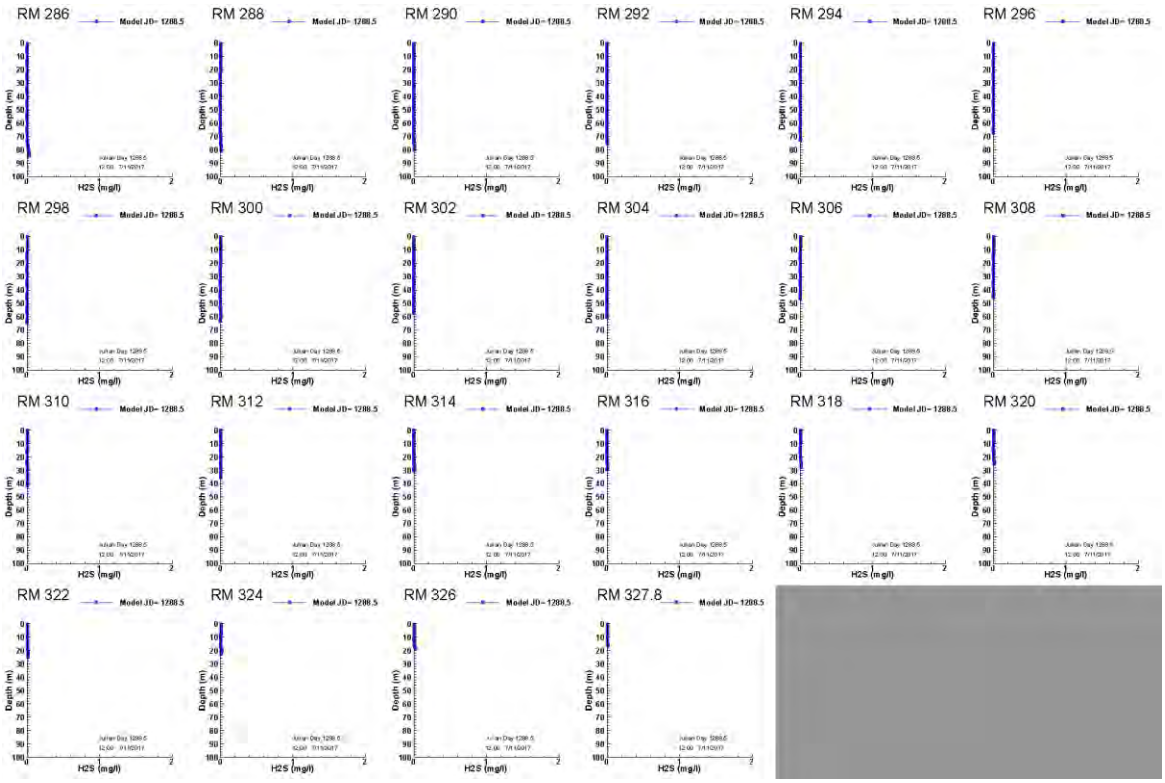


Figure 183. Vertical profiles of hydrogen sulfide compared with data for 7/11/2017.

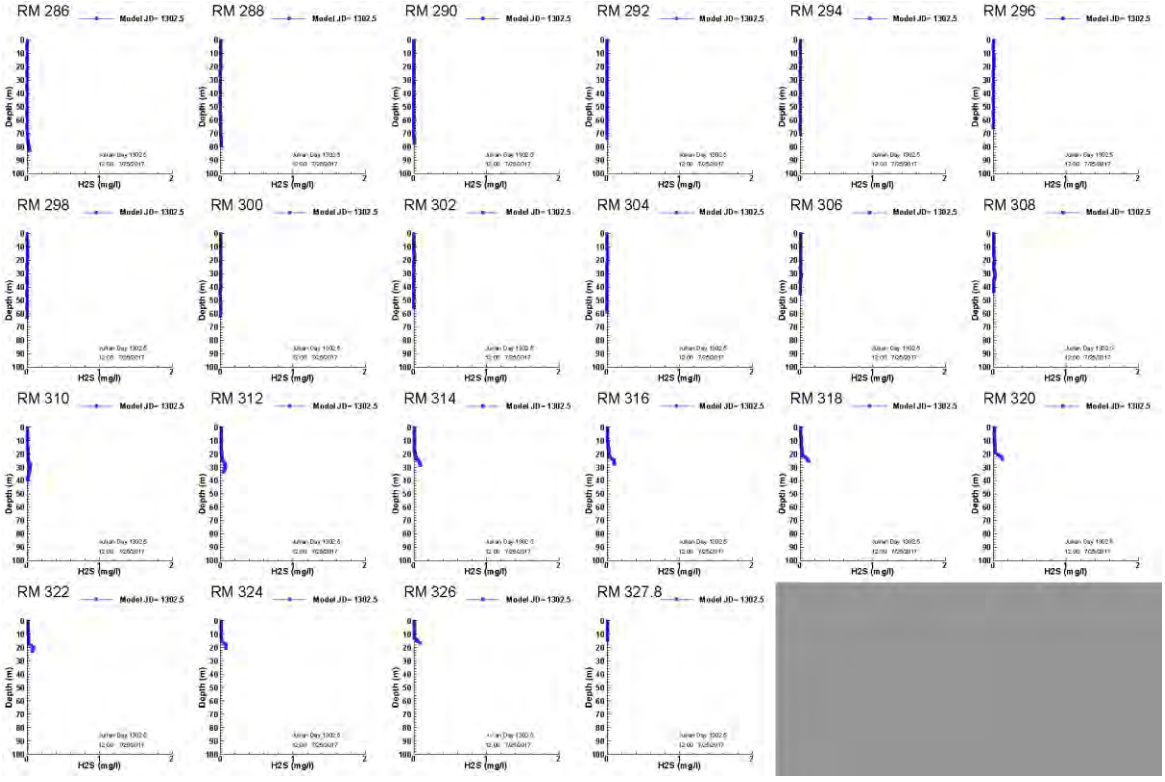


Figure 184. Vertical profiles of hydrogen sulfide compared with data for 7/25/2017.

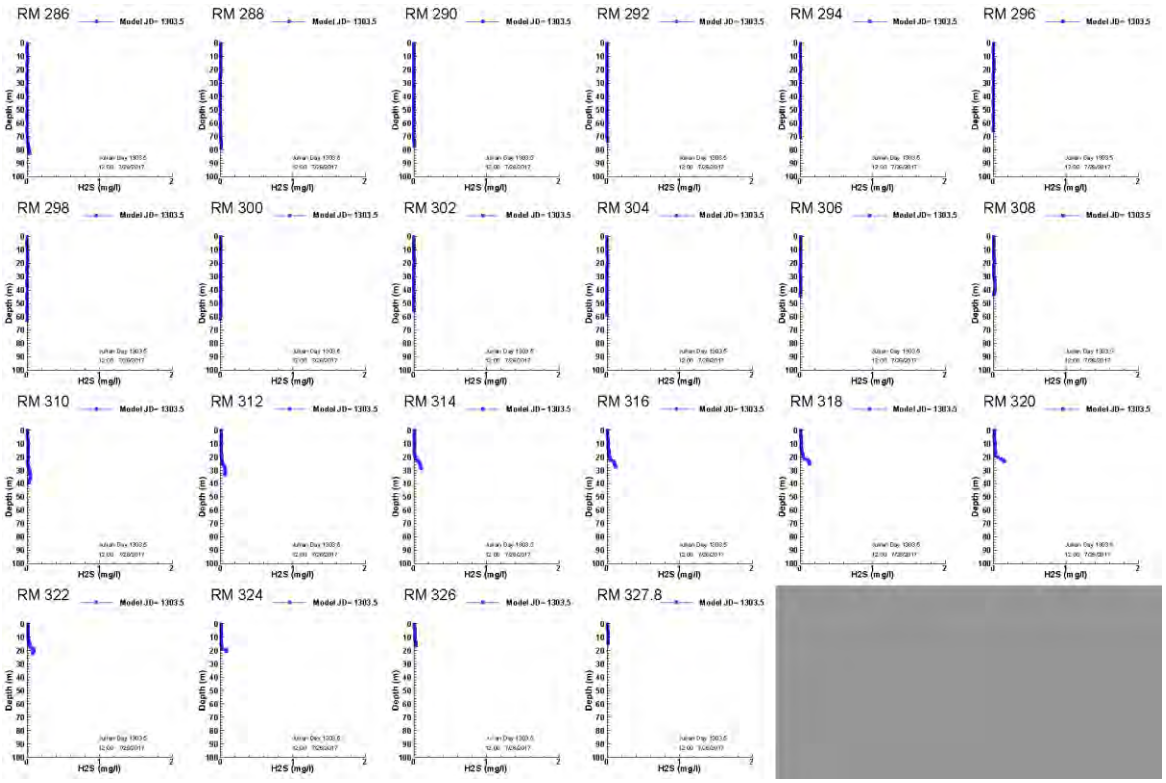


Figure 185. Vertical profiles of hydrogen sulfide compared with data for 7/26/2017.

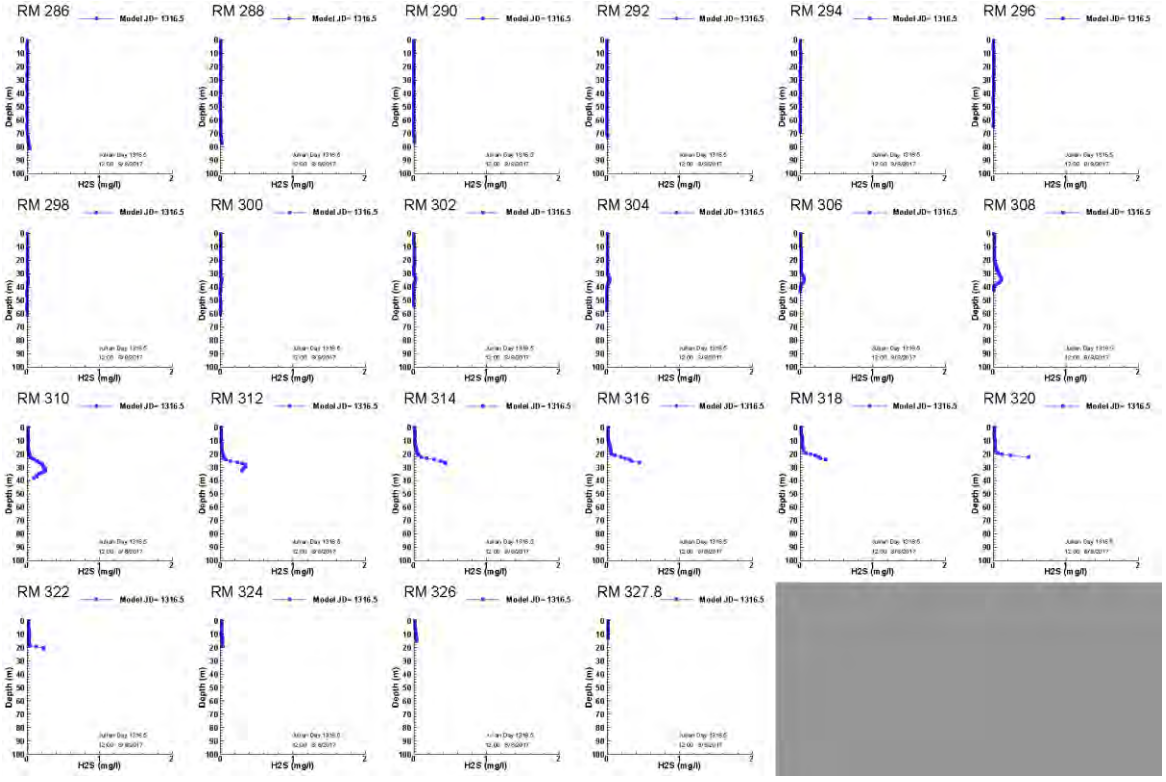


Figure 186. Vertical profiles of hydrogen sulfide compared with data for 8/ 8/2017.

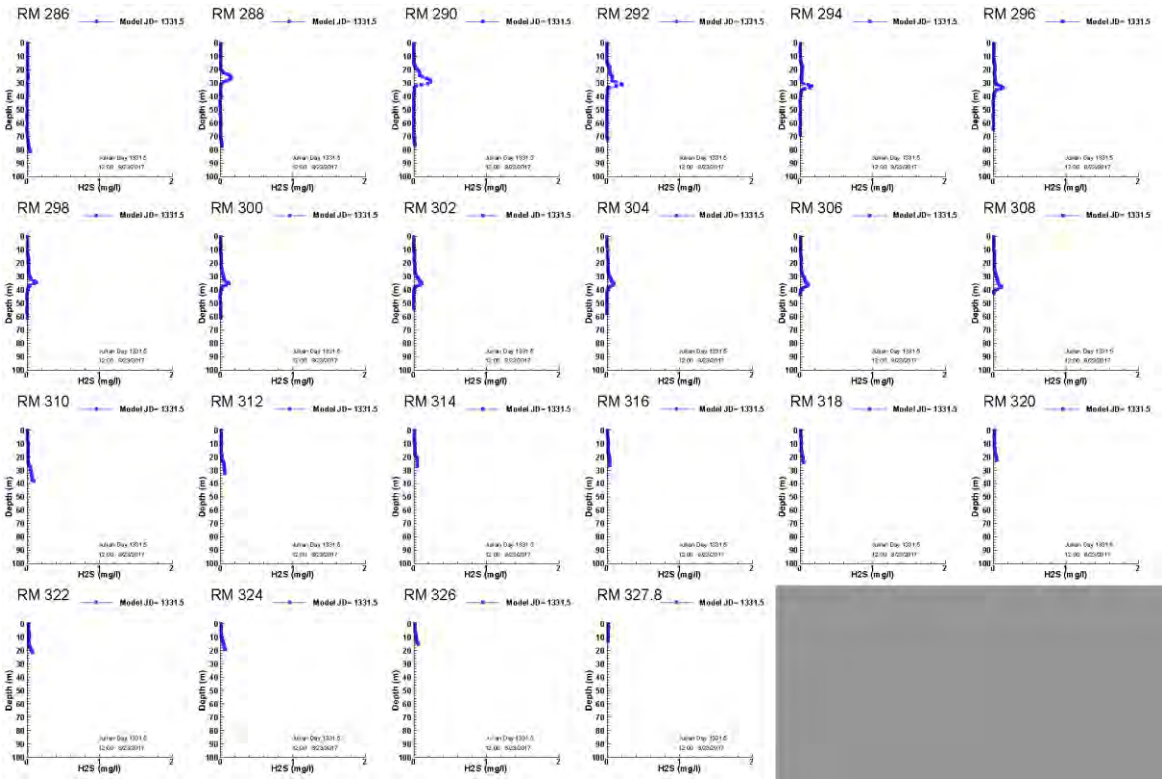


Figure 187. Vertical profiles of hydrogen sulfide compared with data for 8/23/2017.

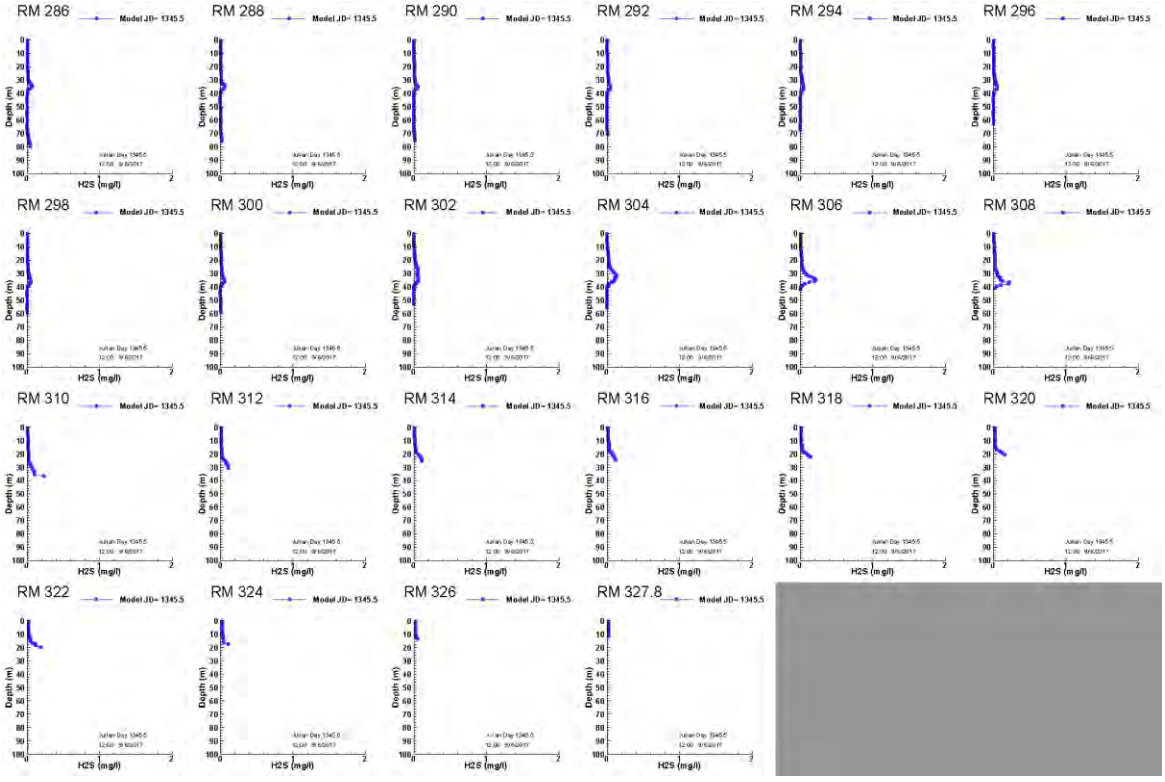


Figure 188. Vertical profiles of hydrogen sulfide compared with data for 9/ 6/2017.

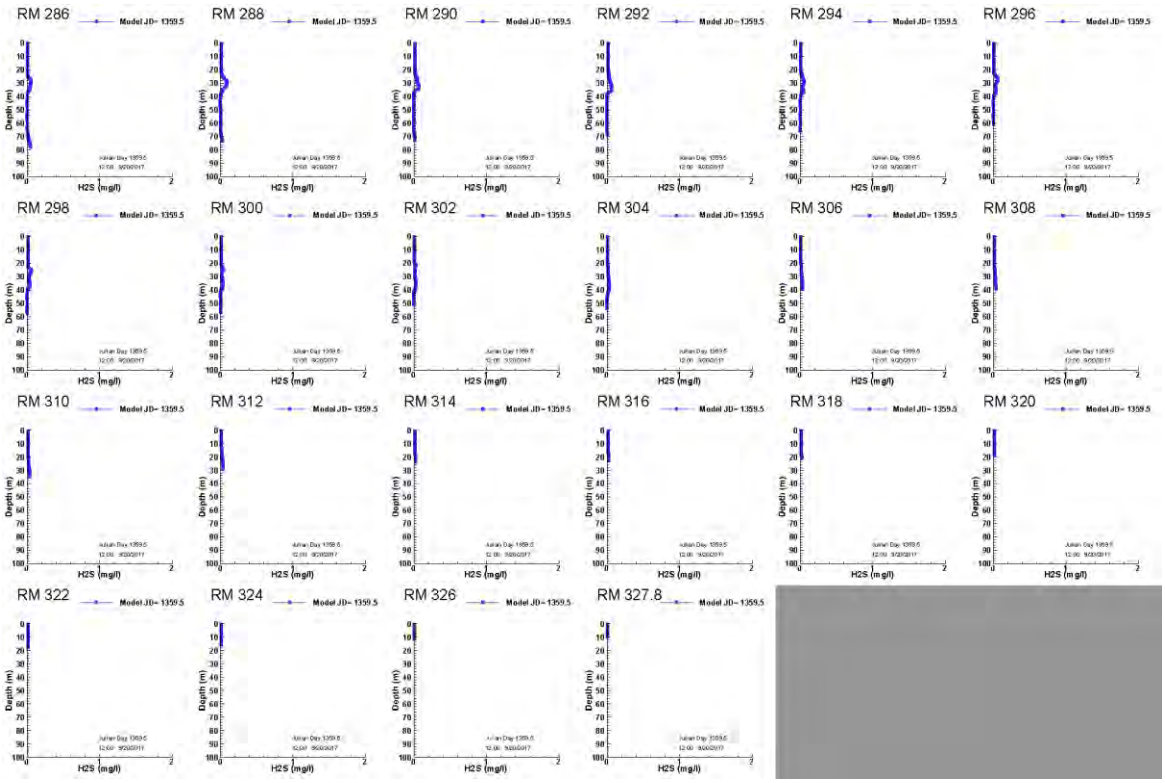


Figure 189. Vertical profiles of hydrogen sulfide compared with data for 9/20/2017.

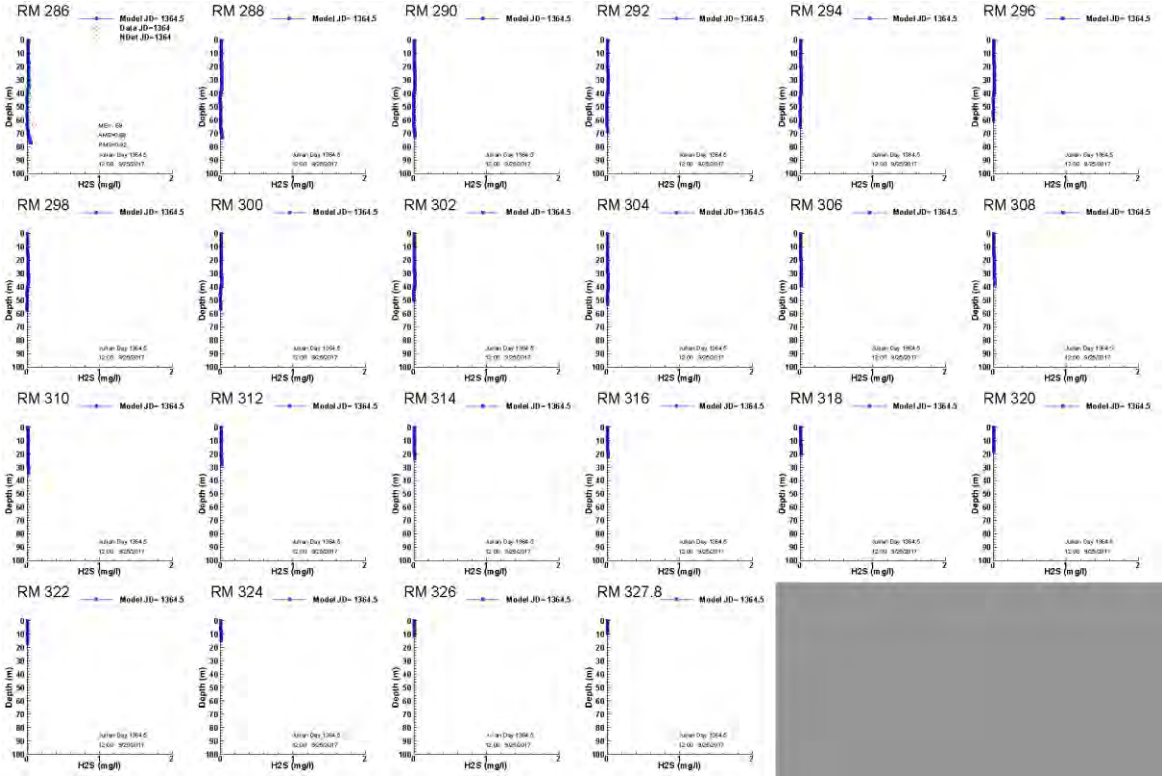


Figure 190. Vertical profiles of hydrogen sulfide compared with data for 9/25/2017.

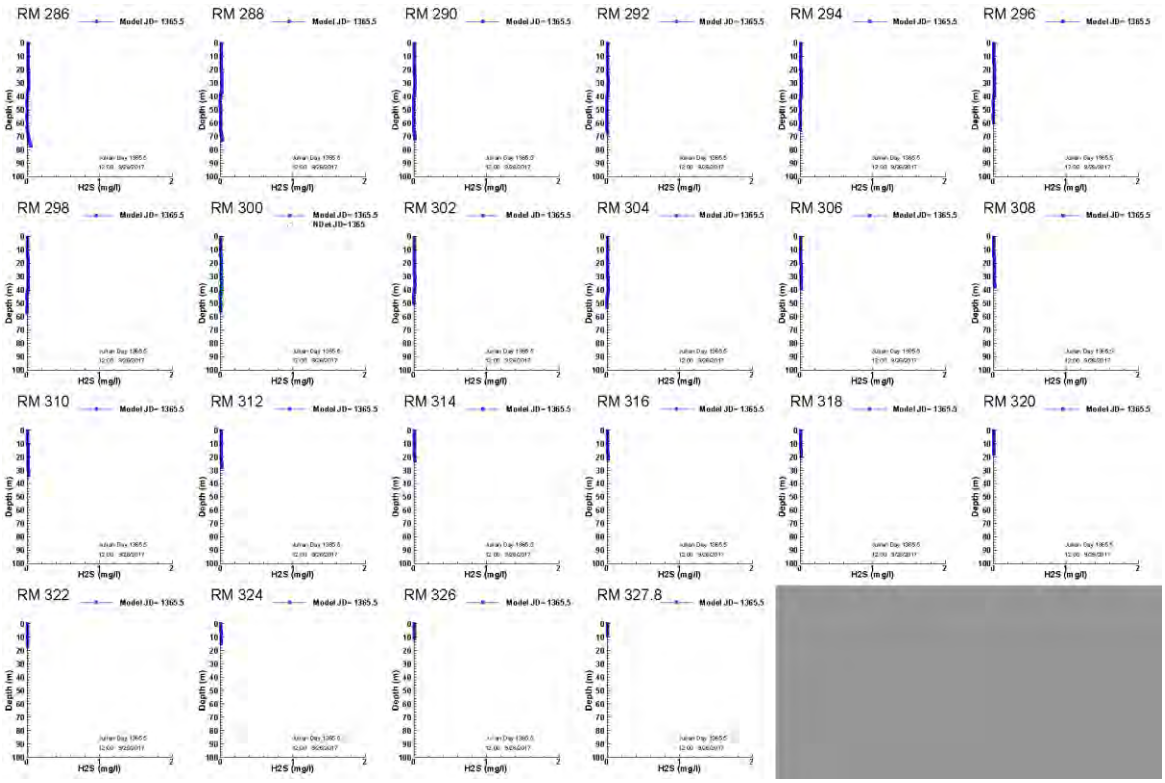


Figure 191. Vertical profiles of hydrogen sulfide compared with data for 9/26/2017.

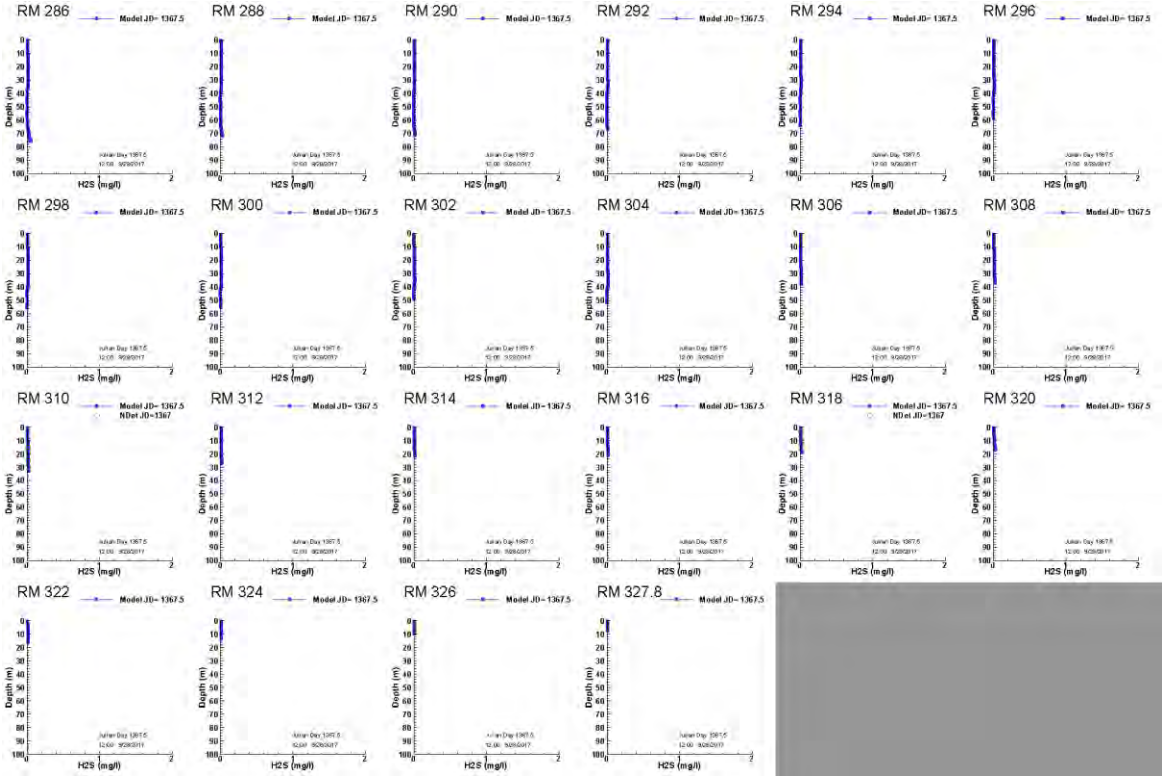


Figure 192. Vertical profiles of hydrogen sulfide compared with data for 9/28/2017.

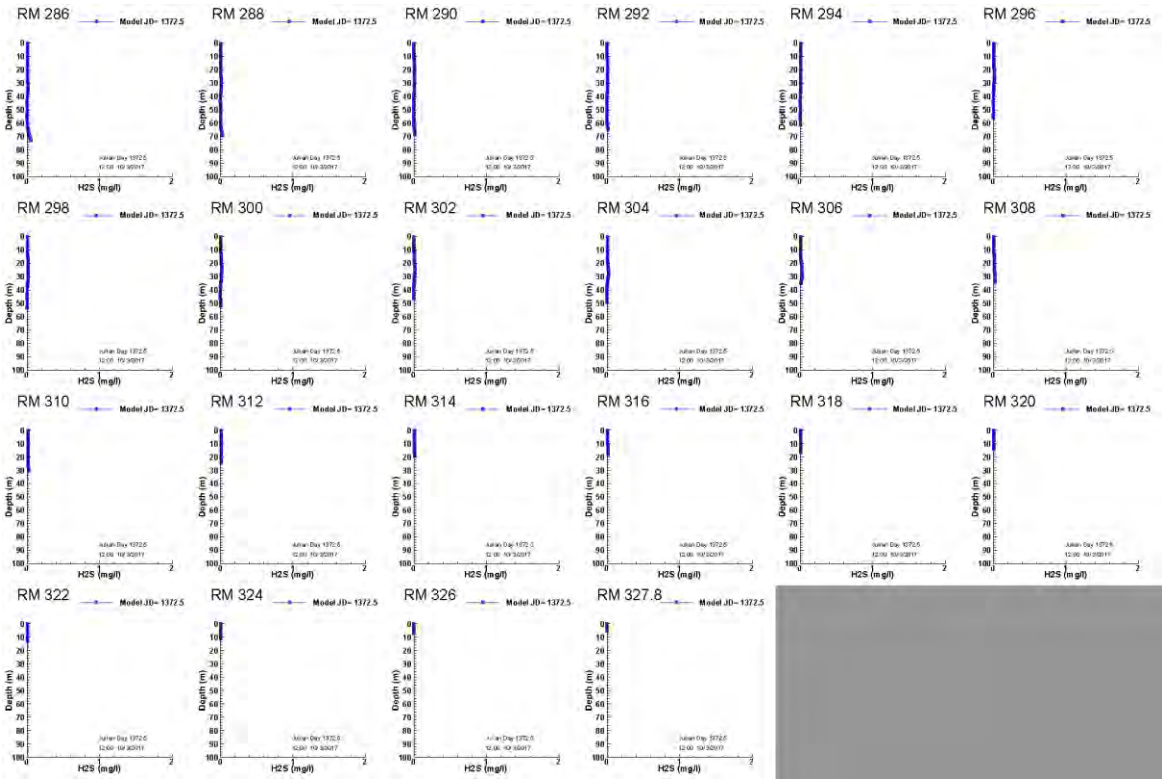


Figure 193. Vertical profiles of hydrogen sulfide compared with data for 10/ 3/2017.

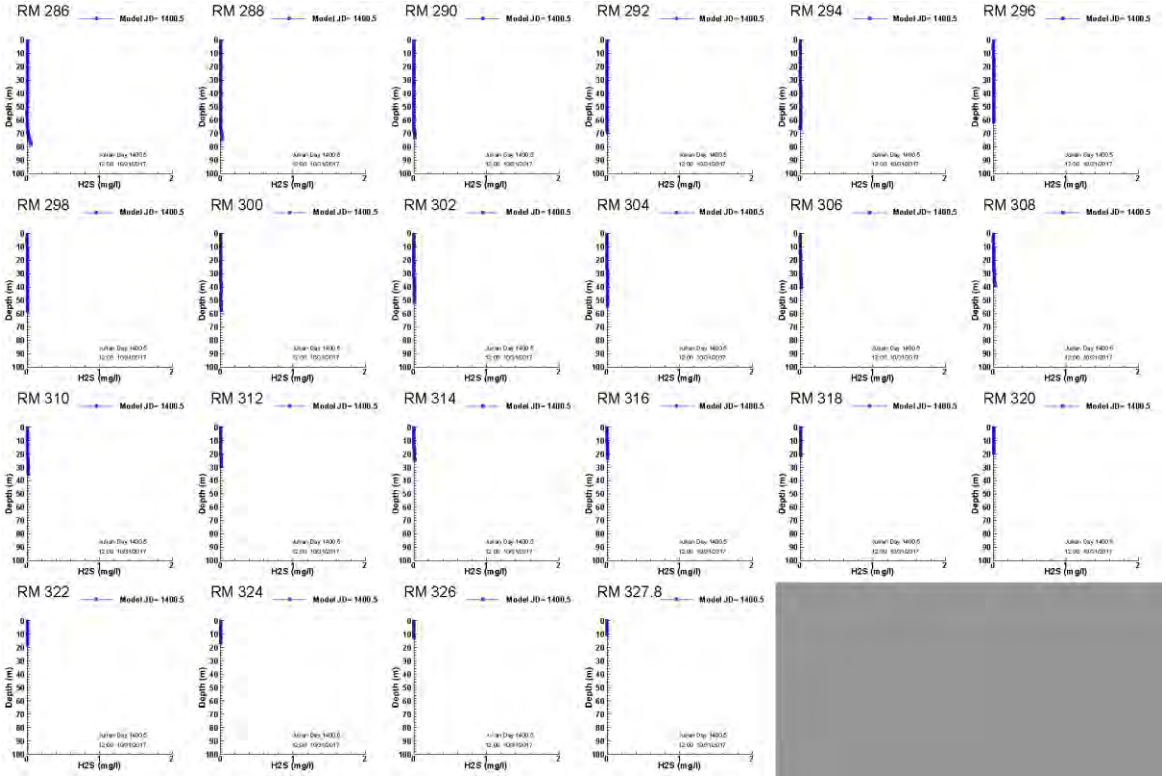


Figure 194. Vertical profiles of hydrogen sulfide compared with data for 10/31/2017.

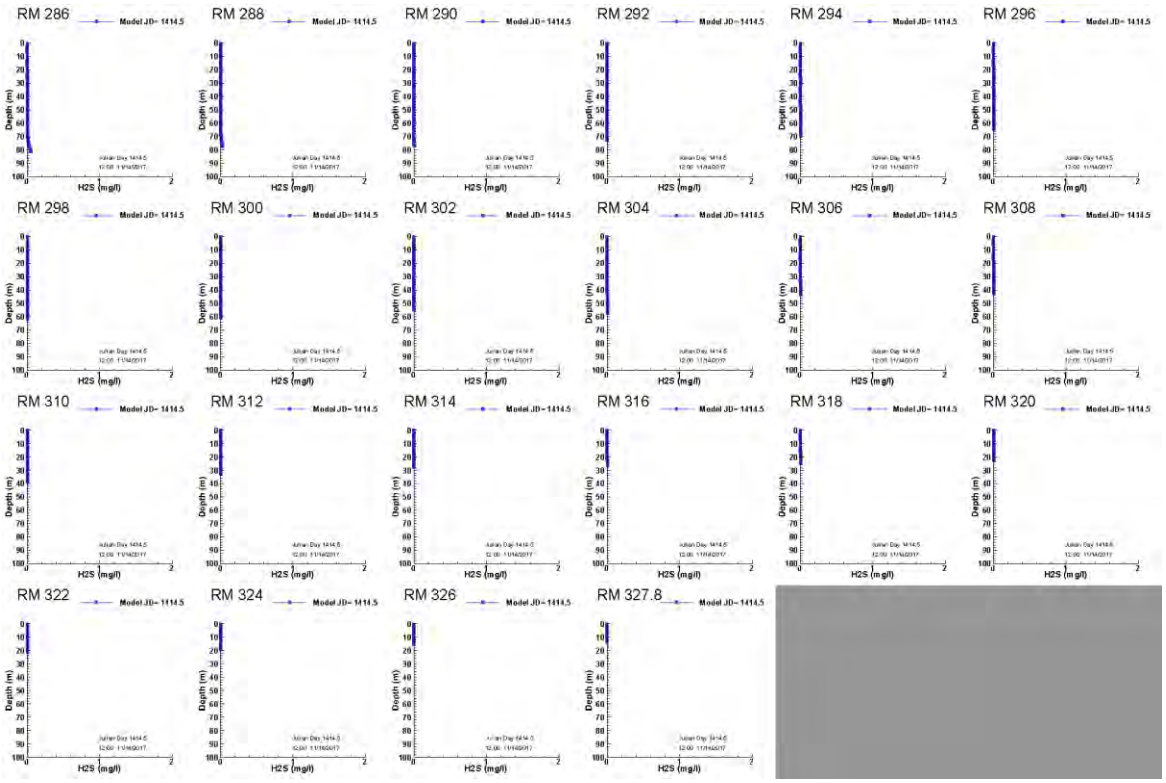


Figure 195. Vertical profiles of hydrogen sulfide compared with data for 11/14/2017.

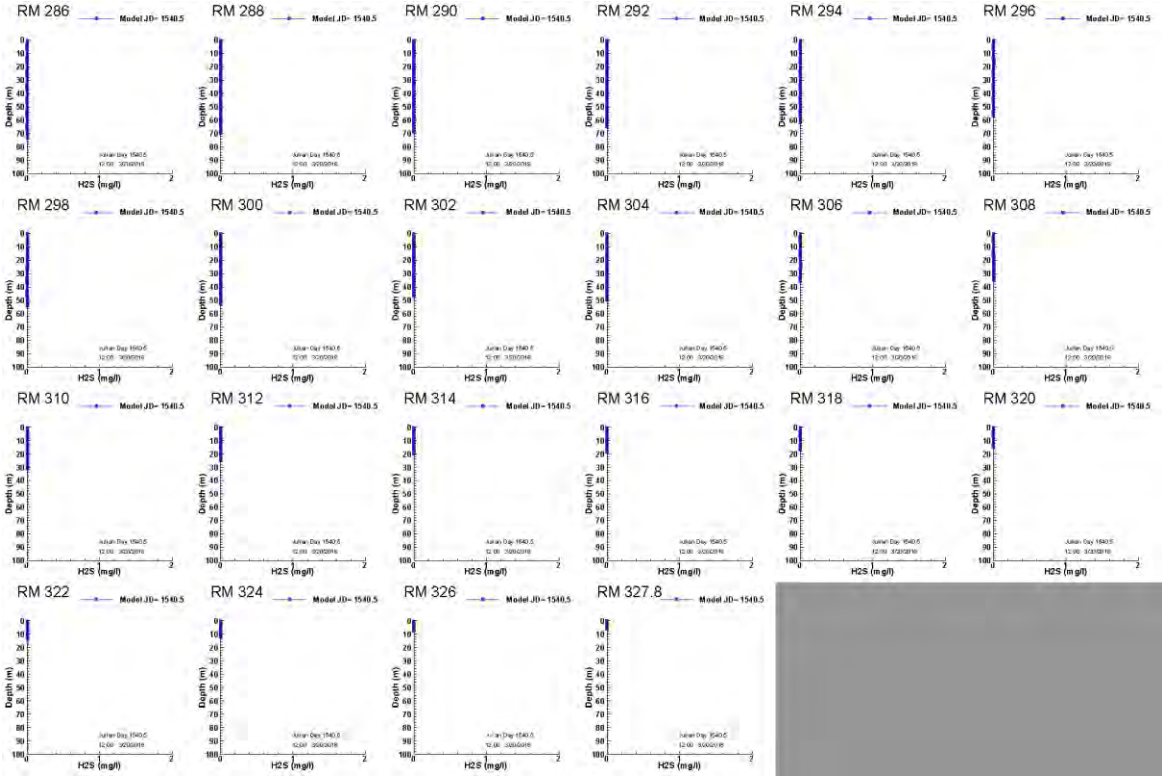


Figure 196. Vertical profiles of hydrogen sulfide compared with data for 3/20/2018.

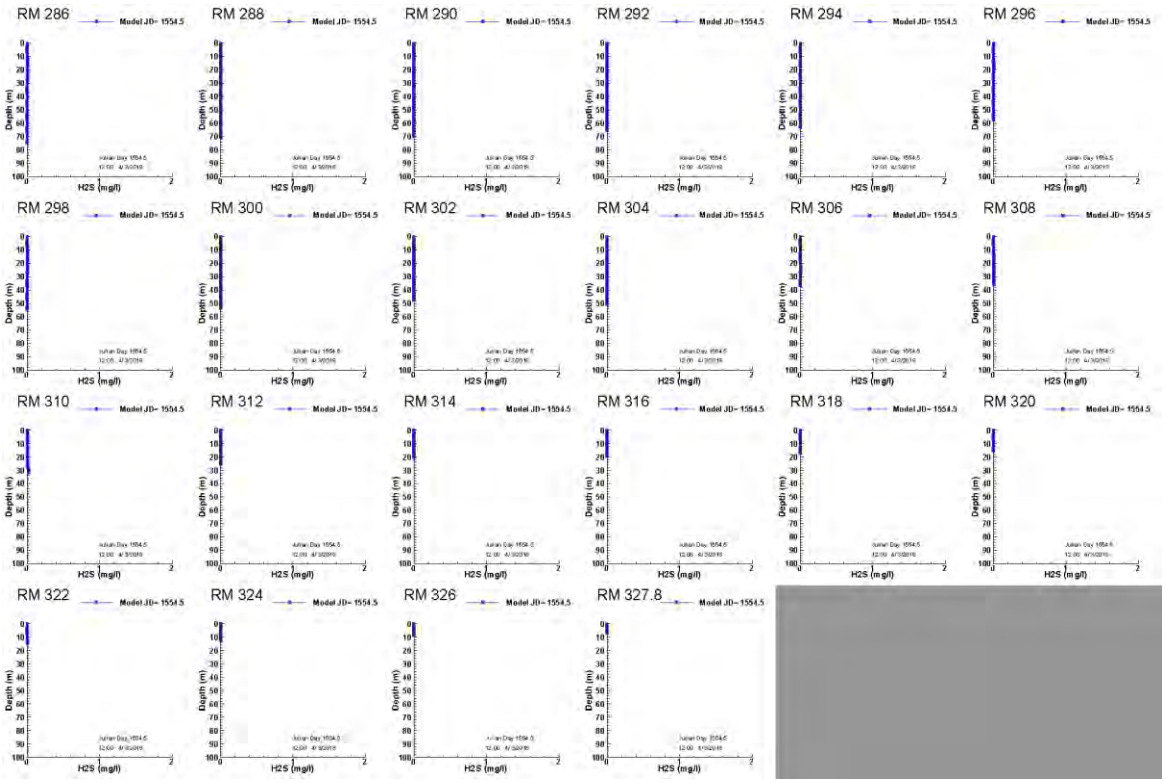


Figure 197. Vertical profiles of hydrogen sulfide compared with data for 4/ 3/2018.

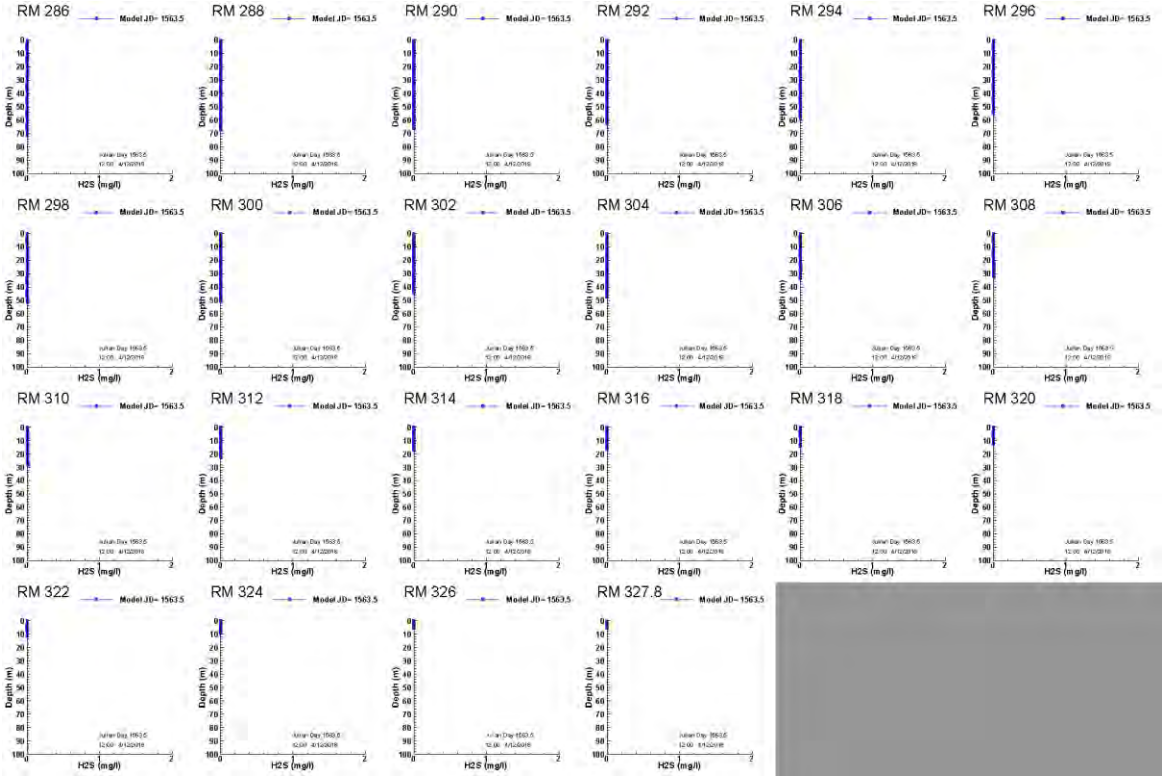


Figure 198. Vertical profiles of hydrogen sulfide compared with data for 4/12/2018.

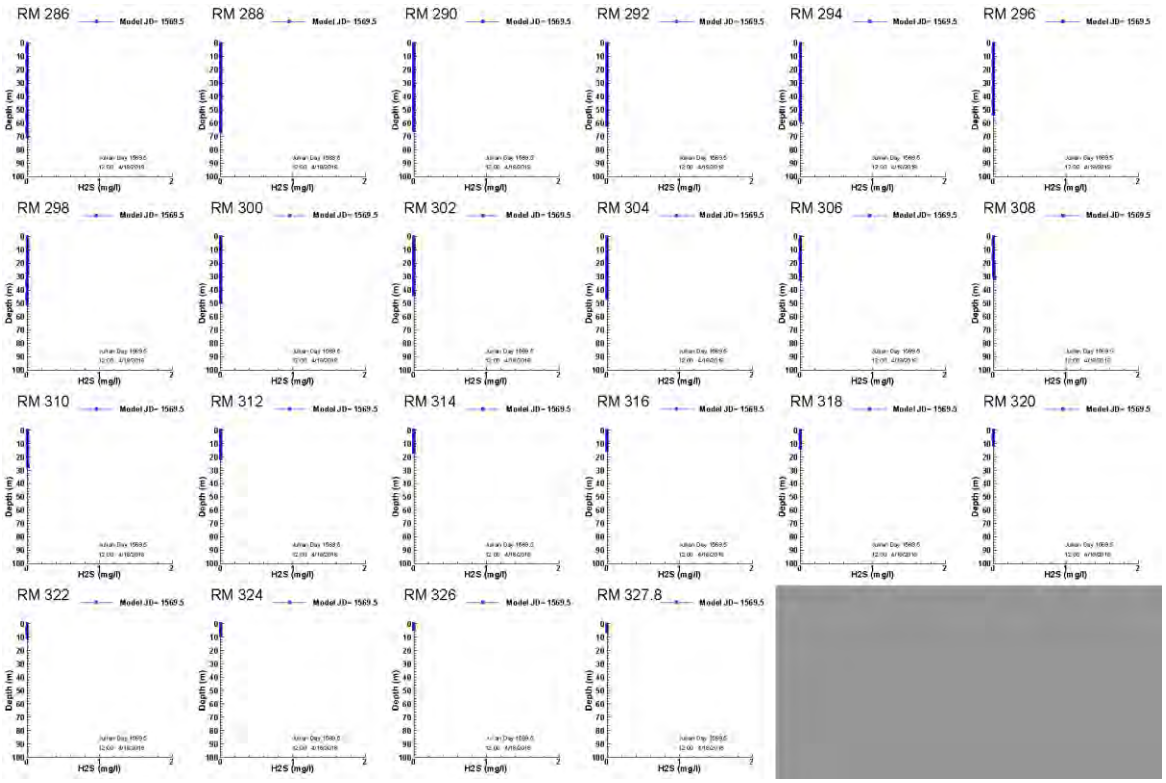


Figure 199. Vertical profiles of hydrogen sulfide compared with data for 4/18/2018.

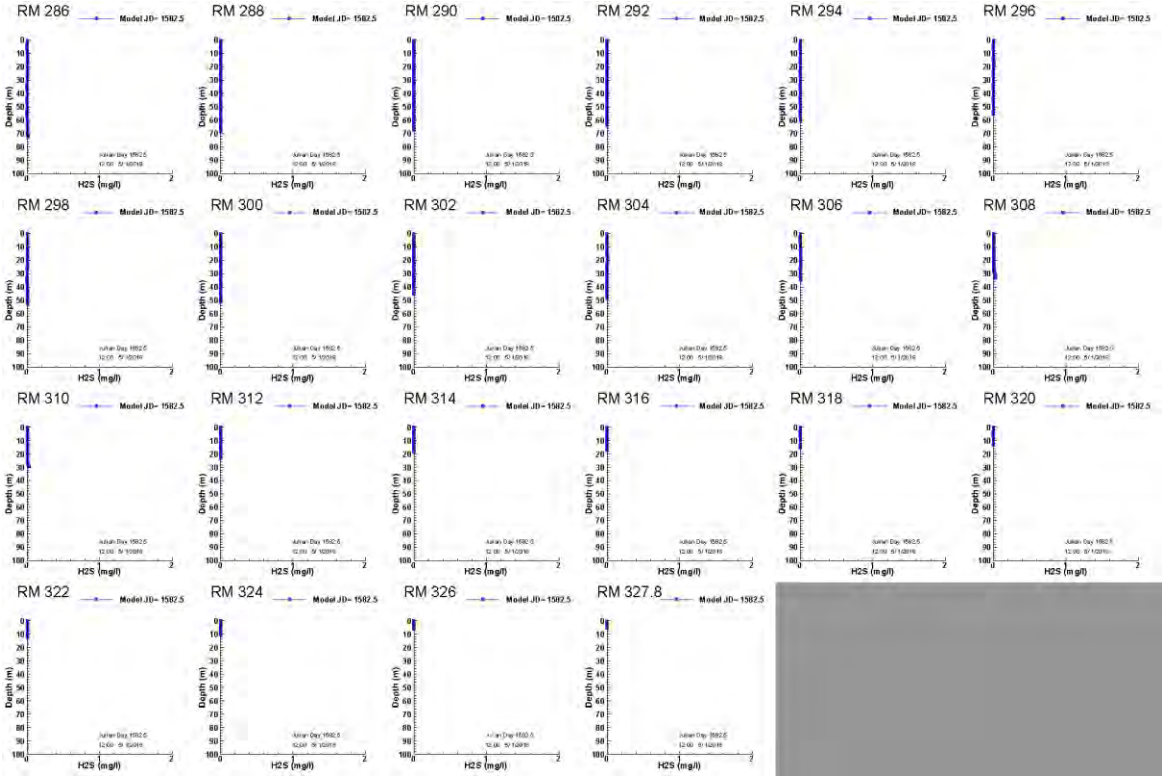


Figure 200. Vertical profiles of hydrogen sulfide compared with data for 5/ 1/2018.

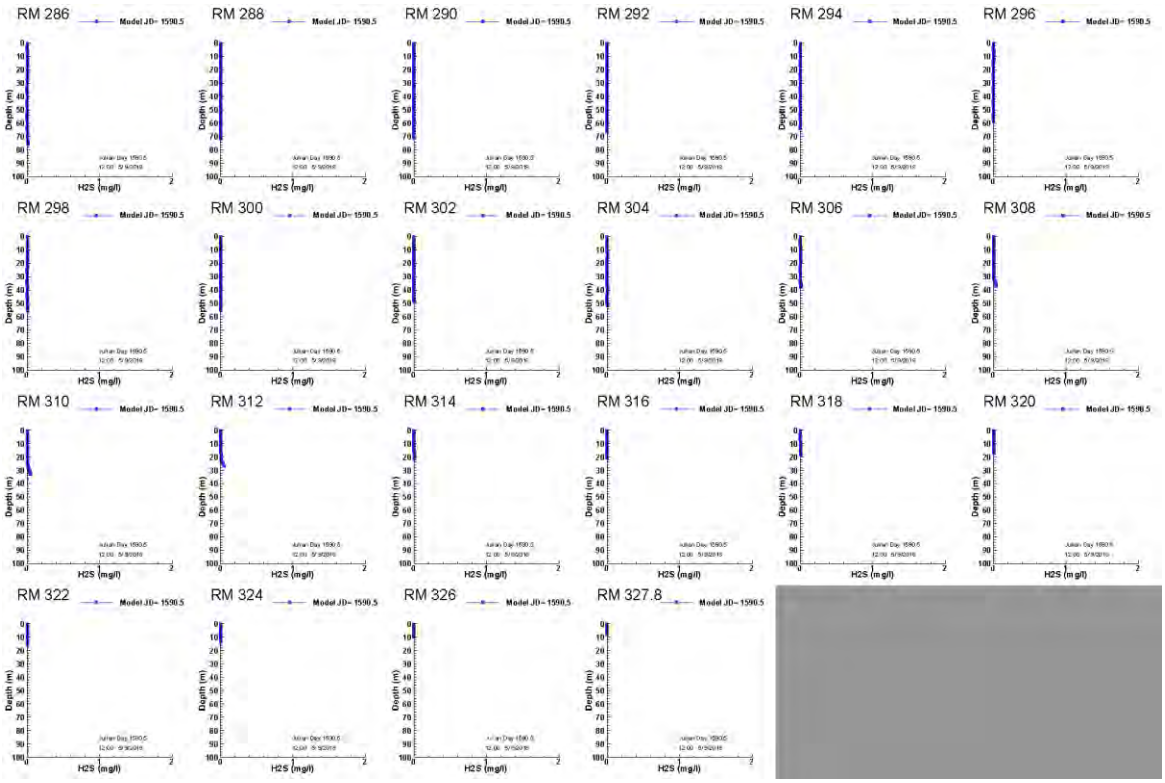


Figure 201. Vertical profiles of hydrogen sulfide compared with data for 5/ 9/2018.

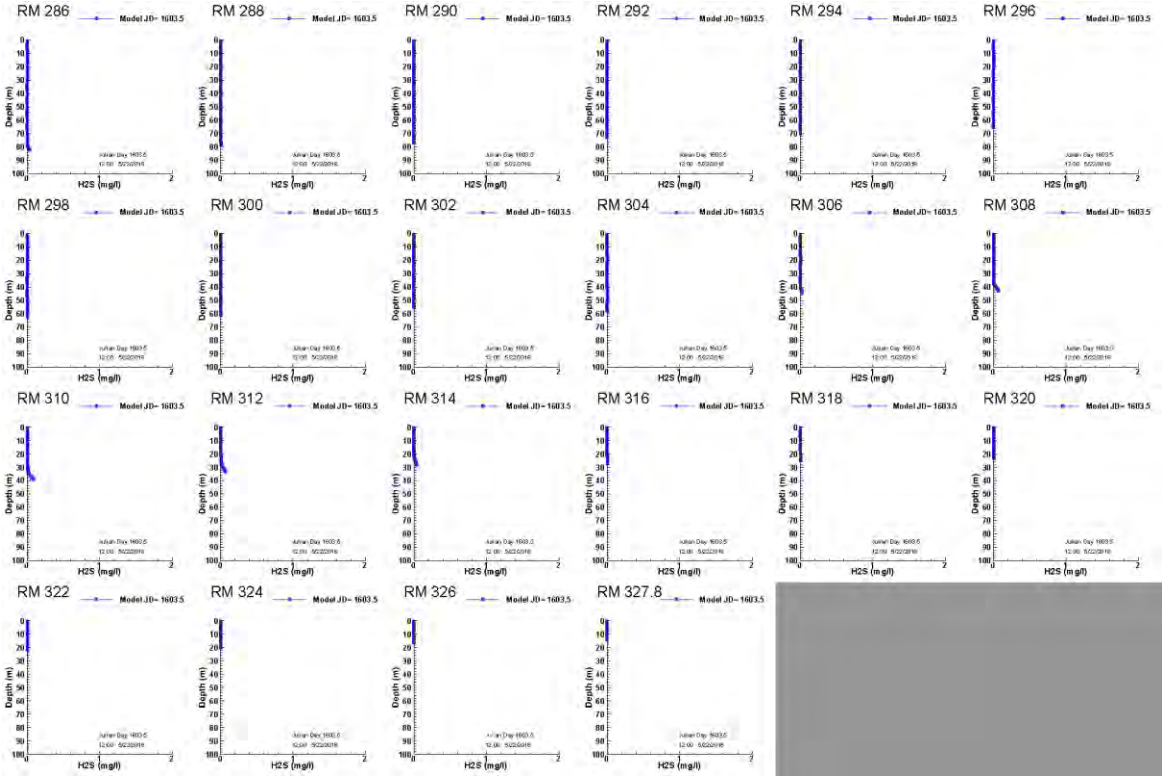


Figure 202. Vertical profiles of hydrogen sulfide compared with data for 5/22/2018.

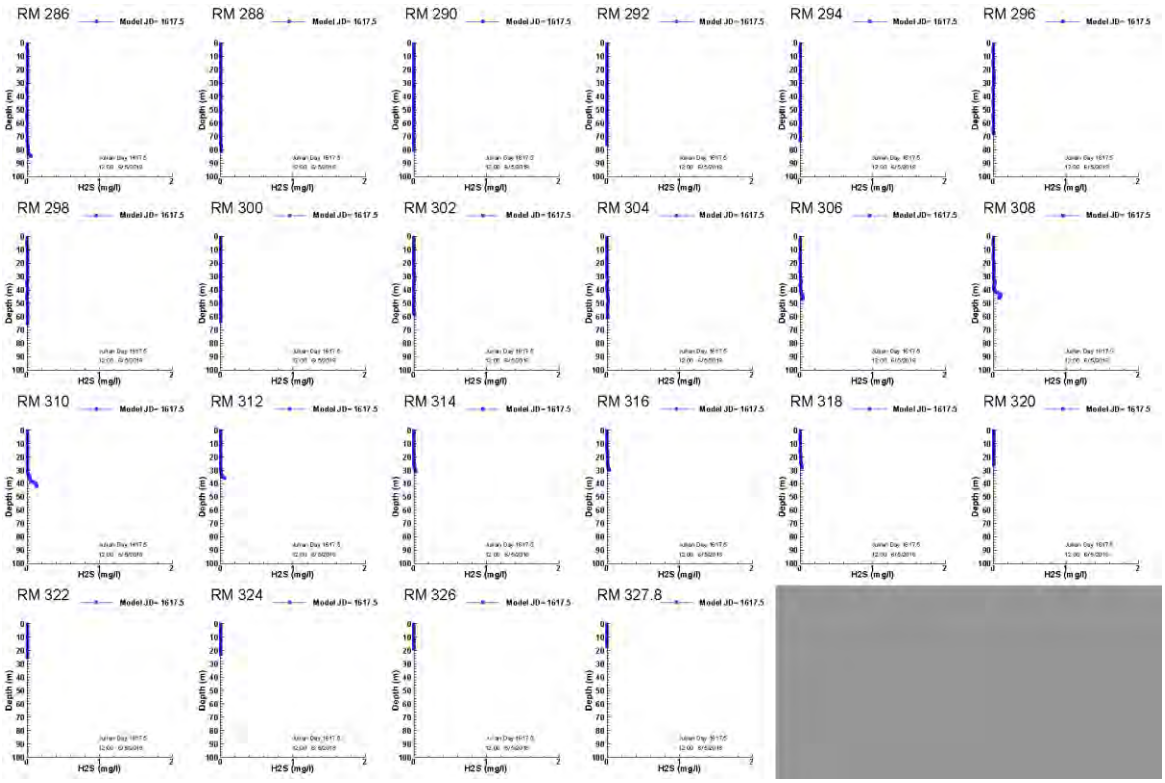


Figure 203. Vertical profiles of hydrogen sulfide compared with data for 6/ 5/2018.

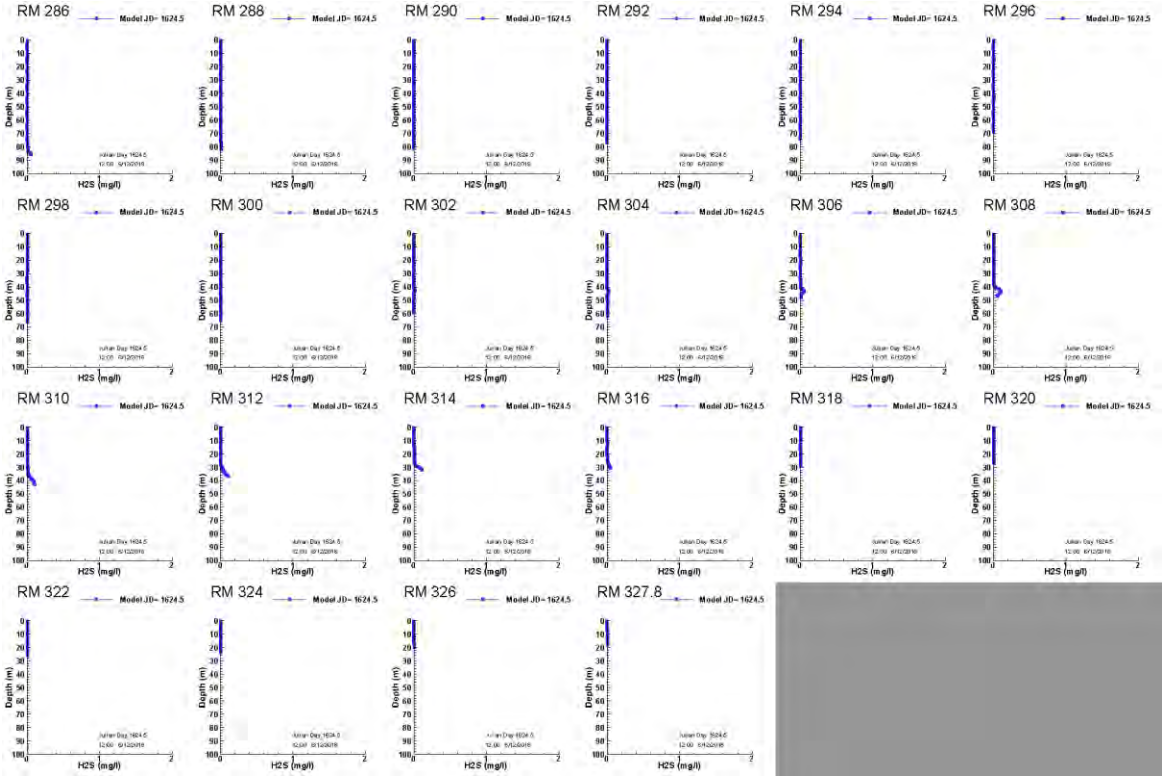


Figure 204. Vertical profiles of hydrogen sulfide compared with data for 6/12/2018.

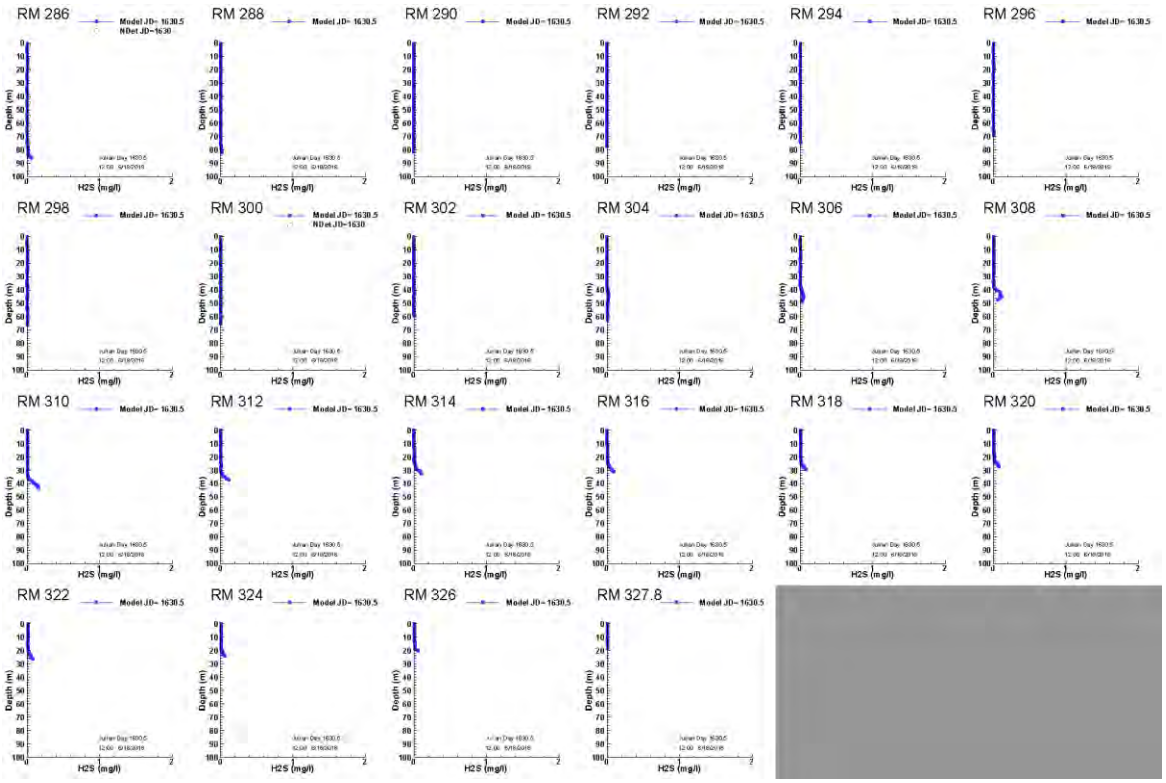


Figure 205. Vertical profiles of hydrogen sulfide compared with data for 6/18/2018.

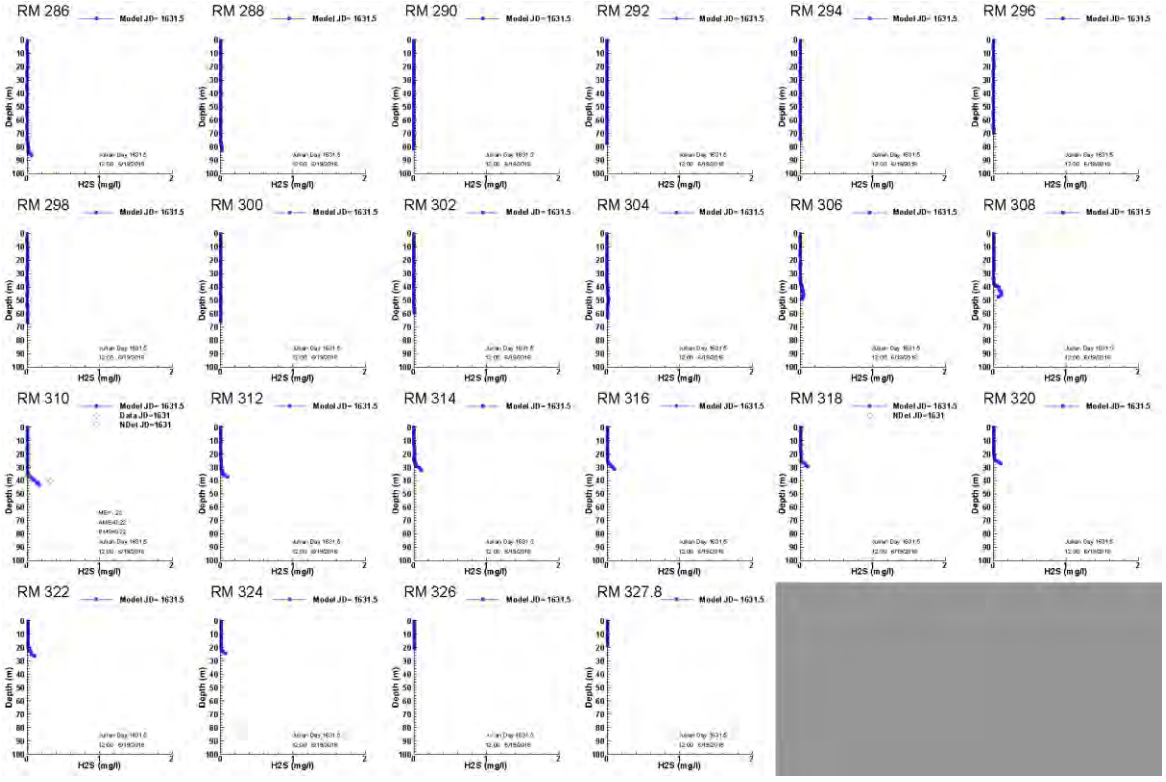


Figure 206. Vertical profiles of hydrogen sulfide compared with data for 6/19/2018.

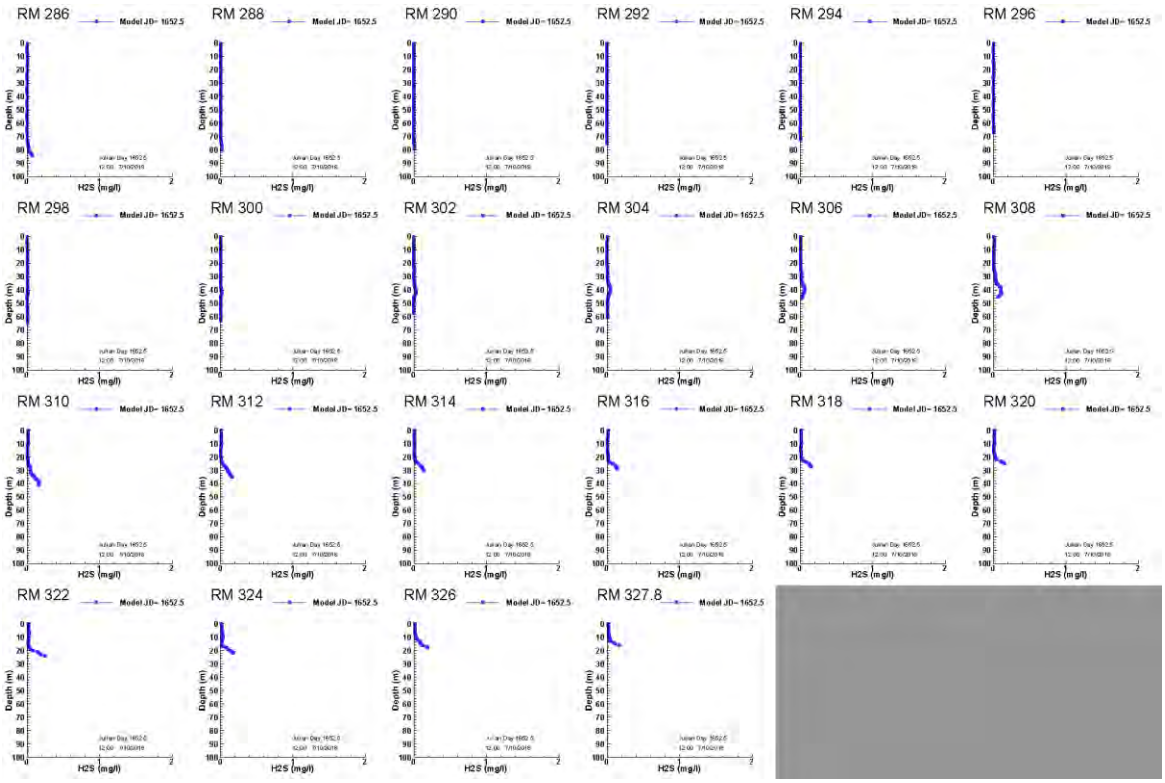


Figure 207. Vertical profiles of hydrogen sulfide compared with data for 7/10/2018.

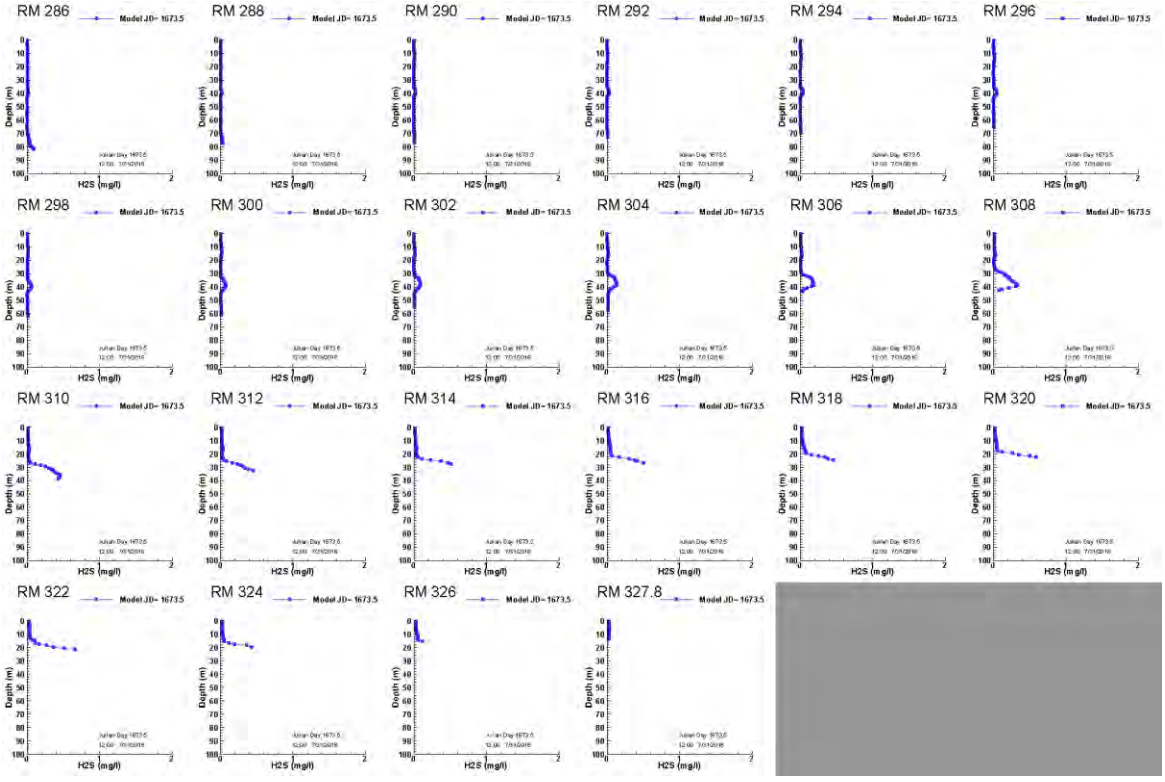


Figure 208. Vertical profiles of hydrogen sulfide compared with data for 7/31/2018.

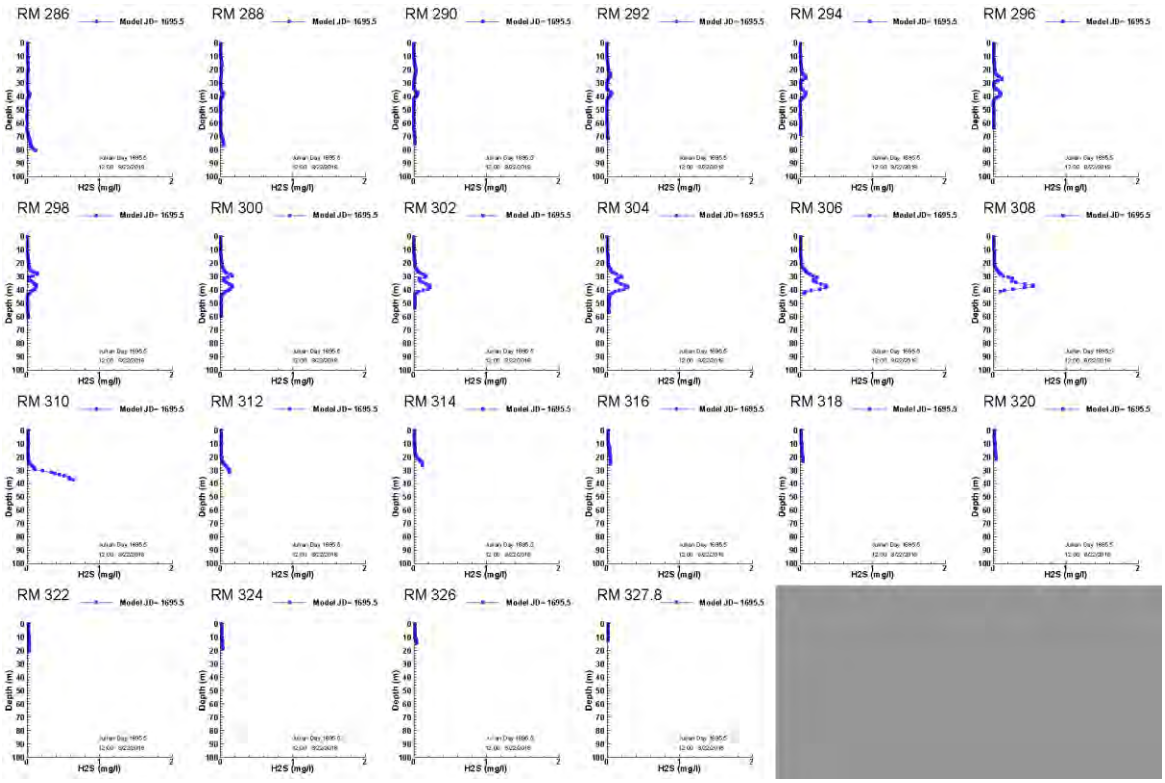


Figure 209. Vertical profiles of hydrogen sulfide compared with data for 8/22/2018.

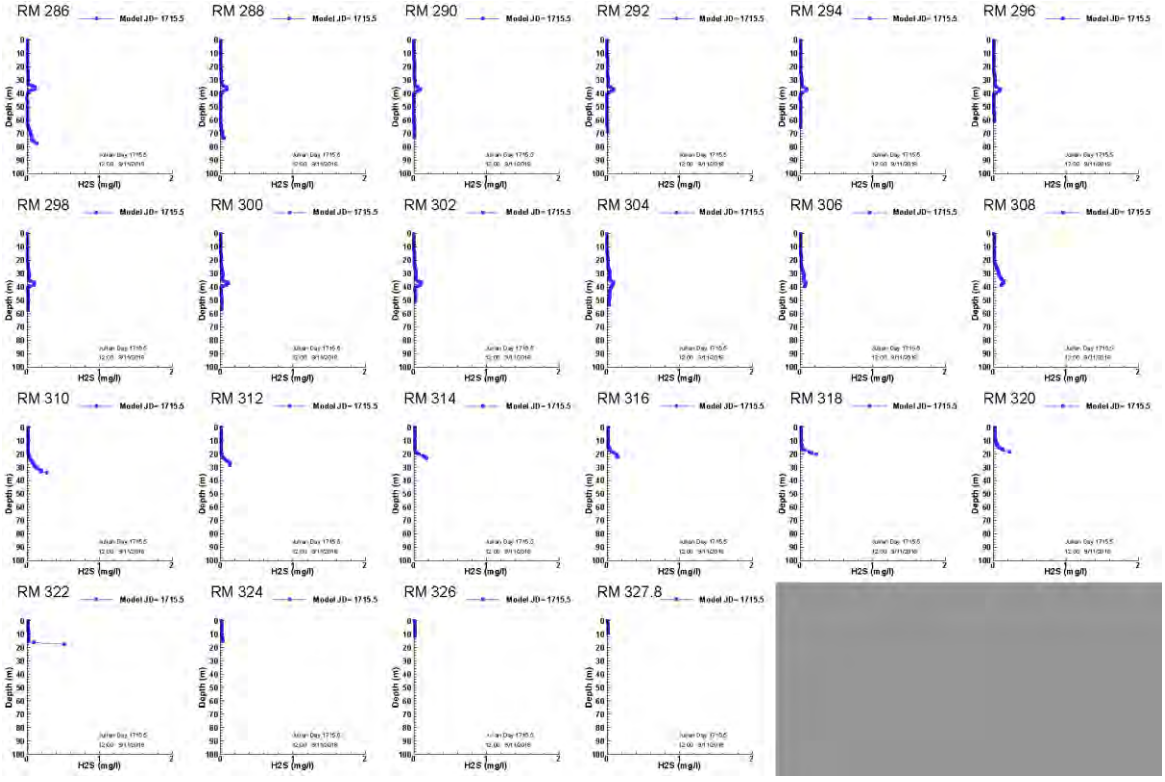


Figure 210. Vertical profiles of hydrogen sulfide compared with data for 9/11/2018.

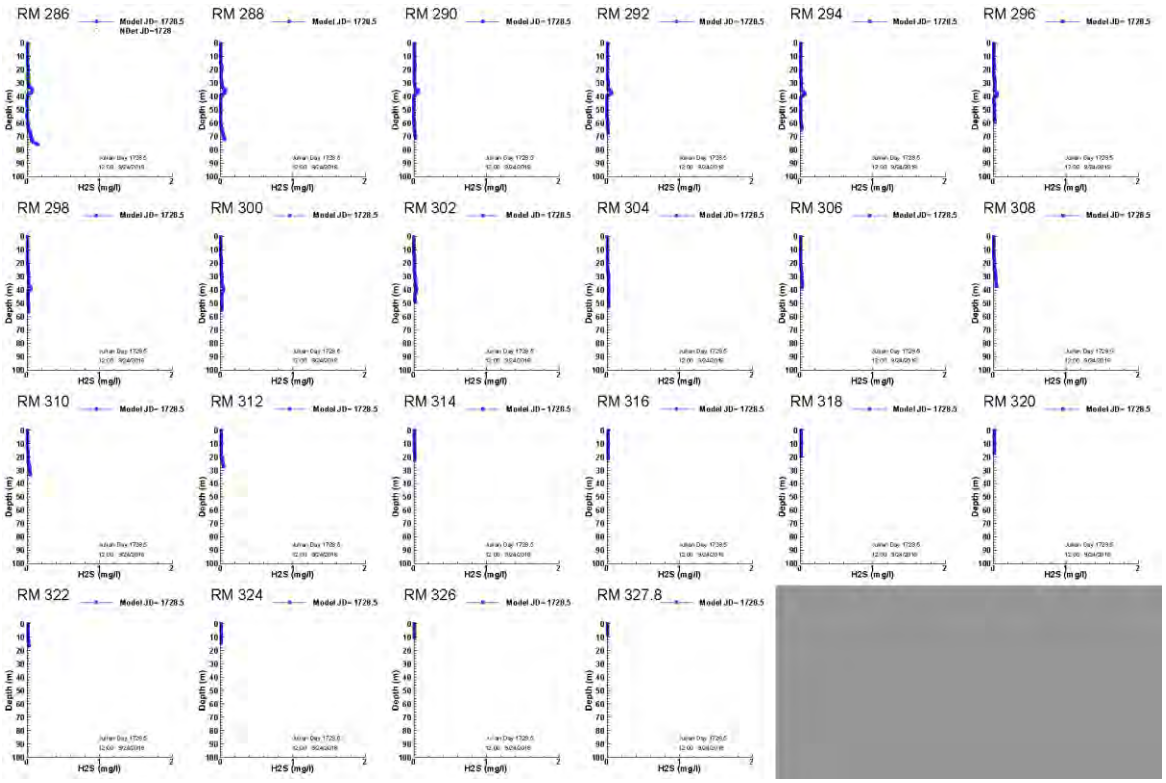


Figure 211. Vertical profiles of hydrogen sulfide compared with data for 9/24/2018.

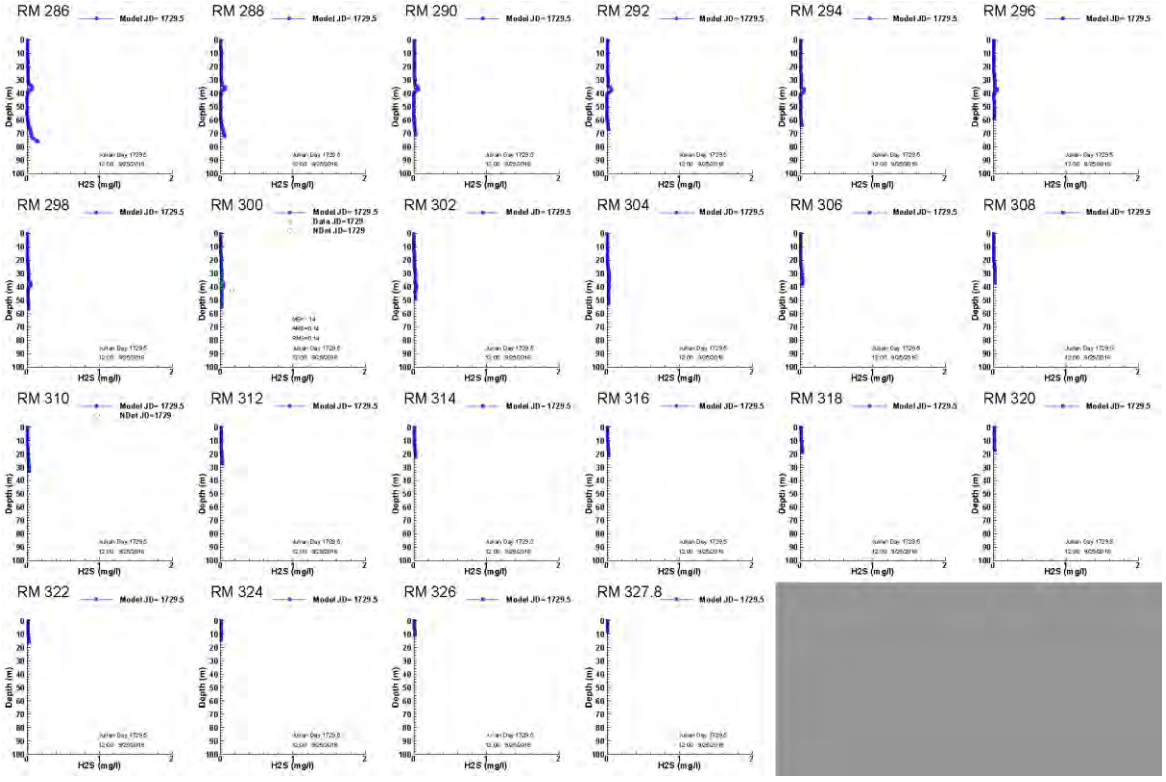


Figure 212. Vertical profiles of hydrogen sulfide compared with data for 9/25/2018.

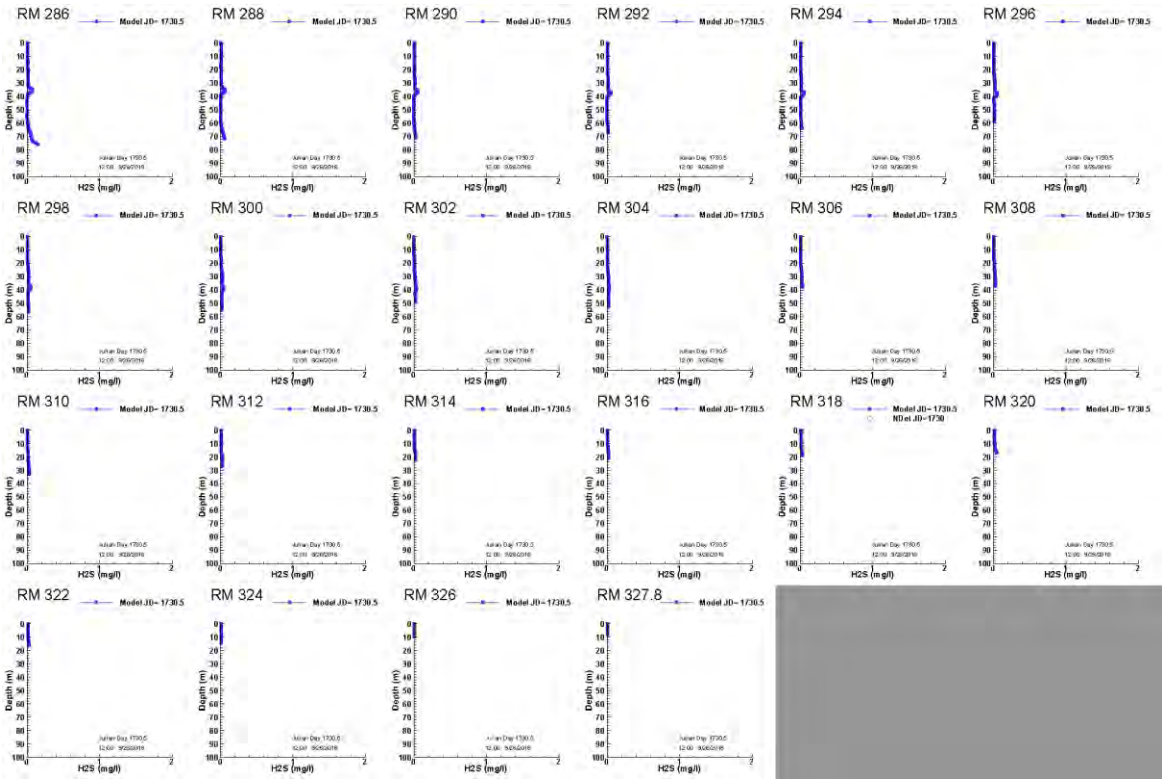


Figure 213. Vertical profiles of hydrogen sulfide compared with data for 9/26/2018.

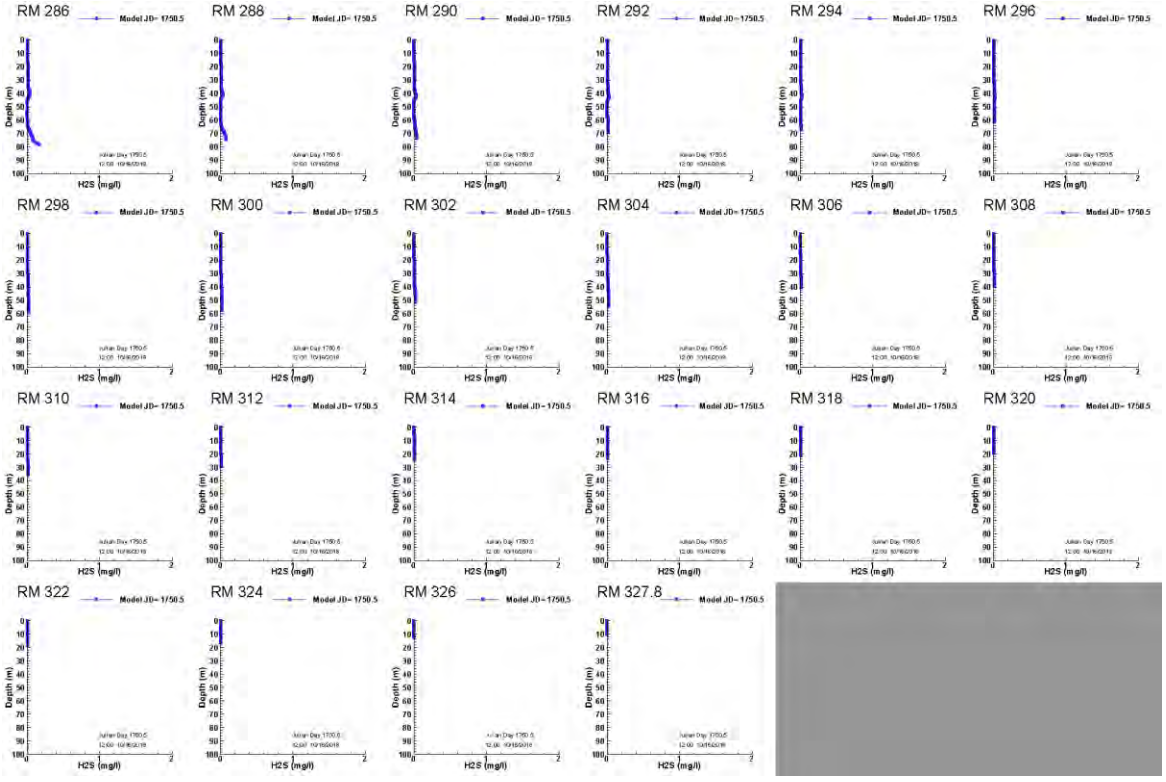


Figure 214. Vertical profiles of hydrogen sulfide compared with data for 10/16/2018.

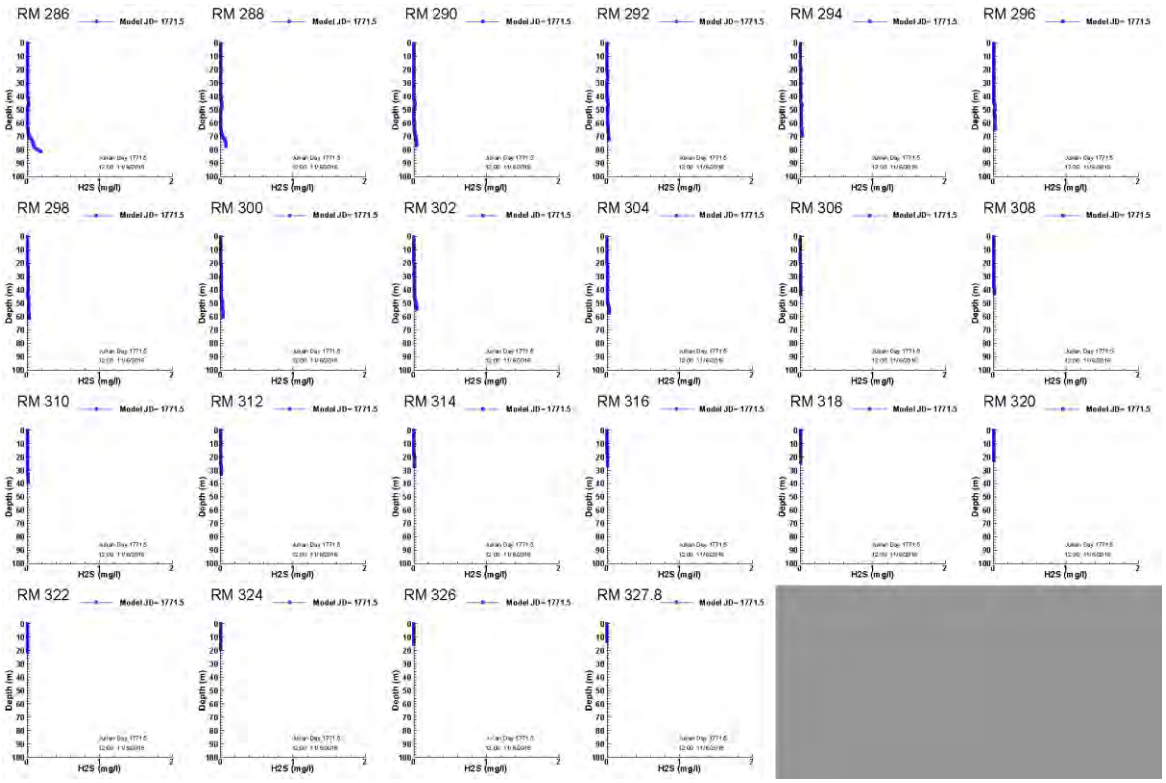


Figure 215. Vertical profiles of hydrogen sulfide compared with data for 11/ 6/2018.

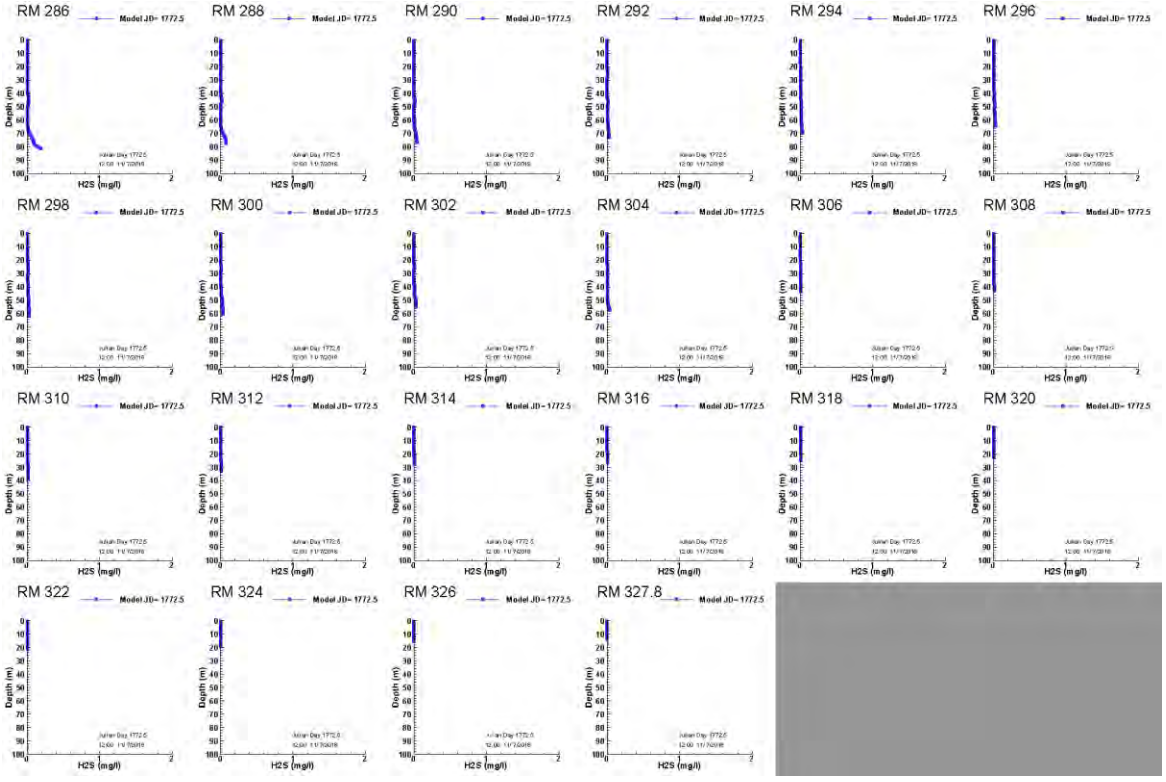


Figure 216. Vertical profiles of hydrogen sulfide compared with data for 11/ 7/2018.

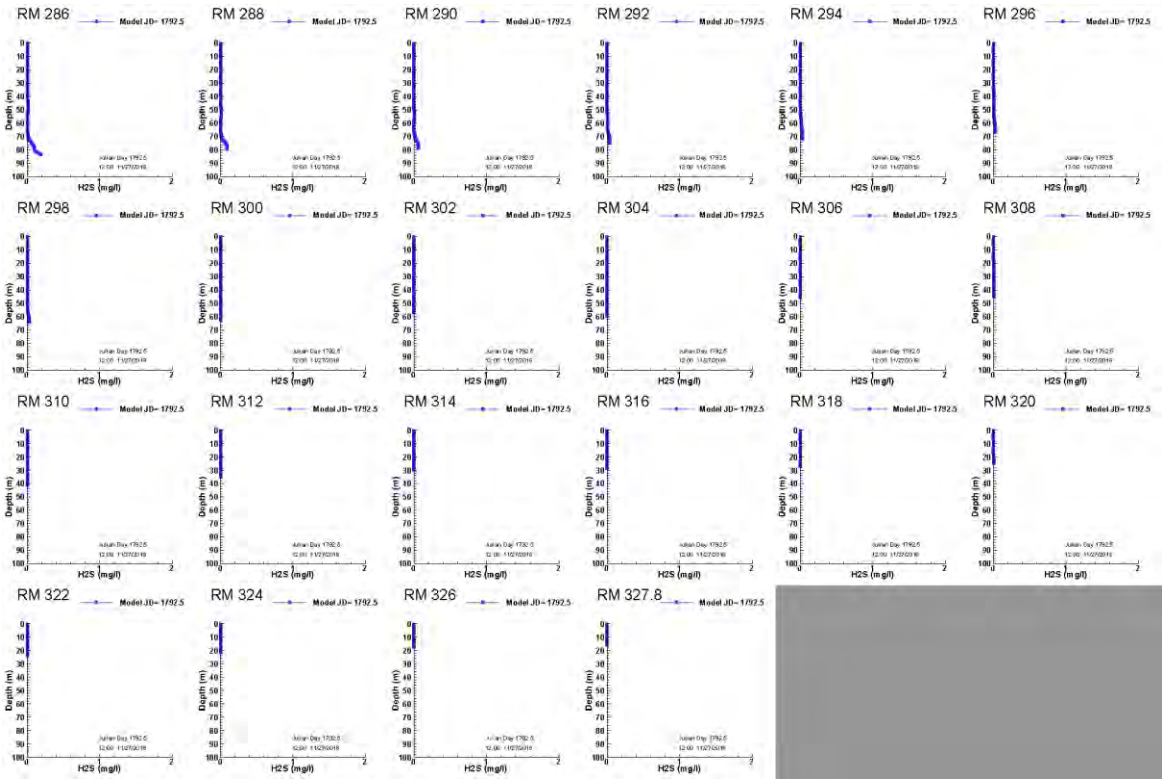


Figure 217. Vertical profiles of hydrogen sulfide compared with data for 11/27/2018.

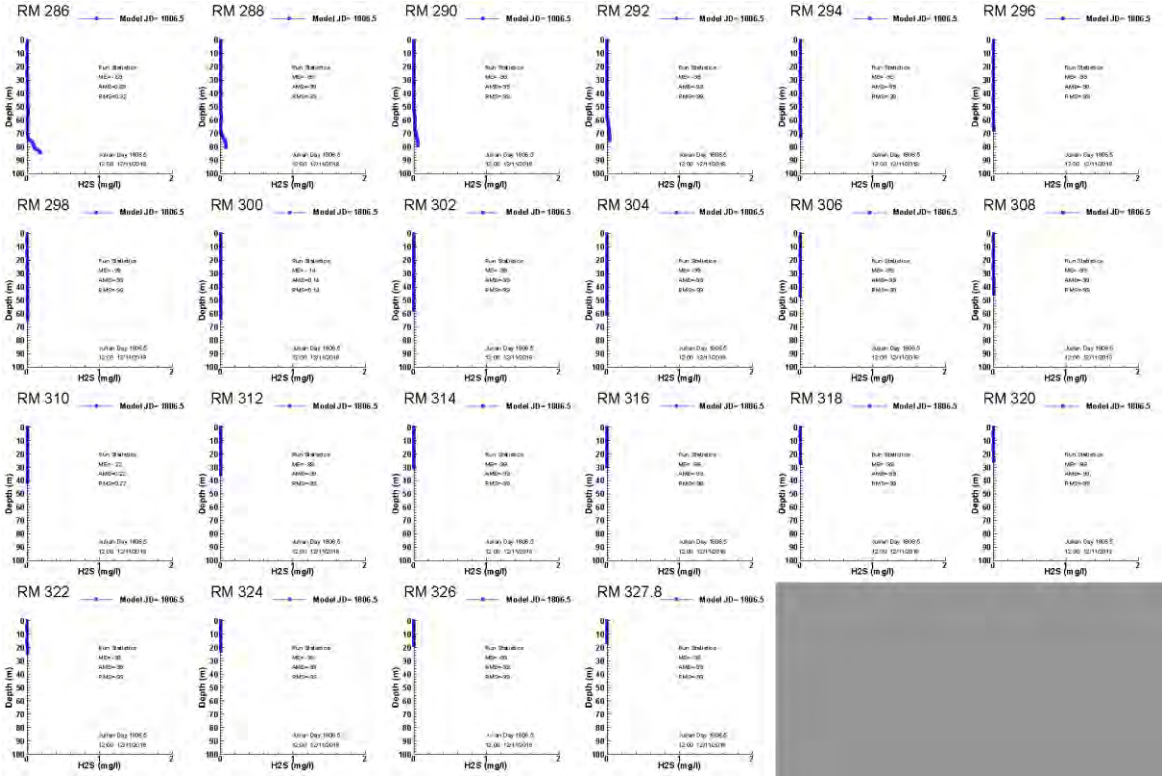


Figure 218. Vertical profiles of hydrogen sulfide compared with data for 12/11/2018.

Sulfate

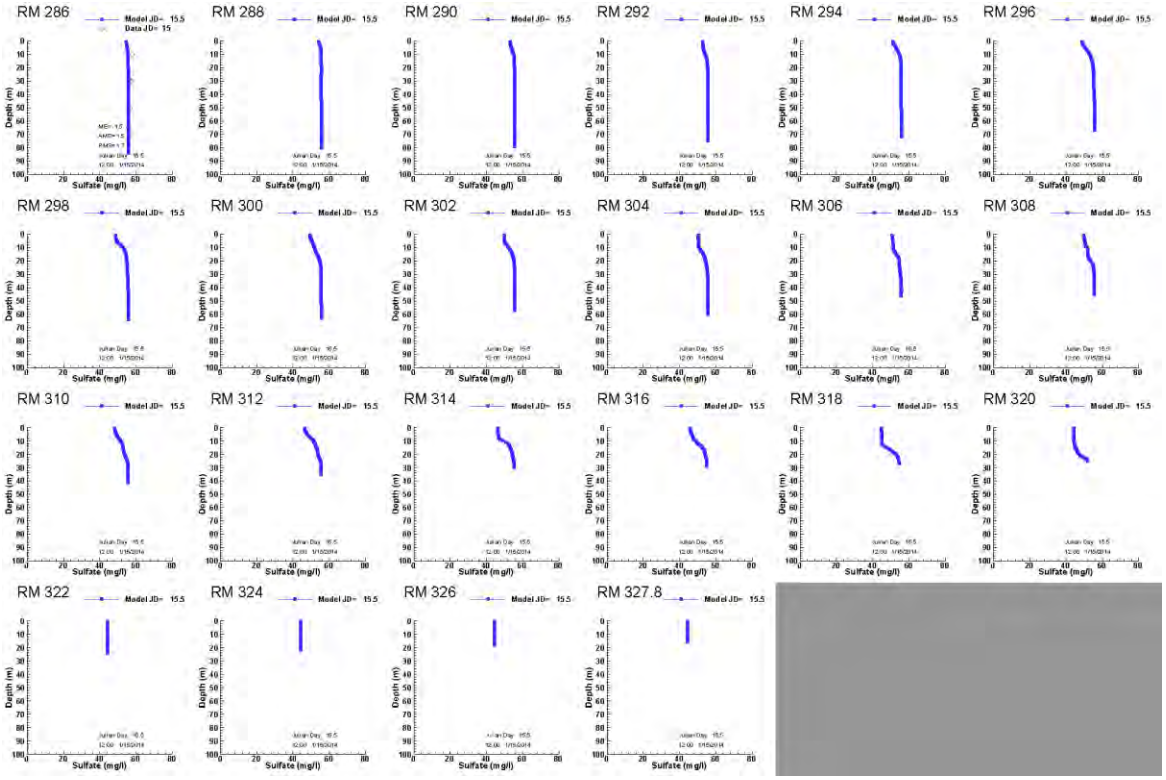


Figure 219. Vertical profiles of sulfate compared with data for 1/15/2014.

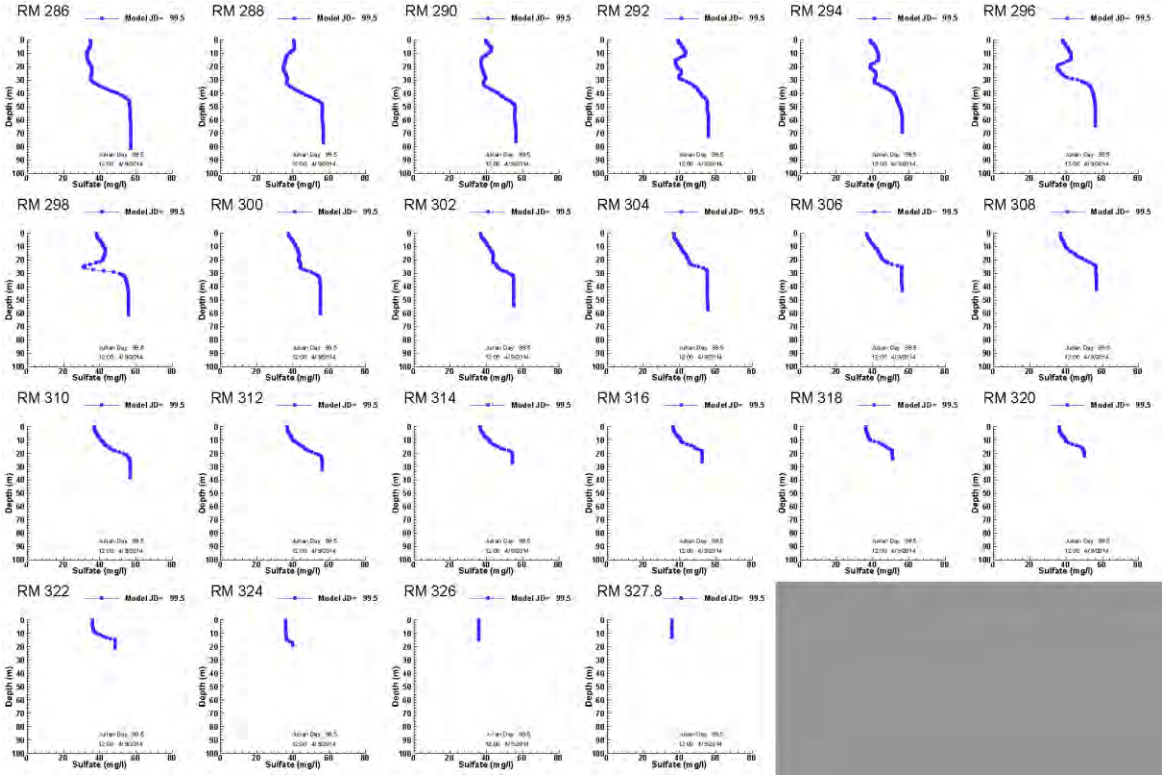


Figure 220. Vertical profiles of sulfate compared with data for 4/ 9/2014.

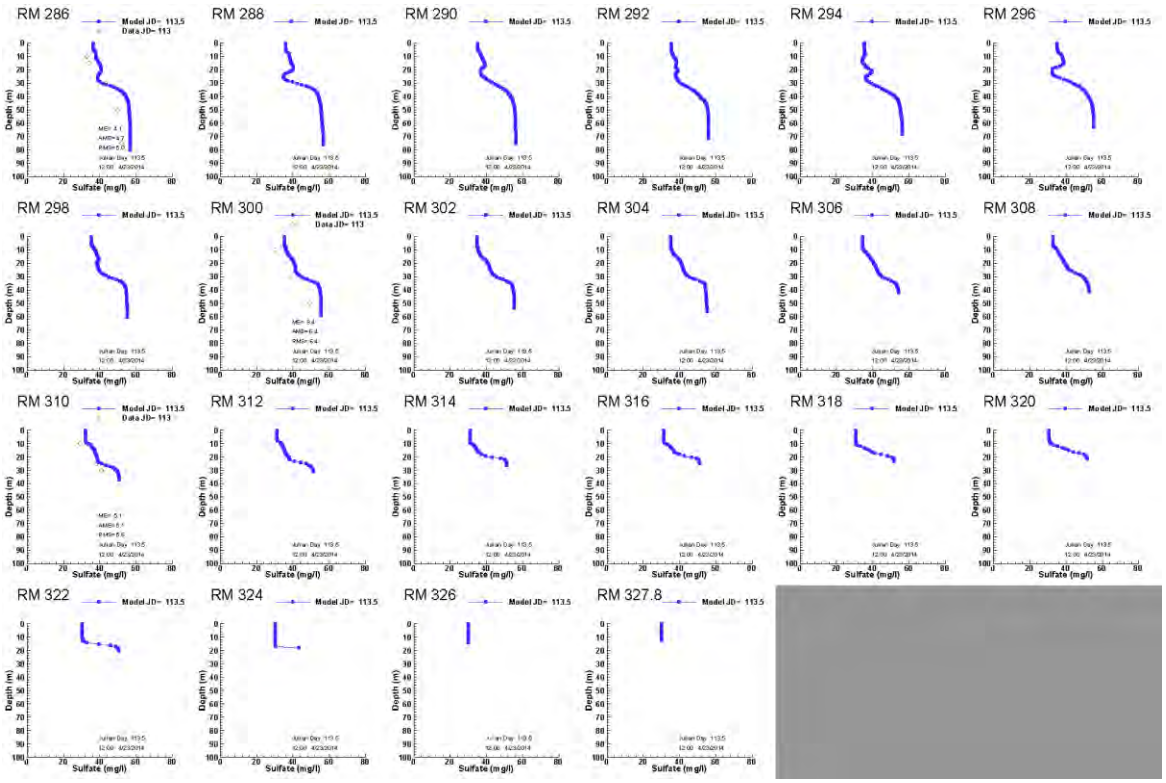


Figure 221. Vertical profiles of sulfate compared with data for 4/23/2014.

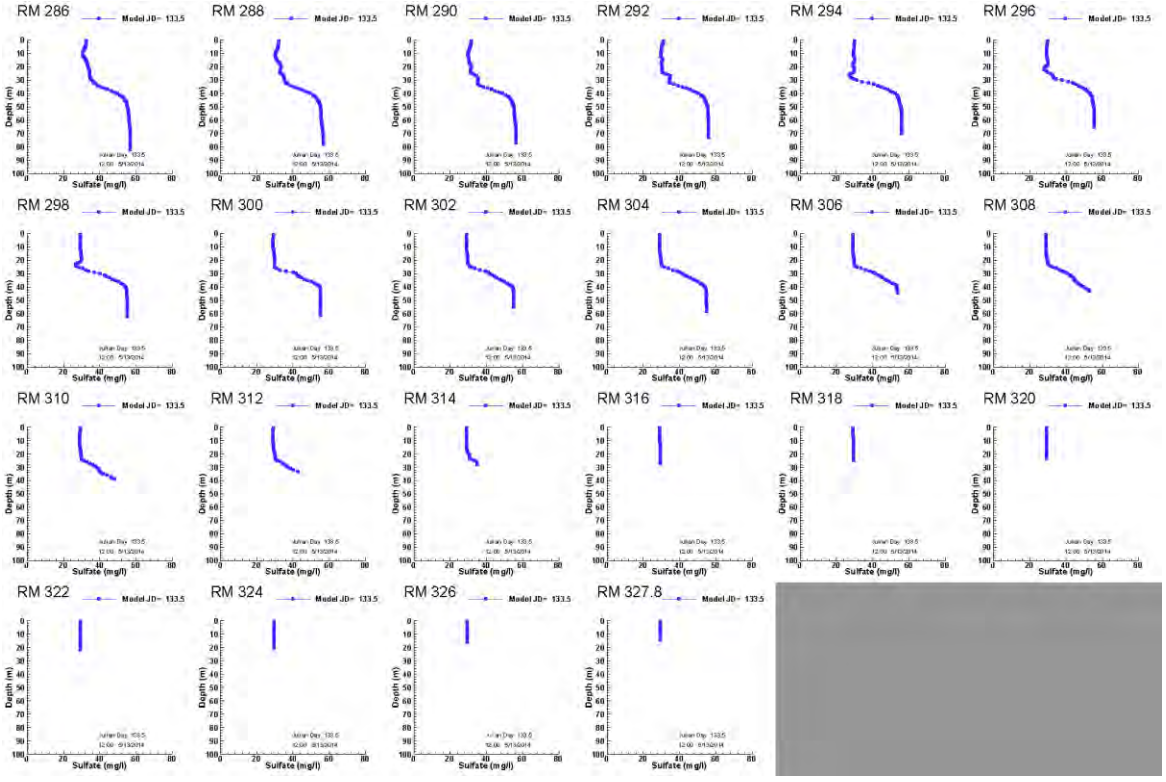


Figure 222. Vertical profiles of sulfate compared with data for 5/13/2014.

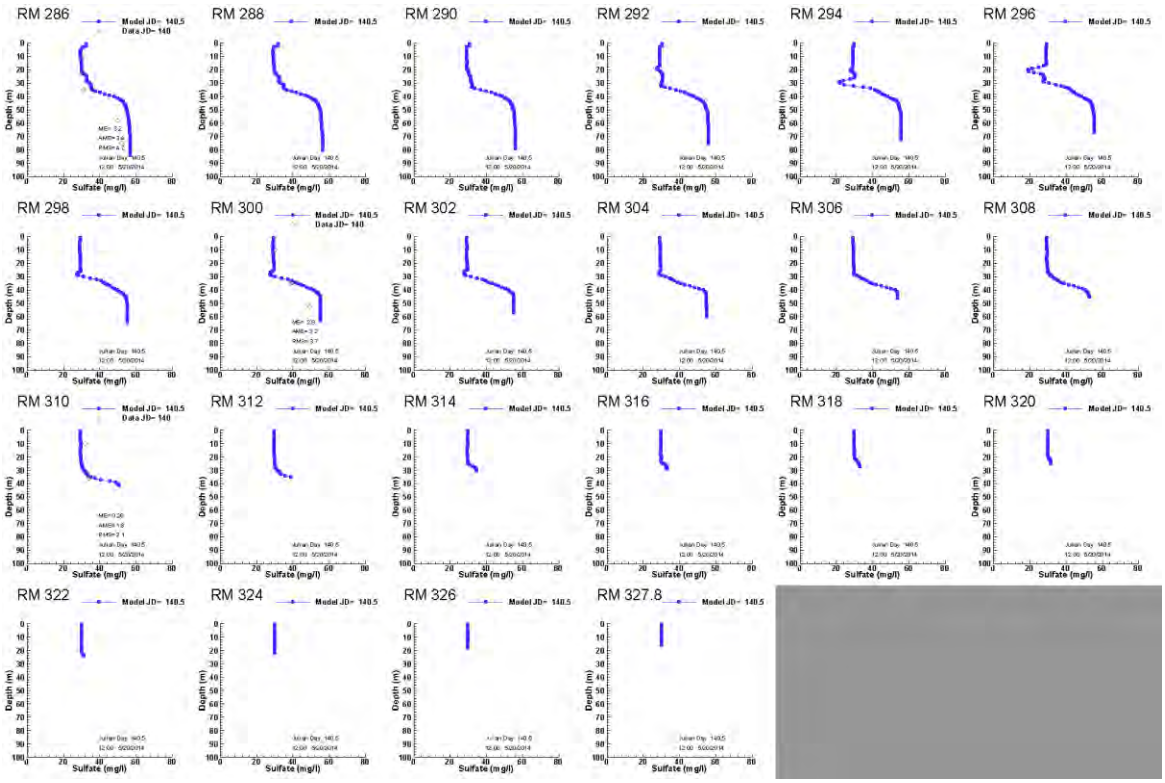


Figure 223. Vertical profiles of sulfate compared with data for 5/20/2014.

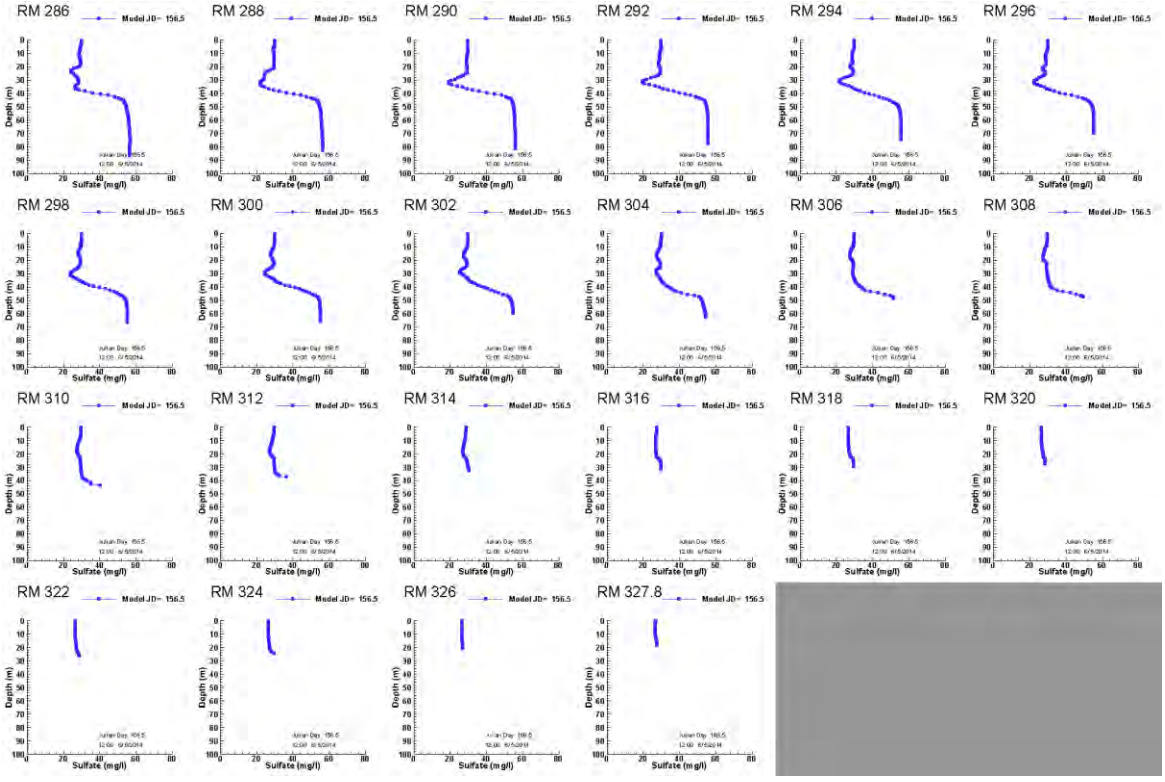


Figure 224. Vertical profiles of sulfate compared with data for 6/ 5/2014.

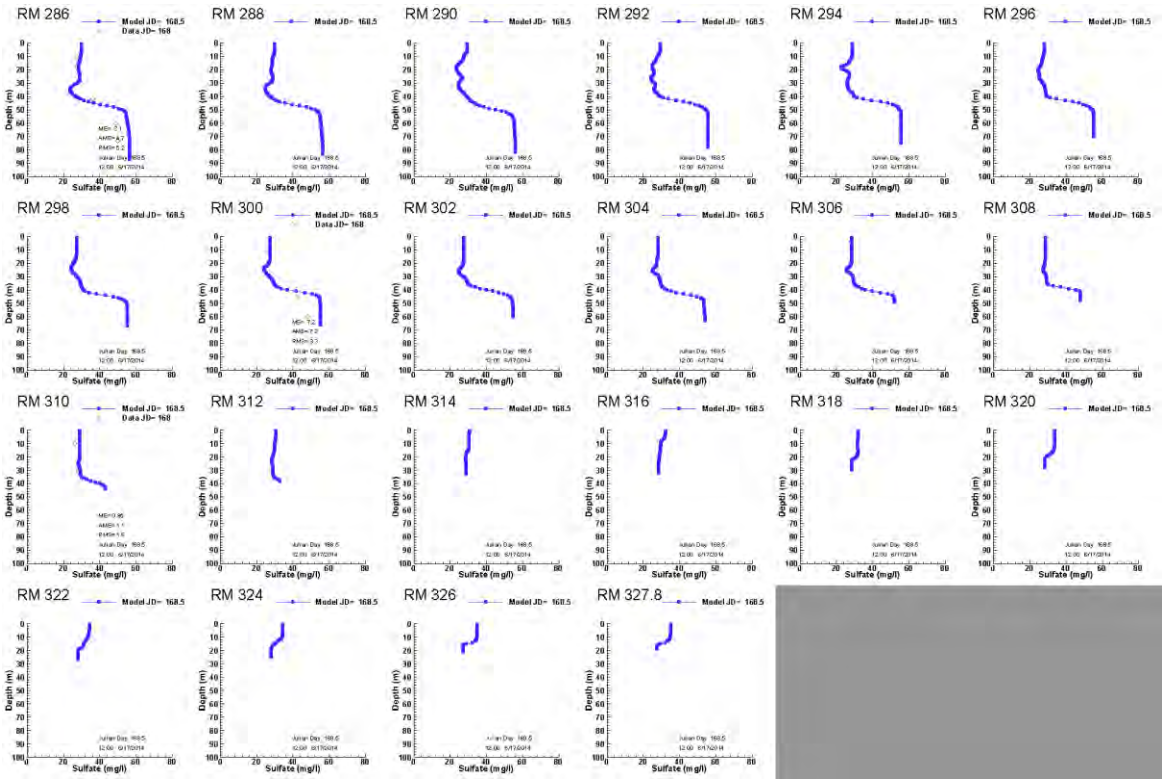


Figure 225. Vertical profiles of sulfate compared with data for 6/17/2014.

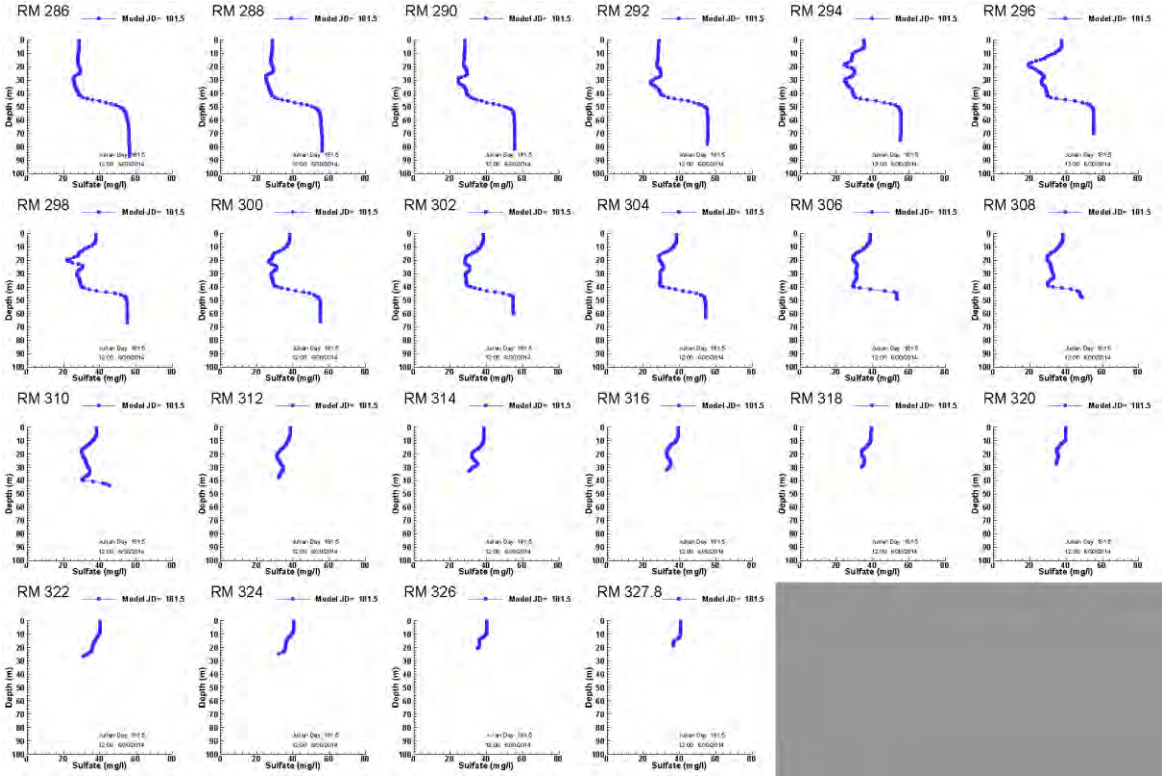


Figure 226. Vertical profiles of sulfate compared with data for 6/30/2014.

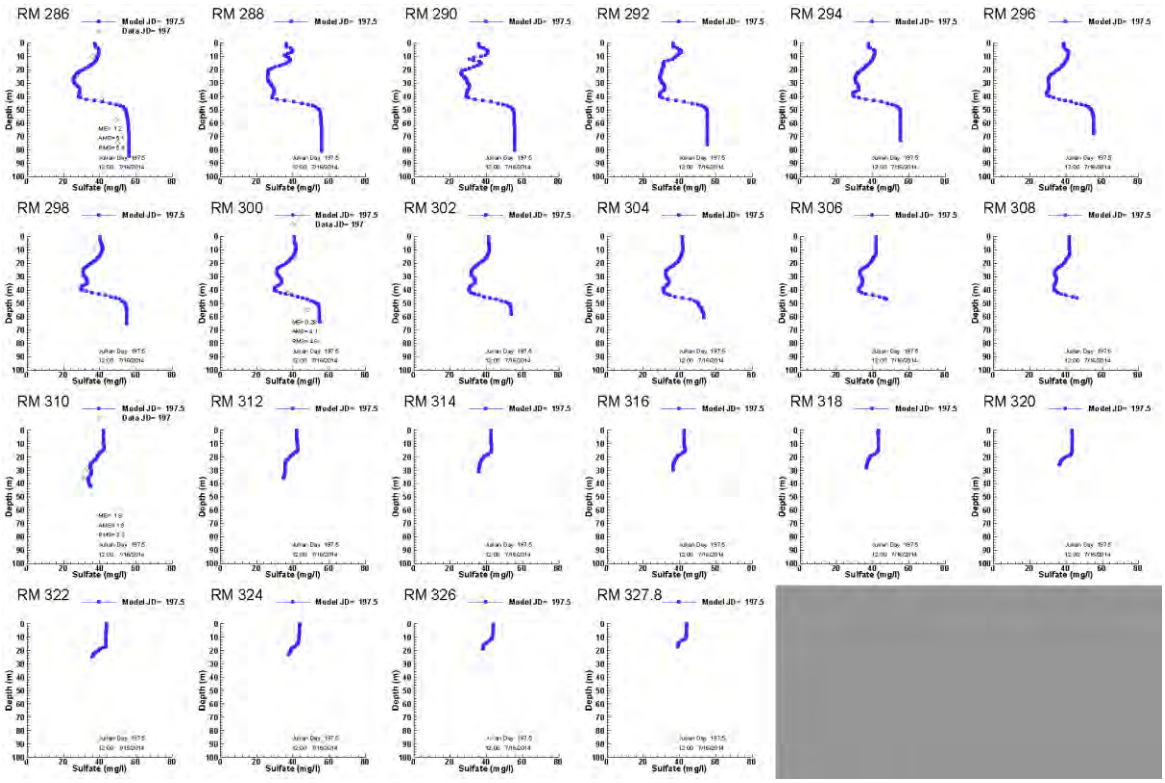


Figure 227. Vertical profiles of sulfate compared with data for 7/16/2014.

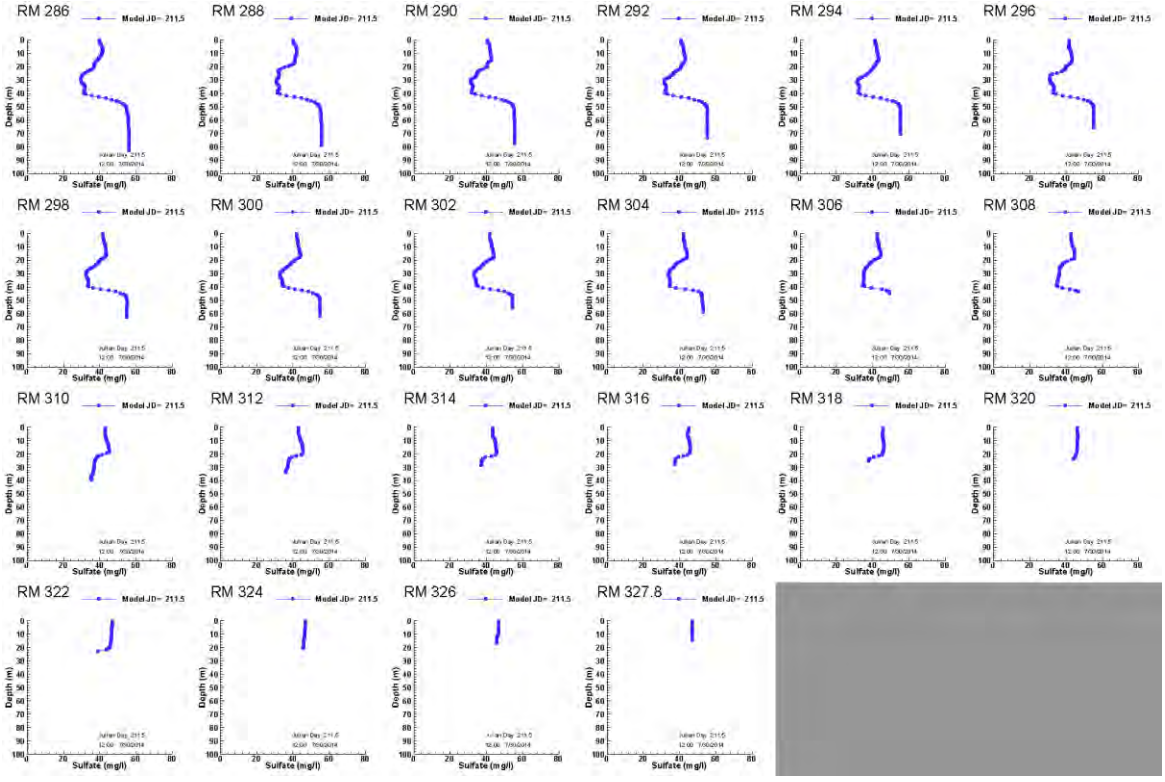


Figure 228. Vertical profiles of sulfate compared with data for 7/30/2014.

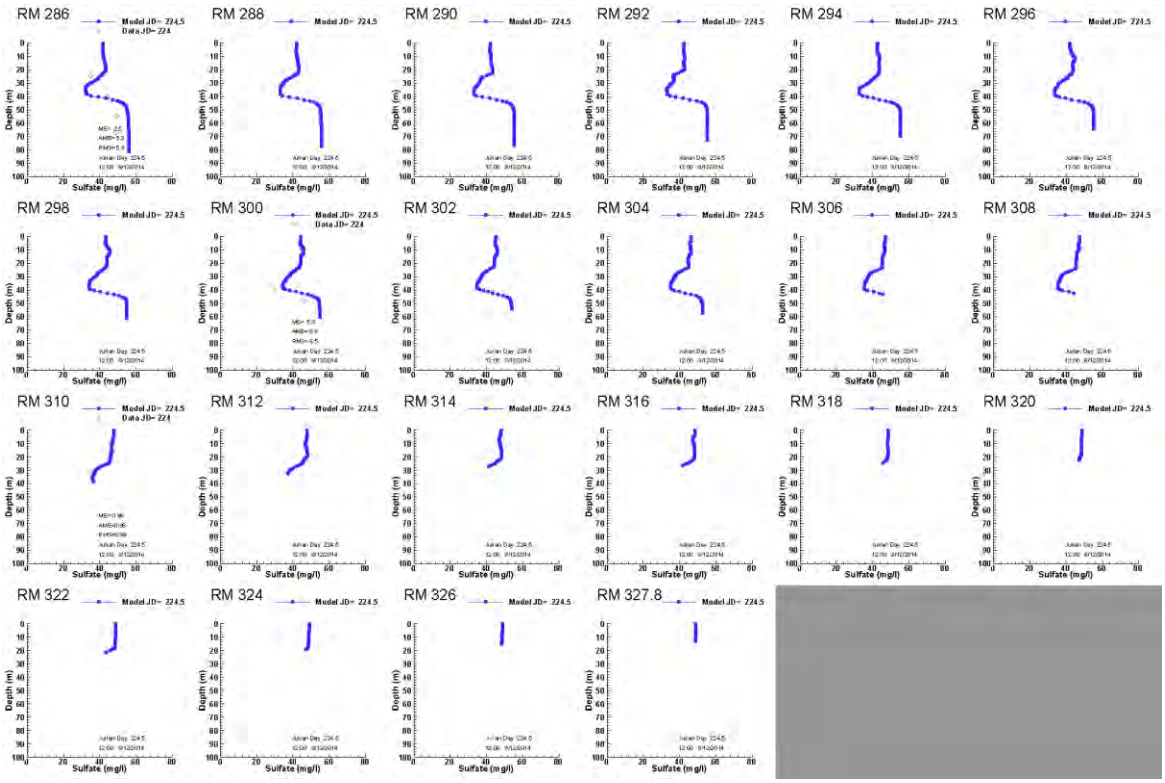


Figure 229. Vertical profiles of sulfate compared with data for 8/12/2014.

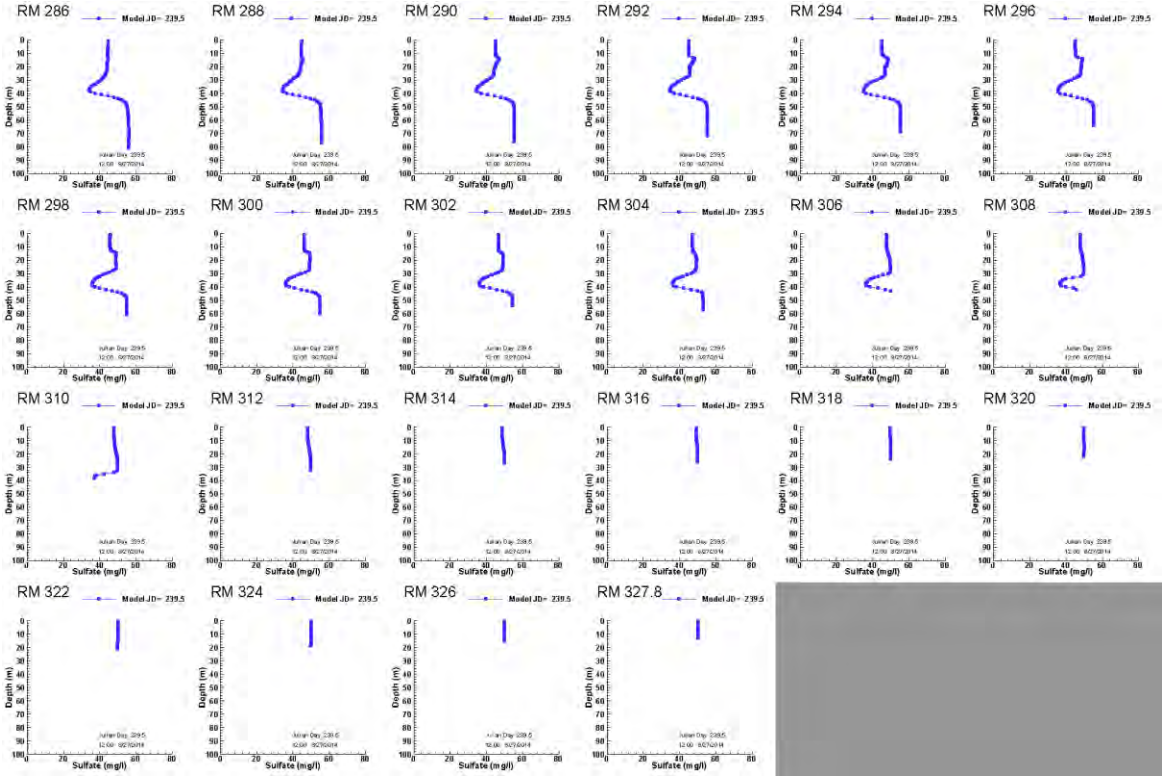


Figure 230. Vertical profiles of sulfate compared with data for 8/27/2014.

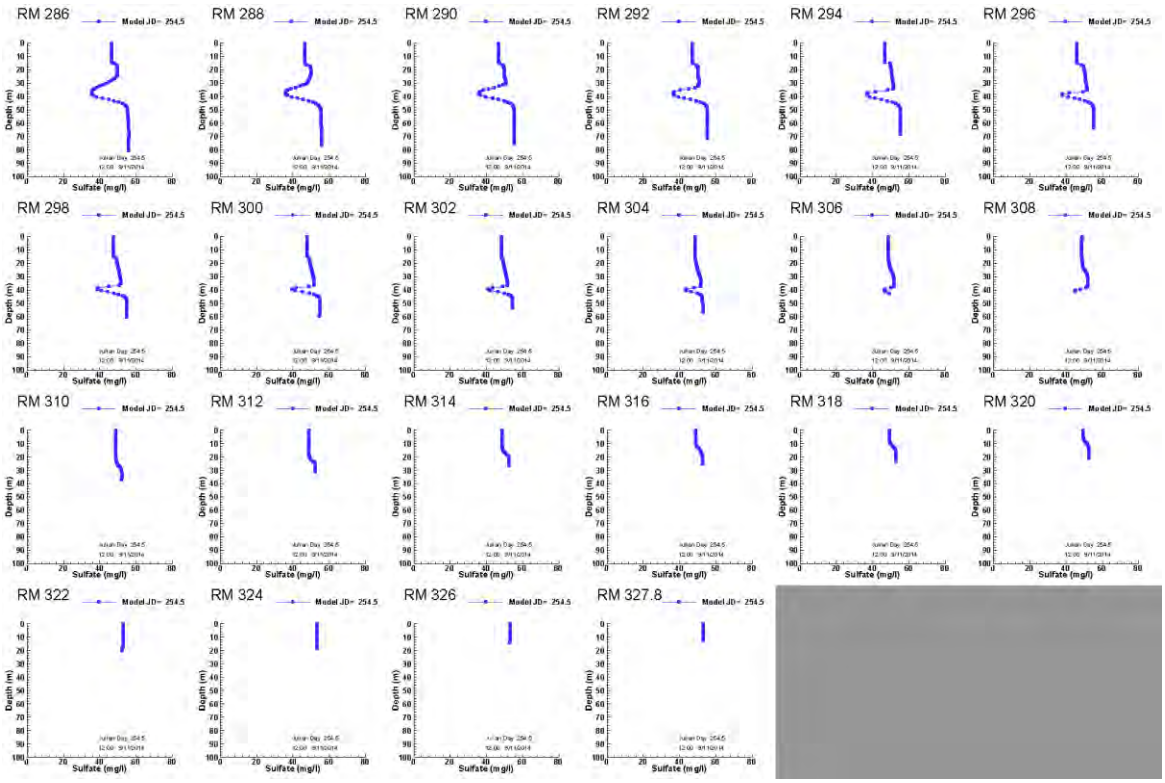


Figure 231. Vertical profiles of sulfate compared with data for 9/11/2014.

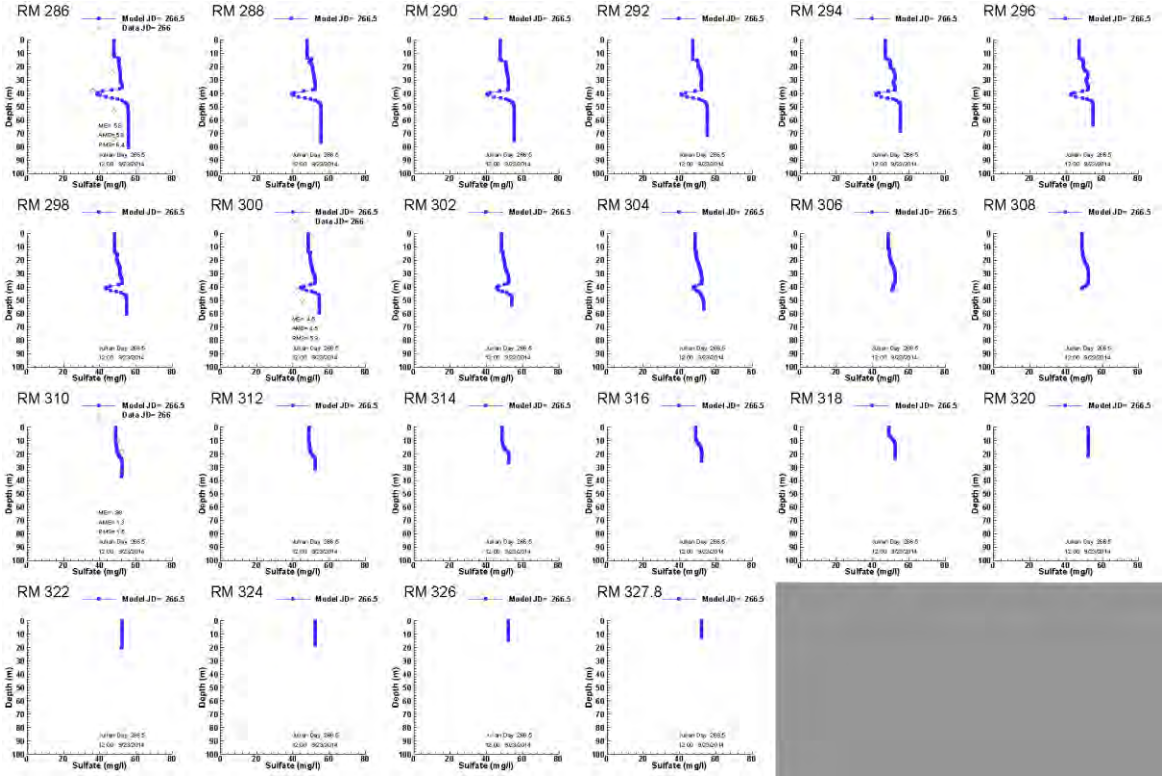


Figure 232. Vertical profiles of sulfate compared with data for 9/23/2014.

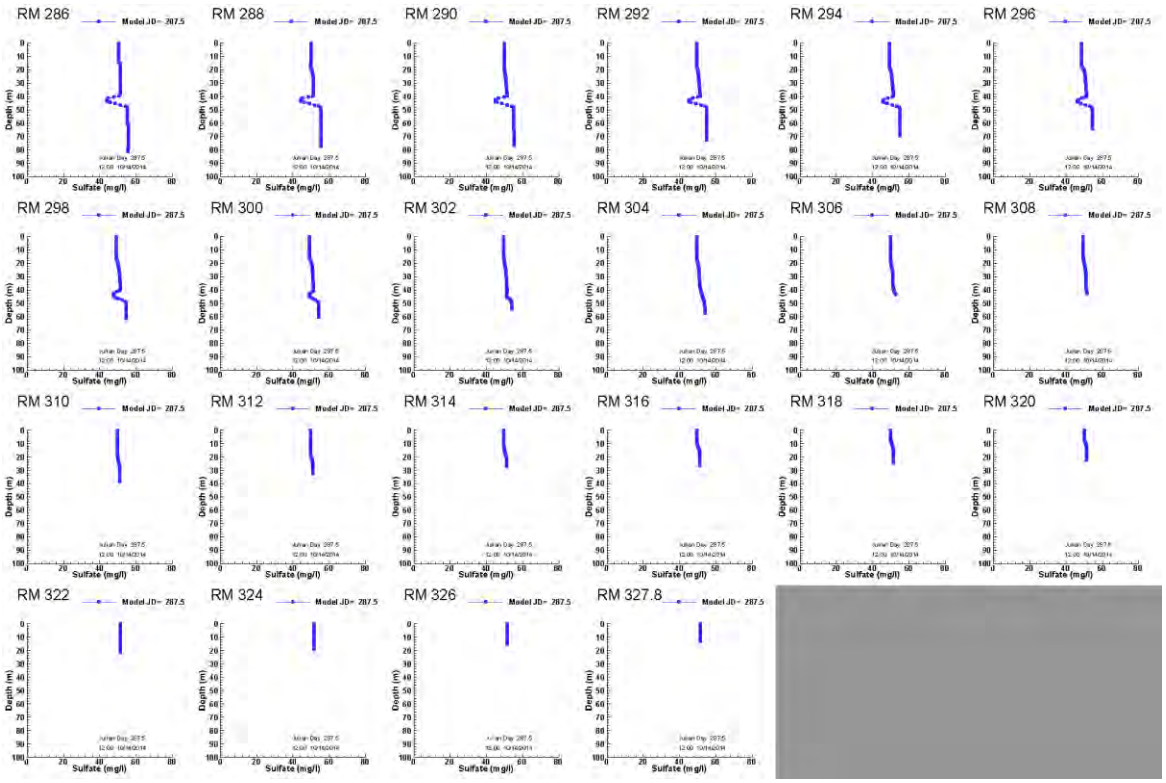


Figure 233. Vertical profiles of sulfate compared with data for 10/14/2014.

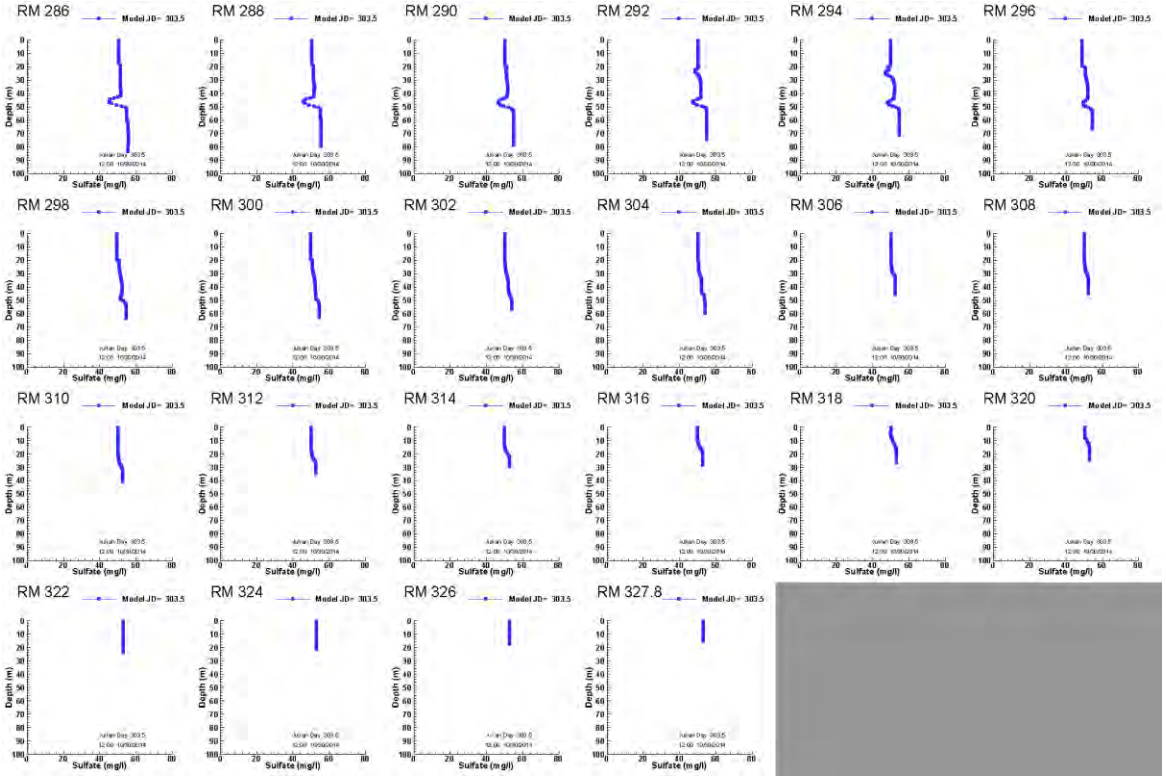


Figure 234. Vertical profiles of sulfate compared with data for 10/30/2014.

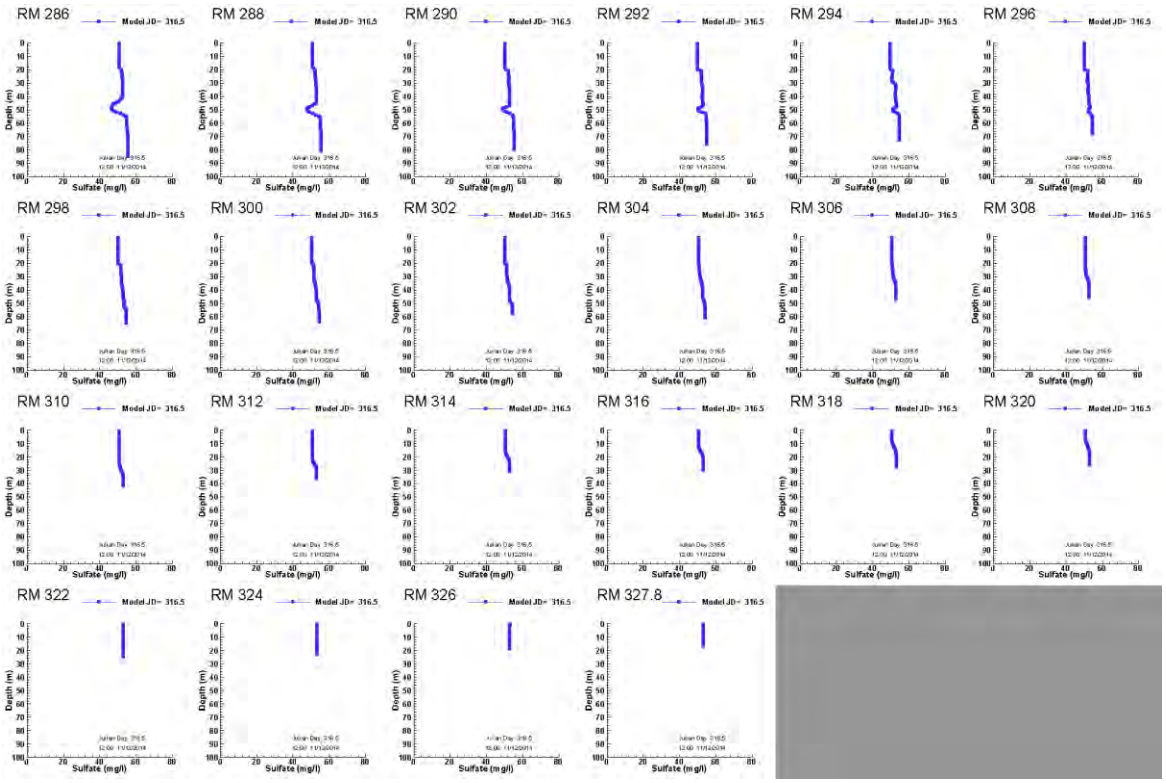


Figure 235. Vertical profiles of sulfate compared with data for 11/12/2014.

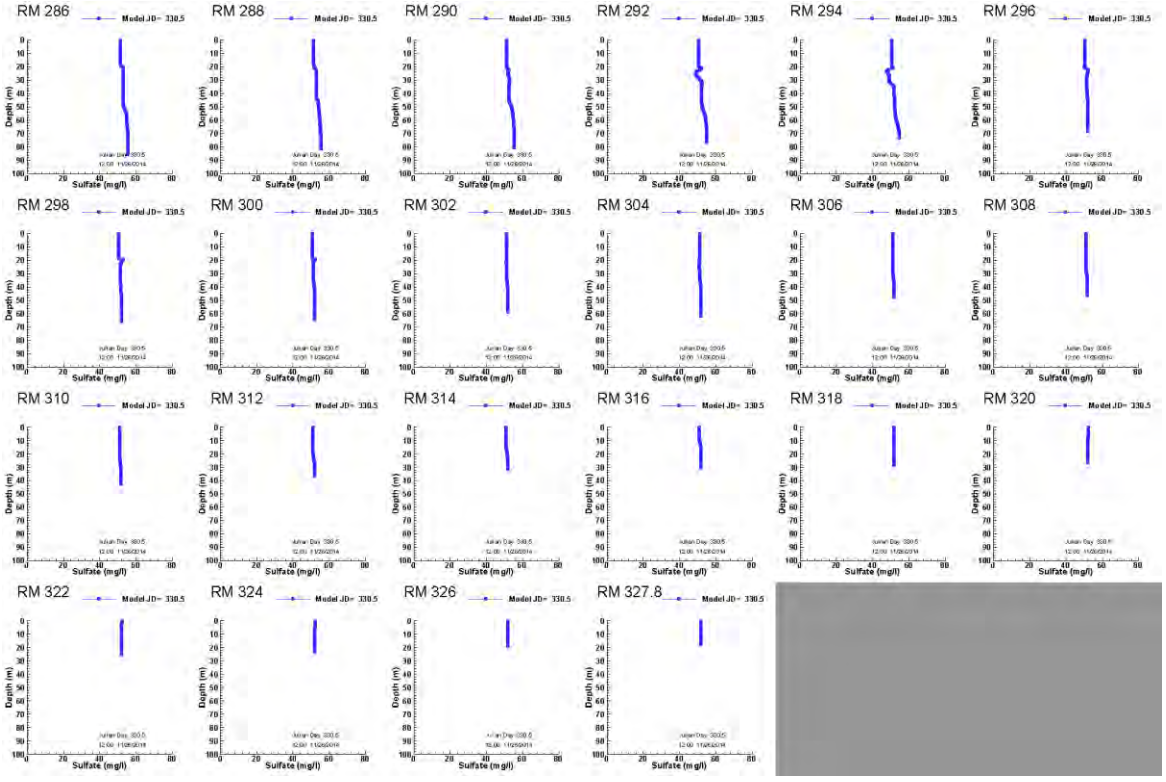


Figure 236. Vertical profiles of sulfate compared with data for 11/26/2014.

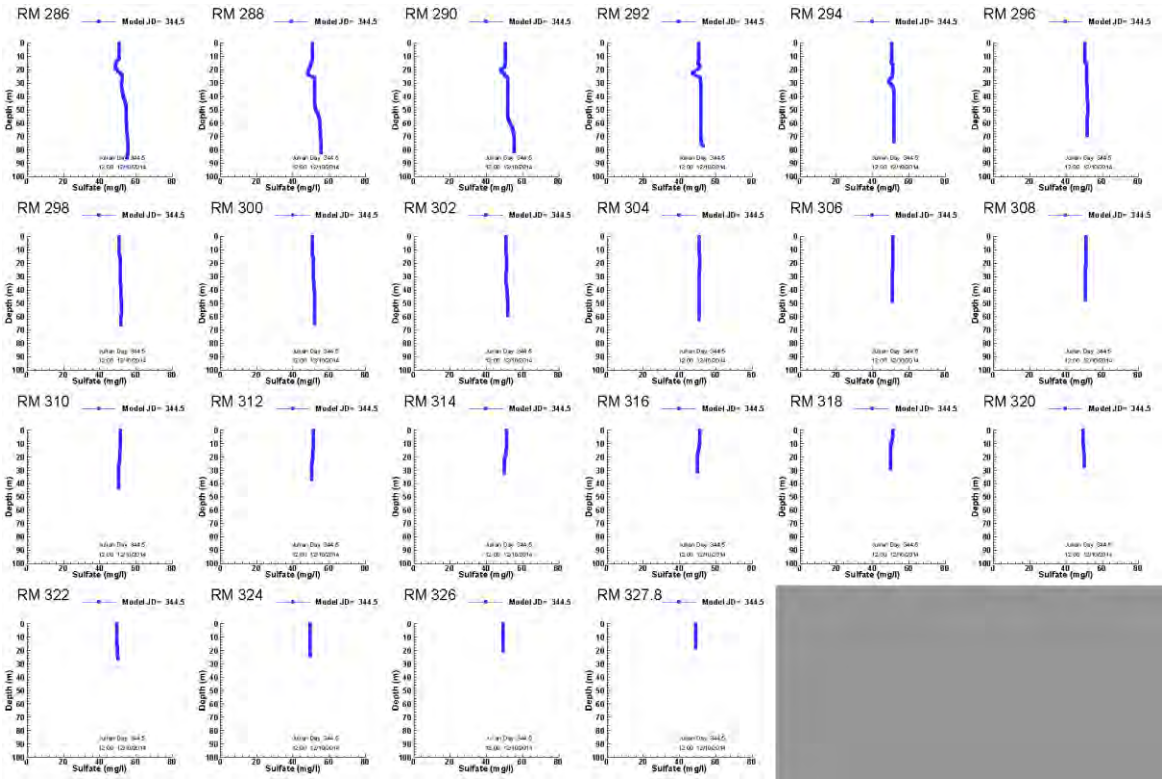


Figure 237. Vertical profiles of sulfate compared with data for 12/10/2014.

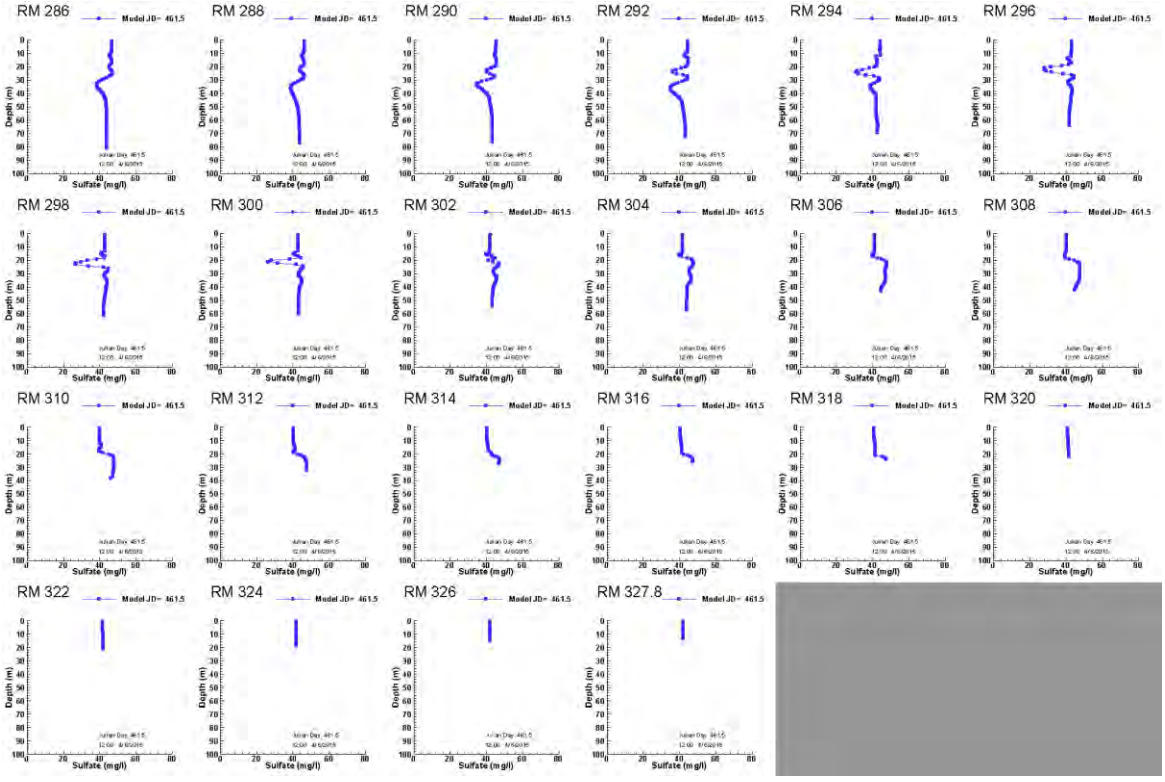


Figure 238. Vertical profiles of sulfate compared with data for 4/ 6/2015.

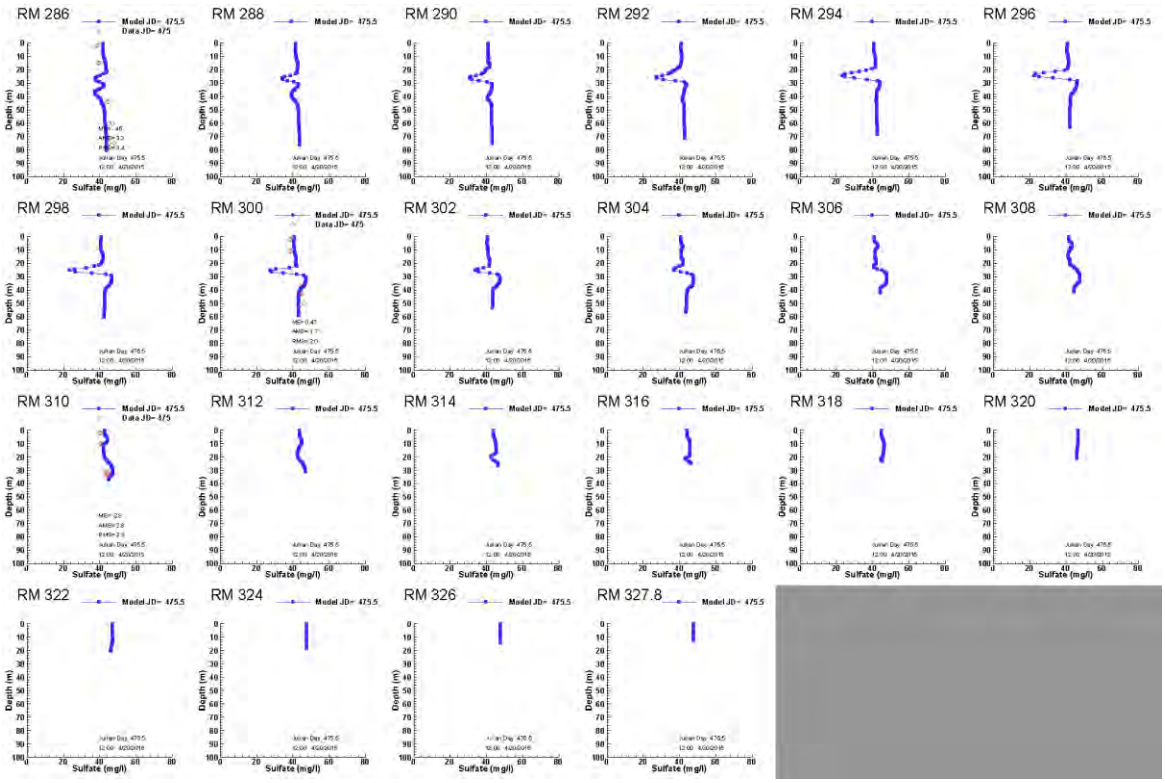


Figure 239. Vertical profiles of sulfate compared with data for 4/20/2015.

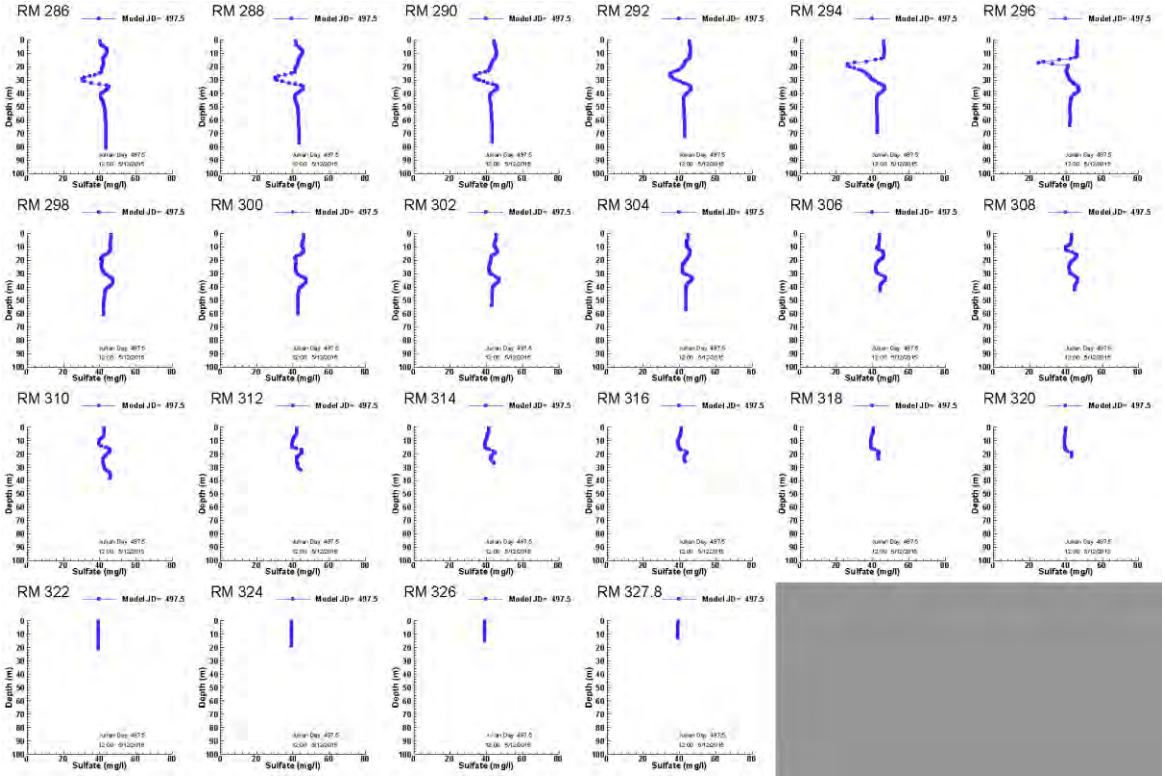


Figure 240. Vertical profiles of sulfate compared with data for 5/12/2015.

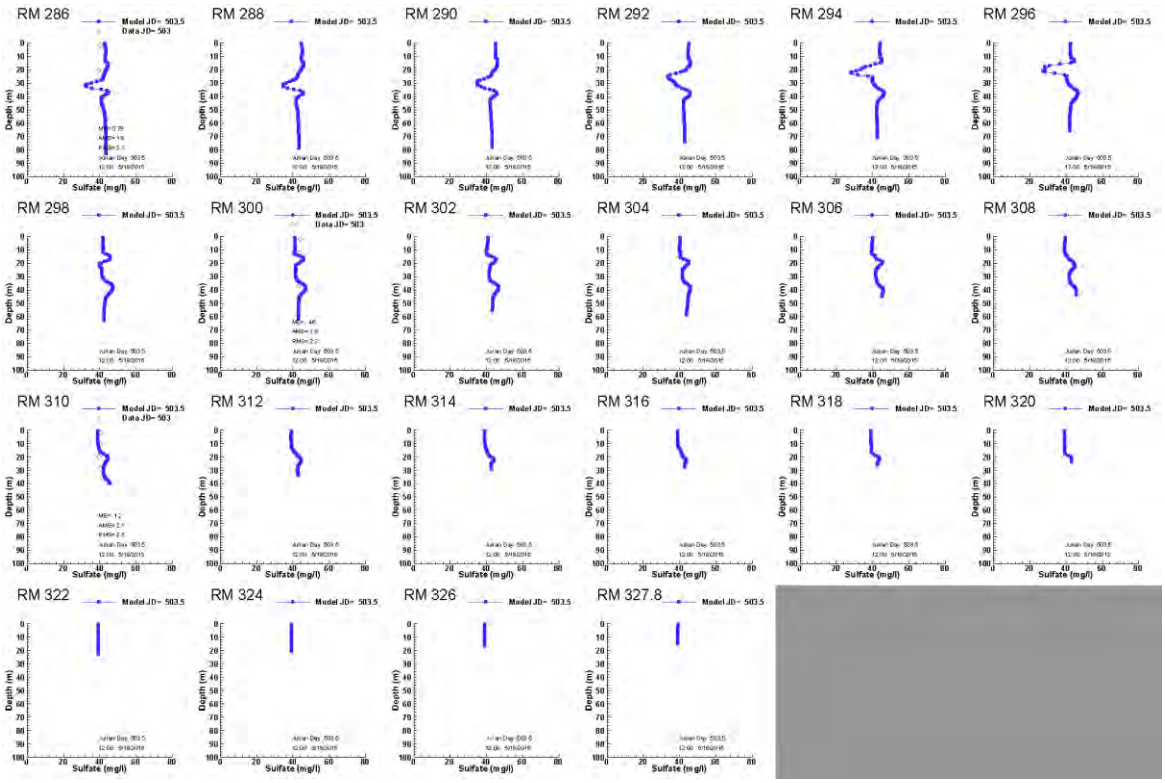


Figure 241. Vertical profiles of sulfate compared with data for 5/18/2015.

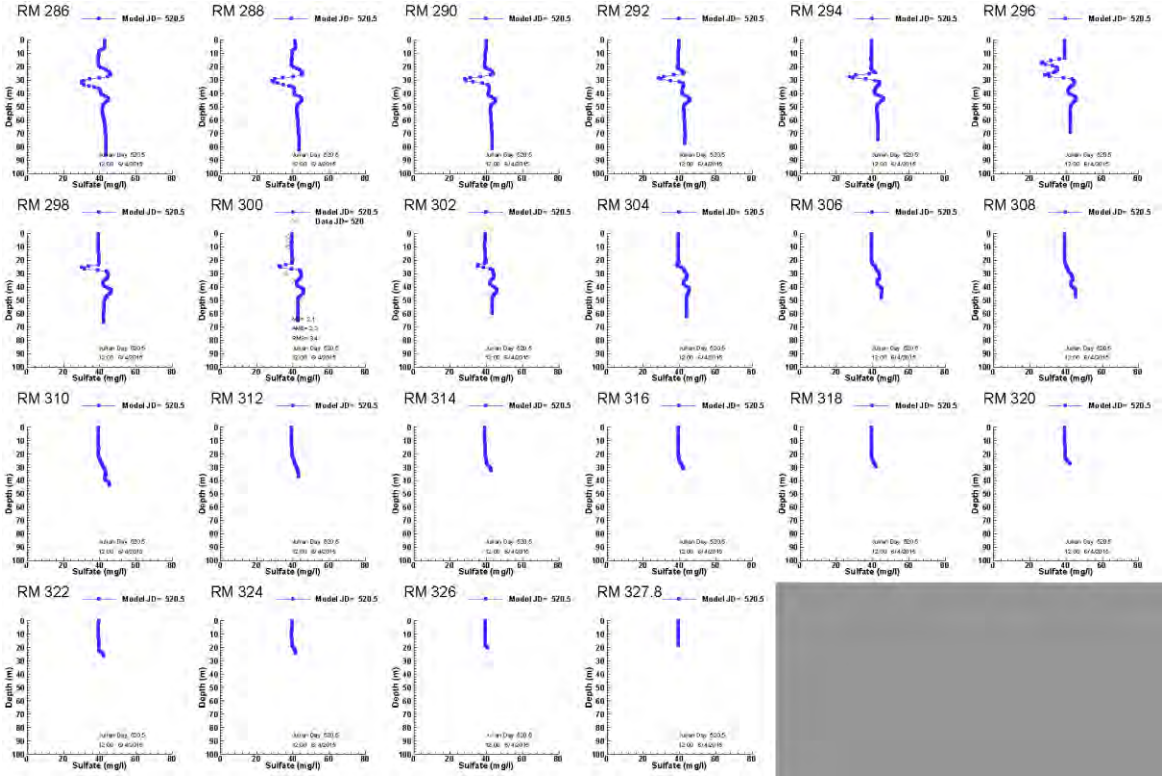


Figure 242. Vertical profiles of sulfate compared with data for 6/ 4/2015.

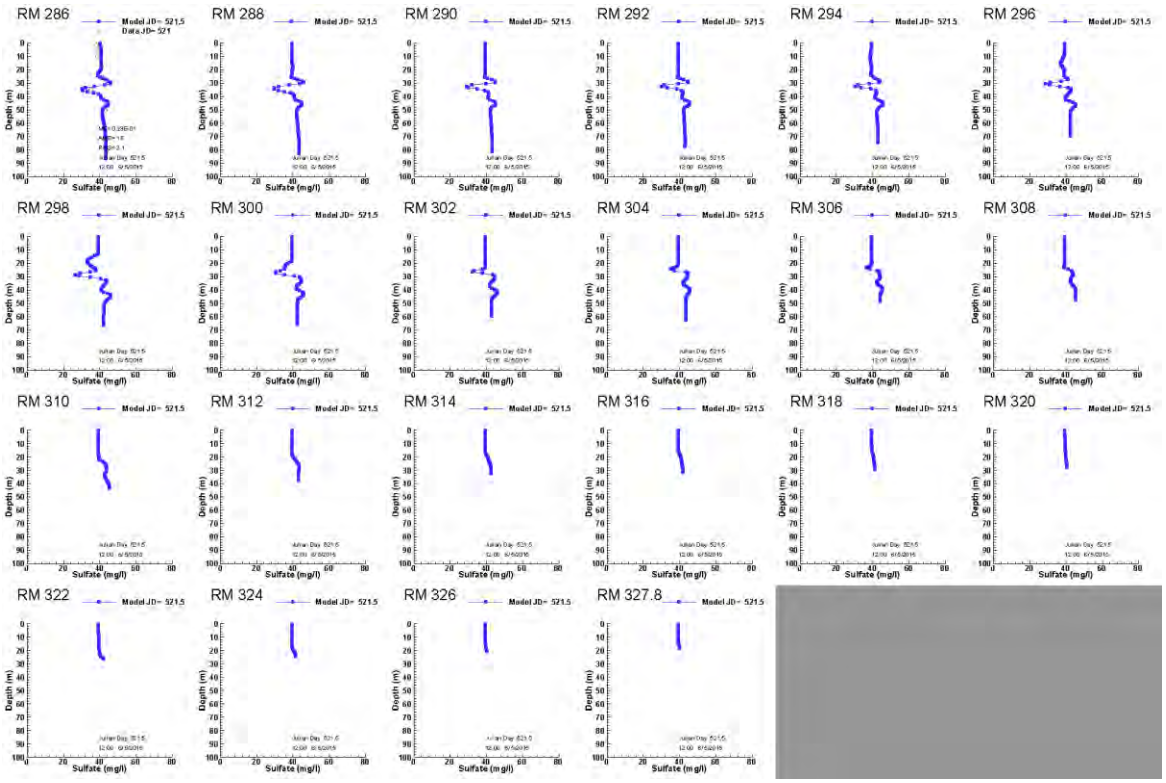


Figure 243. Vertical profiles of sulfate compared with data for 6/ 5/2015.

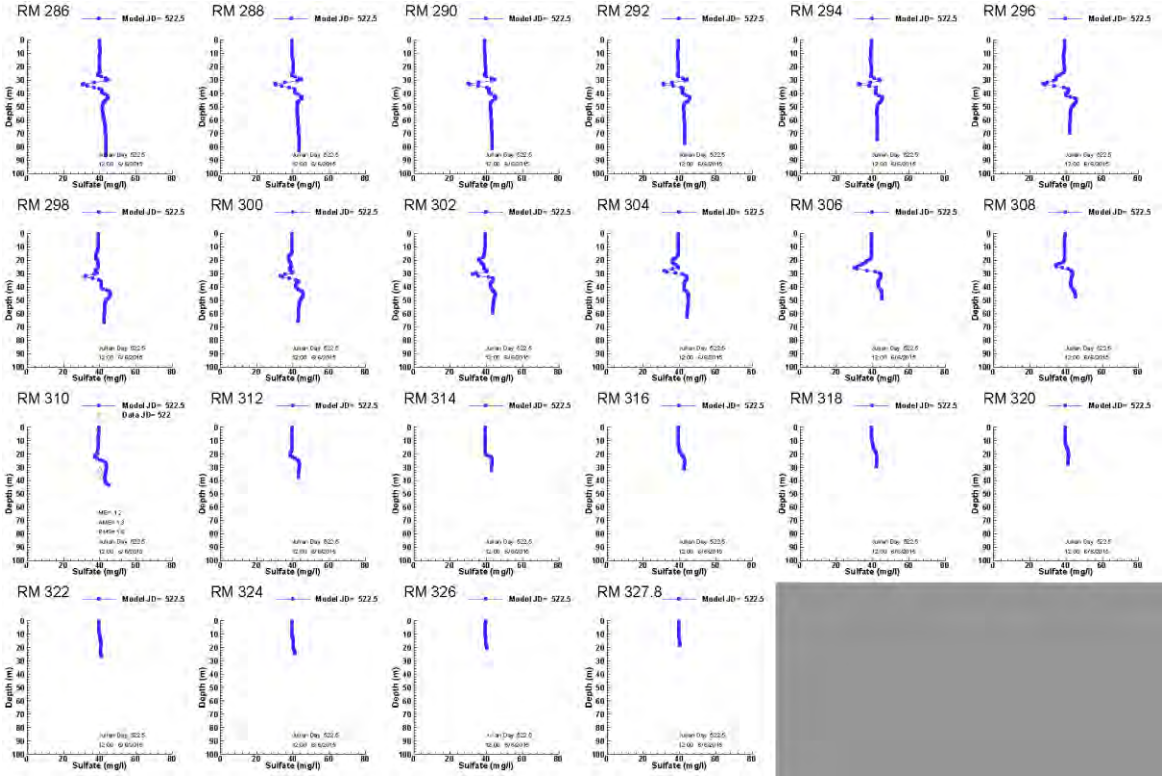


Figure 244. Vertical profiles of sulfate compared with data for 6/ 6/2015.

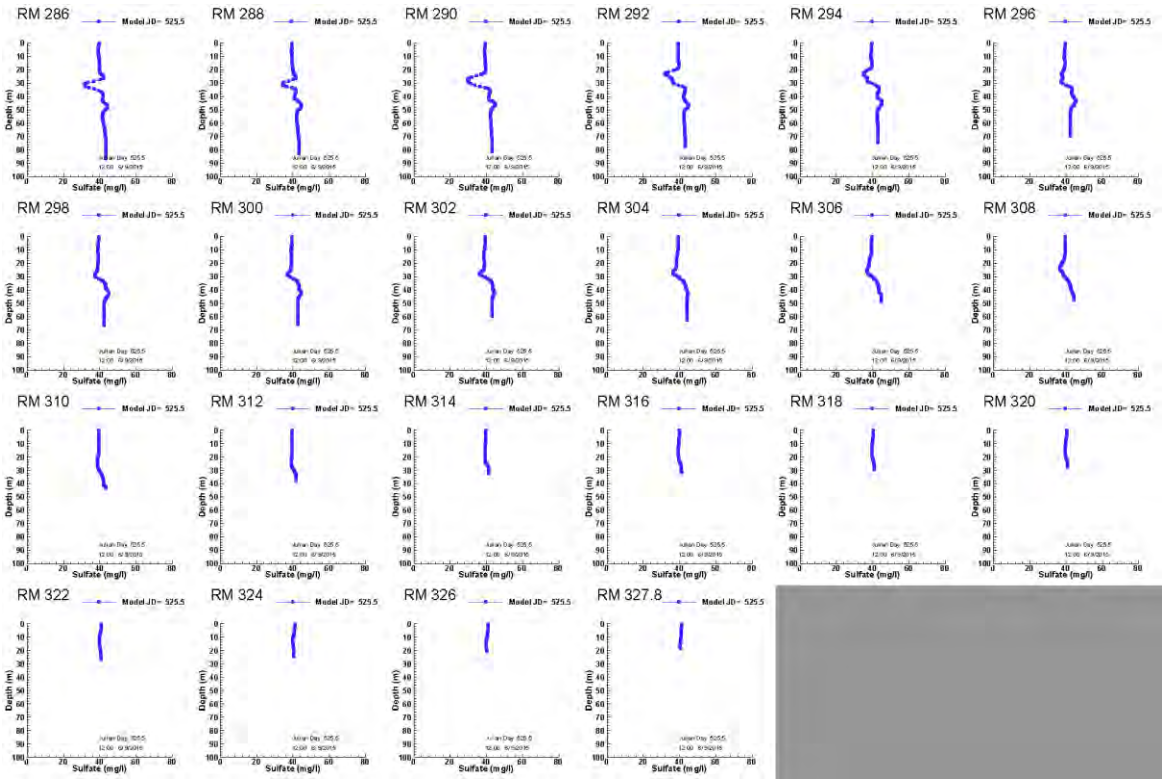


Figure 245. Vertical profiles of sulfate compared with data for 6/ 9/2015.

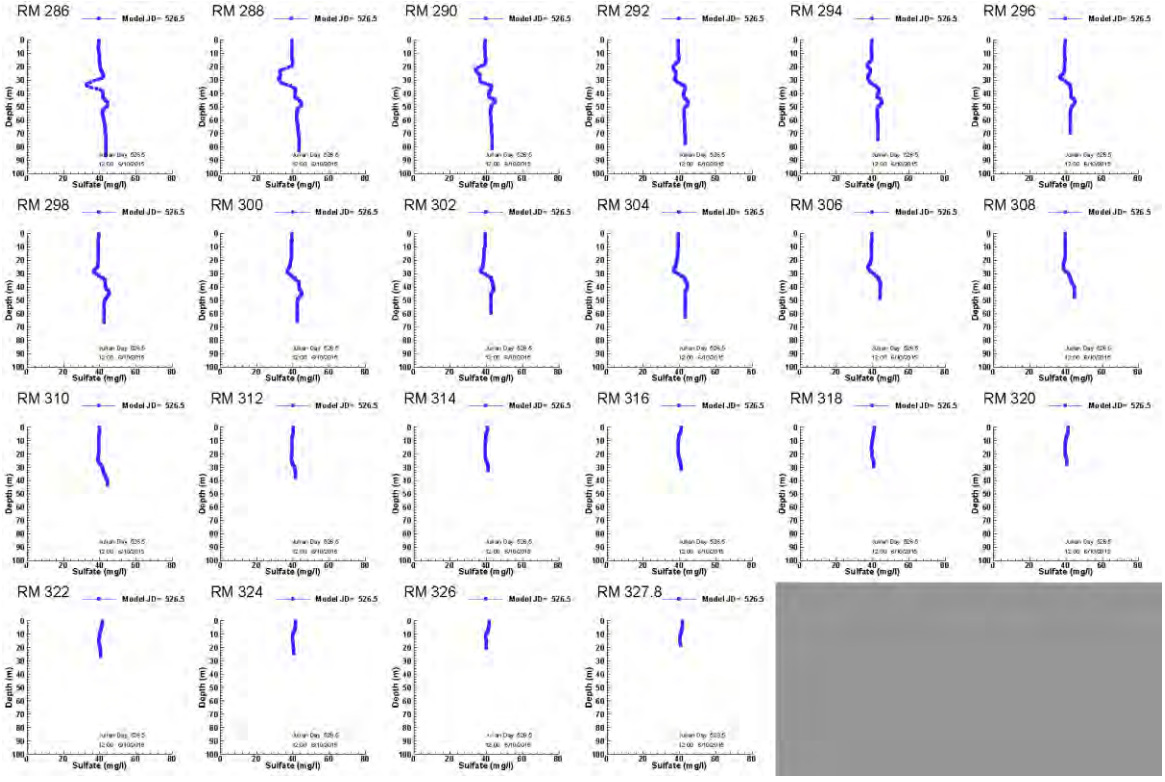


Figure 246. Vertical profiles of sulfate compared with data for 6/10/2015.

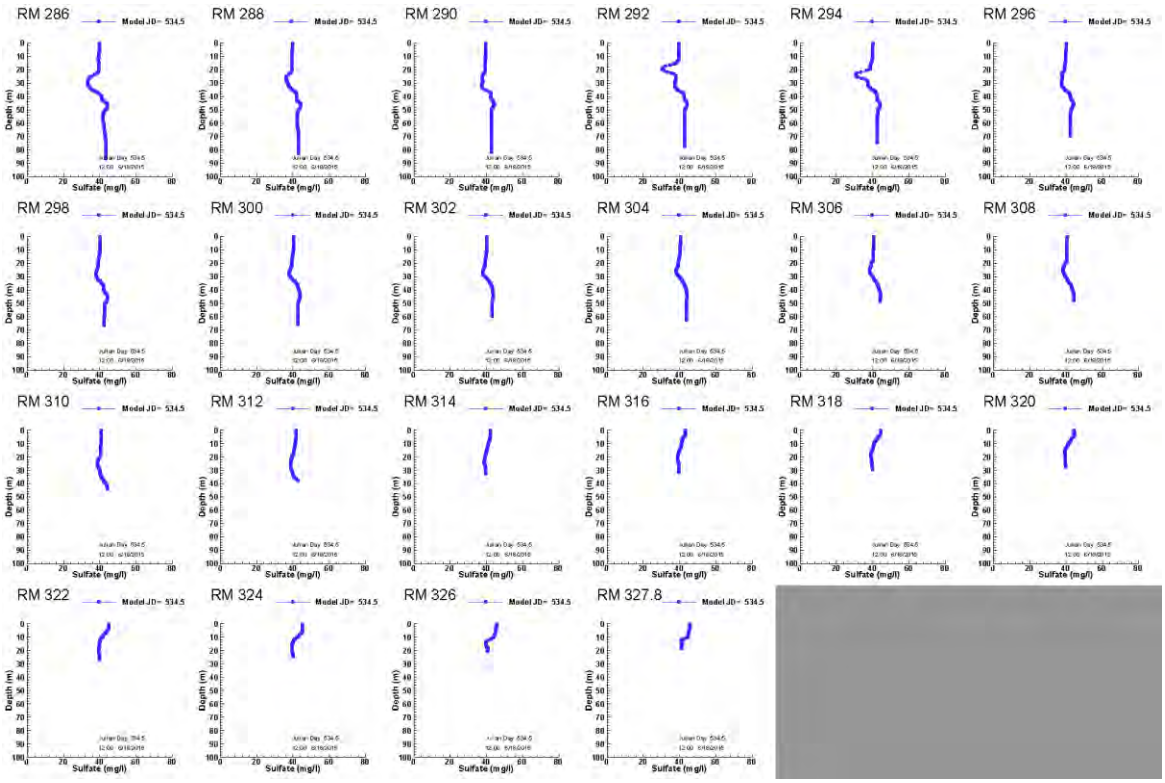


Figure 247. Vertical profiles of sulfate compared with data for 6/18/2015.

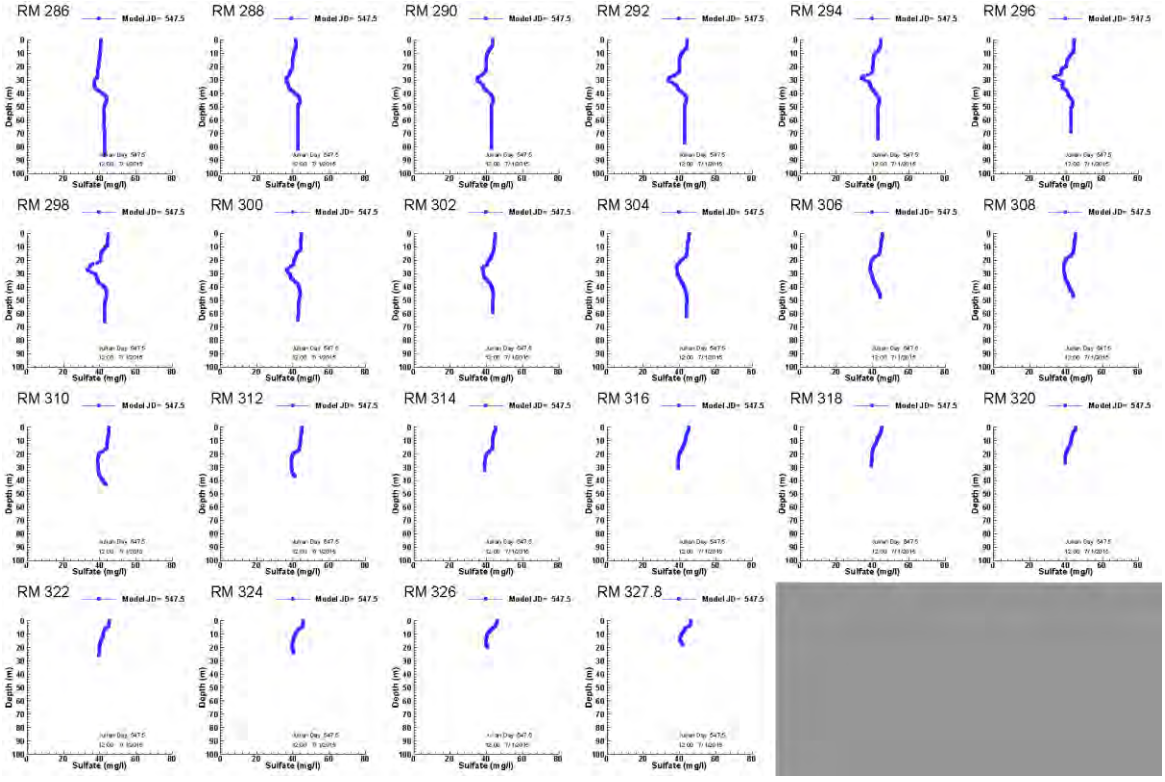


Figure 248. Vertical profiles of sulfate compared with data for 7/ 1/2015.

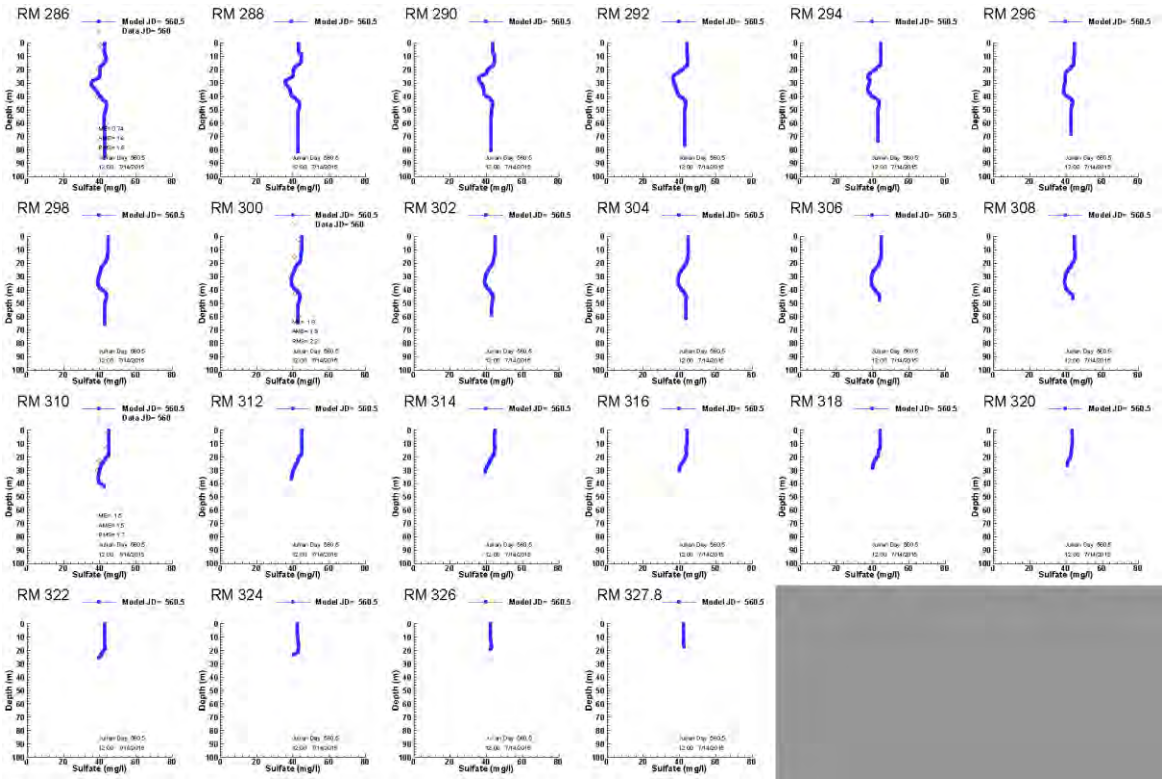


Figure 249. Vertical profiles of sulfate compared with data for 7/14/2015.

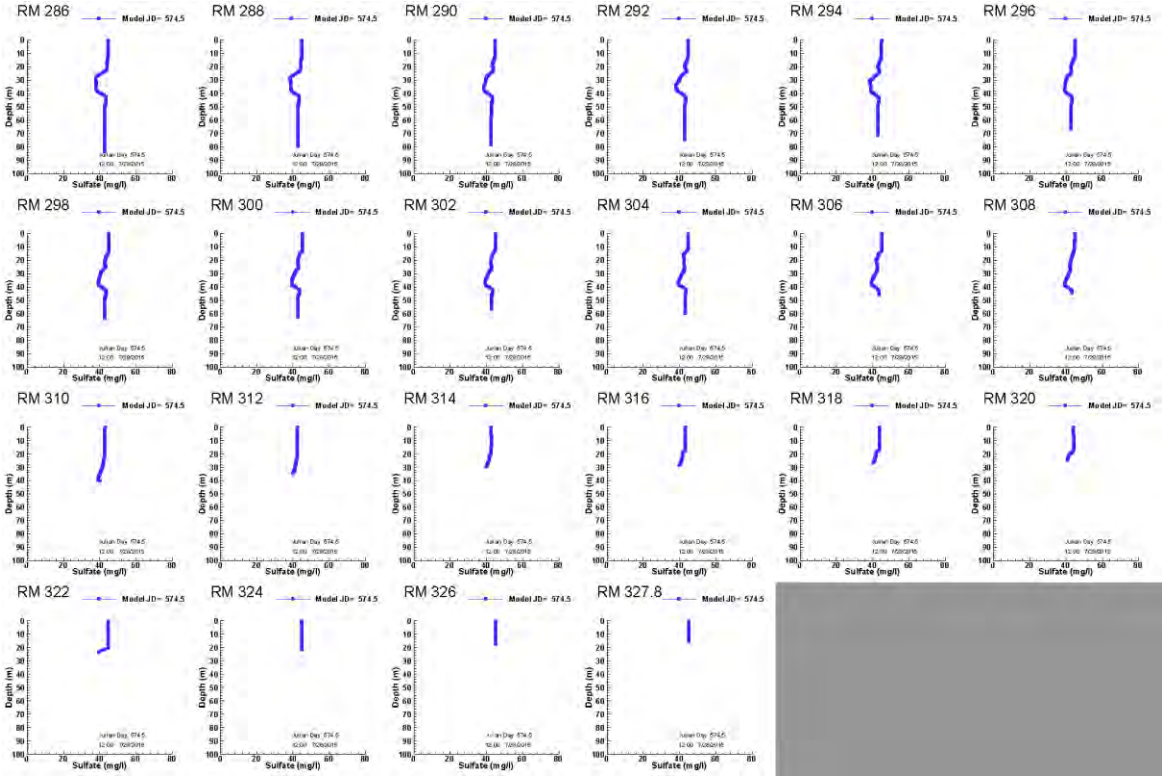


Figure 250. Vertical profiles of sulfate compared with data for 7/28/2015.

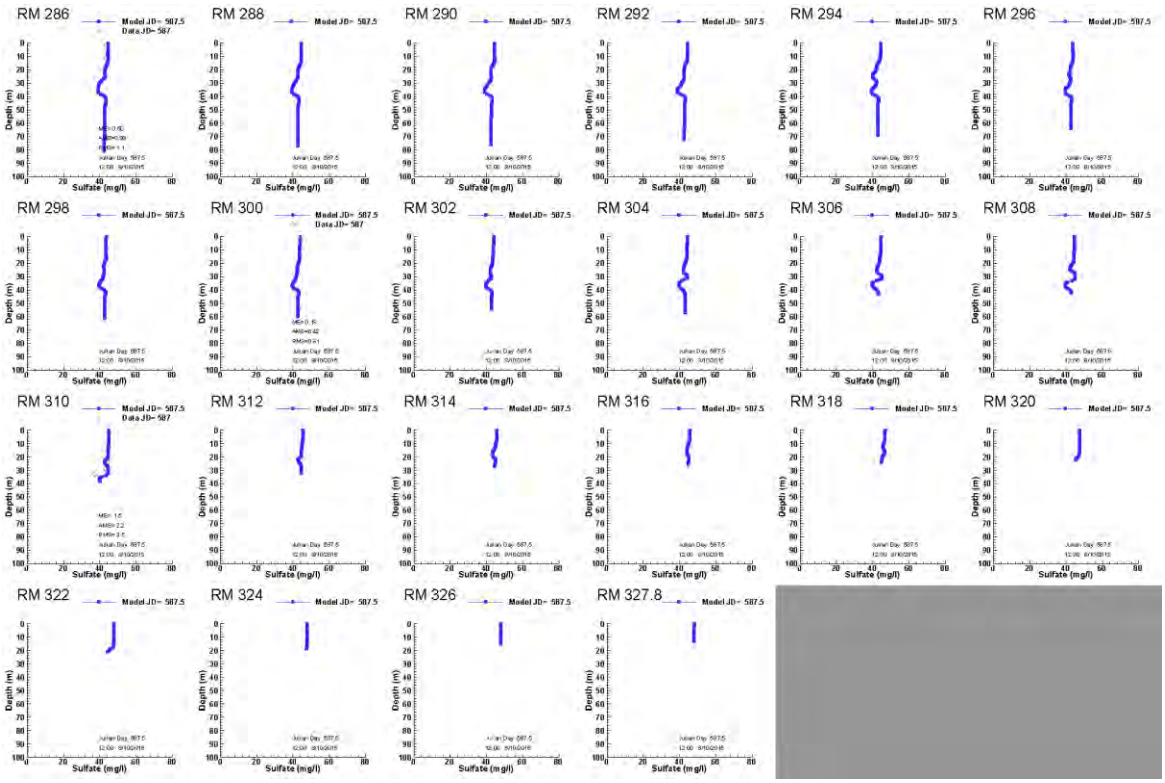


Figure 251. Vertical profiles of sulfate compared with data for 8/10/2015.

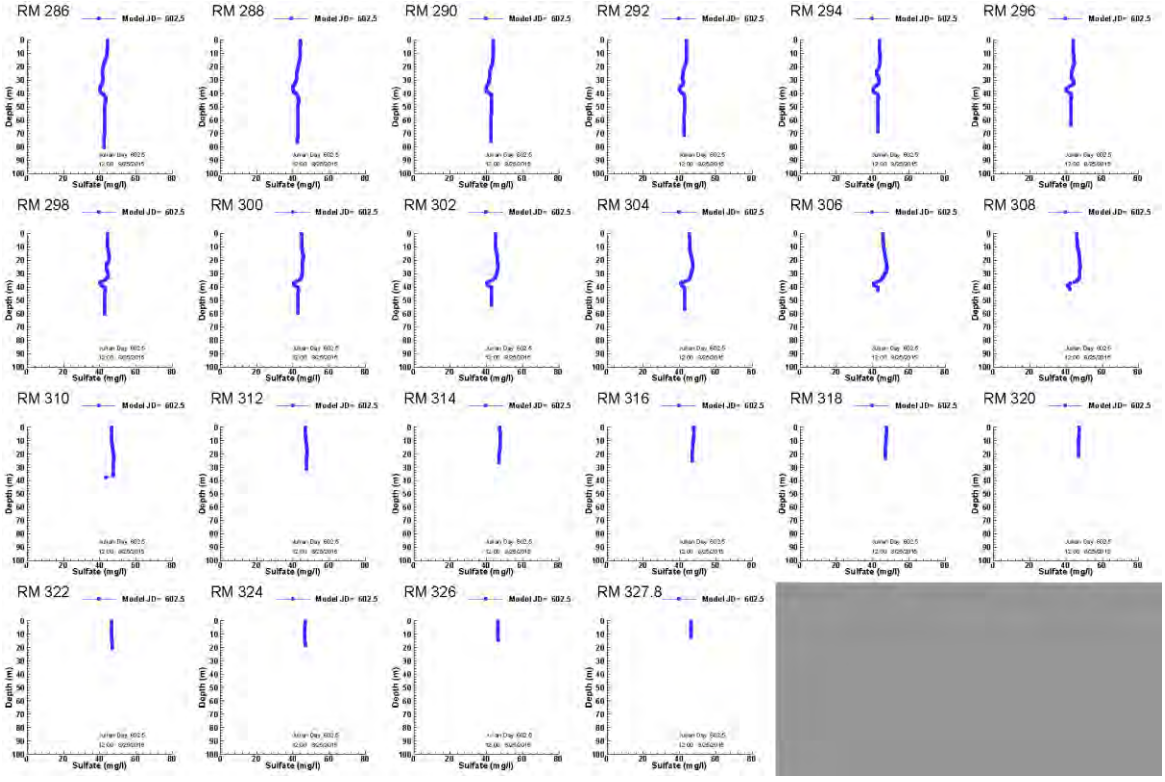


Figure 252. Vertical profiles of sulfate compared with data for 8/25/2015.

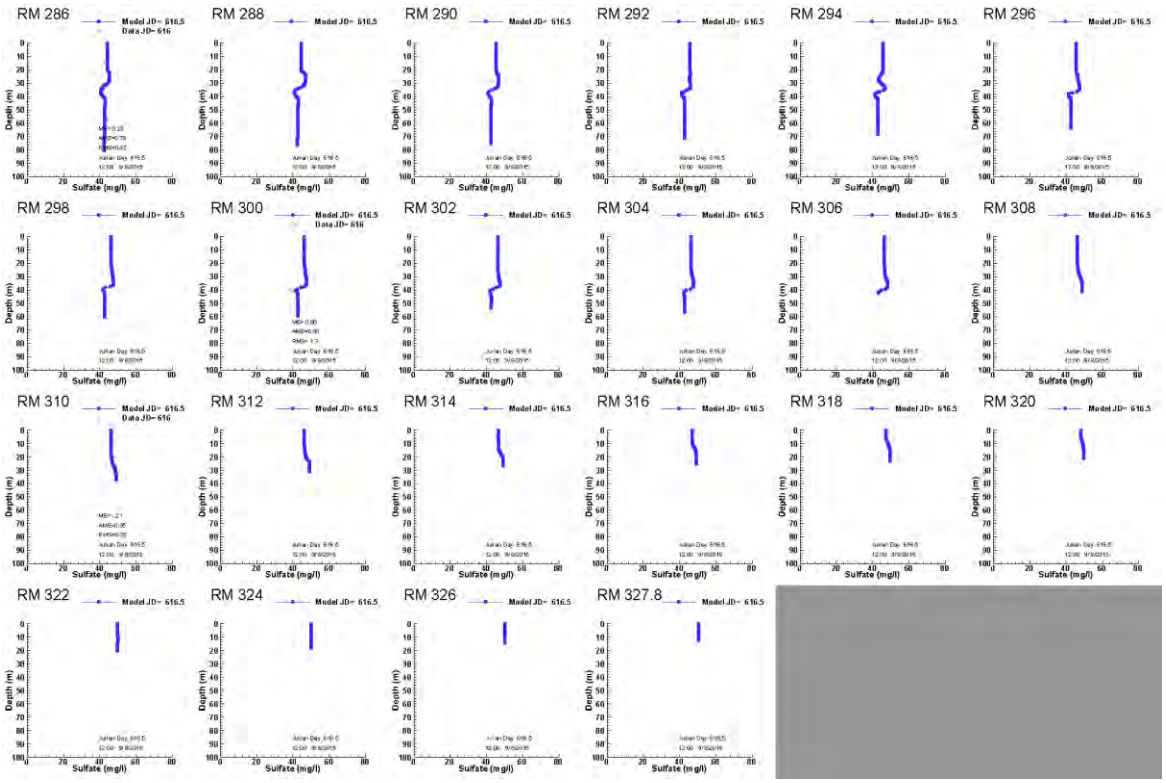


Figure 253. Vertical profiles of sulfate compared with data for 9/ 8/2015.

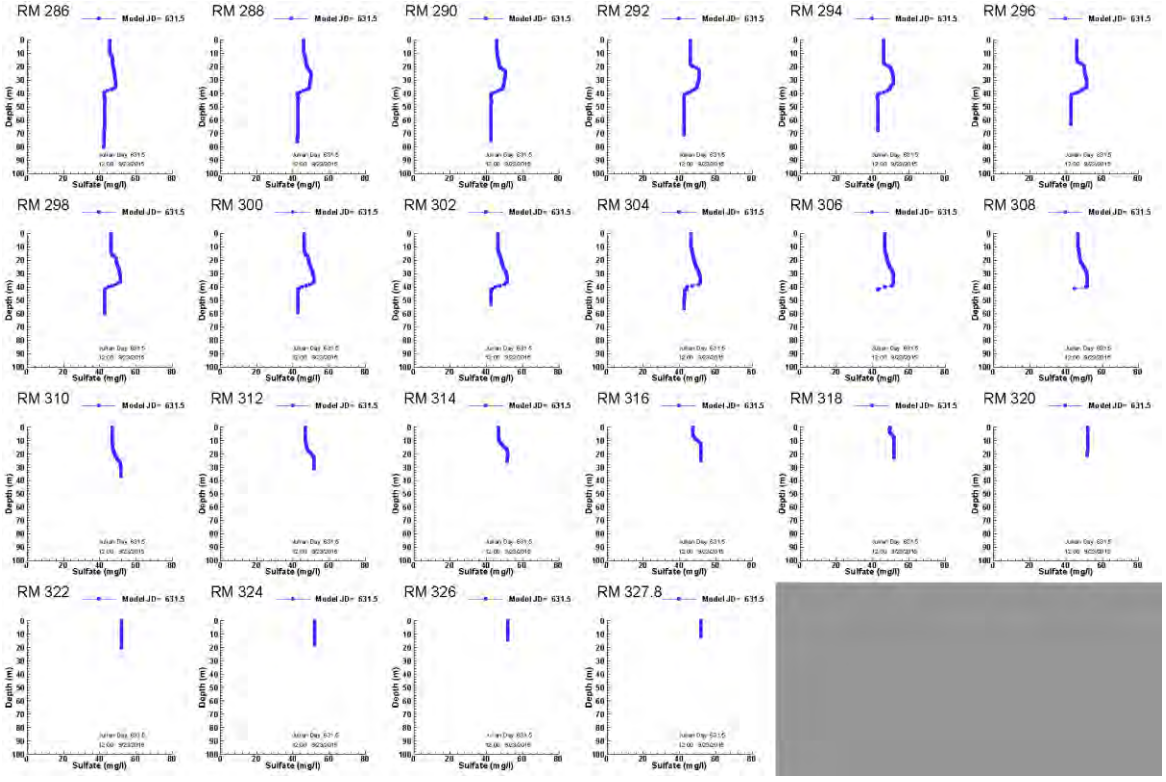


Figure 254. Vertical profiles of sulfate compared with data for 9/23/2015.

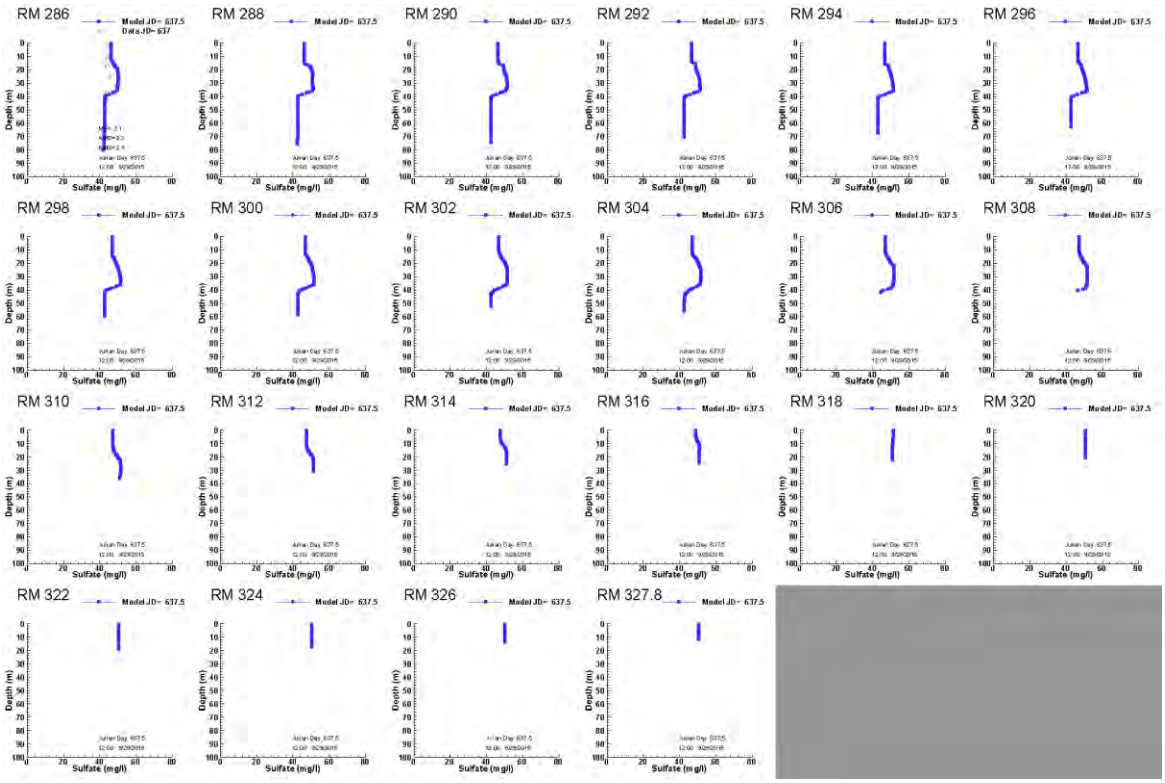


Figure 255. Vertical profiles of sulfate compared with data for 9/29/2015.

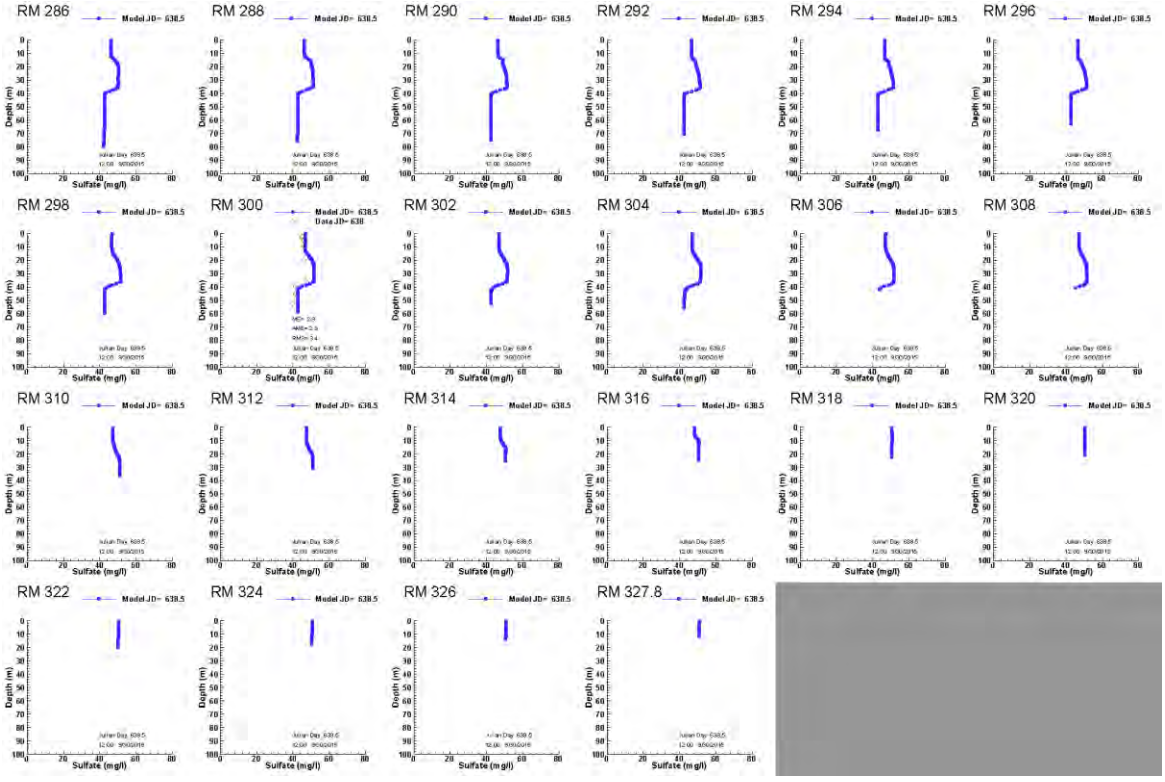


Figure 256. Vertical profiles of sulfate compared with data for 9/30/2015.

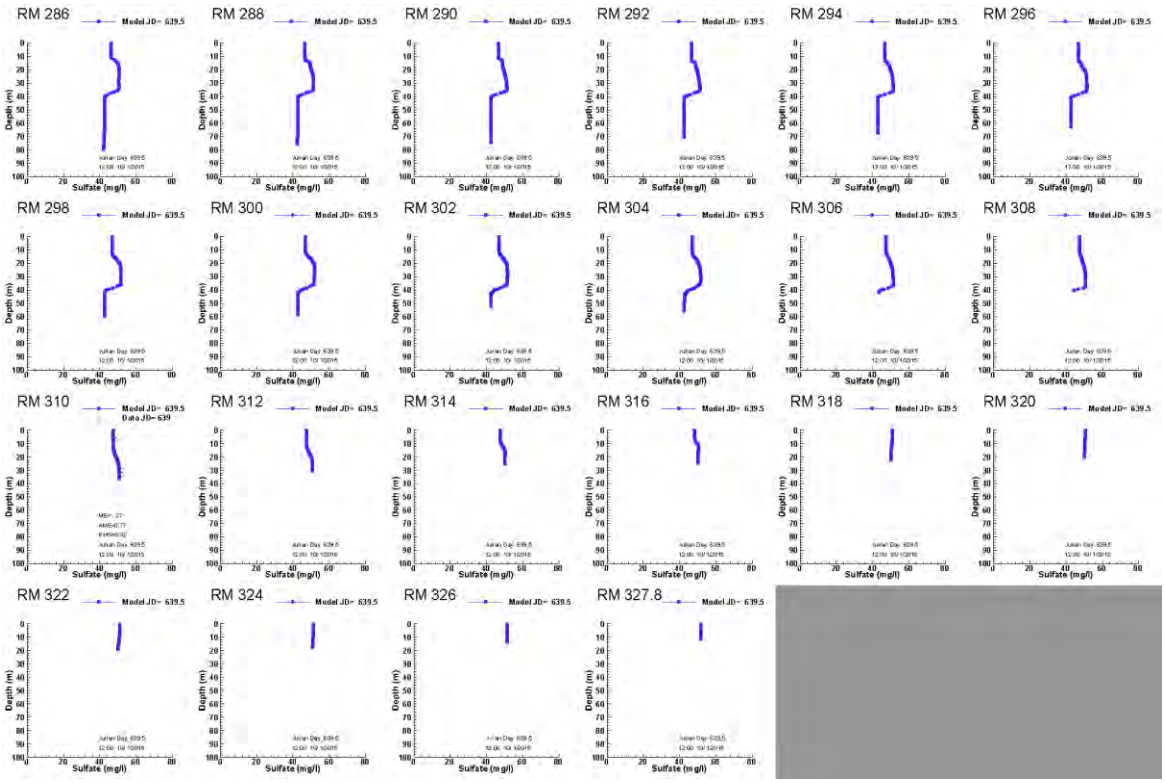


Figure 257. Vertical profiles of sulfate compared with data for 10/ 1/2015.

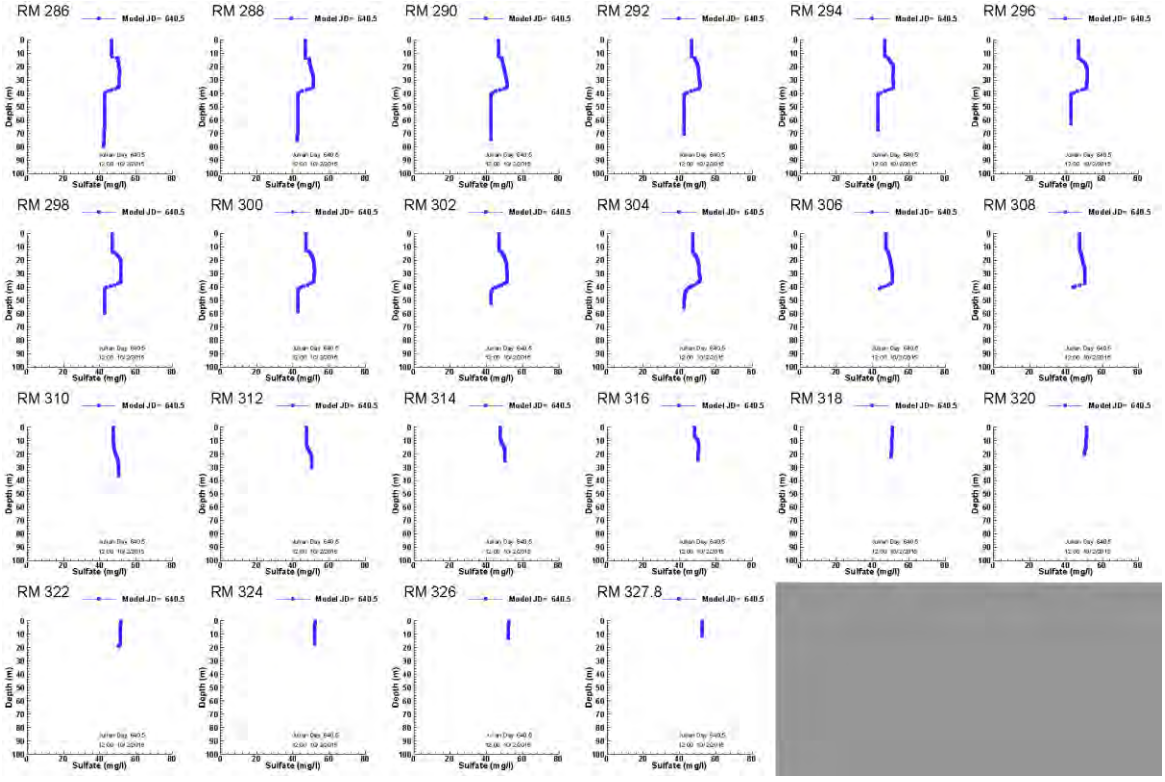


Figure 258. Vertical profiles of sulfate compared with data for 10/ 2/2015.

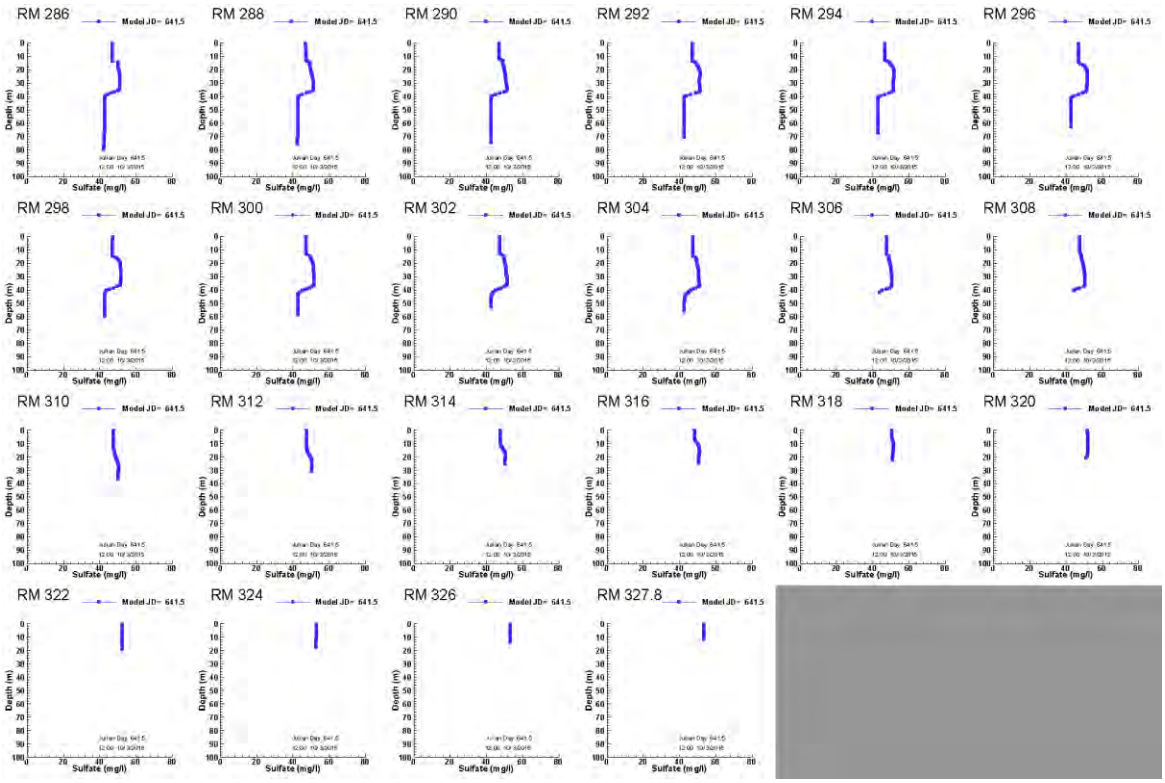


Figure 259. Vertical profiles of sulfate compared with data for 10/ 3/2015.

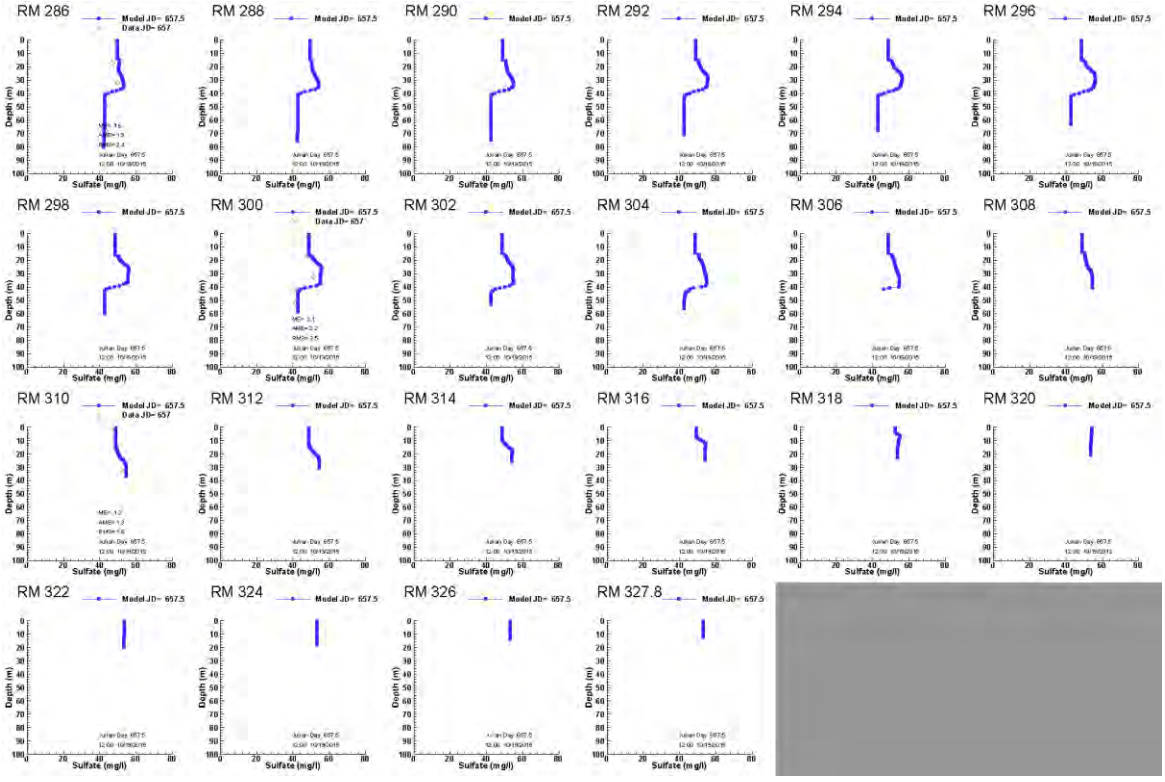


Figure 260. Vertical profiles of sulfate compared with data for 10/19/2015.

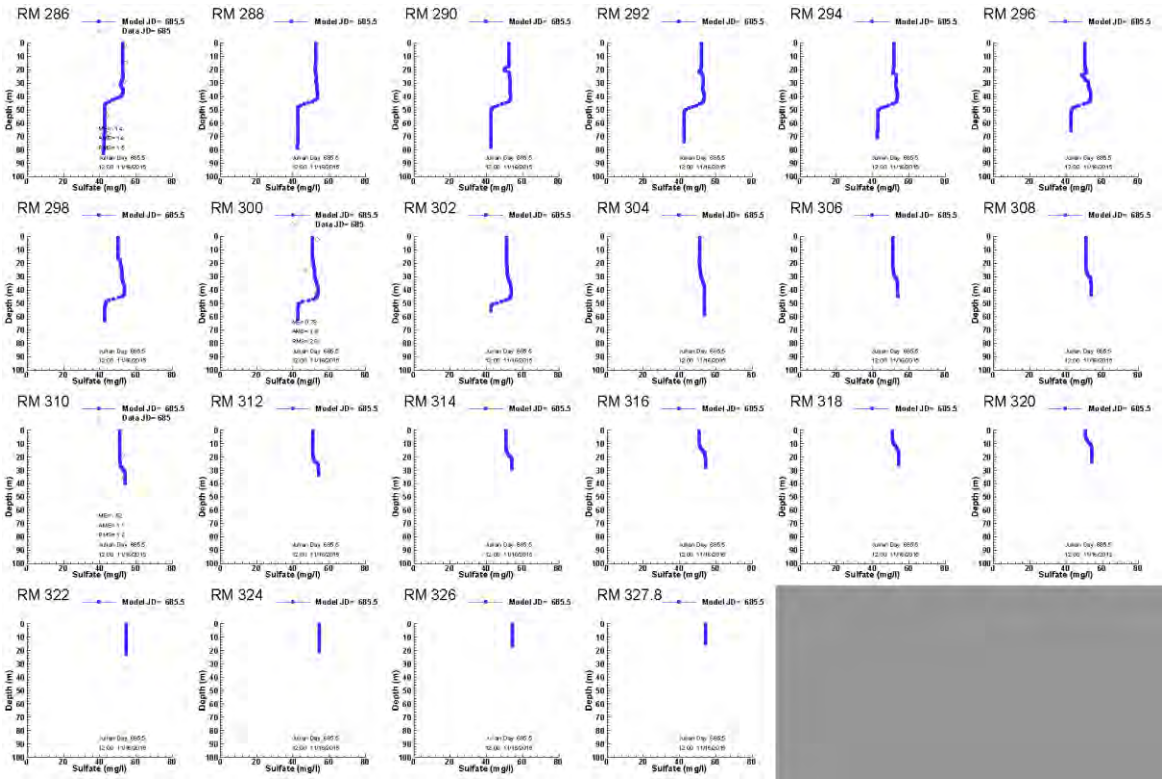


Figure 261. Vertical profiles of sulfate compared with data for 11/16/2015.

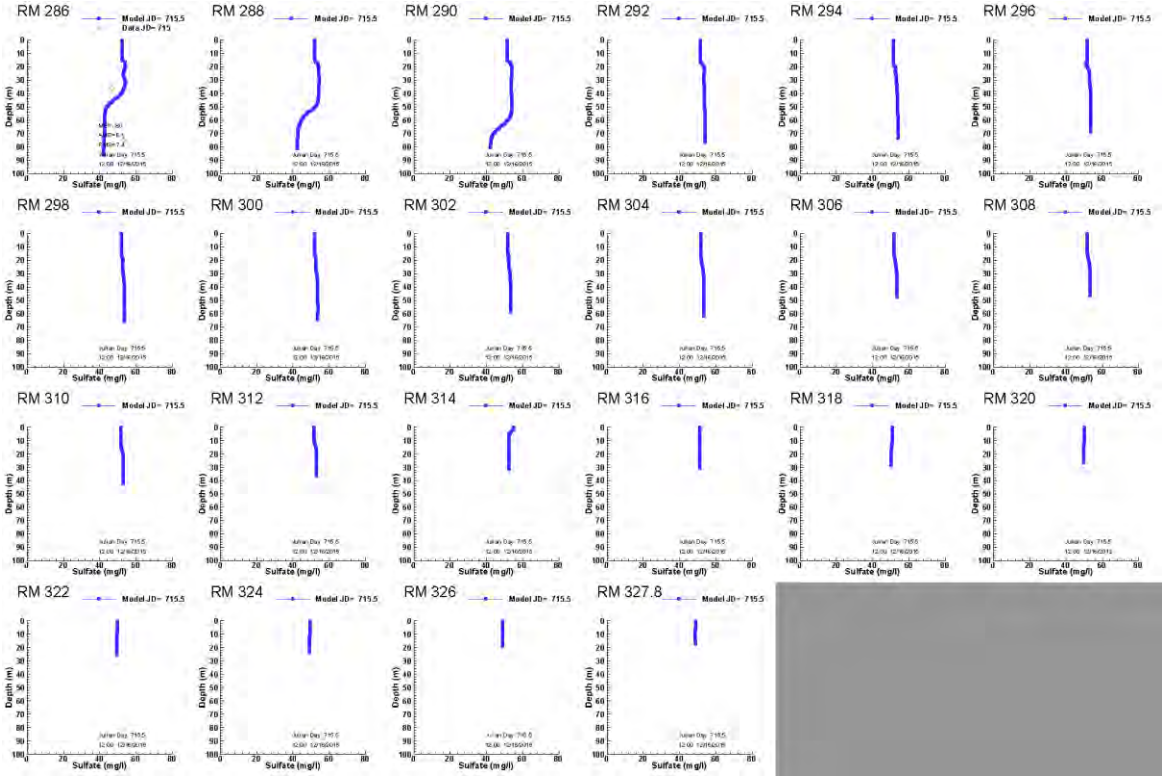


Figure 262. Vertical profiles of sulfate compared with data for 12/16/2015.

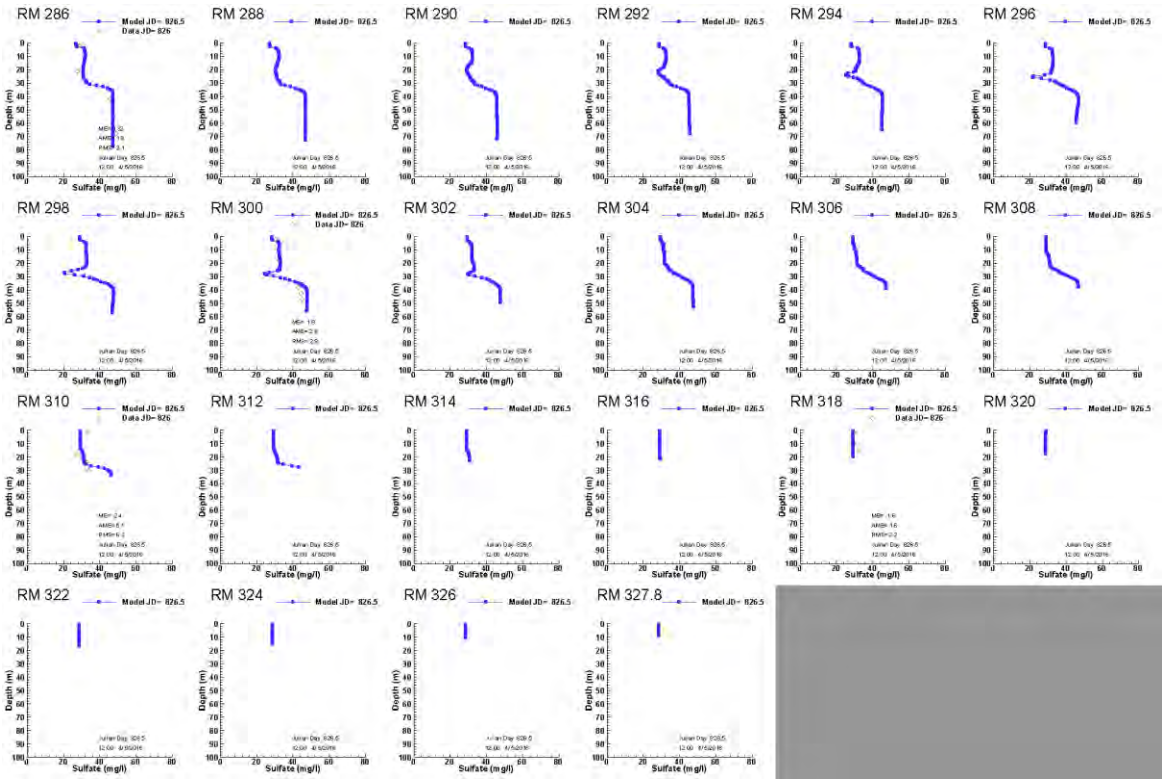


Figure 263. Vertical profiles of sulfate compared with data for 4/ 5/2016.

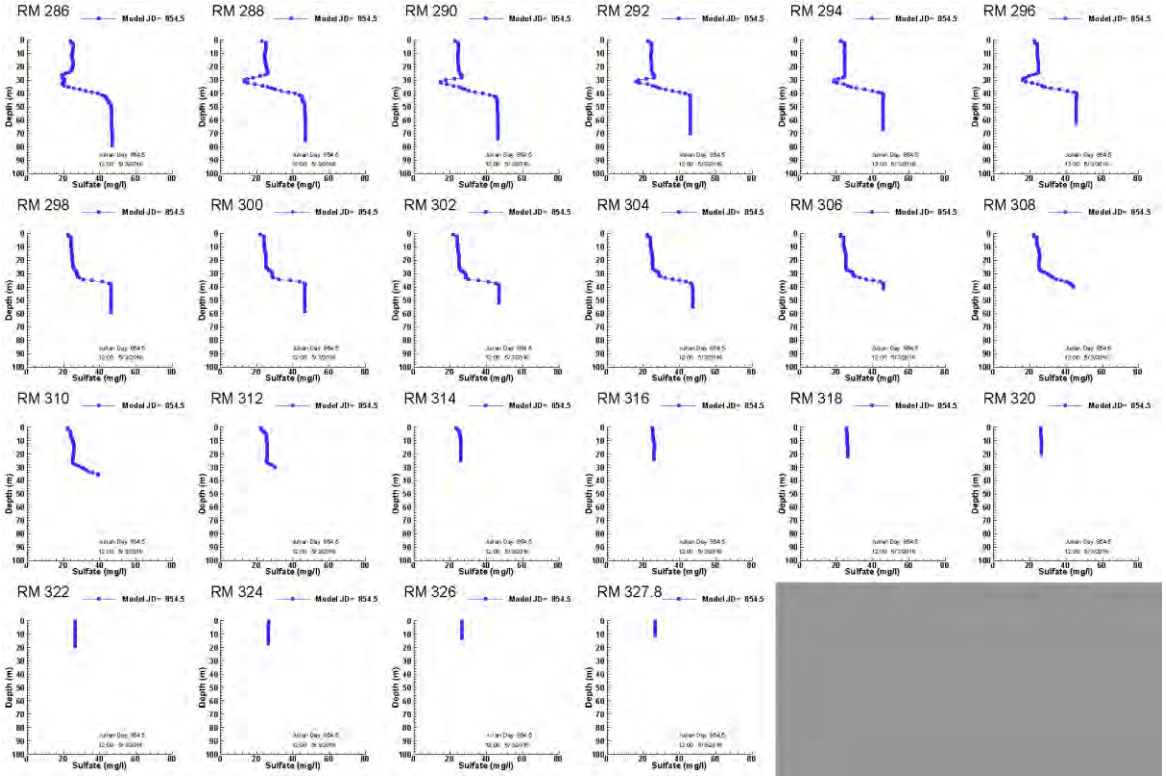


Figure 264. Vertical profiles of sulfate compared with data for 5/ 3/2016.

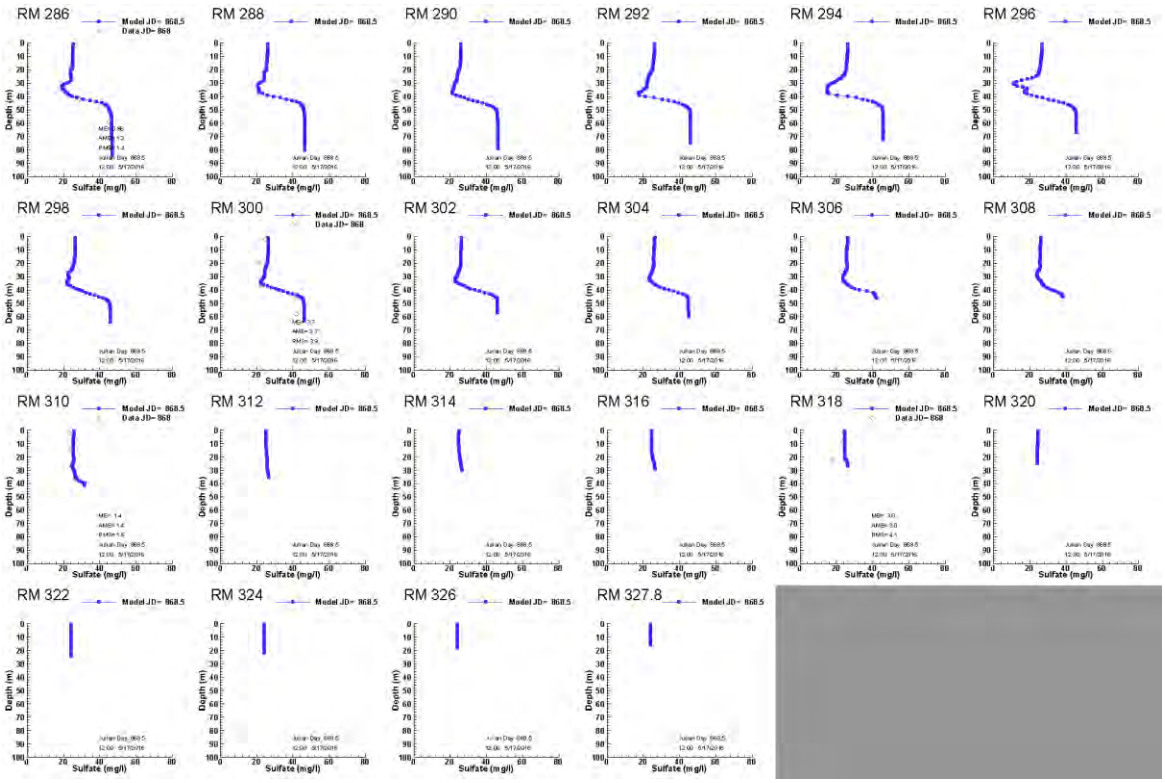


Figure 265. Vertical profiles of sulfate compared with data for 5/17/2016.

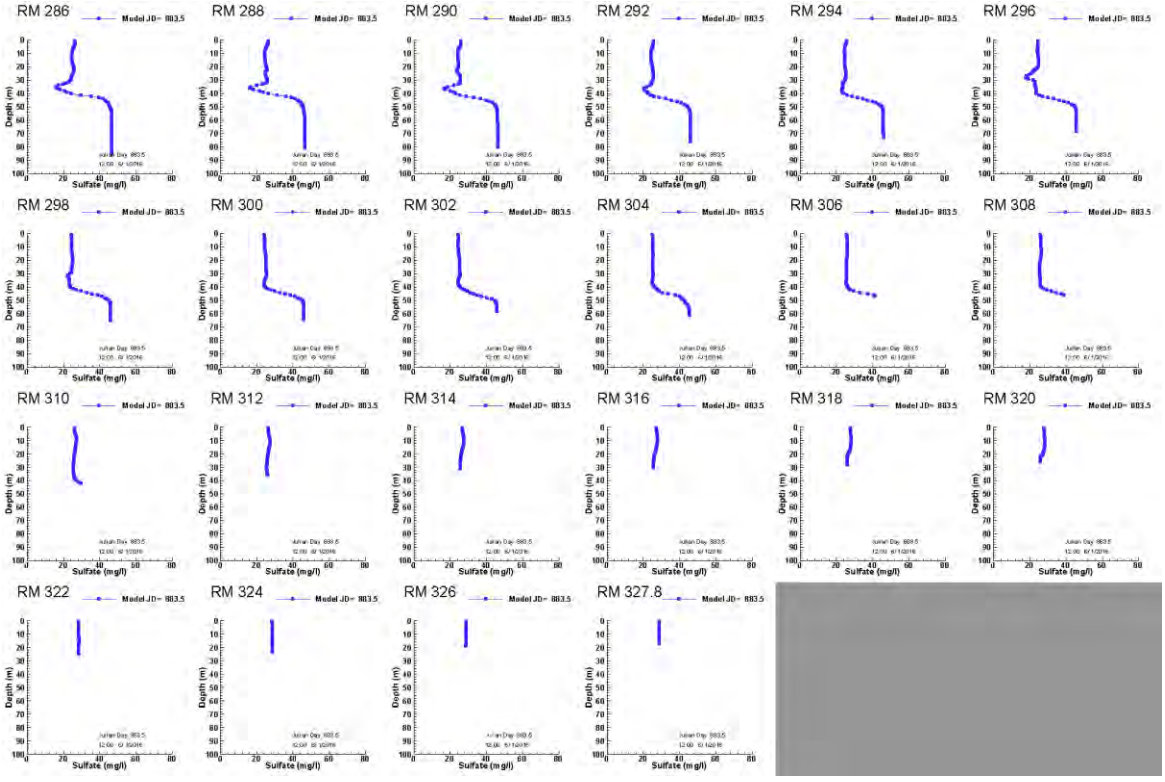


Figure 266. Vertical profiles of sulfate compared with data for 6/ 1/2016.

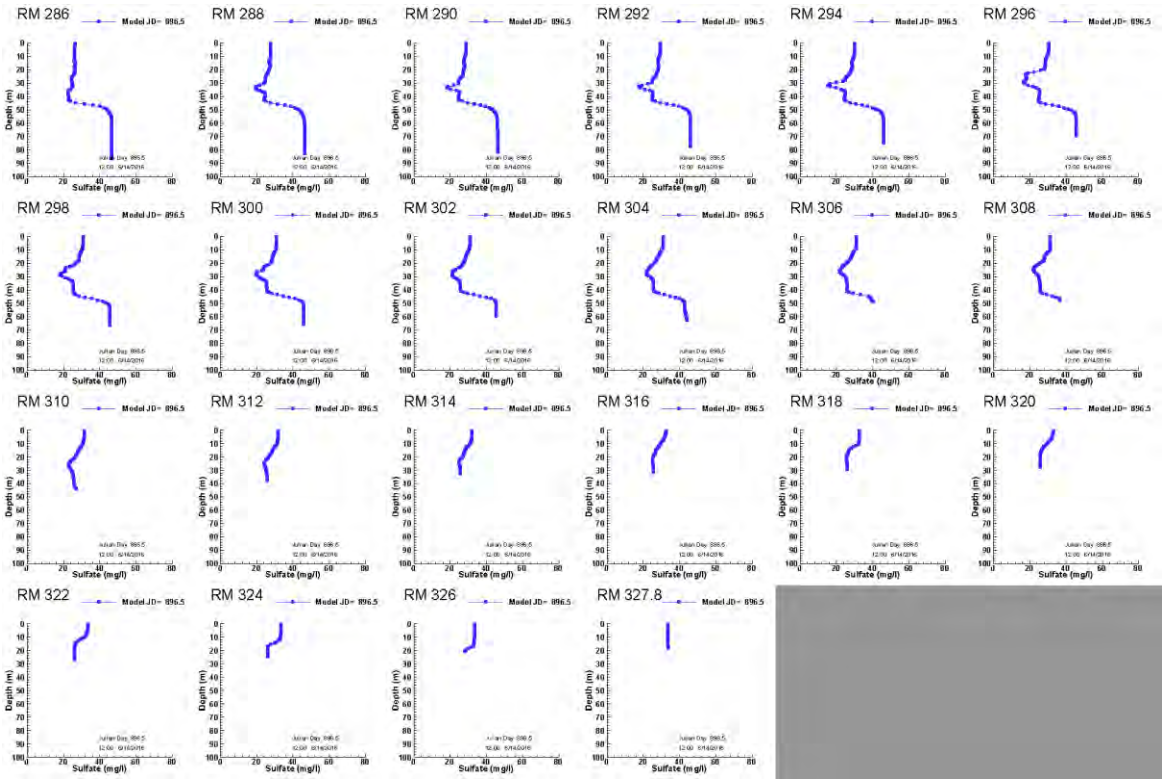


Figure 267. Vertical profiles of sulfate compared with data for 6/14/2016.

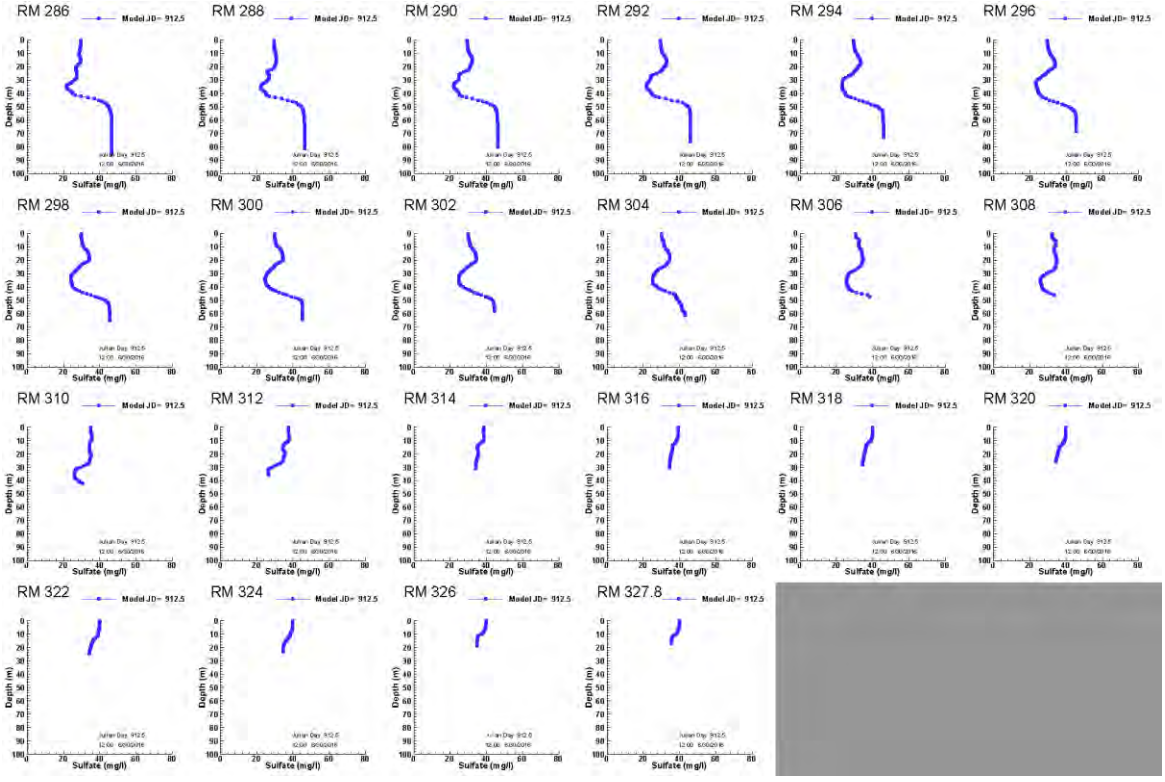


Figure 268. Vertical profiles of sulfate compared with data for 6/30/2016.

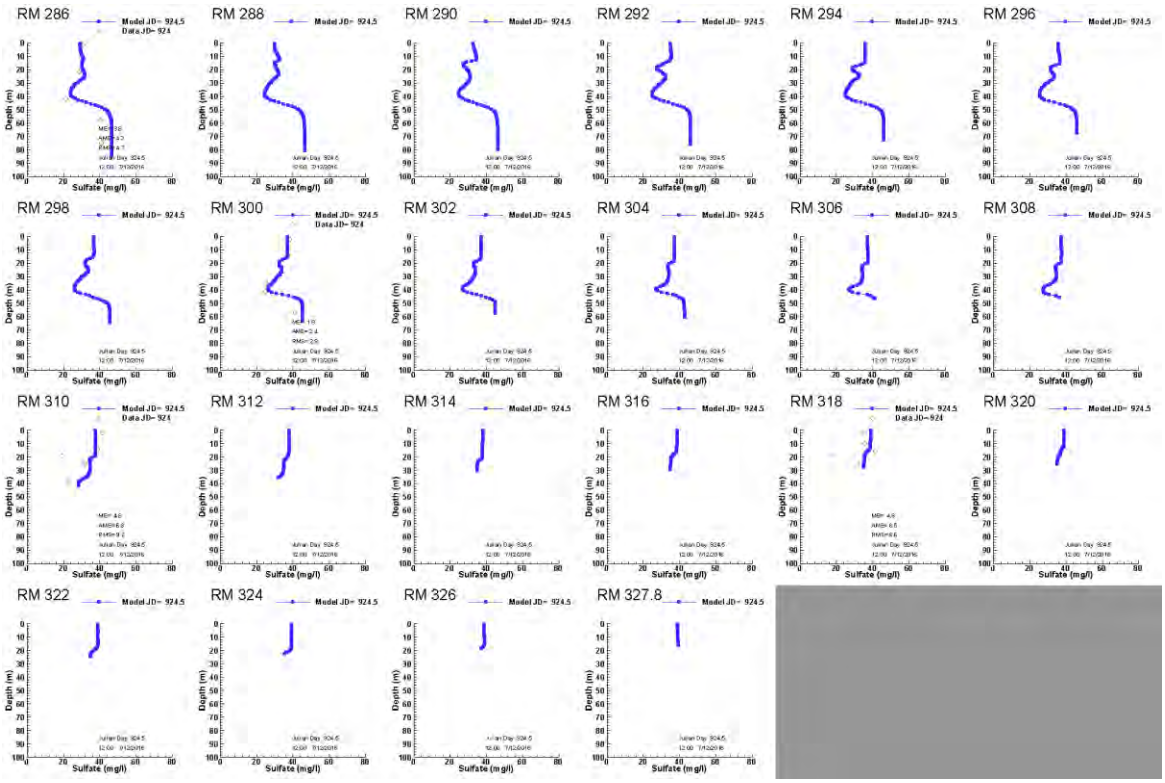


Figure 269. Vertical profiles of sulfate compared with data for 7/12/2016.

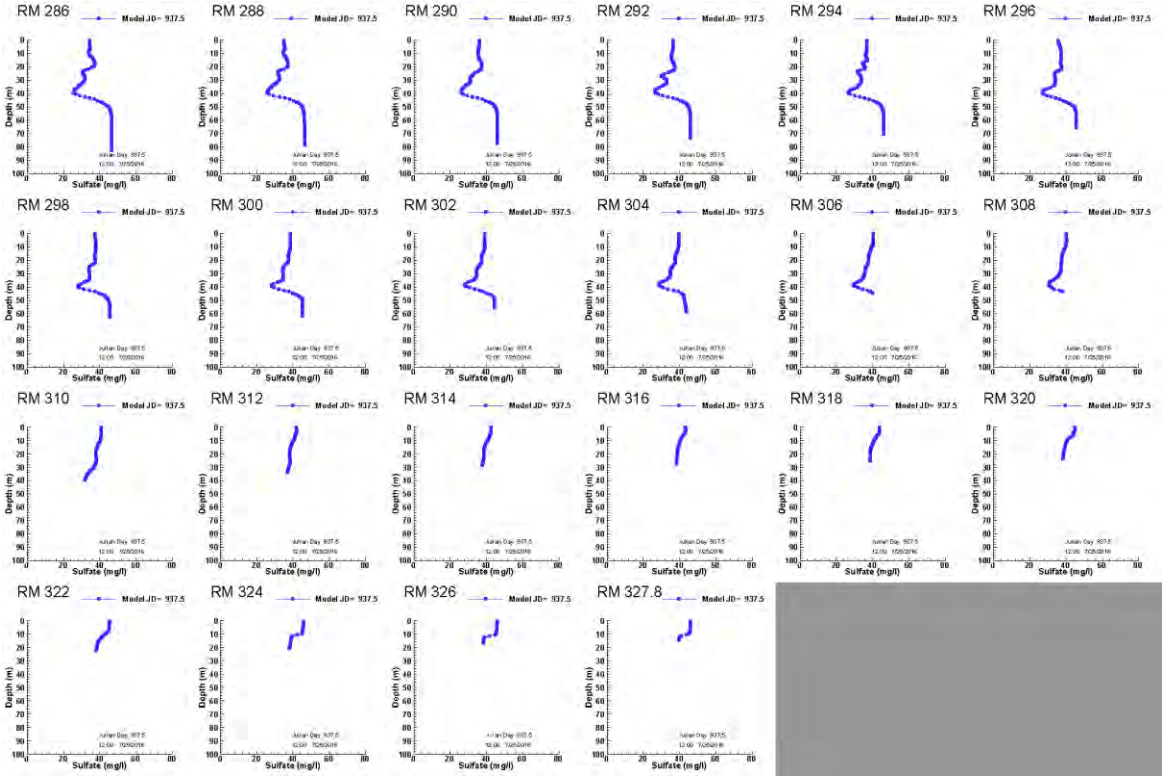


Figure 270. Vertical profiles of sulfate compared with data for 7/25/2016.

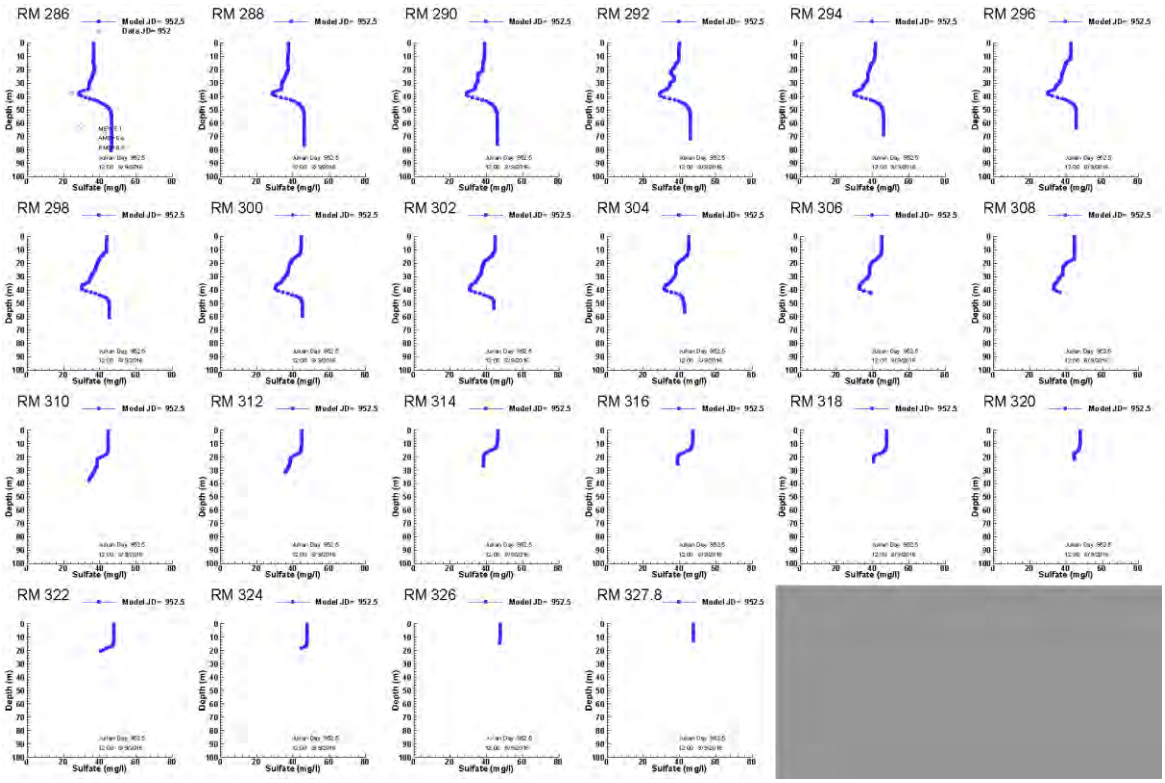


Figure 271. Vertical profiles of sulfate compared with data for 8/ 9/2016.

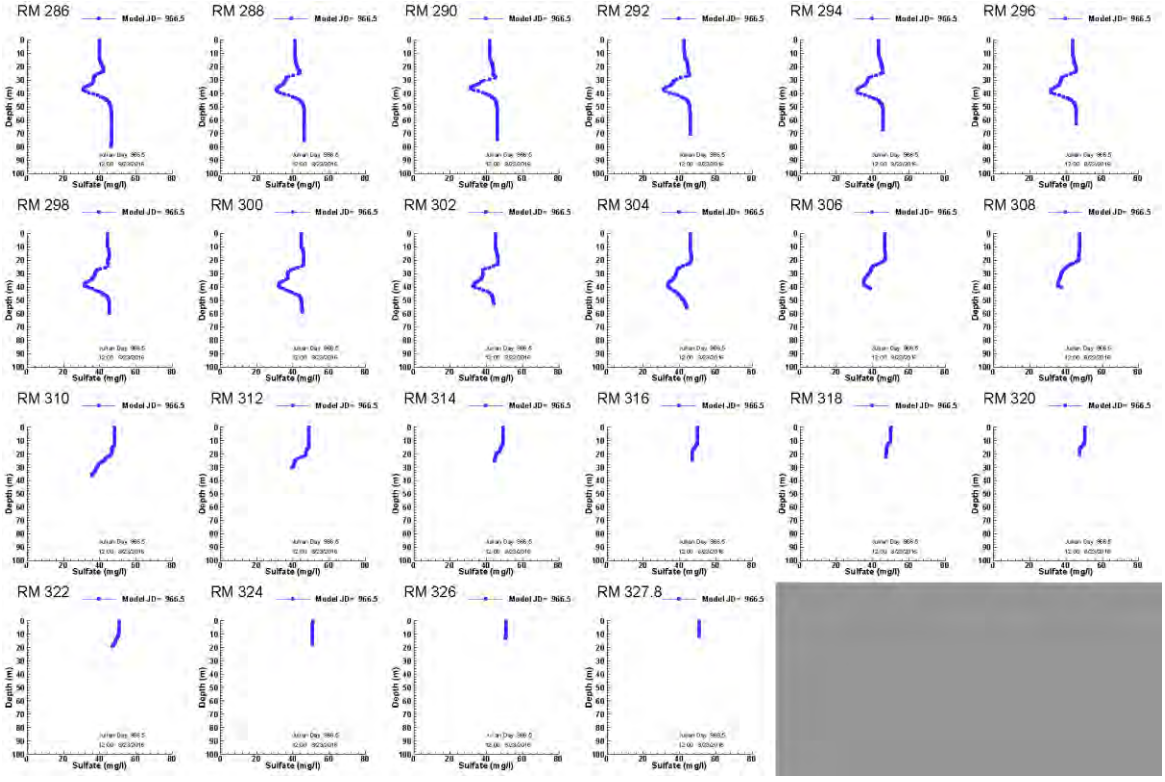


Figure 272. Vertical profiles of sulfate compared with data for 8/23/2016.

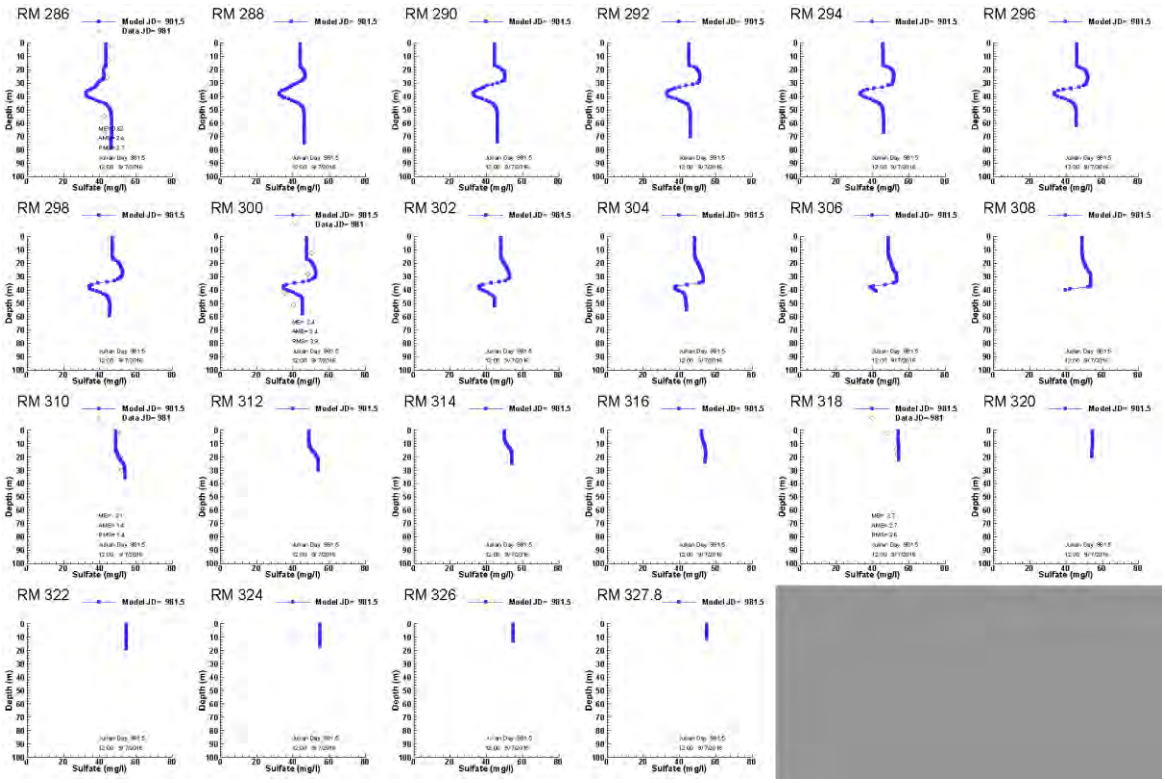


Figure 273. Vertical profiles of sulfate compared with data for 9/ 7/2016.

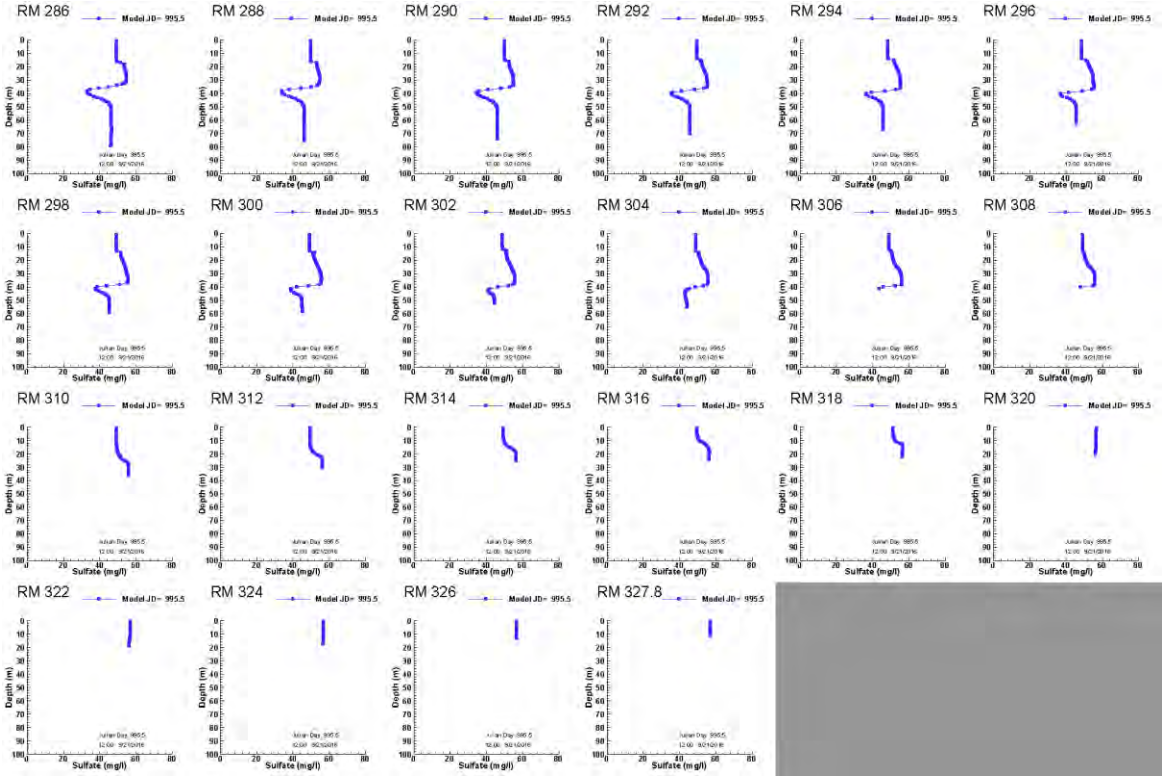


Figure 274. Vertical profiles of sulfate compared with data for 9/21/2016.

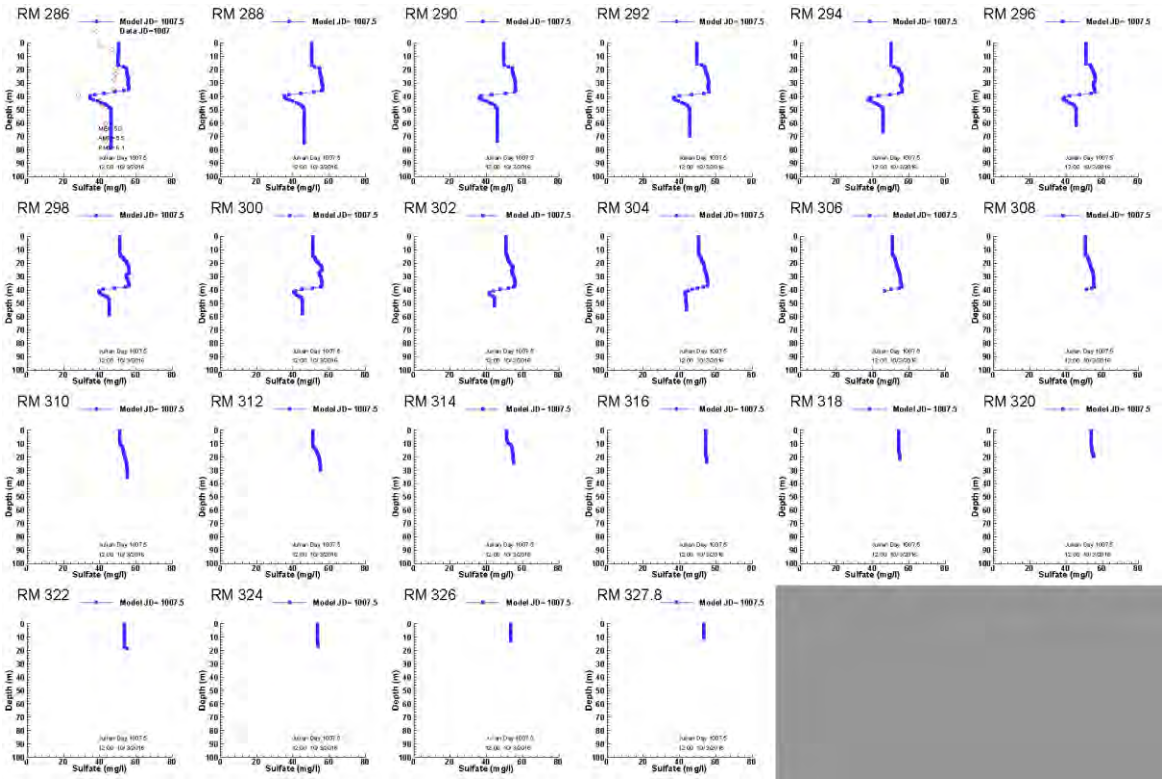


Figure 275. Vertical profiles of sulfate compared with data for 10/ 3/2016.

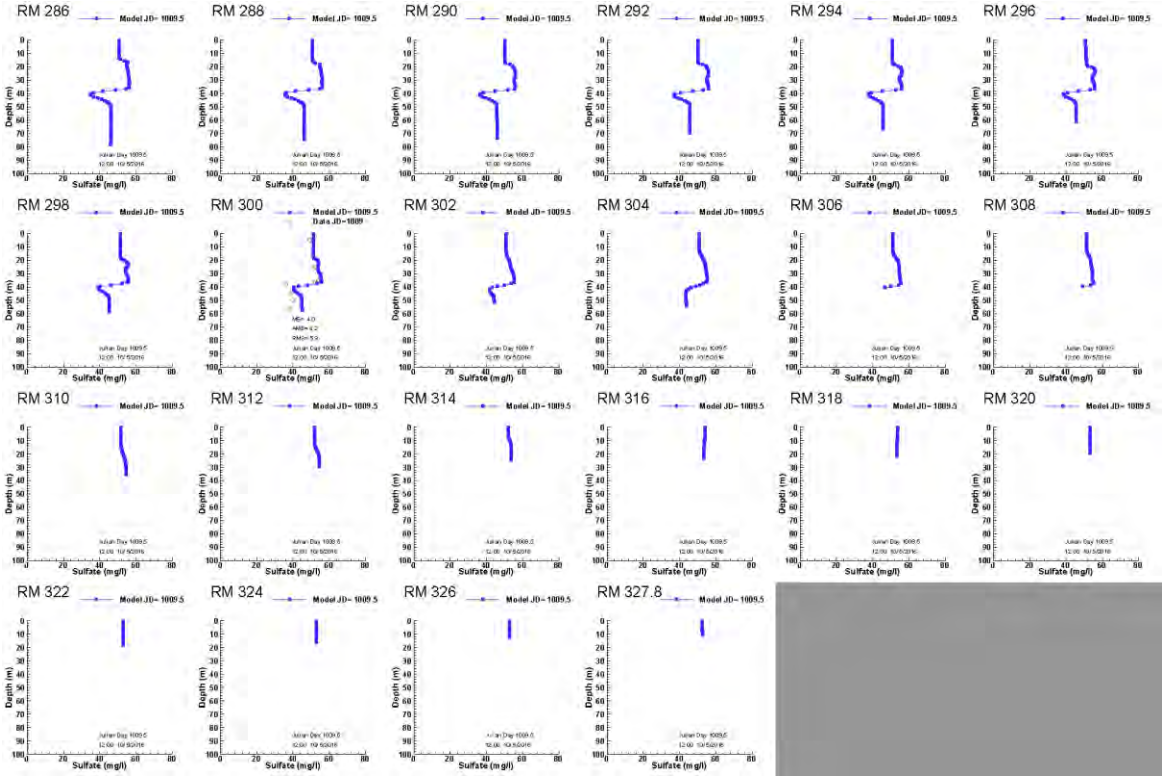


Figure 276. Vertical profiles of sulfate compared with data for 10/ 5/2016.

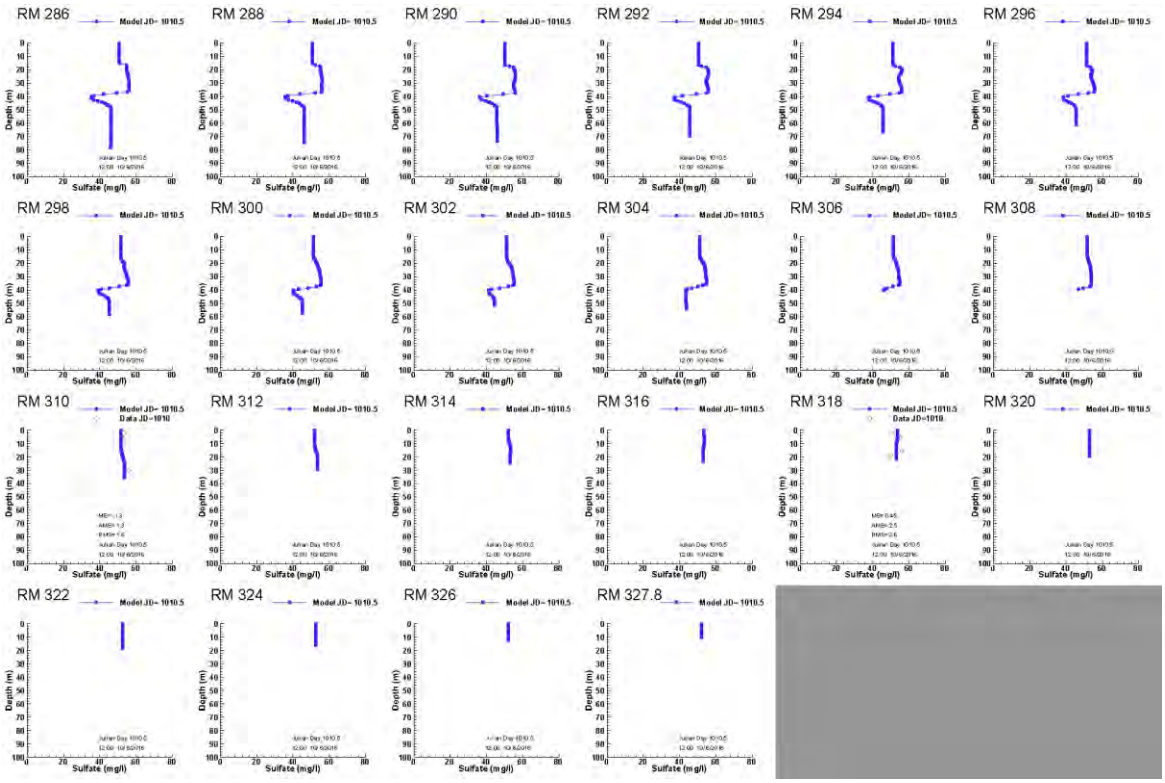


Figure 277. Vertical profiles of sulfate compared with data for 10/ 6/2016.

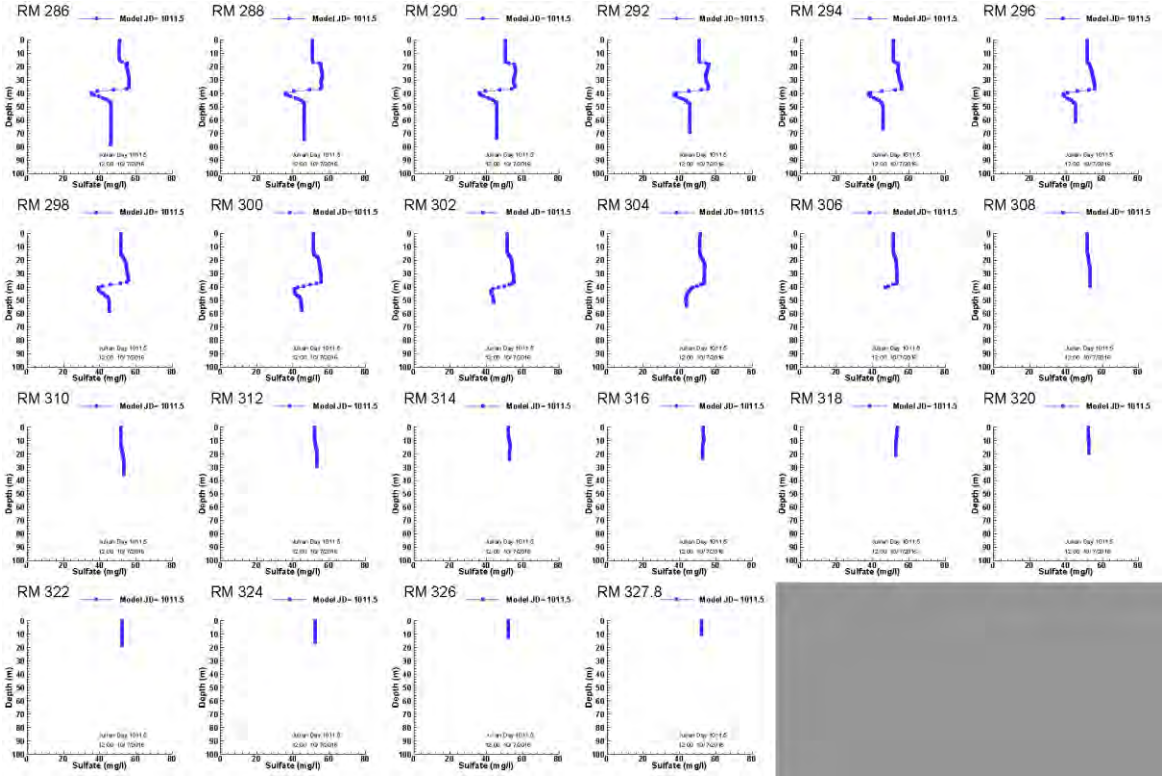


Figure 278. Vertical profiles of sulfate compared with data for 10/ 7/2016.

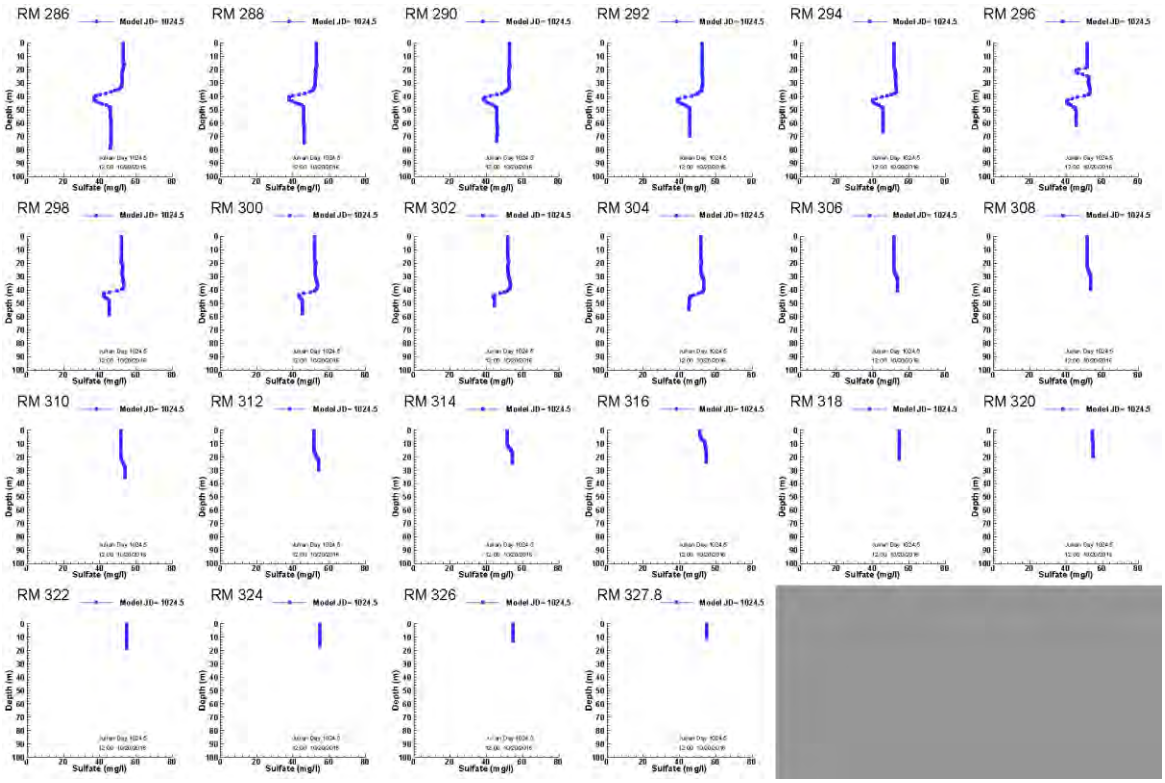


Figure 279. Vertical profiles of sulfate compared with data for 10/20/2016.

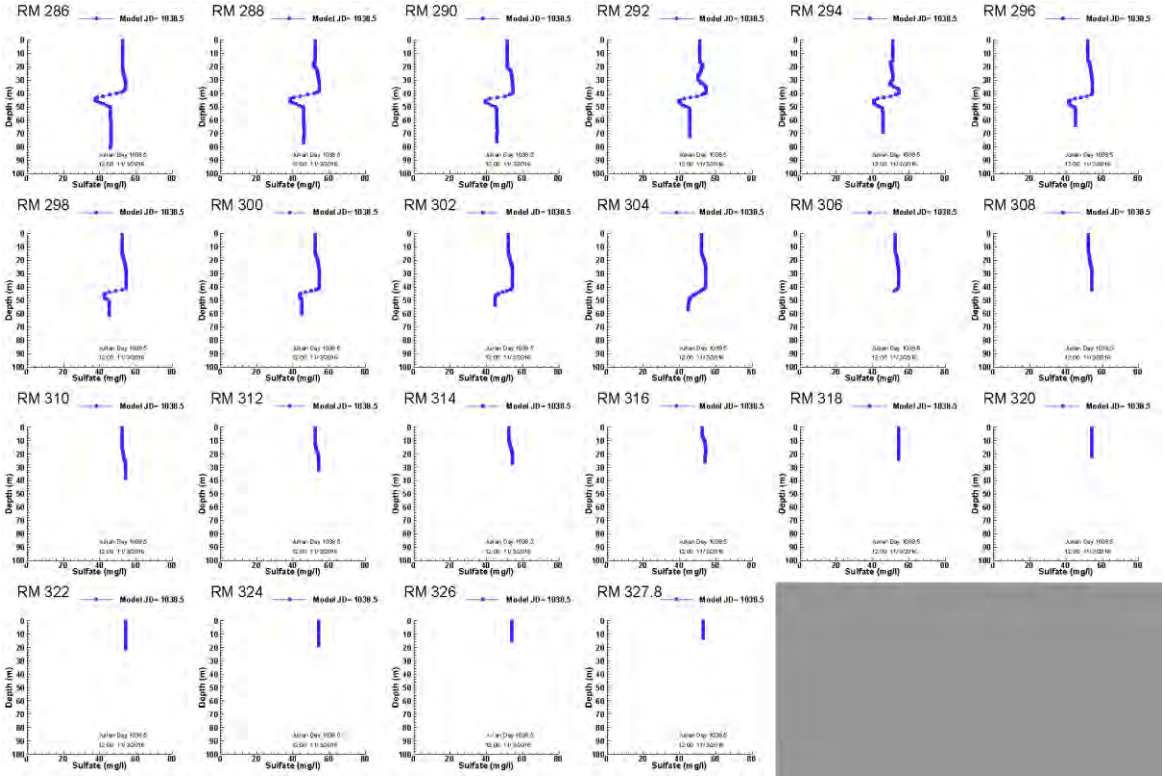


Figure 280. Vertical profiles of sulfate compared with data for 11/ 3/2016.

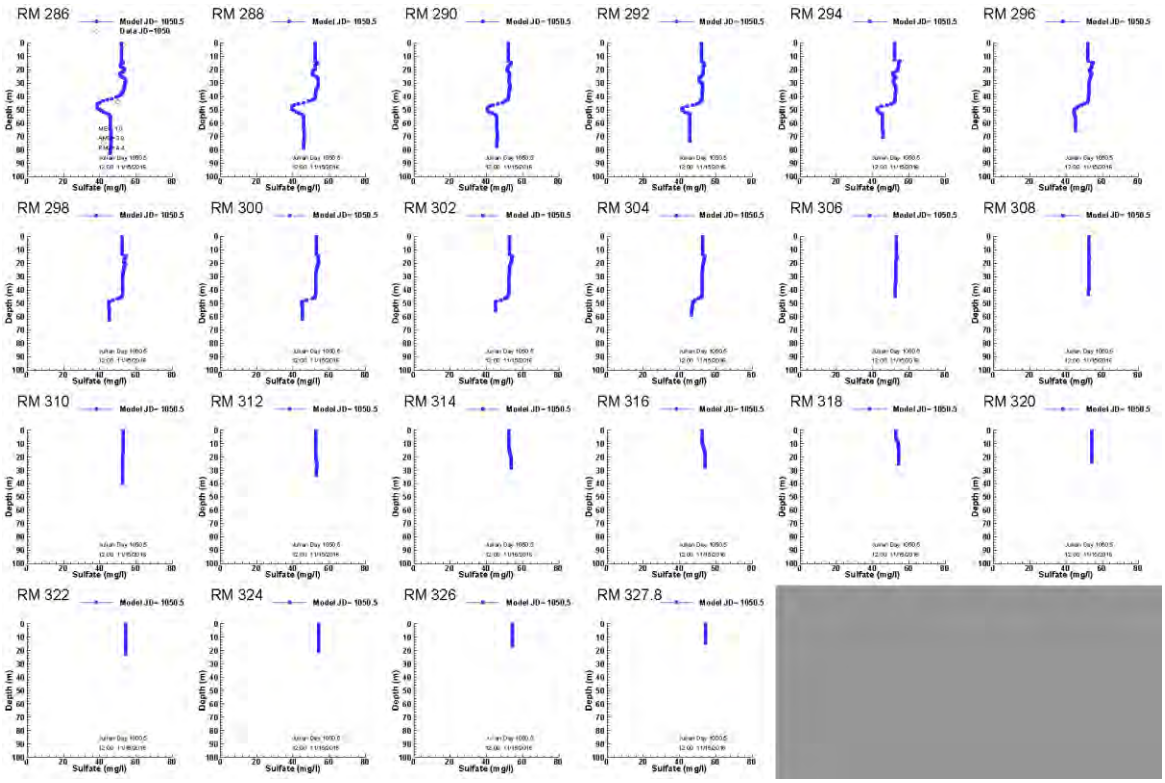


Figure 281. Vertical profiles of sulfate compared with data for 11/15/2016.

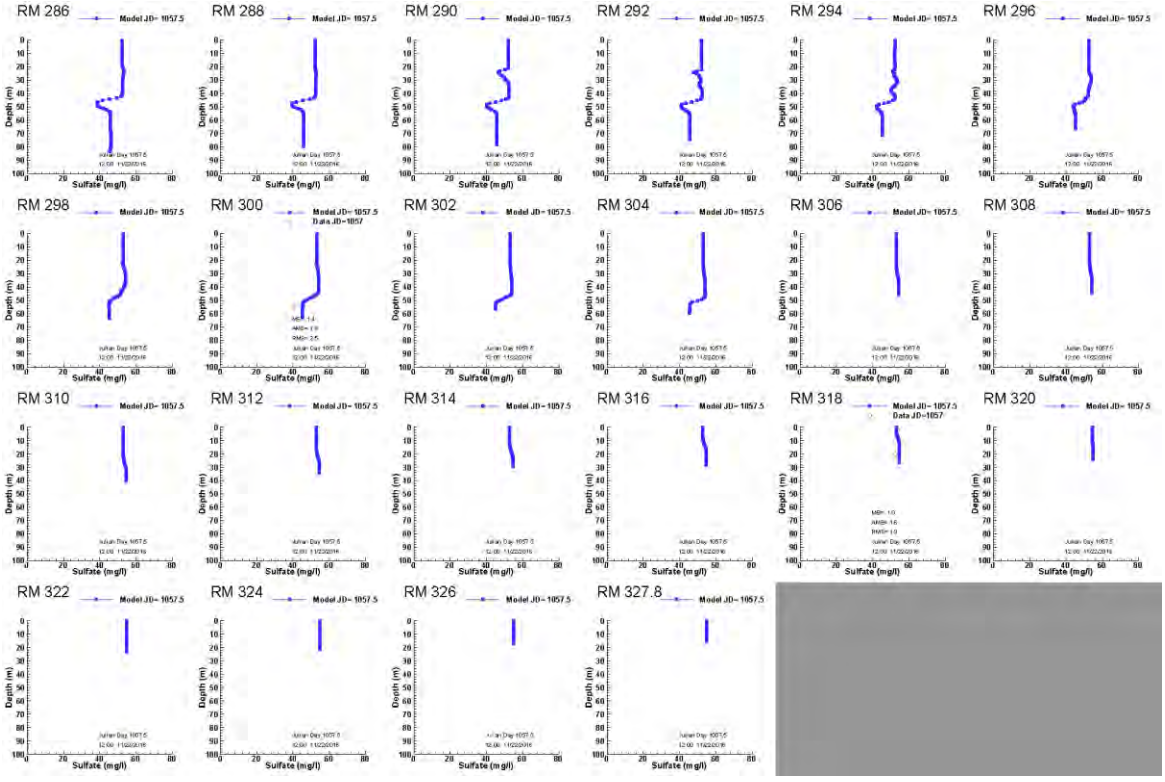


Figure 282. Vertical profiles of sulfate compared with data for 11/22/2016.

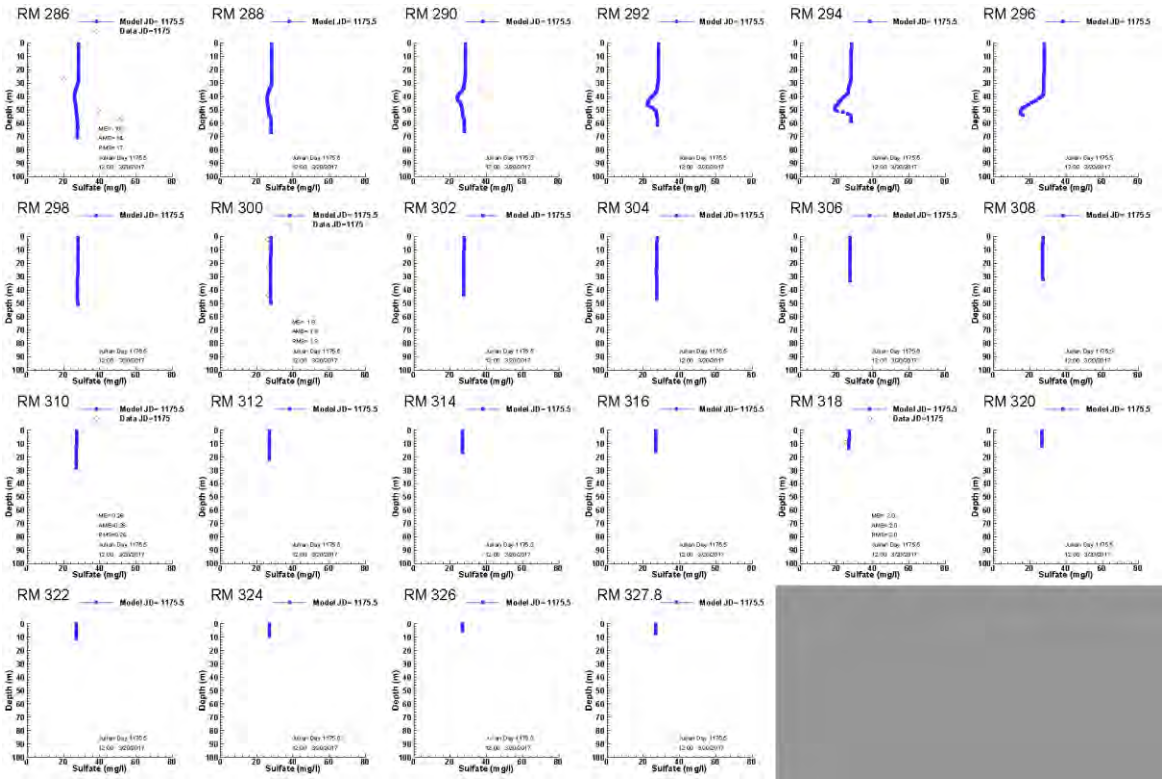


Figure 283. Vertical profiles of sulfate compared with data for 3/20/2017.

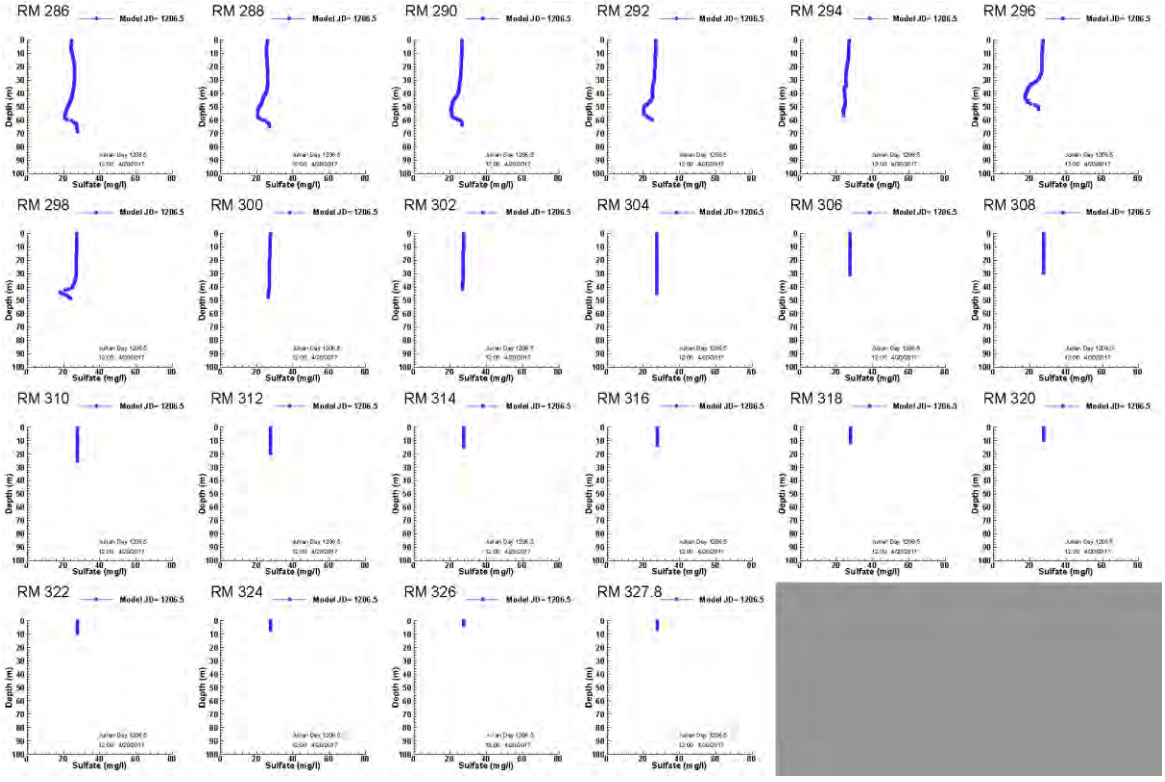


Figure 284. Vertical profiles of sulfate compared with data for 4/20/2017.

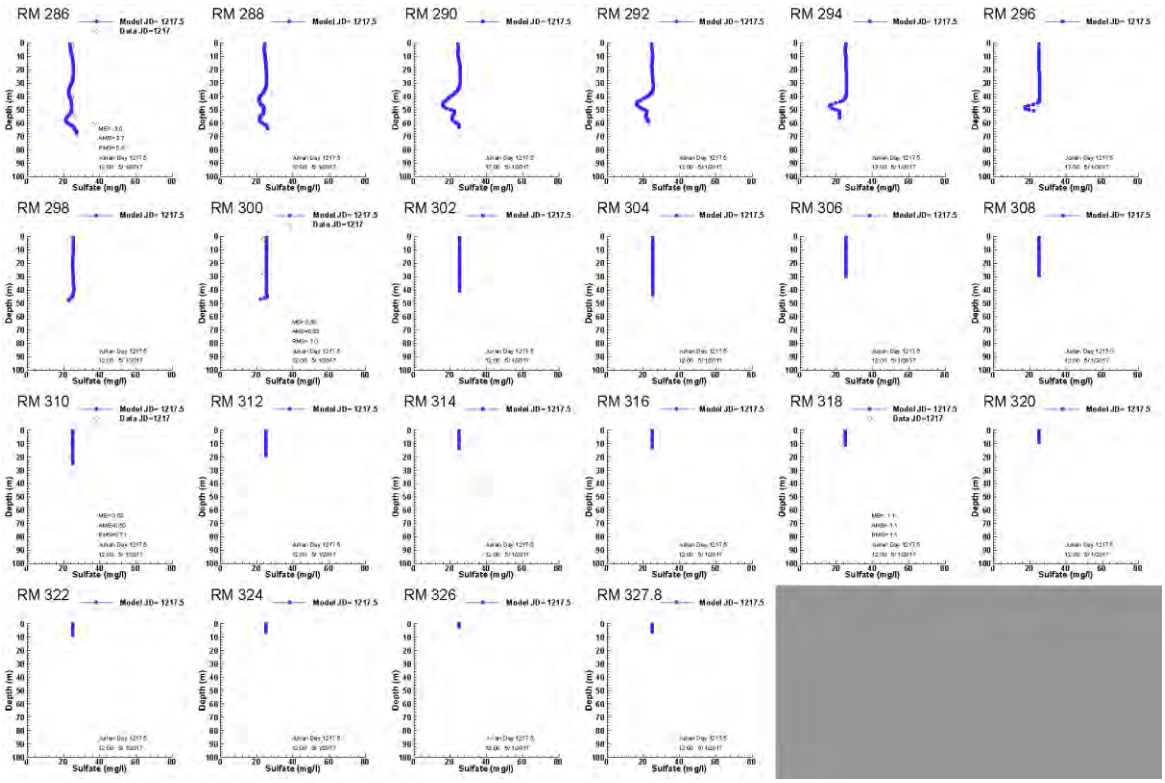


Figure 285. Vertical profiles of sulfate compared with data for 5/ 1/2017.

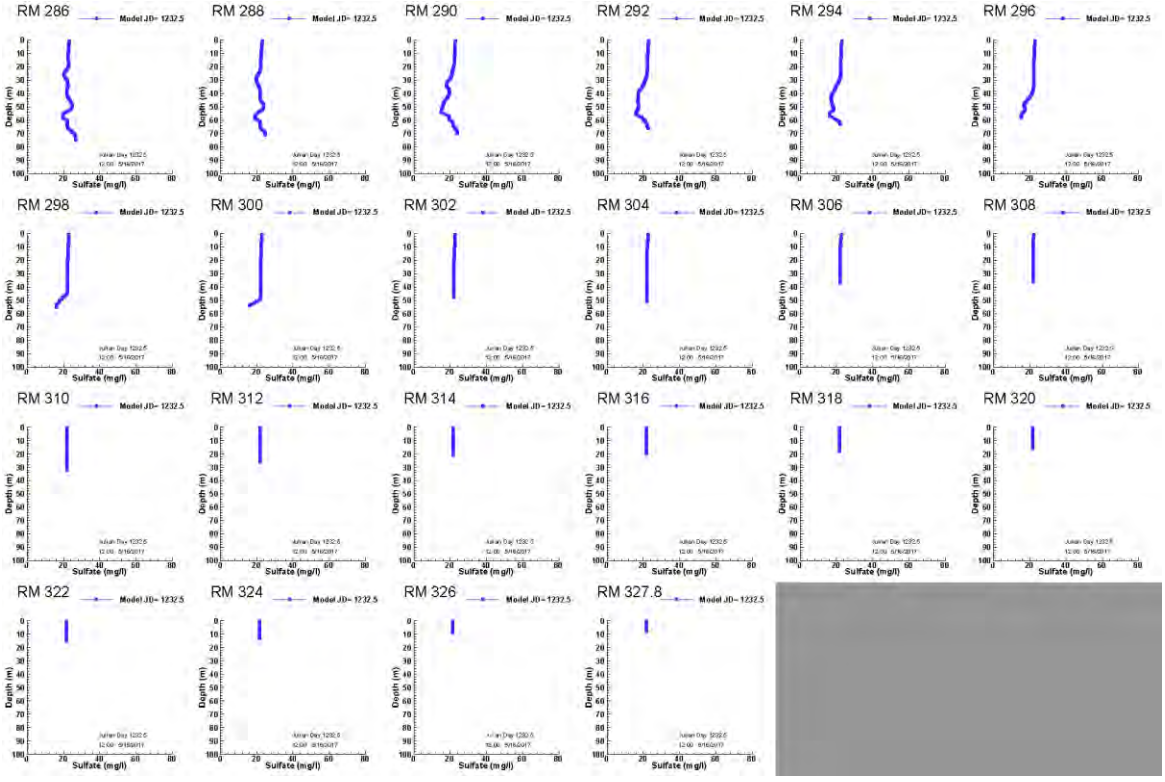


Figure 286. Vertical profiles of sulfate compared with data for 5/16/2017.

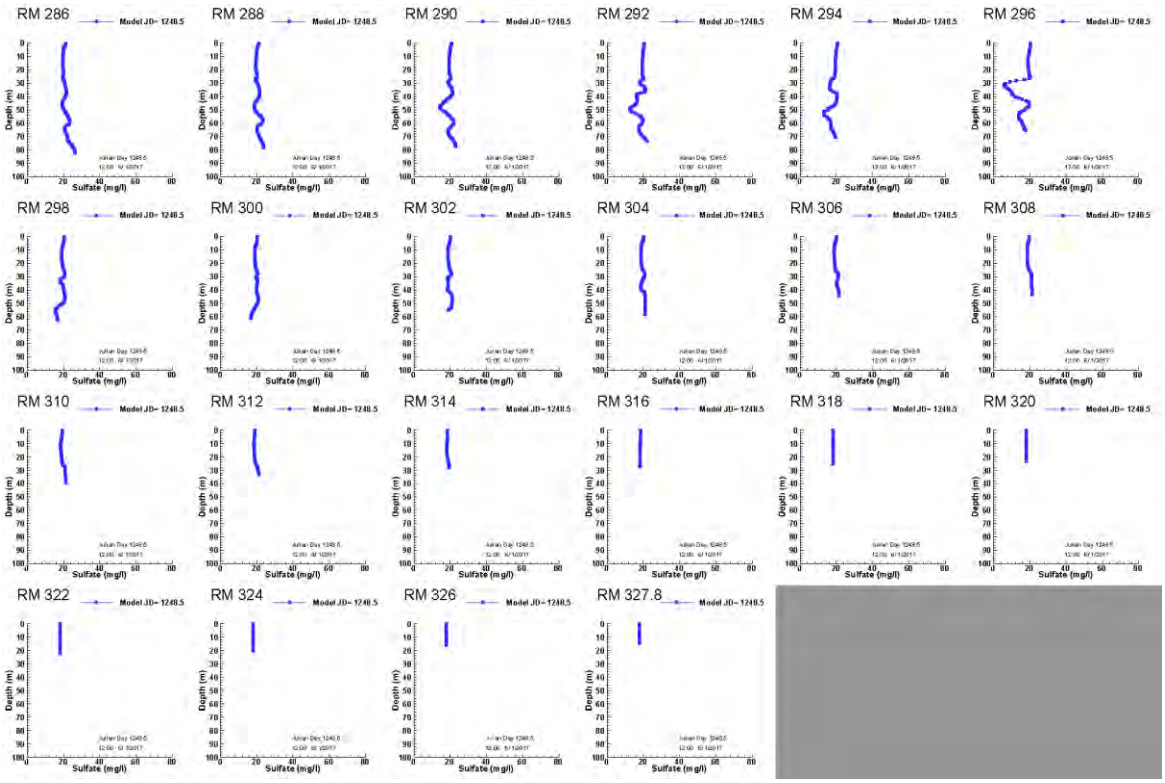


Figure 287. Vertical profiles of sulfate compared with data for 6/ 1/2017.

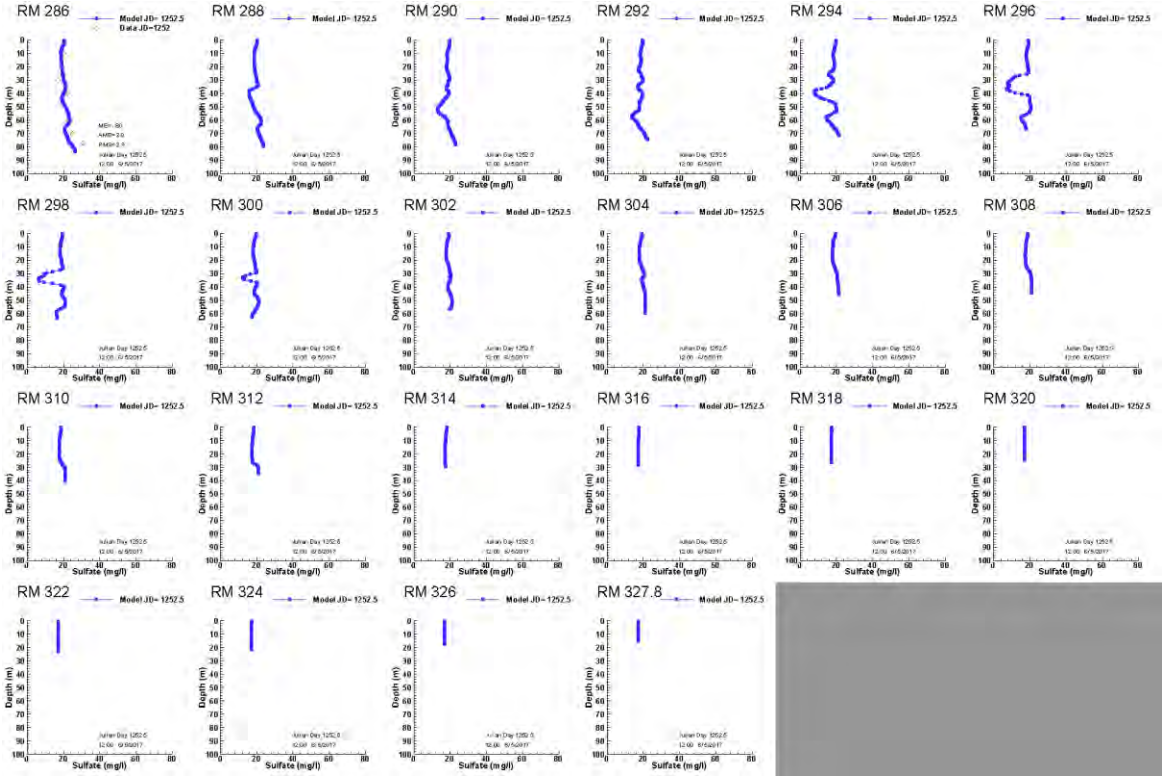


Figure 288. Vertical profiles of sulfate compared with data for 6/ 5/2017.

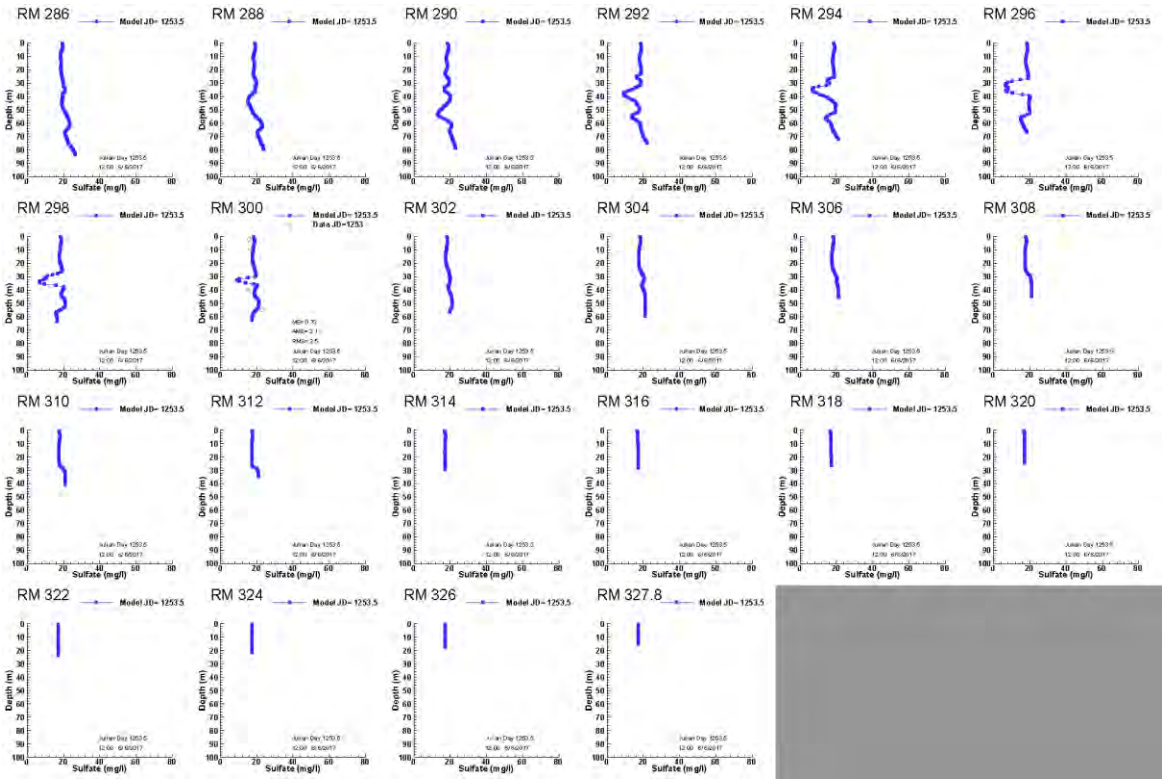


Figure 289. Vertical profiles of sulfate compared with data for 6/ 6/2017.

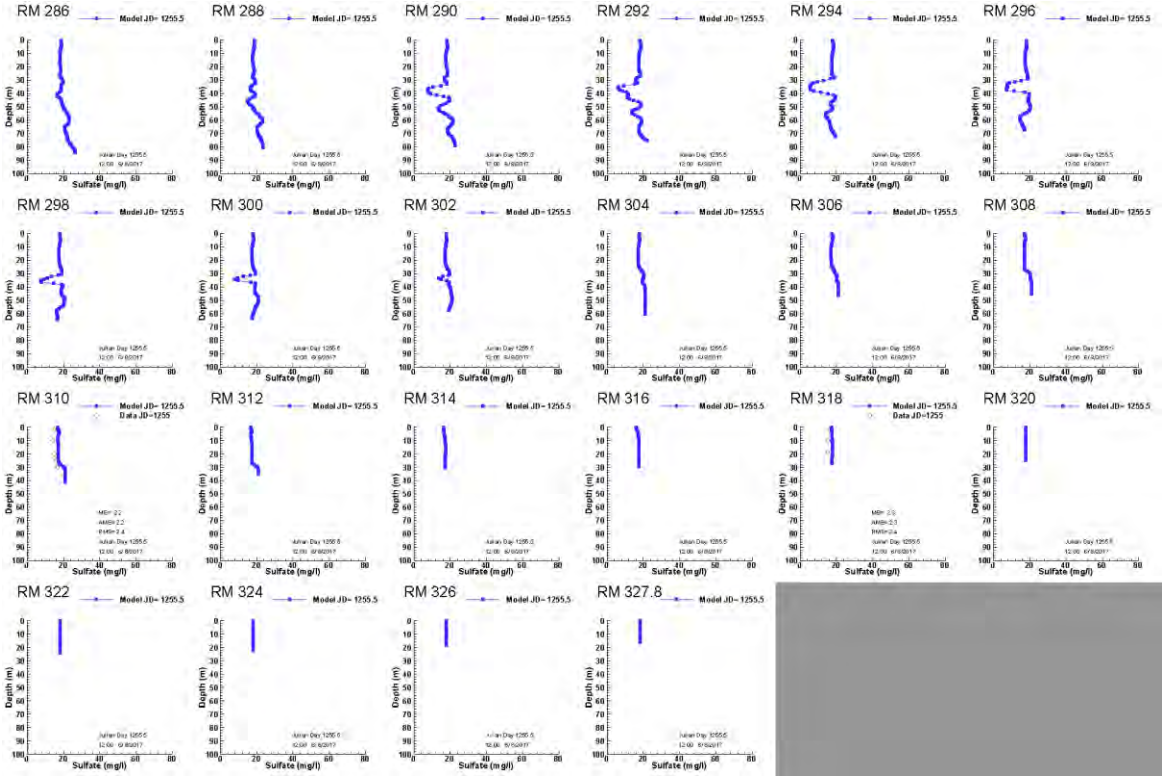


Figure 290. Vertical profiles of sulfate compared with data for 6/ 8/2017.

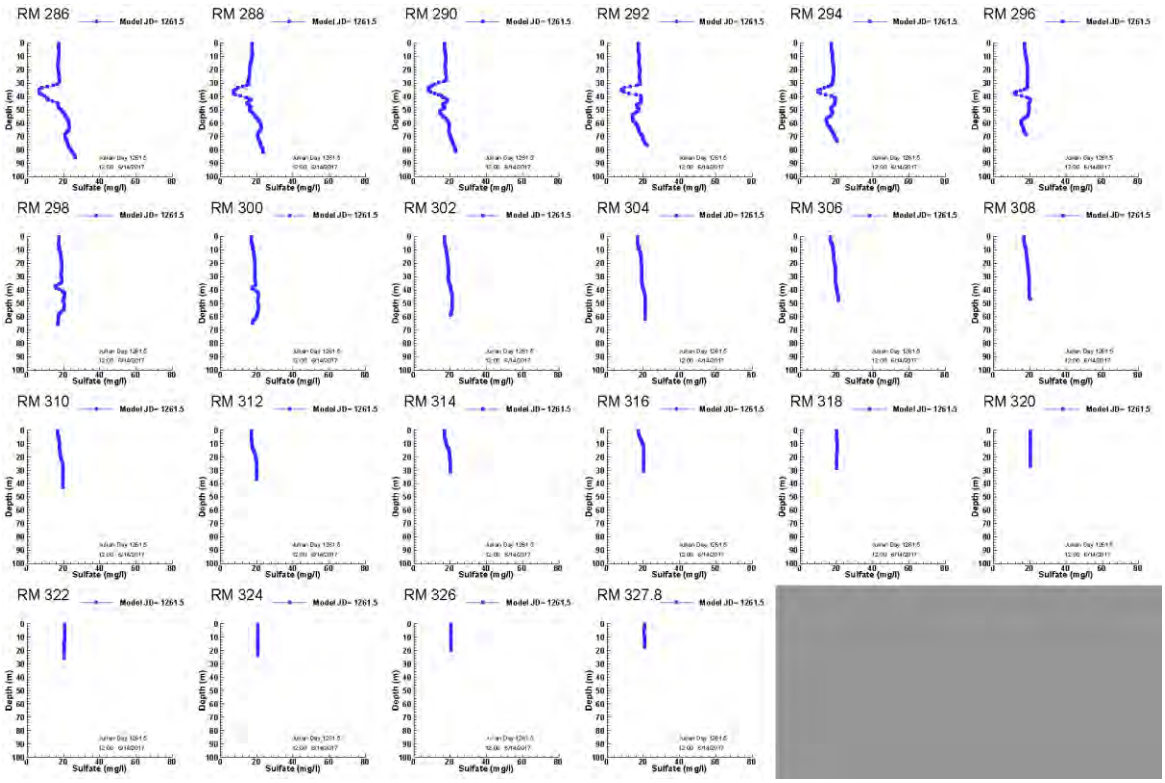


Figure 291. Vertical profiles of sulfate compared with data for 6/14/2017.

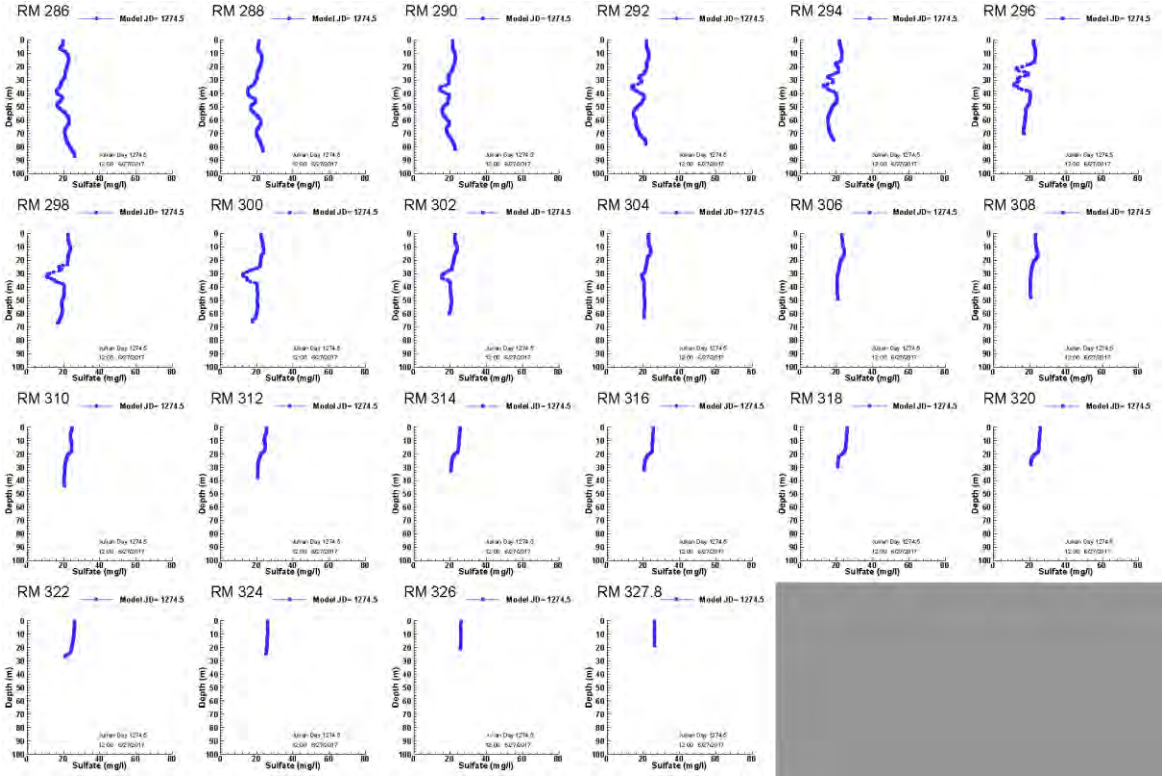


Figure 292. Vertical profiles of sulfate compared with data for 6/27/2017.

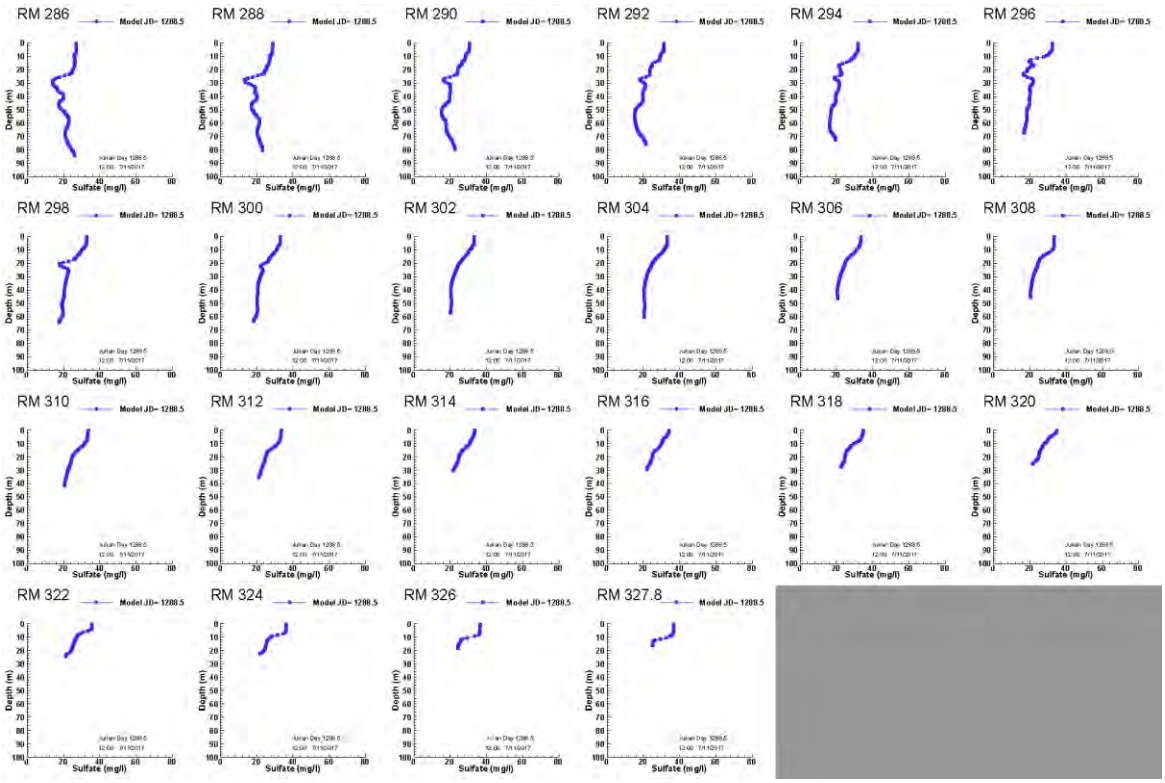


Figure 293. Vertical profiles of sulfate compared with data for 7/11/2017.

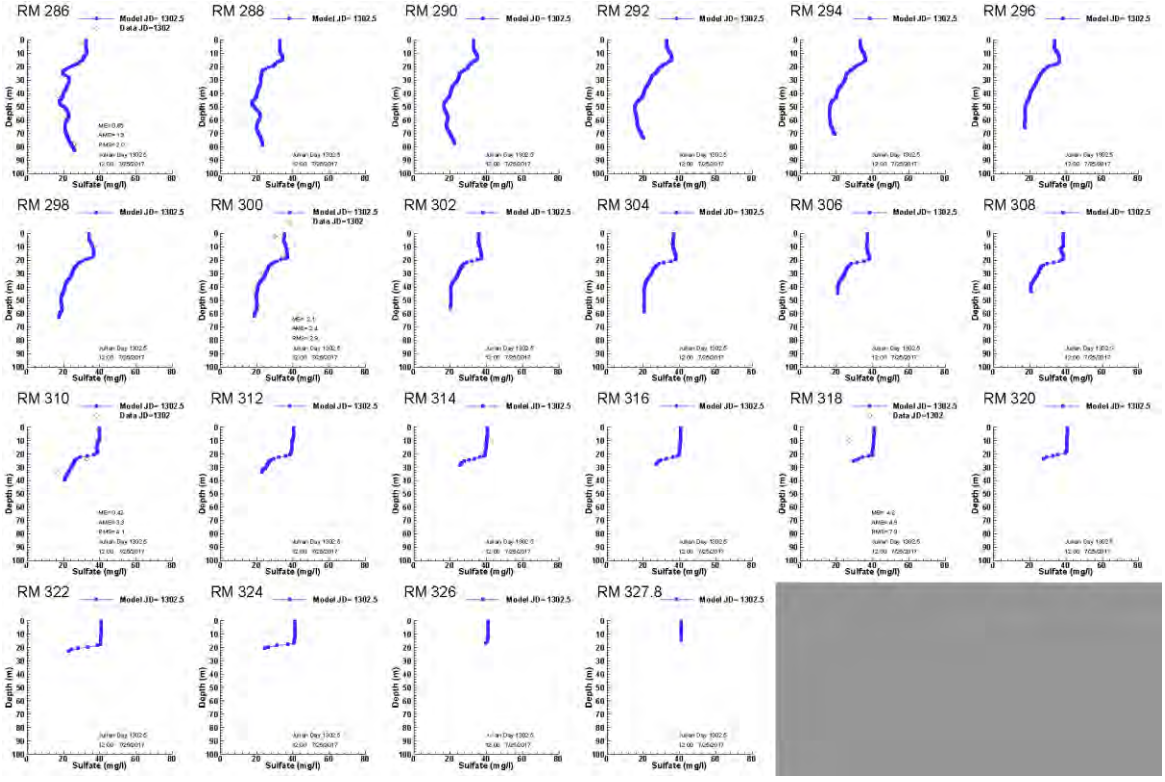


Figure 294. Vertical profiles of sulfate compared with data for 7/25/2017.

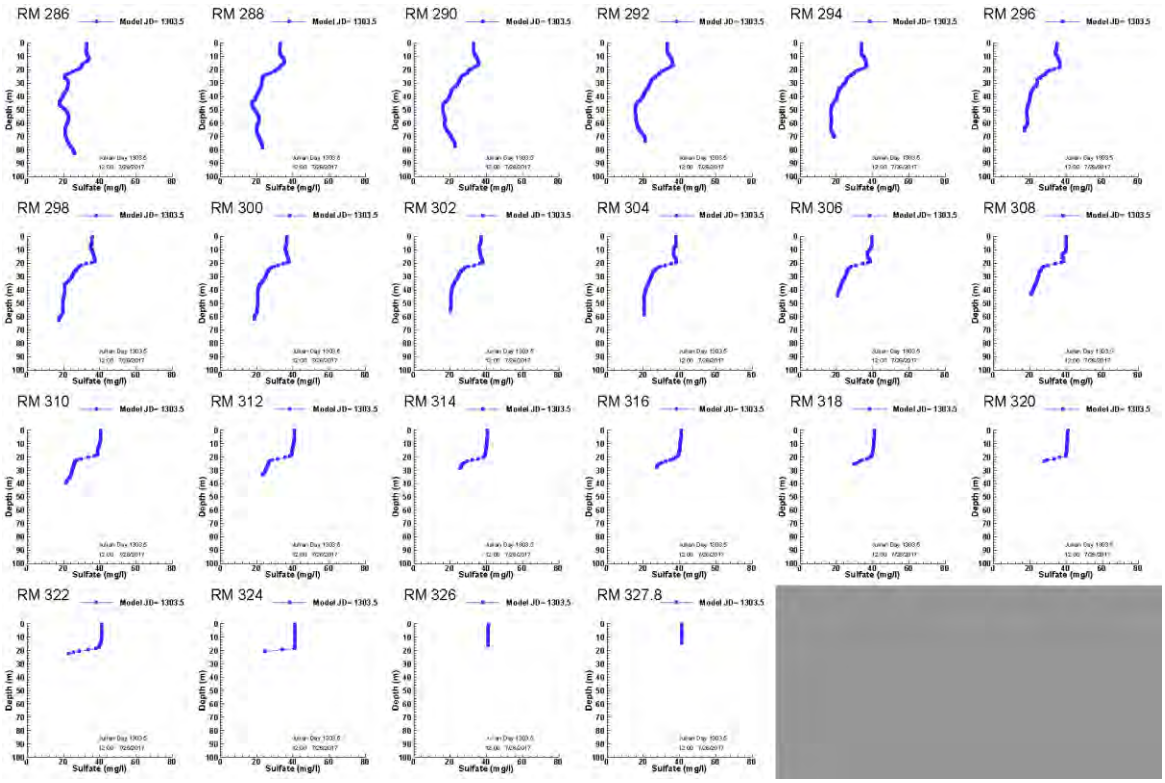


Figure 295. Vertical profiles of sulfate compared with data for 7/26/2017.

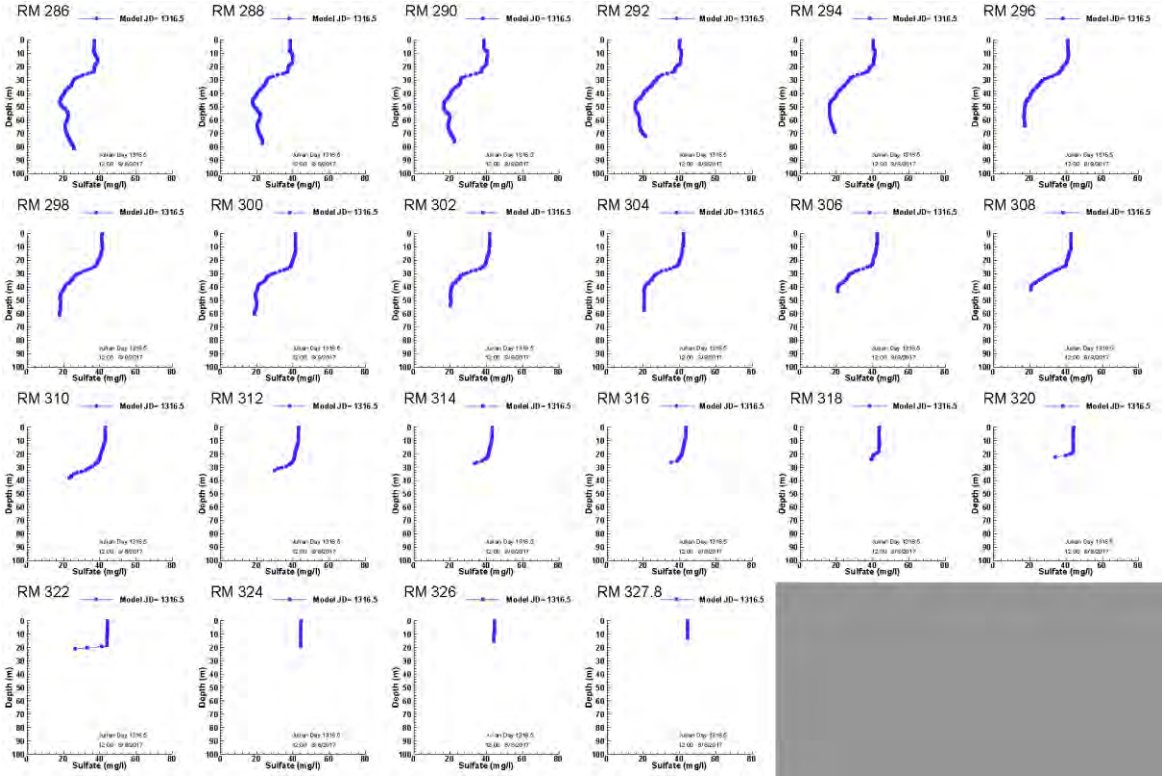


Figure 296. Vertical profiles of sulfate compared with data for 8/ 8/2017.

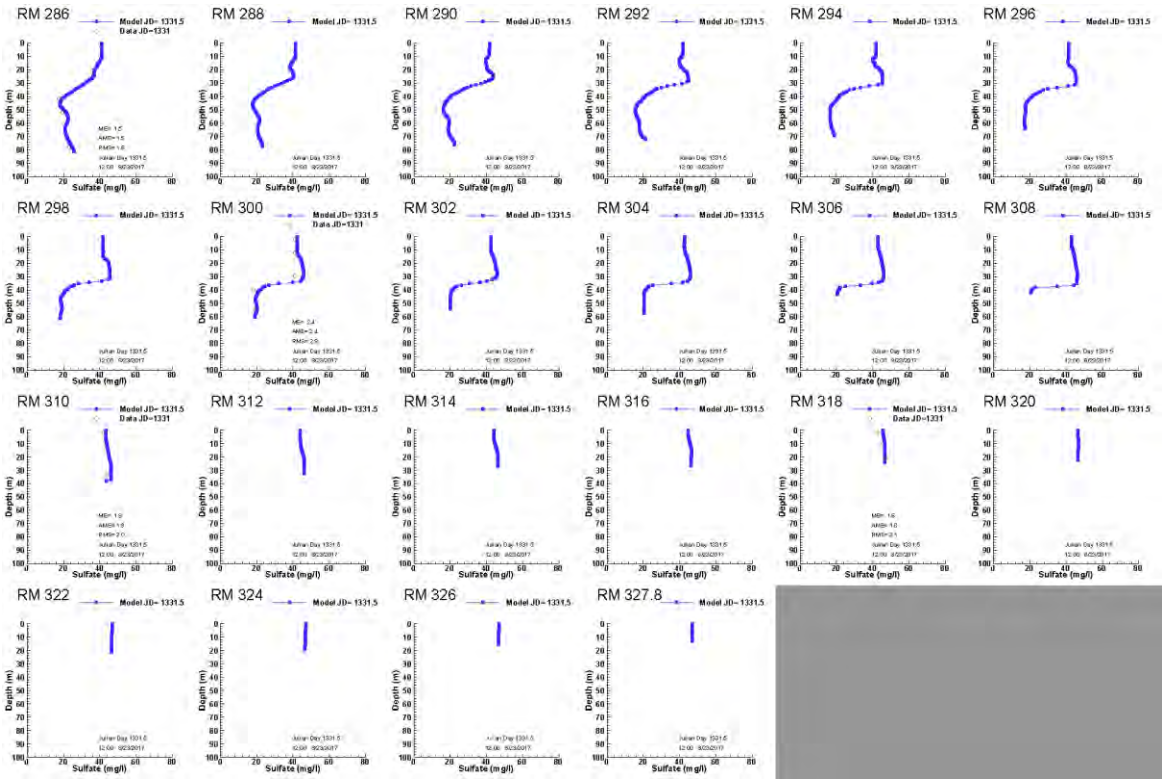


Figure 297. Vertical profiles of sulfate compared with data for 8/23/2017.

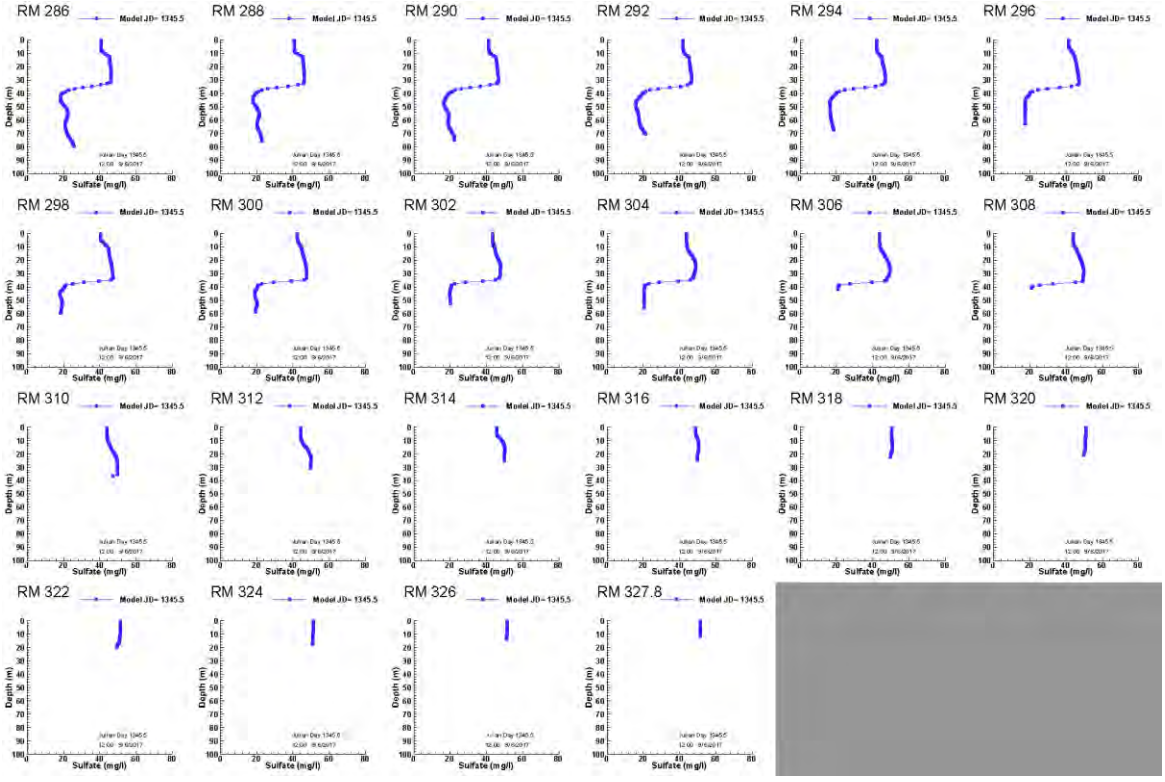


Figure 298. Vertical profiles of sulfate compared with data for 9/ 6/2017.

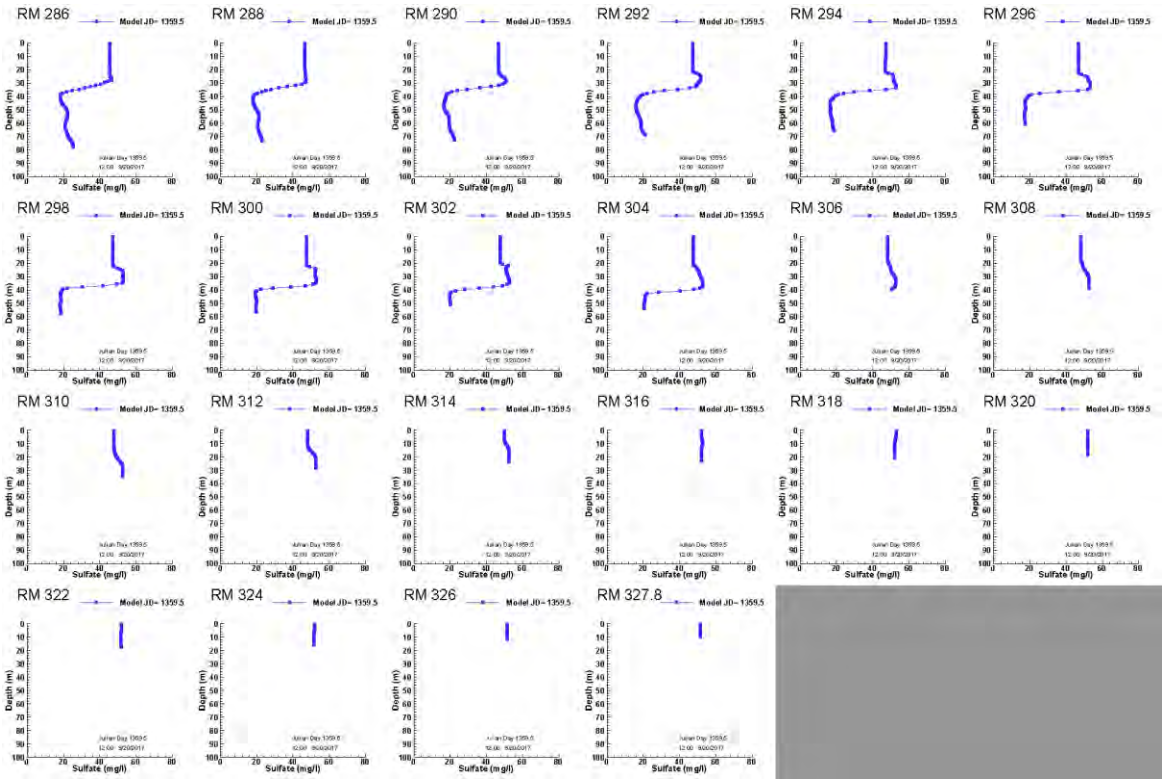


Figure 299. Vertical profiles of sulfate compared with data for 9/20/2017.

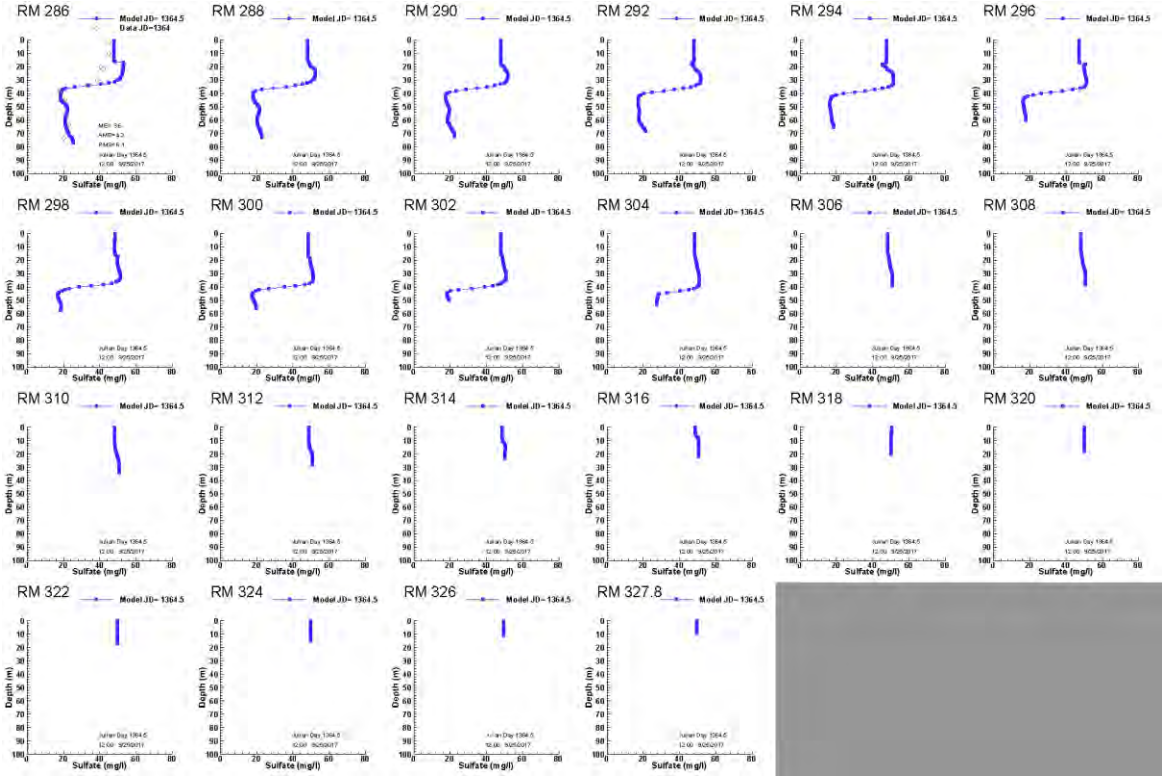


Figure 300. Vertical profiles of sulfate compared with data for 9/25/2017.

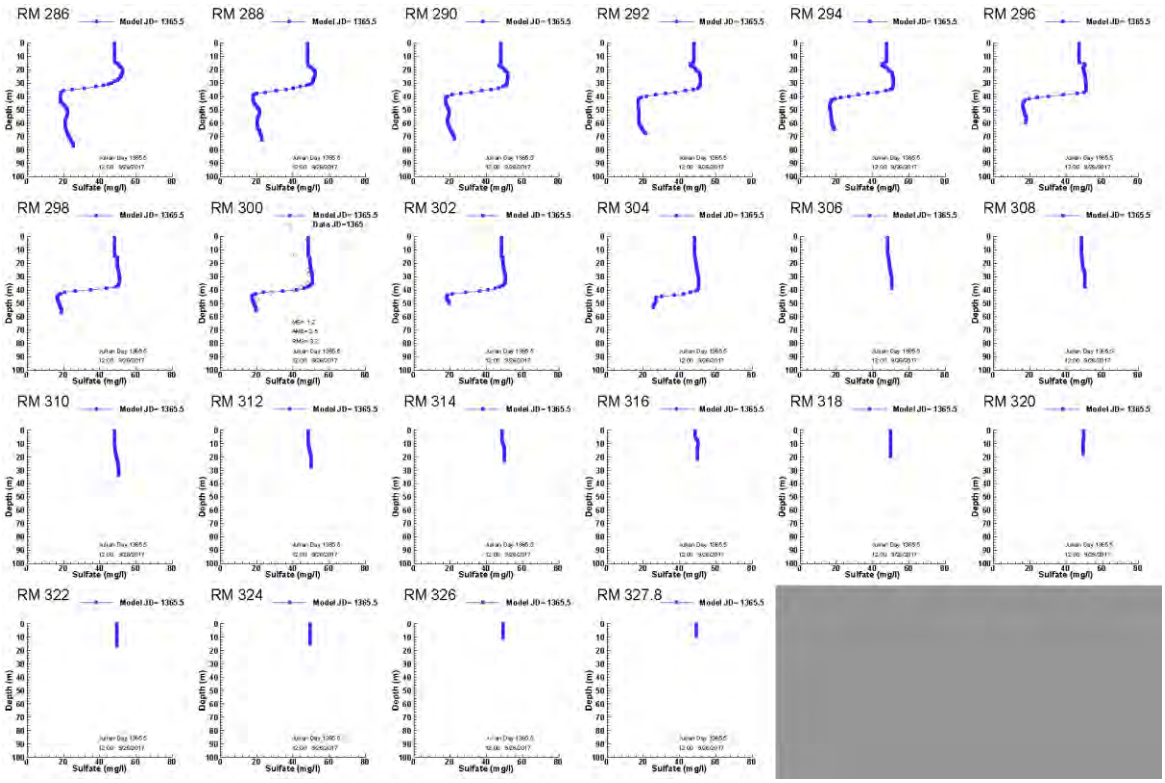


Figure 301. Vertical profiles of sulfate compared with data for 9/26/2017.

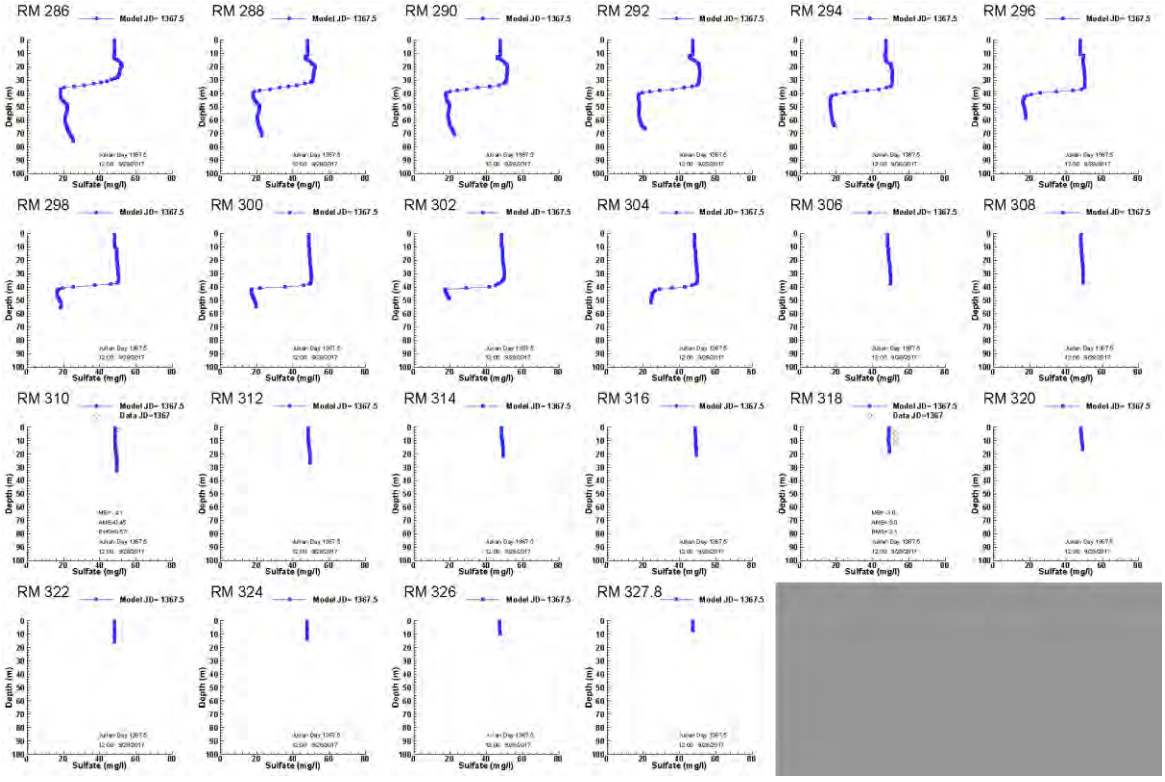


Figure 302. Vertical profiles of sulfate compared with data for 9/28/2017.

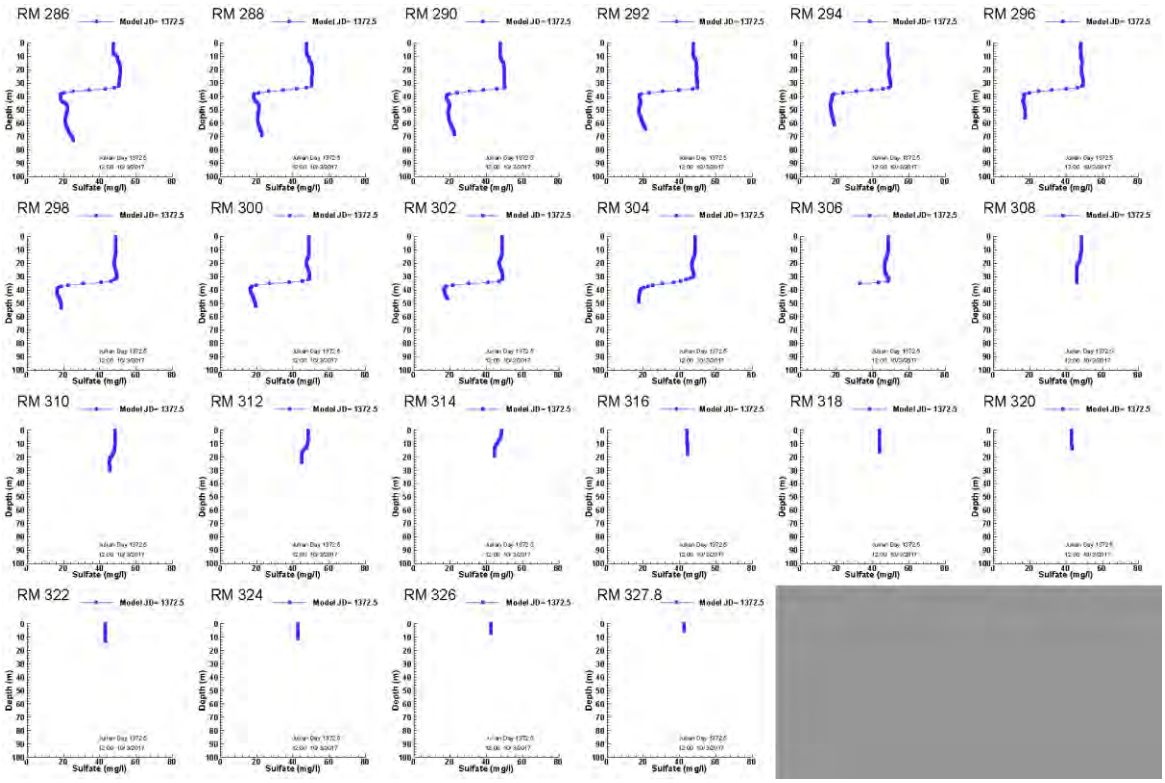


Figure 303. Vertical profiles of sulfate compared with data for 10/ 3/2017.

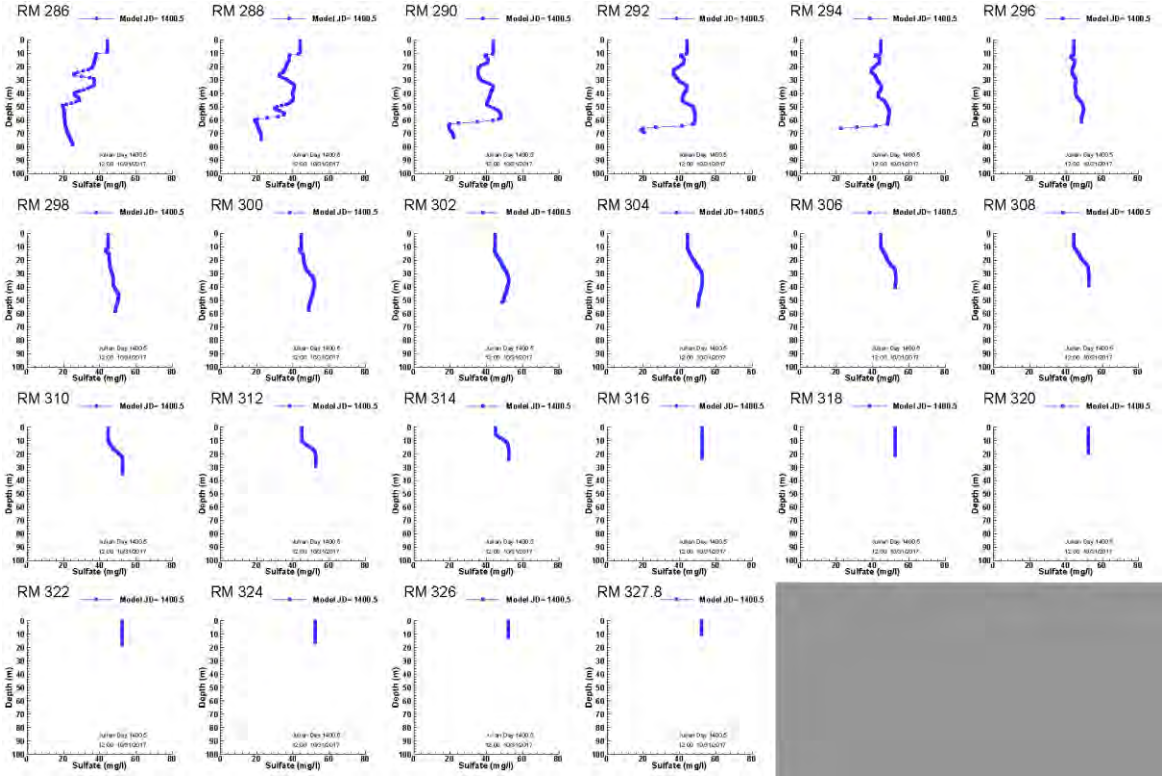


Figure 304. Vertical profiles of sulfate compared with data for 10/31/2017.

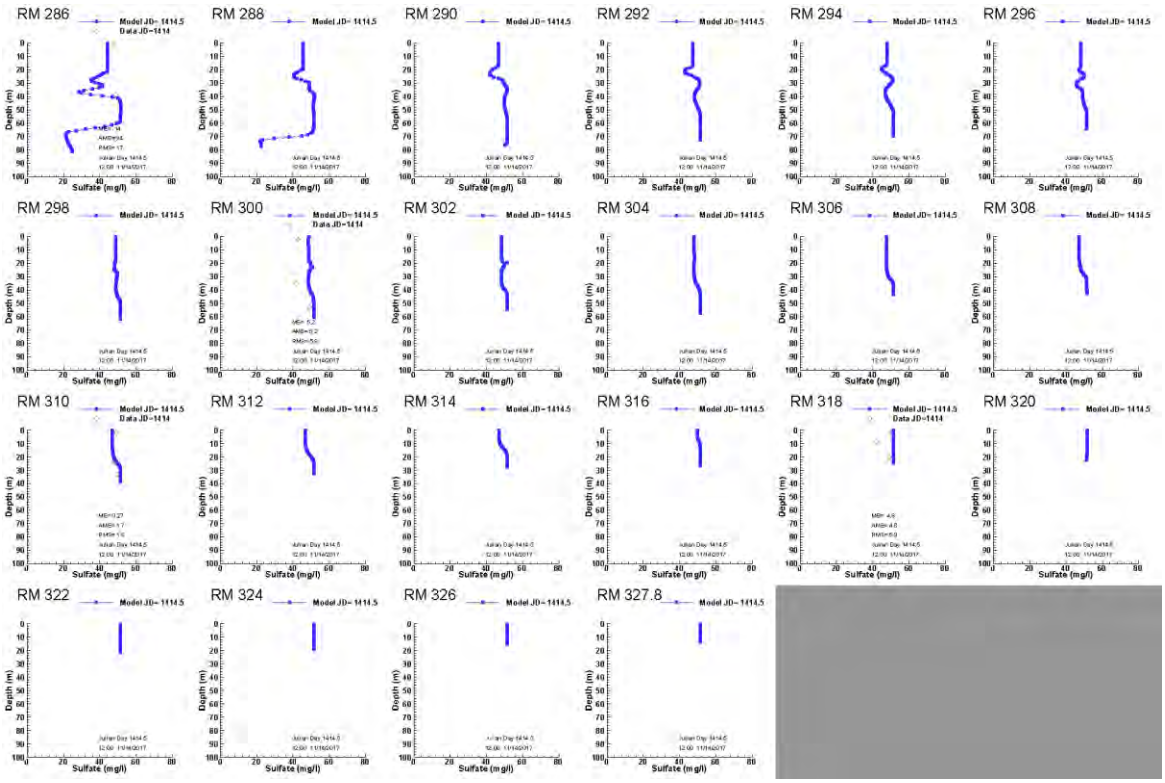


Figure 305. Vertical profiles of sulfate compared with data for 11/14/2017.

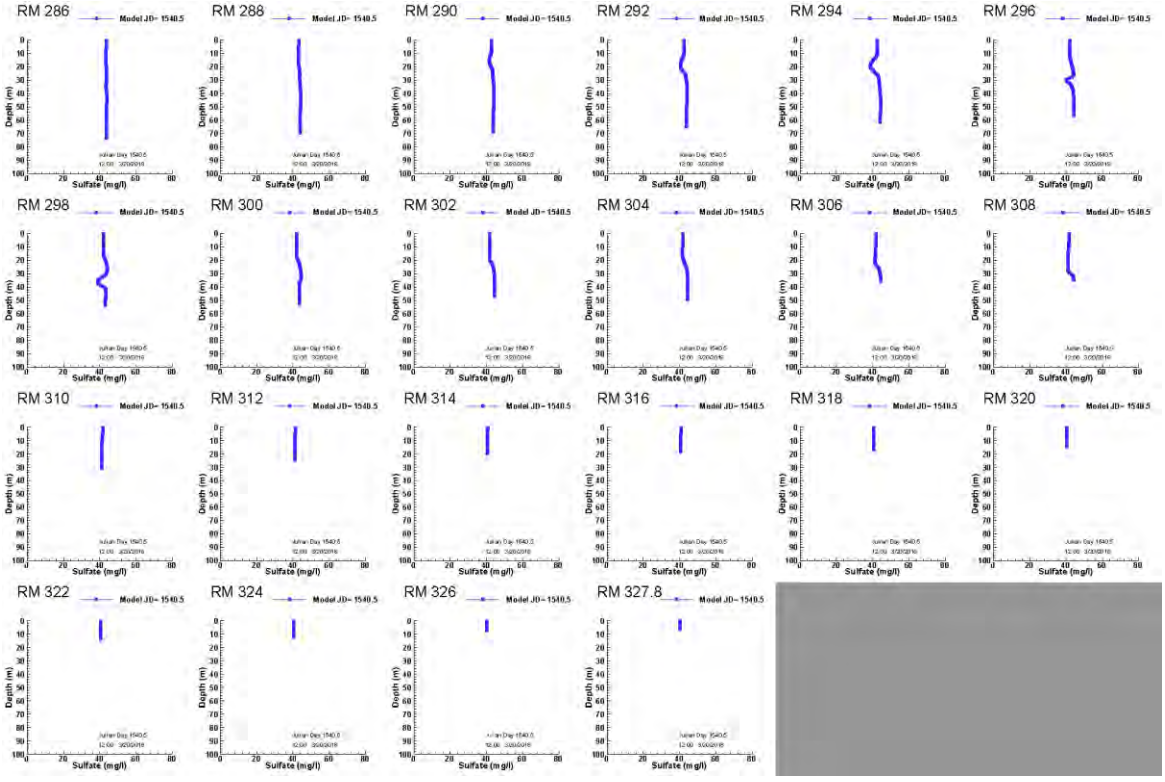


Figure 306. Vertical profiles of sulfate compared with data for 3/20/2018.

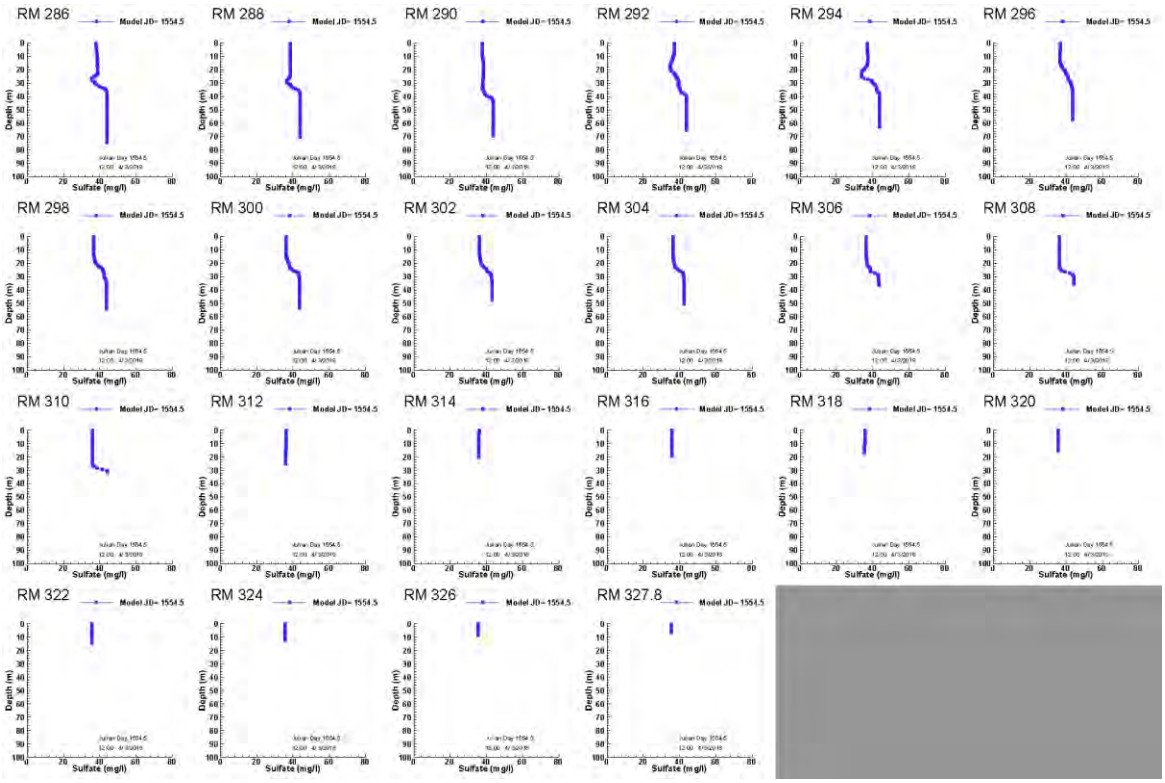


Figure 307. Vertical profiles of sulfate compared with data for 4/ 3/2018.

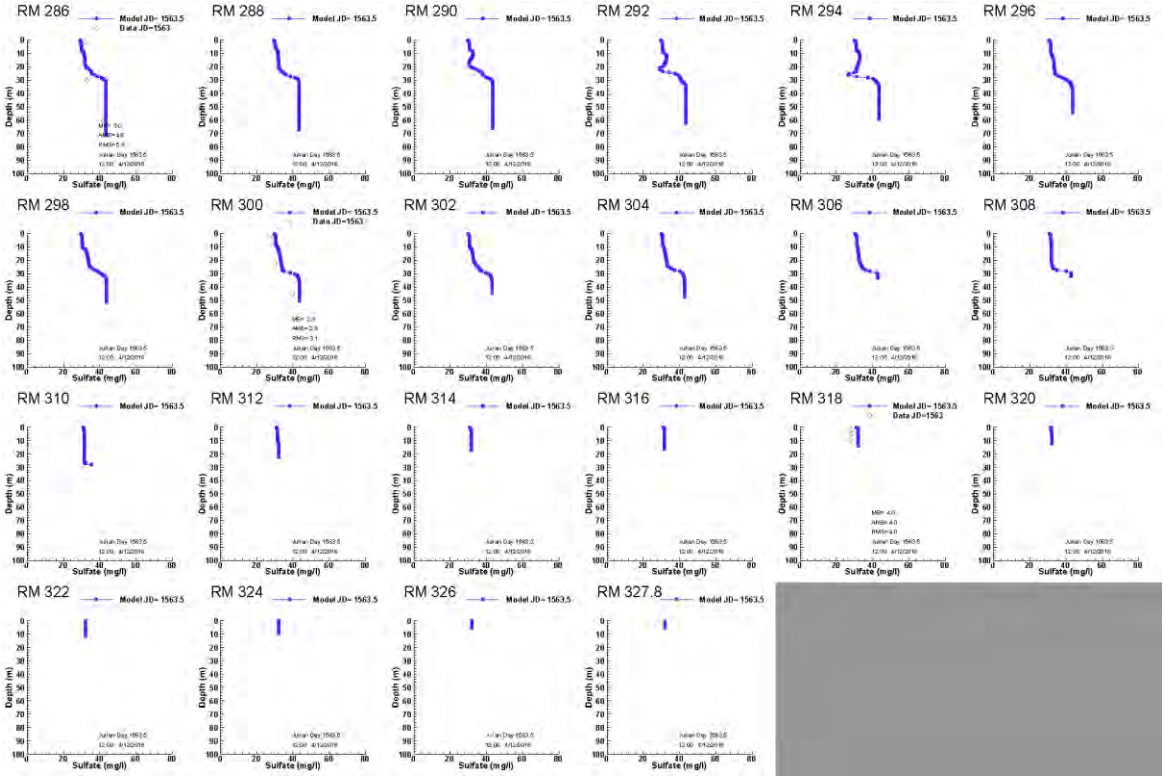


Figure 308. Vertical profiles of sulfate compared with data for 4/12/2018.

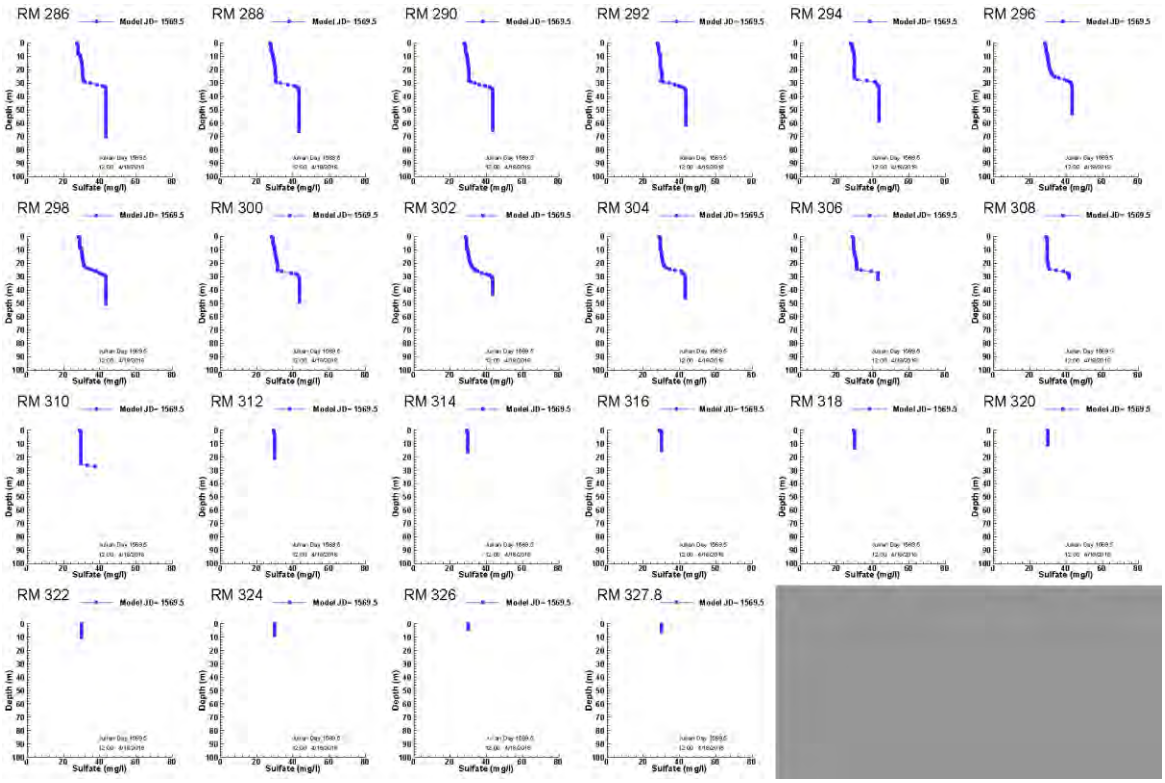


Figure 309. Vertical profiles of sulfate compared with data for 4/18/2018.

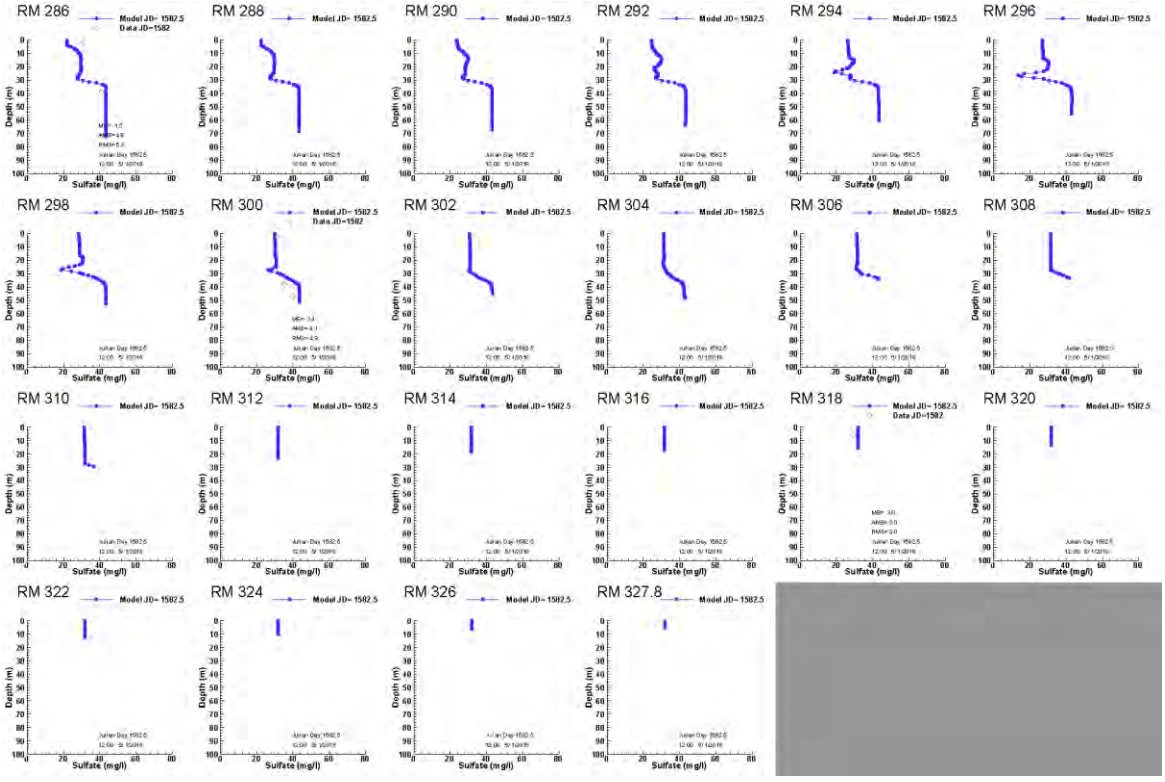


Figure 310. Vertical profiles of sulfate compared with data for 5/ 1/2018.

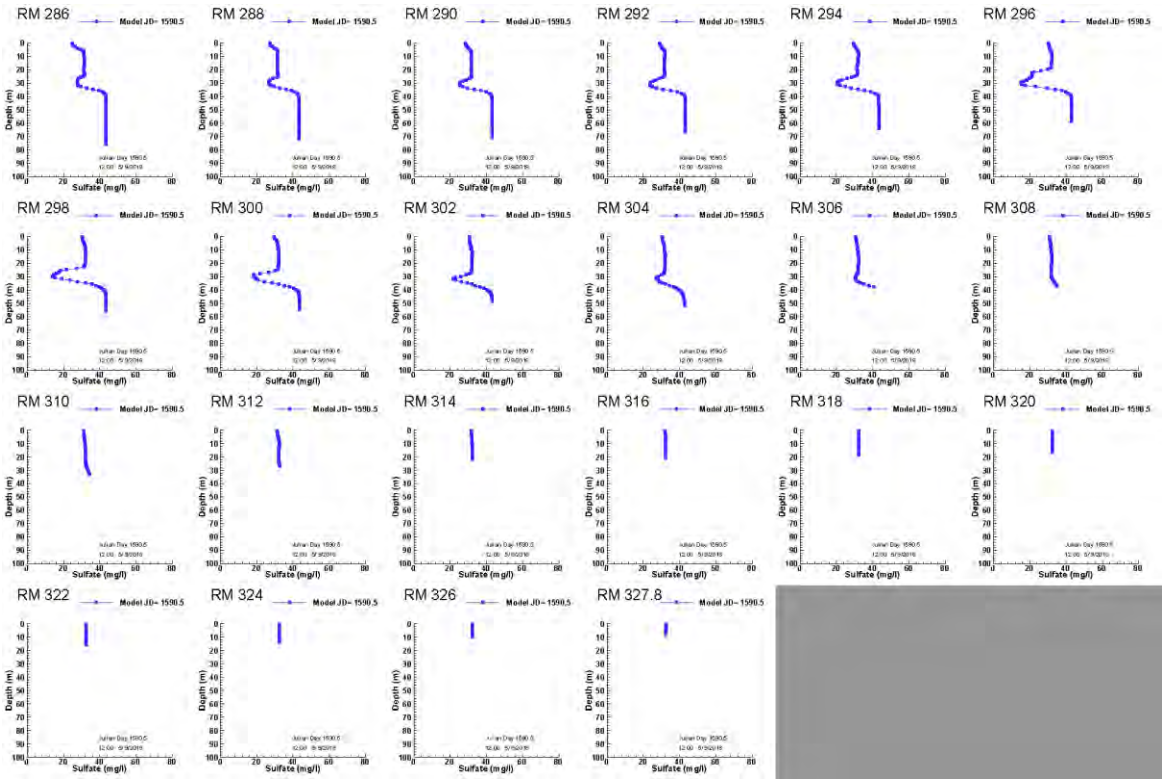


Figure 311. Vertical profiles of sulfate compared with data for 5/ 9/2018.

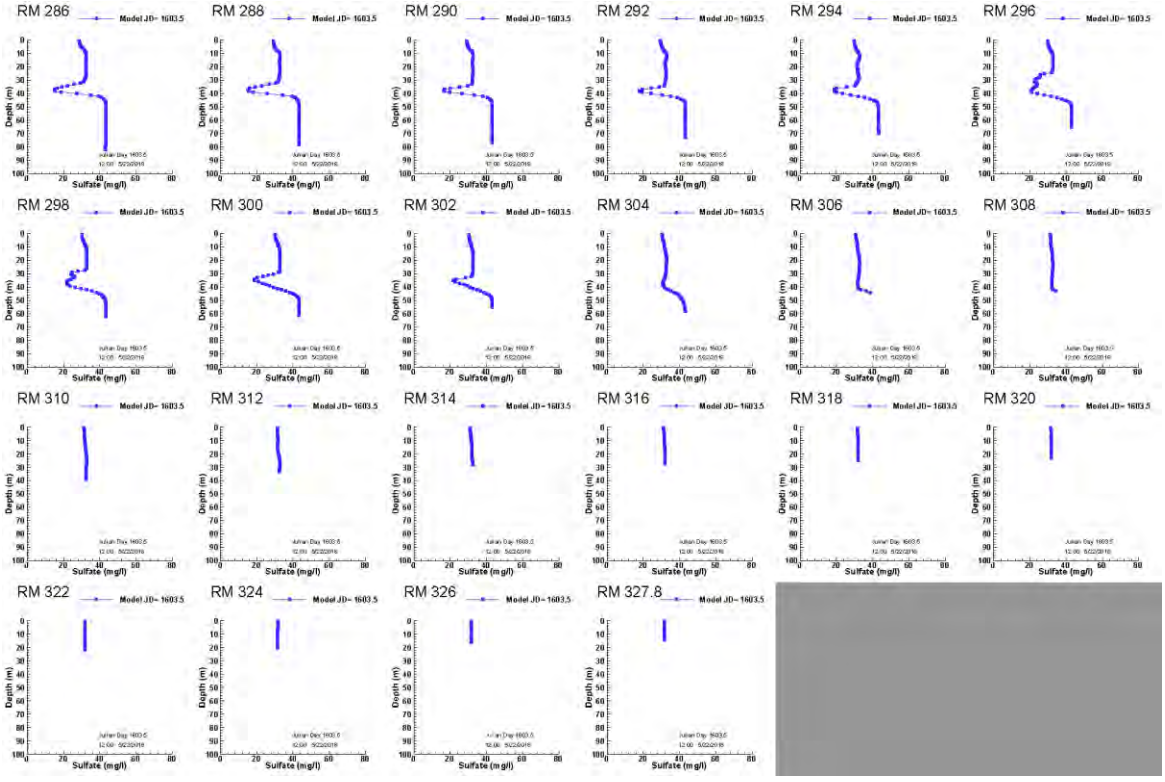


Figure 312. Vertical profiles of sulfate compared with data for 5/22/2018.

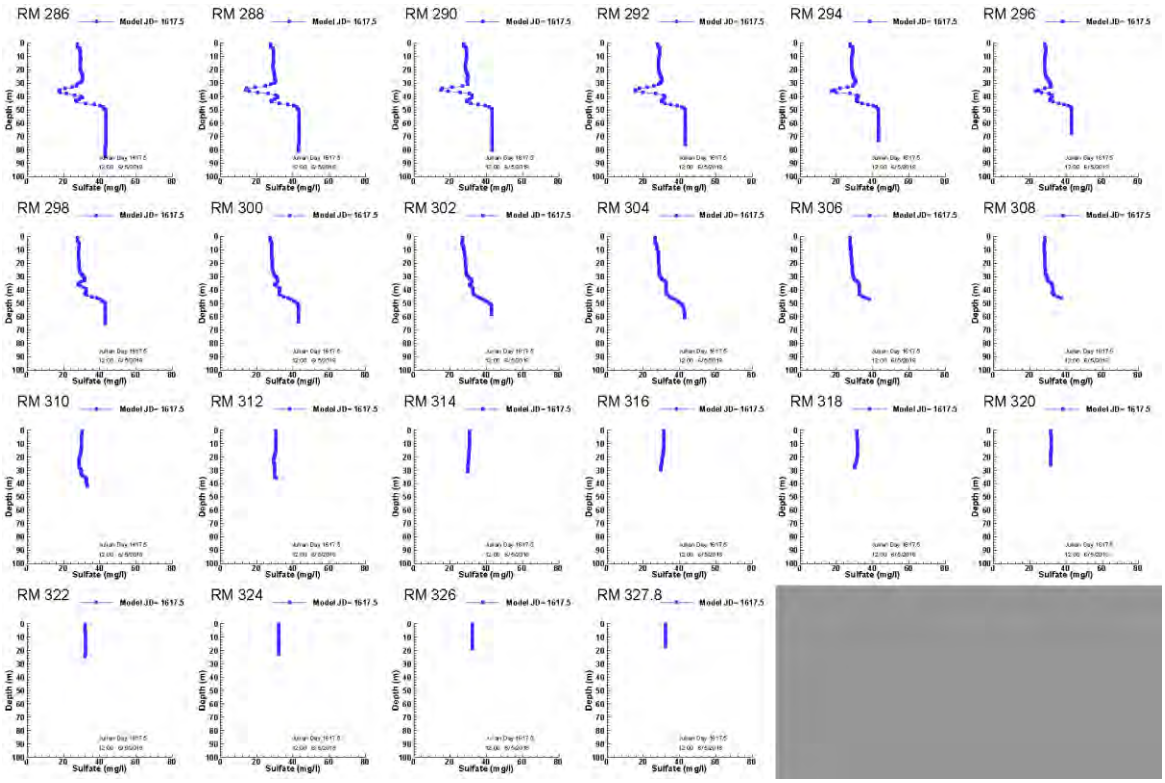


Figure 313. Vertical profiles of sulfate compared with data for 6/ 5/2018.

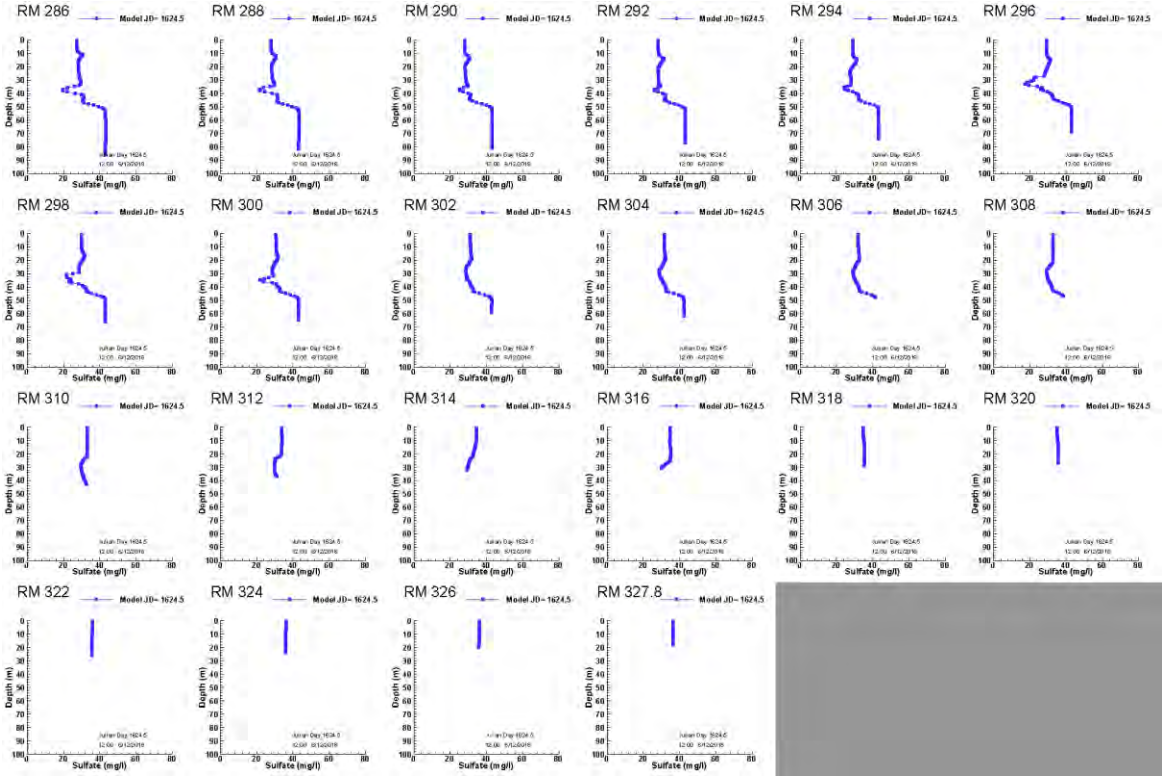


Figure 314. Vertical profiles of sulfate compared with data for 6/12/2018.

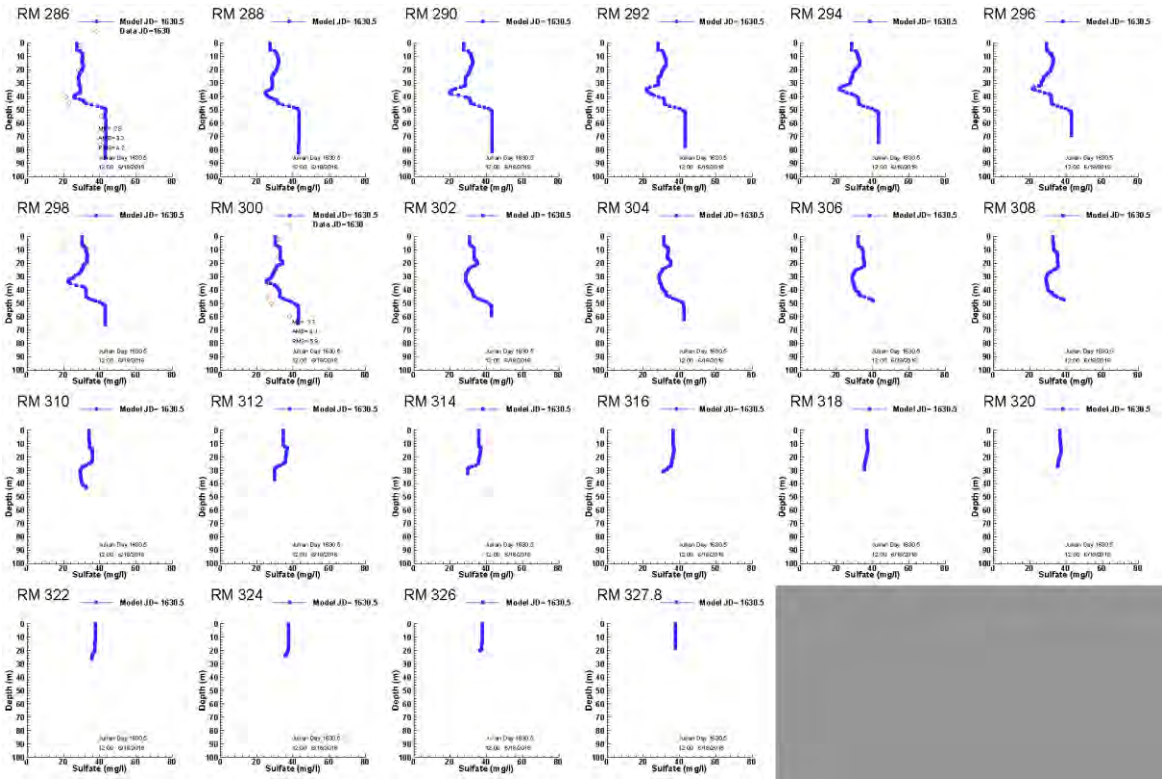


Figure 315. Vertical profiles of sulfate compared with data for 6/18/2018.

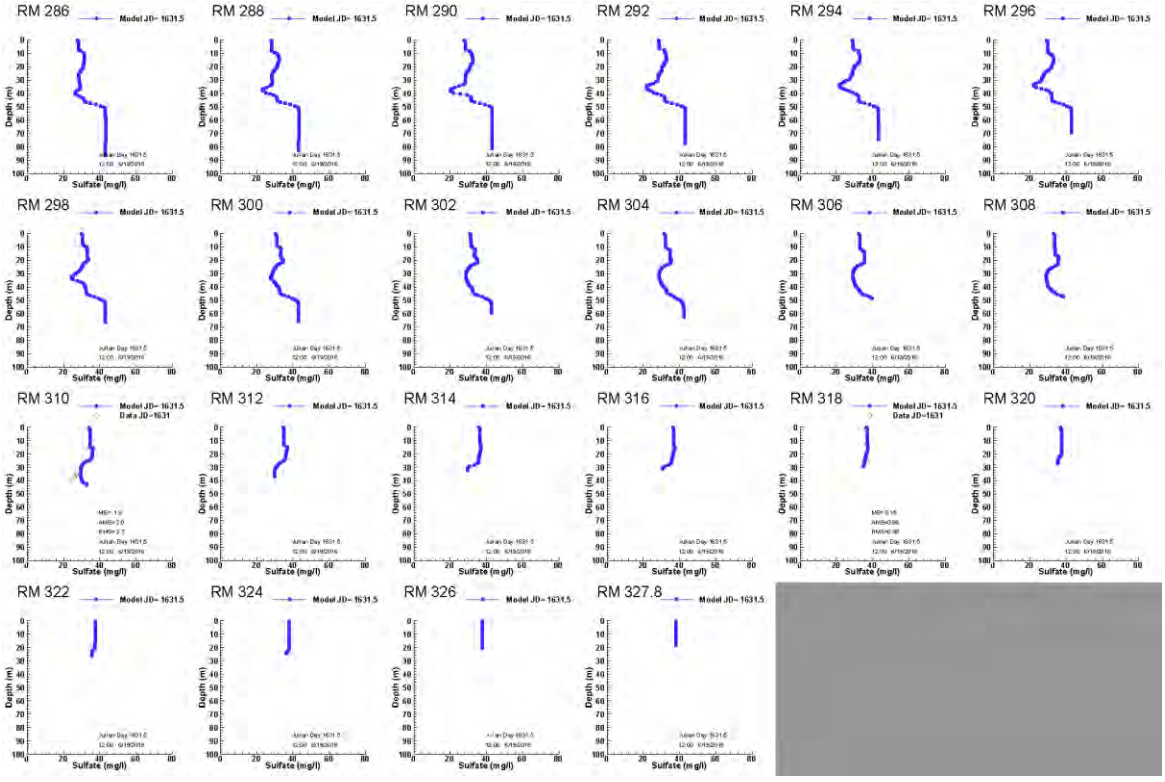


Figure 316. Vertical profiles of sulfate compared with data for 6/19/2018.

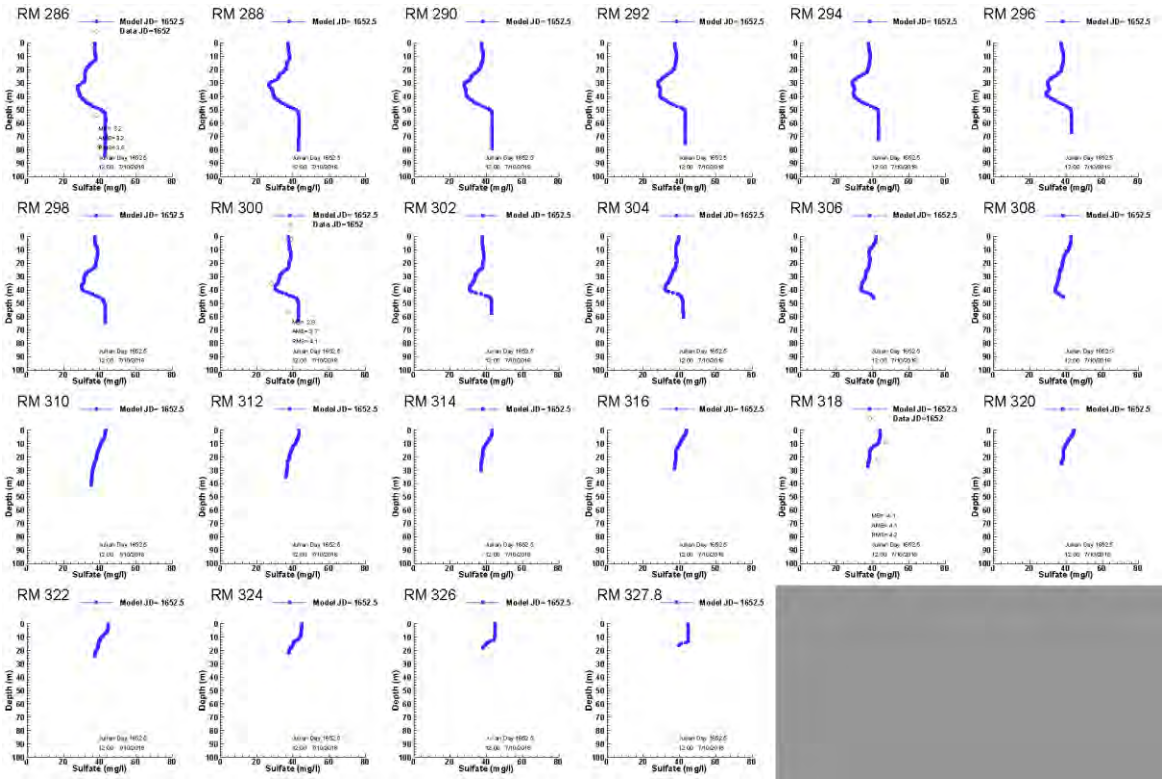


Figure 317. Vertical profiles of sulfate compared with data for 7/10/2018.

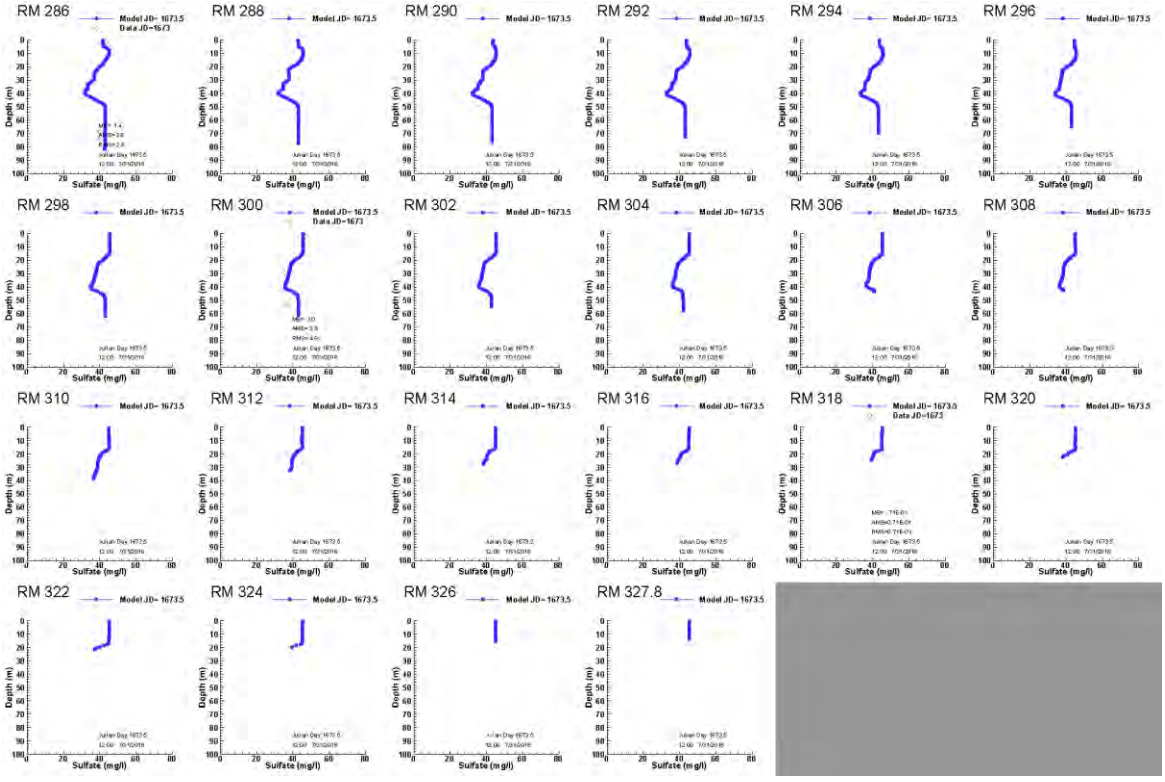


Figure 318. Vertical profiles of sulfate compared with data for 7/31/2018.

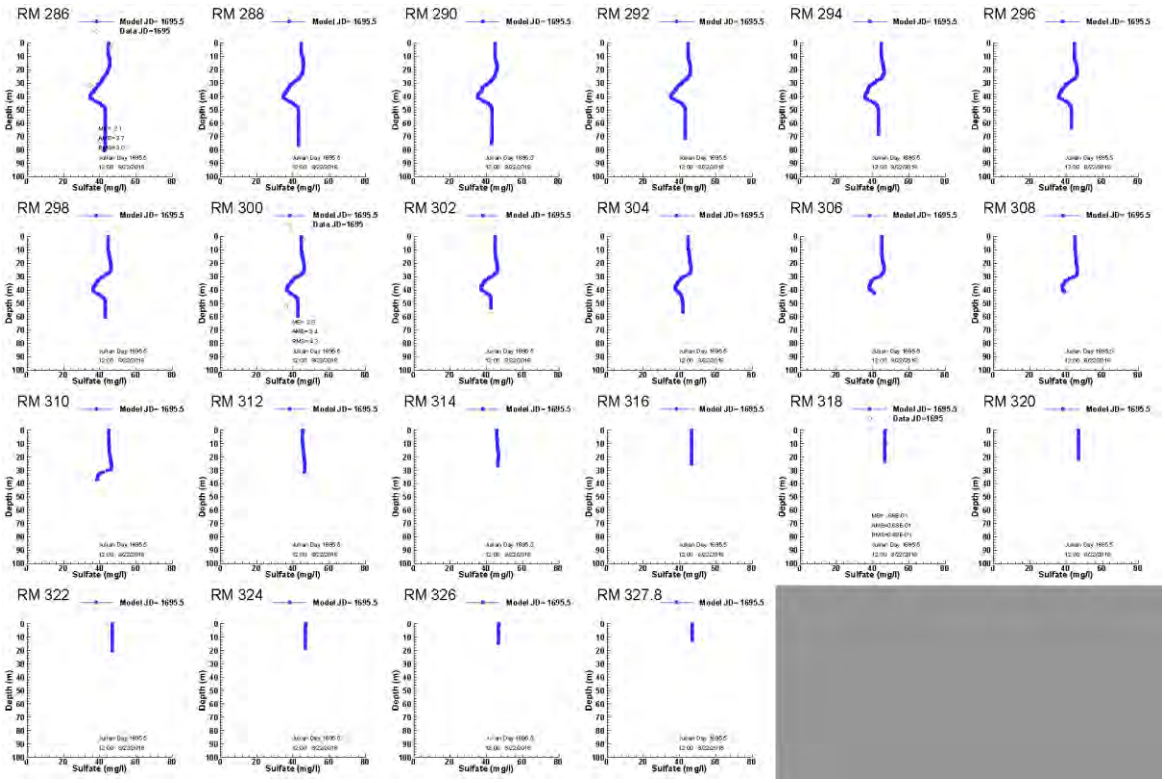


Figure 319. Vertical profiles of sulfate compared with data for 8/22/2018.

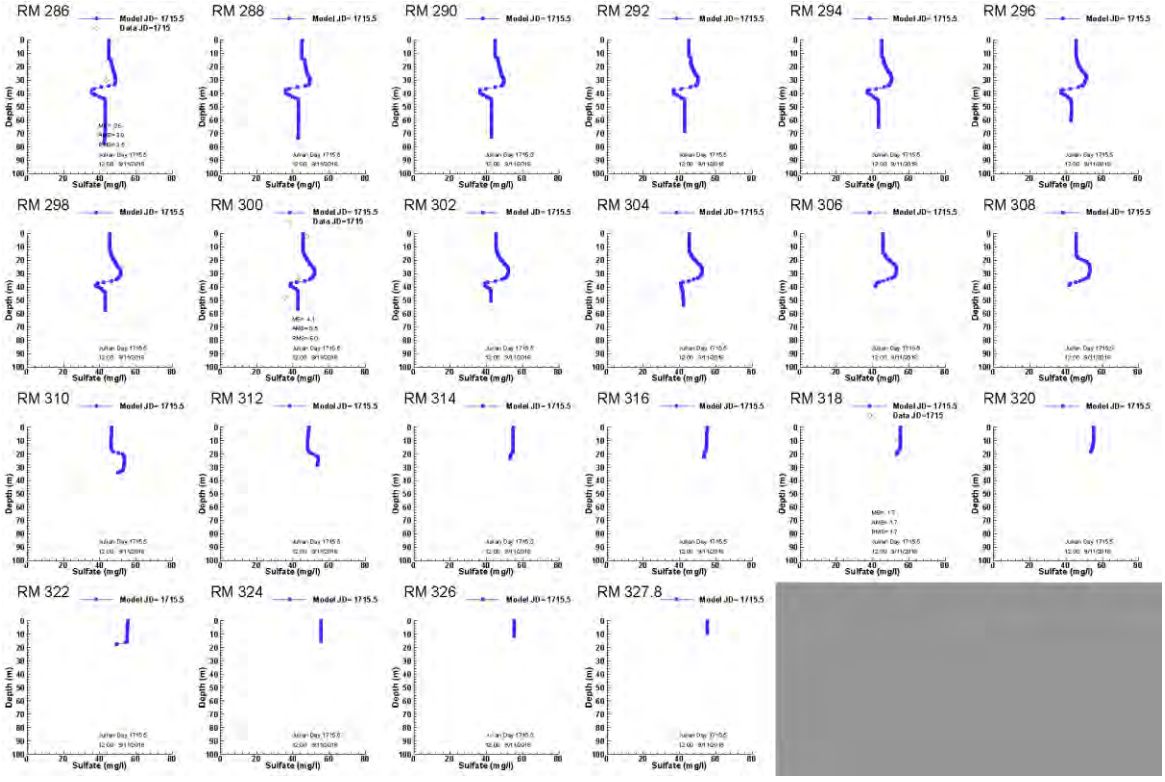


Figure 320. Vertical profiles of sulfate compared with data for 9/11/2018.

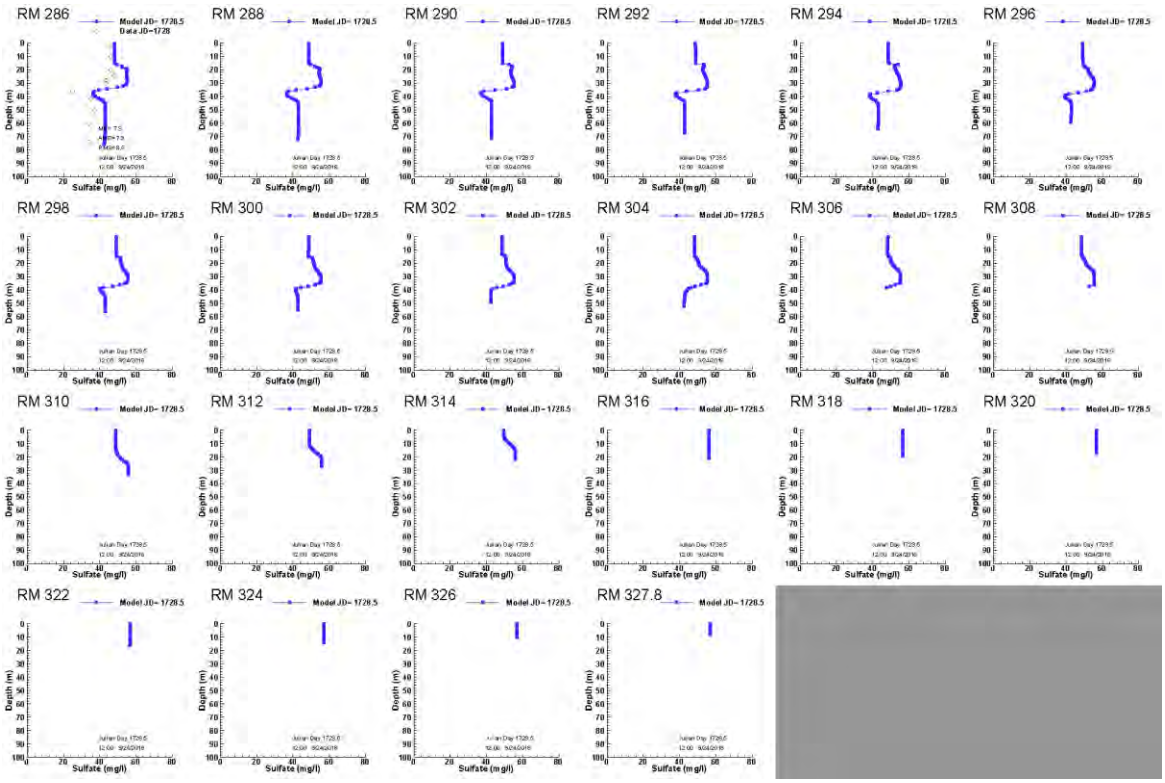


Figure 321. Vertical profiles of sulfate compared with data for 9/24/2018.

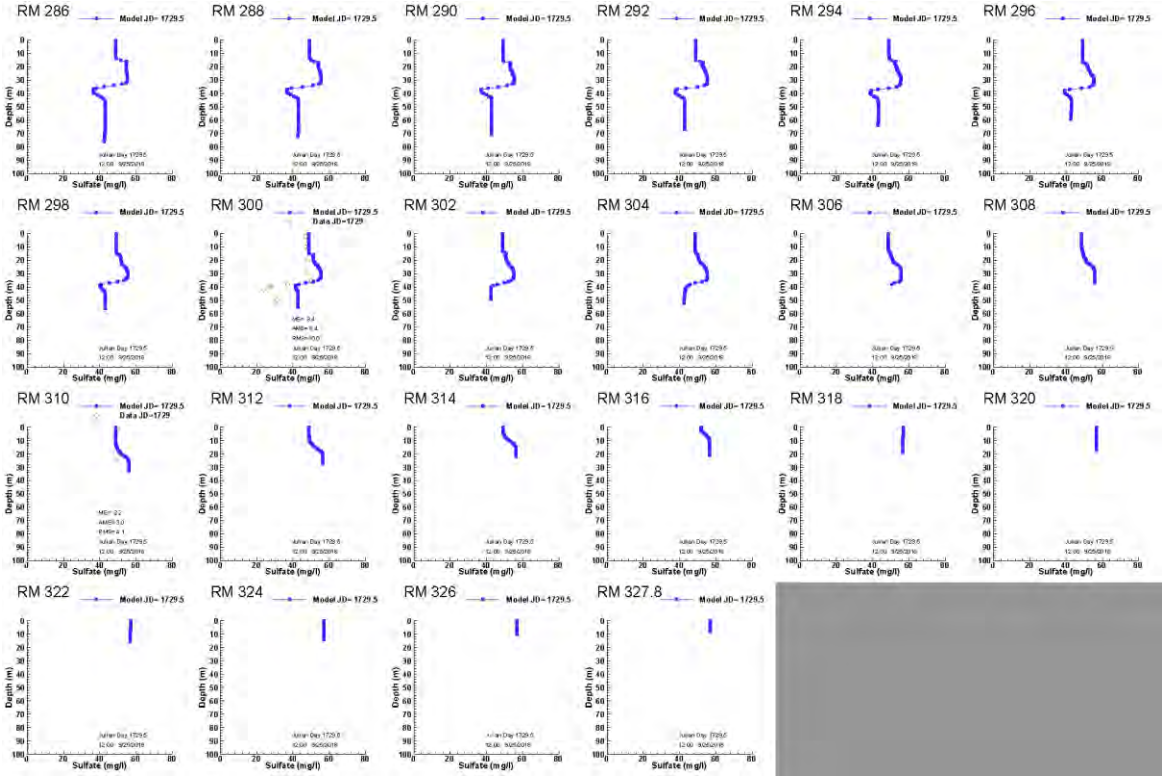


Figure 322. Vertical profiles of sulfate compared with data for 9/25/2018.

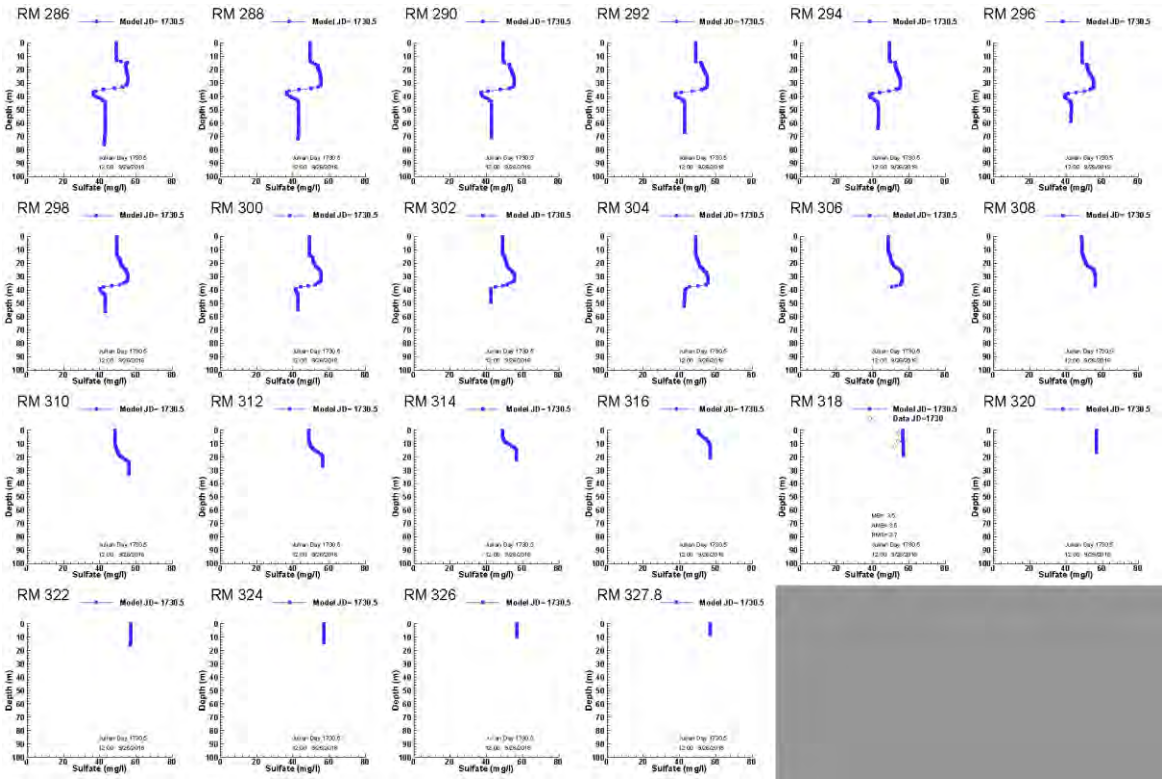


Figure 323. Vertical profiles of sulfate compared with data for 9/26/2018.

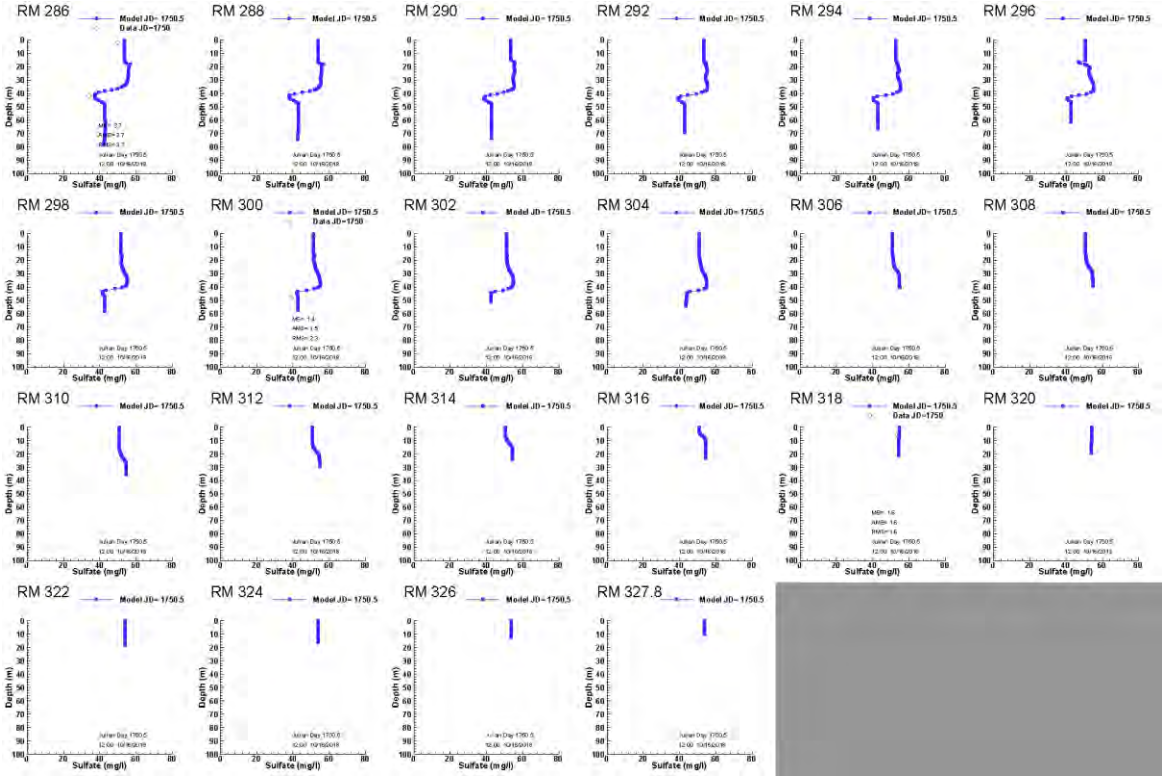


Figure 324. Vertical profiles of sulfate compared with data for 10/16/2018.

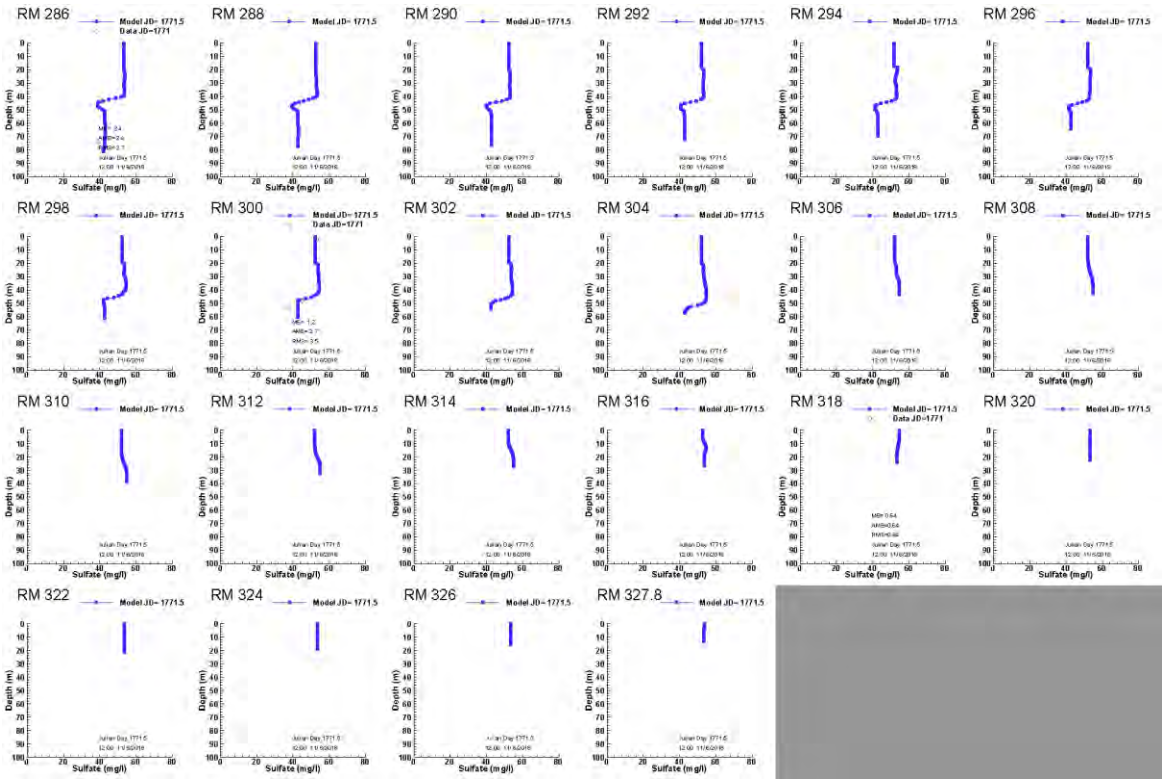


Figure 325. Vertical profiles of sulfate compared with data for 11/ 6/2018.

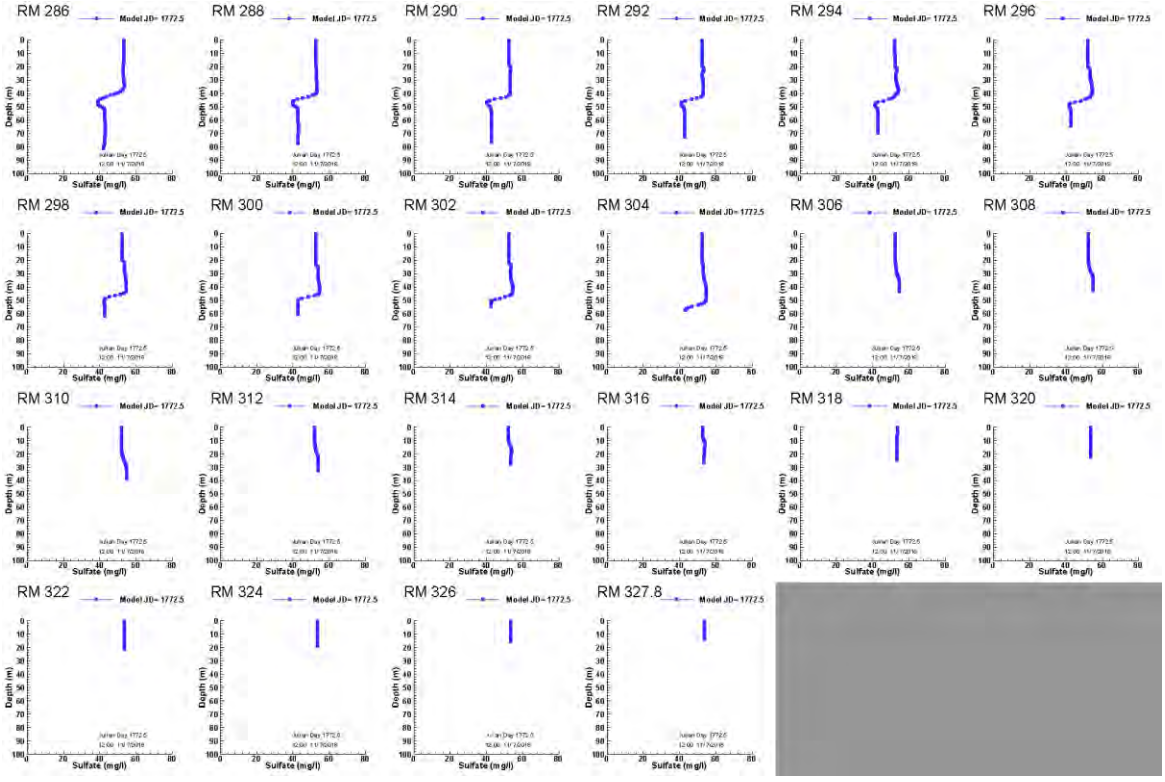


Figure 326. Vertical profiles of sulfate compared with data for 11/ 7/2018.

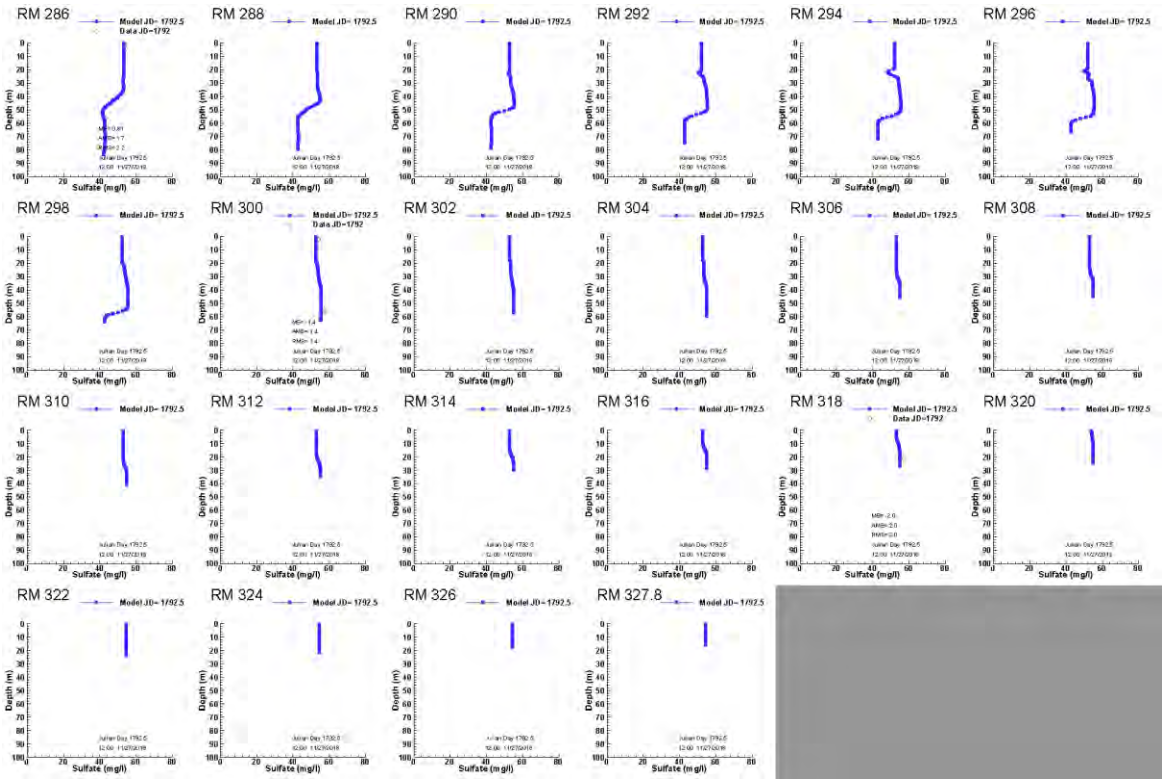


Figure 327. Vertical profiles of sulfate compared with data for 11/27/2018.

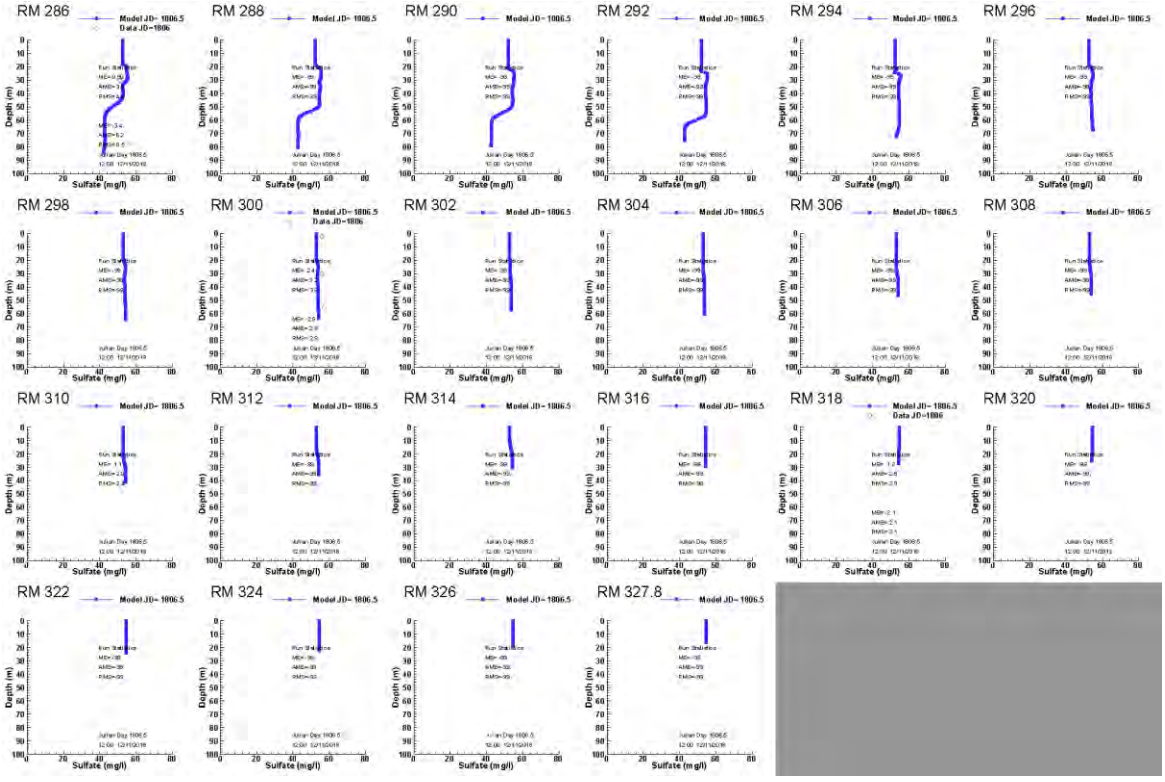


Figure 328. Vertical profiles of sulfate compared with data for 12/11/2018.

Fe(II)

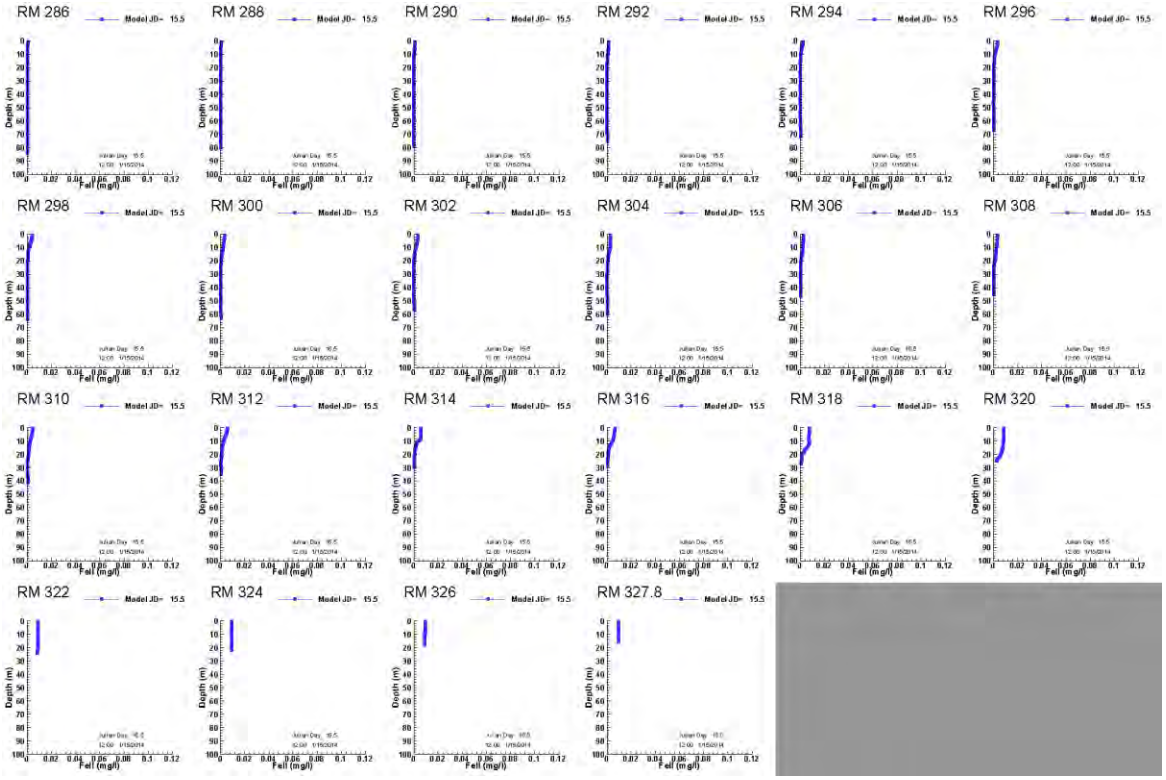


Figure 329. Vertical profiles of Fe(II) compared with data for 1/15/2014.

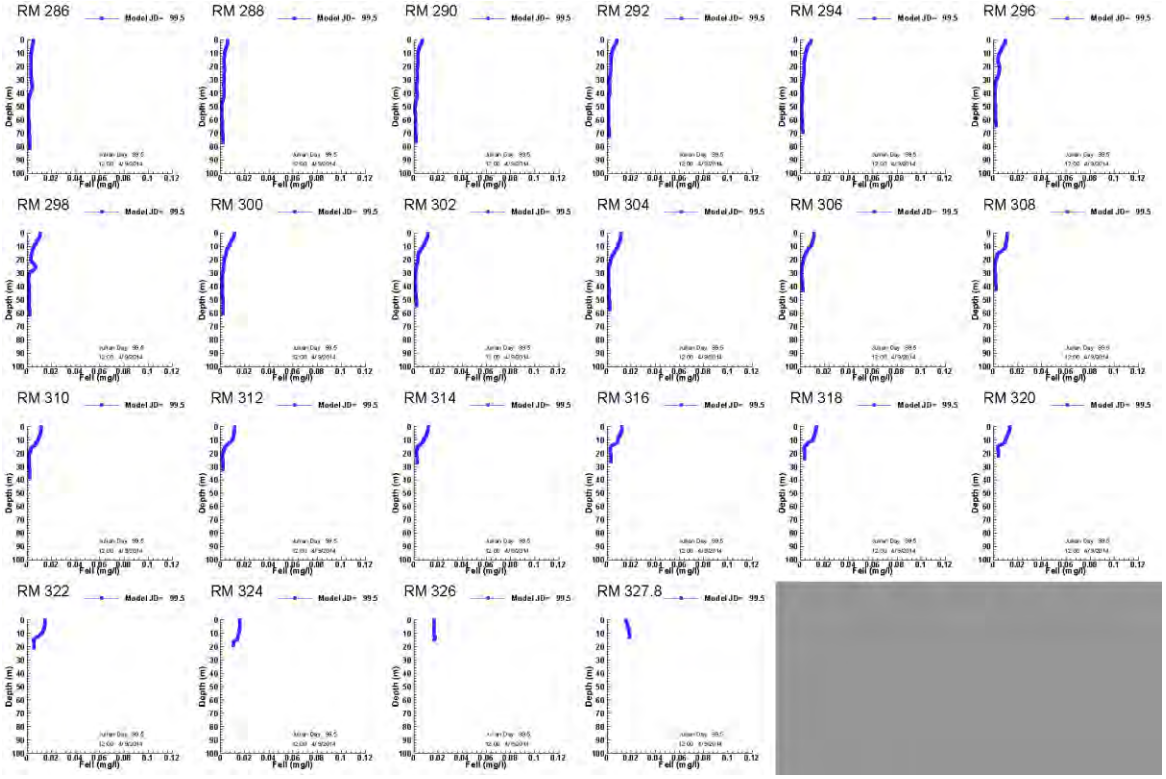


Figure 330. Vertical profiles of Fe(II) compared with data for 4/ 9/2014.

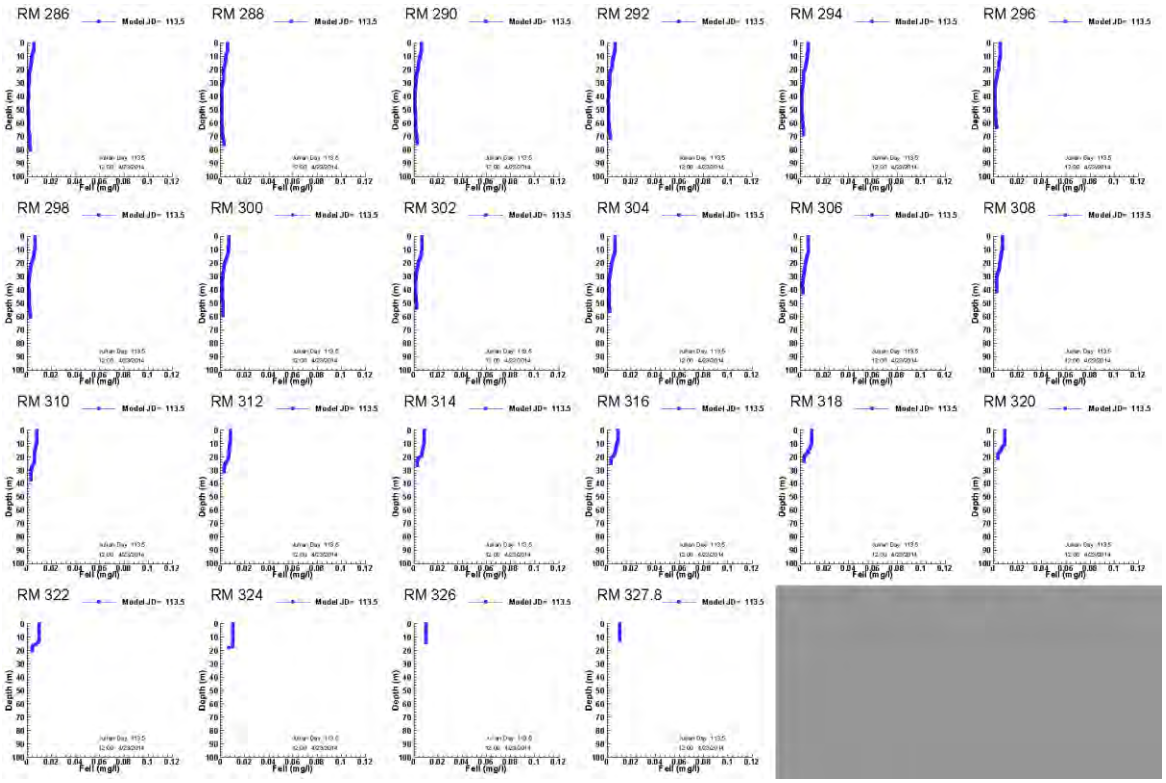


Figure 331. Vertical profiles of Fe(II) compared with data for 4/23/2014.

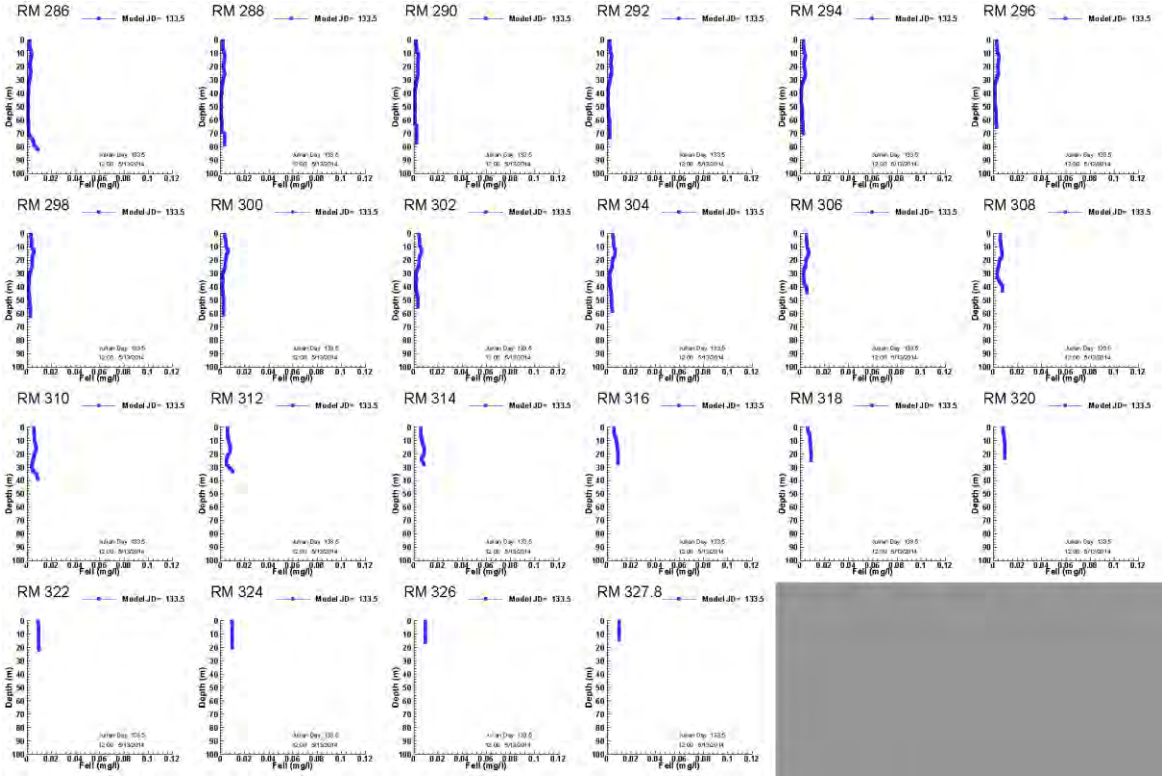


Figure 332. Vertical profiles of Fe(II) compared with data for 5/13/2014.

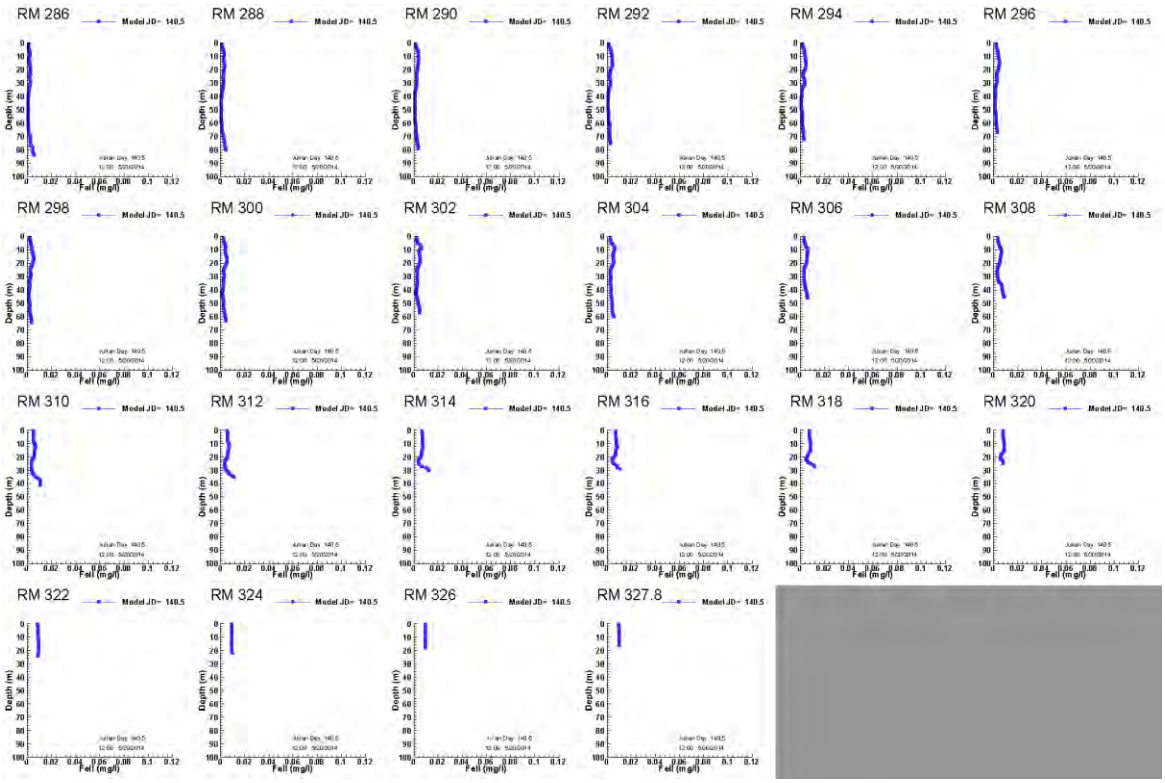


Figure 333. Vertical profiles of Fe(II) compared with data for 5/20/2014.

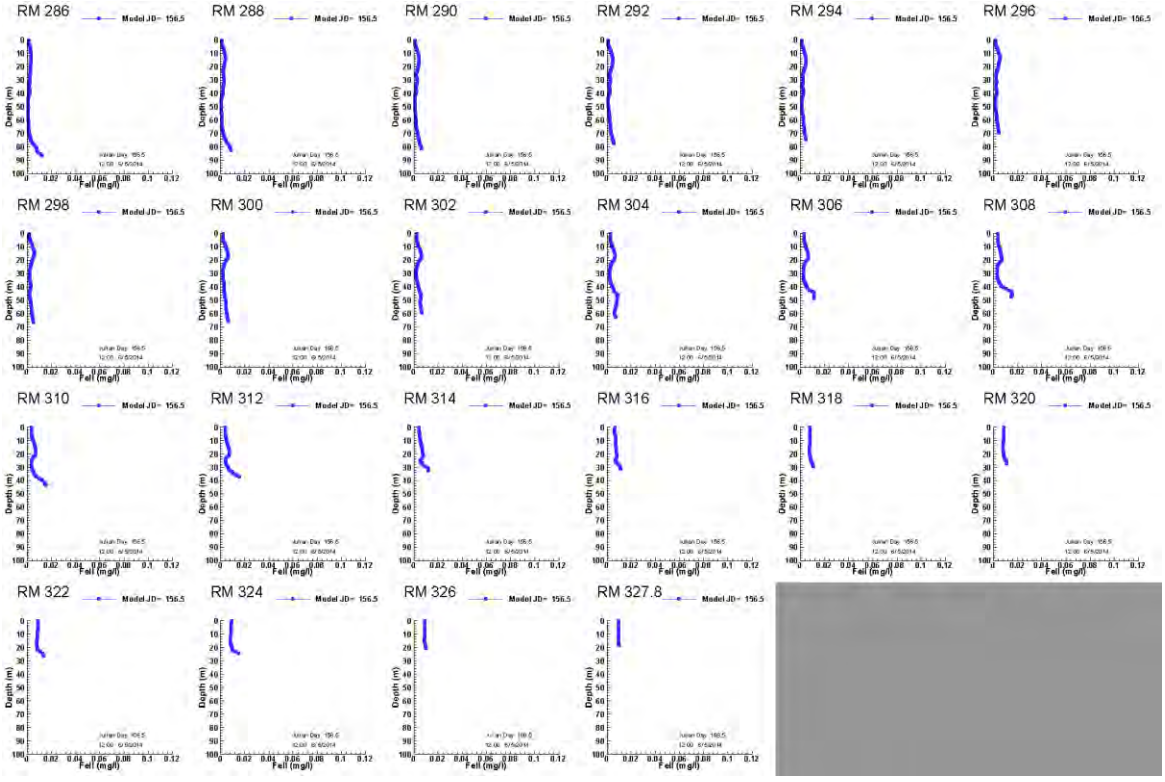


Figure 334. Vertical profiles of Fe(II) compared with data for 6/ 5/2014.

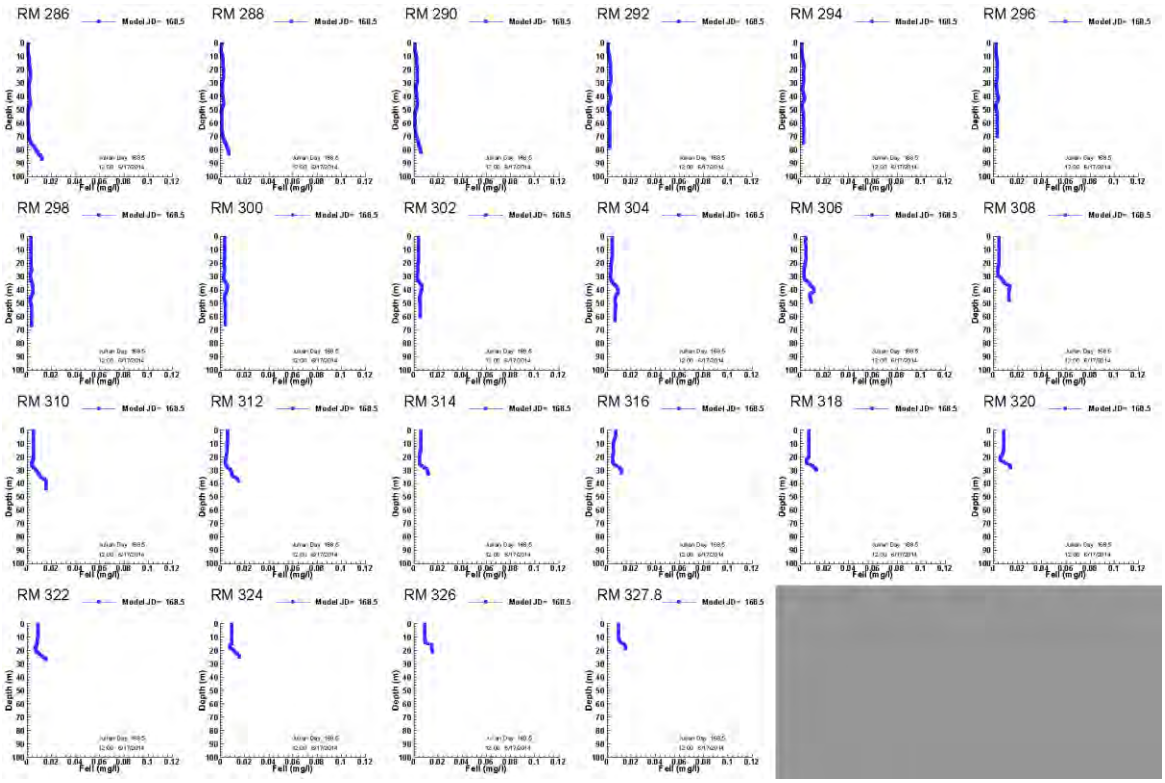


Figure 335. Vertical profiles of Fe(II) compared with data for 6/17/2014.

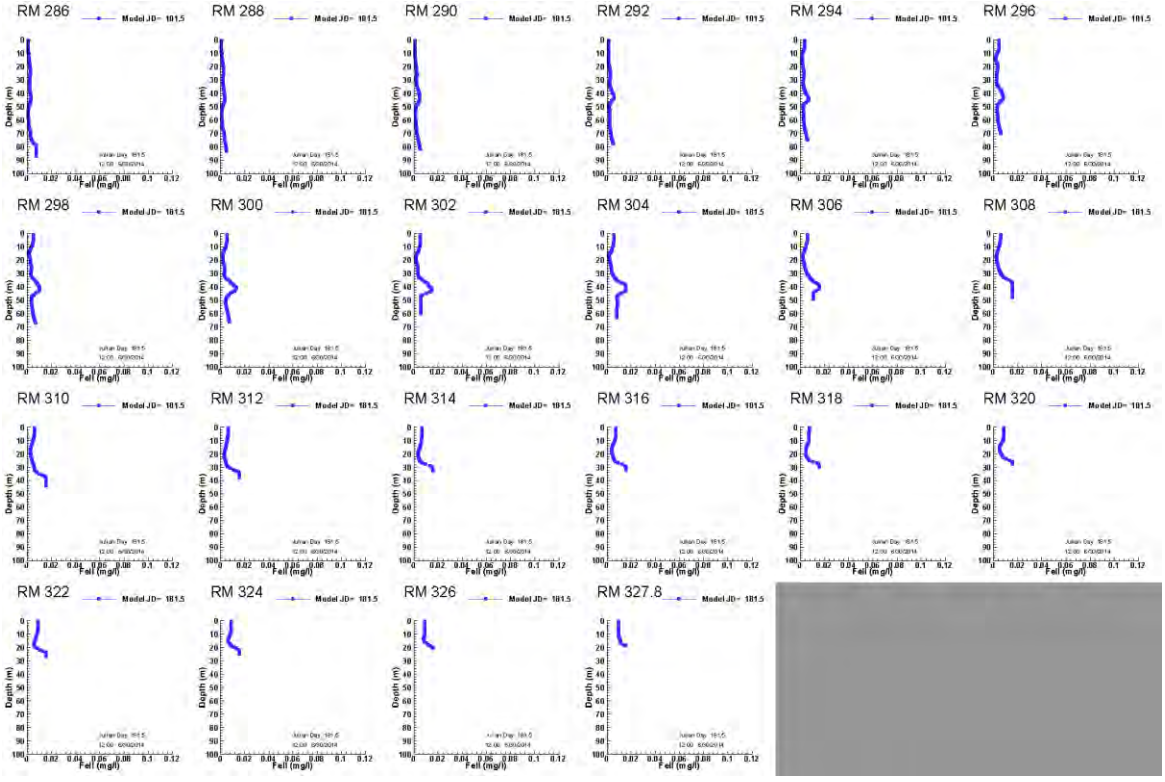


Figure 336. Vertical profiles of Fe(II) compared with data for 6/30/2014.

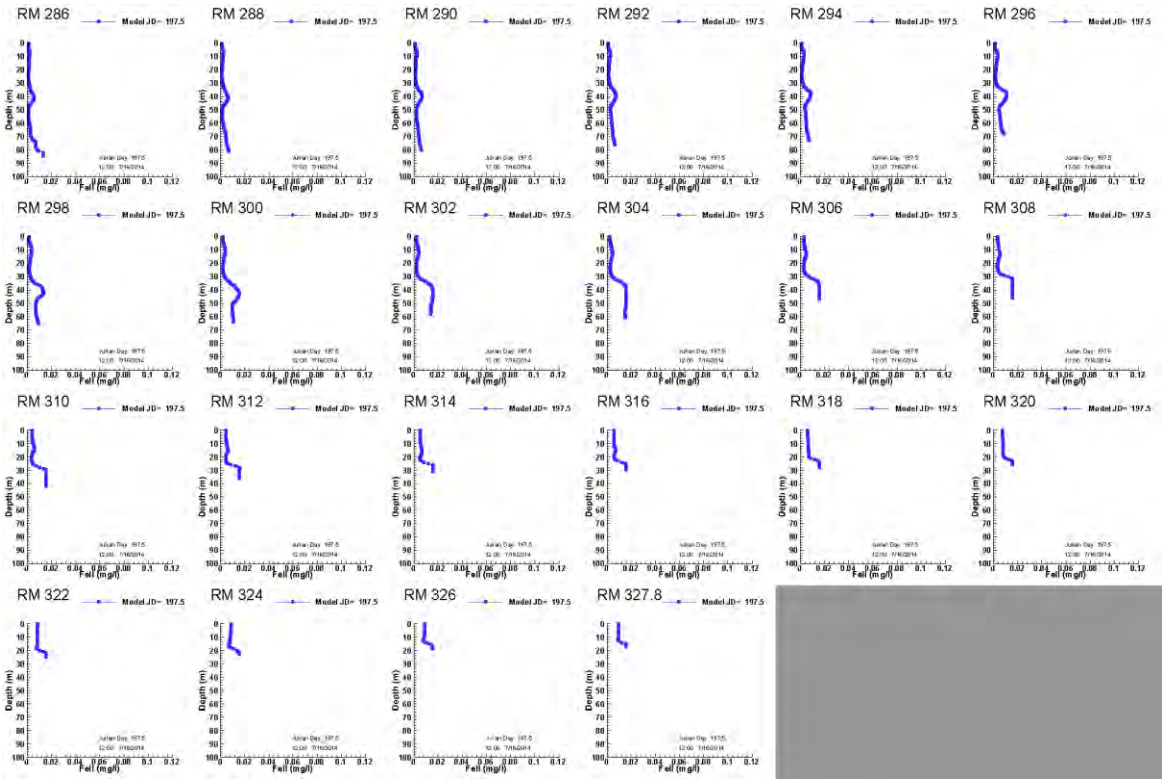


Figure 337. Vertical profiles of Fe(II) compared with data for 7/16/2014.

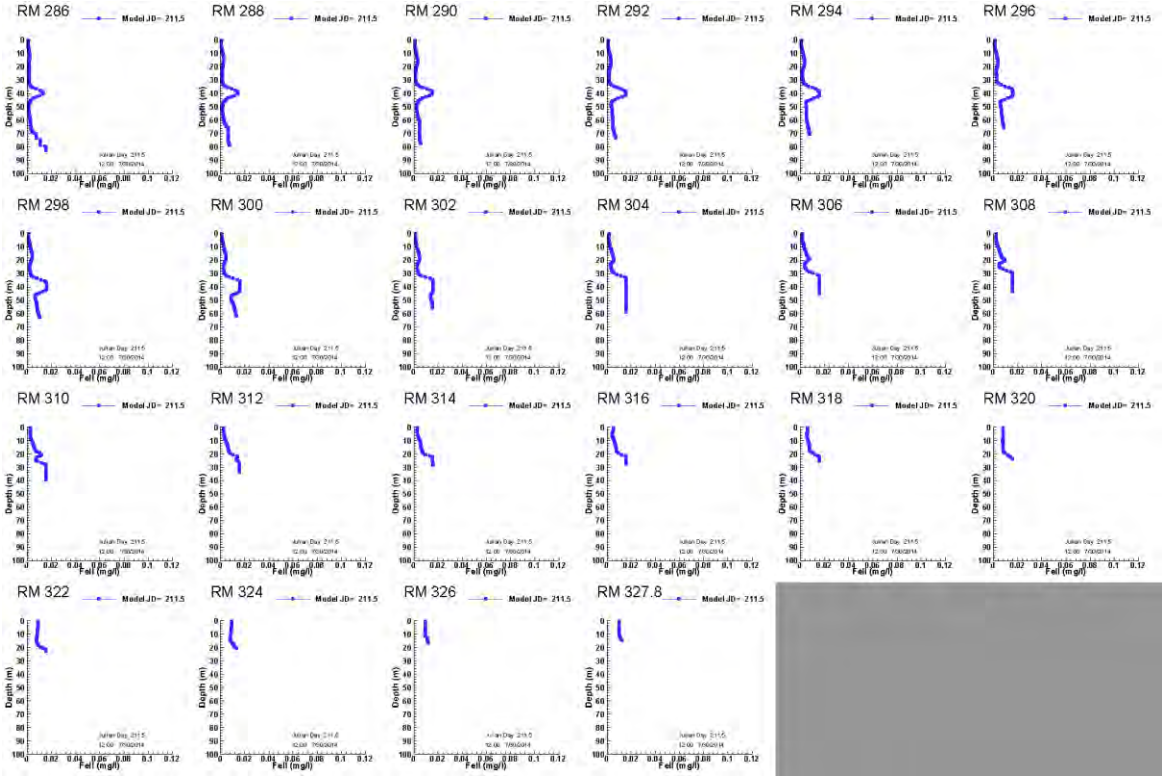


Figure 338. Vertical profiles of Fe(II) compared with data for 7/30/2014.

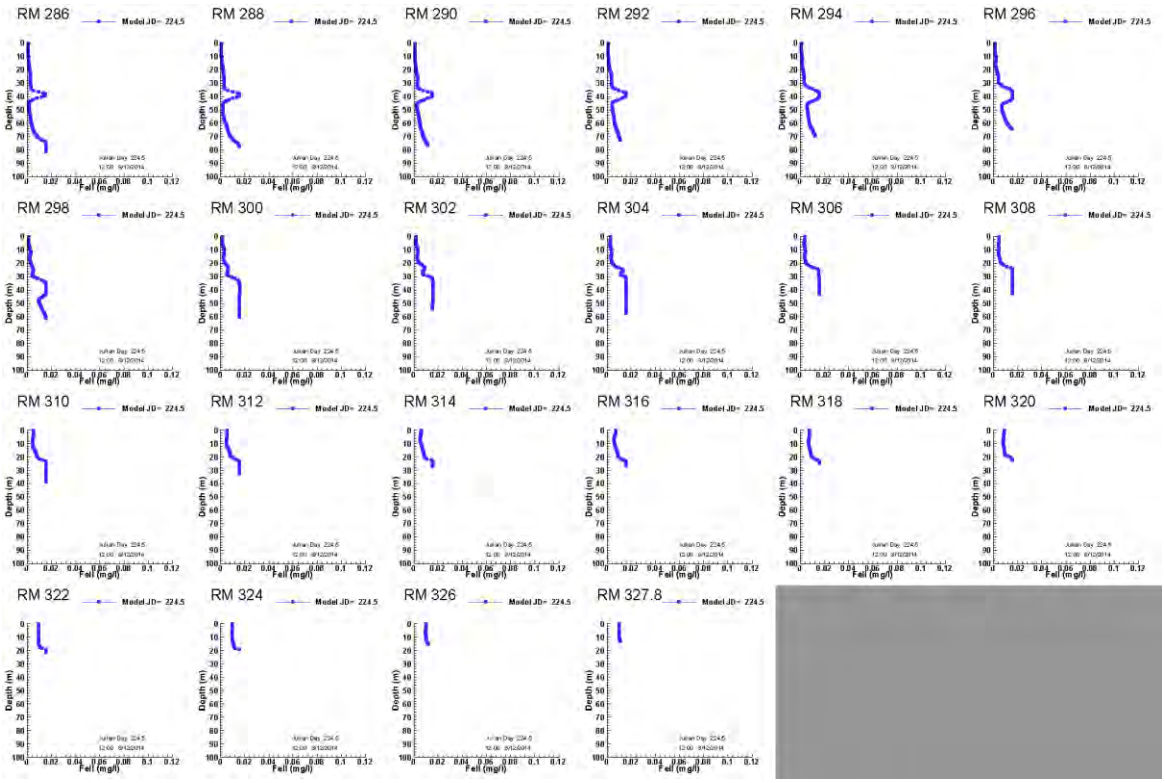


Figure 339. Vertical profiles of Fe(II) compared with data for 8/12/2014.

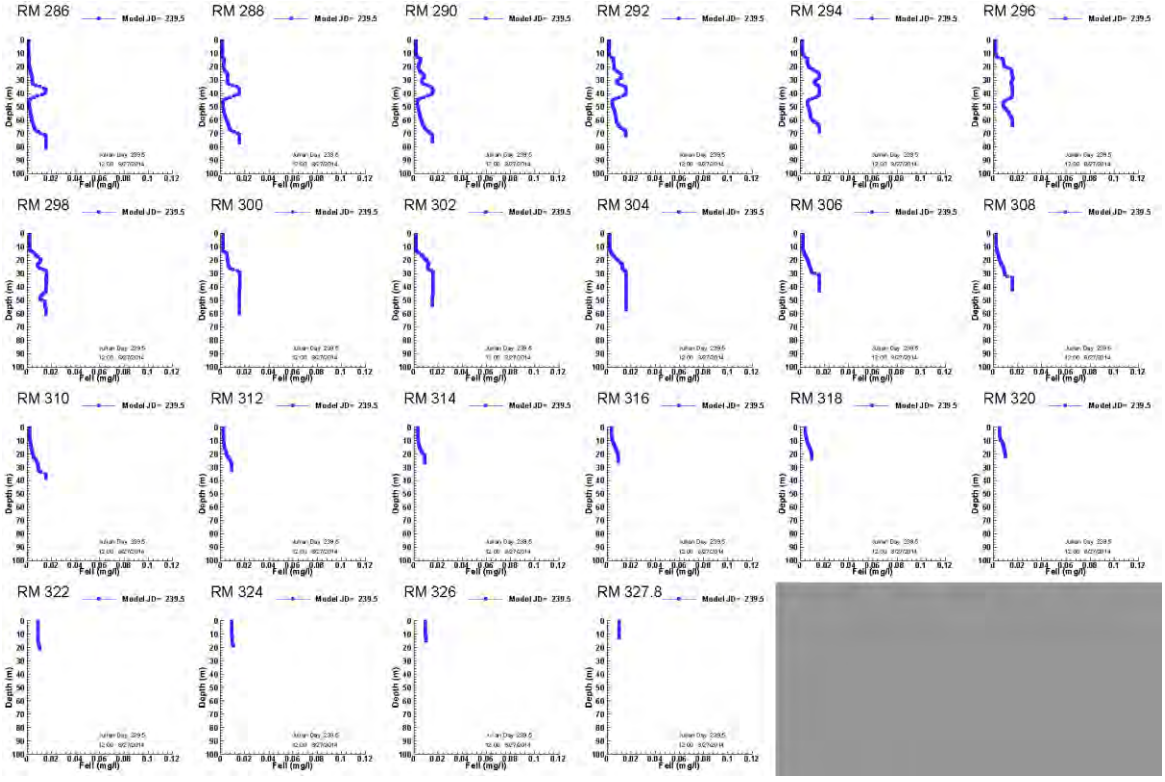


Figure 340. Vertical profiles of Fe(II) compared with data for 8/27/2014.

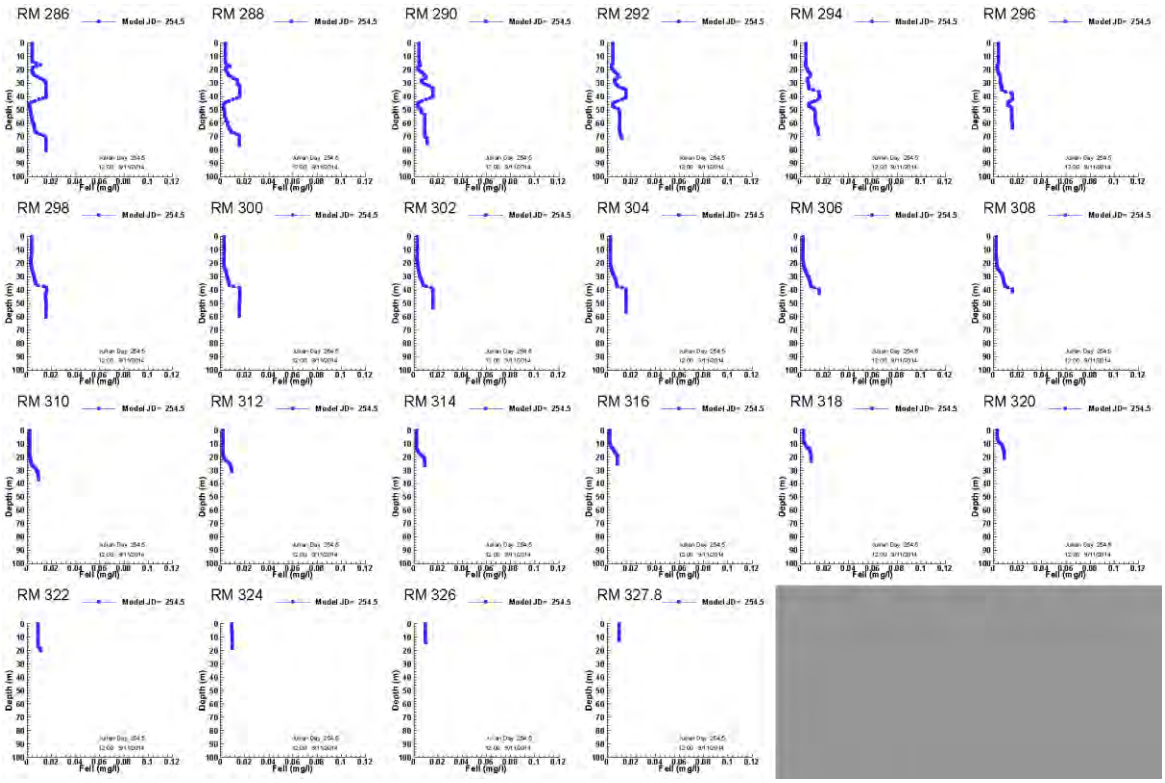


Figure 341. Vertical profiles of Fe(II) compared with data for 9/11/2014.

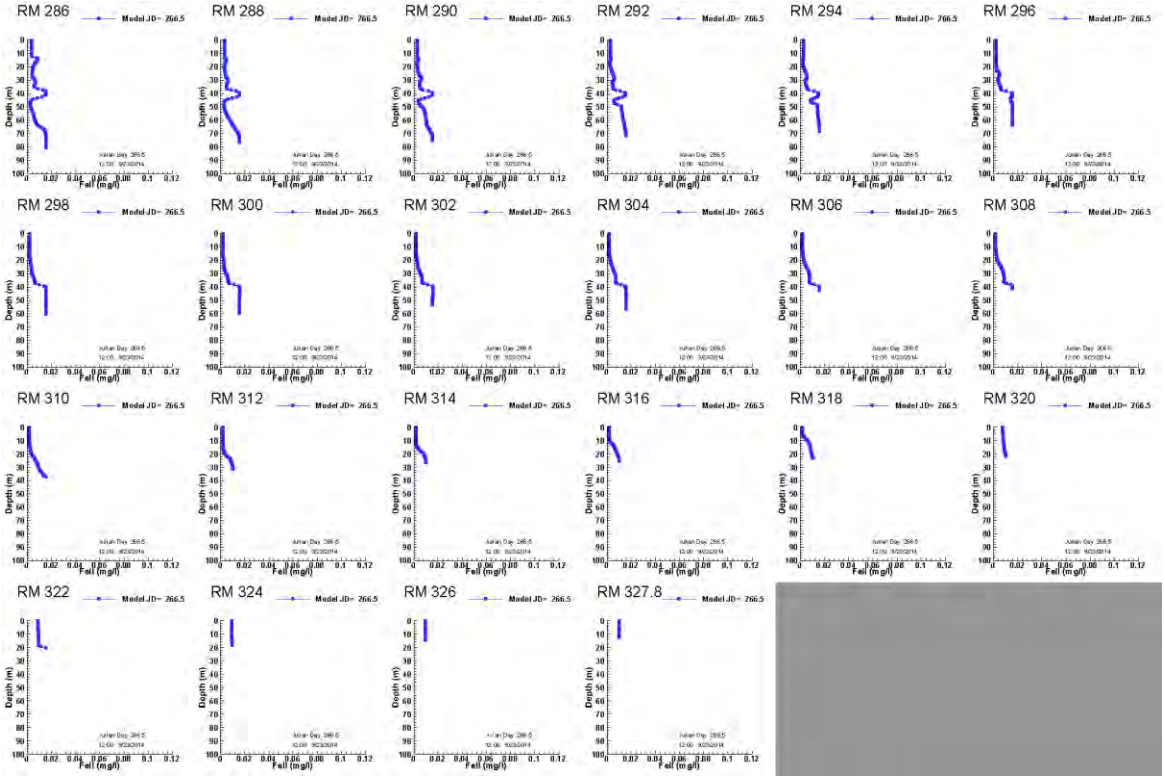


Figure 342. Vertical profiles of Fe(II) compared with data for 9/23/2014.

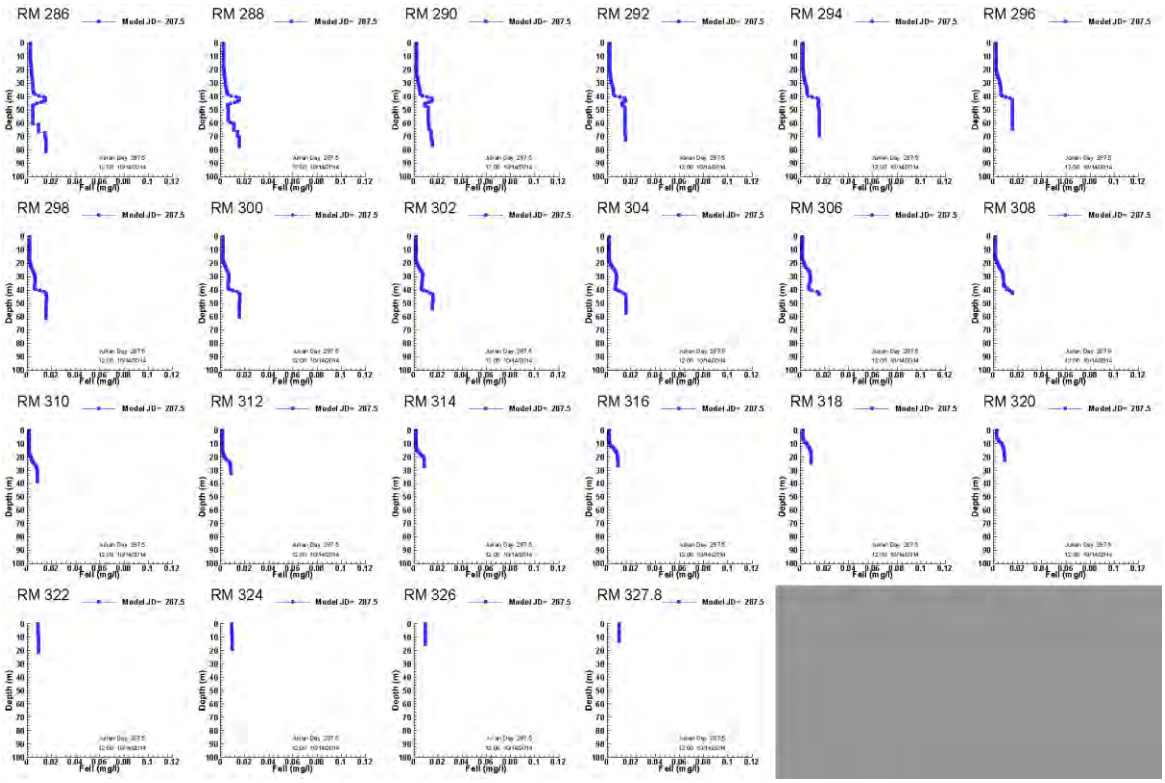


Figure 343. Vertical profiles of Fe(II) compared with data for 10/14/2014.

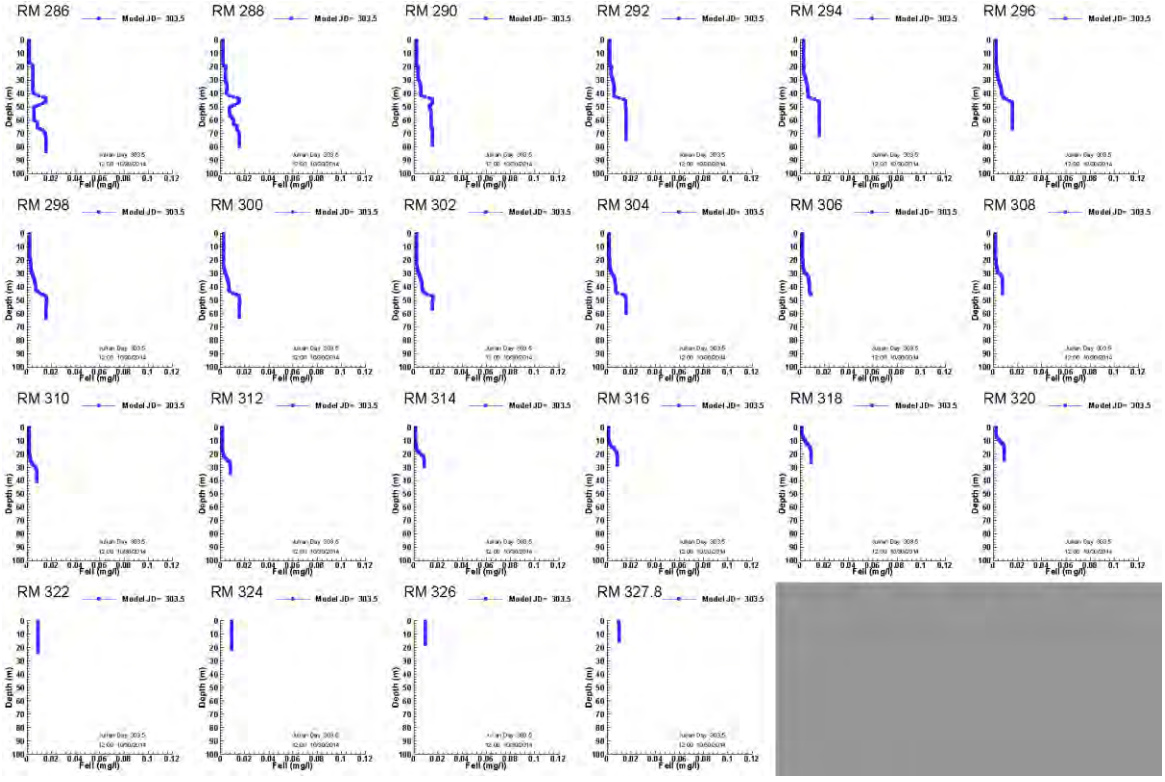


Figure 344. Vertical profiles of Fe(II) compared with data for 10/30/2014.

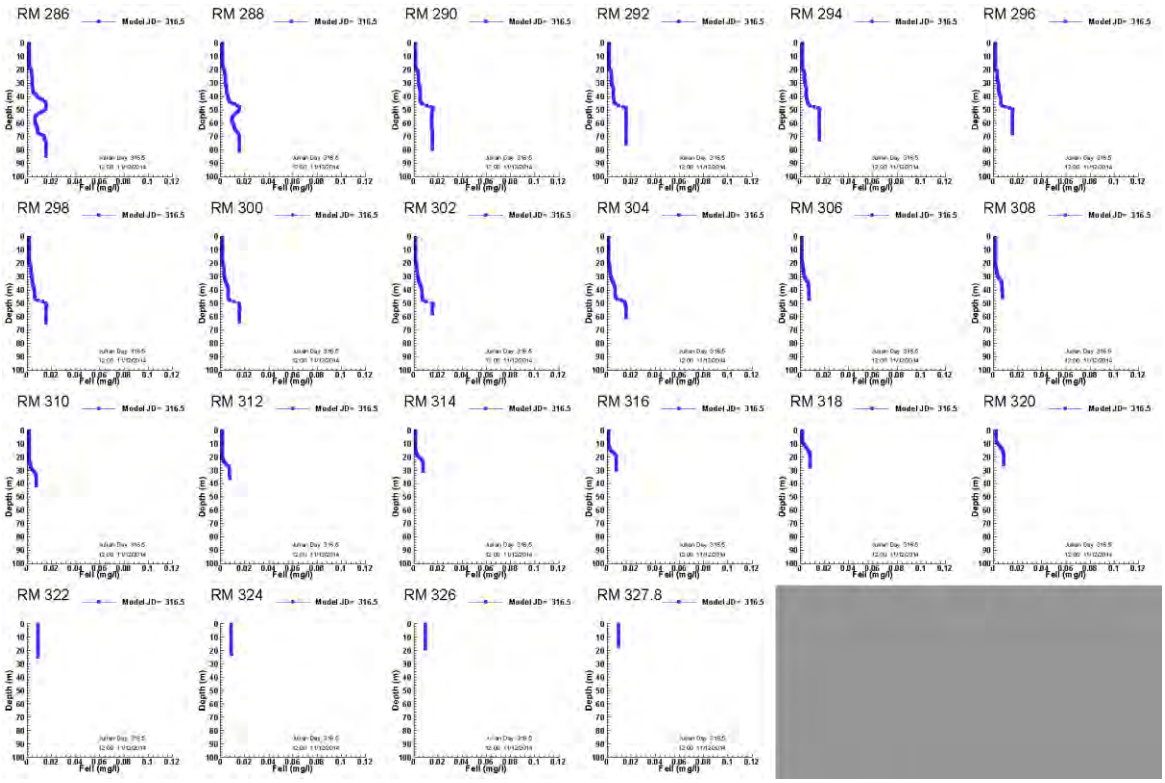


Figure 345. Vertical profiles of Fe(II) compared with data for 11/12/2014.

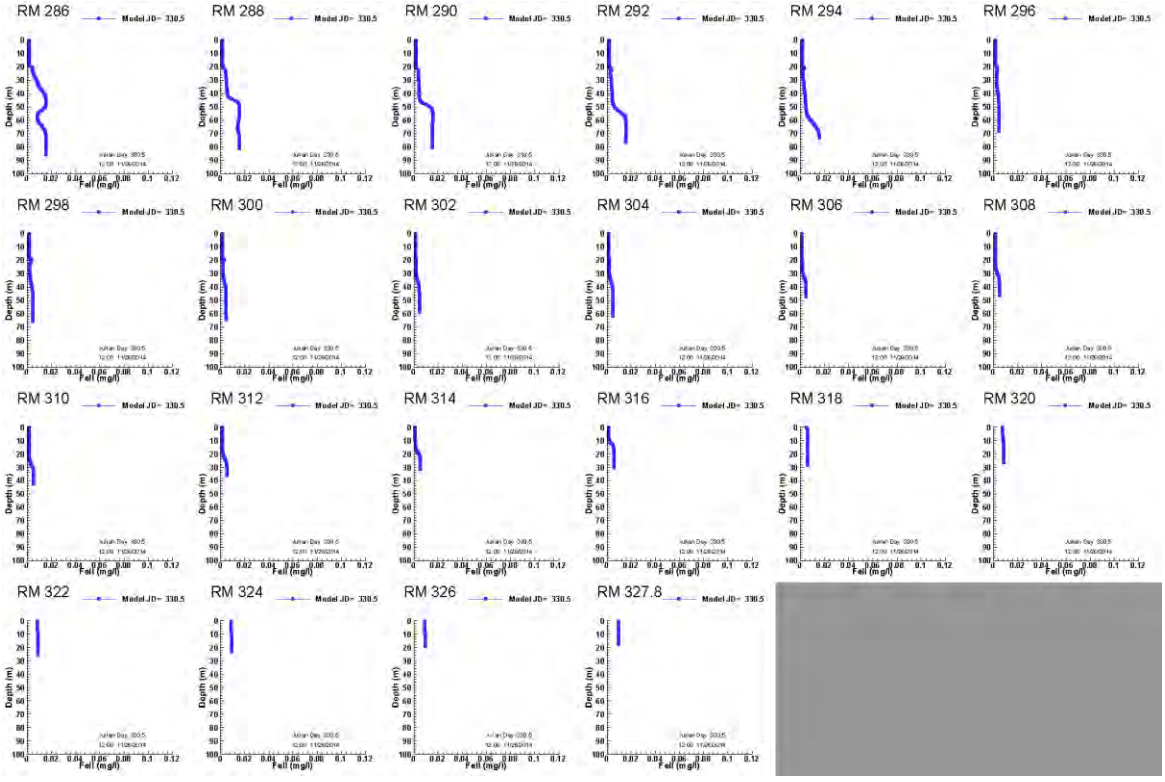


Figure 346. Vertical profiles of Fe(II) compared with data for 11/26/2014.

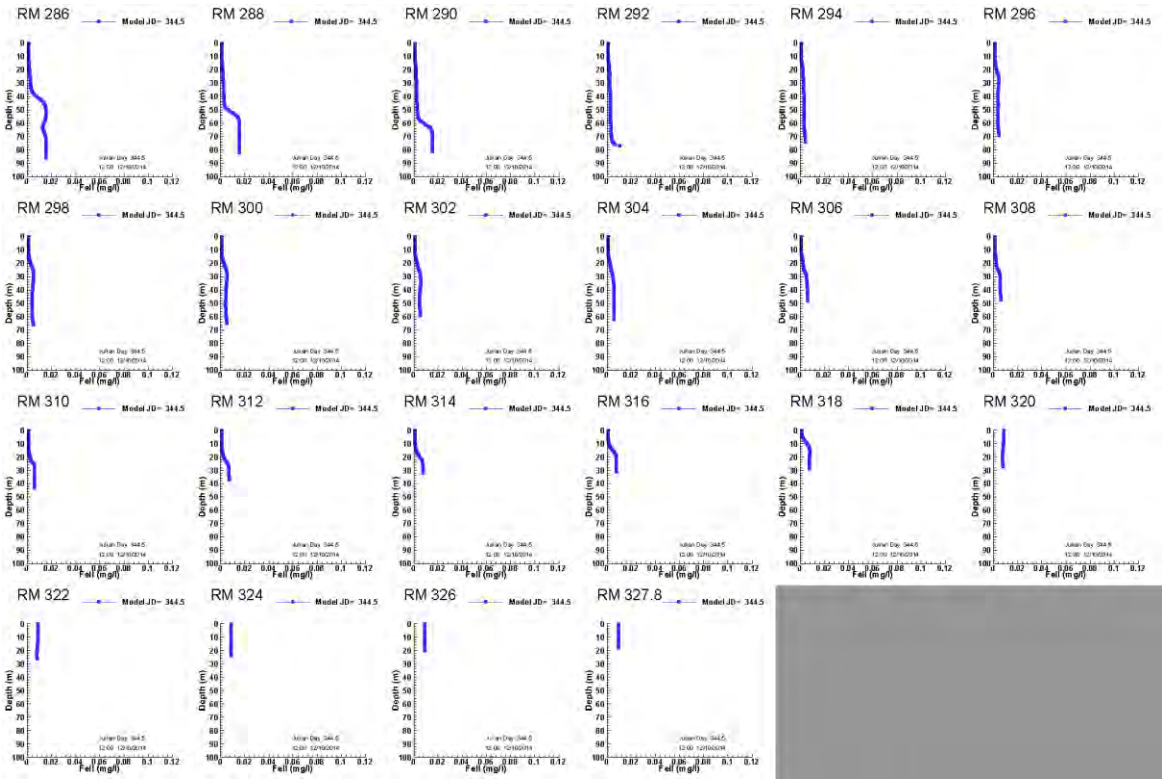


Figure 347. Vertical profiles of Fe(II) compared with data for 12/10/2014.

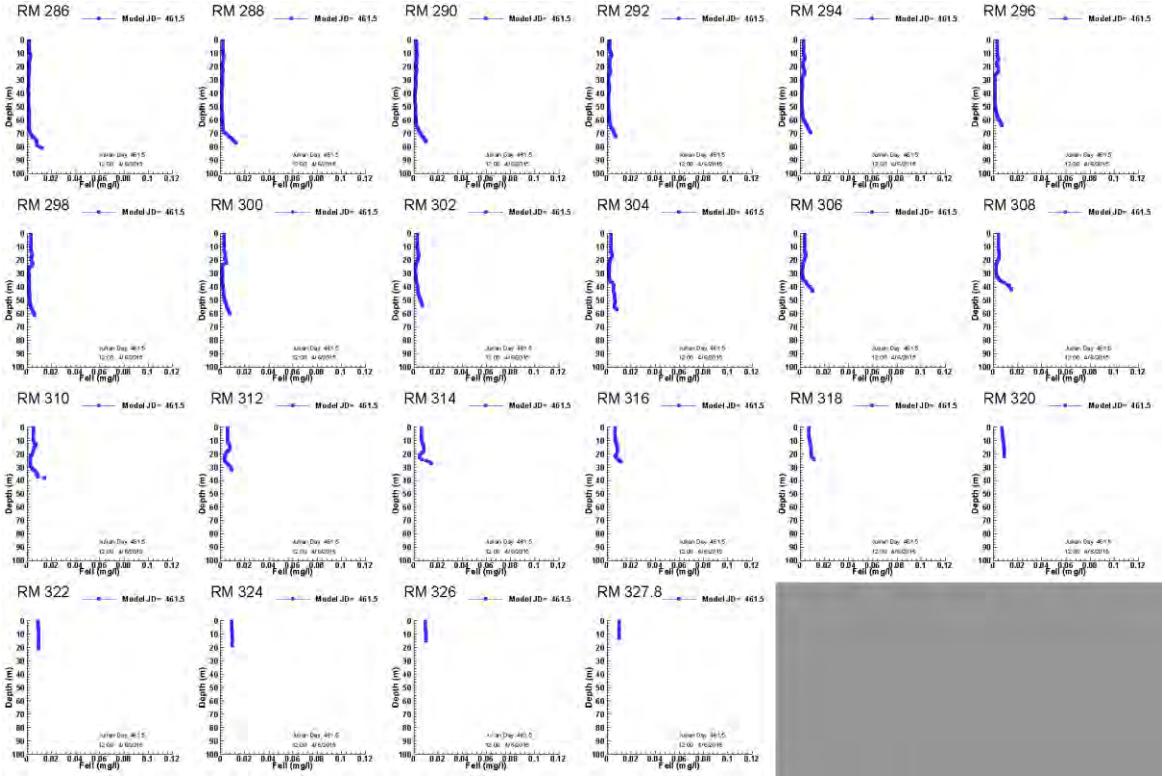


Figure 348. Vertical profiles of Fe(II) compared with data for 4/ 6/2015.

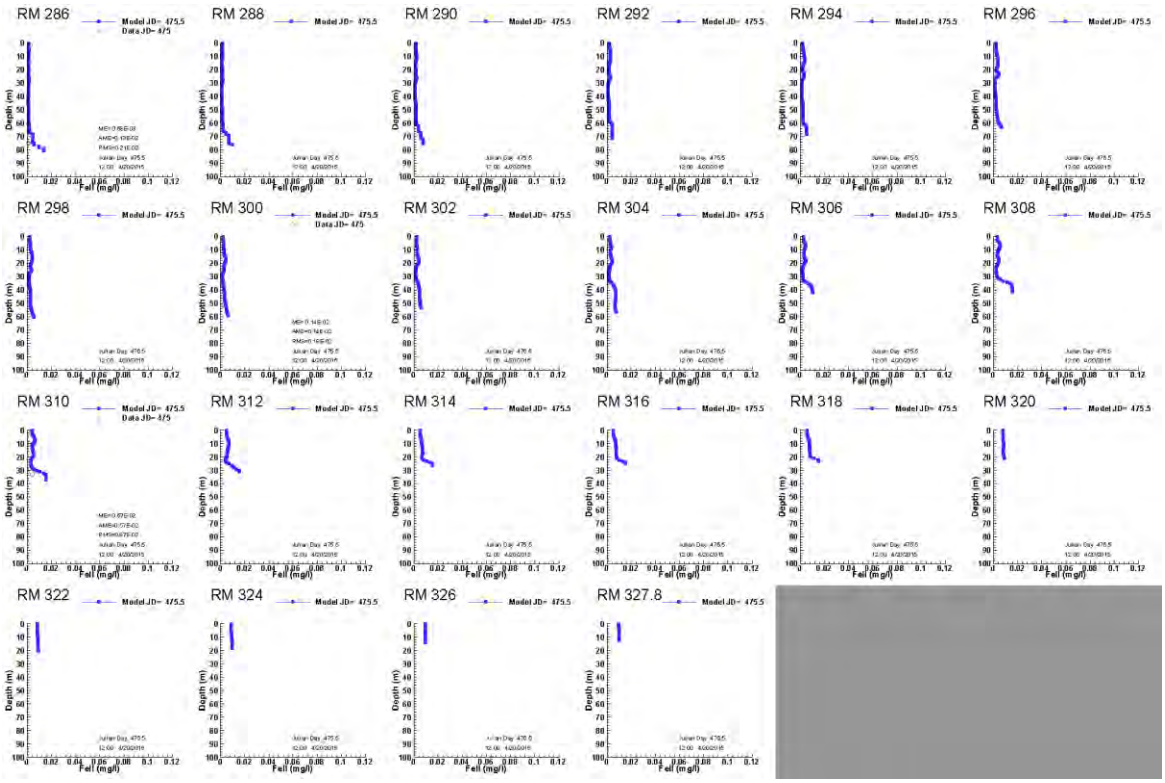


Figure 349. Vertical profiles of Fe(II) compared with data for 4/20/2015.

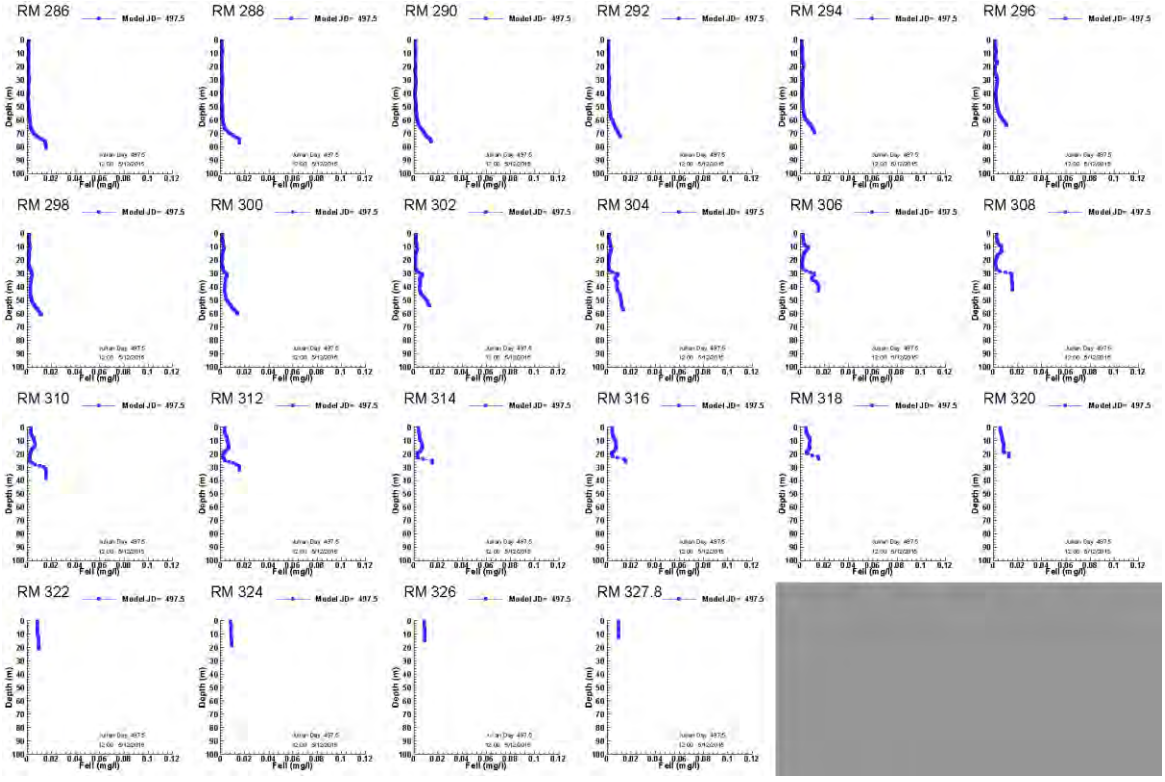


Figure 350. Vertical profiles of Fe(II) compared with data for 5/12/2015.

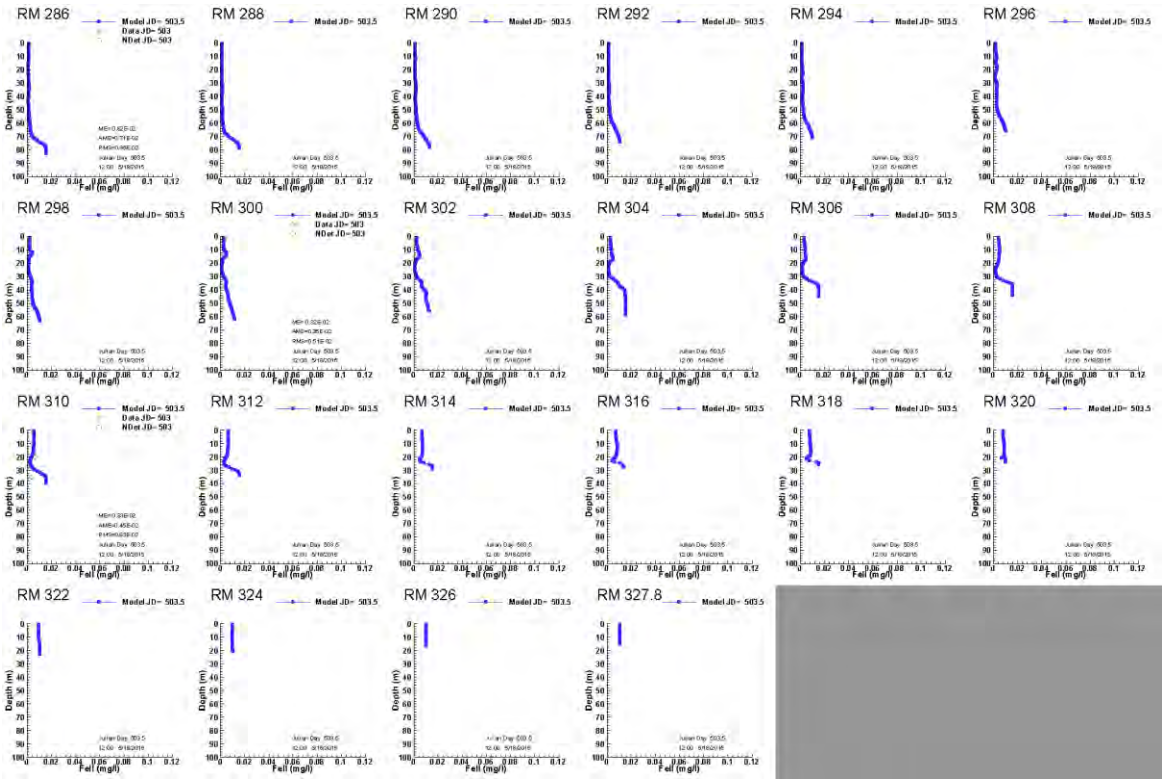


Figure 351. Vertical profiles of Fe(II) compared with data for 5/18/2015.

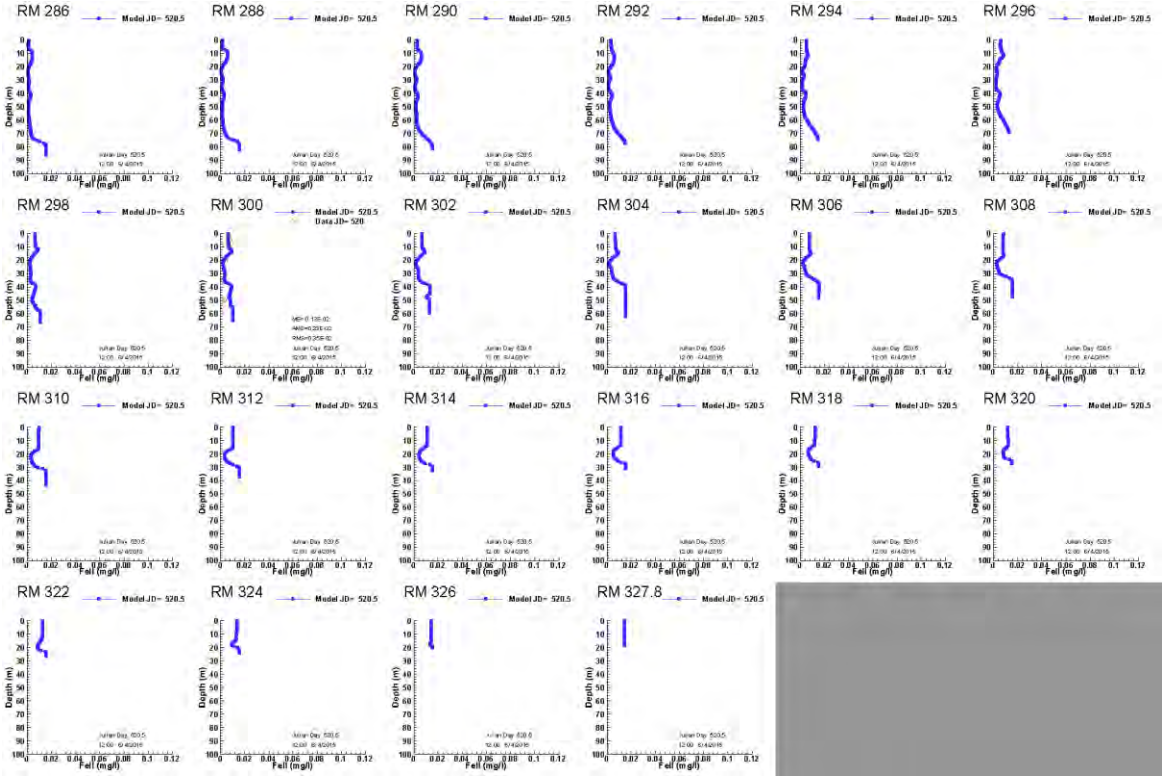


Figure 352. Vertical profiles of Fe(II) compared with data for 6/ 4/2015.

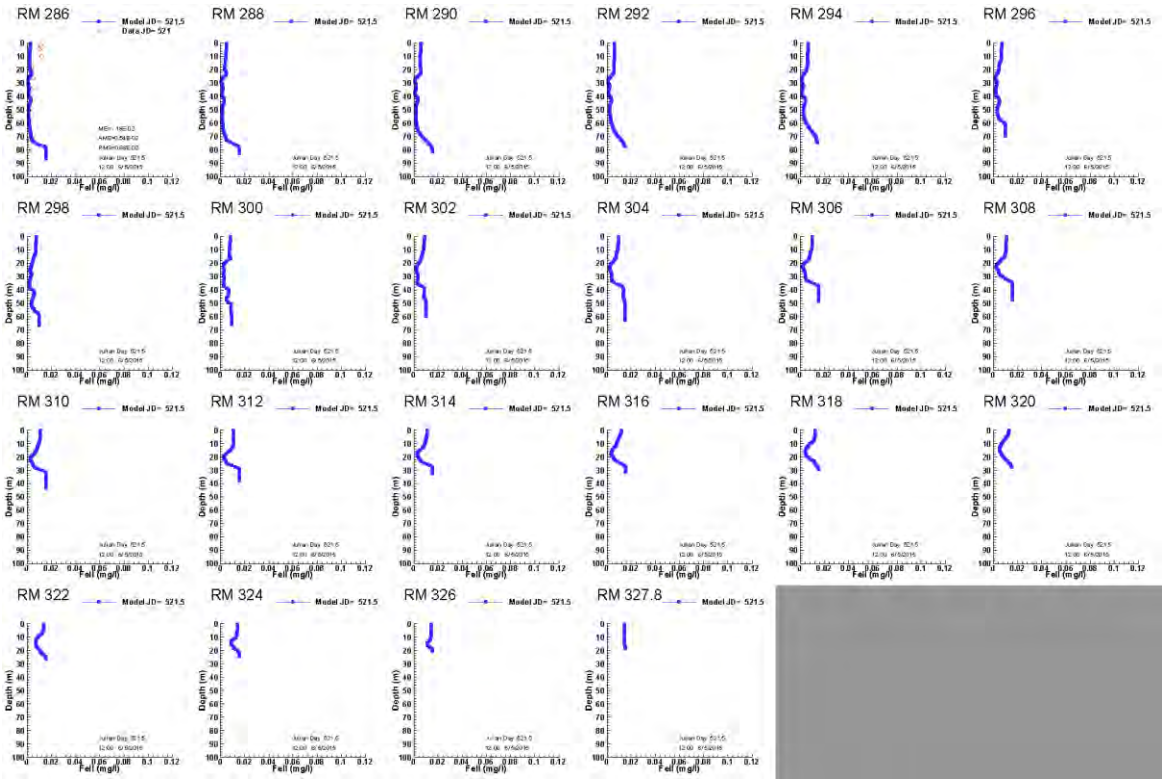


Figure 353. Vertical profiles of Fe(II) compared with data for 6/ 5/2015.

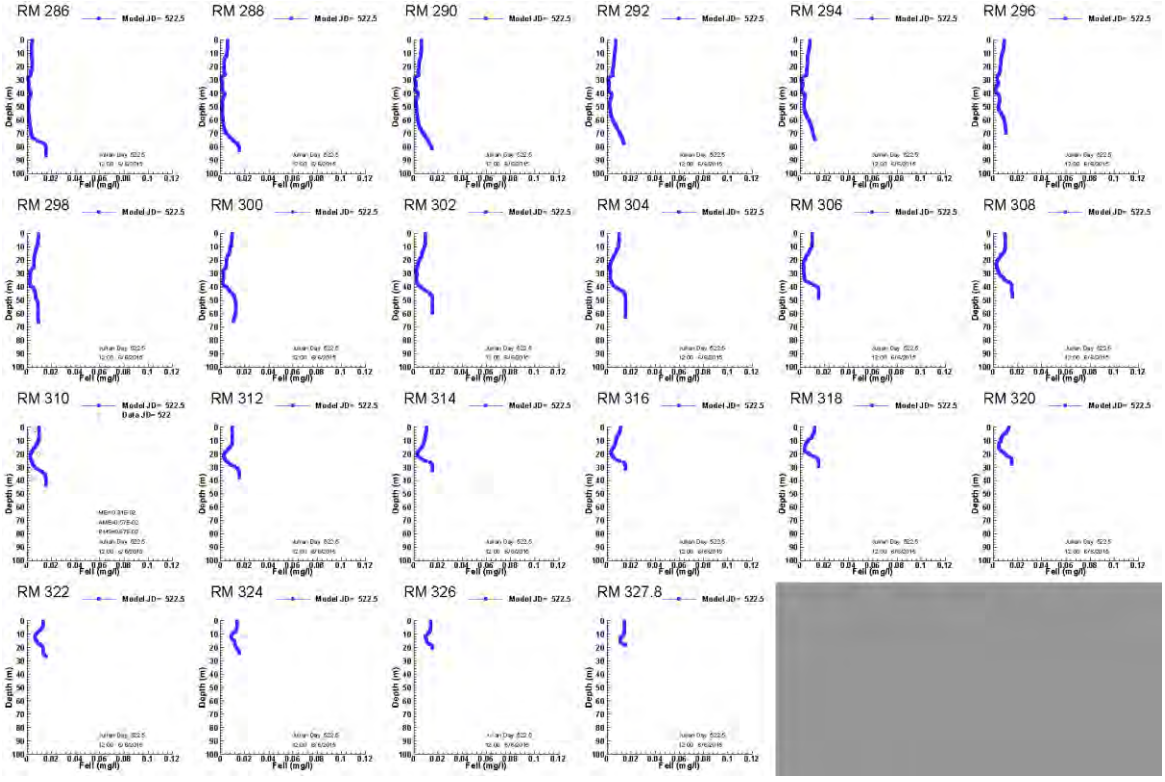


Figure 354. Vertical profiles of Fe(II) compared with data for 6/ 6/2015.

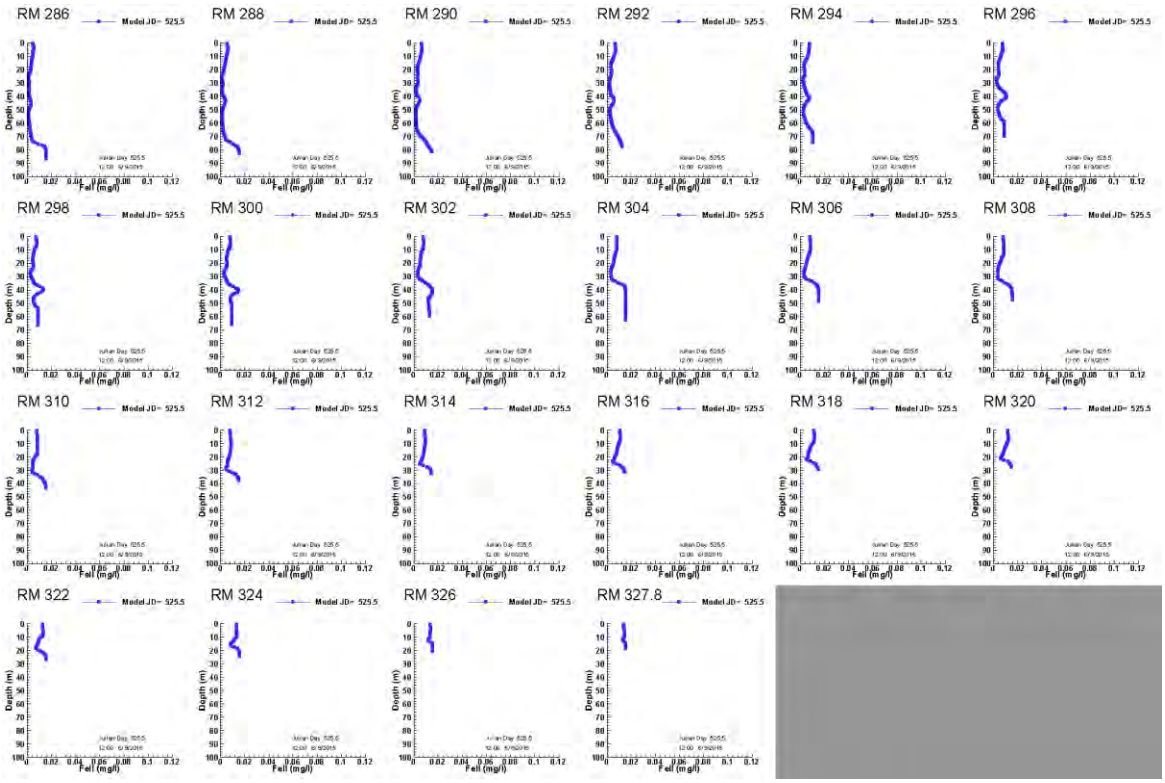


Figure 355. Vertical profiles of Fe(II) compared with data for 6/ 9/2015.

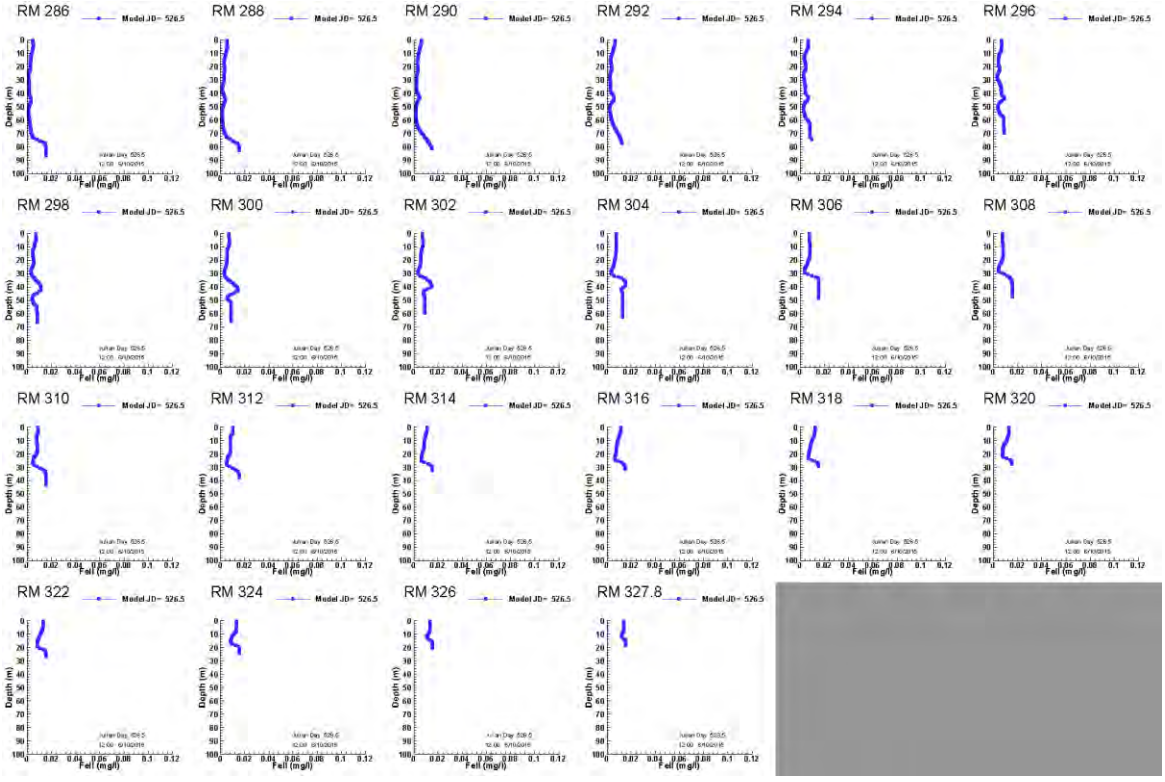


Figure 356. Vertical profiles of Fe(II) compared with data for 6/10/2015.

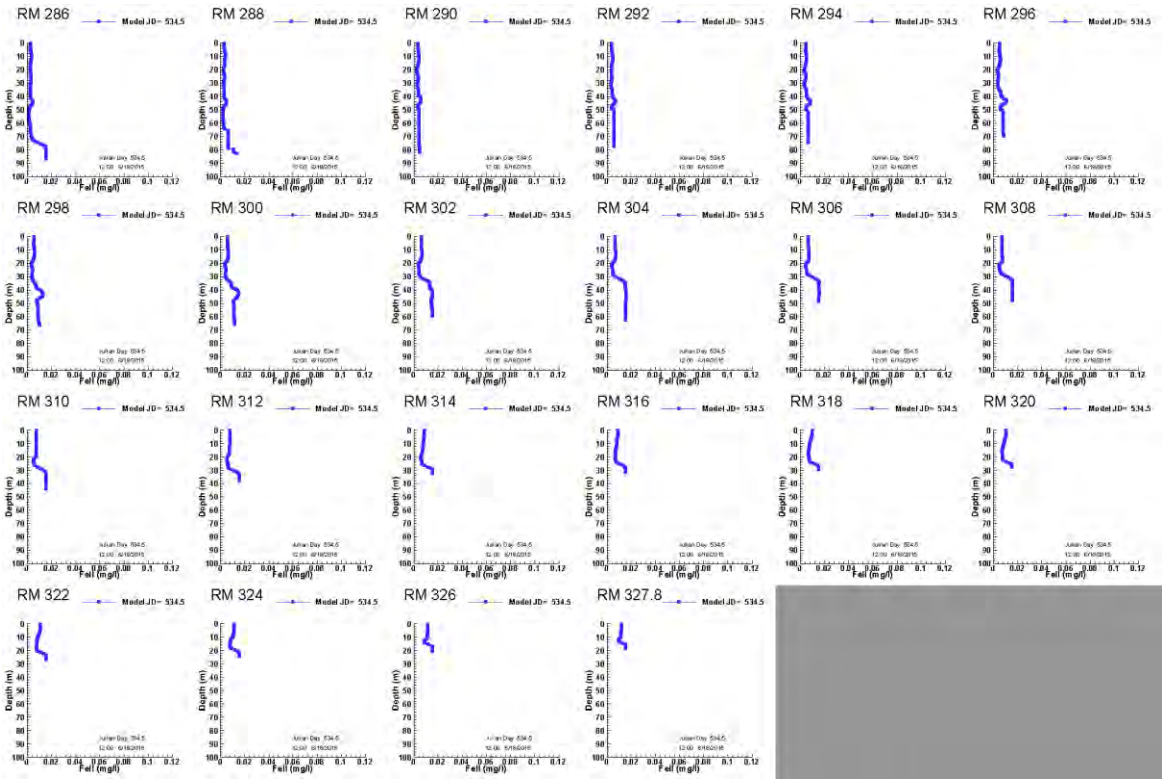


Figure 357. Vertical profiles of Fe(II) compared with data for 6/18/2015.

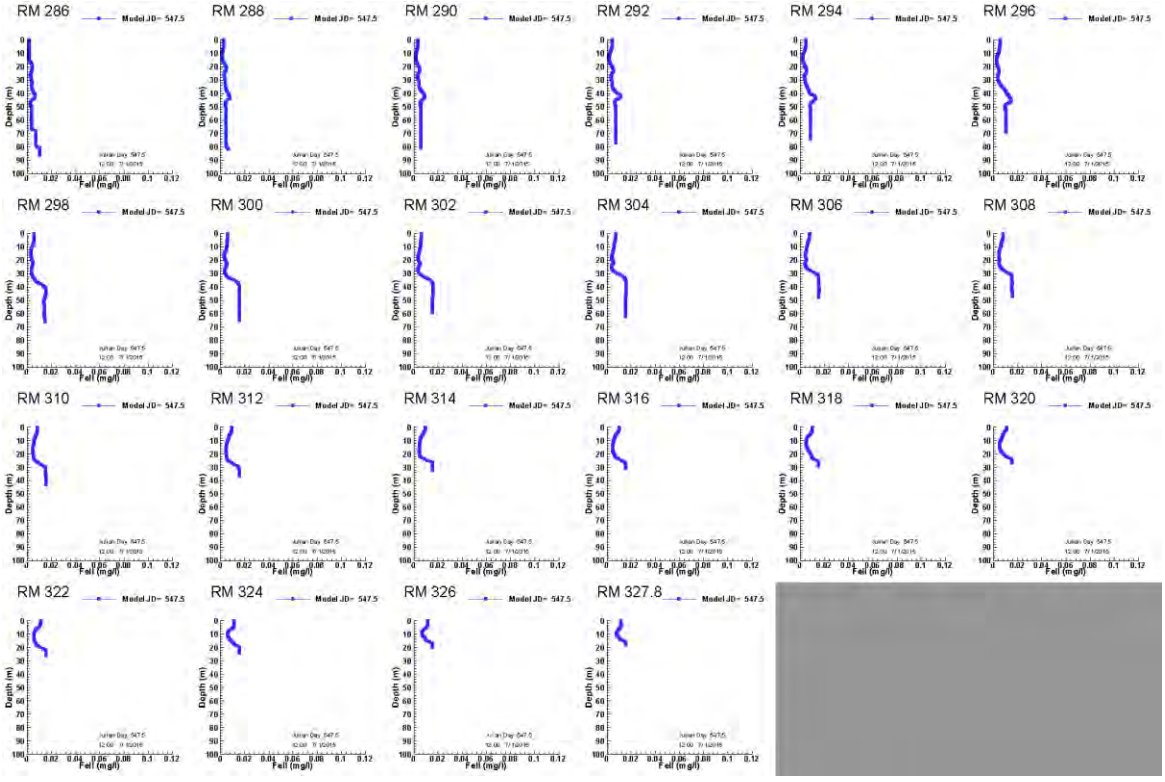


Figure 358. Vertical profiles of Fe(II) compared with data for 7/ 1/2015.

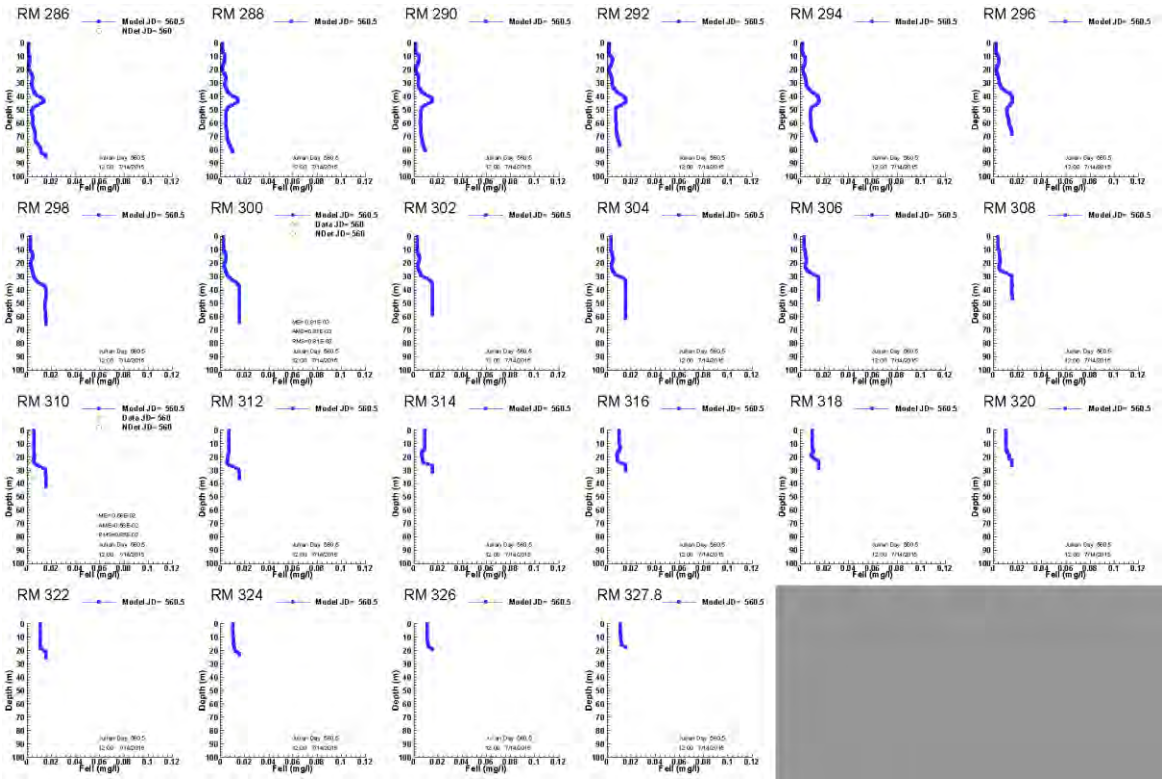


Figure 359. Vertical profiles of Fe(II) compared with data for 7/14/2015.

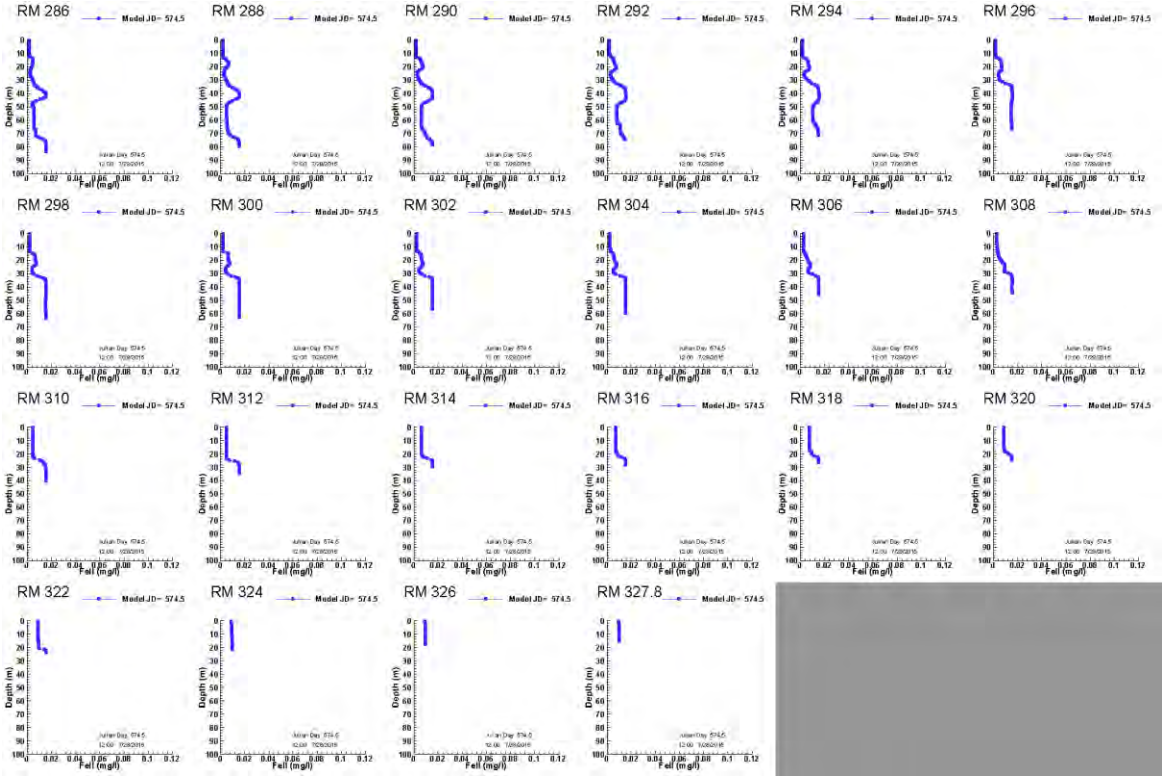


Figure 360. Vertical profiles of Fe(II) compared with data for 7/28/2015.

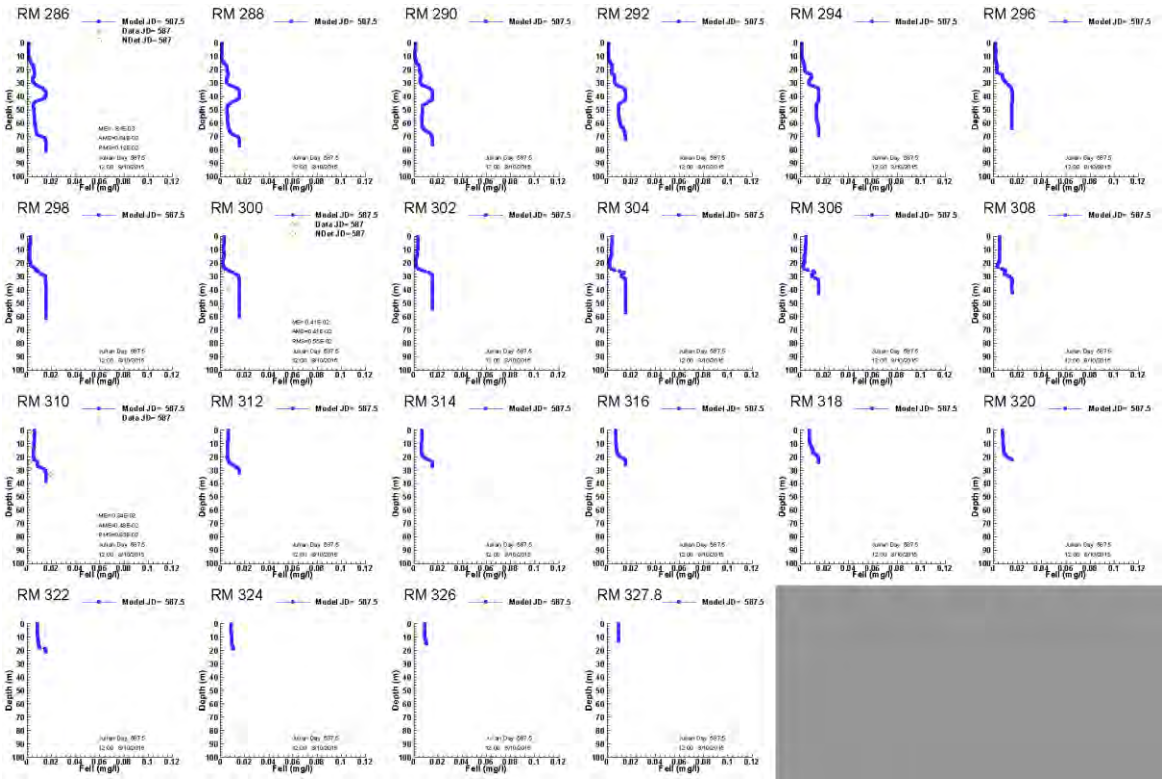


Figure 361. Vertical profiles of Fe(II) compared with data for 8/10/2015.

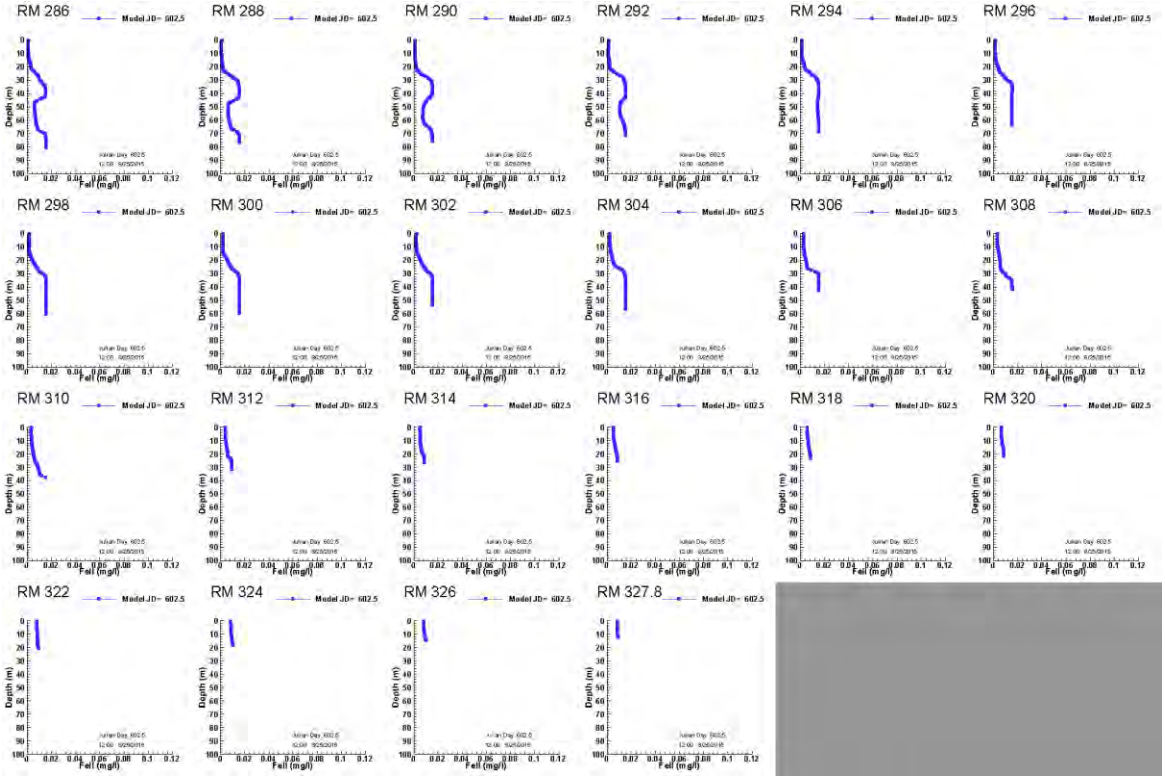


Figure 362. Vertical profiles of Fe(II) compared with data for 8/25/2015.

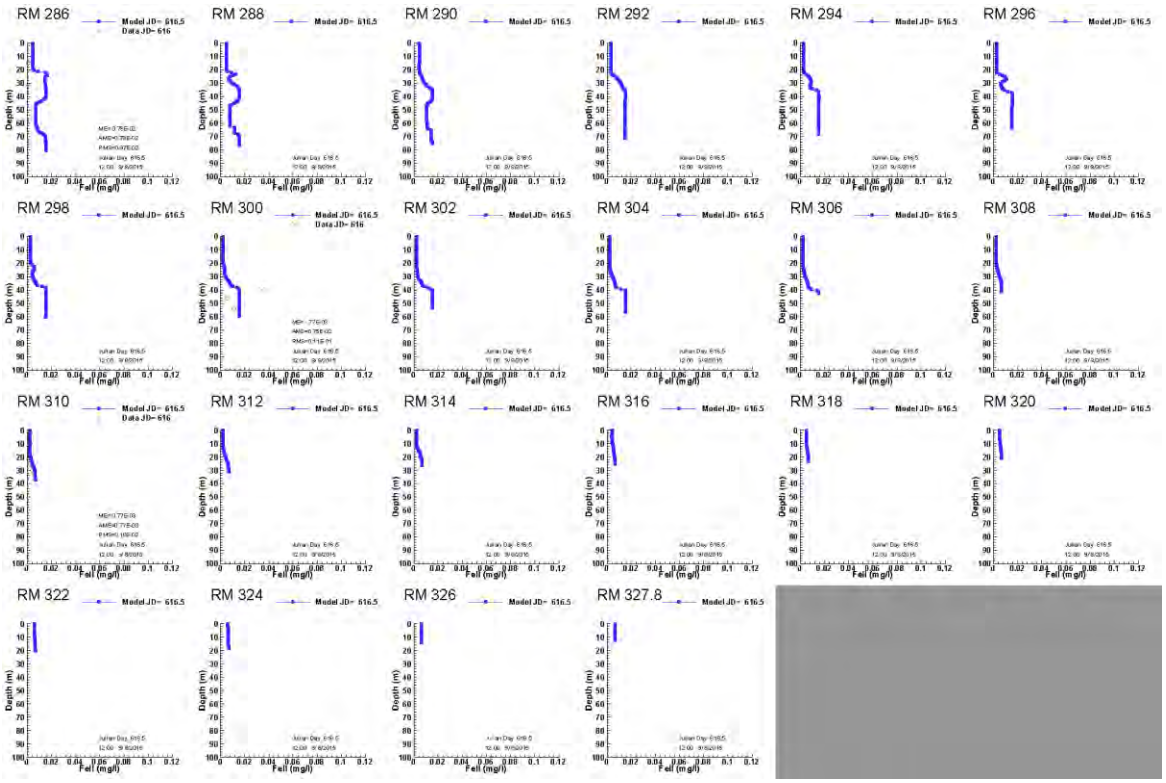


Figure 363. Vertical profiles of Fe(II) compared with data for 9/ 8/2015.

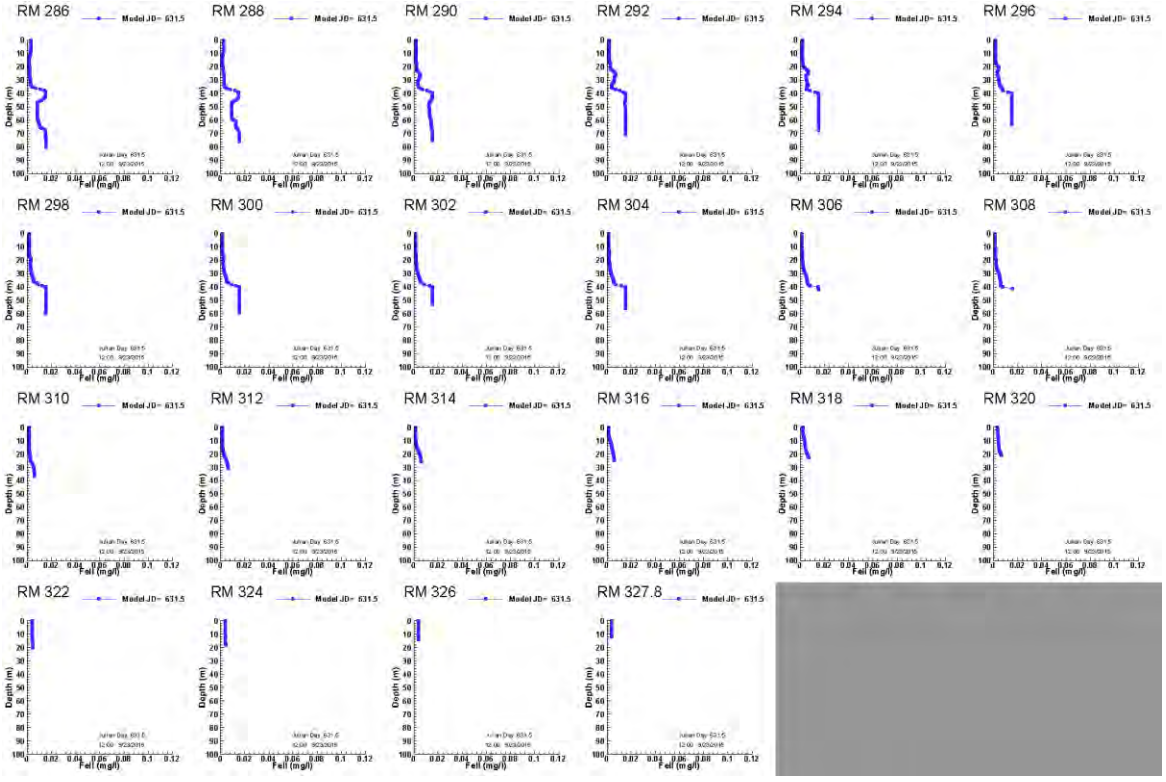


Figure 364. Vertical profiles of Fe(II) compared with data for 9/23/2015.

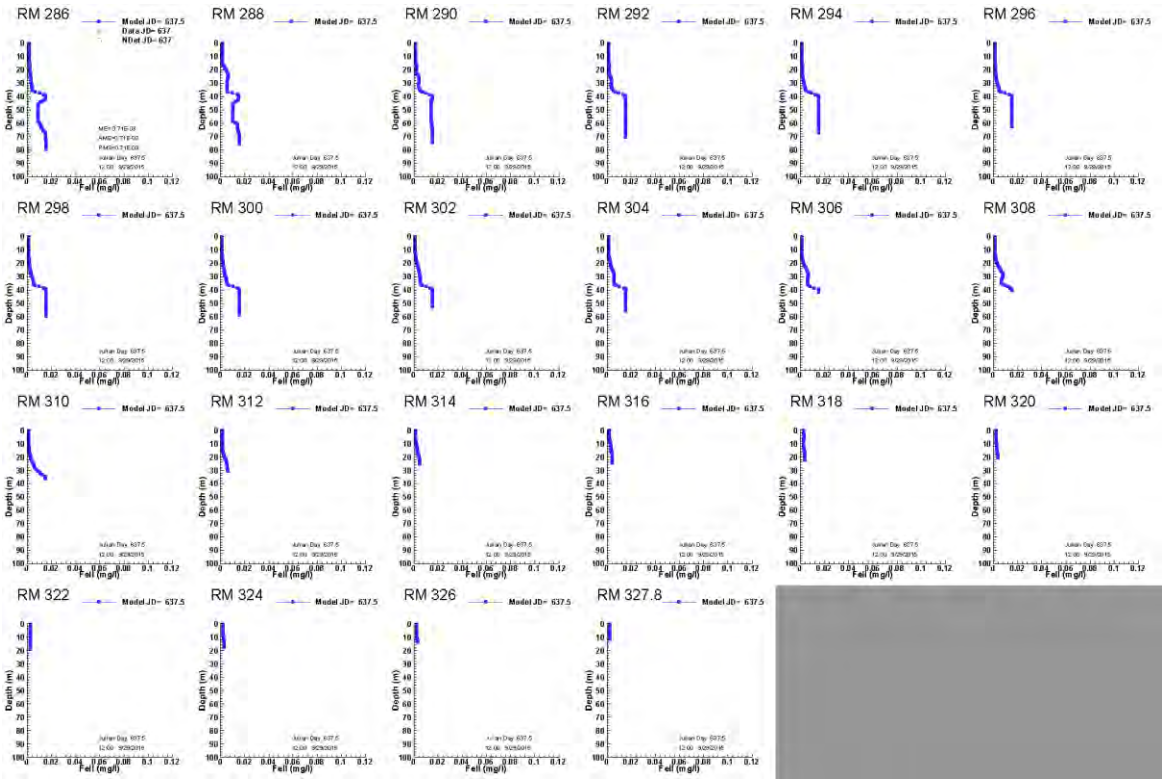


Figure 365. Vertical profiles of Fe(II) compared with data for 9/29/2015.

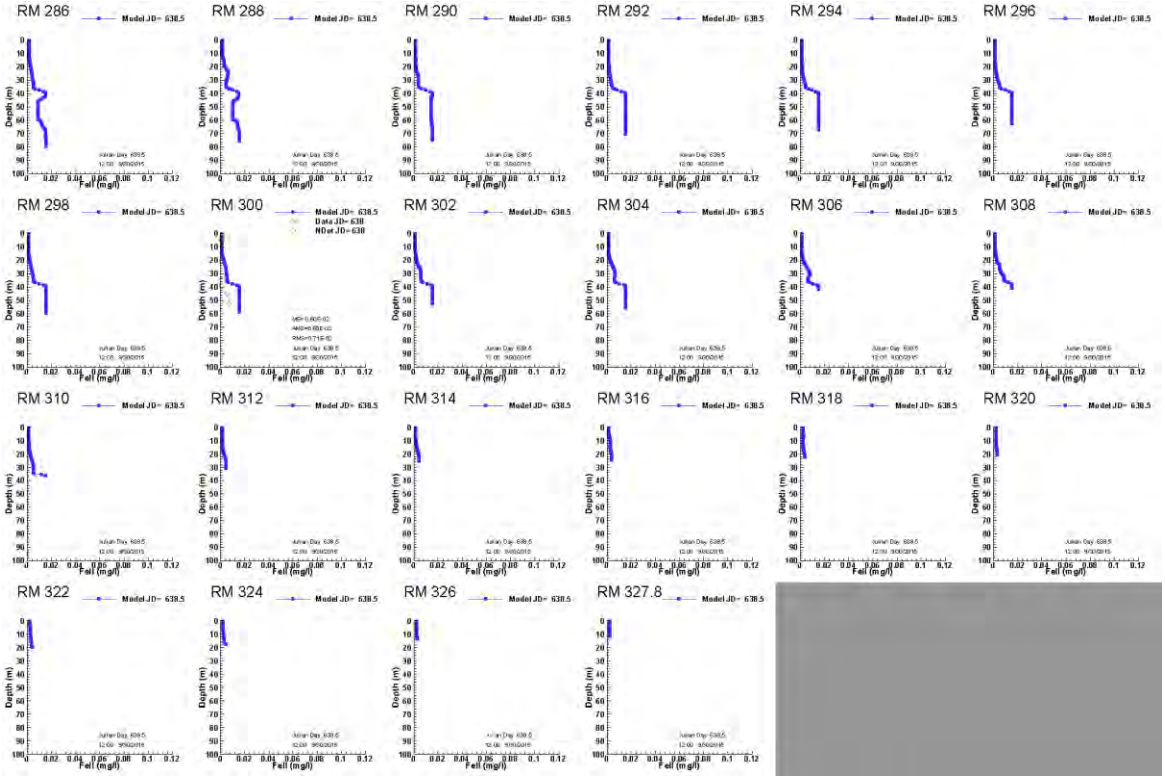


Figure 366. Vertical profiles of Fe(II) compared with data for 9/30/2015.

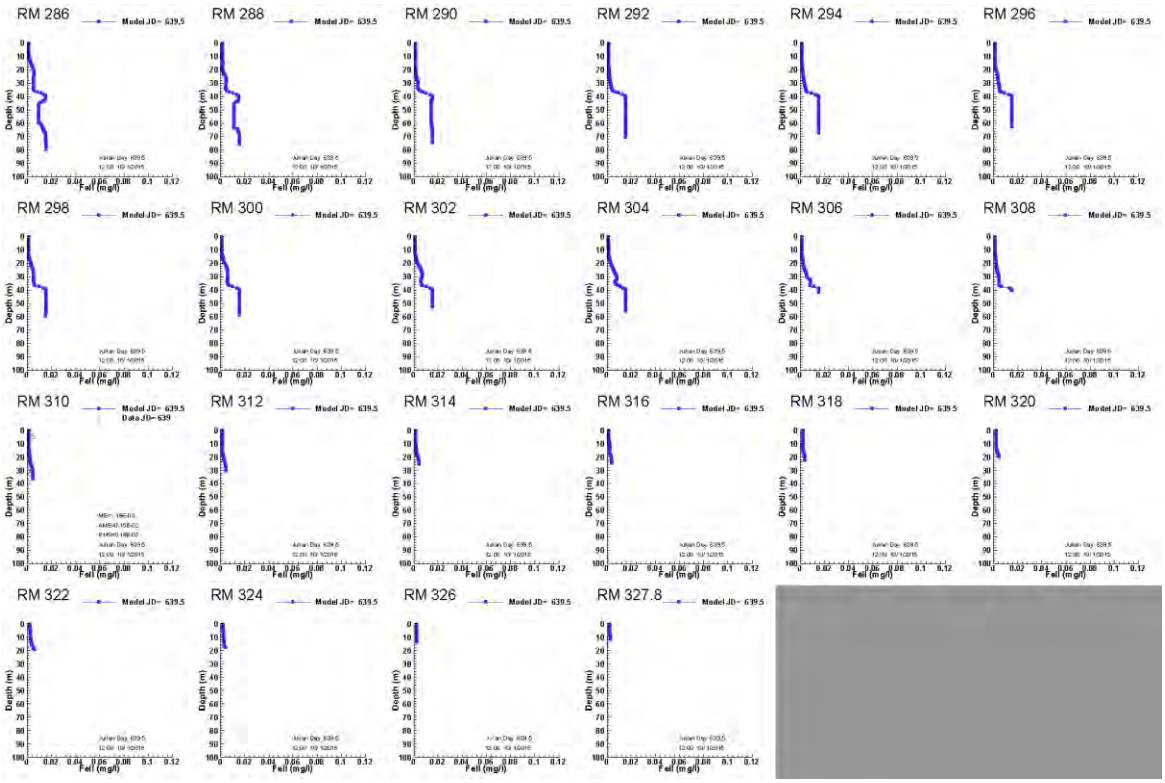


Figure 367. Vertical profiles of Fe(II) compared with data for 10/ 1/2015.

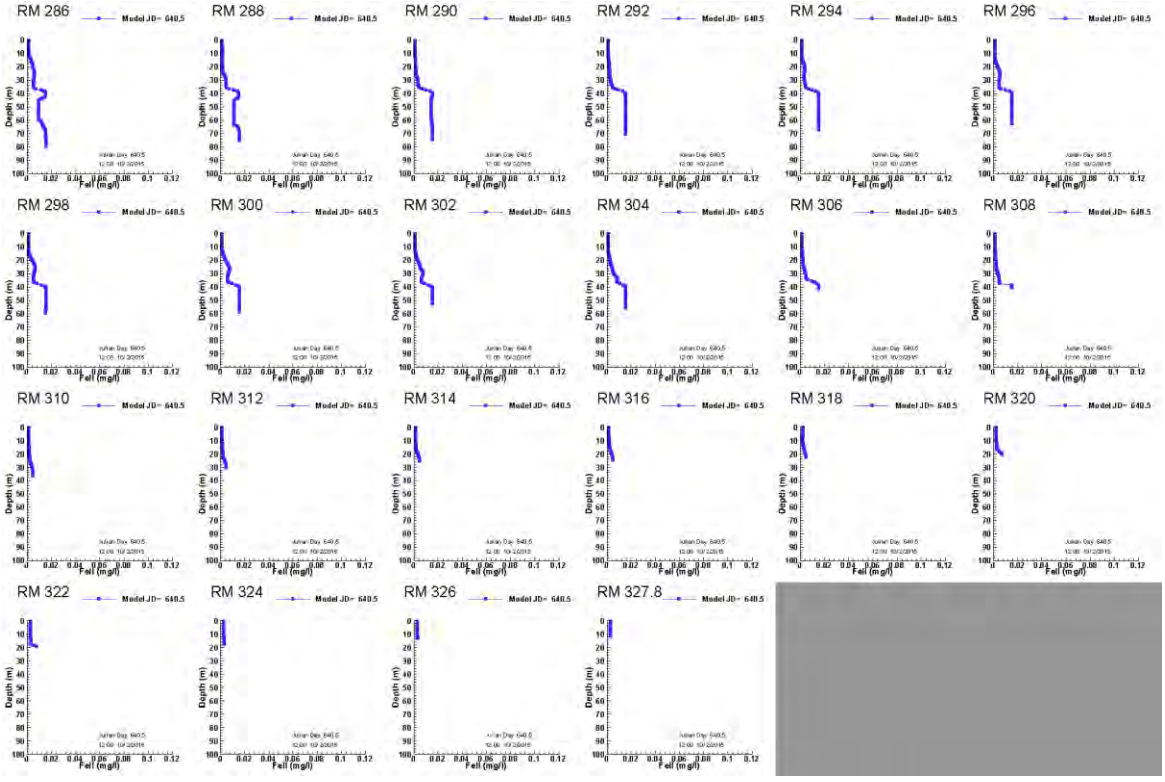


Figure 368. Vertical profiles of Fe(II) compared with data for 10/ 2/2015.

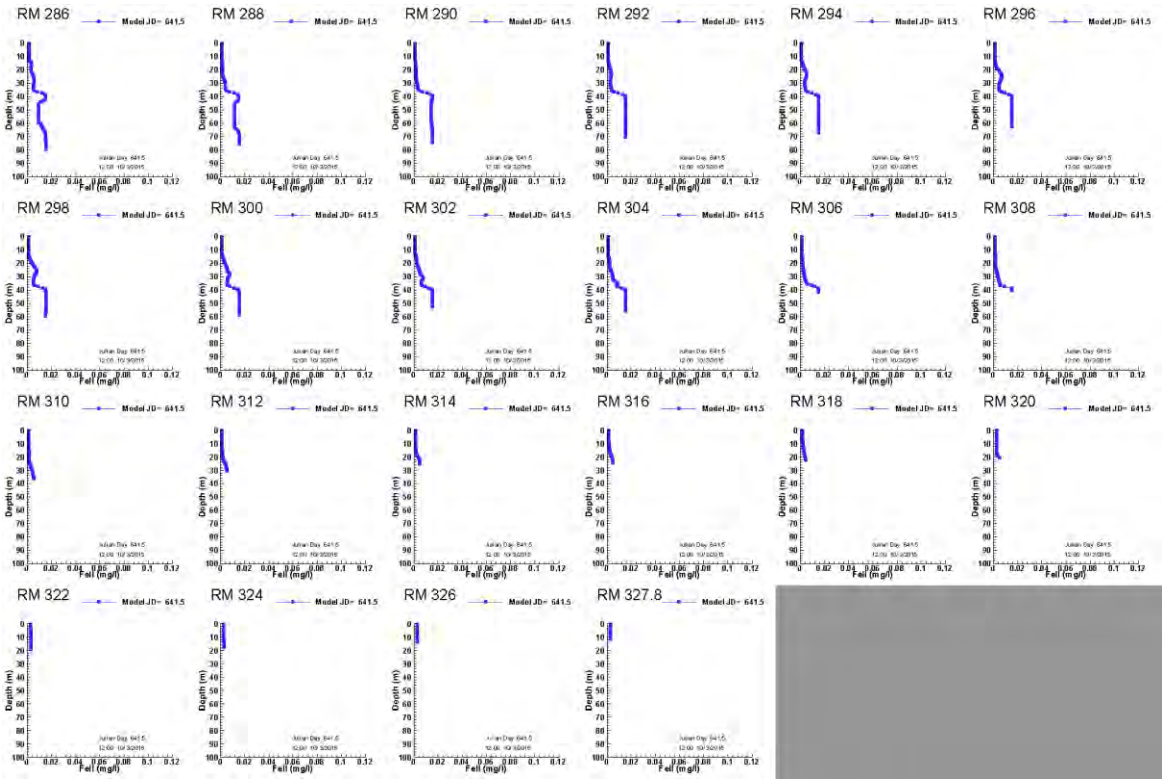


Figure 369. Vertical profiles of Fe(II) compared with data for 10/ 3/2015.

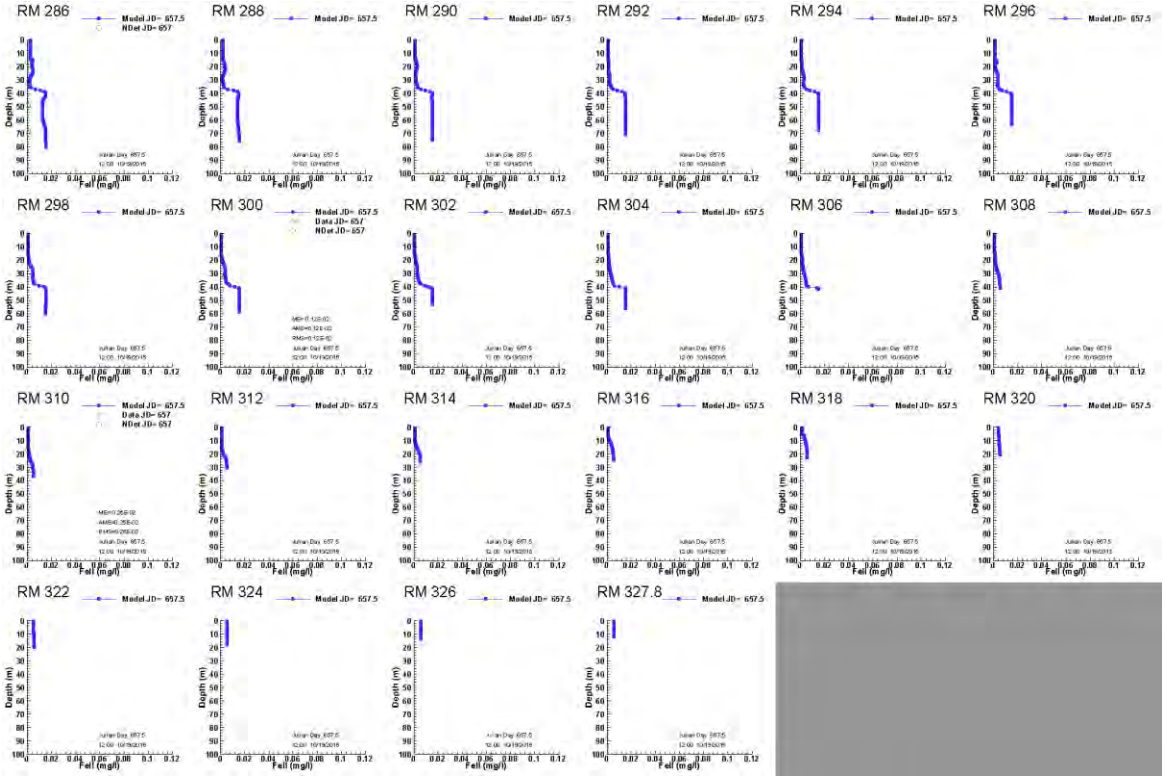


Figure 370. Vertical profiles of Fe(II) compared with data for 10/19/2015.

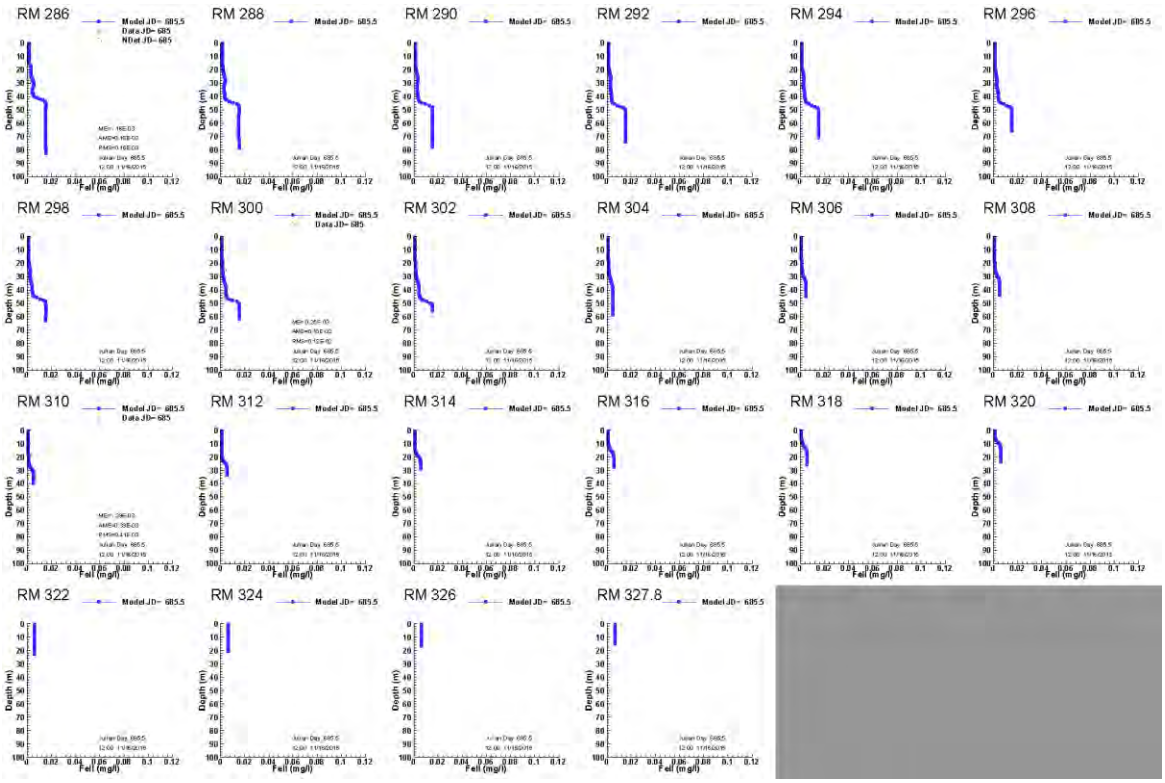


Figure 371. Vertical profiles of Fe(II) compared with data for 11/16/2015.

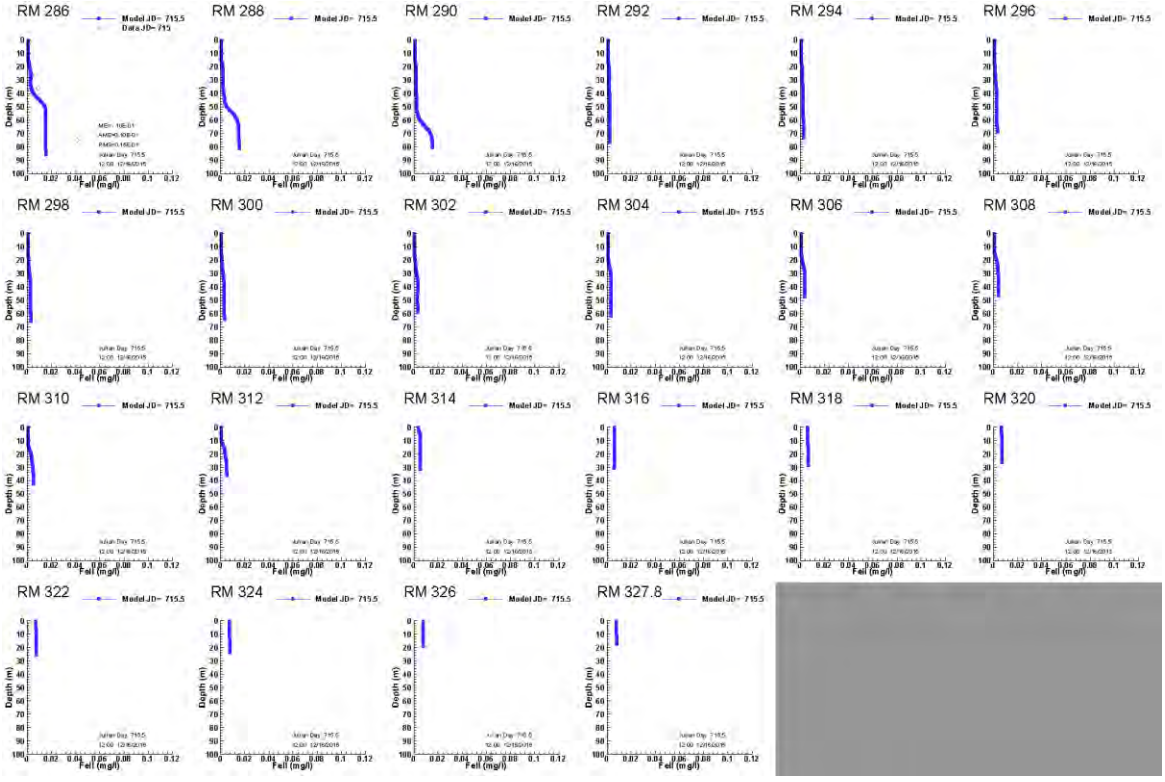


Figure 372. Vertical profiles of Fe(II) compared with data for 12/16/2015.

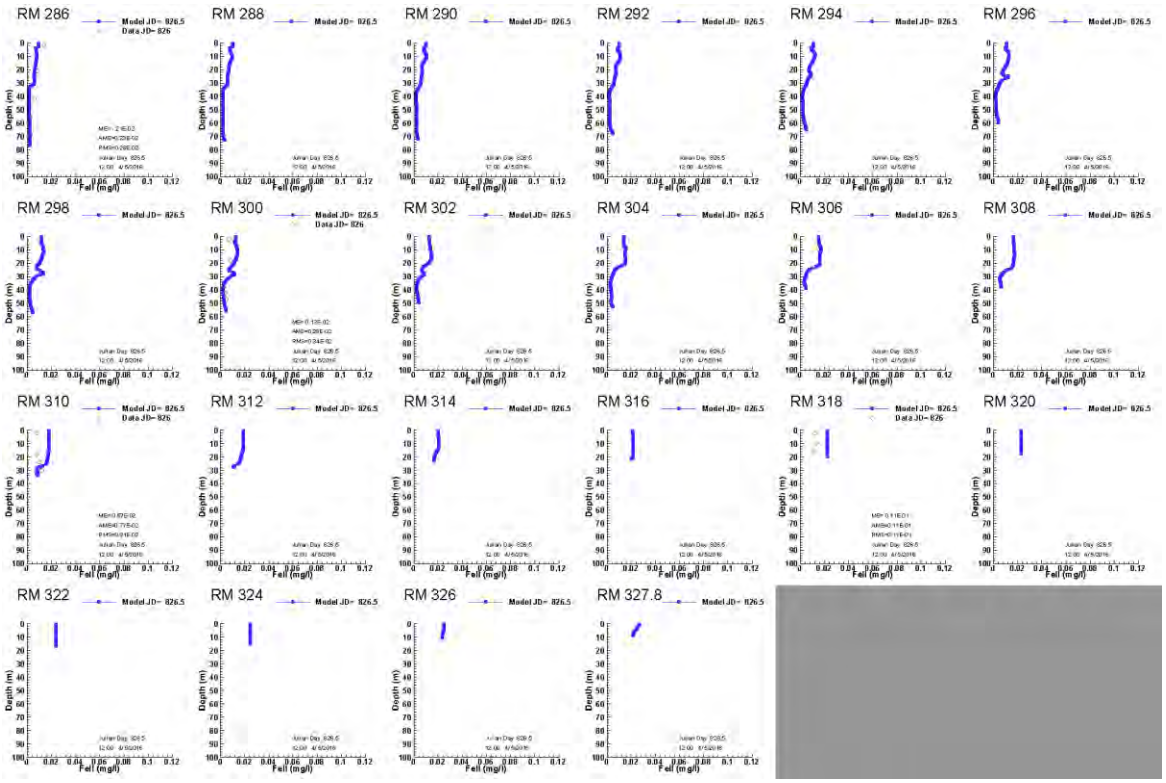


Figure 373. Vertical profiles of Fe(II) compared with data for 4/ 5/2016.

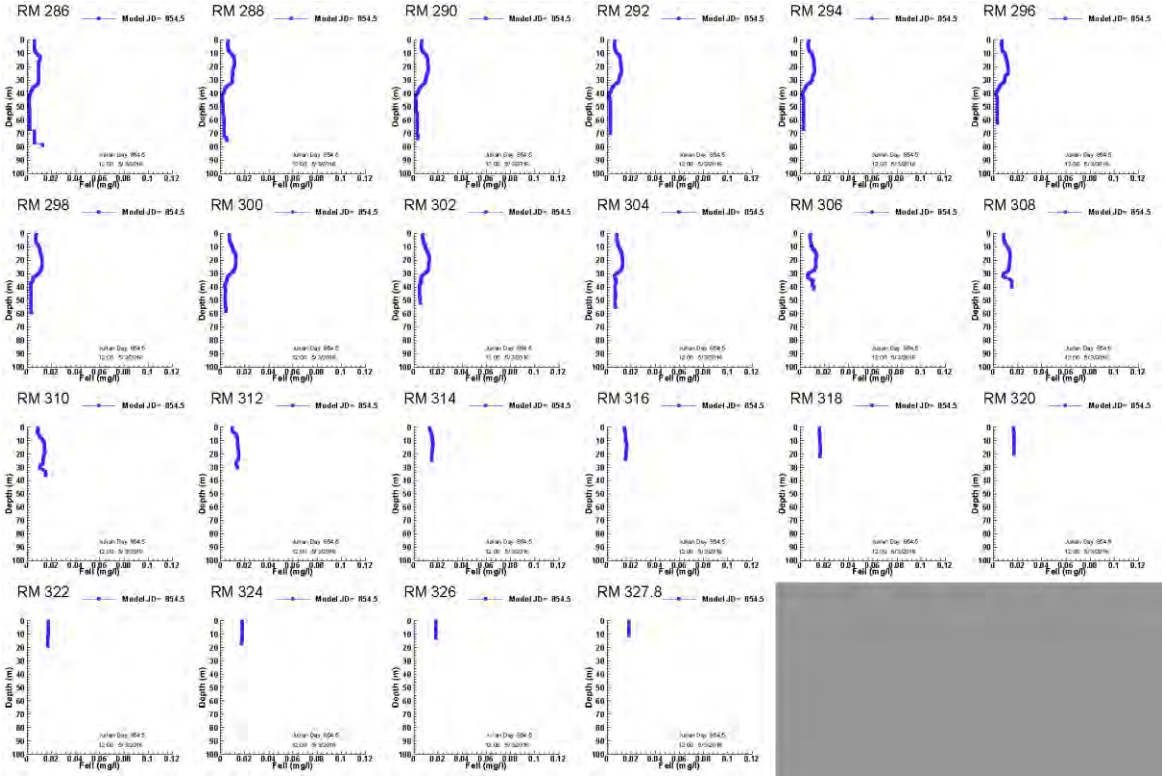


Figure 374. Vertical profiles of Fe(II) compared with data for 5/ 3/2016.

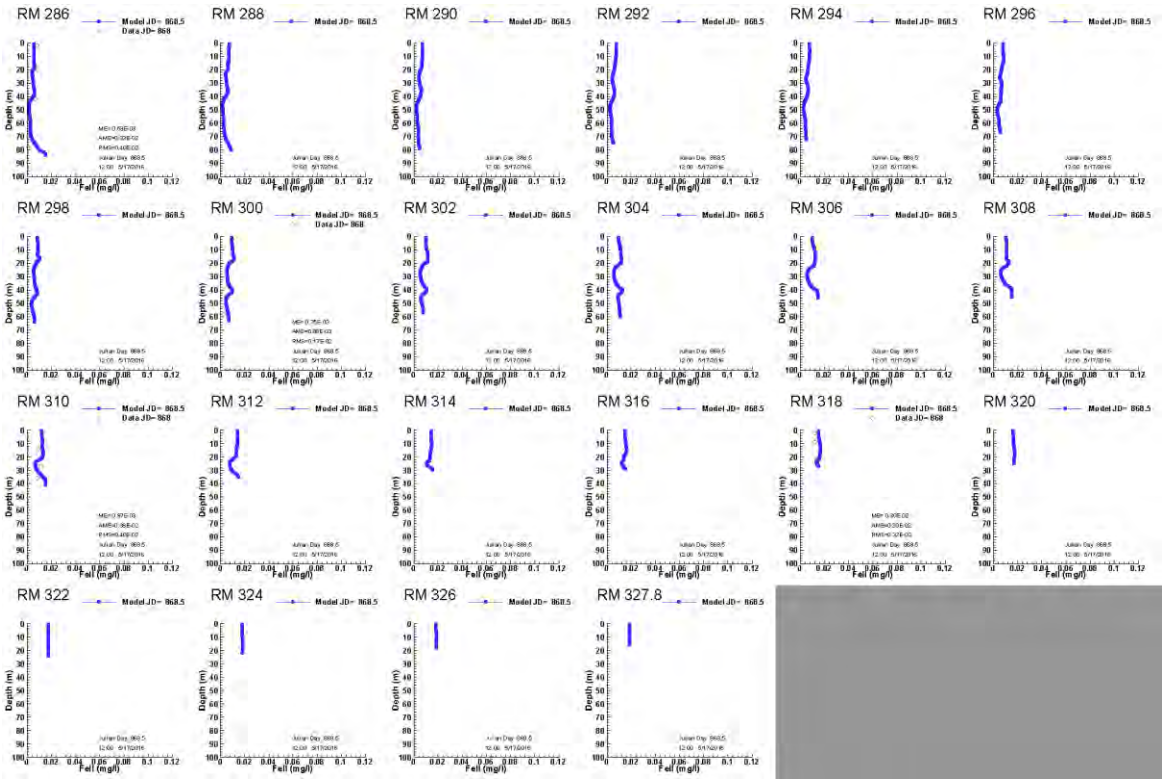


Figure 375. Vertical profiles of Fe(II) compared with data for 5/17/2016.

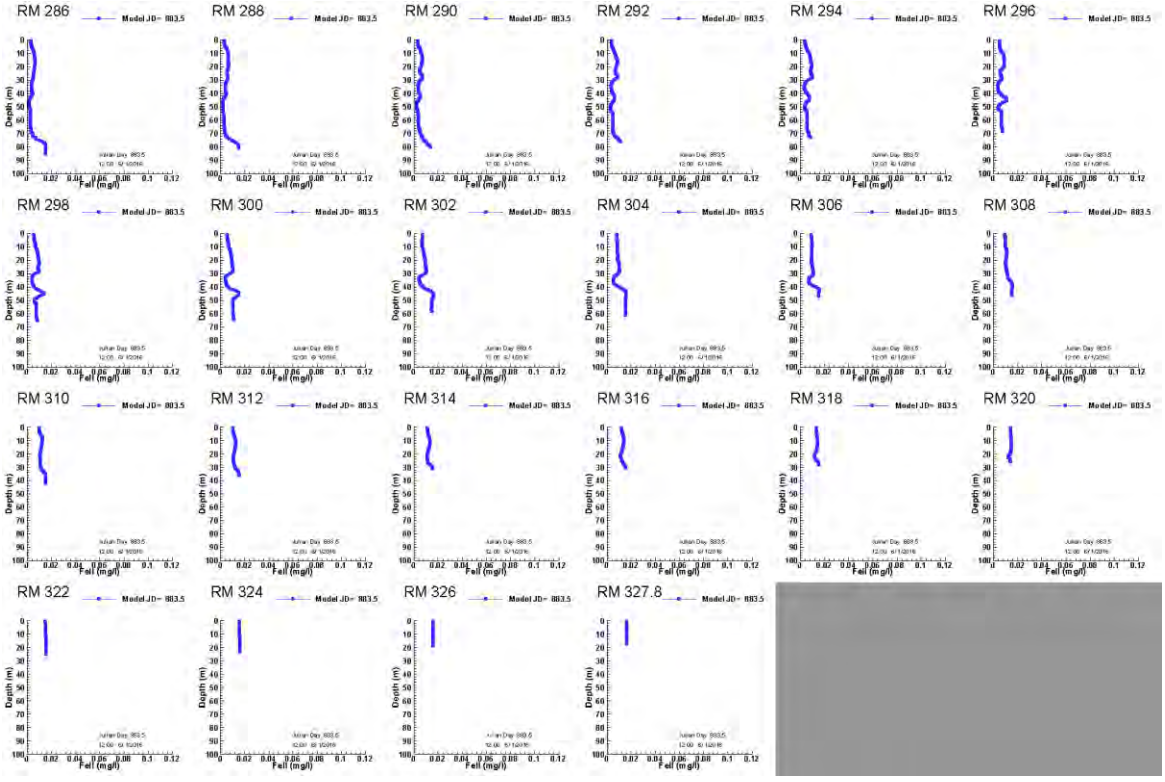


Figure 376. Vertical profiles of Fe(II) compared with data for 6/ 1/2016.

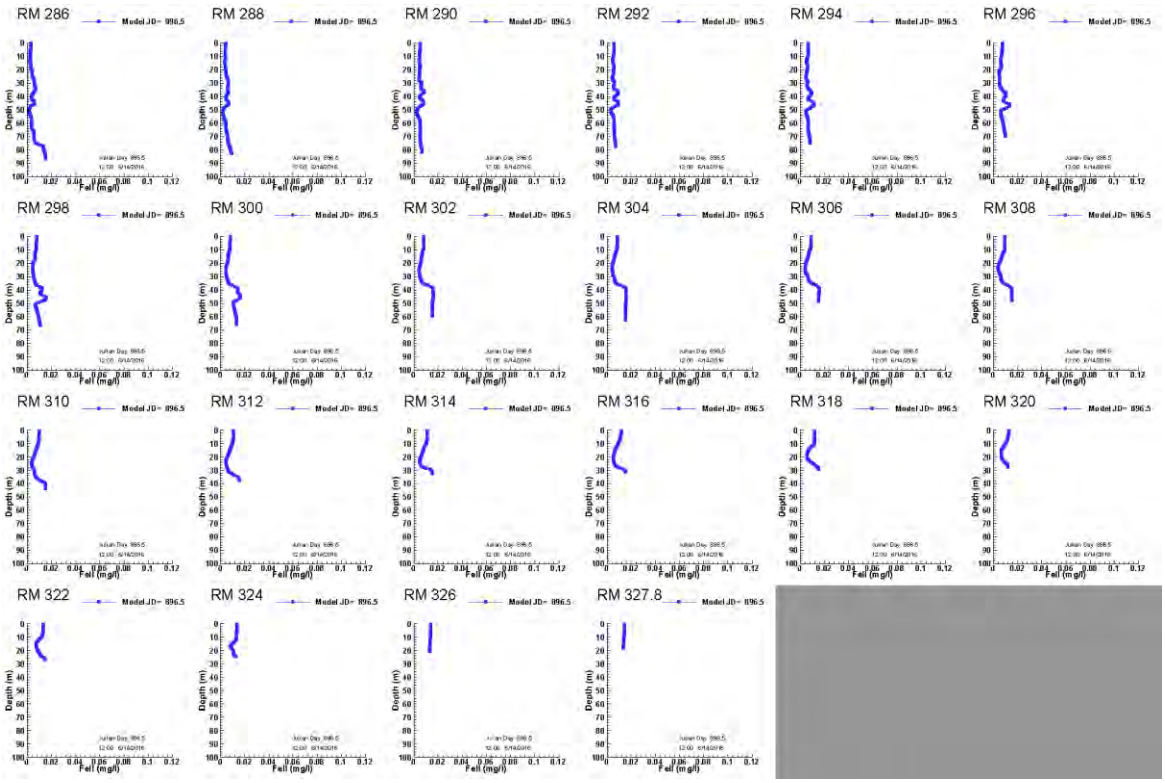


Figure 377. Vertical profiles of Fe(II) compared with data for 6/14/2016.

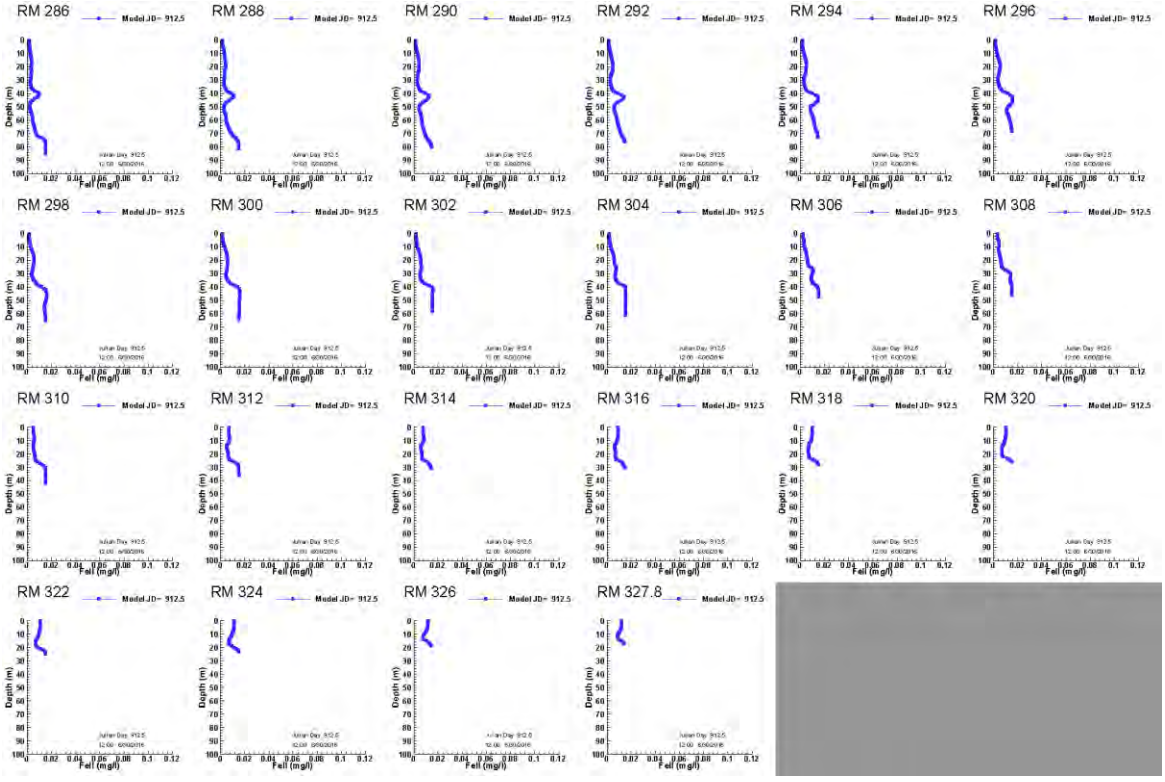


Figure 378. Vertical profiles of Fe(II) compared with data for 6/30/2016.

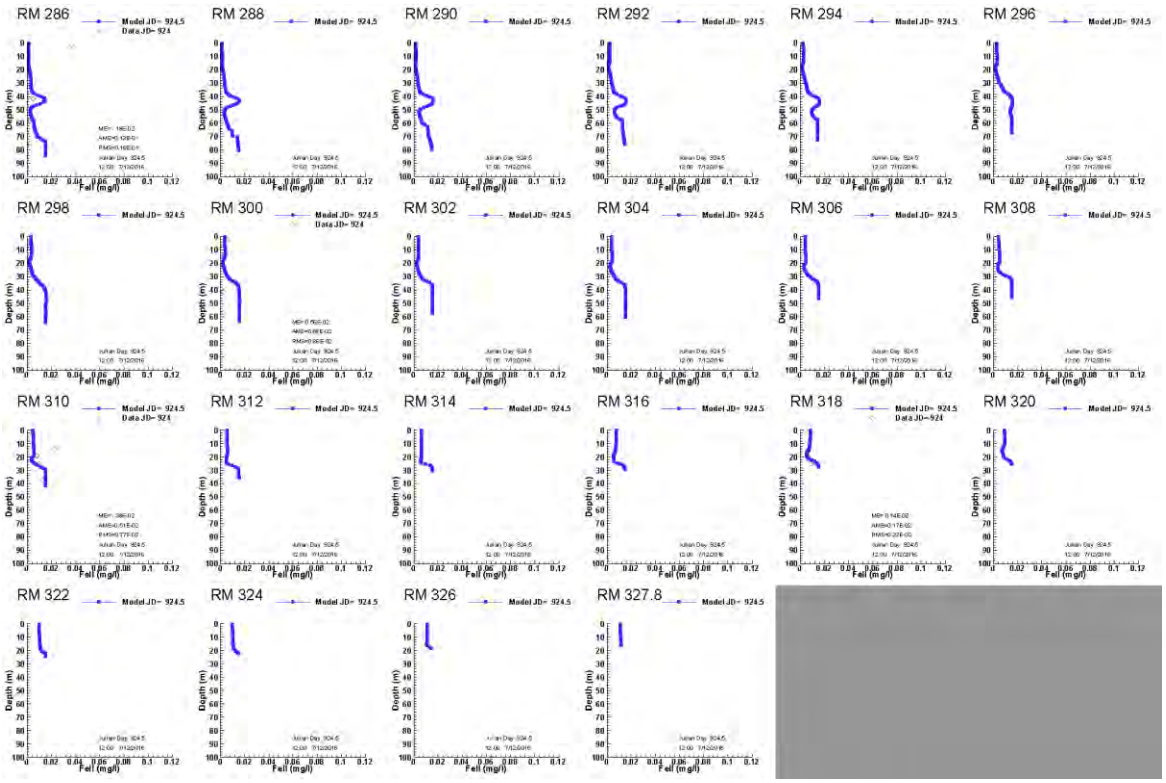


Figure 379. Vertical profiles of Fe(II) compared with data for 7/12/2016.

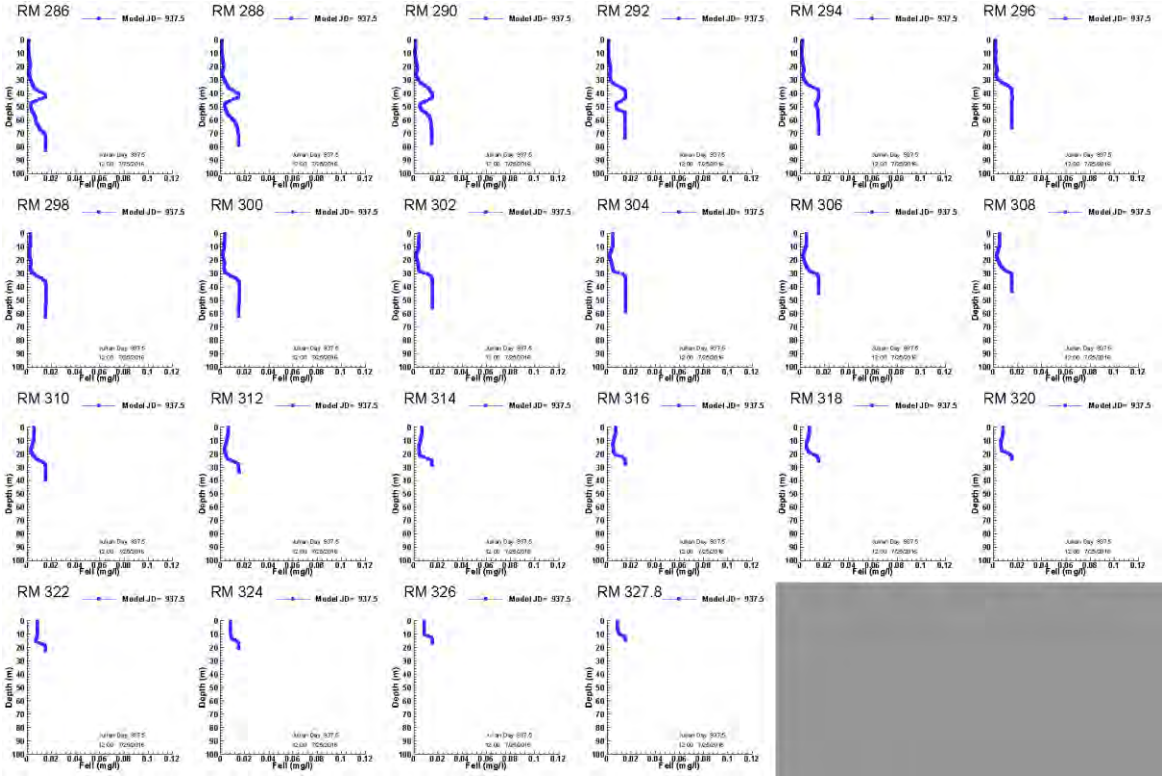


Figure 380. Vertical profiles of Fe(II) compared with data for 7/25/2016.

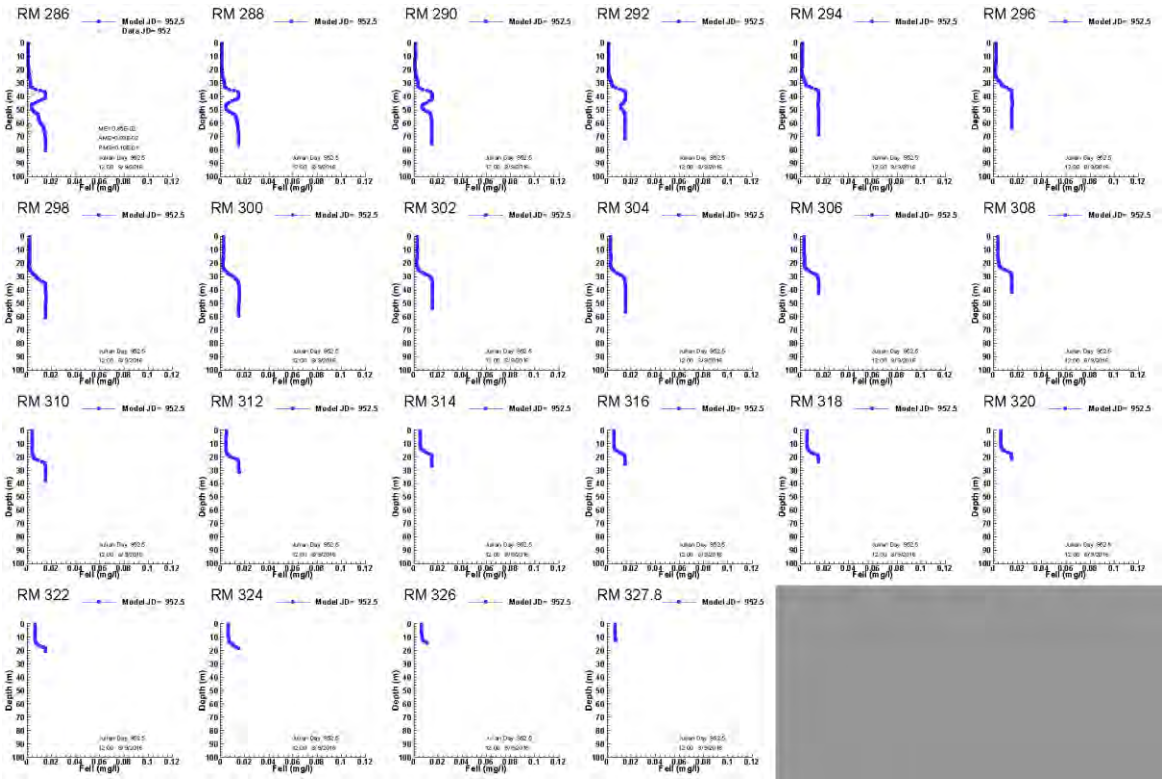


Figure 381. Vertical profiles of Fe(II) compared with data for 8/ 9/2016.

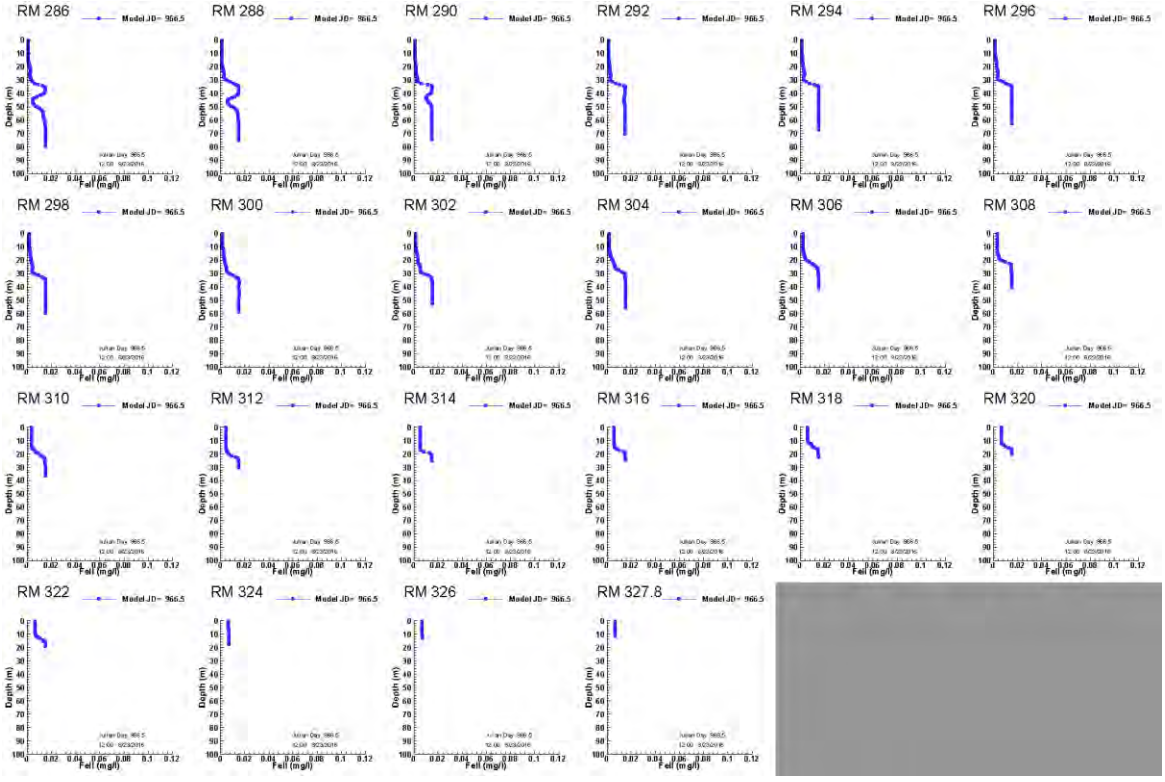


Figure 382. Vertical profiles of Fe(II) compared with data for 8/23/2016.

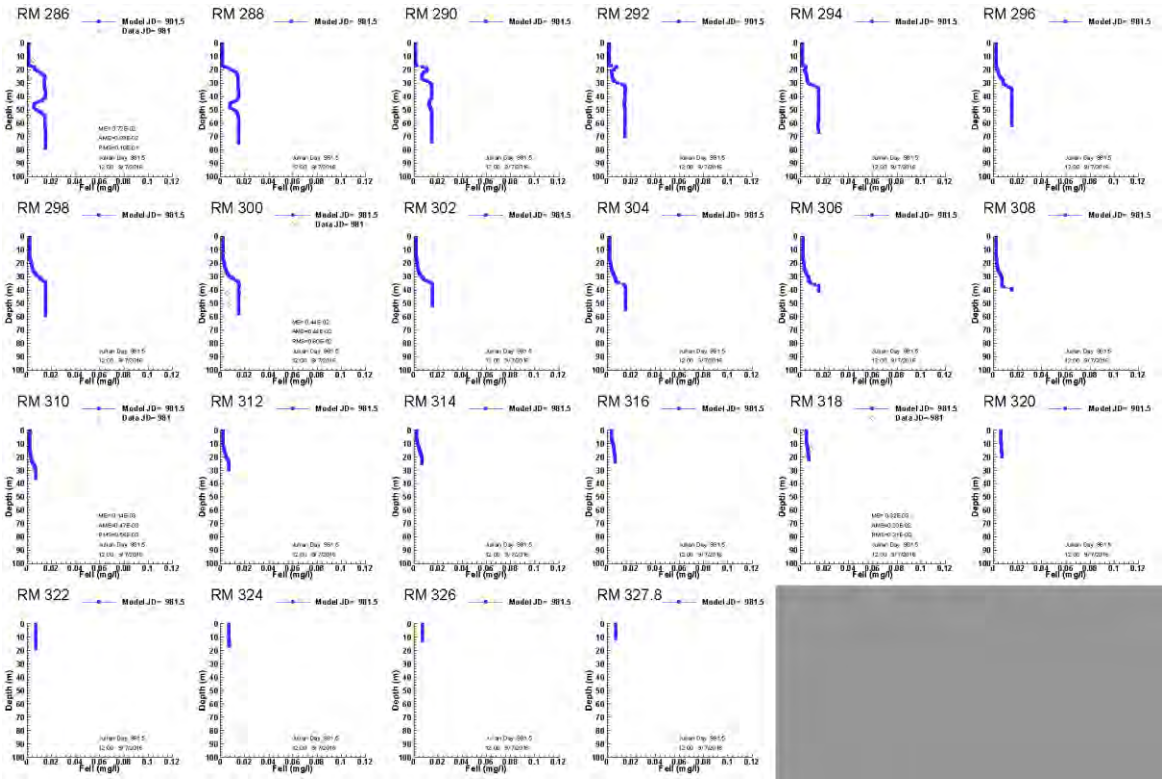


Figure 383. Vertical profiles of Fe(II) compared with data for 9/ 7/2016.

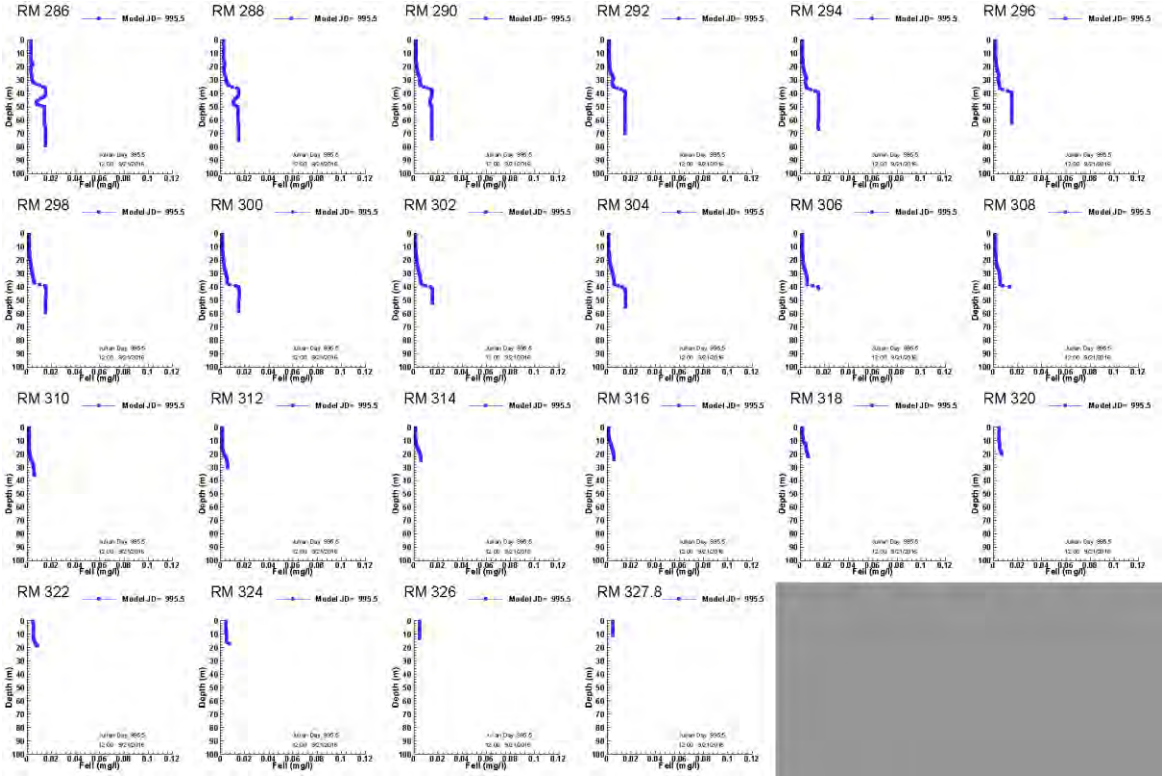


Figure 384. Vertical profiles of Fe(II) compared with data for 9/21/2016.

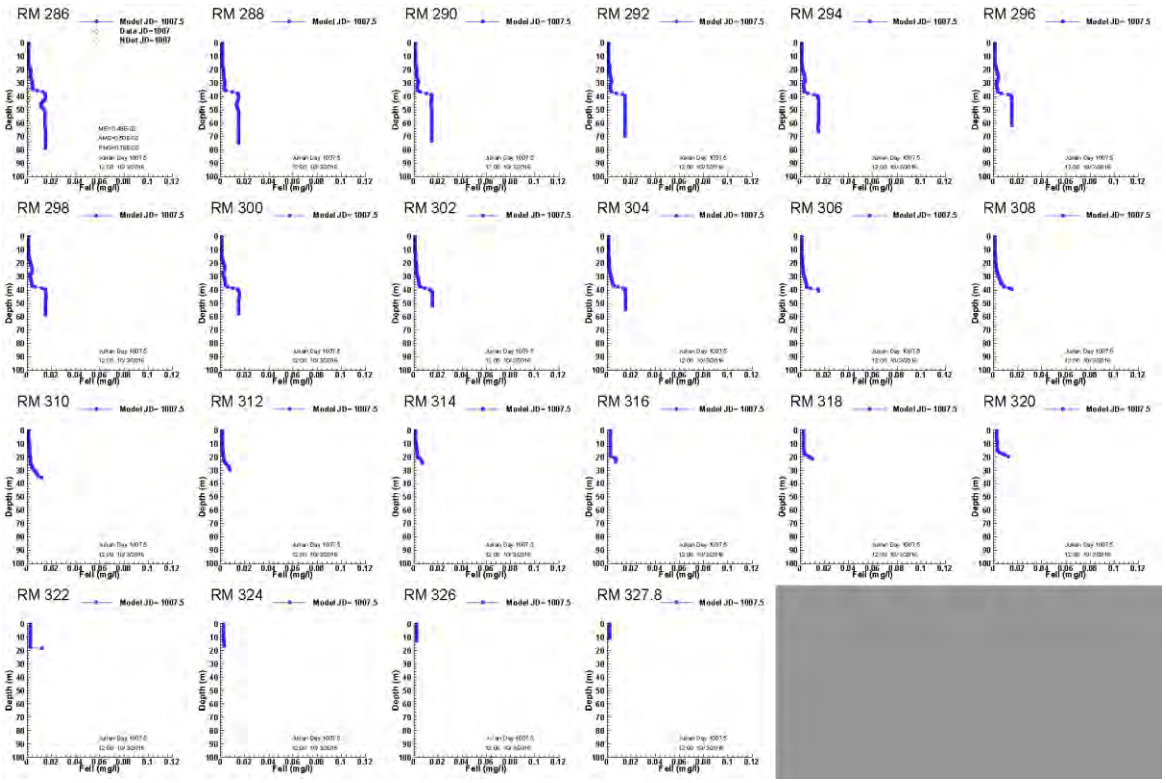


Figure 385. Vertical profiles of Fe(II) compared with data for 10/ 3/2016.

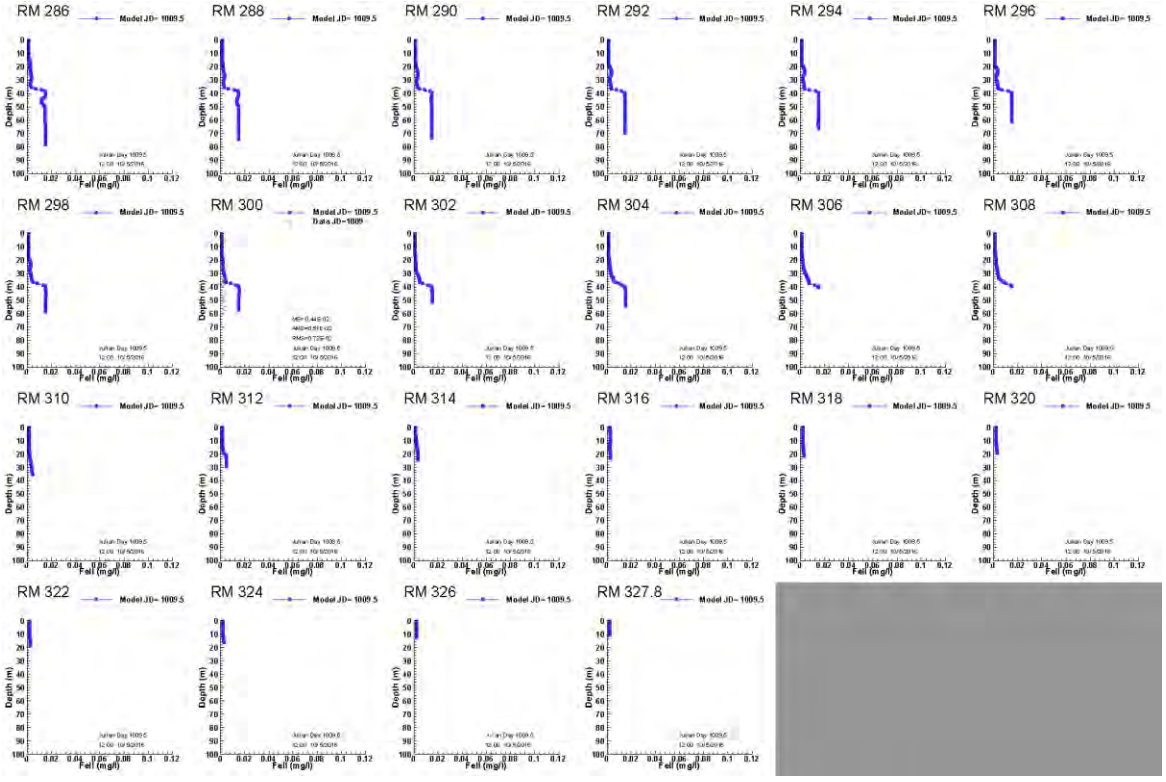


Figure 386. Vertical profiles of Fe(II) compared with data for 10/ 5/2016.

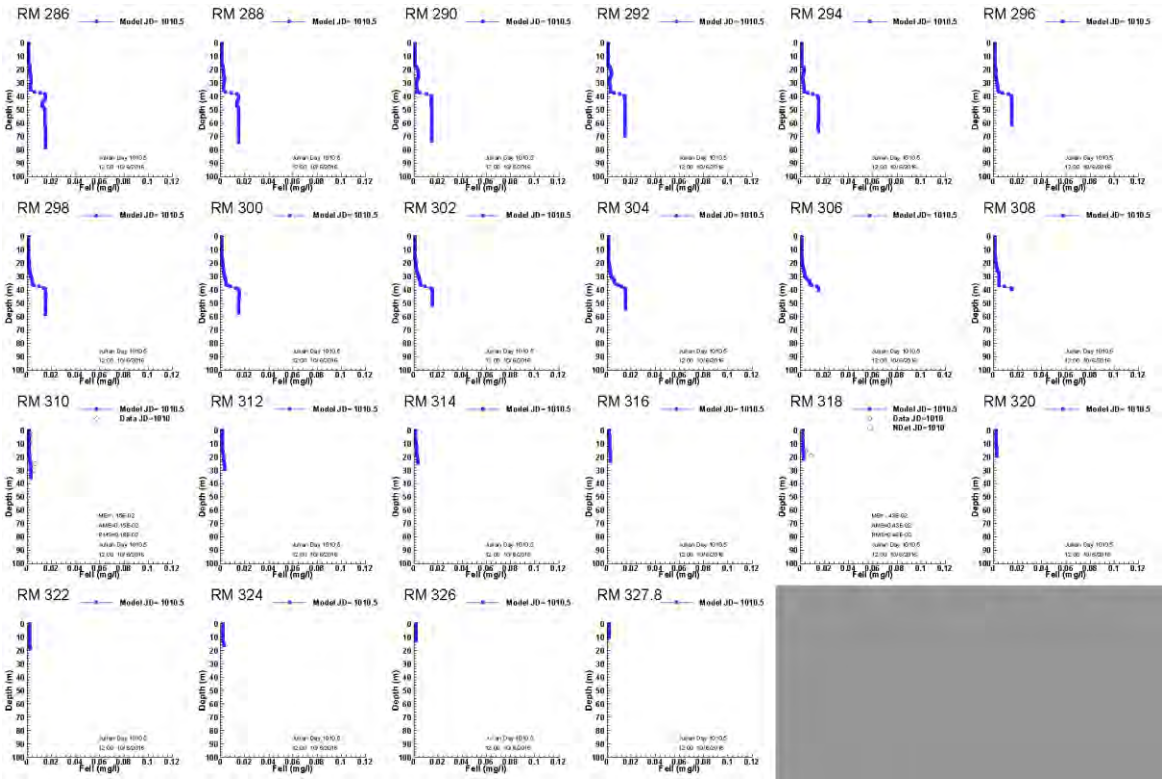


Figure 387. Vertical profiles of Fe(II) compared with data for 10/ 6/2016.

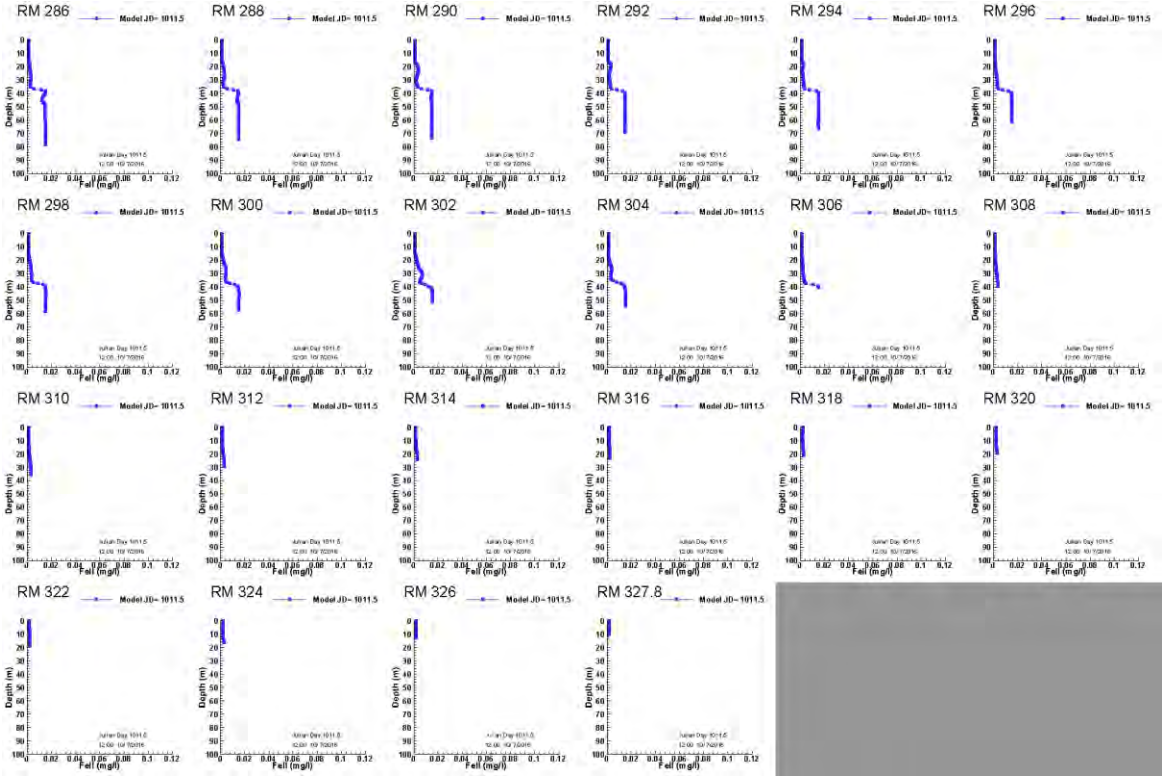


Figure 388. Vertical profiles of Fe(II) compared with data for 10/ 7/2016.

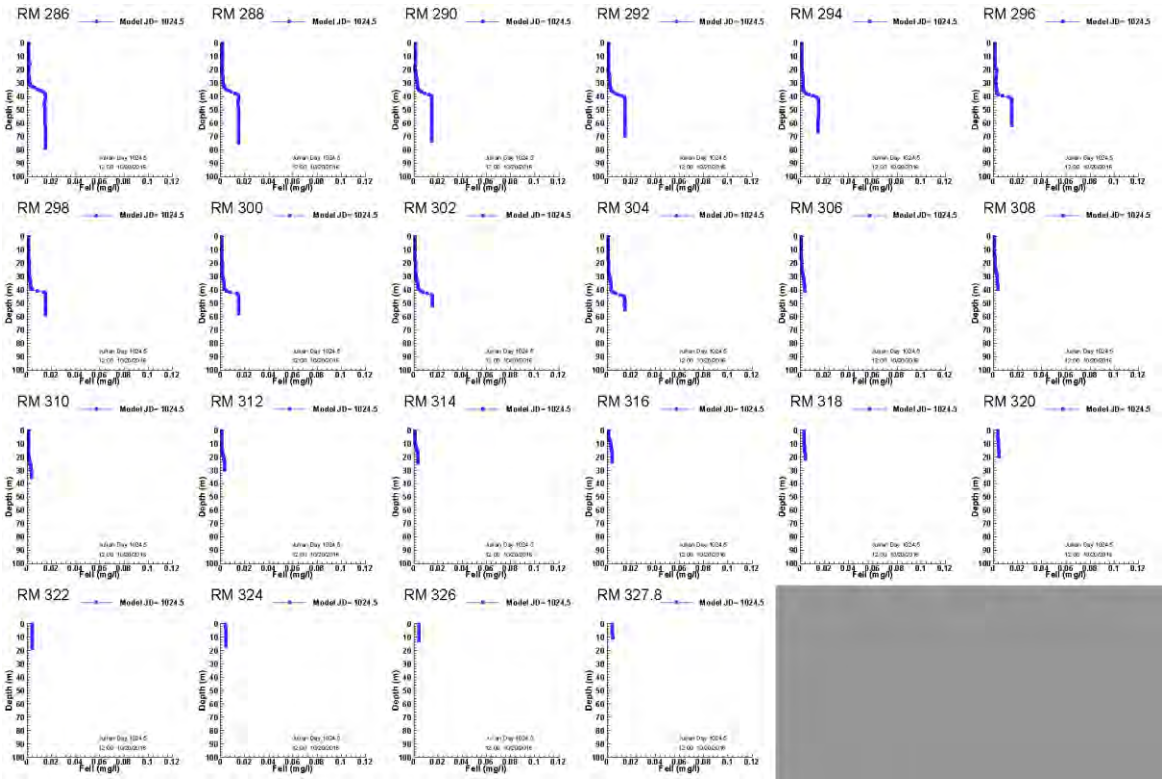


Figure 389. Vertical profiles of Fe(II) compared with data for 10/20/2016.

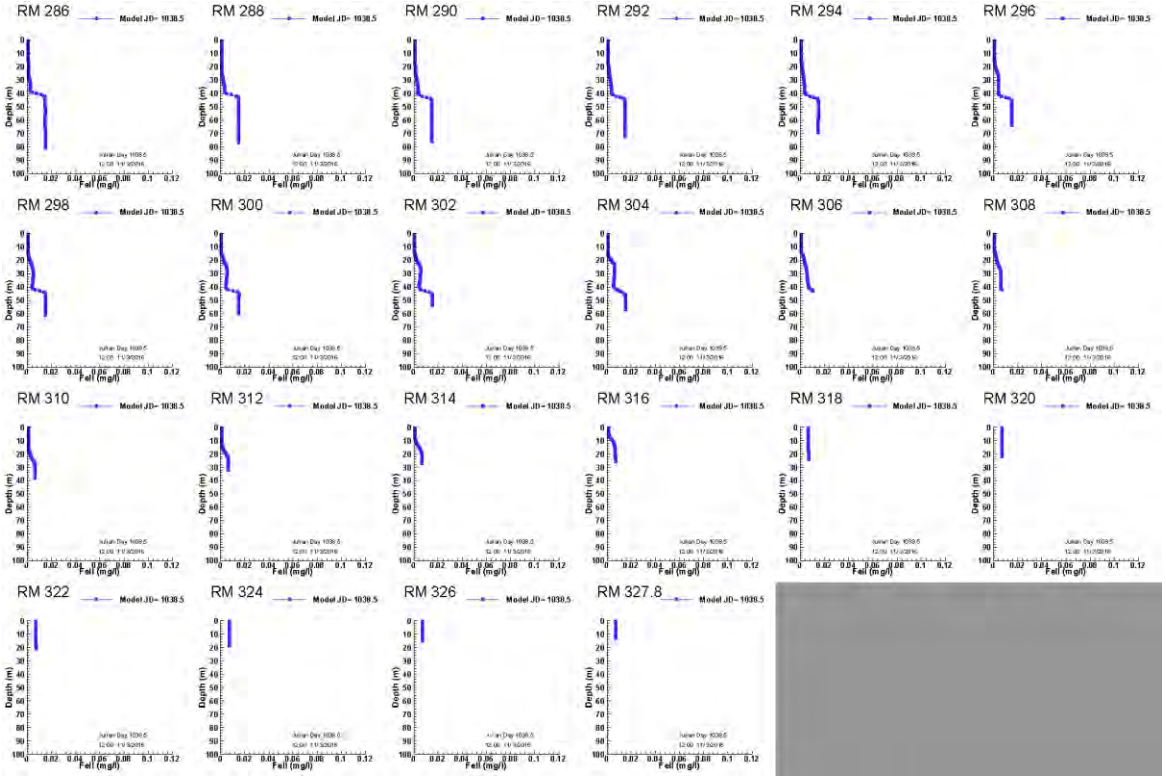


Figure 390. Vertical profiles of Fe(II) compared with data for 11/ 3/2016.

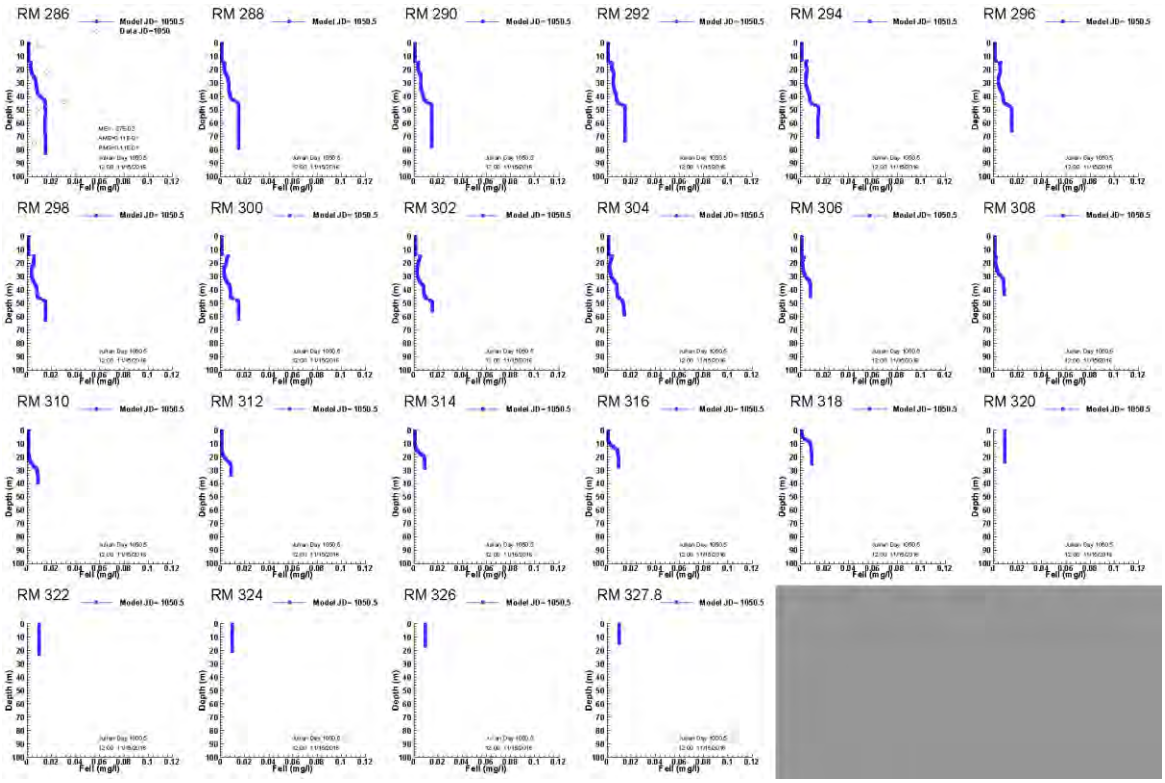


Figure 391. Vertical profiles of Fe(II) compared with data for 11/15/2016.

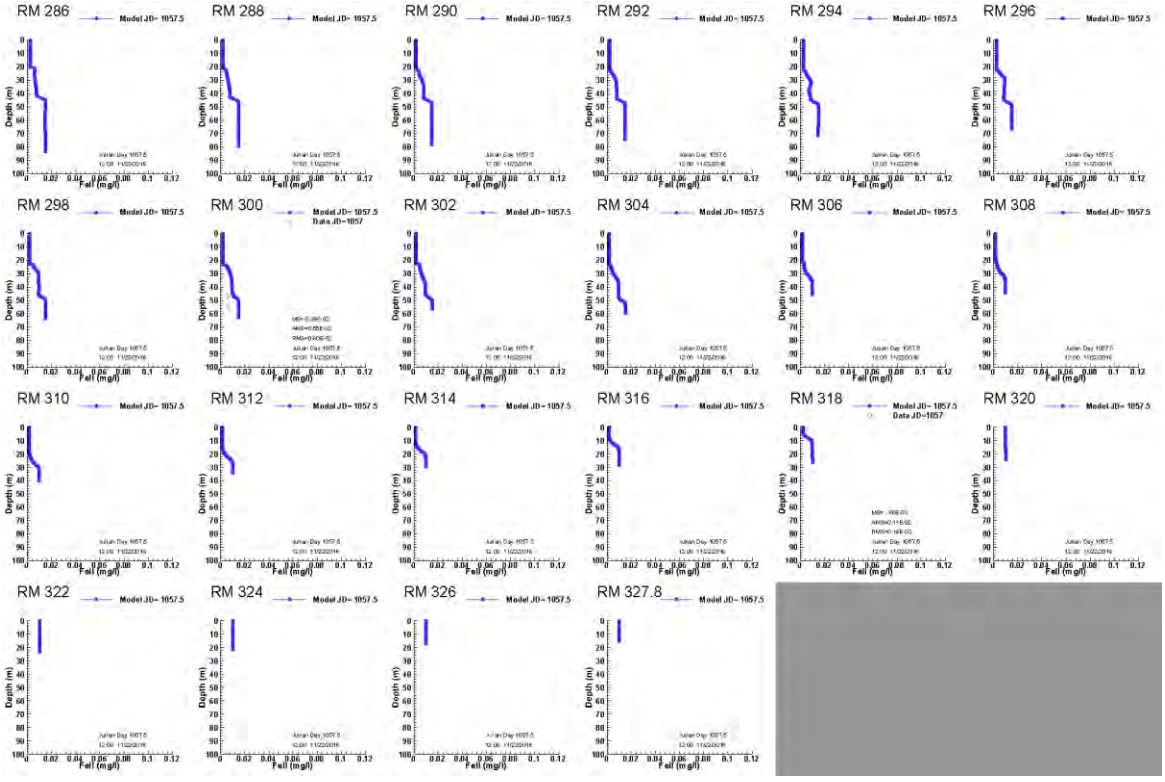


Figure 392. Vertical profiles of Fe(II) compared with data for 11/22/2016.

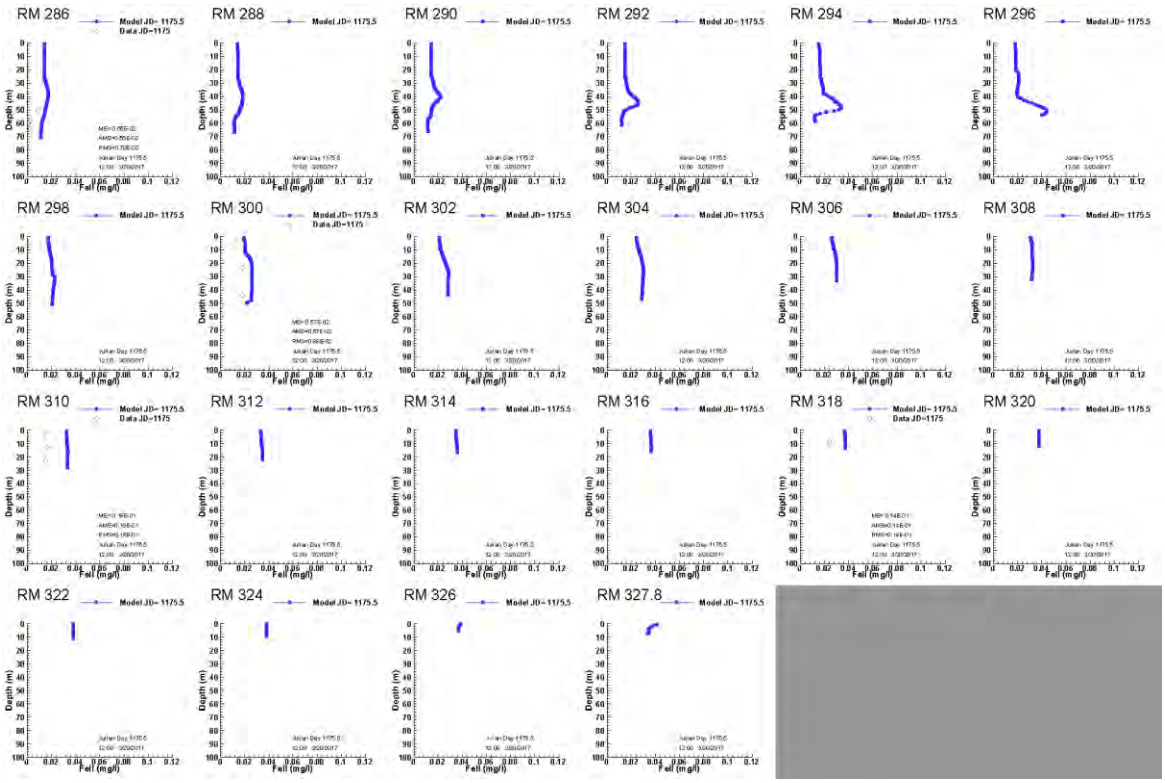


Figure 393. Vertical profiles of Fe(II) compared with data for 3/20/2017.

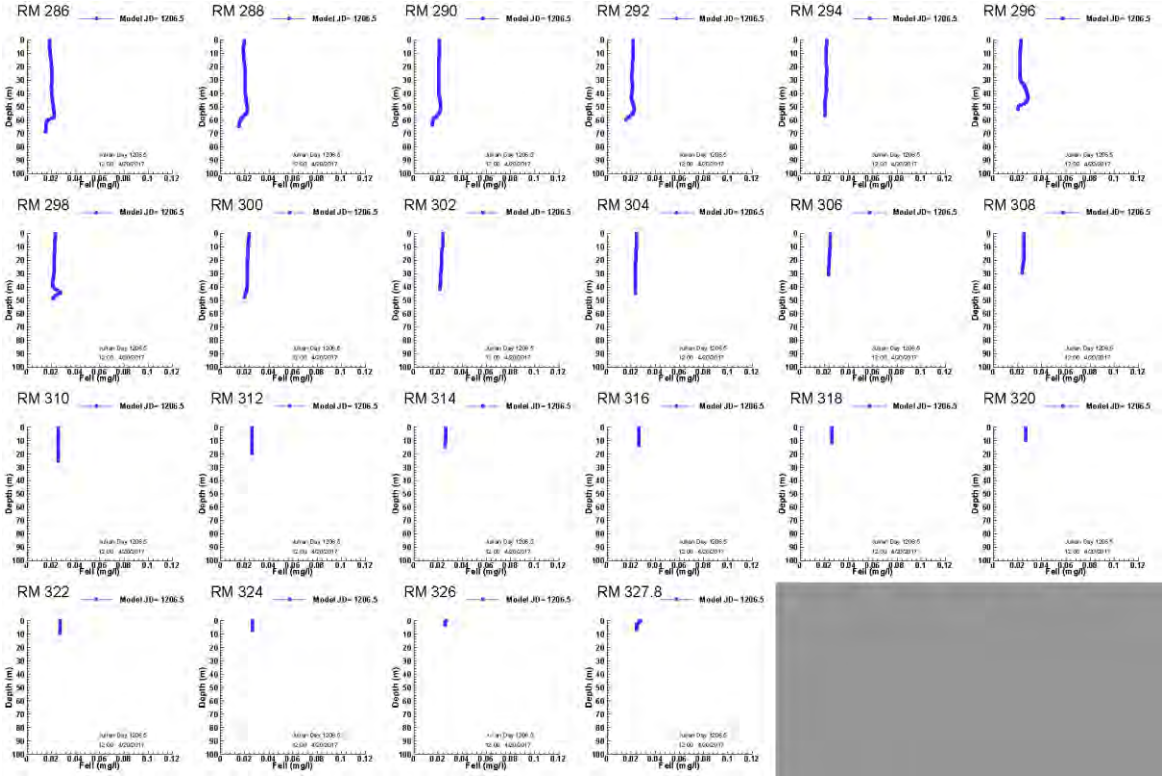


Figure 394. Vertical profiles of Fe(II) compared with data for 4/20/2017.

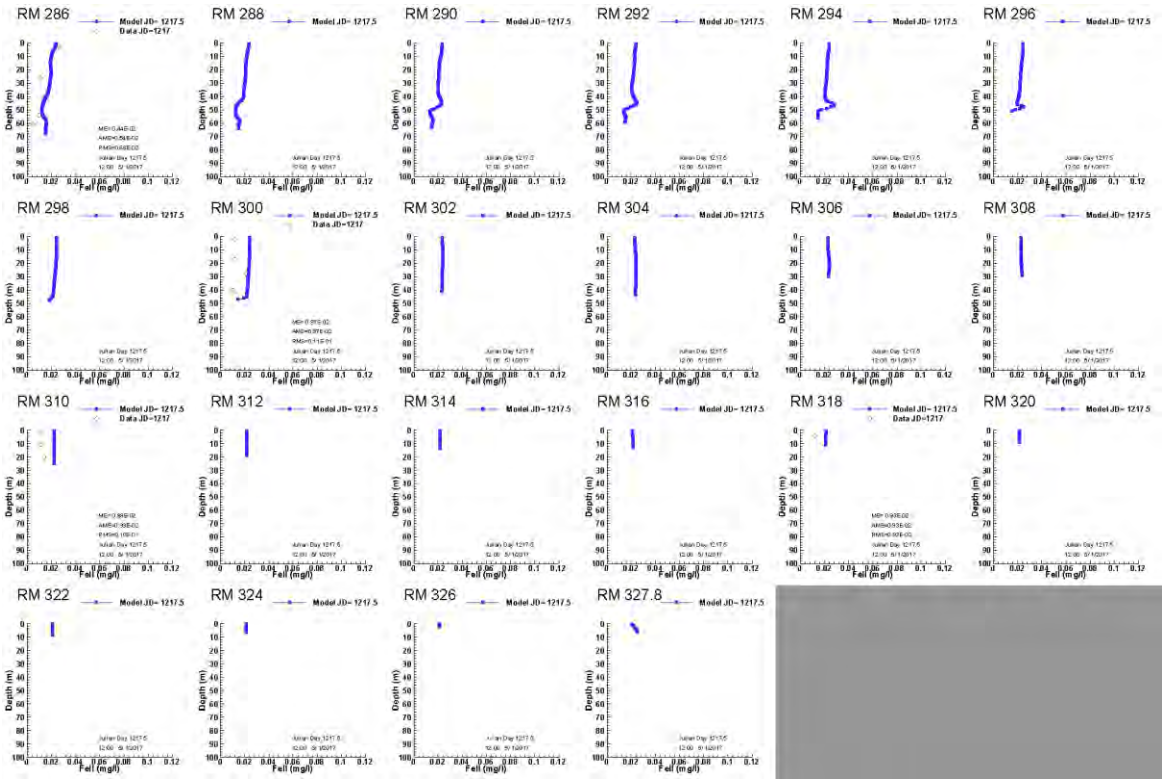


Figure 395. Vertical profiles of Fe(II) compared with data for 5/ 1/2017.

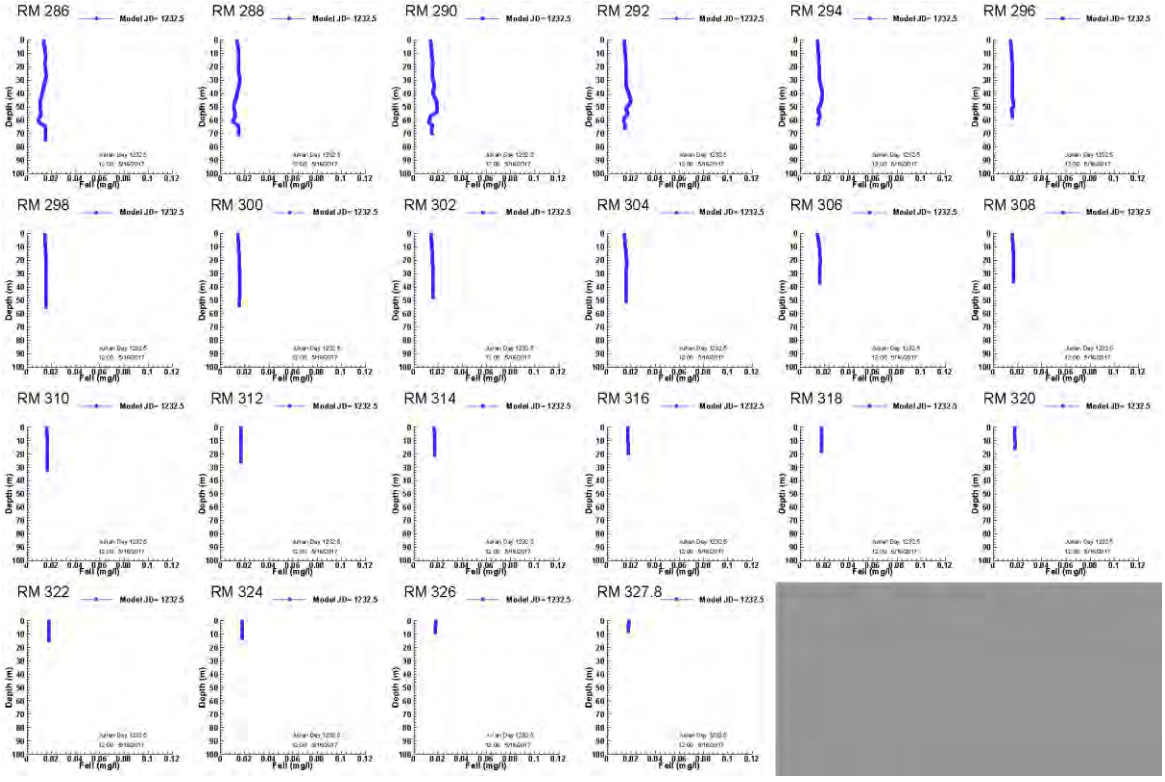


Figure 396. Vertical profiles of Fe(II) compared with data for 5/16/2017.

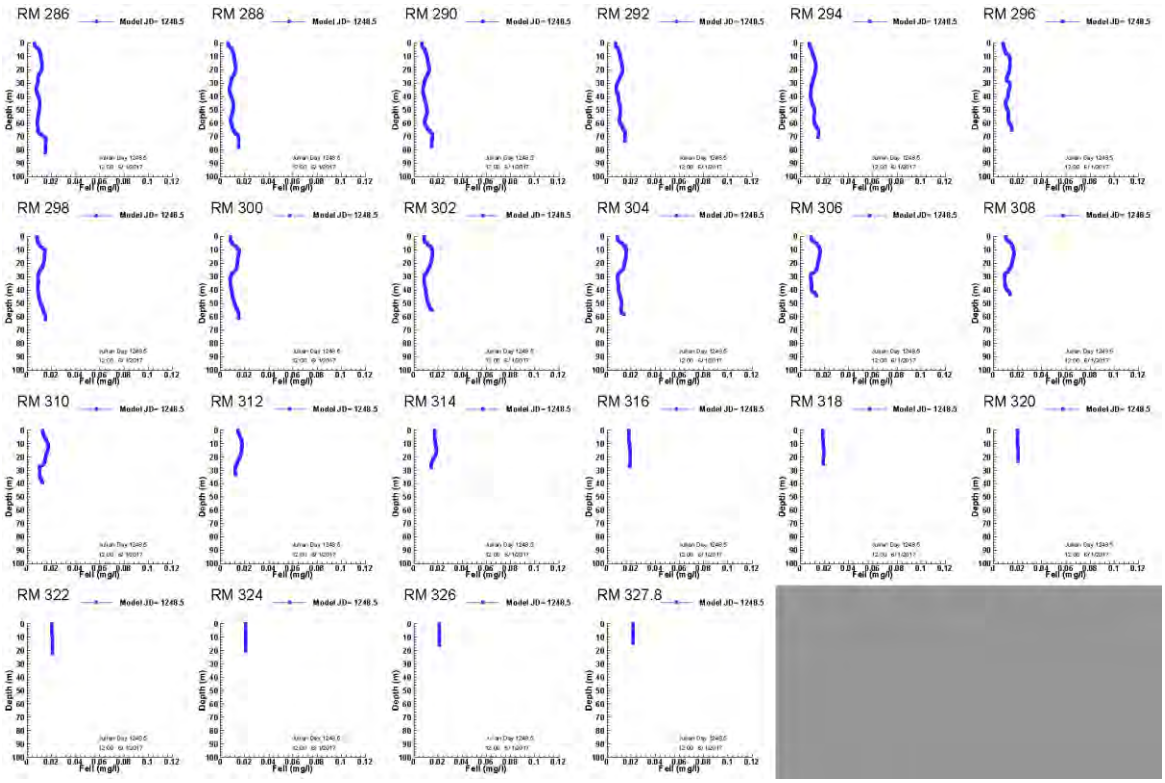


Figure 397. Vertical profiles of Fe(II) compared with data for 6/ 1/2017.

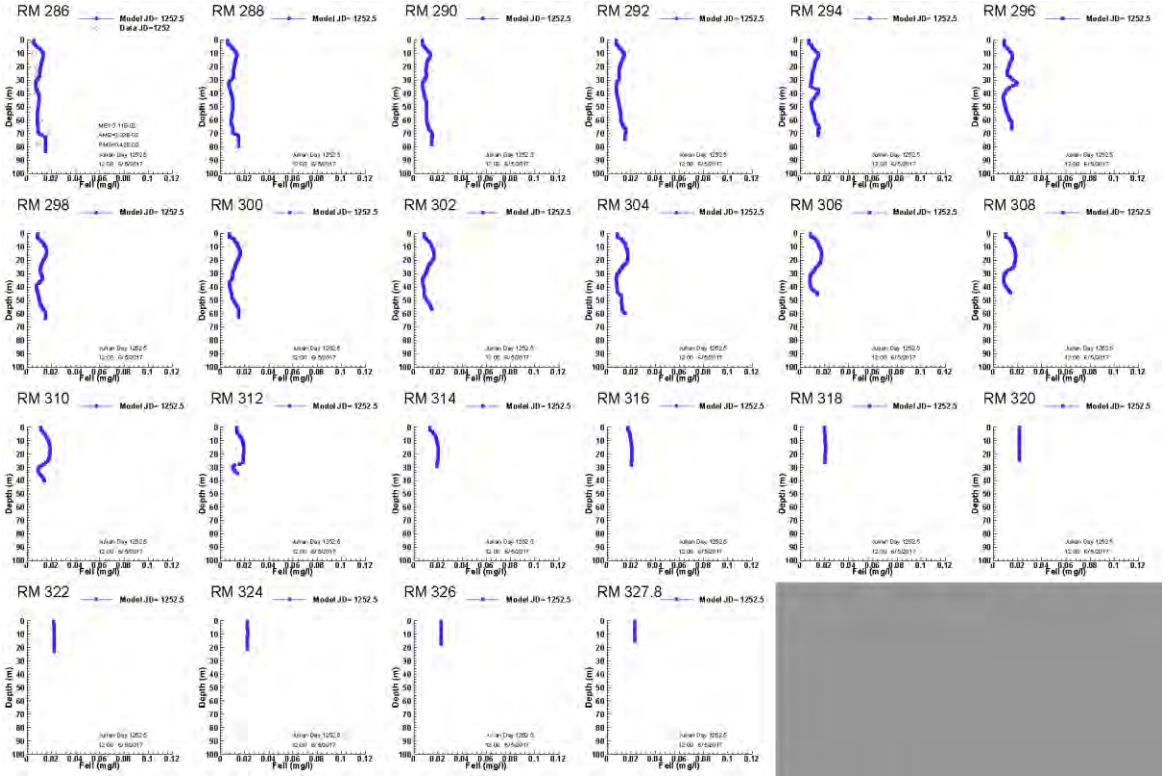


Figure 398. Vertical profiles of Fe(II) compared with data for 6/ 5/2017.

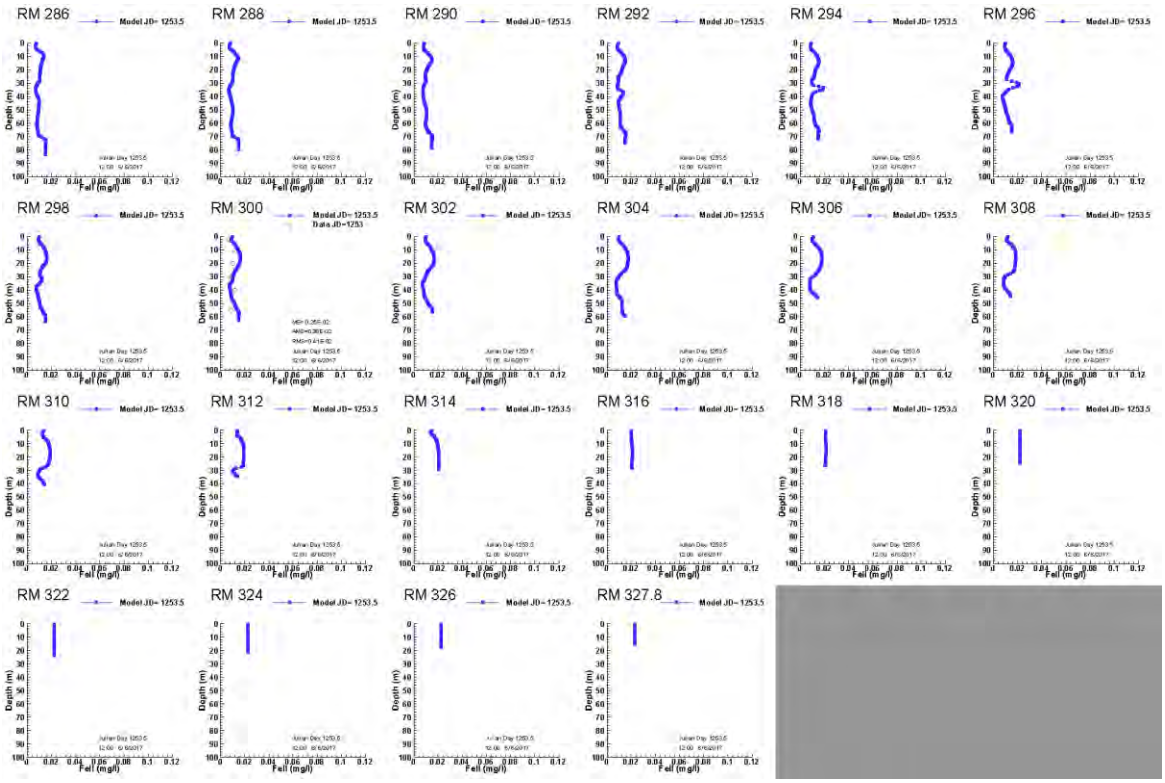


Figure 399. Vertical profiles of Fe(II) compared with data for 6/ 6/2017.

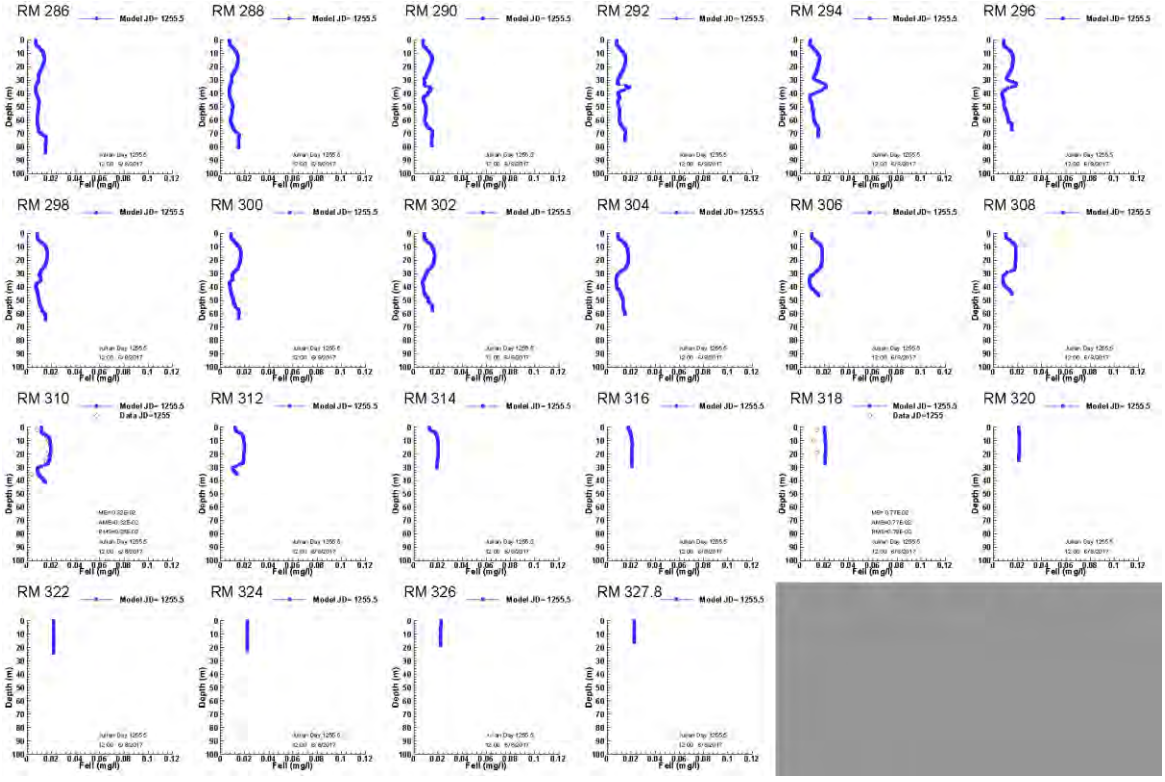


Figure 400. Vertical profiles of Fe(II) compared with data for 6/ 8/2017.

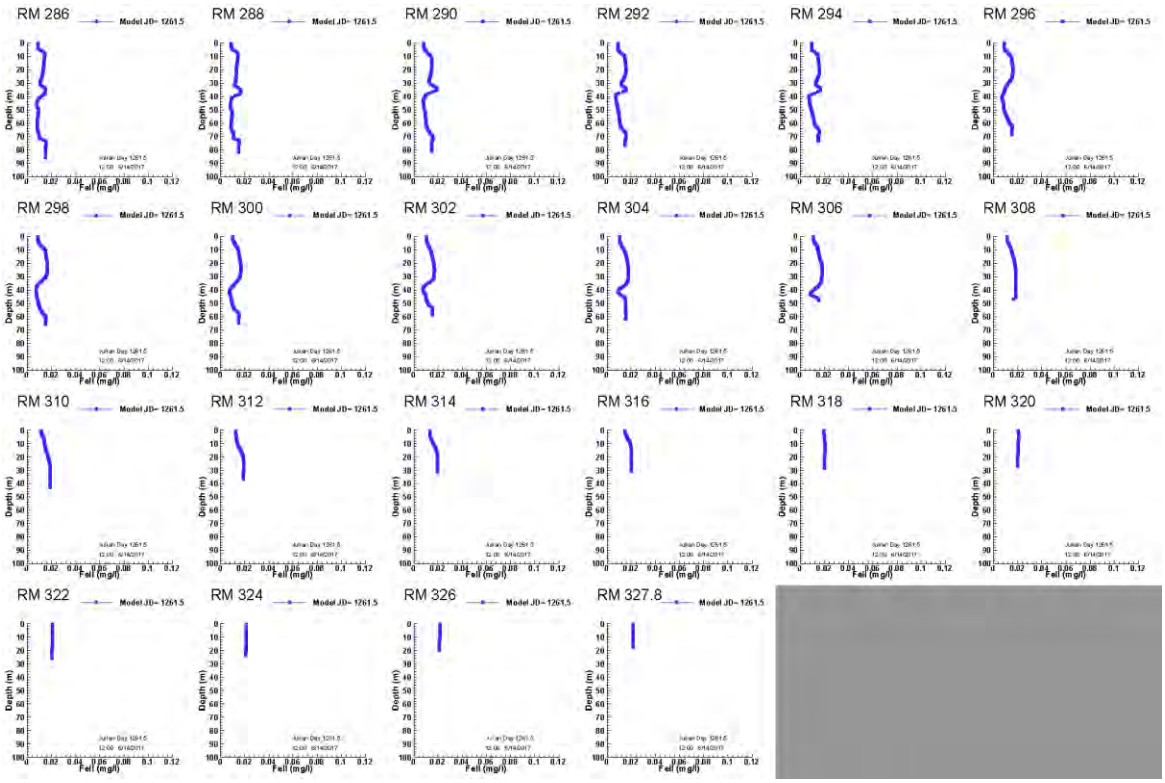


Figure 401. Vertical profiles of Fe(II) compared with data for 6/14/2017.

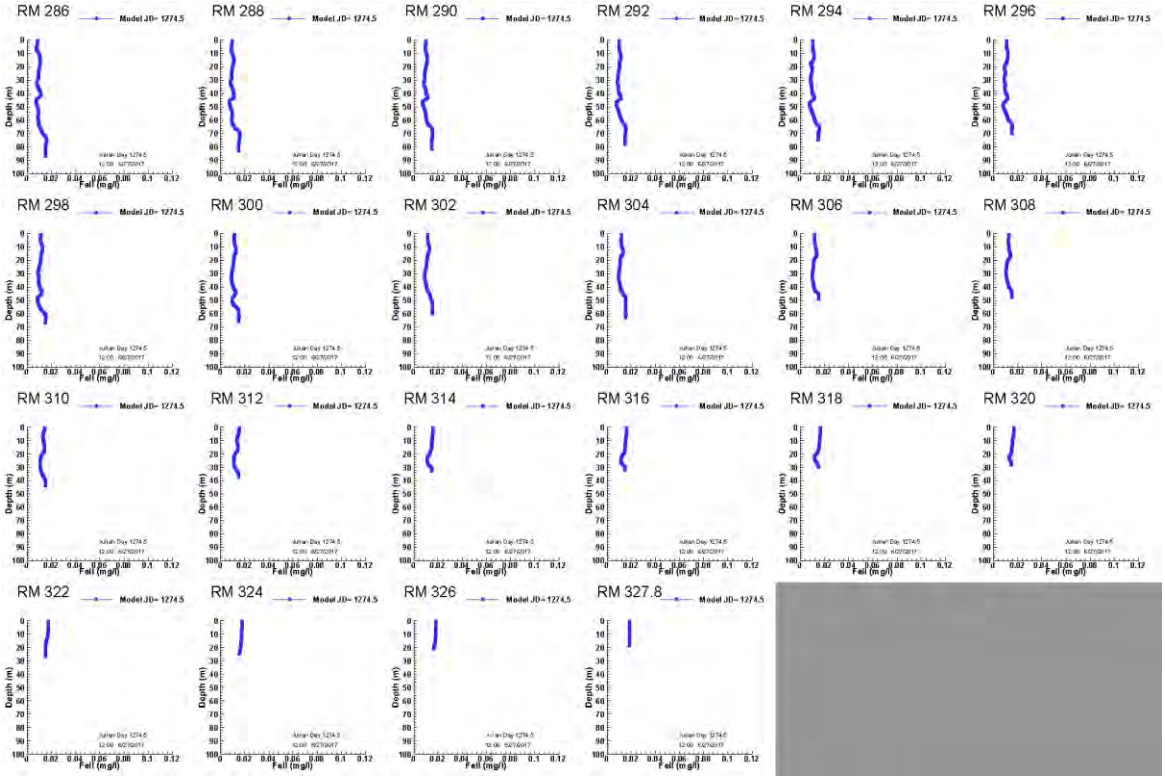


Figure 402. Vertical profiles of Fe(II) compared with data for 6/27/2017.

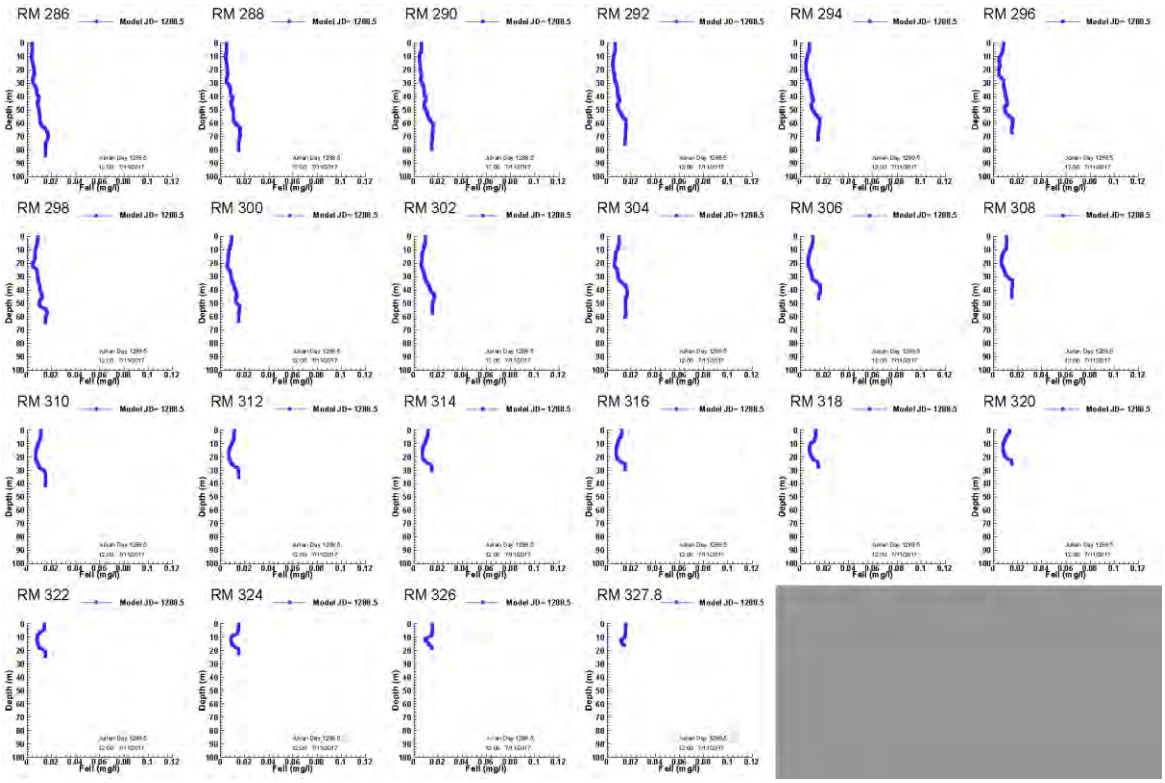


Figure 403. Vertical profiles of Fe(II) compared with data for 7/11/2017.

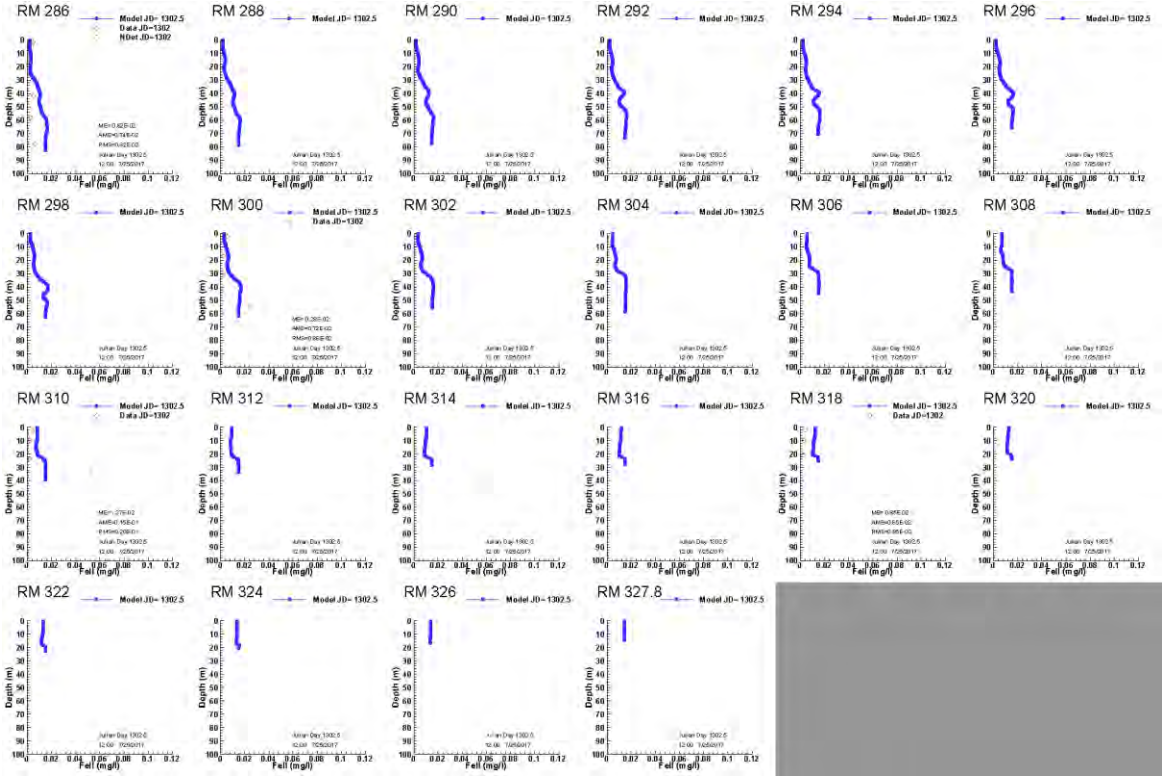


Figure 404. Vertical profiles of Fe(II) compared with data for 7/25/2017.

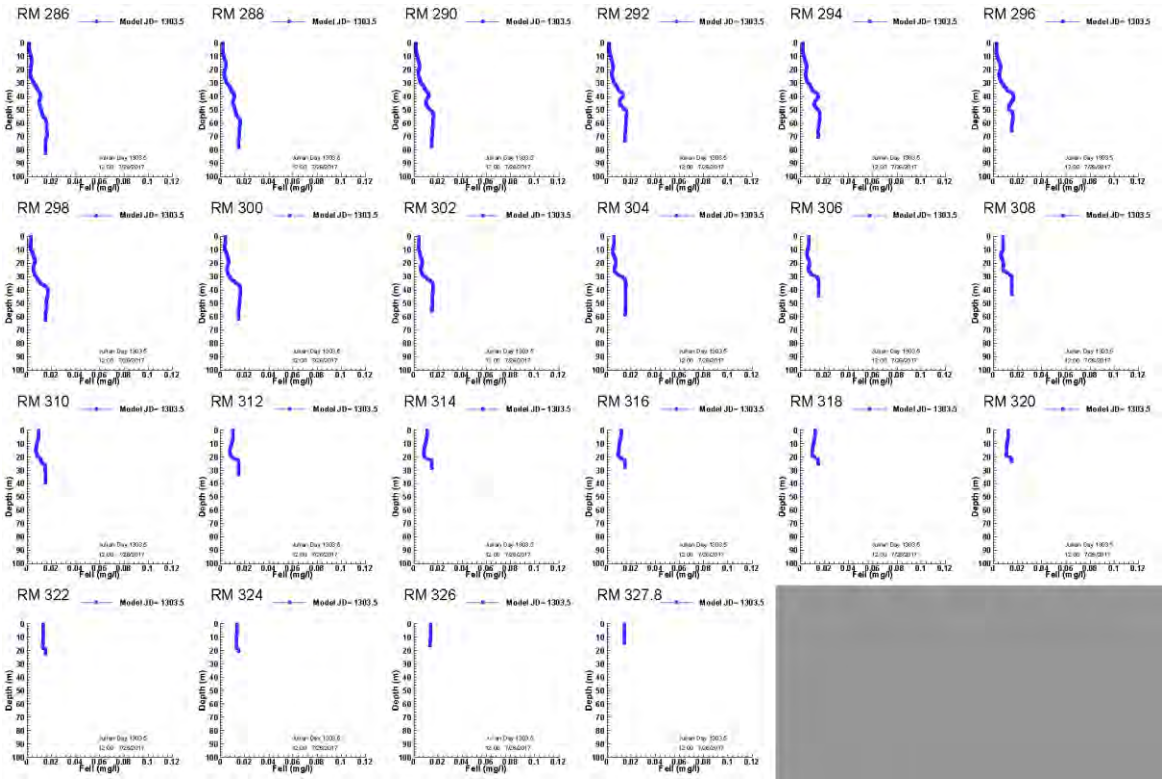


Figure 405. Vertical profiles of Fe(II) compared with data for 7/26/2017.

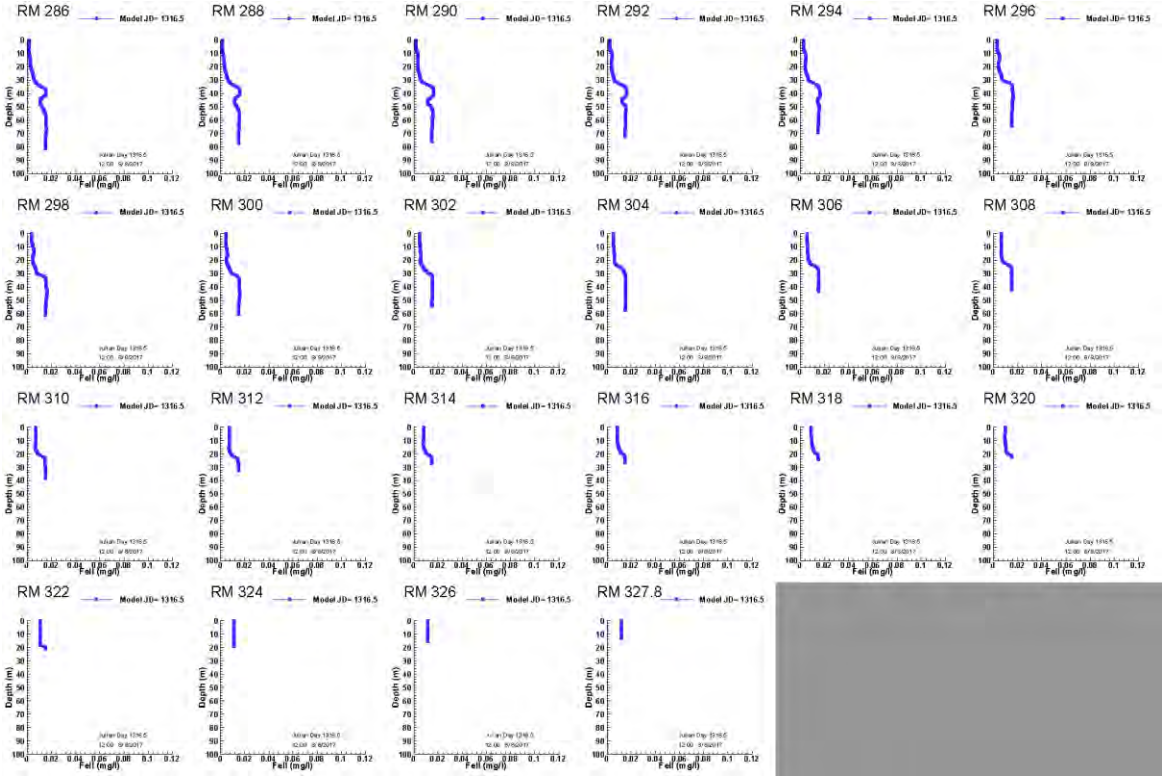


Figure 406. Vertical profiles of Fe(II) compared with data for 8/ 8/2017.

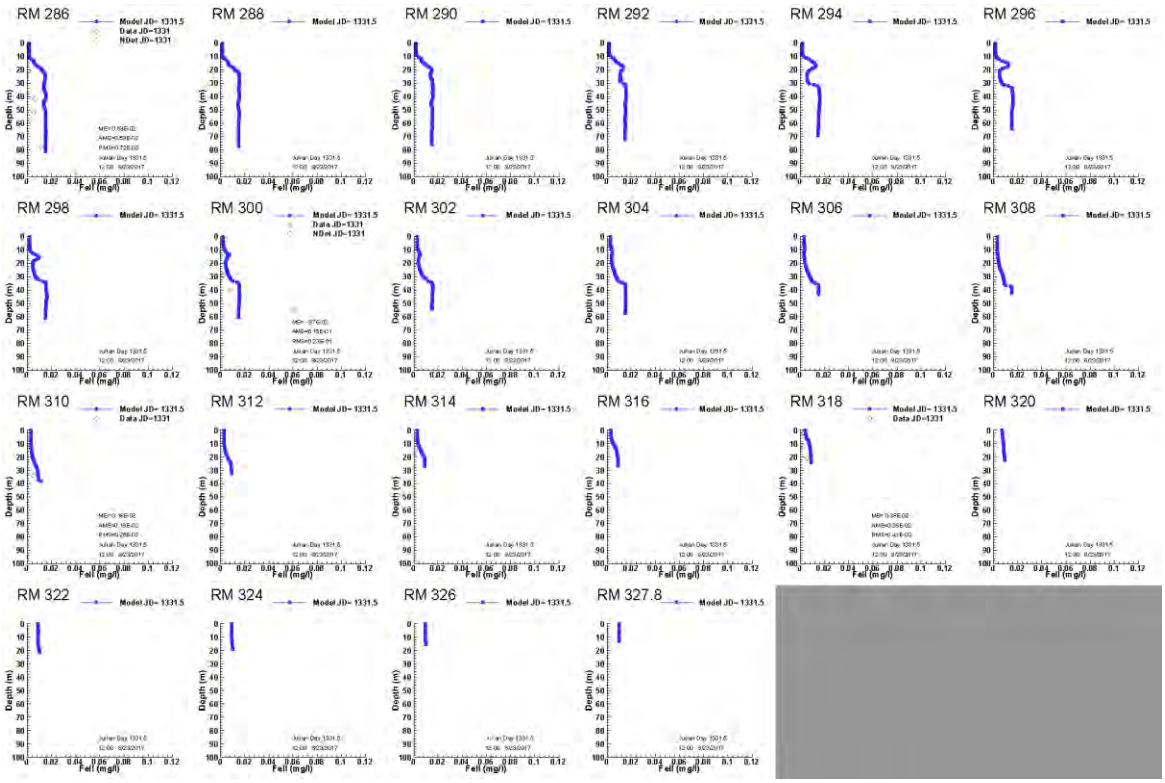


Figure 407. Vertical profiles of Fe(II) compared with data for 8/23/2017.

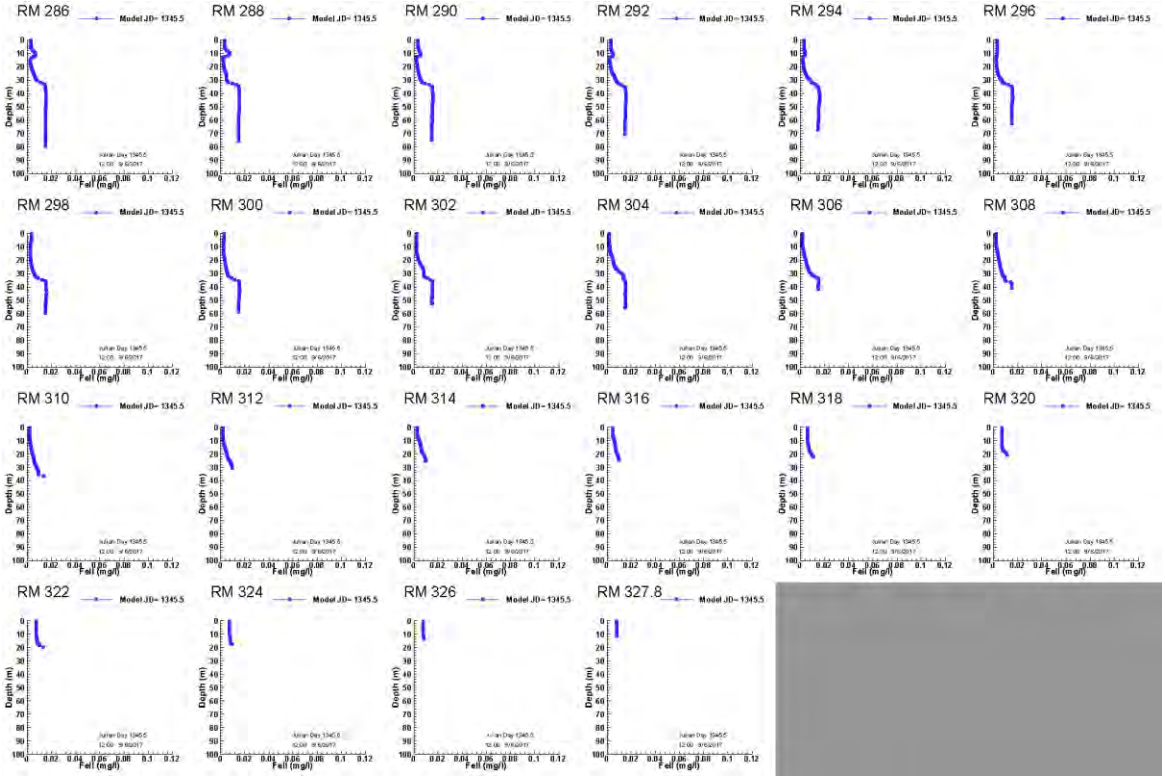


Figure 408. Vertical profiles of Fe(II) compared with data for 9/ 6/2017.

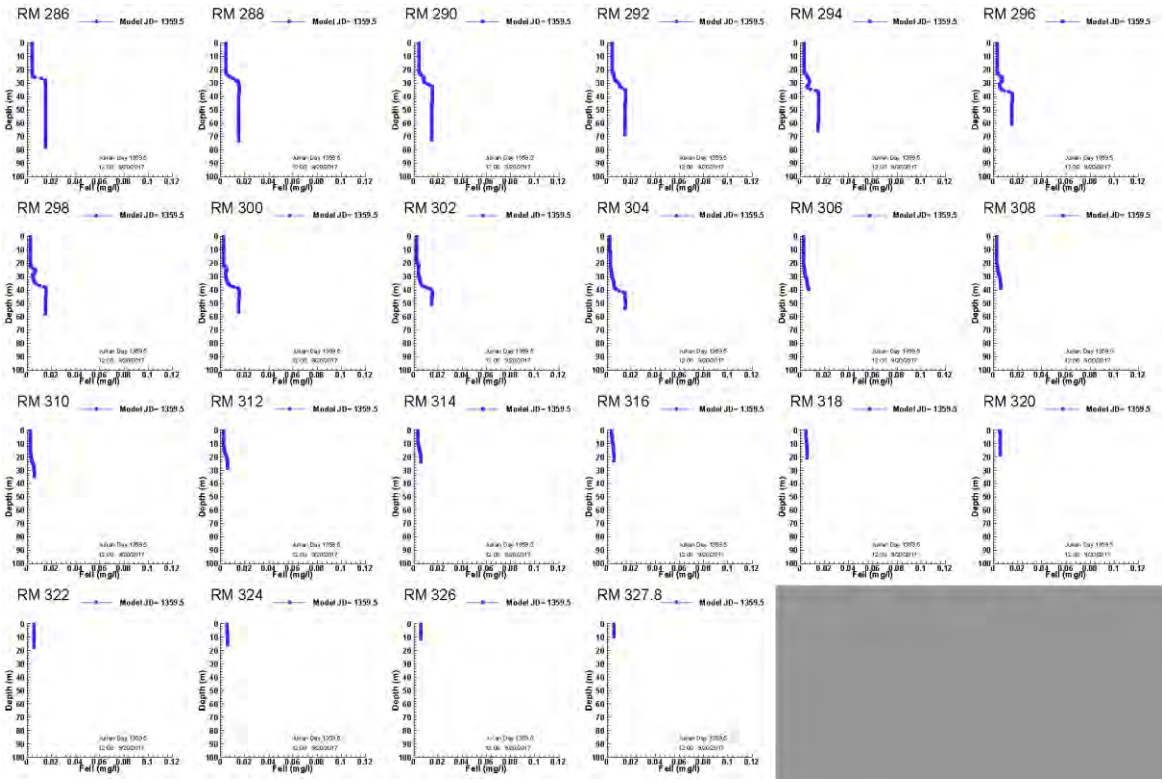


Figure 409. Vertical profiles of Fe(II) compared with data for 9/20/2017.

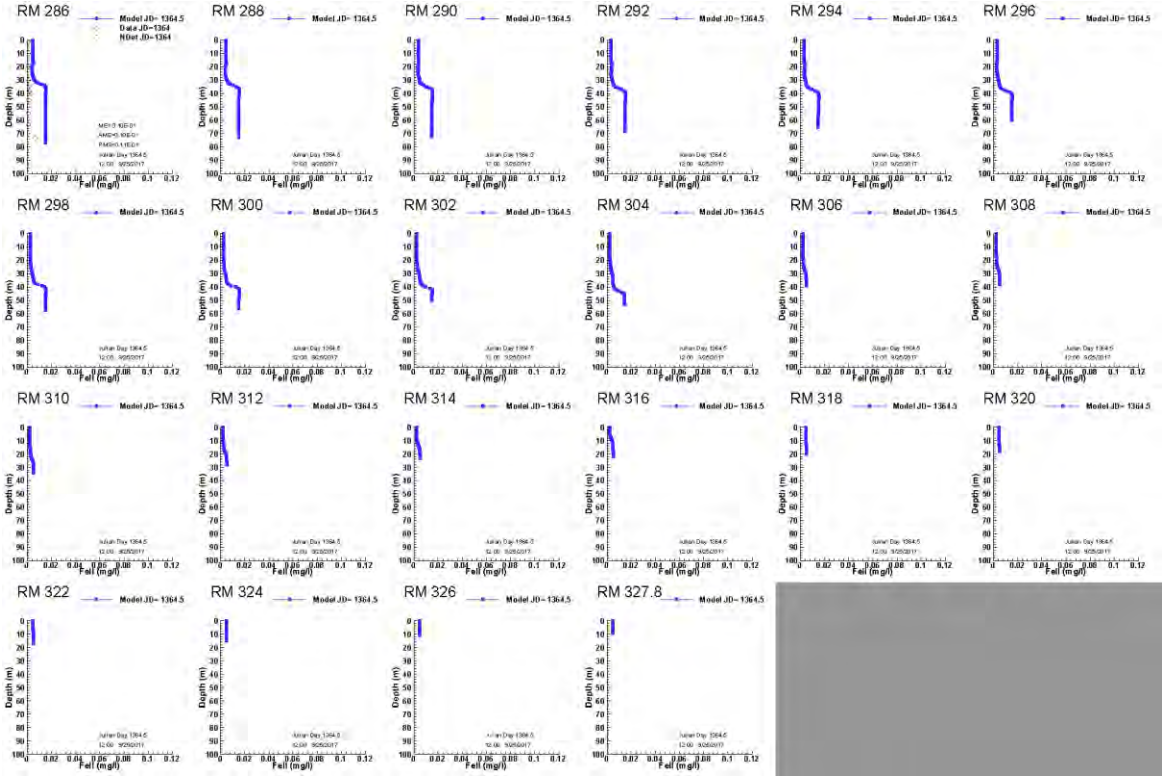


Figure 410. Vertical profiles of Fe(II) compared with data for 9/25/2017.

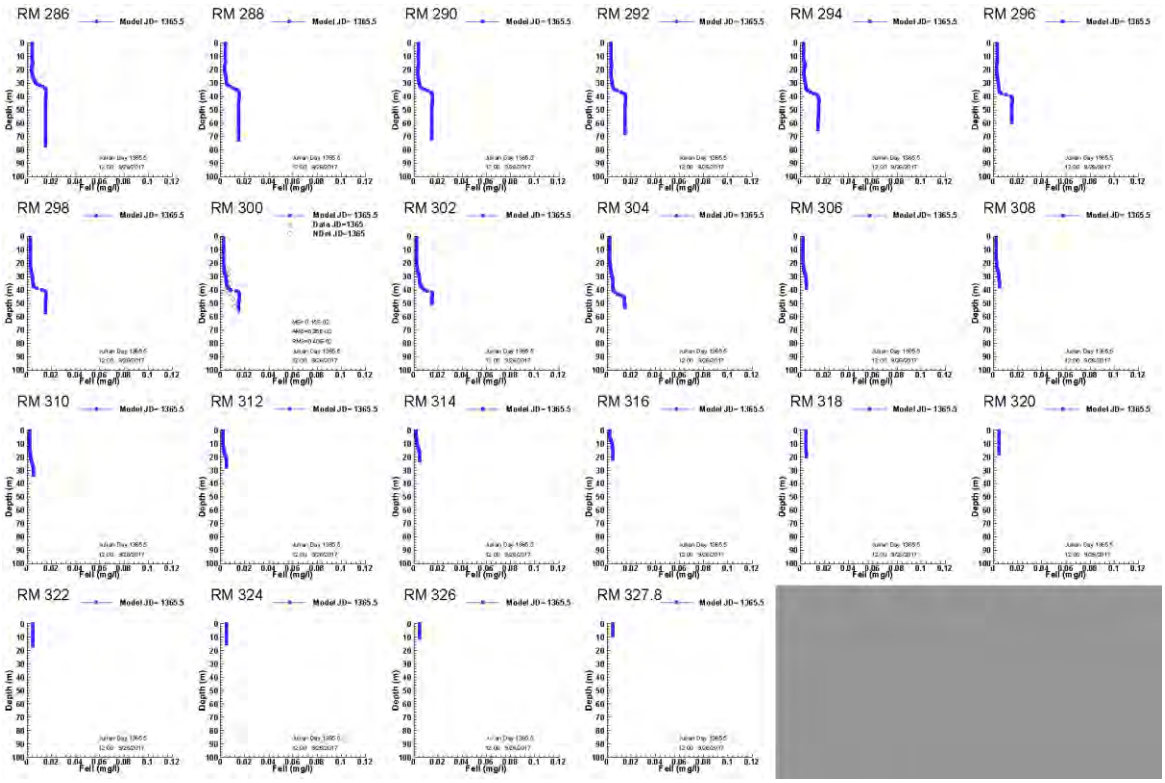


Figure 411. Vertical profiles of Fe(II) compared with data for 9/26/2017.

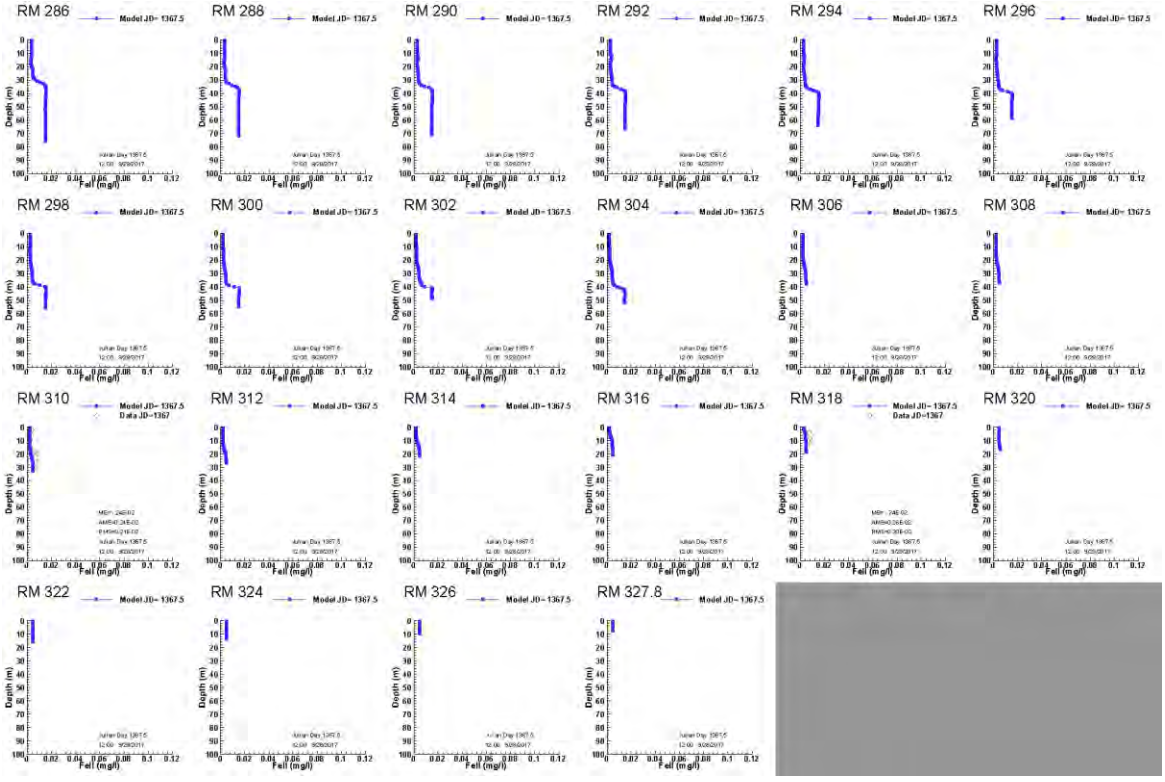


Figure 412. Vertical profiles of Fe(II) compared with data for 9/28/2017.

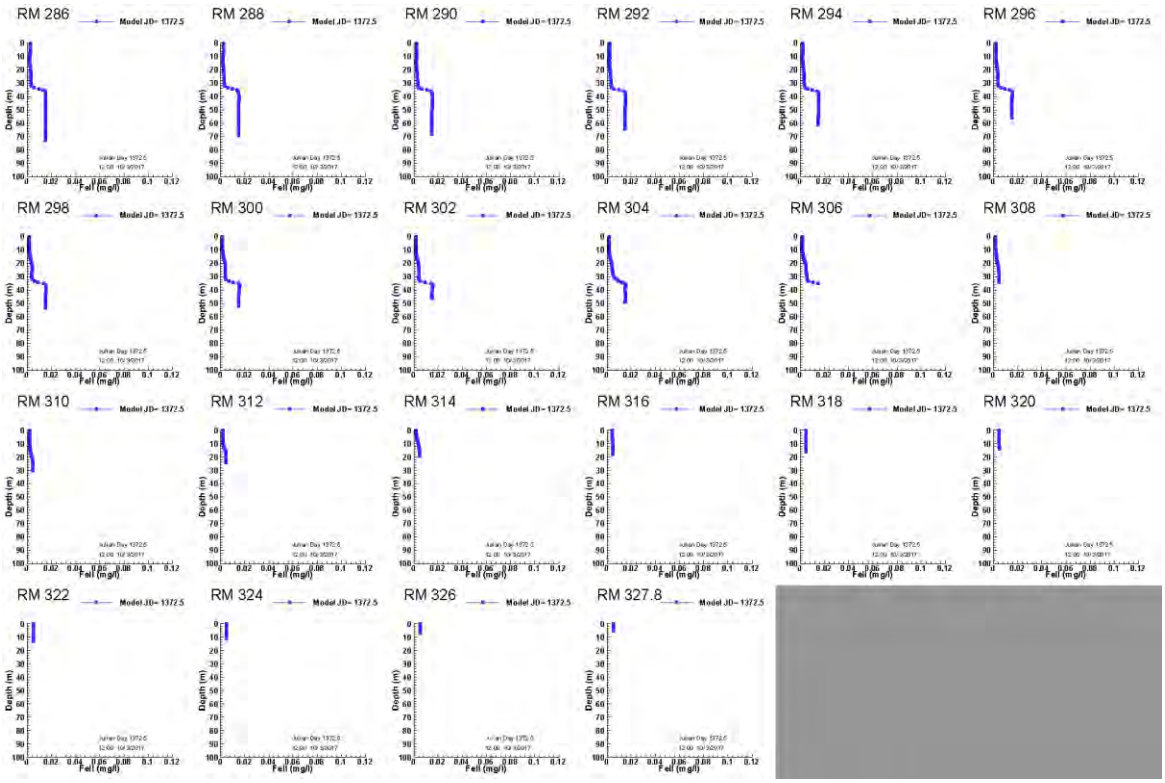


Figure 413. Vertical profiles of Fe(II) compared with data for 10/ 3/2017.

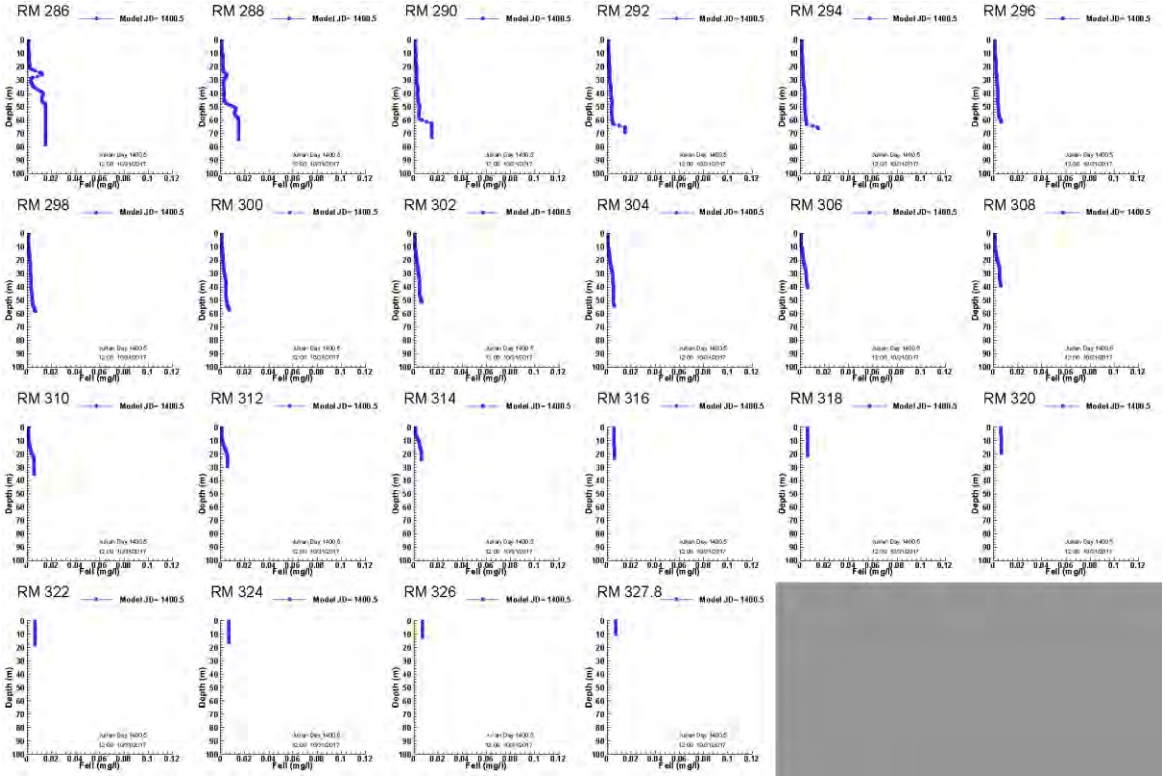


Figure 414. Vertical profiles of Fe(II) compared with data for 10/31/2017.

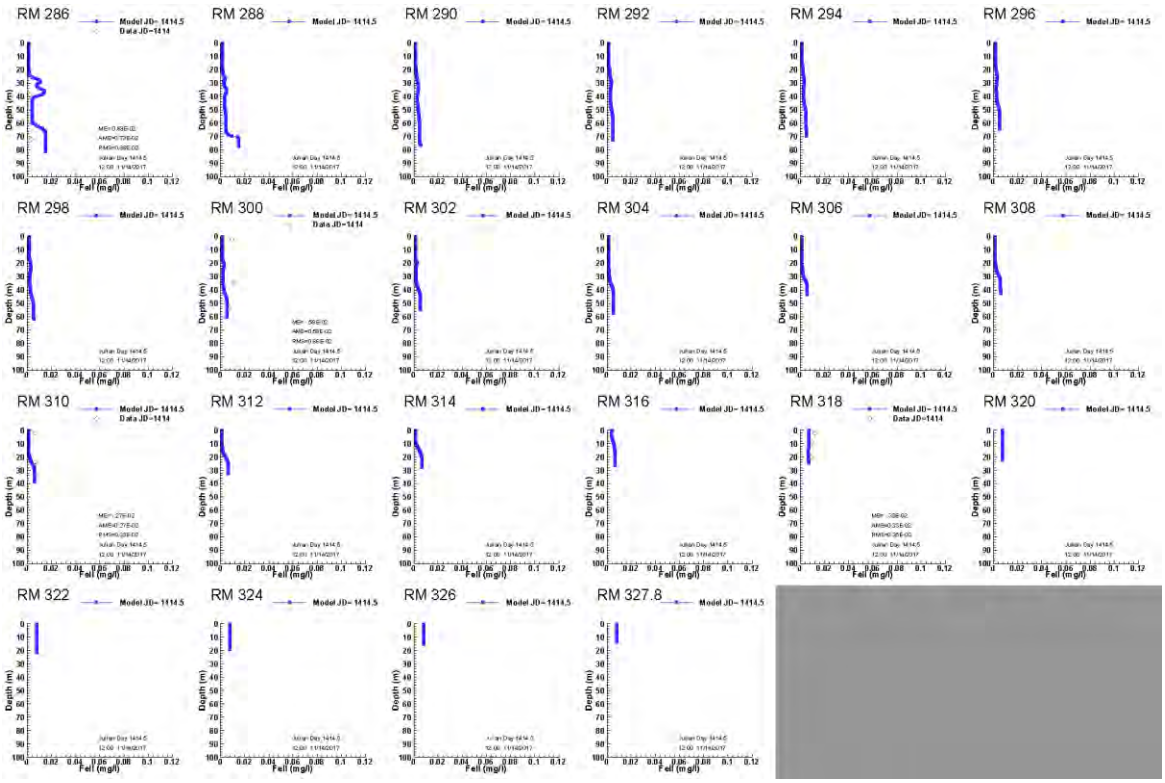


Figure 415. Vertical profiles of Fe(II) compared with data for 11/14/2017.

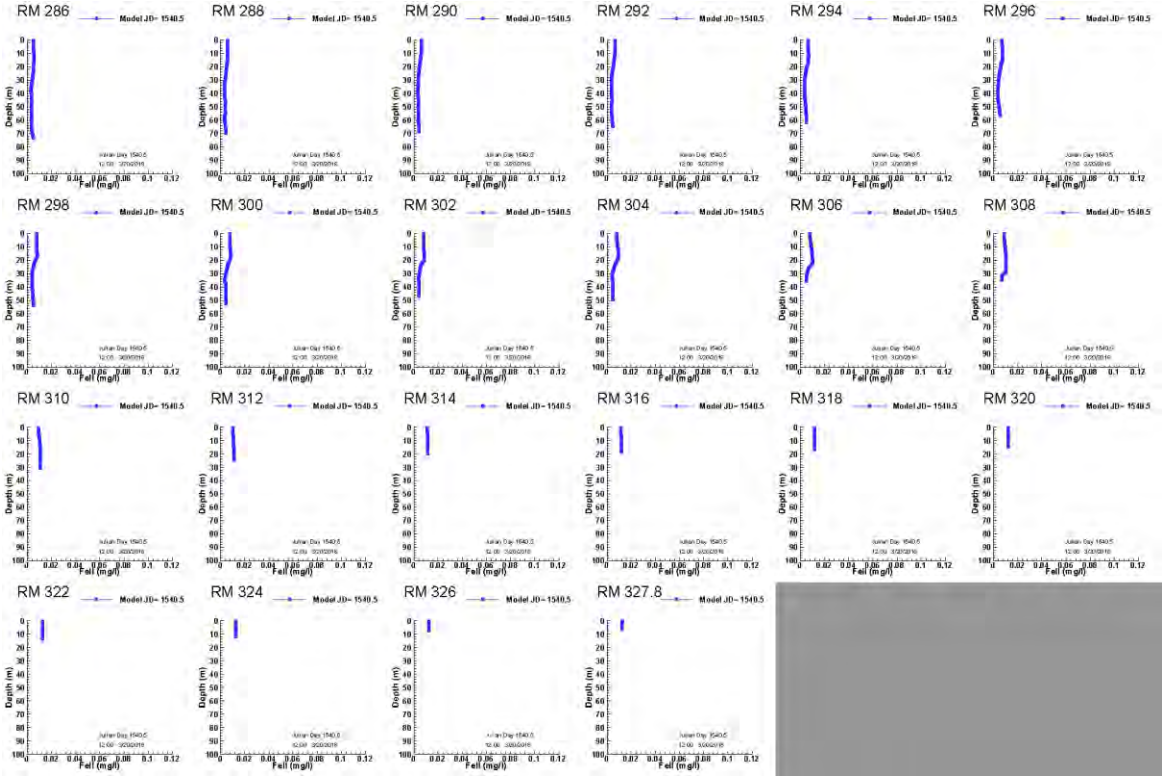


Figure 416. Vertical profiles of Fe(II) compared with data for 3/20/2018.

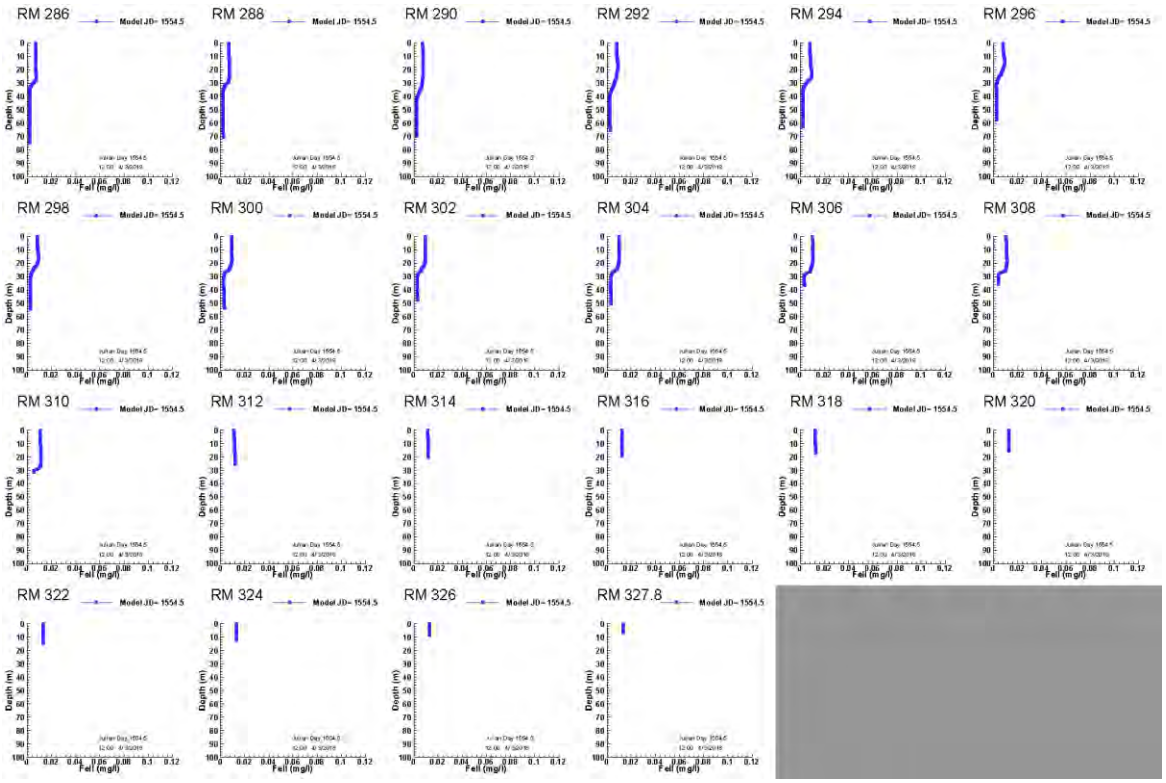


Figure 417. Vertical profiles of Fe(II) compared with data for 4/ 3/2018.

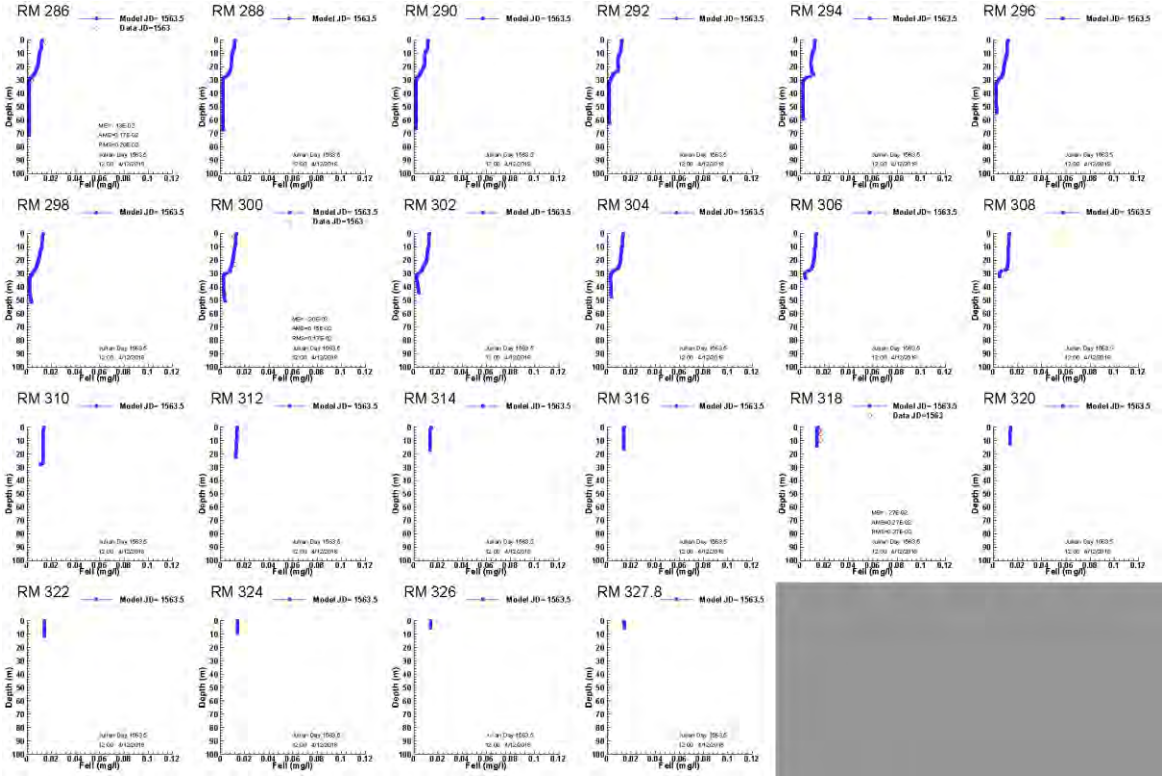


Figure 418. Vertical profiles of Fe(II) compared with data for 4/12/2018.

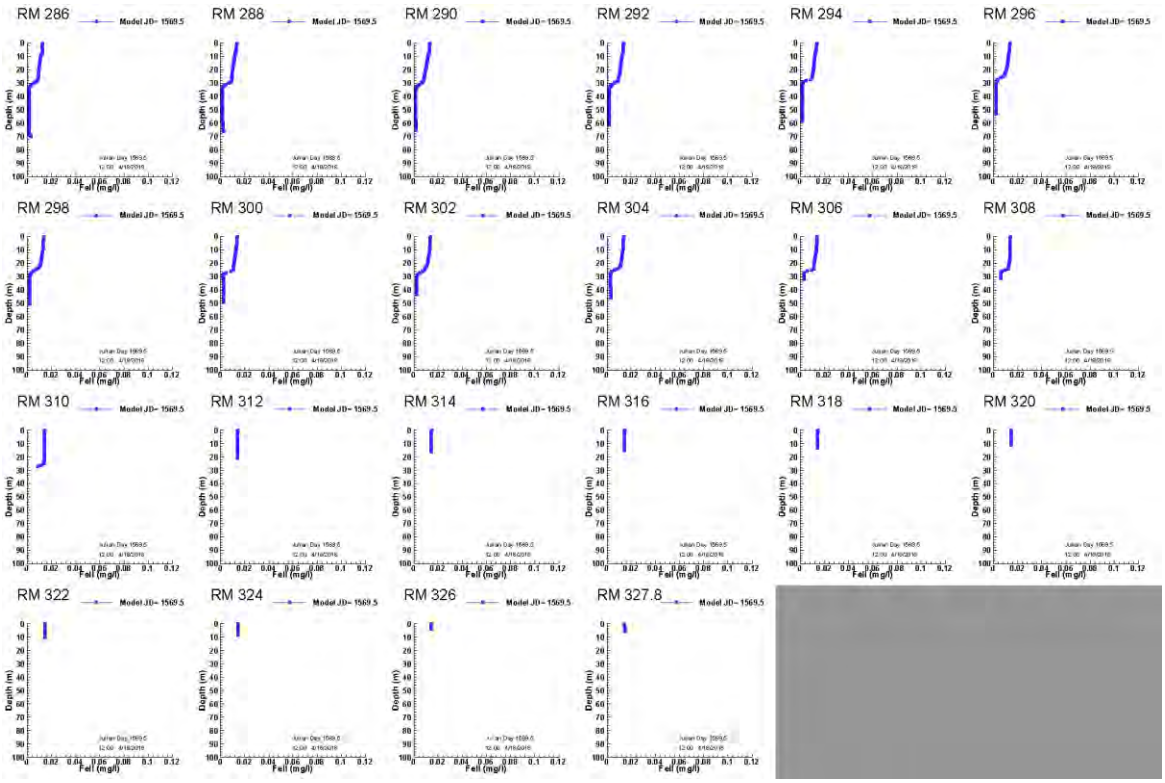


Figure 419. Vertical profiles of Fe(II) compared with data for 4/18/2018.

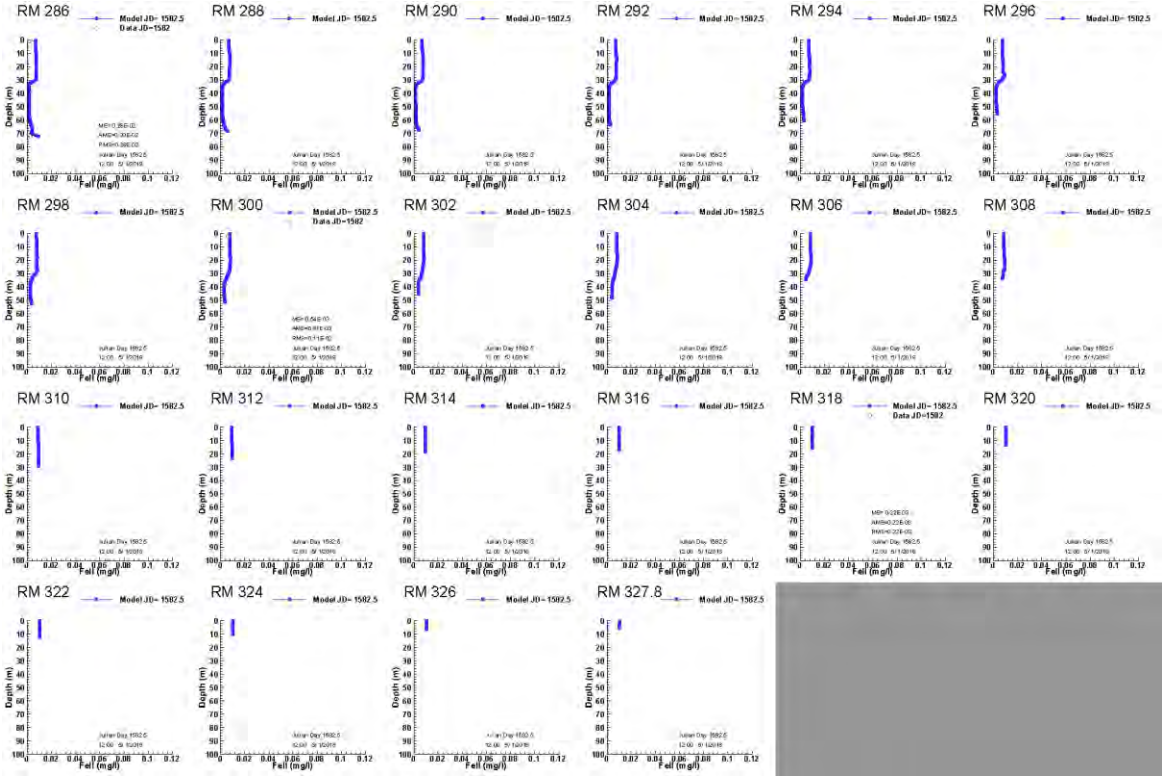


Figure 420. Vertical profiles of Fe(II) compared with data for 5/ 1/2018.

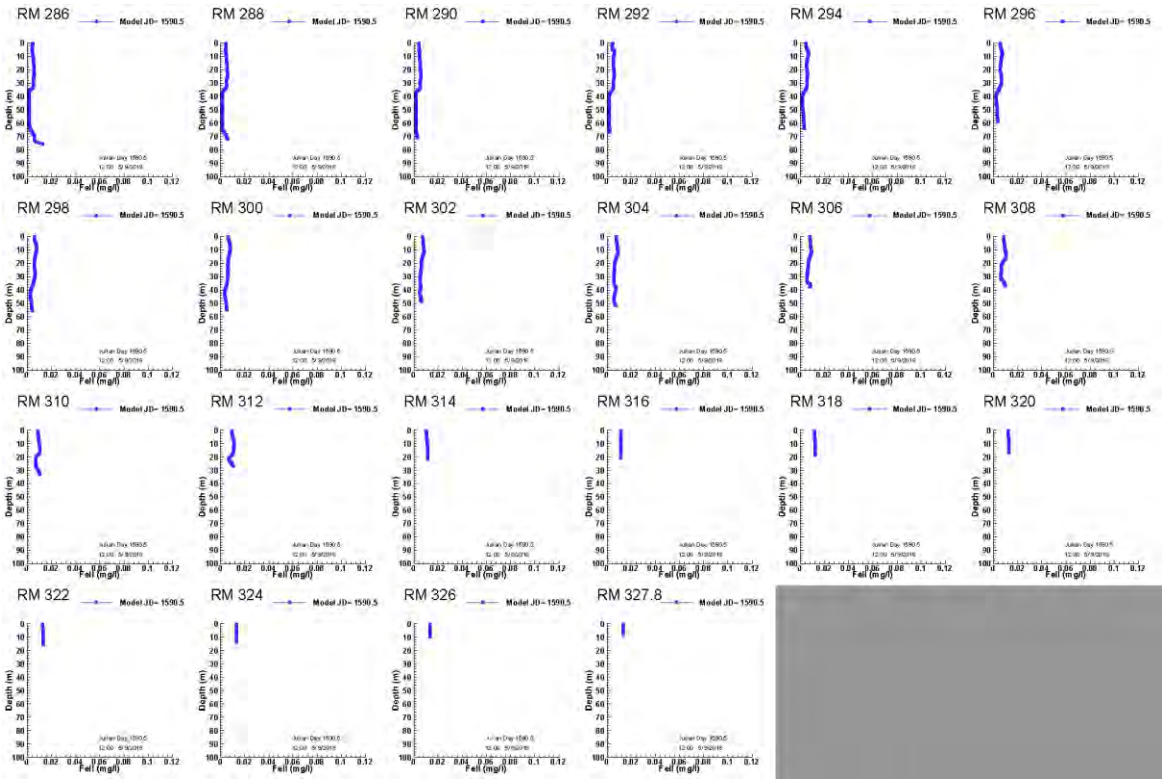


Figure 421. Vertical profiles of Fe(II) compared with data for 5/ 9/2018.

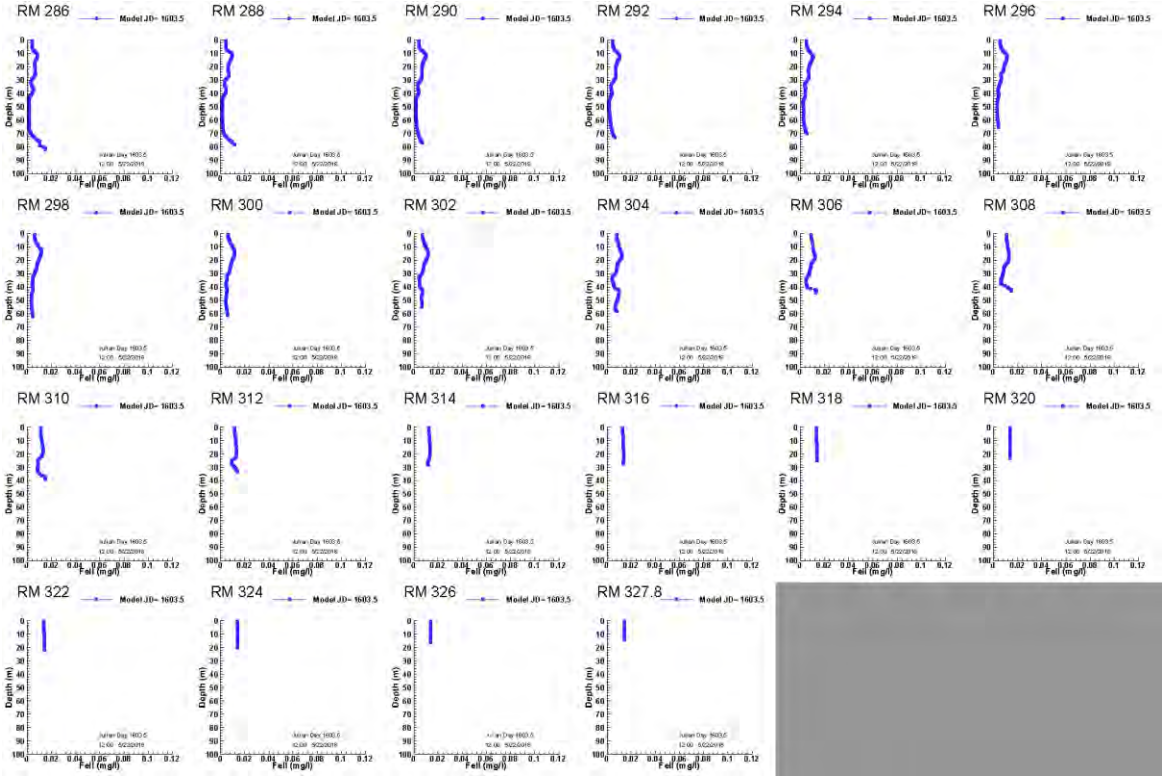


Figure 422. Vertical profiles of Fe(II) compared with data for 5/22/2018.

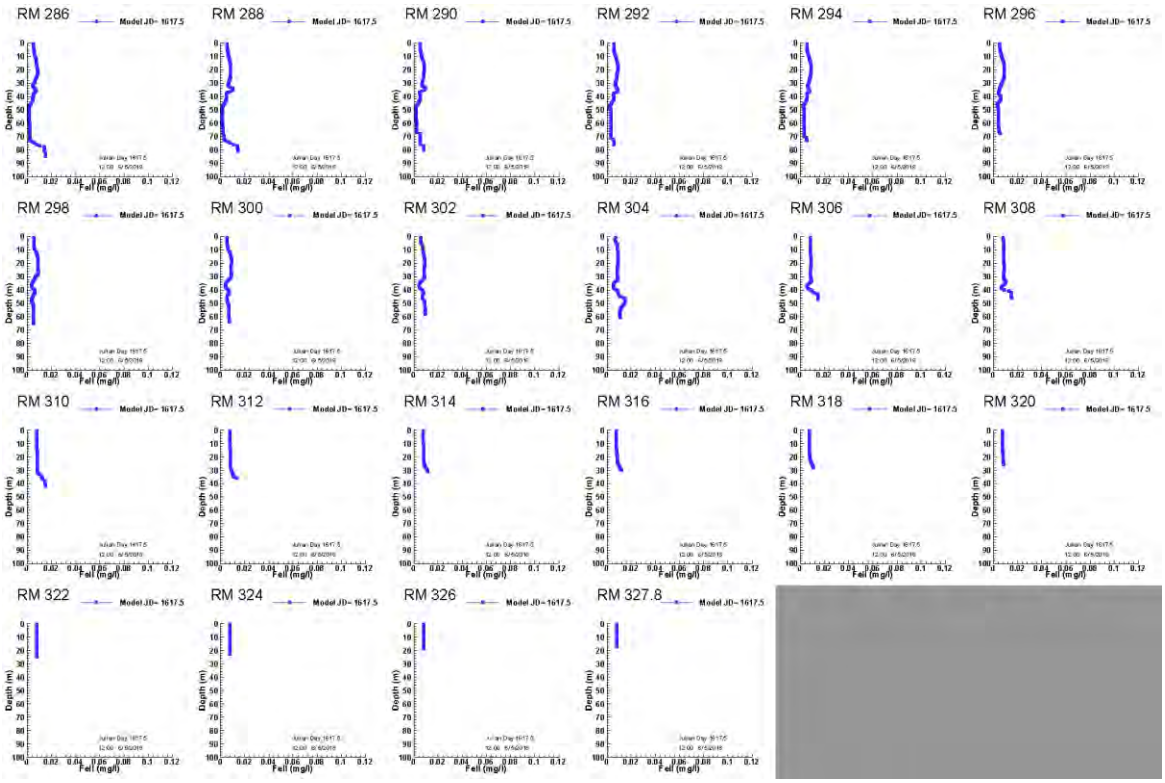


Figure 423. Vertical profiles of Fe(II) compared with data for 6/ 5/2018.

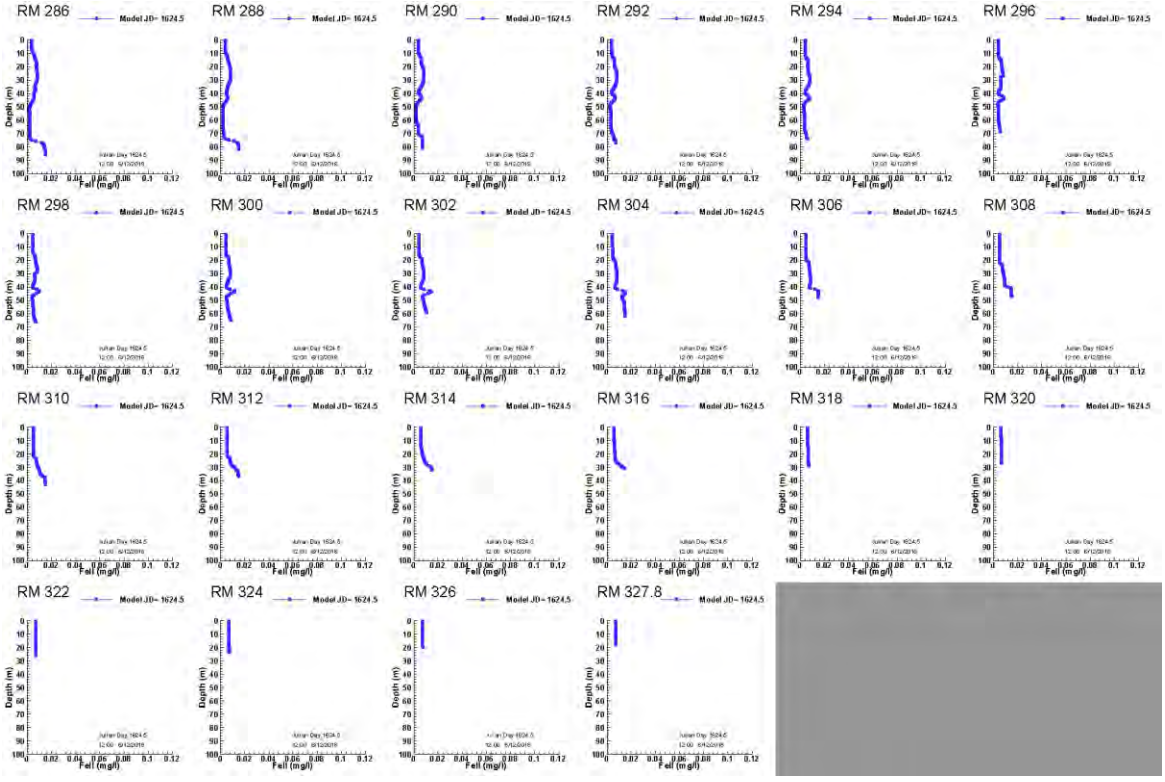


Figure 424. Vertical profiles of Fe(II) compared with data for 6/12/2018.

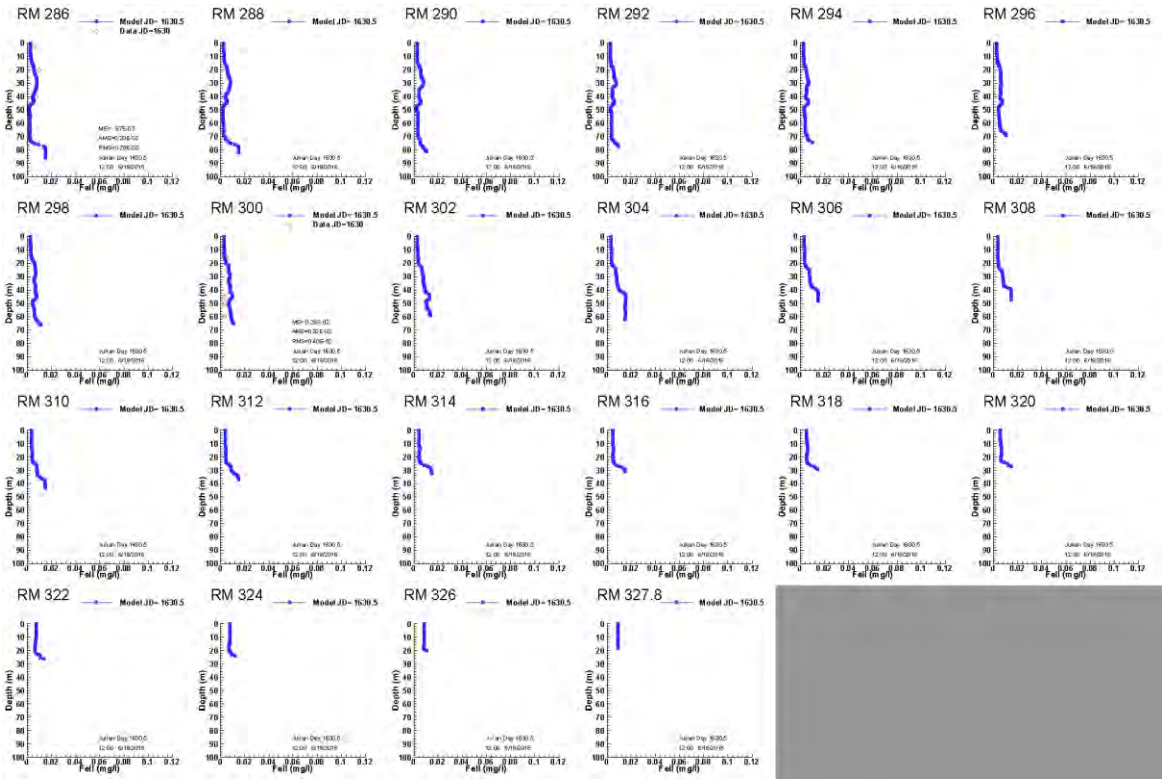


Figure 425. Vertical profiles of Fe(II) compared with data for 6/18/2018.

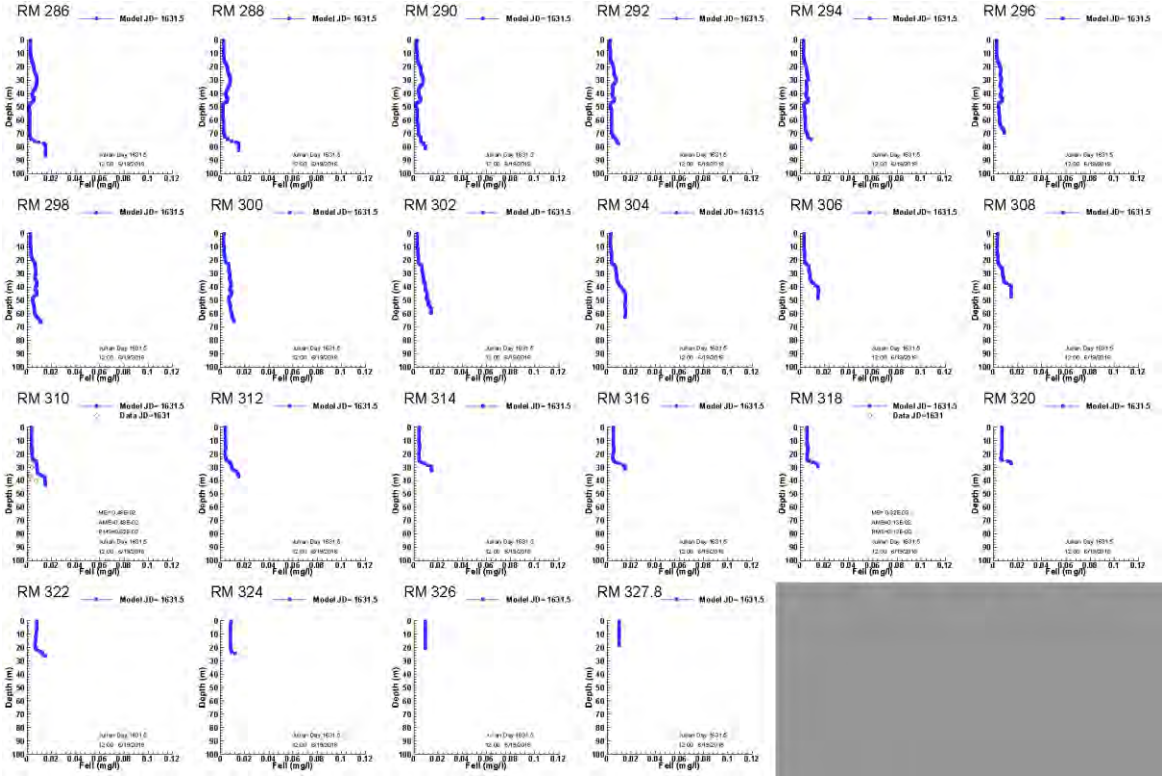


Figure 426. Vertical profiles of Fe(II) compared with data for 6/19/2018.

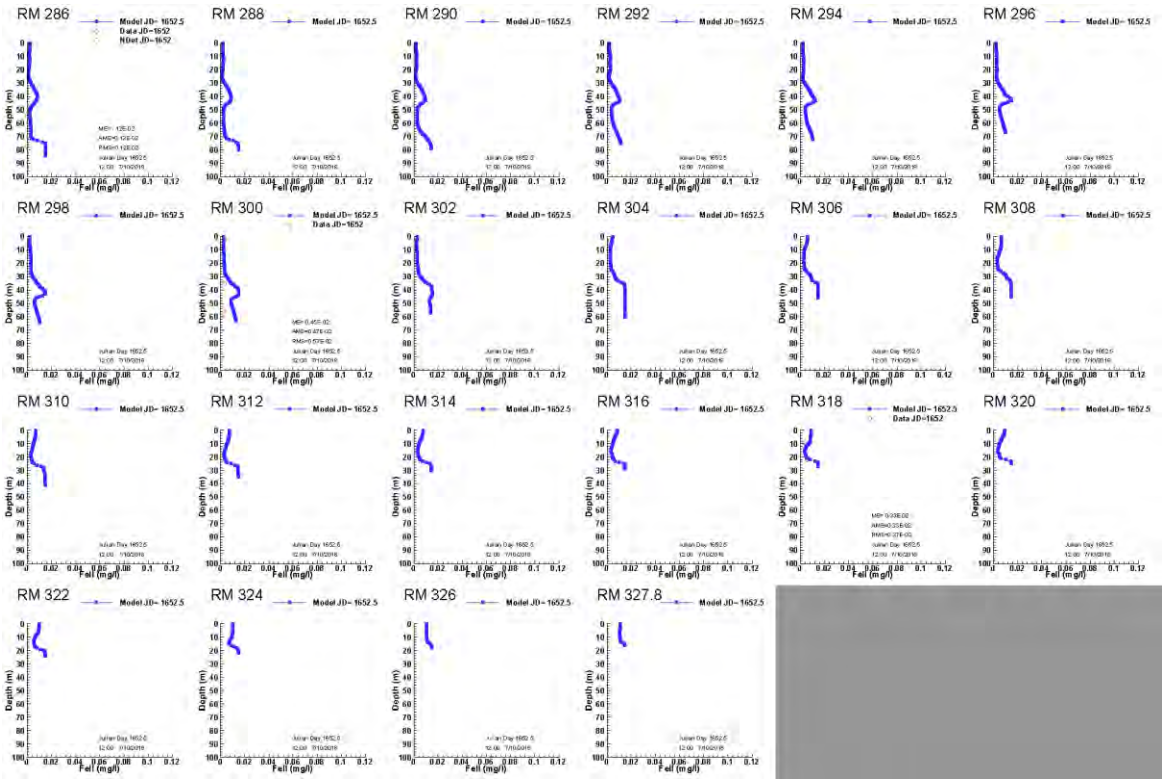


Figure 427. Vertical profiles of Fe(II) compared with data for 7/10/2018.

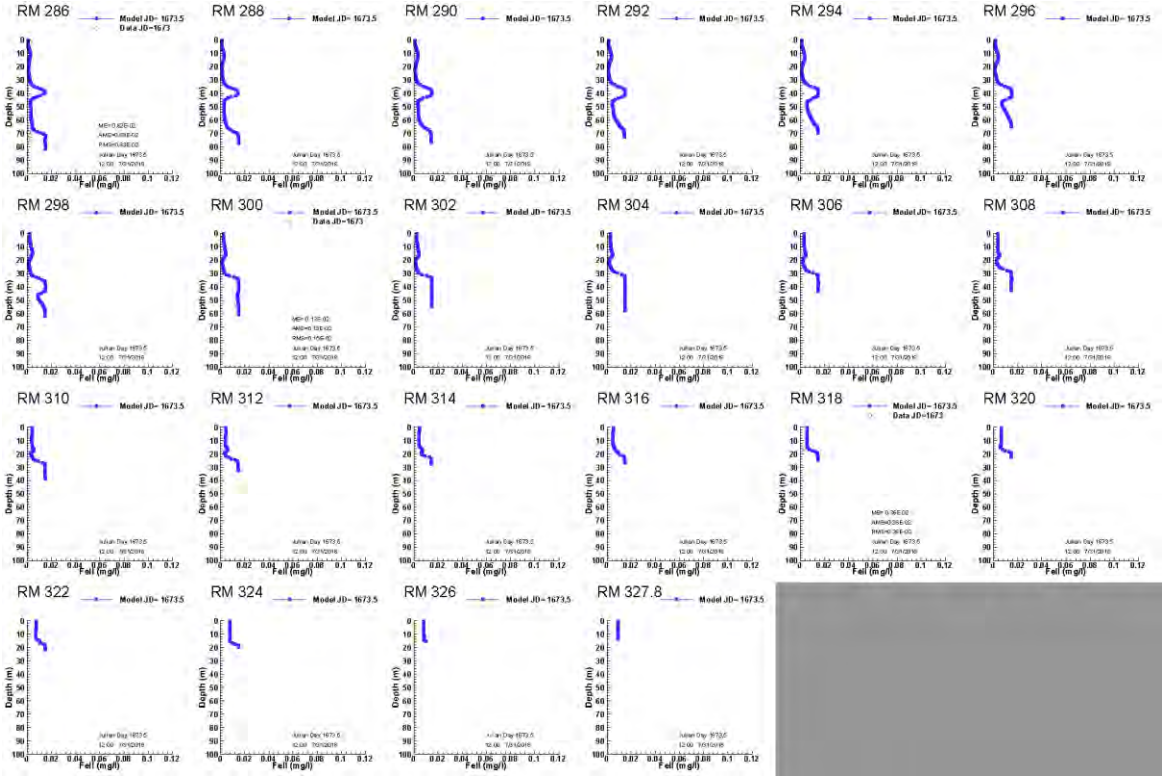


Figure 428. Vertical profiles of Fe(II) compared with data for 7/31/2018.

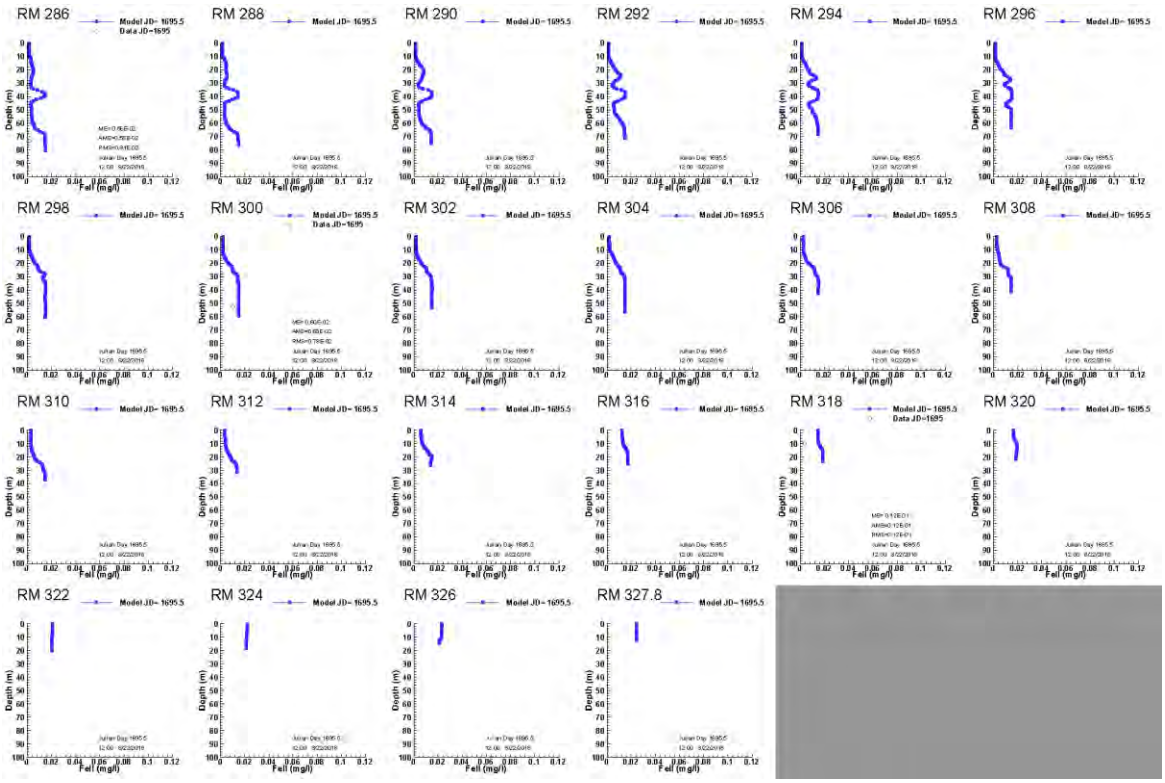


Figure 429. Vertical profiles of Fe(II) compared with data for 8/22/2018.

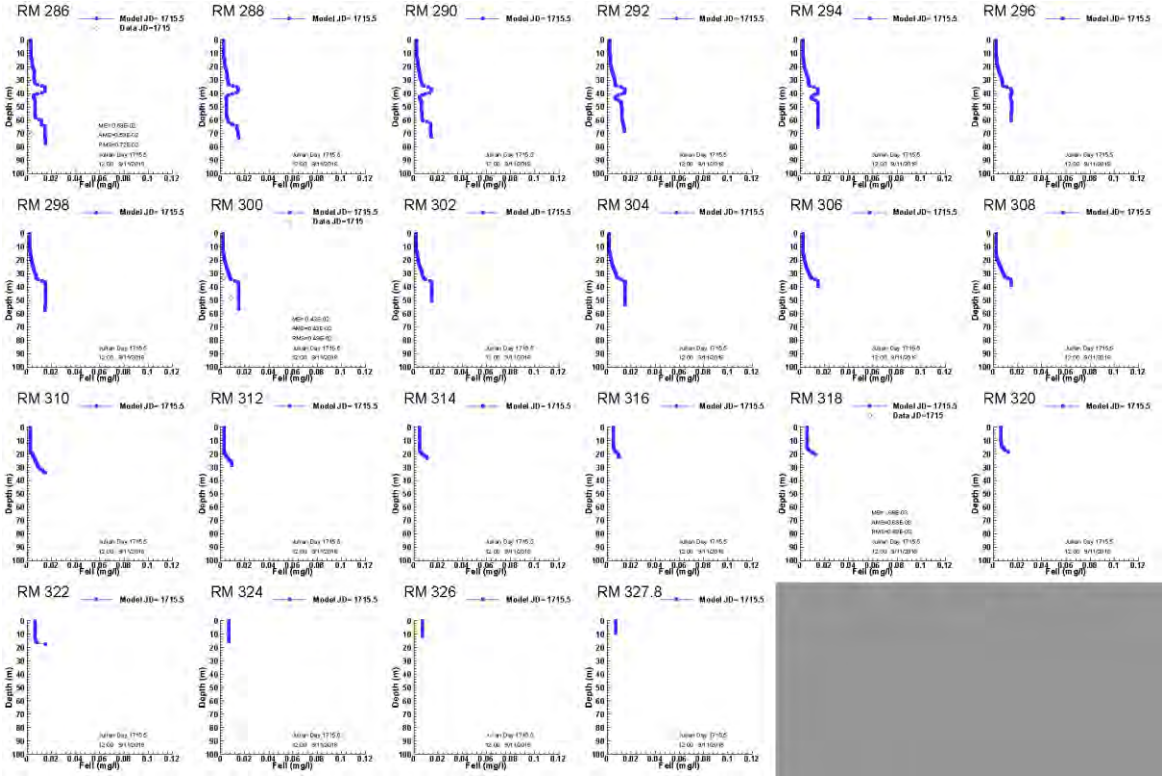


Figure 430. Vertical profiles of Fe(II) compared with data for 9/11/2018.

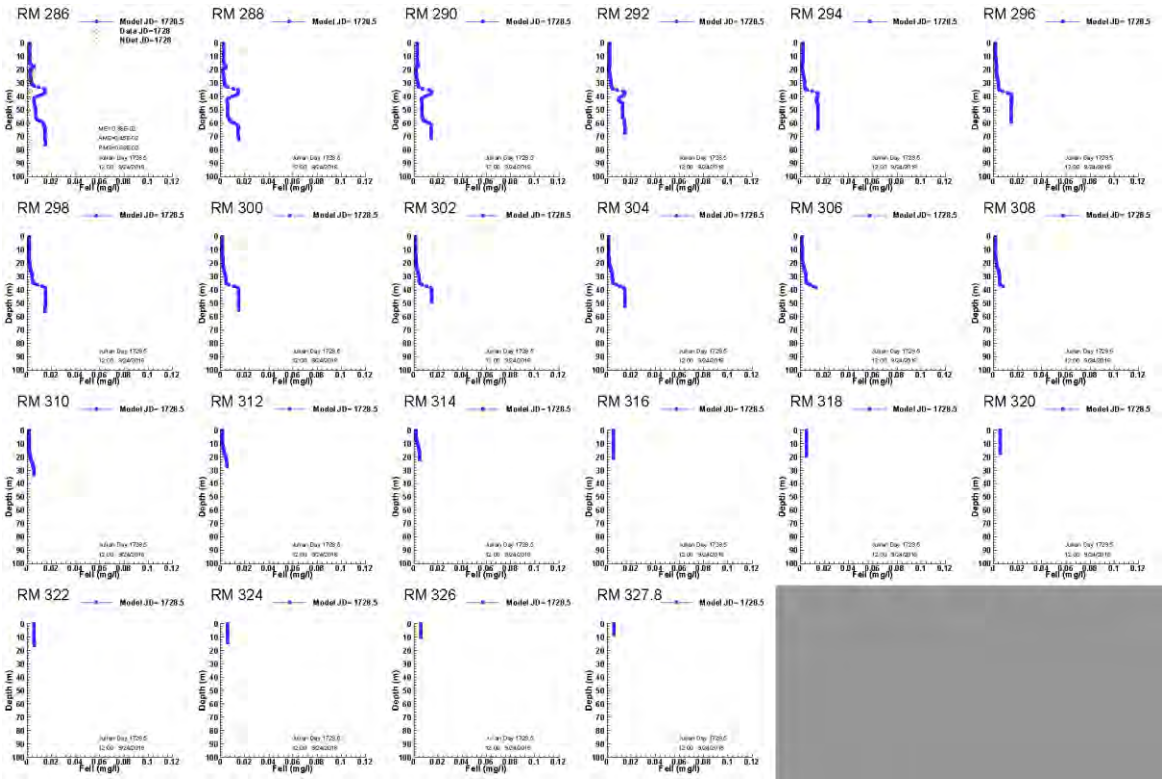


Figure 431. Vertical profiles of Fe(II) compared with data for 9/24/2018.

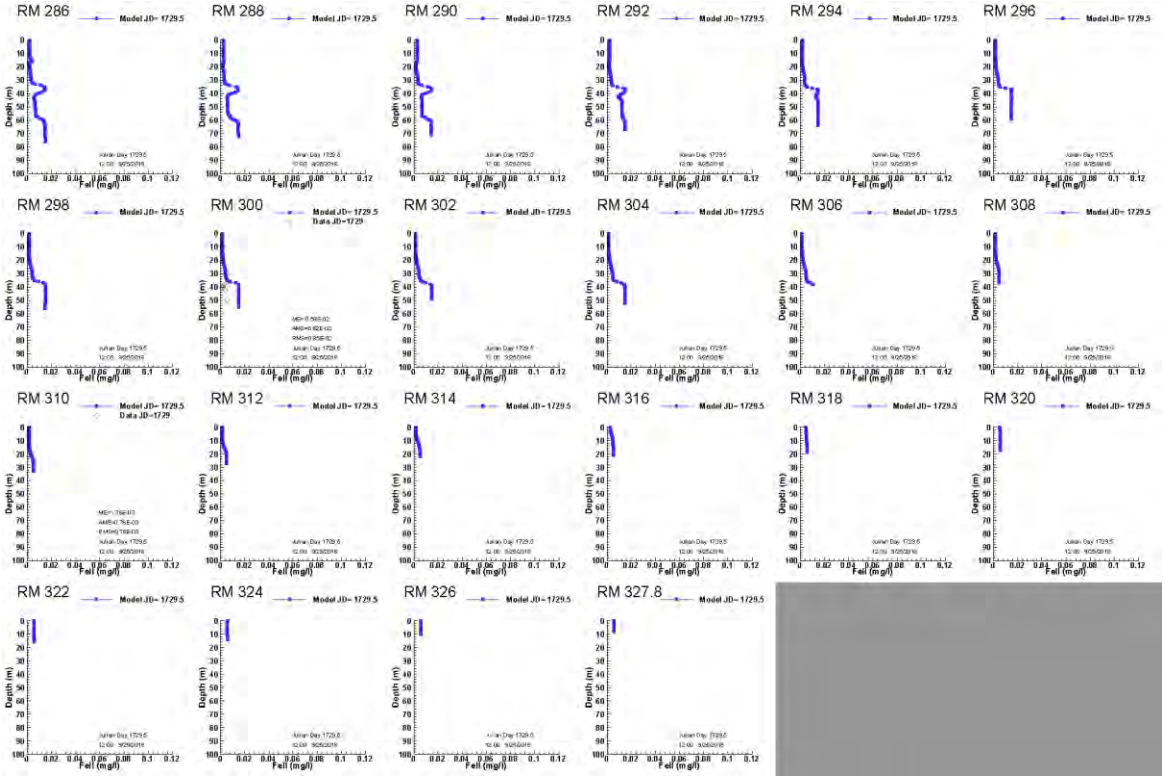


Figure 432. Vertical profiles of Fe(II) compared with data for 9/25/2018.

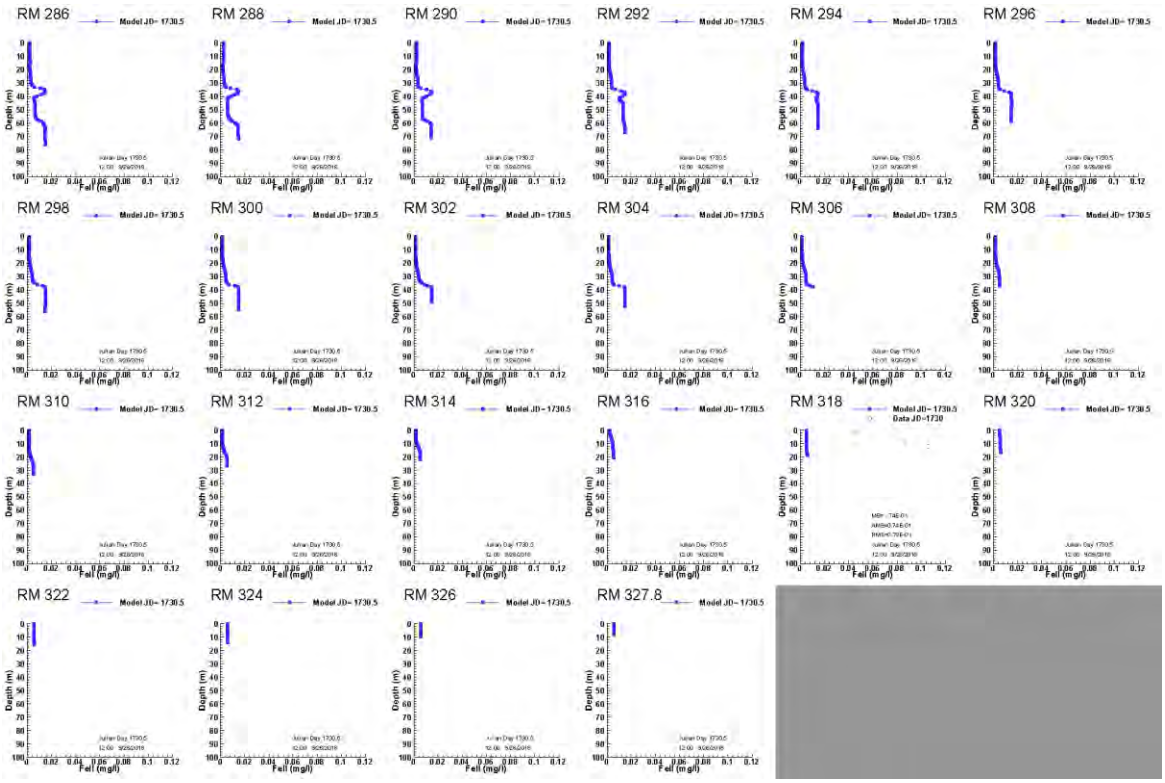


Figure 433. Vertical profiles of Fe(II) compared with data for 9/26/2018.

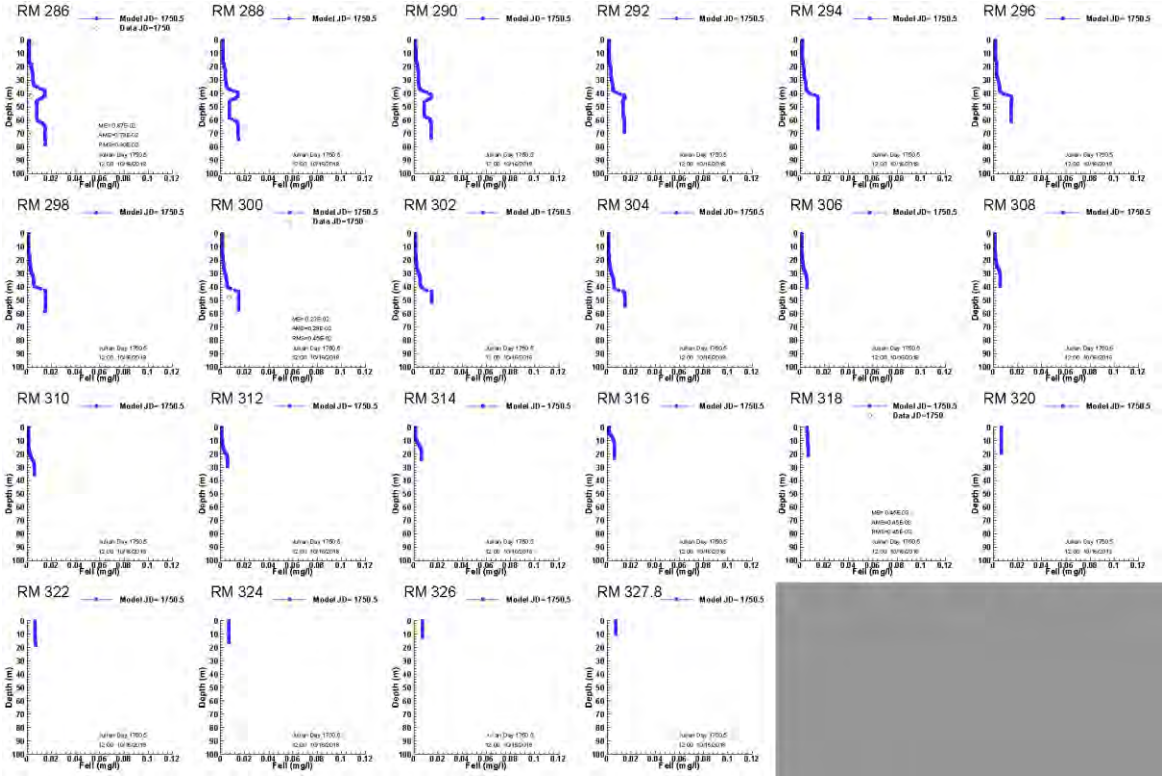


Figure 434. Vertical profiles of Fe(II) compared with data for 10/16/2018.

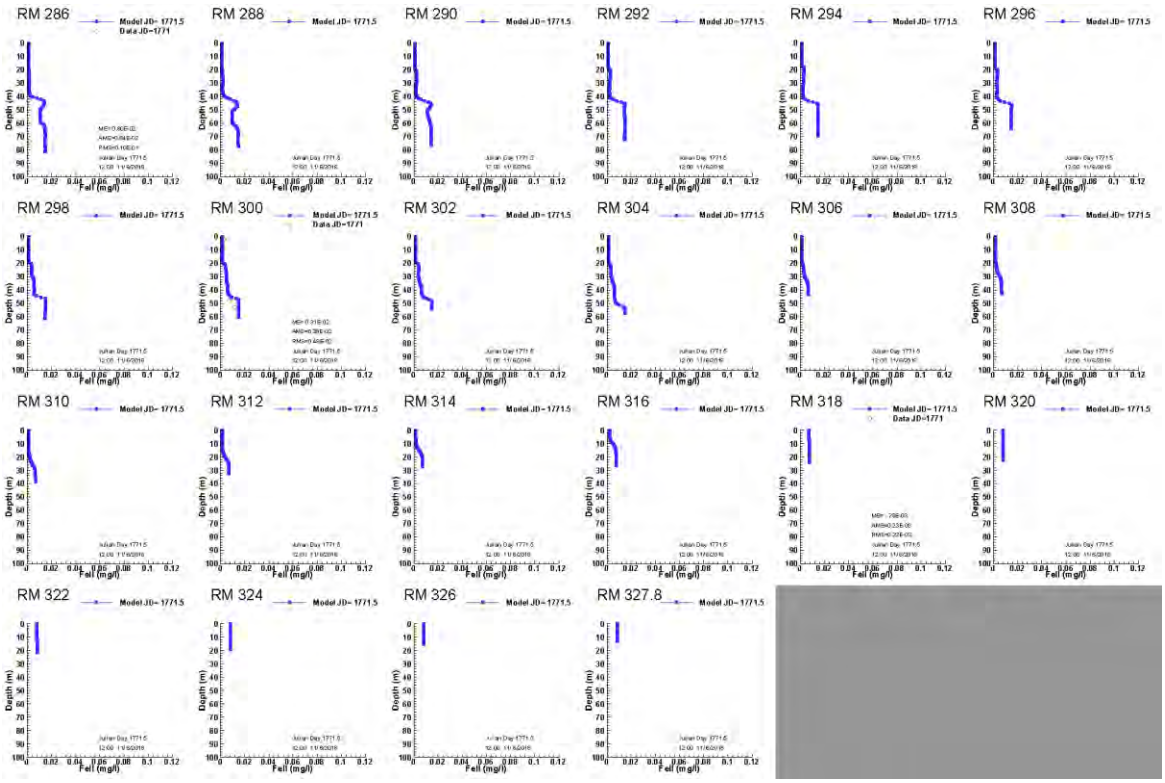


Figure 435. Vertical profiles of Fe(II) compared with data for 11/ 6/2018.

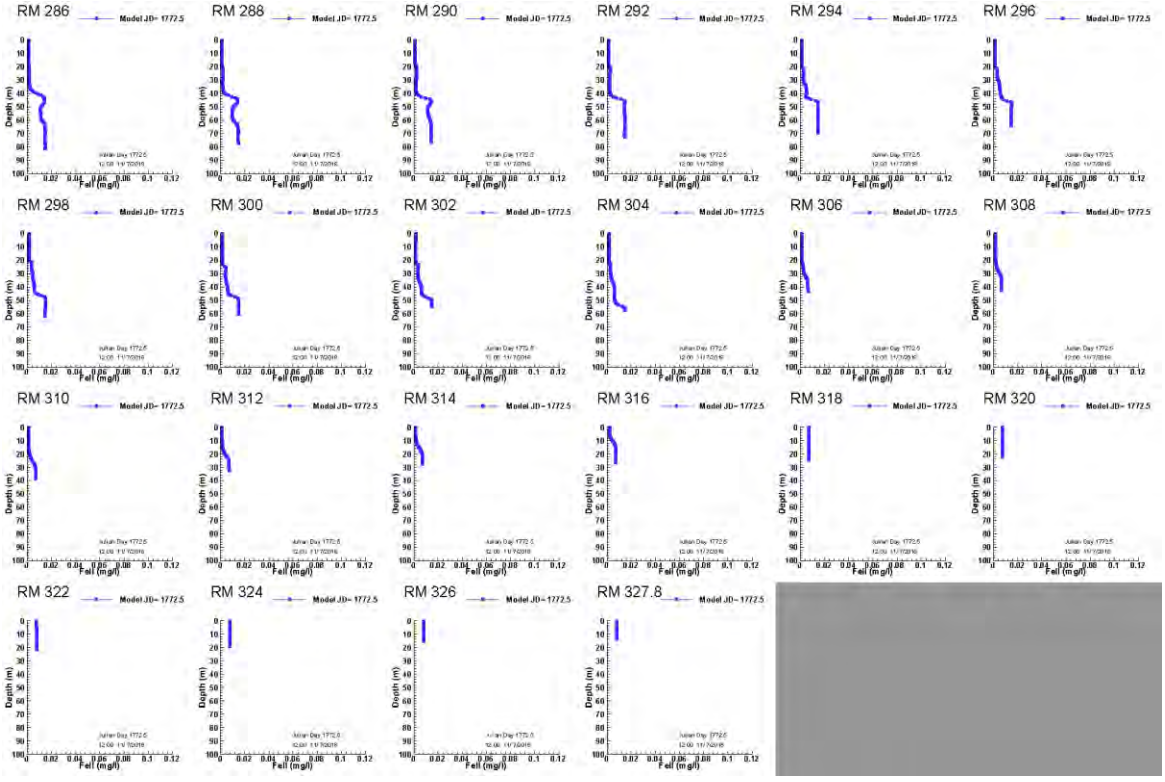


Figure 436. Vertical profiles of Fe(II) compared with data for 11/ 7/2018.

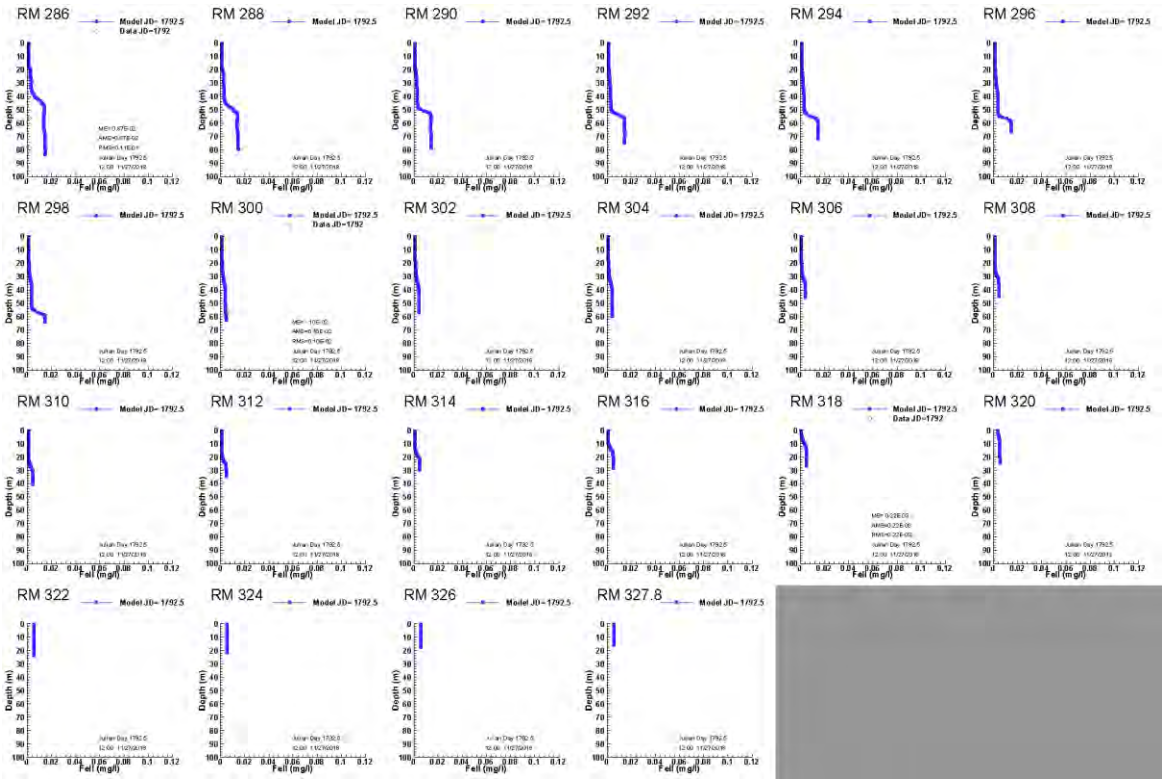


Figure 437. Vertical profiles of Fe(II) compared with data for 11/27/2018.

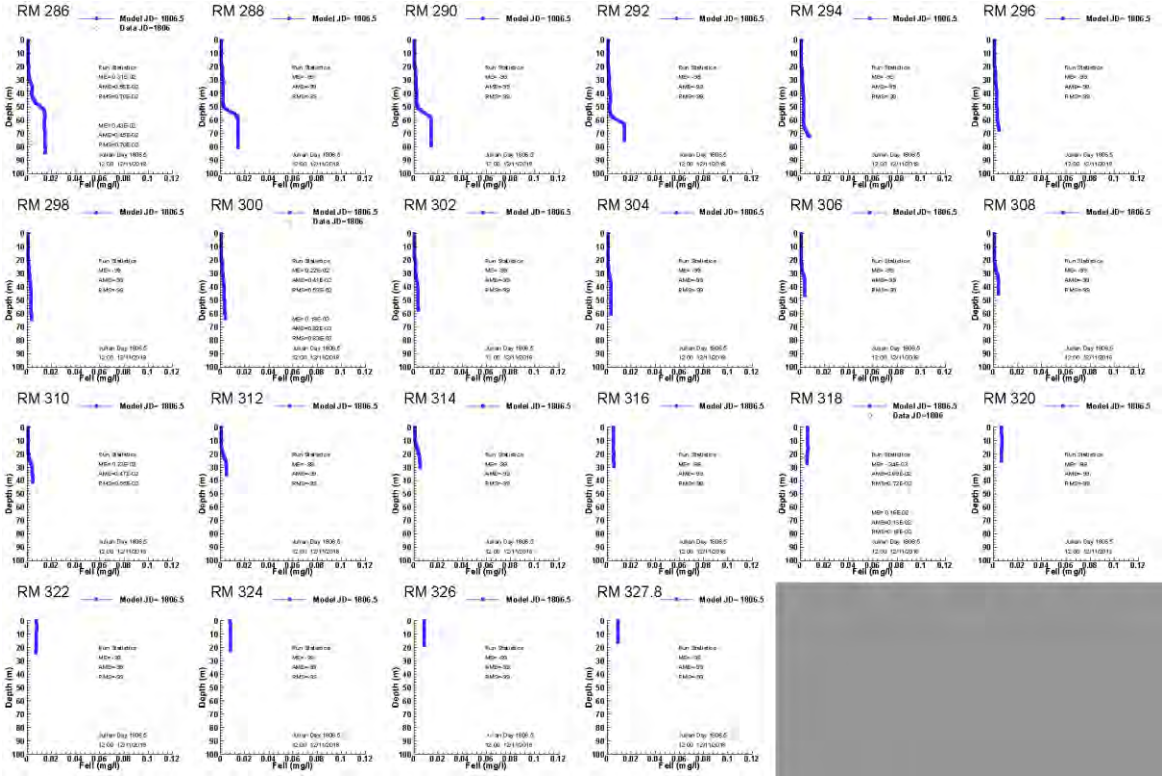


Figure 438. Vertical profiles of Fe(II) compared with data for 12/11/2018.

FeOOH

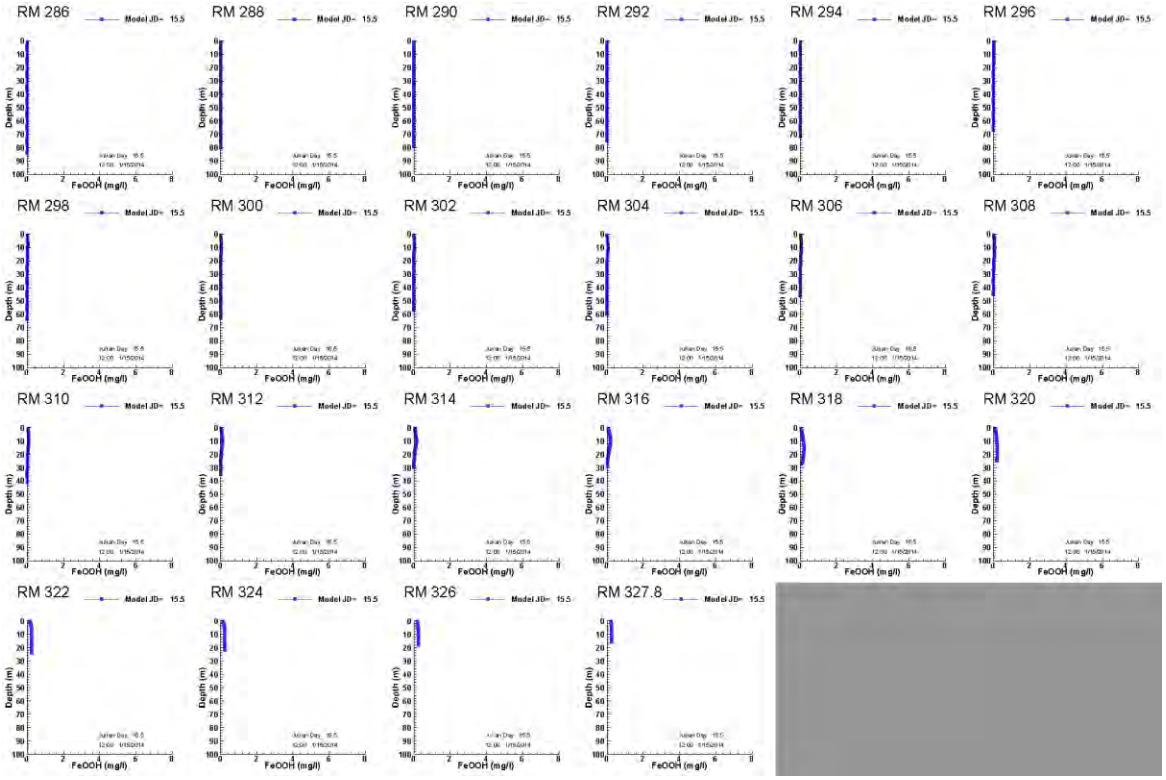


Figure 439. Vertical profiles of FeOOH compared with data for 1/15/2014.

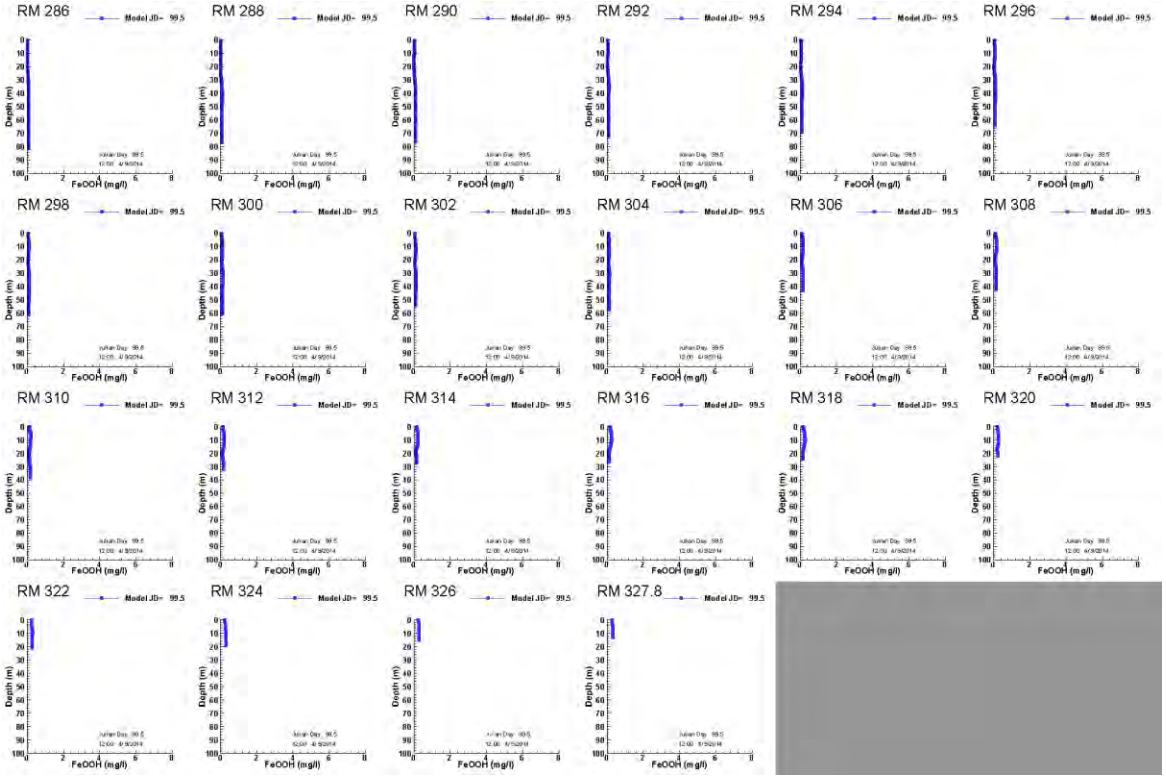


Figure 440. Vertical profiles of FeOOH compared with data for 4/ 9/2014.

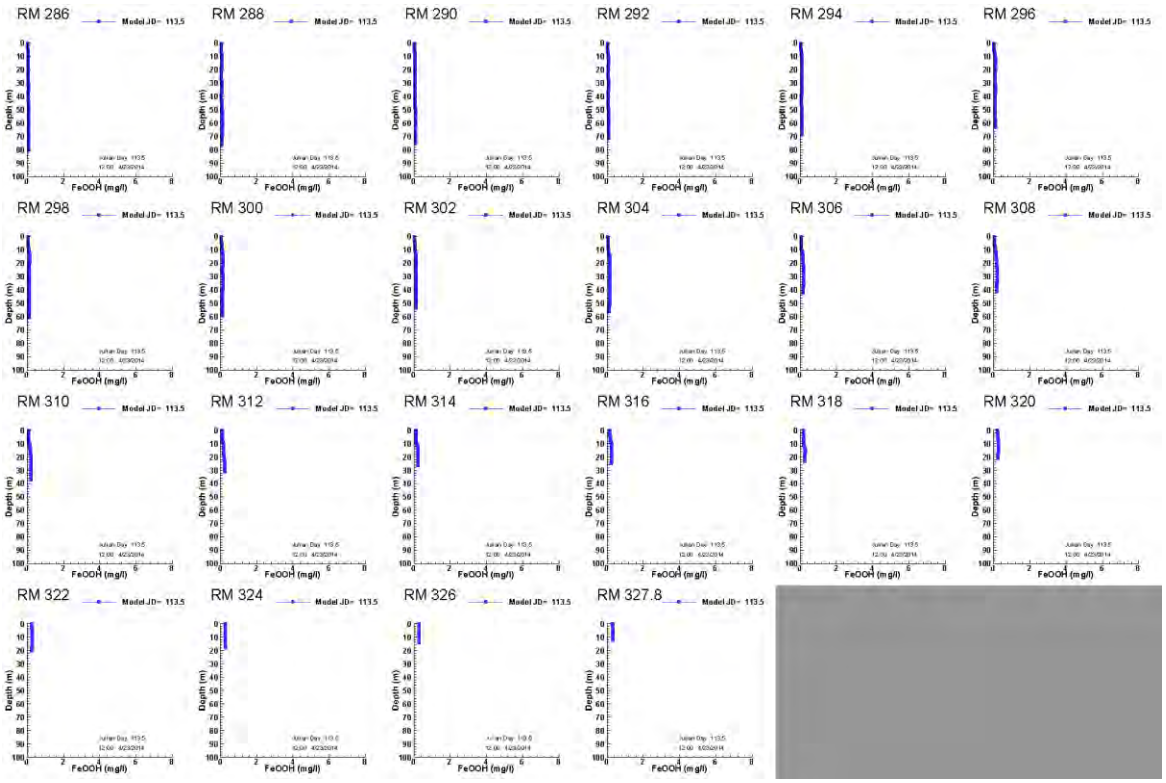


Figure 441. Vertical profiles of FeOOH compared with data for 4/23/2014.

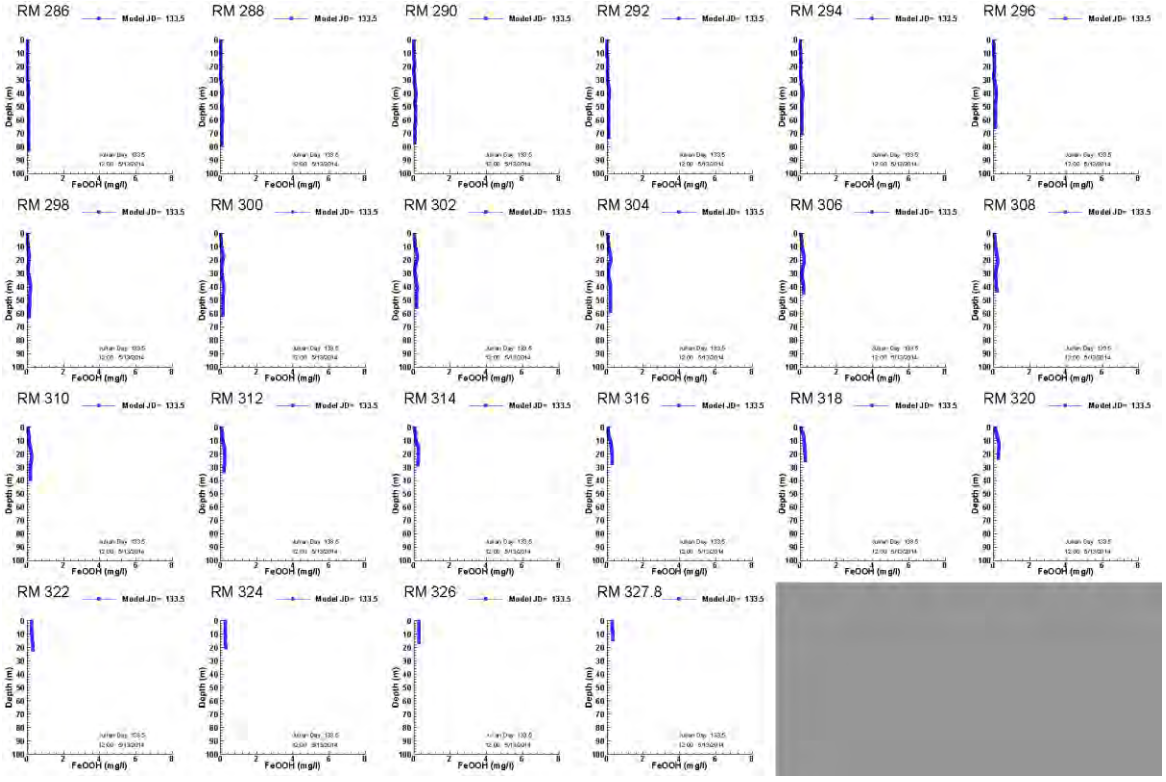


Figure 442. Vertical profiles of FeOOH compared with data for 5/13/2014.

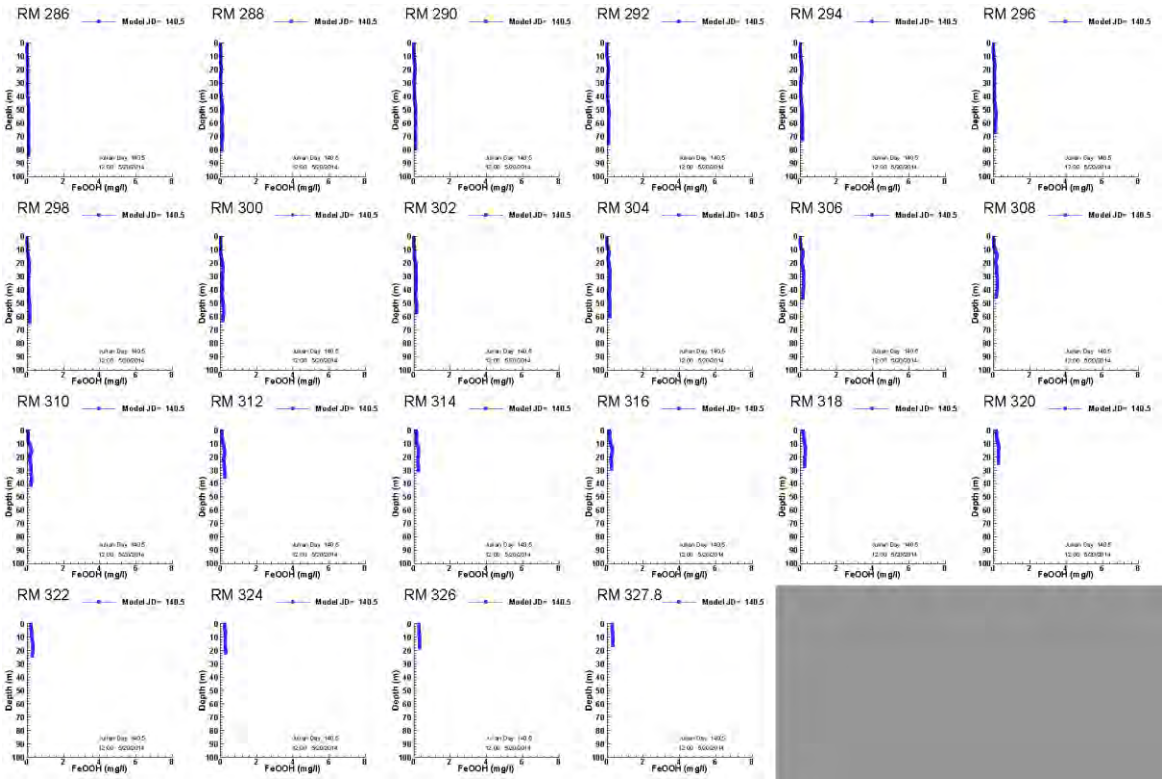


Figure 443. Vertical profiles of FeOOH compared with data for 5/20/2014.

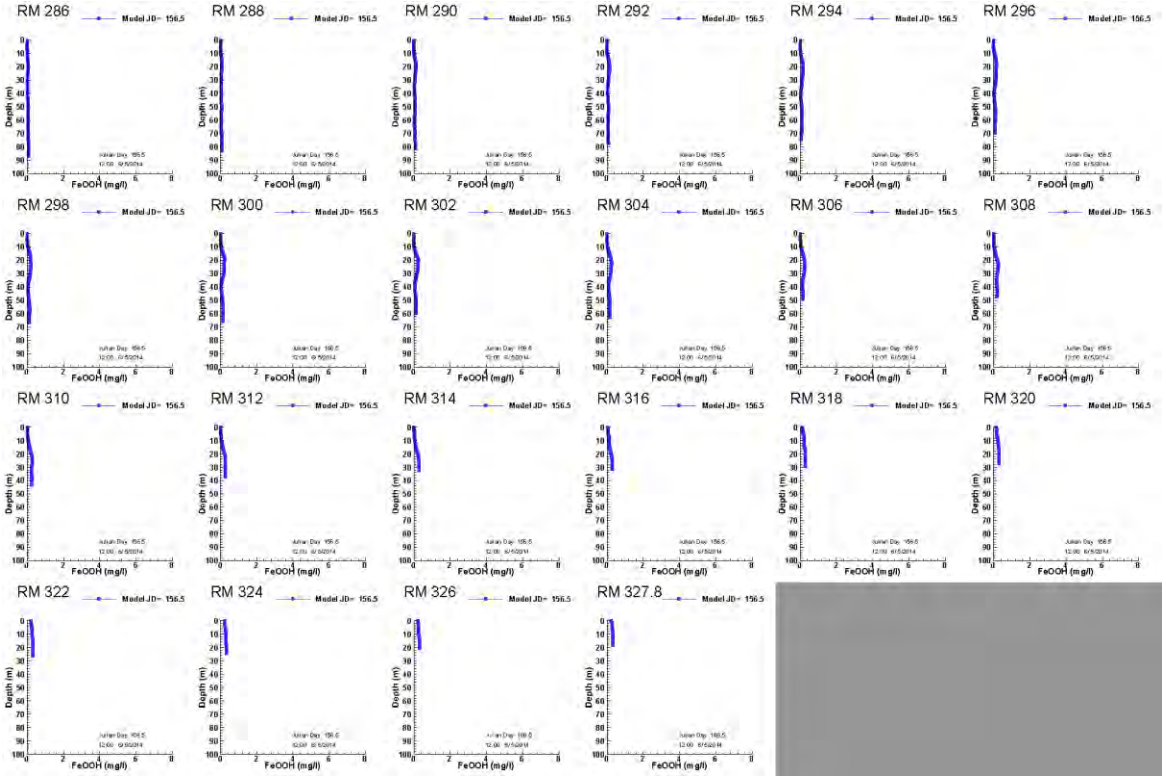


Figure 444. Vertical profiles of FeOOH compared with data for 6/ 5/2014.

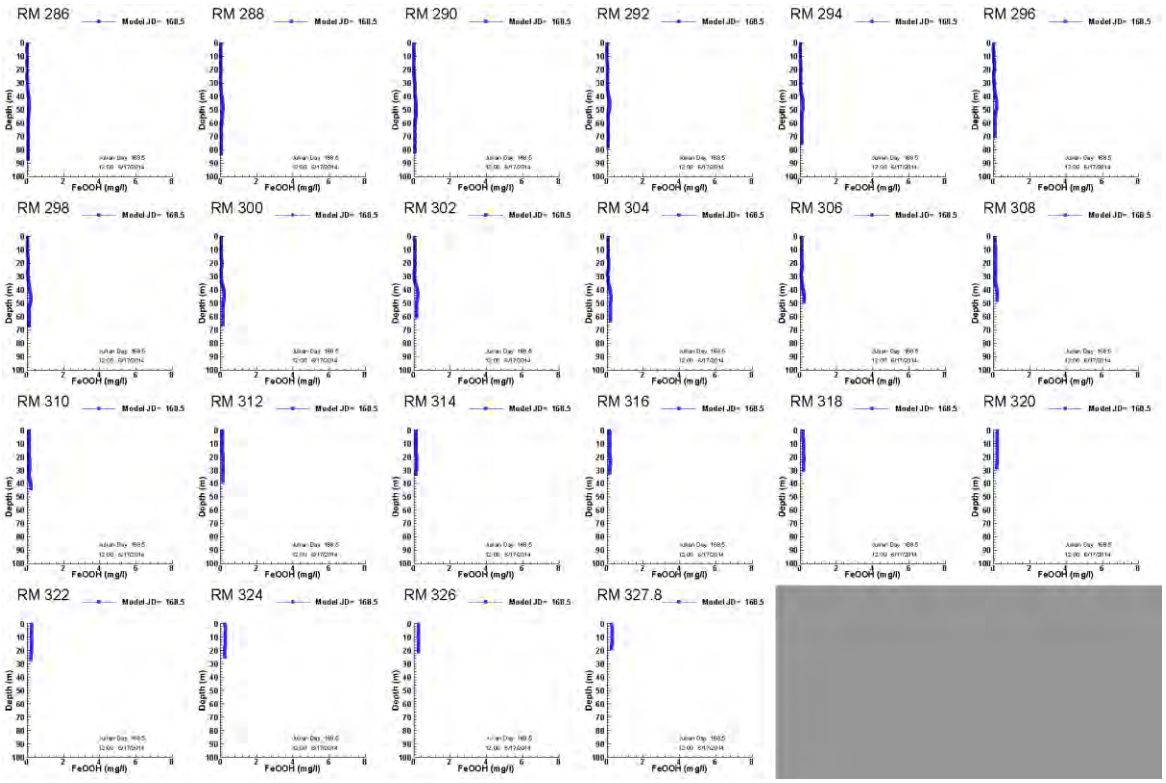


Figure 445. Vertical profiles of FeOOH compared with data for 6/17/2014.

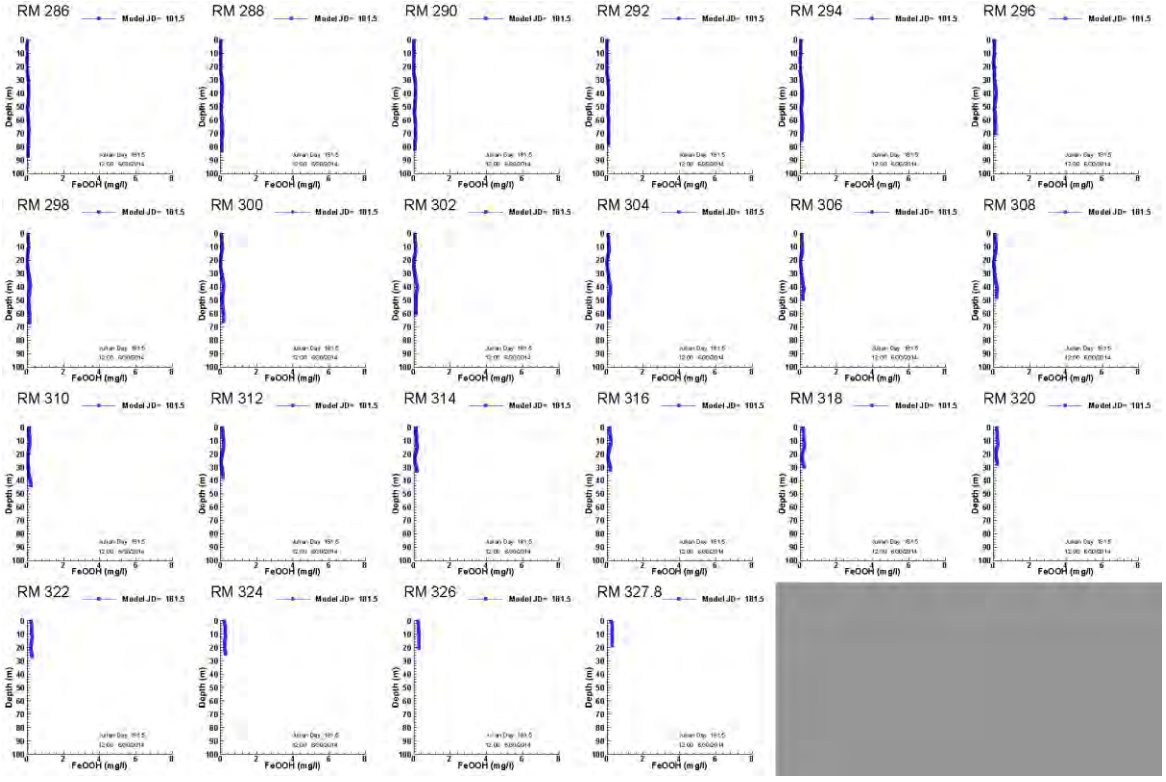


Figure 446. Vertical profiles of FeOOH compared with data for 6/30/2014.

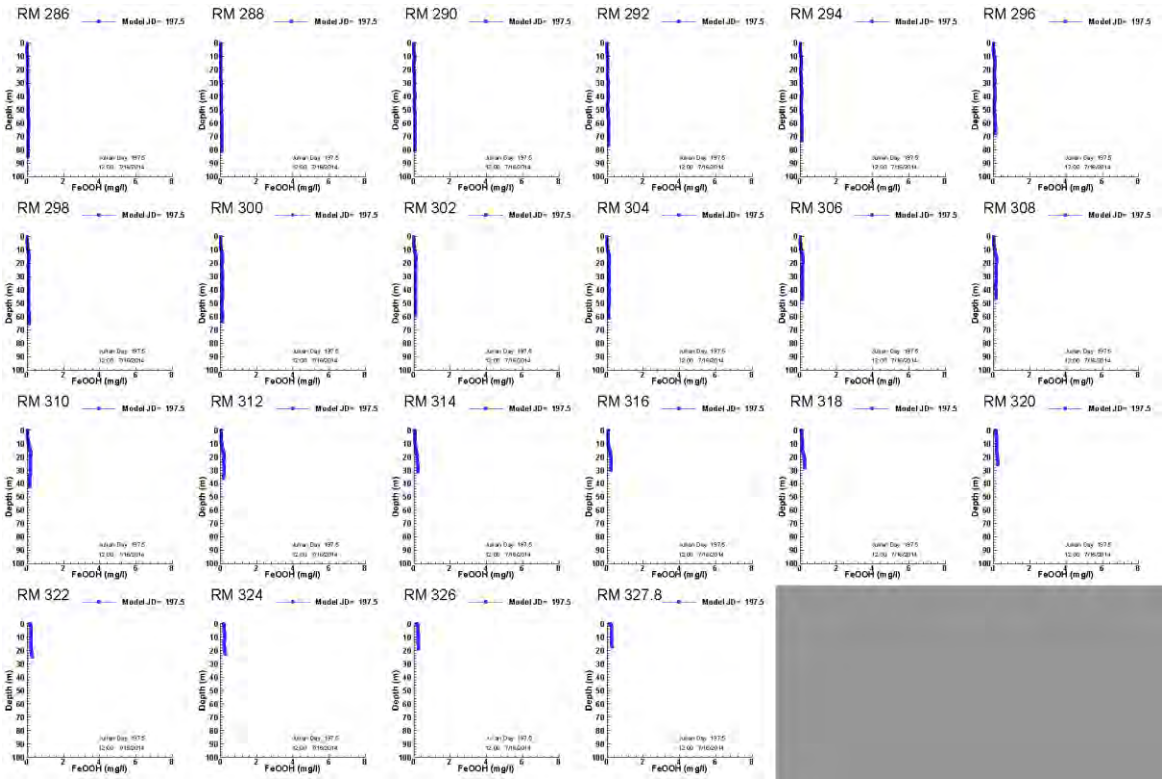


Figure 447. Vertical profiles of FeOOH compared with data for 7/16/2014.

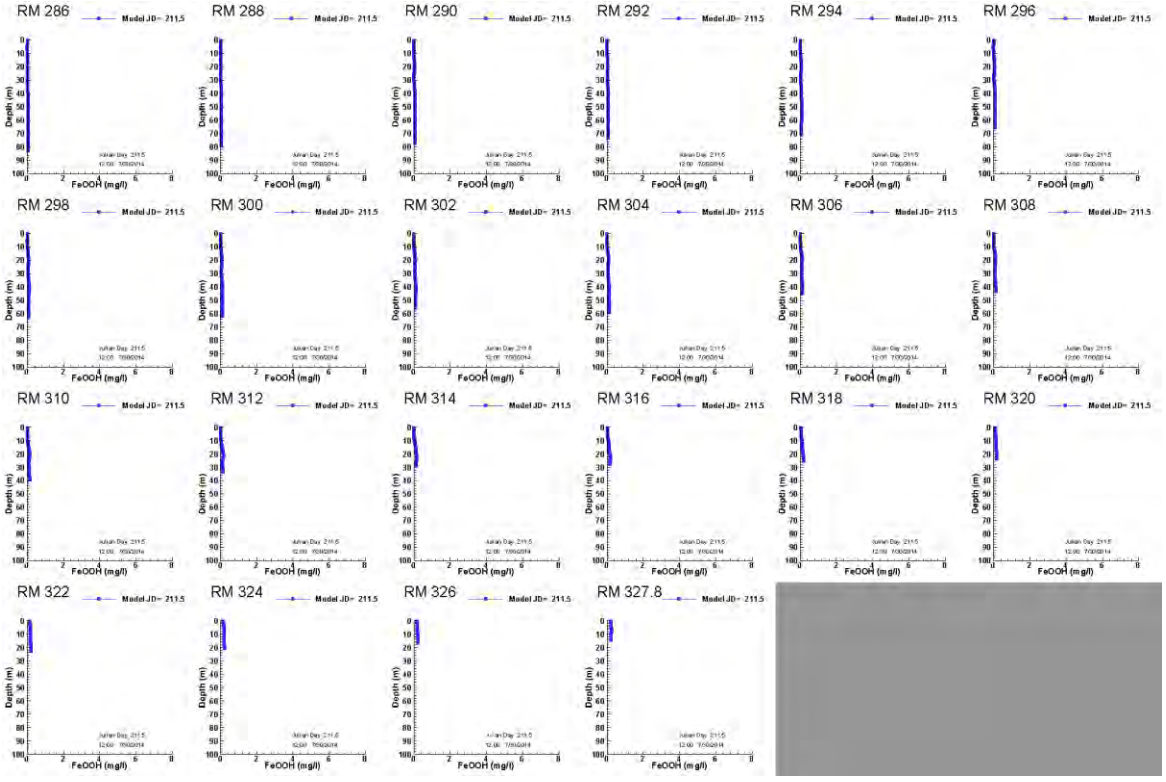


Figure 448. Vertical profiles of FeOOH compared with data for 7/30/2014.

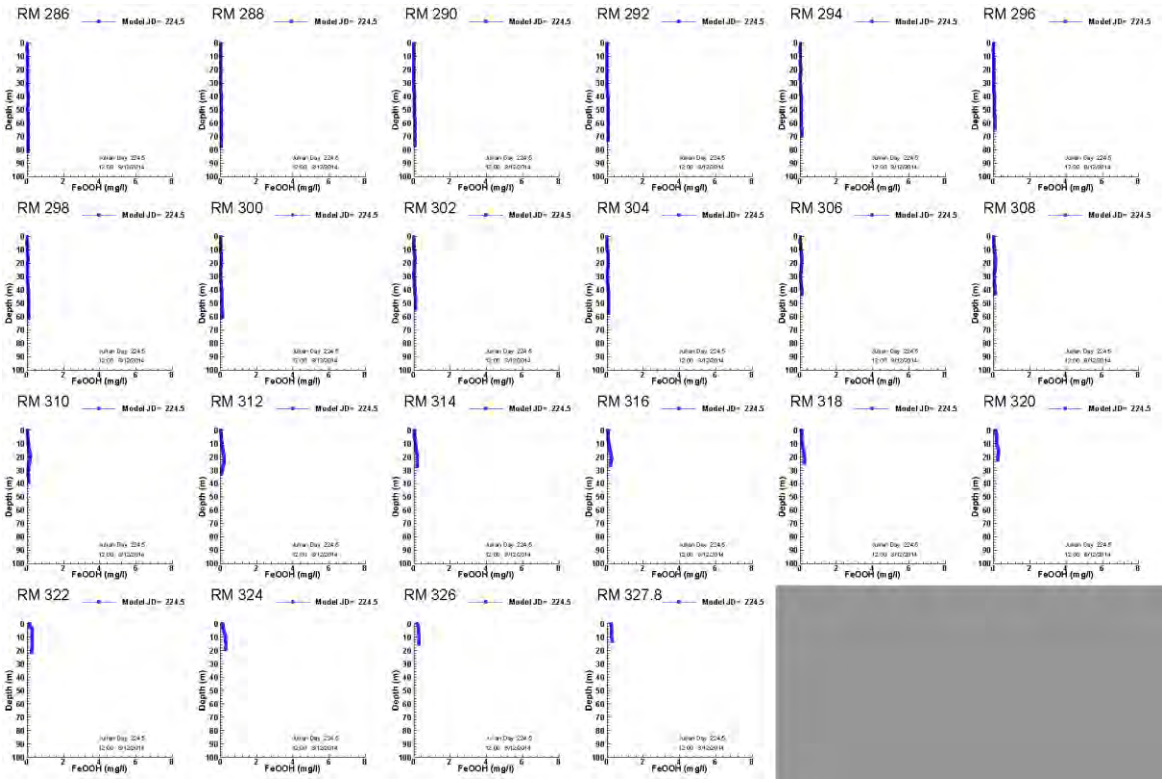


Figure 449. Vertical profiles of FeOOH compared with data for 8/12/2014.

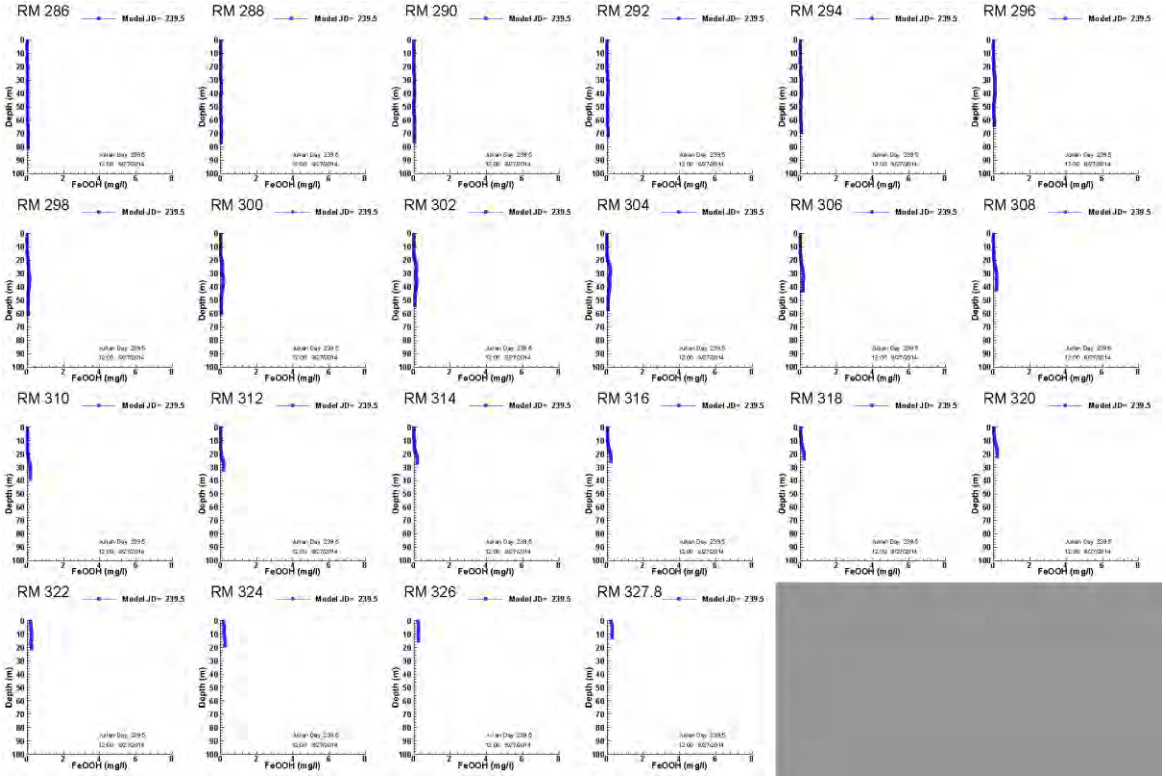


Figure 450. Vertical profiles of FeOOH compared with data for 8/27/2014.

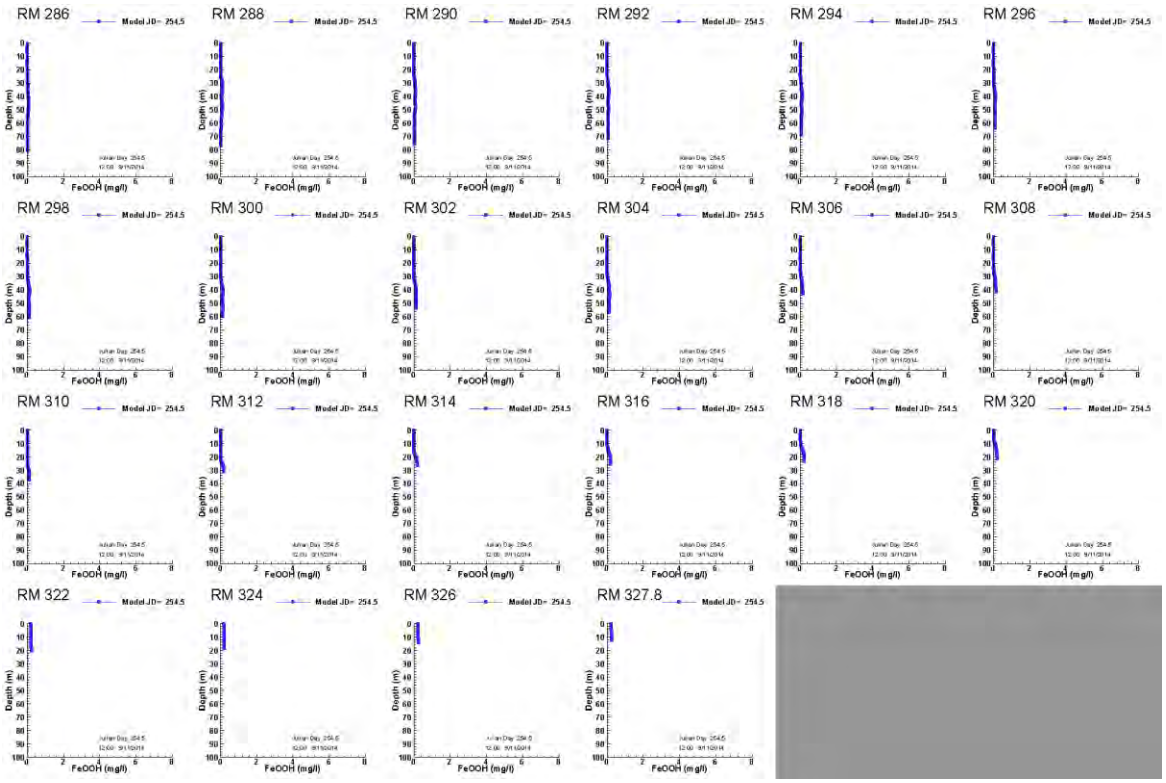


Figure 451. Vertical profiles of FeOOH compared with data for 9/11/2014.

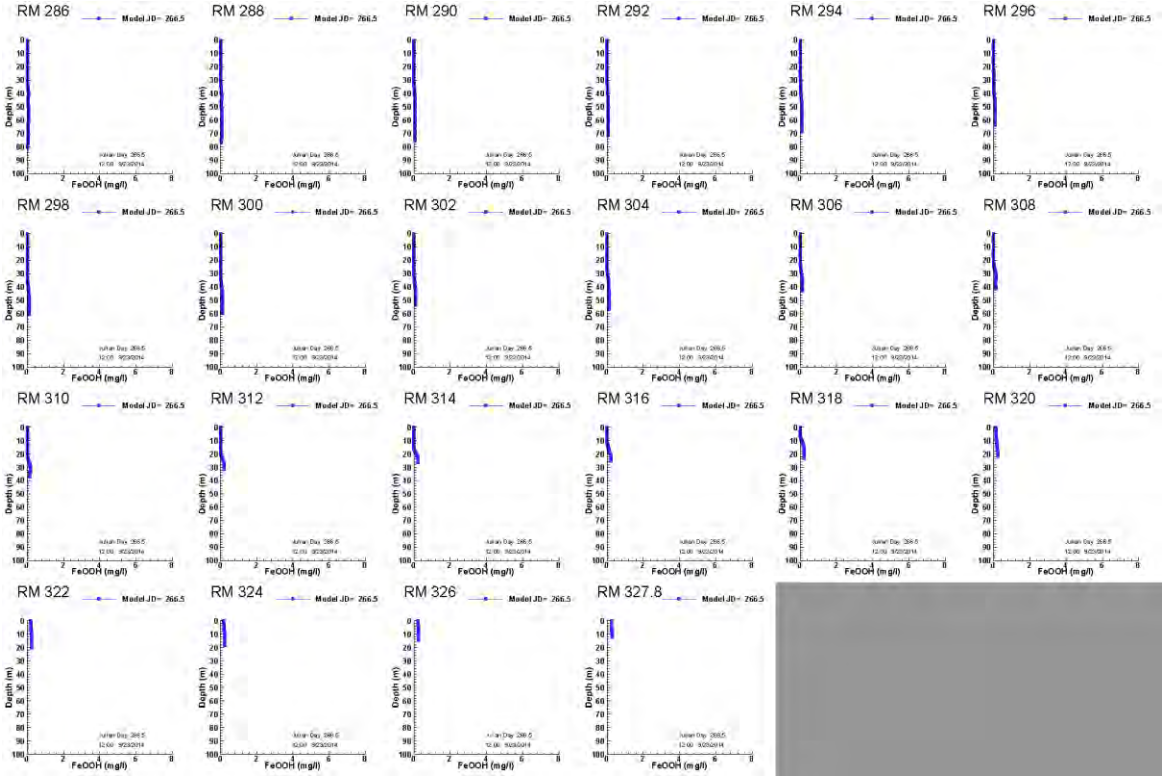


Figure 452. Vertical profiles of FeOOH compared with data for 9/23/2014.

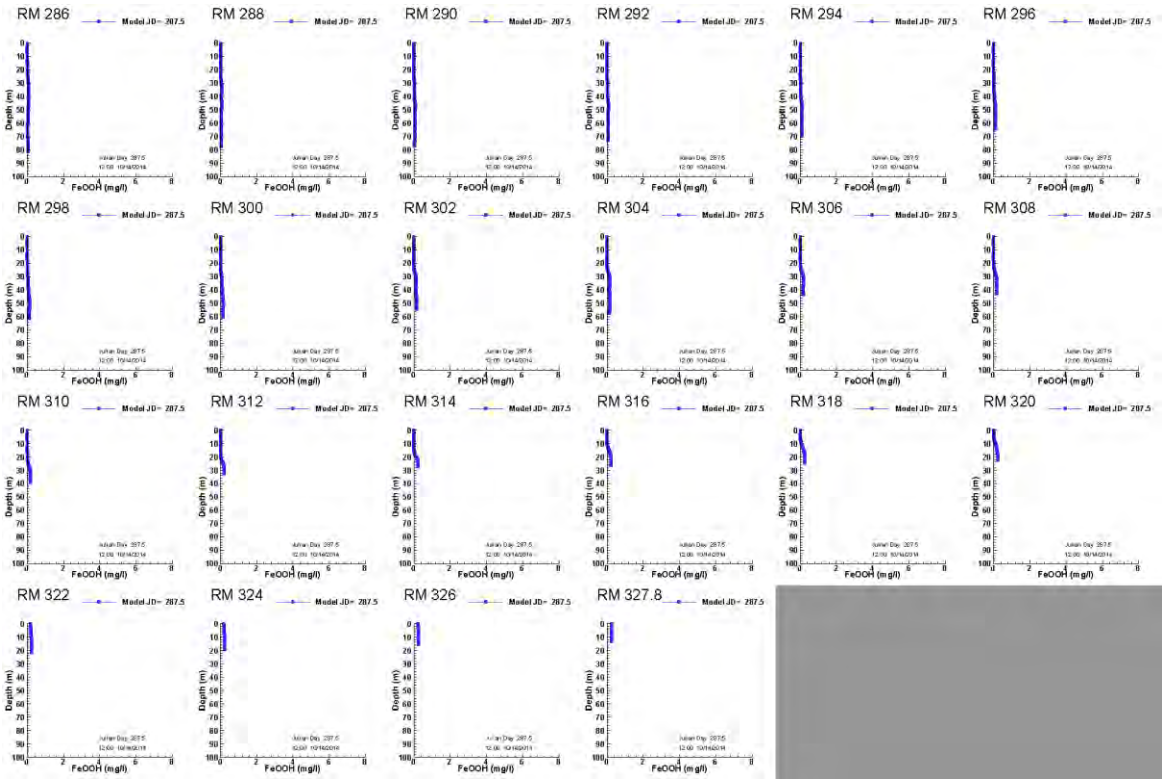


Figure 453. Vertical profiles of FeOOH compared with data for 10/14/2014.

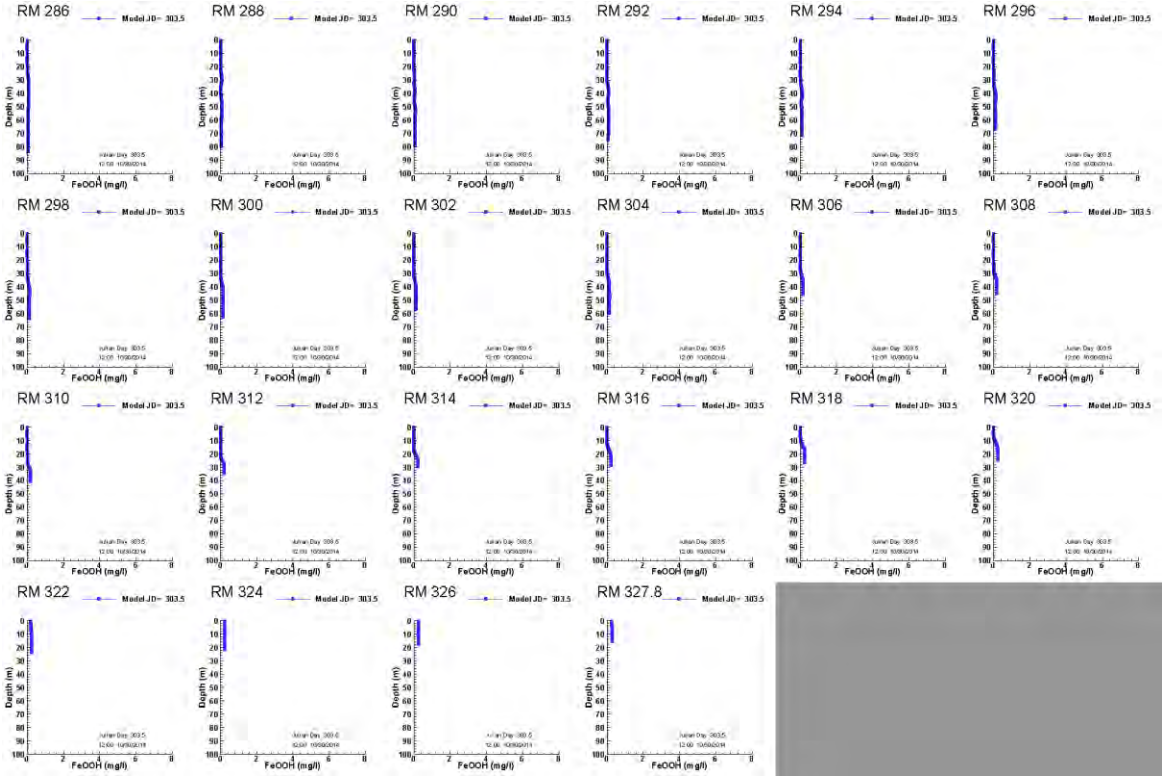


Figure 454. Vertical profiles of FeOOH compared with data for 10/30/2014.

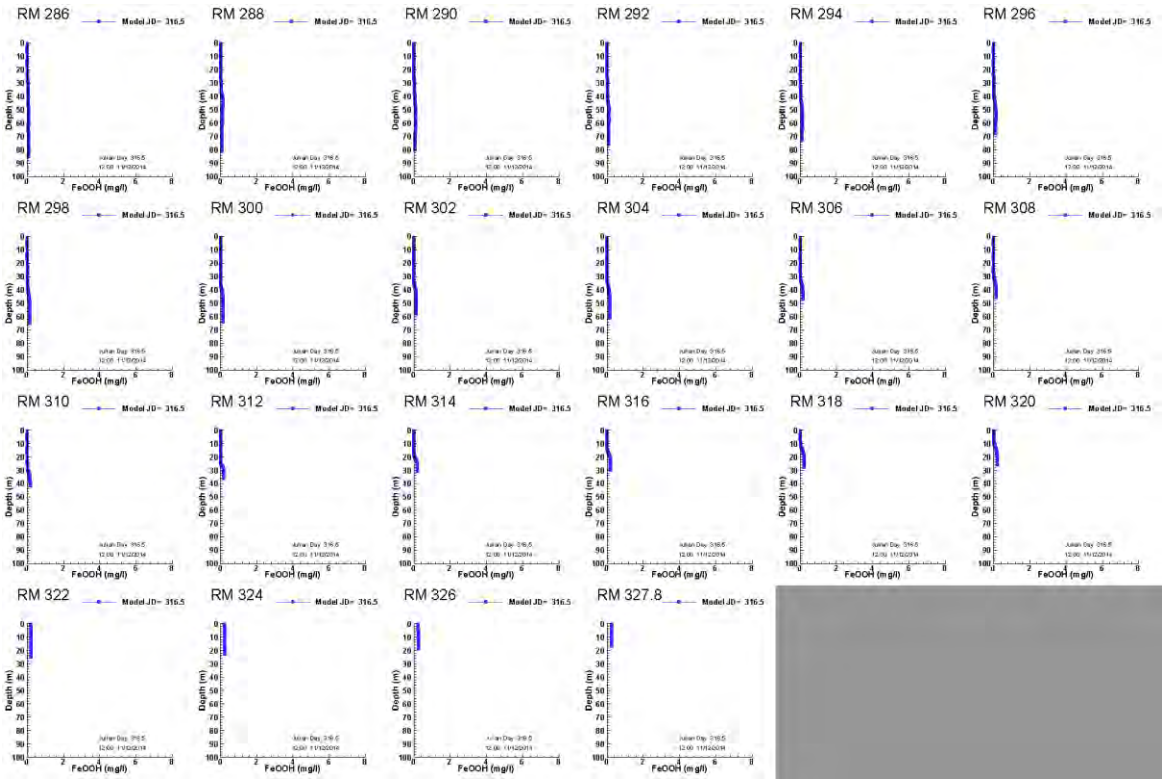


Figure 455. Vertical profiles of FeOOH compared with data for 11/12/2014.

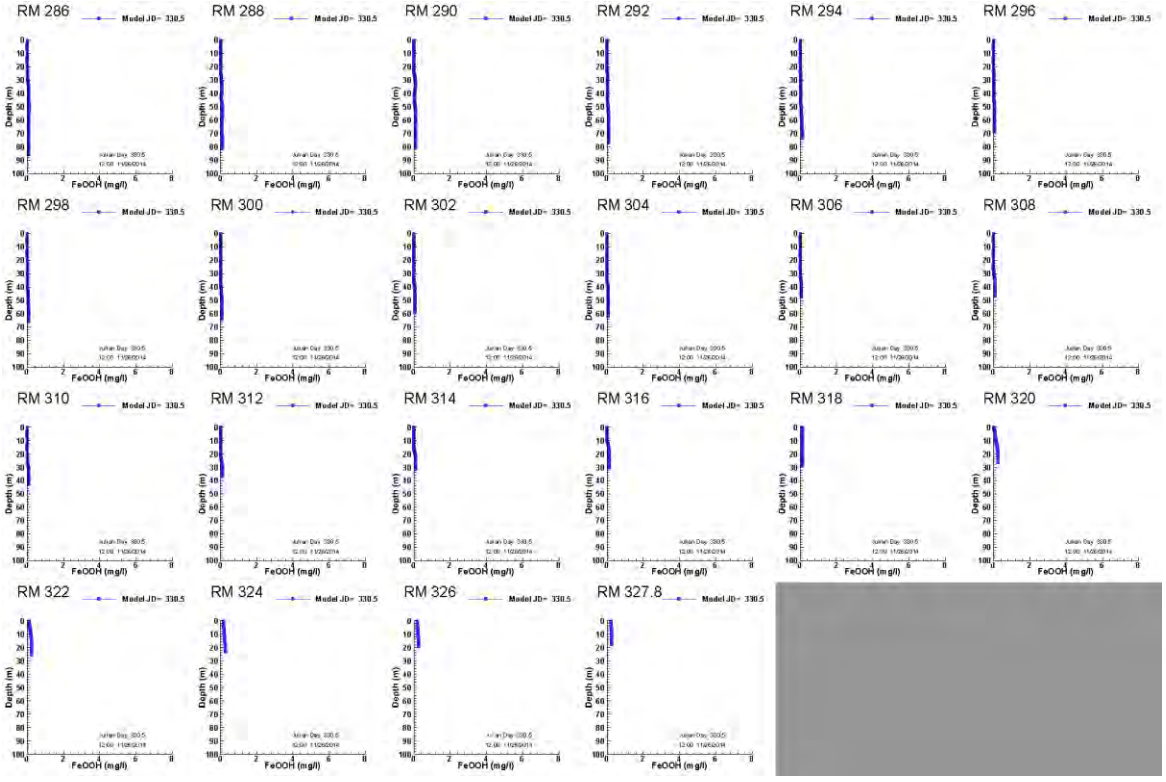


Figure 456. Vertical profiles of FeOOH compared with data for 11/26/2014.

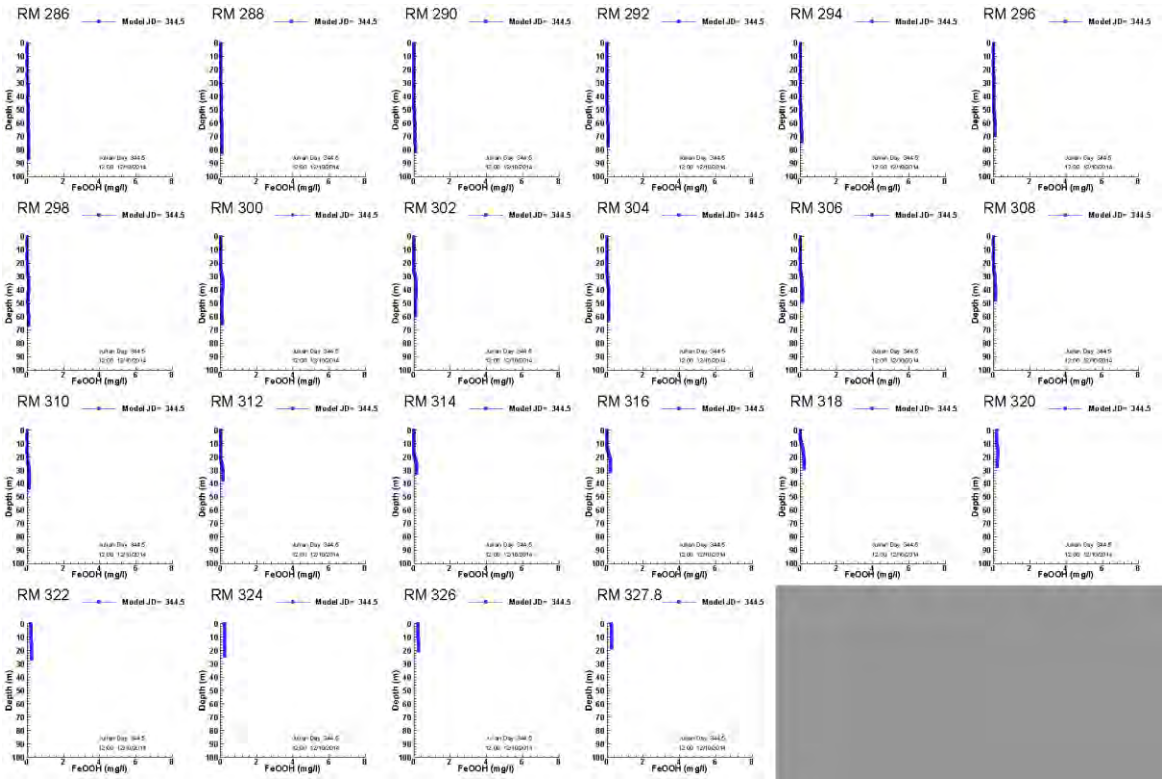


Figure 457. Vertical profiles of FeOOH compared with data for 12/10/2014.

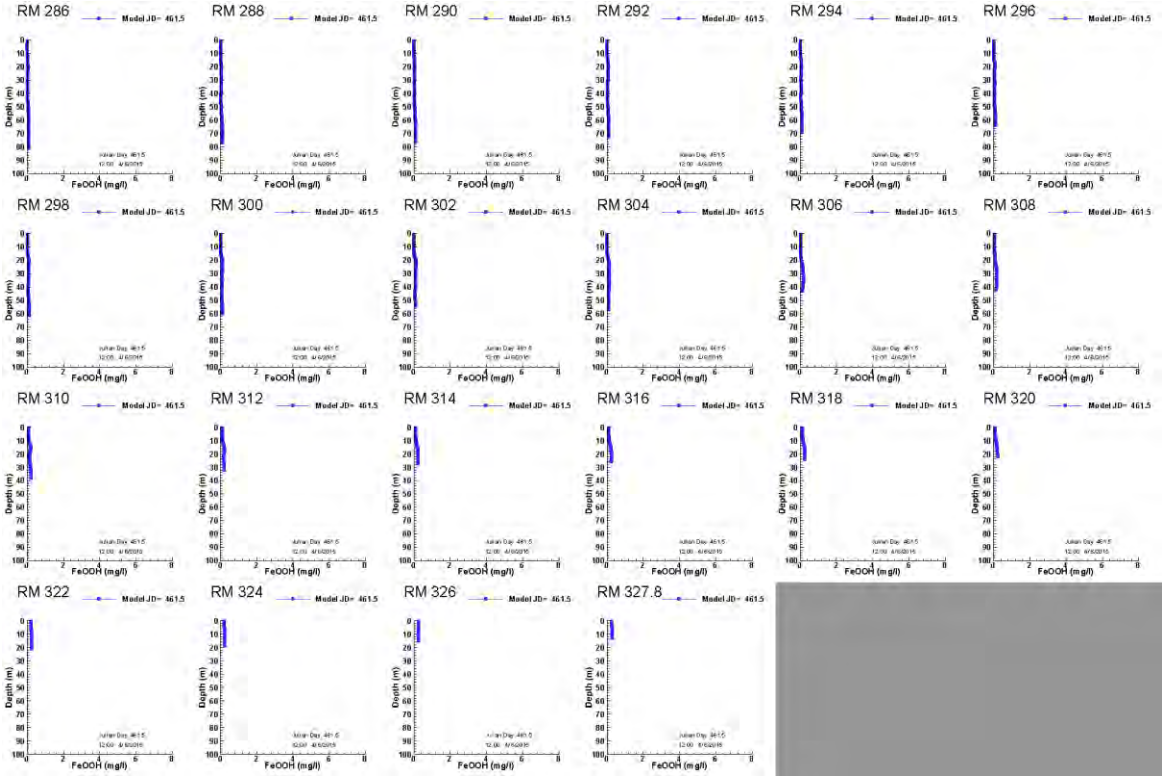


Figure 458. Vertical profiles of FeOOH compared with data for 4/ 6/2015.

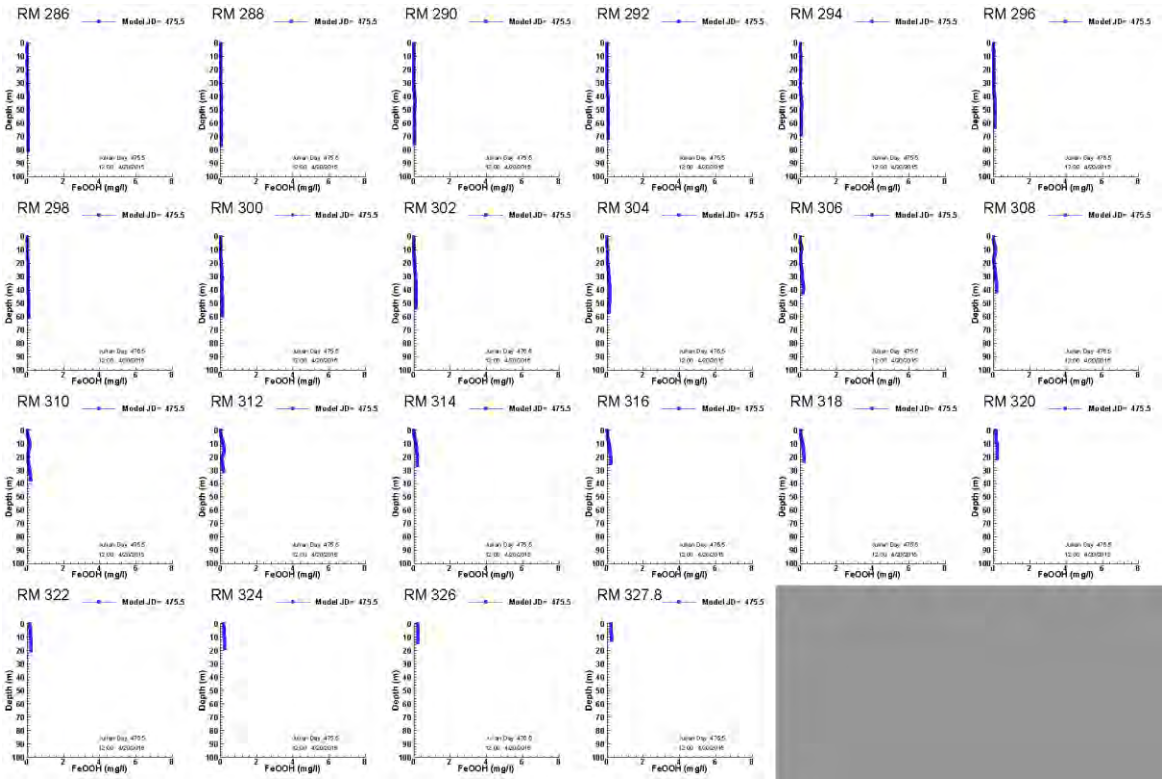


Figure 459. Vertical profiles of FeOOH compared with data for 4/20/2015.

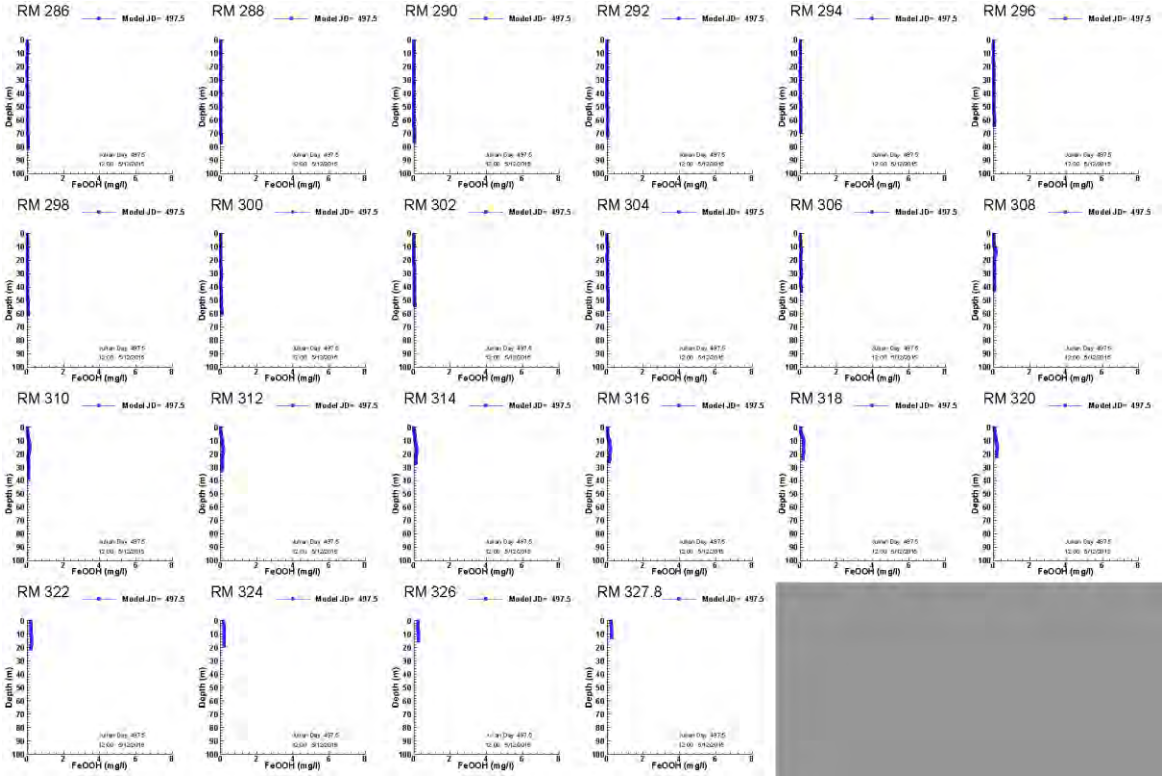


Figure 460. Vertical profiles of FeOOH compared with data for 5/12/2015.

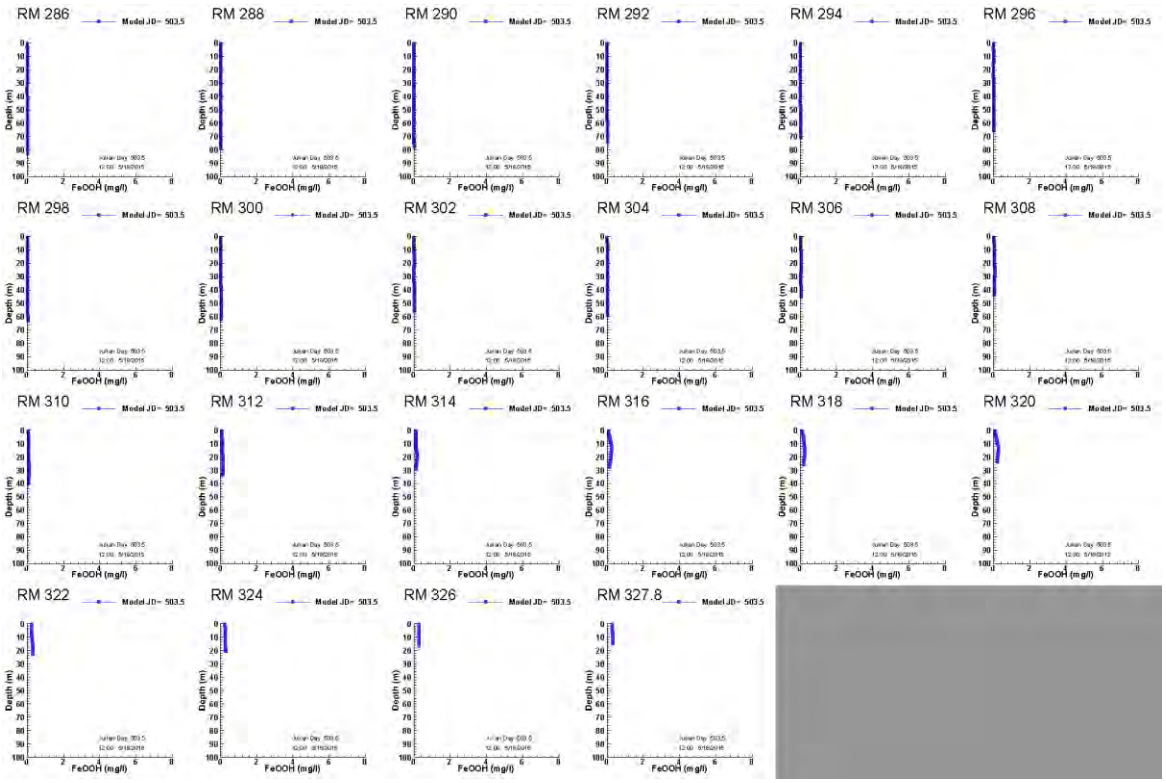


Figure 461. Vertical profiles of FeOOH compared with data for 5/18/2015.

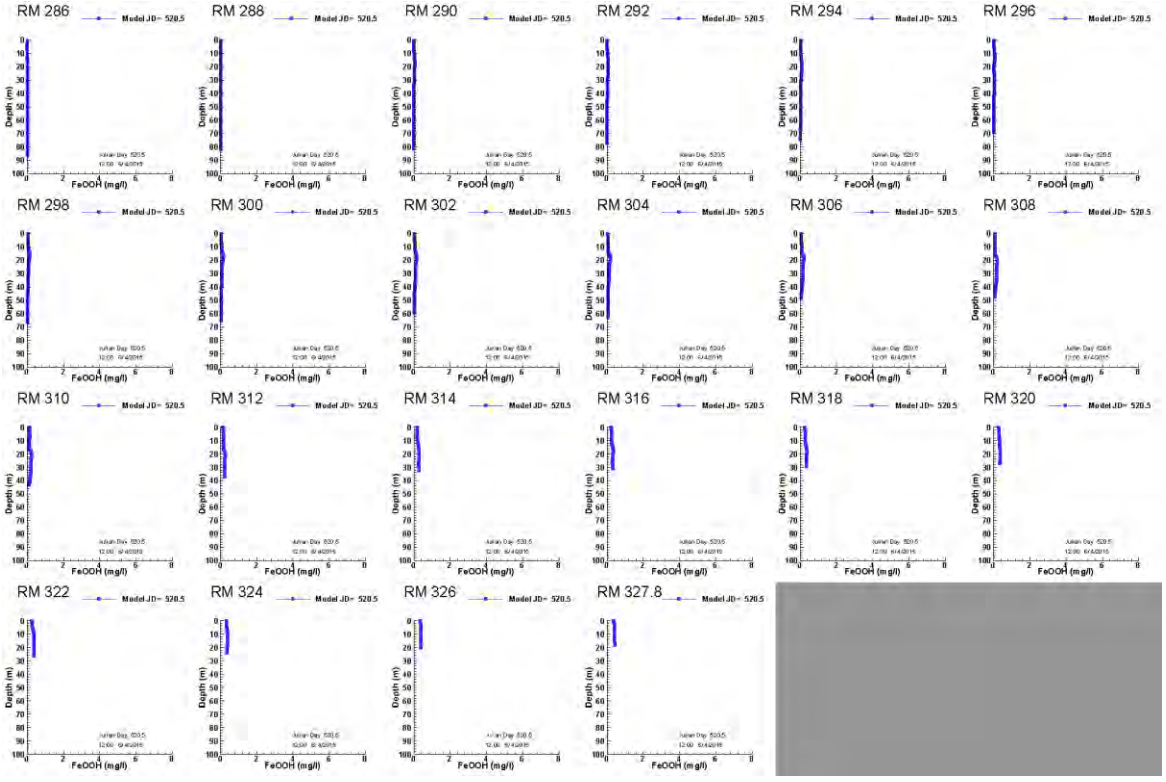


Figure 462. Vertical profiles of FeOOH compared with data for 6/ 4/2015.

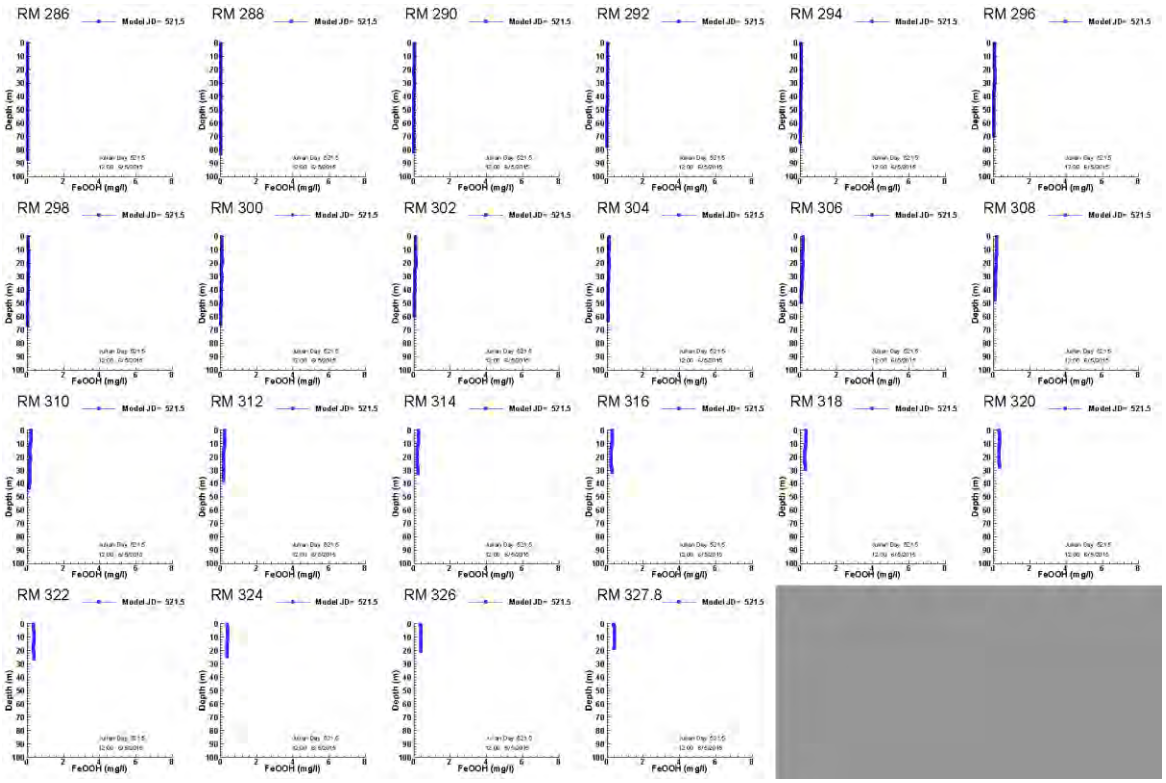


Figure 463. Vertical profiles of FeOOH compared with data for 6/ 5/2015.

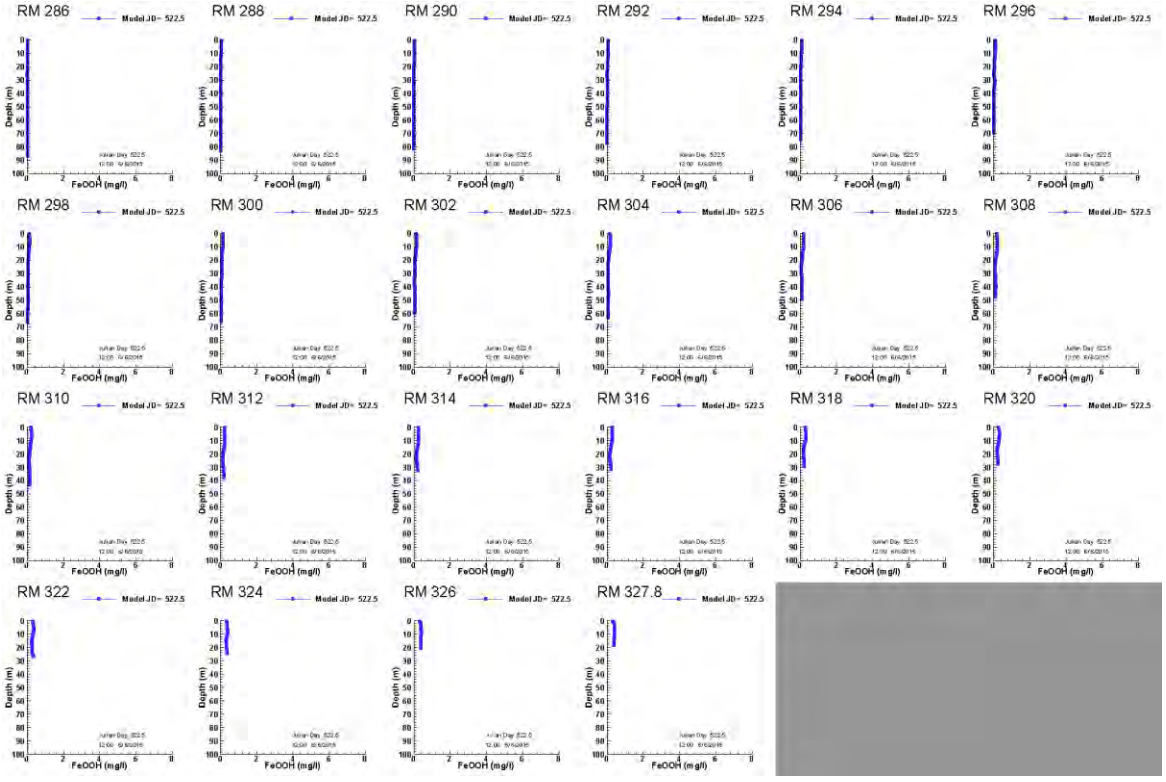


Figure 464. Vertical profiles of FeOOH compared with data for 6/ 6/2015.

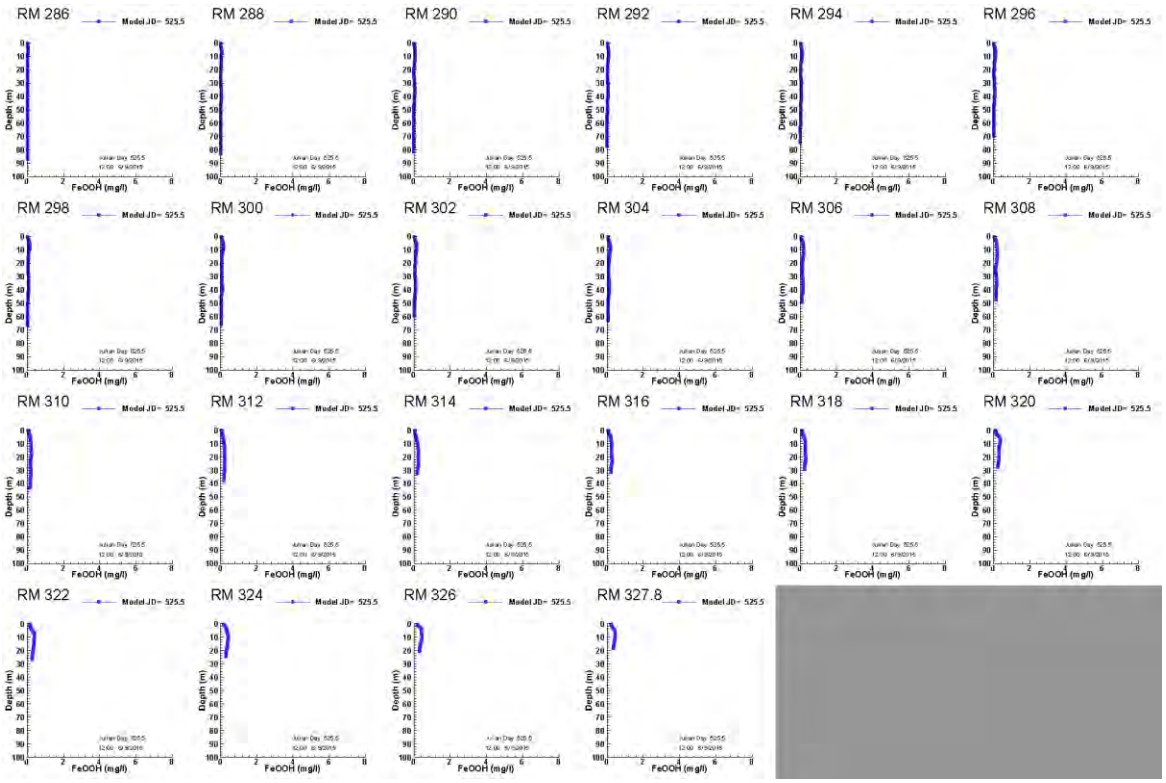


Figure 465. Vertical profiles of FeOOH compared with data for 6/ 9/2015.

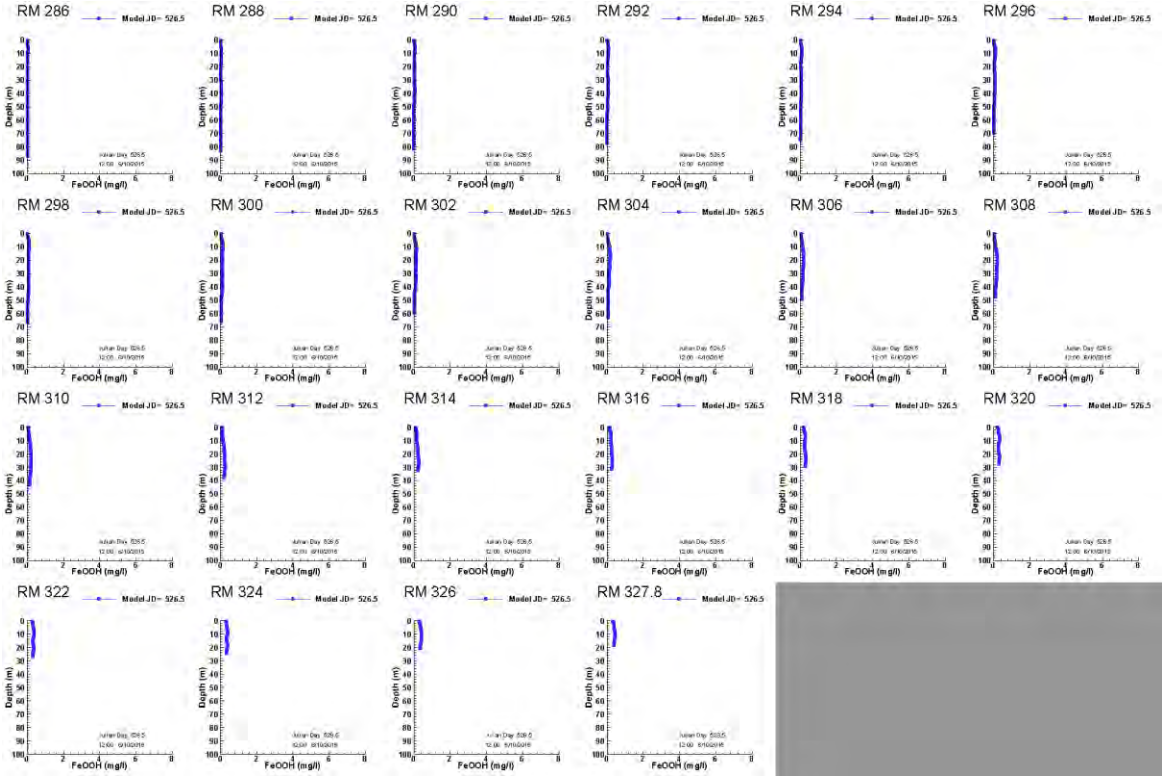


Figure 466. Vertical profiles of FeOOH compared with data for 6/10/2015.

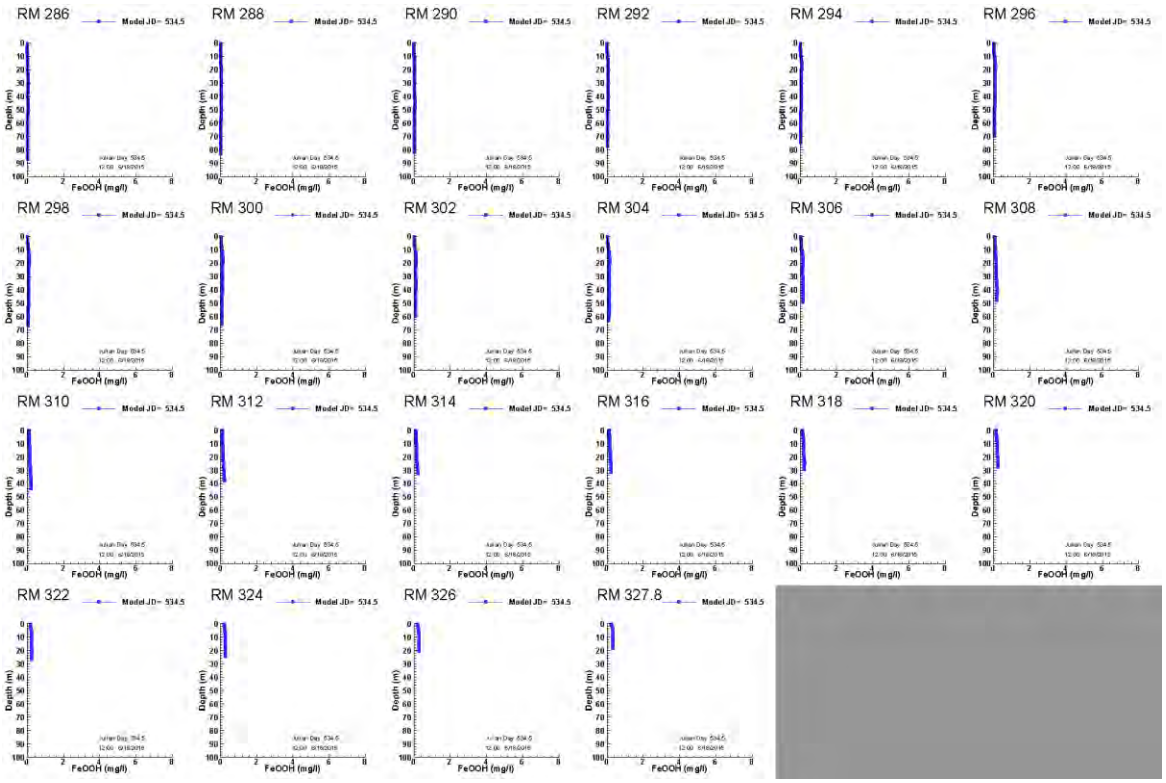


Figure 467. Vertical profiles of FeOOH compared with data for 6/18/2015.

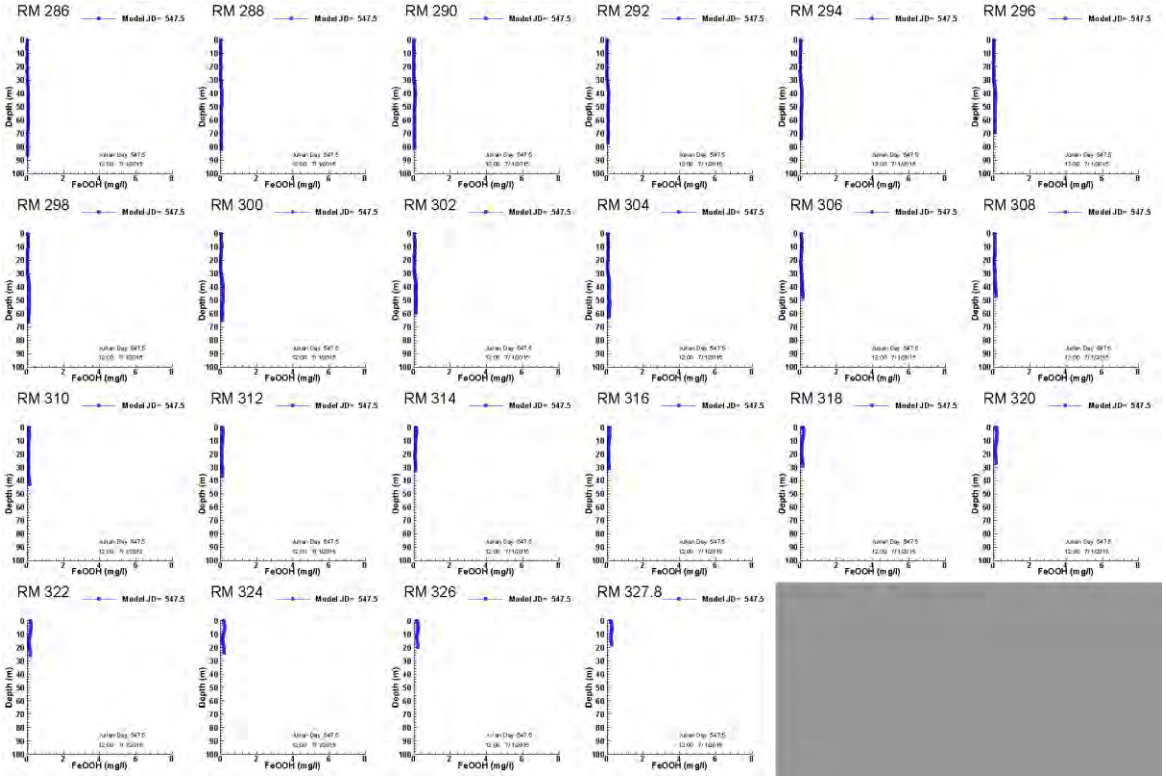


Figure 468. Vertical profiles of FeOOH compared with data for 7/ 1/2015.

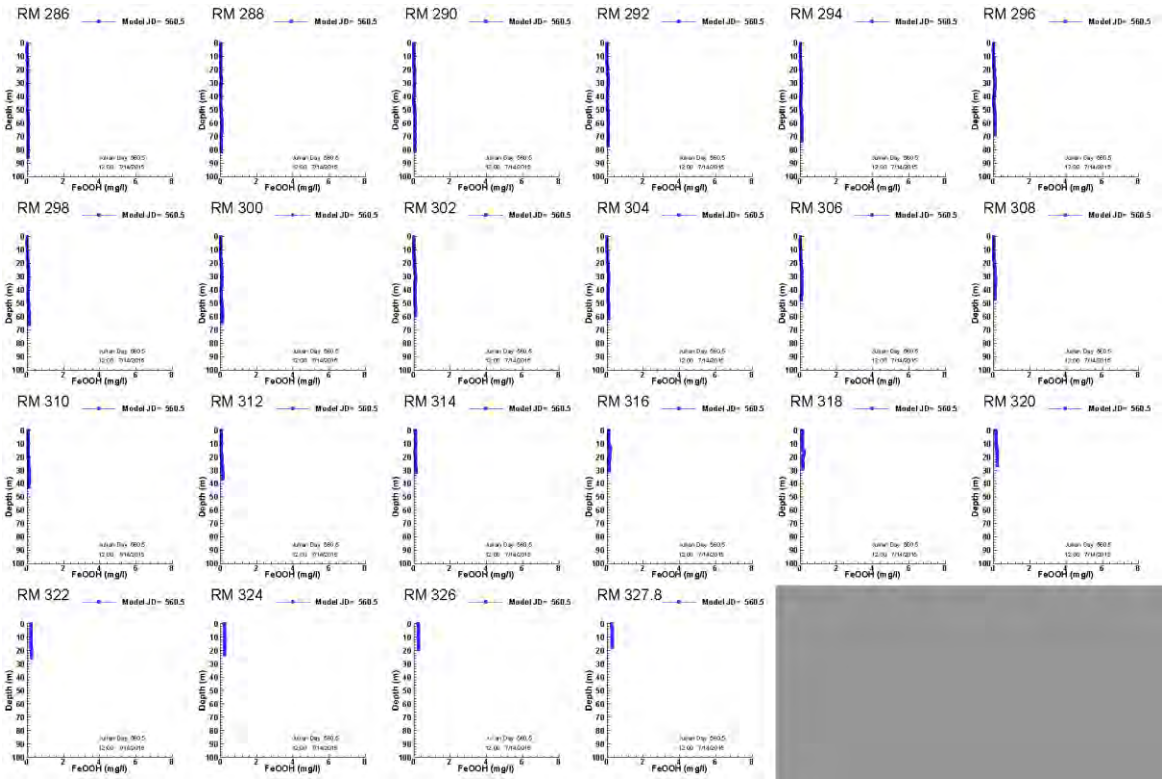


Figure 469. Vertical profiles of FeOOH compared with data for 7/14/2015.

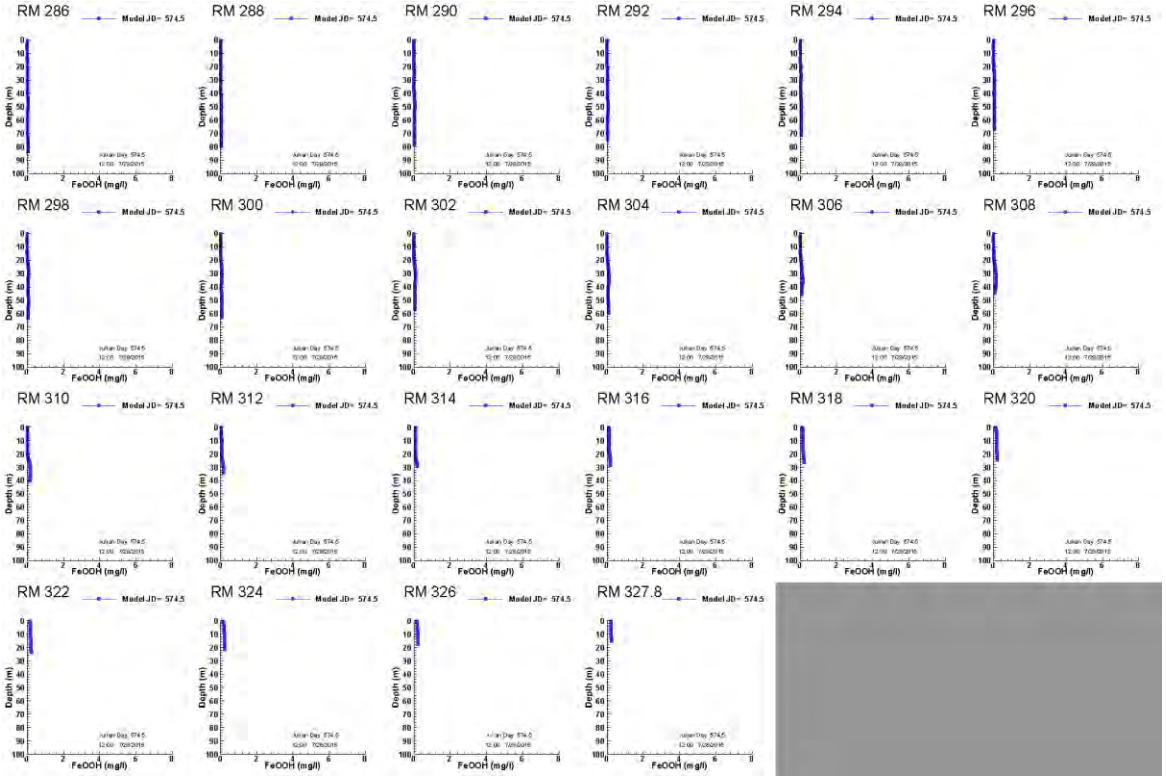


Figure 470. Vertical profiles of FeOOH compared with data for 7/28/2015.

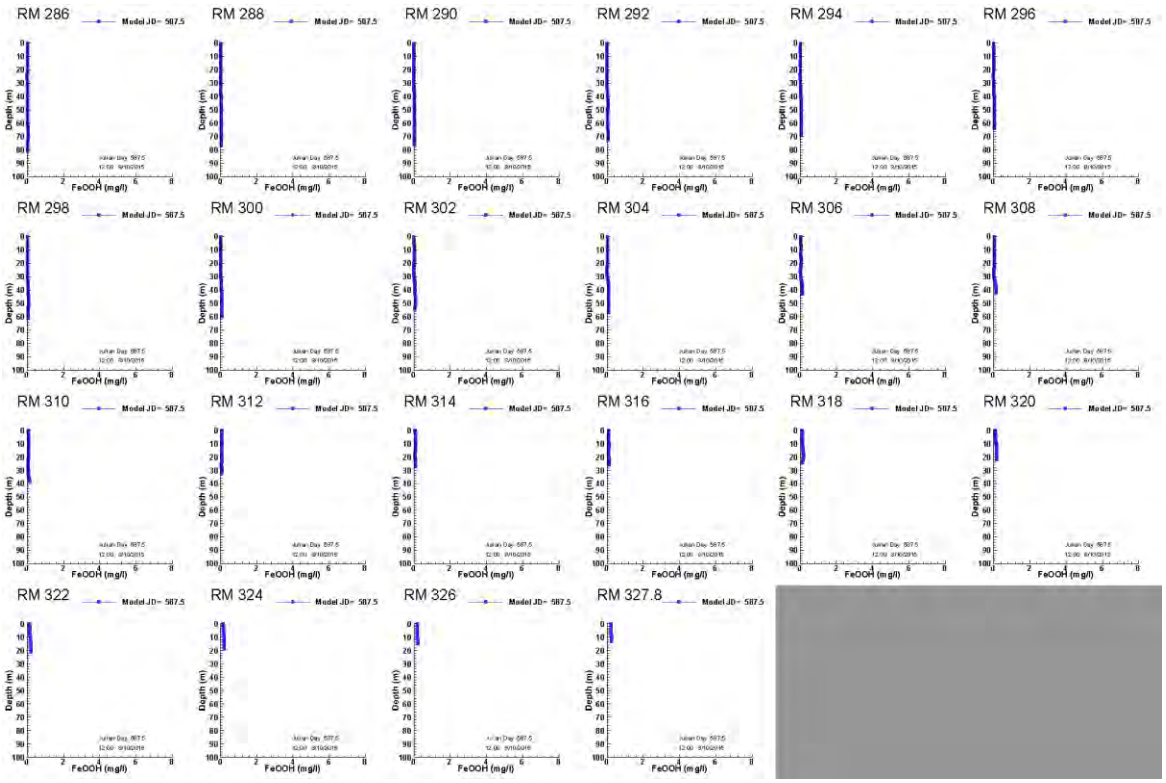


Figure 471. Vertical profiles of FeOOH compared with data for 8/10/2015.

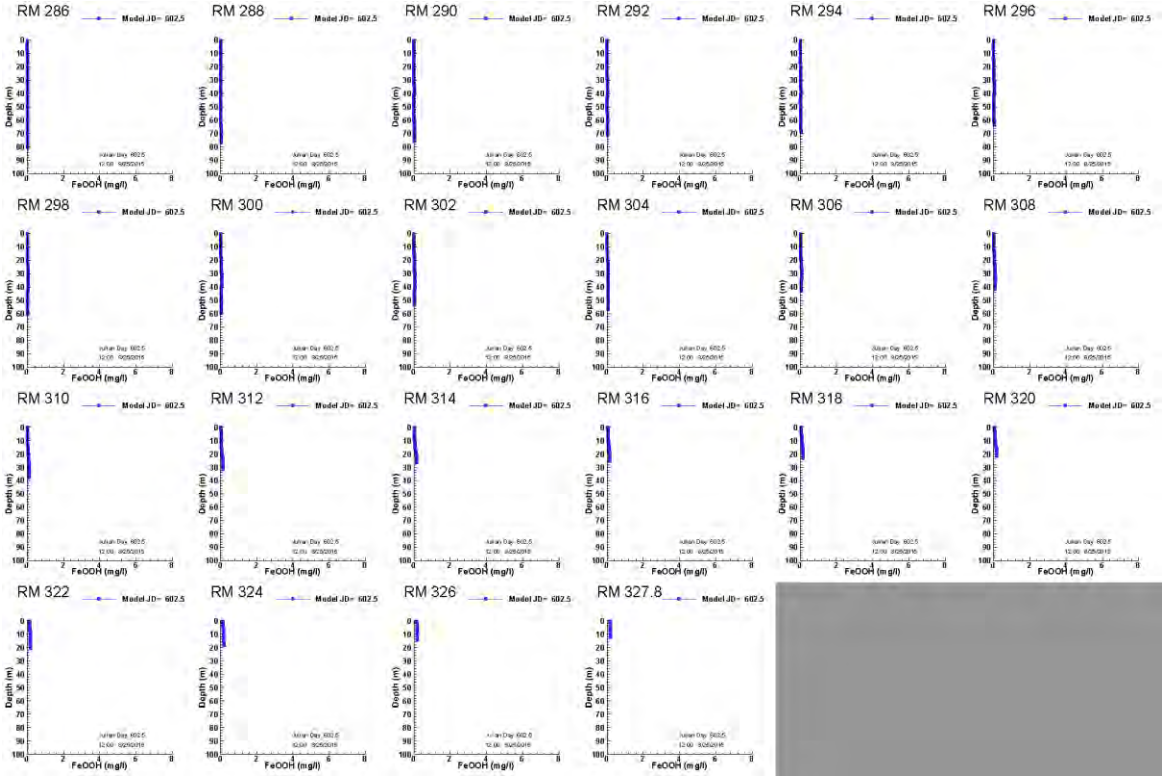


Figure 472. Vertical profiles of FeOOH compared with data for 8/25/2015.

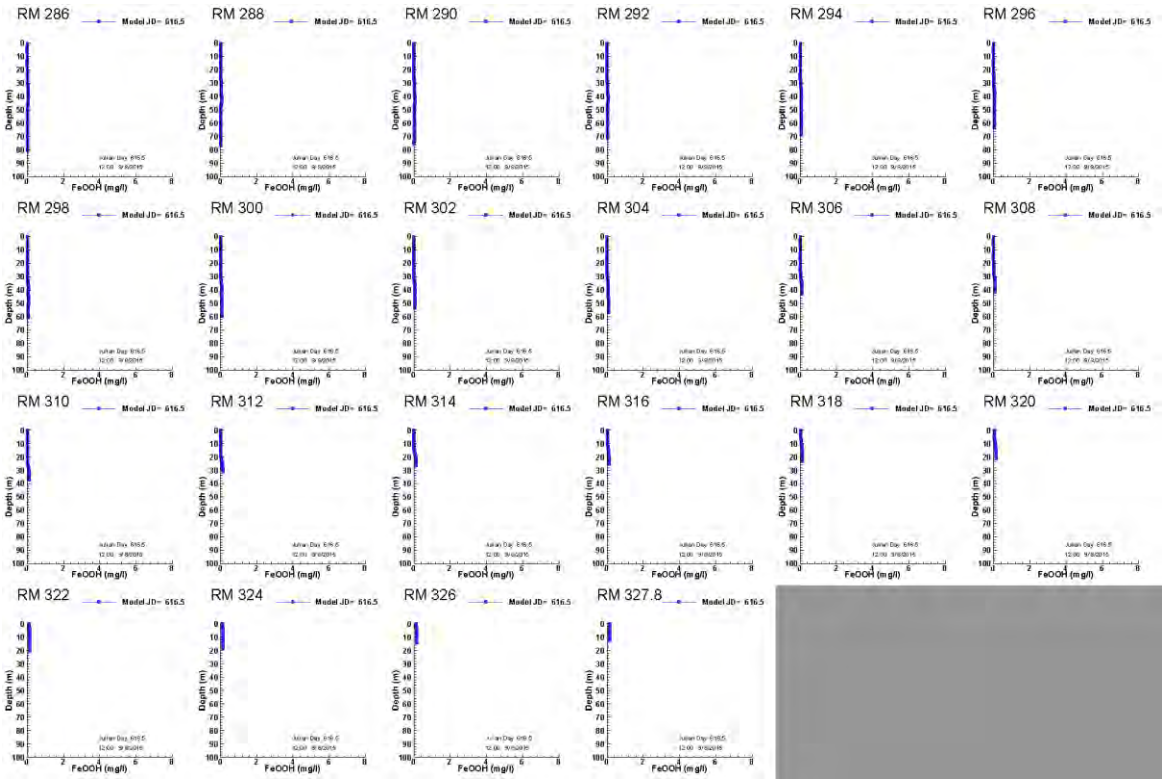


Figure 473. Vertical profiles of FeOOH compared with data for 9/ 8/2015.

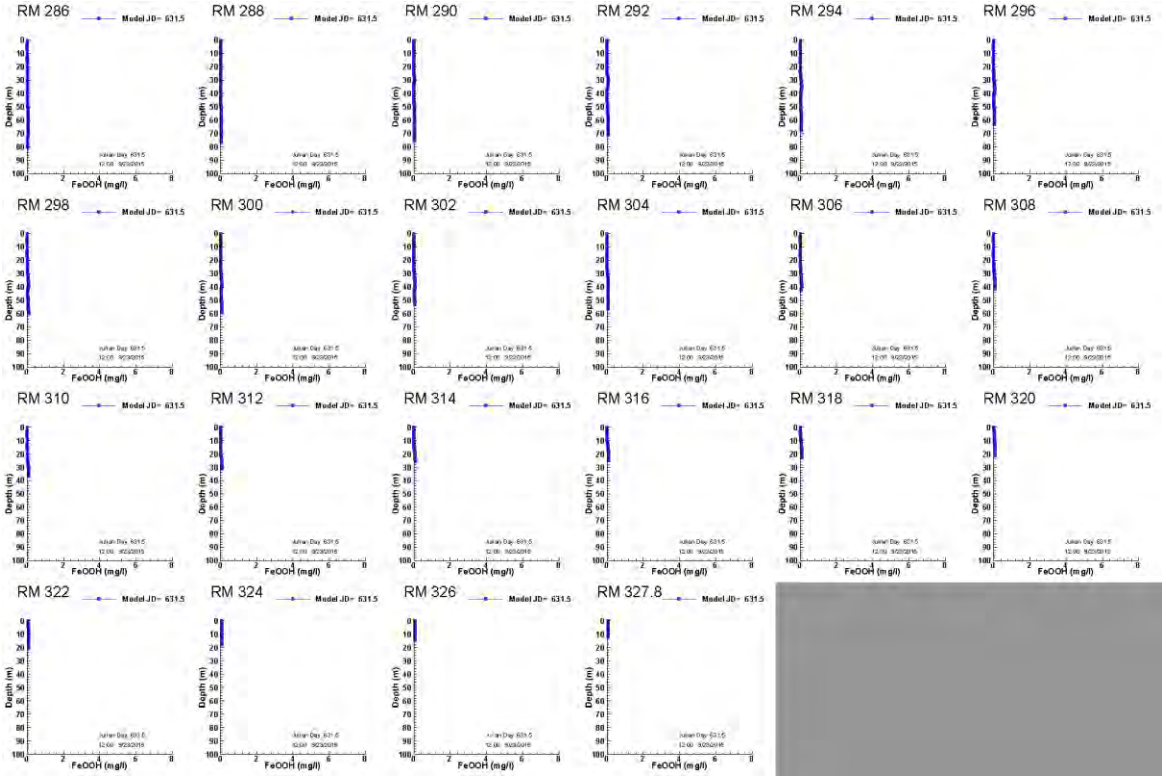


Figure 474. Vertical profiles of FeOOH compared with data for 9/23/2015.

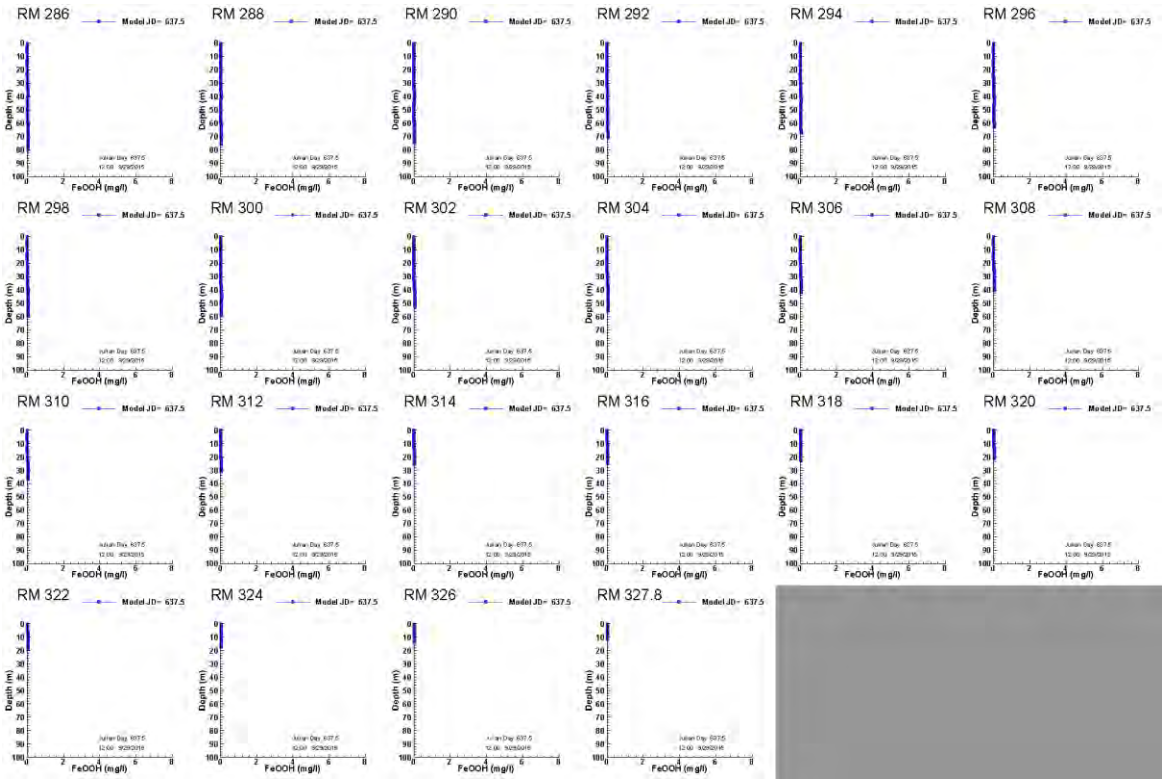


Figure 475. Vertical profiles of FeOOH compared with data for 9/29/2015.

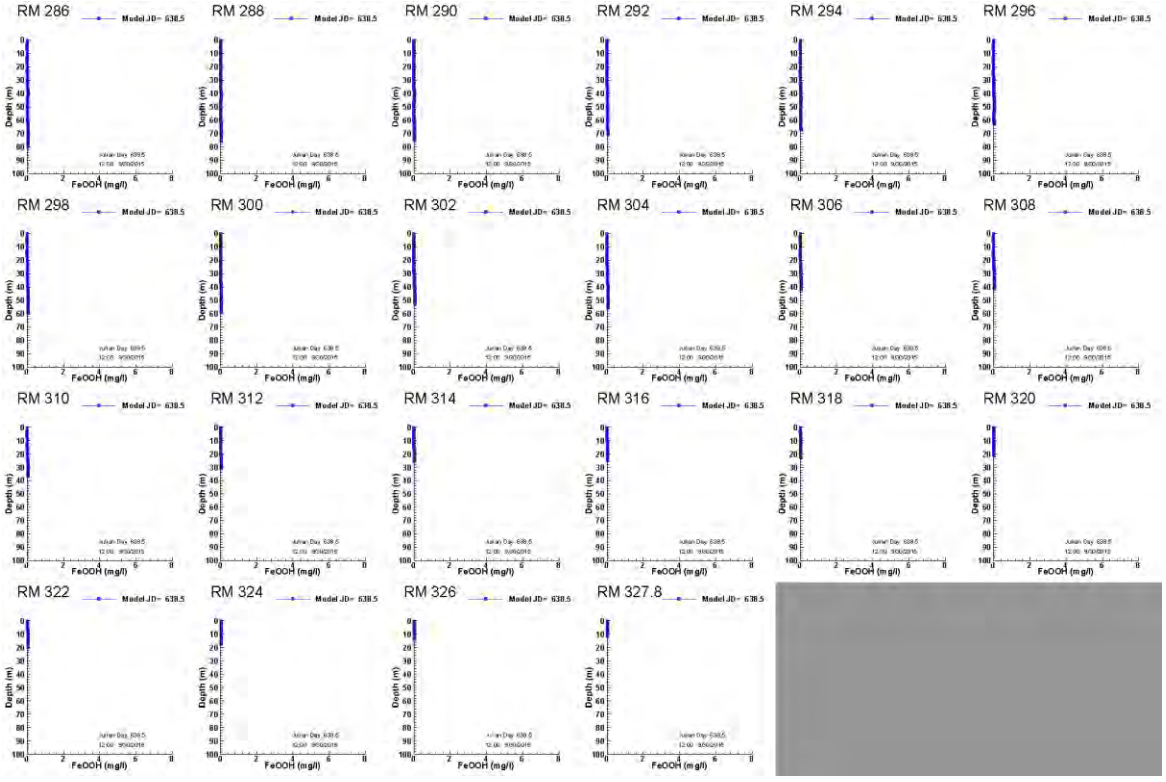


Figure 476. Vertical profiles of FeOOH compared with data for 9/30/2015.

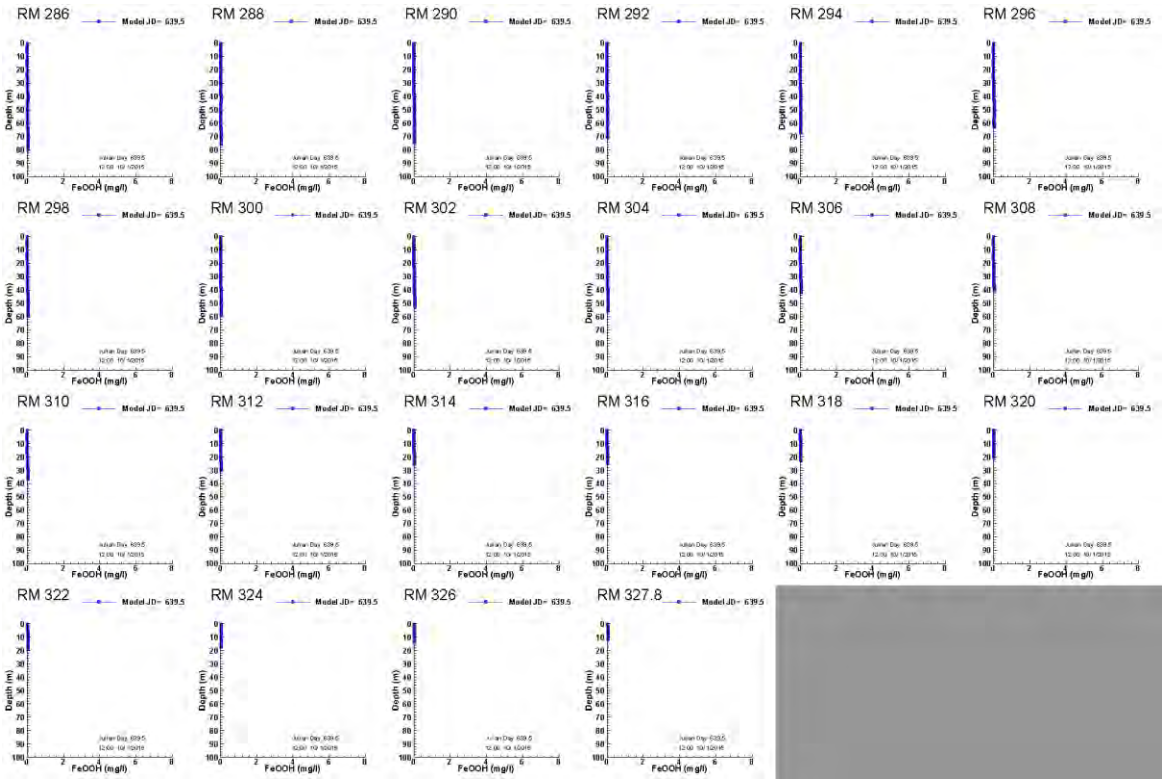


Figure 477. Vertical profiles of FeOOH compared with data for 10/ 1/2015.

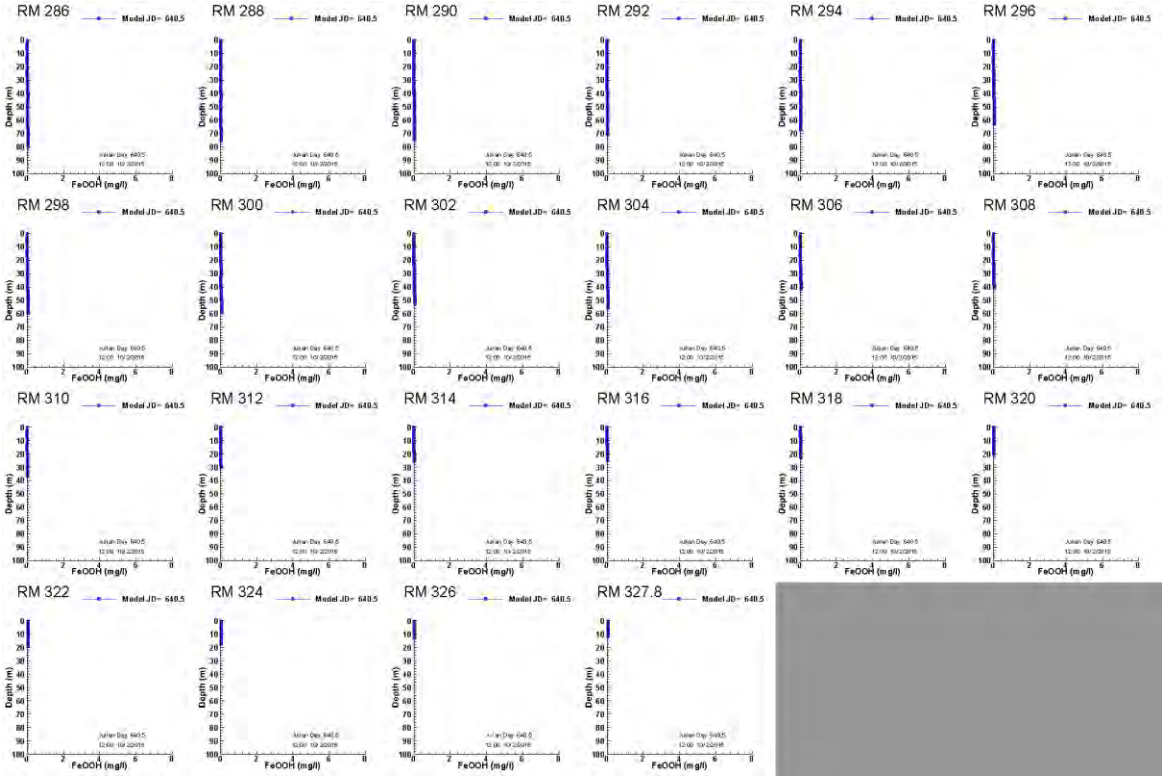


Figure 478. Vertical profiles of FeOOH compared with data for 10/ 2/2015.

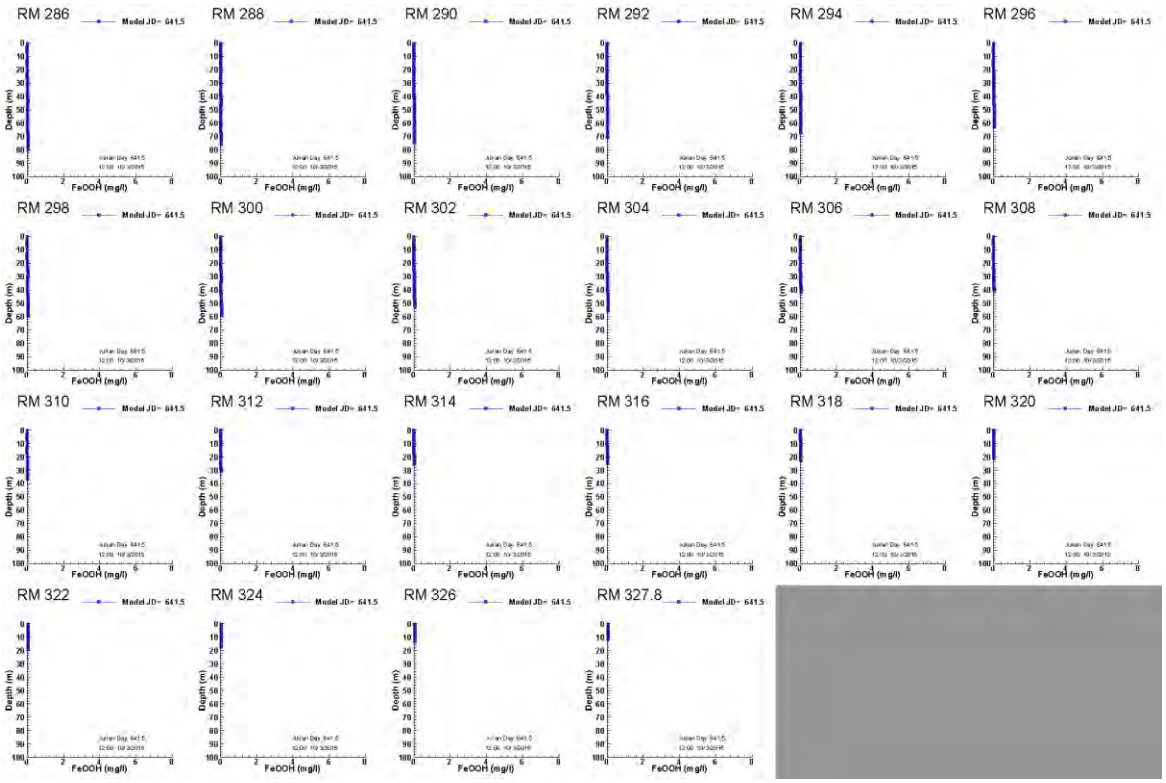


Figure 479. Vertical profiles of FeOOH compared with data for 10/ 3/2015.

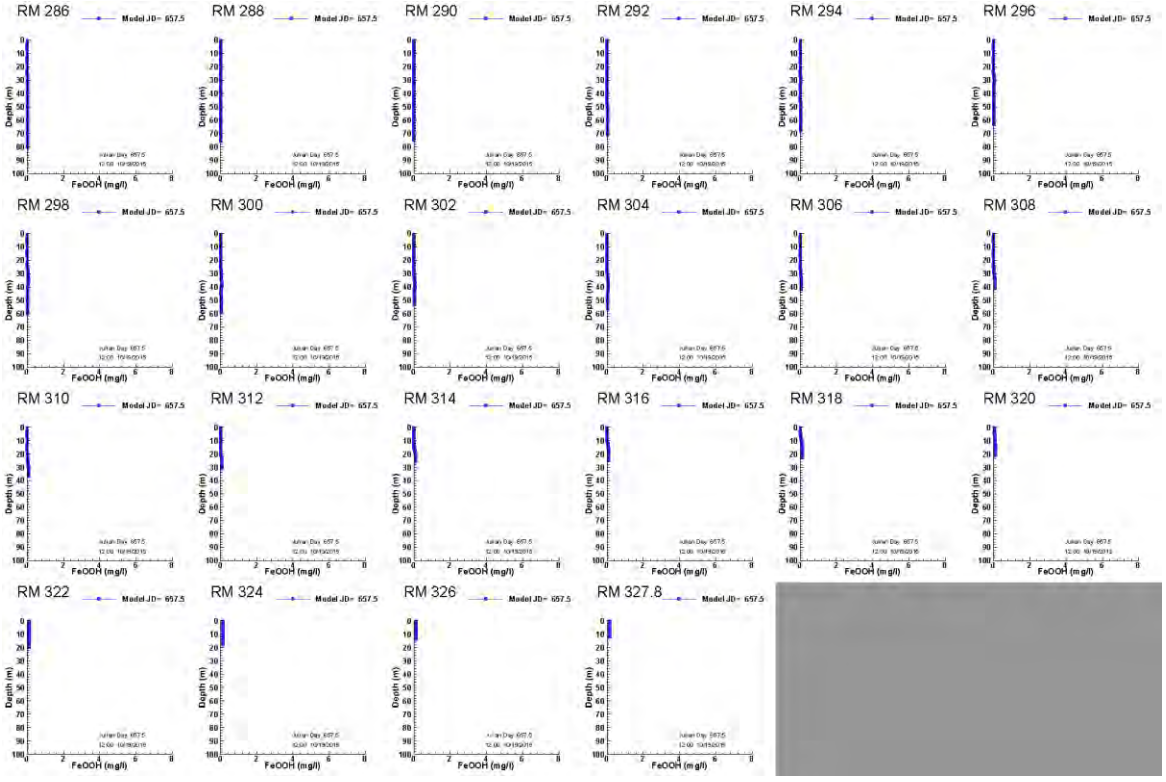


Figure 480. Vertical profiles of FeOOH compared with data for 10/19/2015.

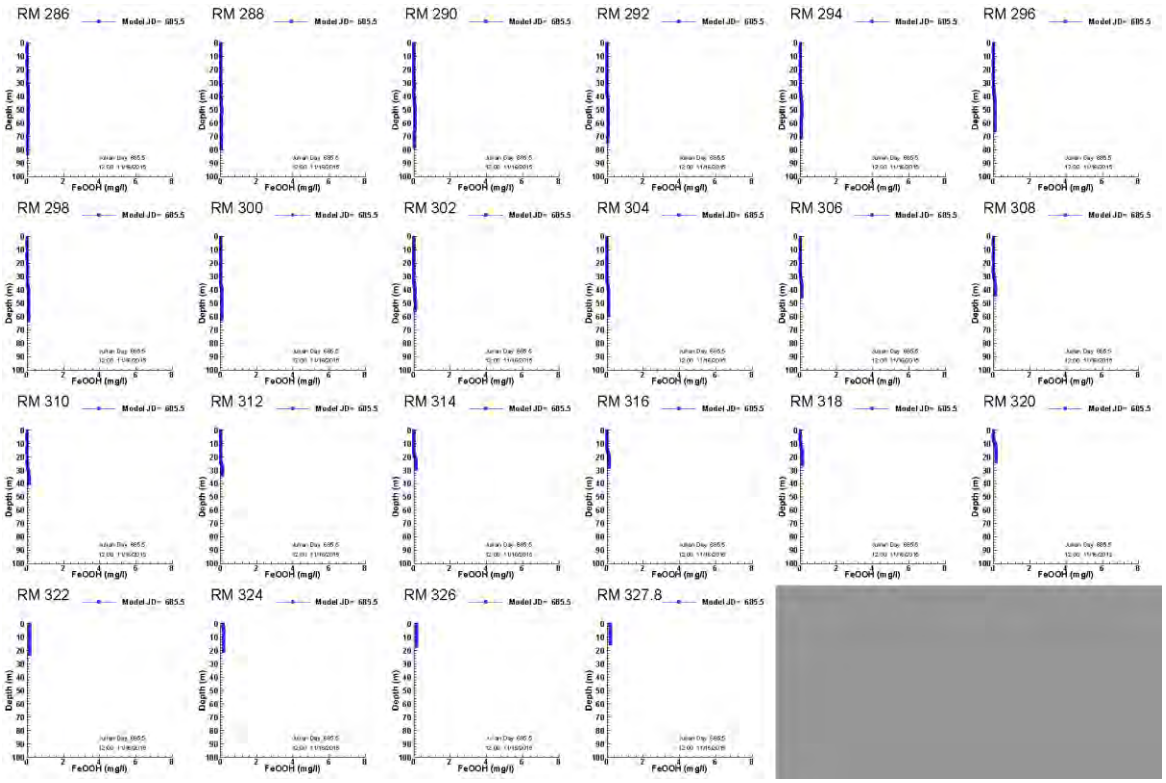


Figure 481. Vertical profiles of FeOOH compared with data for 11/16/2015.

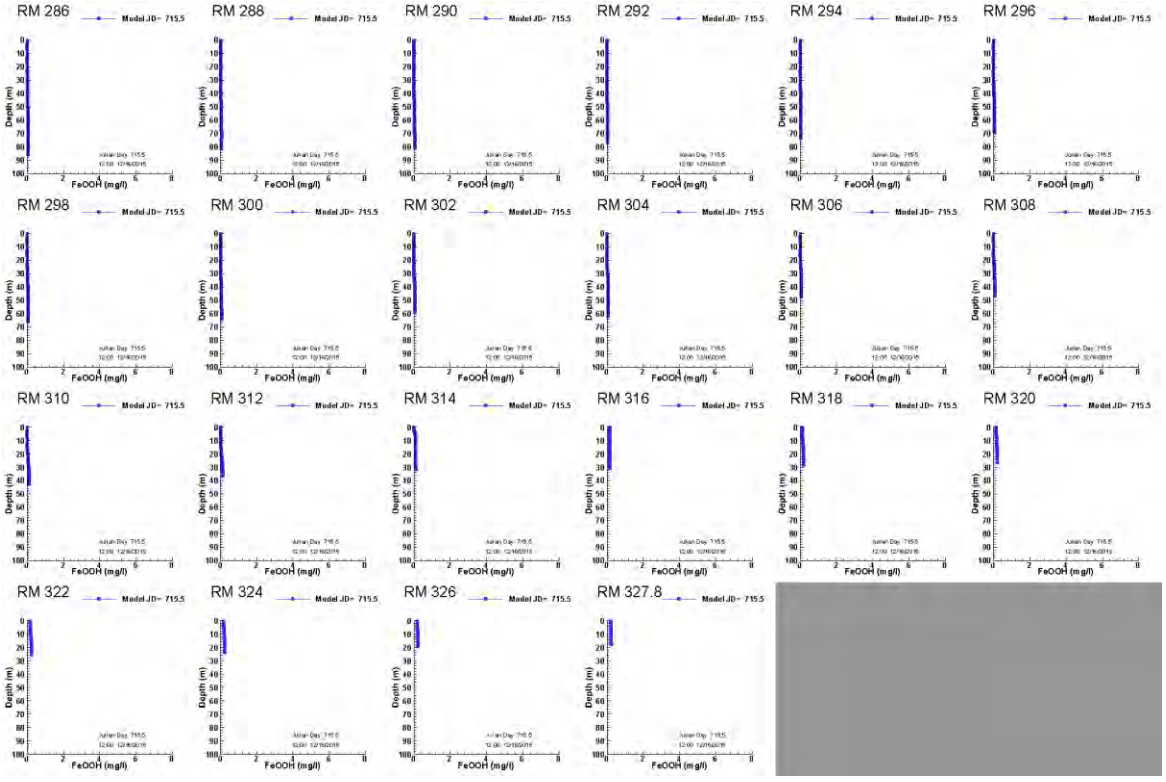


Figure 482. Vertical profiles of FeOOH compared with data for 12/16/2015.

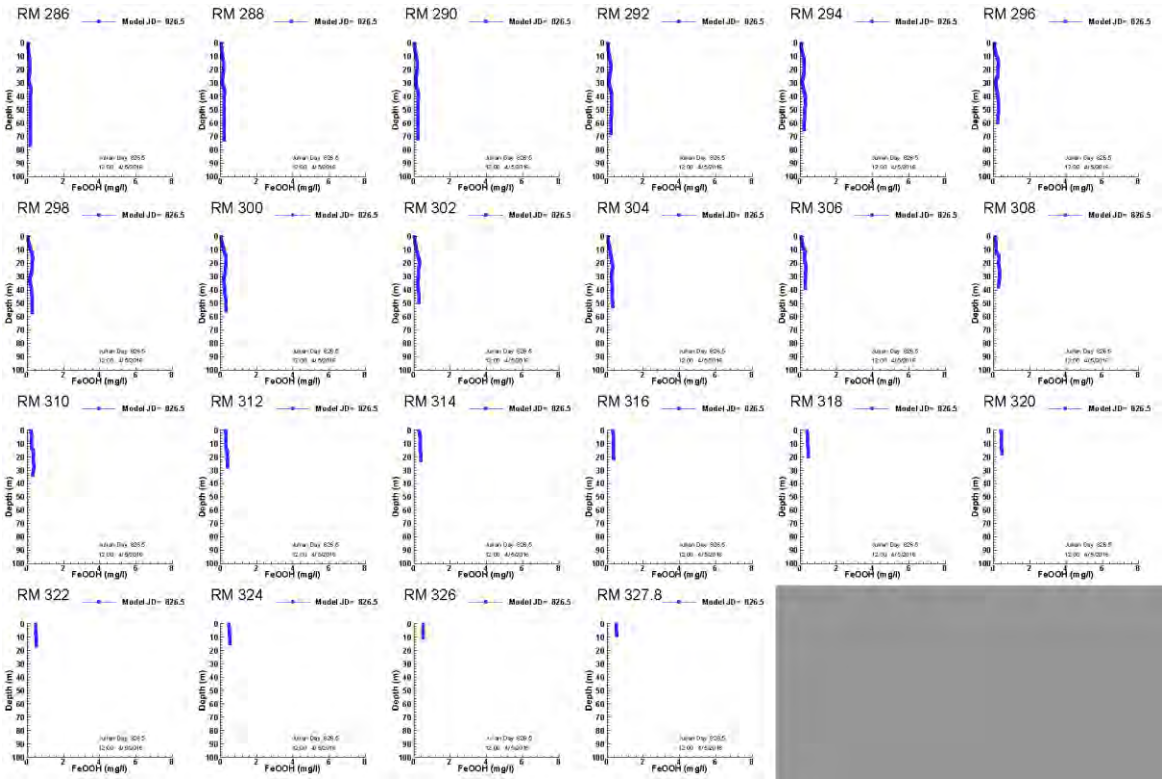


Figure 483. Vertical profiles of FeOOH compared with data for 4/ 5/2016.

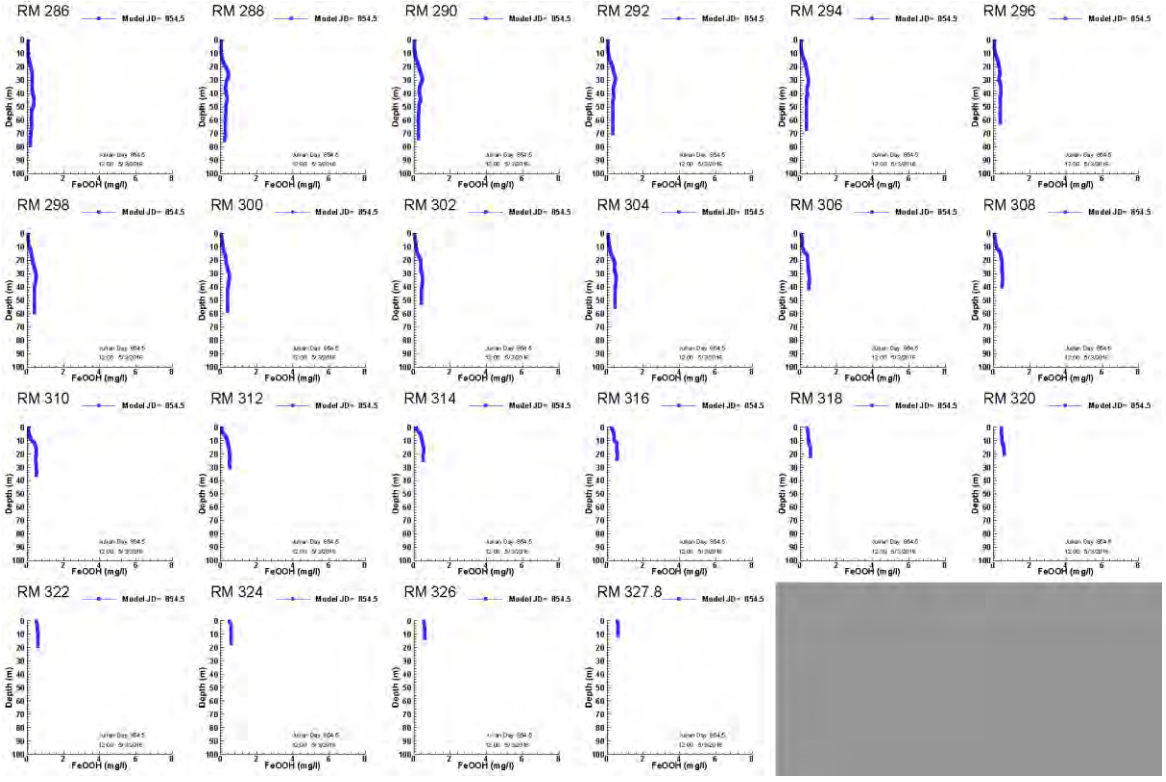


Figure 484. Vertical profiles of FeOOH compared with data for 5/ 3/2016.

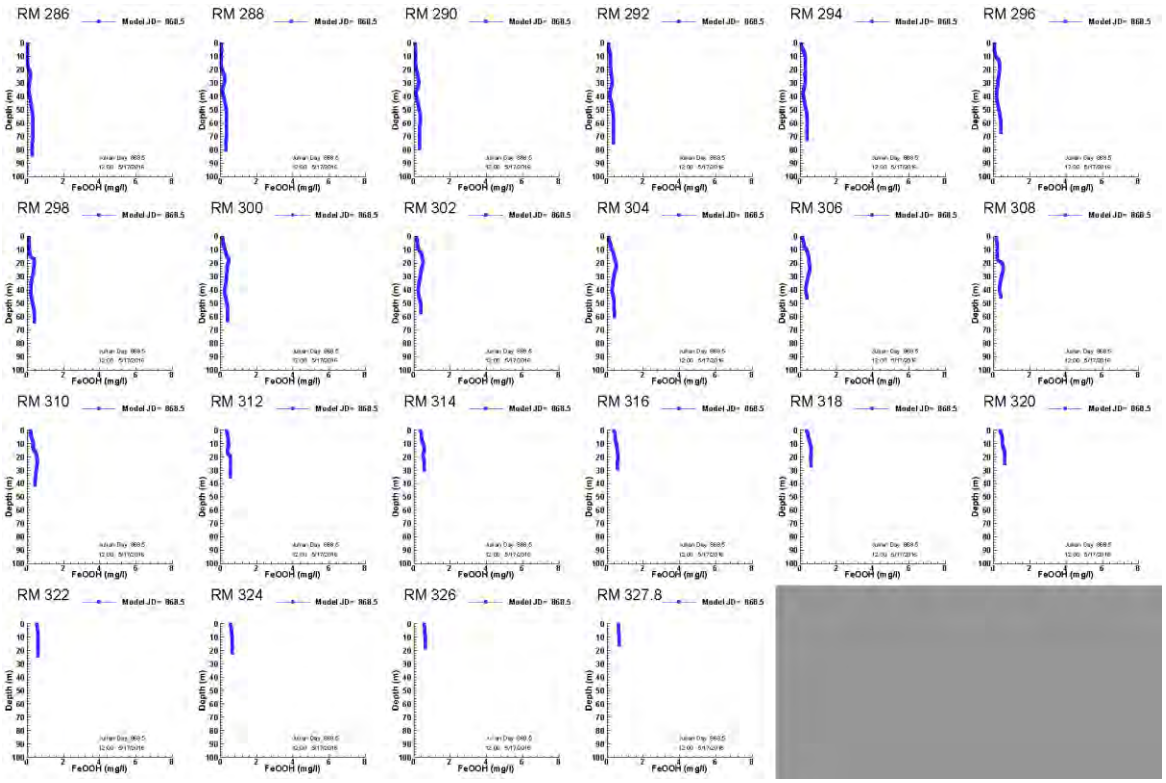


Figure 485. Vertical profiles of FeOOH compared with data for 5/17/2016.

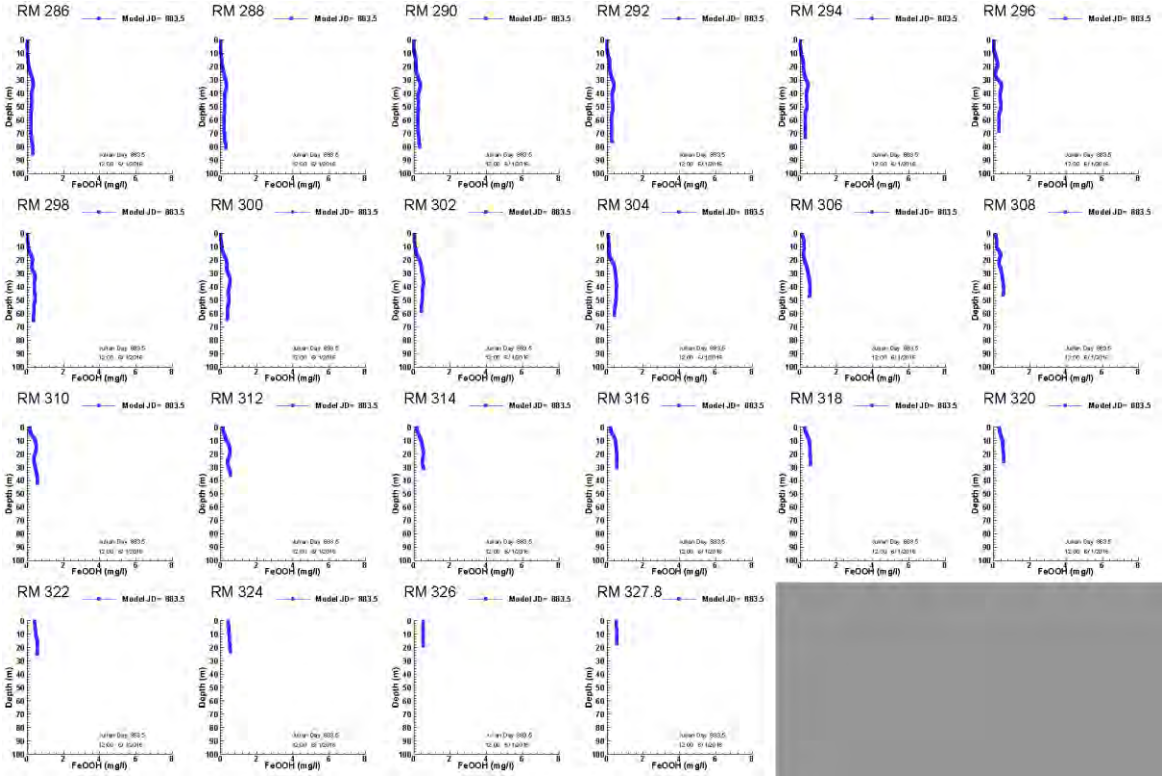


Figure 486. Vertical profiles of FeOOH compared with data for 6/ 1/2016.

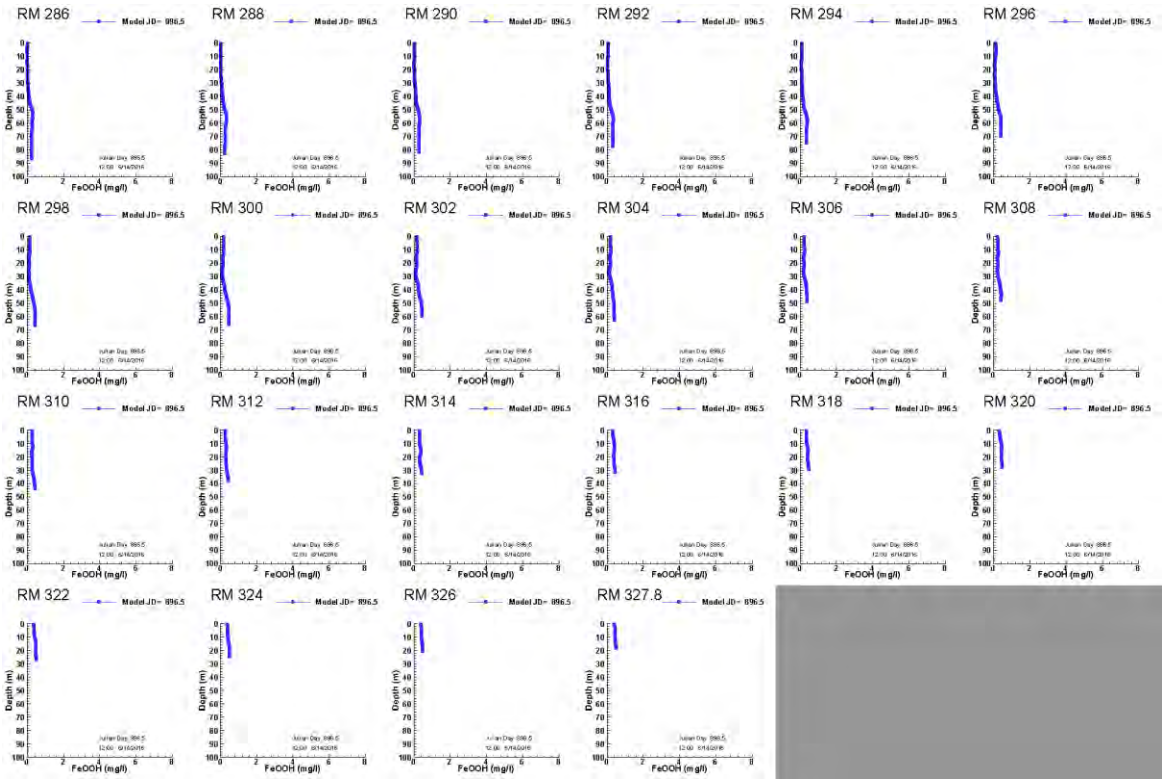


Figure 487. Vertical profiles of FeOOH compared with data for 6/14/2016.

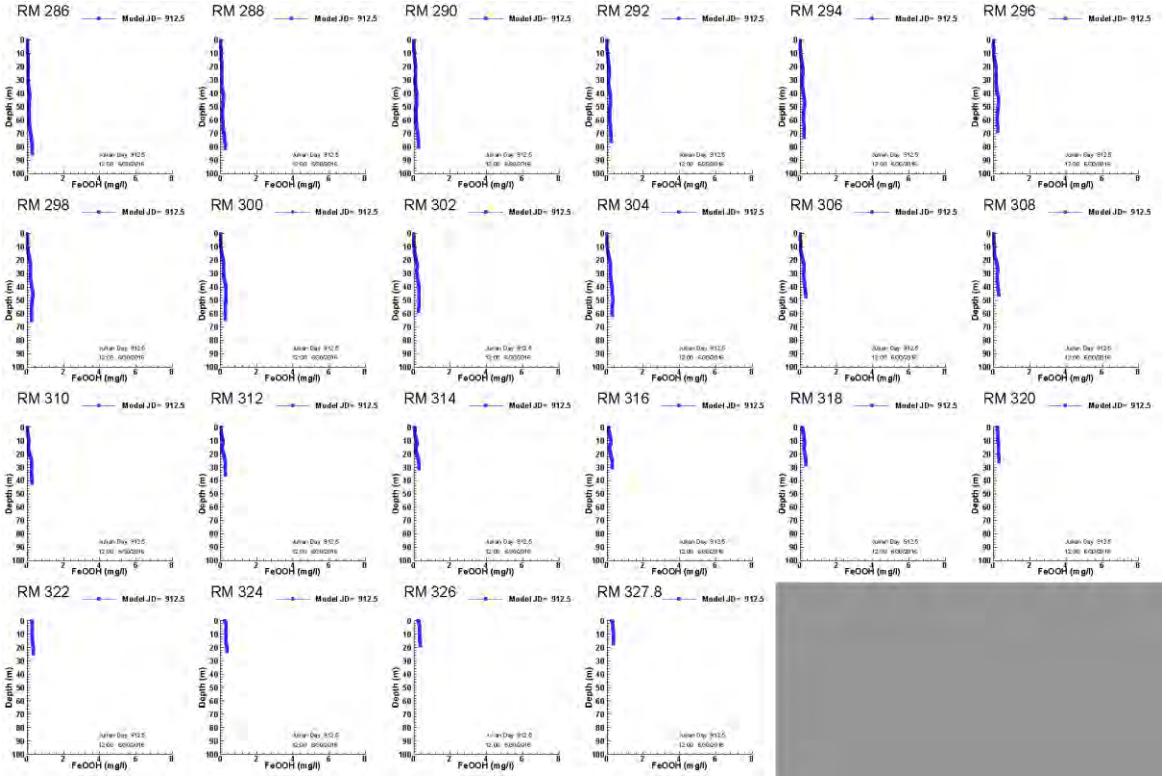


Figure 488. Vertical profiles of FeOOH compared with data for 6/30/2016.

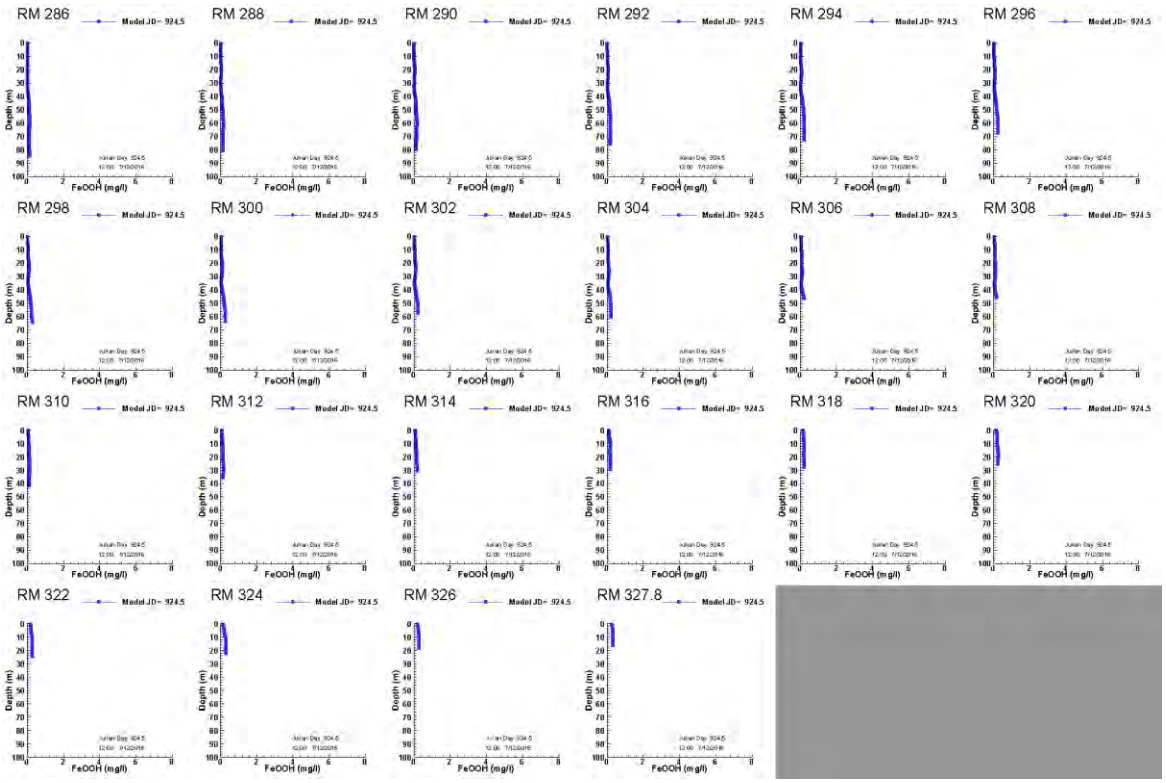


Figure 489. Vertical profiles of FeOOH compared with data for 7/12/2016.

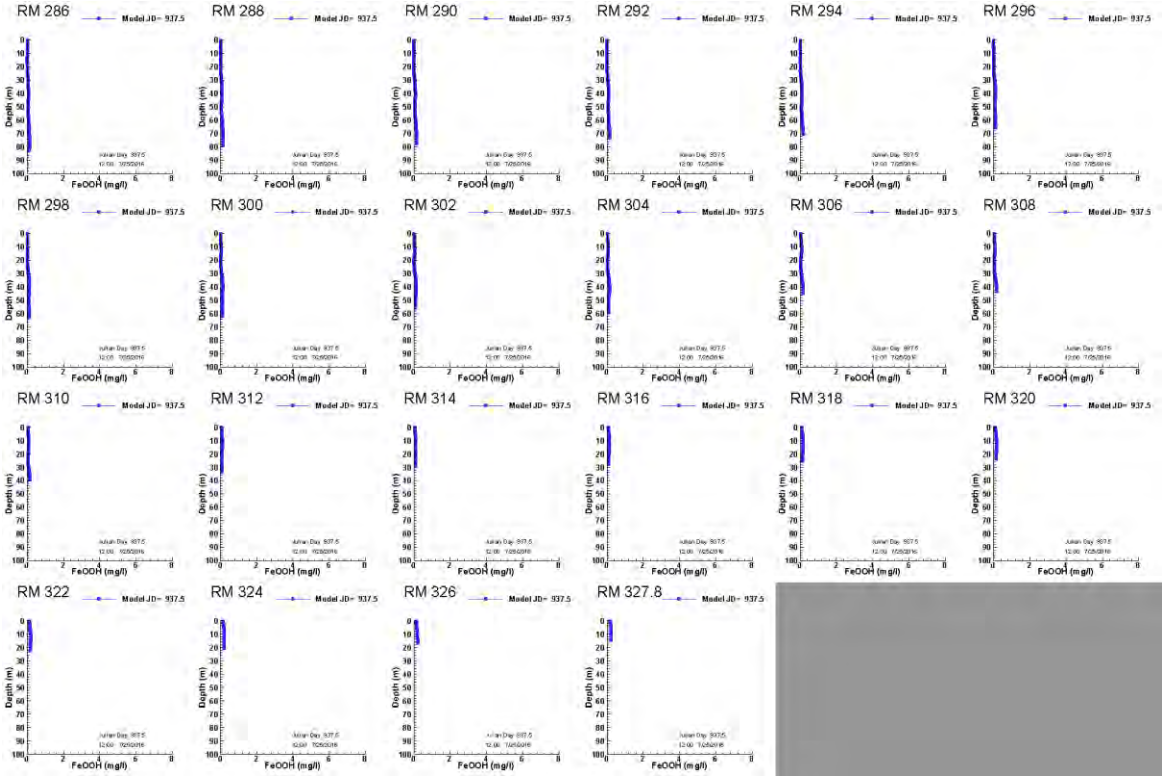


Figure 490. Vertical profiles of FeOOH compared with data for 7/25/2016.

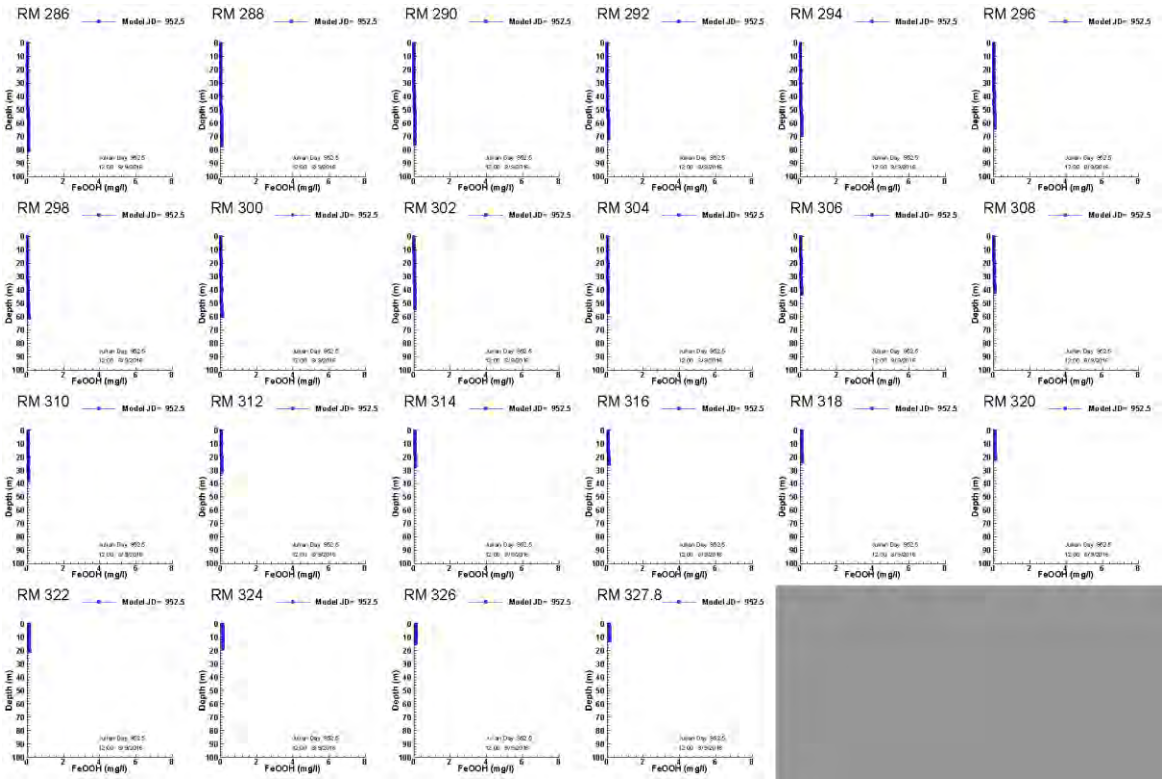


Figure 491. Vertical profiles of FeOOH compared with data for 8/ 9/2016.

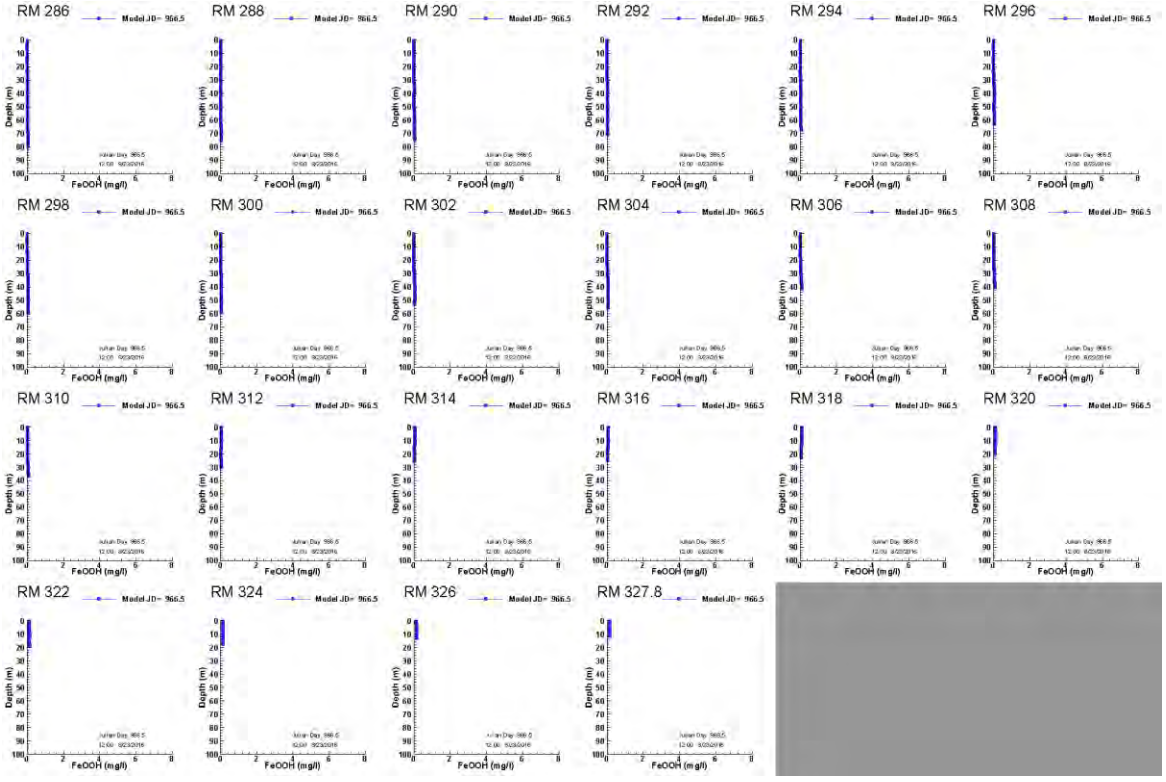


Figure 492. Vertical profiles of FeOOH compared with data for 8/23/2016.

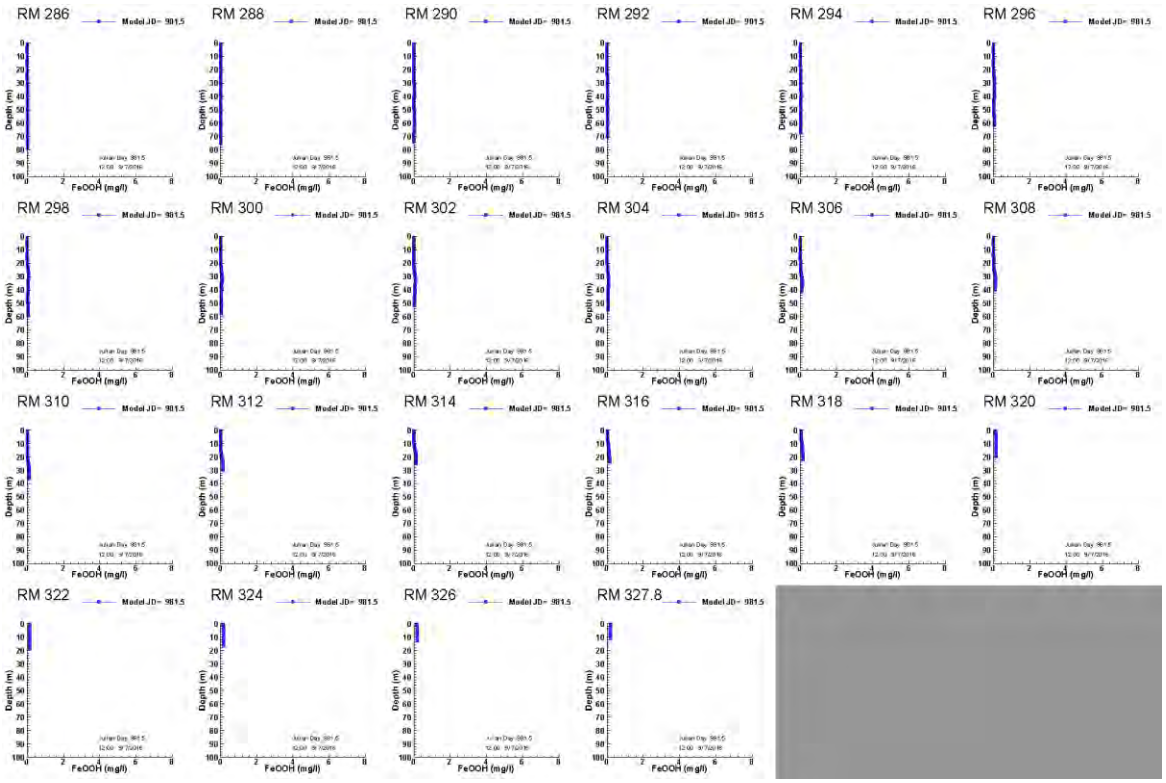


Figure 493. Vertical profiles of FeOOH compared with data for 9/ 7/2016.

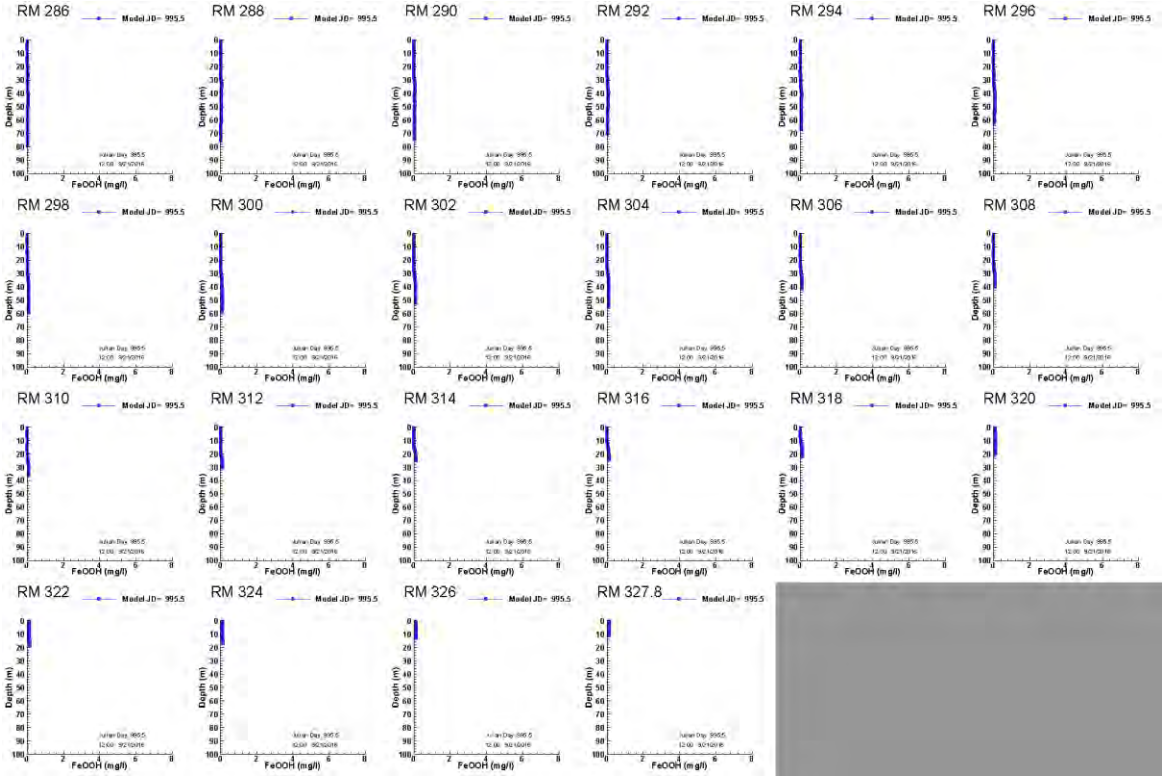


Figure 494. Vertical profiles of FeOOH compared with data for 9/21/2016.

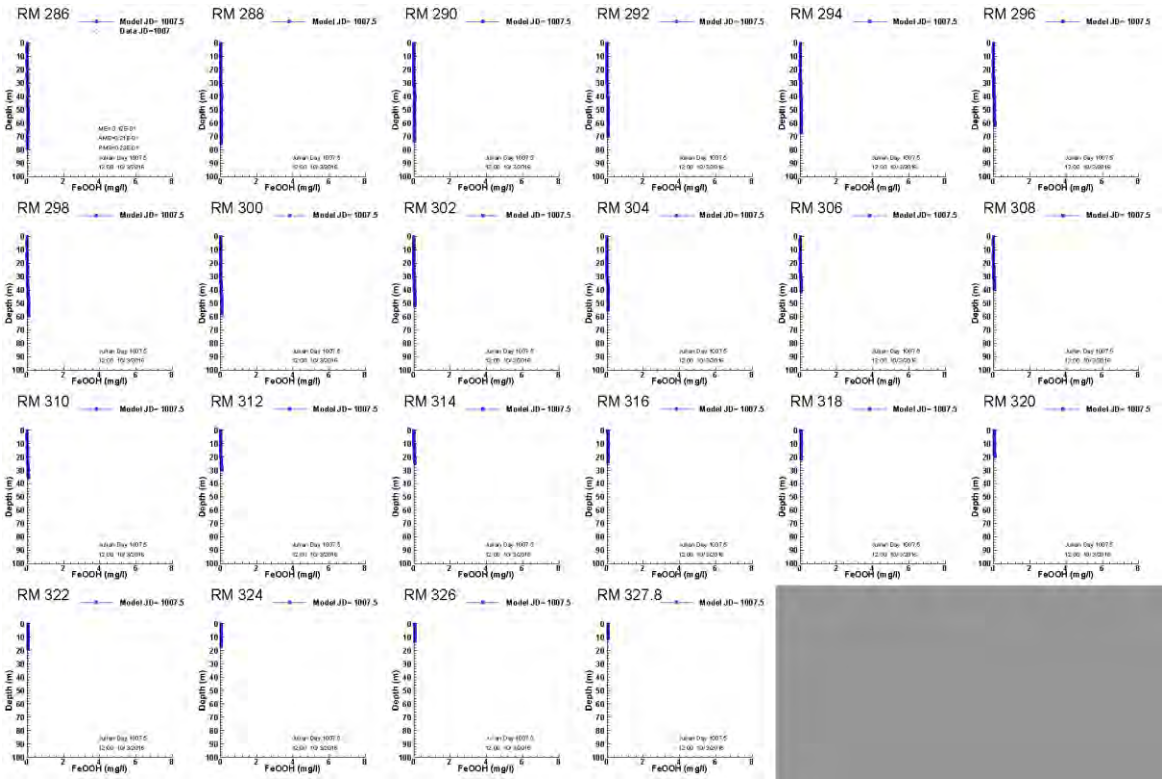


Figure 495. Vertical profiles of FeOOH compared with data for 10/ 3/2016.

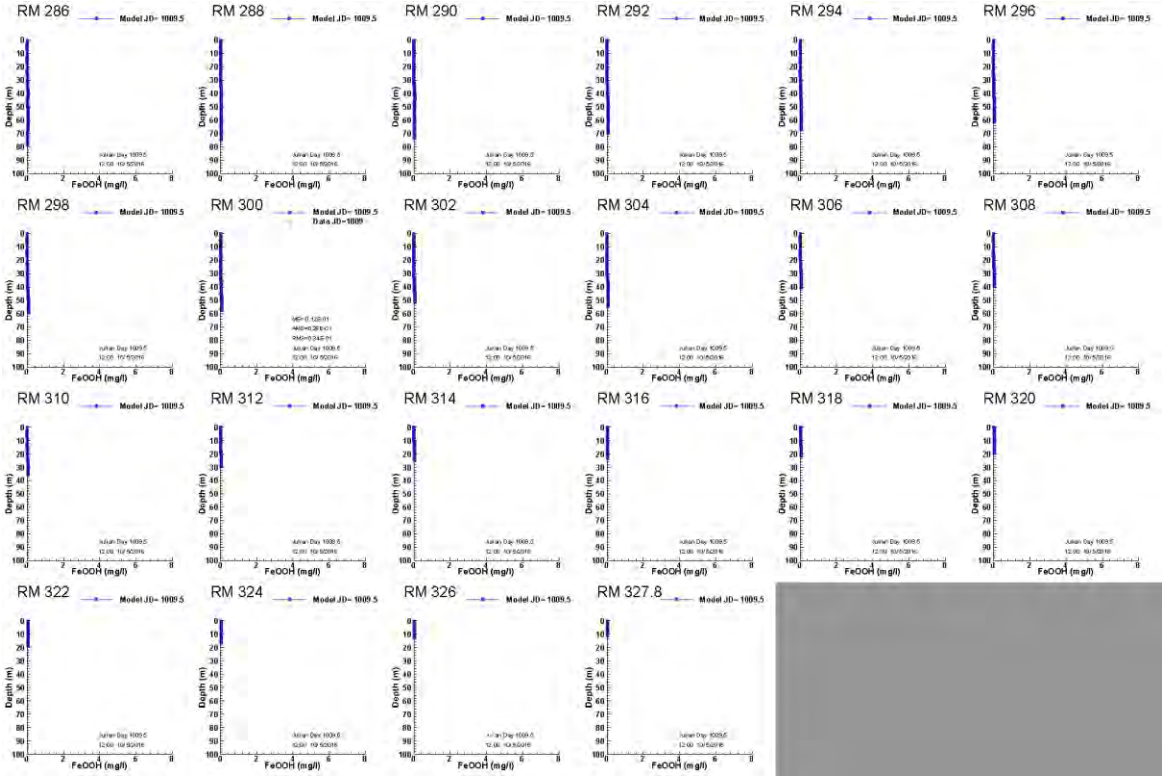


Figure 496. Vertical profiles of FeOOH compared with data for 10/ 5/2016.

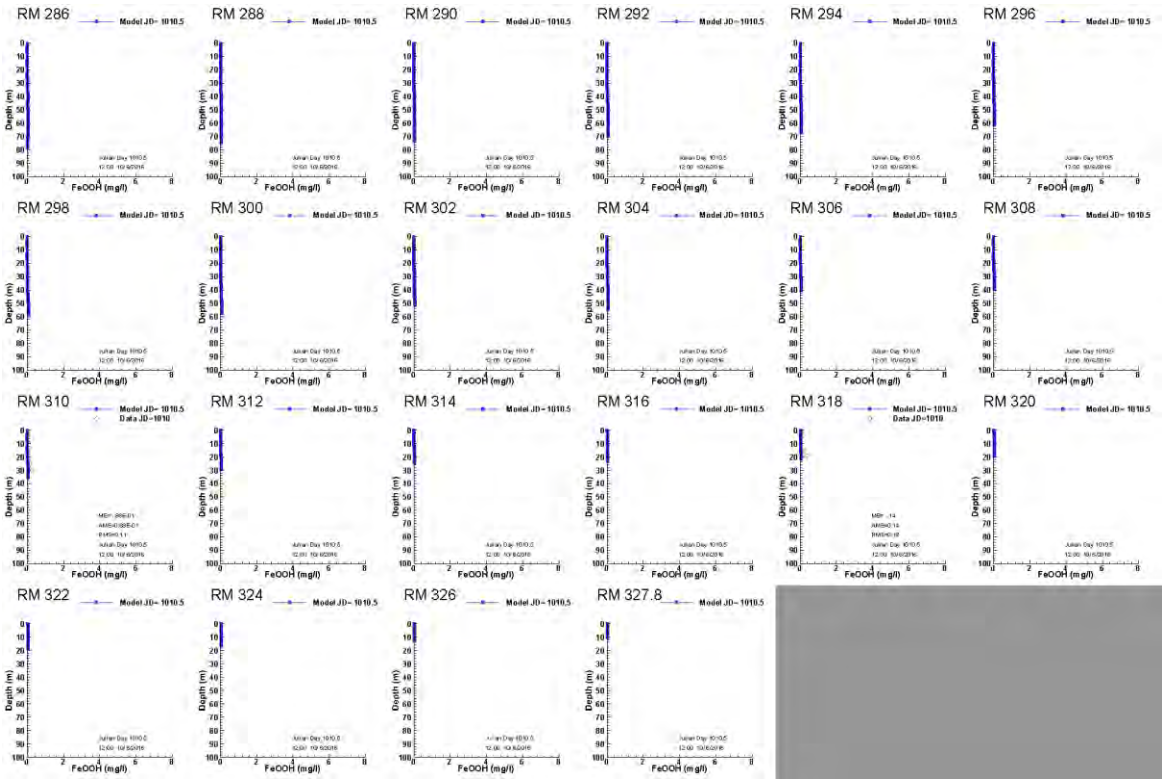


Figure 497. Vertical profiles of FeOOH compared with data for 10/ 6/2016.

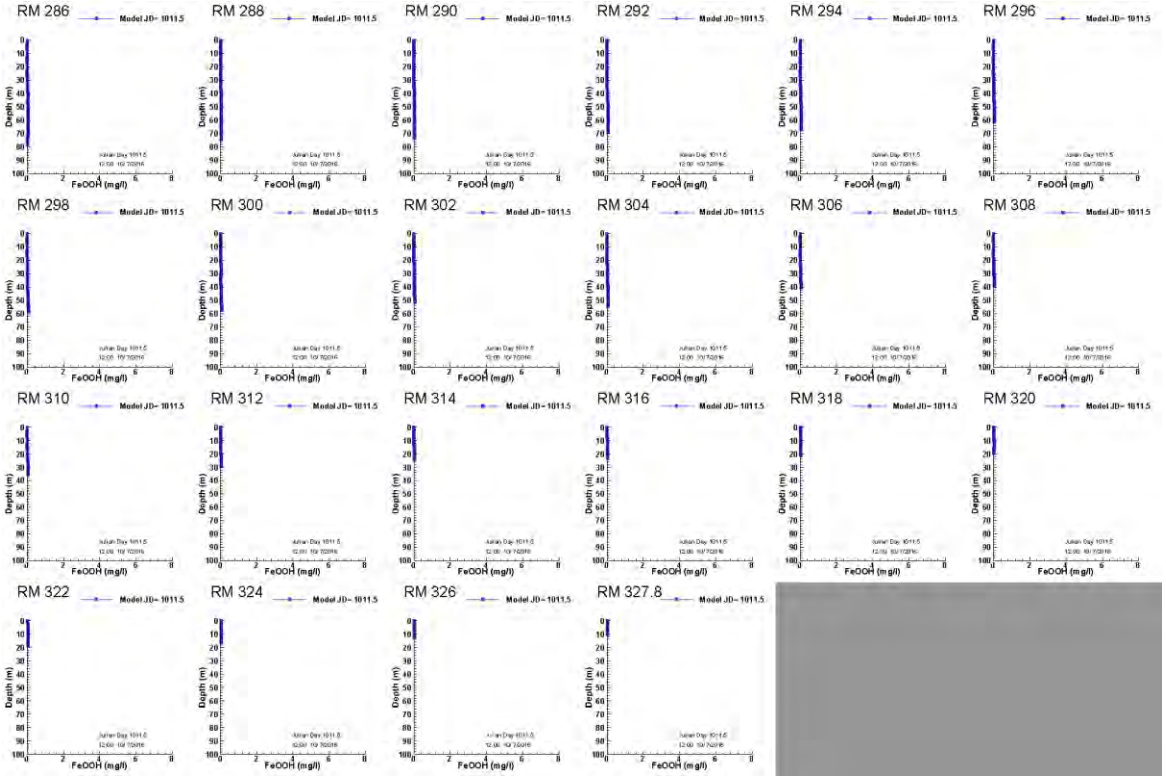


Figure 498. Vertical profiles of FeOOH compared with data for 10/ 7/2016.

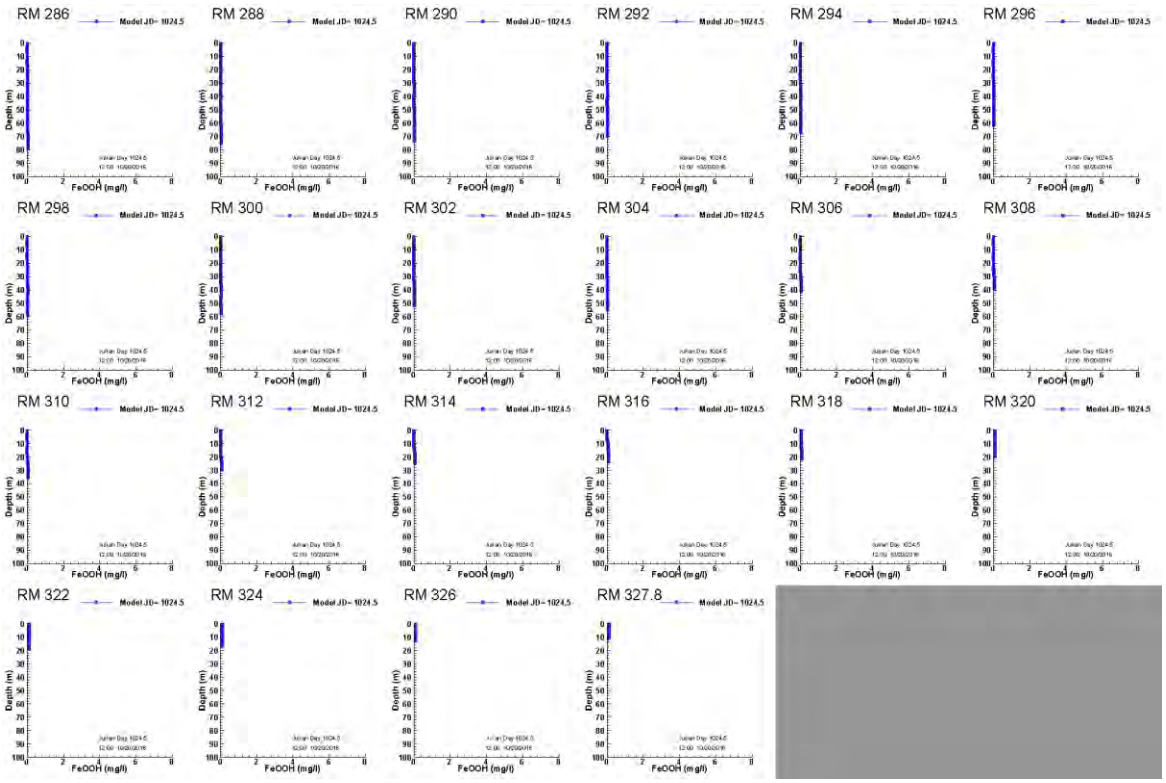


Figure 499. Vertical profiles of FeOOH compared with data for 10/20/2016.

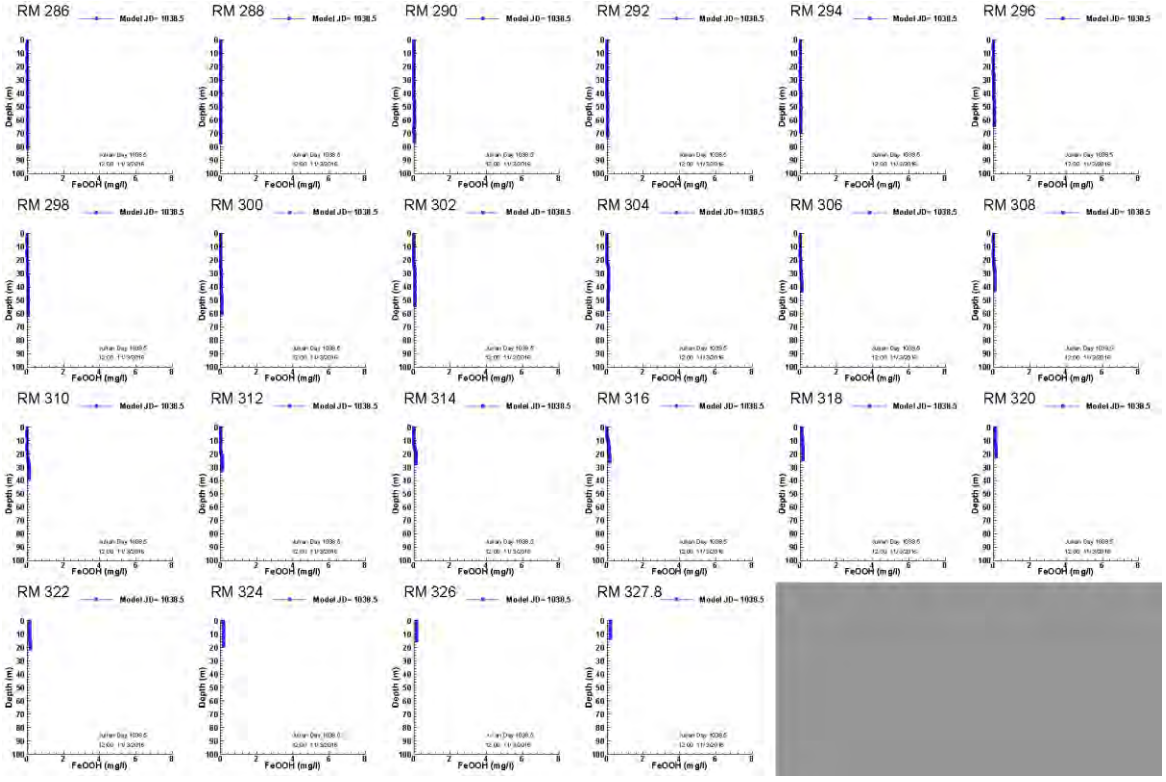


Figure 500. Vertical profiles of FeOOH compared with data for 11/ 3/2016.

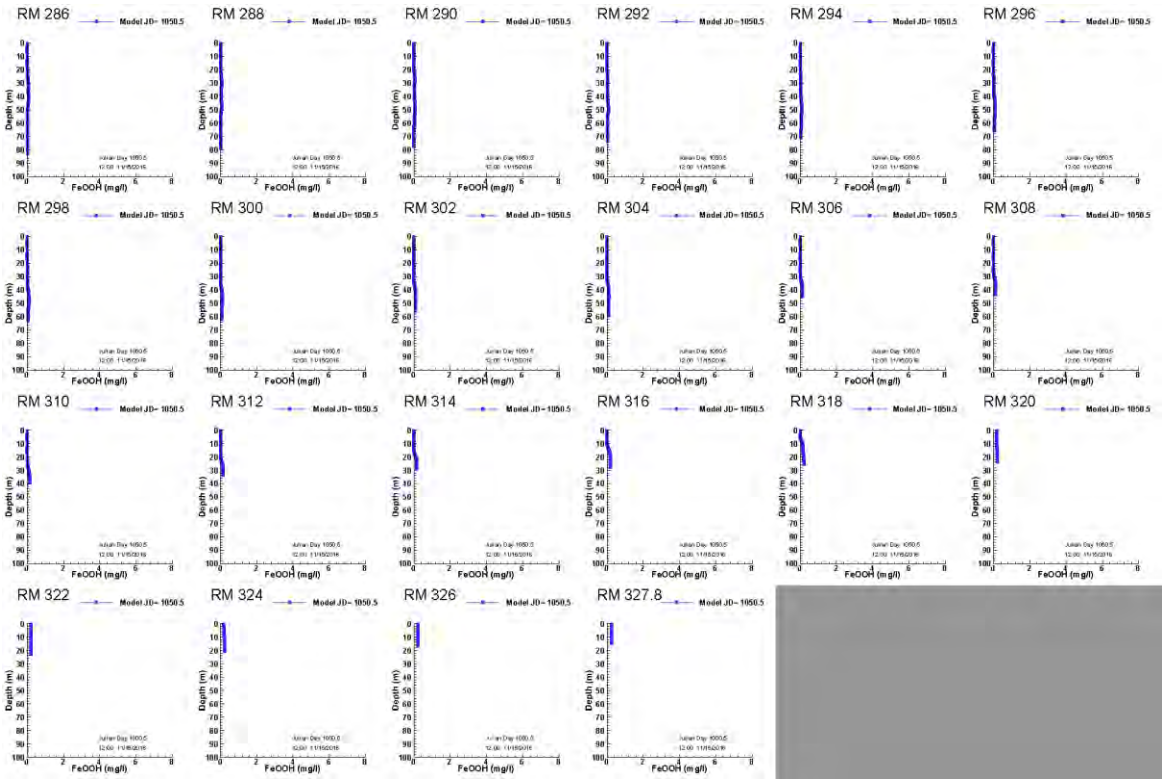


Figure 501. Vertical profiles of FeOOH compared with data for 11/15/2016.

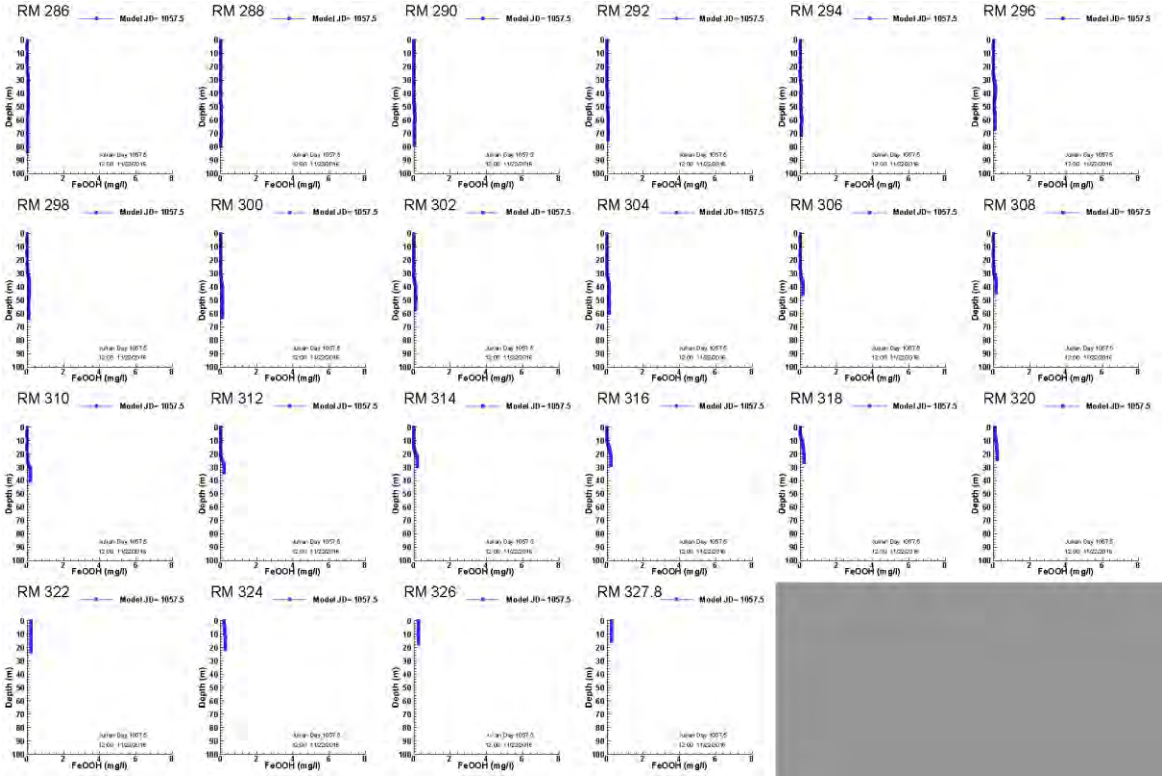


Figure 502. Vertical profiles of FeOOH compared with data for 11/22/2016.

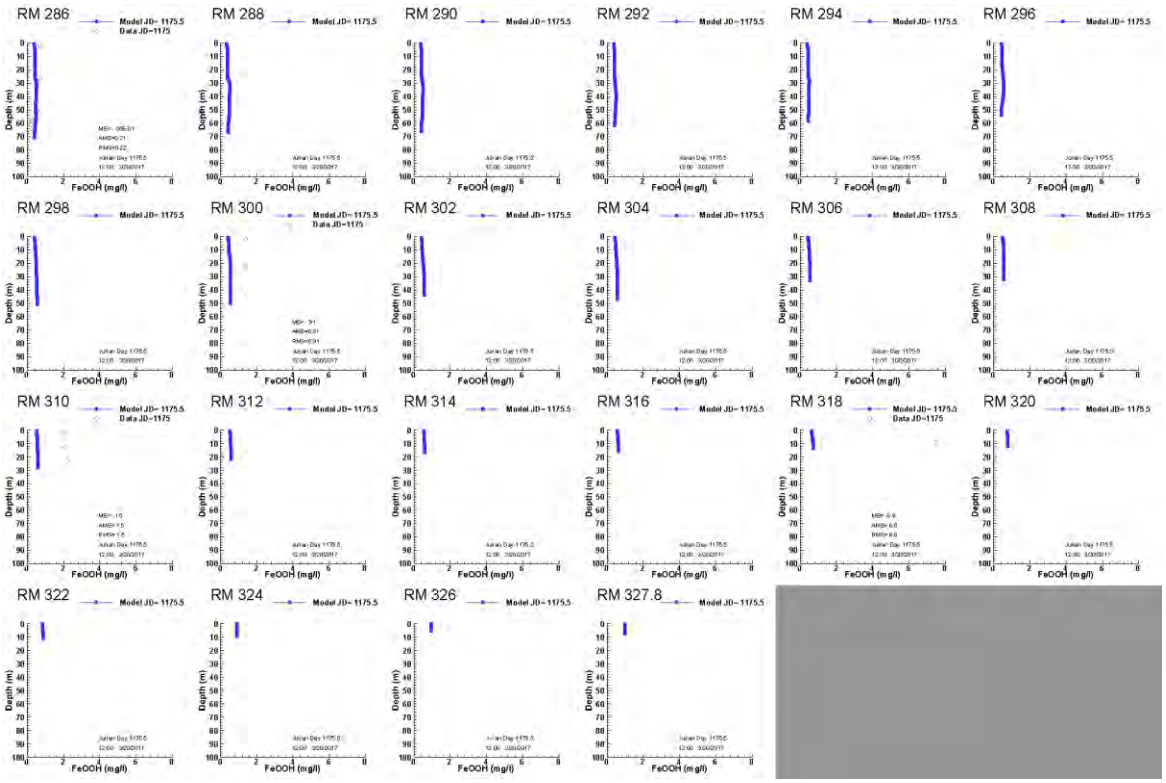


Figure 503. Vertical profiles of FeOOH compared with data for 3/20/2017.

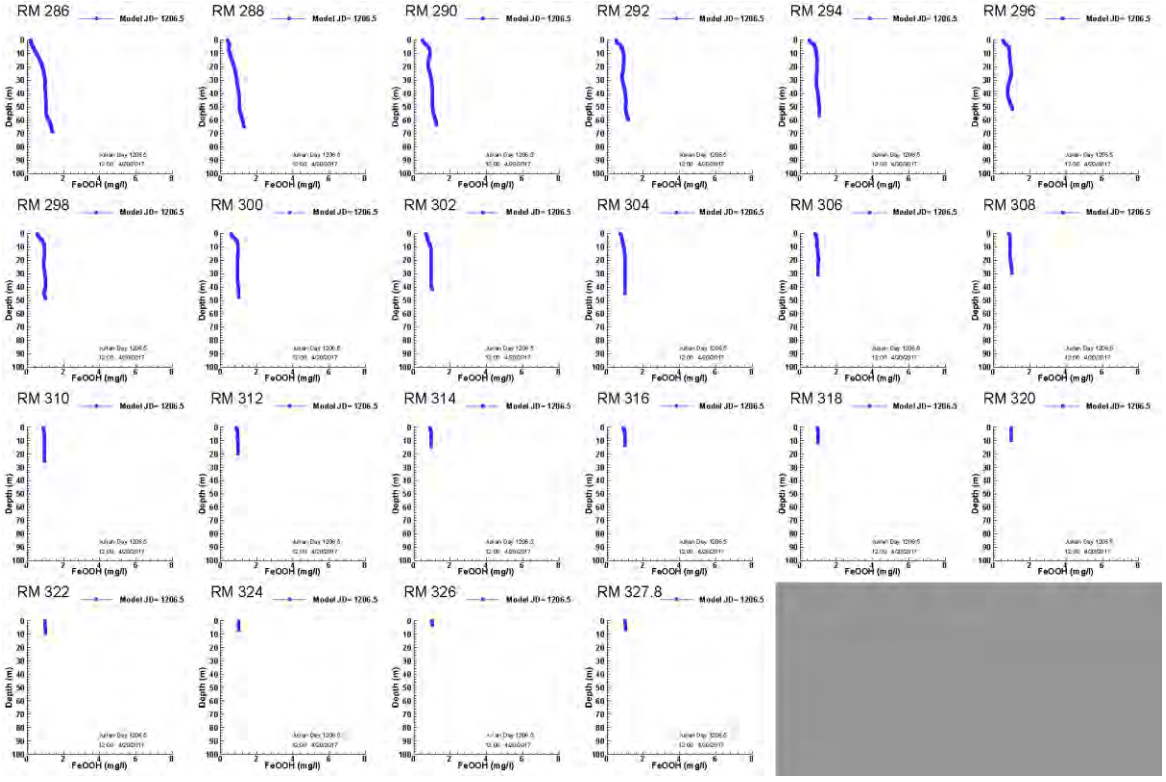


Figure 504. Vertical profiles of FeOOH compared with data for 4/20/2017.

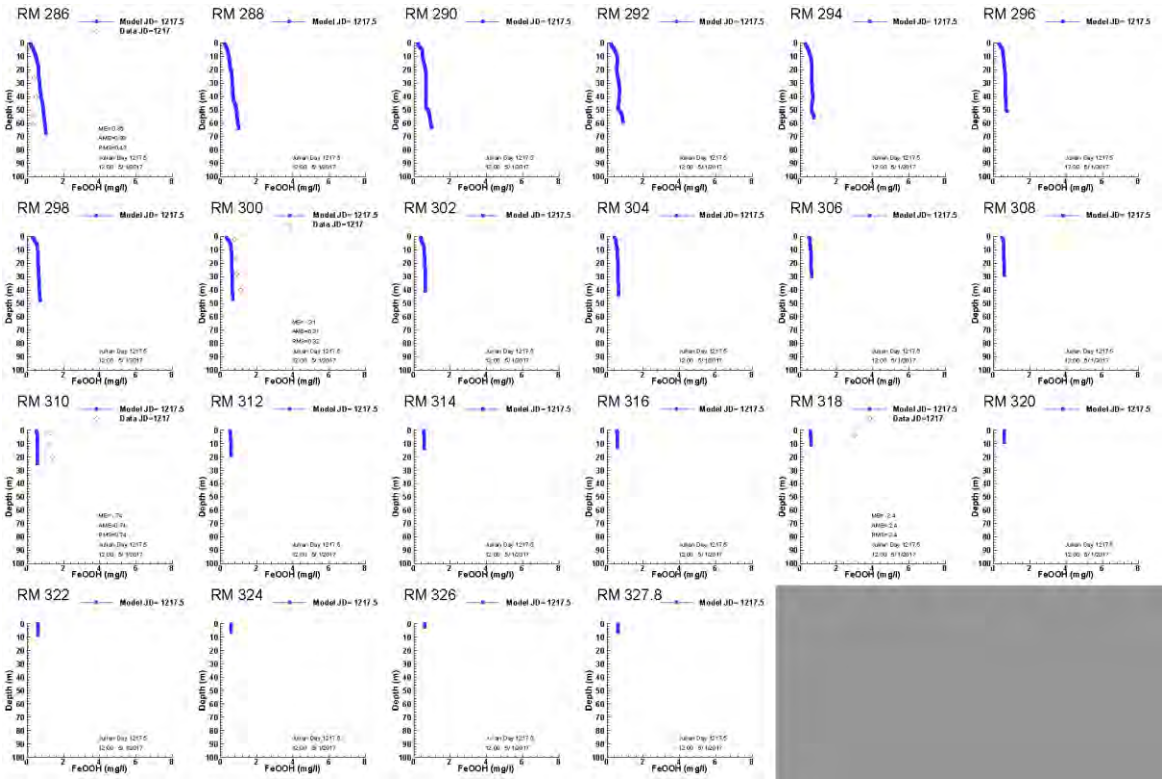


Figure 505. Vertical profiles of FeOOH compared with data for 5/ 1/2017.

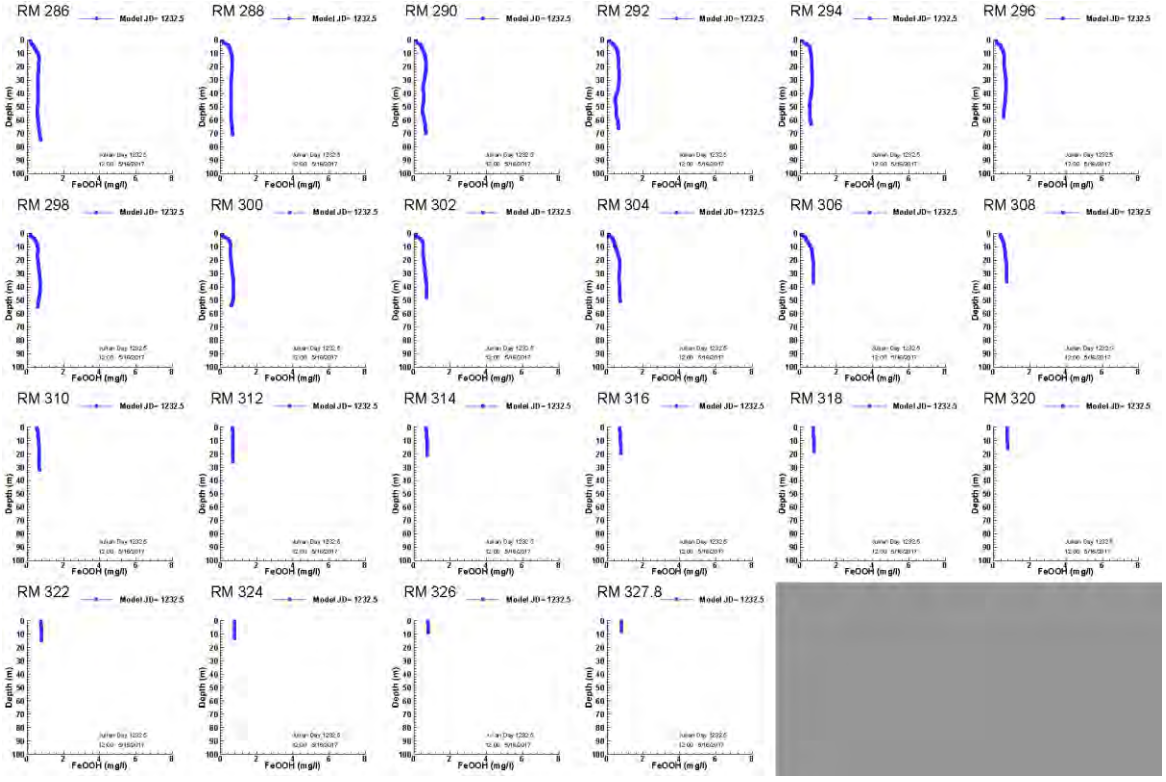


Figure 506. Vertical profiles of FeOOH compared with data for 5/16/2017.

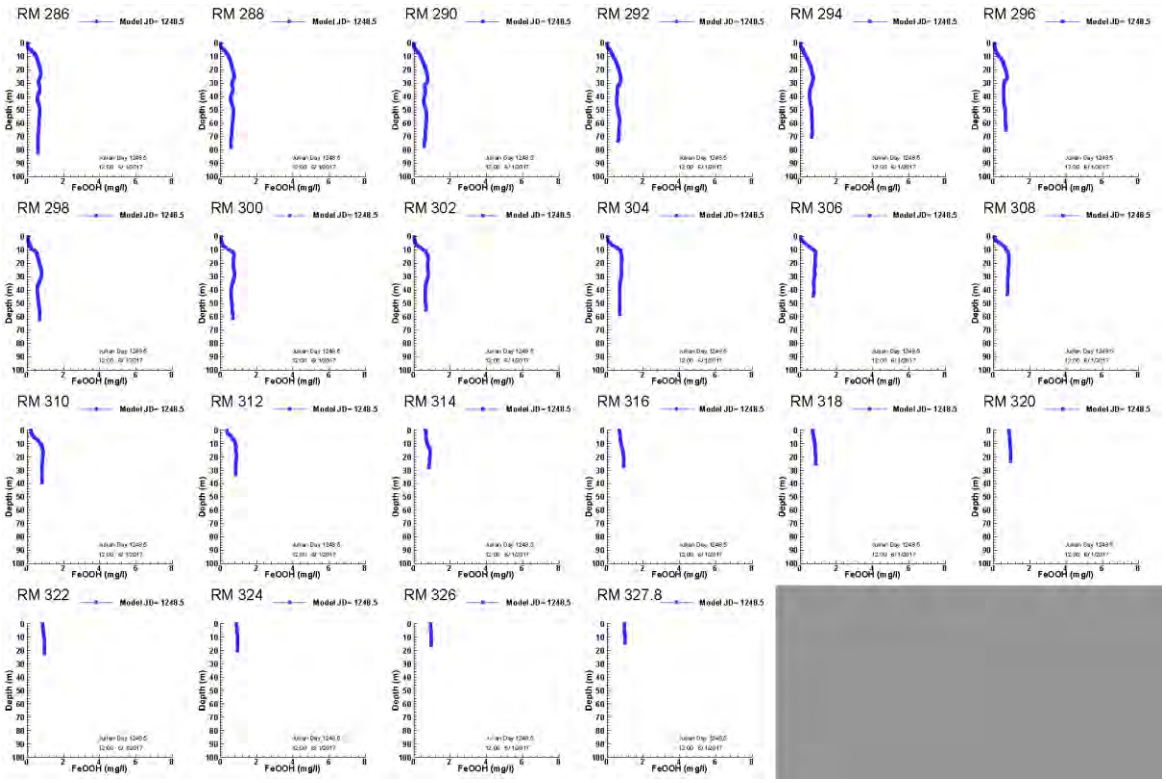


Figure 507. Vertical profiles of FeOOH compared with data for 6/ 1/2017.

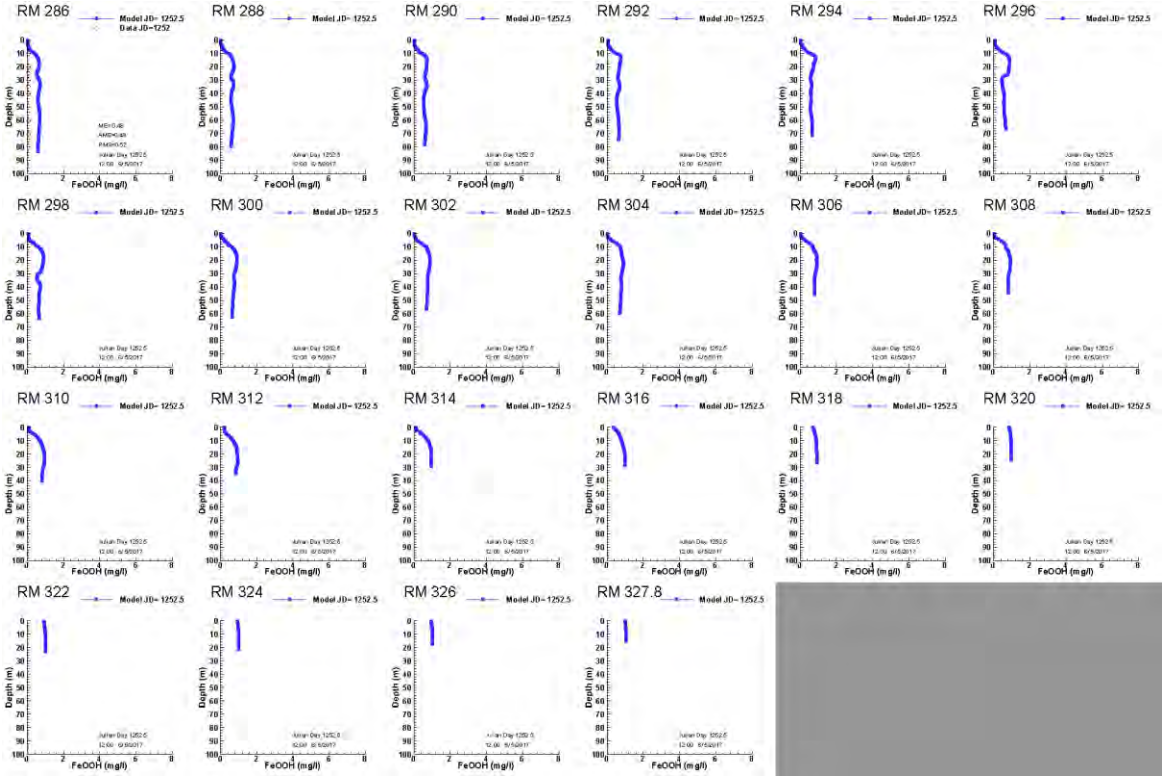


Figure 508. Vertical profiles of FeOOH compared with data for 6/ 5/2017.

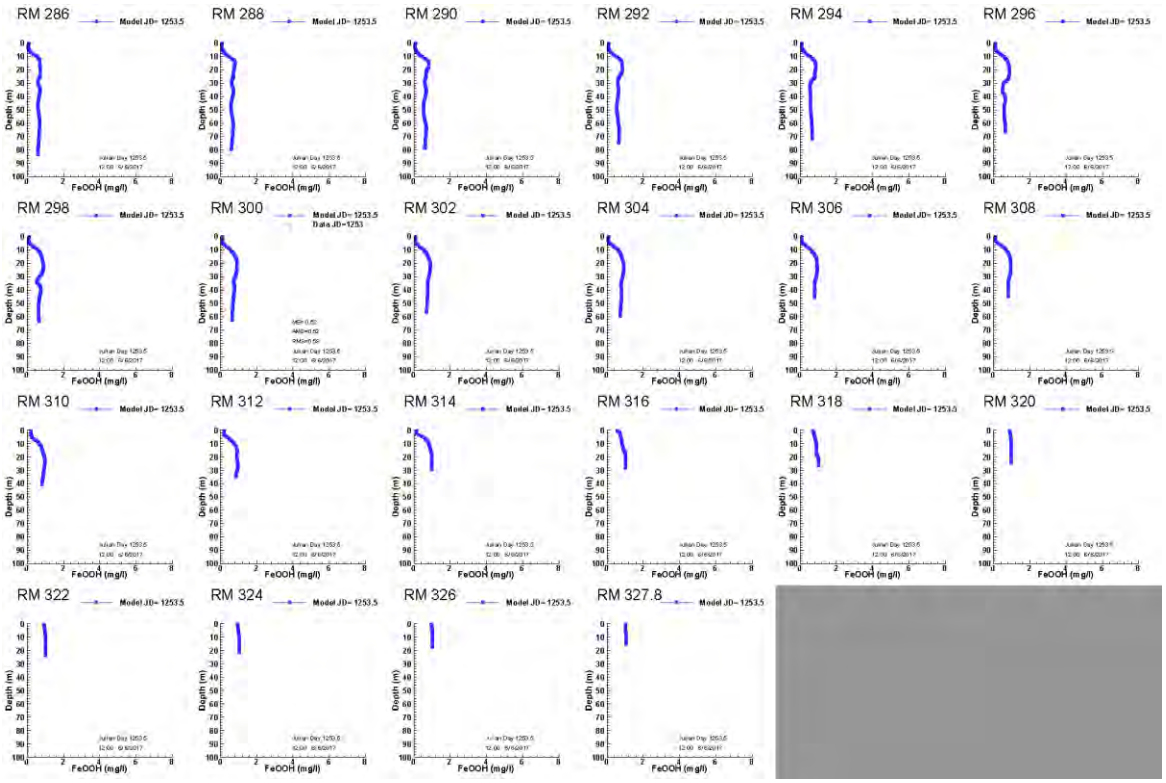


Figure 509. Vertical profiles of FeOOH compared with data for 6/ 6/2017.

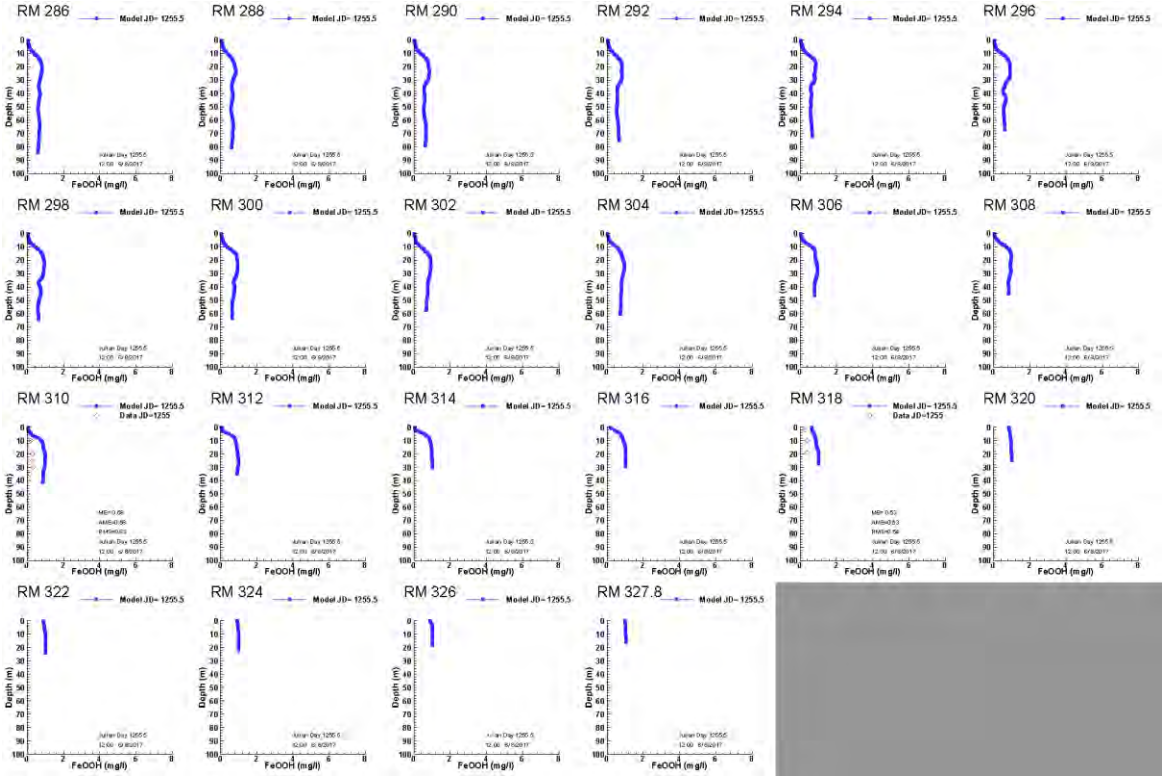


Figure 510. Vertical profiles of FeOOH compared with data for 6/ 8/2017.

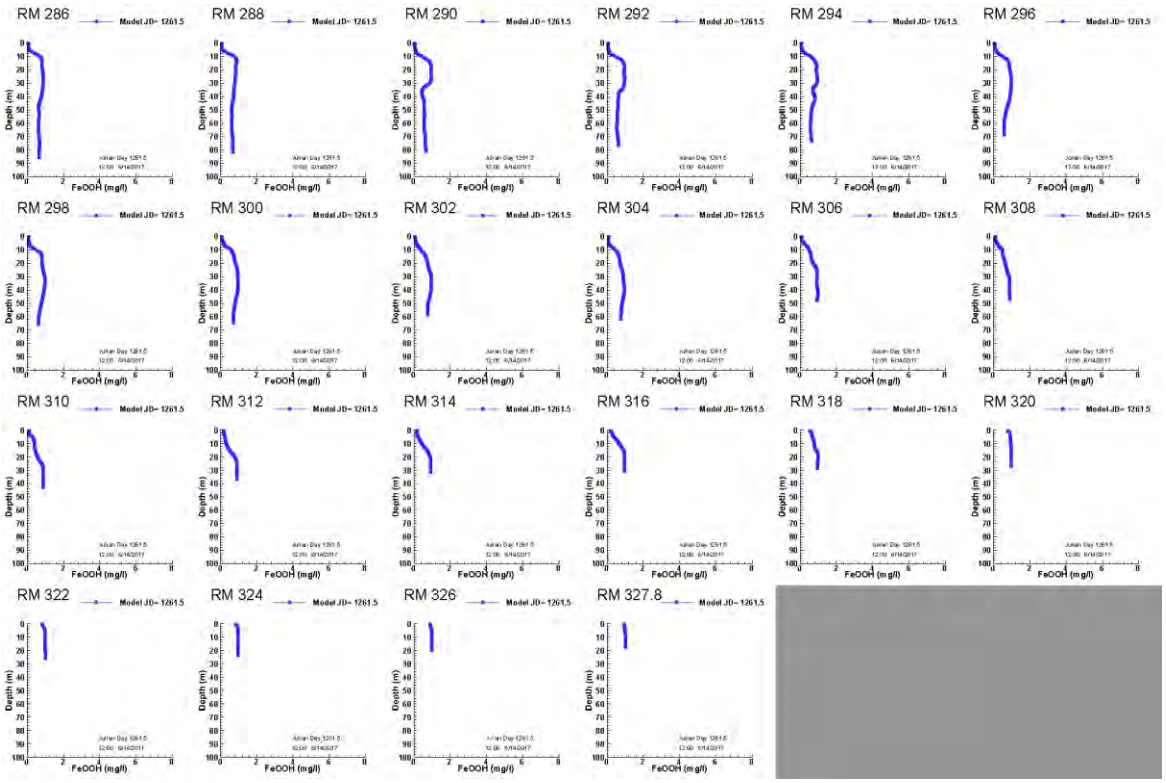


Figure 511. Vertical profiles of FeOOH compared with data for 6/14/2017.

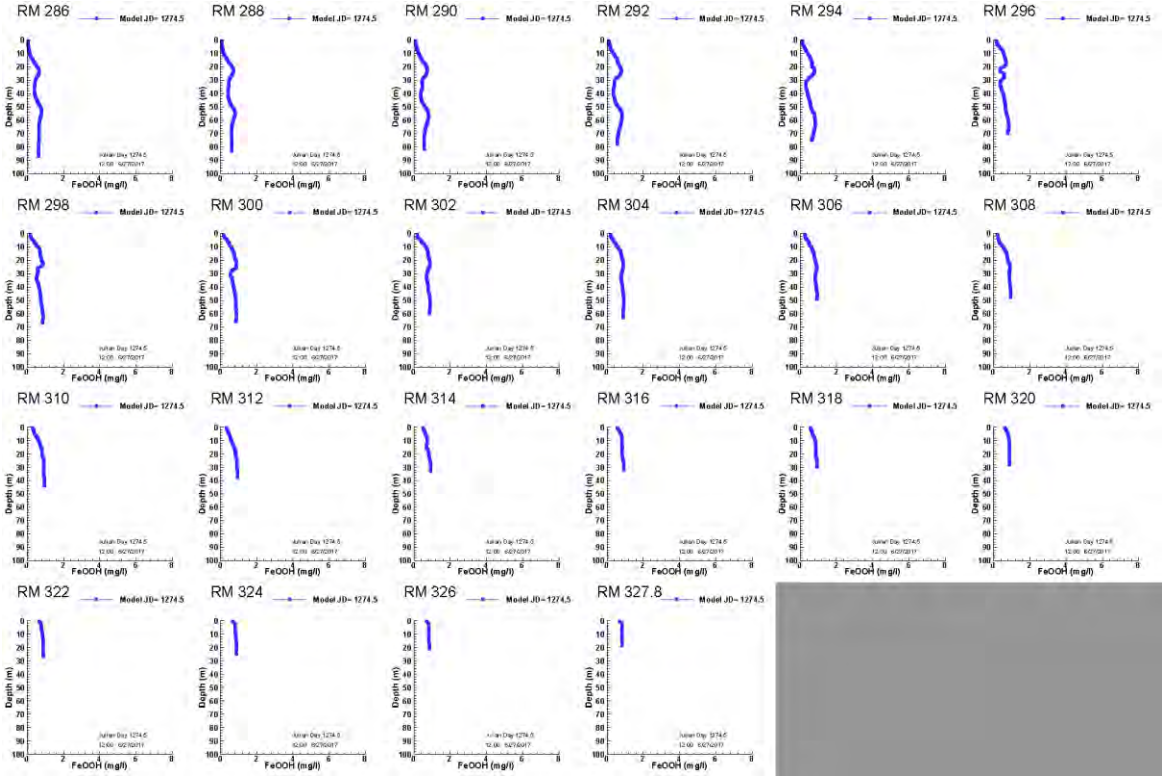


Figure 512. Vertical profiles of FeOOH compared with data for 6/27/2017.

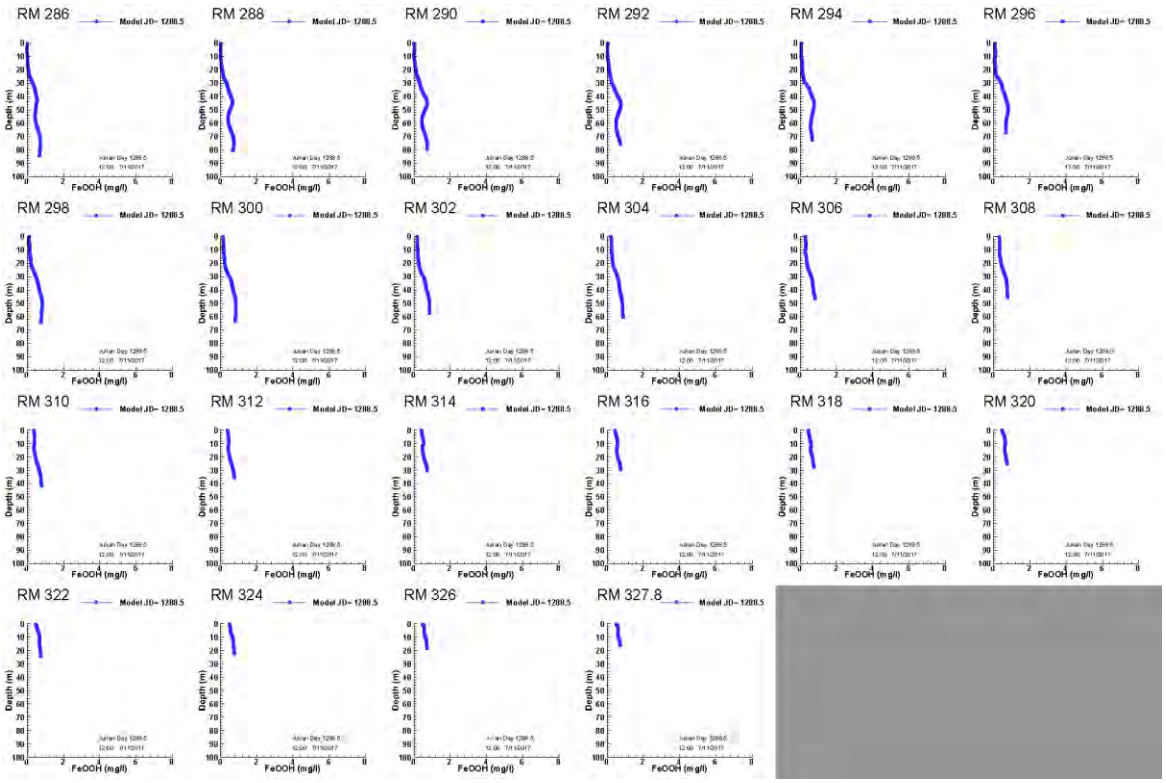


Figure 513. Vertical profiles of FeOOH compared with data for 7/11/2017.

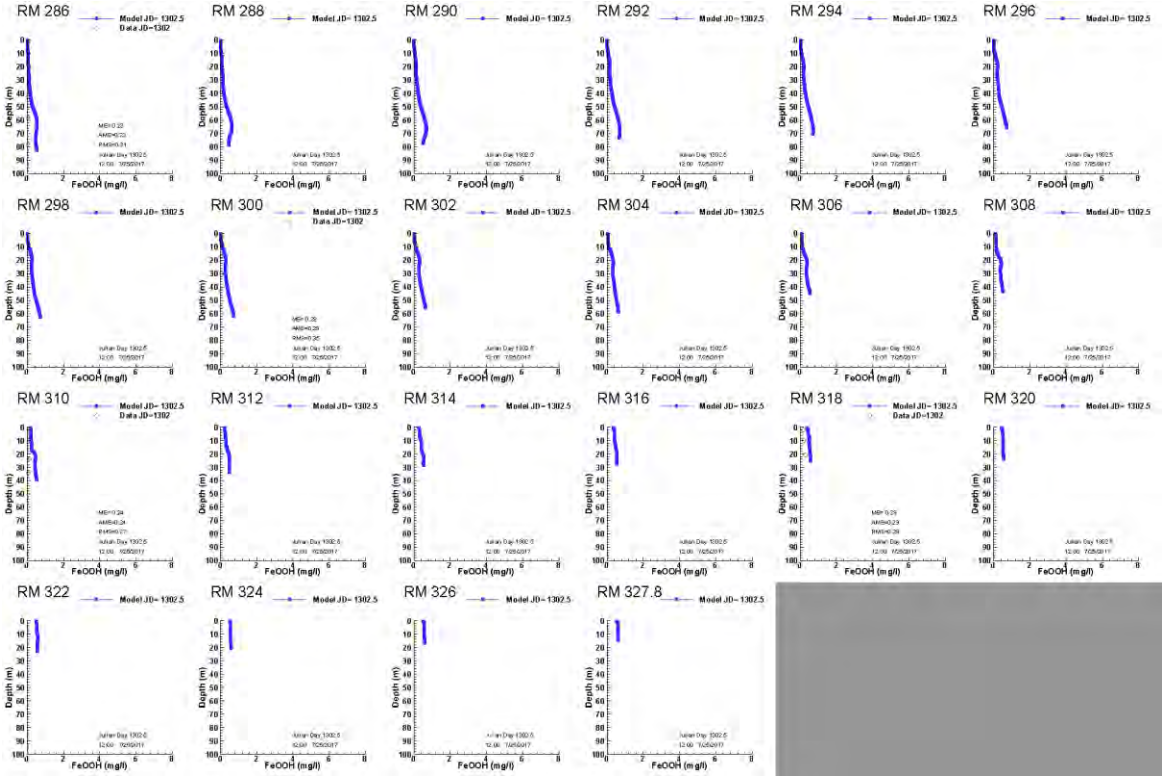


Figure 514. Vertical profiles of FeOOH compared with data for 7/25/2017.

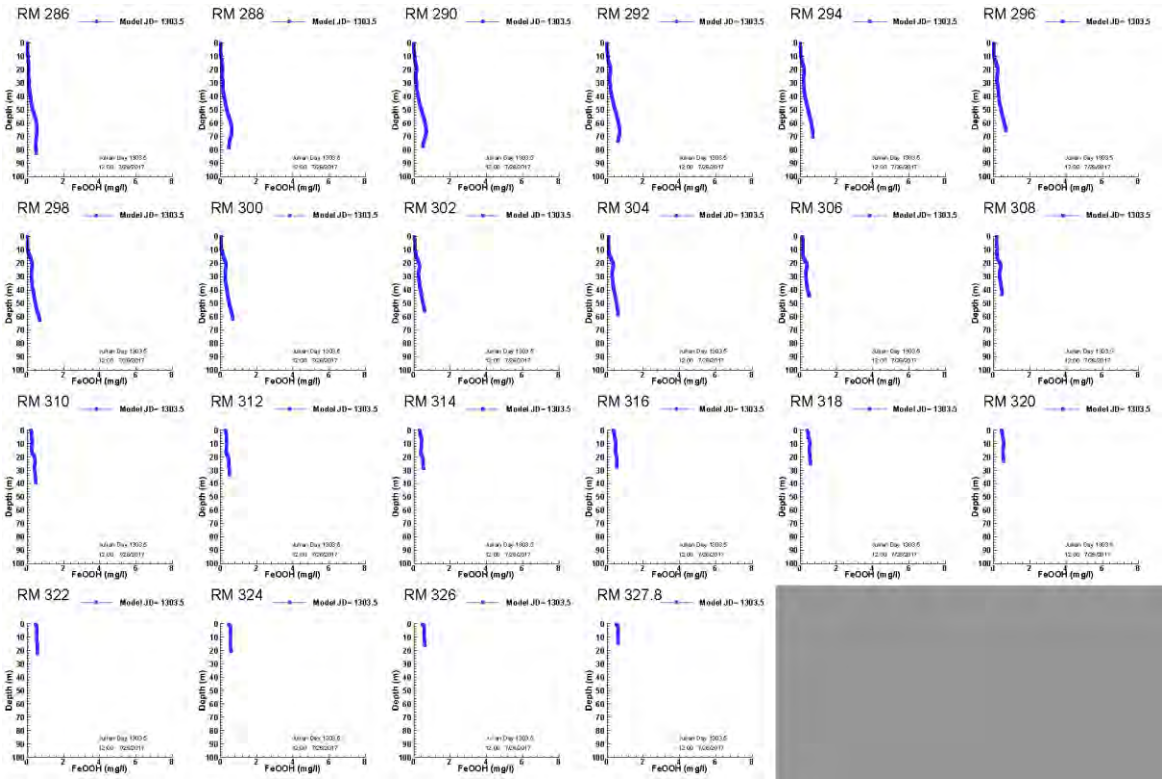


Figure 515. Vertical profiles of FeOOH compared with data for 7/26/2017.

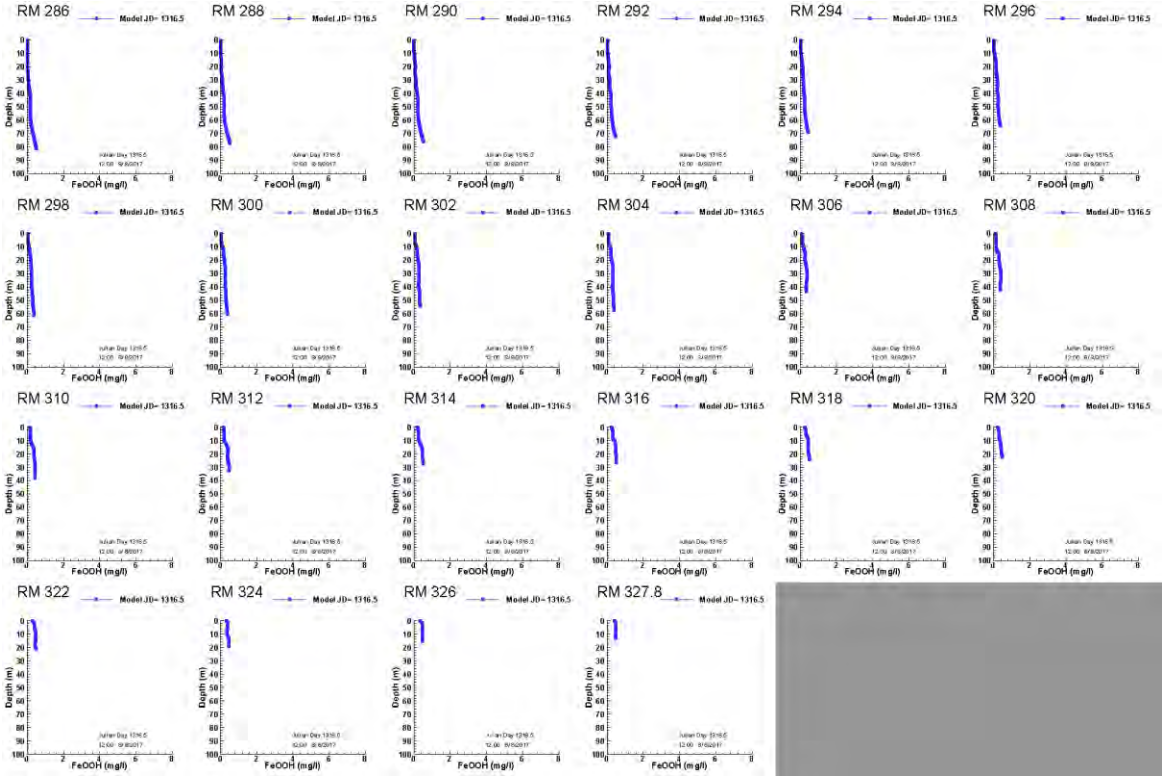


Figure 516. Vertical profiles of FeOOH compared with data for 8/ 8/2017.

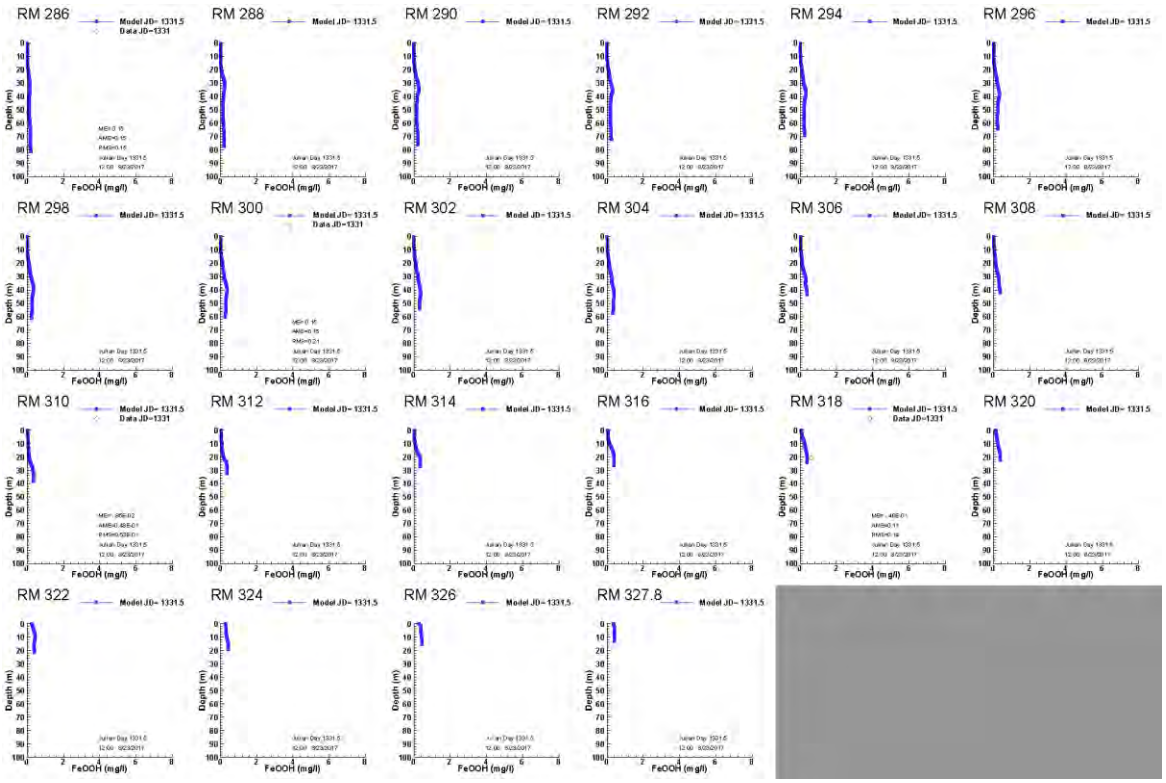


Figure 517. Vertical profiles of FeOOH compared with data for 8/23/2017.

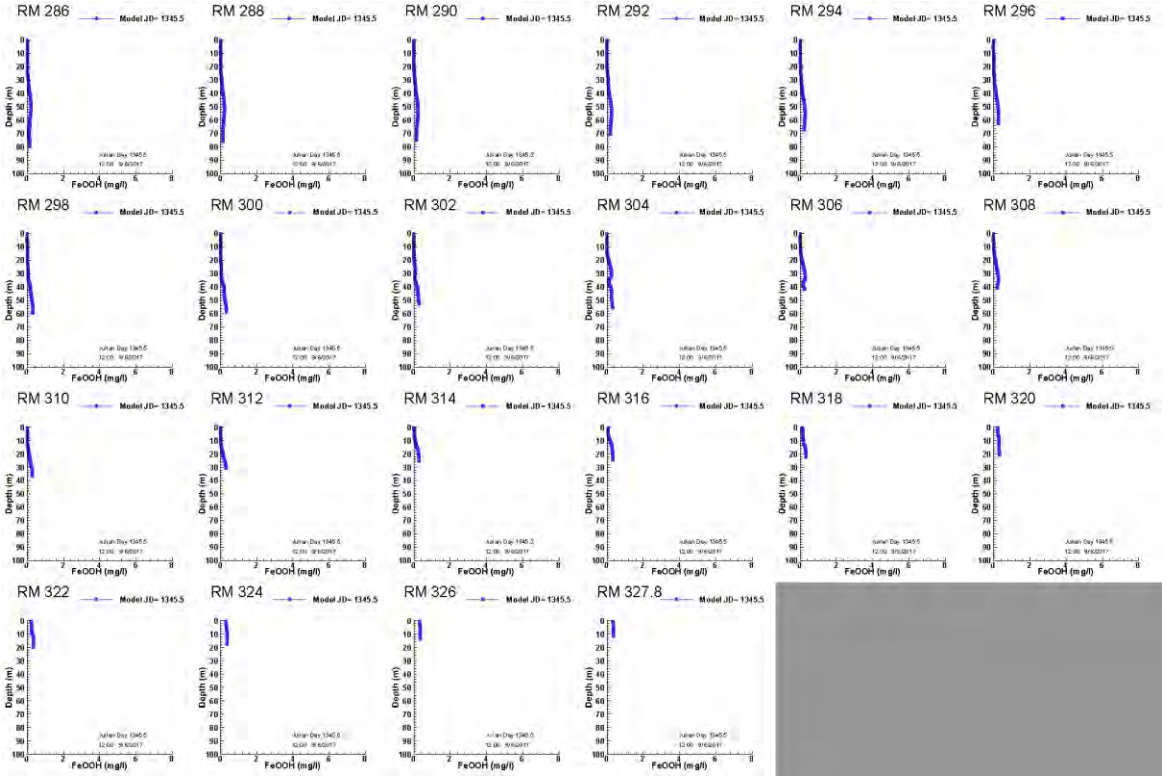


Figure 518. Vertical profiles of FeOOH compared with data for 9/ 6/2017.

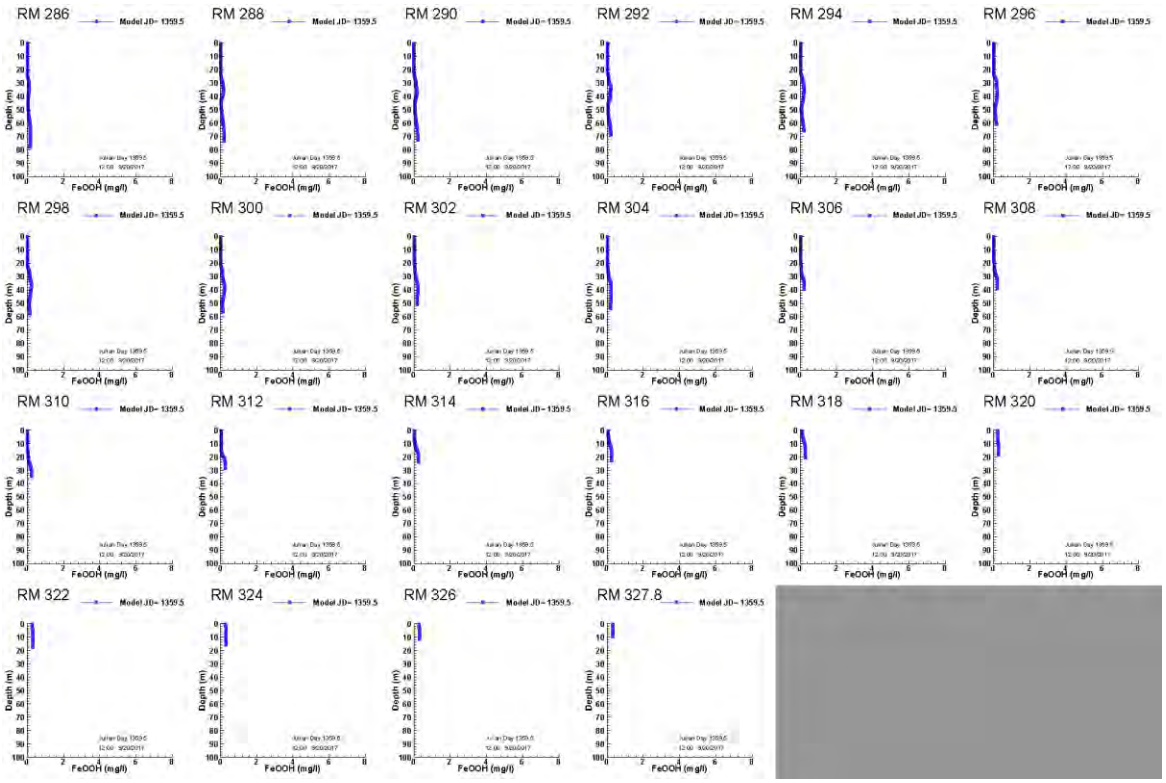


Figure 519. Vertical profiles of FeOOH compared with data for 9/20/2017.

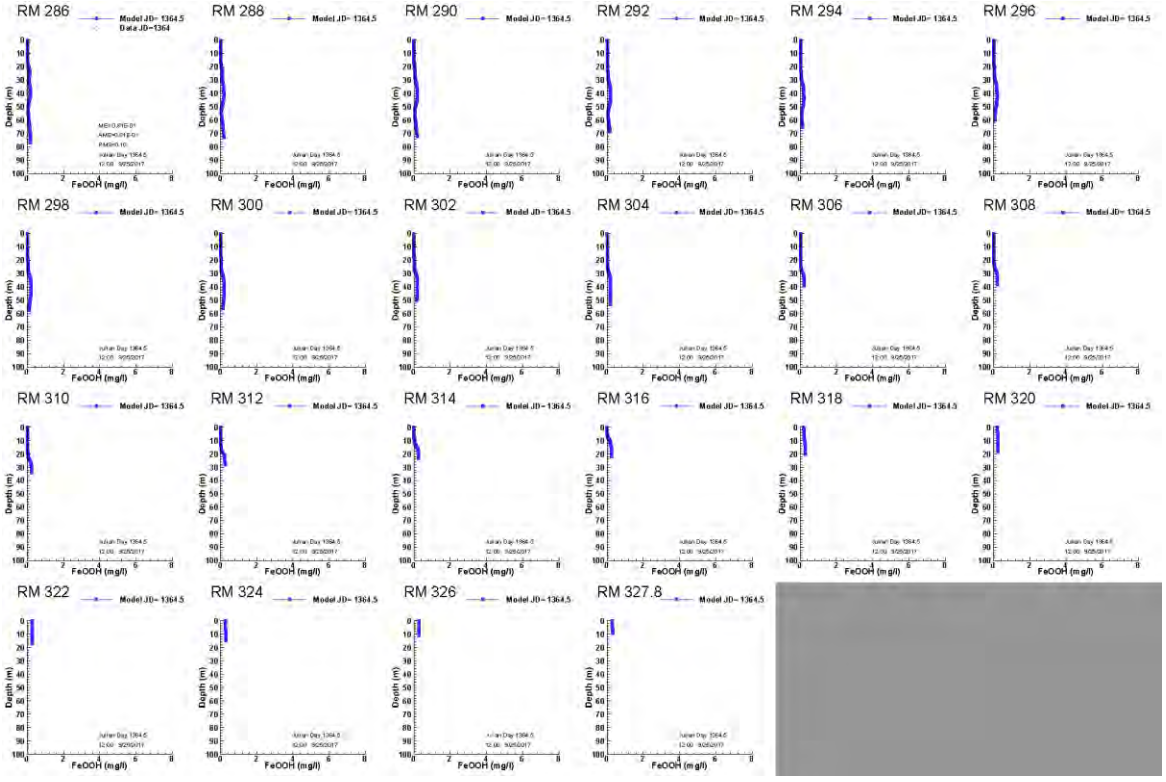


Figure 520. Vertical profiles of FeOOH compared with data for 9/25/2017.

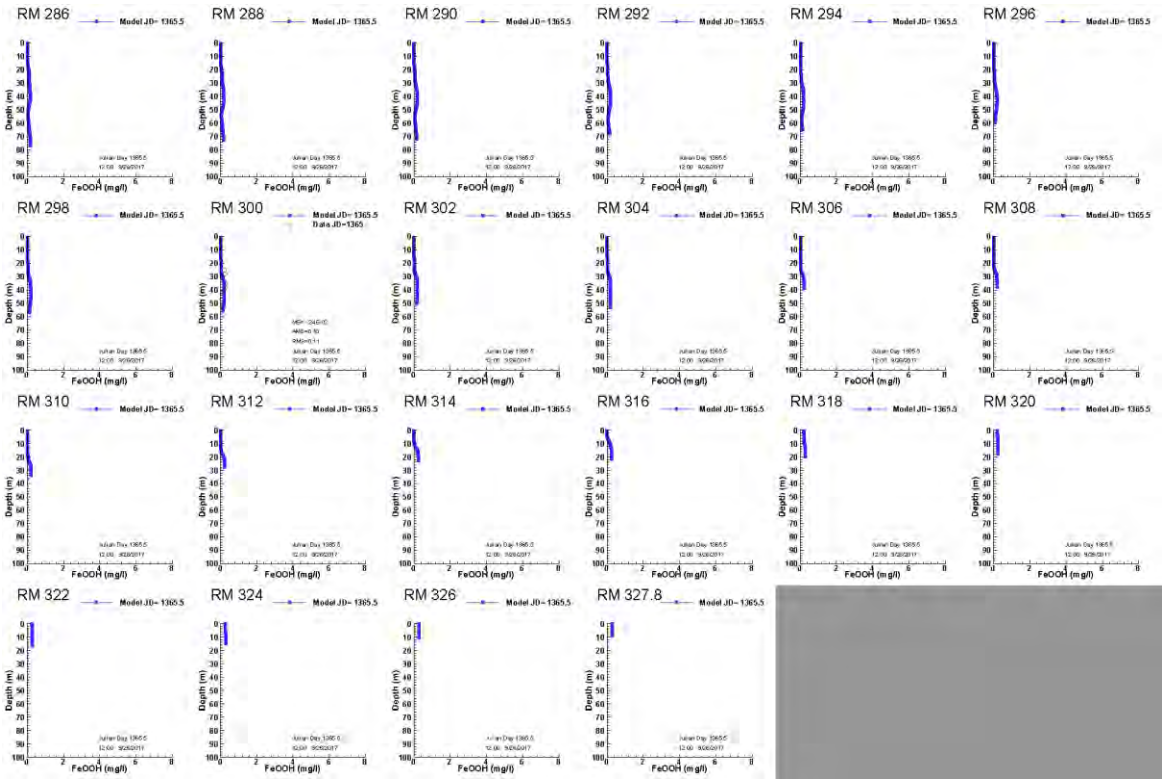


Figure 521. Vertical profiles of FeOOH compared with data for 9/26/2017.

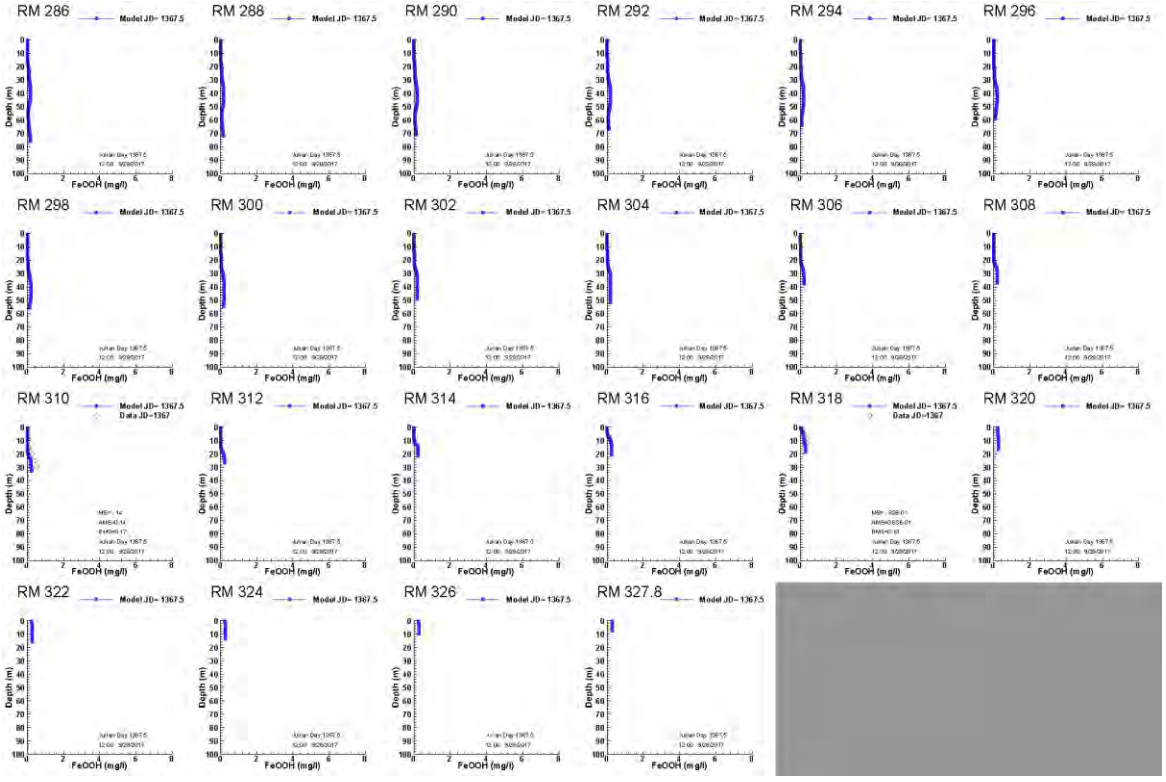


Figure 522. Vertical profiles of FeOOH compared with data for 9/28/2017.

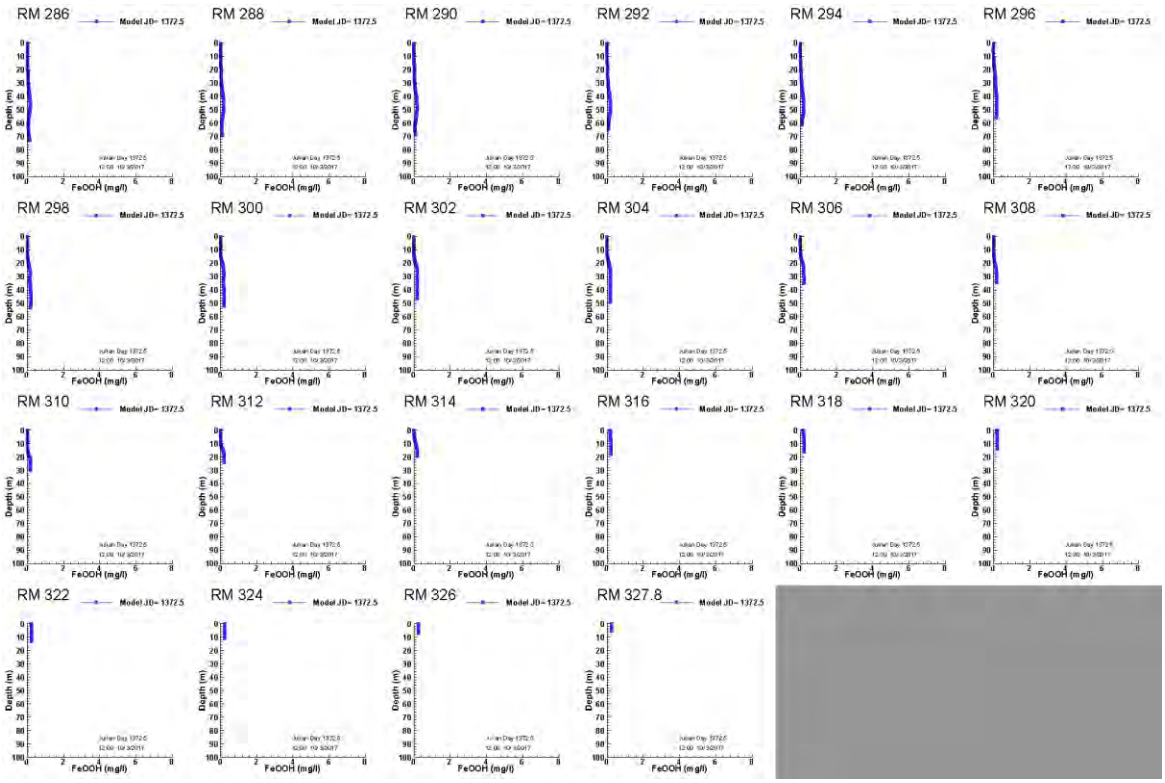


Figure 523. Vertical profiles of FeOOH compared with data for 10/ 3/2017.

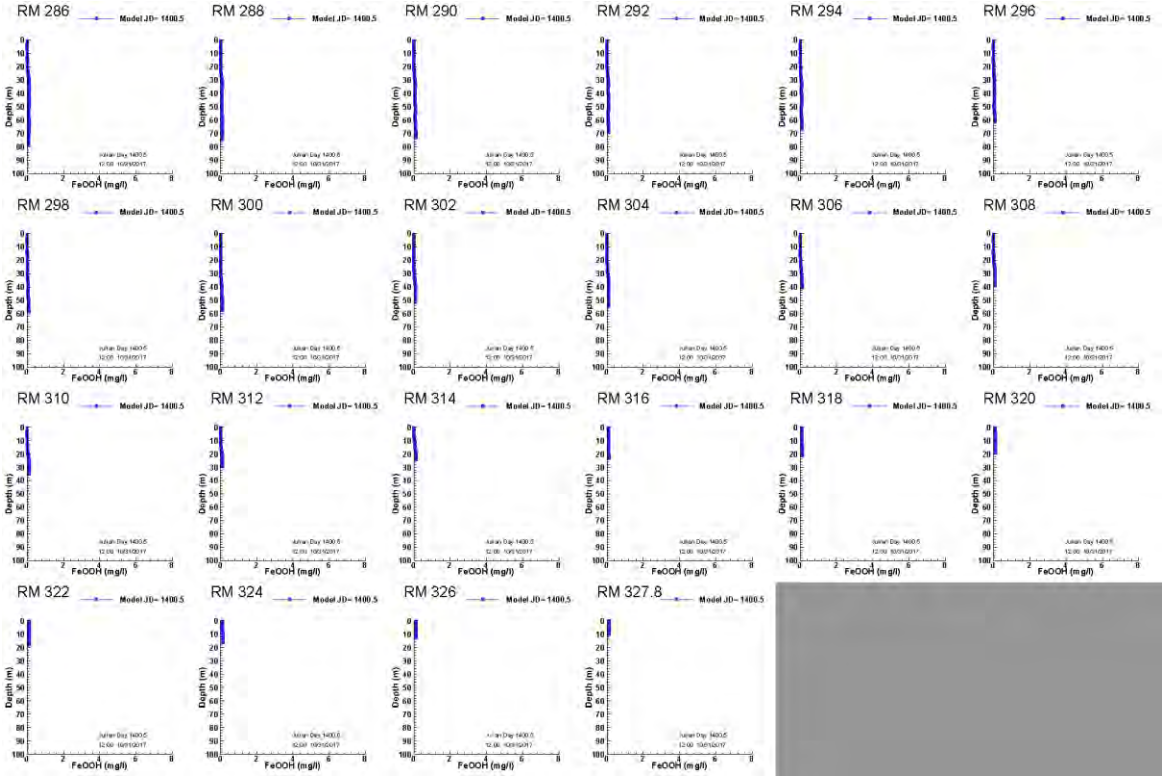


Figure 524. Vertical profiles of FeOOH compared with data for 10/31/2017.

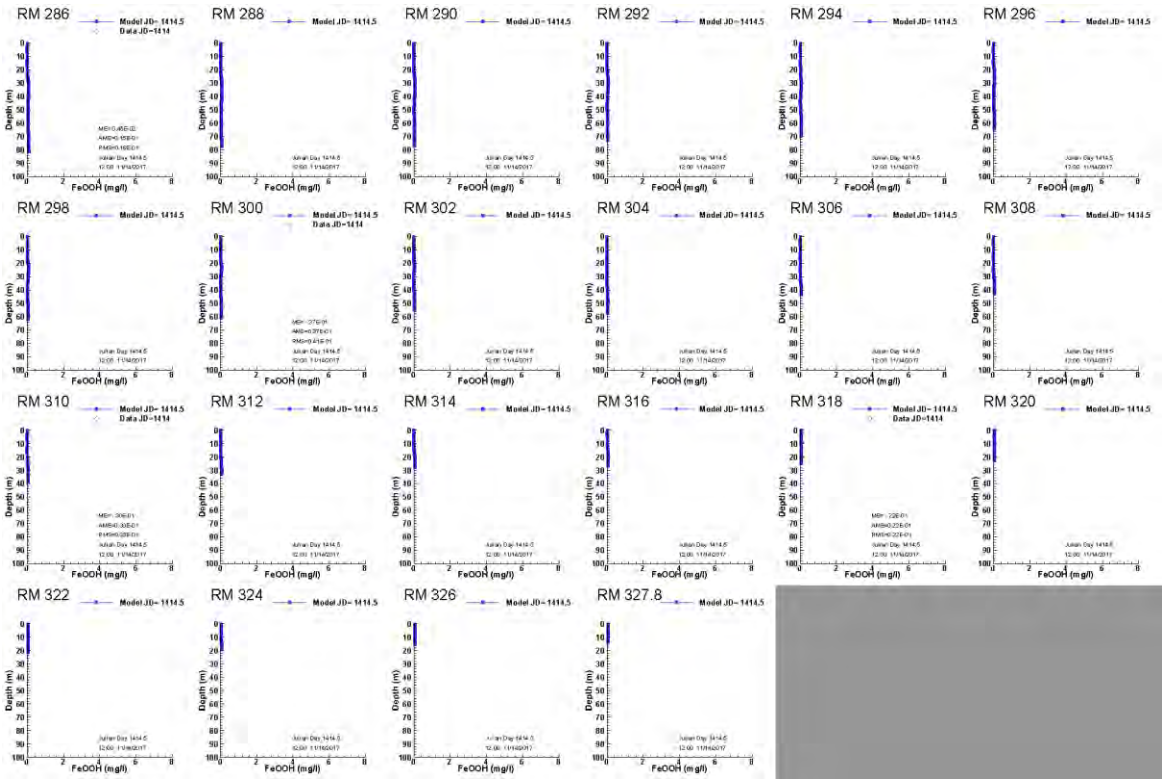


Figure 525. Vertical profiles of FeOOH compared with data for 11/14/2017.

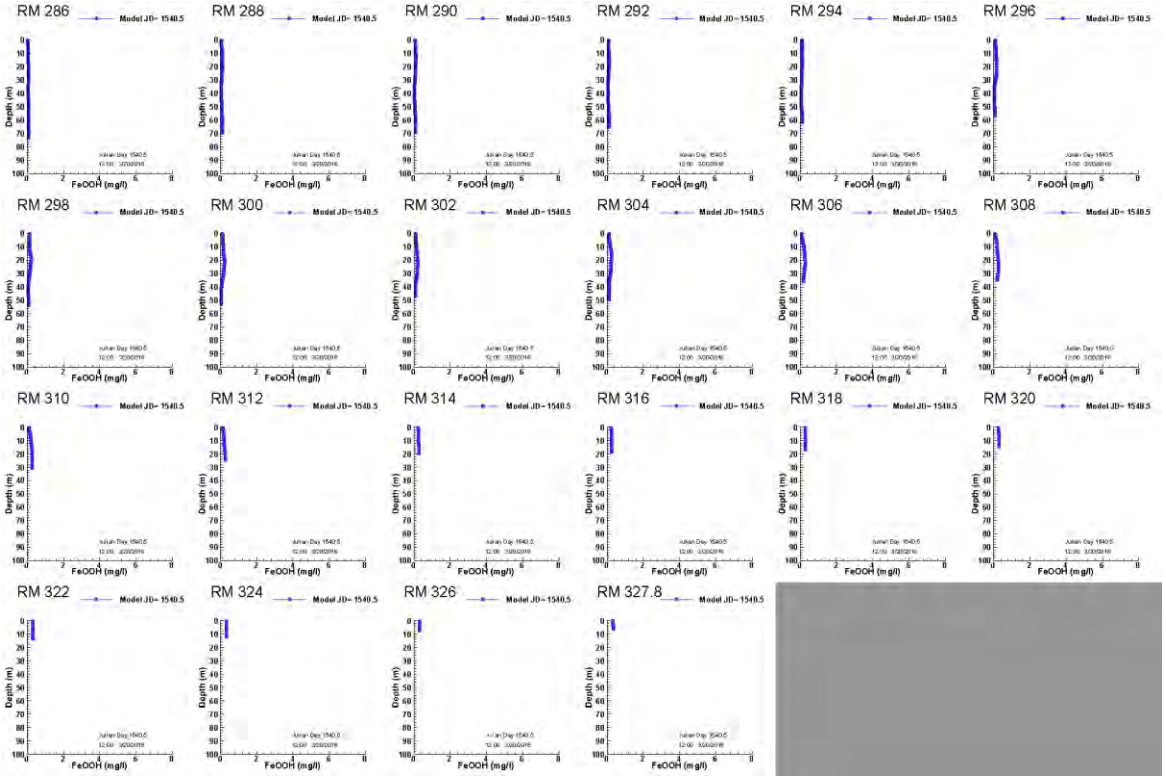


Figure 526. Vertical profiles of FeOOH compared with data for 3/20/2018.

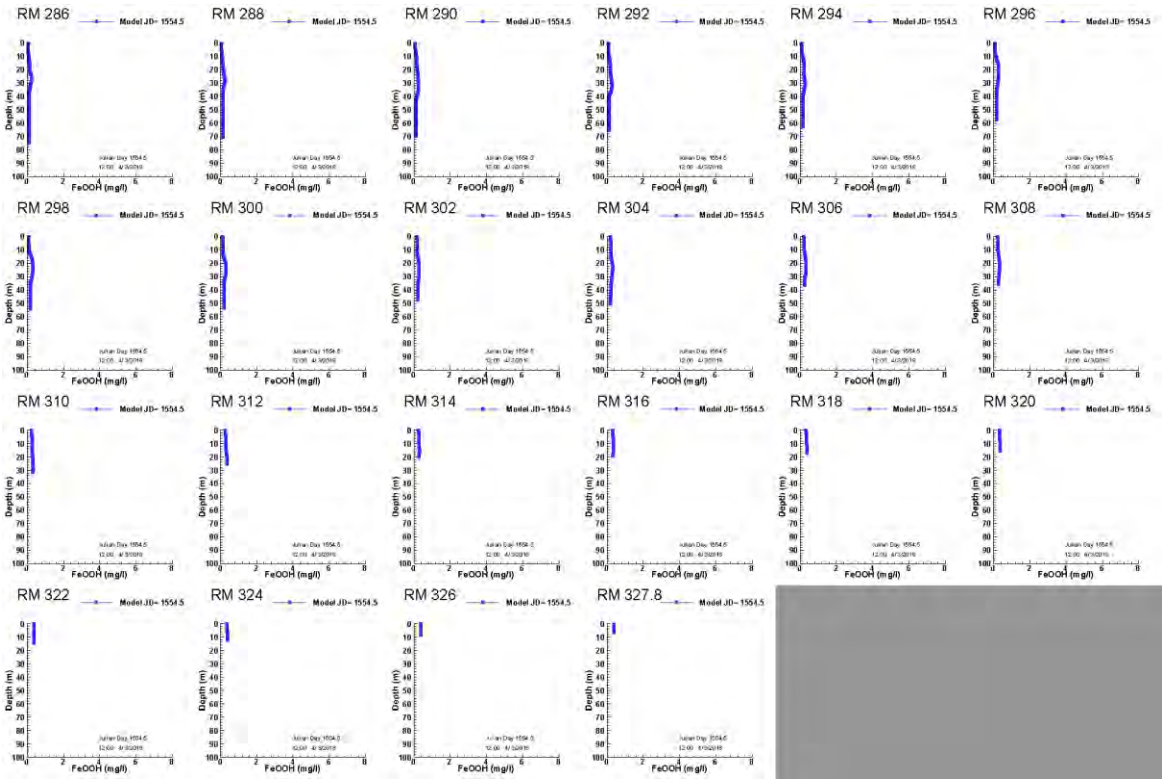


Figure 527. Vertical profiles of FeOOH compared with data for 4/ 3/2018.

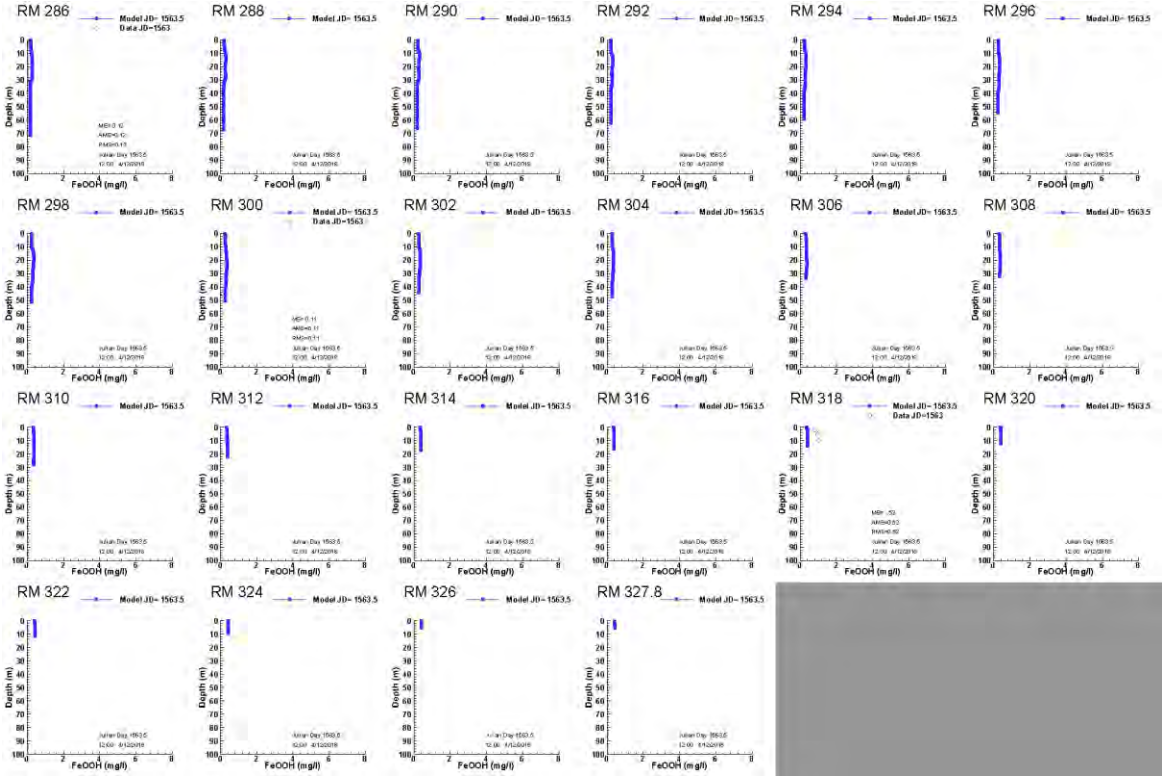


Figure 528. Vertical profiles of FeOOH compared with data for 4/12/2018.

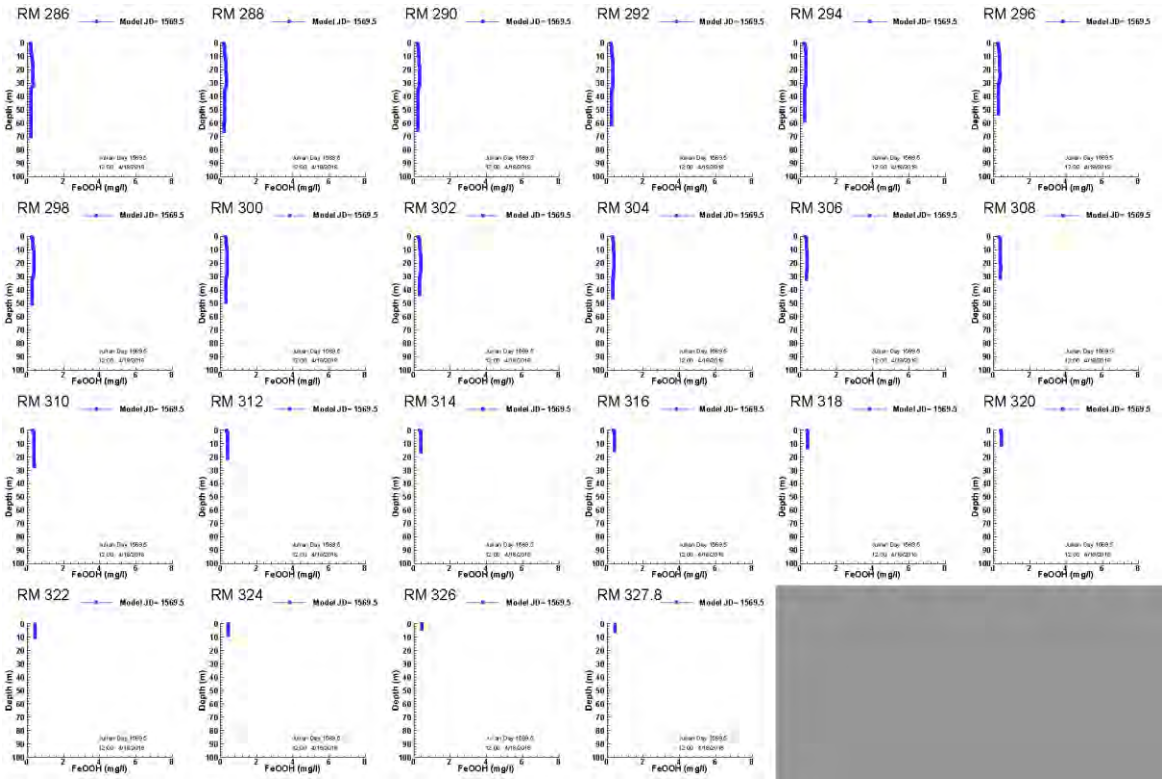


Figure 529. Vertical profiles of FeOOH compared with data for 4/18/2018.

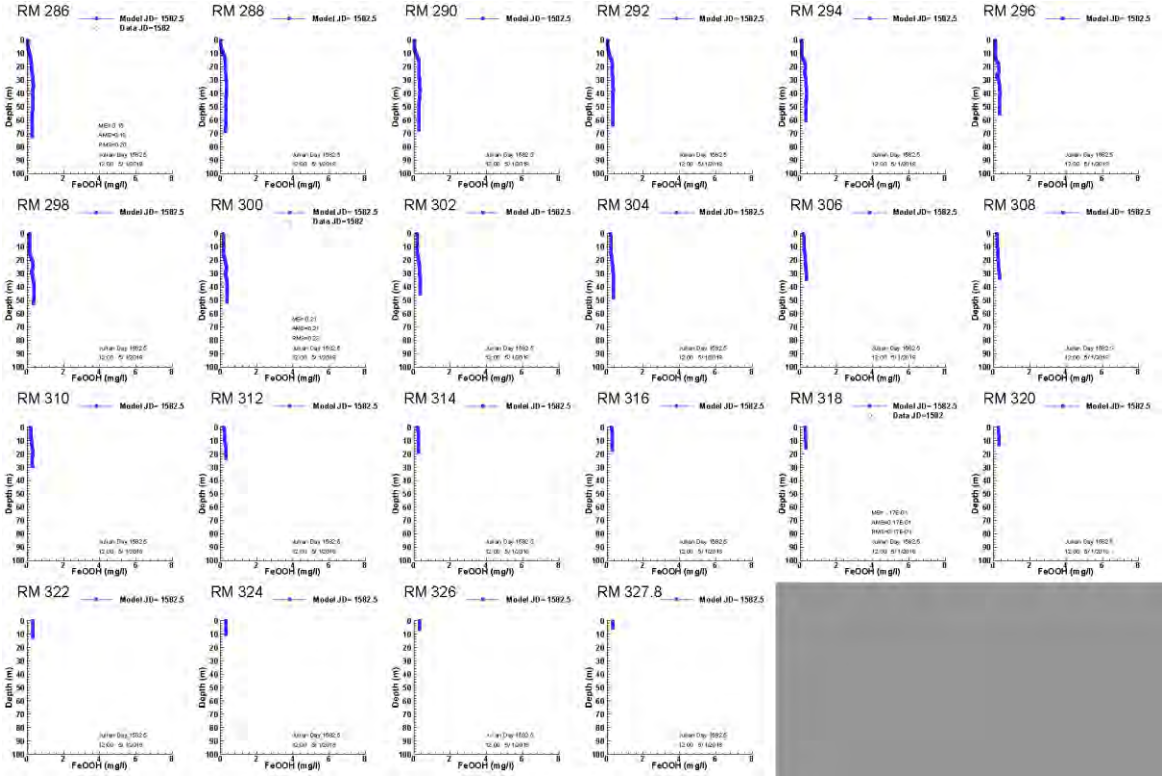


Figure 530. Vertical profiles of FeOOH compared with data for 5/ 1/2018.

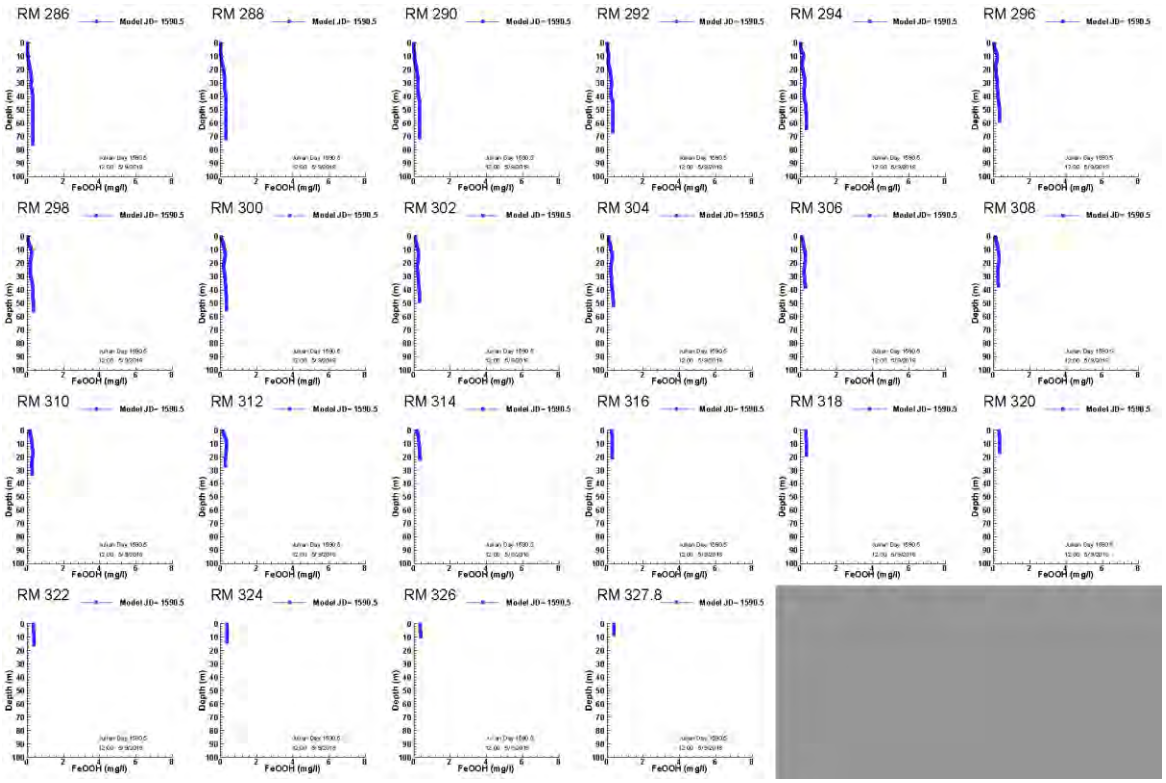


Figure 531. Vertical profiles of FeOOH compared with data for 5/ 9/2018.

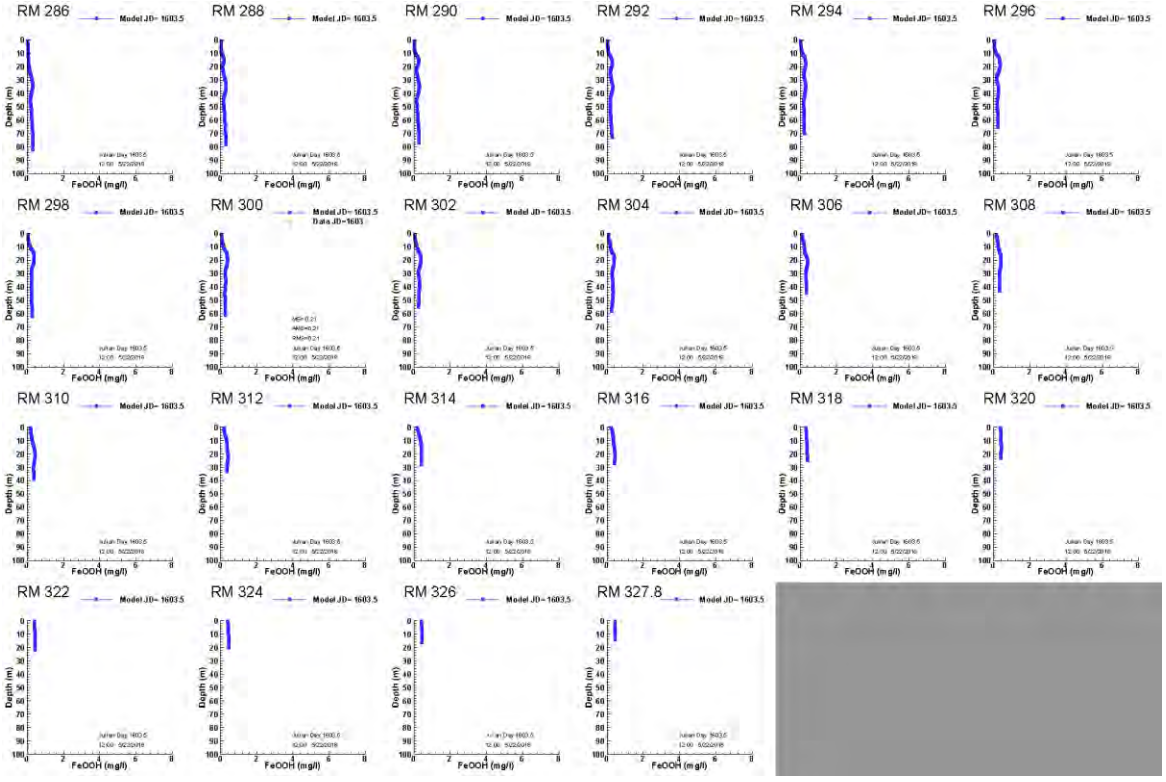


Figure 532. Vertical profiles of FeOOH compared with data for 5/22/2018.

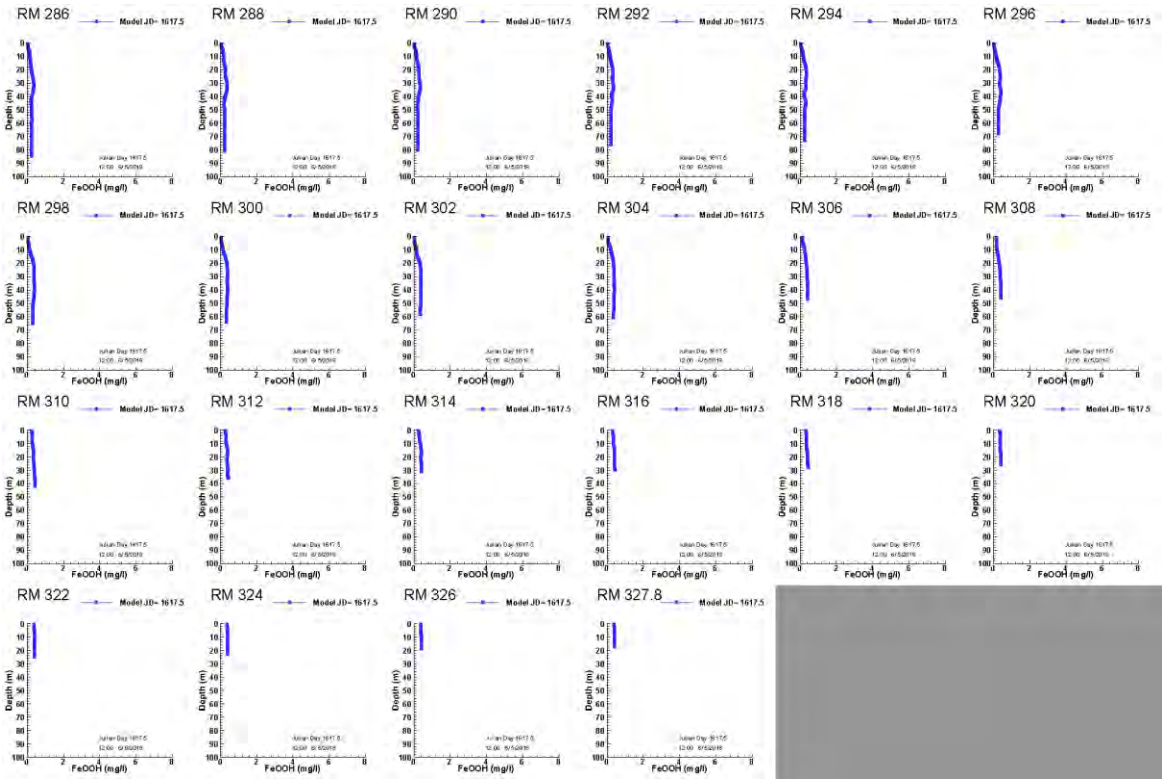


Figure 533. Vertical profiles of FeOOH compared with data for 6/ 5/2018.

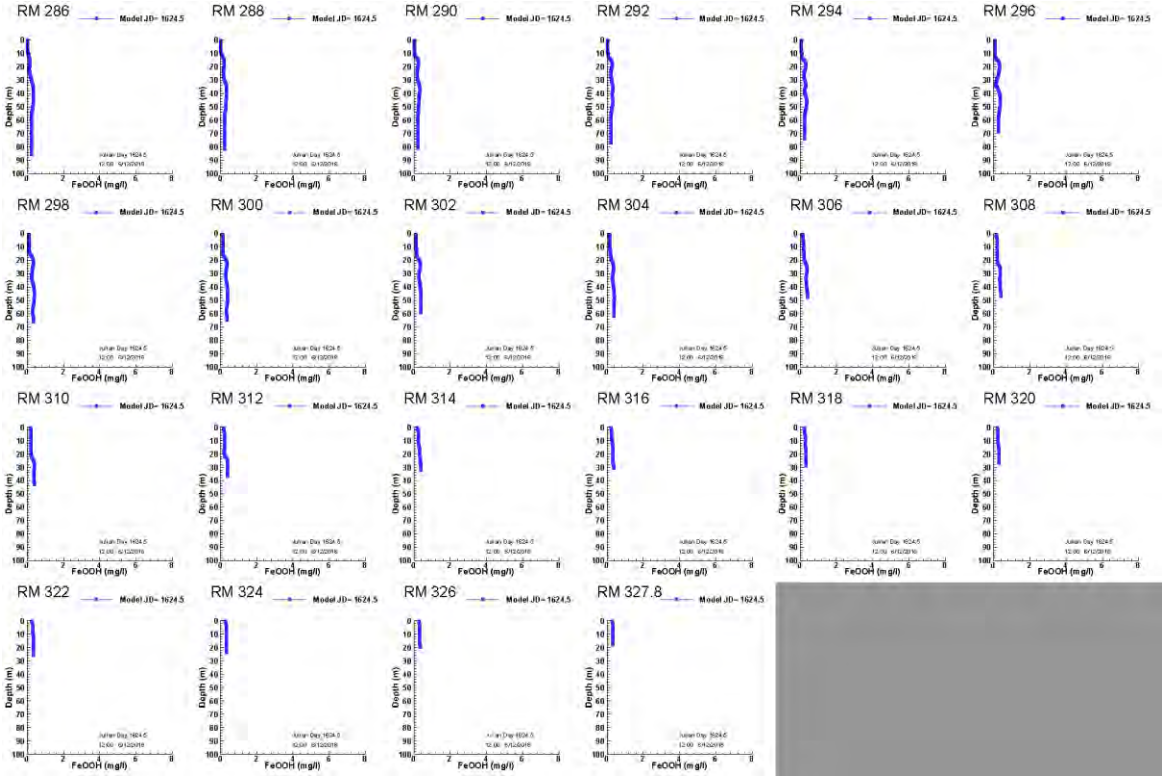


Figure 534. Vertical profiles of FeOOH compared with data for 6/12/2018.

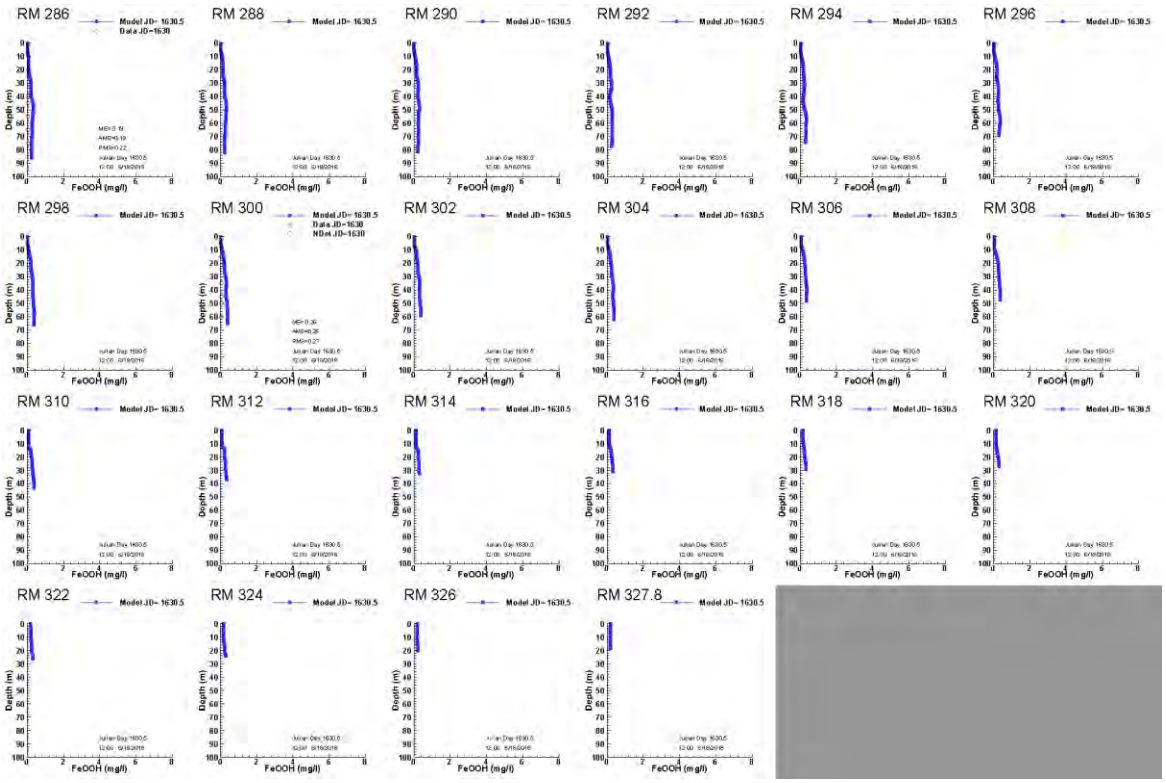


Figure 535. Vertical profiles of FeOOH compared with data for 6/18/2018.

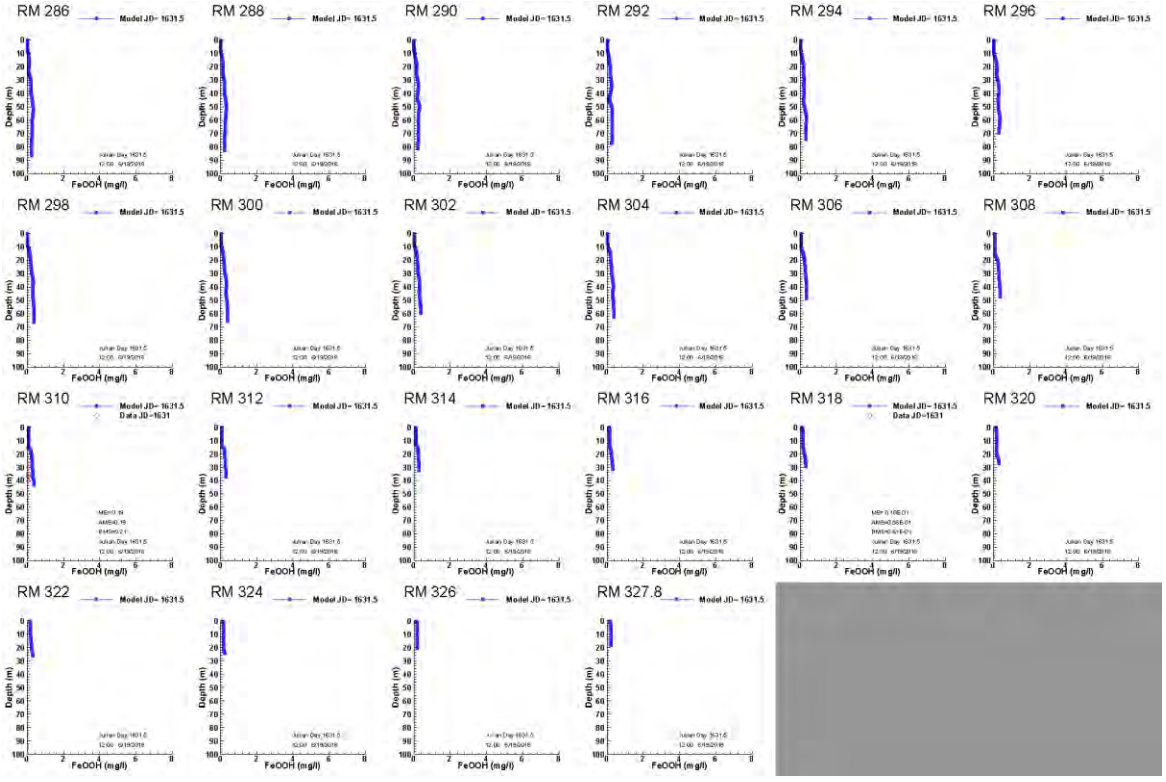


Figure 536. Vertical profiles of FeOOH compared with data for 6/19/2018.

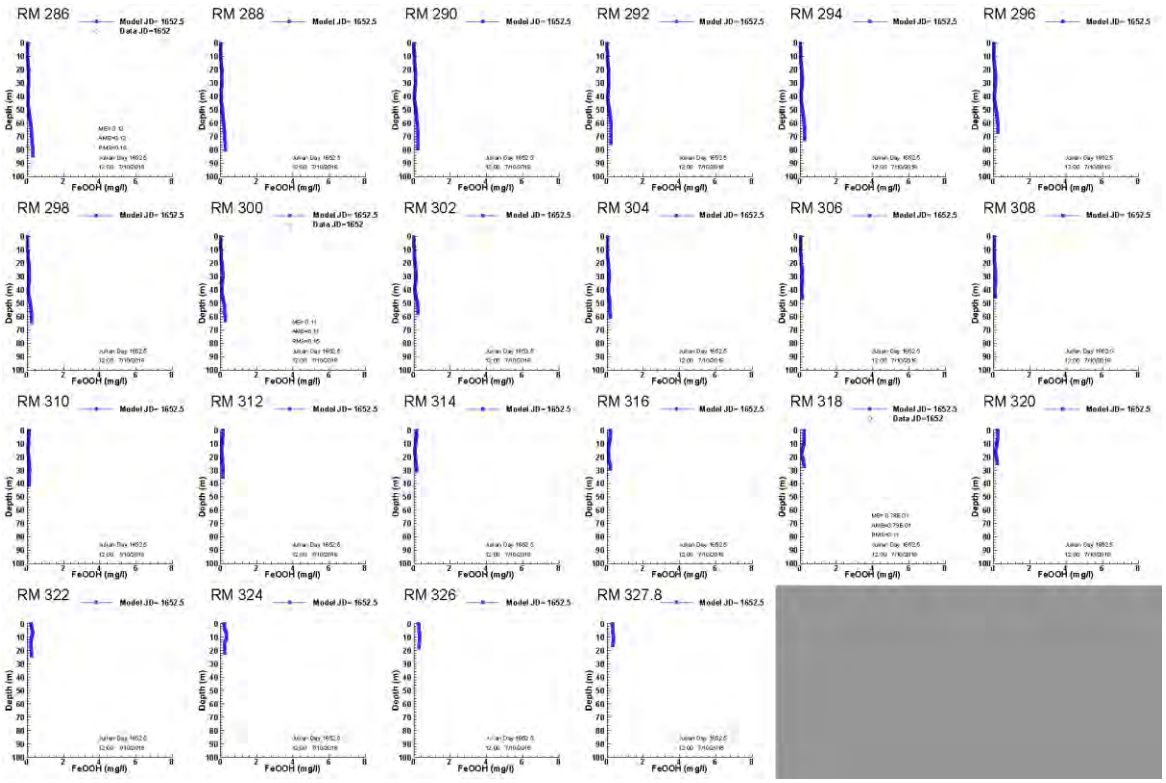


Figure 537. Vertical profiles of FeOOH compared with data for 7/10/2018.

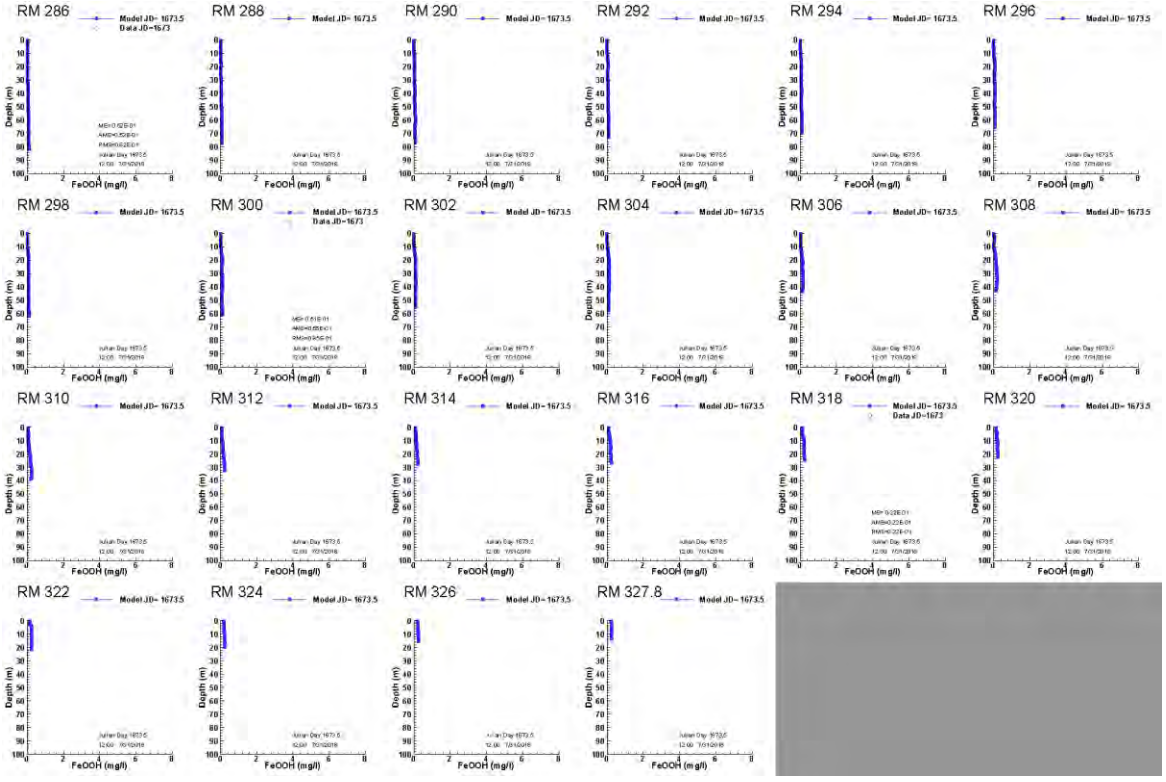


Figure 538. Vertical profiles of FeOOH compared with data for 7/31/2018.

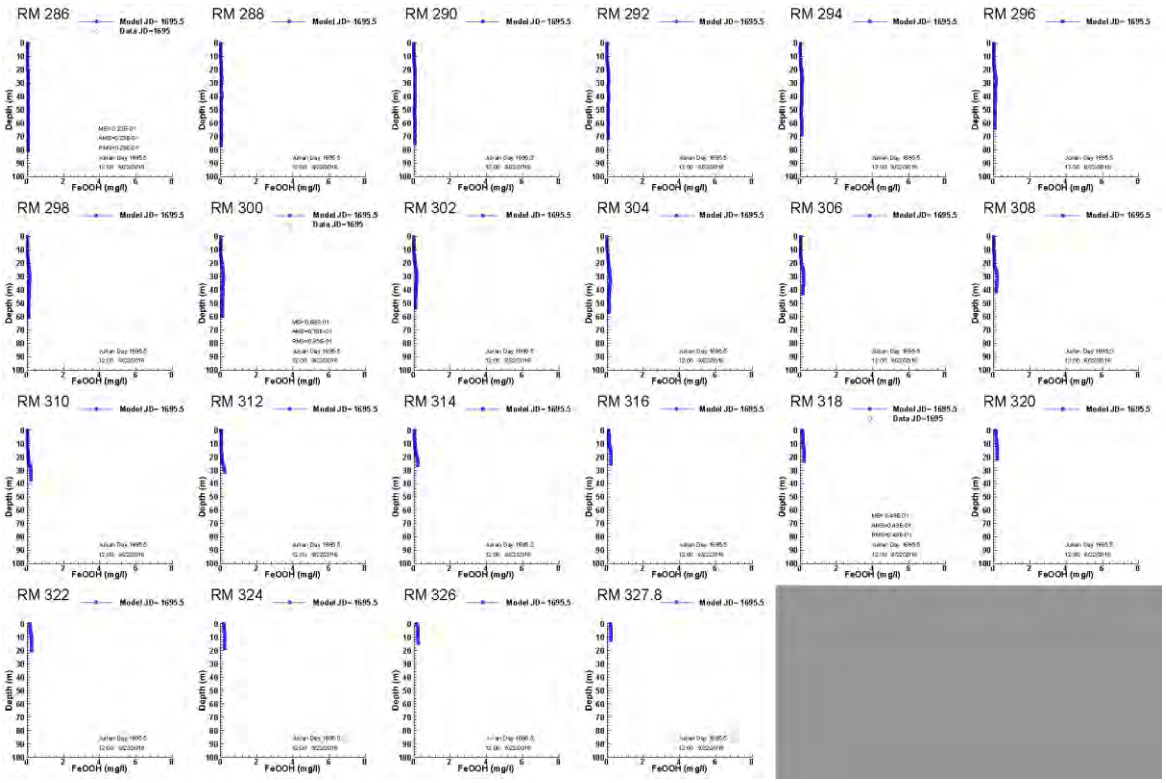


Figure 539. Vertical profiles of FeOOH compared with data for 8/22/2018.

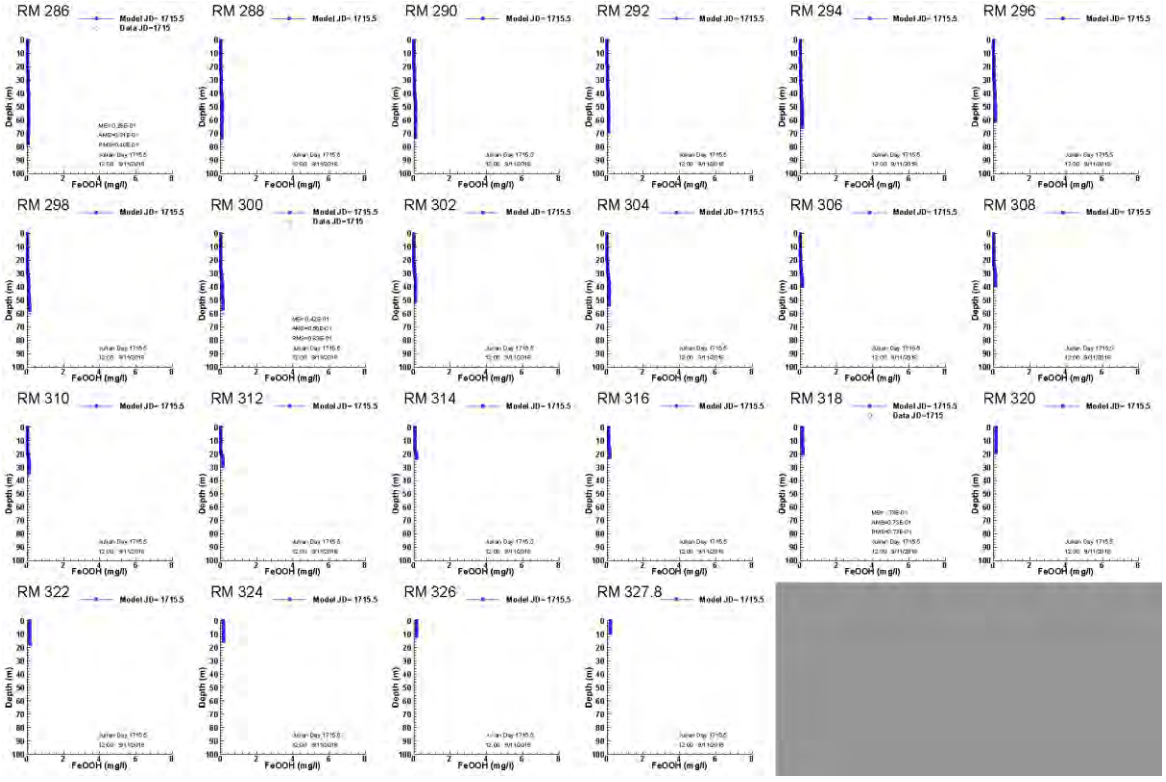


Figure 540. Vertical profiles of FeOOH compared with data for 9/11/2018.

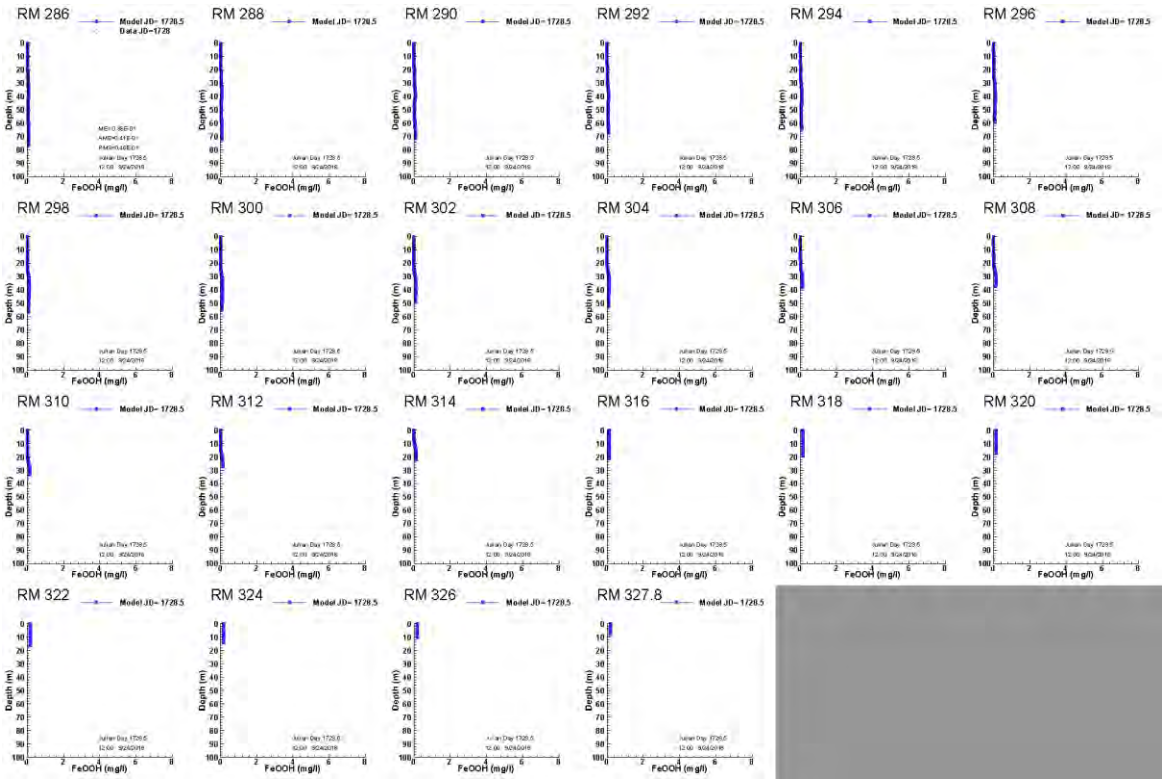


Figure 541. Vertical profiles of FeOOH compared with data for 9/24/2018.

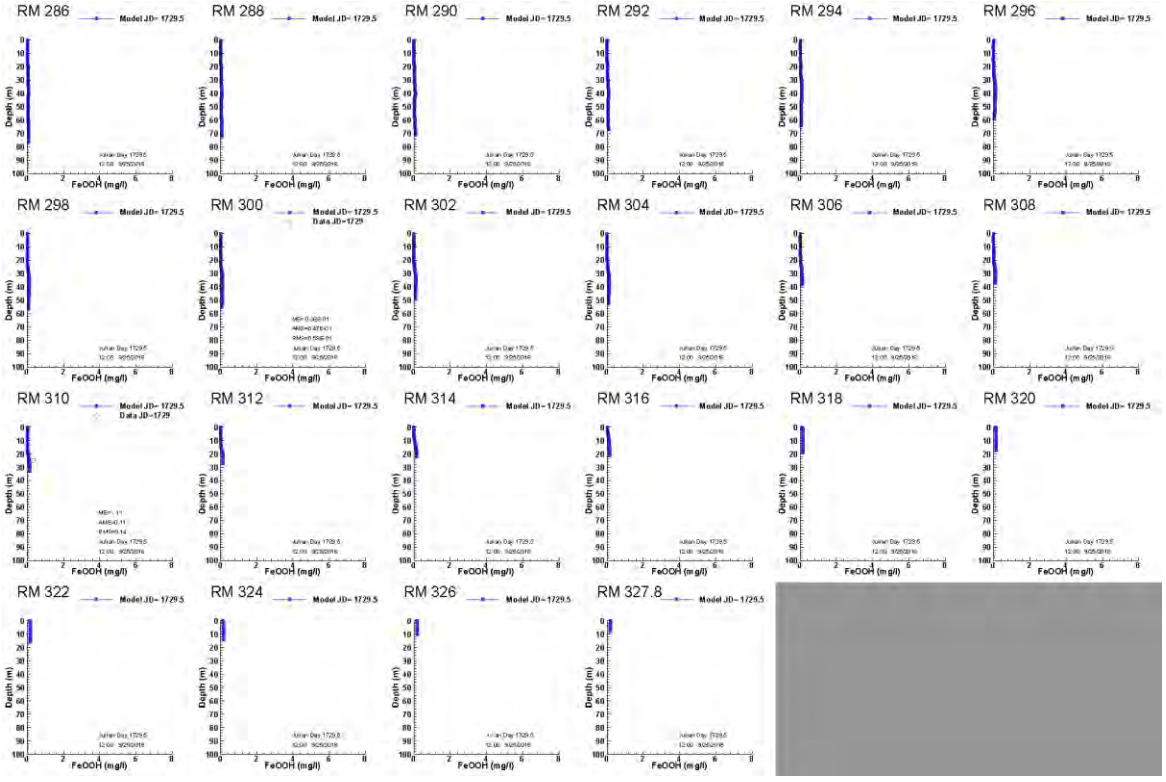


Figure 542. Vertical profiles of FeOOH compared with data for 9/25/2018.

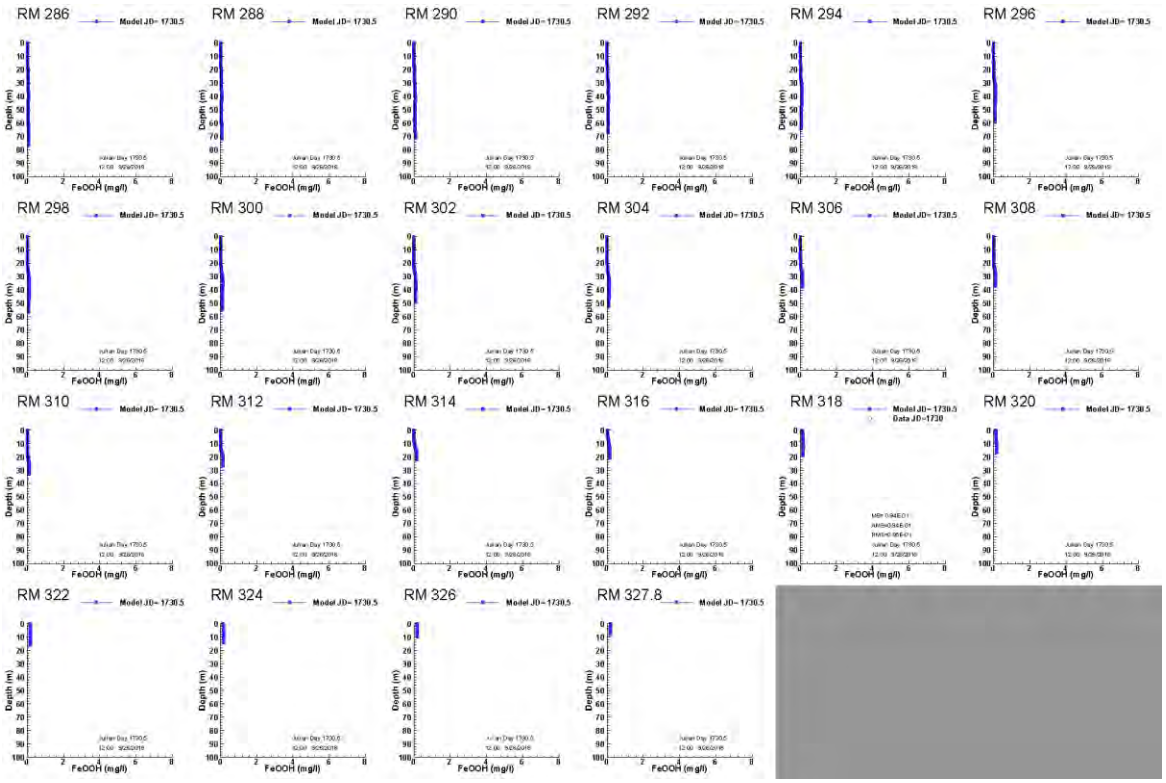


Figure 543. Vertical profiles of FeOOH compared with data for 9/26/2018.

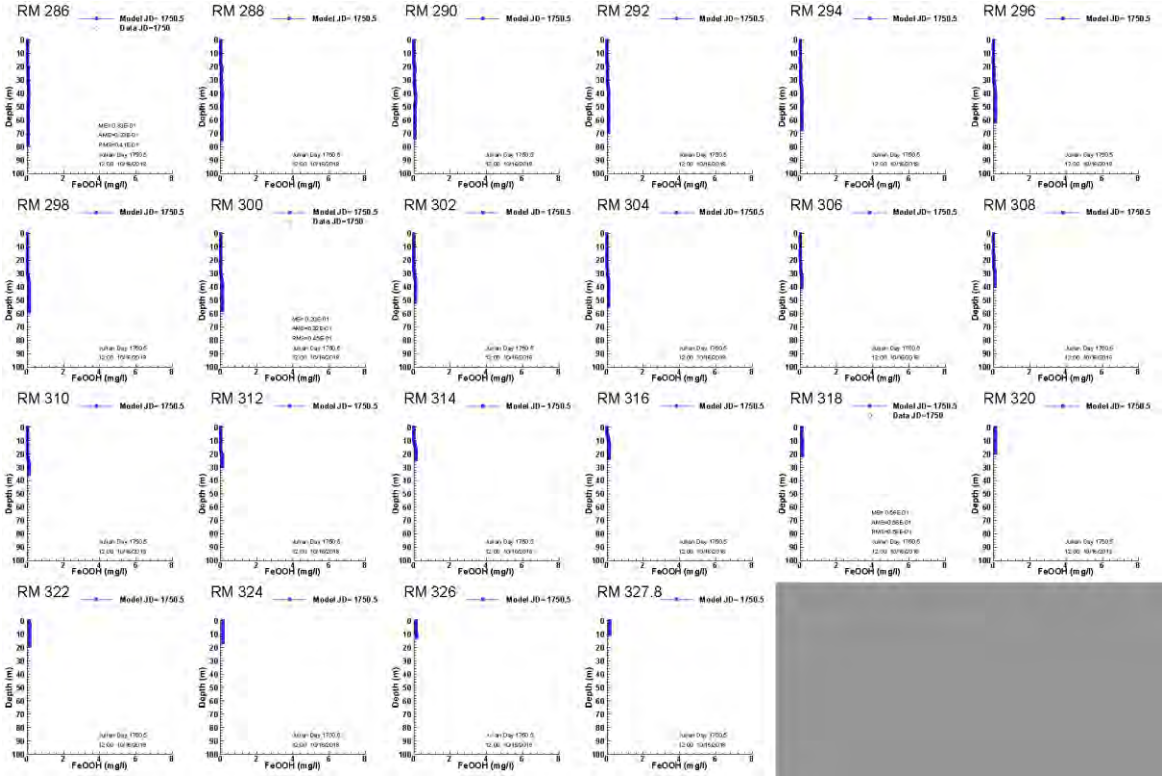


Figure 544. Vertical profiles of FeOOH compared with data for 10/16/2018.

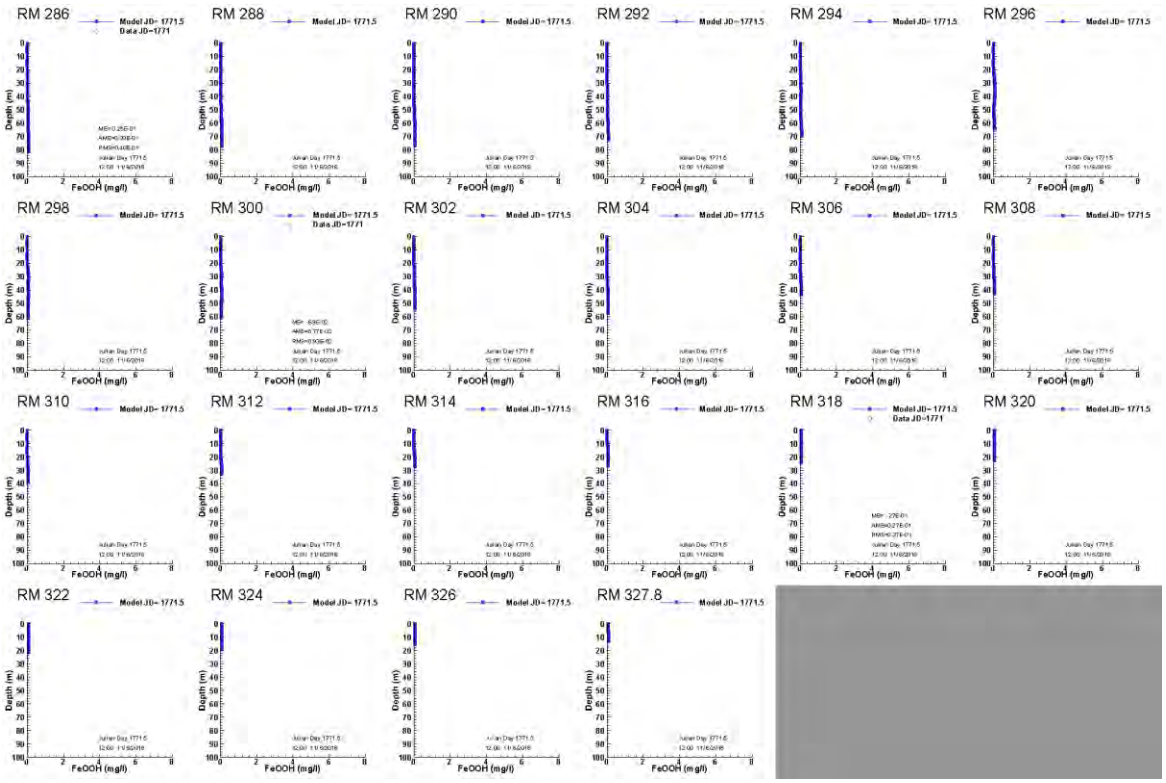


Figure 545. Vertical profiles of FeOOH compared with data for 11/ 6/2018.

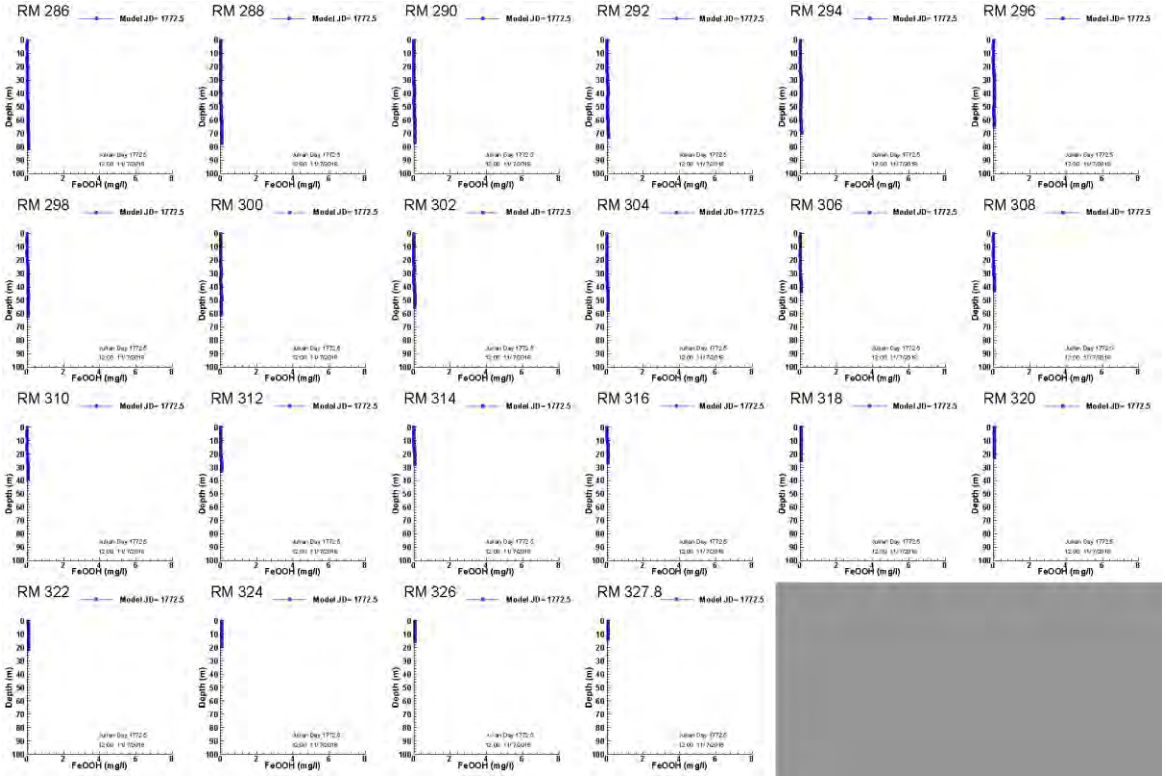


Figure 546. Vertical profiles of FeOOH compared with data for 11/ 7/2018.

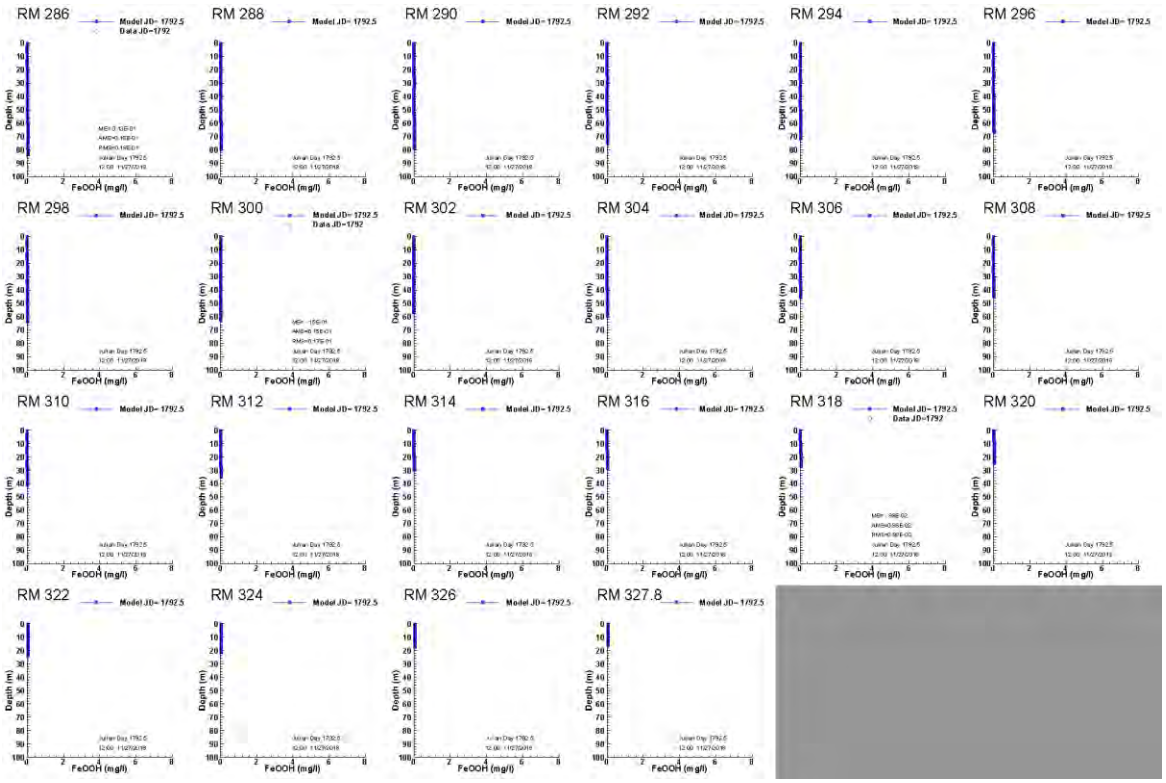


Figure 547. Vertical profiles of FeOOH compared with data for 11/27/2018.

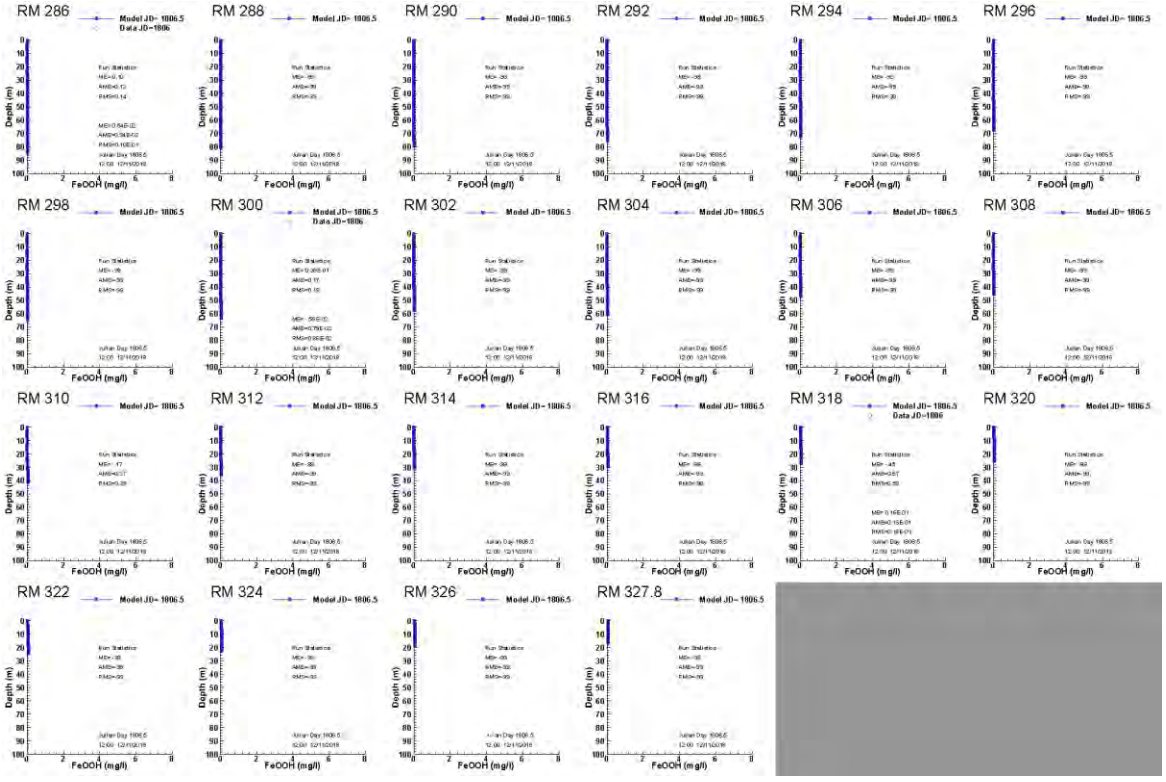


Figure 548. Vertical profiles of FeOOH compared with data for 12/11/2018.

Mn(II)

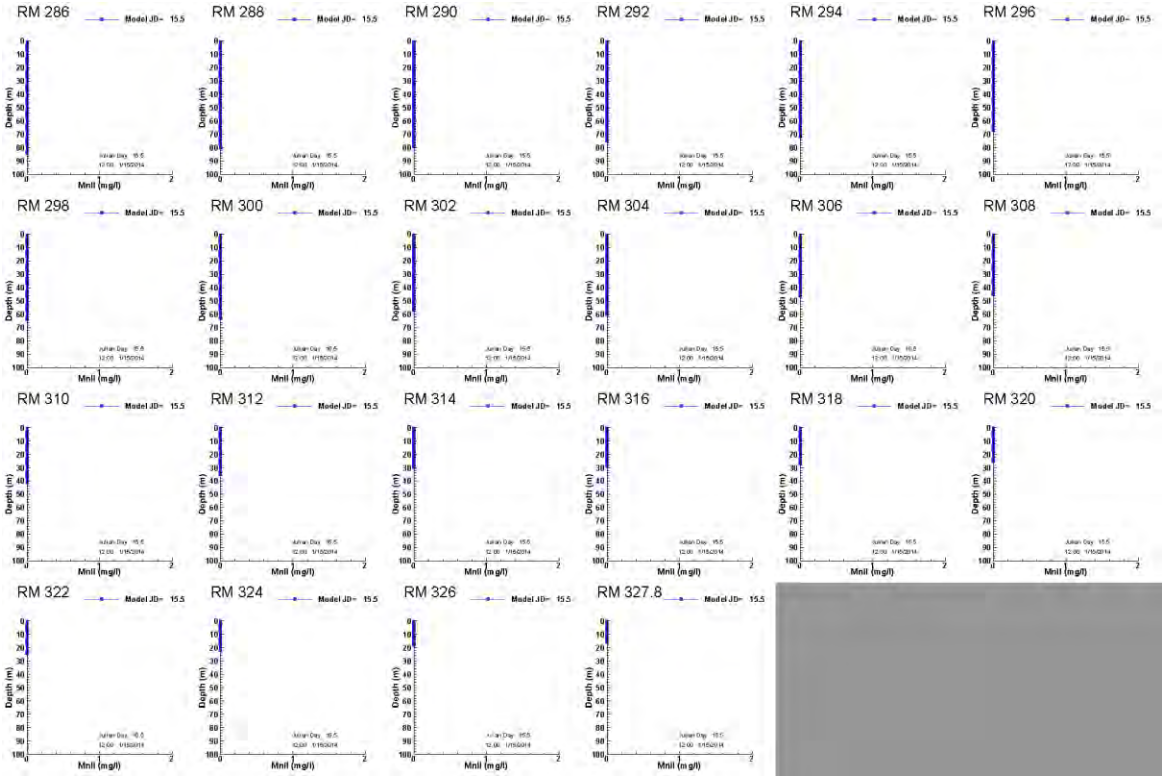


Figure 549. Vertical profiles of Mn(II) compared with data for 1/15/2014.

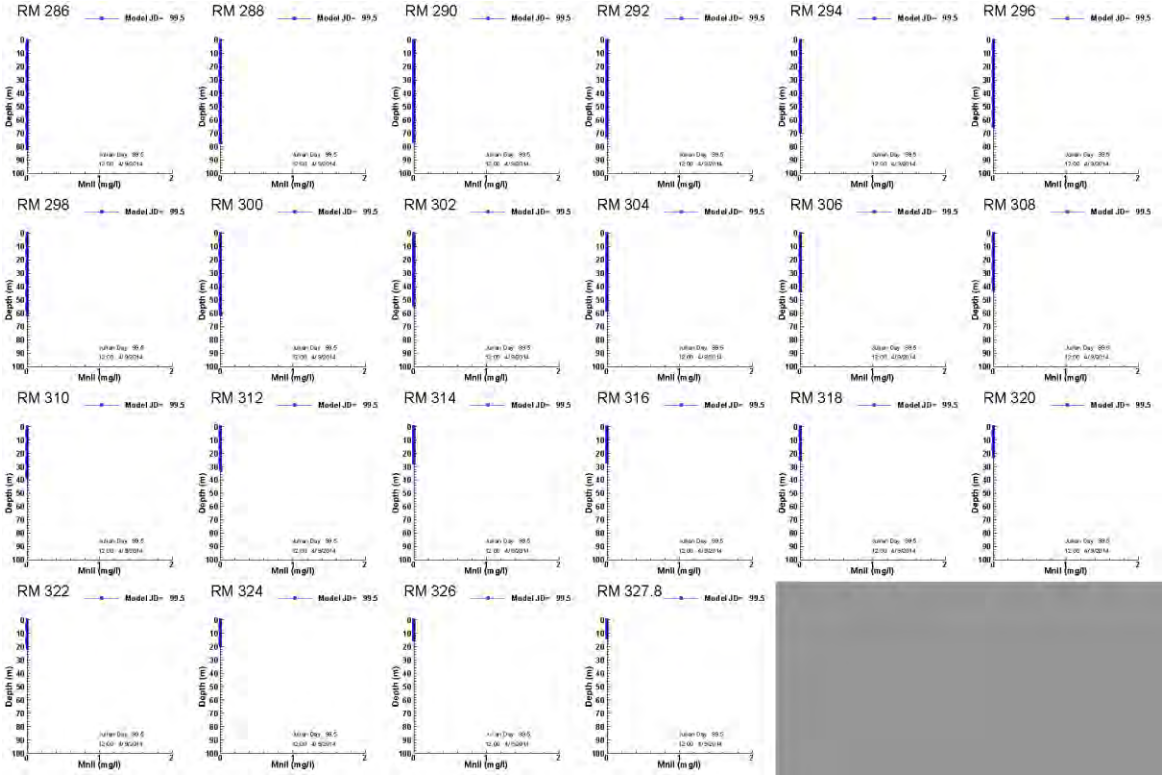


Figure 550. Vertical profiles of Mn(II) compared with data for 4/ 9/2014.

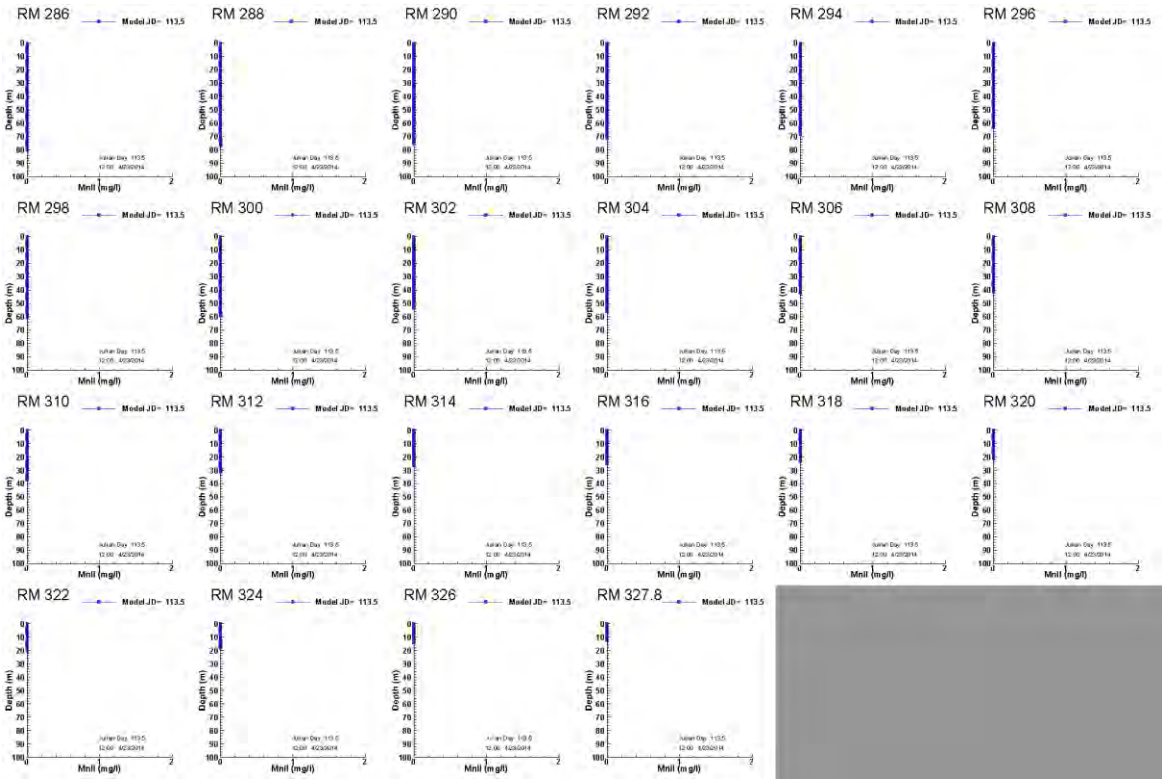


Figure 551. Vertical profiles of Mn(II) compared with data for 4/23/2014.

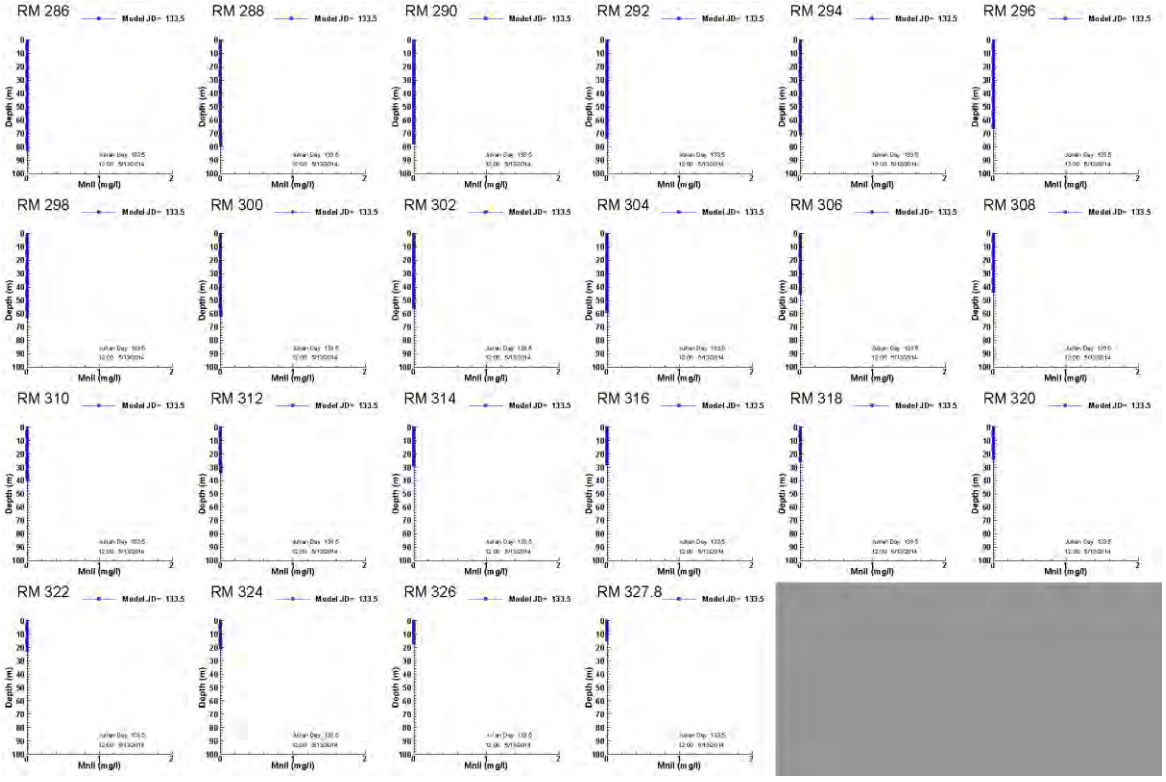


Figure 552. Vertical profiles of Mn(II) compared with data for 5/13/2014.

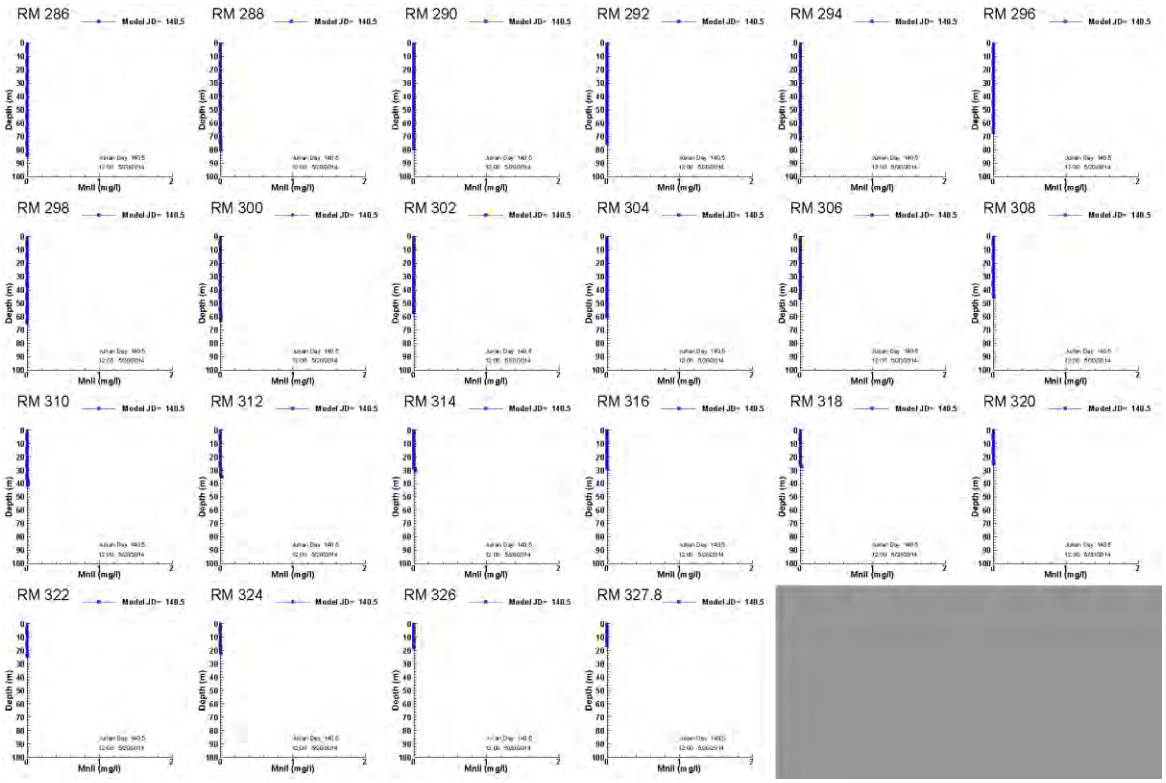


Figure 553. Vertical profiles of Mn(II) compared with data for 5/20/2014.

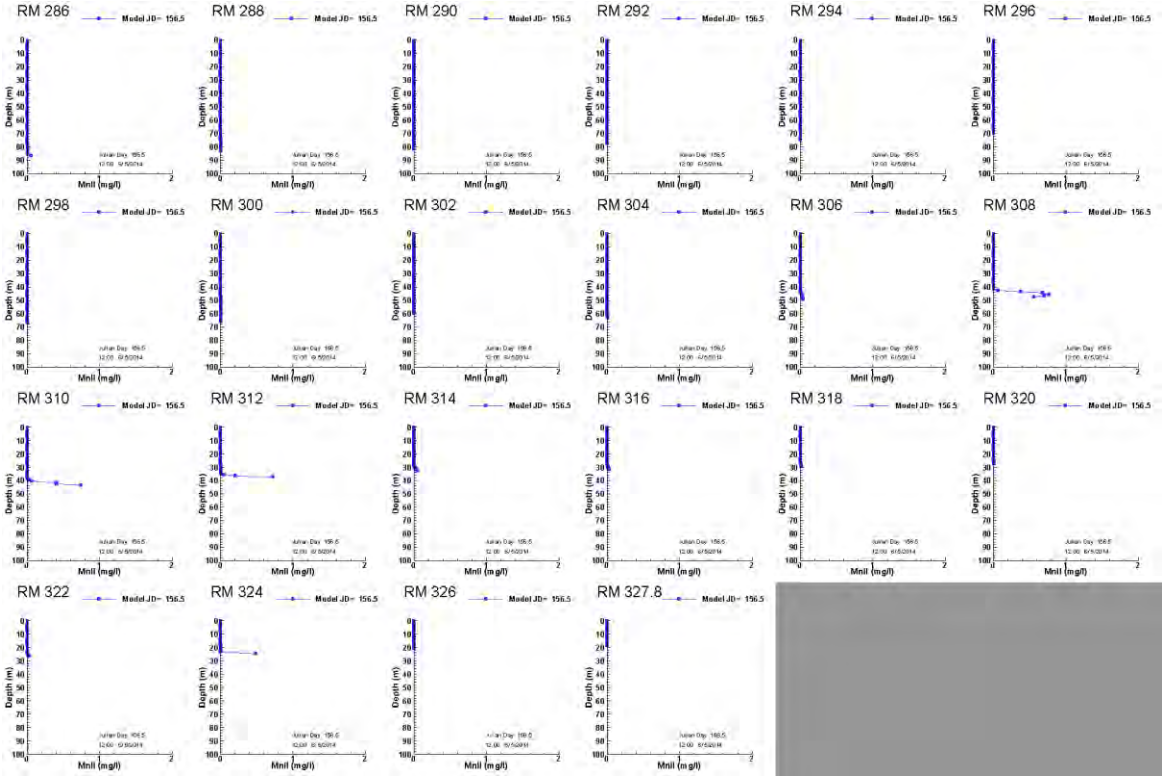


Figure 554. Vertical profiles of Mn(II) compared with data for 6/ 5/2014.

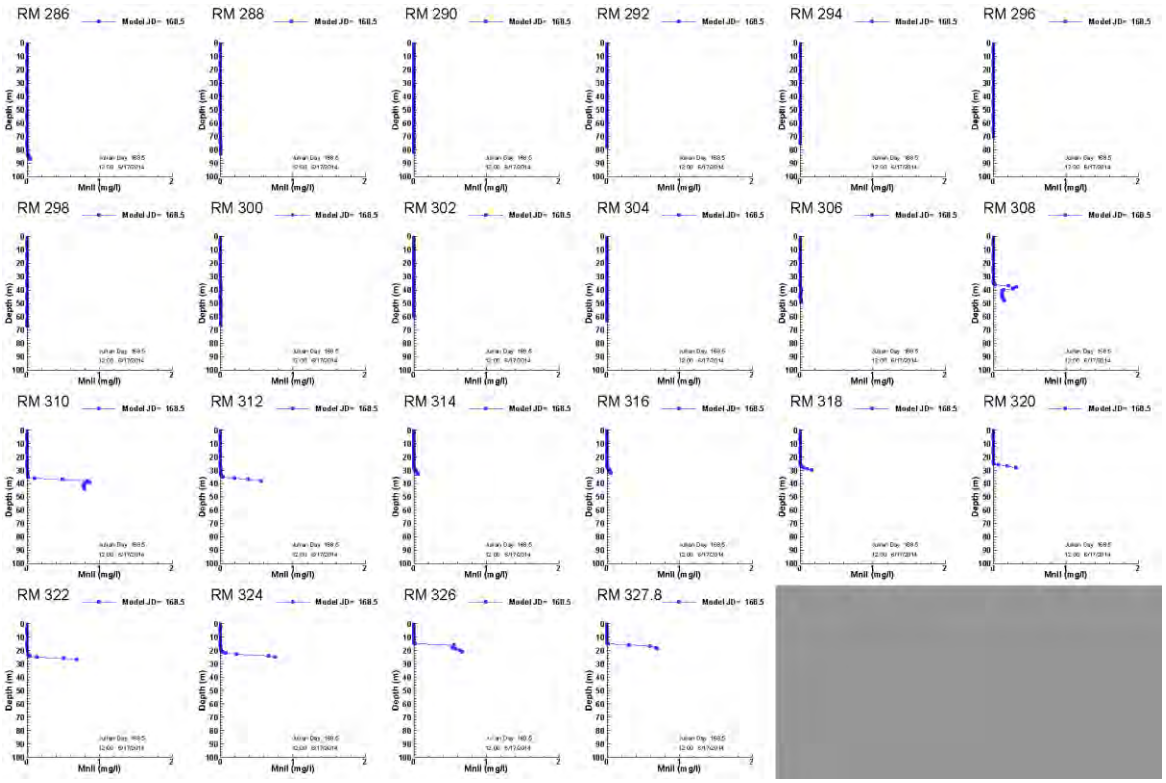


Figure 555. Vertical profiles of Mn(II) compared with data for 6/17/2014.

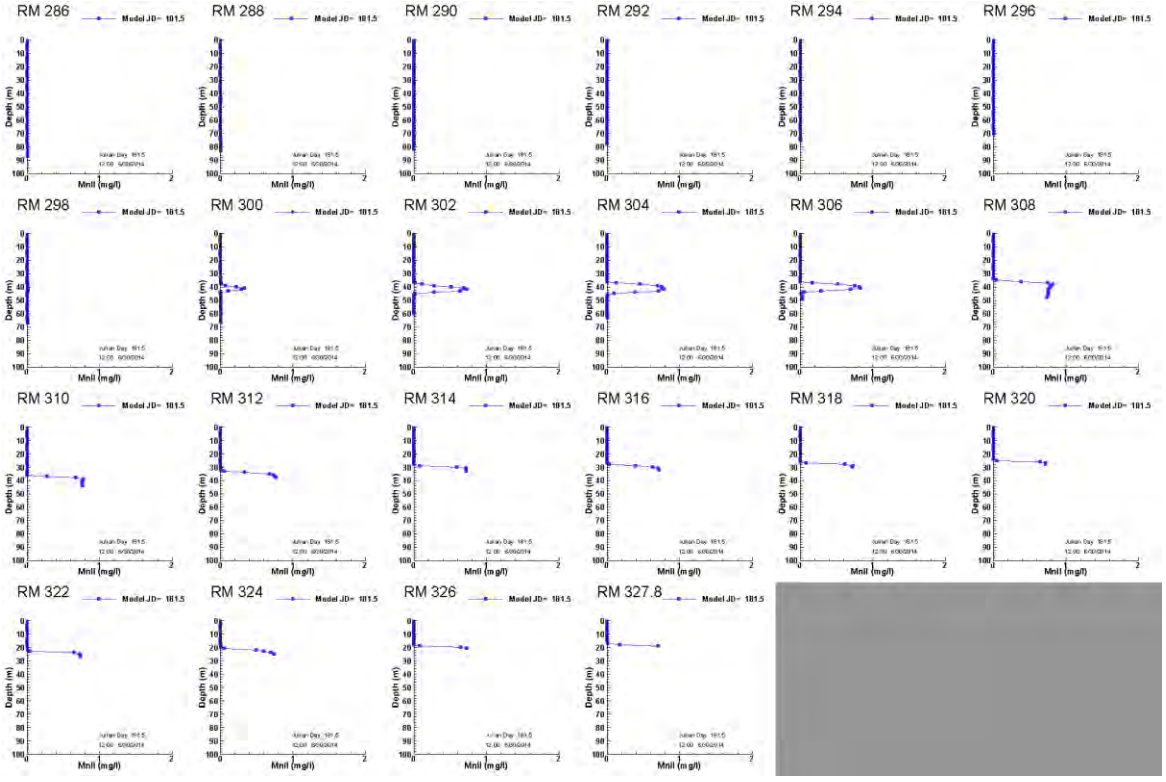


Figure 556. Vertical profiles of Mn(II) compared with data for 6/30/2014.

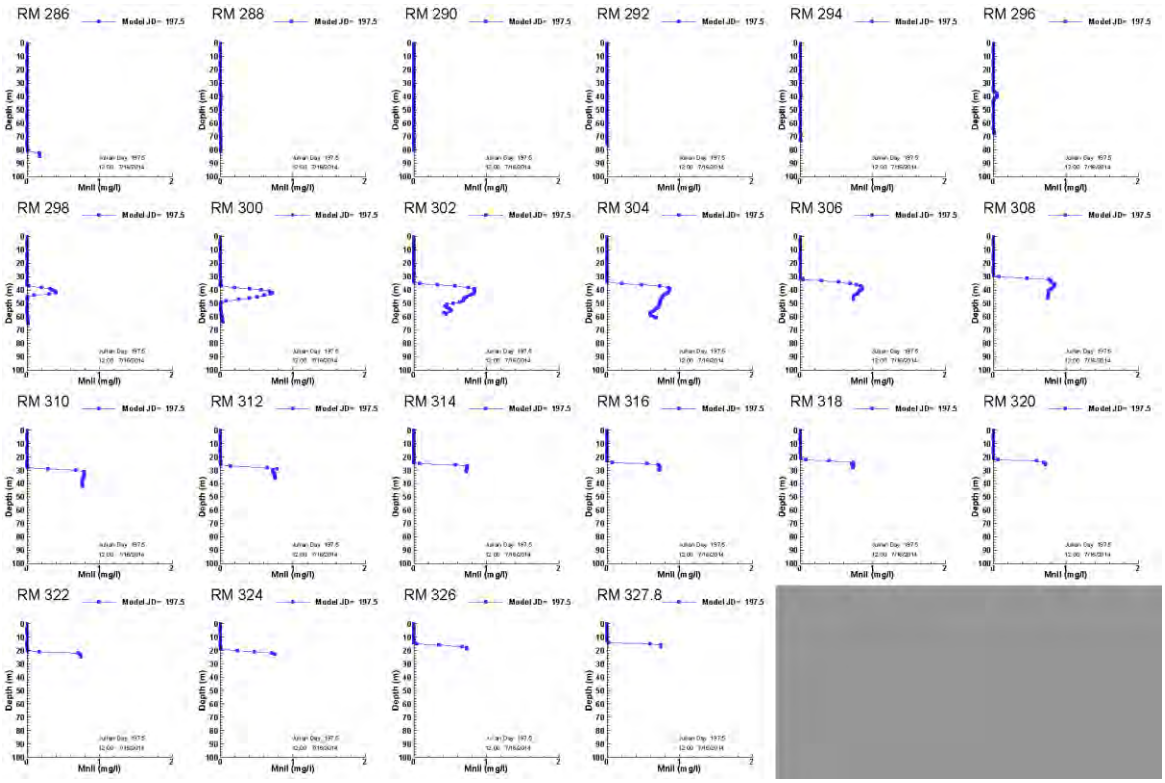


Figure 557. Vertical profiles of Mn(II) compared with data for 7/16/2014.

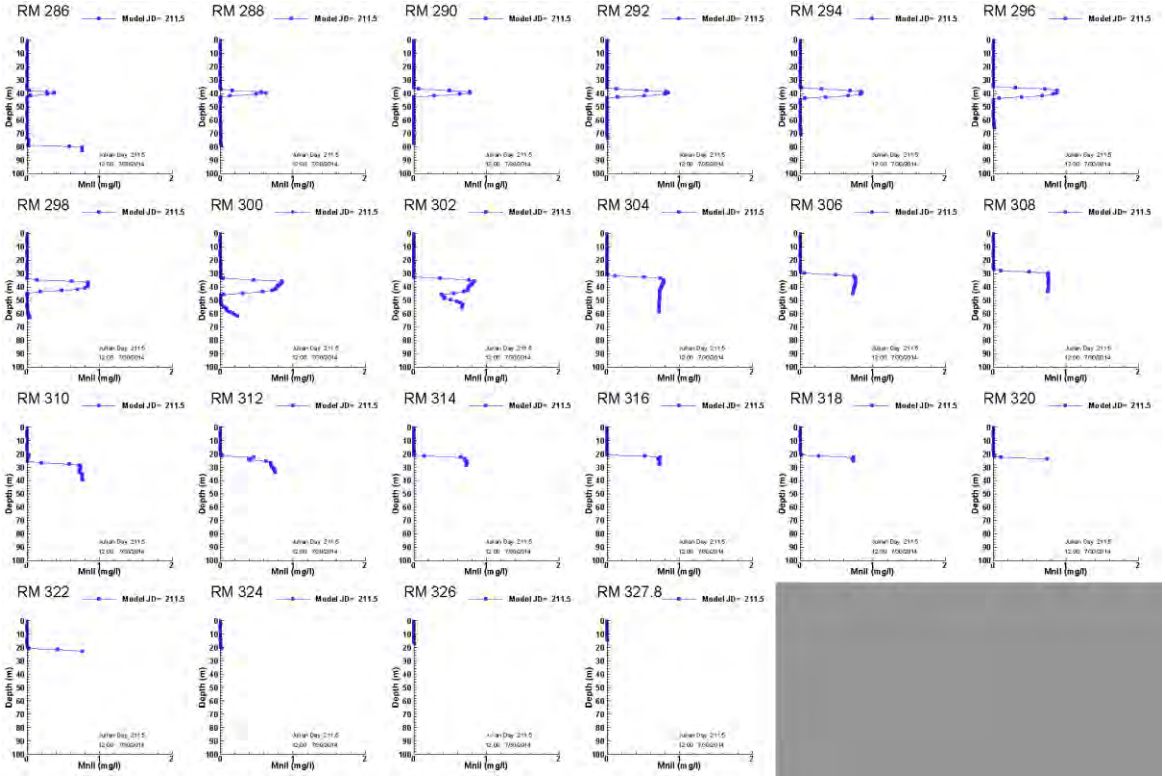


Figure 558. Vertical profiles of Mn(II) compared with data for 7/30/2014.

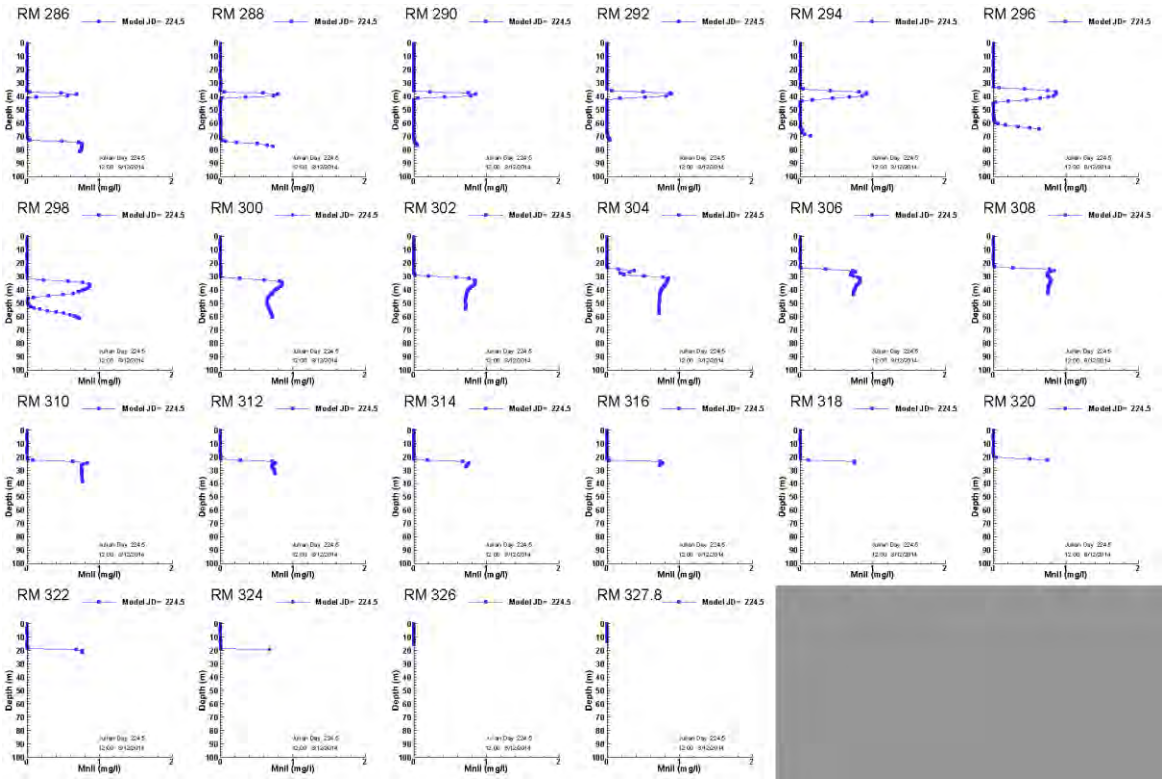


Figure 559. Vertical profiles of Mn(II) compared with data for 8/12/2014.

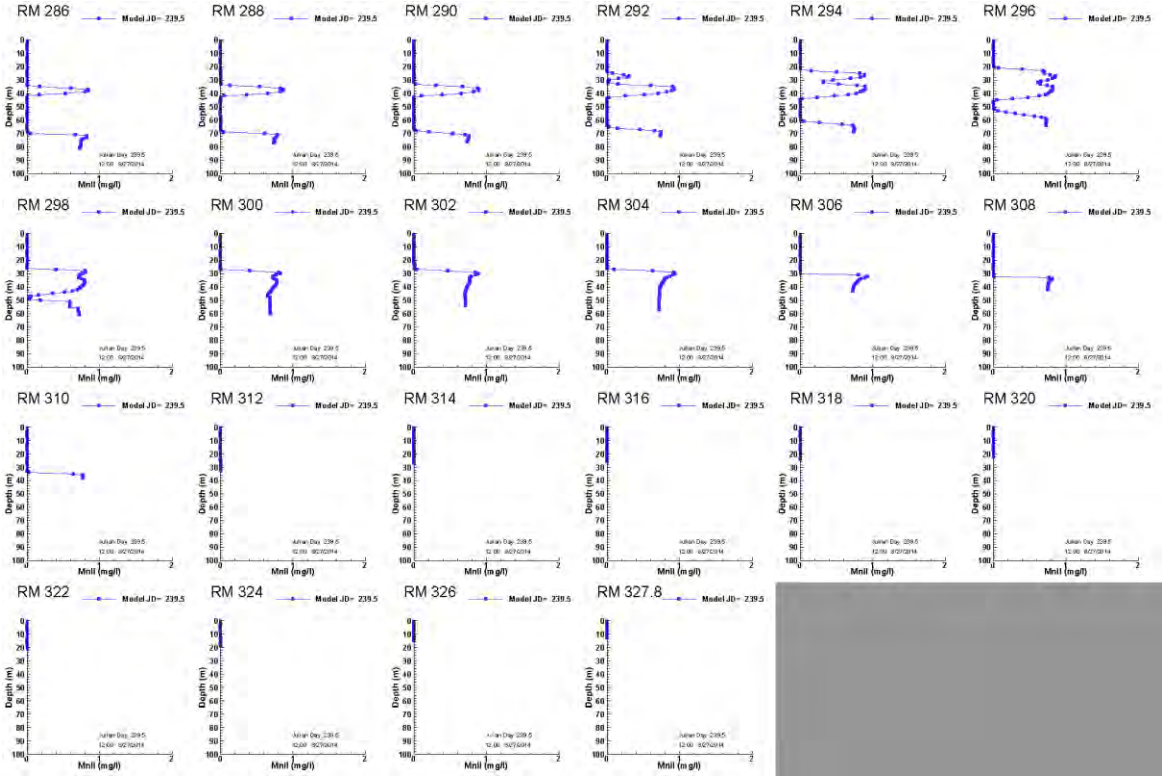


Figure 560. Vertical profiles of Mn(II) compared with data for 8/27/2014.

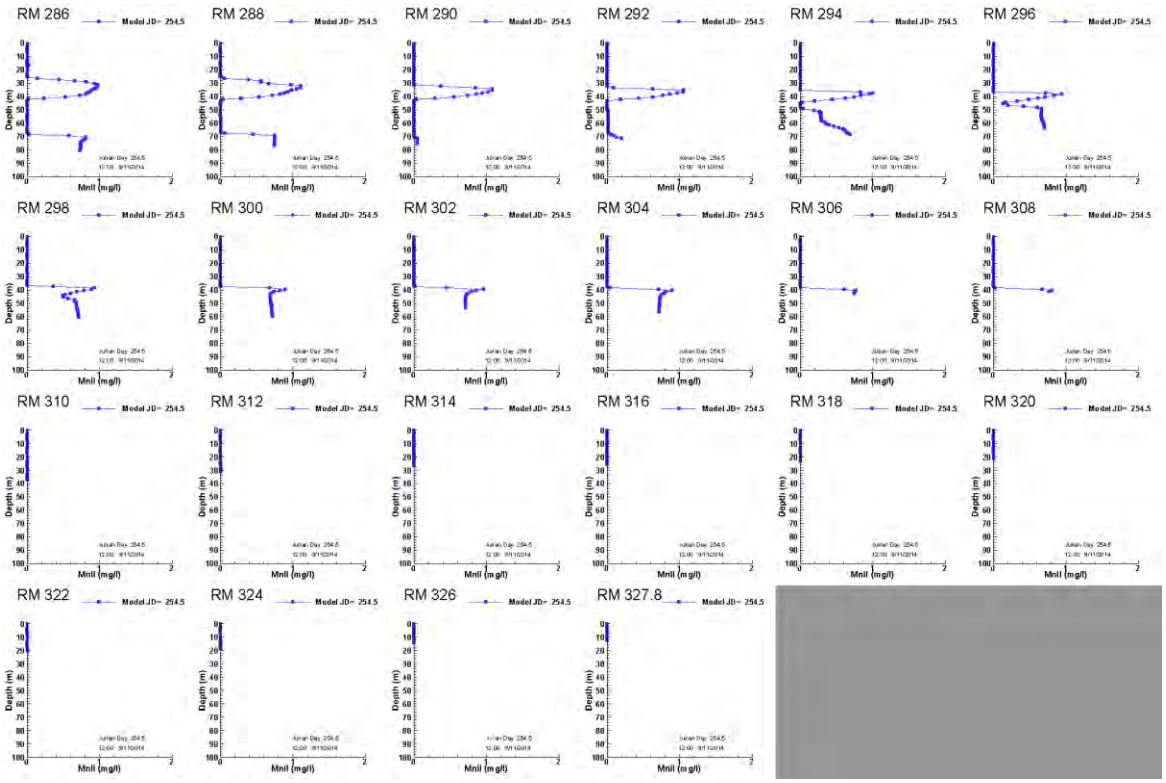


Figure 561. Vertical profiles of Mn(II) compared with data for 9/11/2014.

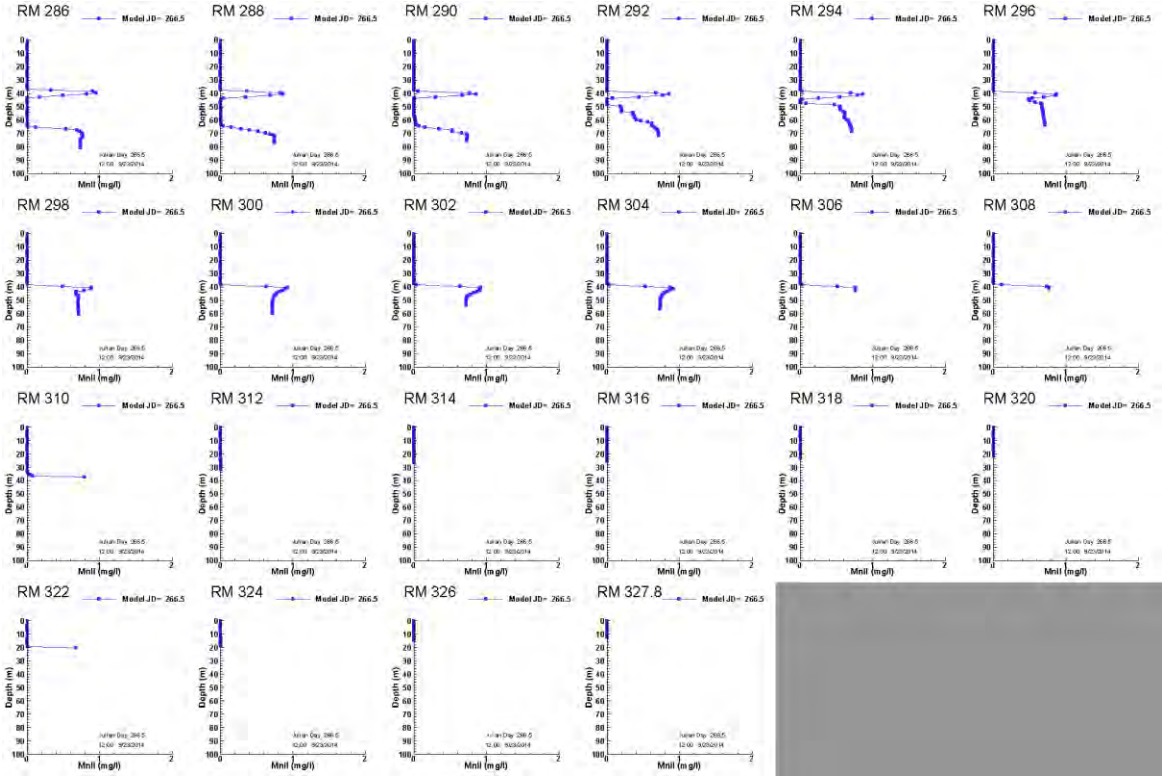


Figure 562. Vertical profiles of Mn(II) compared with data for 9/23/2014.

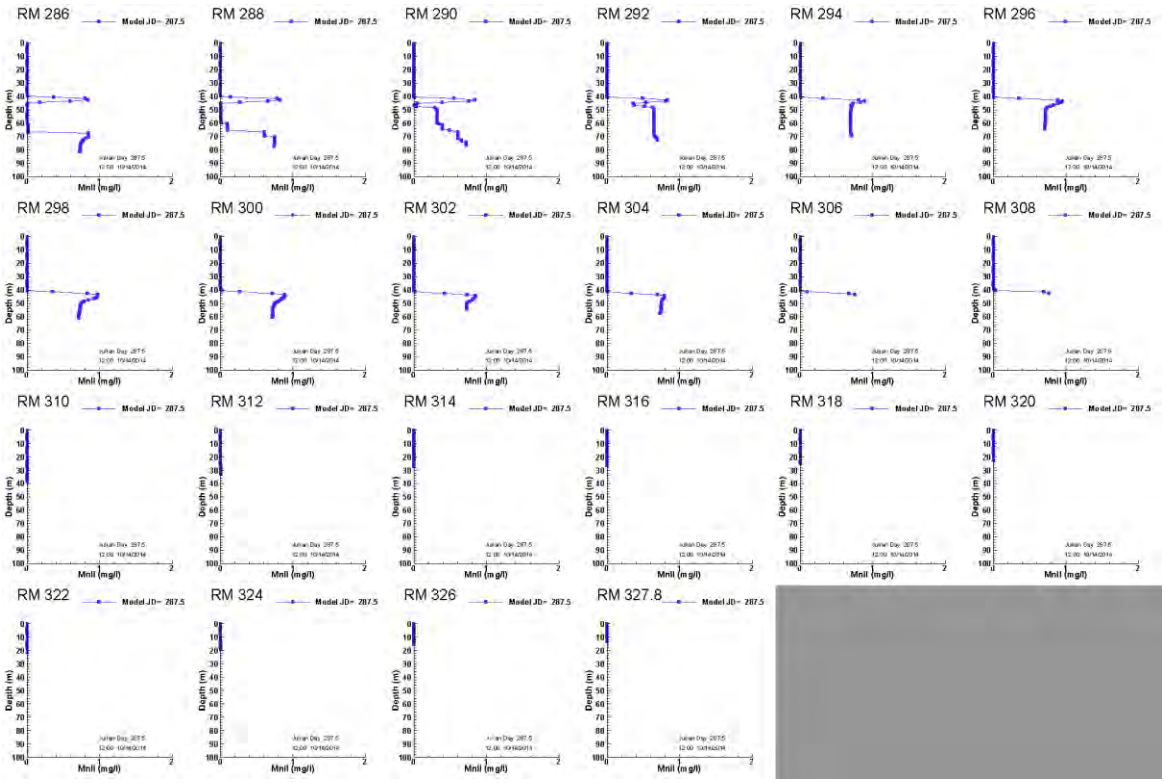


Figure 563. Vertical profiles of Mn(II) compared with data for 10/14/2014.

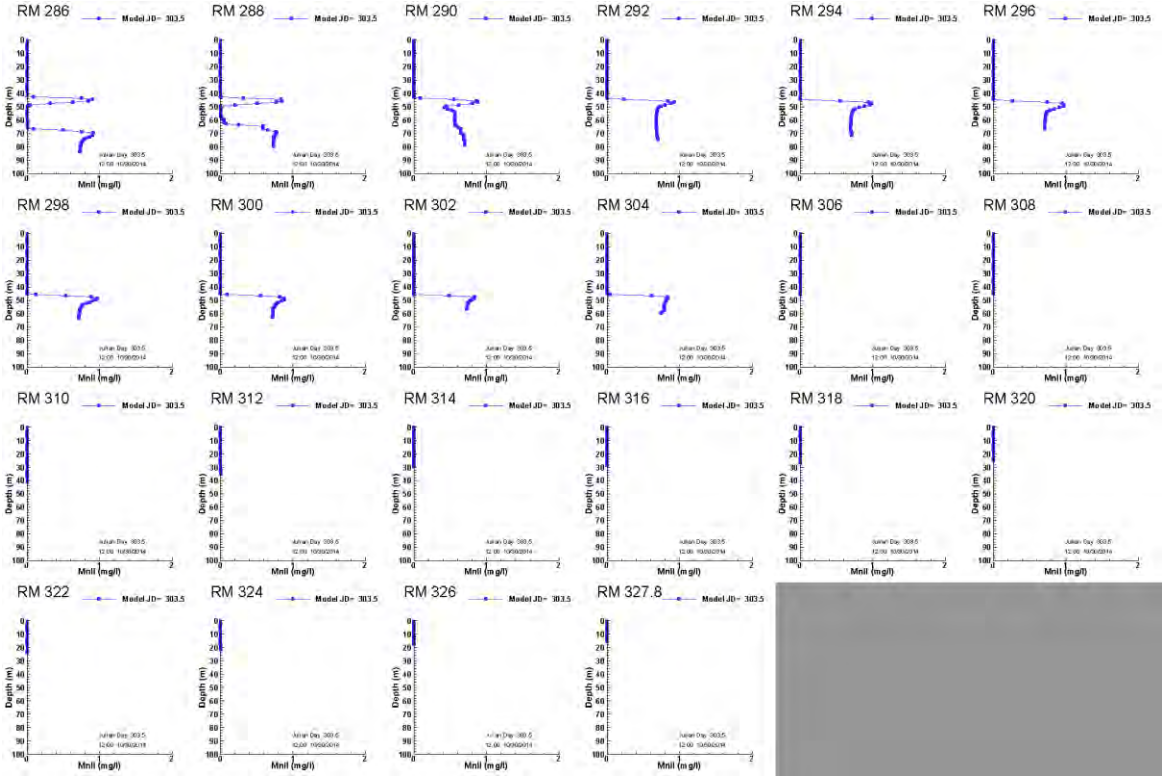


Figure 564. Vertical profiles of Mn(II) compared with data for 10/30/2014.

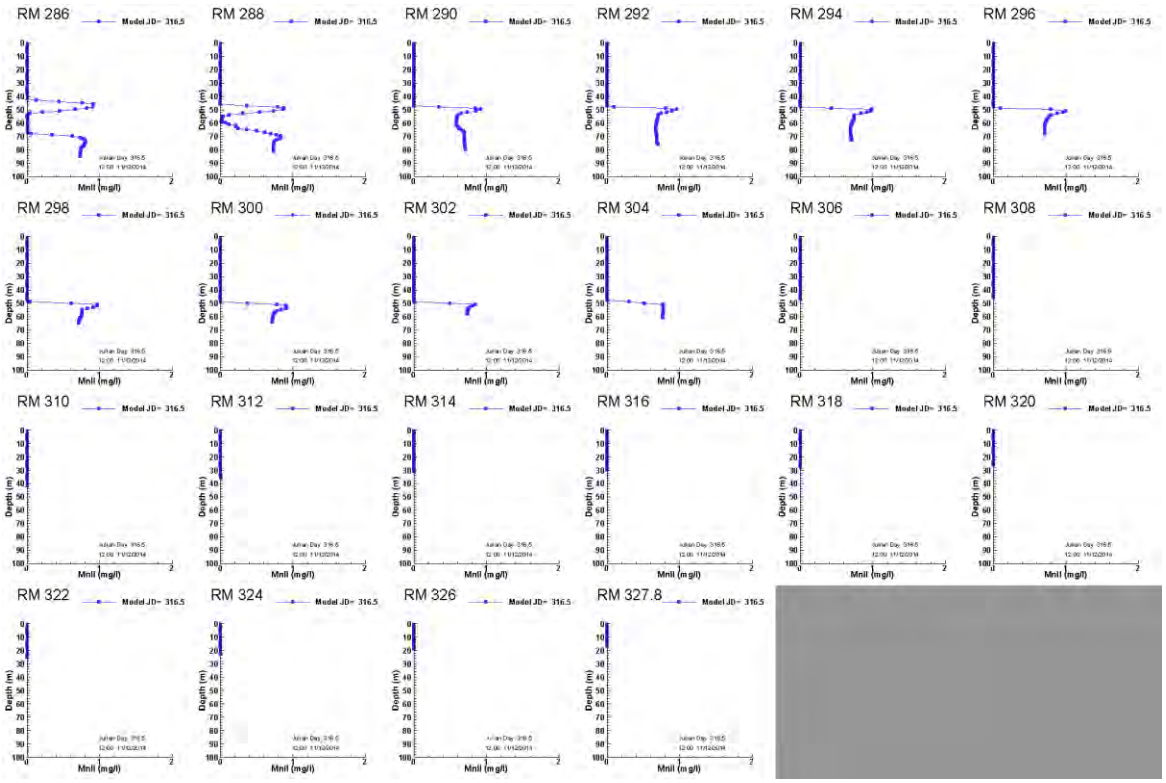


Figure 565. Vertical profiles of Mn(II) compared with data for 11/12/2014.

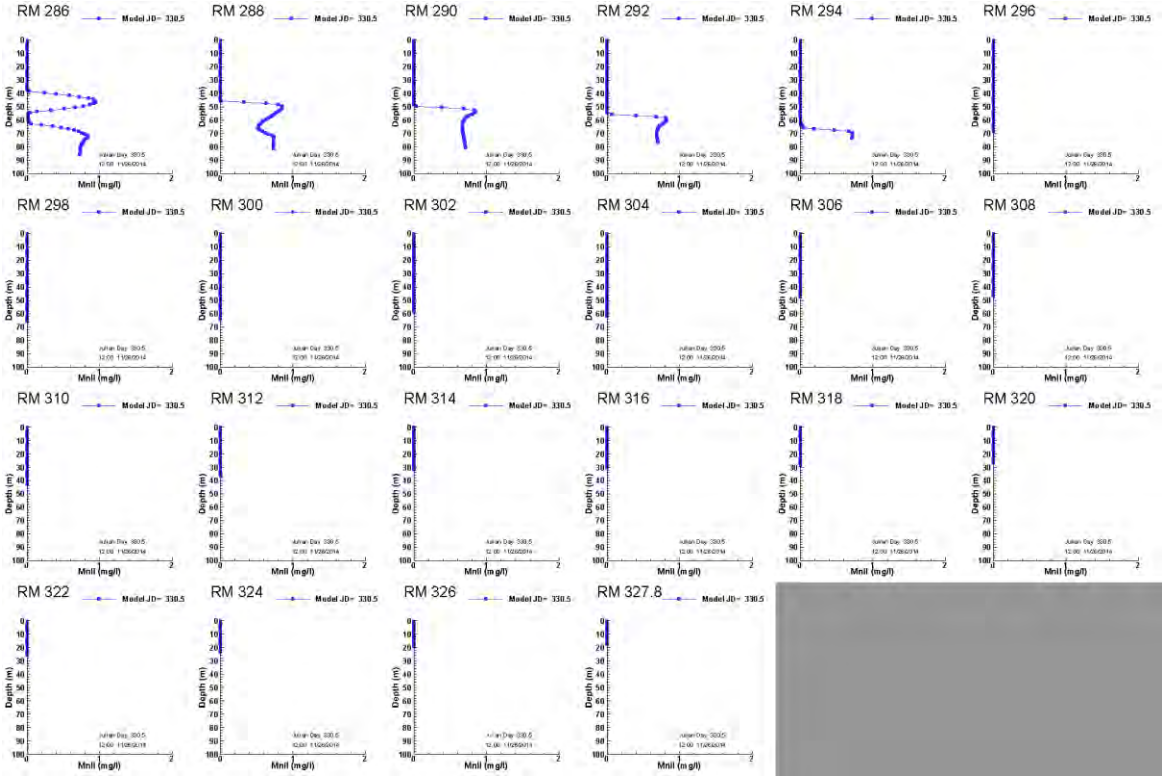


Figure 566. Vertical profiles of Mn(II) compared with data for 11/26/2014.

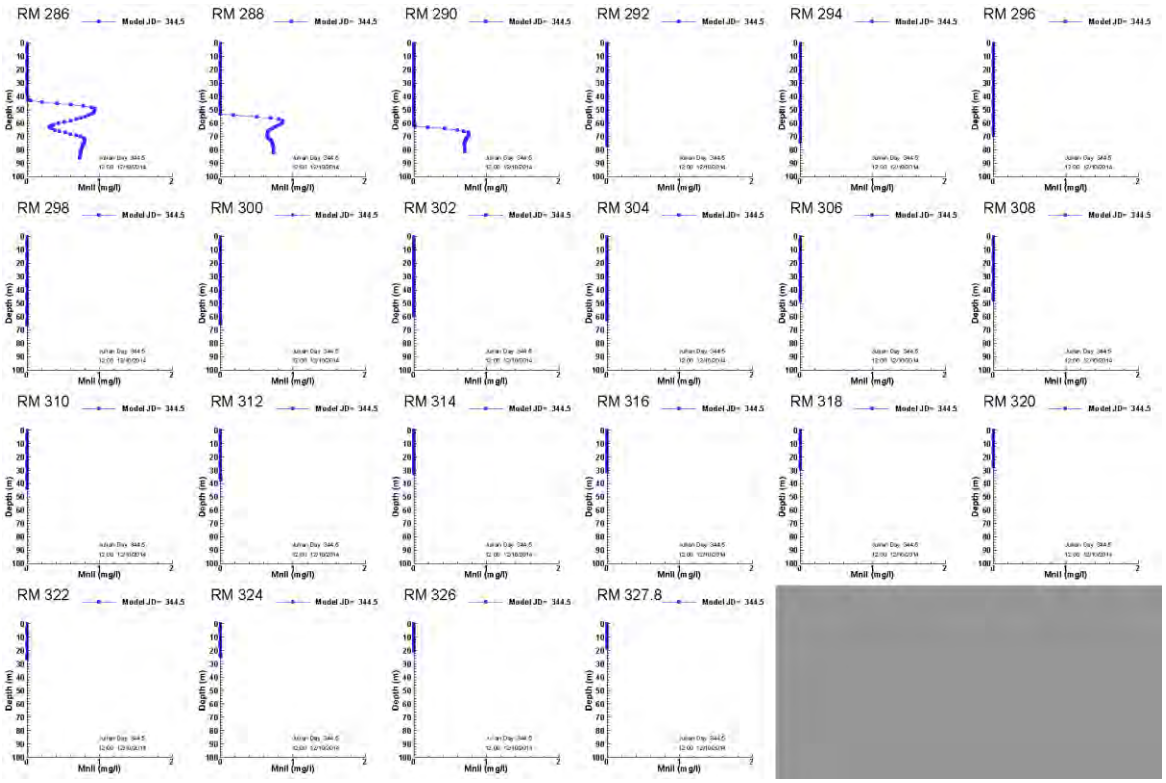


Figure 567. Vertical profiles of Mn(II) compared with data for 12/10/2014.

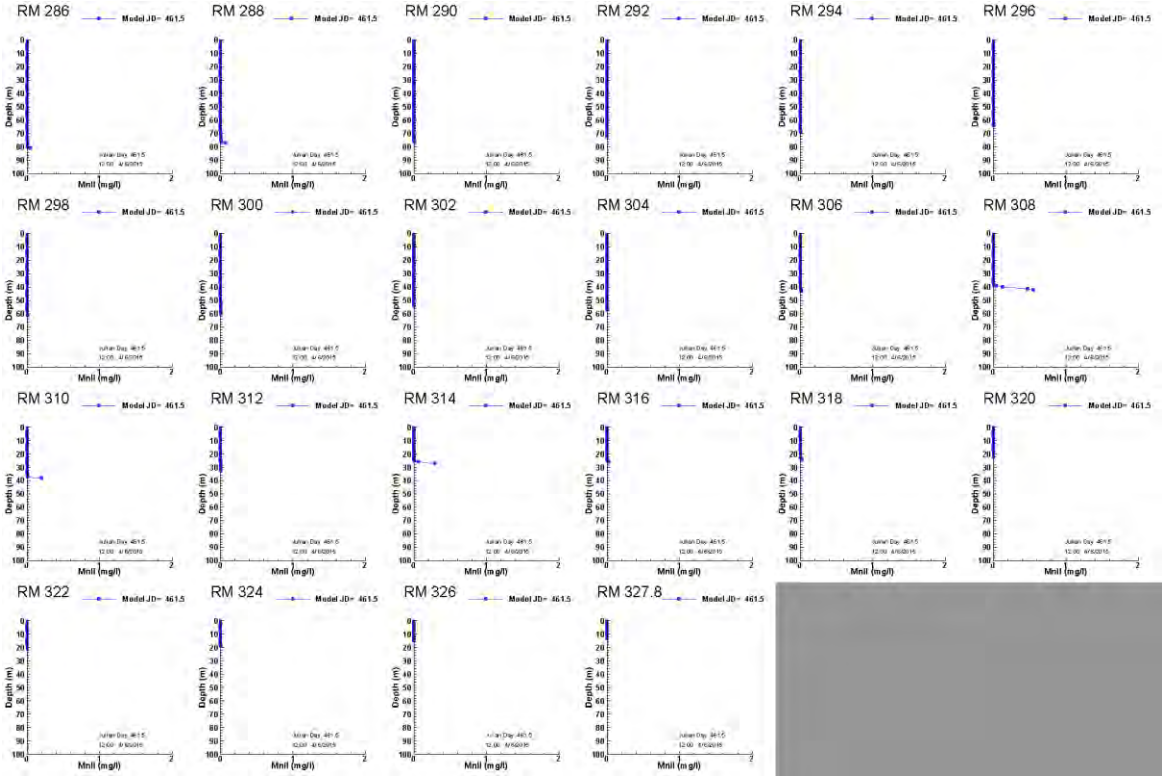


Figure 568. Vertical profiles of Mn(II) compared with data for 4/ 6/2015.

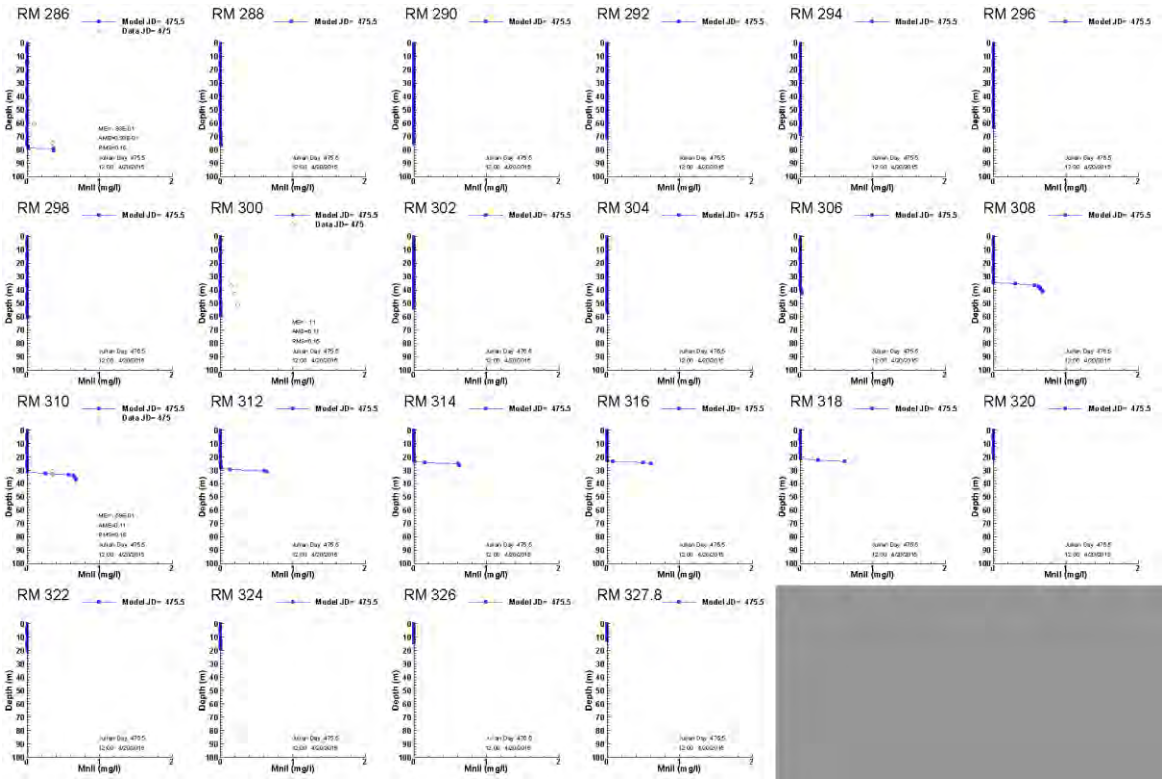


Figure 569. Vertical profiles of Mn(II) compared with data for 4/20/2015.

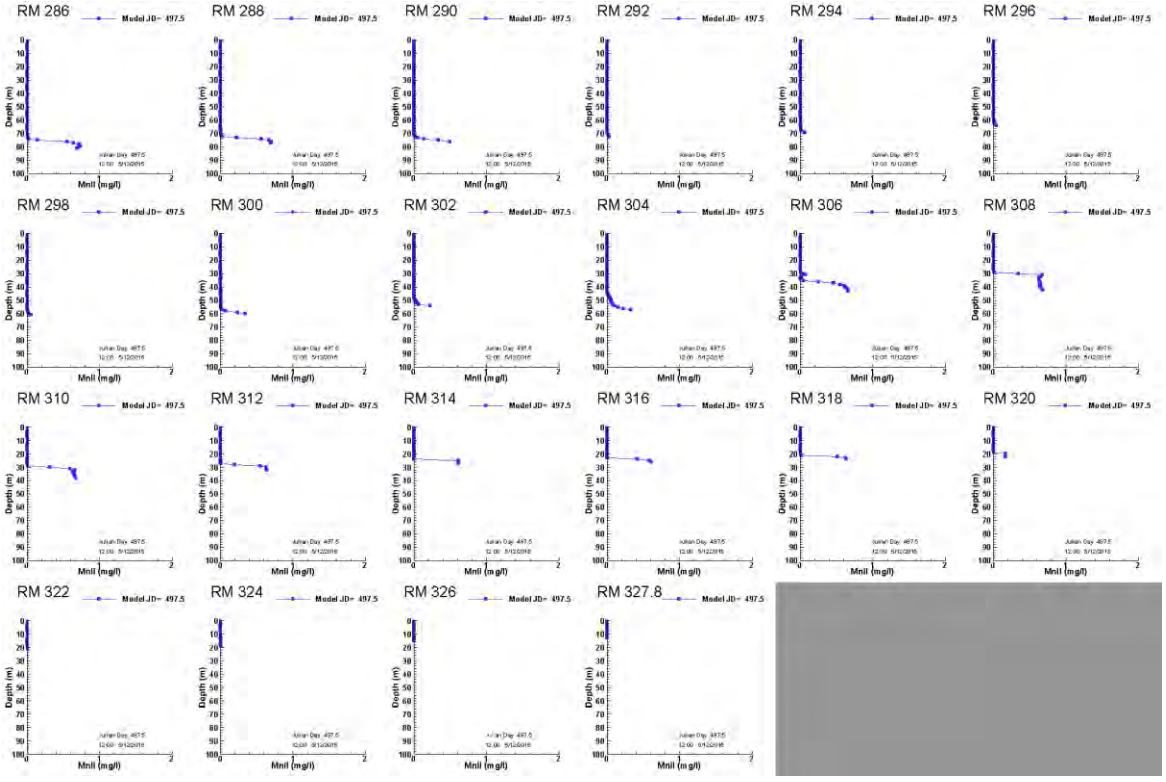


Figure 570. Vertical profiles of Mn(II) compared with data for 5/12/2015.

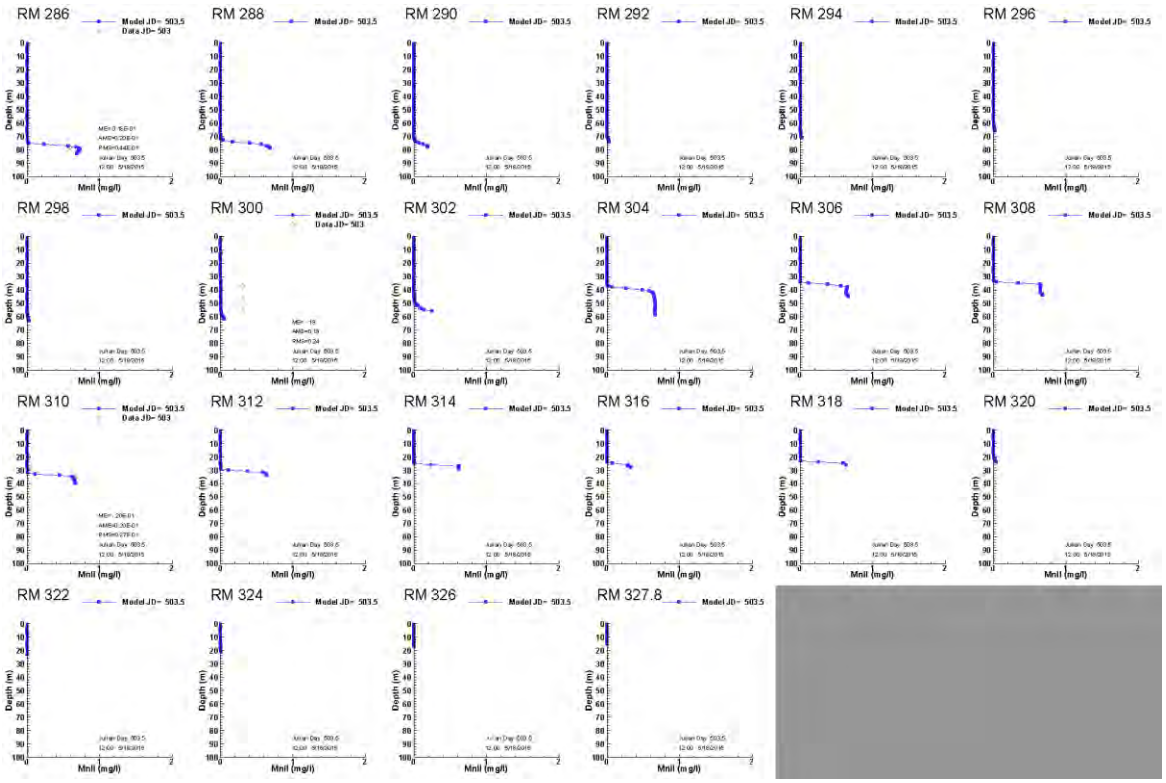


Figure 571. Vertical profiles of Mn(II) compared with data for 5/18/2015.

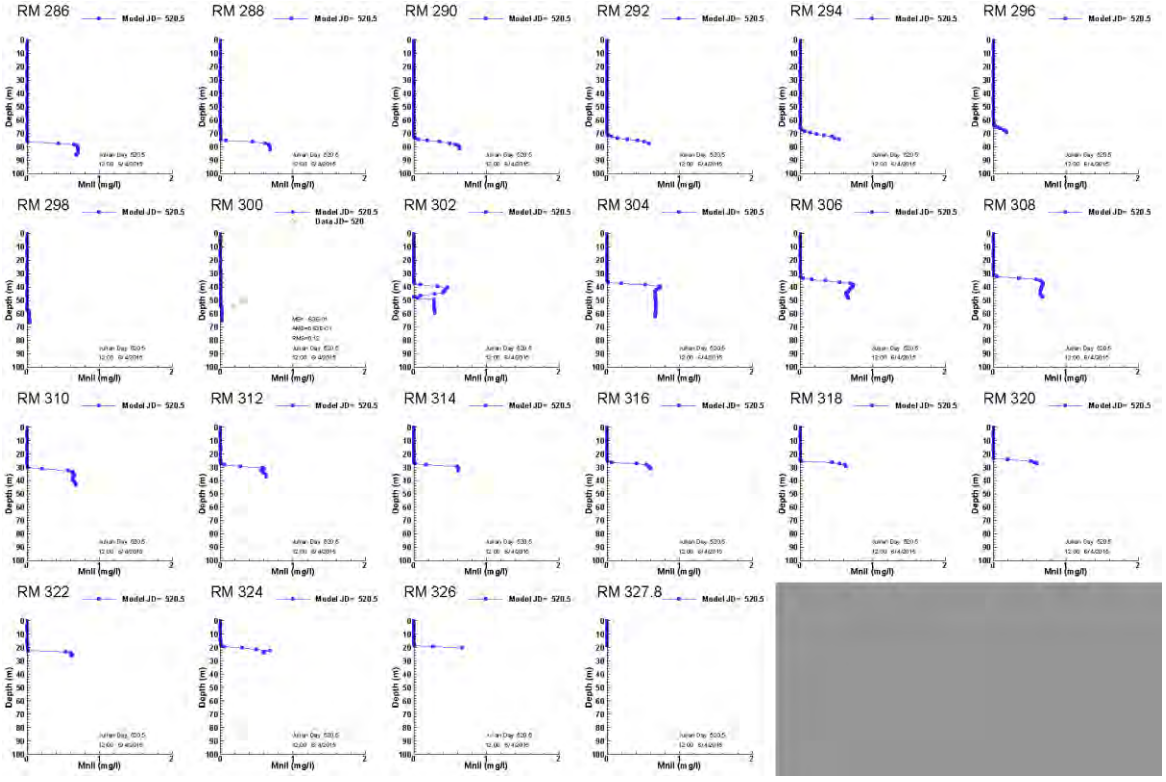


Figure 572. Vertical profiles of Mn(II) compared with data for 6/ 4/2015.

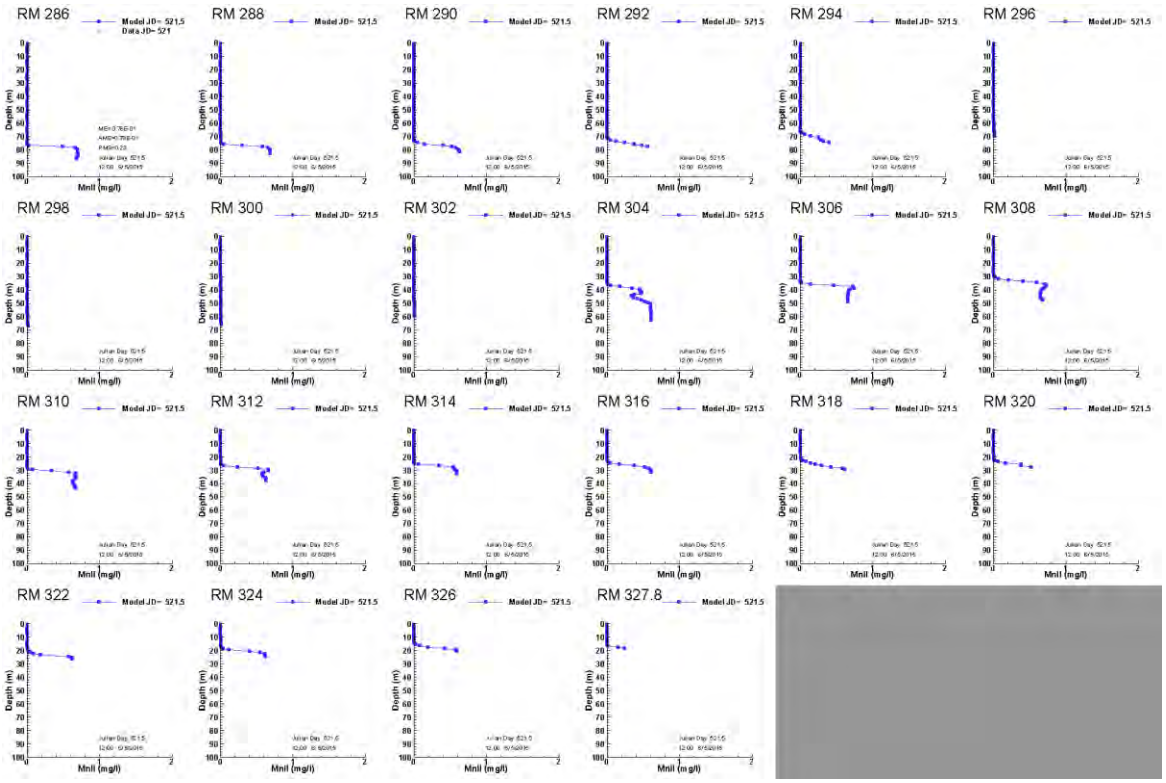


Figure 573. Vertical profiles of Mn(II) compared with data for 6/ 5/2015.

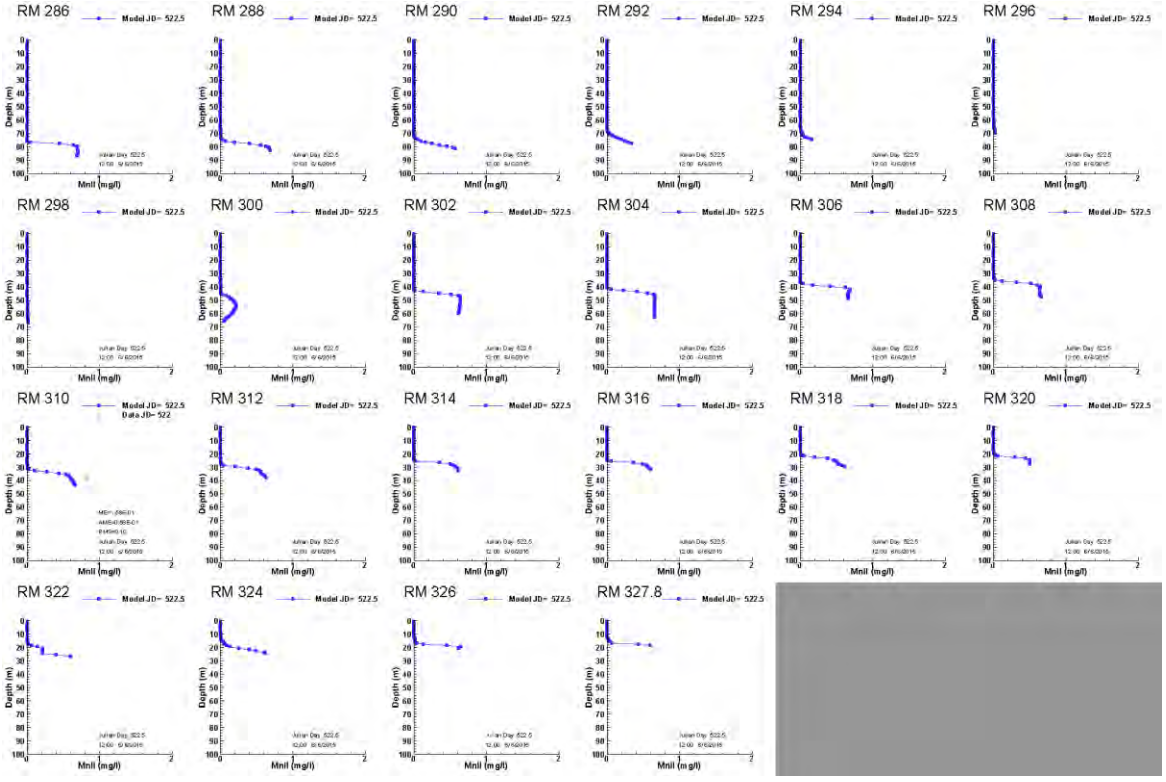


Figure 574. Vertical profiles of Mn(II) compared with data for 6/ 6/2015.

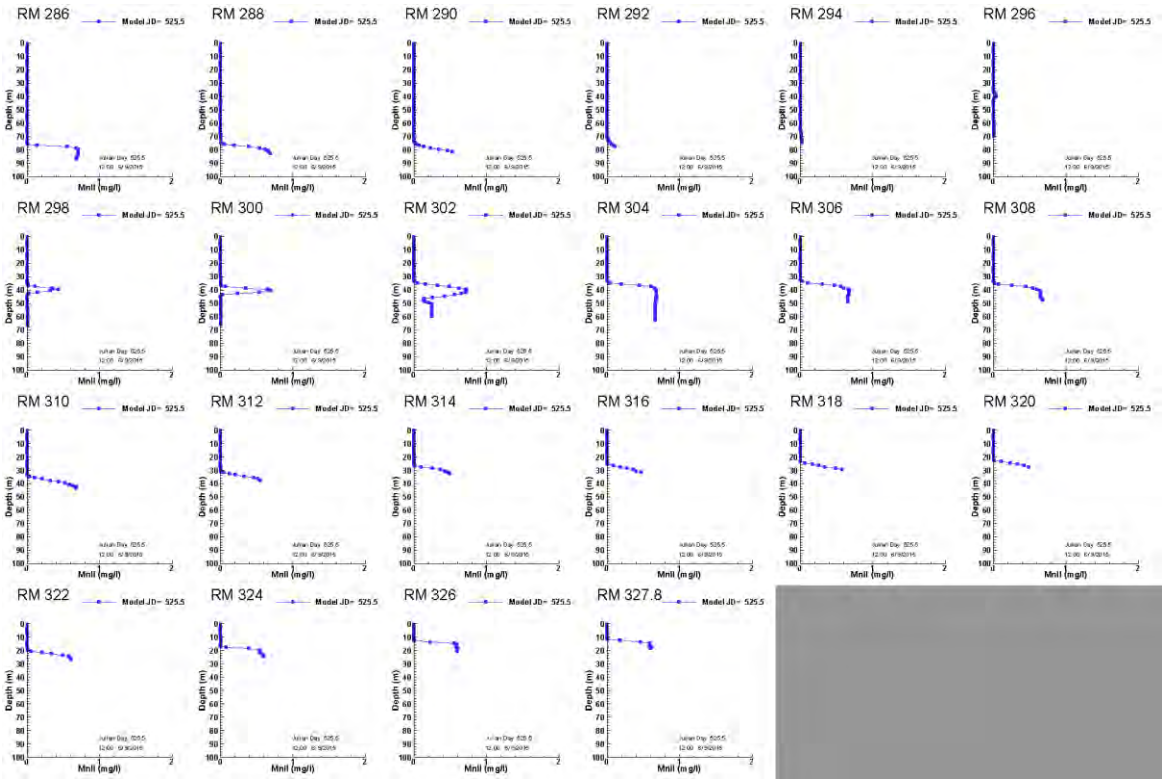


Figure 575. Vertical profiles of Mn(II) compared with data for 6/ 9/2015.

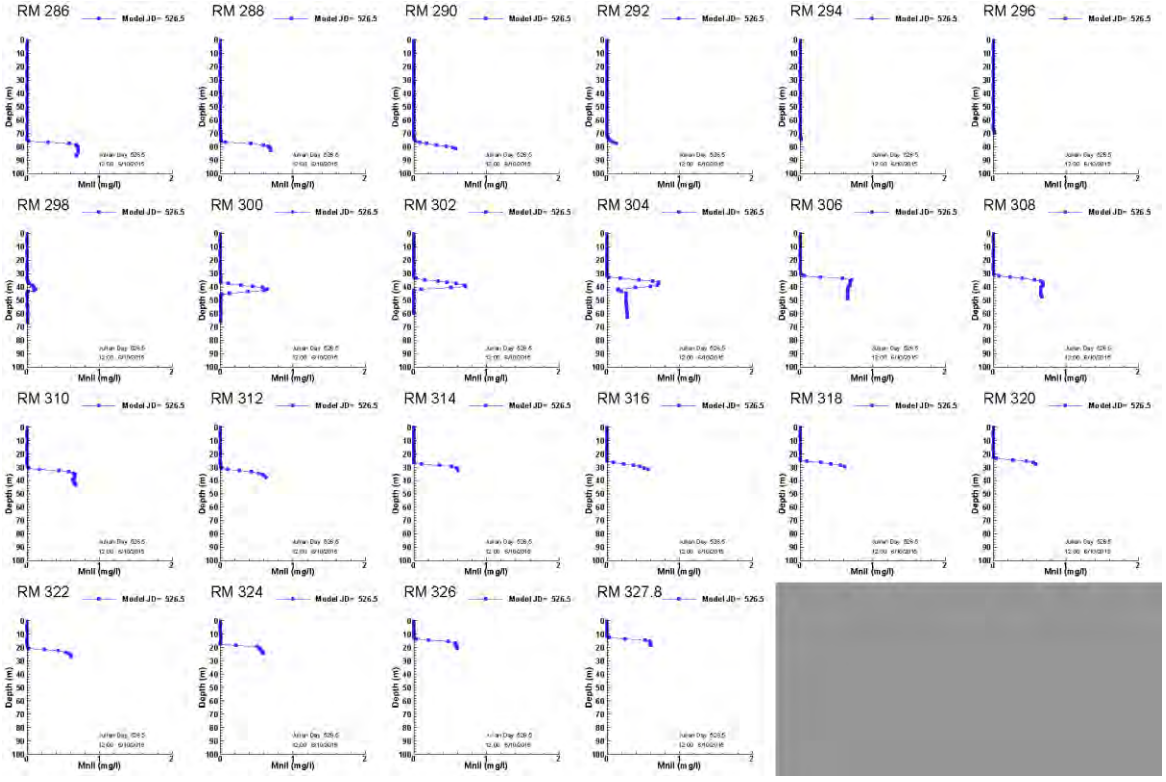


Figure 576. Vertical profiles of Mn(II) compared with data for 6/10/2015.

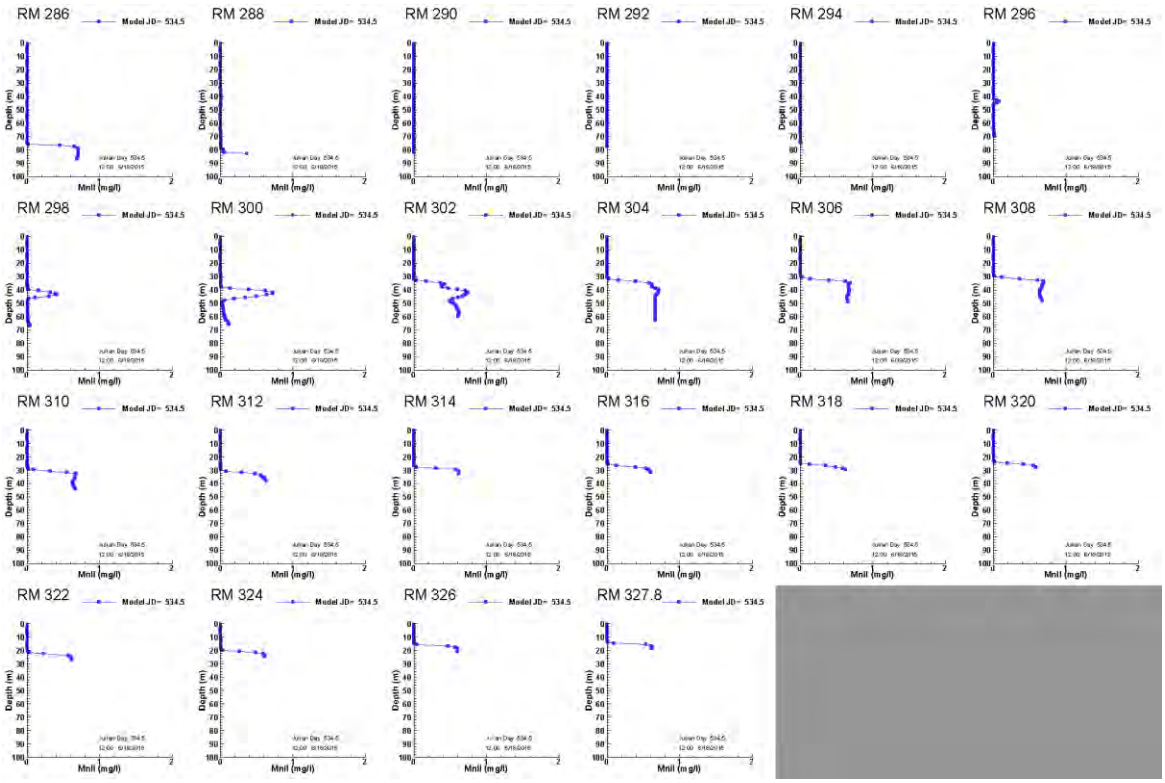


Figure 577. Vertical profiles of Mn(II) compared with data for 6/18/2015.

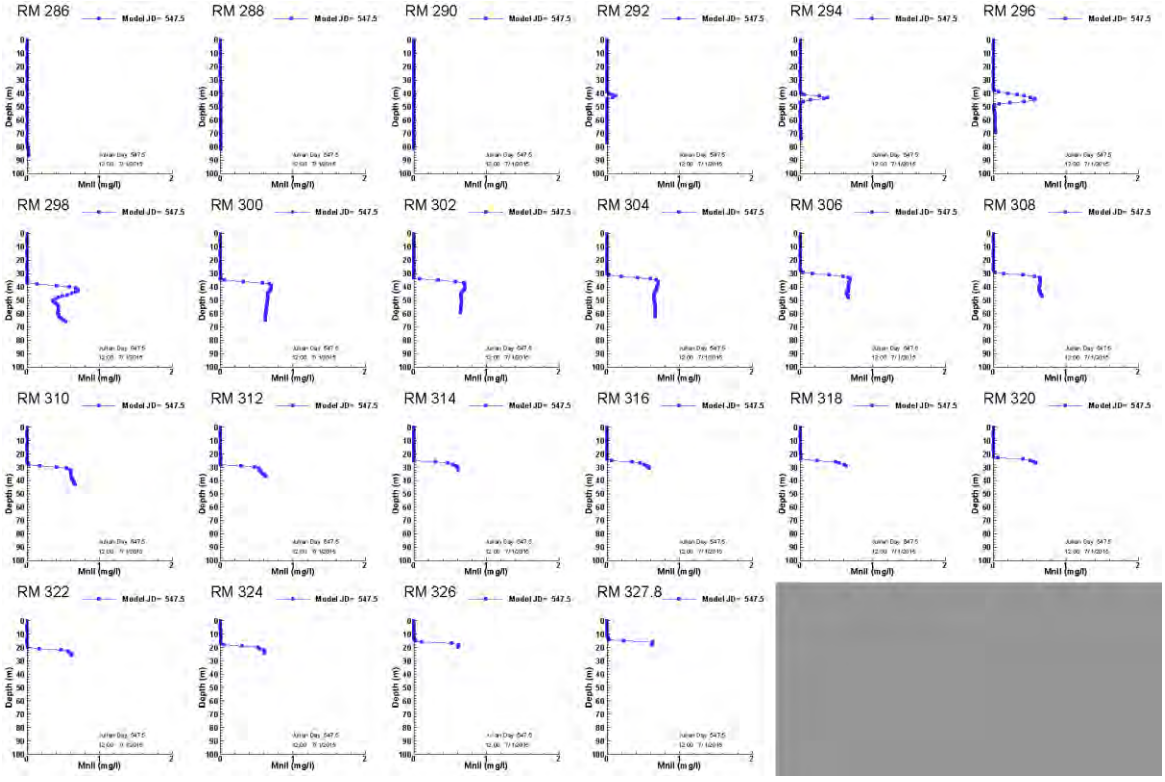


Figure 578. Vertical profiles of Mn(II) compared with data for 7/ 1/2015.

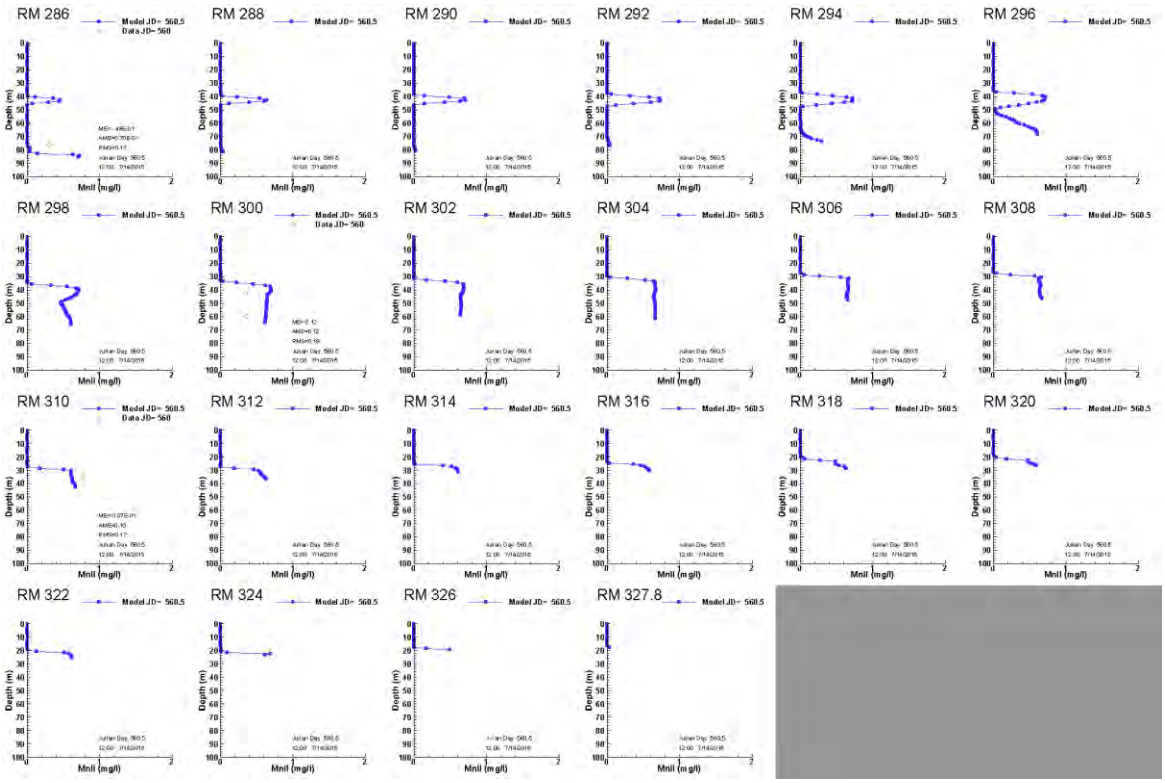


Figure 579. Vertical profiles of Mn(II) compared with data for 7/14/2015.

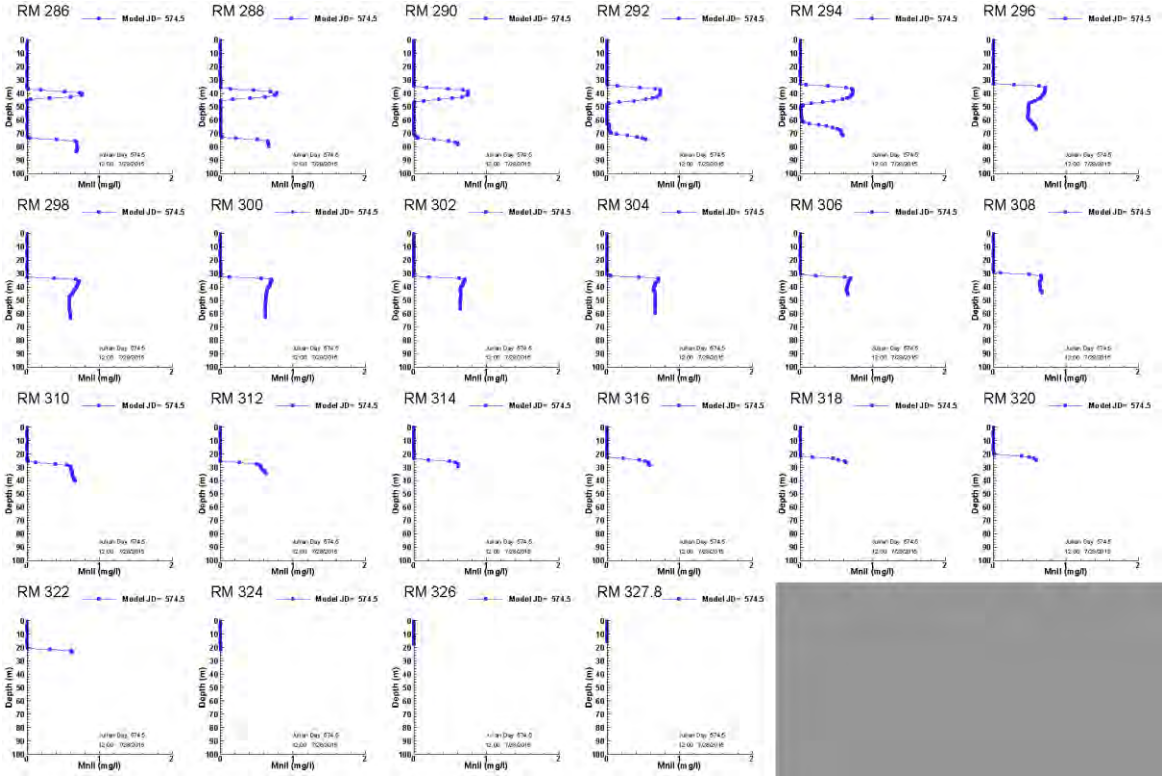


Figure 580. Vertical profiles of Mn(II) compared with data for 7/28/2015.

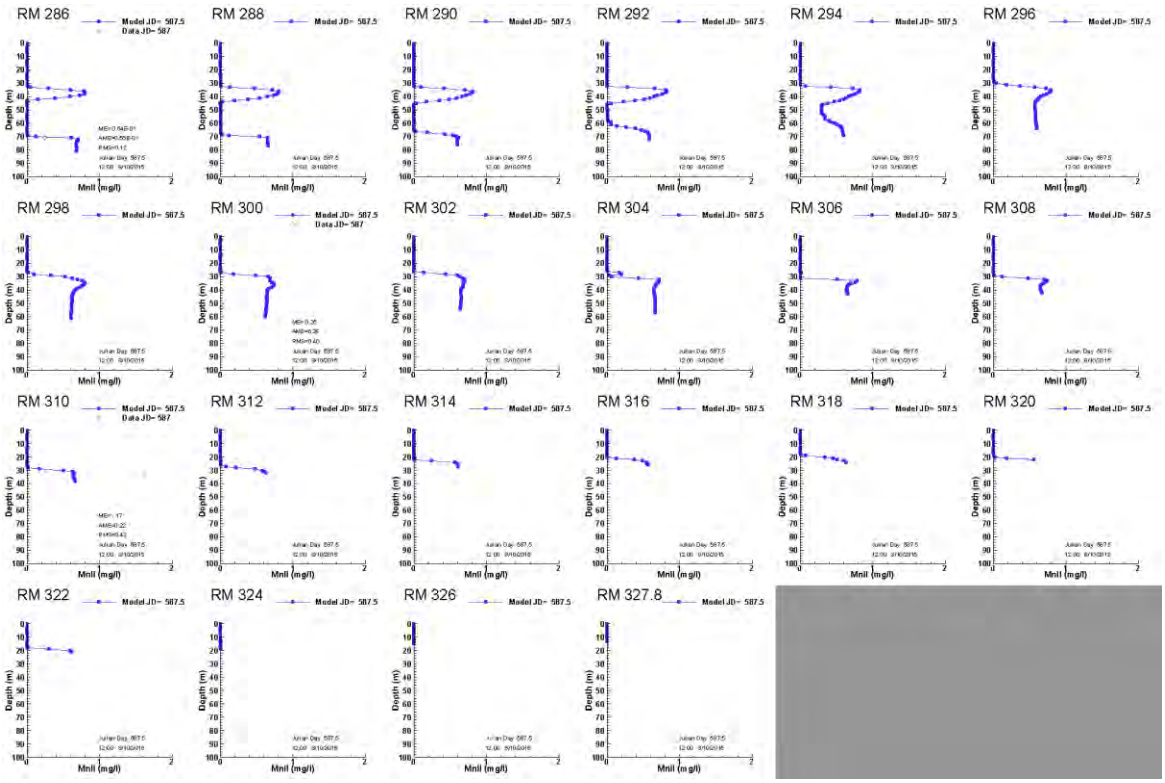


Figure 581. Vertical profiles of Mn(II) compared with data for 8/10/2015.

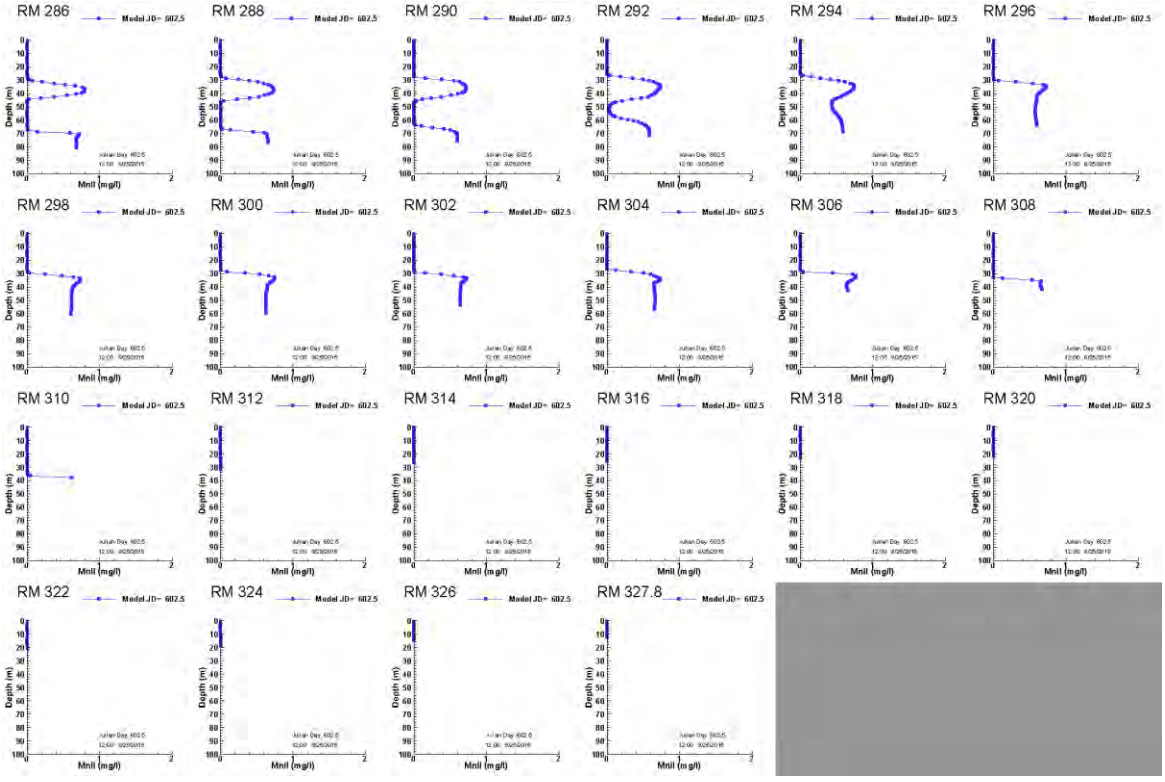


Figure 582. Vertical profiles of Mn(II) compared with data for 8/25/2015.

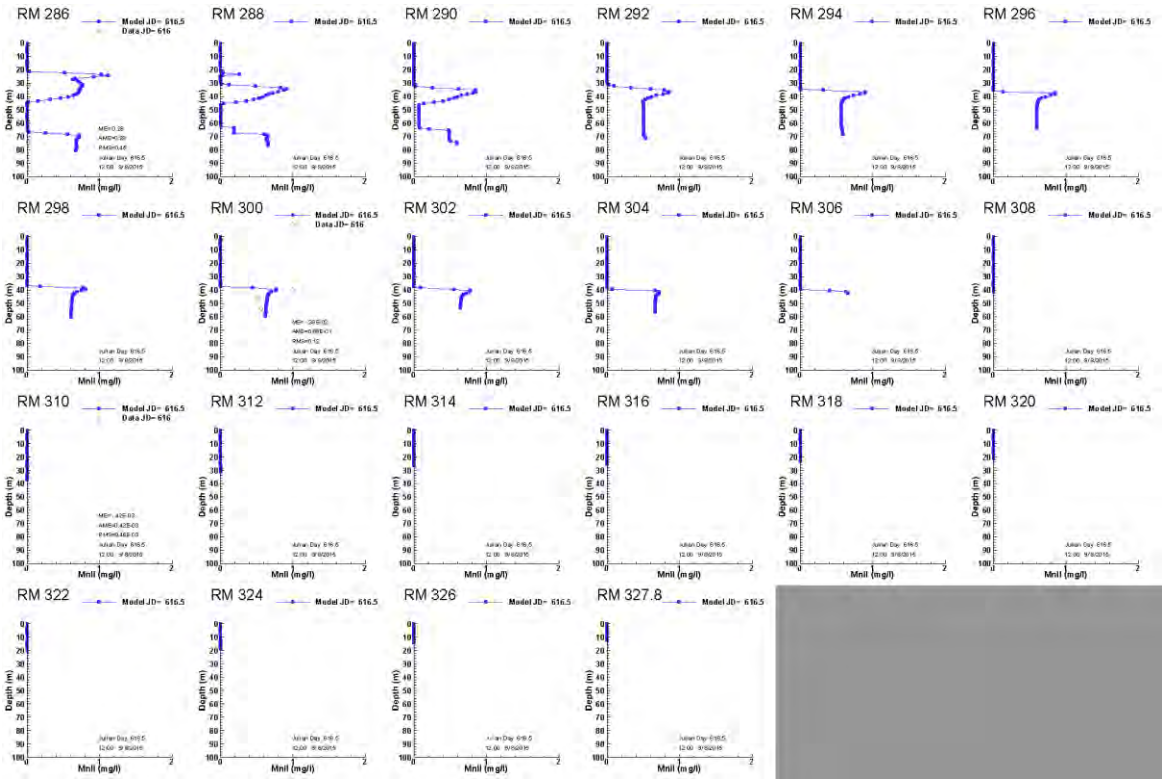


Figure 583. Vertical profiles of Mn(II) compared with data for 9/ 8/2015.

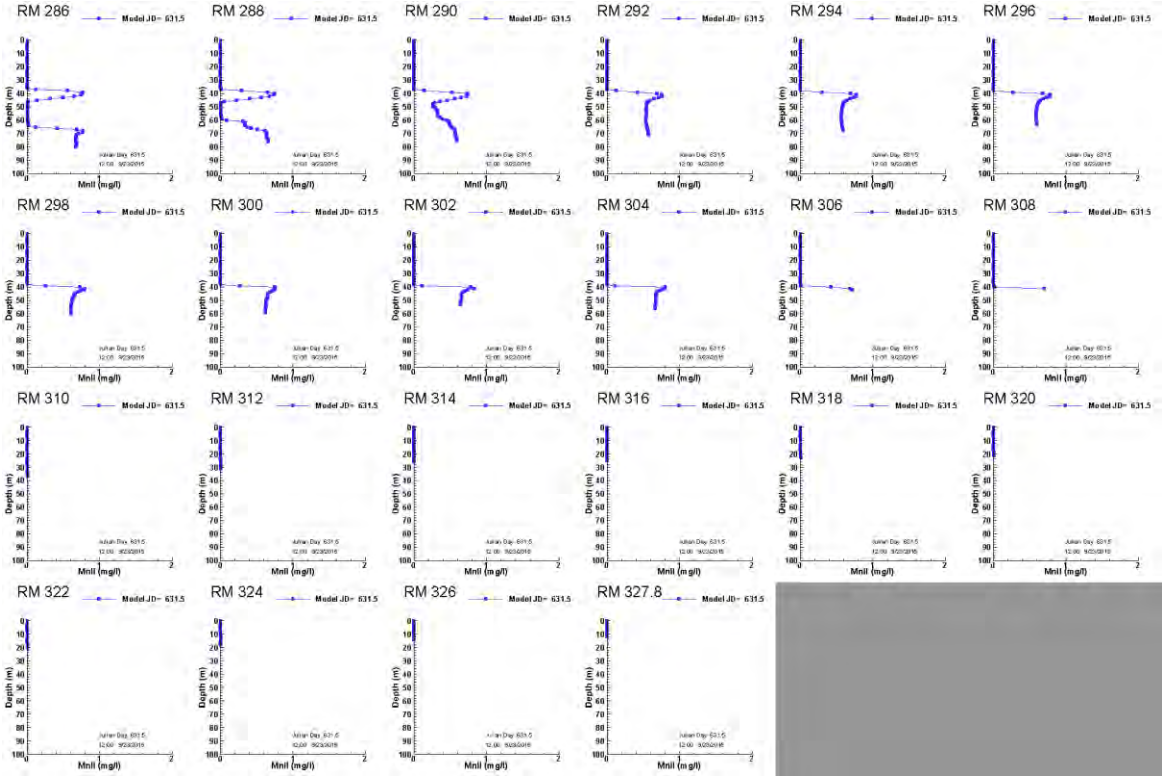


Figure 584. Vertical profiles of Mn(II) compared with data for 9/23/2015.

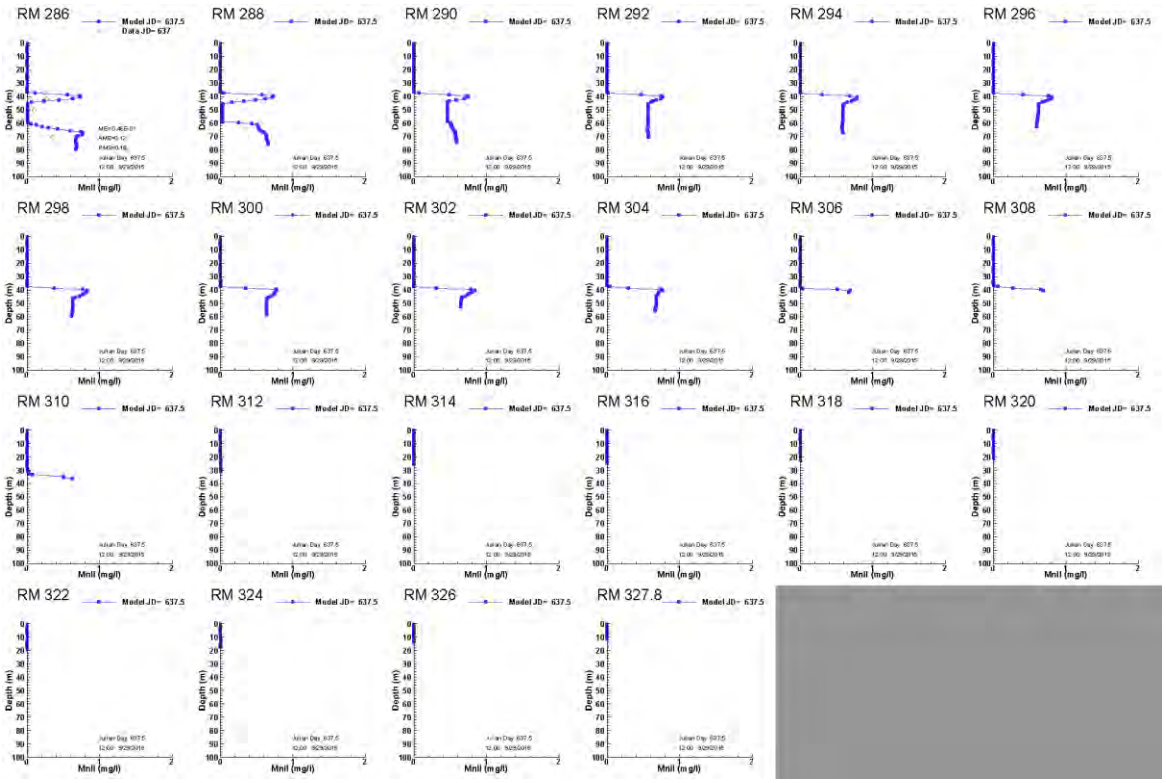


Figure 585. Vertical profiles of Mn(II) compared with data for 9/29/2015.

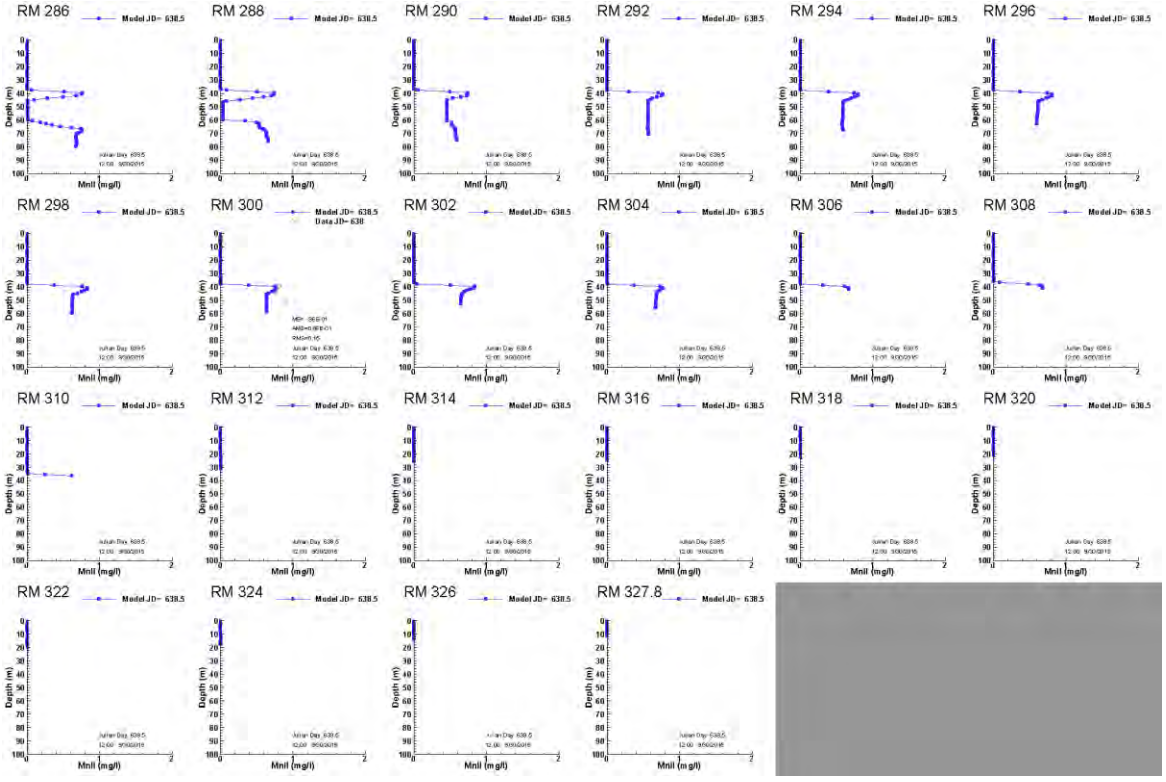


Figure 586. Vertical profiles of Mn(II) compared with data for 9/30/2015.

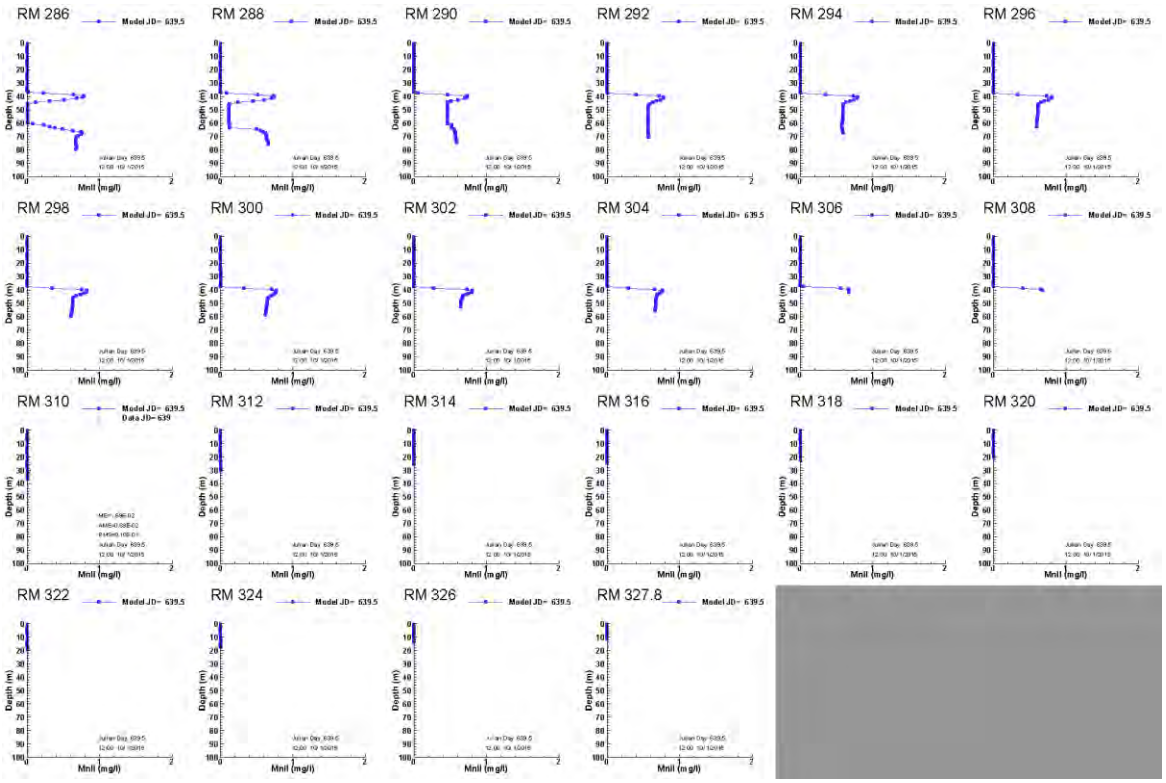


Figure 587. Vertical profiles of Mn(II) compared with data for 10/ 1/2015.

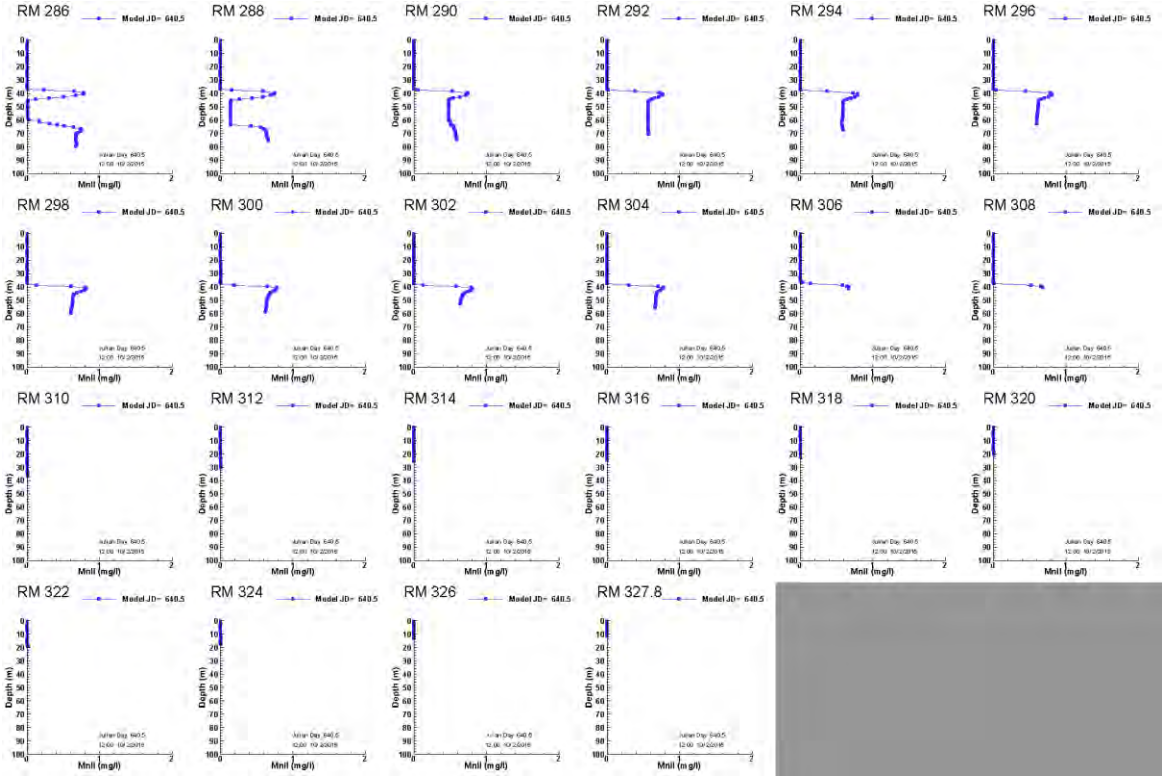


Figure 588. Vertical profiles of Mn(II) compared with data for 10/ 2/2015.

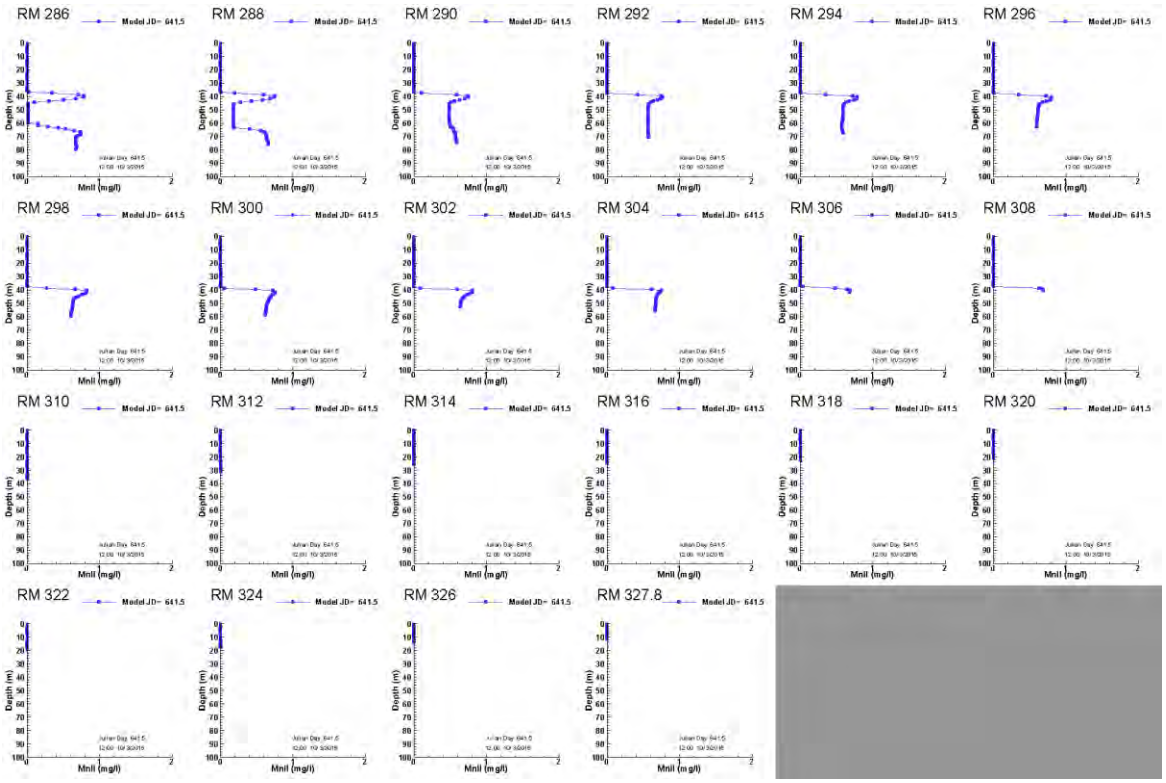


Figure 589. Vertical profiles of Mn(II) compared with data for 10/ 3/2015.

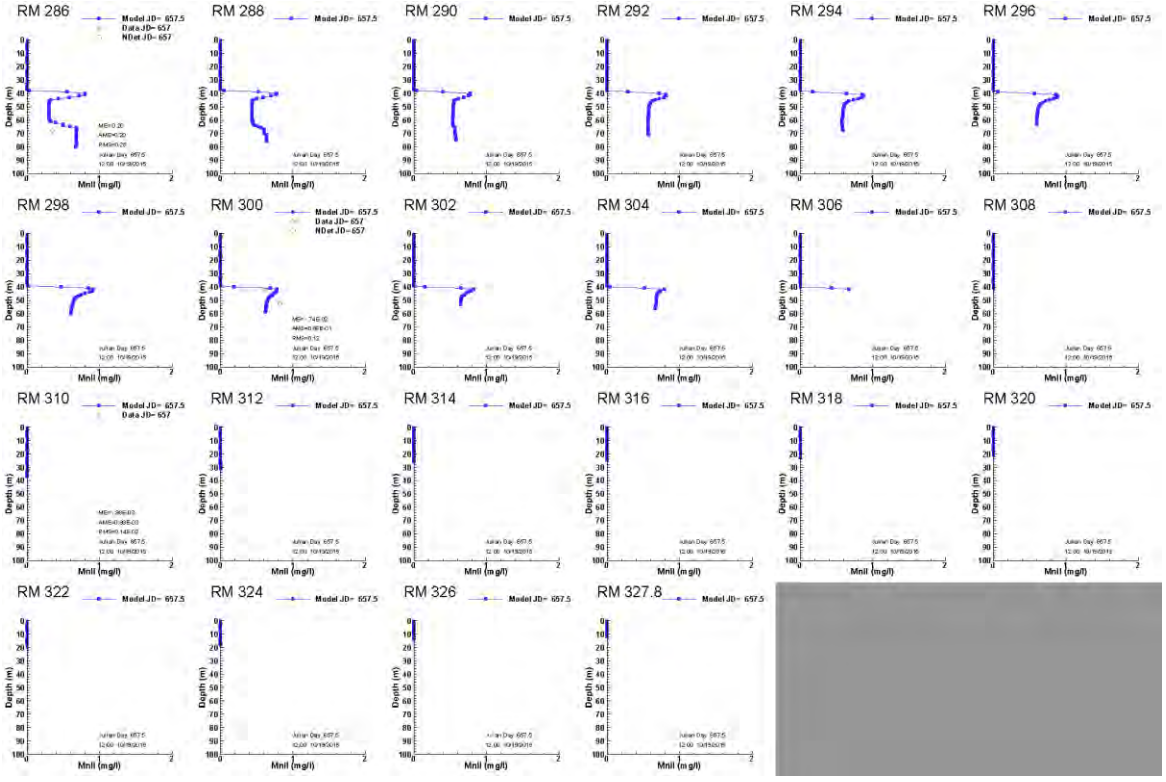


Figure 590. Vertical profiles of Mn(II) compared with data for 10/19/2015.

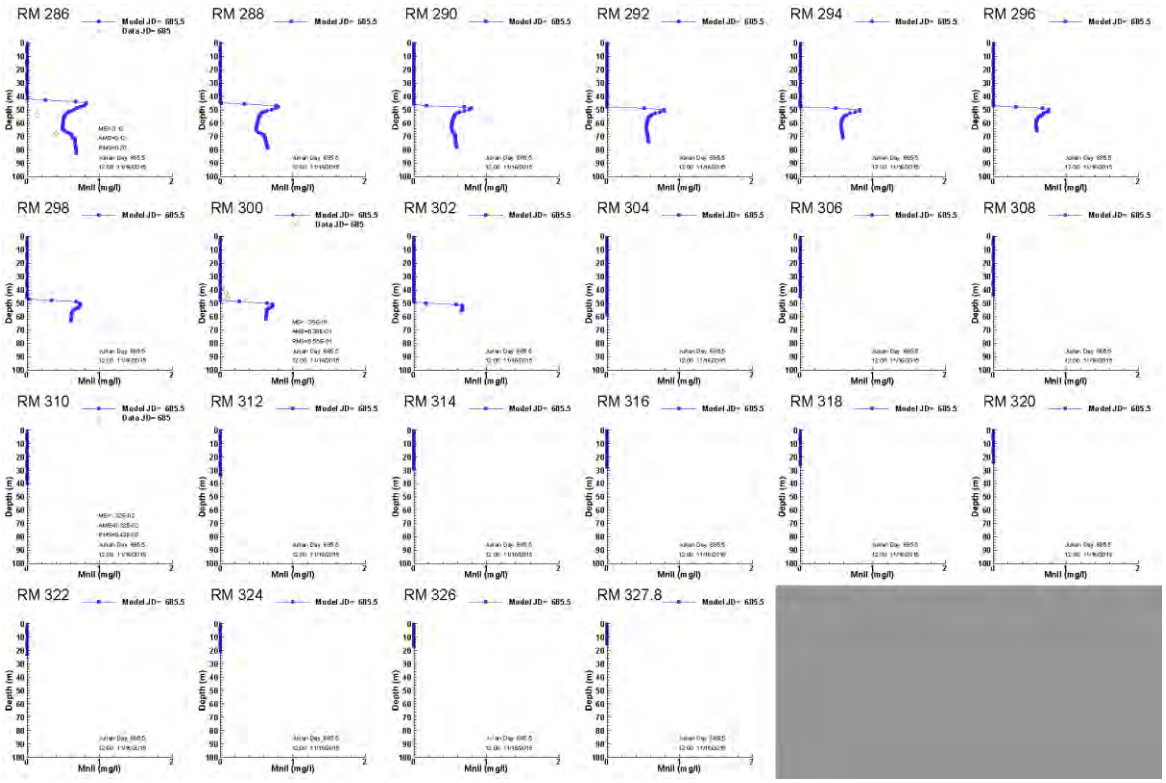


Figure 591. Vertical profiles of Mn(II) compared with data for 11/16/2015.

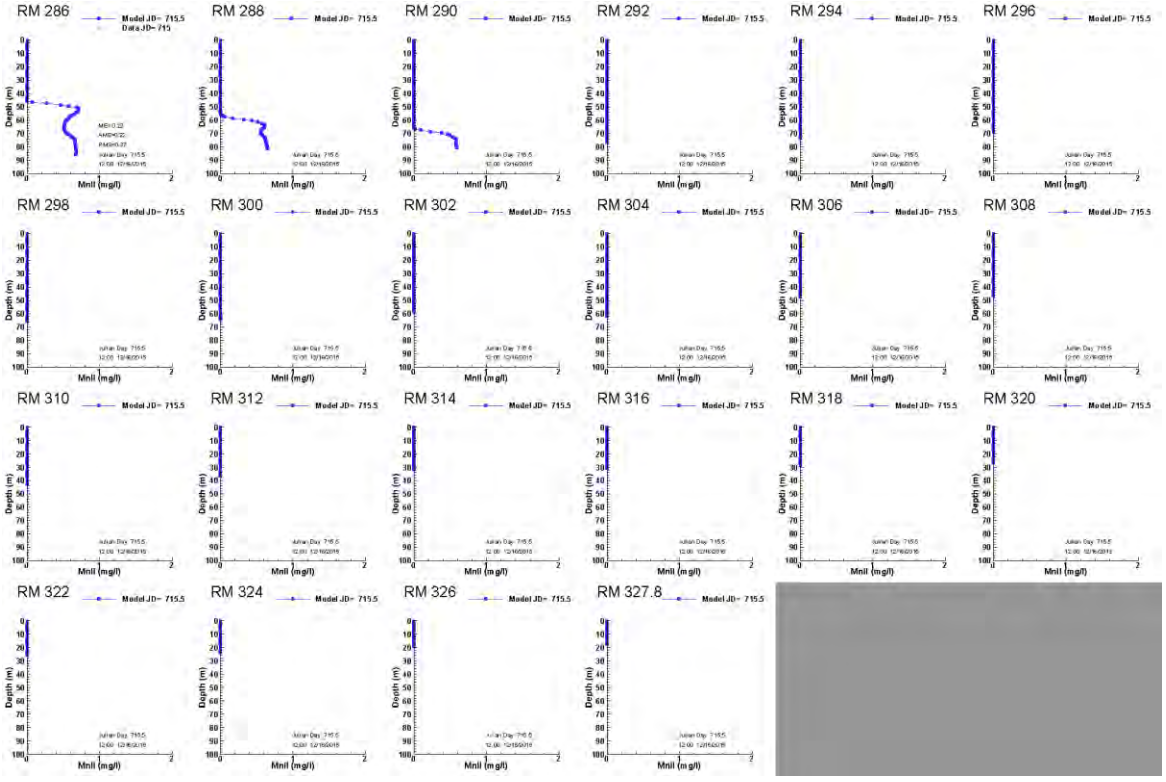


Figure 592. Vertical profiles of Mn(II) compared with data for 12/16/2015.

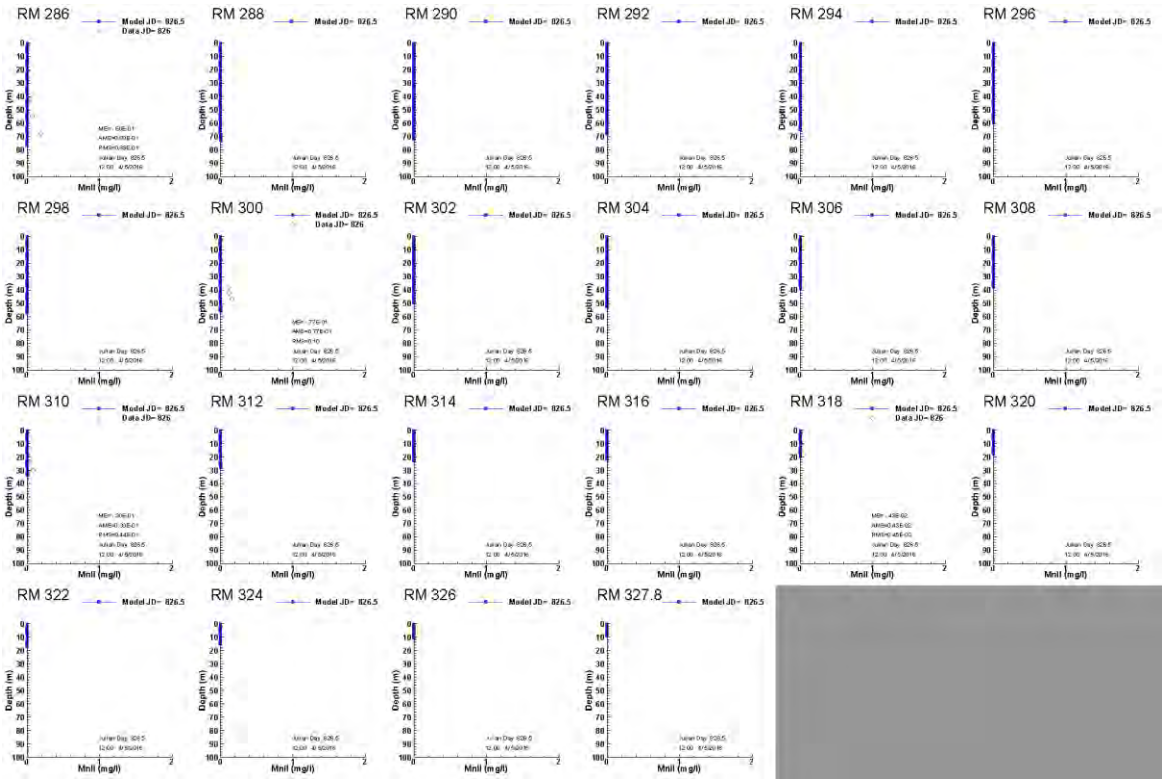


Figure 593. Vertical profiles of Mn(II) compared with data for 4/ 5/2016.

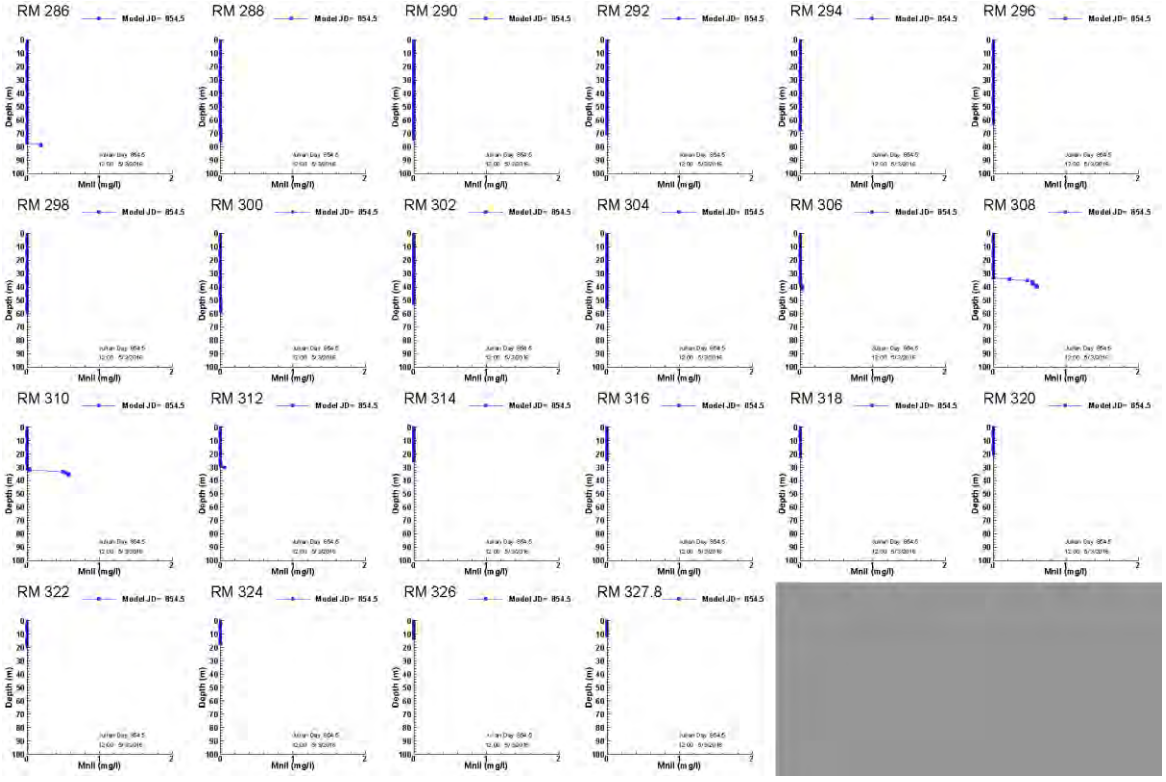


Figure 594. Vertical profiles of Mn(II) compared with data for 5/ 3/2016.

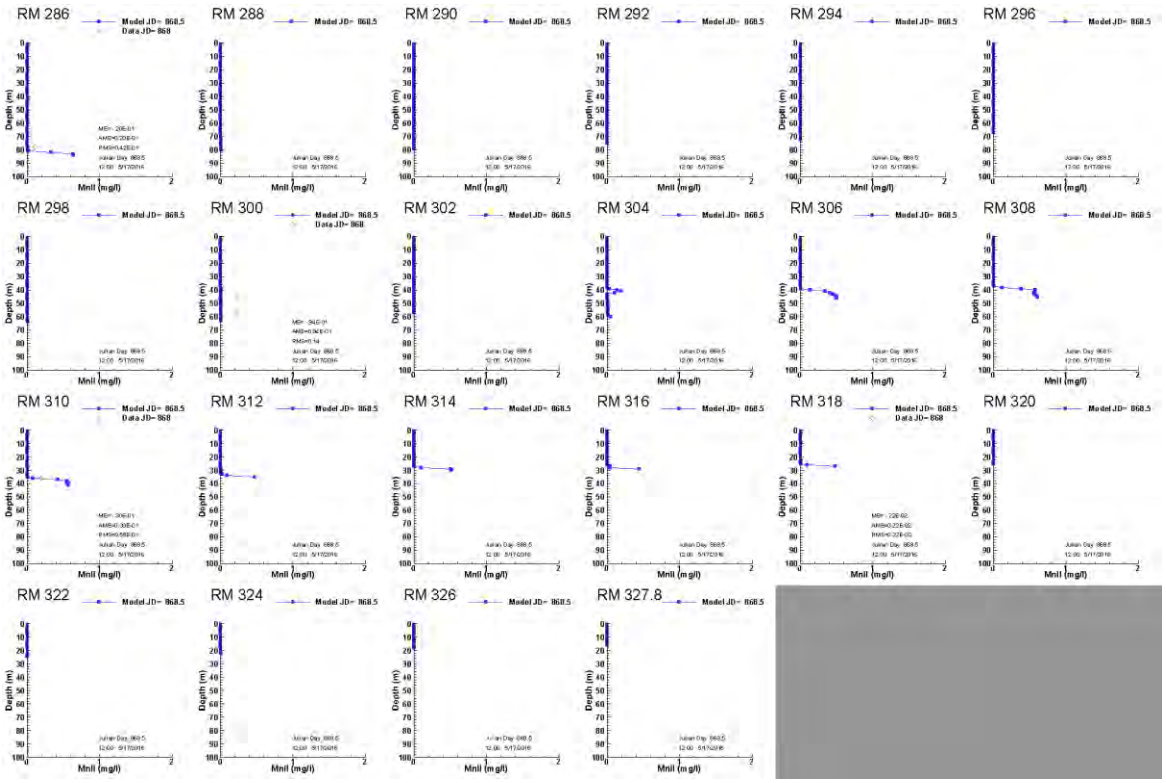


Figure 595. Vertical profiles of Mn(II) compared with data for 5/17/2016.

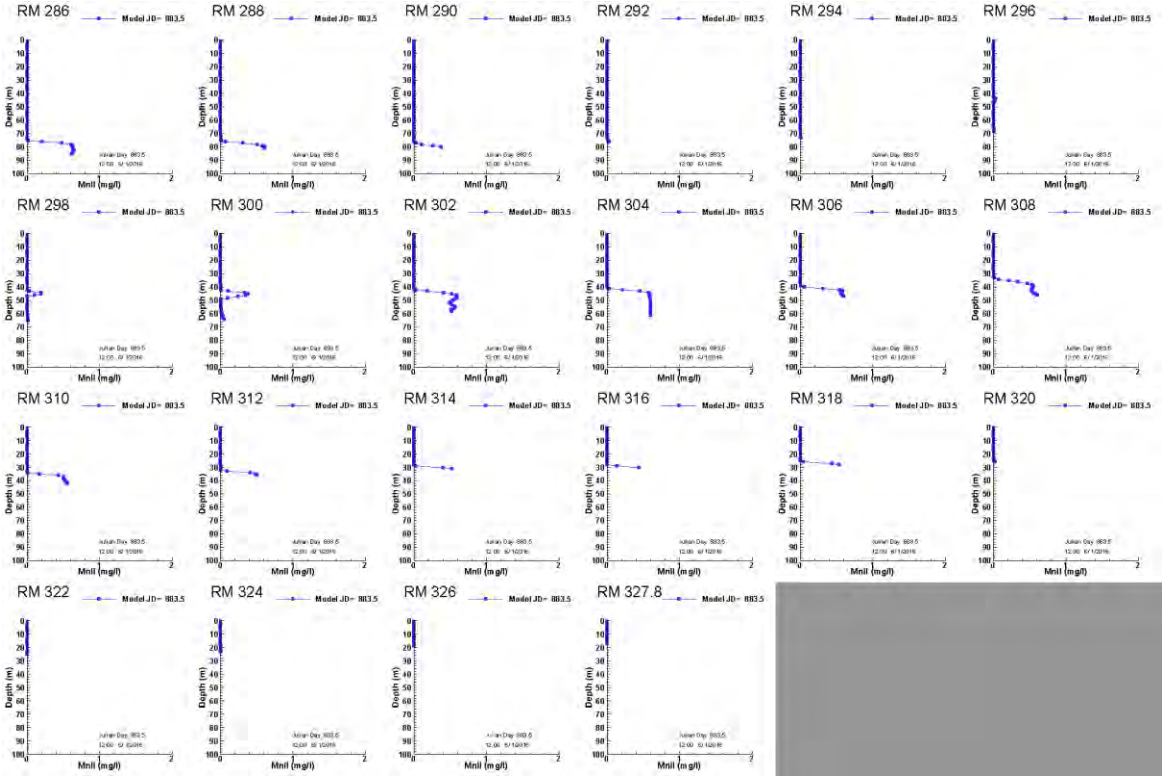


Figure 596. Vertical profiles of Mn(II) compared with data for 6/ 1/2016.

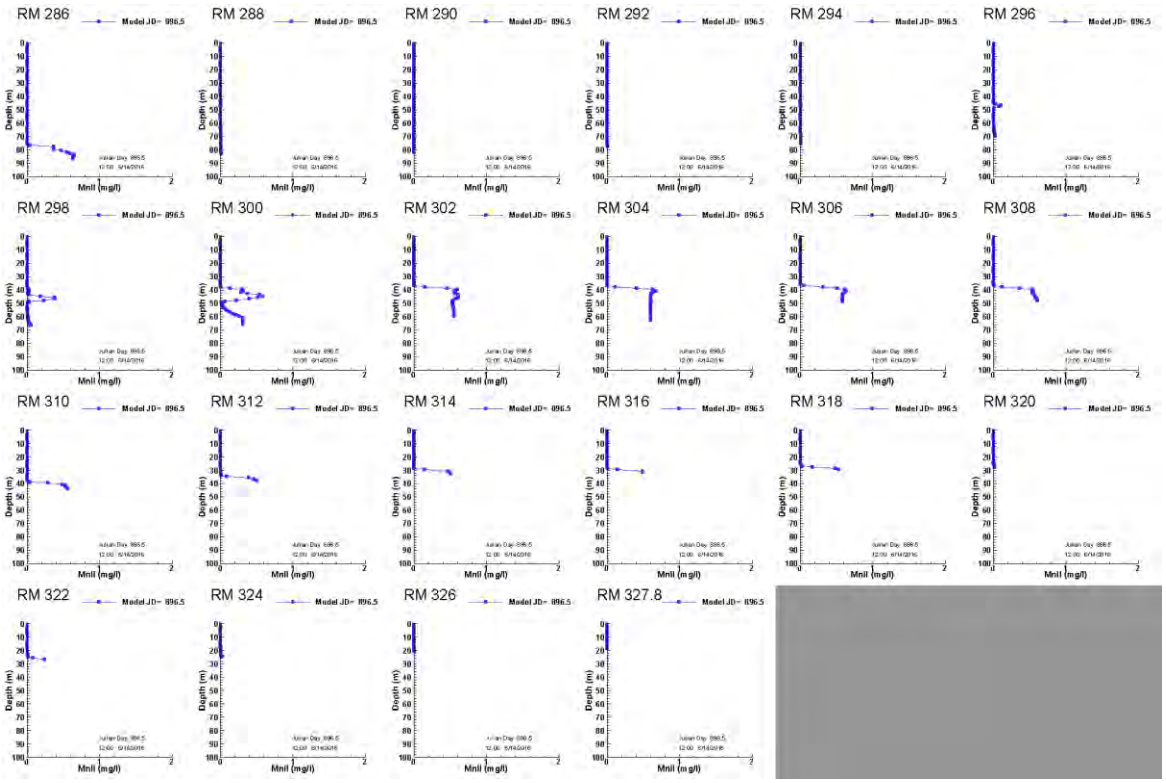


Figure 597. Vertical profiles of Mn(II) compared with data for 6/14/2016.

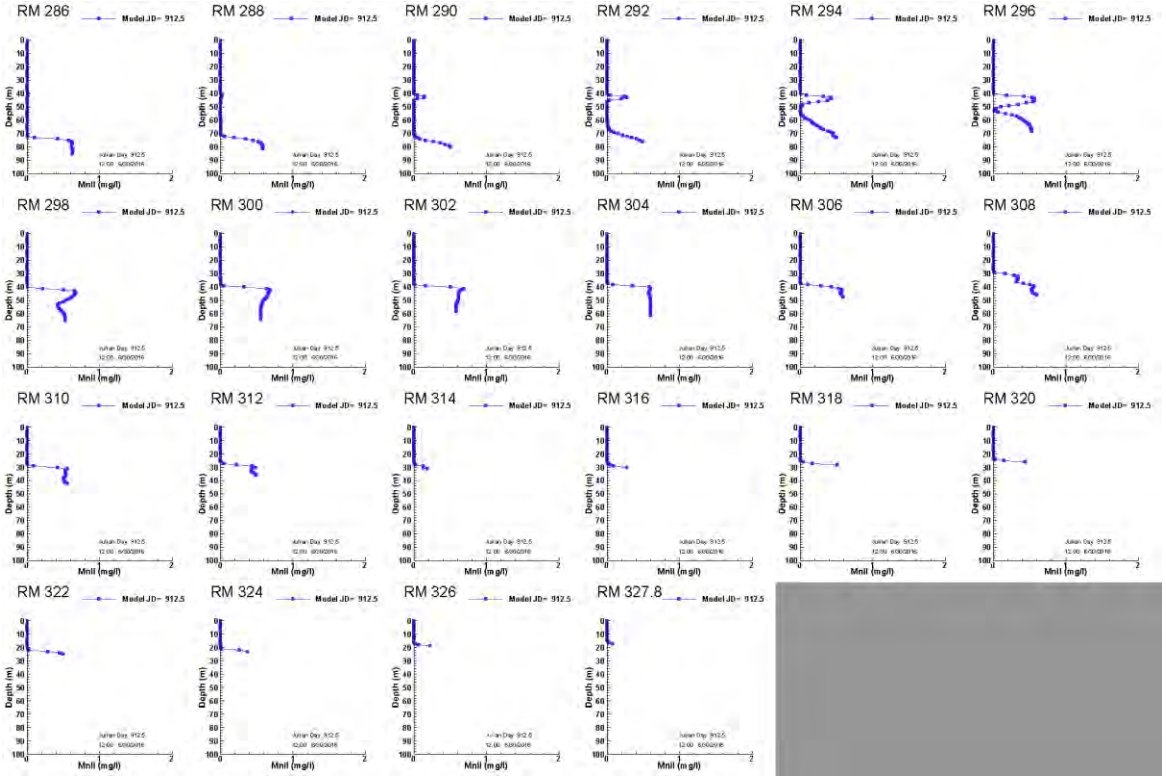


Figure 598. Vertical profiles of Mn(II) compared with data for 6/30/2016.

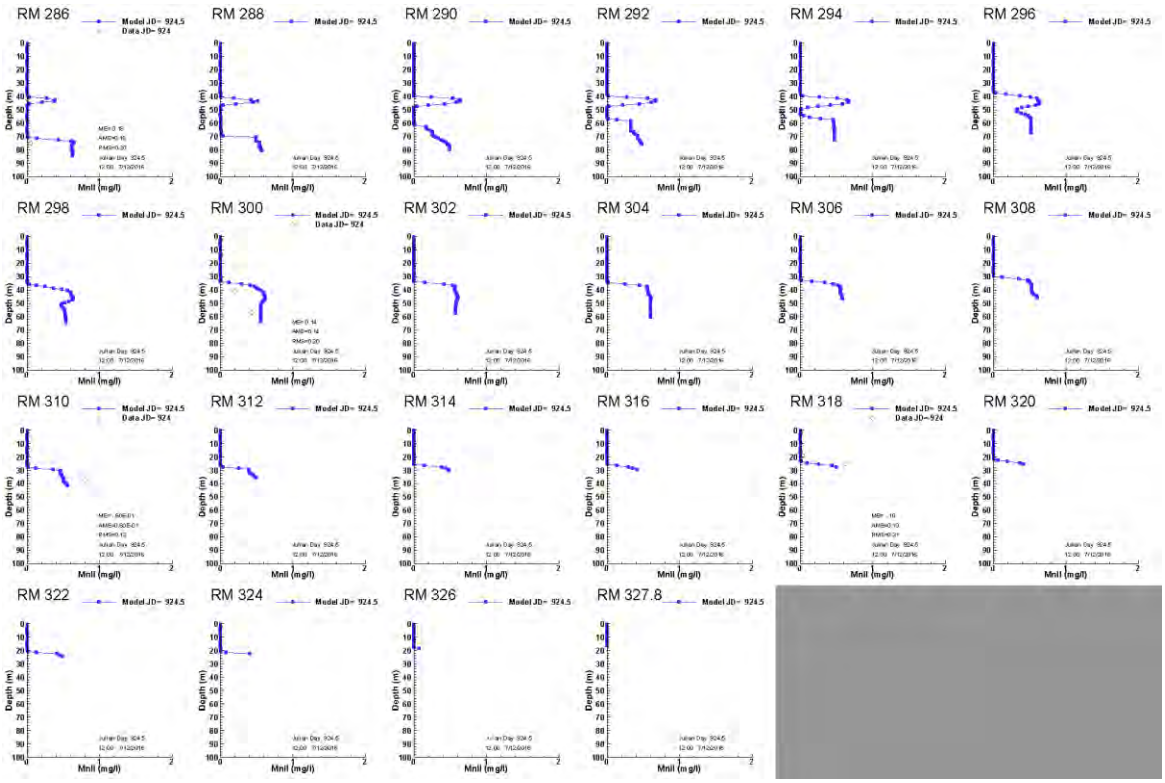


Figure 599. Vertical profiles of Mn(II) compared with data for 7/12/2016.

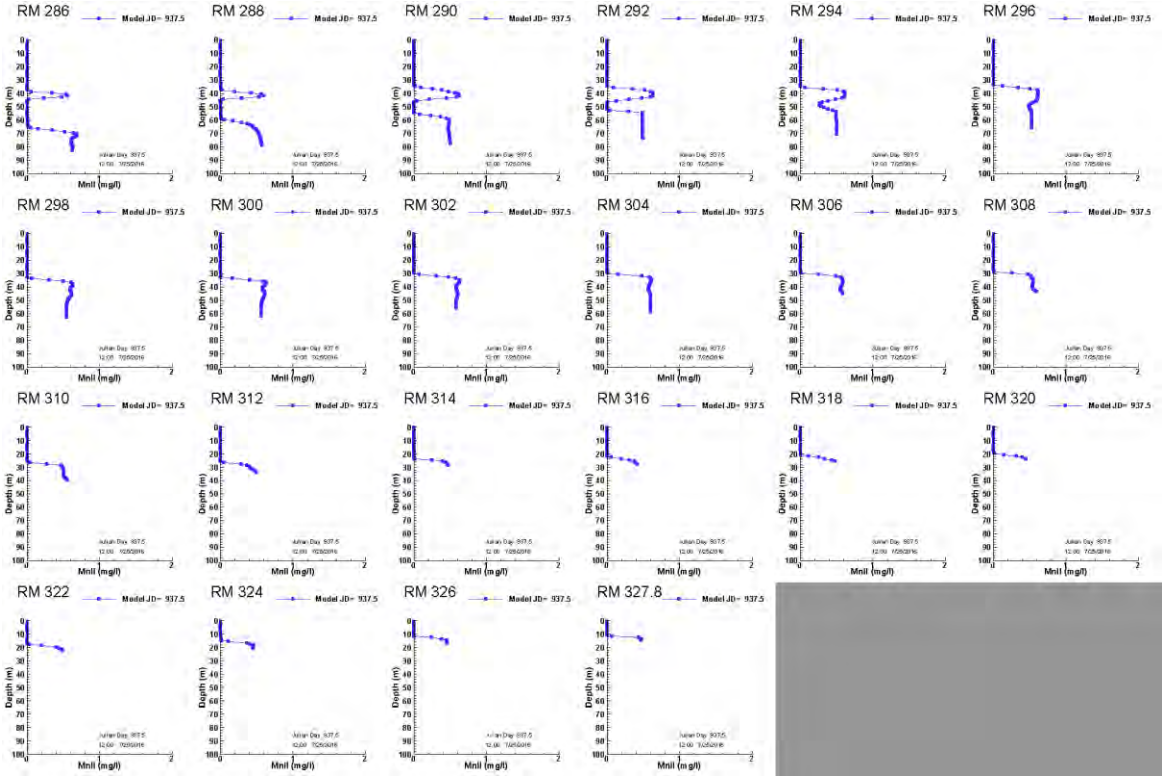


Figure 600. Vertical profiles of Mn(II) compared with data for 7/25/2016.

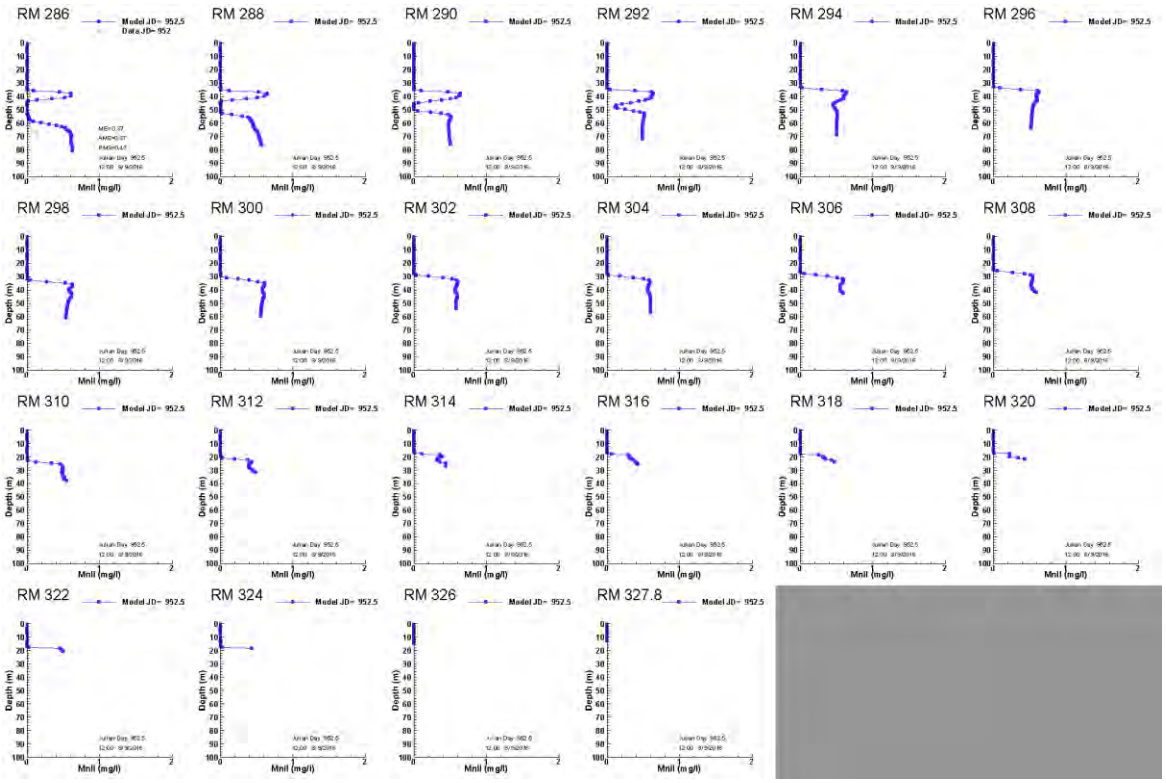


Figure 601. Vertical profiles of Mn(II) compared with data for 8/ 9/2016.

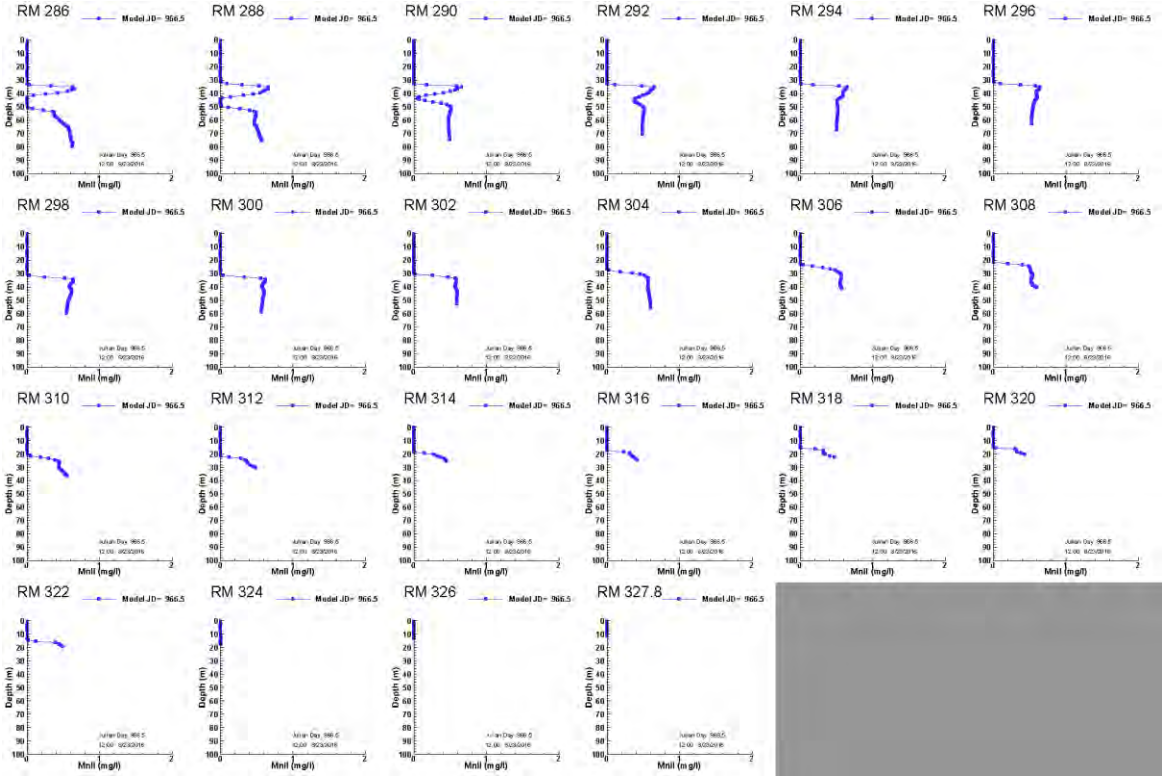


Figure 602. Vertical profiles of Mn(II) compared with data for 8/23/2016.

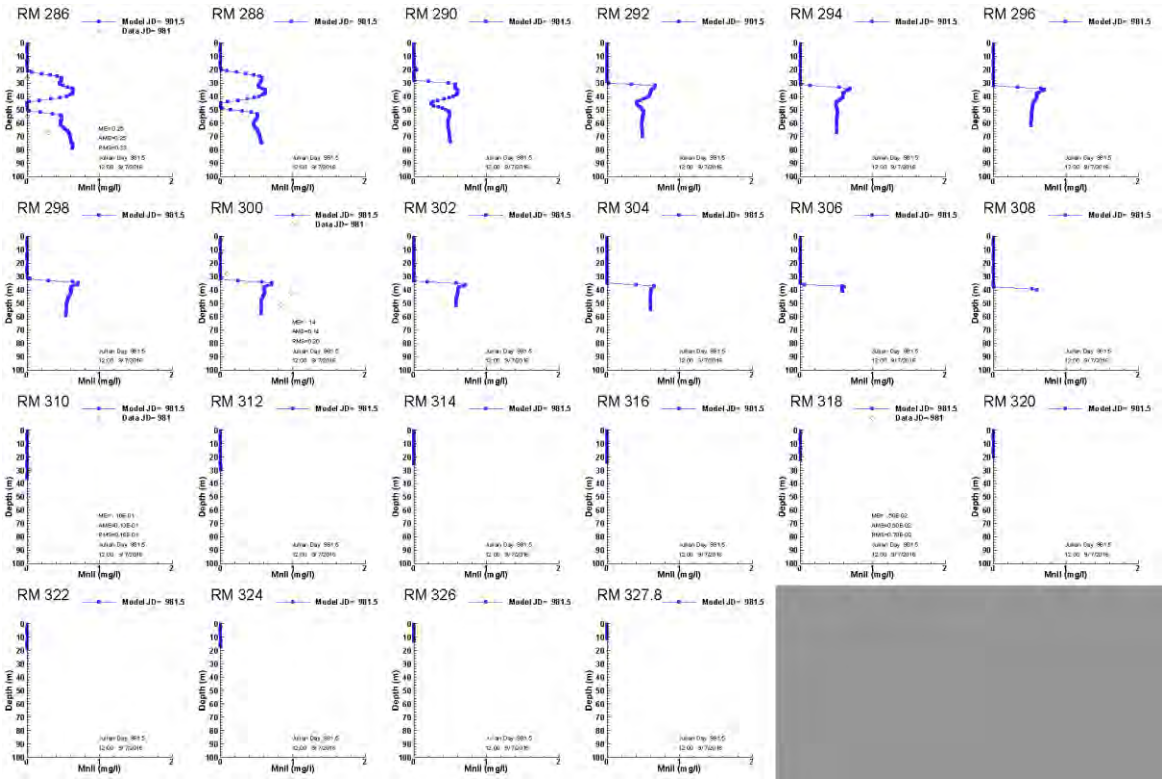


Figure 603. Vertical profiles of Mn(II) compared with data for 9/ 7/2016.

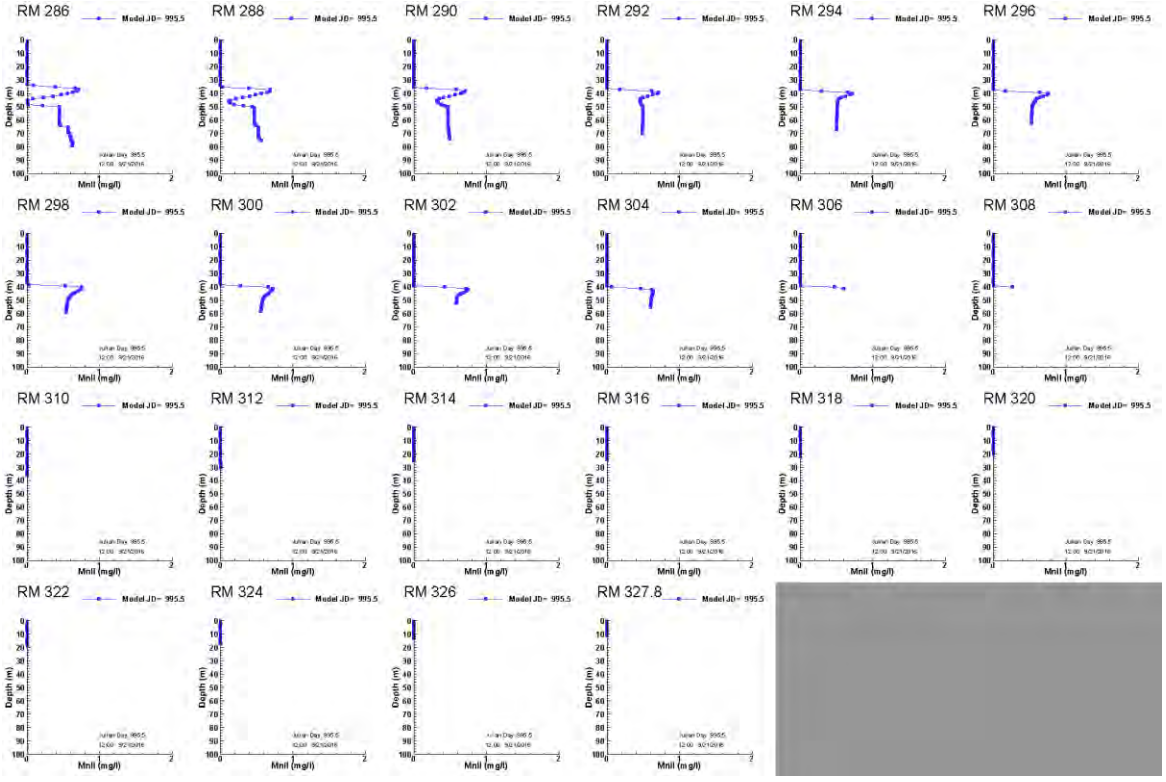


Figure 604. Vertical profiles of Mn(II) compared with data for 9/21/2016.

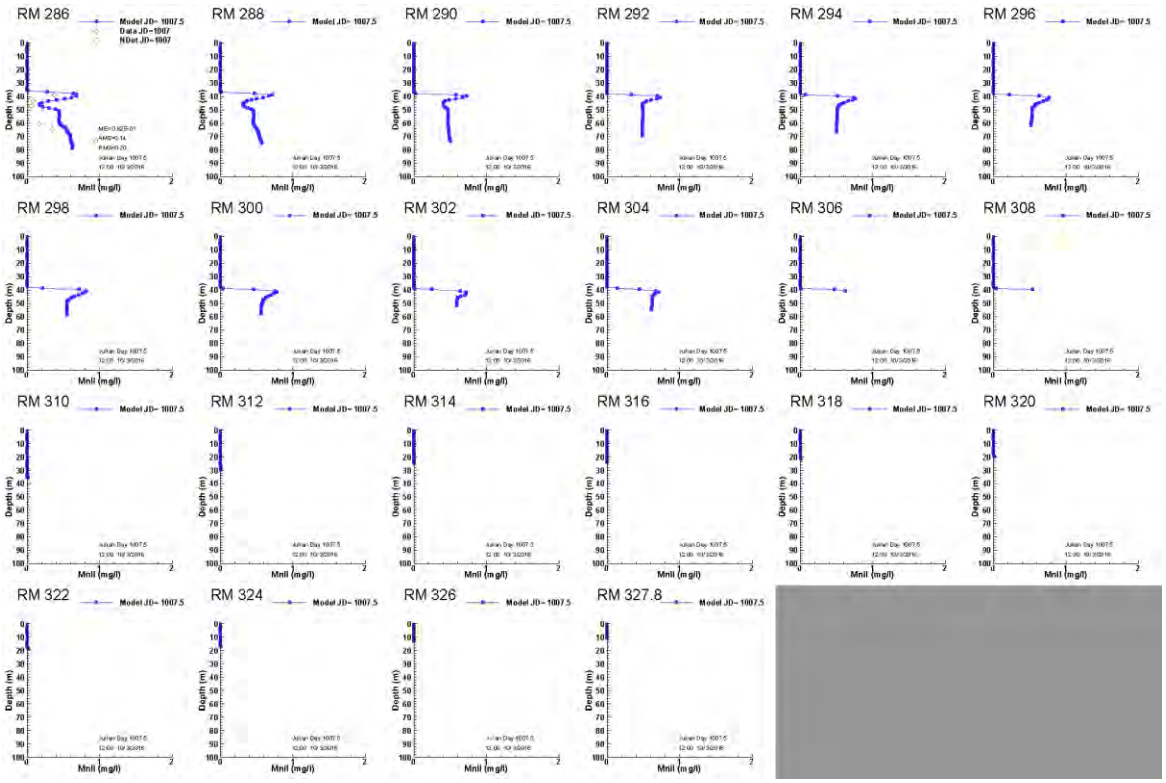


Figure 605. Vertical profiles of Mn(II) compared with data for 10/ 3/2016.

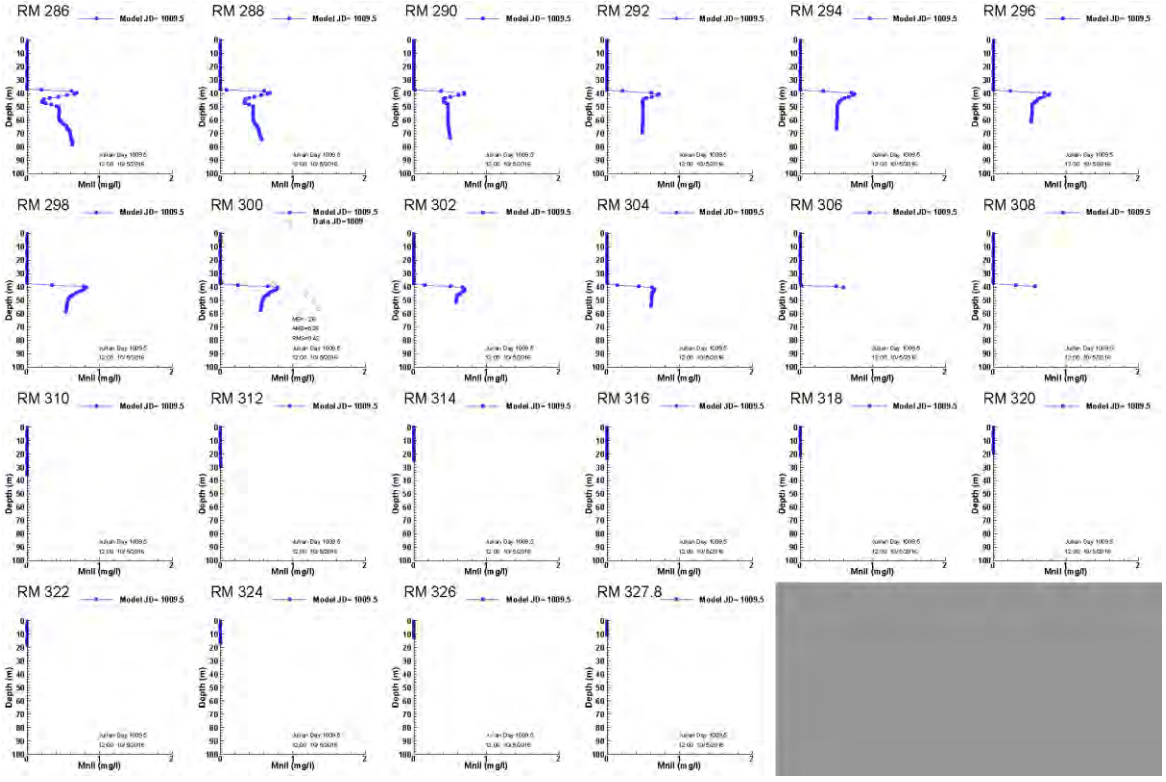


Figure 606. Vertical profiles of Mn(II) compared with data for 10/ 5/2016.

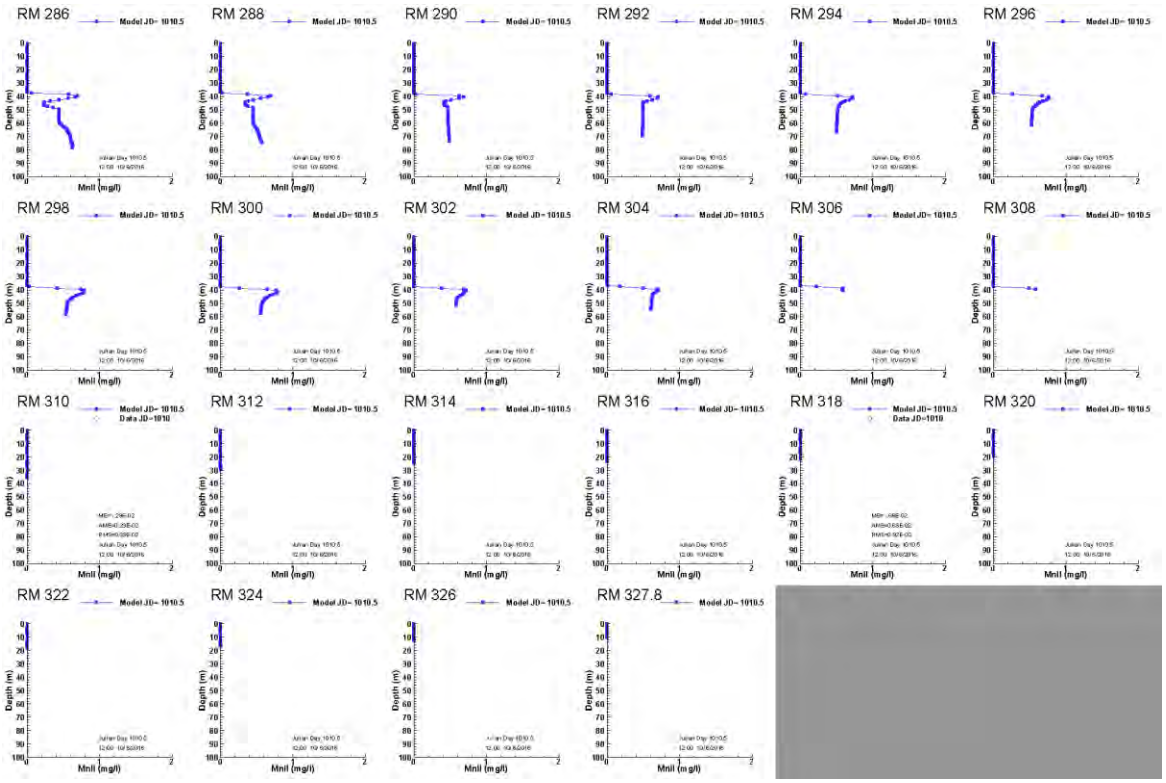


Figure 607. Vertical profiles of Mn(II) compared with data for 10/ 6/2016.

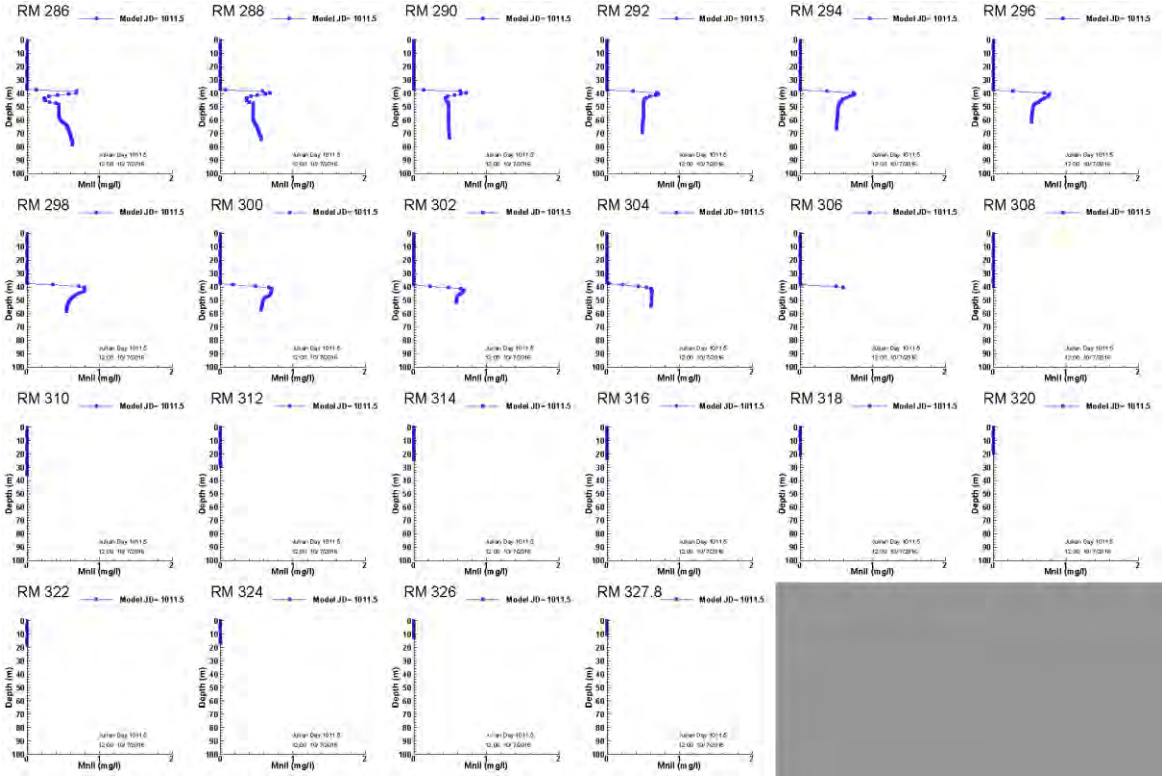


Figure 608. Vertical profiles of Mn(II) compared with data for 10/ 7/2016.

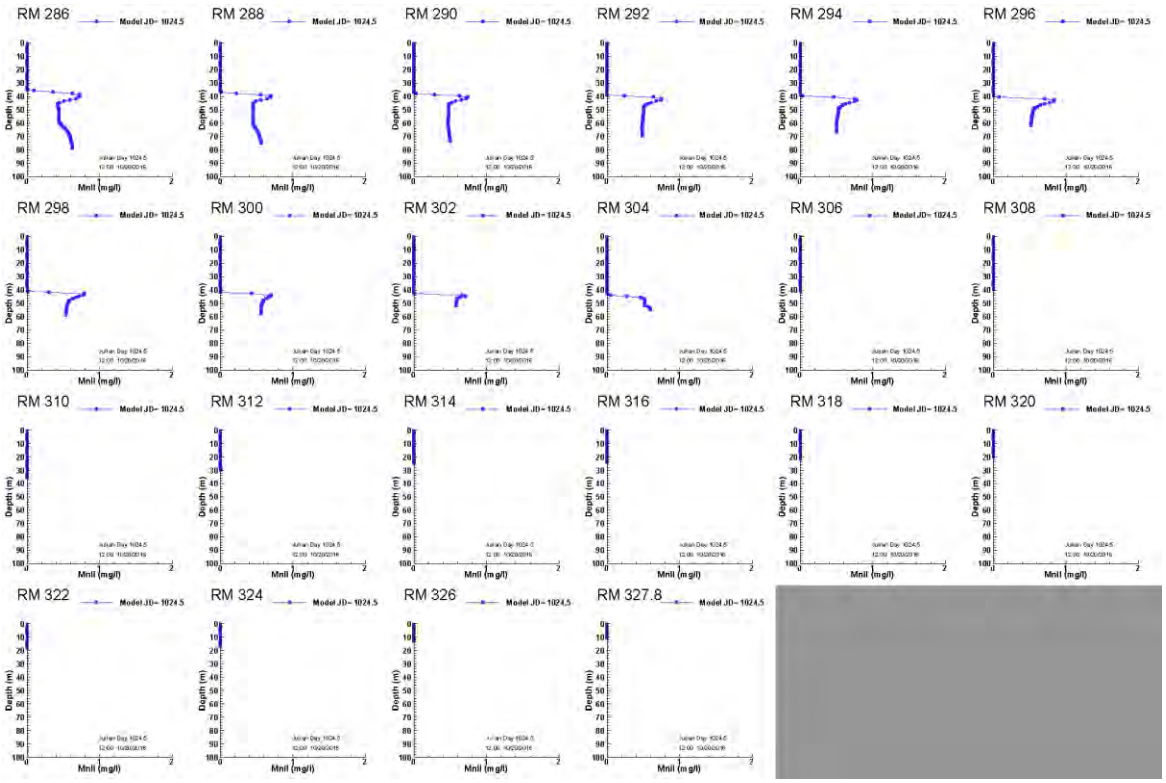


Figure 609. Vertical profiles of Mn(II) compared with data for 10/20/2016.

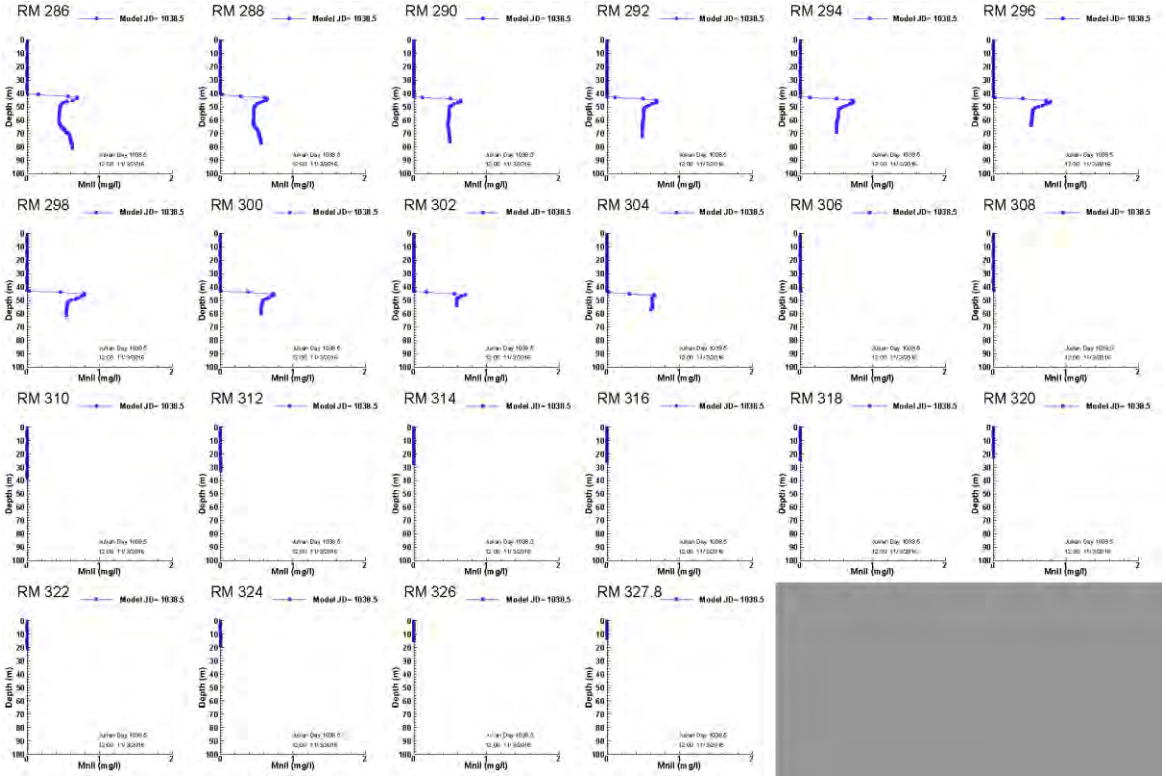


Figure 610. Vertical profiles of Mn(II) compared with data for 11/ 3/2016.

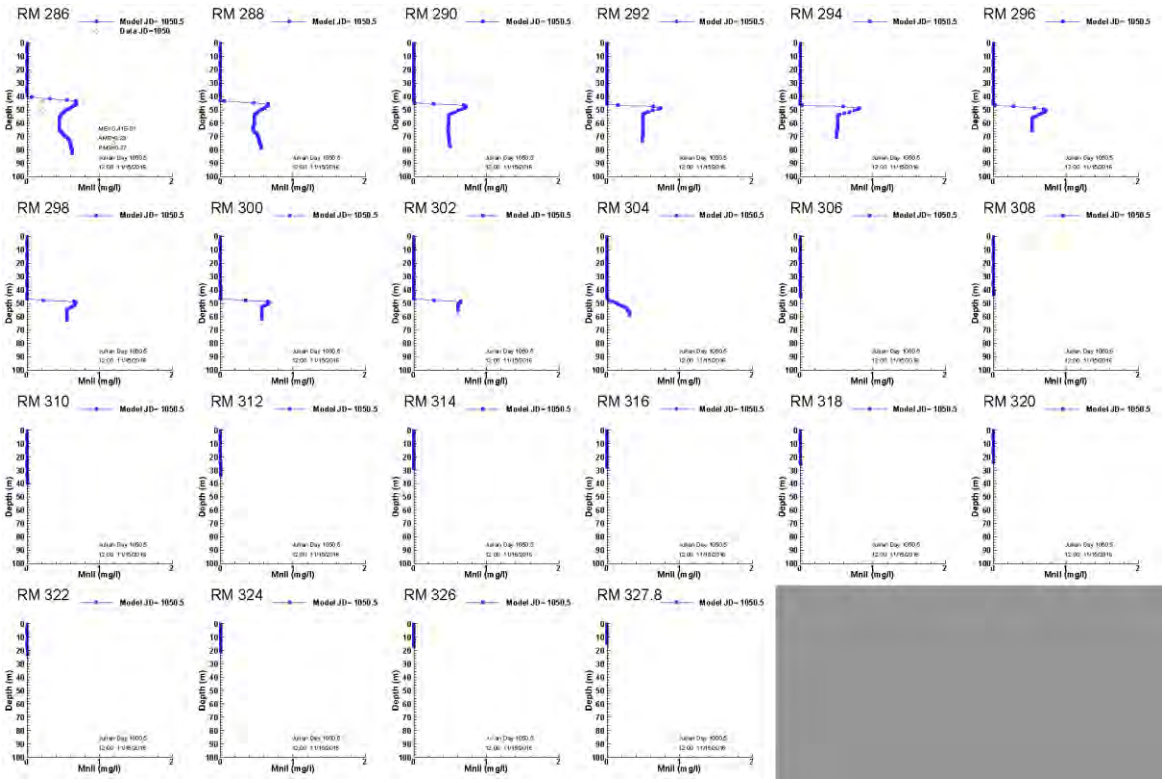


Figure 611. Vertical profiles of Mn(II) compared with data for 11/15/2016.

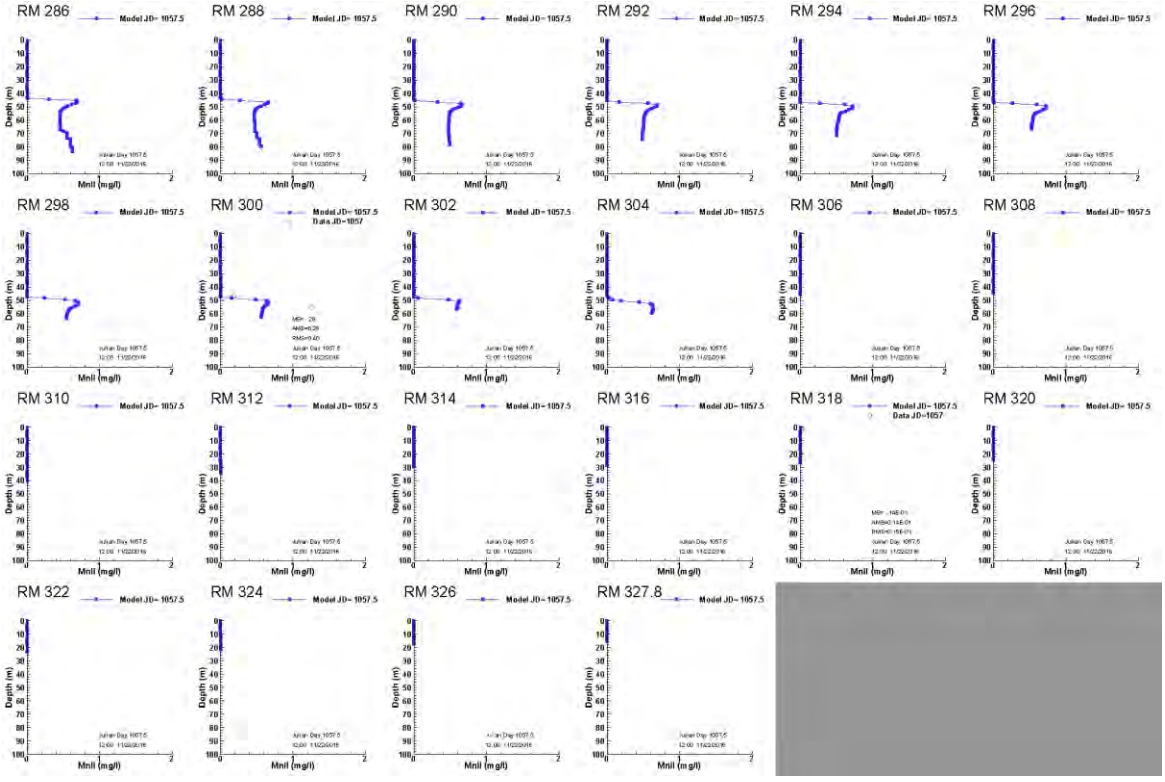


Figure 612. Vertical profiles of Mn(II) compared with data for 11/22/2016.

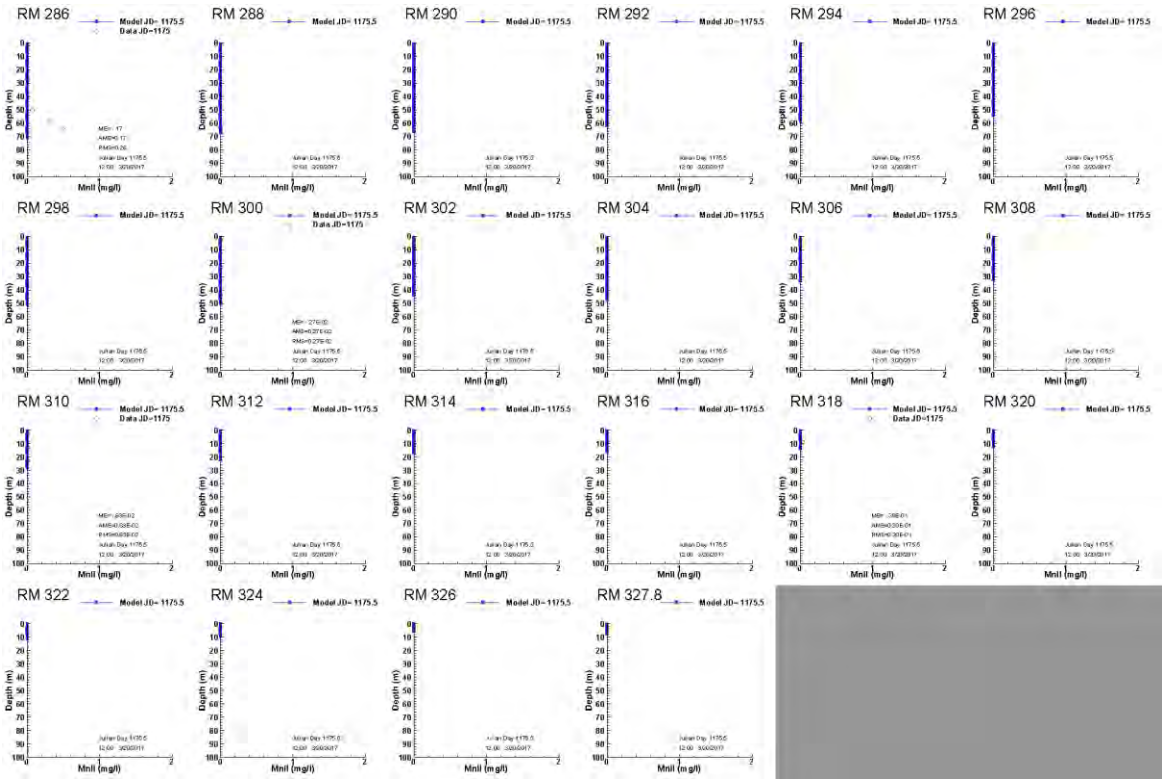


Figure 613. Vertical profiles of Mn(II) compared with data for 3/20/2017.

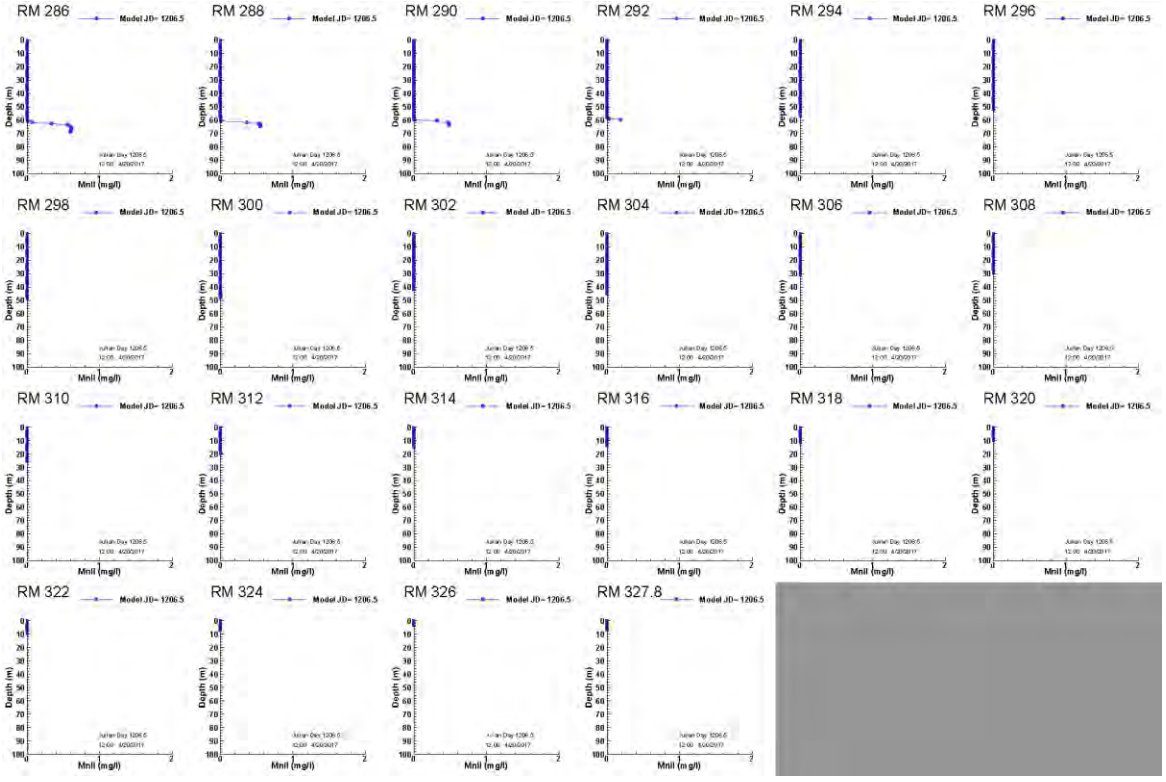


Figure 614. Vertical profiles of Mn(II) compared with data for 4/20/2017.

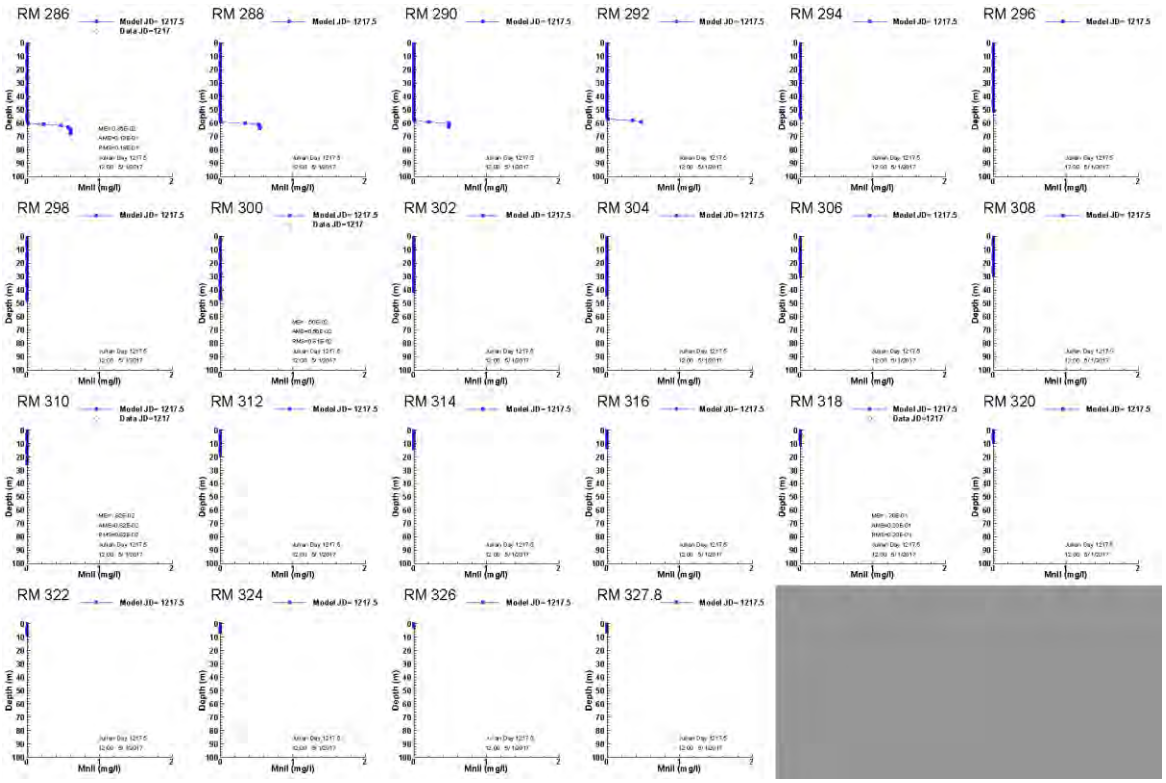


Figure 615. Vertical profiles of Mn(II) compared with data for 5/ 1/2017.

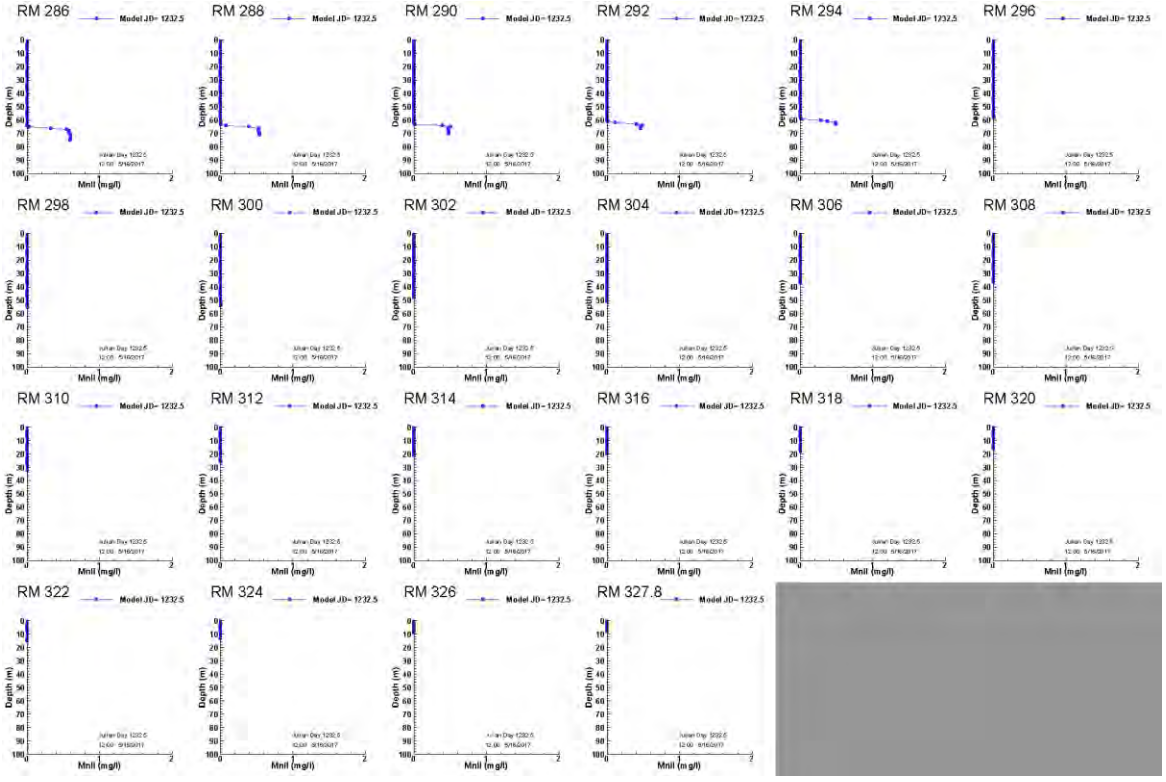


Figure 616. Vertical profiles of Mn(II) compared with data for 5/16/2017.

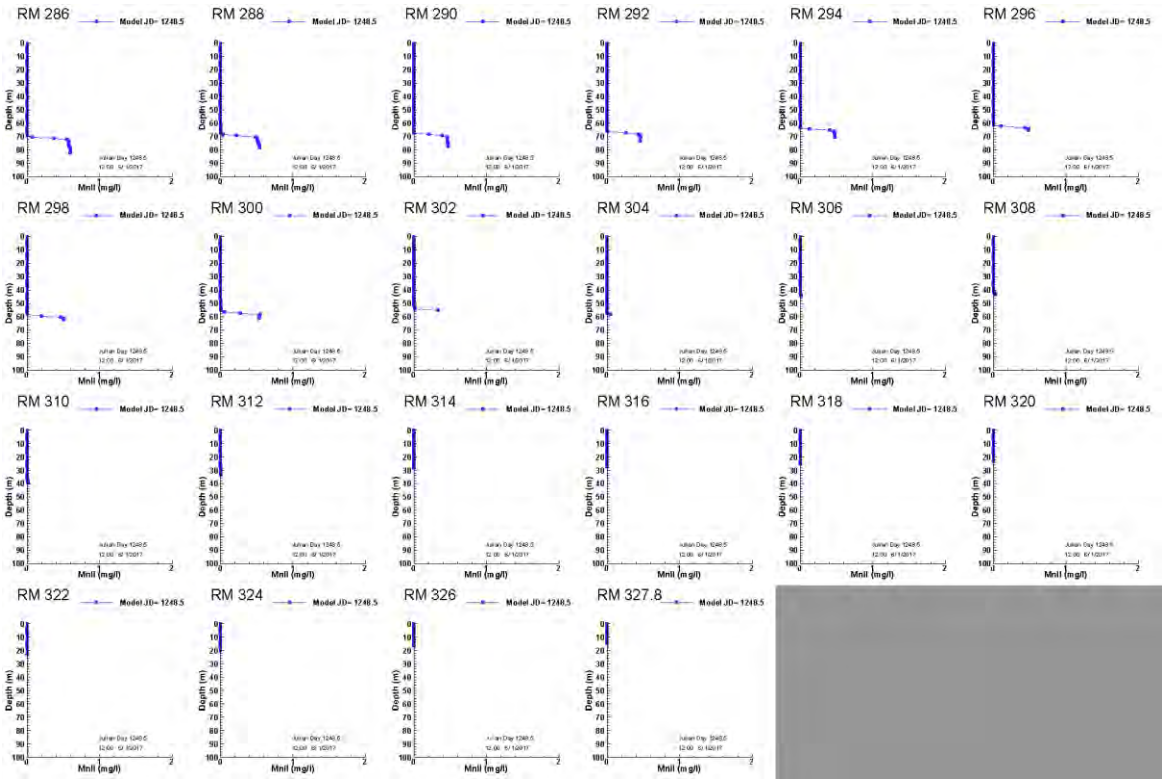


Figure 617. Vertical profiles of Mn(II) compared with data for 6/ 1/2017.

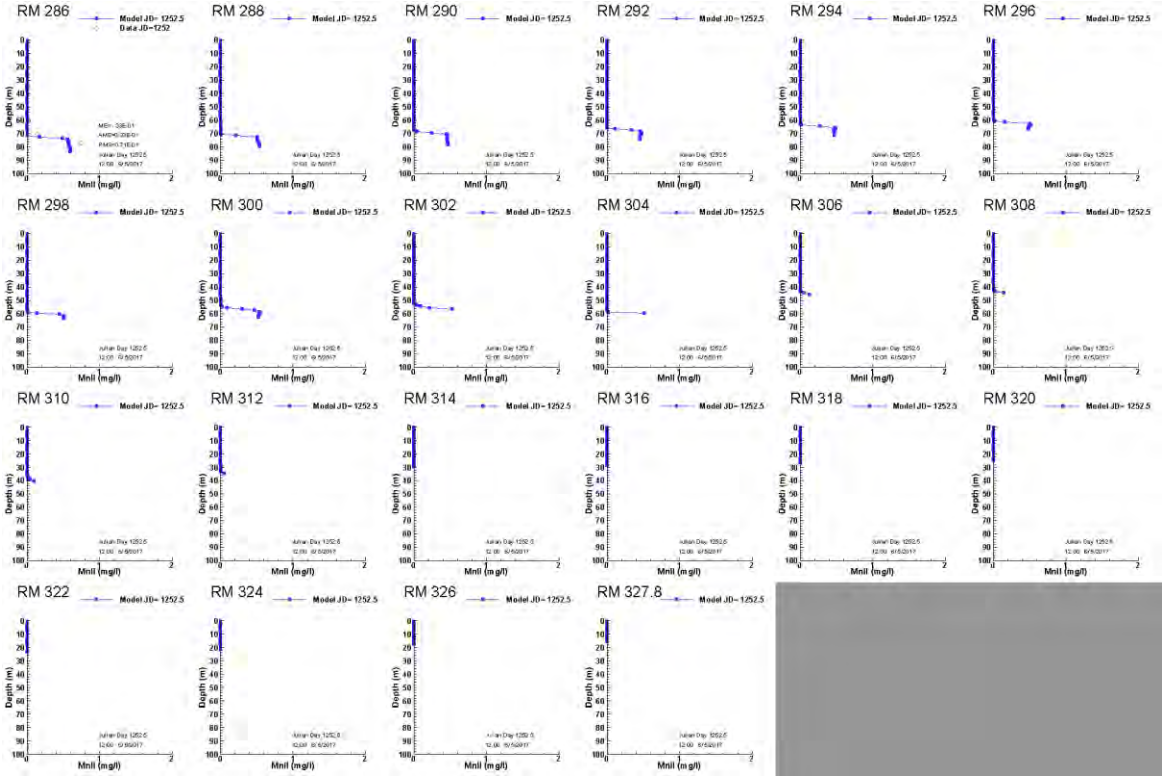


Figure 618. Vertical profiles of Mn(II) compared with data for 6/ 5/2017.

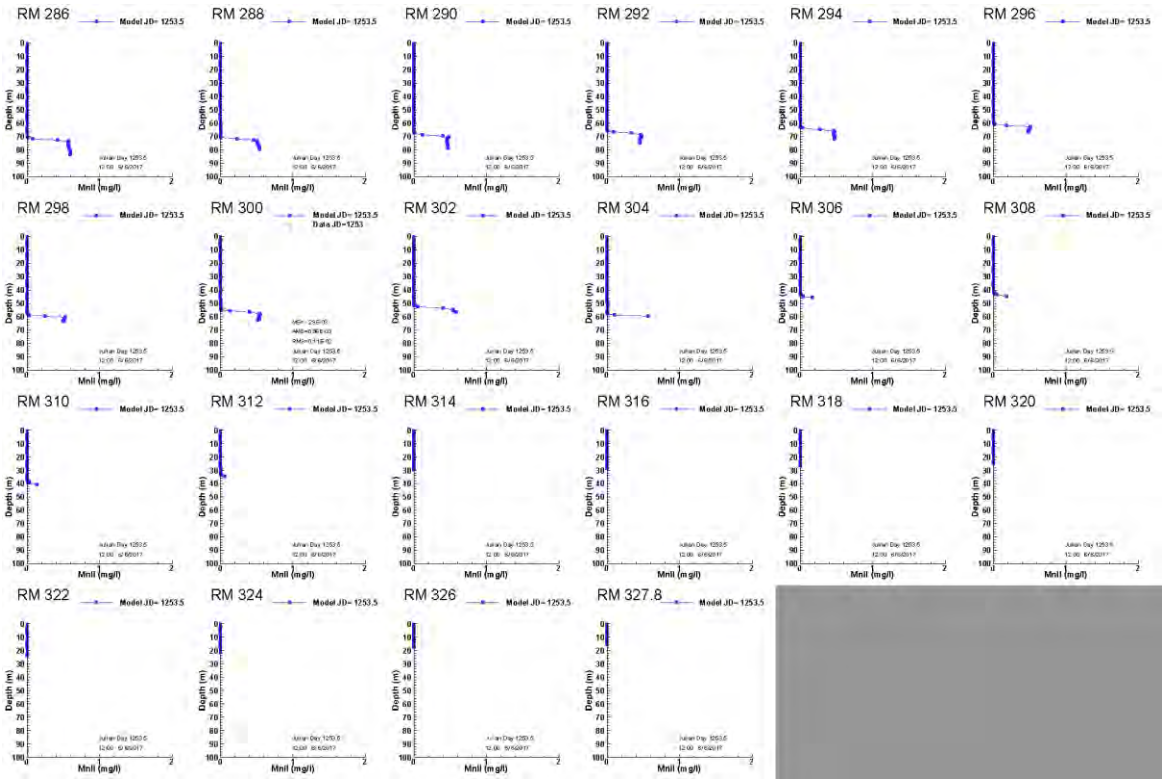


Figure 619. Vertical profiles of Mn(II) compared with data for 6/ 6/2017.

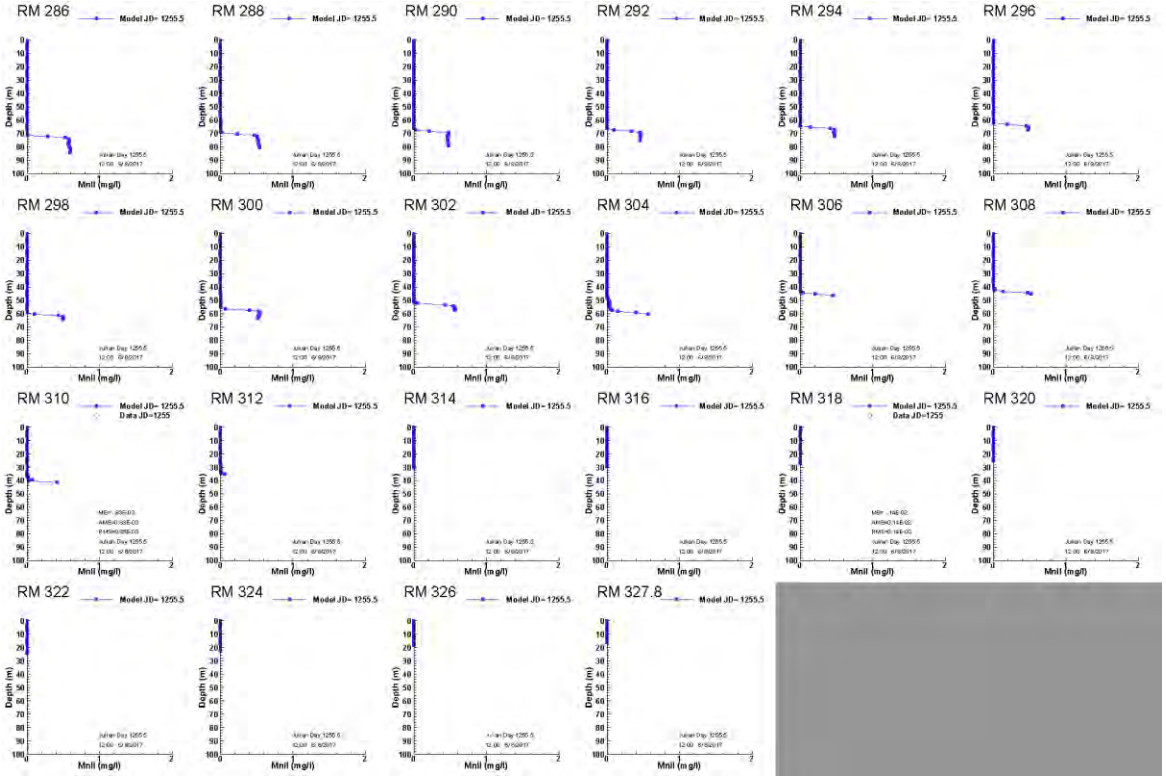


Figure 620. Vertical profiles of Mn(II) compared with data for 6/ 8/2017.

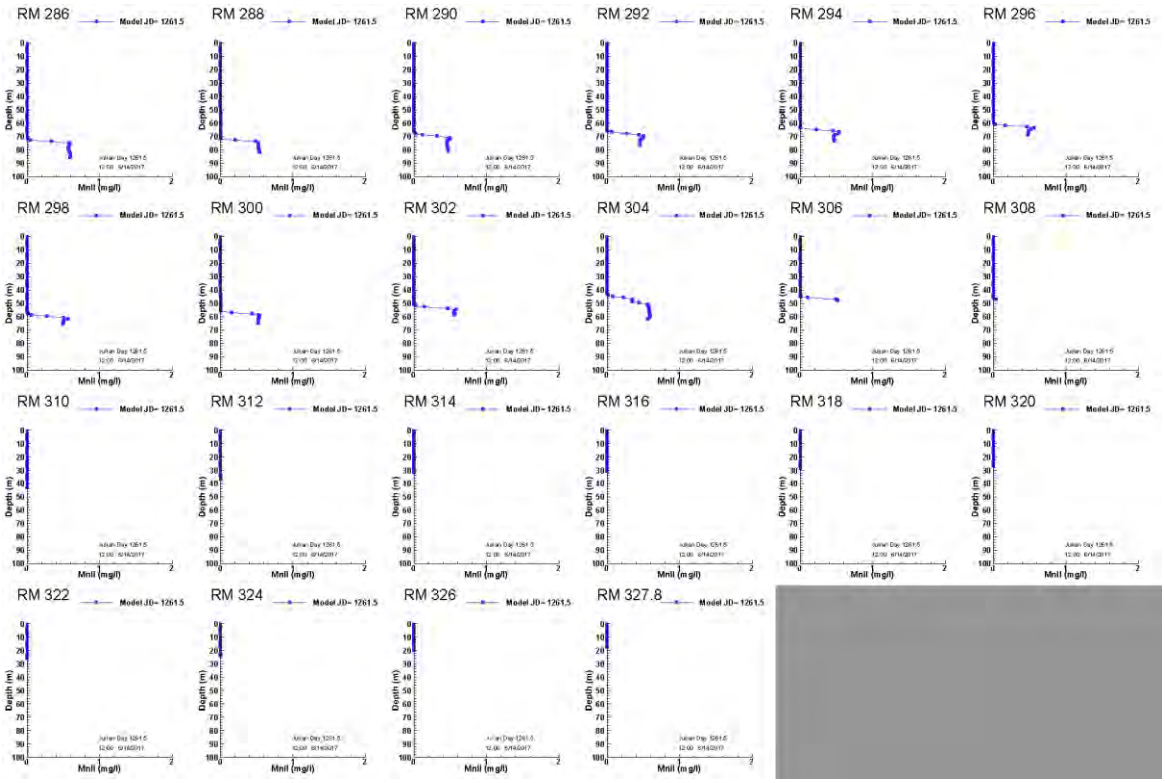


Figure 621. Vertical profiles of Mn(II) compared with data for 6/14/2017.

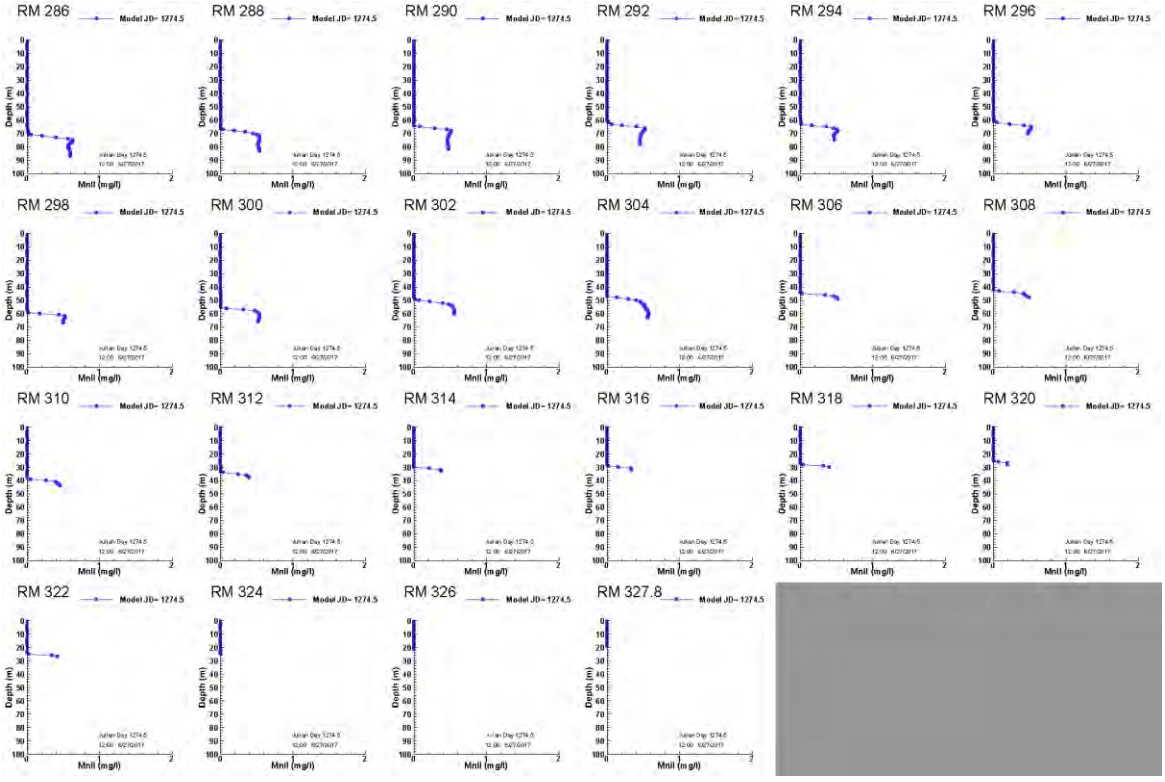


Figure 622. Vertical profiles of Mn(II) compared with data for 6/27/2017.

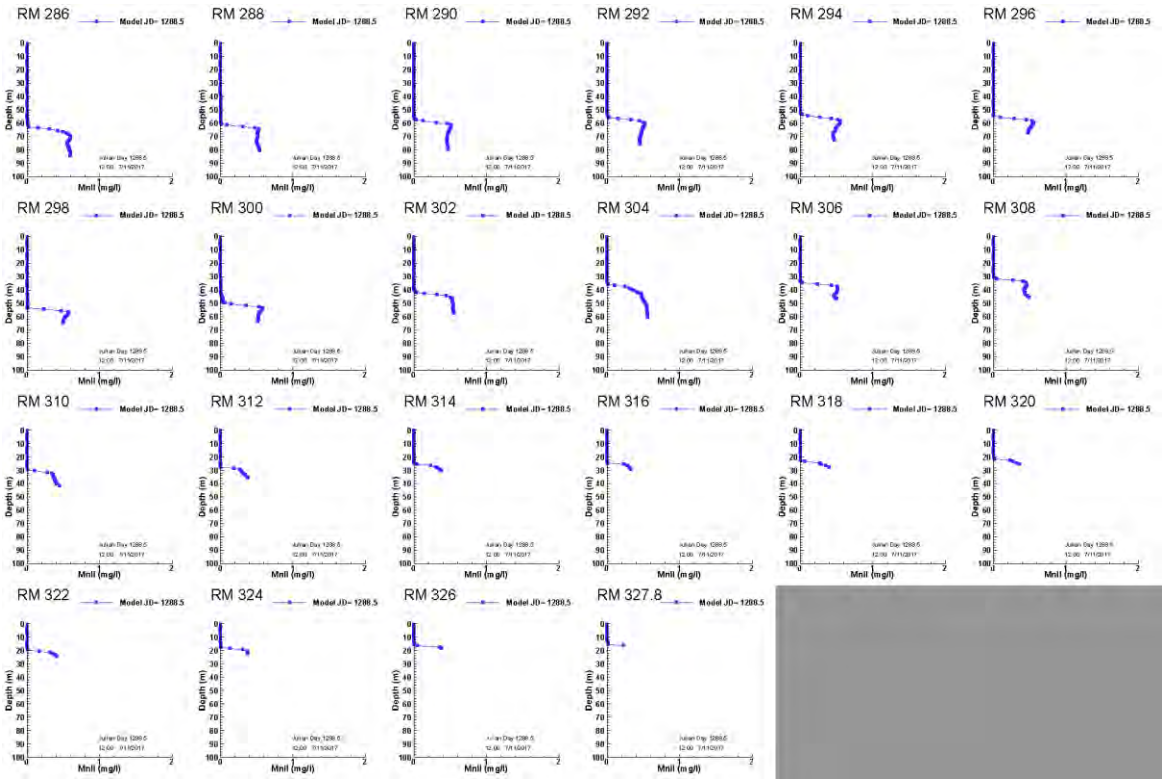


Figure 623. Vertical profiles of Mn(II) compared with data for 7/11/2017.

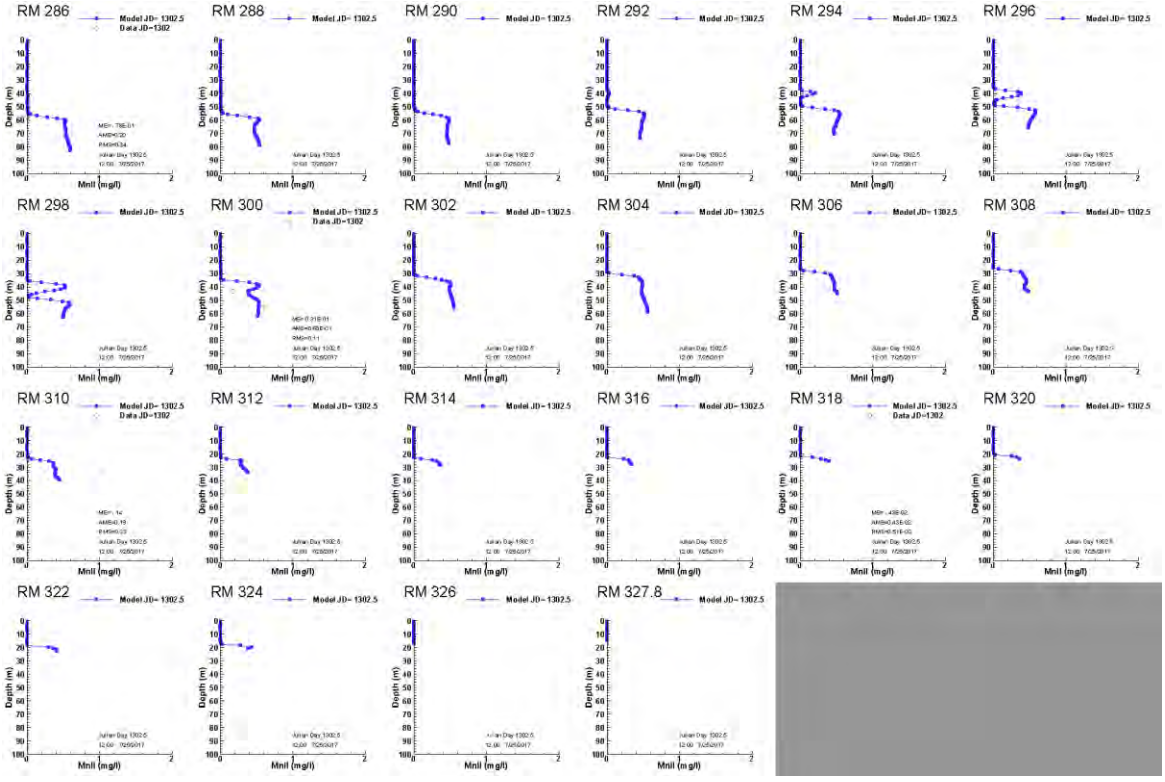


Figure 624. Vertical profiles of Mn(II) compared with data for 7/25/2017.

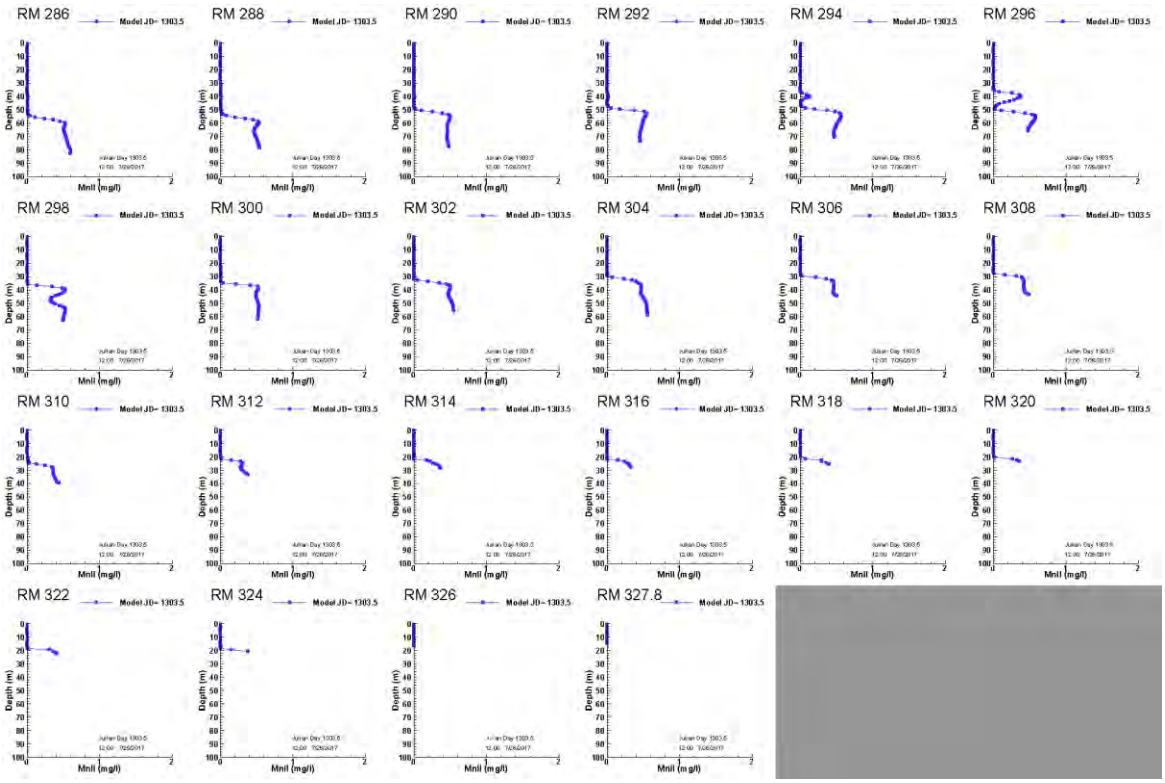


Figure 625. Vertical profiles of Mn(II) compared with data for 7/26/2017.

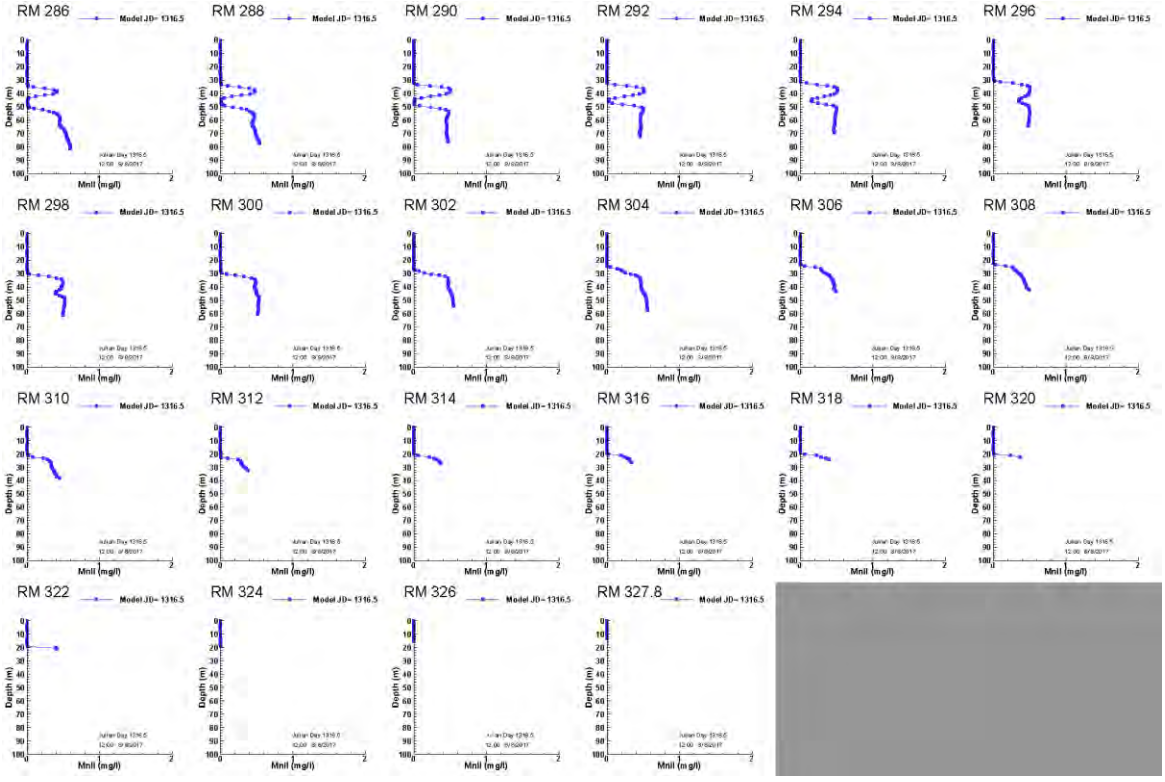


Figure 626. Vertical profiles of Mn(II) compared with data for 8/ 8/2017.

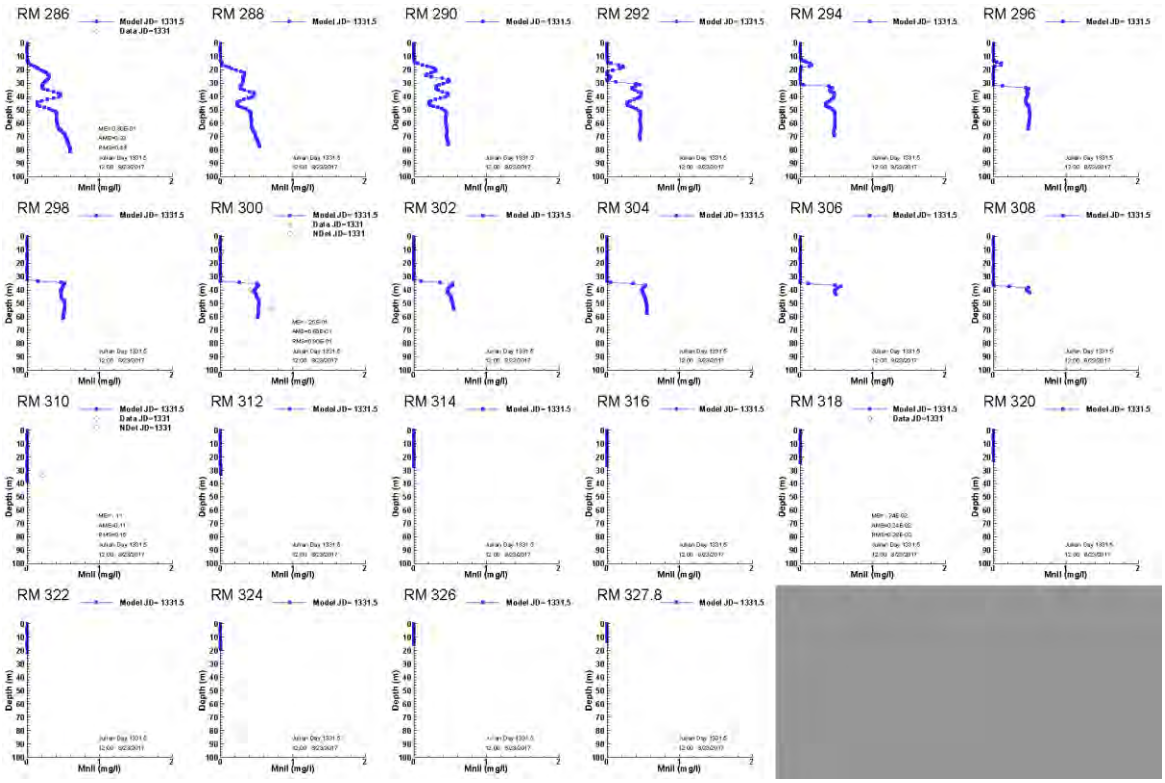


Figure 627. Vertical profiles of Mn(II) compared with data for 8/23/2017.

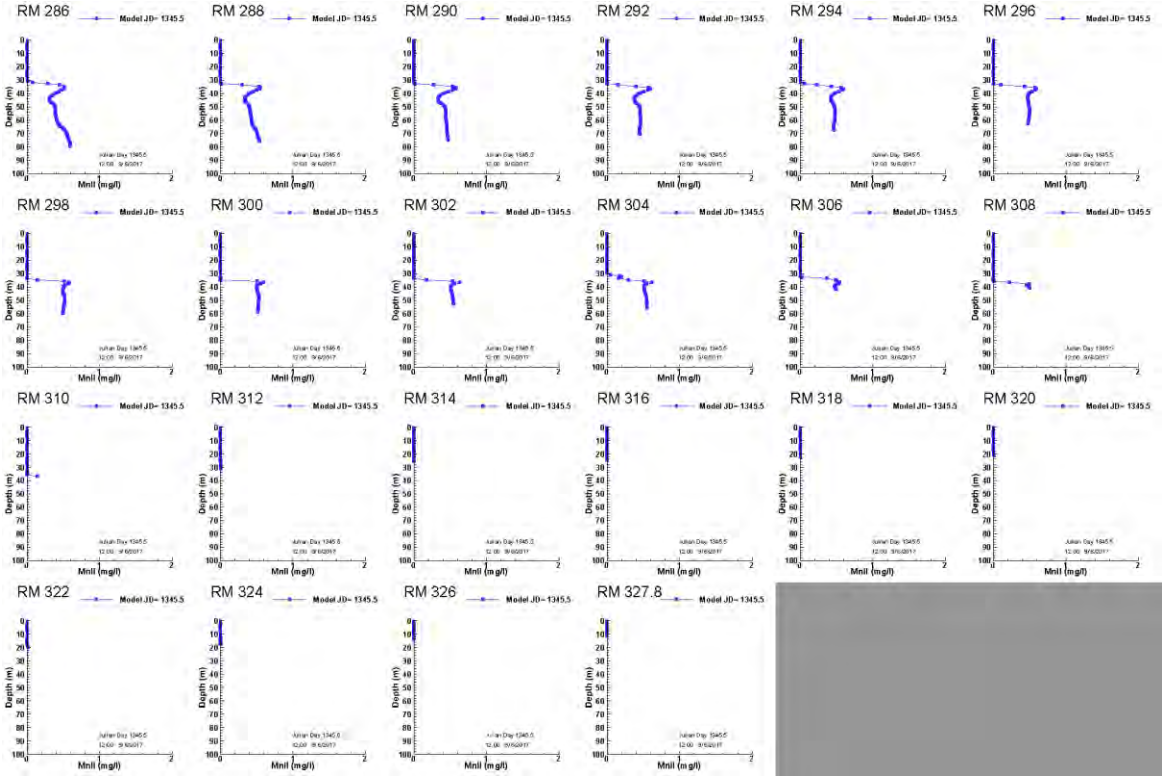


Figure 628. Vertical profiles of Mn(II) compared with data for 9/ 6/2017.

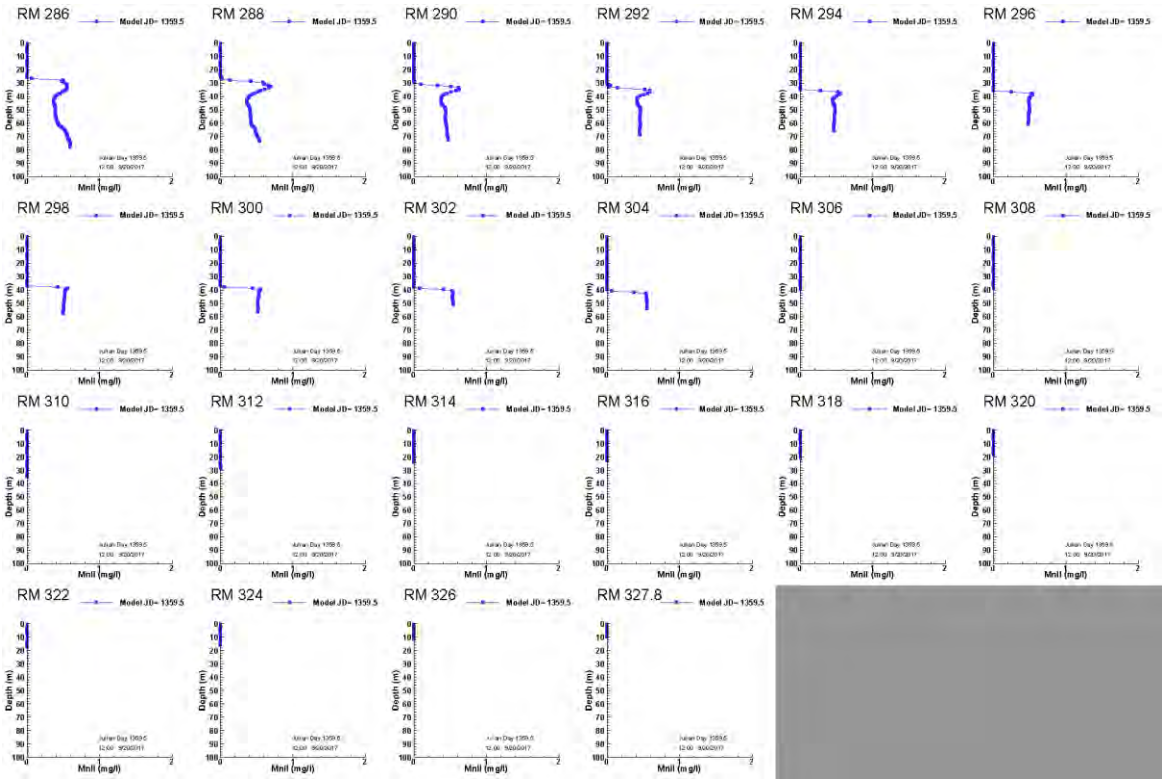


Figure 629. Vertical profiles of Mn(II) compared with data for 9/20/2017.

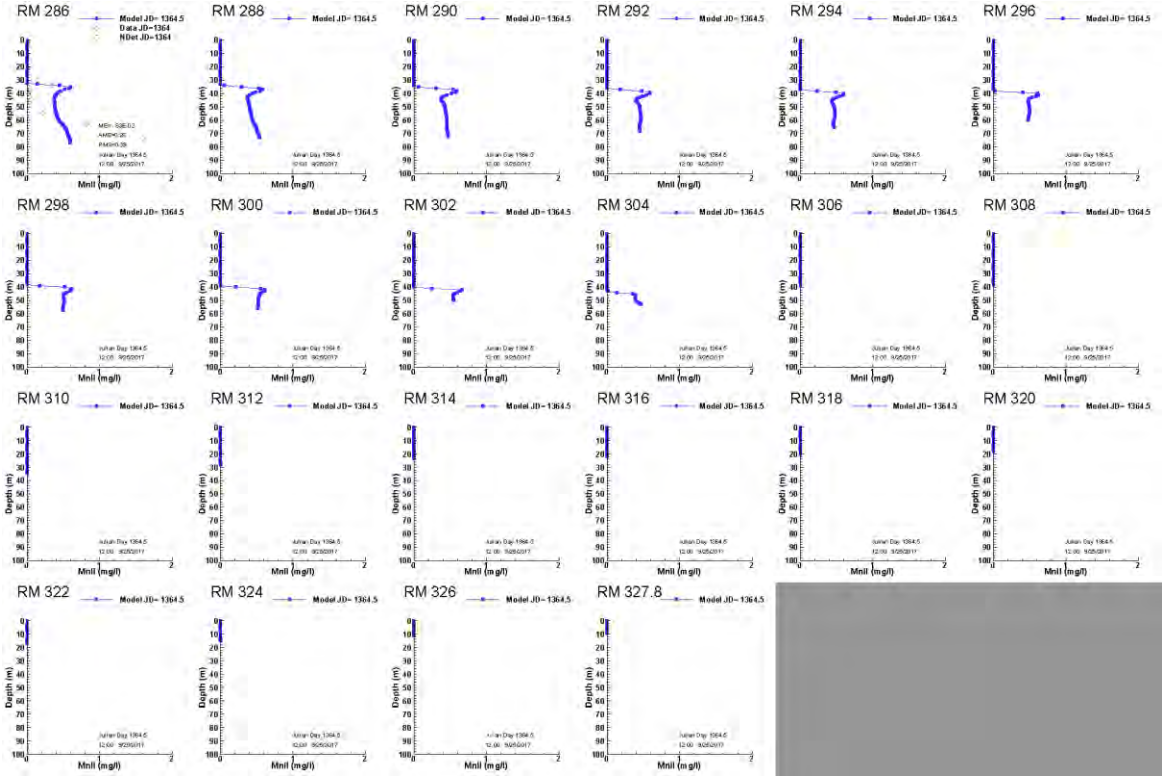


Figure 630. Vertical profiles of Mn(II) compared with data for 9/25/2017.

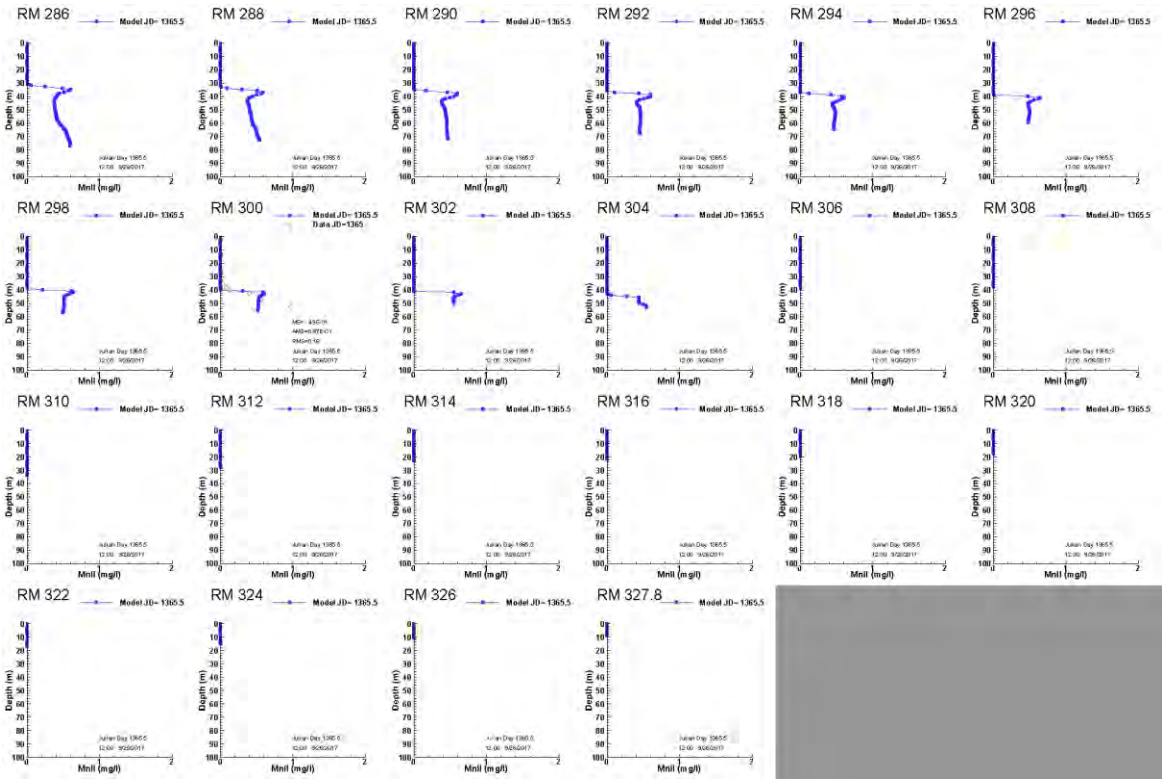


Figure 631. Vertical profiles of Mn(II) compared with data for 9/26/2017.

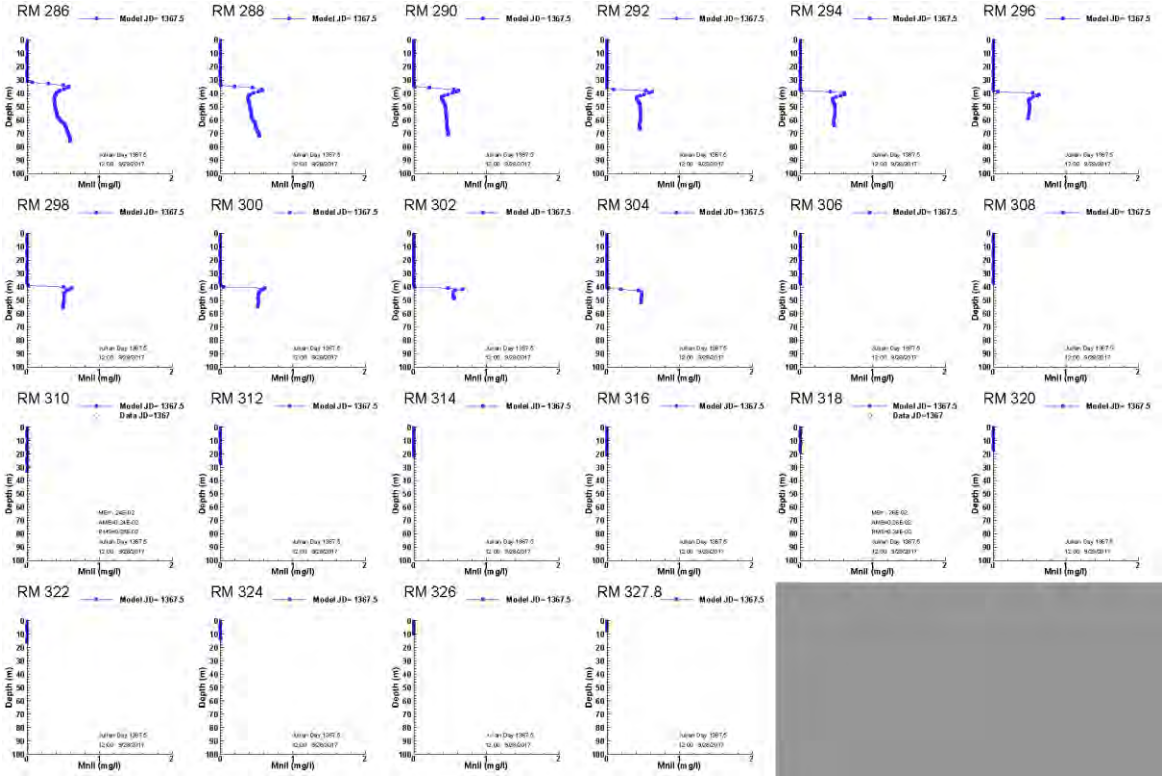


Figure 632. Vertical profiles of Mn(II) compared with data for 9/28/2017.

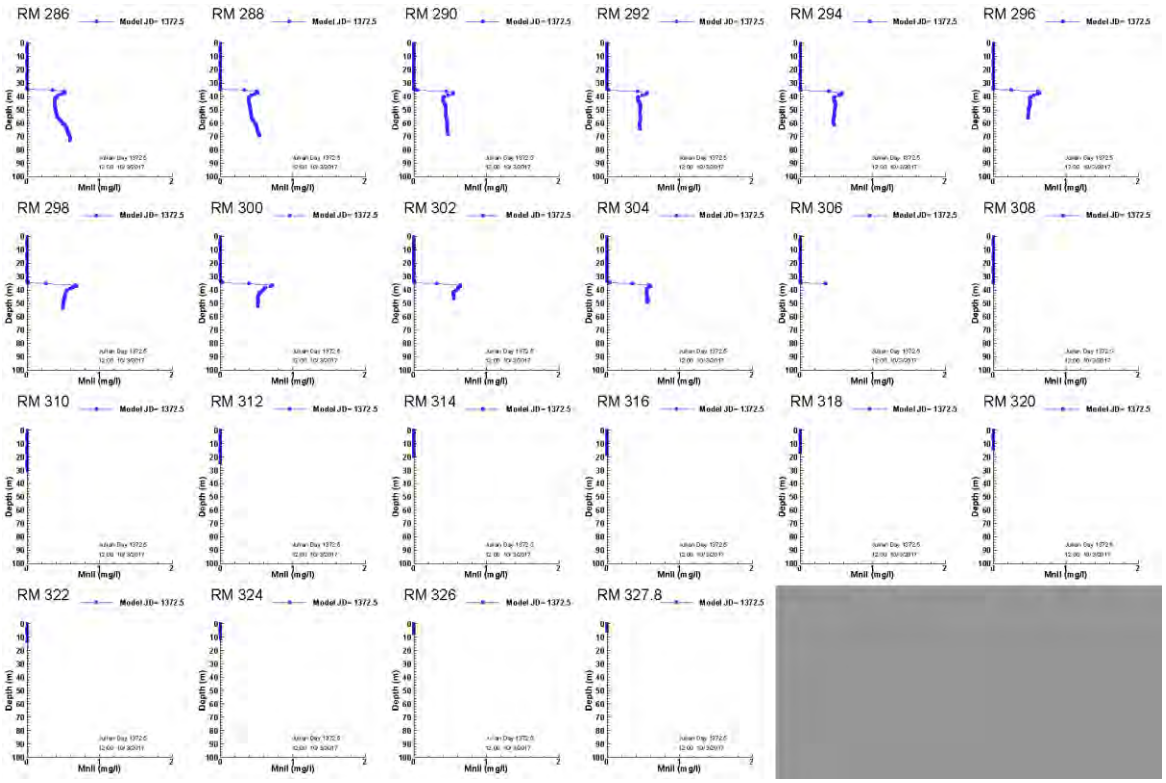


Figure 633. Vertical profiles of Mn(II) compared with data for 10/ 3/2017.

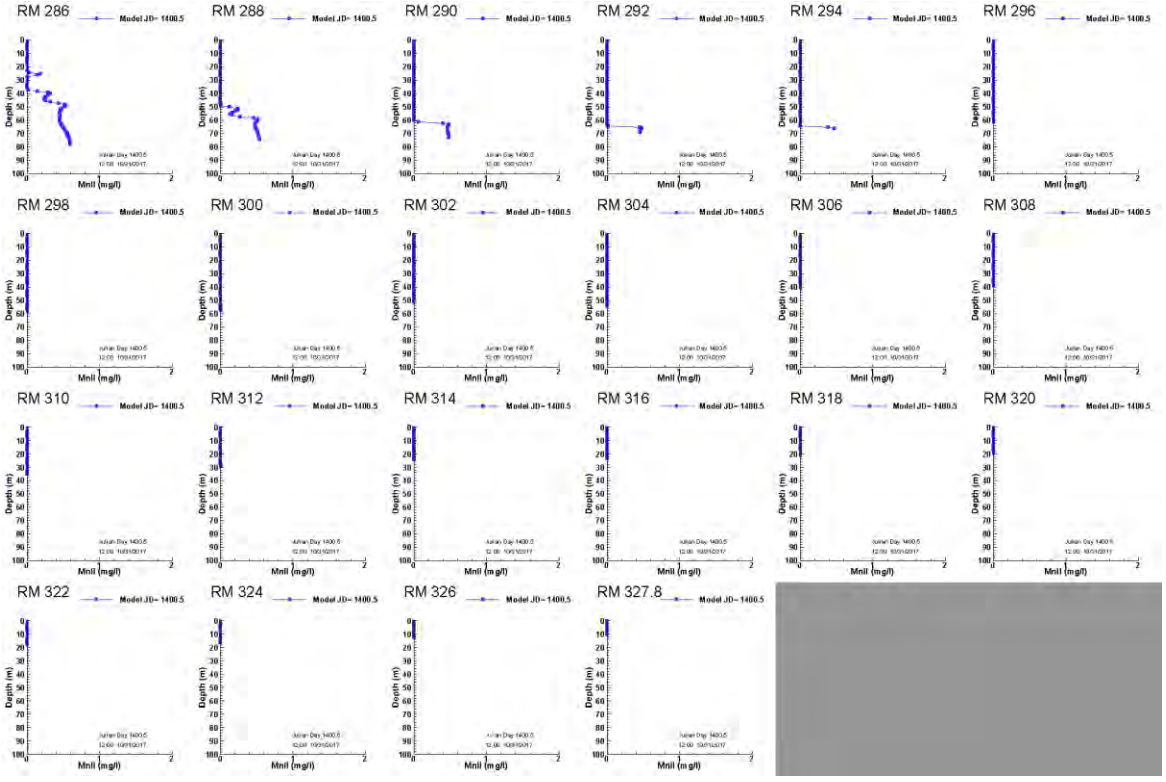


Figure 634. Vertical profiles of Mn(II) compared with data for 10/31/2017.

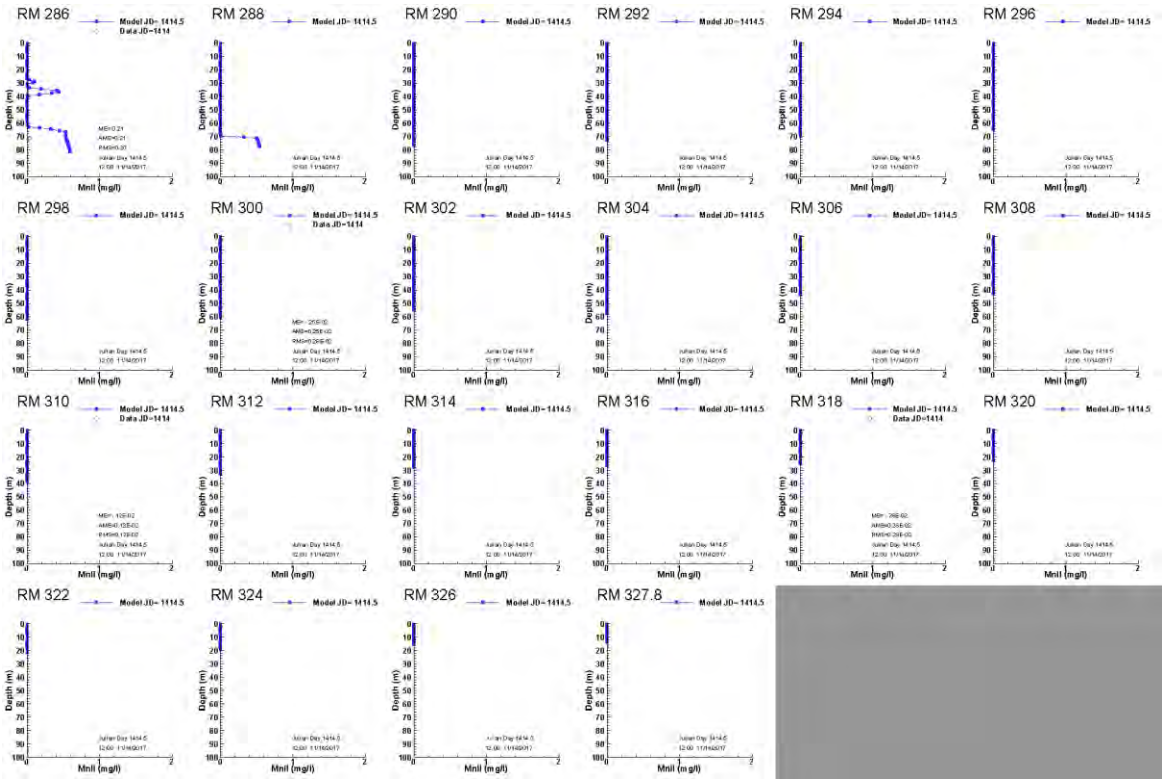


Figure 635. Vertical profiles of Mn(II) compared with data for 11/14/2017.

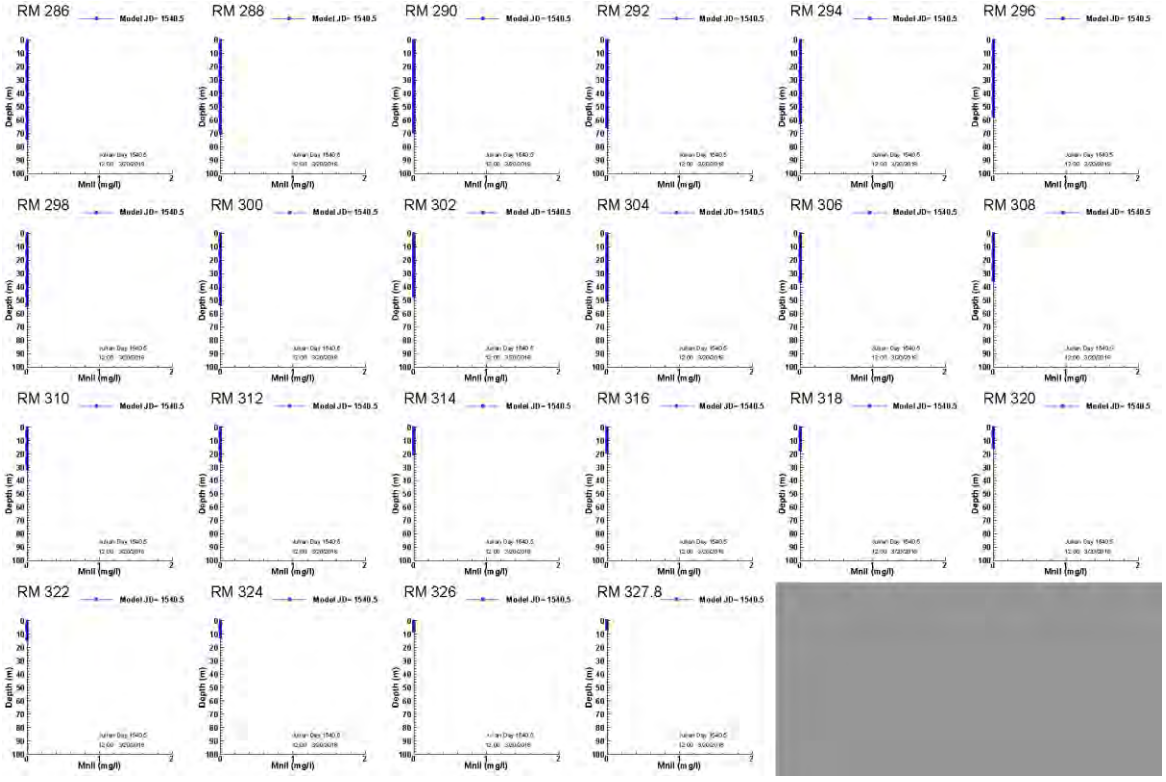


Figure 636. Vertical profiles of Mn(II) compared with data for 3/20/2018.

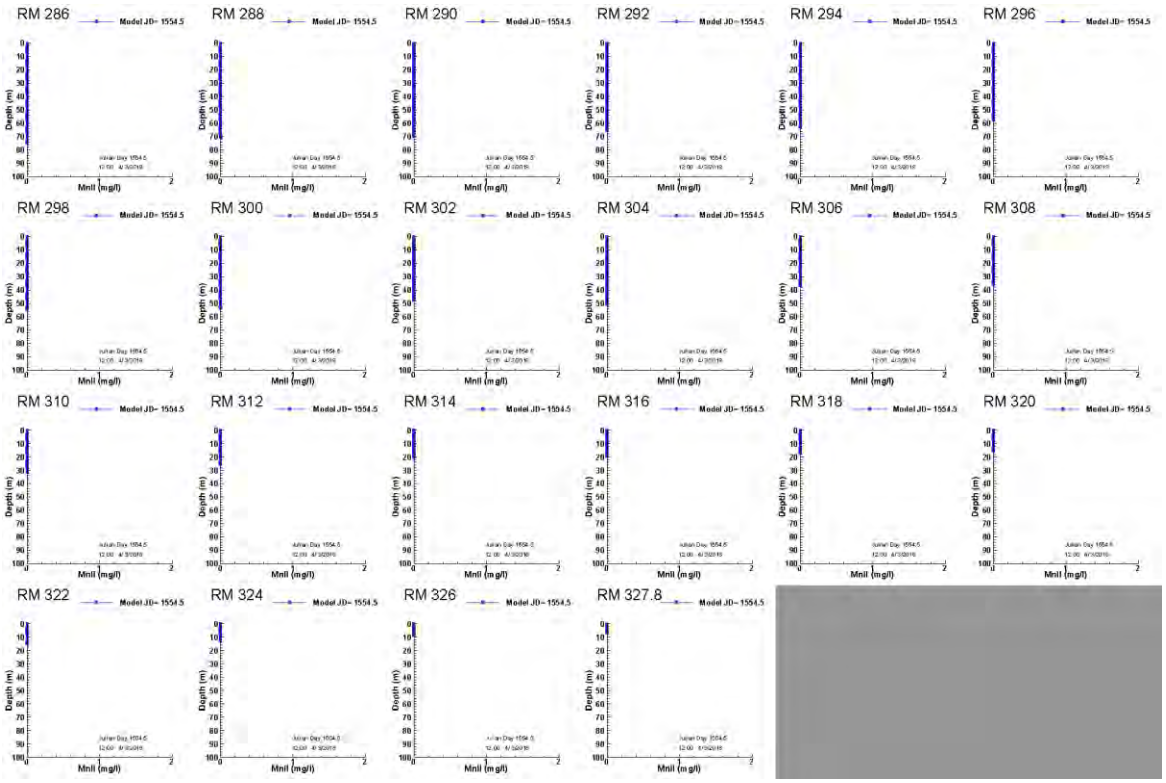


Figure 637. Vertical profiles of Mn(II) compared with data for 4/ 3/2018.

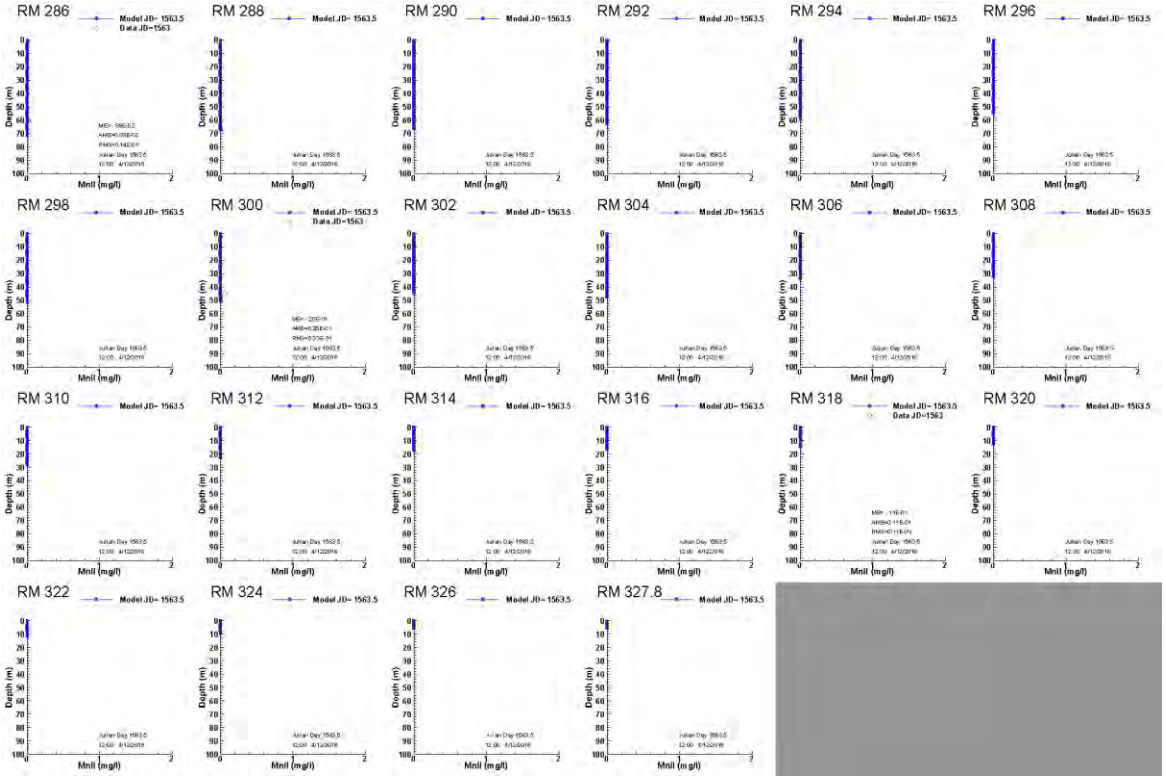


Figure 638. Vertical profiles of Mn(II) compared with data for 4/12/2018.

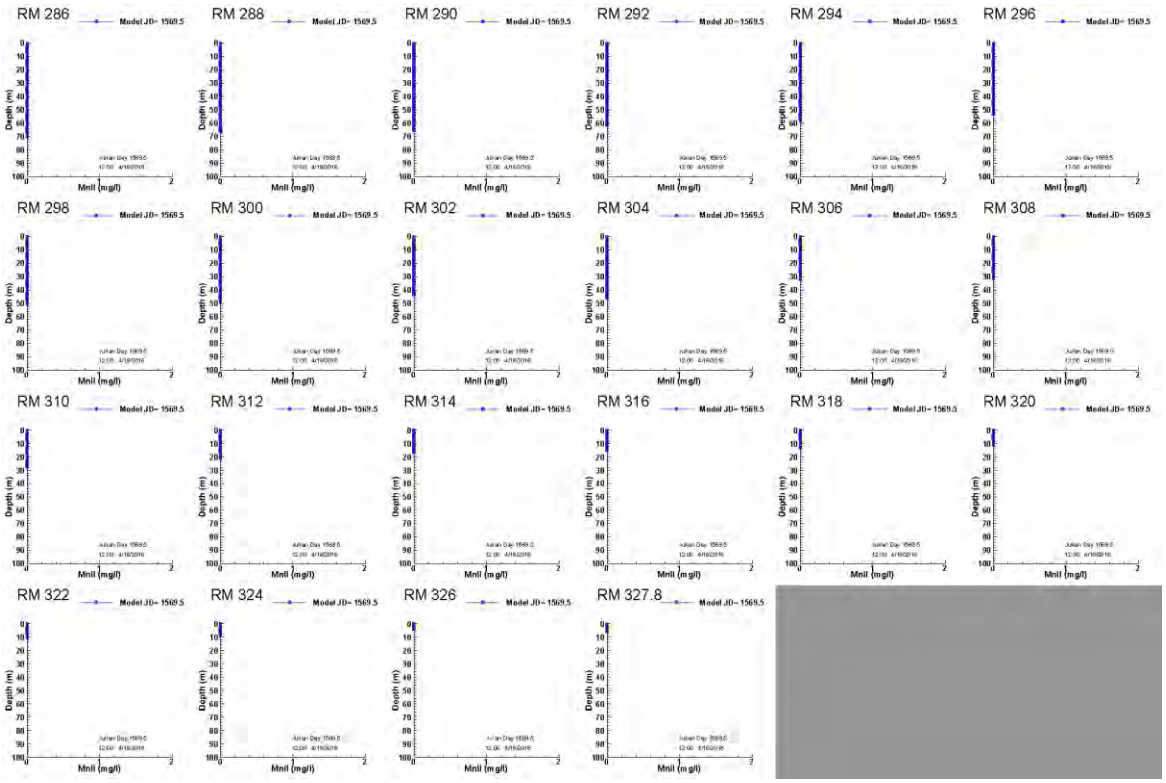


Figure 639. Vertical profiles of Mn(II) compared with data for 4/18/2018.

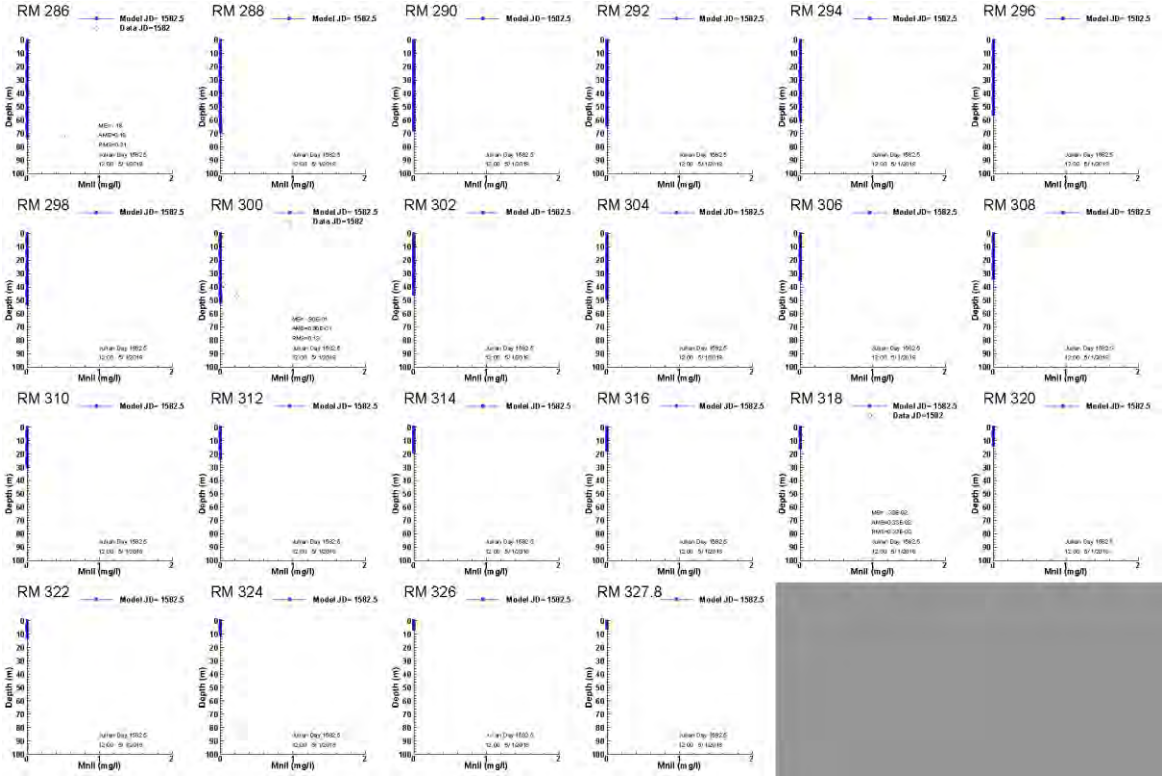


Figure 640. Vertical profiles of Mn(II) compared with data for 5/ 1/2018.

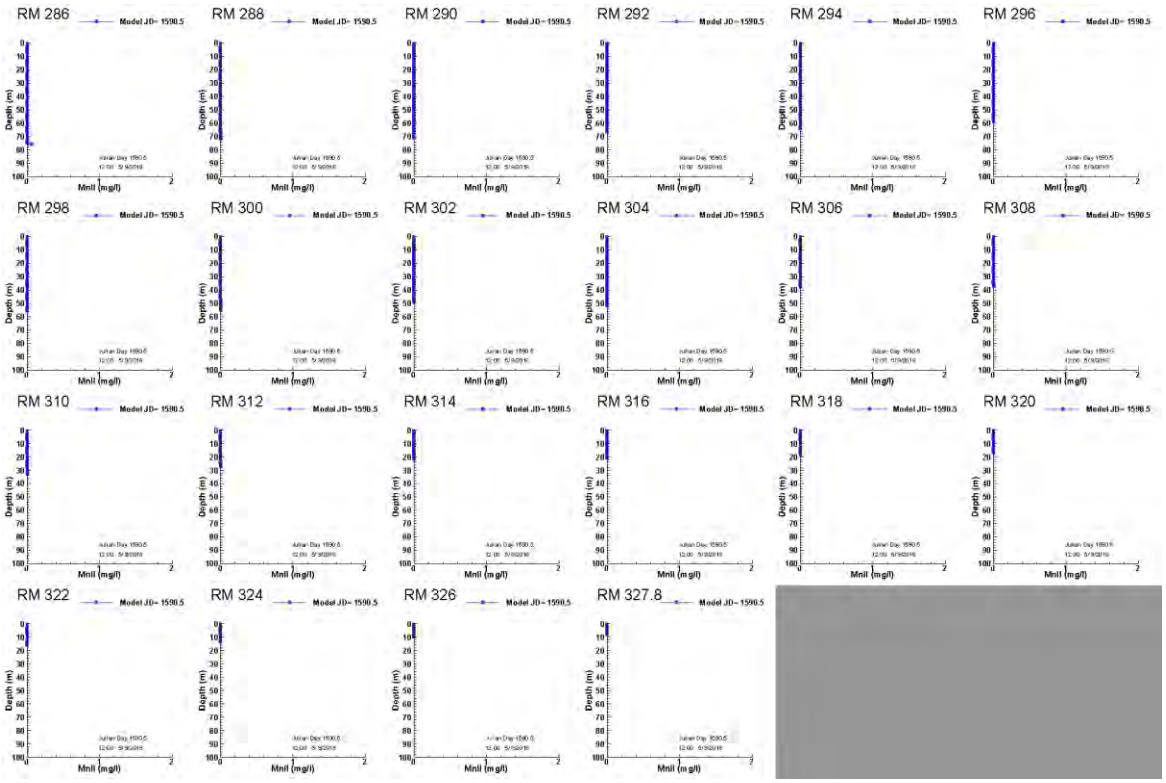


Figure 641. Vertical profiles of Mn(II) compared with data for 5/ 9/2018.

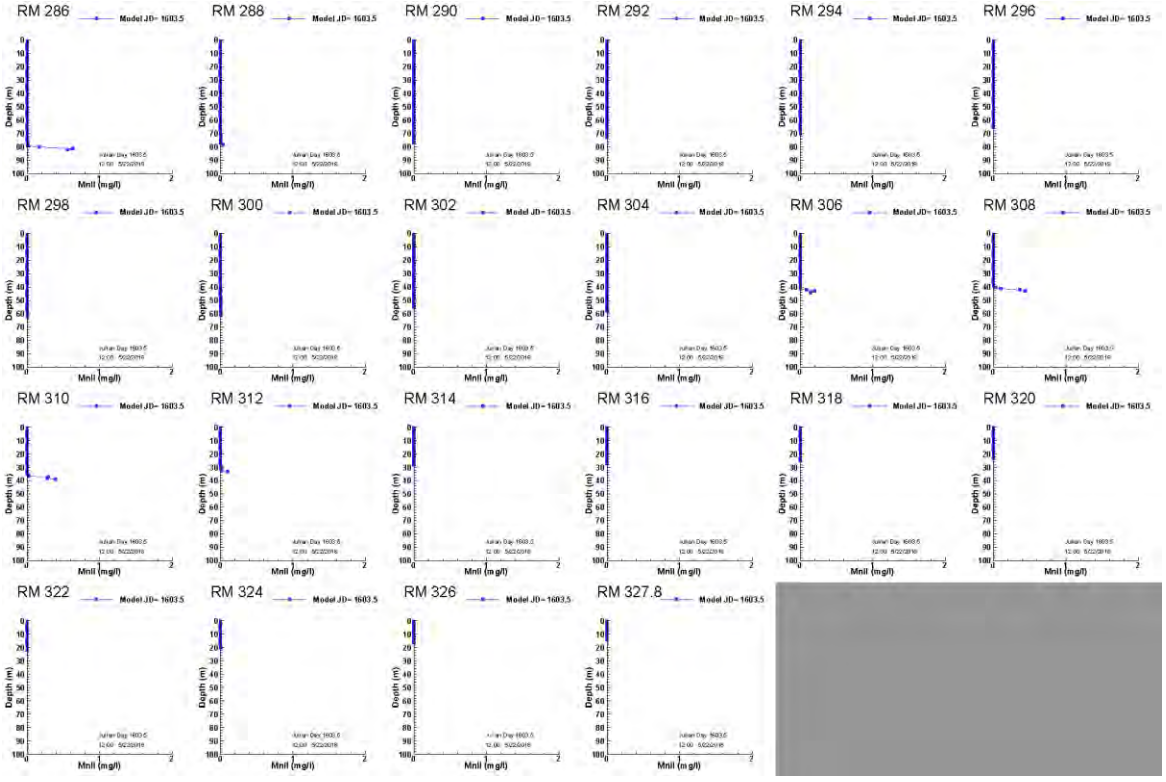


Figure 642. Vertical profiles of Mn(II) compared with data for 5/22/2018.

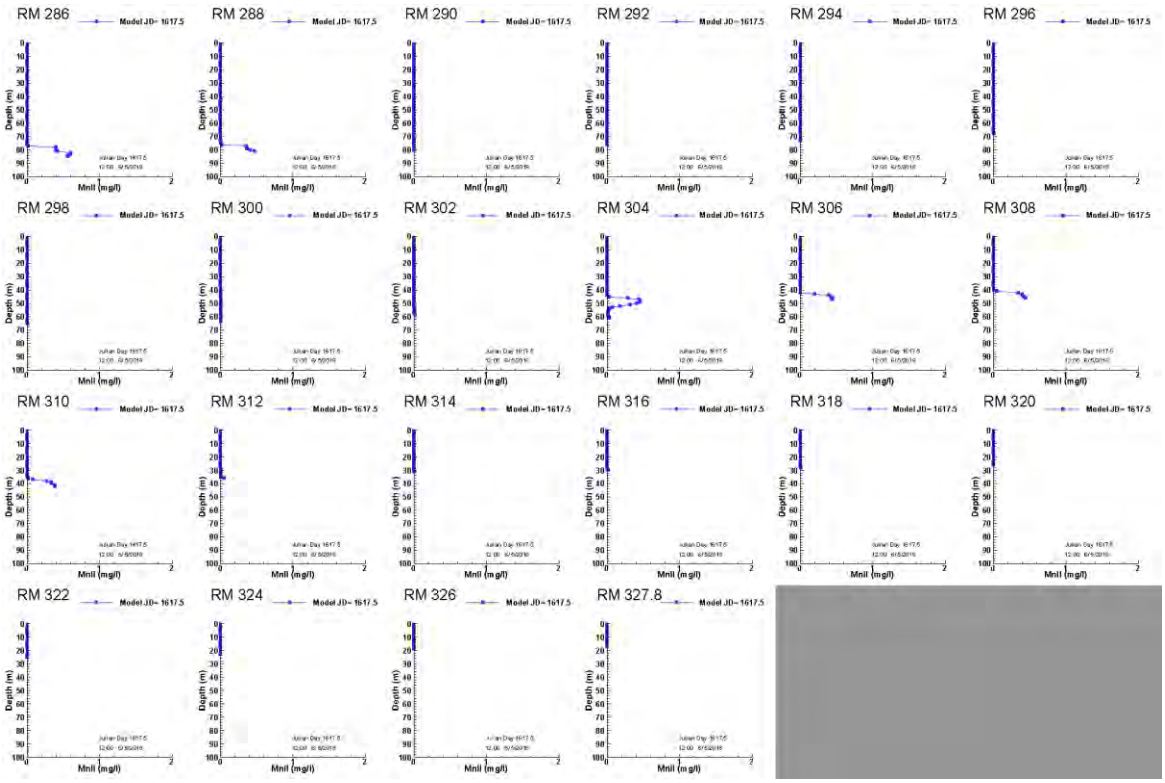


Figure 643. Vertical profiles of Mn(II) compared with data for 6/ 5/2018.

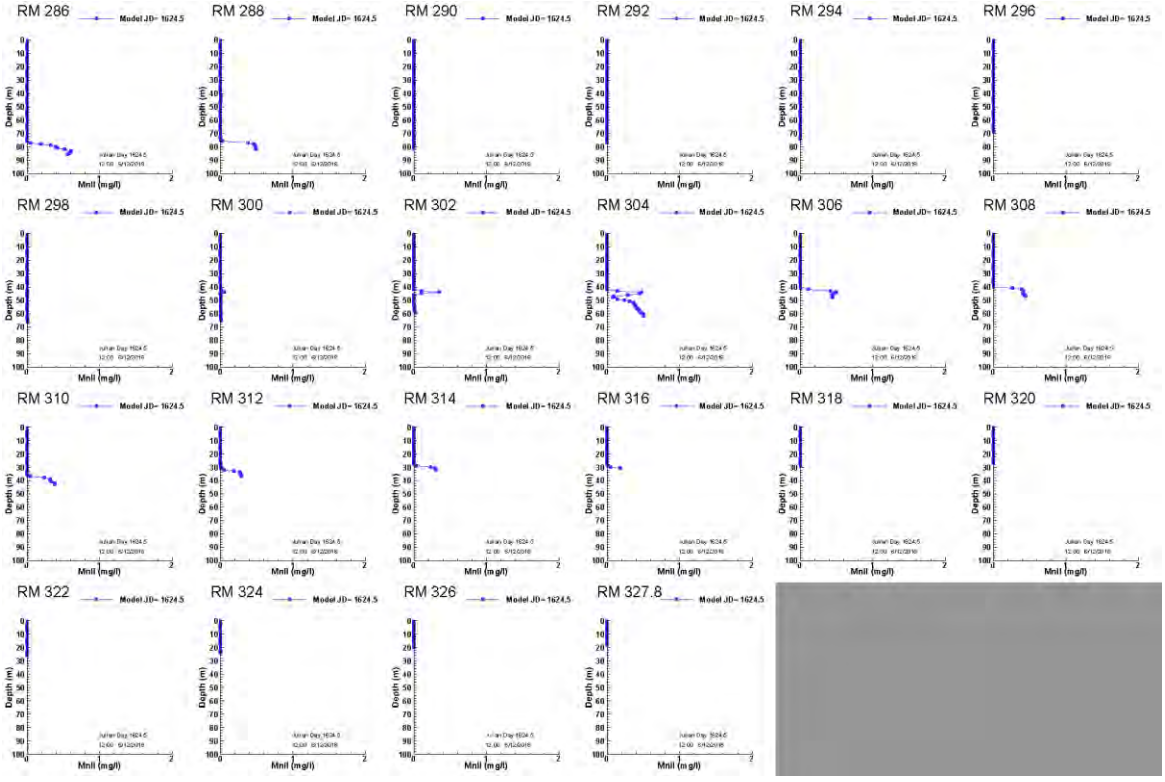


Figure 644. Vertical profiles of Mn(II) compared with data for 6/12/2018.

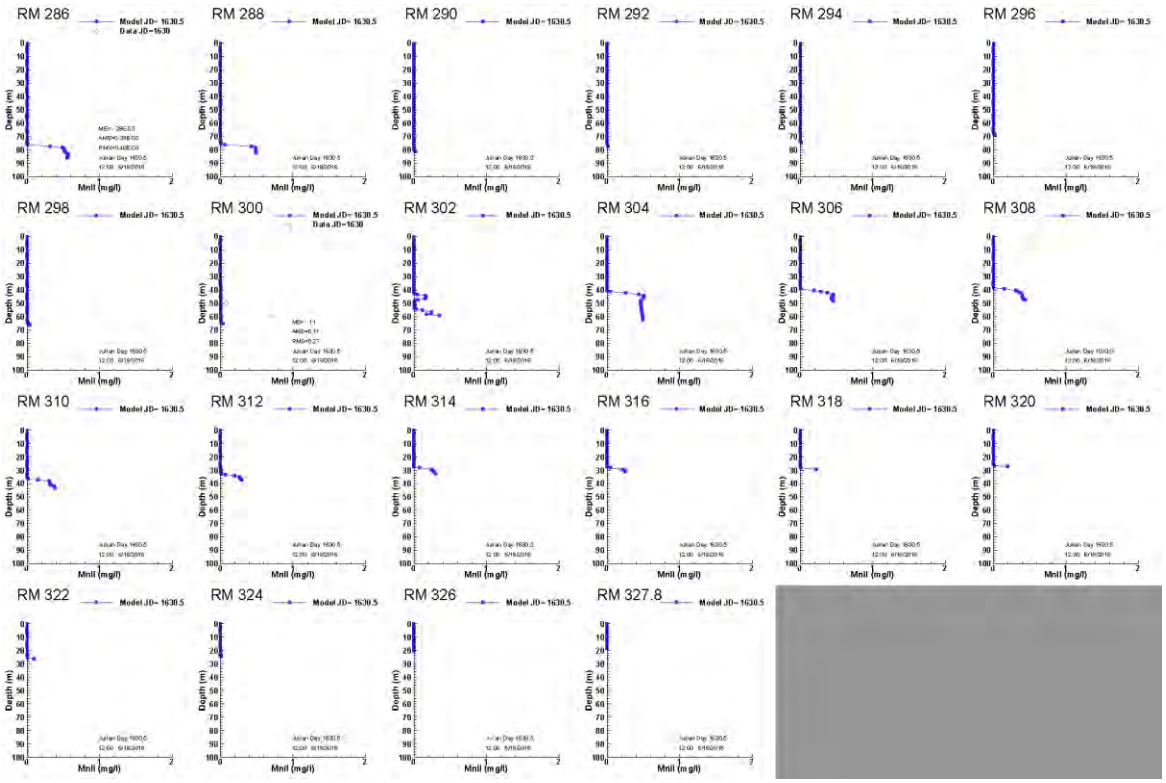


Figure 645. Vertical profiles of Mn(II) compared with data for 6/18/2018.

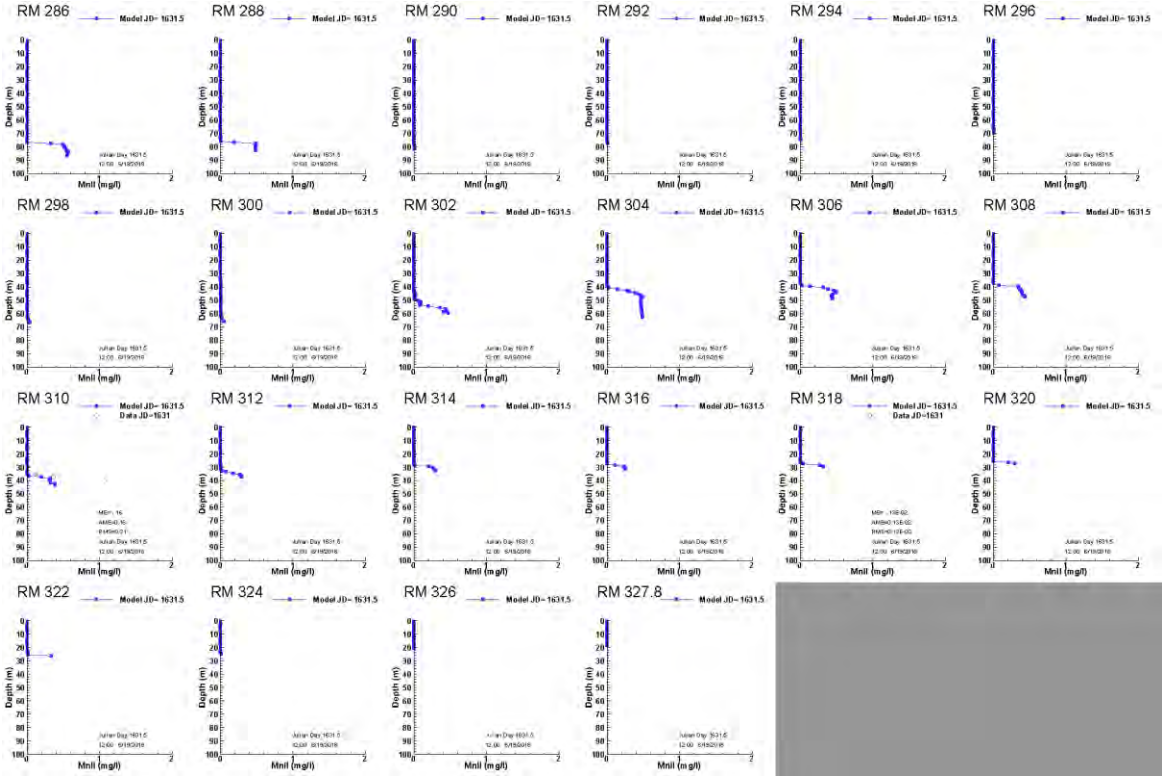


Figure 646. Vertical profiles of Mn(II) compared with data for 6/19/2018.

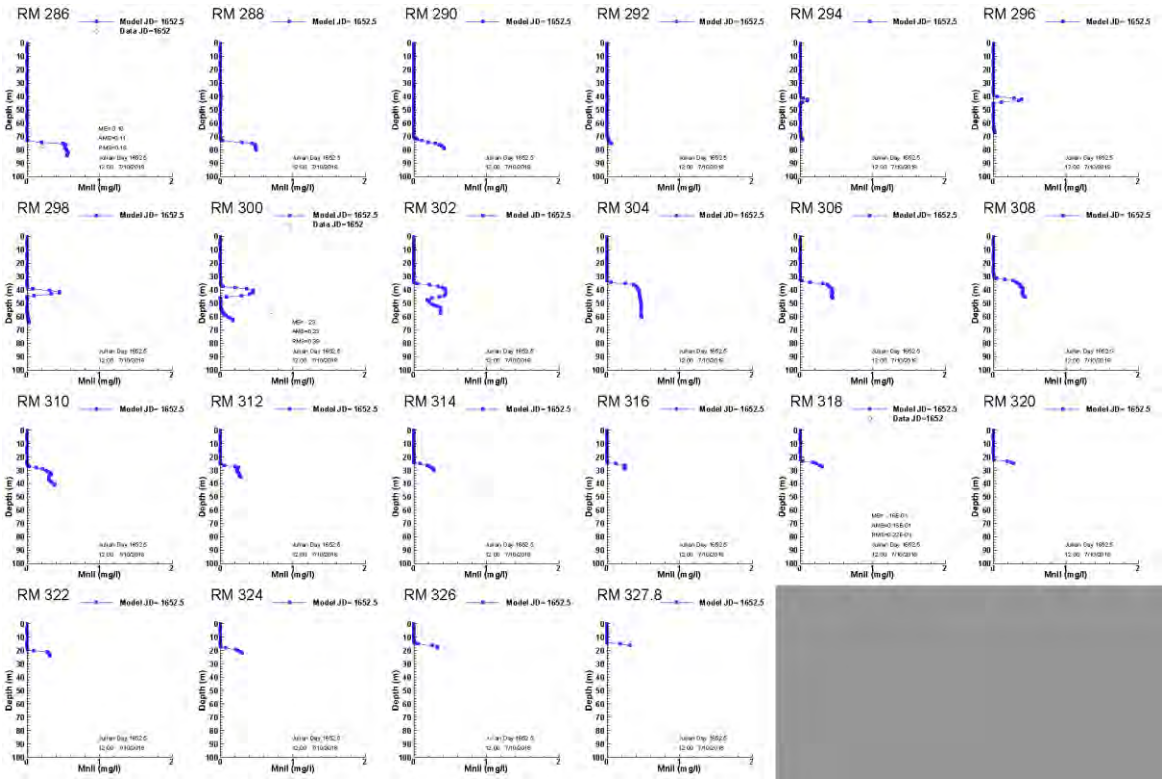


Figure 647. Vertical profiles of Mn(II) compared with data for 7/10/2018.

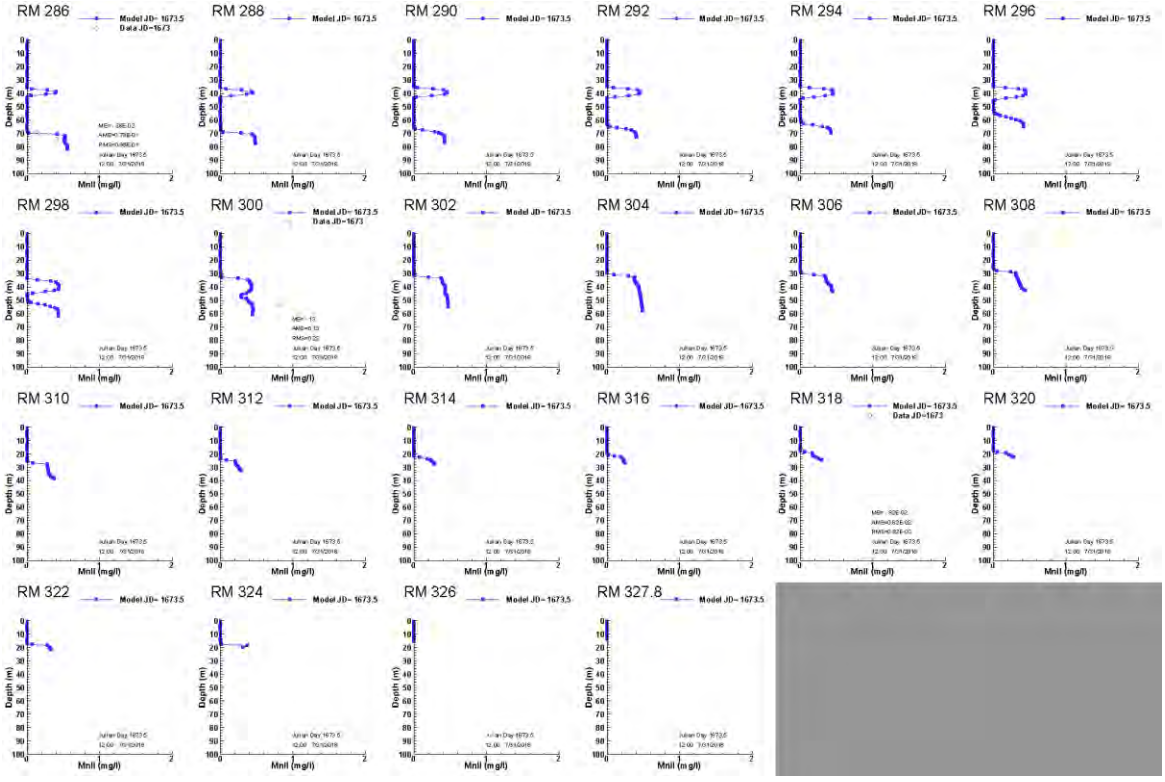


Figure 648. Vertical profiles of Mn(II) compared with data for 7/31/2018.

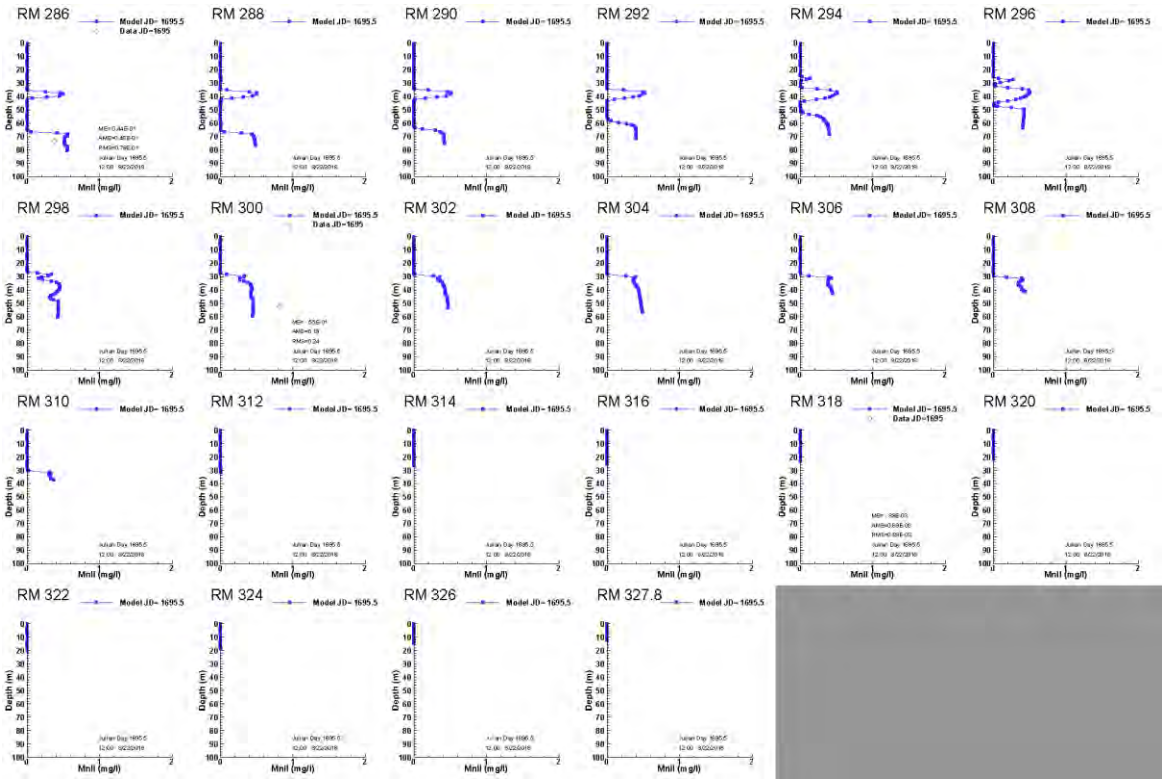


Figure 649. Vertical profiles of Mn(II) compared with data for 8/22/2018.

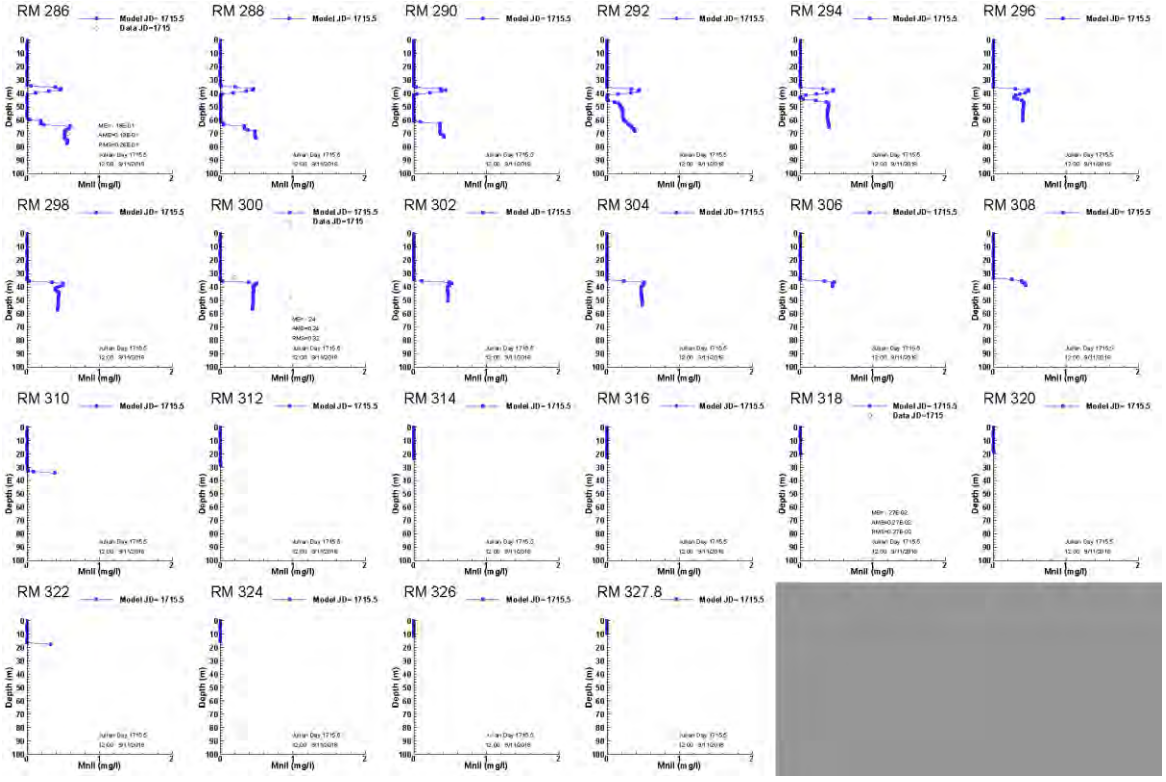


Figure 650. Vertical profiles of Mn(II) compared with data for 9/11/2018.

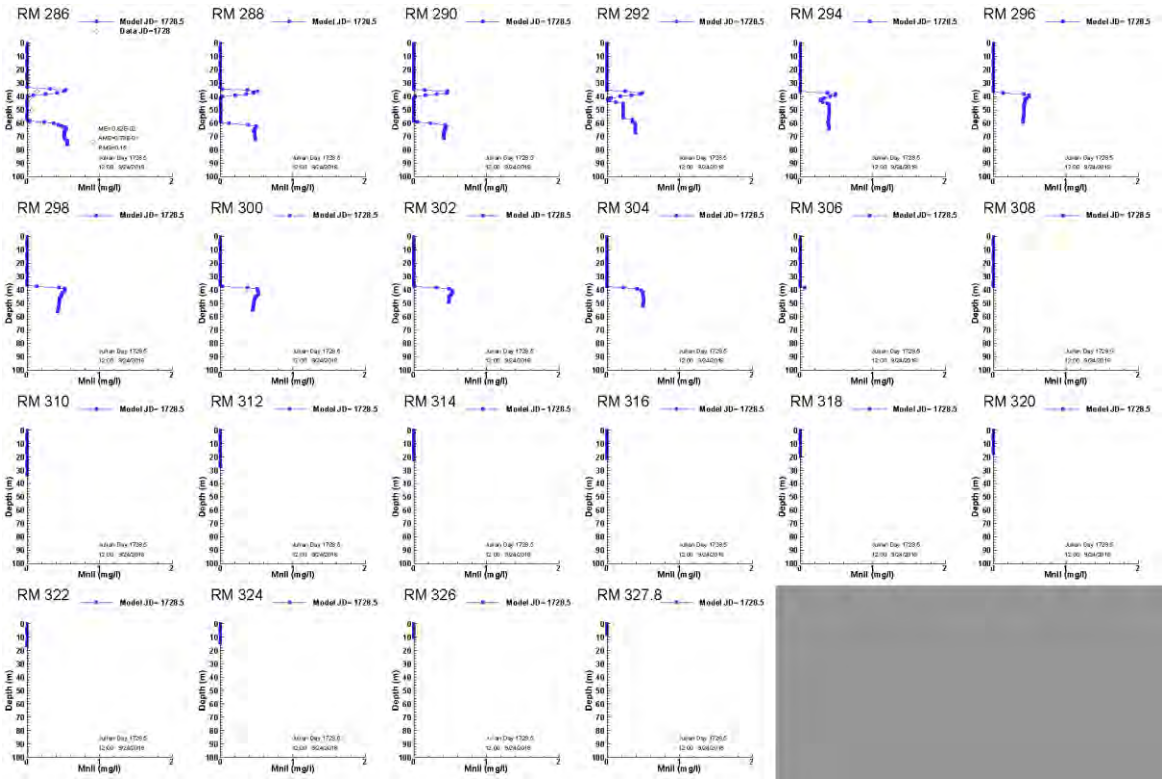


Figure 651. Vertical profiles of Mn(II) compared with data for 9/24/2018.

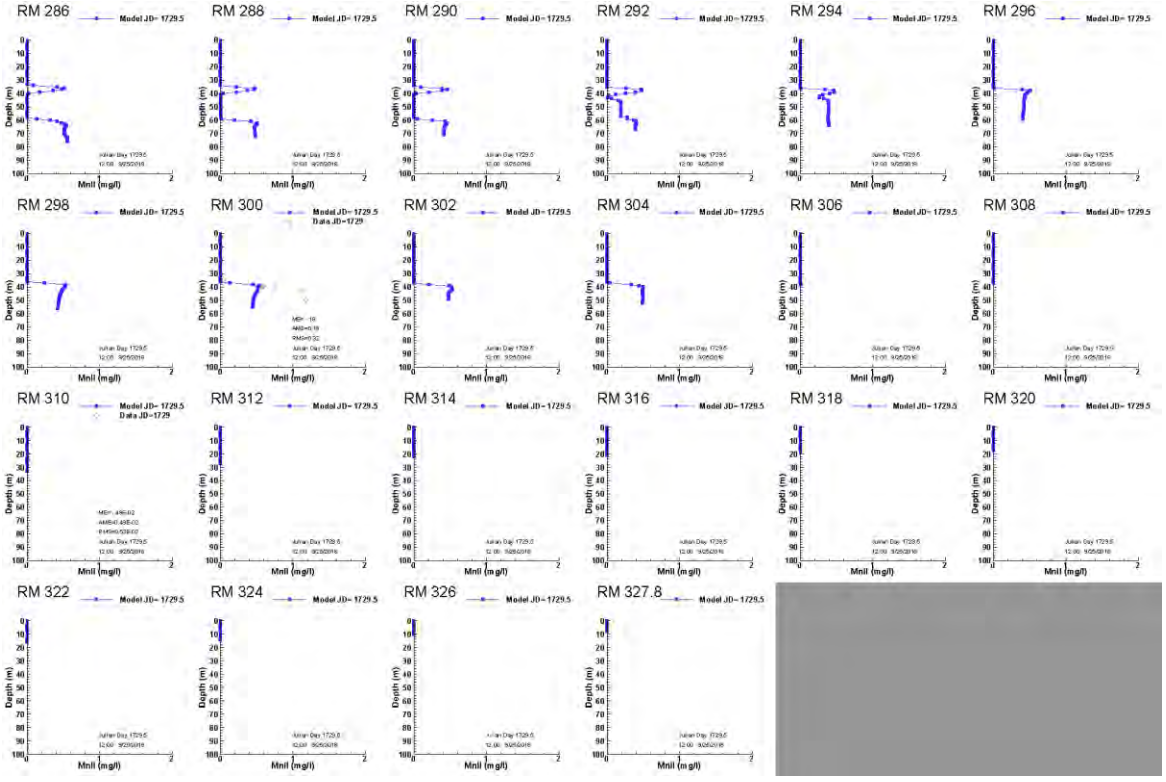


Figure 652. Vertical profiles of Mn(II) compared with data for 9/25/2018.

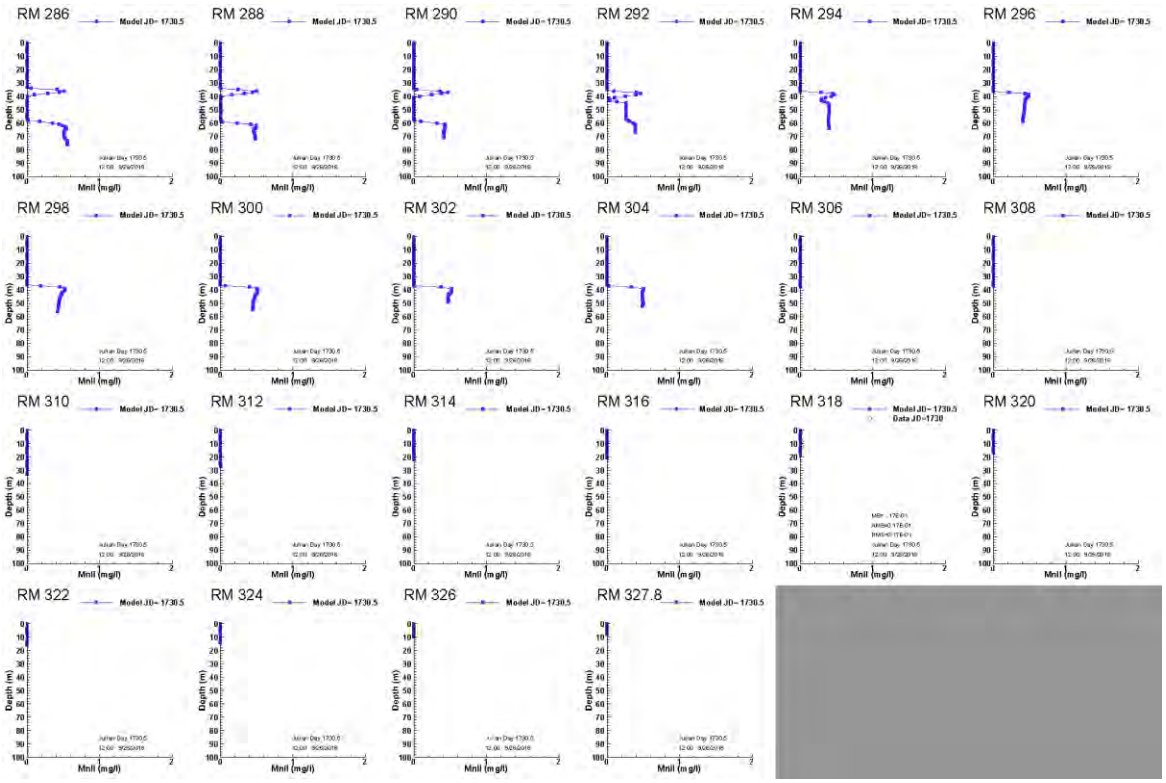


Figure 653. Vertical profiles of Mn(II) compared with data for 9/26/2018.

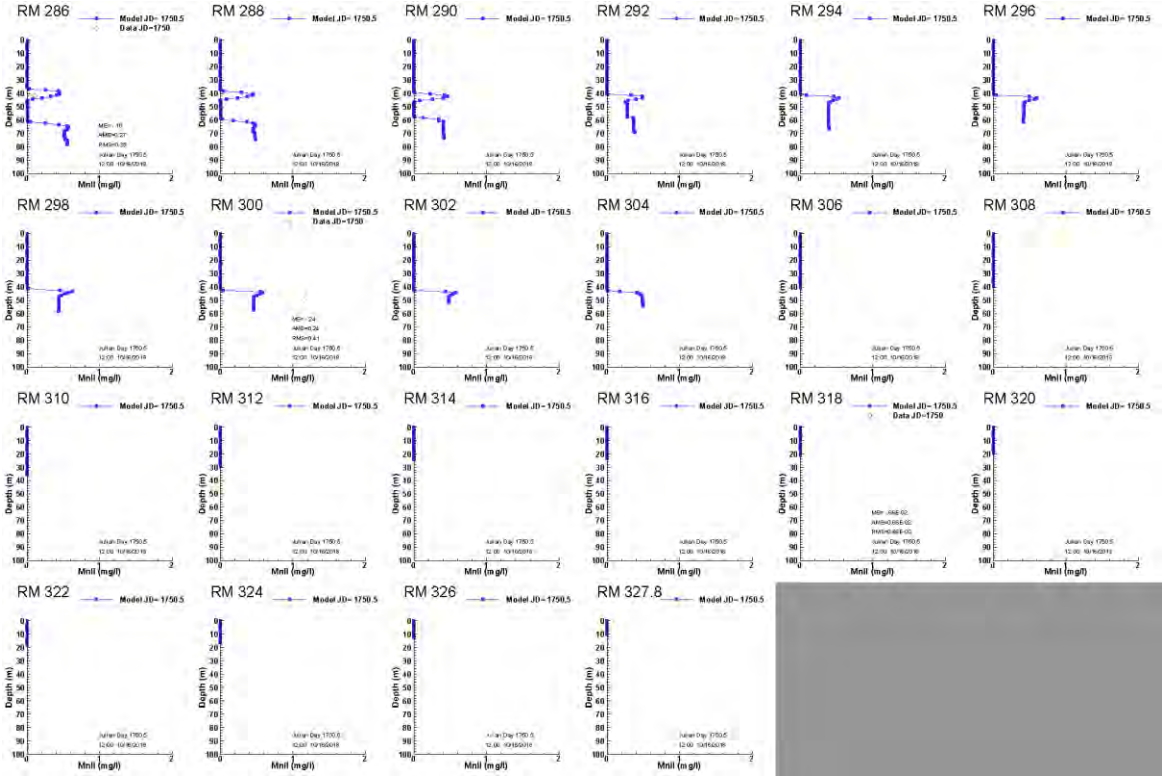


Figure 654. Vertical profiles of Mn(II) compared with data for 10/16/2018.

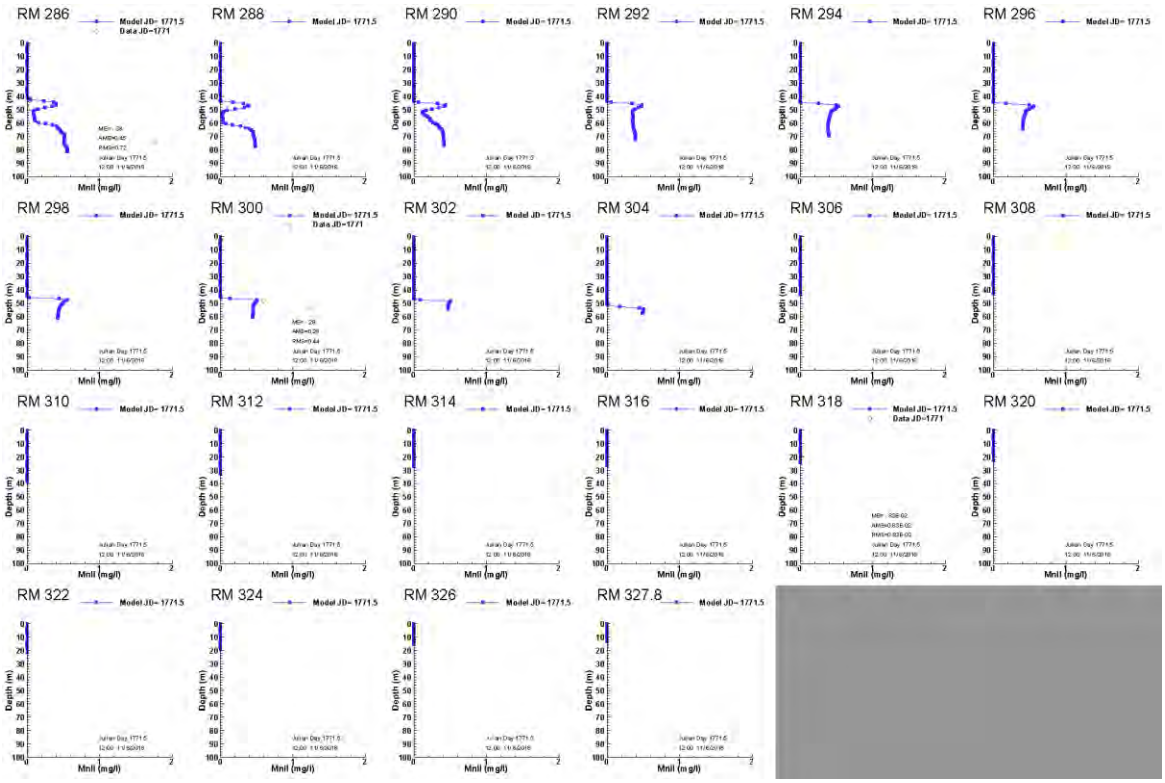


Figure 655. Vertical profiles of Mn(II) compared with data for 11/ 6/2018.

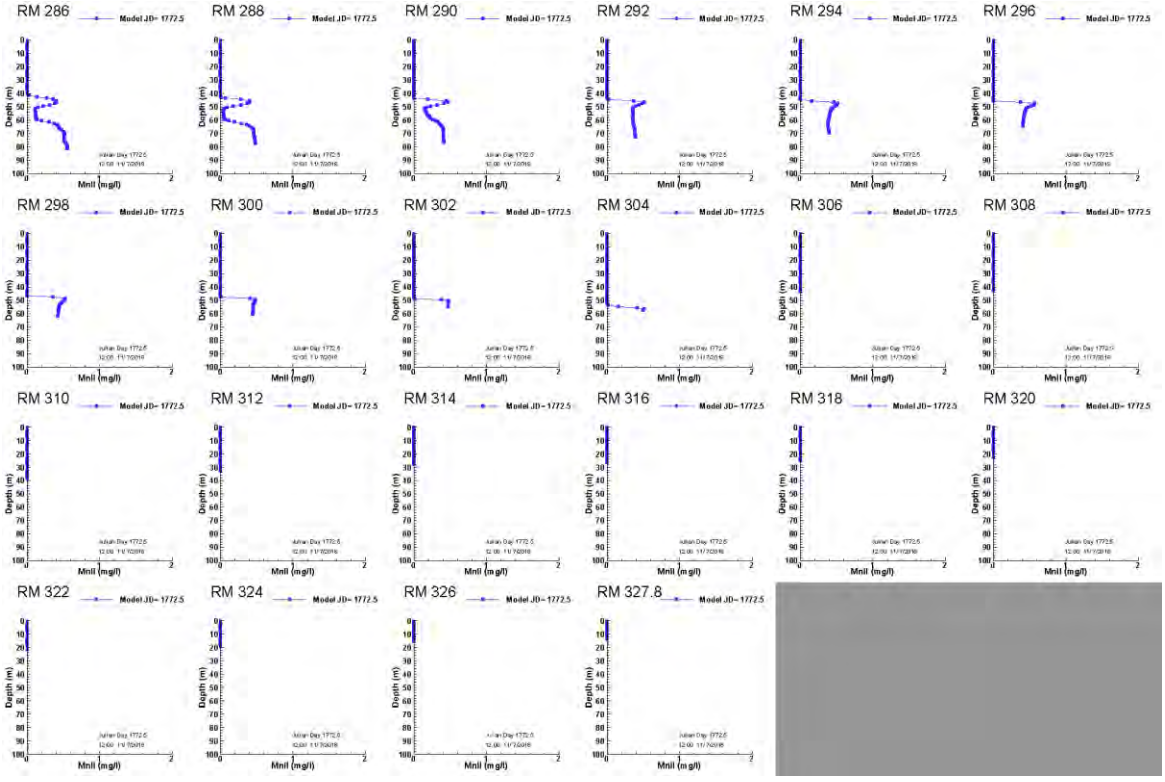


Figure 656. Vertical profiles of Mn(II) compared with data for 11/ 7/2018.

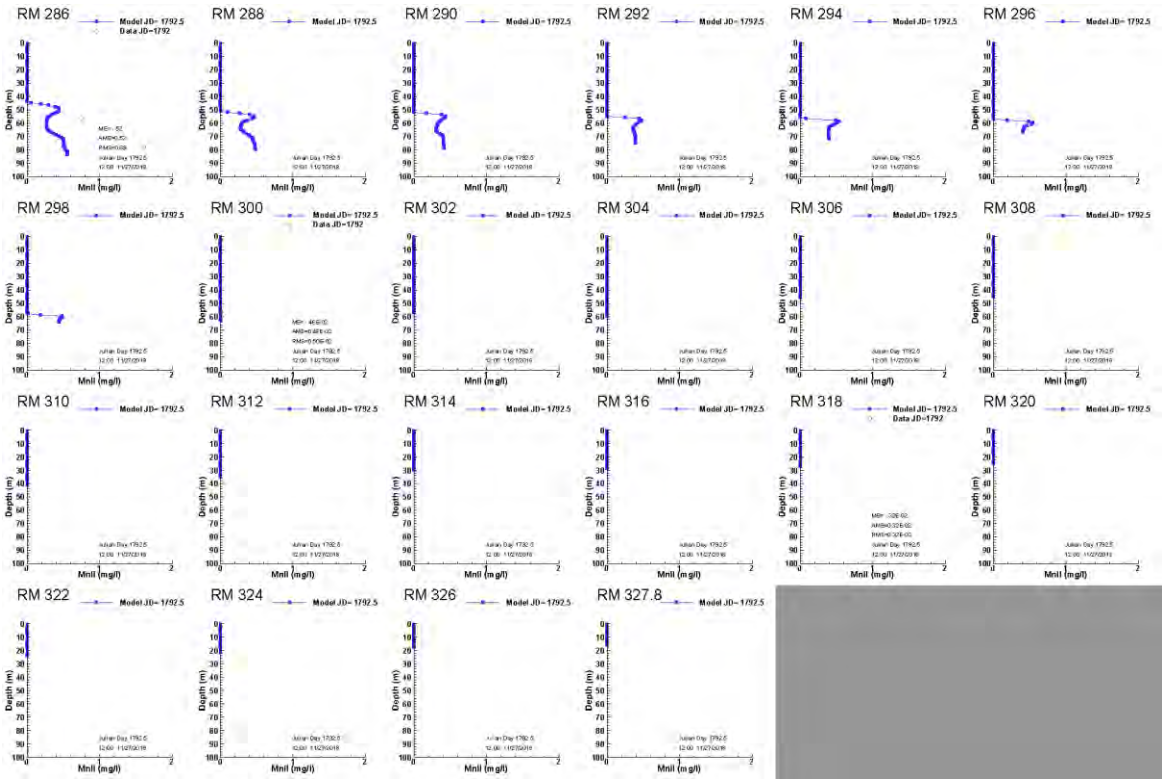


Figure 657. Vertical profiles of Mn(II) compared with data for 11/27/2018.

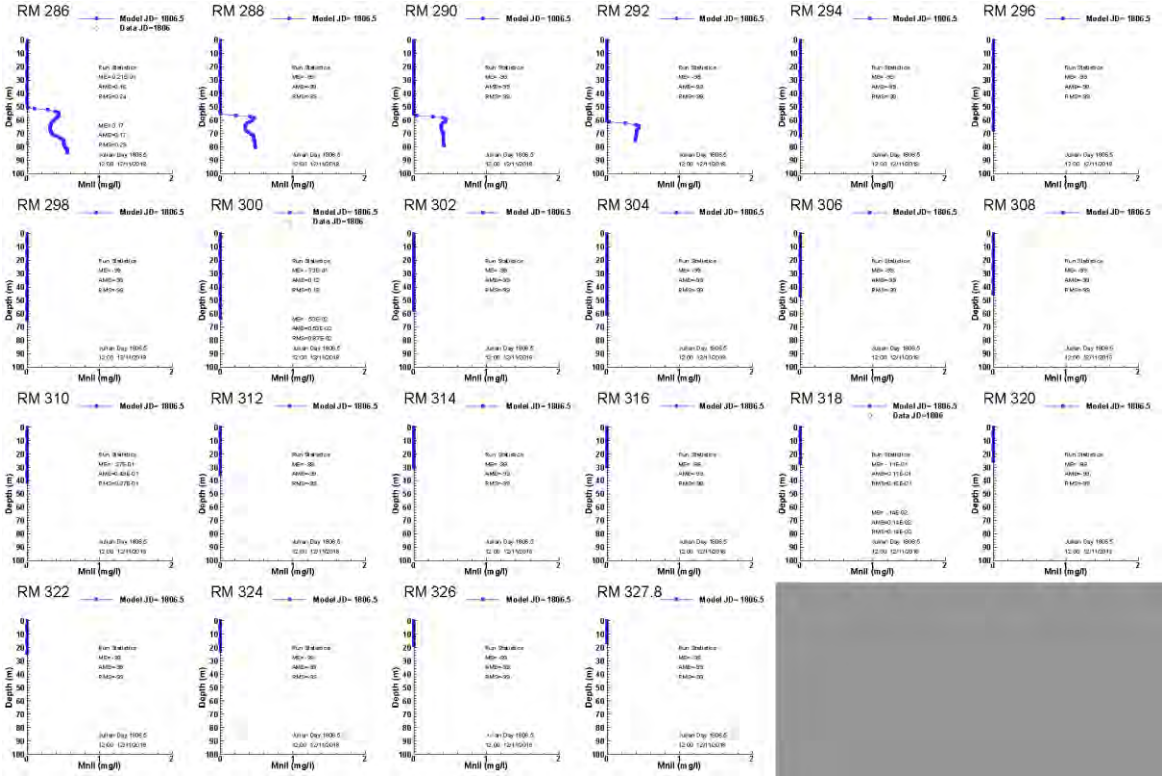


Figure 658. Vertical profiles of Mn(II) compared with data for 12/11/2018.

MnO2

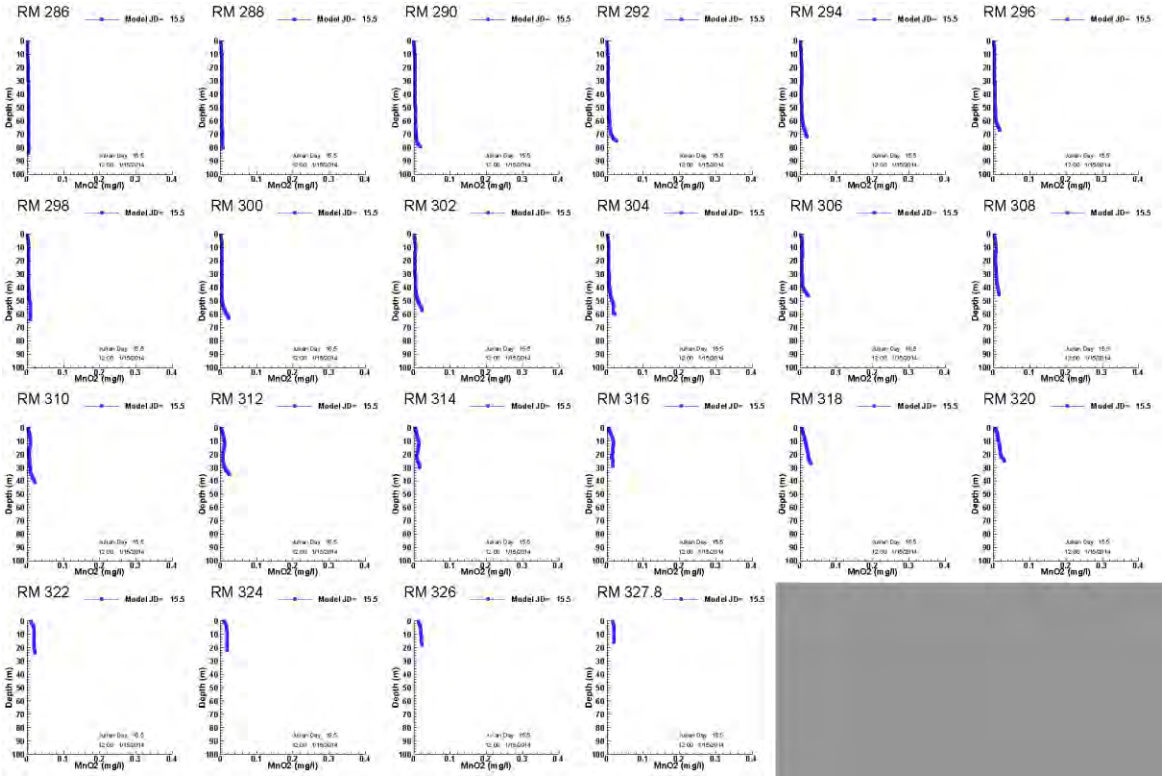


Figure 659. Vertical profiles of MnO2 compared with data for 1/15/2014.

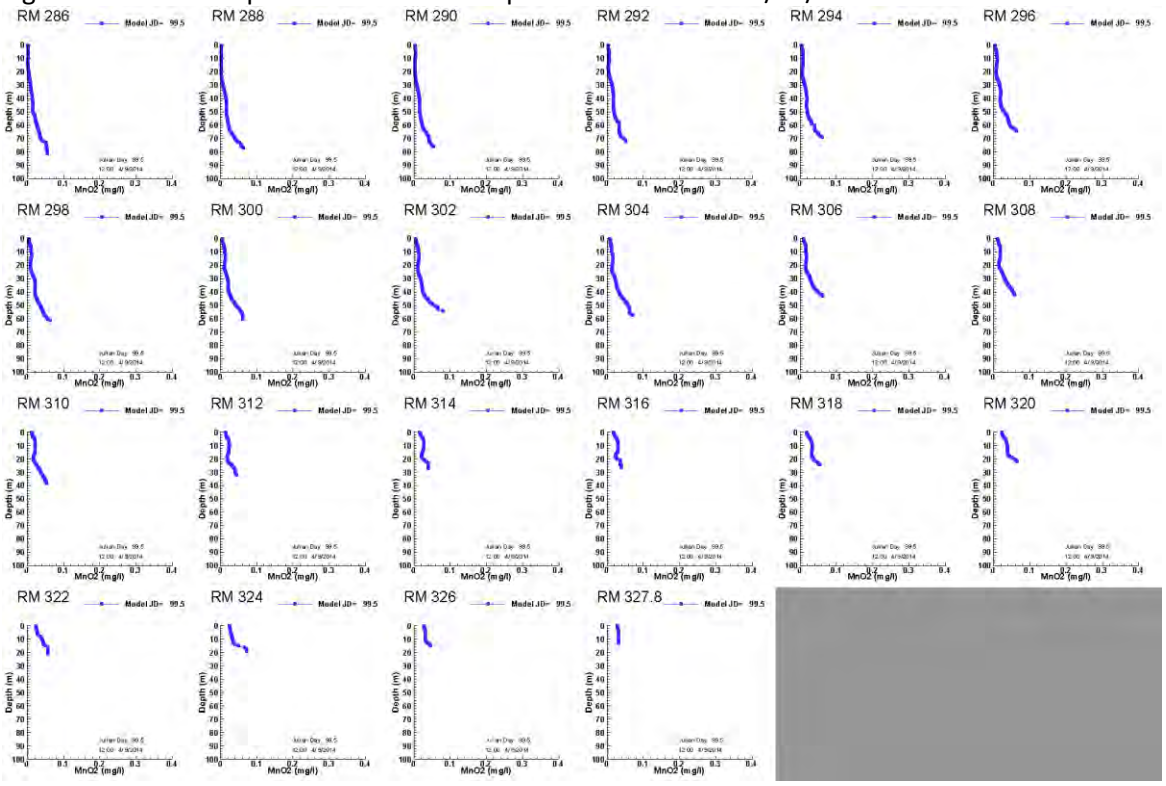


Figure 660. Vertical profiles of MnO2 compared with data for 4/ 9/2014.

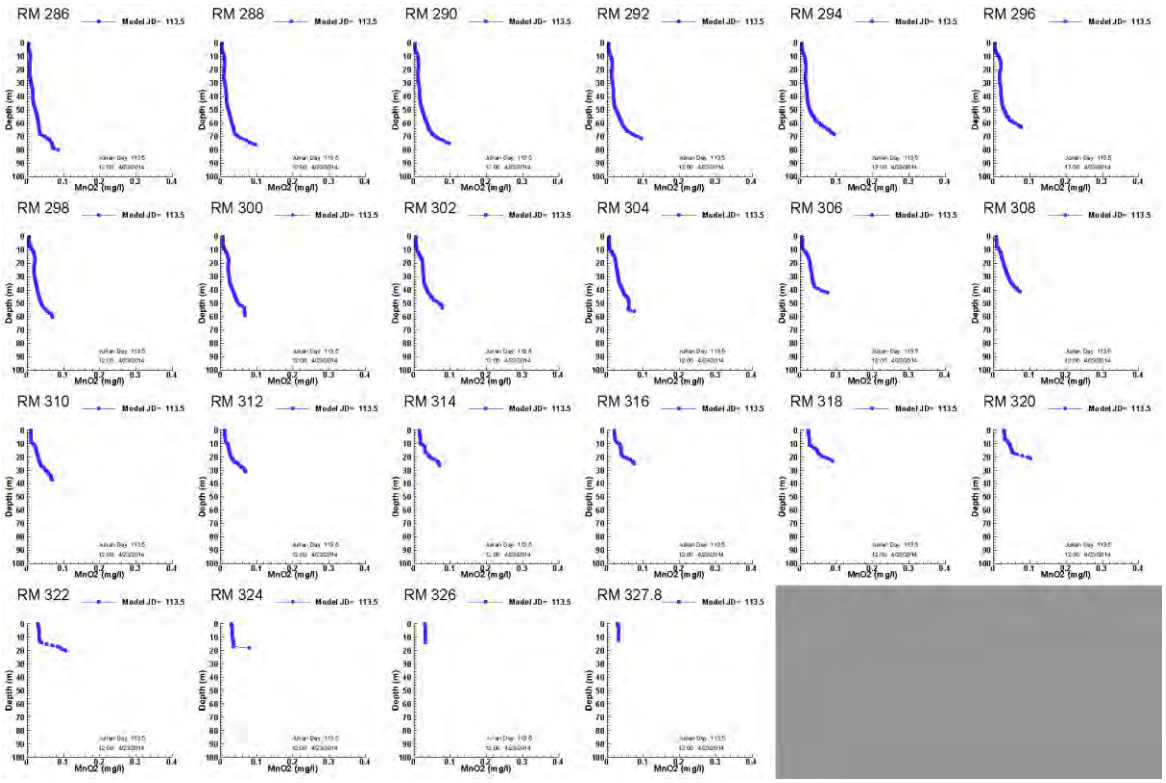


Figure 661. Vertical profiles of MnO2 compared with data for 4/23/2014.

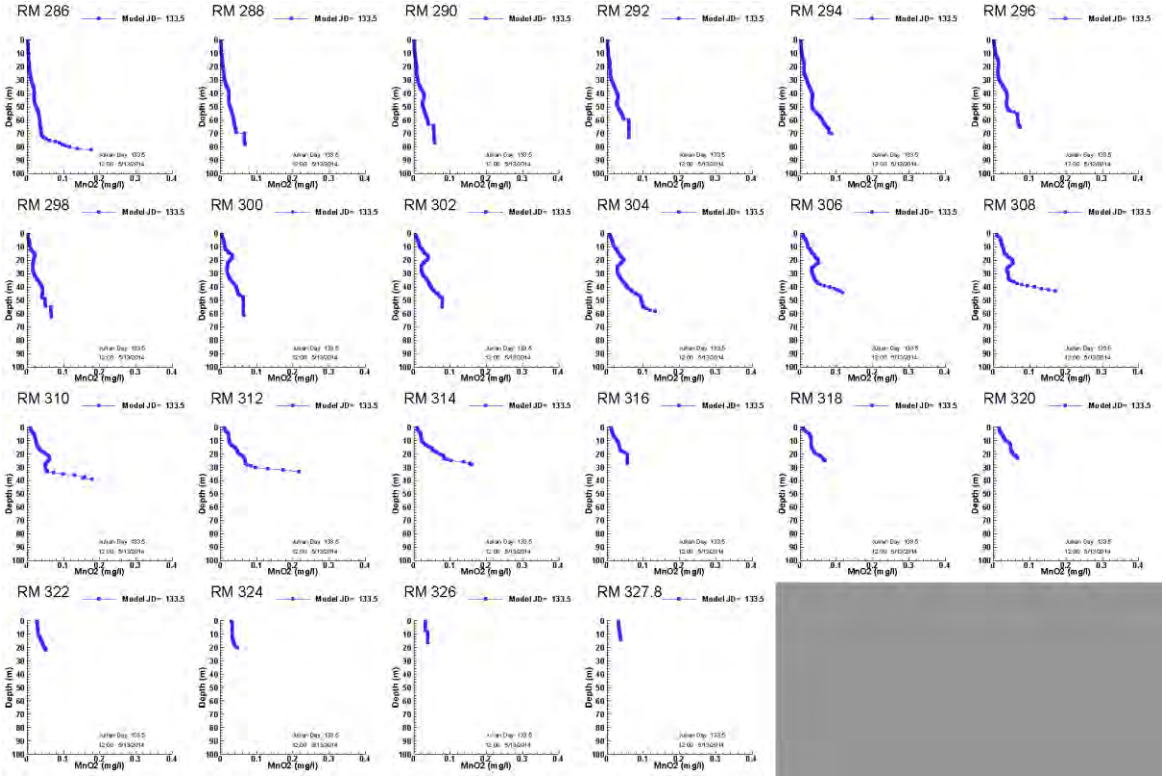


Figure 662. Vertical profiles of MnO2 compared with data for 5/13/2014.

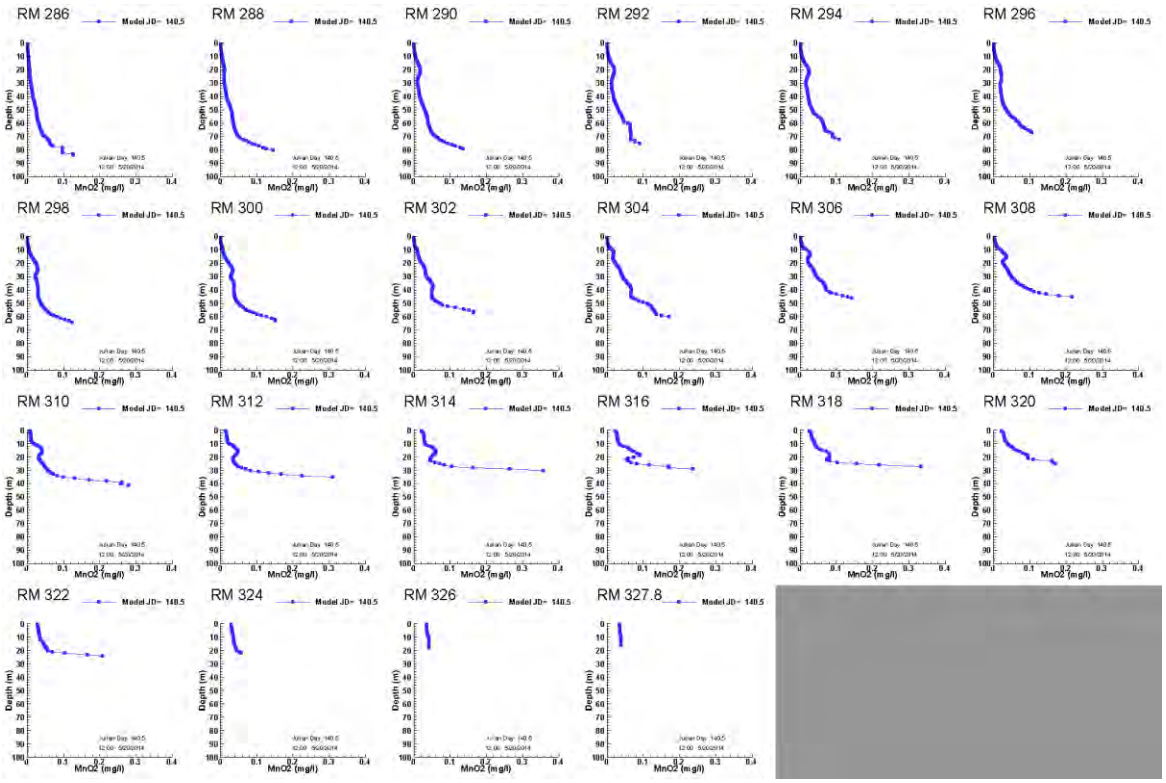


Figure 663. Vertical profiles of MnO2 compared with data for 5/20/2014.

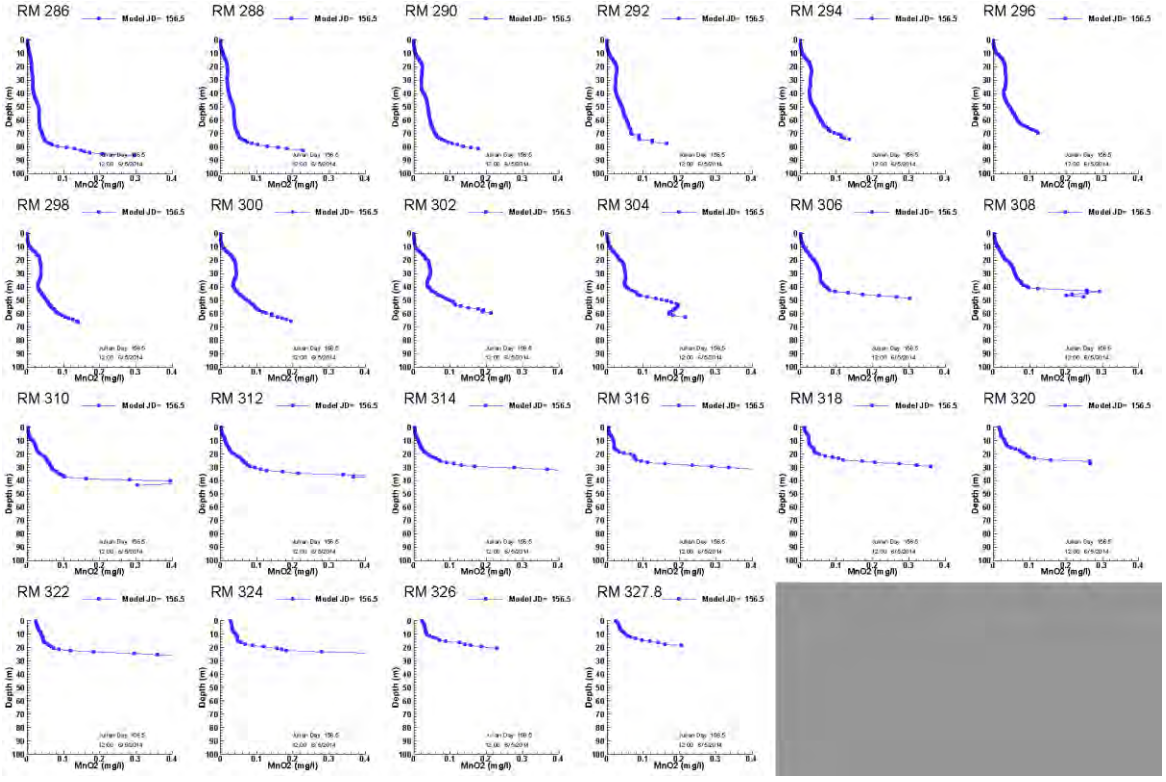


Figure 664. Vertical profiles of MnO2 compared with data for 6/ 5/2014.

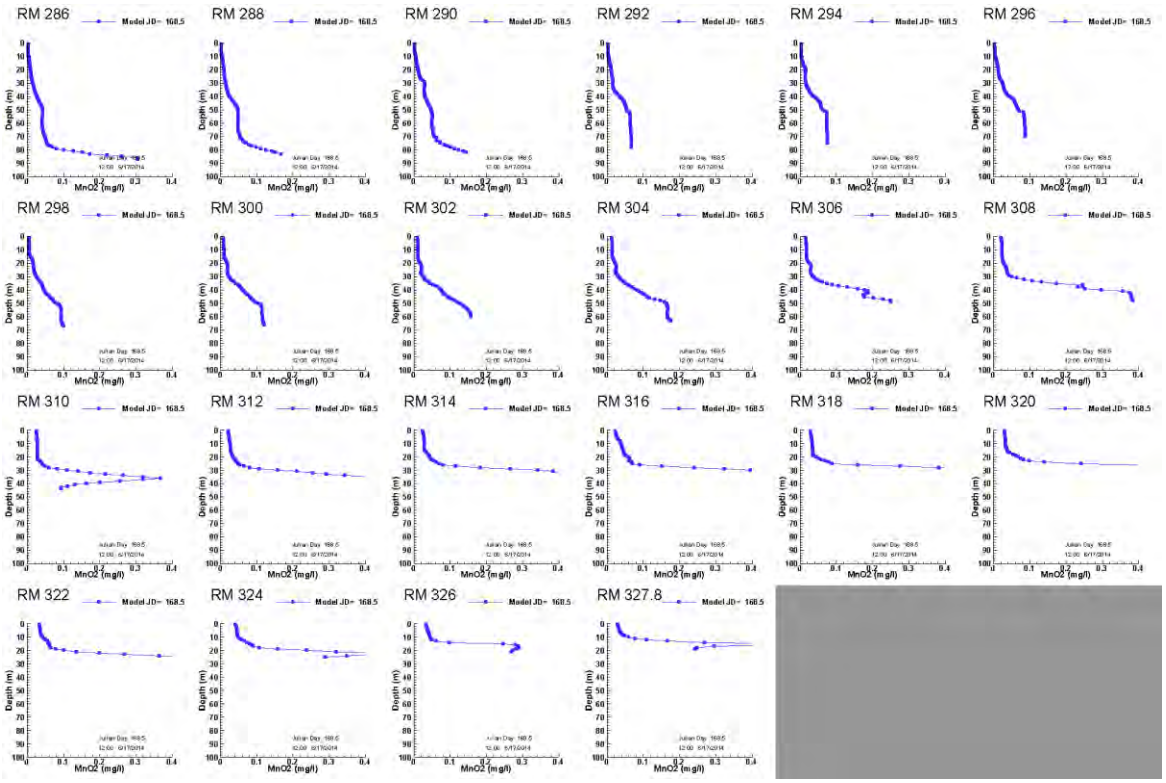


Figure 665. Vertical profiles of MnO2 compared with data for 6/17/2014.

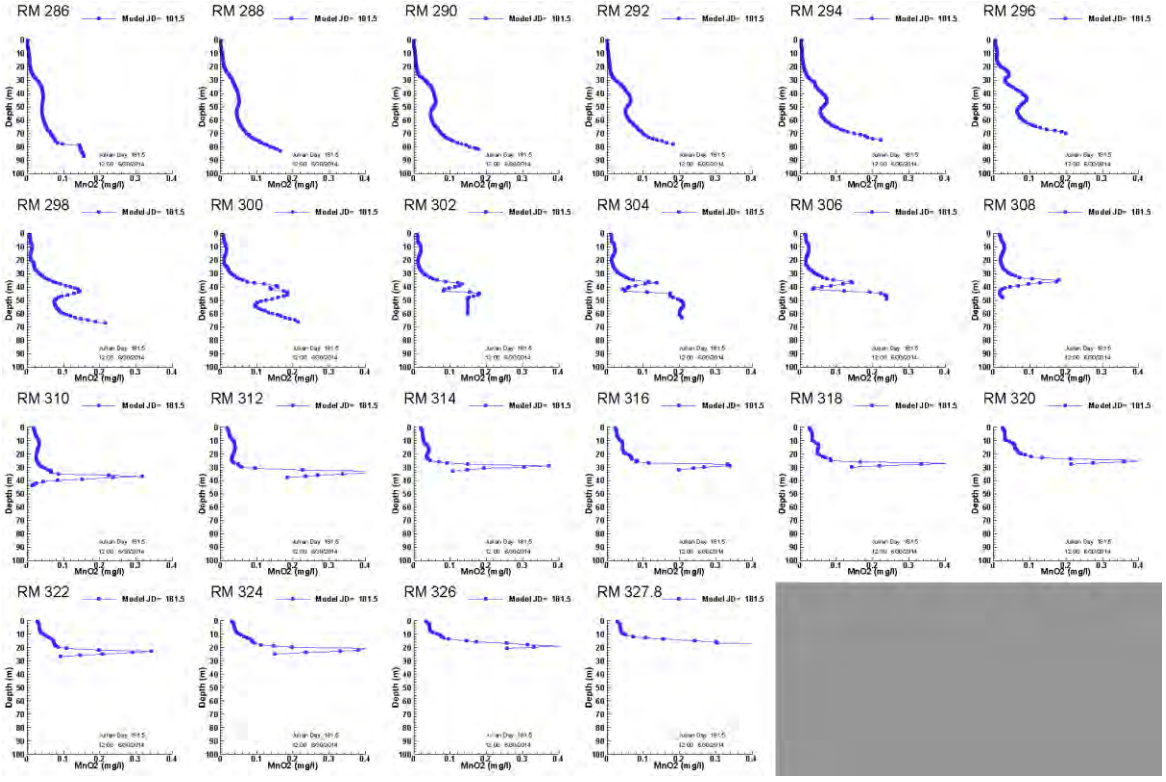


Figure 666. Vertical profiles of MnO2 compared with data for 6/30/2014.

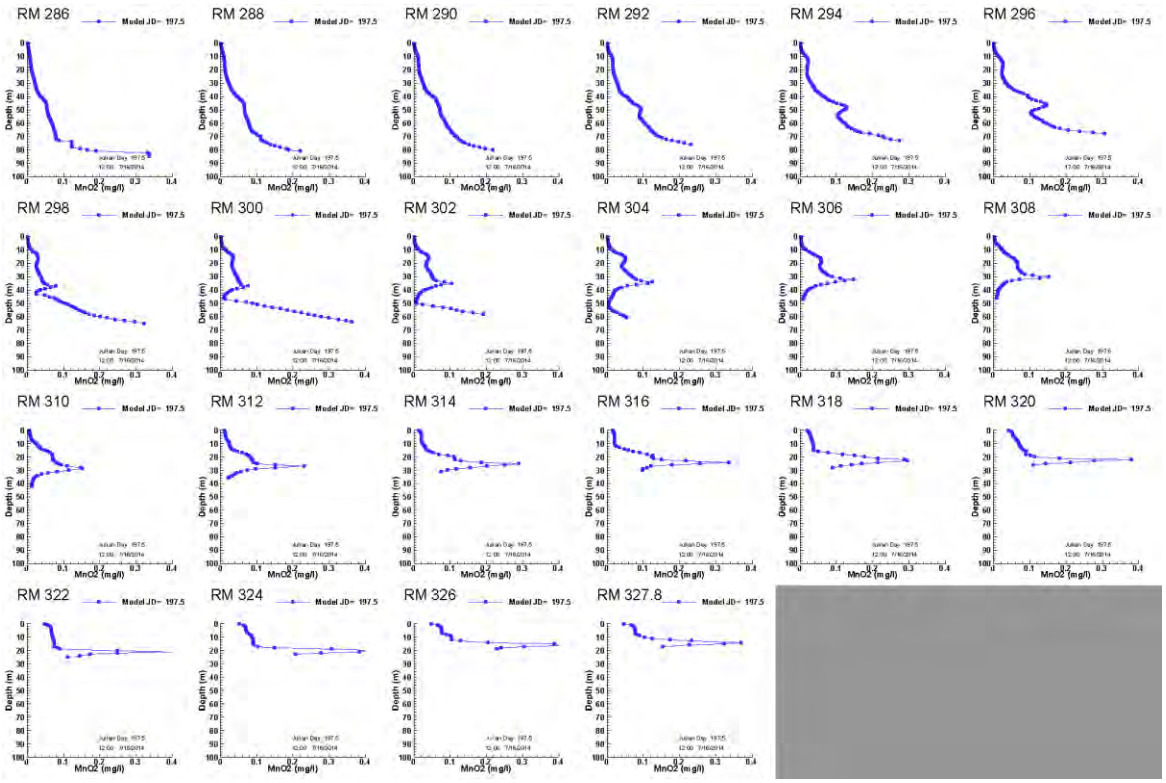


Figure 667. Vertical profiles of MnO2 compared with data for 7/16/2014.

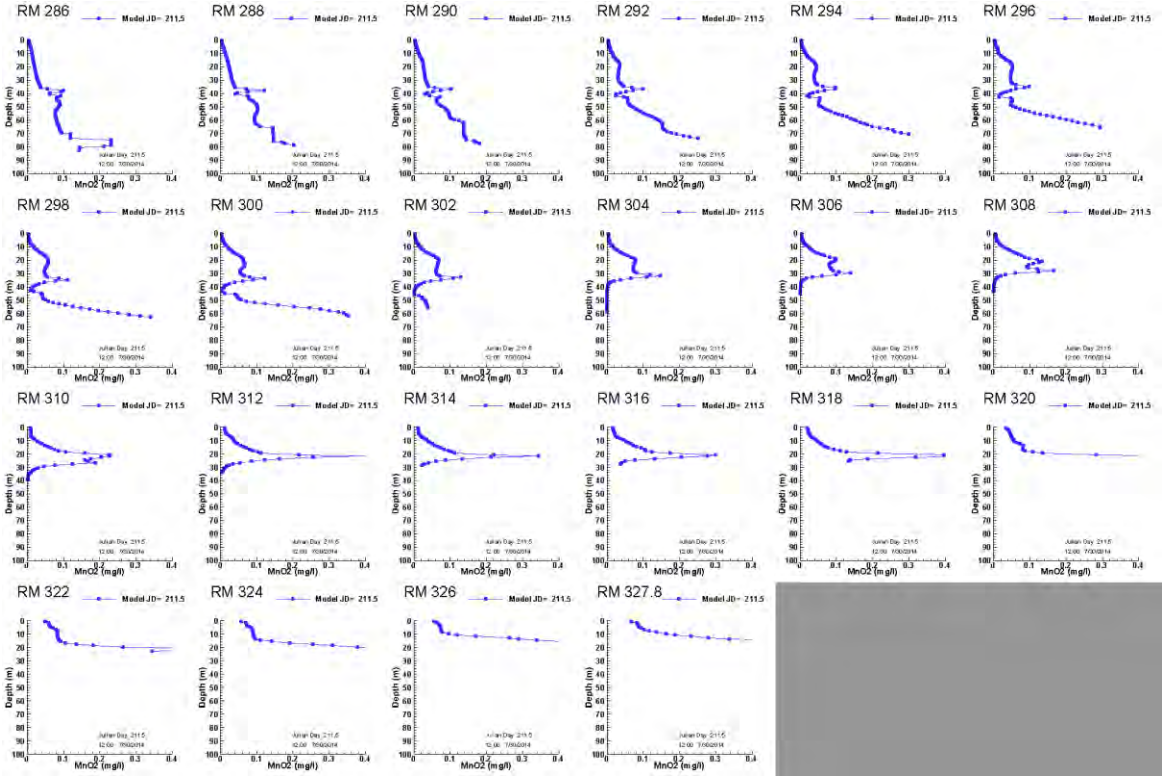


Figure 668. Vertical profiles of MnO2 compared with data for 7/30/2014.

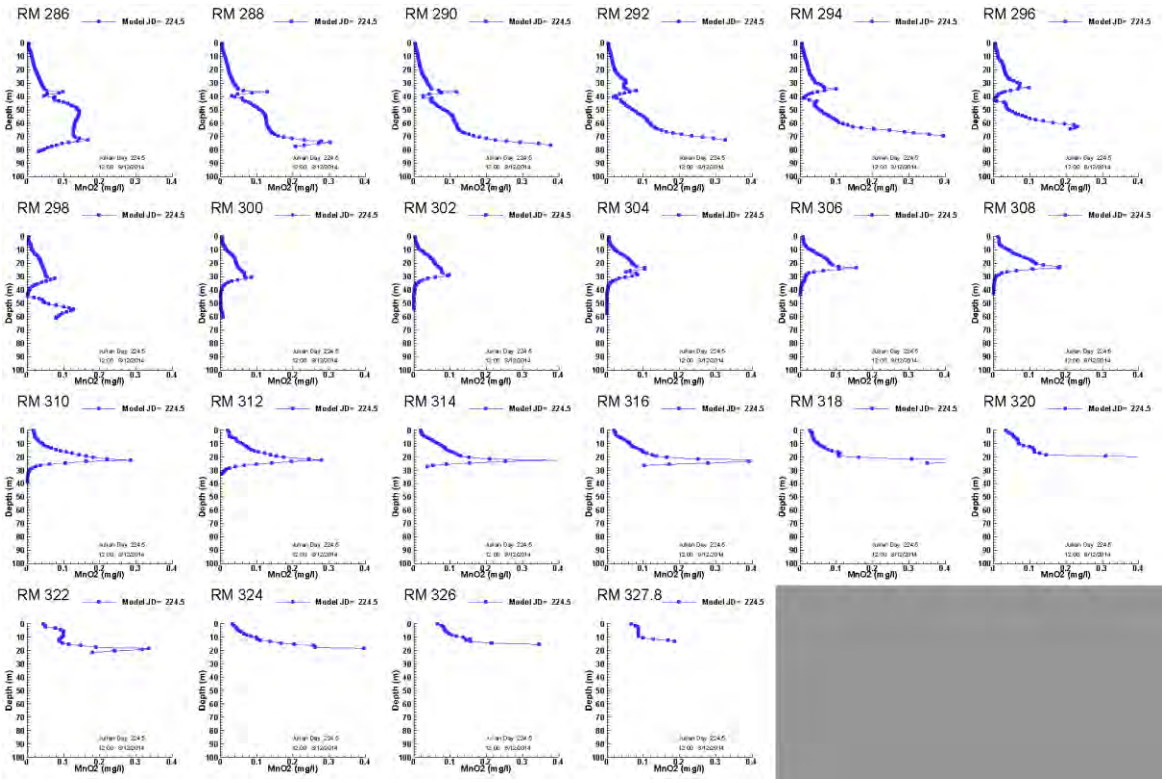


Figure 669. Vertical profiles of MnO2 compared with data for 8/12/2014.

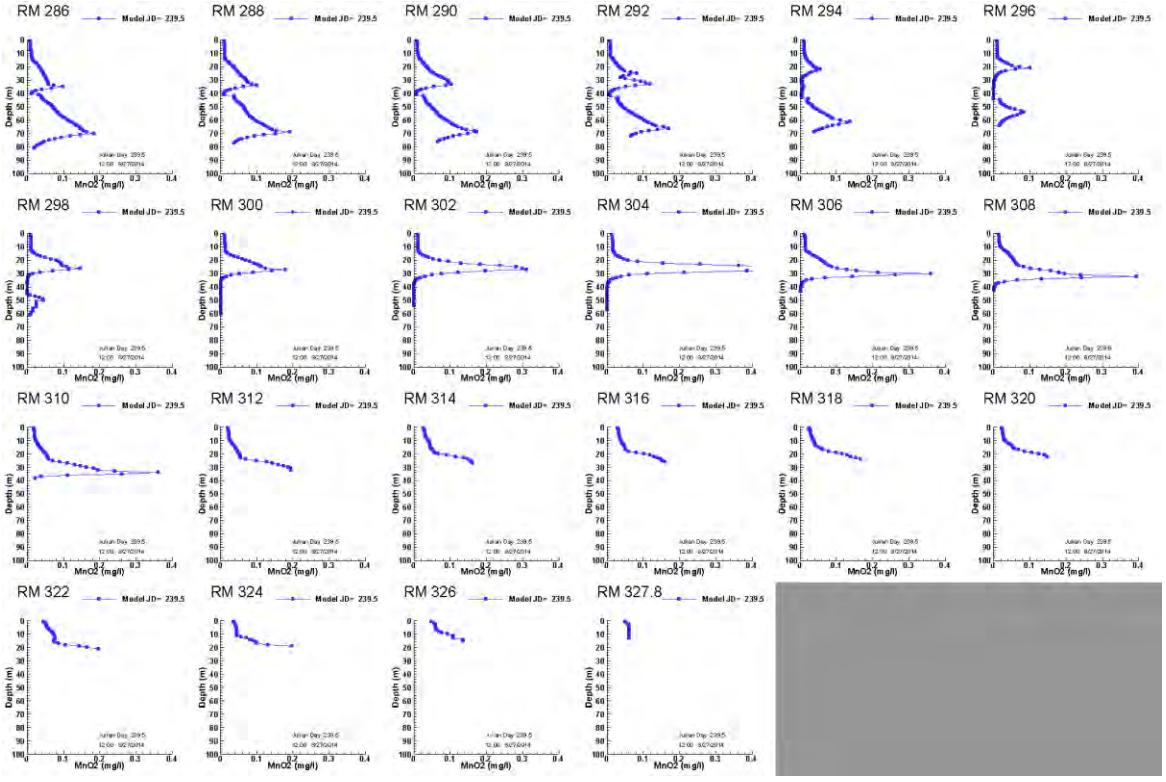


Figure 670. Vertical profiles of MnO2 compared with data for 8/27/2014.

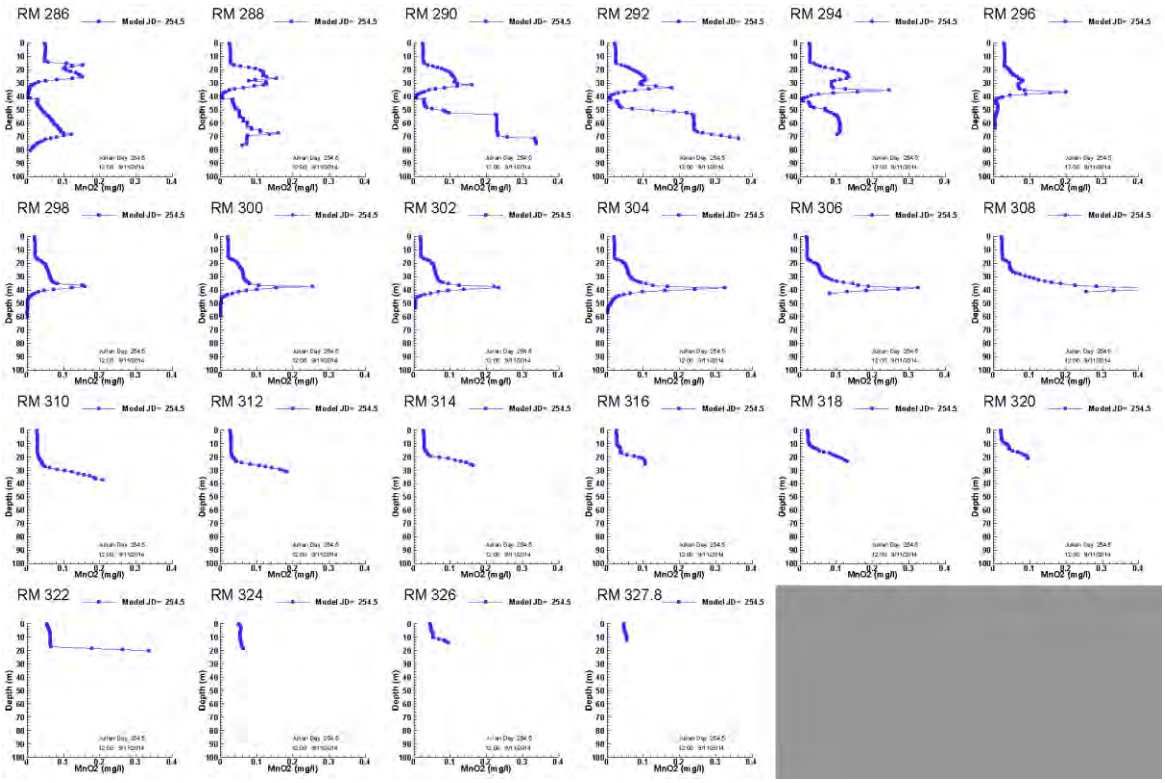


Figure 671. Vertical profiles of MnO2 compared with data for 9/11/2014.

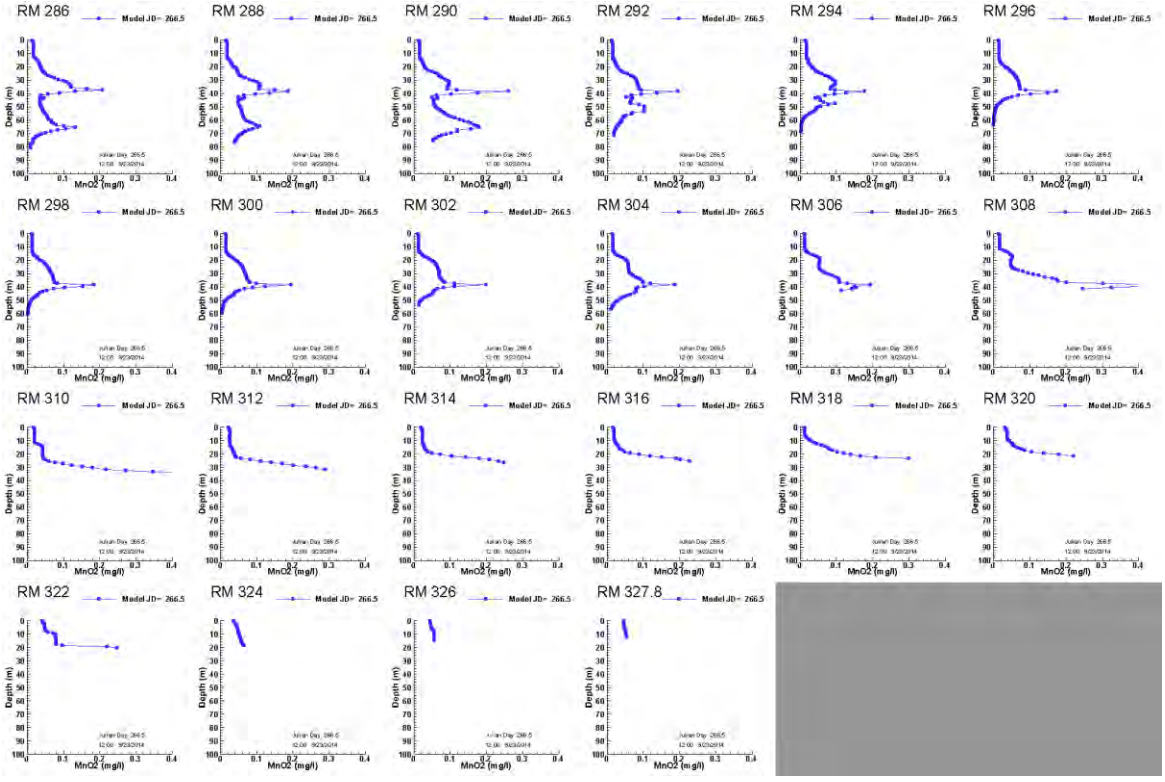


Figure 672. Vertical profiles of MnO2 compared with data for 9/23/2014.

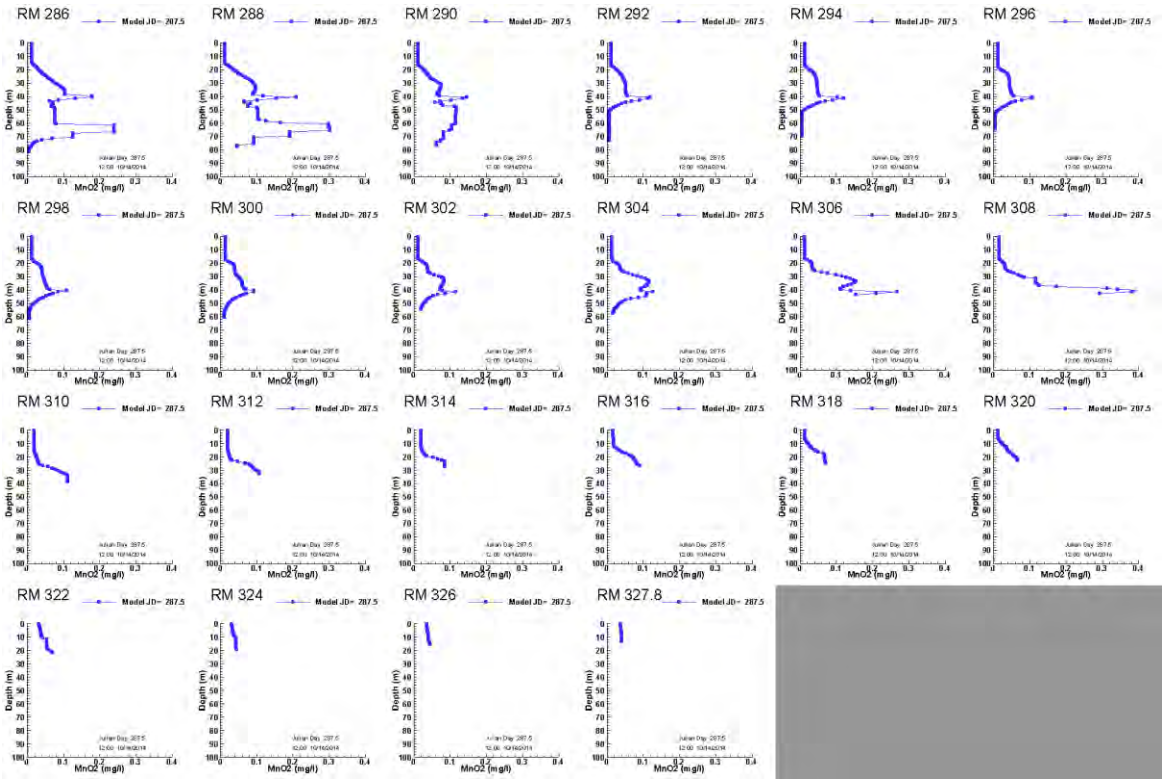


Figure 673. Vertical profiles of MnO2 compared with data for 10/14/2014.

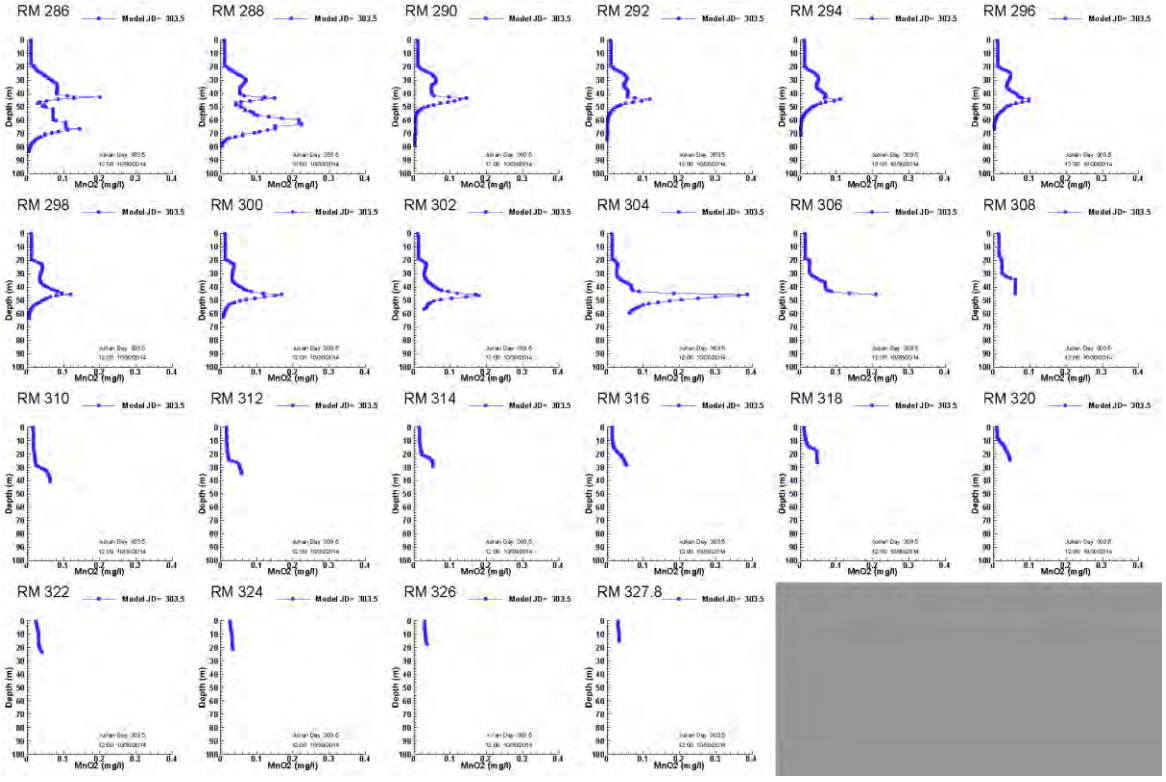


Figure 674. Vertical profiles of MnO2 compared with data for 10/30/2014.

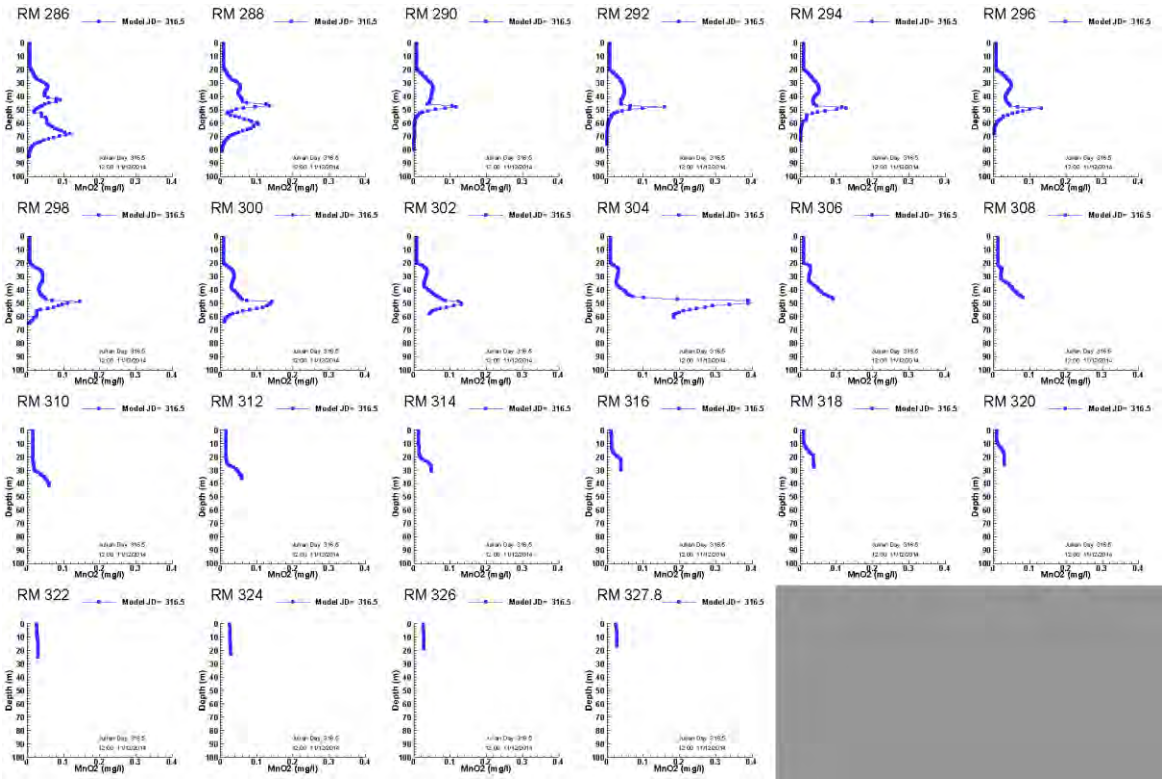


Figure 675. Vertical profiles of MnO2 compared with data for 11/12/2014.

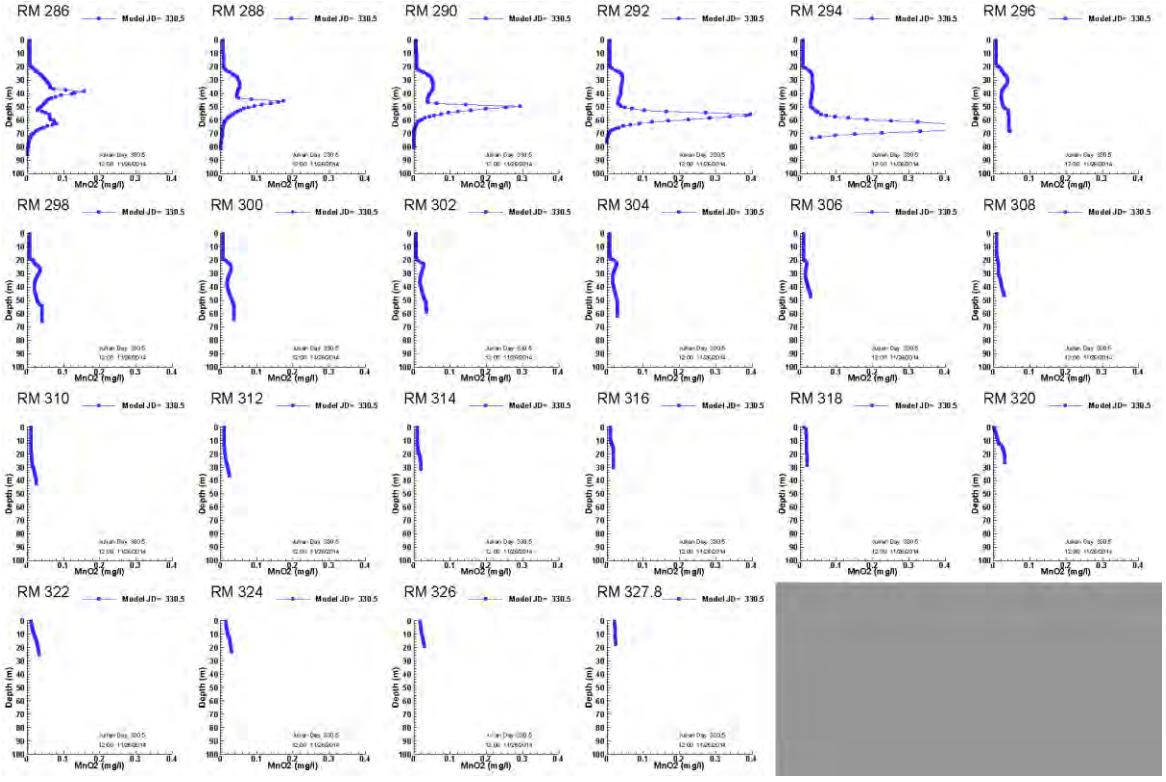


Figure 676. Vertical profiles of MnO2 compared with data for 11/26/2014.

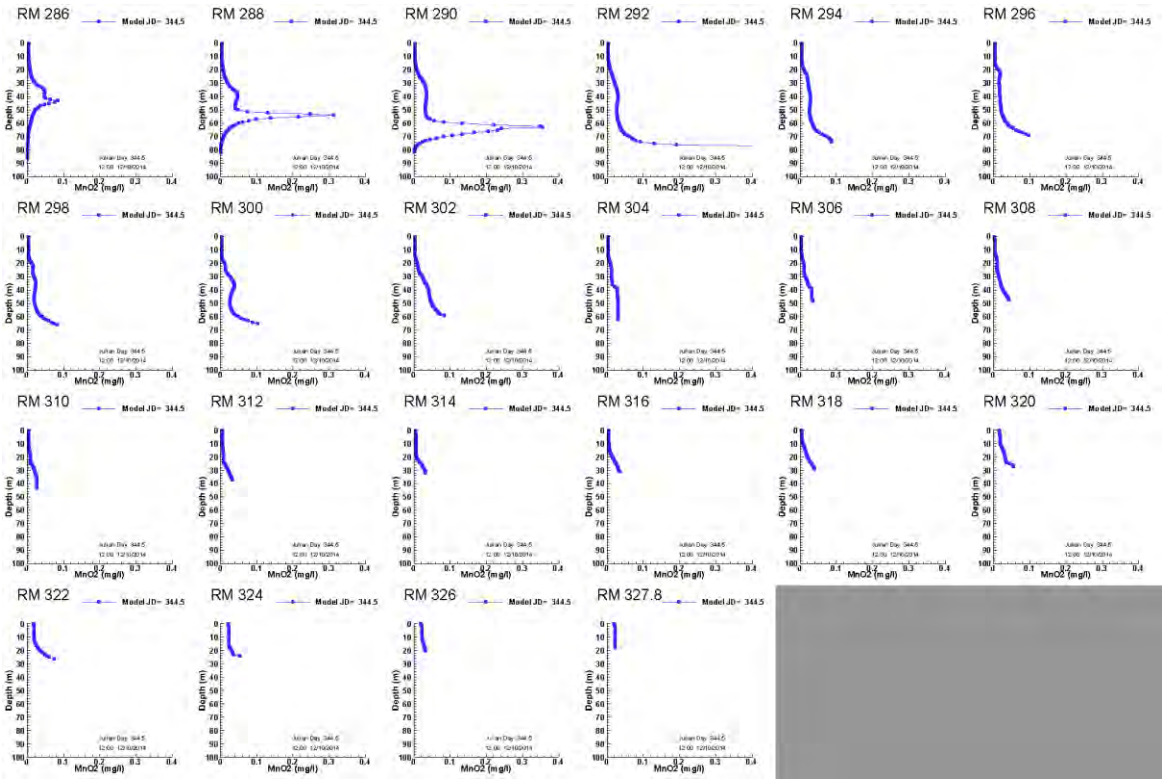


Figure 677. Vertical profiles of MnO2 compared with data for 12/10/2014.

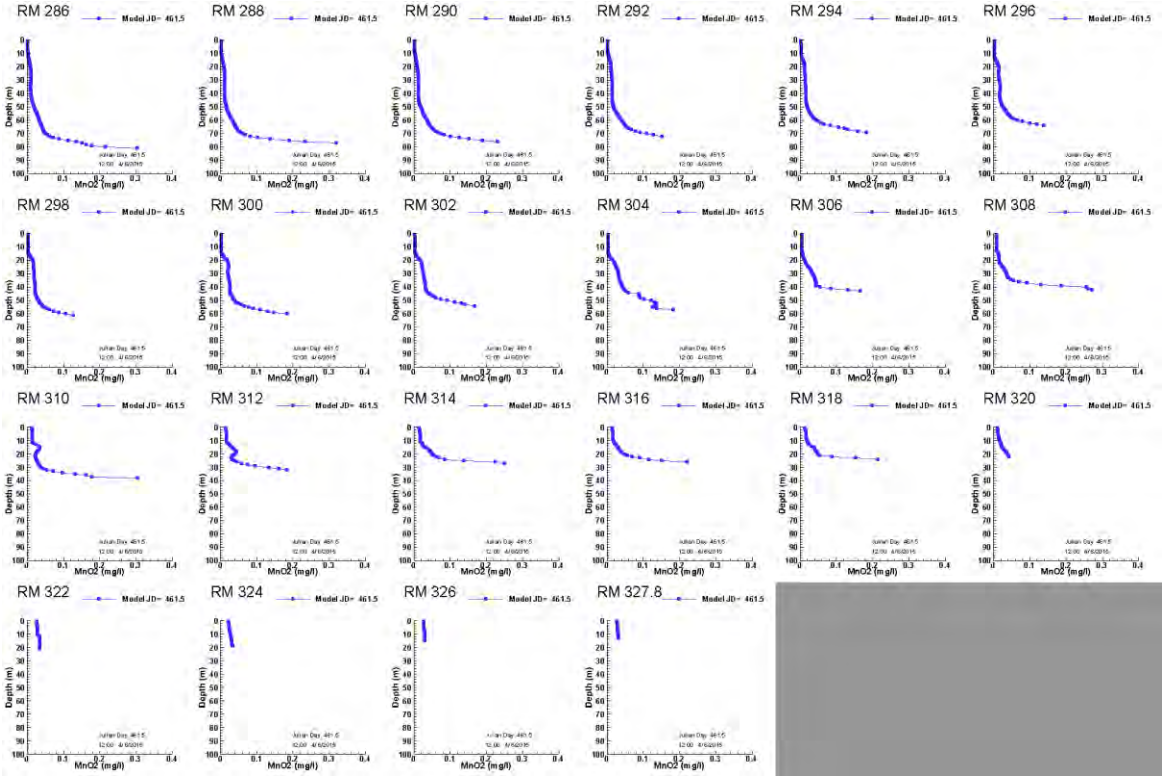


Figure 678. Vertical profiles of MnO2 compared with data for 4/ 6/2015.

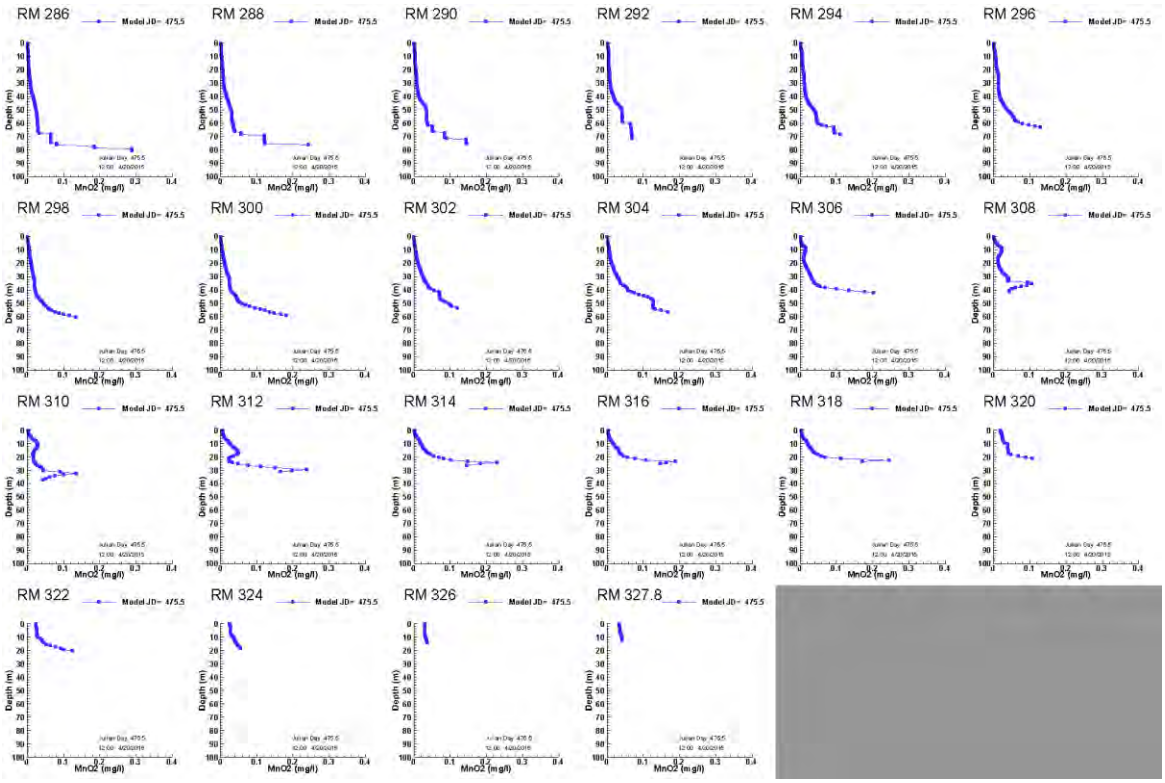


Figure 679. Vertical profiles of MnO2 compared with data for 4/20/2015.

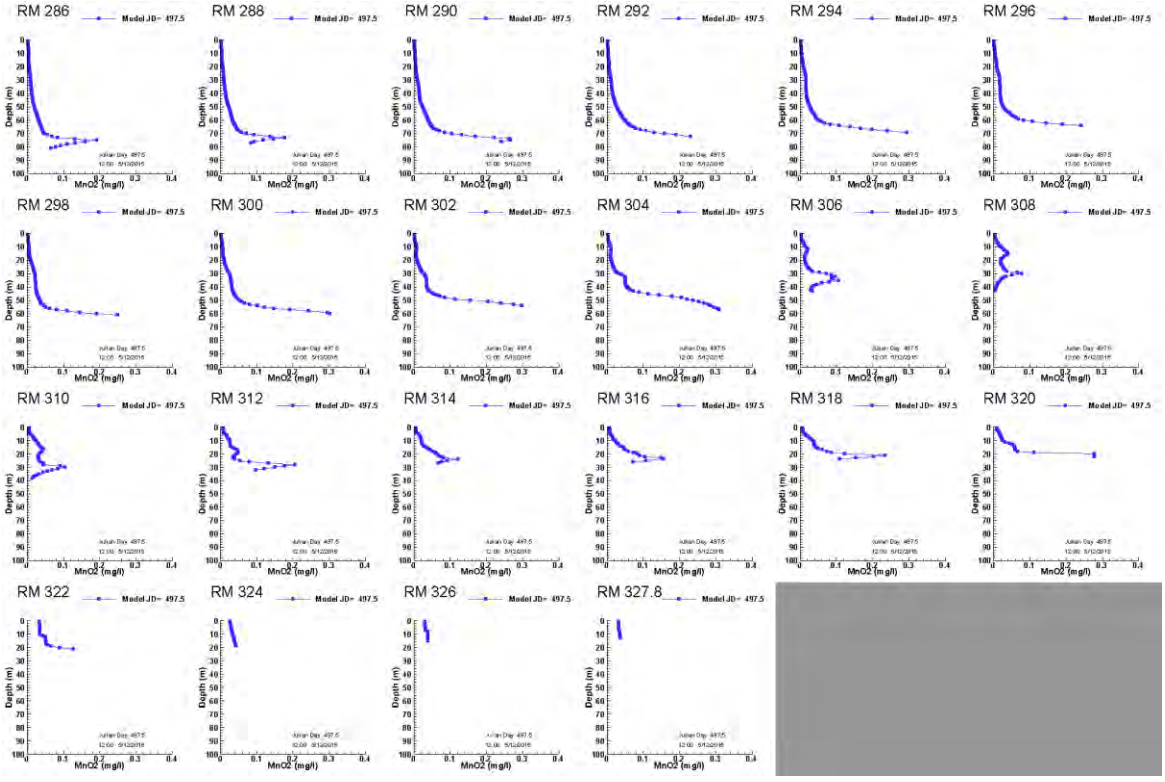


Figure 680. Vertical profiles of MnO2 compared with data for 5/12/2015.

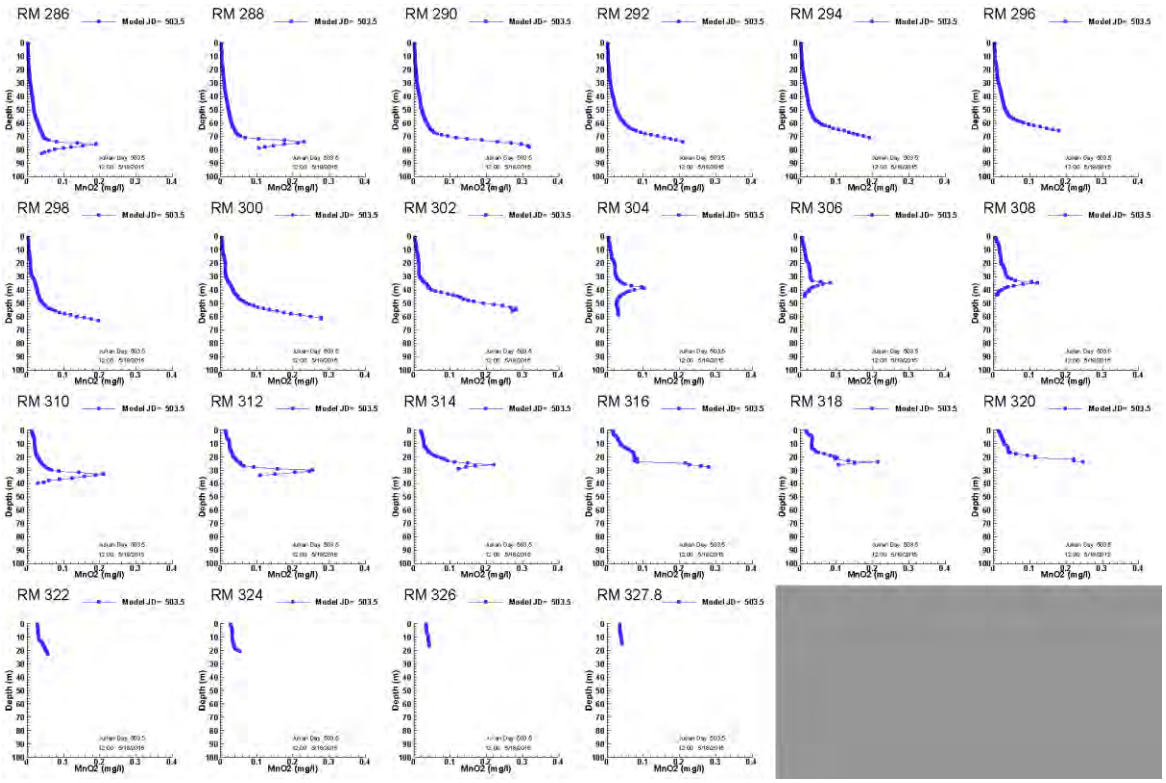


Figure 681. Vertical profiles of MnO2 compared with data for 5/18/2015.

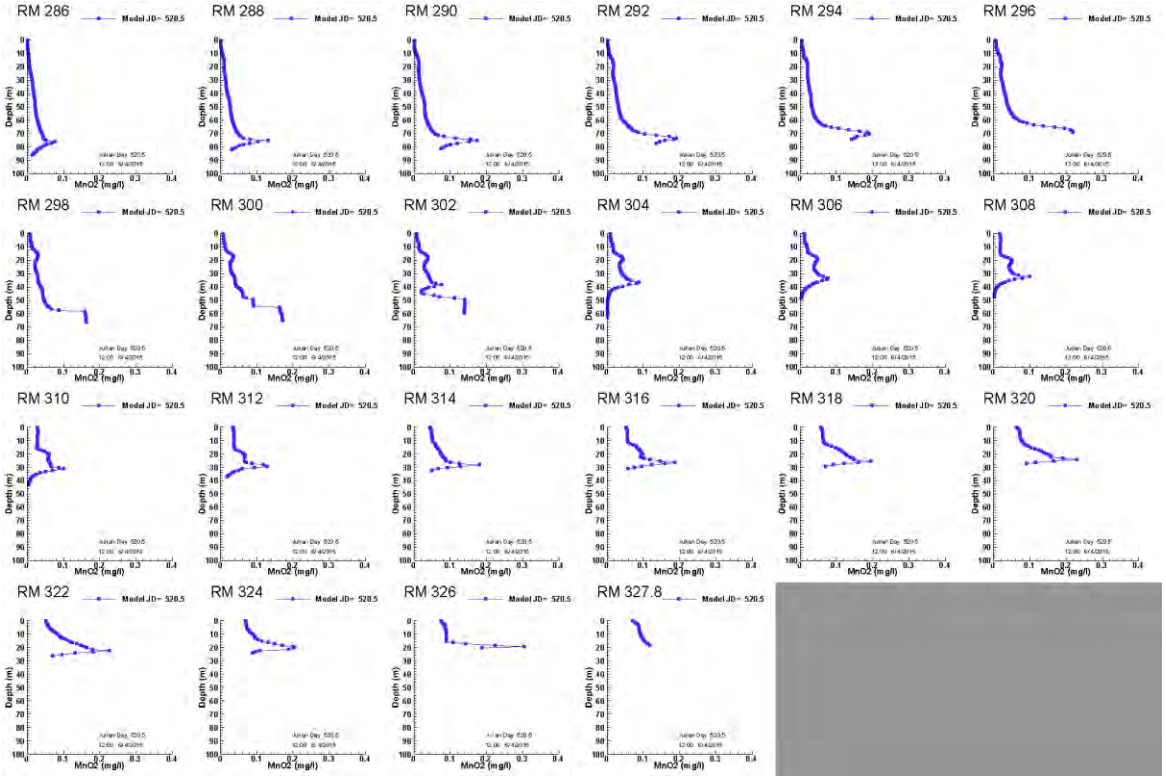


Figure 682. Vertical profiles of MnO2 compared with data for 6/ 4/2015.

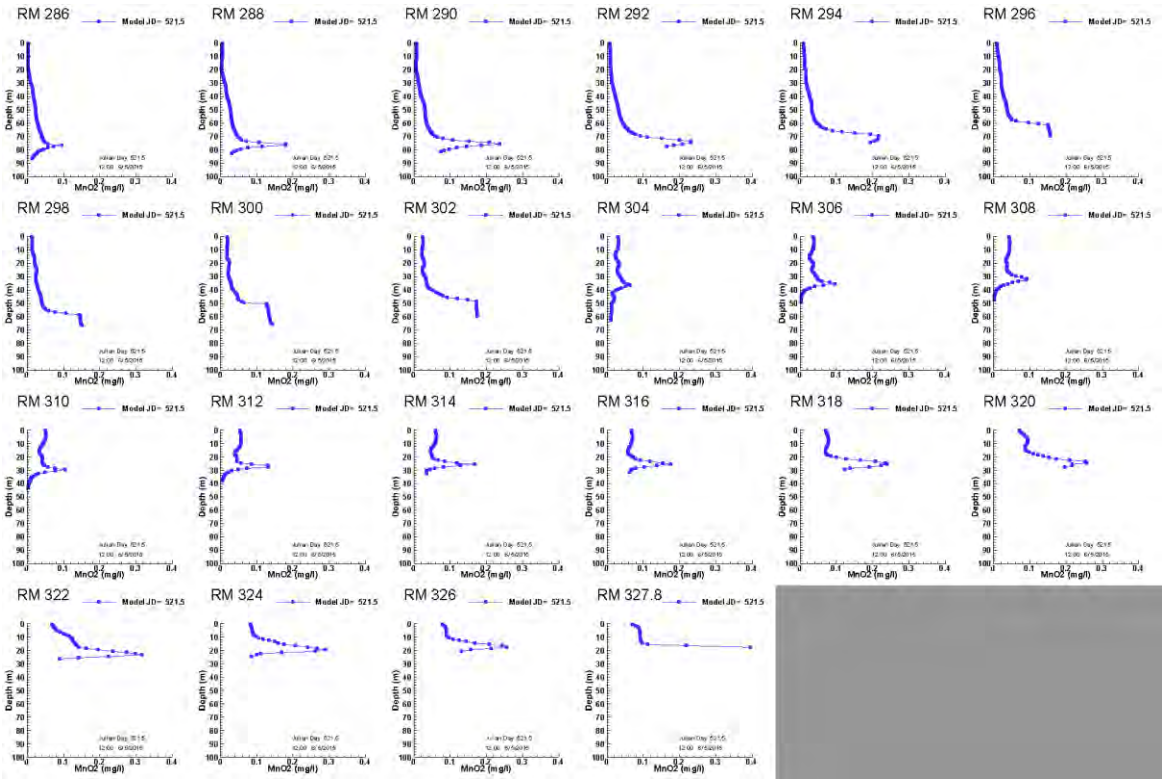


Figure 683. Vertical profiles of MnO2 compared with data for 6/ 5/2015.

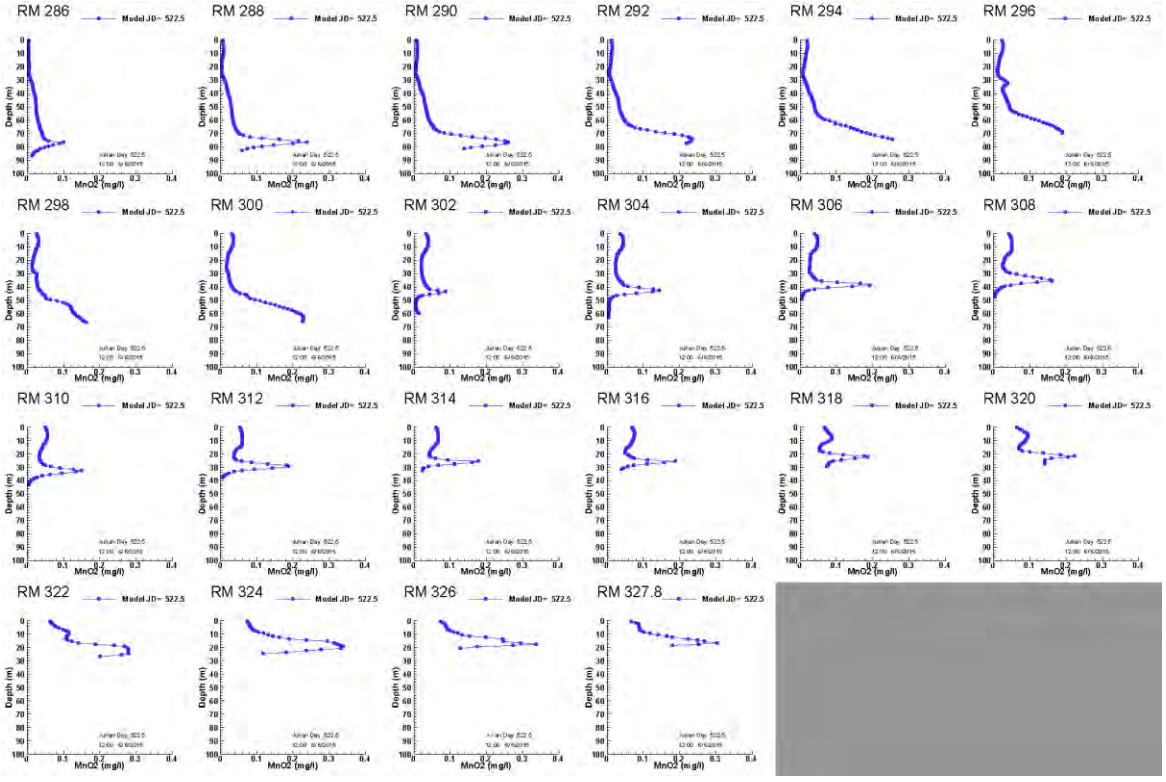


Figure 684. Vertical profiles of MnO2 compared with data for 6/ 6/2015.

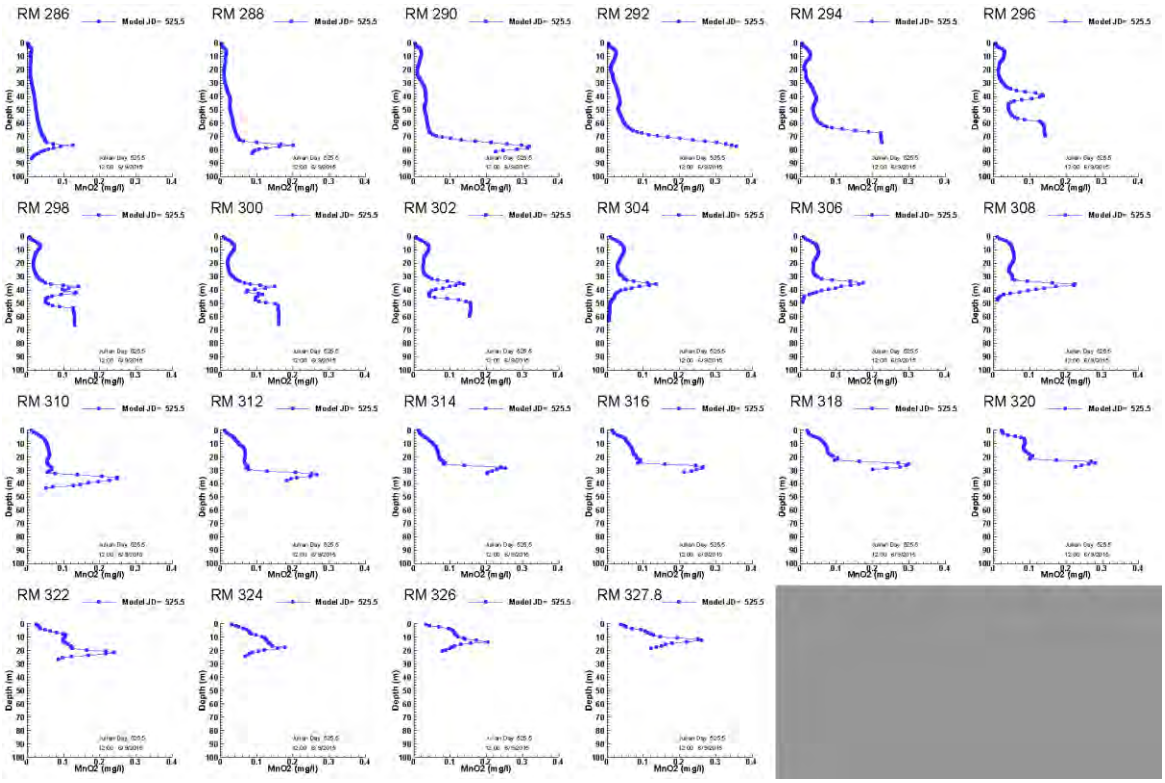


Figure 685. Vertical profiles of MnO2 compared with data for 6/ 9/2015.

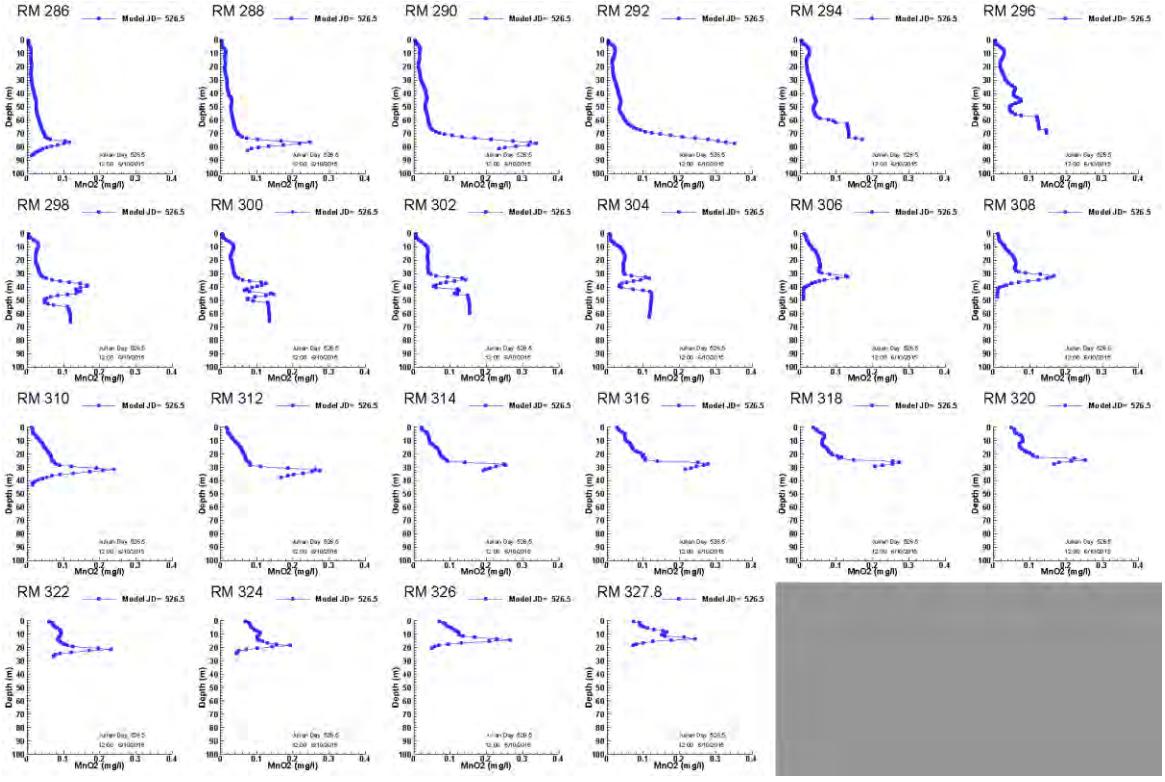


Figure 686. Vertical profiles of MnO2 compared with data for 6/10/2015.

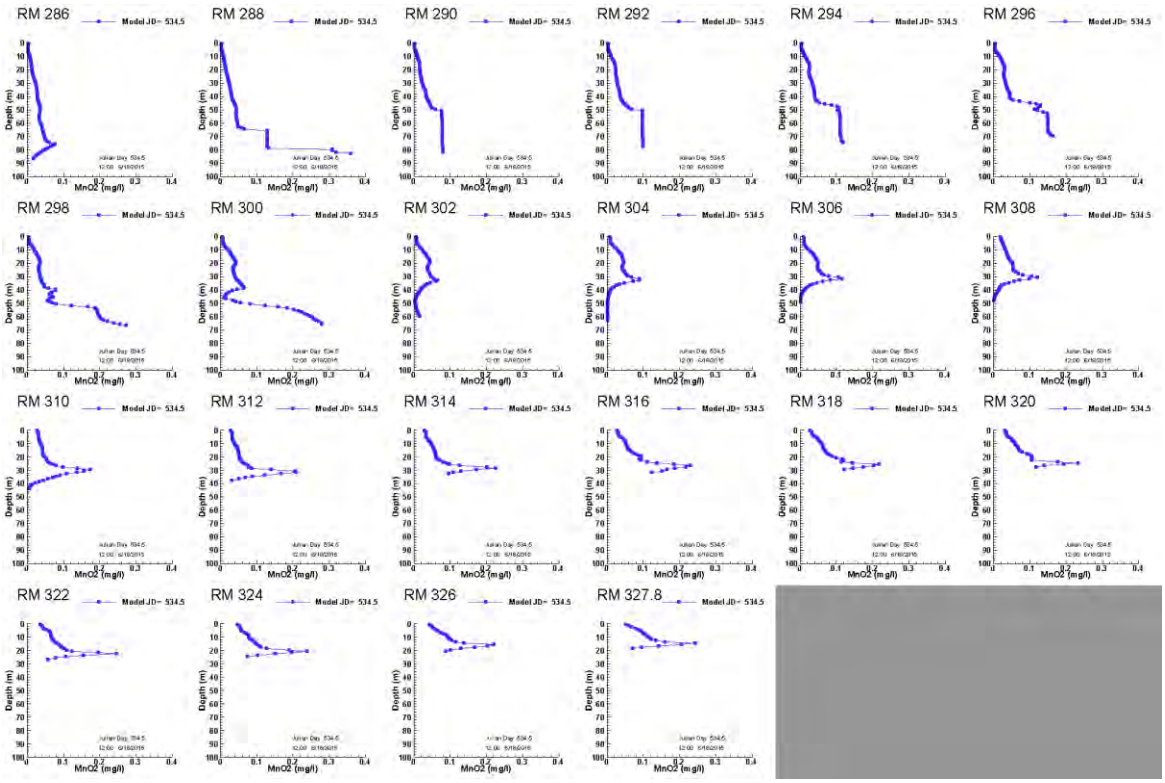


Figure 687. Vertical profiles of MnO2 compared with data for 6/18/2015.

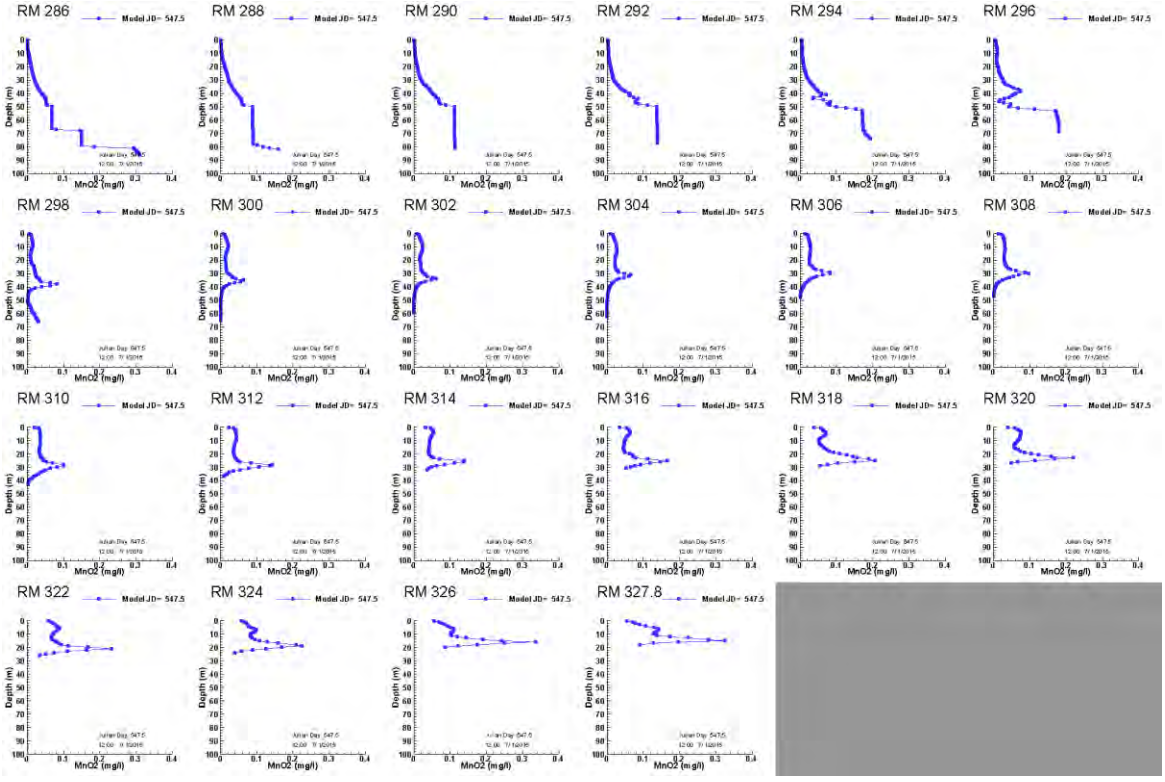


Figure 688. Vertical profiles of MnO2 compared with data for 7/ 1/2015.

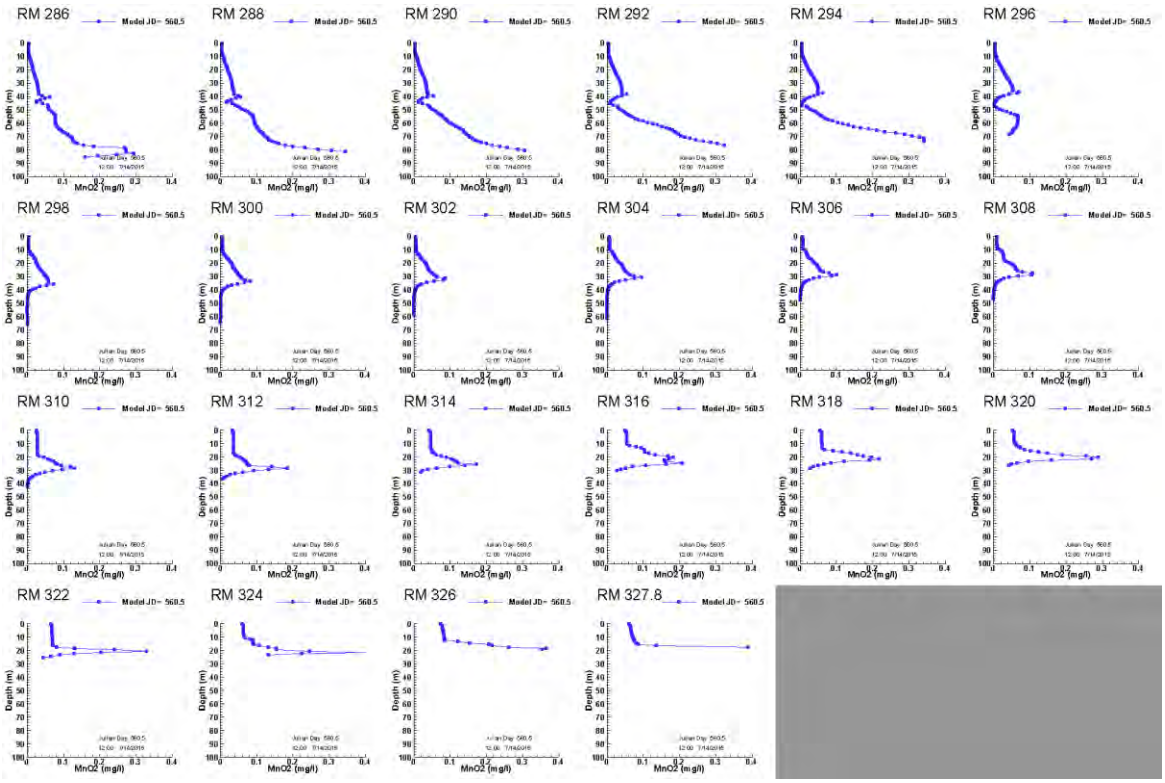


Figure 689. Vertical profiles of MnO2 compared with data for 7/14/2015.

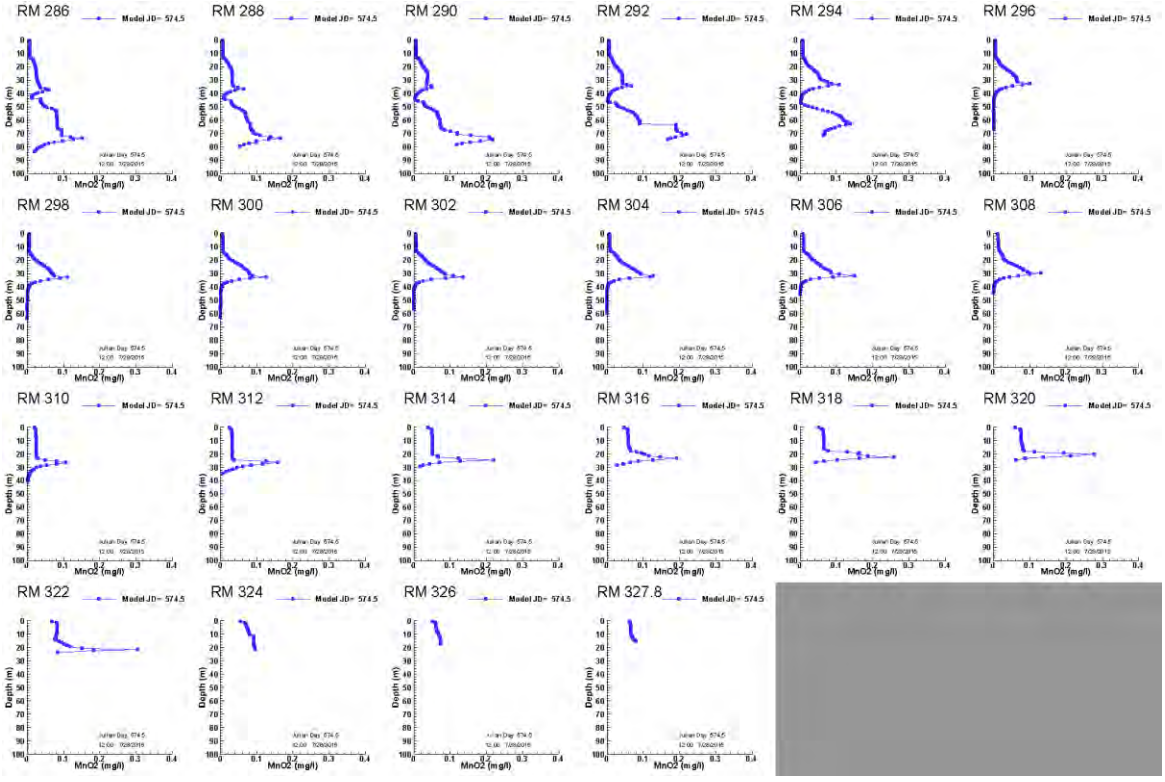


Figure 690. Vertical profiles of MnO2 compared with data for 7/28/2015.

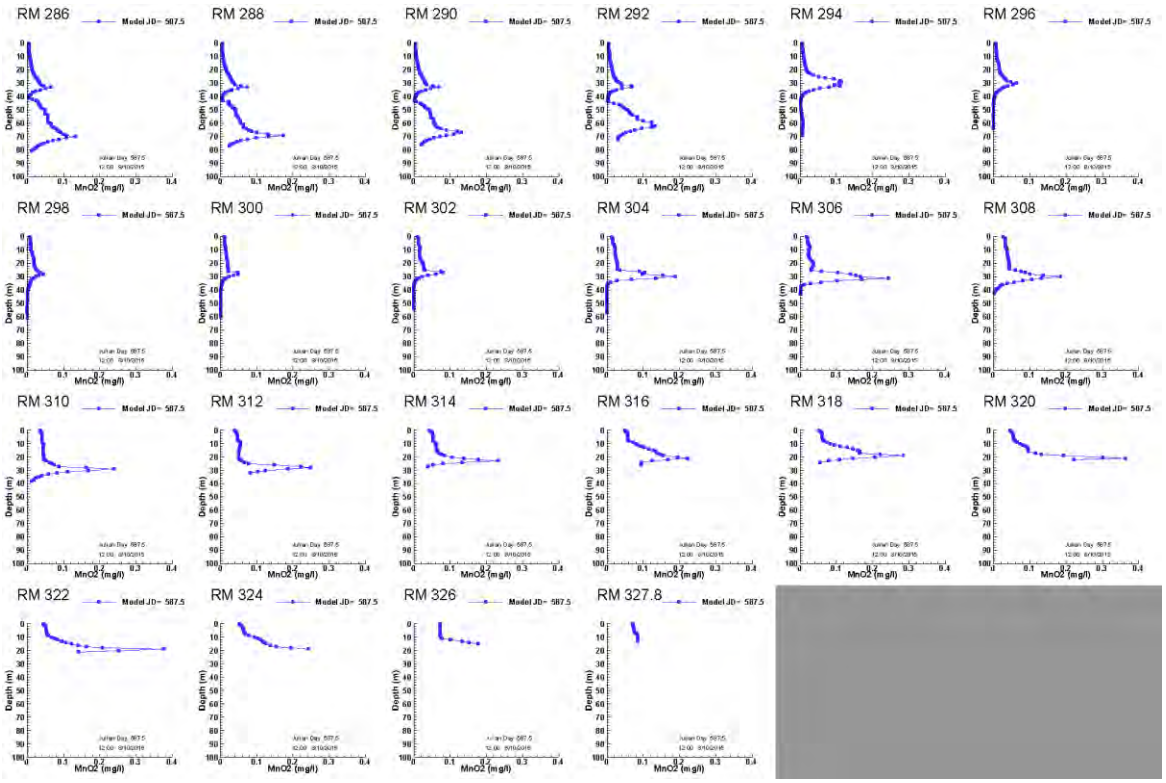


Figure 691. Vertical profiles of MnO2 compared with data for 8/10/2015.

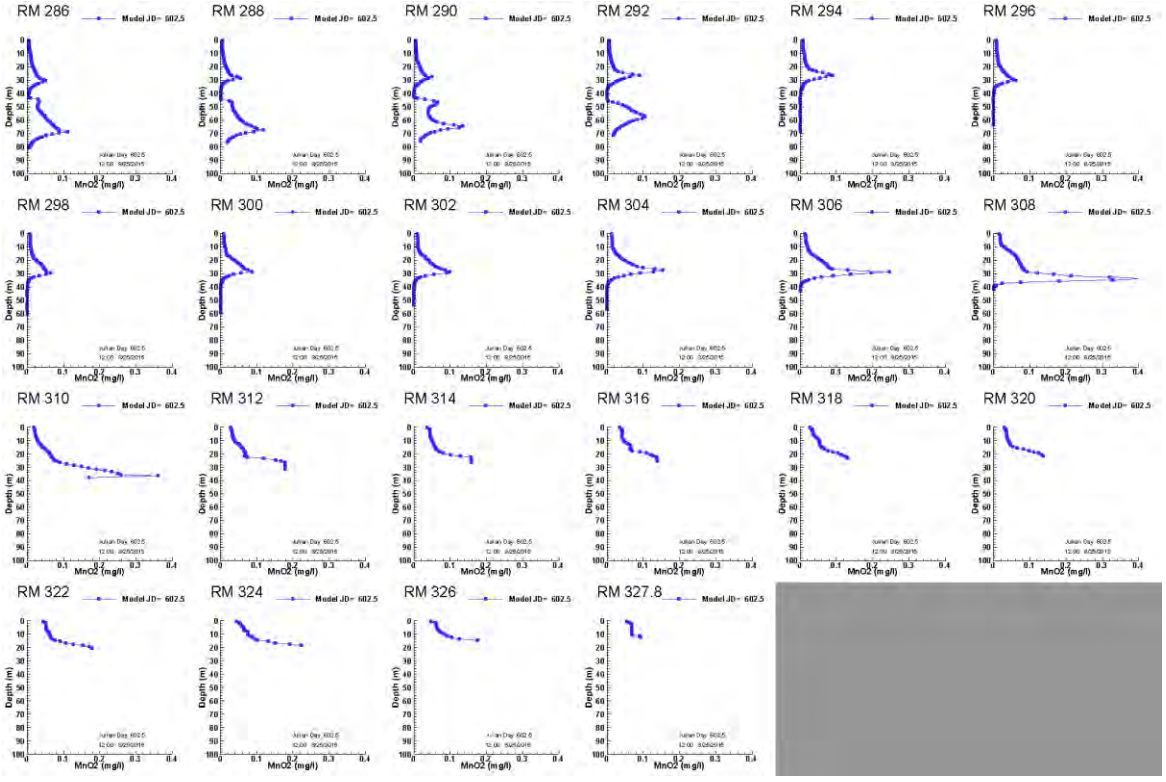


Figure 692. Vertical profiles of MnO2 compared with data for 8/25/2015.

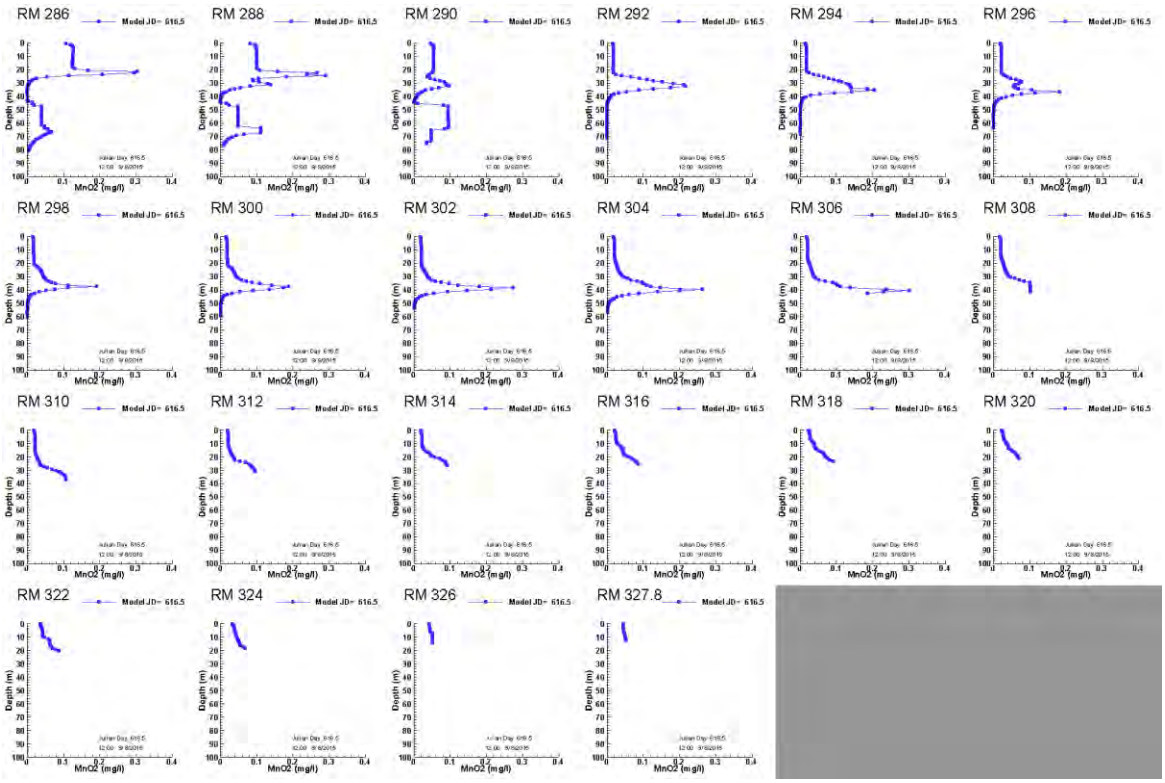


Figure 693. Vertical profiles of MnO2 compared with data for 9/ 8/2015.

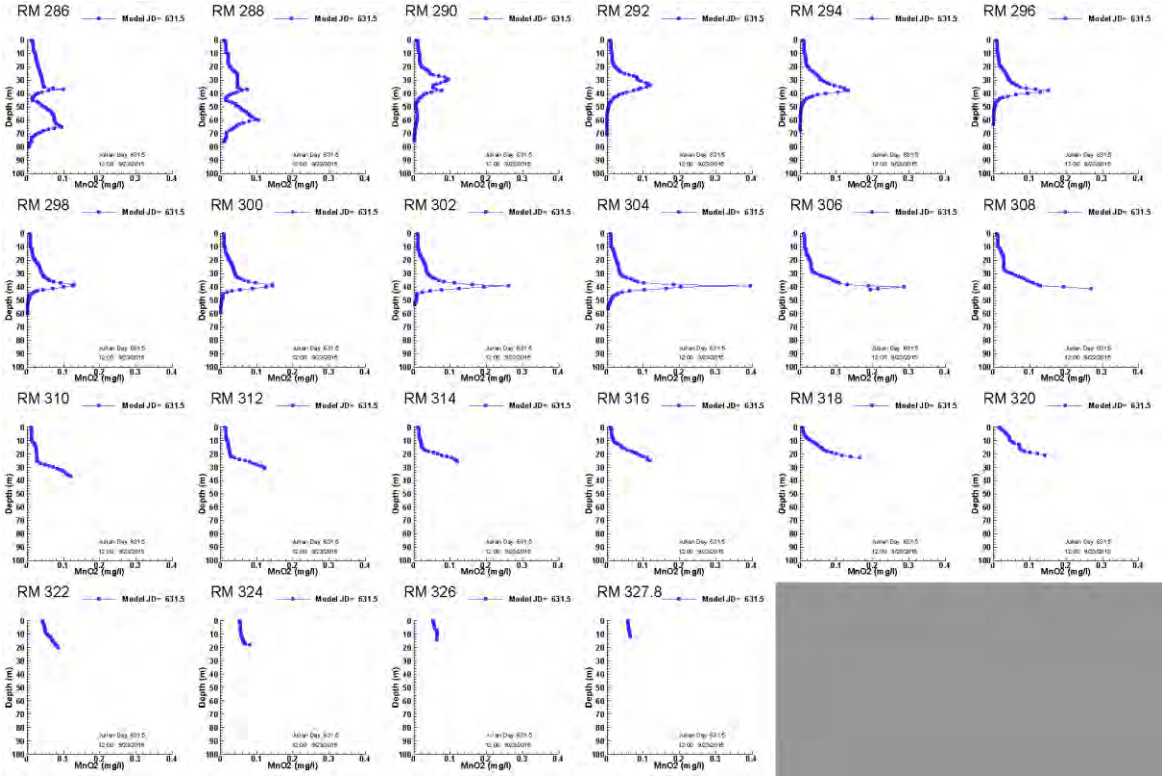


Figure 694. Vertical profiles of MnO2 compared with data for 9/23/2015.

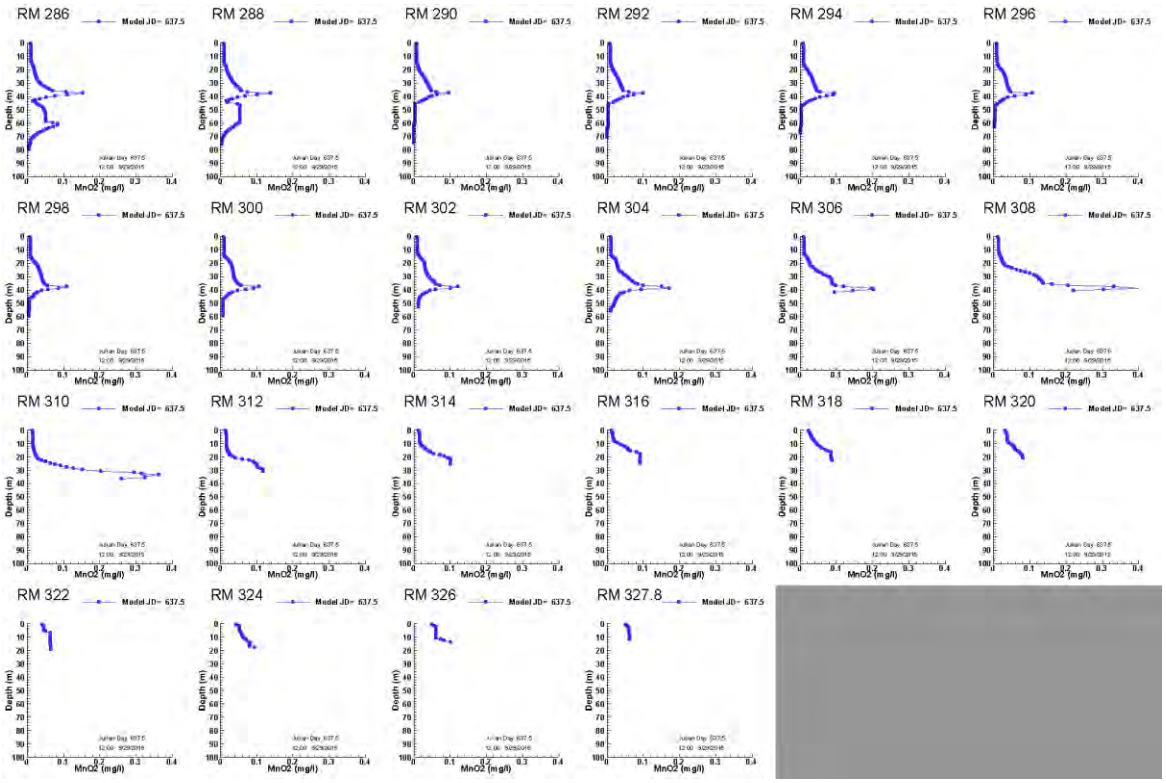


Figure 695. Vertical profiles of MnO2 compared with data for 9/29/2015.

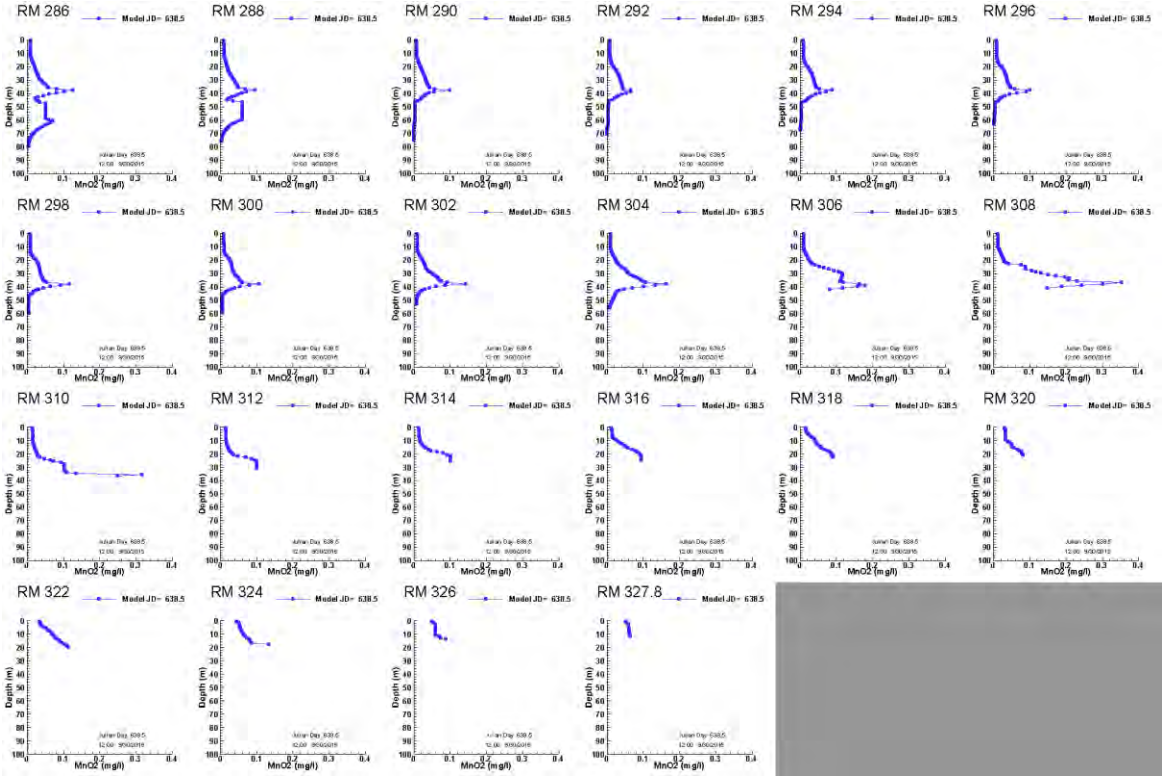


Figure 696. Vertical profiles of MnO2 compared with data for 9/30/2015.

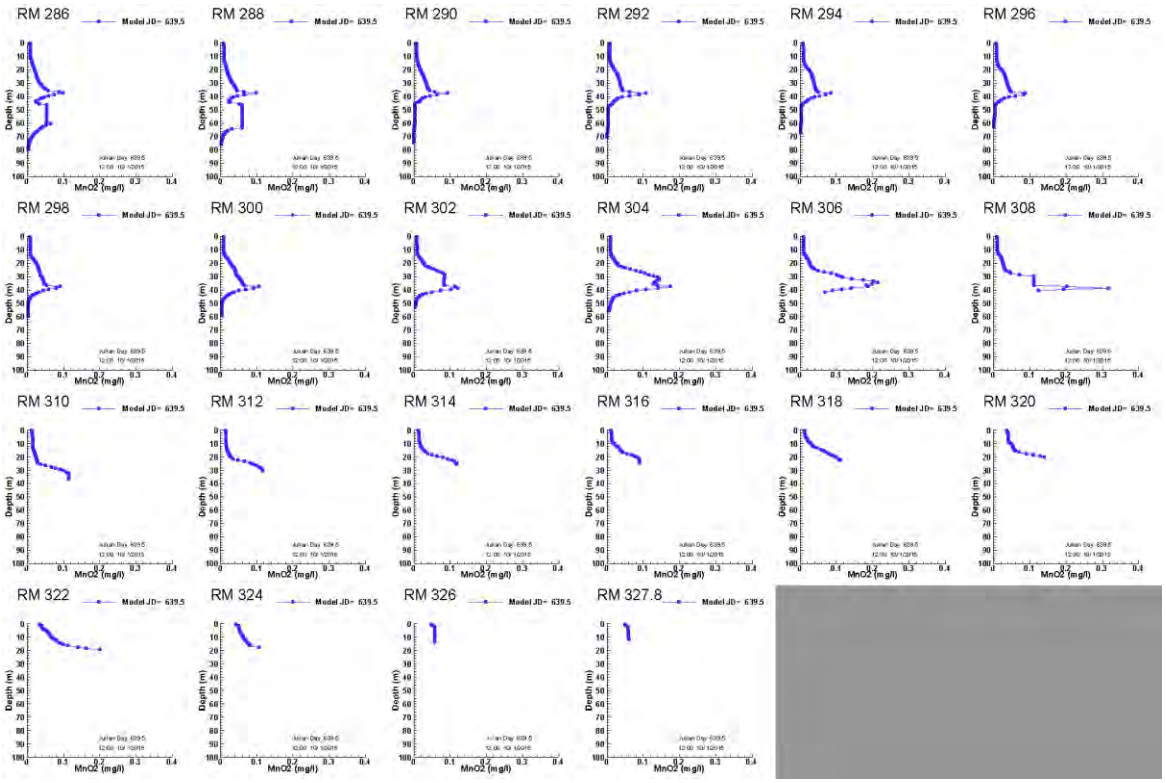


Figure 697. Vertical profiles of MnO2 compared with data for 10/ 1/2015.

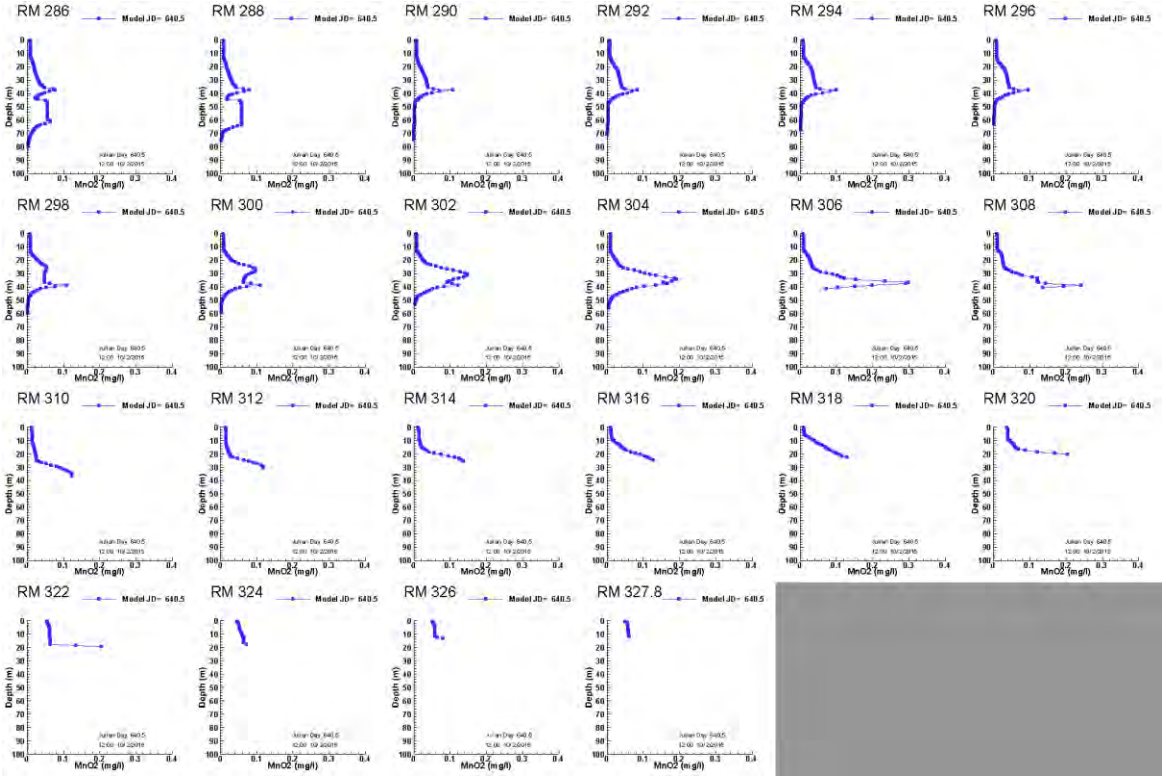


Figure 698. Vertical profiles of MnO2 compared with data for 10/ 2/2015.

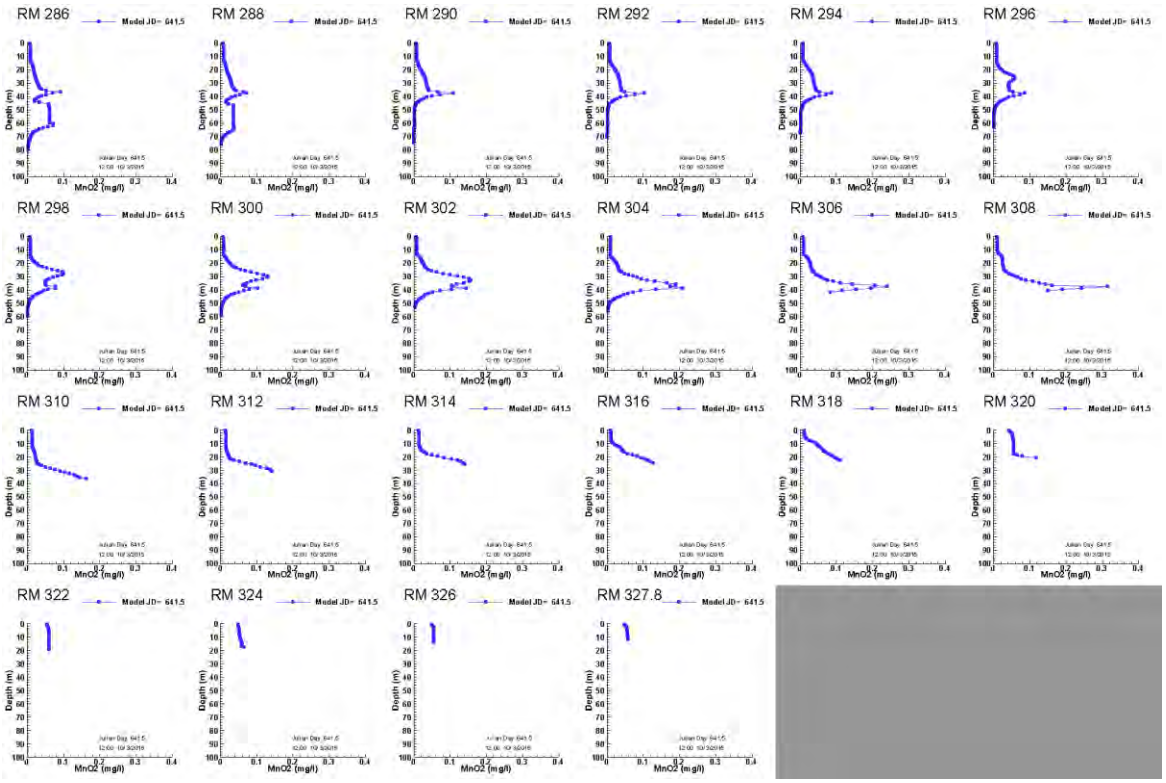


Figure 699. Vertical profiles of MnO2 compared with data for 10/ 3/2015.

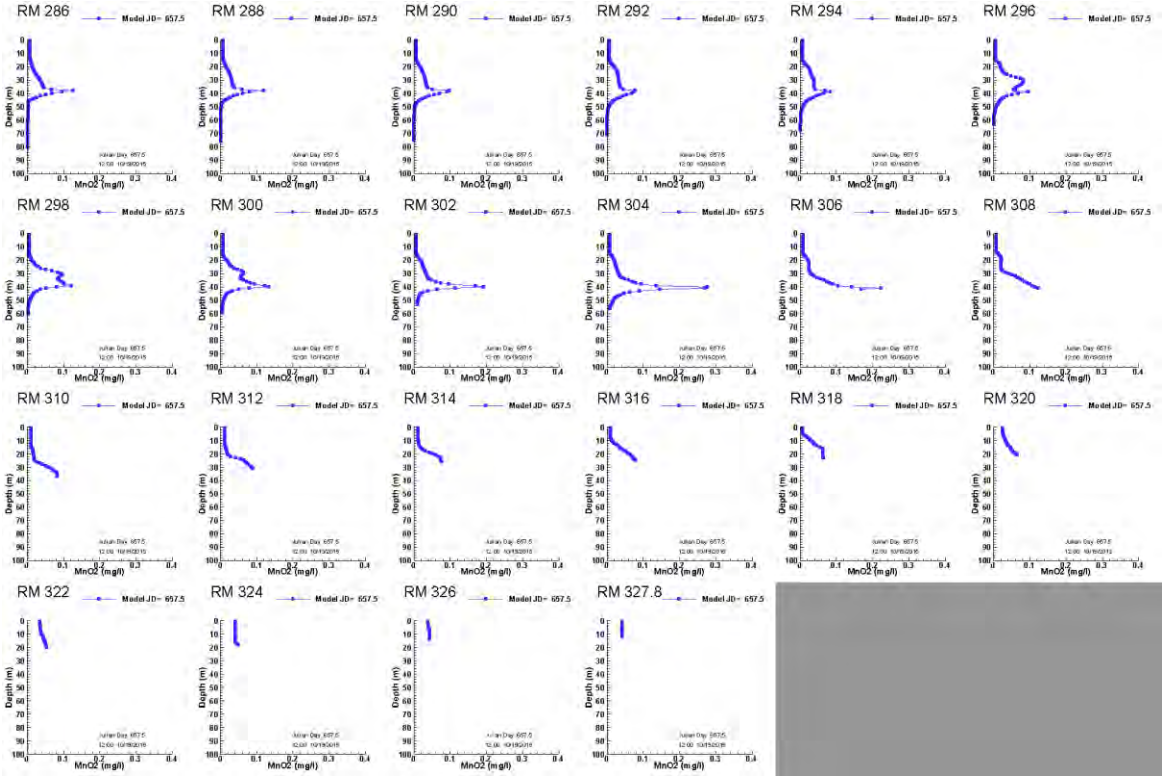


Figure 700. Vertical profiles of MnO2 compared with data for 10/19/2015.

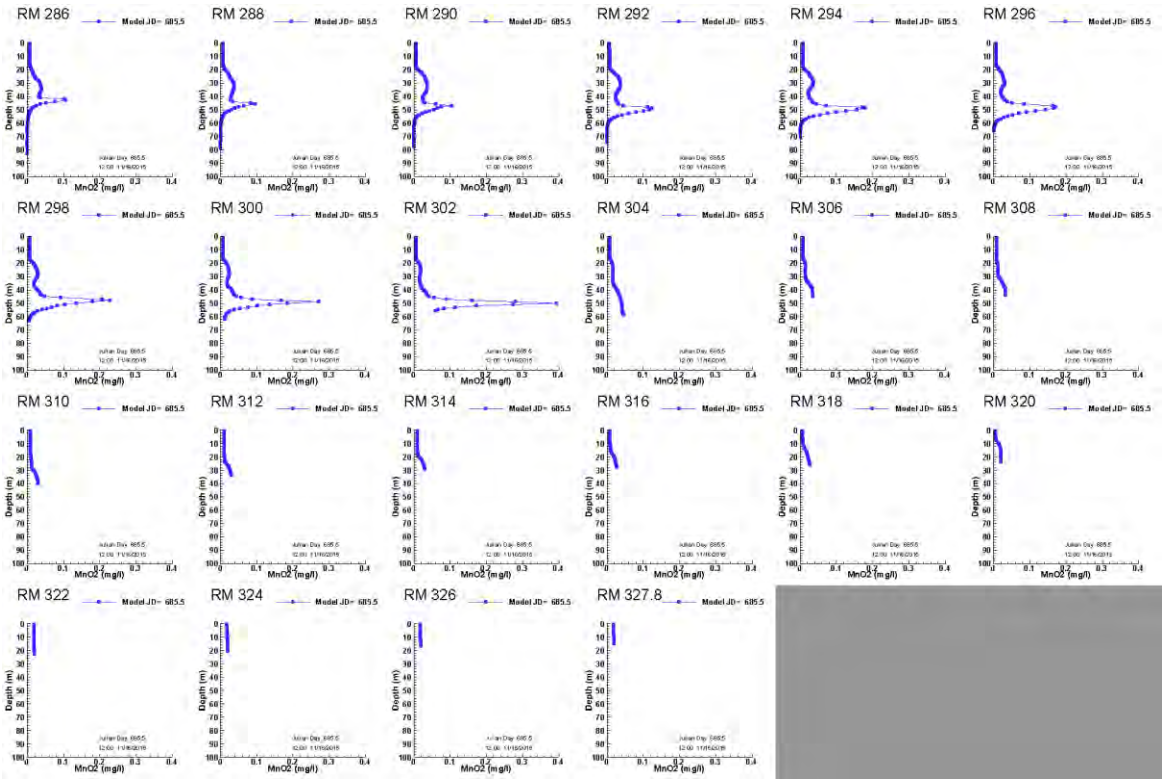


Figure 701. Vertical profiles of MnO2 compared with data for 11/16/2015.

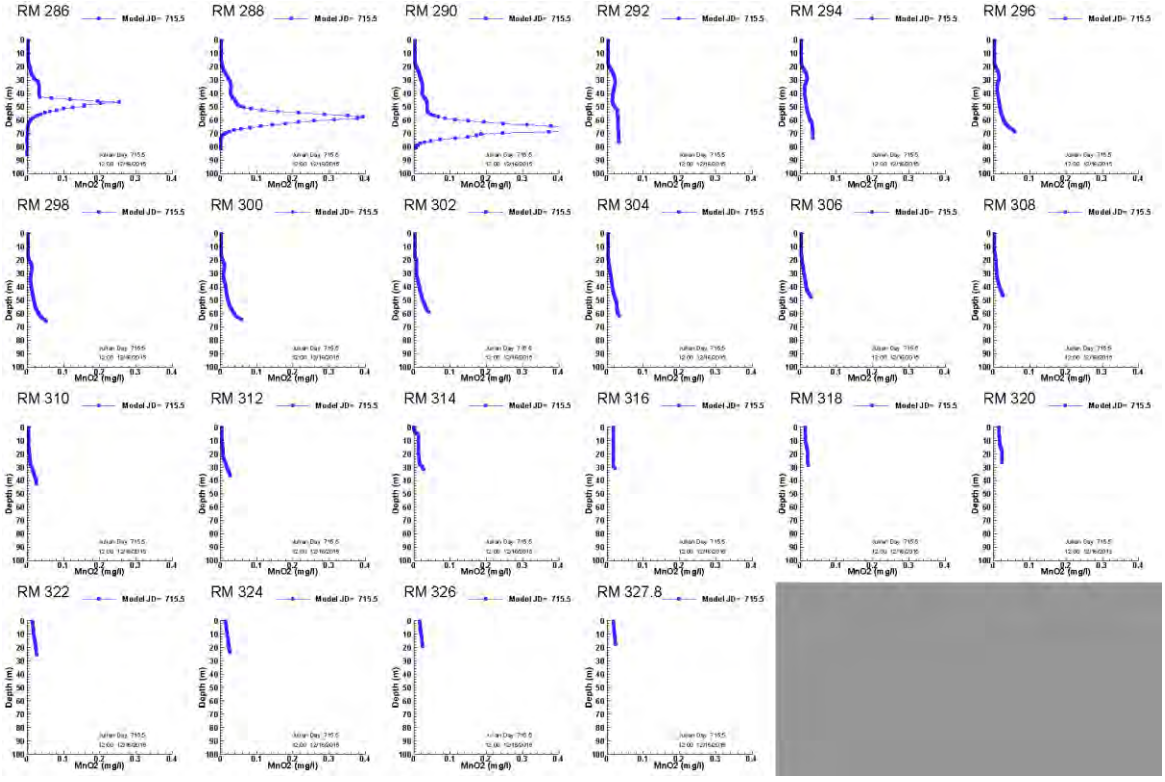


Figure 702. Vertical profiles of MnO2 compared with data for 12/16/2015.

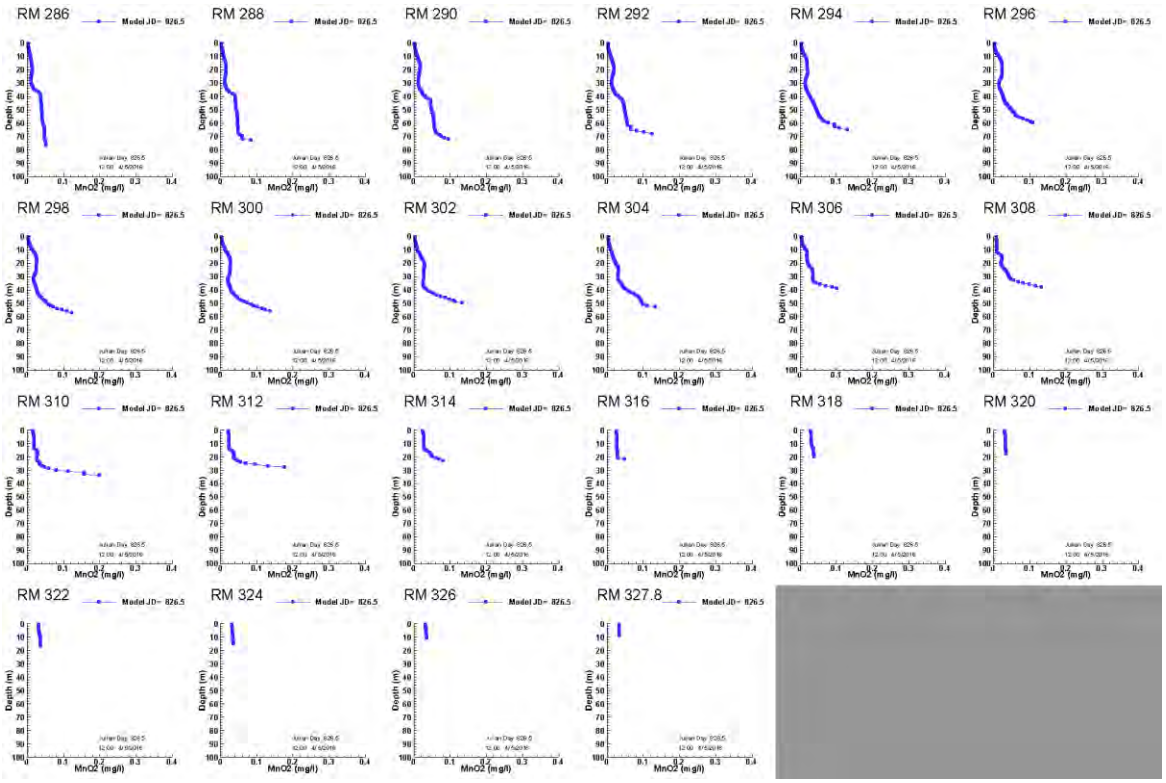


Figure 703. Vertical profiles of MnO2 compared with data for 4/ 5/2016.

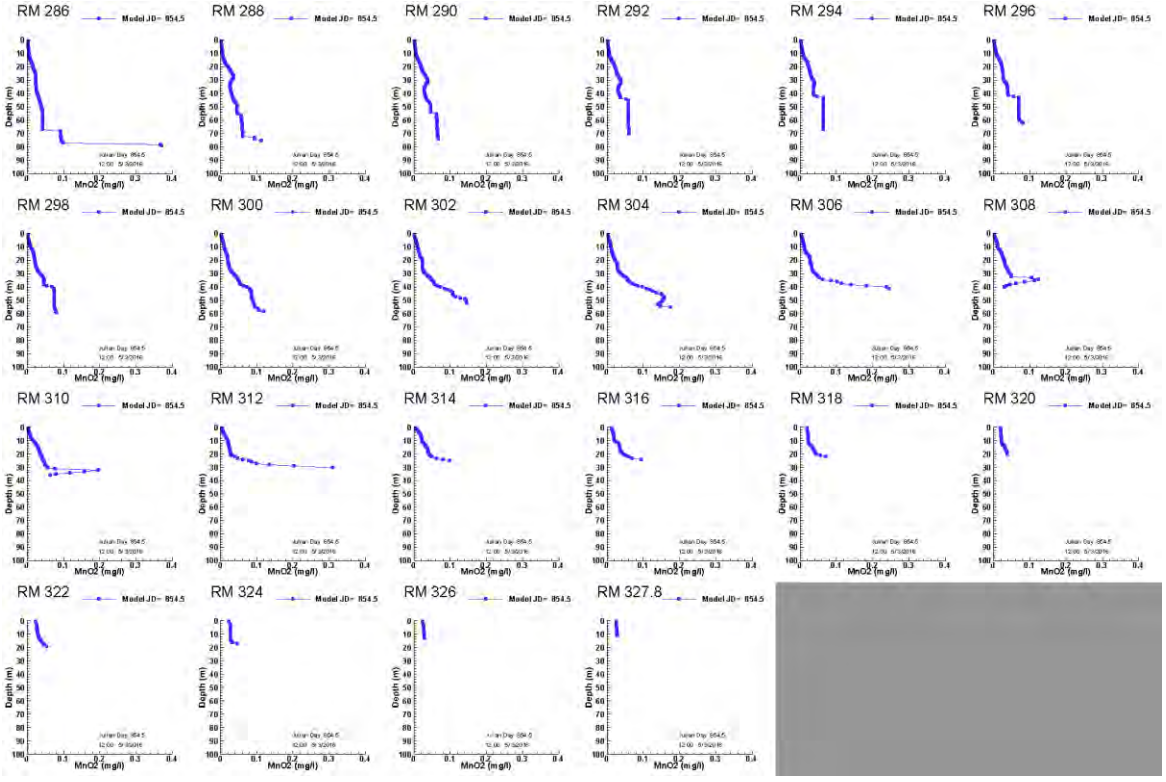


Figure 704. Vertical profiles of MnO2 compared with data for 5/ 3/2016.

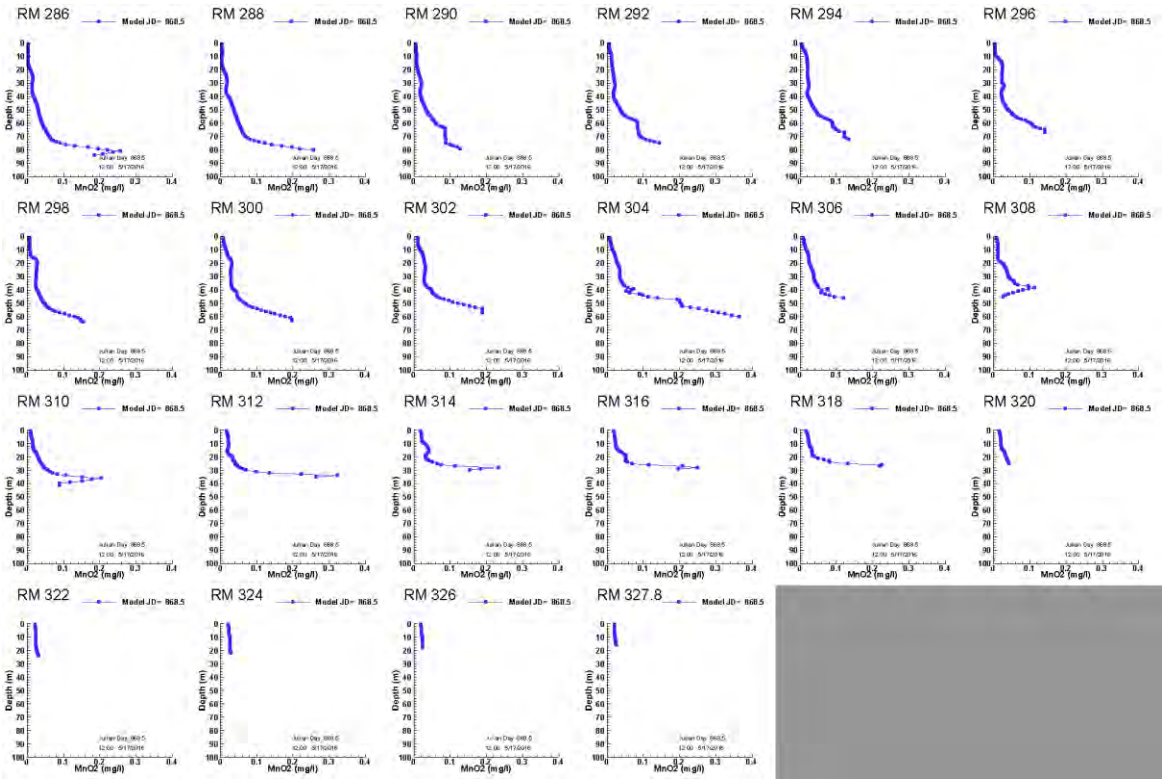


Figure 705. Vertical profiles of MnO2 compared with data for 5/17/2016.

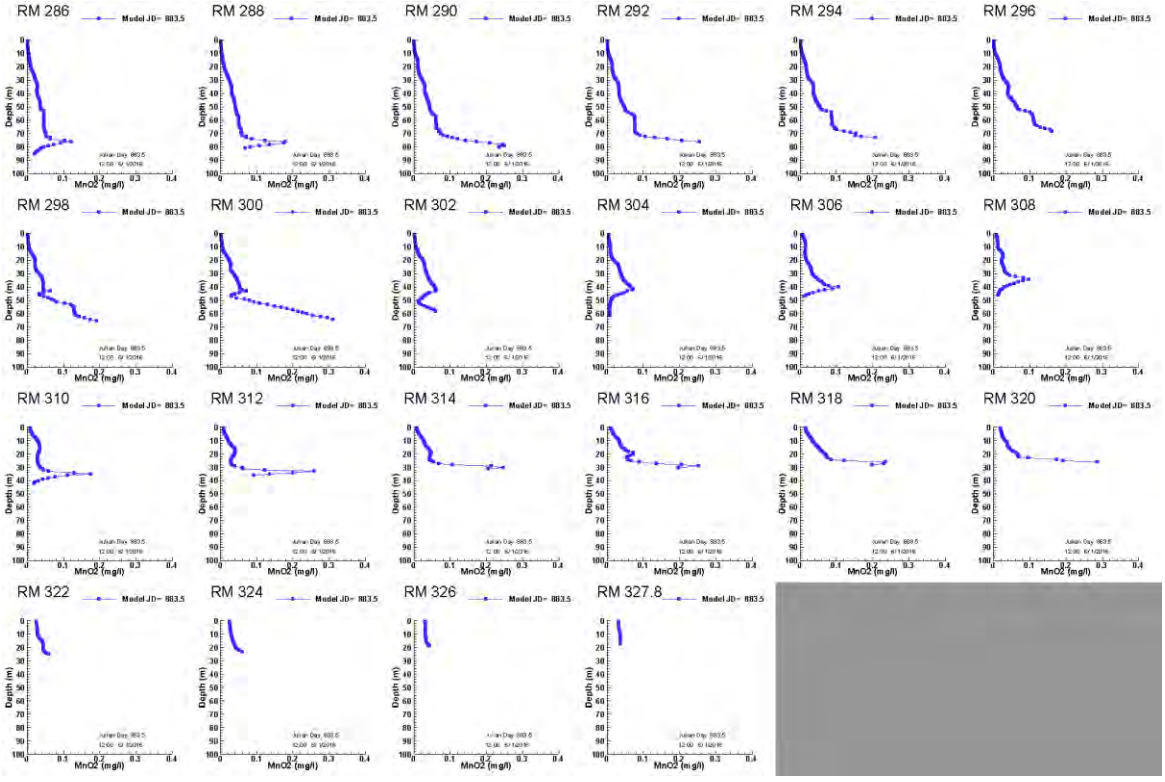


Figure 706. Vertical profiles of MnO2 compared with data for 6/ 1/2016.

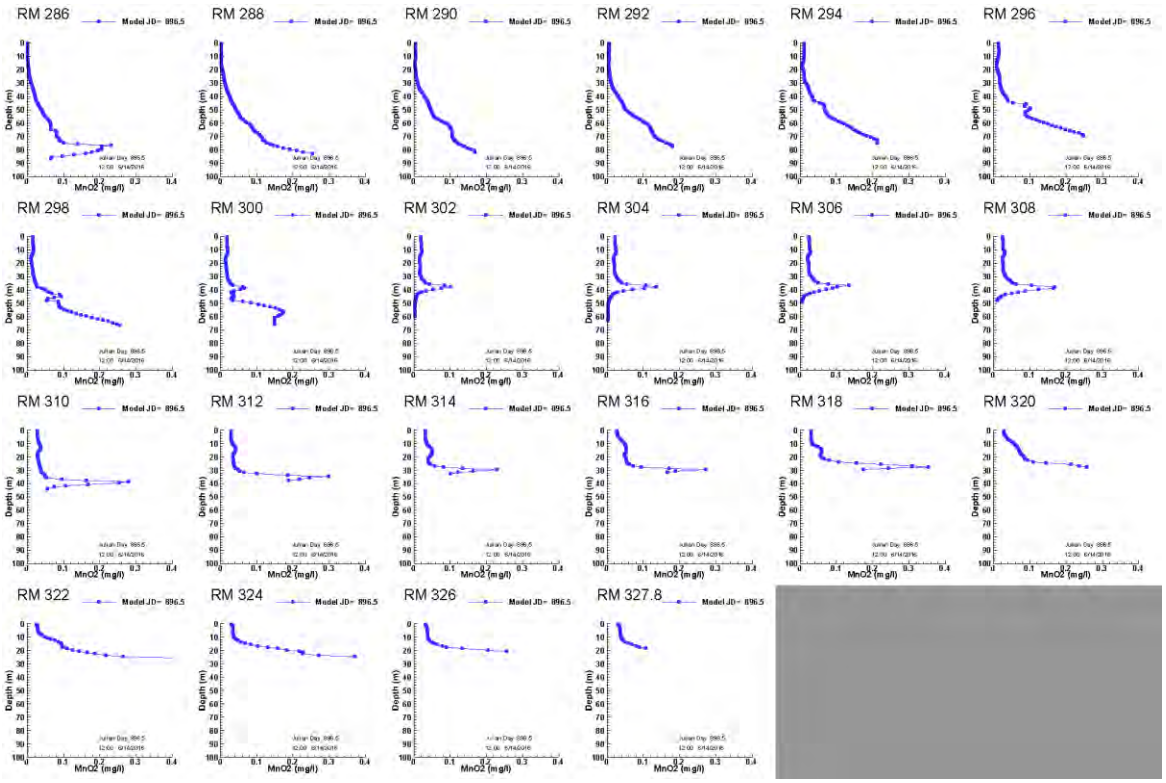


Figure 707. Vertical profiles of MnO2 compared with data for 6/14/2016.

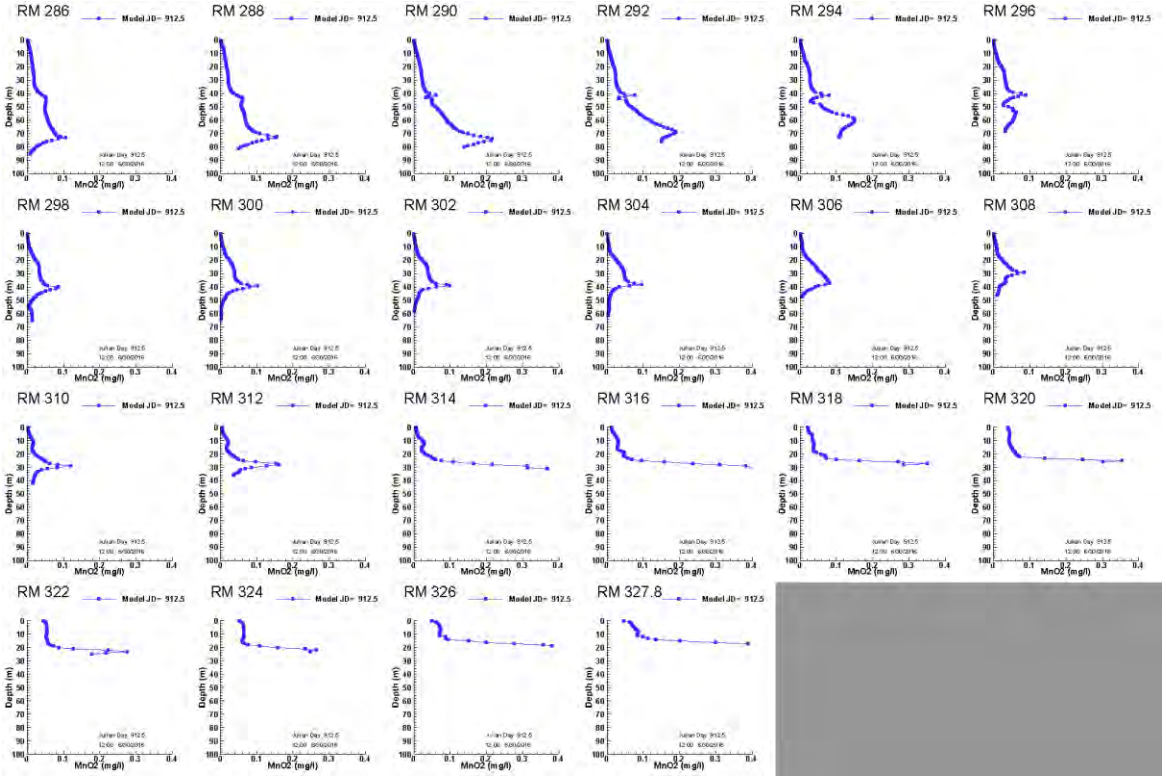


Figure 708. Vertical profiles of MnO2 compared with data for 6/30/2016.

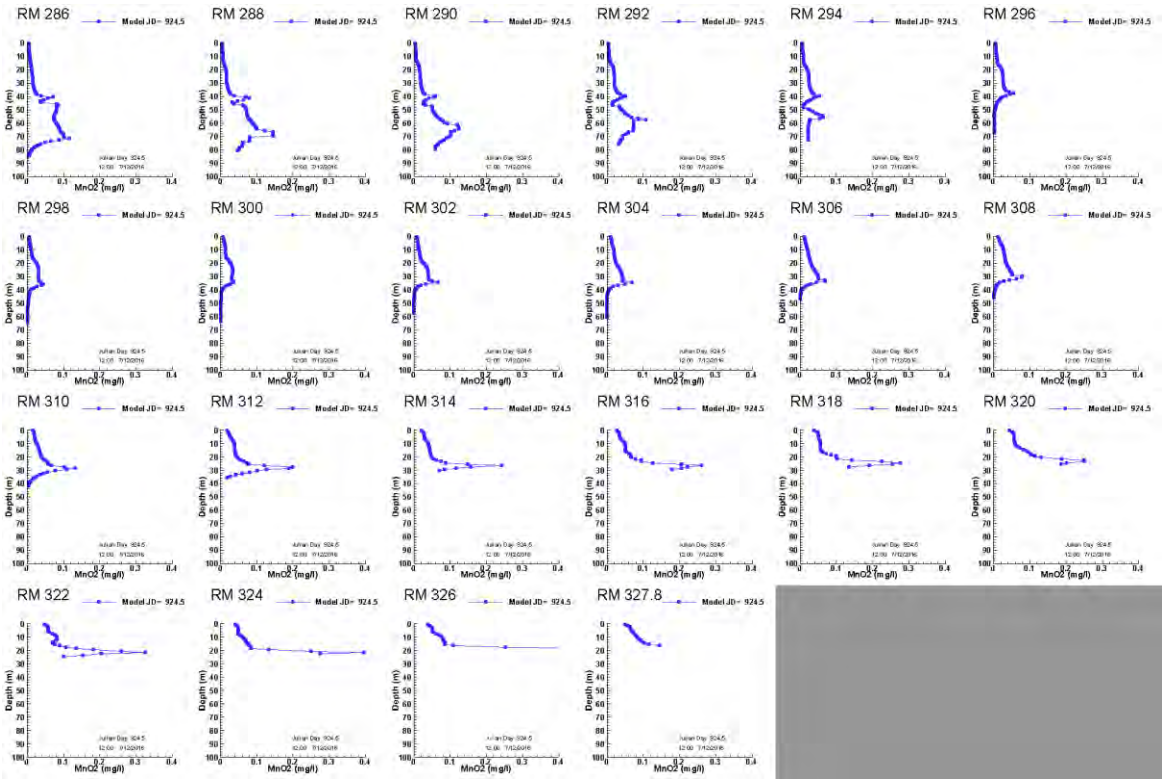


Figure 709. Vertical profiles of MnO2 compared with data for 7/12/2016.

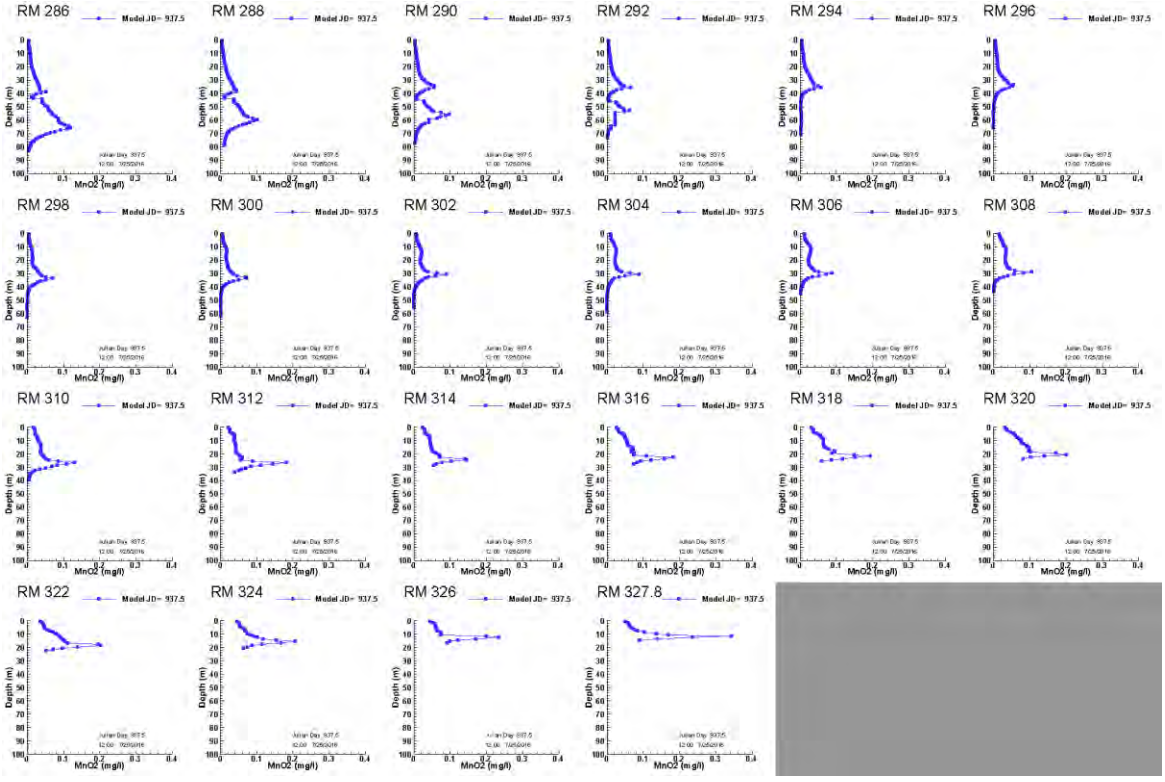


Figure 710. Vertical profiles of MnO2 compared with data for 7/25/2016.

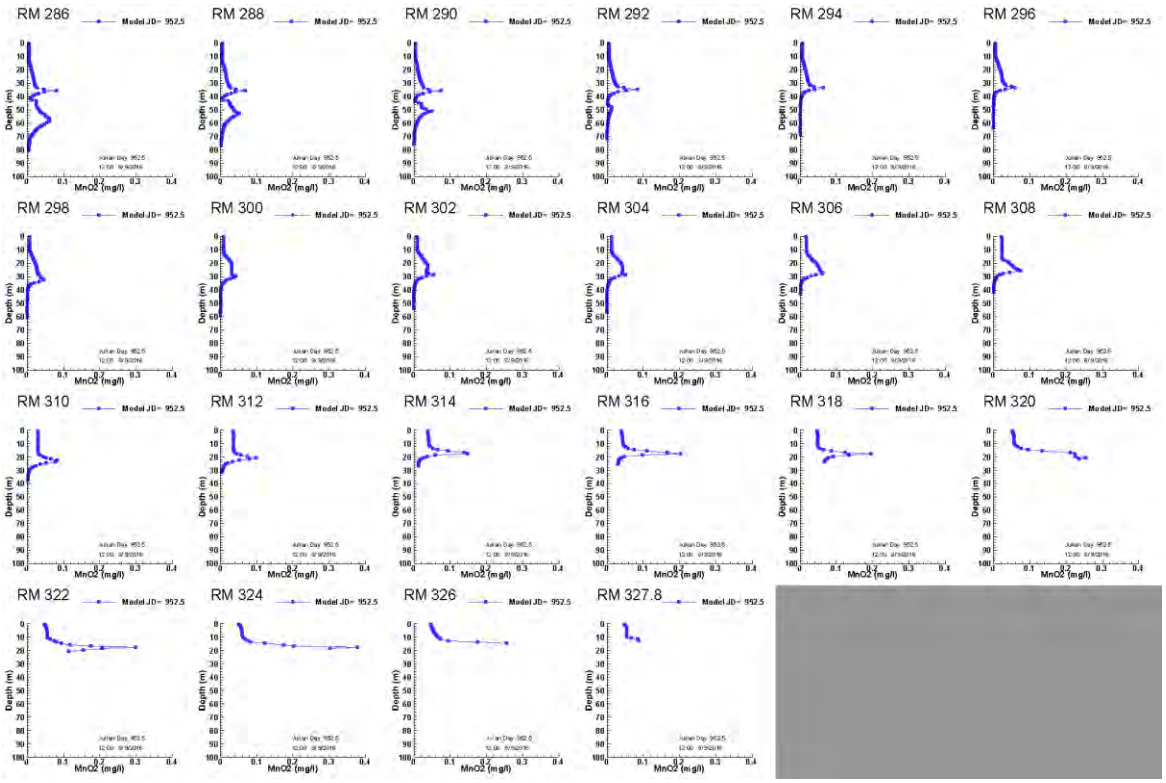


Figure 711. Vertical profiles of MnO2 compared with data for 8/ 9/2016.

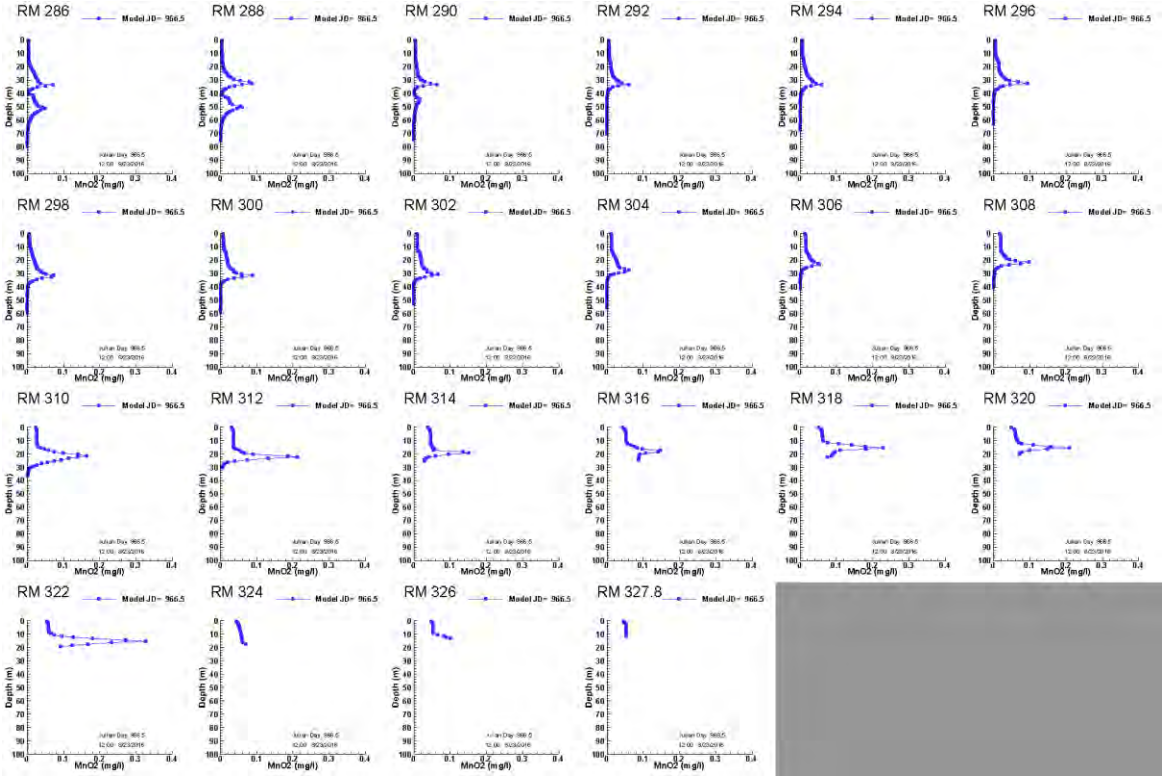


Figure 712. Vertical profiles of MnO2 compared with data for 8/23/2016.

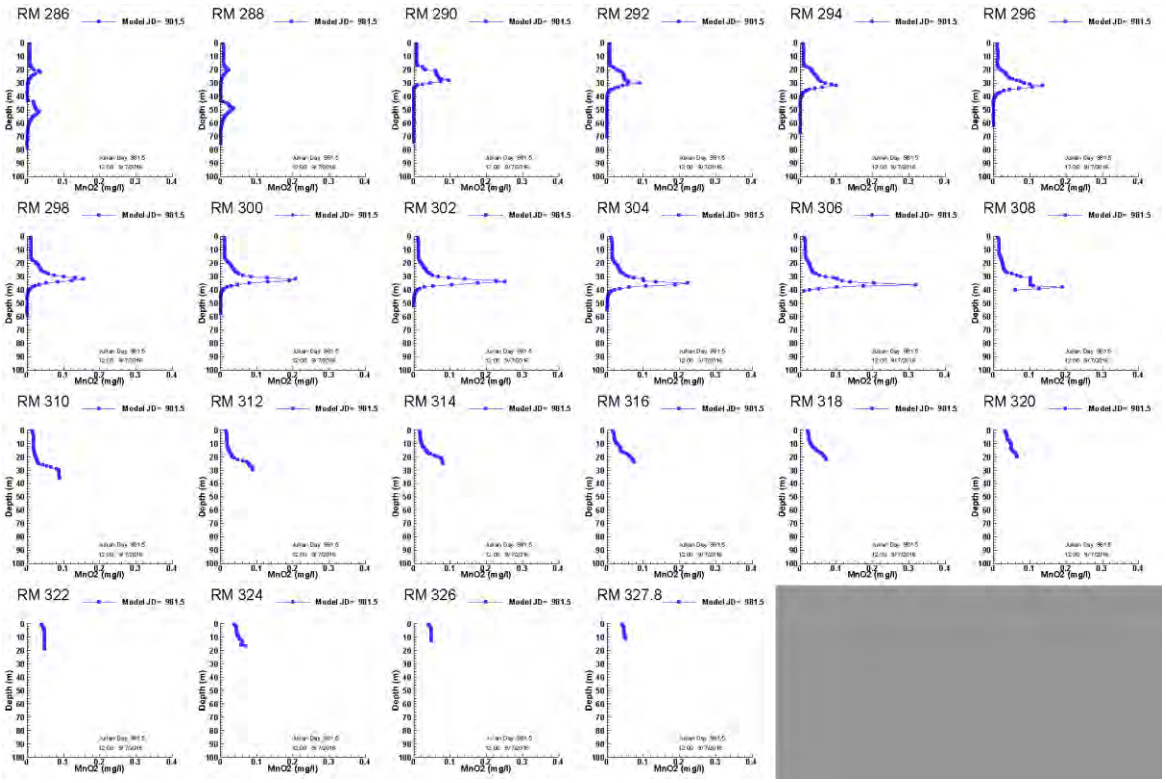


Figure 713. Vertical profiles of MnO2 compared with data for 9/ 7/2016.

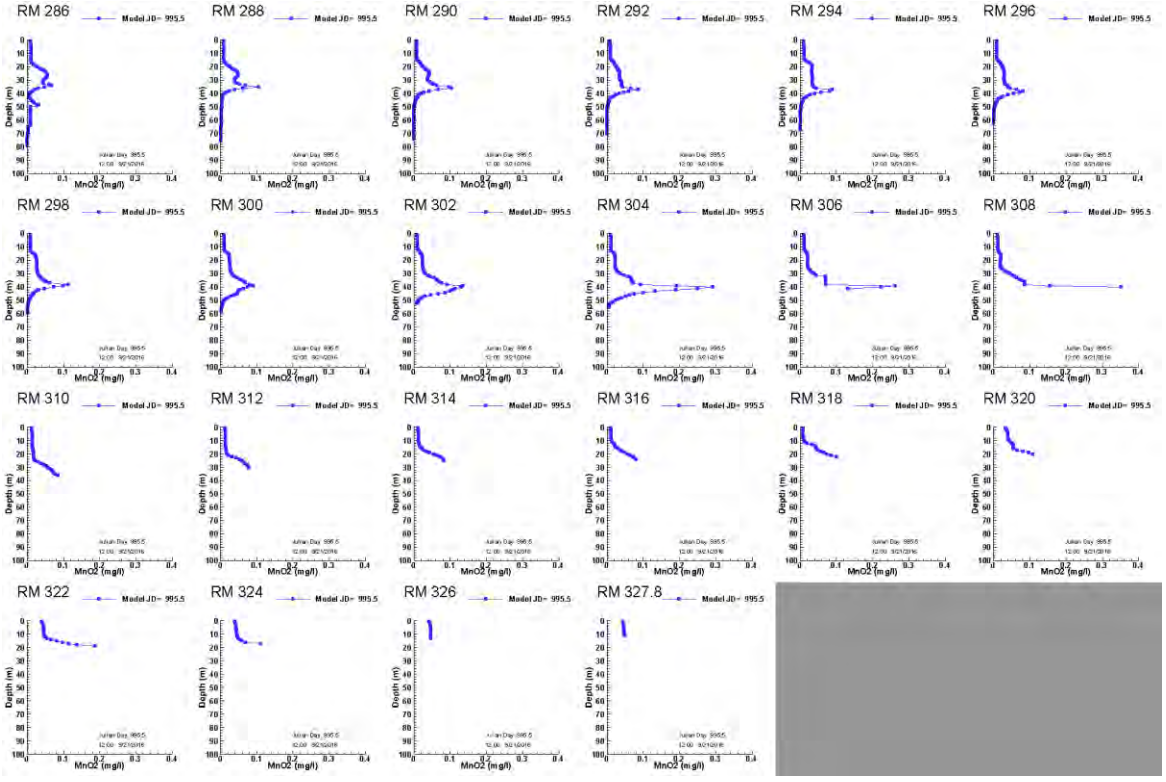


Figure 714. Vertical profiles of MnO2 compared with data for 9/21/2016.

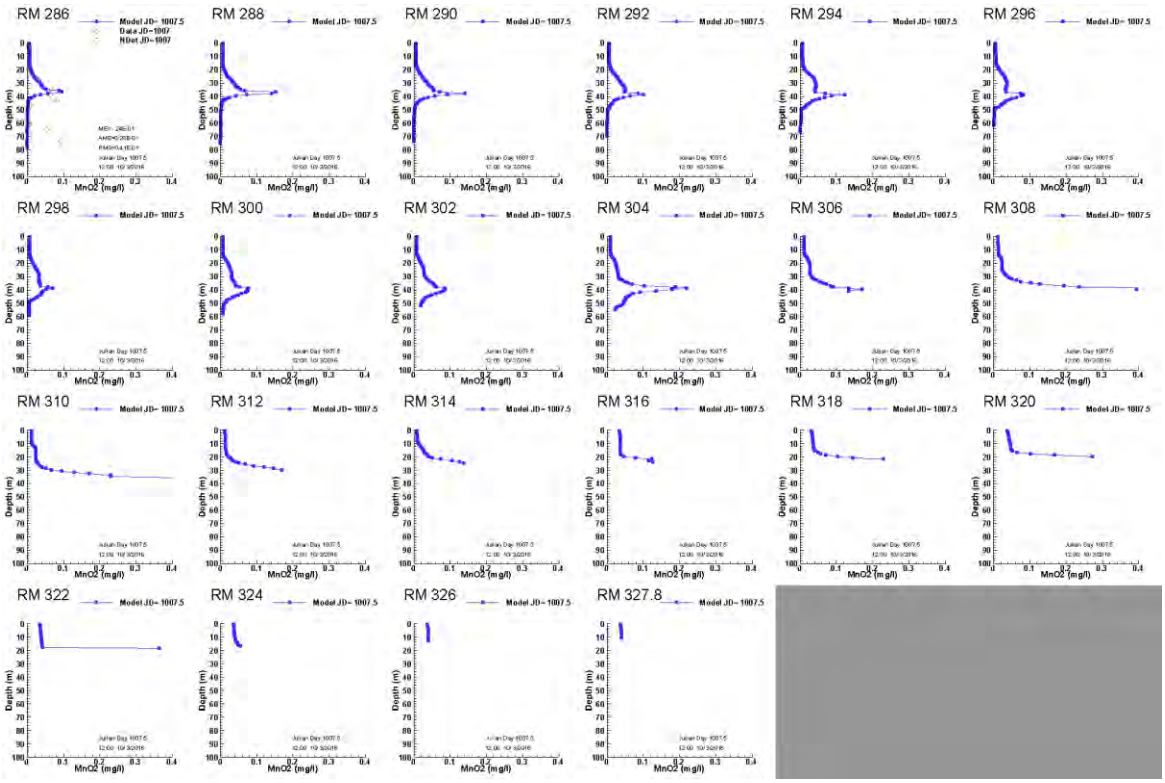


Figure 715. Vertical profiles of MnO2 compared with data for 10/ 3/2016.

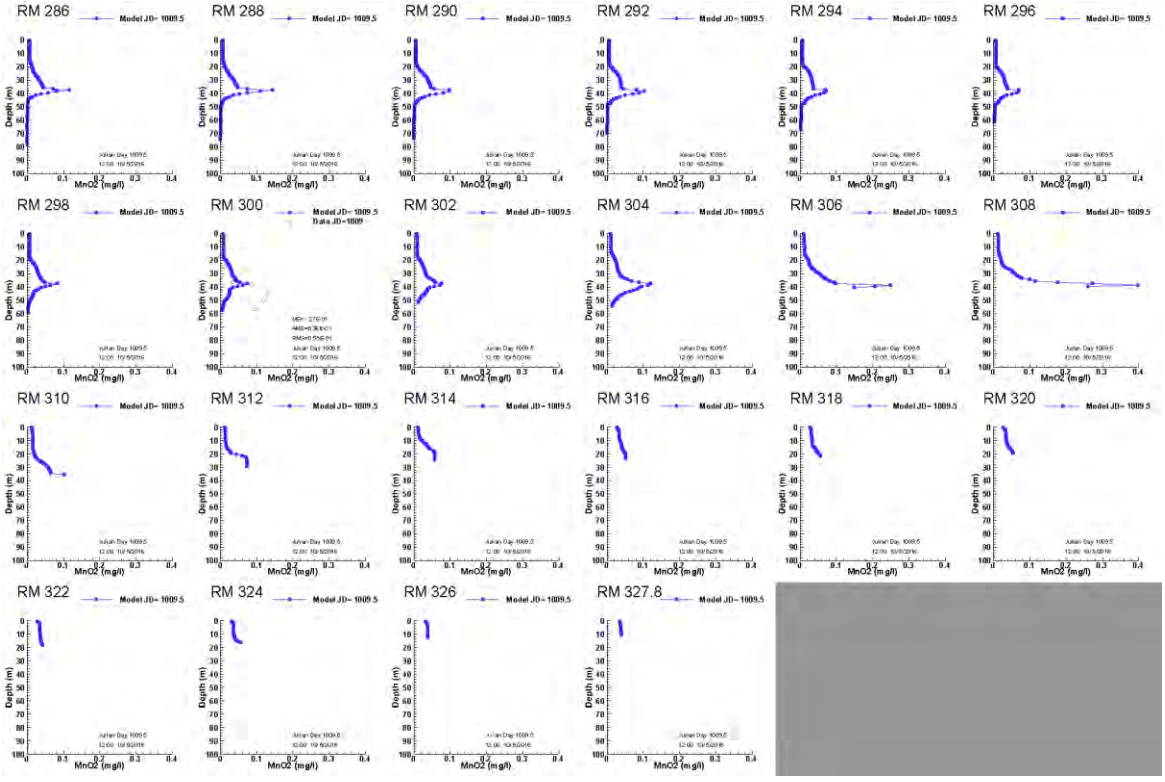


Figure 716. Vertical profiles of MnO2 compared with data for 10/ 5/2016.

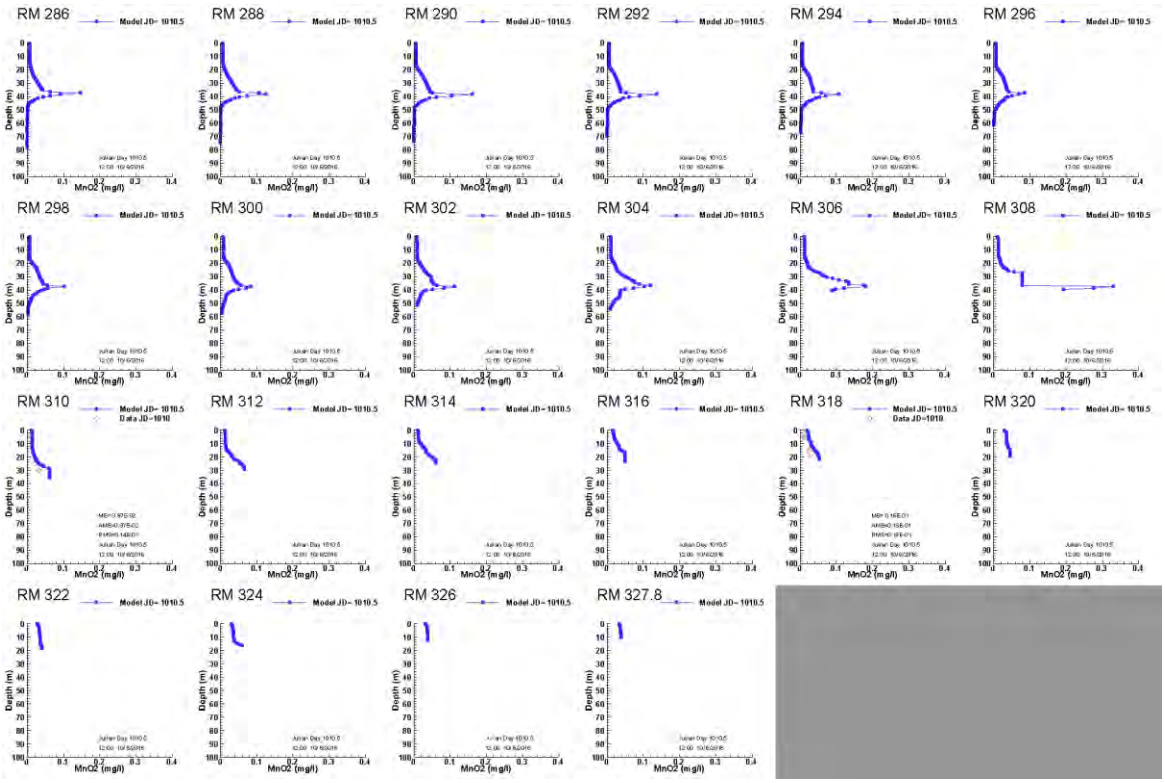


Figure 717. Vertical profiles of MnO2 compared with data for 10/ 6/2016.

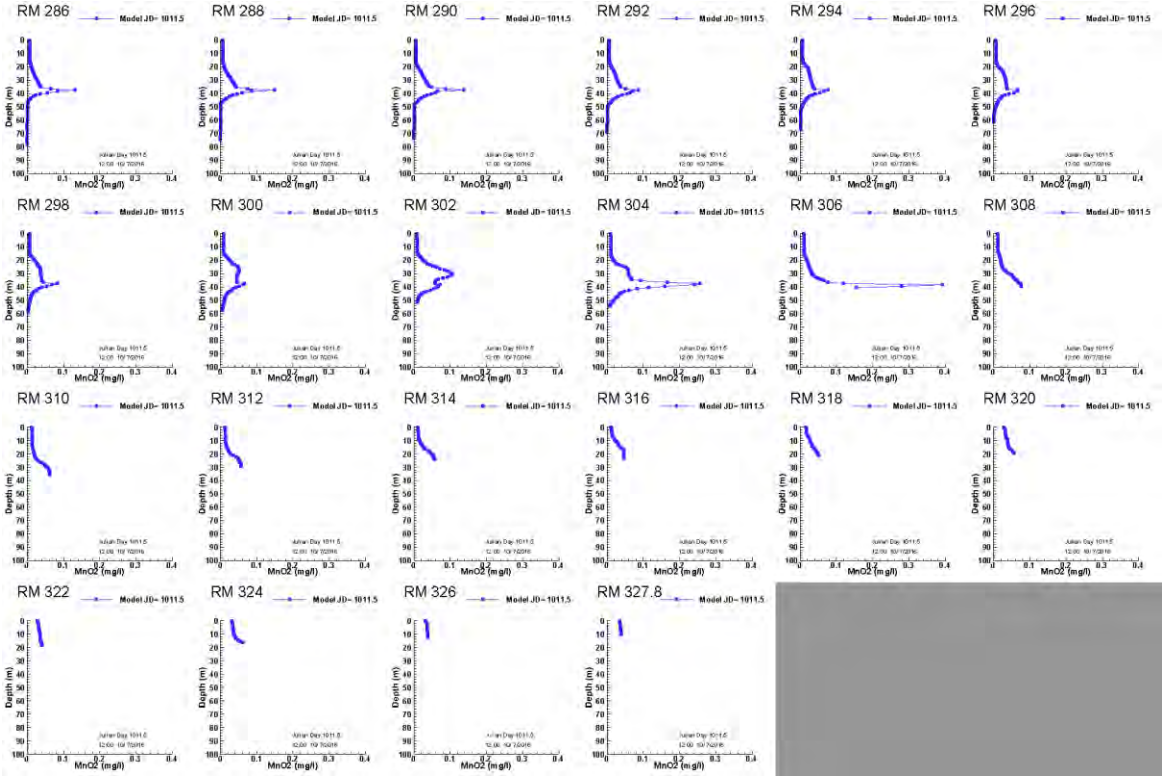


Figure 718. Vertical profiles of MnO2 compared with data for 10/ 7/2016.

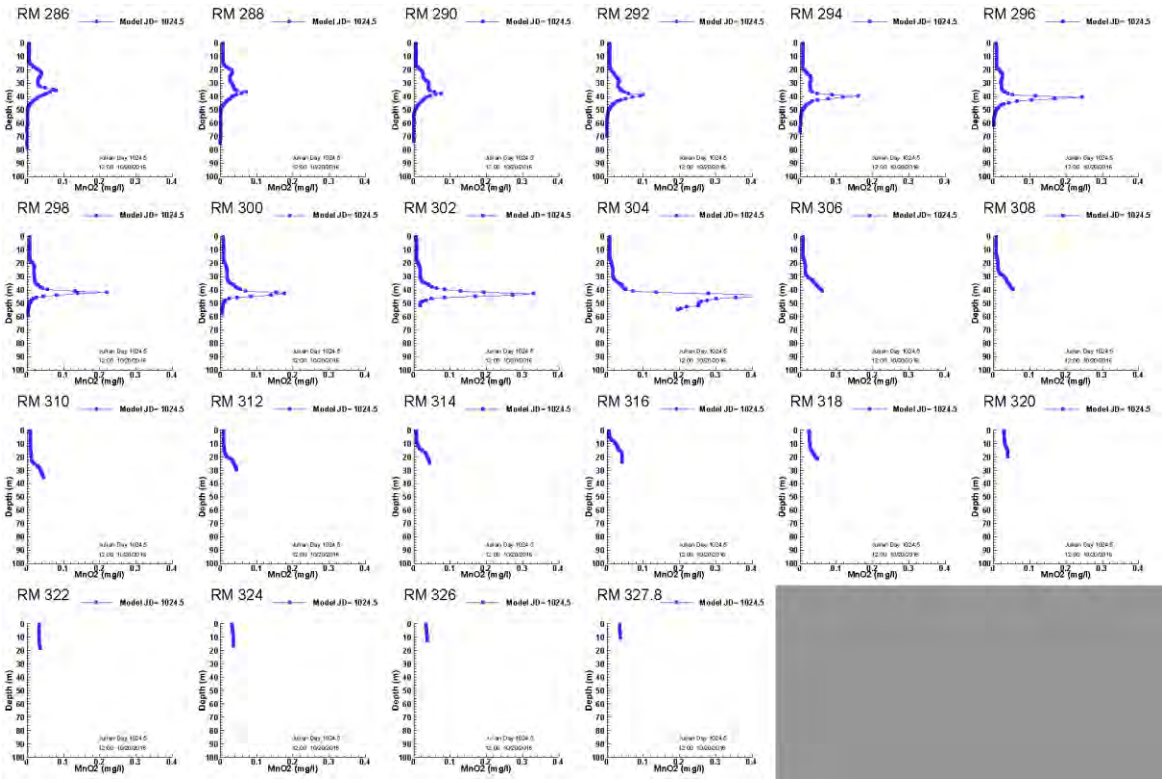


Figure 719. Vertical profiles of MnO2 compared with data for 10/20/2016.

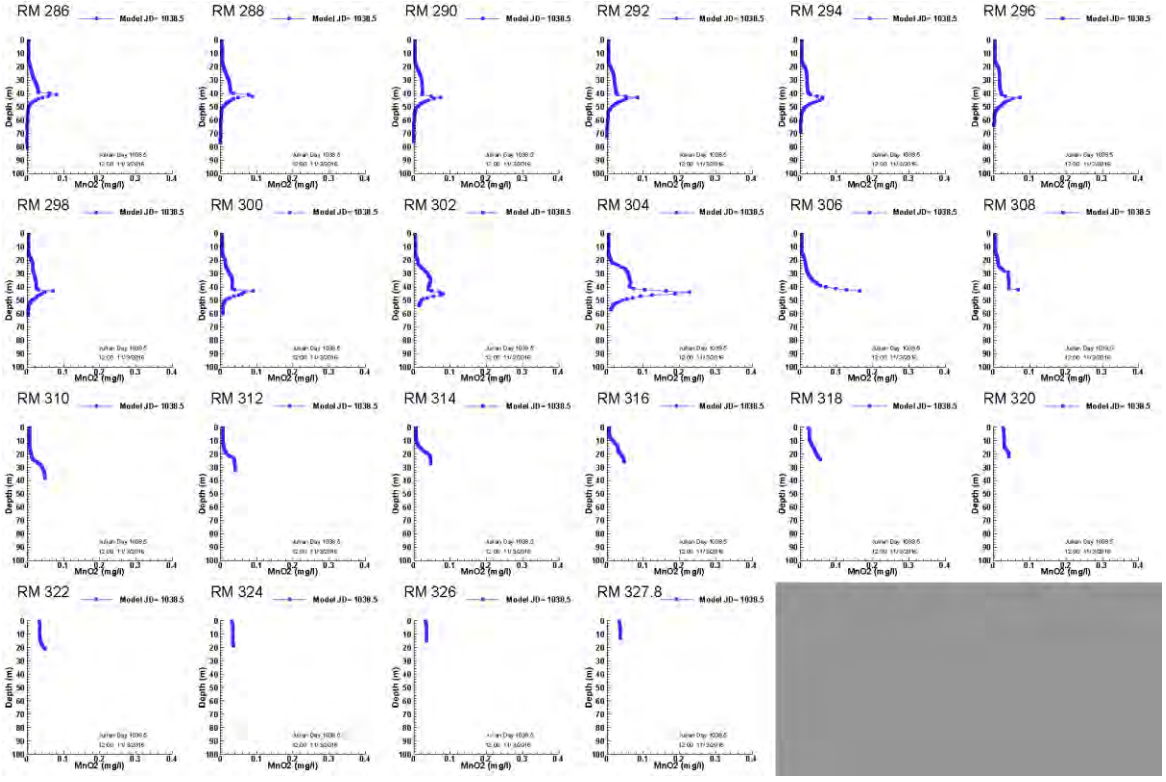


Figure 720. Vertical profiles of MnO2 compared with data for 11/ 3/2016.

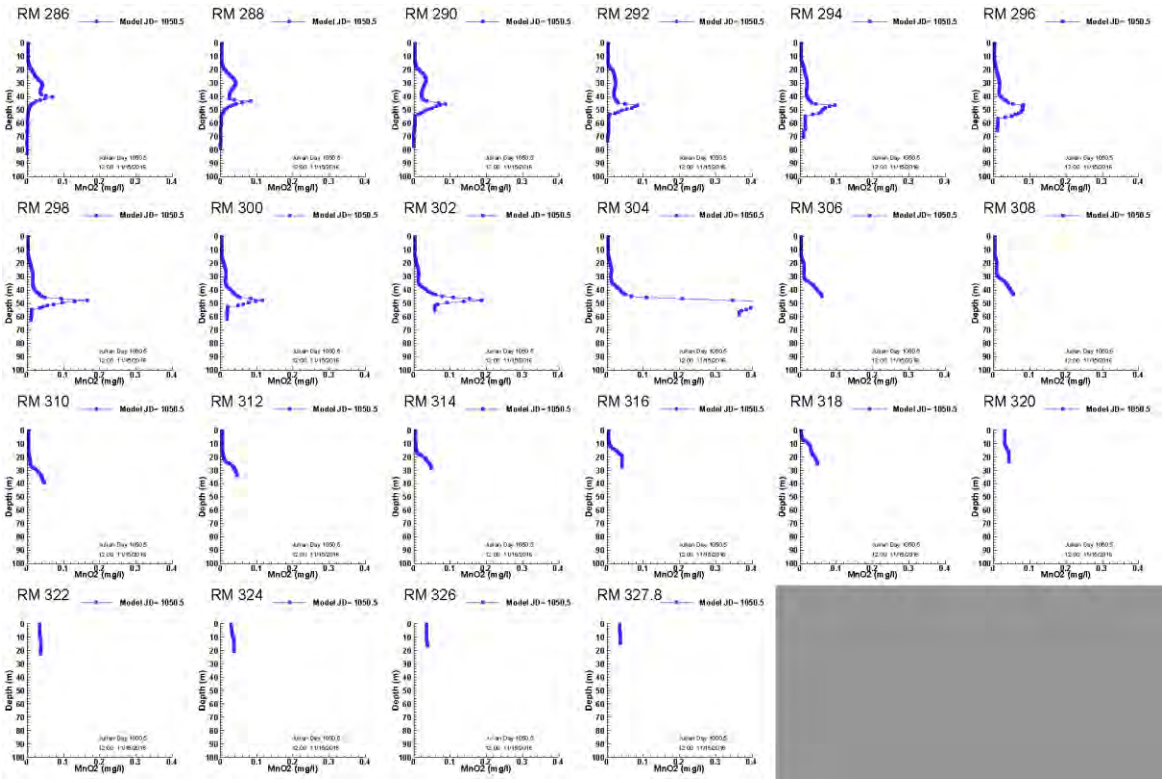


Figure 721. Vertical profiles of MnO2 compared with data for 11/15/2016.

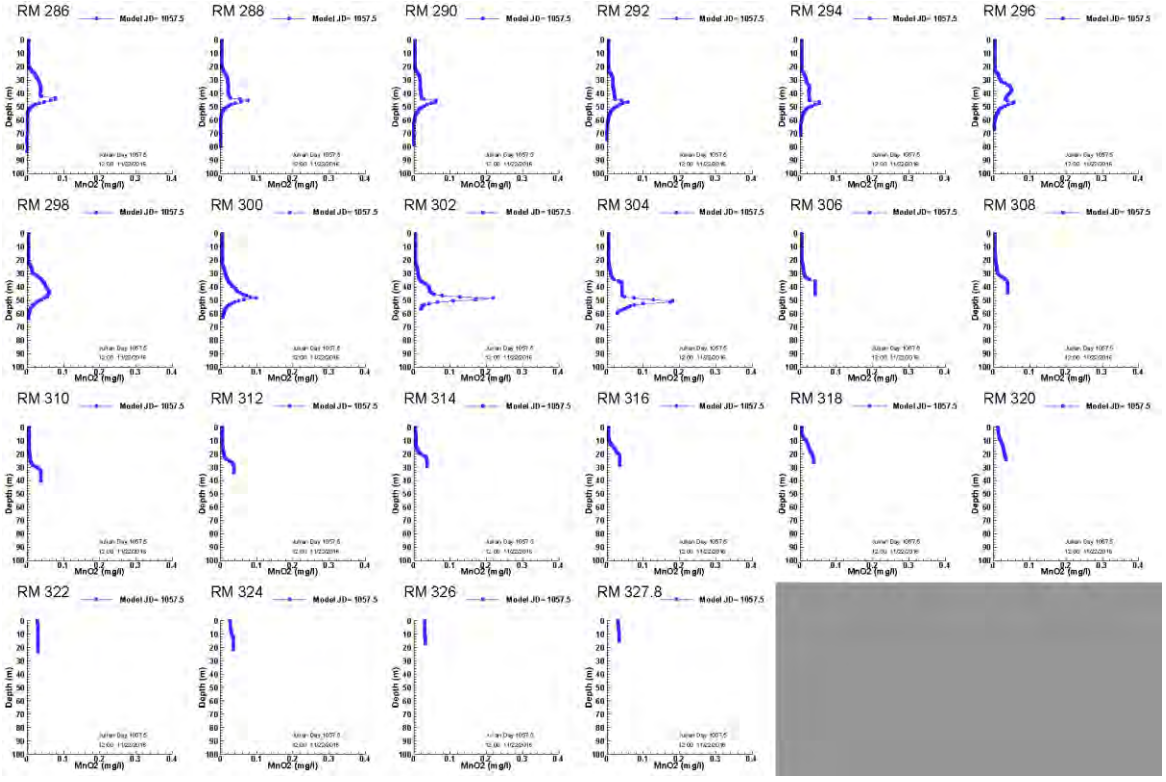


Figure 722. Vertical profiles of MnO2 compared with data for 11/22/2016.

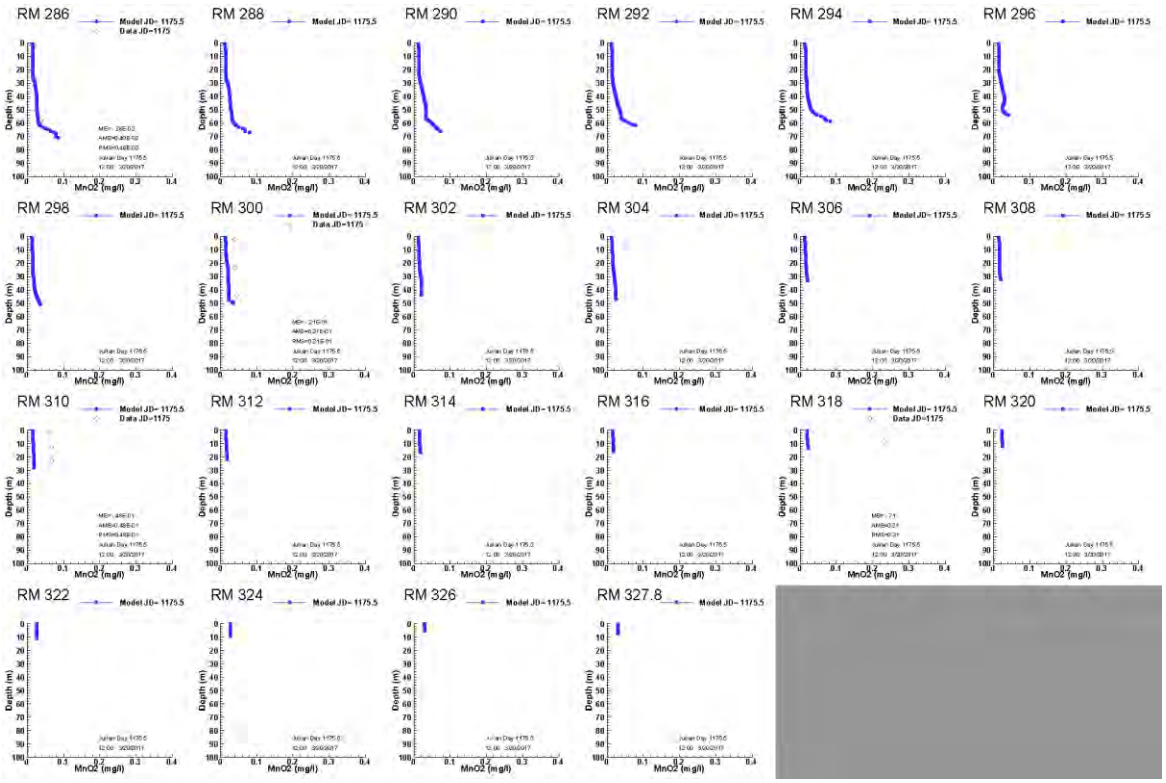


Figure 723. Vertical profiles of MnO2 compared with data for 3/20/2017.

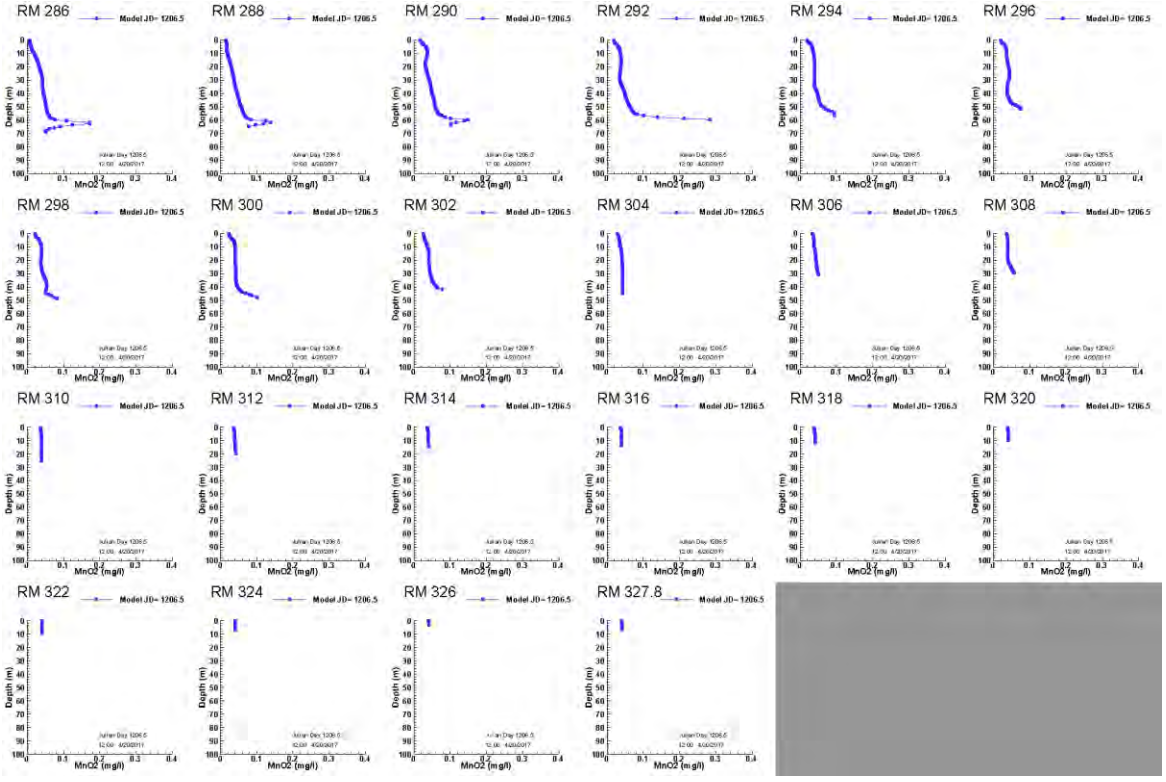


Figure 724. Vertical profiles of MnO2 compared with data for 4/20/2017.

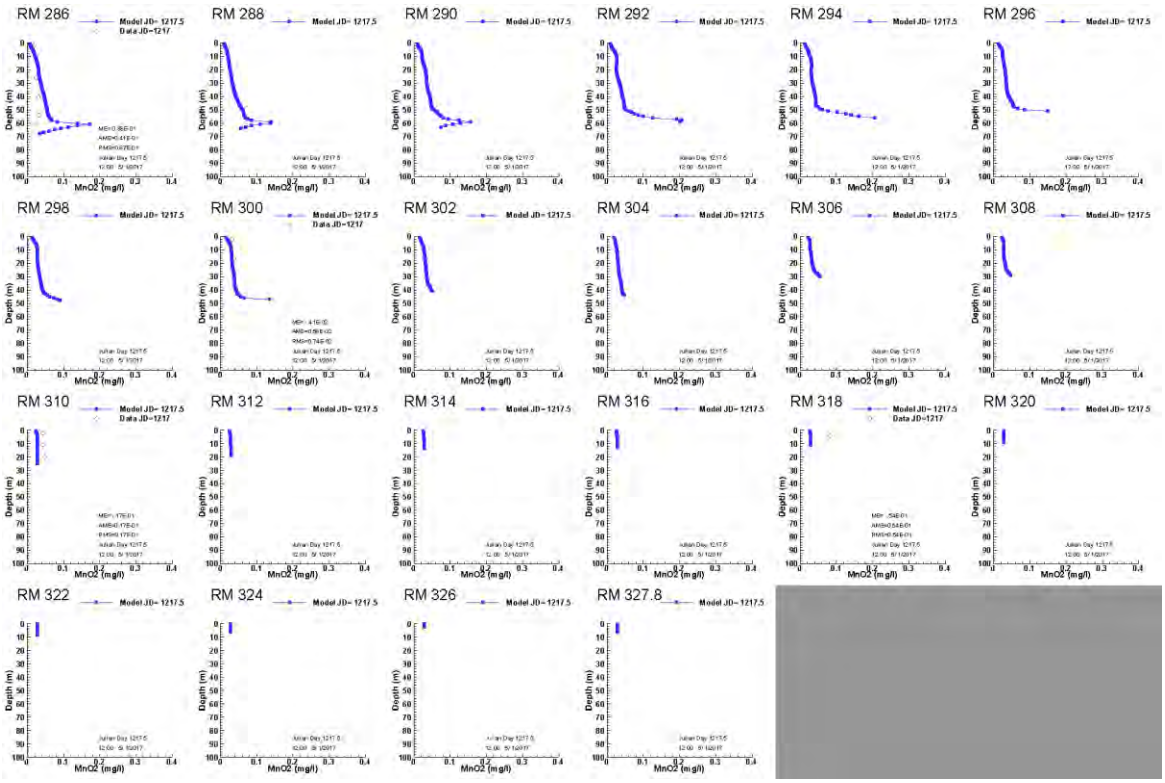


Figure 725. Vertical profiles of MnO2 compared with data for 5/ 1/2017.

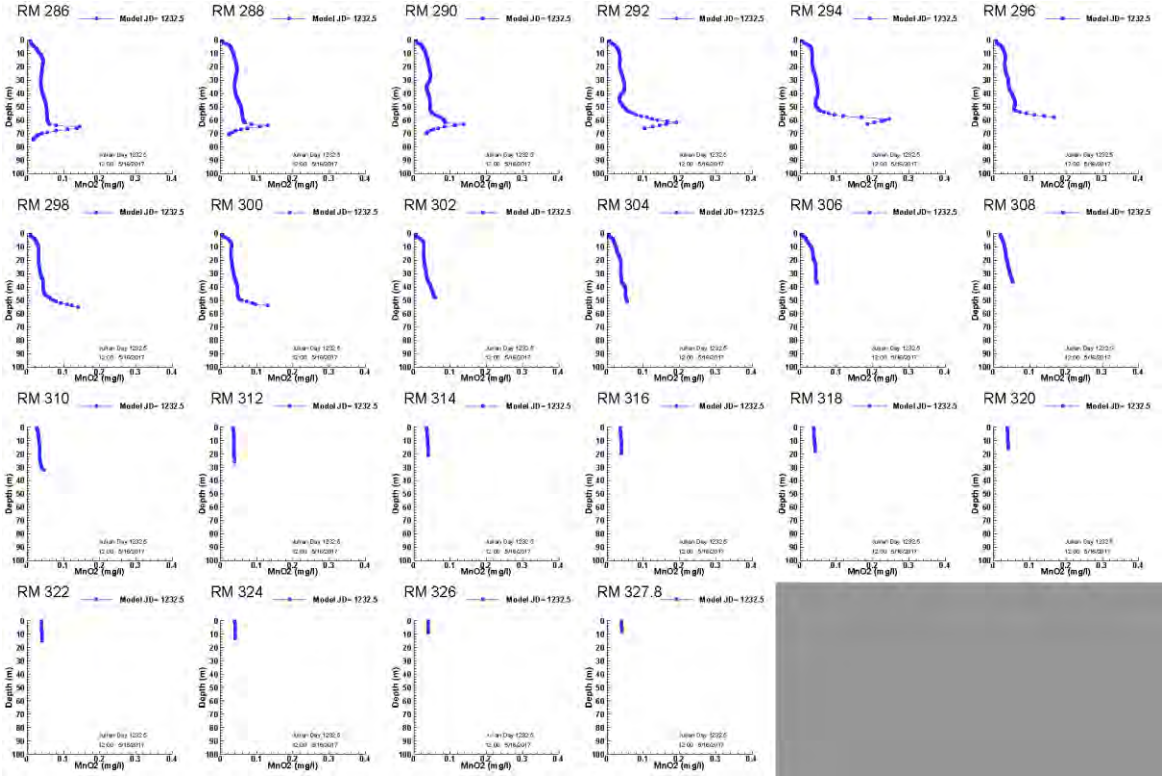


Figure 726. Vertical profiles of MnO2 compared with data for 5/16/2017.

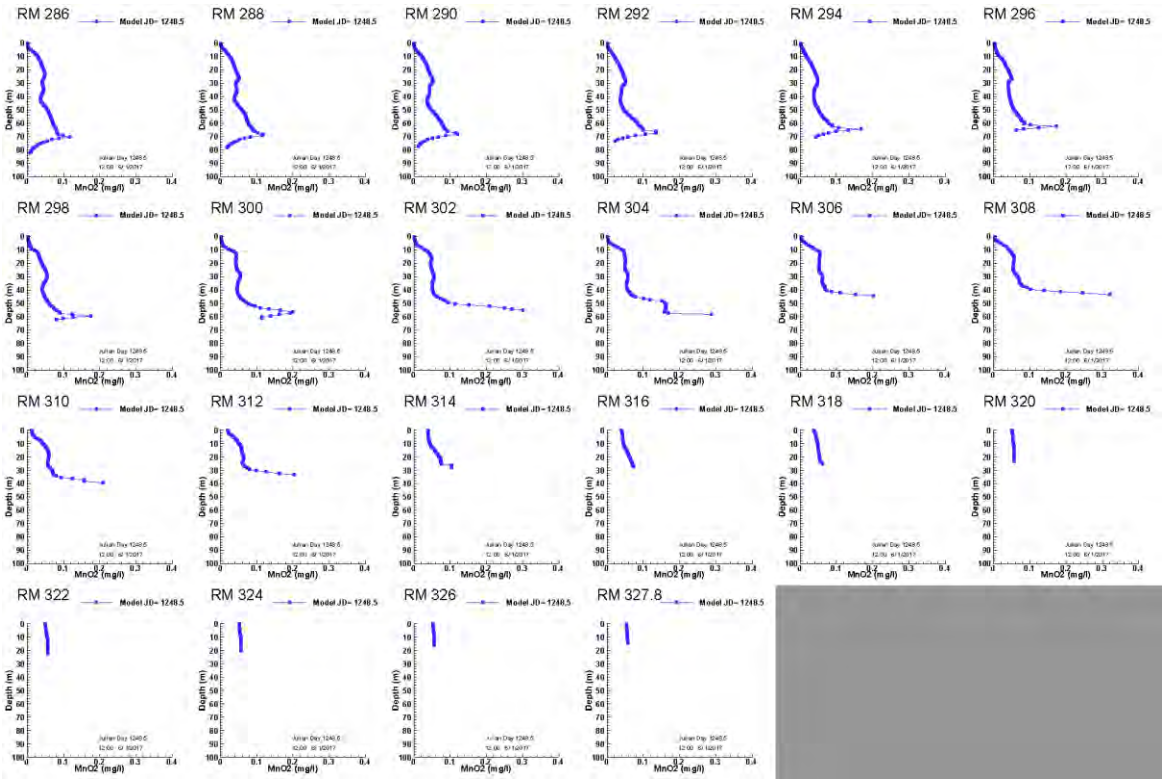


Figure 727. Vertical profiles of MnO2 compared with data for 6/ 1/2017.

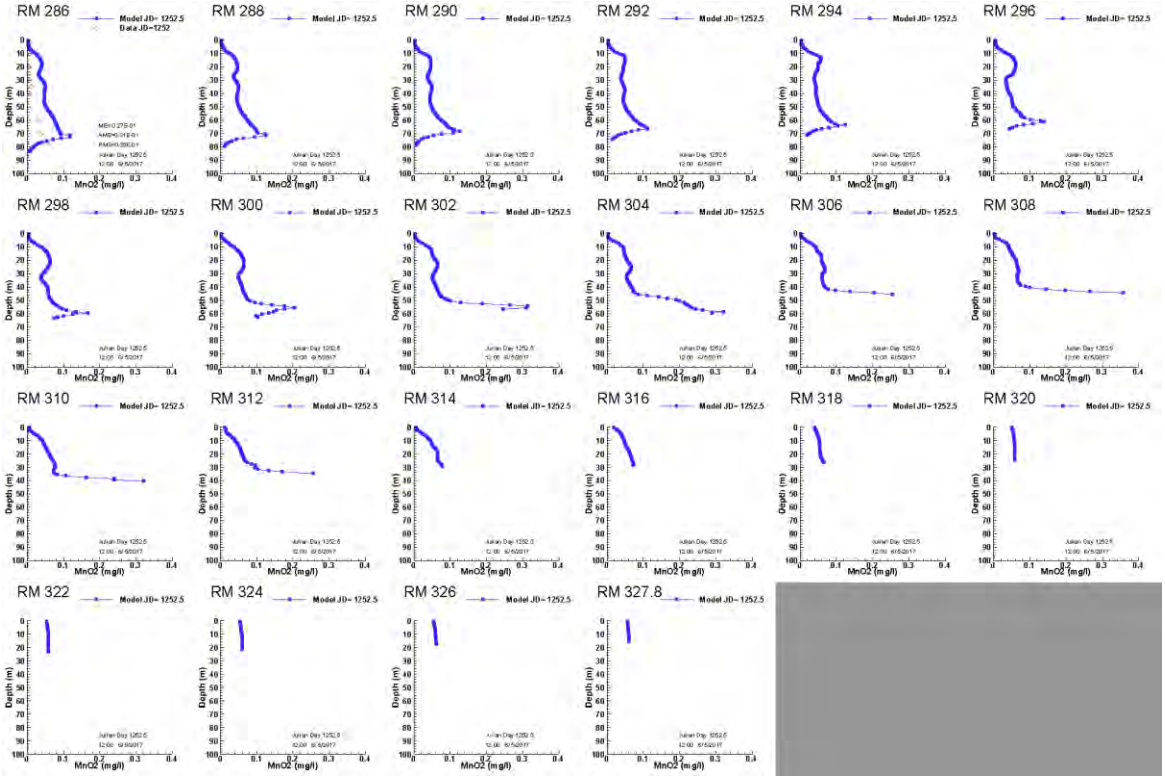


Figure 728. Vertical profiles of MnO2 compared with data for 6/ 5/2017.

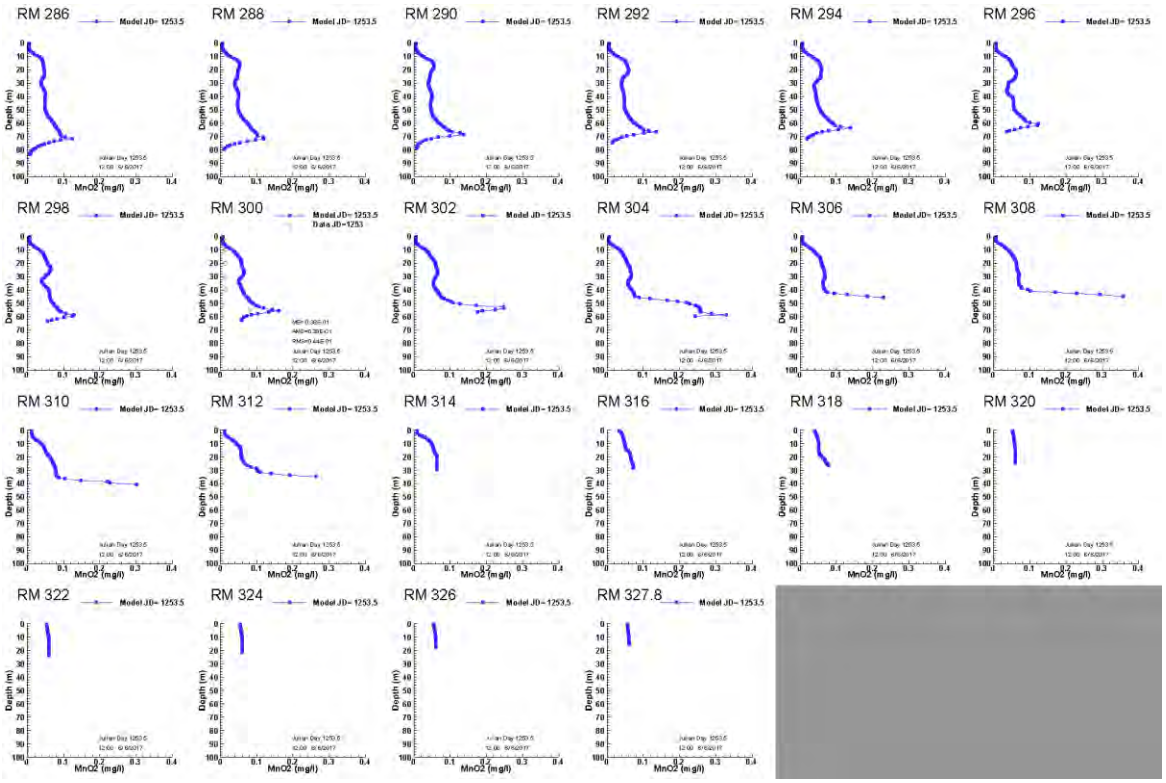


Figure 729. Vertical profiles of MnO2 compared with data for 6/ 6/2017.

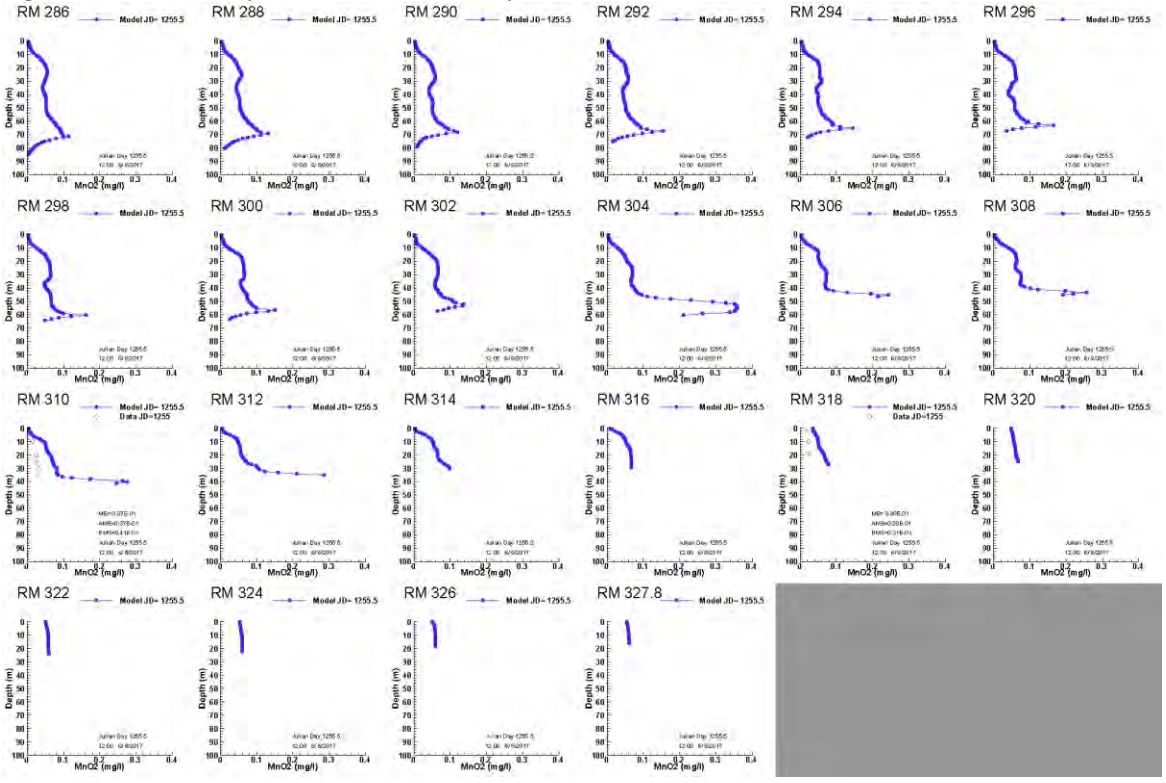


Figure 730. Vertical profiles of MnO2 compared with data for 6/ 8/2017.

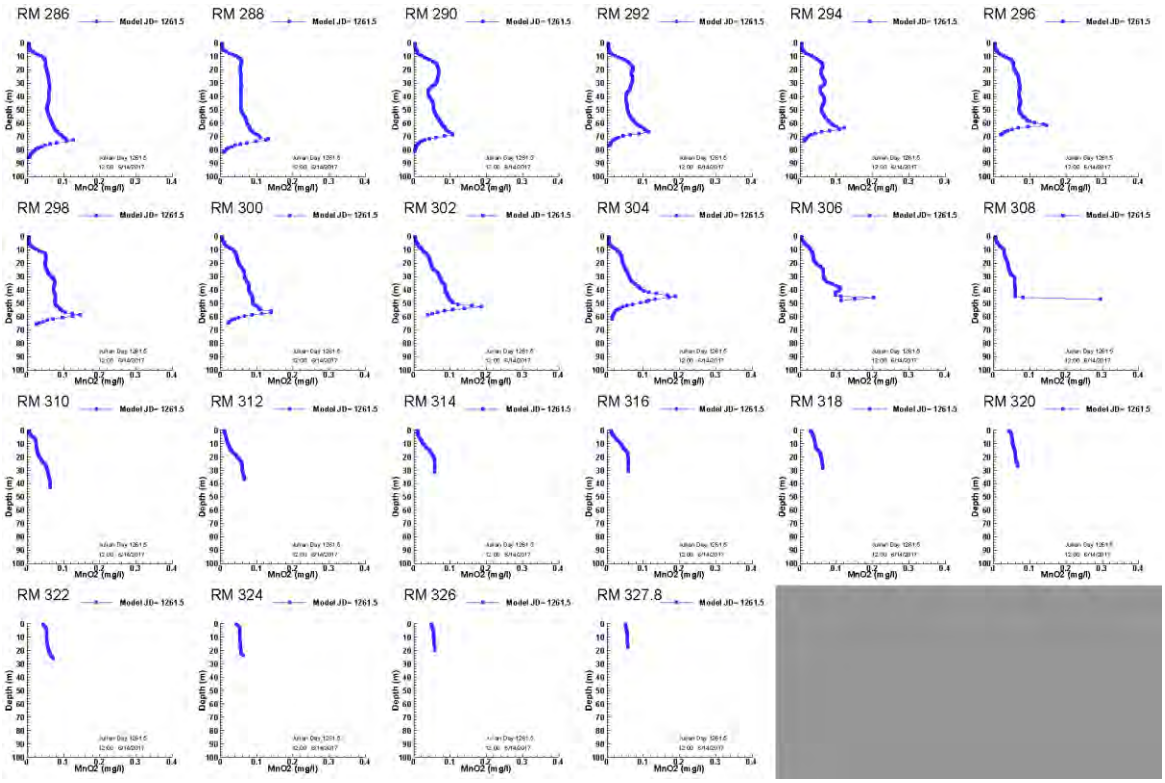


Figure 731. Vertical profiles of MnO2 compared with data for 6/14/2017.

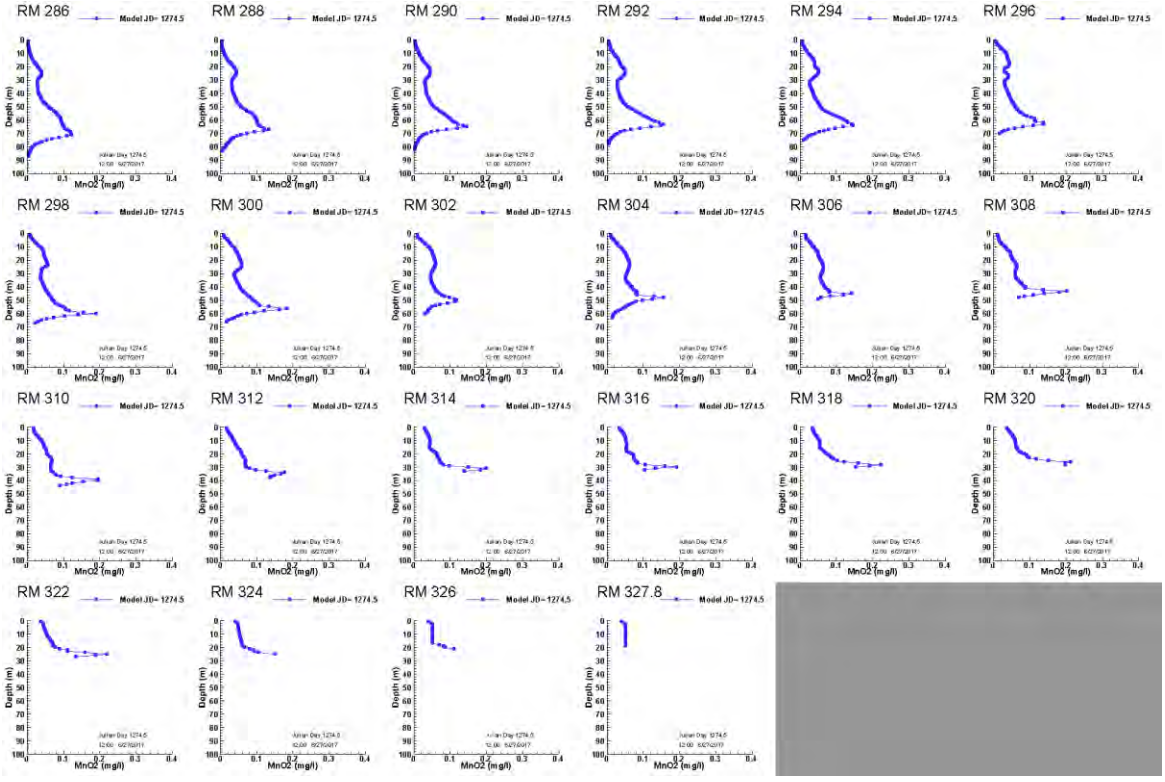


Figure 732. Vertical profiles of MnO2 compared with data for 6/27/2017.

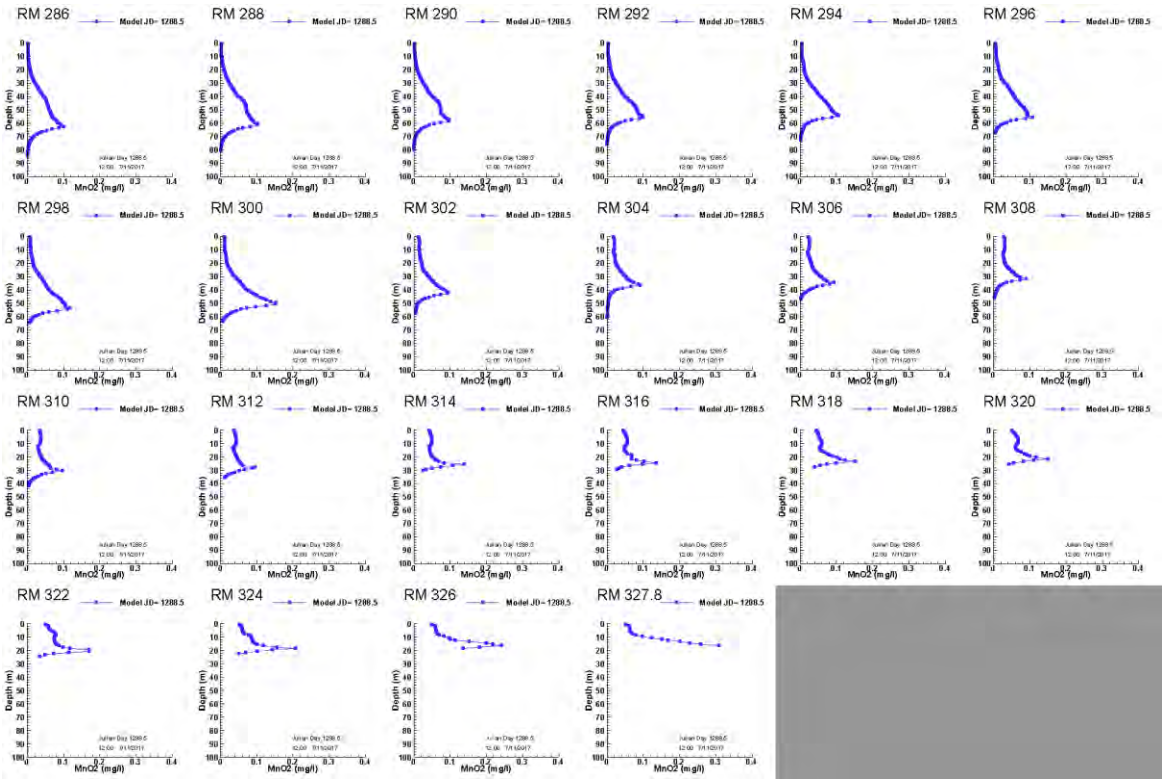


Figure 733. Vertical profiles of MnO2 compared with data for 7/11/2017.

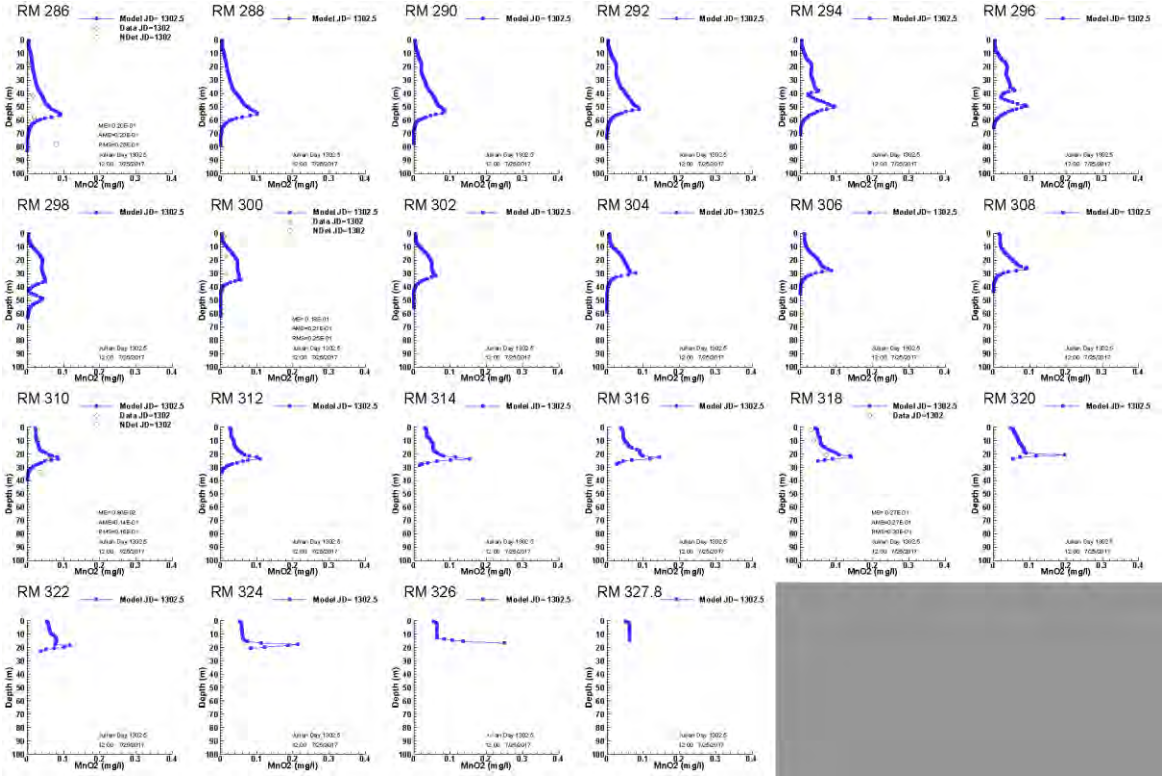


Figure 734. Vertical profiles of MnO2 compared with data for 7/25/2017.

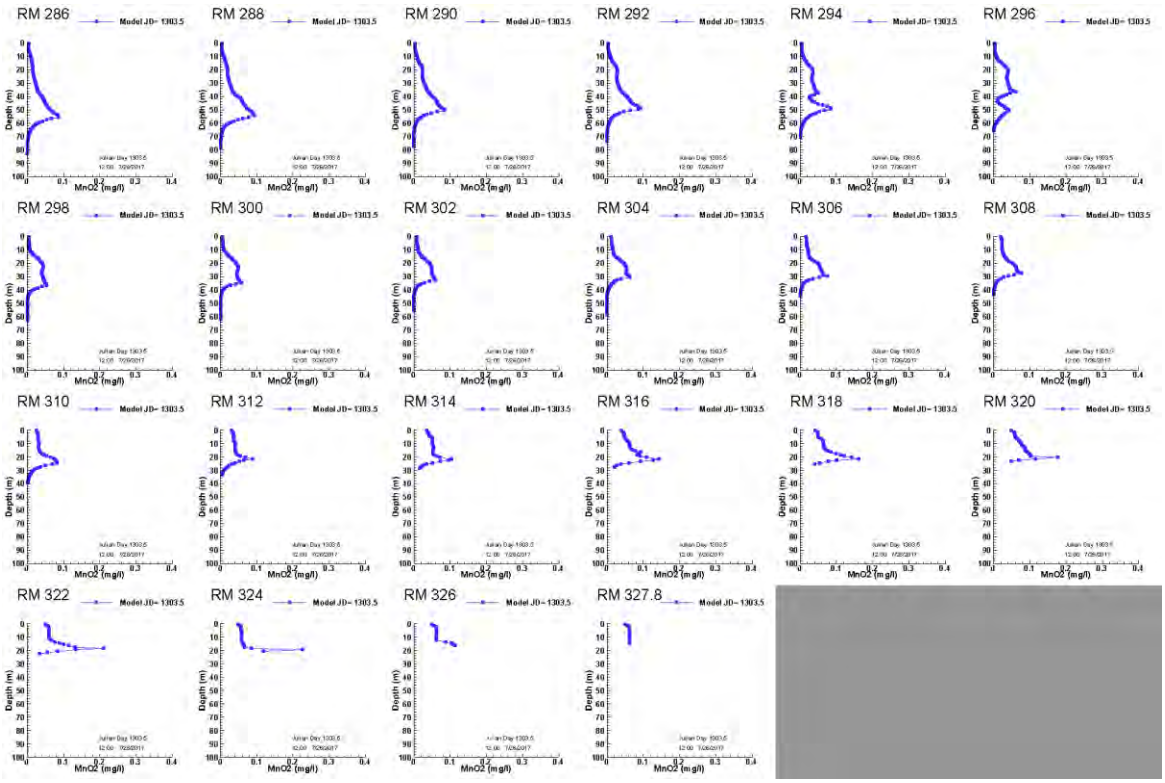


Figure 735. Vertical profiles of MnO2 compared with data for 7/26/2017.

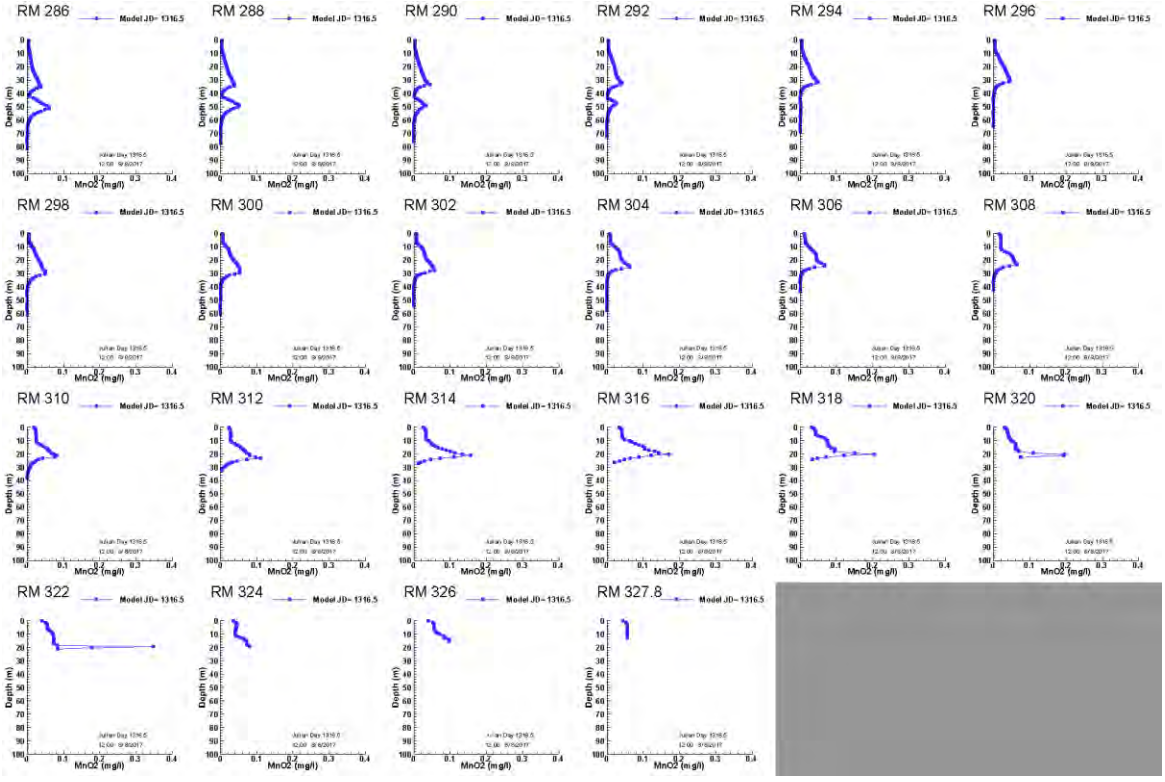


Figure 736. Vertical profiles of MnO2 compared with data for 8/ 8/2017.

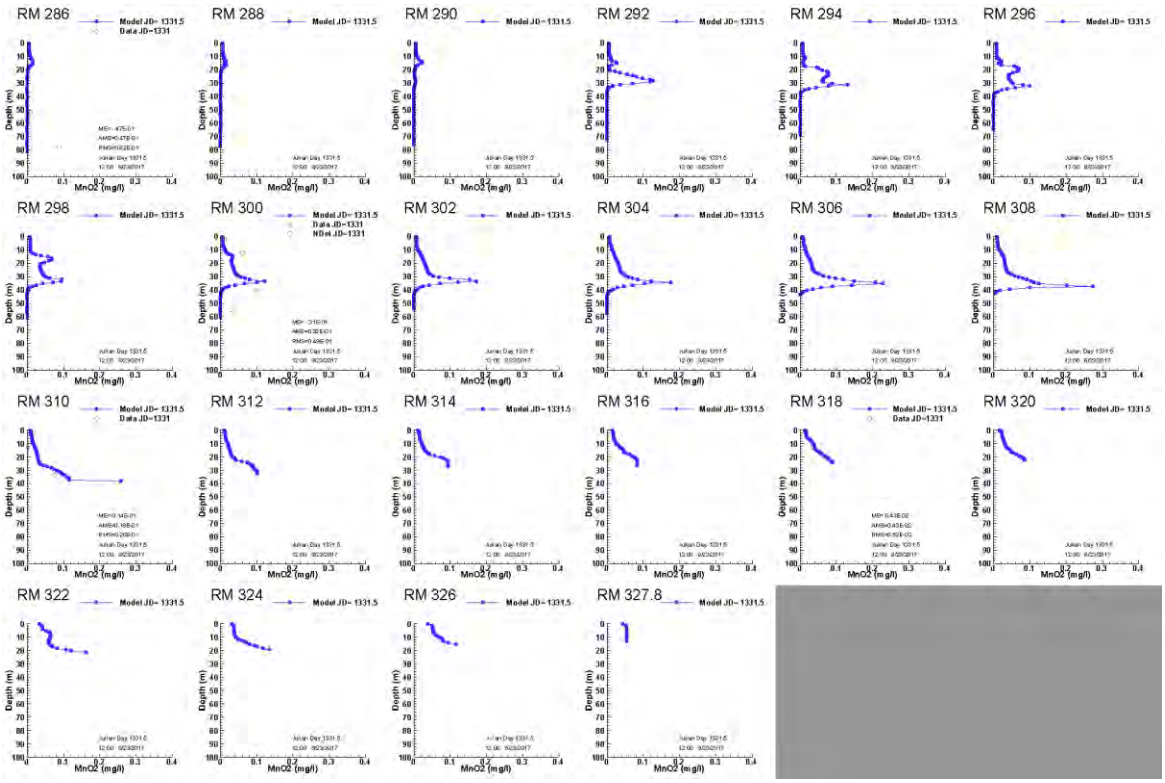


Figure 737. Vertical profiles of MnO2 compared with data for 8/23/2017.

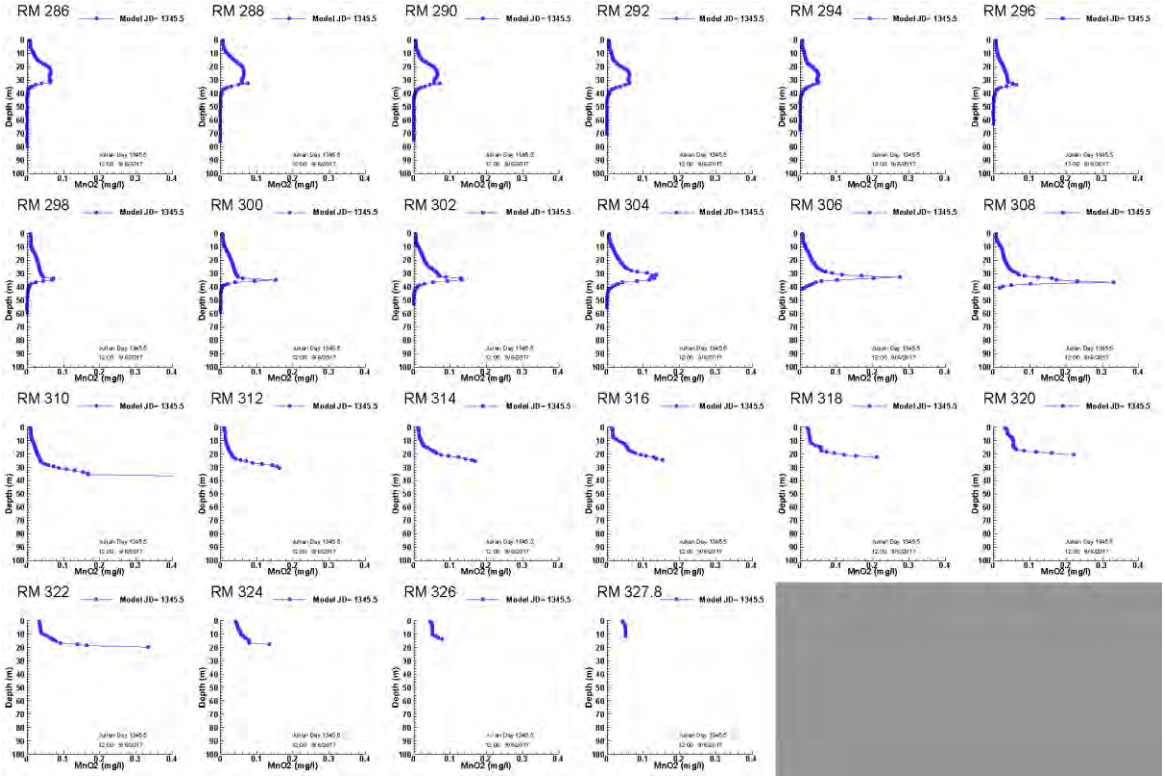


Figure 738. Vertical profiles of MnO2 compared with data for 9/ 6/2017.

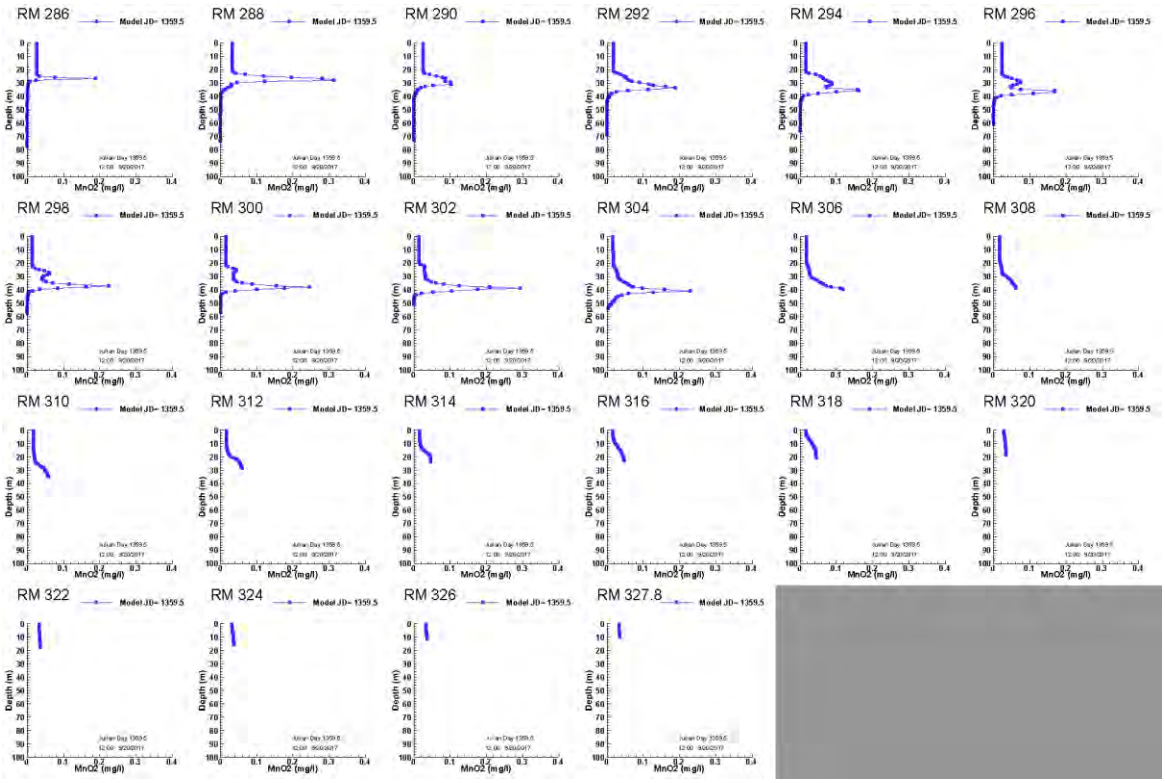


Figure 739. Vertical profiles of MnO2 compared with data for 9/20/2017.

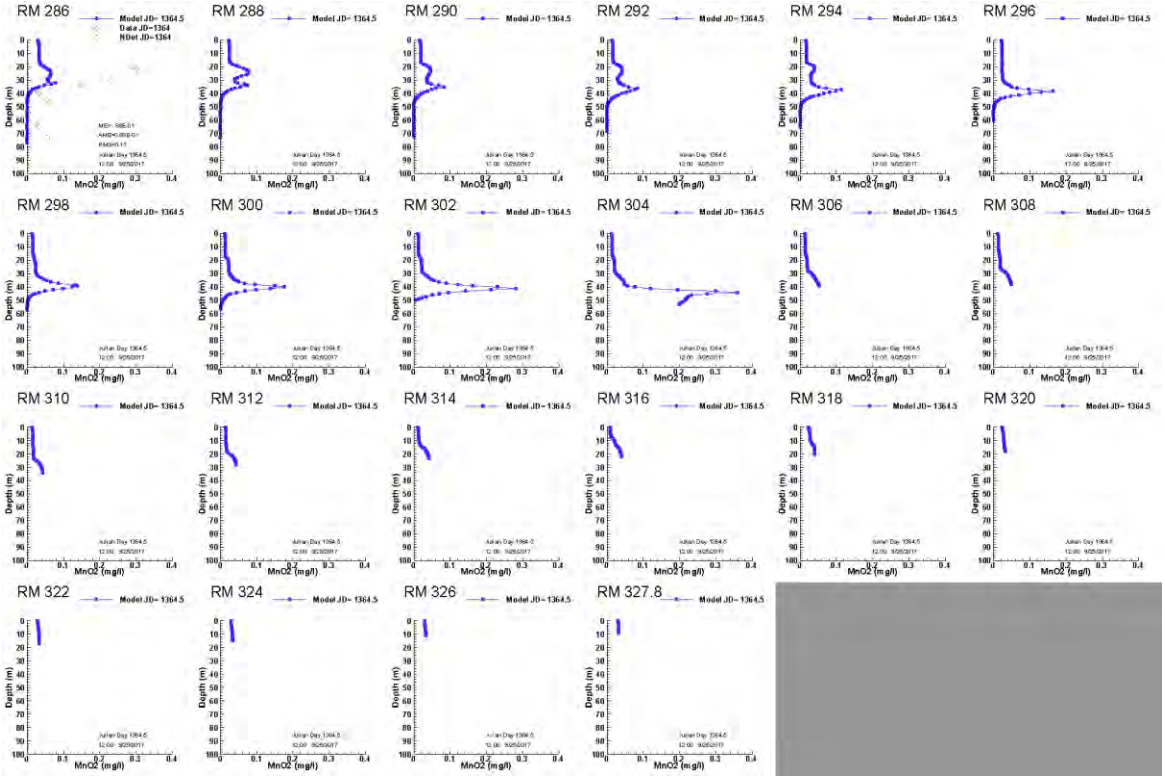


Figure 740. Vertical profiles of MnO2 compared with data for 9/25/2017.

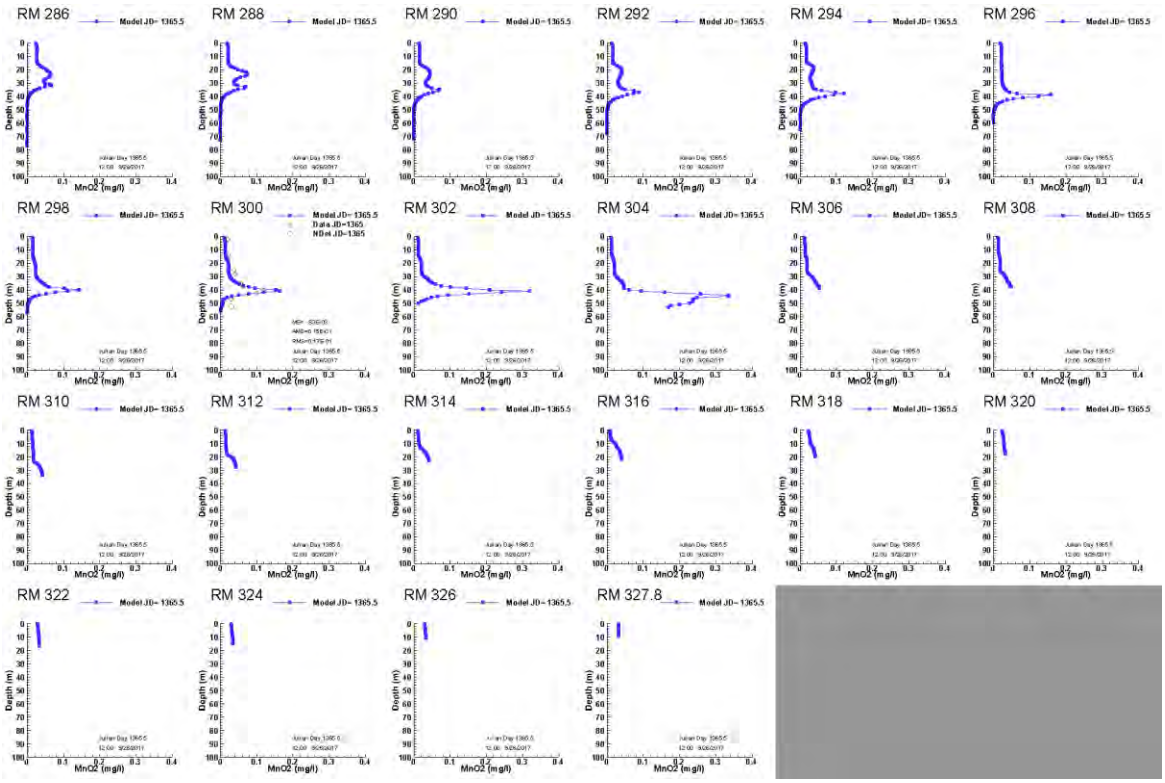


Figure 741. Vertical profiles of MnO2 compared with data for 9/26/2017.

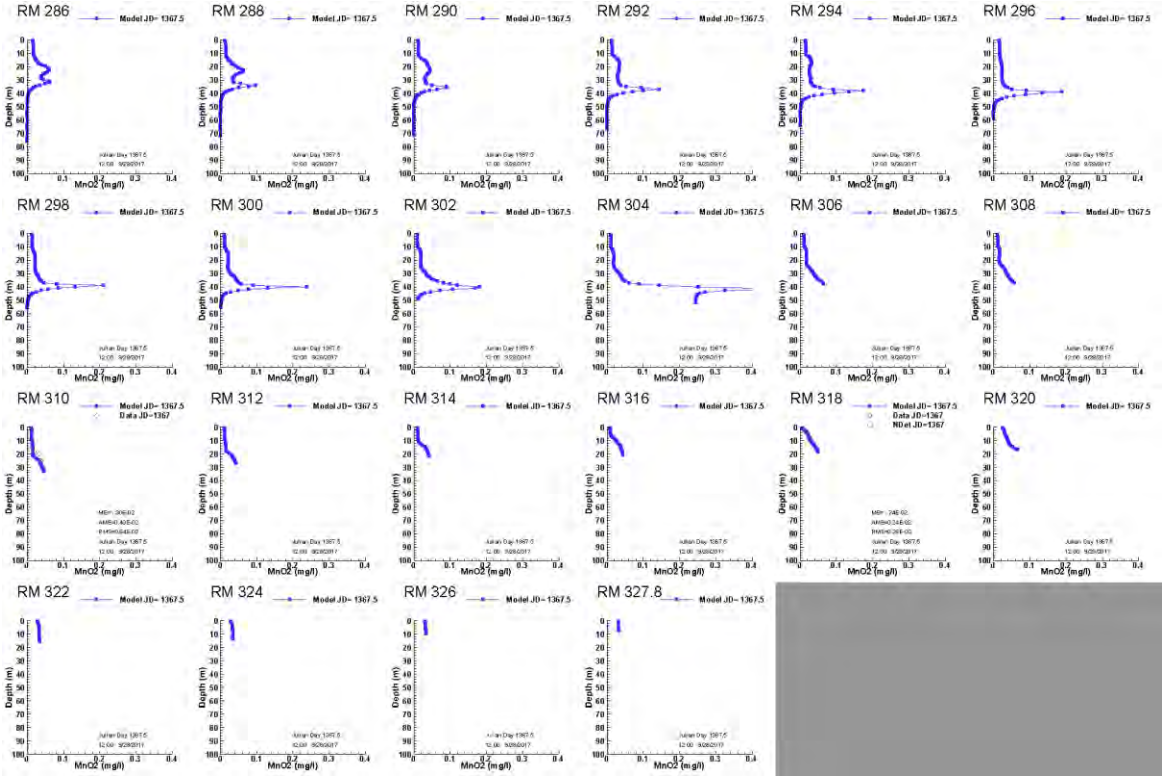


Figure 742. Vertical profiles of MnO2 compared with data for 9/28/2017.

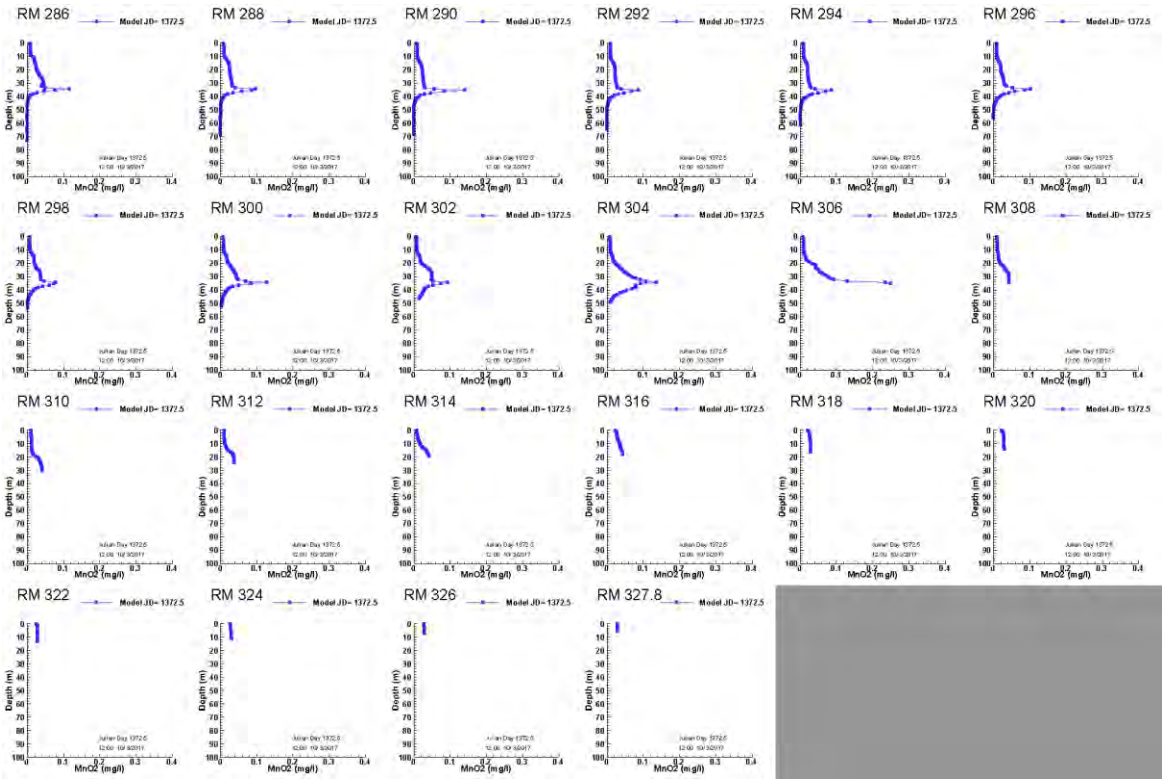


Figure 743. Vertical profiles of MnO2 compared with data for 10/ 3/2017.

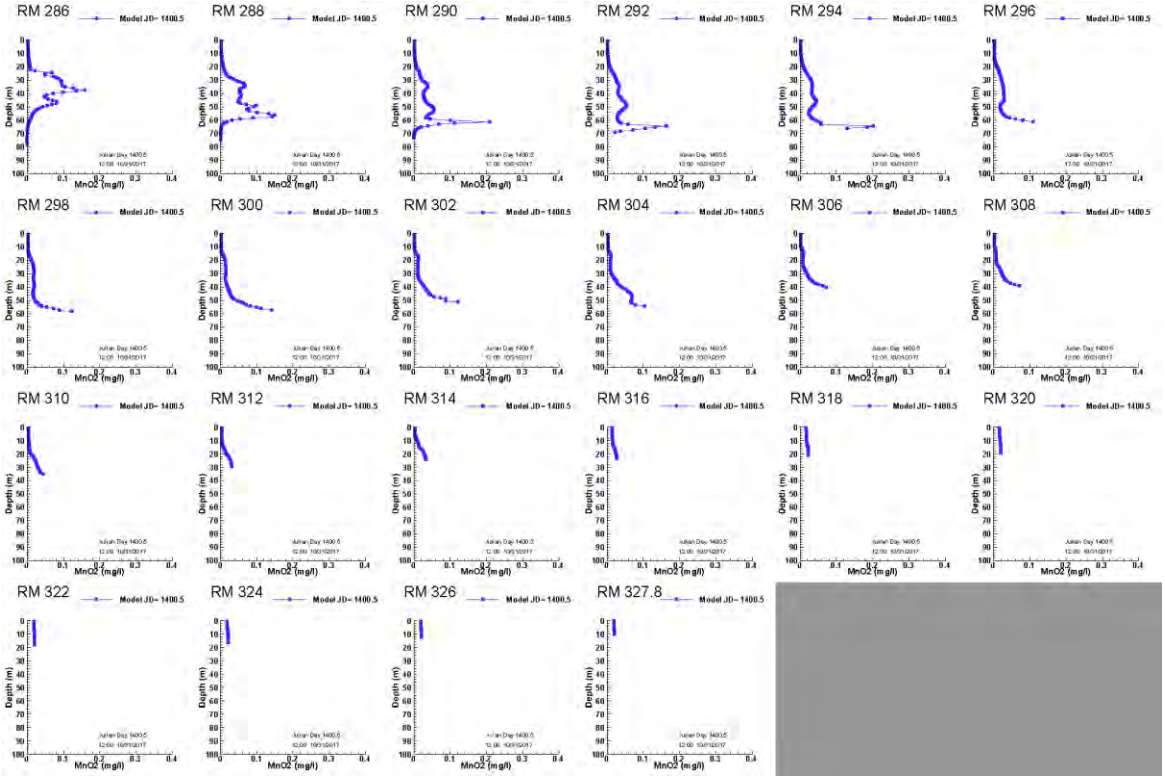


Figure 744. Vertical profiles of MnO2 compared with data for 10/31/2017.

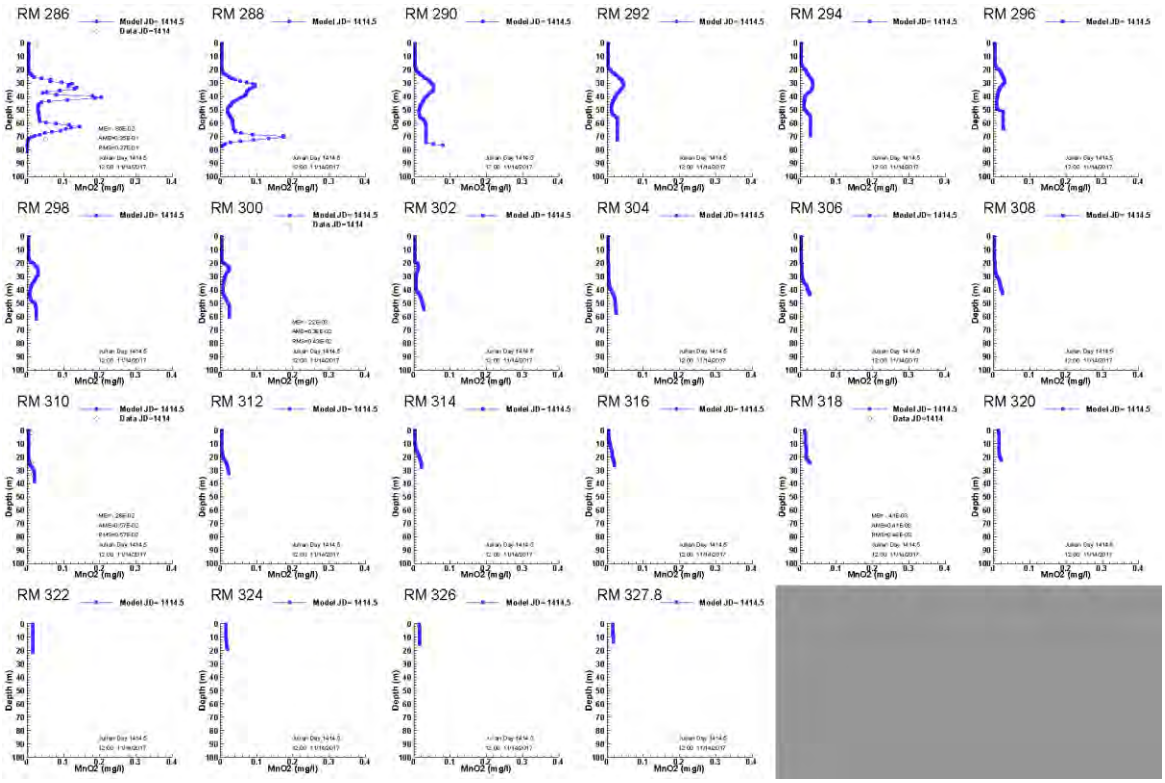


Figure 745. Vertical profiles of MnO2 compared with data for 11/14/2017.

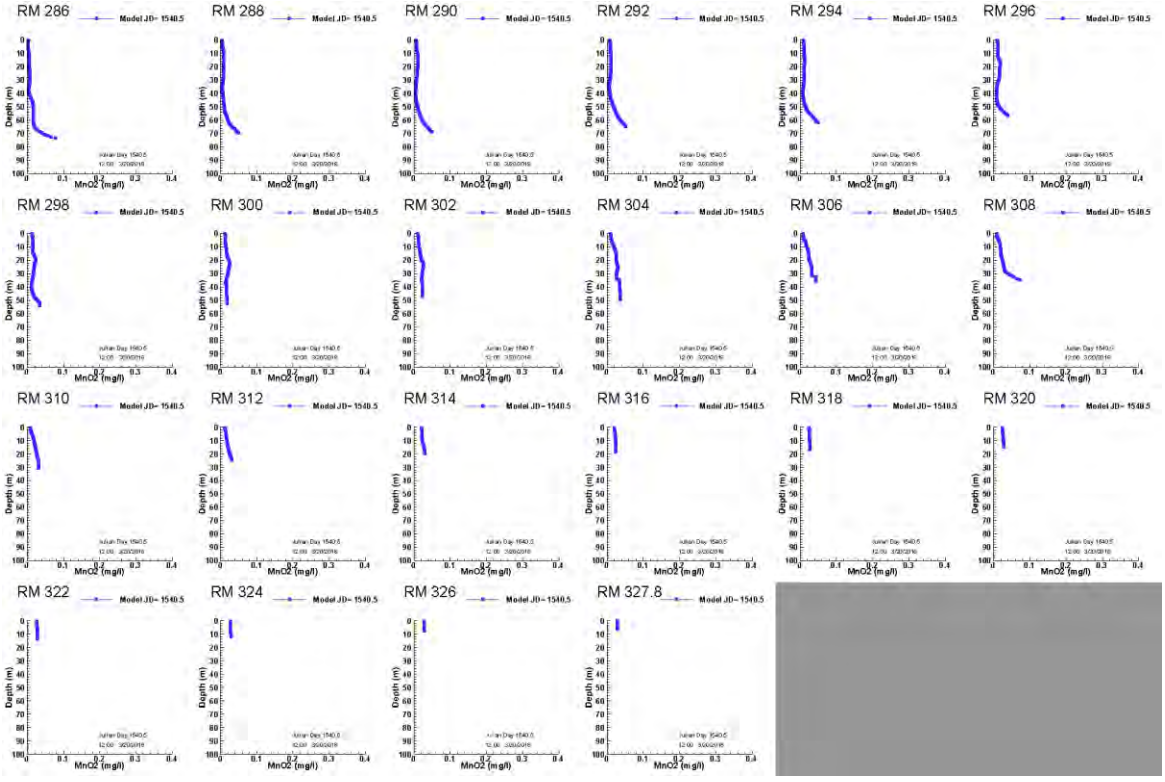


Figure 746. Vertical profiles of MnO2 compared with data for 3/20/2018.

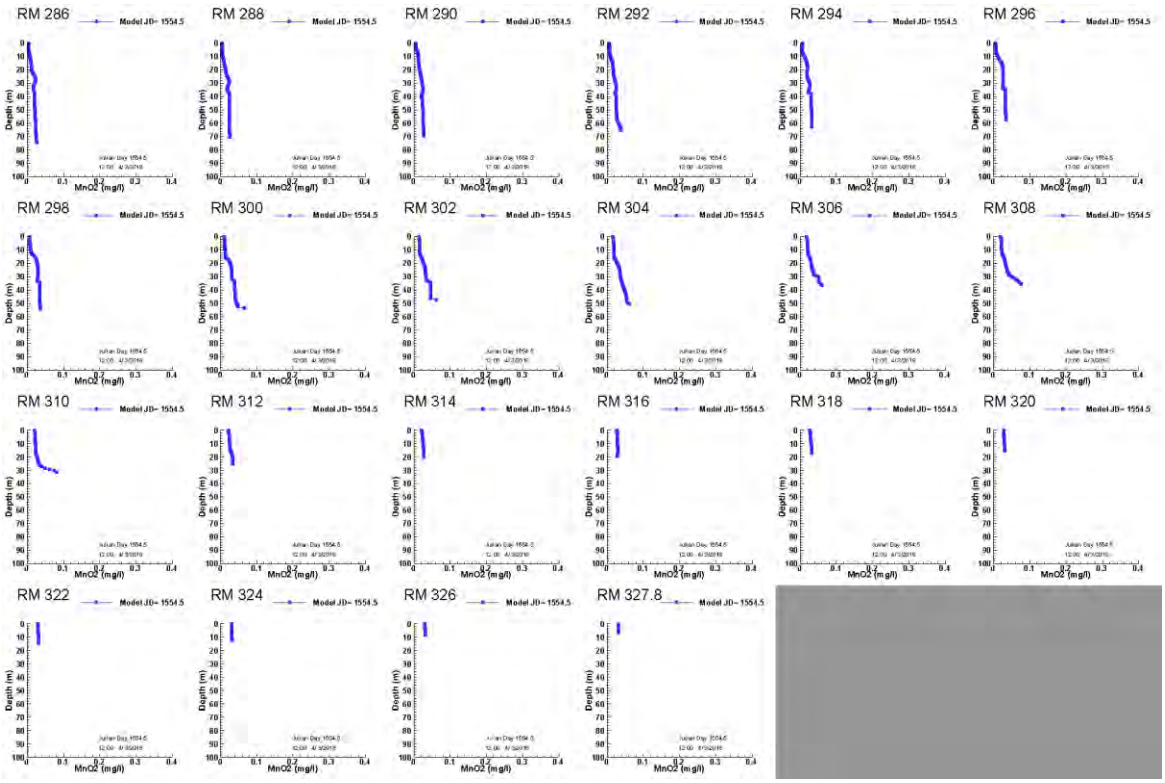


Figure 747. Vertical profiles of MnO2 compared with data for 4/ 3/2018.

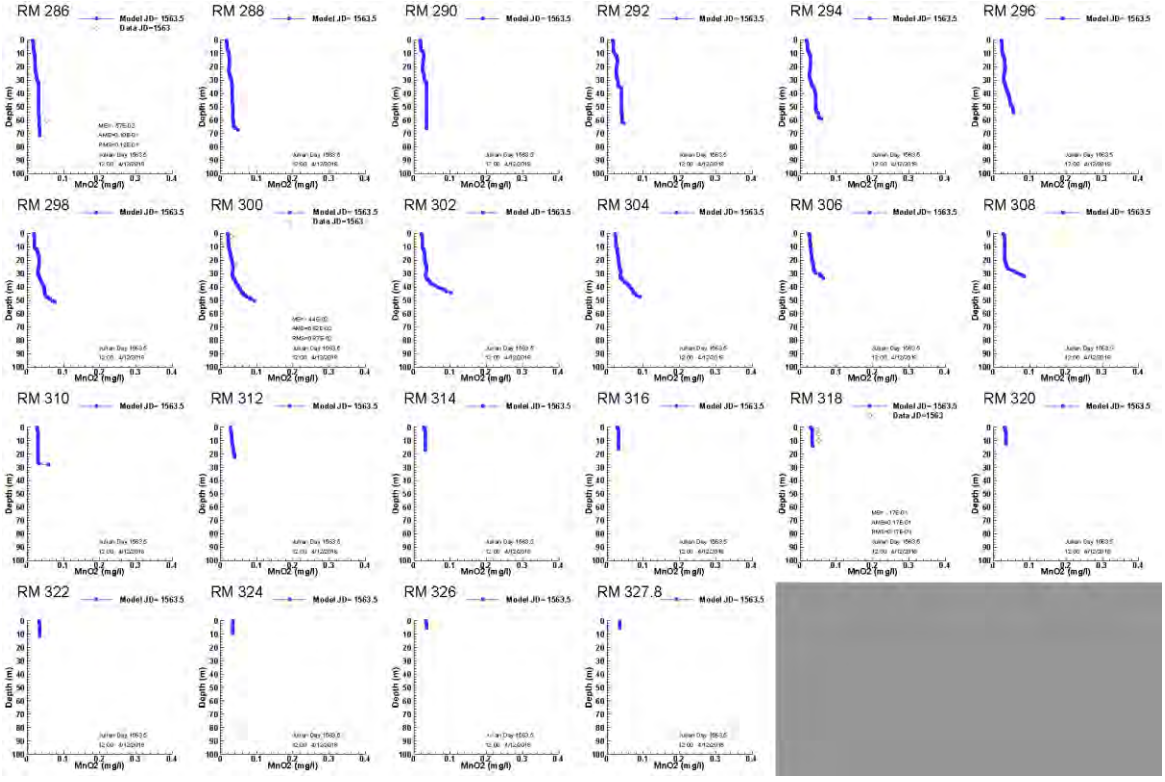


Figure 748. Vertical profiles of MnO2 compared with data for 4/12/2018.

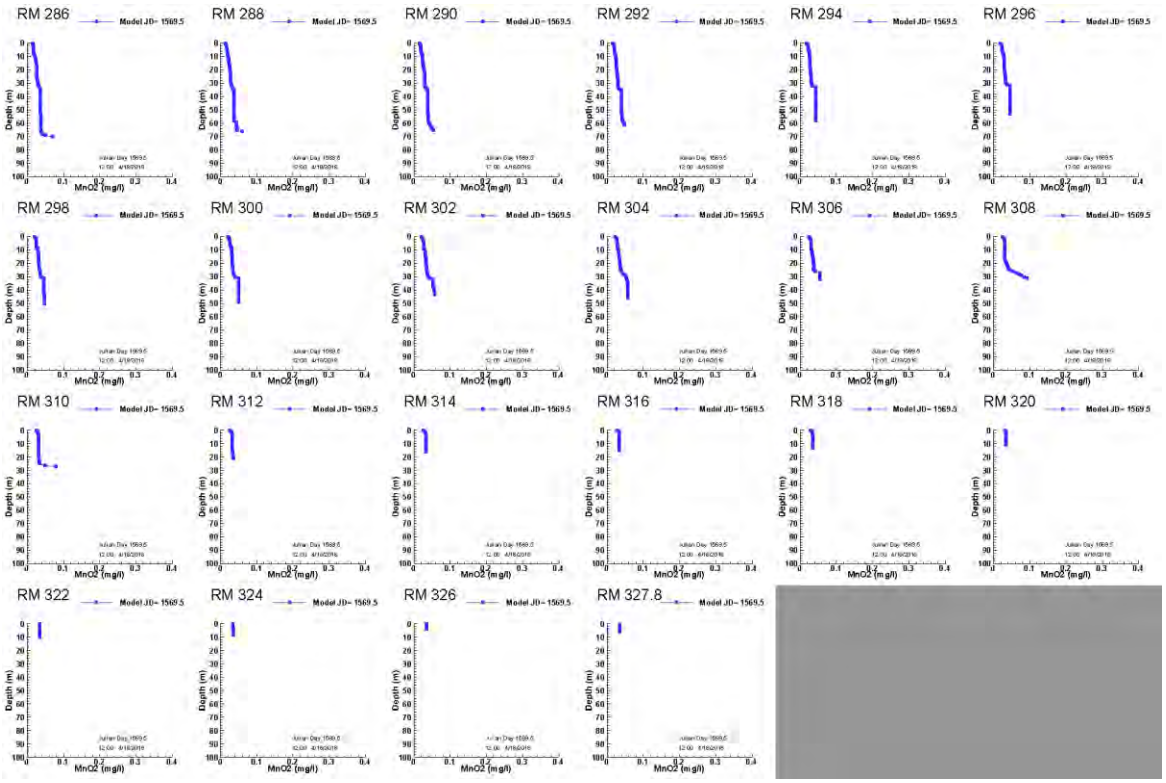


Figure 749. Vertical profiles of MnO2 compared with data for 4/18/2018.

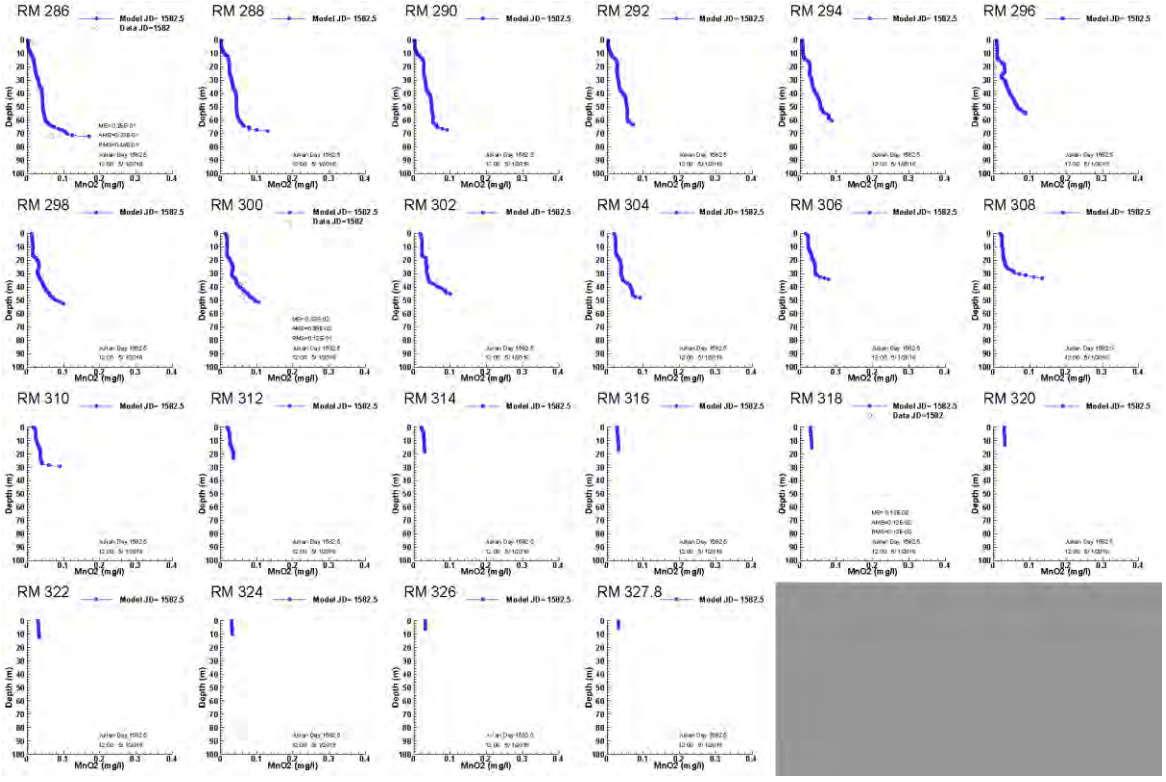


Figure 750. Vertical profiles of MnO2 compared with data for 5/ 1/2018.

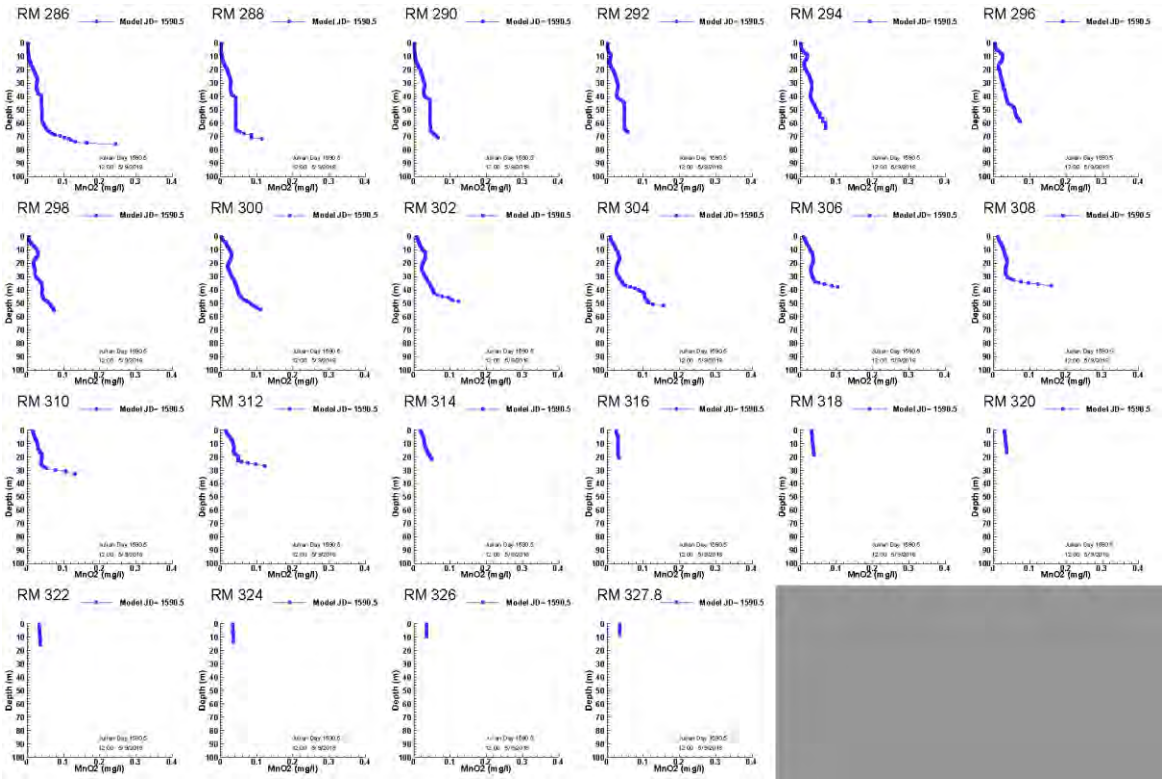


Figure 751. Vertical profiles of MnO2 compared with data for 5/ 9/2018.

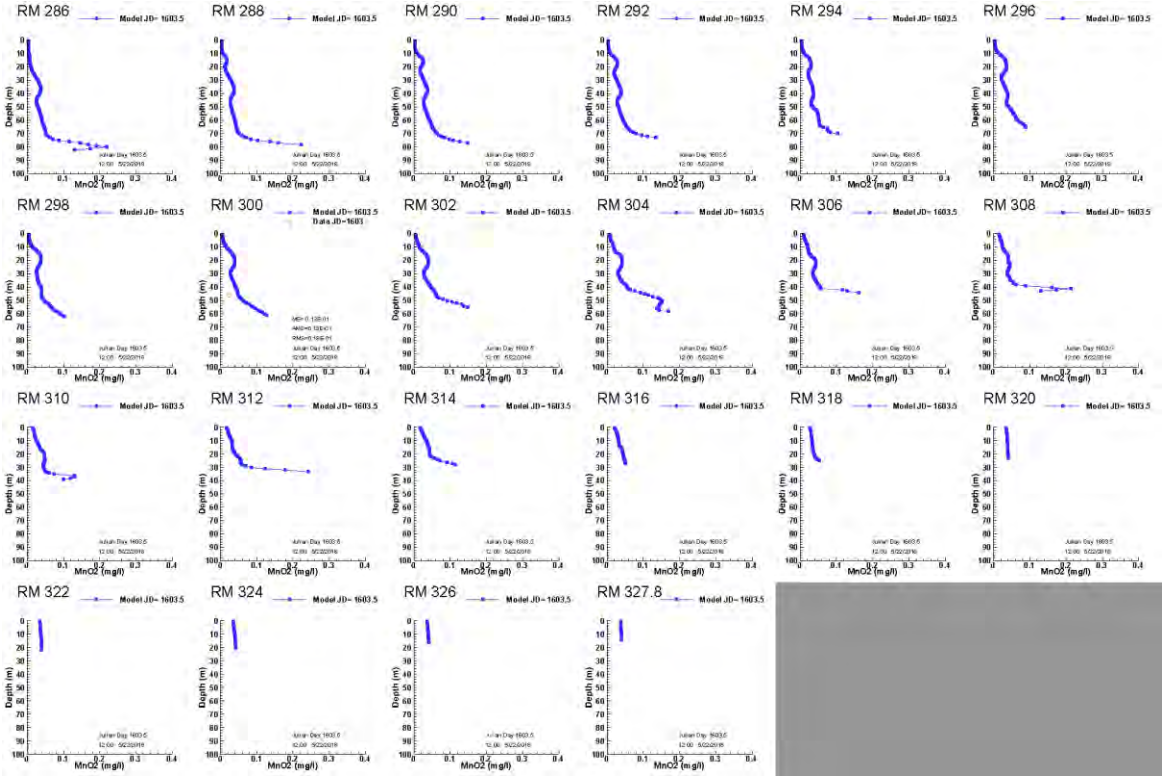


Figure 752. Vertical profiles of MnO2 compared with data for 5/22/2018.

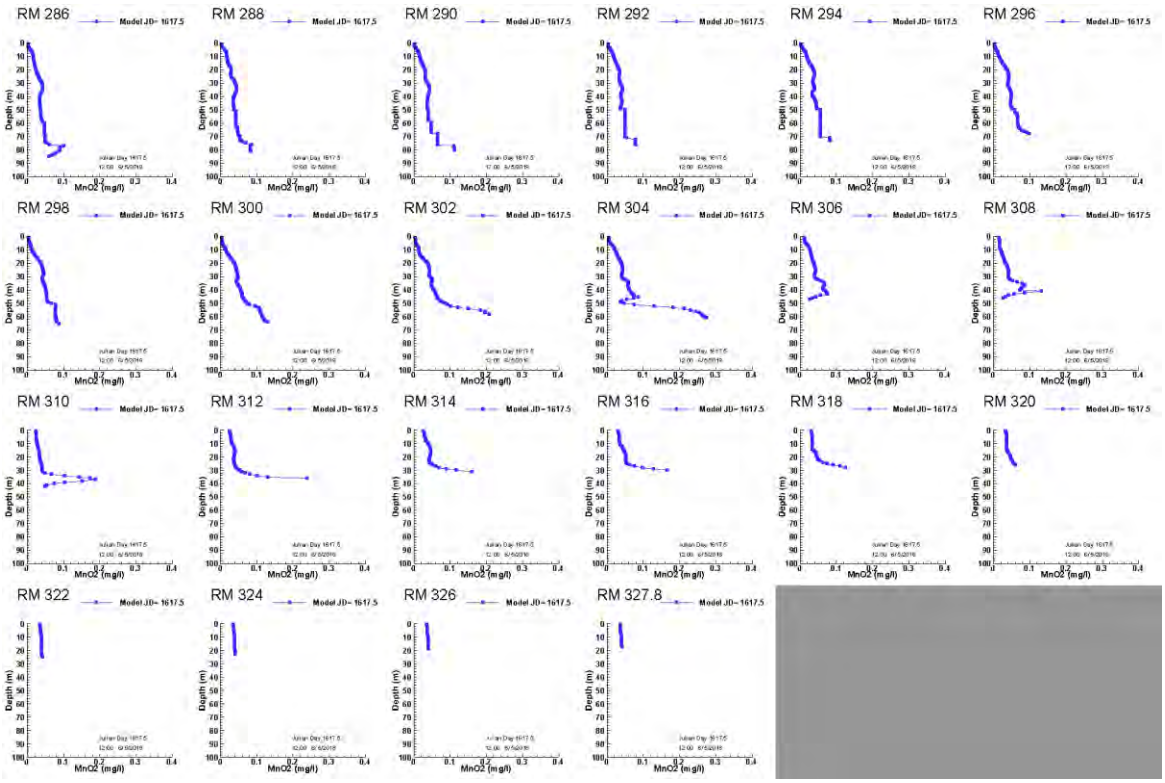


Figure 753. Vertical profiles of MnO2 compared with data for 6/ 5/2018.

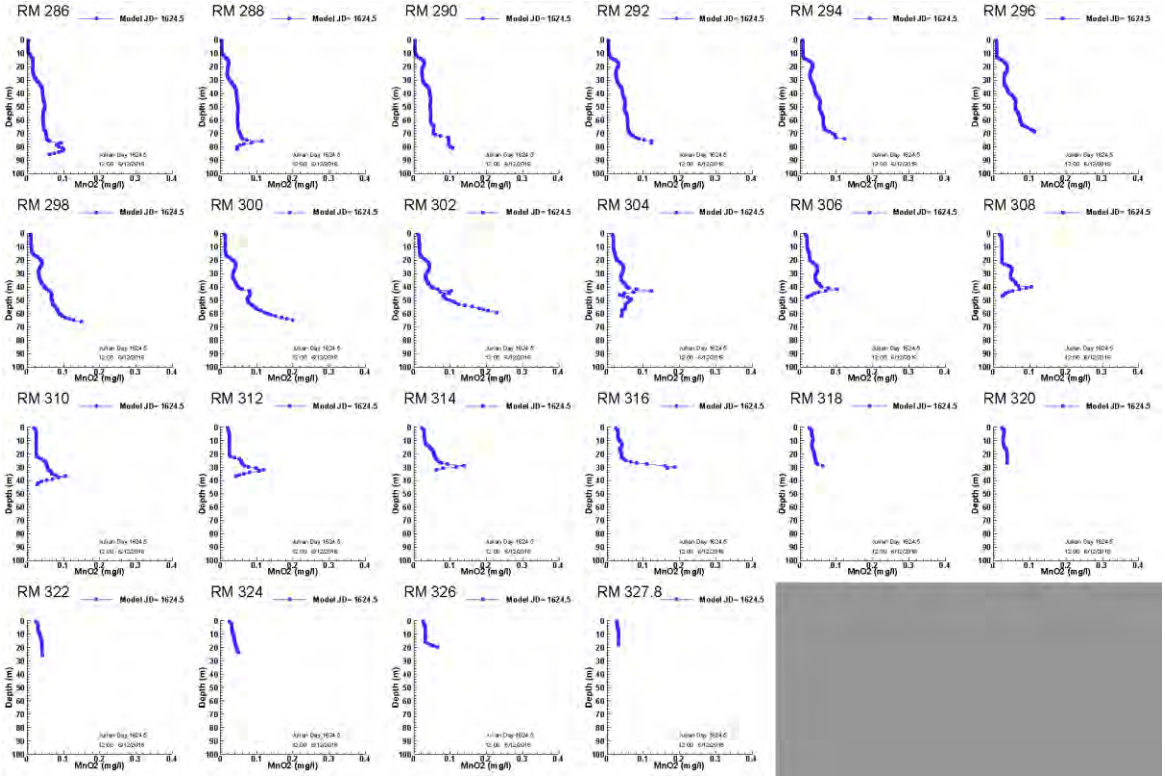


Figure 754. Vertical profiles of MnO2 compared with data for 6/12/2018.

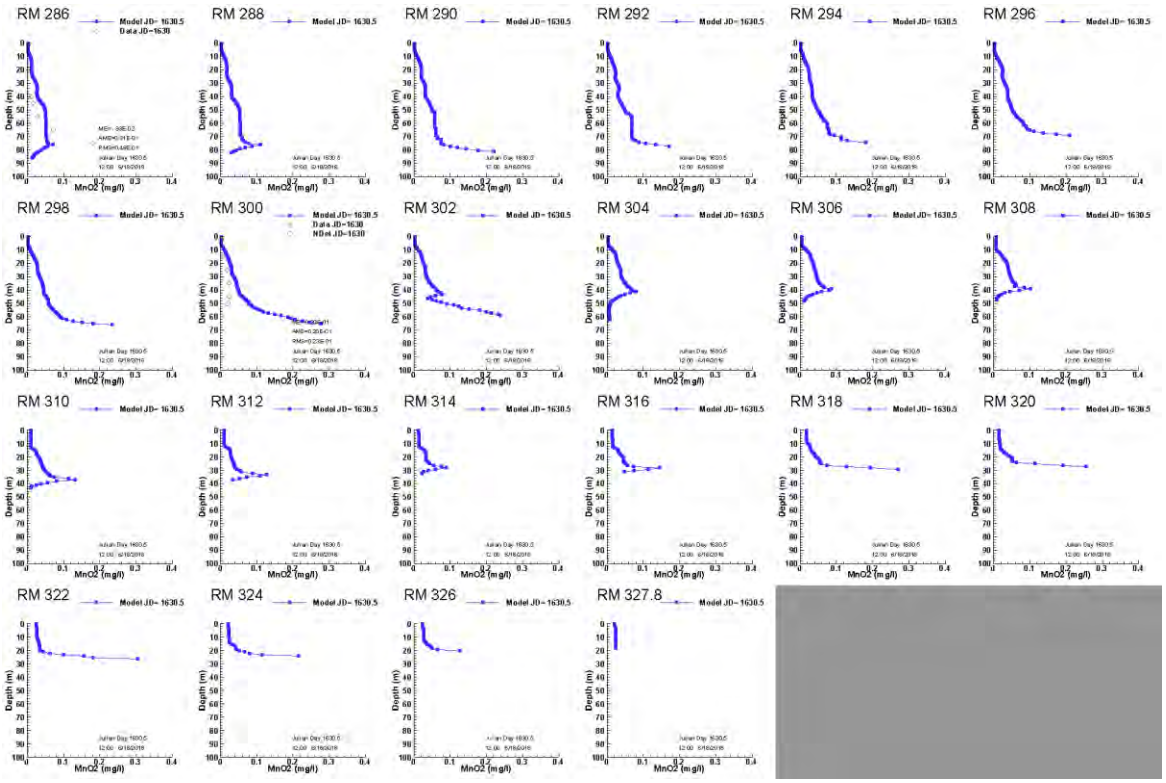


Figure 755. Vertical profiles of MnO2 compared with data for 6/18/2018.

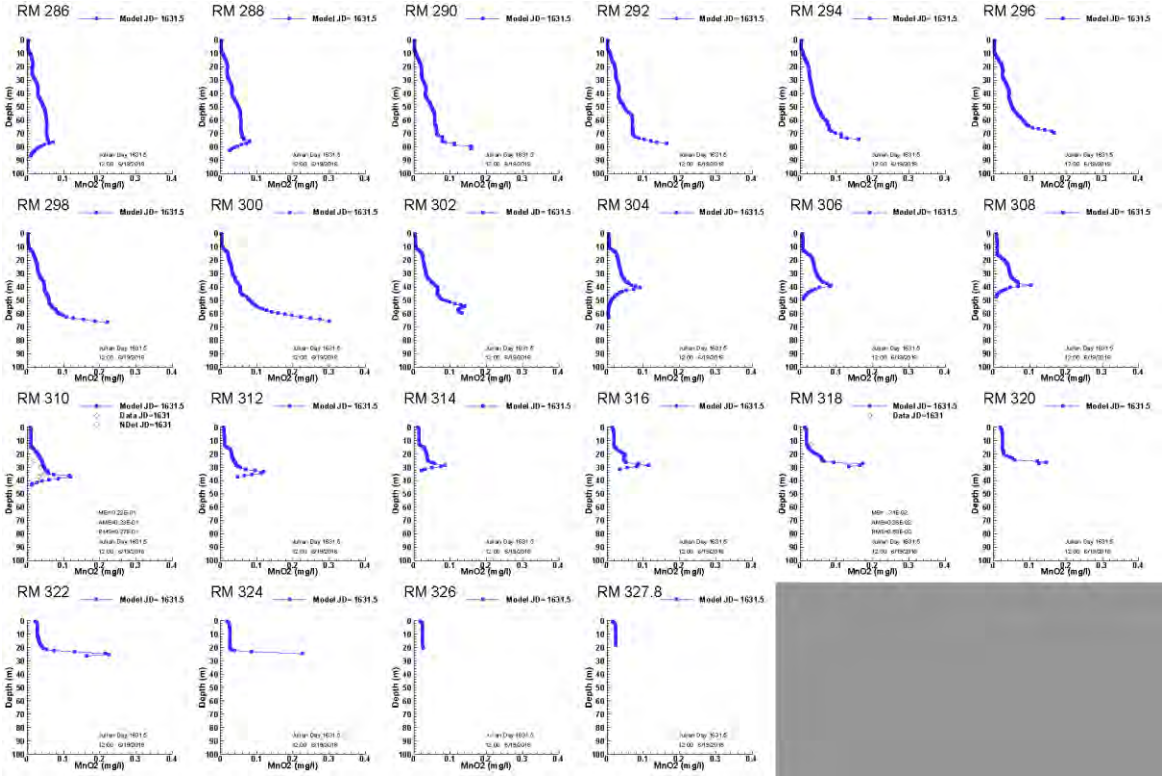


Figure 756. Vertical profiles of MnO2 compared with data for 6/19/2018.

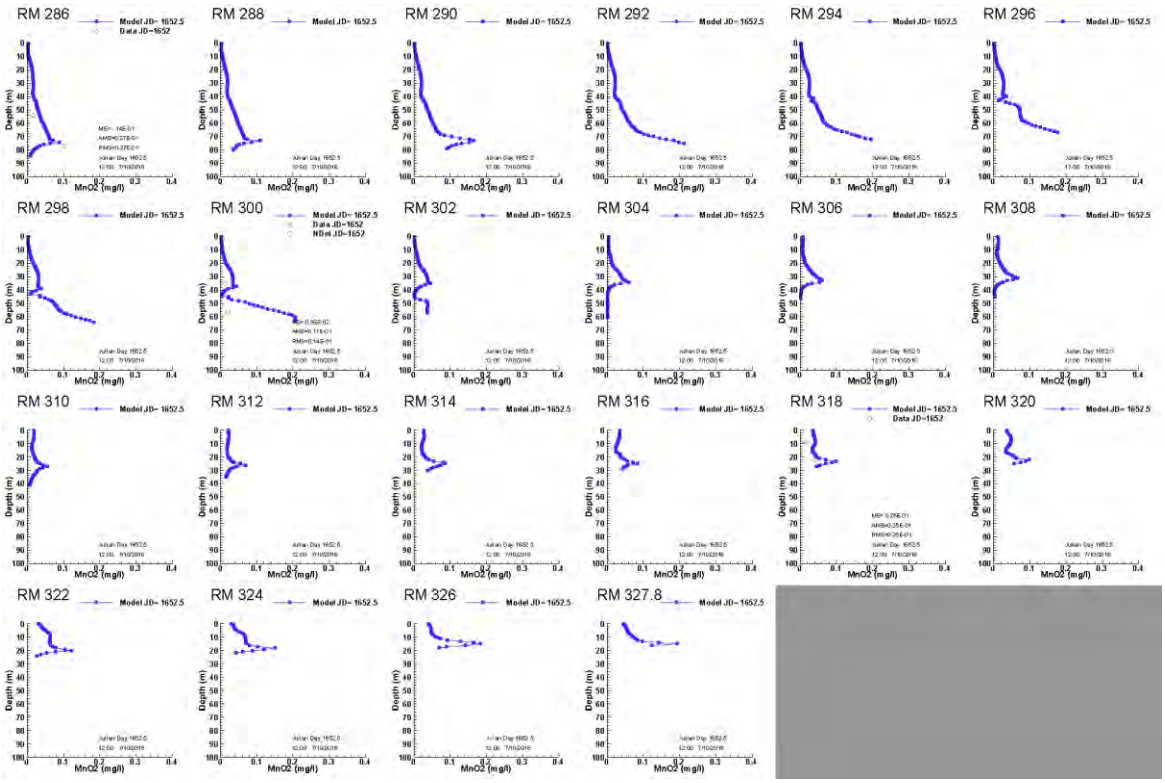


Figure 757. Vertical profiles of MnO2 compared with data for 7/10/2018.

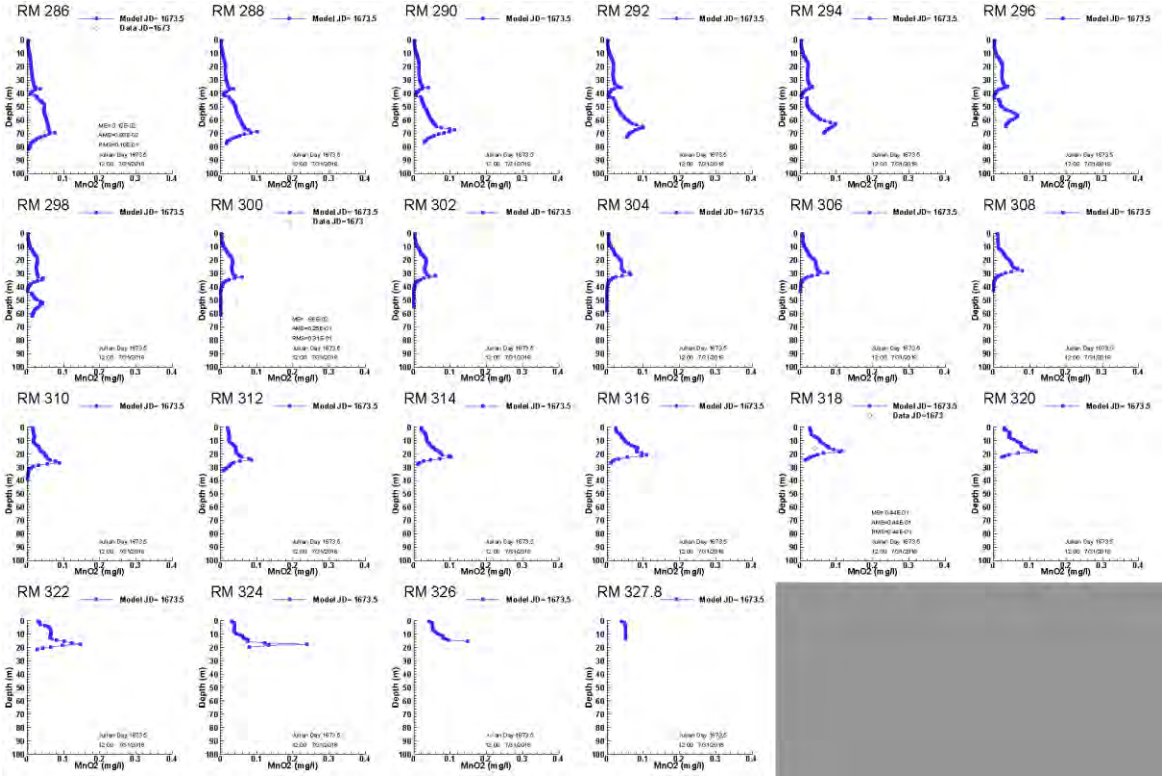


Figure 758. Vertical profiles of MnO2 compared with data for 7/31/2018.

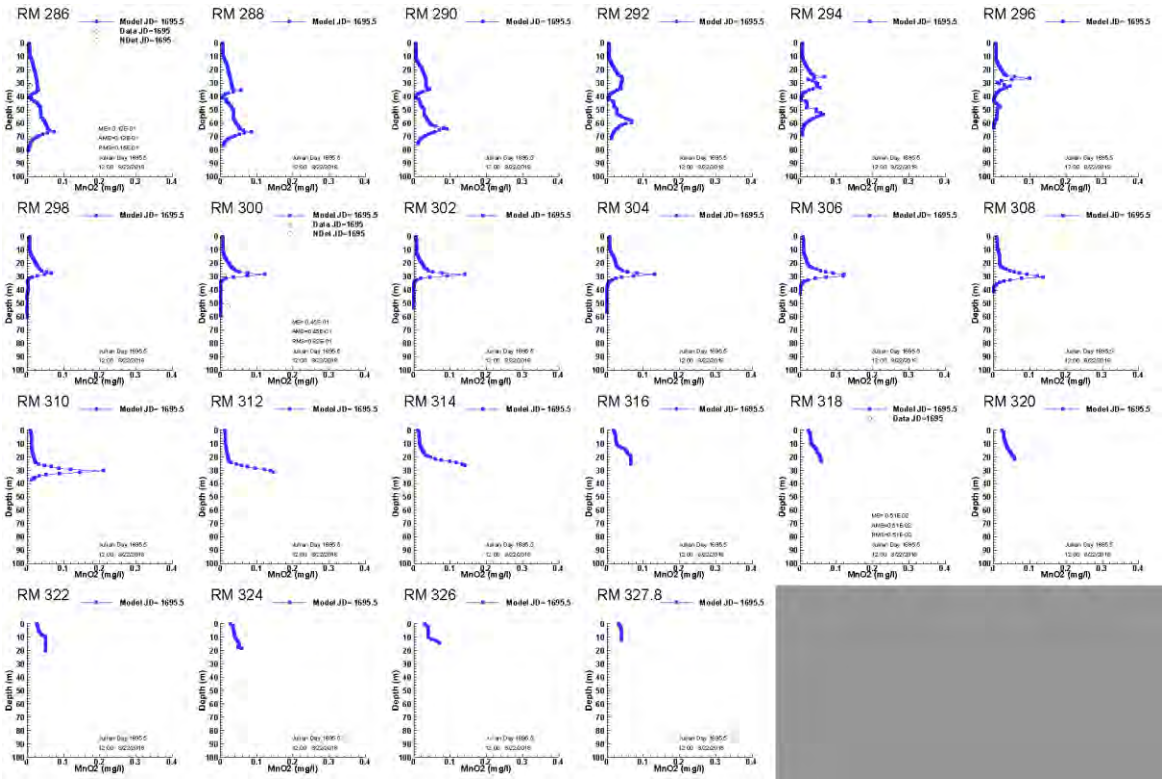


Figure 759. Vertical profiles of MnO2 compared with data for 8/22/2018.

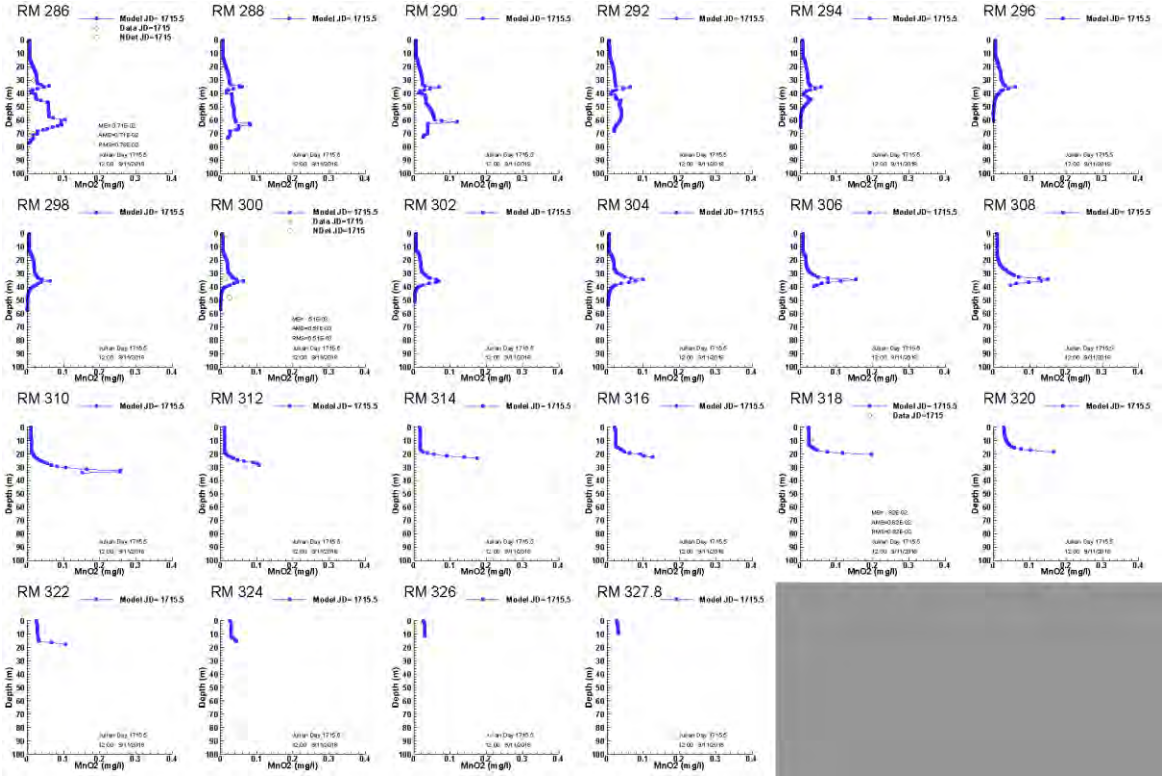


Figure 760. Vertical profiles of MnO2 compared with data for 9/11/2018.

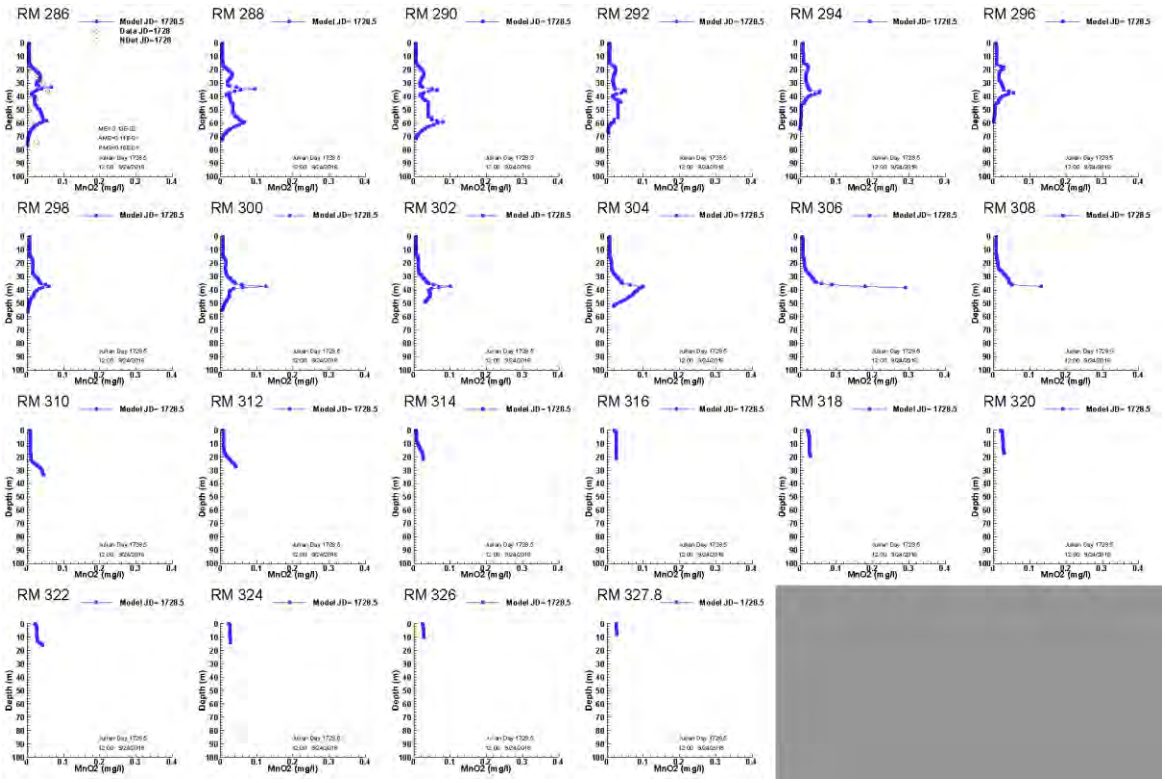


Figure 761. Vertical profiles of MnO2 compared with data for 9/24/2018.

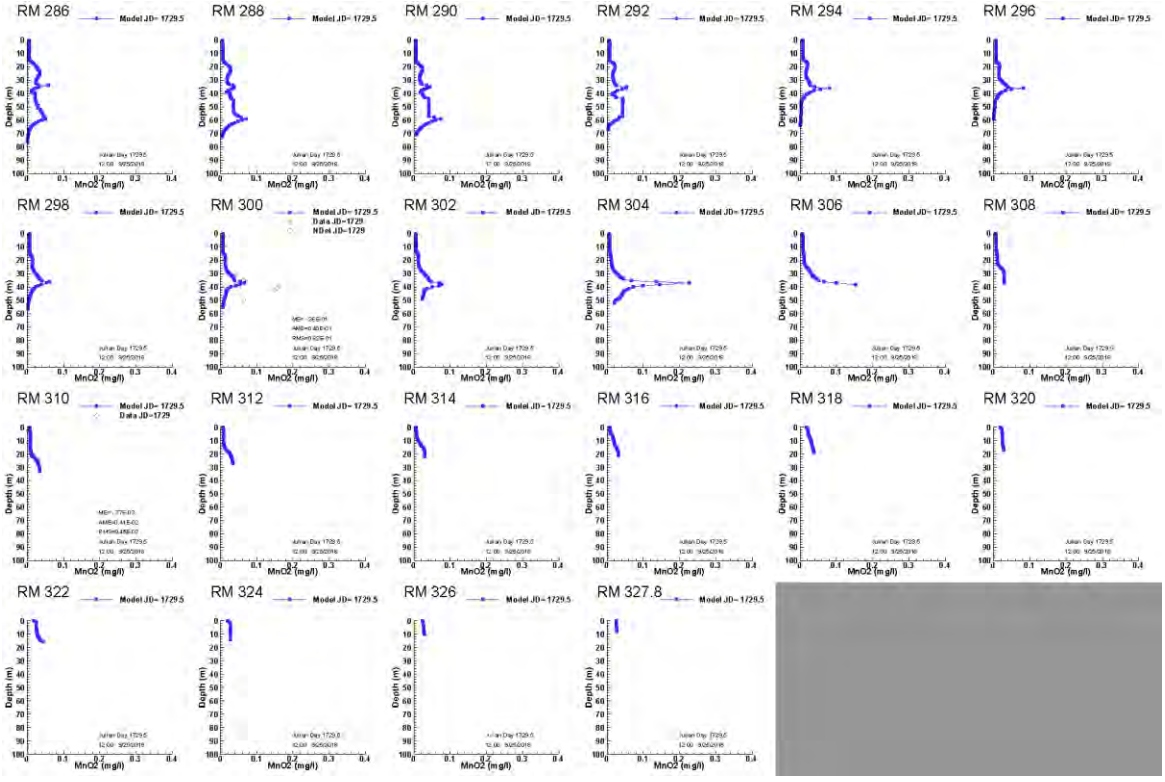


Figure 762. Vertical profiles of MnO2 compared with data for 9/25/2018.

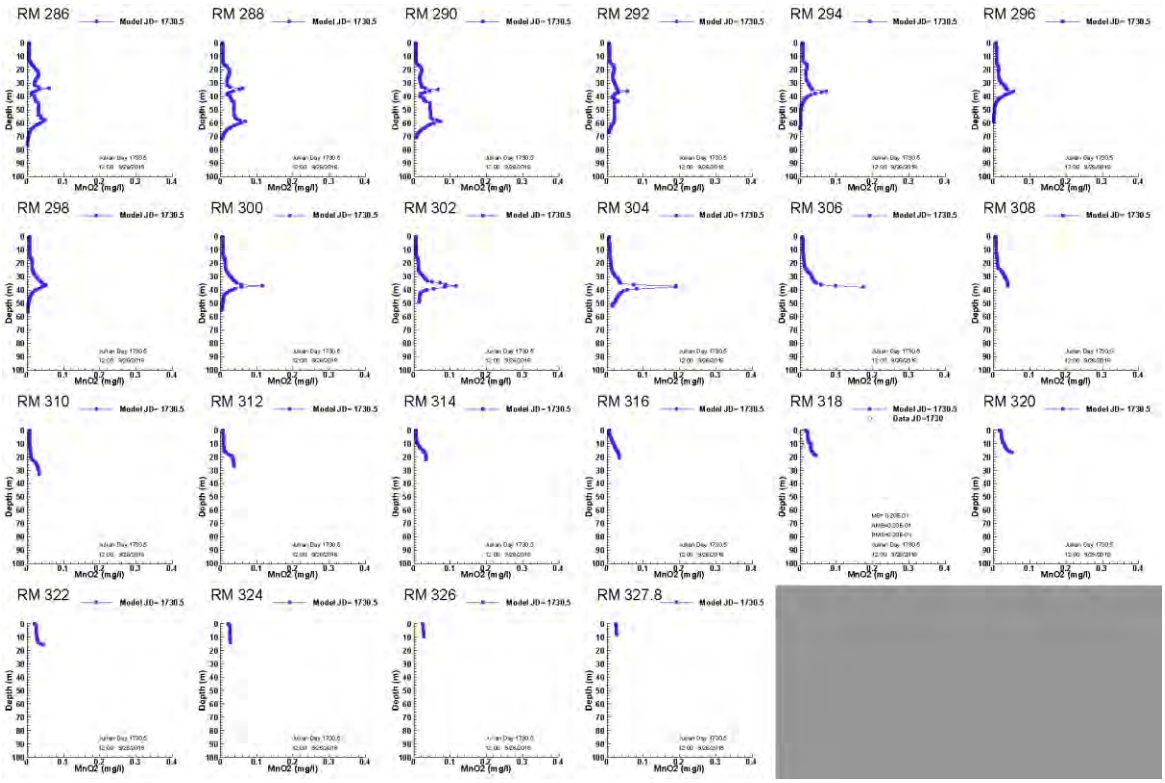


Figure 763. Vertical profiles of MnO2 compared with data for 9/26/2018.

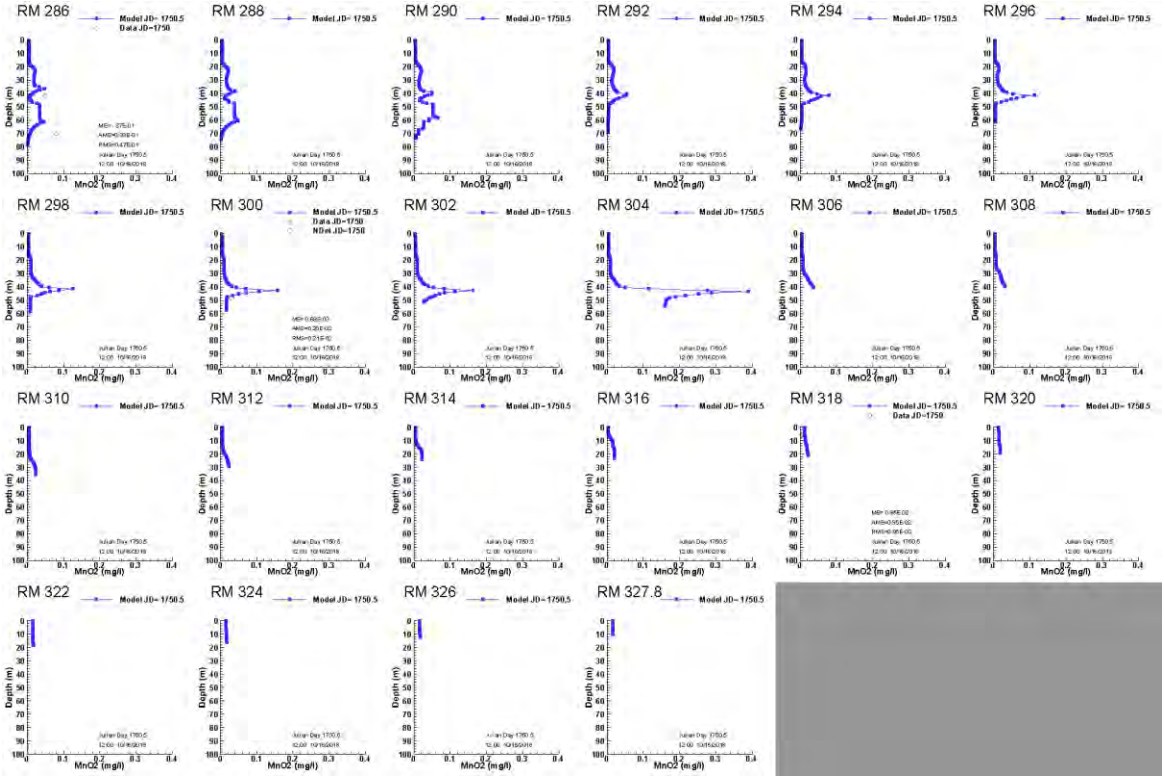


Figure 764. Vertical profiles of MnO2 compared with data for 10/16/2018.

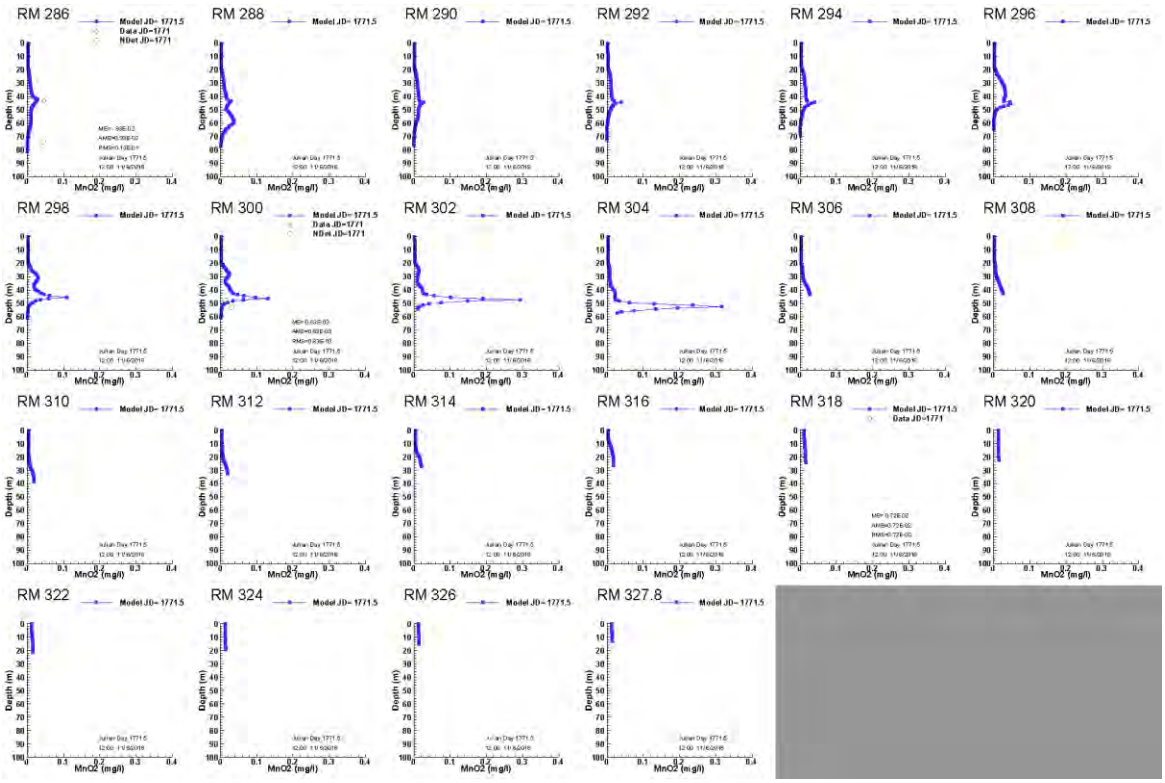


Figure 765. Vertical profiles of MnO2 compared with data for 11/ 6/2018.

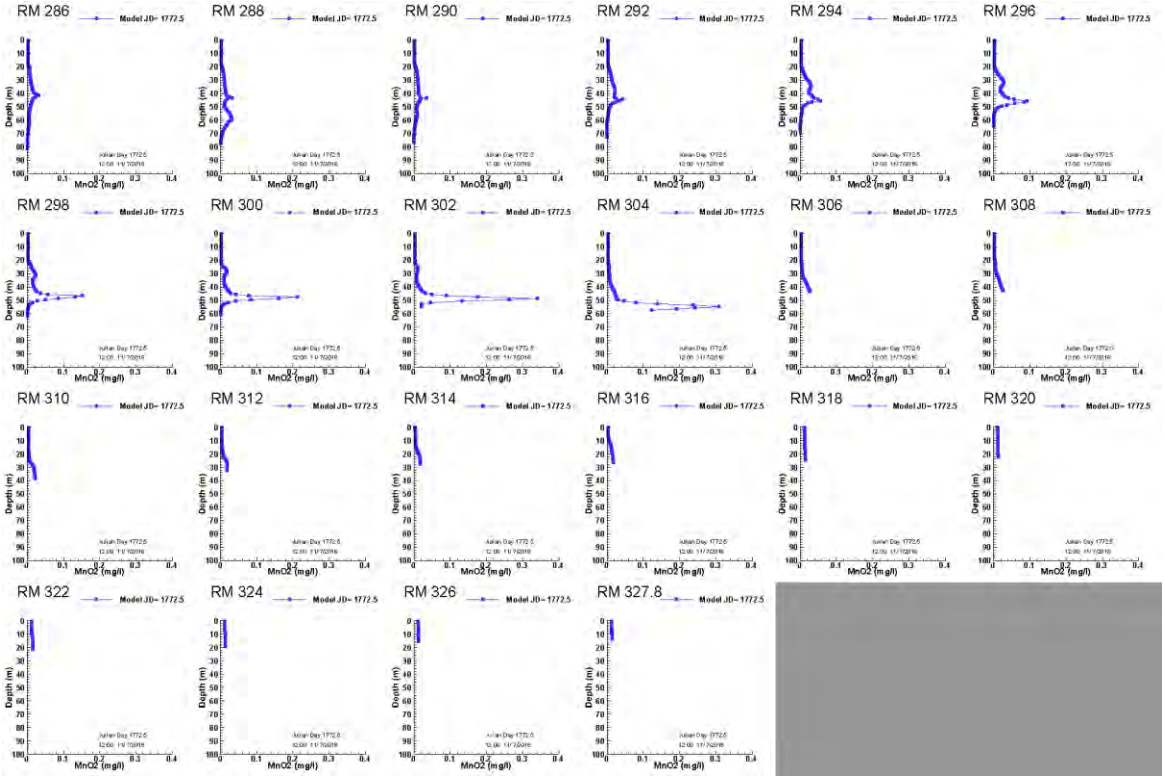


Figure 766. Vertical profiles of MnO2 compared with data for 11/ 7/2018.

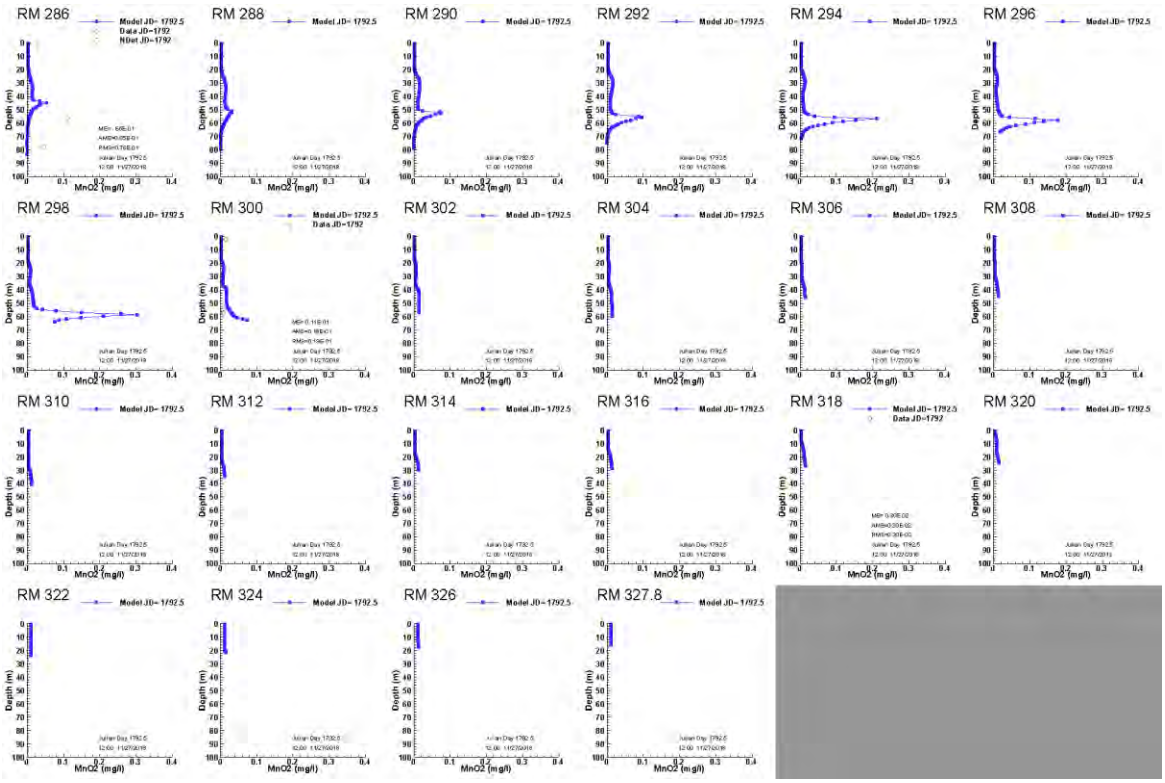


Figure 767. Vertical profiles of MnO2 compared with data for 11/27/2018.

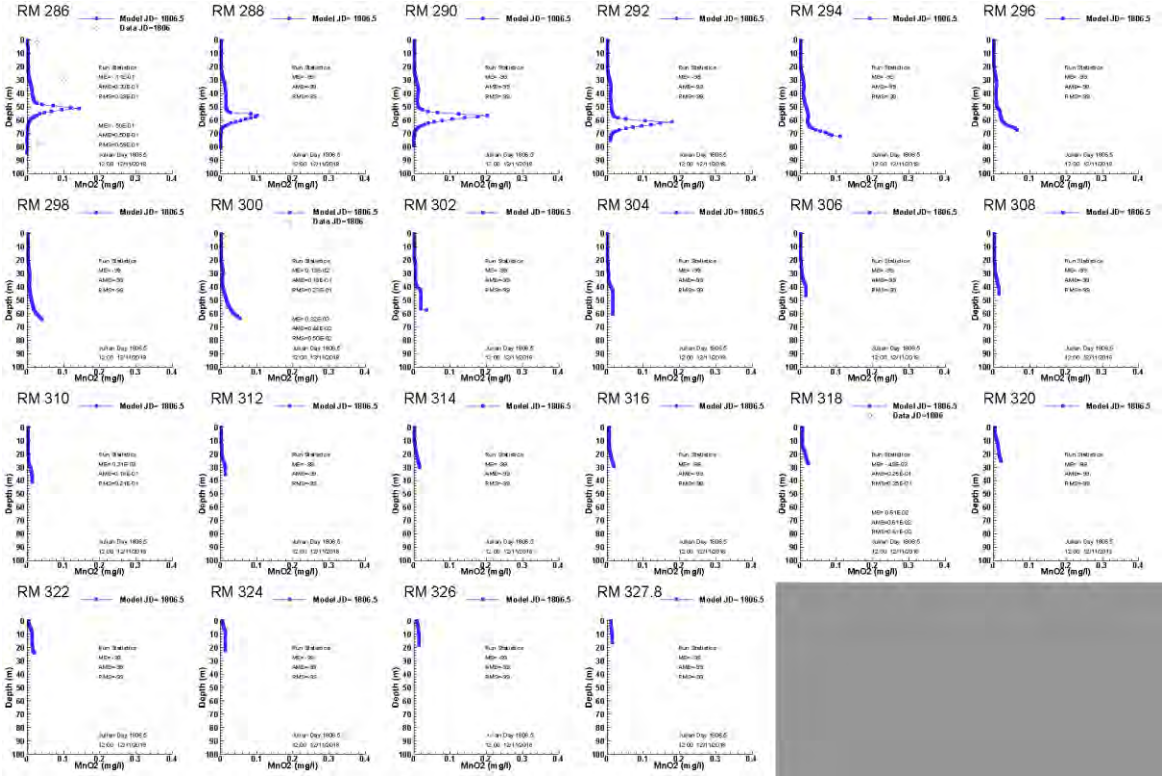


Figure 768. Vertical profiles of MnO2 compared with data for 12/11/2018.

Orthophosphate

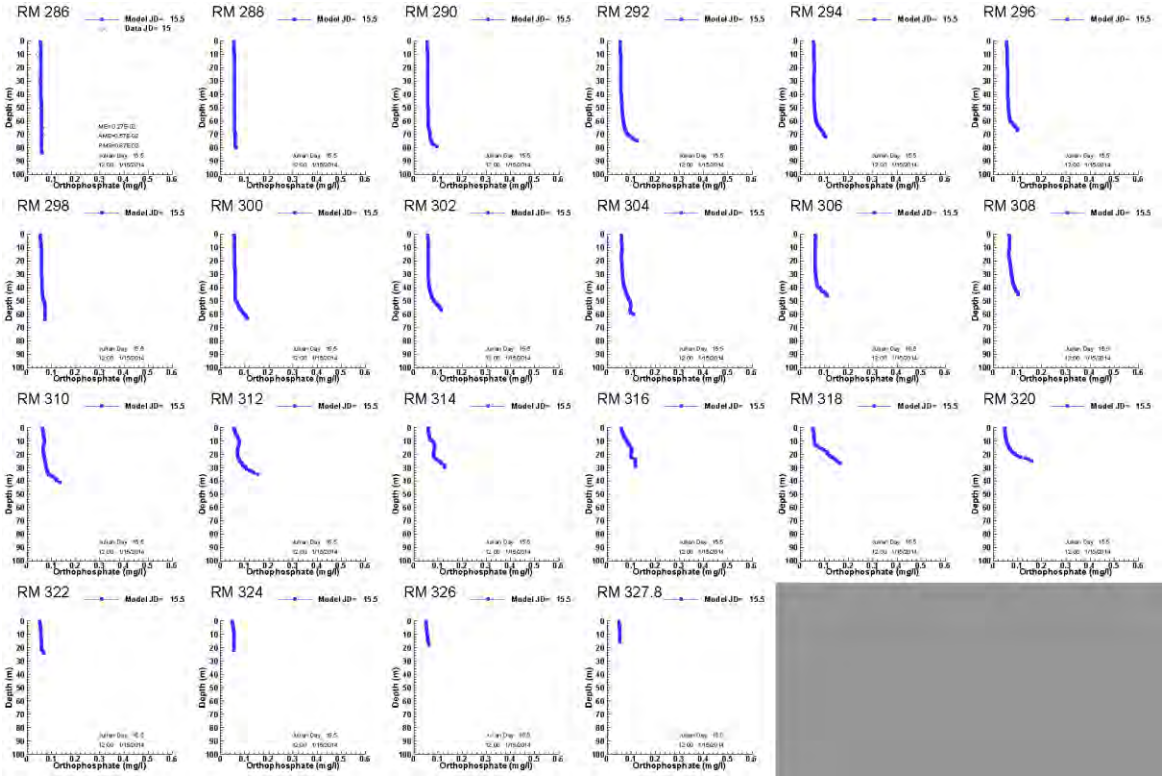


Figure 769. Vertical profiles of orthophosphate compared with data for 1/15/2014.

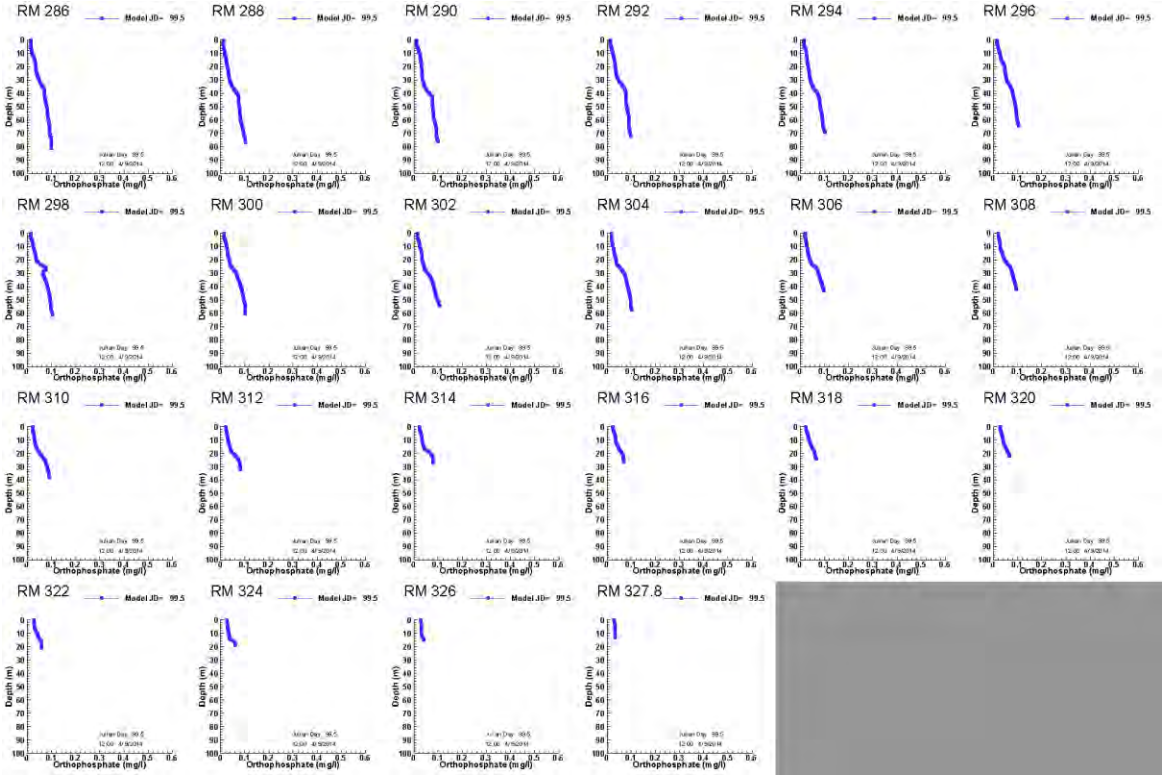


Figure 770. Vertical profiles of orthophosphate compared with data for 4/ 9/2014.

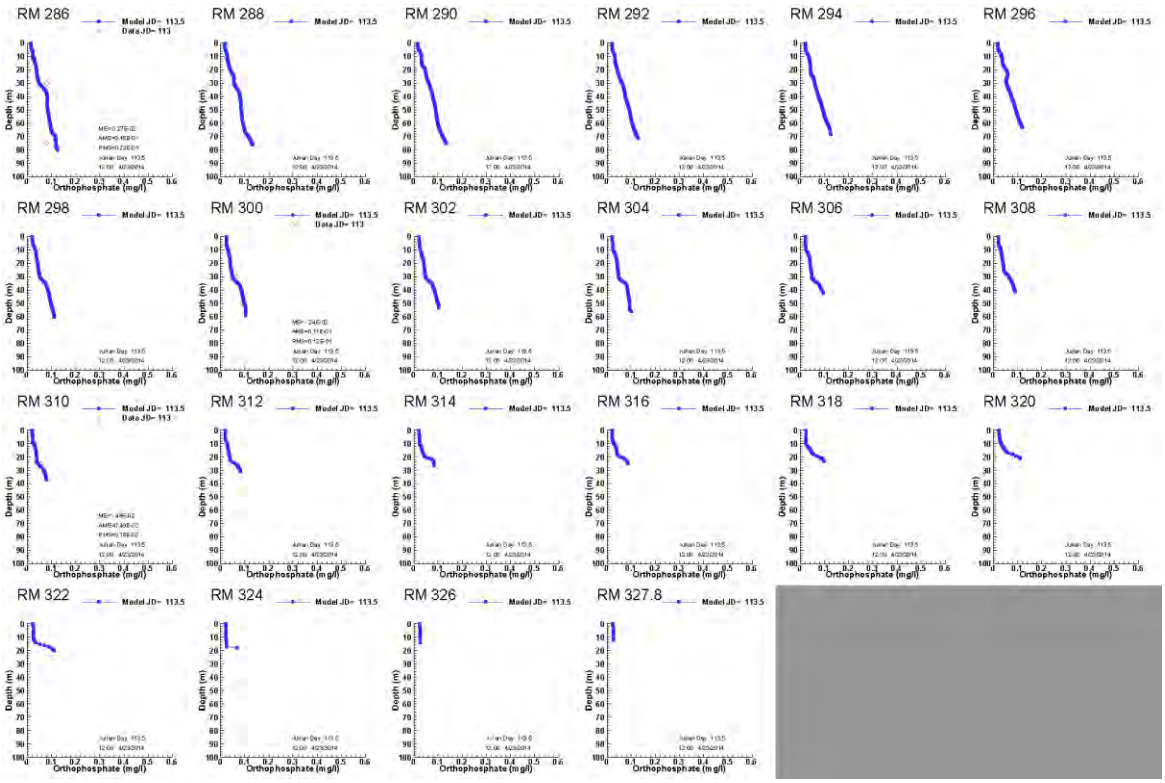


Figure 771. Vertical profiles of orthophosphate compared with data for 4/23/2014.

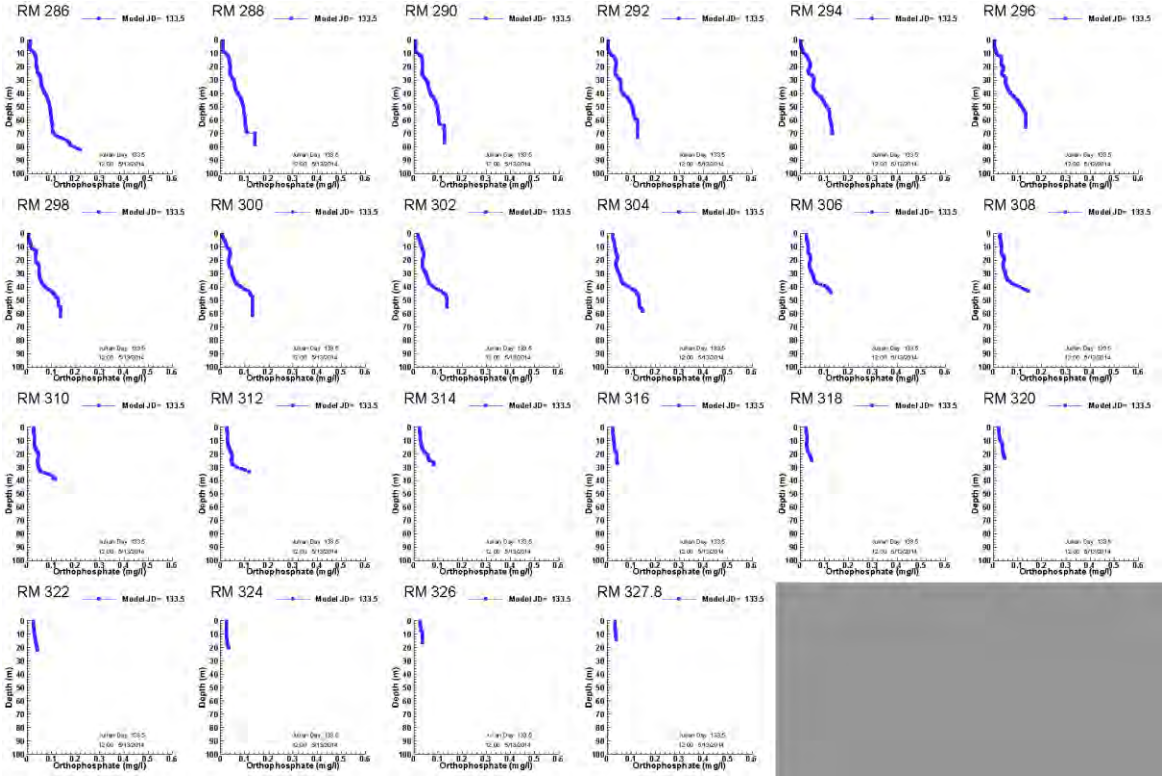


Figure 772. Vertical profiles of orthophosphate compared with data for 5/13/2014.

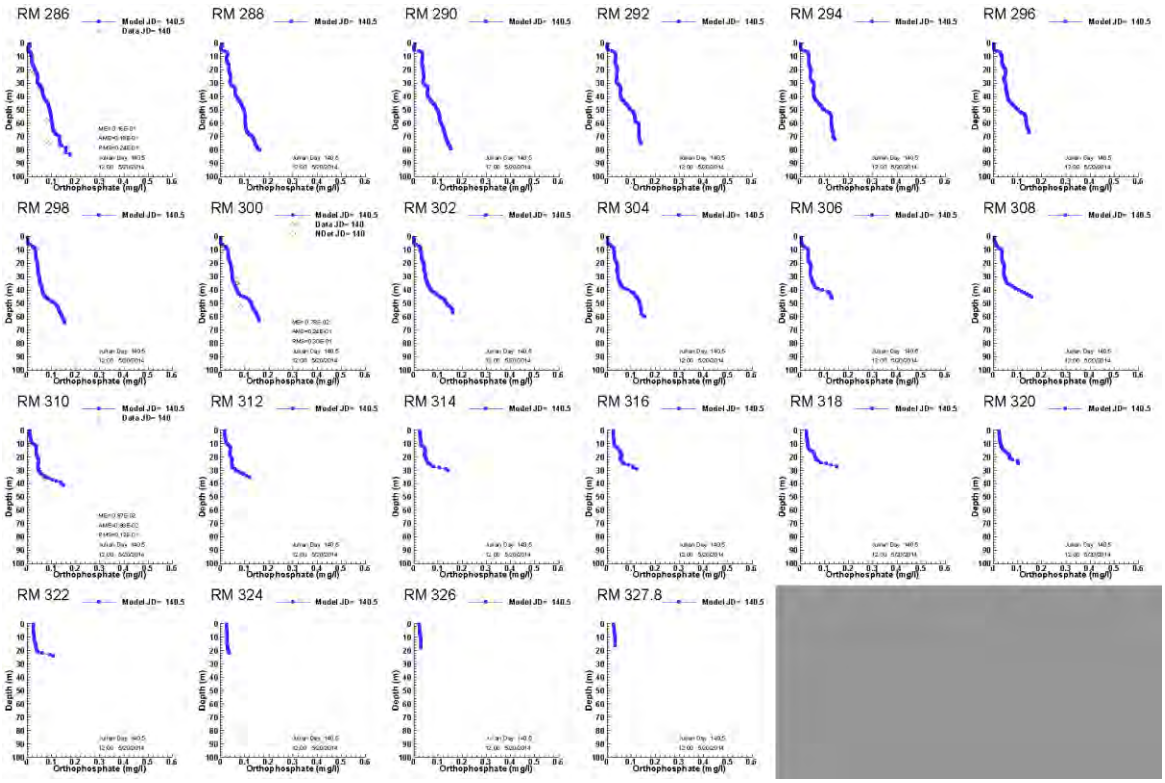


Figure 773. Vertical profiles of orthophosphate compared with data for 5/20/2014.

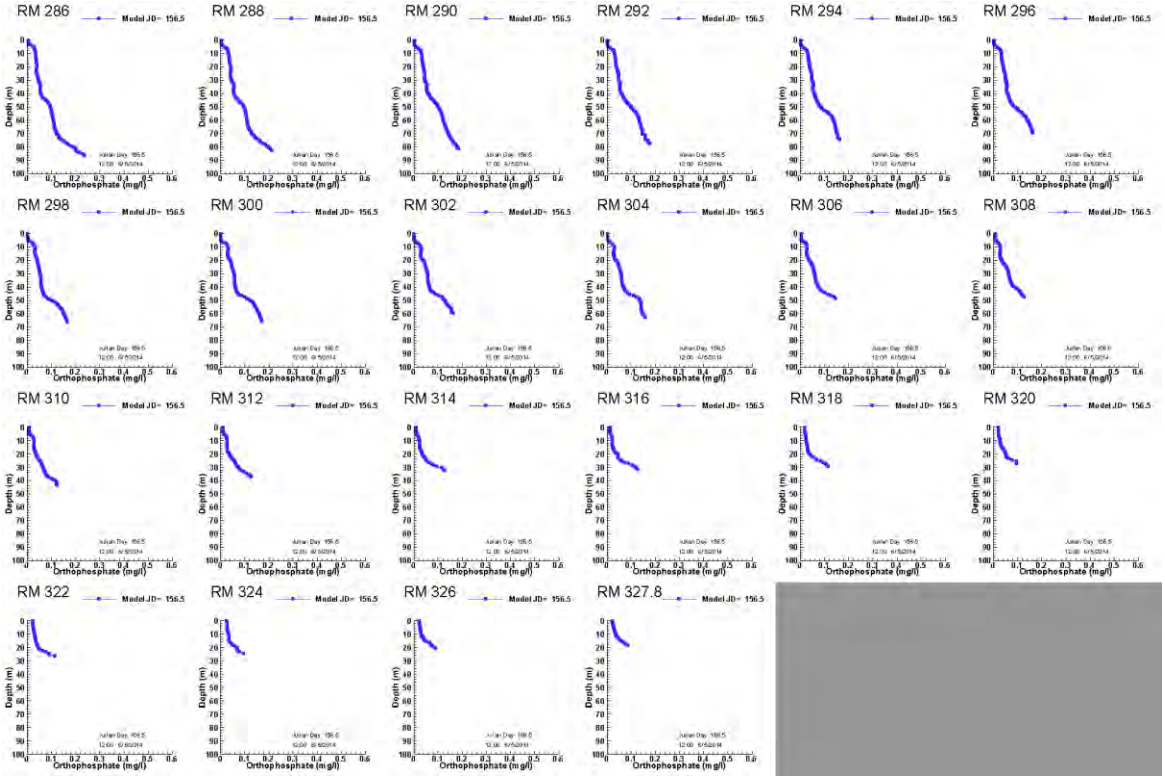


Figure 774. Vertical profiles of orthophosphate compared with data for 6/ 5/2014.

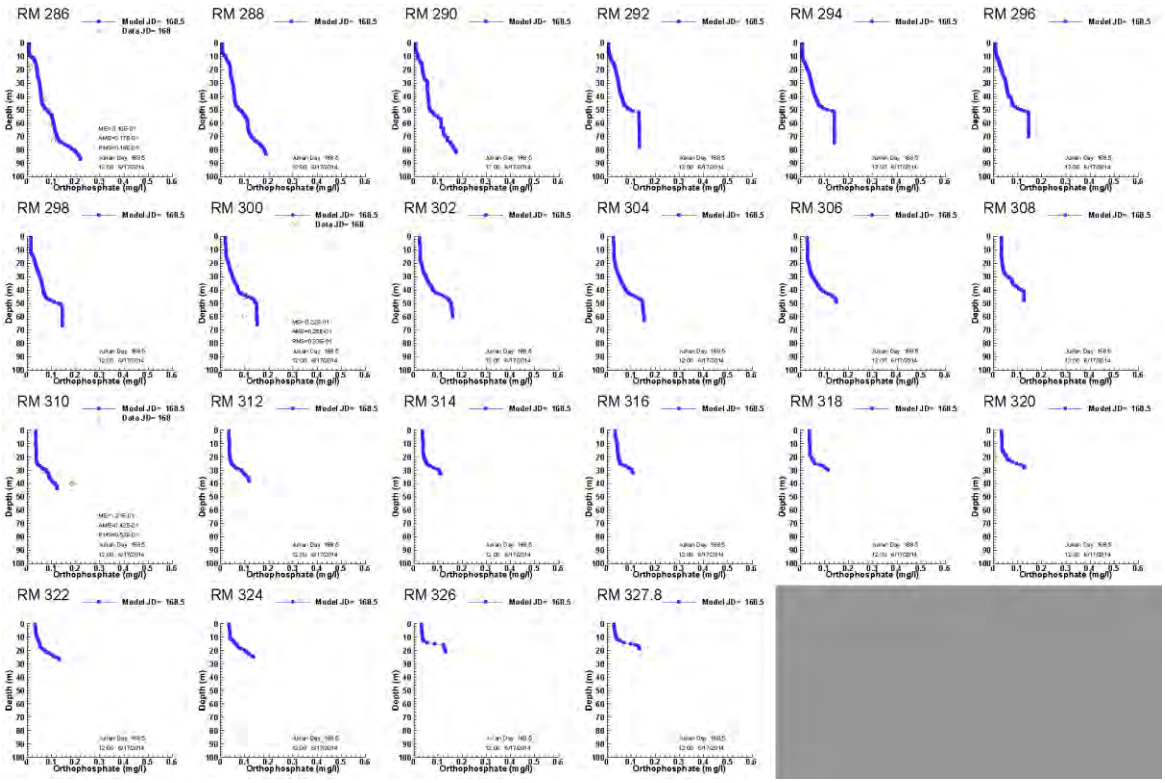


Figure 775. Vertical profiles of orthophosphate compared with data for 6/17/2014.

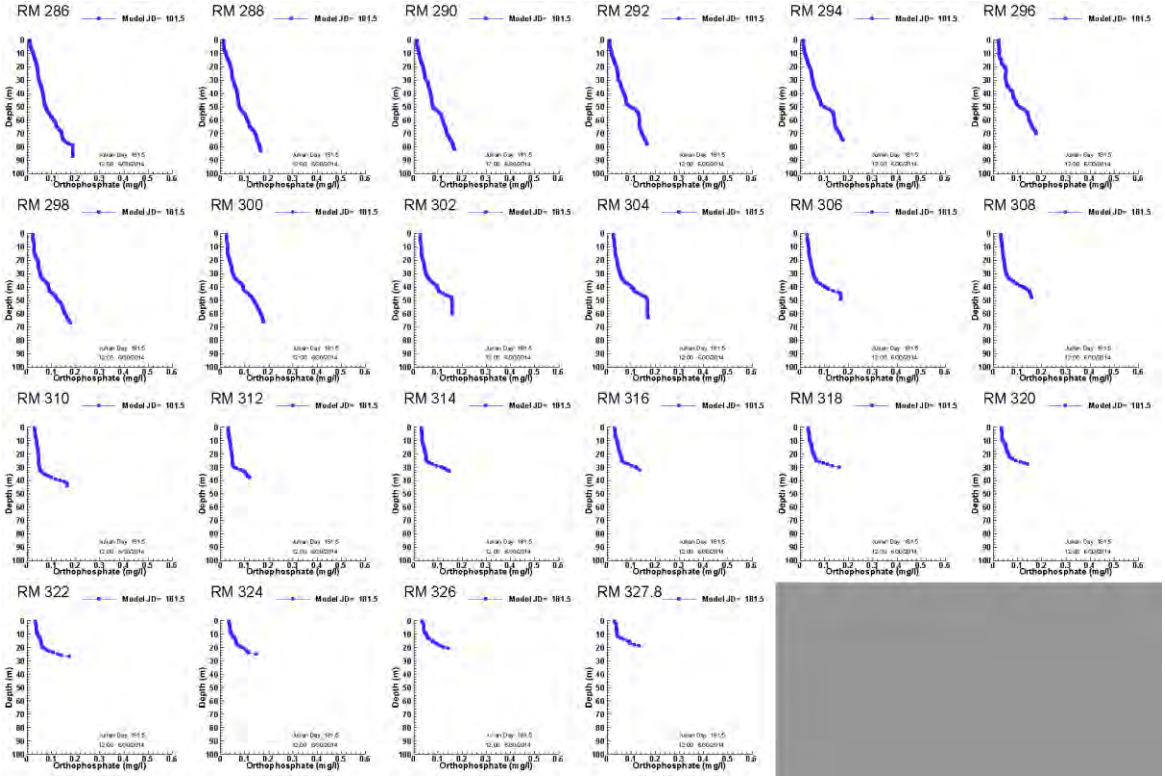


Figure 776. Vertical profiles of orthophosphate compared with data for 6/30/2014.

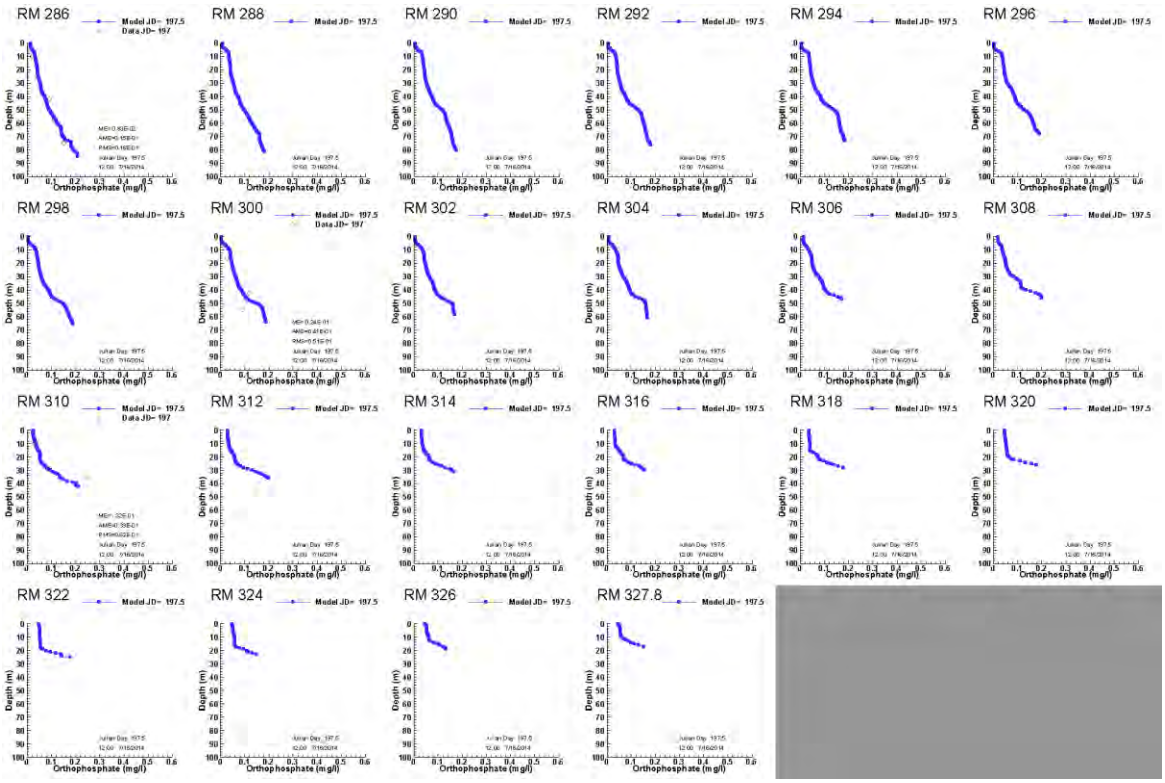


Figure 777. Vertical profiles of orthophosphate compared with data for 7/16/2014.

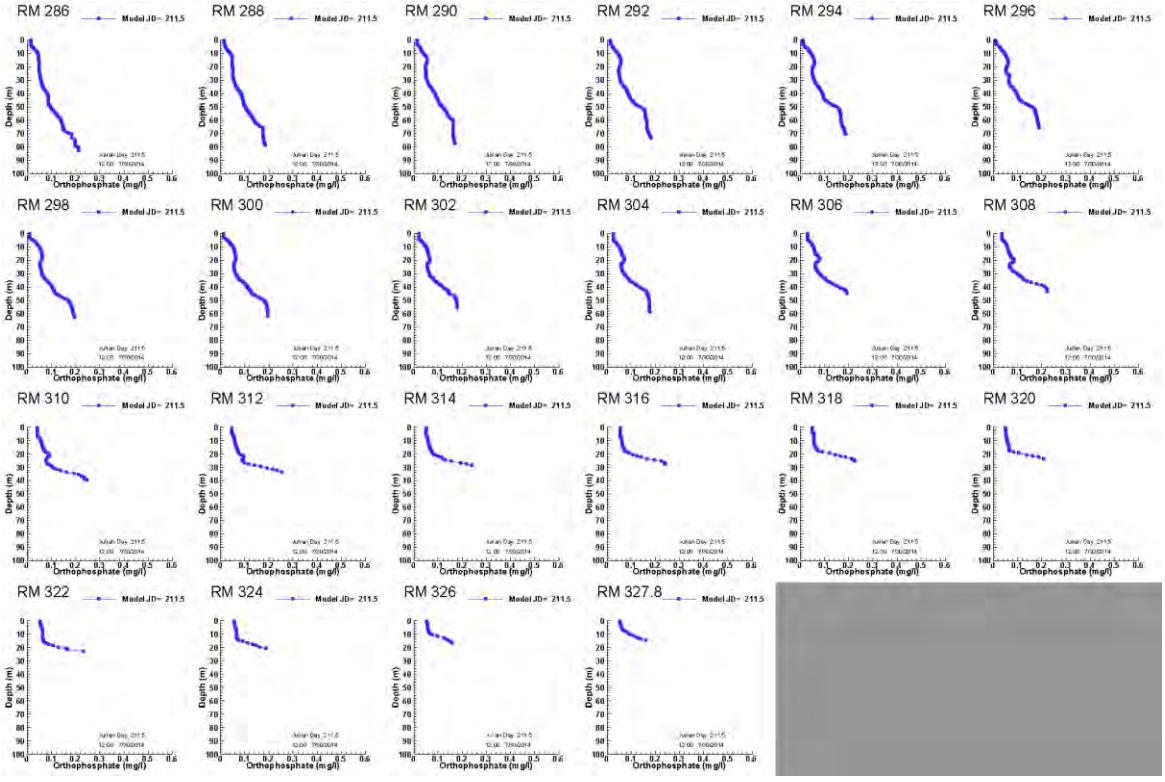


Figure 778. Vertical profiles of orthophosphate compared with data for 7/30/2014.

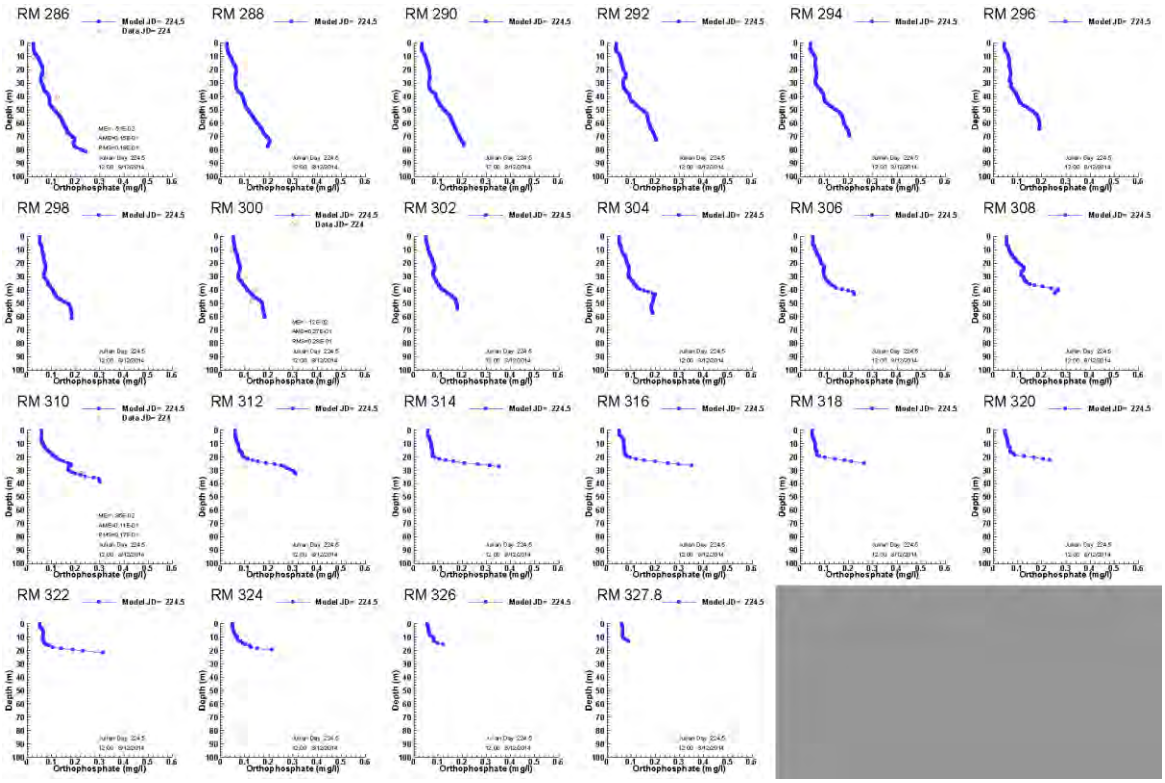


Figure 779. Vertical profiles of orthophosphate compared with data for 8/12/2014.

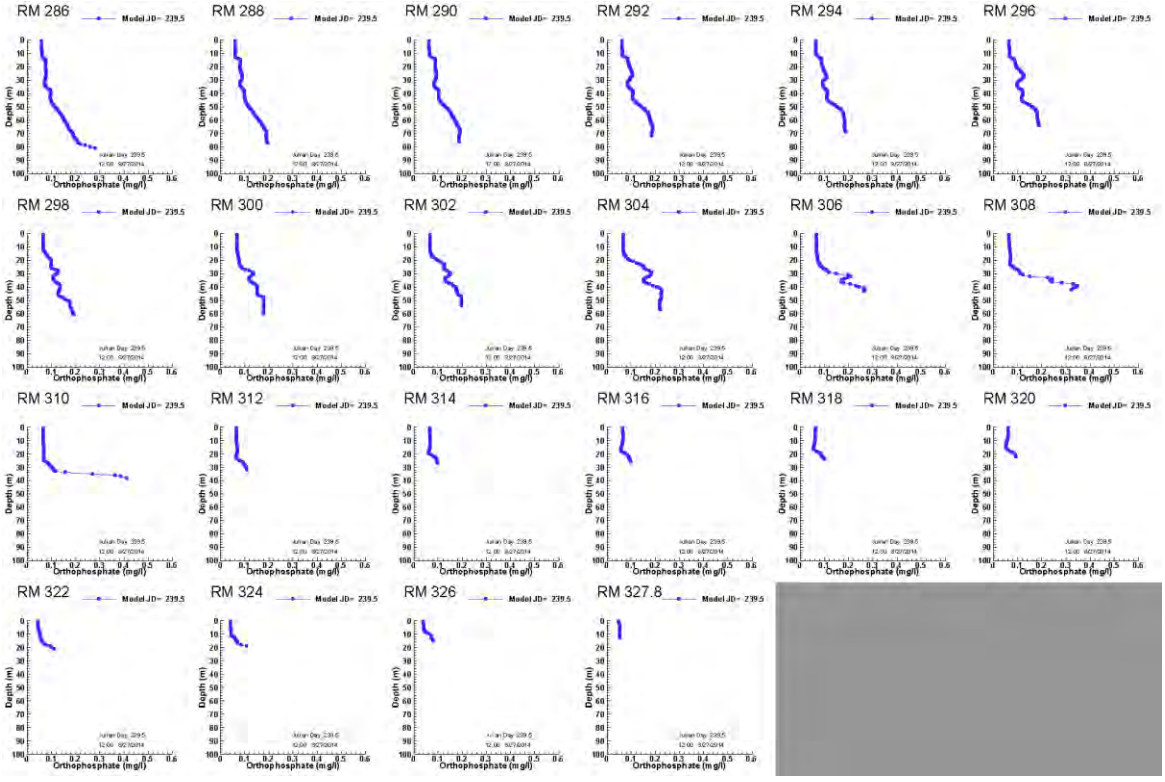


Figure 780. Vertical profiles of orthophosphate compared with data for 8/27/2014.

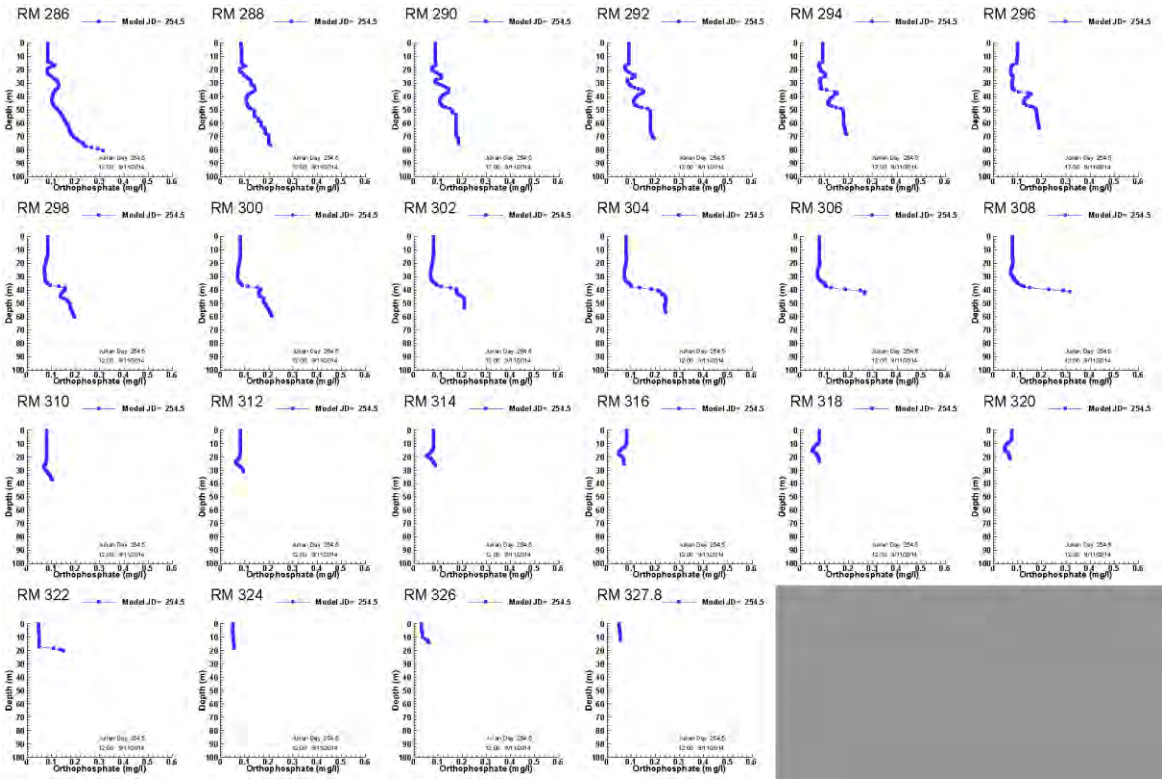


Figure 781. Vertical profiles of orthophosphate compared with data for 9/11/2014.

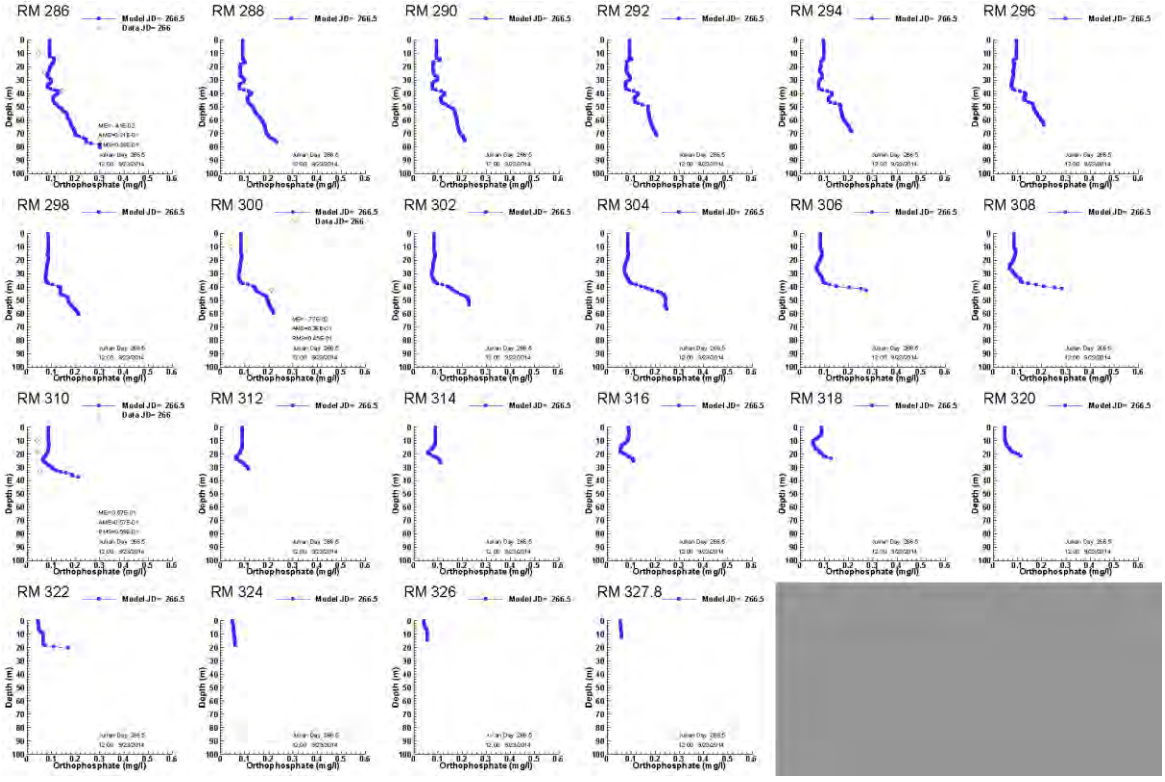


Figure 782. Vertical profiles of orthophosphate compared with data for 9/23/2014.

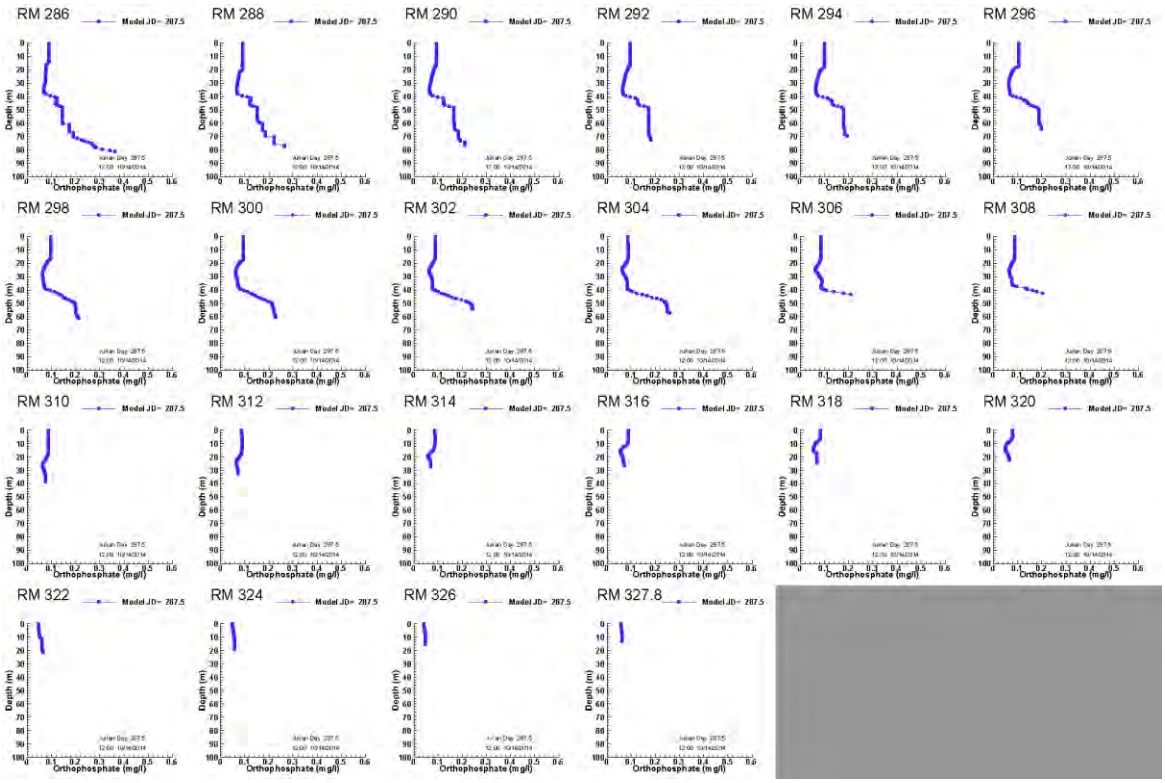


Figure 783. Vertical profiles of orthophosphate compared with data for 10/14/2014.

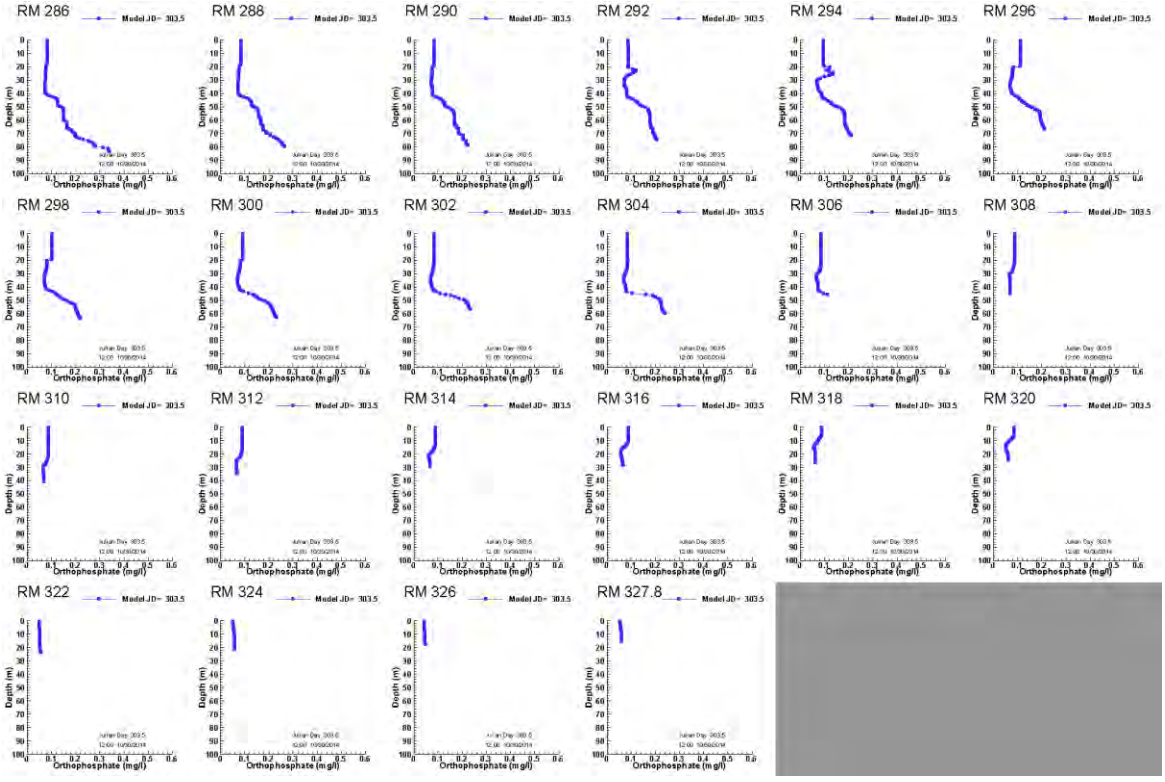


Figure 784. Vertical profiles of orthophosphate compared with data for 10/30/2014.

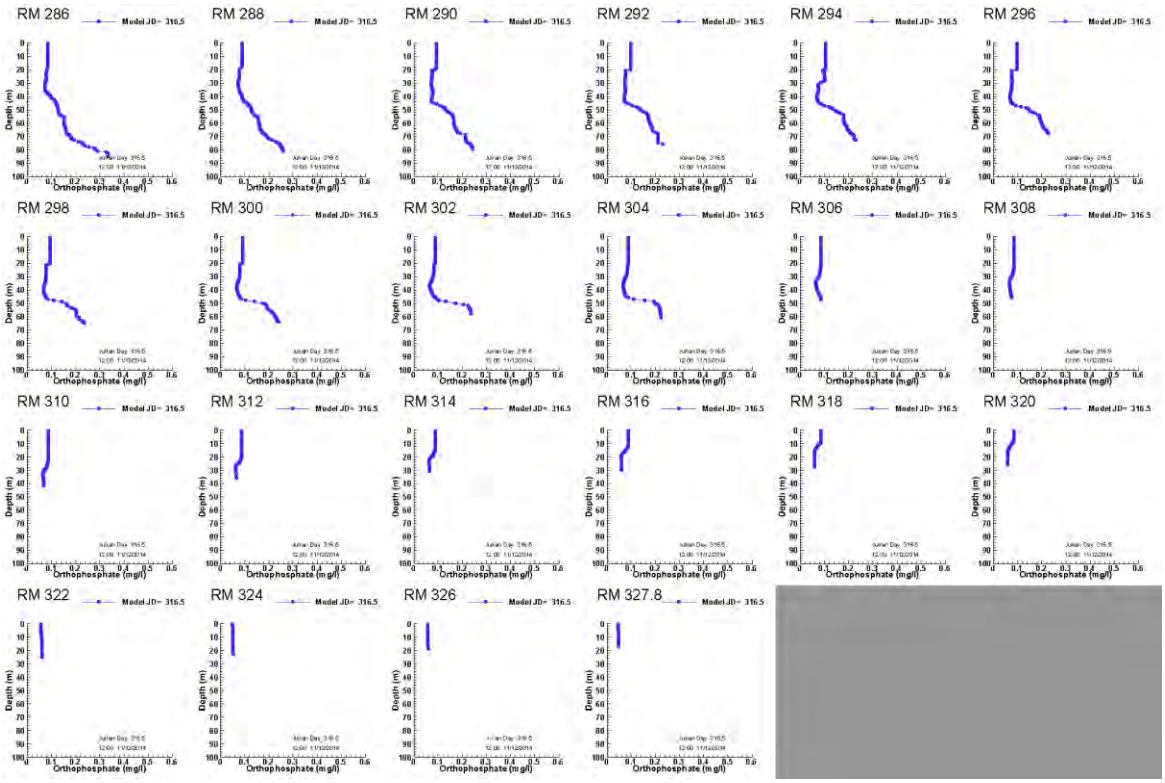


Figure 785. Vertical profiles of orthophosphate compared with data for 11/12/2014.

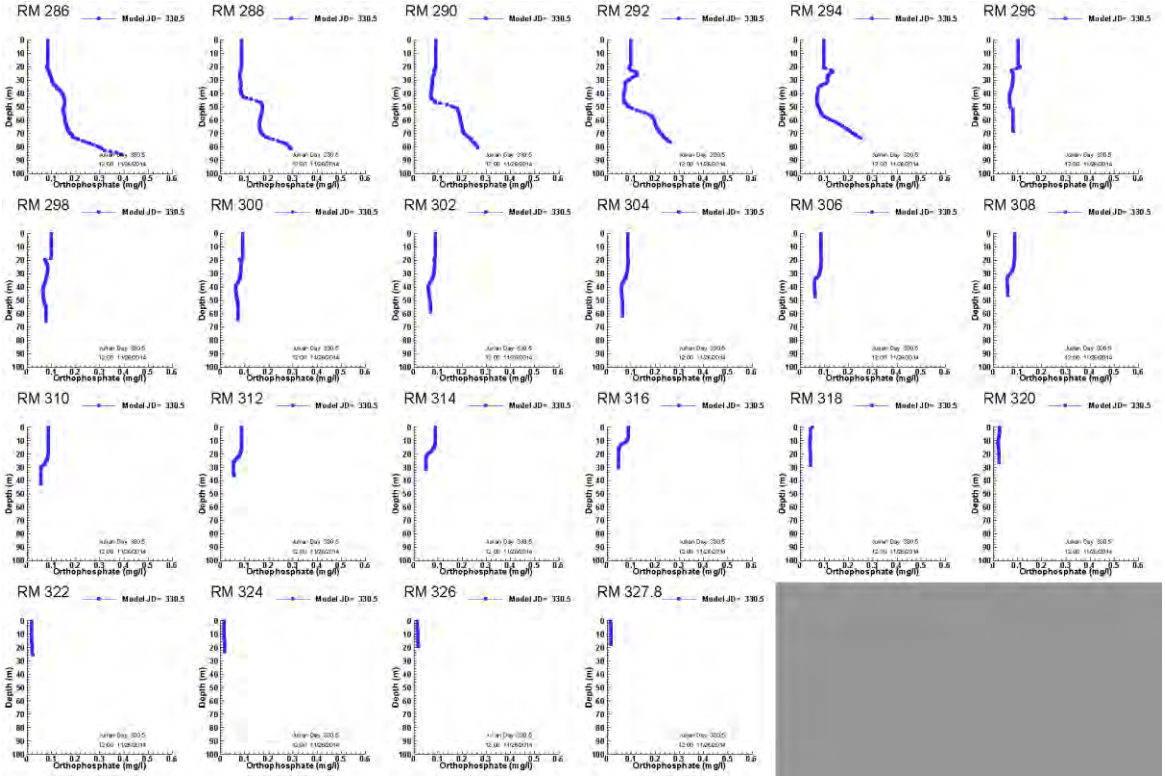


Figure 786. Vertical profiles of orthophosphate compared with data for 11/26/2014.

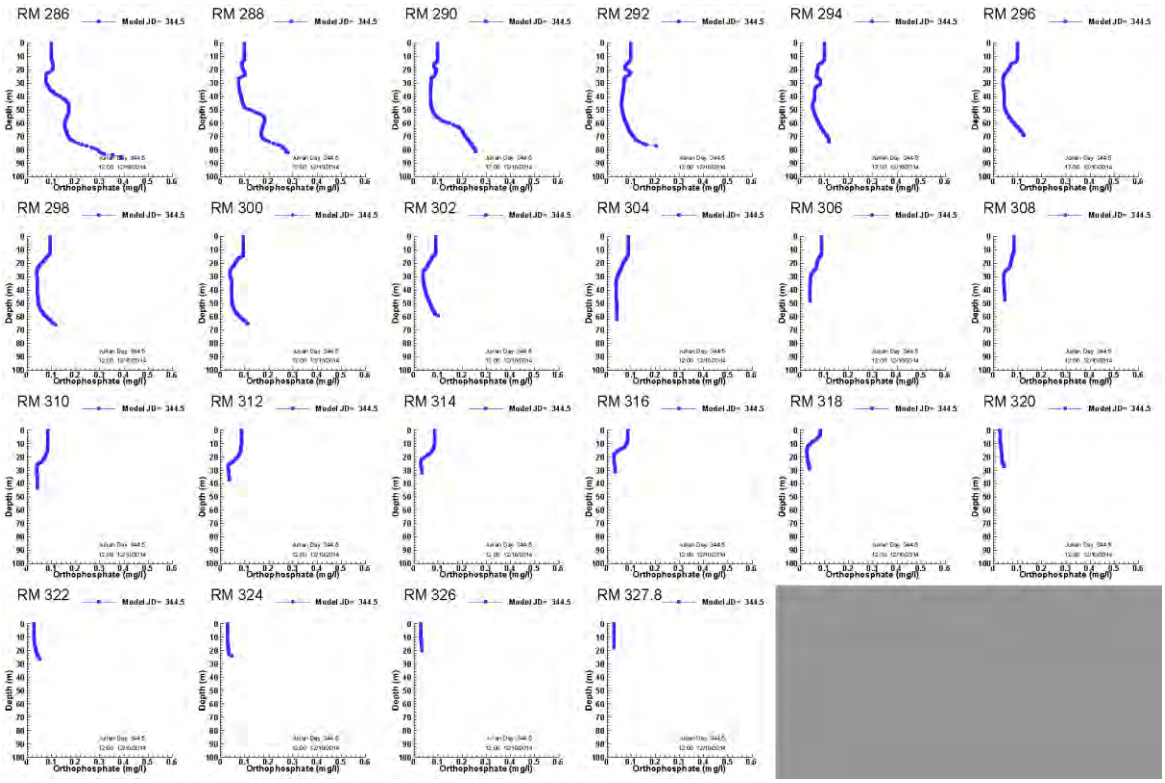


Figure 787. Vertical profiles of orthophosphate compared with data for 12/10/2014.

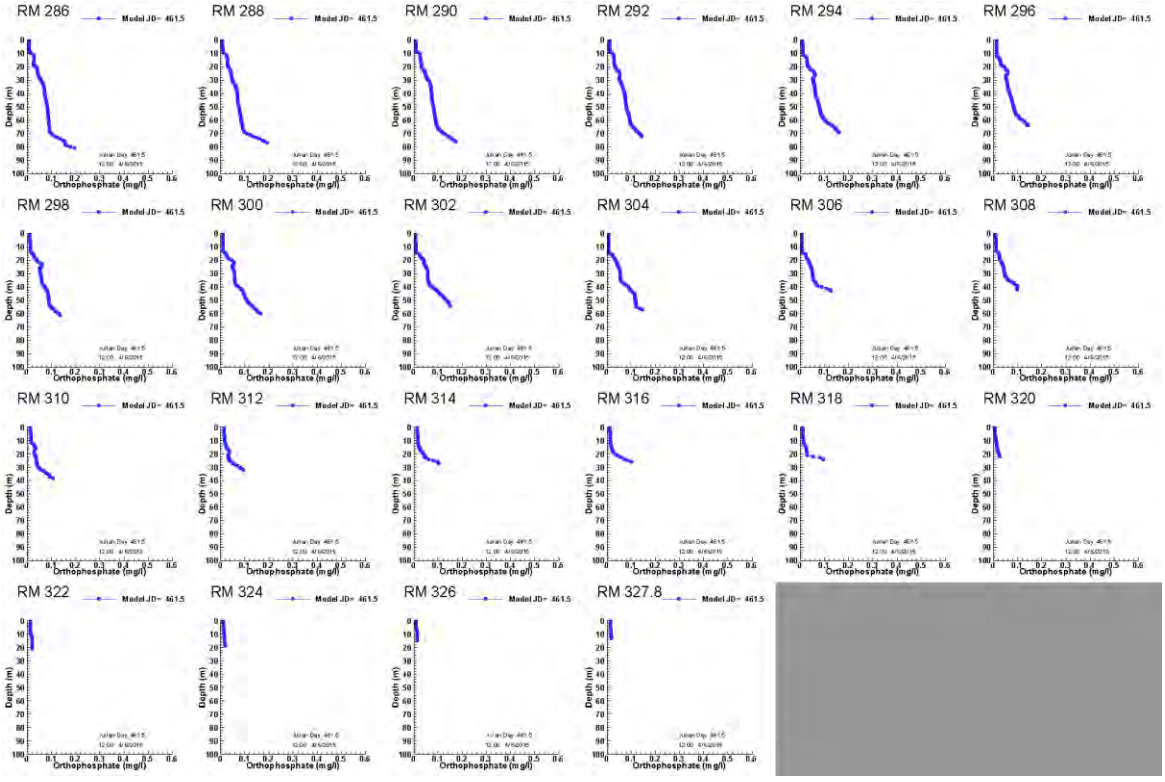


Figure 788. Vertical profiles of orthophosphate compared with data for 4/ 6/2015.

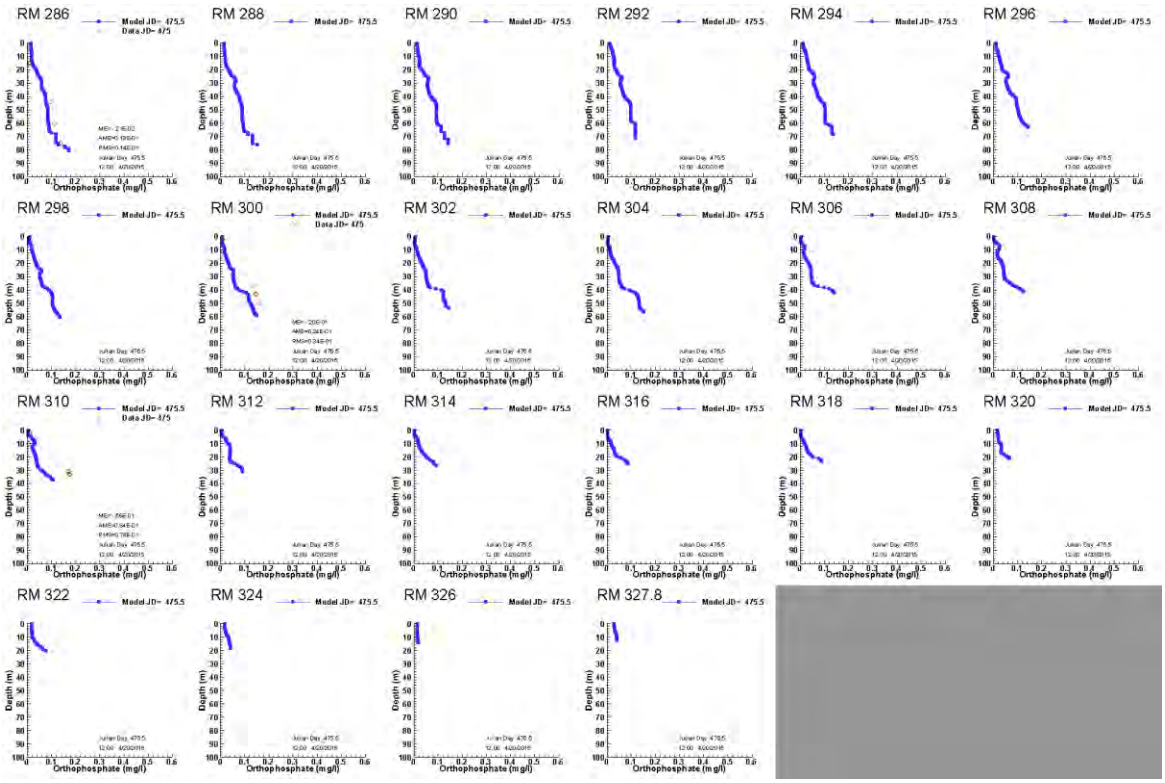


Figure 789. Vertical profiles of orthophosphate compared with data for 4/20/2015.

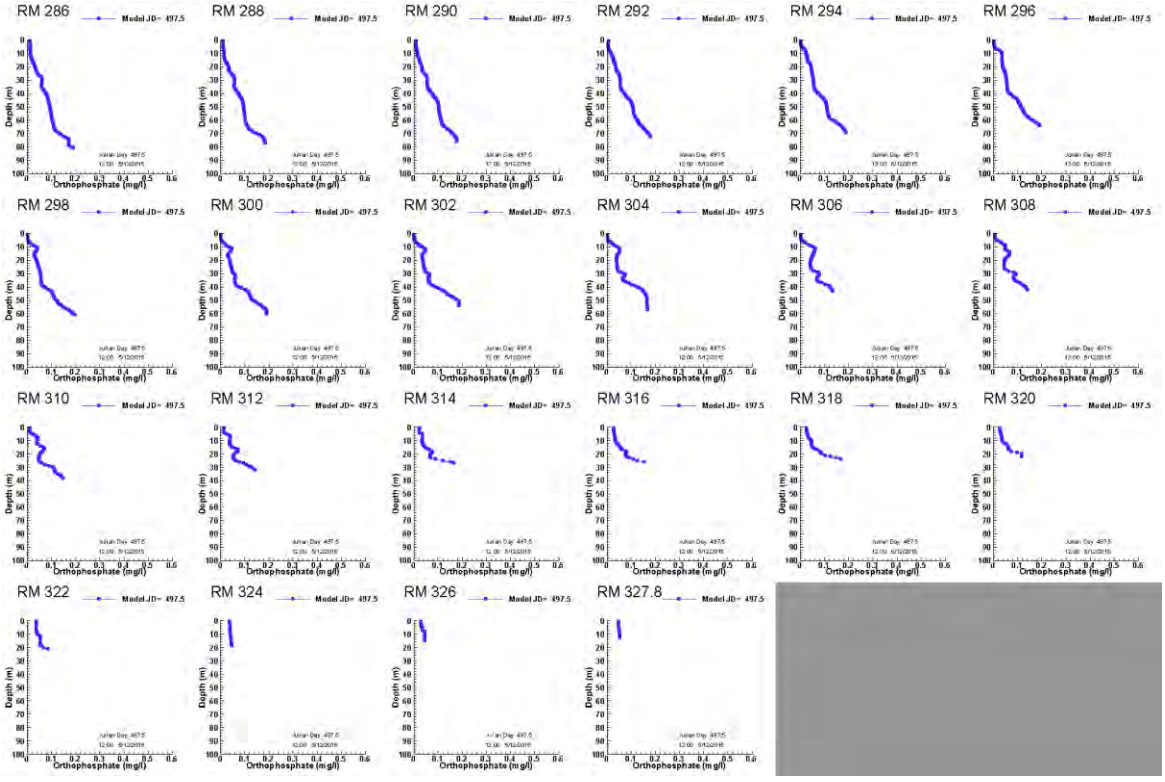


Figure 790. Vertical profiles of orthophosphate compared with data for 5/12/2015.

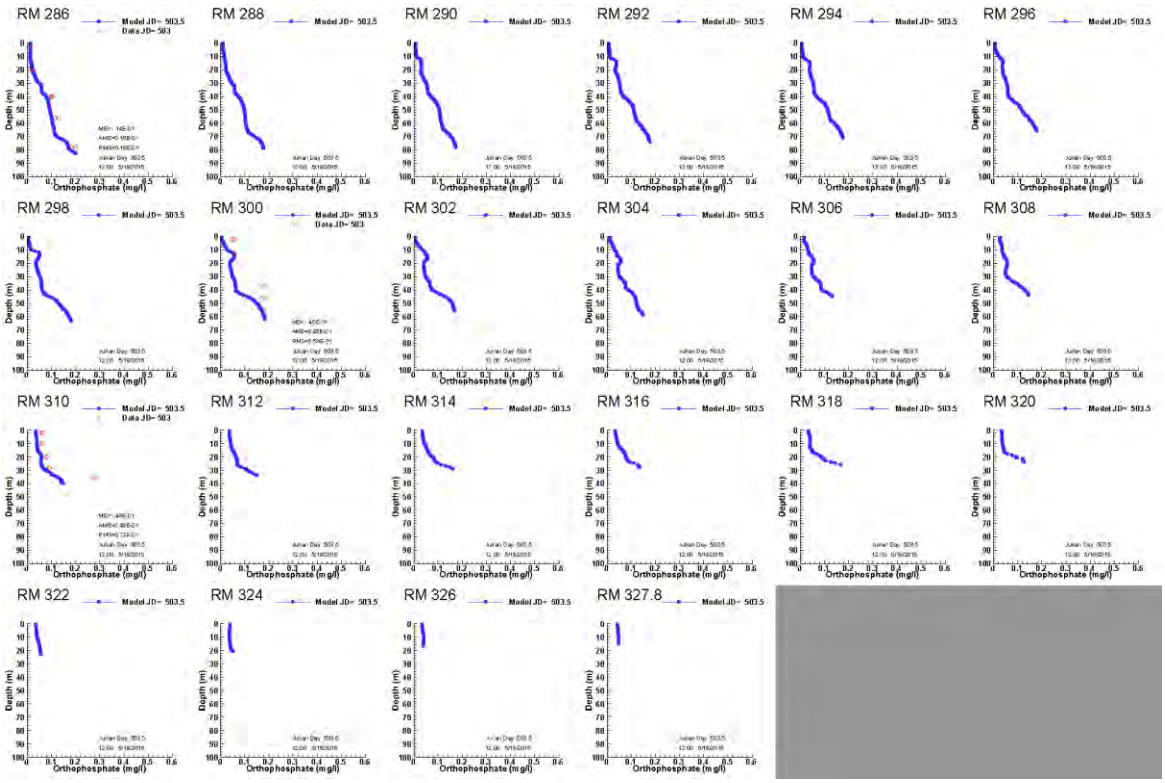


Figure 791. Vertical profiles of orthophosphate compared with data for 5/18/2015.

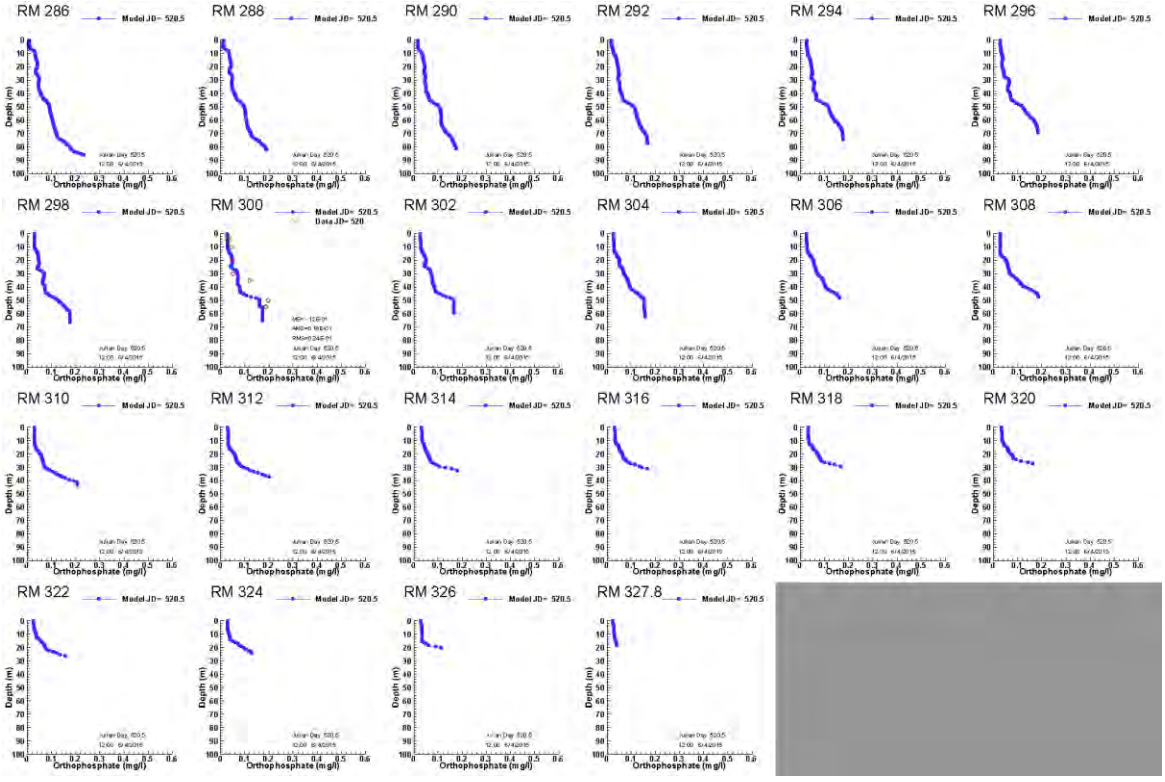


Figure 792. Vertical profiles of orthophosphate compared with data for 6/ 4/2015.

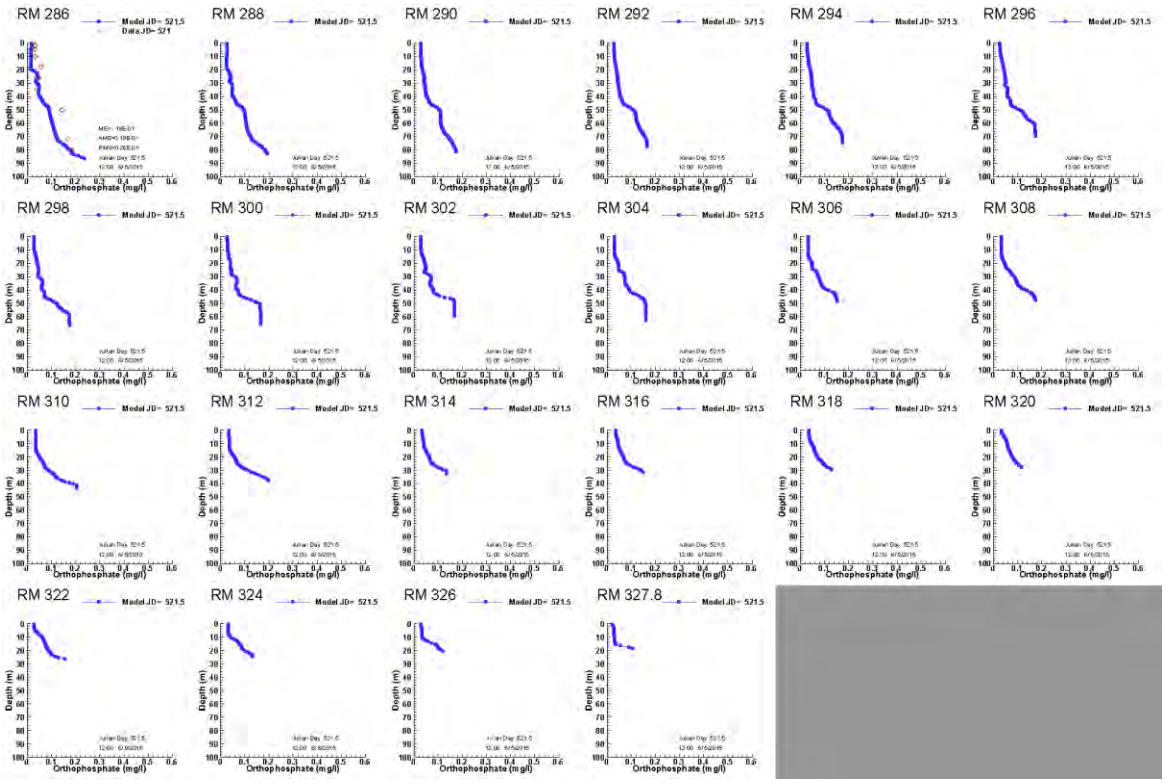


Figure 793. Vertical profiles of orthophosphate compared with data for 6/ 5/2015.

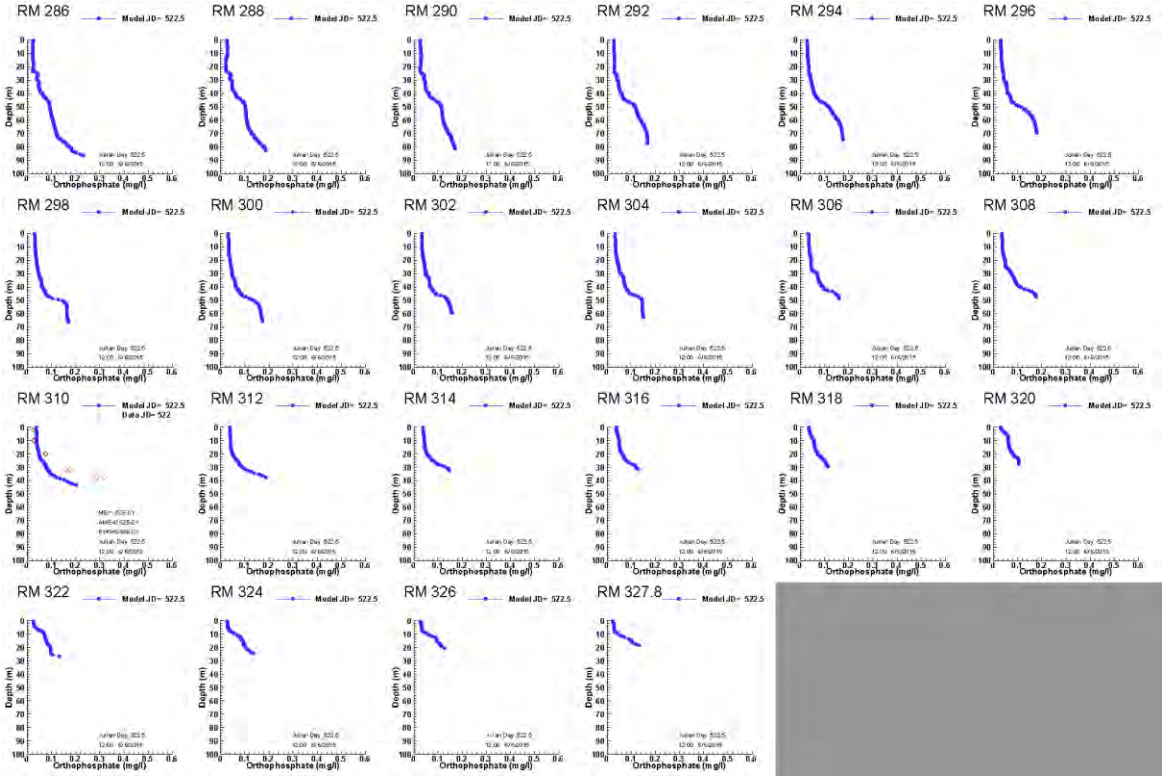


Figure 794. Vertical profiles of orthophosphate compared with data for 6/ 6/2015.

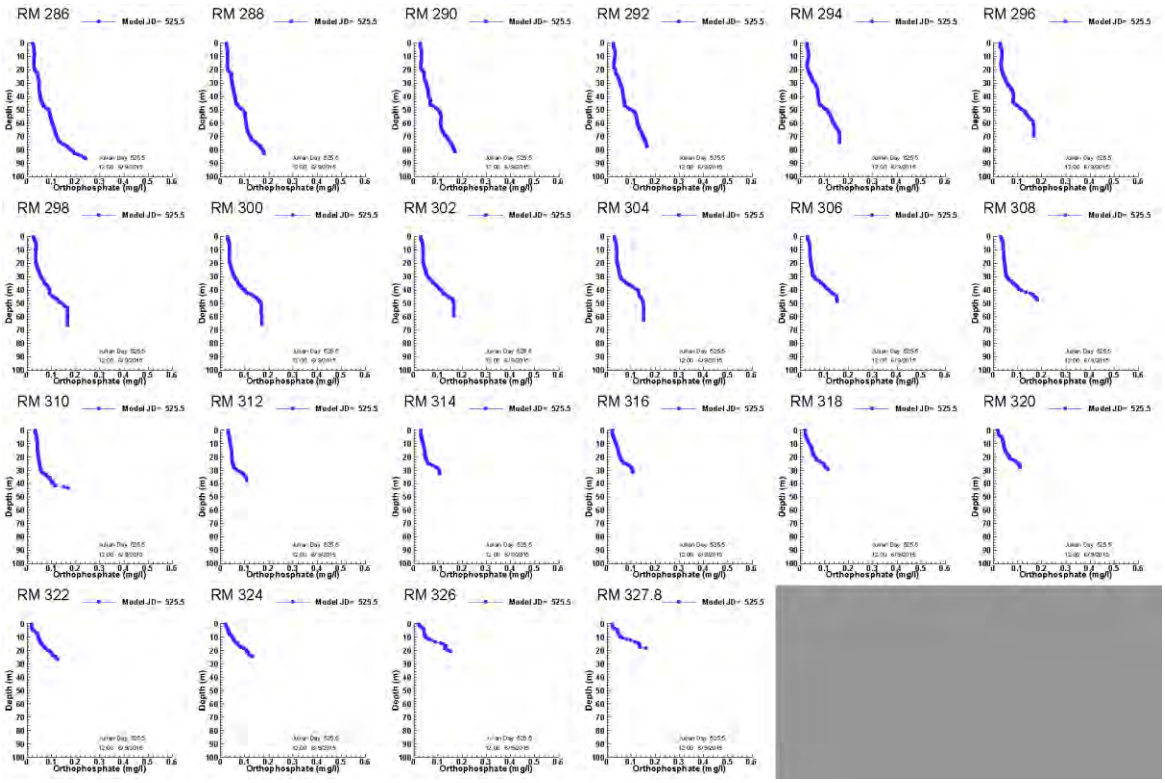


Figure 795. Vertical profiles of orthophosphate compared with data for 6/ 9/2015.

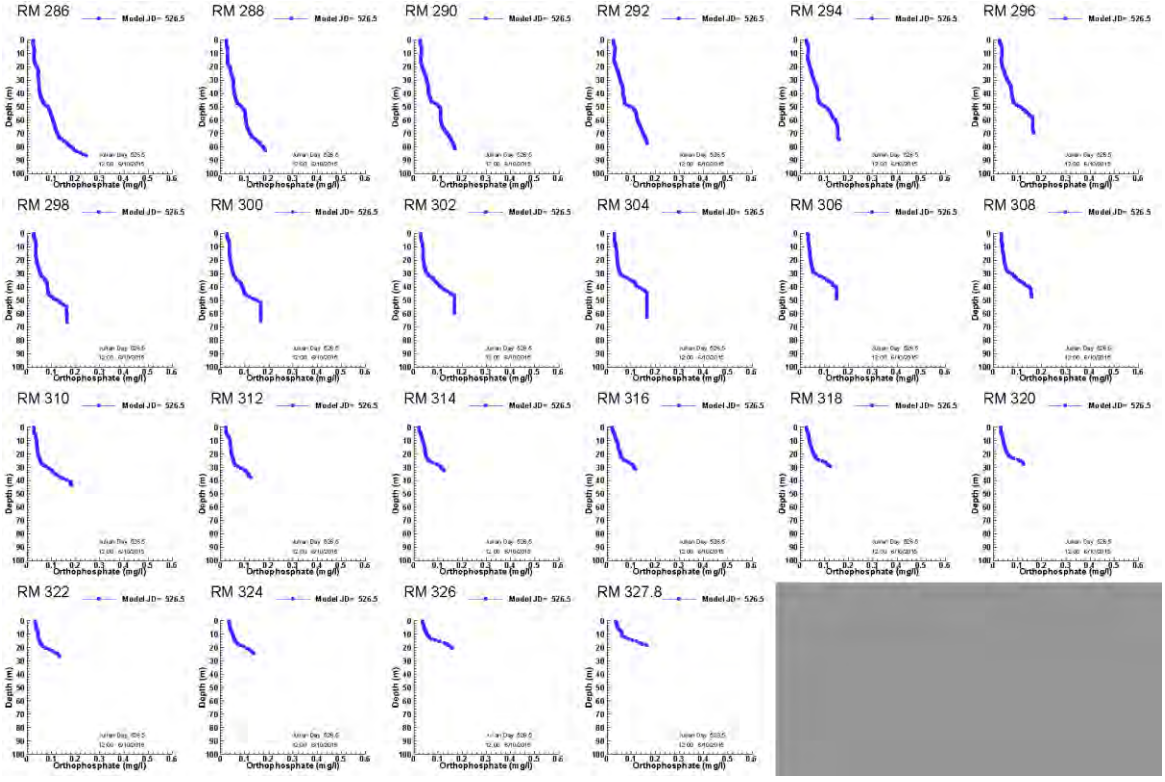


Figure 796. Vertical profiles of orthophosphate compared with data for 6/10/2015.

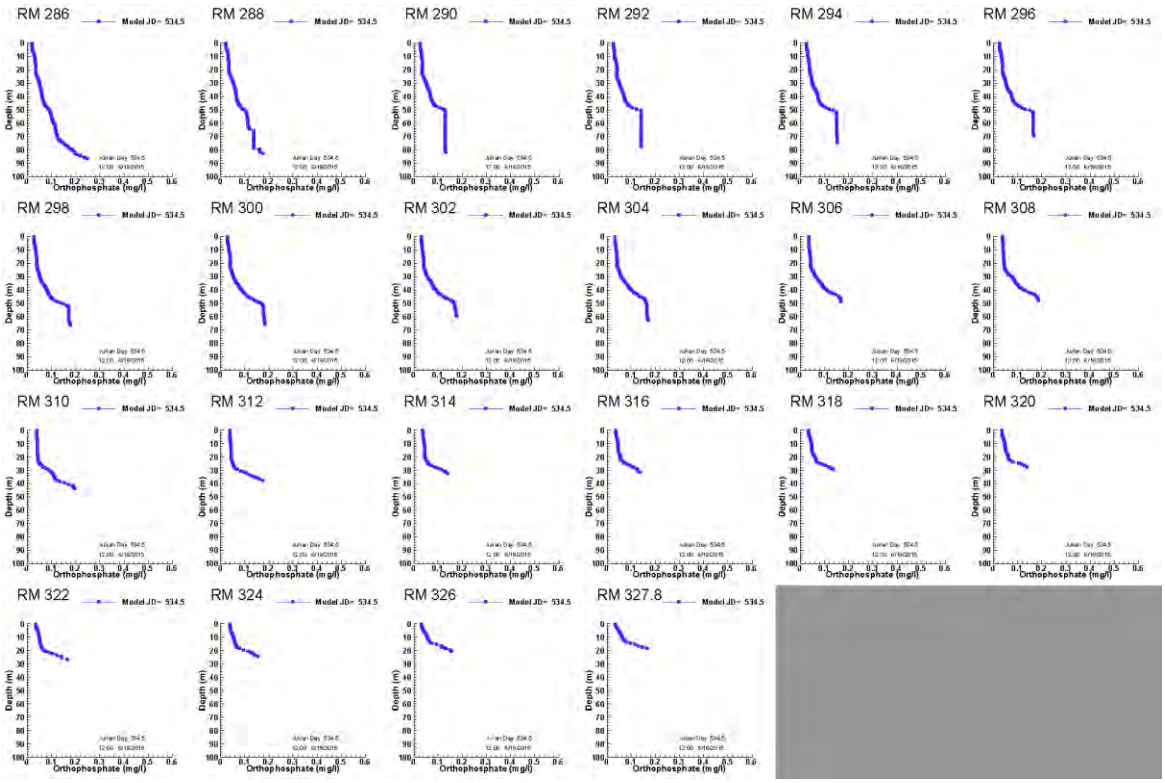


Figure 797. Vertical profiles of orthophosphate compared with data for 6/18/2015.

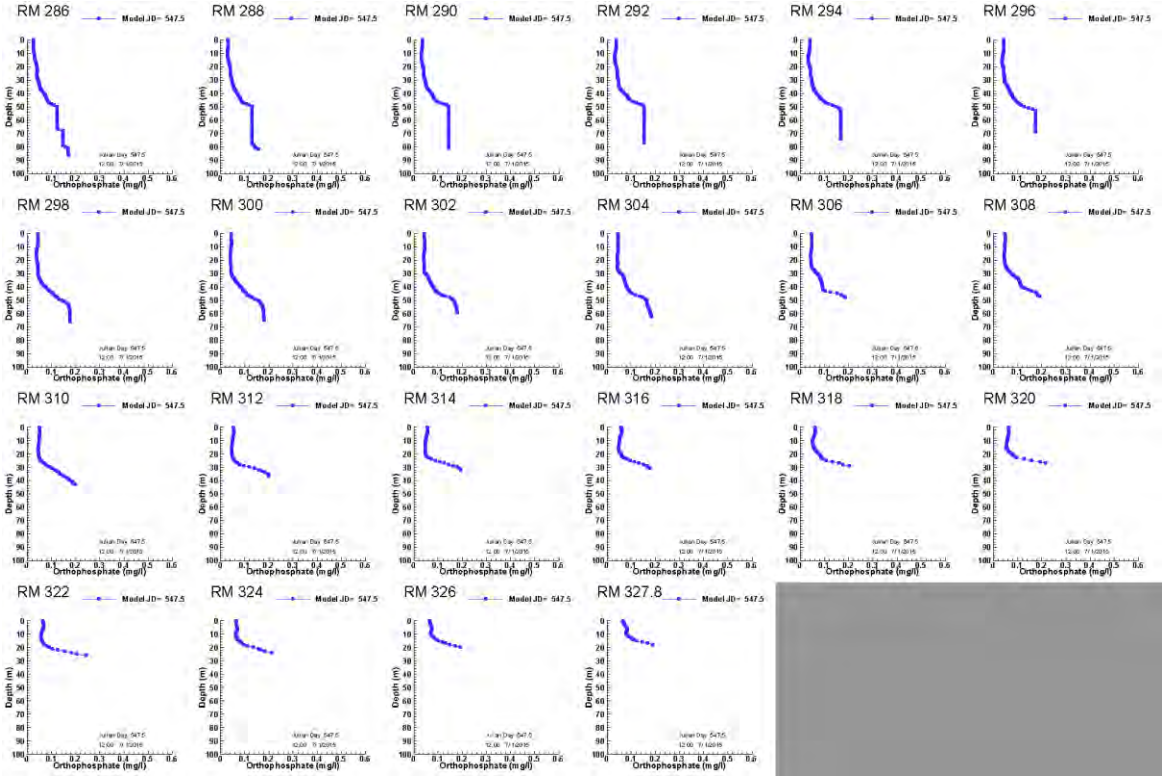


Figure 798. Vertical profiles of orthophosphate compared with data for 7/ 1/2015.

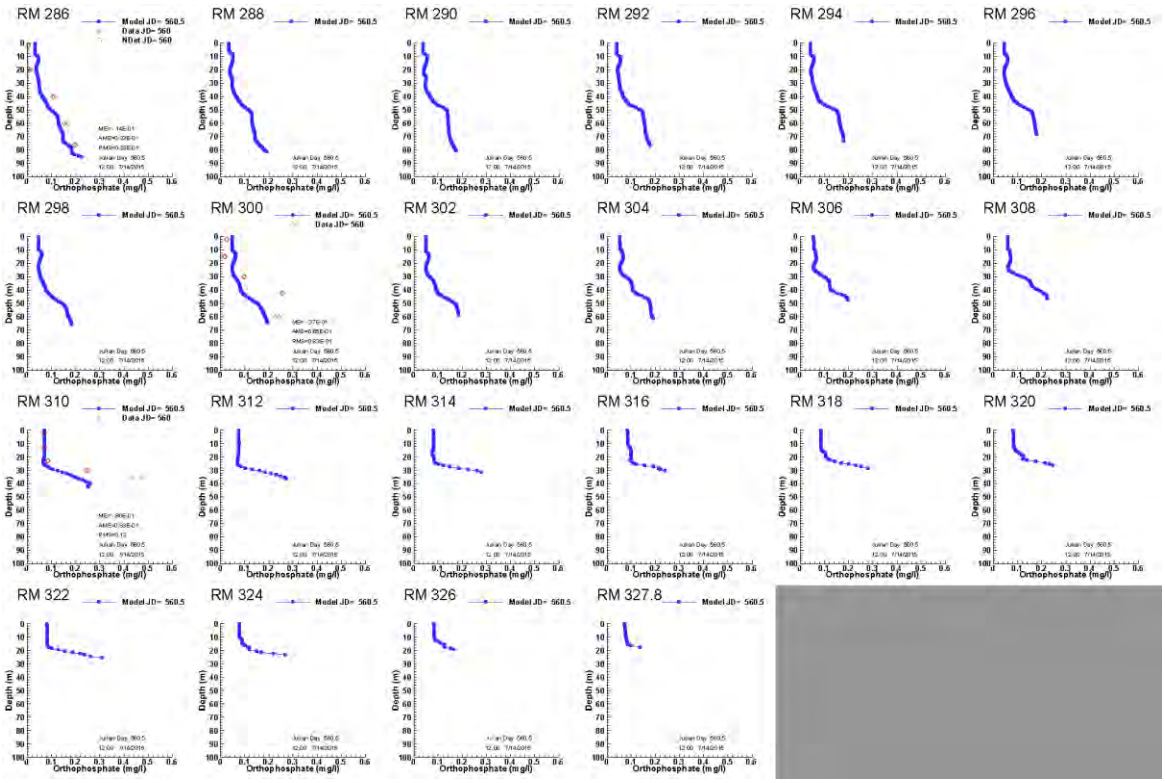


Figure 799. Vertical profiles of orthophosphate compared with data for 7/14/2015.

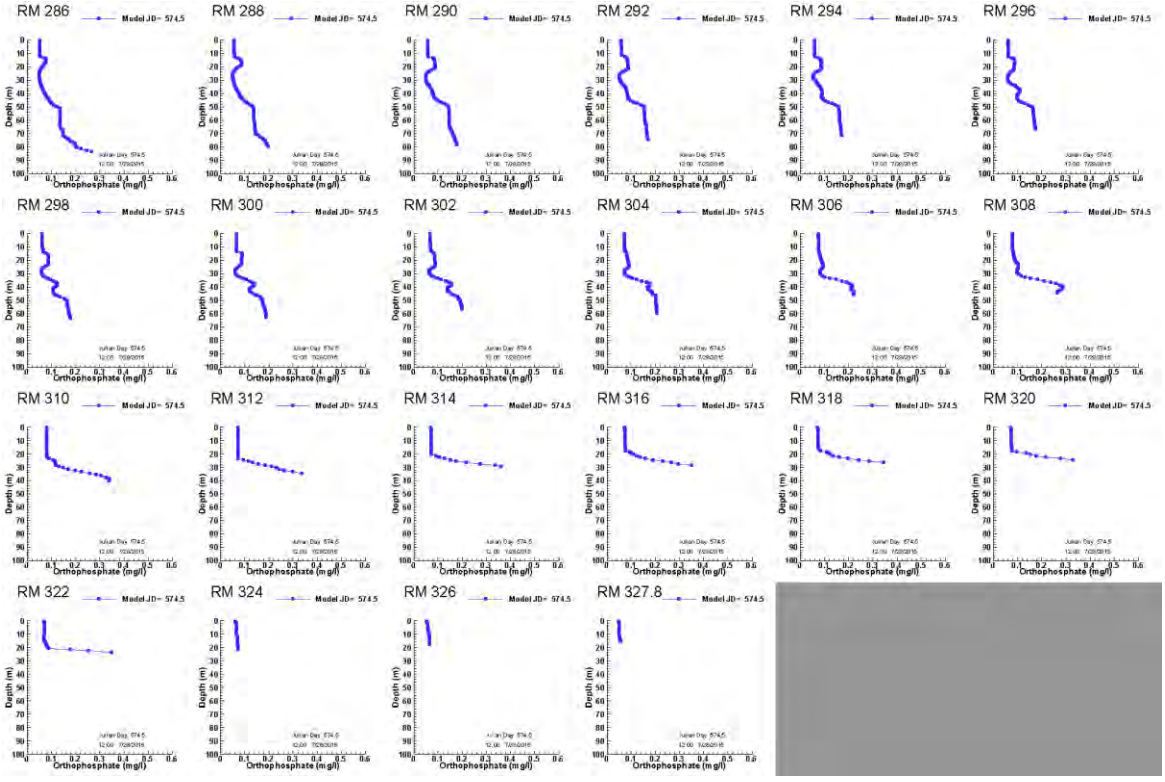


Figure 800. Vertical profiles of orthophosphate compared with data for 7/28/2015.

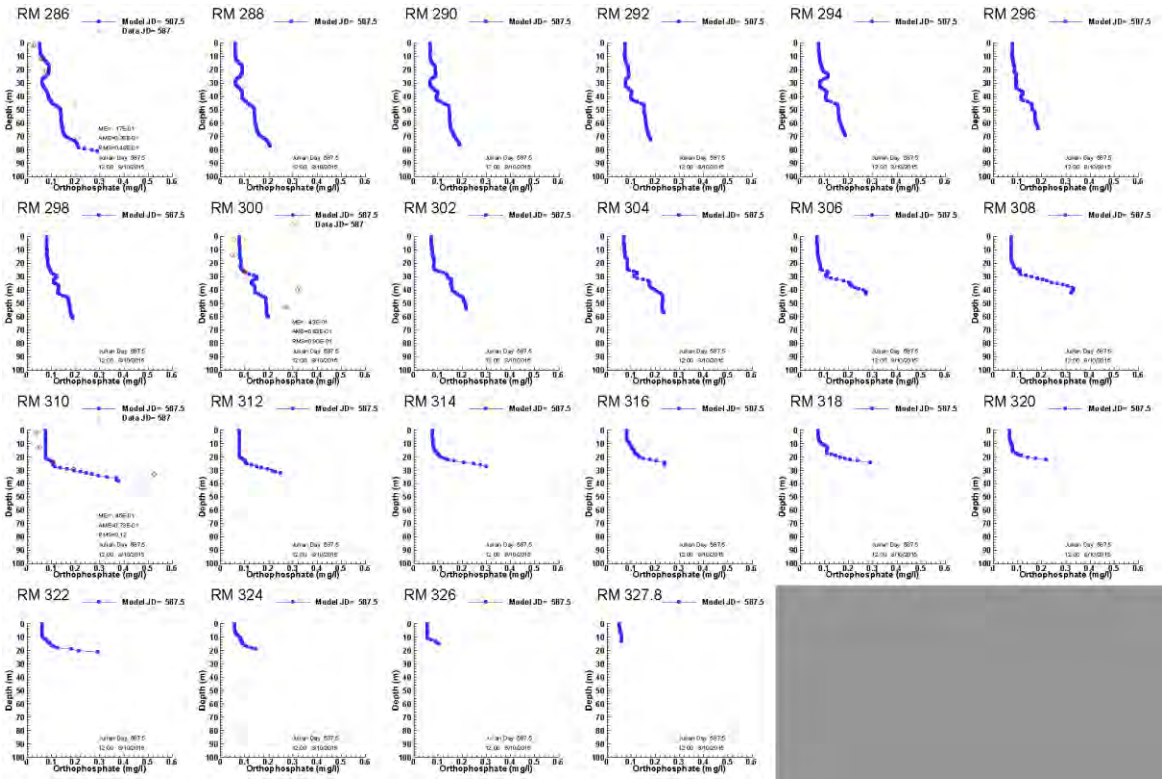


Figure 801. Vertical profiles of orthophosphate compared with data for 8/10/2015.

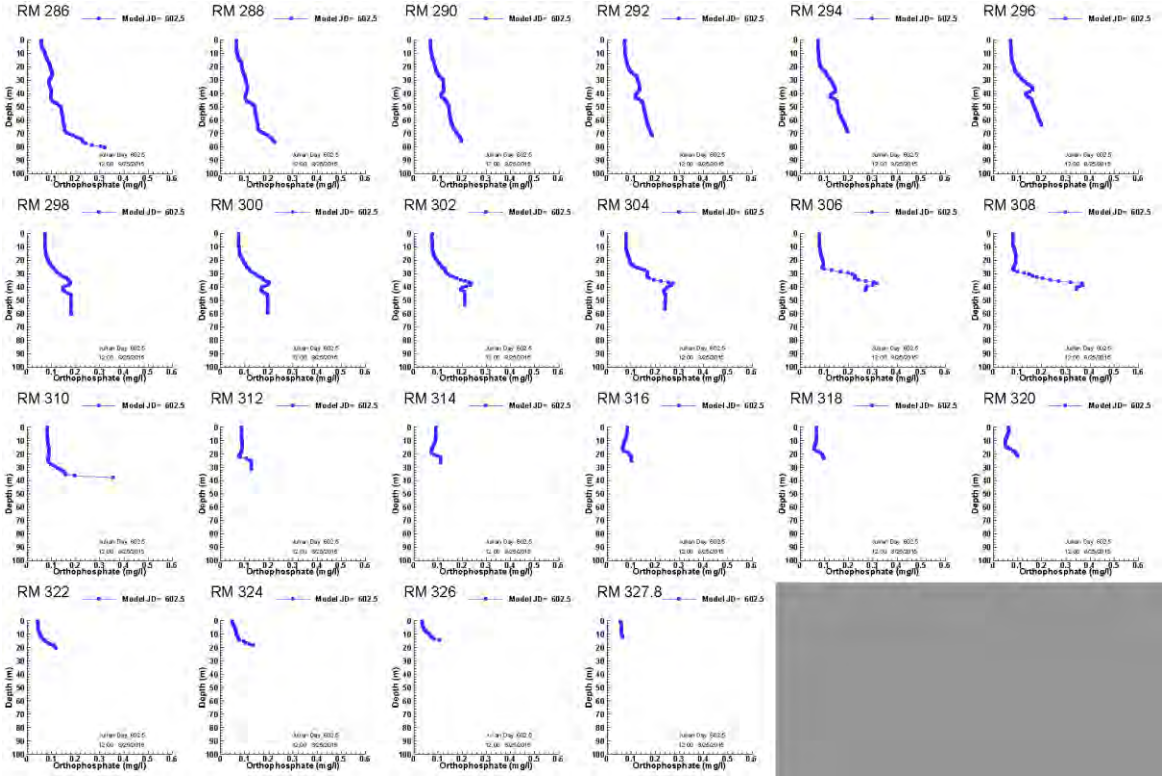


Figure 802. Vertical profiles of orthophosphate compared with data for 8/25/2015.

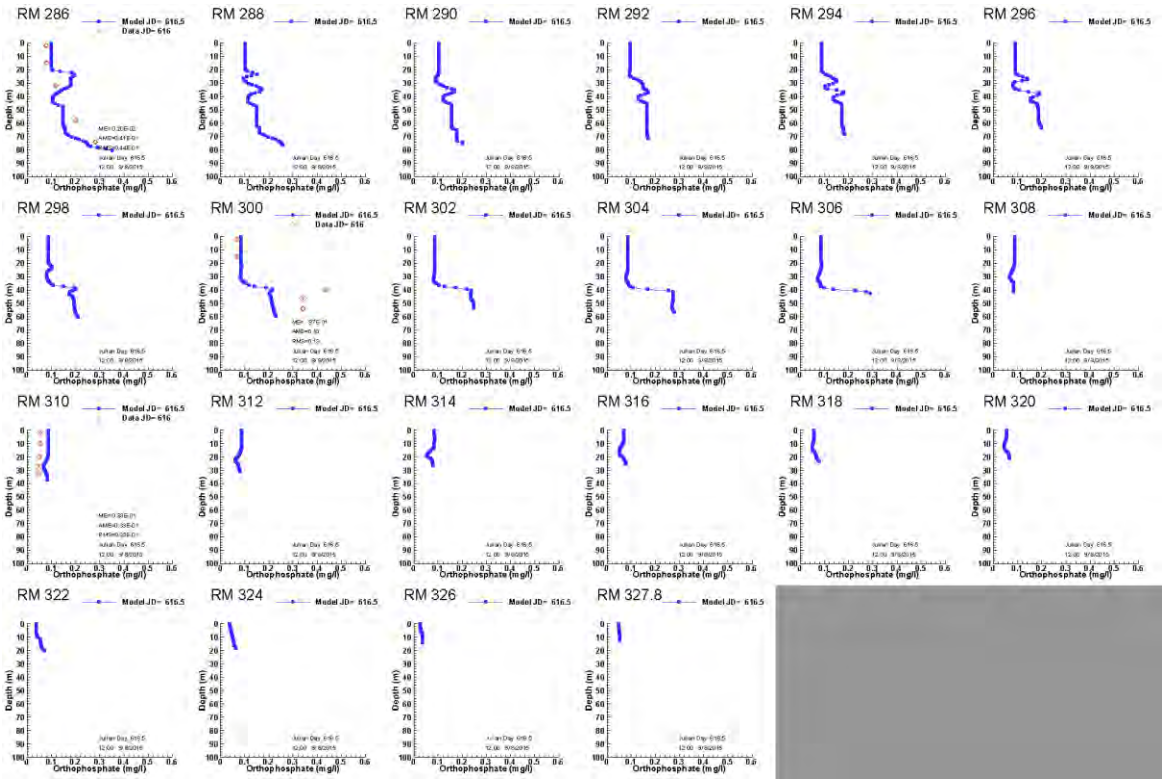


Figure 803. Vertical profiles of orthophosphate compared with data for 9/ 8/2015.

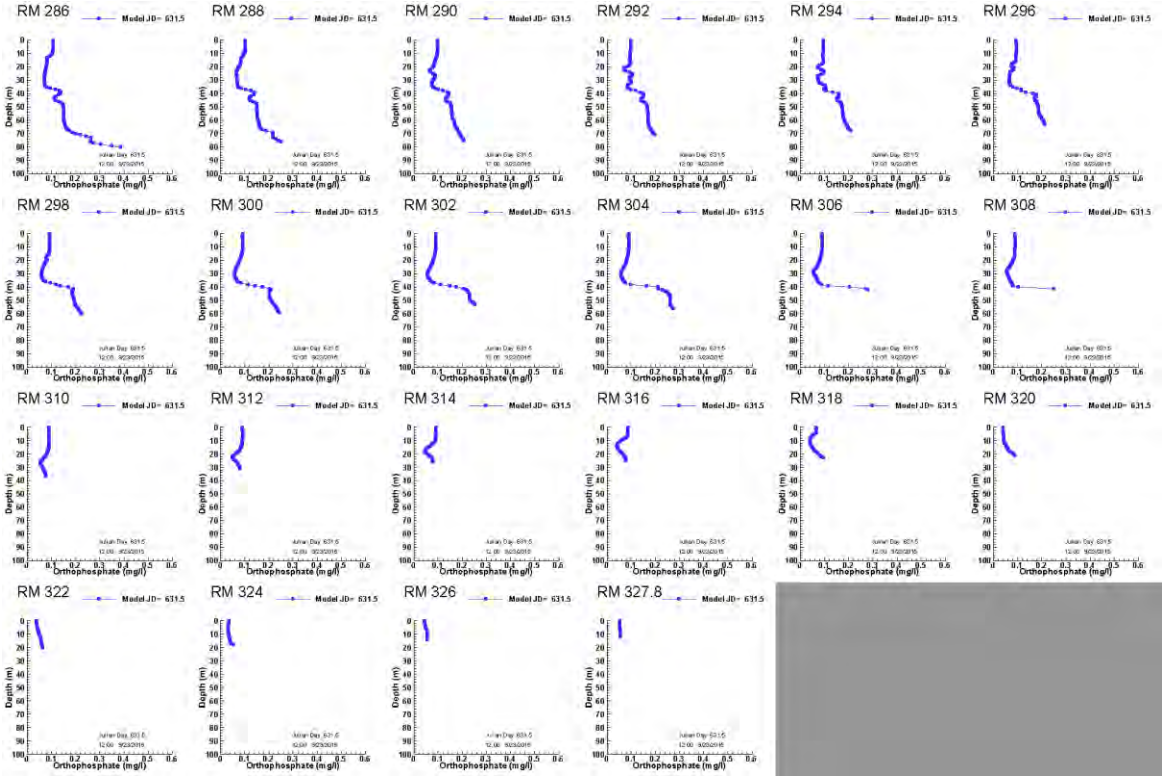


Figure 804. Vertical profiles of orthophosphate compared with data for 9/23/2015.

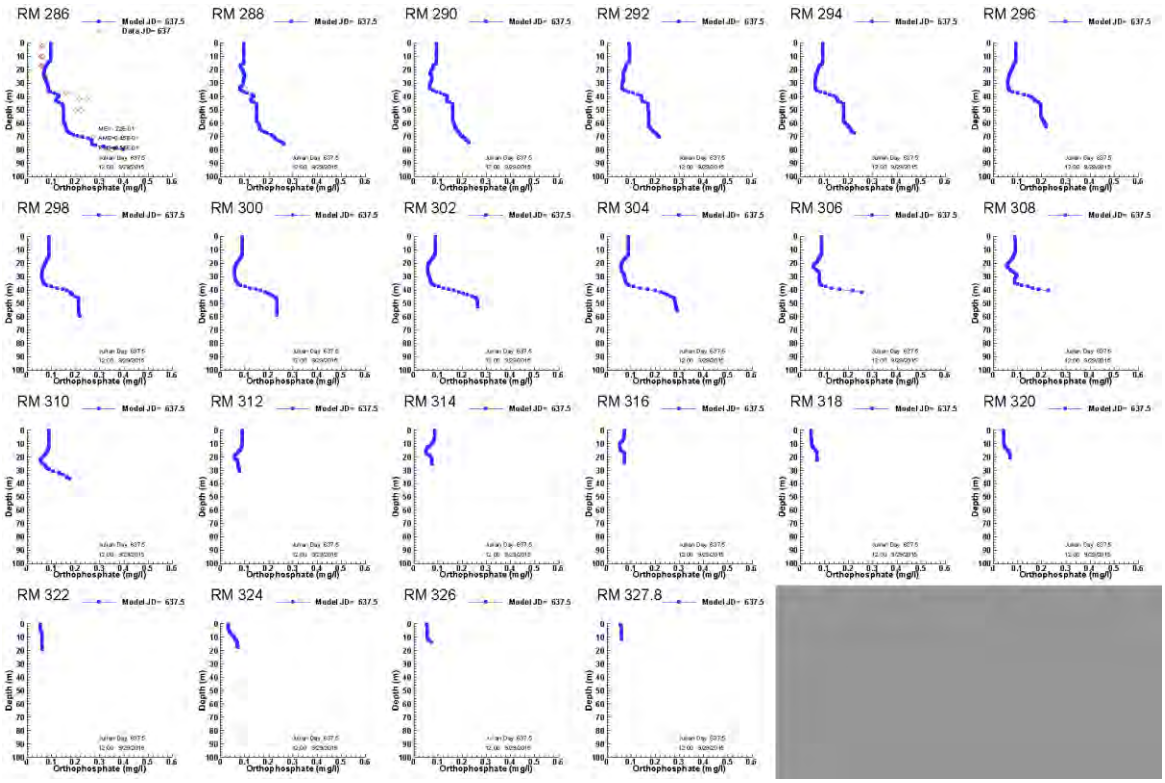


Figure 805. Vertical profiles of orthophosphate compared with data for 9/29/2015.

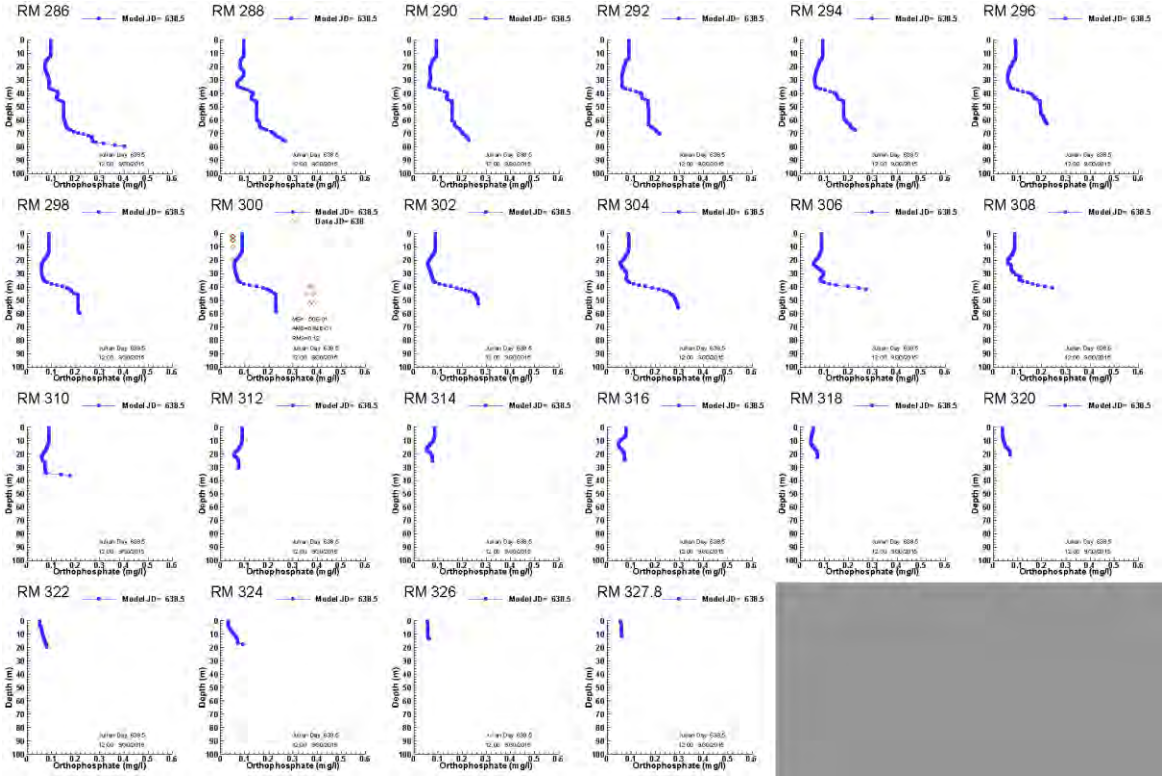


Figure 806. Vertical profiles of orthophosphate compared with data for 9/30/2015.

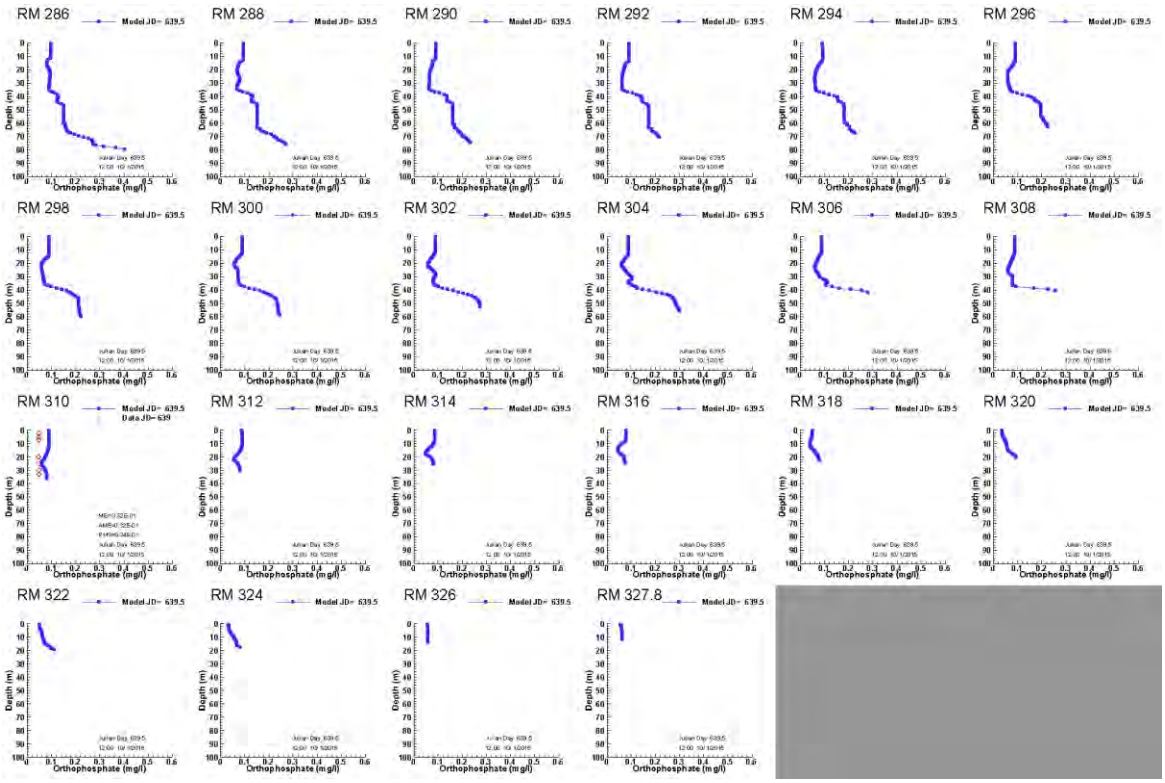


Figure 807. Vertical profiles of orthophosphate compared with data for 10/ 1/2015.

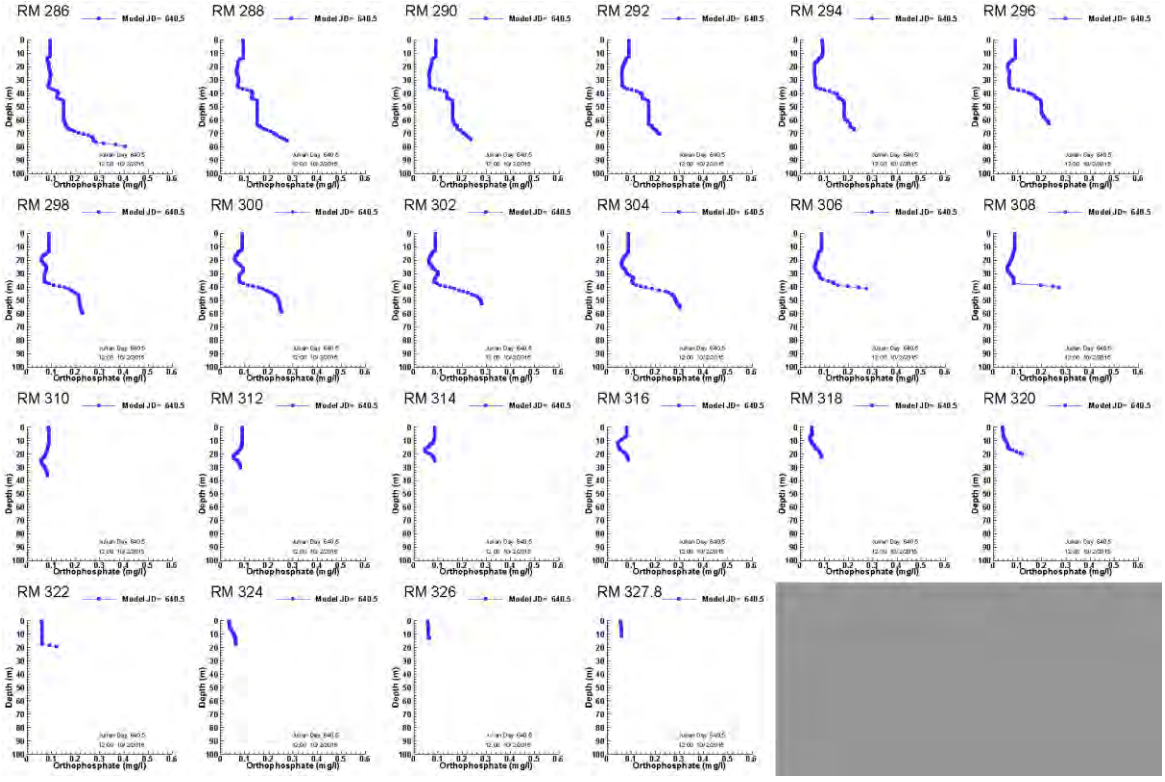


Figure 808. Vertical profiles of orthophosphate compared with data for 10/ 2/2015.

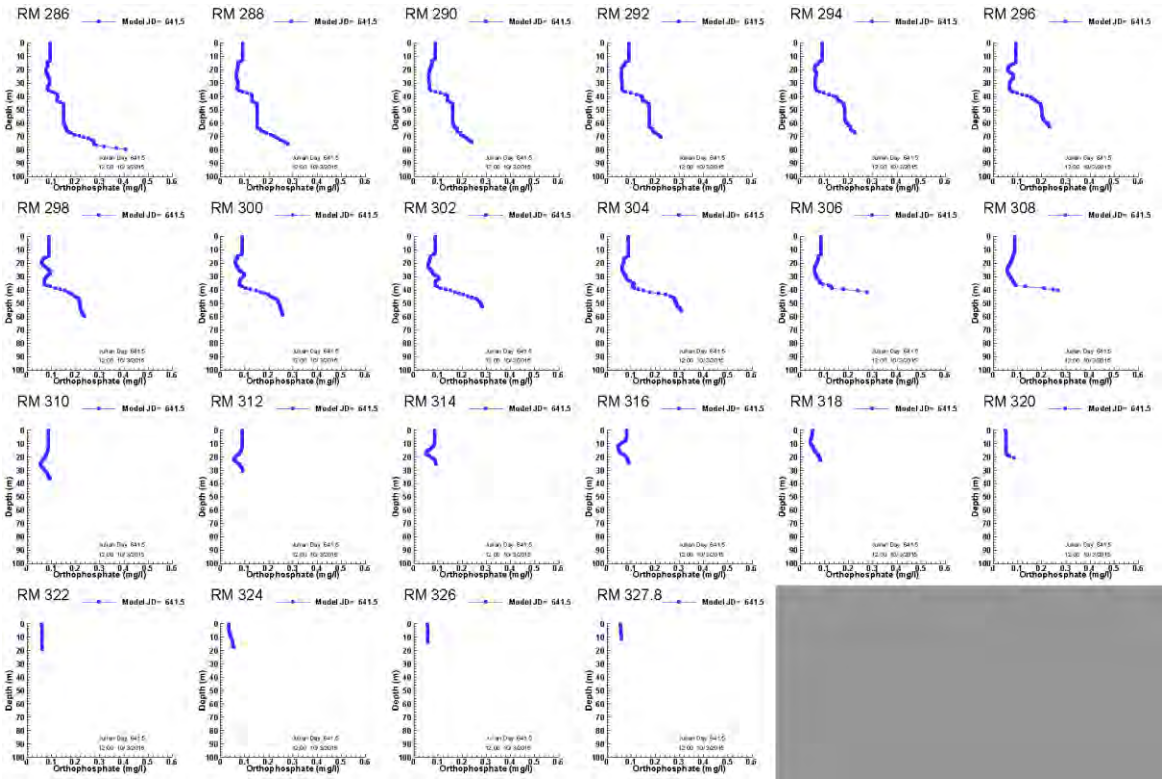


Figure 809. Vertical profiles of orthophosphate compared with data for 10/ 3/2015.

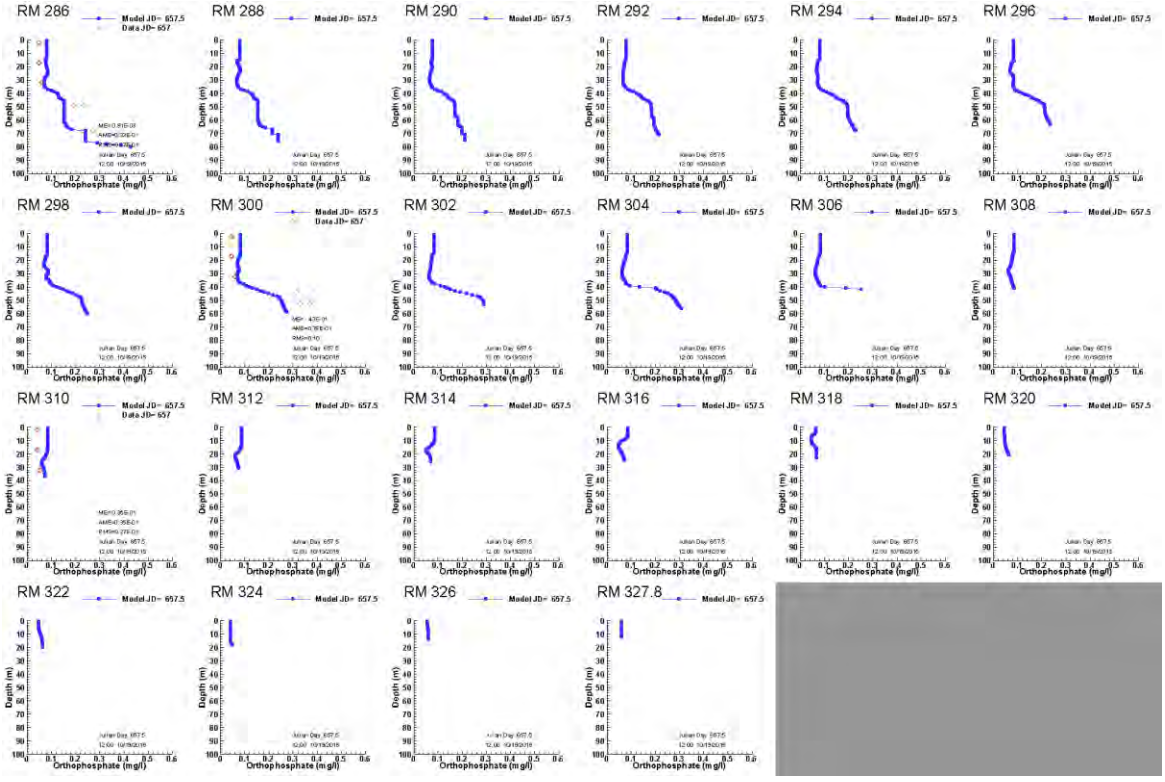


Figure 810. Vertical profiles of orthophosphate compared with data for 10/19/2015.

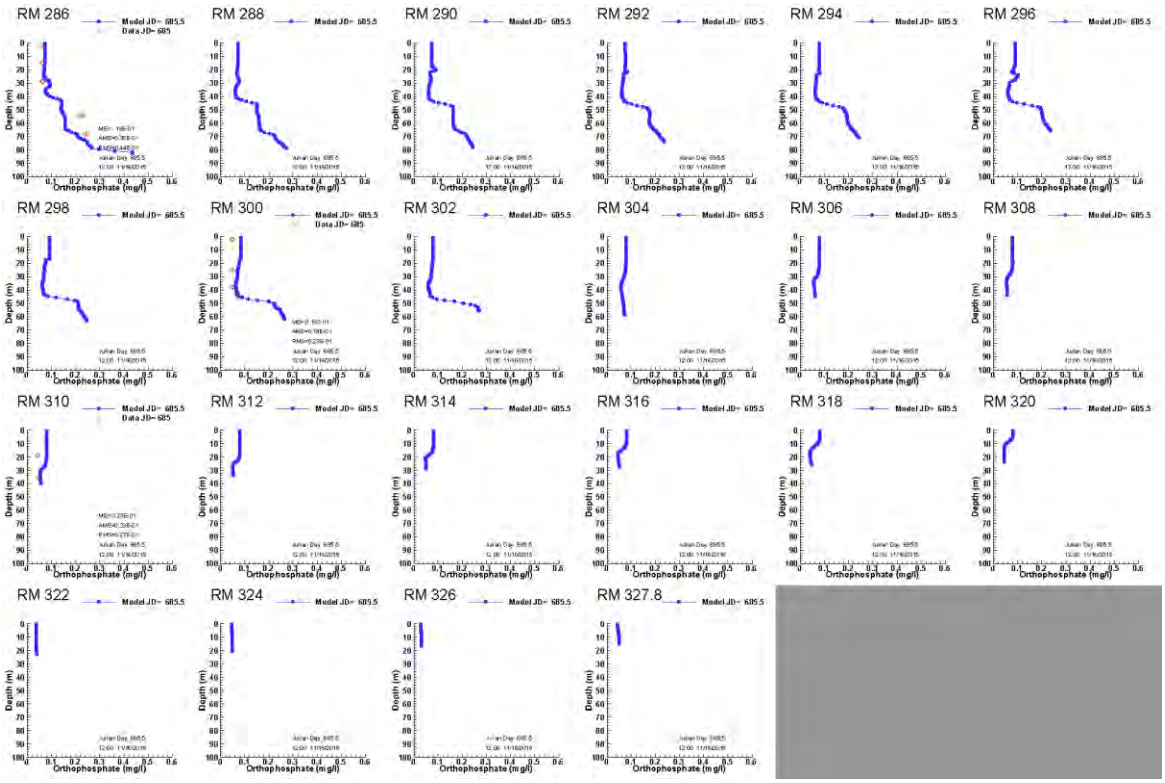


Figure 811. Vertical profiles of orthophosphate compared with data for 11/16/2015.

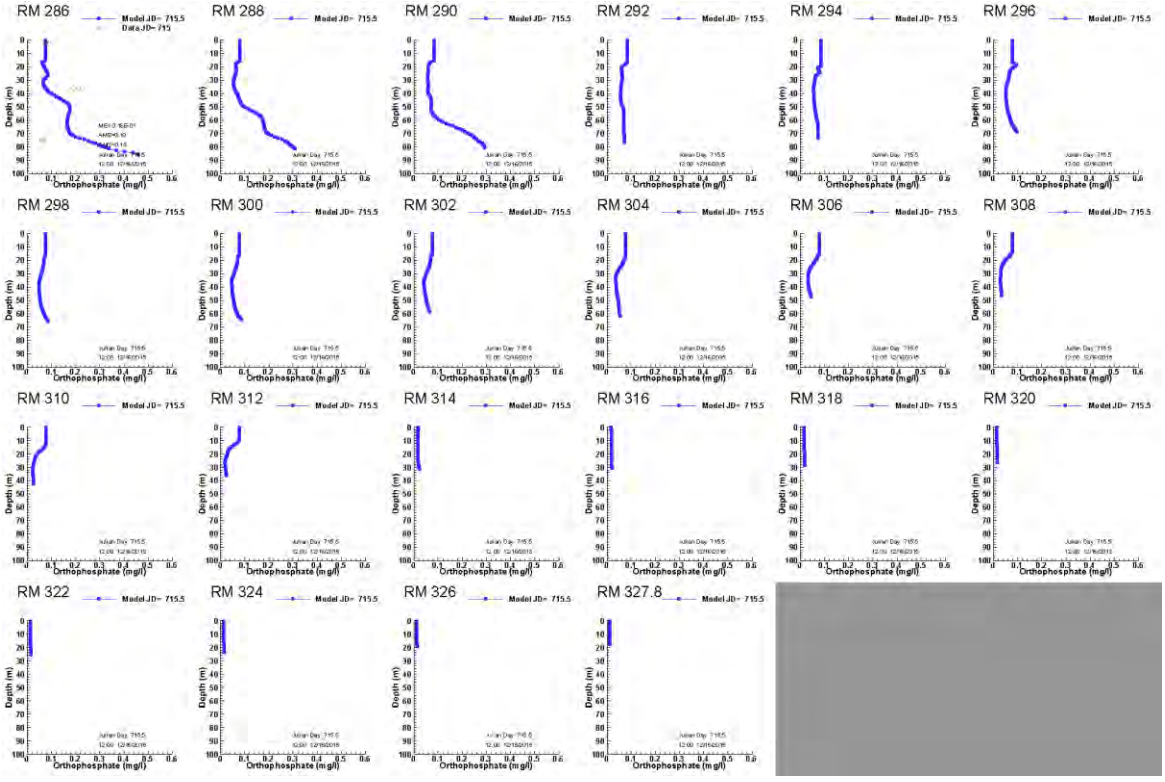


Figure 812. Vertical profiles of orthophosphate compared with data for 12/16/2015.

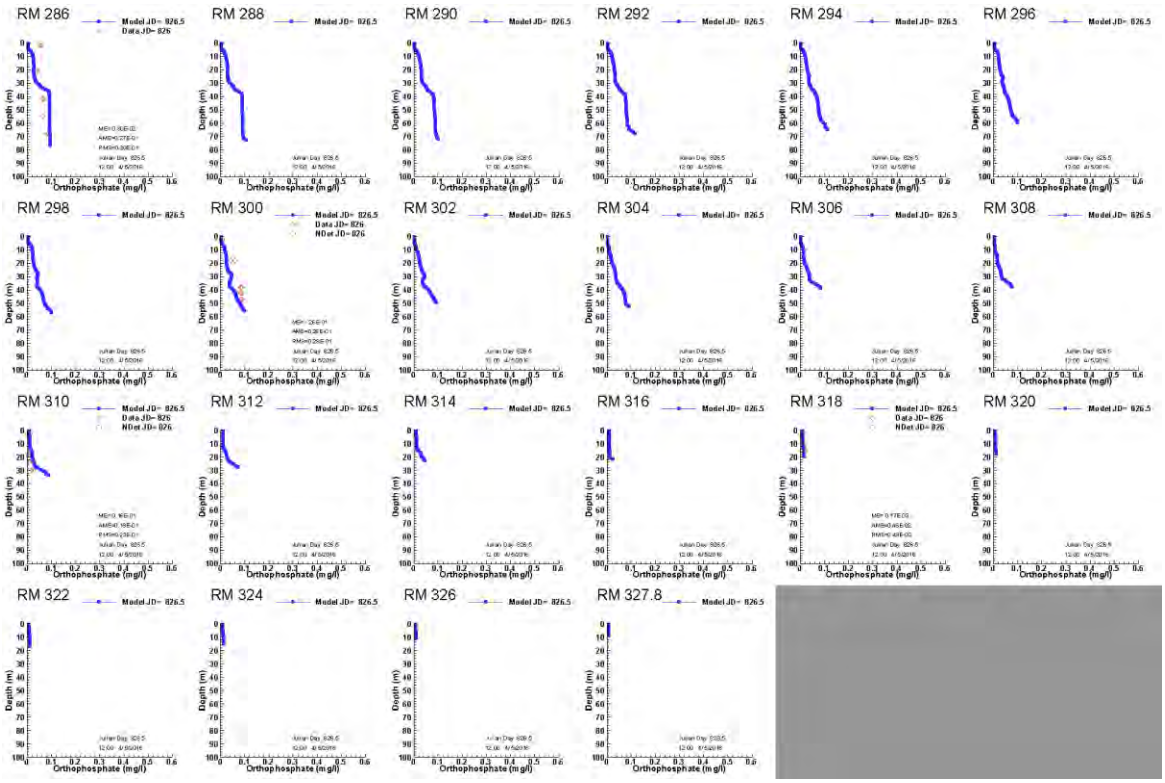


Figure 813. Vertical profiles of orthophosphate compared with data for 4/ 5/2016.

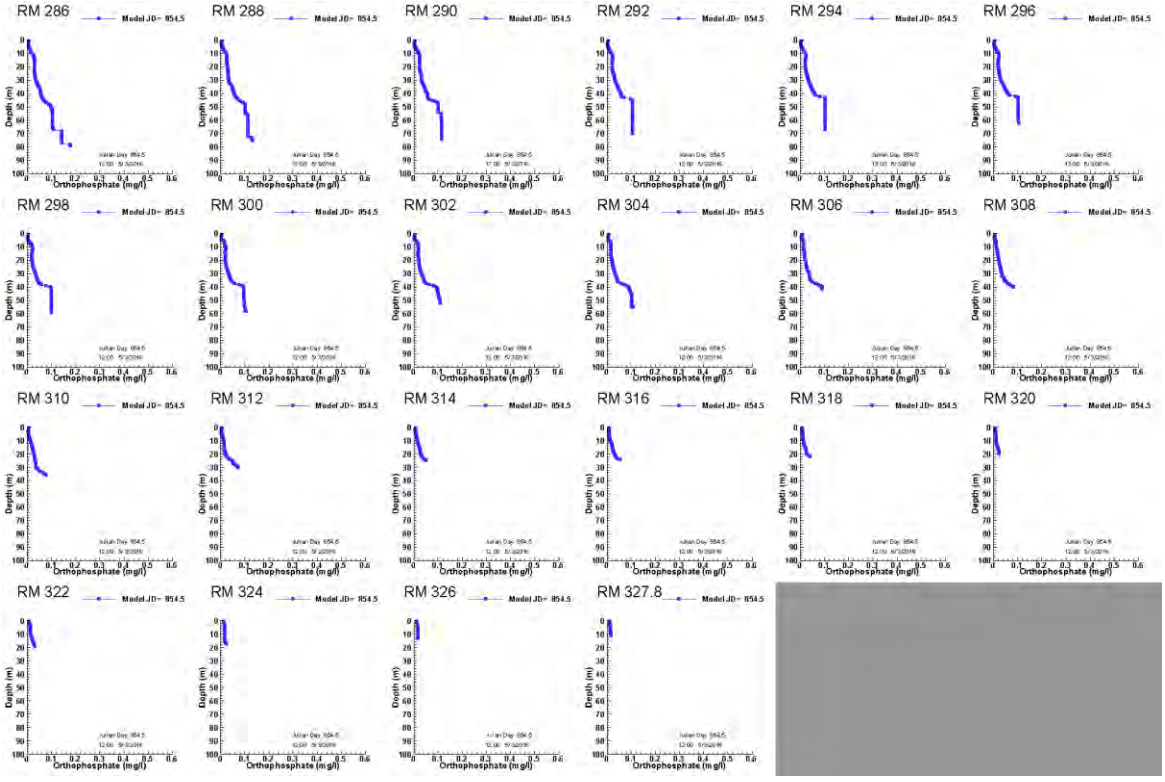


Figure 814. Vertical profiles of orthophosphate compared with data for 5/ 3/2016.

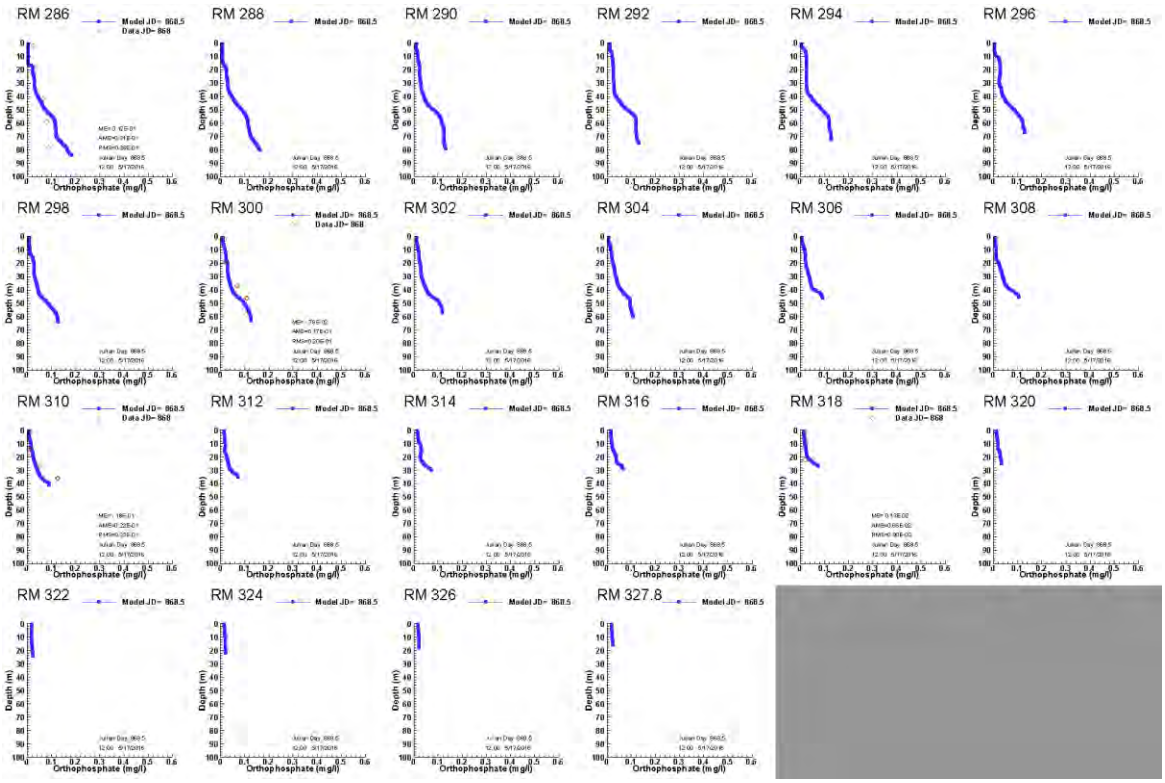


Figure 815. Vertical profiles of orthophosphate compared with data for 5/17/2016.

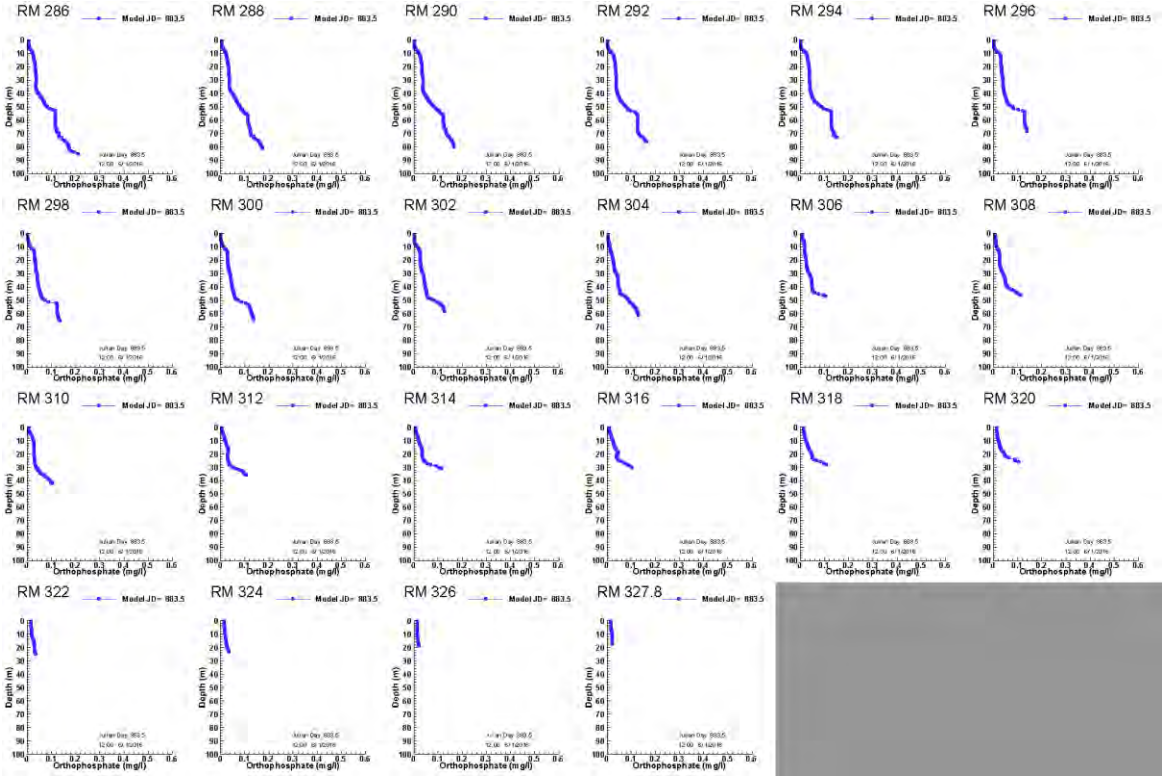


Figure 816. Vertical profiles of orthophosphate compared with data for 6/ 1/2016.

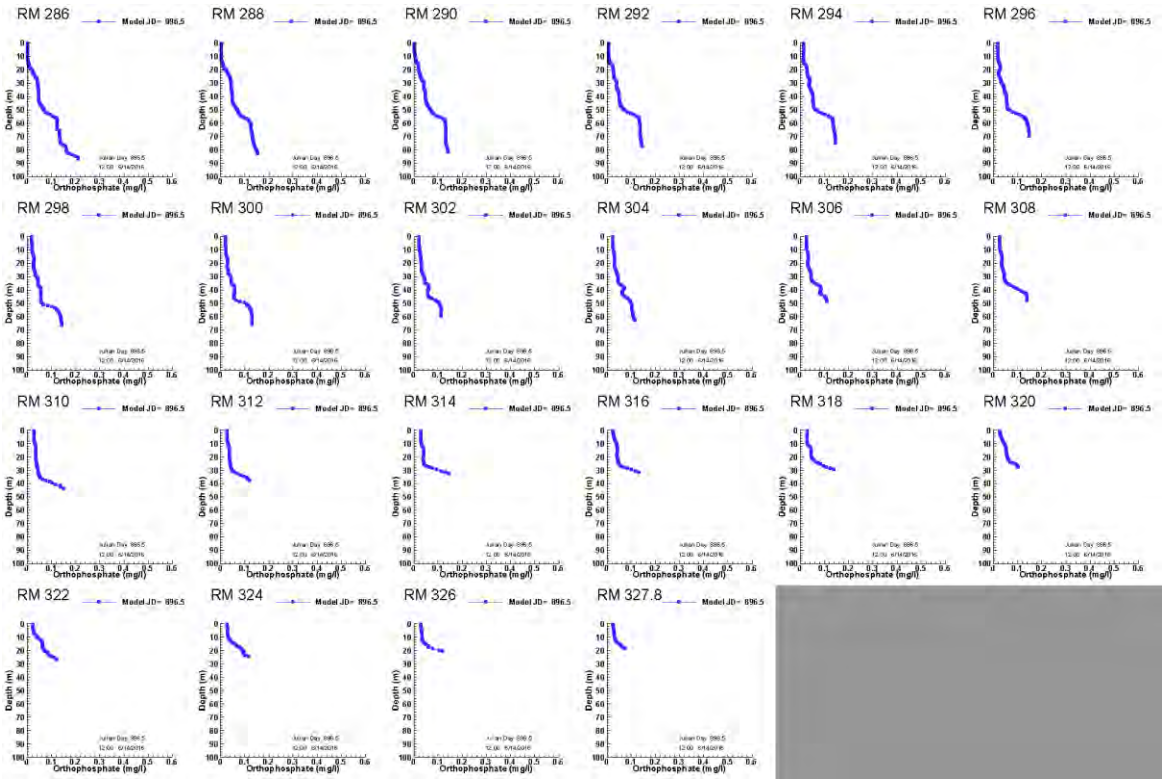


Figure 817. Vertical profiles of orthophosphate compared with data for 6/14/2016.

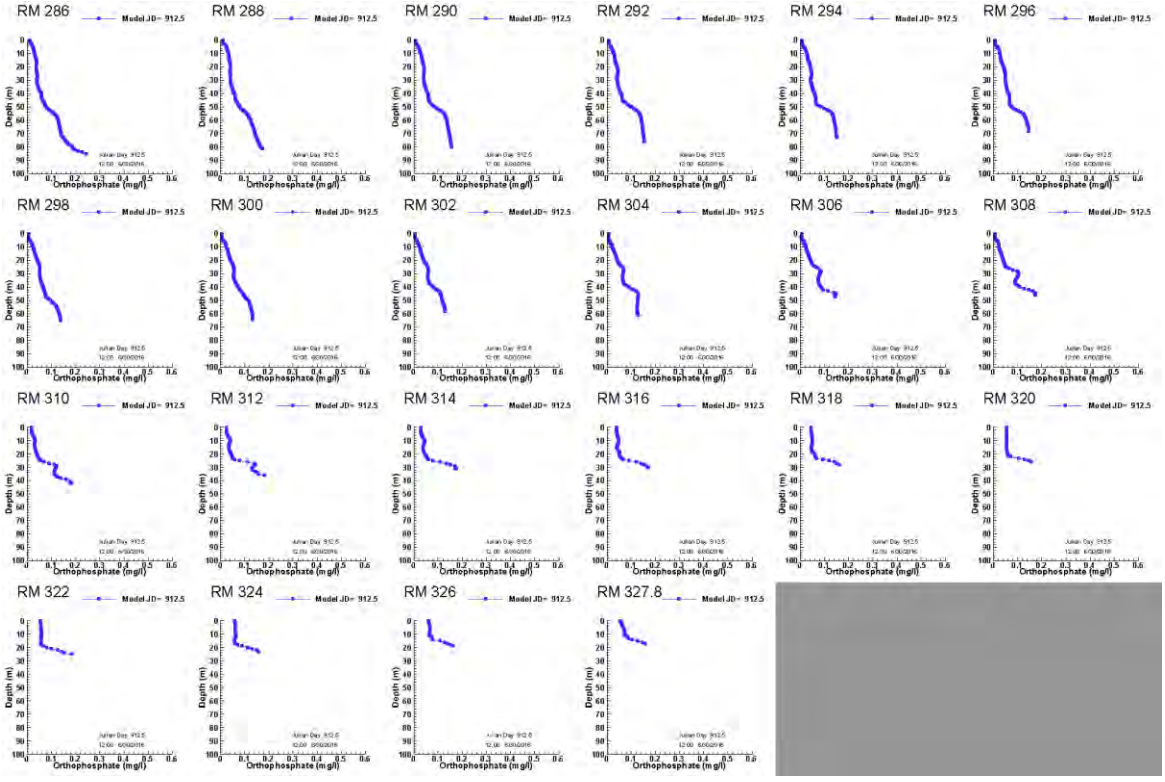


Figure 818. Vertical profiles of orthophosphate compared with data for 6/30/2016.

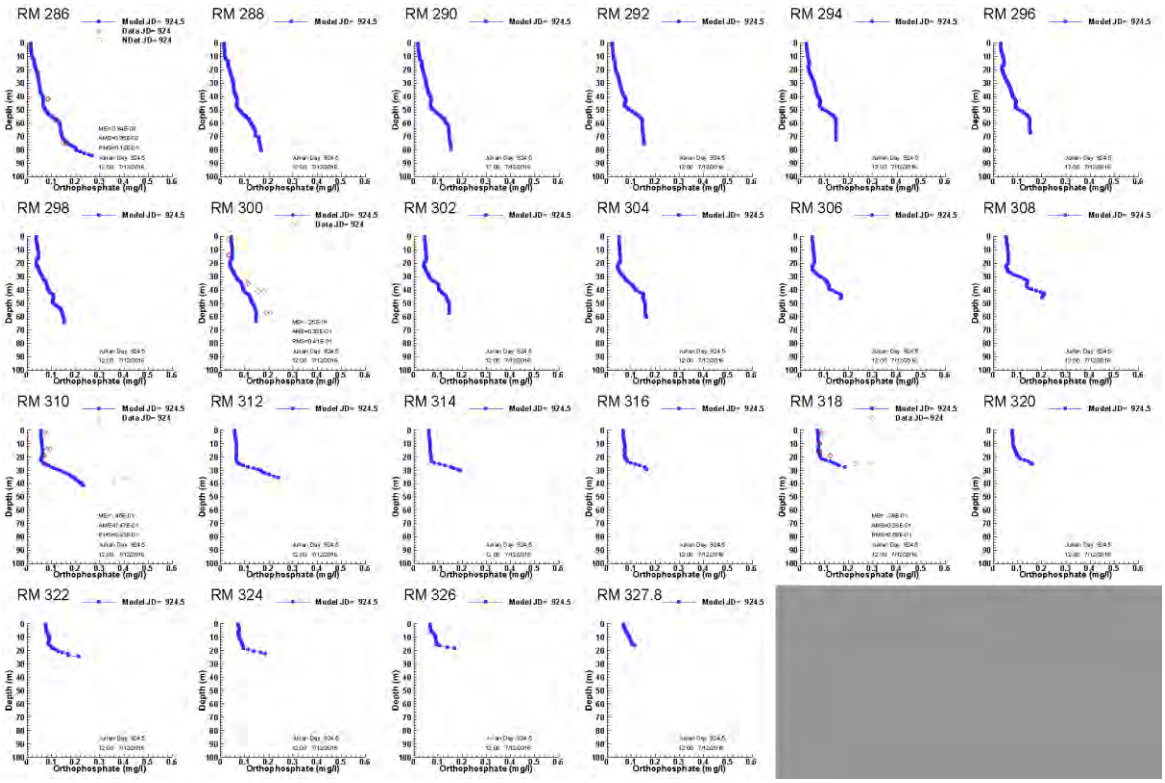


Figure 819. Vertical profiles of orthophosphate compared with data for 7/12/2016.

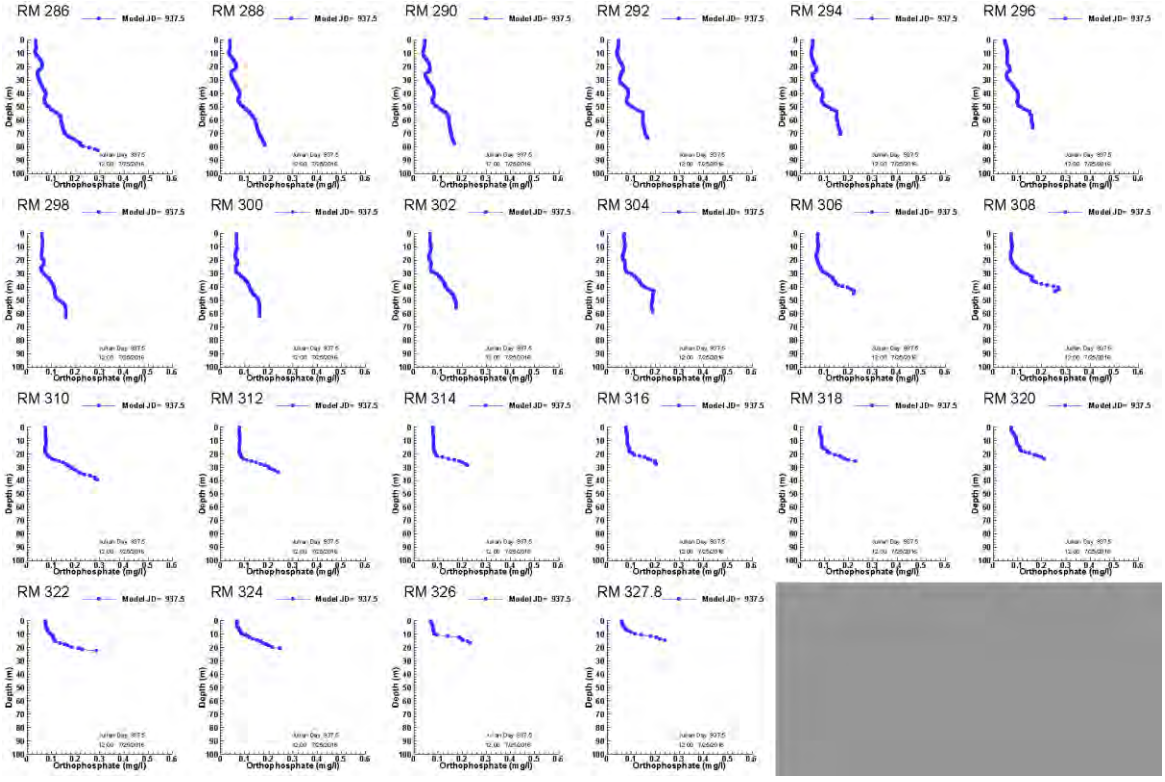


Figure 820. Vertical profiles of orthophosphate compared with data for 7/25/2016.

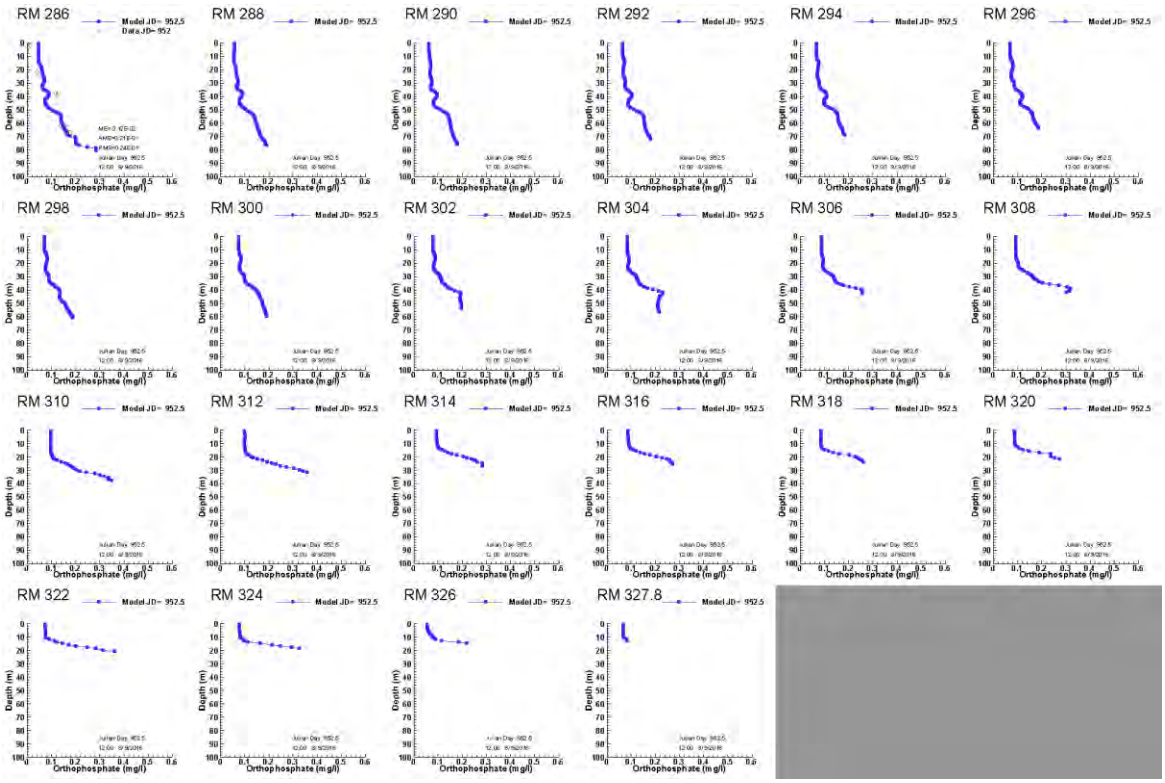


Figure 821. Vertical profiles of orthophosphate compared with data for 8/ 9/2016.

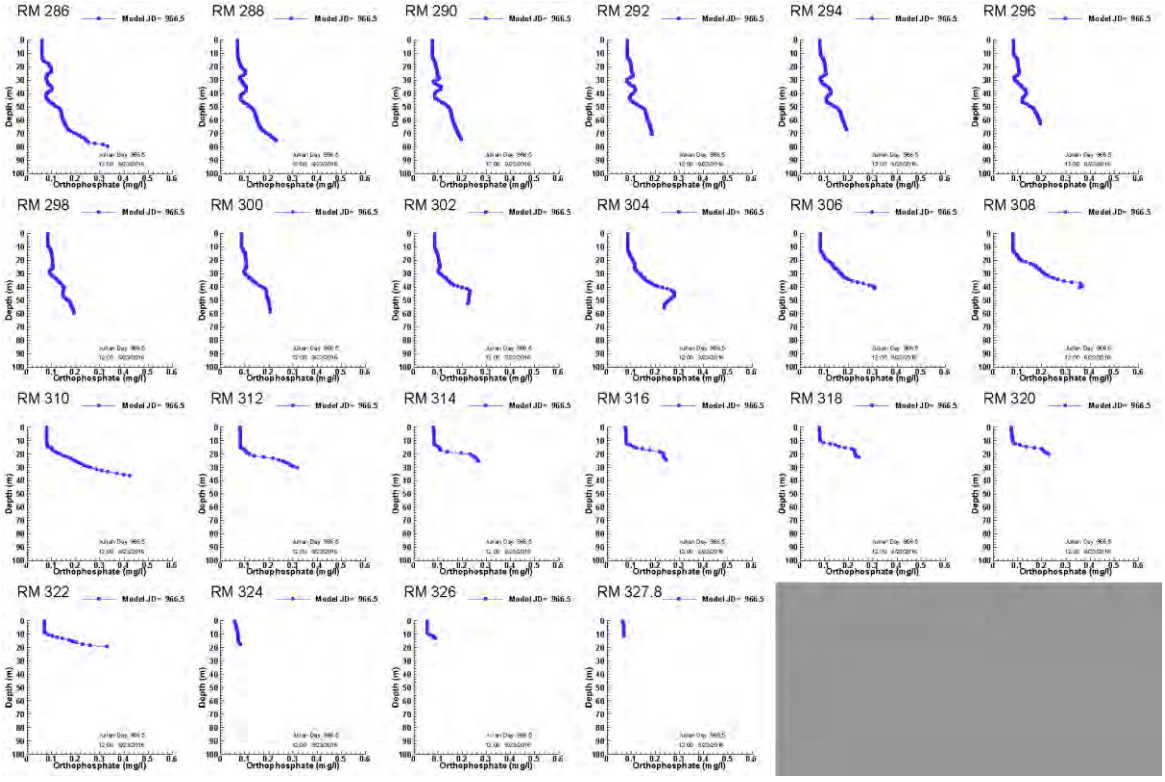


Figure 822. Vertical profiles of orthophosphate compared with data for 8/23/2016.

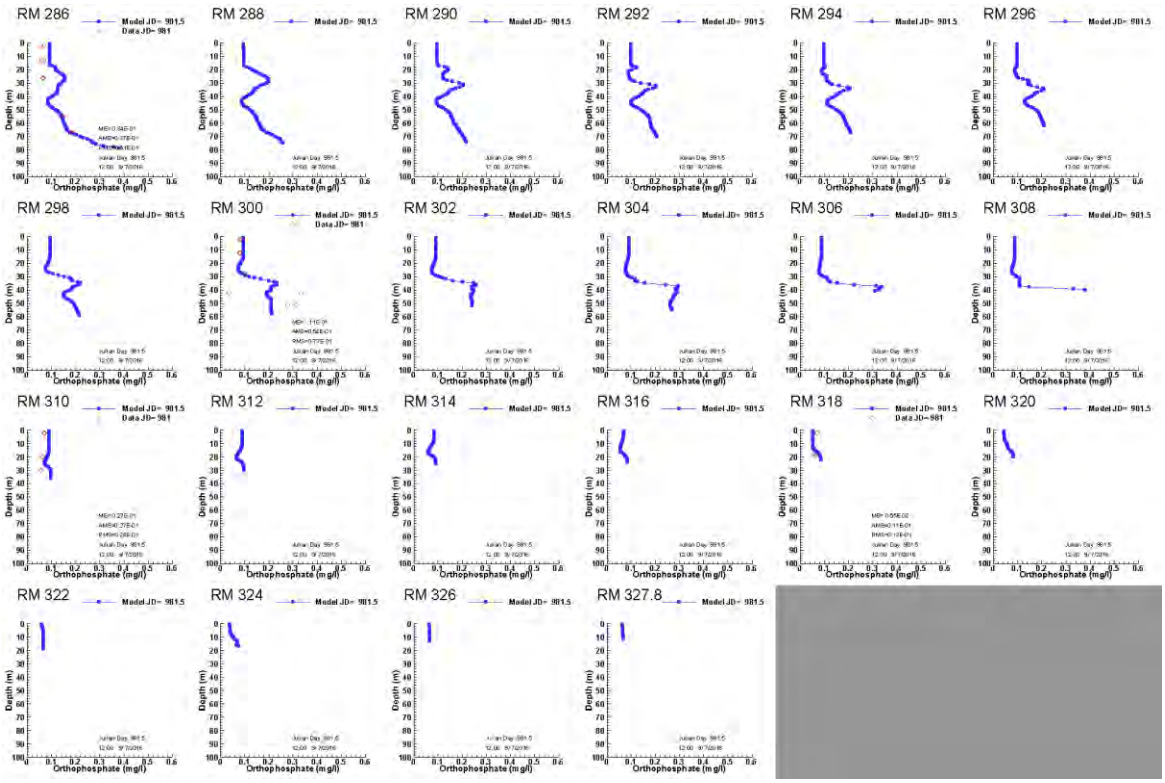


Figure 823. Vertical profiles of orthophosphate compared with data for 9/ 7/2016.

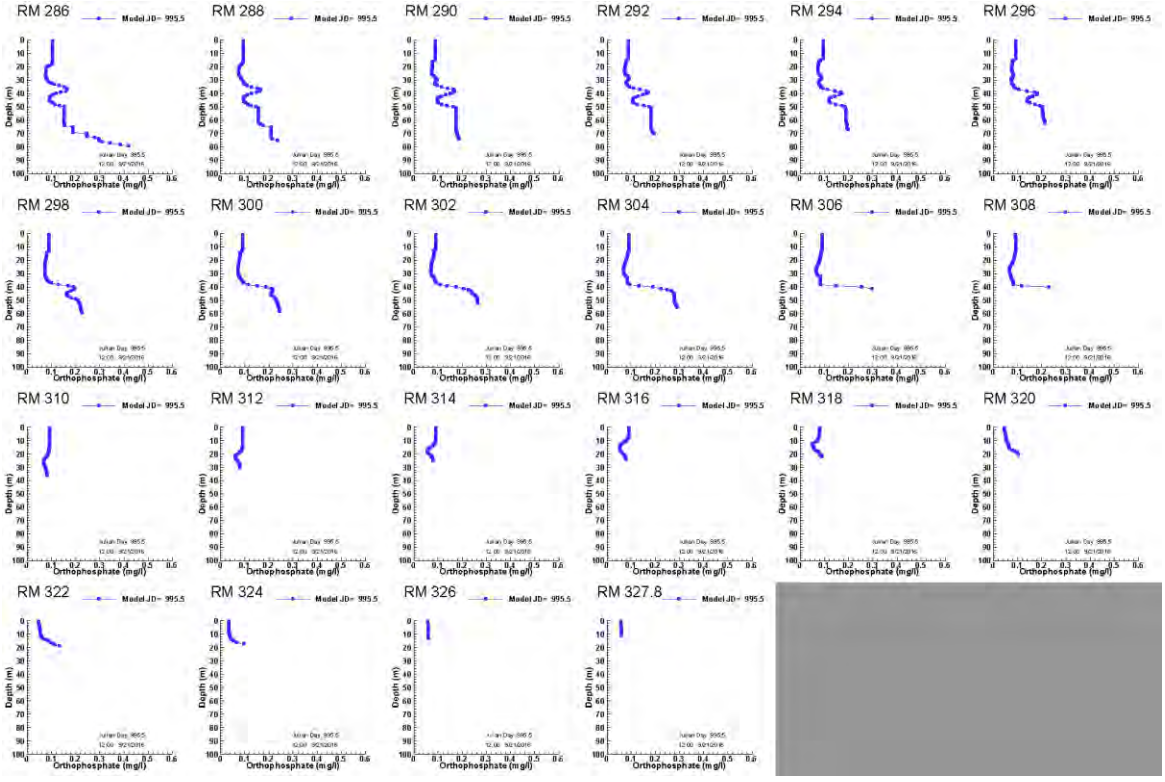


Figure 824. Vertical profiles of orthophosphate compared with data for 9/21/2016.

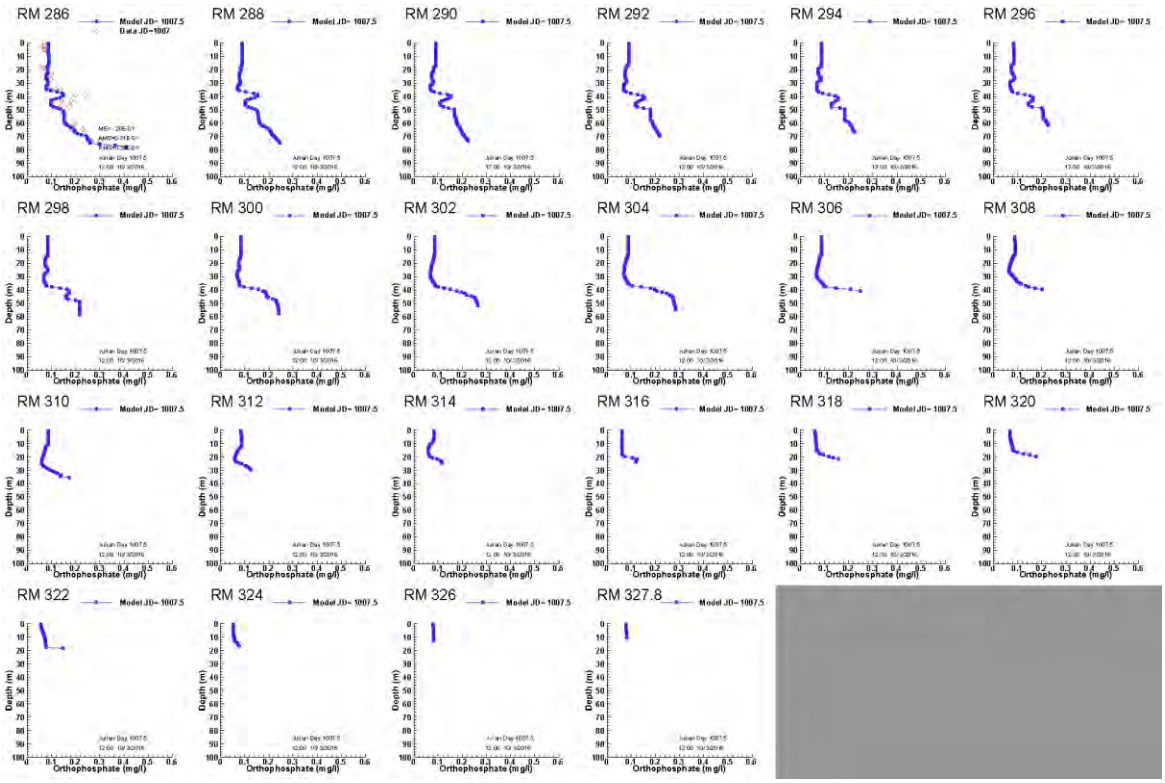


Figure 825. Vertical profiles of orthophosphate compared with data for 10/ 3/2016.

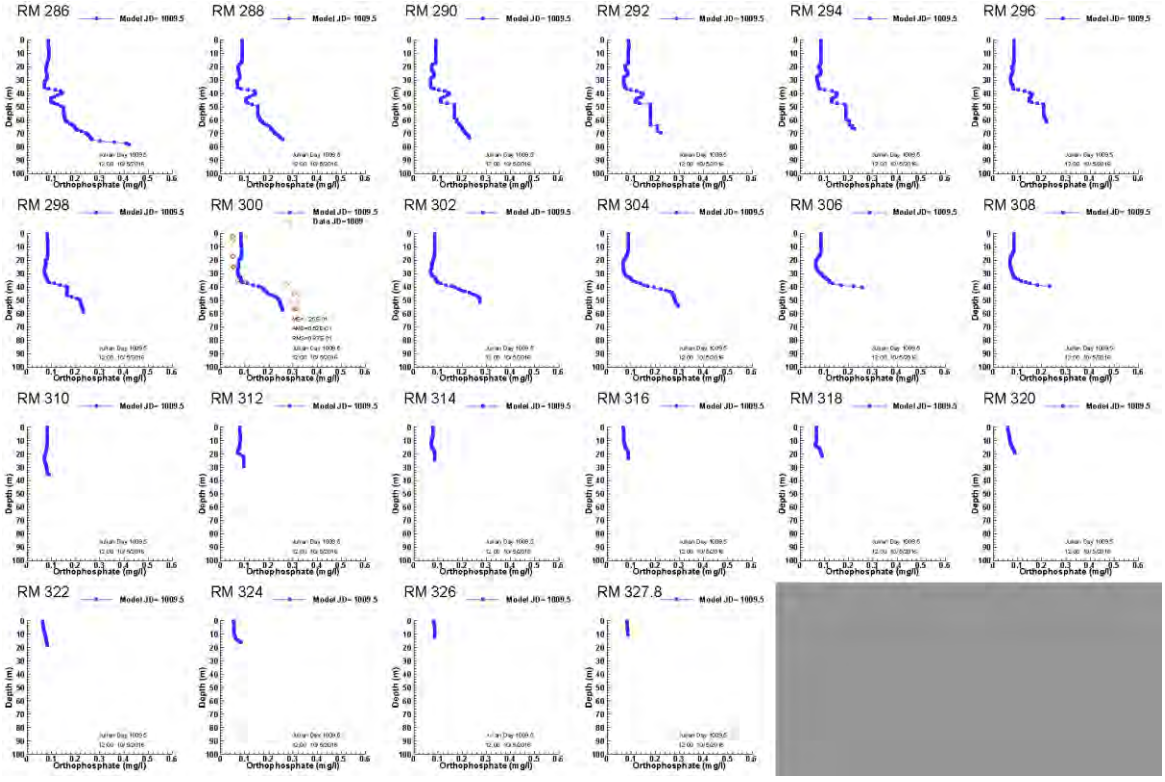


Figure 826. Vertical profiles of orthophosphate compared with data for 10/ 5/2016.

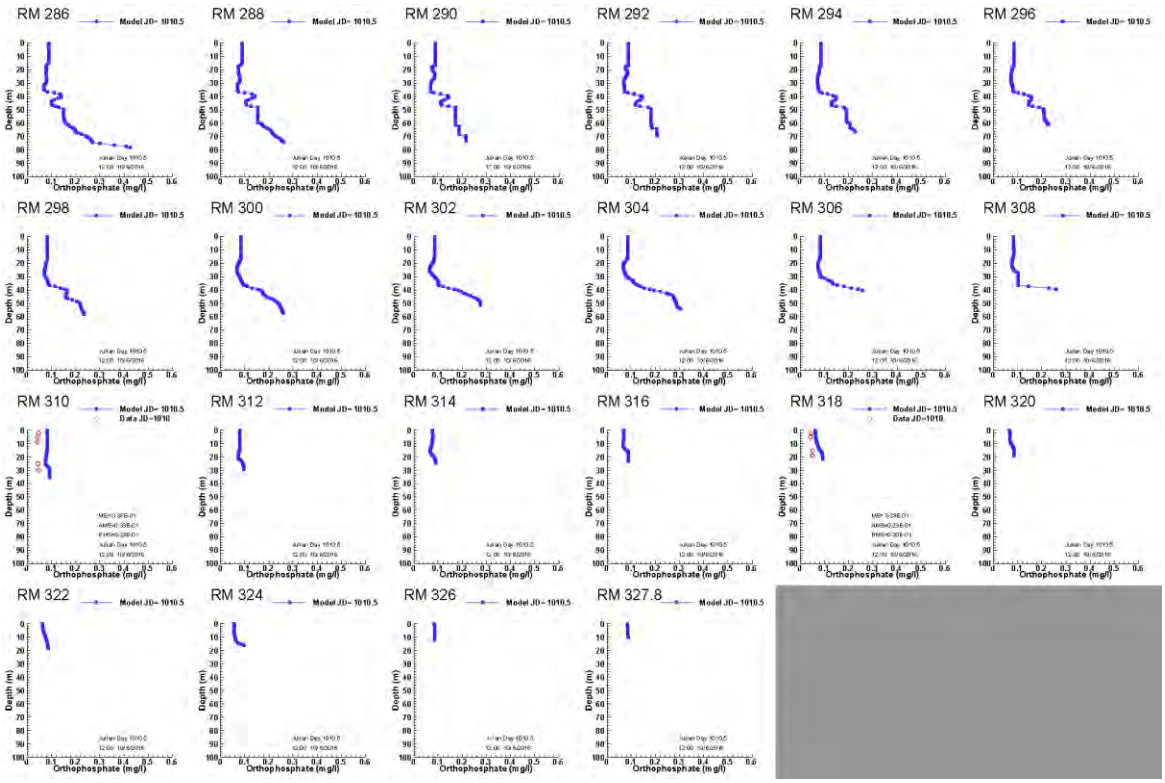


Figure 827. Vertical profiles of orthophosphate compared with data for 10/ 6/2016.

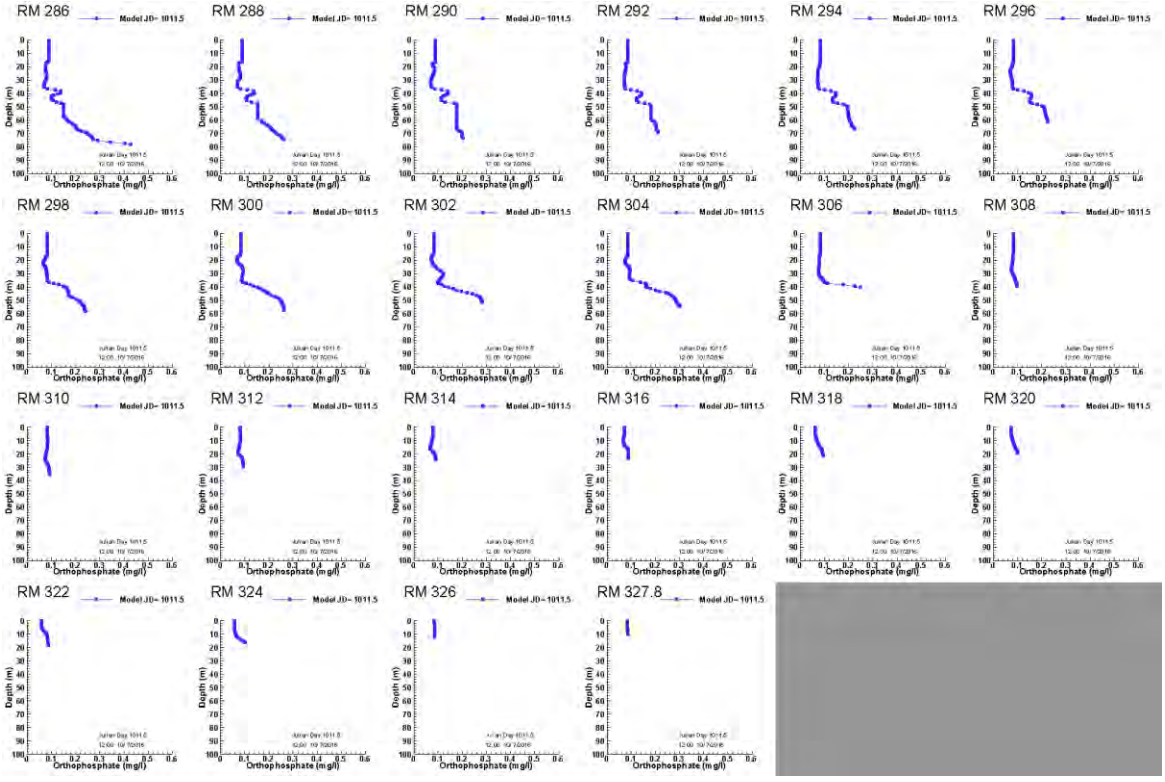


Figure 828. Vertical profiles of orthophosphate compared with data for 10/ 7/2016.

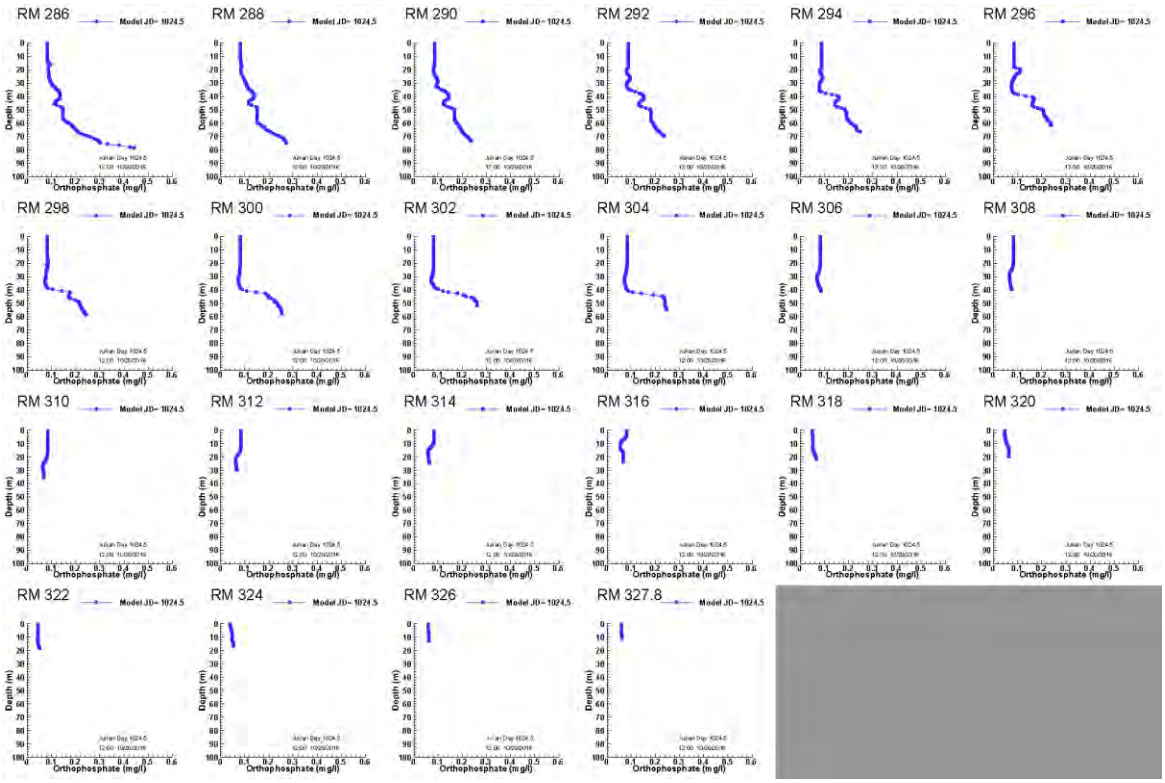


Figure 829. Vertical profiles of orthophosphate compared with data for 10/20/2016.

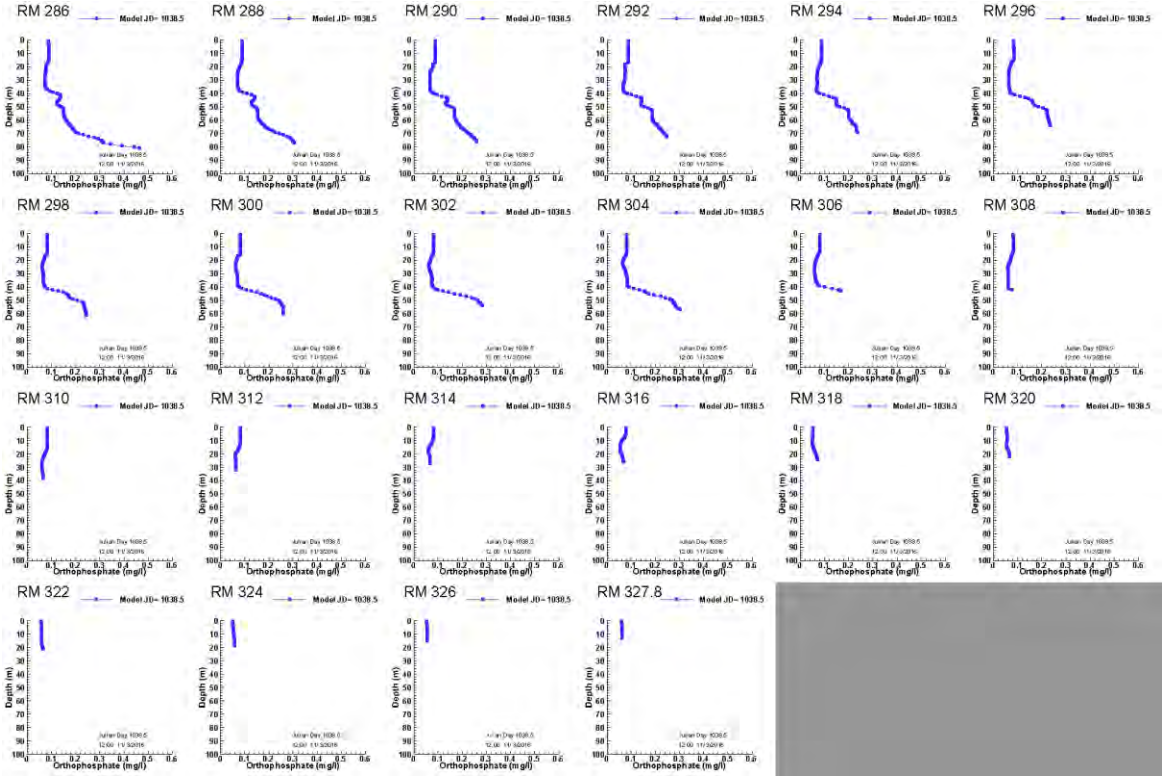


Figure 830. Vertical profiles of orthophosphate compared with data for 11/ 3/2016.

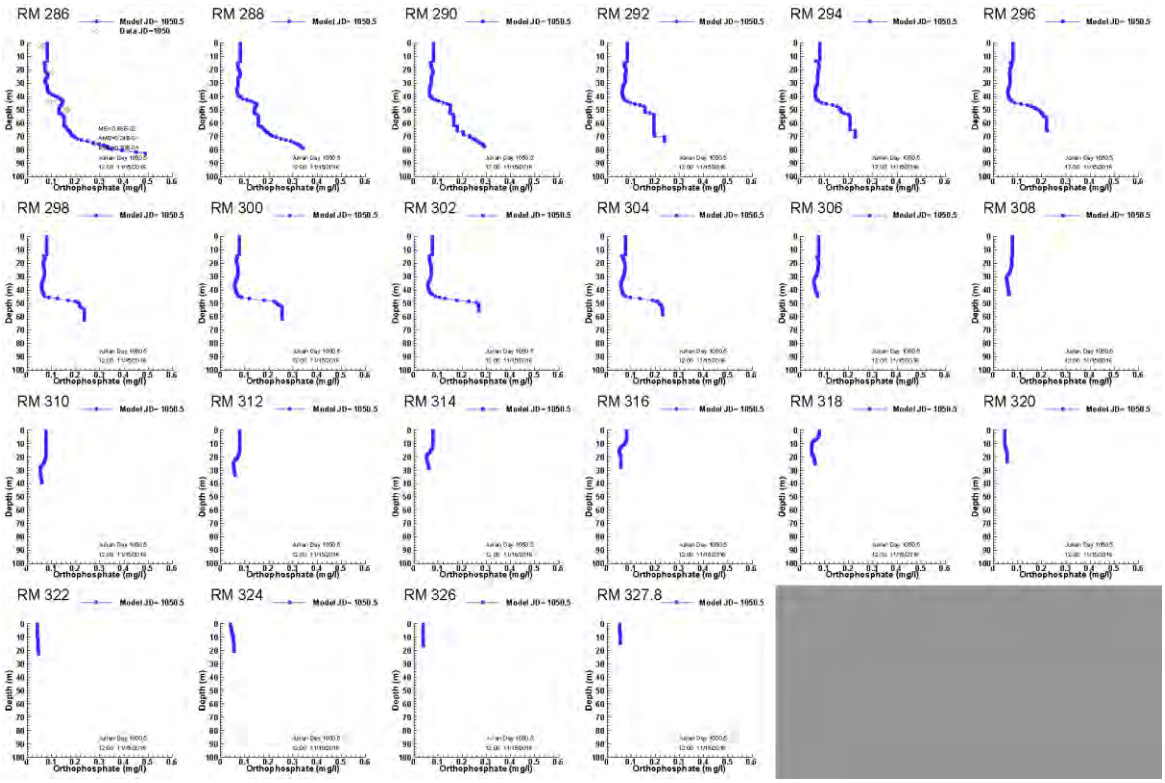


Figure 831. Vertical profiles of orthophosphate compared with data for 11/15/2016.

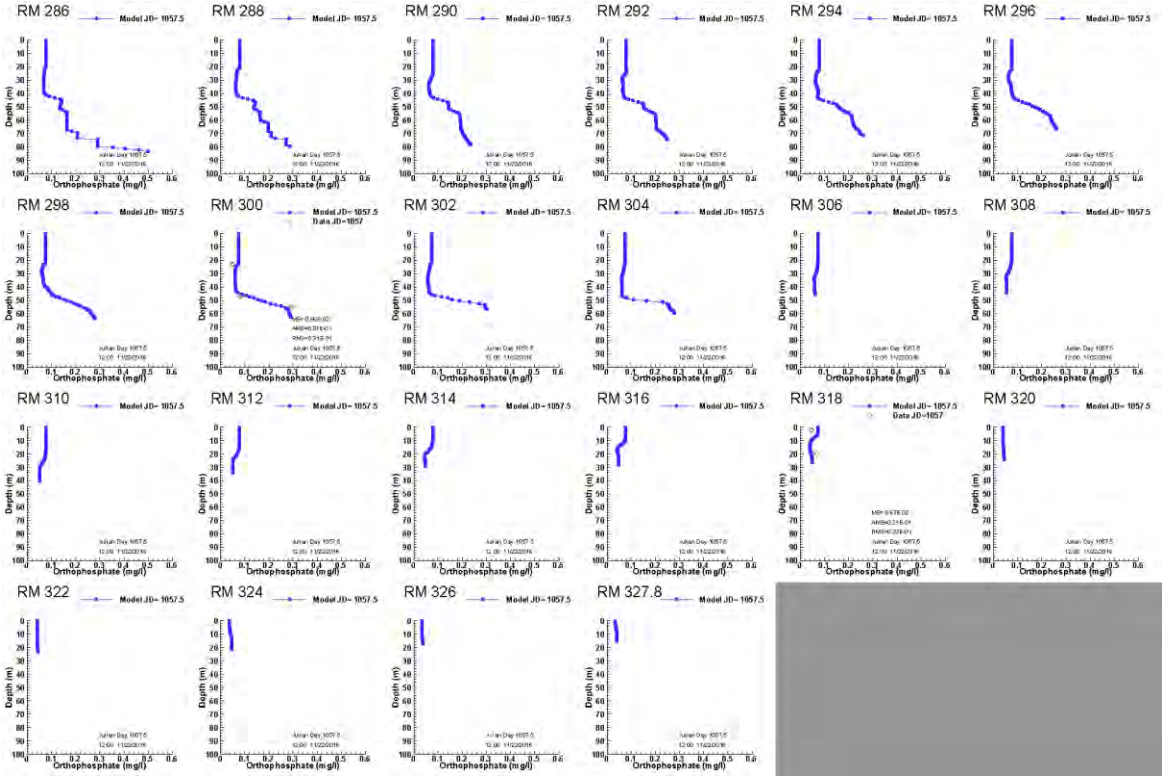


Figure 832. Vertical profiles of orthophosphate compared with data for 11/22/2016.

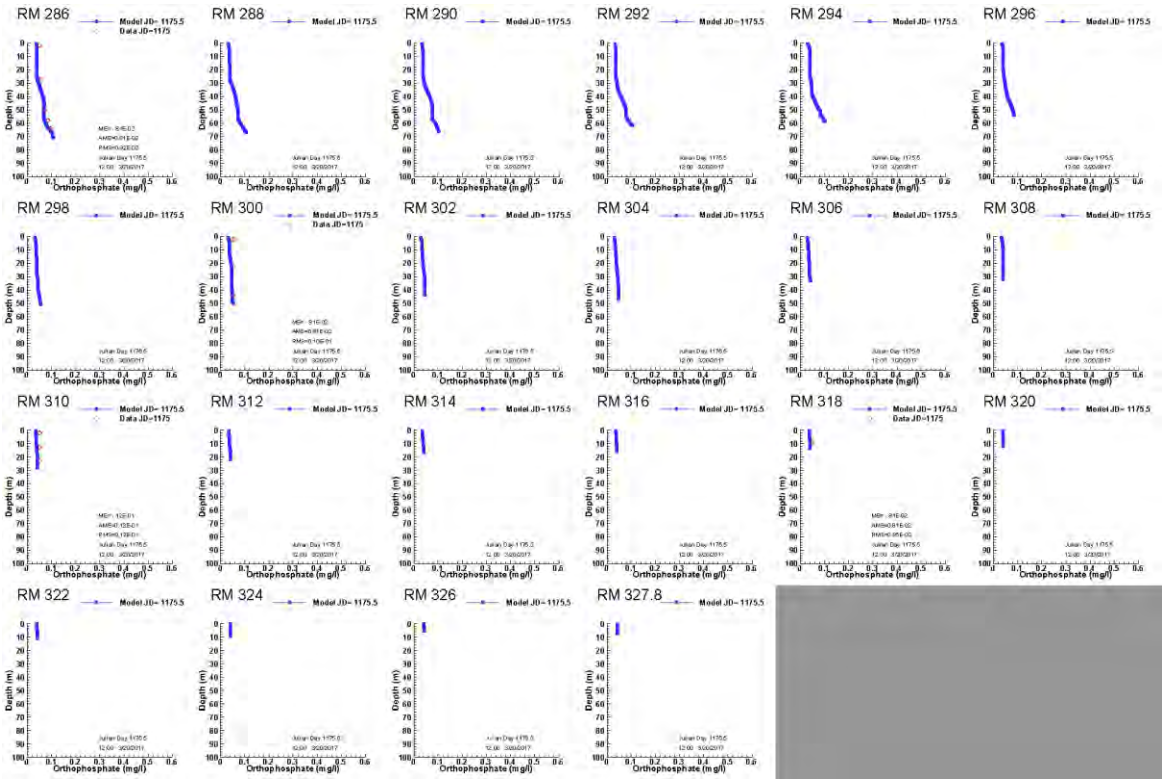


Figure 833. Vertical profiles of orthophosphate compared with data for 3/20/2017.

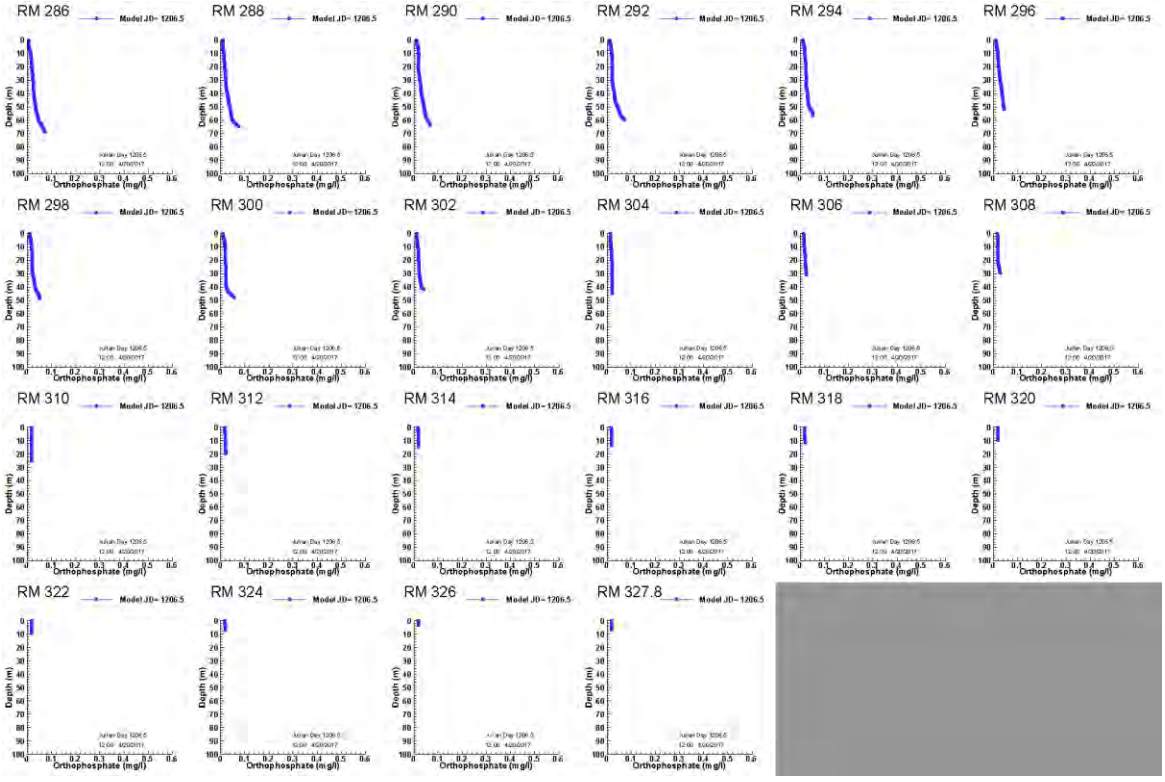


Figure 834. Vertical profiles of orthophosphate compared with data for 4/20/2017.

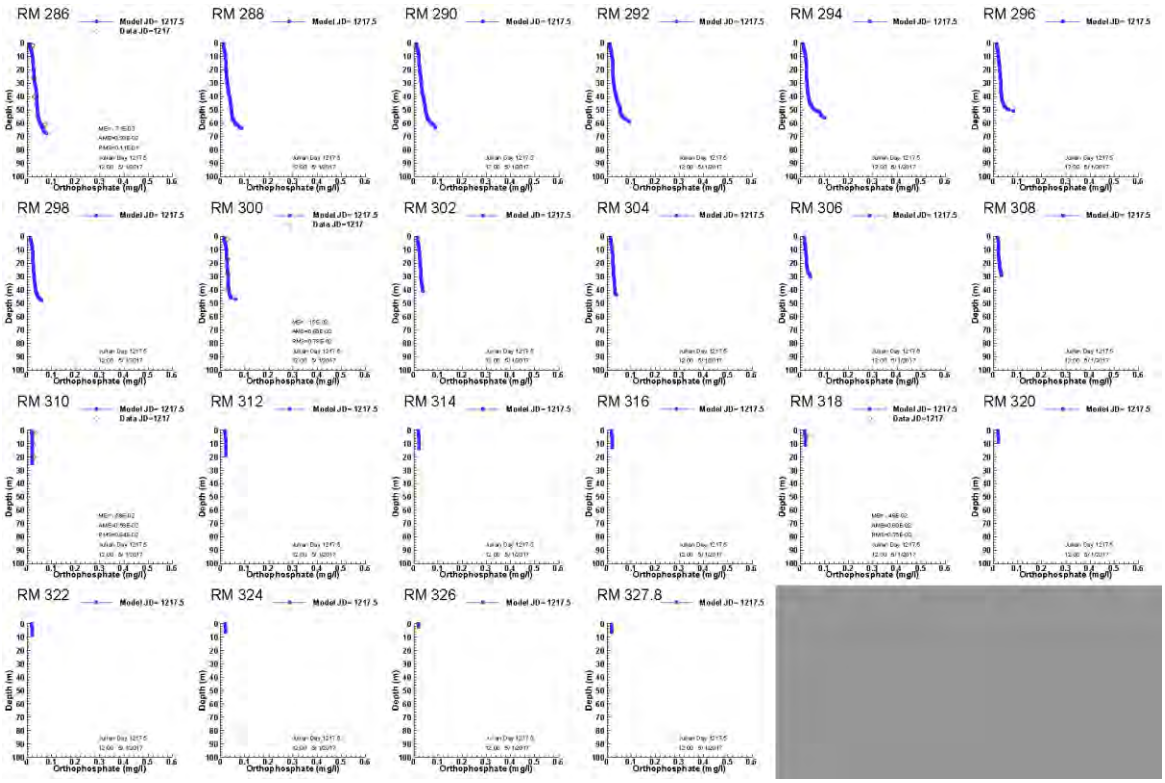


Figure 835. Vertical profiles of orthophosphate compared with data for 5/ 1/2017.

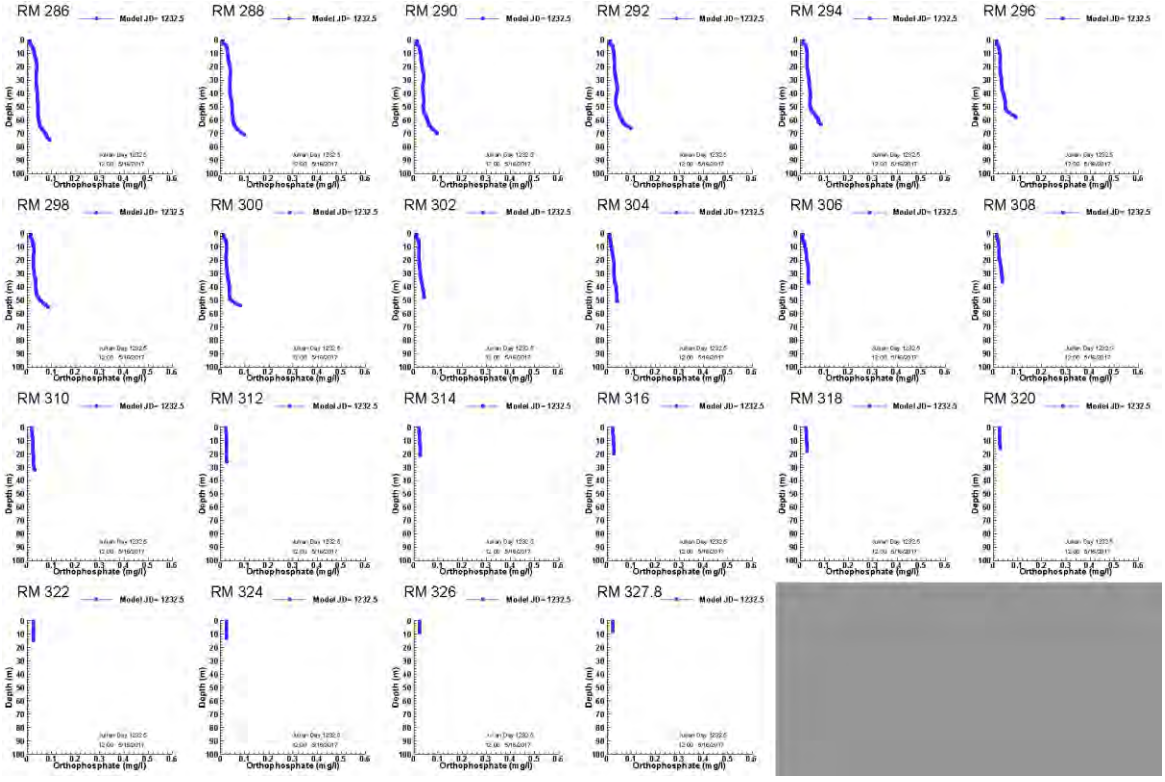


Figure 836. Vertical profiles of orthophosphate compared with data for 5/16/2017.

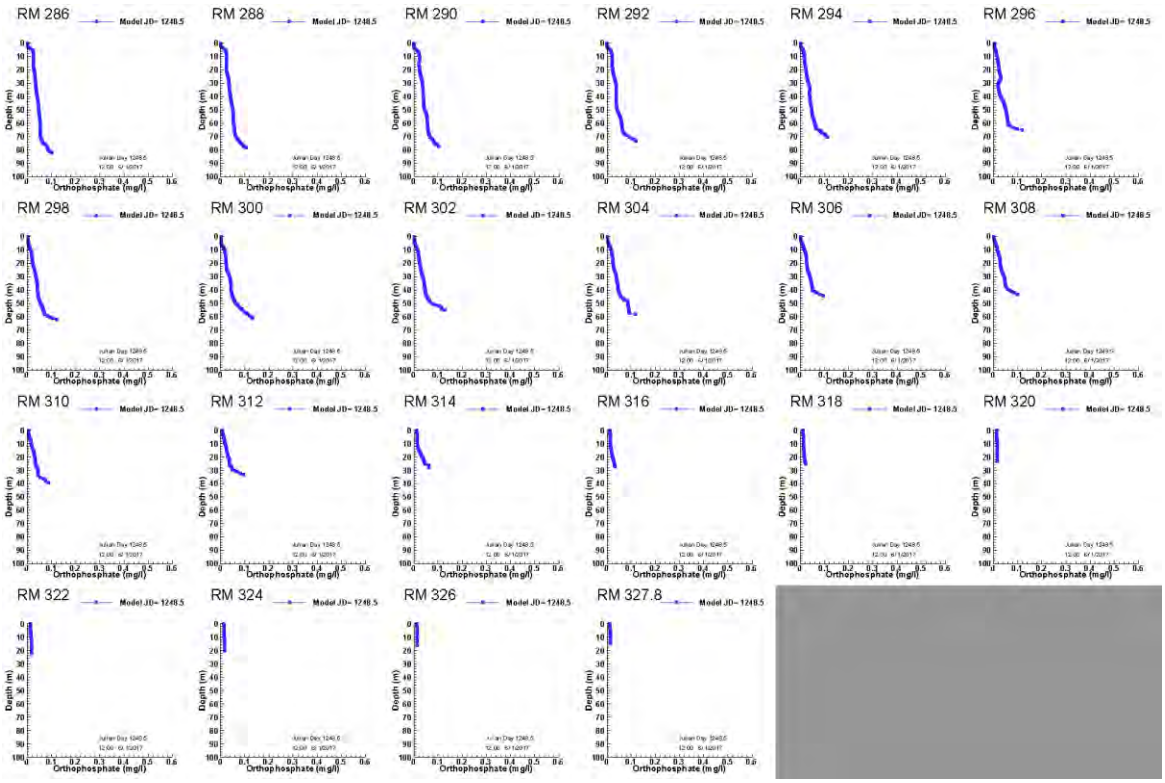


Figure 837. Vertical profiles of orthophosphate compared with data for 6/ 1/2017.

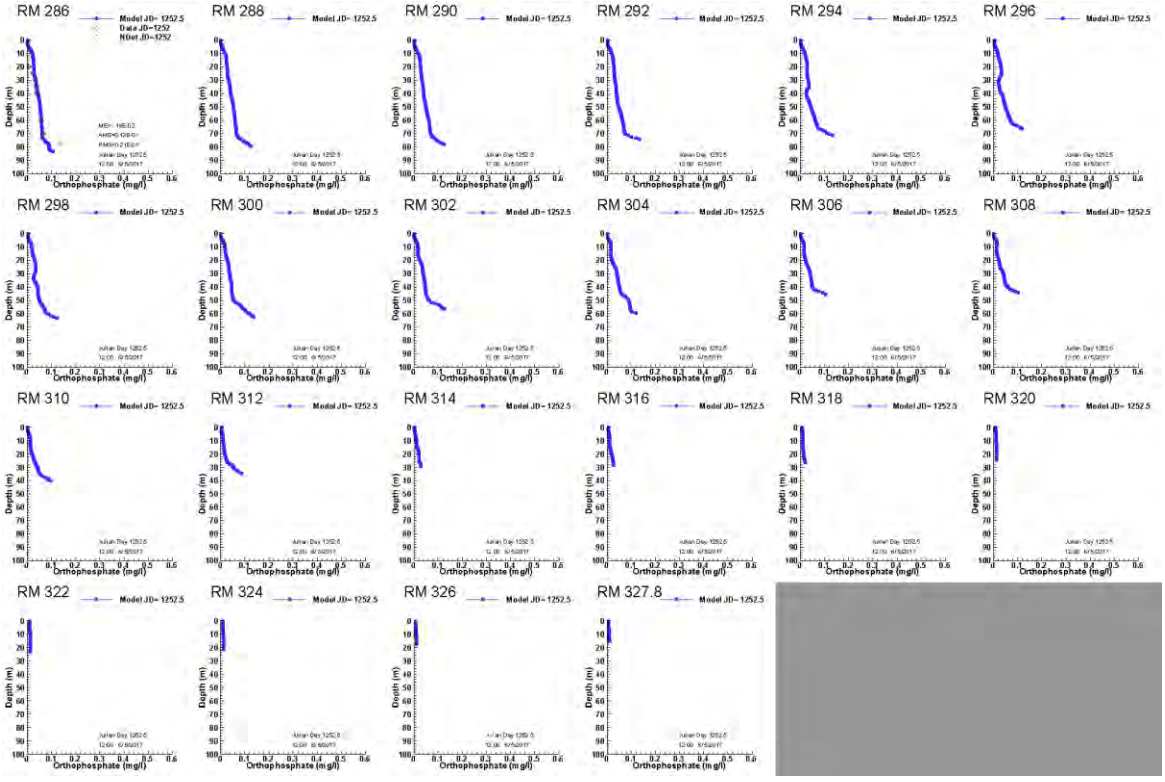


Figure 838. Vertical profiles of orthophosphate compared with data for 6/ 5/2017.

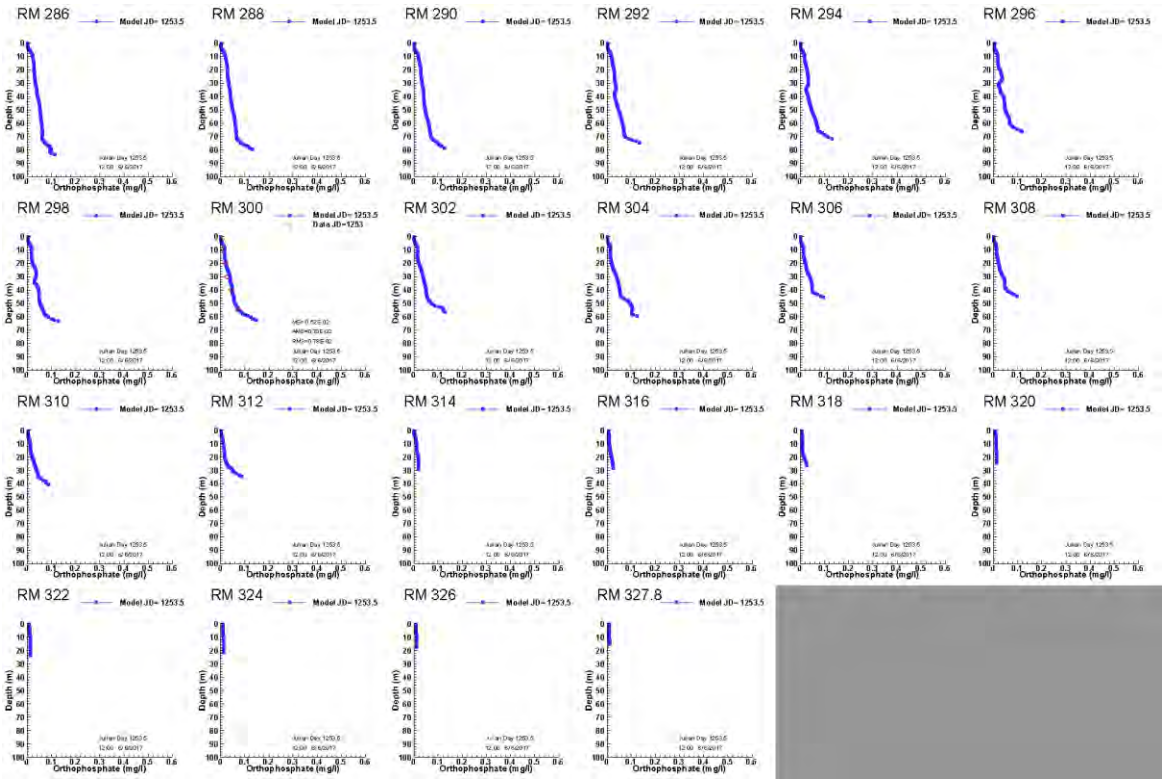


Figure 839. Vertical profiles of orthophosphate compared with data for 6/ 6/2017.

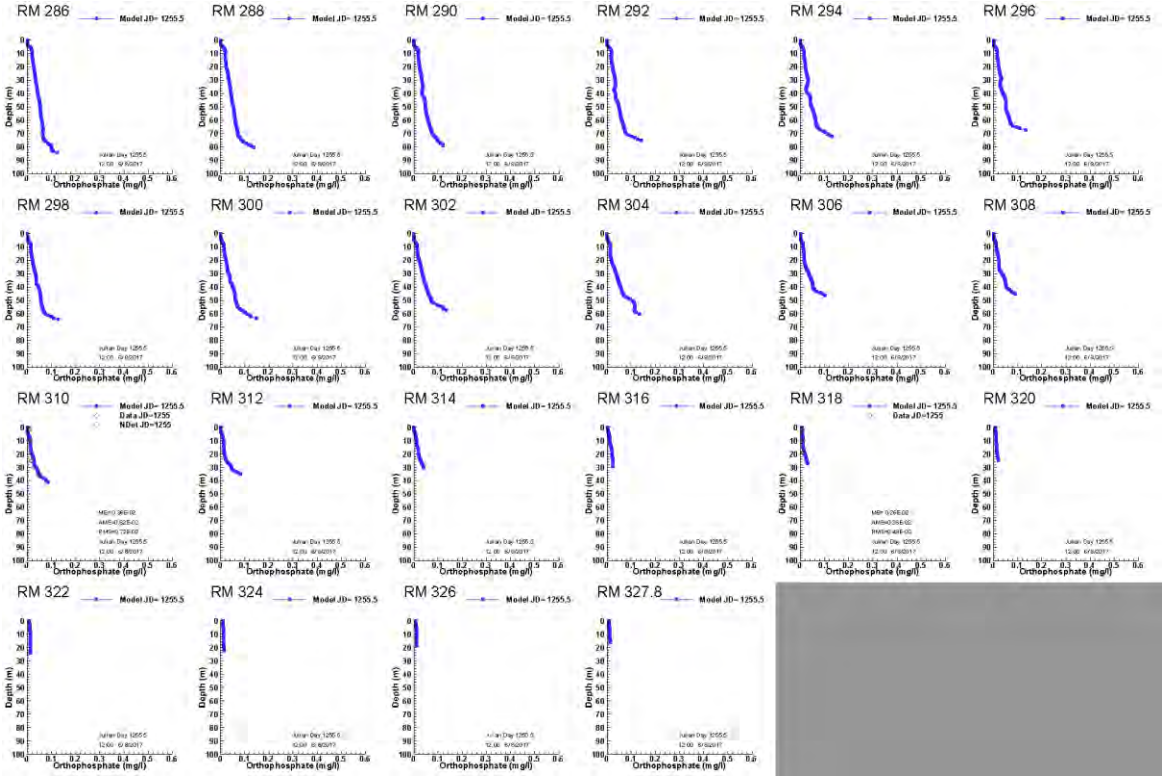


Figure 840. Vertical profiles of orthophosphate compared with data for 6/ 8/2017.

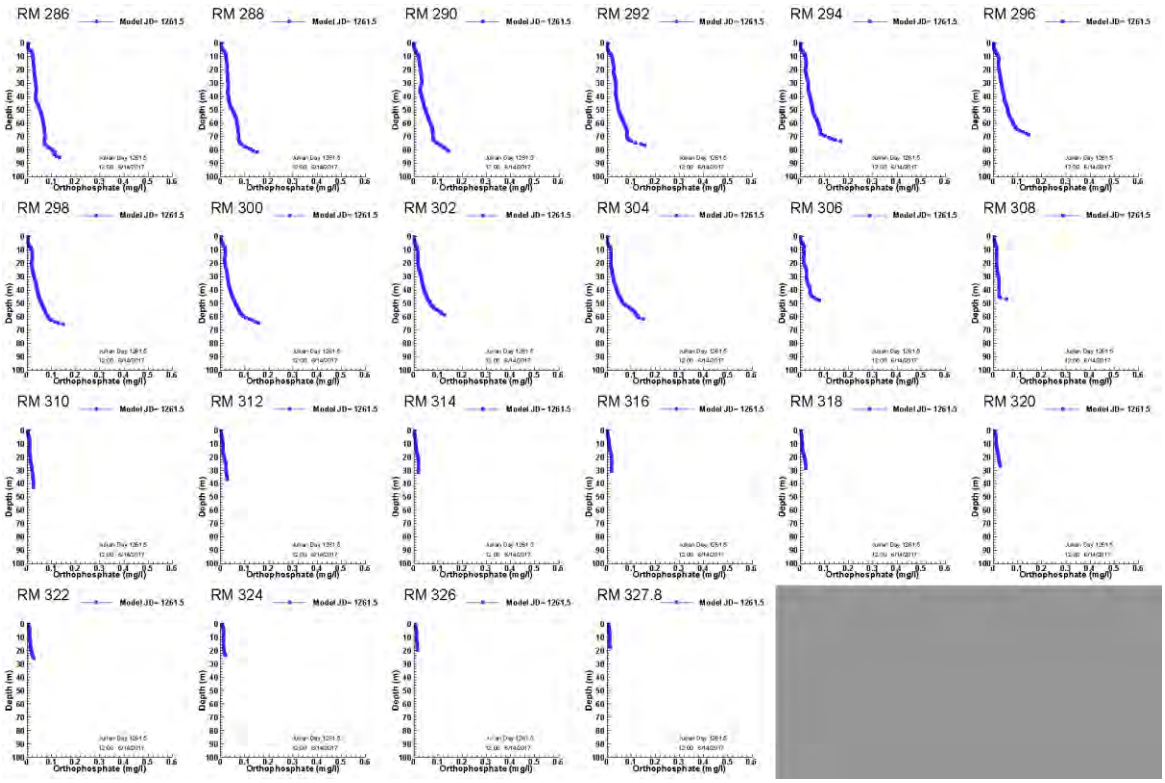


Figure 841. Vertical profiles of orthophosphate compared with data for 6/14/2017.

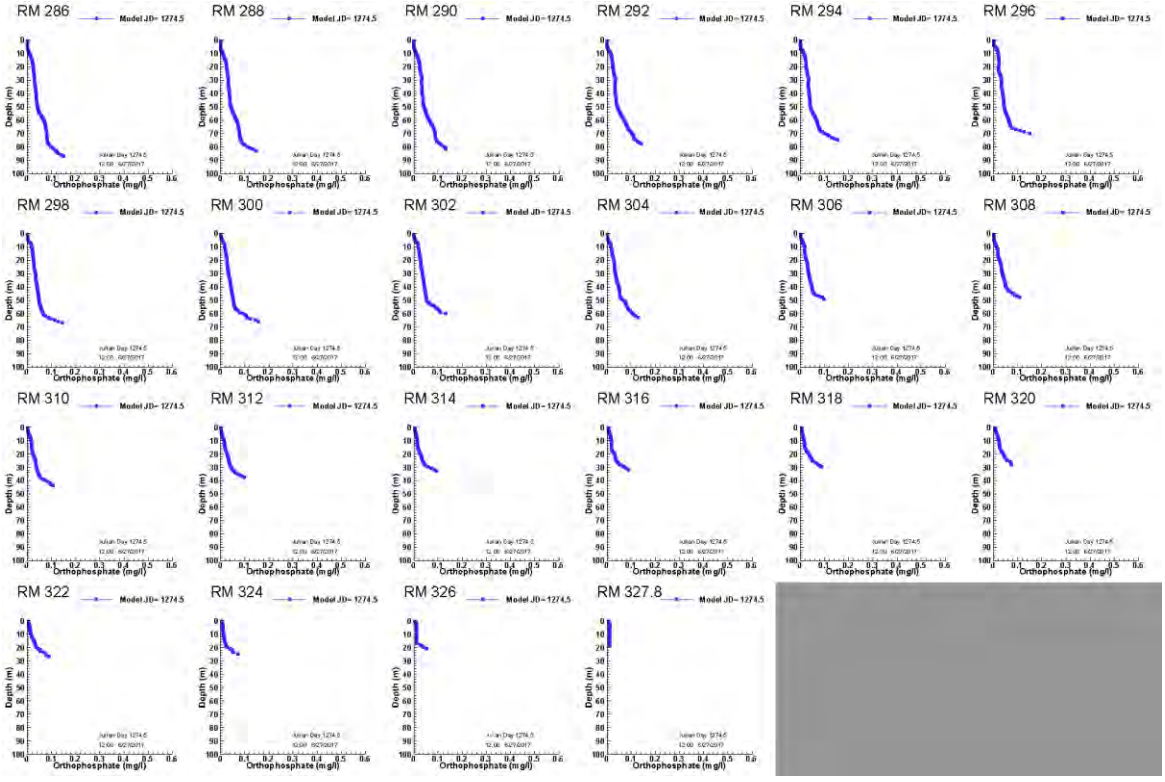


Figure 842. Vertical profiles of orthophosphate compared with data for 6/27/2017.

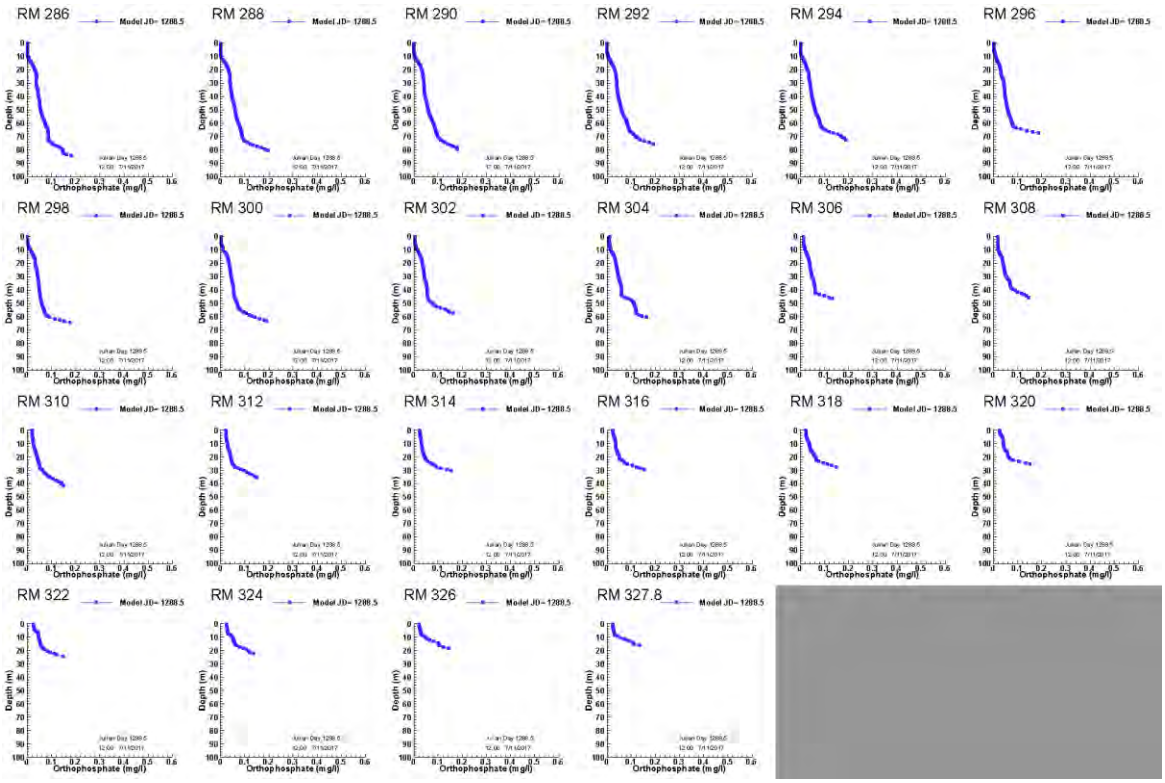


Figure 843. Vertical profiles of orthophosphate compared with data for 7/11/2017.

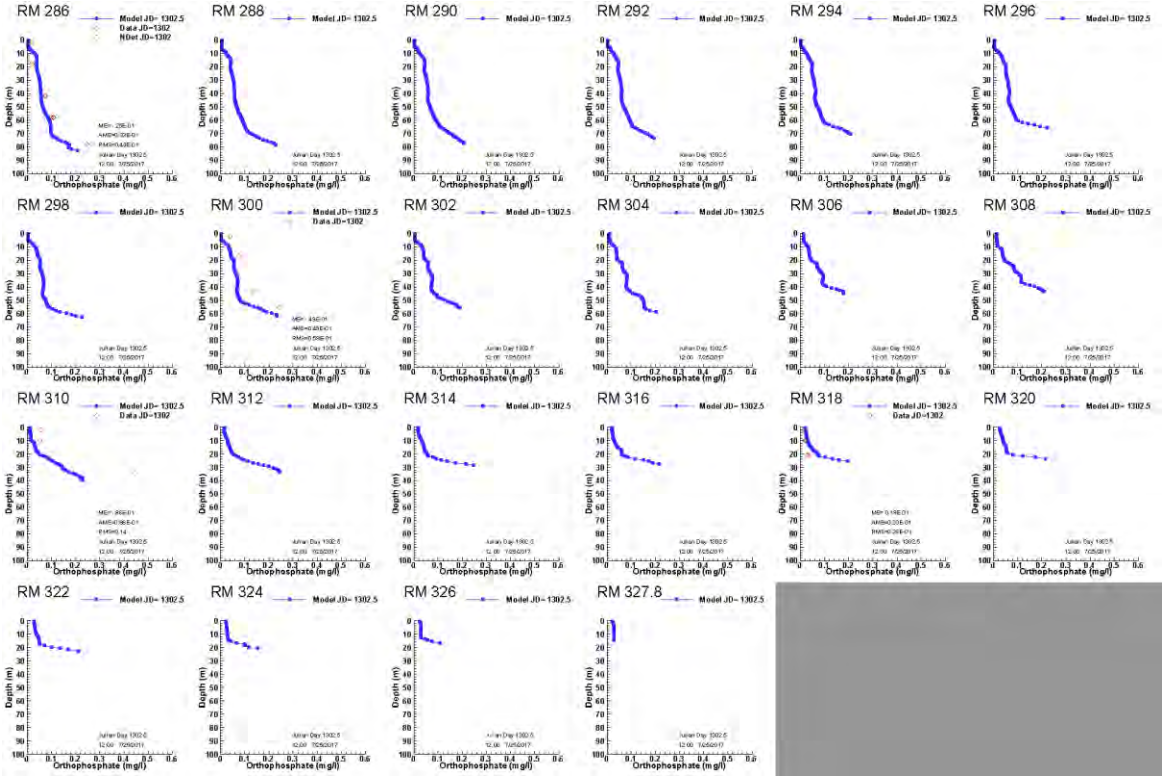


Figure 844. Vertical profiles of orthophosphate compared with data for 7/25/2017.

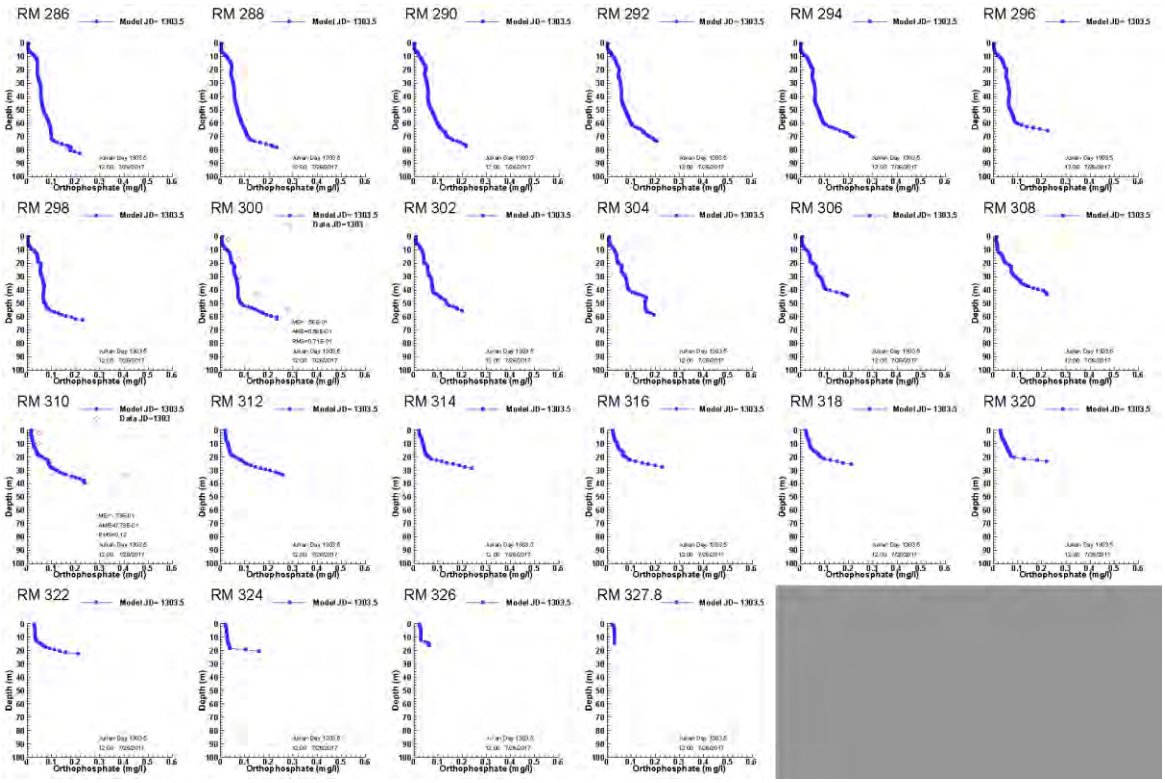


Figure 845. Vertical profiles of orthophosphate compared with data for 7/26/2017.

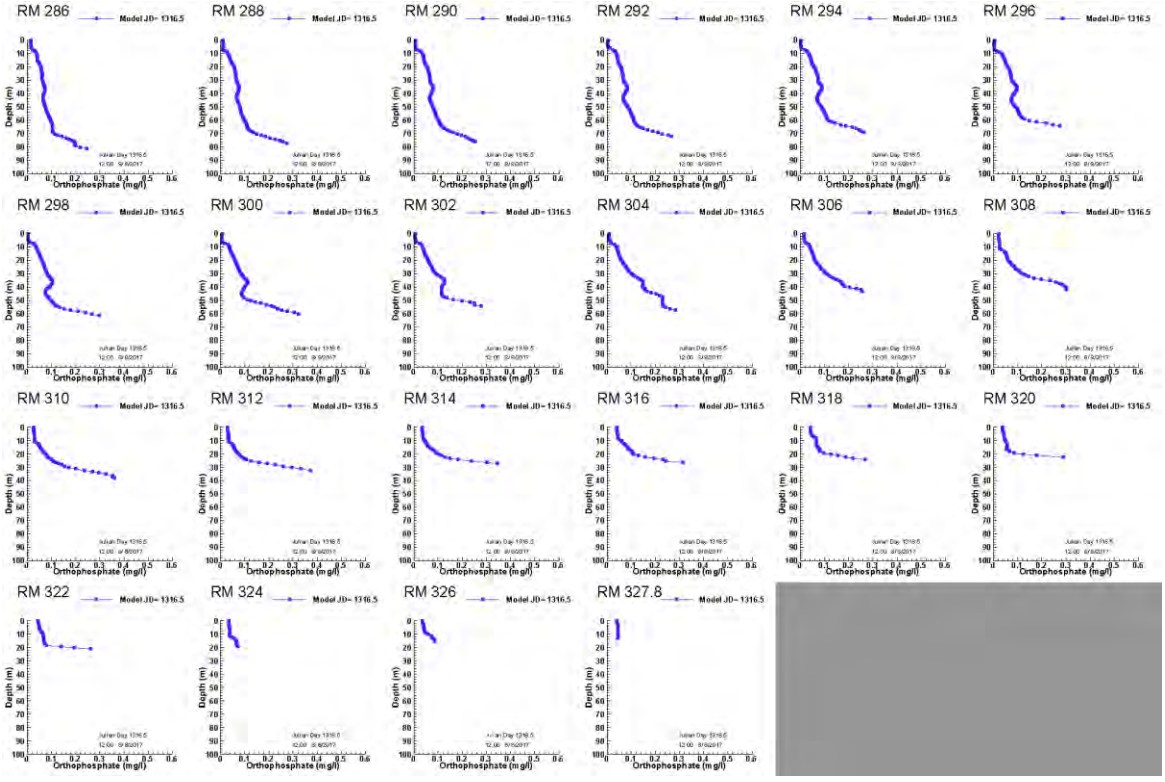


Figure 846. Vertical profiles of orthophosphate compared with data for 8/ 8/2017.

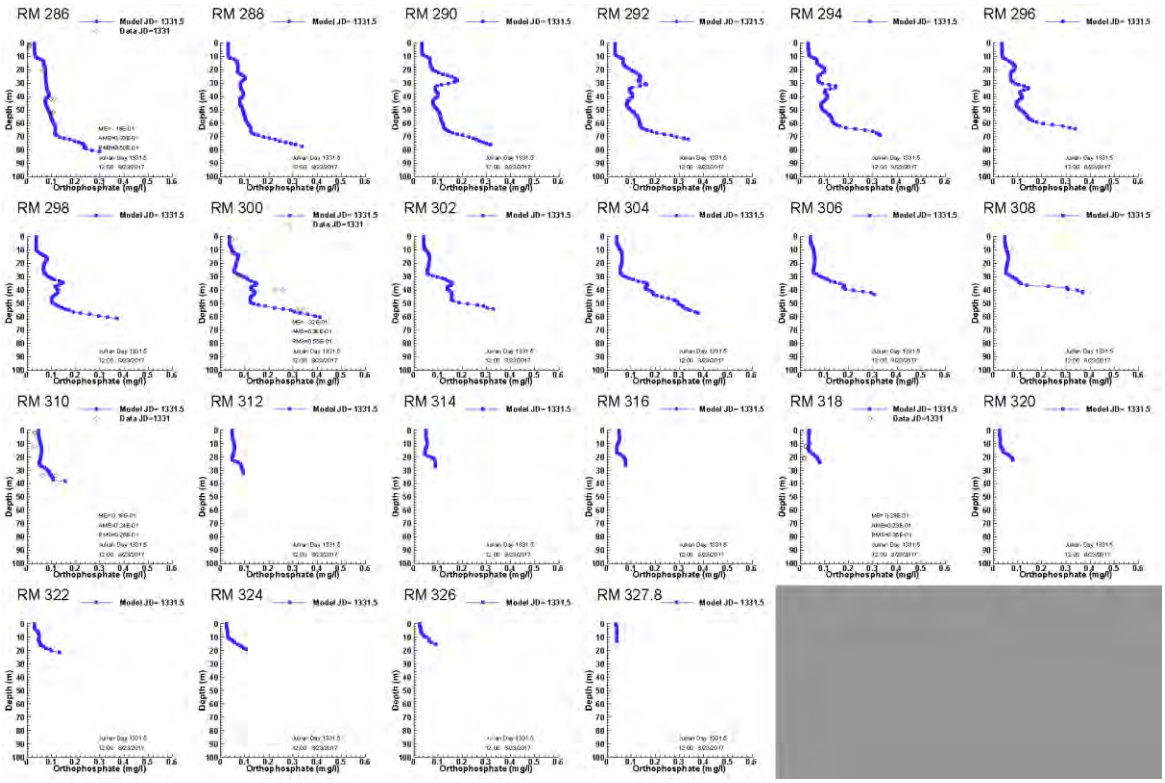


Figure 847. Vertical profiles of orthophosphate compared with data for 8/23/2017.

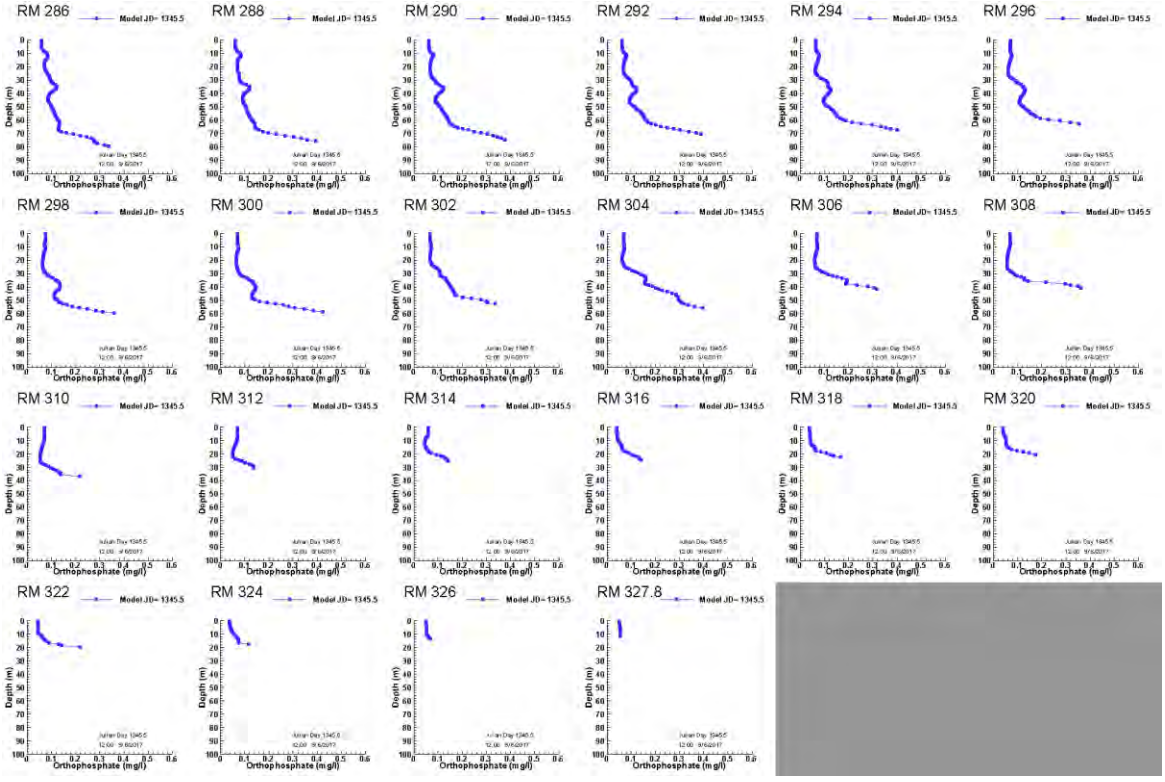


Figure 848. Vertical profiles of orthophosphate compared with data for 9/ 6/2017.

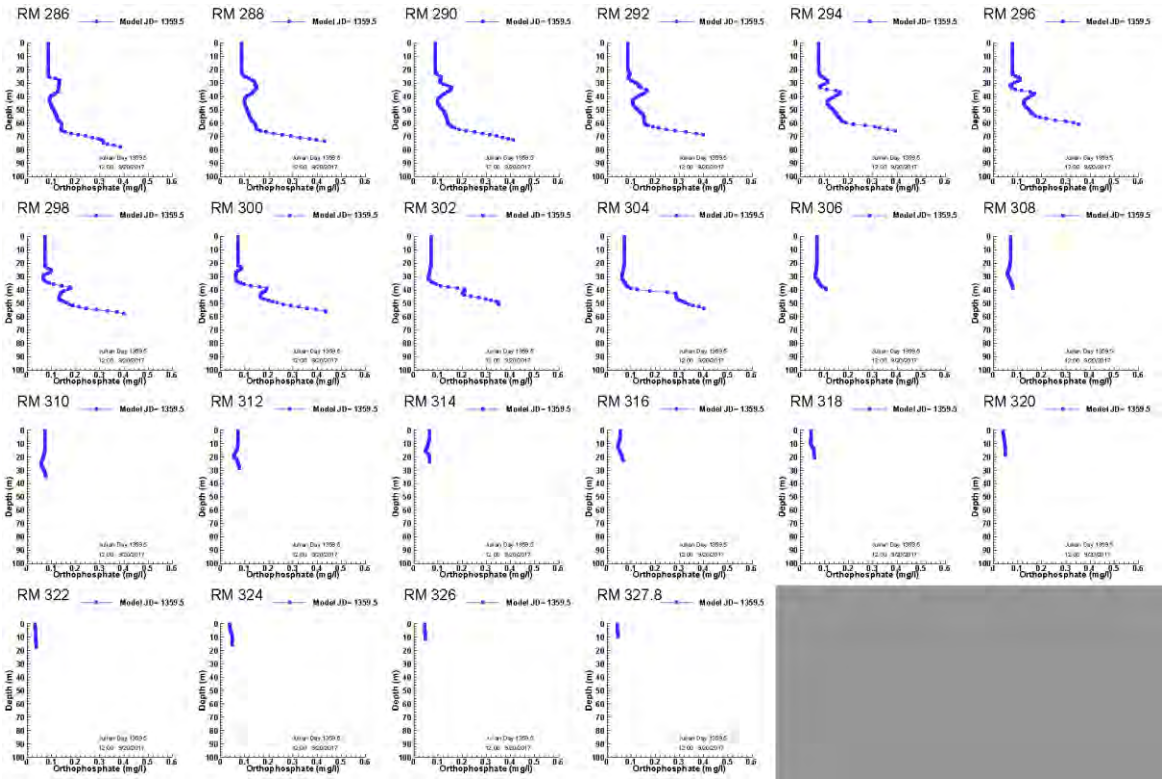


Figure 849. Vertical profiles of orthophosphate compared with data for 9/20/2017.

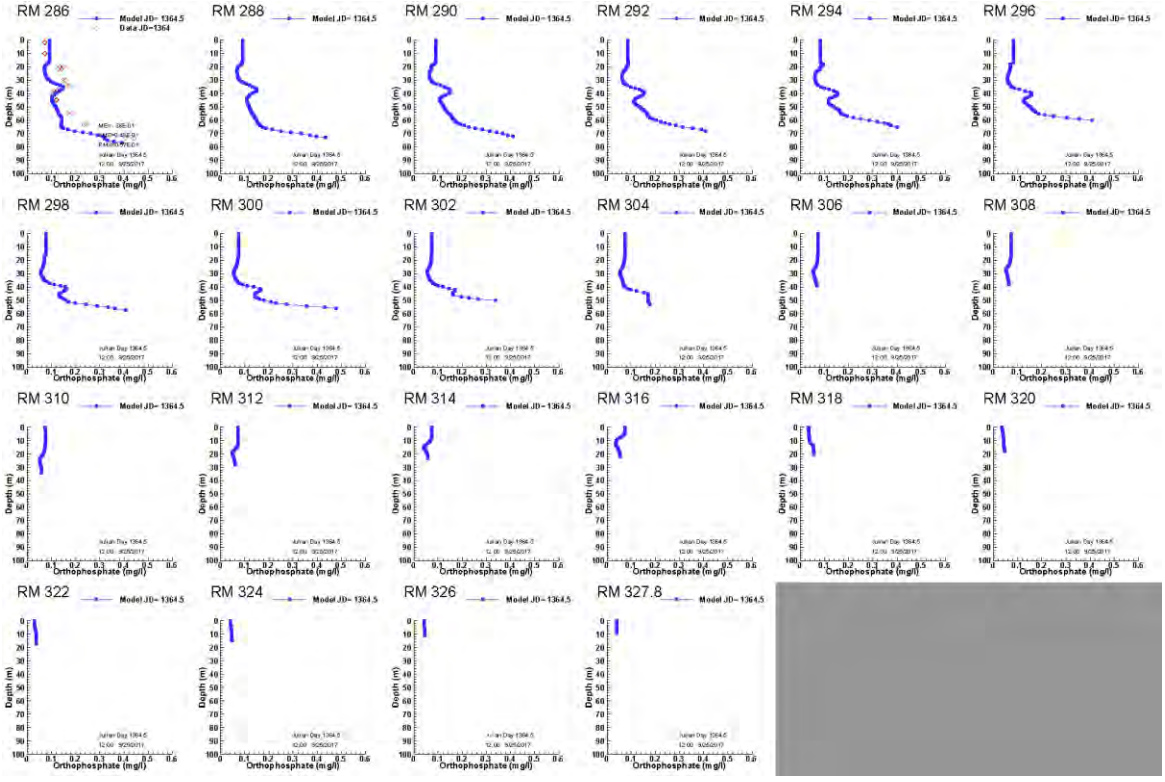


Figure 850. Vertical profiles of orthophosphate compared with data for 9/25/2017.

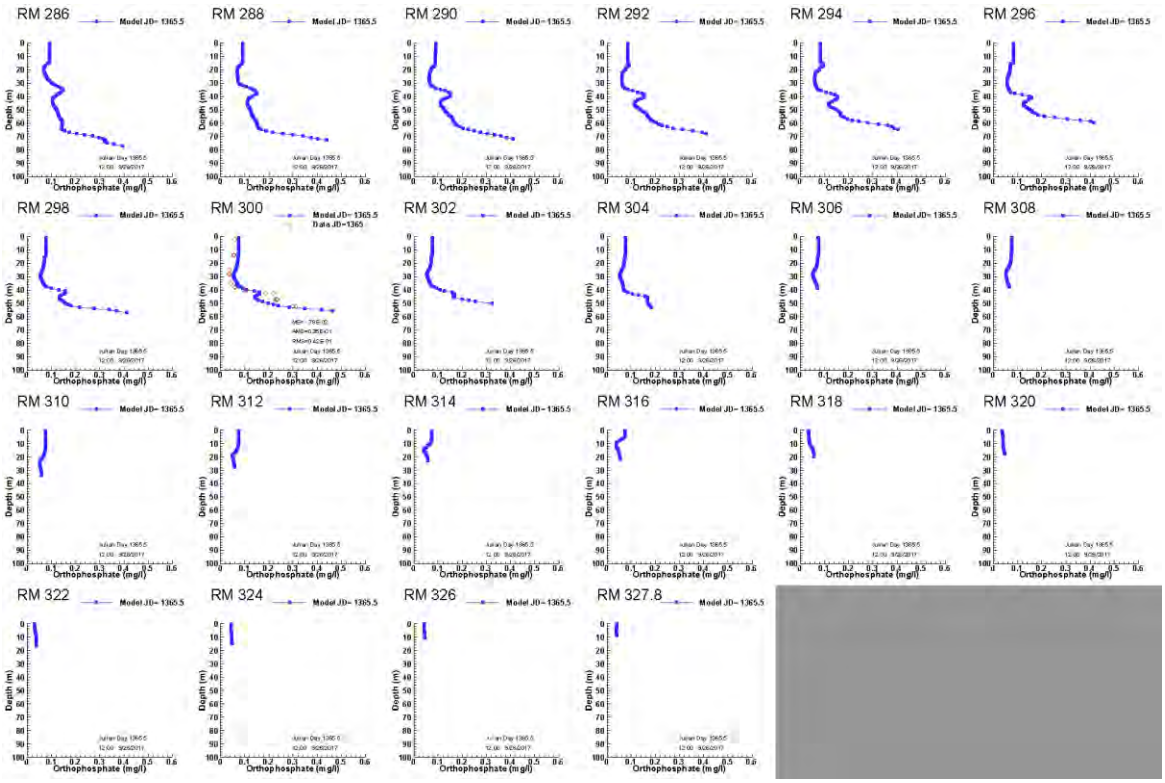


Figure 851. Vertical profiles of orthophosphate compared with data for 9/26/2017.

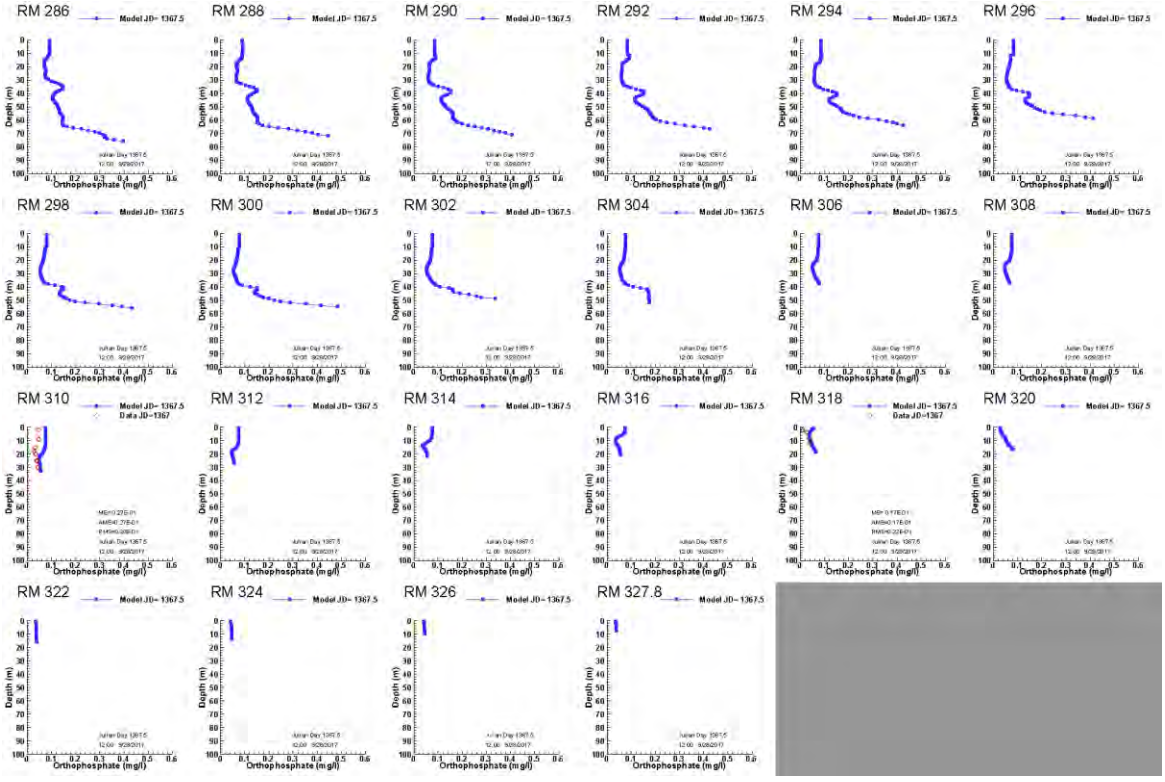


Figure 852. Vertical profiles of orthophosphate compared with data for 9/28/2017.

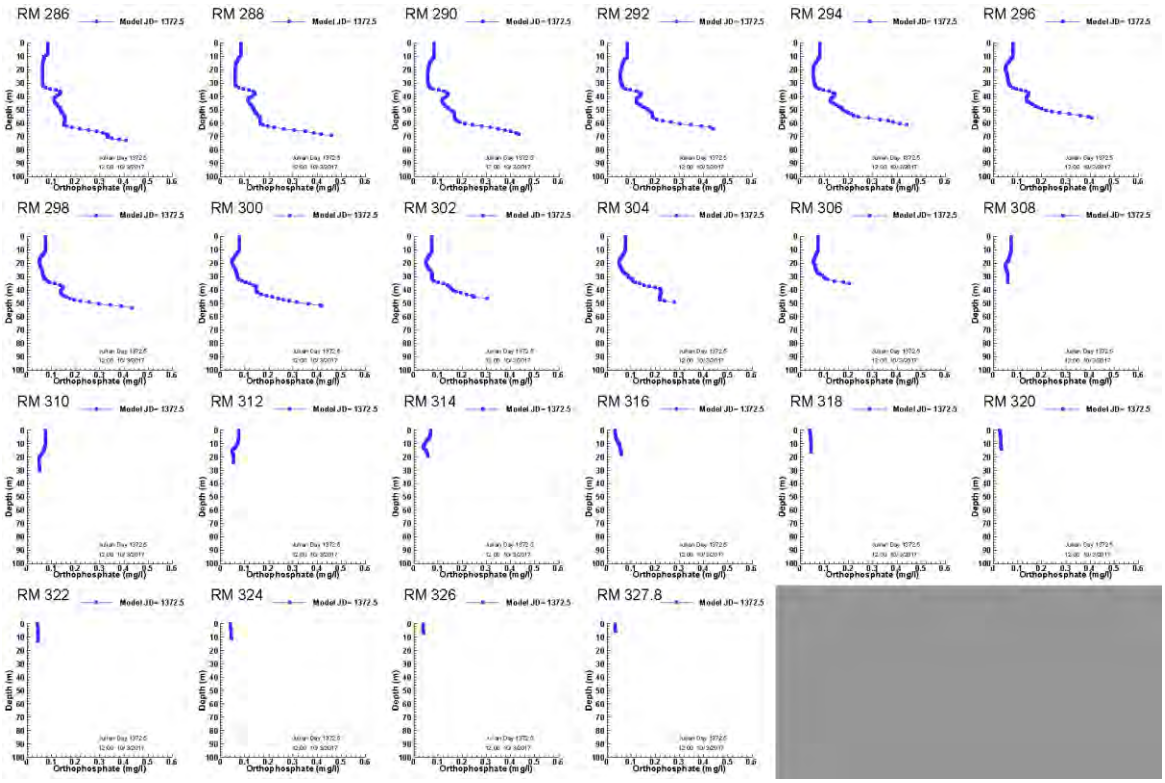


Figure 853. Vertical profiles of orthophosphate compared with data for 10/ 3/2017.

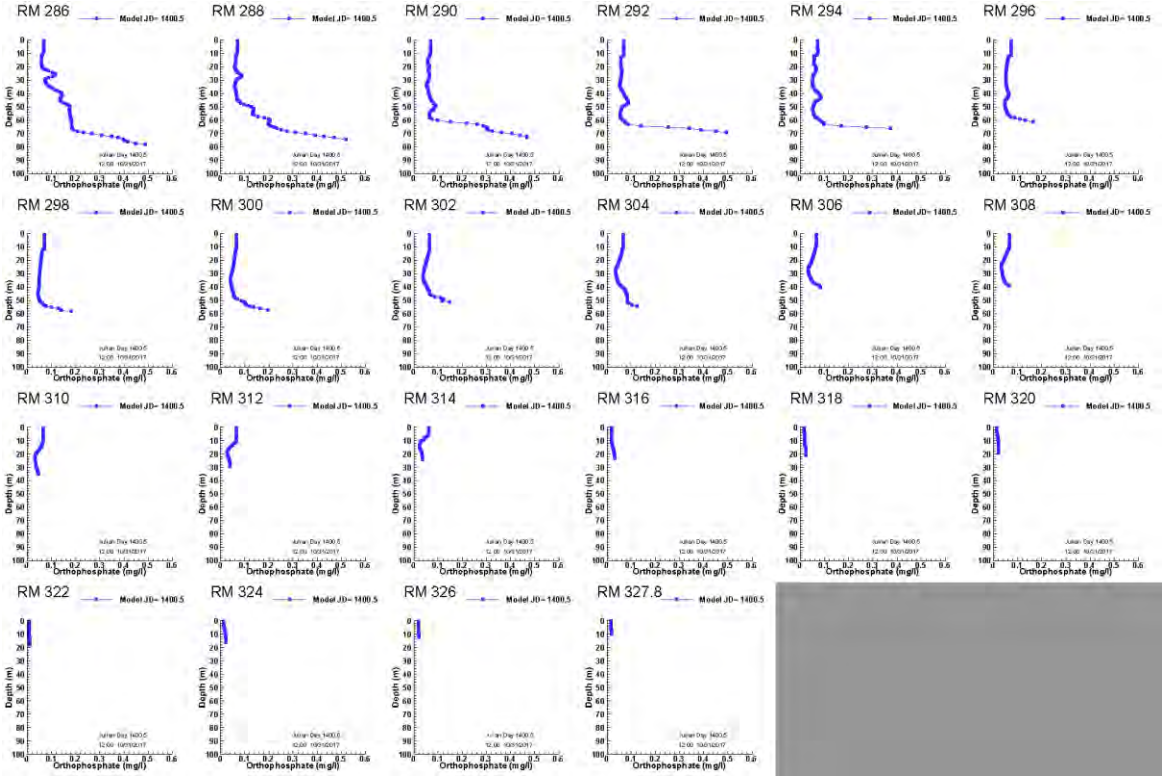


Figure 854. Vertical profiles of orthophosphate compared with data for 10/31/2017.

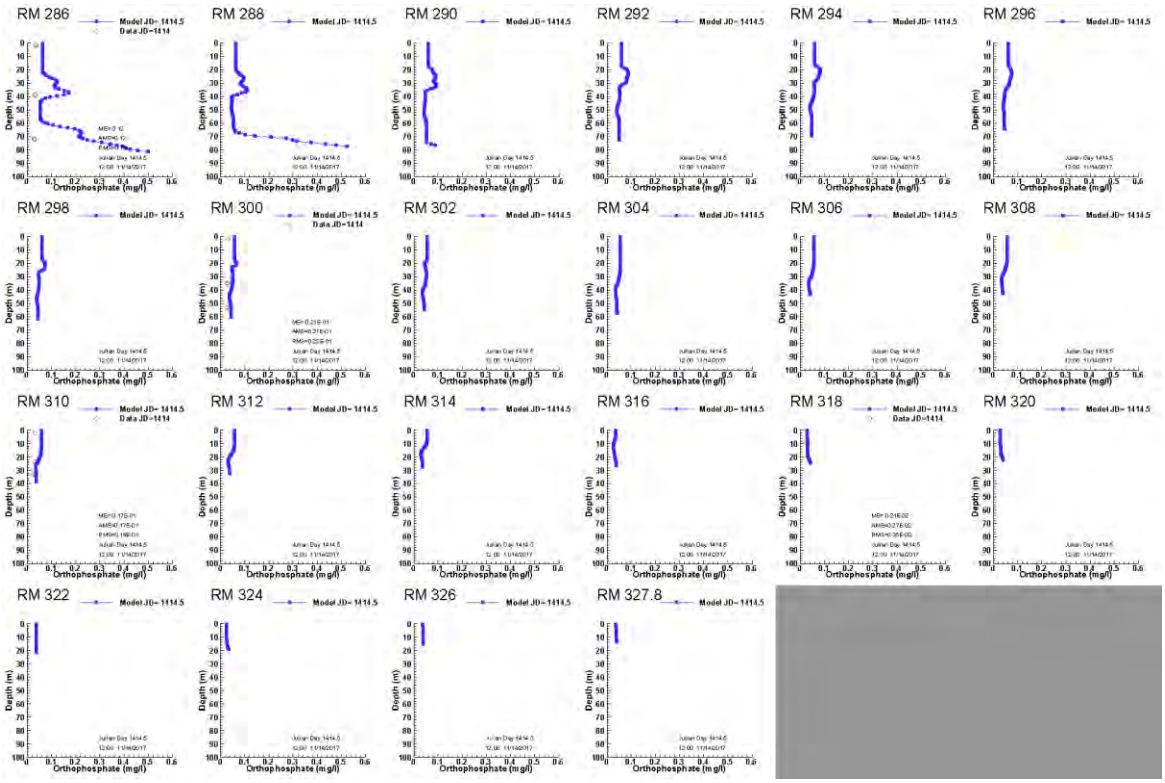


Figure 855. Vertical profiles of orthophosphate compared with data for 11/14/2017.

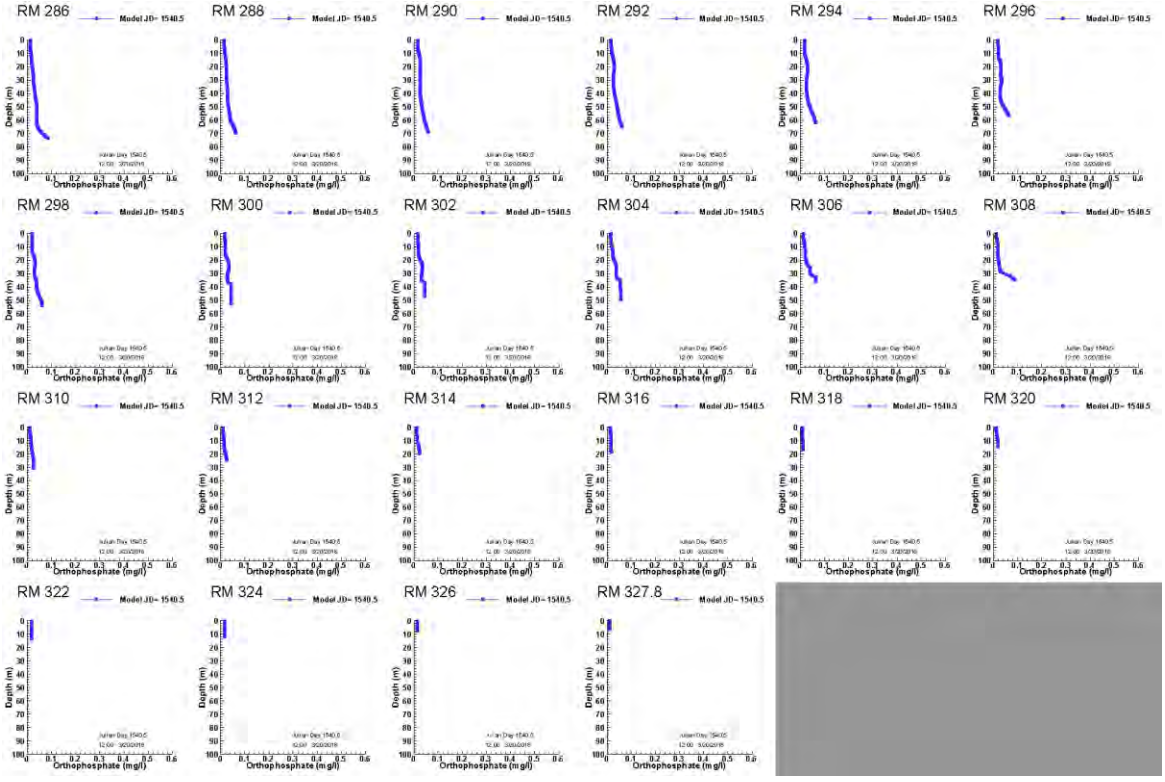


Figure 856. Vertical profiles of orthophosphate compared with data for 3/20/2018.

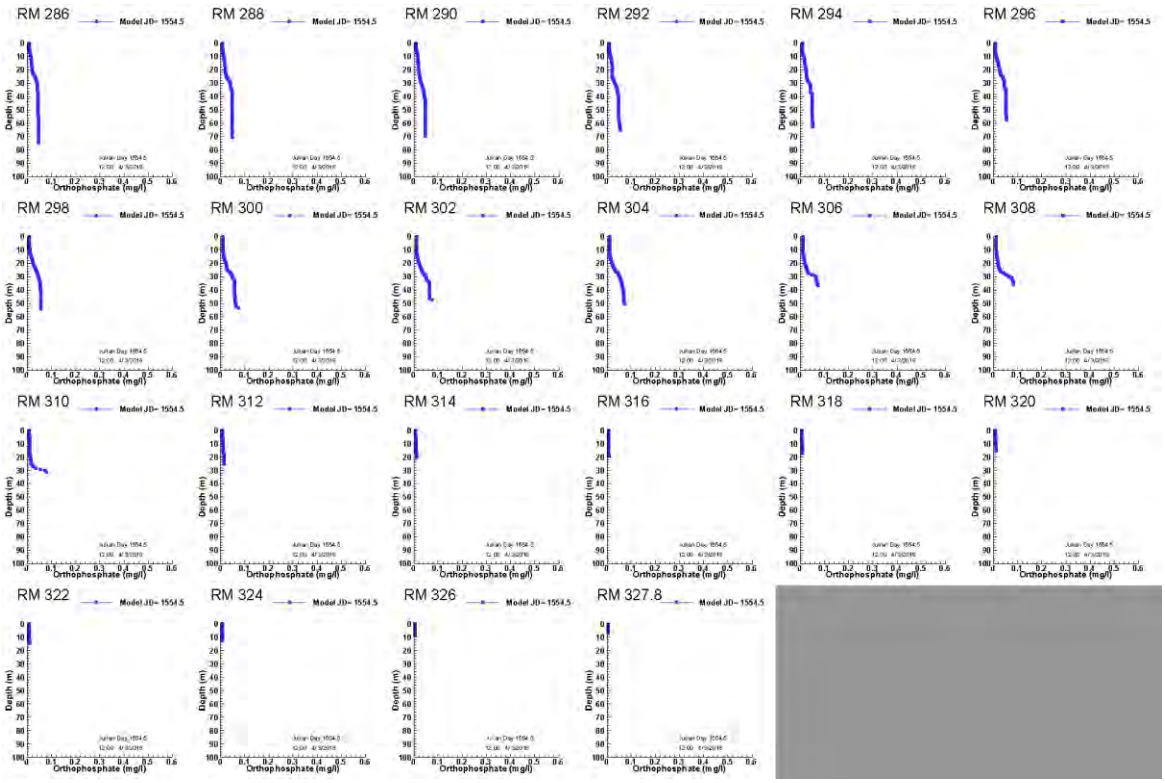


Figure 857. Vertical profiles of orthophosphate compared with data for 4/ 3/2018.

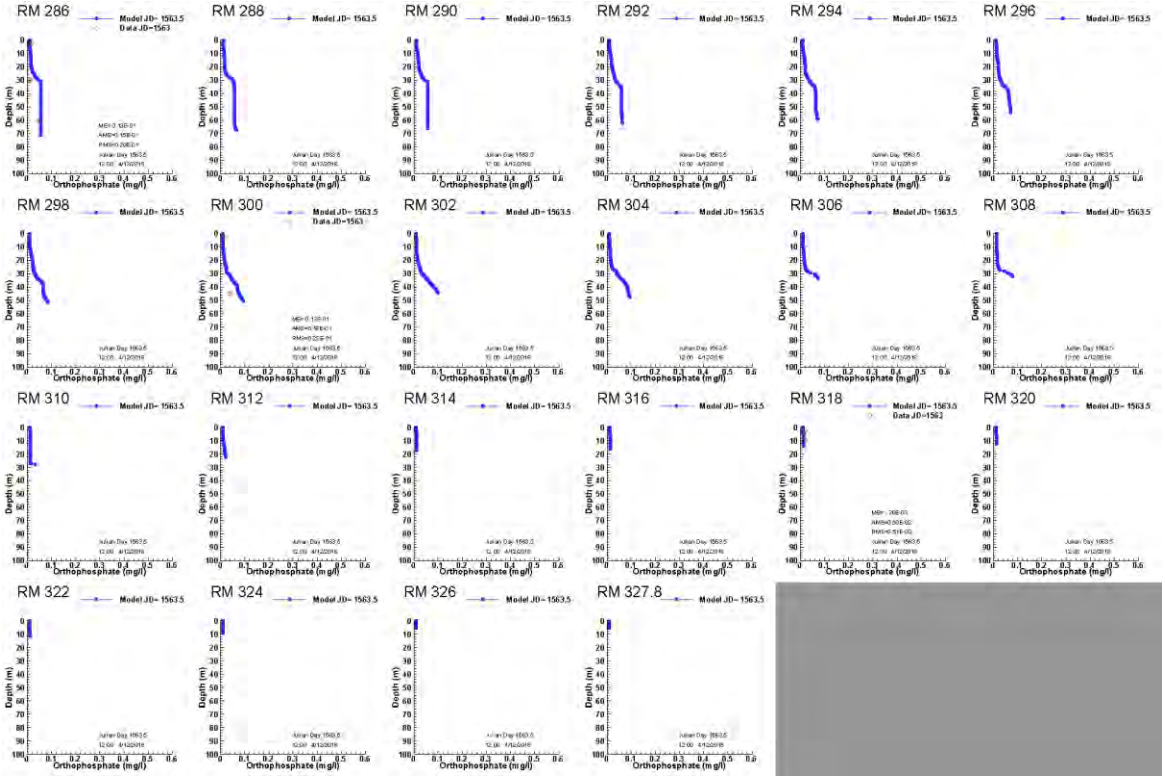


Figure 858. Vertical profiles of orthophosphate compared with data for 4/12/2018.

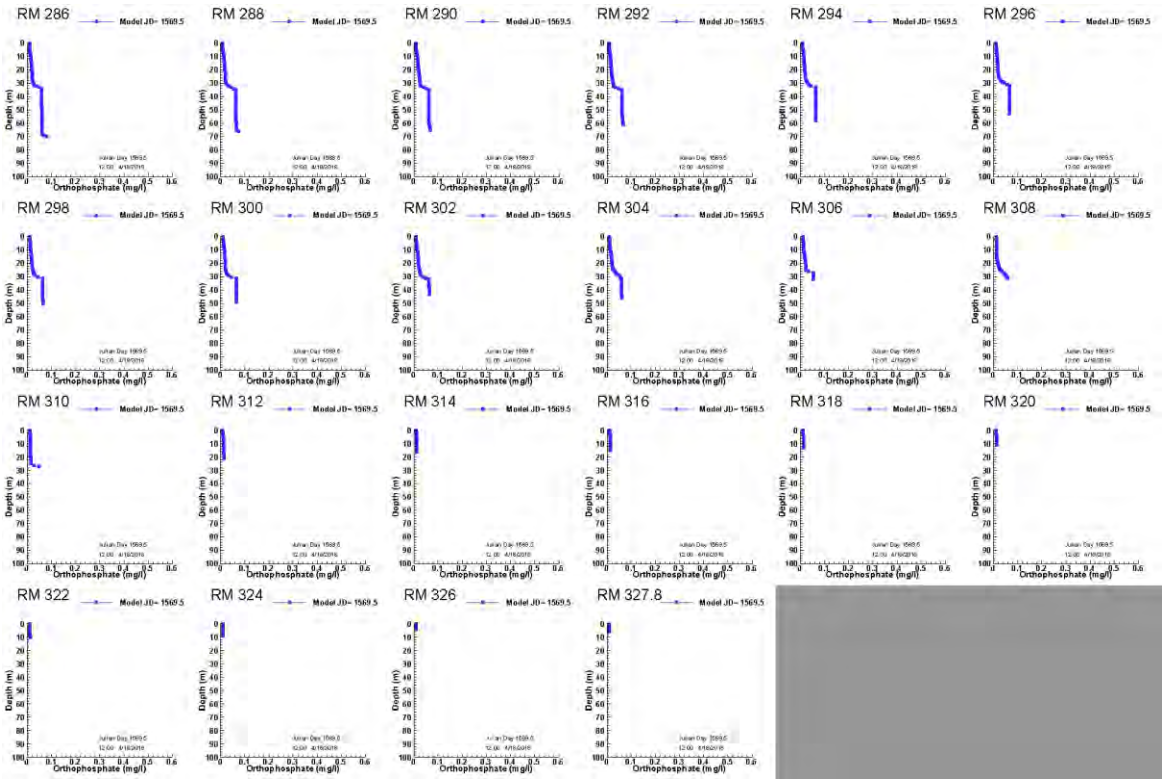


Figure 859. Vertical profiles of orthophosphate compared with data for 4/18/2018.

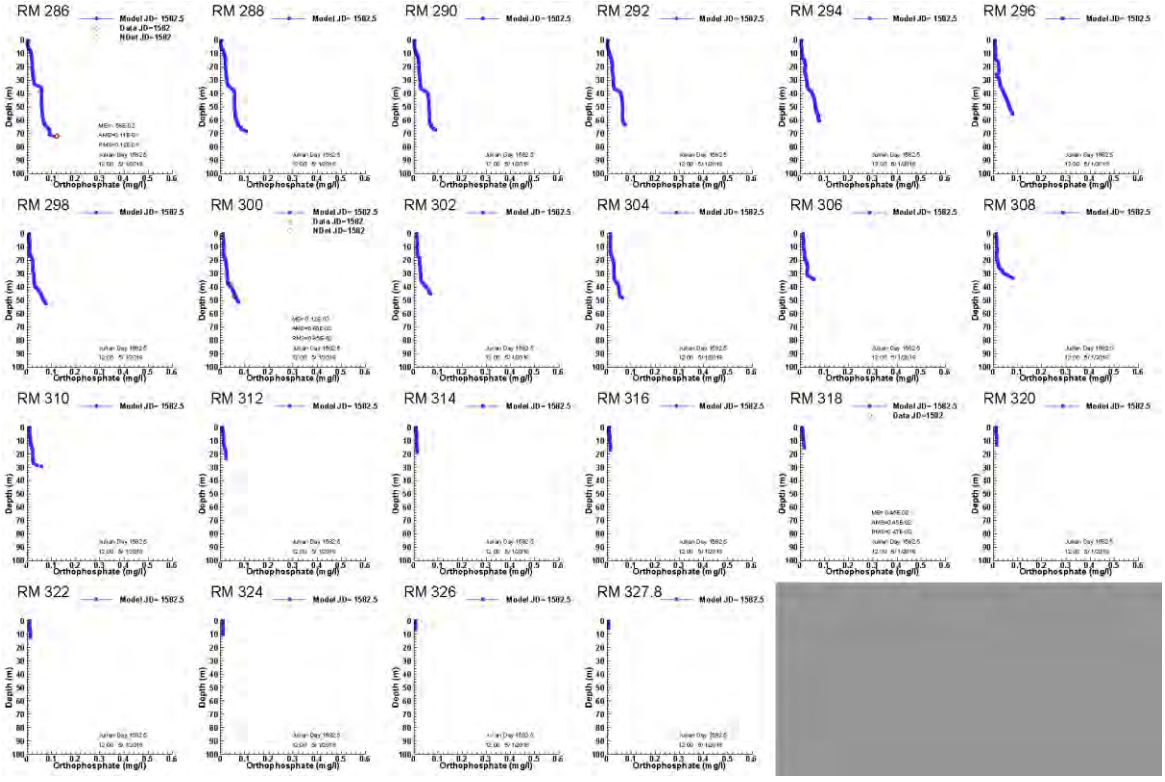


Figure 860. Vertical profiles of orthophosphate compared with data for 5/ 1/2018.

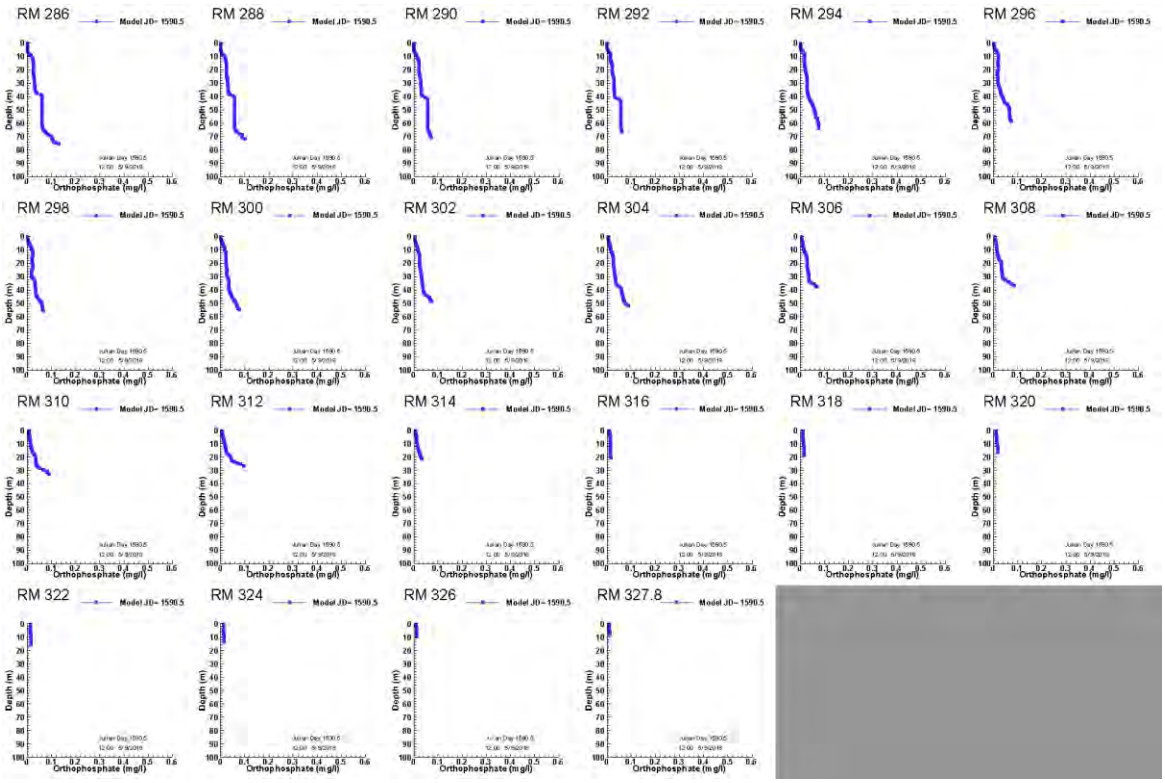


Figure 861. Vertical profiles of orthophosphate compared with data for 5/ 9/2018.

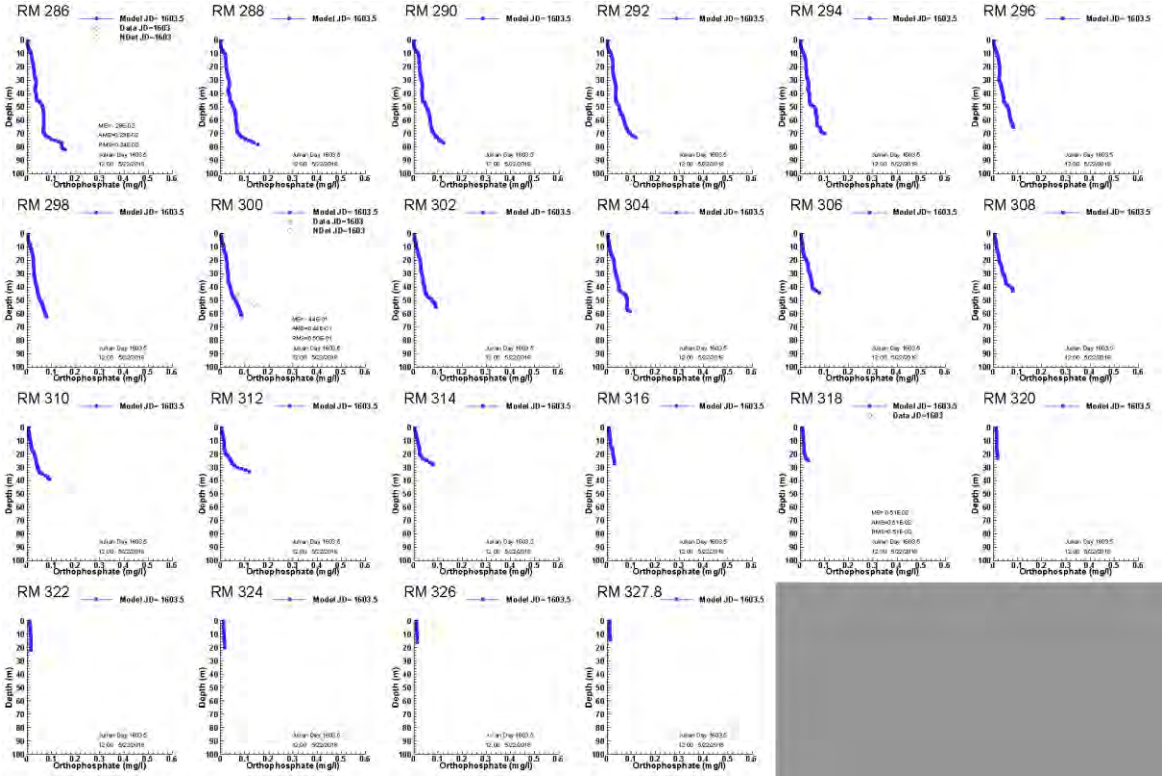


Figure 862. Vertical profiles of orthophosphate compared with data for 5/22/2018.

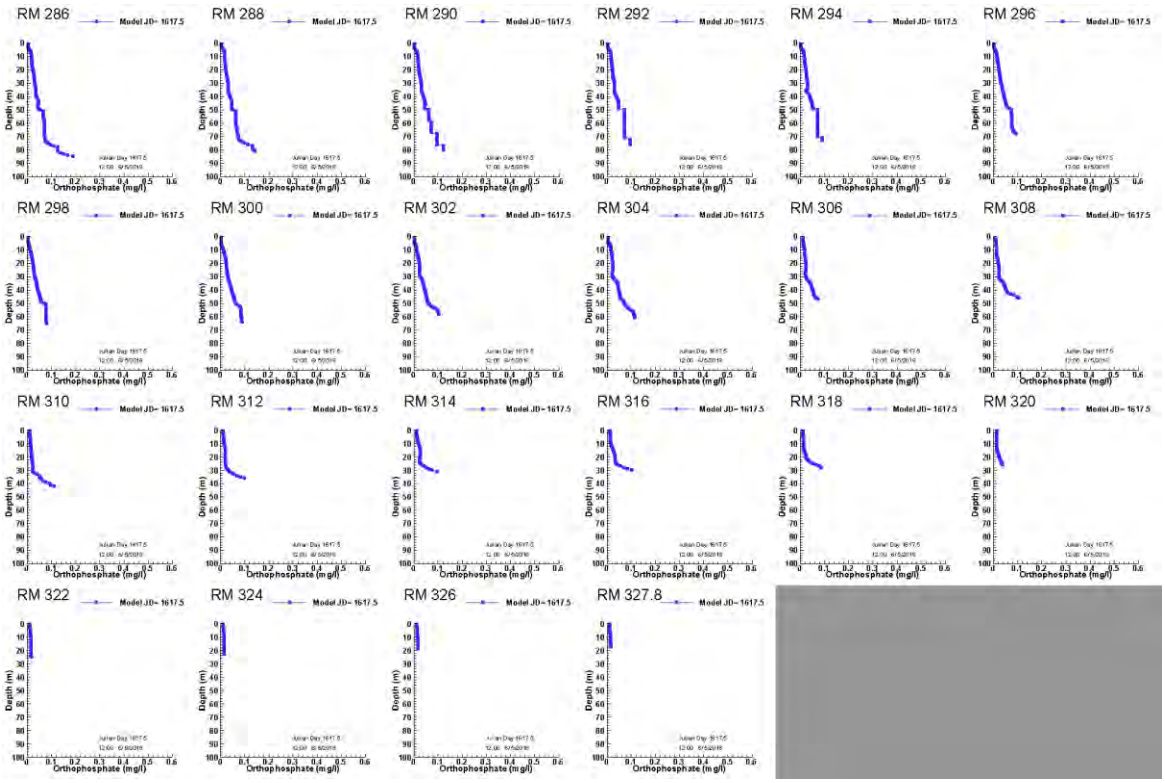


Figure 863. Vertical profiles of orthophosphate compared with data for 6/ 5/2018.

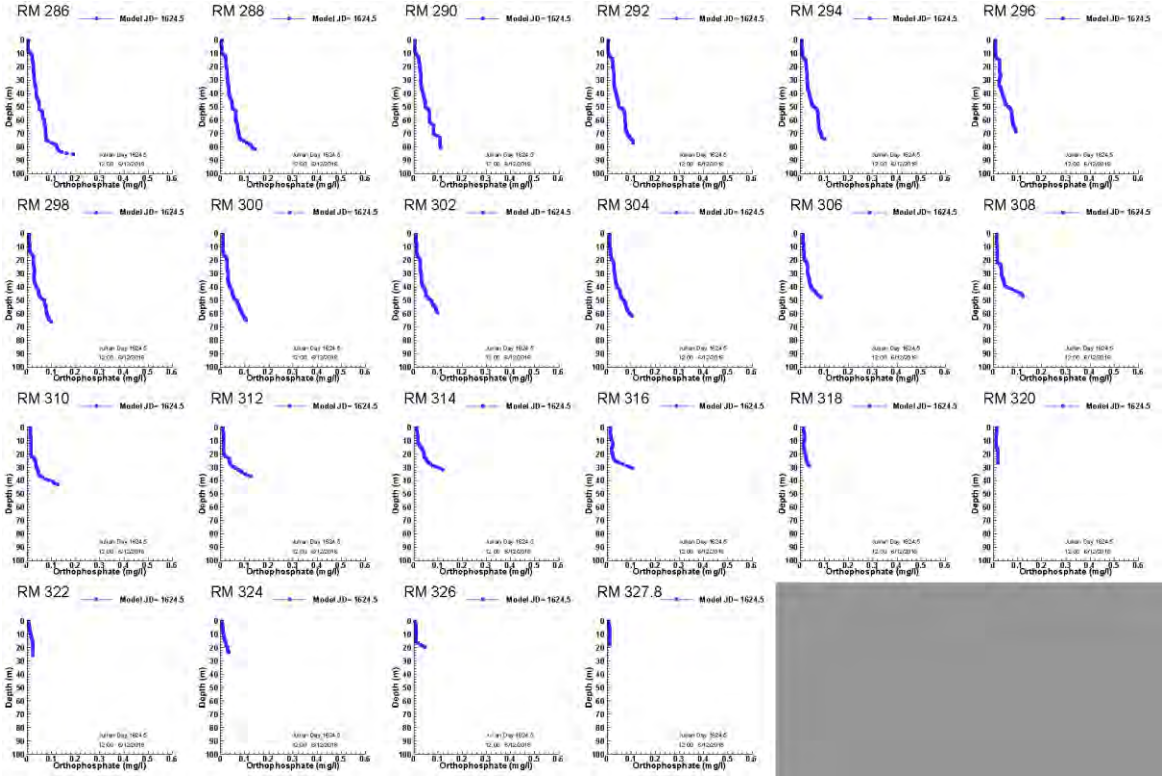


Figure 864. Vertical profiles of orthophosphate compared with data for 6/12/2018.

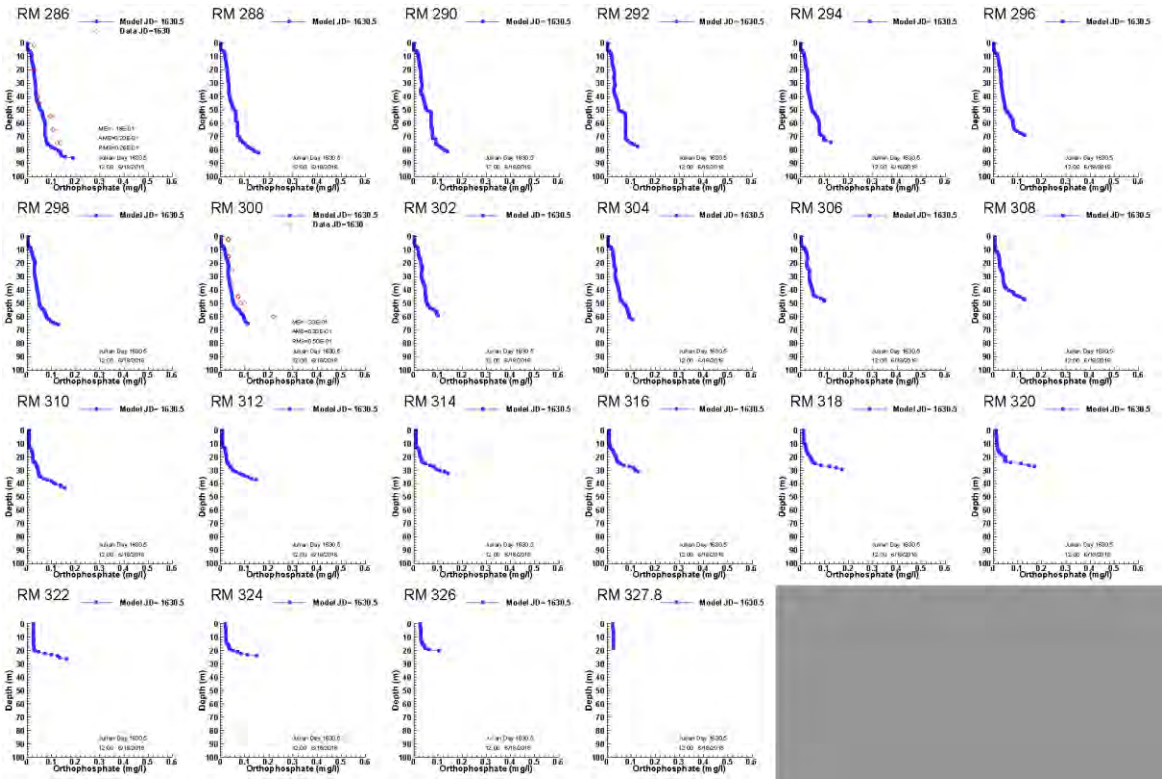


Figure 865. Vertical profiles of orthophosphate compared with data for 6/18/2018.

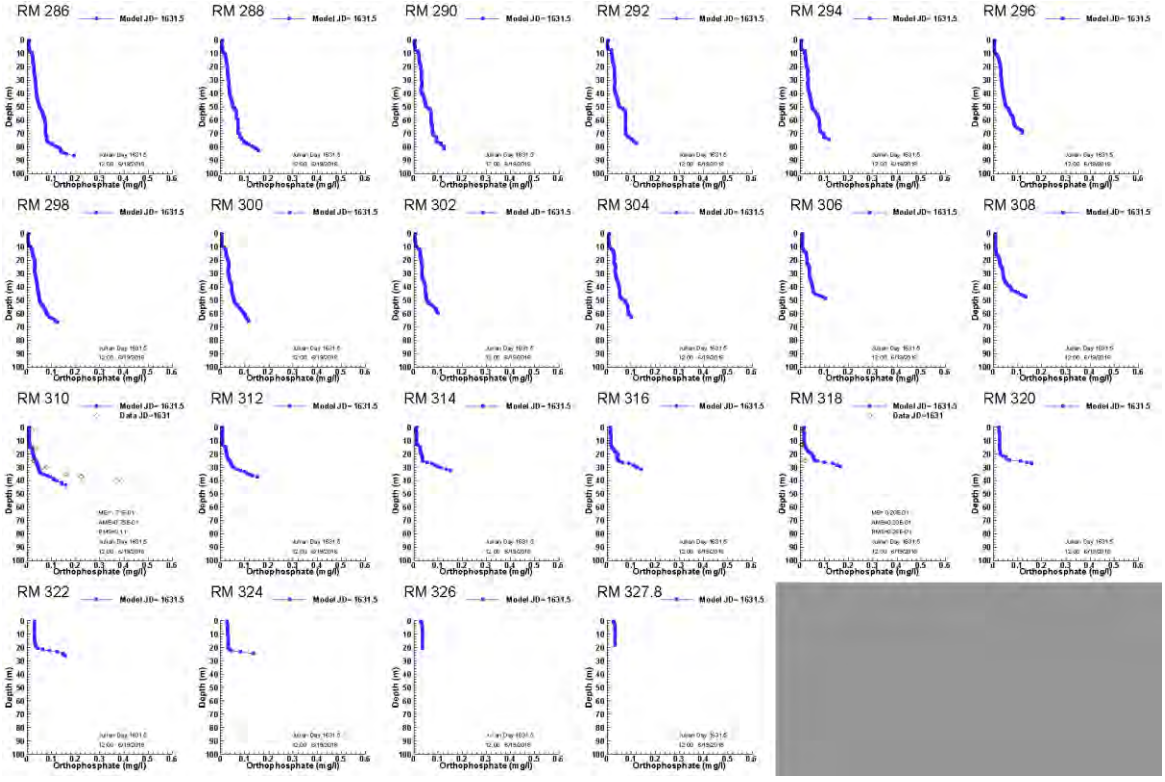


Figure 866. Vertical profiles of orthophosphate compared with data for 6/19/2018.

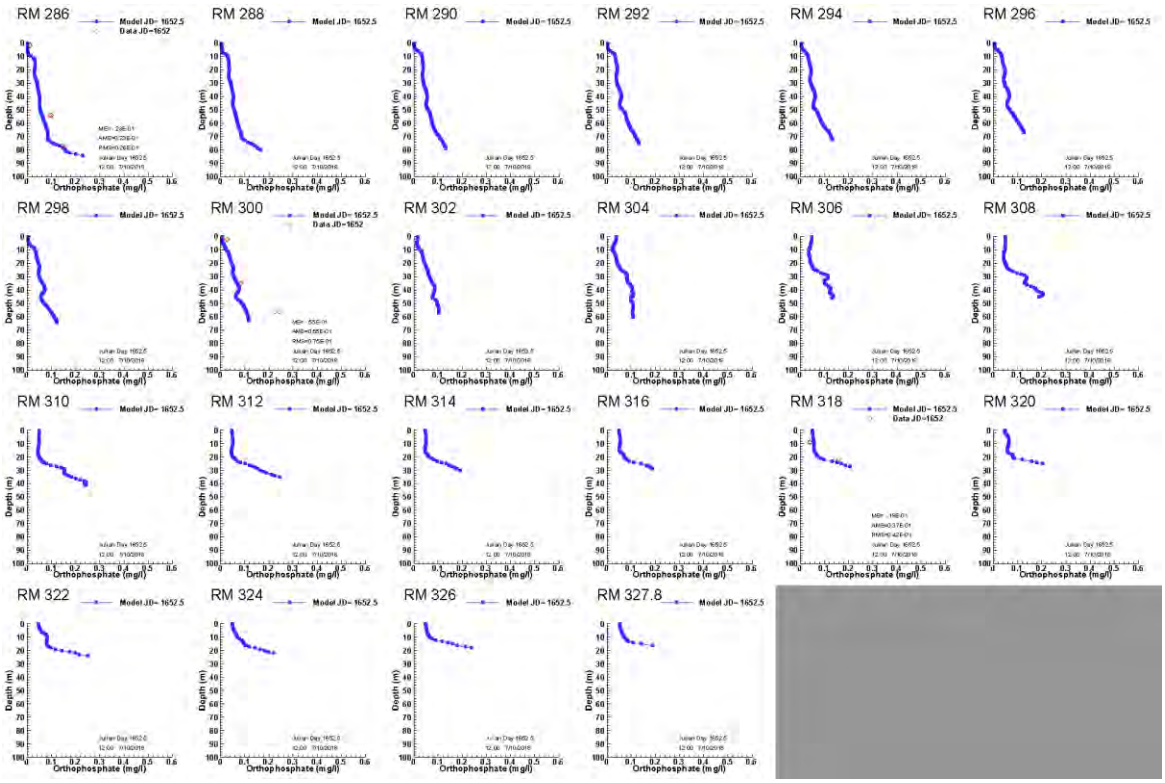


Figure 867. Vertical profiles of orthophosphate compared with data for 7/10/2018.

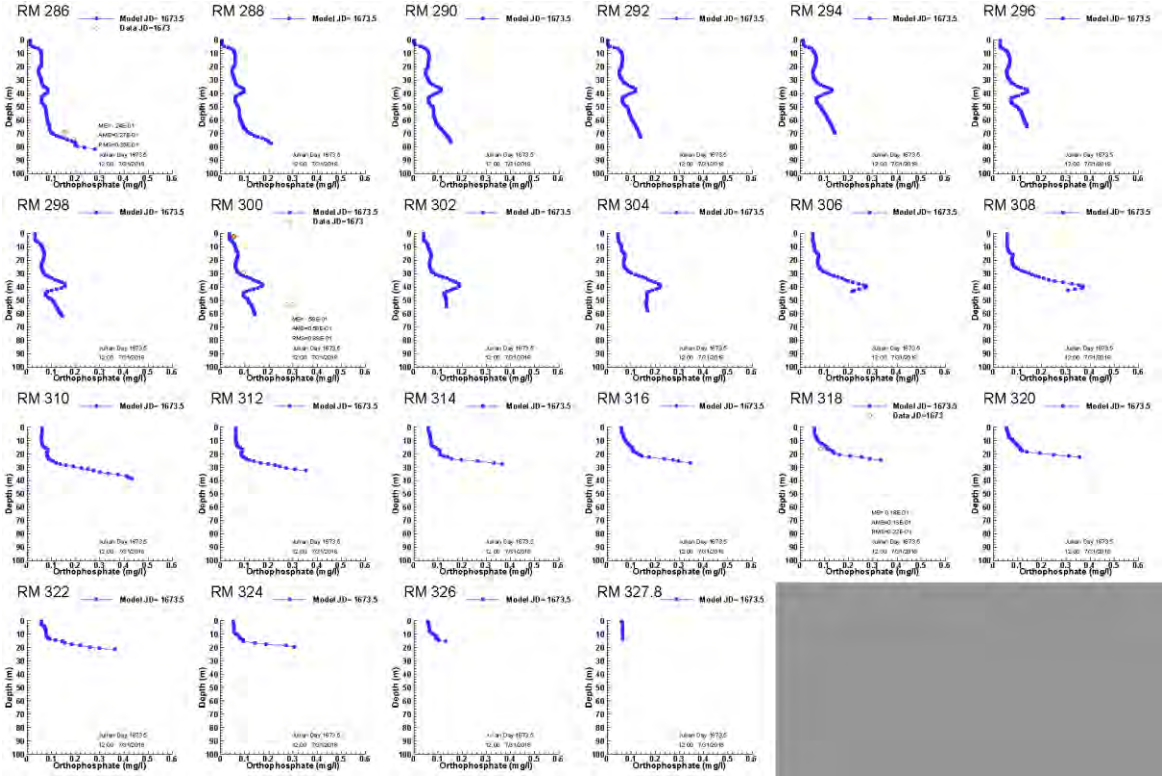


Figure 868. Vertical profiles of orthophosphate compared with data for 7/31/2018.

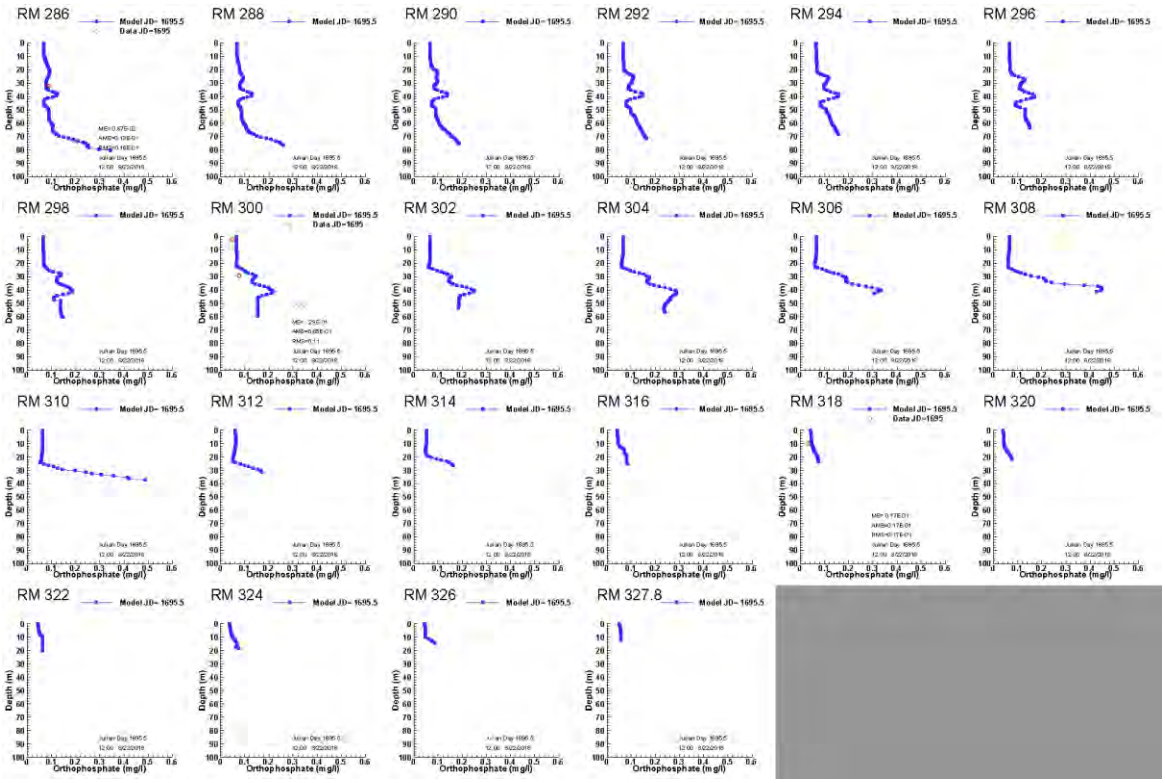


Figure 869. Vertical profiles of orthophosphate compared with data for 8/22/2018.

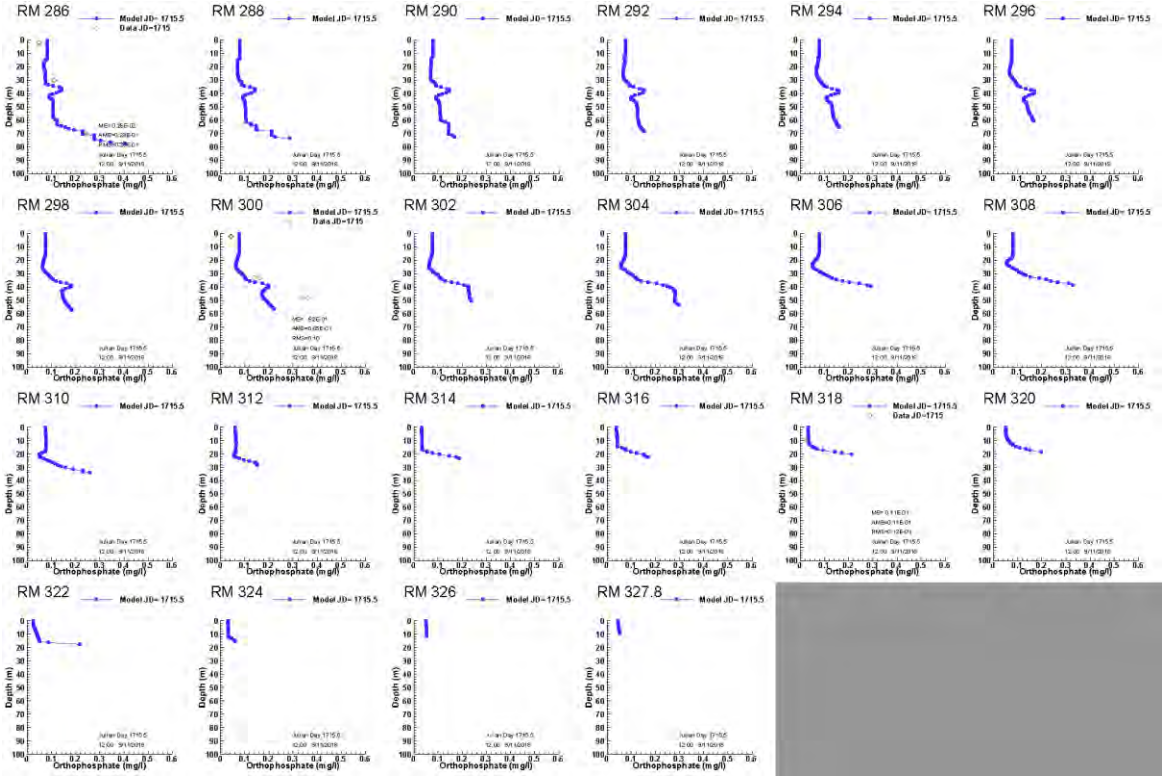


Figure 870. Vertical profiles of orthophosphate compared with data for 9/11/2018.

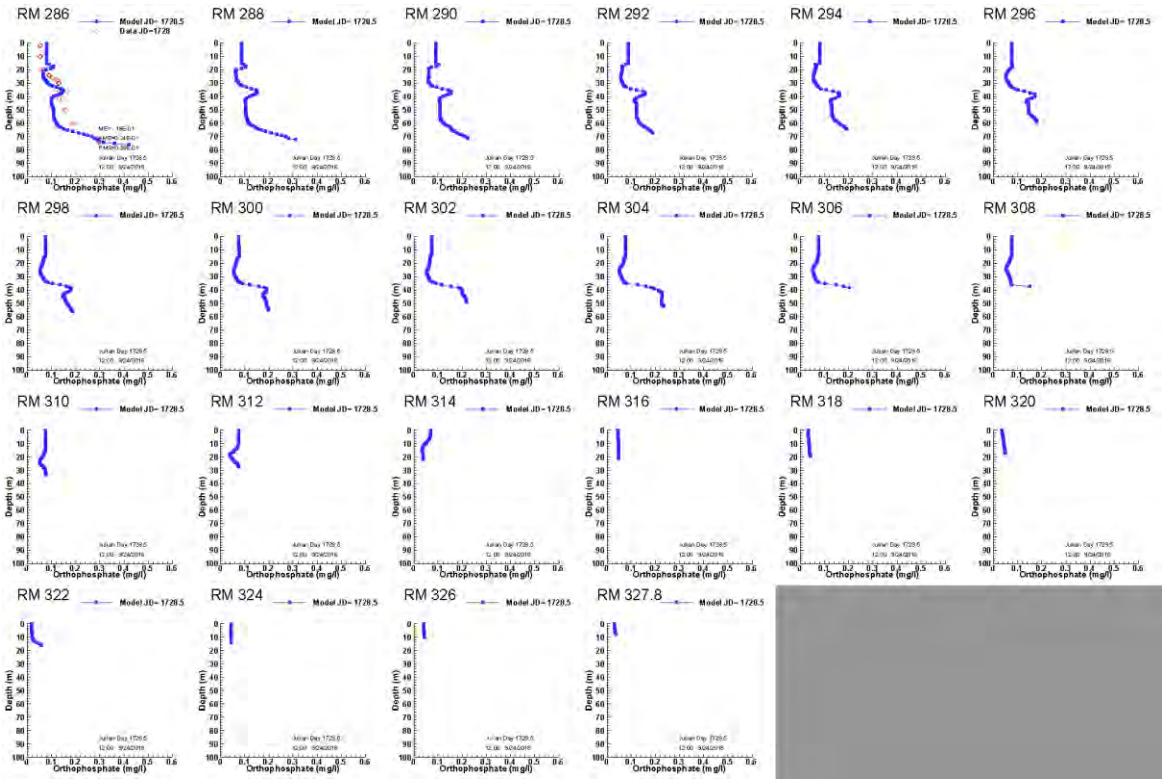


Figure 871. Vertical profiles of orthophosphate compared with data for 9/24/2018.

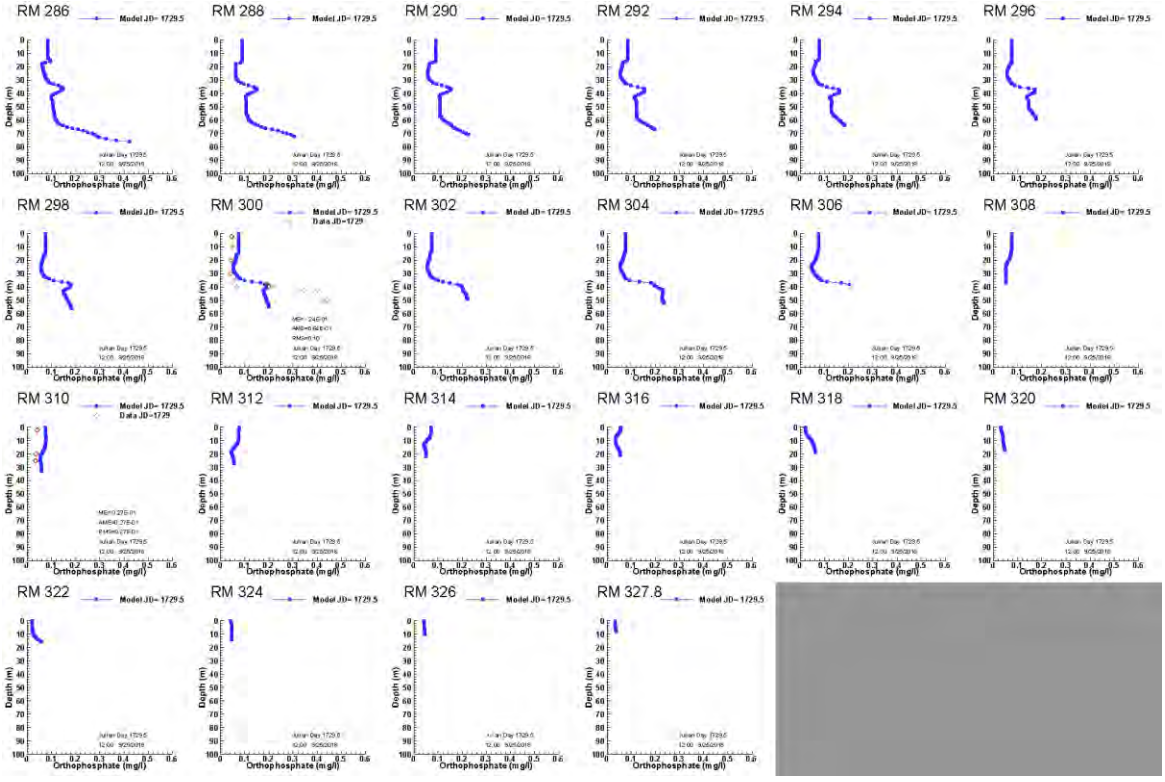


Figure 872. Vertical profiles of orthophosphate compared with data for 9/25/2018.

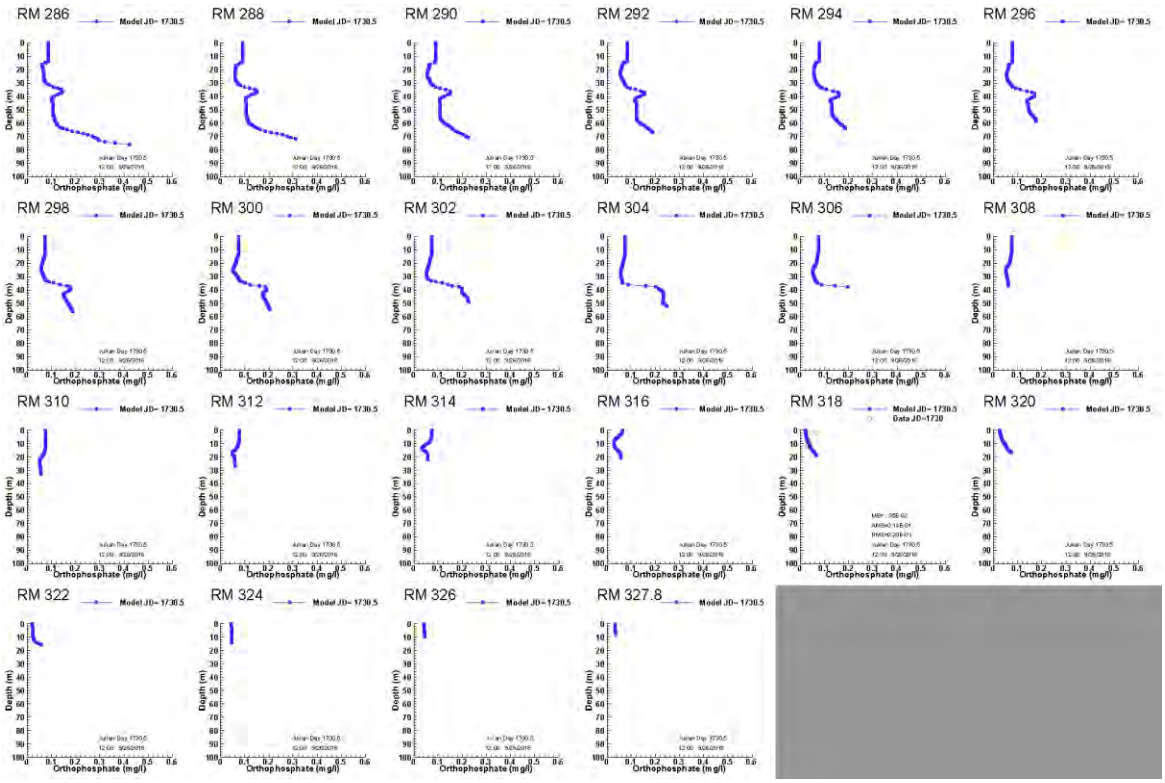


Figure 873. Vertical profiles of orthophosphate compared with data for 9/26/2018.

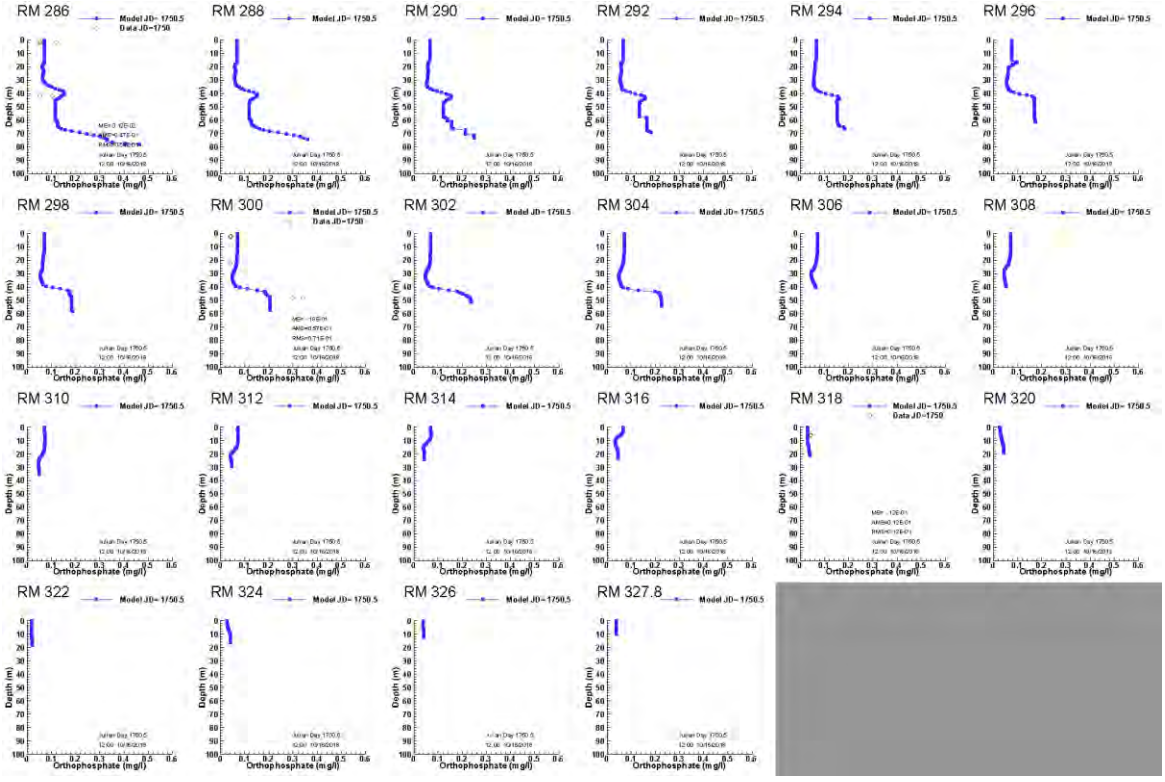


Figure 874. Vertical profiles of orthophosphate compared with data for 10/16/2018.

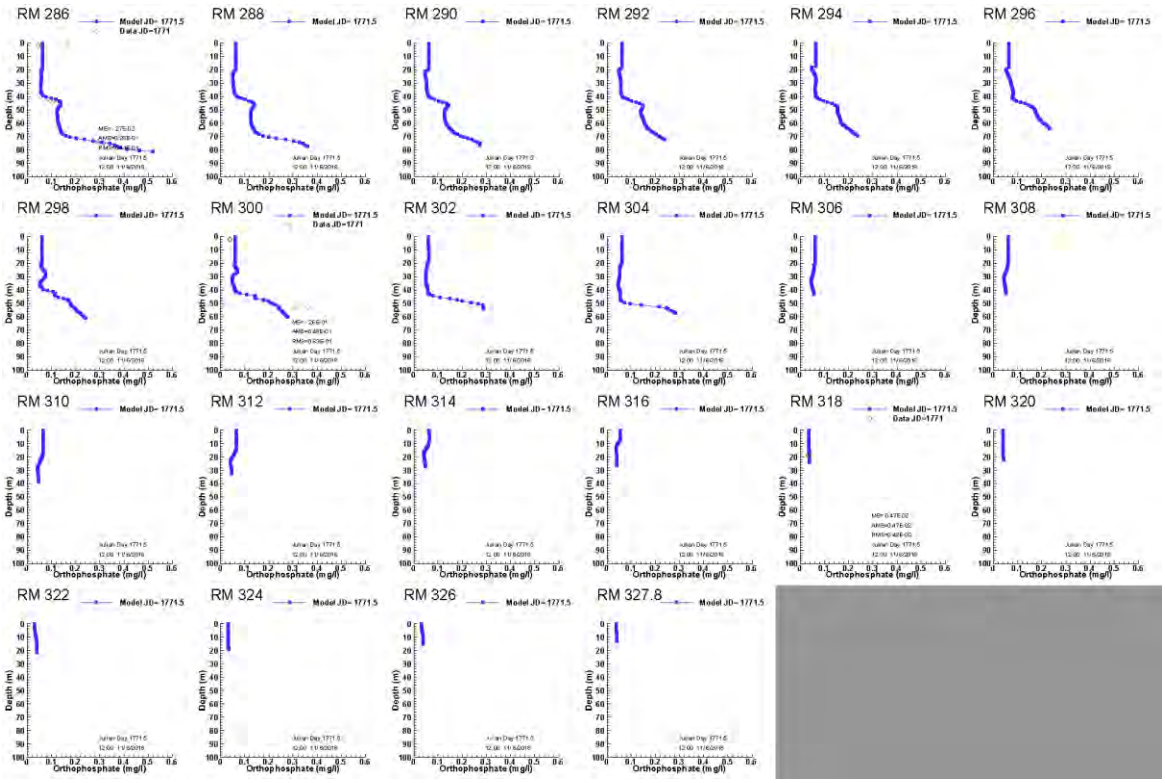


Figure 875. Vertical profiles of orthophosphate compared with data for 11/ 6/2018.

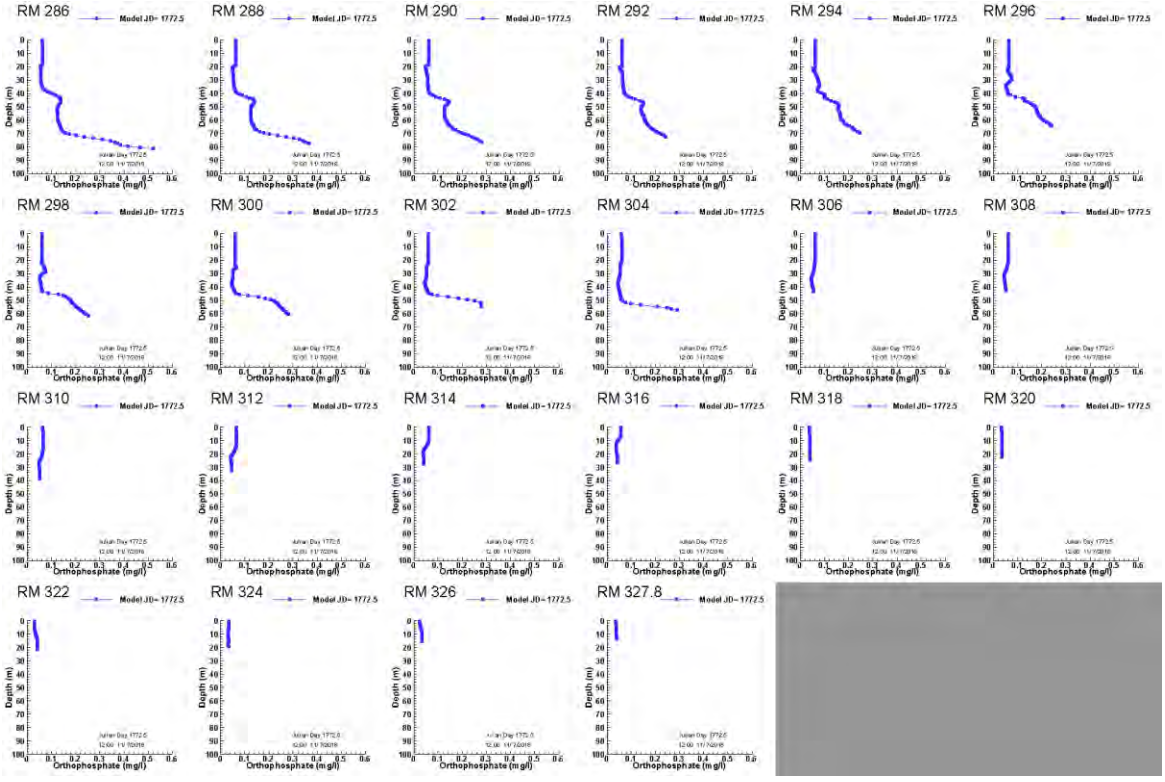


Figure 876. Vertical profiles of orthophosphate compared with data for 11/ 7/2018.

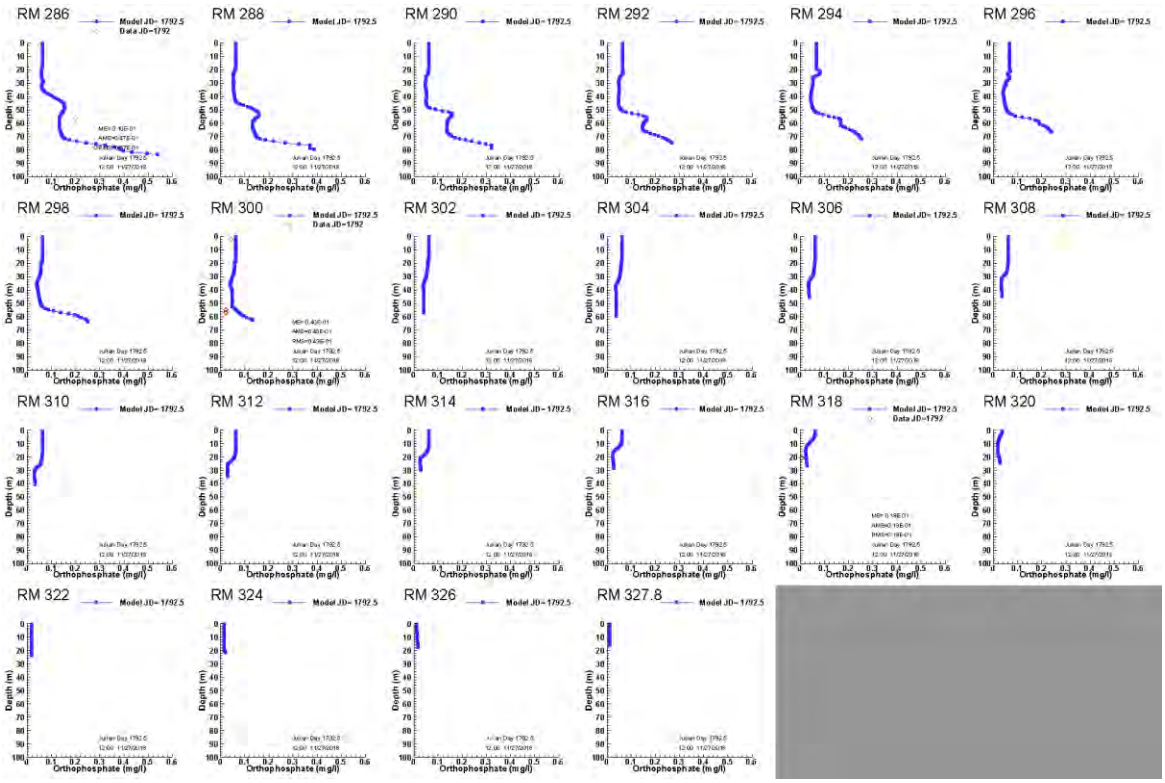


Figure 877. Vertical profiles of orthophosphate compared with data for 11/27/2018.

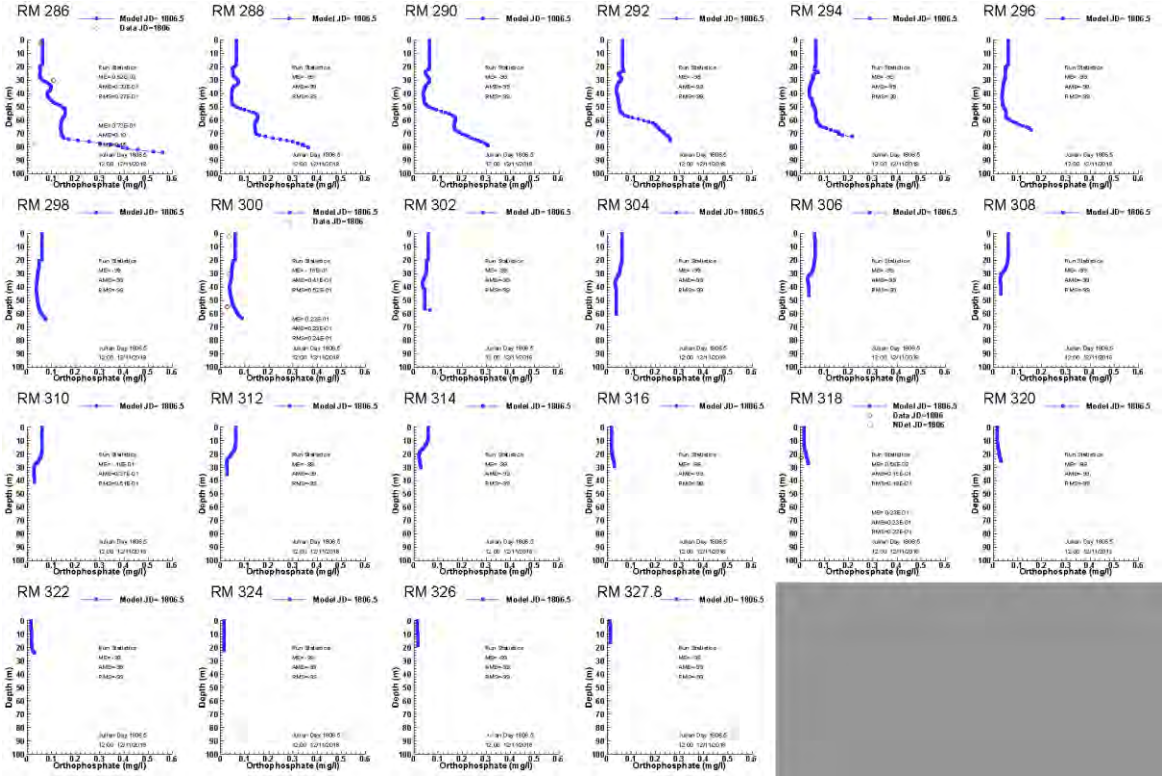


Figure 878. Vertical profiles of orthophosphate compared with data for 12/11/2018.

Ammonia Nitrogen

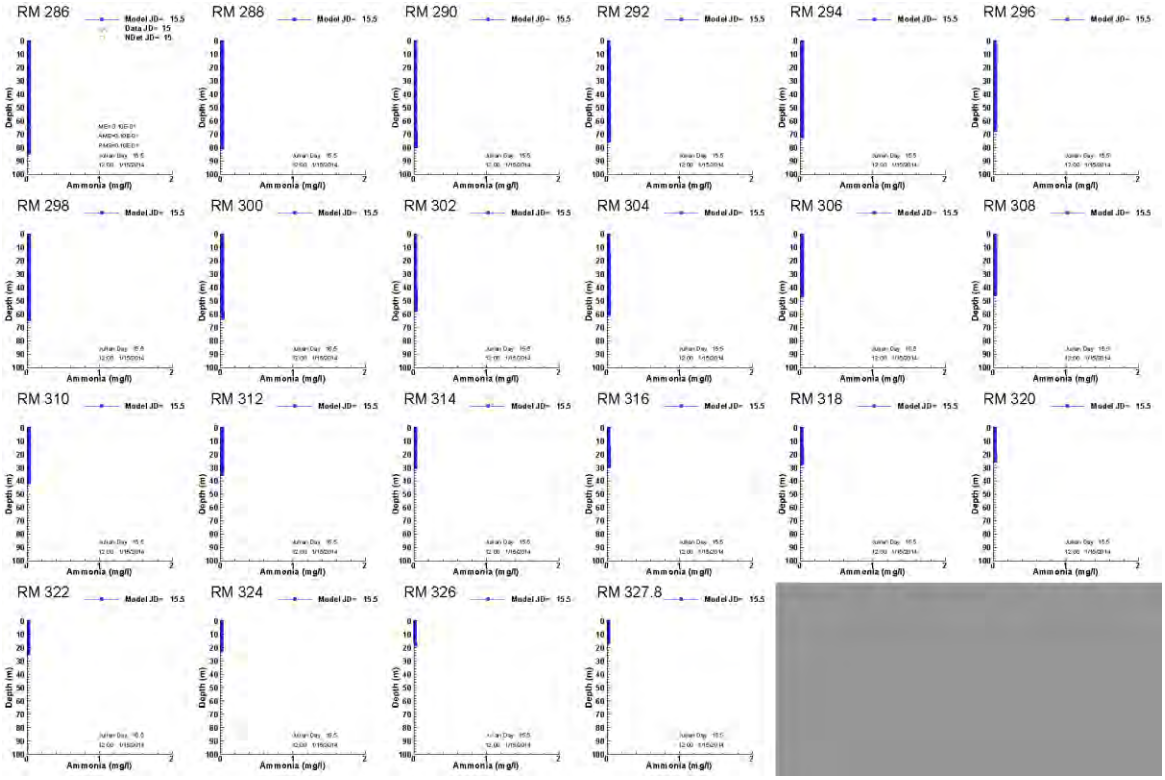


Figure 879. Vertical profiles of ammonia nitrogen compared with data for 1/15/2014.

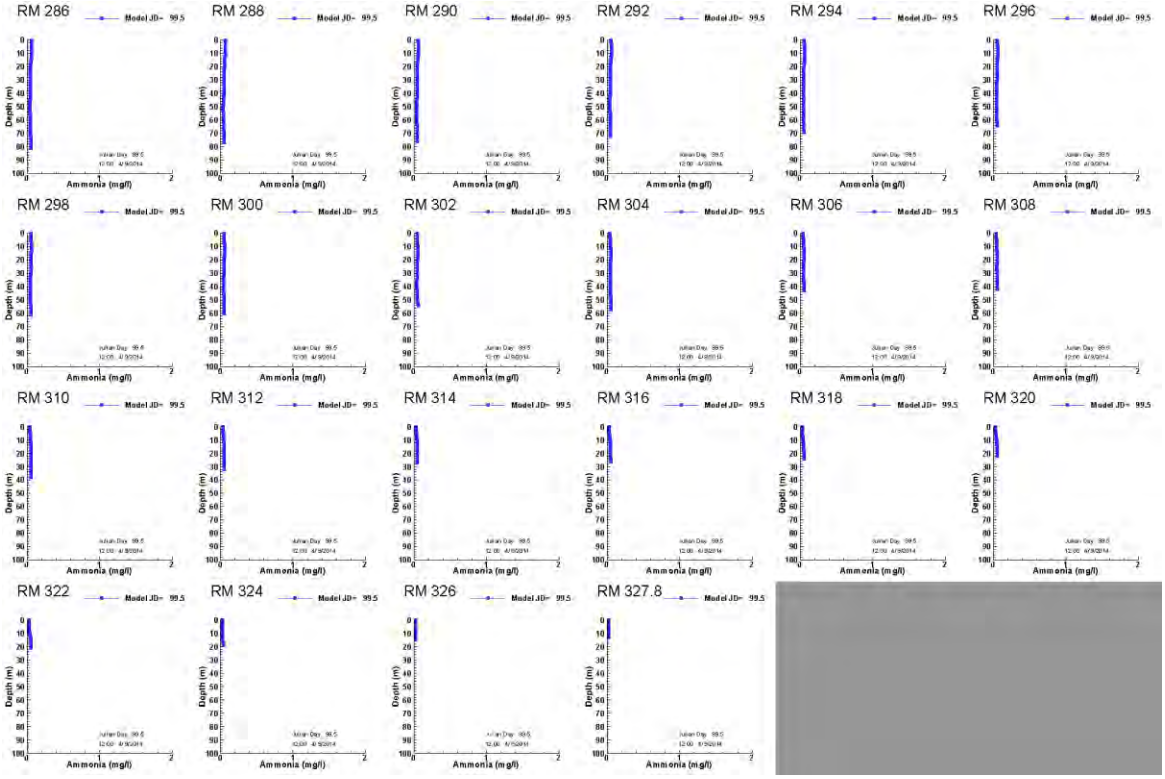


Figure 880. Vertical profiles of ammonia nitrogen compared with data for 4/ 9/2014.

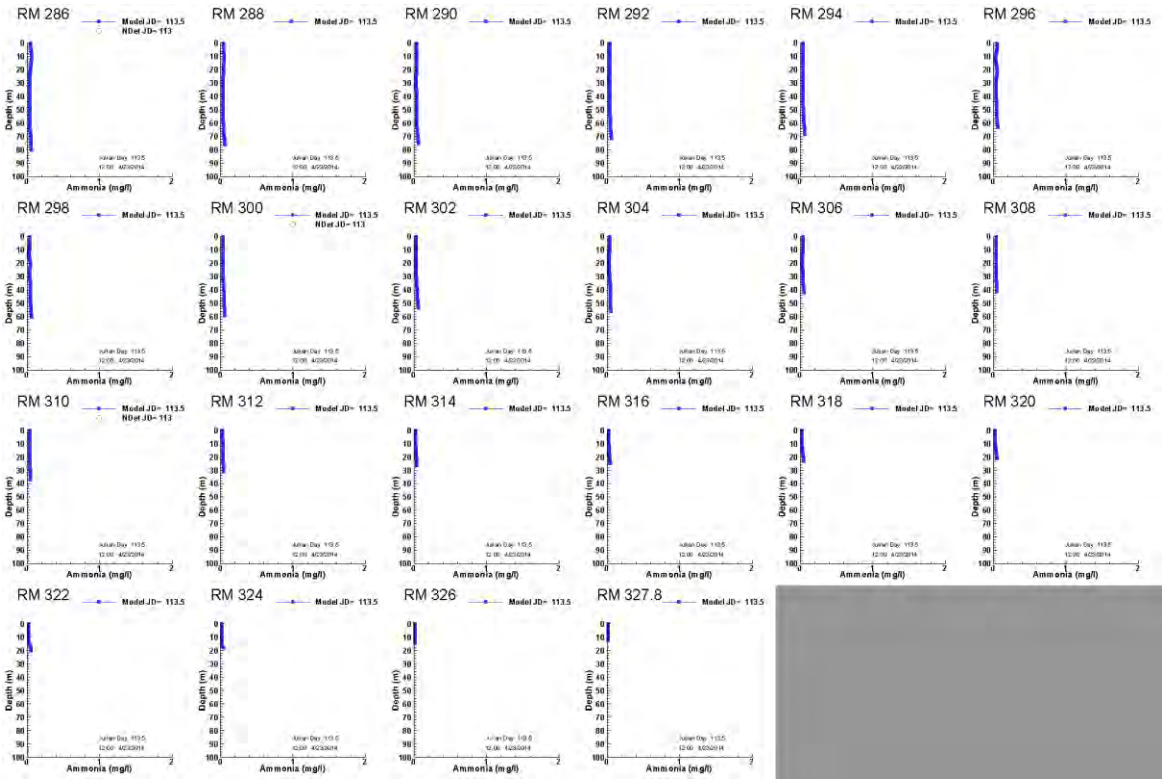


Figure 881. Vertical profiles of ammonia nitrogen compared with data for 4/23/2014.

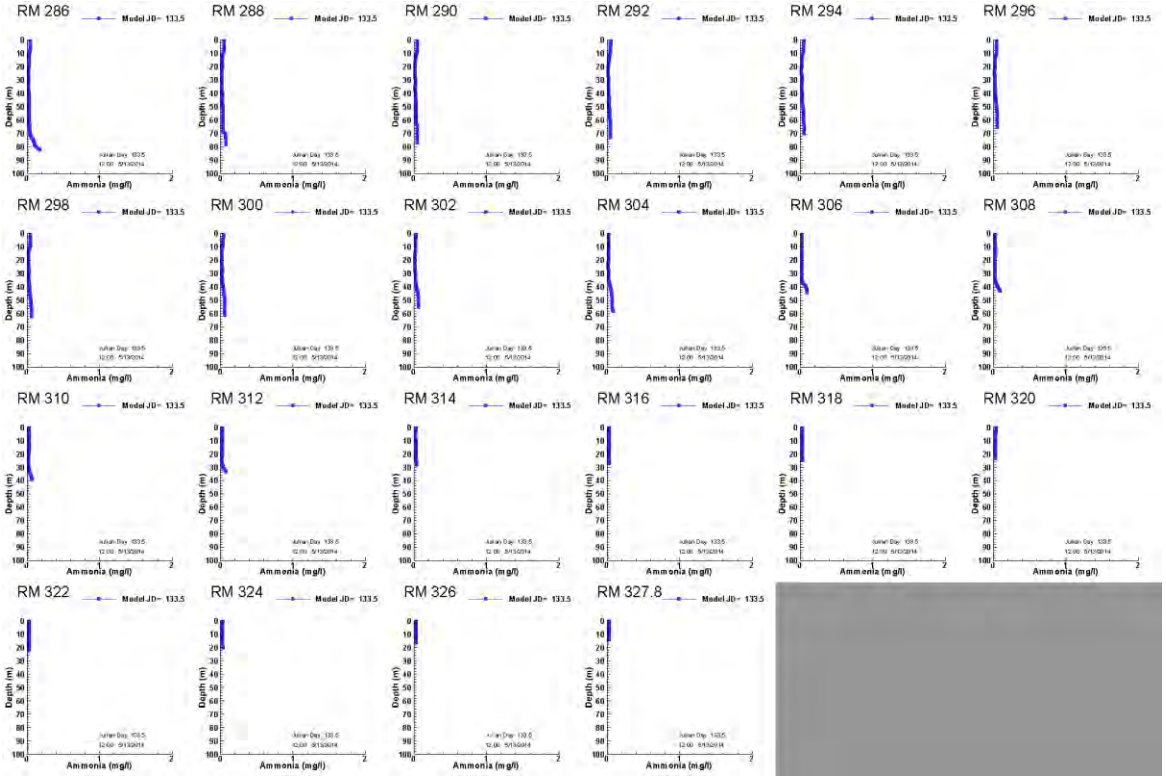


Figure 882. Vertical profiles of ammonia nitrogen compared with data for 5/13/2014.

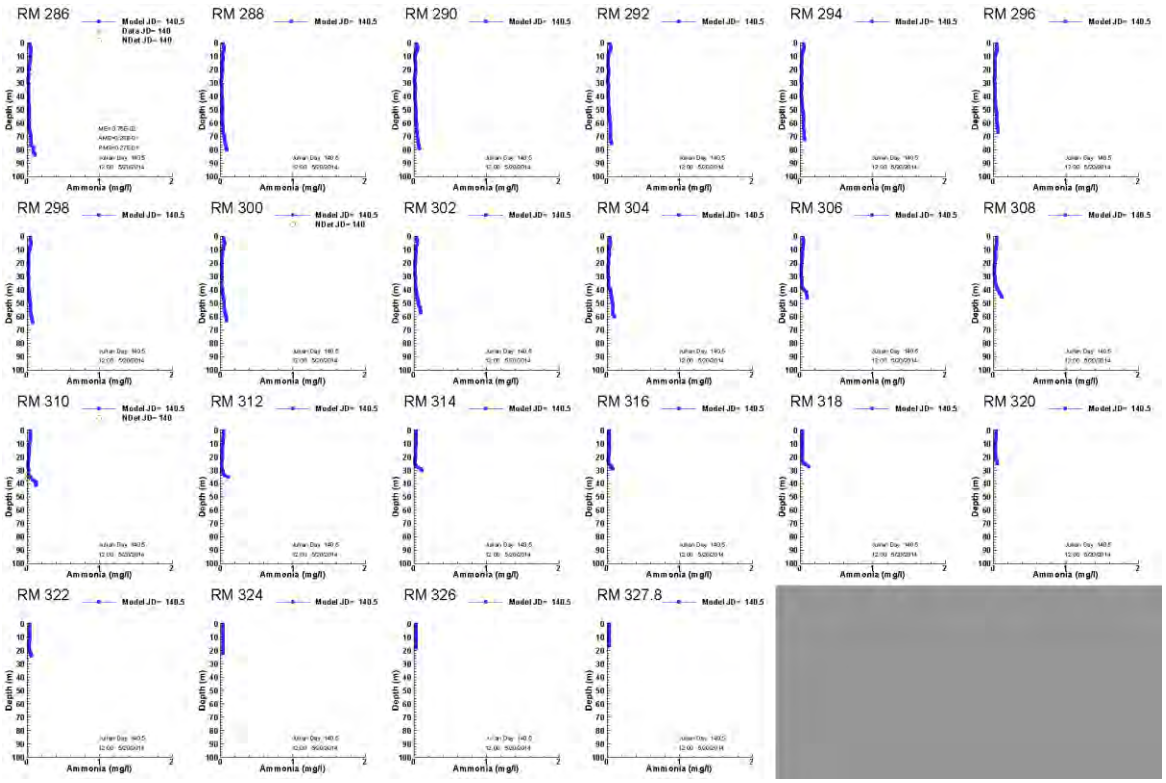


Figure 883. Vertical profiles of ammonia nitrogen compared with data for 5/20/2014.

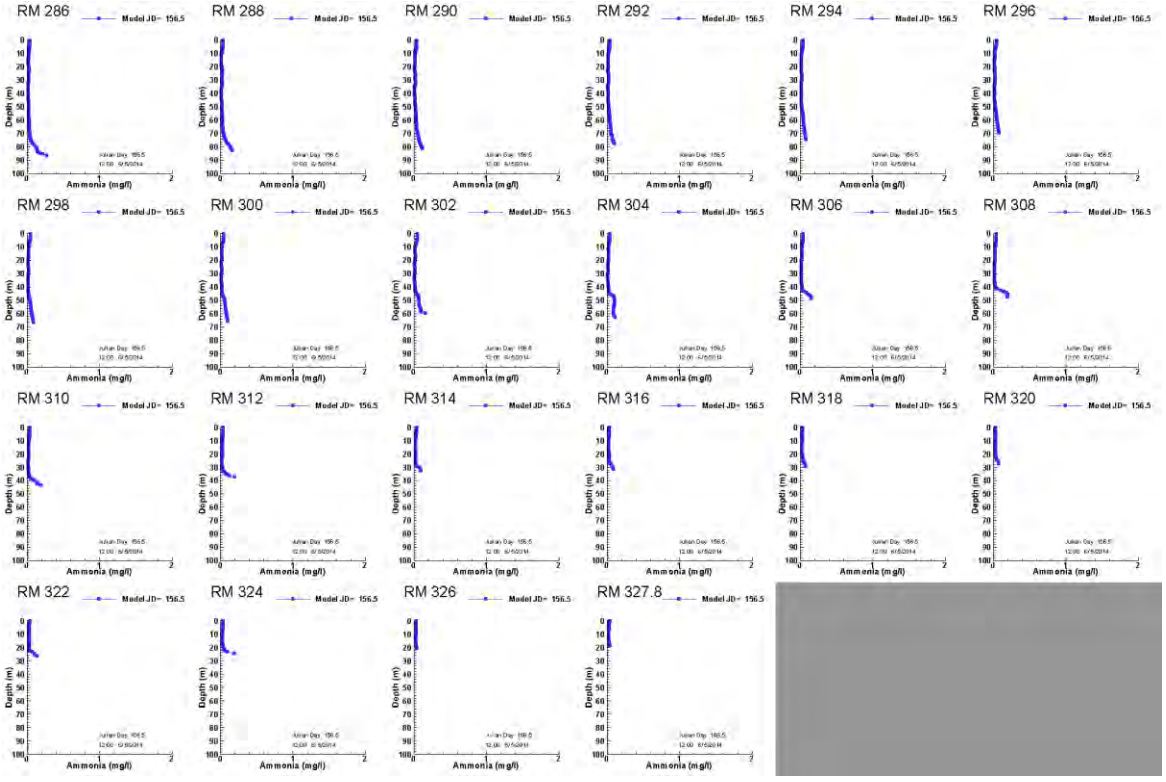


Figure 884. Vertical profiles of ammonia nitrogen compared with data for 6/ 5/2014.

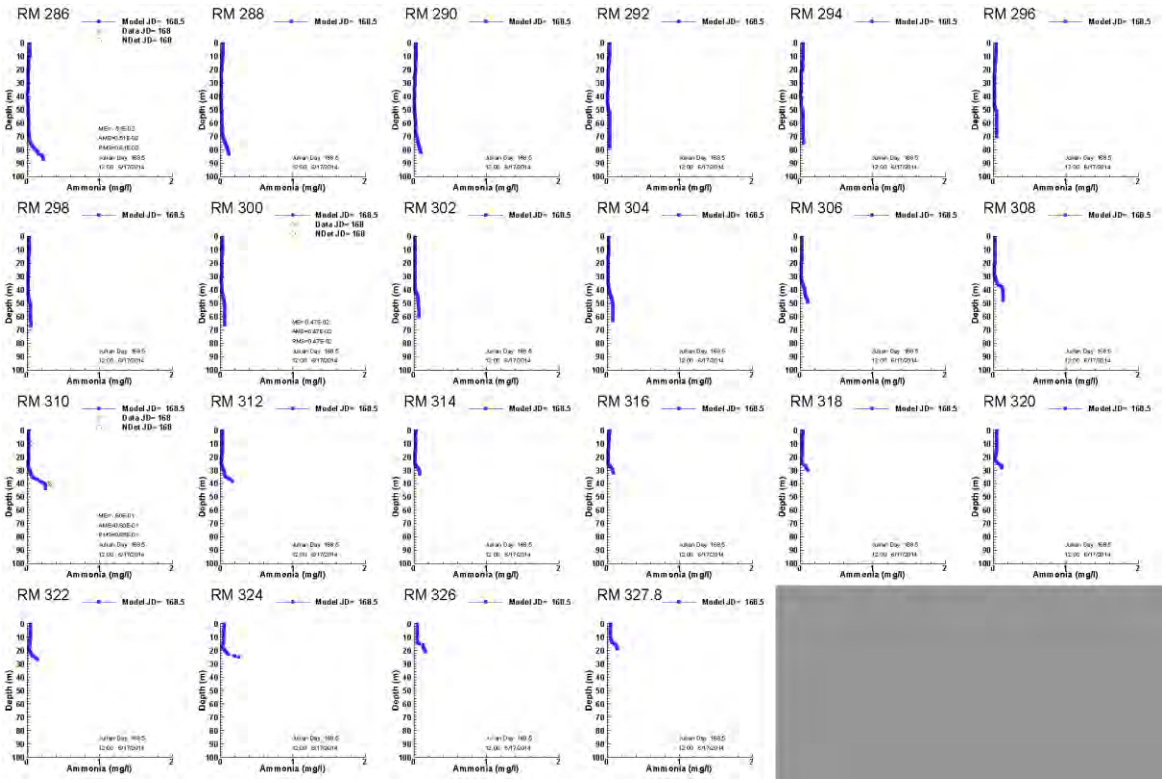


Figure 885. Vertical profiles of ammonia nitrogen compared with data for 6/17/2014.

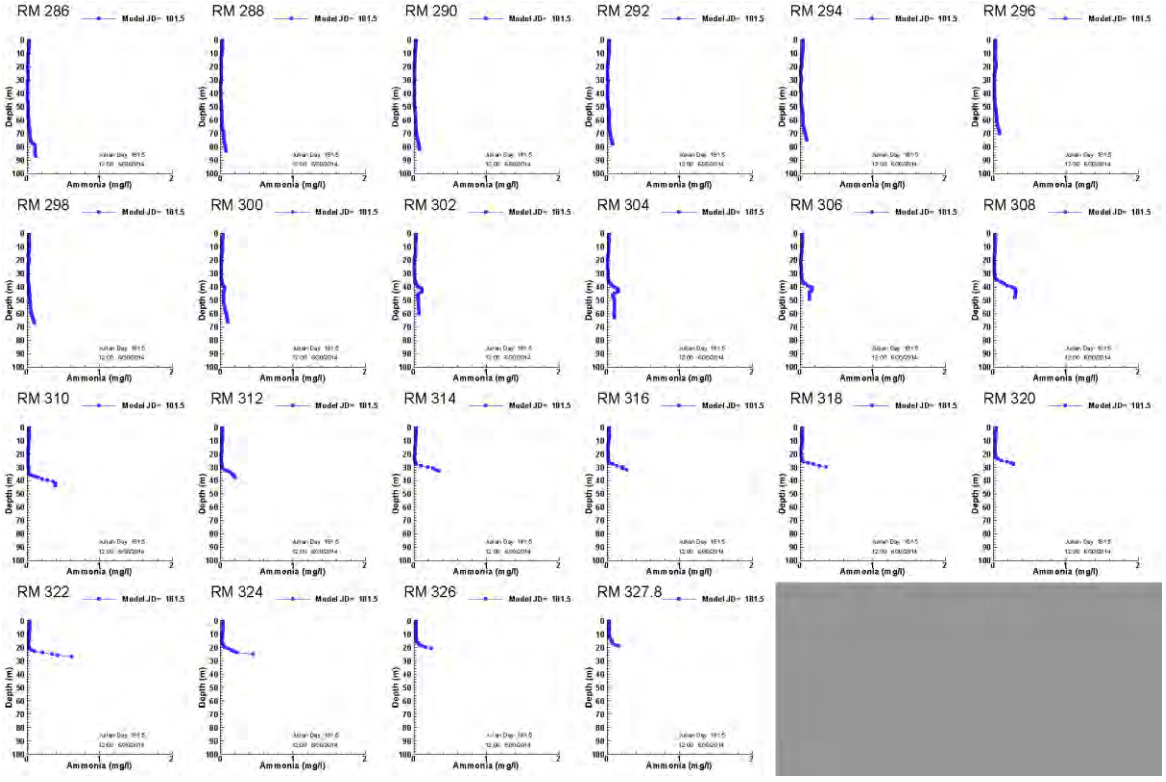


Figure 886. Vertical profiles of ammonia nitrogen compared with data for 6/30/2014.

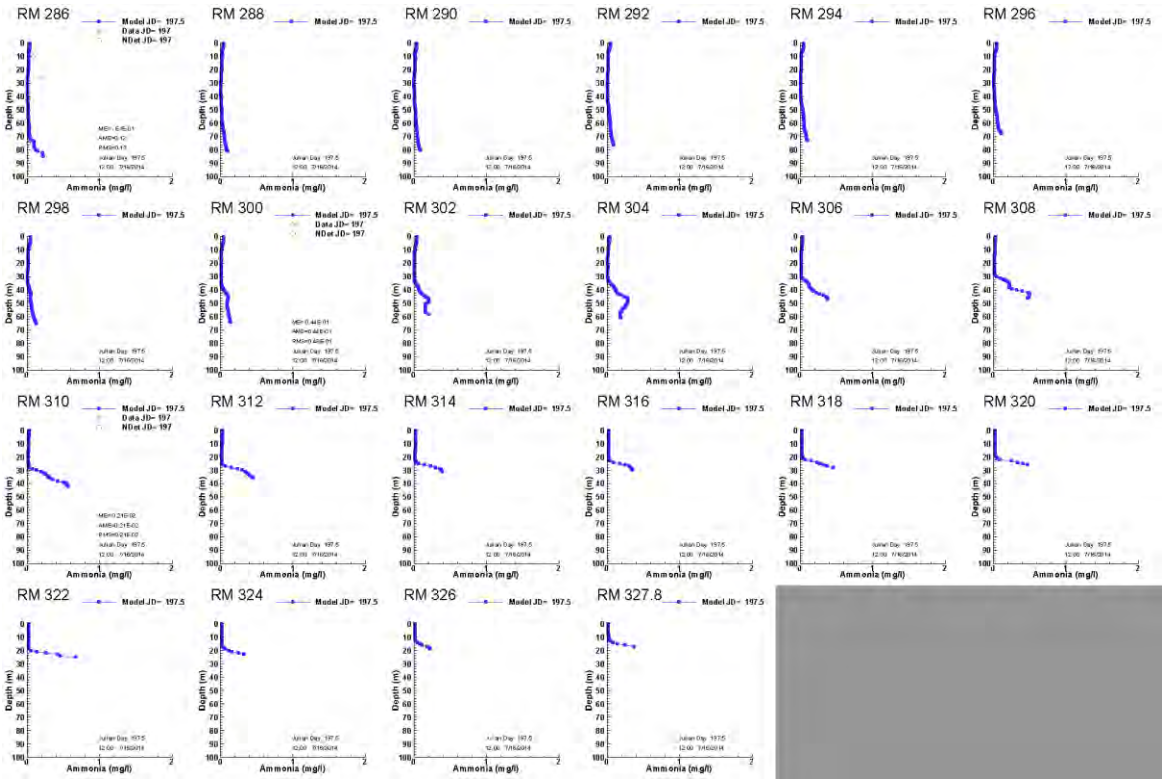


Figure 887. Vertical profiles of ammonia nitrogen compared with data for 7/16/2014.

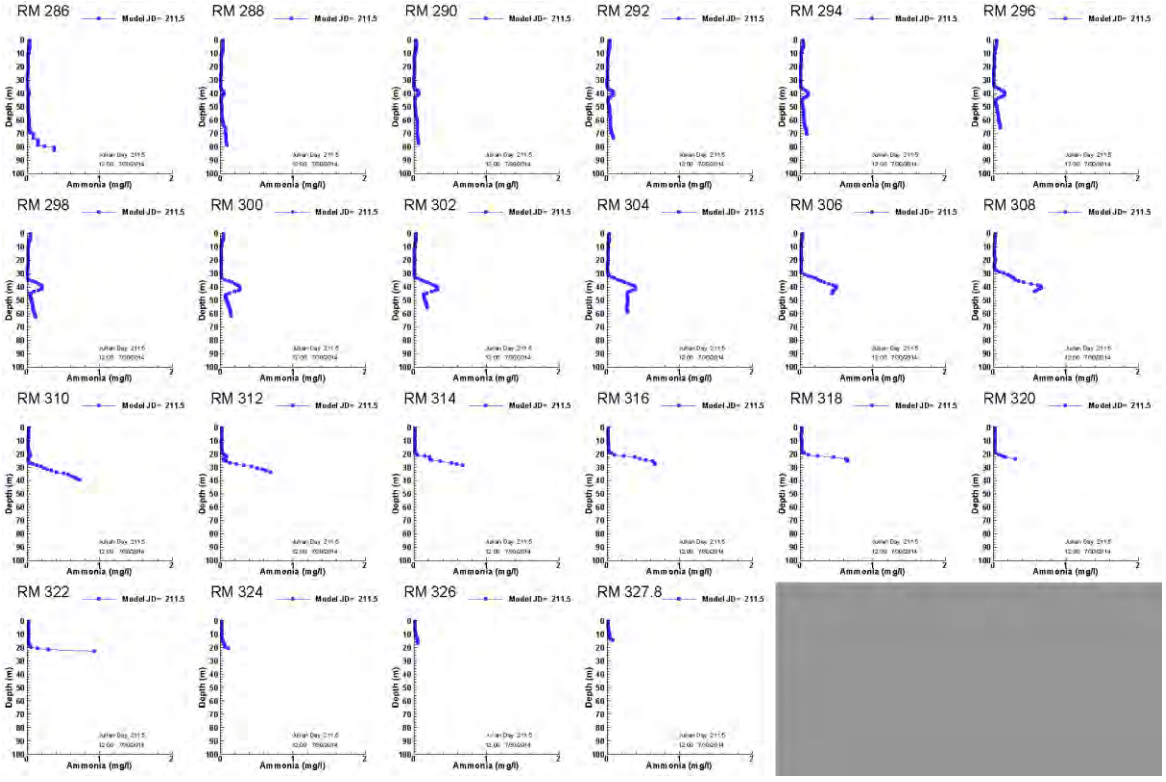


Figure 888. Vertical profiles of ammonia nitrogen compared with data for 7/30/2014.

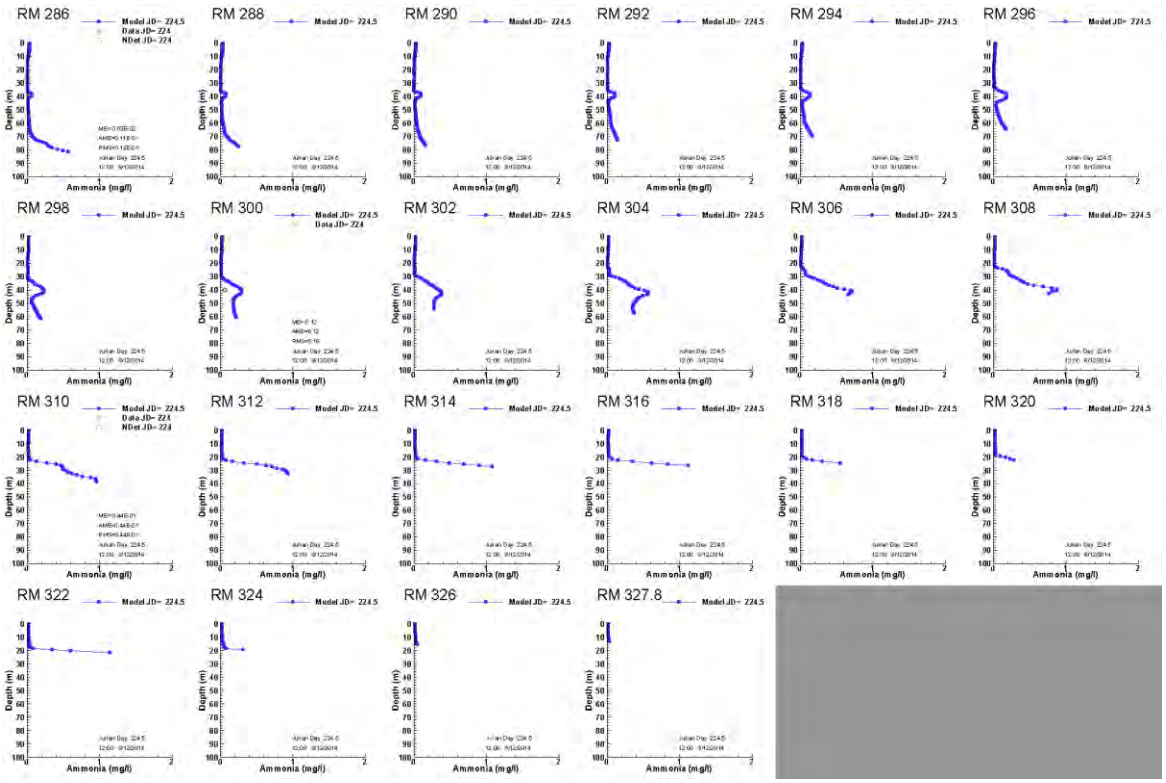


Figure 889. Vertical profiles of ammonia nitrogen compared with data for 8/12/2014.

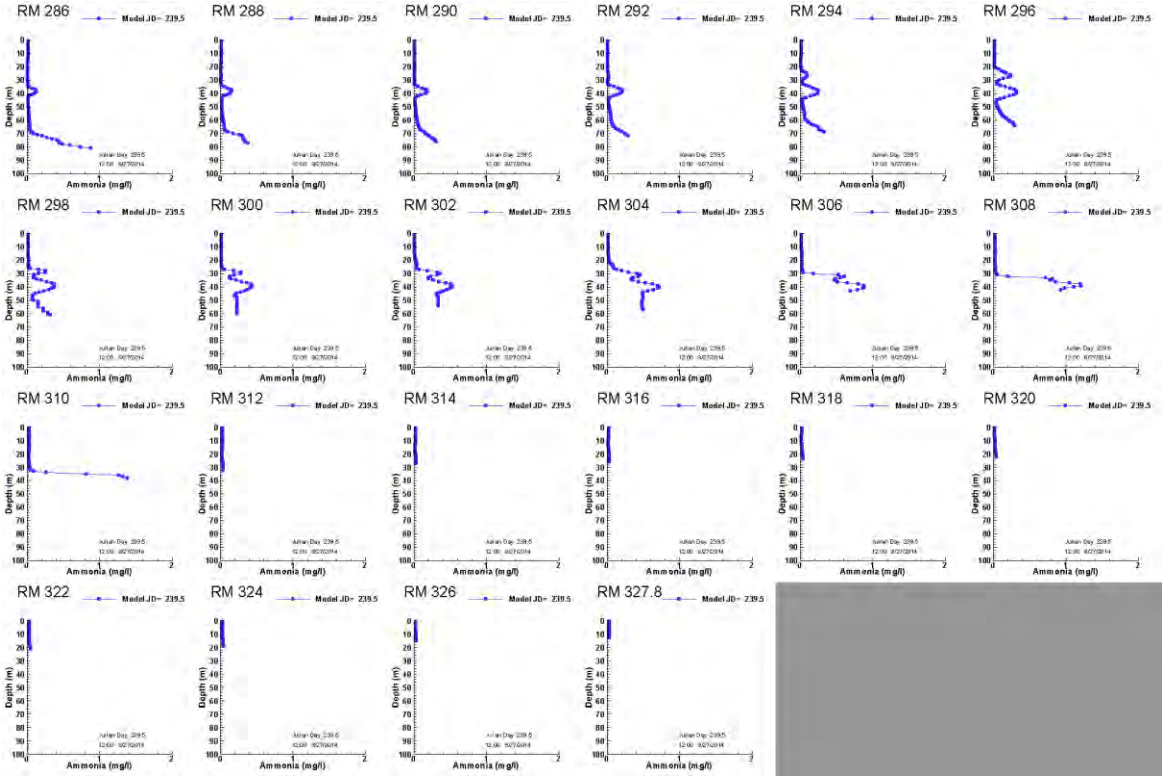


Figure 890. Vertical profiles of ammonia nitrogen compared with data for 8/27/2014.

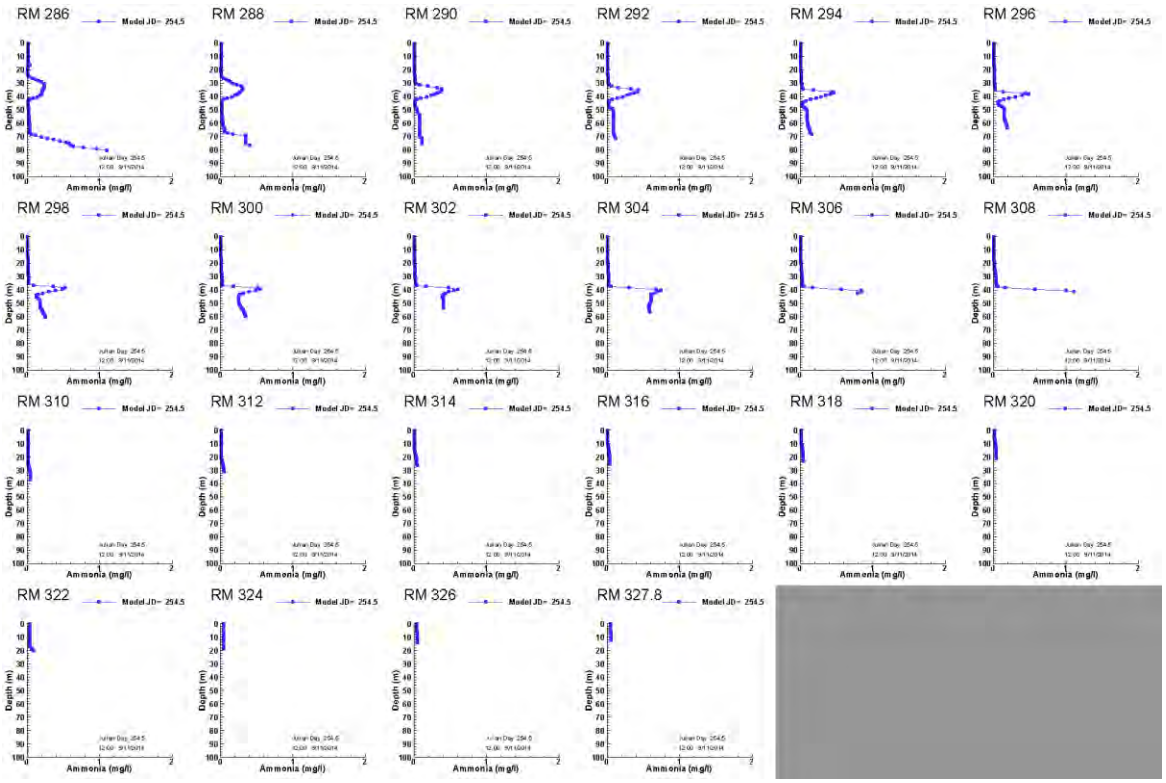


Figure 891. Vertical profiles of ammonia nitrogen compared with data for 9/11/2014.

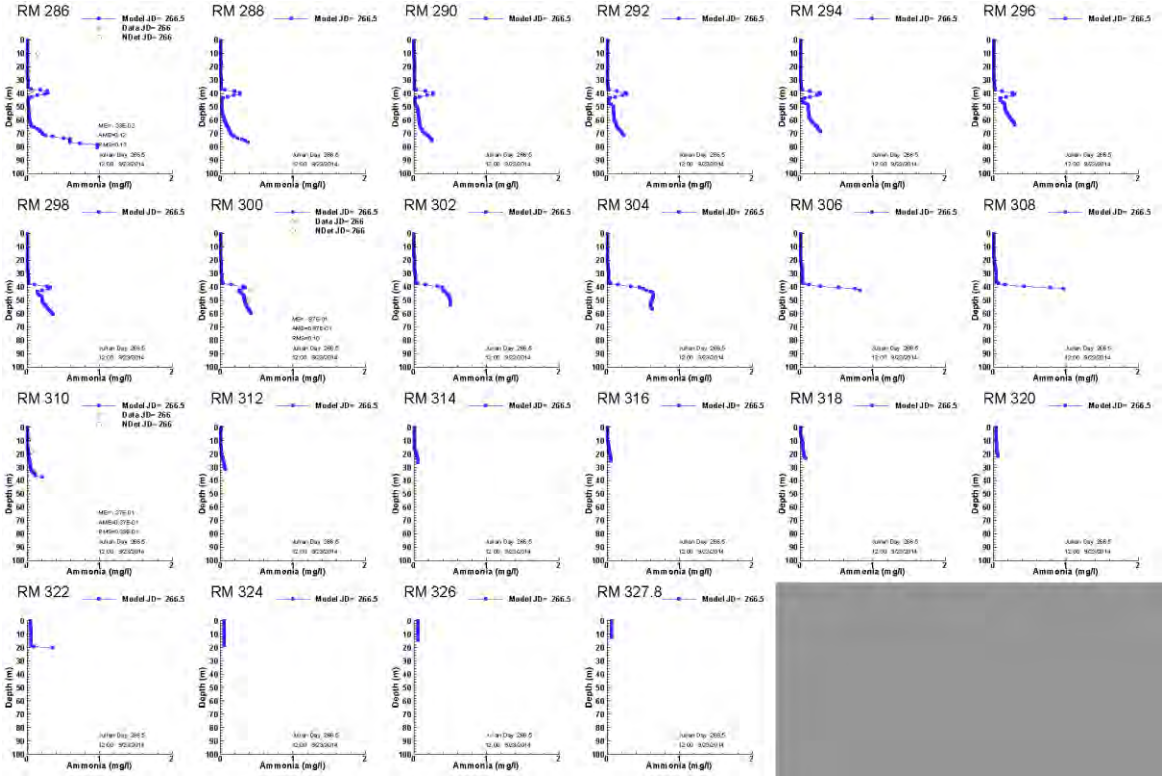


Figure 892. Vertical profiles of ammonia nitrogen compared with data for 9/23/2014.

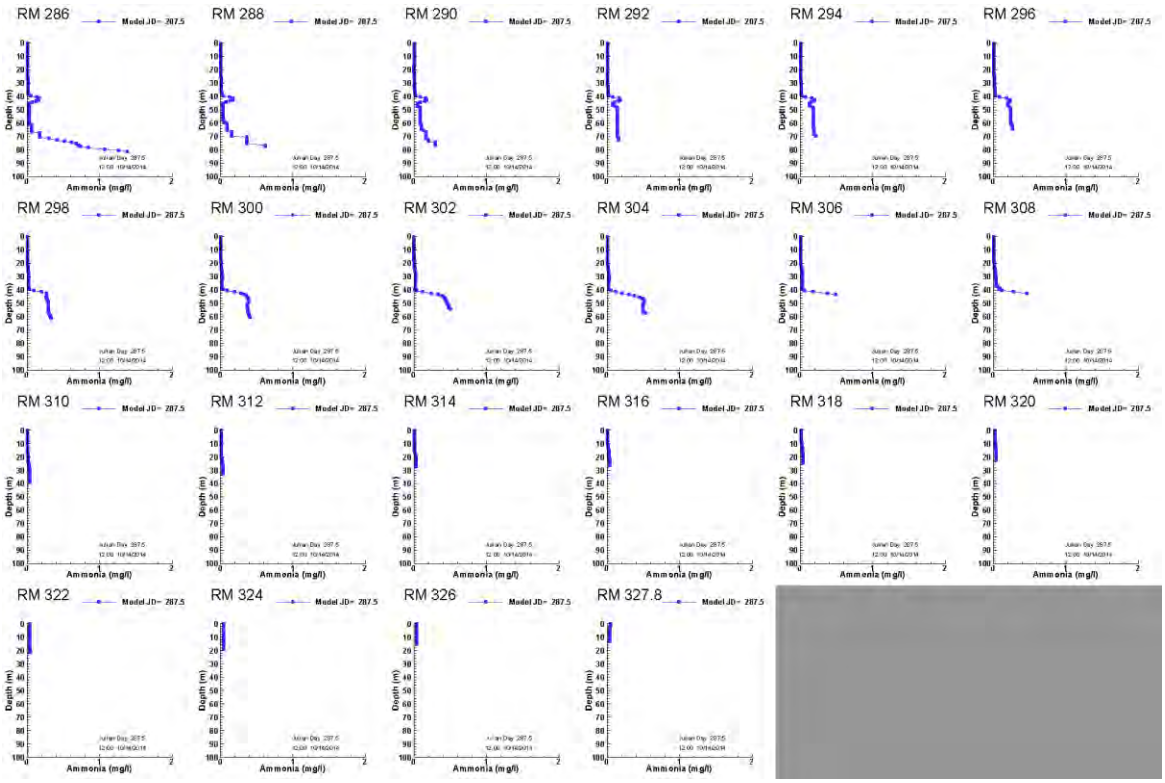


Figure 893. Vertical profiles of ammonia nitrogen compared with data for 10/14/2014.

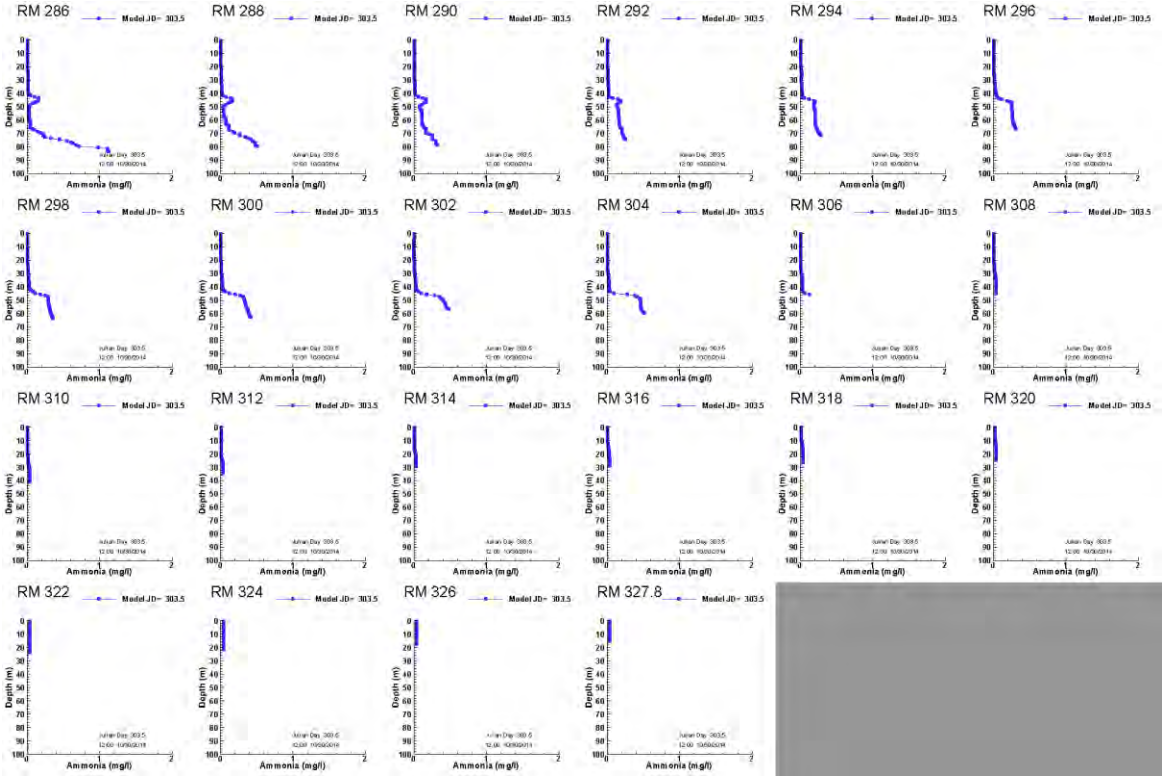


Figure 894. Vertical profiles of ammonia nitrogen compared with data for 10/30/2014.

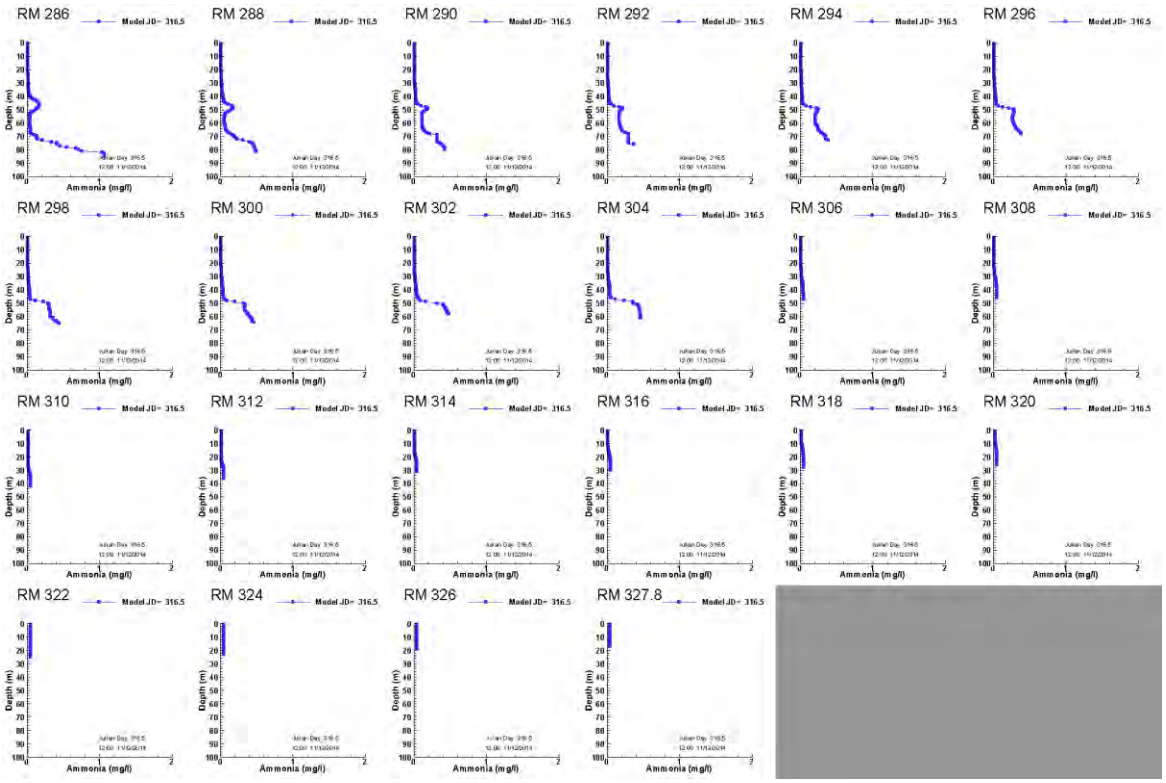


Figure 895. Vertical profiles of ammonia nitrogen compared with data for 11/12/2014.

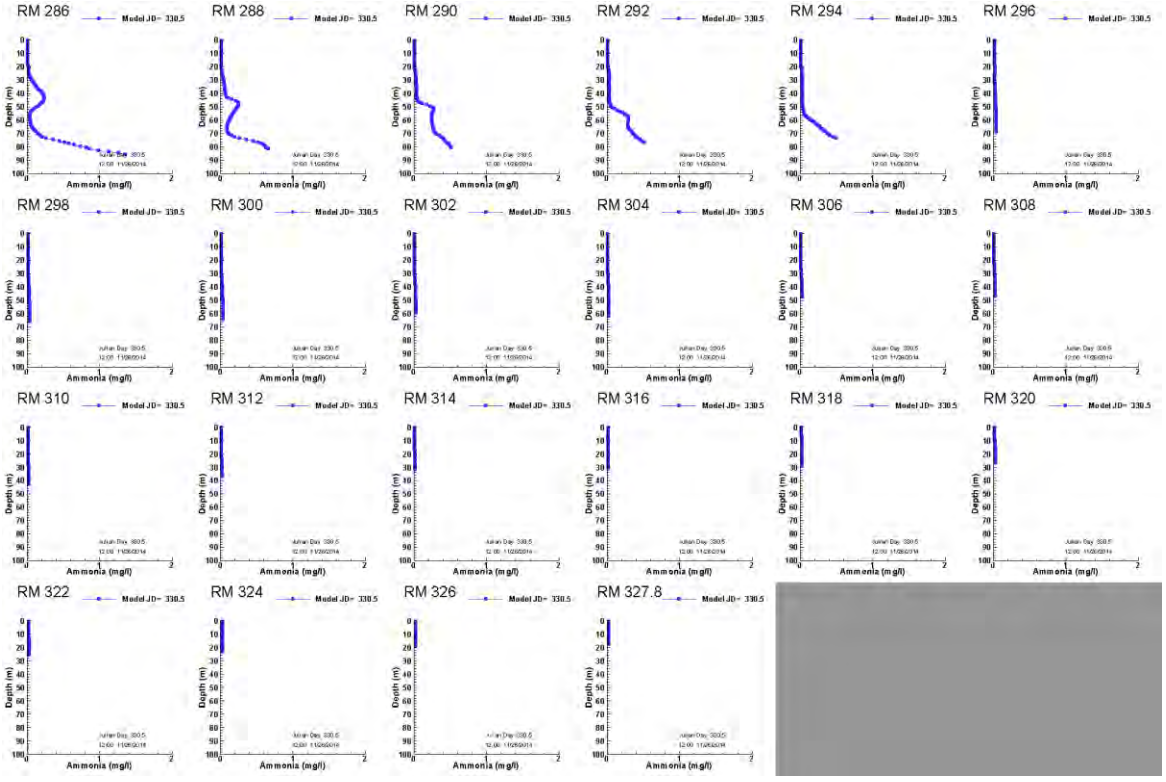


Figure 896. Vertical profiles of ammonia nitrogen compared with data for 11/26/2014.

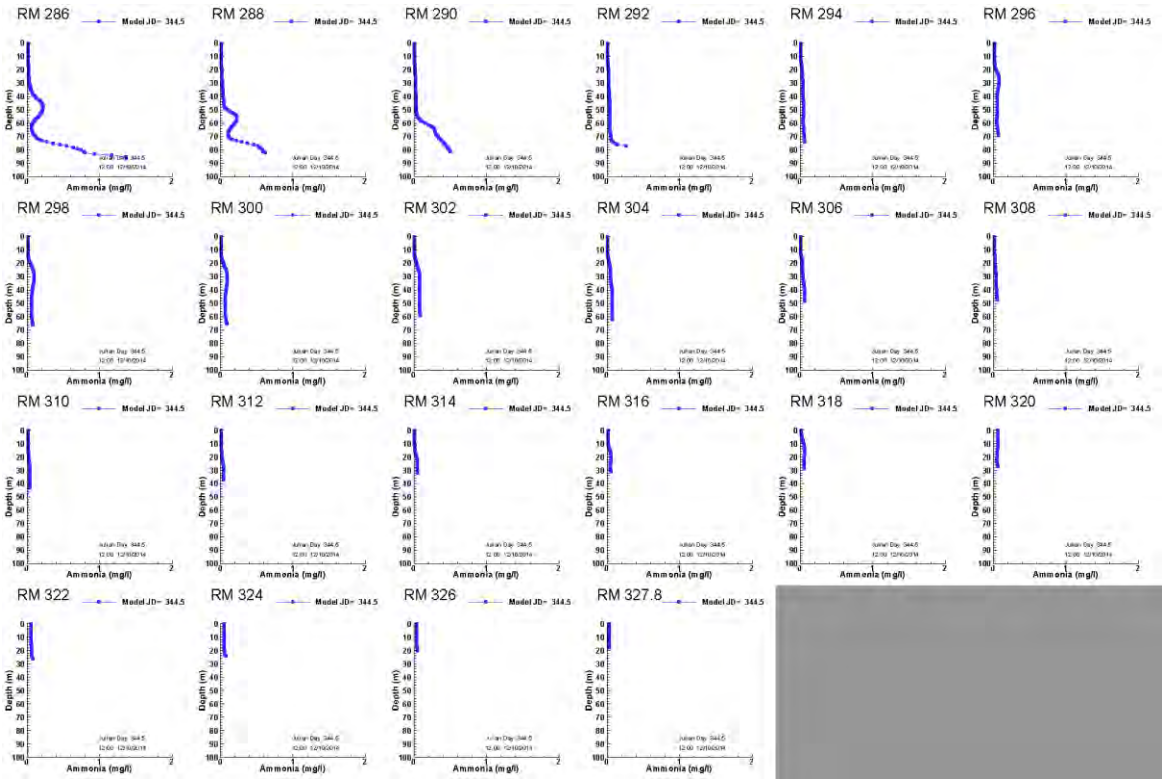


Figure 897. Vertical profiles of ammonia nitrogen compared with data for 12/10/2014.

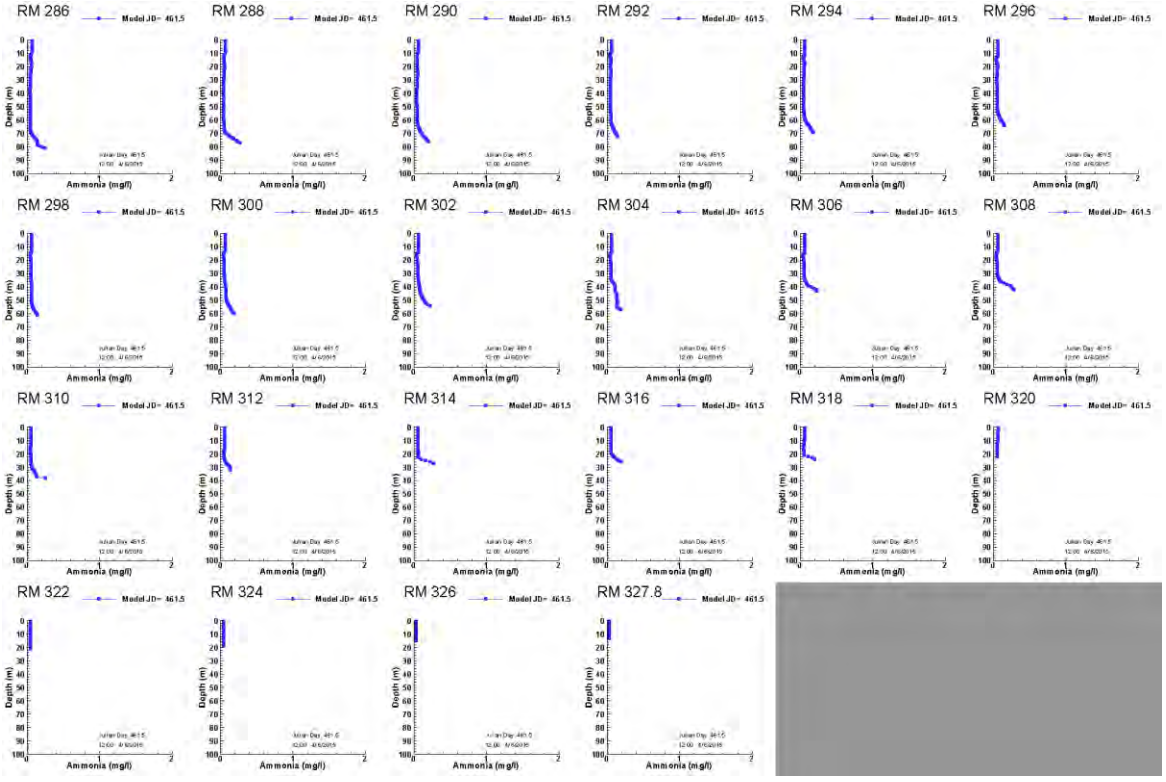


Figure 898. Vertical profiles of ammonia nitrogen compared with data for 4/ 6/2015.

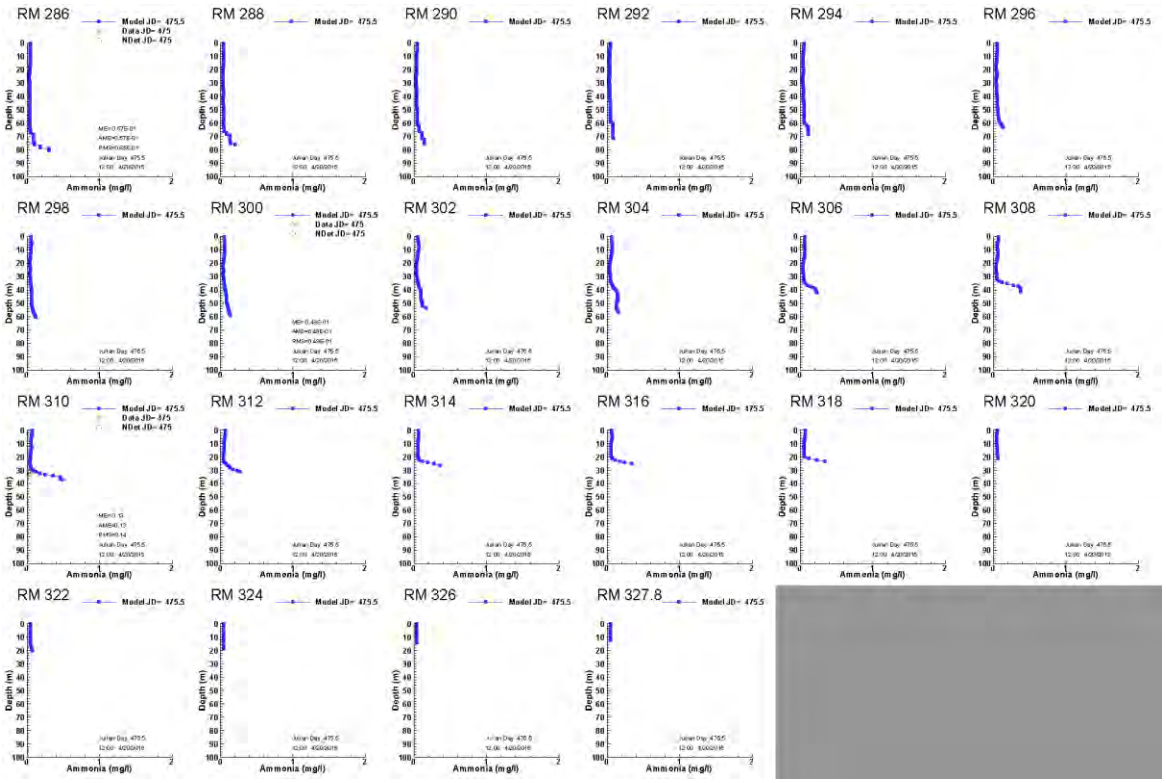


Figure 899. Vertical profiles of ammonia nitrogen compared with data for 4/20/2015.

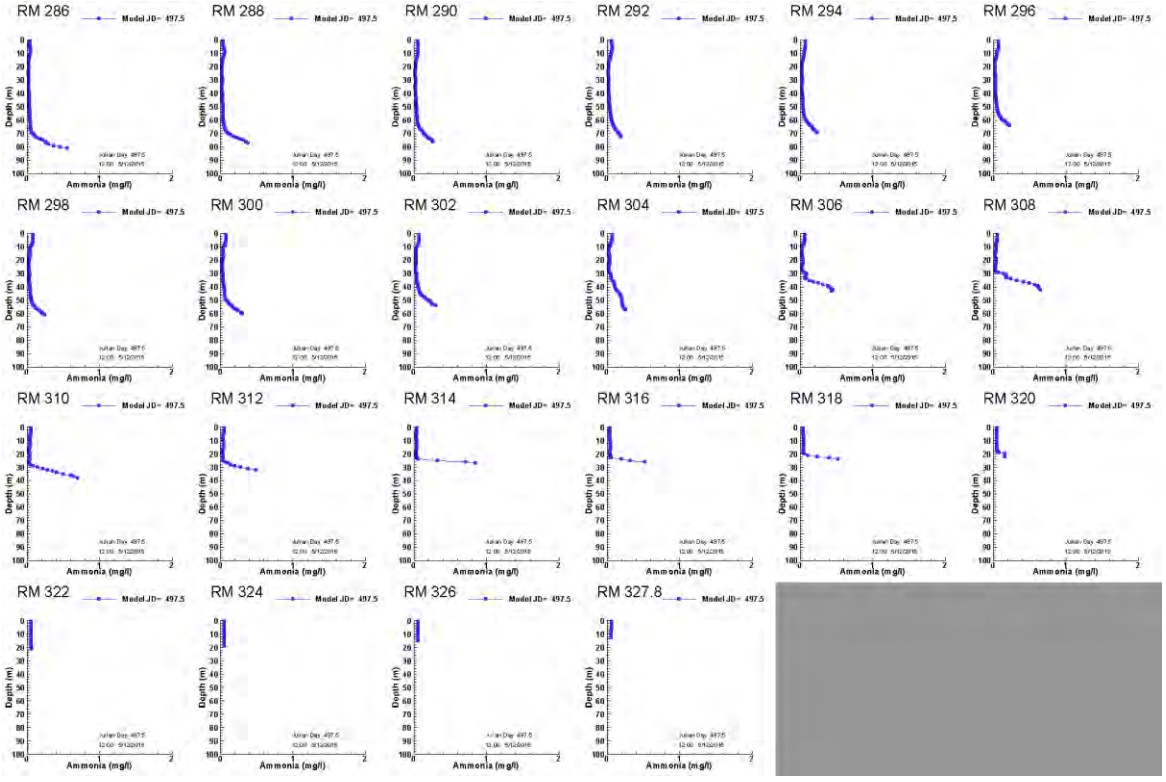


Figure 900. Vertical profiles of ammonia nitrogen compared with data for 5/12/2015.

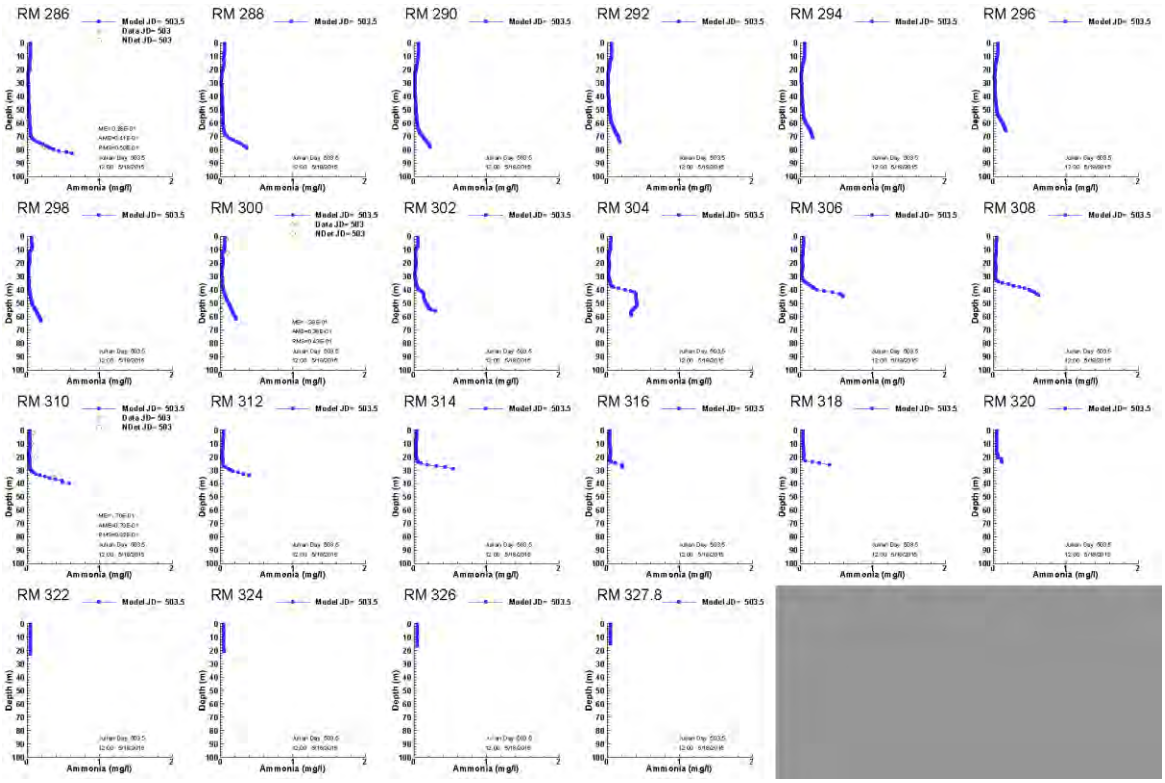


Figure 901. Vertical profiles of ammonia nitrogen compared with data for 5/18/2015.

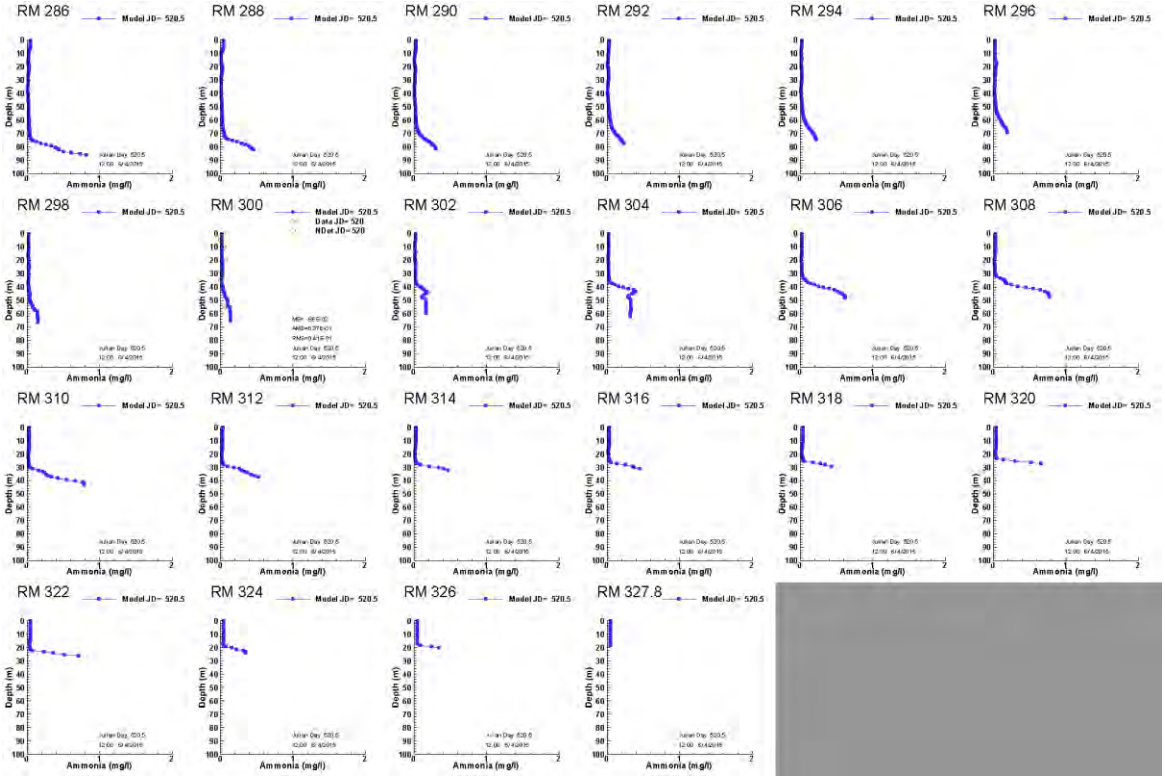


Figure 902. Vertical profiles of ammonia nitrogen compared with data for 6/ 4/2015.

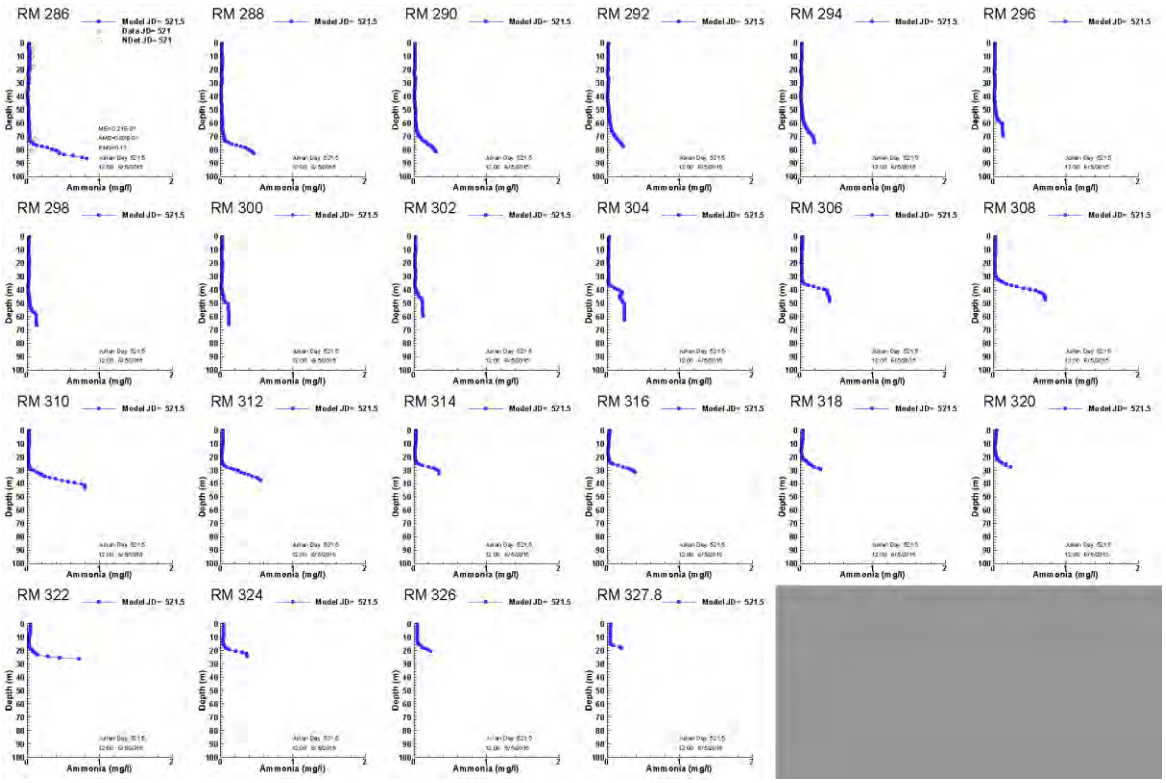


Figure 903. Vertical profiles of ammonia nitrogen compared with data for 6/ 5/2015.

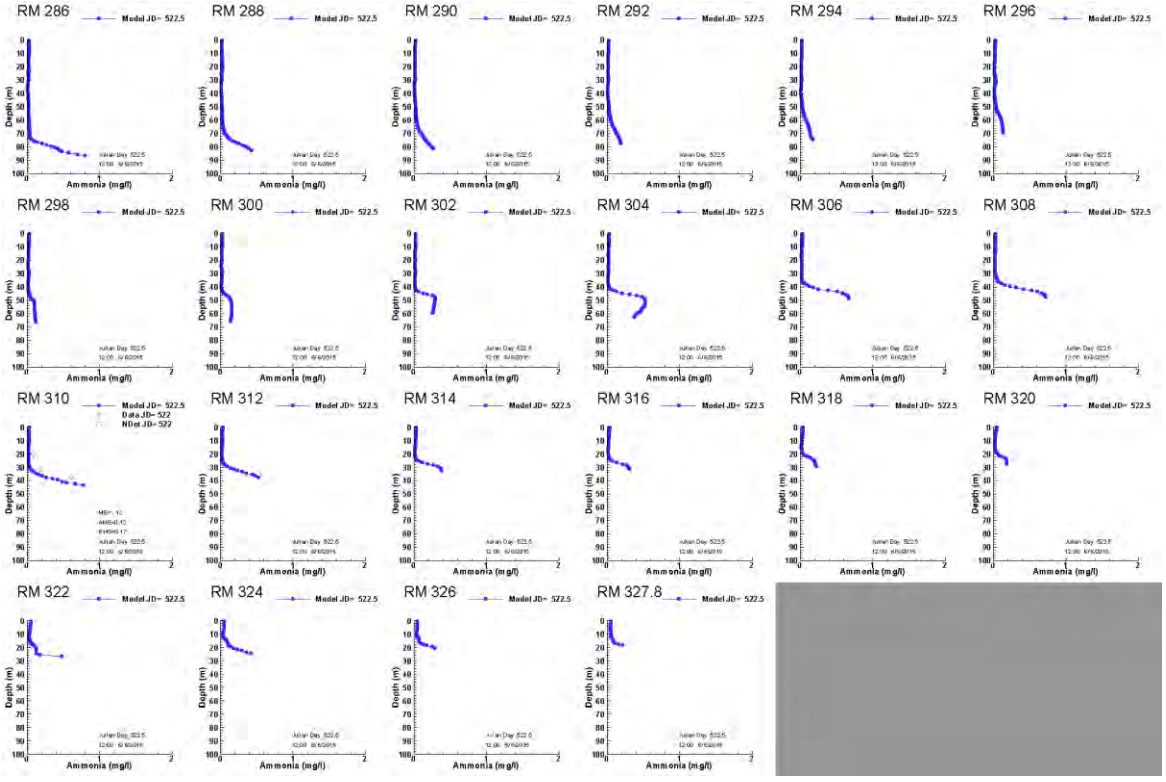


Figure 904. Vertical profiles of ammonia nitrogen compared with data for 6/ 6/2015.

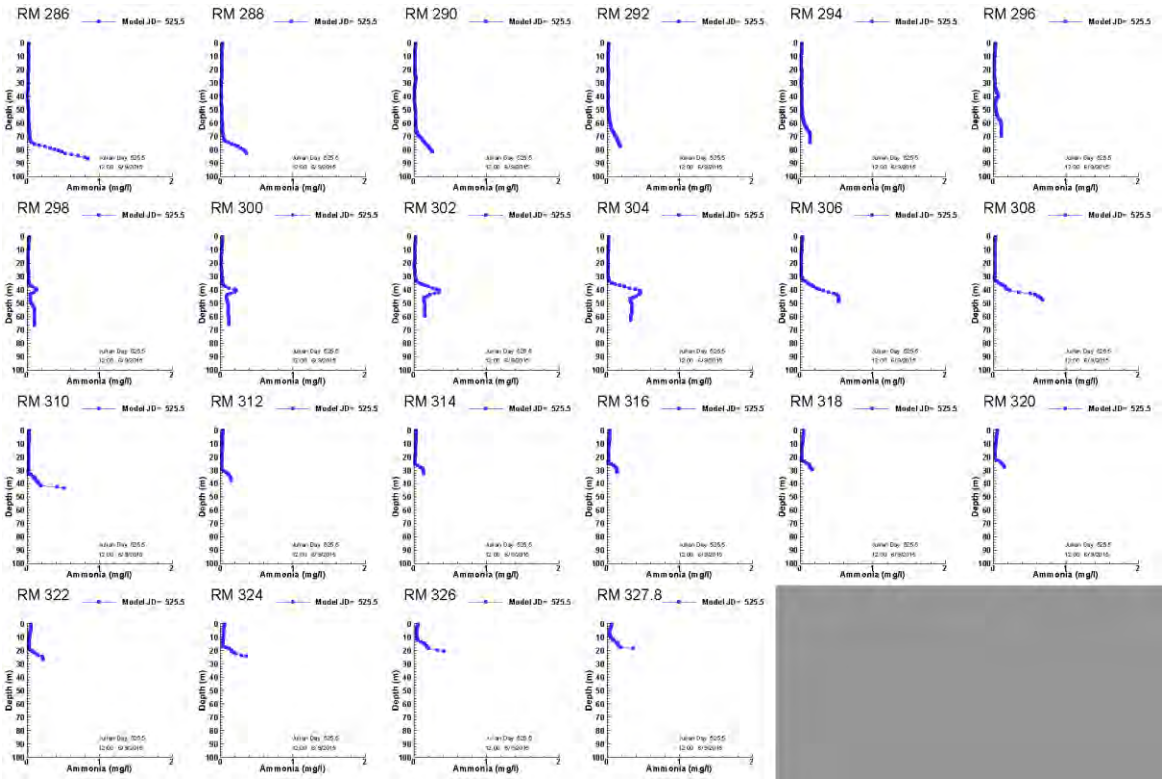


Figure 905. Vertical profiles of ammonia nitrogen compared with data for 6/ 9/2015.

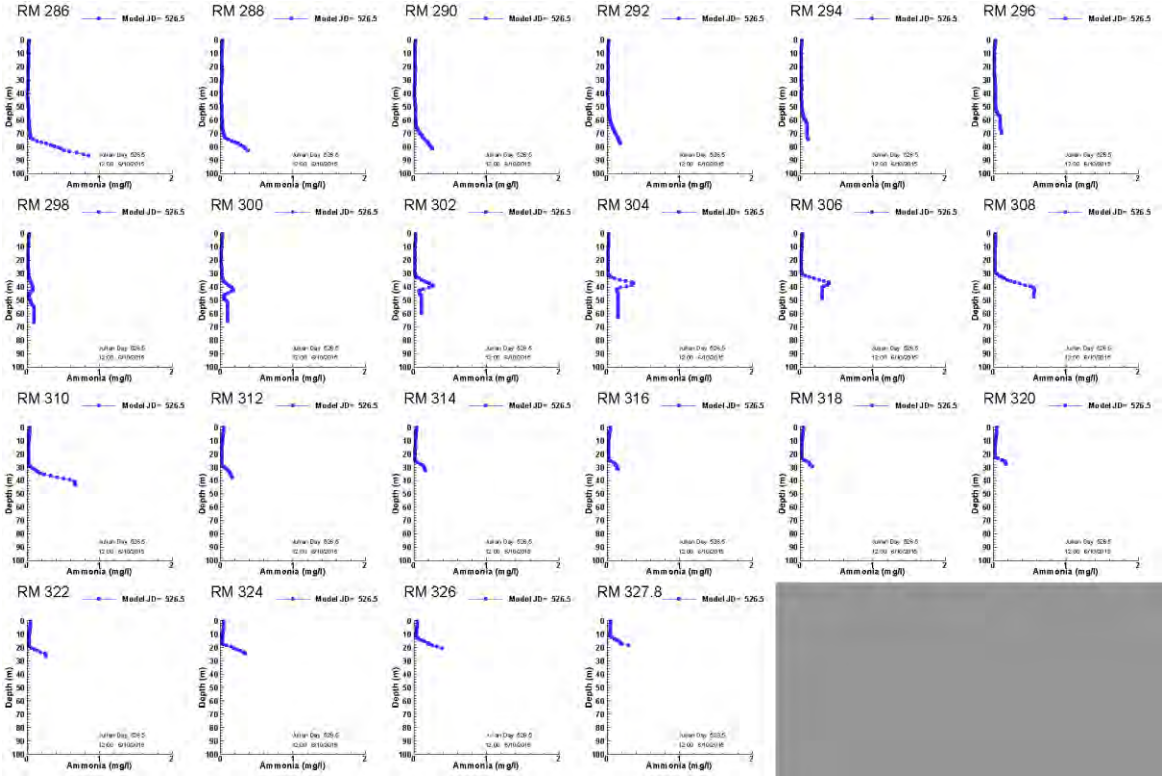


Figure 906. Vertical profiles of ammonia nitrogen compared with data for 6/10/2015.

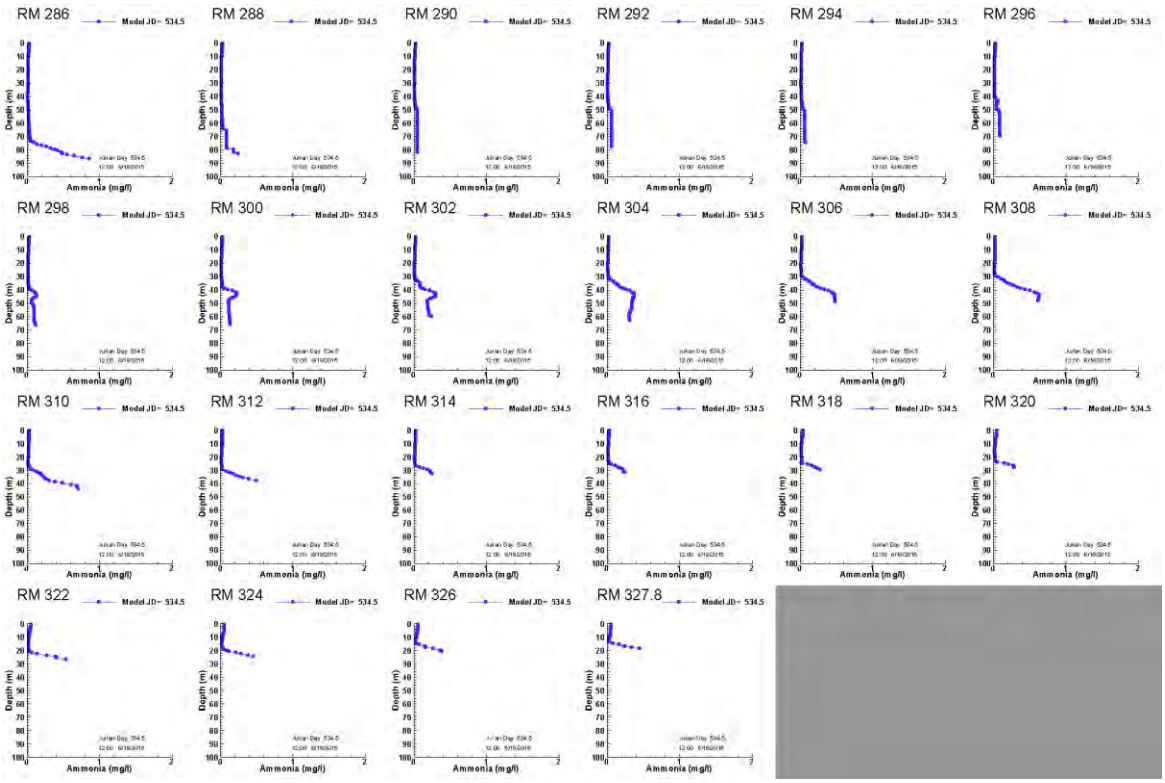


Figure 907. Vertical profiles of ammonia nitrogen compared with data for 6/18/2015.

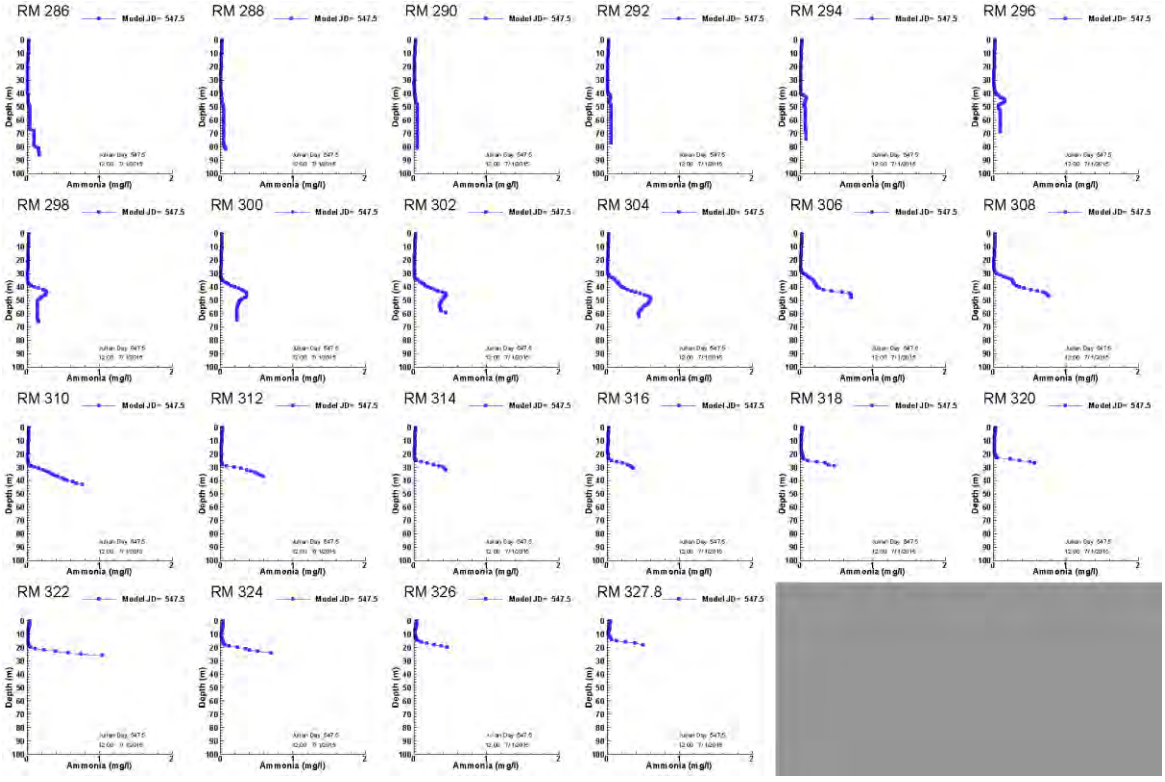


Figure 908. Vertical profiles of ammonia nitrogen compared with data for 7/ 1/2015.

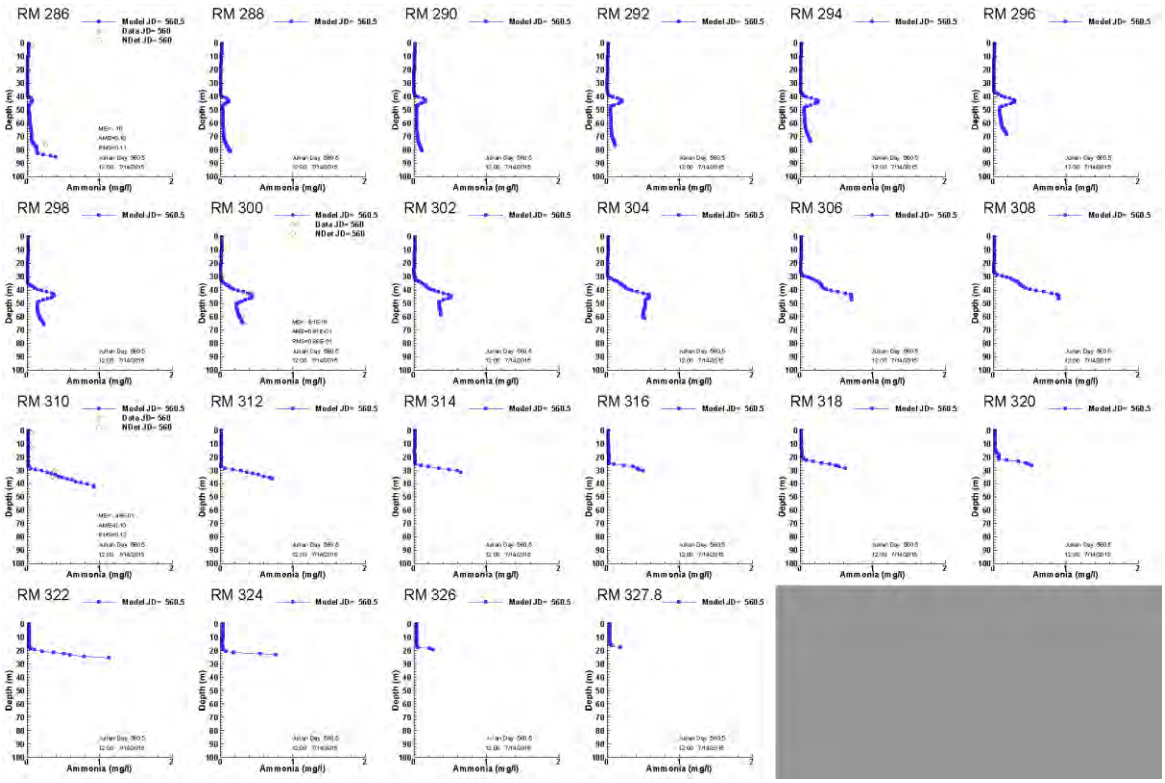


Figure 909. Vertical profiles of ammonia nitrogen compared with data for 7/14/2015.

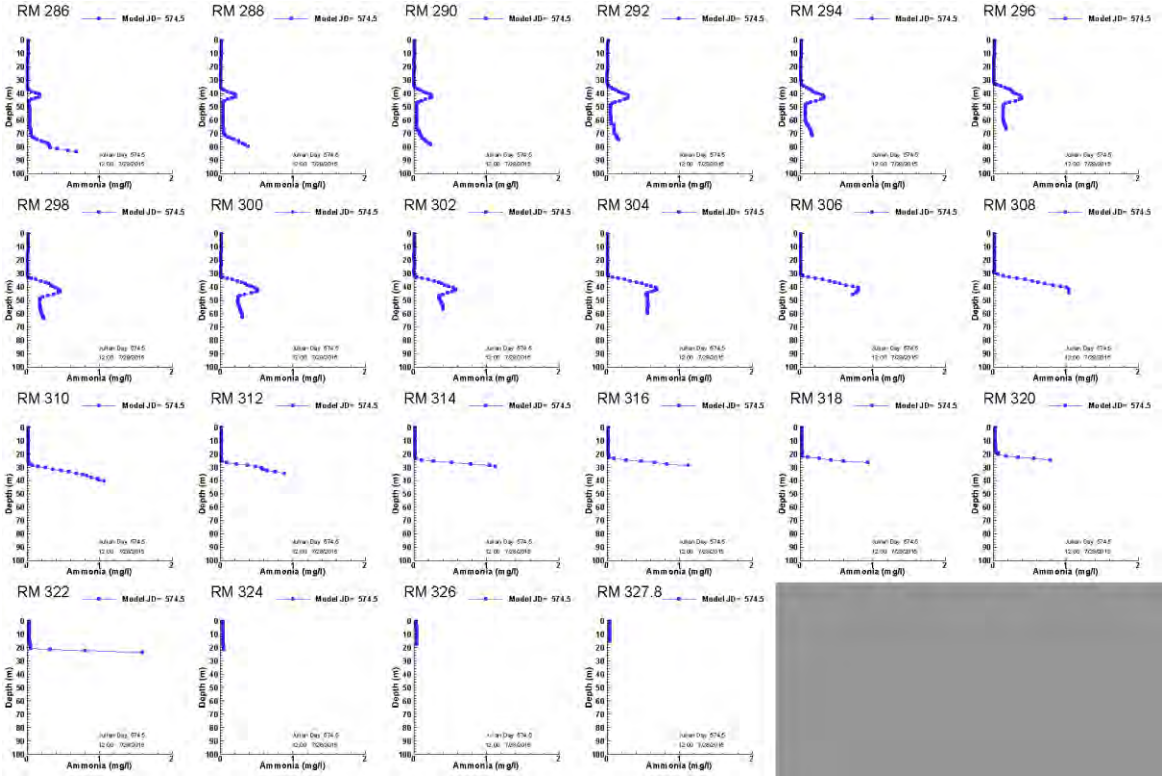


Figure 910. Vertical profiles of ammonia nitrogen compared with data for 7/28/2015.

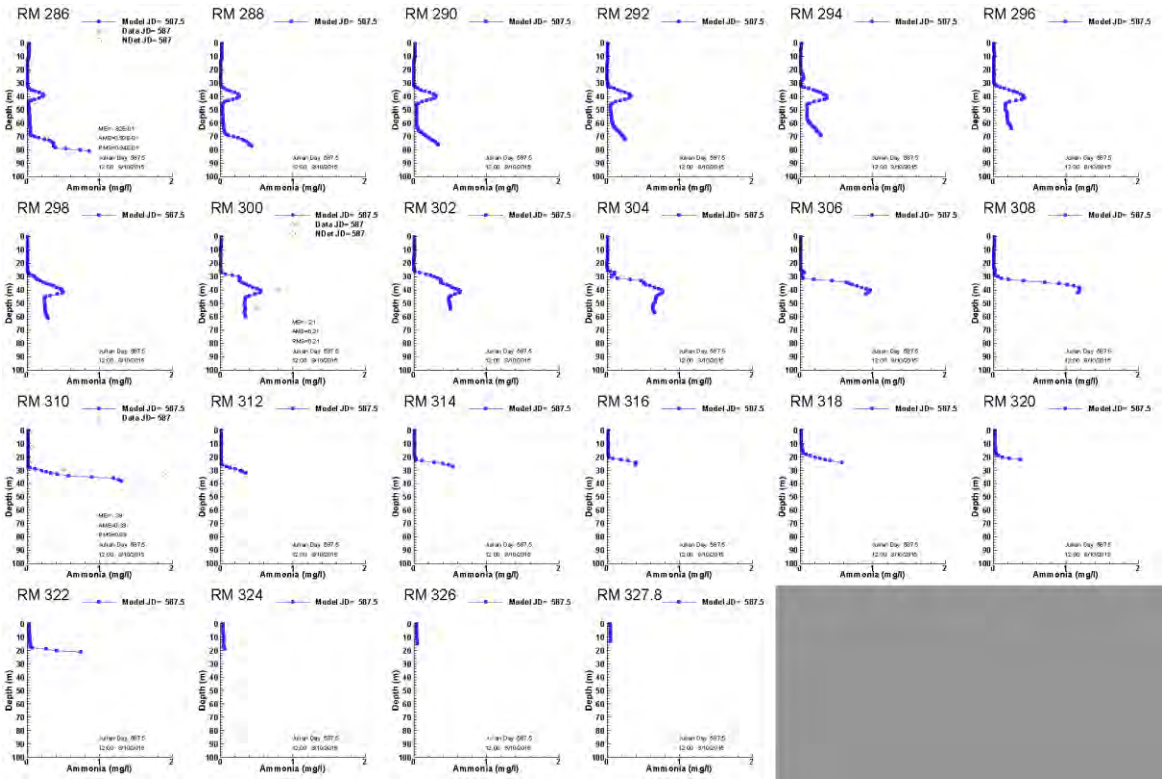


Figure 911. Vertical profiles of ammonia nitrogen compared with data for 8/10/2015.

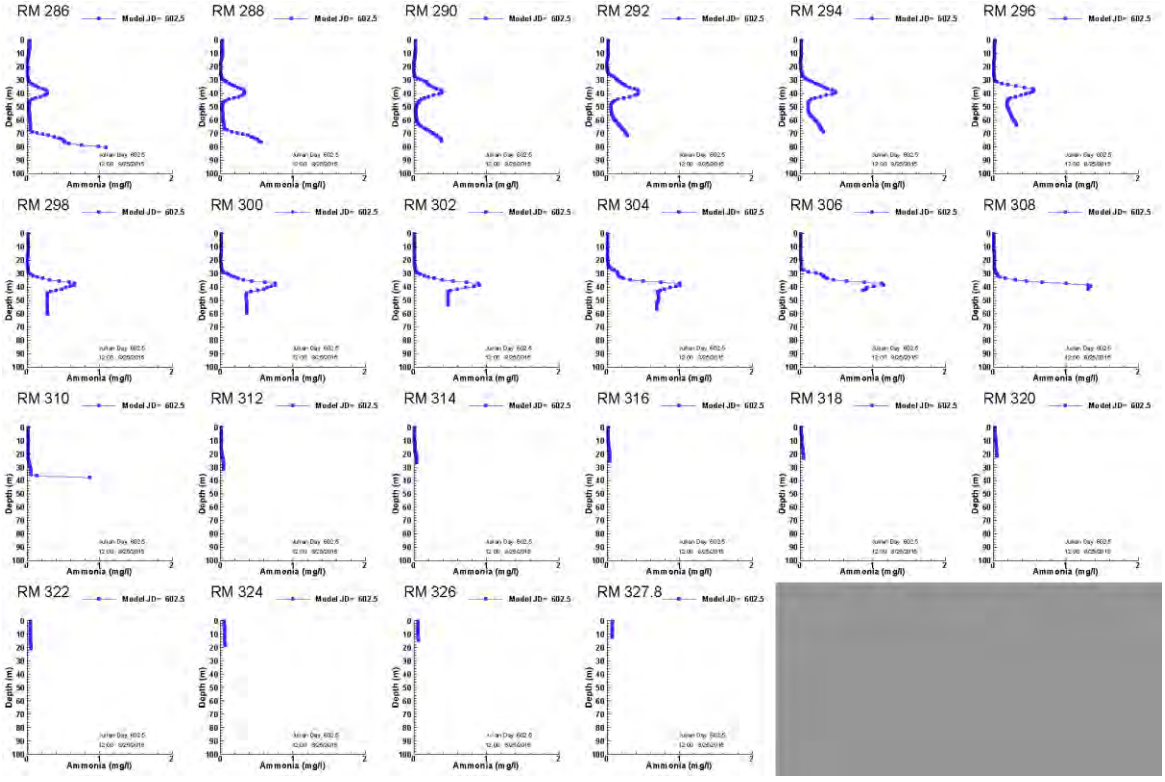


Figure 912. Vertical profiles of ammonia nitrogen compared with data for 8/25/2015.

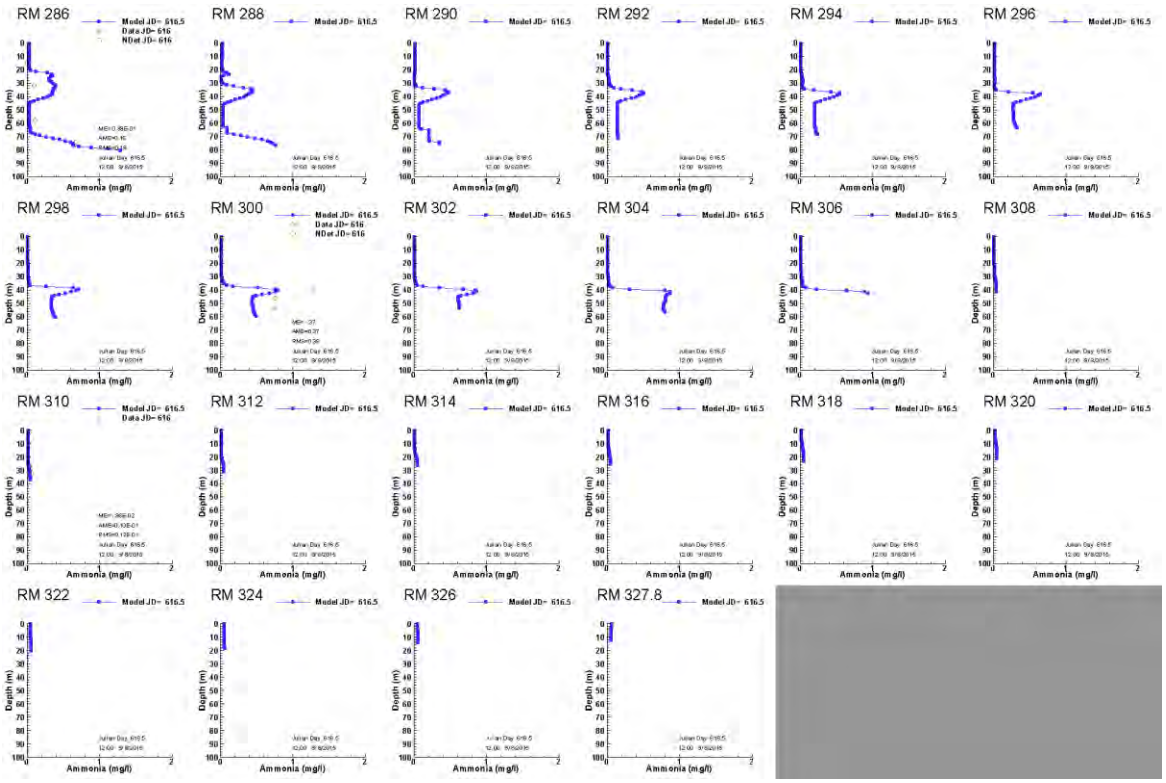


Figure 913. Vertical profiles of ammonia nitrogen compared with data for 9/ 8/2015.

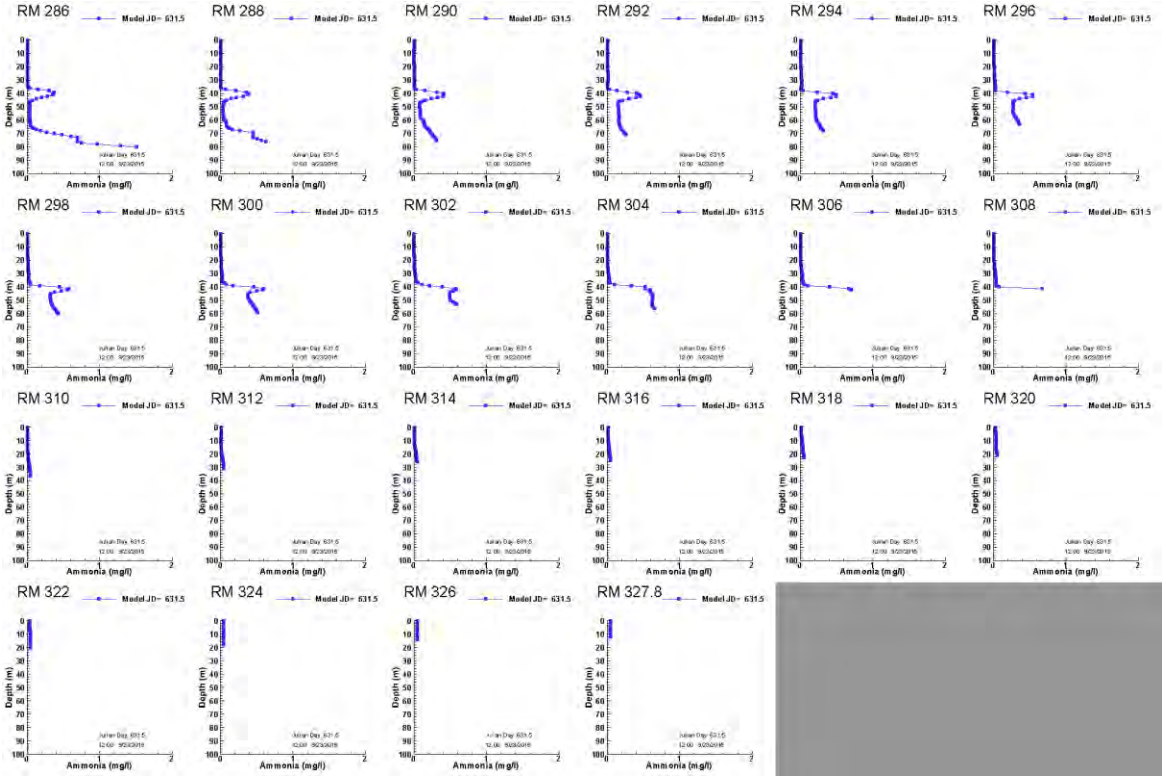


Figure 914. Vertical profiles of ammonia nitrogen compared with data for 9/23/2015.

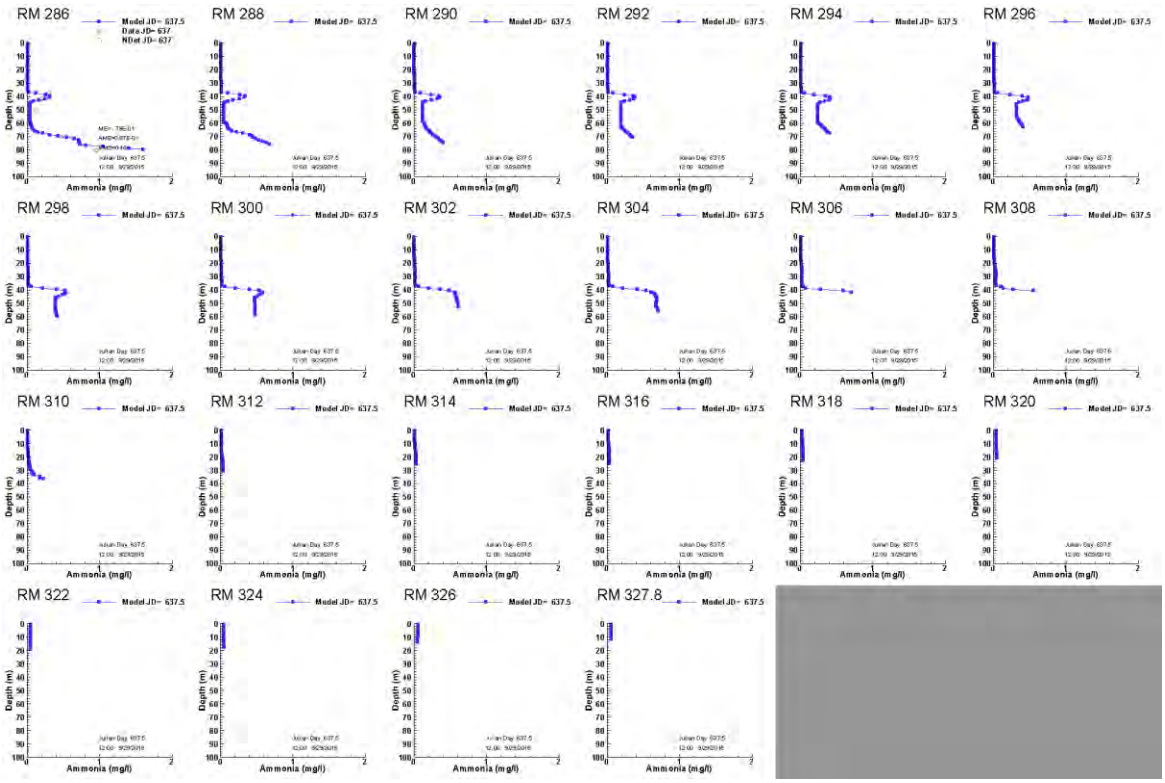


Figure 915. Vertical profiles of ammonia nitrogen compared with data for 9/29/2015.

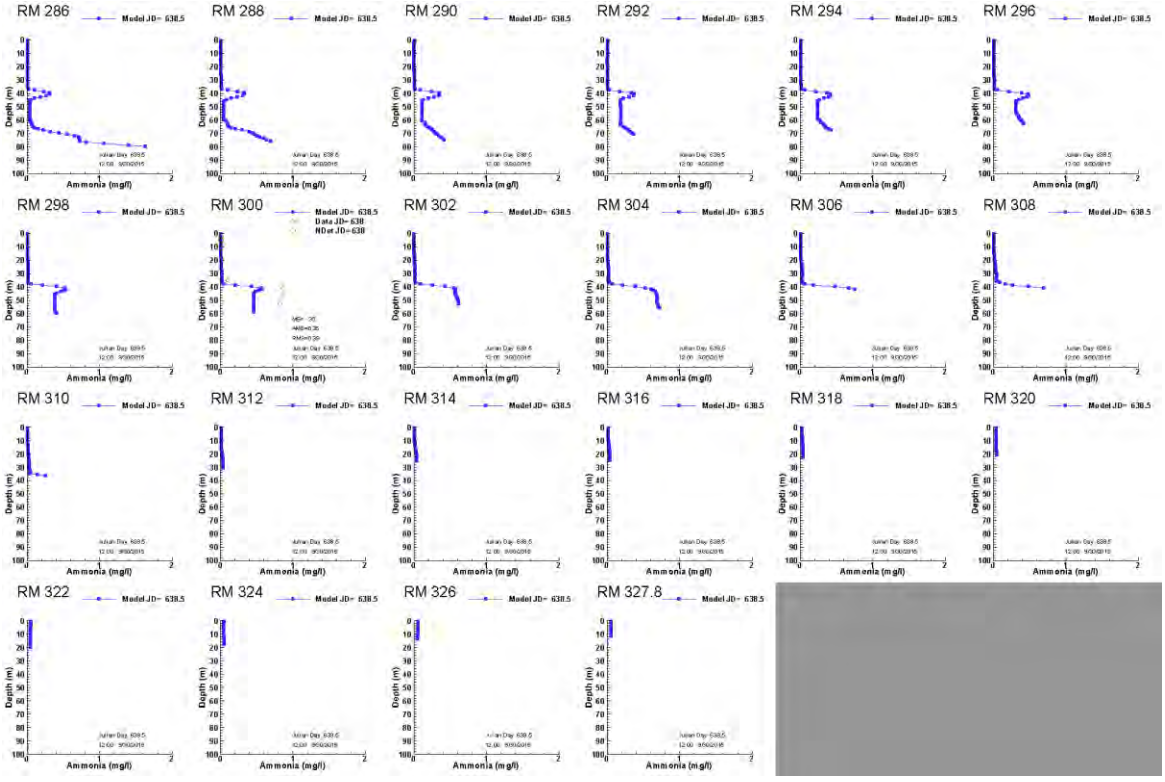


Figure 916. Vertical profiles of ammonia nitrogen compared with data for 9/30/2015.

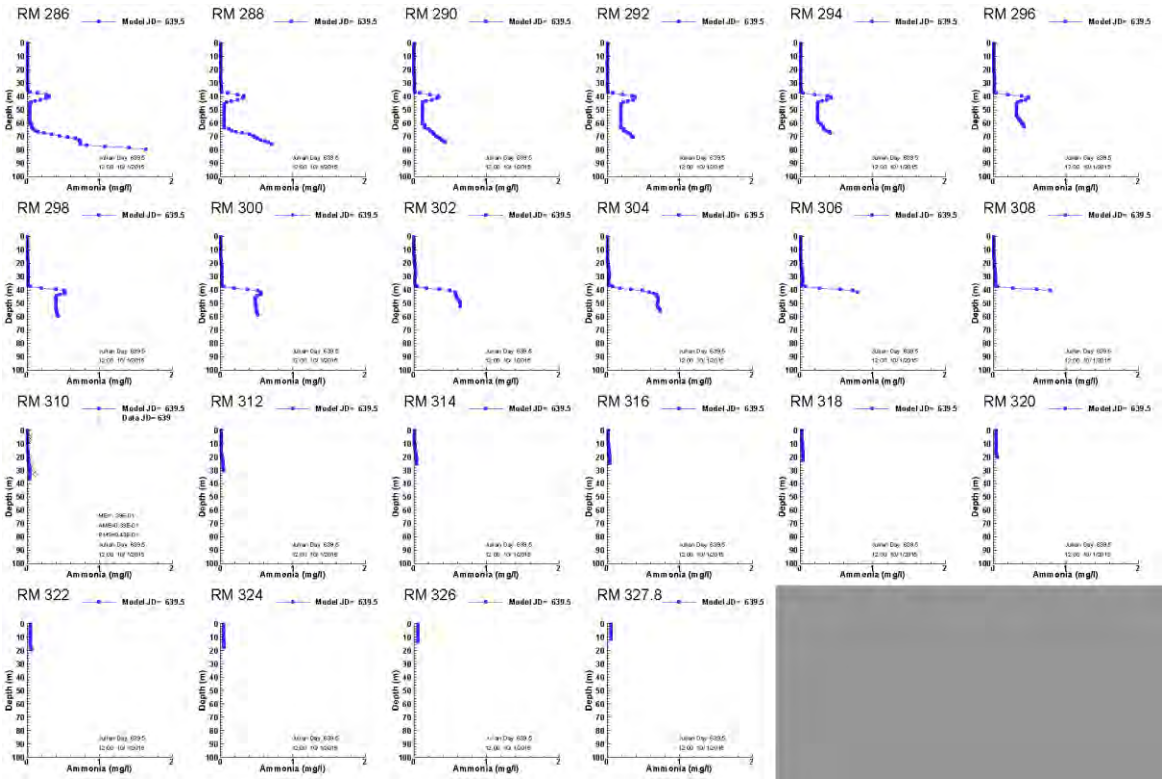


Figure 917. Vertical profiles of ammonia nitrogen compared with data for 10/ 1/2015.

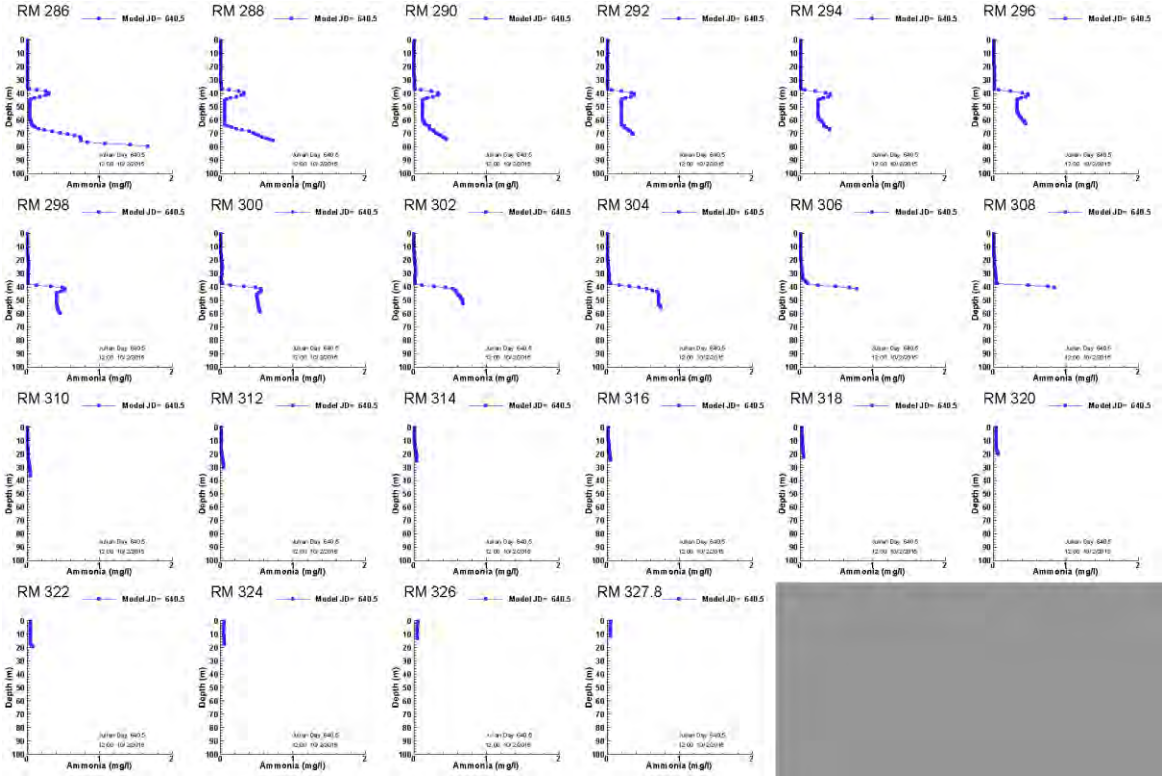


Figure 918. Vertical profiles of ammonia nitrogen compared with data for 10/ 2/2015.

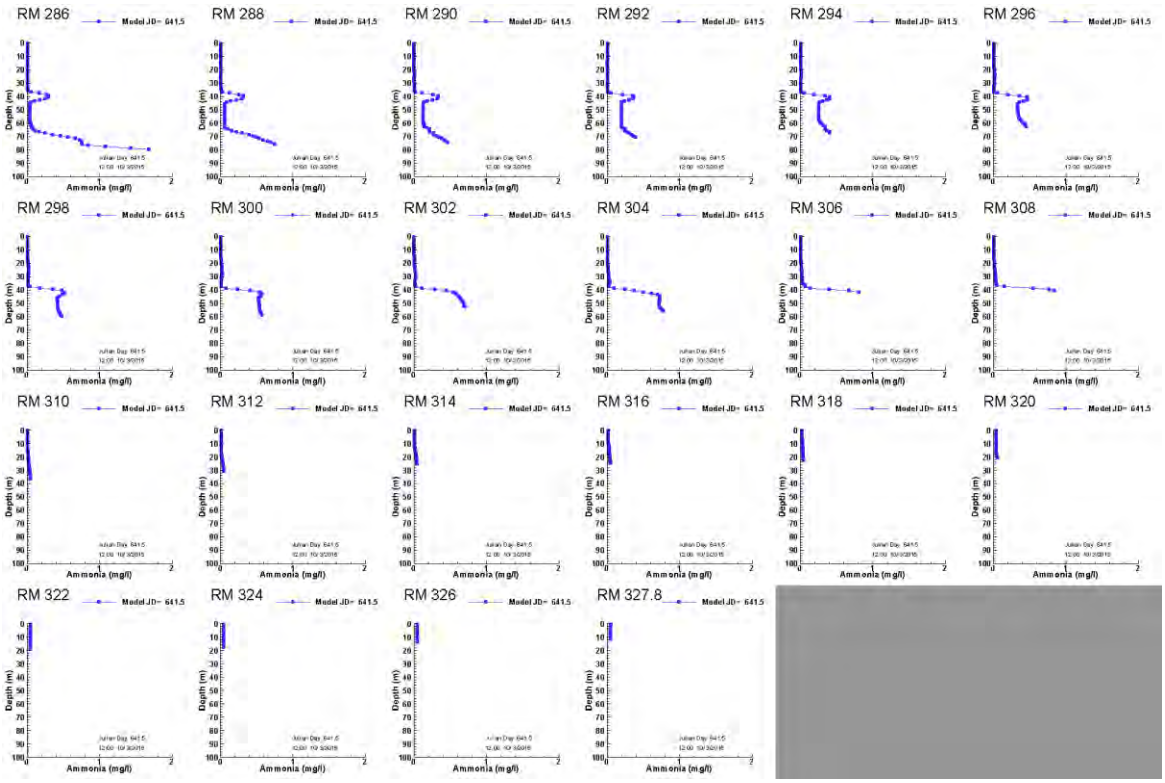


Figure 919. Vertical profiles of ammonia nitrogen compared with data for 10/ 3/2015.

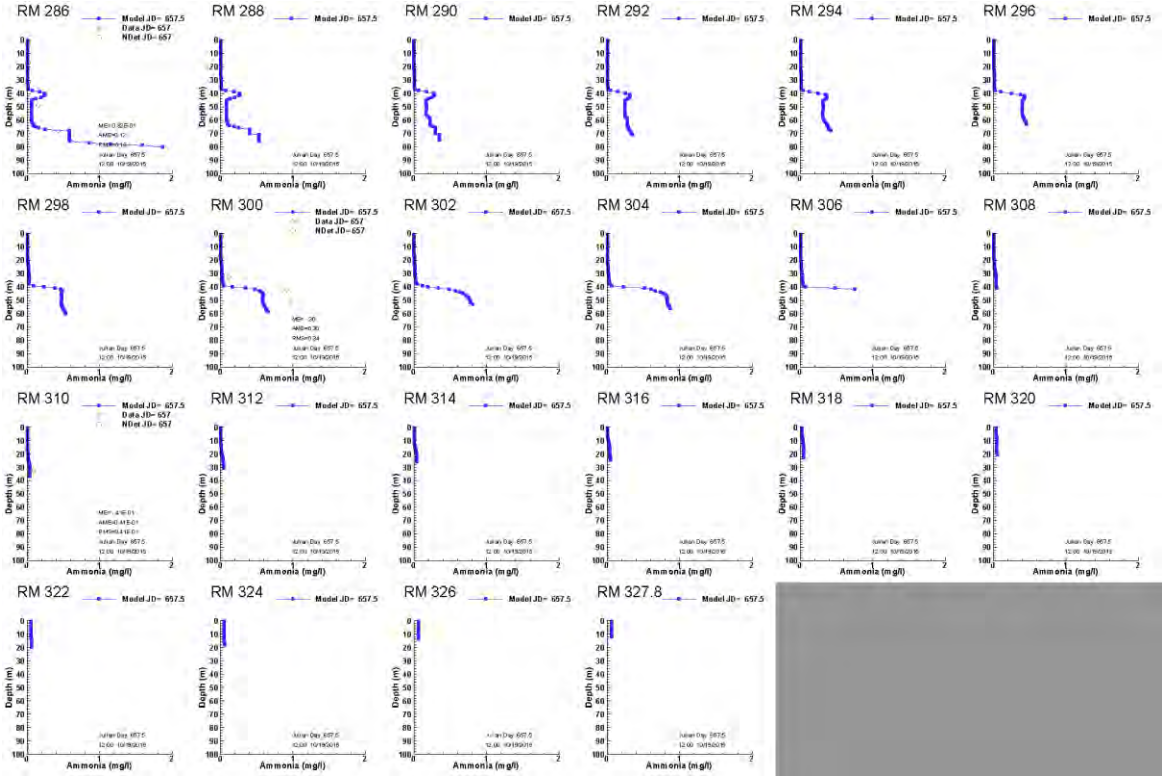


Figure 920. Vertical profiles of ammonia nitrogen compared with data for 10/19/2015.

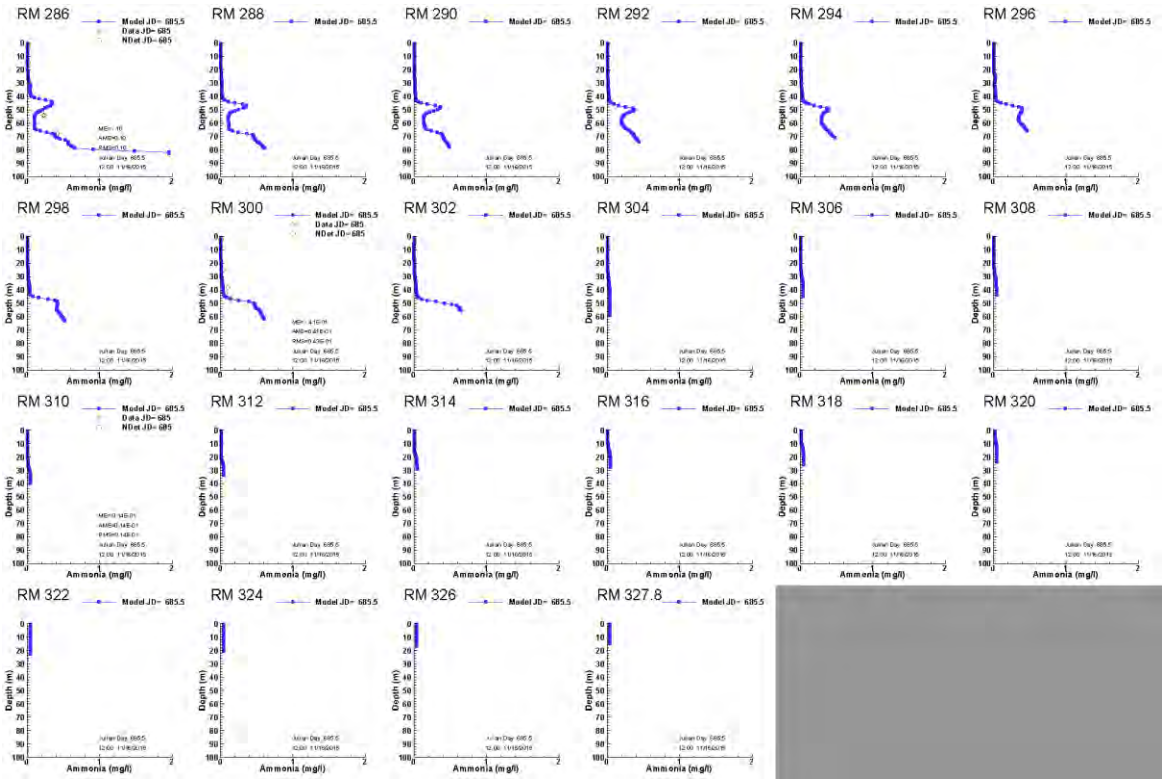


Figure 921. Vertical profiles of ammonia nitrogen compared with data for 11/16/2015.

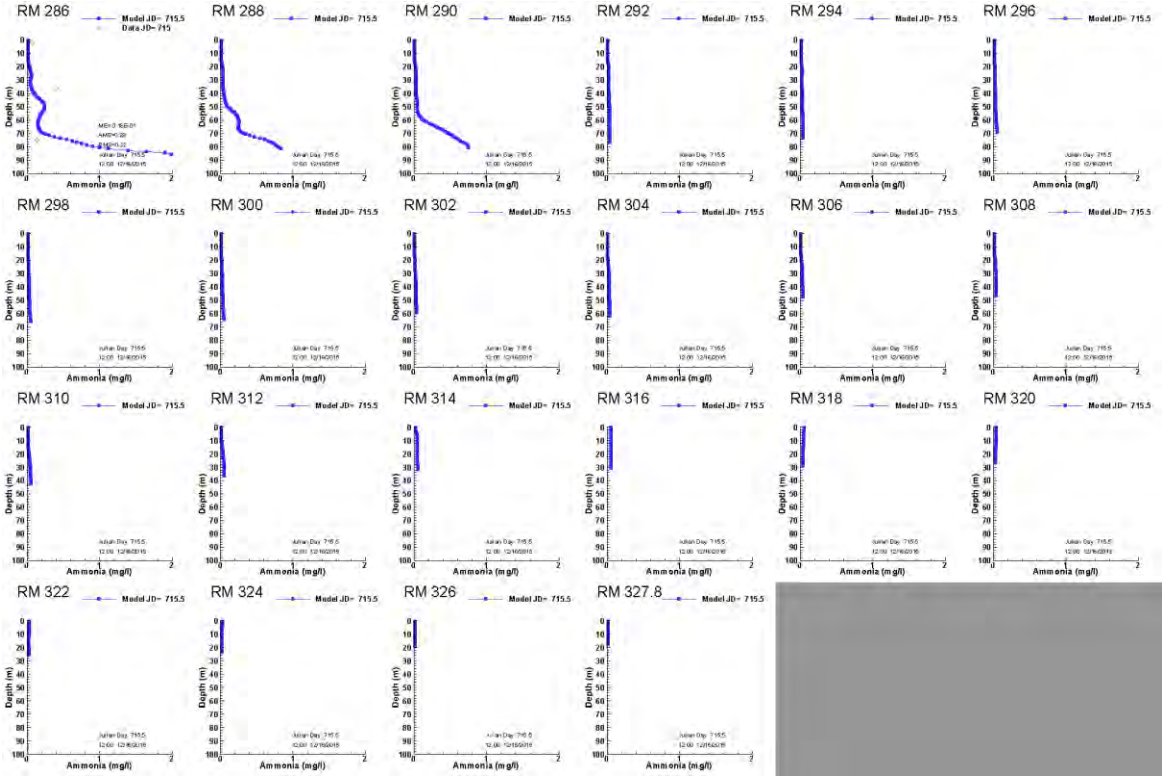


Figure 922. Vertical profiles of ammonia nitrogen compared with data for 12/16/2015.

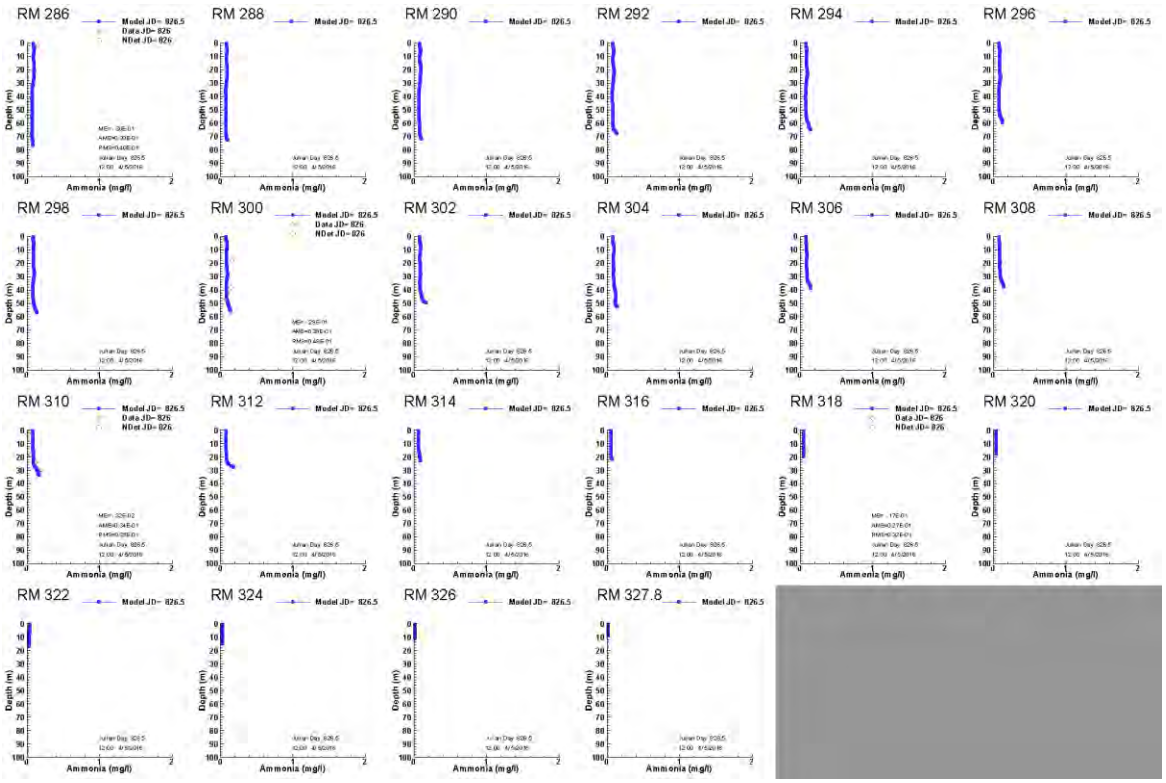


Figure 923. Vertical profiles of ammonia nitrogen compared with data for 4/ 5/2016.

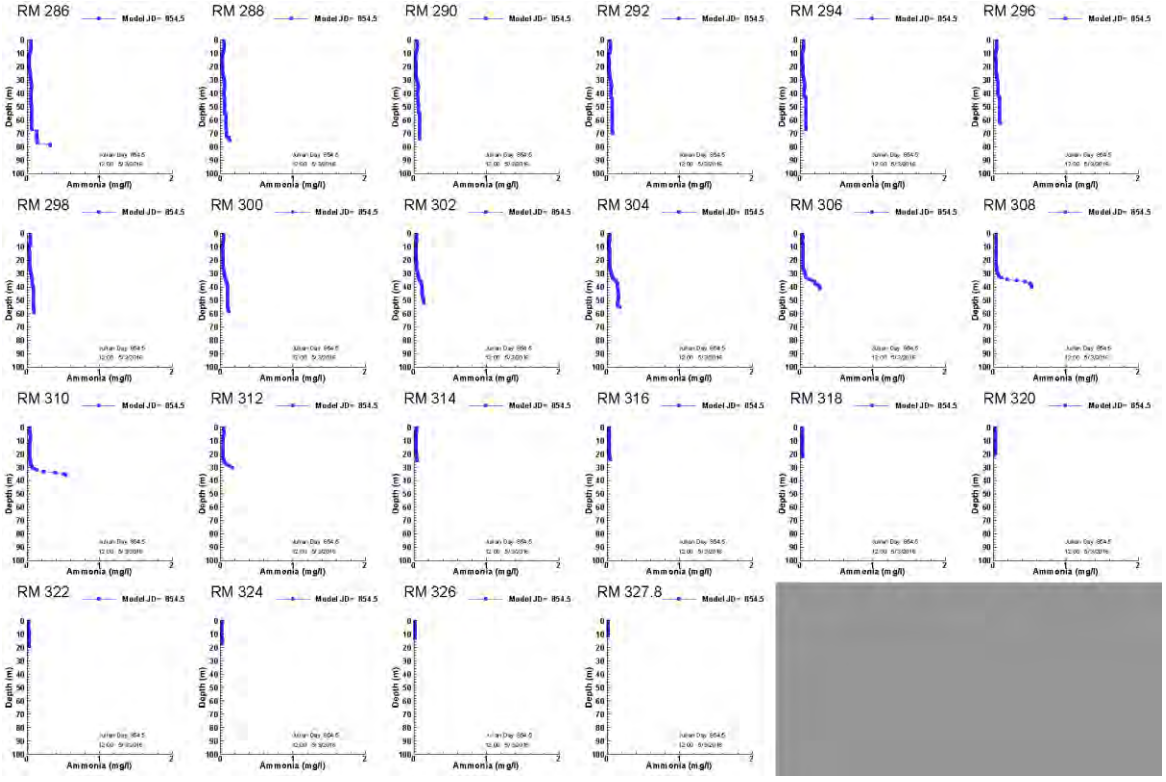


Figure 924. Vertical profiles of ammonia nitrogen compared with data for 5/ 3/2016.

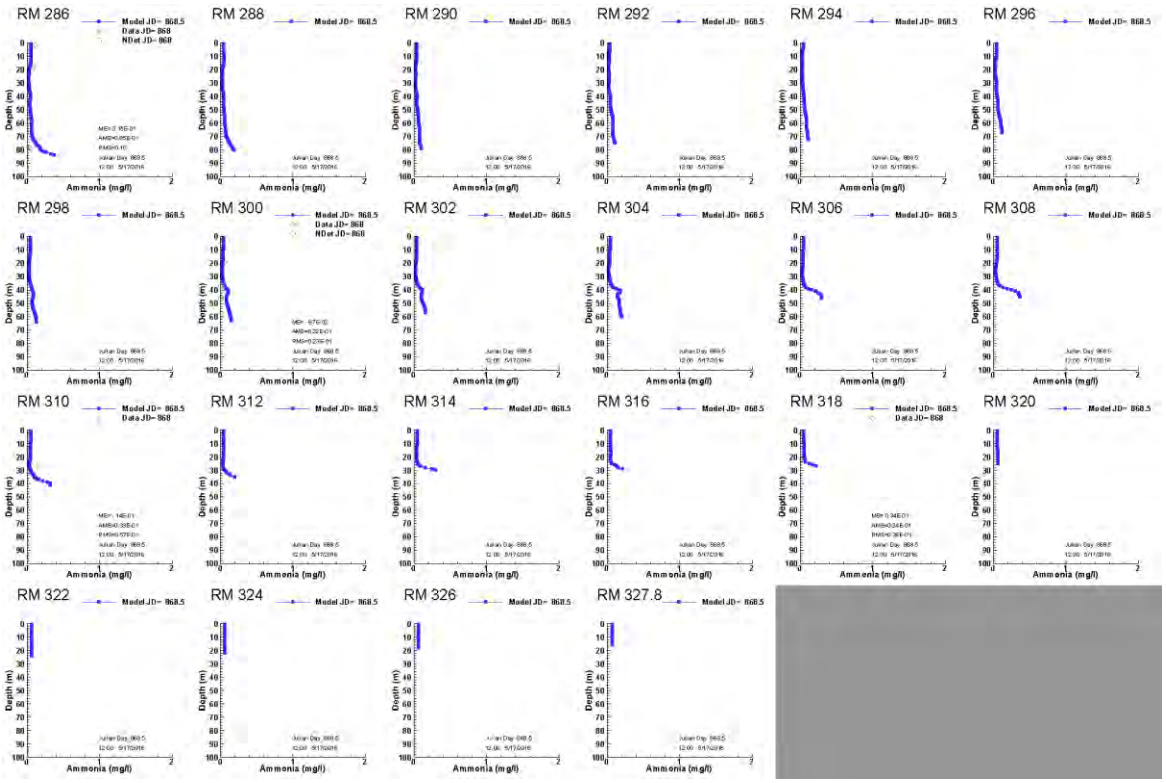


Figure 925. Vertical profiles of ammonia nitrogen compared with data for 5/17/2016.

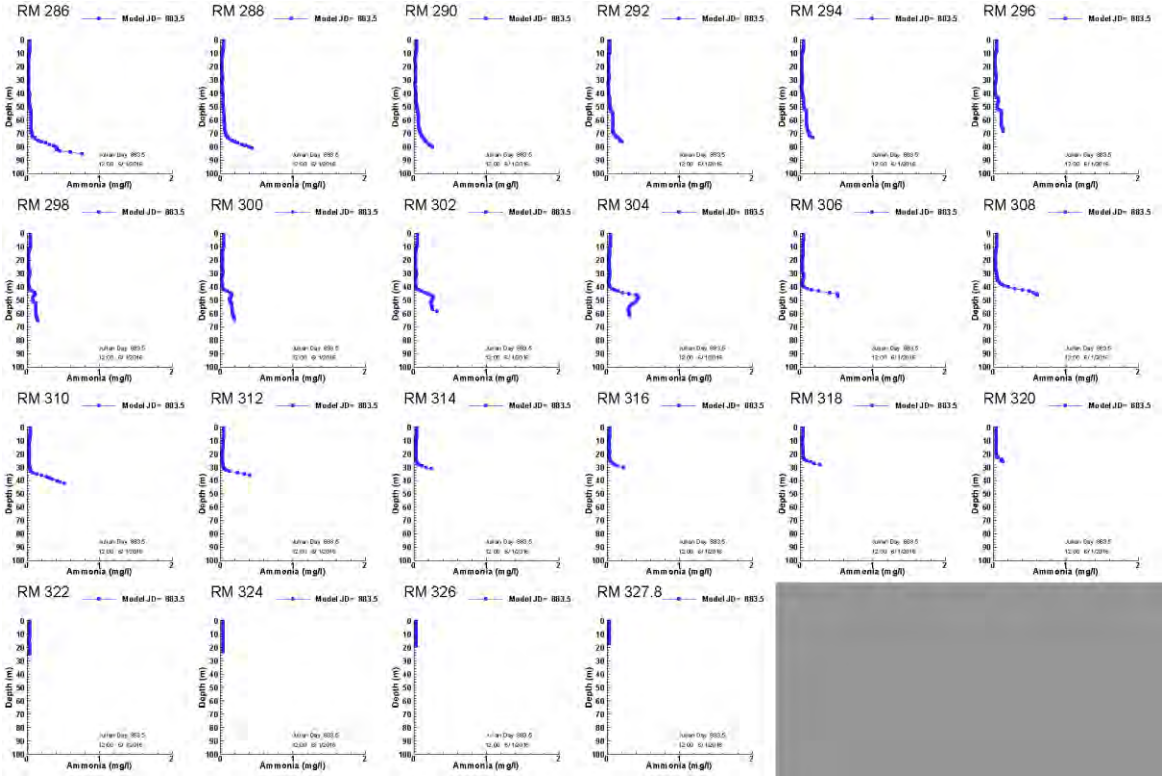


Figure 926. Vertical profiles of ammonia nitrogen compared with data for 6/ 1/2016.

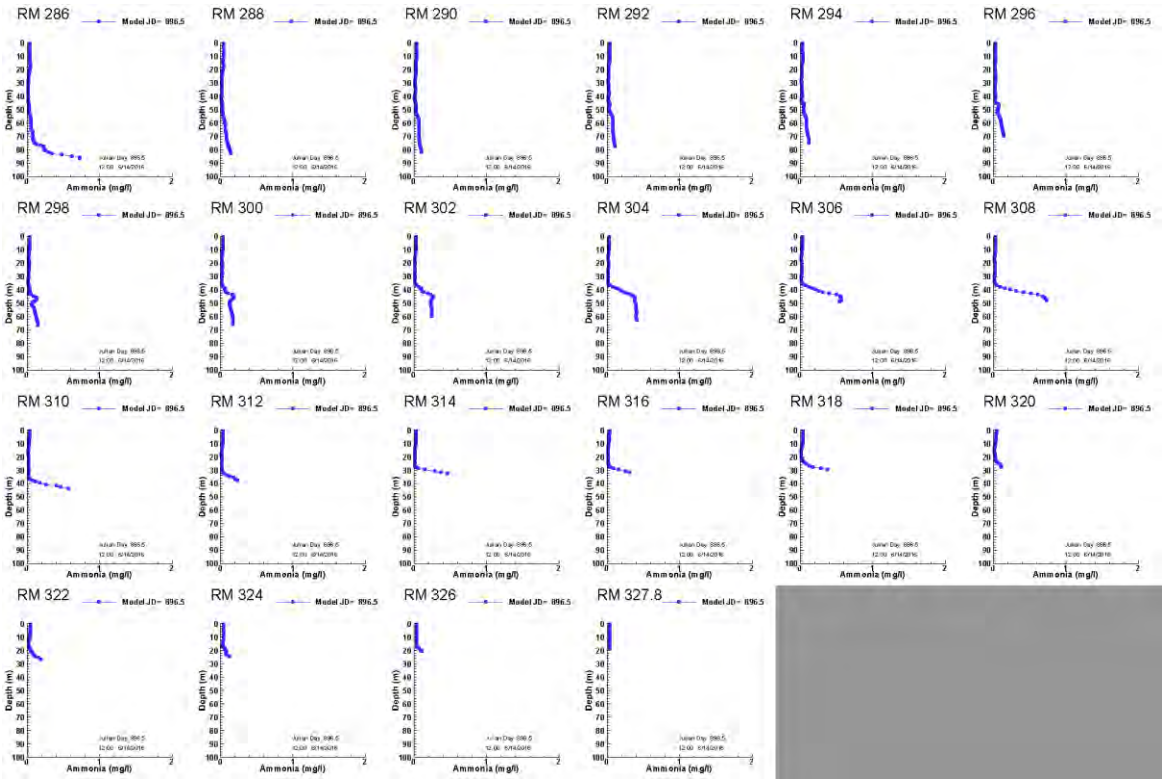


Figure 927. Vertical profiles of ammonia nitrogen compared with data for 6/14/2016.

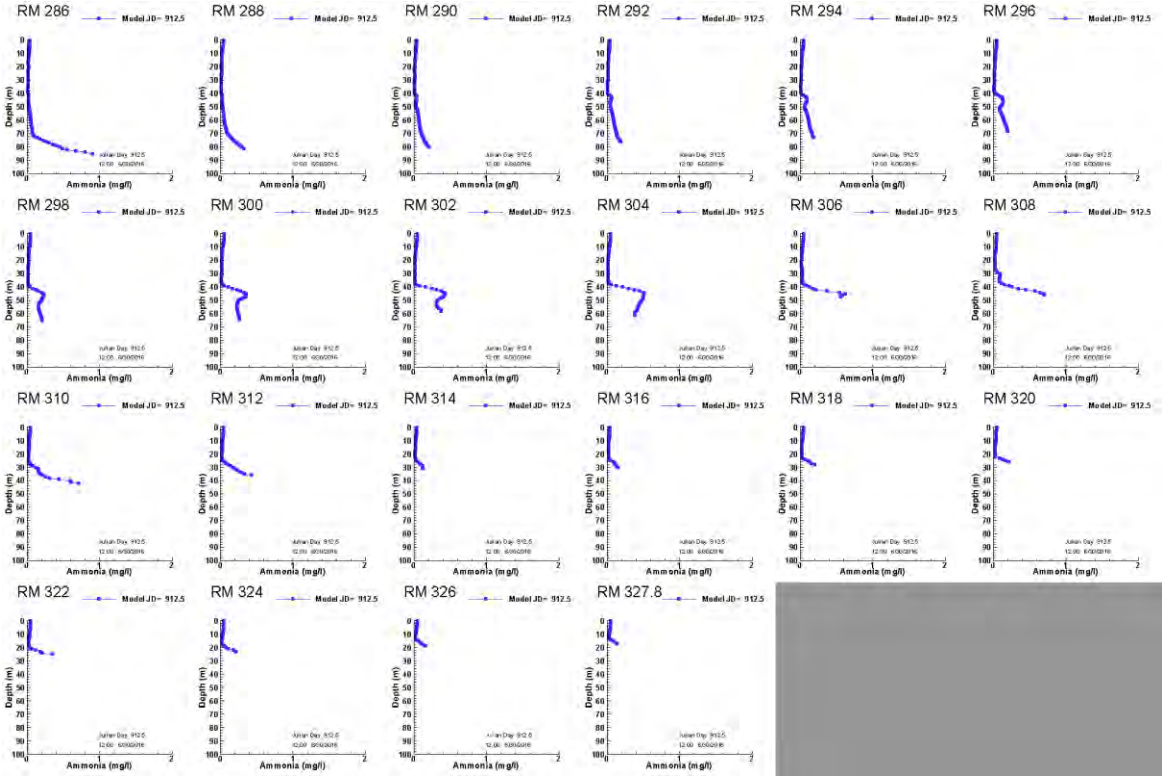


Figure 928. Vertical profiles of ammonia nitrogen compared with data for 6/30/2016.

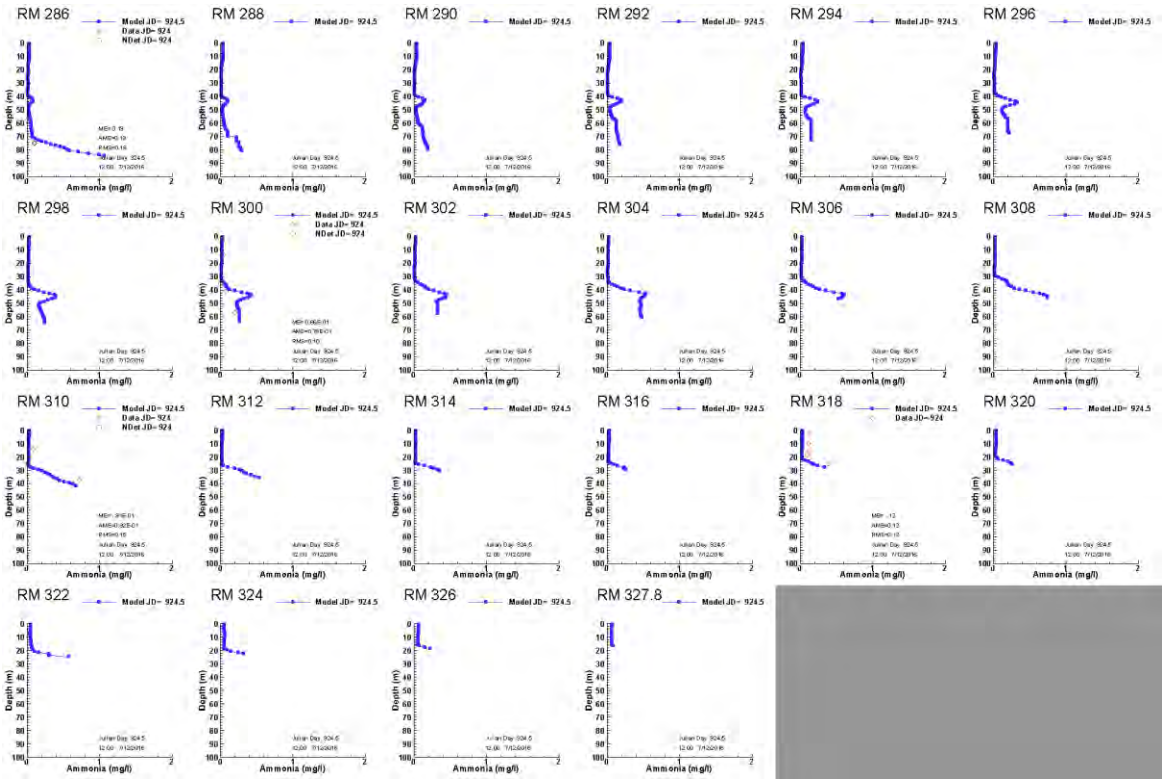


Figure 929. Vertical profiles of ammonia nitrogen compared with data for 7/12/2016.

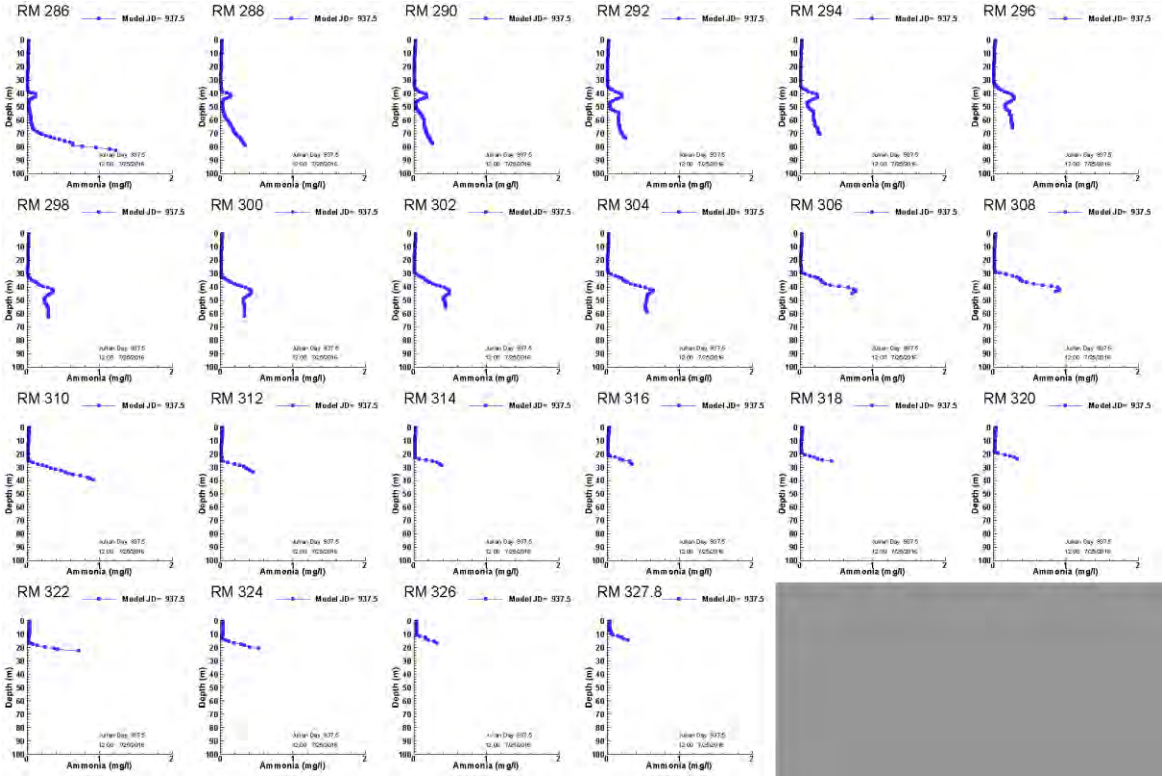


Figure 930. Vertical profiles of ammonia nitrogen compared with data for 7/25/2016.

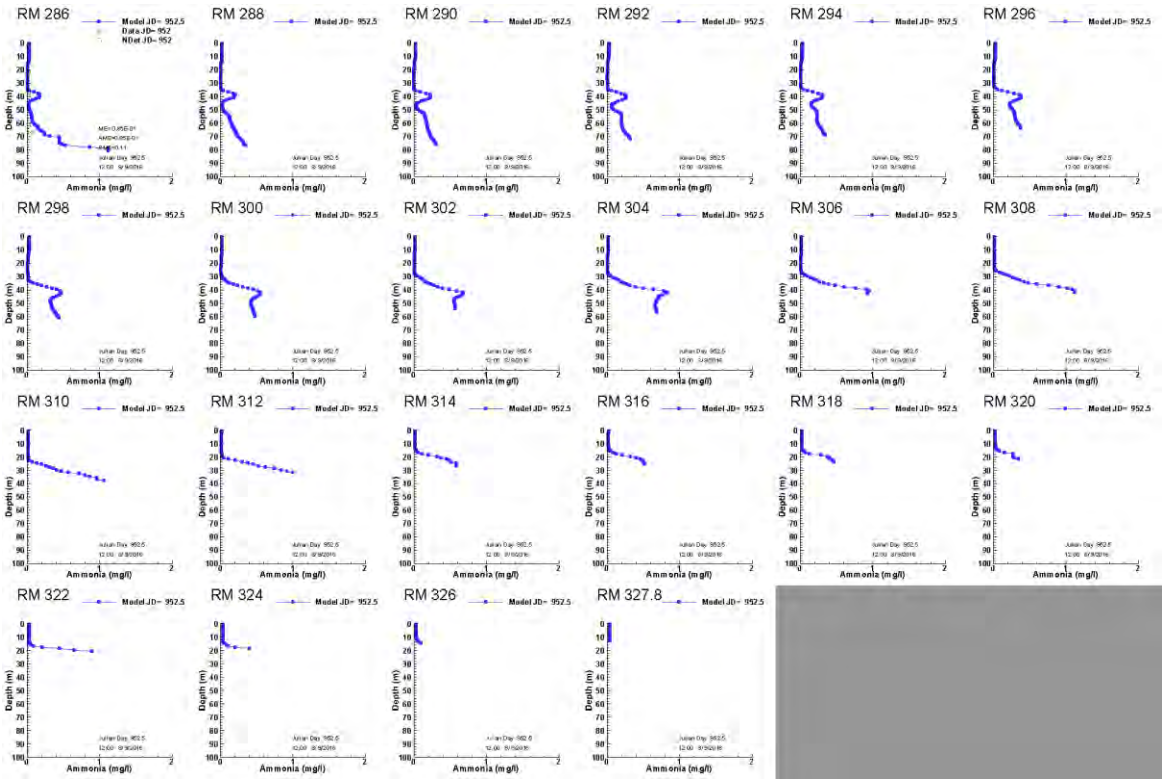


Figure 931. Vertical profiles of ammonia nitrogen compared with data for 8/ 9/2016.

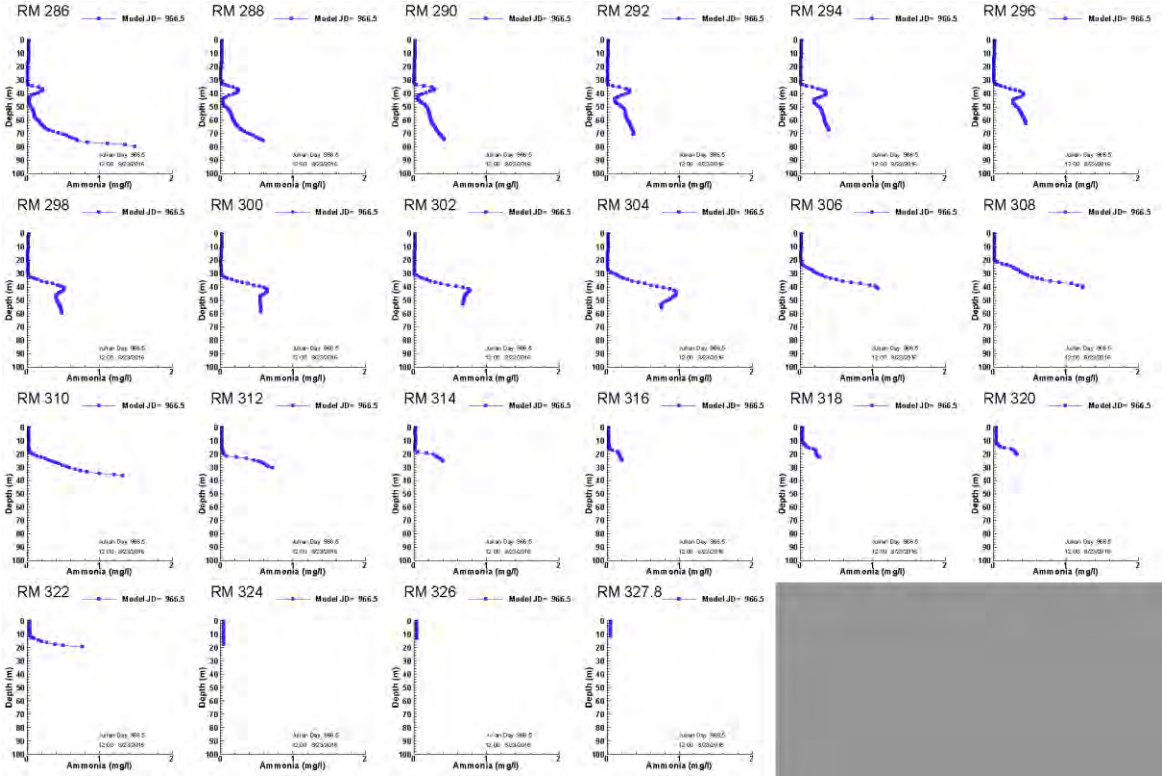


Figure 932. Vertical profiles of ammonia nitrogen compared with data for 8/23/2016.

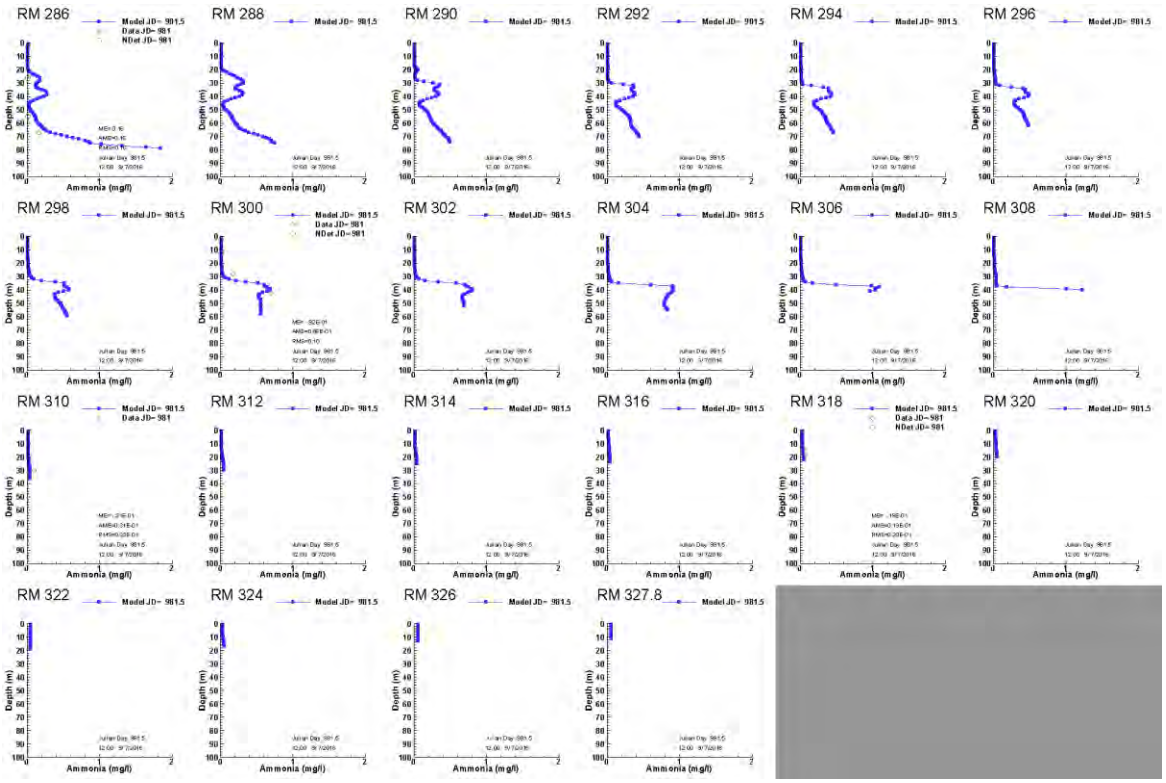


Figure 933. Vertical profiles of ammonia nitrogen compared with data for 9/ 7/2016.

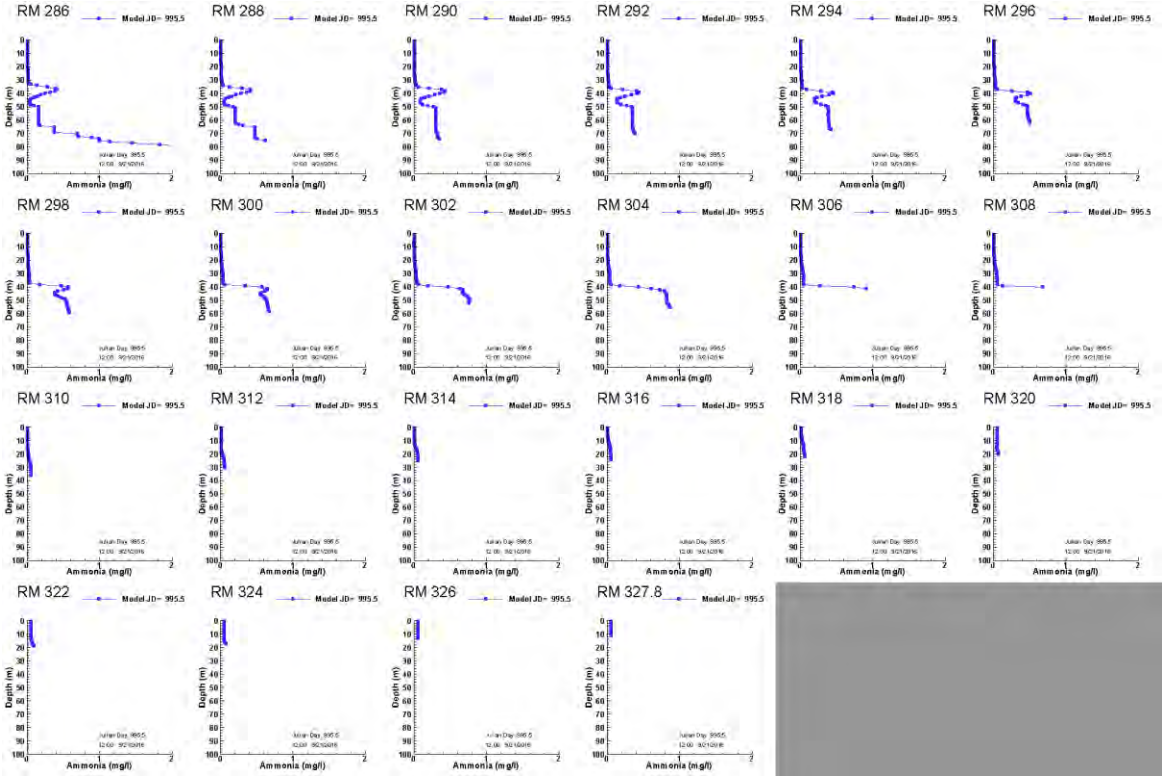


Figure 934. Vertical profiles of ammonia nitrogen compared with data for 9/21/2016.

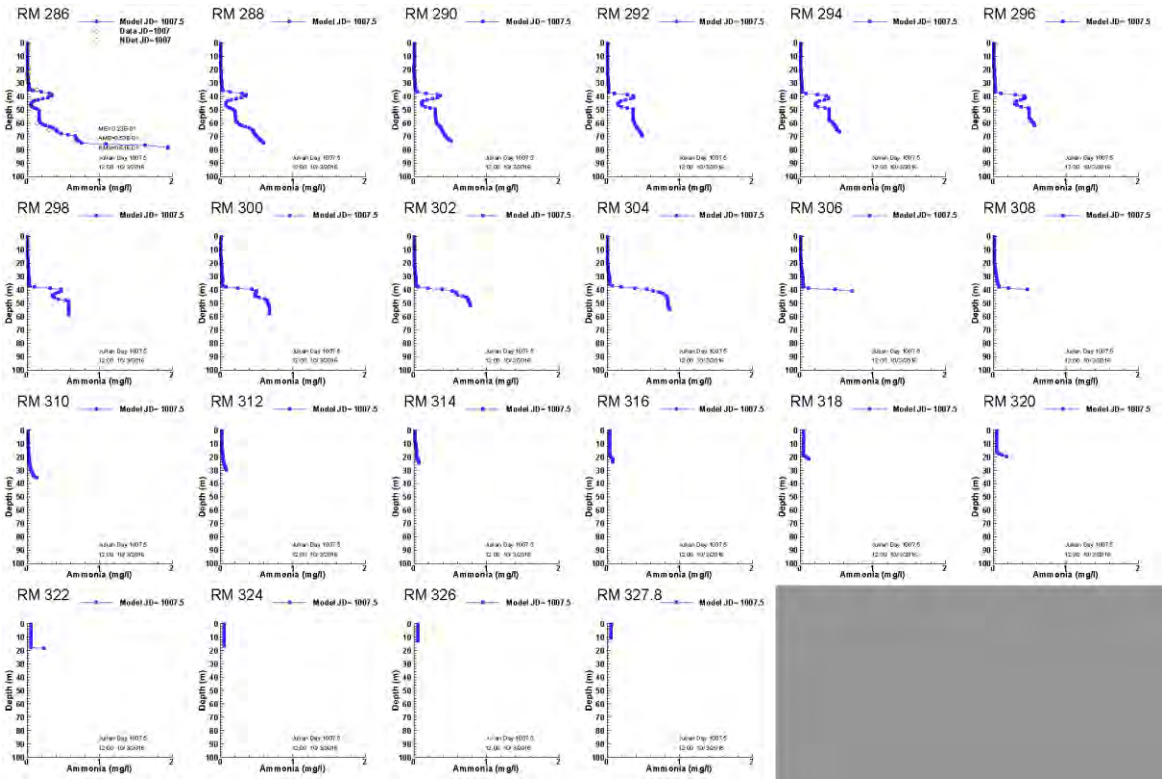


Figure 935. Vertical profiles of ammonia nitrogen compared with data for 10/ 3/2016.

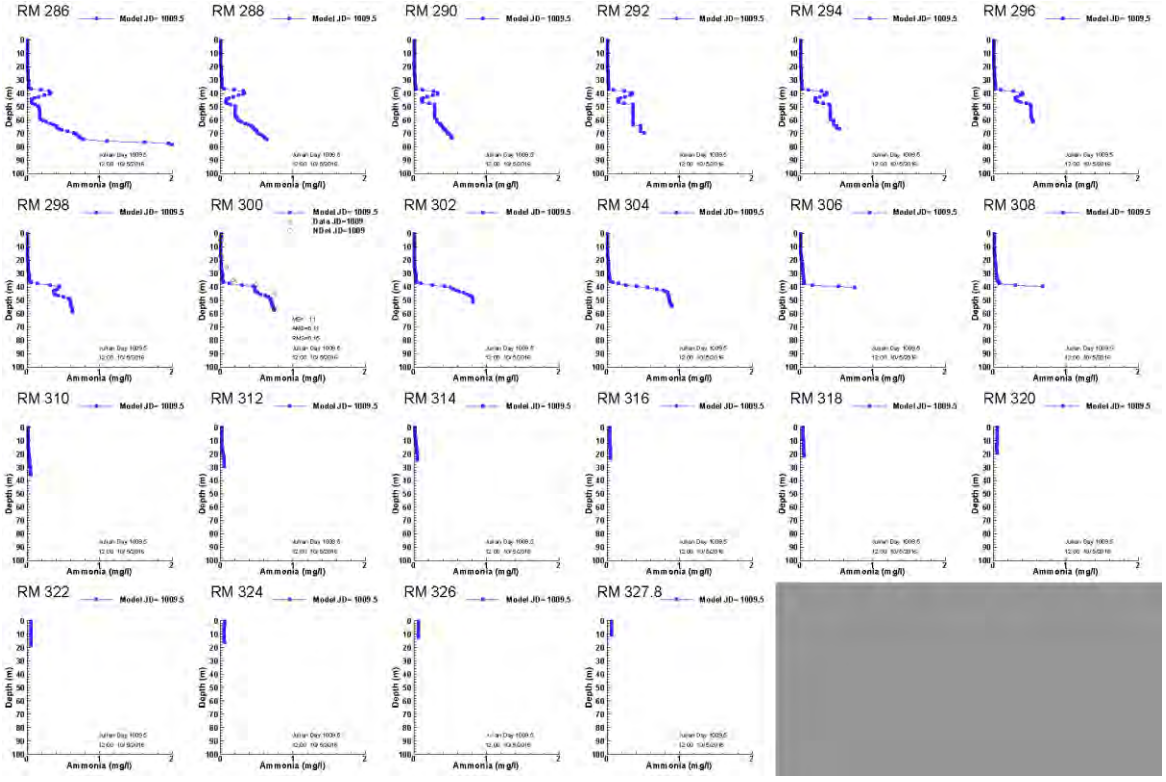


Figure 936. Vertical profiles of ammonia nitrogen compared with data for 10/ 5/2016.

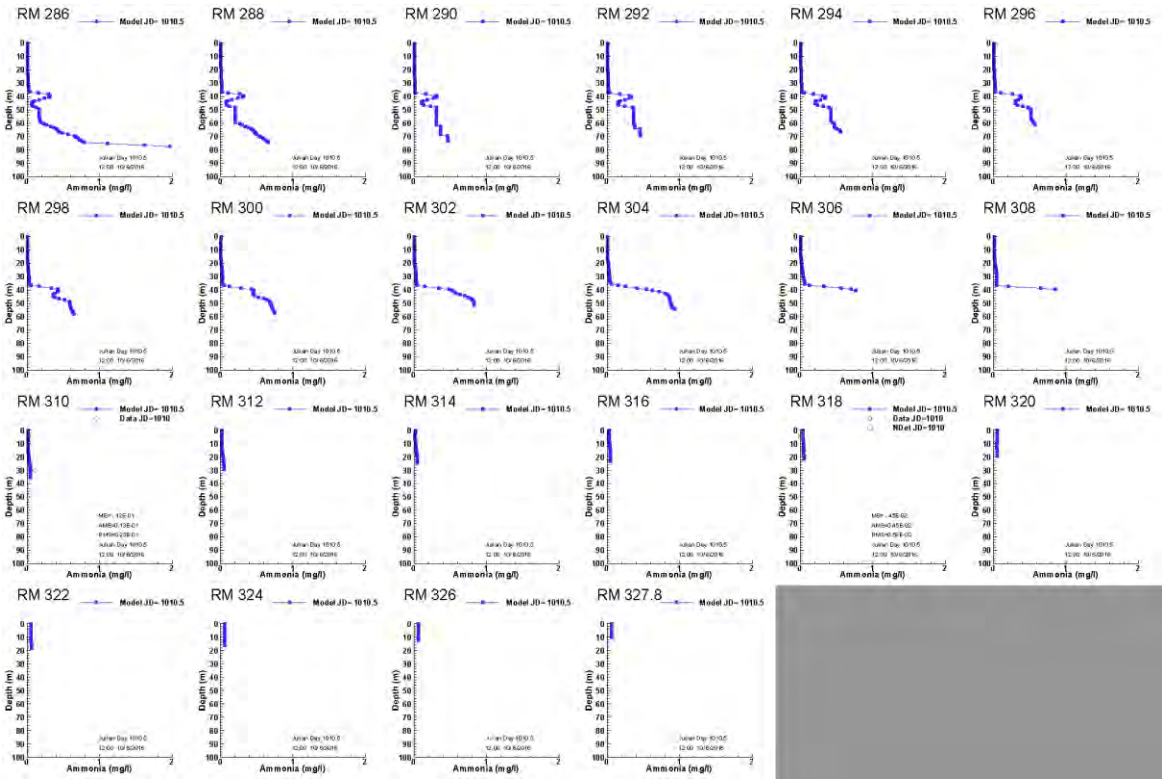


Figure 937. Vertical profiles of ammonia nitrogen compared with data for 10/ 6/2016.

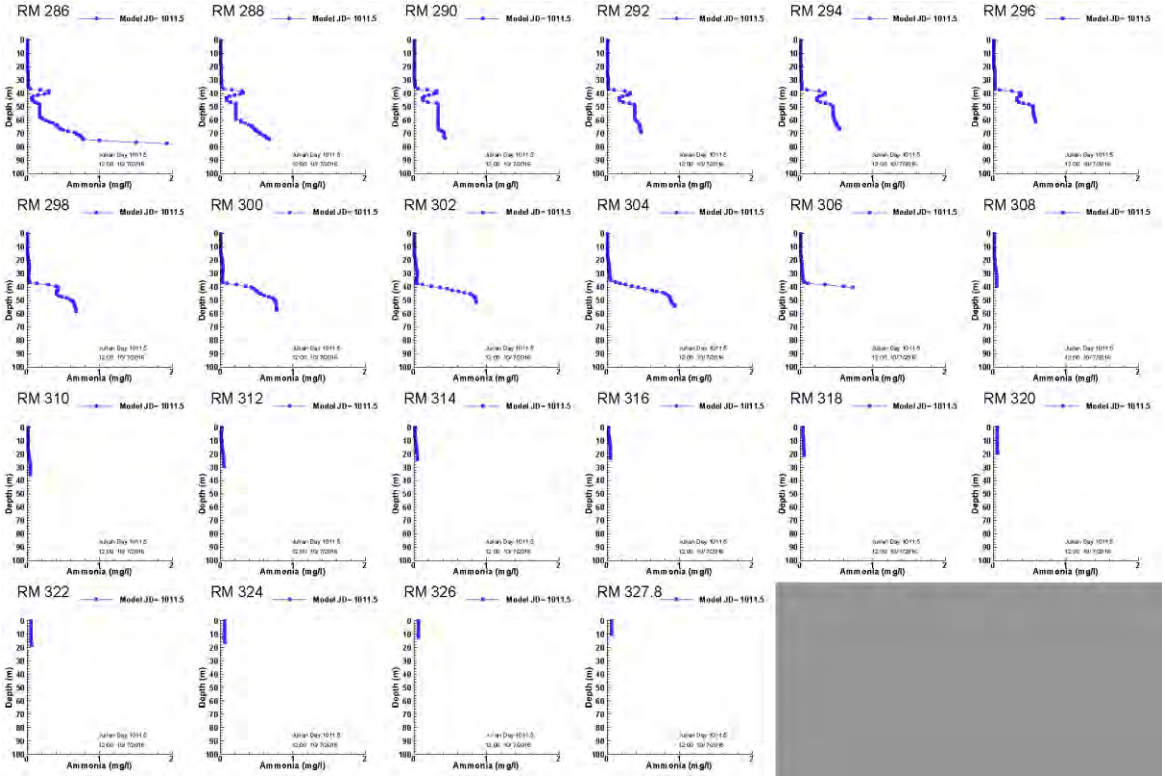


Figure 938. Vertical profiles of ammonia nitrogen compared with data for 10/ 7/2016.

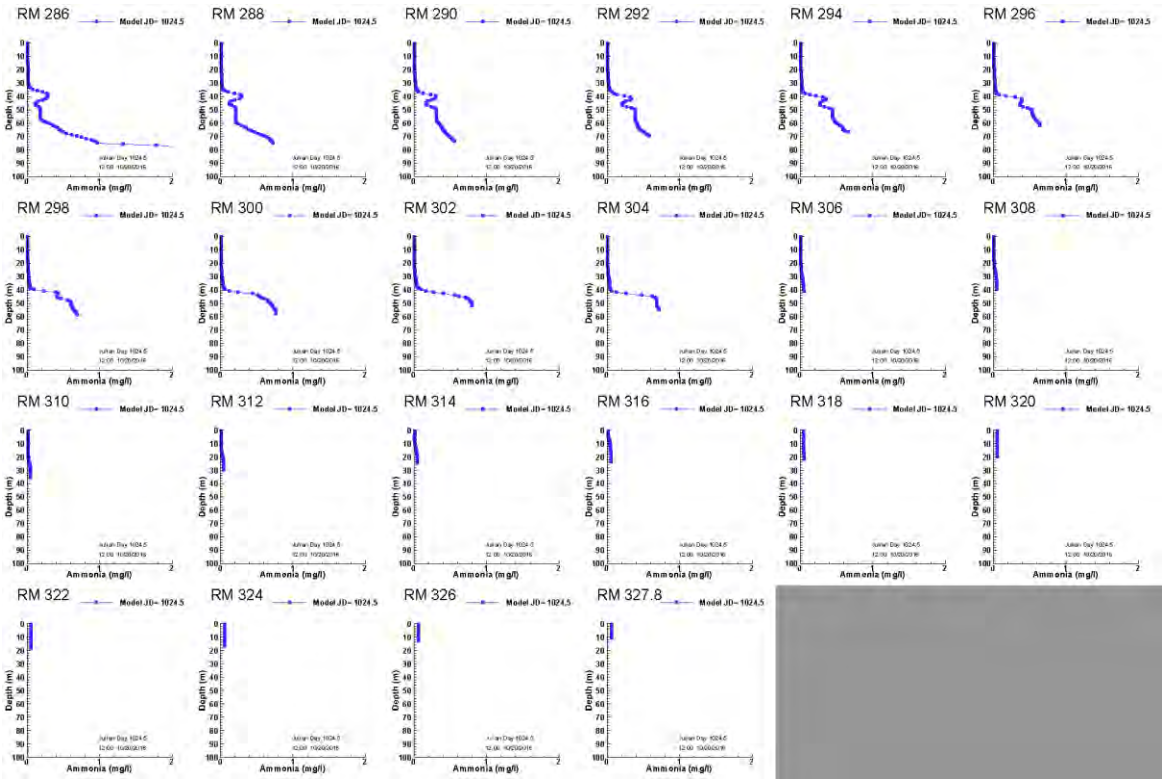


Figure 939. Vertical profiles of ammonia nitrogen compared with data for 10/20/2016.

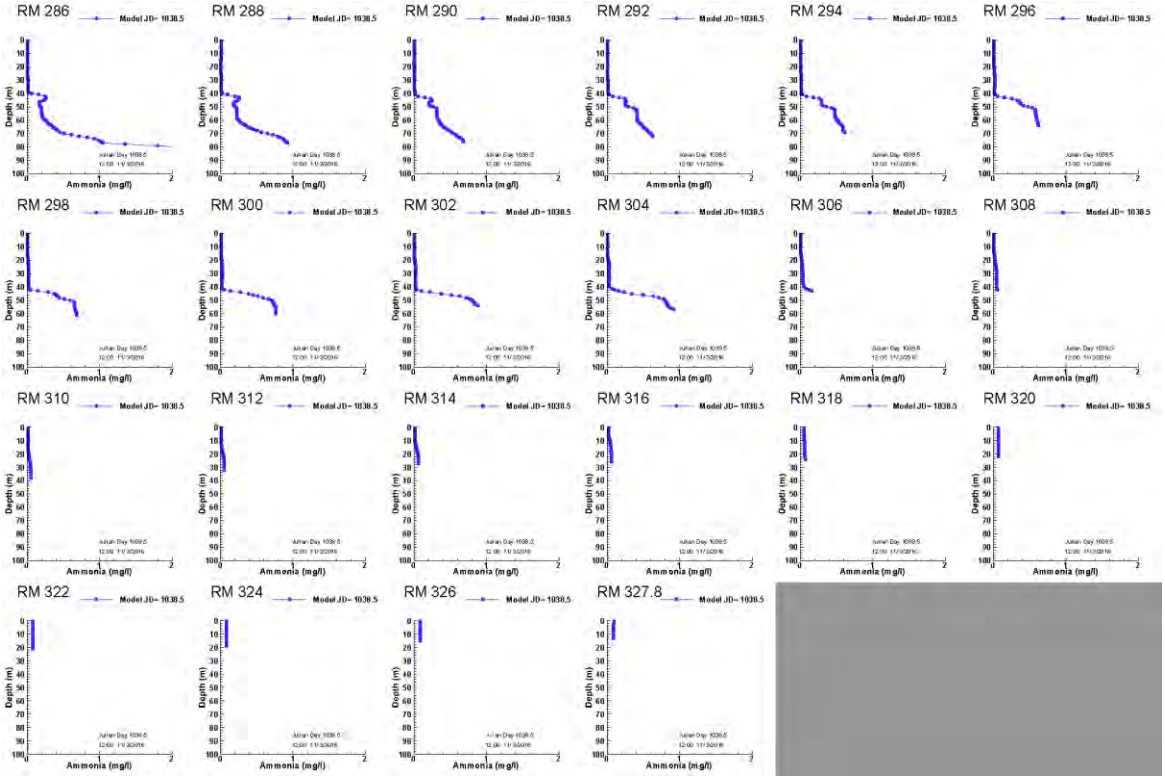


Figure 940. Vertical profiles of ammonia nitrogen compared with data for 11/ 3/2016.

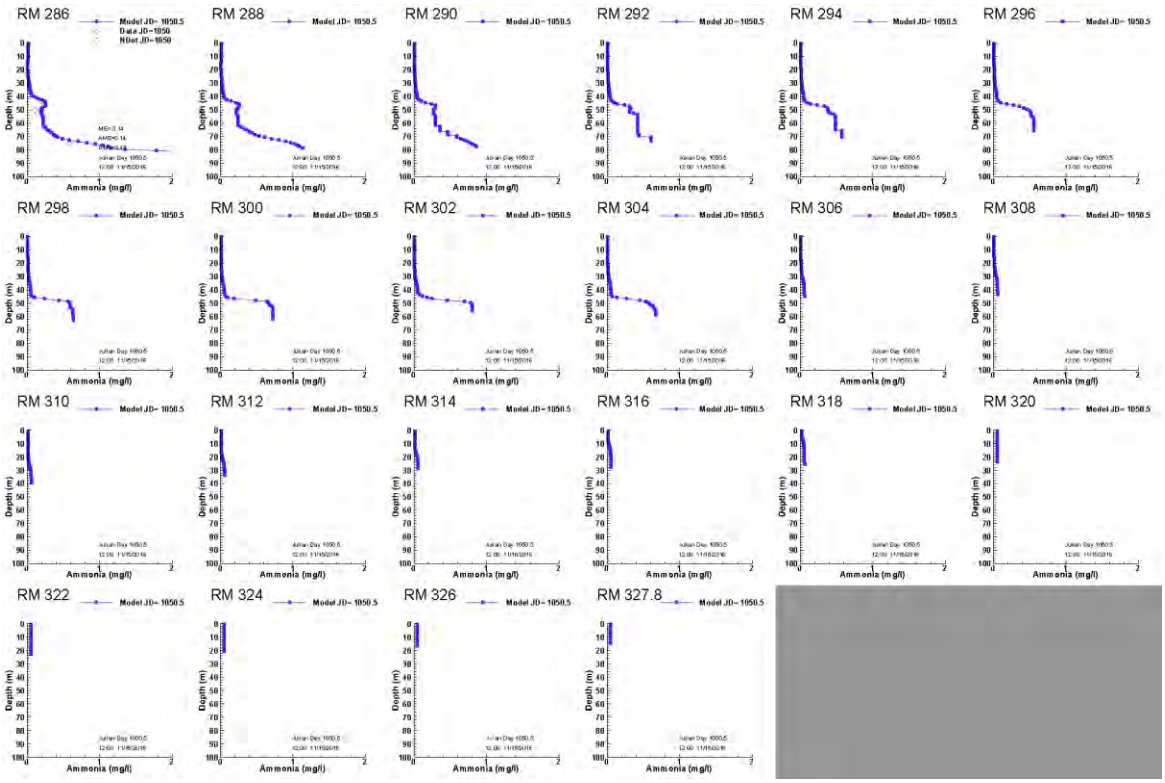


Figure 941. Vertical profiles of ammonia nitrogen compared with data for 11/15/2016.

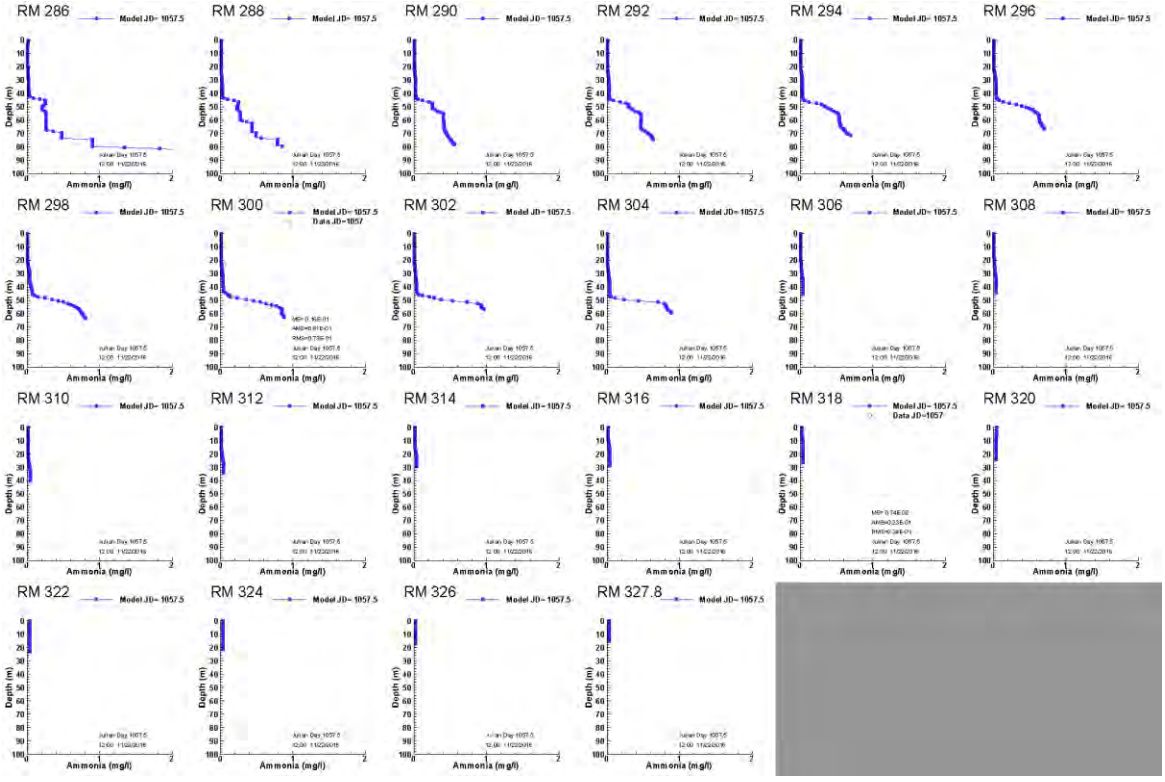


Figure 942. Vertical profiles of ammonia nitrogen compared with data for 11/22/2016.

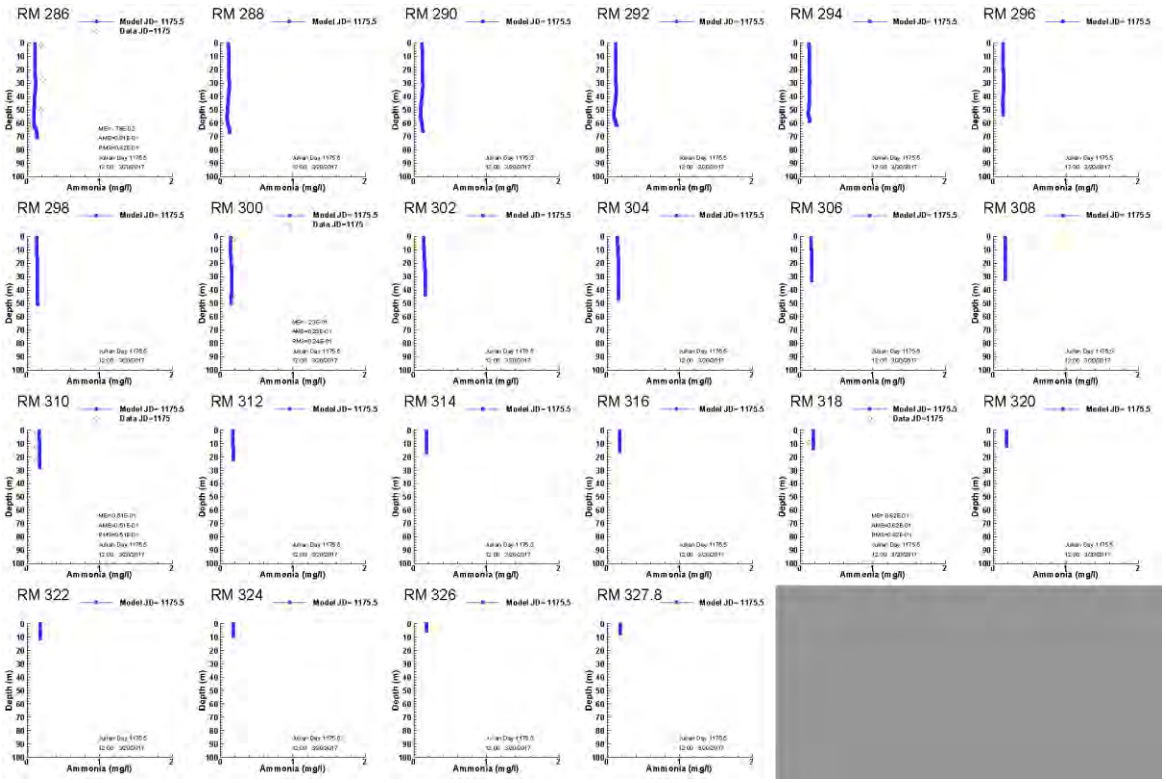


Figure 943. Vertical profiles of ammonia nitrogen compared with data for 3/20/2017.

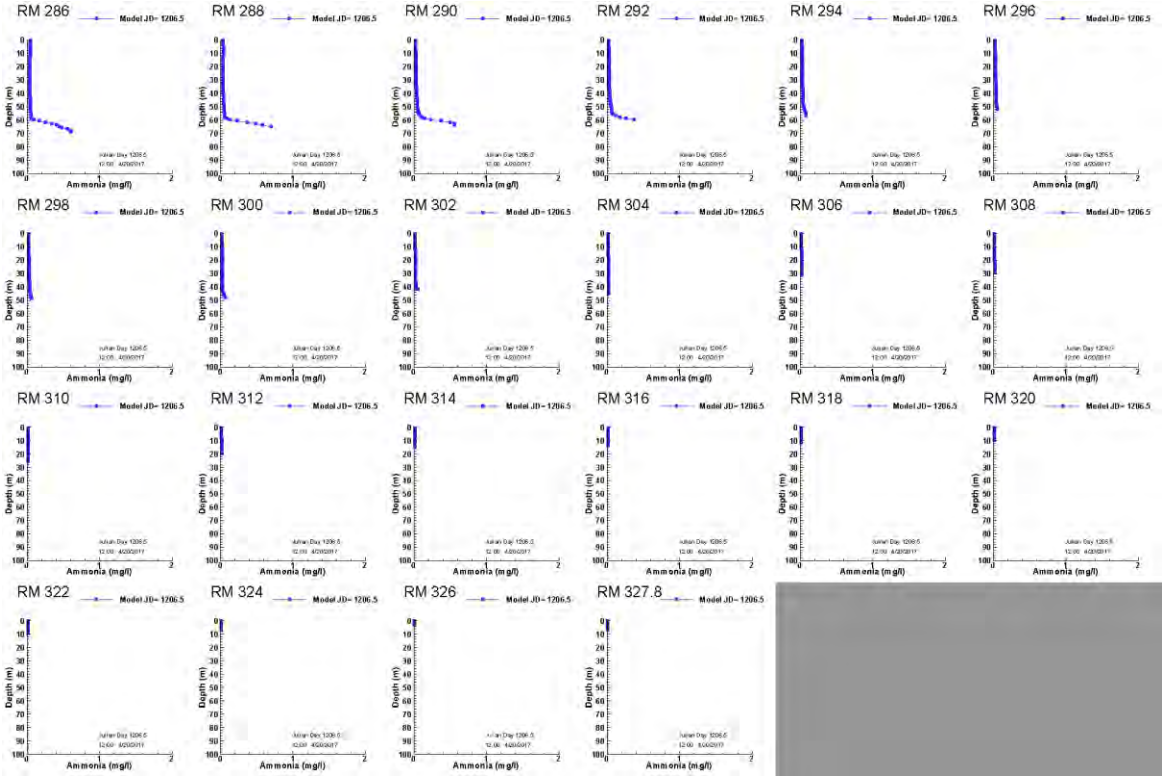


Figure 944. Vertical profiles of ammonia nitrogen compared with data for 4/20/2017.

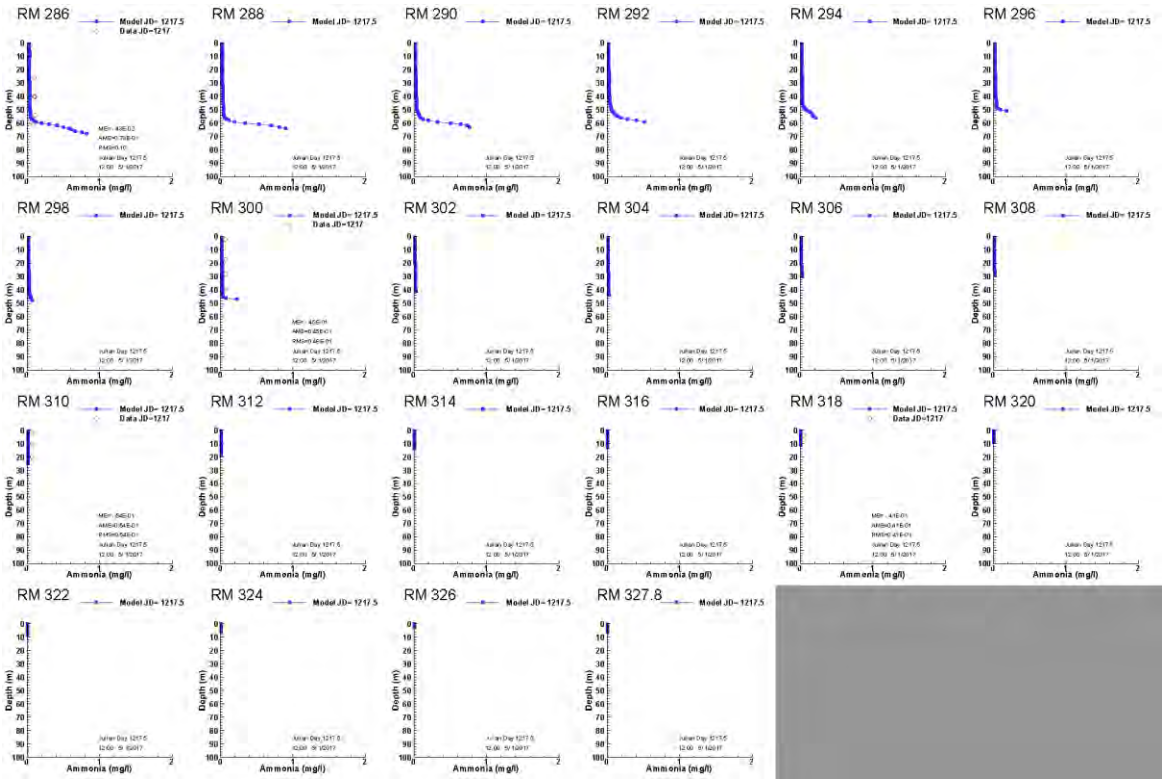


Figure 945. Vertical profiles of ammonia nitrogen compared with data for 5/ 1/2017.

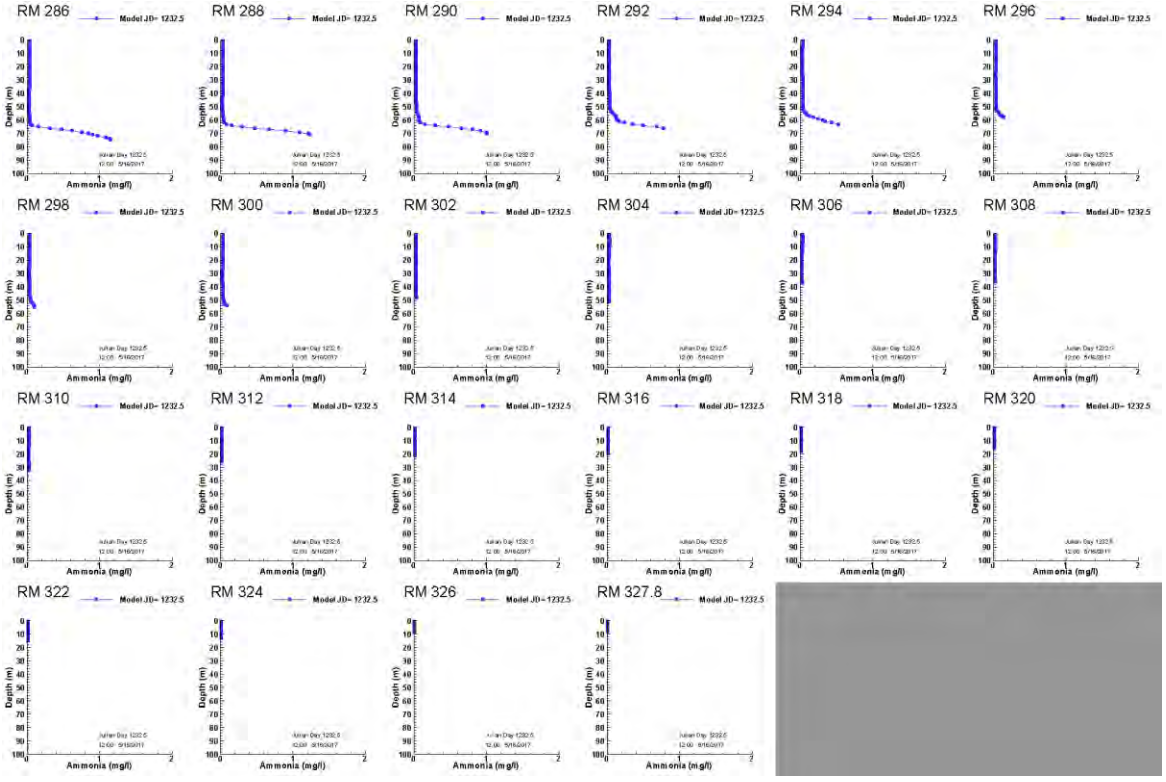


Figure 946. Vertical profiles of ammonia nitrogen compared with data for 5/16/2017.

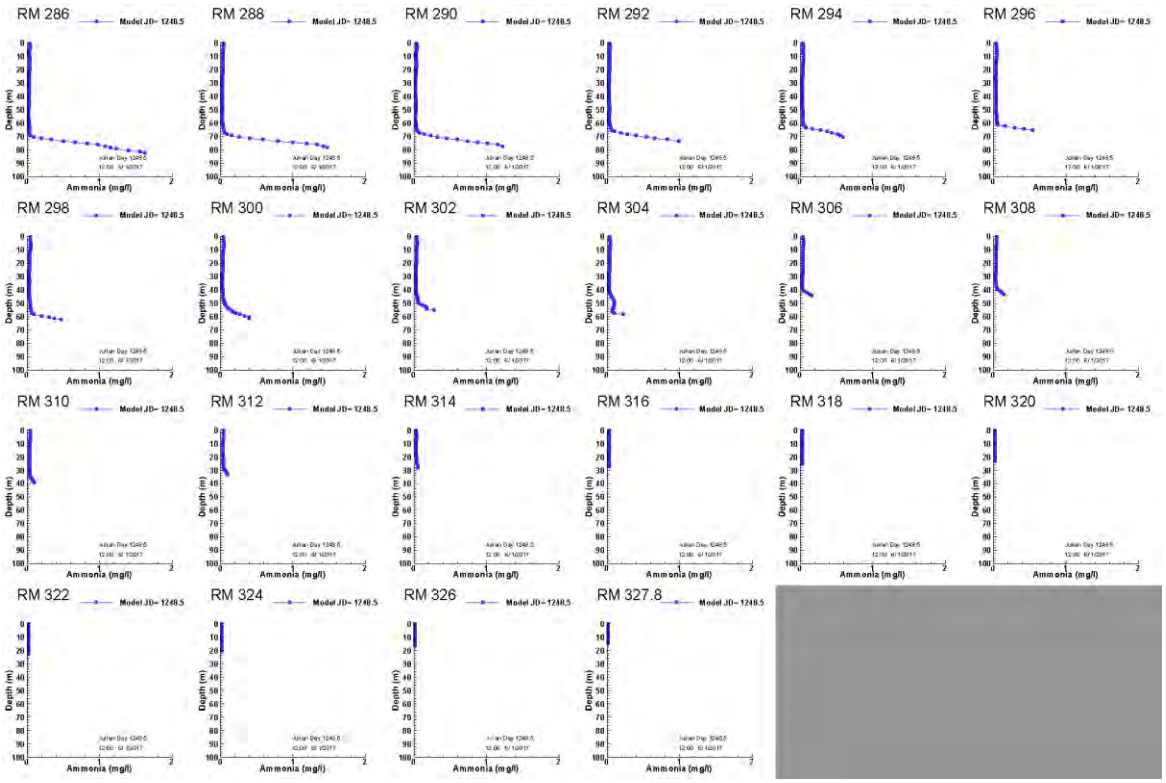


Figure 947. Vertical profiles of ammonia nitrogen compared with data for 6/ 1/2017.

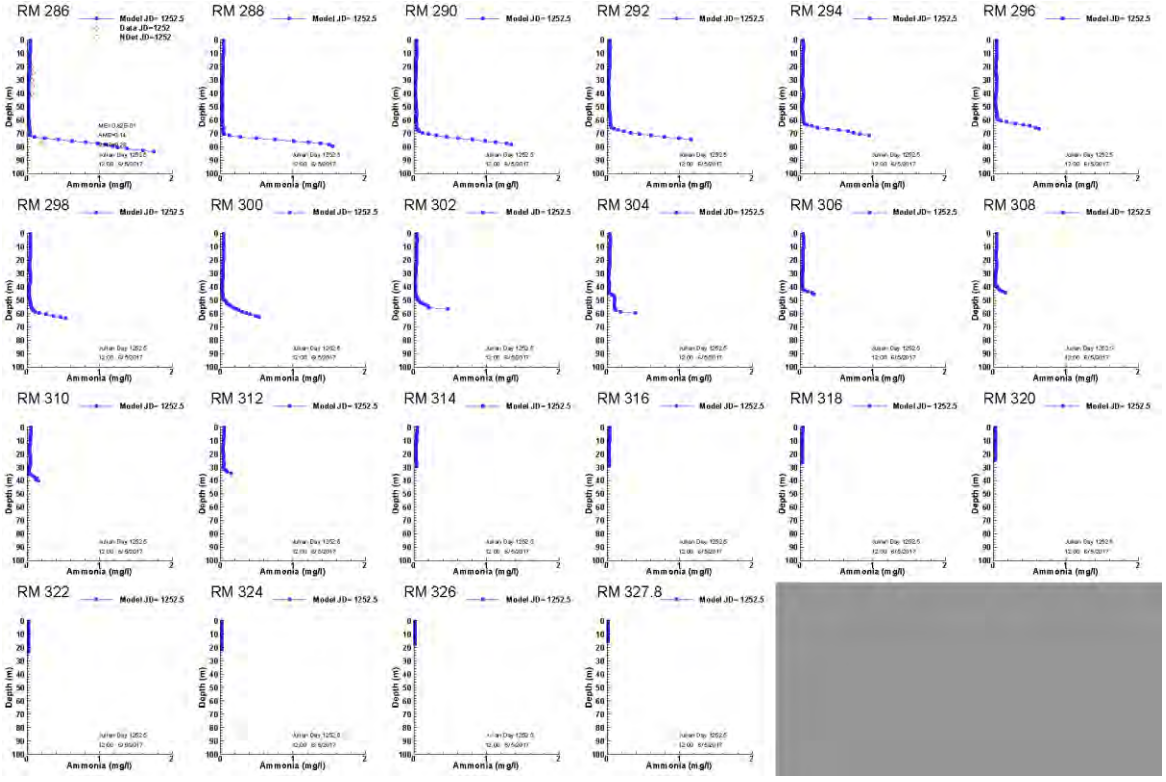


Figure 948. Vertical profiles of ammonia nitrogen compared with data for 6/ 5/2017.

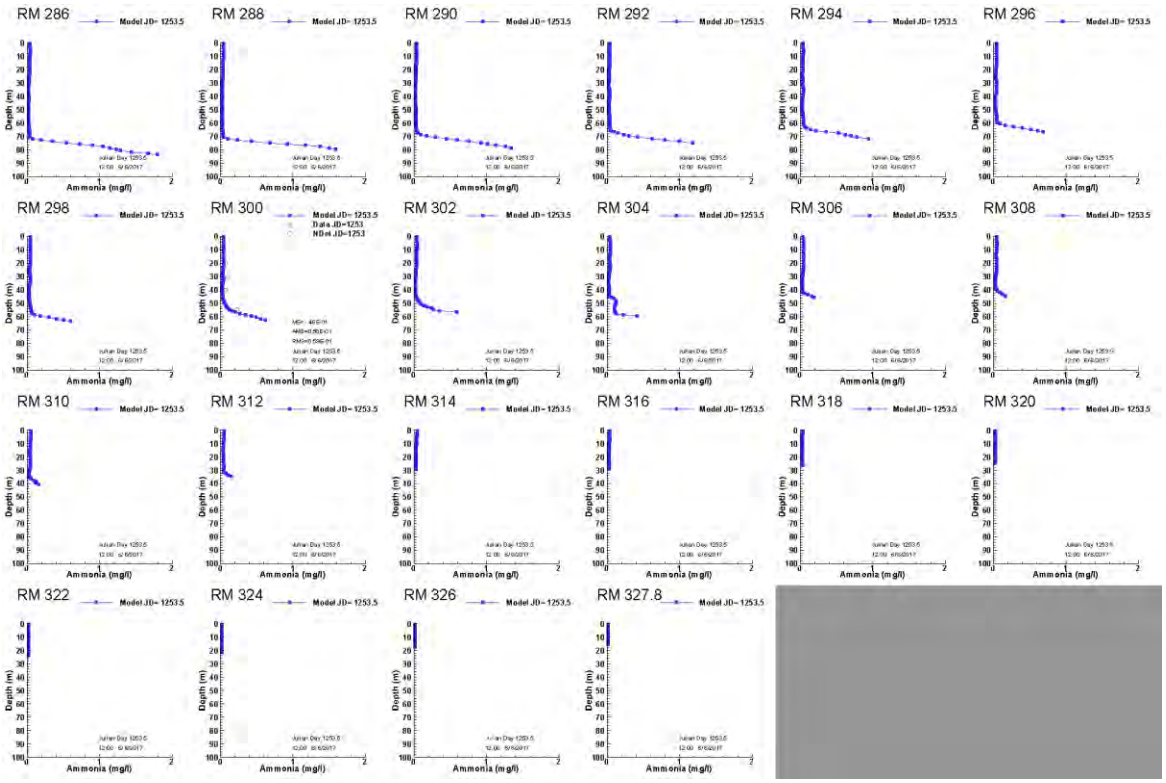


Figure 949. Vertical profiles of ammonia nitrogen compared with data for 6/ 6/2017.

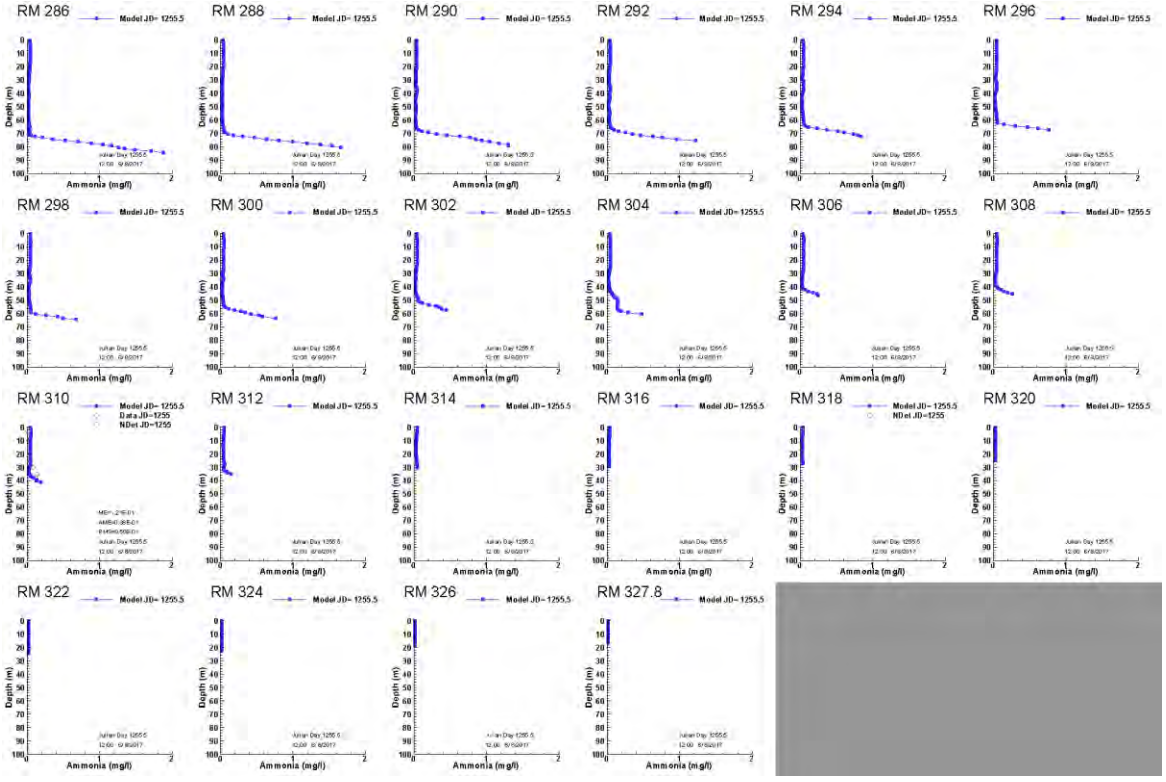


Figure 950. Vertical profiles of ammonia nitrogen compared with data for 6/ 8/2017.

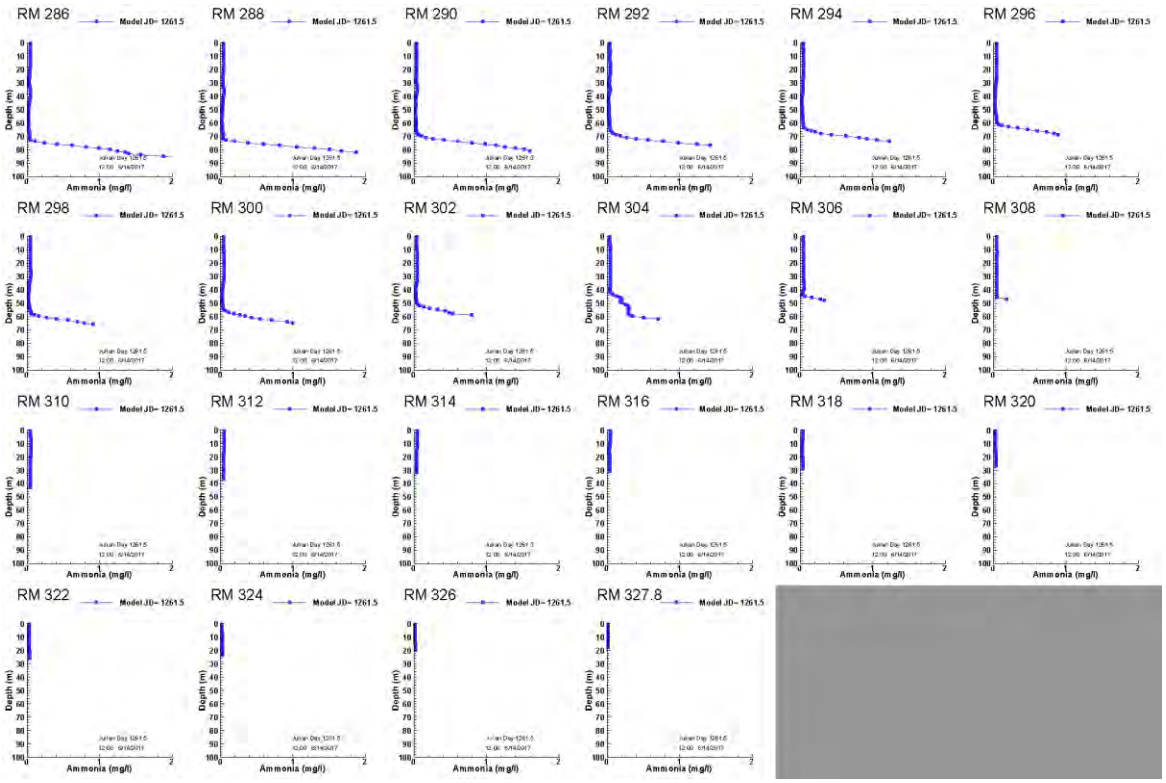


Figure 951. Vertical profiles of ammonia nitrogen compared with data for 6/14/2017.

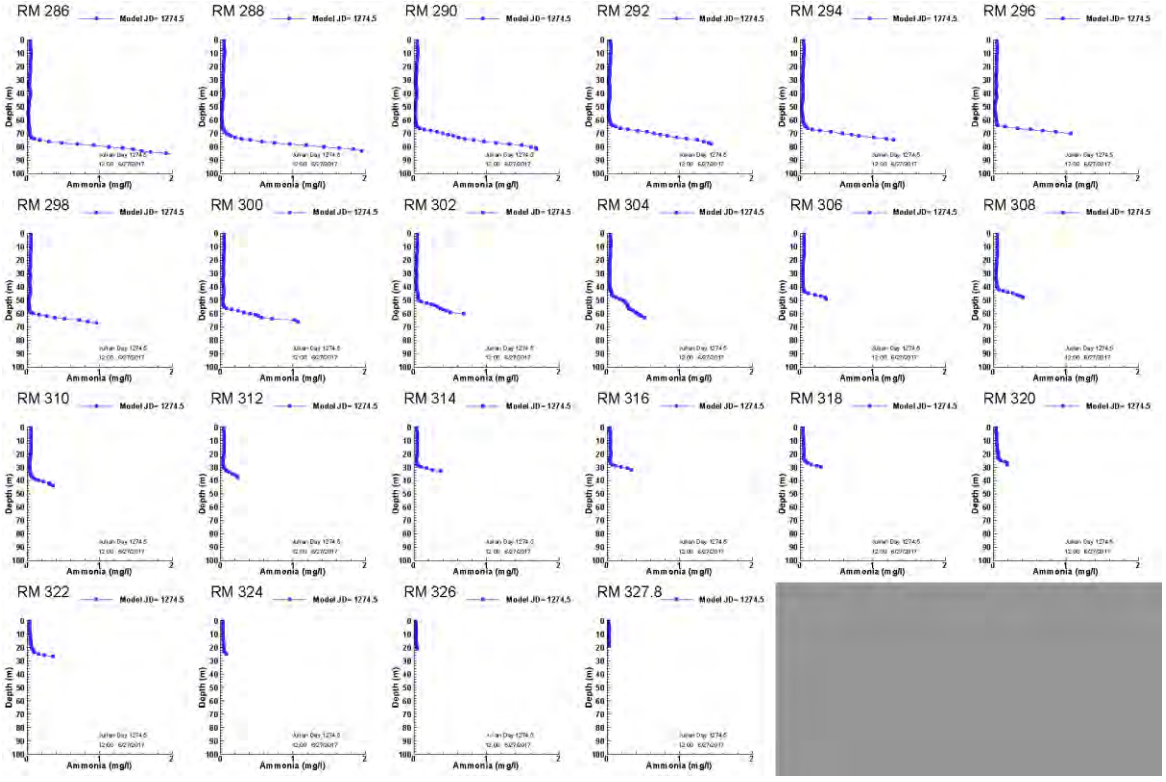


Figure 952. Vertical profiles of ammonia nitrogen compared with data for 6/27/2017.

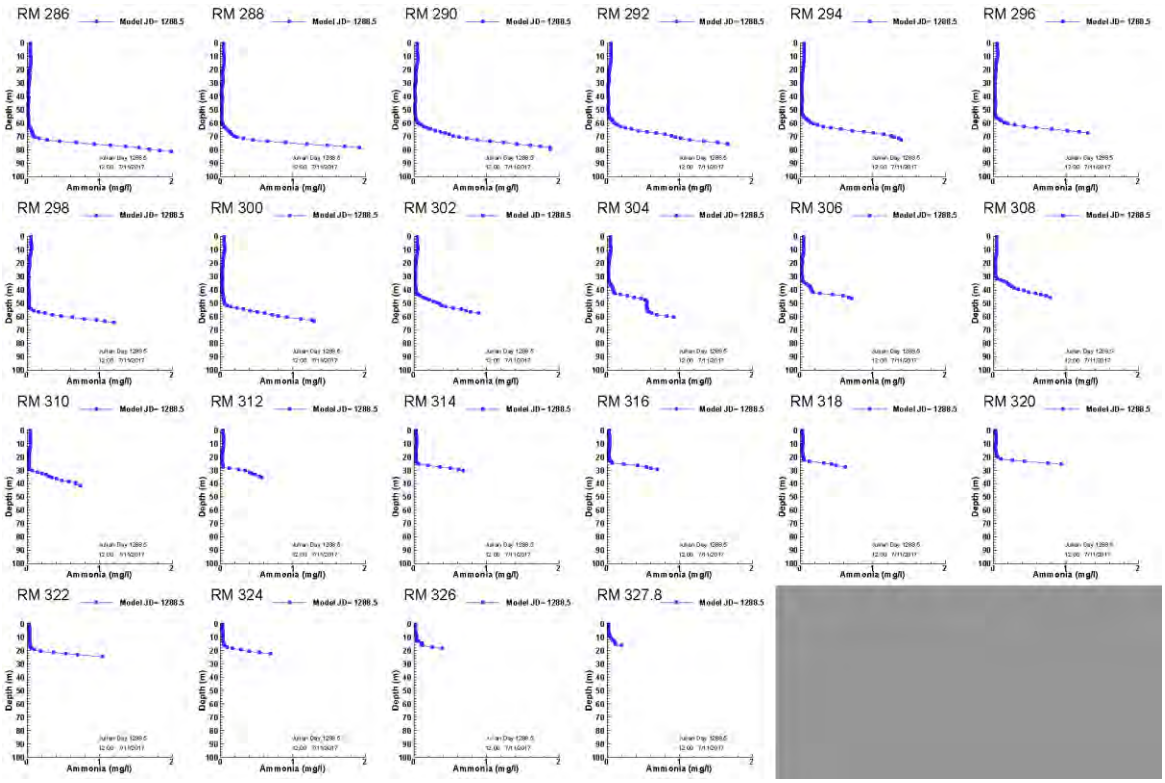


Figure 953. Vertical profiles of ammonia nitrogen compared with data for 7/11/2017.

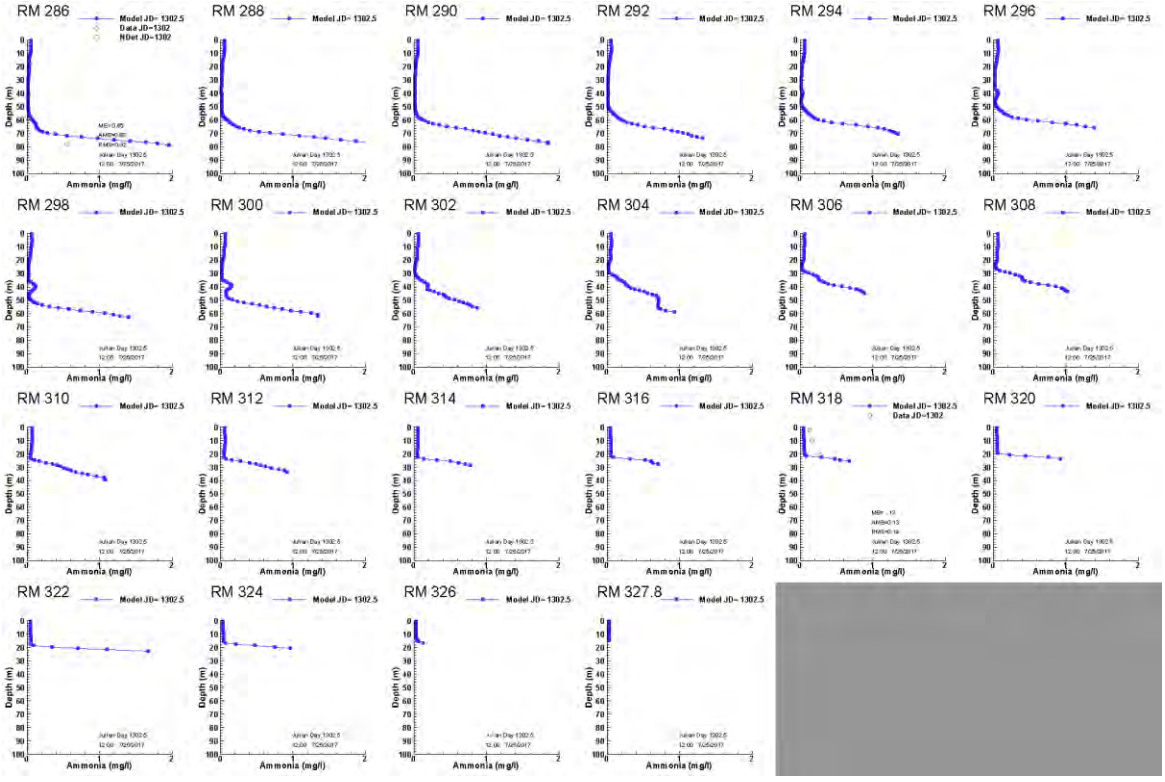


Figure 954. Vertical profiles of ammonia nitrogen compared with data for 7/25/2017.

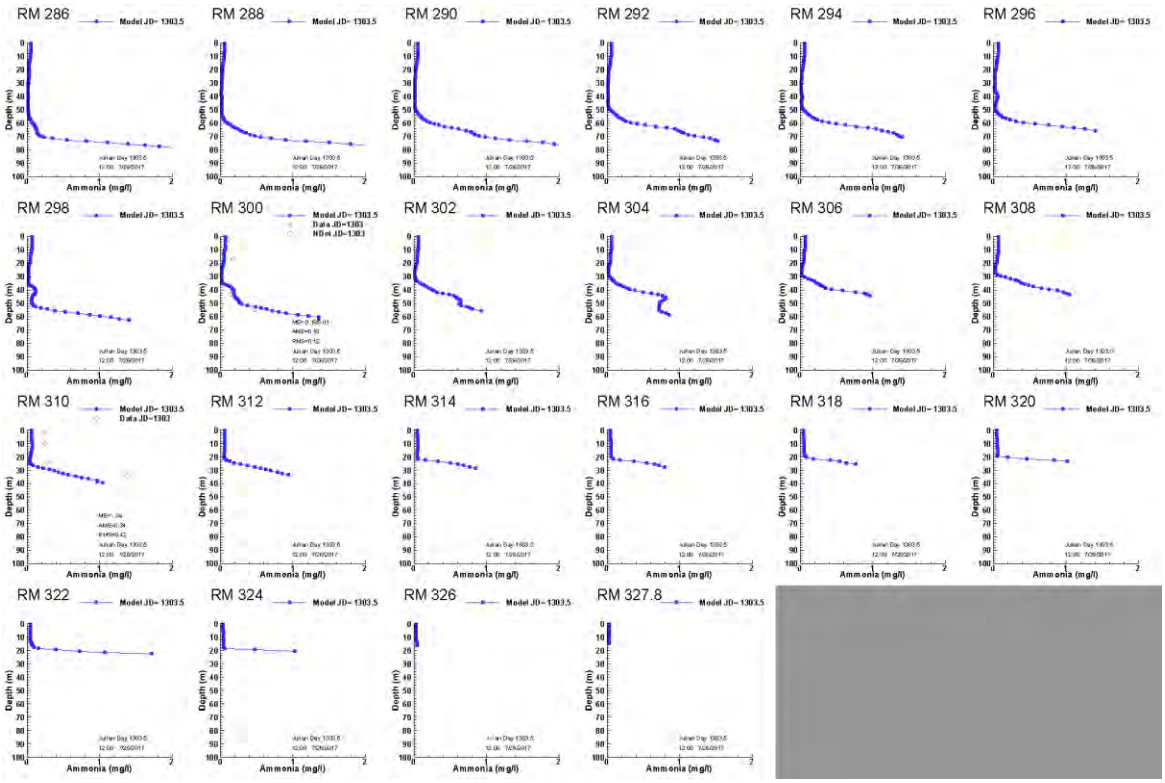


Figure 955. Vertical profiles of ammonia nitrogen compared with data for 7/26/2017.

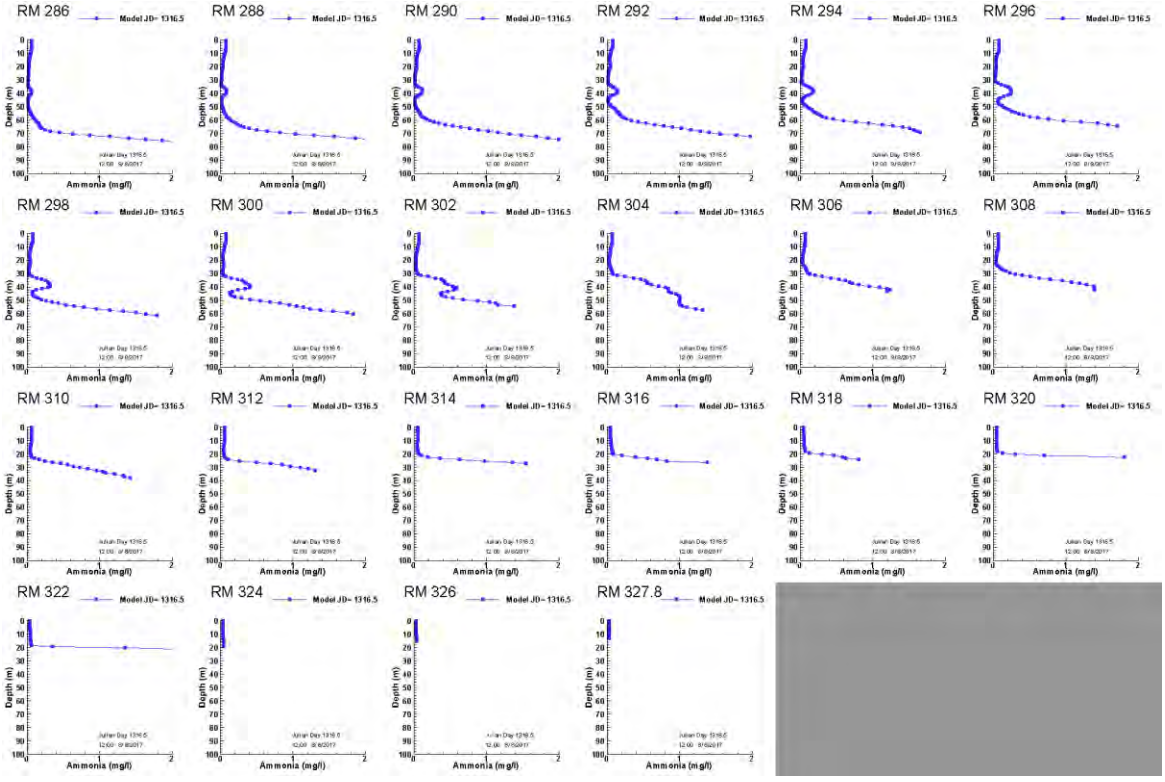


Figure 956. Vertical profiles of ammonia nitrogen compared with data for 8/ 8/2017.

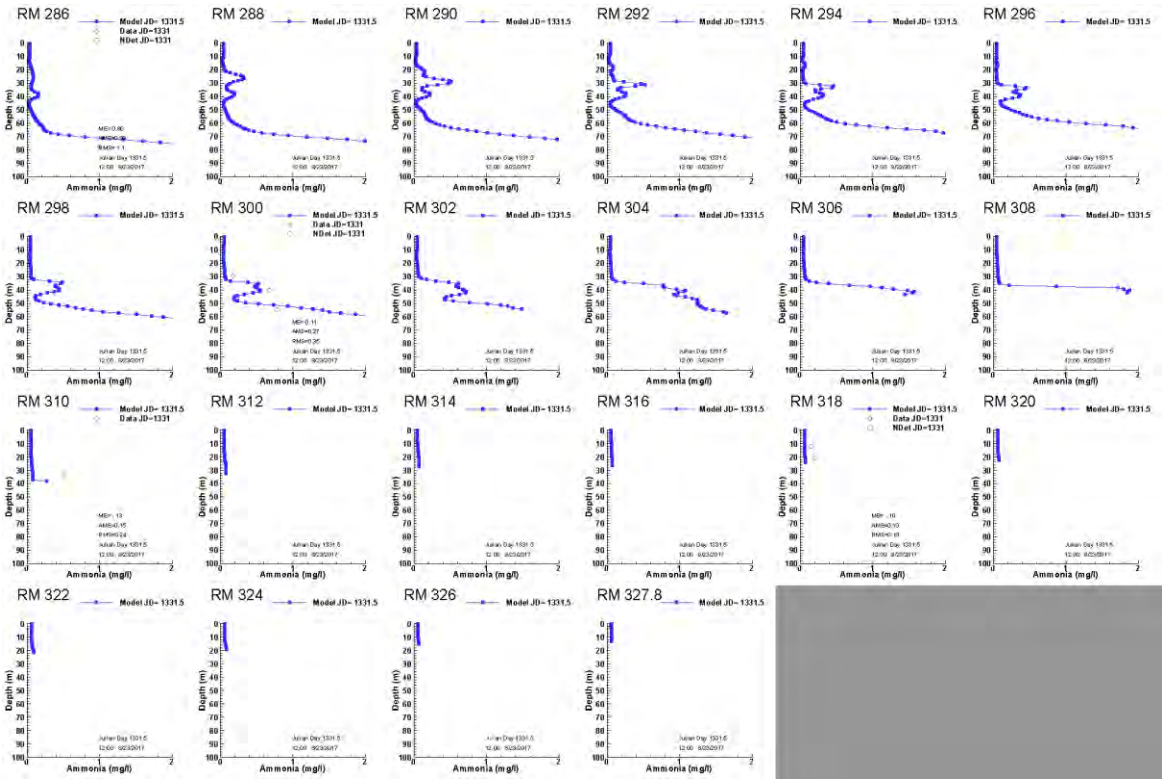


Figure 957. Vertical profiles of ammonia nitrogen compared with data for 8/23/2017.

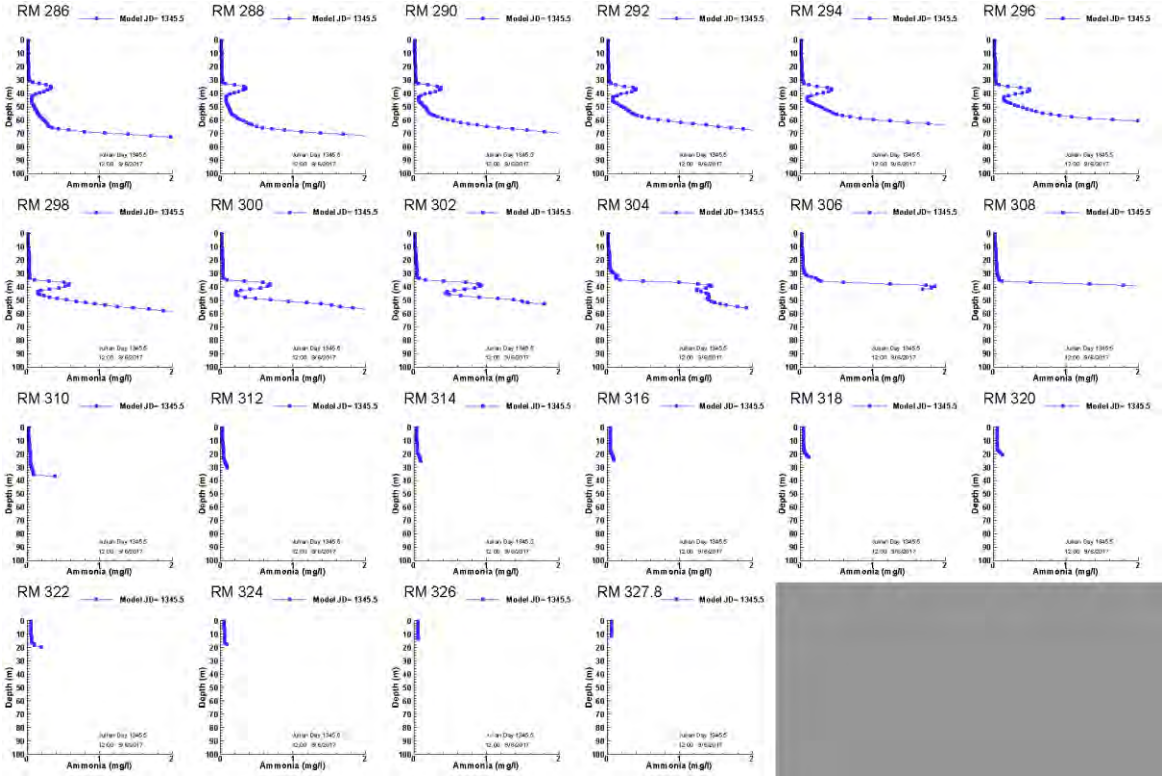


Figure 958. Vertical profiles of ammonia nitrogen compared with data for 9/ 6/2017.

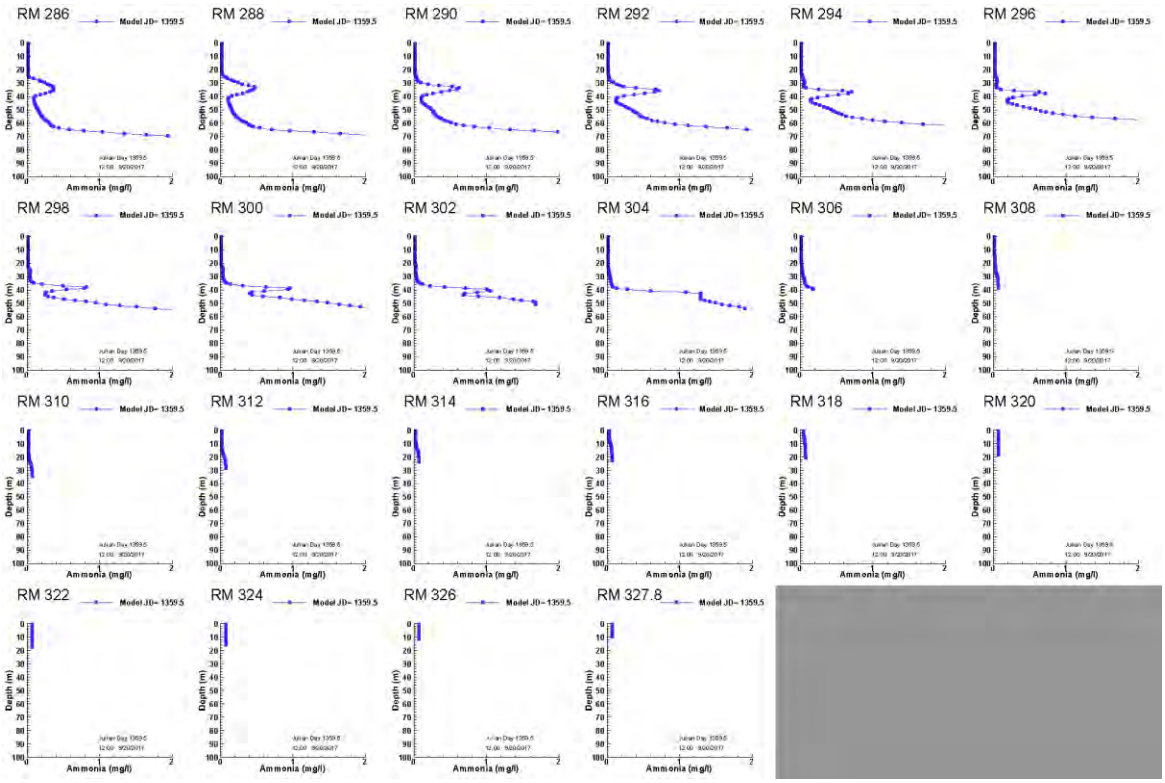


Figure 959. Vertical profiles of ammonia nitrogen compared with data for 9/20/2017.

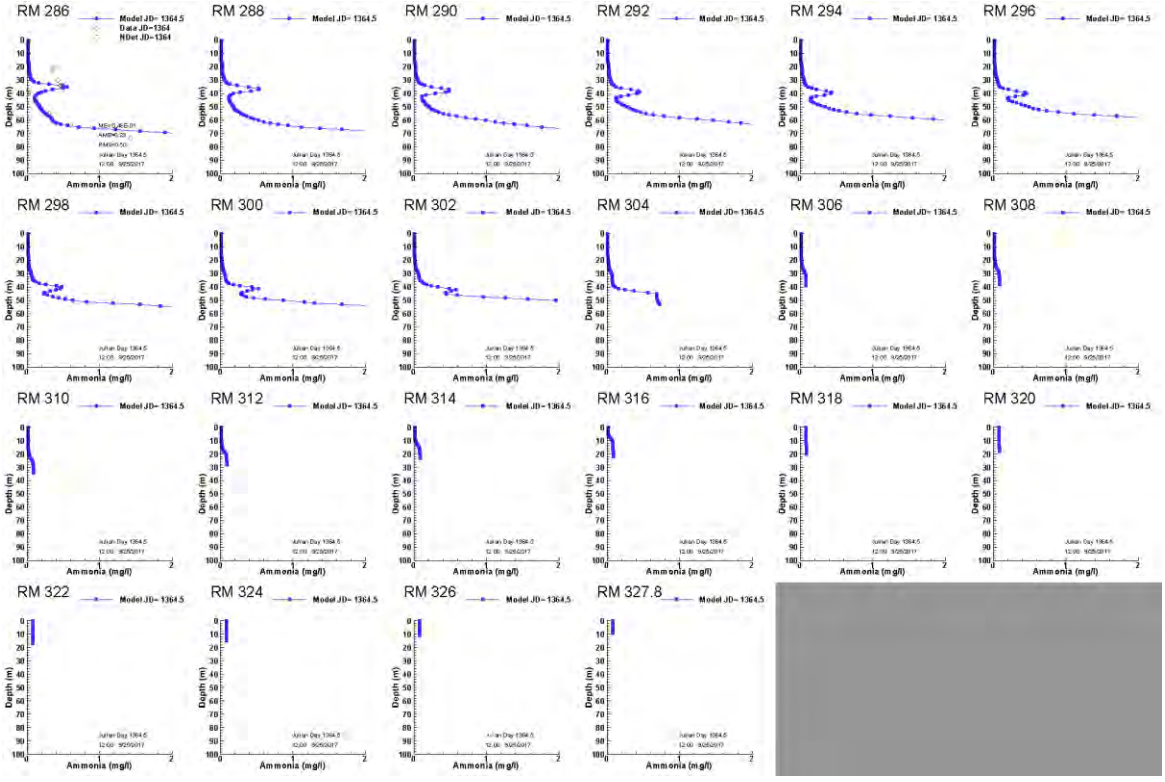


Figure 960. Vertical profiles of ammonia nitrogen compared with data for 9/25/2017.

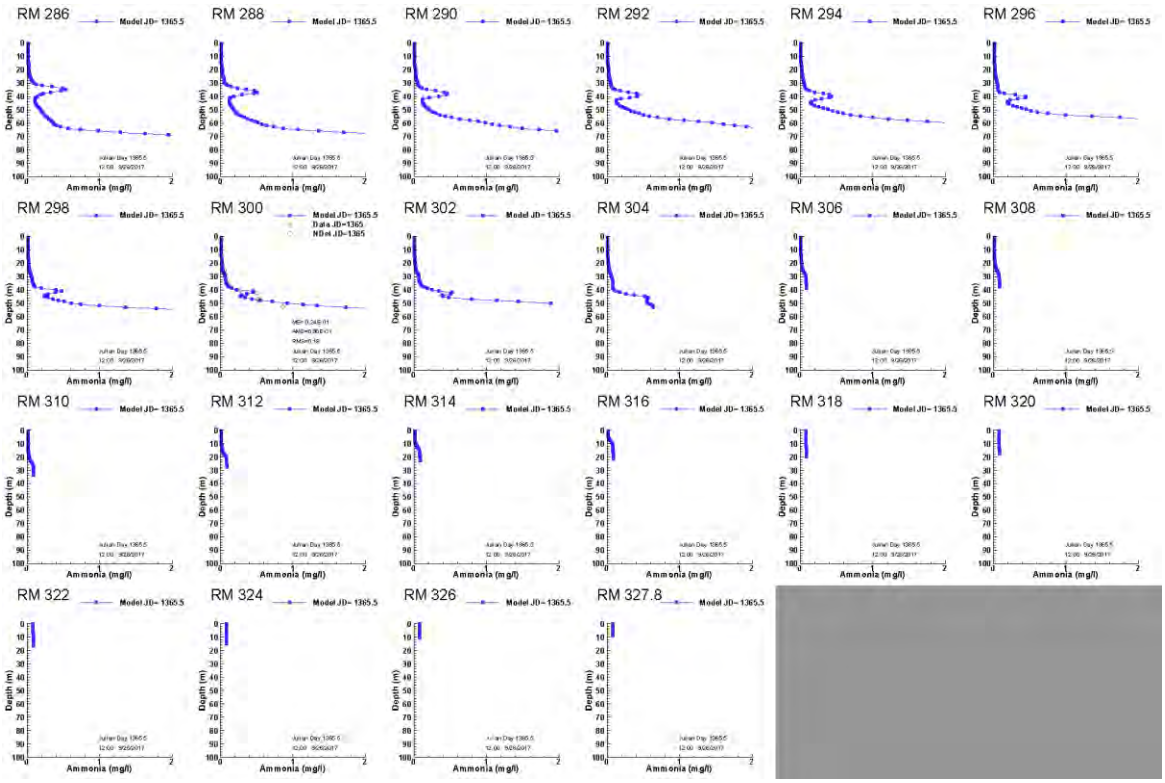


Figure 961. Vertical profiles of ammonia nitrogen compared with data for 9/26/2017.

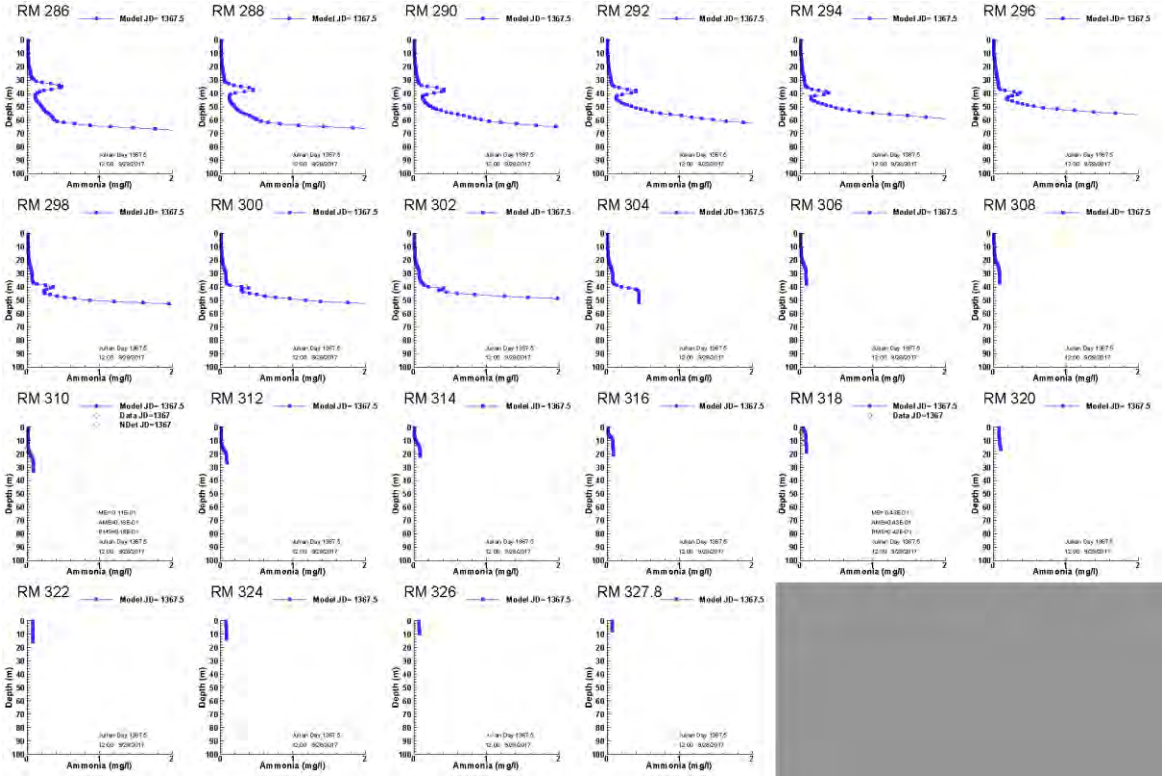


Figure 962. Vertical profiles of ammonia nitrogen compared with data for 9/28/2017.

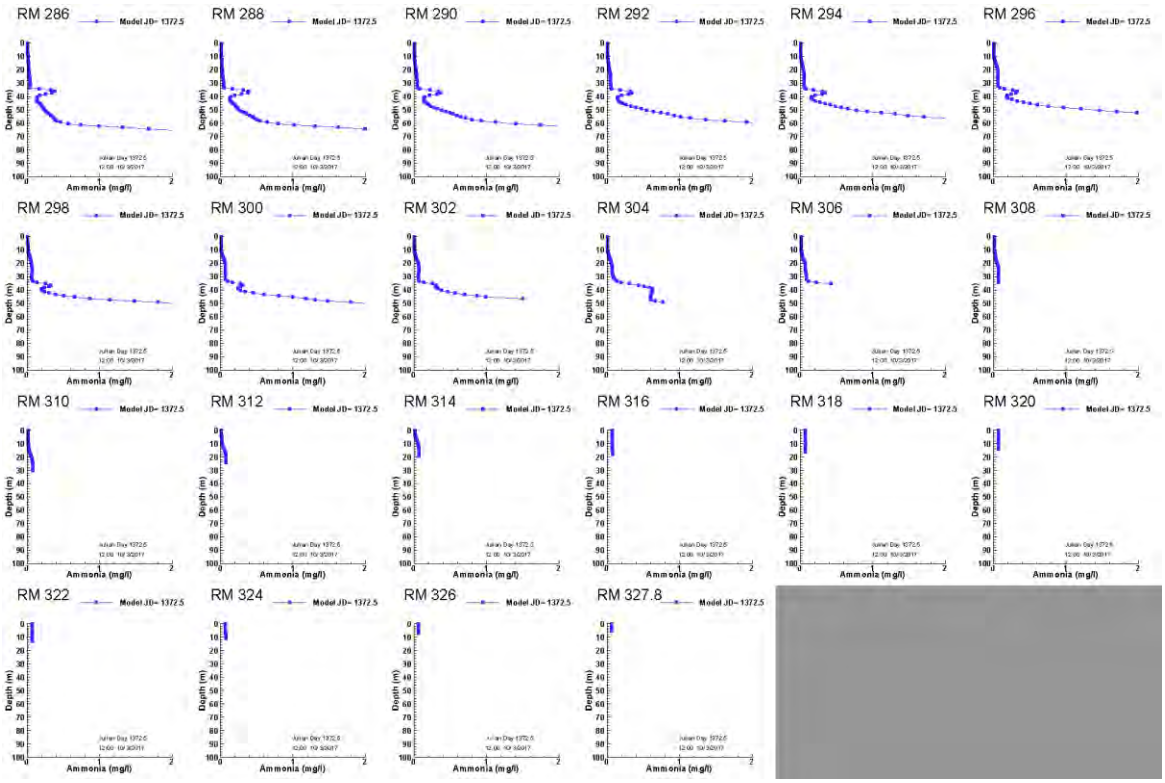


Figure 963. Vertical profiles of ammonia nitrogen compared with data for 10/ 3/2017.

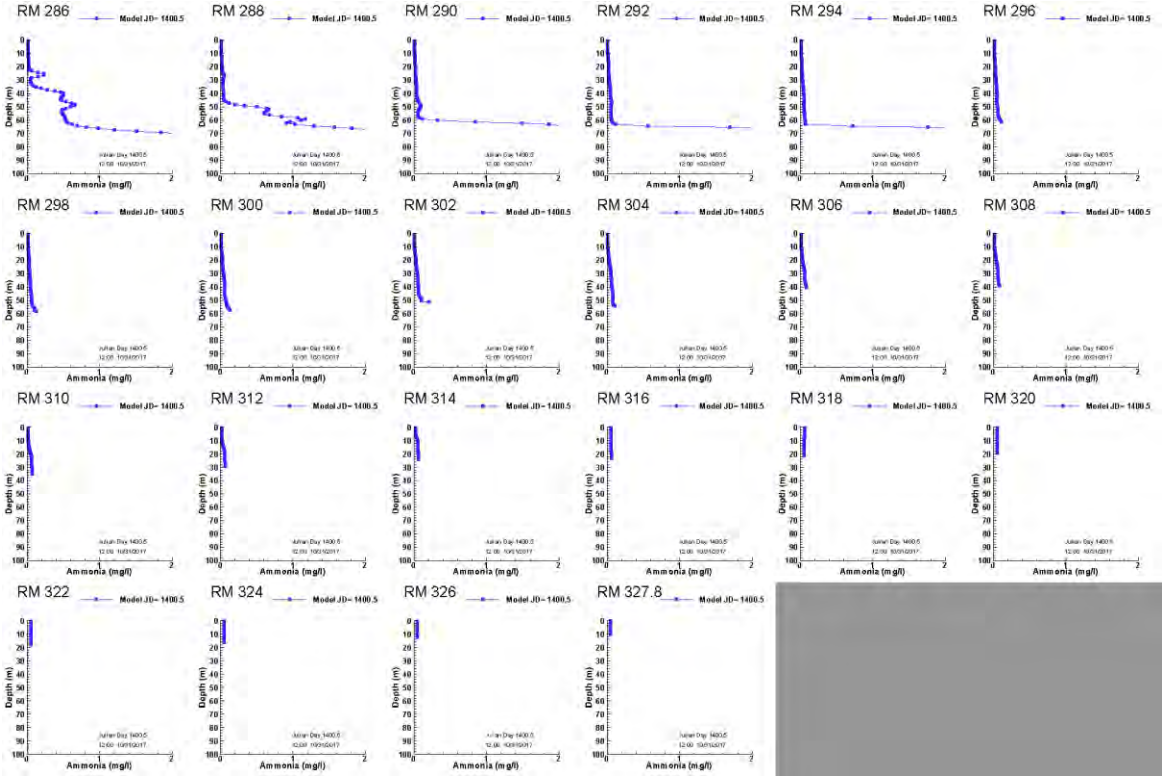


Figure 964. Vertical profiles of ammonia nitrogen compared with data for 10/31/2017.

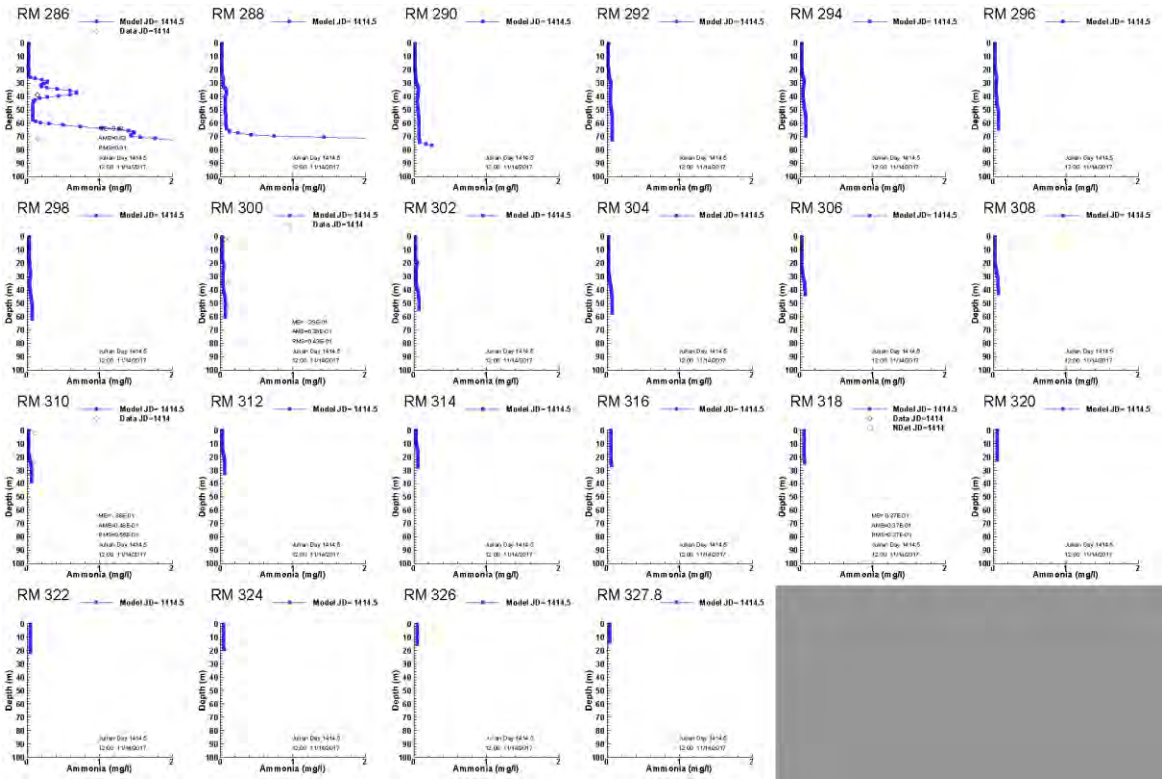


Figure 965. Vertical profiles of ammonia nitrogen compared with data for 11/14/2017.

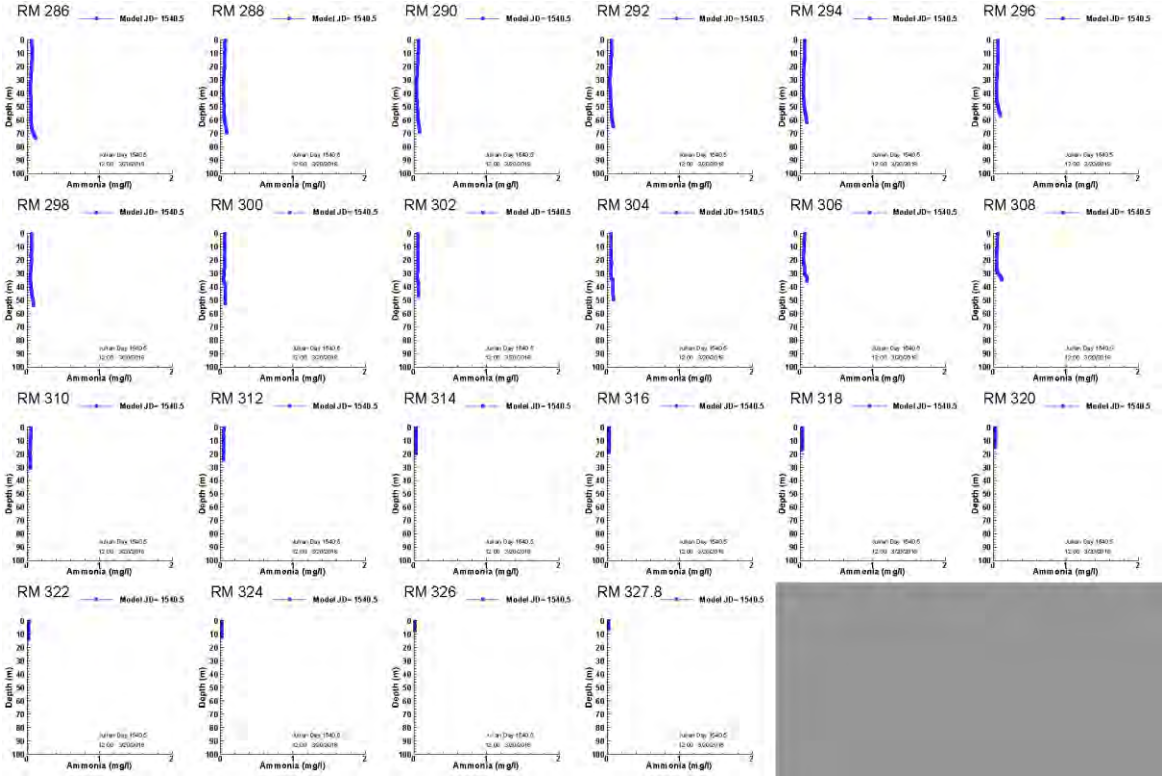


Figure 966. Vertical profiles of ammonia nitrogen compared with data for 3/20/2018.

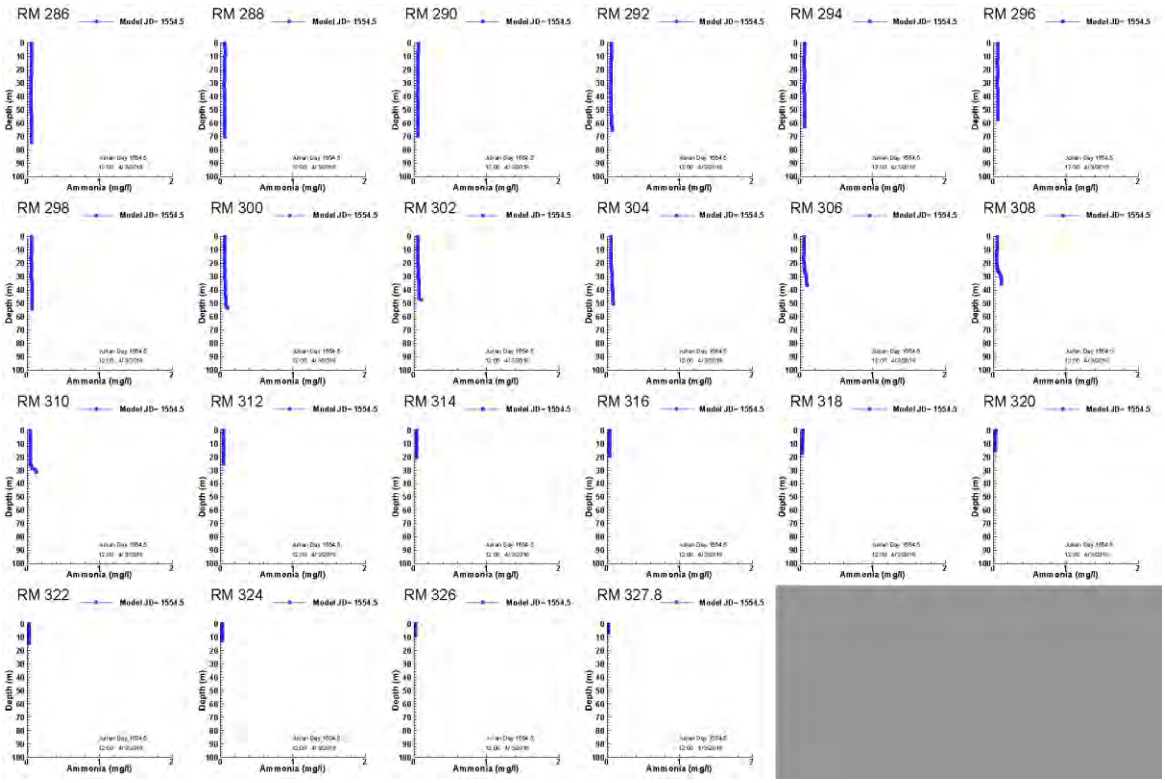


Figure 967. Vertical profiles of ammonia nitrogen compared with data for 4/ 3/2018.

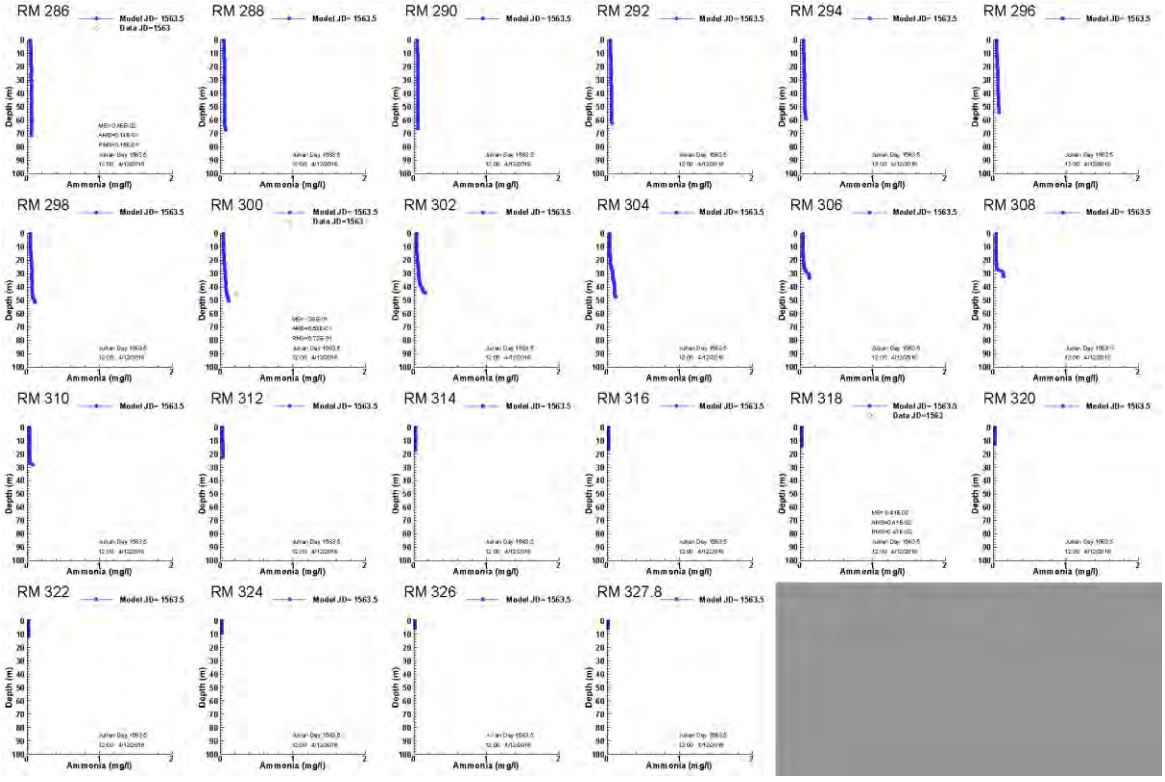


Figure 968. Vertical profiles of ammonia nitrogen compared with data for 4/12/2018.

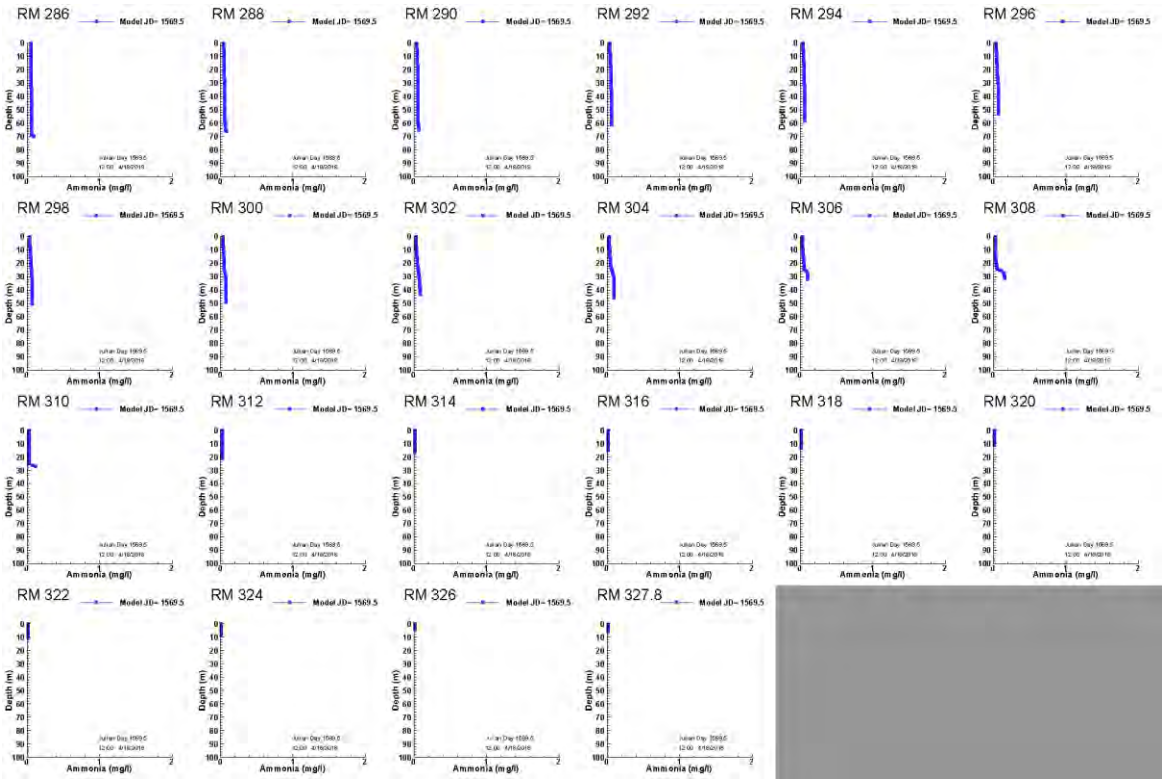


Figure 969. Vertical profiles of ammonia nitrogen compared with data for 4/18/2018.

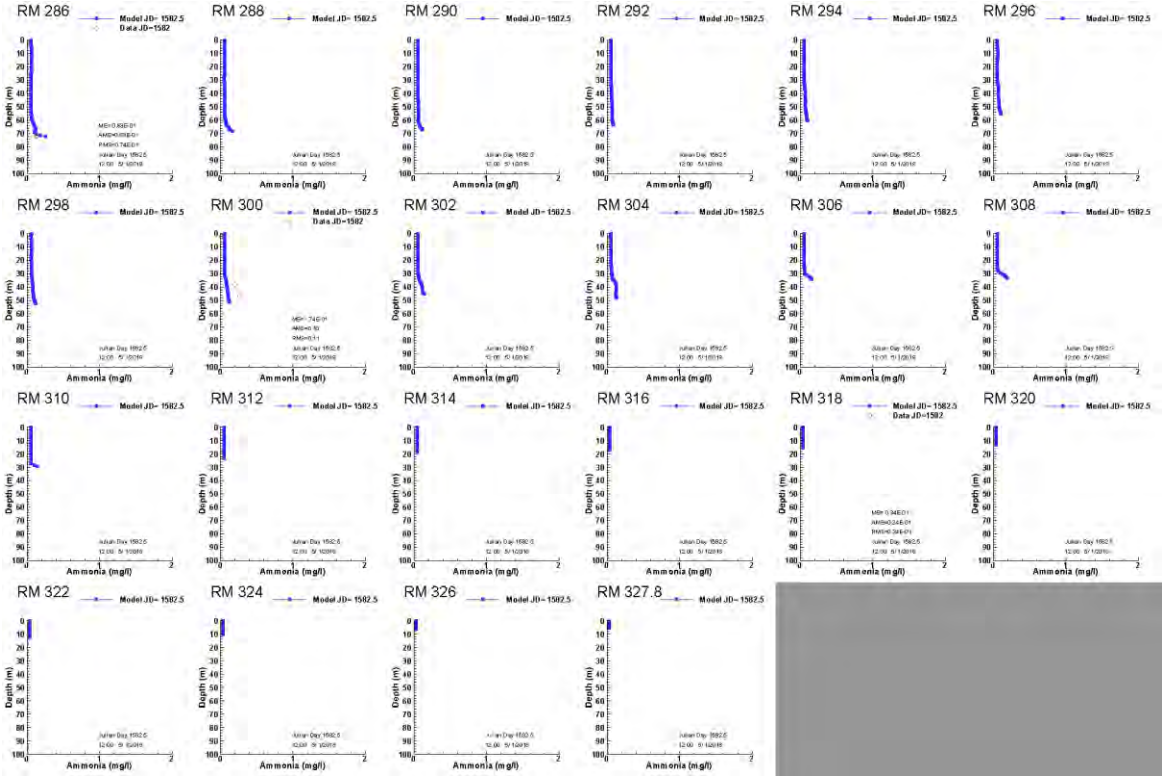


Figure 970. Vertical profiles of ammonia nitrogen compared with data for 5/ 1/2018.

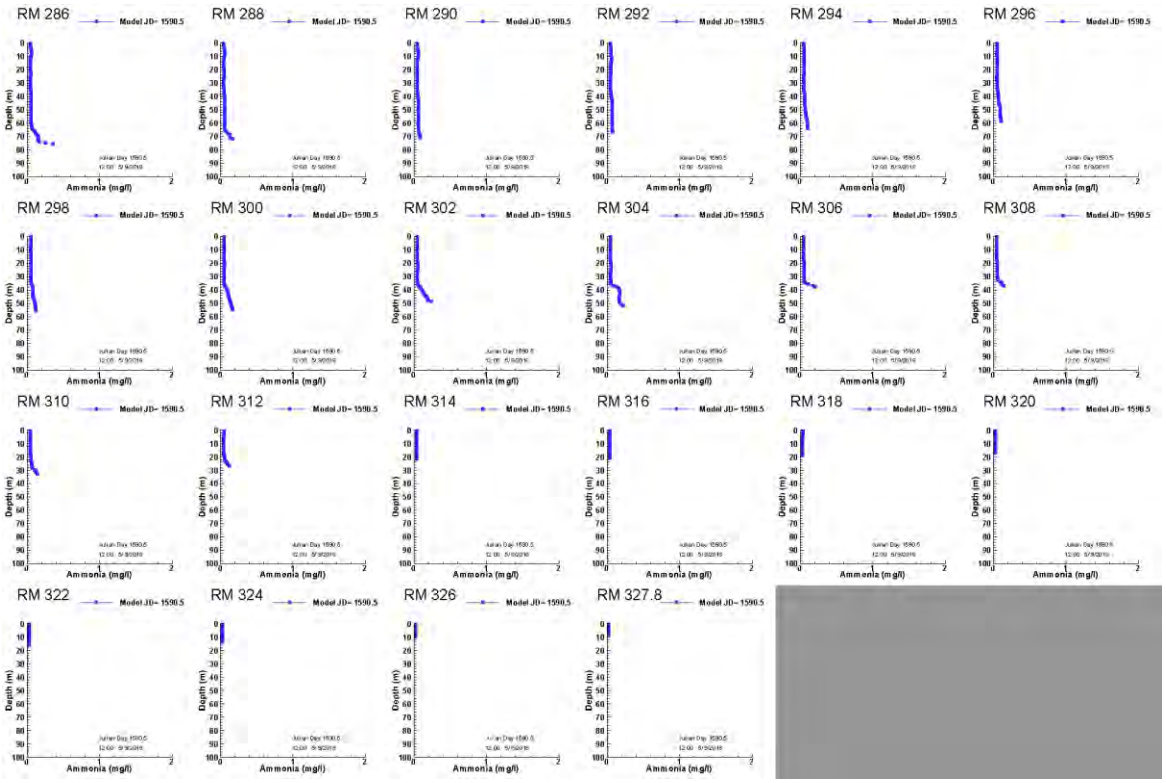


Figure 971. Vertical profiles of ammonia nitrogen compared with data for 5/ 9/2018.

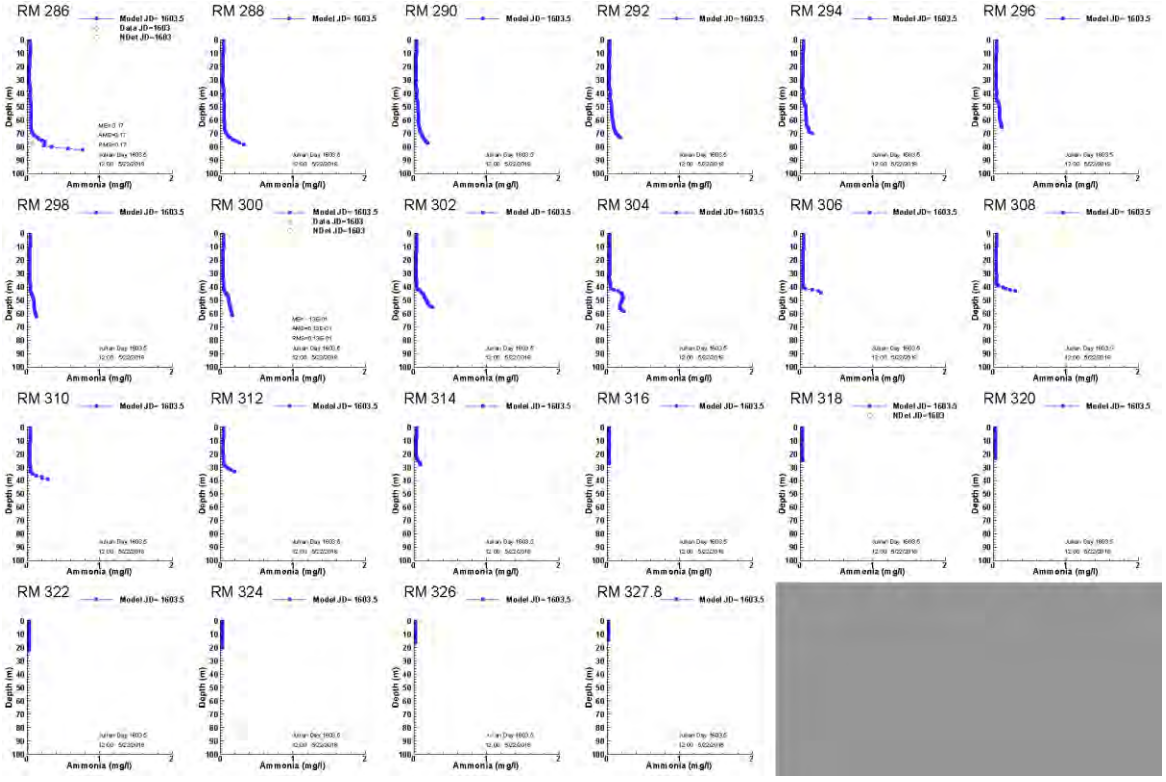


Figure 972. Vertical profiles of ammonia nitrogen compared with data for 5/22/2018.

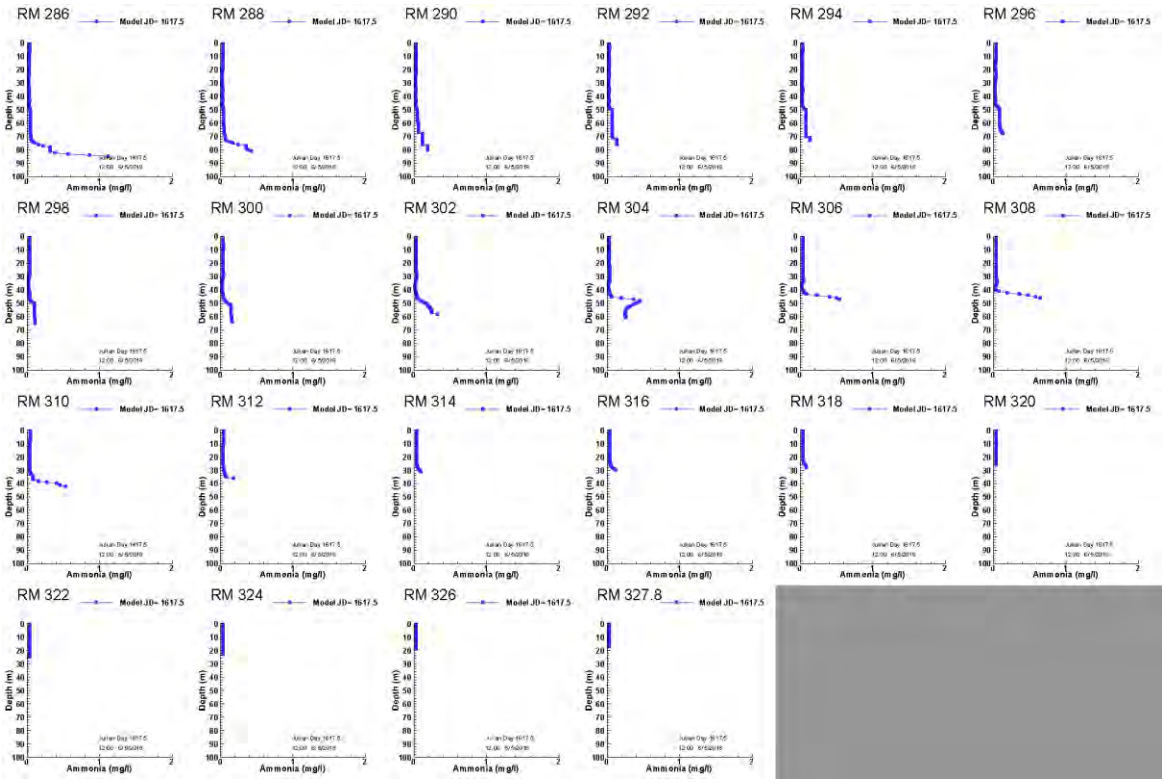


Figure 973. Vertical profiles of ammonia nitrogen compared with data for 6/ 5/2018.

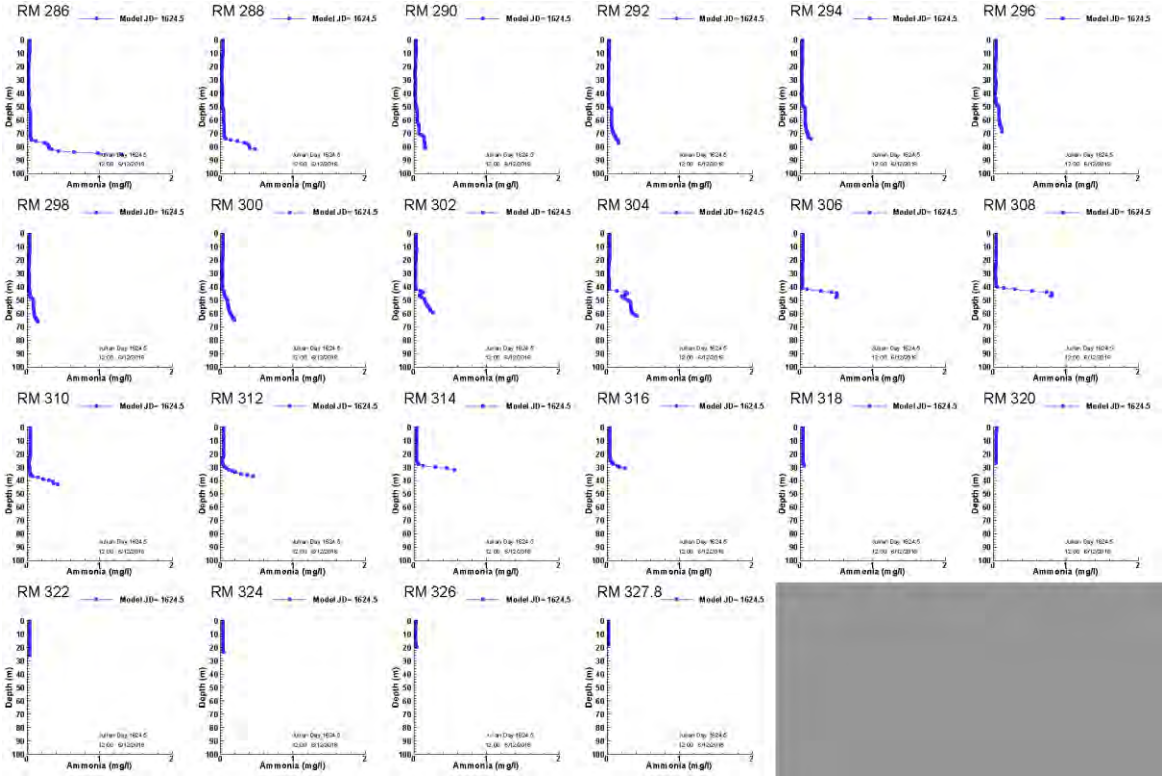


Figure 974. Vertical profiles of ammonia nitrogen compared with data for 6/12/2018.

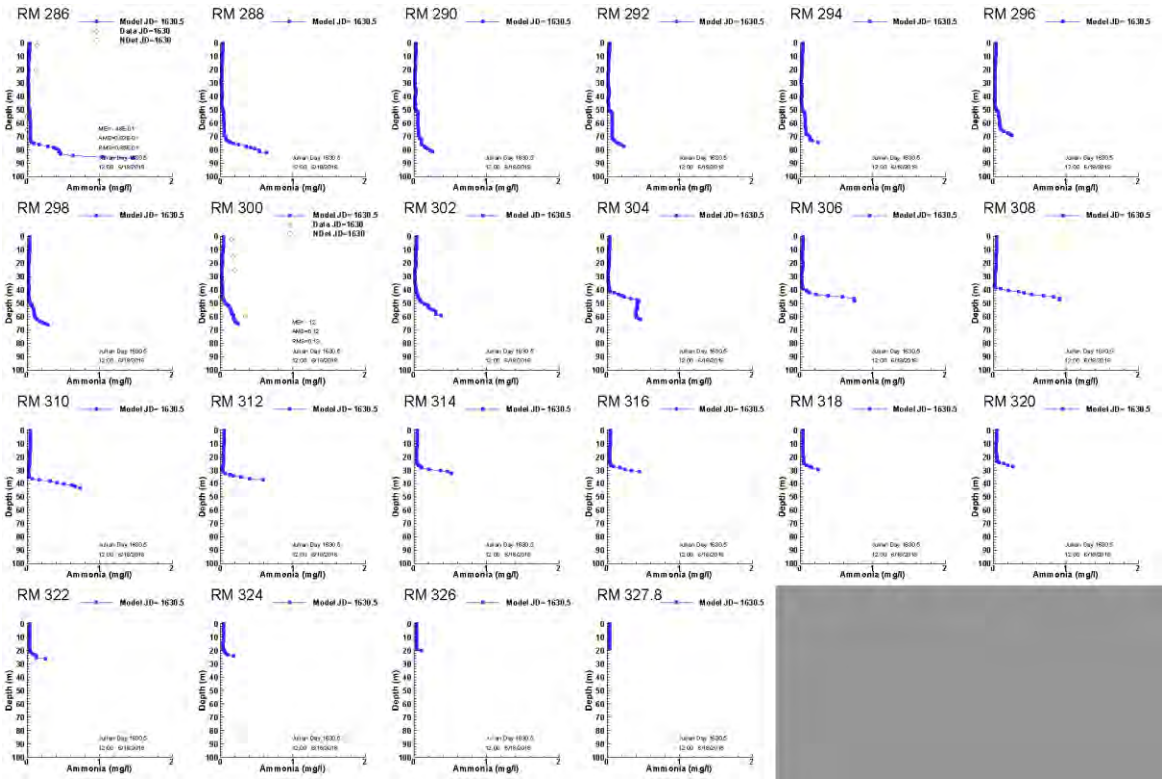


Figure 975. Vertical profiles of ammonia nitrogen compared with data for 6/18/2018.

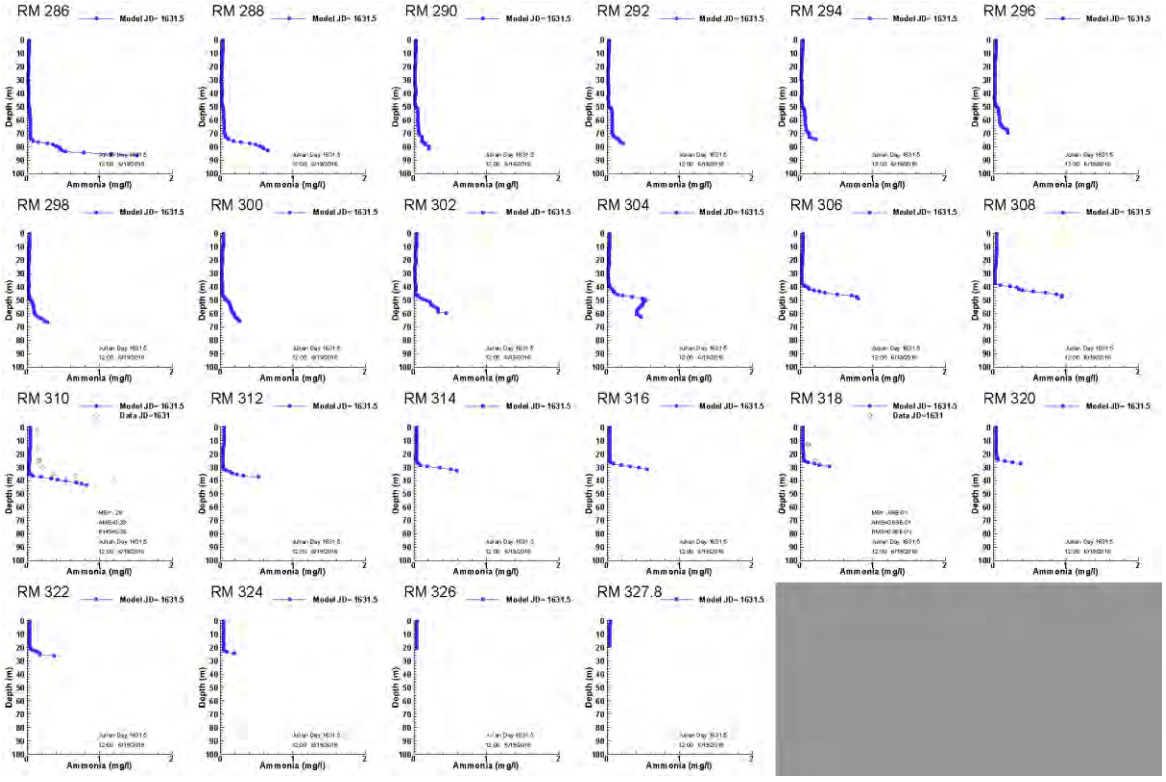


Figure 976. Vertical profiles of ammonia nitrogen compared with data for 6/19/2018.

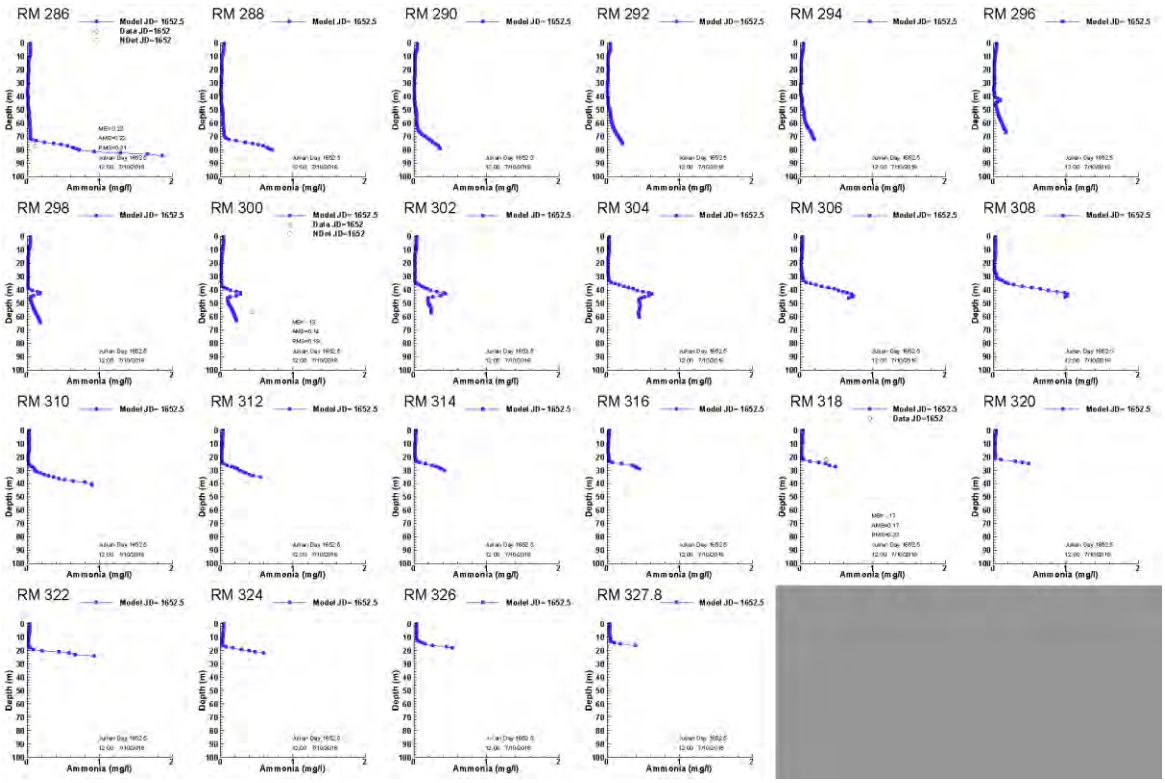


Figure 977. Vertical profiles of ammonia nitrogen compared with data for 7/10/2018.

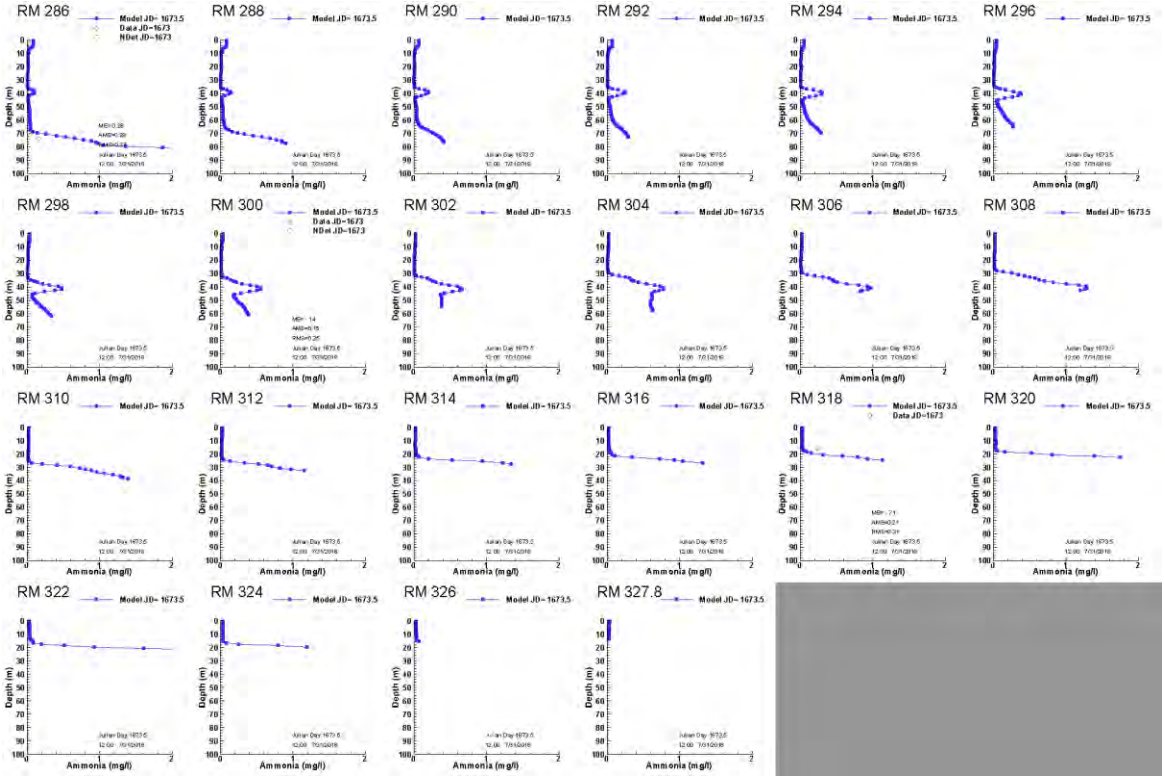


Figure 978. Vertical profiles of ammonia nitrogen compared with data for 7/31/2018.

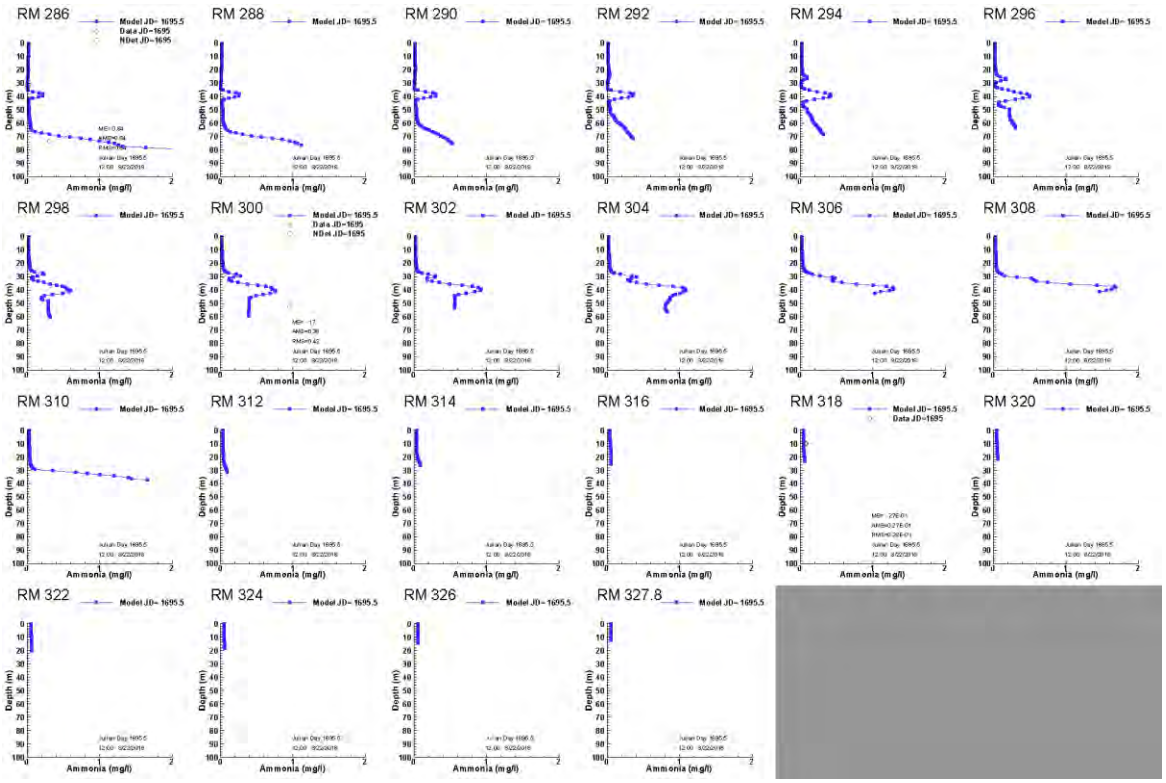


Figure 979. Vertical profiles of ammonia nitrogen compared with data for 8/22/2018.

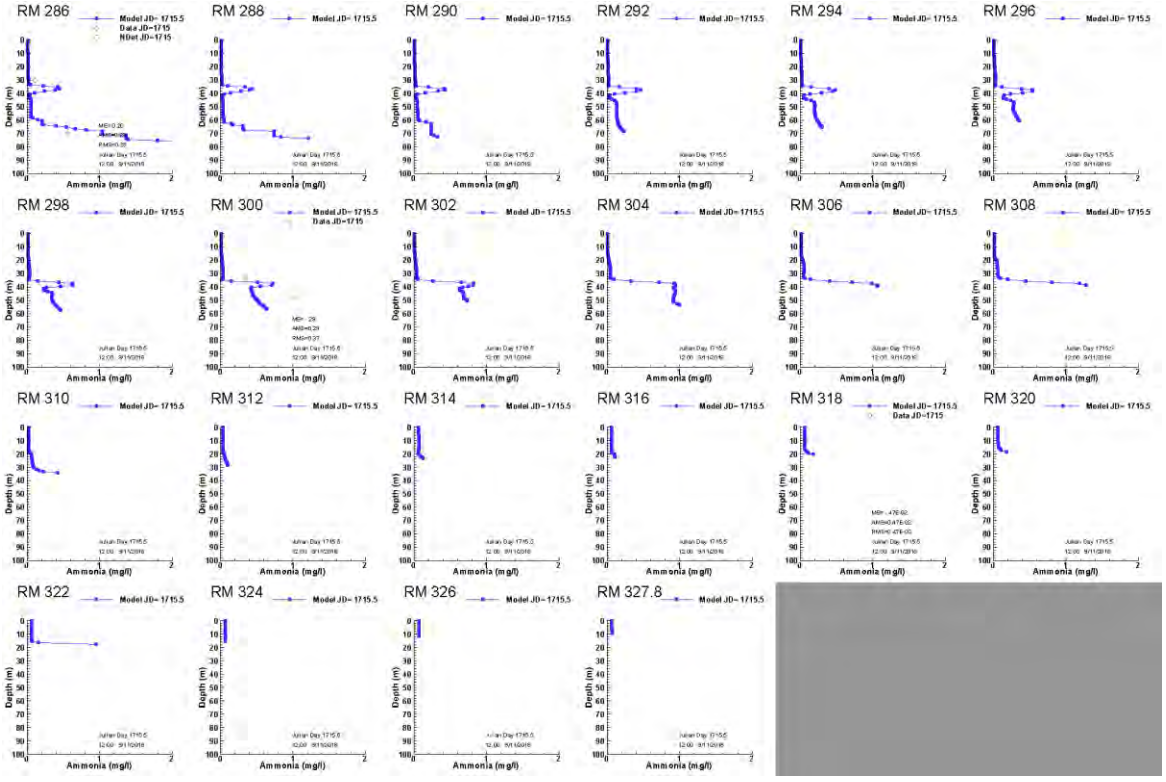


Figure 980. Vertical profiles of ammonia nitrogen compared with data for 9/11/2018.

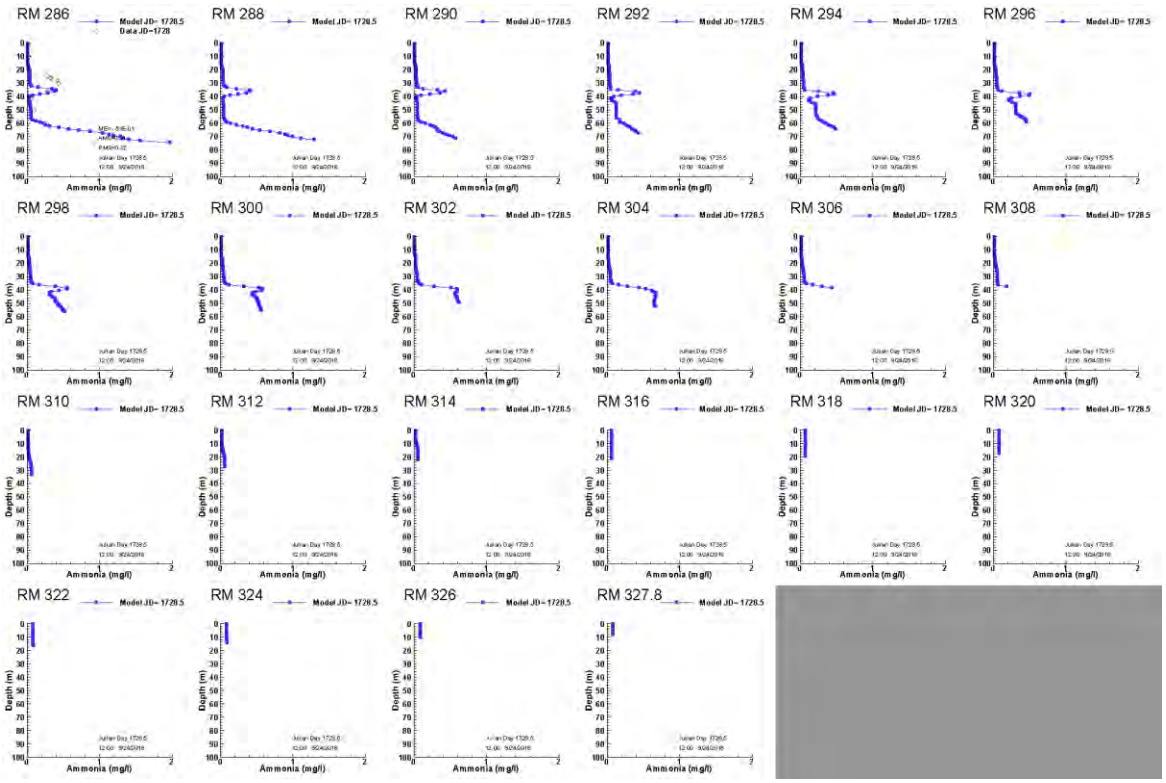


Figure 981. Vertical profiles of ammonia nitrogen compared with data for 9/24/2018.

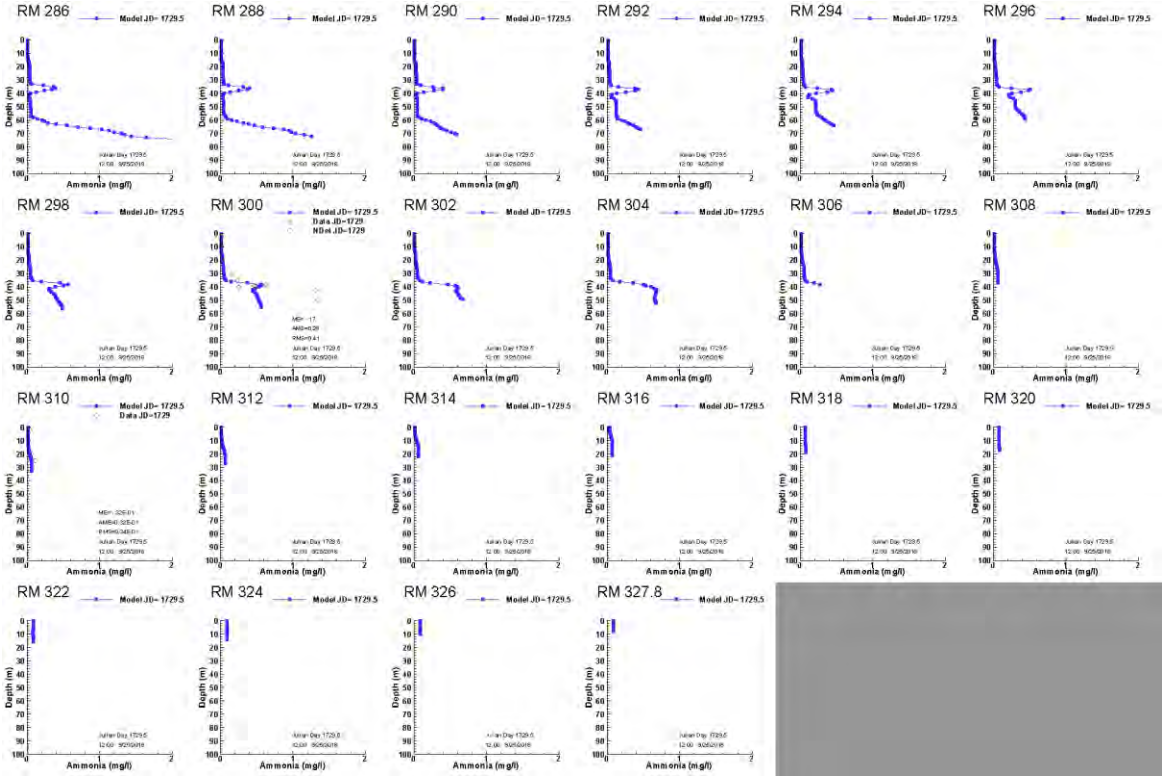


Figure 982. Vertical profiles of ammonia nitrogen compared with data for 9/25/2018.

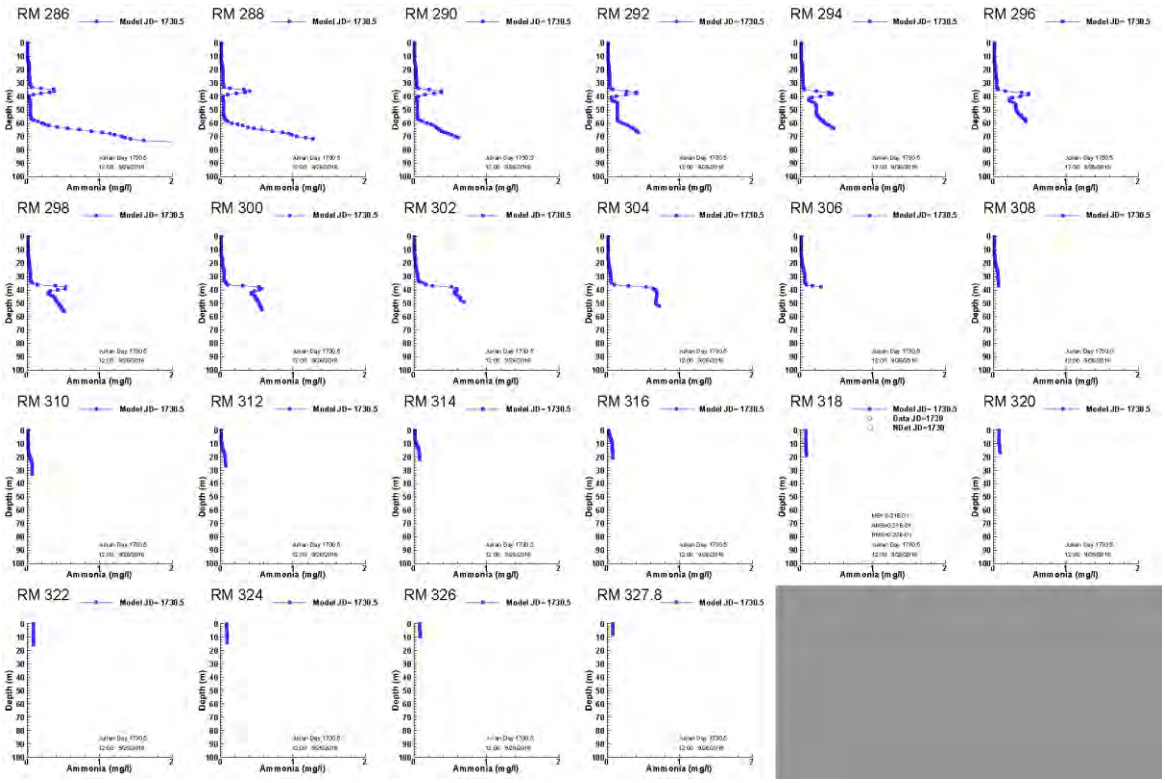


Figure 983. Vertical profiles of ammonia nitrogen compared with data for 9/26/2018.

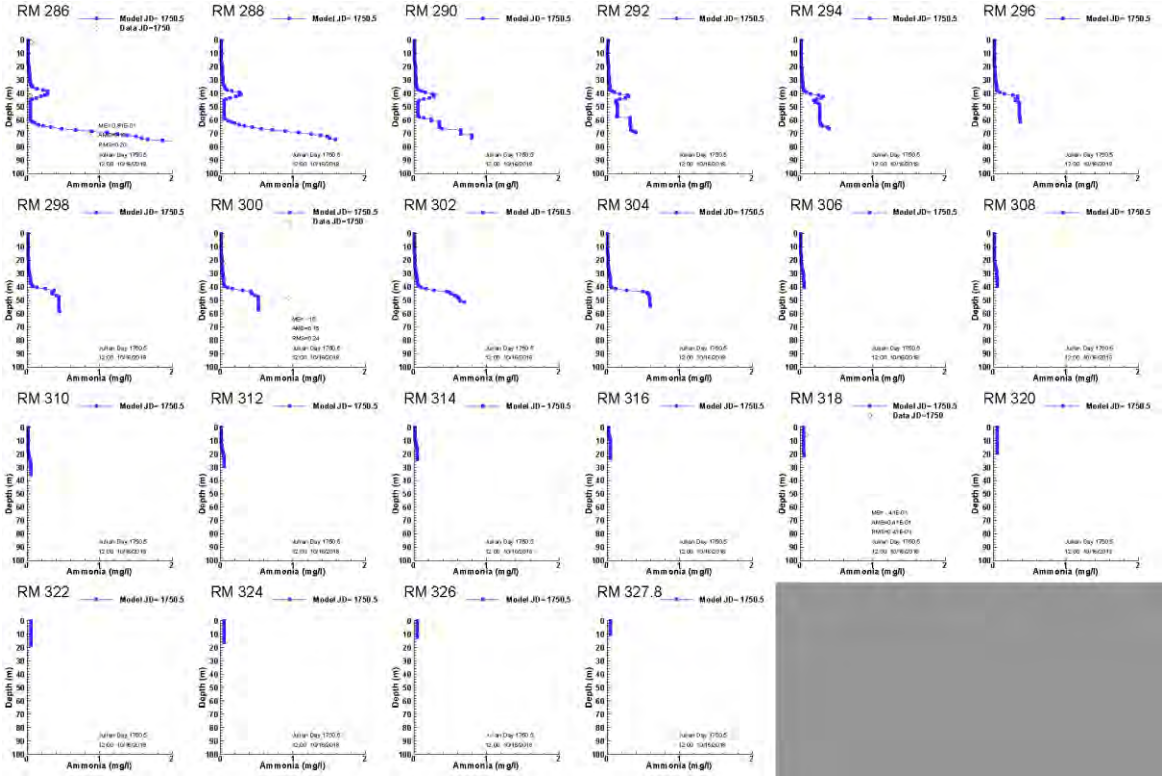


Figure 984. Vertical profiles of ammonia nitrogen compared with data for 10/16/2018.

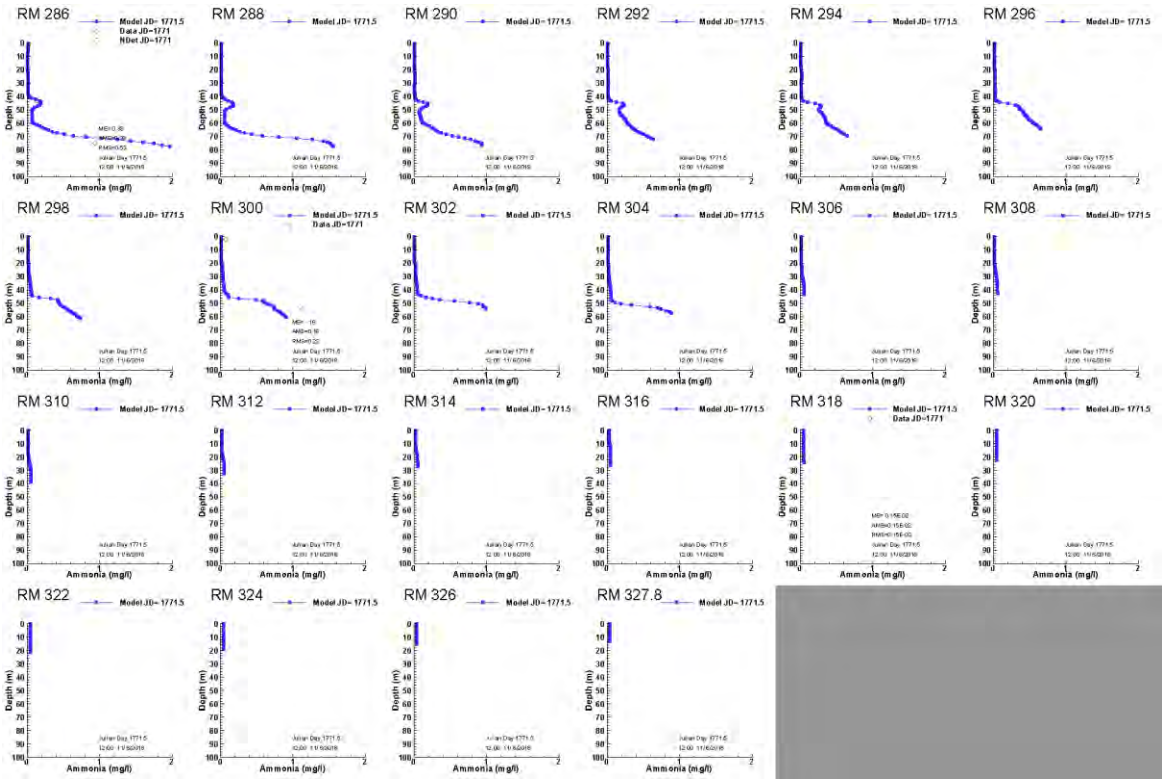


Figure 985. Vertical profiles of ammonia nitrogen compared with data for 11/ 6/2018.

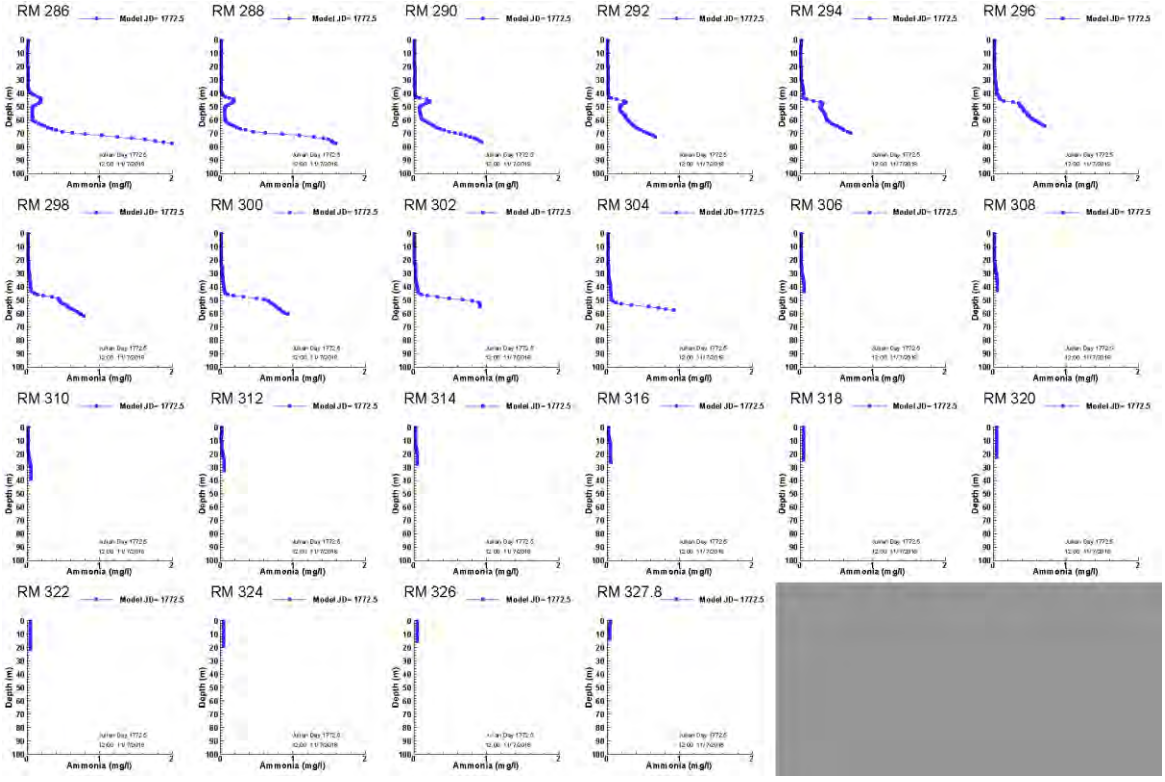


Figure 986. Vertical profiles of ammonia nitrogen compared with data for 11/ 7/2018.

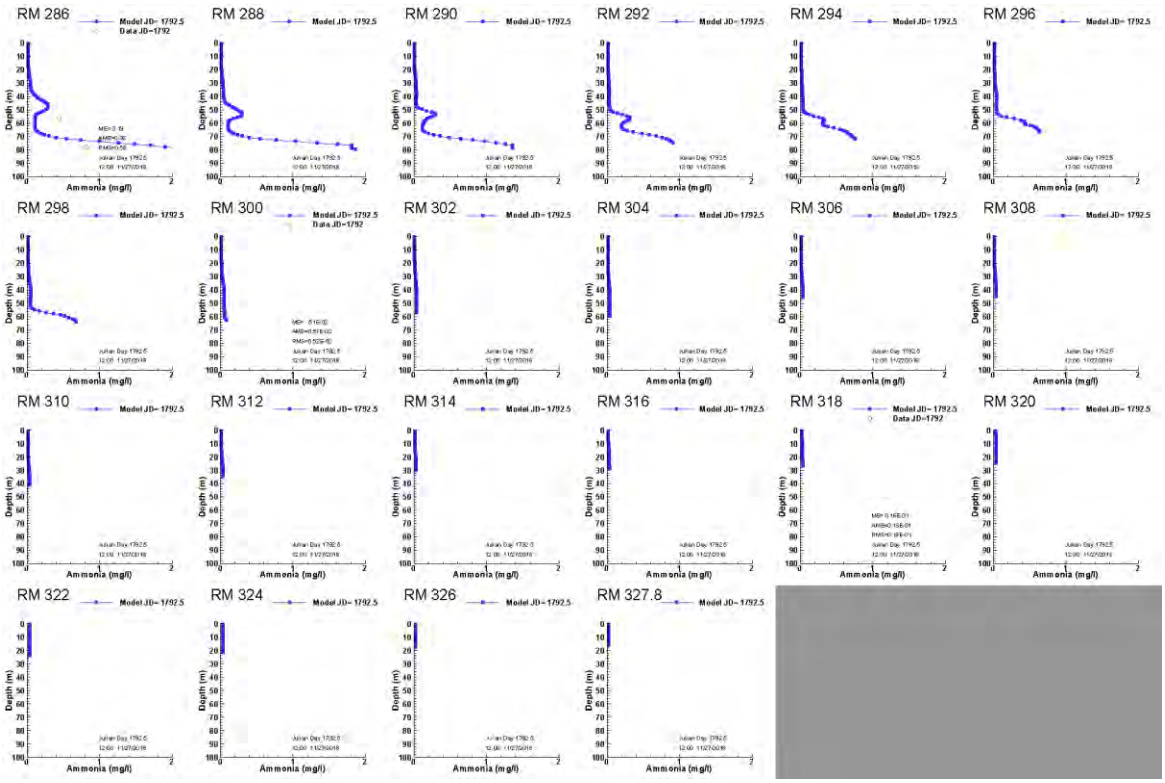


Figure 987. Vertical profiles of ammonia nitrogen compared with data for 11/27/2018.

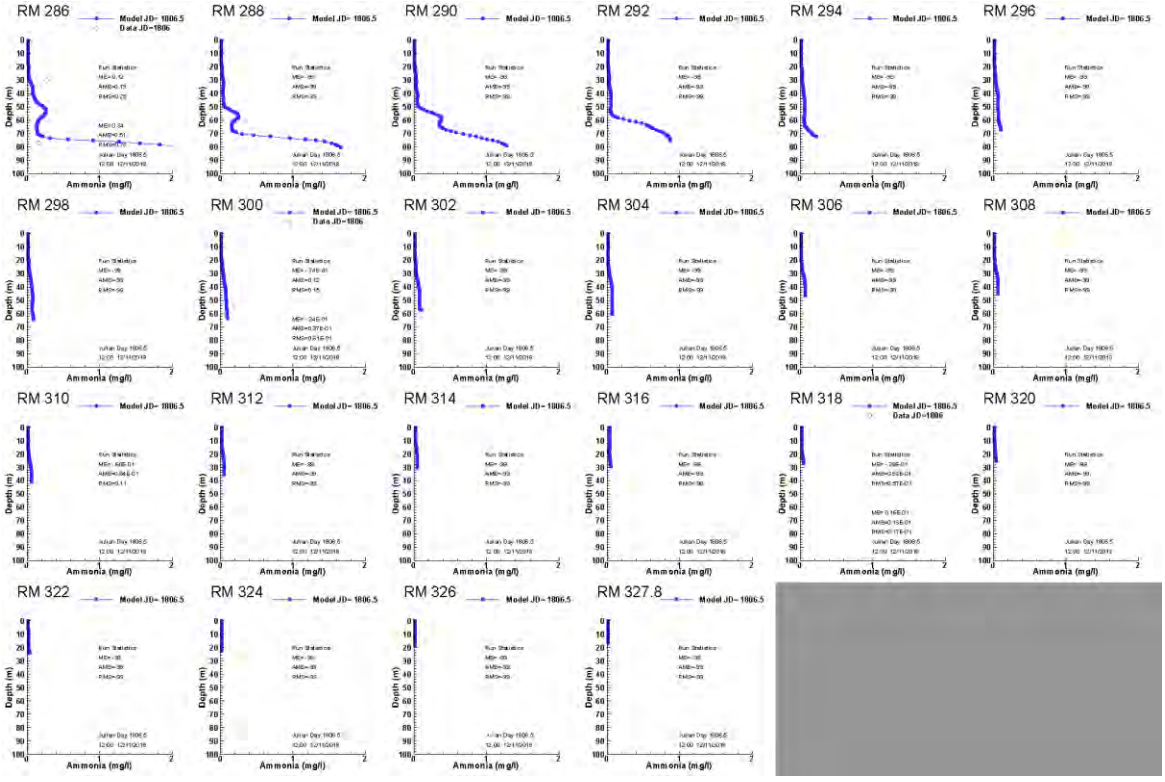


Figure 988. Vertical profiles of ammonia nitrogen compared with data for 12/11/2018.

Nitrate Nitrogen

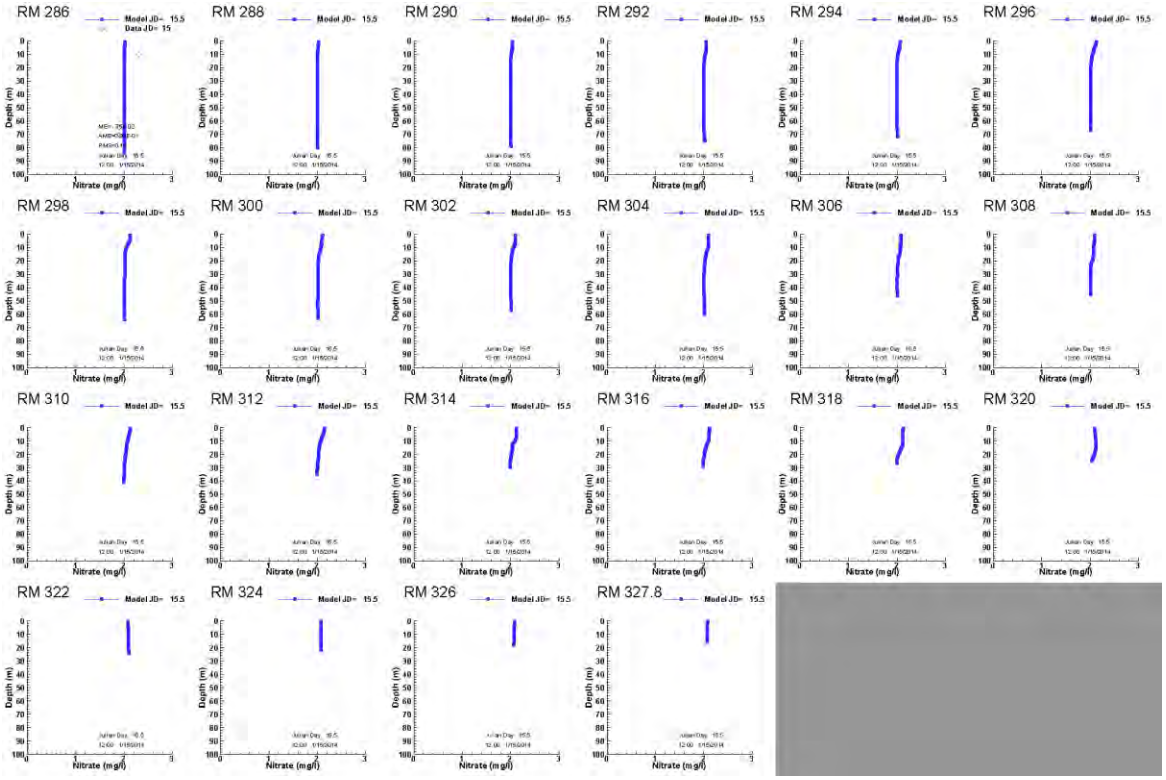


Figure 989. Vertical profiles of NOxN compared with data for 1/15/2014.

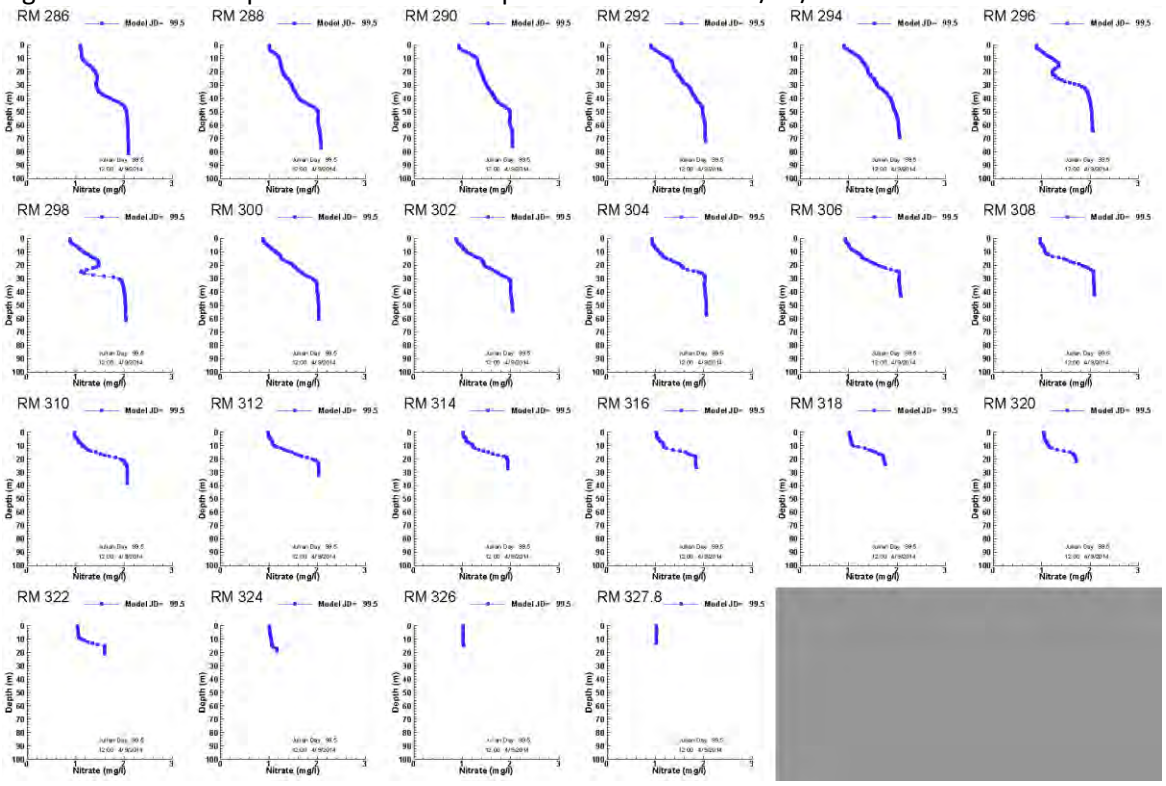


Figure 990. Vertical profiles of NOxN compared with data for 4/ 9/2014.

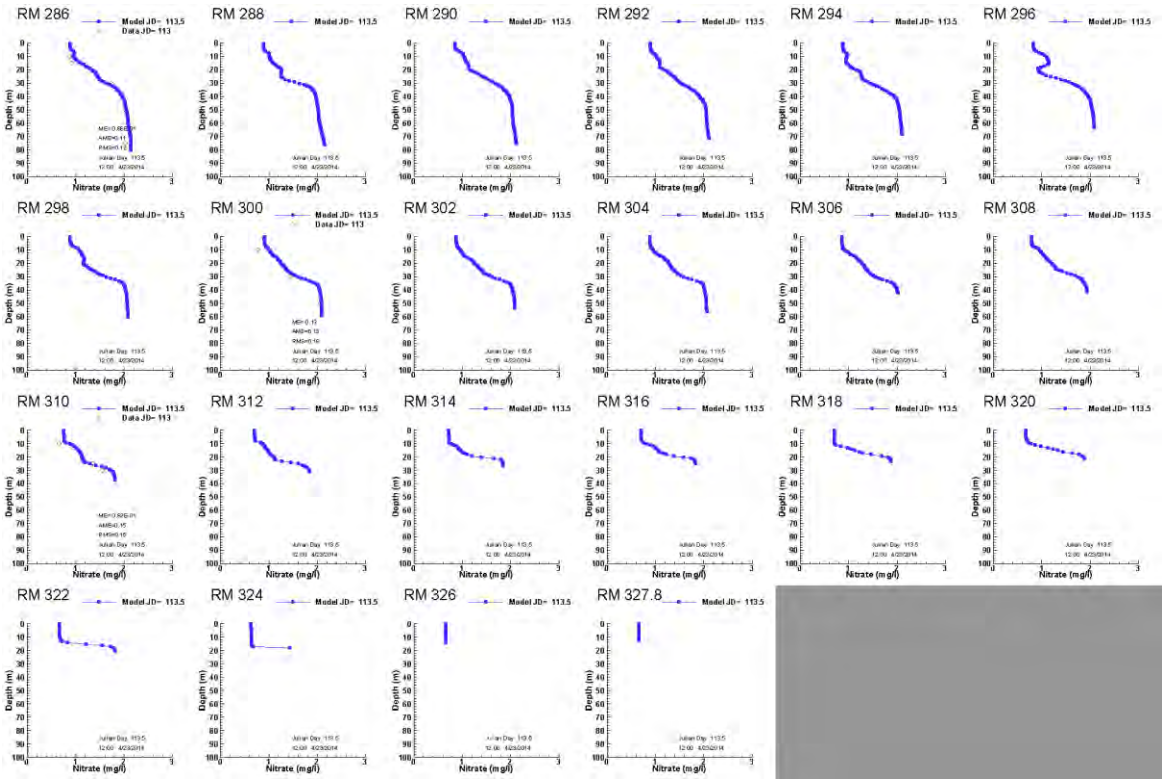


Figure 991. Vertical profiles of NOxN compared with data for 4/23/2014.

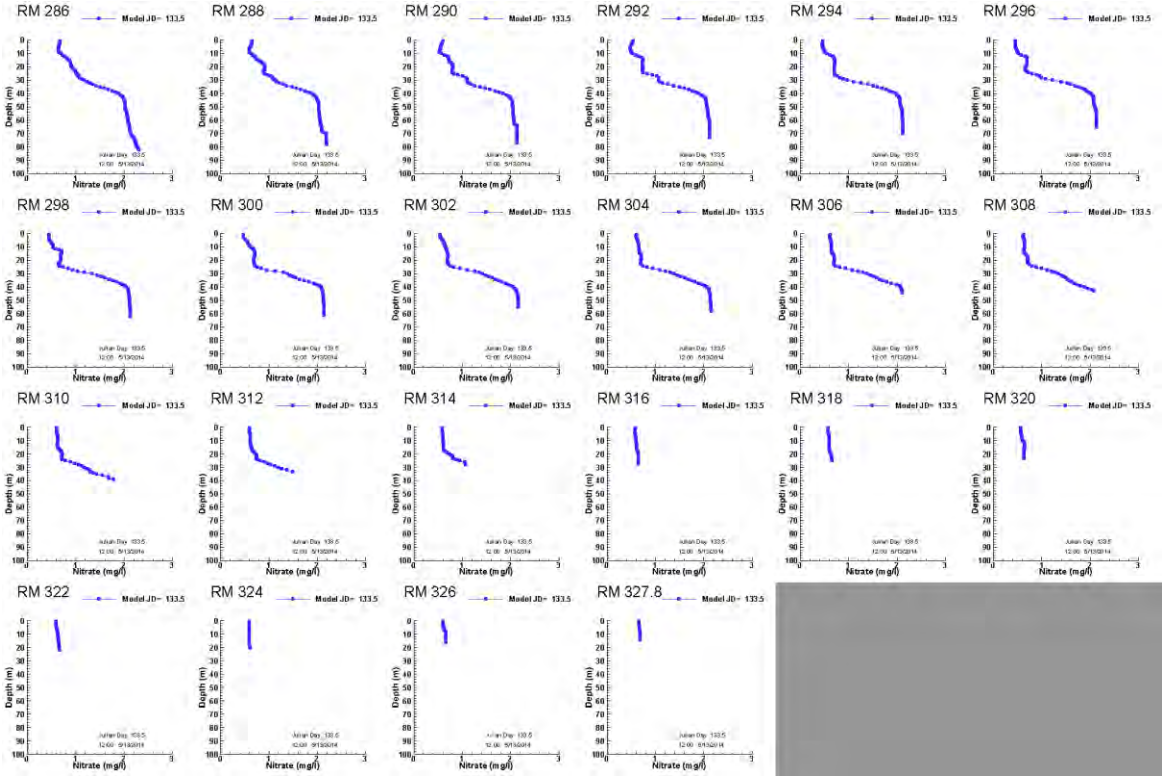


Figure 992. Vertical profiles of NOxN compared with data for 5/13/2014.

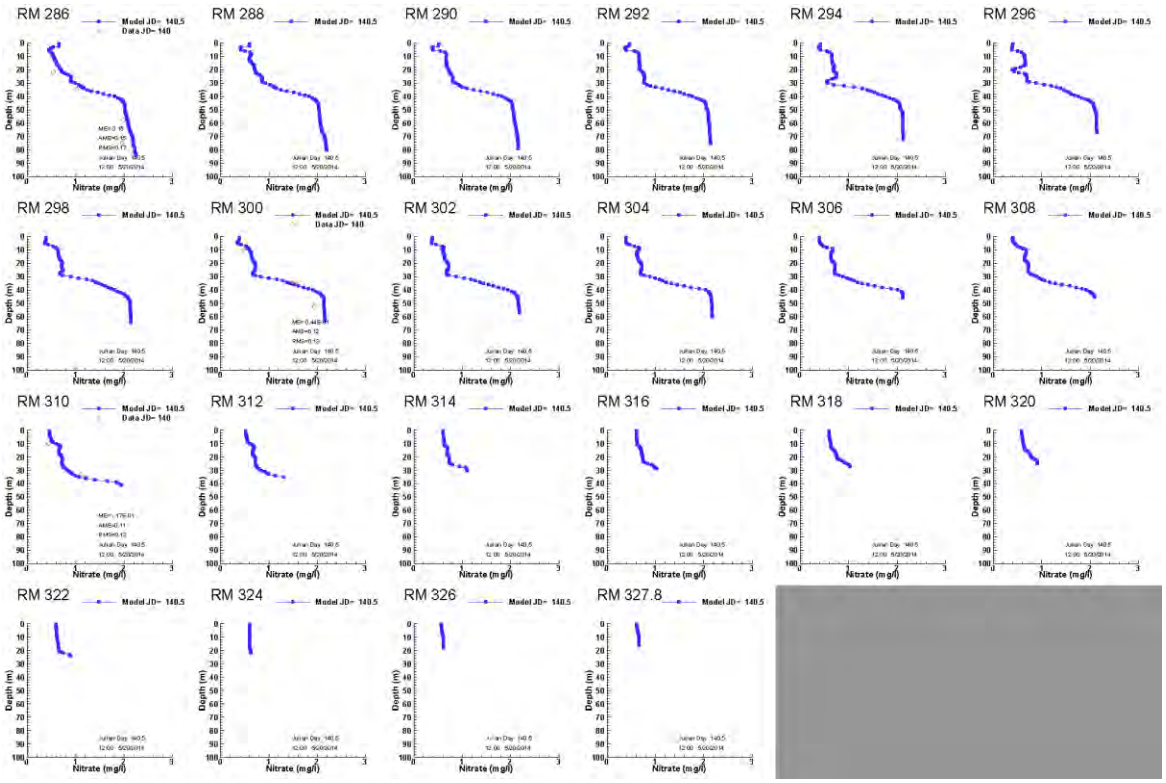


Figure 993. Vertical profiles of NOxN compared with data for 5/20/2014.

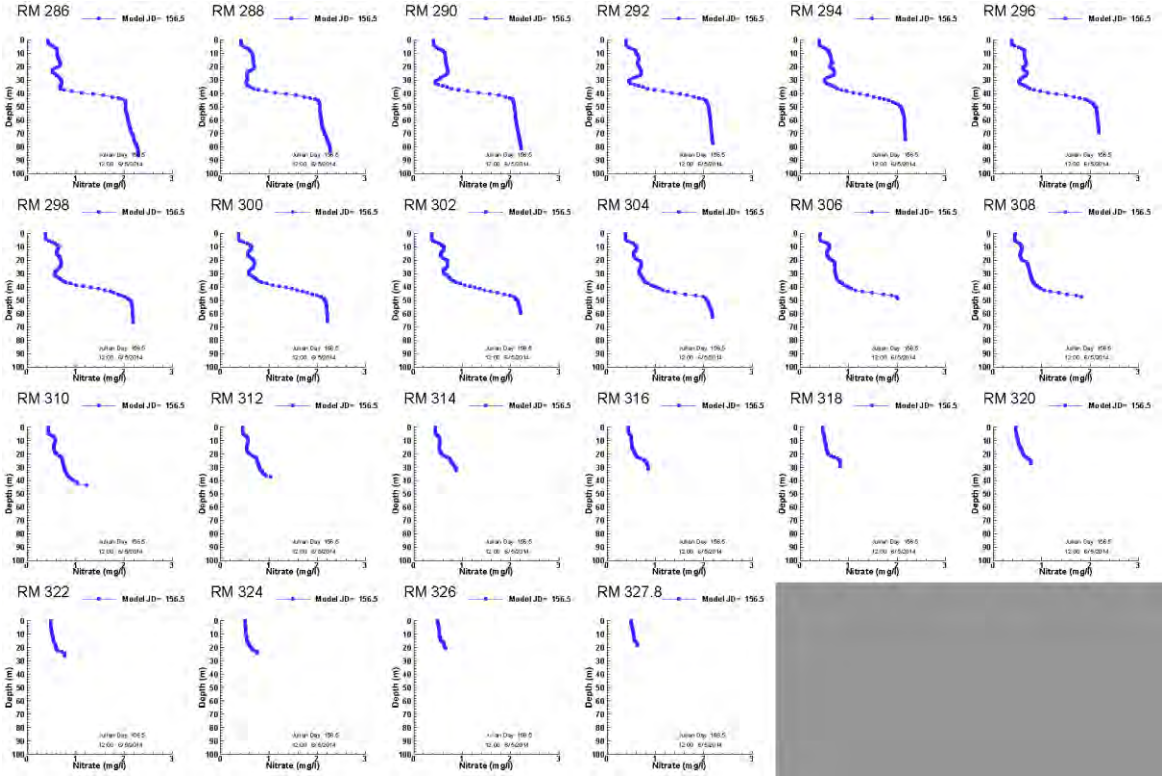


Figure 994. Vertical profiles of NOxN compared with data for 6/ 5/2014.

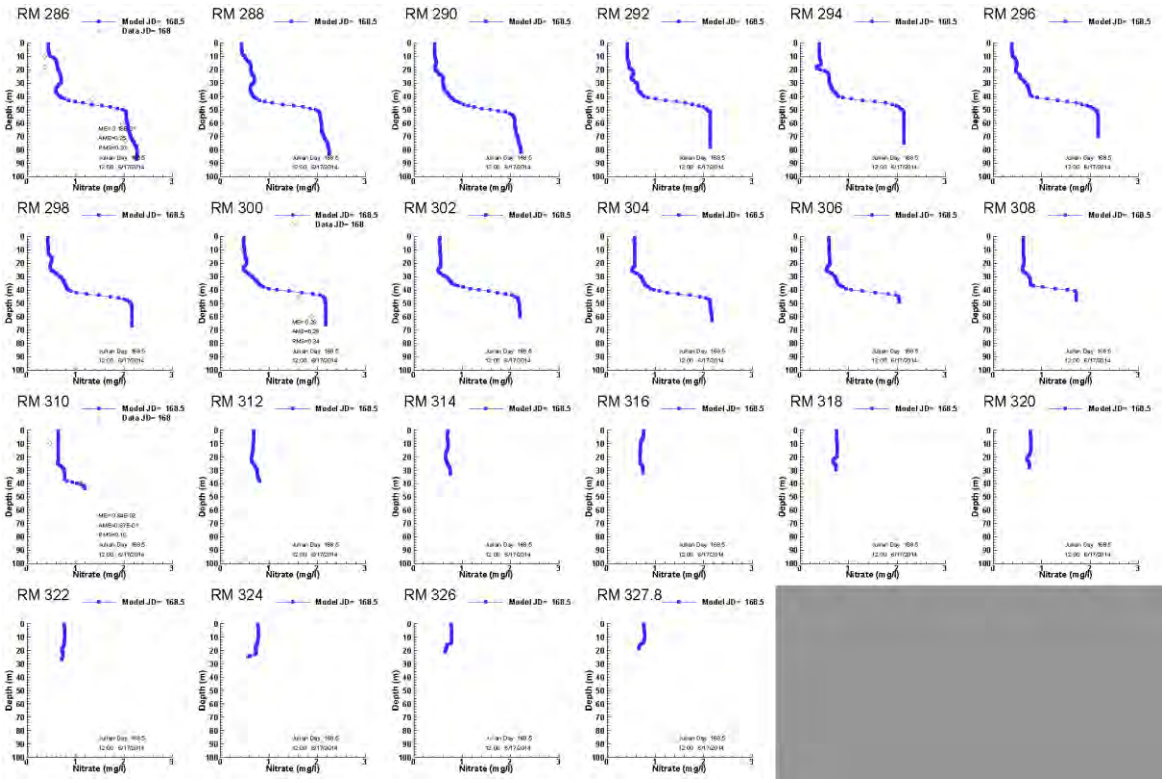


Figure 995. Vertical profiles of NOxN compared with data for 6/17/2014.

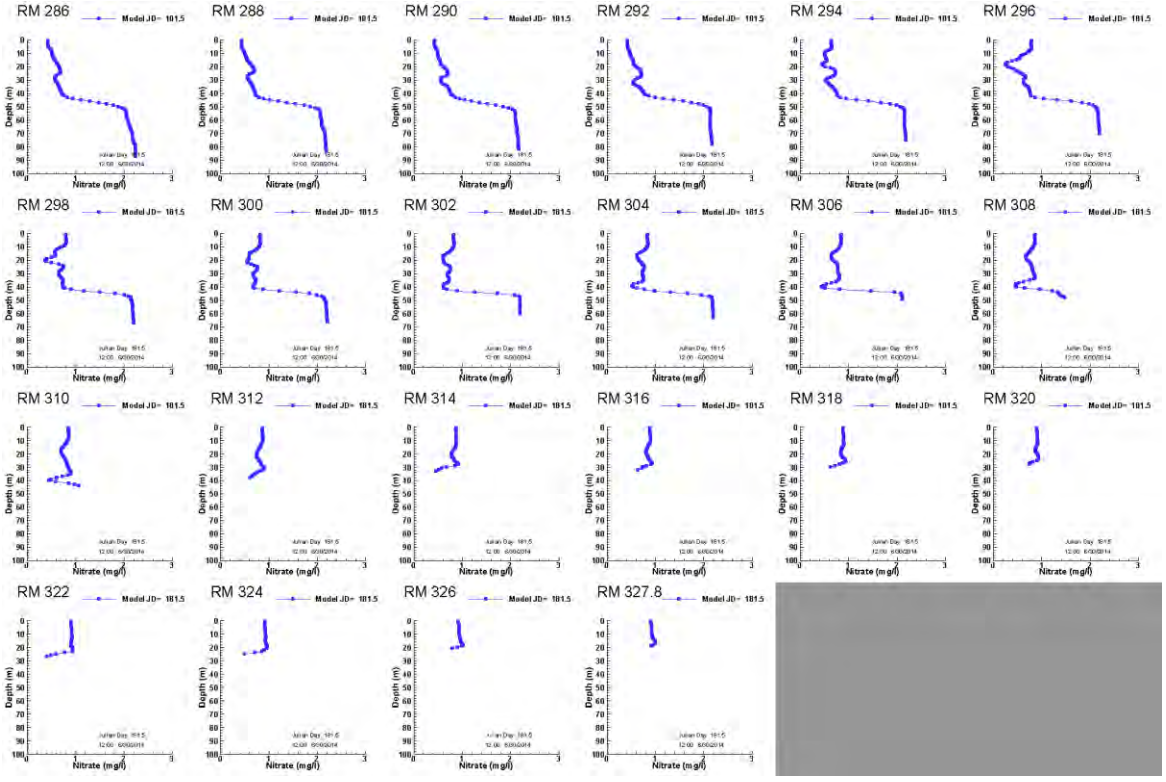


Figure 996. Vertical profiles of NOxN compared with data for 6/30/2014.

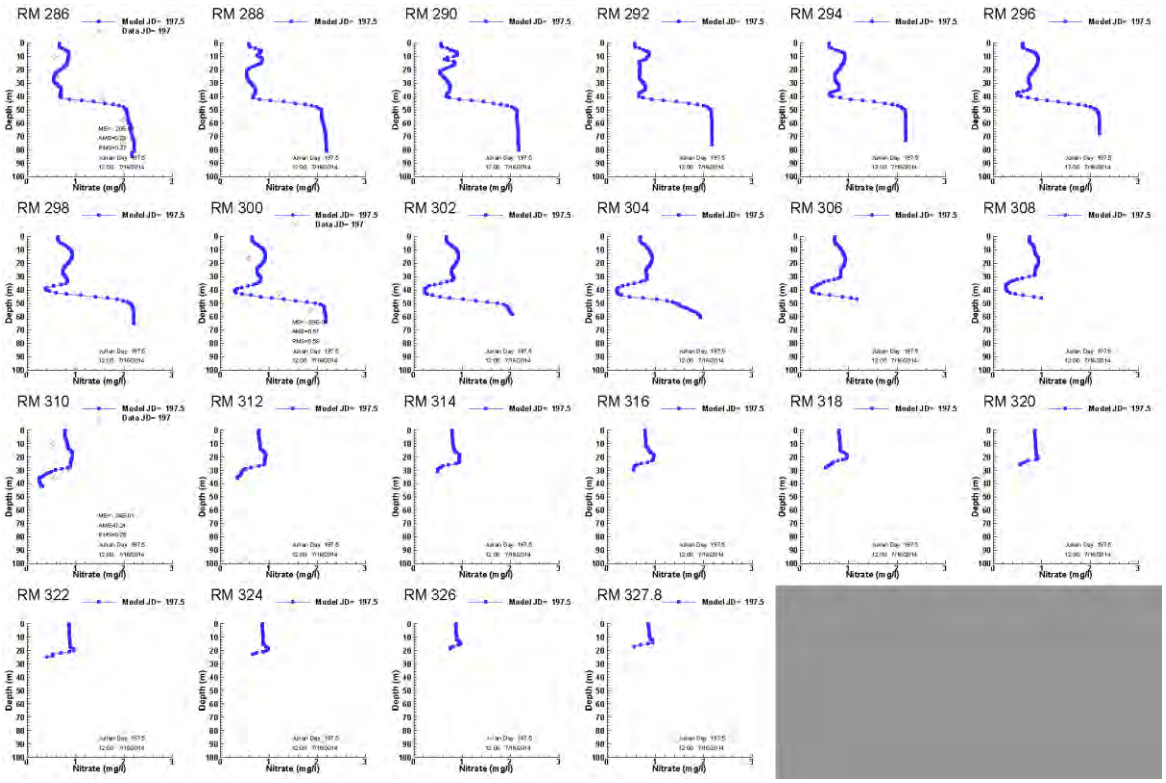


Figure 997. Vertical profiles of NOxN compared with data for 7/16/2014.

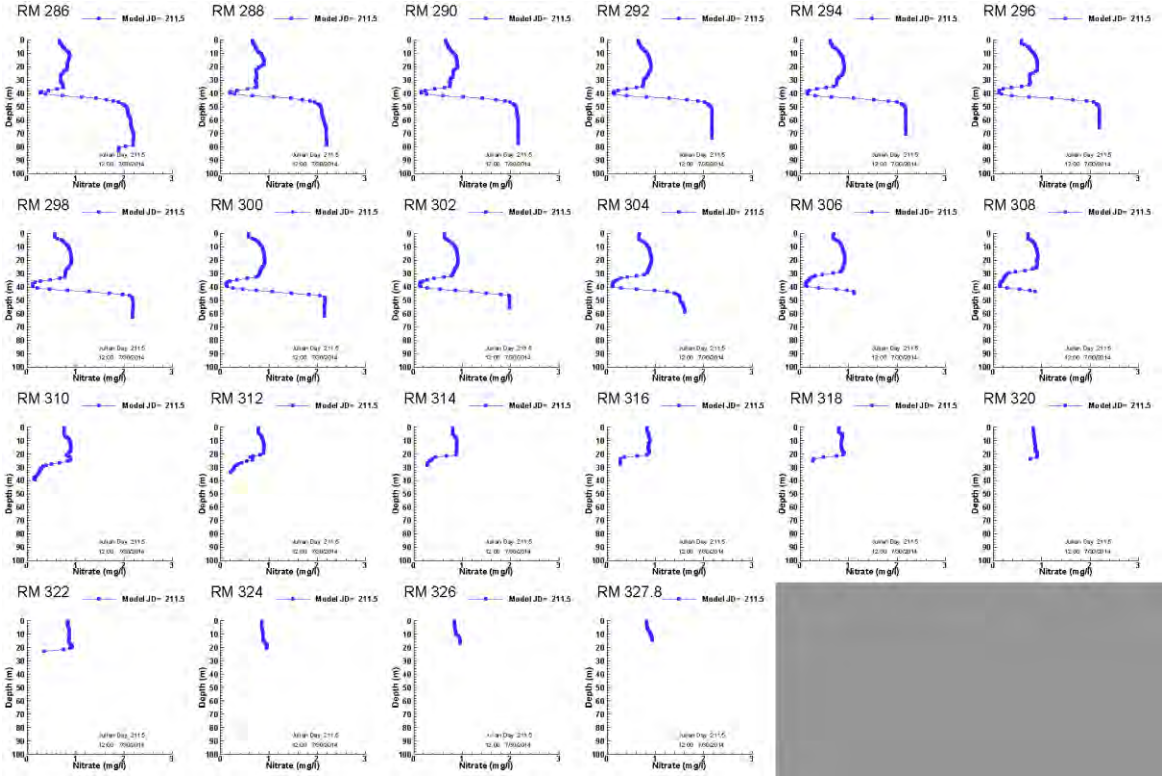


Figure 998. Vertical profiles of NOxN compared with data for 7/30/2014.

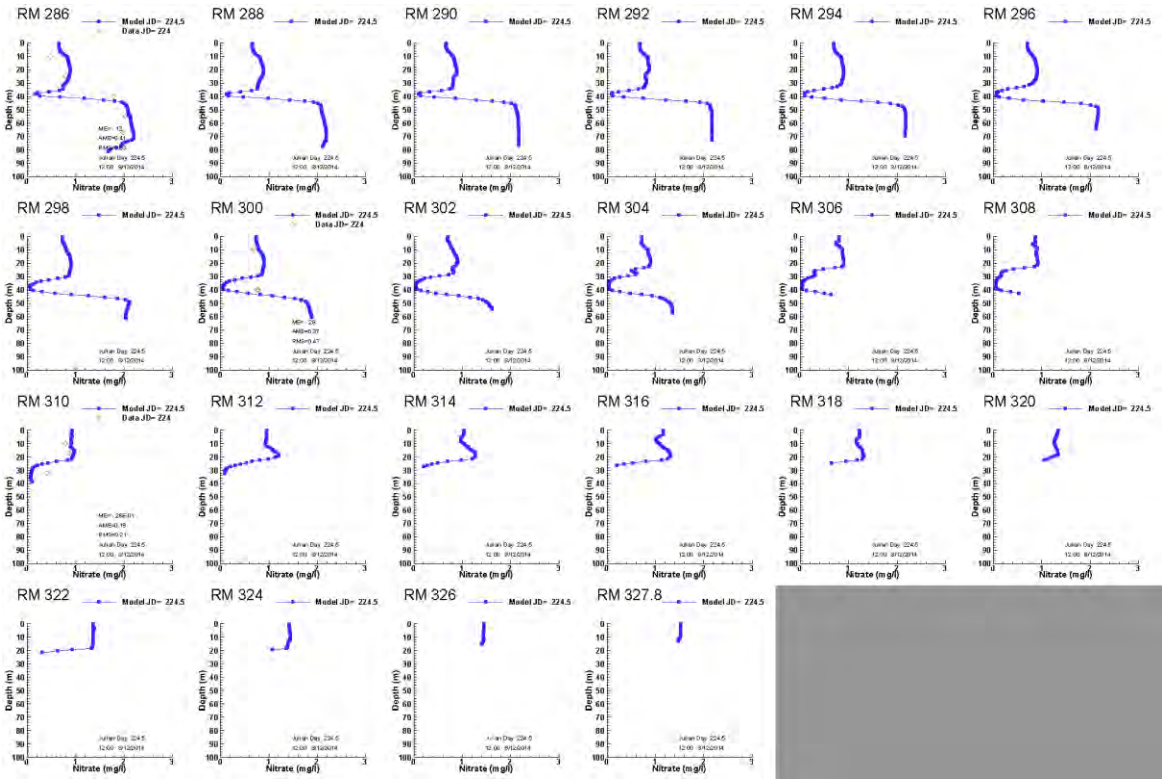


Figure 999. Vertical profiles of NOxN compared with data for 8/12/2014.

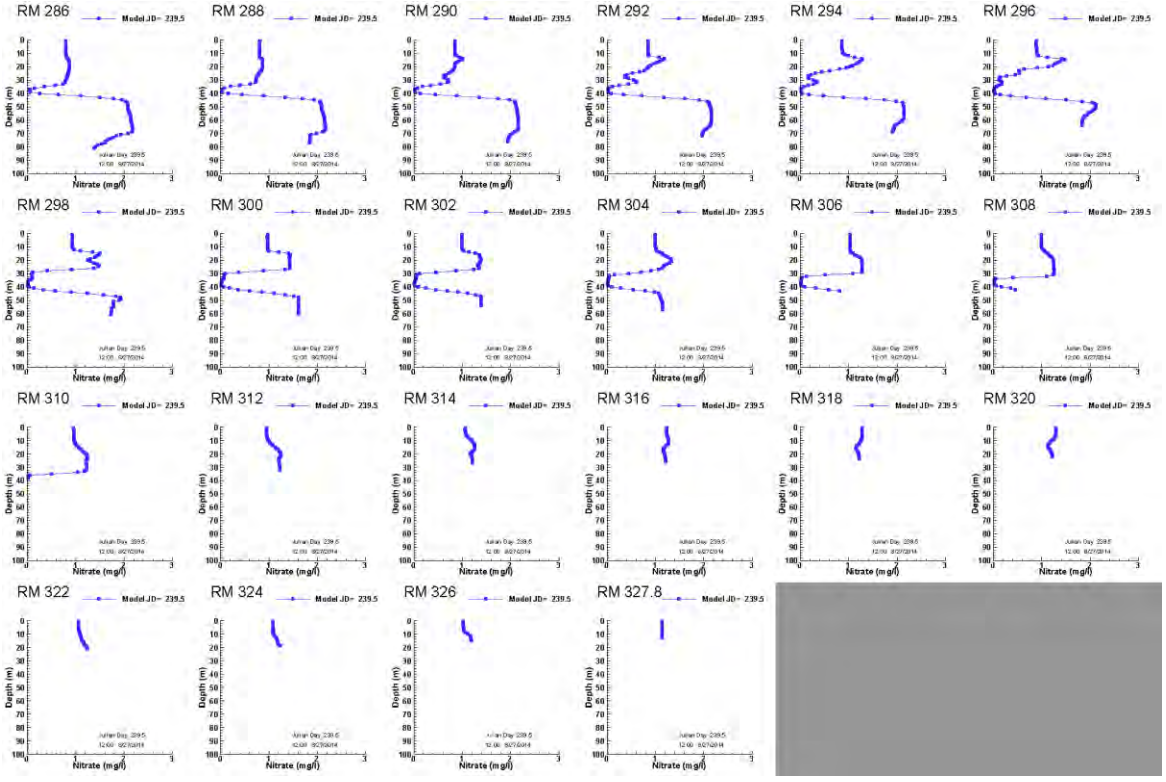


Figure 1000. Vertical profiles of NOxN compared with data for 8/27/2014.

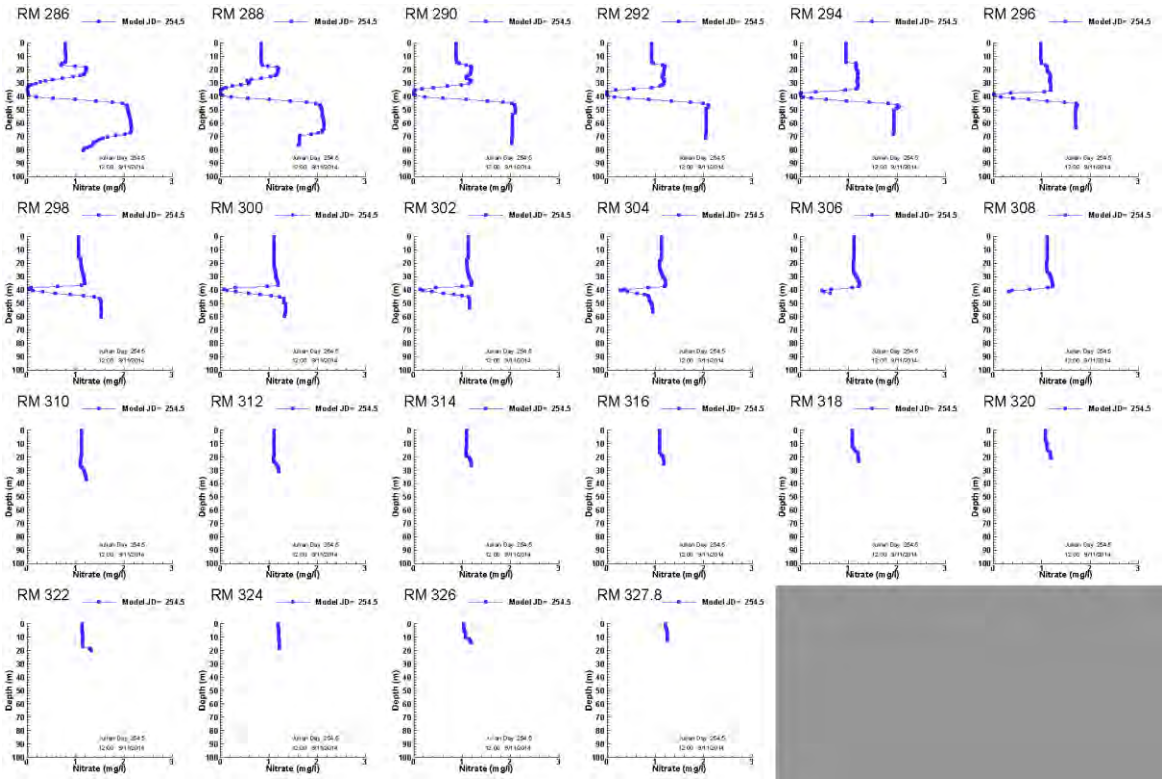


Figure 1001. Vertical profiles of NOxN compared with data for 9/11/2014.

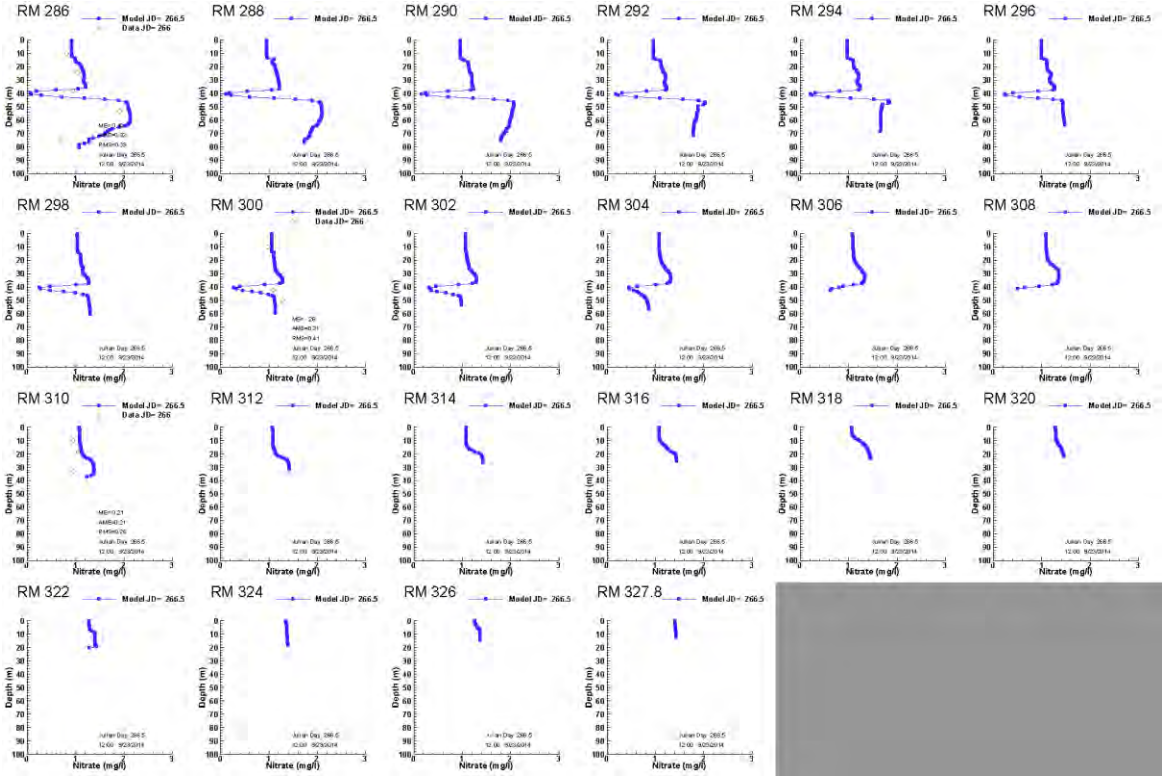


Figure 1002. Vertical profiles of NOxN compared with data for 9/23/2014.

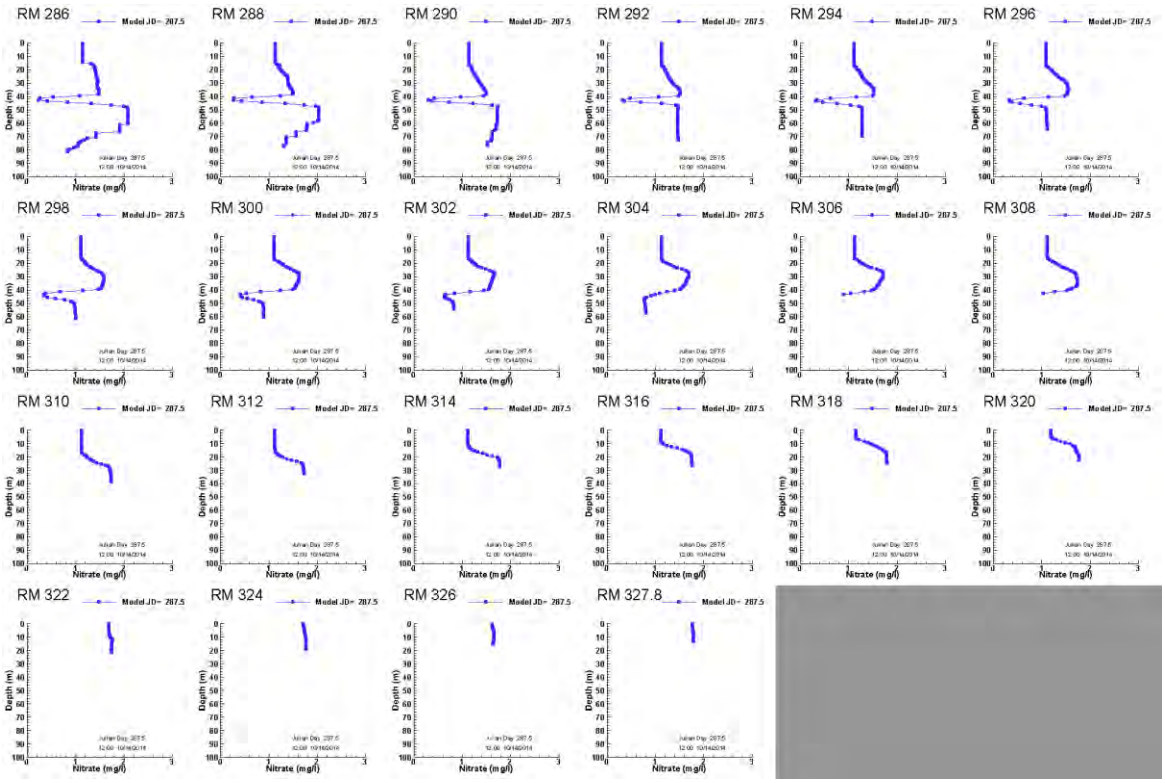


Figure 1003. Vertical profiles of NOxN compared with data for 10/14/2014.

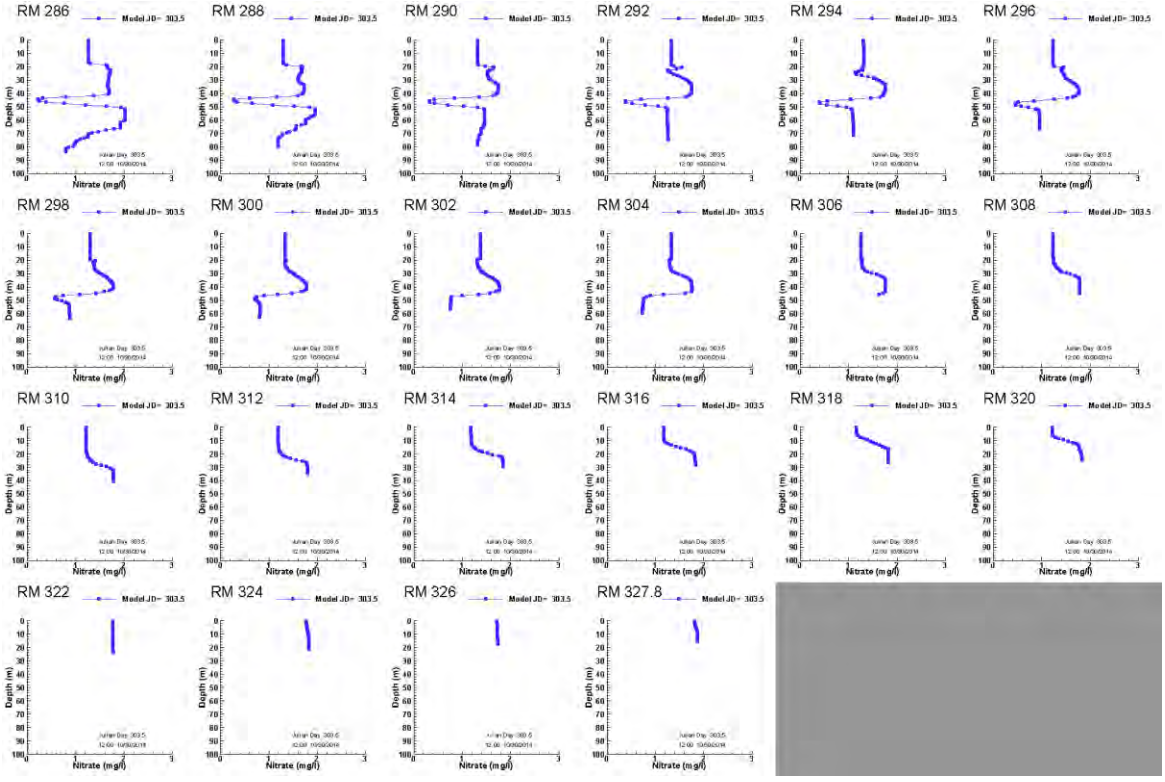


Figure 1004. Vertical profiles of NOxN compared with data for 10/30/2014.

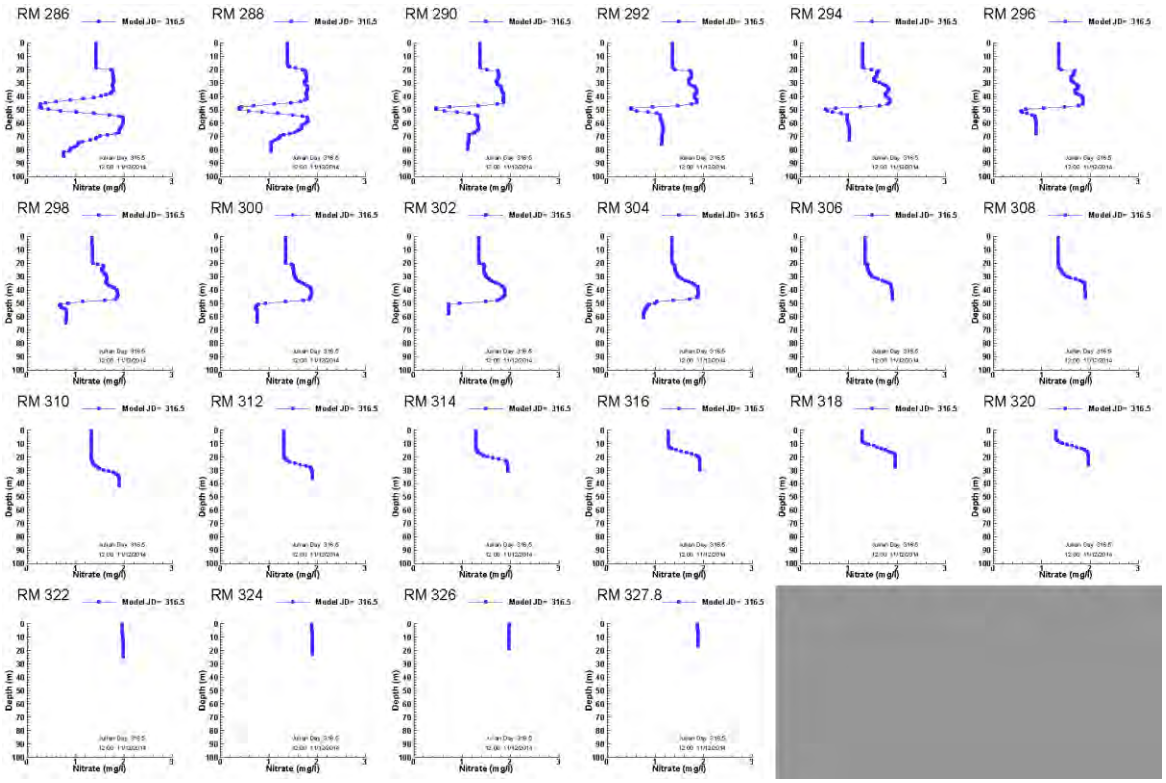


Figure 1005. Vertical profiles of NOxN compared with data for 11/12/2014.

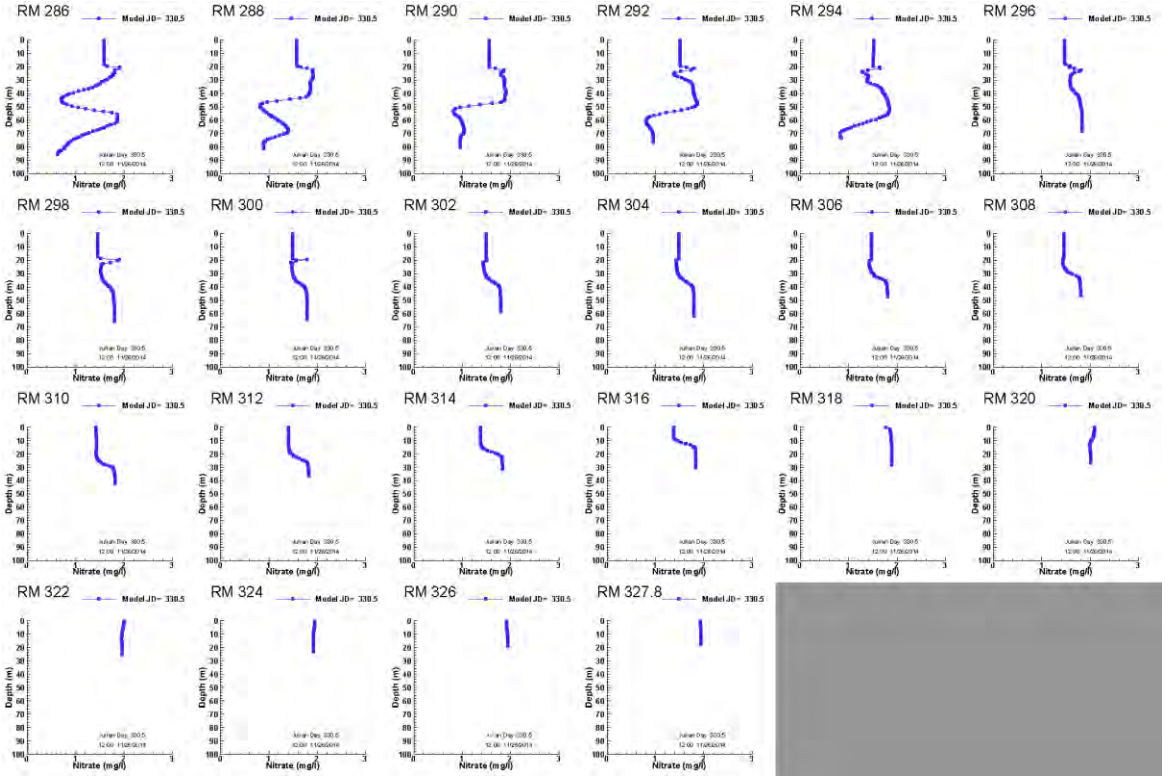


Figure 1006. Vertical profiles of NOxN compared with data for 11/26/2014.

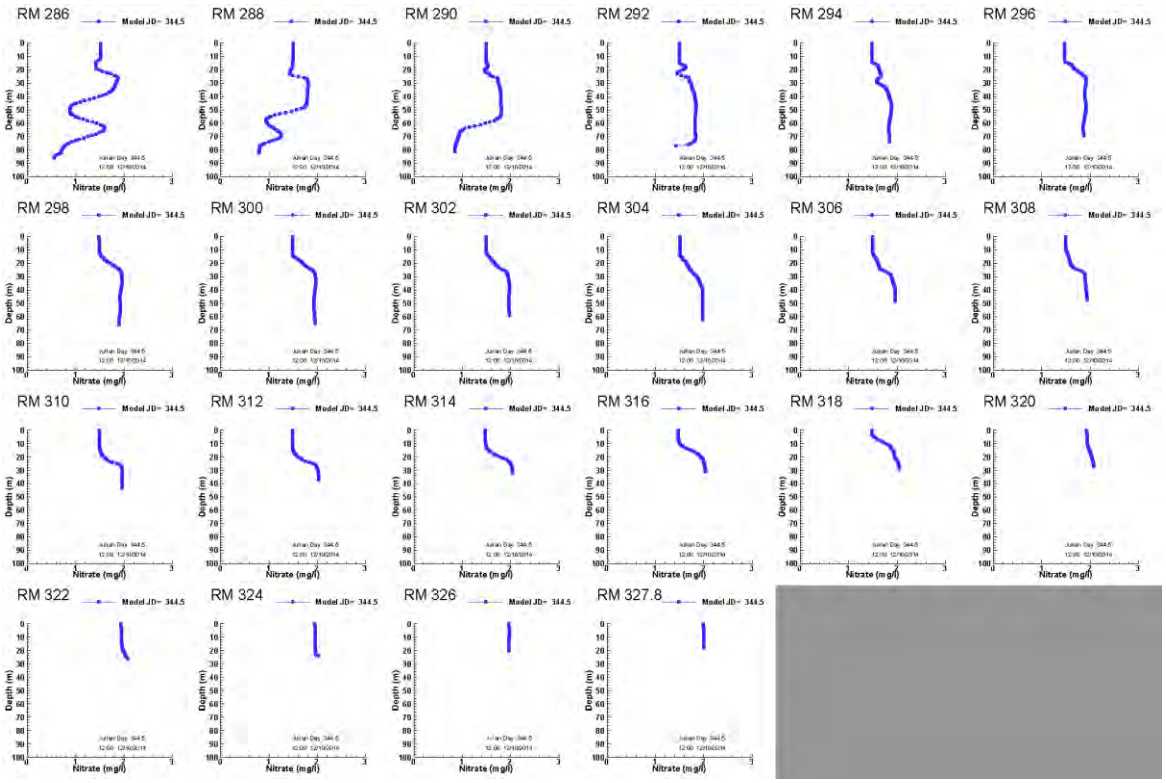


Figure 1007. Vertical profiles of NOxN compared with data for 12/10/2014.

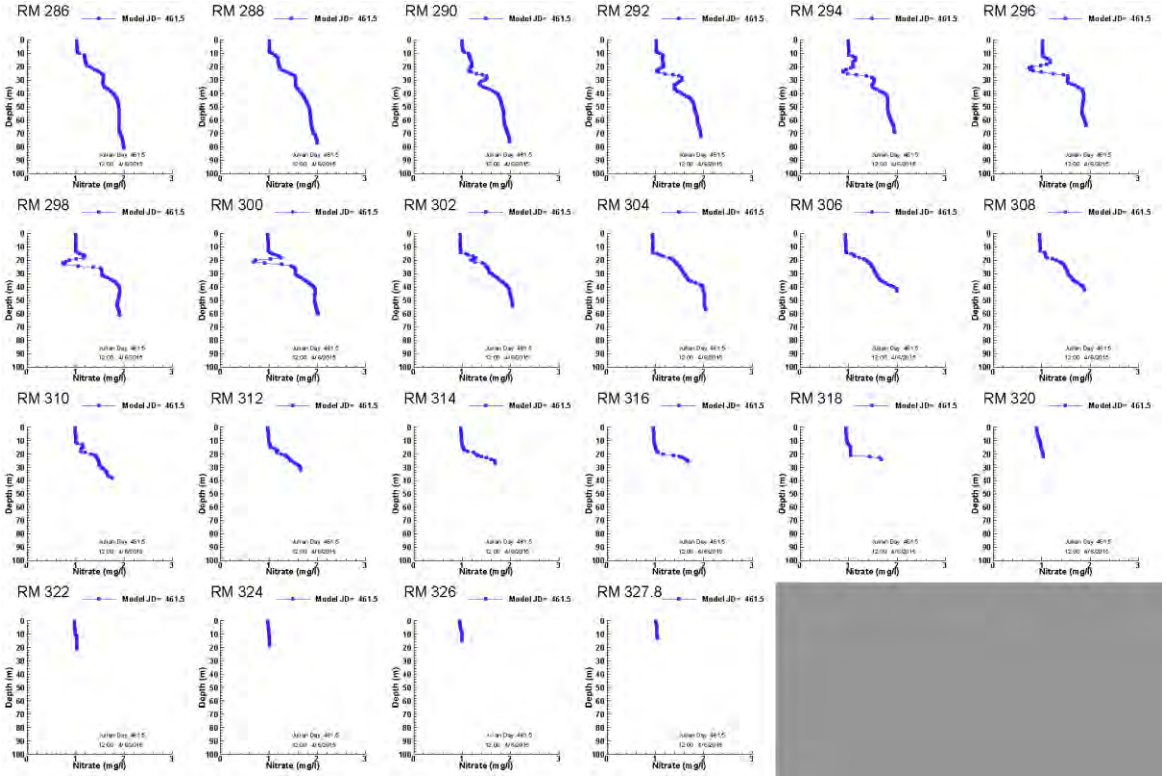


Figure 1008. Vertical profiles of NOxN compared with data for 4/ 6/2015.

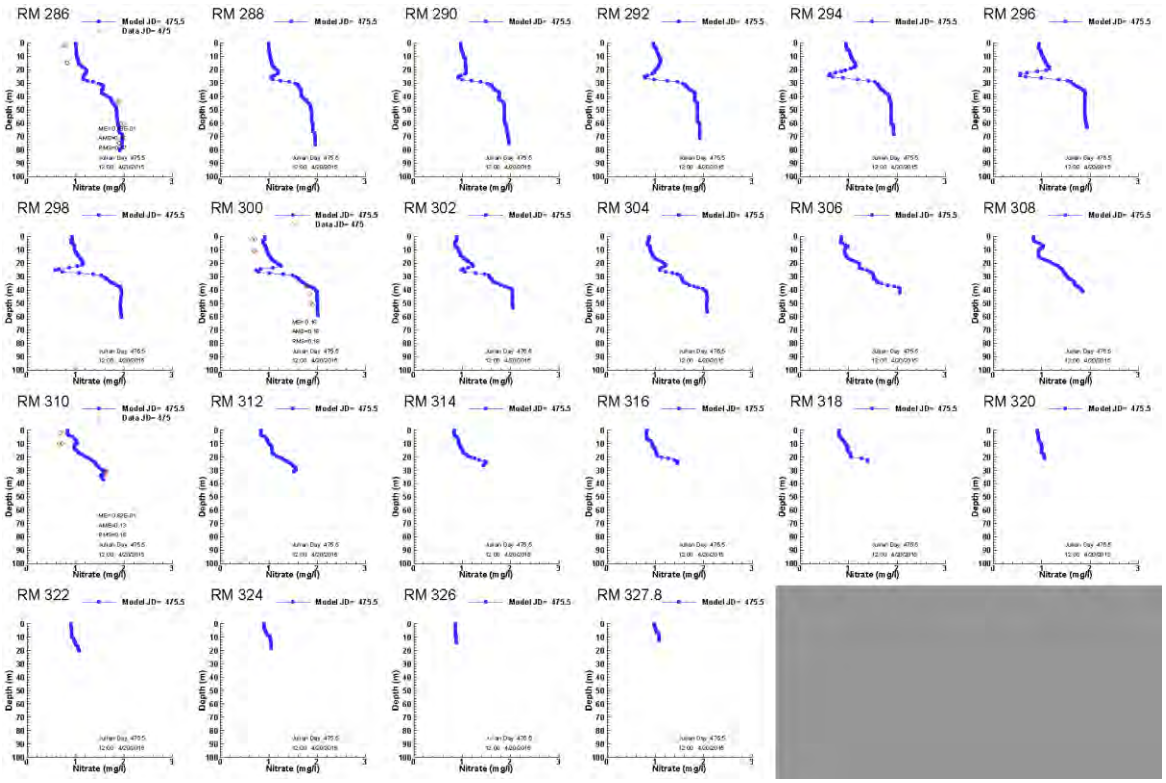


Figure 1009. Vertical profiles of NOxN compared with data for 4/20/2015.

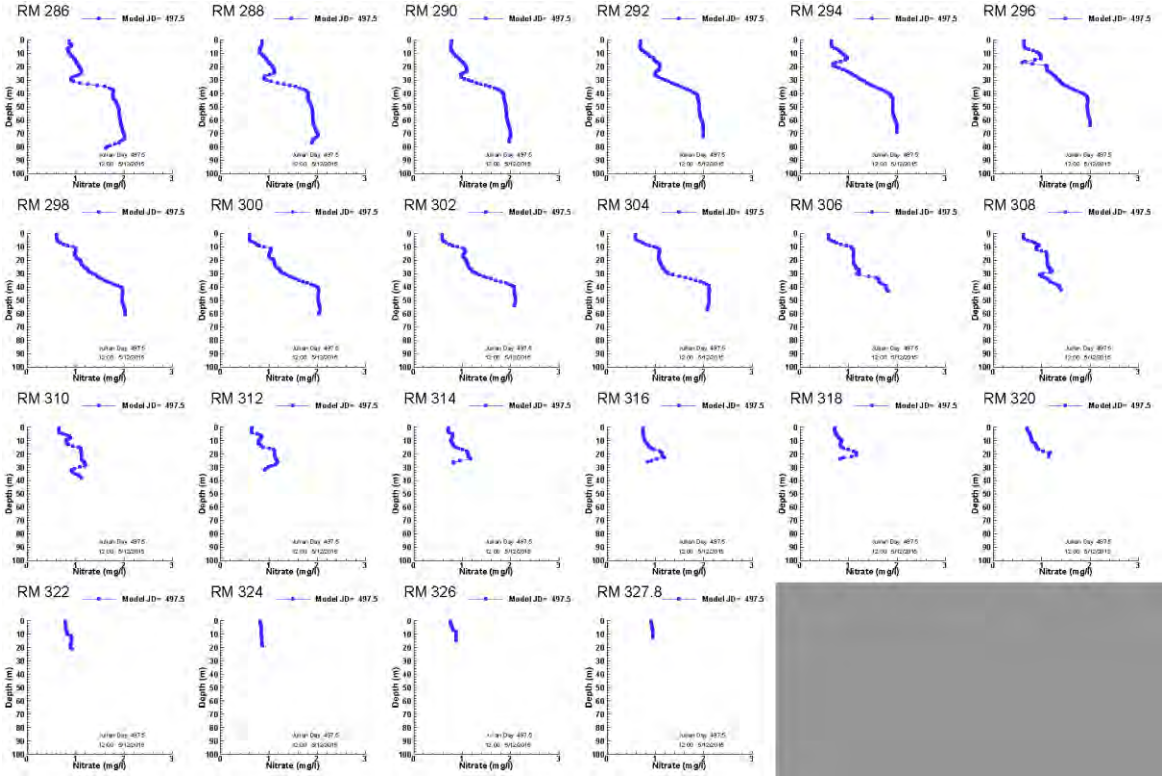


Figure 1010. Vertical profiles of NOxN compared with data for 5/12/2015.

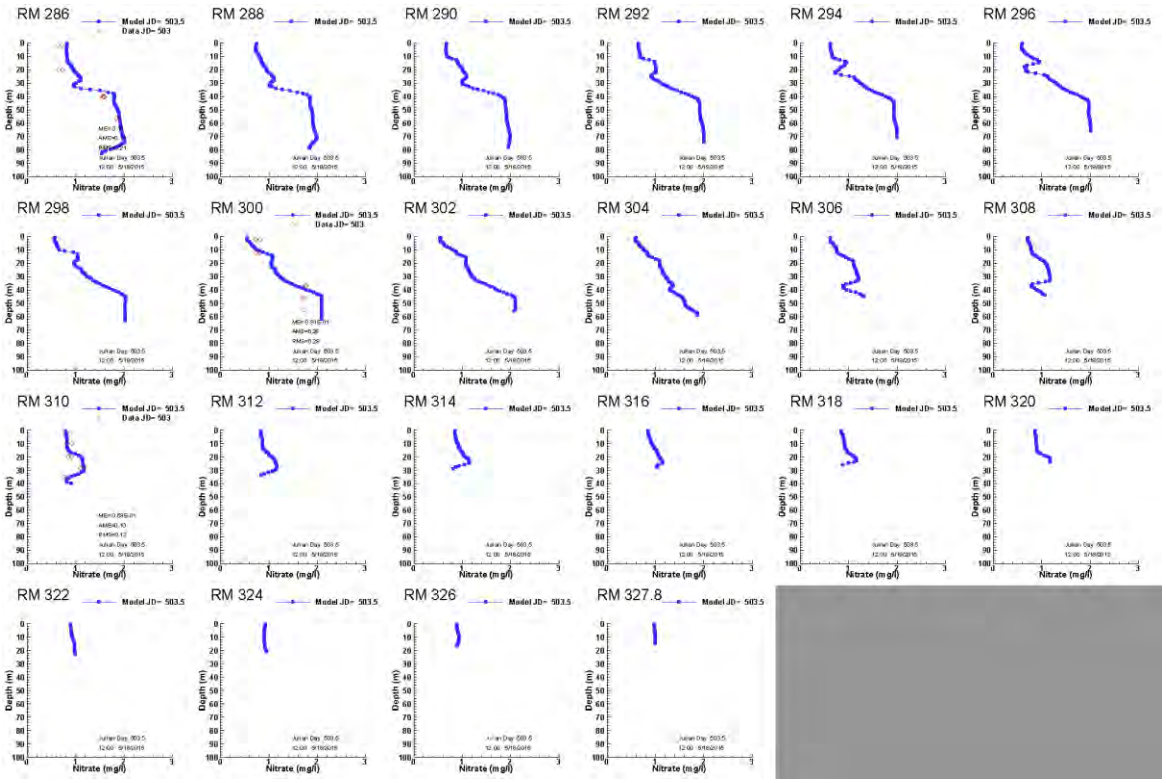


Figure 1011. Vertical profiles of NOxN compared with data for 5/18/2015.

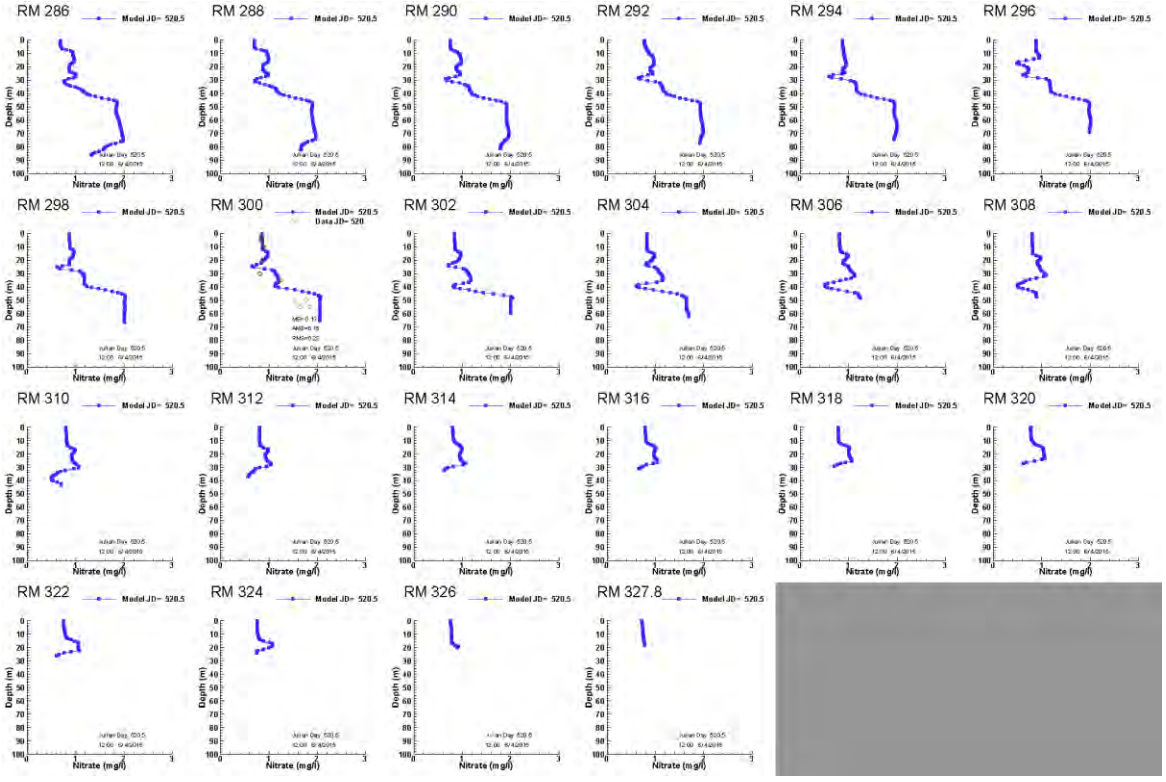


Figure 1012. Vertical profiles of NOxN compared with data for 6/ 4/2015.

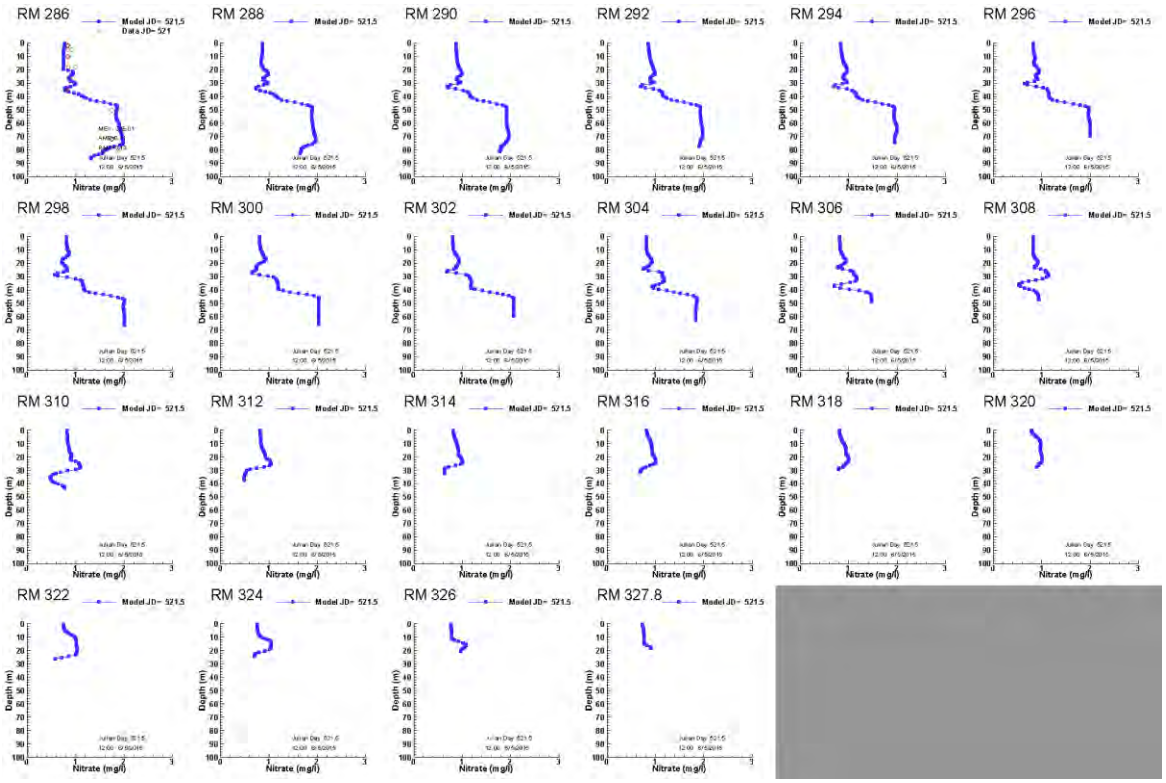


Figure 1013. Vertical profiles of NOxN compared with data for 6/ 5/2015.

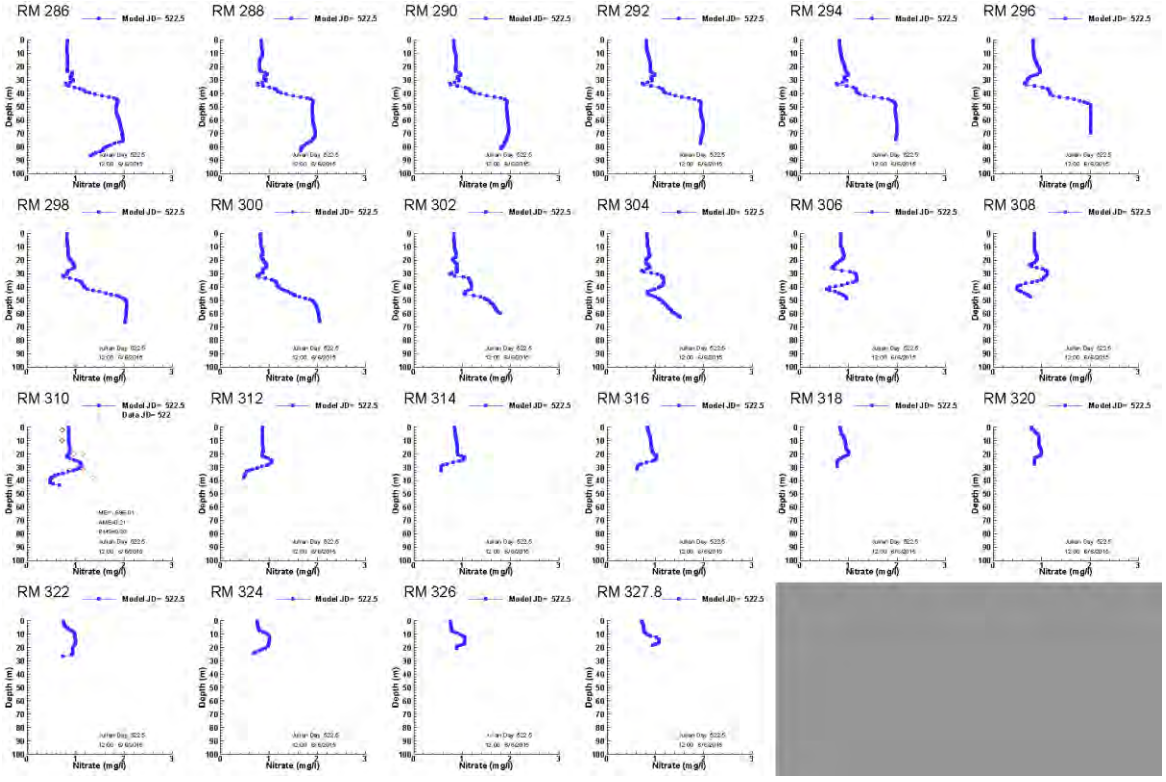


Figure 1014. Vertical profiles of NOxN compared with data for 6/ 6/2015.

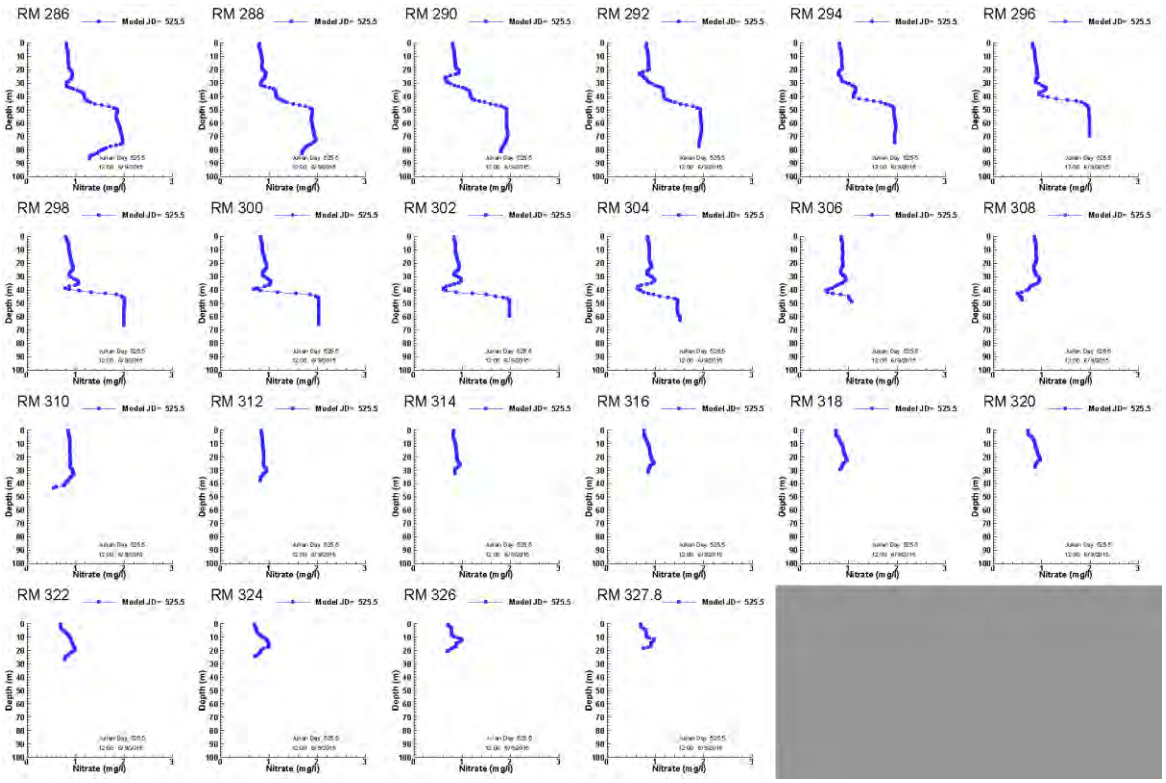


Figure 1015. Vertical profiles of NOxN compared with data for 6/ 9/2015.

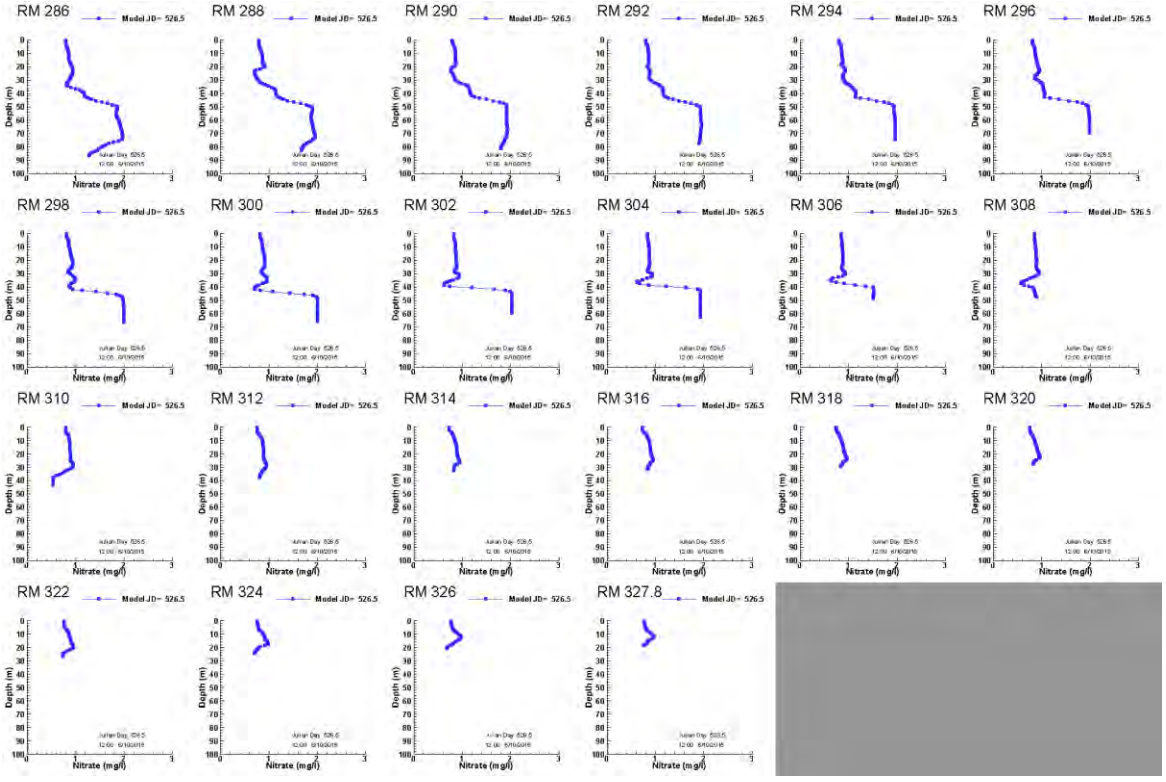


Figure 1016. Vertical profiles of NOxN compared with data for 6/10/2015.

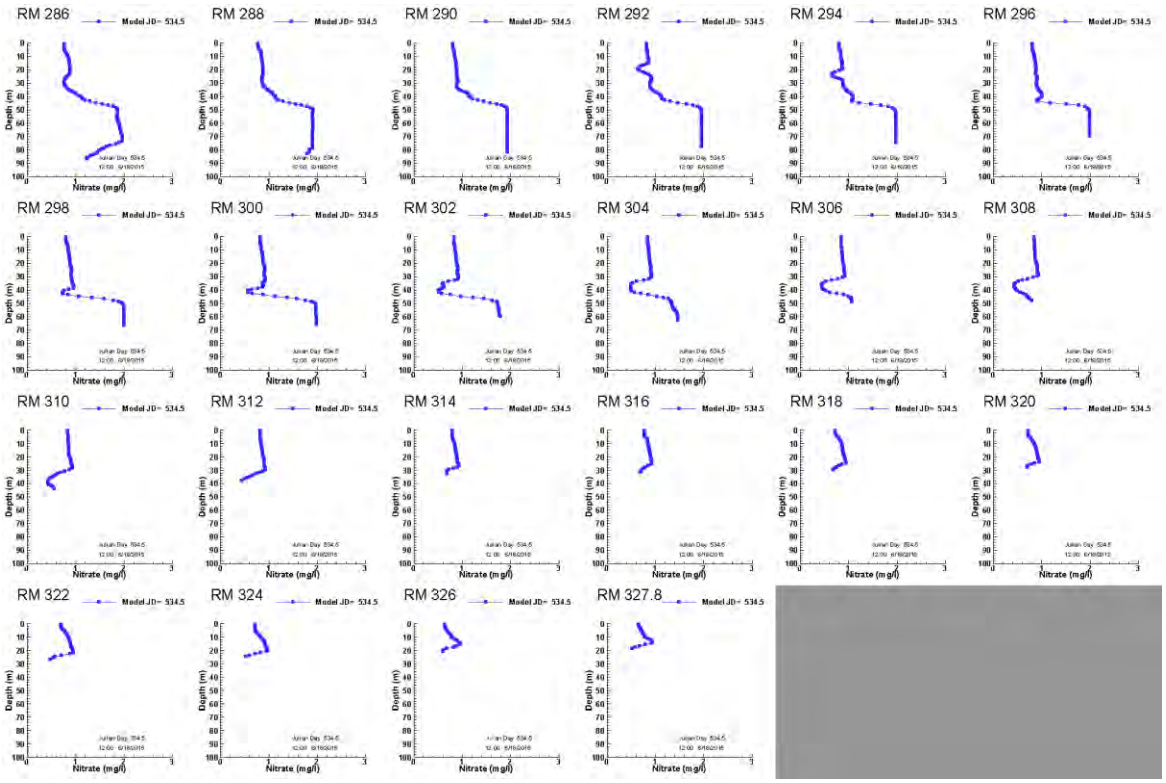


Figure 1017. Vertical profiles of NOxN compared with data for 6/18/2015.

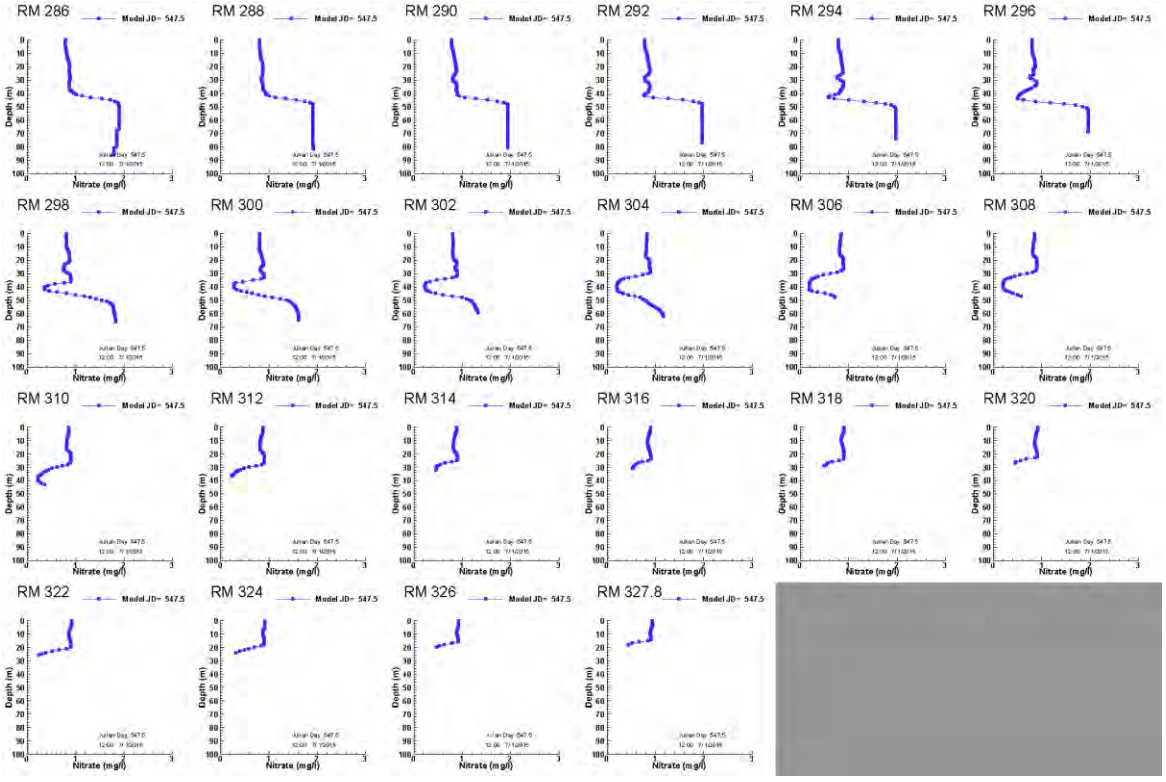


Figure 1018. Vertical profiles of NOxN compared with data for 7/ 1/2015.

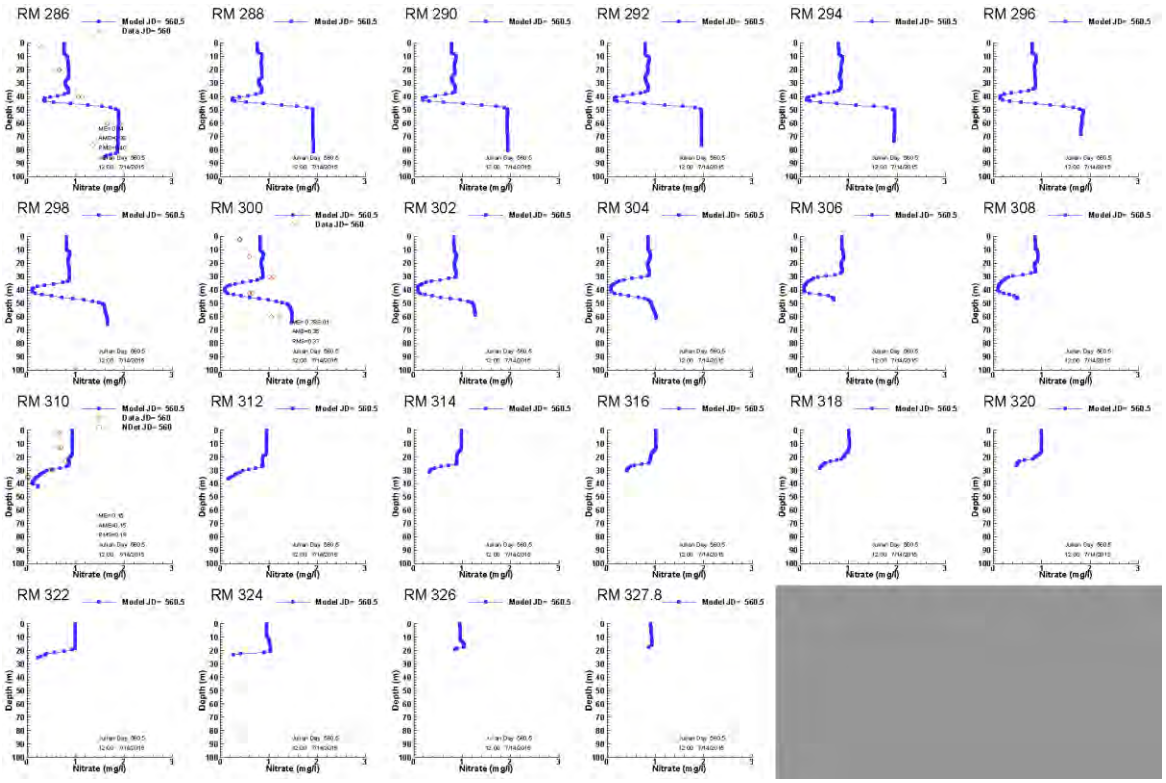


Figure 1019. Vertical profiles of NOxN compared with data for 7/14/2015.

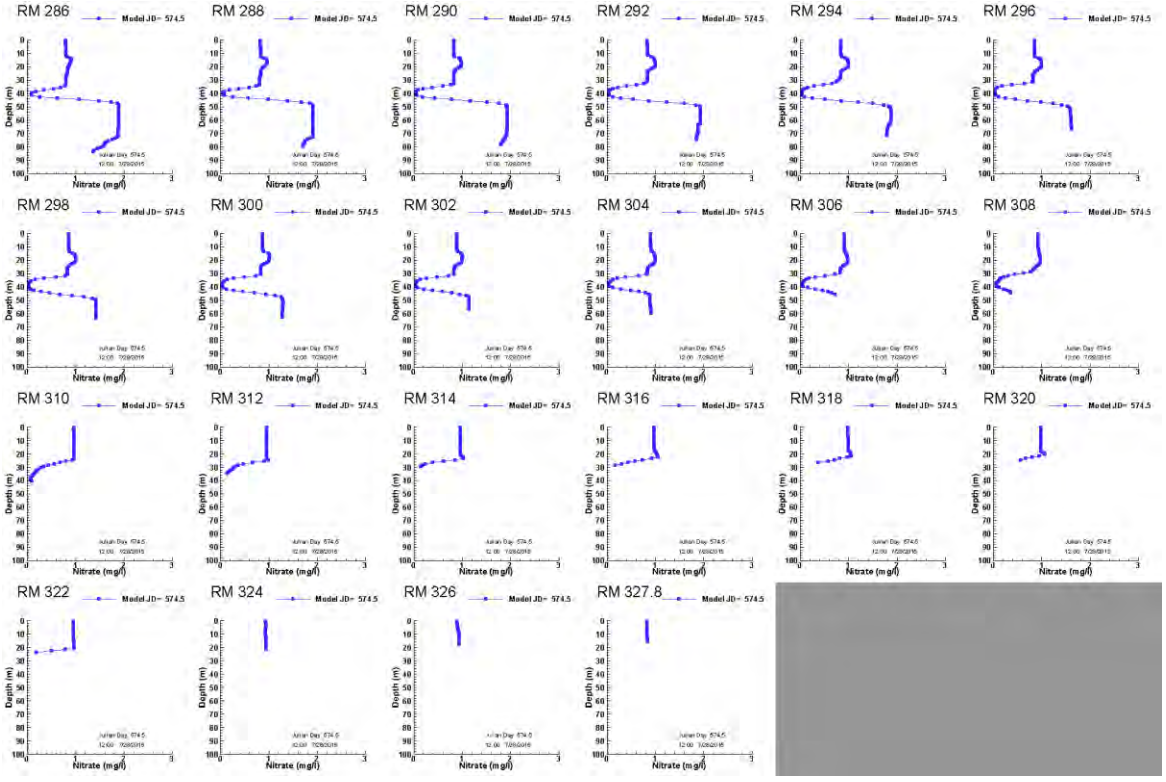


Figure 1020. Vertical profiles of NOxN compared with data for 7/28/2015.

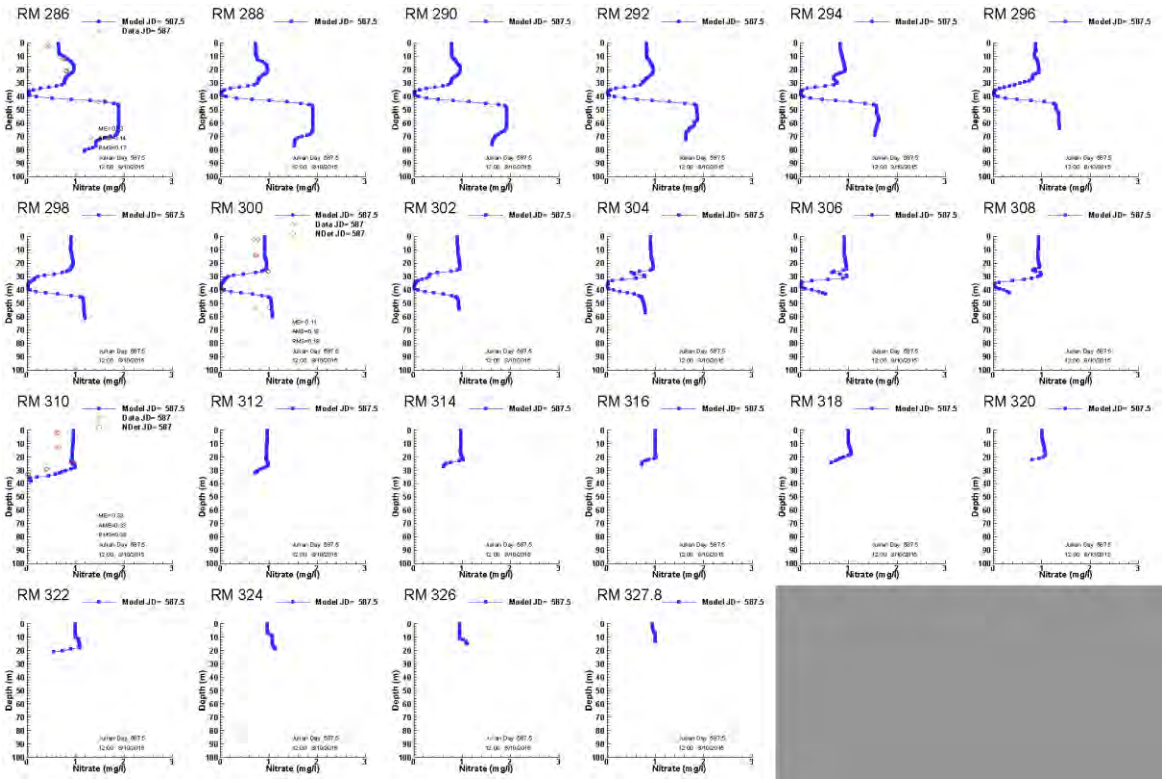


Figure 1021. Vertical profiles of NOxN compared with data for 8/10/2015.

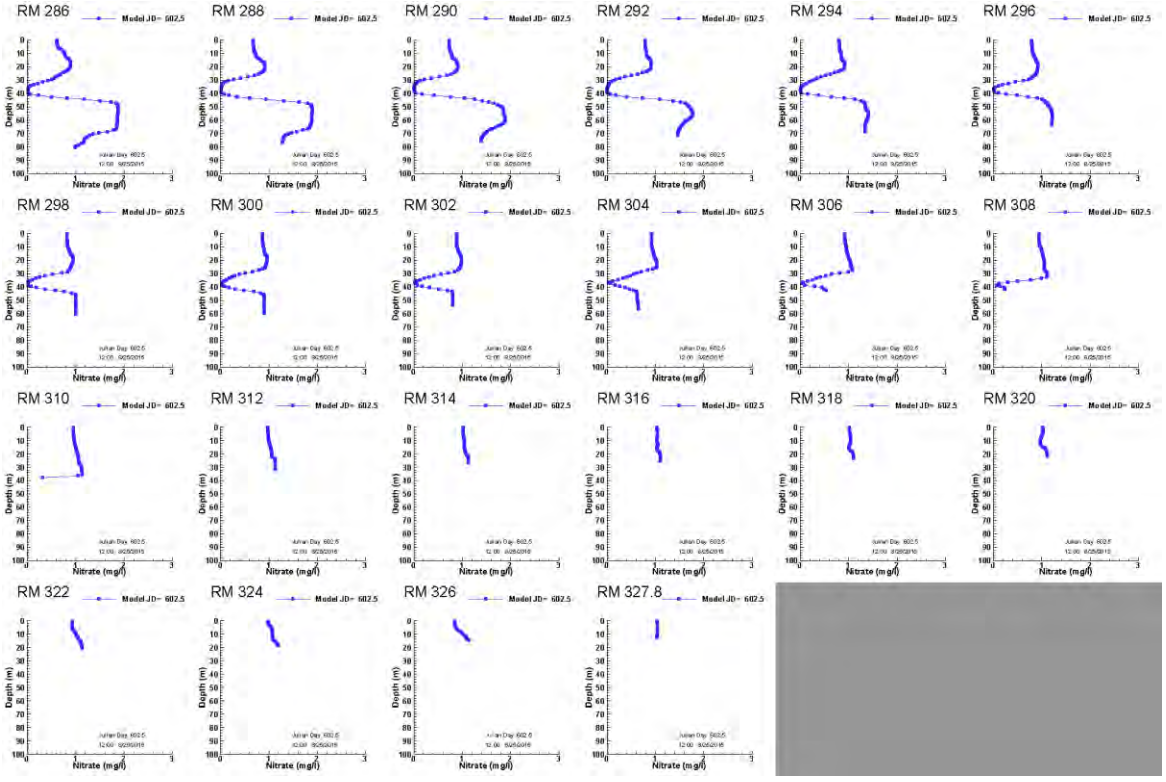


Figure 1022. Vertical profiles of NOxN compared with data for 8/25/2015.

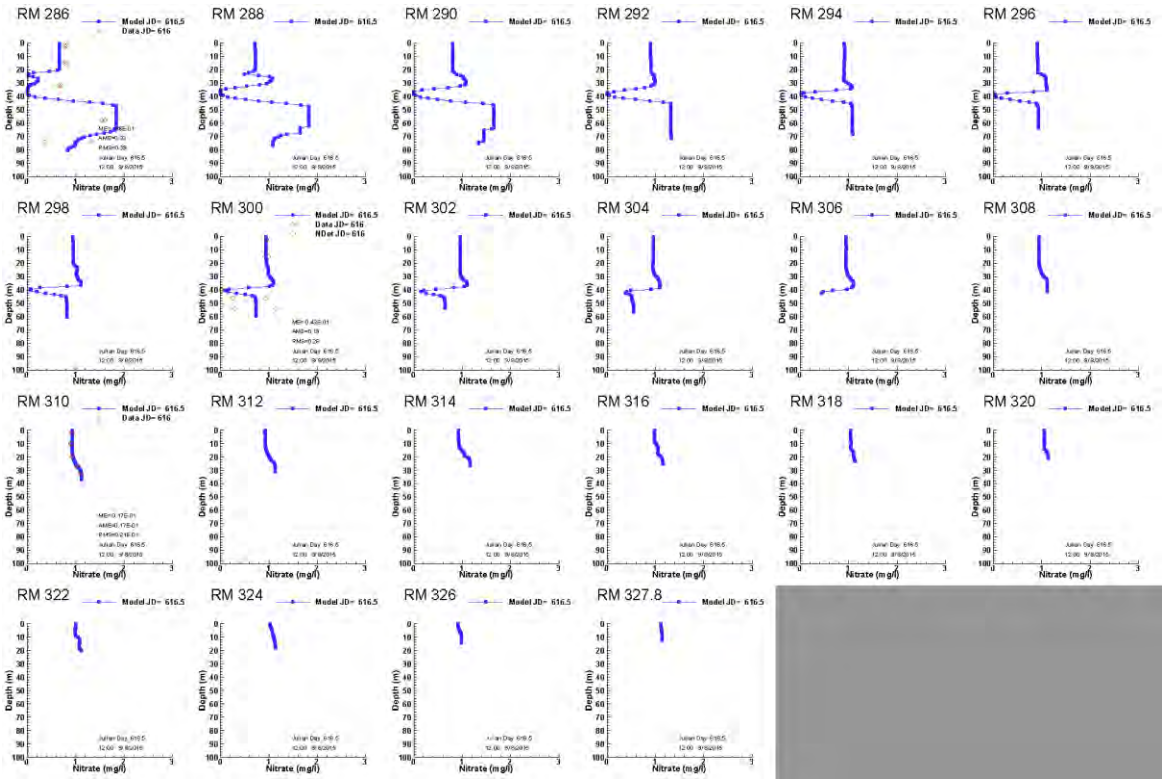


Figure 1023. Vertical profiles of NOxN compared with data for 9/ 8/2015.

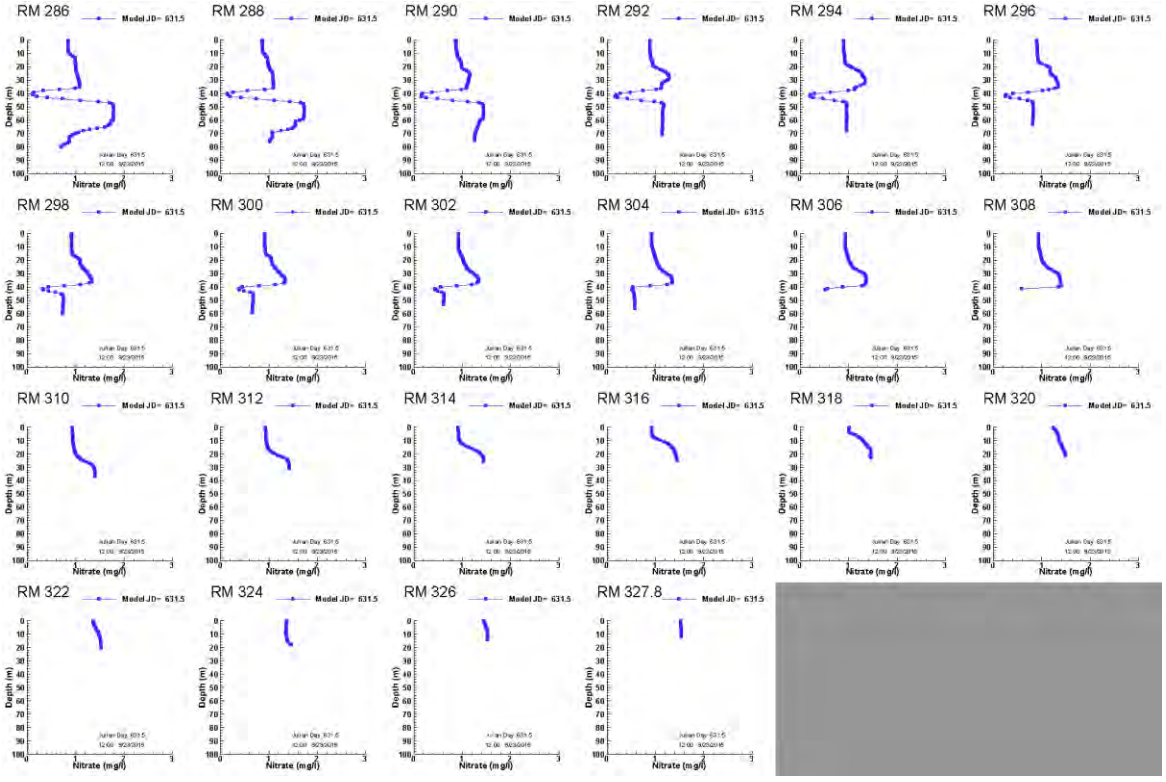


Figure 1024. Vertical profiles of NOxN compared with data for 9/23/2015.

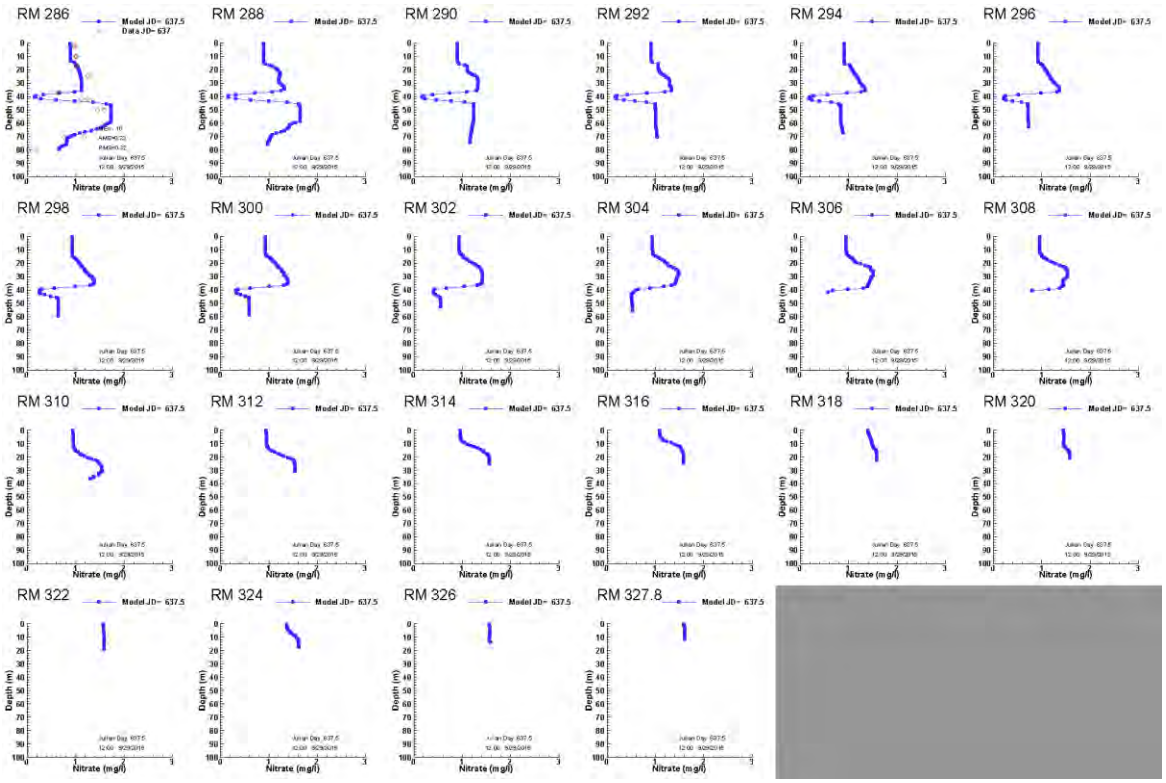


Figure 1025. Vertical profiles of NOxN compared with data for 9/29/2015.

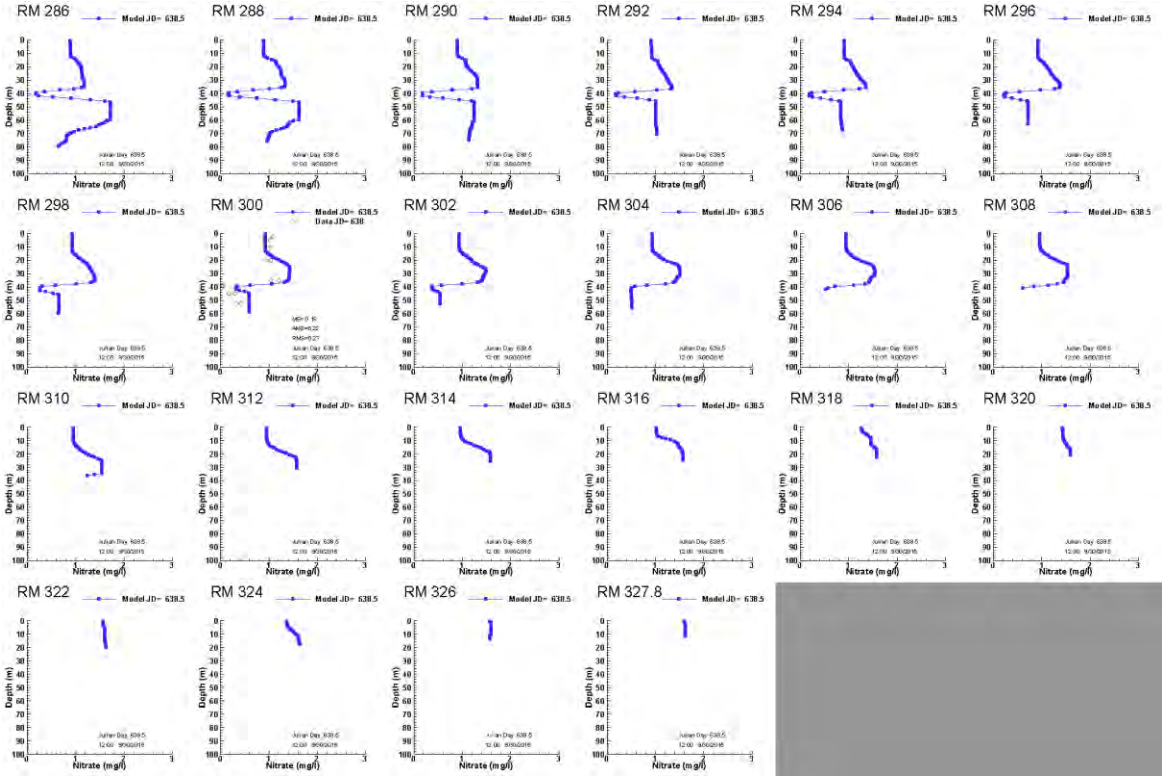


Figure 1026. Vertical profiles of NOxN compared with data for 9/30/2015.

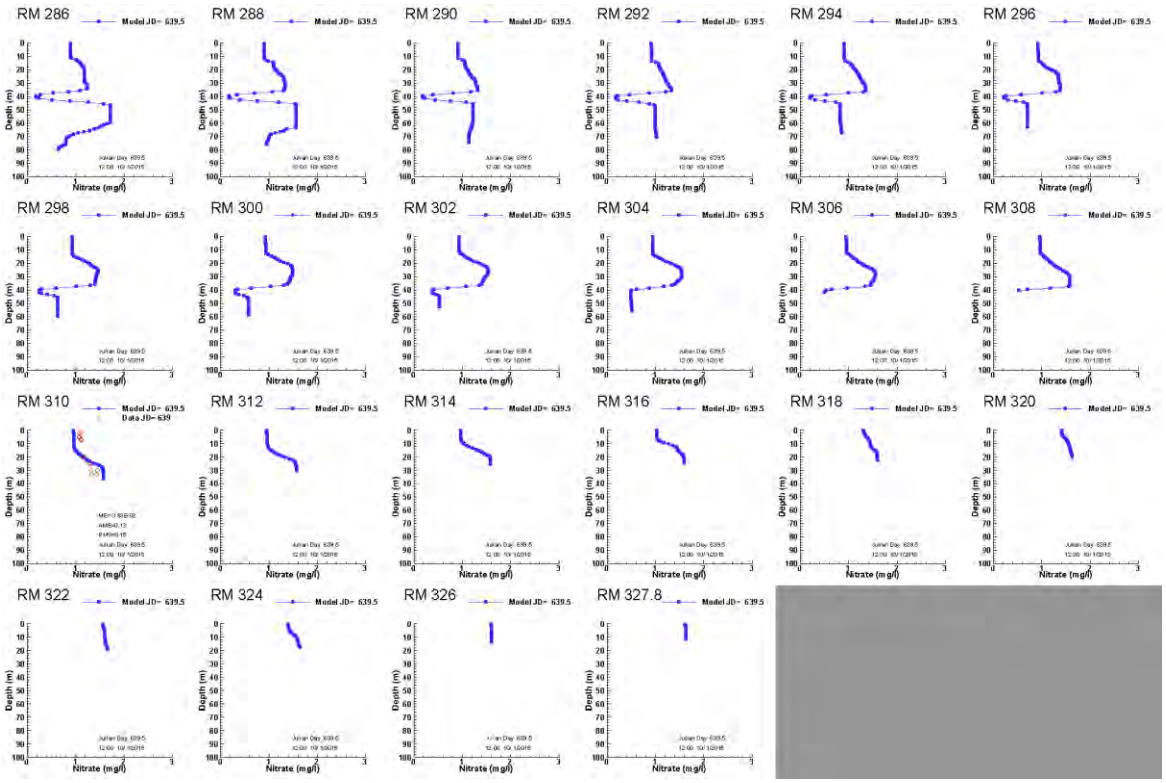


Figure 1027. Vertical profiles of NOxN compared with data for 10/ 1/2015.

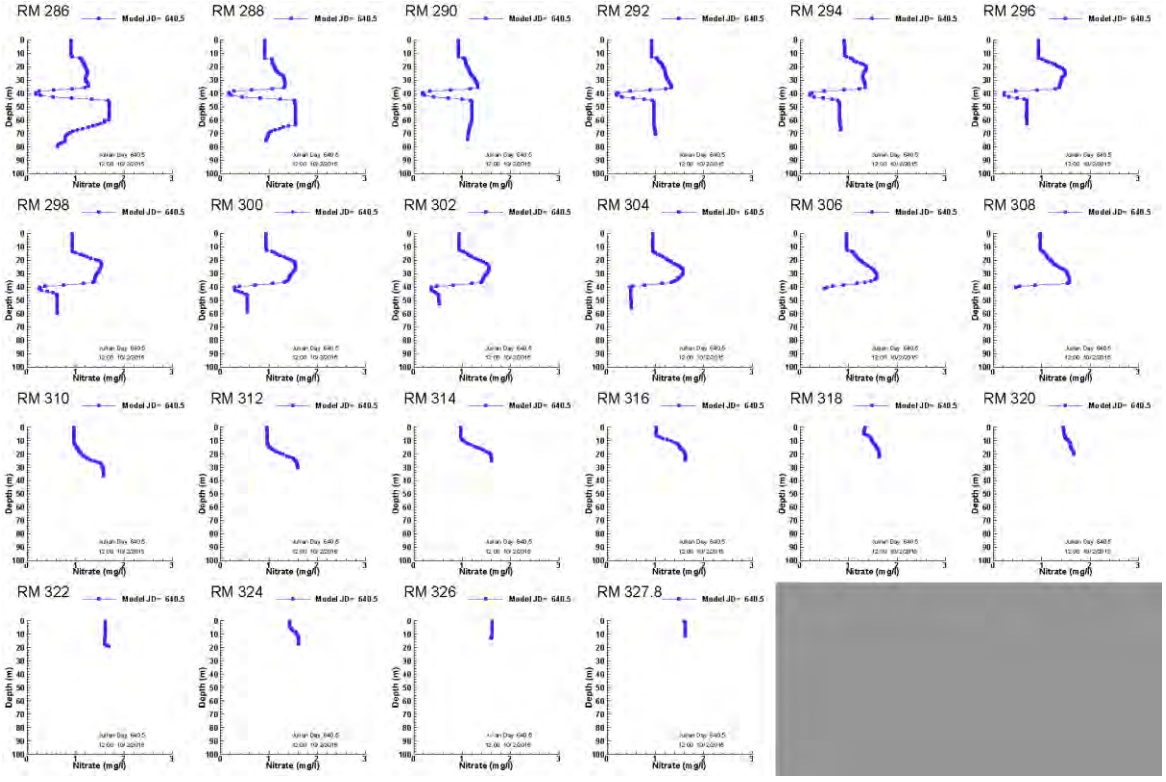


Figure 1028. Vertical profiles of NOxN compared with data for 10/ 2/2015.

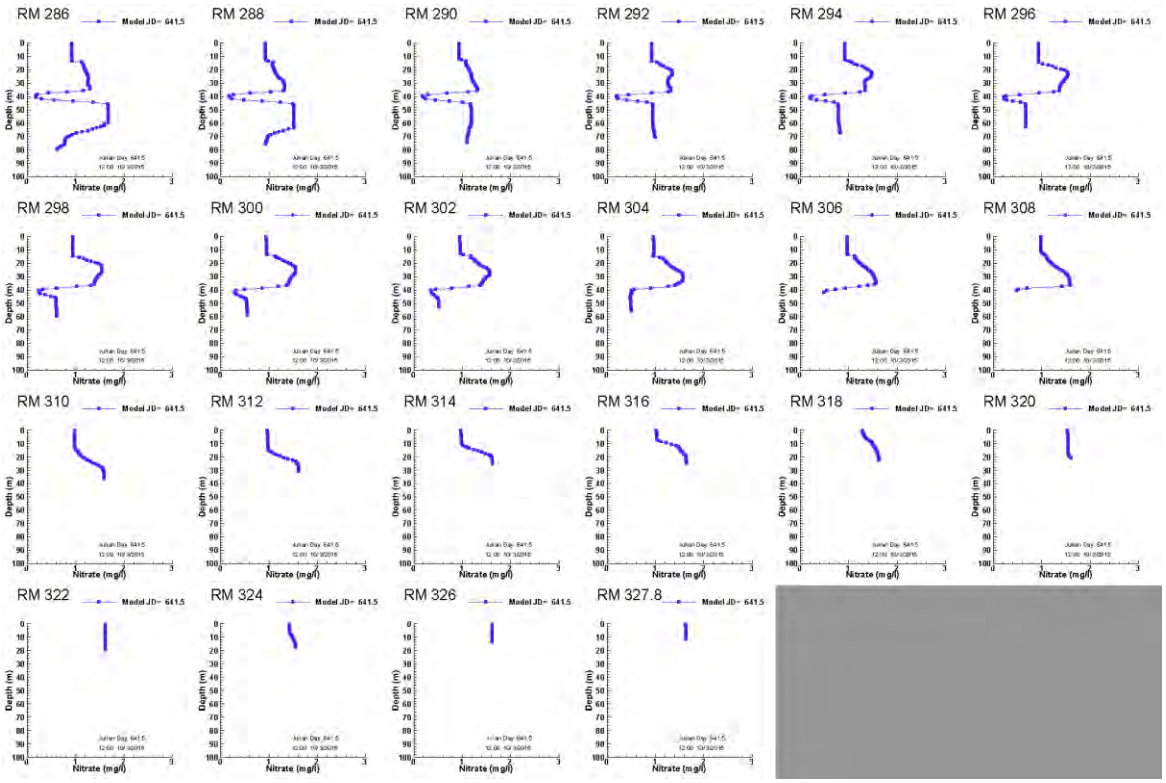


Figure 1029. Vertical profiles of NOxN compared with data for 10/ 3/2015.

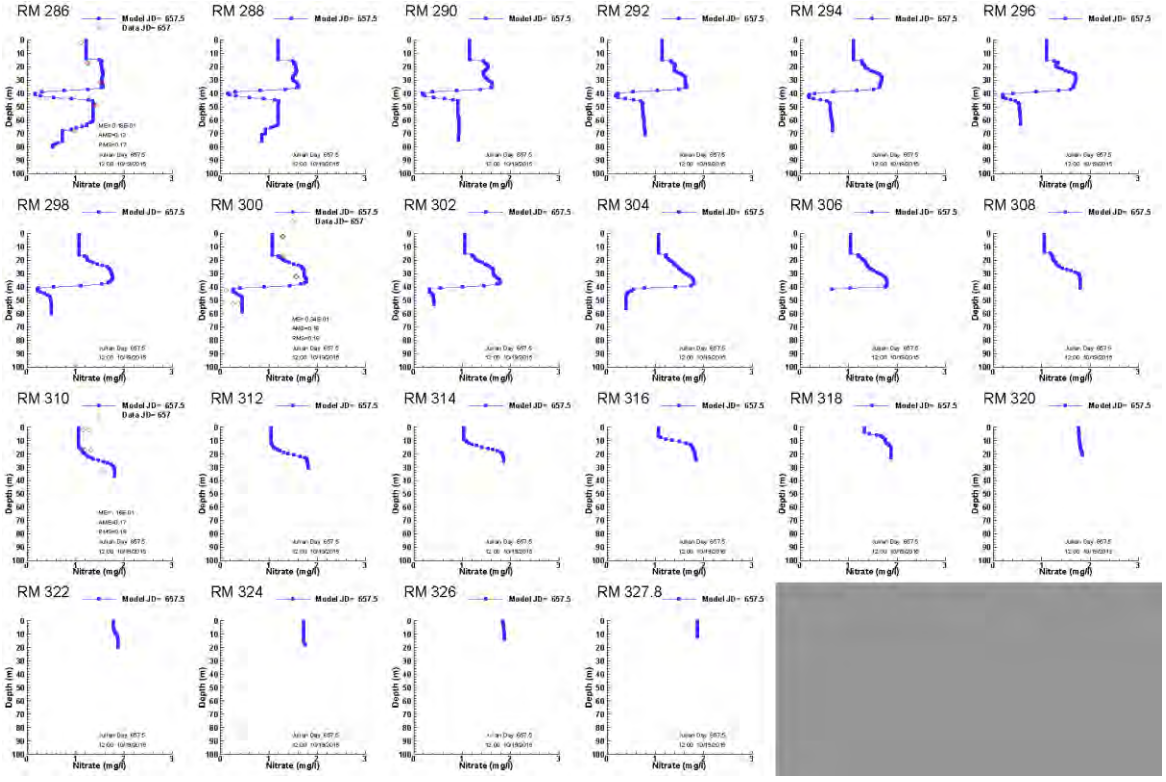


Figure 1030. Vertical profiles of NOxN compared with data for 10/19/2015.

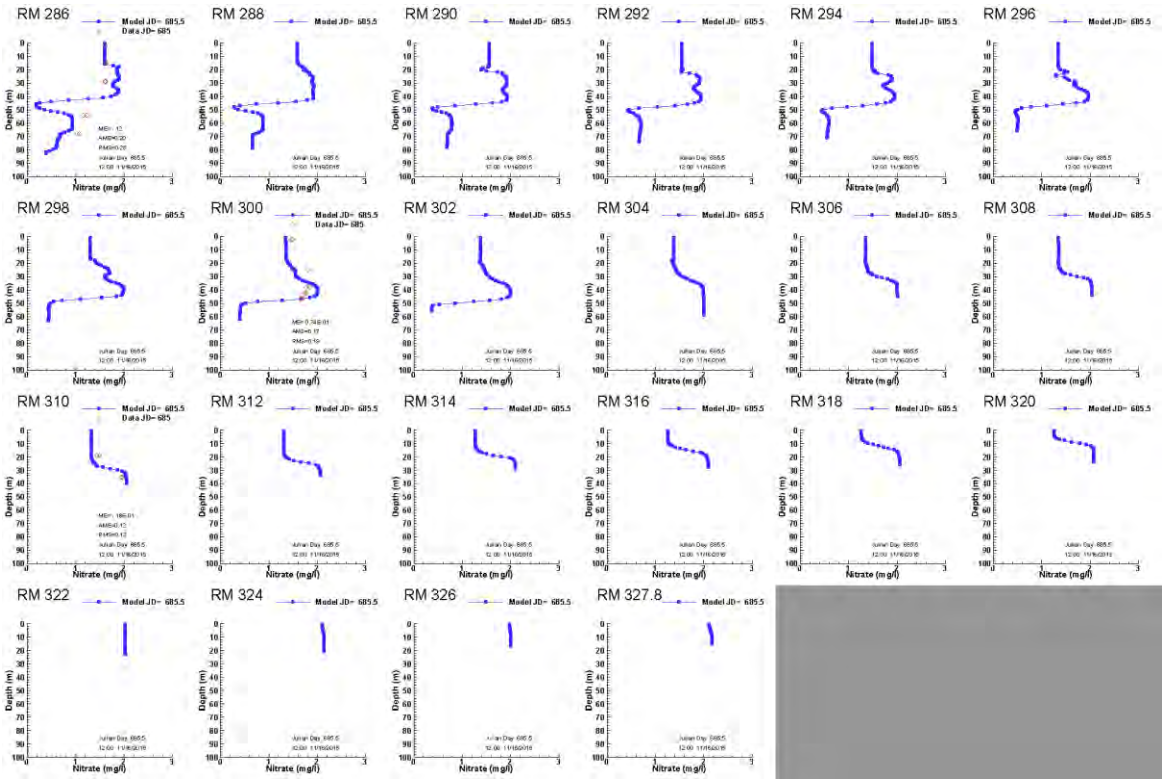


Figure 1031. Vertical profiles of NOxN compared with data for 11/16/2015.

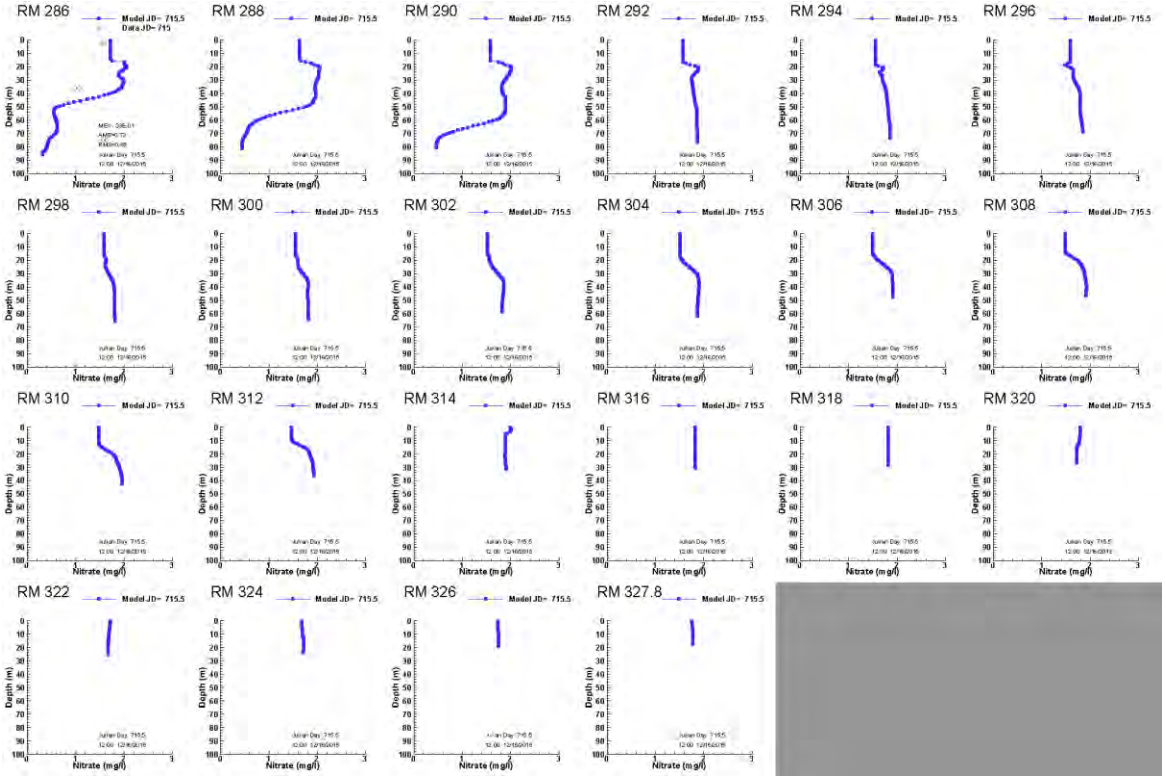


Figure 1032. Vertical profiles of NOxN compared with data for 12/16/2015.

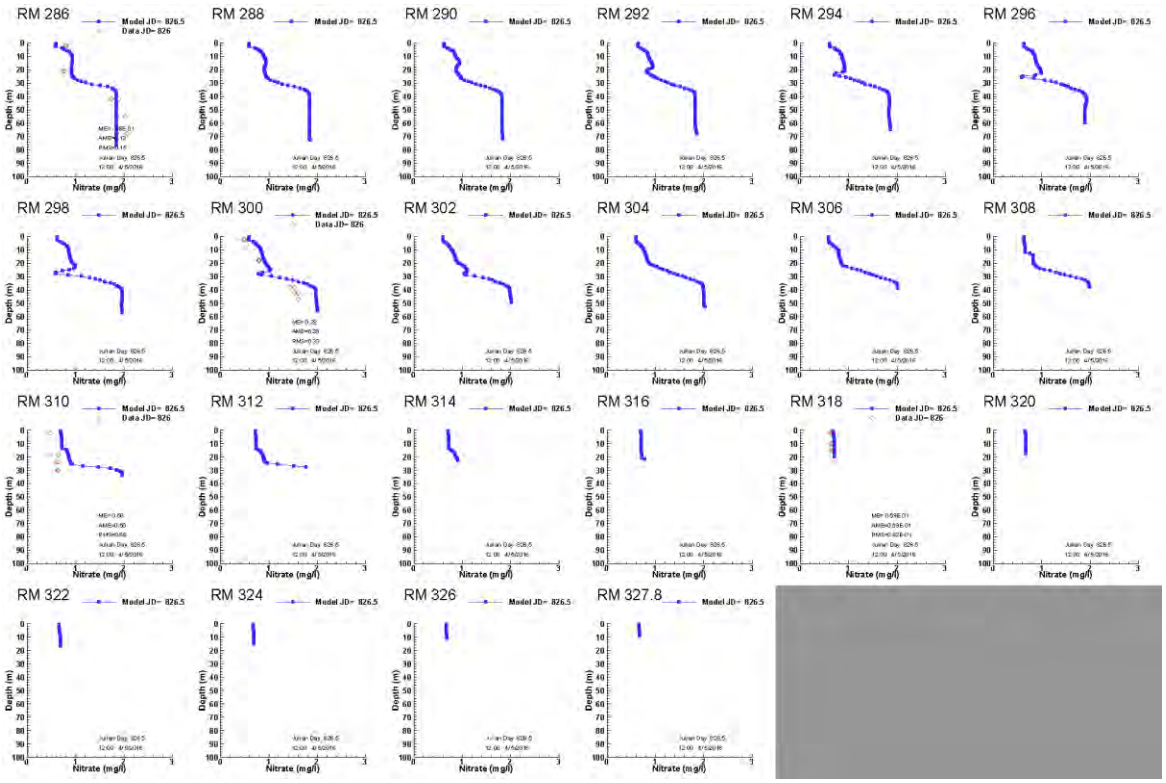


Figure 1033. Vertical profiles of NOxN compared with data for 4/ 5/2016.

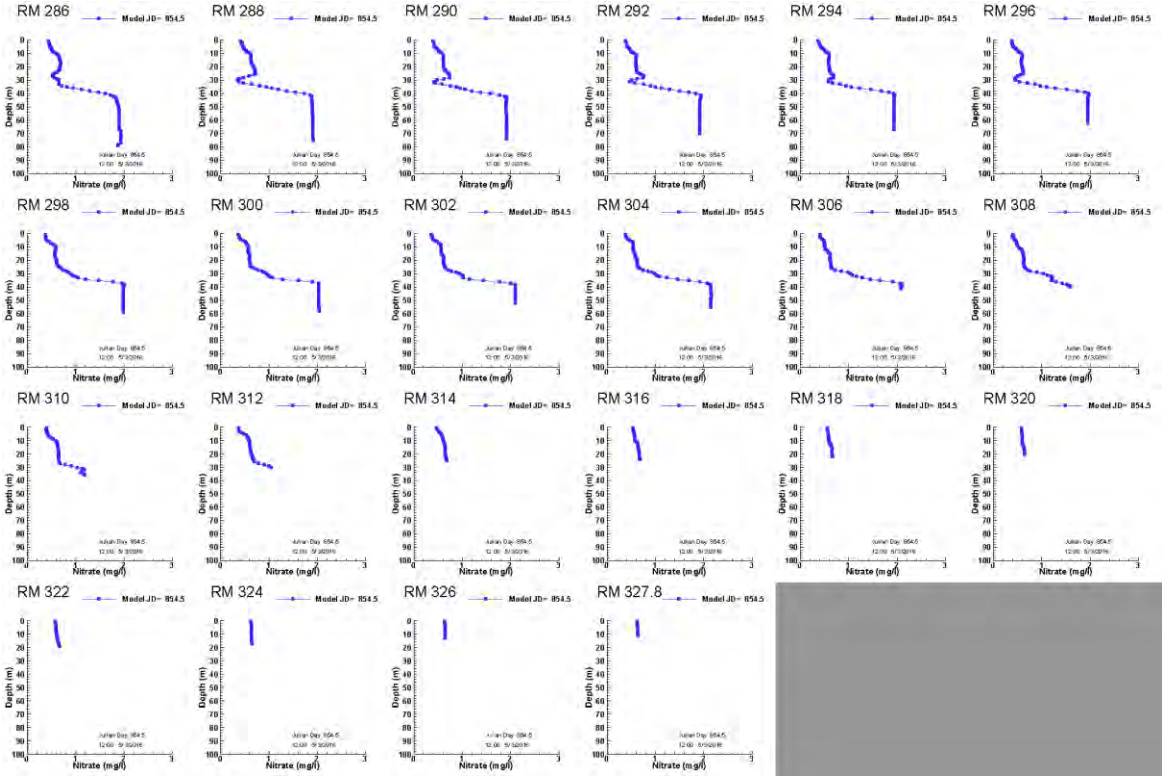


Figure 1034. Vertical profiles of NOxN compared with data for 5/ 3/2016.

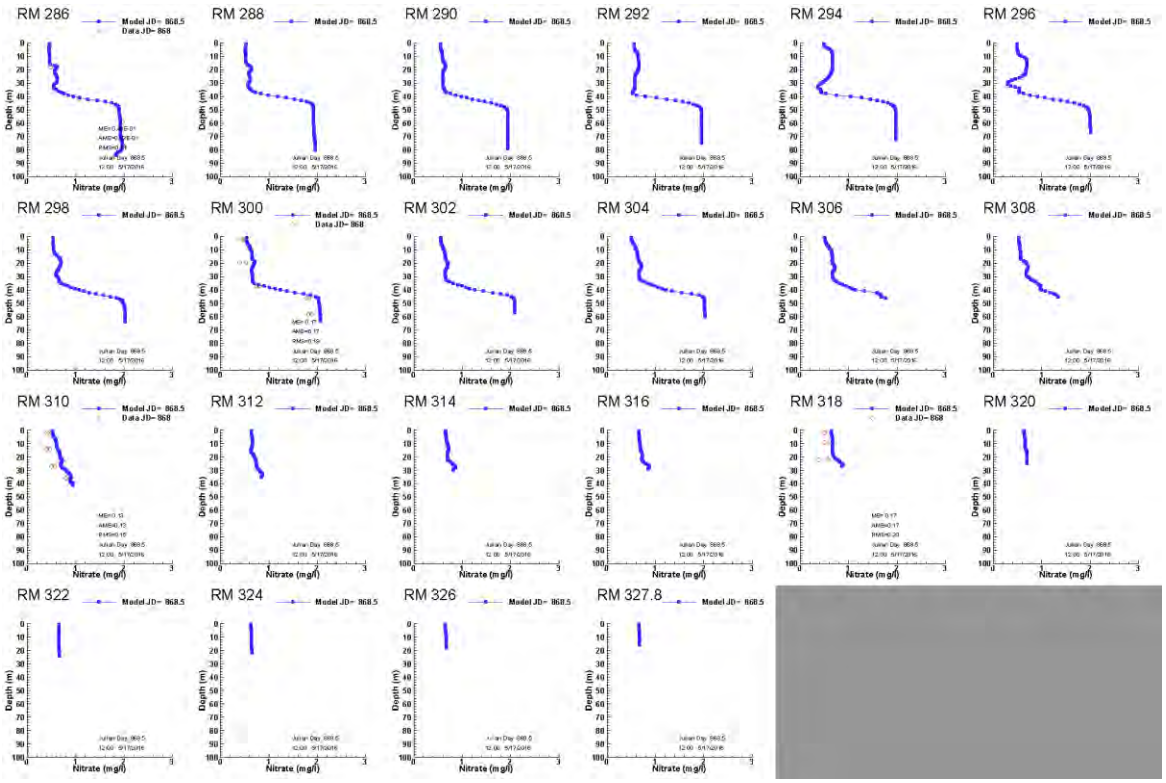


Figure 1035. Vertical profiles of NOxN compared with data for 5/17/2016.

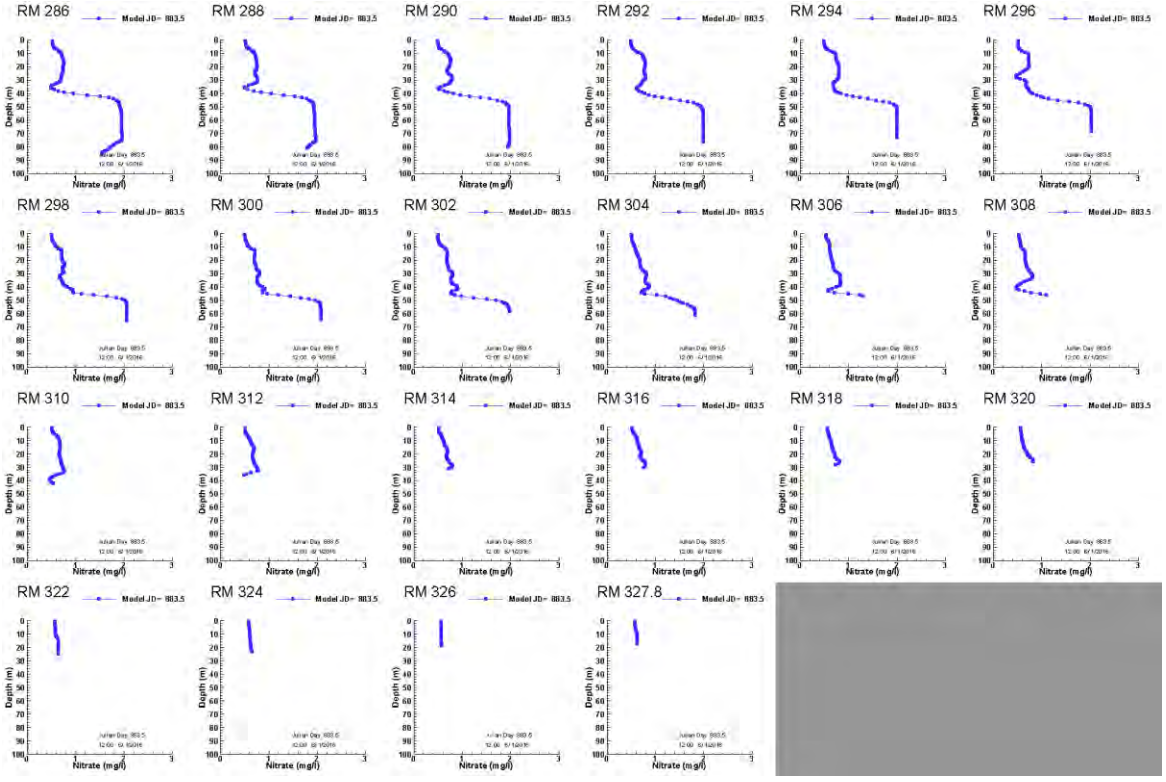


Figure 1036. Vertical profiles of NOxN compared with data for 6/ 1/2016.

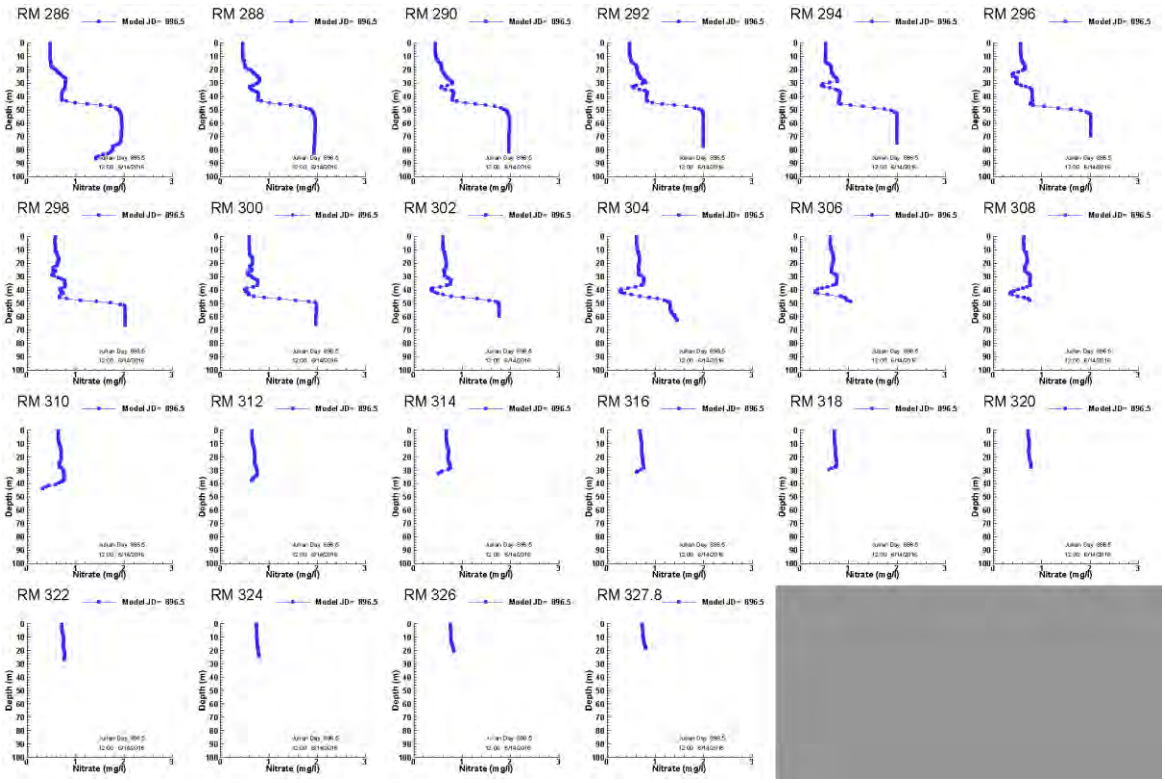


Figure 1037. Vertical profiles of NOxN compared with data for 6/14/2016.

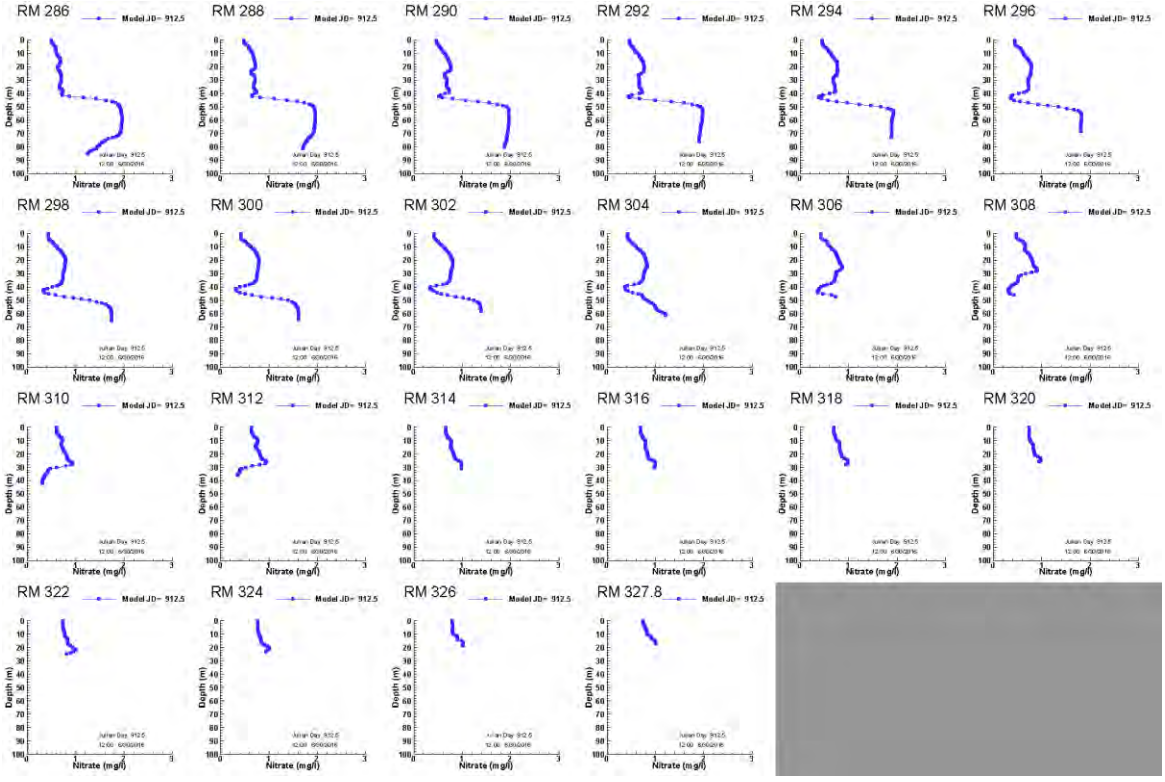


Figure 1038. Vertical profiles of NOxN compared with data for 6/30/2016.

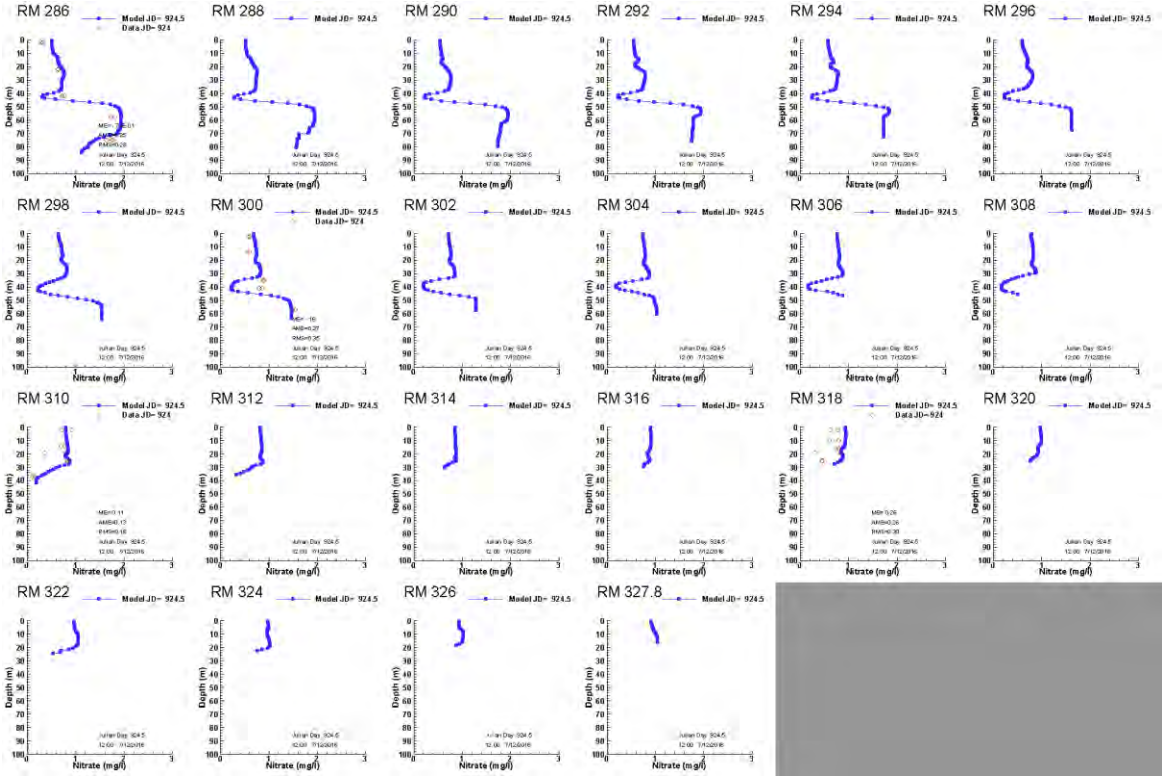


Figure 1039. Vertical profiles of NOxN compared with data for 7/12/2016.

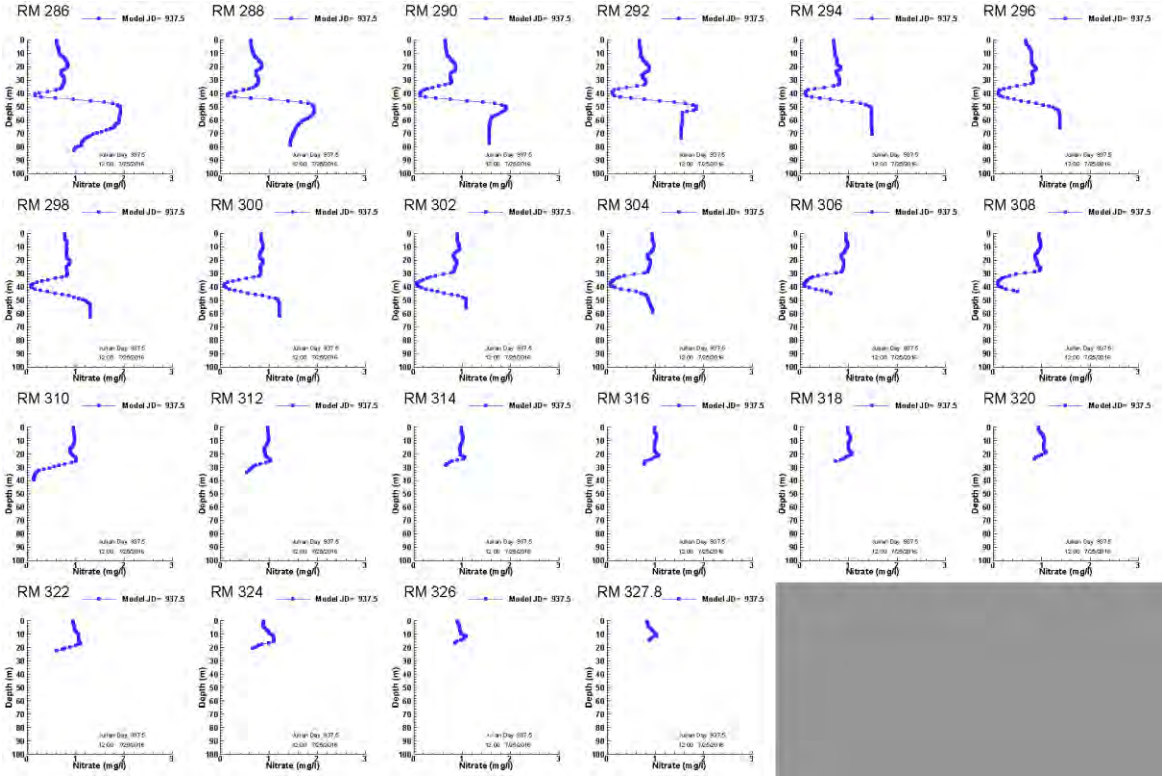


Figure 1040. Vertical profiles of NOxN compared with data for 7/25/2016.

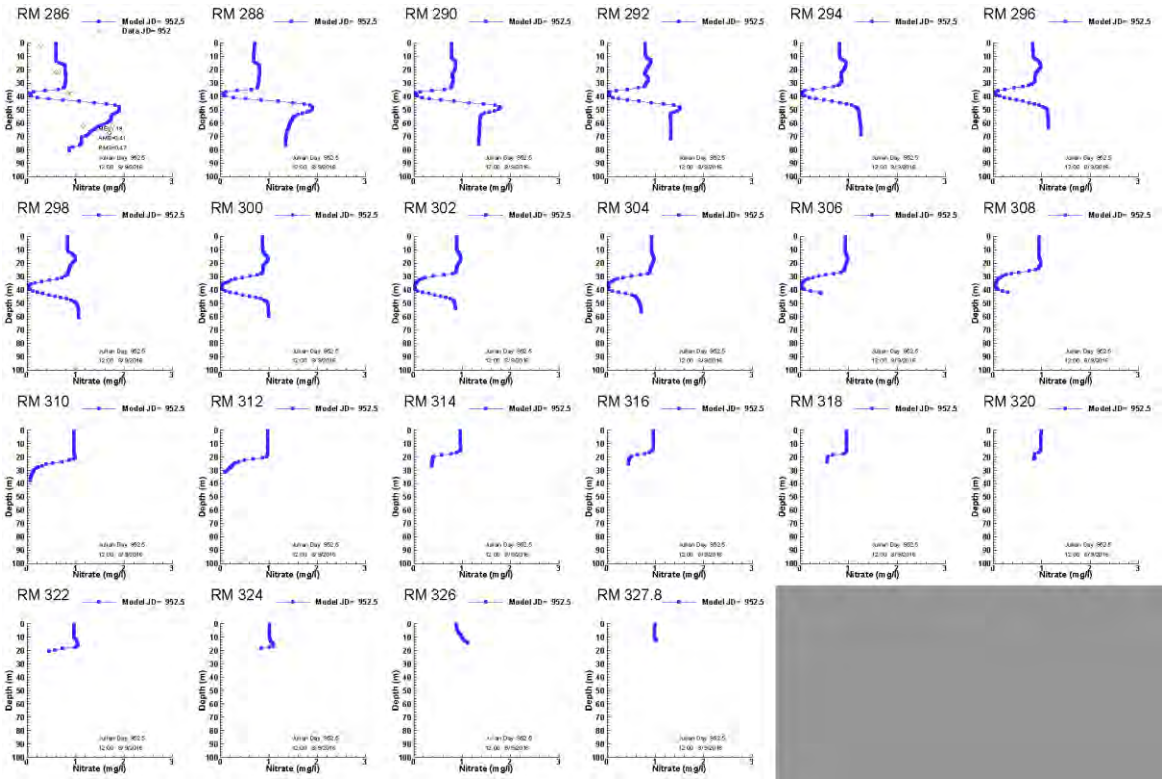


Figure 1041. Vertical profiles of NOxN compared with data for 8/ 9/2016.

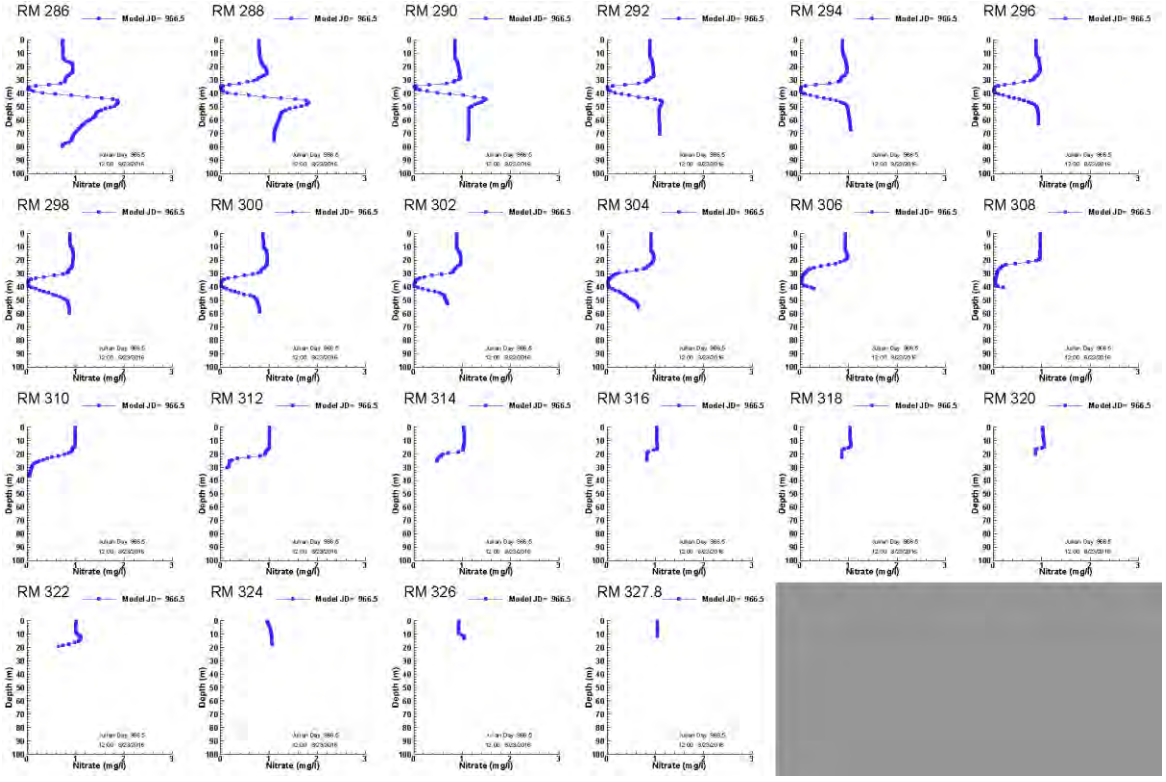


Figure 1042. Vertical profiles of NOxN compared with data for 8/23/2016.

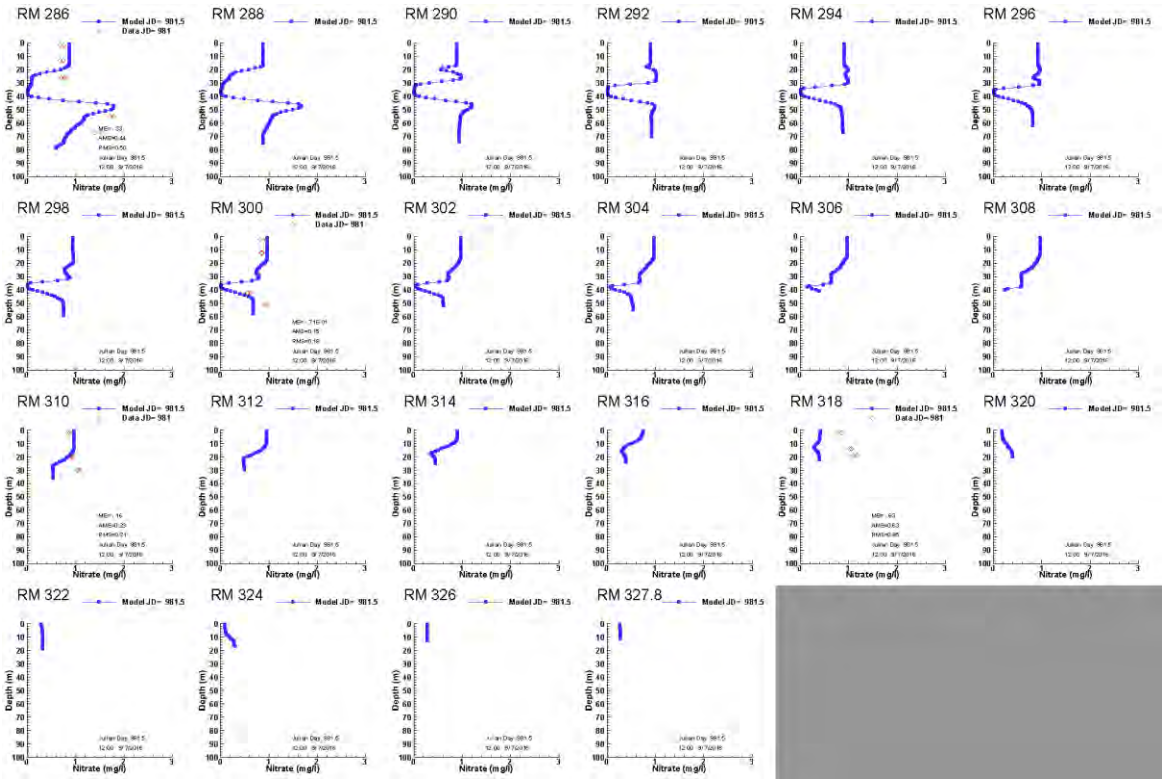


Figure 1043. Vertical profiles of NOxN compared with data for 9/ 7/2016.

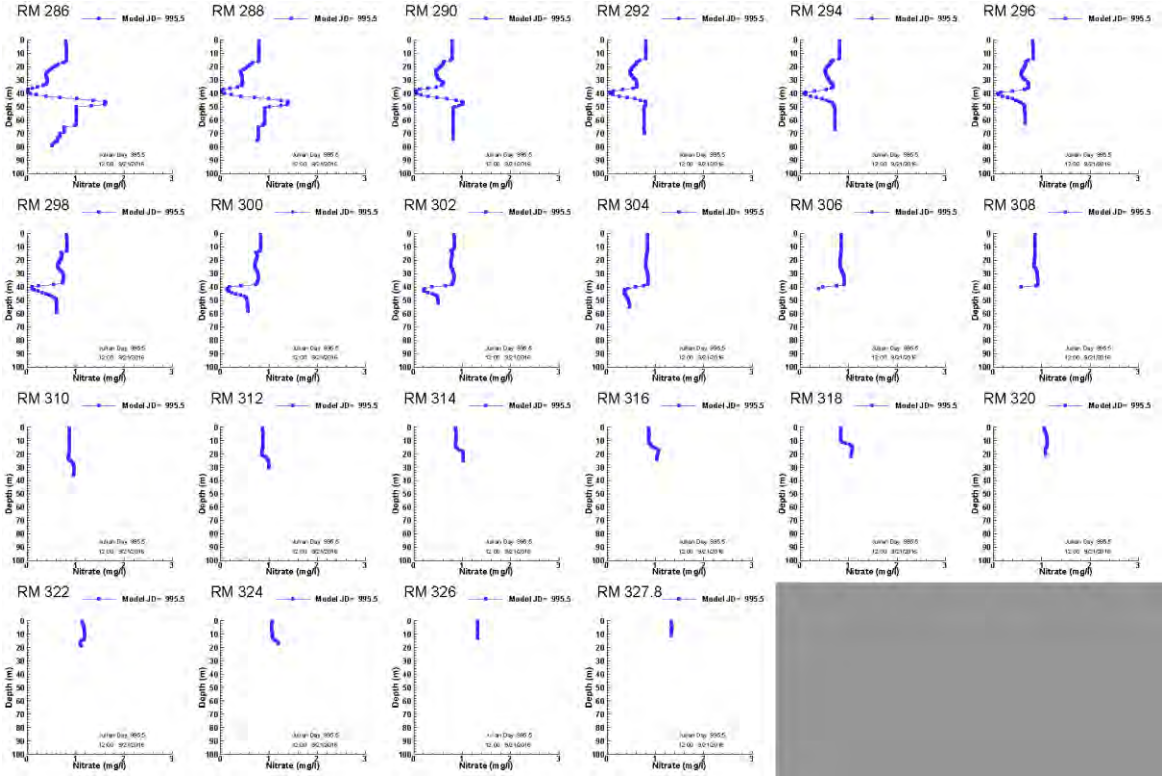


Figure 1044. Vertical profiles of NOxN compared with data for 9/21/2016.

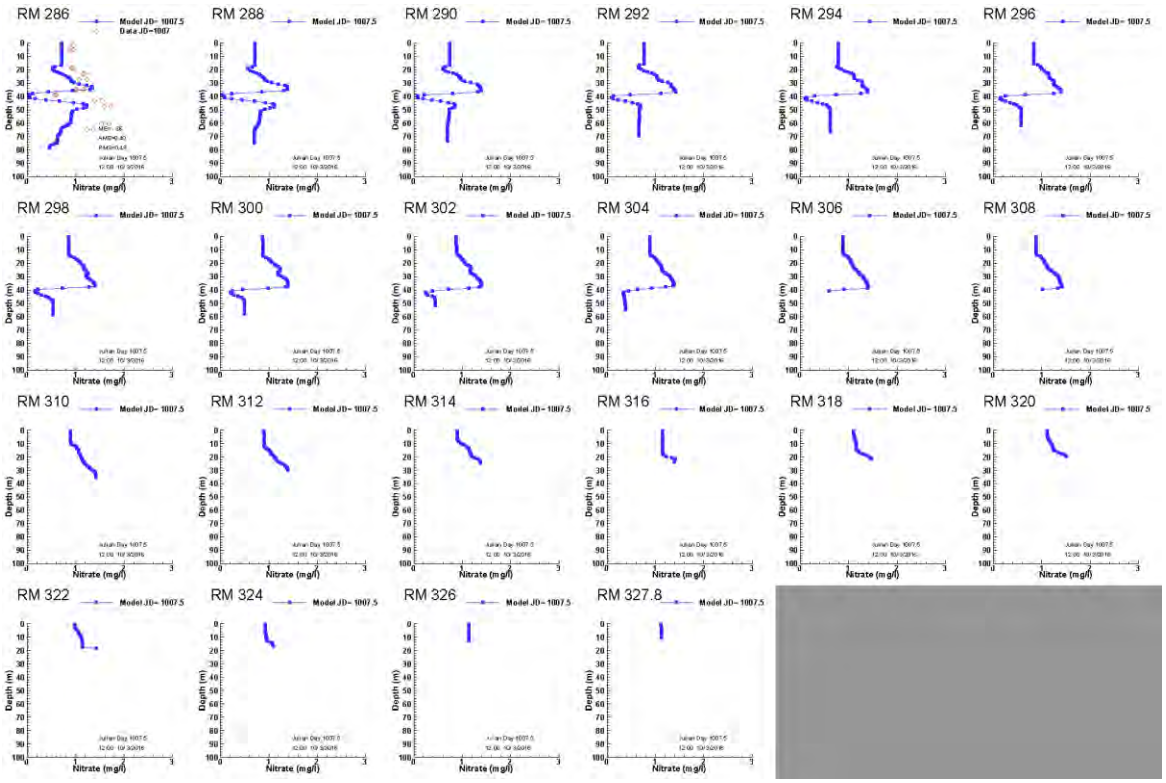


Figure 1045. Vertical profiles of NOxN compared with data for 10/ 3/2016.

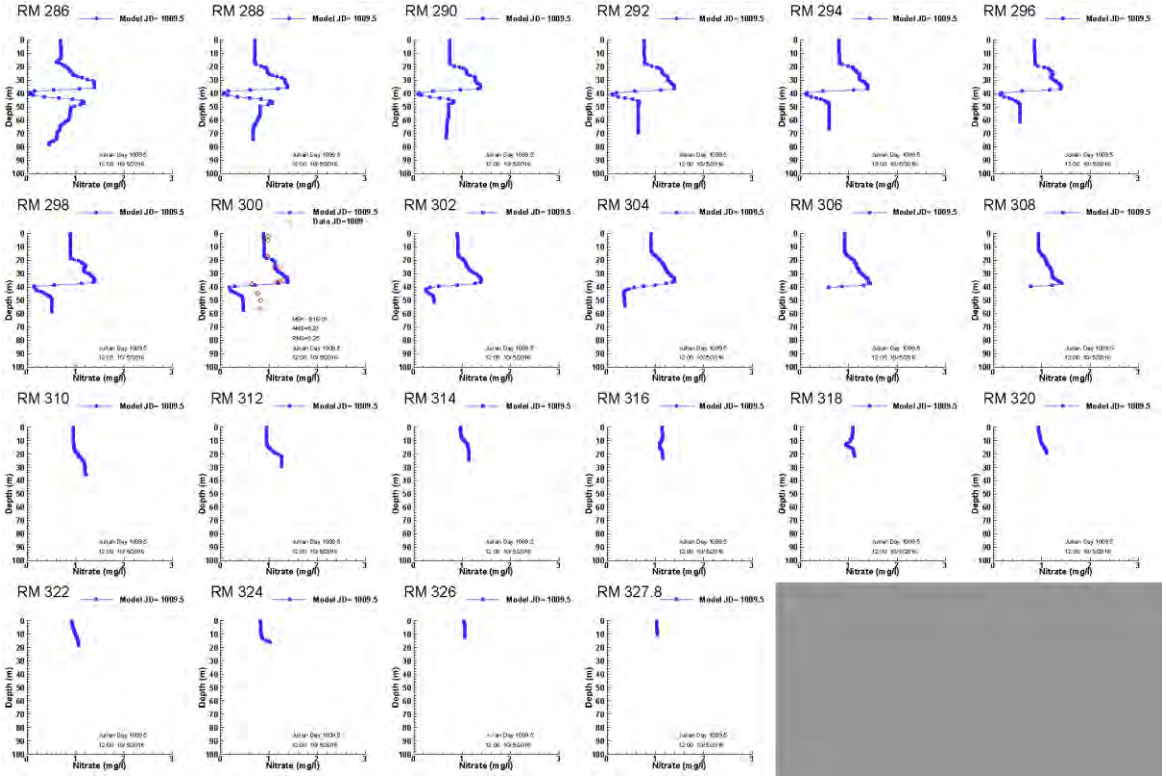


Figure 1046. Vertical profiles of NOxN compared with data for 10/ 5/2016.

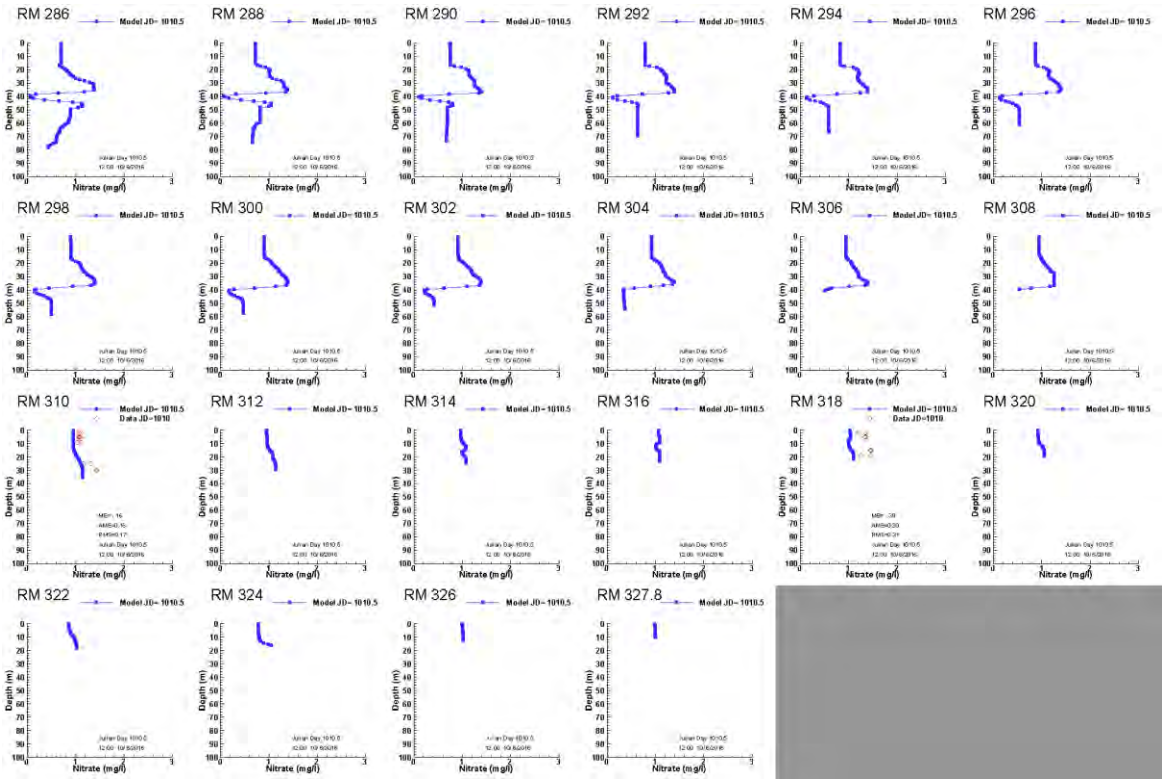


Figure 1047. Vertical profiles of NOxN compared with data for 10/ 6/2016.

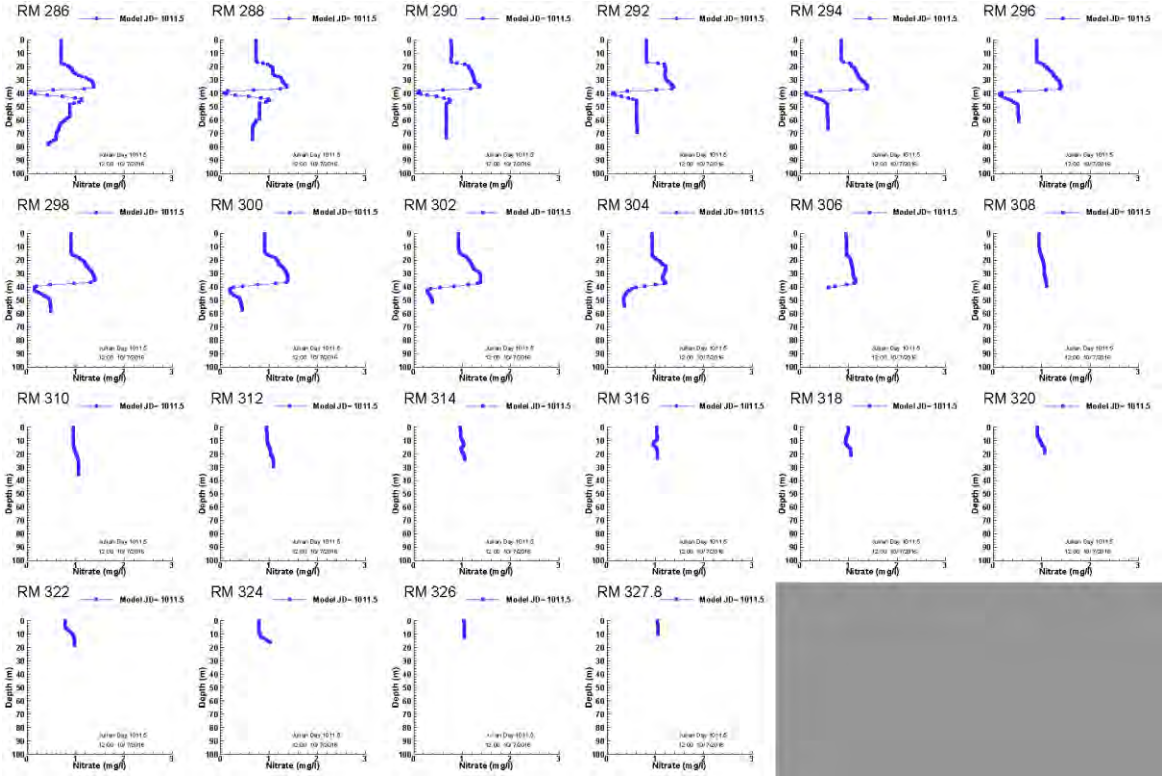


Figure 1048. Vertical profiles of NOxN compared with data for 10/ 7/2016.

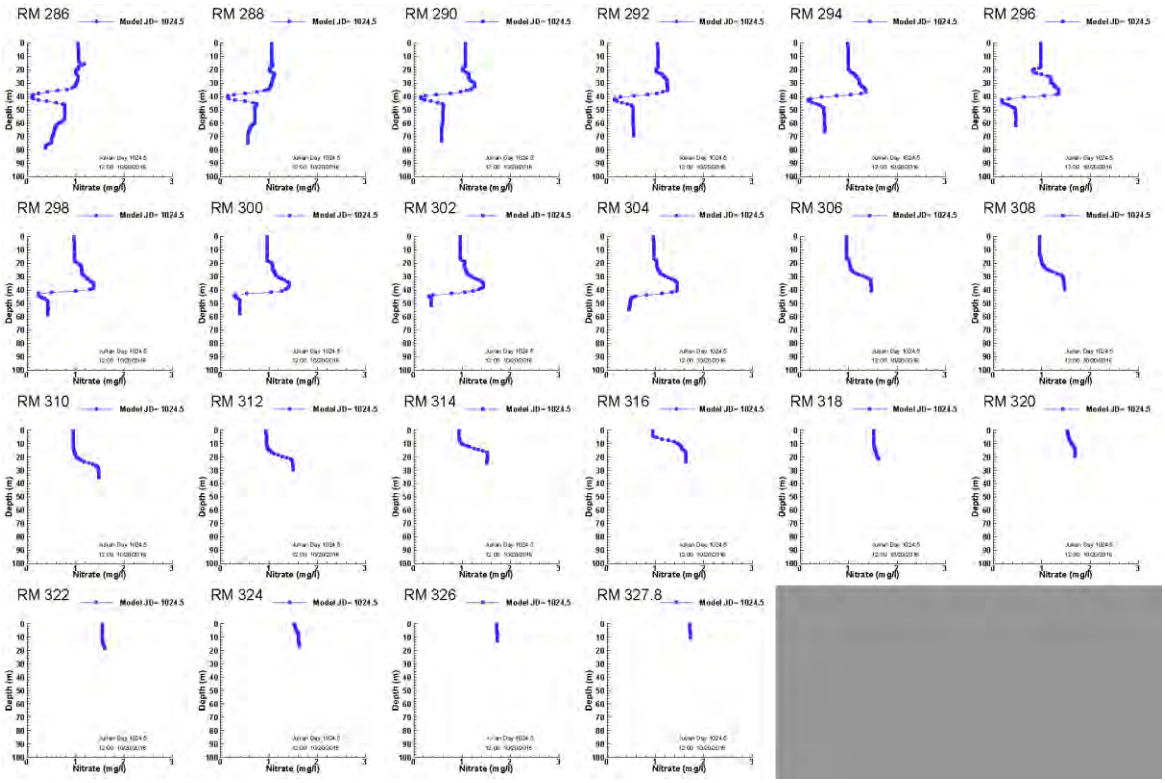


Figure 1049. Vertical profiles of NOxN compared with data for 10/20/2016.

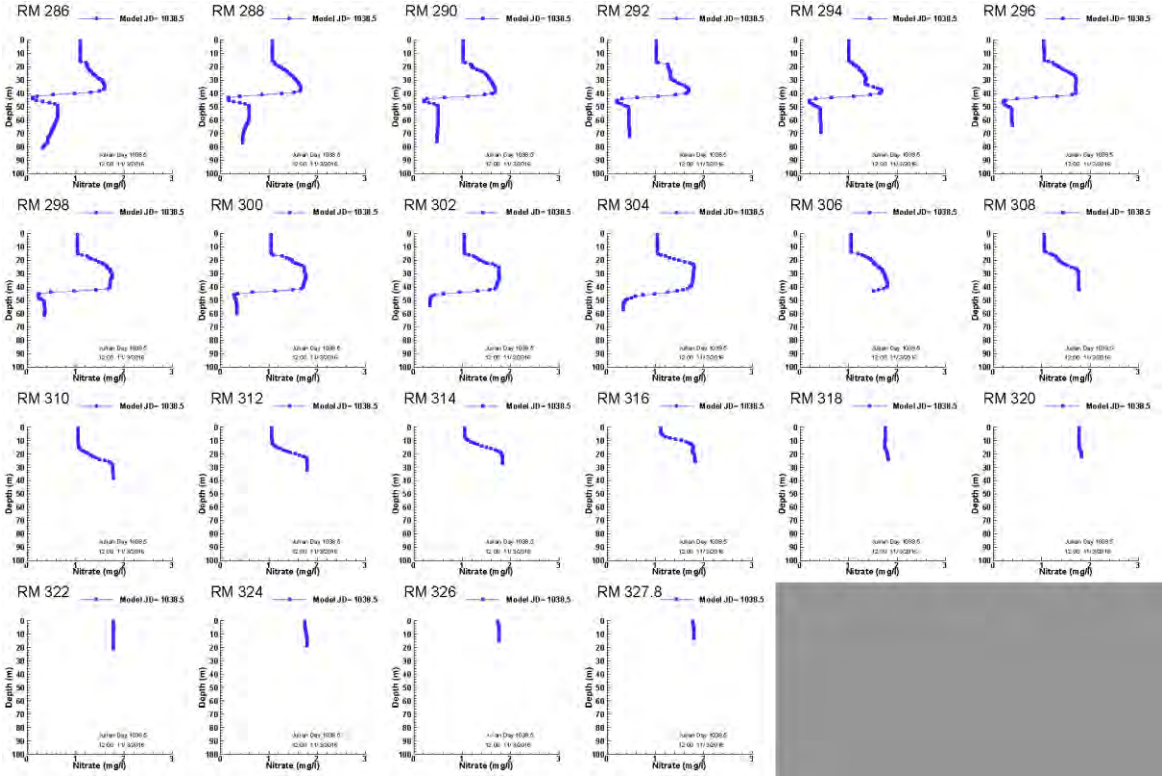


Figure 1050. Vertical profiles of NOxN compared with data for 11/ 3/2016.

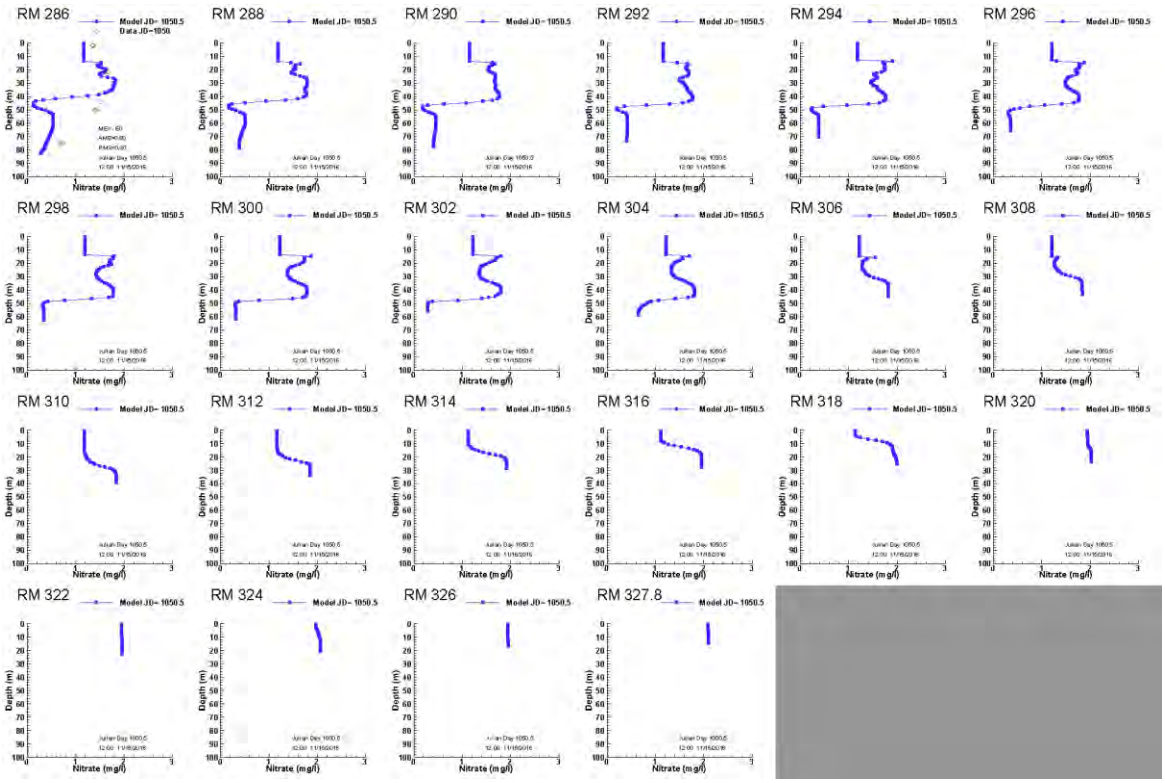


Figure 1051. Vertical profiles of NOxN compared with data for 11/15/2016.

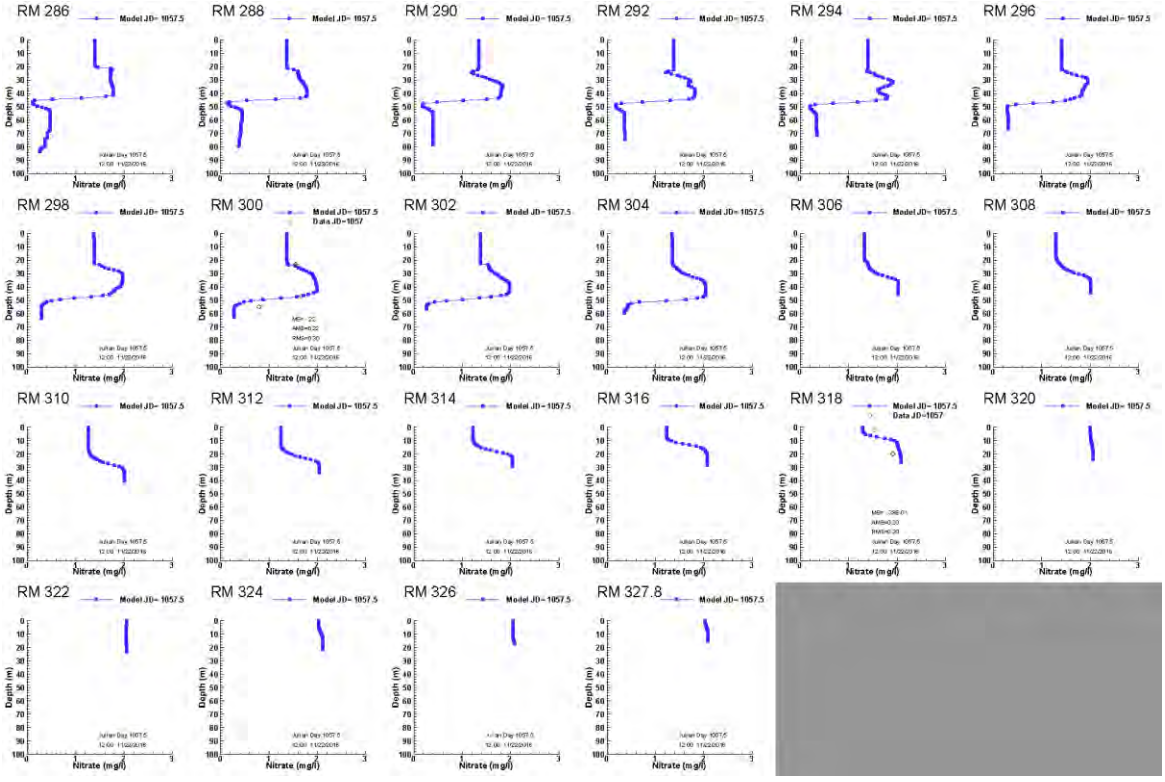


Figure 1052. Vertical profiles of NOxN compared with data for 11/22/2016.

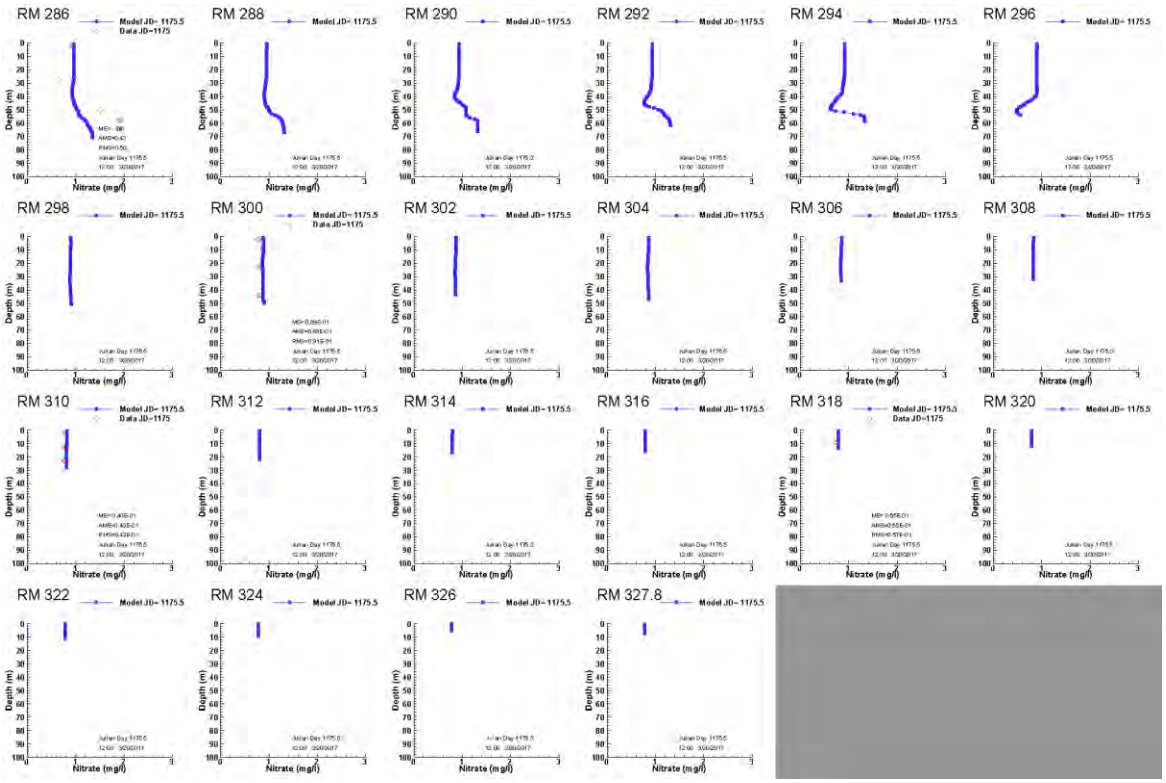


Figure 1053. Vertical profiles of NOxN compared with data for 3/20/2017.

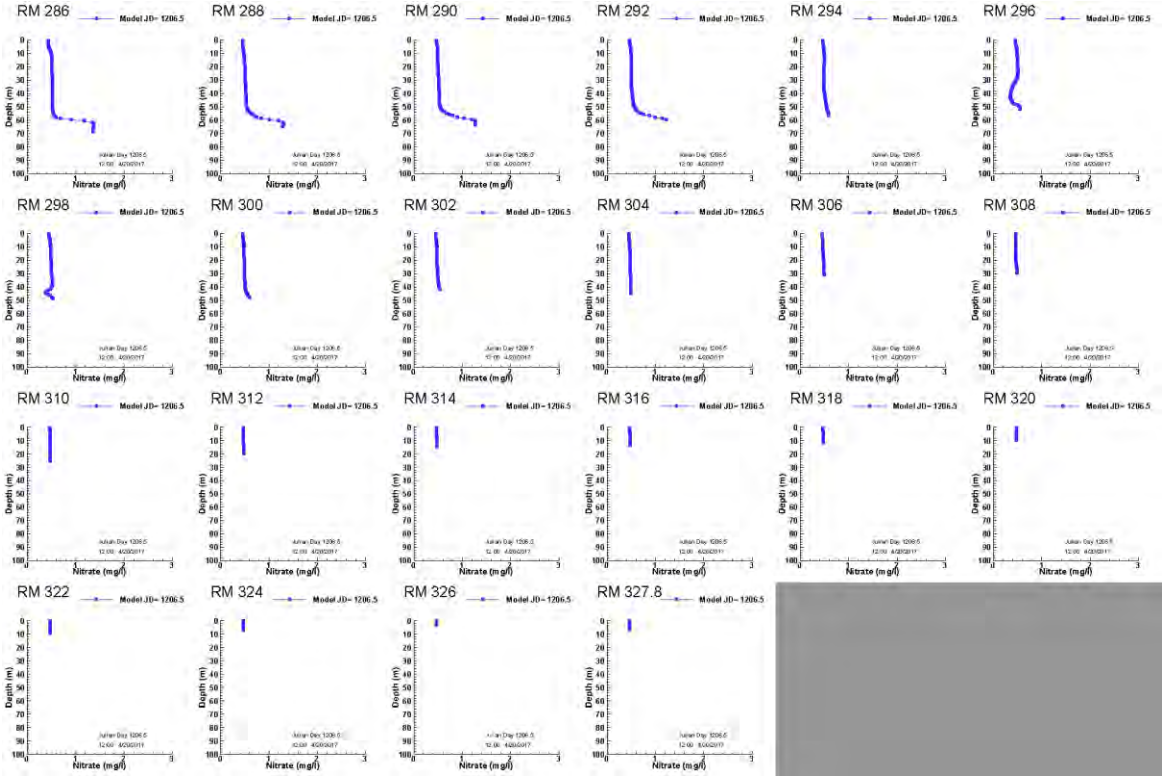


Figure 1054. Vertical profiles of NOxN compared with data for 4/20/2017.

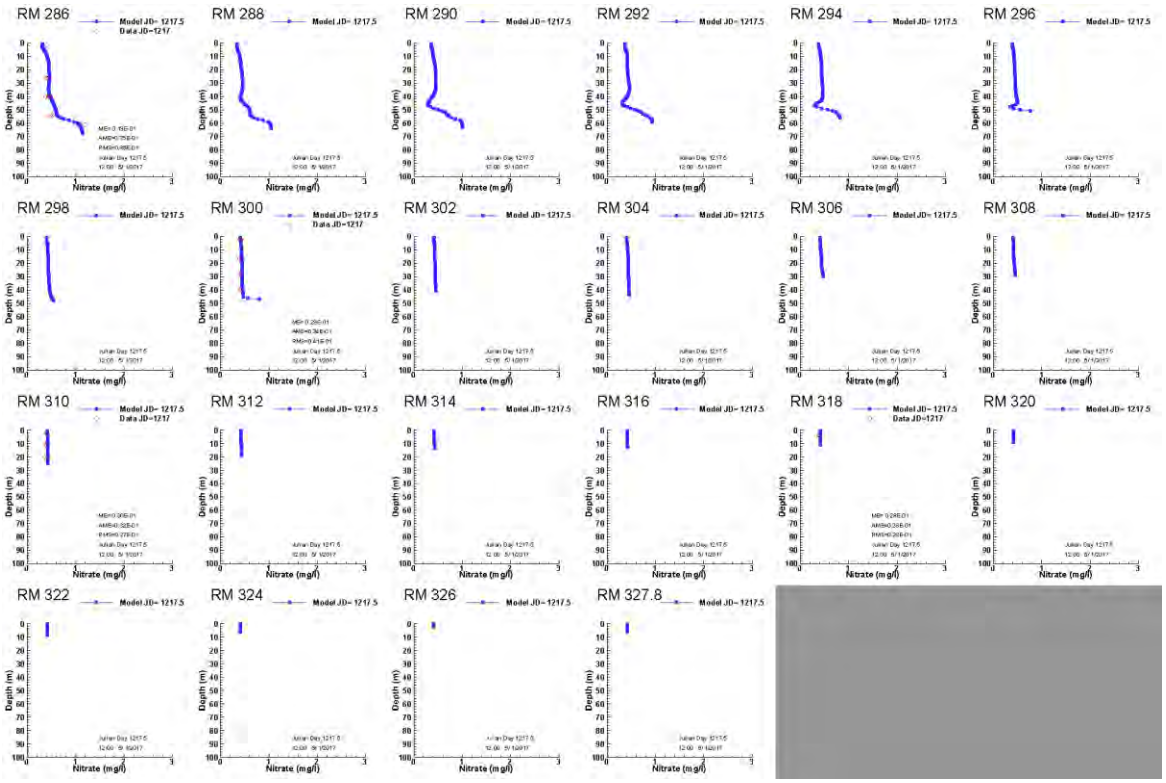


Figure 1055. Vertical profiles of NOxN compared with data for 5/ 1/2017.

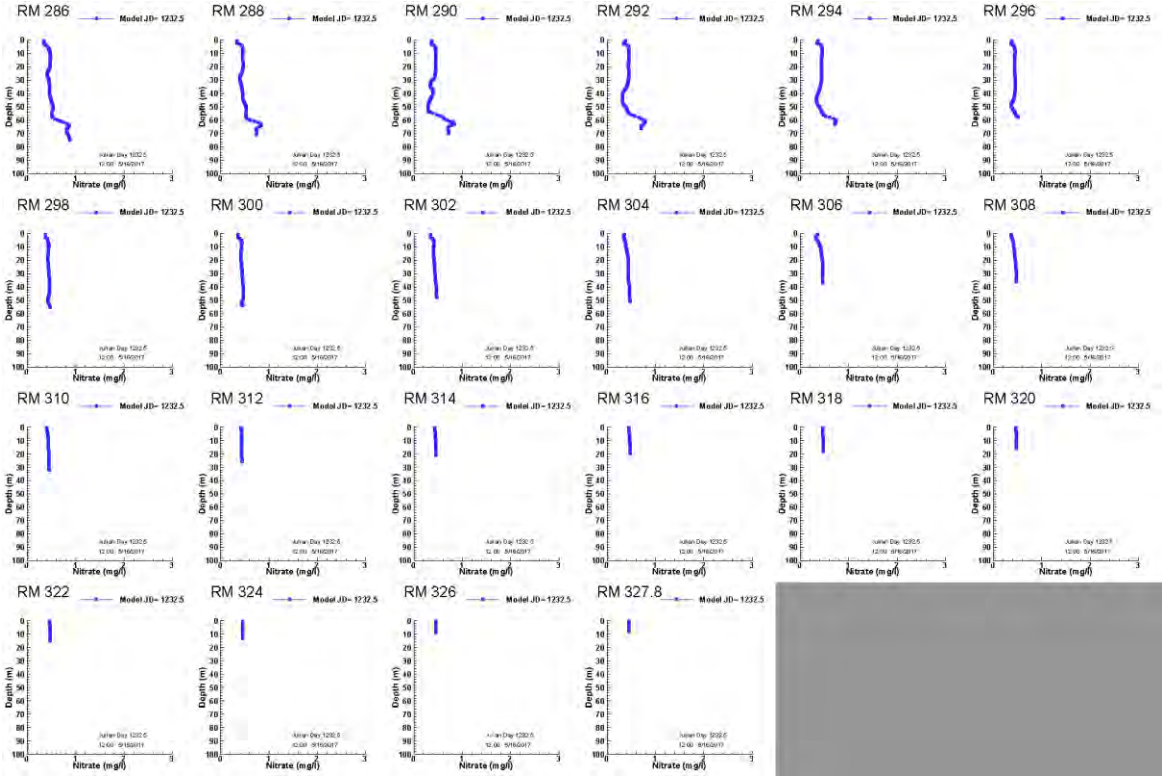


Figure 1056. Vertical profiles of NOxN compared with data for 5/16/2017.

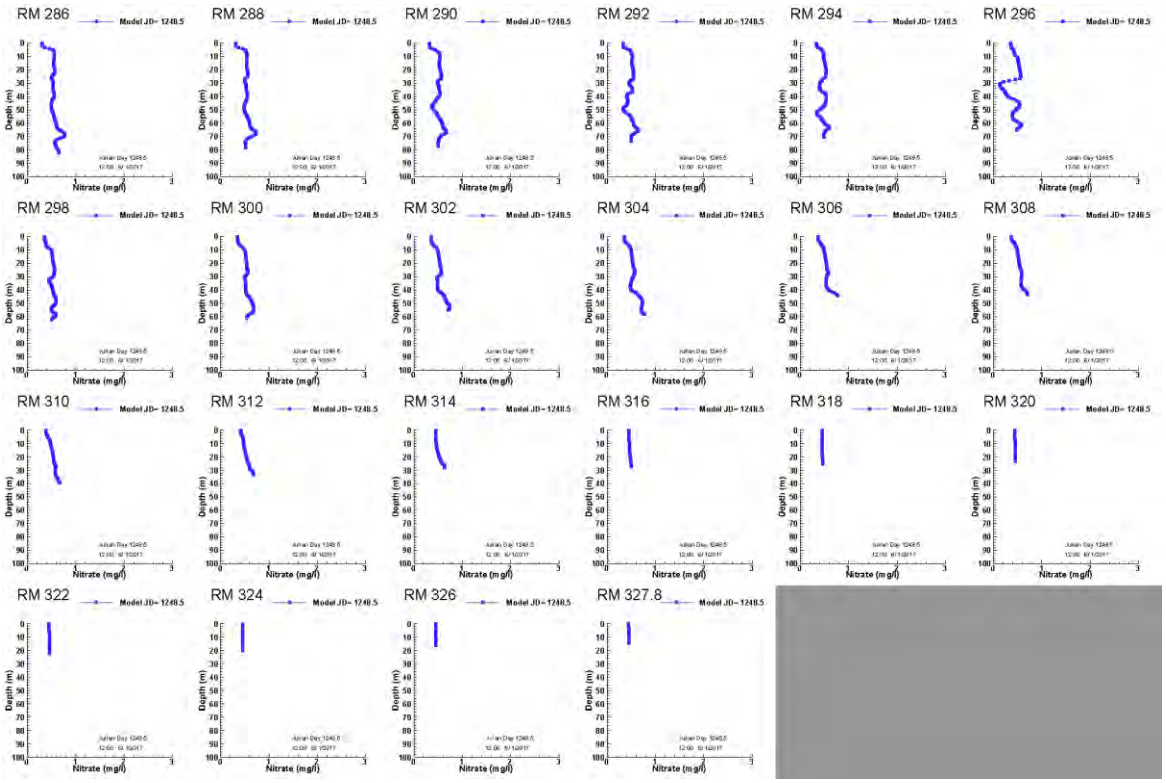


Figure 1057. Vertical profiles of NOxN compared with data for 6/ 1/2017.

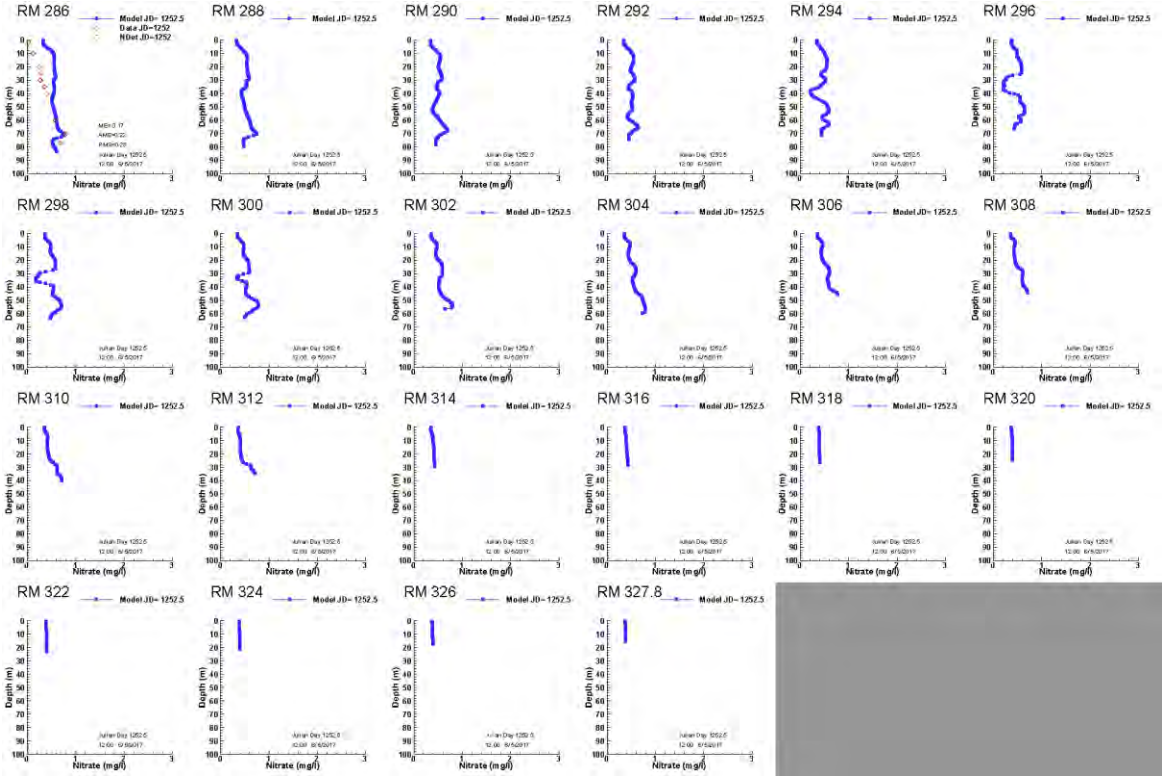


Figure 1058. Vertical profiles of NOxN compared with data for 6/ 5/2017.

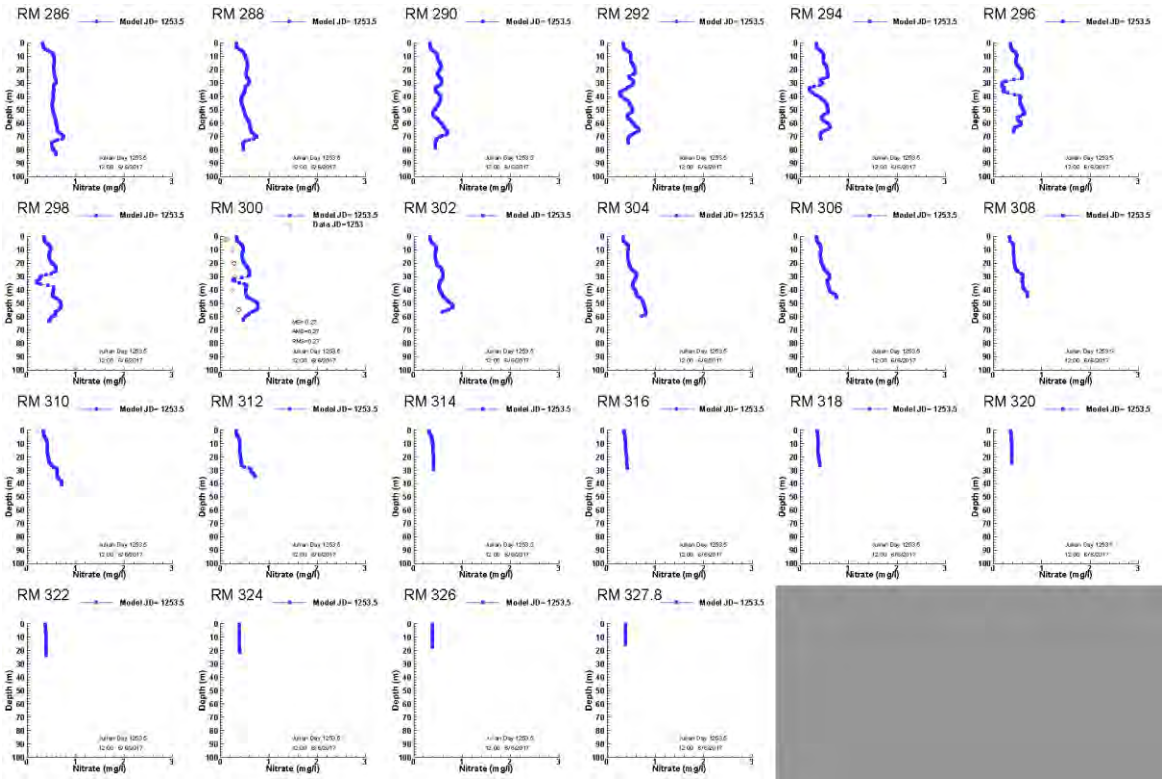


Figure 1059. Vertical profiles of NOxN compared with data for 6/ 6/2017.

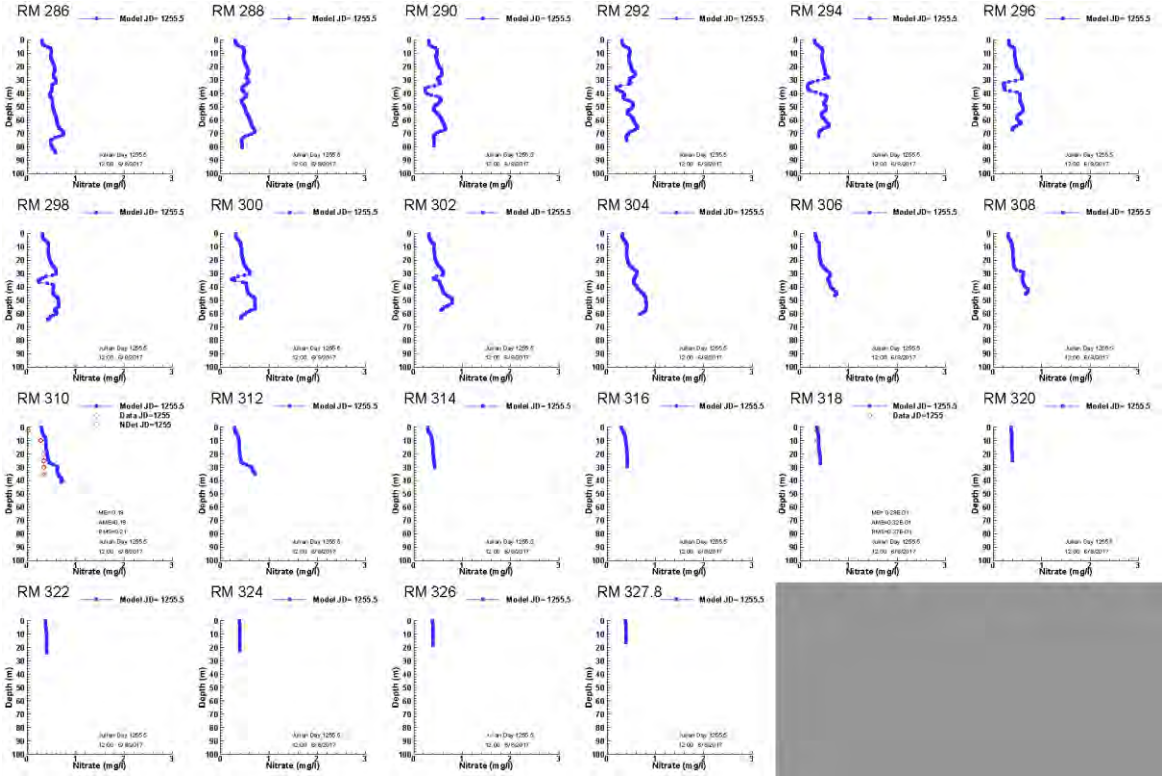


Figure 1060. Vertical profiles of NOxN compared with data for 6/ 8/2017.

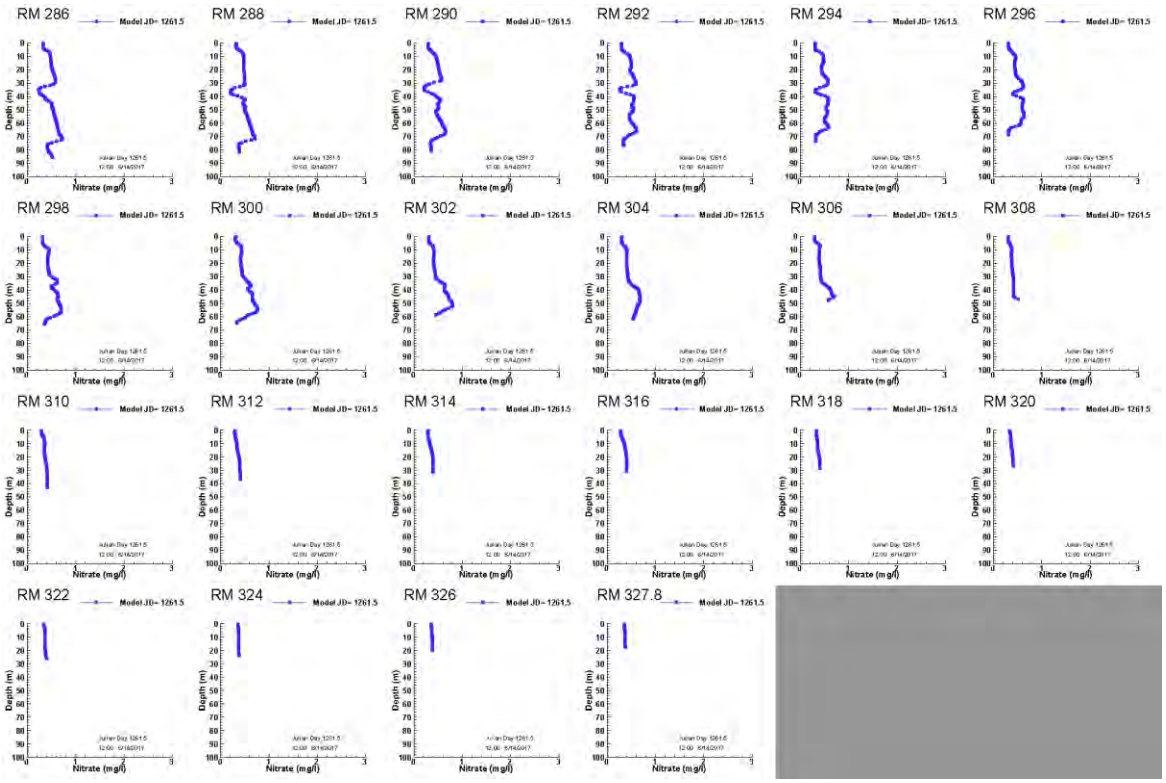


Figure 1061. Vertical profiles of NOxN compared with data for 6/14/2017.

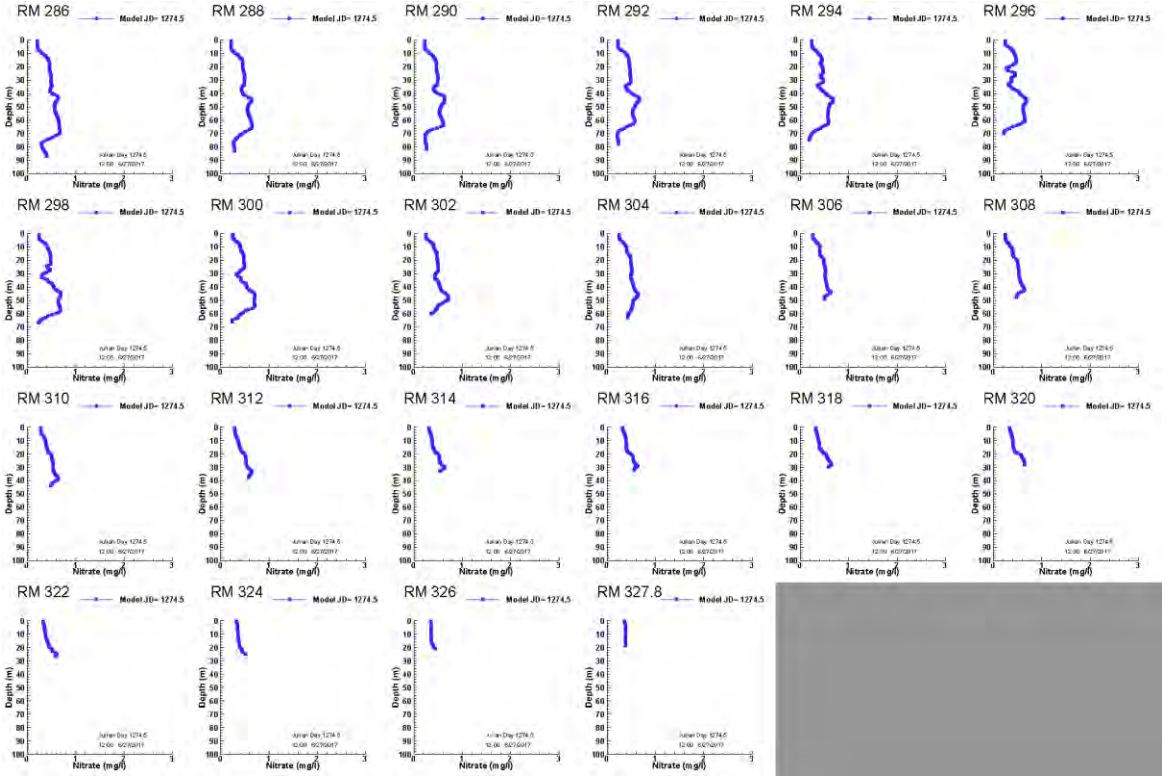


Figure 1062. Vertical profiles of NOxN compared with data for 6/27/2017.

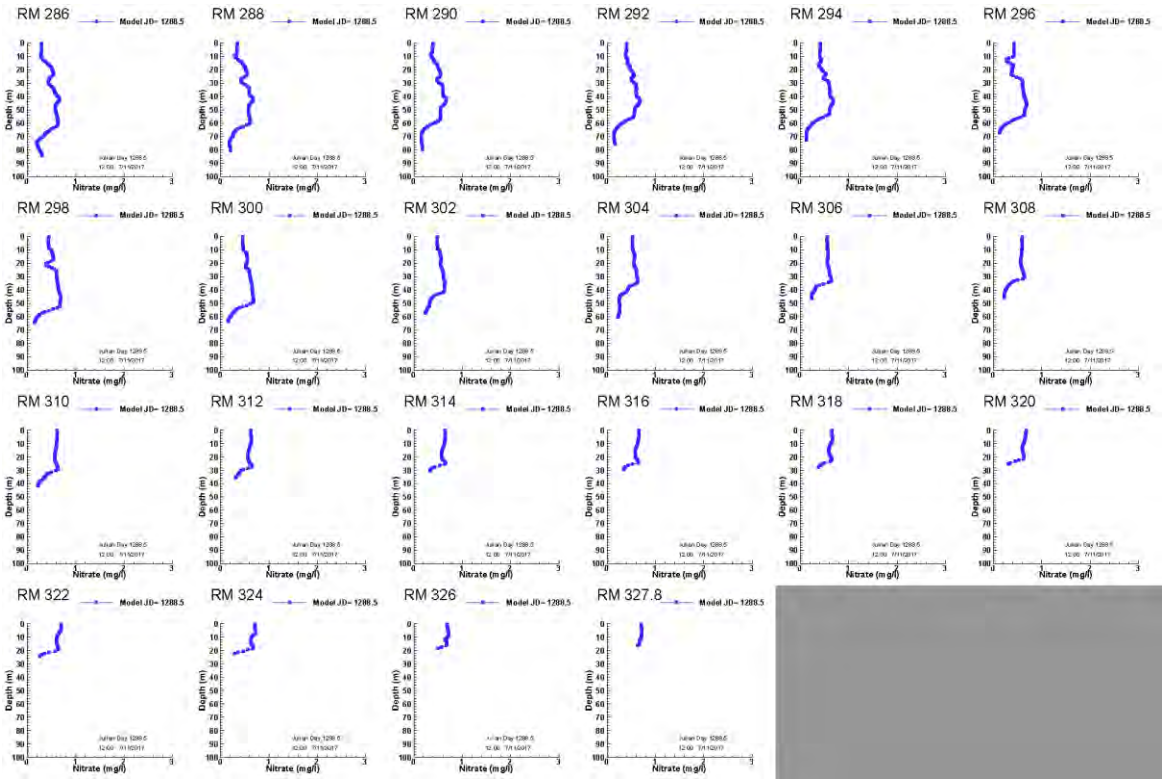


Figure 1063. Vertical profiles of NOxN compared with data for 7/11/2017.

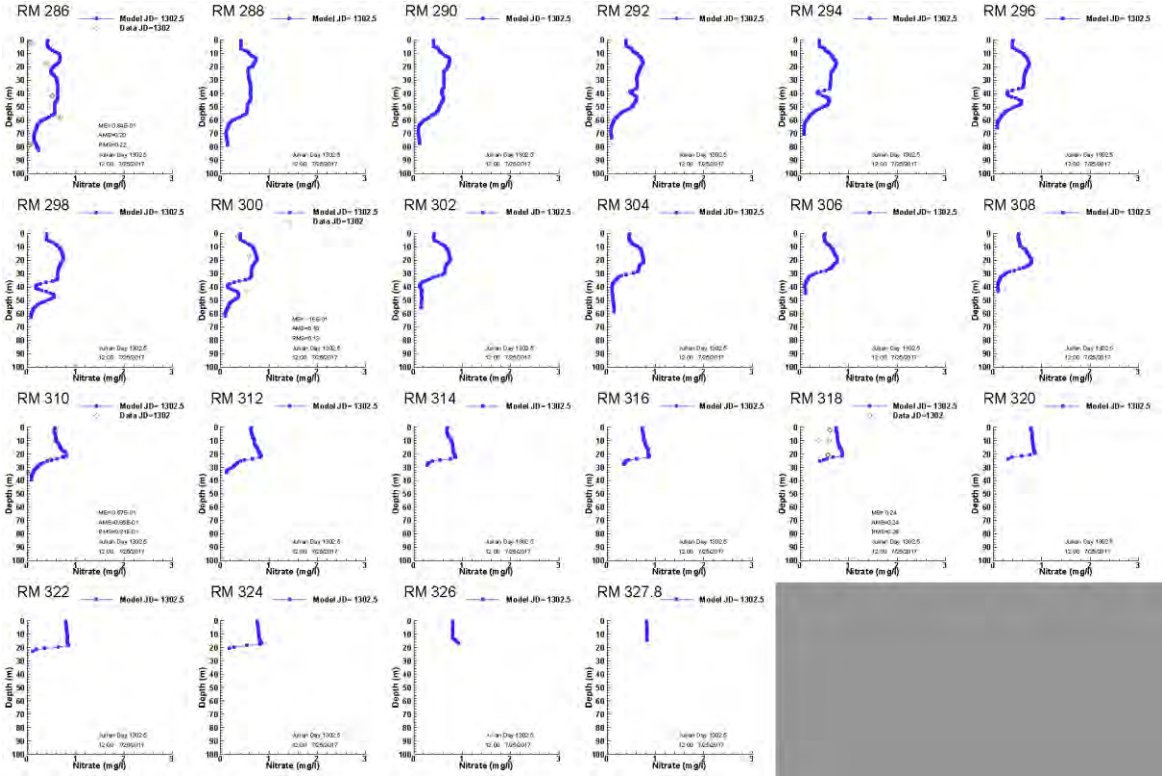


Figure 1064. Vertical profiles of NOxN compared with data for 7/25/2017.

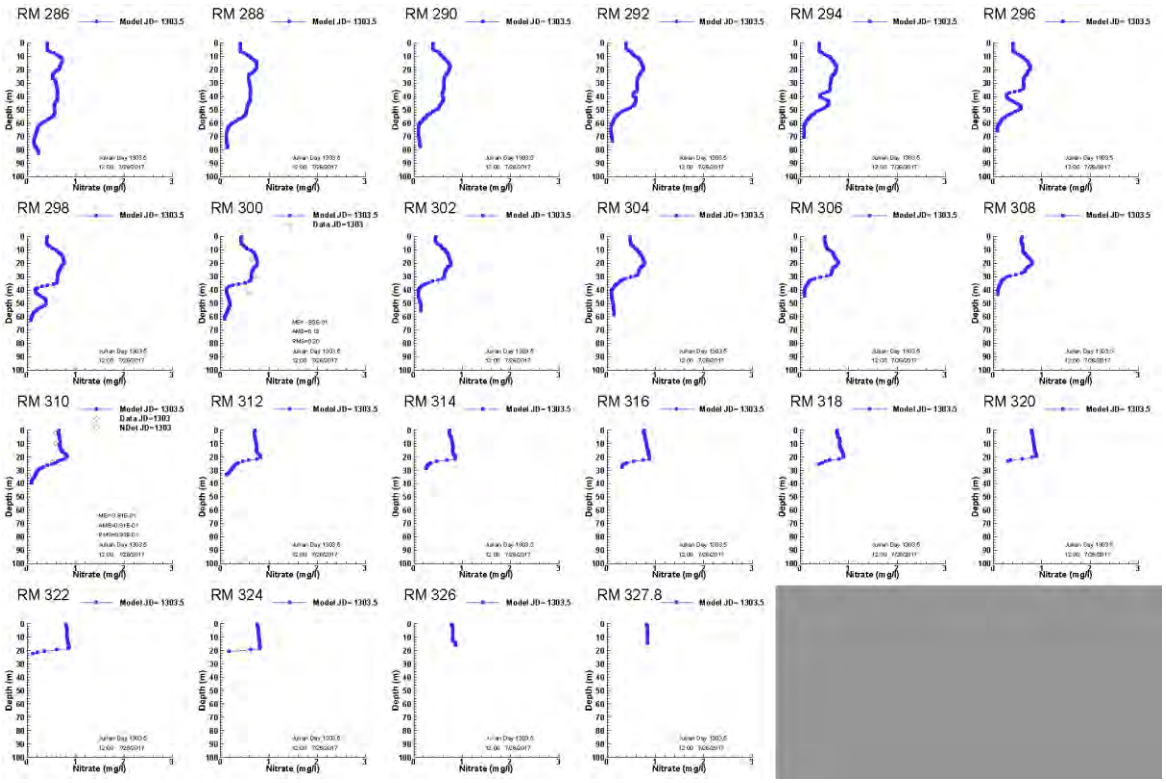


Figure 1065. Vertical profiles of NOxN compared with data for 7/26/2017.

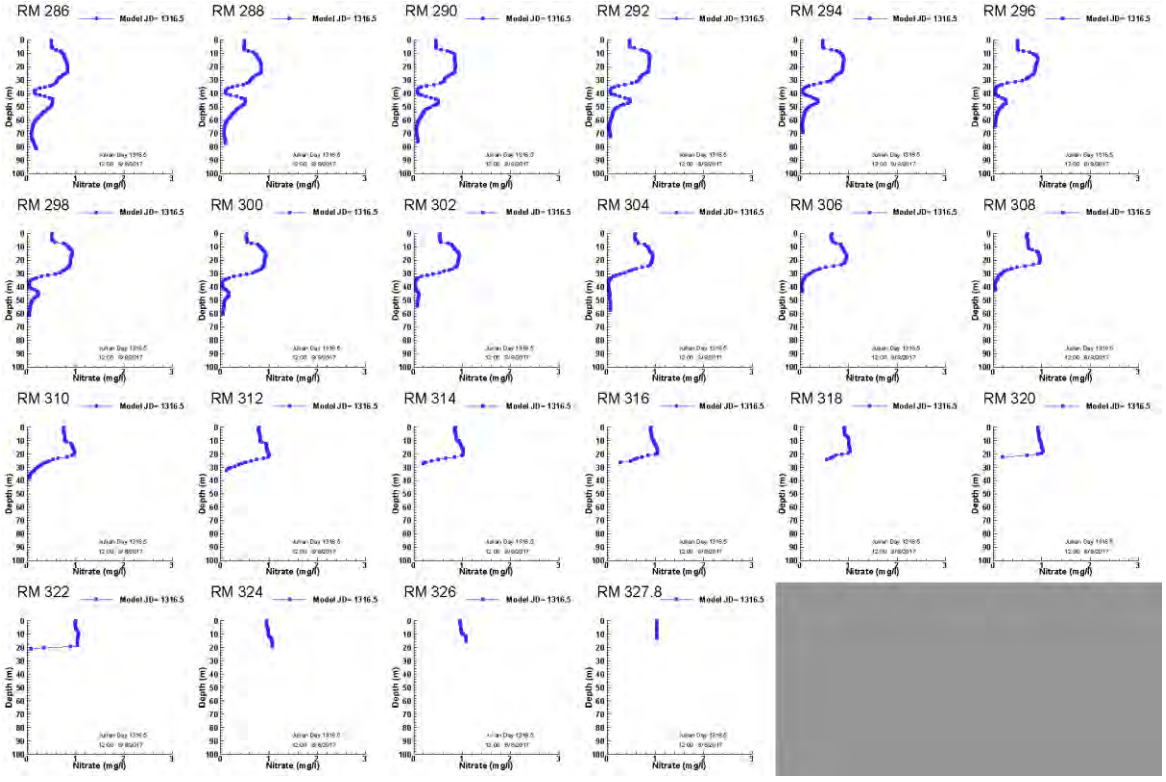


Figure 1066. Vertical profiles of NOxN compared with data for 8/ 8/2017.

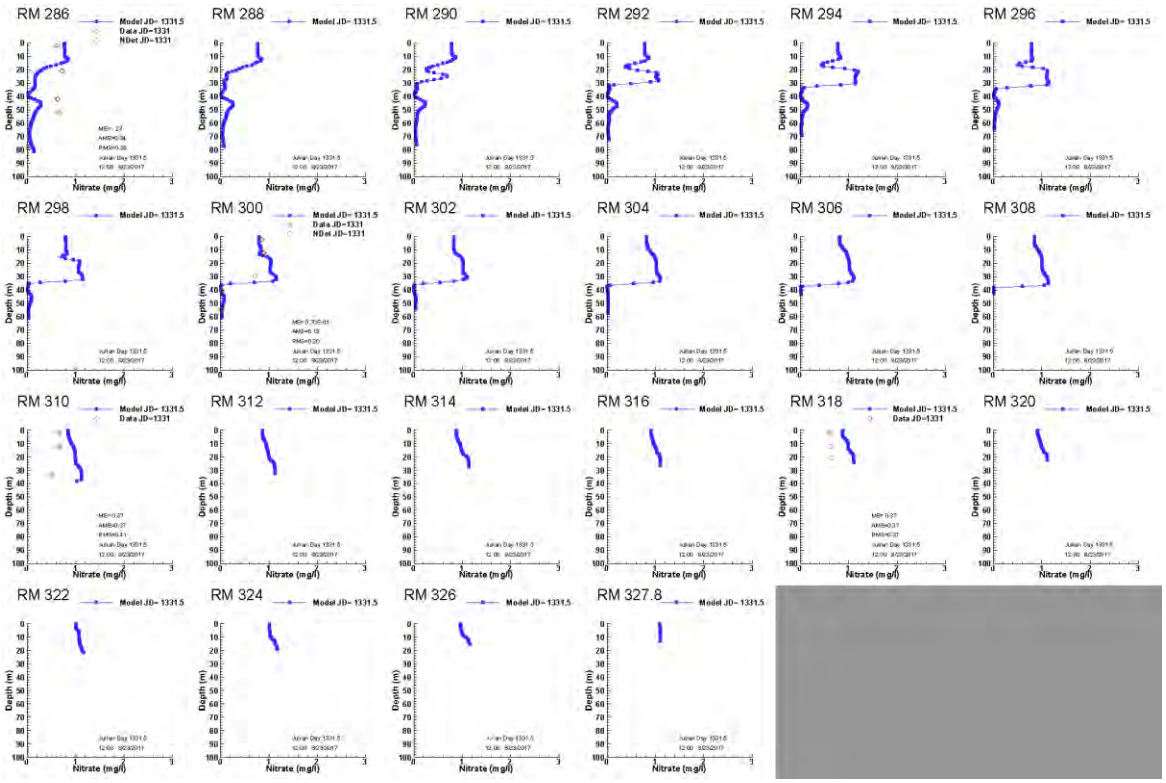


Figure 1067. Vertical profiles of NOxN compared with data for 8/23/2017.

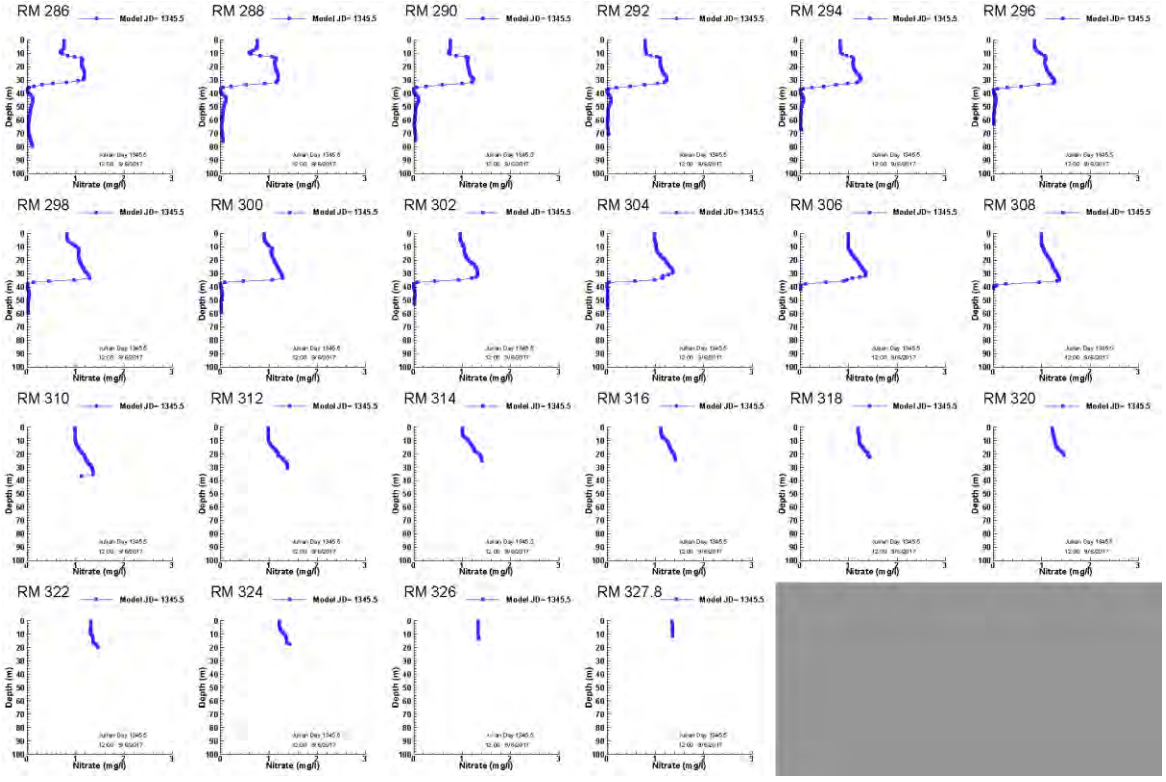


Figure 1068. Vertical profiles of NOxN compared with data for 9/ 6/2017.

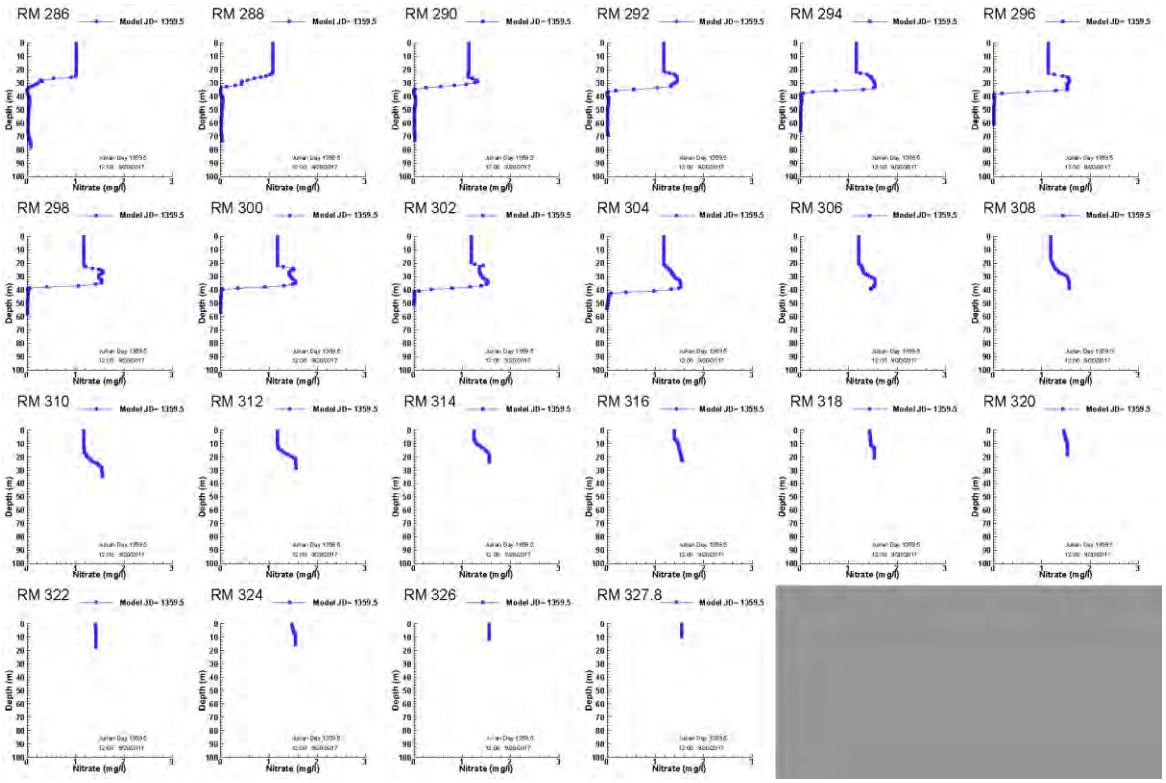


Figure 1069. Vertical profiles of NOxN compared with data for 9/20/2017.

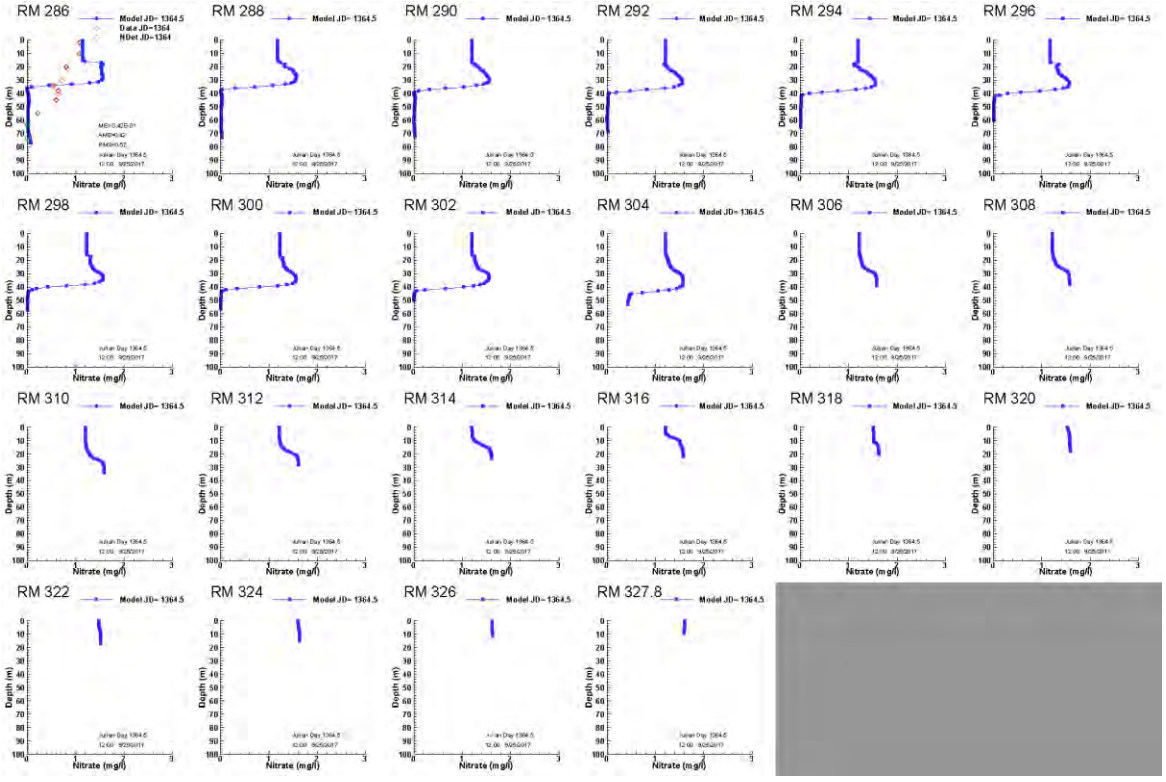


Figure 1070. Vertical profiles of NOxN compared with data for 9/25/2017.

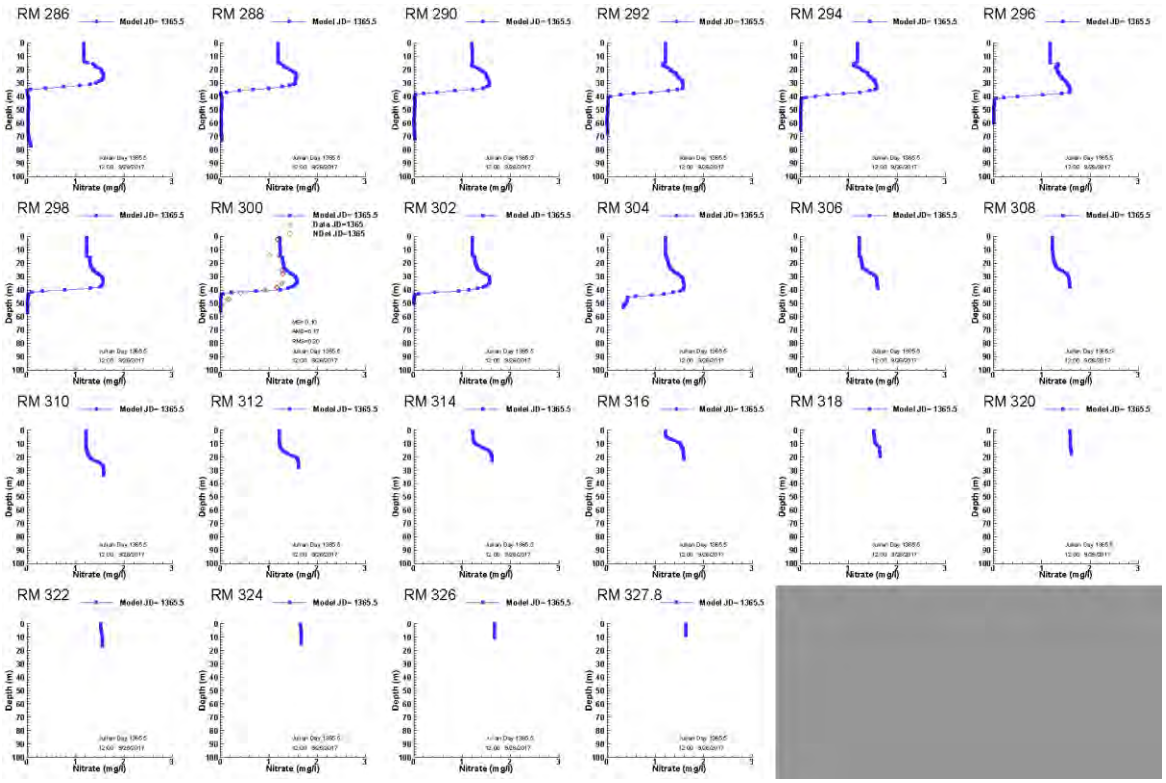


Figure 1071. Vertical profiles of NOxN compared with data for 9/26/2017.

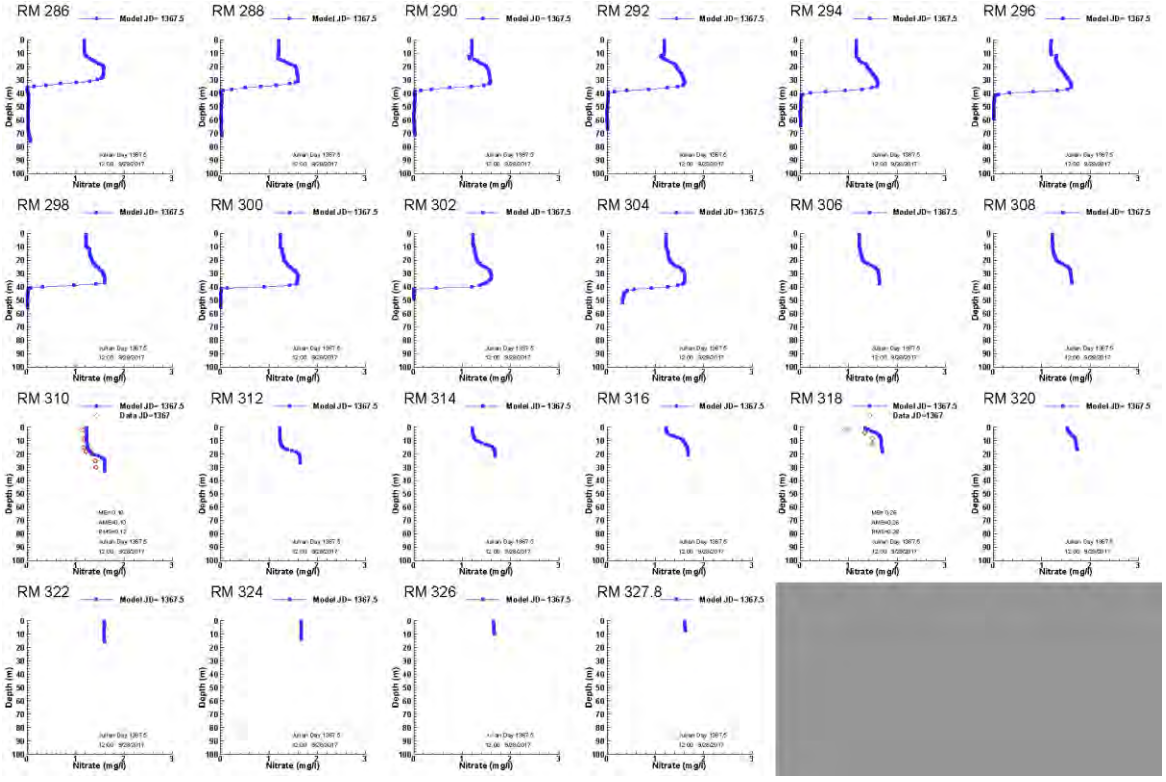


Figure 1072. Vertical profiles of NOxN compared with data for 9/28/2017.

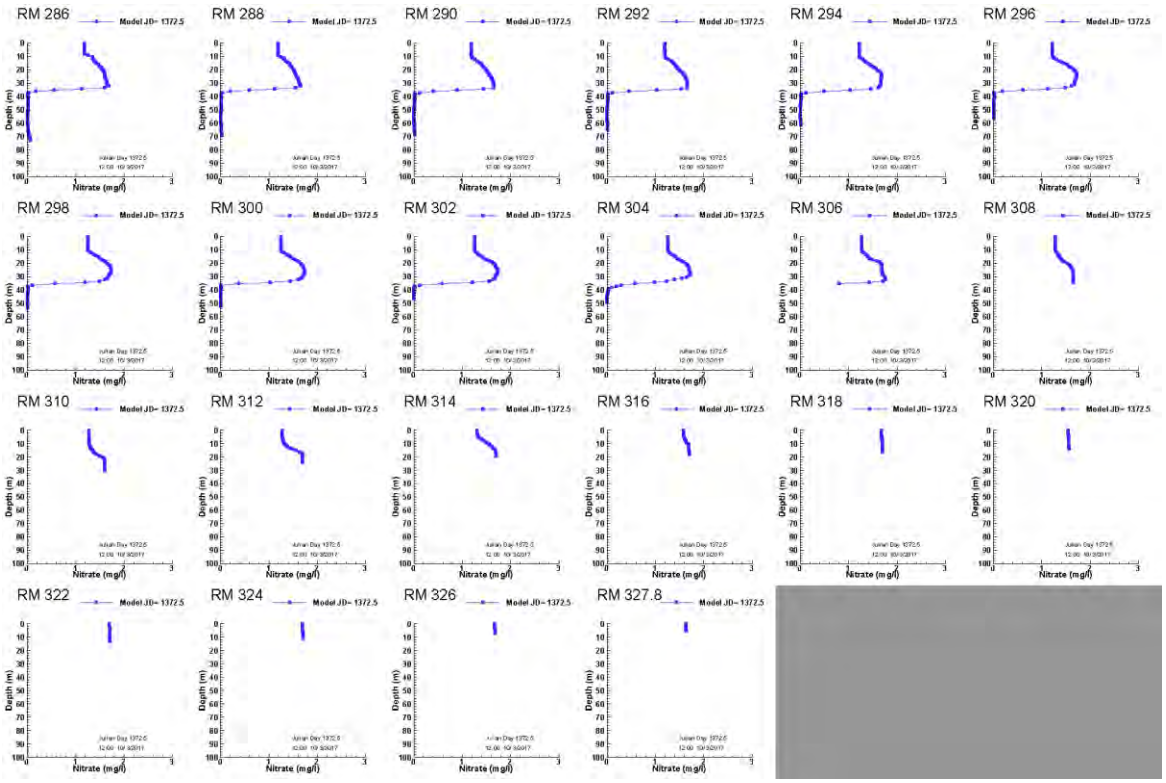


Figure 1073. Vertical profiles of NOxN compared with data for 10/ 3/2017.

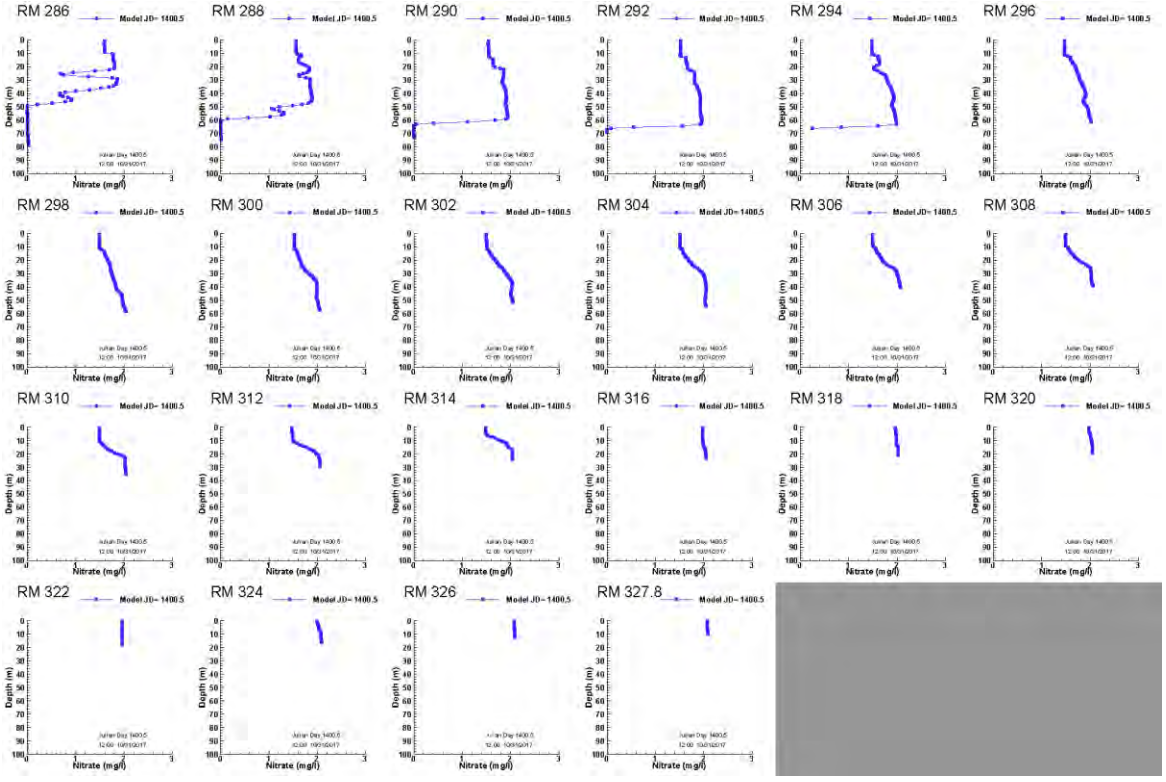


Figure 1074. Vertical profiles of NOxN compared with data for 10/31/2017.

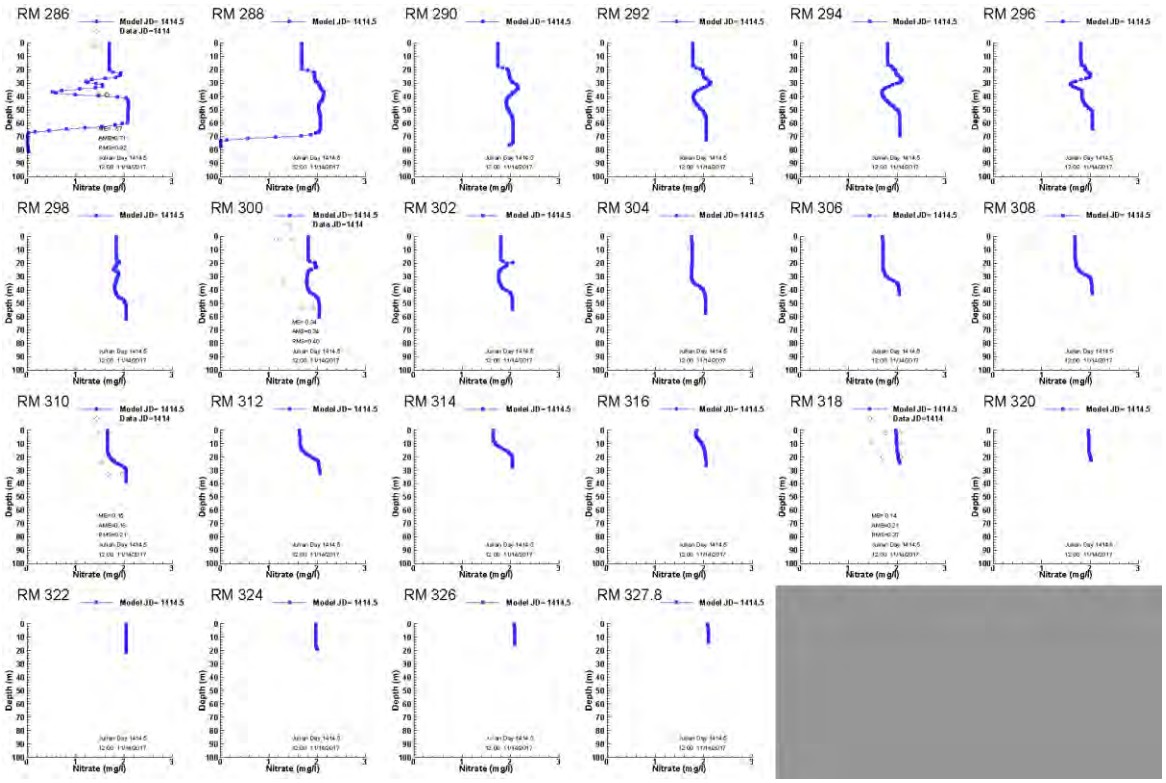


Figure 1075. Vertical profiles of NOxN compared with data for 11/14/2017.

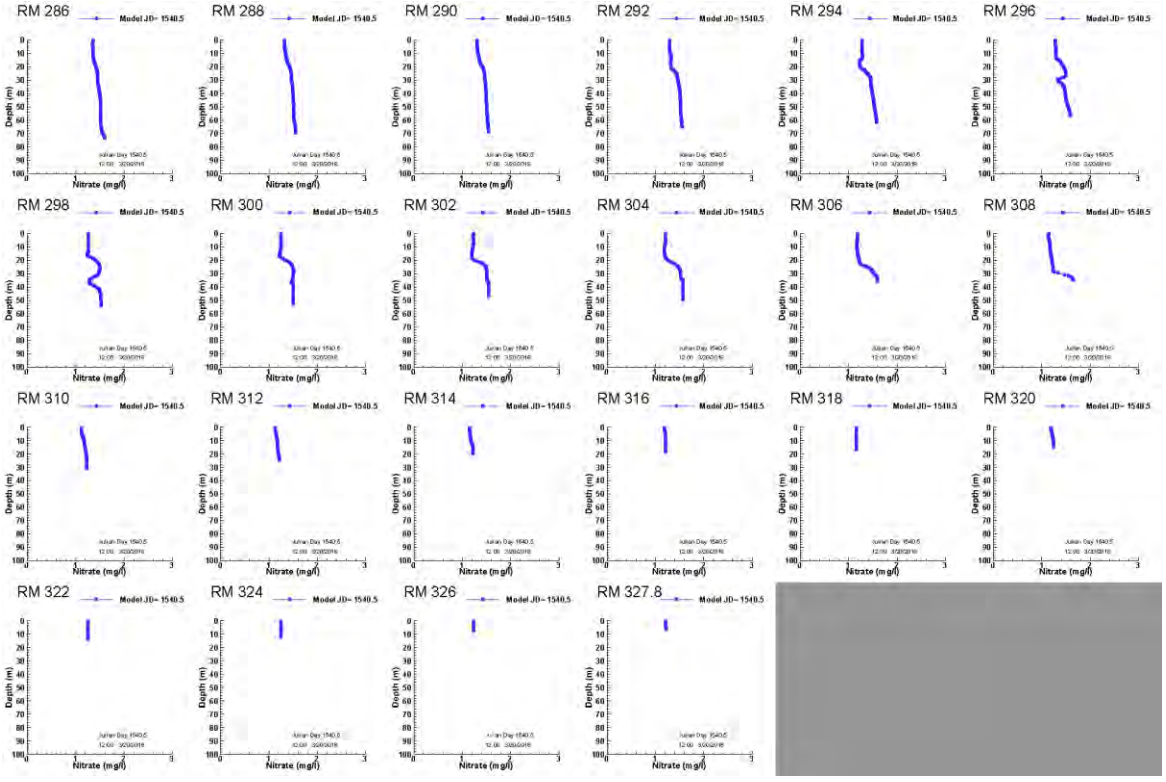


Figure 1076. Vertical profiles of NOxN compared with data for 3/20/2018.

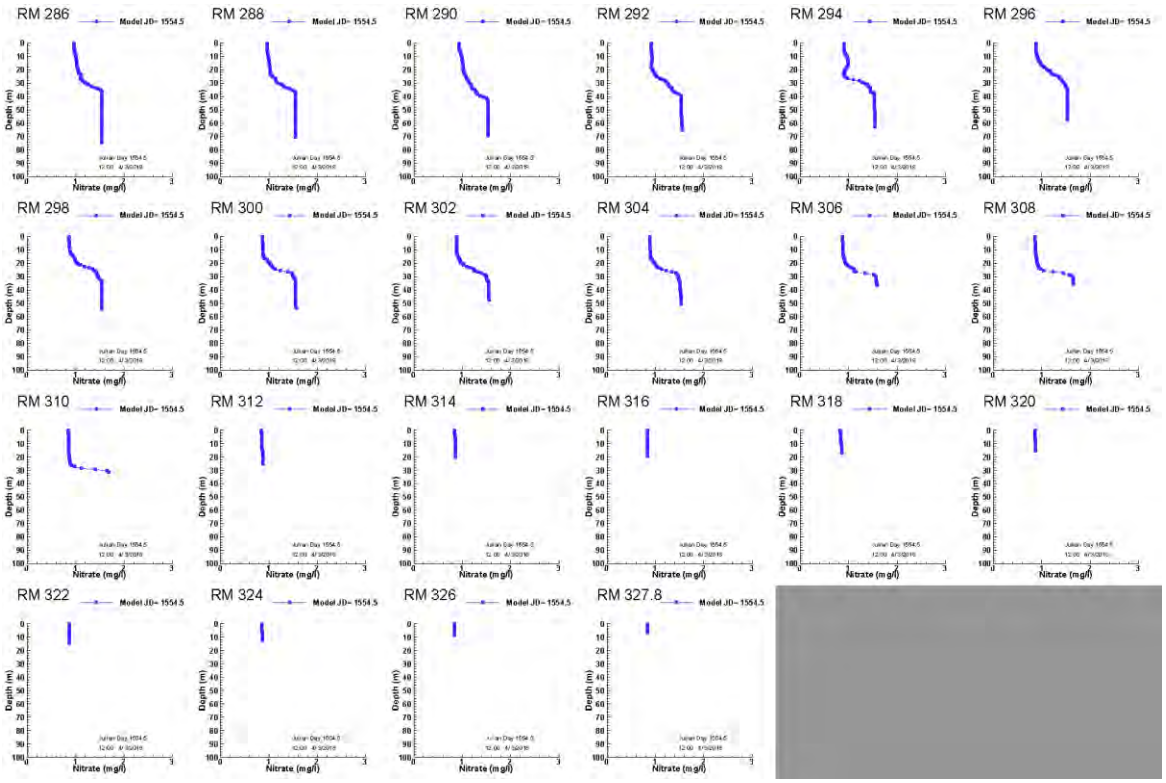


Figure 1077. Vertical profiles of NOxN compared with data for 4/ 3/2018.

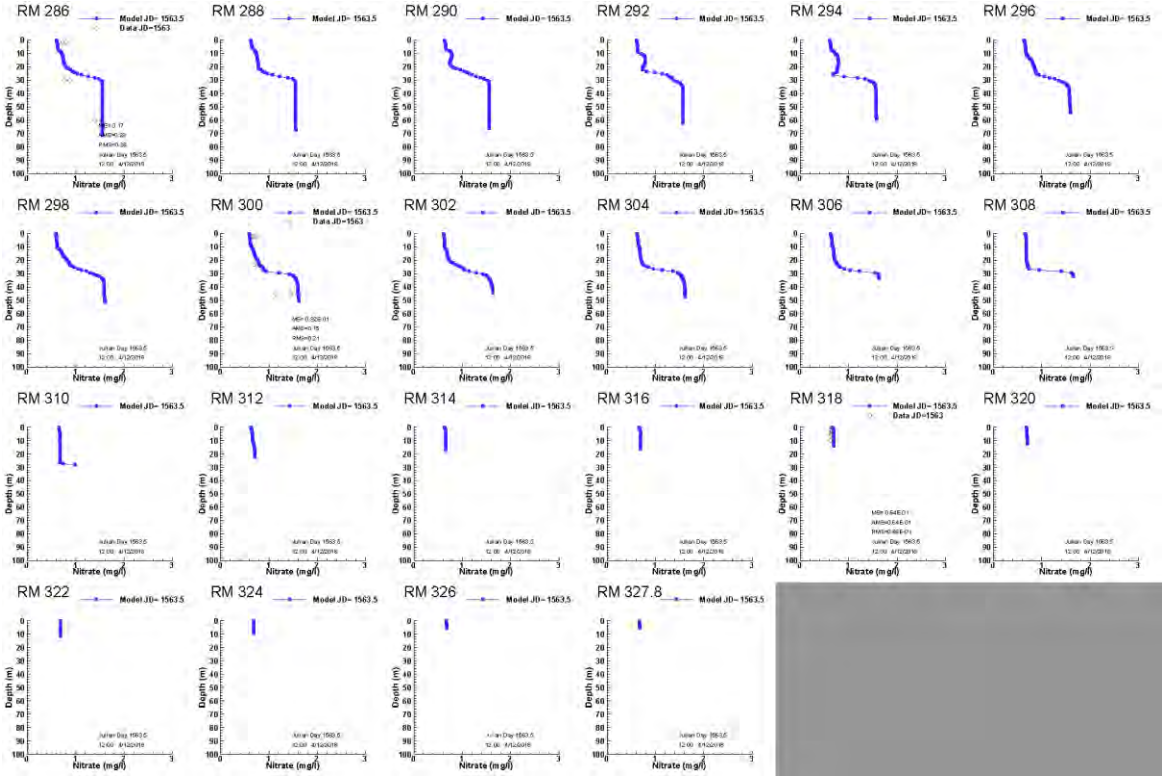


Figure 1078. Vertical profiles of NOxN compared with data for 4/12/2018.

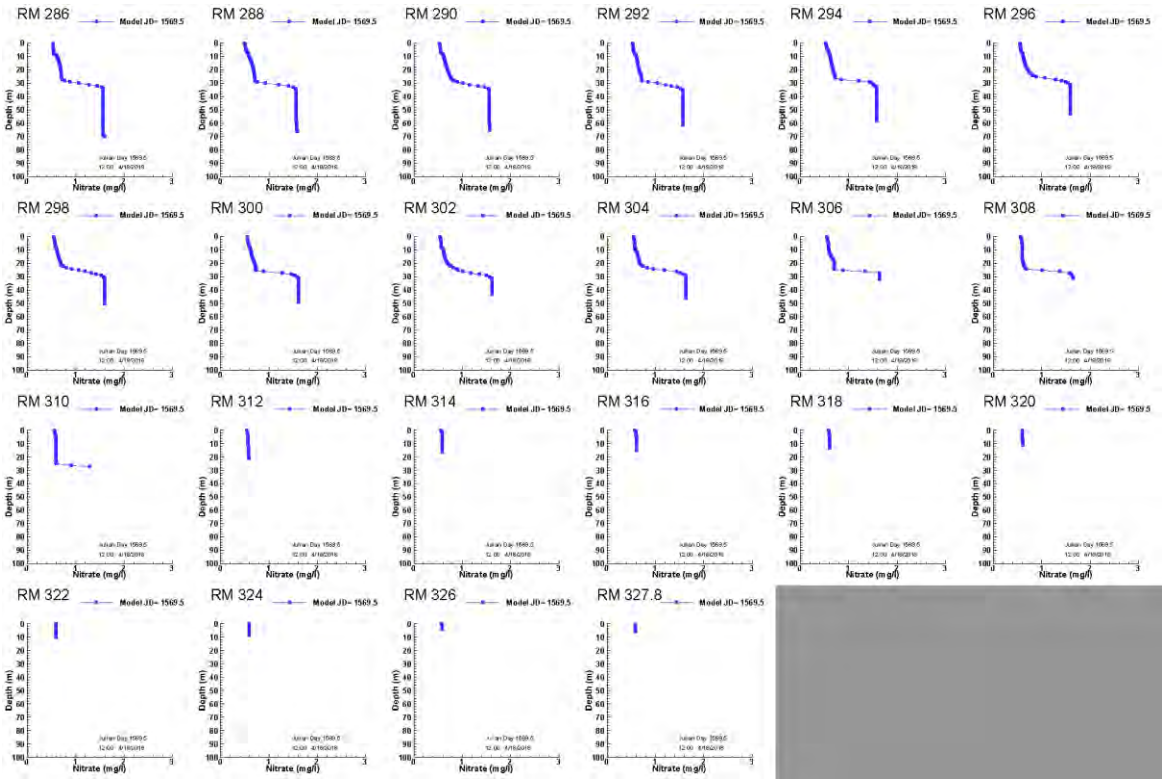


Figure 1079. Vertical profiles of NOxN compared with data for 4/18/2018.

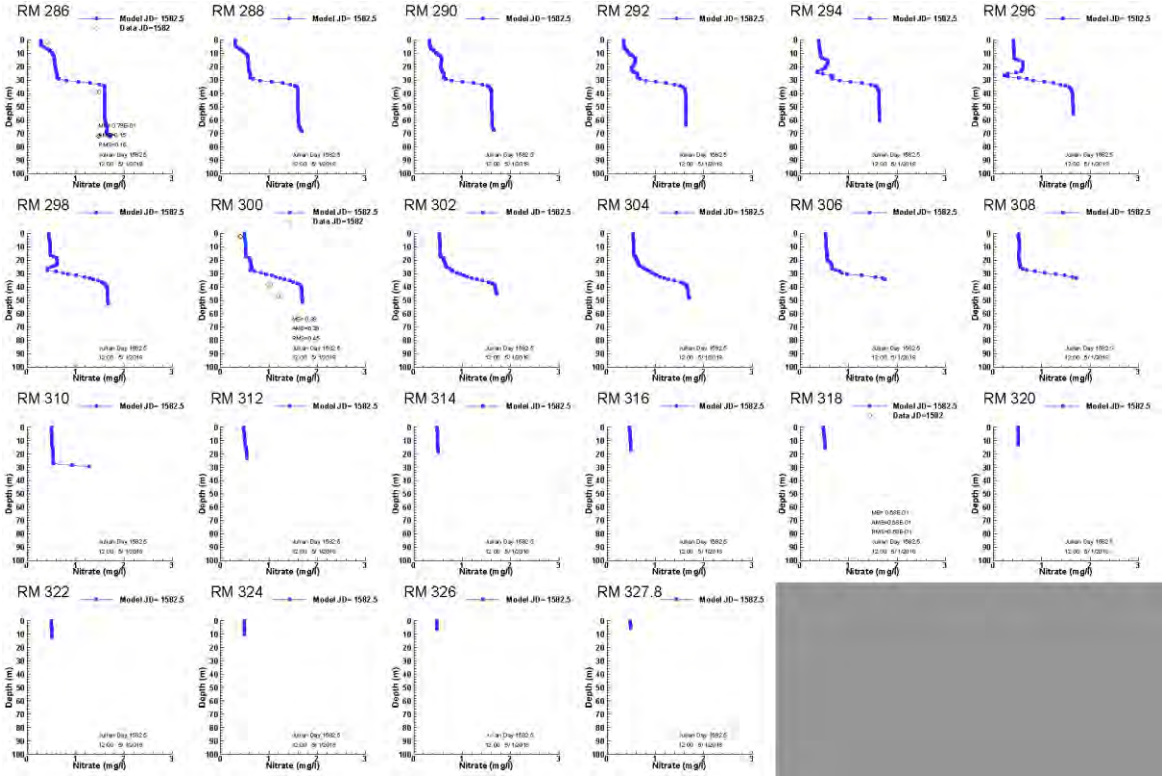


Figure 1080. Vertical profiles of NOxN compared with data for 5/ 1/2018.

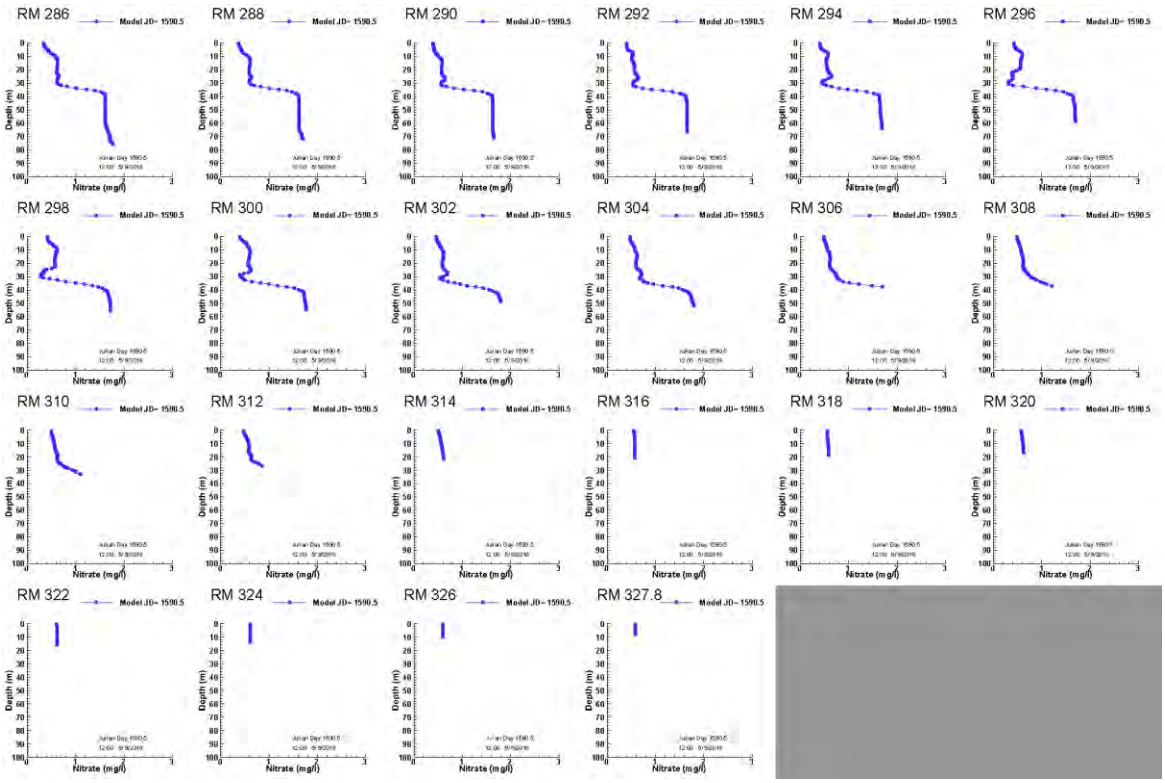


Figure 1081. Vertical profiles of NOxN compared with data for 5/ 9/2018.

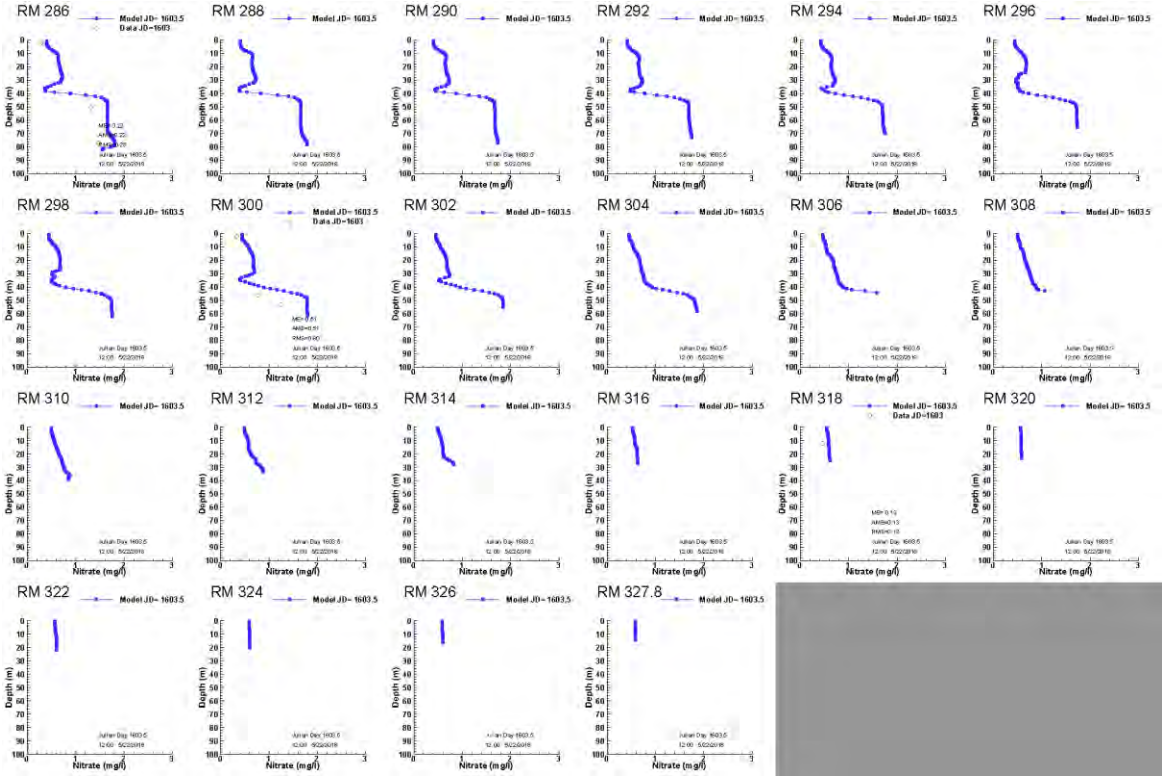


Figure 1082. Vertical profiles of NOxN compared with data for 5/22/2018.

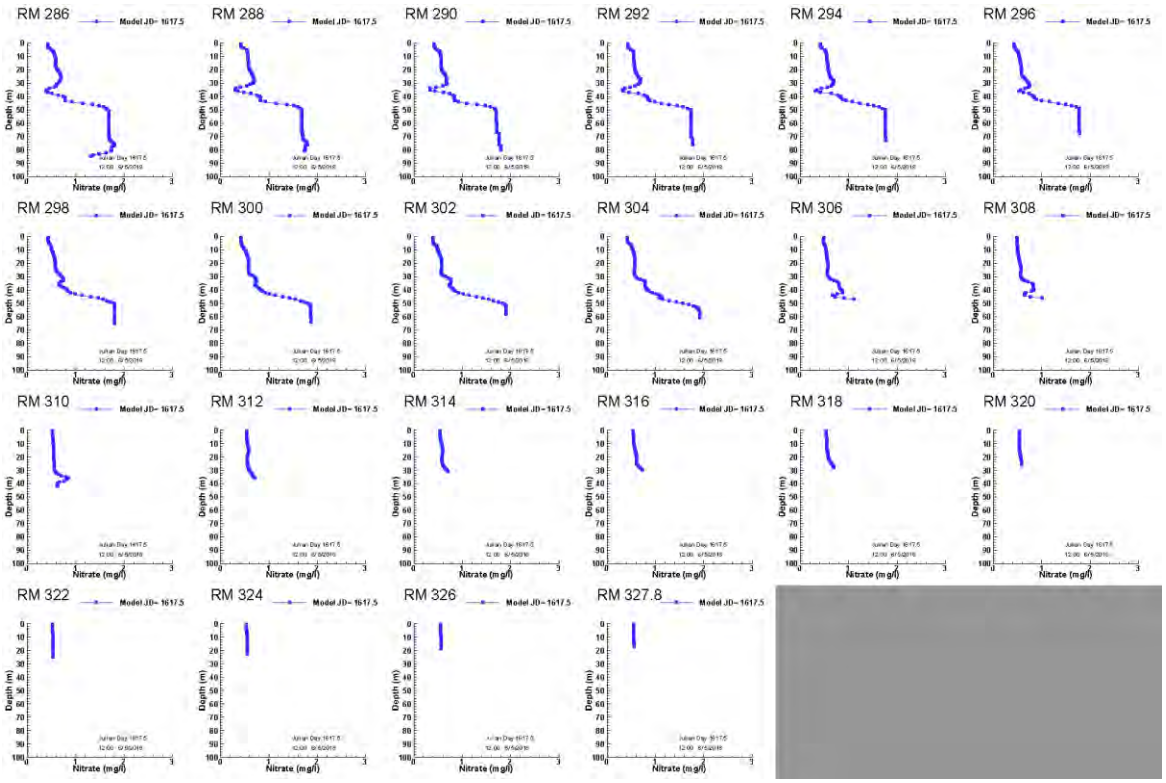


Figure 1083. Vertical profiles of NOxN compared with data for 6/ 5/2018.

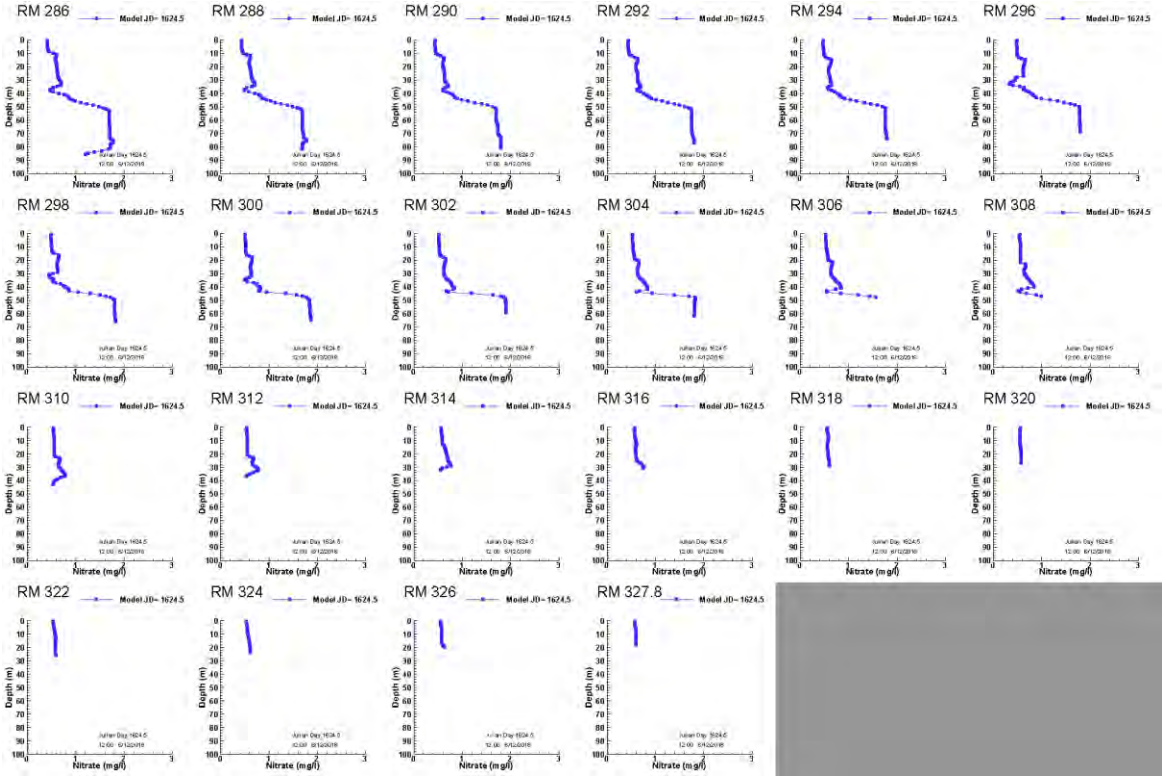


Figure 1084. Vertical profiles of NOxN compared with data for 6/12/2018.

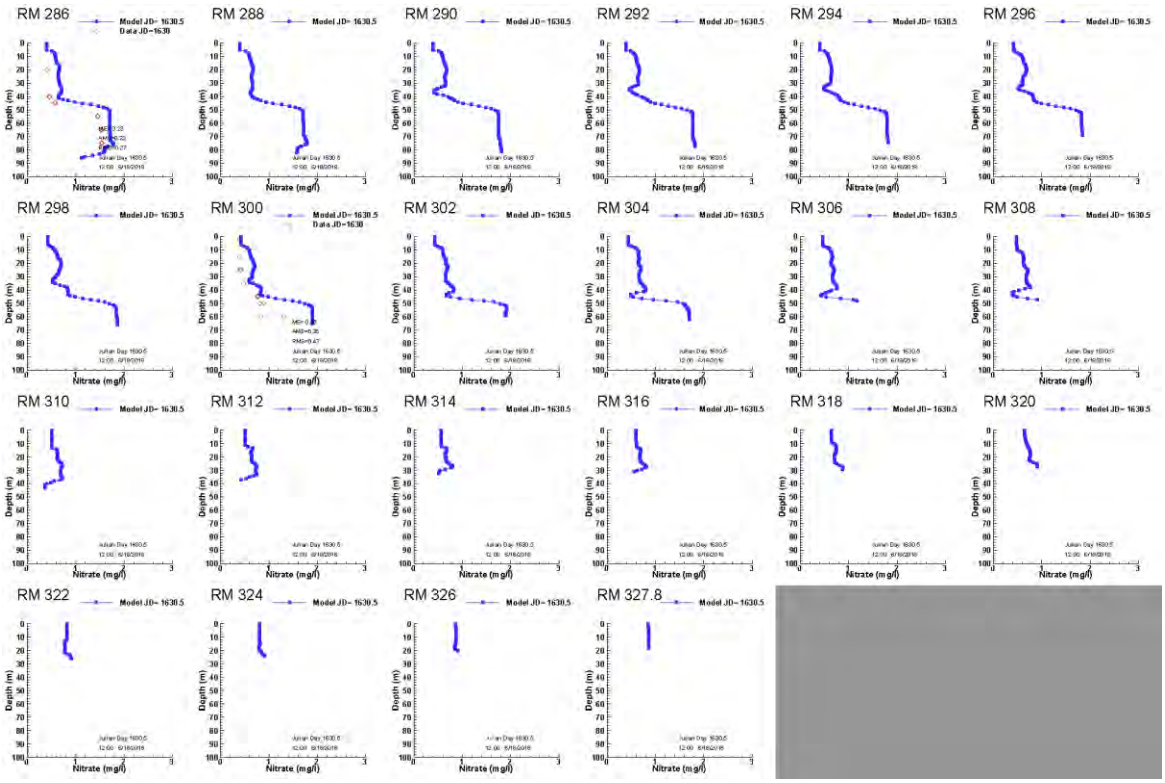


Figure 1085. Vertical profiles of NOxN compared with data for 6/18/2018.

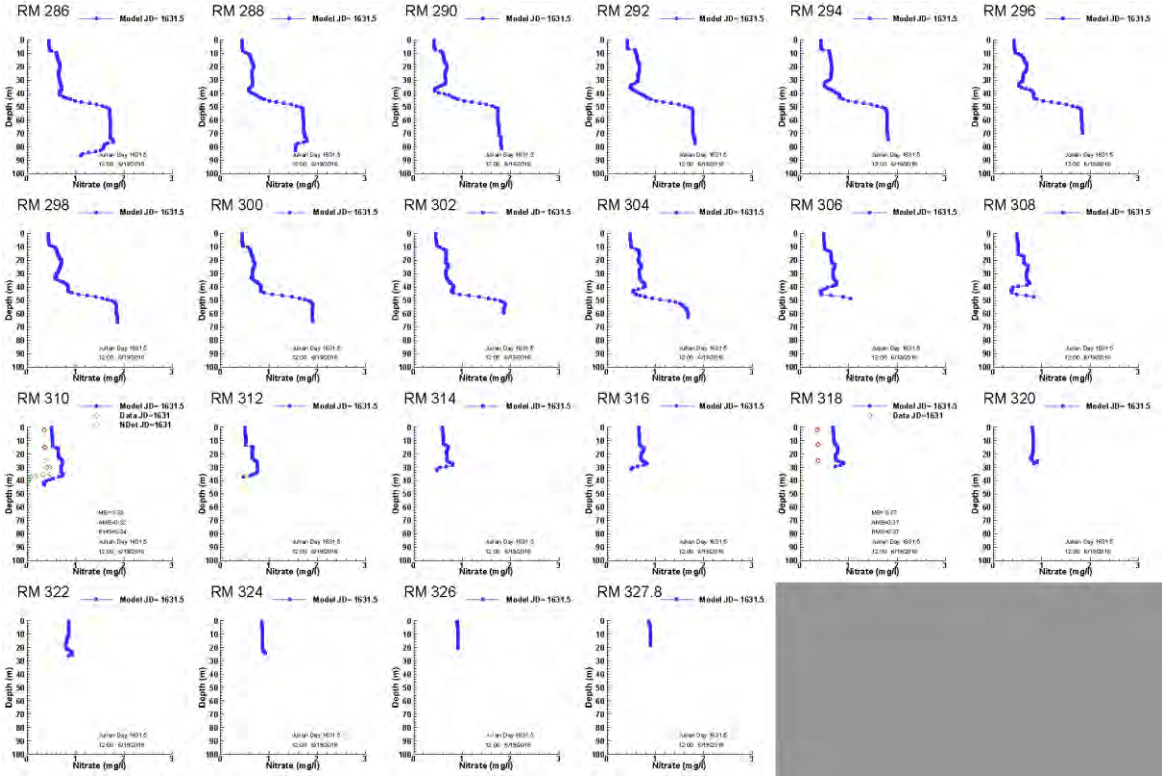


Figure 1086. Vertical profiles of NOxN compared with data for 6/19/2018.

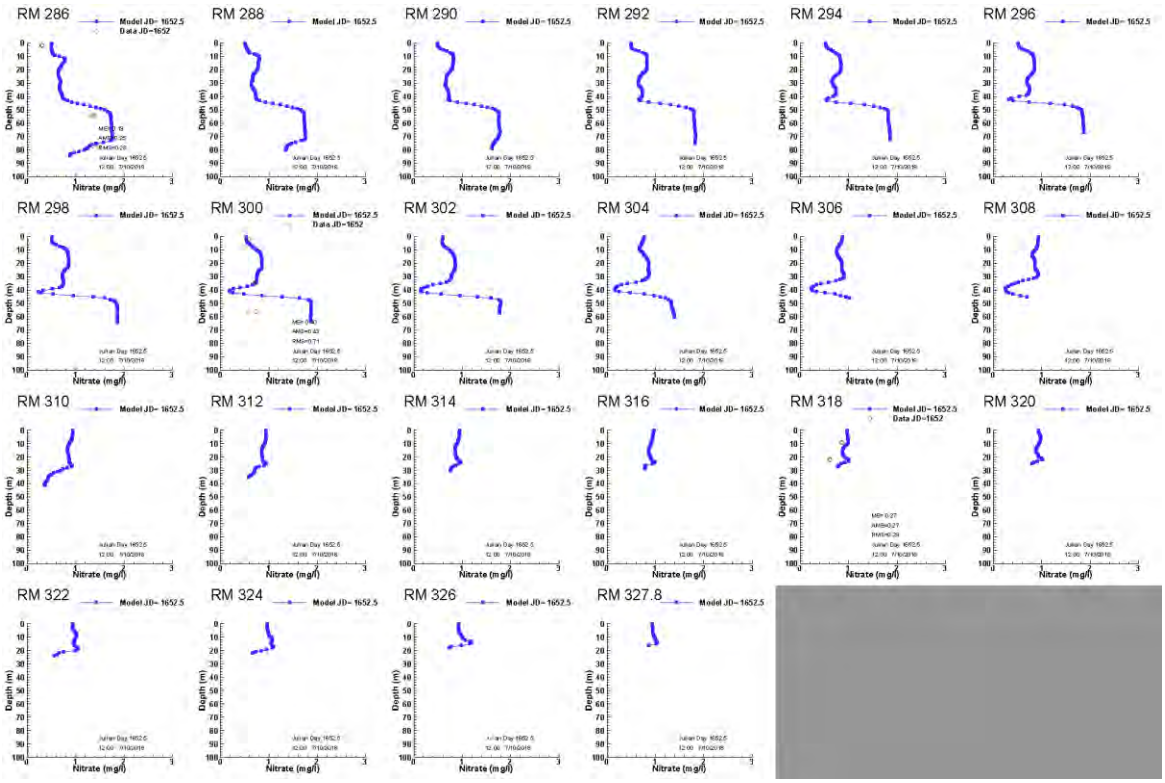


Figure 1087. Vertical profiles of NOxN compared with data for 7/10/2018.

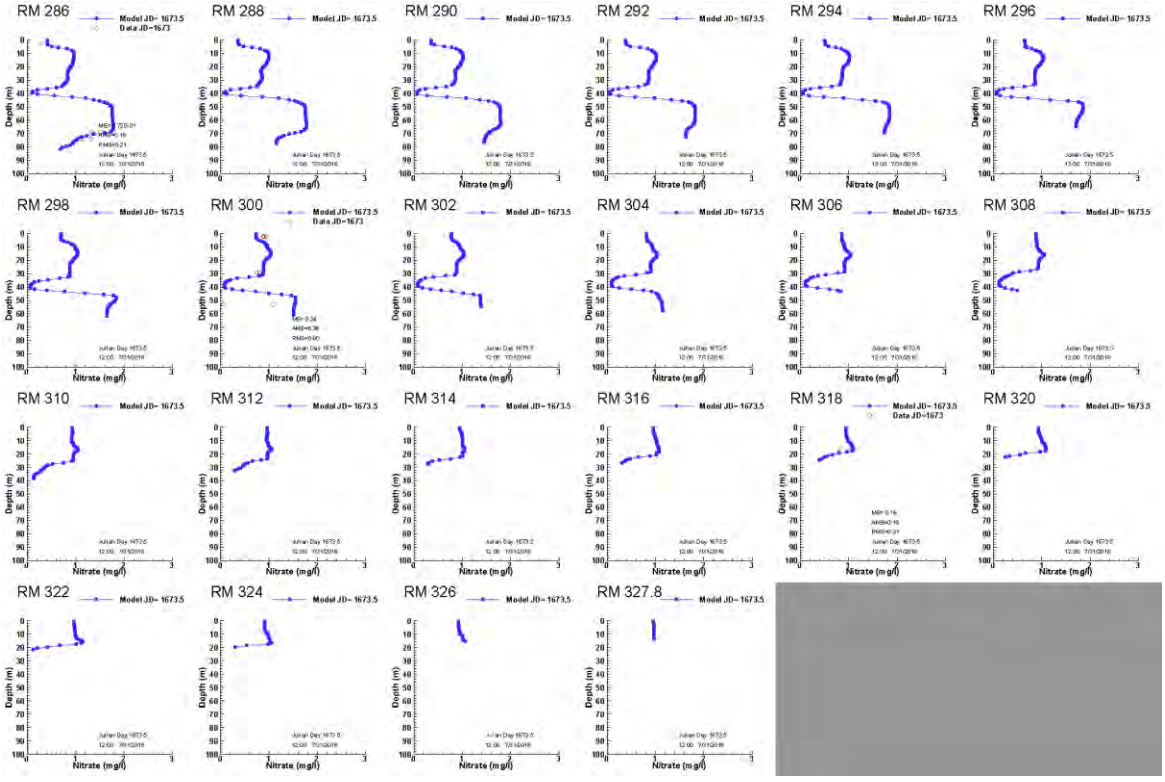


Figure 1088. Vertical profiles of NOxN compared with data for 7/31/2018.

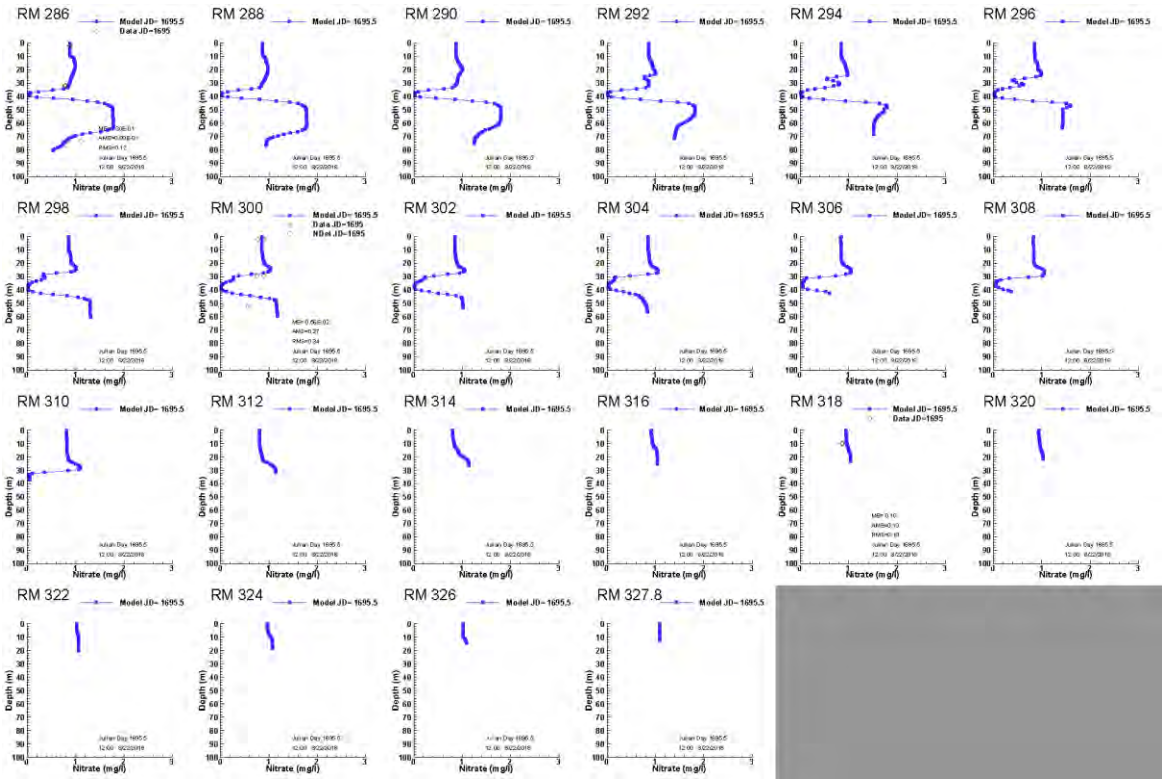


Figure 1089. Vertical profiles of NOxN compared with data for 8/22/2018.

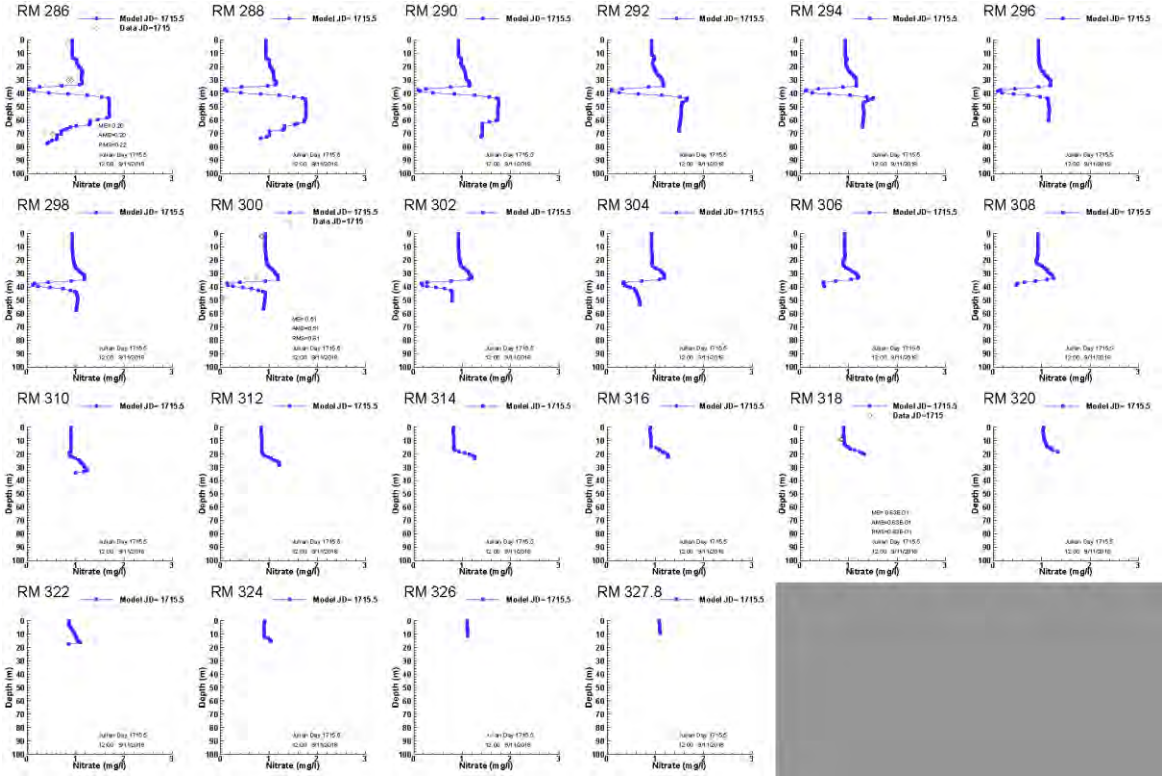


Figure 1090. Vertical profiles of NOxN compared with data for 9/11/2018.

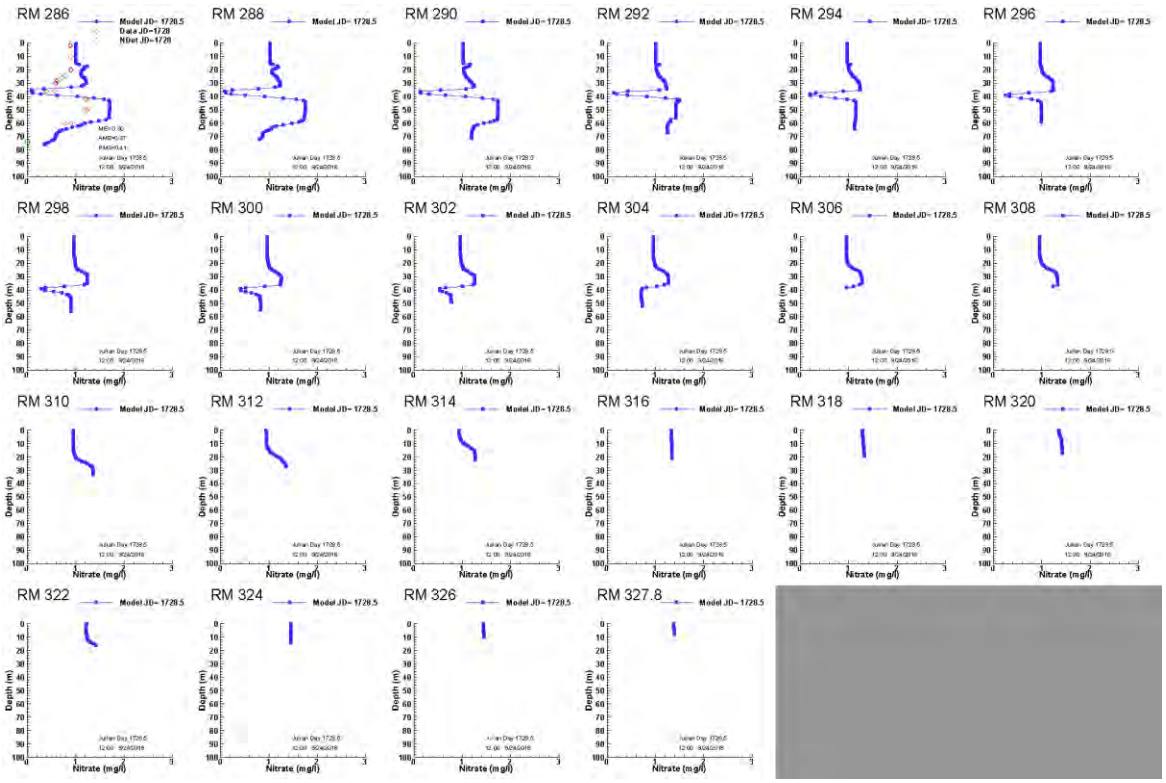


Figure 1091. Vertical profiles of NOxN compared with data for 9/24/2018.

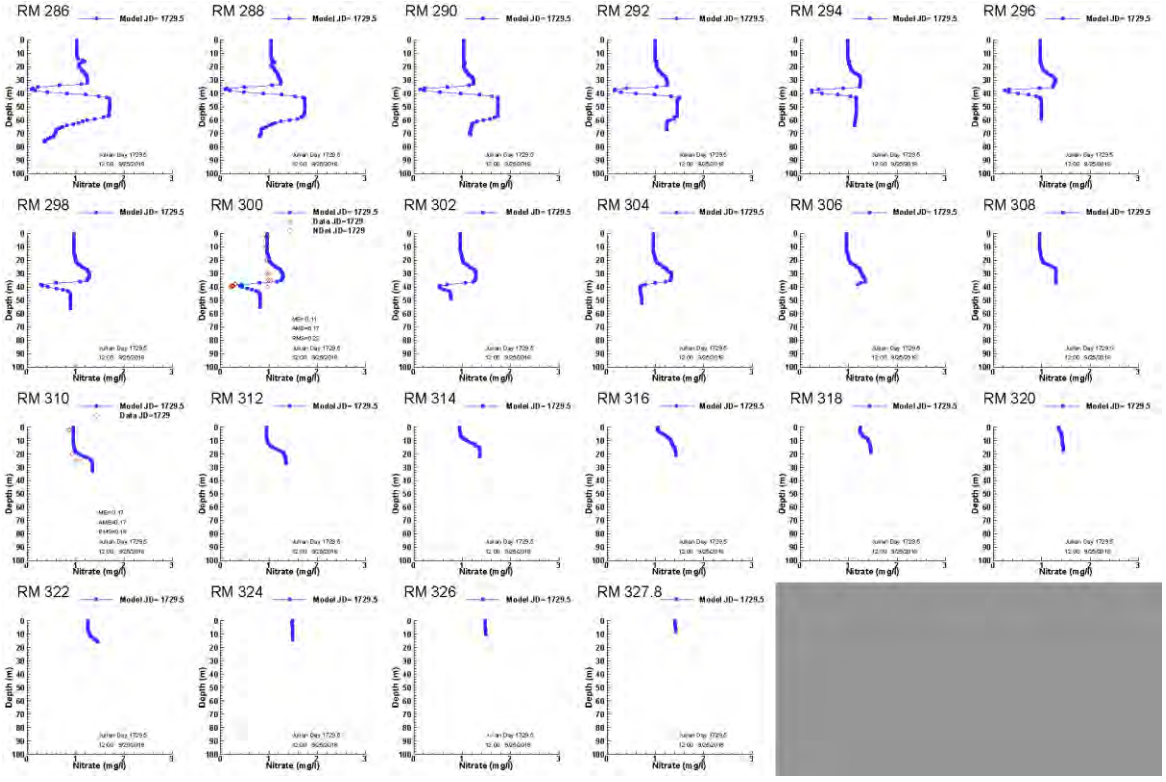


Figure 1092. Vertical profiles of NOxN compared with data for 9/25/2018.

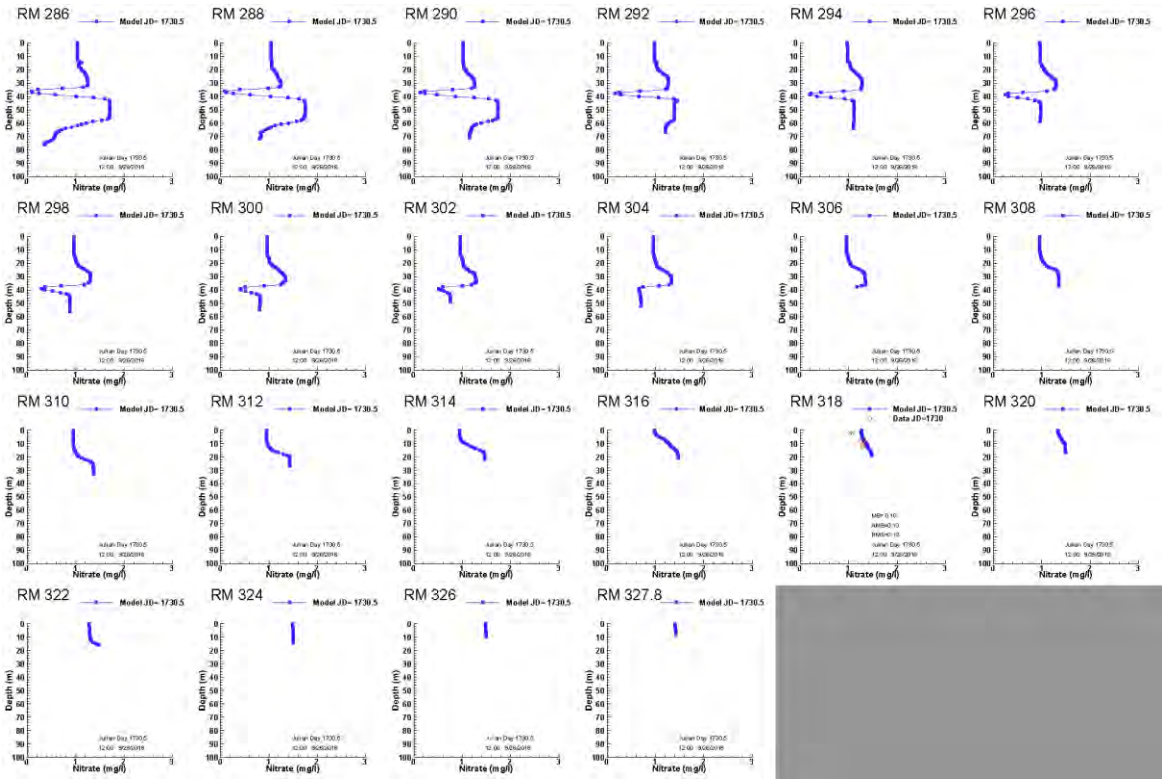


Figure 1093. Vertical profiles of NOxN compared with data for 9/26/2018.

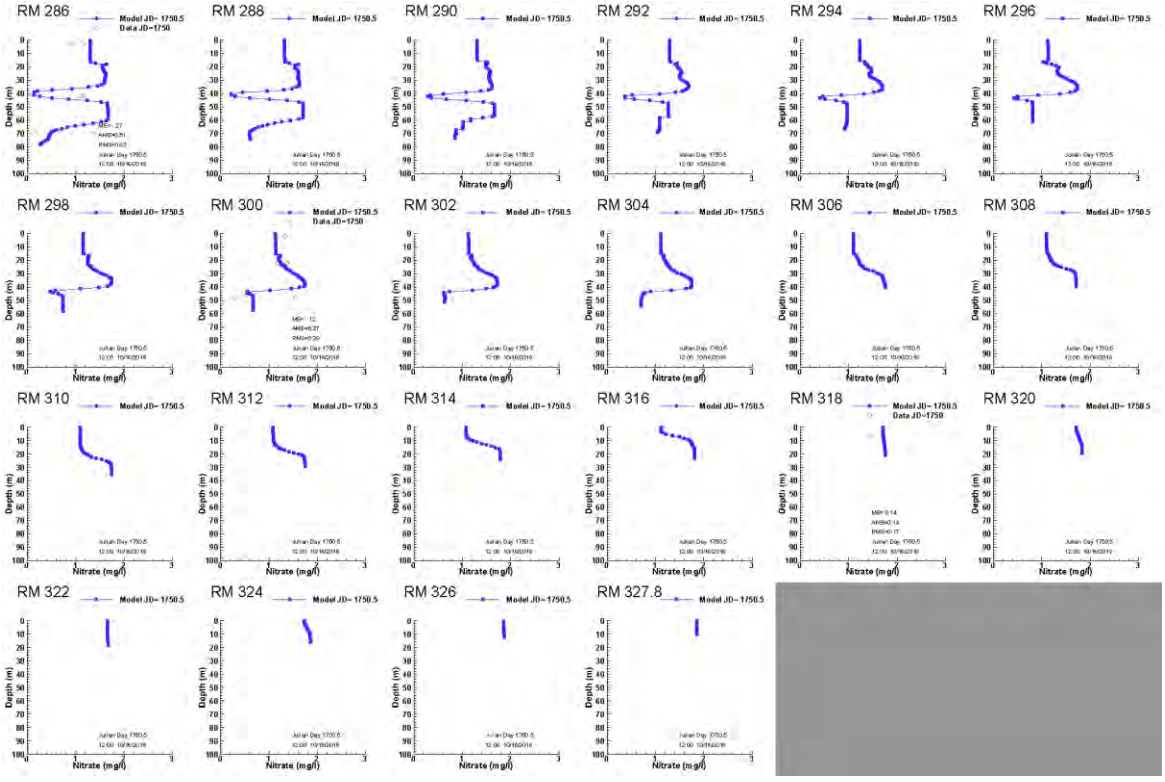


Figure 1094. Vertical profiles of NOxN compared with data for 10/16/2018.

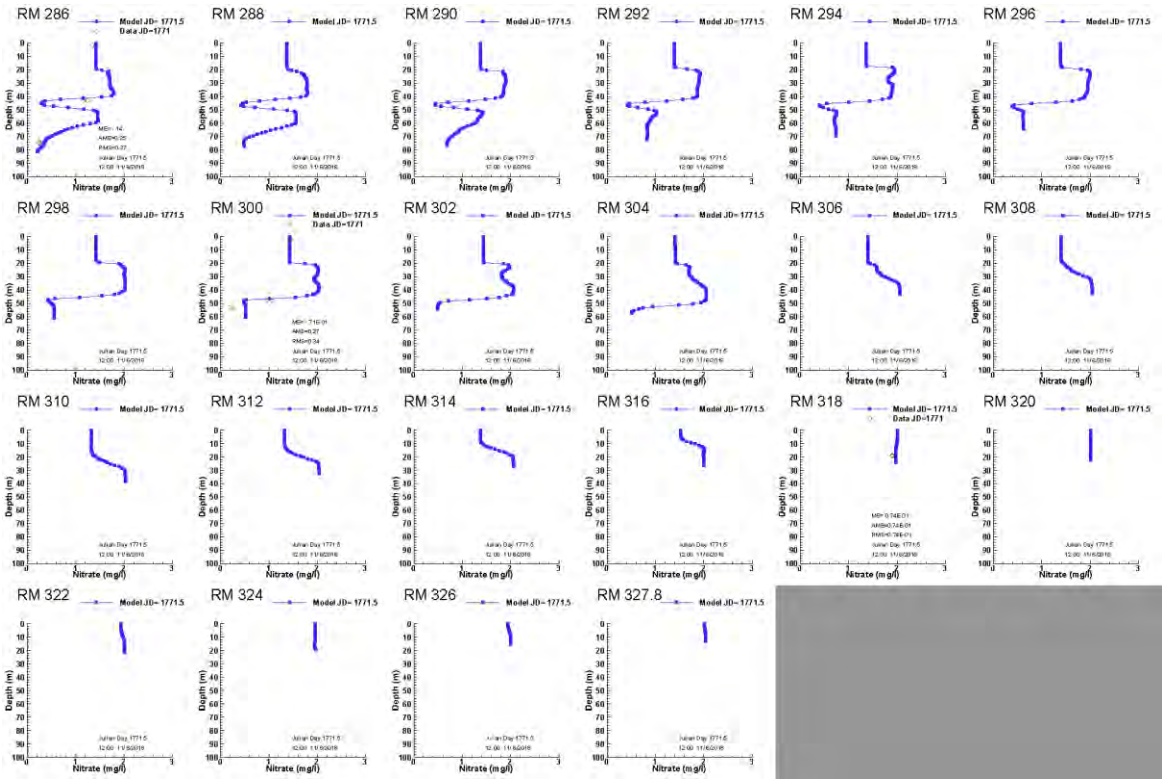


Figure 1095. Vertical profiles of NOxN compared with data for 11/ 6/2018.

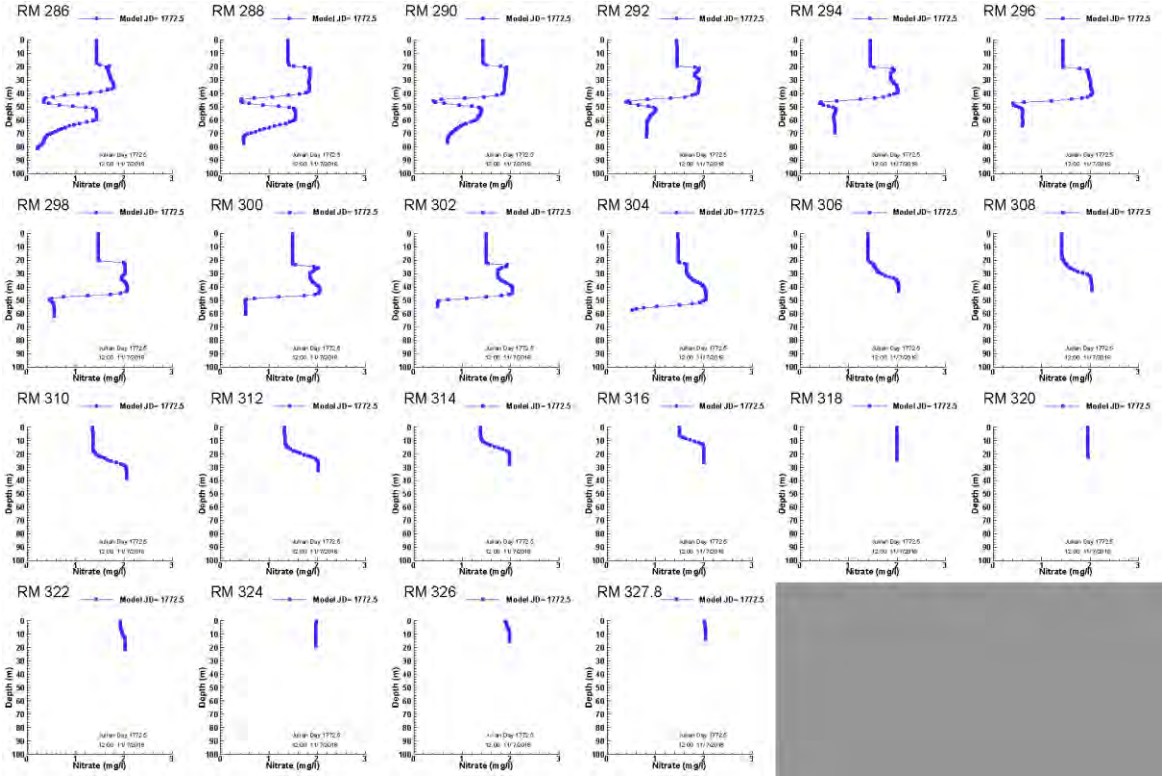


Figure 1096. Vertical profiles of NOxN compared with data for 11/ 7/2018.

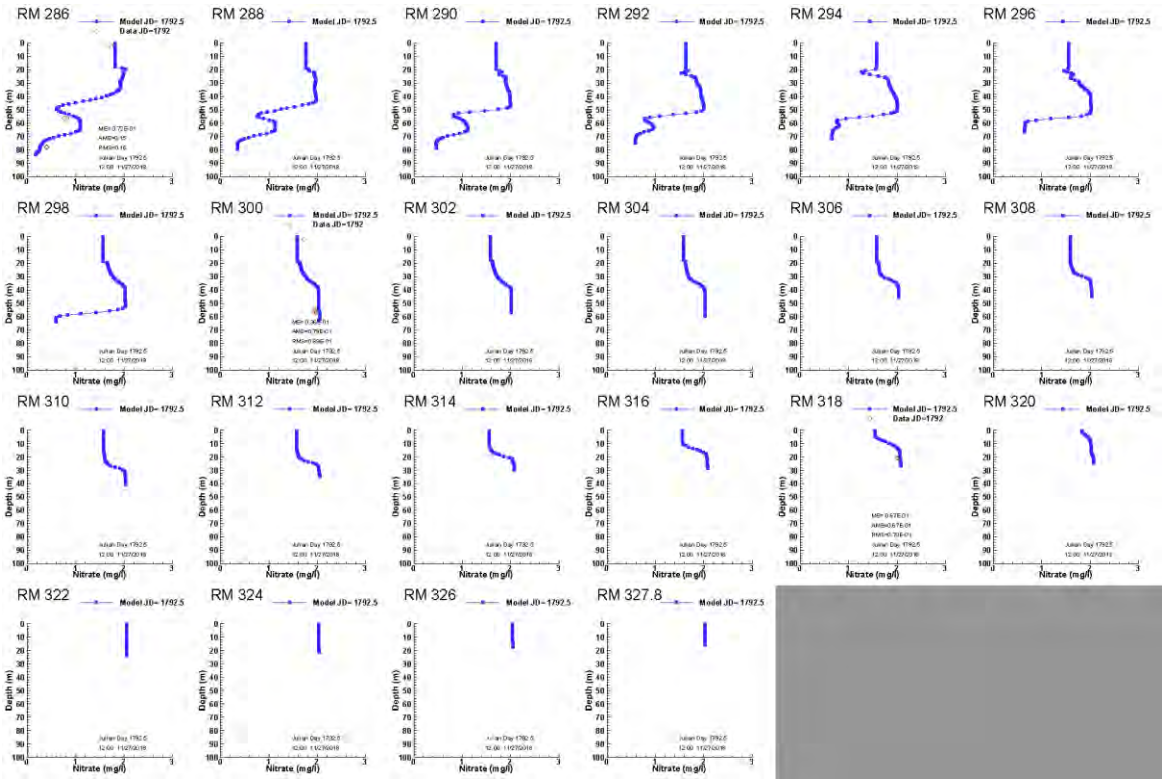


Figure 1097. Vertical profiles of NOxN compared with data for 11/27/2018.

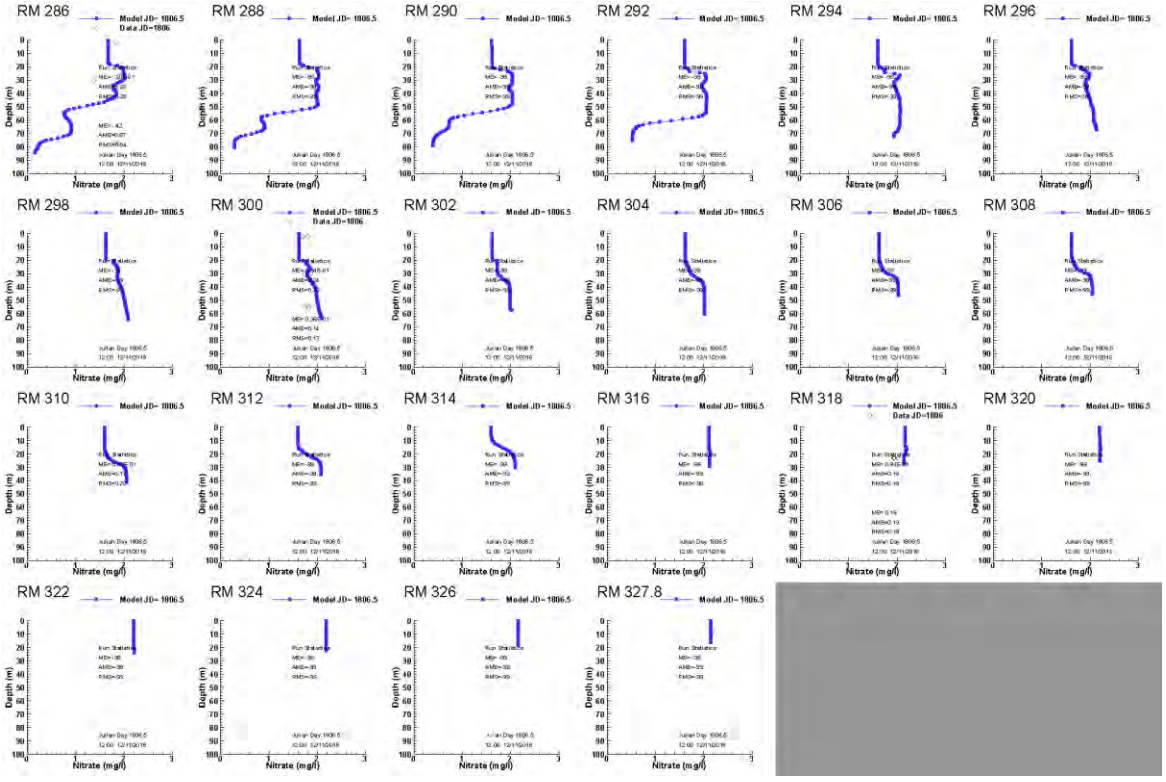


Figure 1098. Vertical profiles of NOxN compared with data for 12/11/2018.

Dissolved Oxygen

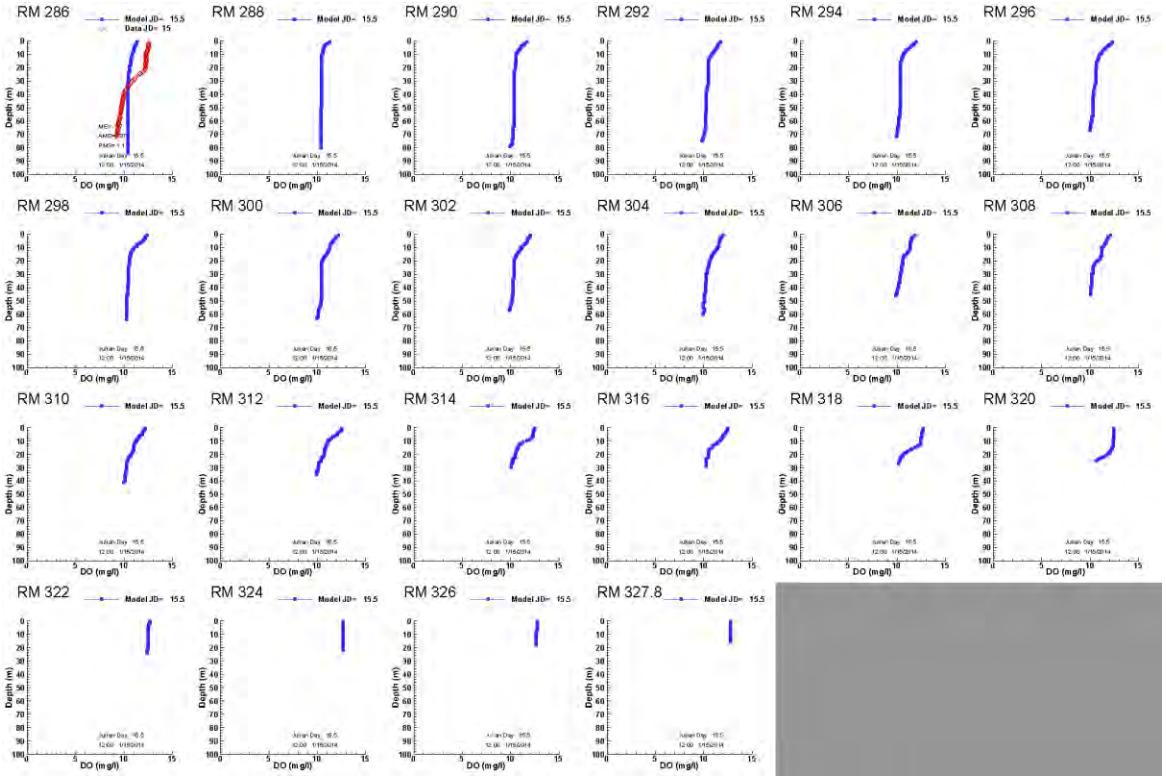


Figure 1099. Vertical profiles of DO compared with data for 1/15/2014.

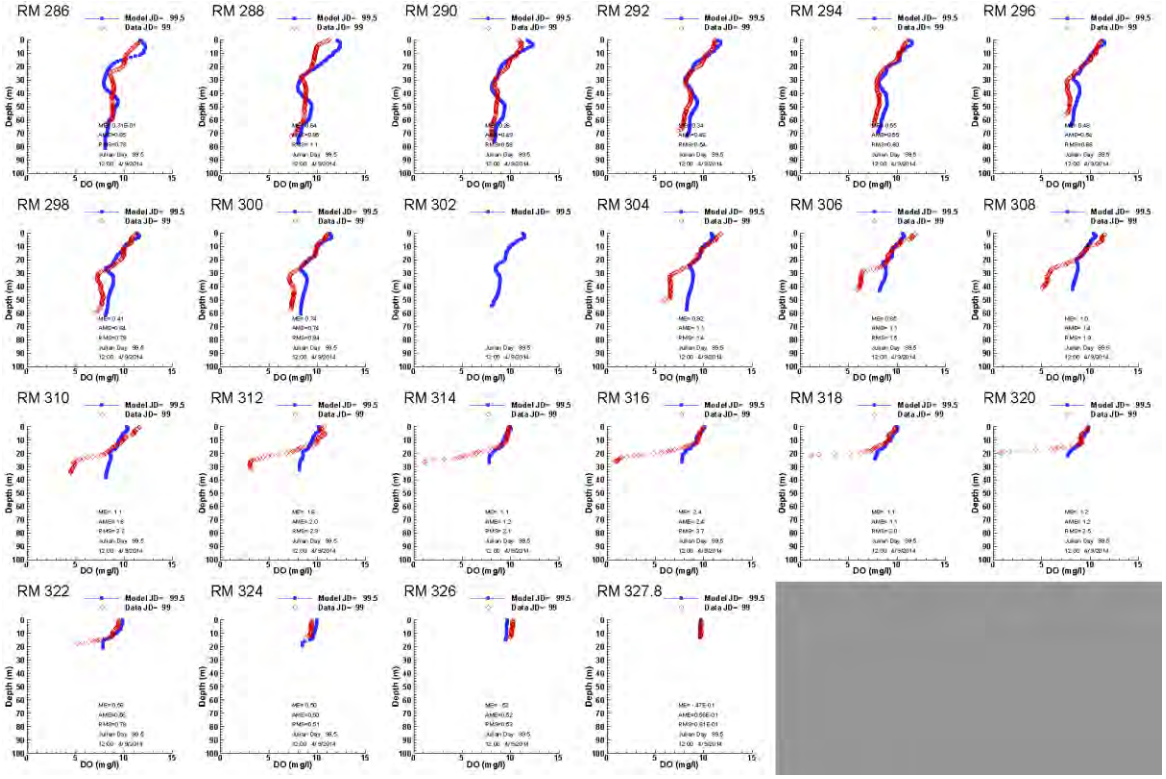


Figure 1100. Vertical profiles of DO compared with data for 4/ 9/2014.

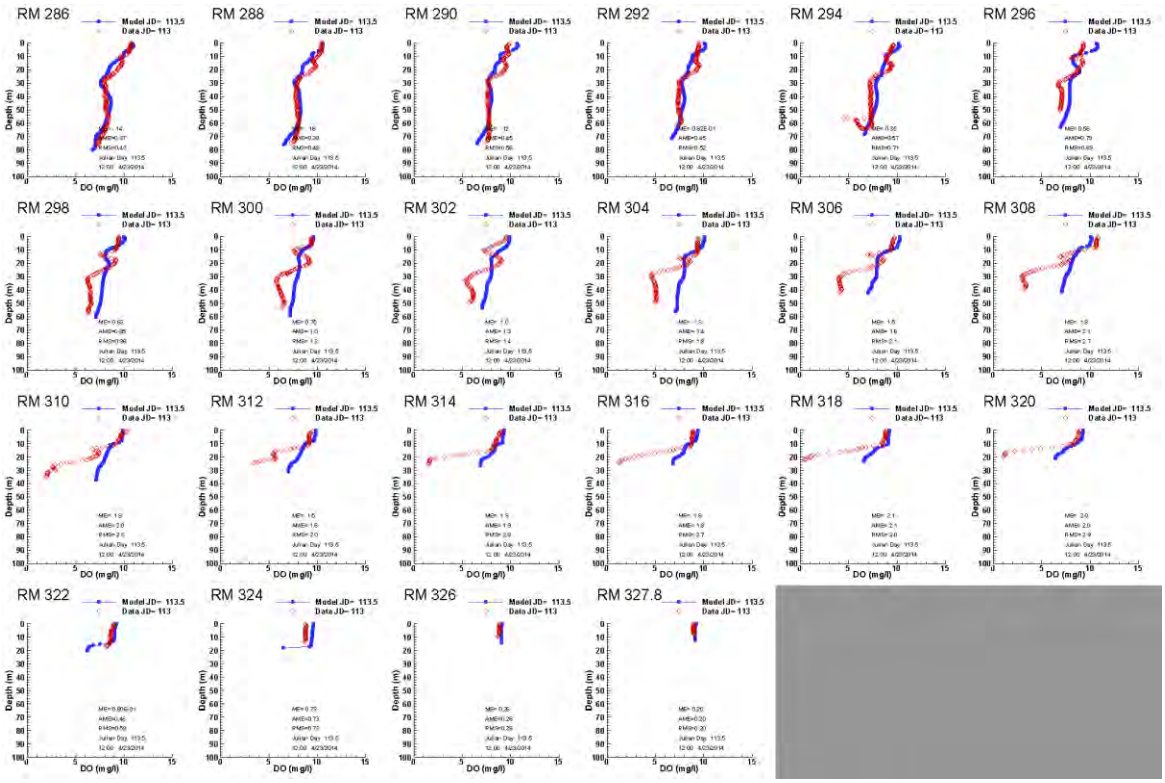


Figure 1101. Vertical profiles of DO compared with data for 4/23/2014.

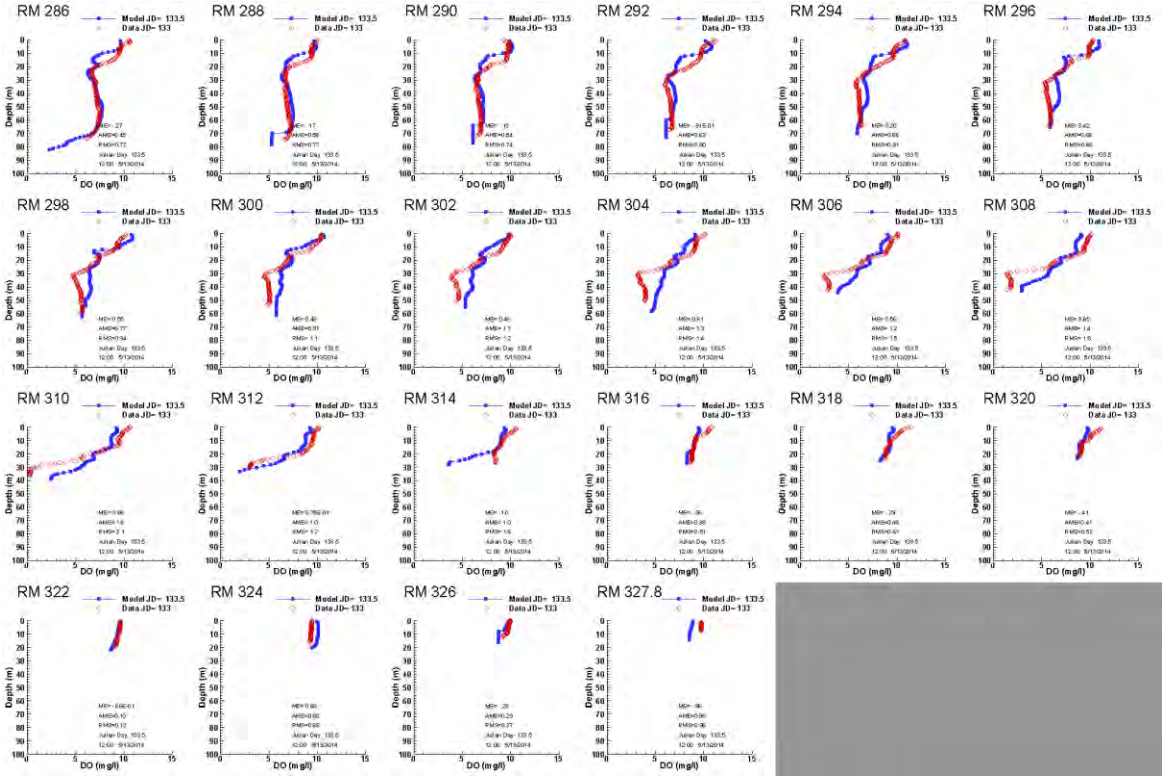


Figure 1102. Vertical profiles of DO compared with data for 5/13/2014.

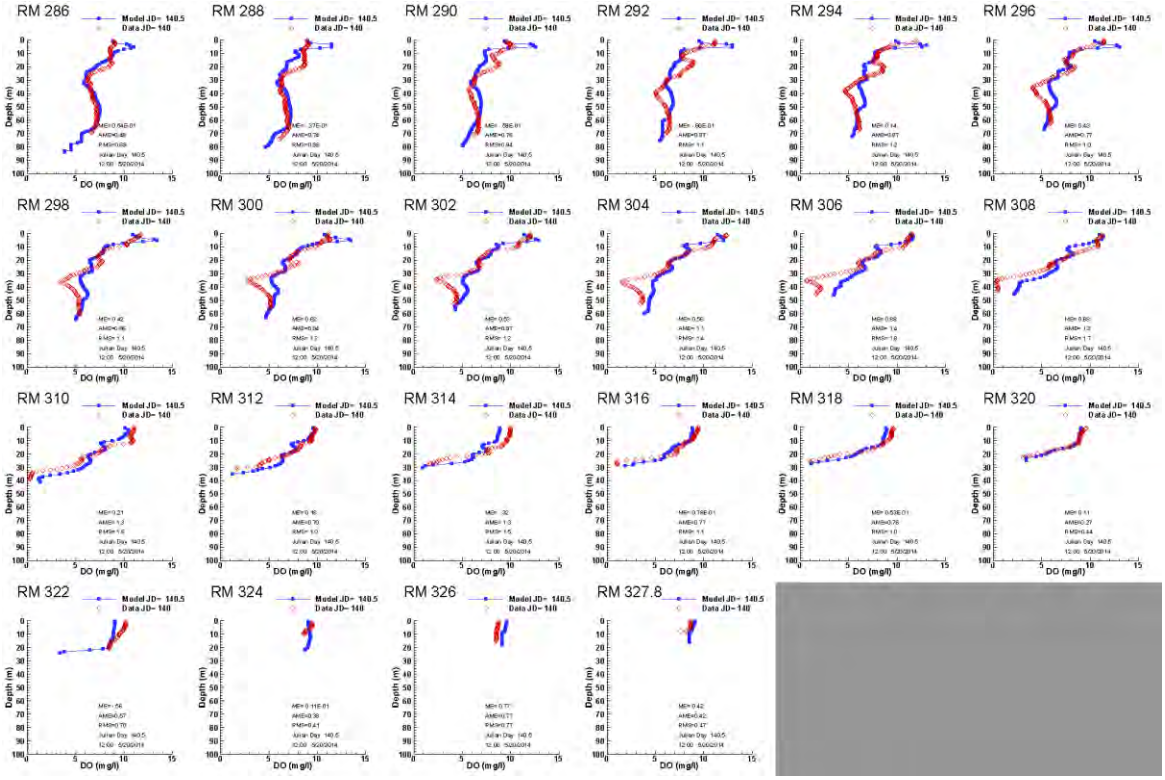


Figure 1103. Vertical profiles of DO compared with data for 5/20/2014.

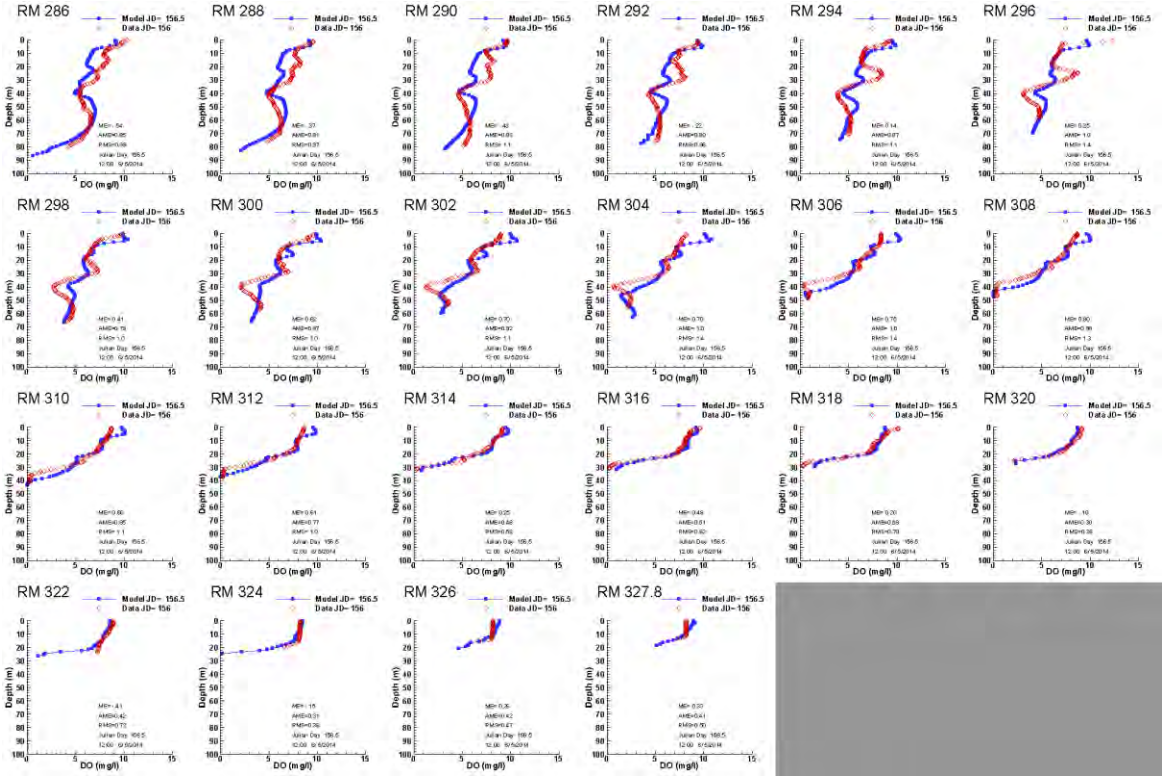


Figure 1104. Vertical profiles of DO compared with data for 6/ 5/2014.

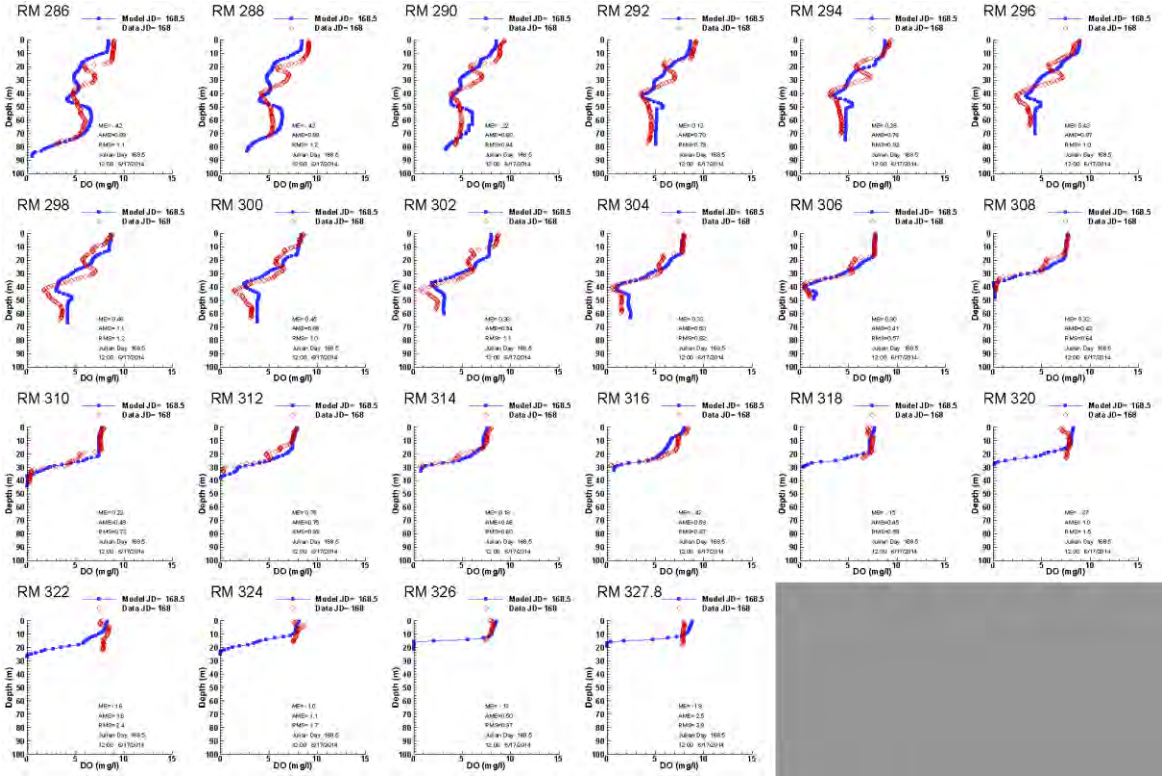


Figure 1105. Vertical profiles of DO compared with data for 6/17/2014.

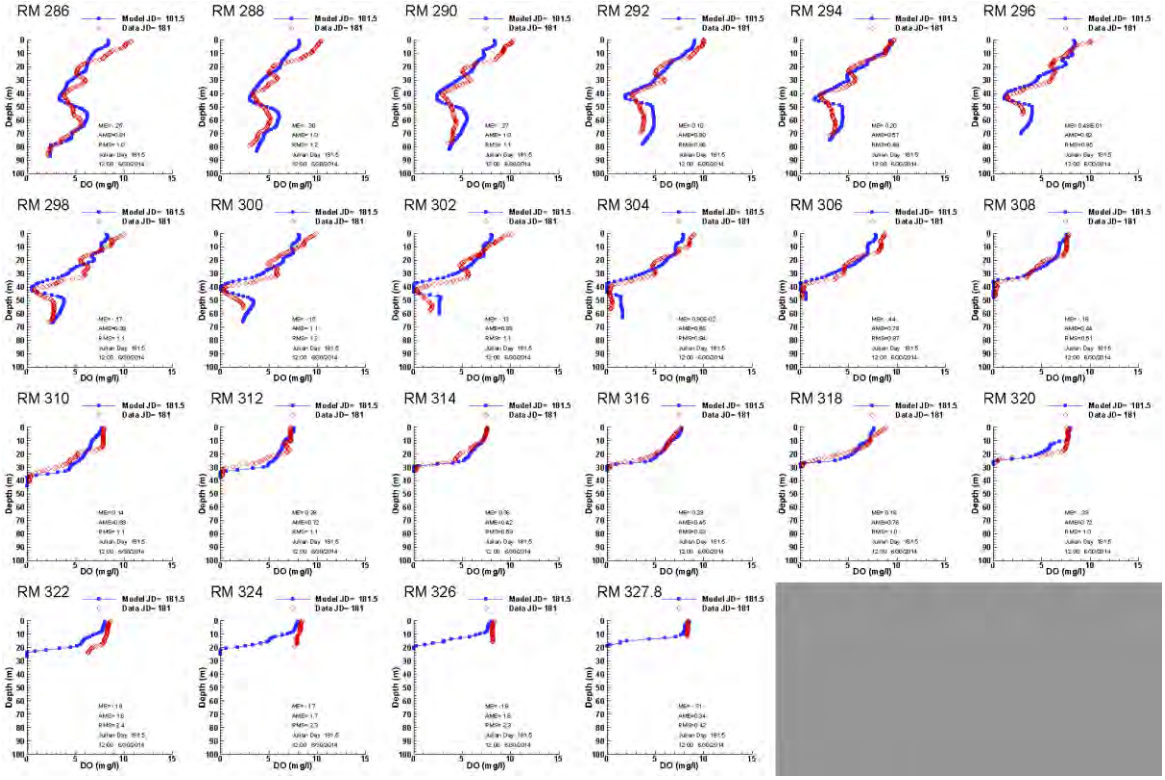


Figure 1106. Vertical profiles of DO compared with data for 6/30/2014.

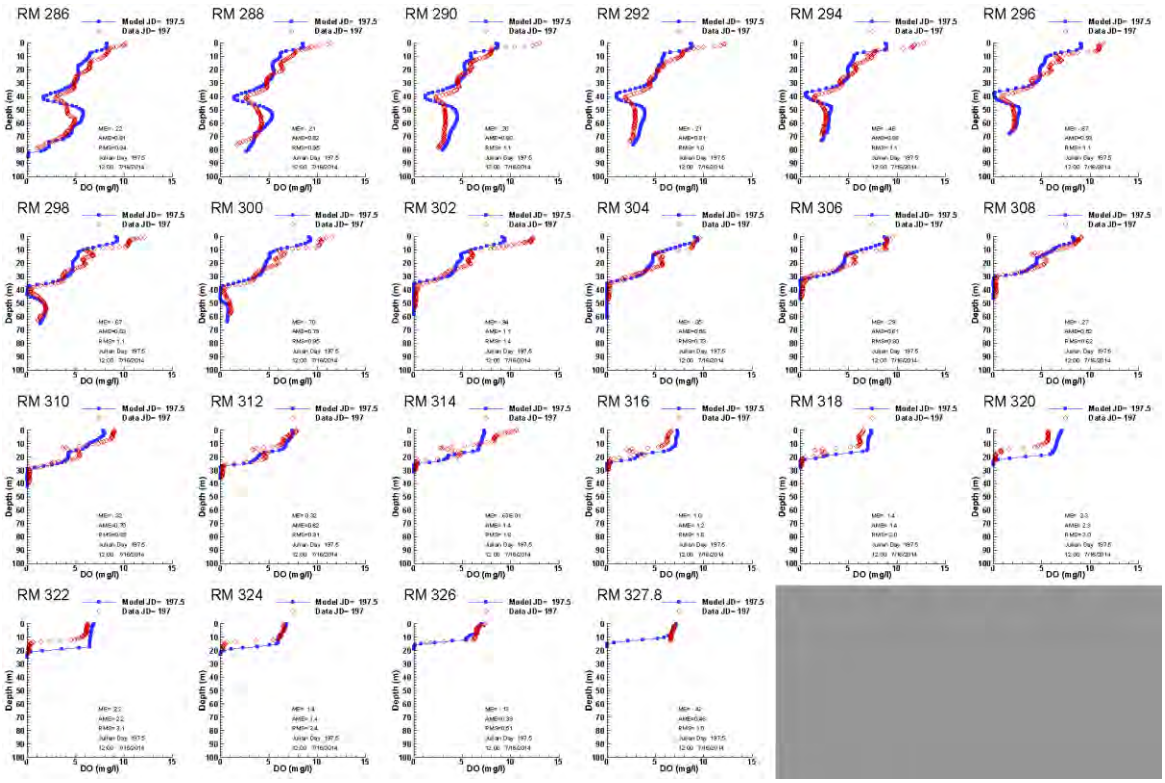


Figure 1107. Vertical profiles of DO compared with data for 7/16/2014.

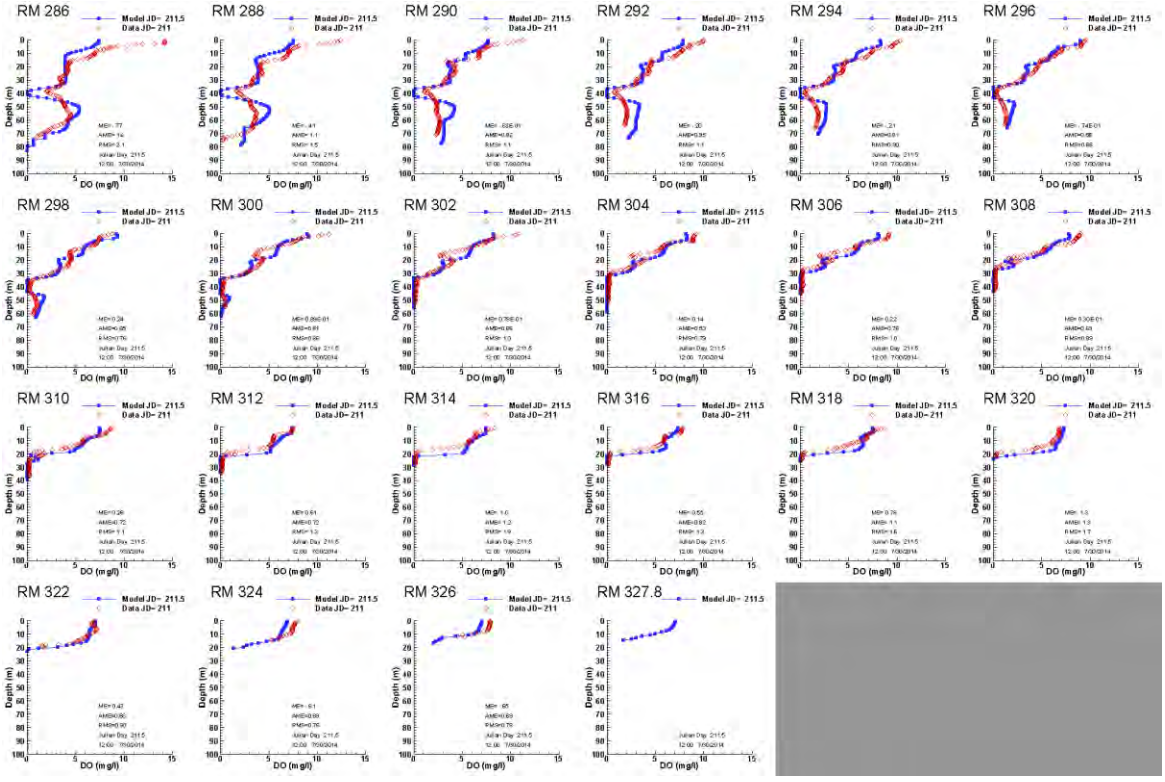


Figure 1108. Vertical profiles of DO compared with data for 7/30/2014.

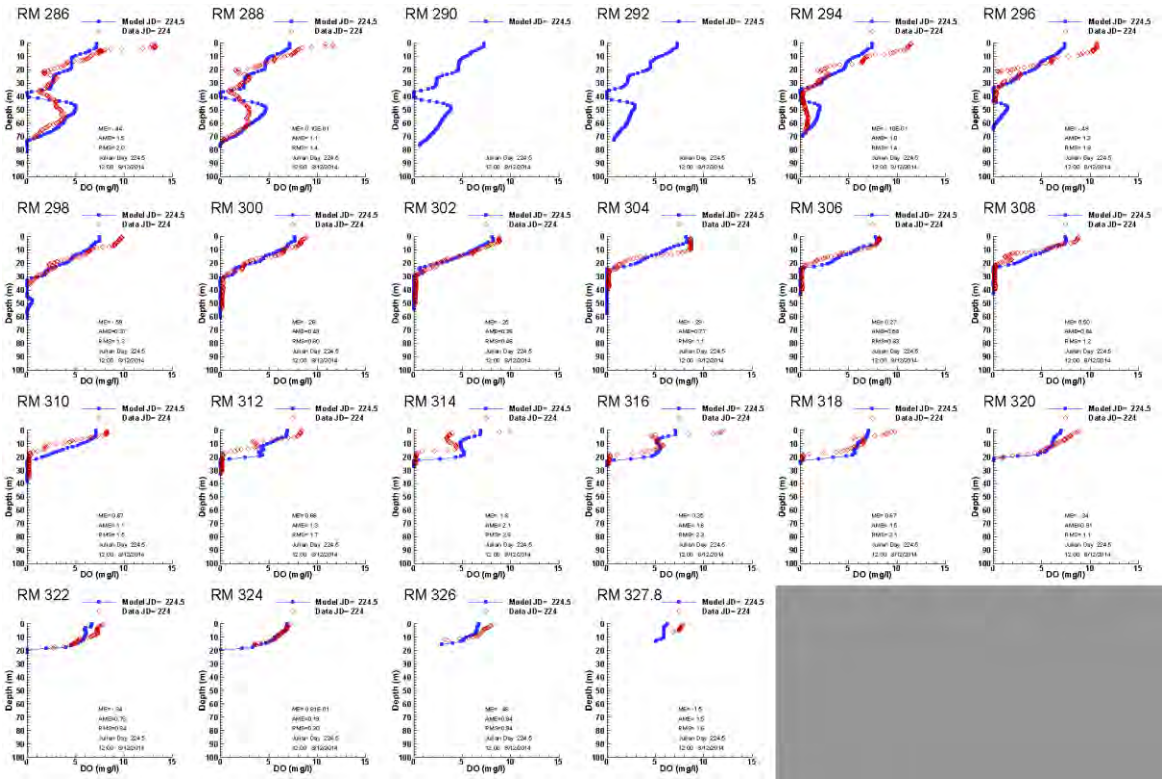


Figure 1109. Vertical profiles of DO compared with data for 8/12/2014.

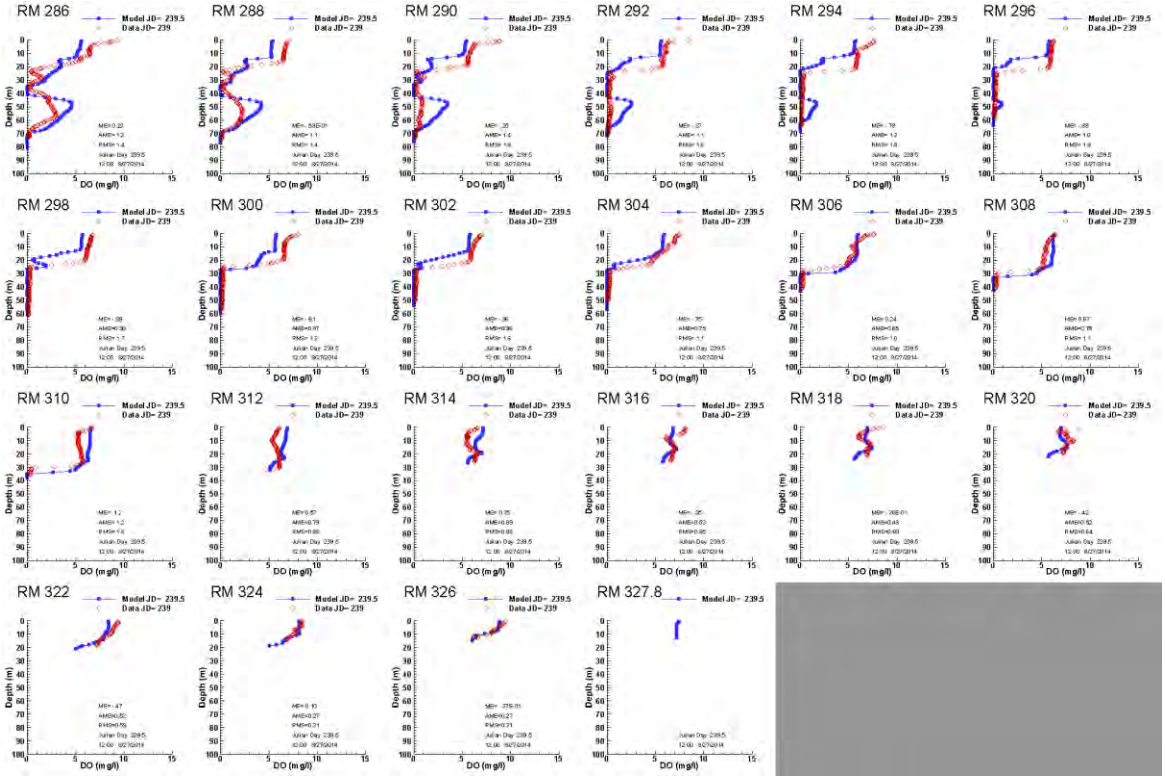


Figure 1110. Vertical profiles of DO compared with data for 8/27/2014.

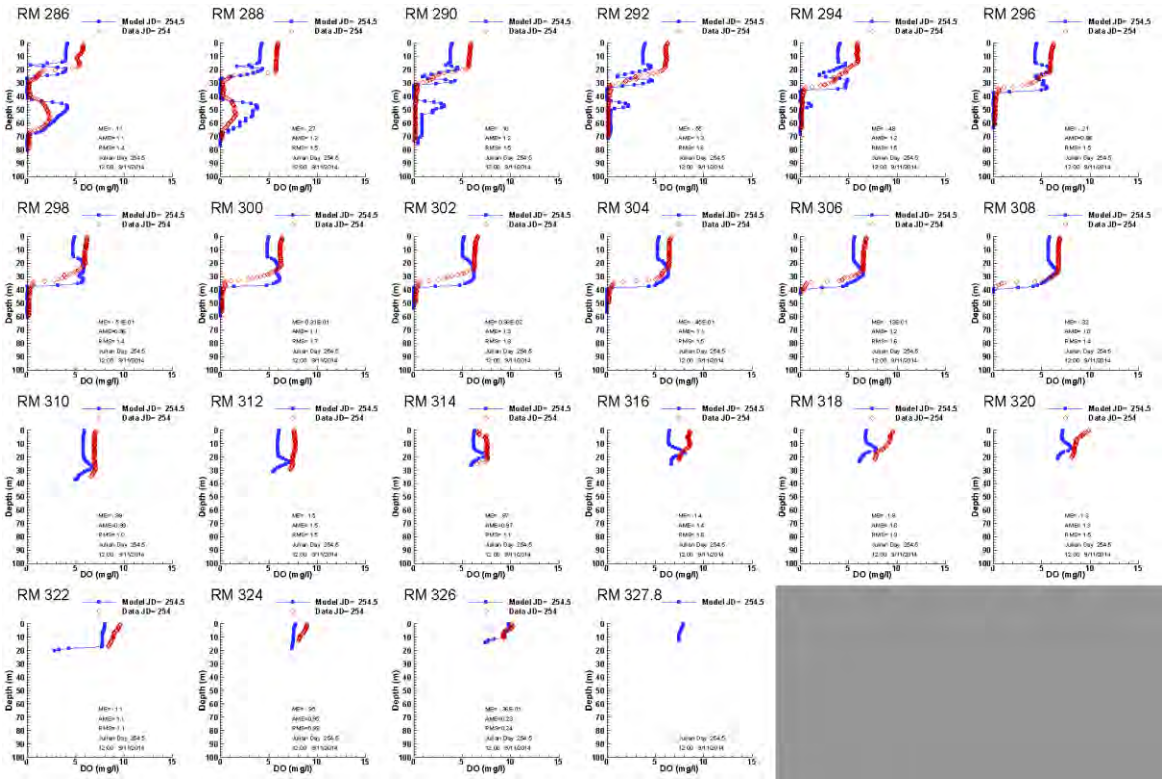


Figure 1111. Vertical profiles of DO compared with data for 9/11/2014.

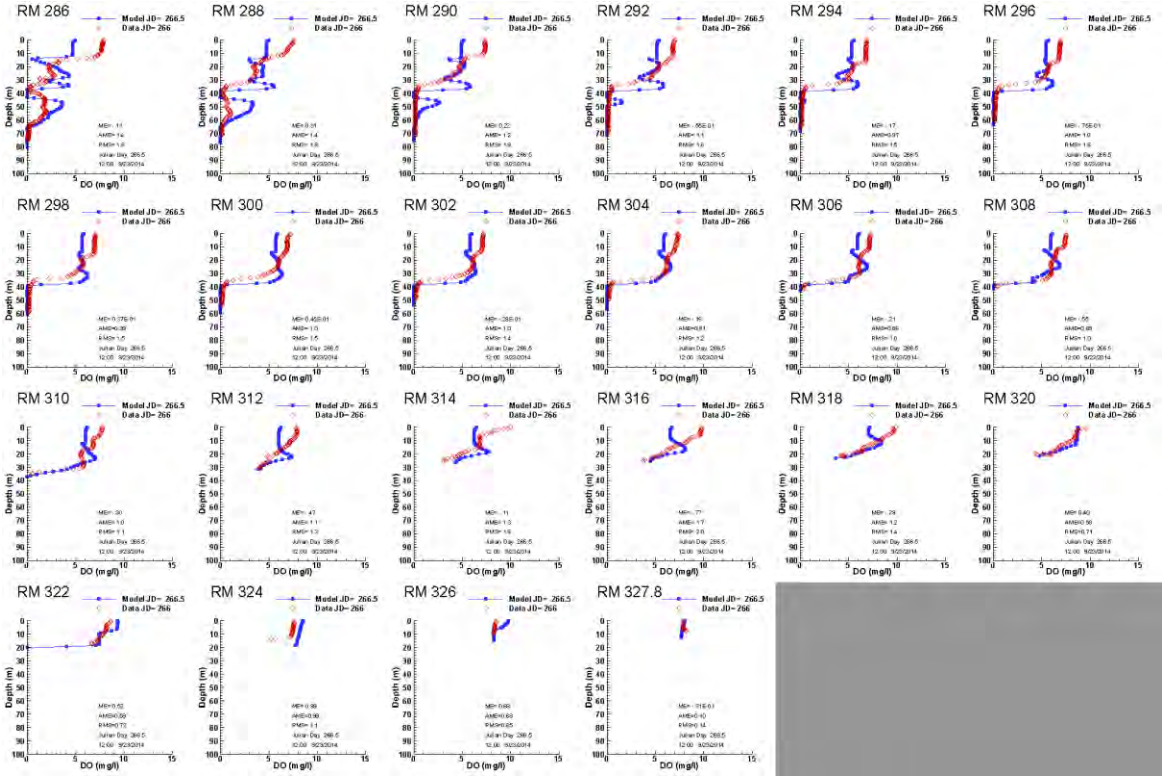


Figure 1112. Vertical profiles of DO compared with data for 9/23/2014.

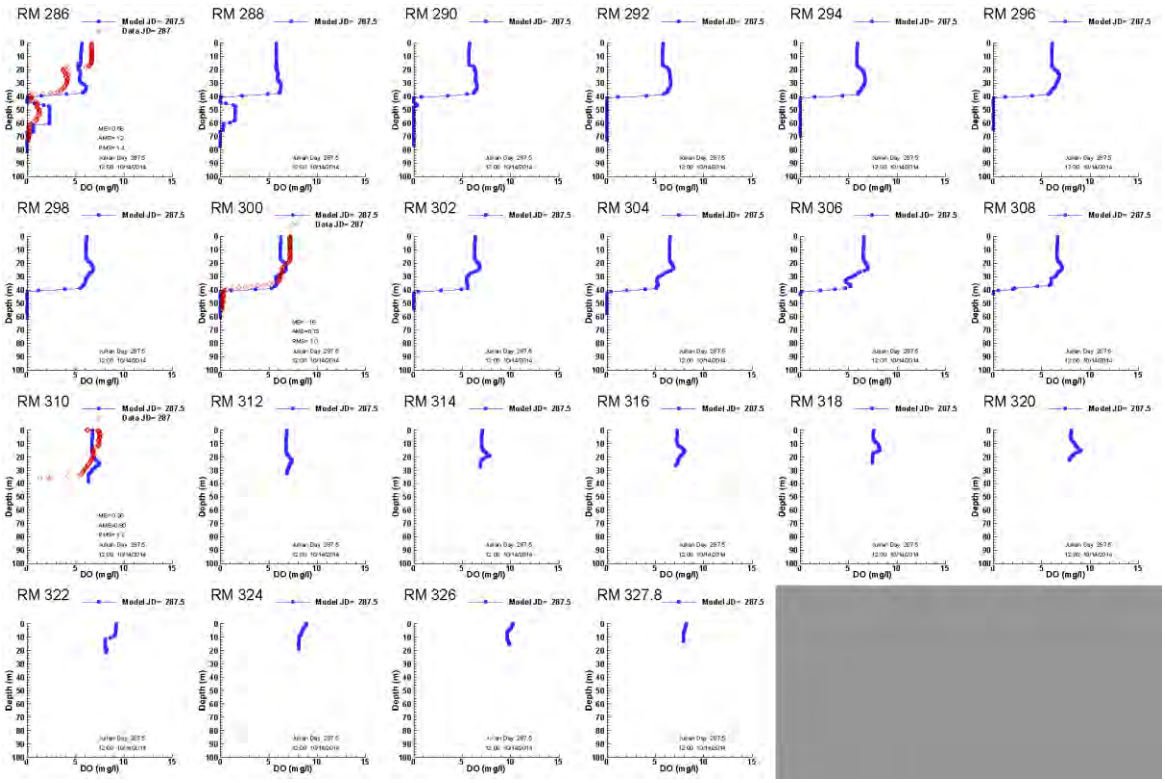


Figure 1113. Vertical profiles of DO compared with data for 10/14/2014.

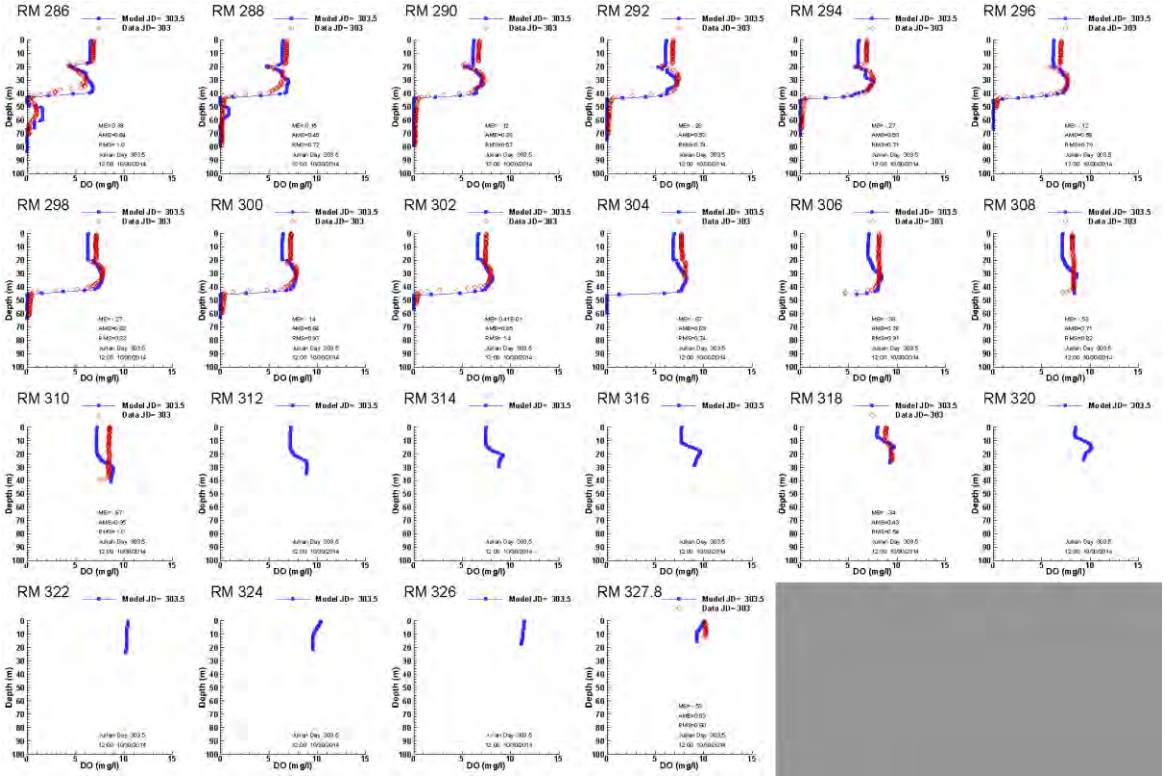


Figure 1114. Vertical profiles of DO compared with data for 10/30/2014.

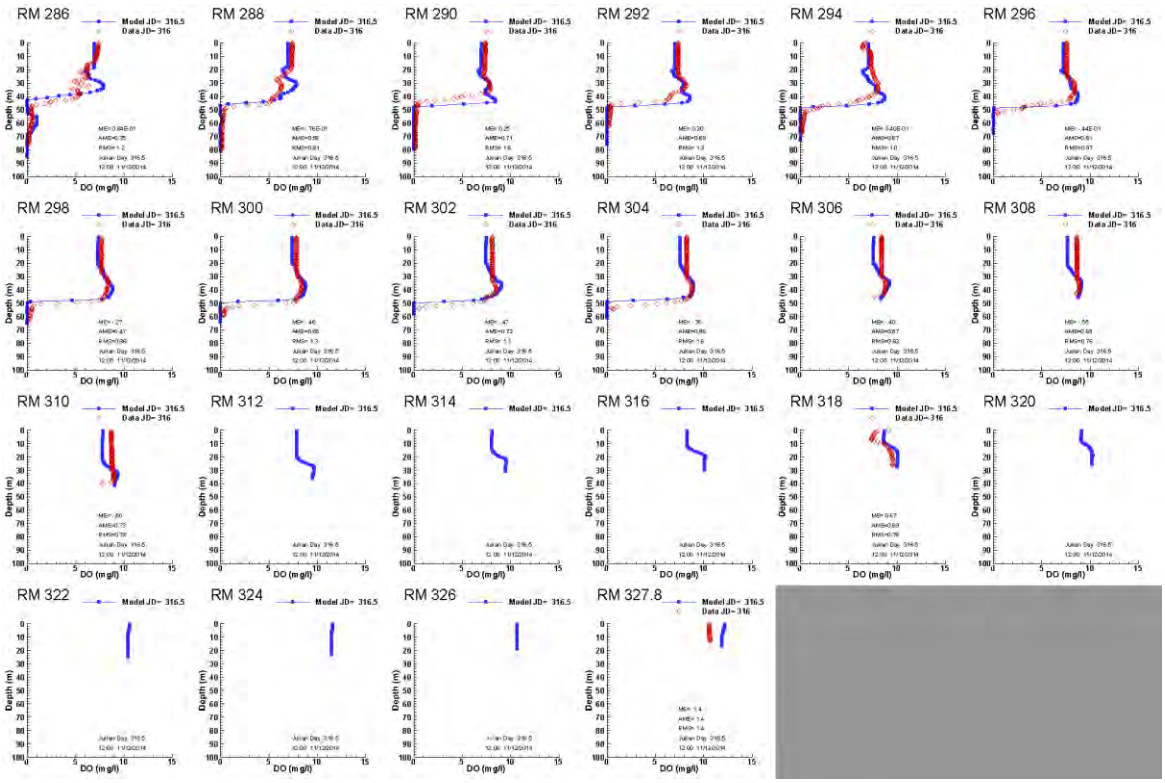


Figure 1115. Vertical profiles of DO compared with data for 11/12/2014.

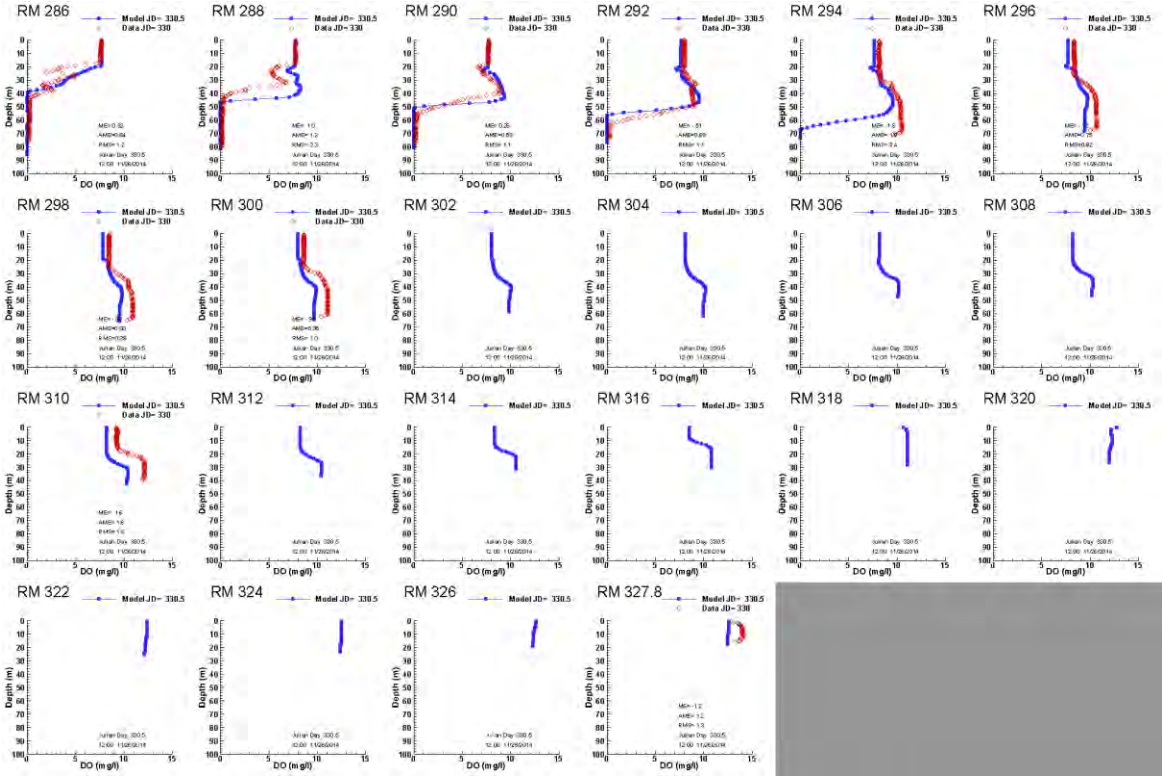


Figure 1116. Vertical profiles of DO compared with data for 11/26/2014.

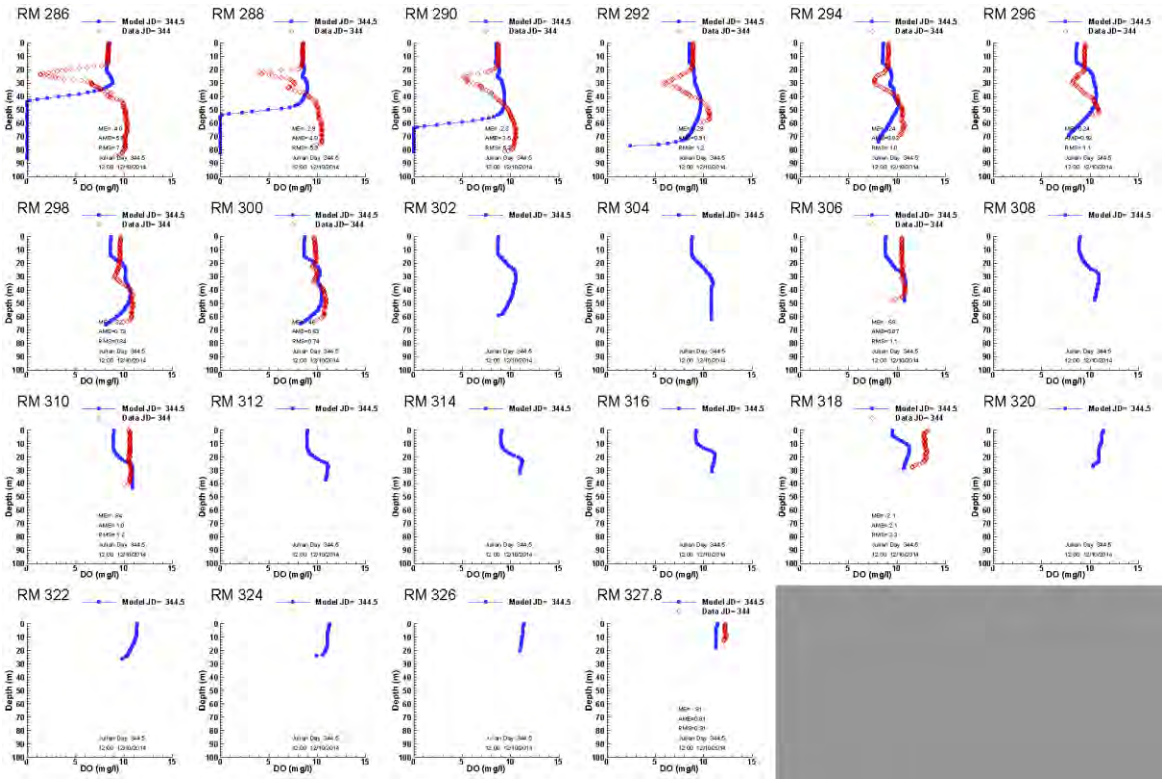


Figure 1117. Vertical profiles of DO compared with data for 12/10/2014.

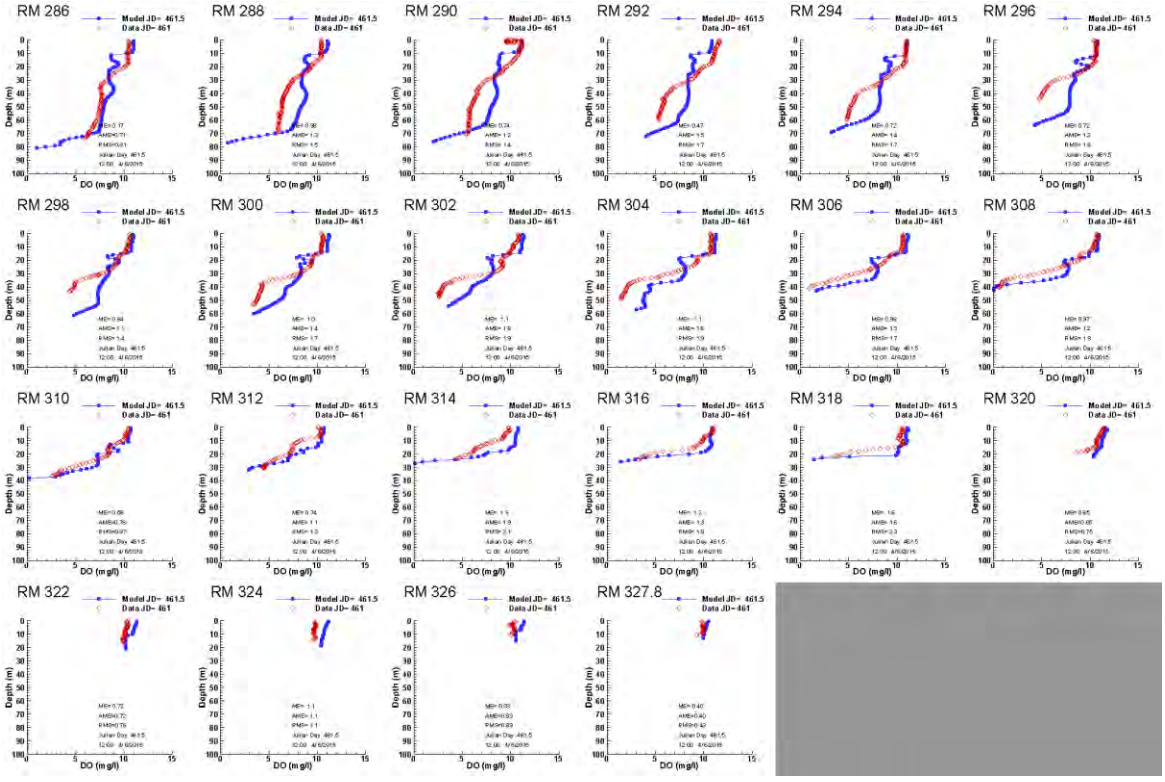


Figure 1118. Vertical profiles of DO compared with data for 4/ 6/2015.

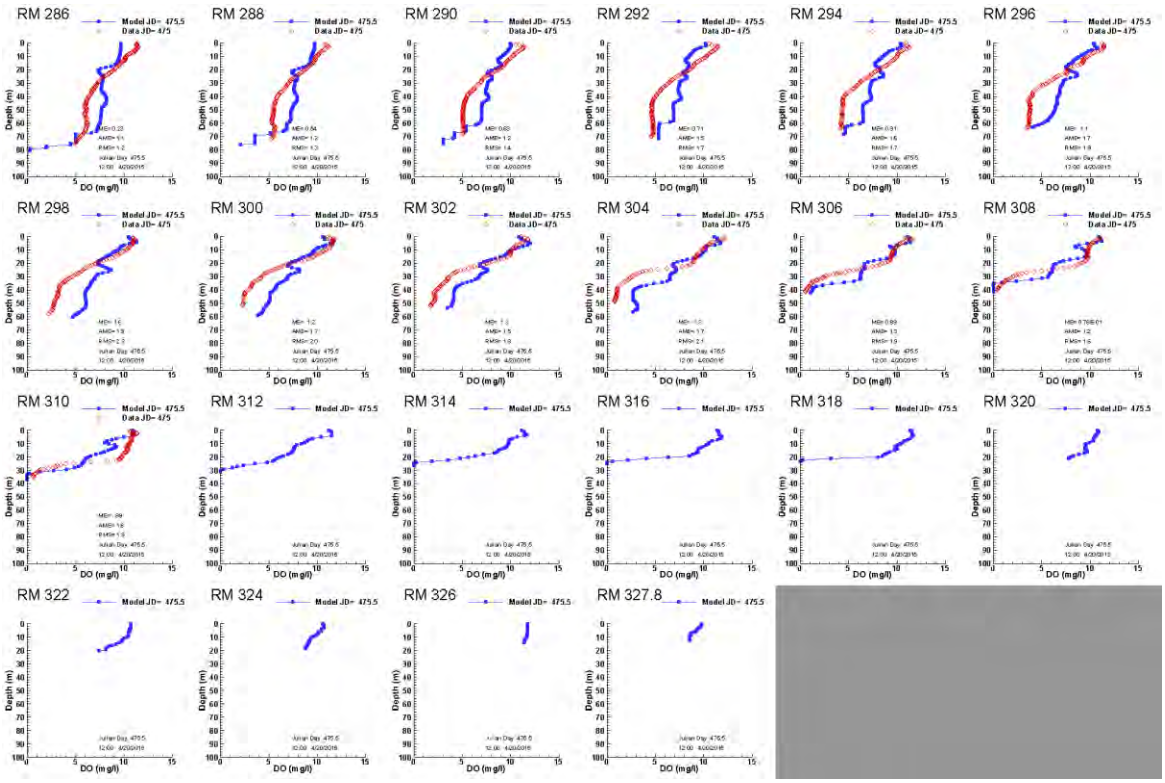


Figure 1119. Vertical profiles of DO compared with data for 4/20/2015.

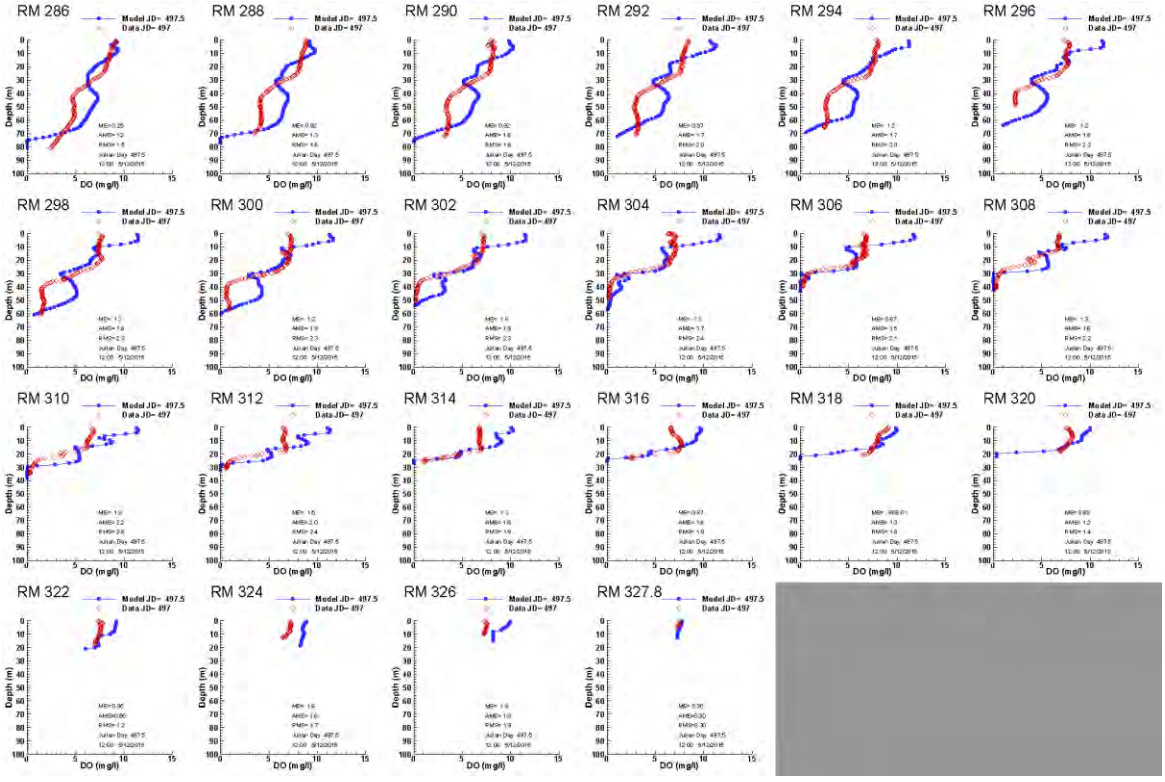


Figure 1120. Vertical profiles of DO compared with data for 5/12/2015.

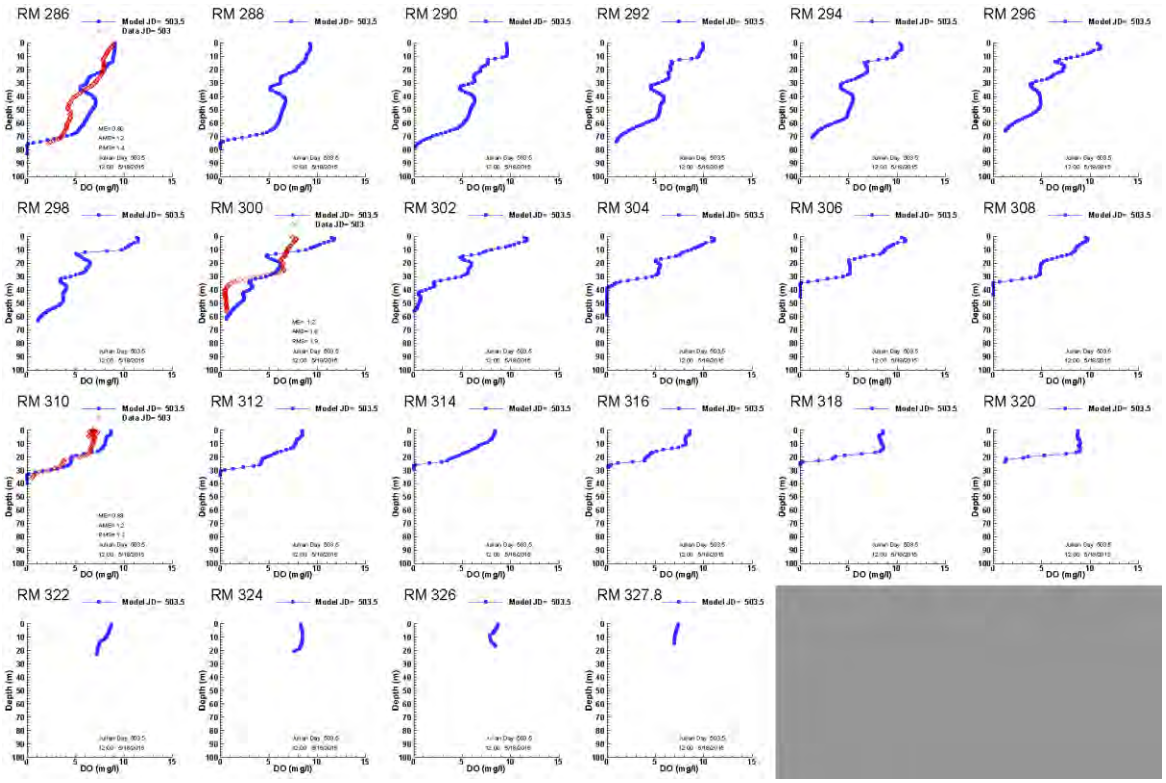


Figure 1121. Vertical profiles of DO compared with data for 5/18/2015.

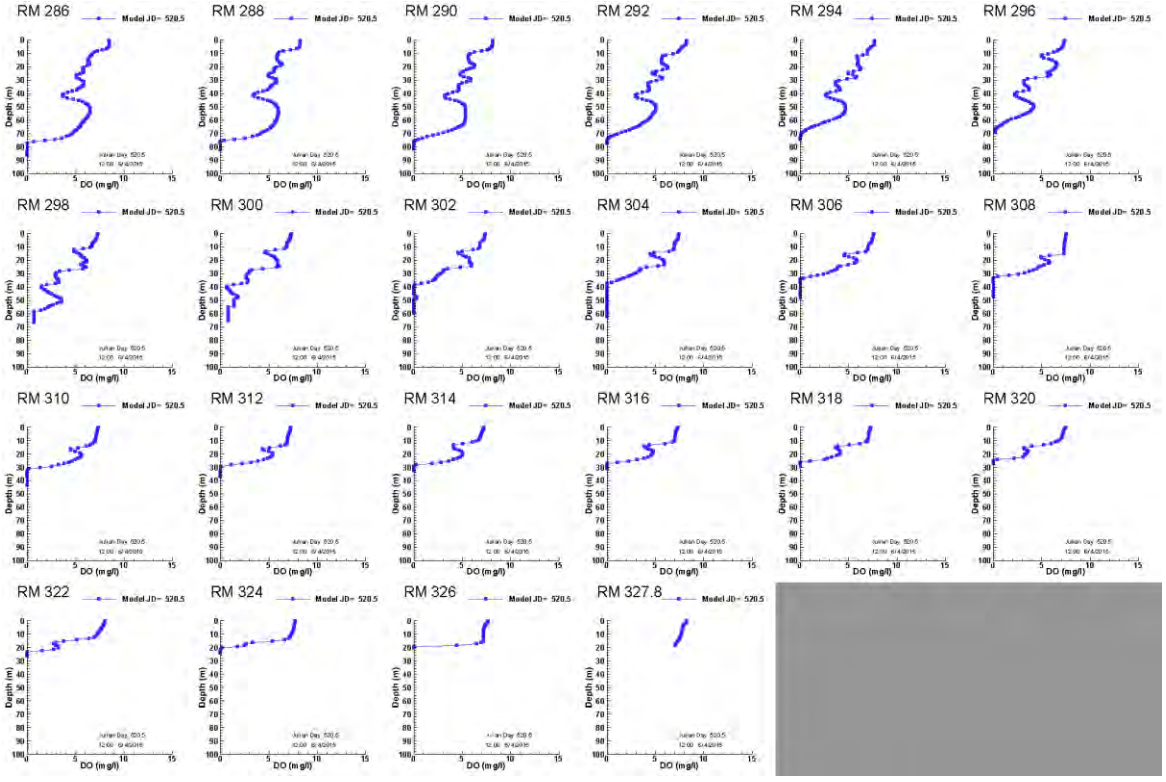


Figure 1122. Vertical profiles of DO compared with data for 6/ 4/2015.

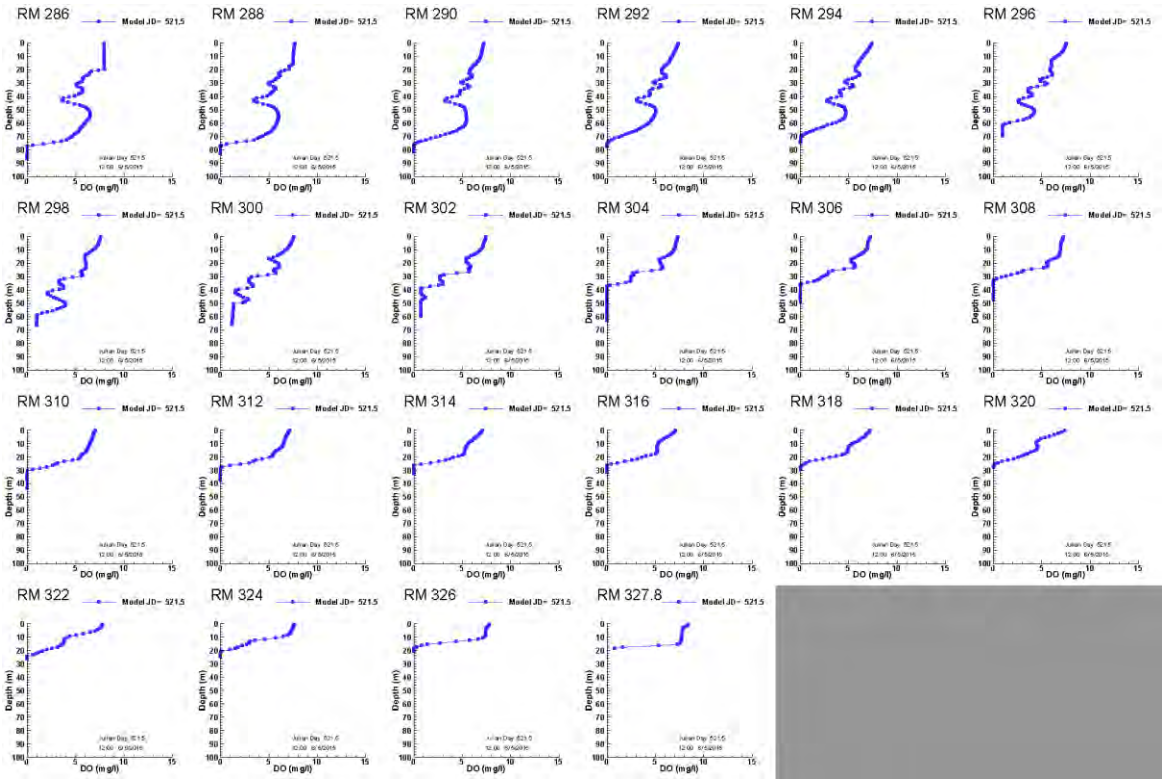


Figure 1123. Vertical profiles of DO compared with data for 6/ 5/2015.

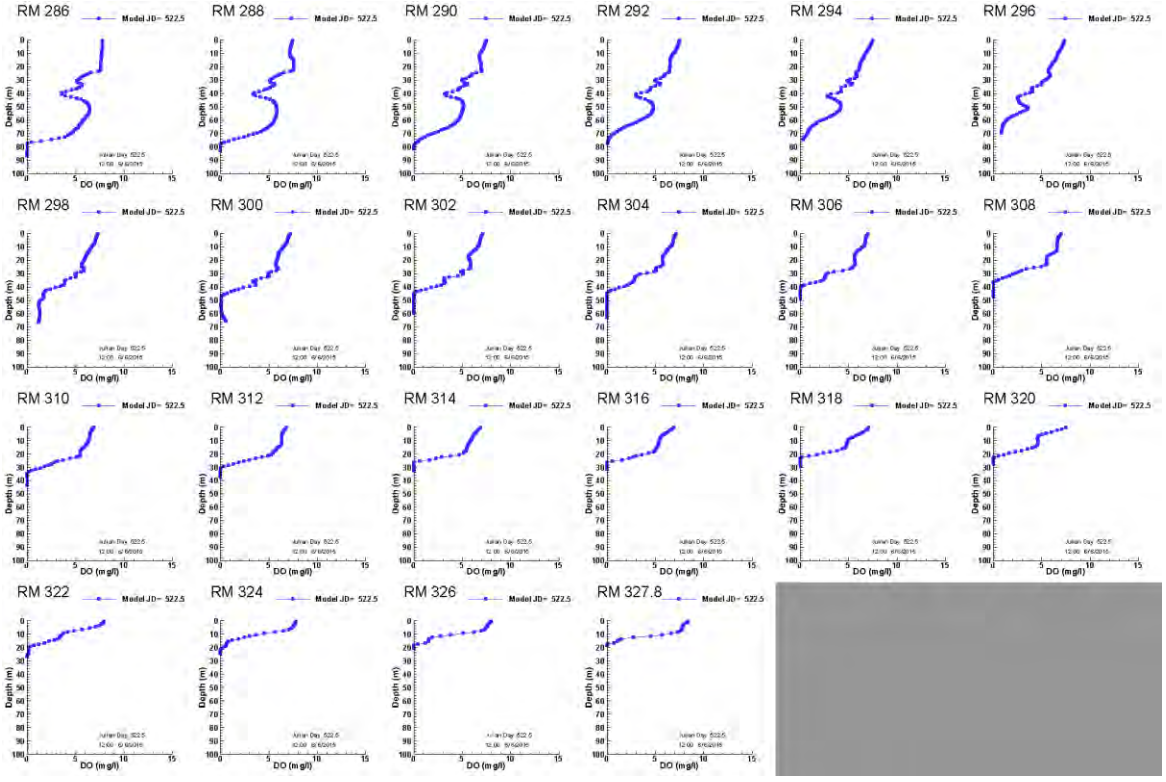


Figure 1124. Vertical profiles of DO compared with data for 6/ 6/2015.

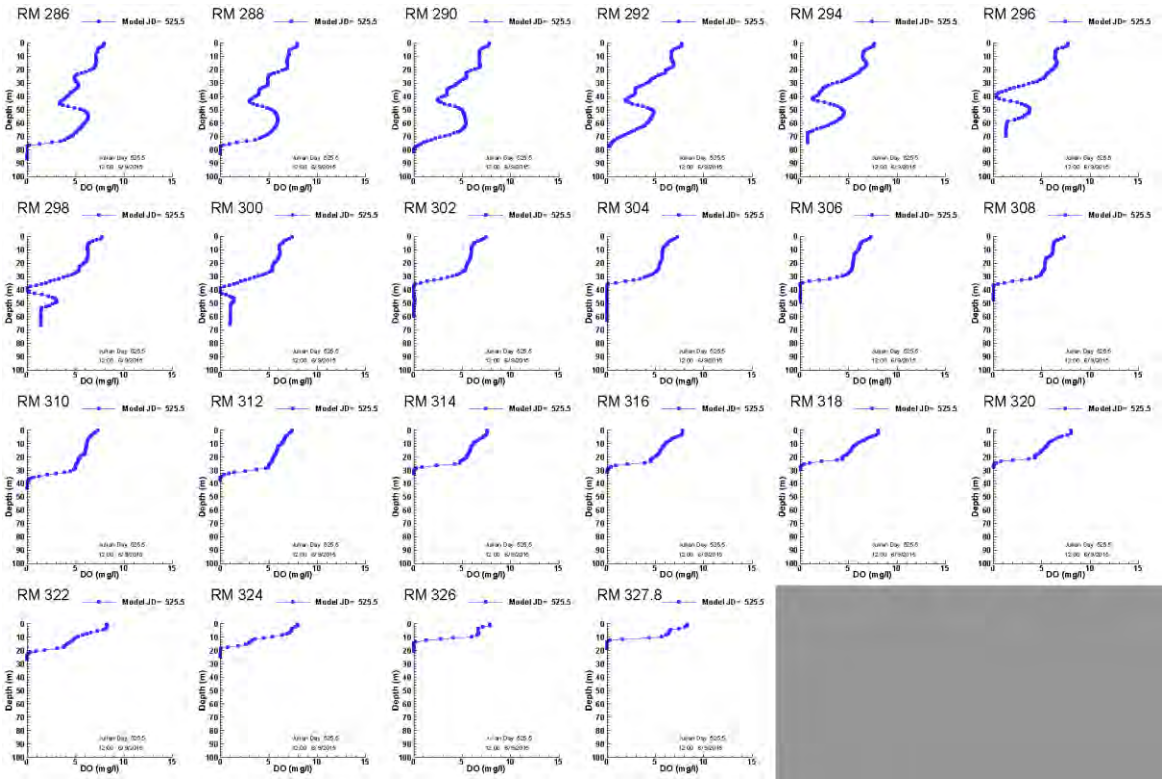


Figure 1125. Vertical profiles of DO compared with data for 6/ 9/2015.

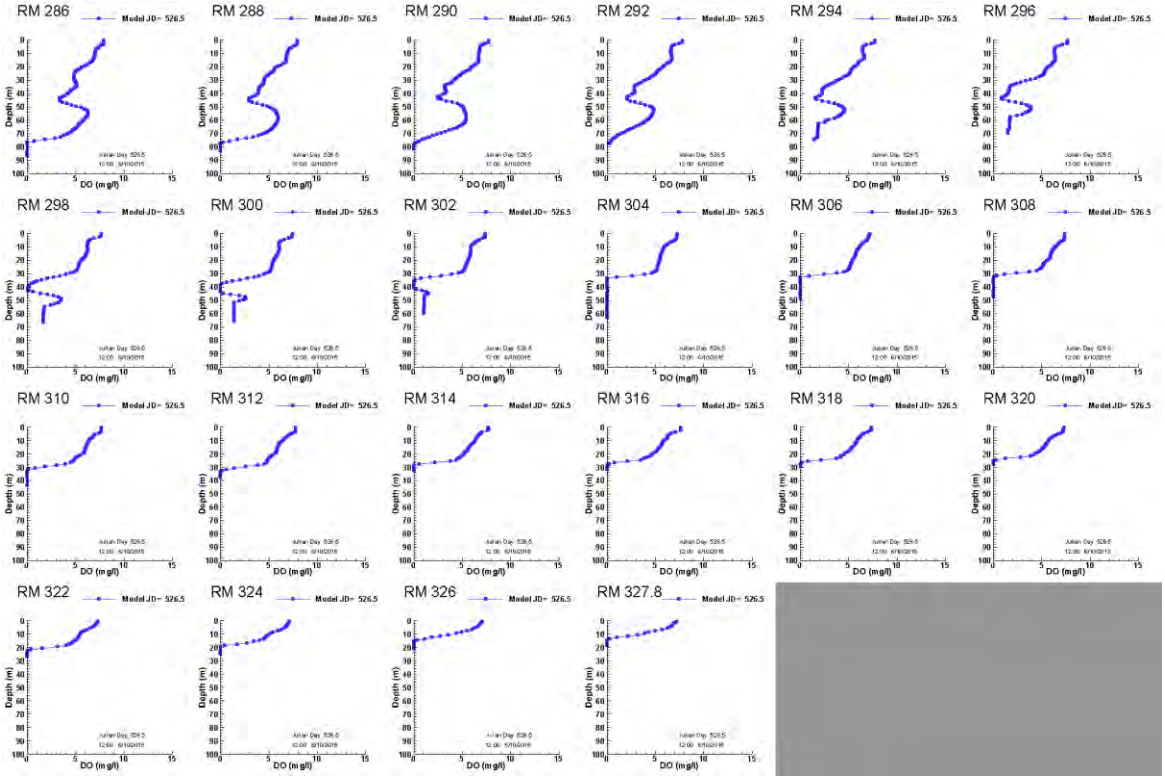


Figure 1126. Vertical profiles of DO compared with data for 6/10/2015.

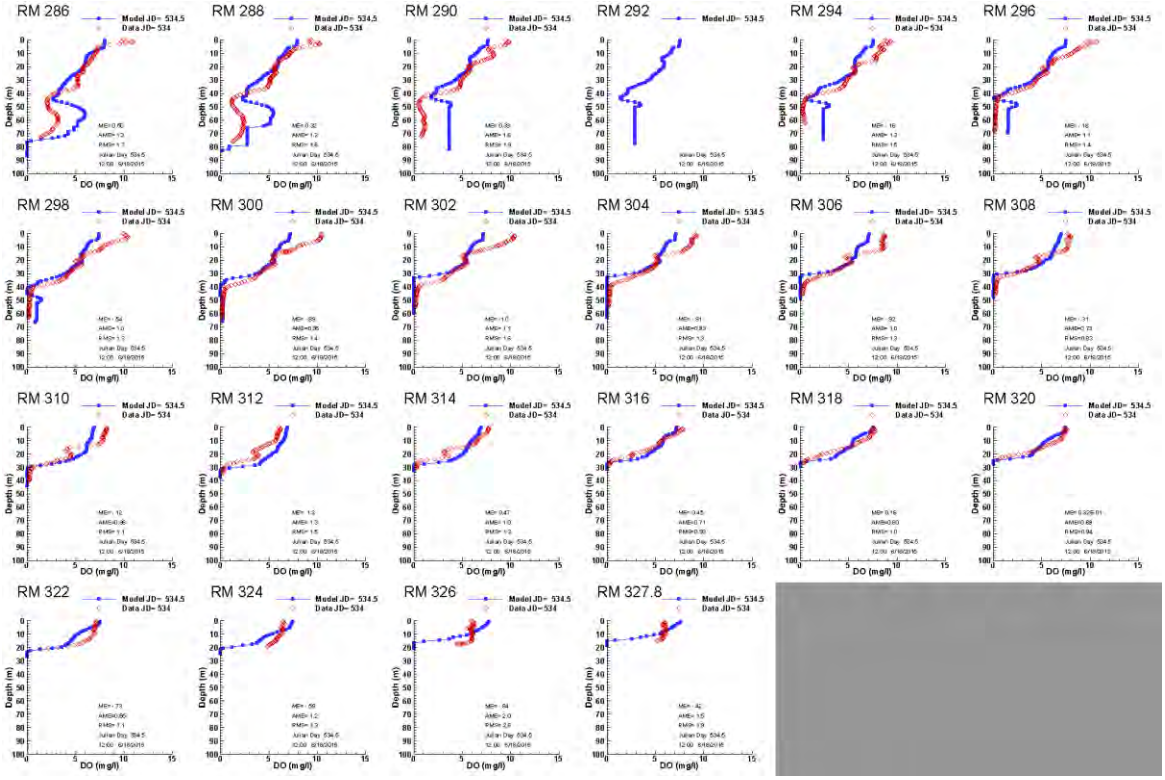


Figure 1127. Vertical profiles of DO compared with data for 6/18/2015.

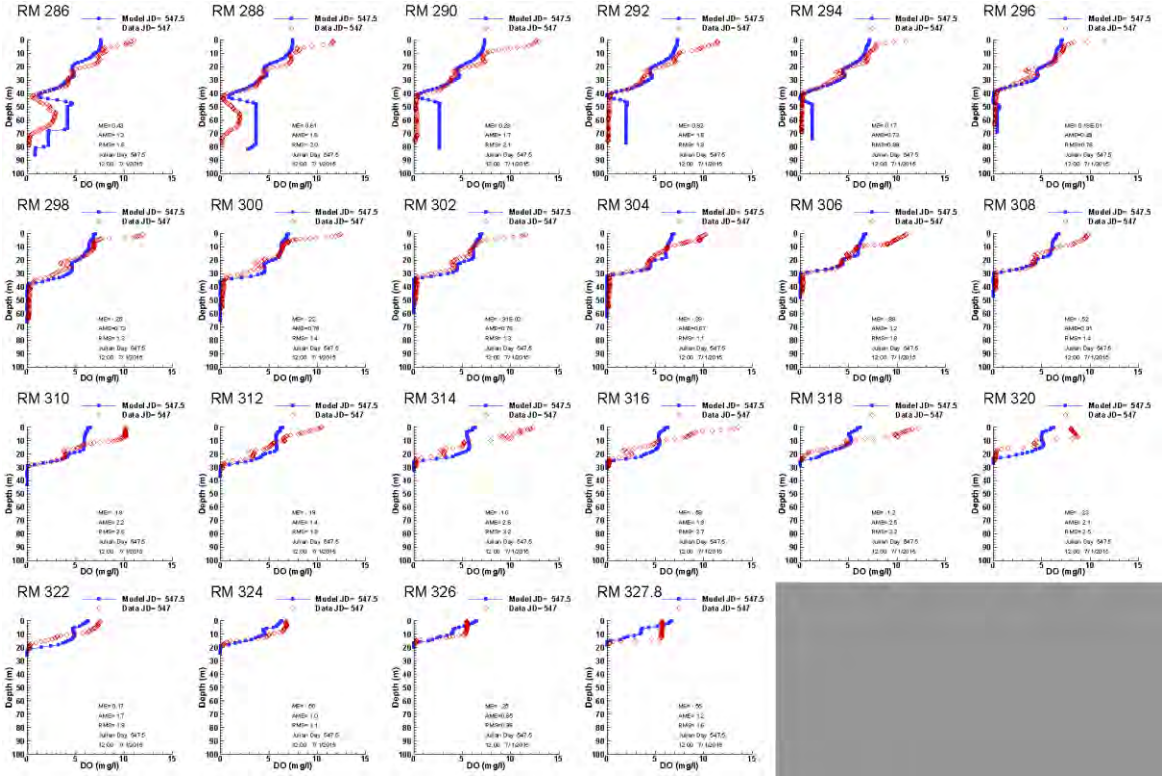


Figure 1128. Vertical profiles of DO compared with data for 7/ 1/2015.

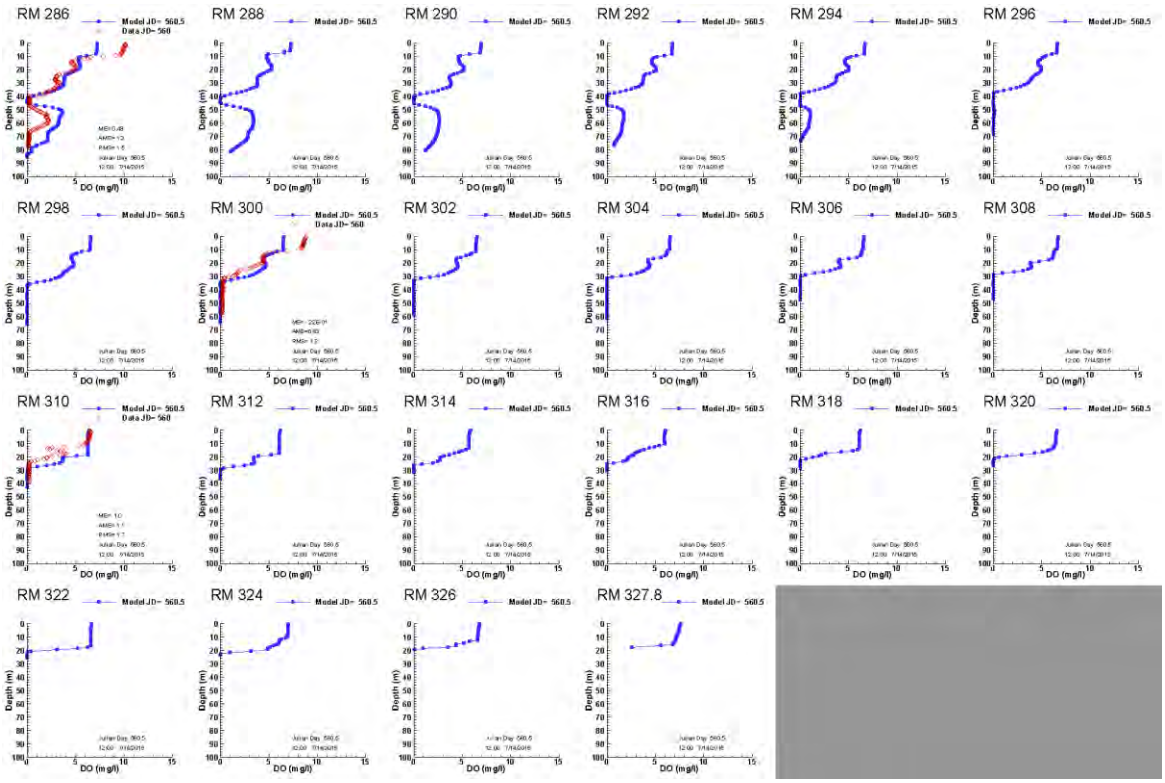


Figure 1129. Vertical profiles of DO compared with data for 7/14/2015.

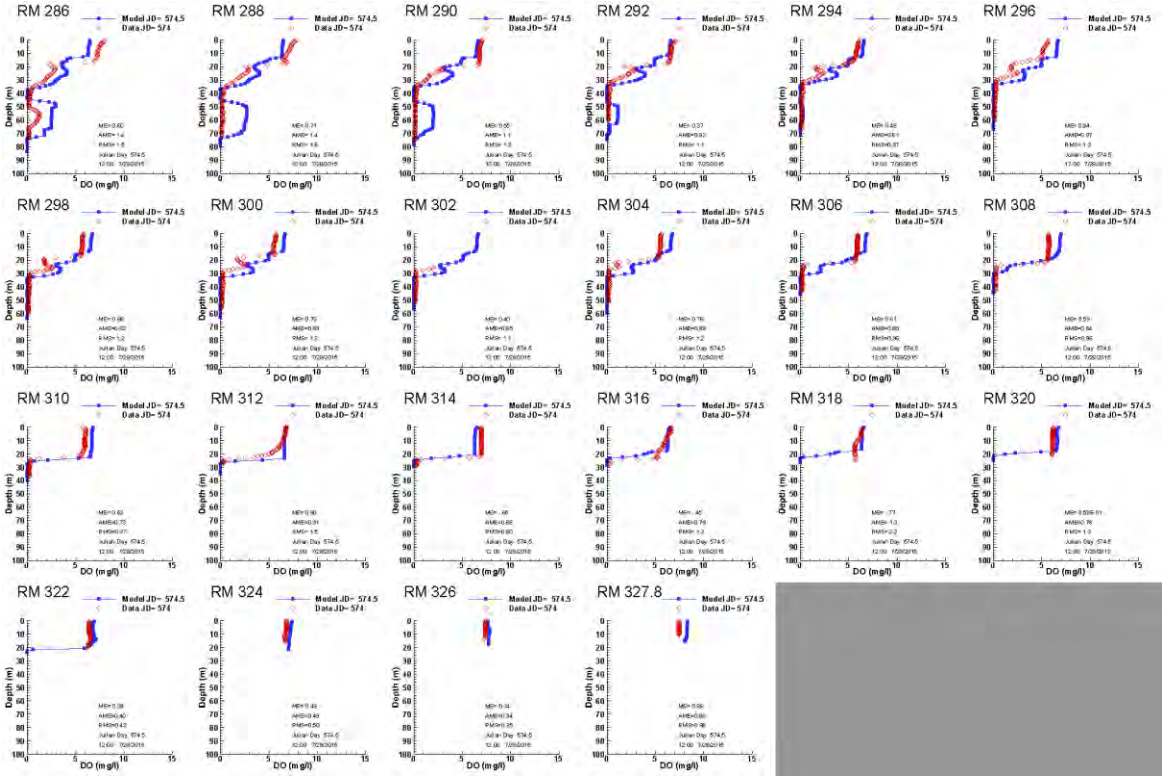


Figure 1130. Vertical profiles of DO compared with data for 7/28/2015.

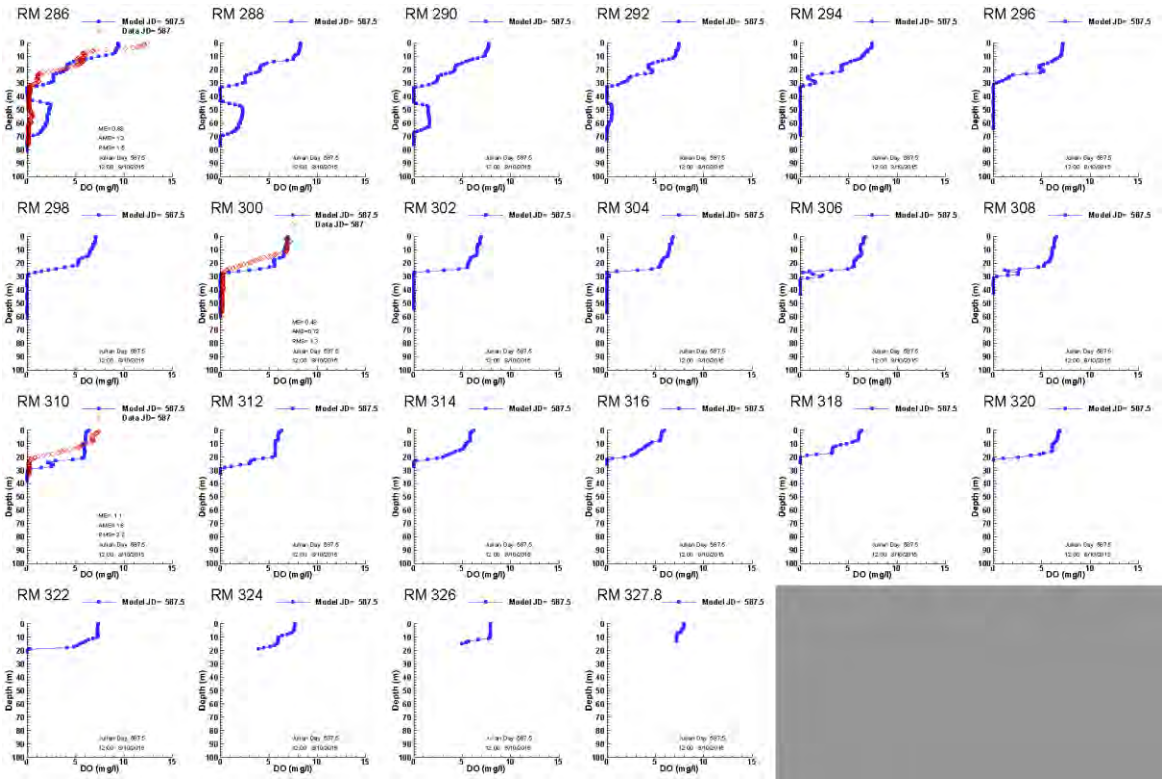


Figure 1131. Vertical profiles of DO compared with data for 8/10/2015.

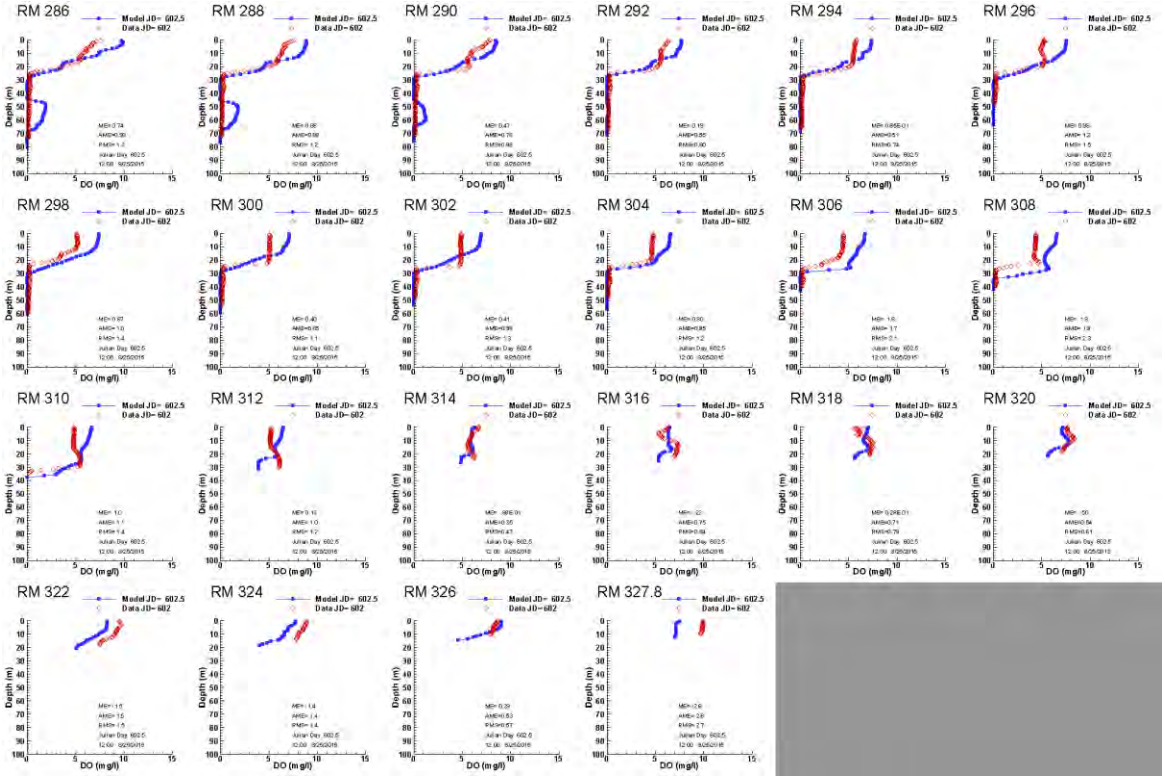


Figure 1132. Vertical profiles of DO compared with data for 8/25/2015.

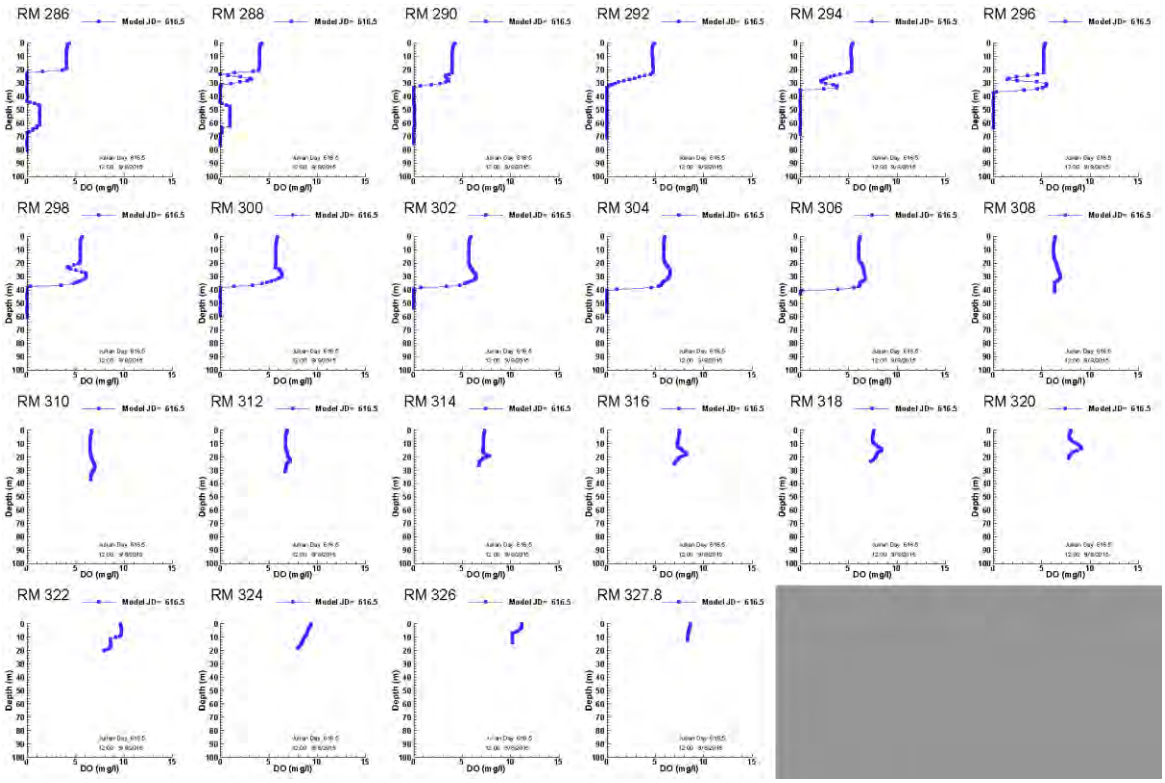


Figure 1133. Vertical profiles of DO compared with data for 9/ 8/2015.

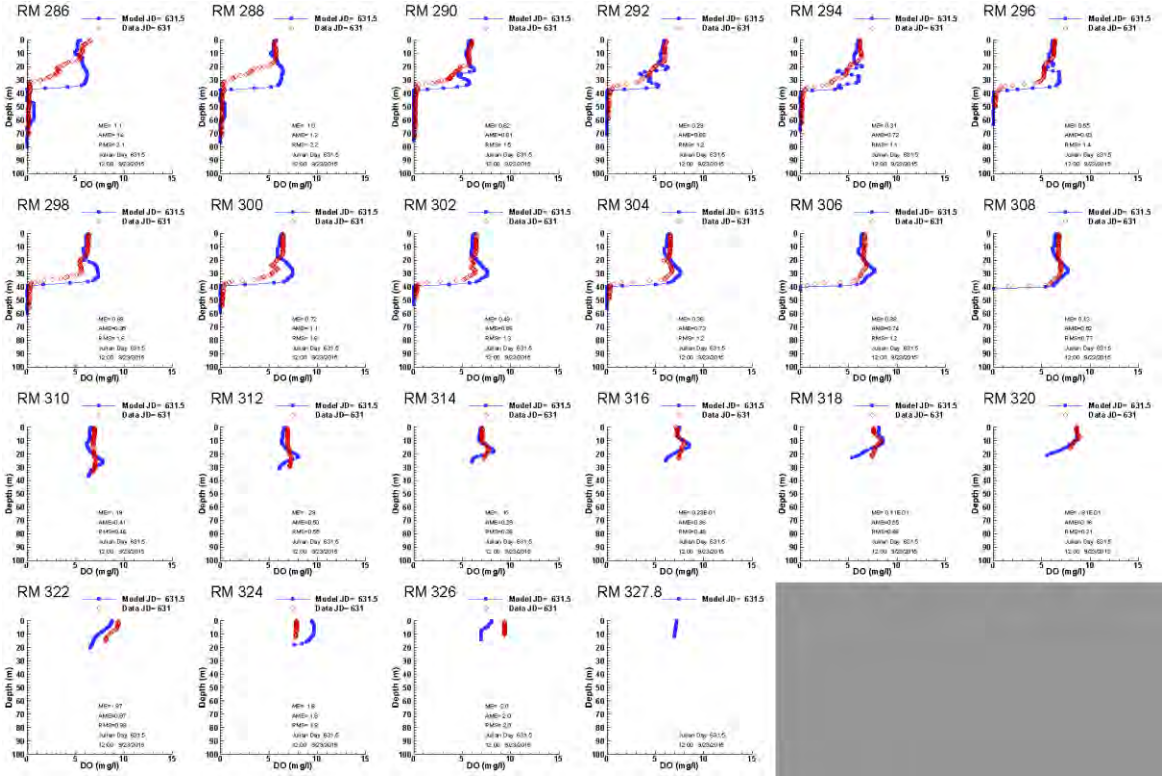


Figure 1134. Vertical profiles of DO compared with data for 9/23/2015.

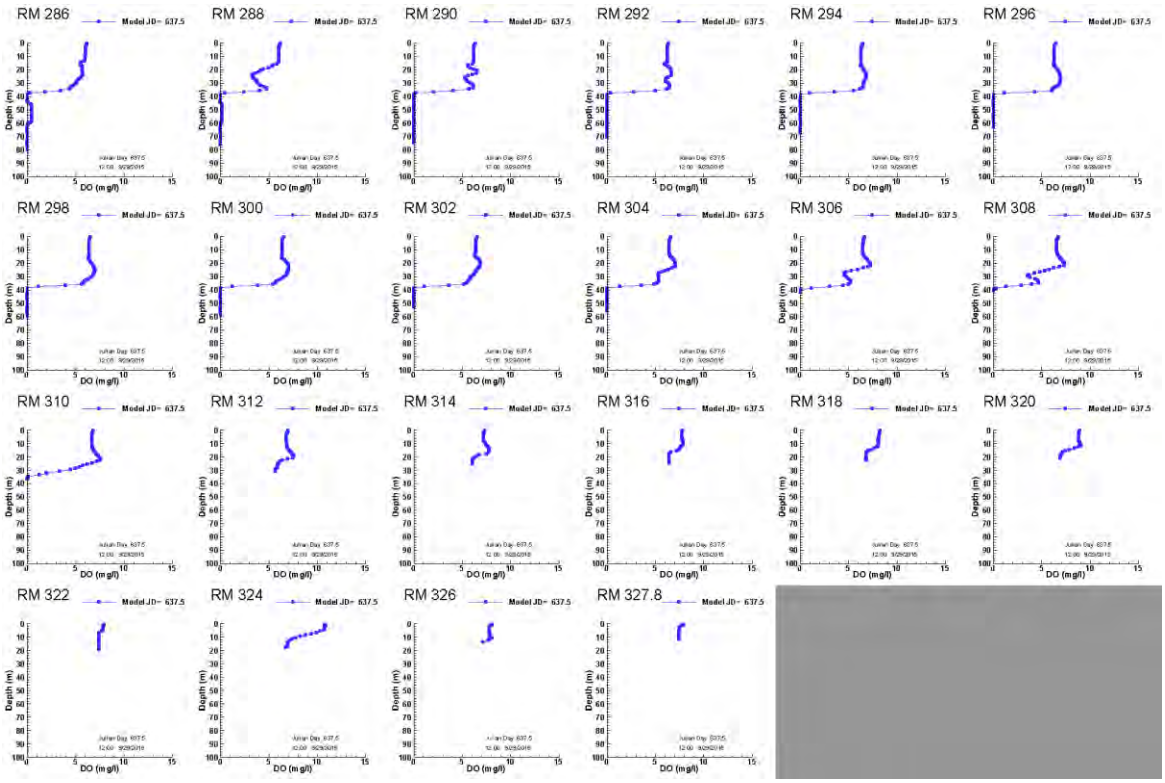


Figure 1135. Vertical profiles of DO compared with data for 9/29/2015.

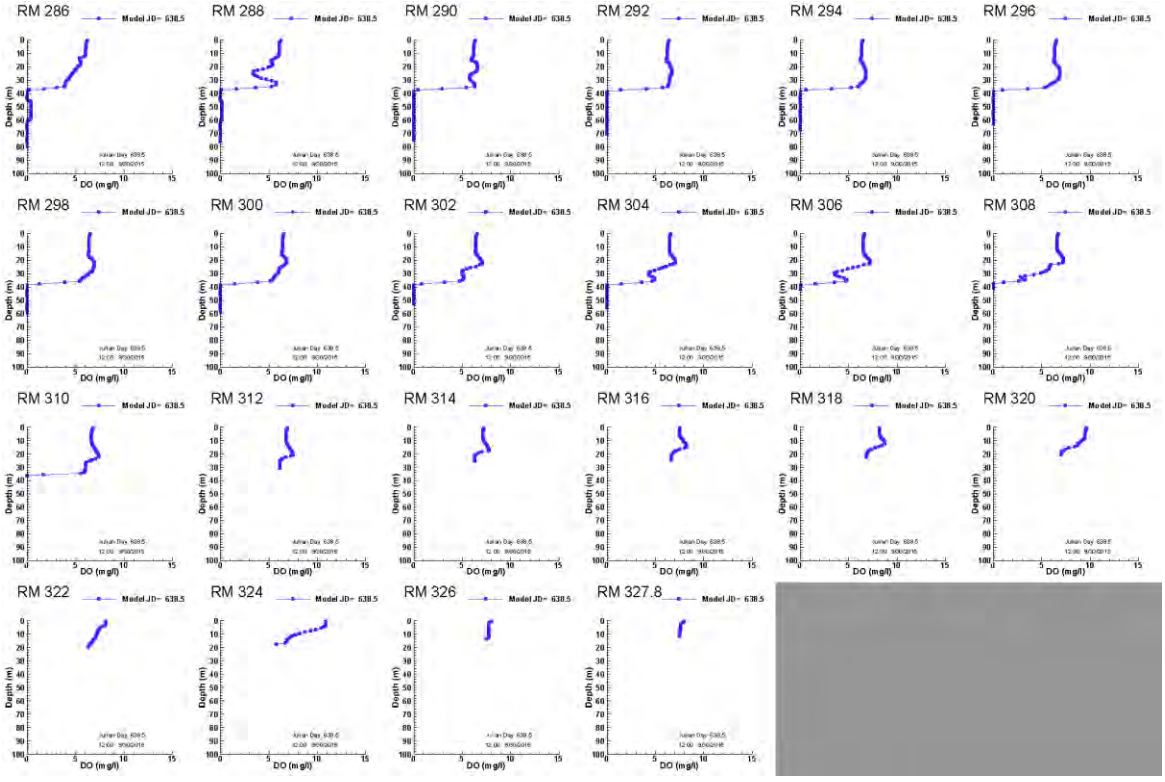


Figure 1136. Vertical profiles of DO compared with data for 9/30/2015.

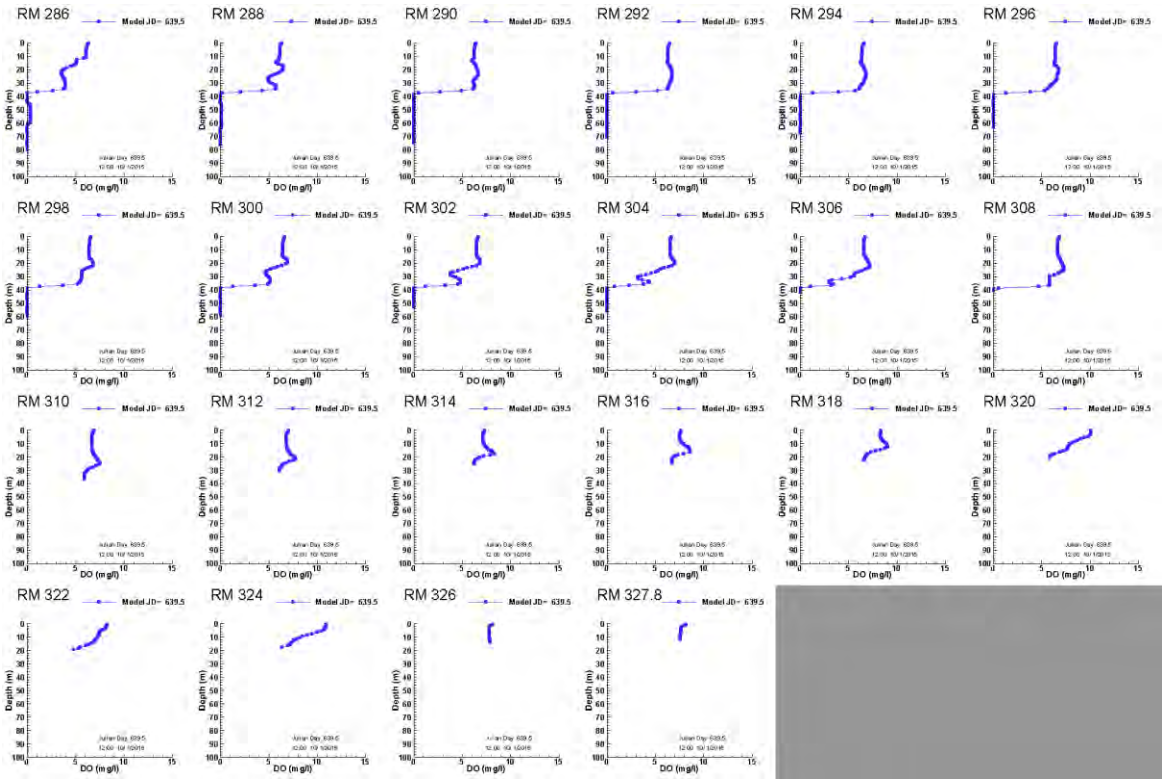


Figure 1137. Vertical profiles of DO compared with data for 10/ 1/2015.

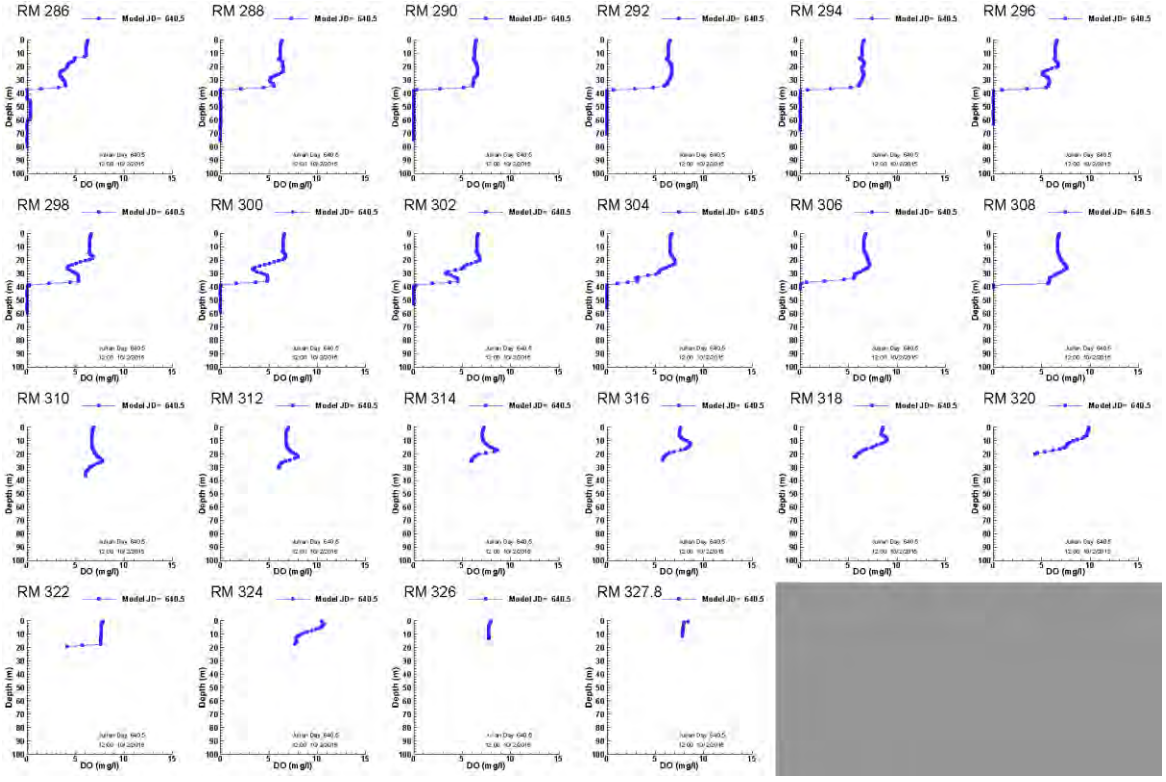


Figure 1138. Vertical profiles of DO compared with data for 10/ 2/2015.

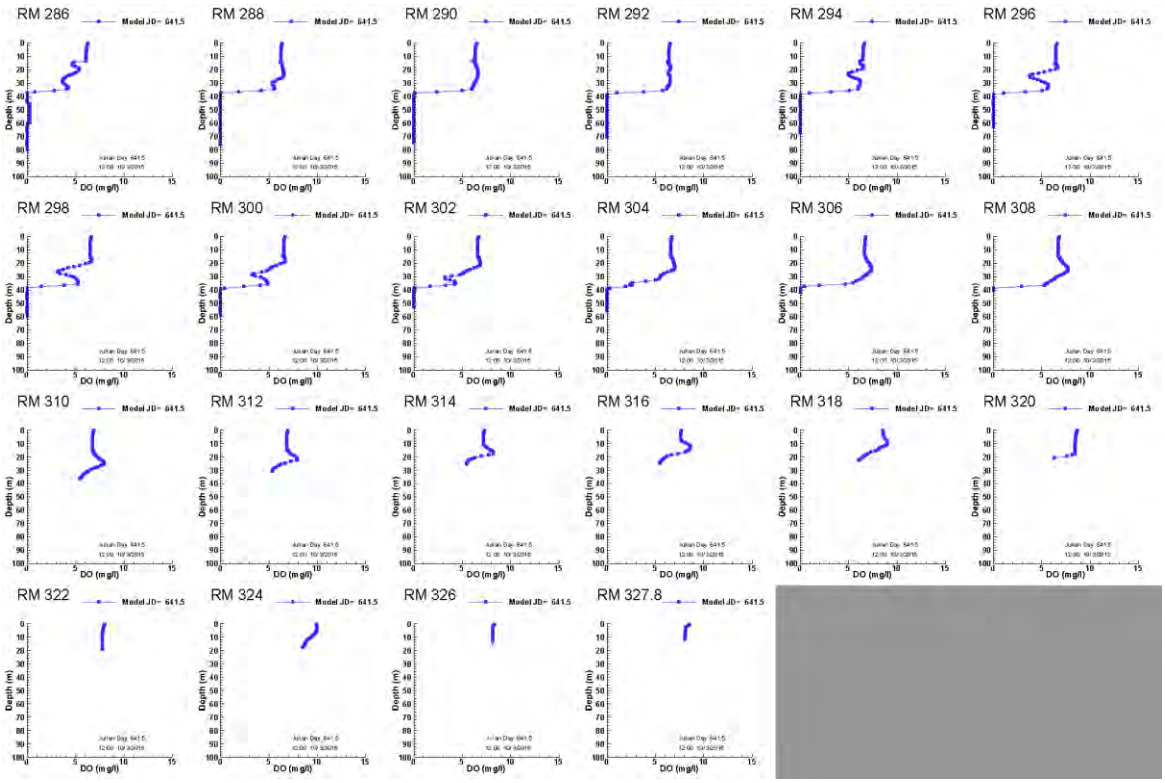


Figure 1139. Vertical profiles of DO compared with data for 10/ 3/2015.

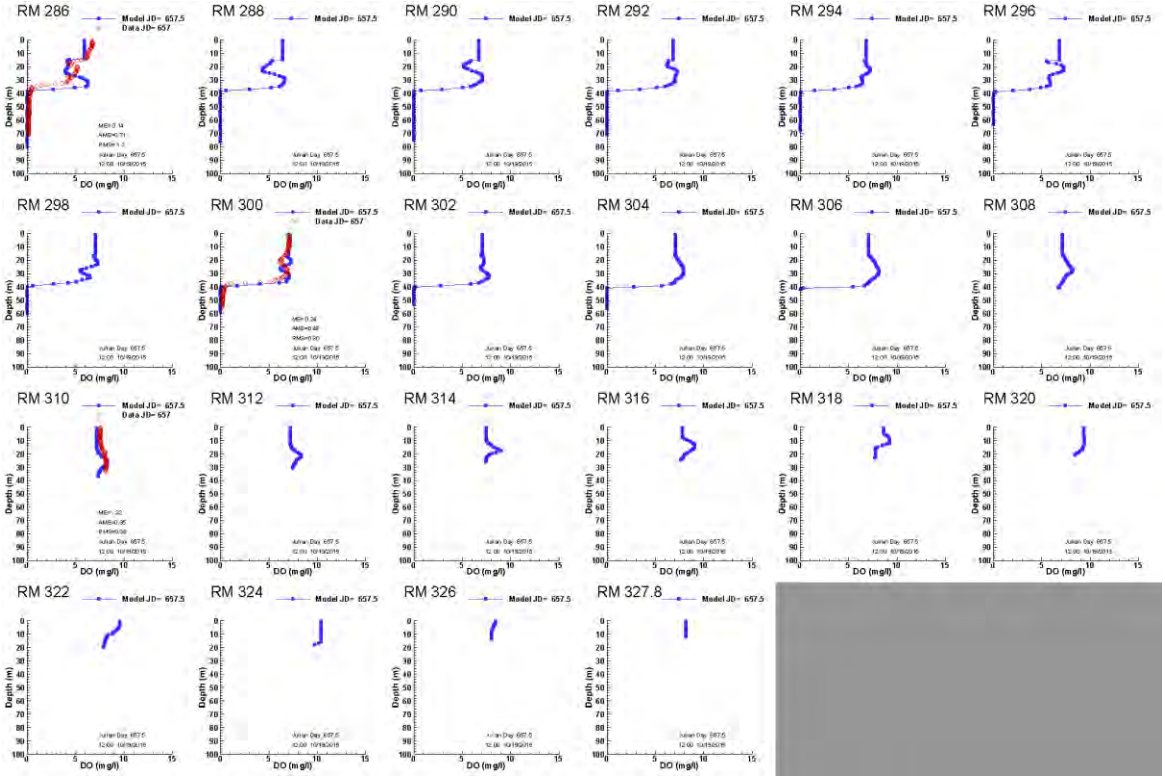


Figure 1140. Vertical profiles of DO compared with data for 10/19/2015.

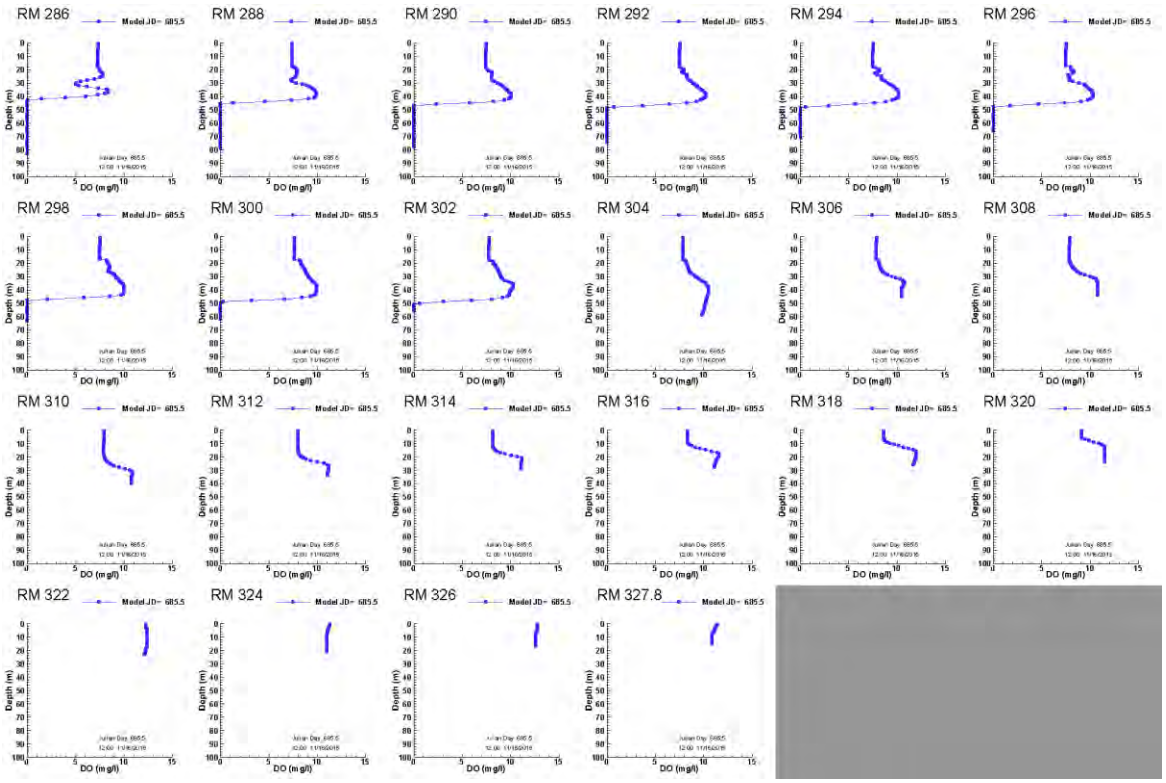


Figure 1141. Vertical profiles of DO compared with data for 11/16/2015.

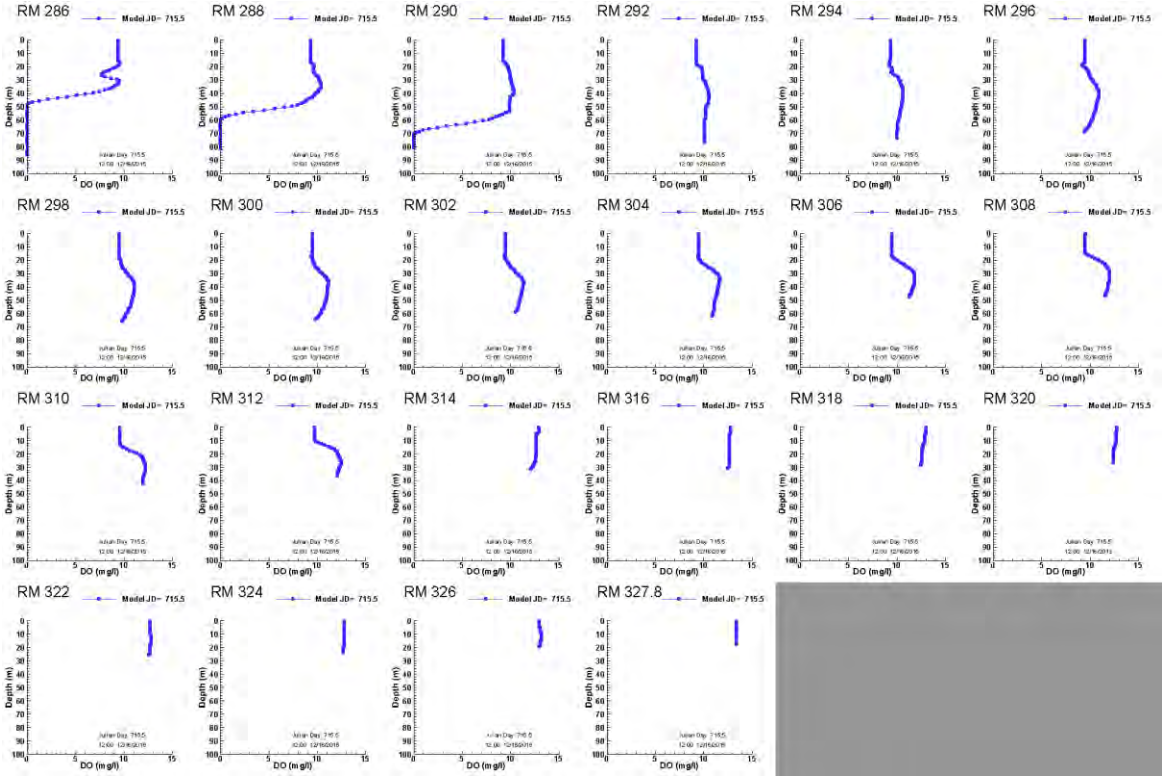


Figure 1142. Vertical profiles of DO compared with data for 12/16/2015.

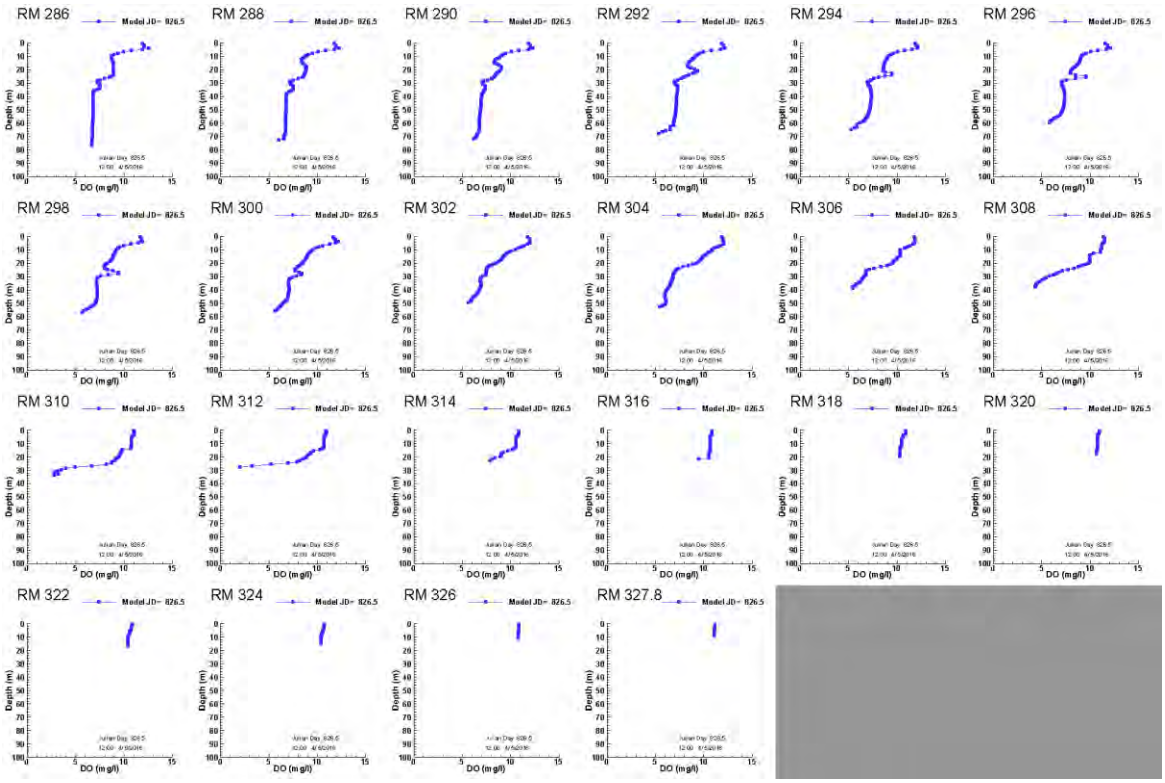


Figure 1143. Vertical profiles of DO compared with data for 4/ 5/2016.

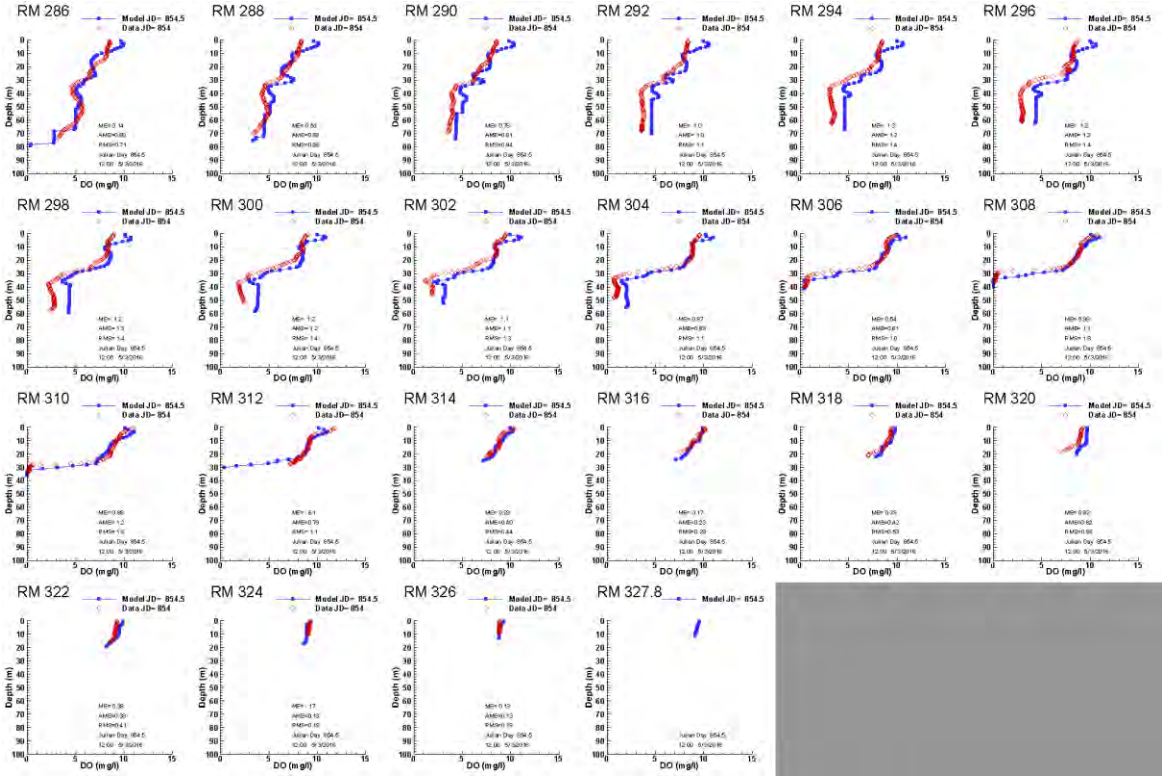


Figure 1144. Vertical profiles of DO compared with data for 5/ 3/2016.

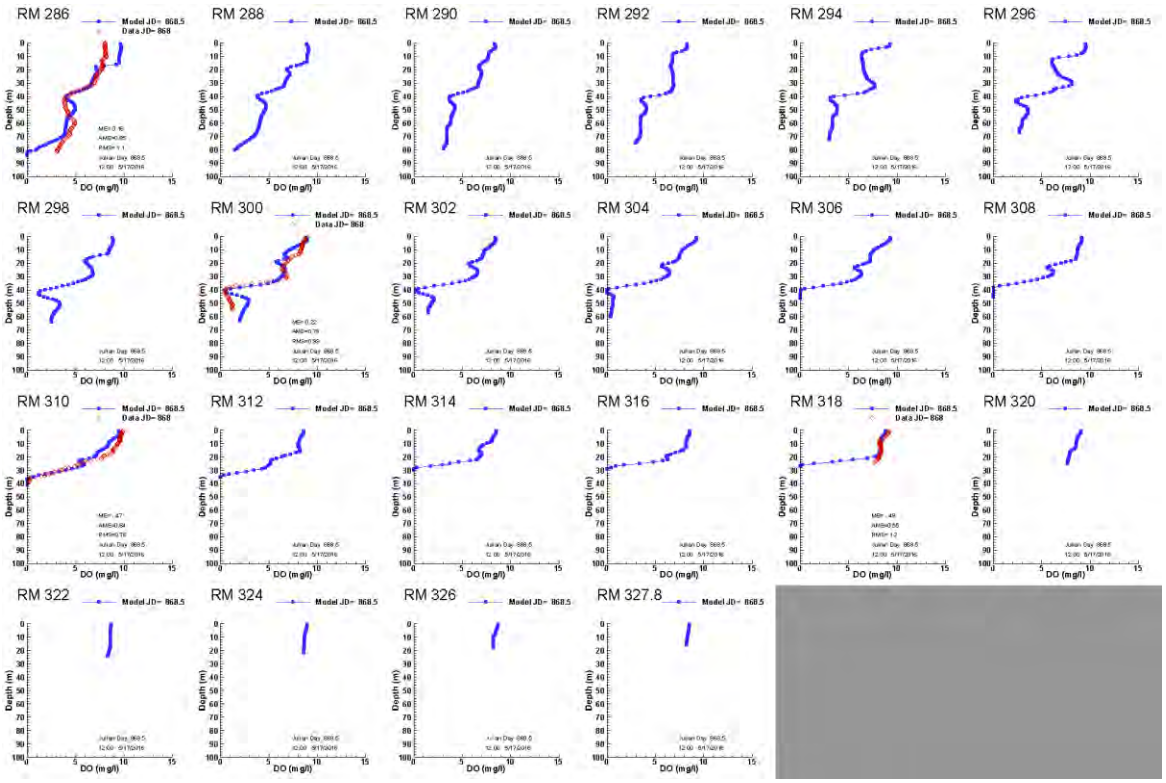


Figure 1145. Vertical profiles of DO compared with data for 5/17/2016.

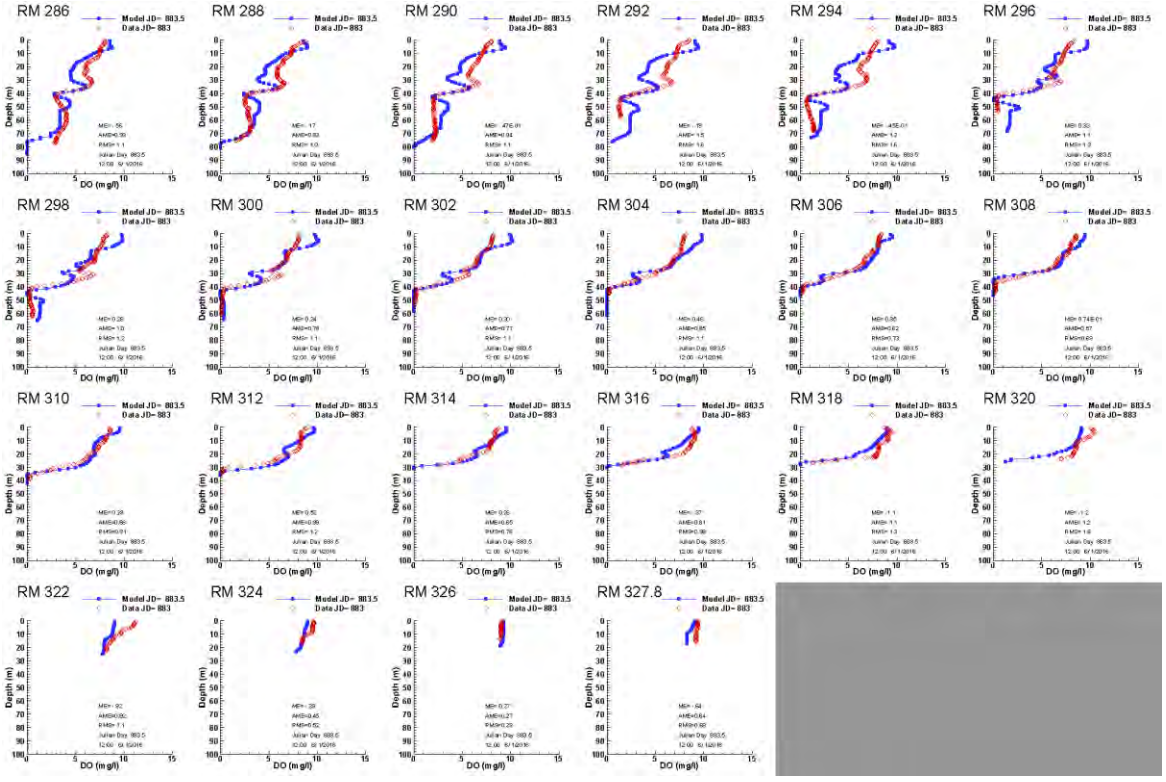


Figure 1146. Vertical profiles of DO compared with data for 6/ 1/2016.

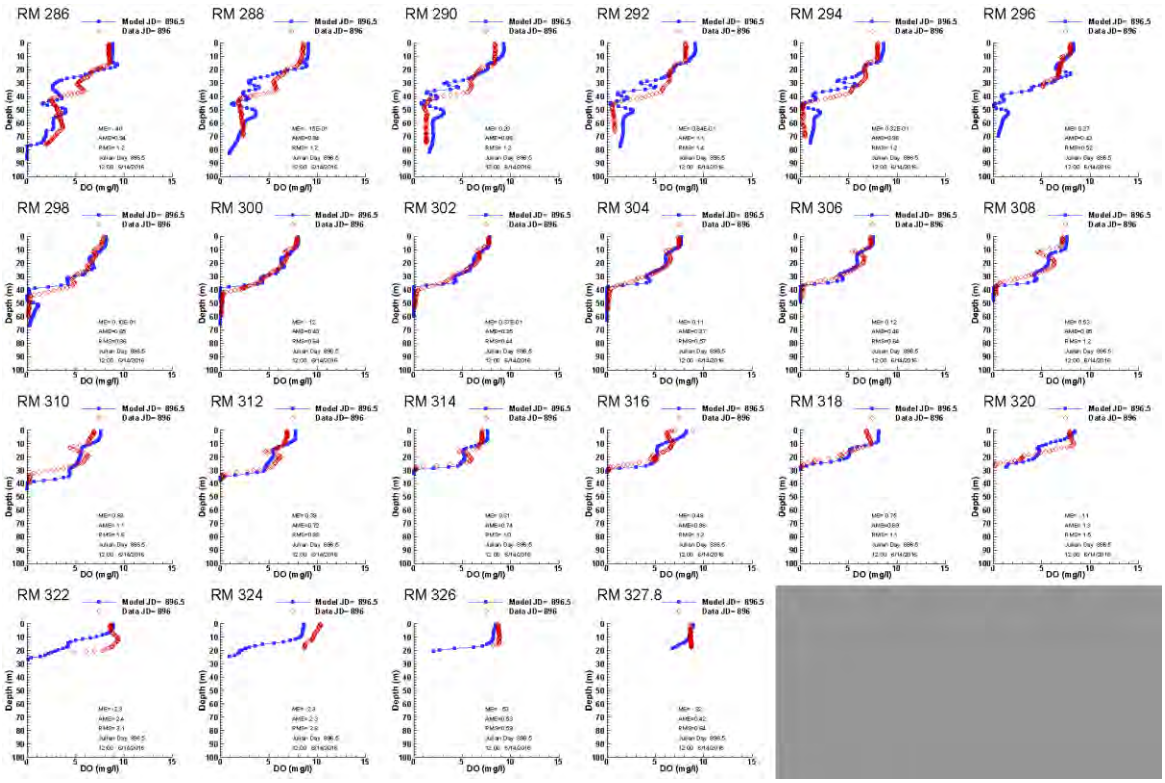


Figure 1147. Vertical profiles of DO compared with data for 6/14/2016.

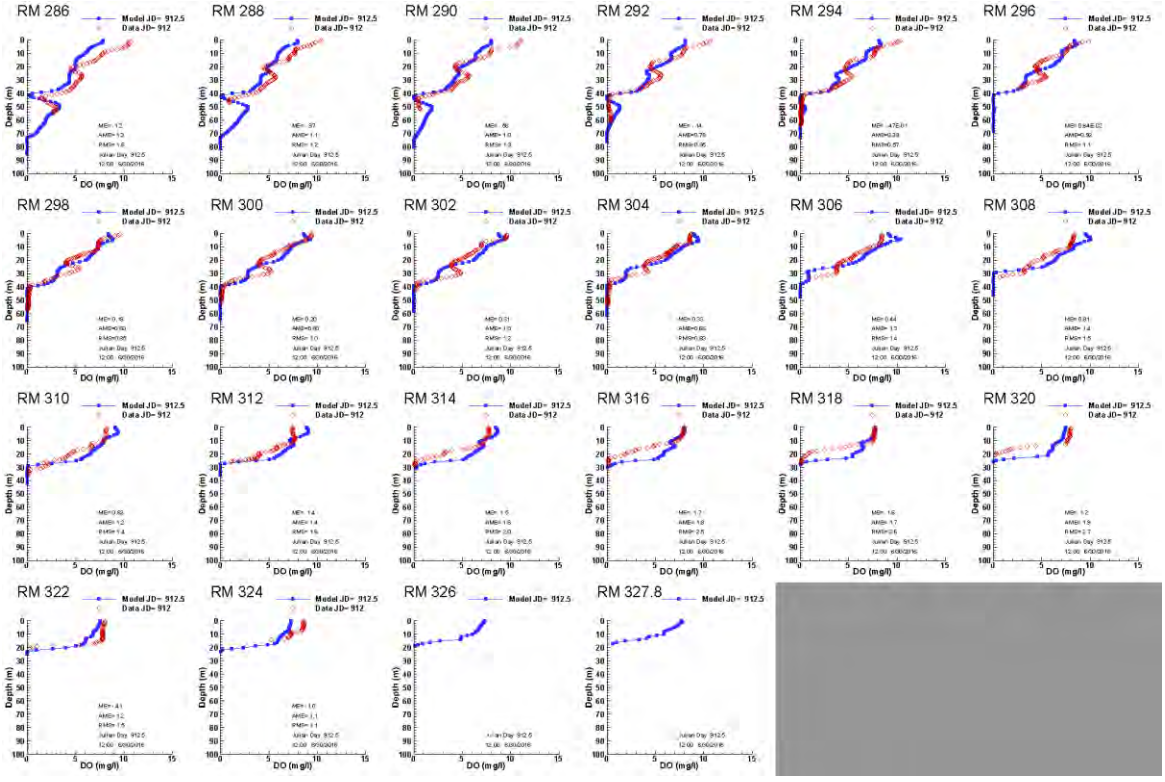


Figure 1148. Vertical profiles of DO compared with data for 6/30/2016.

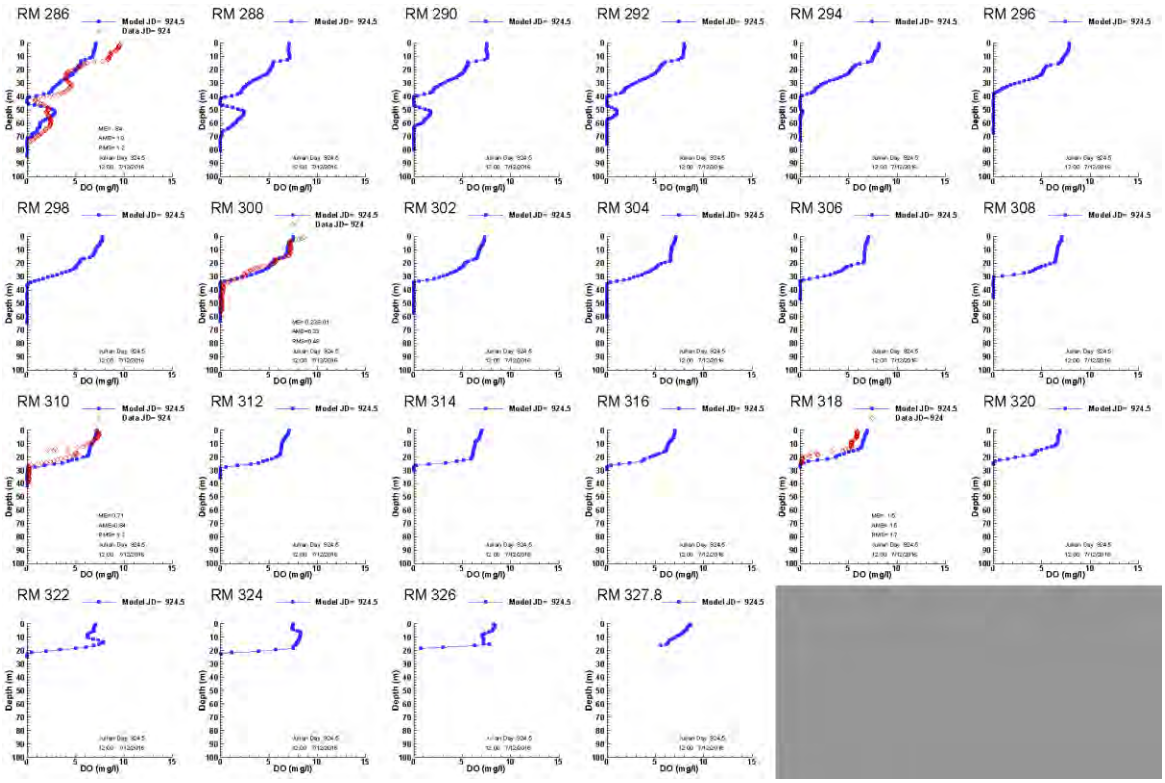


Figure 1149. Vertical profiles of DO compared with data for 7/12/2016.

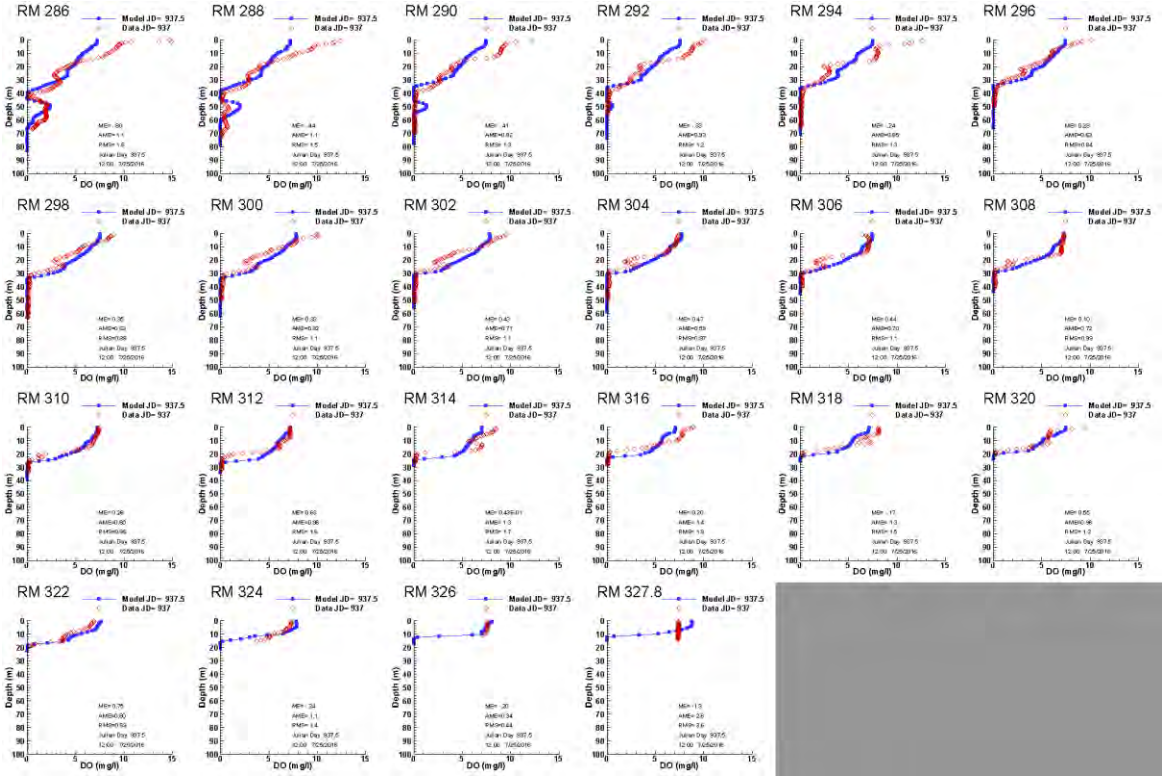


Figure 1150. Vertical profiles of DO compared with data for 7/25/2016.

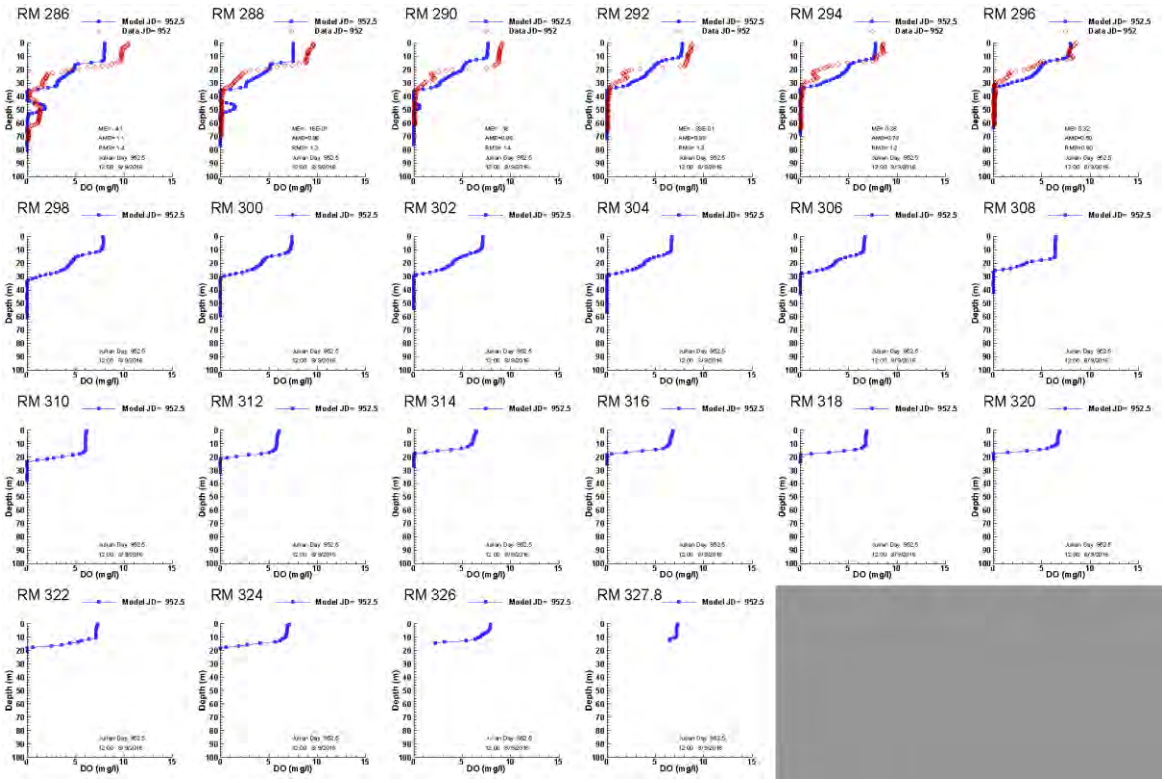


Figure 1151. Vertical profiles of DO compared with data for 8/ 9/2016.

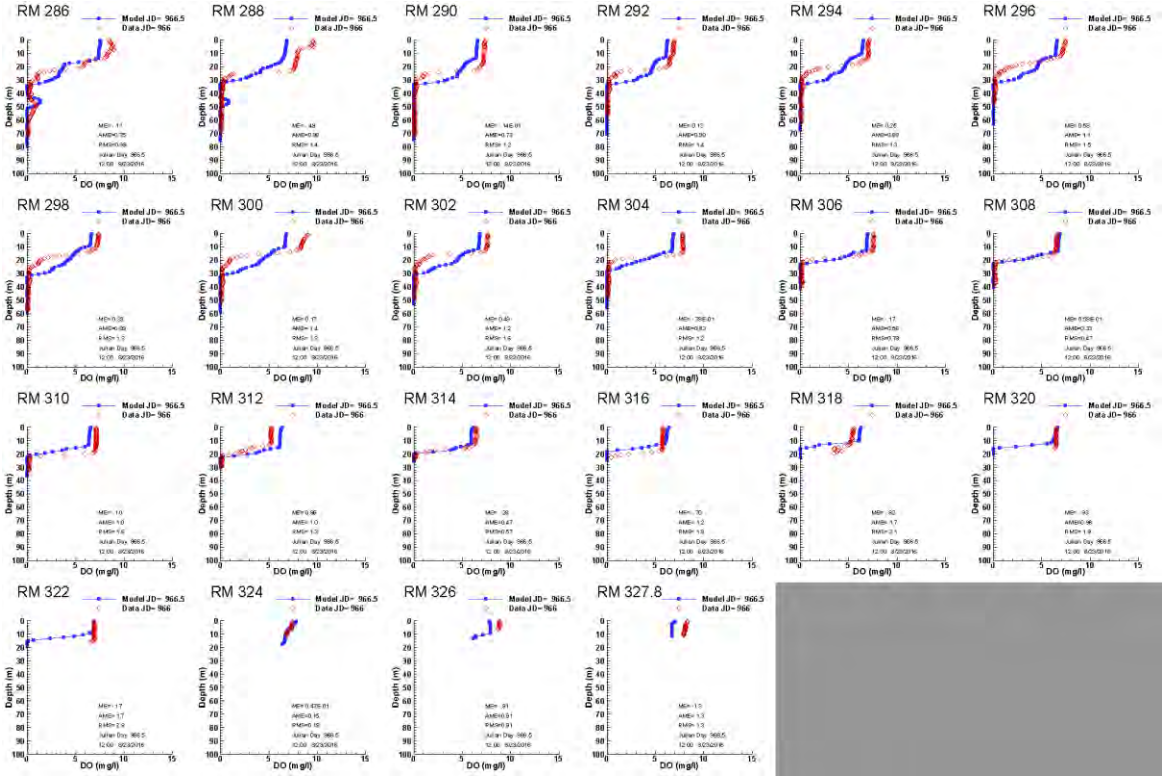


Figure 1152. Vertical profiles of DO compared with data for 8/23/2016.

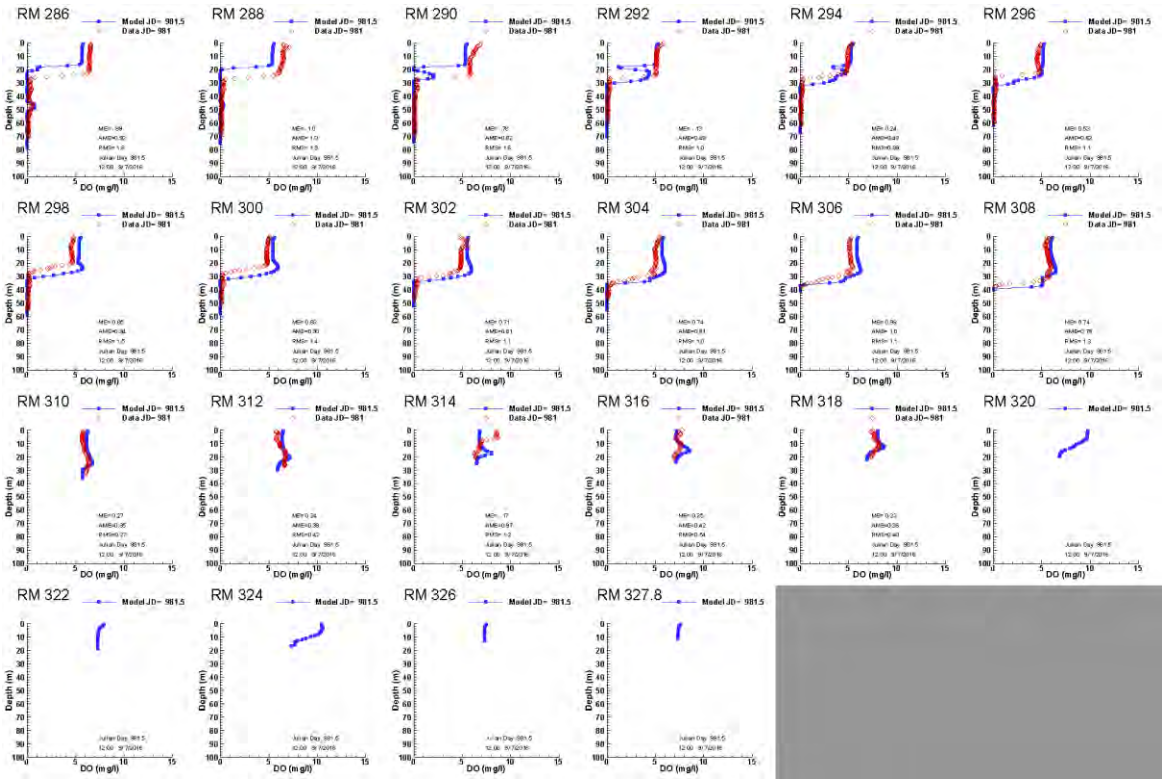


Figure 1153. Vertical profiles of DO compared with data for 9/ 7/2016.

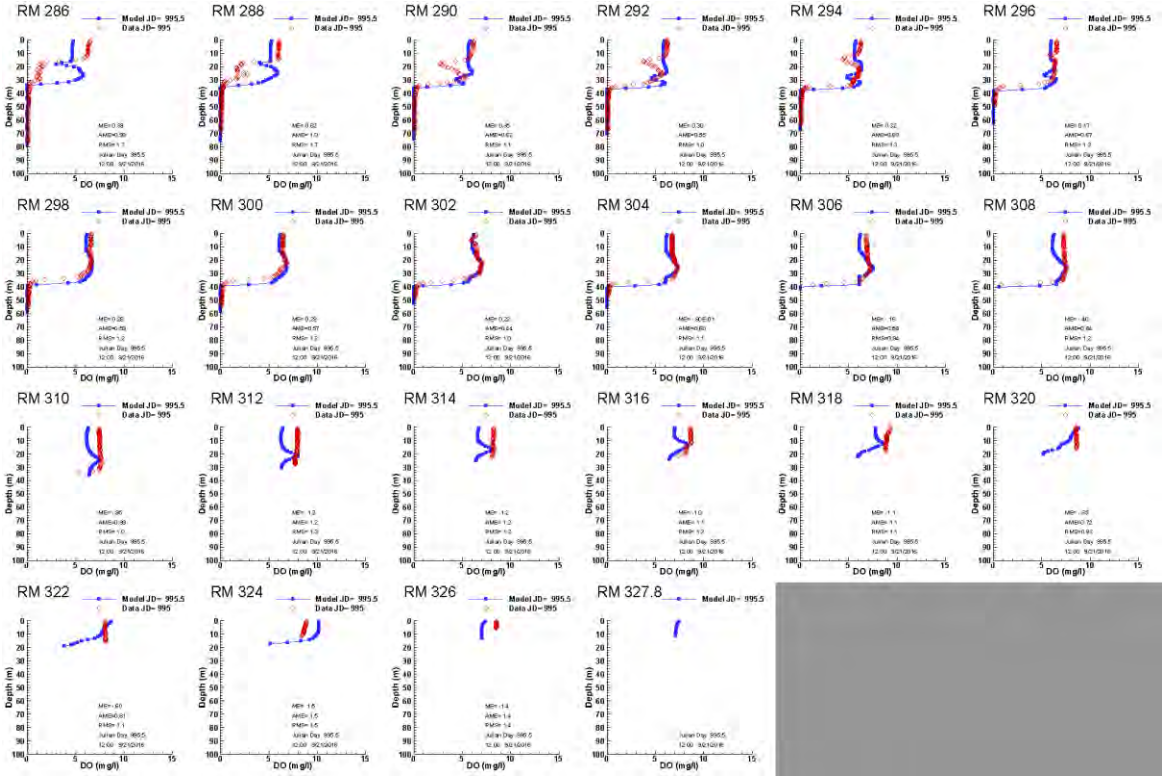


Figure 1154. Vertical profiles of DO compared with data for 9/21/2016.

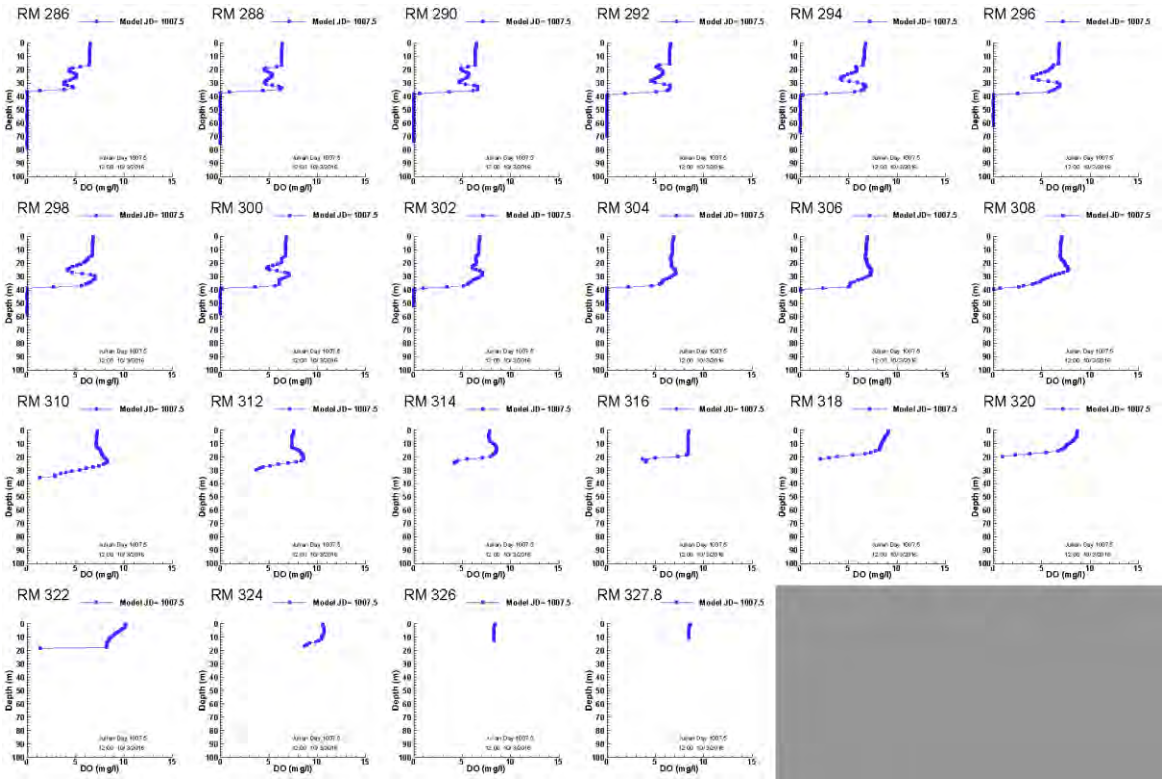


Figure 1155. Vertical profiles of DO compared with data for 10/ 3/2016.

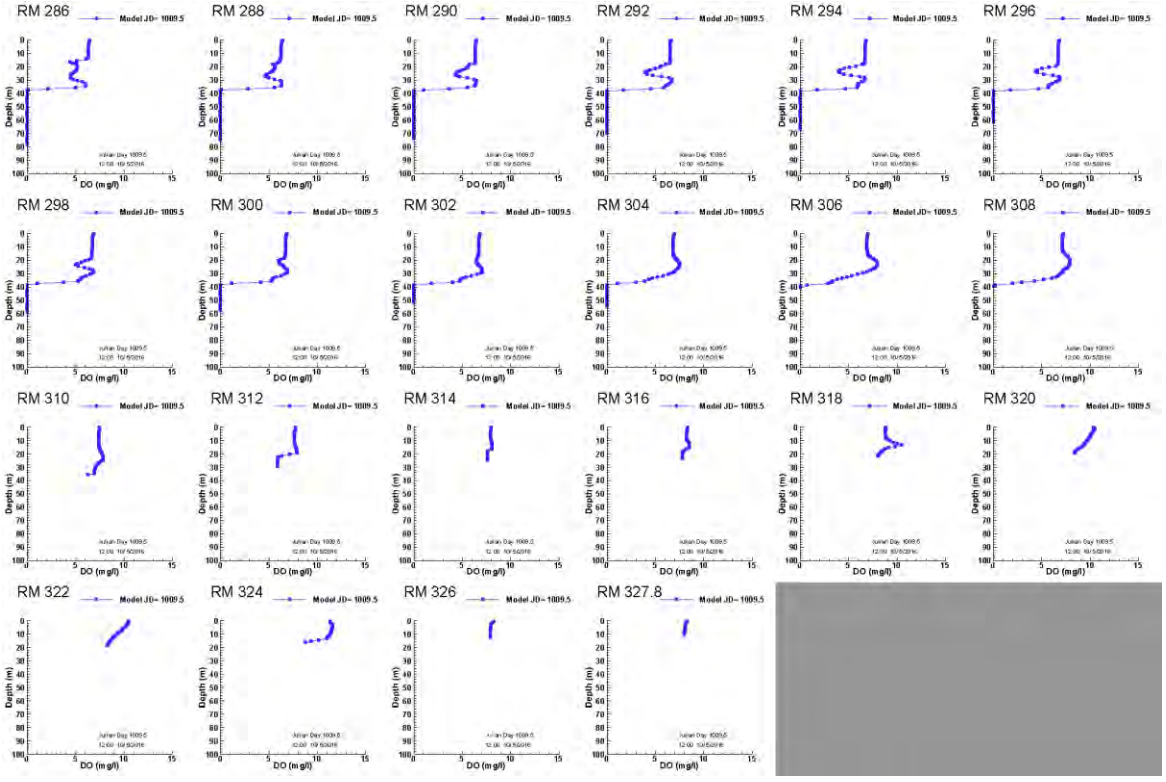


Figure 1156. Vertical profiles of DO compared with data for 10/ 5/2016.

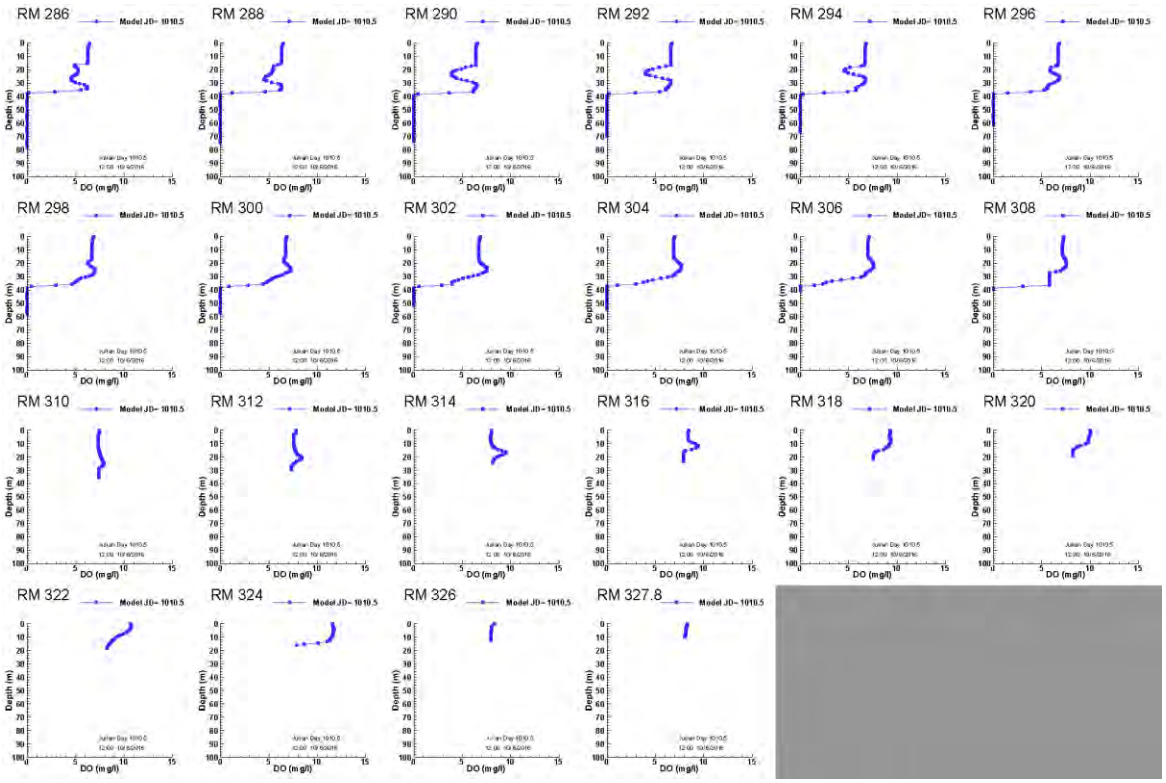


Figure 1157. Vertical profiles of DO compared with data for 10/ 6/2016.

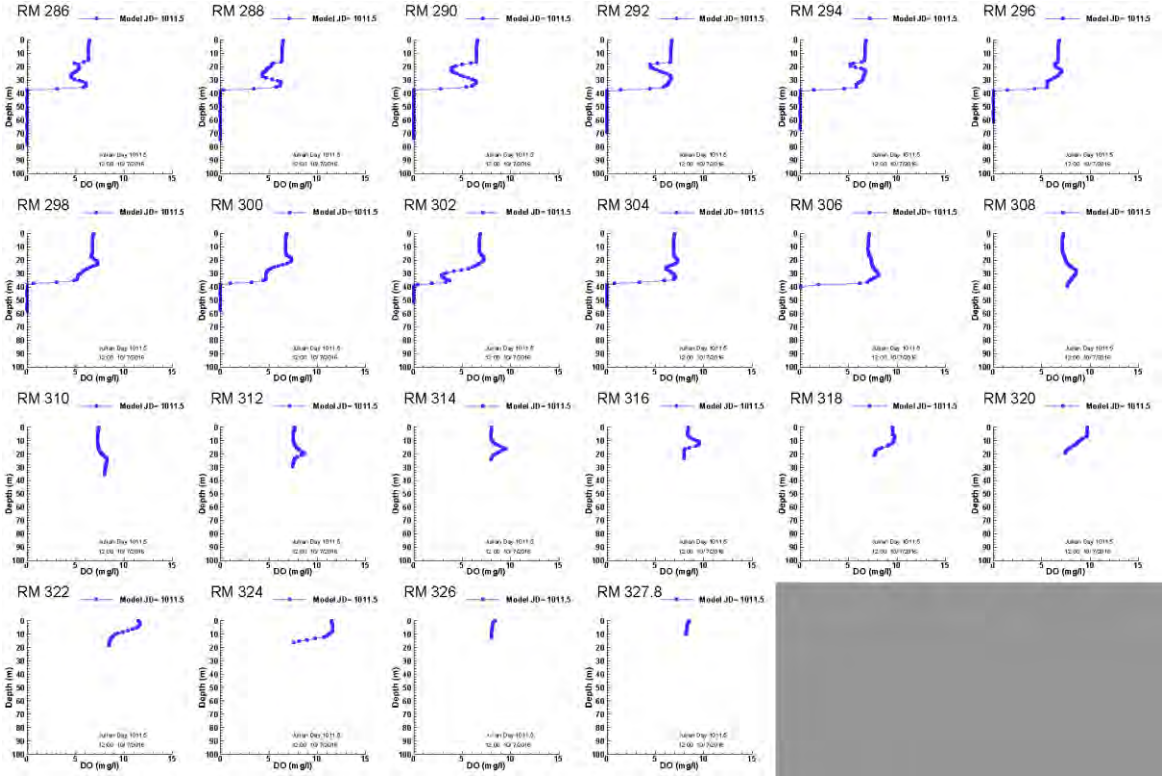


Figure 1158. Vertical profiles of DO compared with data for 10/ 7/2016.

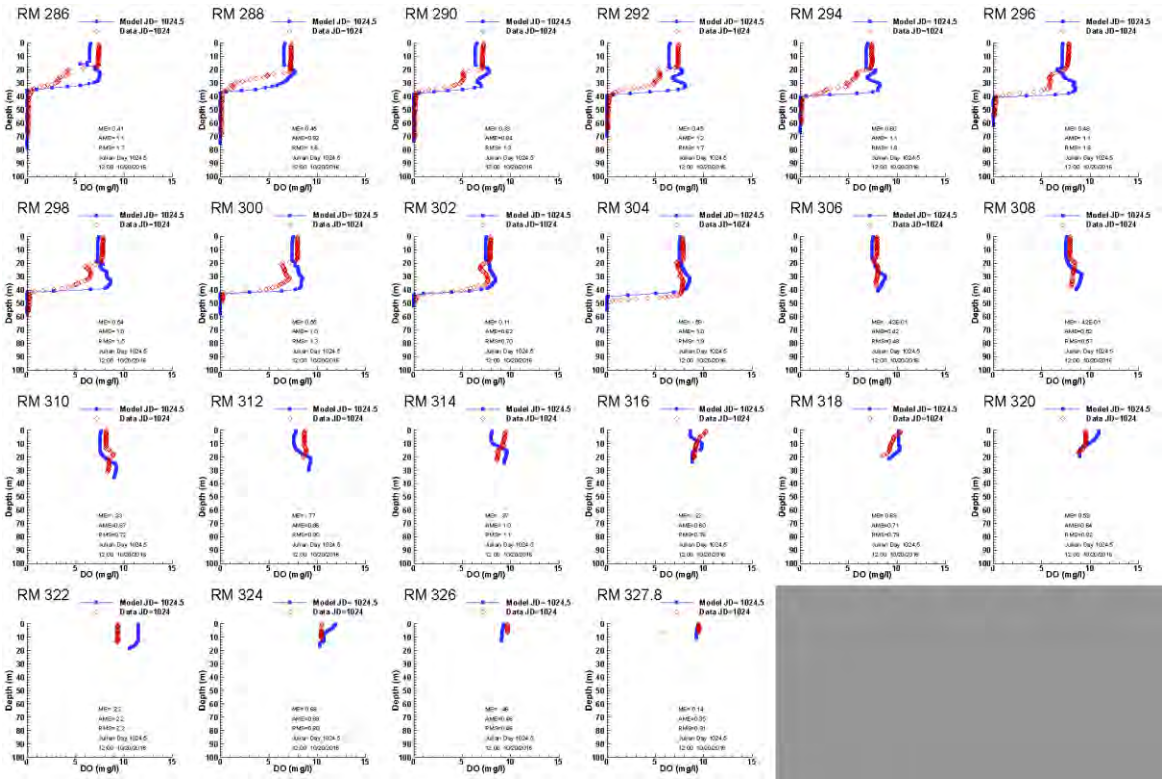


Figure 1159. Vertical profiles of DO compared with data for 10/20/2016.

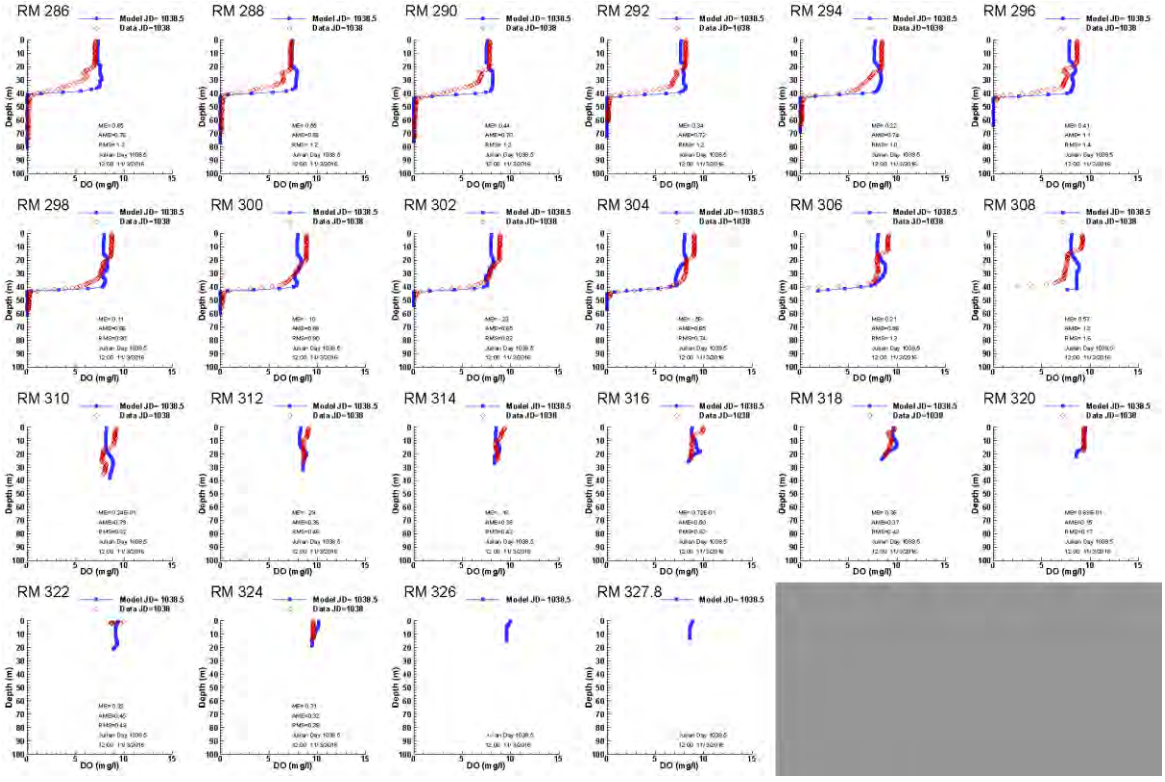


Figure 1160. Vertical profiles of DO compared with data for 11/ 3/2016.

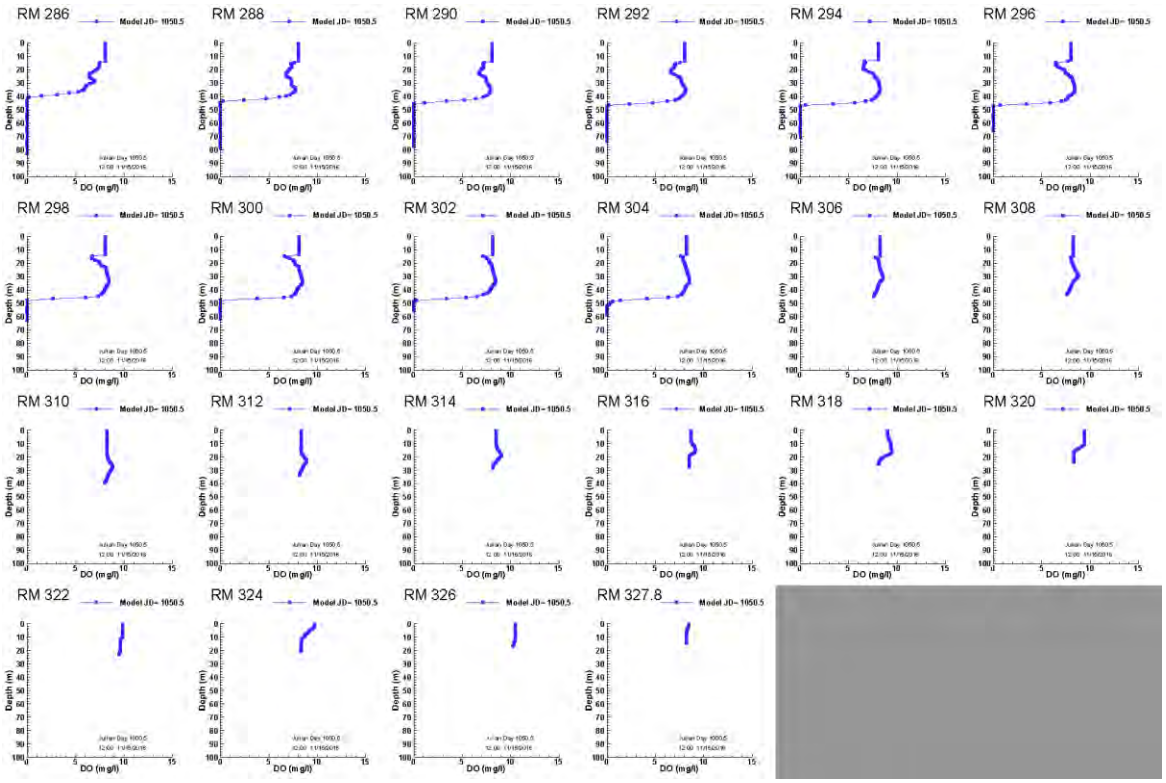


Figure 1161. Vertical profiles of DO compared with data for 11/15/2016.

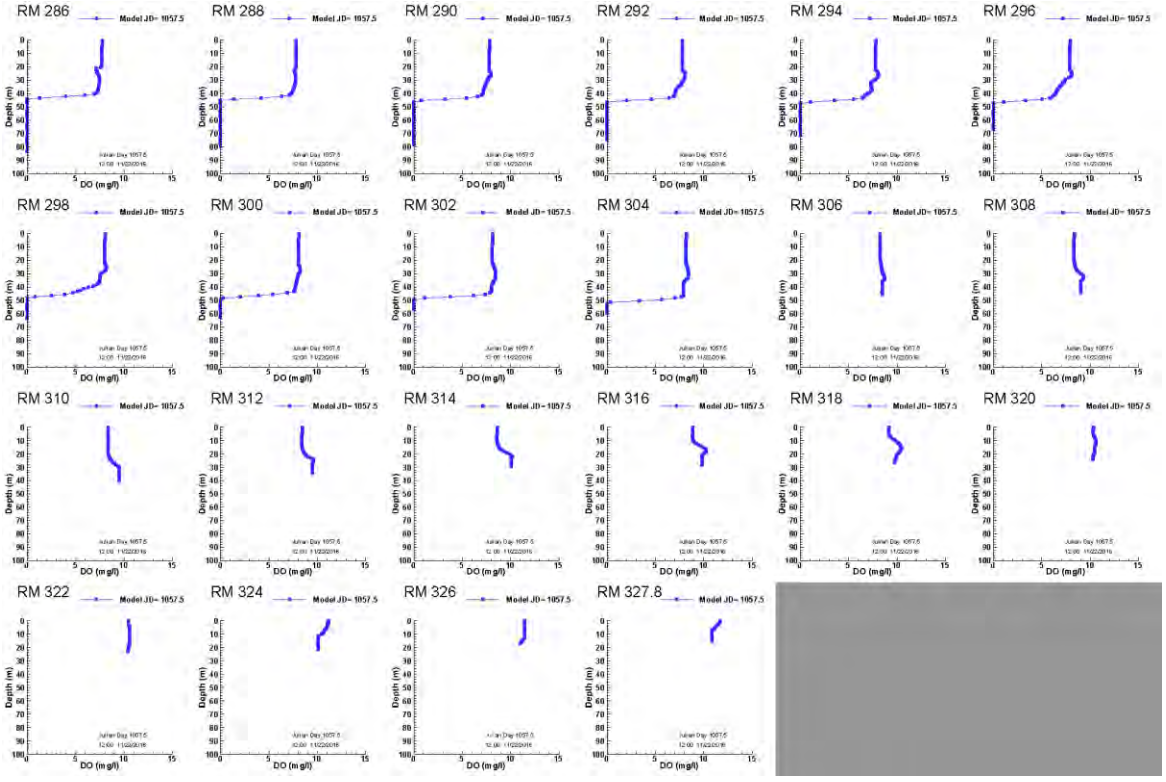


Figure 1162. Vertical profiles of DO compared with data for 11/22/2016.

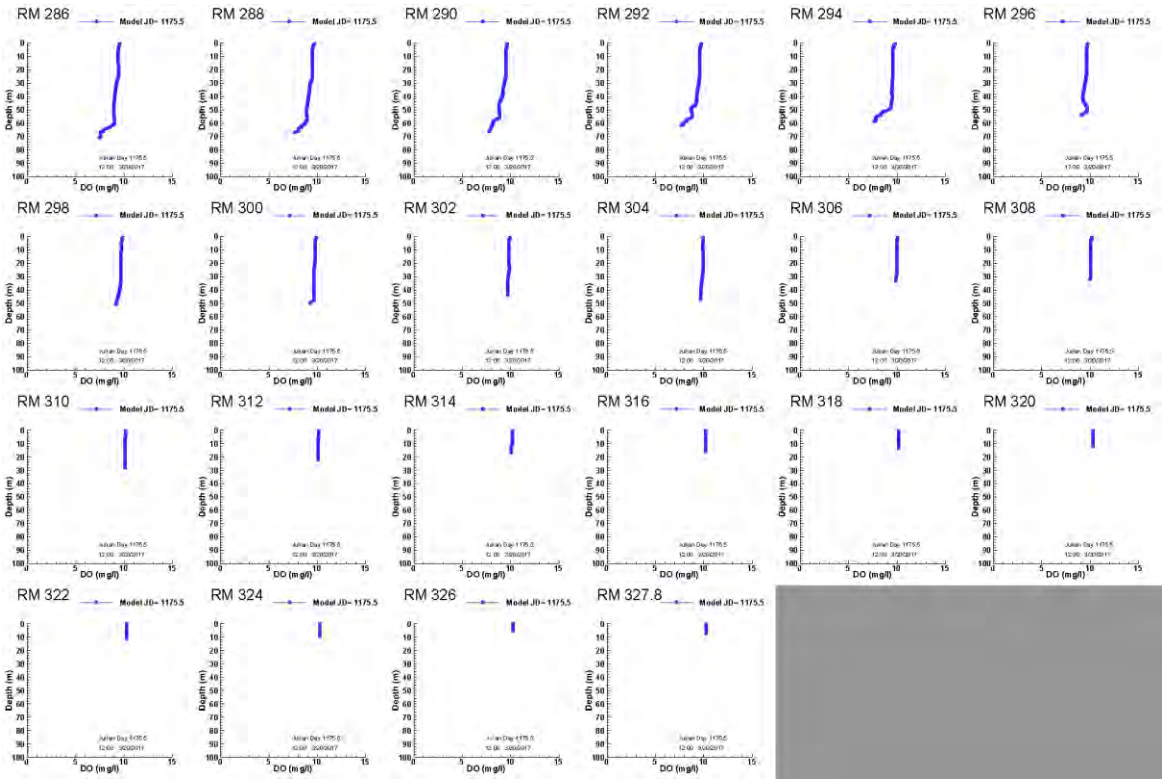


Figure 1163. Vertical profiles of DO compared with data for 3/20/2017.

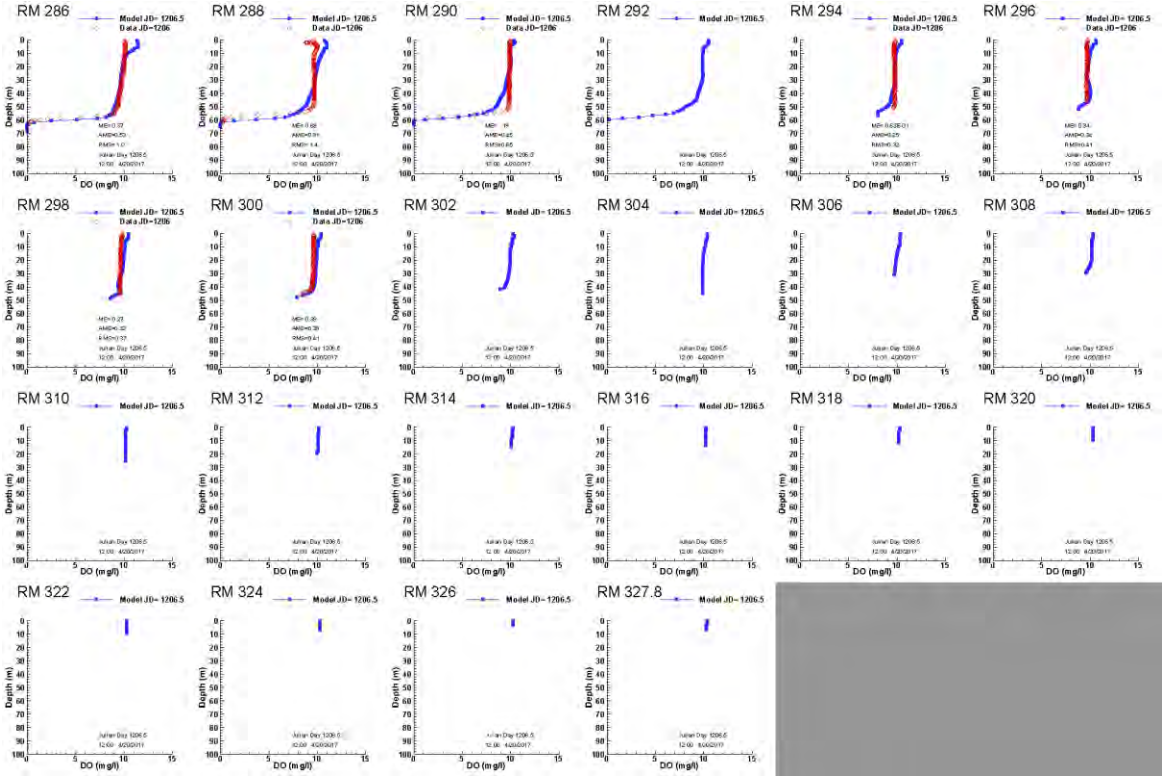


Figure 1164. Vertical profiles of DO compared with data for 4/20/2017.

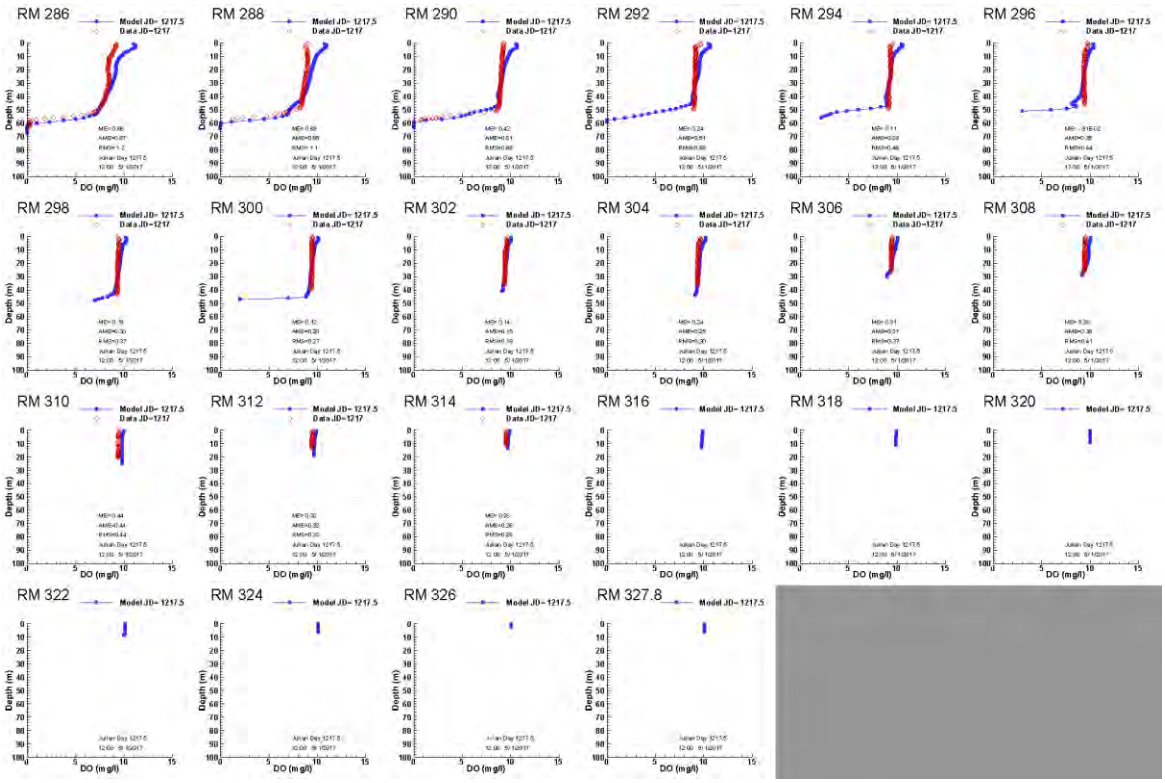


Figure 1165. Vertical profiles of DO compared with data for 5/ 1/2017.

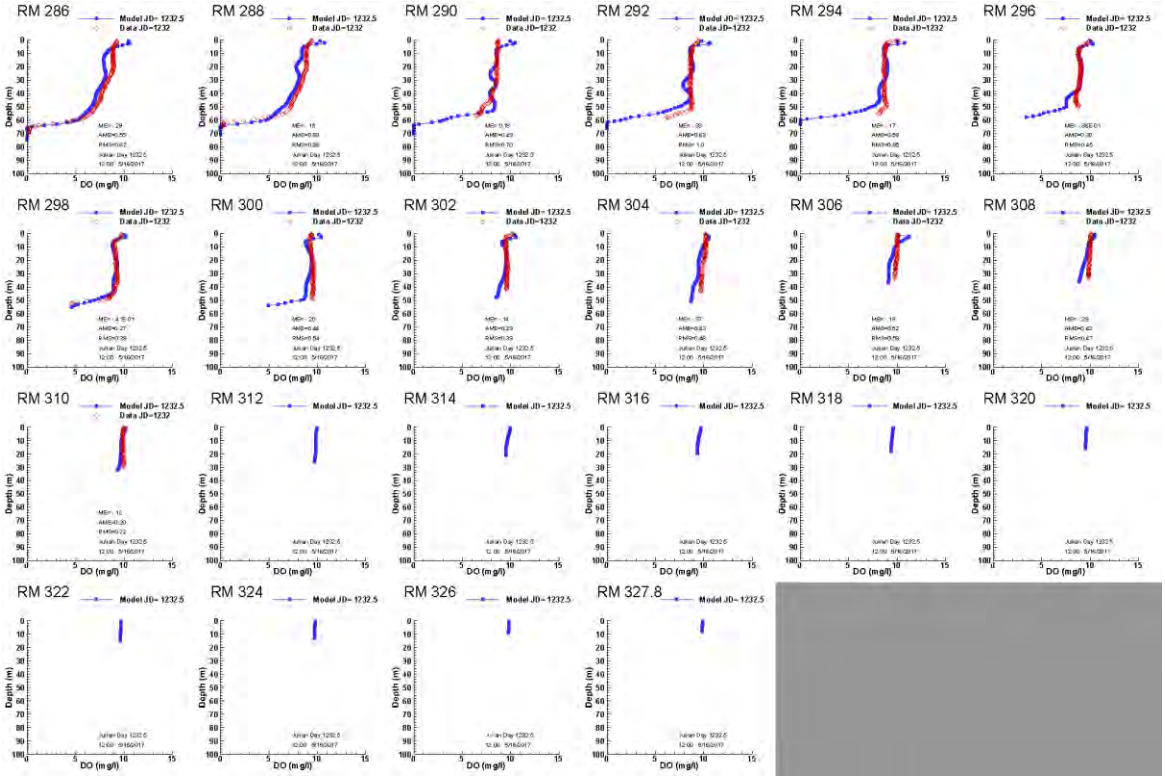


Figure 1166. Vertical profiles of DO compared with data for 5/16/2017.

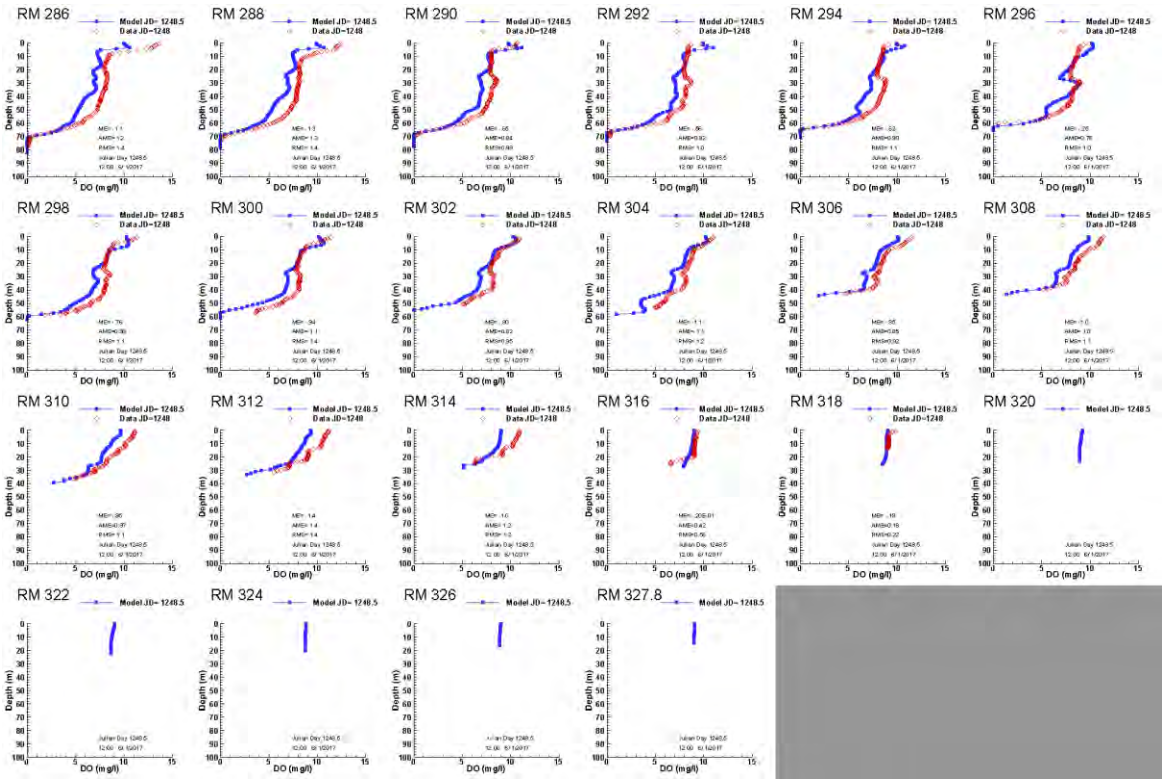


Figure 1167. Vertical profiles of DO compared with data for 6/ 1/2017.

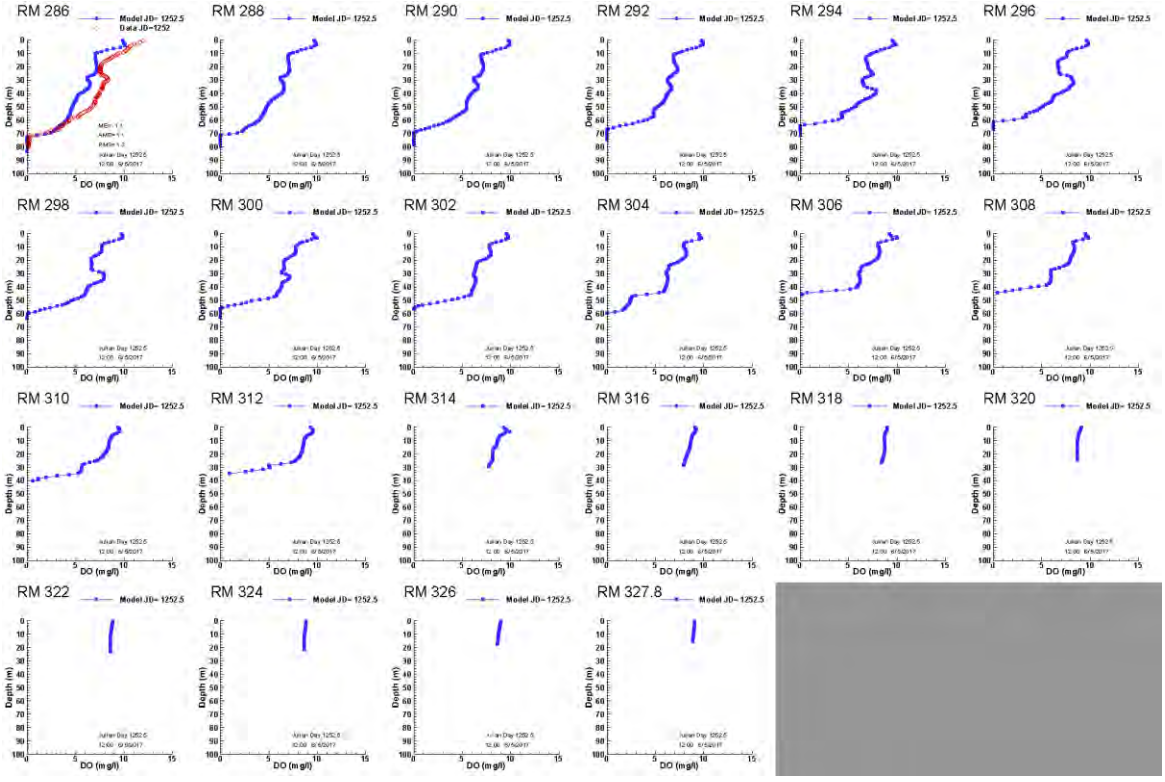


Figure 1168. Vertical profiles of DO compared with data for 6/ 5/2017.

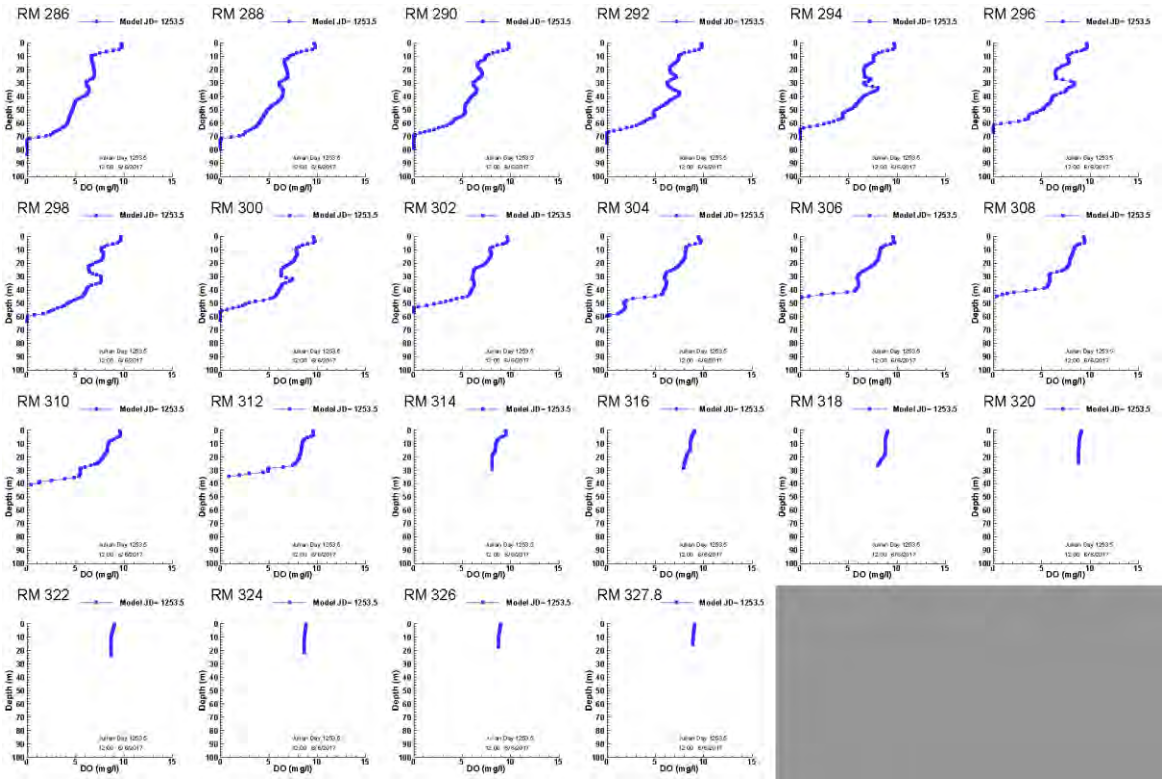


Figure 1169. Vertical profiles of DO compared with data for 6/ 6/2017.

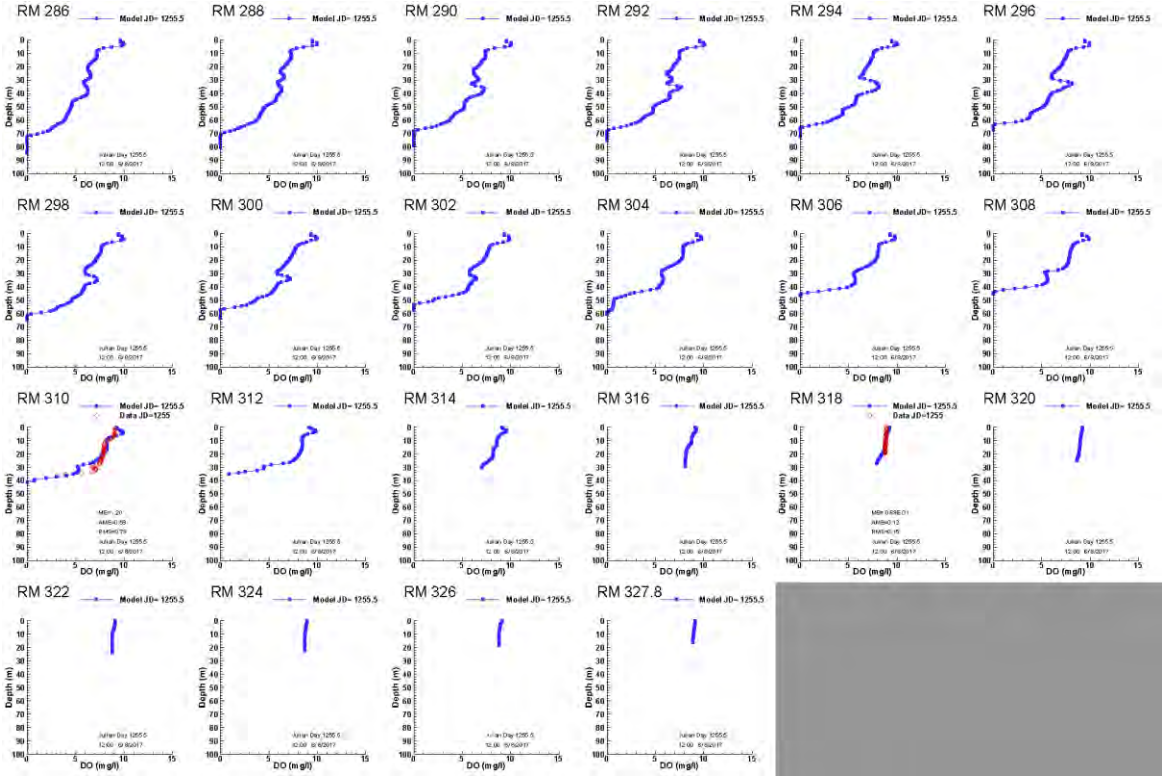


Figure 1170. Vertical profiles of DO compared with data for 6/ 8/2017.

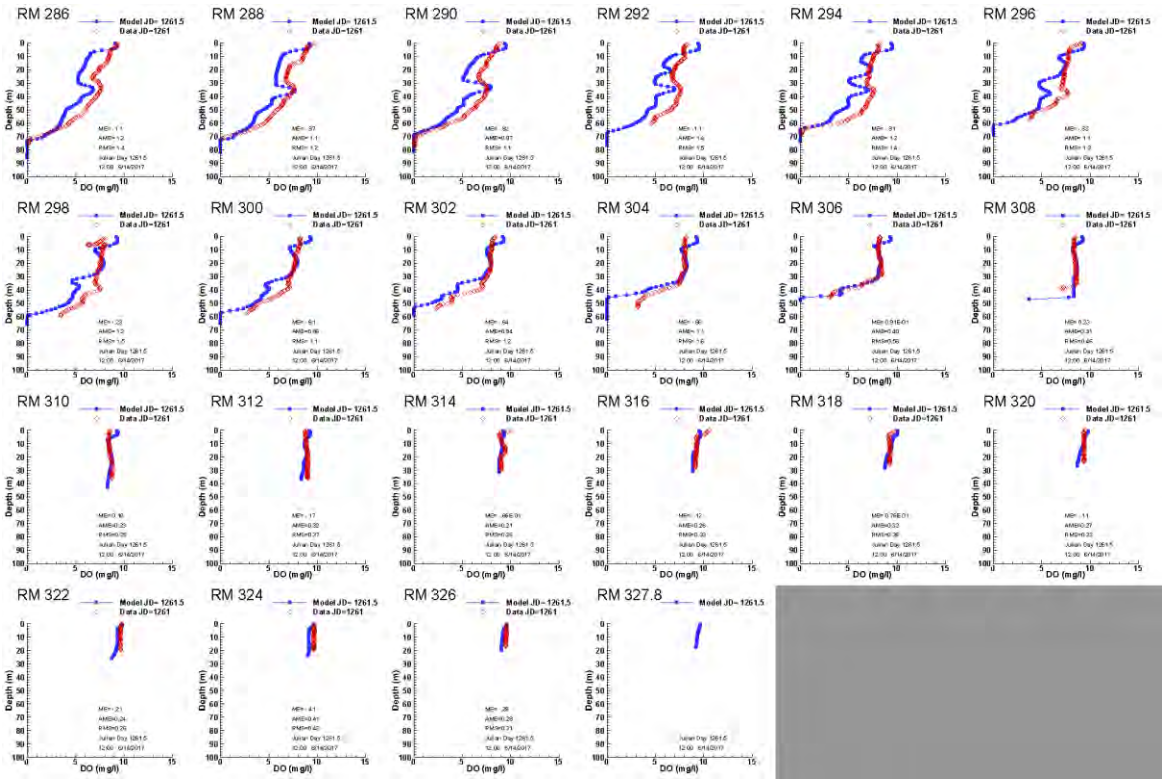


Figure 1171. Vertical profiles of DO compared with data for 6/14/2017.

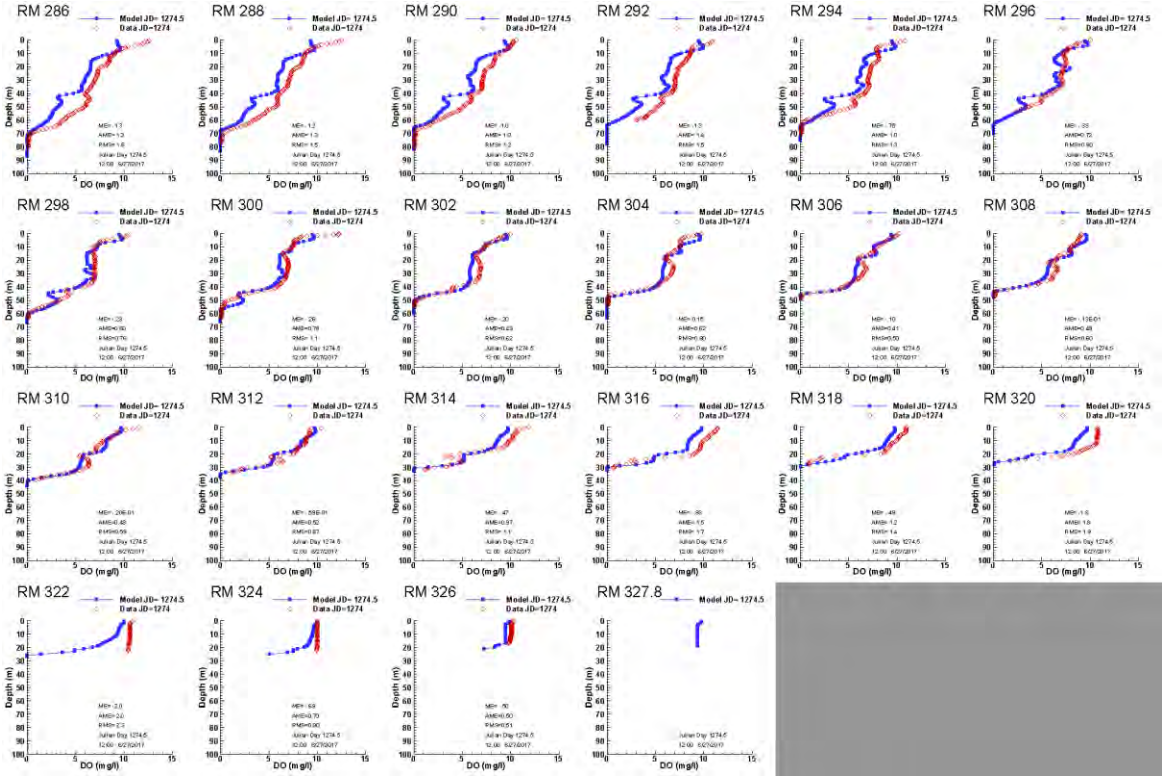


Figure 1172. Vertical profiles of DO compared with data for 6/27/2017.

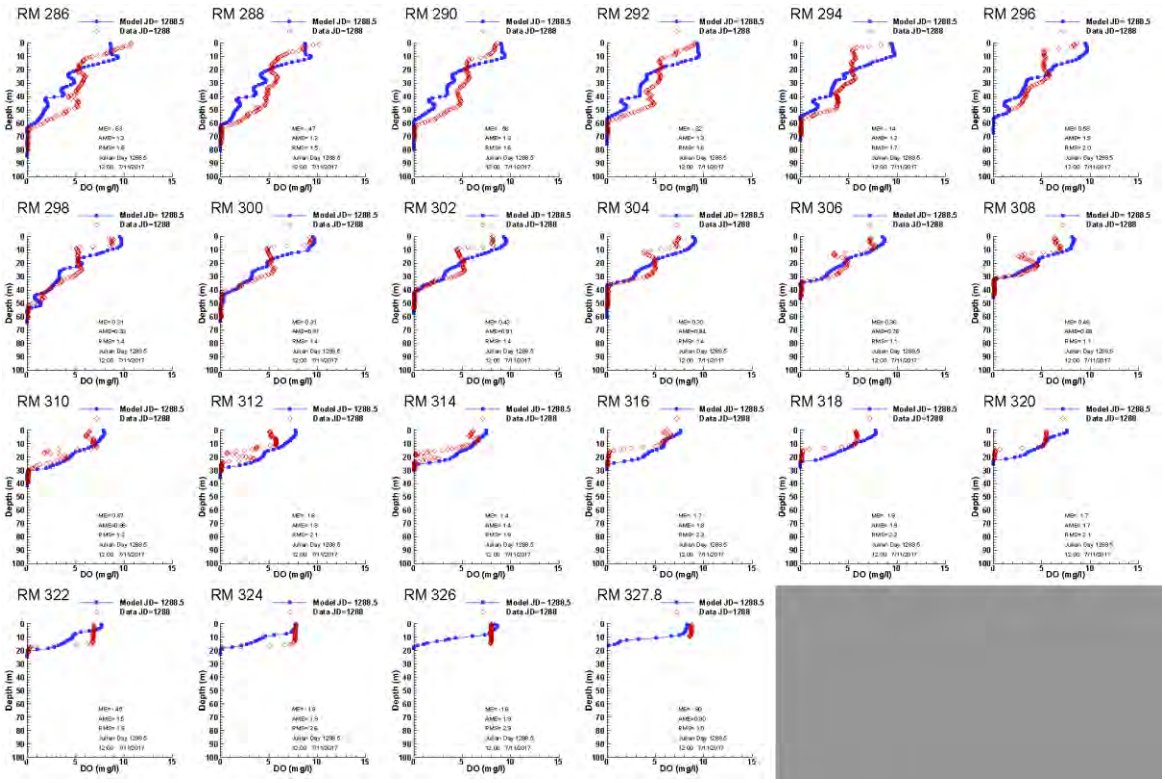


Figure 1173. Vertical profiles of DO compared with data for 7/11/2017.

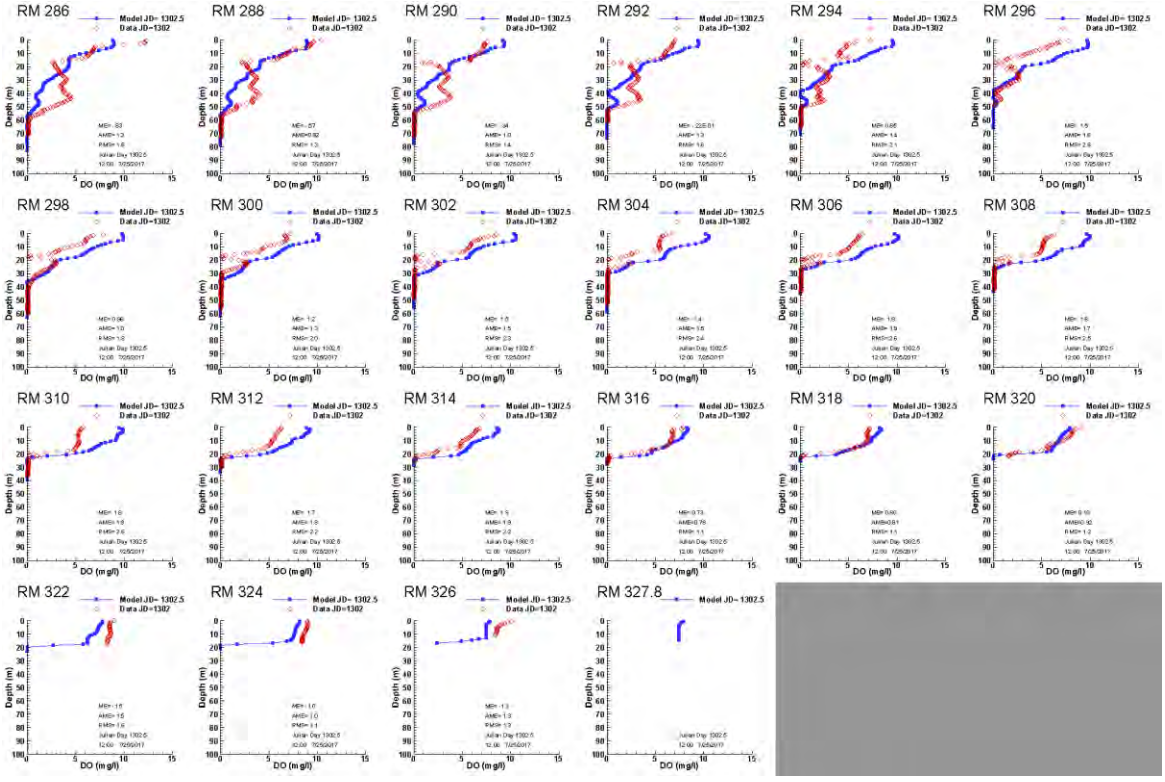


Figure 1174. Vertical profiles of DO compared with data for 7/25/2017.

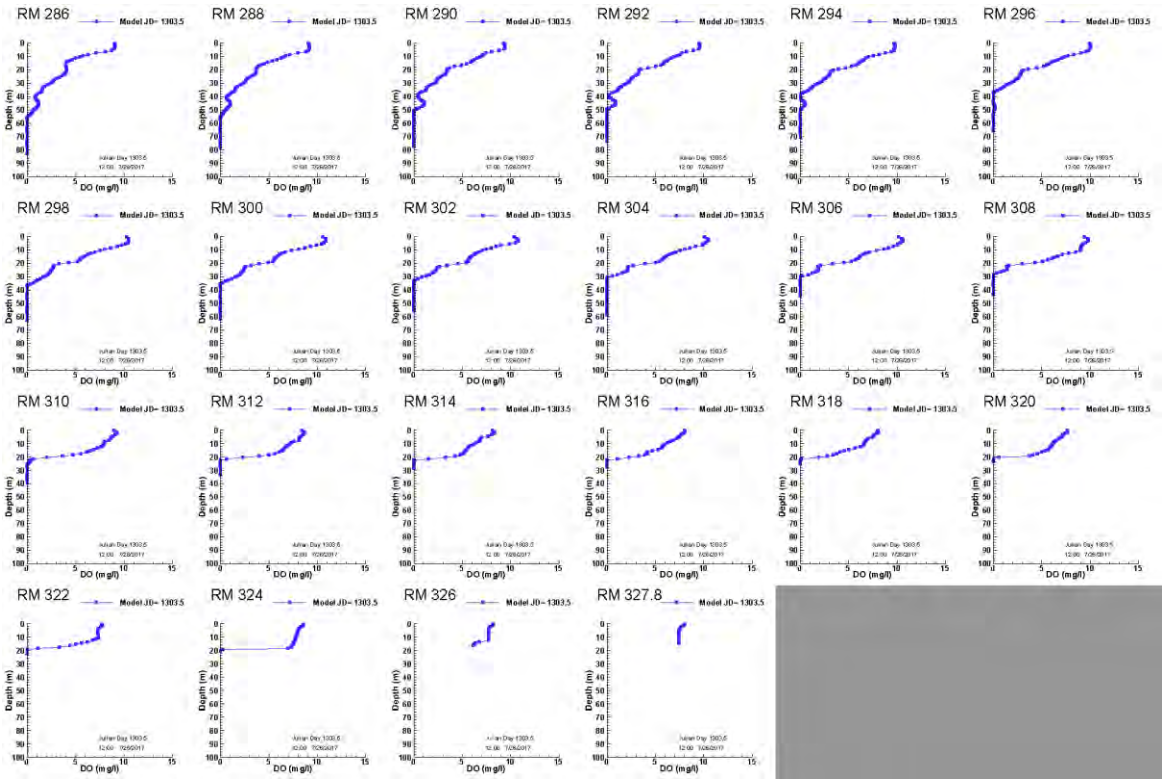


Figure 1175. Vertical profiles of DO compared with data for 7/26/2017.

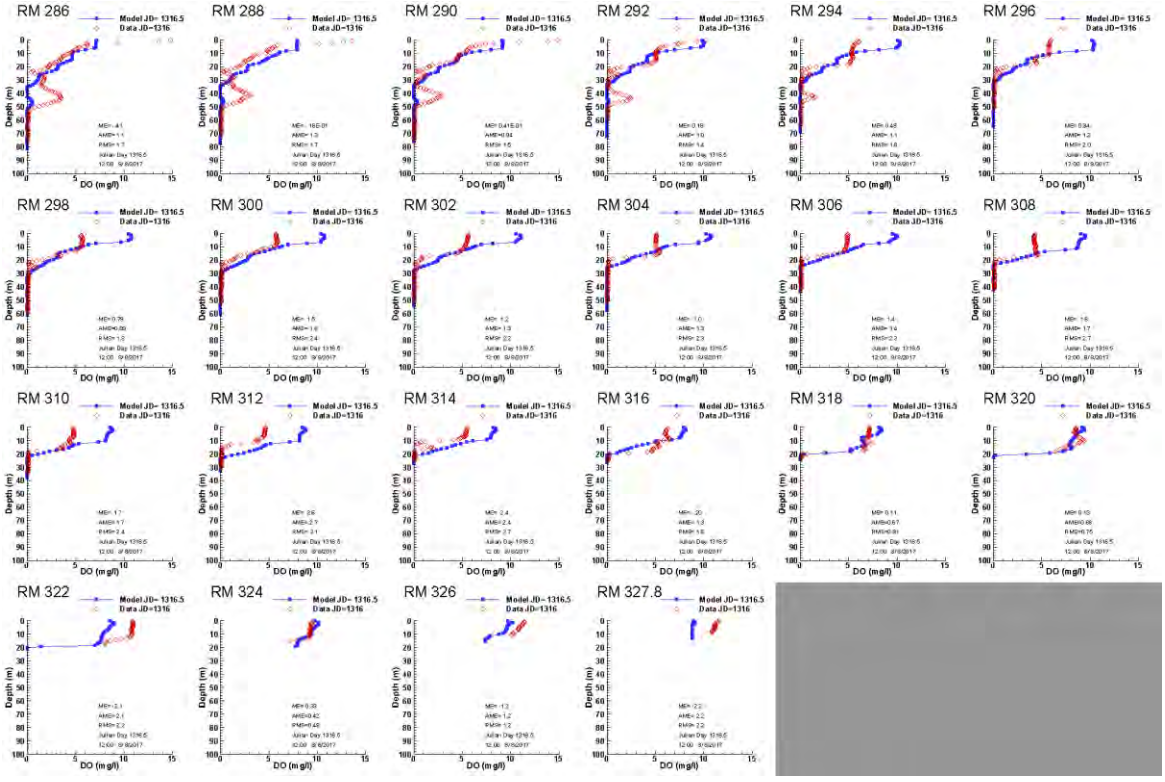


Figure 1176. Vertical profiles of DO compared with data for 8/ 8/2017.

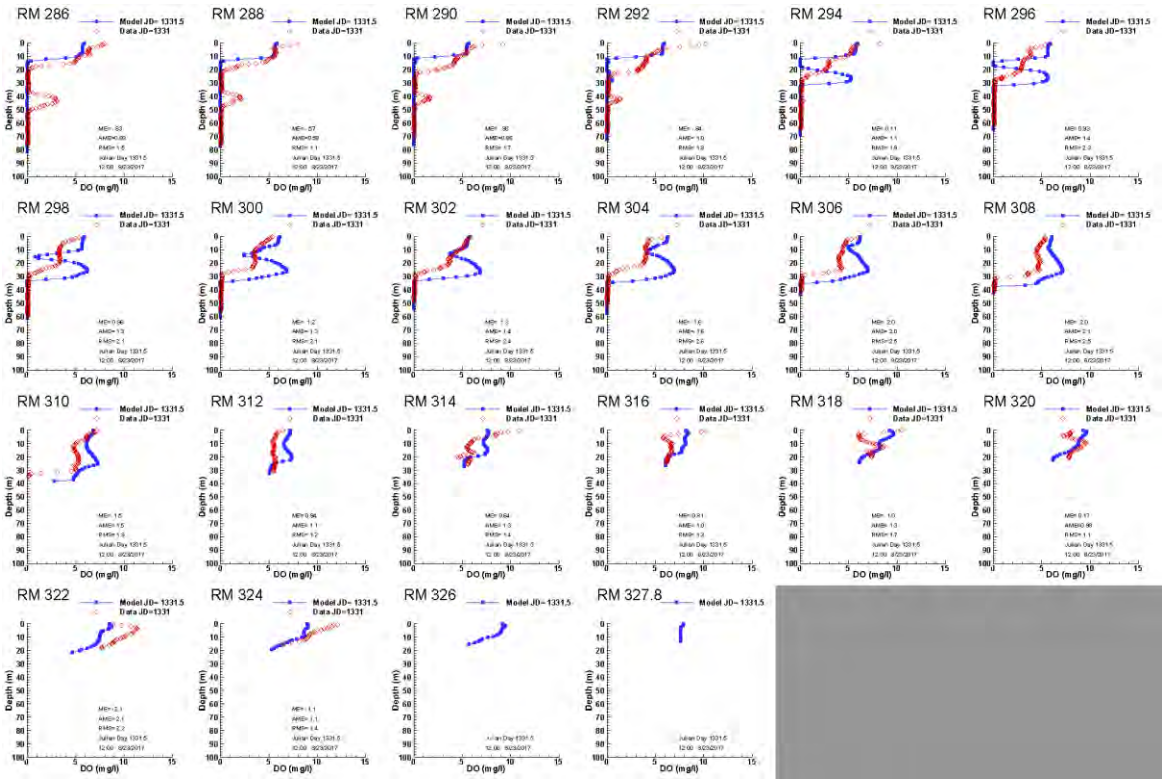


Figure 1177. Vertical profiles of DO compared with data for 8/23/2017.

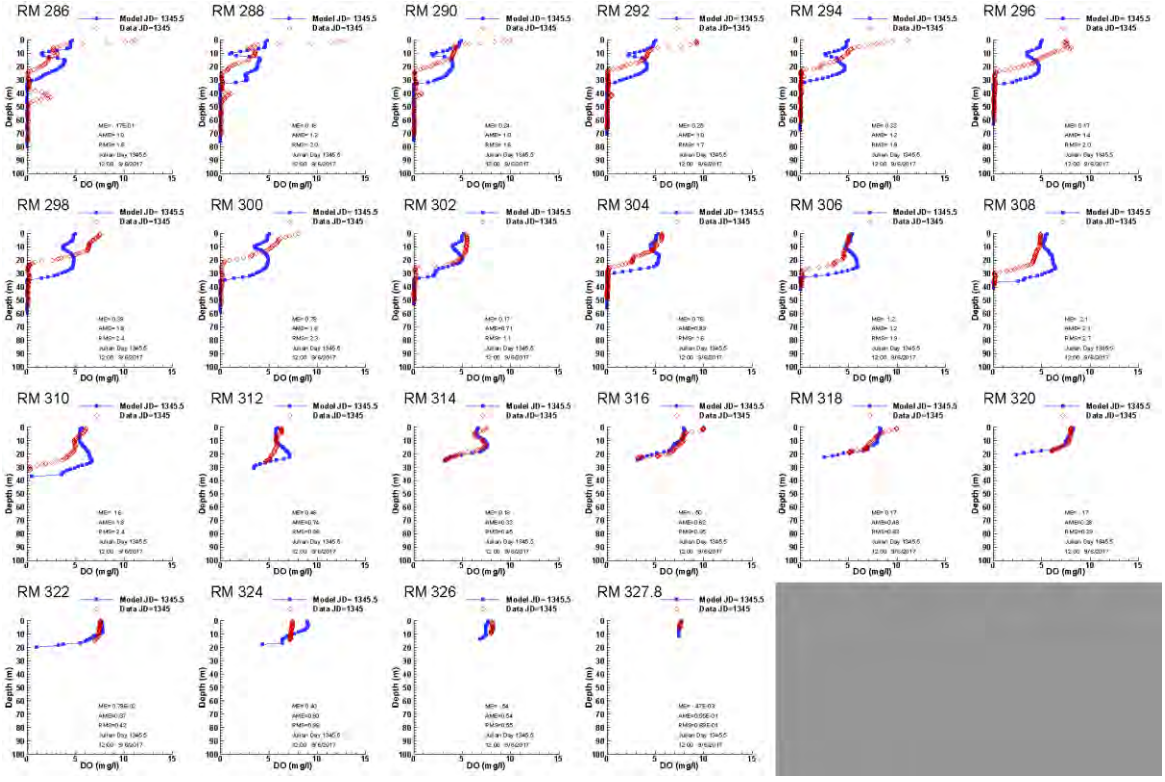


Figure 1178. Vertical profiles of DO compared with data for 9/ 6/2017.

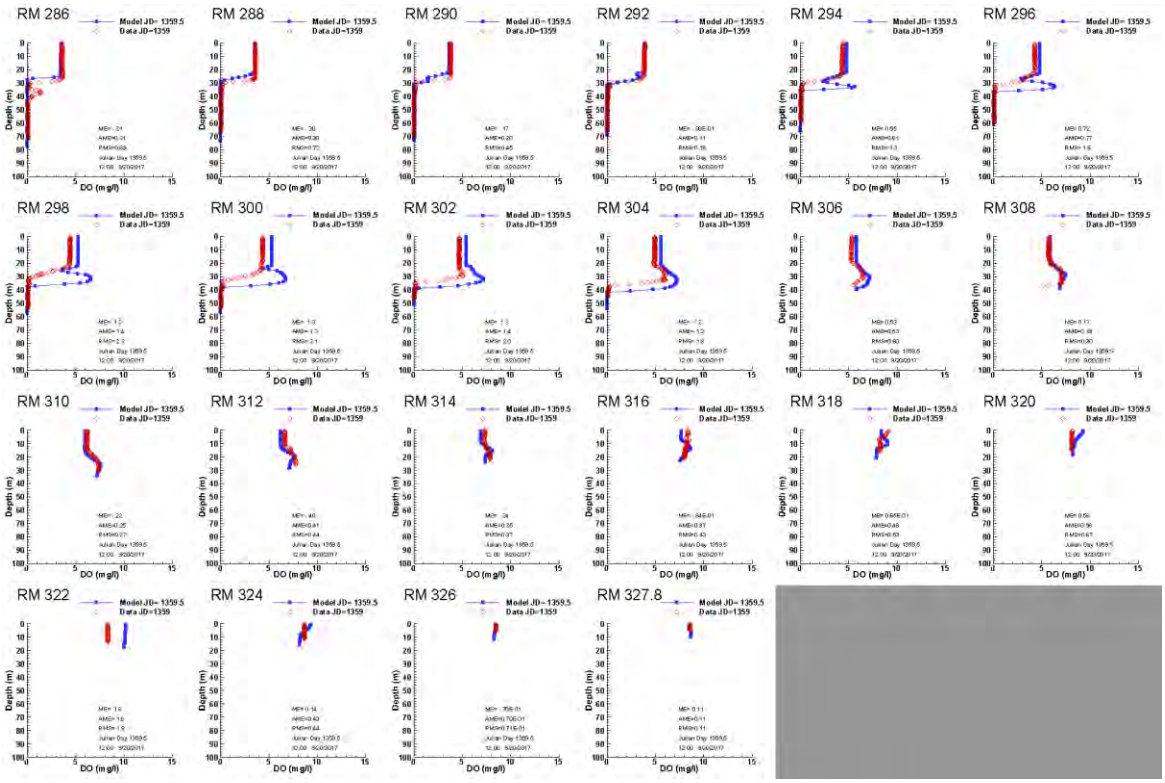


Figure 1179. Vertical profiles of DO compared with data for 9/20/2017.

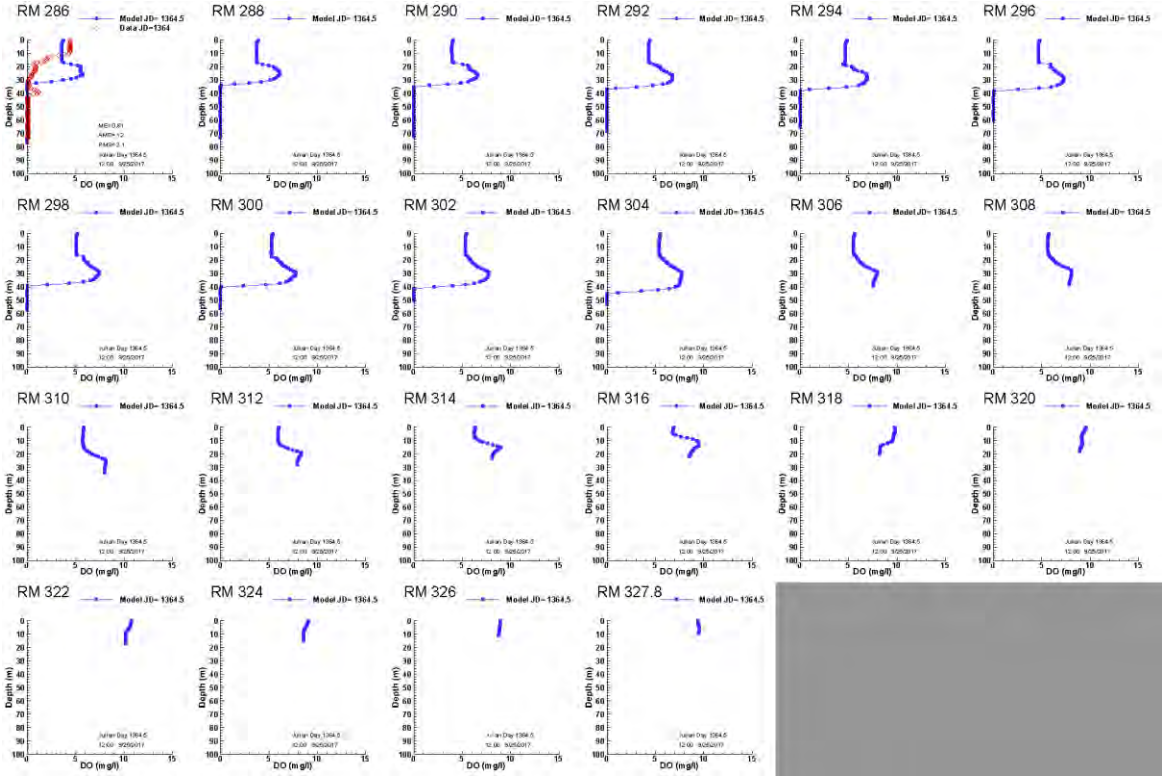


Figure 1180. Vertical profiles of DO compared with data for 9/25/2017.

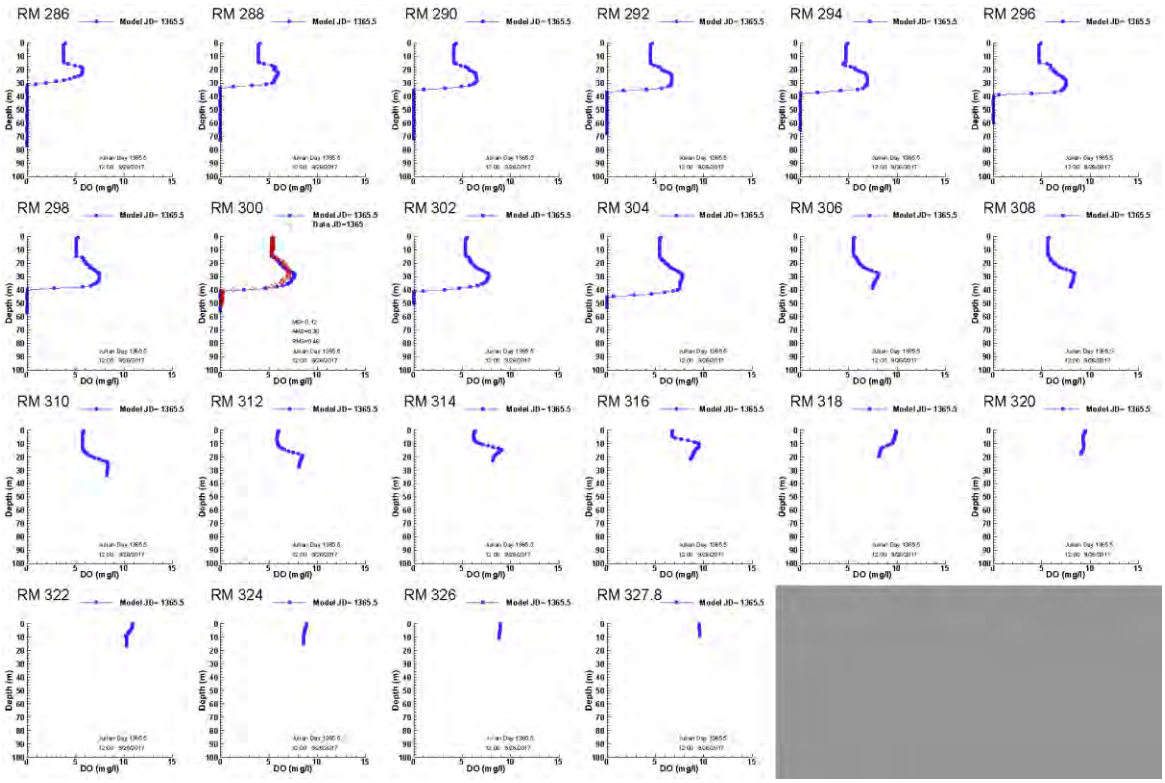


Figure 1181. Vertical profiles of DO compared with data for 9/26/2017.

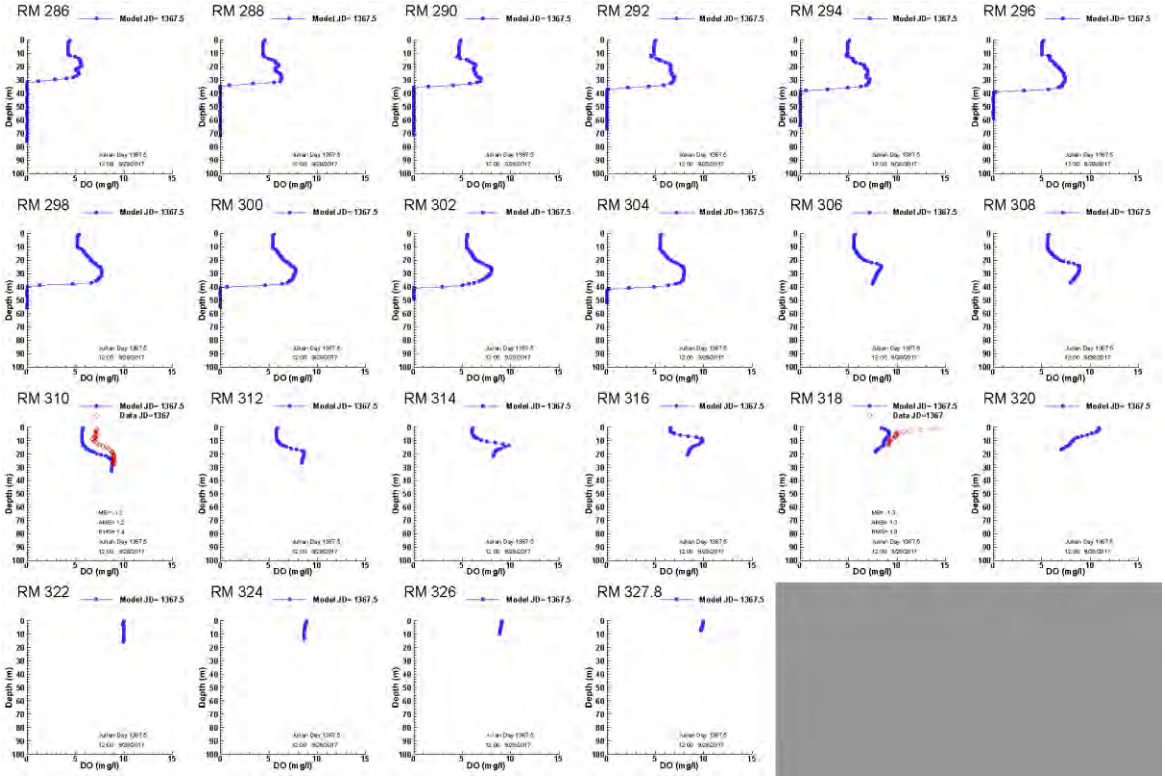


Figure 1182. Vertical profiles of DO compared with data for 9/28/2017.

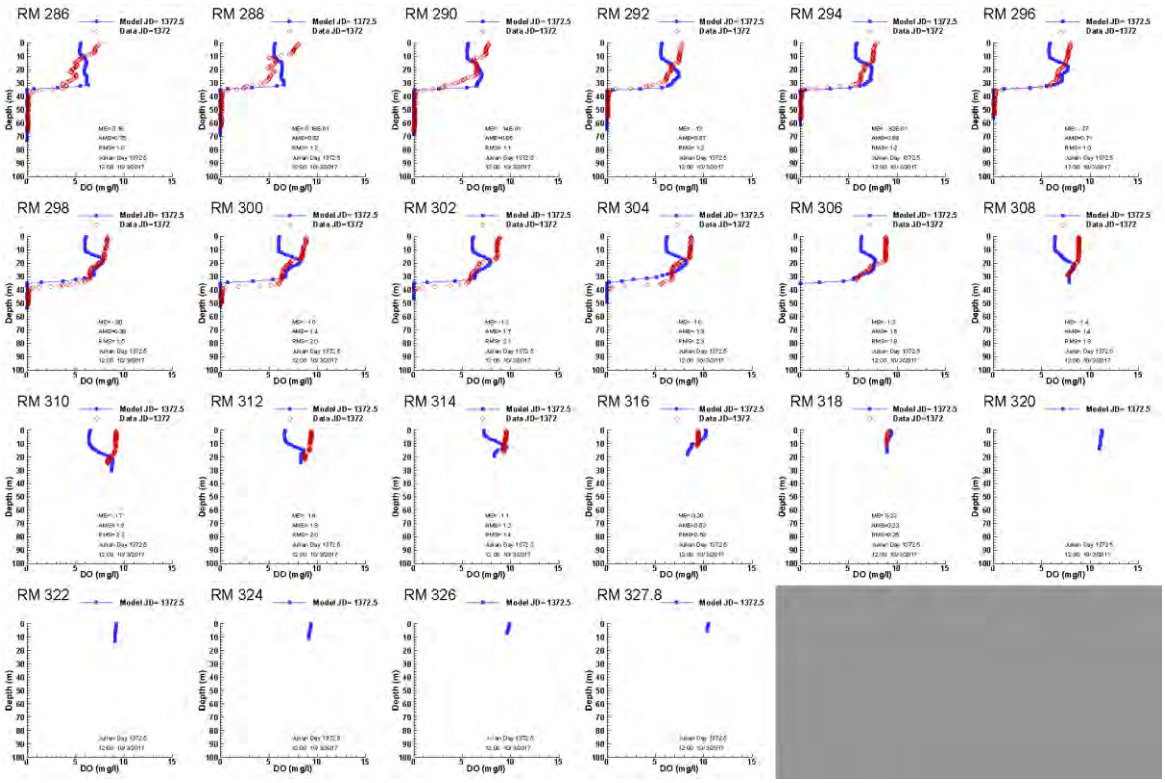


Figure 1183. Vertical profiles of DO compared with data for 10/ 3/2017.

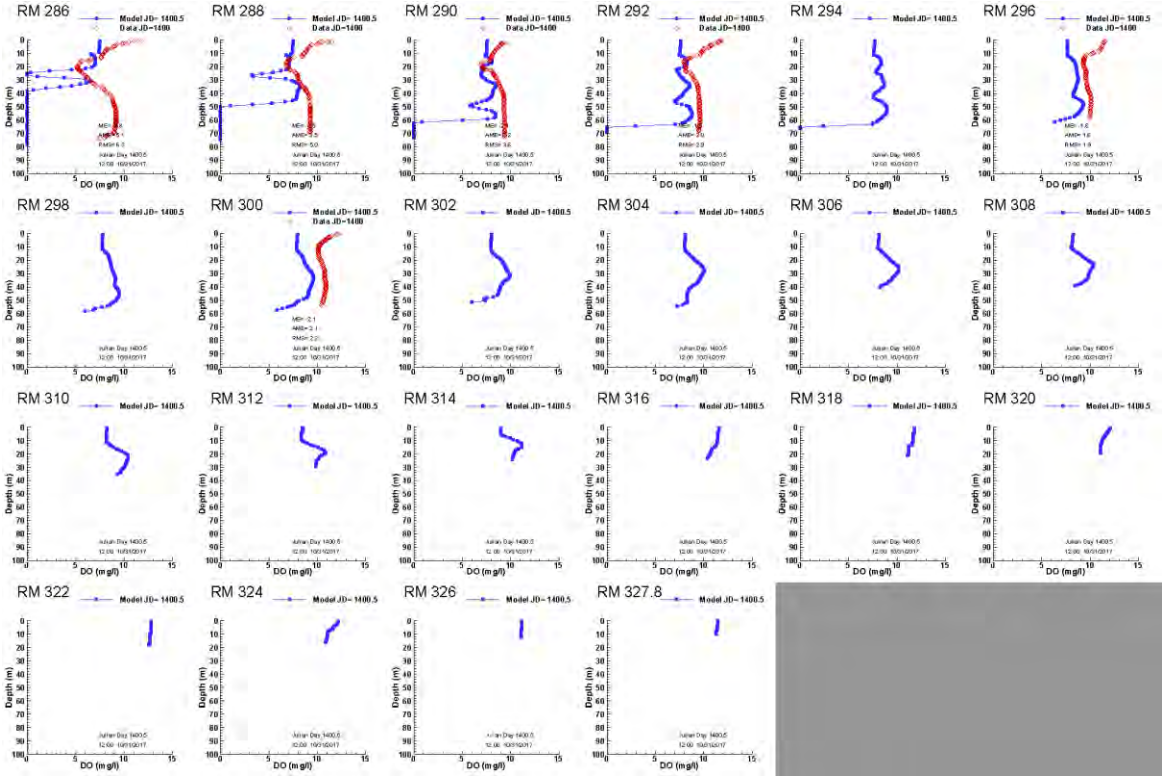


Figure 1184. Vertical profiles of DO compared with data for 10/31/2017.

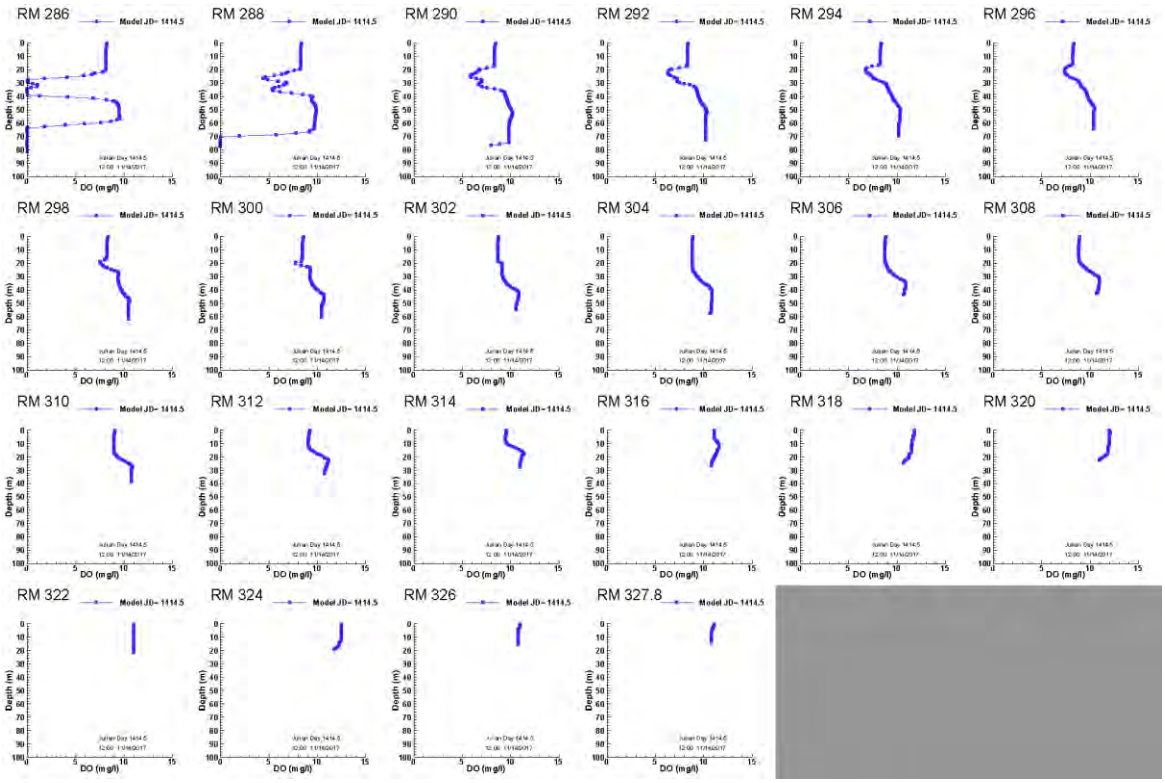


Figure 1185. Vertical profiles of DO compared with data for 11/14/2017.

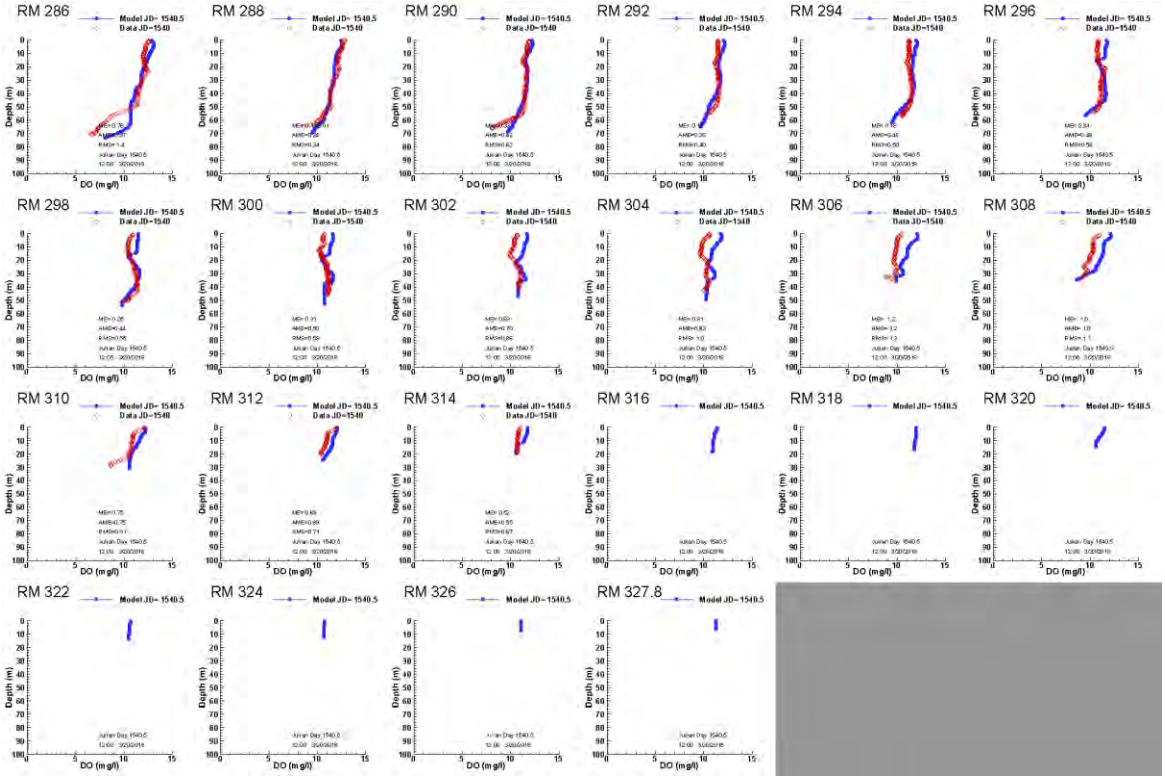


Figure 1186. Vertical profiles of DO compared with data for 3/20/2018.

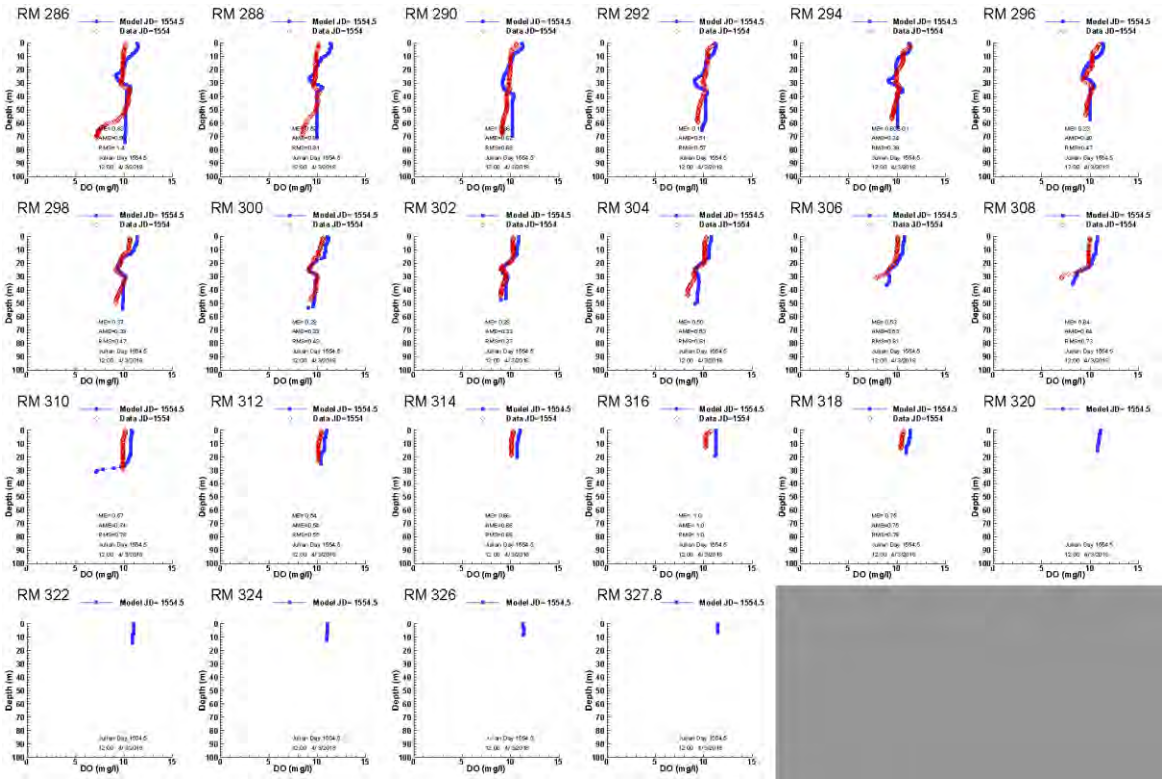


Figure 1187. Vertical profiles of DO compared with data for 4/ 3/2018.

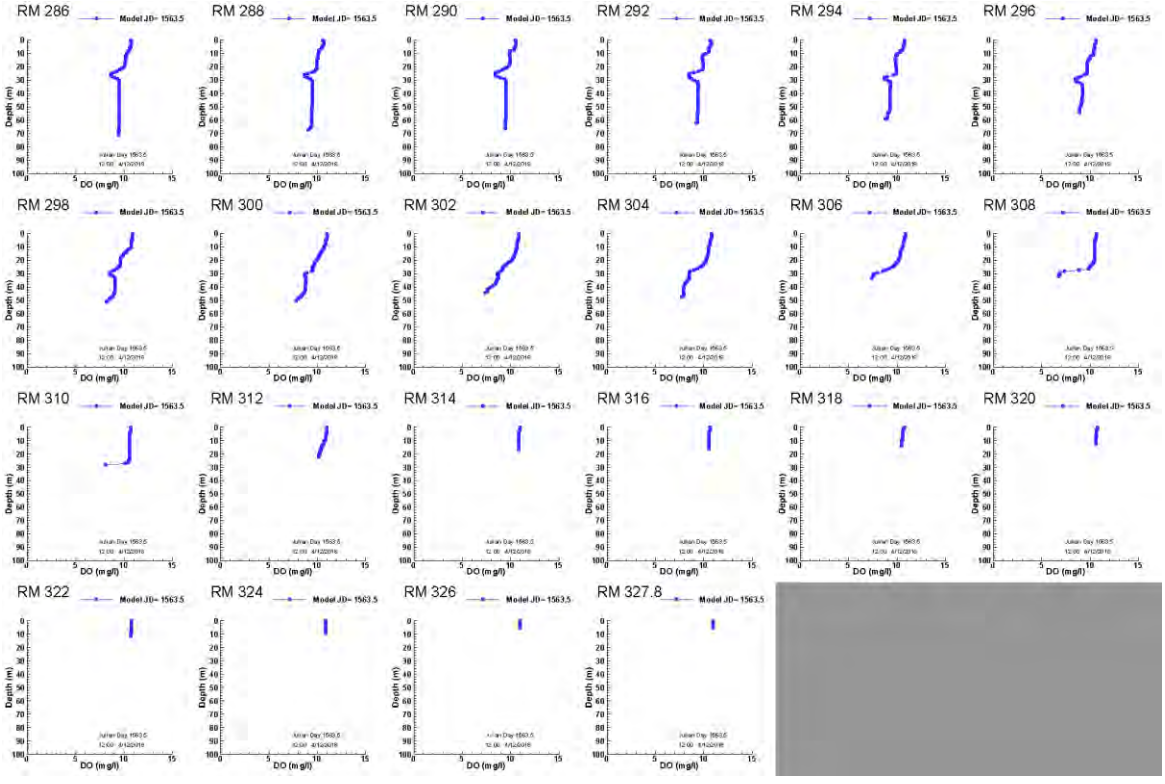


Figure 1188. Vertical profiles of DO compared with data for 4/12/2018.

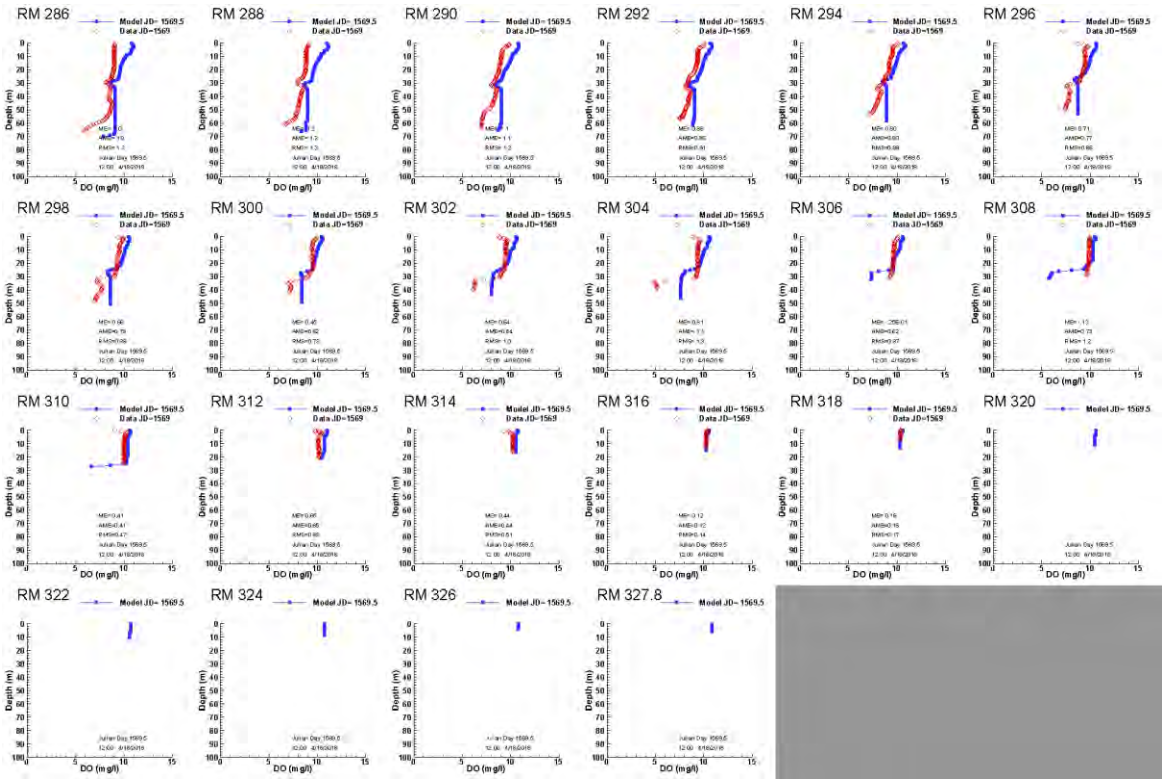


Figure 1189. Vertical profiles of DO compared with data for 4/18/2018.

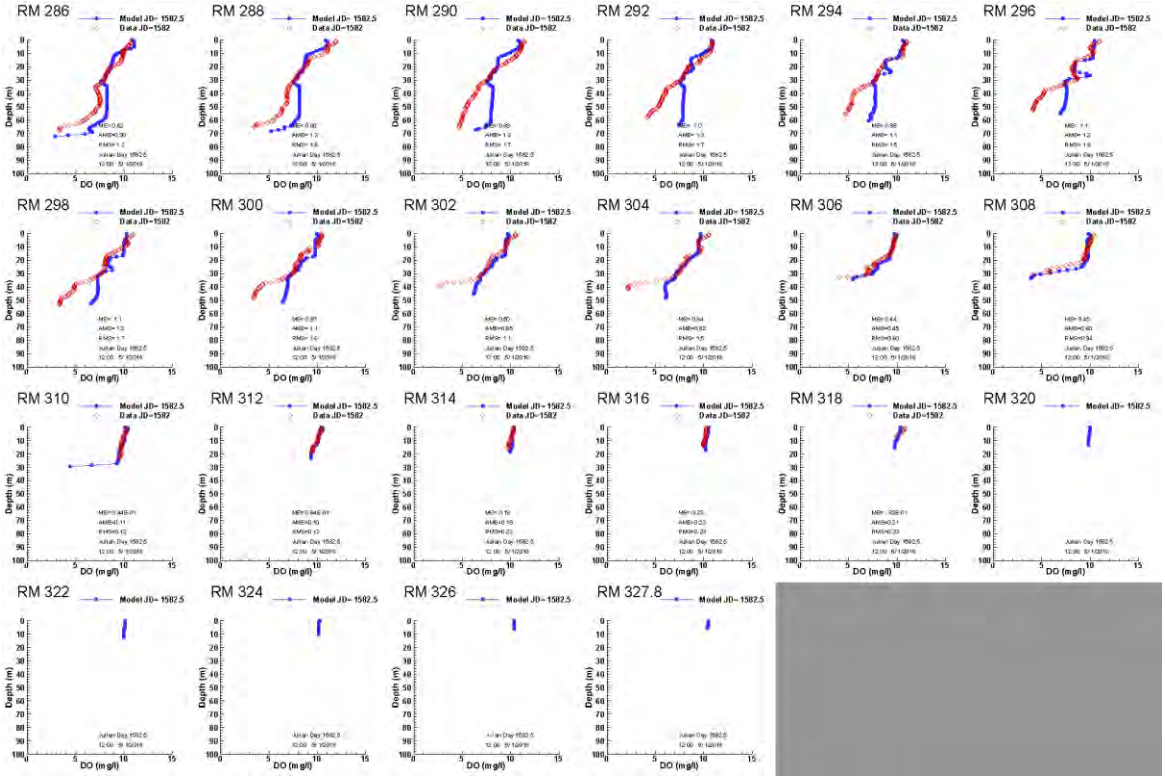


Figure 1190. Vertical profiles of DO compared with data for 5/ 1/2018.

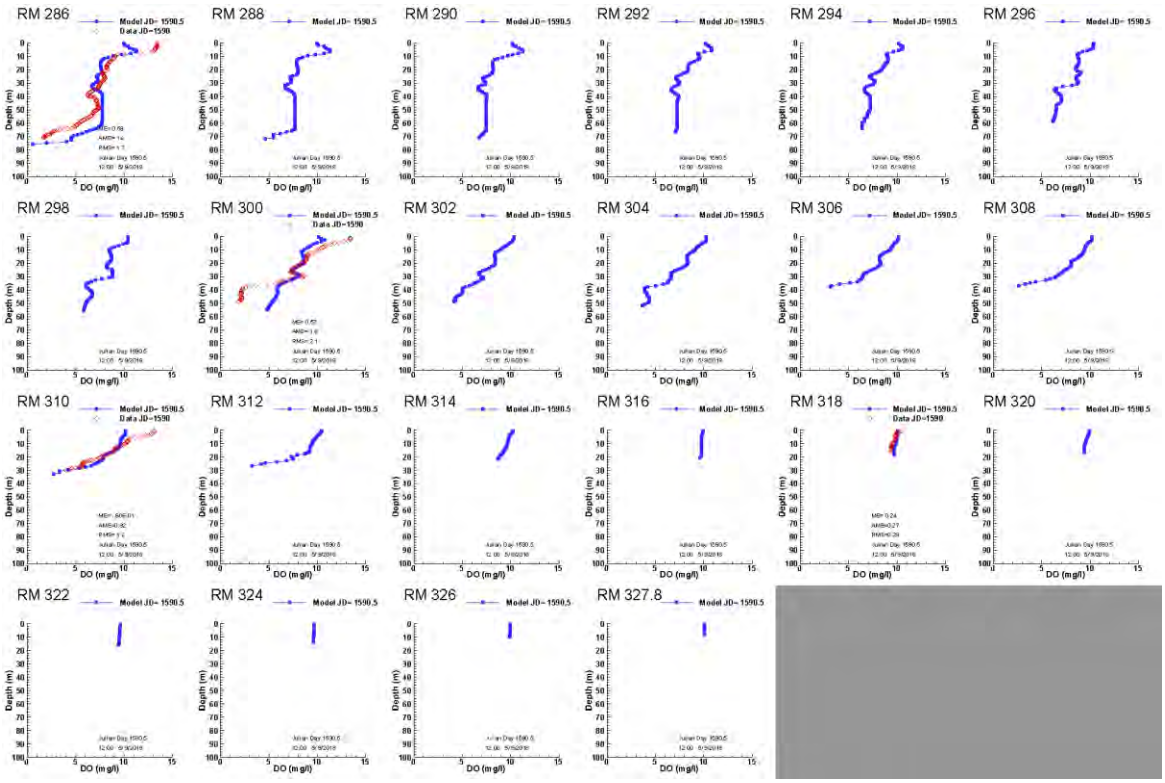


Figure 1191. Vertical profiles of DO compared with data for 5/ 9/2018.

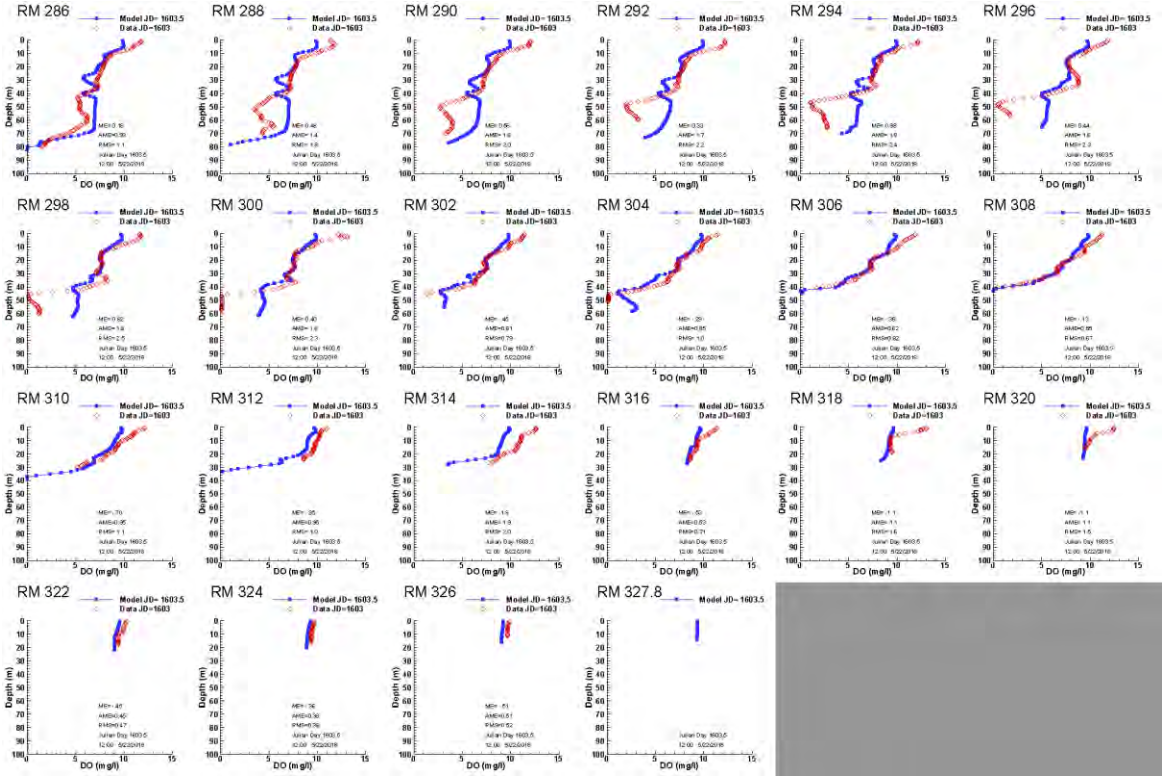


Figure 1192. Vertical profiles of DO compared with data for 5/22/2018.

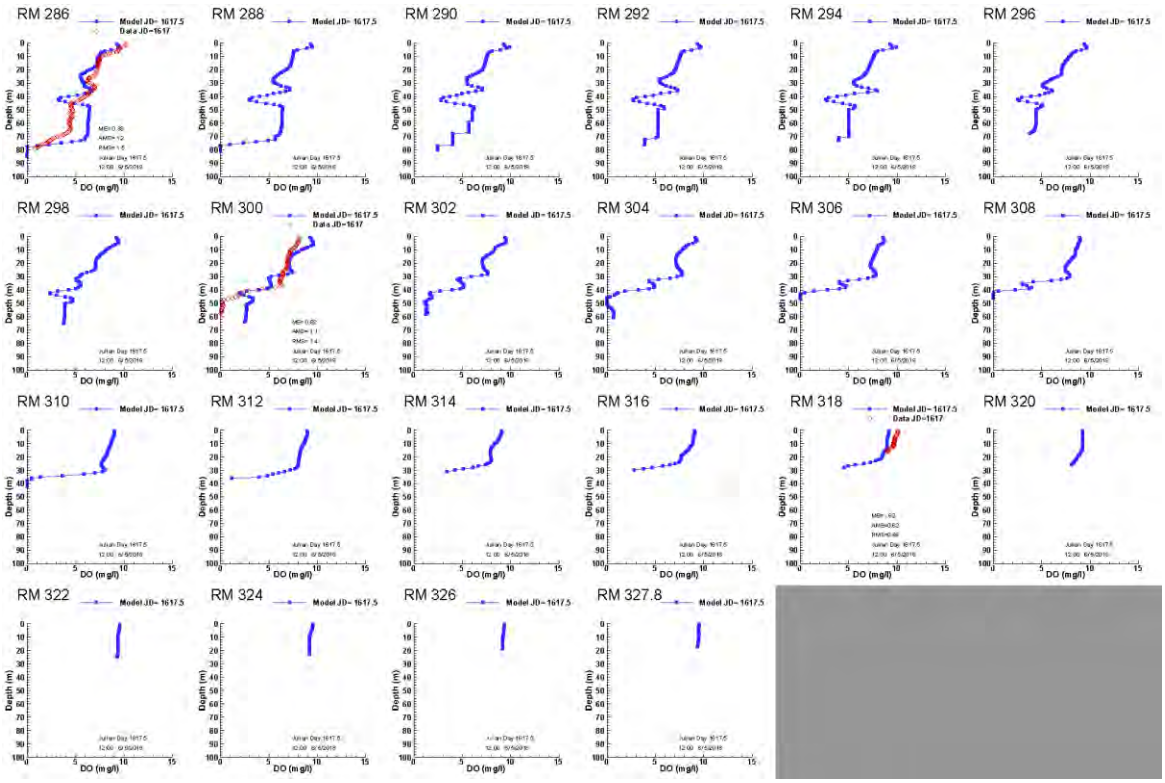


Figure 1193. Vertical profiles of DO compared with data for 6/ 5/2018.

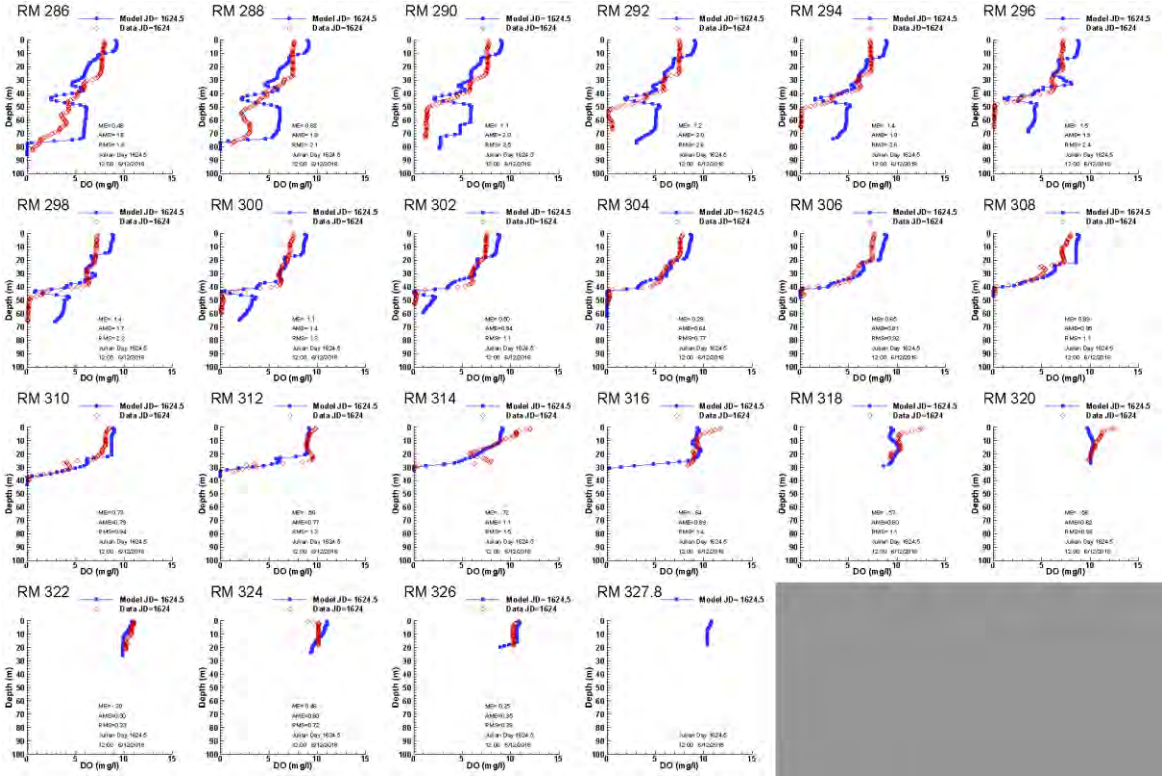


Figure 1194. Vertical profiles of DO compared with data for 6/12/2018.

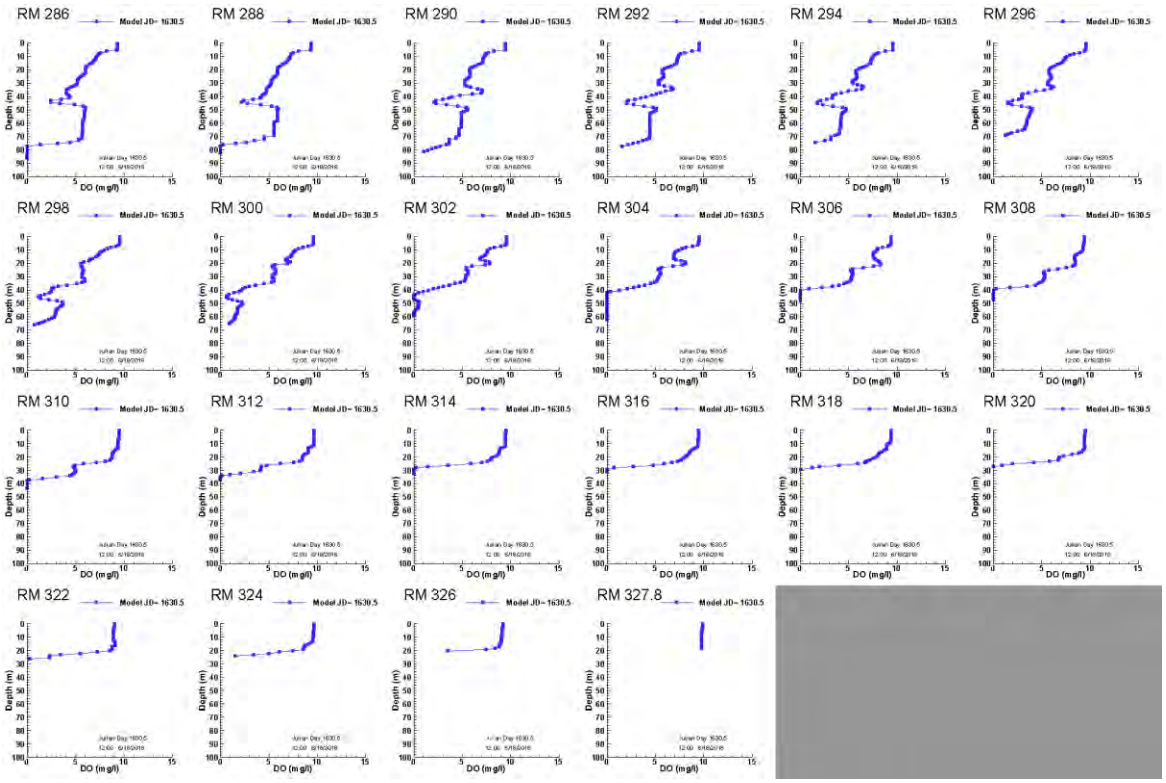


Figure 1195. Vertical profiles of DO compared with data for 6/18/2018.

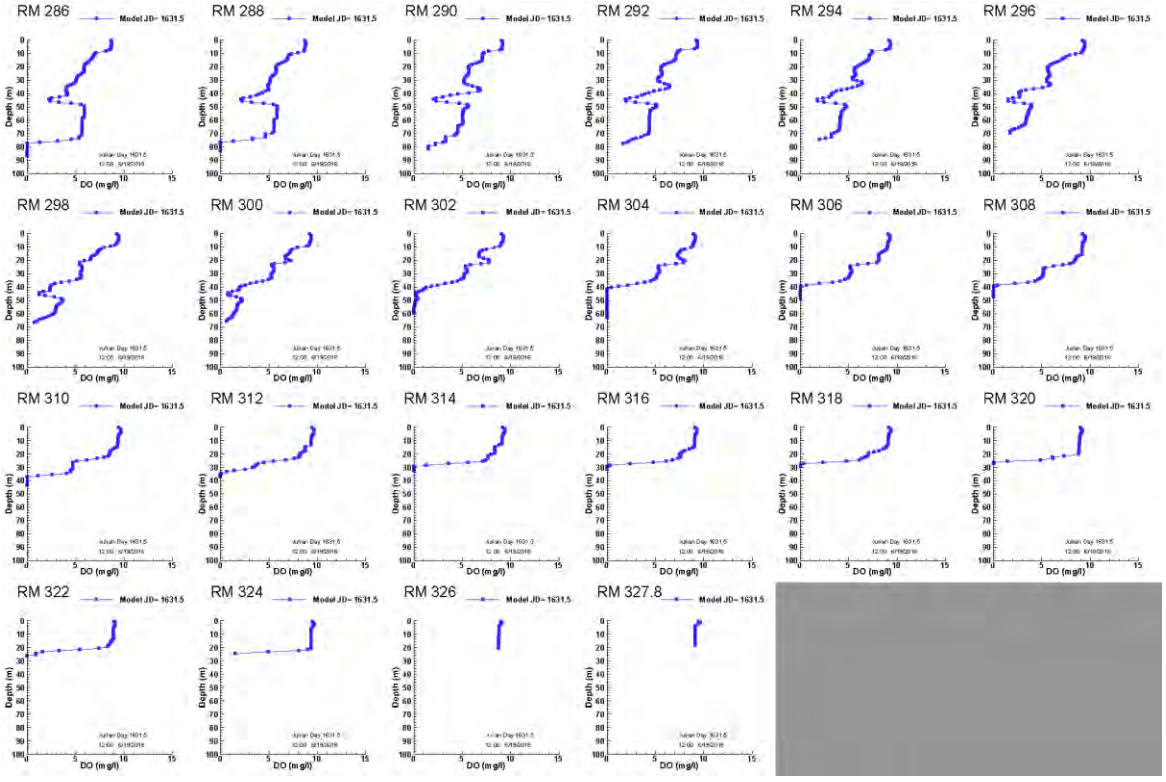


Figure 1196. Vertical profiles of DO compared with data for 6/19/2018.

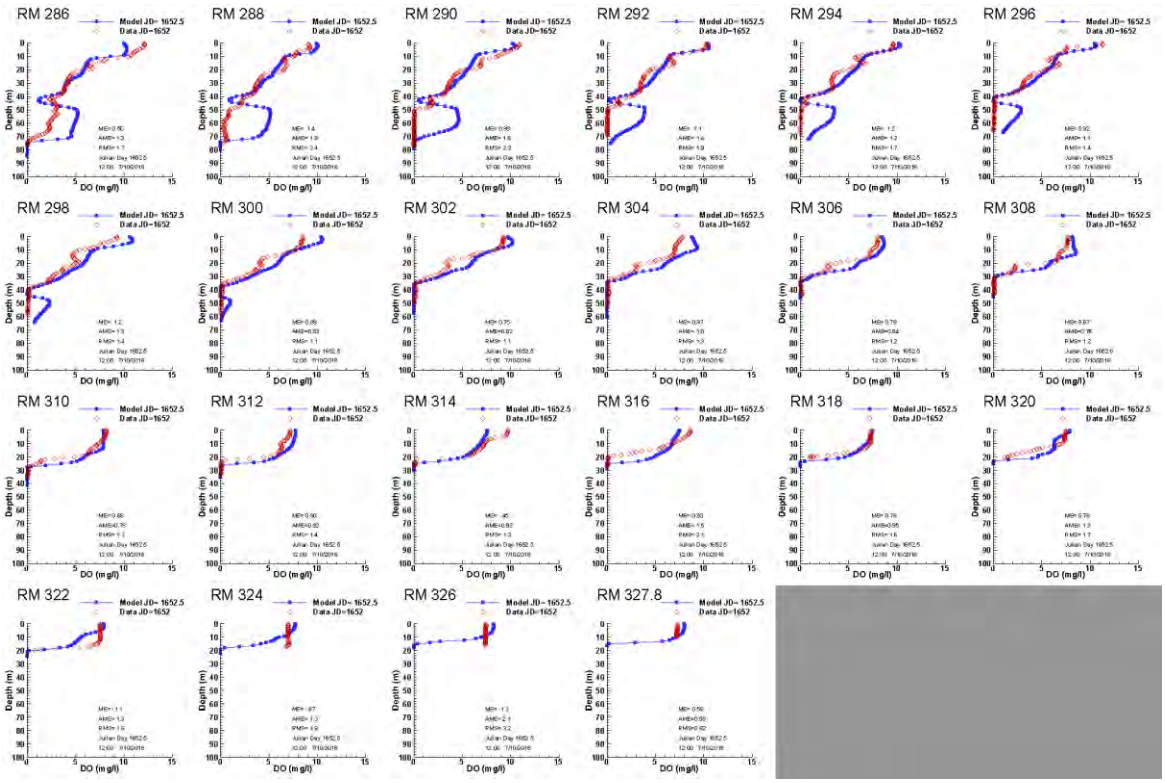


Figure 1197. Vertical profiles of DO compared with data for 7/10/2018.

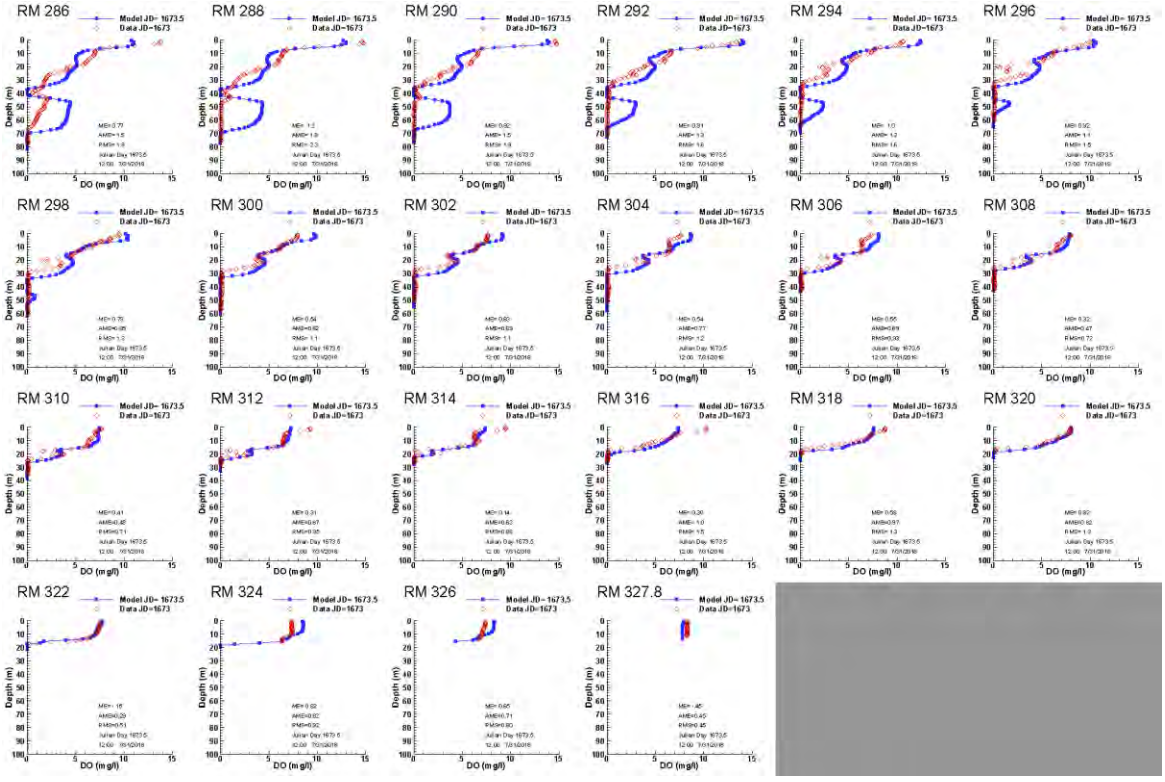


Figure 1198. Vertical profiles of DO compared with data for 7/31/2018.

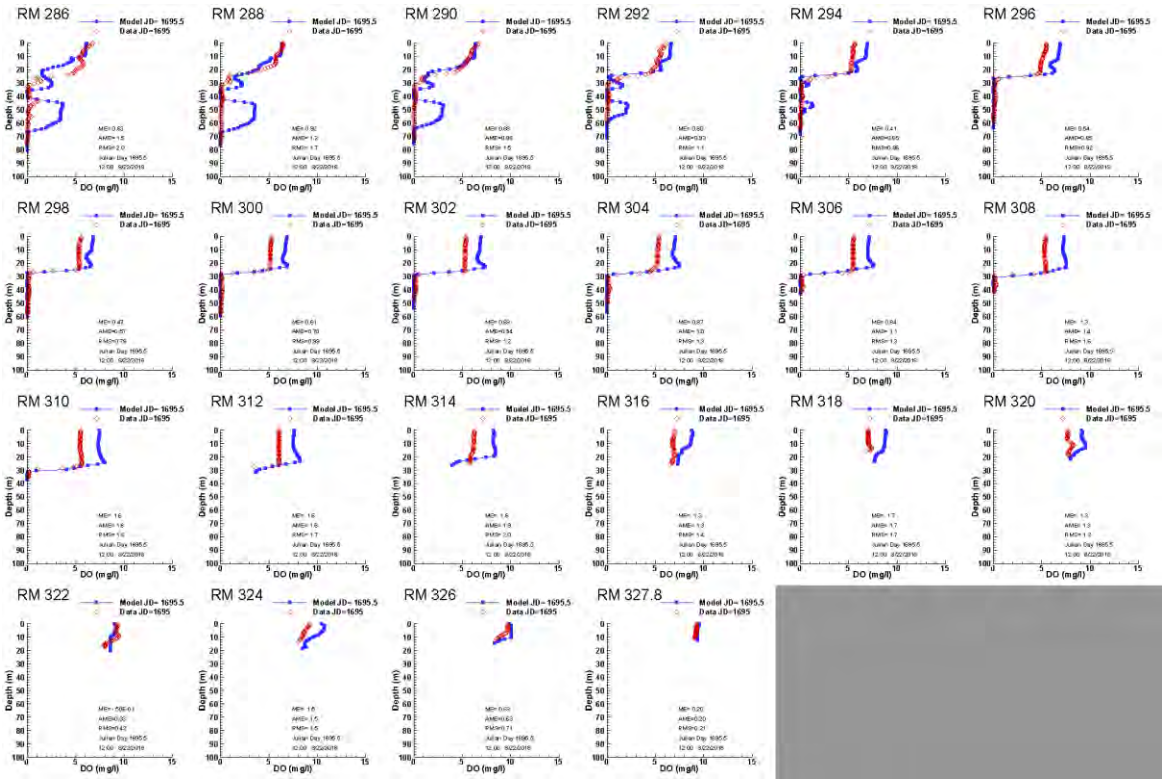


Figure 1199. Vertical profiles of DO compared with data for 8/22/2018.

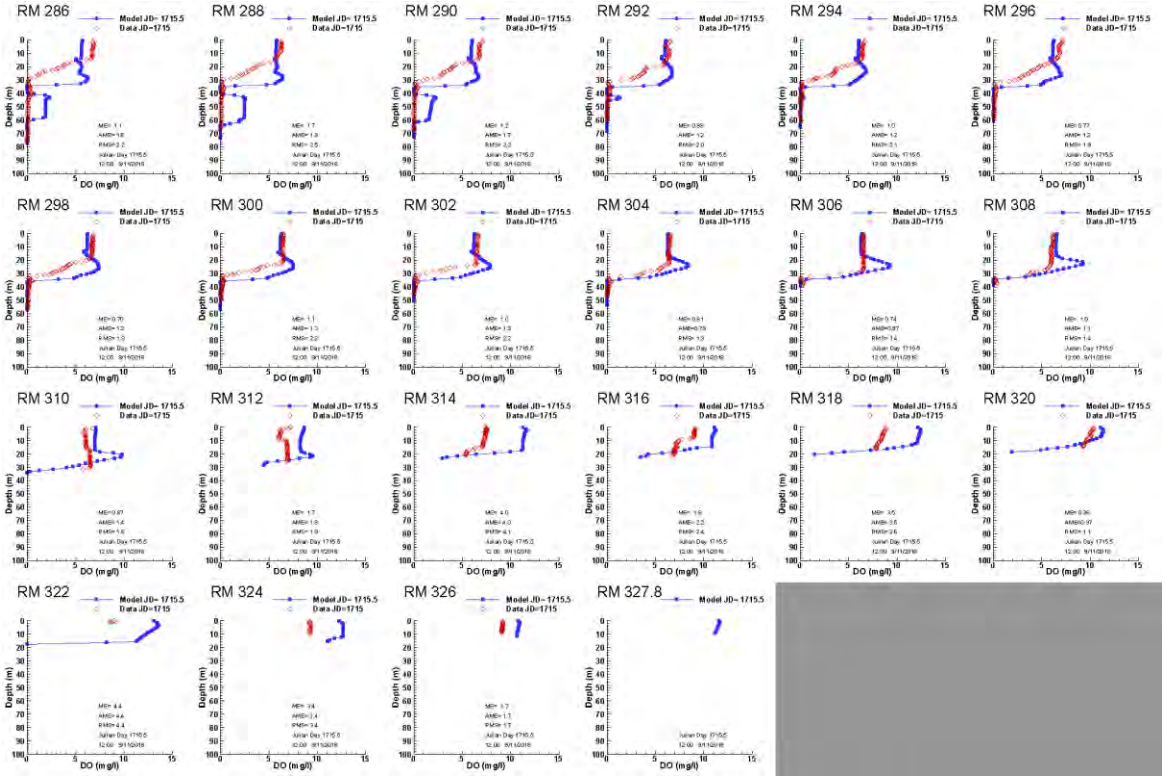


Figure 1200. Vertical profiles of DO compared with data for 9/11/2018.

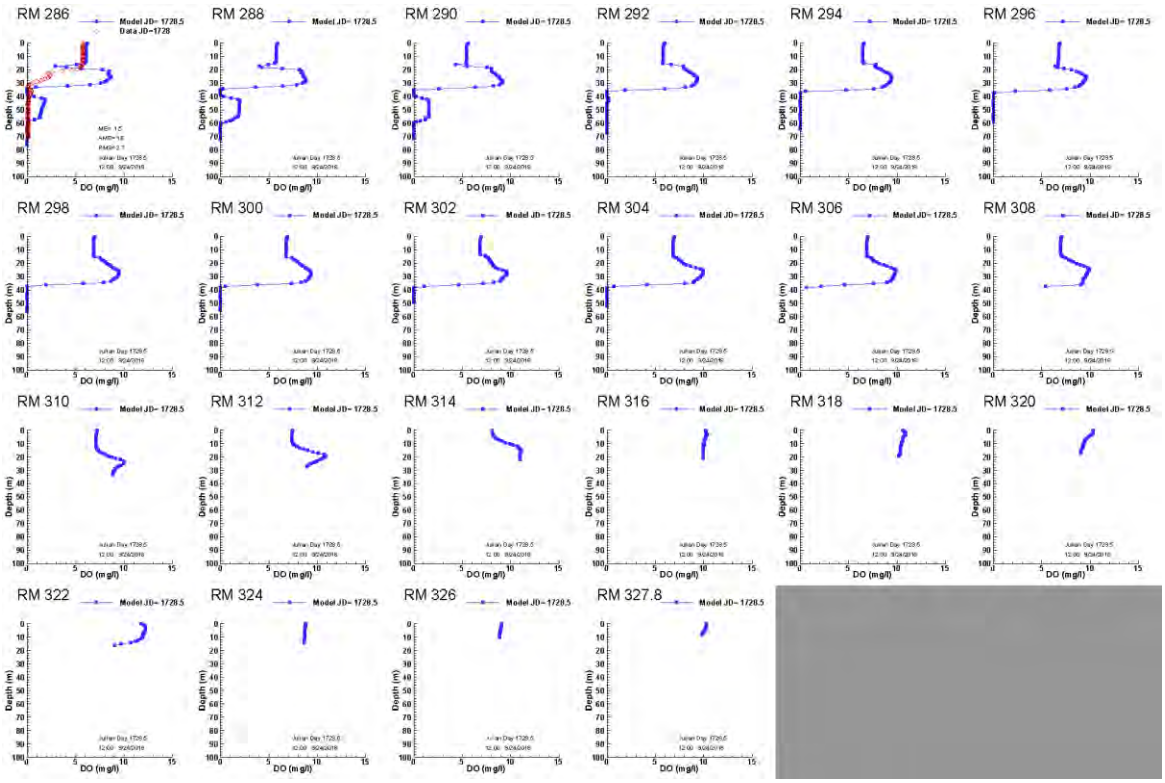


Figure 1201. Vertical profiles of DO compared with data for 9/24/2018.

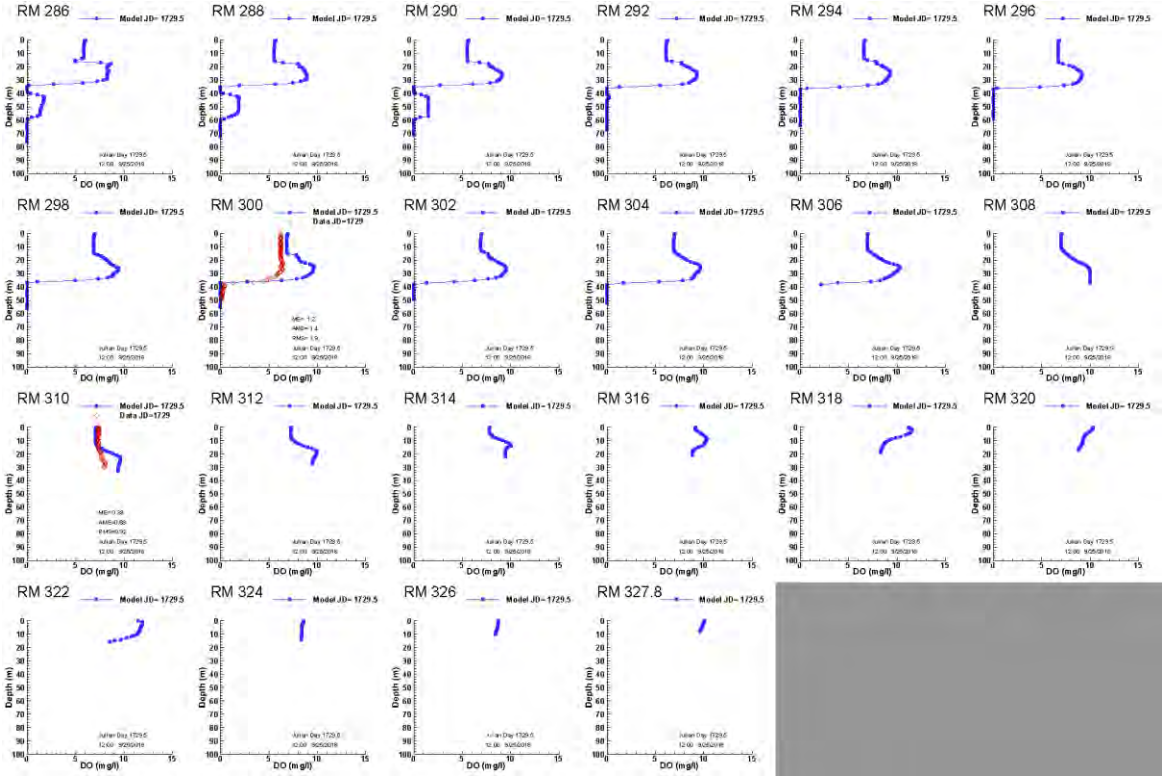


Figure 1202. Vertical profiles of DO compared with data for 9/25/2018.

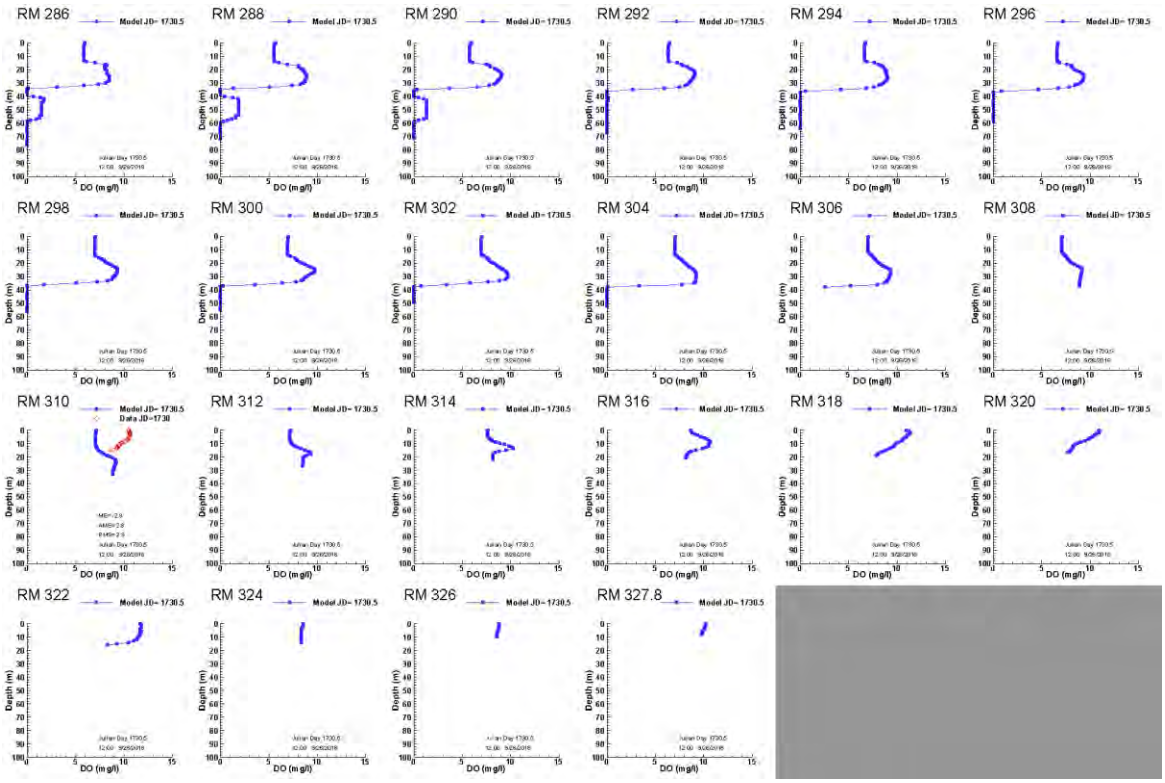


Figure 1203. Vertical profiles of DO compared with data for 9/26/2018.

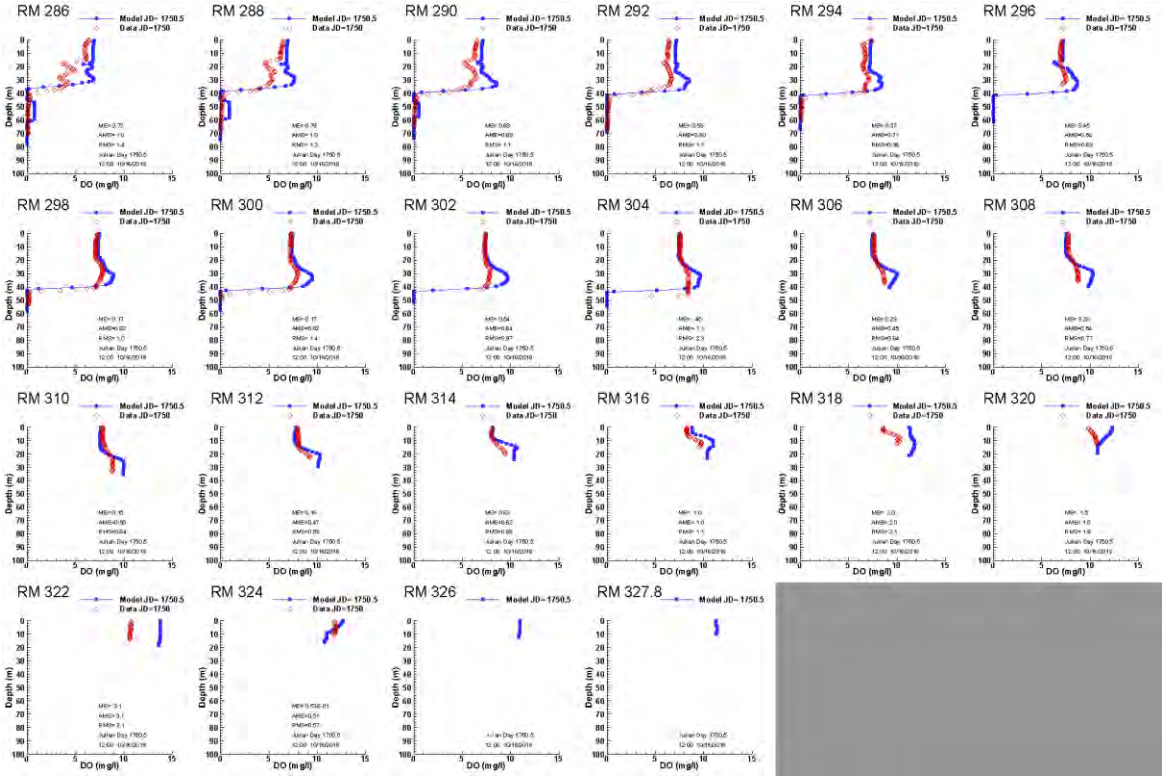


Figure 1204. Vertical profiles of DO compared with data for 10/16/2018.

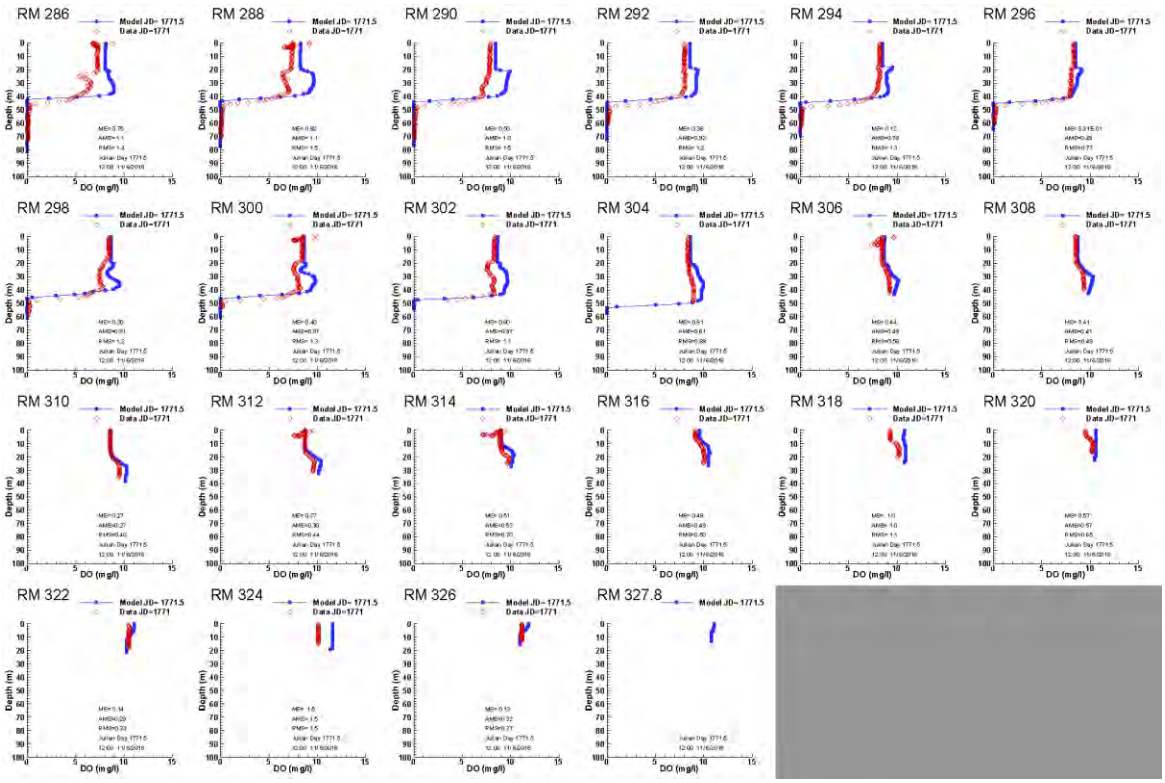


Figure 1205. Vertical profiles of DO compared with data for 11/ 6/2018.

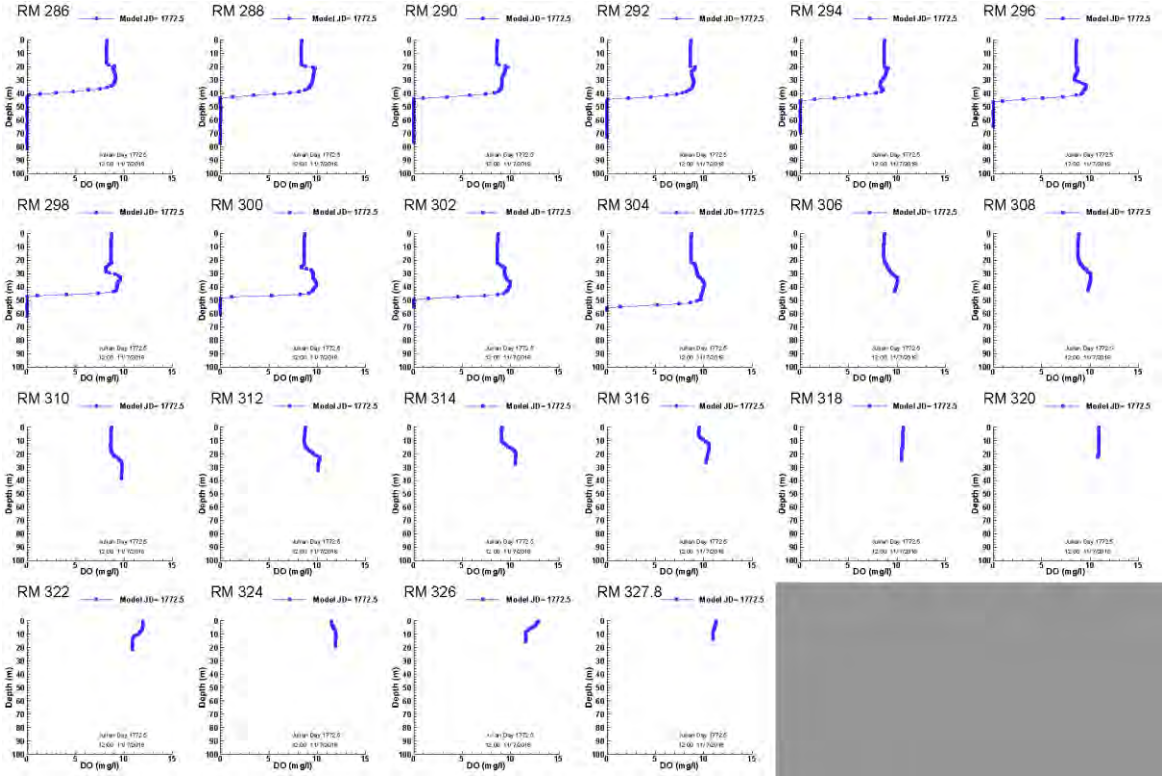


Figure 1206. Vertical profiles of DO compared with data for 11/ 7/2018.

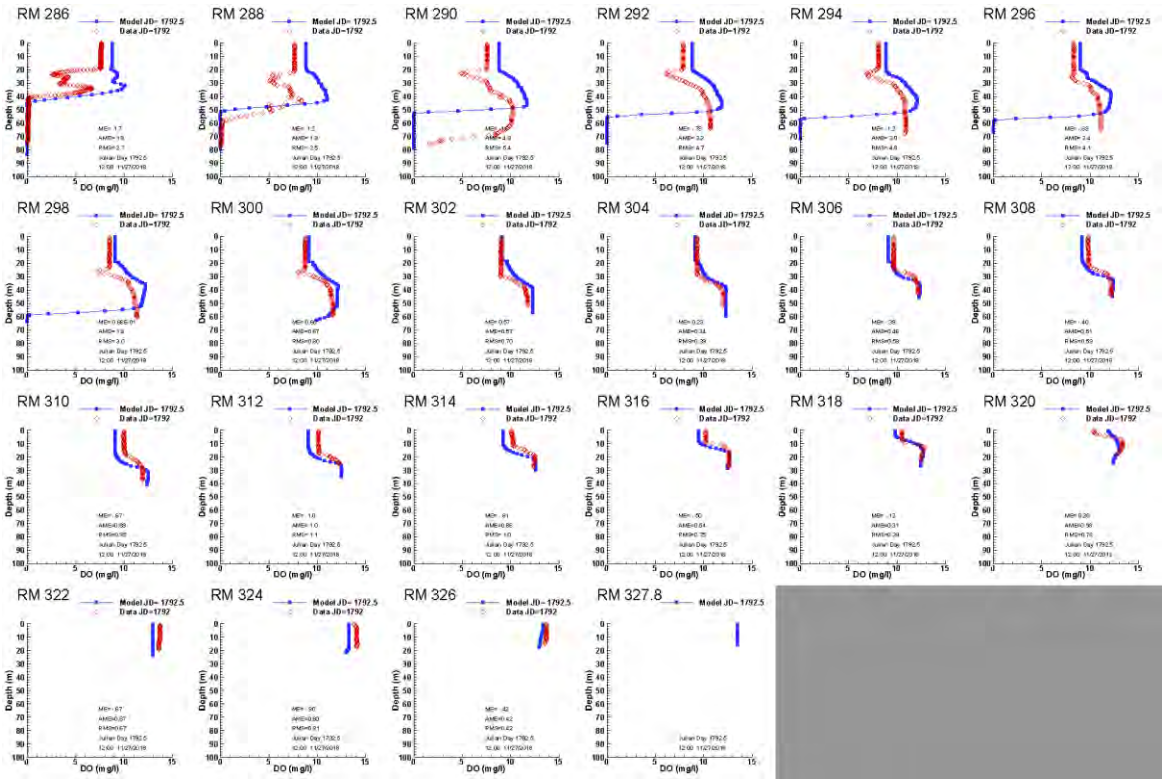


Figure 1207. Vertical profiles of DO compared with data for 11/27/2018.

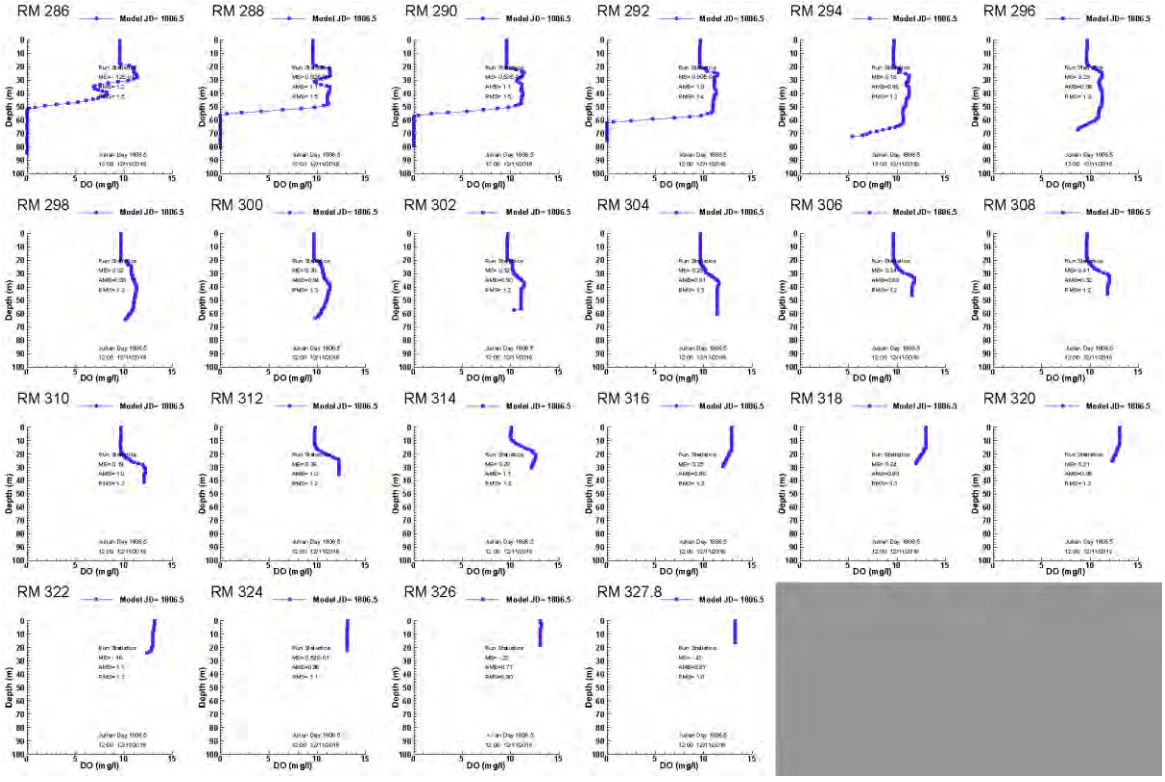


Figure 1208. Vertical profiles of DO compared with data for 12/11/2018.

Total Inorganic Carbon

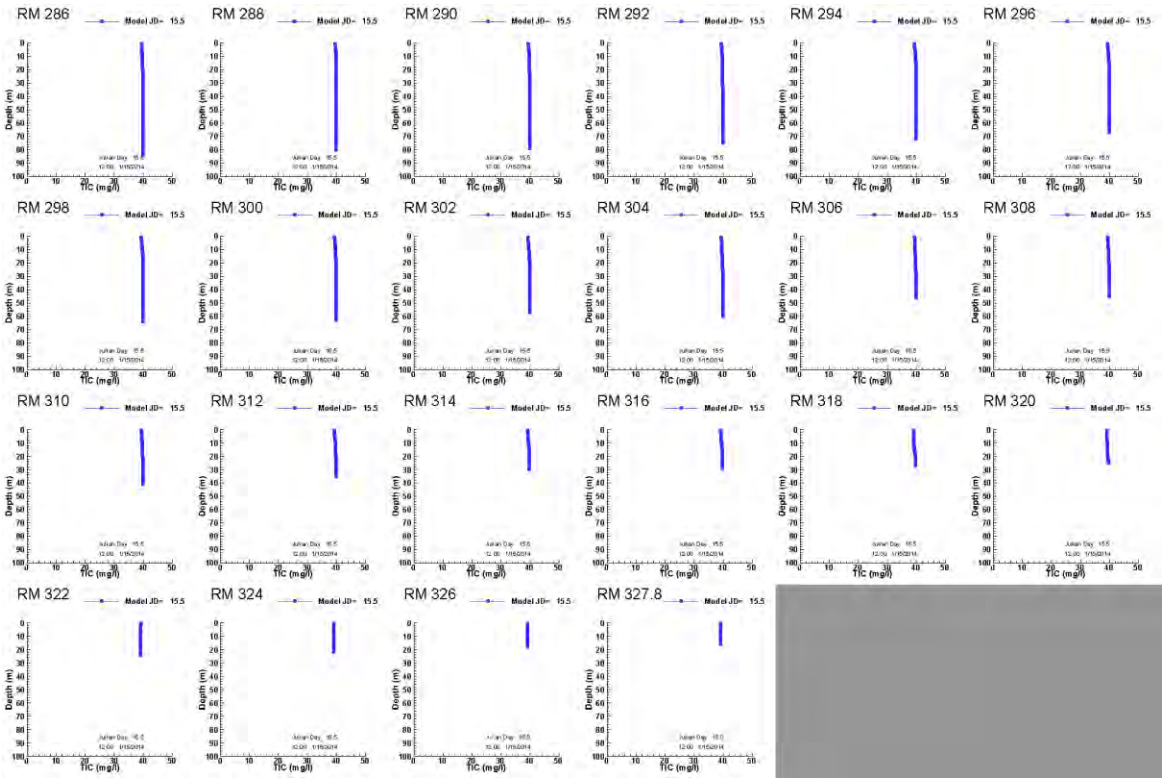


Figure 1209. Vertical profiles of TIC compared with data for 1/15/2014.

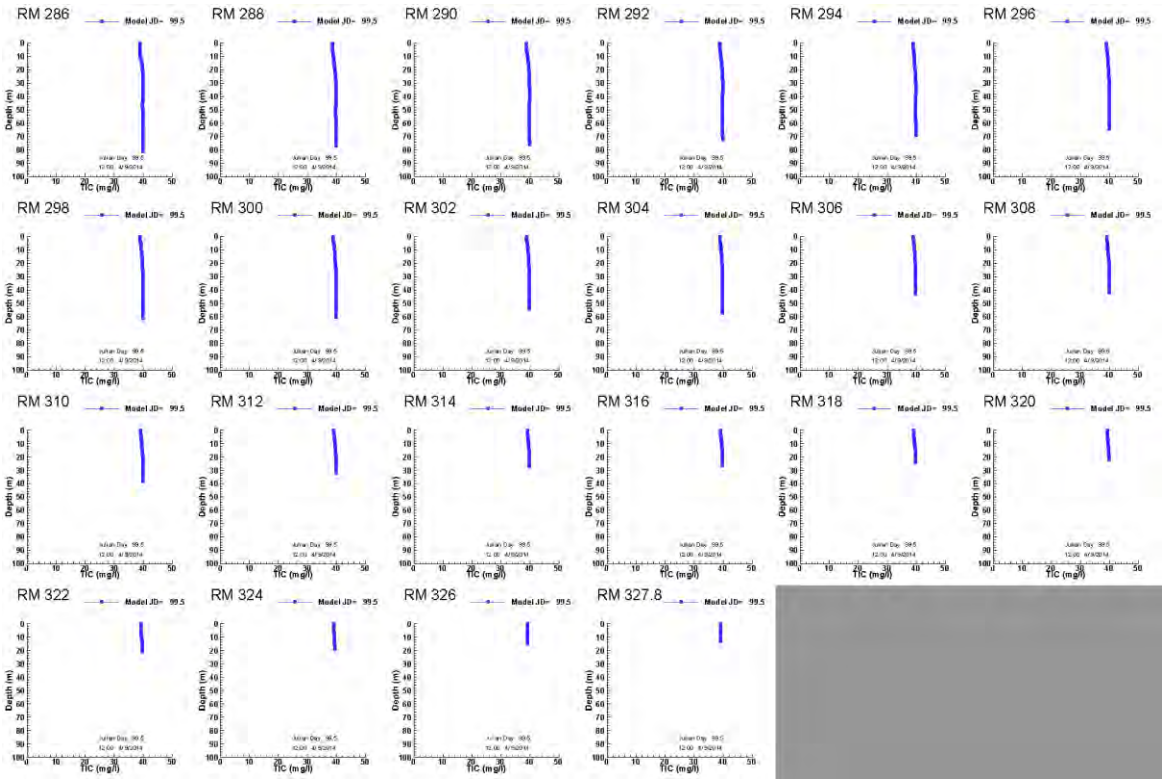


Figure 1210. Vertical profiles of TIC compared with data for 4/ 9/2014.

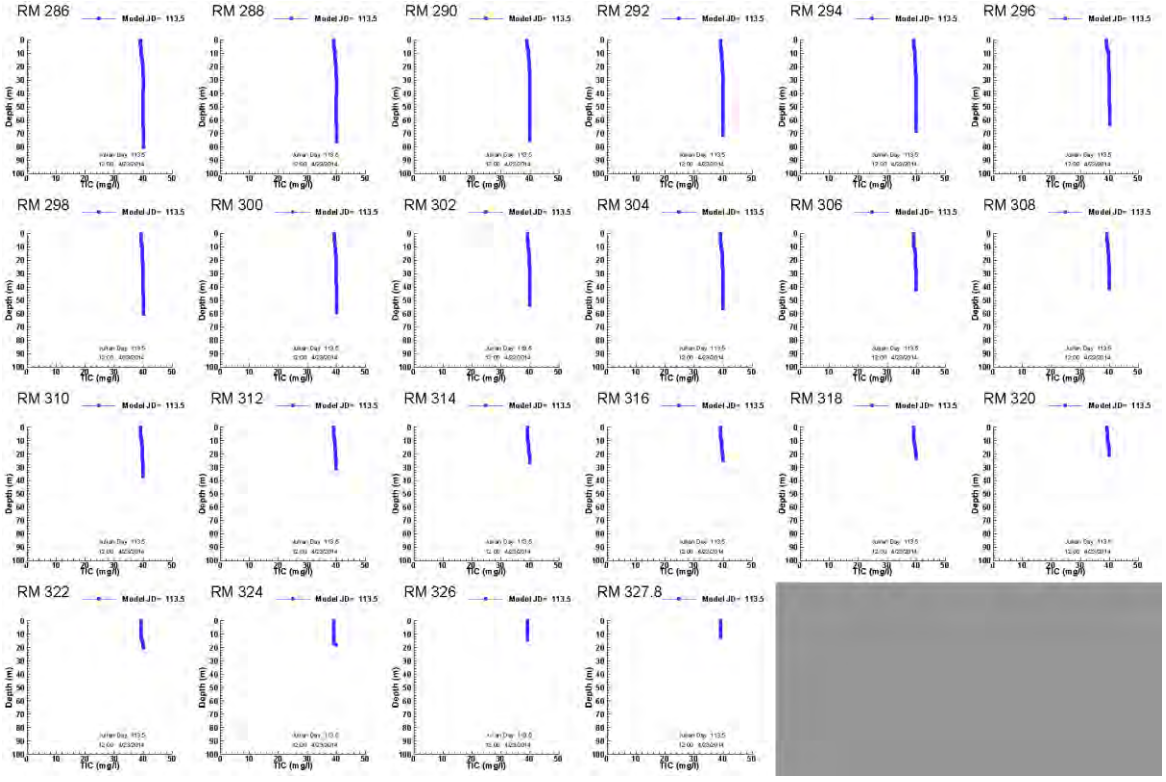


Figure 1211. Vertical profiles of TIC compared with data for 4/23/2014.

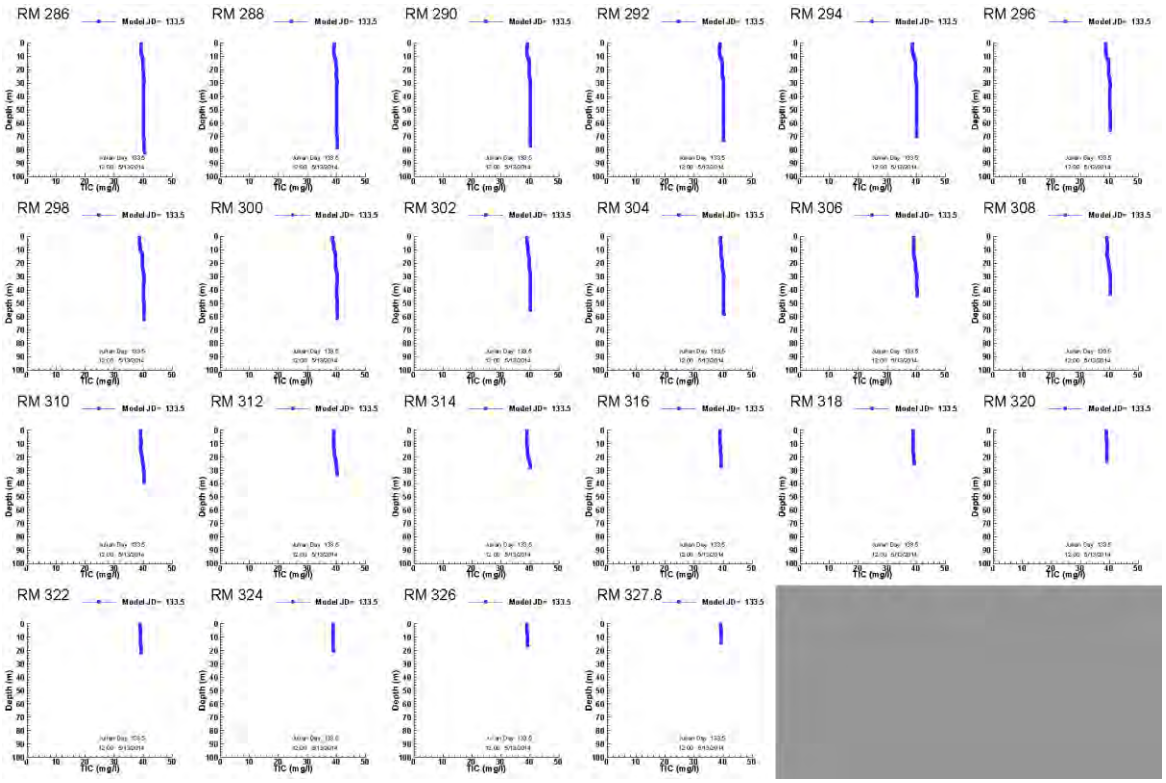


Figure 1212. Vertical profiles of TIC compared with data for 5/13/2014.

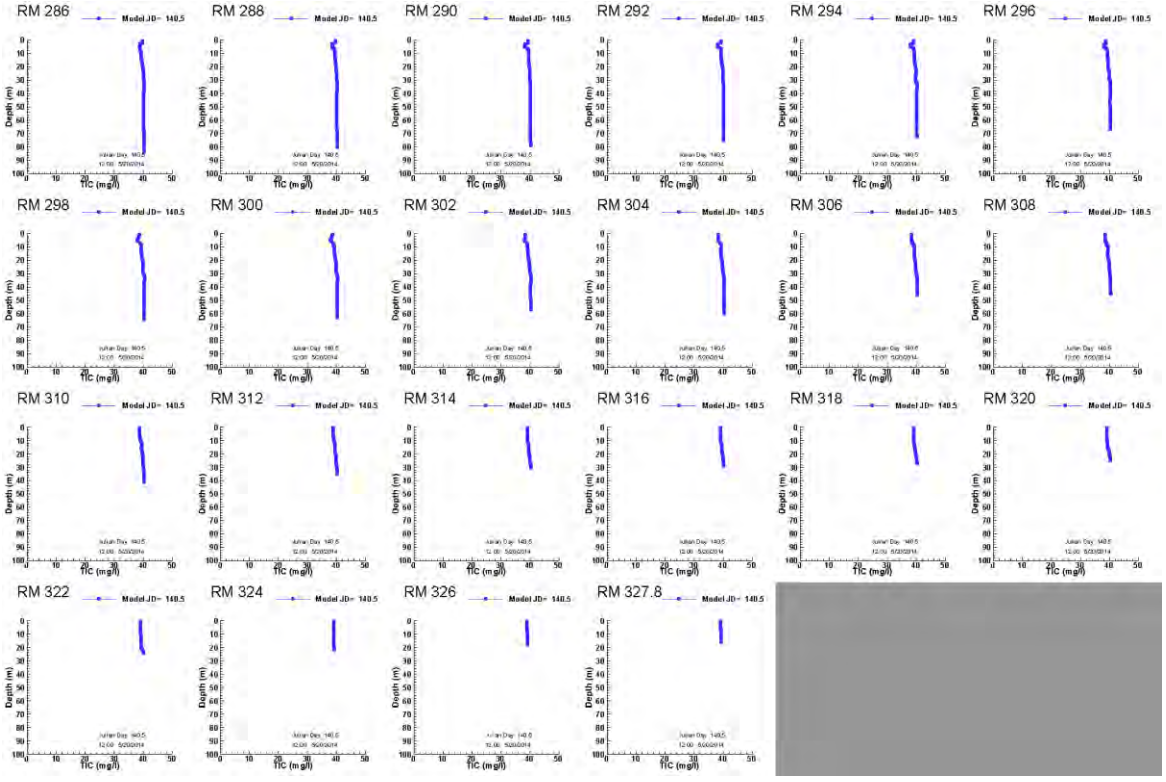


Figure 1213. Vertical profiles of TIC compared with data for 5/20/2014.

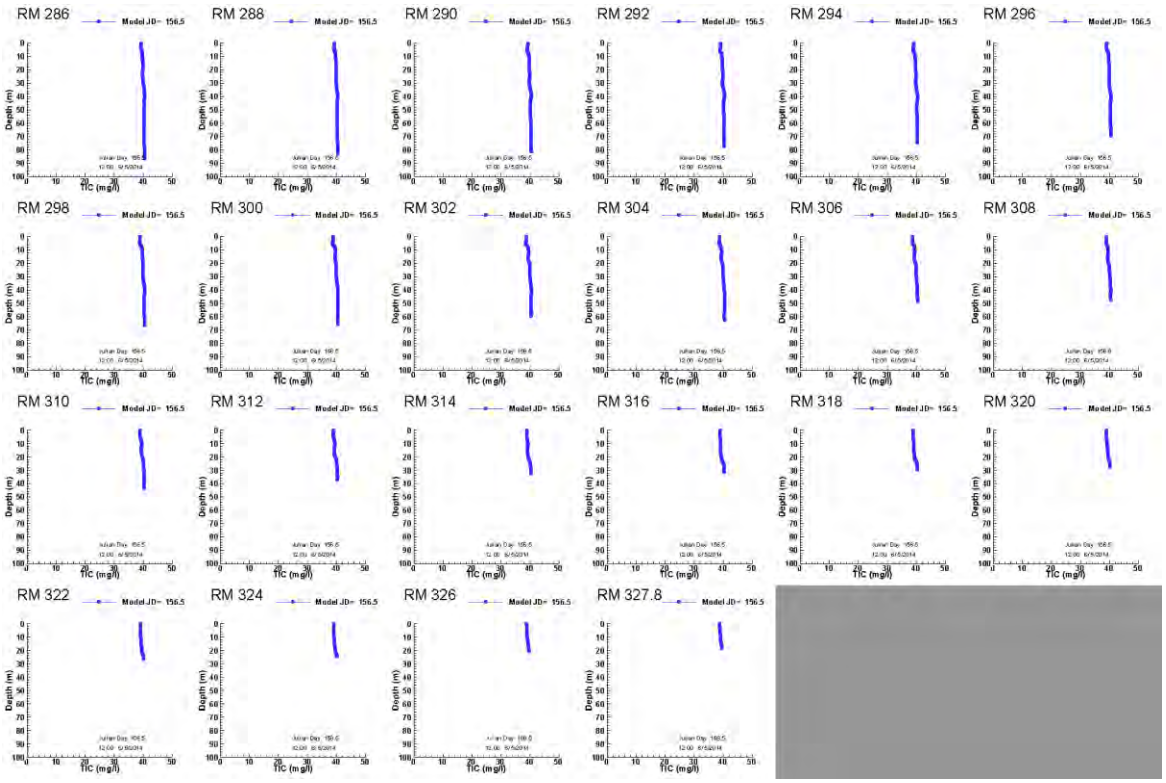


Figure 1214. Vertical profiles of TIC compared with data for 6/ 5/2014.

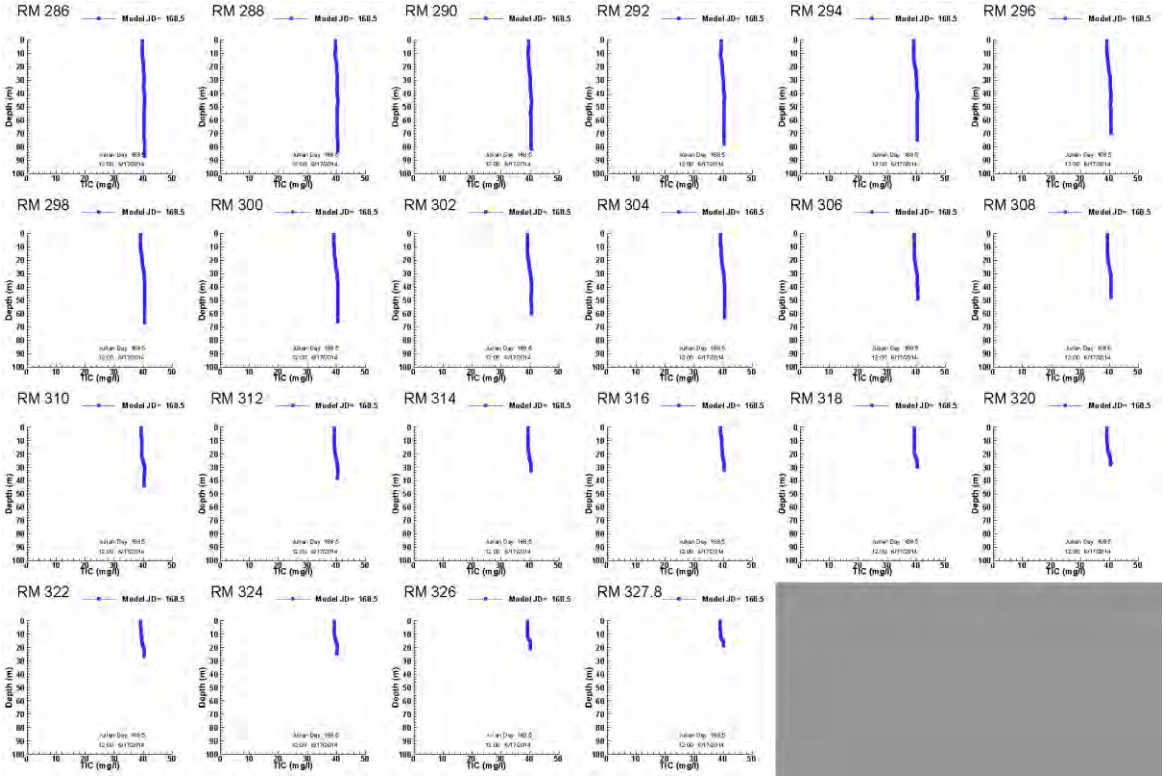


Figure 1215. Vertical profiles of TIC compared with data for 6/17/2014.

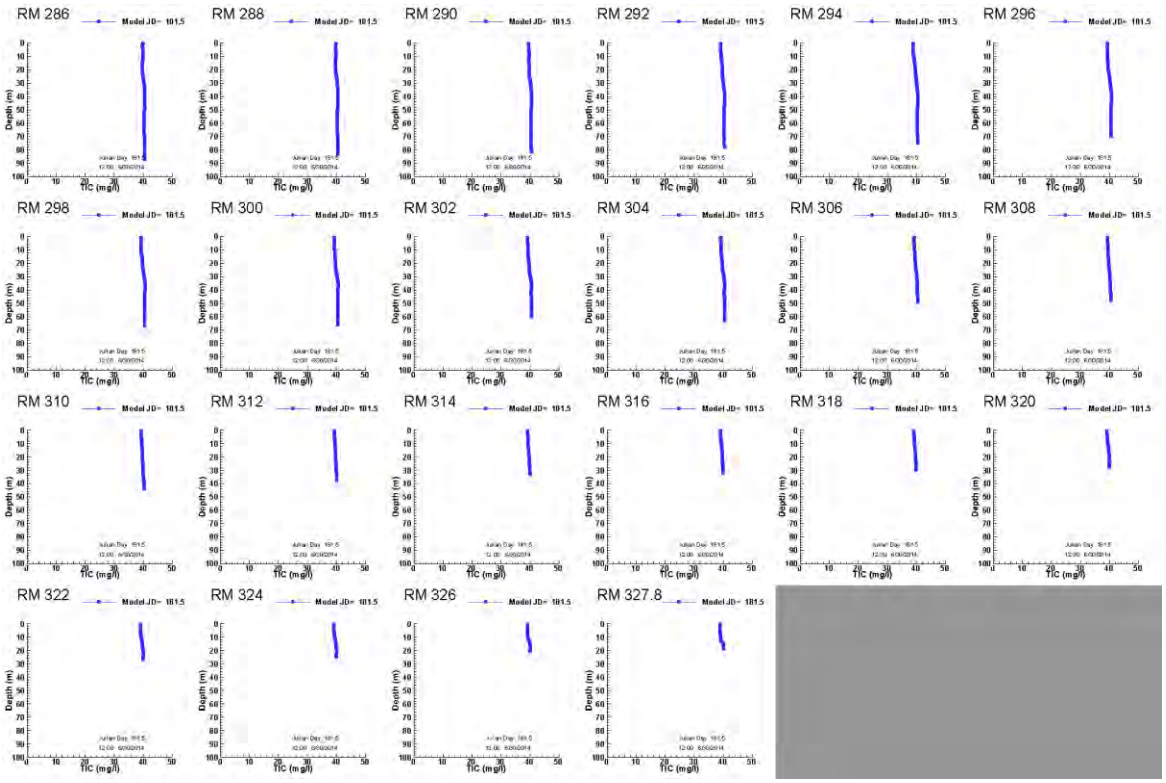


Figure 1216. Vertical profiles of TIC compared with data for 6/30/2014.

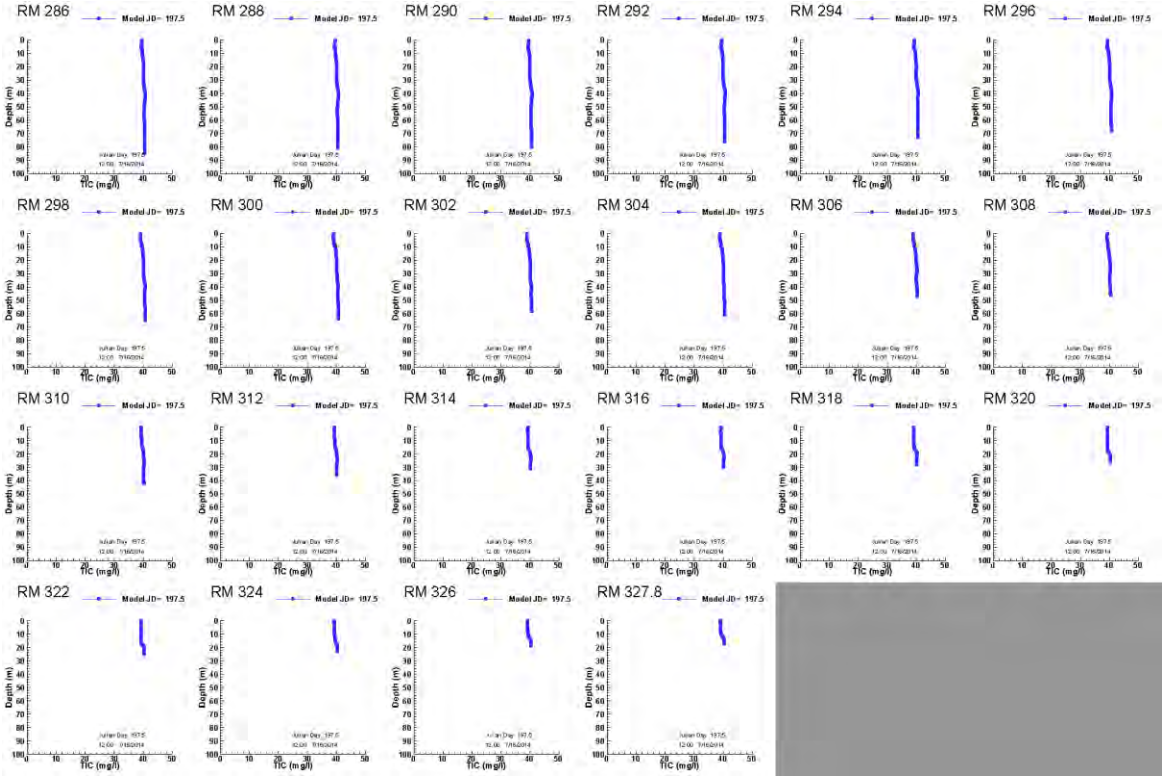


Figure 1217. Vertical profiles of TIC compared with data for 7/16/2014.

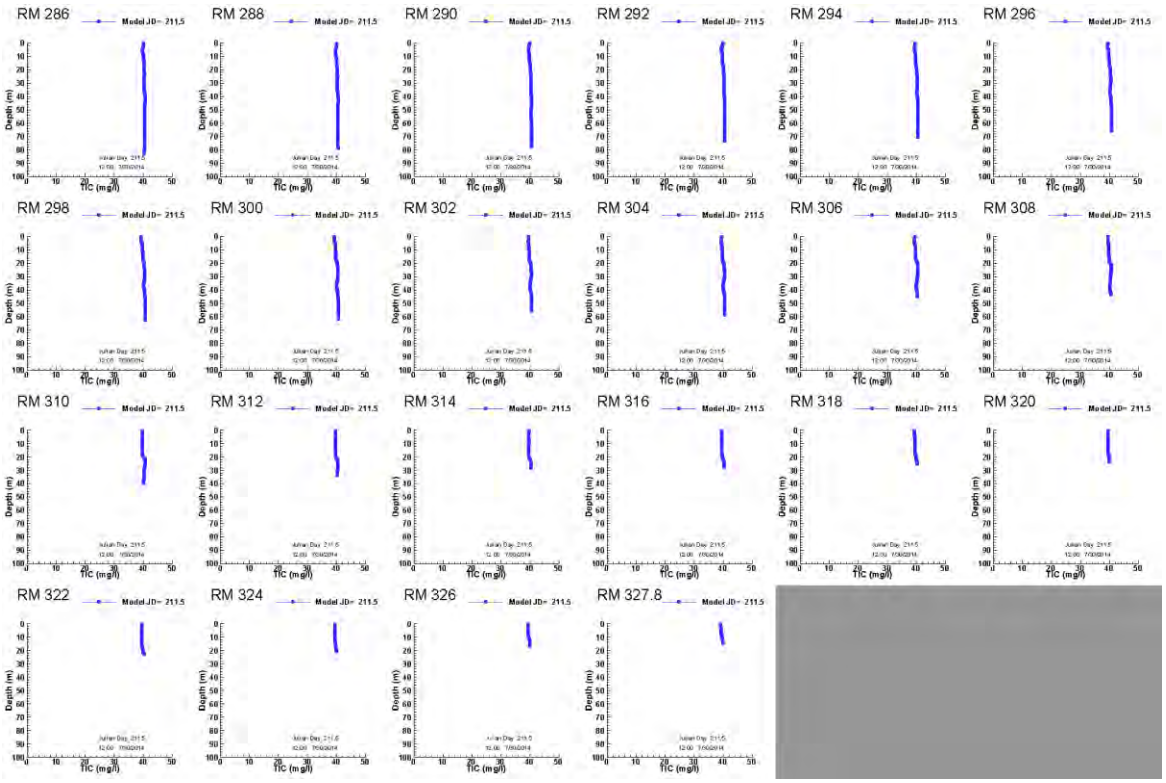


Figure 1218. Vertical profiles of TIC compared with data for 7/30/2014.

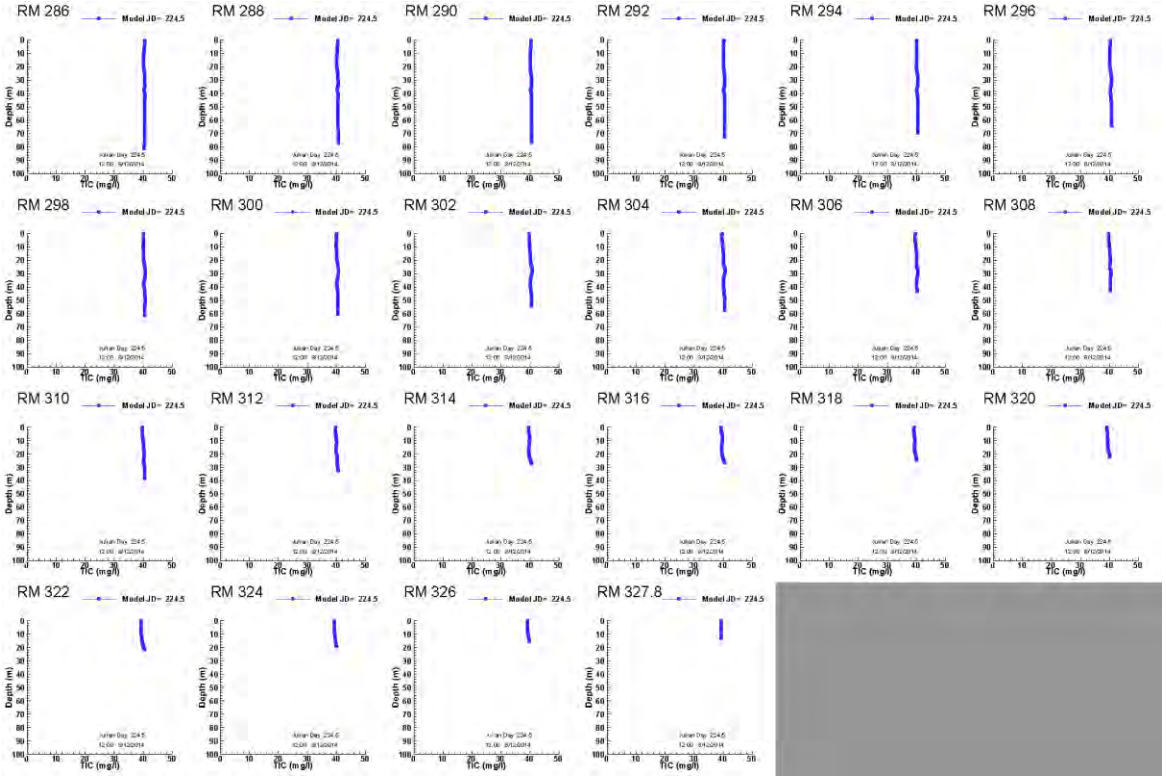


Figure 1219. Vertical profiles of TIC compared with data for 8/12/2014.

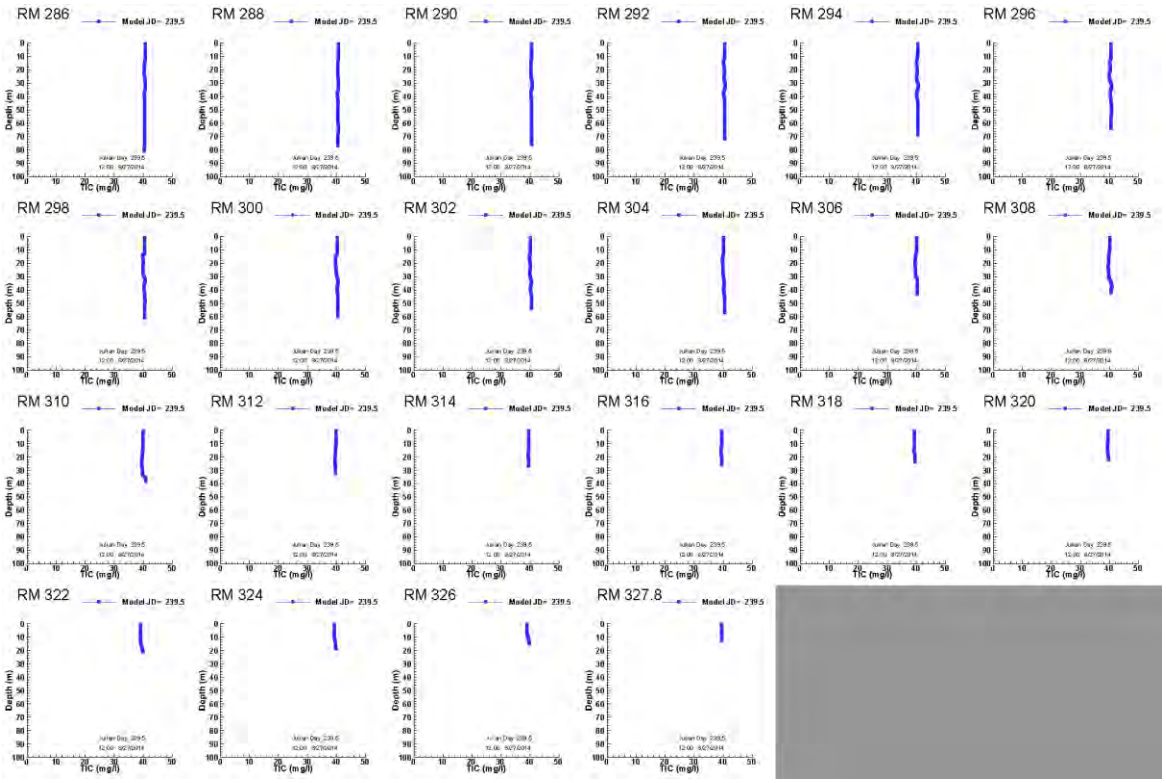


Figure 1220. Vertical profiles of TIC compared with data for 8/27/2014.

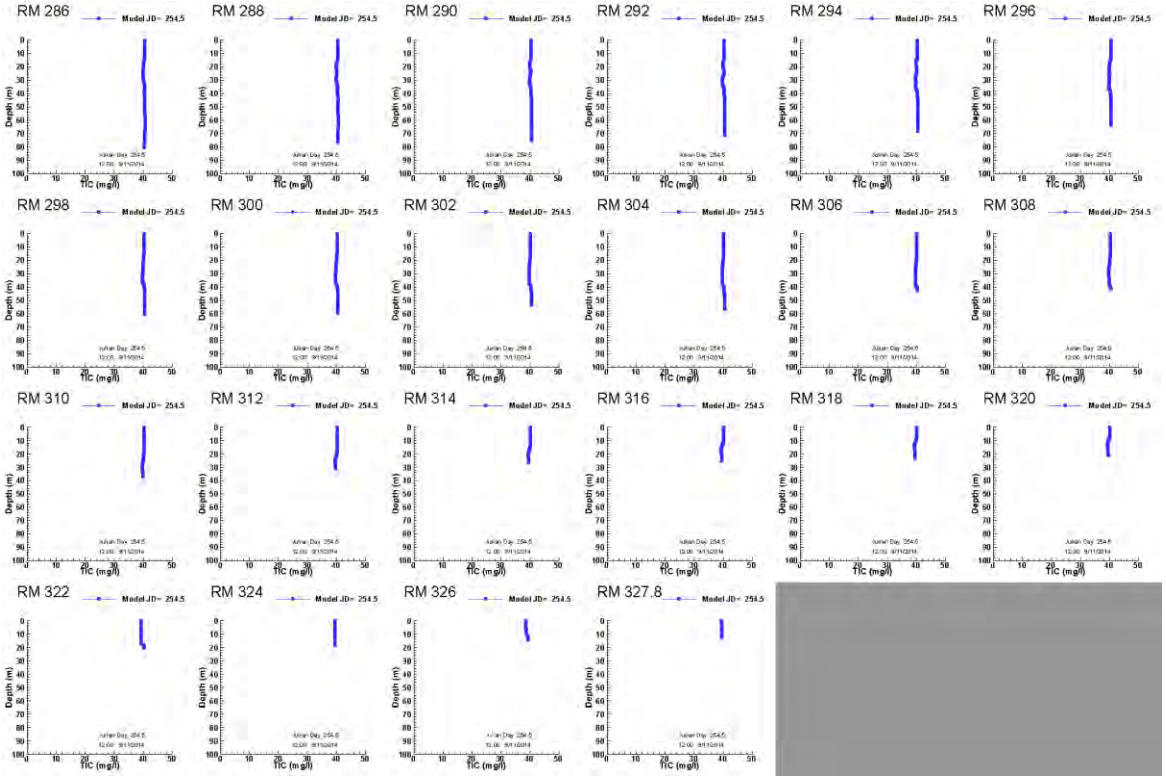


Figure 1221. Vertical profiles of TIC compared with data for 9/11/2014.

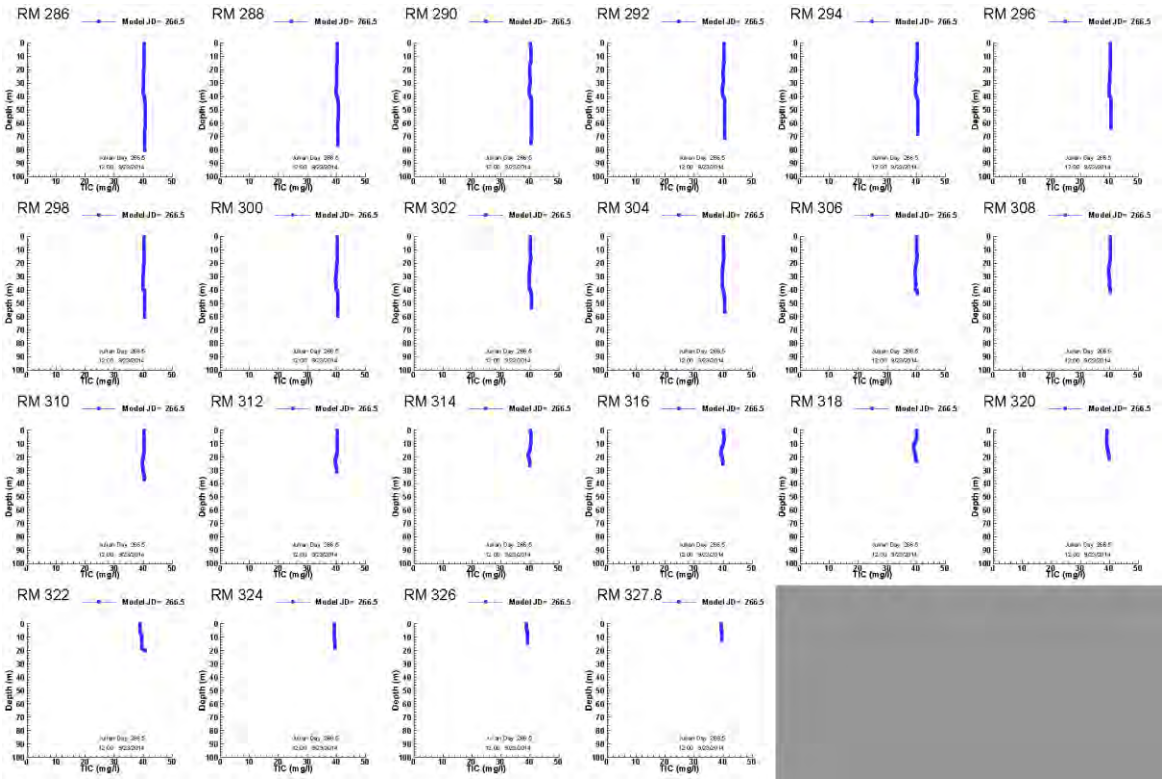


Figure 1222. Vertical profiles of TIC compared with data for 9/23/2014.

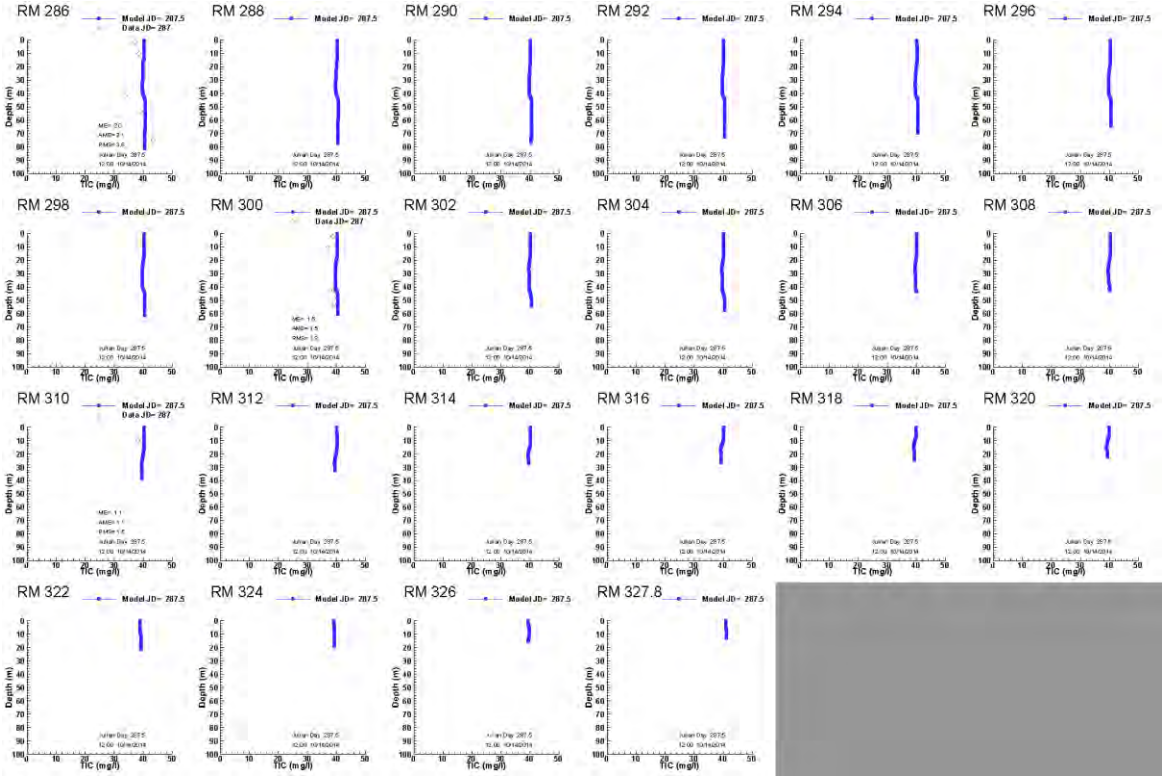


Figure 1223. Vertical profiles of TIC compared with data for 10/14/2014.

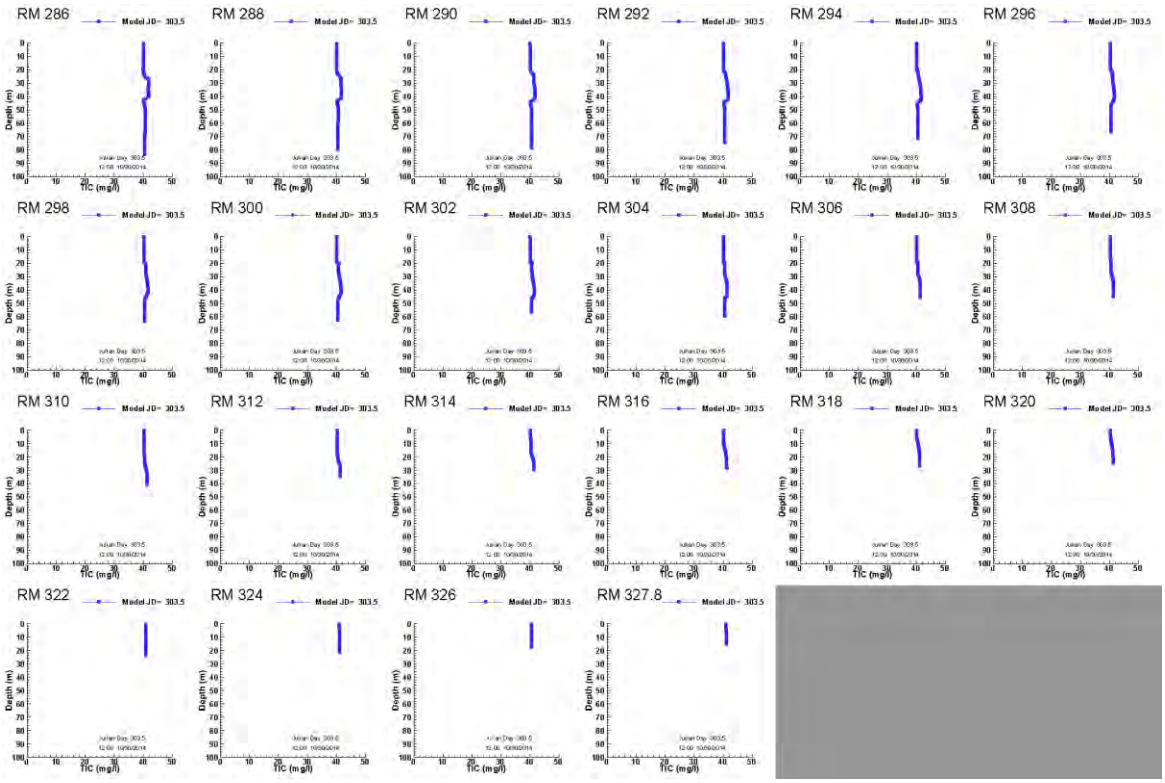


Figure 1224. Vertical profiles of TIC compared with data for 10/30/2014.

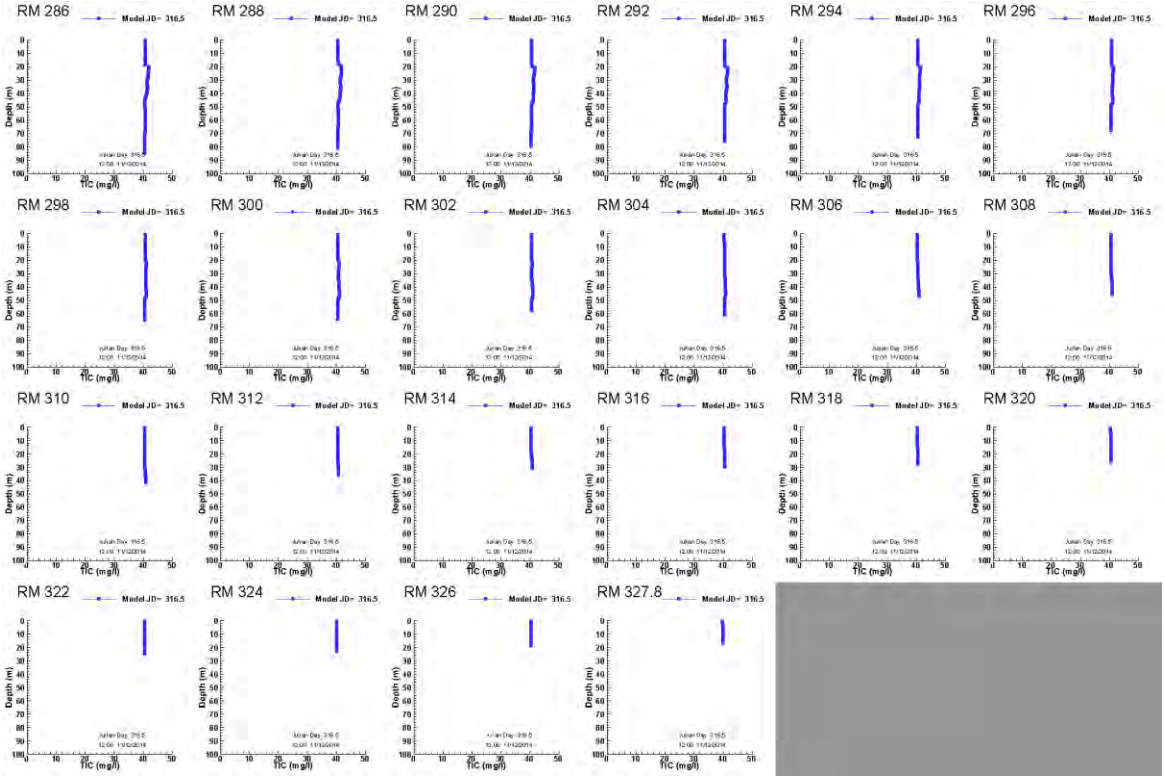


Figure 1225. Vertical profiles of TIC compared with data for 11/12/2014.

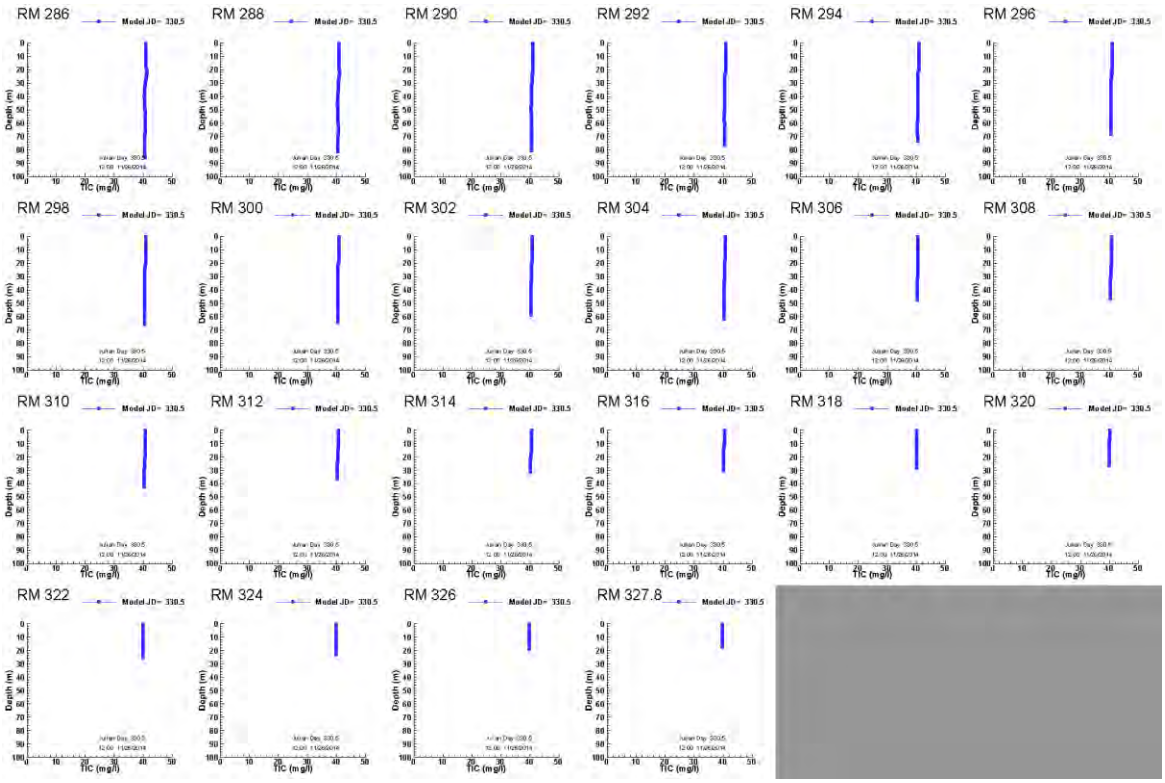


Figure 1226. Vertical profiles of TIC compared with data for 11/26/2014.

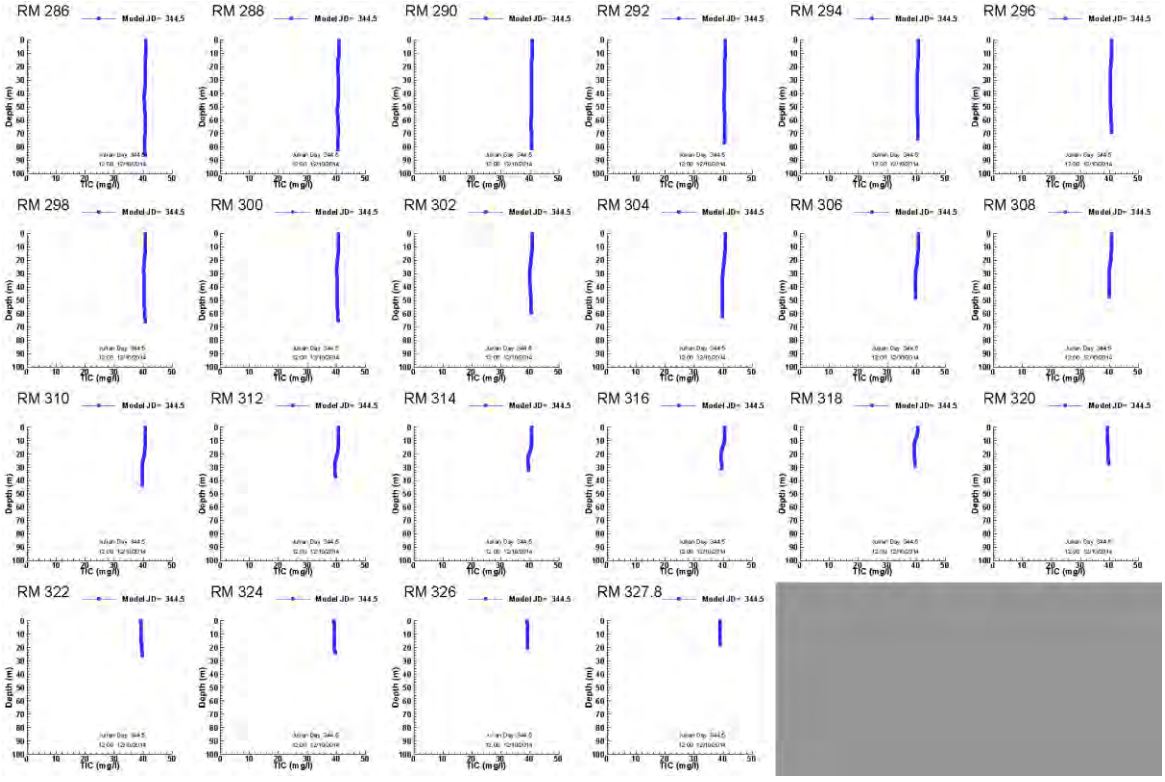


Figure 1227. Vertical profiles of TIC compared with data for 12/10/2014.

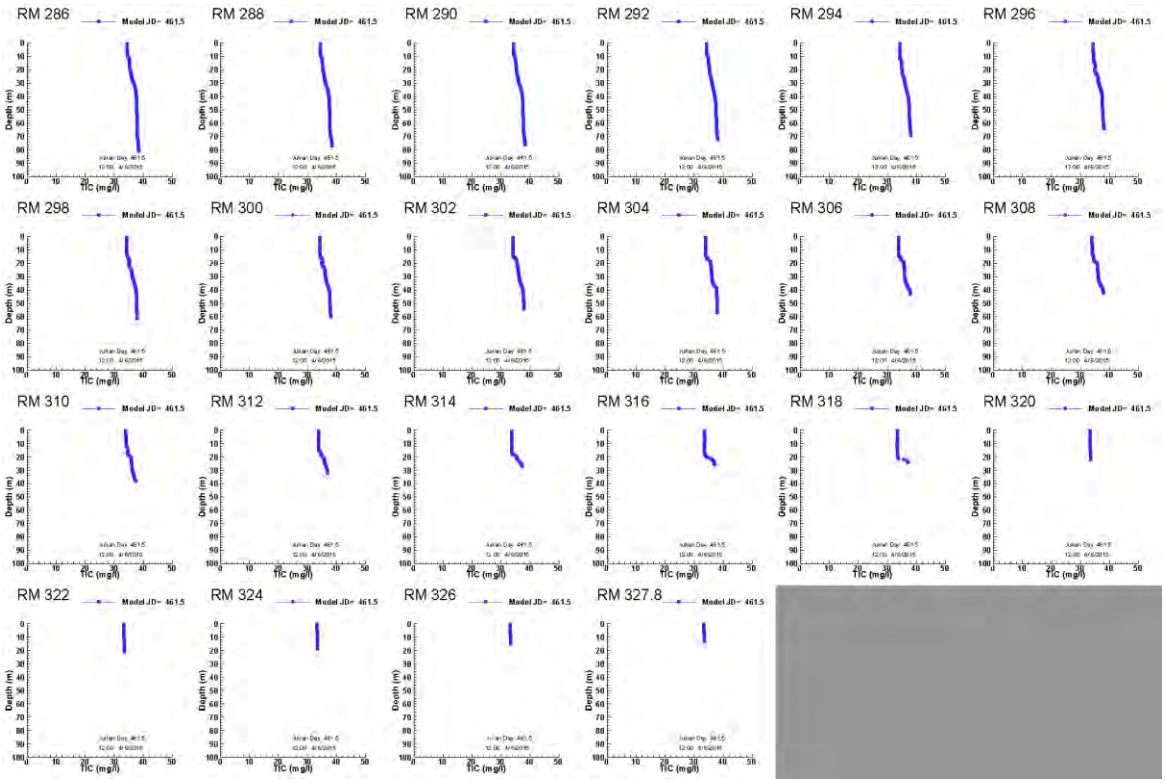


Figure 1228. Vertical profiles of TIC compared with data for 4/ 6/2015.

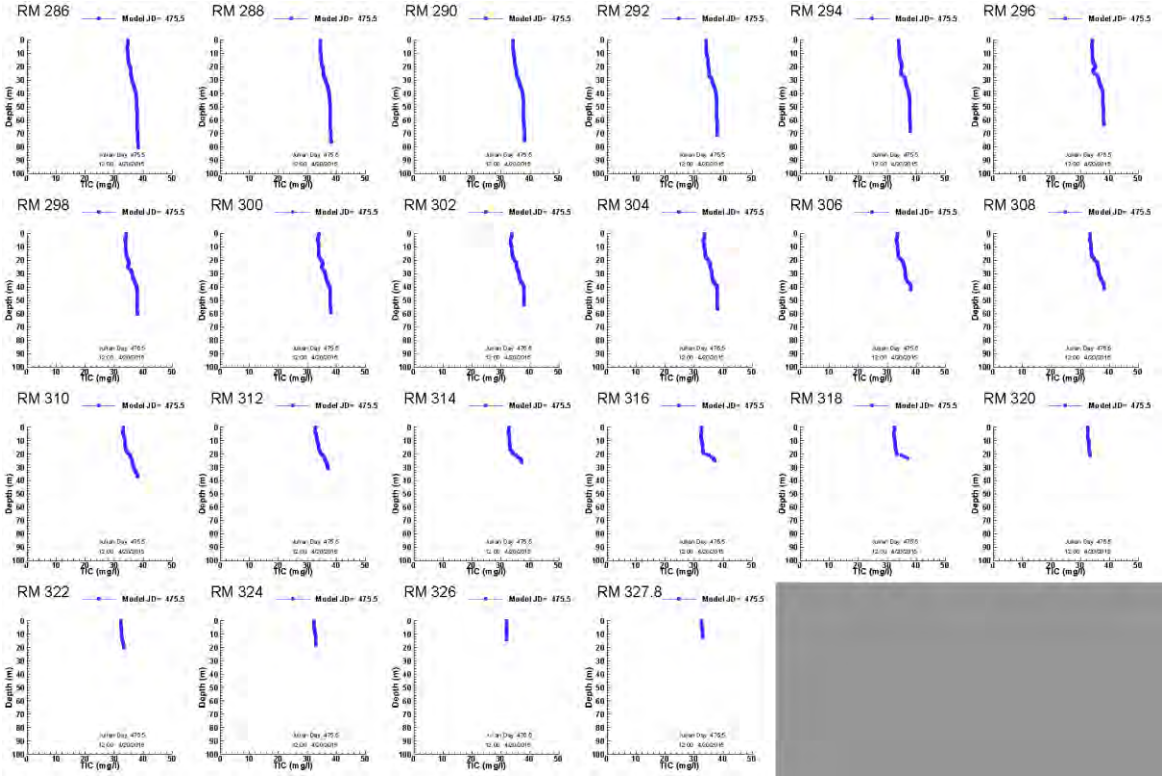


Figure 1229. Vertical profiles of TIC compared with data for 4/20/2015.

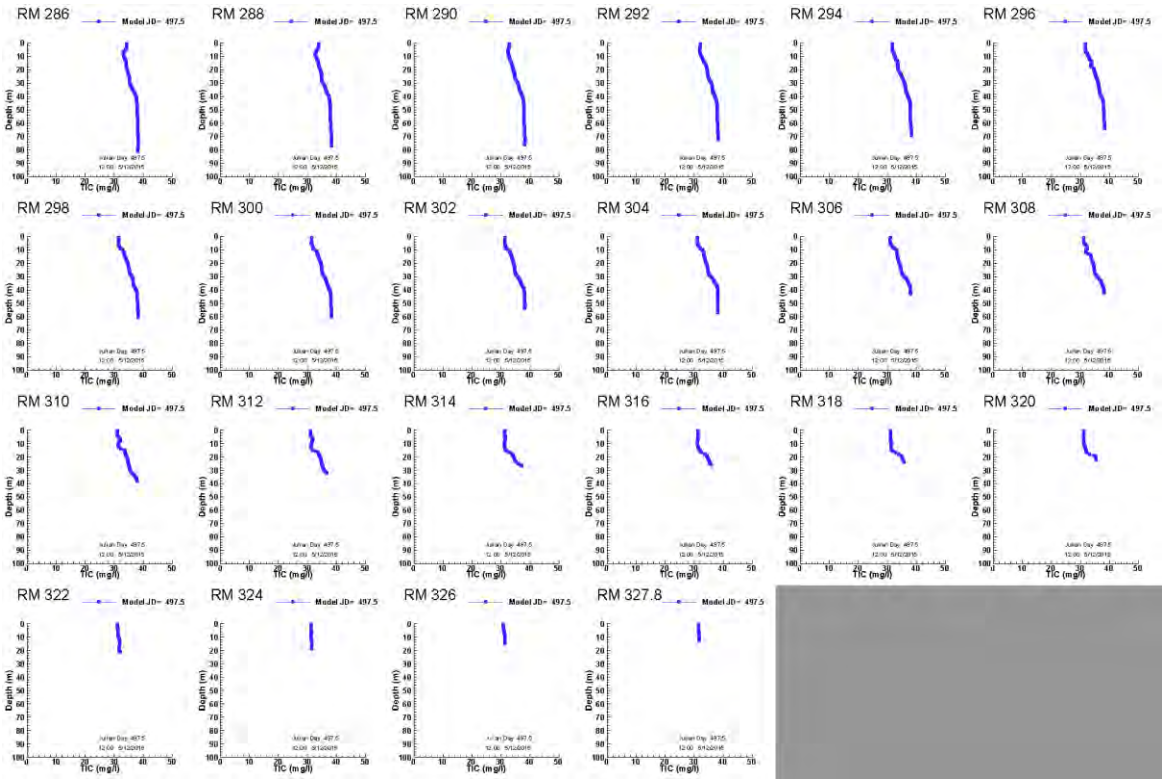


Figure 1230. Vertical profiles of TIC compared with data for 5/12/2015.

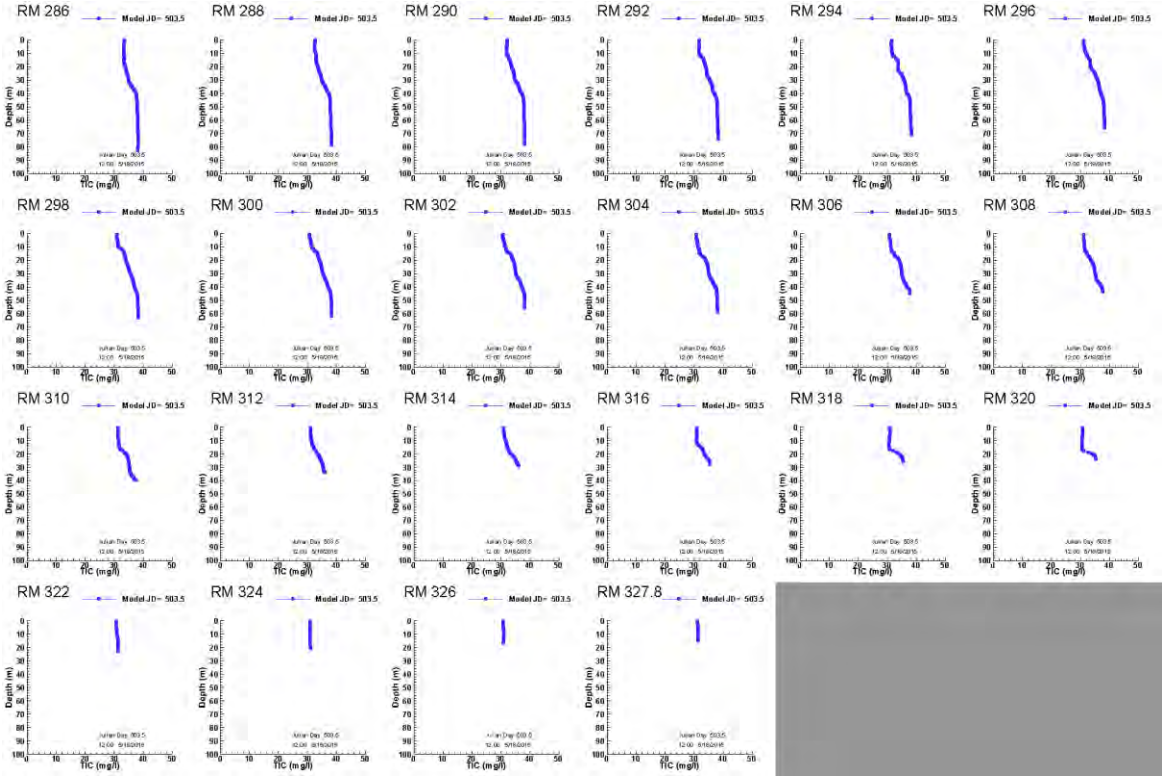


Figure 1231. Vertical profiles of TIC compared with data for 5/18/2015.

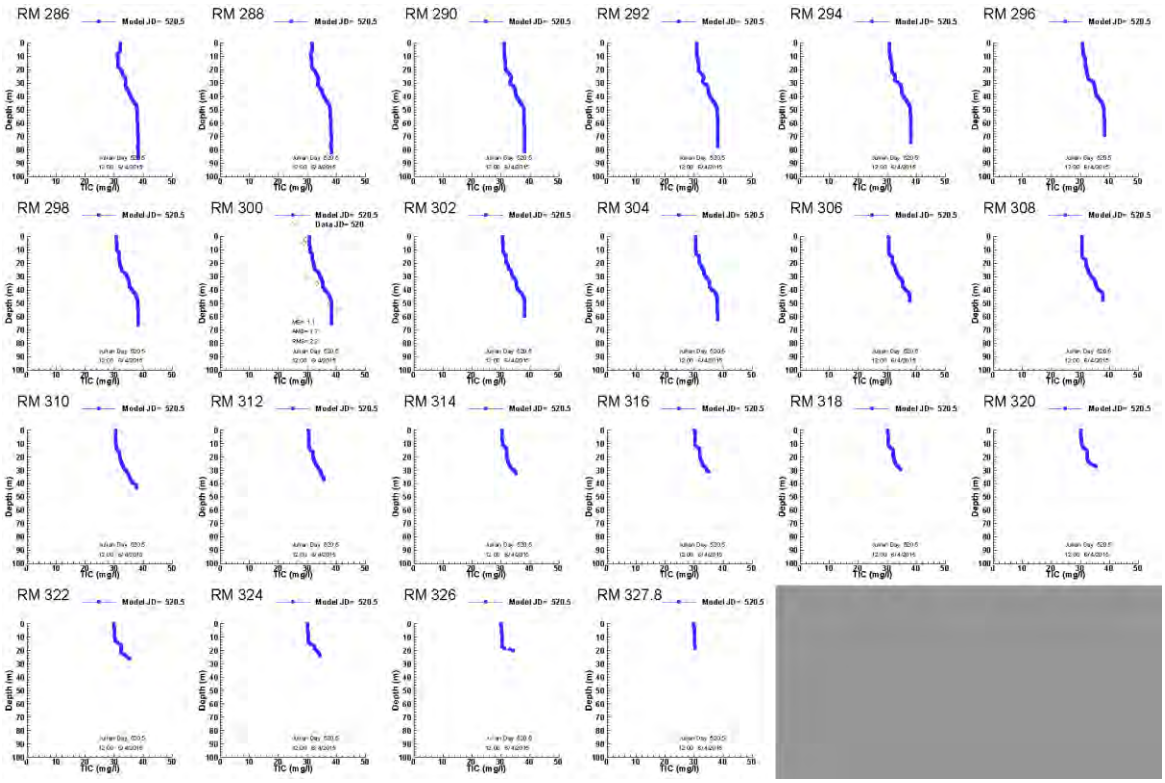


Figure 1232. Vertical profiles of TIC compared with data for 6/ 4/2015.

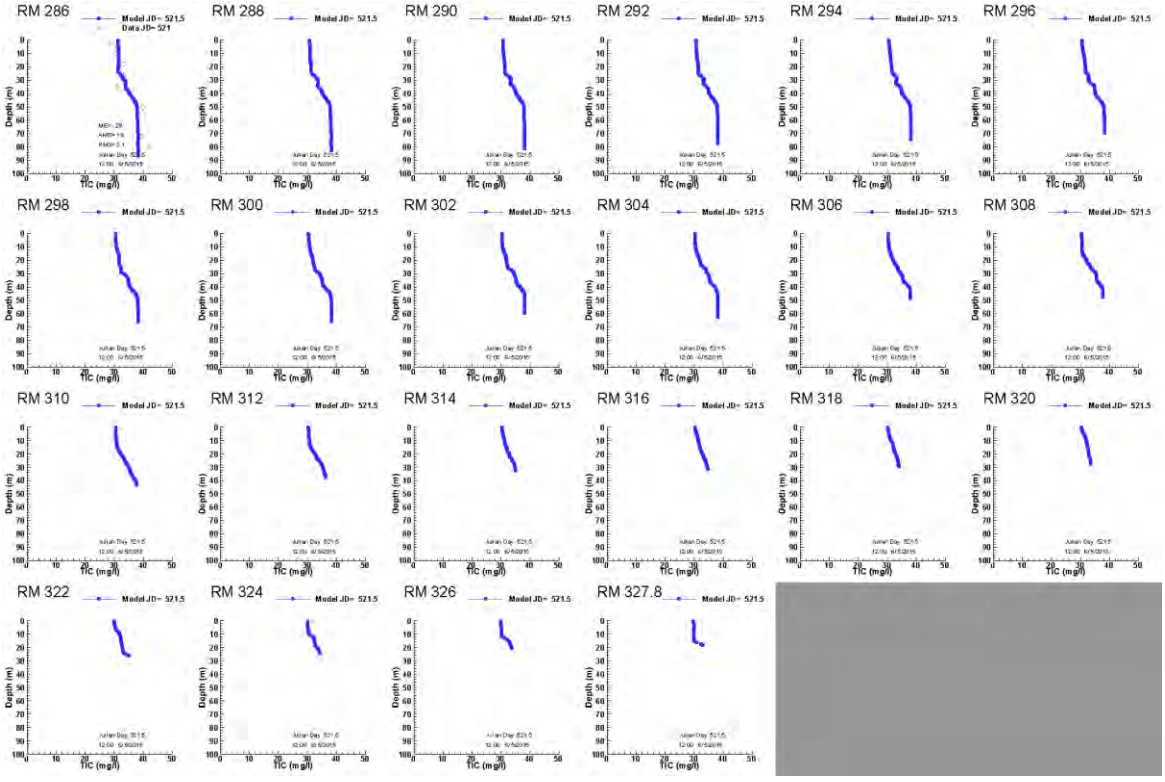


Figure 1233. Vertical profiles of TIC compared with data for 6/ 5/2015.

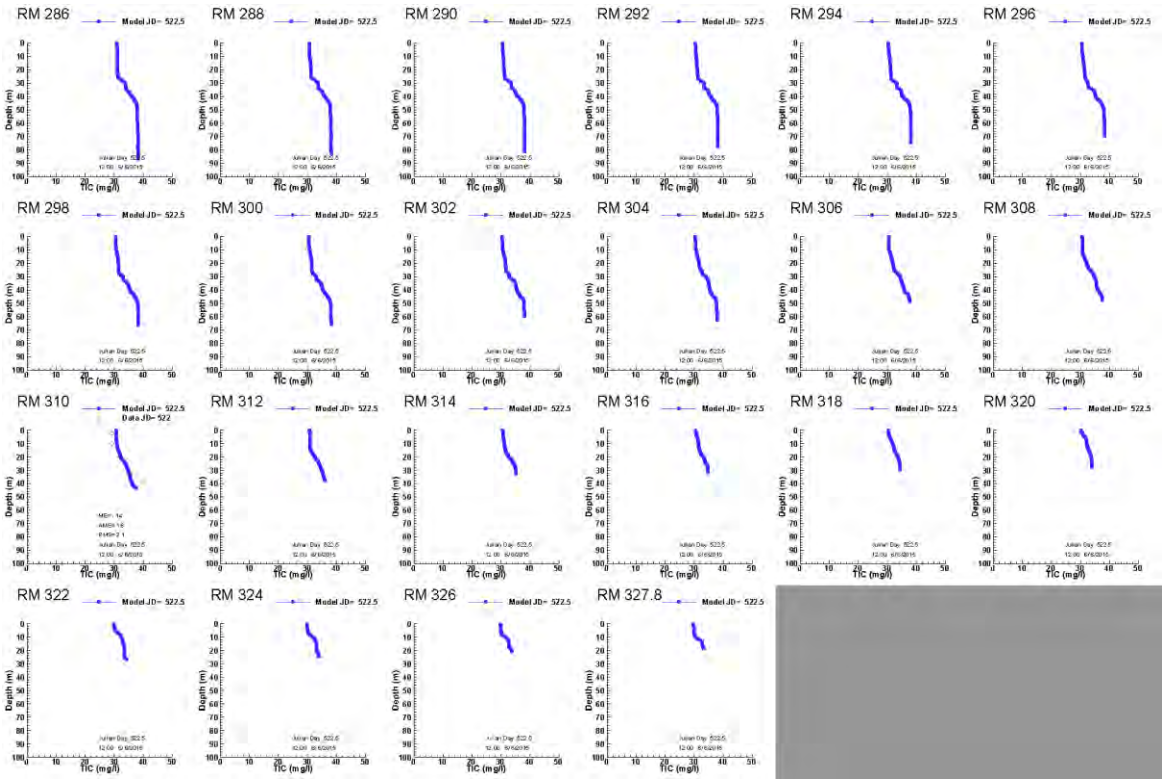


Figure 1234. Vertical profiles of TIC compared with data for 6/ 6/2015.

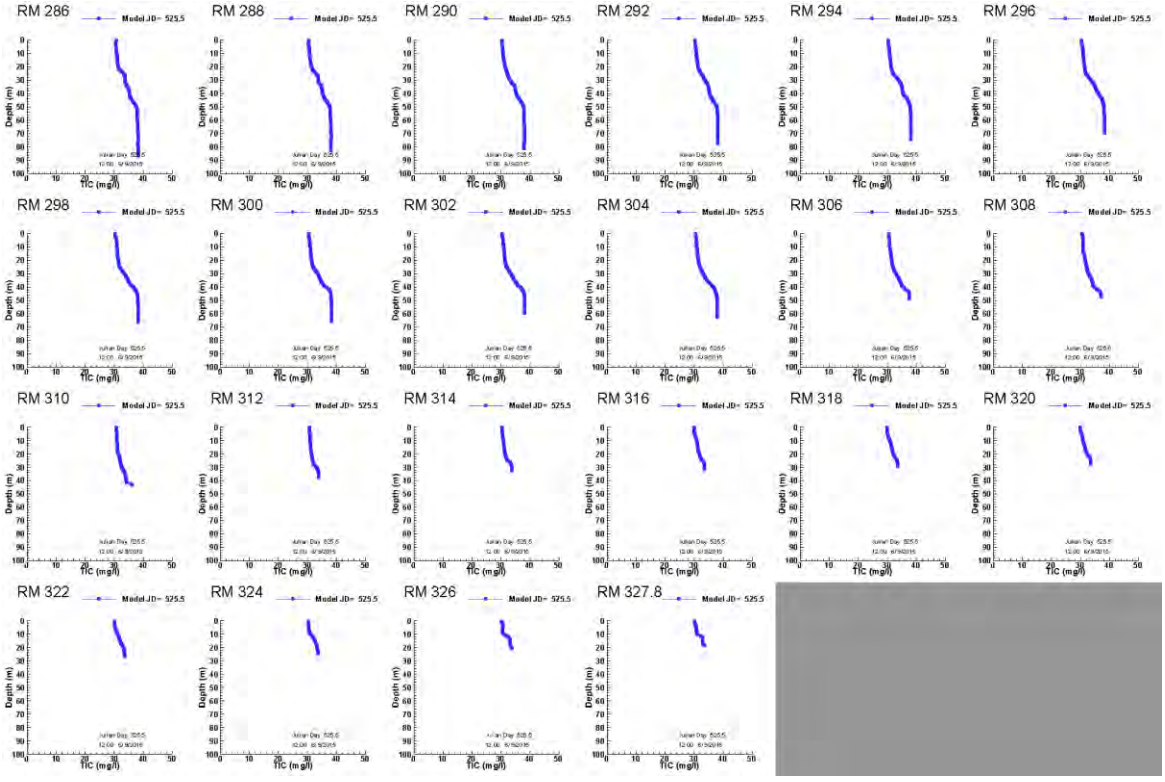


Figure 1235. Vertical profiles of TIC compared with data for 6/ 9/2015.

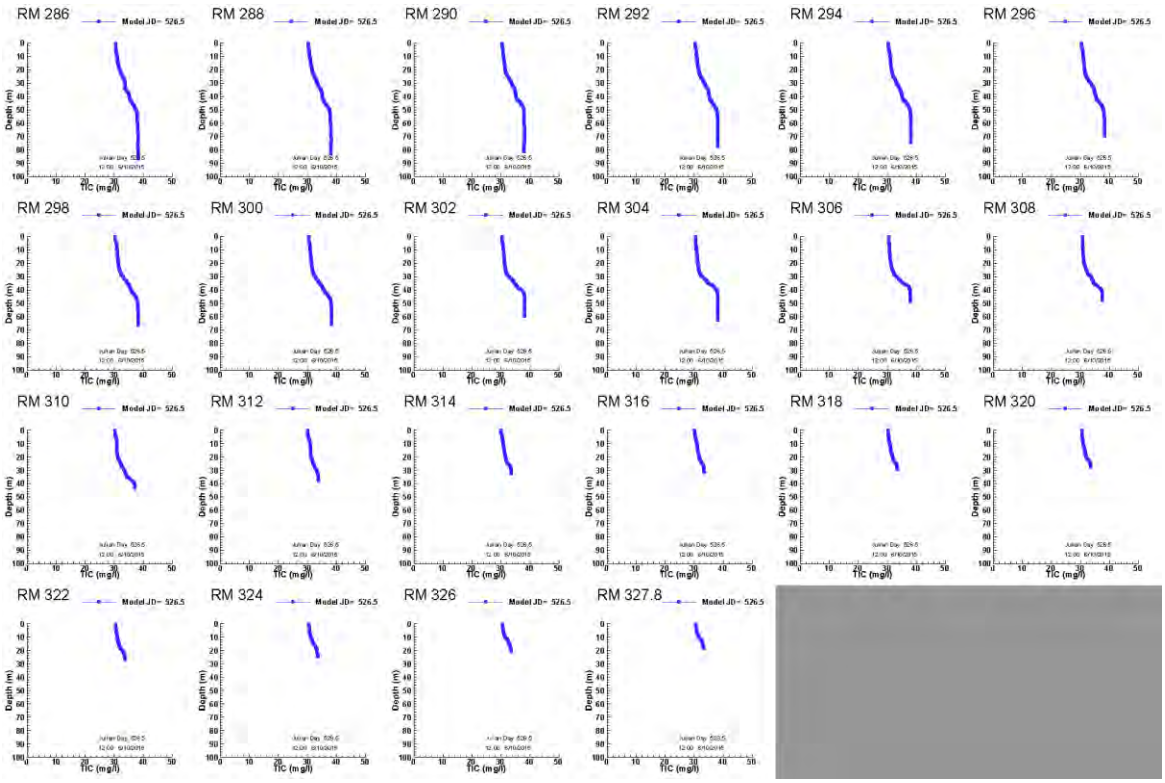


Figure 1236. Vertical profiles of TIC compared with data for 6/10/2015.

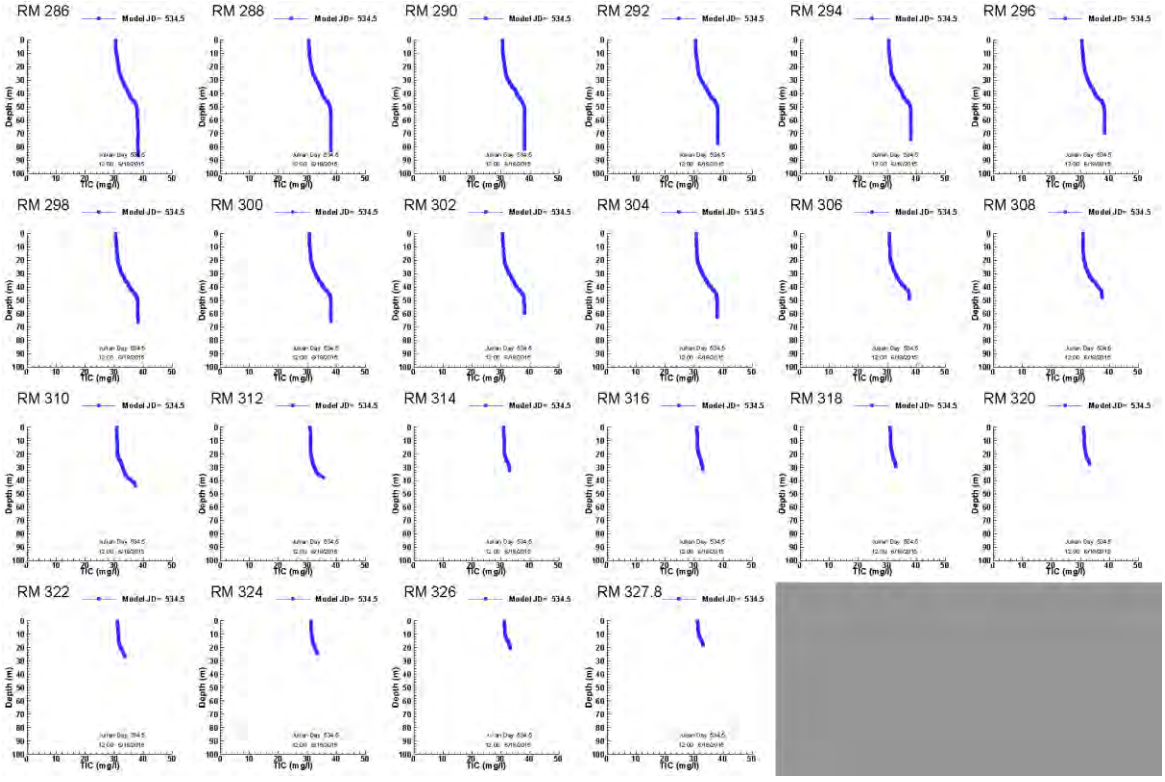


Figure 1237. Vertical profiles of TIC compared with data for 6/18/2015.

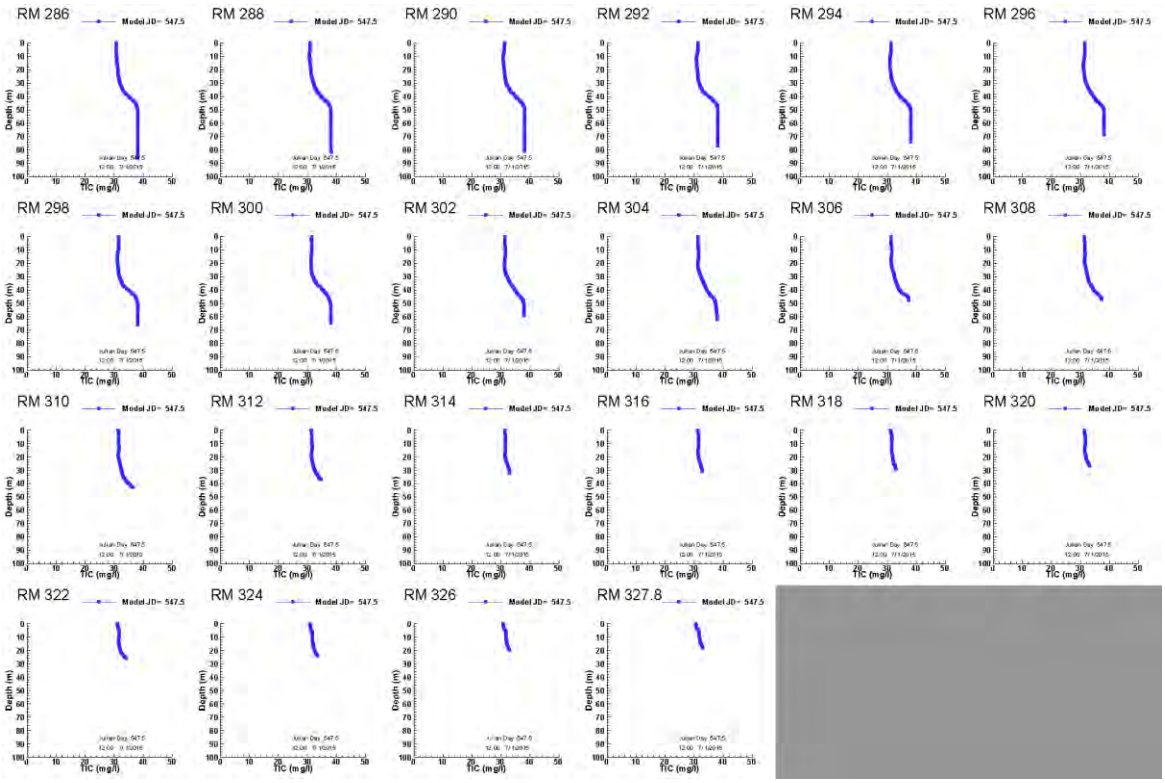


Figure 1238. Vertical profiles of TIC compared with data for 7/ 1/2015.

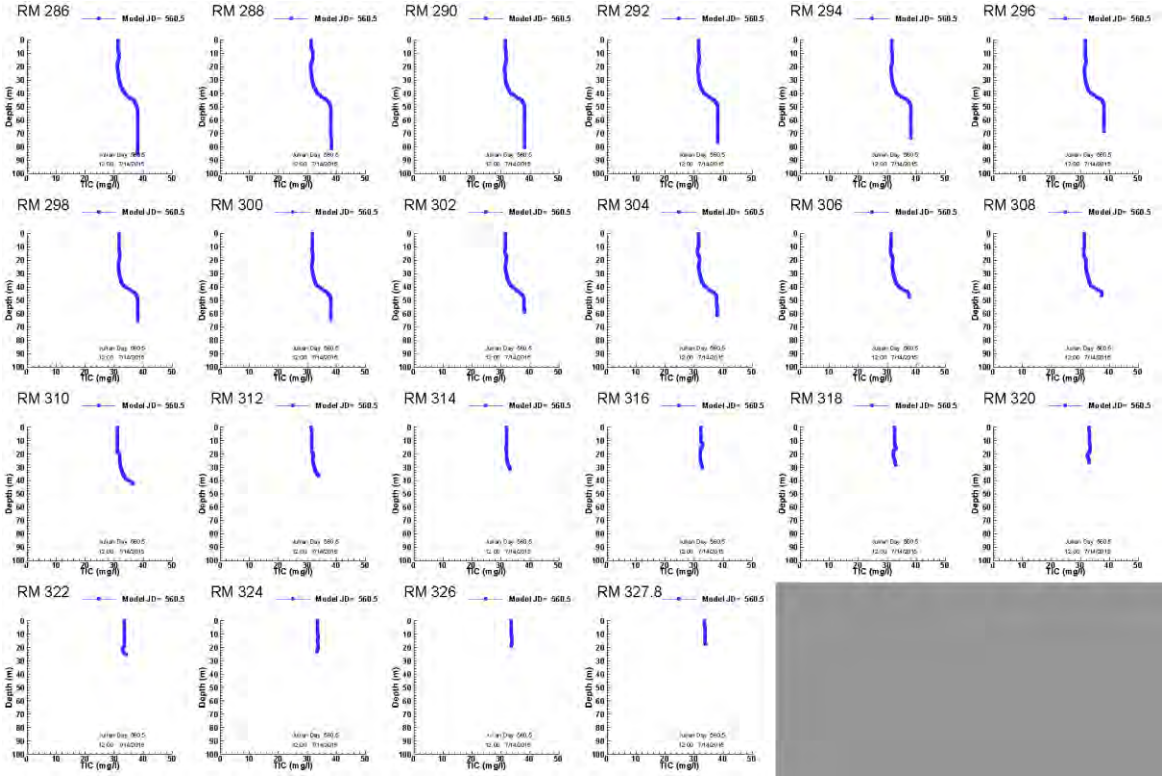


Figure 1239. Vertical profiles of TIC compared with data for 7/14/2015.

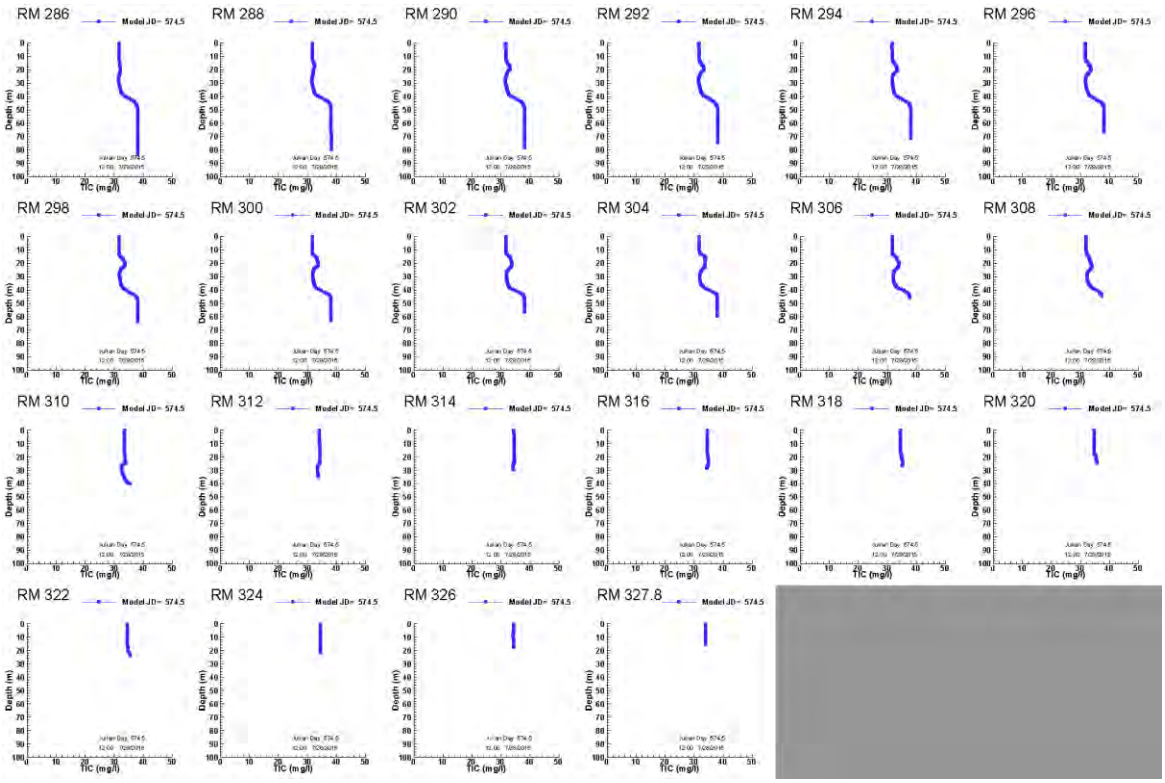


Figure 1240. Vertical profiles of TIC compared with data for 7/28/2015.

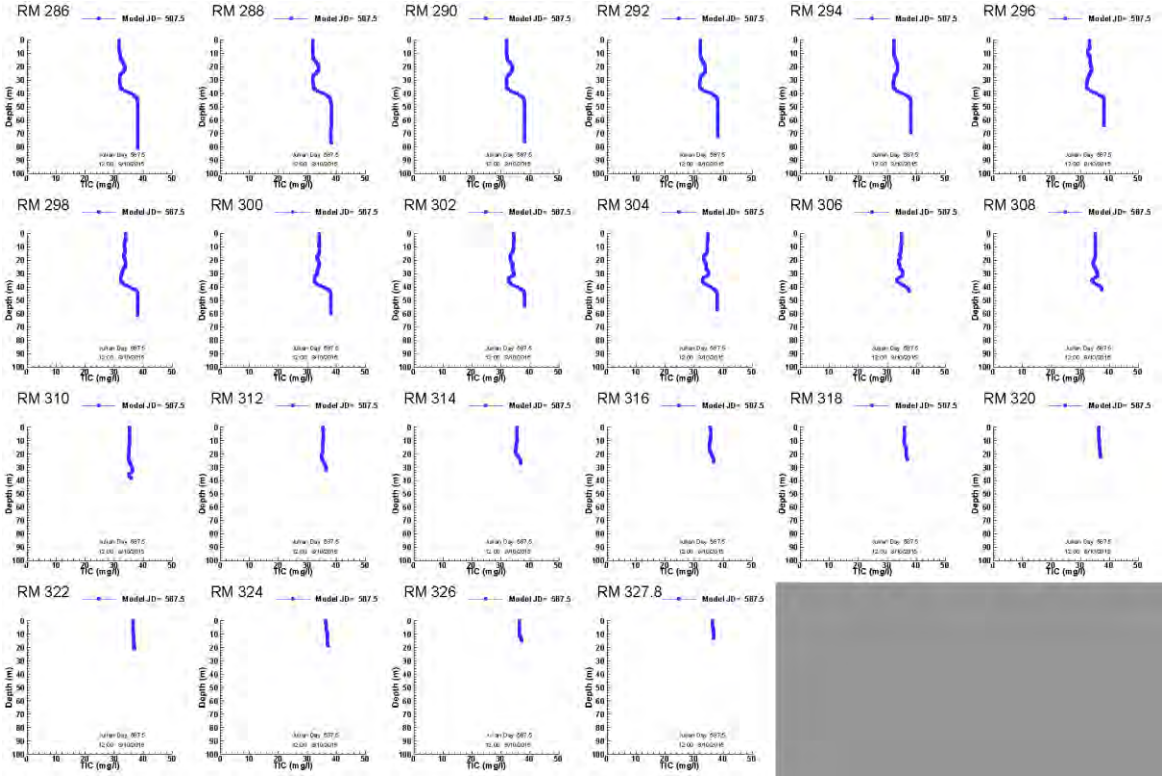


Figure 1241. Vertical profiles of TIC compared with data for 8/10/2015.

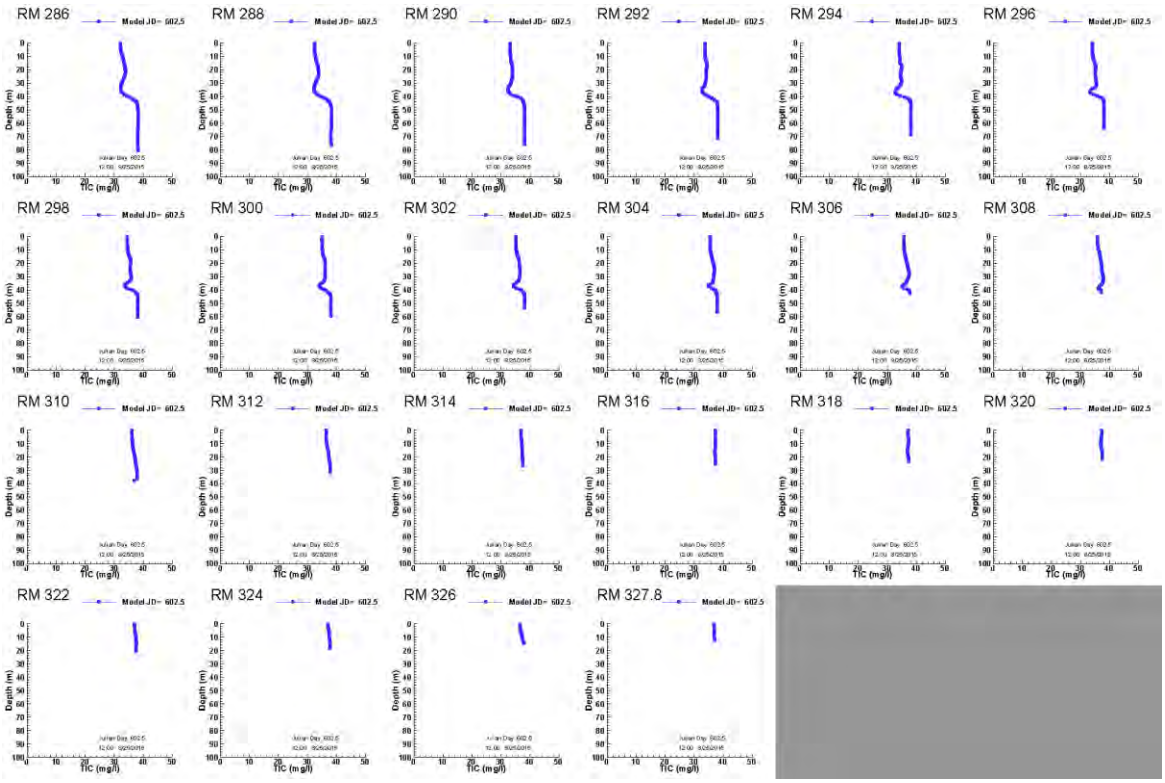


Figure 1242. Vertical profiles of TIC compared with data for 8/25/2015.

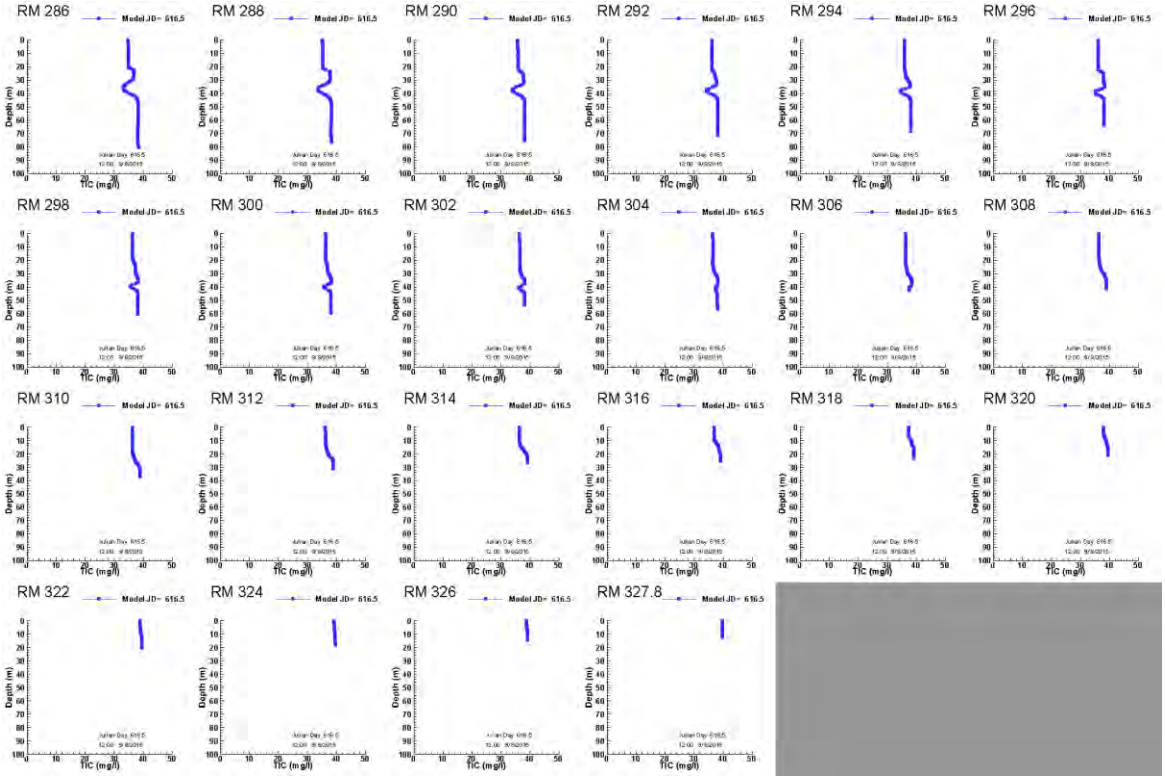


Figure 1243. Vertical profiles of TIC compared with data for 9/ 8/2015.

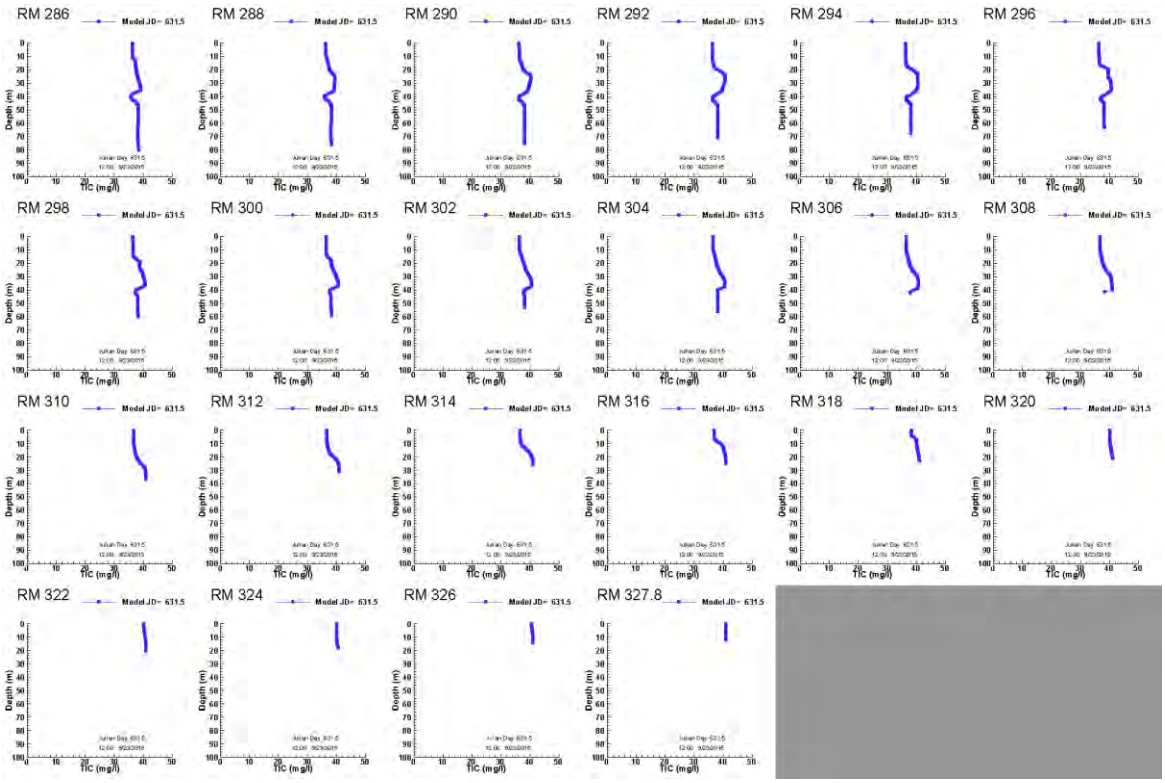


Figure 1244. Vertical profiles of TIC compared with data for 9/23/2015.

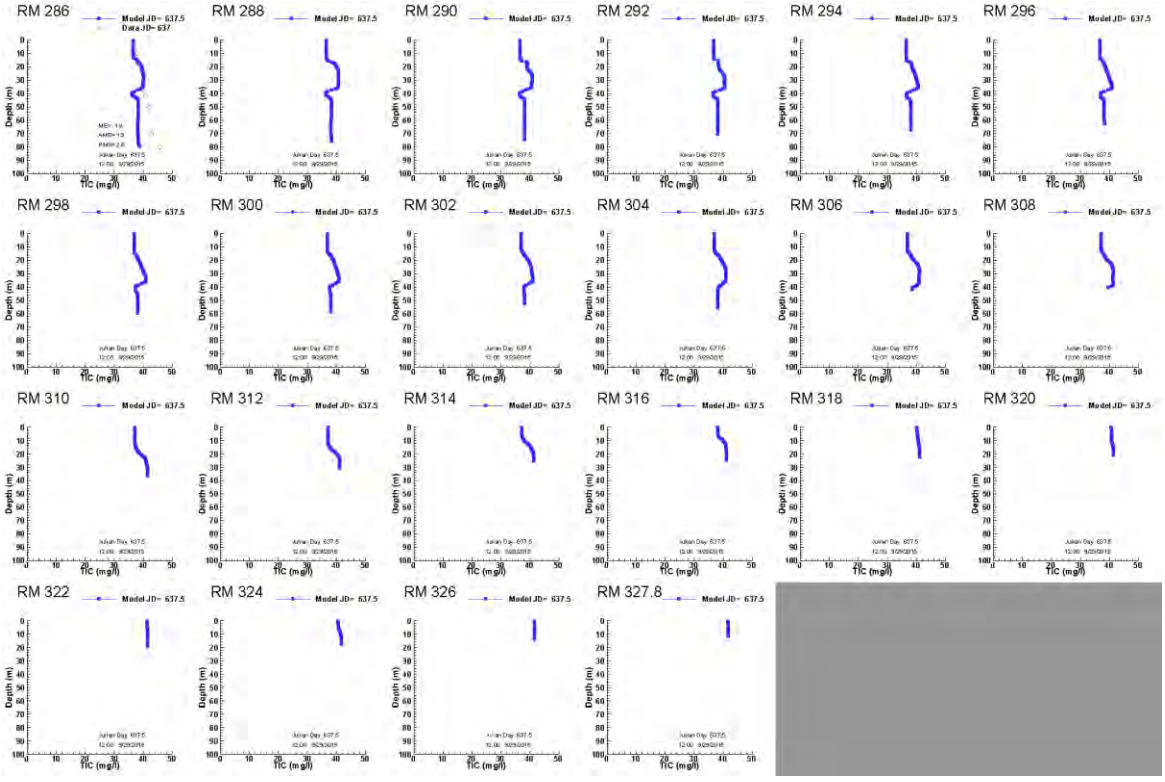


Figure 1245. Vertical profiles of TIC compared with data for 9/29/2015.

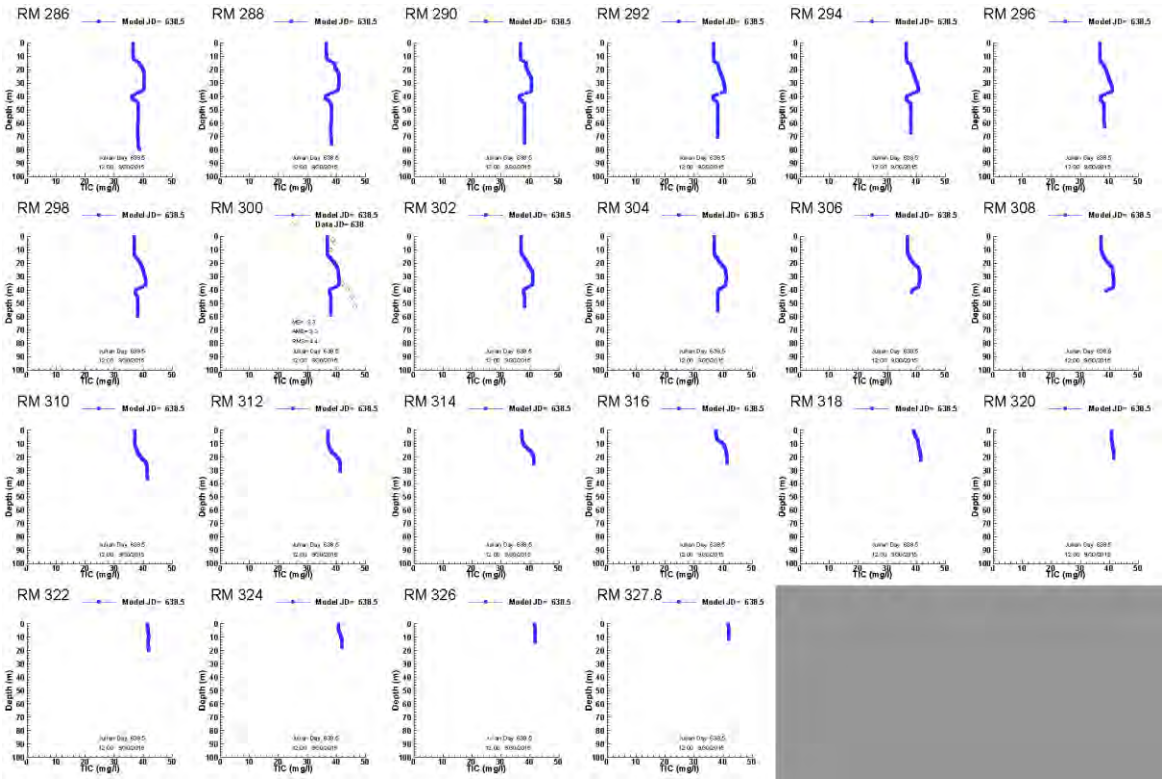


Figure 1246. Vertical profiles of TIC compared with data for 9/30/2015.

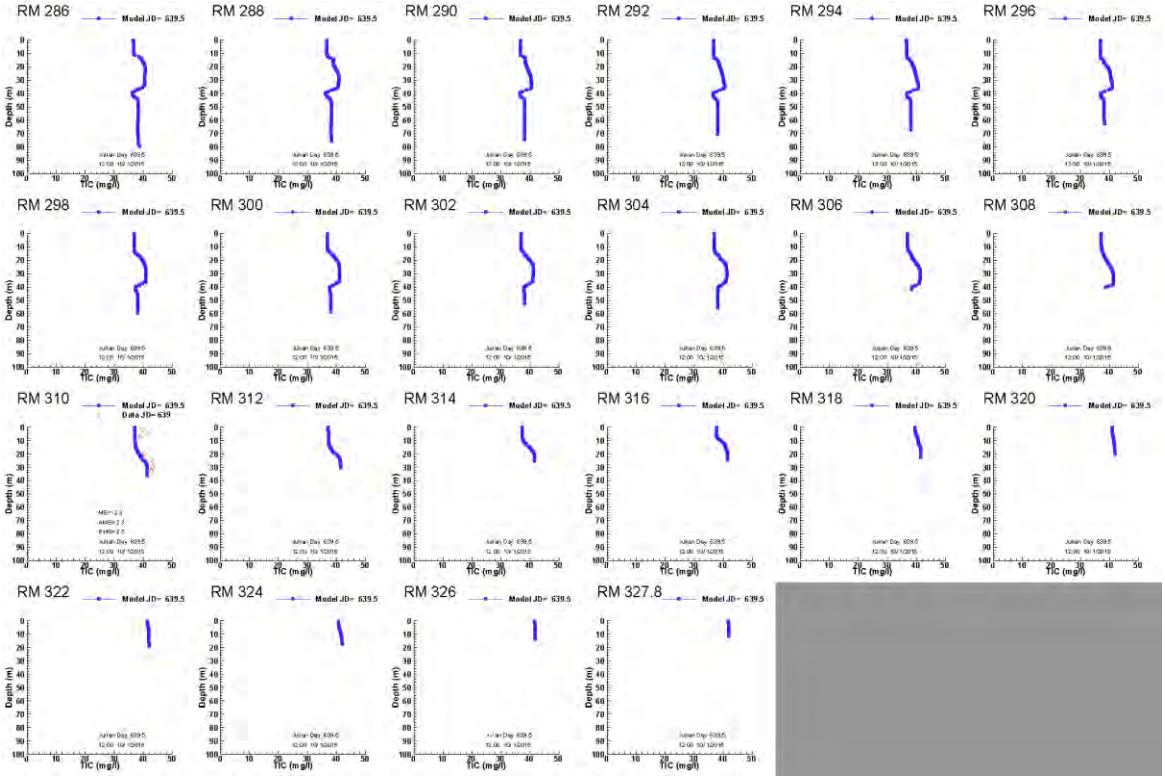


Figure 1247. Vertical profiles of TIC compared with data for 10/ 1/2015.

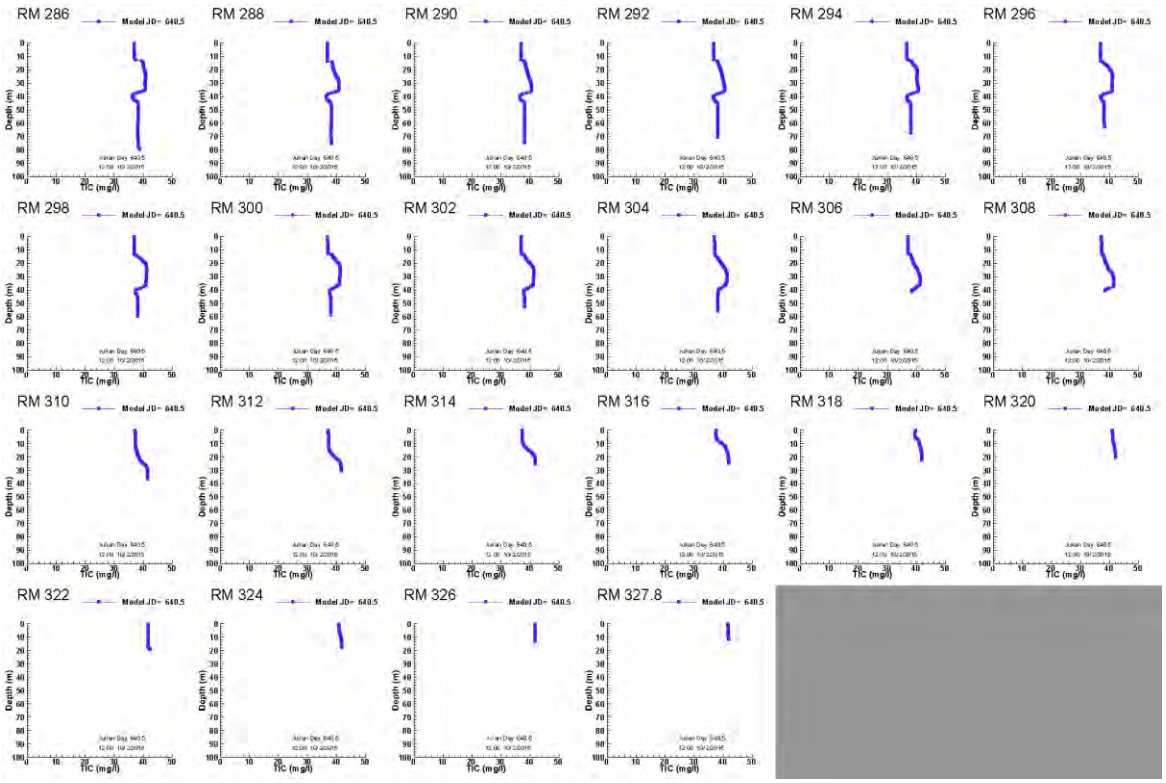


Figure 1248. Vertical profiles of TIC compared with data for 10/ 2/2015.

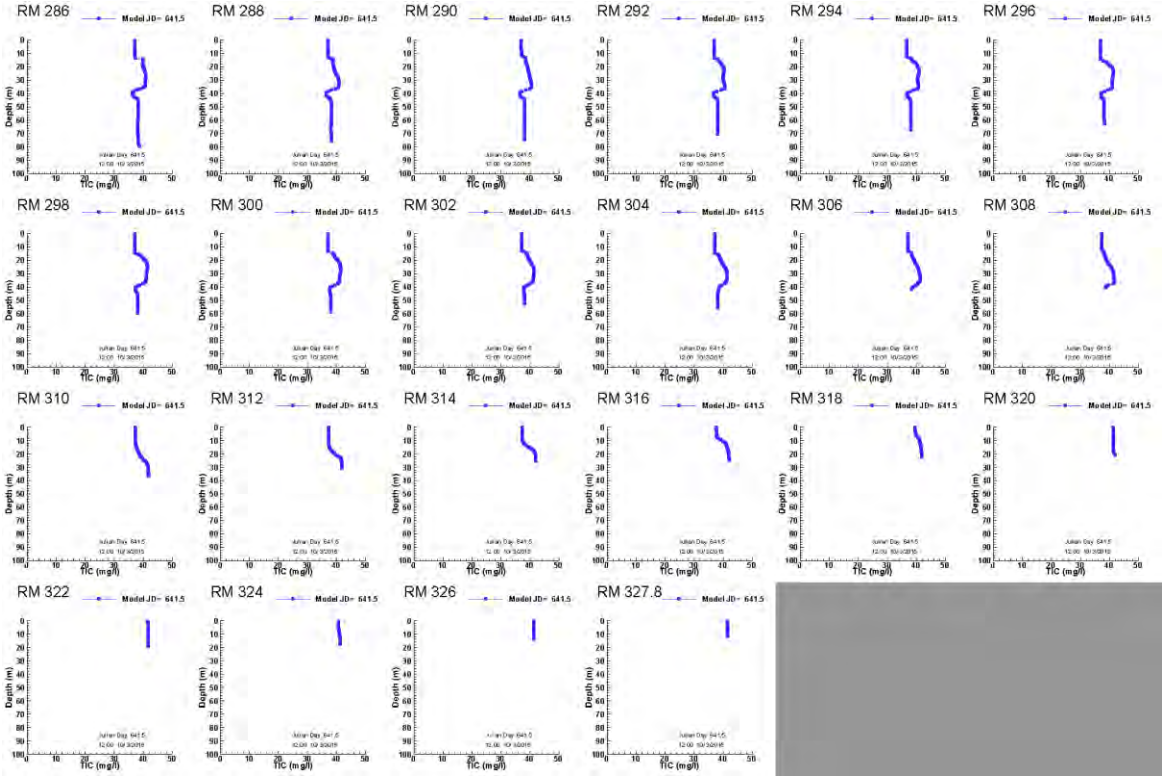


Figure 1249. Vertical profiles of TIC compared with data for 10/ 3/2015.

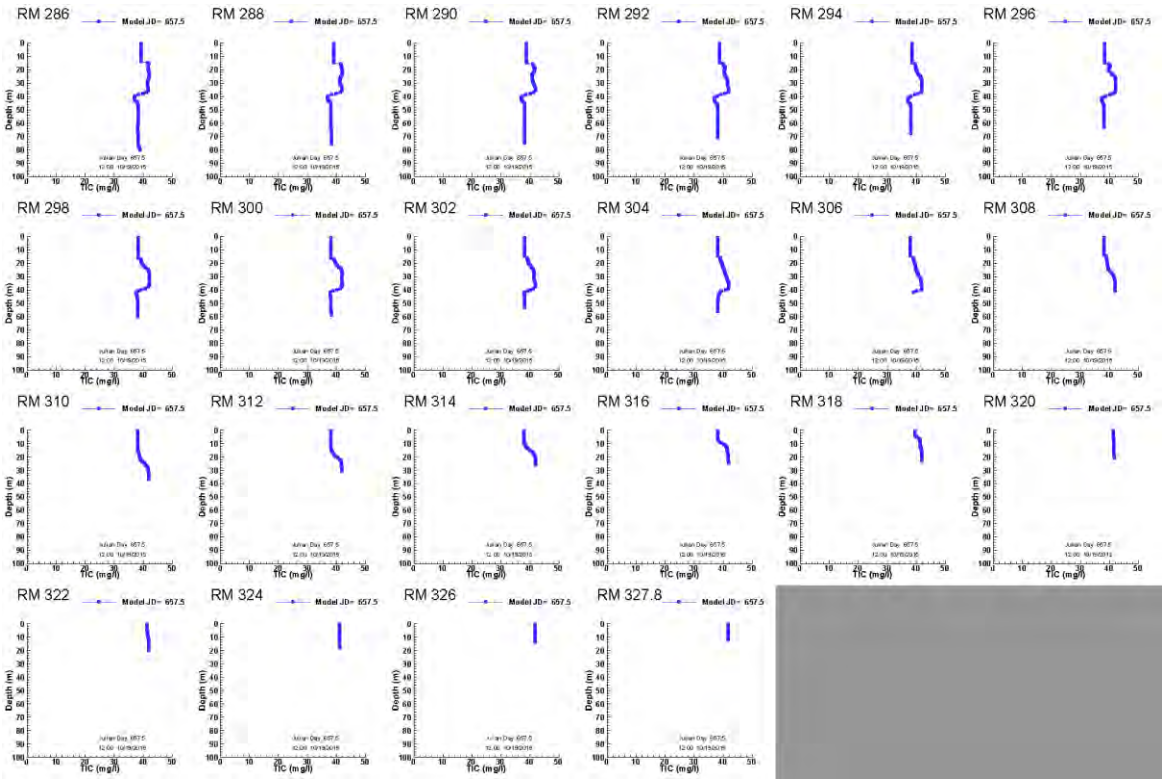


Figure 1250. Vertical profiles of TIC compared with data for 10/19/2015.

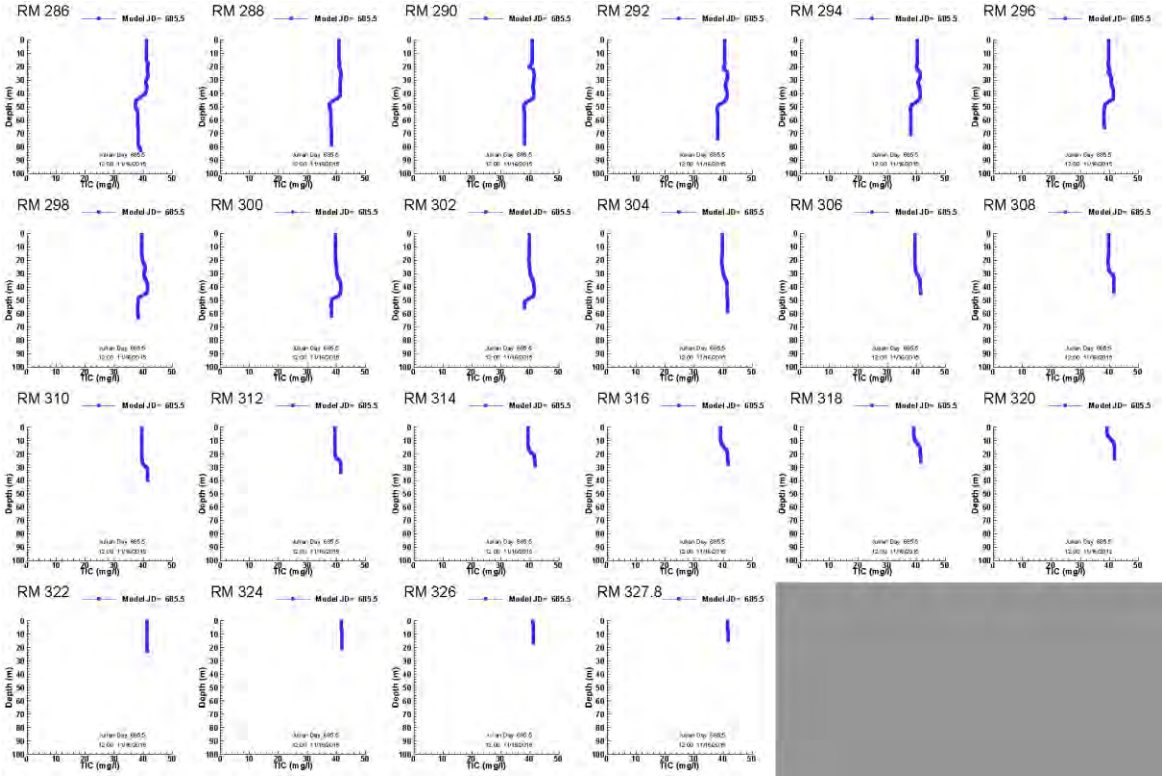


Figure 1251. Vertical profiles of TIC compared with data for 11/16/2015.

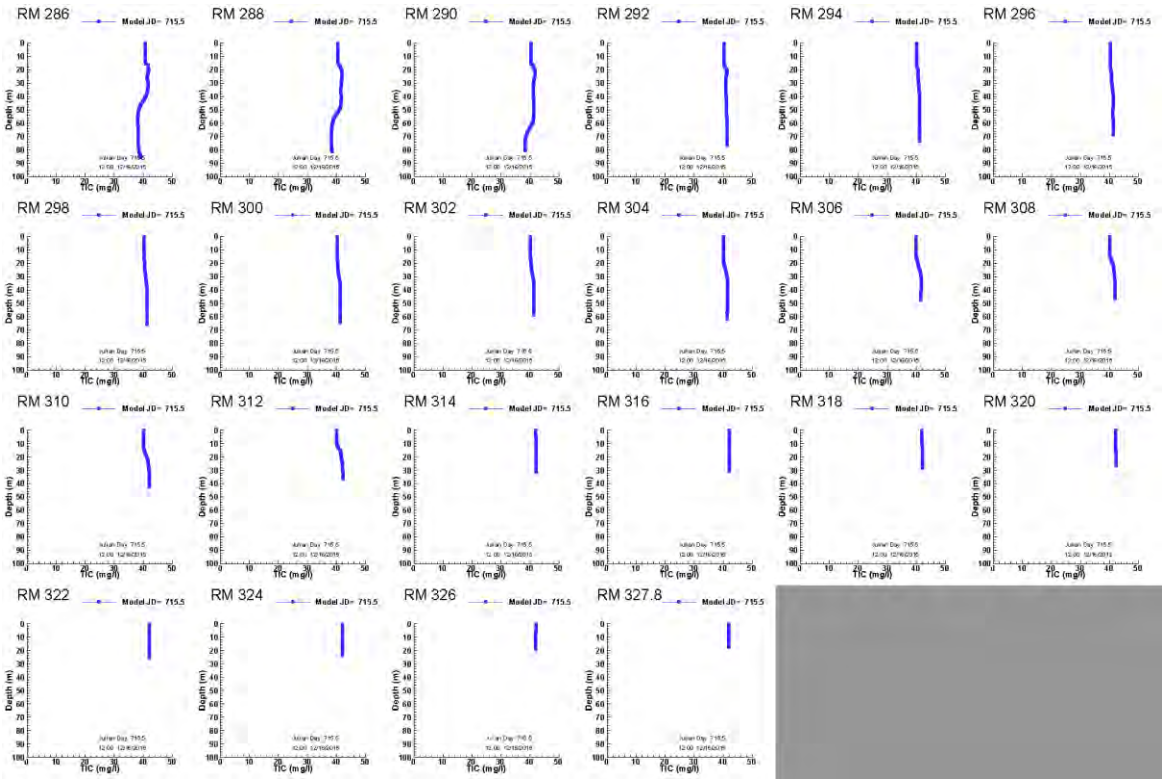


Figure 1252. Vertical profiles of TIC compared with data for 12/16/2015.

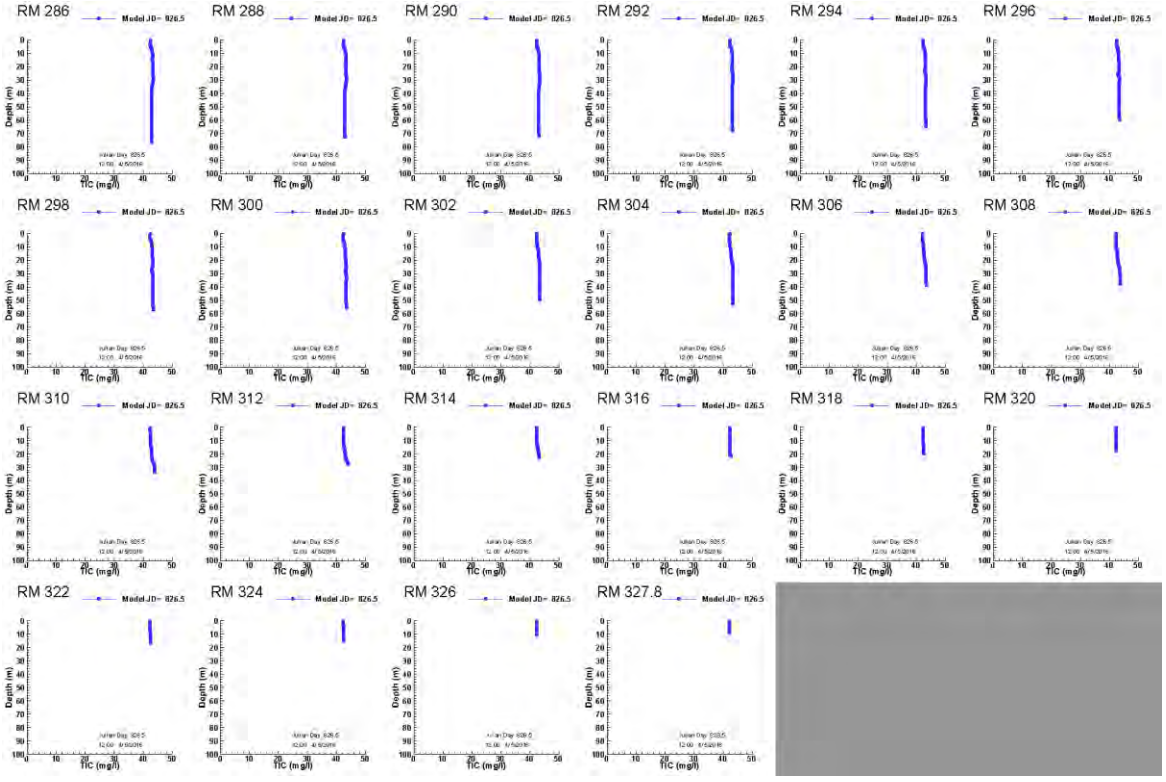


Figure 1253. Vertical profiles of TIC compared with data for 4/ 5/2016.

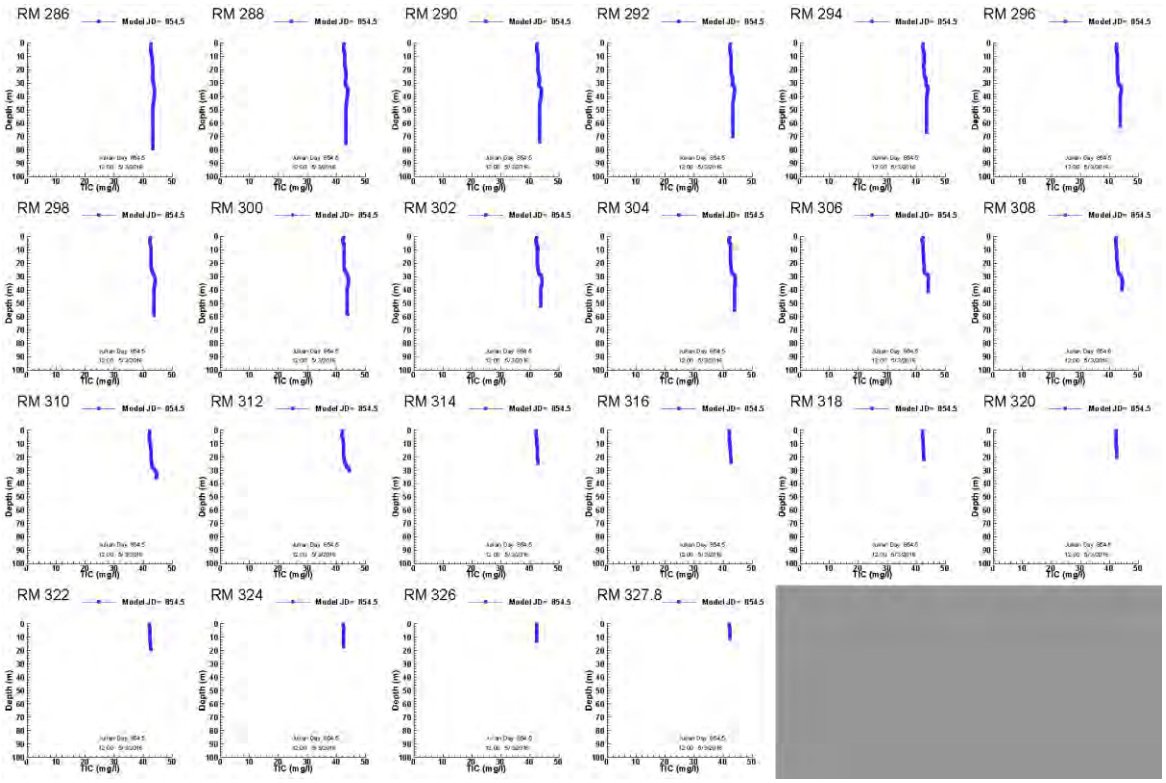


Figure 1254. Vertical profiles of TIC compared with data for 5/ 3/2016.

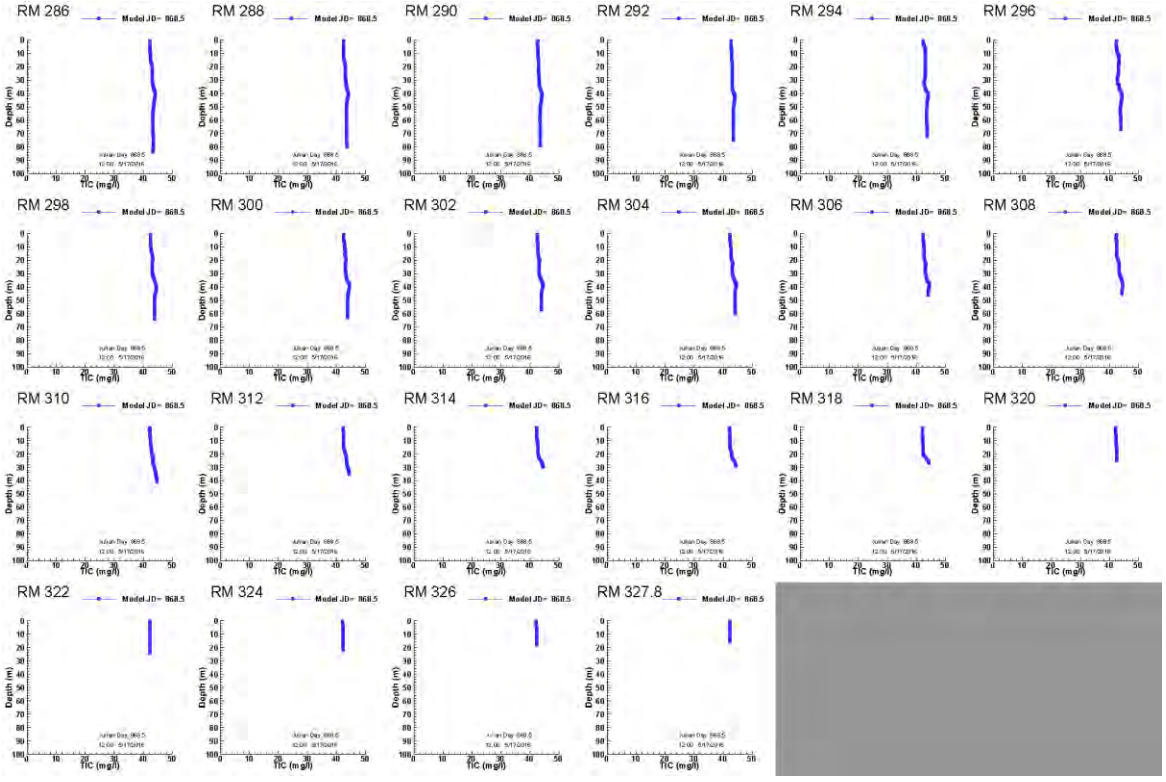


Figure 1255. Vertical profiles of TIC compared with data for 5/17/2016.

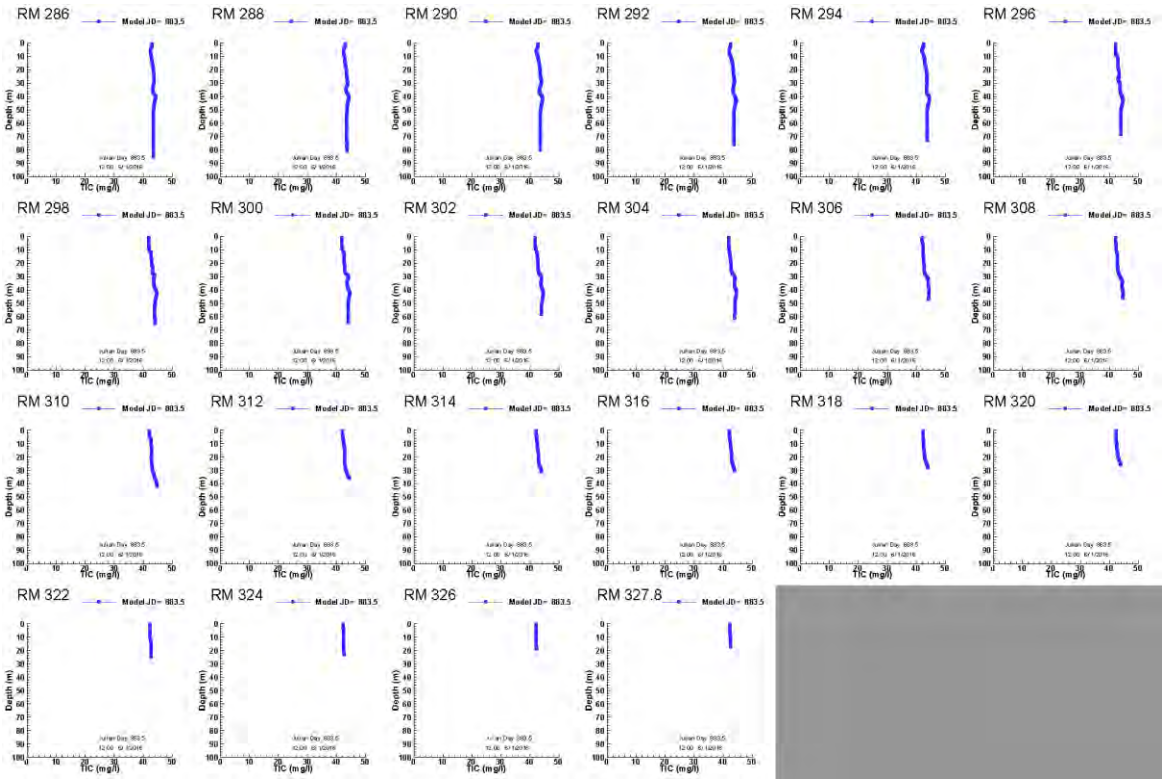


Figure 1256. Vertical profiles of TIC compared with data for 6/ 1/2016.

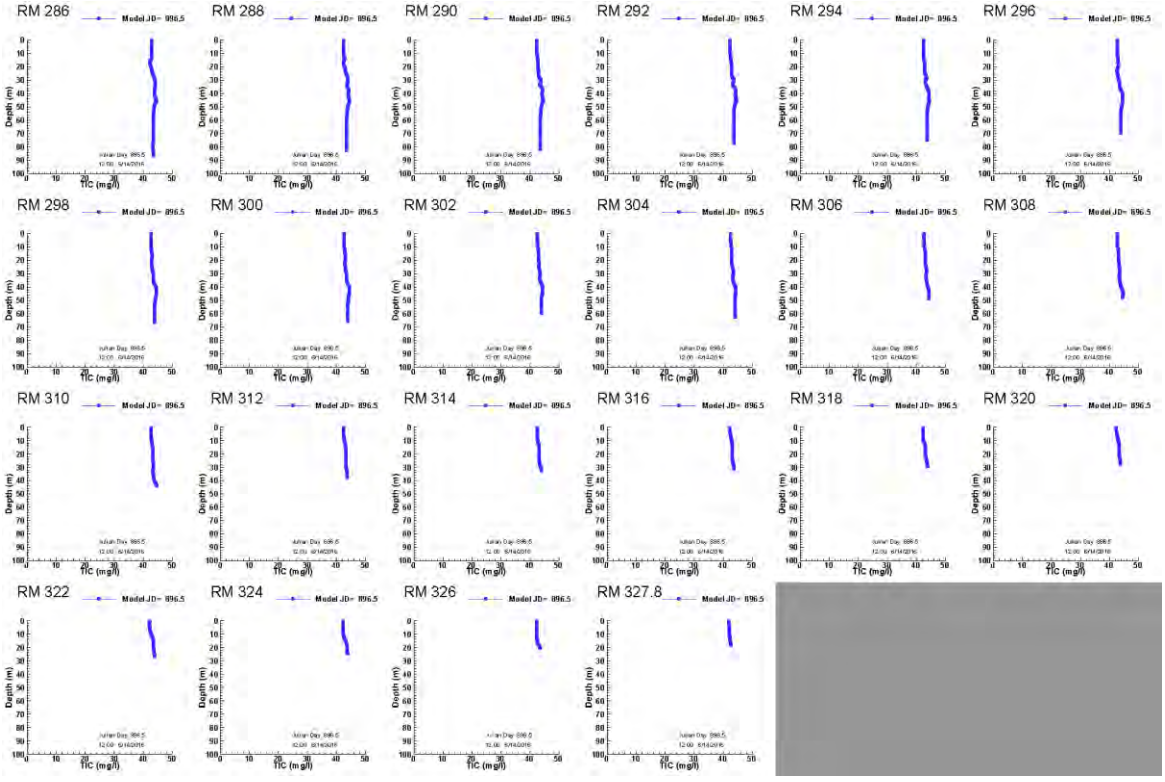


Figure 1257. Vertical profiles of TIC compared with data for 6/14/2016.

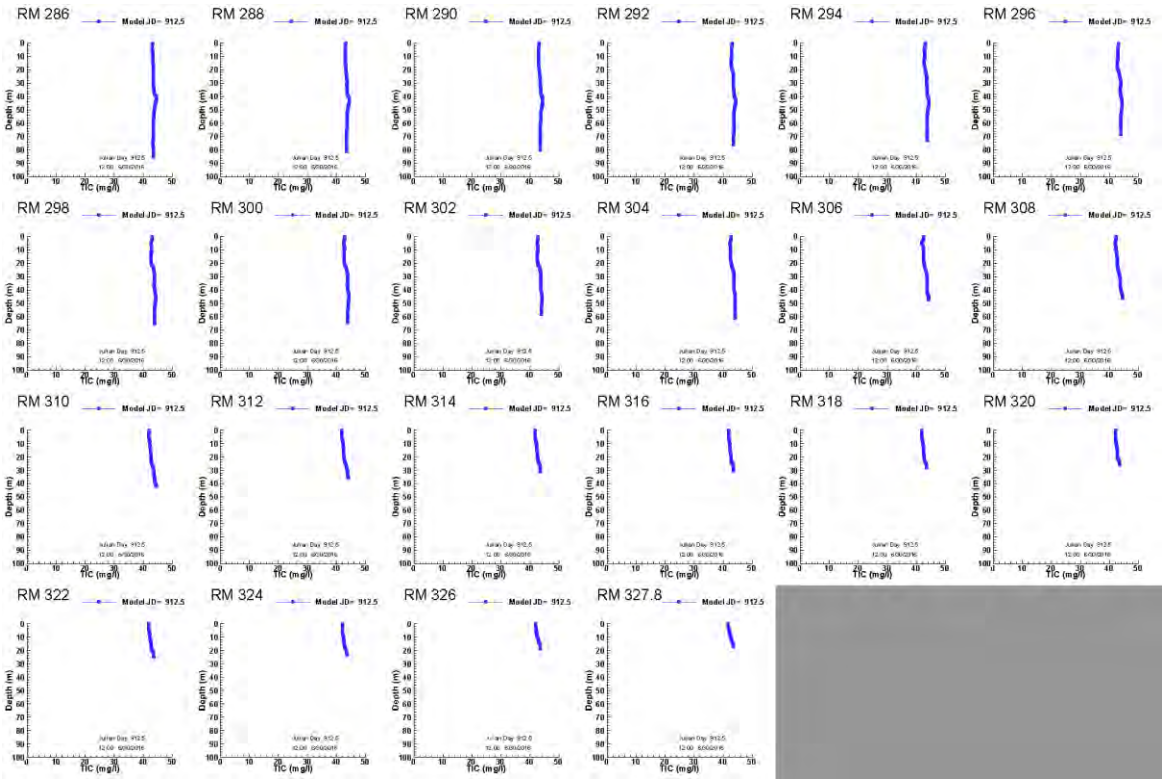


Figure 1258. Vertical profiles of TIC compared with data for 6/30/2016.

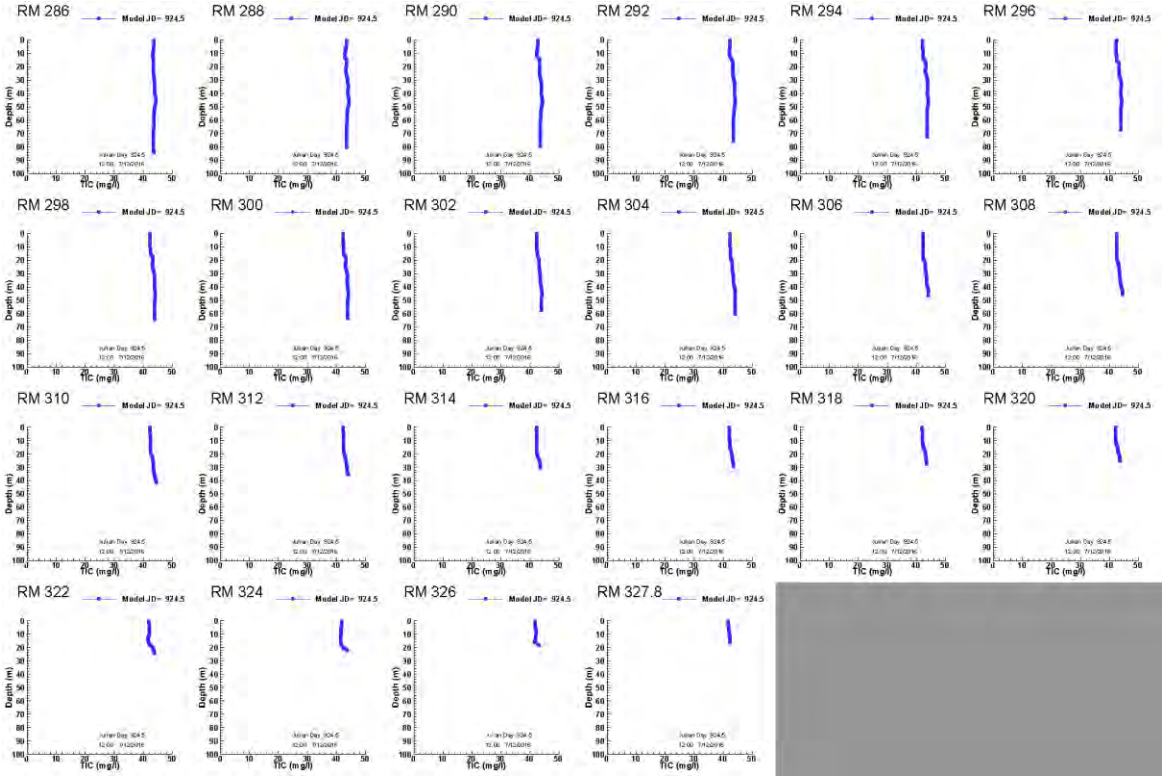


Figure 1259. Vertical profiles of TIC compared with data for 7/12/2016.

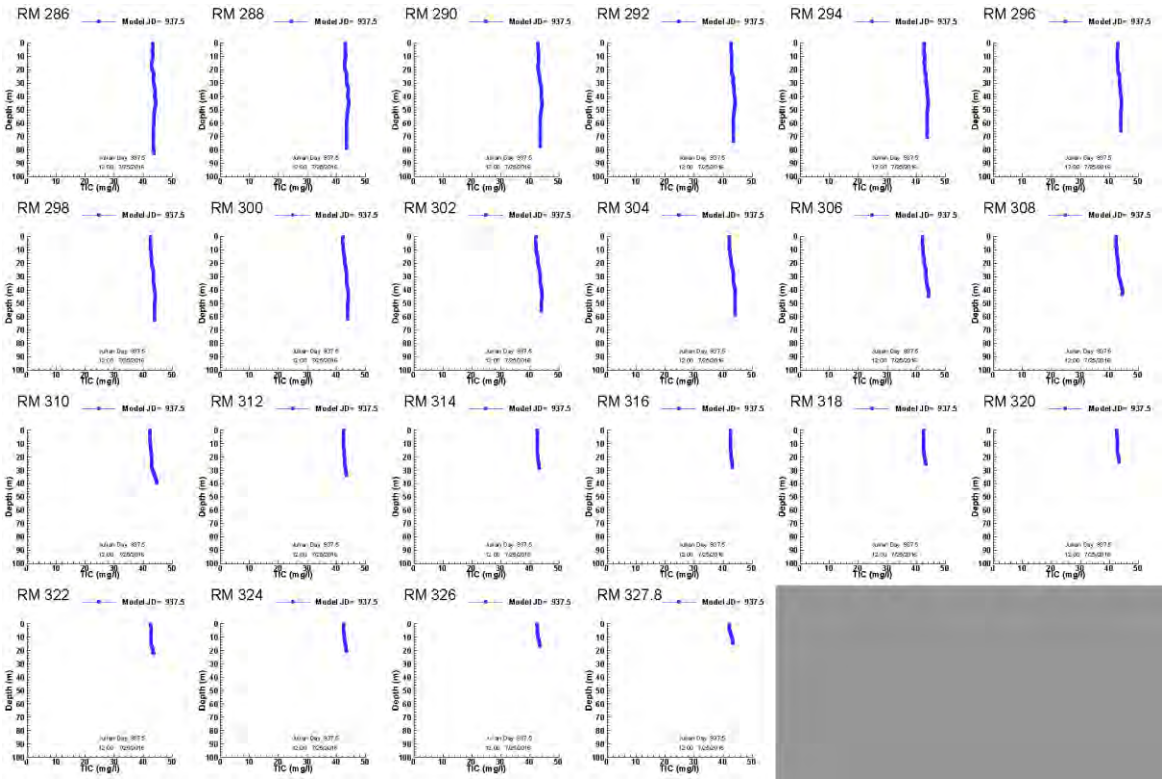


Figure 1260. Vertical profiles of TIC compared with data for 7/25/2016.

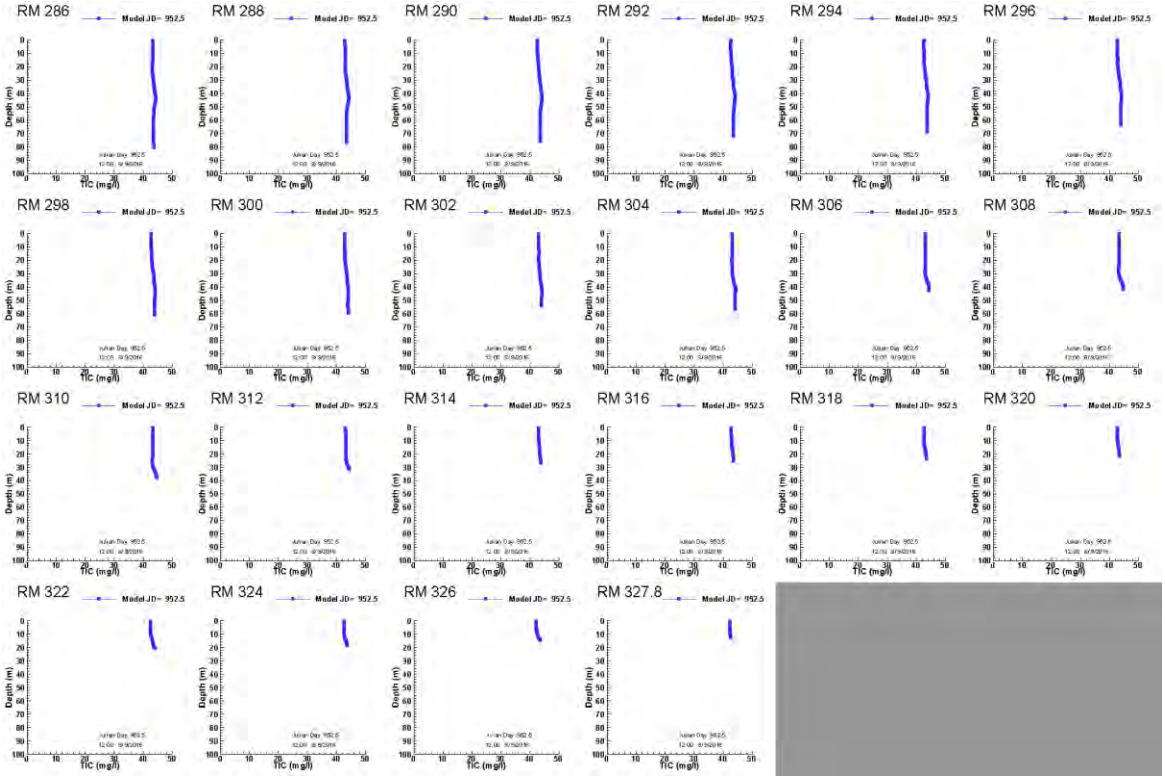


Figure 1261. Vertical profiles of TIC compared with data for 8/ 9/2016.

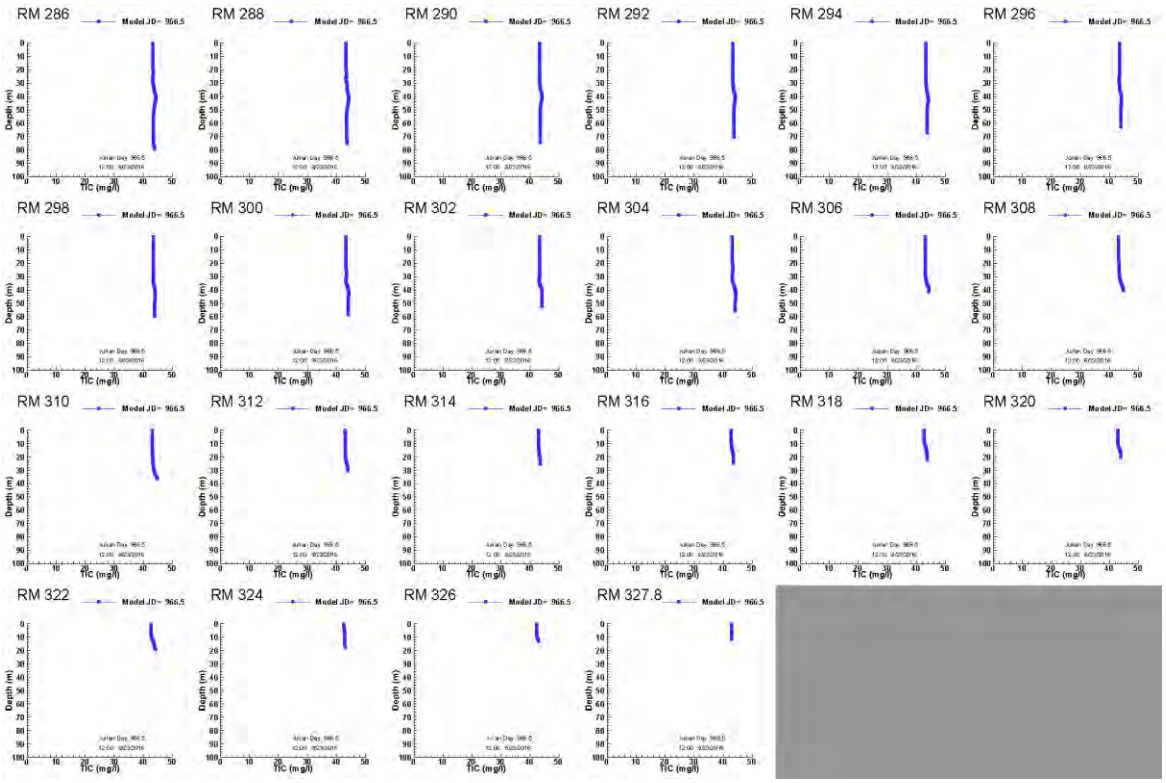


Figure 1262. Vertical profiles of TIC compared with data for 8/23/2016.

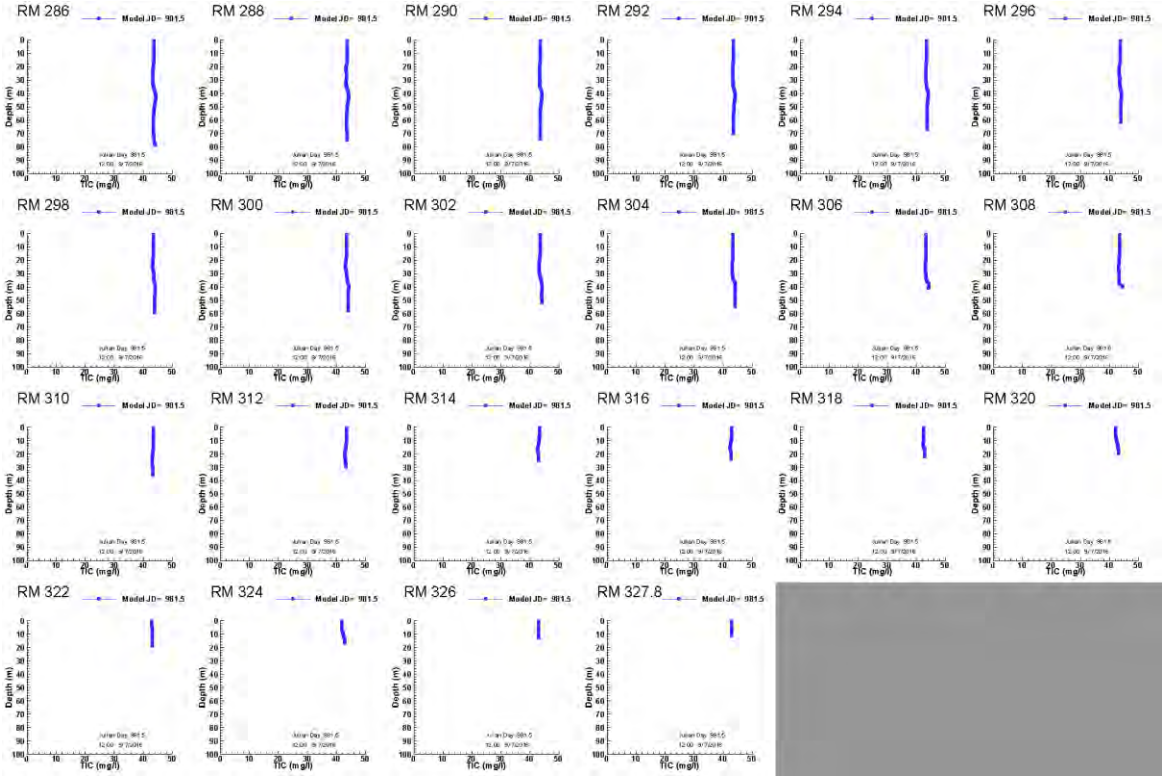


Figure 1263. Vertical profiles of TIC compared with data for 9/ 7/2016.

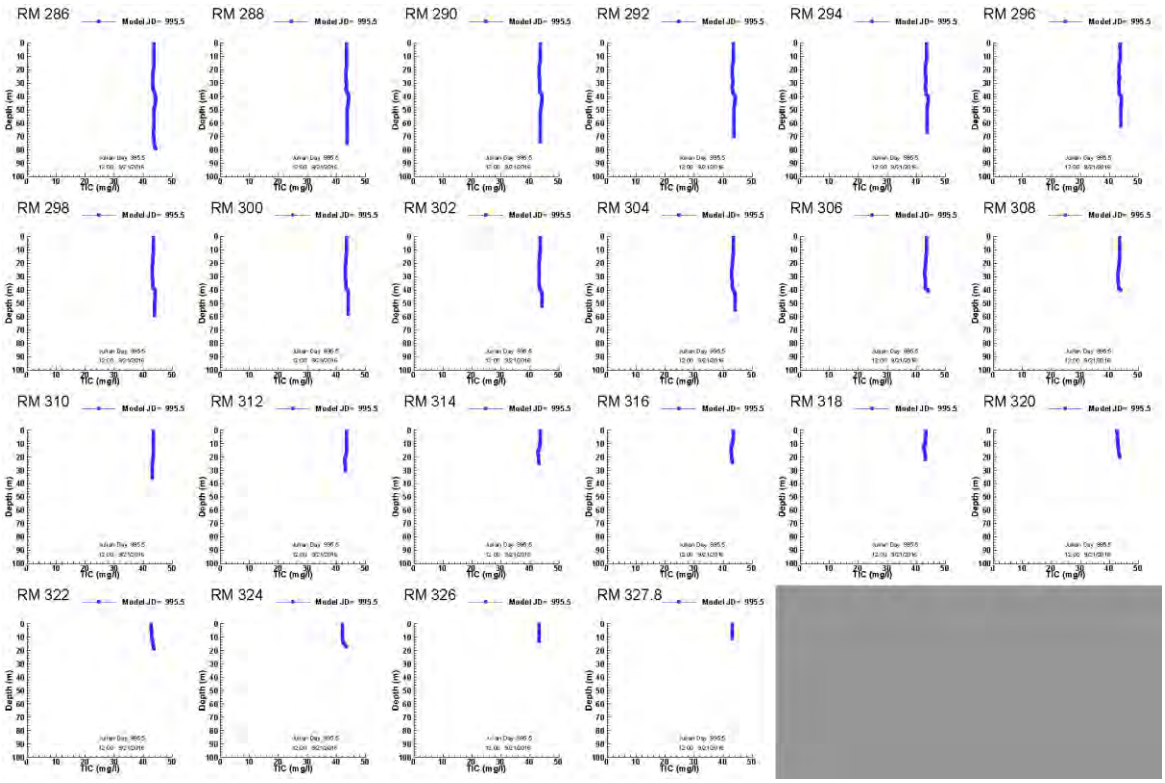


Figure 1264. Vertical profiles of TIC compared with data for 9/21/2016.

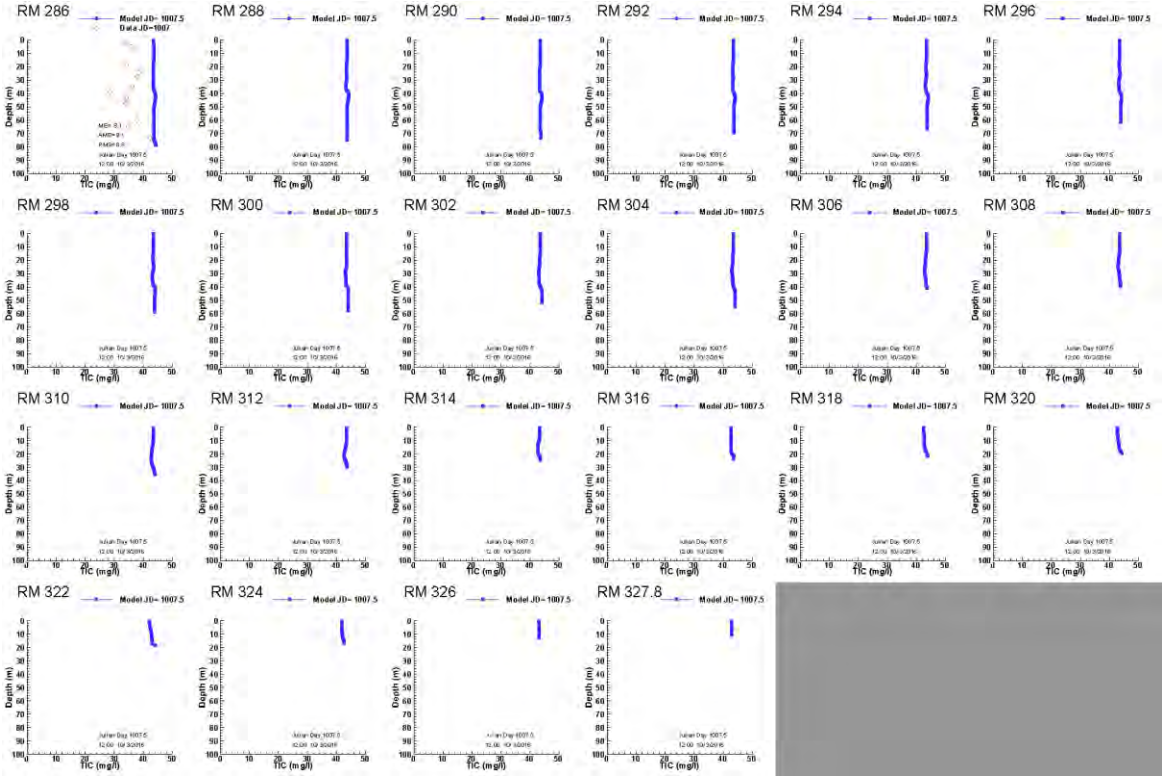


Figure 1265. Vertical profiles of TIC compared with data for 10/ 3/2016.

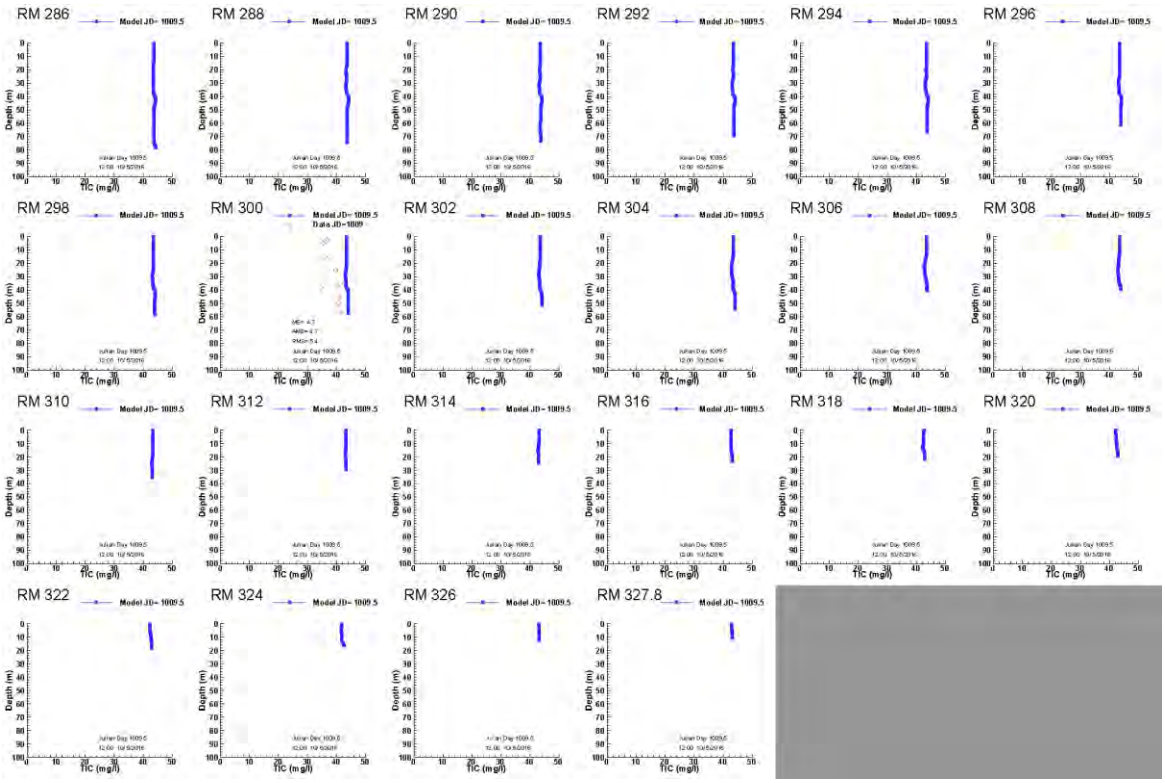


Figure 1266. Vertical profiles of TIC compared with data for 10/ 5/2016.

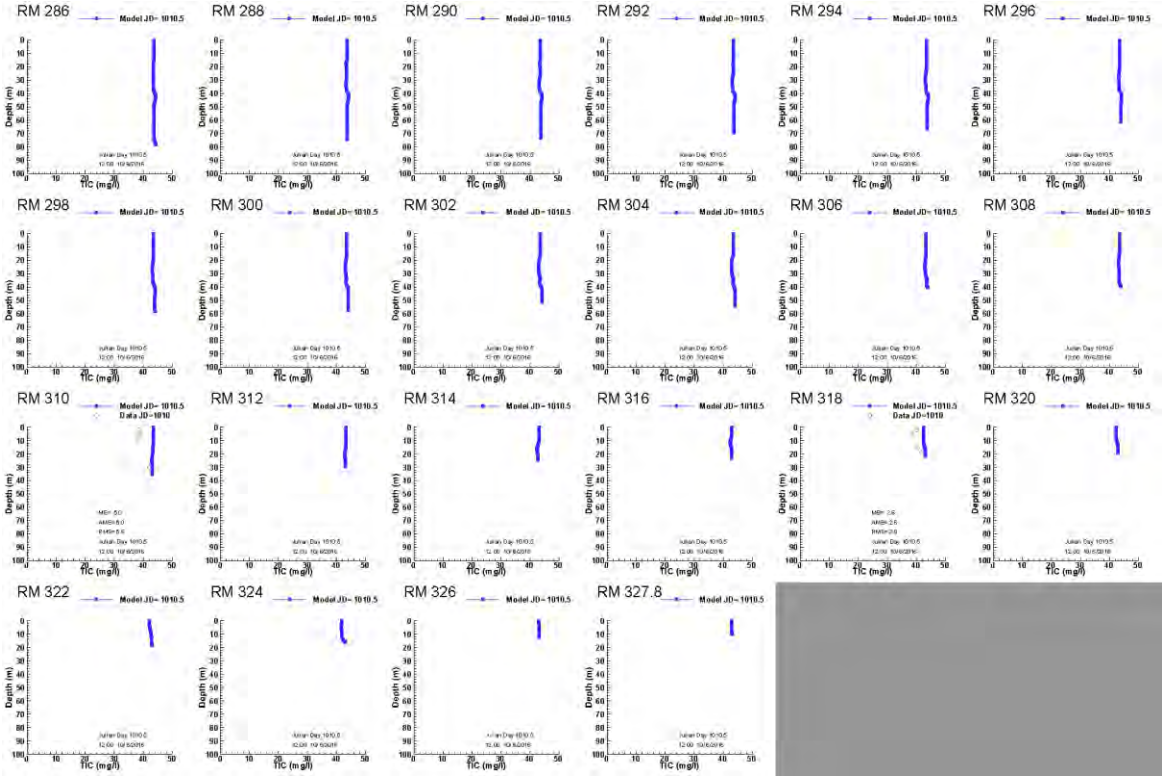


Figure 1267. Vertical profiles of TIC compared with data for 10/ 6/2016.

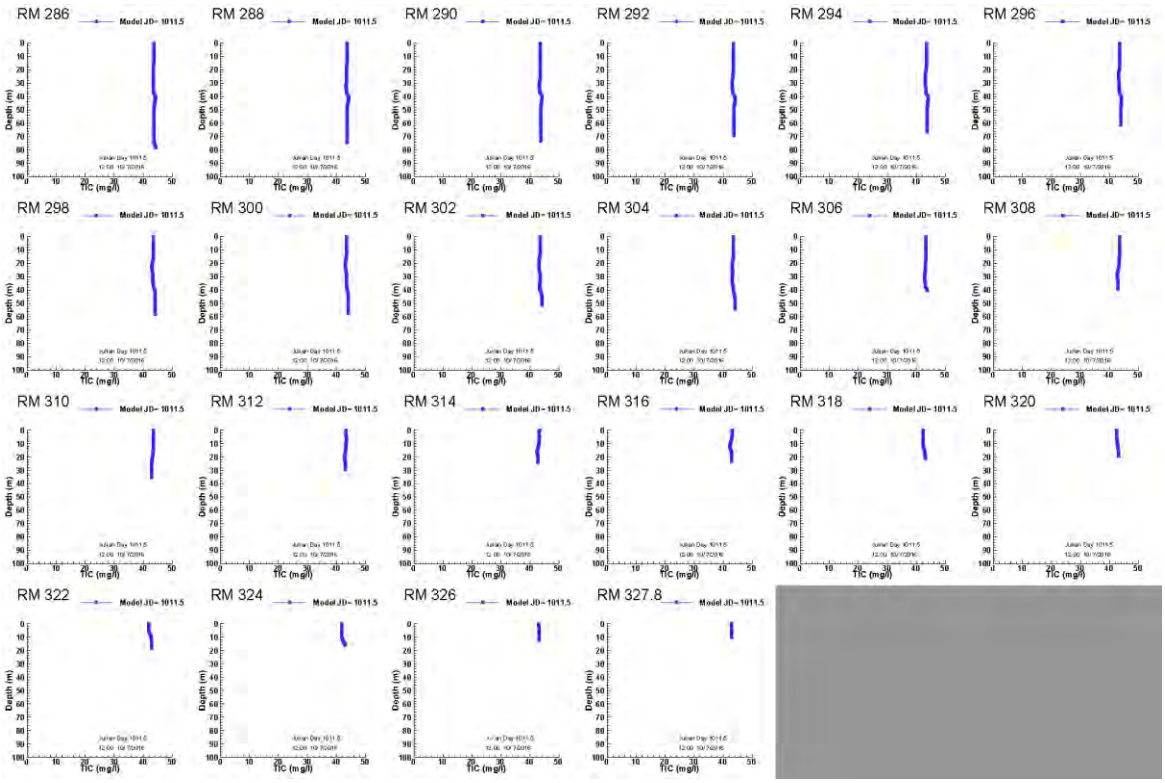


Figure 1268. Vertical profiles of TIC compared with data for 10/ 7/2016.

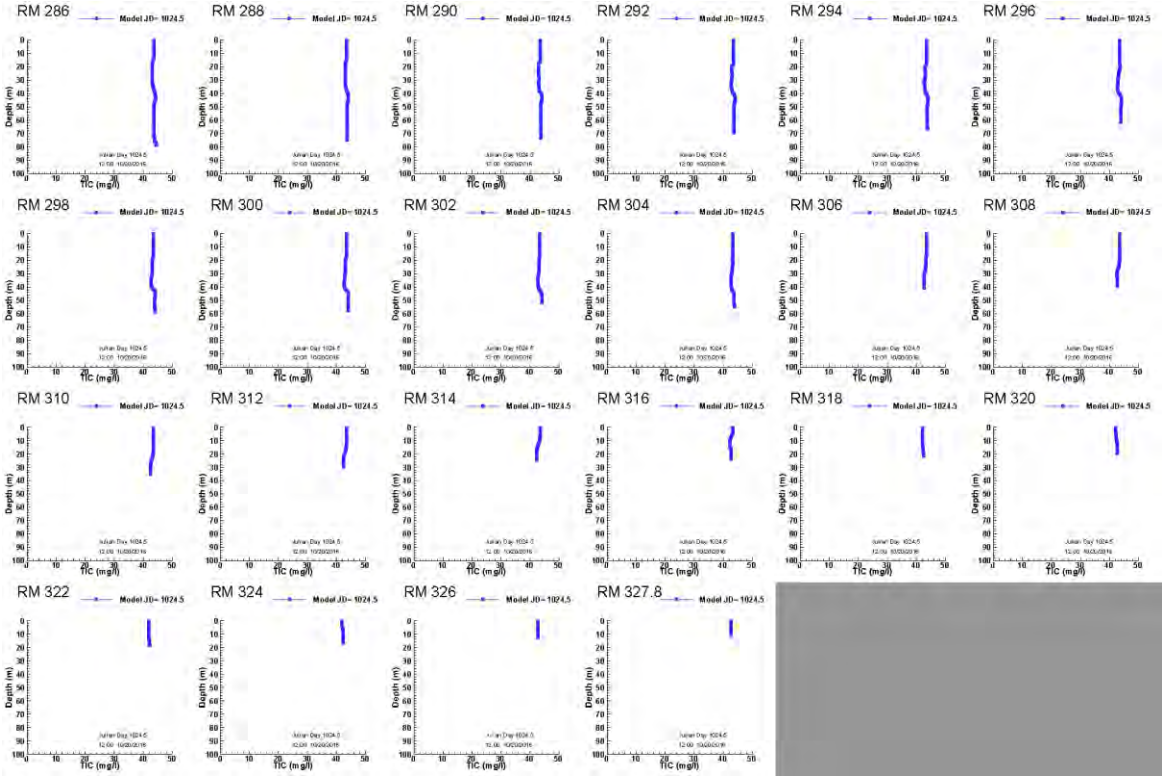


Figure 1269. Vertical profiles of TIC compared with data for 10/20/2016.

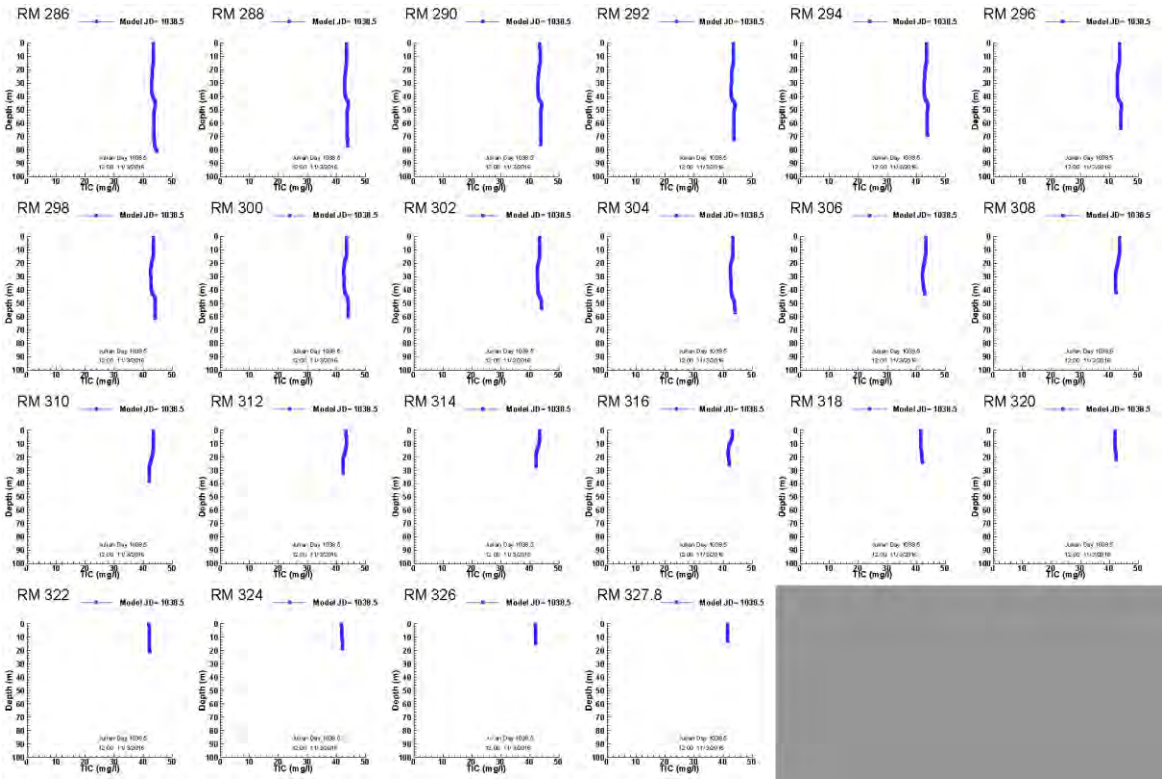


Figure 1270. Vertical profiles of TIC compared with data for 11/ 3/2016.

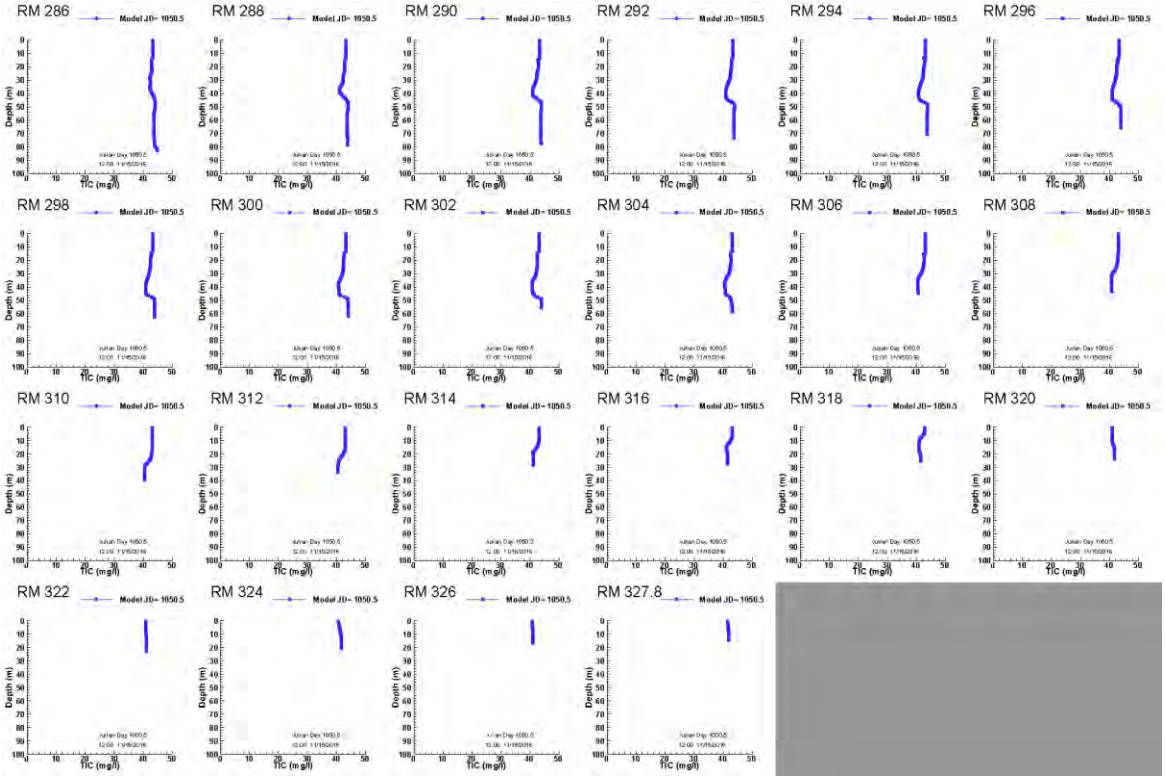


Figure 1271. Vertical profiles of TIC compared with data for 11/15/2016.

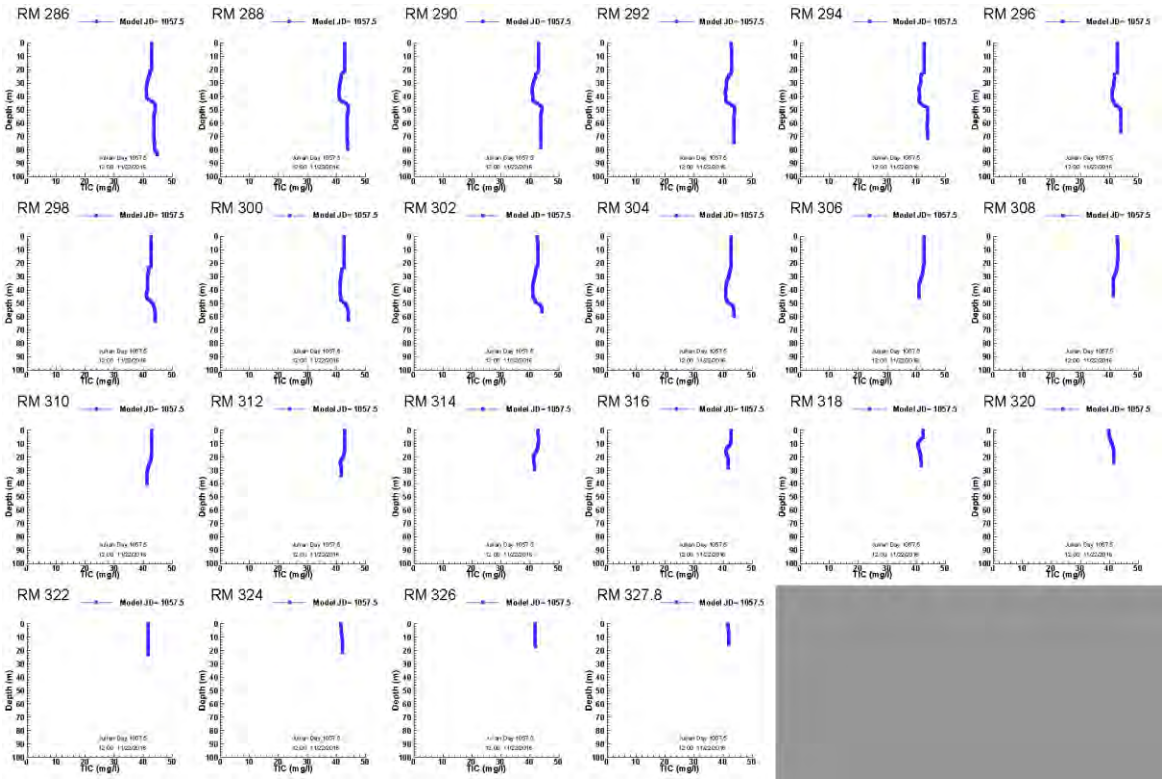


Figure 1272. Vertical profiles of TIC compared with data for 11/22/2016.

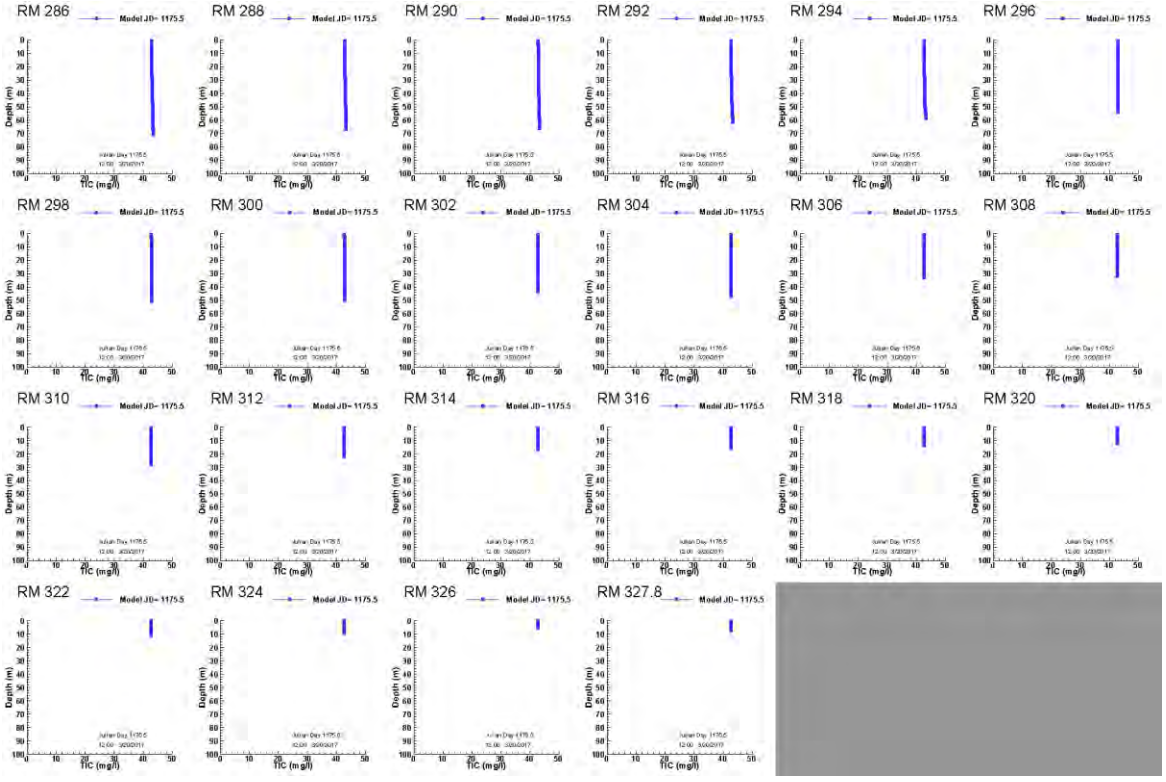


Figure 1273. Vertical profiles of TIC compared with data for 3/20/2017.

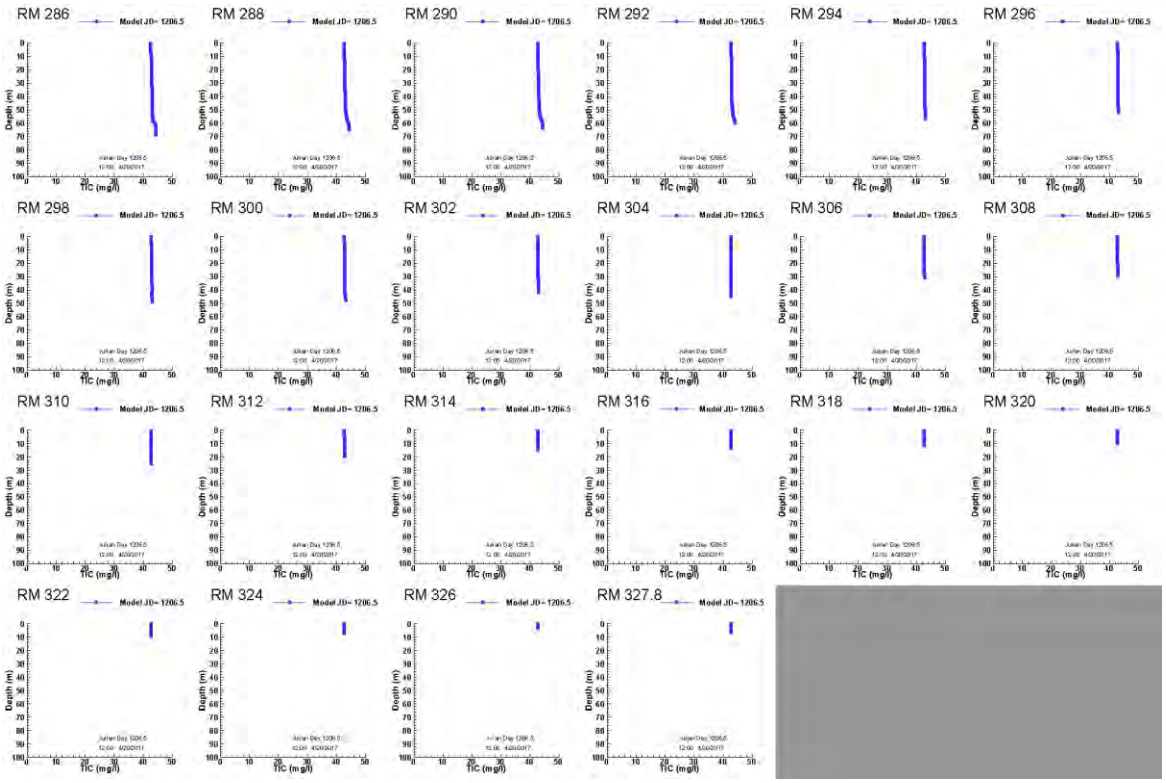


Figure 1274. Vertical profiles of TIC compared with data for 4/20/2017.

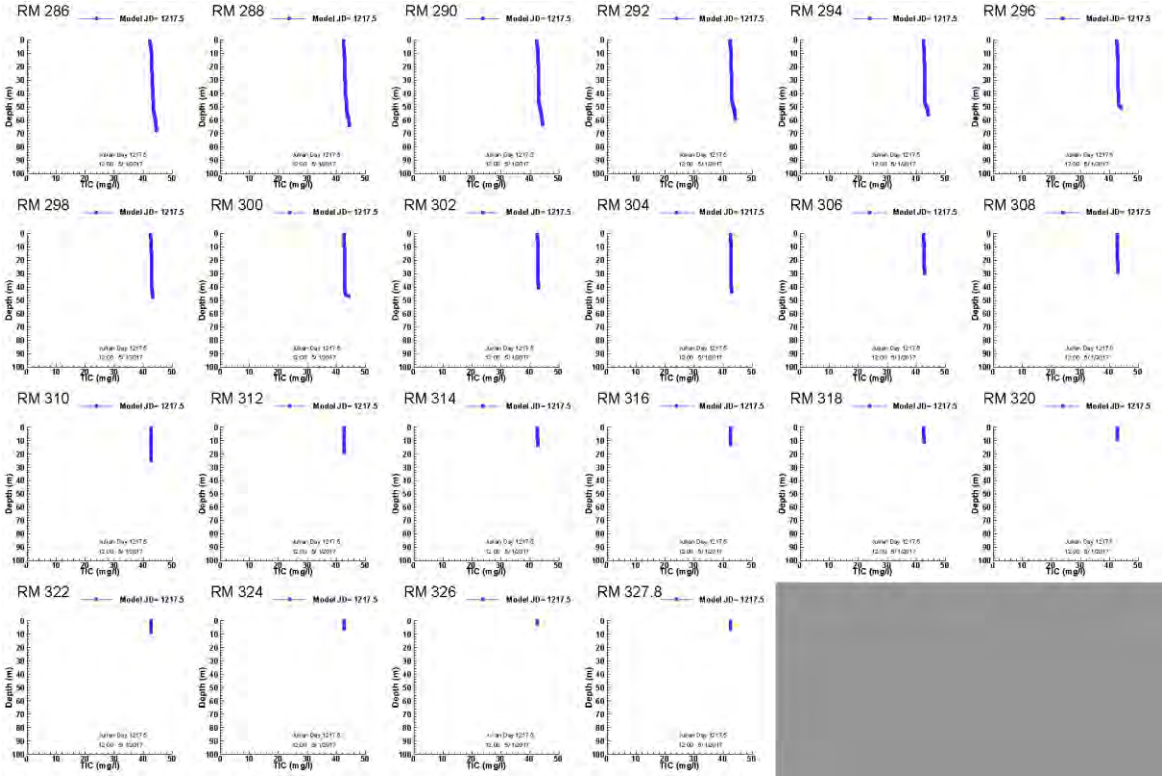


Figure 1275. Vertical profiles of TIC compared with data for 5/ 1/2017.

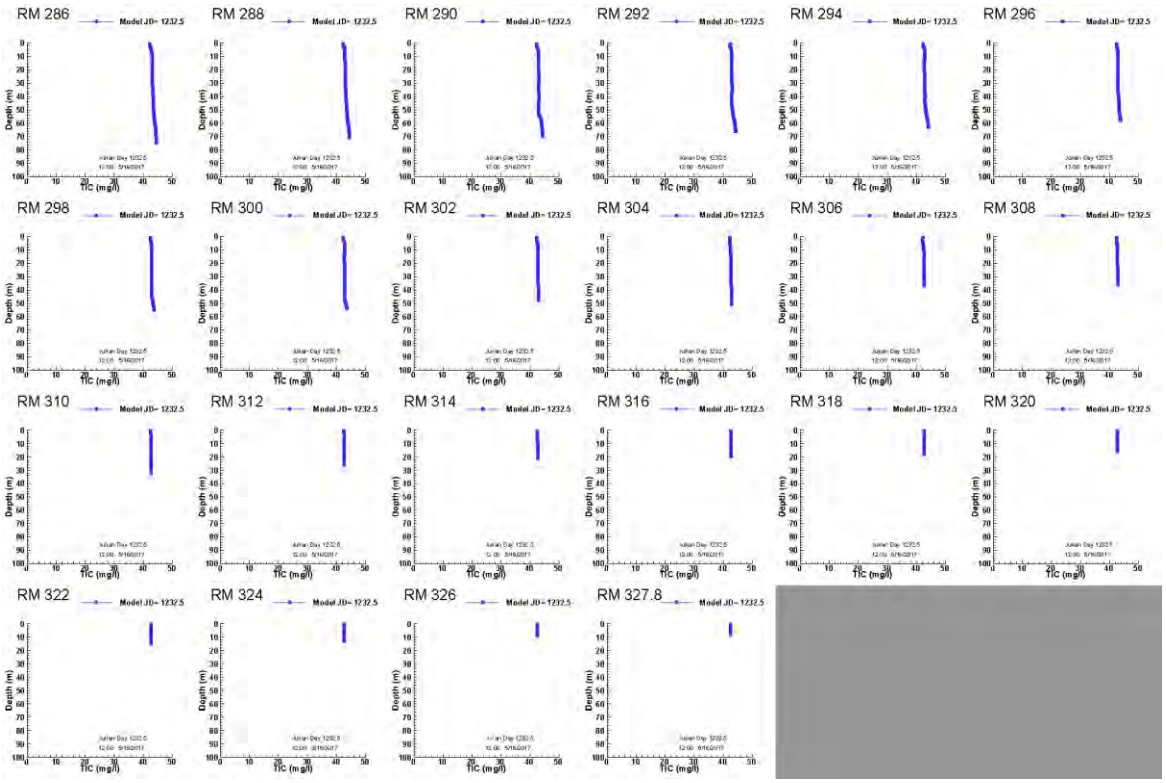


Figure 1276. Vertical profiles of TIC compared with data for 5/16/2017.

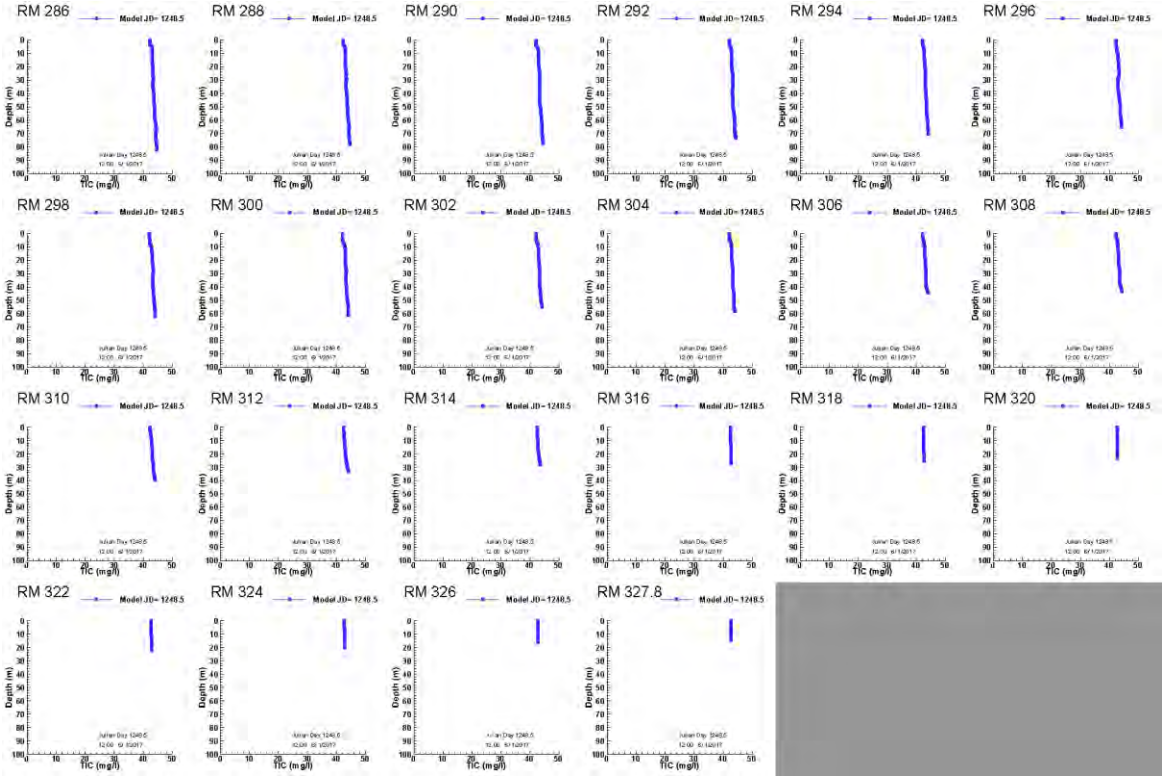


Figure 1277. Vertical profiles of TIC compared with data for 6/ 1/2017.

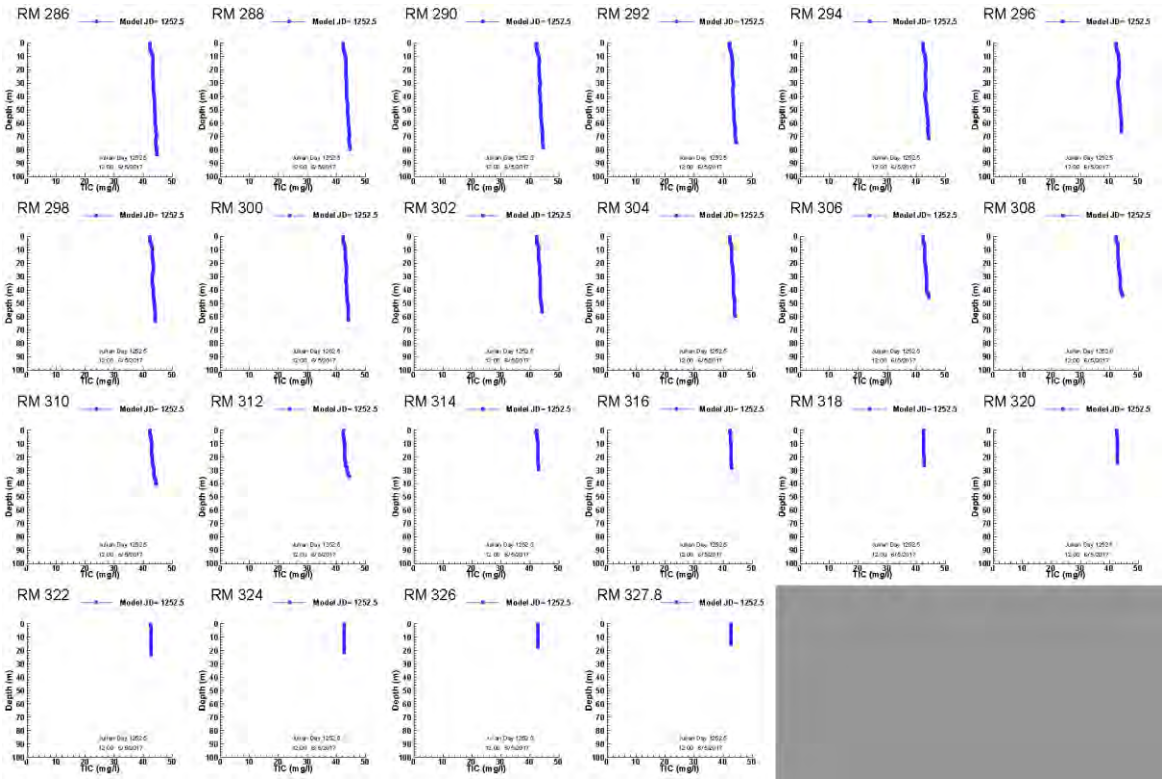


Figure 1278. Vertical profiles of TIC compared with data for 6/ 5/2017.

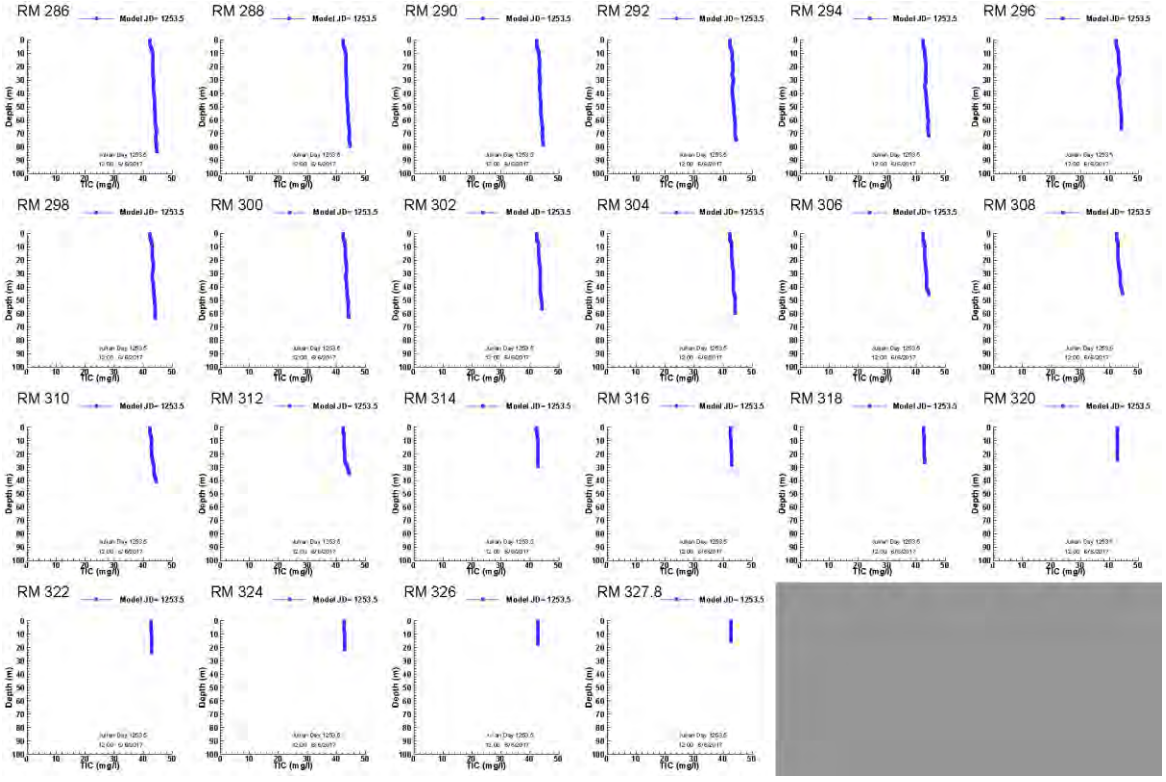


Figure 1279. Vertical profiles of TIC compared with data for 6/ 6/2017.

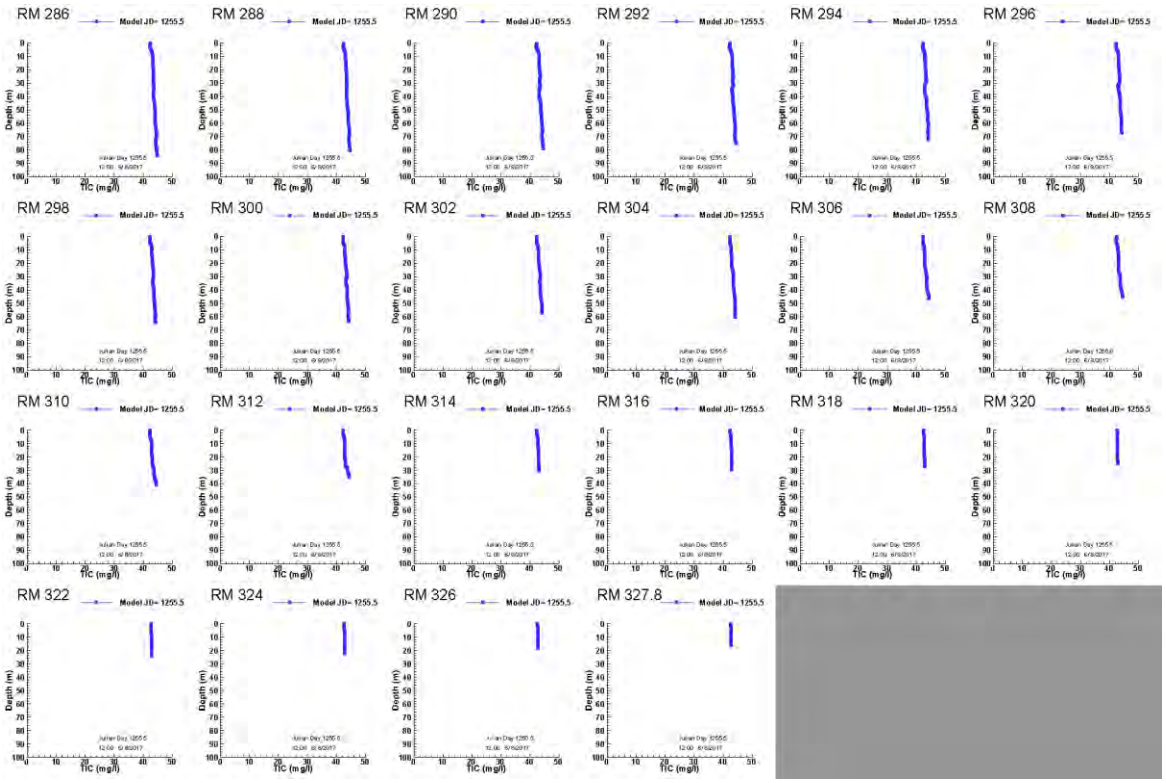


Figure 1280. Vertical profiles of TIC compared with data for 6/ 8/2017.

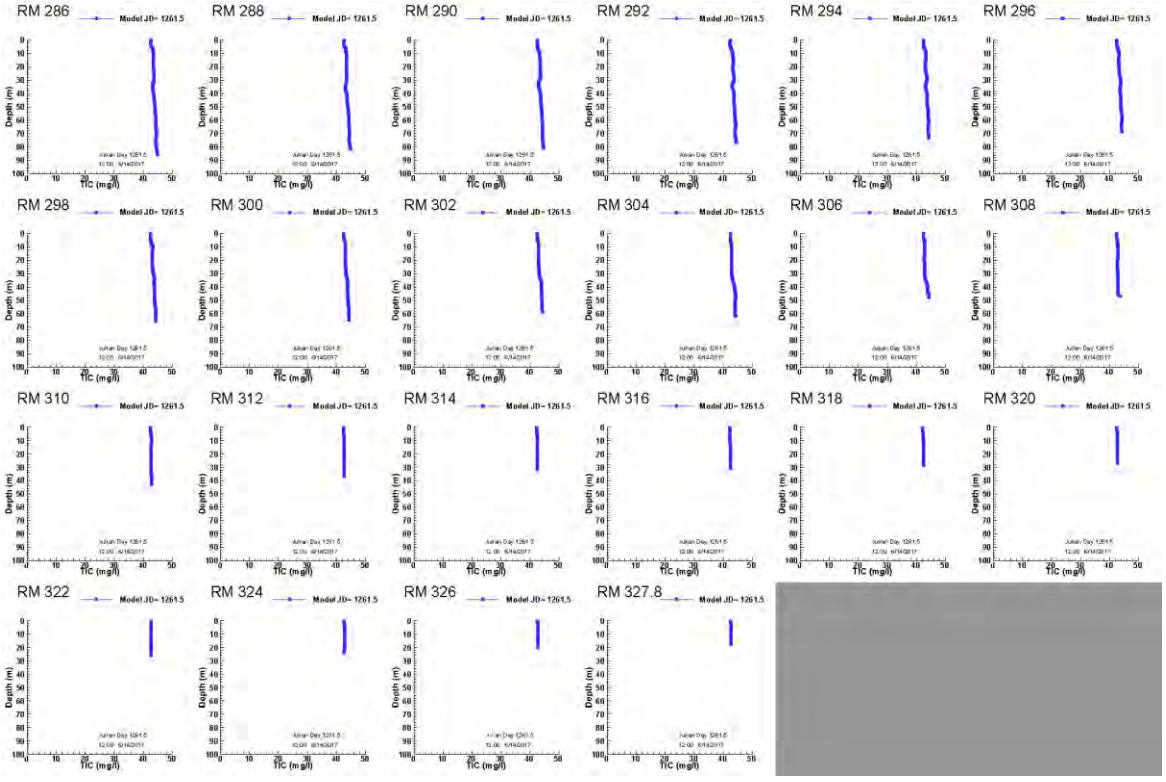


Figure 1281. Vertical profiles of TIC compared with data for 6/14/2017.

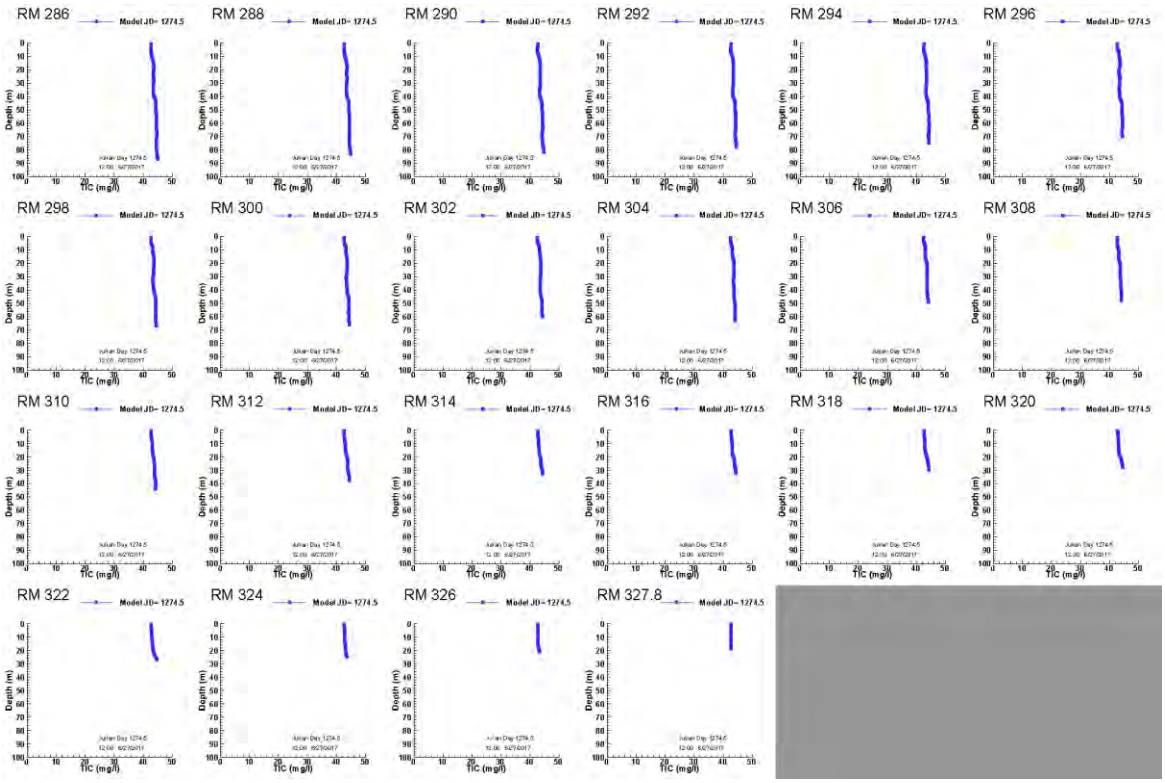


Figure 1282. Vertical profiles of TIC compared with data for 6/27/2017.

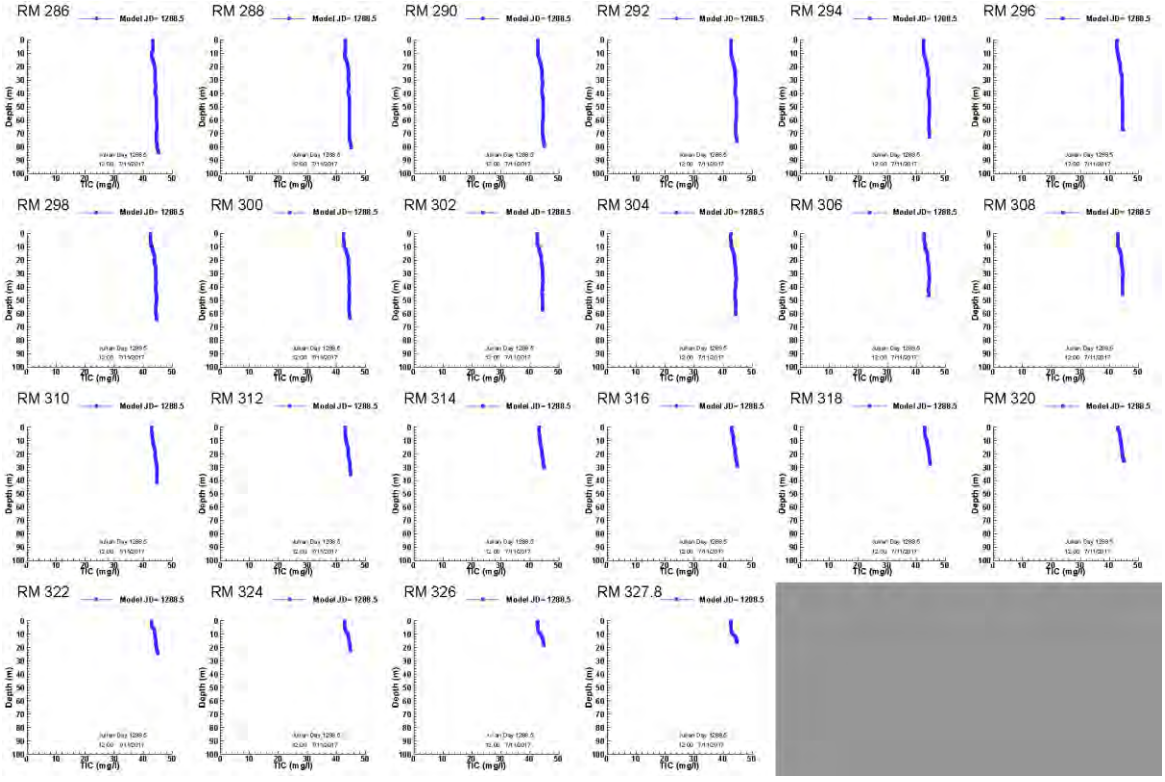


Figure 1283. Vertical profiles of TIC compared with data for 7/11/2017.

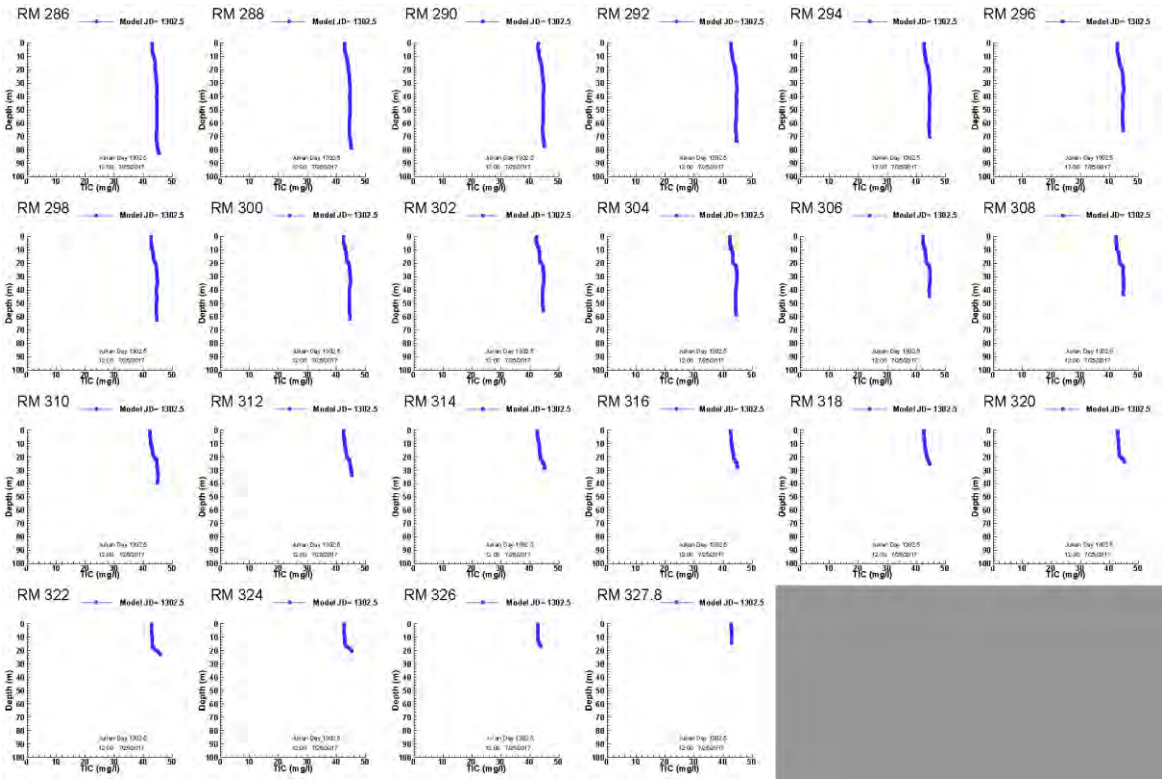


Figure 1284. Vertical profiles of TIC compared with data for 7/25/2017.

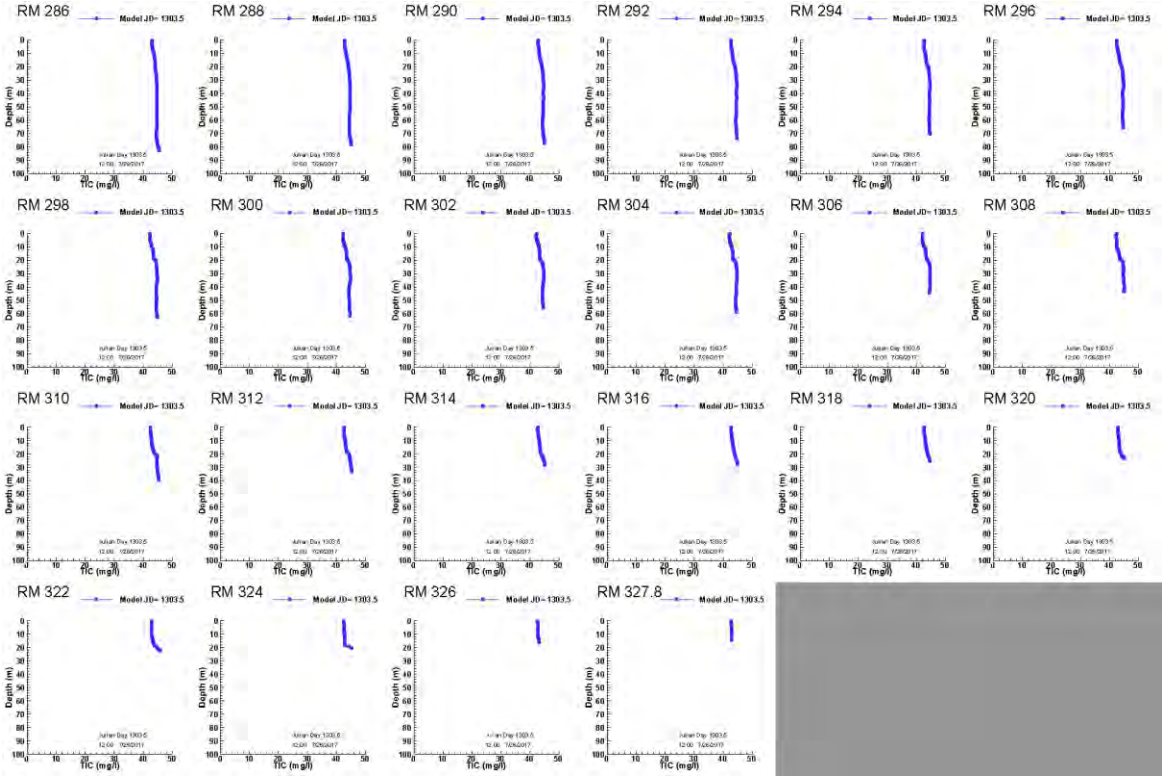


Figure 1285. Vertical profiles of TIC compared with data for 7/26/2017.

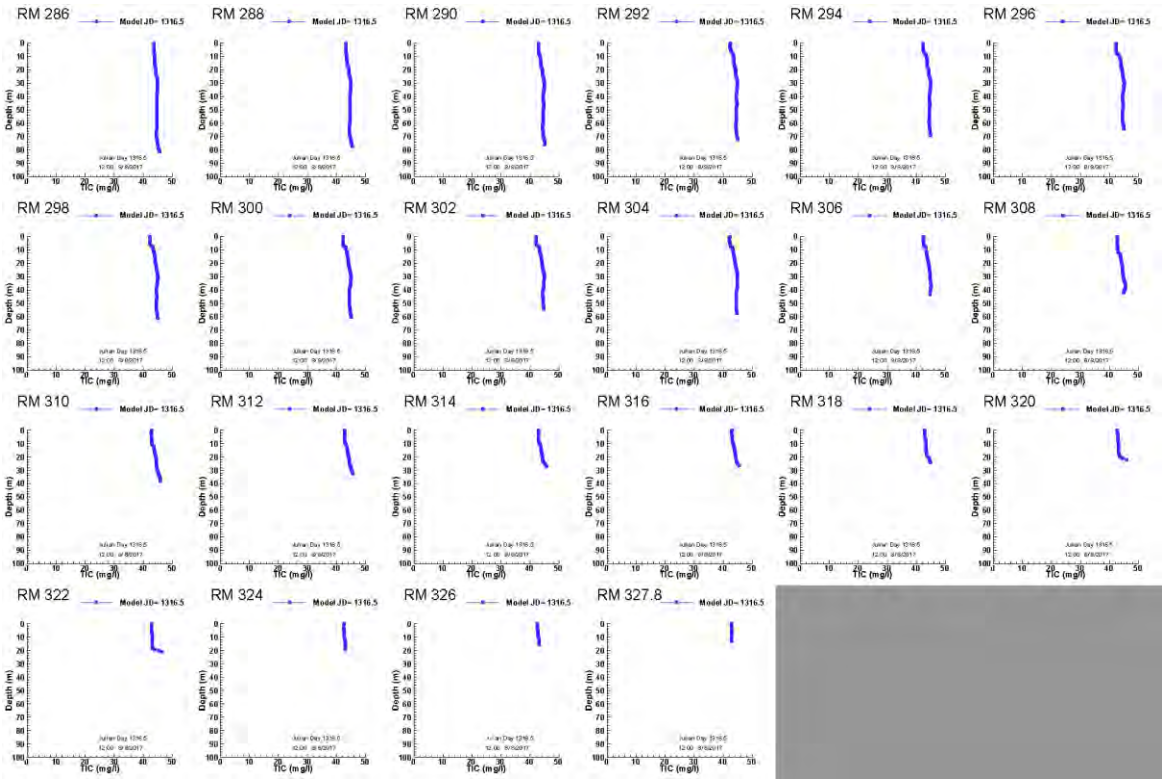


Figure 1286. Vertical profiles of TIC compared with data for 8/ 8/2017.

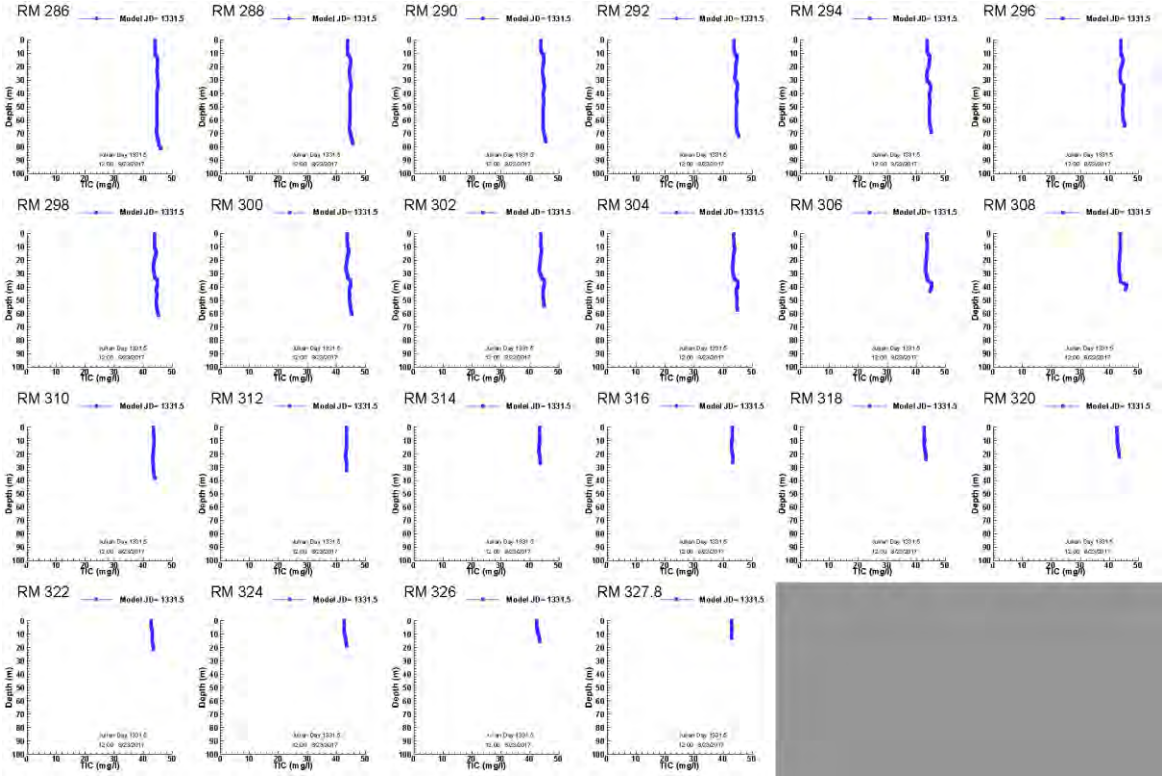


Figure 1287. Vertical profiles of TIC compared with data for 8/23/2017.

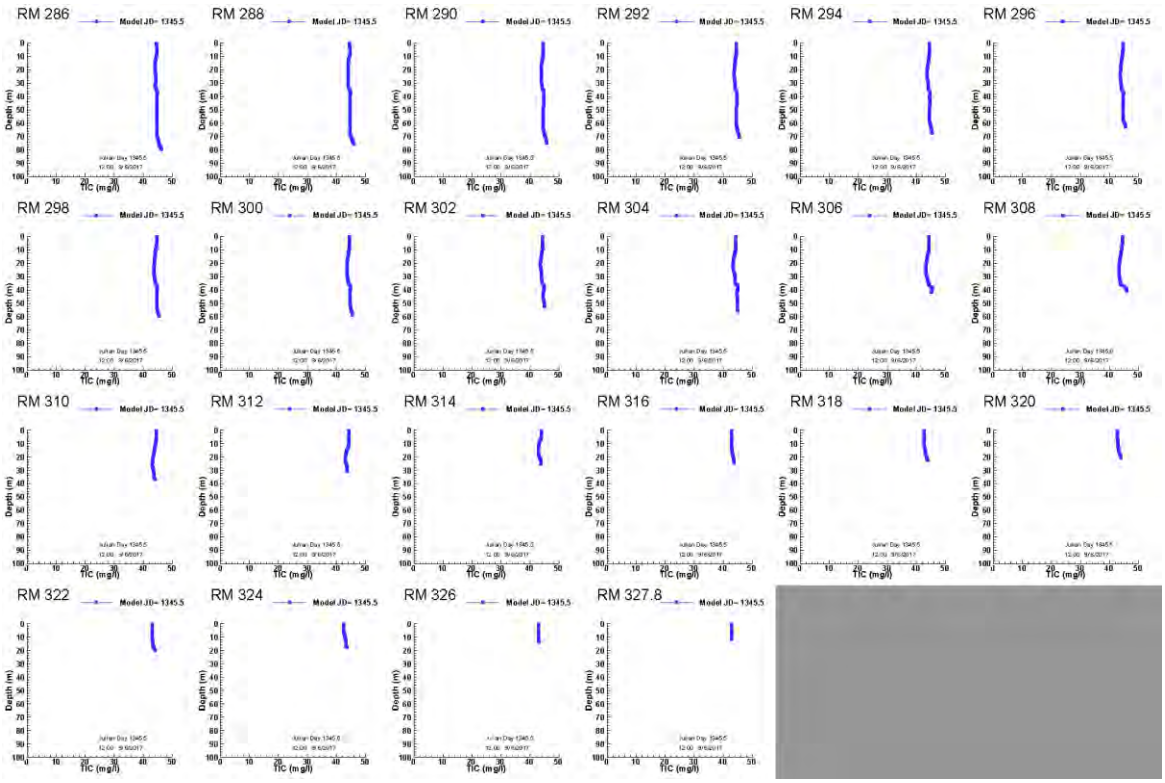


Figure 1288. Vertical profiles of TIC compared with data for 9/ 6/2017.

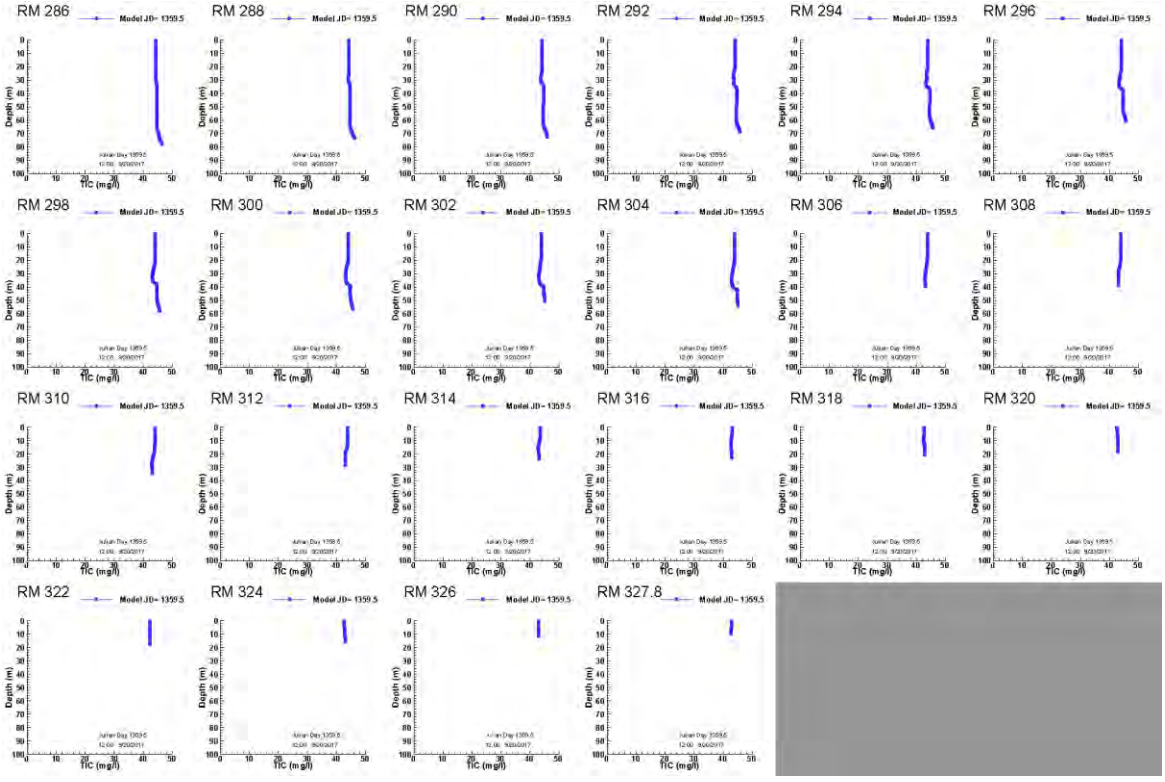


Figure 1289. Vertical profiles of TIC compared with data for 9/20/2017.

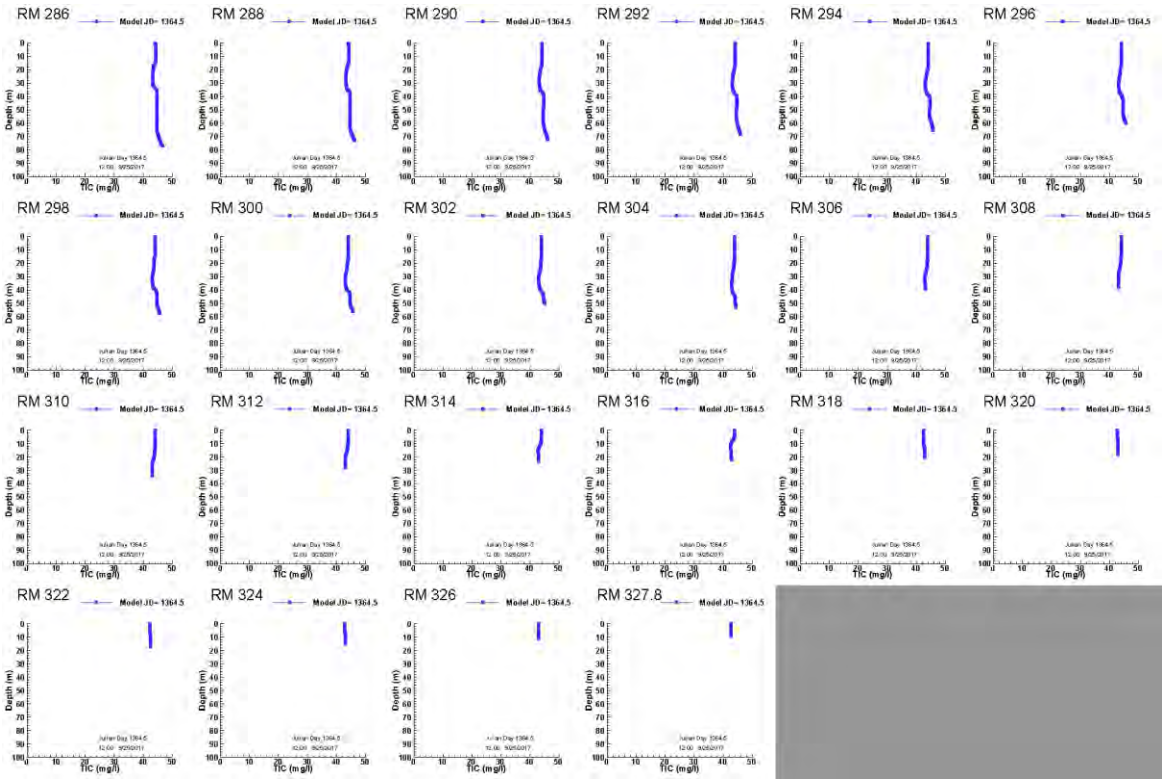


Figure 1290. Vertical profiles of TIC compared with data for 9/25/2017.

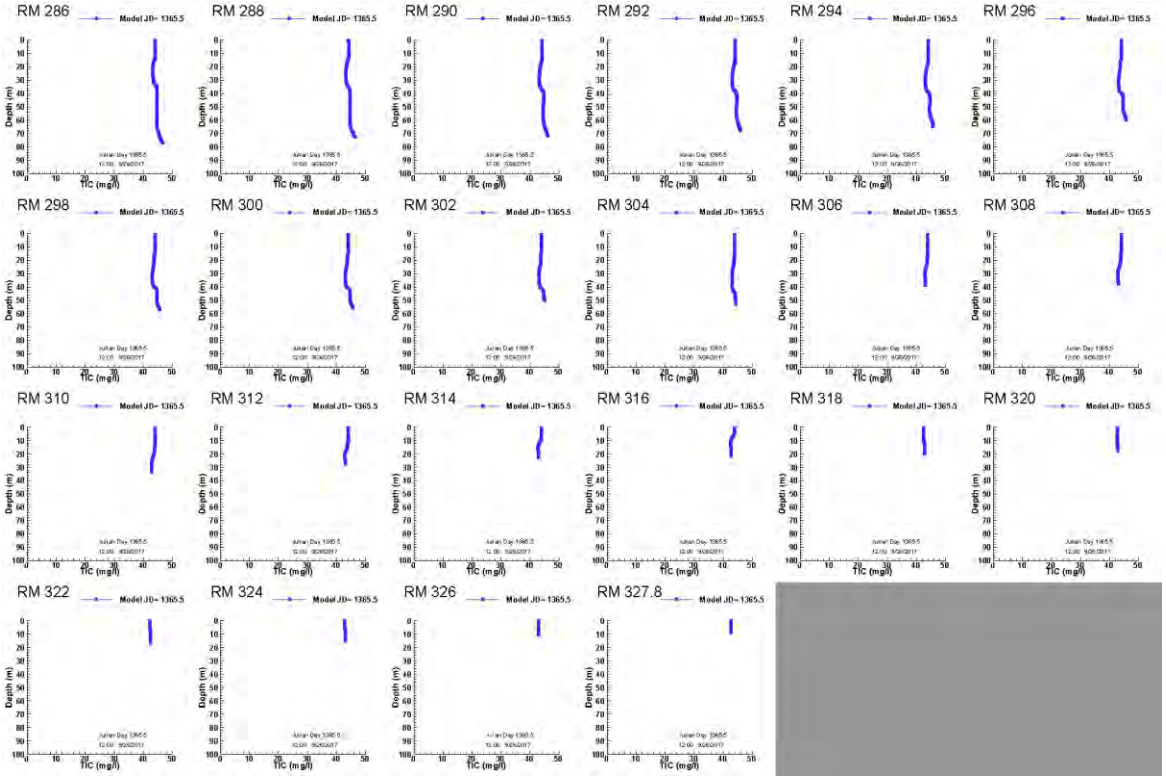


Figure 1291. Vertical profiles of TIC compared with data for 9/26/2017.

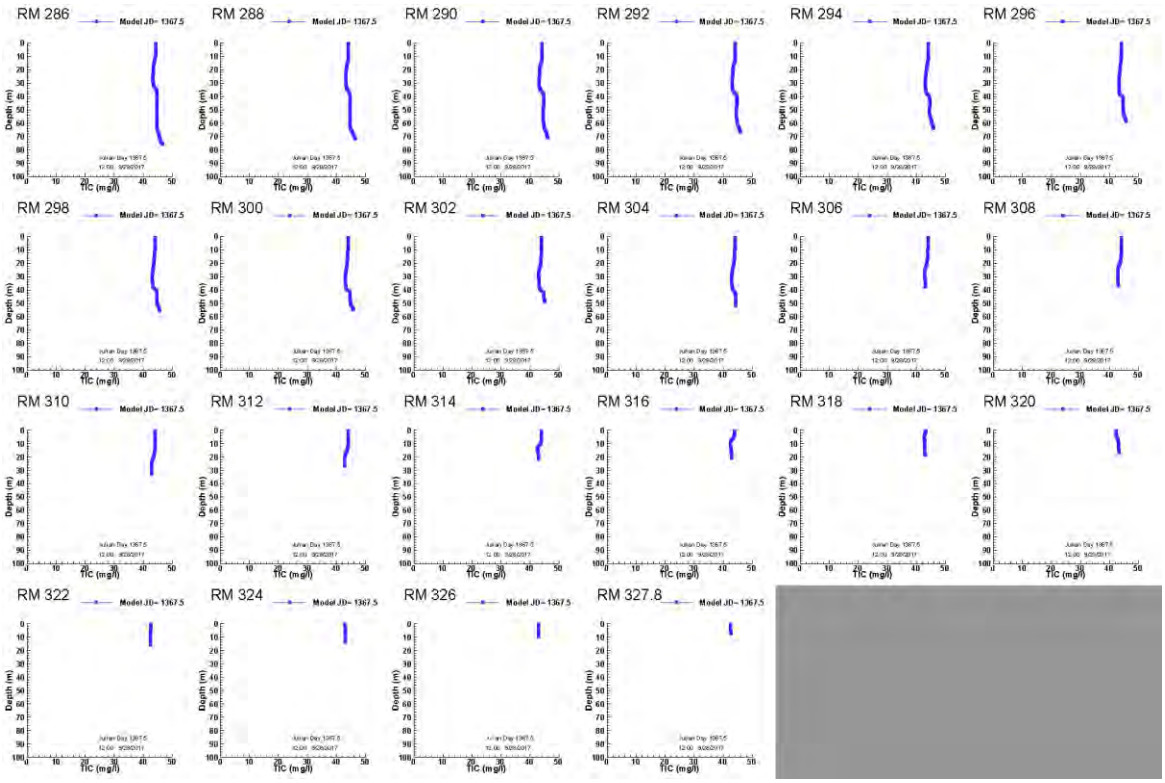


Figure 1292. Vertical profiles of TIC compared with data for 9/28/2017.

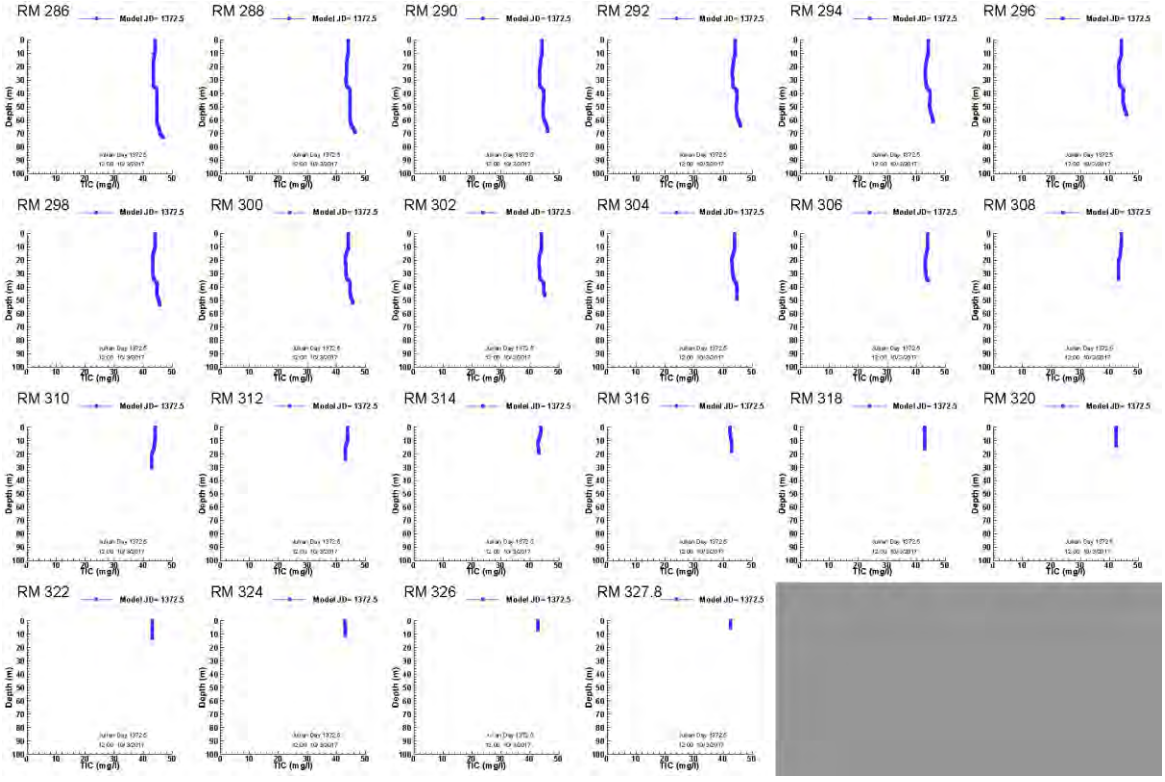


Figure 1293. Vertical profiles of TIC compared with data for 10/ 3/2017.

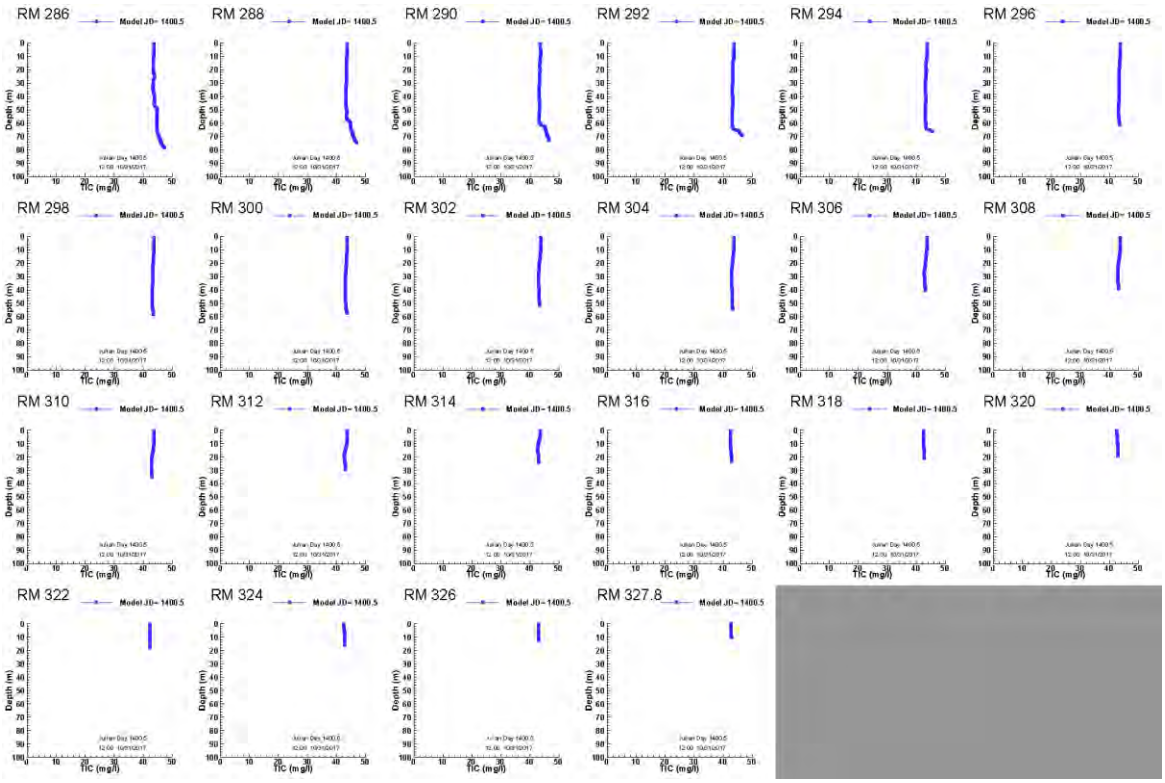


Figure 1294. Vertical profiles of TIC compared with data for 10/31/2017.

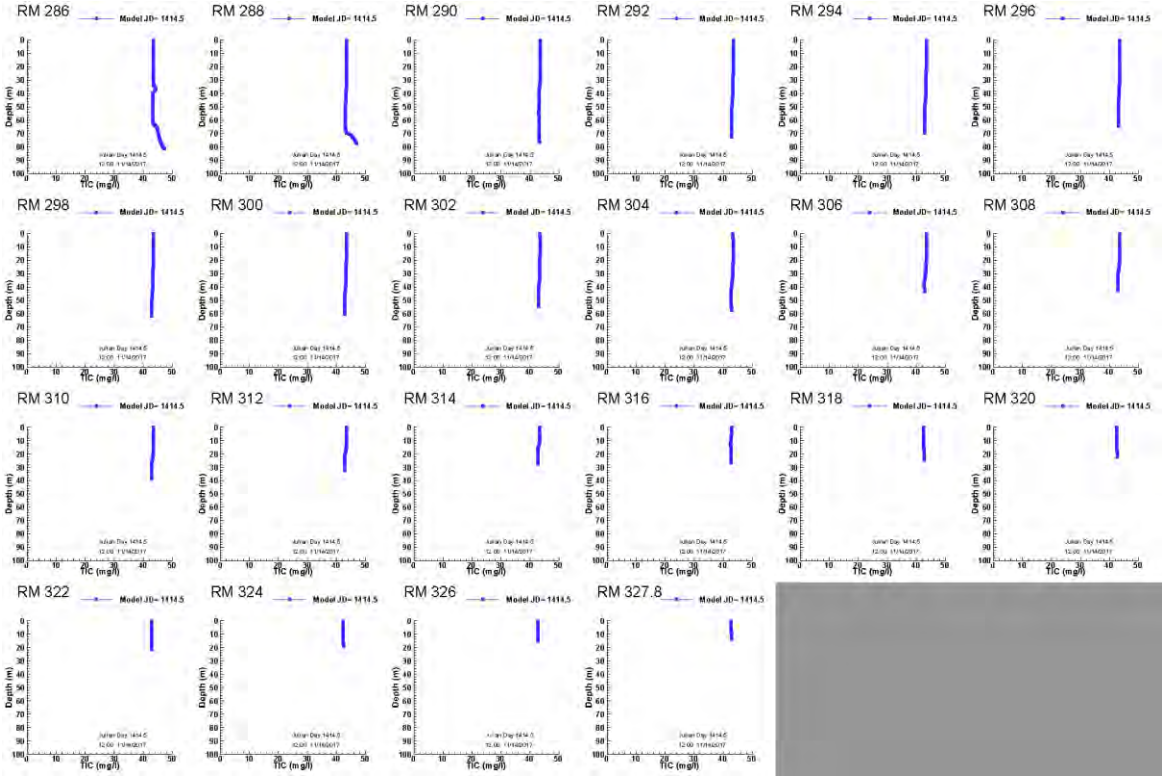


Figure 1295. Vertical profiles of TIC compared with data for 11/14/2017.

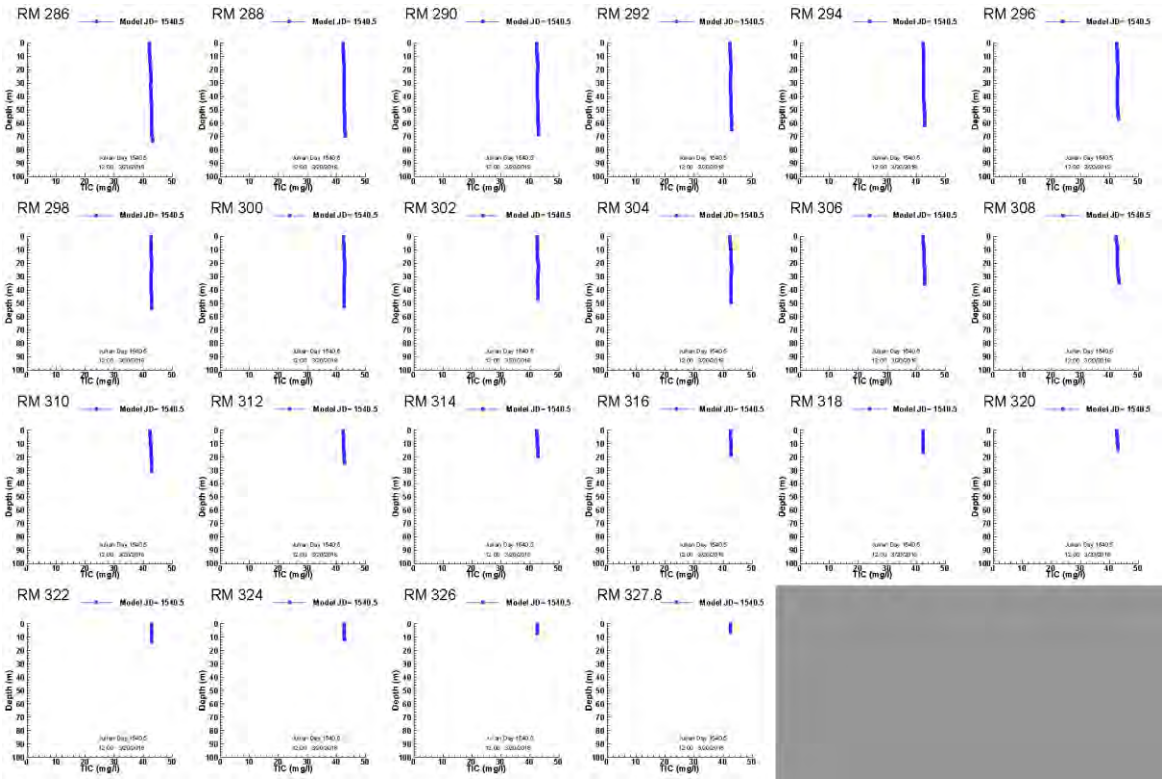


Figure 1296. Vertical profiles of TIC compared with data for 3/20/2018.

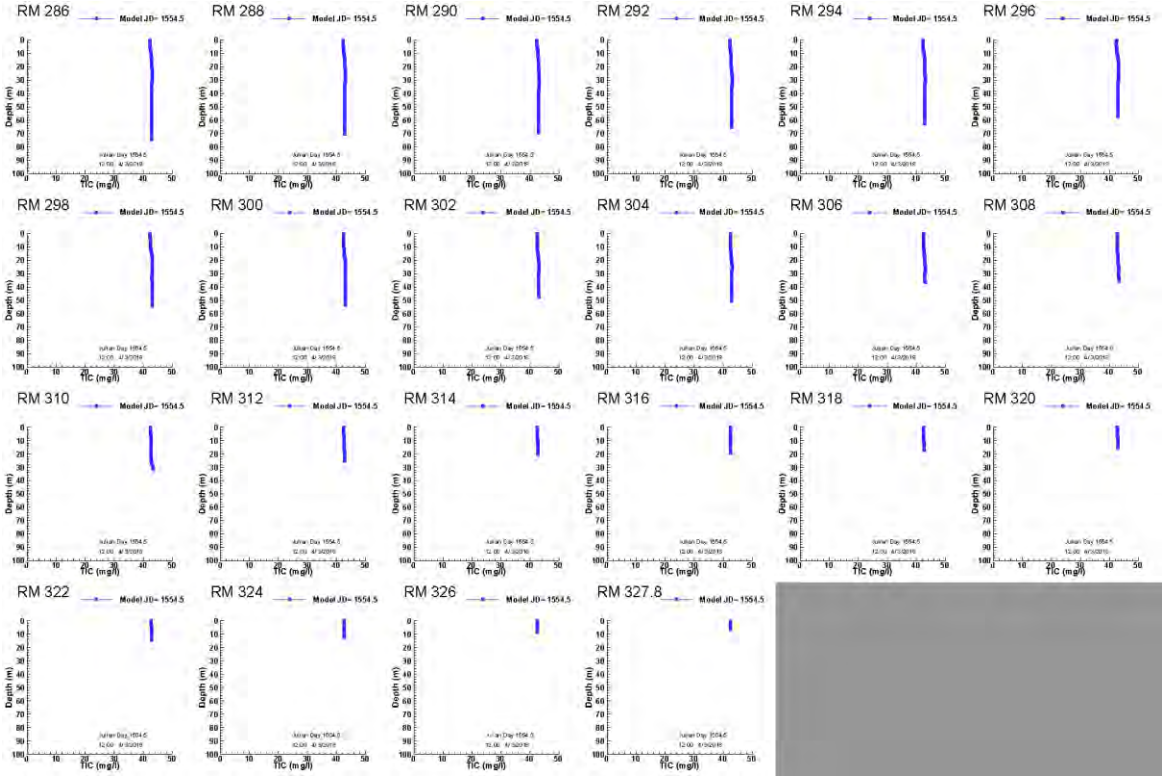


Figure 1297. Vertical profiles of TIC compared with data for 4/ 3/2018.

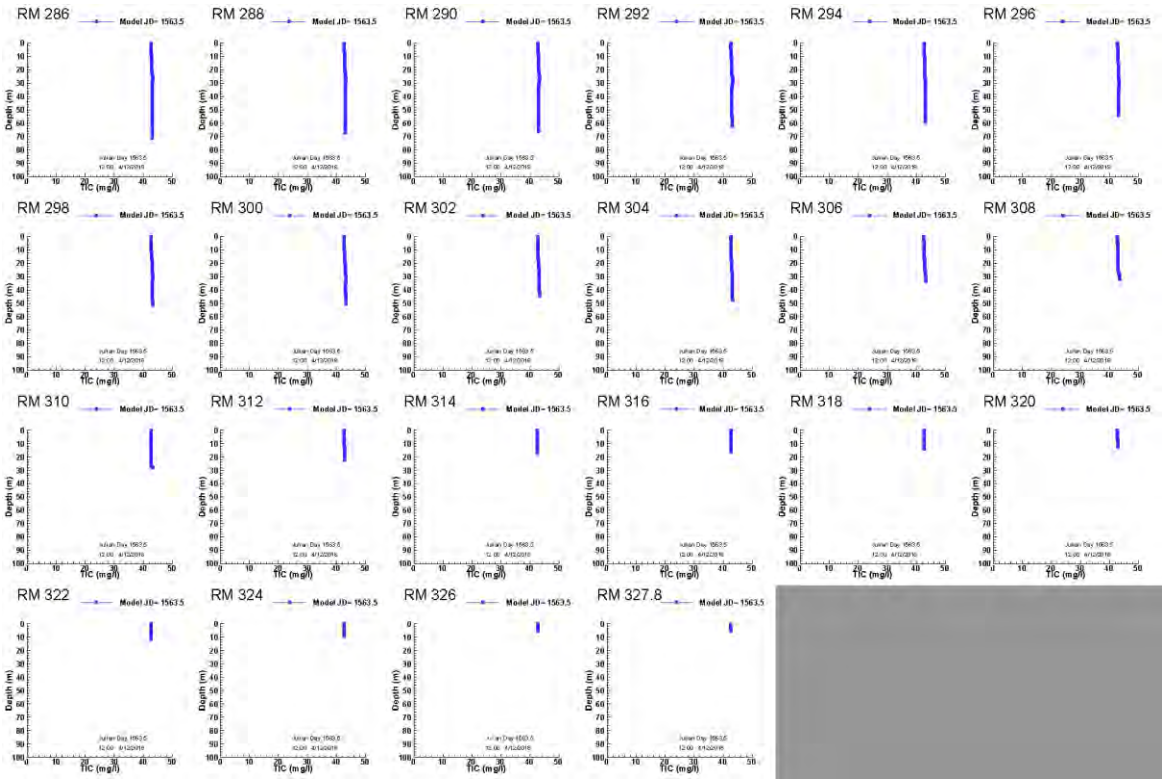


Figure 1298. Vertical profiles of TIC compared with data for 4/12/2018.

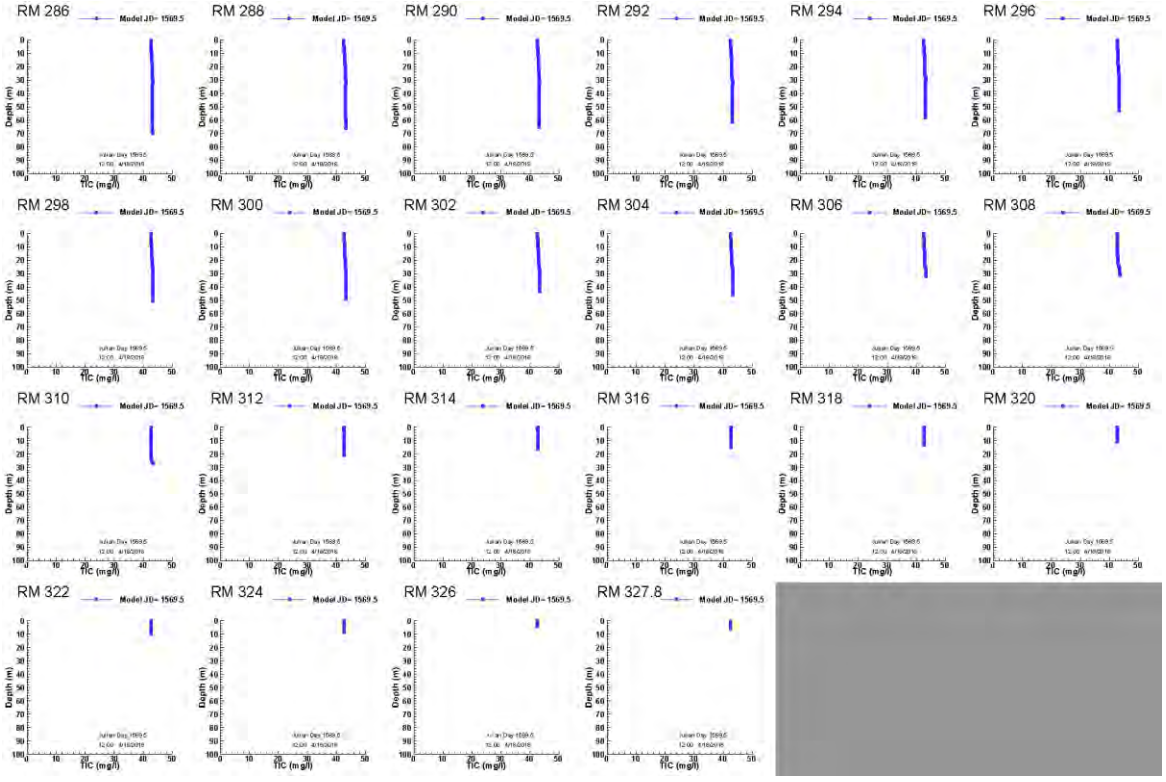


Figure 1299. Vertical profiles of TIC compared with data for 4/18/2018.

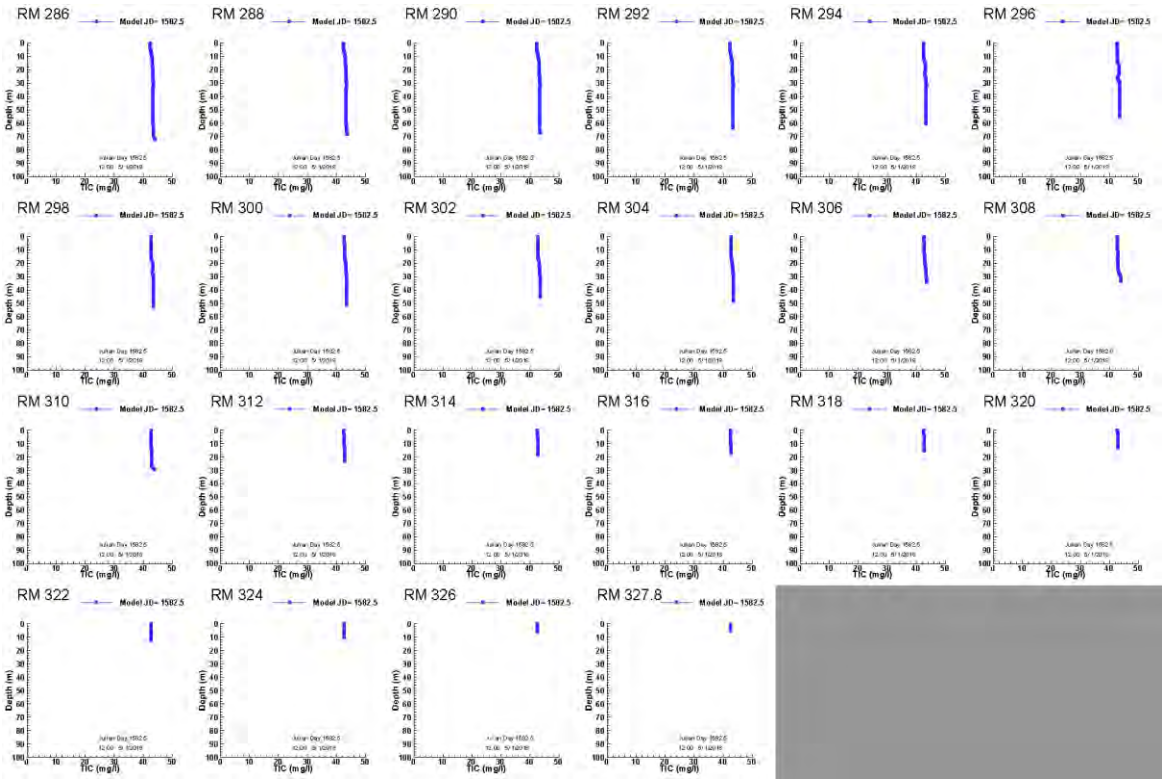


Figure 1300. Vertical profiles of TIC compared with data for 5/ 1/2018.

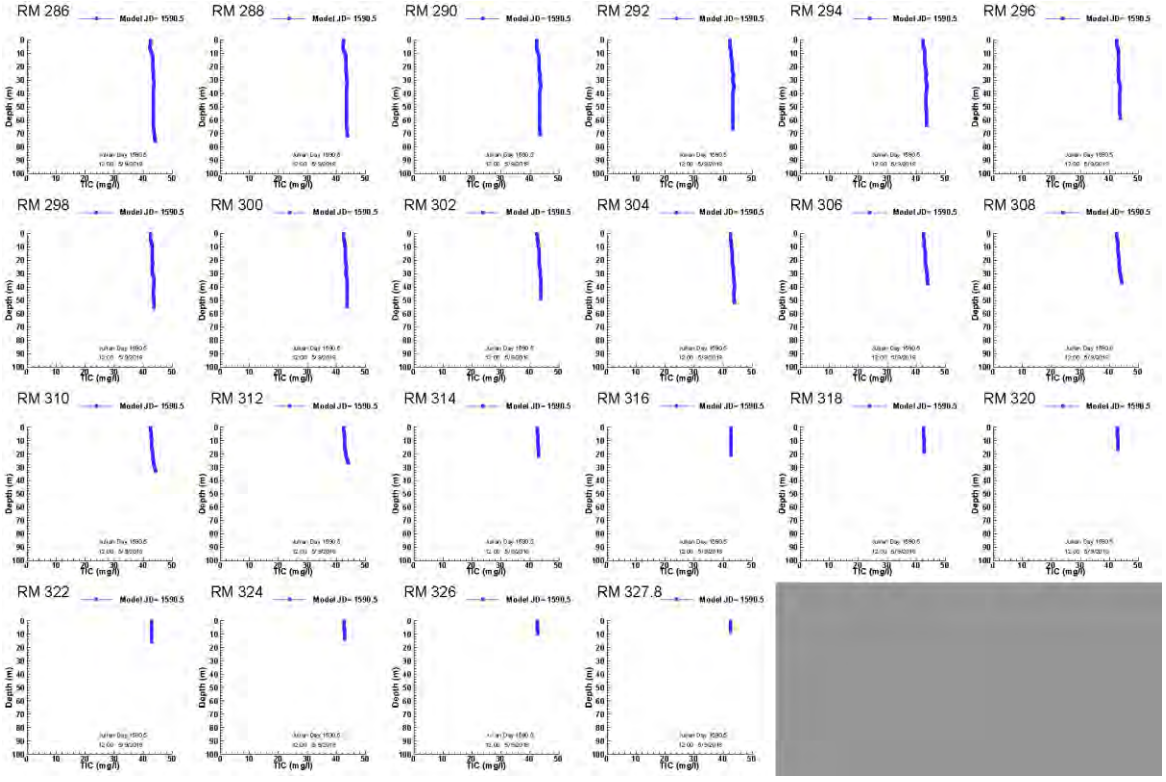


Figure 1301. Vertical profiles of TIC compared with data for 5/ 9/2018.

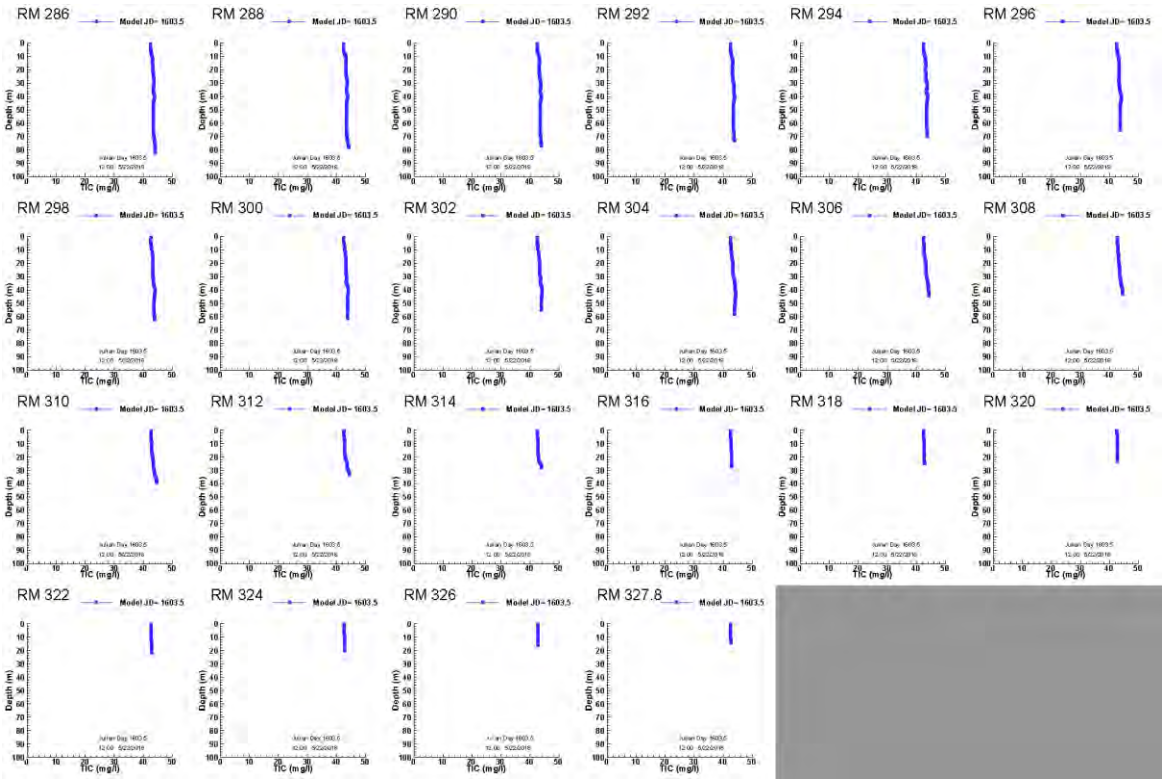


Figure 1302. Vertical profiles of TIC compared with data for 5/22/2018.

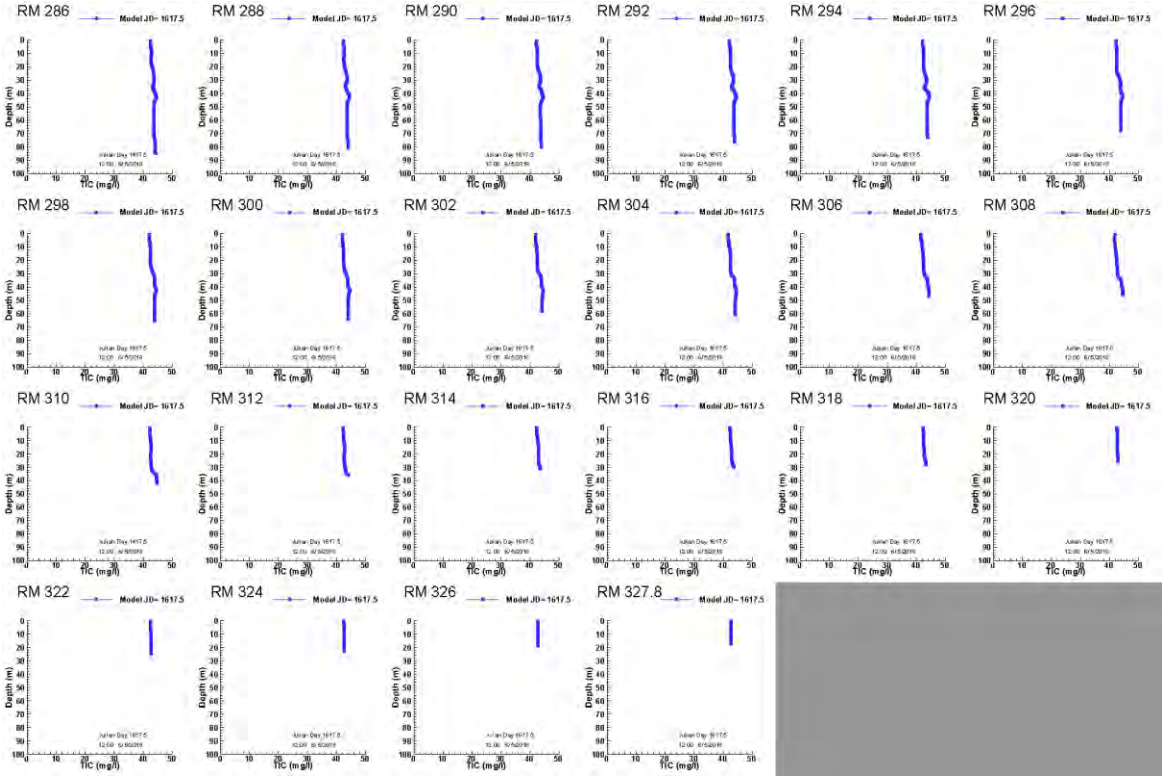


Figure 1303. Vertical profiles of TIC compared with data for 6/ 5/2018.

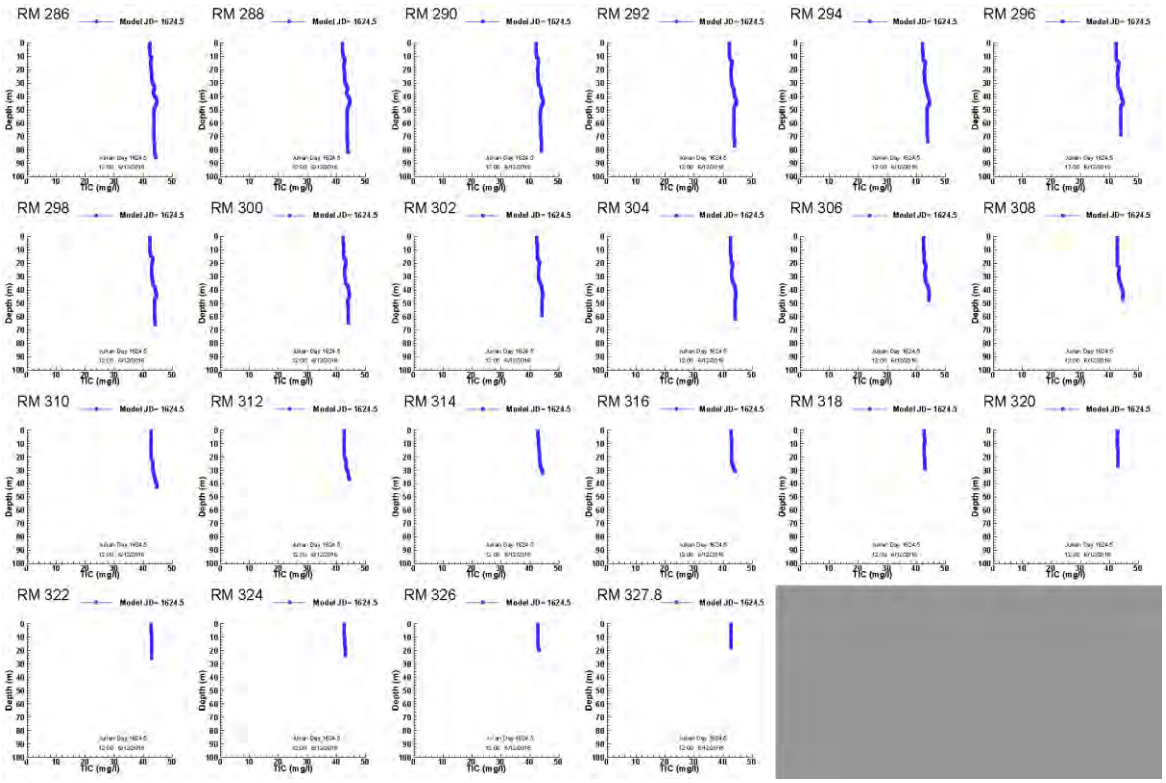


Figure 1304. Vertical profiles of TIC compared with data for 6/12/2018.

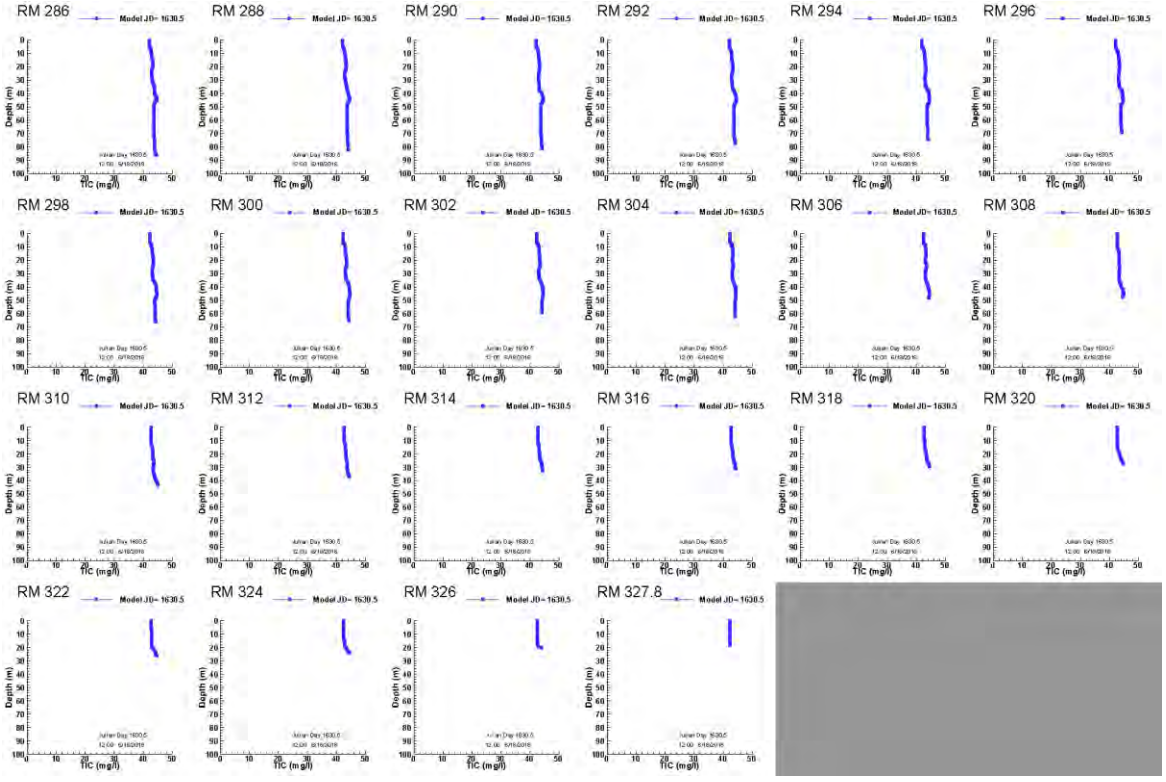


Figure 1305. Vertical profiles of TIC compared with data for 6/18/2018.

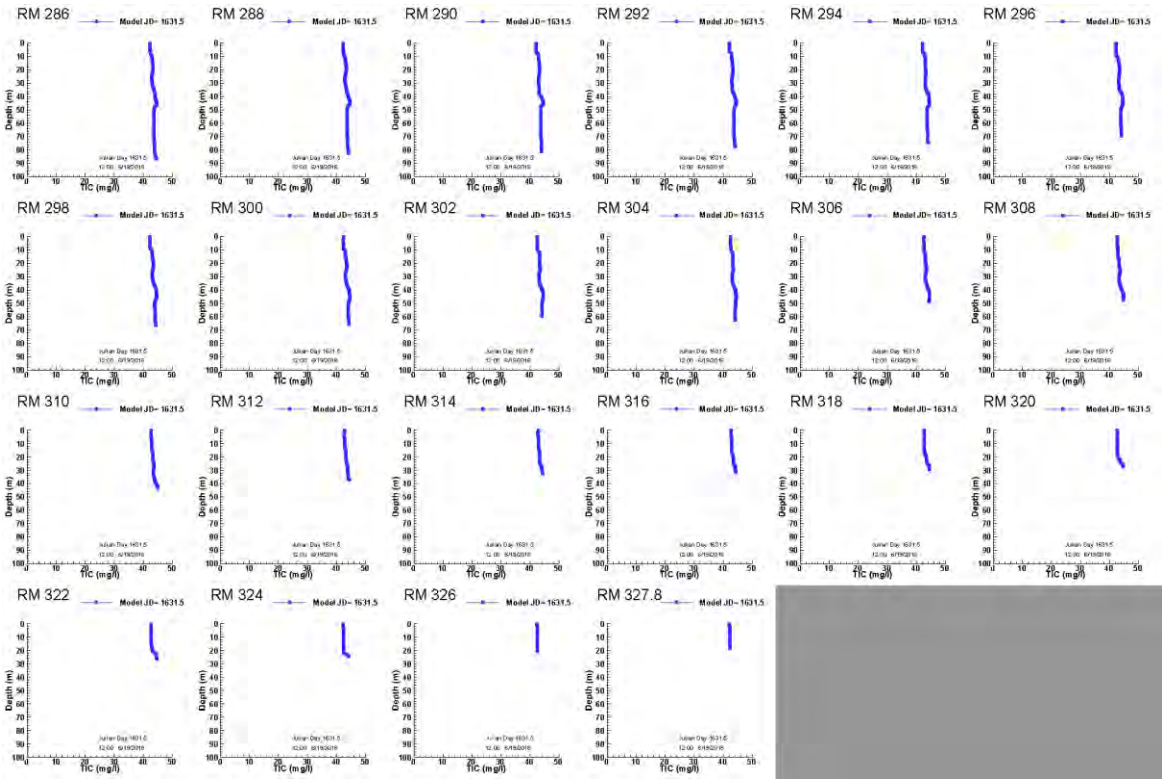


Figure 1306. Vertical profiles of TIC compared with data for 6/19/2018.

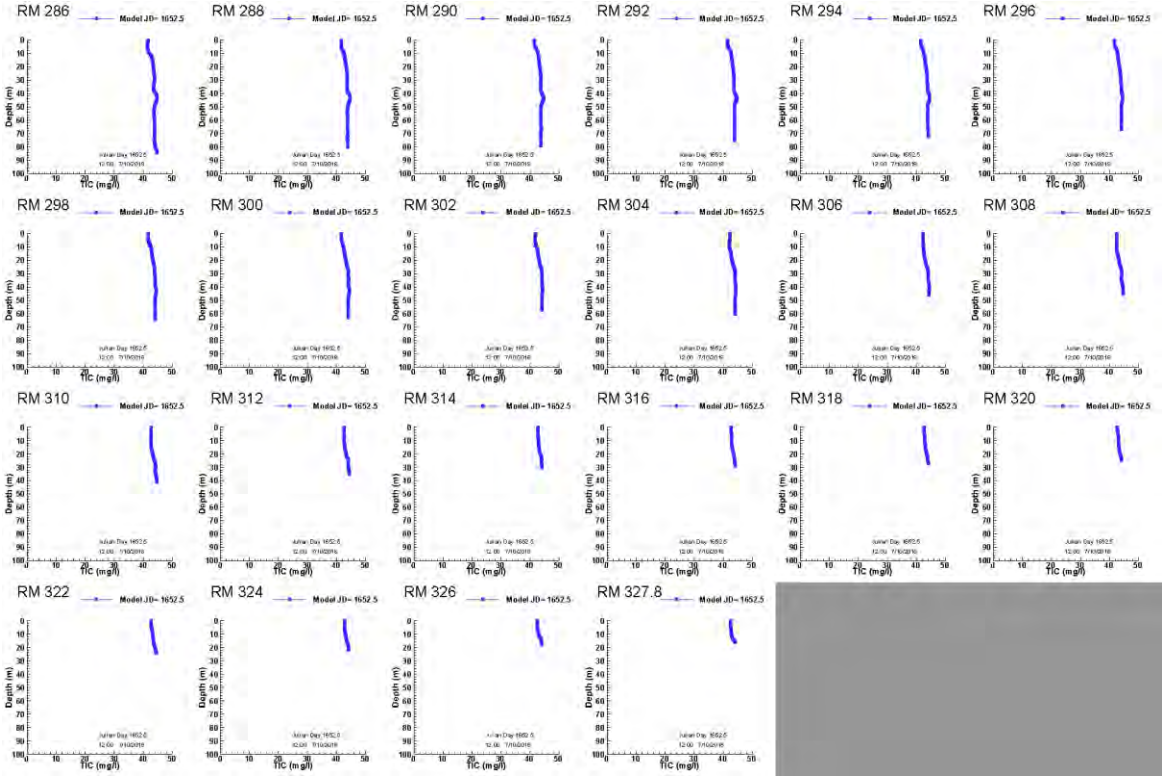


Figure 1307. Vertical profiles of TIC compared with data for 7/10/2018.

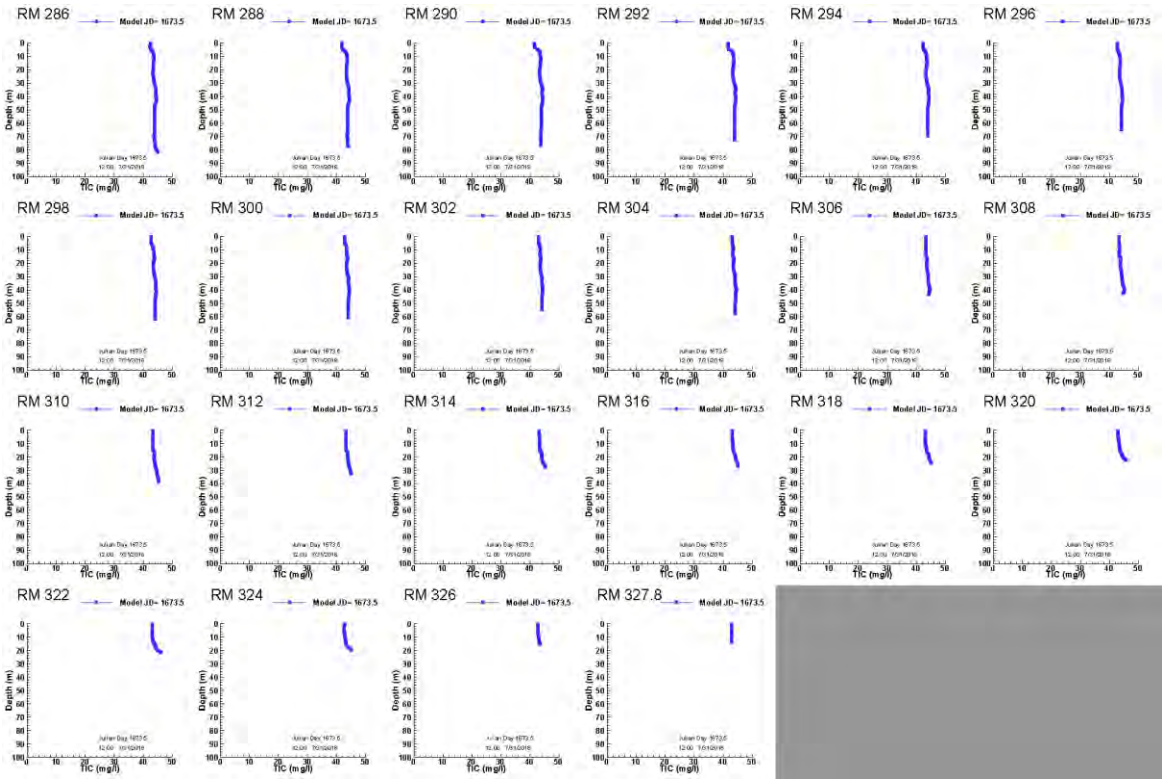


Figure 1308. Vertical profiles of TIC compared with data for 7/31/2018.

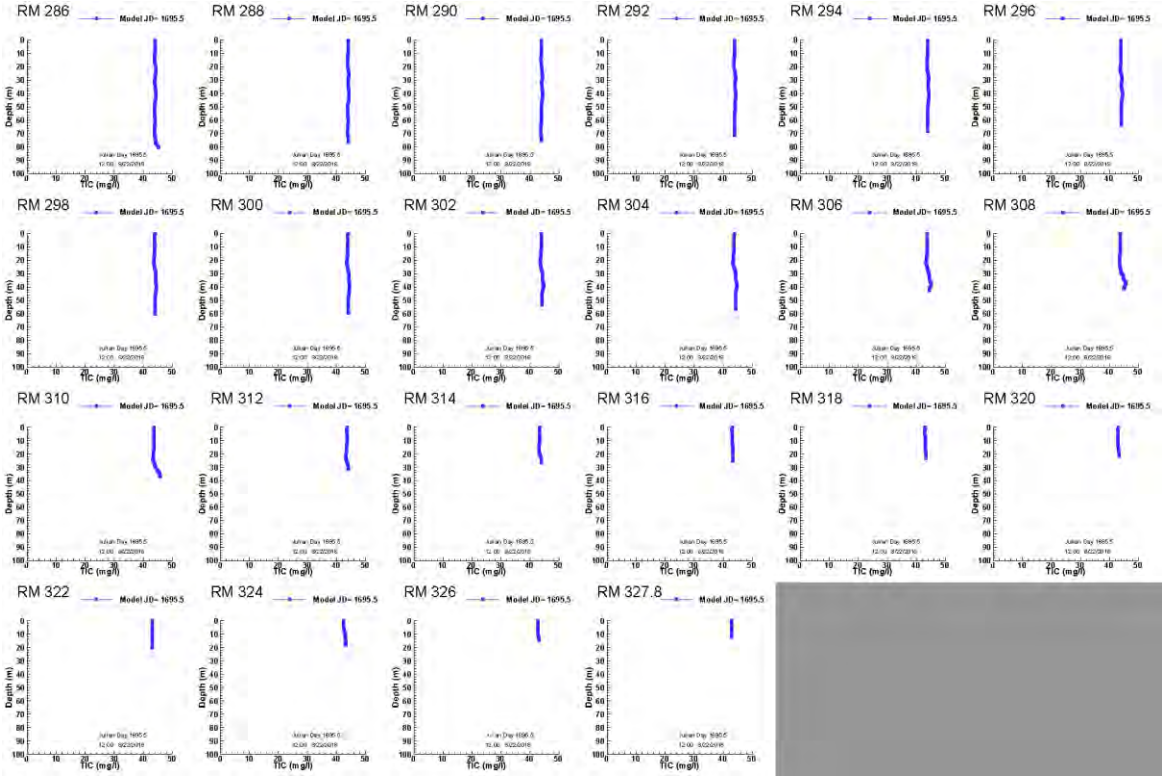


Figure 1309. Vertical profiles of TIC compared with data for 8/22/2018.

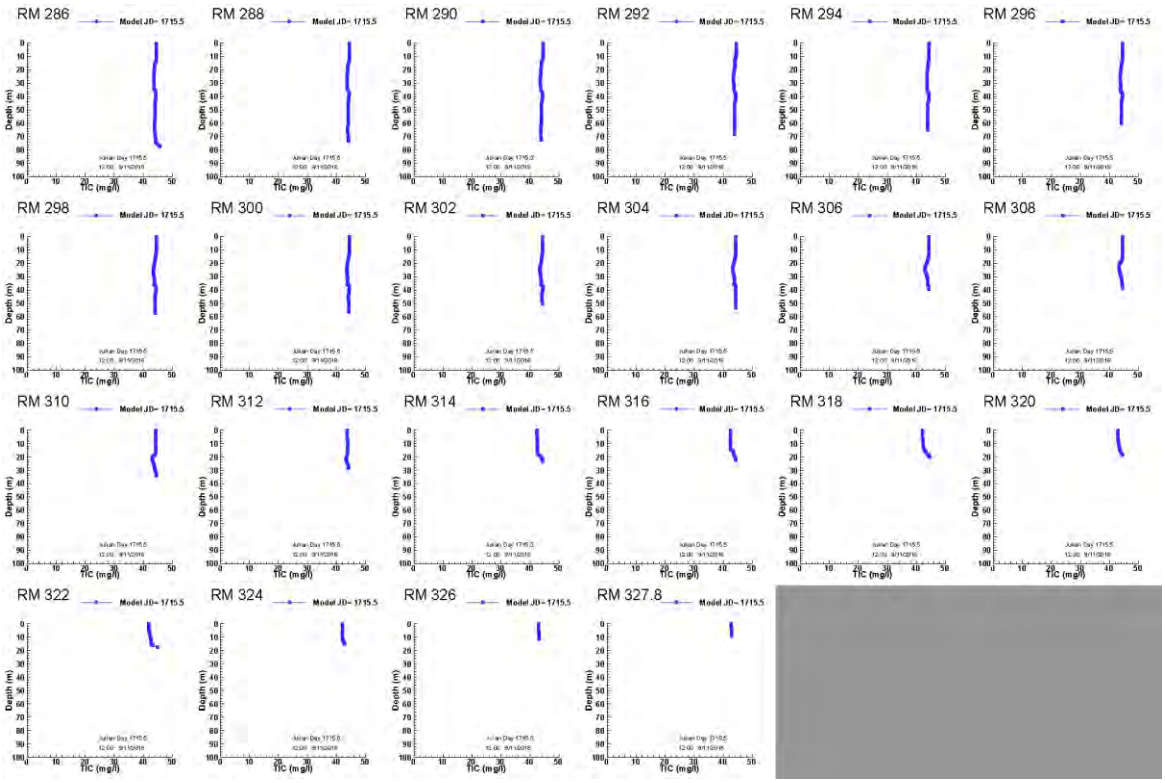


Figure 1310. Vertical profiles of TIC compared with data for 9/11/2018.

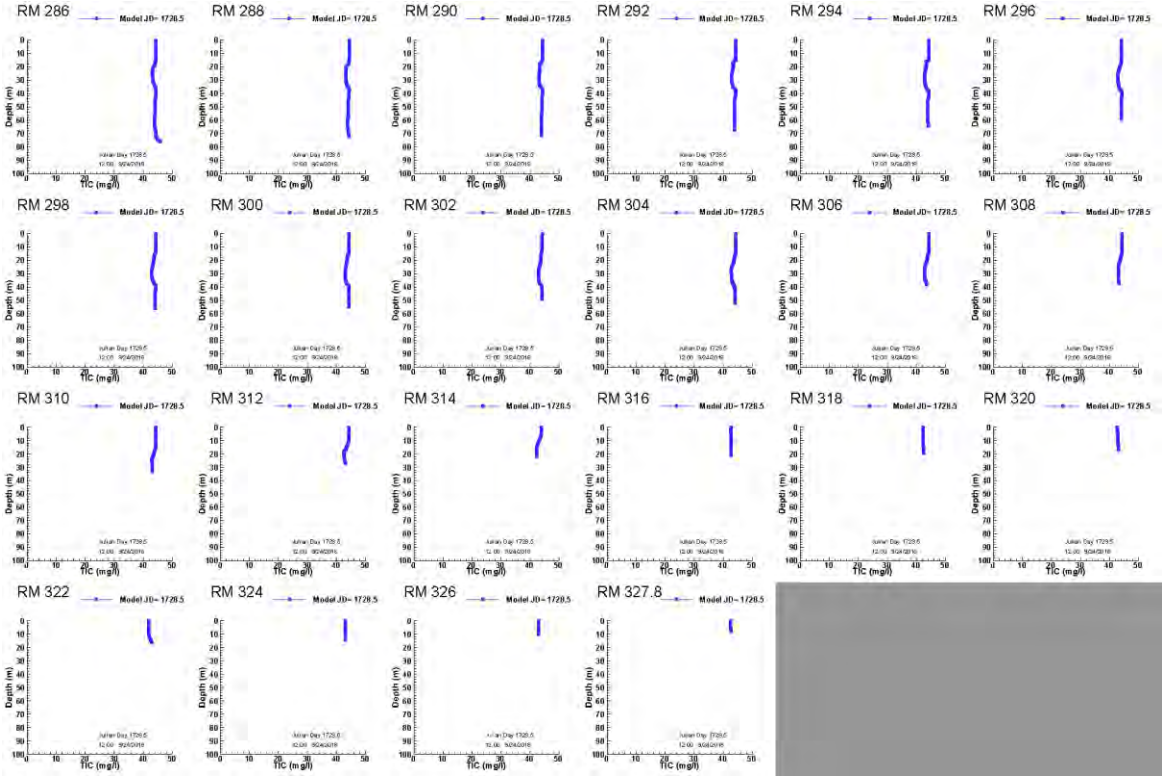


Figure 1311. Vertical profiles of TIC compared with data for 9/24/2018.

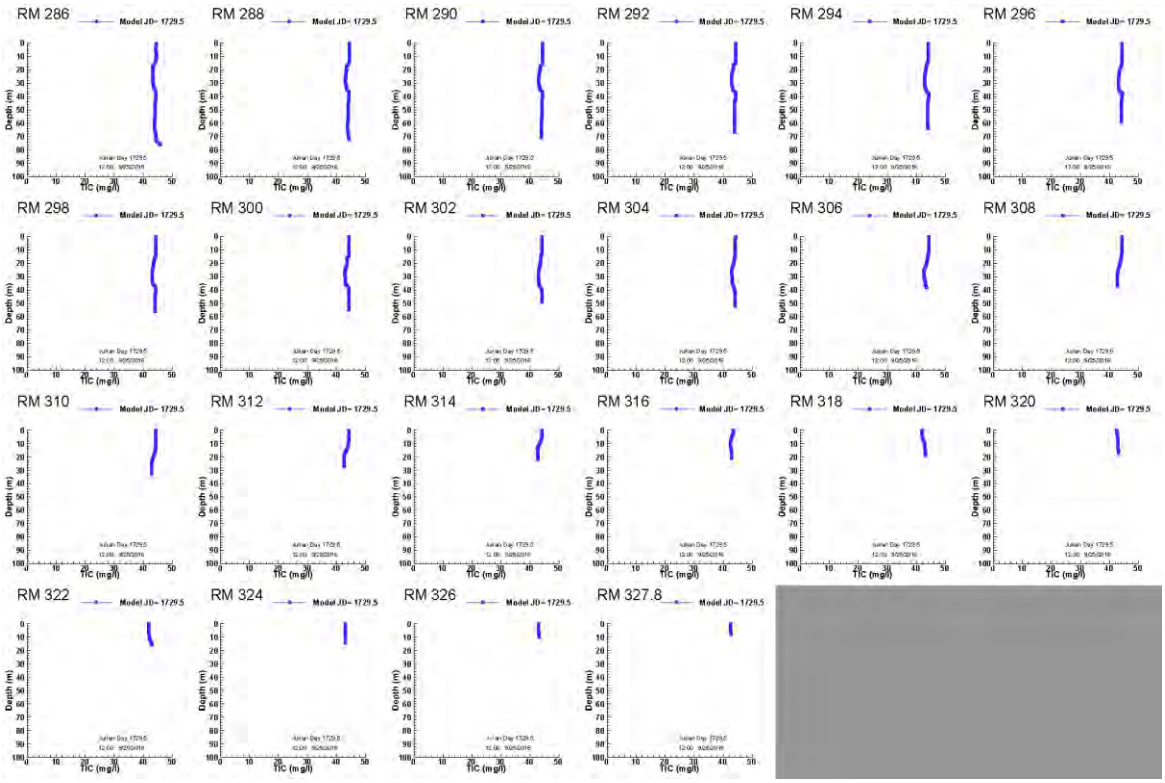


Figure 1312. Vertical profiles of TIC compared with data for 9/25/2018.

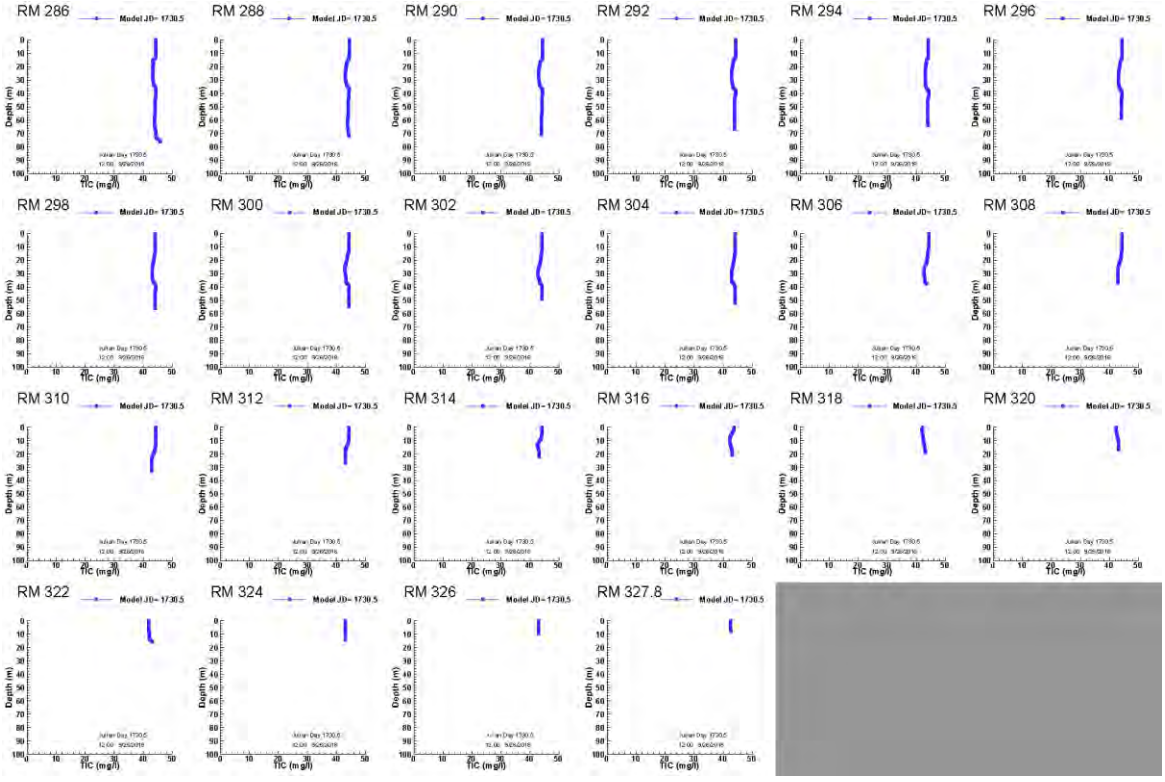


Figure 1313. Vertical profiles of TIC compared with data for 9/26/2018.

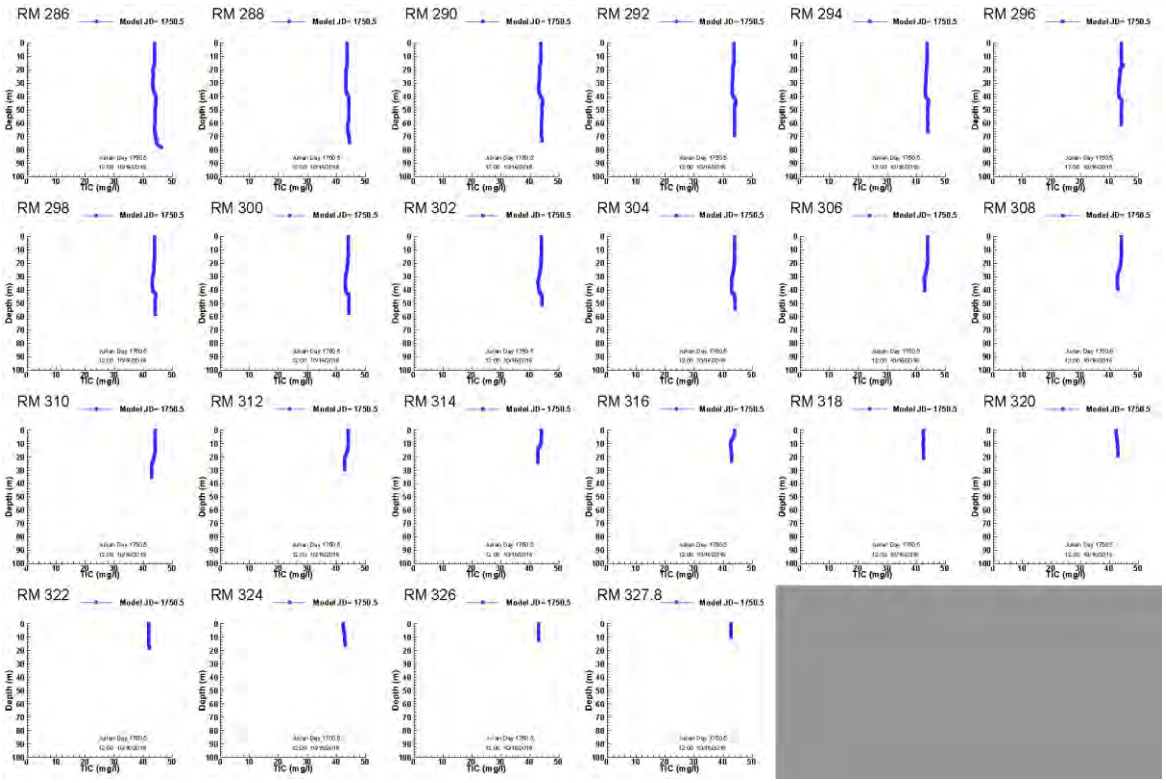


Figure 1314. Vertical profiles of TIC compared with data for 10/16/2018.

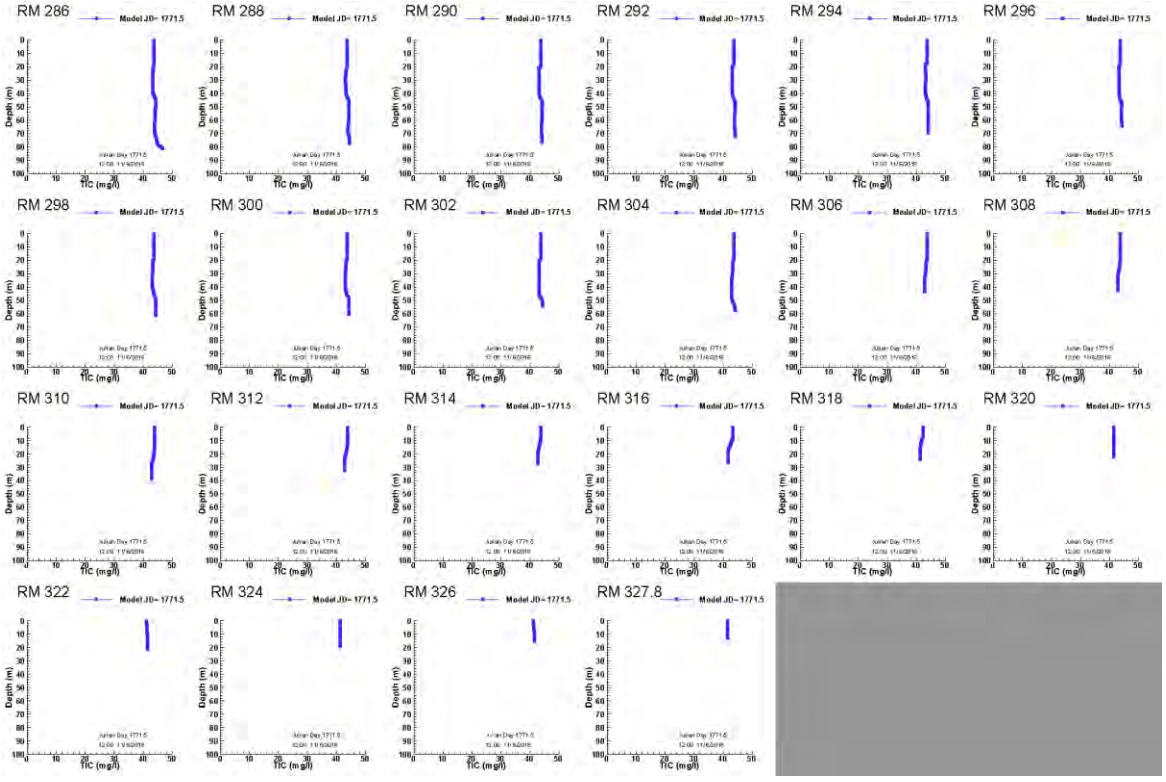


Figure 1315. Vertical profiles of TIC compared with data for 11/ 6/2018.

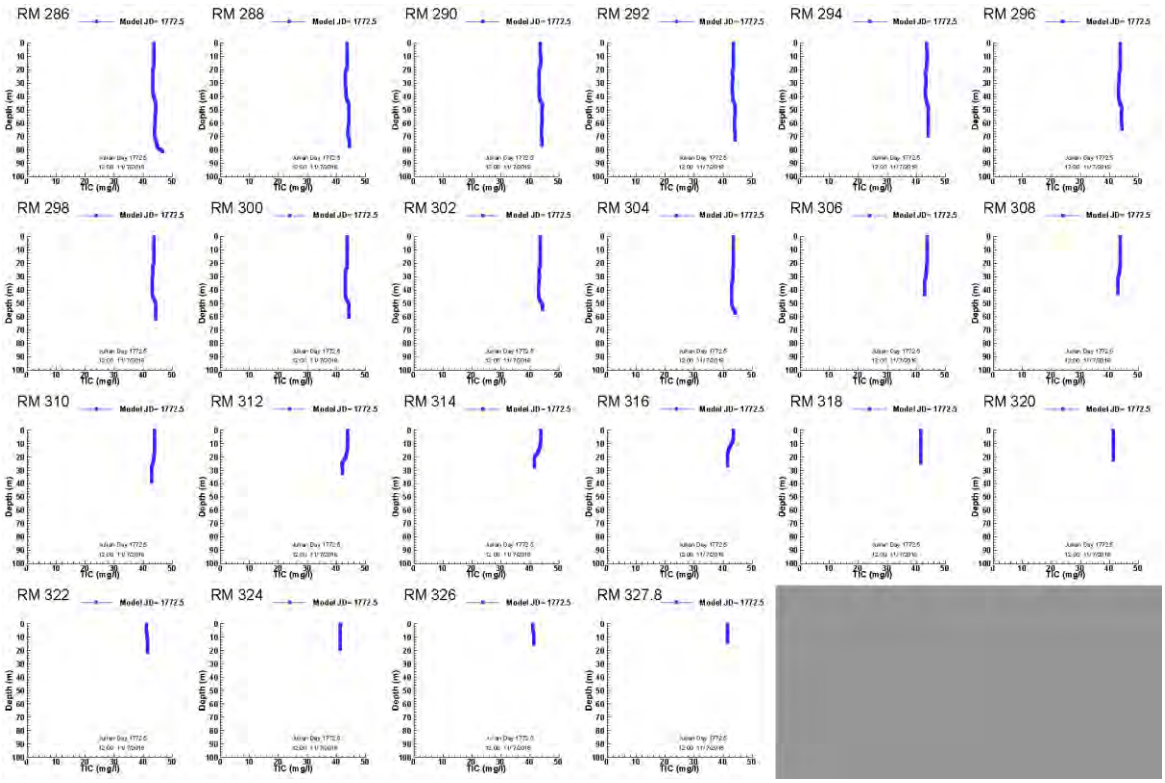


Figure 1316. Vertical profiles of TIC compared with data for 11/ 7/2018.

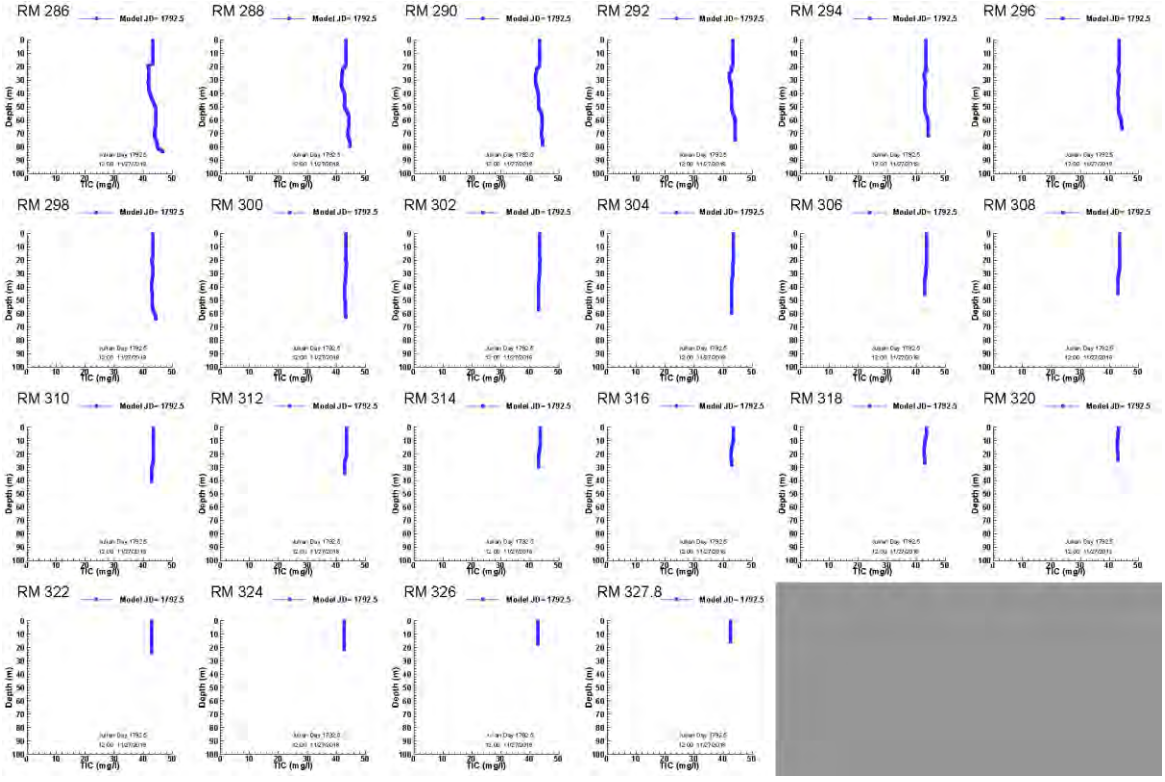


Figure 1317. Vertical profiles of TIC compared with data for 11/27/2018.

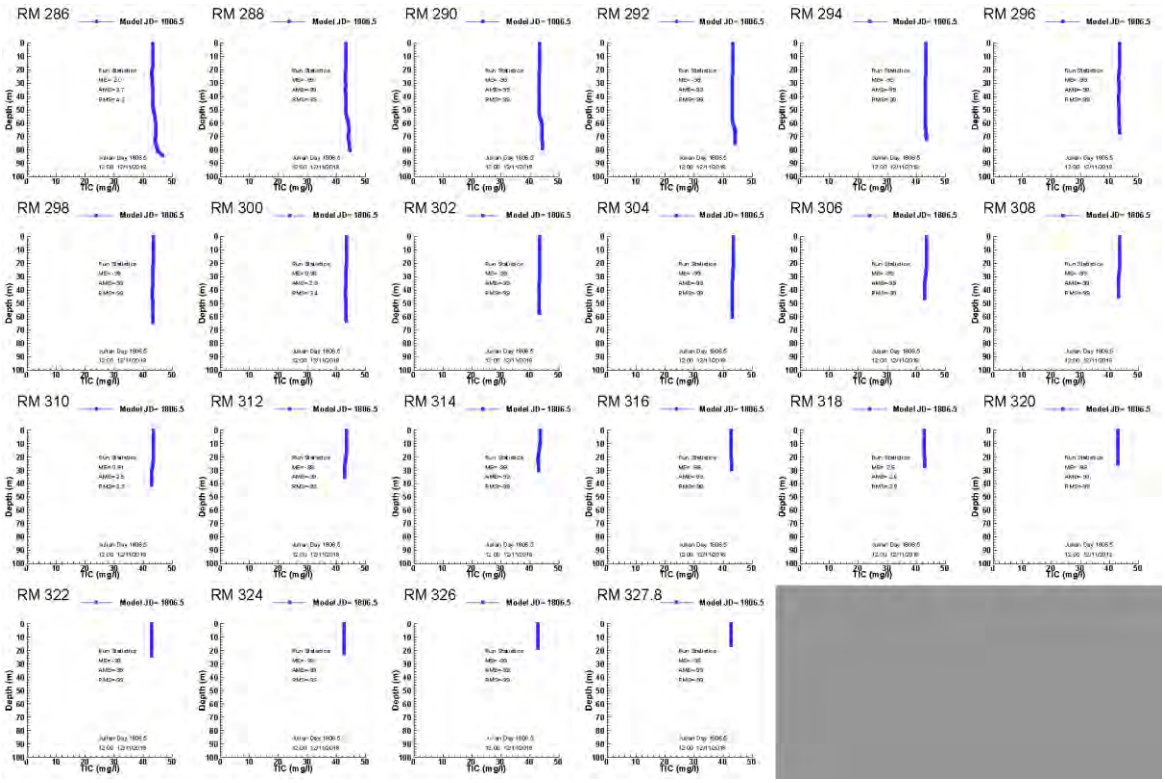


Figure 1318. Vertical profiles of TIC compared with data for 12/11/2018.

Zooplankton

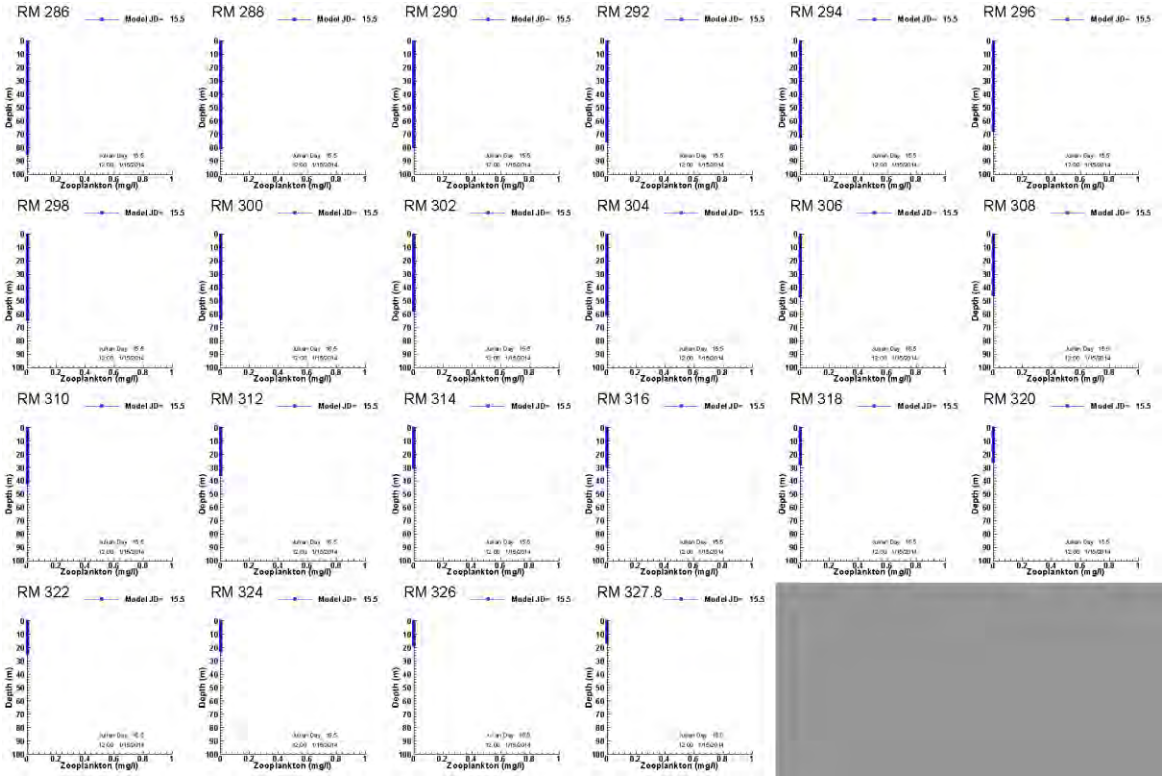


Figure 1319. Vertical profiles of zooplankton compared with data for 1/15/2014.

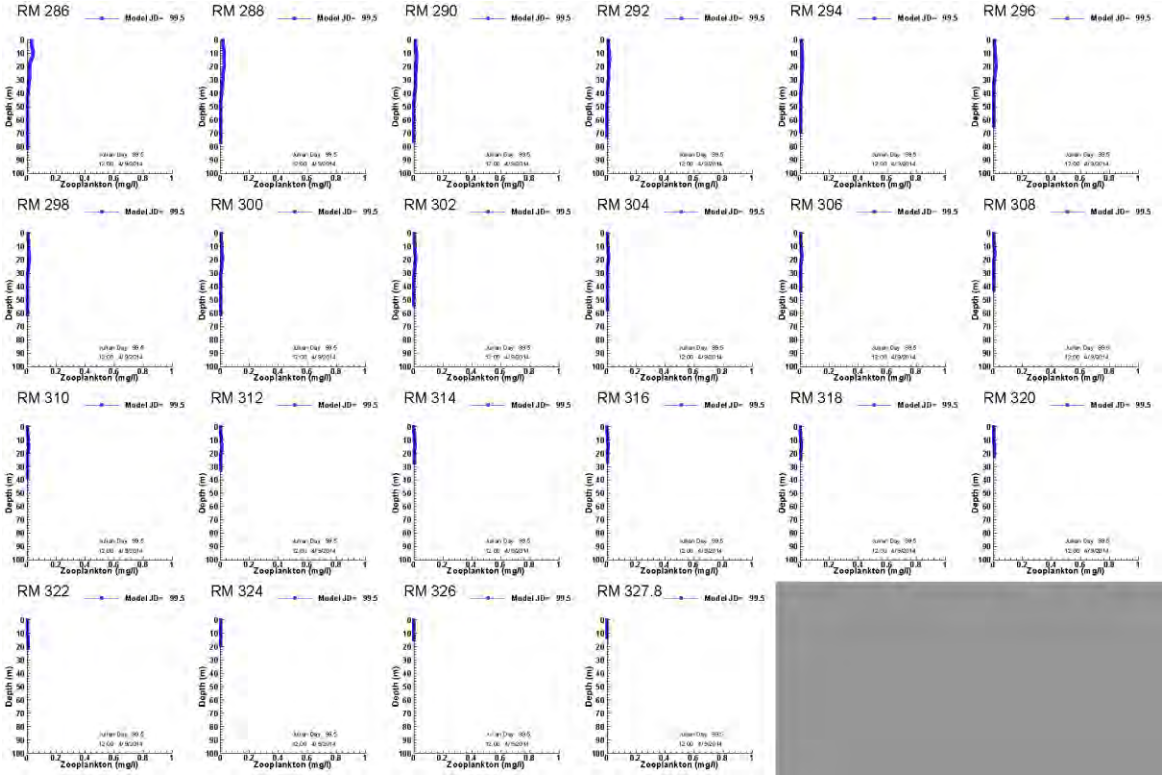


Figure 1320. Vertical profiles of zooplankton compared with data for 4/ 9/2014.

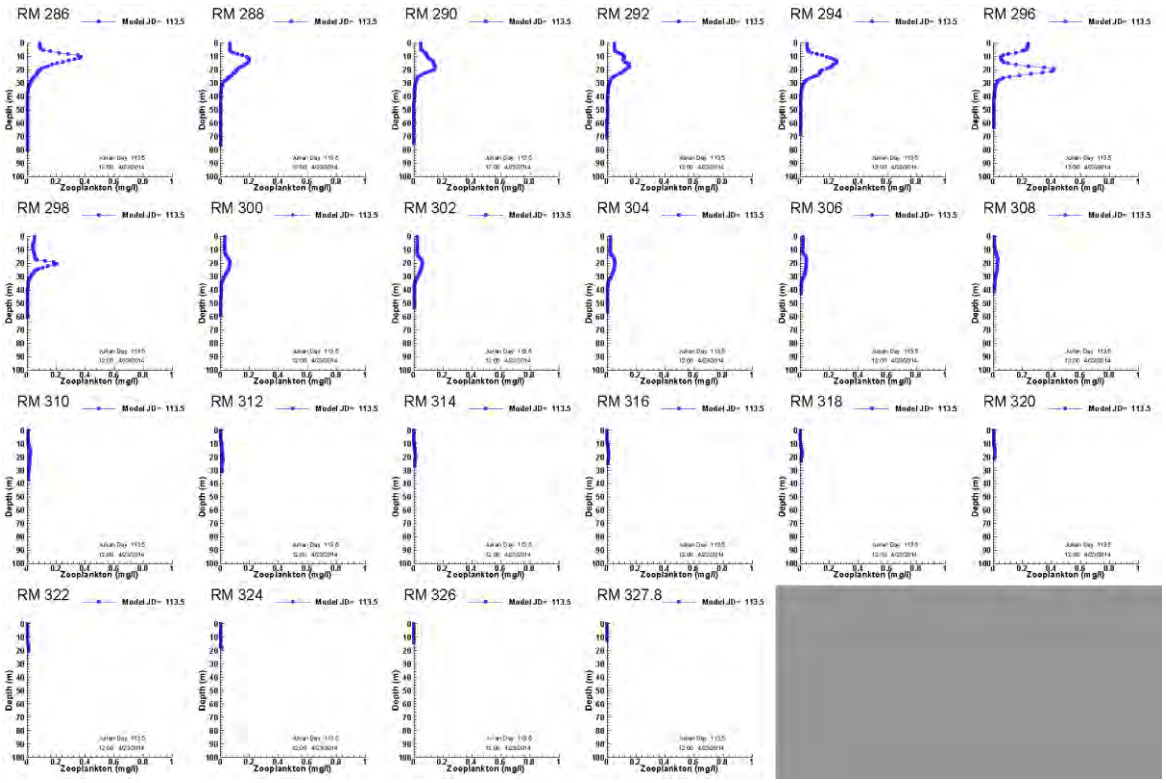


Figure 1321. Vertical profiles of zooplankton compared with data for 4/23/2014.

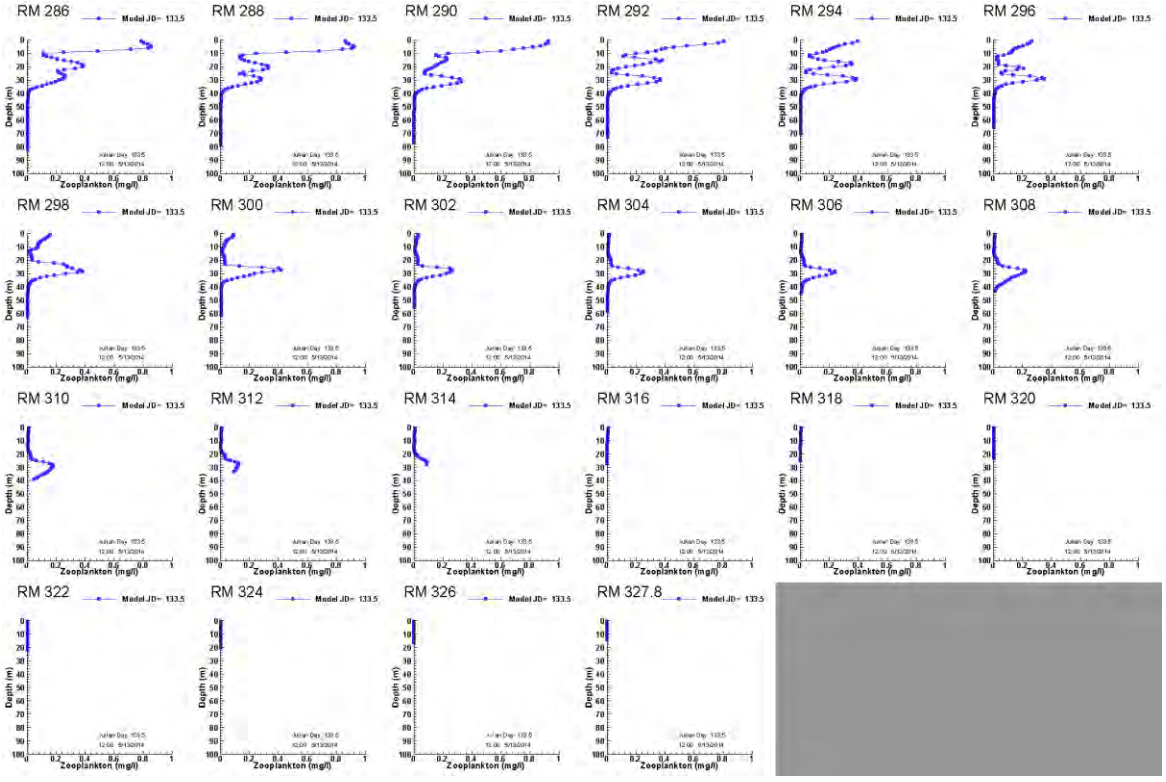


Figure 1322. Vertical profiles of zooplankton compared with data for 5/13/2014.

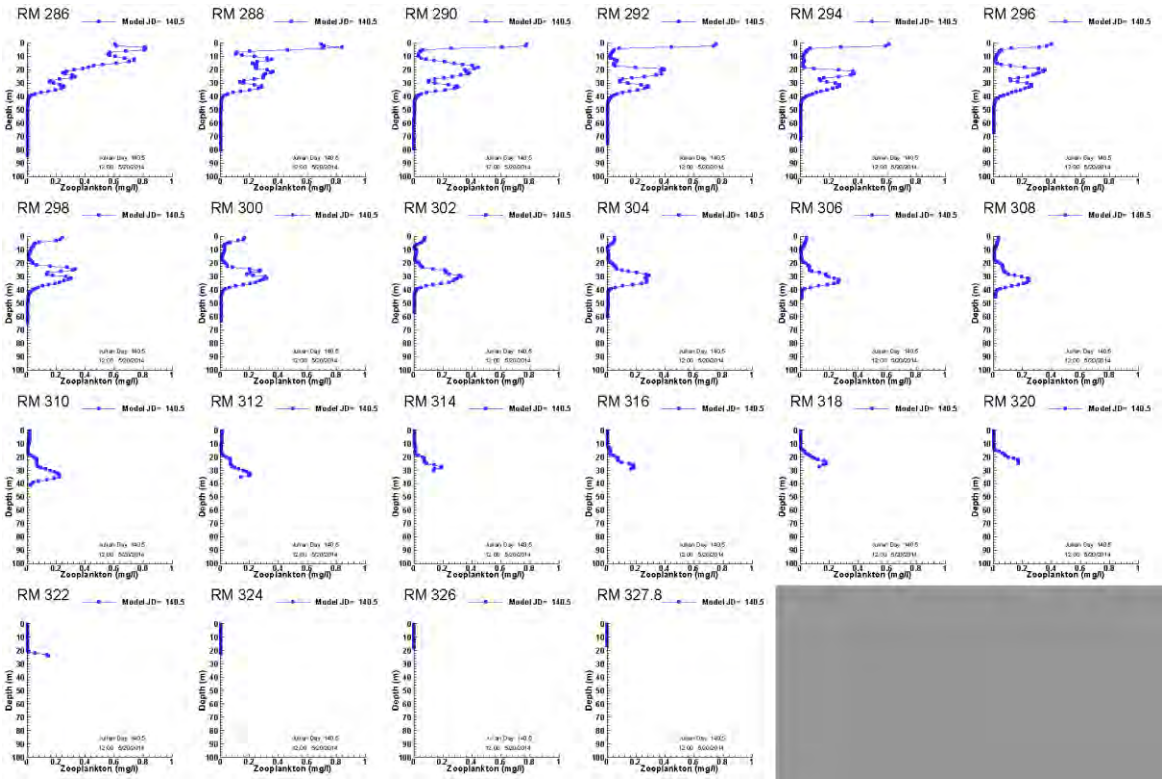


Figure 1323. Vertical profiles of zooplankton compared with data for 5/20/2014.

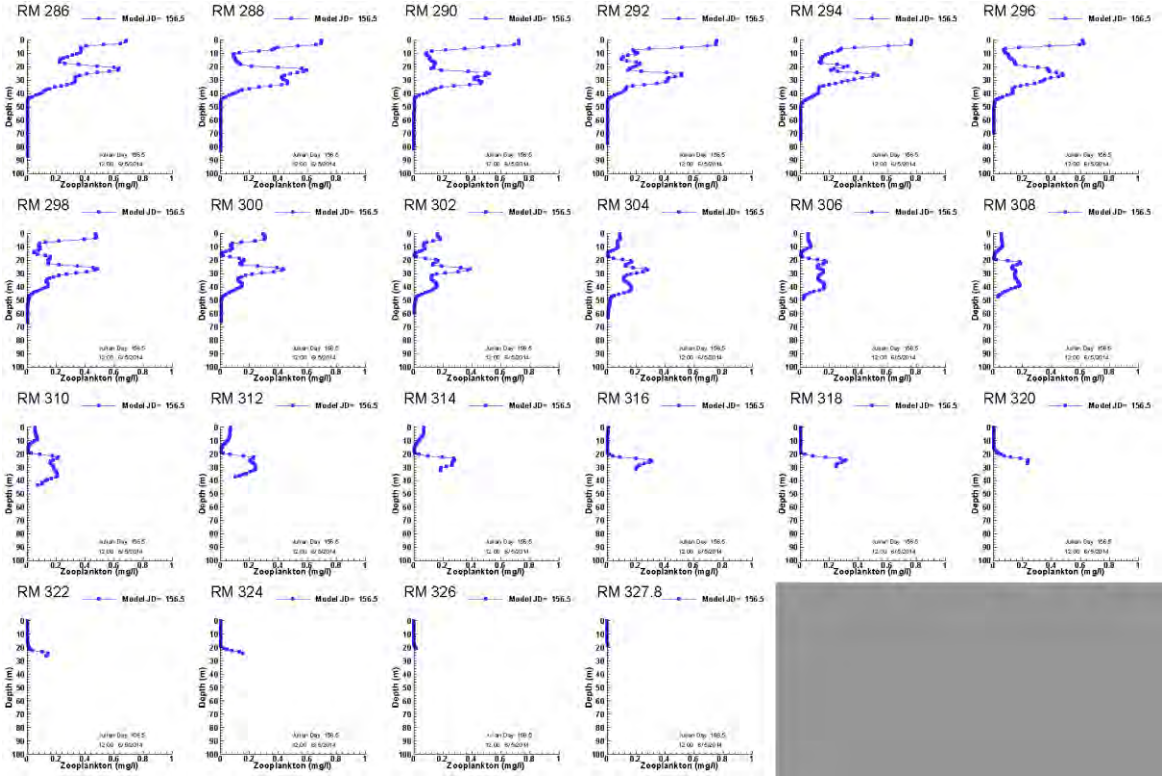


Figure 1324. Vertical profiles of zooplankton compared with data for 6/ 5/2014.

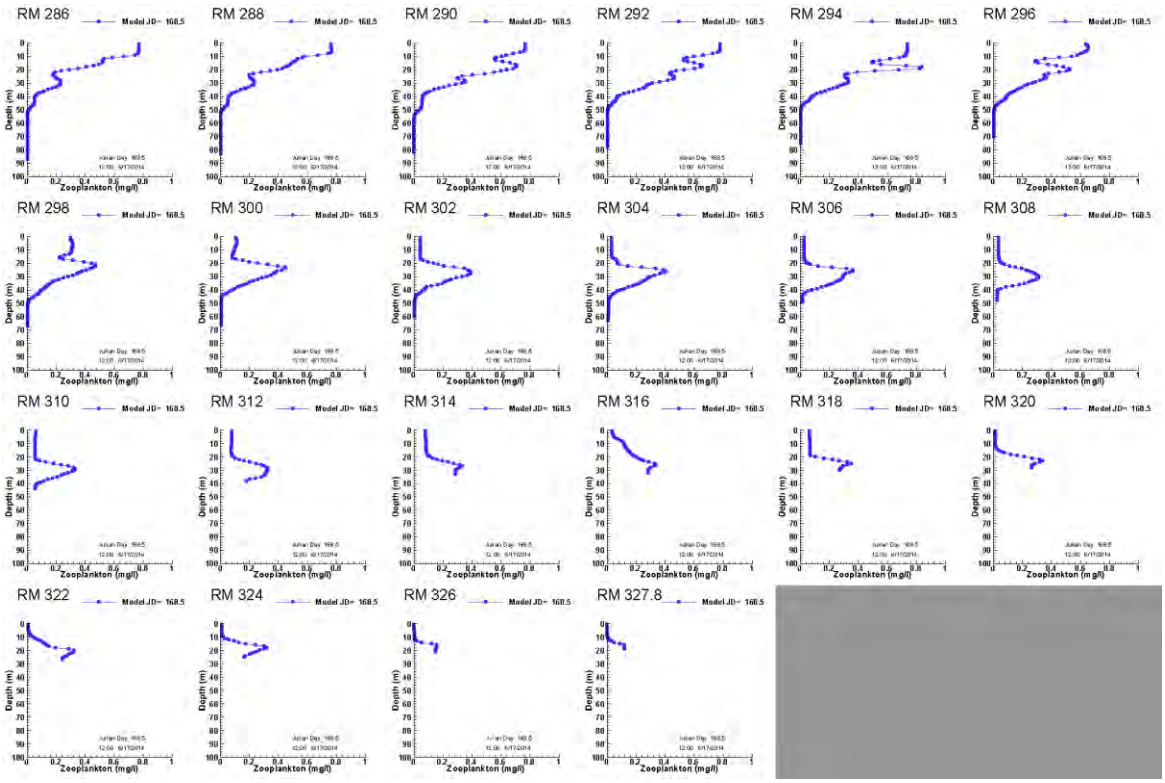


Figure 1325. Vertical profiles of zooplankton compared with data for 6/17/2014.

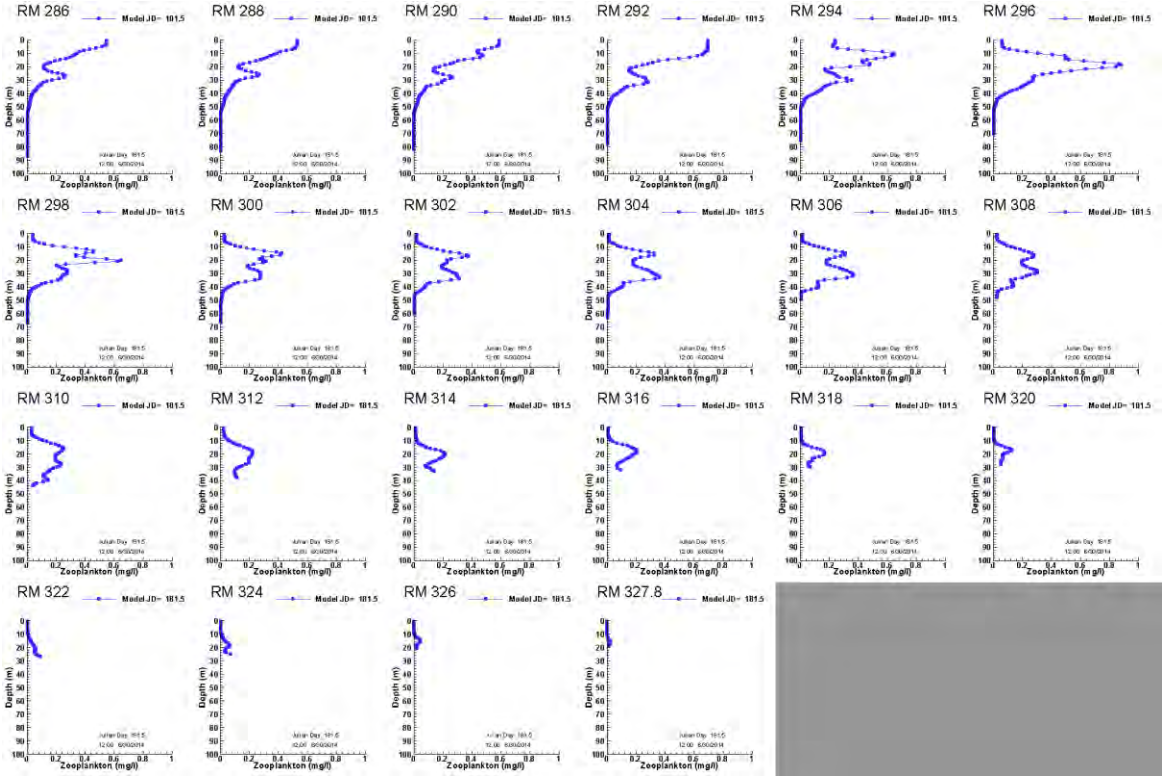


Figure 1326. Vertical profiles of zooplankton compared with data for 6/30/2014.

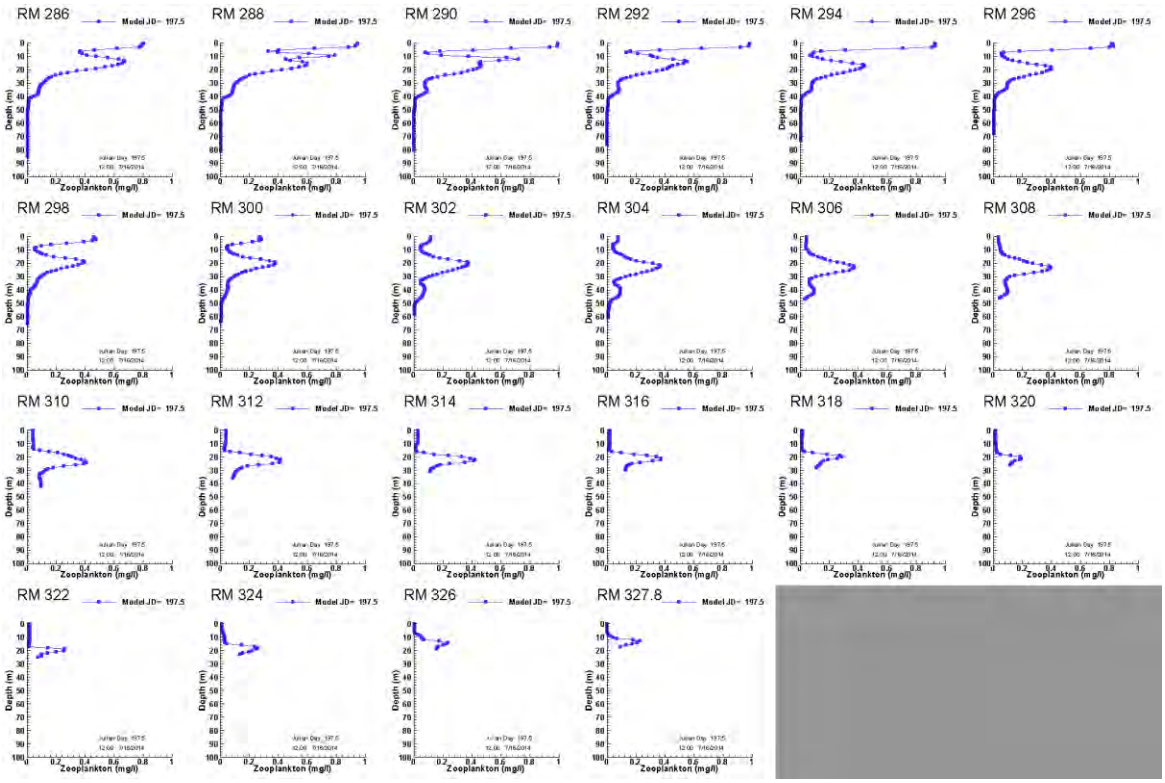


Figure 1327. Vertical profiles of zooplankton compared with data for 7/16/2014.

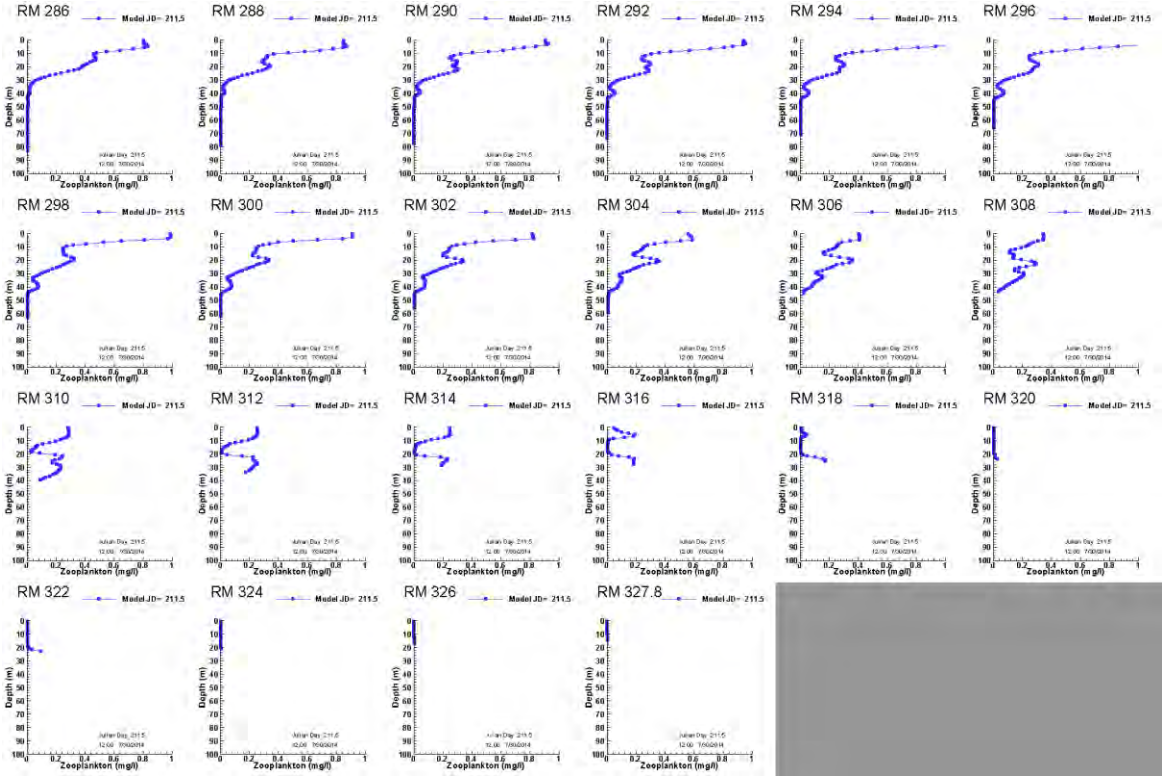


Figure 1328. Vertical profiles of zooplankton compared with data for 7/30/2014.

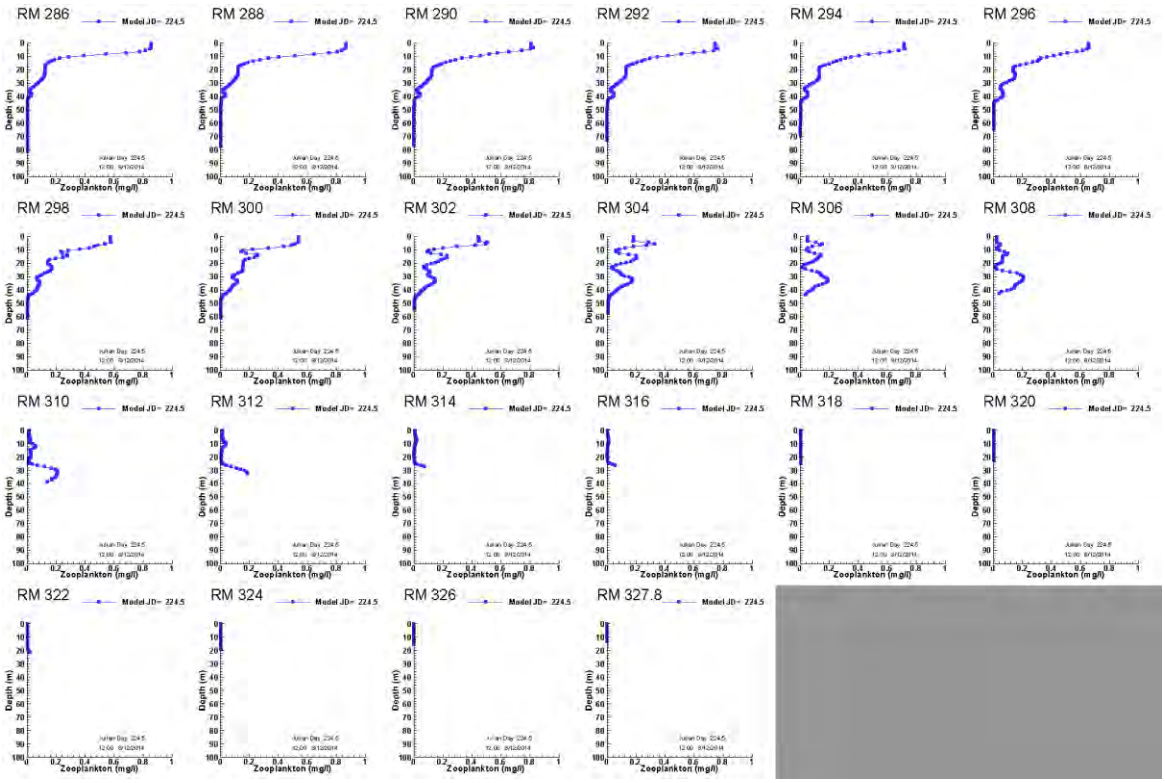


Figure 1329. Vertical profiles of zooplankton compared with data for 8/12/2014.

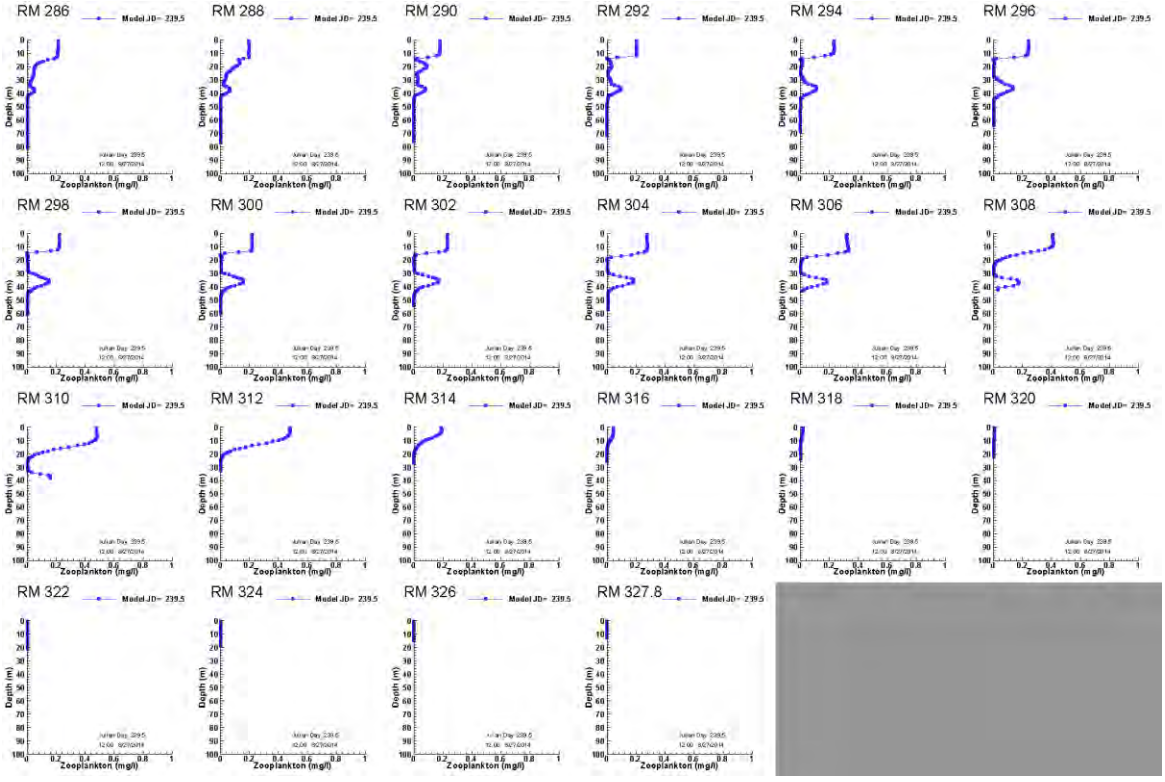


Figure 1330. Vertical profiles of zooplankton compared with data for 8/27/2014.

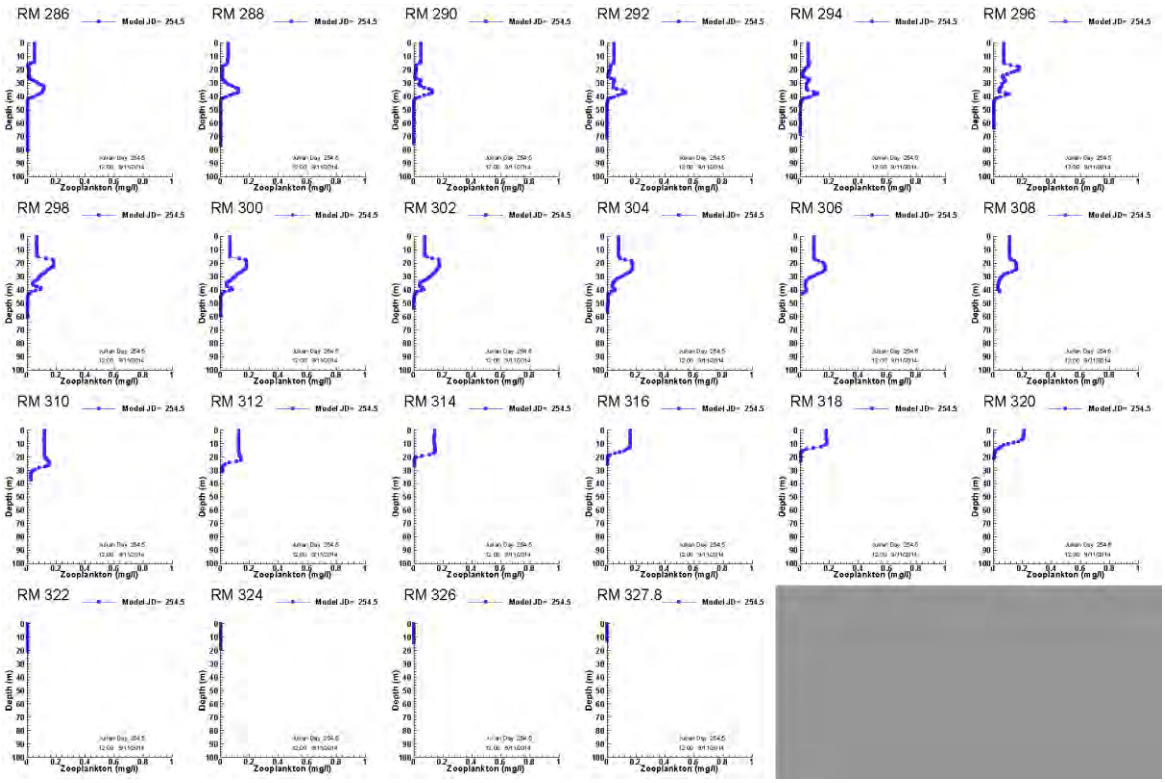


Figure 1331. Vertical profiles of zooplankton compared with data for 9/11/2014.

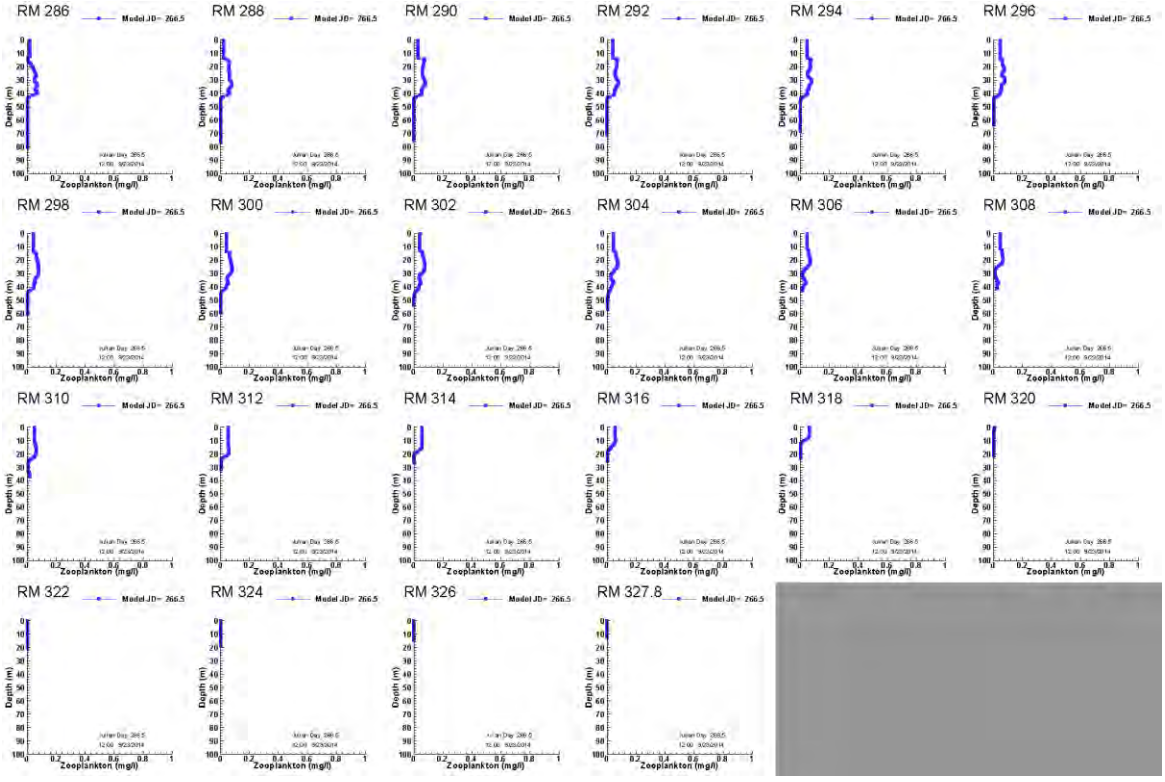


Figure 1332. Vertical profiles of zooplankton compared with data for 9/23/2014.

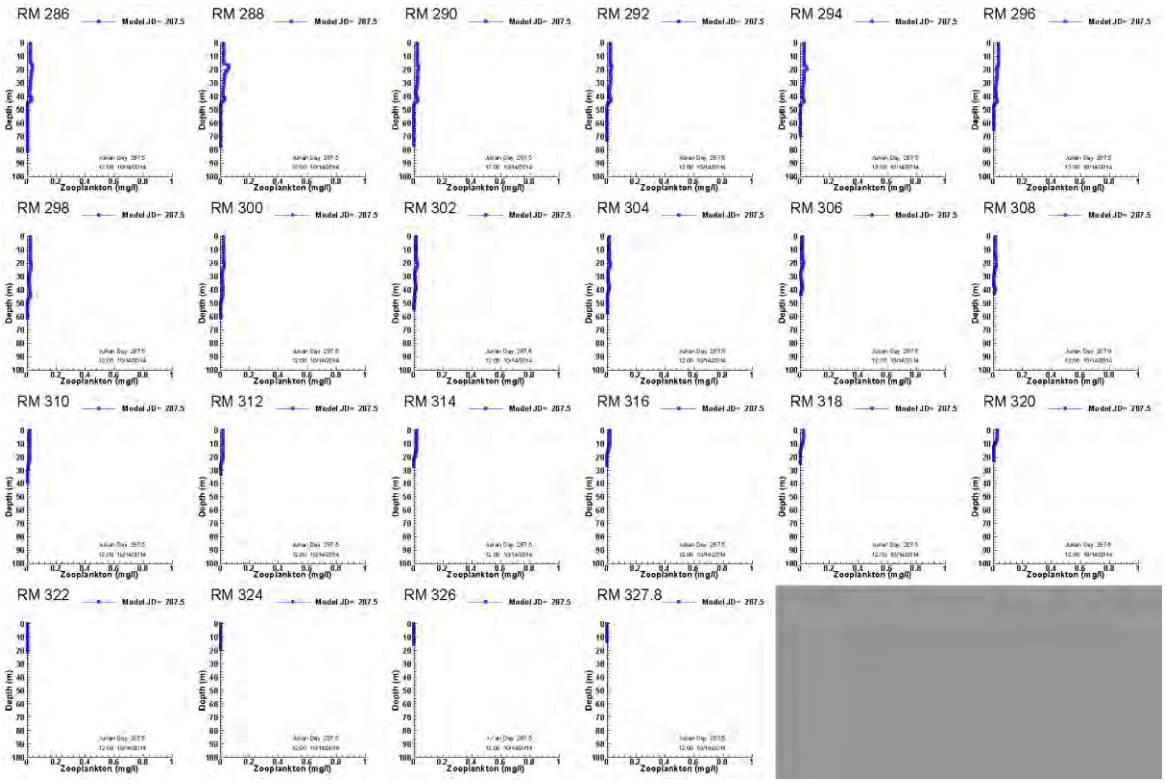


Figure 1333. Vertical profiles of zooplankton compared with data for 10/14/2014.

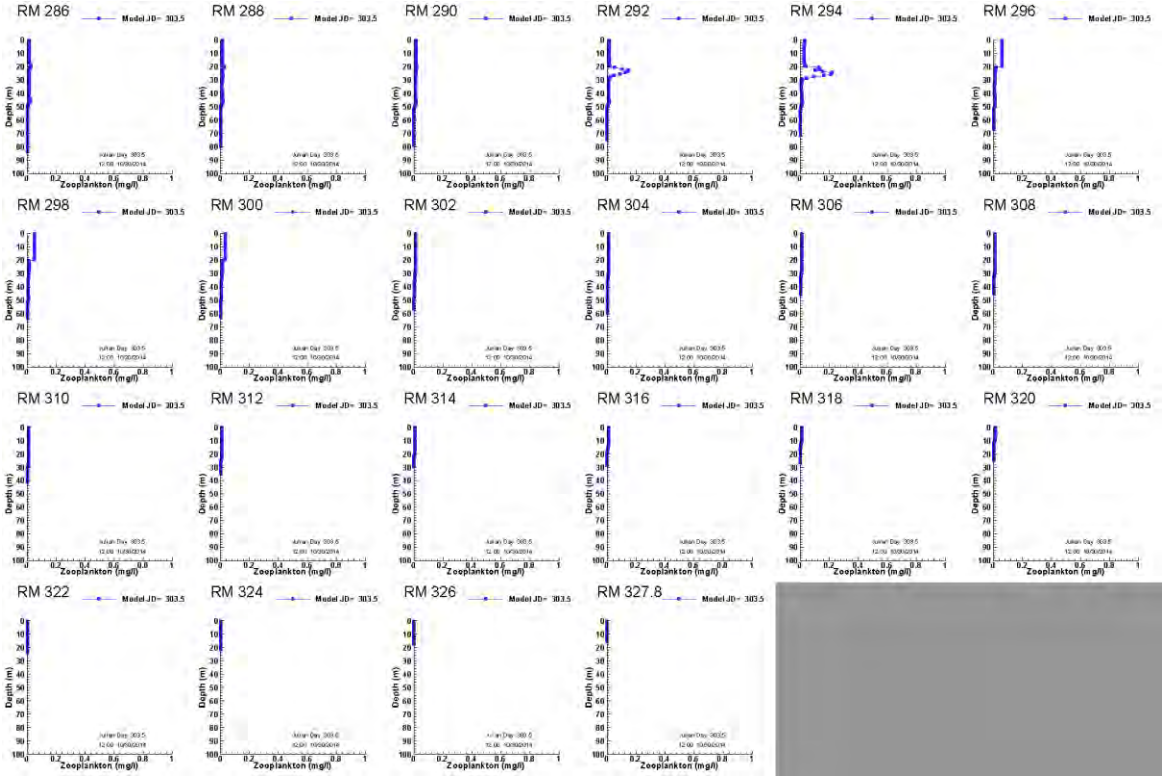


Figure 1334. Vertical profiles of zooplankton compared with data for 10/30/2014.

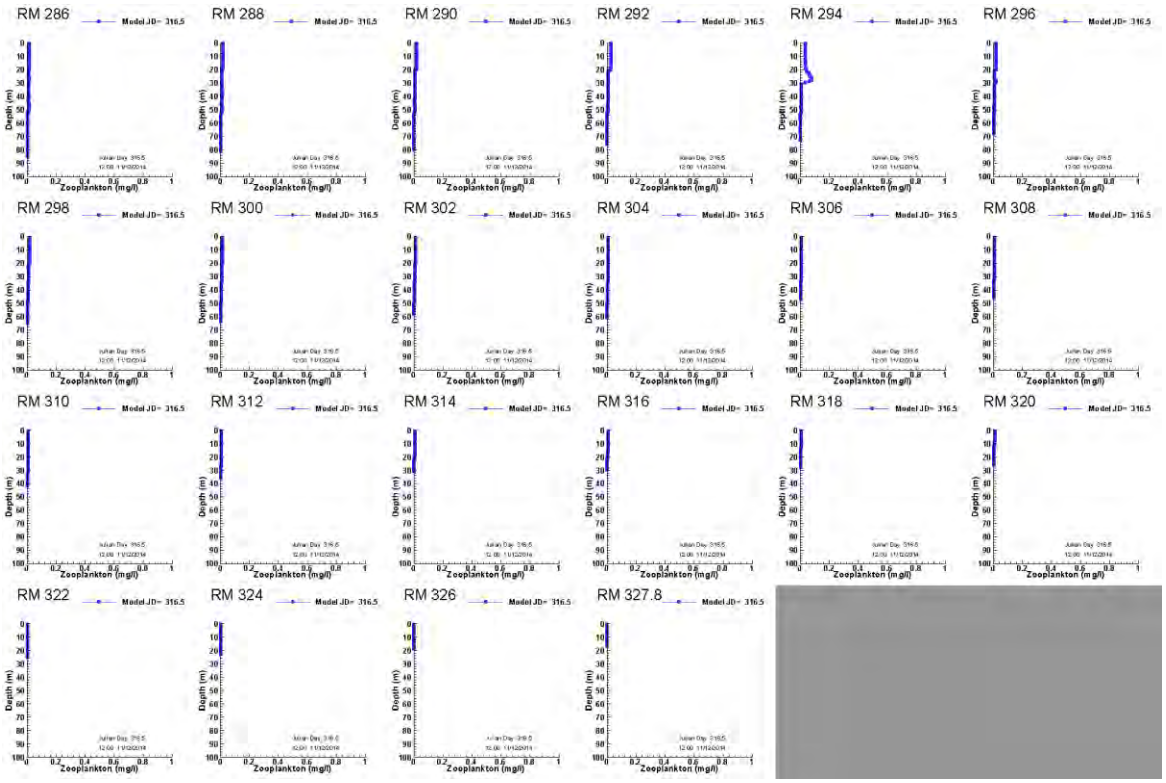


Figure 1335. Vertical profiles of zooplankton compared with data for 11/12/2014.

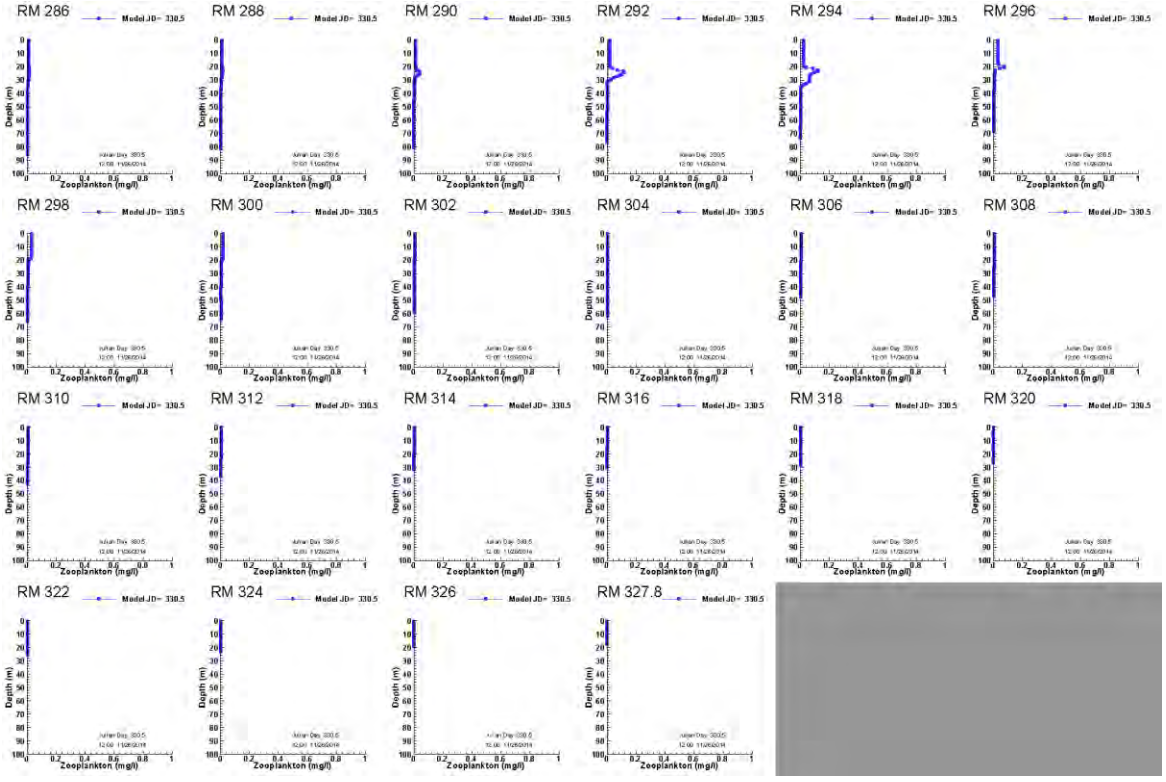


Figure 1336. Vertical profiles of zooplankton compared with data for 11/26/2014.

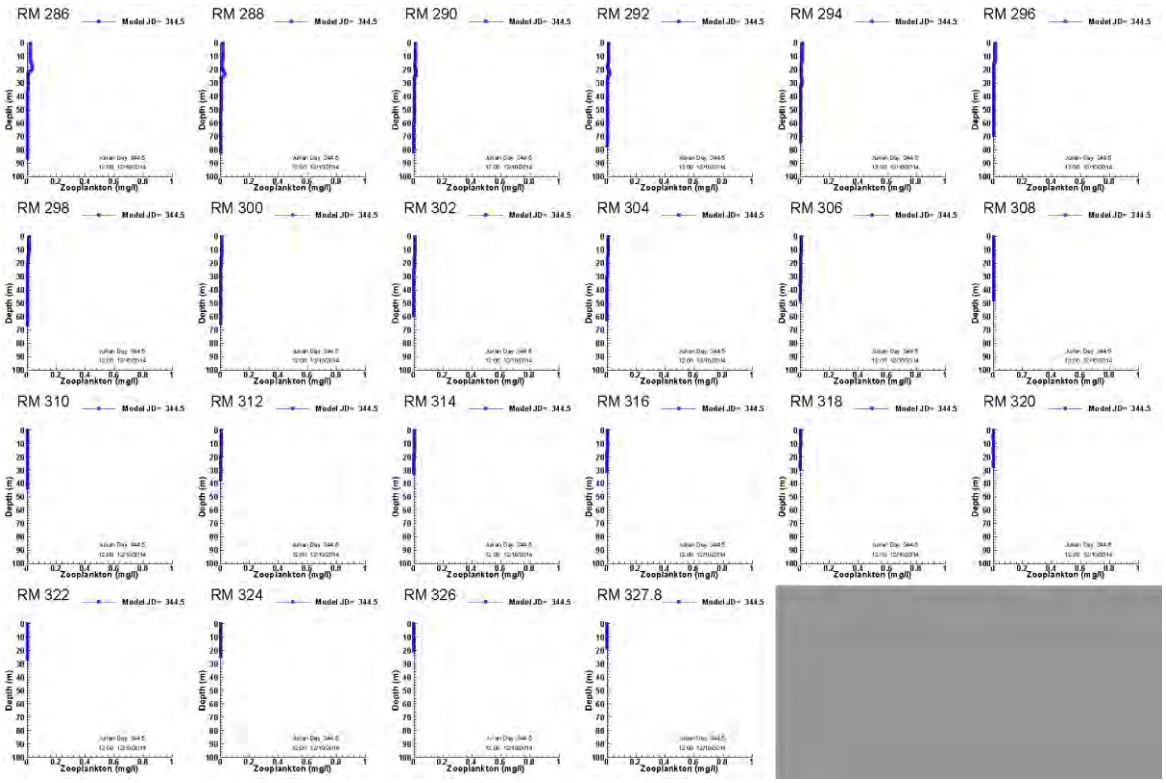


Figure 1337. Vertical profiles of zooplankton compared with data for 12/10/2014.

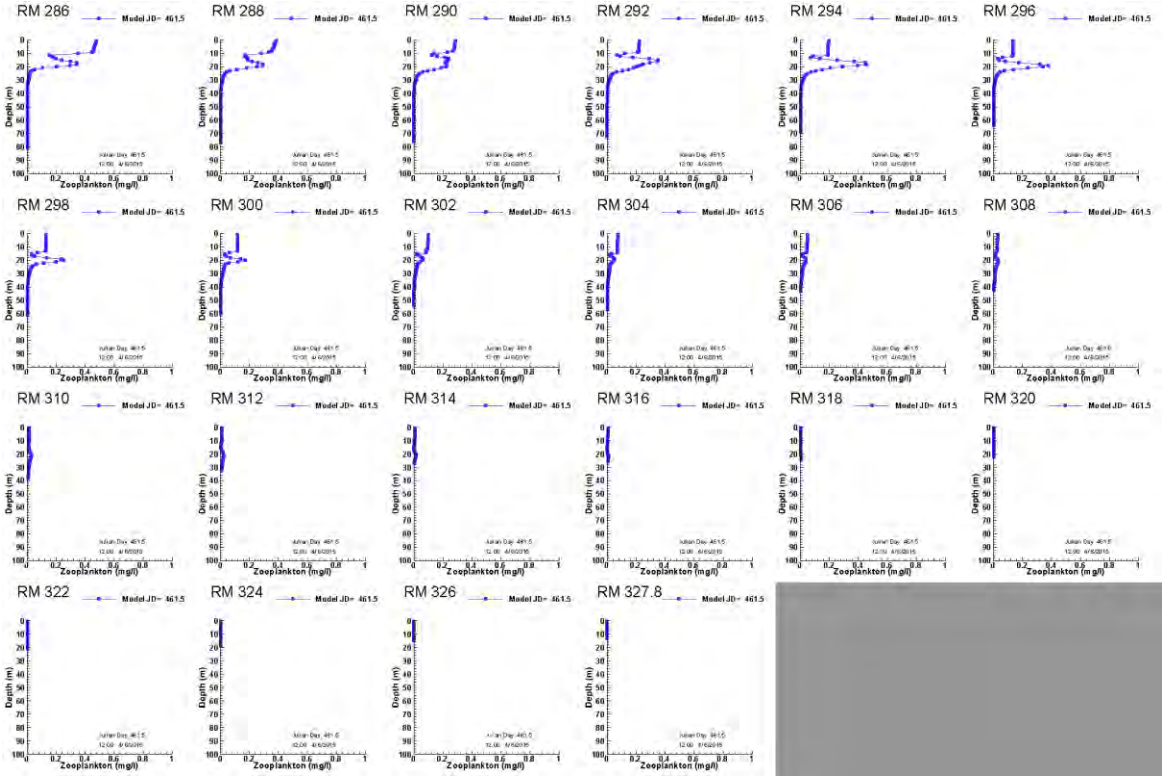


Figure 1338. Vertical profiles of zooplankton compared with data for 4/ 6/2015.

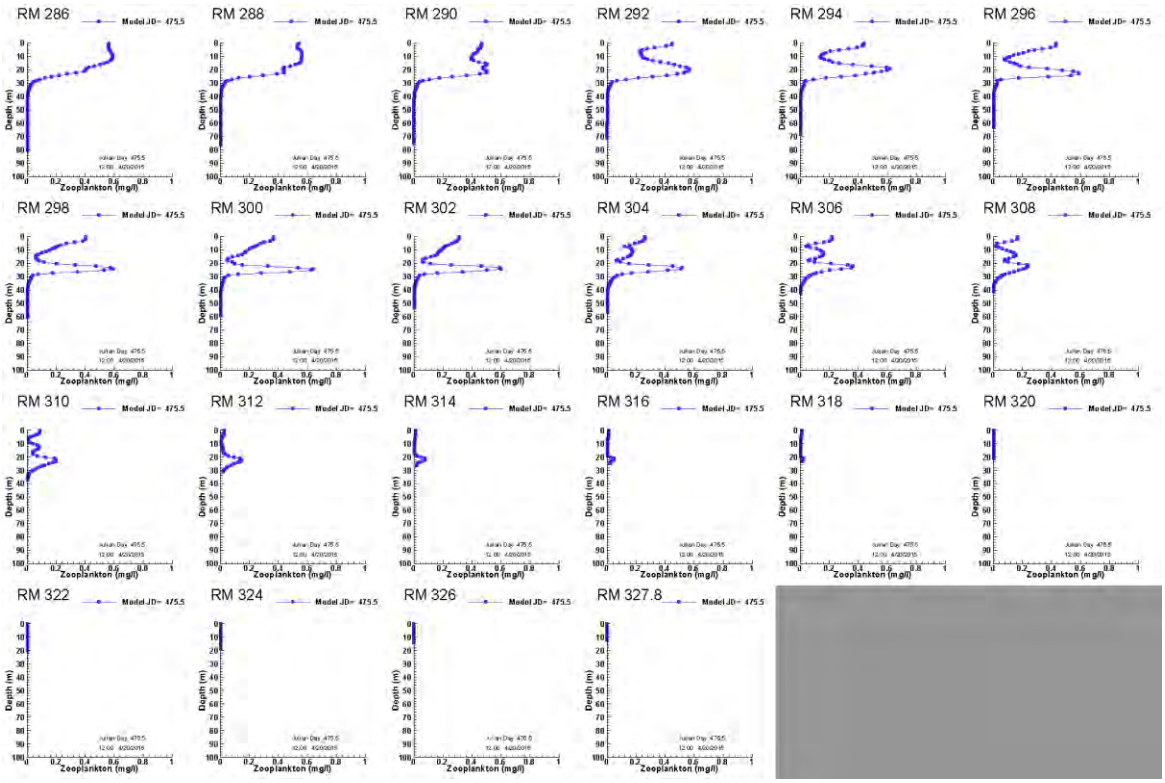


Figure 1339. Vertical profiles of zooplankton compared with data for 4/20/2015.

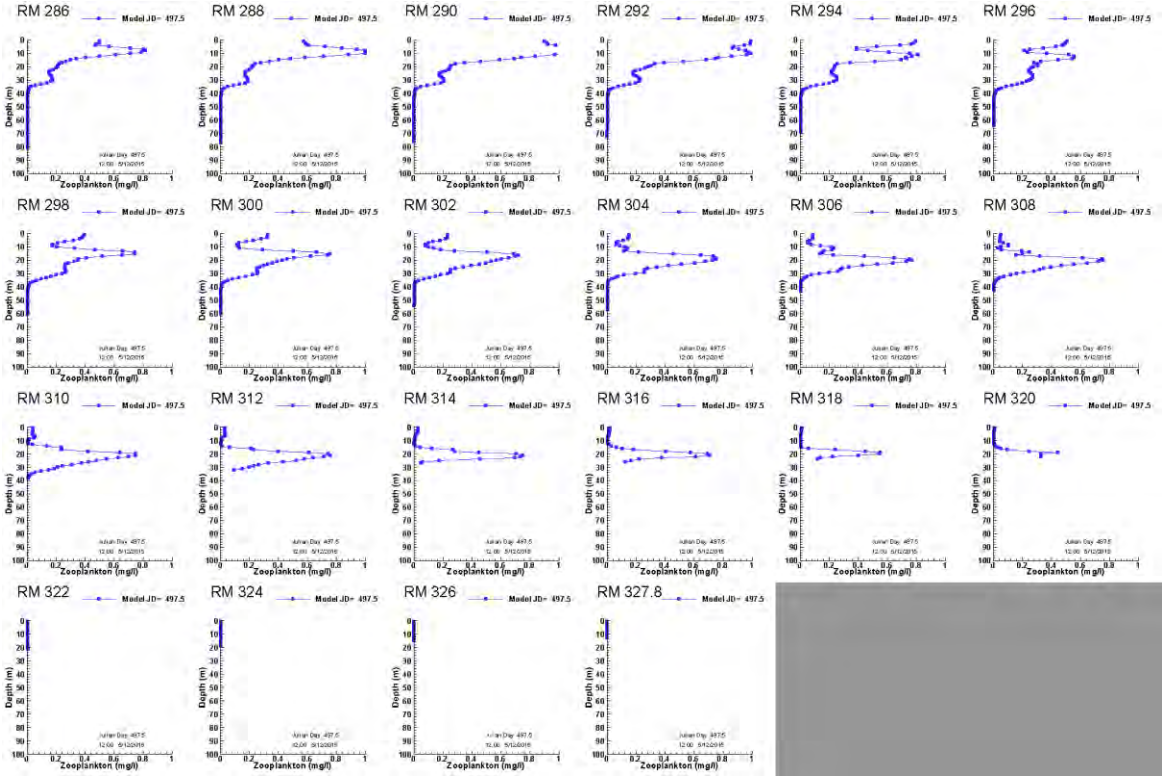


Figure 1340. Vertical profiles of zooplankton compared with data for 5/12/2015.

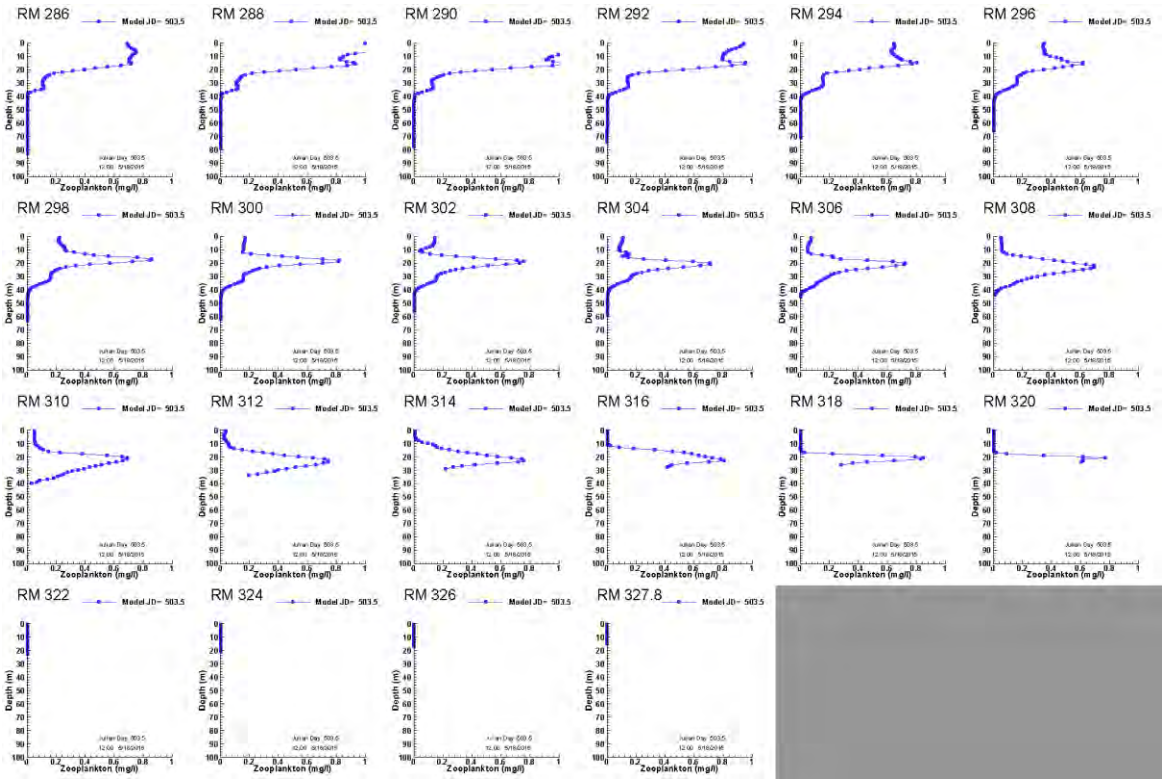


Figure 1341. Vertical profiles of zooplankton compared with data for 5/18/2015.

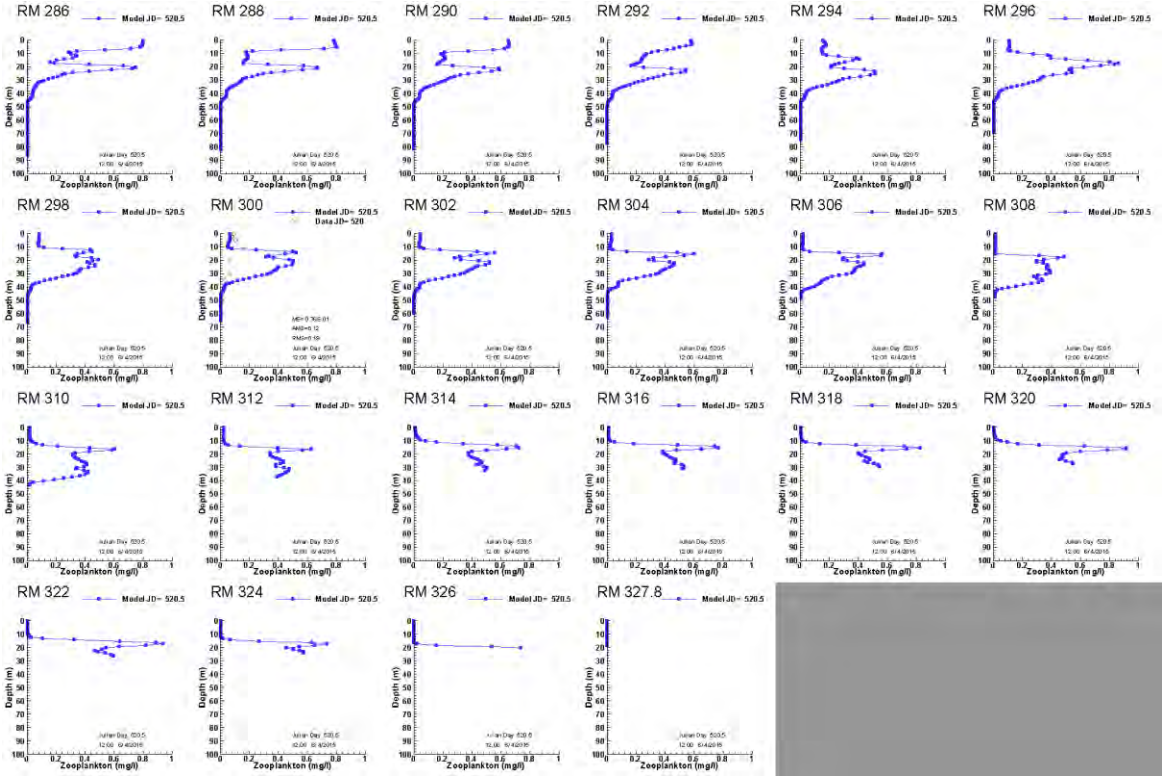


Figure 1342. Vertical profiles of zooplankton compared with data for 6/ 4/2015.

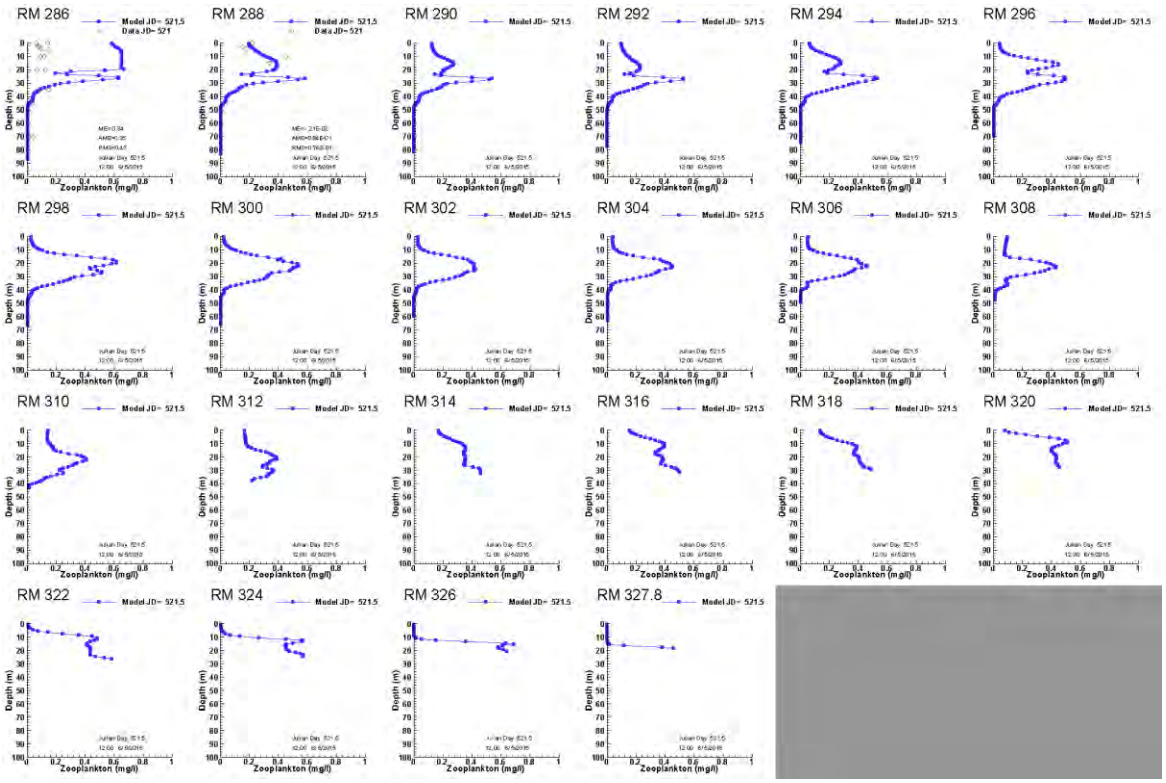


Figure 1343. Vertical profiles of zooplankton compared with data for 6/ 5/2015.

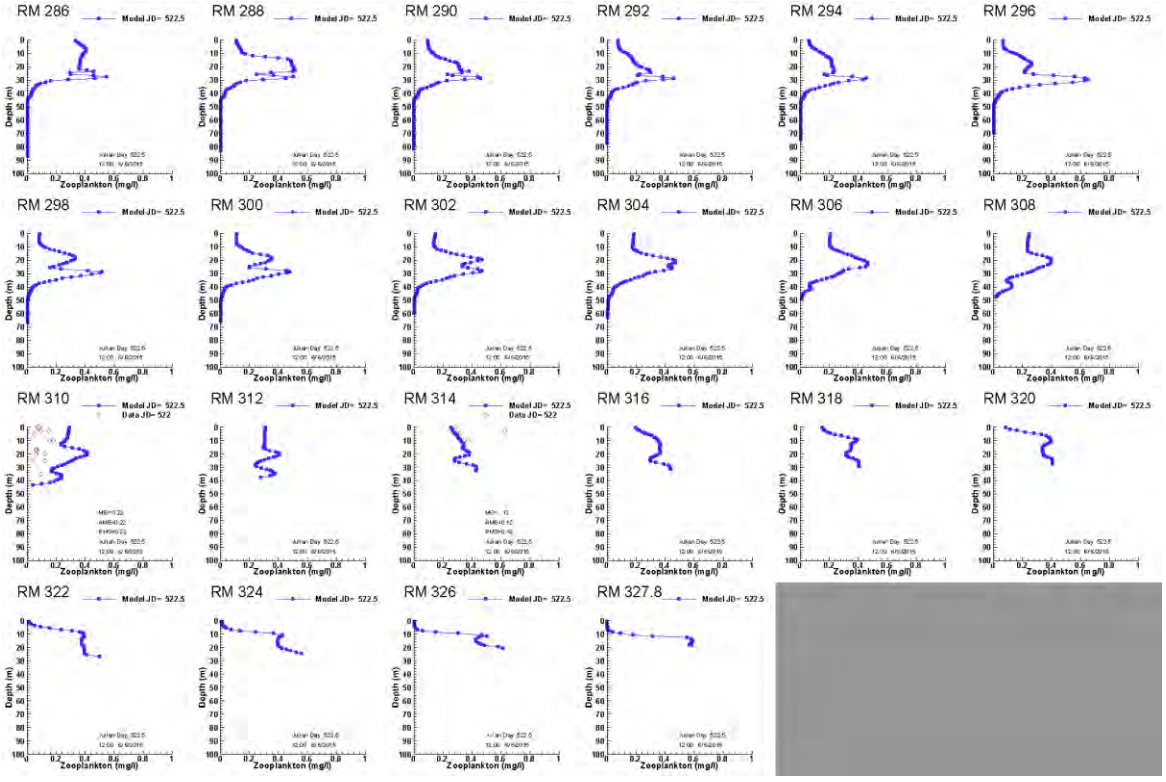


Figure 1344. Vertical profiles of zooplankton compared with data for 6/ 6/2015.

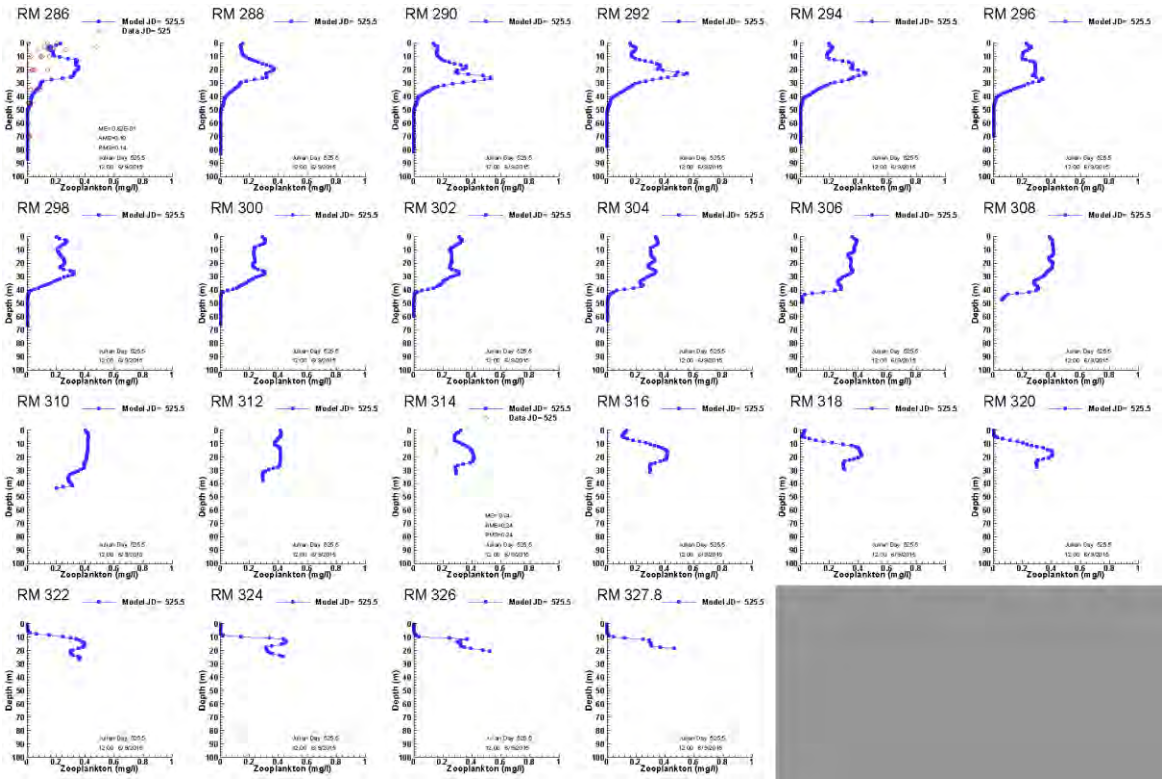


Figure 1345. Vertical profiles of zooplankton compared with data for 6/ 9/2015.

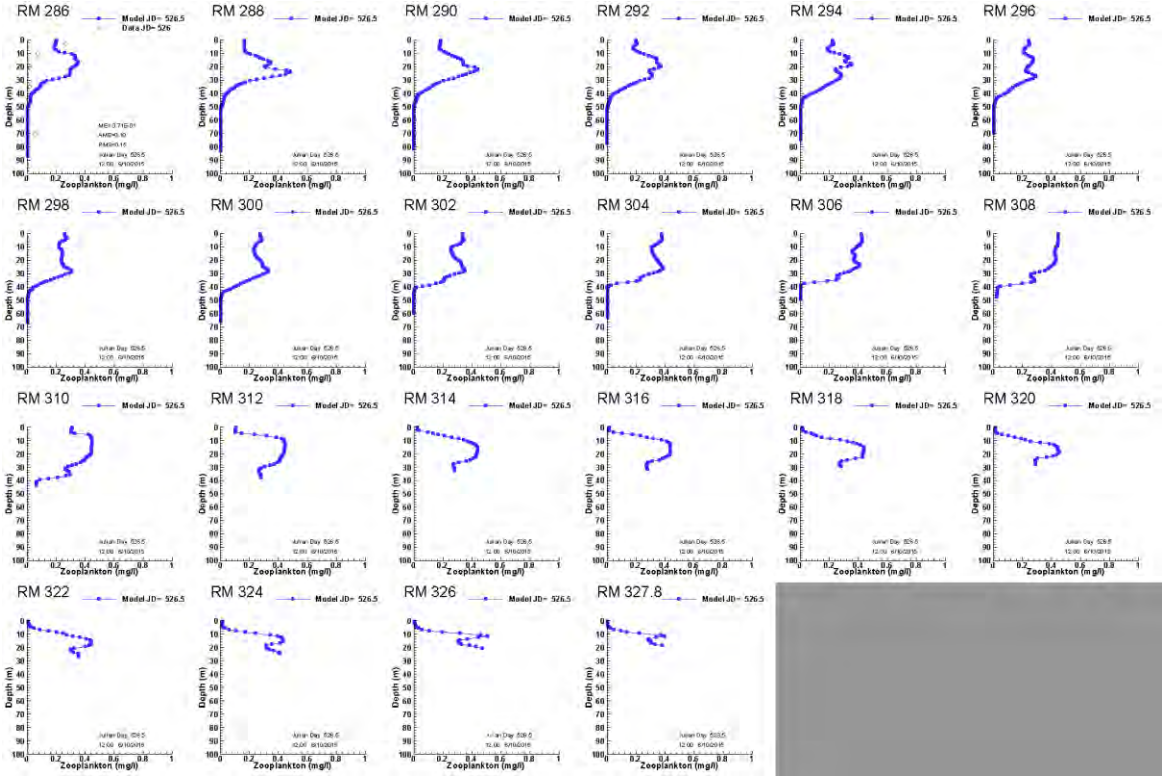


Figure 1346. Vertical profiles of zooplankton compared with data for 6/10/2015.

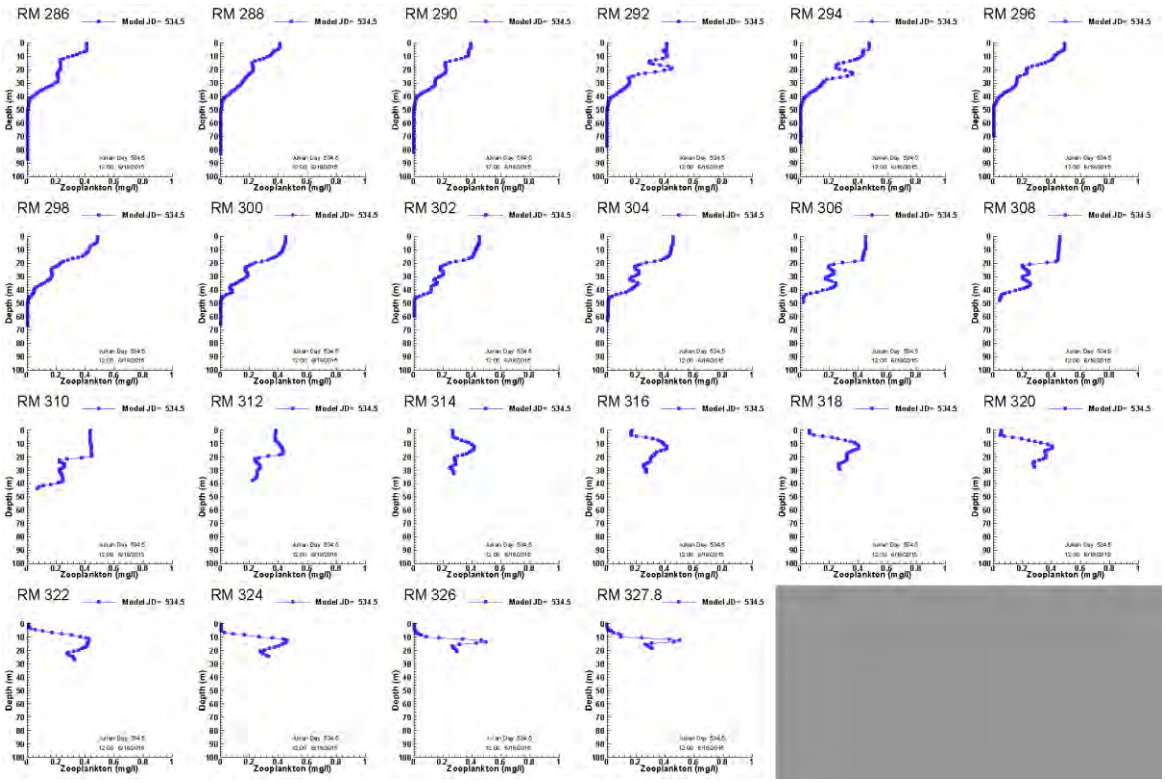


Figure 1347. Vertical profiles of zooplankton compared with data for 6/18/2015.

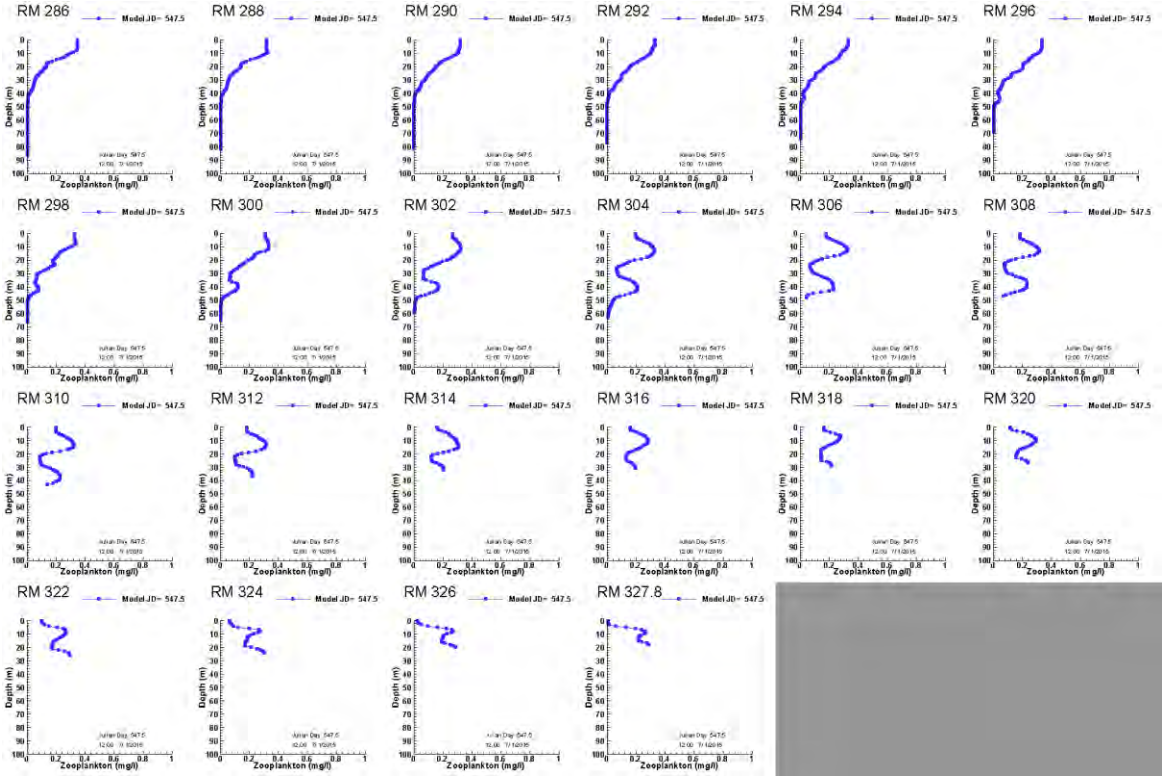


Figure 1348. Vertical profiles of zooplankton compared with data for 7/ 1/2015.

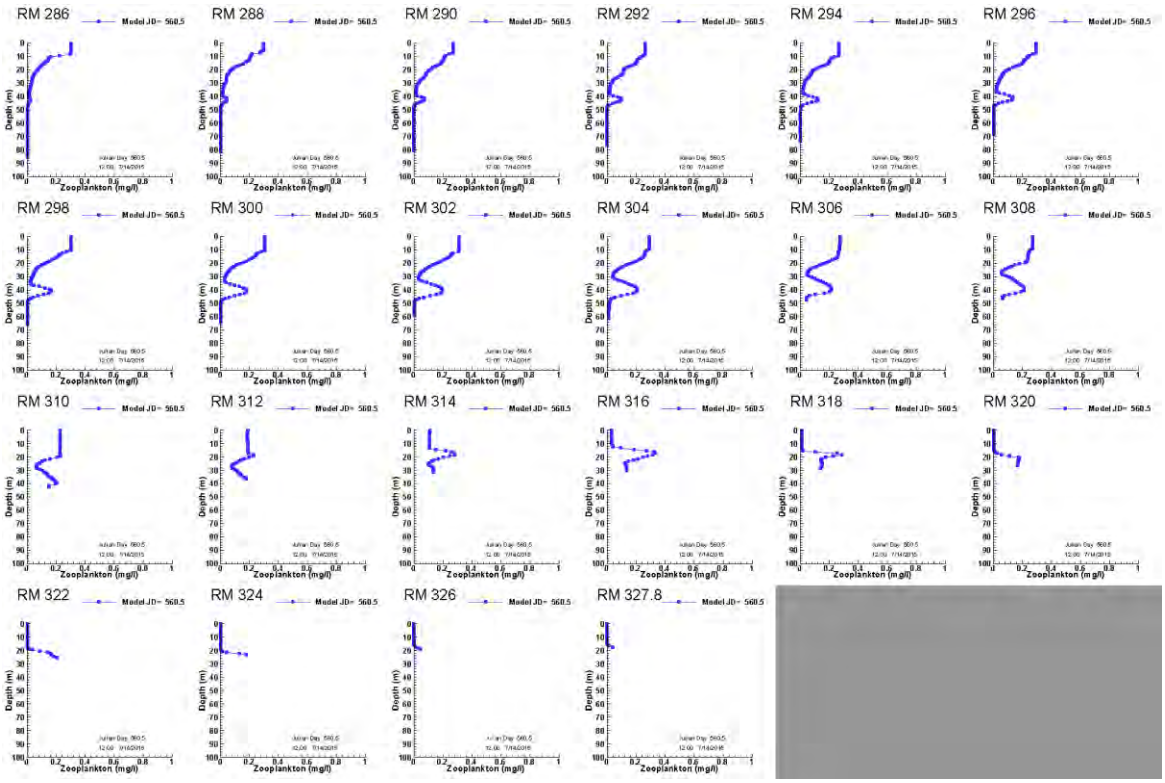


Figure 1349. Vertical profiles of zooplankton compared with data for 7/14/2015.

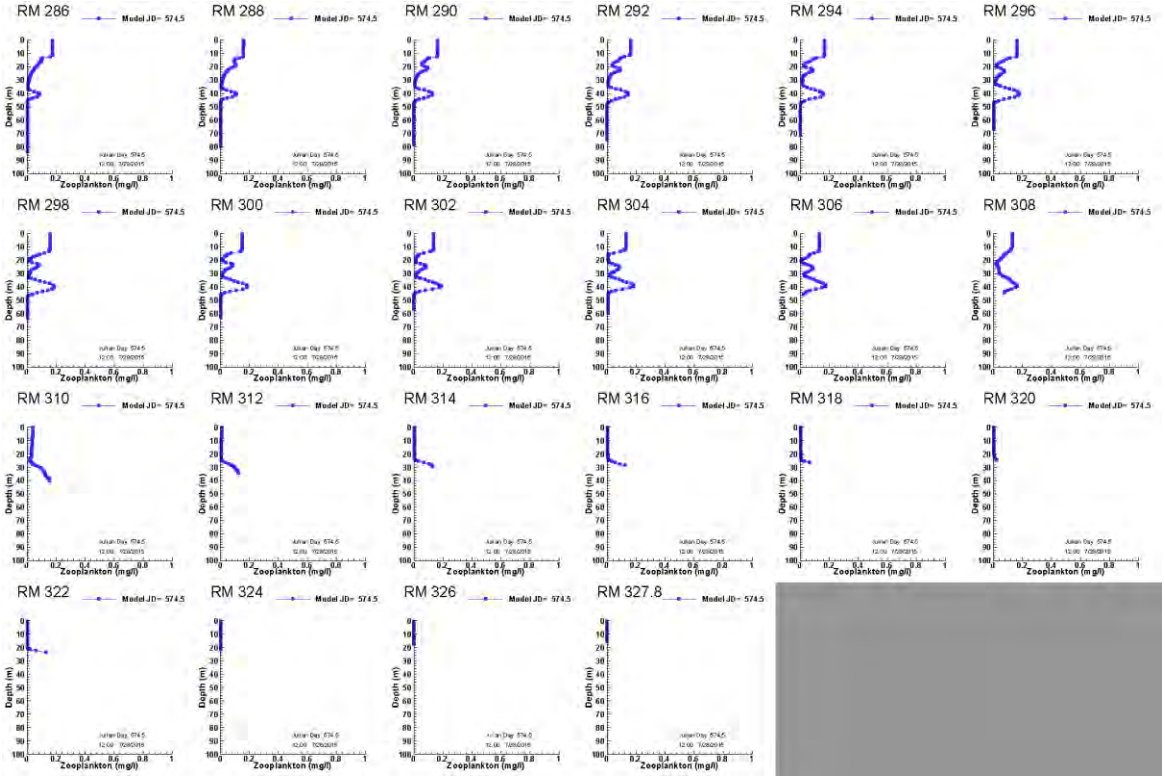


Figure 1350. Vertical profiles of zooplankton compared with data for 7/28/2015.

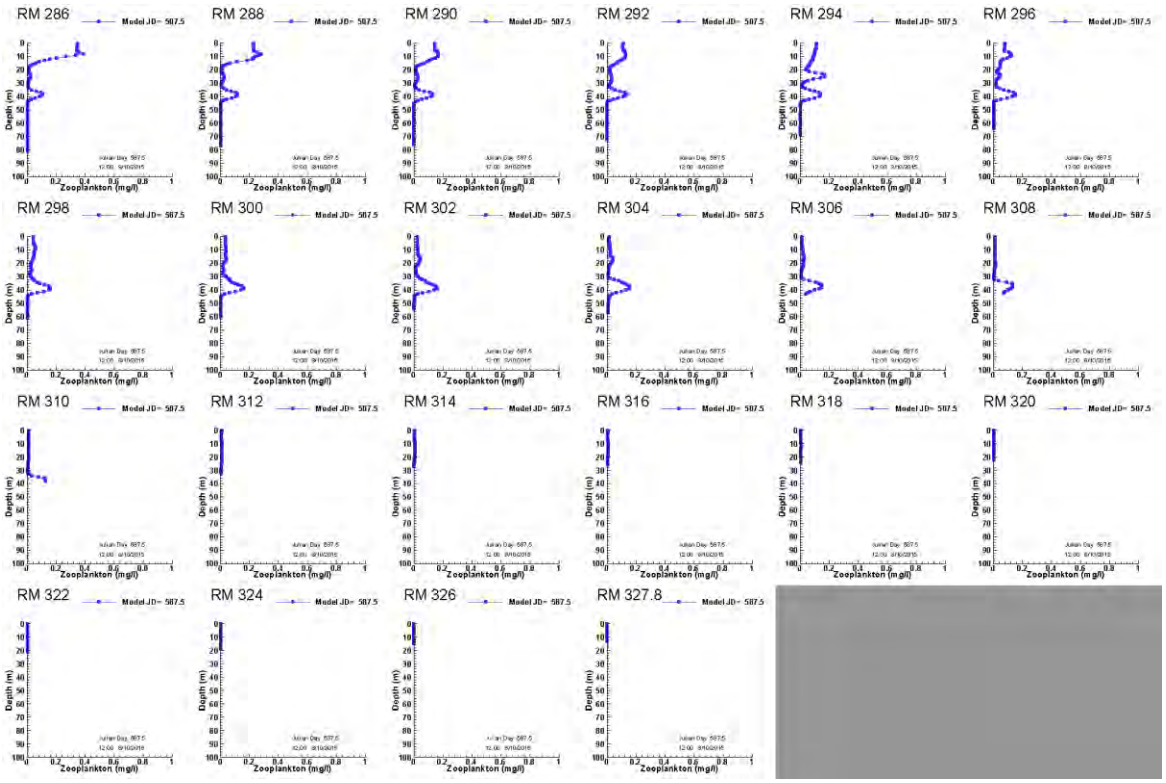


Figure 1351. Vertical profiles of zooplankton compared with data for 8/10/2015.

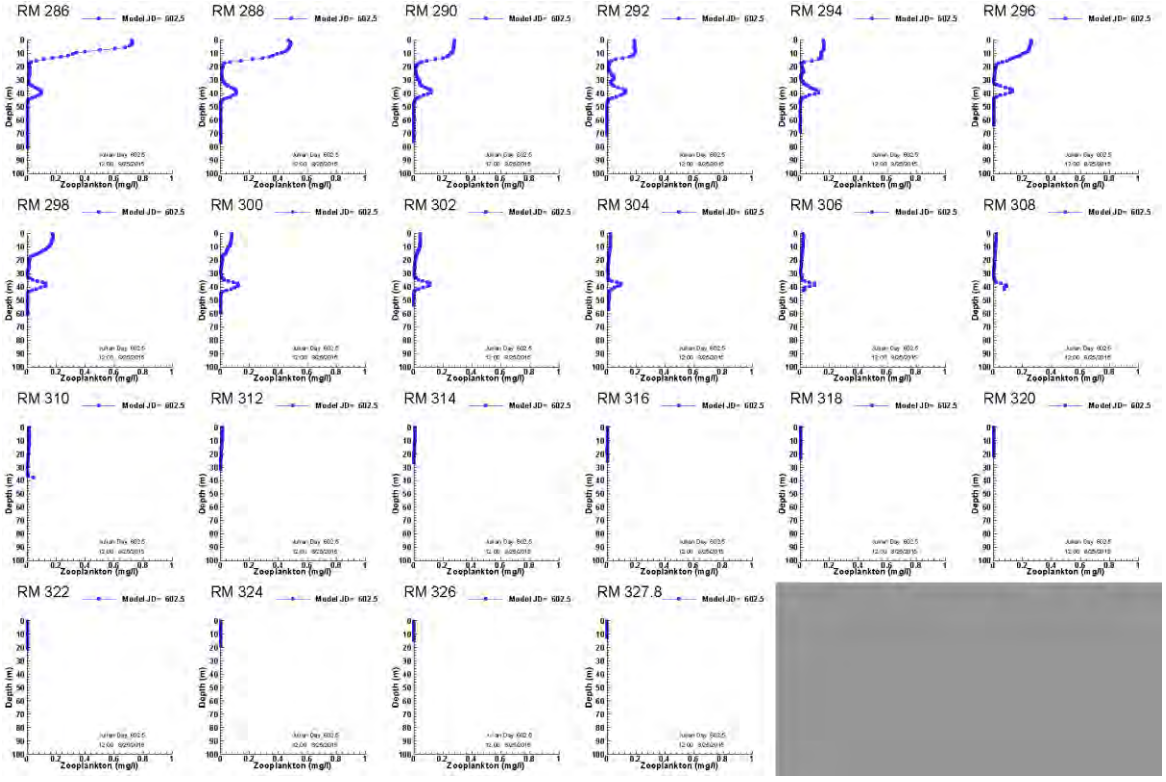


Figure 1352. Vertical profiles of zooplankton compared with data for 8/25/2015.

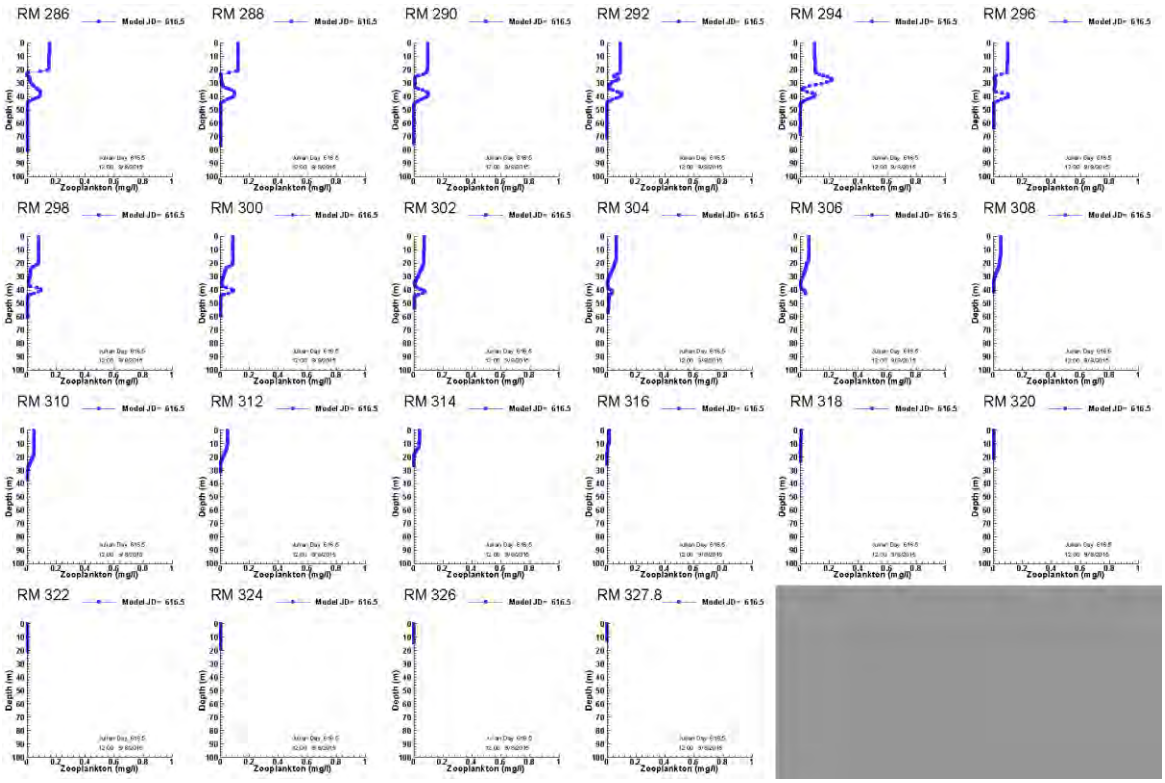


Figure 1353. Vertical profiles of zooplankton compared with data for 9/ 8/2015.

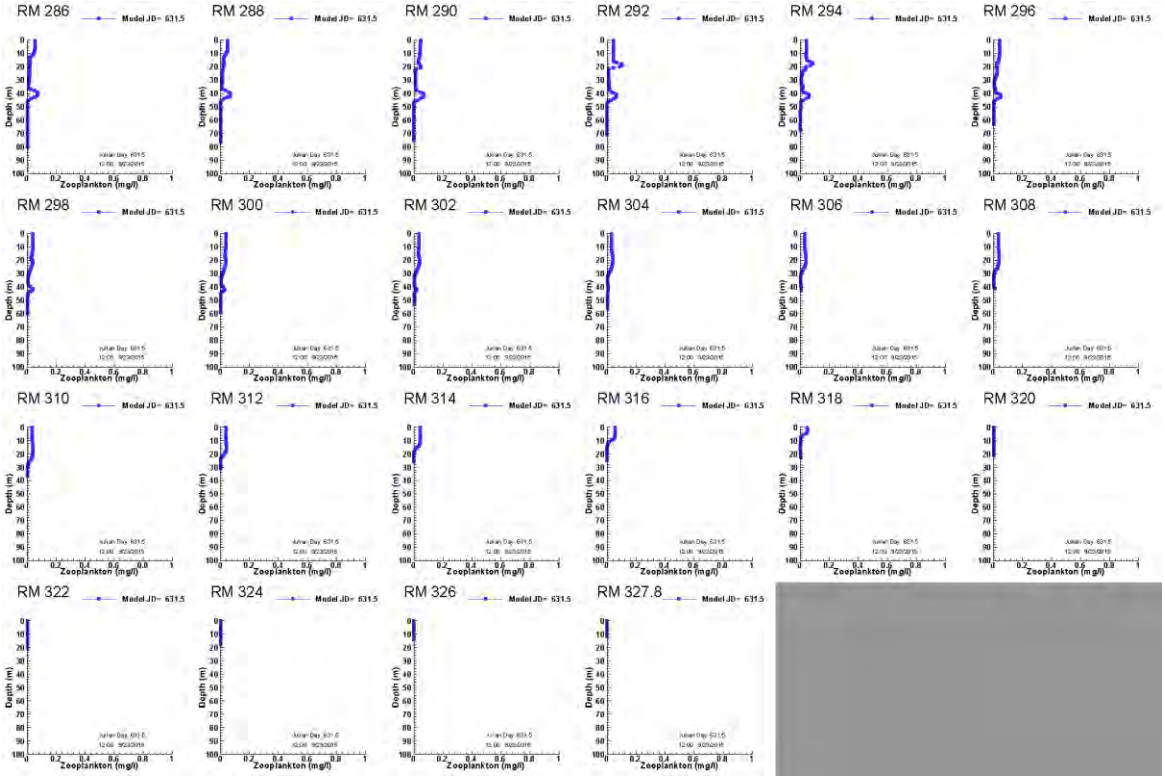


Figure 1354. Vertical profiles of zooplankton compared with data for 9/23/2015.

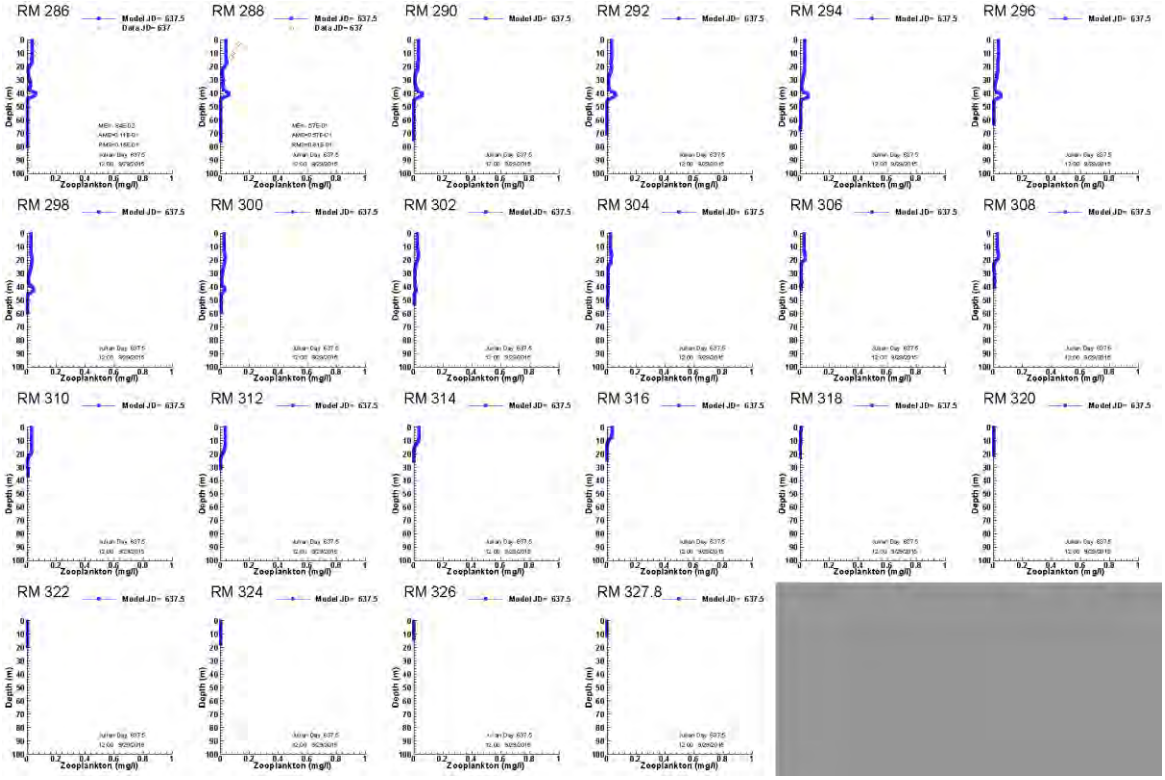


Figure 1355. Vertical profiles of zooplankton compared with data for 9/29/2015.

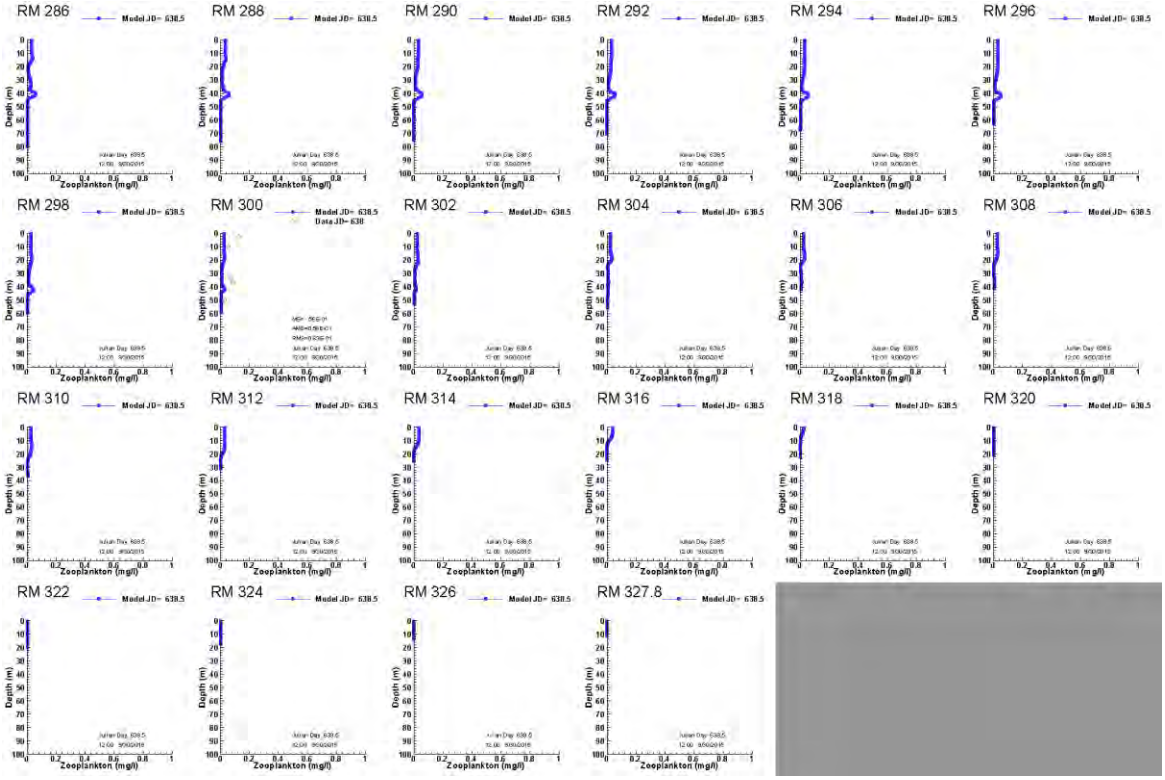


Figure 1356. Vertical profiles of zooplankton compared with data for 9/30/2015.

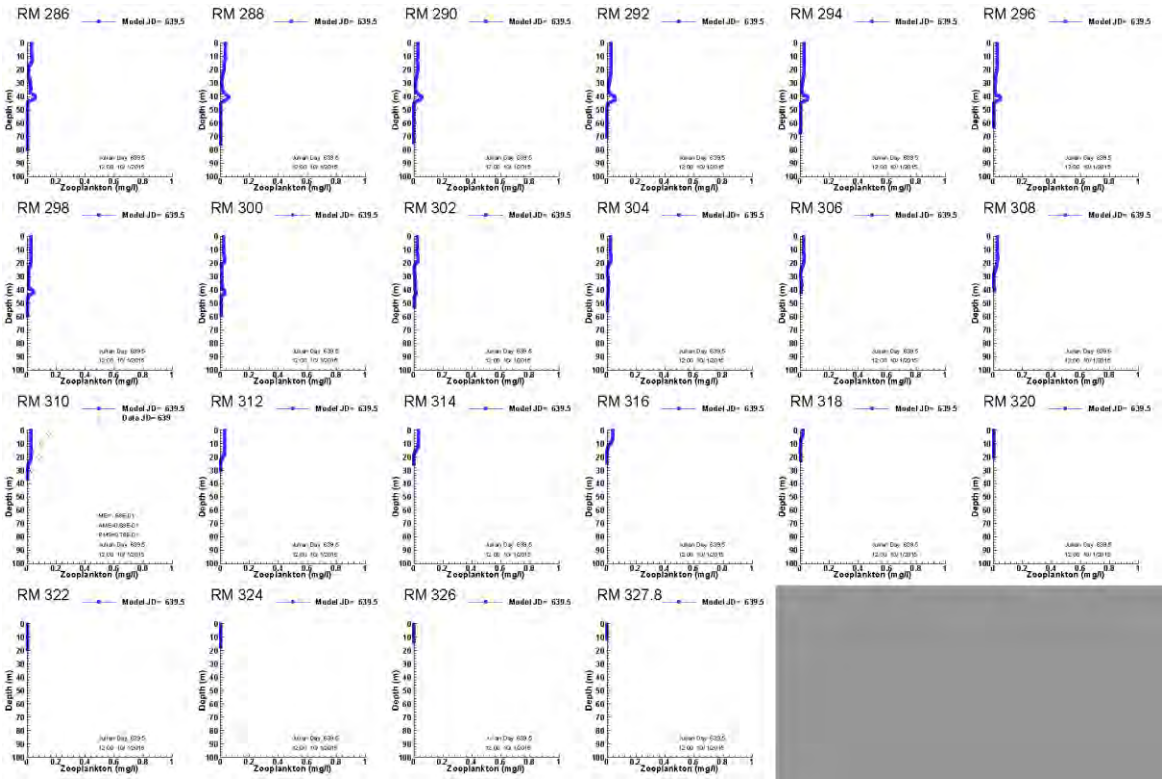


Figure 1357. Vertical profiles of zooplankton compared with data for 10/ 1/2015.

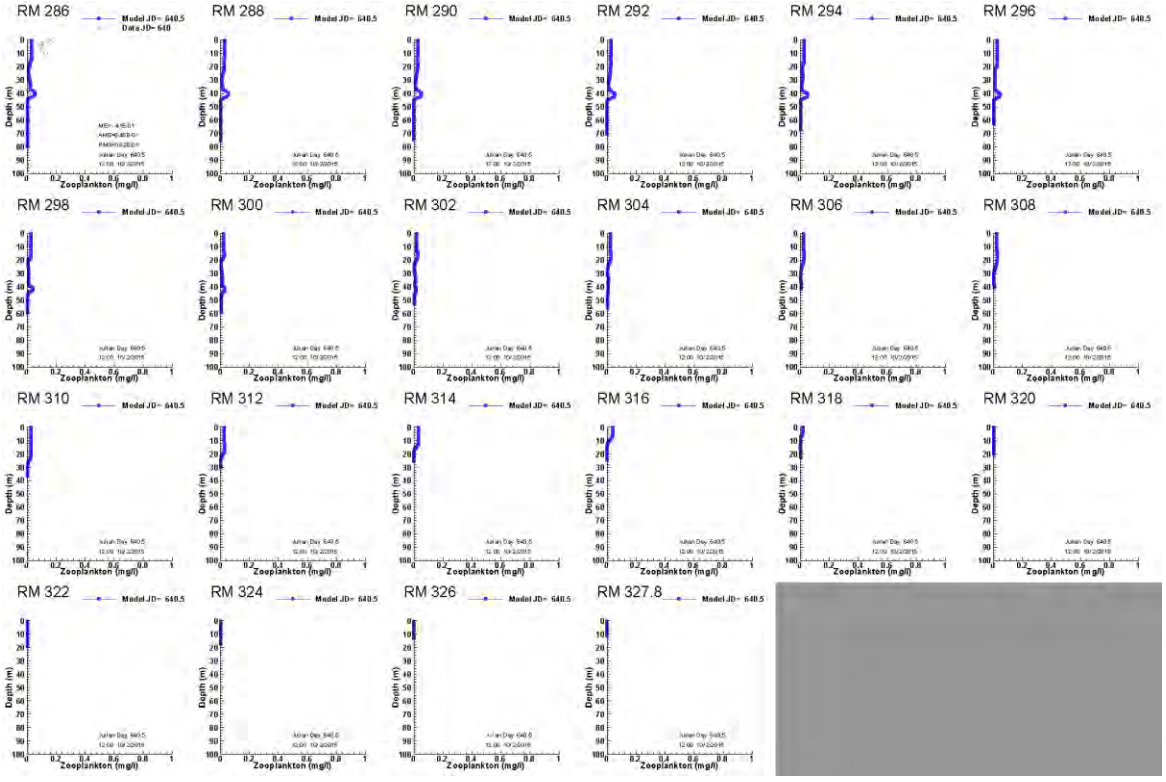


Figure 1358. Vertical profiles of zooplankton compared with data for 10/ 2/2015.

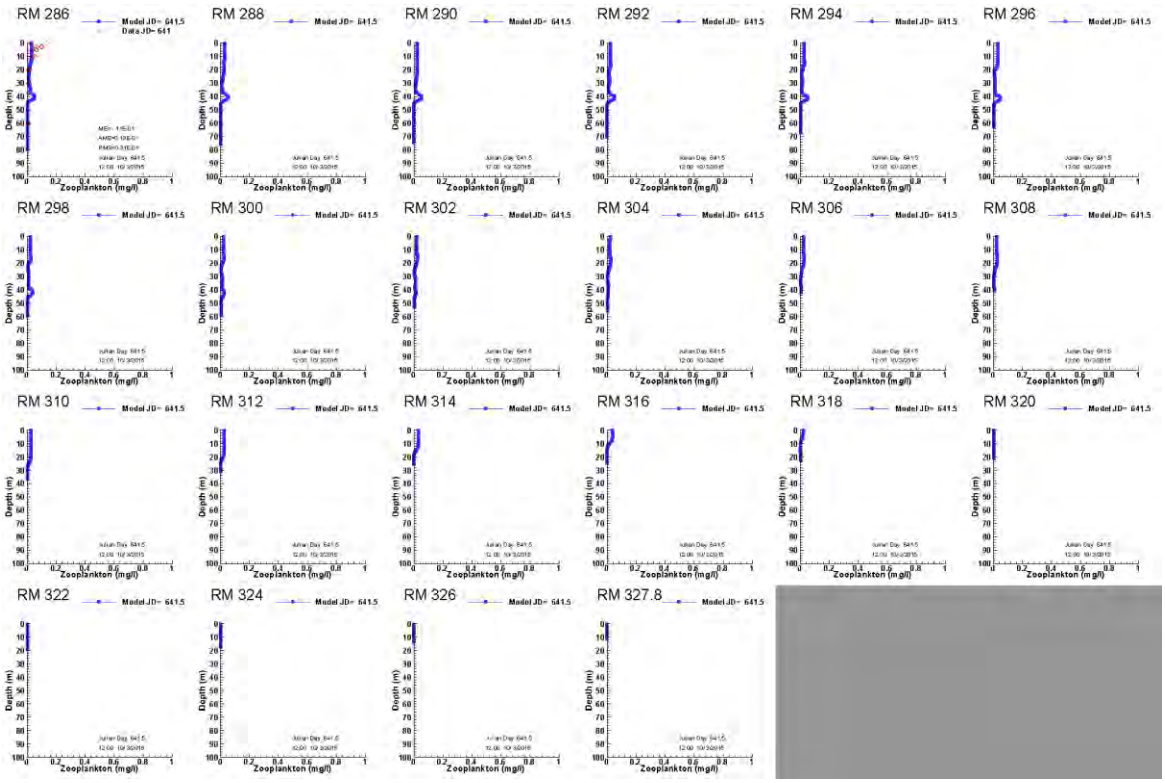


Figure 1359. Vertical profiles of zooplankton compared with data for 10/ 3/2015.

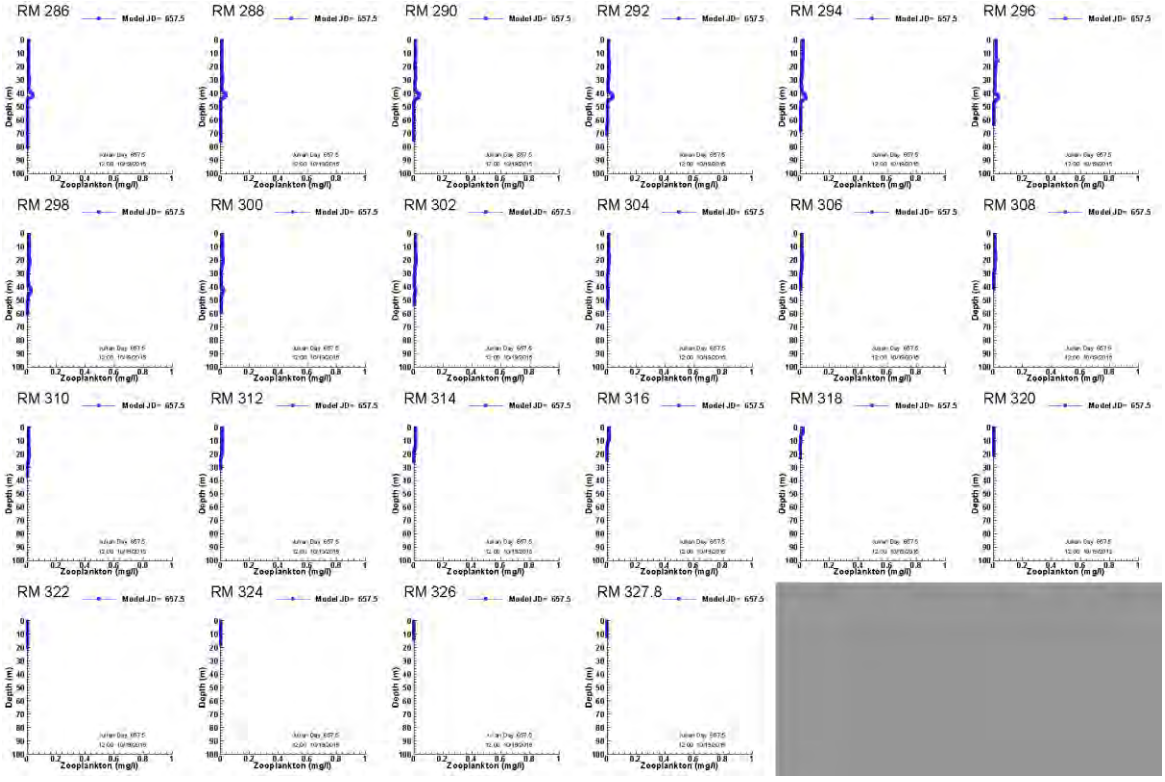


Figure 1360. Vertical profiles of zooplankton compared with data for 10/19/2015.

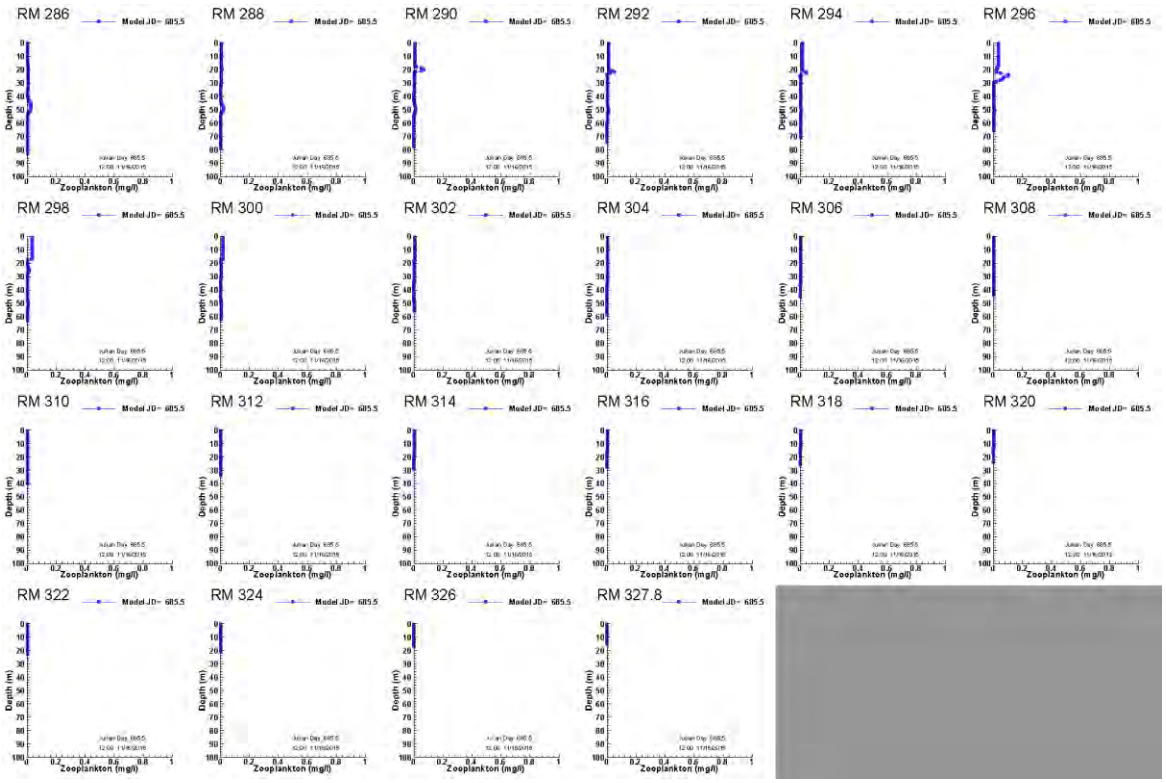


Figure 1361. Vertical profiles of zooplankton compared with data for 11/16/2015.

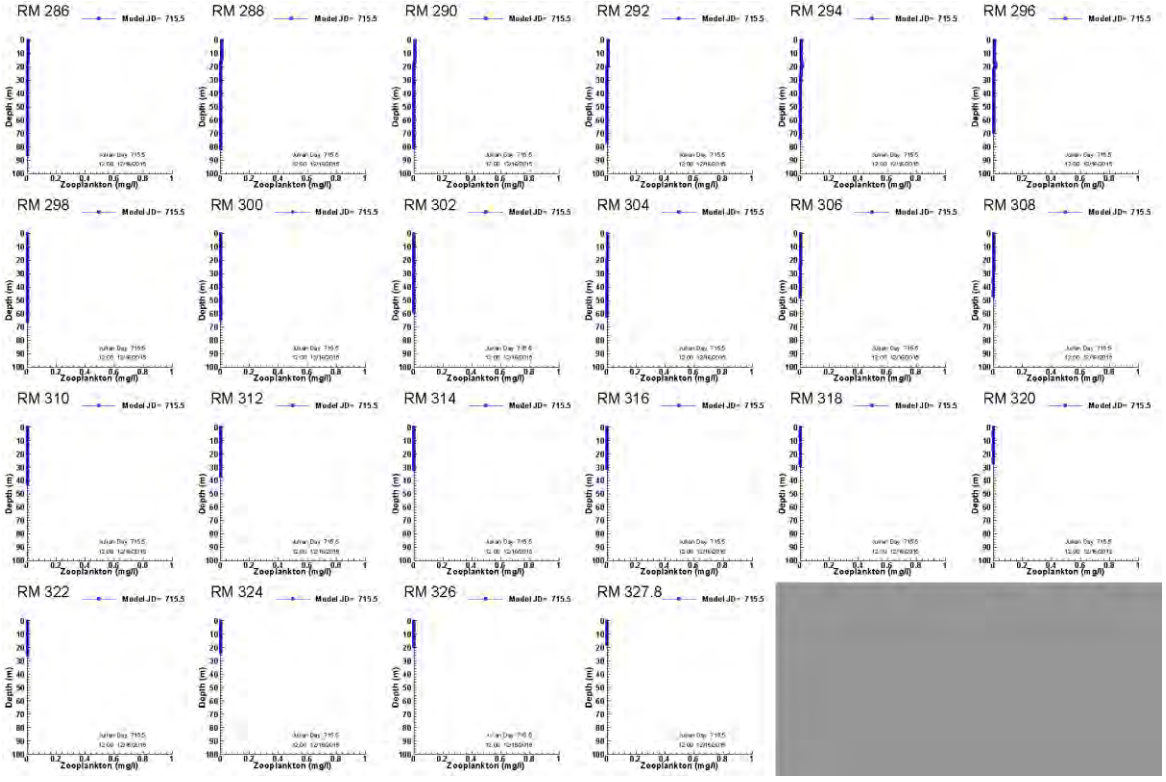


Figure 1362. Vertical profiles of zooplankton compared with data for 12/16/2015.

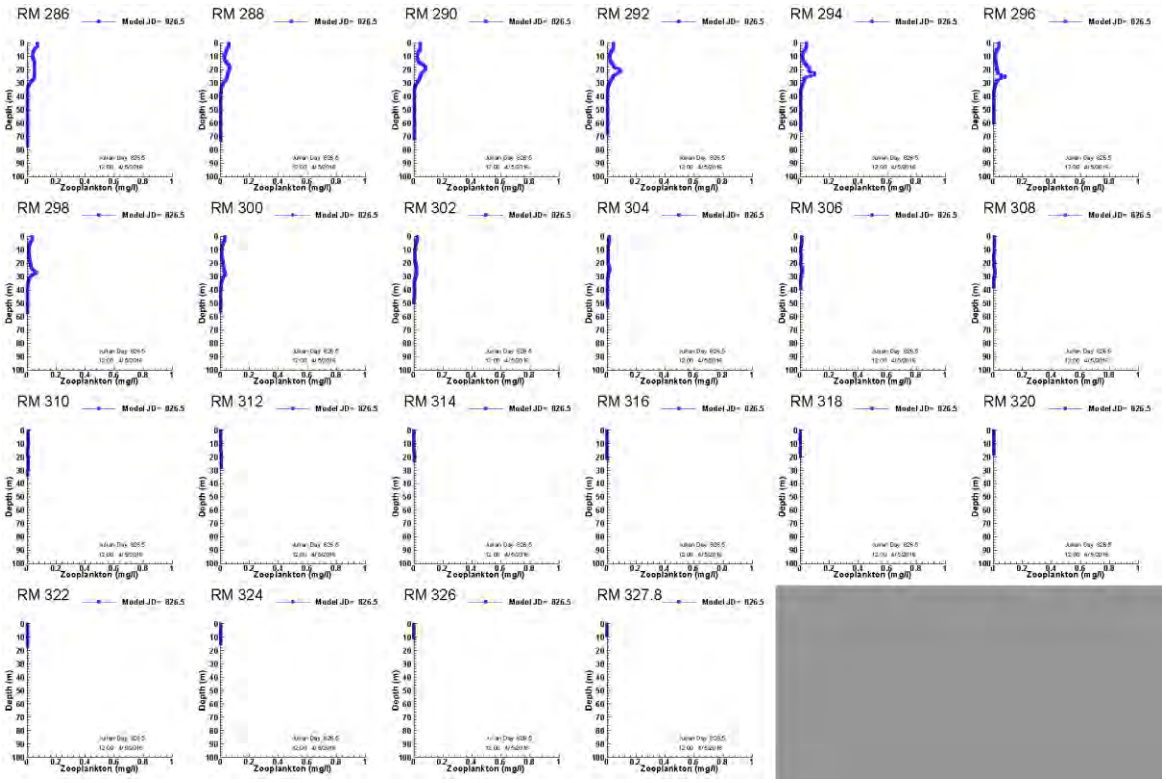


Figure 1363. Vertical profiles of zooplankton compared with data for 4/ 5/2016.

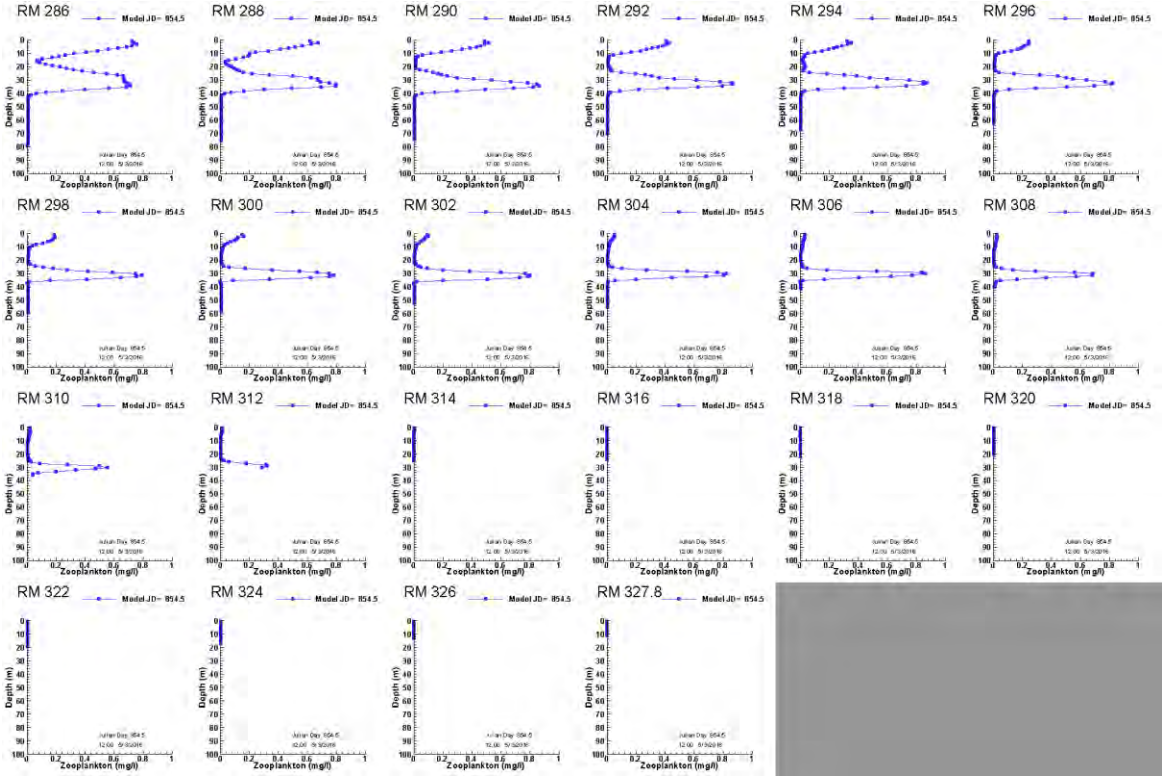


Figure 1364. Vertical profiles of zooplankton compared with data for 5/ 3/2016.

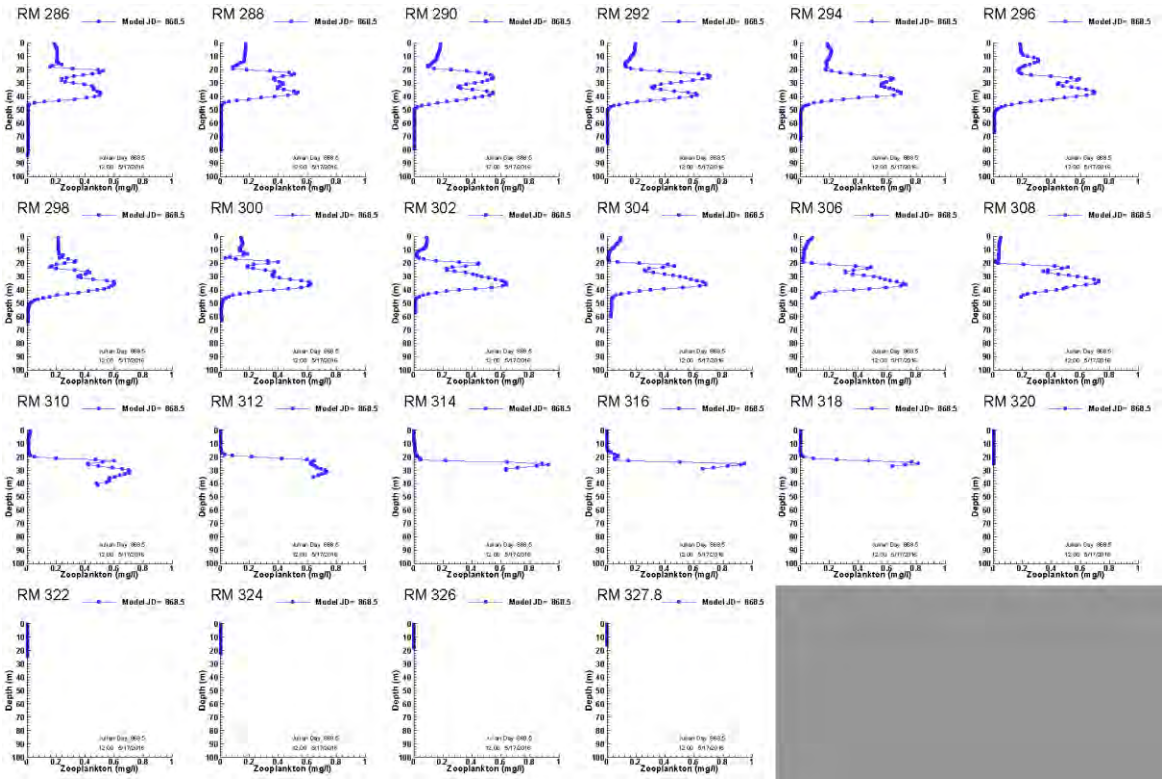


Figure 1365. Vertical profiles of zooplankton compared with data for 5/17/2016.

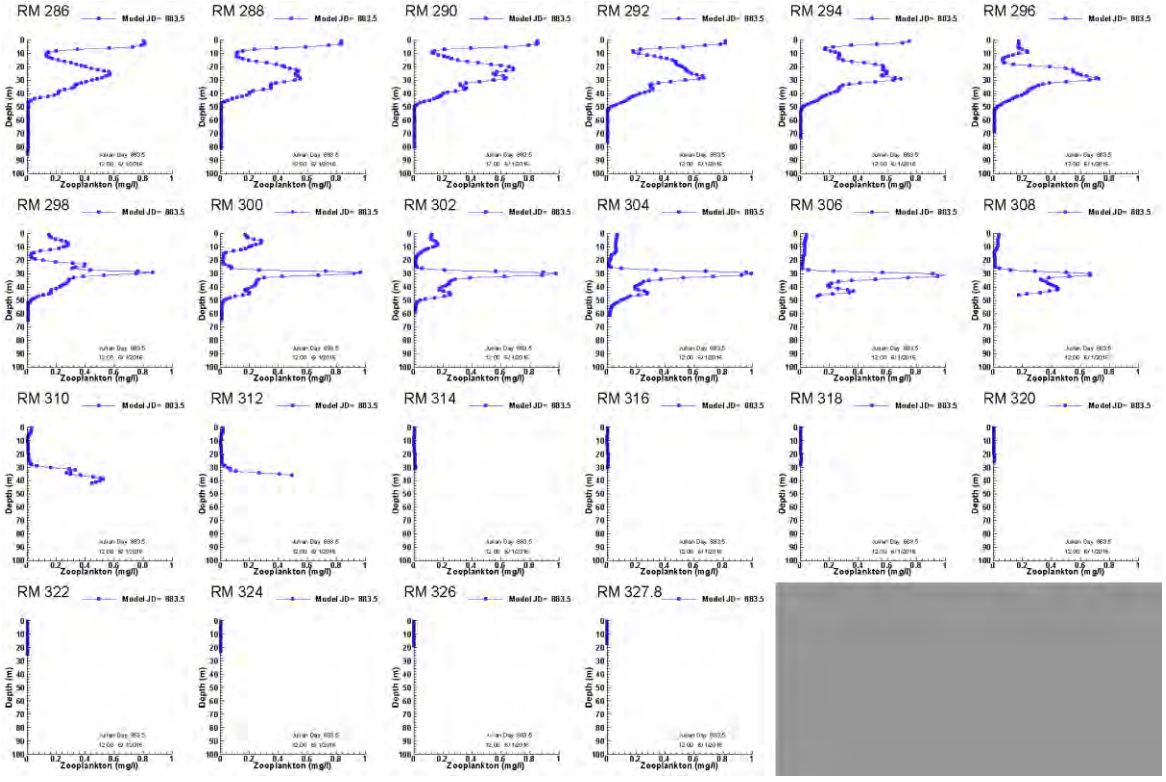


Figure 1366. Vertical profiles of zooplankton compared with data for 6/ 1/2016.

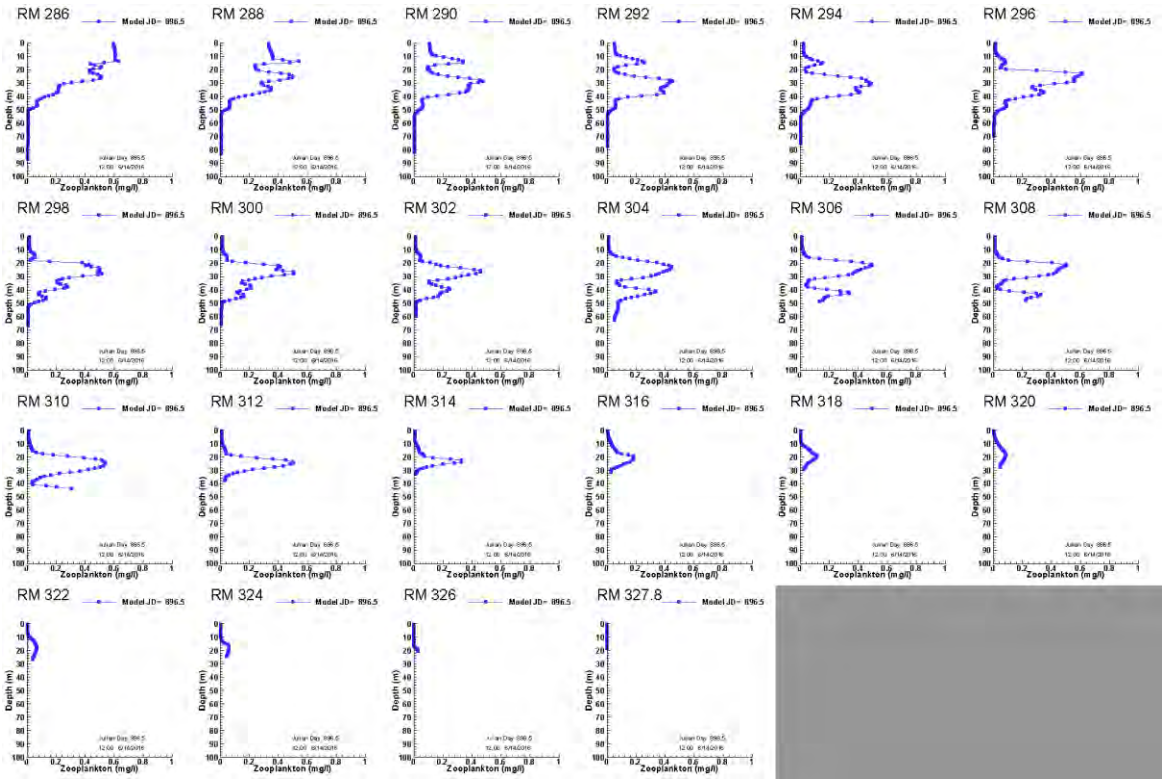


Figure 1367. Vertical profiles of zooplankton compared with data for 6/14/2016.

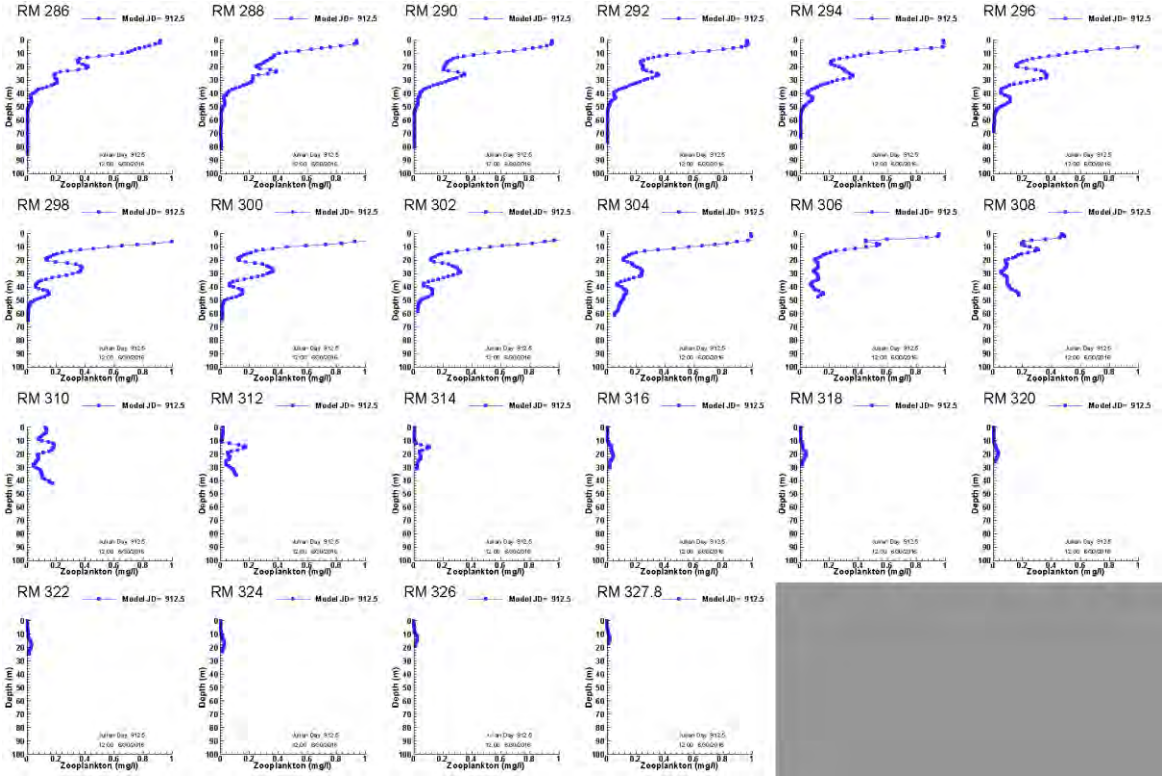


Figure 1368. Vertical profiles of zooplankton compared with data for 6/30/2016.

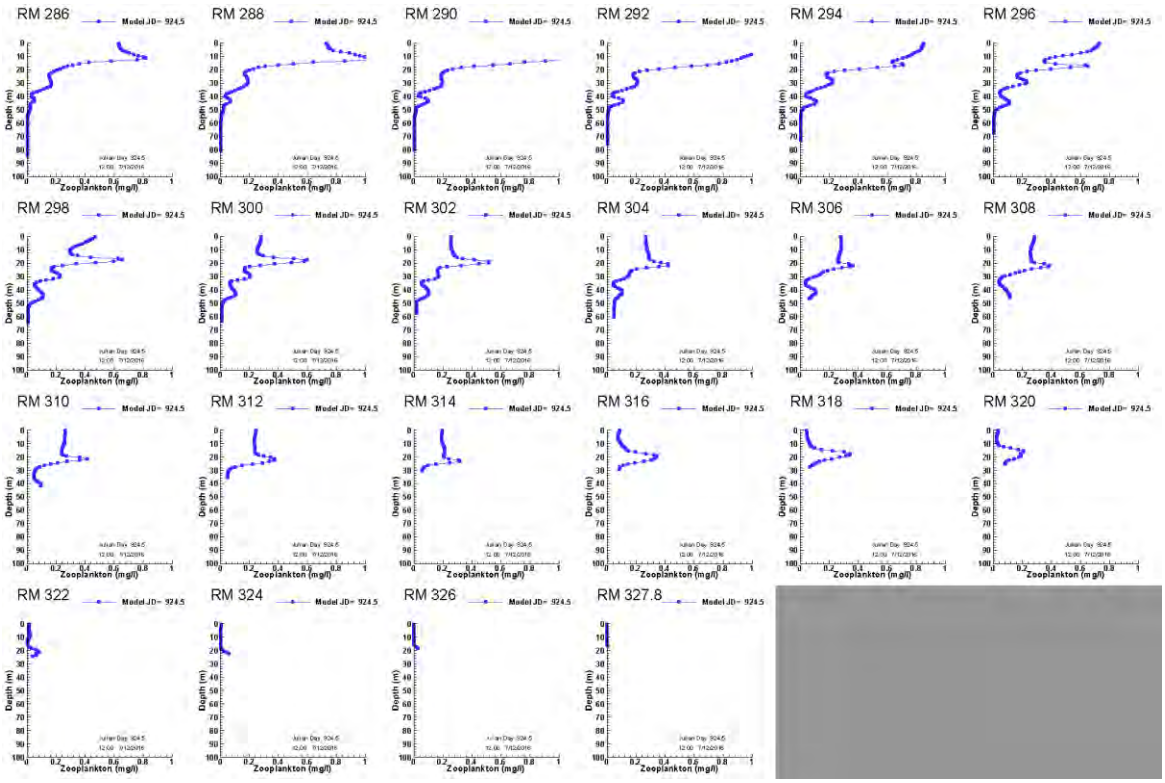


Figure 1369. Vertical profiles of zooplankton compared with data for 7/12/2016.

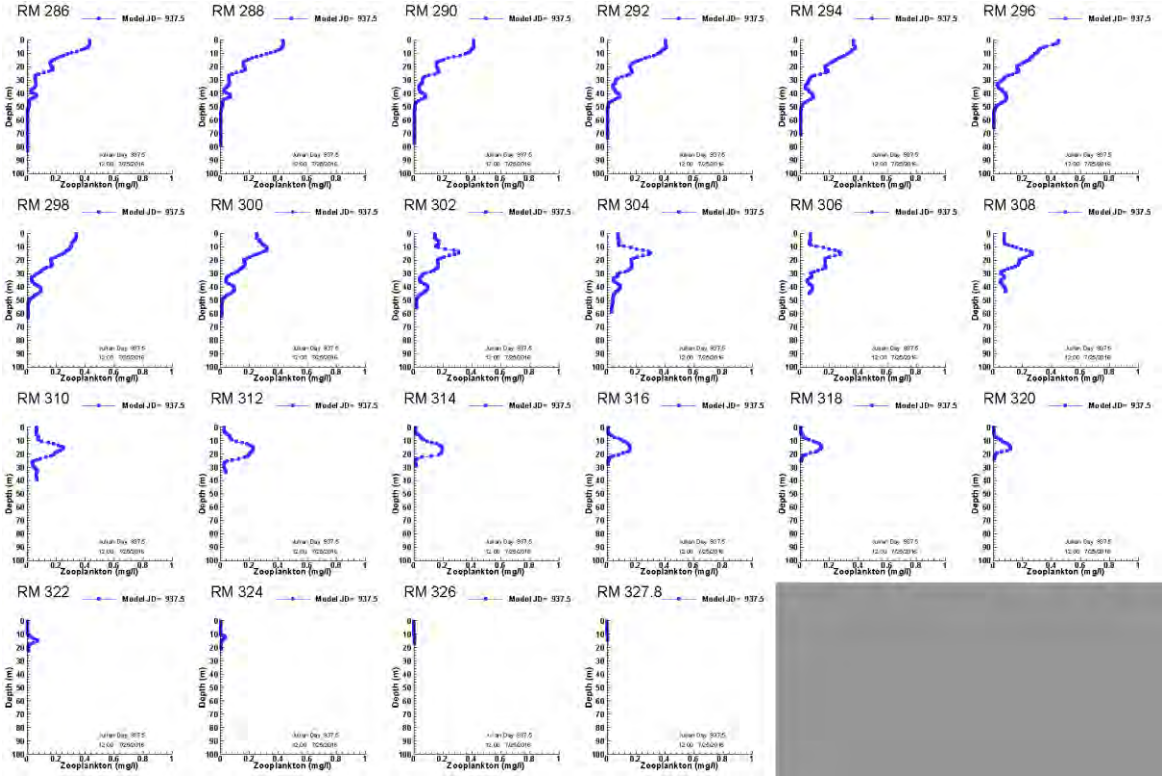


Figure 1370. Vertical profiles of zooplankton compared with data for 7/25/2016.

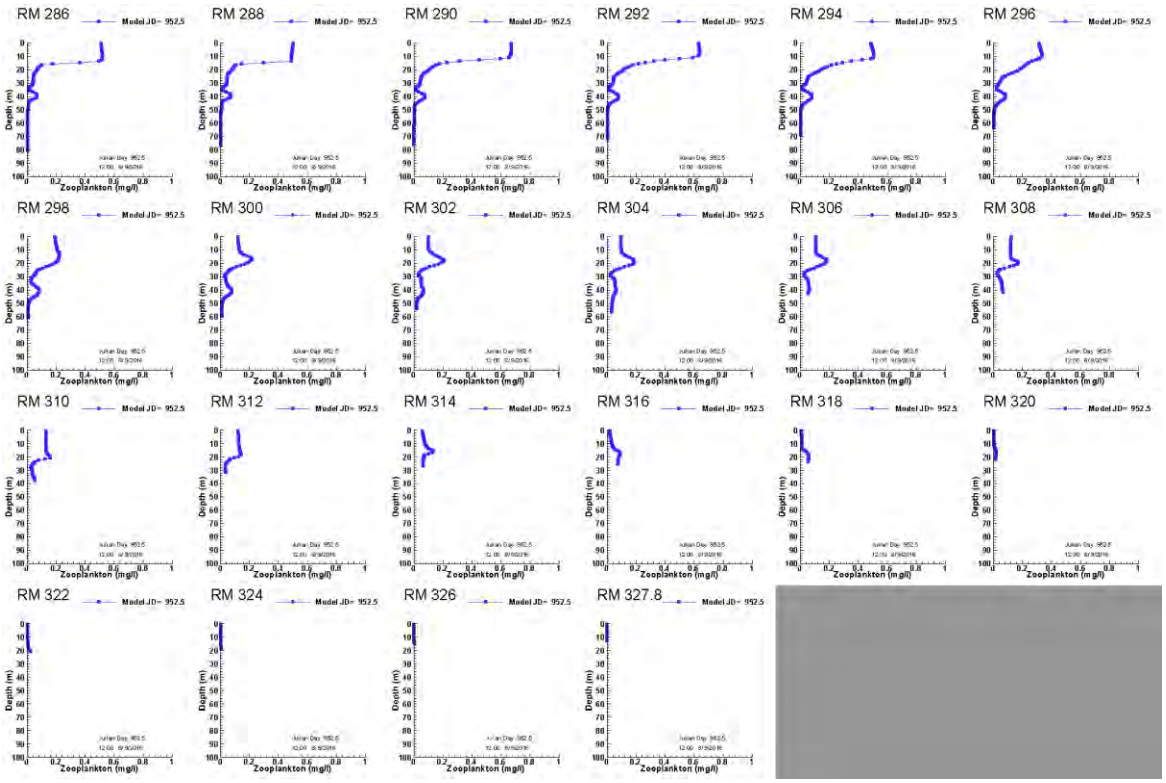


Figure 1371. Vertical profiles of zooplankton compared with data for 8/ 9/2016.

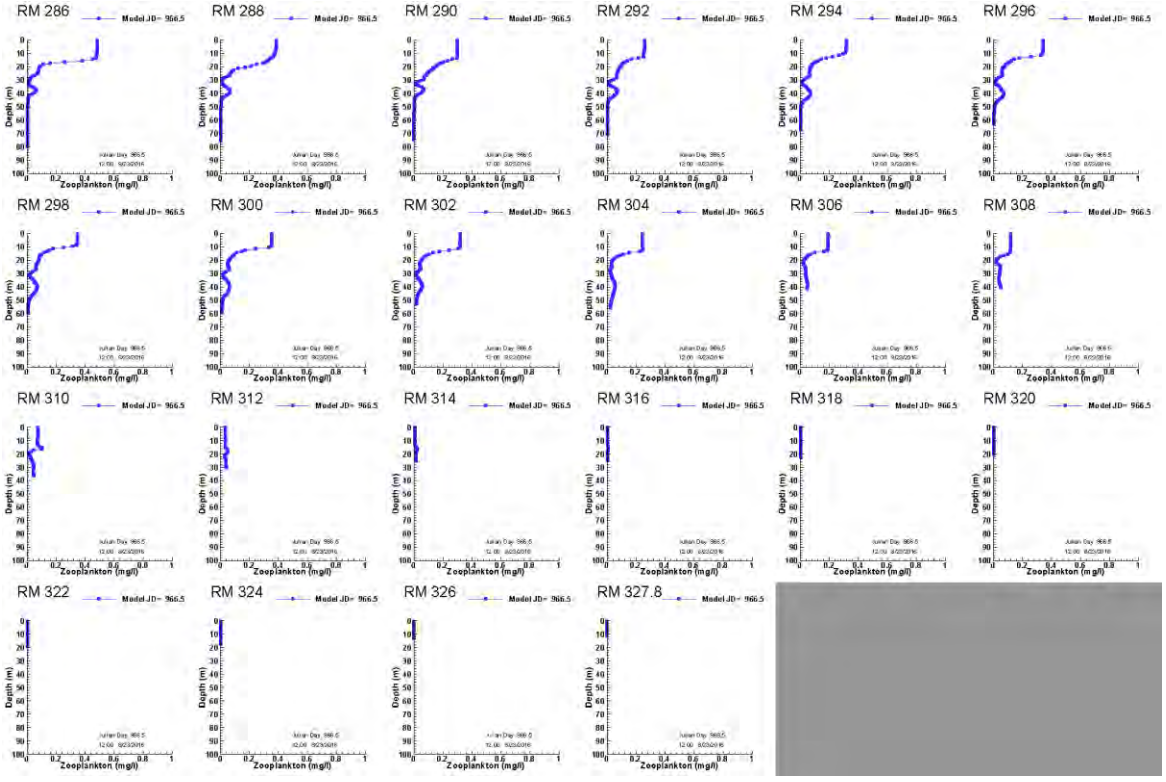


Figure 1372. Vertical profiles of zooplankton compared with data for 8/23/2016.

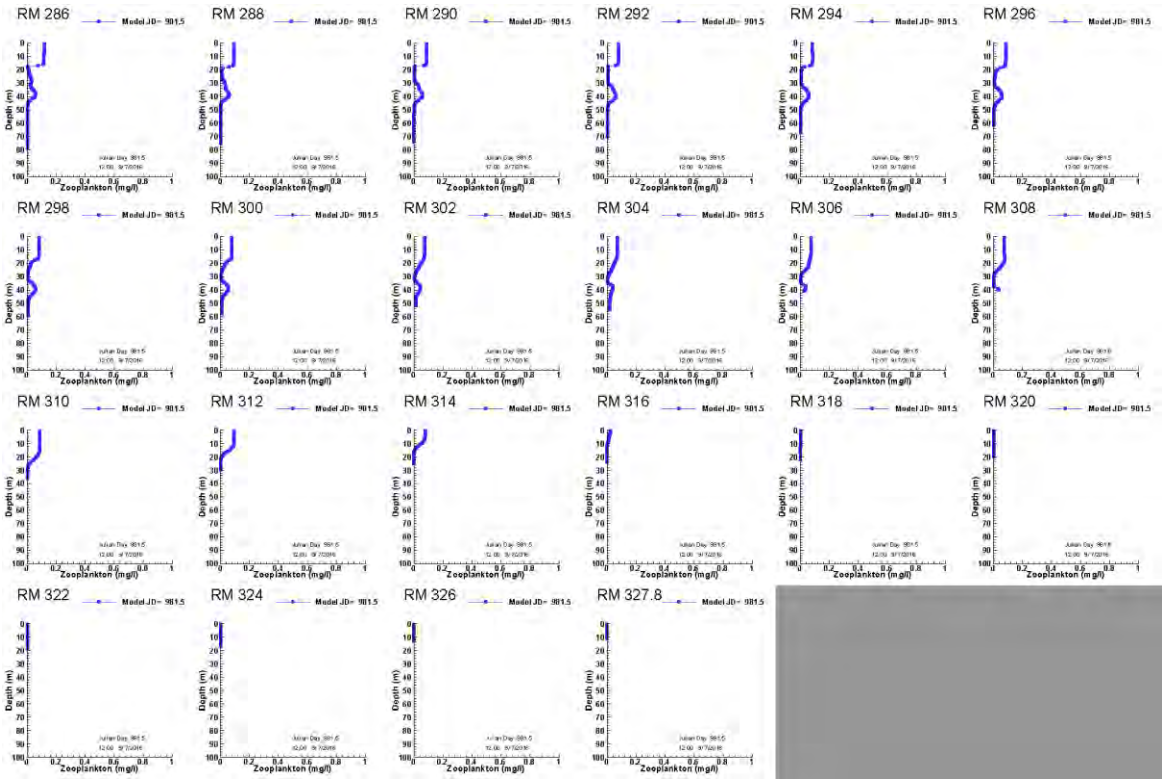


Figure 1373. Vertical profiles of zooplankton compared with data for 9/ 7/2016.

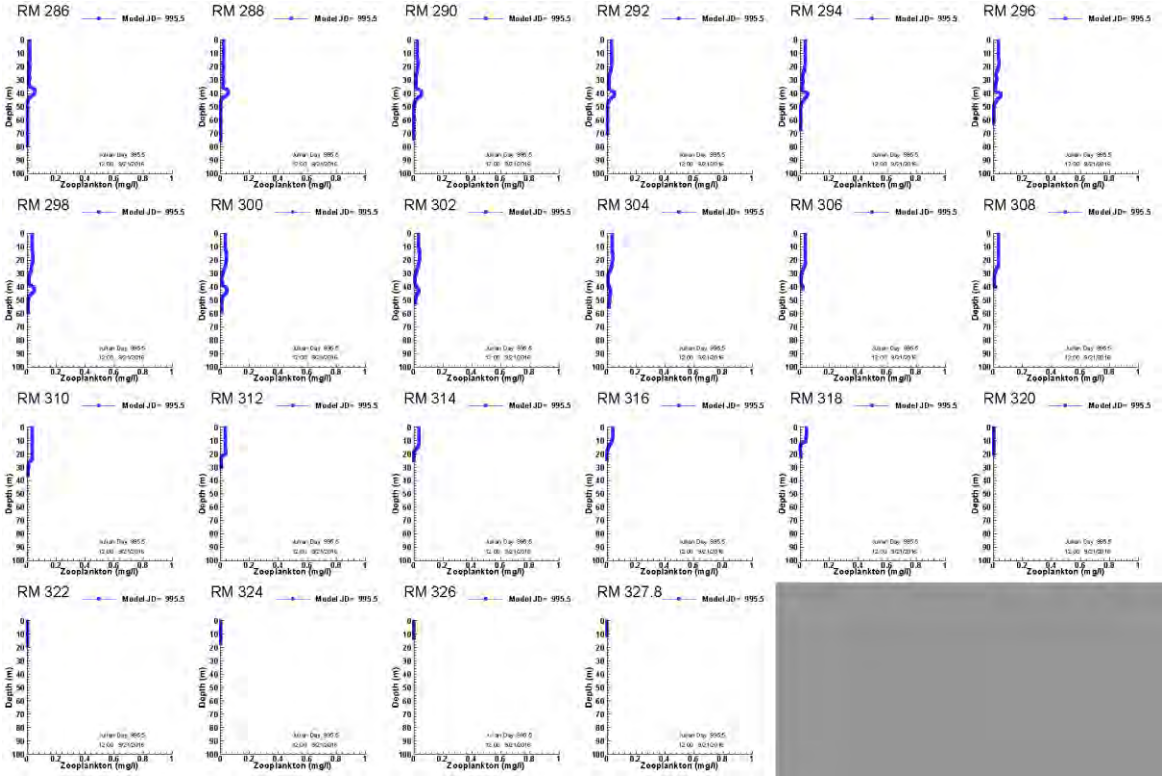


Figure 1374. Vertical profiles of zooplankton compared with data for 9/21/2016.

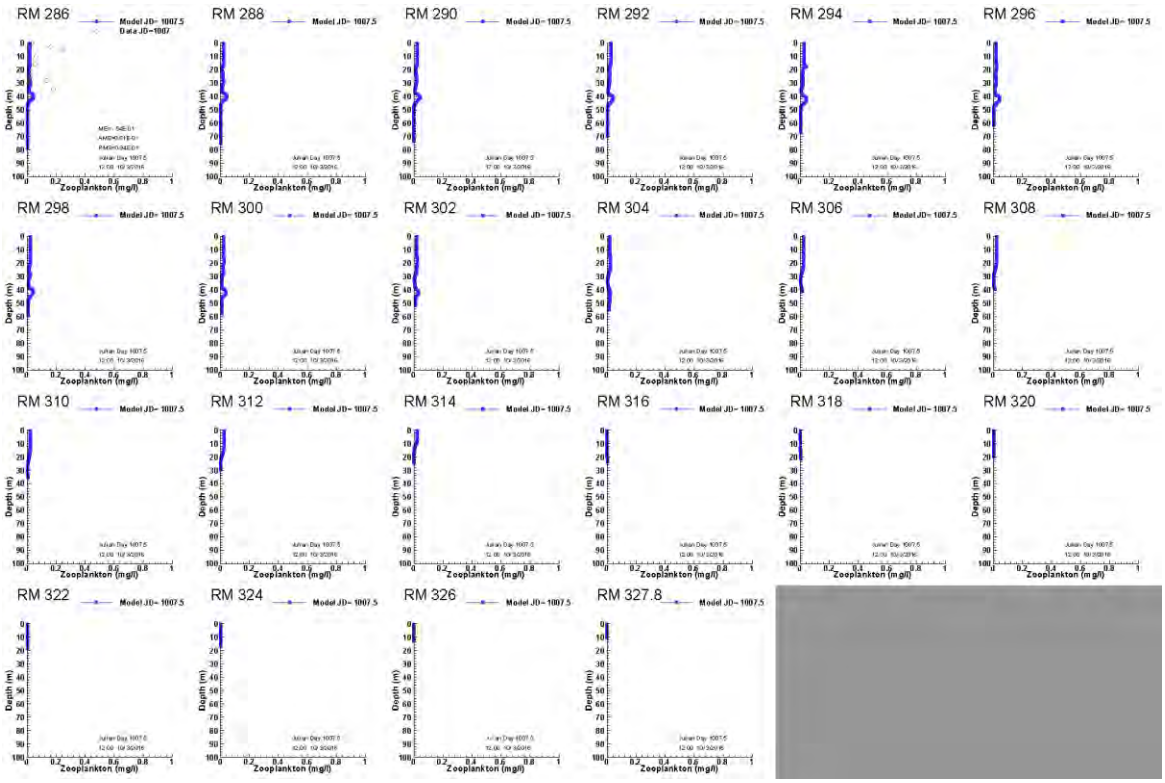


Figure 1375. Vertical profiles of zooplankton compared with data for 10/ 3/2016.

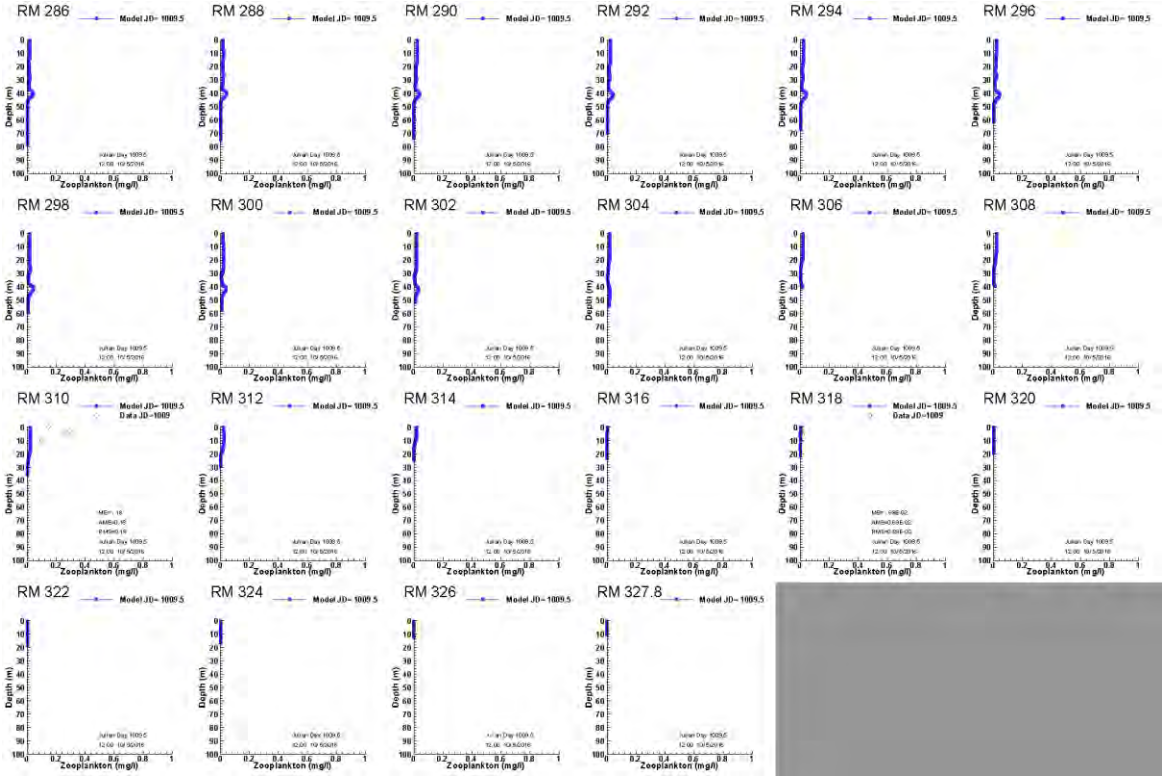


Figure 1376. Vertical profiles of zooplankton compared with data for 10/ 5/2016.

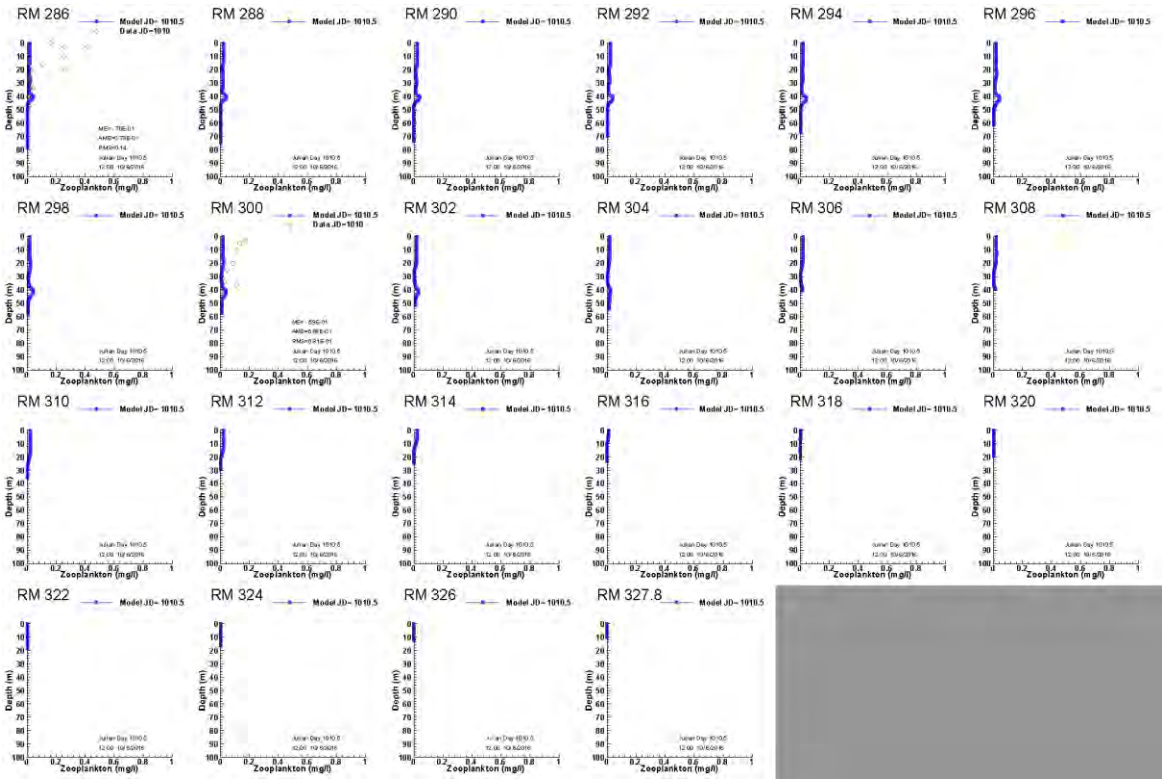


Figure 1377. Vertical profiles of zooplankton compared with data for 10/ 6/2016.

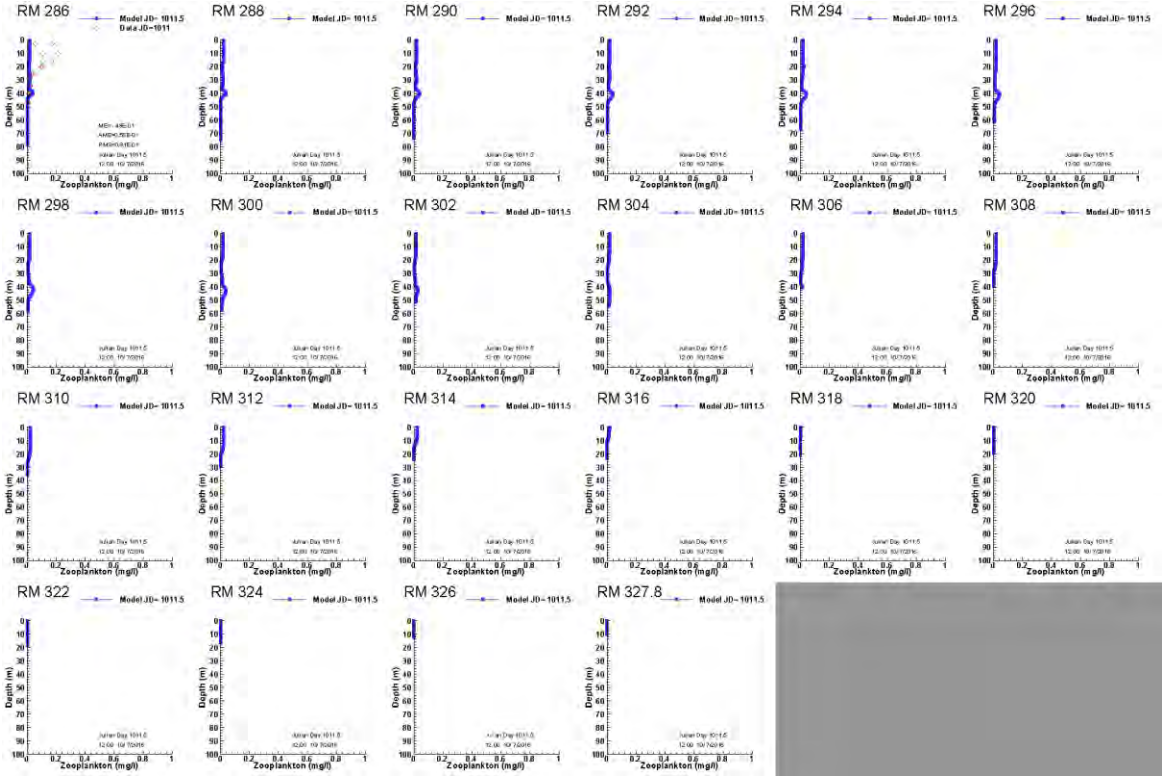


Figure 1378. Vertical profiles of zooplankton compared with data for 10/ 7/2016.

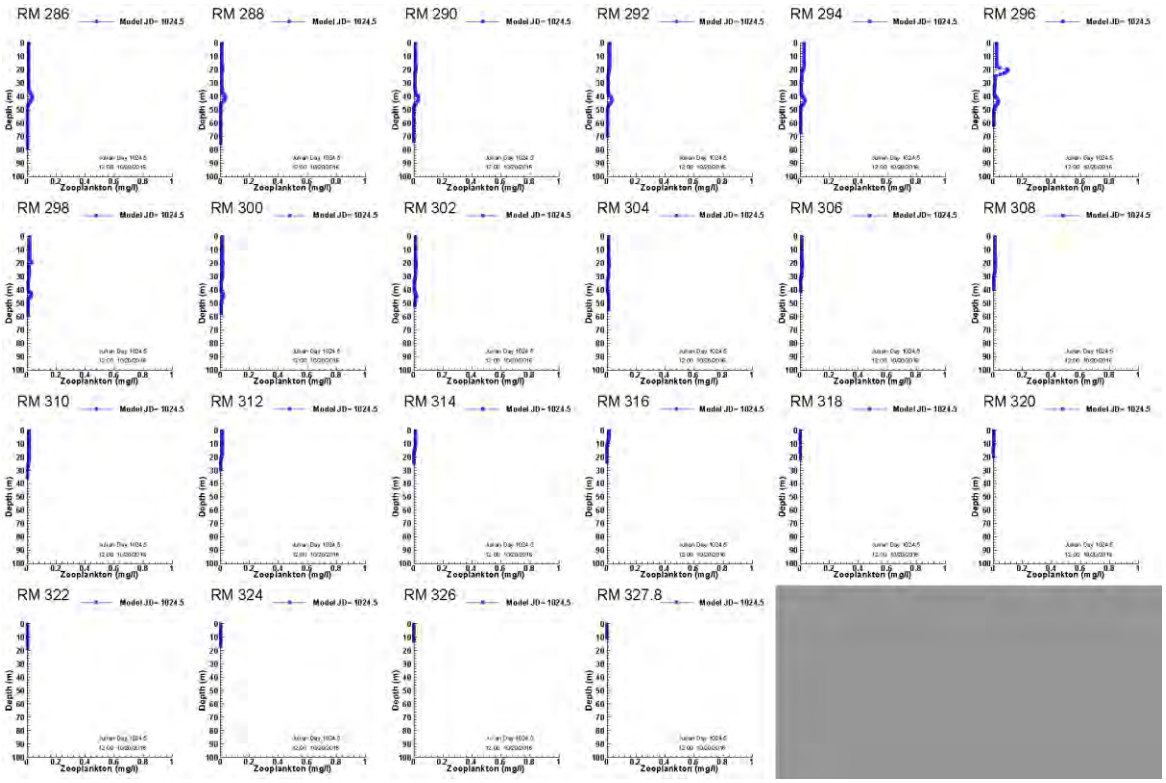


Figure 1379. Vertical profiles of zooplankton compared with data for 10/20/2016.

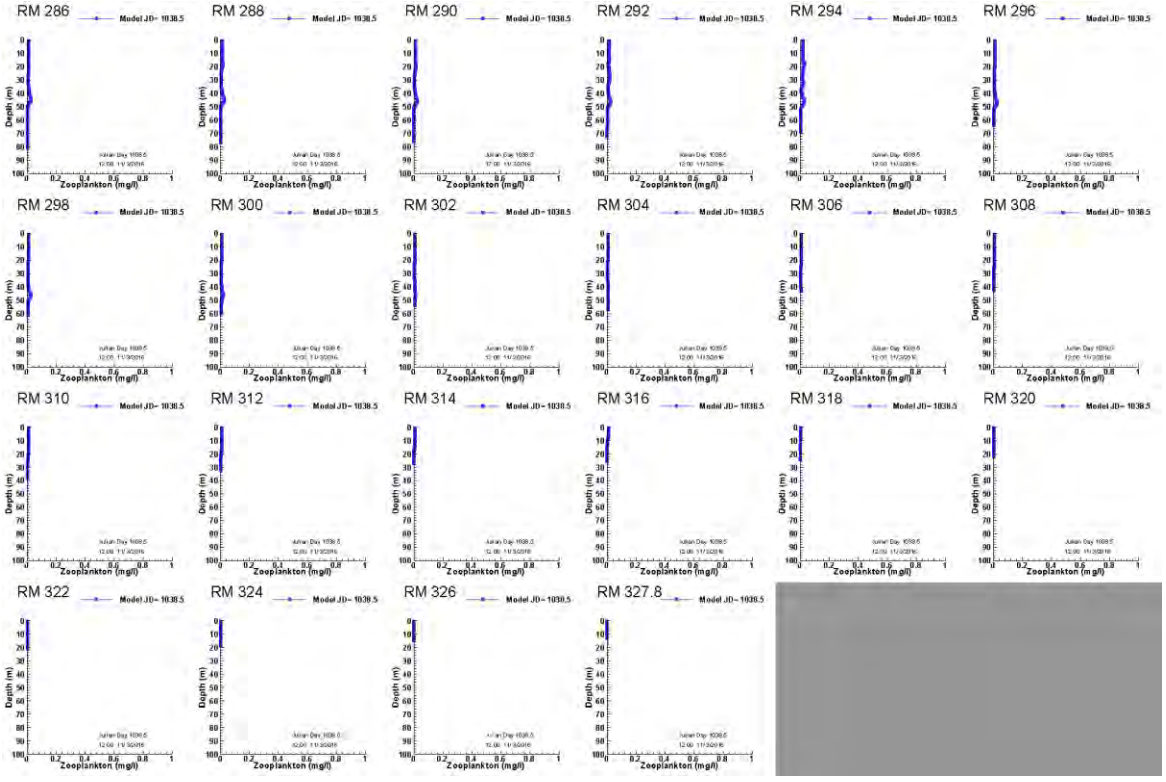


Figure 1380. Vertical profiles of zooplankton compared with data for 11/ 3/2016.

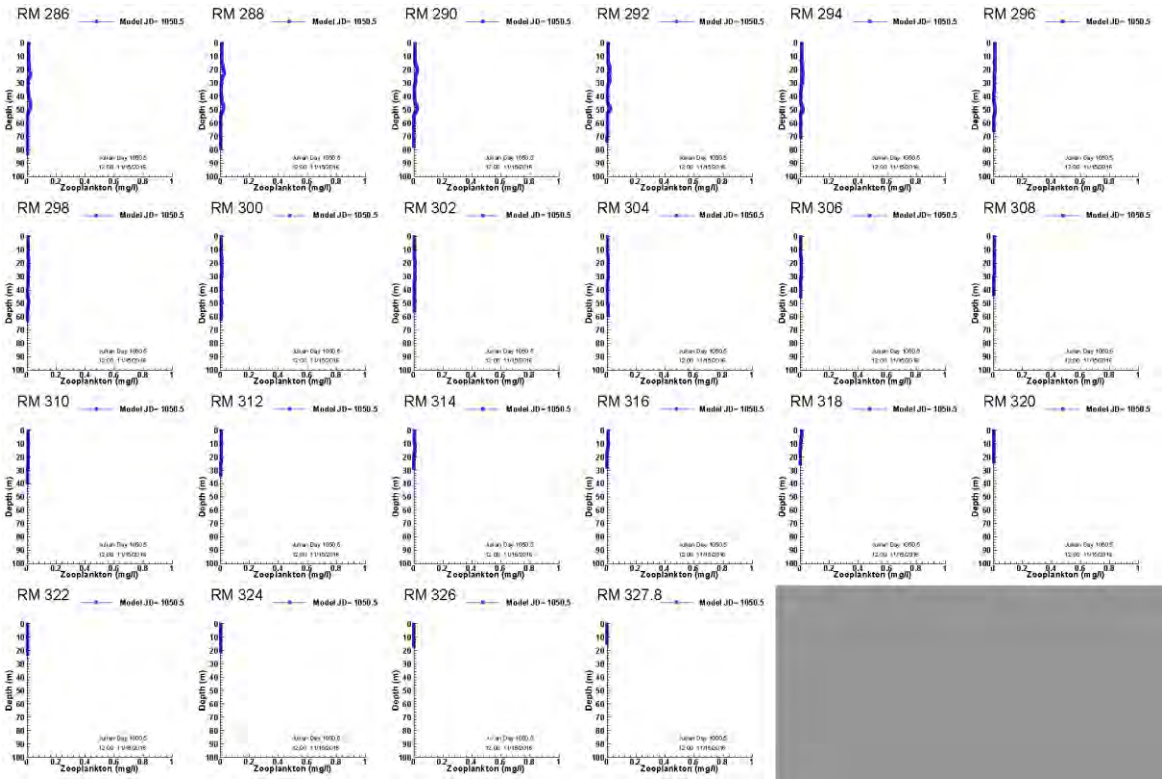


Figure 1381. Vertical profiles of zooplankton compared with data for 11/15/2016.

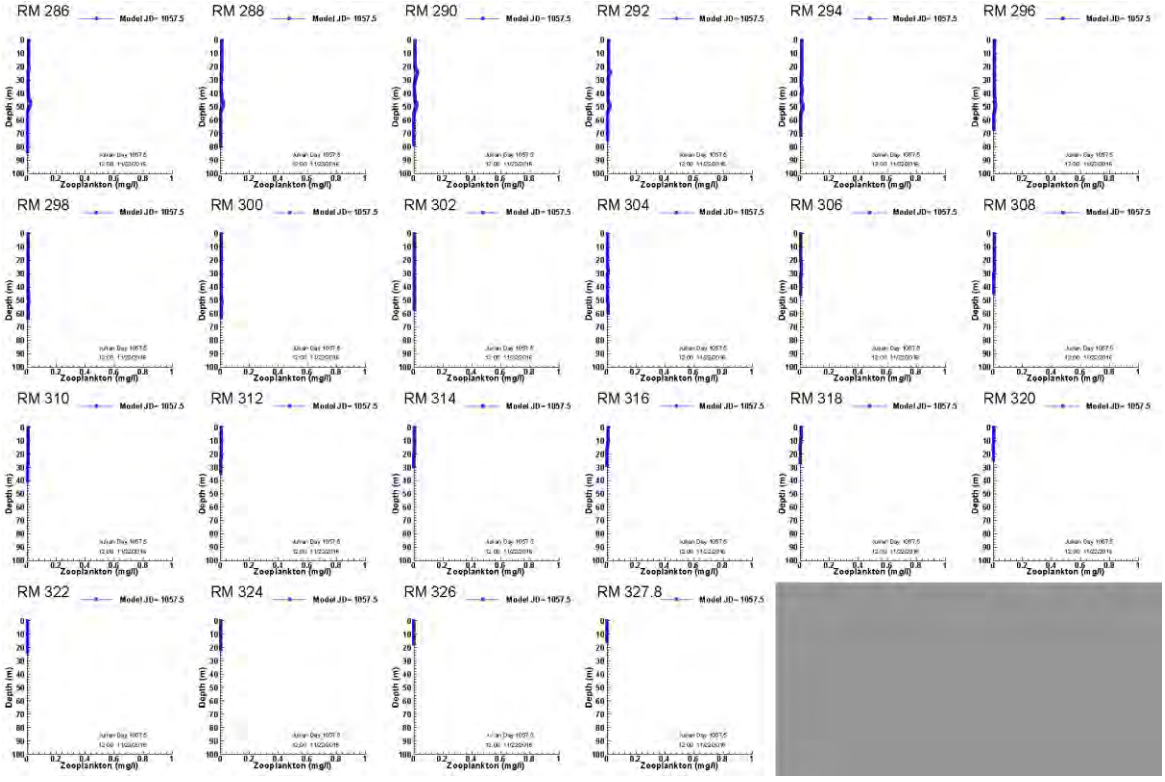


Figure 1382. Vertical profiles of zooplankton compared with data for 11/22/2016.

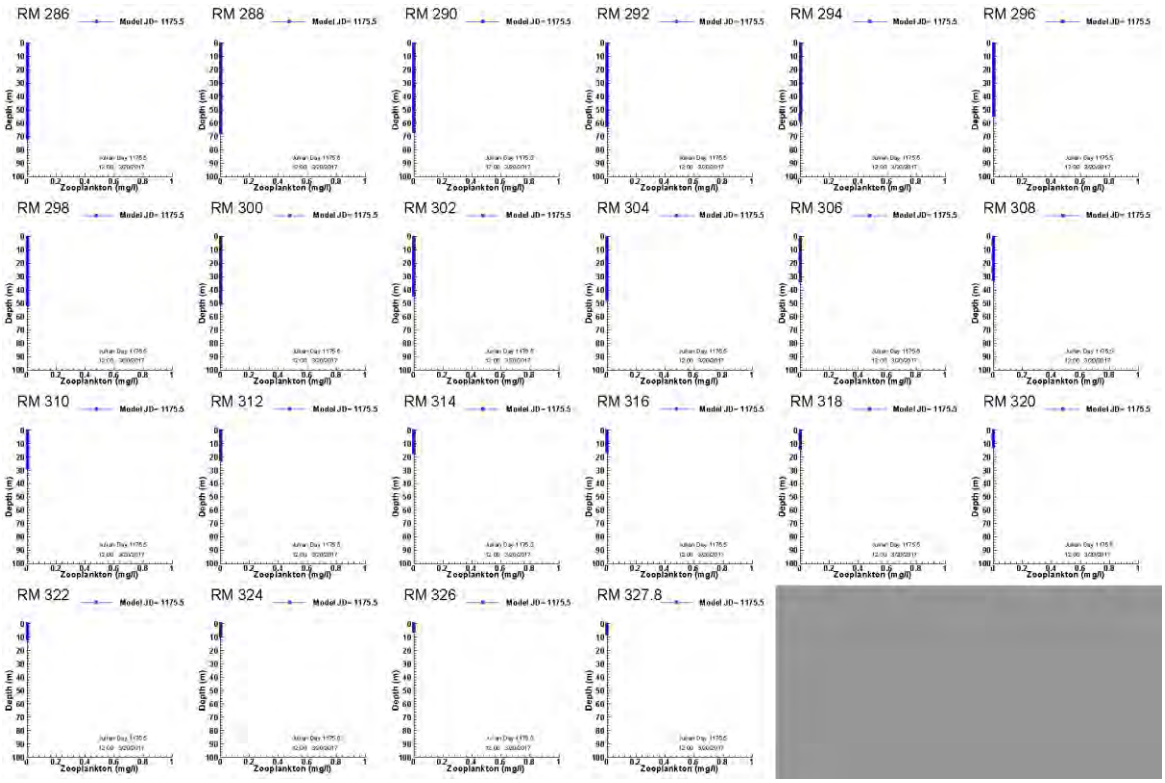


Figure 1383. Vertical profiles of zooplankton compared with data for 3/20/2017.

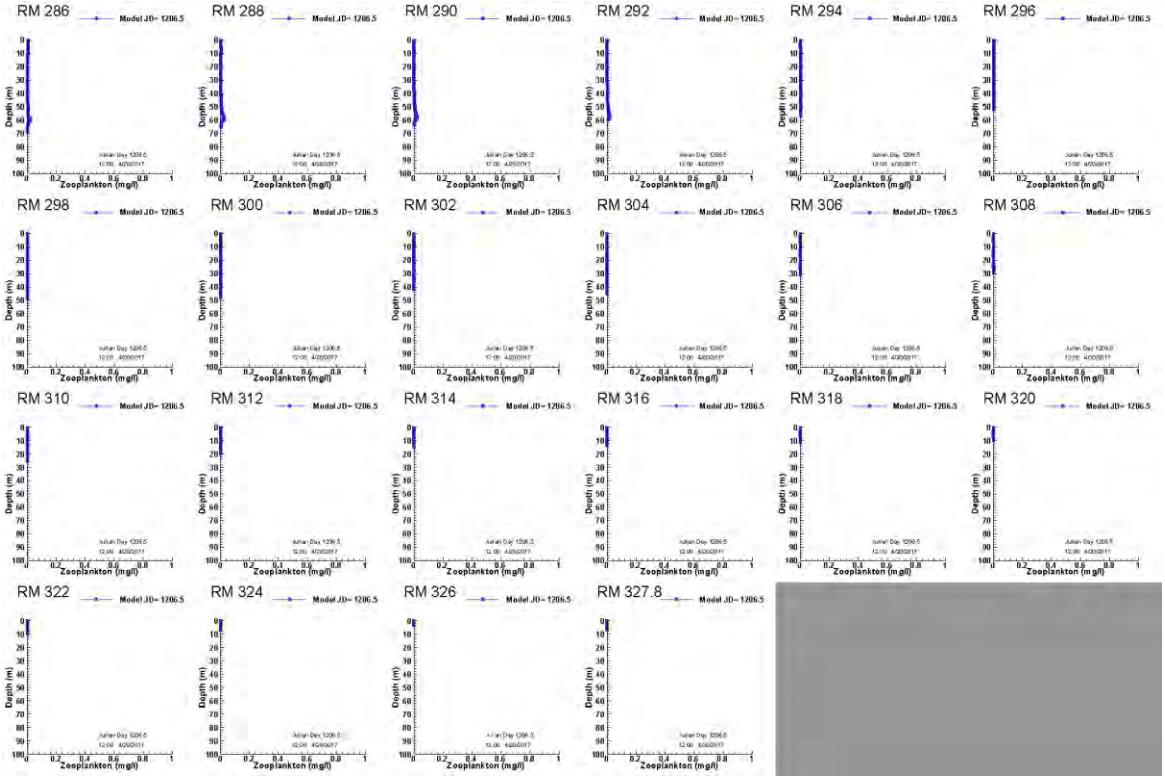


Figure 1384. Vertical profiles of zooplankton compared with data for 4/20/2017.

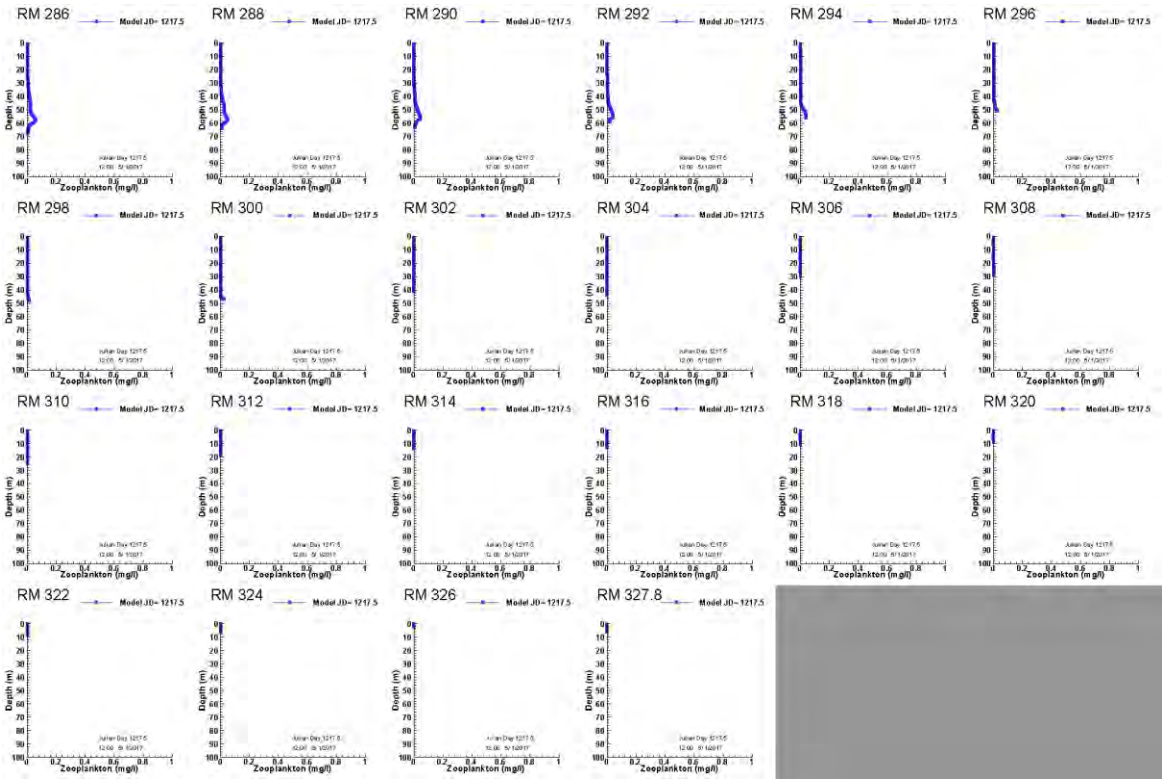


Figure 1385. Vertical profiles of zooplankton compared with data for 5/ 1/2017.

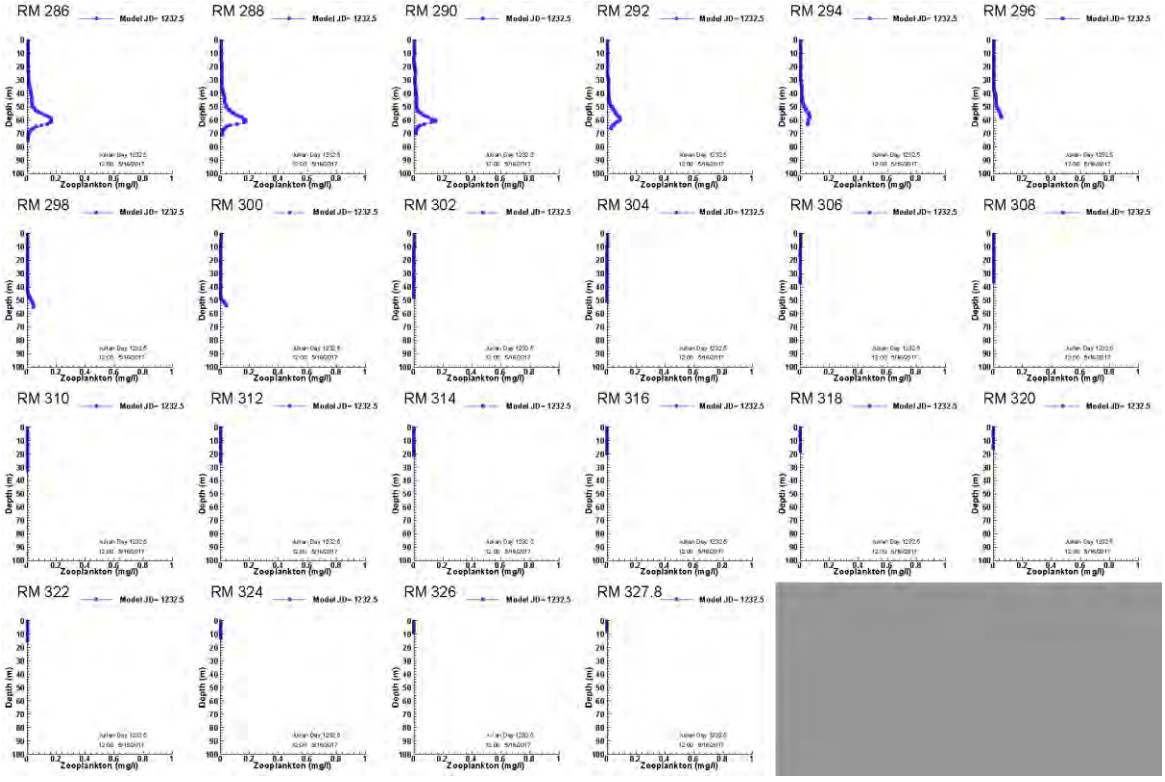


Figure 1386. Vertical profiles of zooplankton compared with data for 5/16/2017.

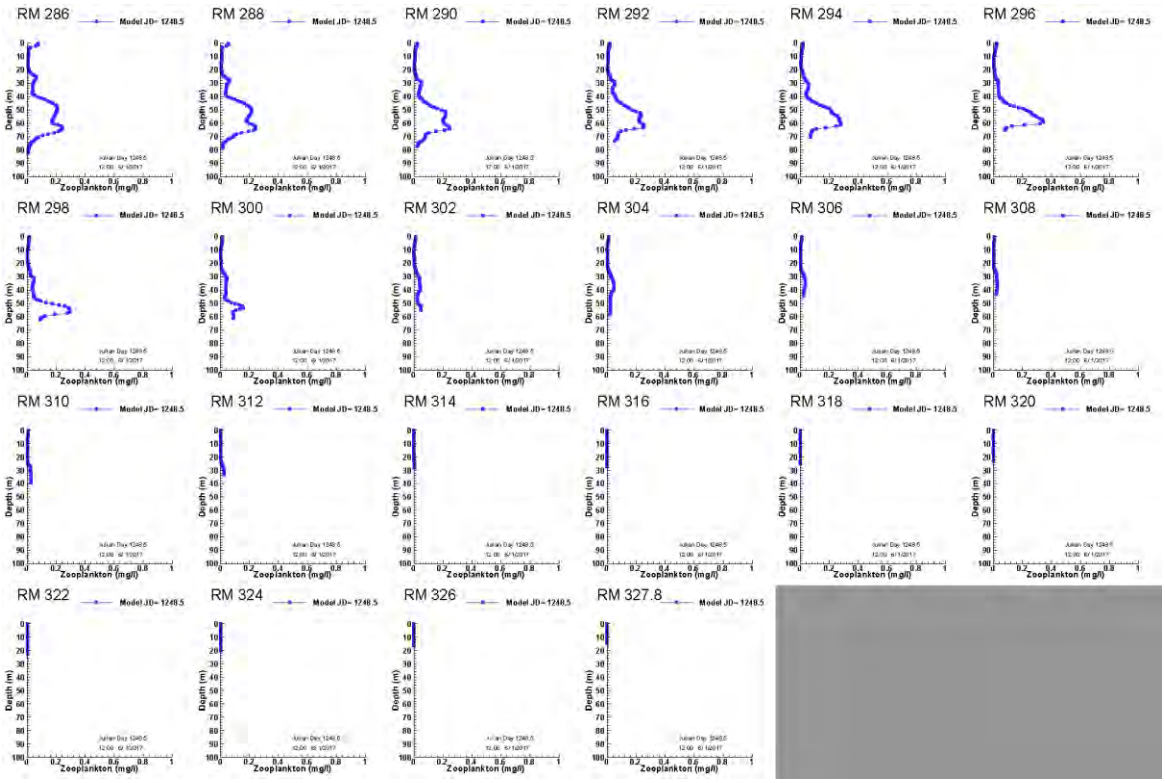


Figure 1387. Vertical profiles of zooplankton compared with data for 6/ 1/2017.

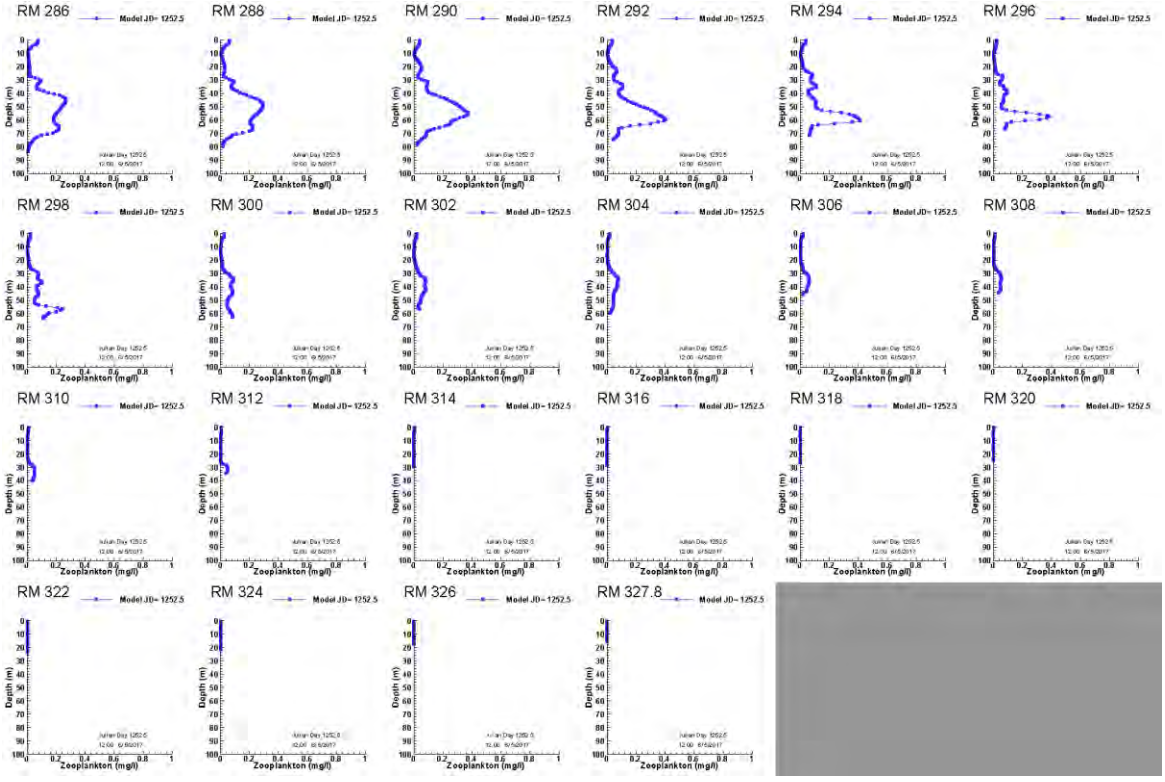


Figure 1388. Vertical profiles of zooplankton compared with data for 6/ 5/2017.

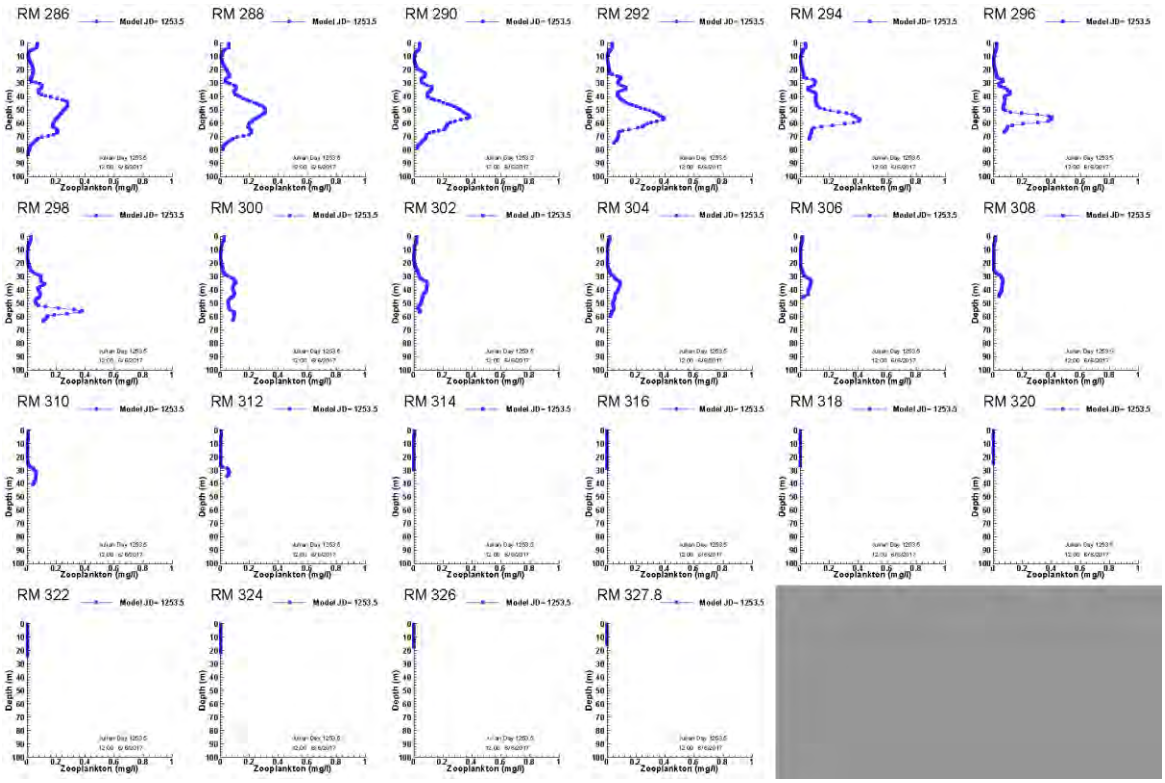


Figure 1389. Vertical profiles of zooplankton compared with data for 6/ 6/2017.

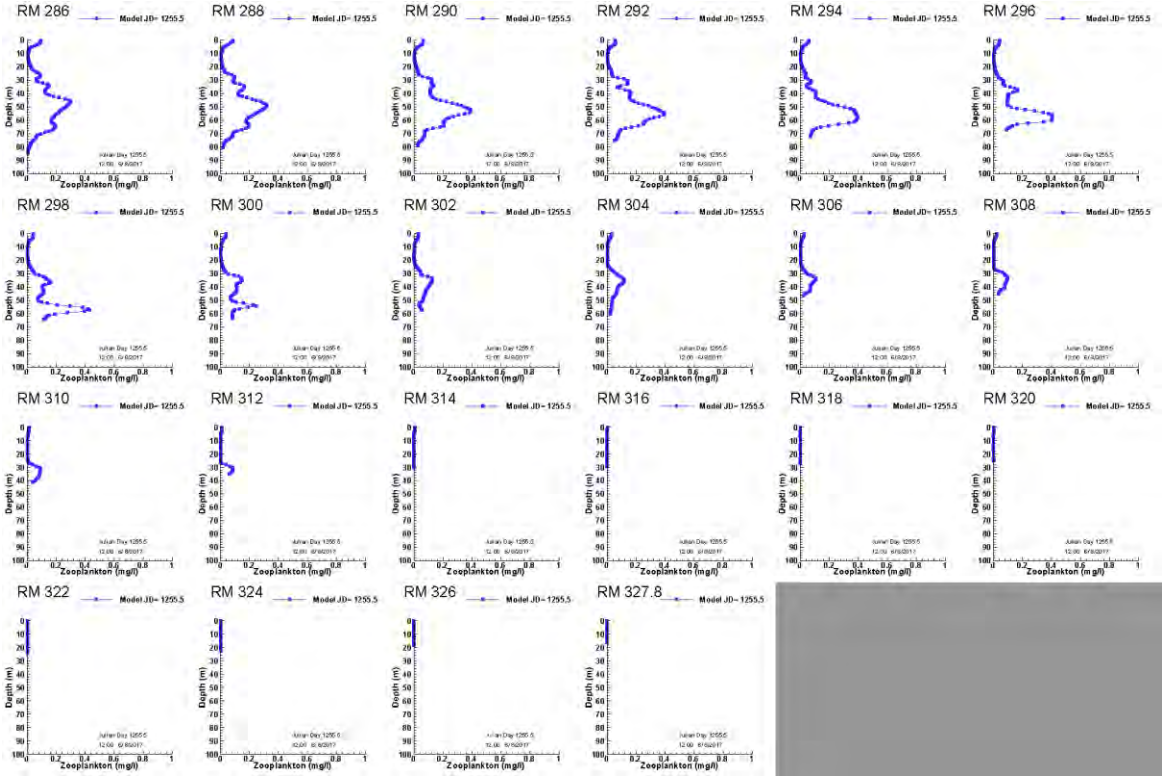


Figure 1390. Vertical profiles of zooplankton compared with data for 6/ 8/2017.

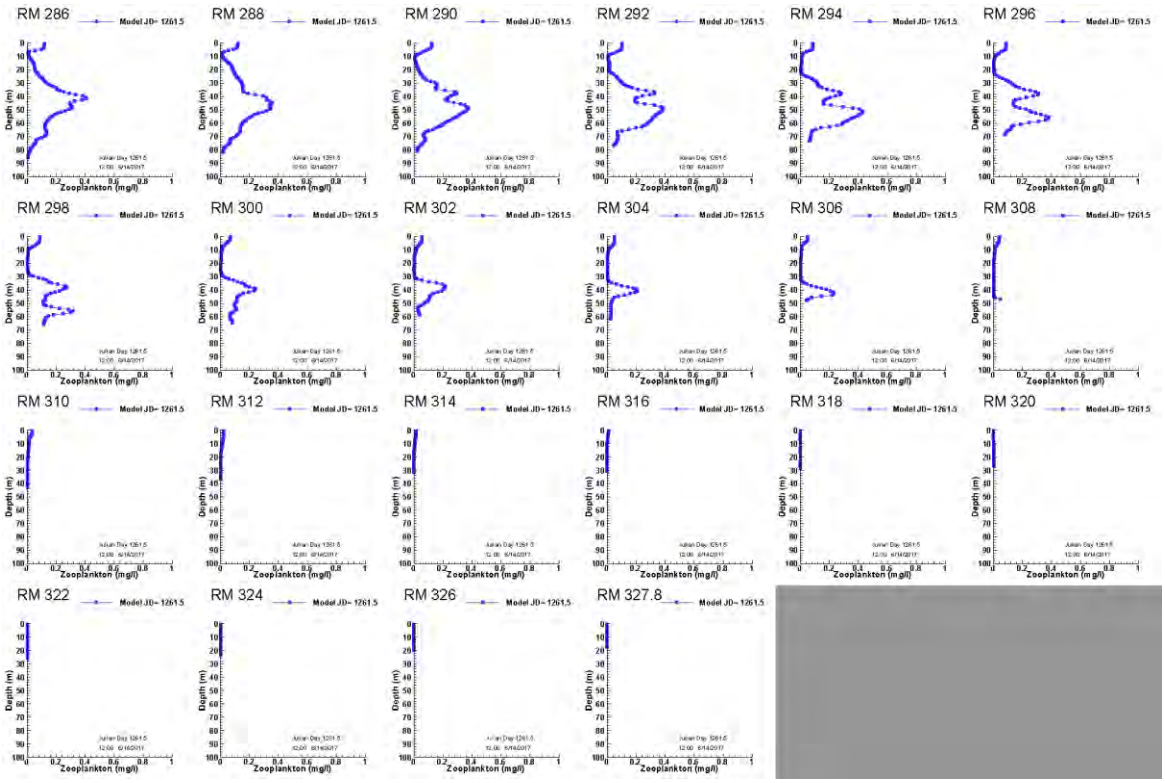


Figure 1391. Vertical profiles of zooplankton compared with data for 6/14/2017.

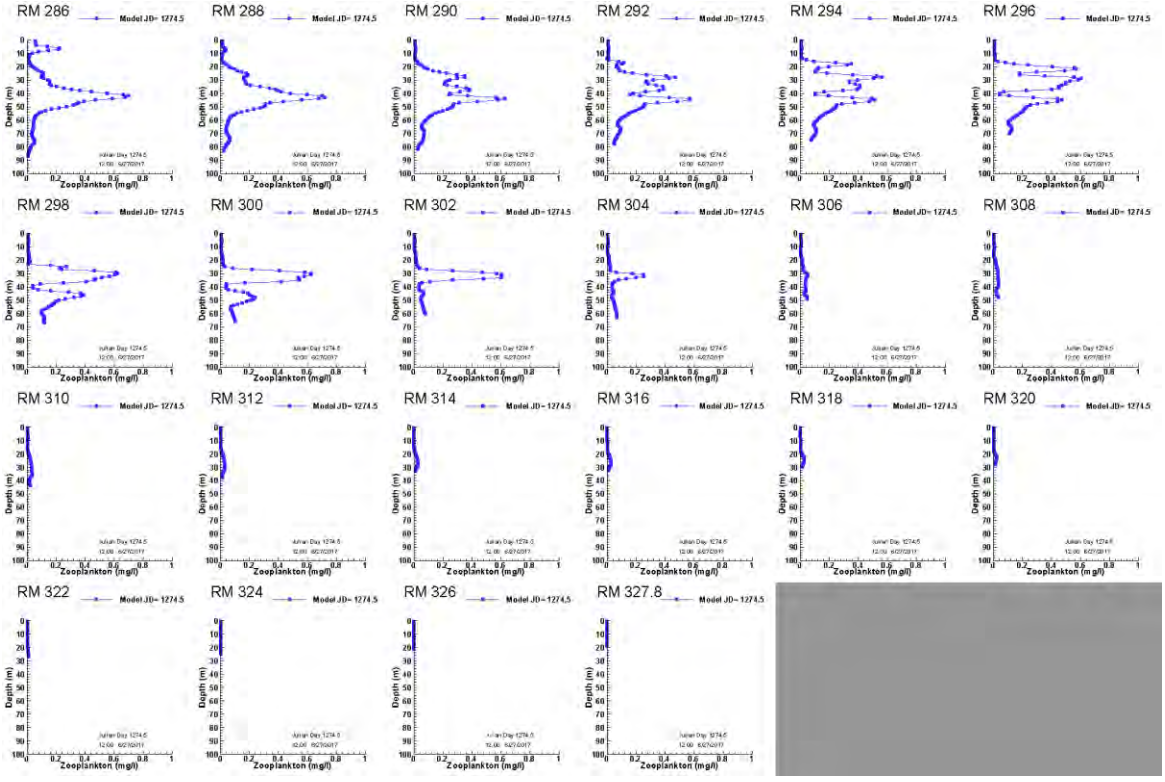


Figure 1392. Vertical profiles of zooplankton compared with data for 6/27/2017.

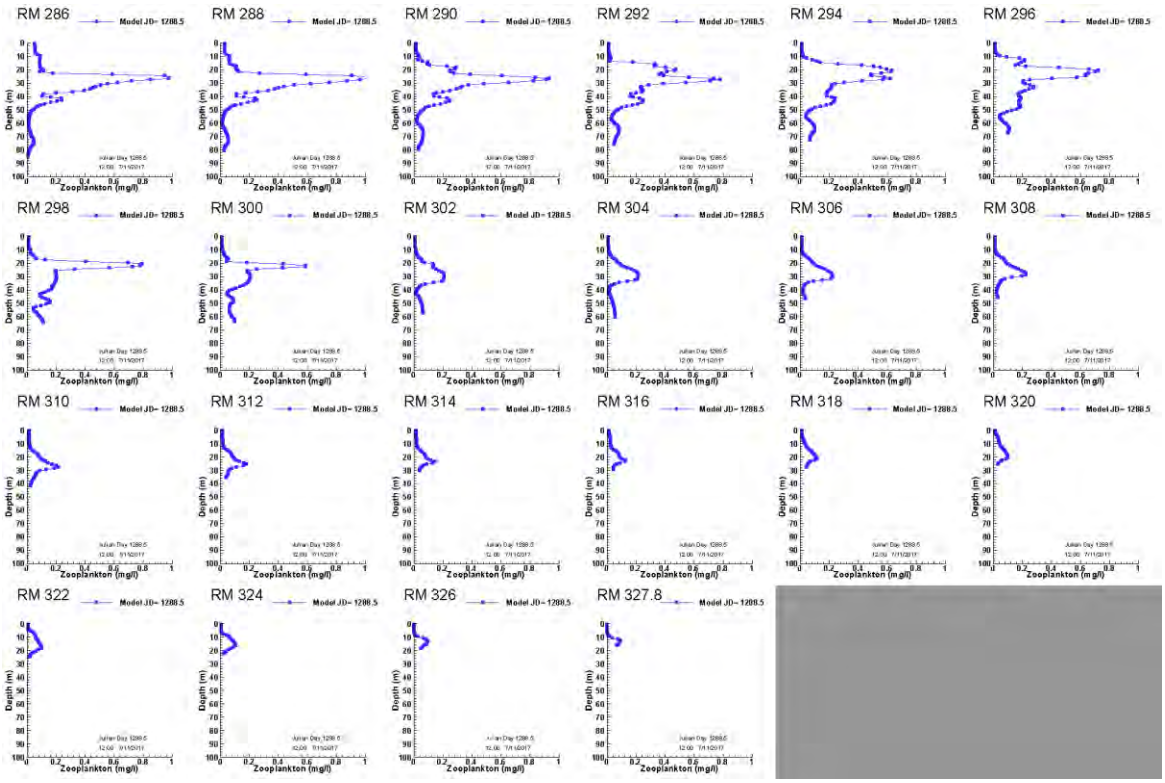


Figure 1393. Vertical profiles of zooplankton compared with data for 7/11/2017.

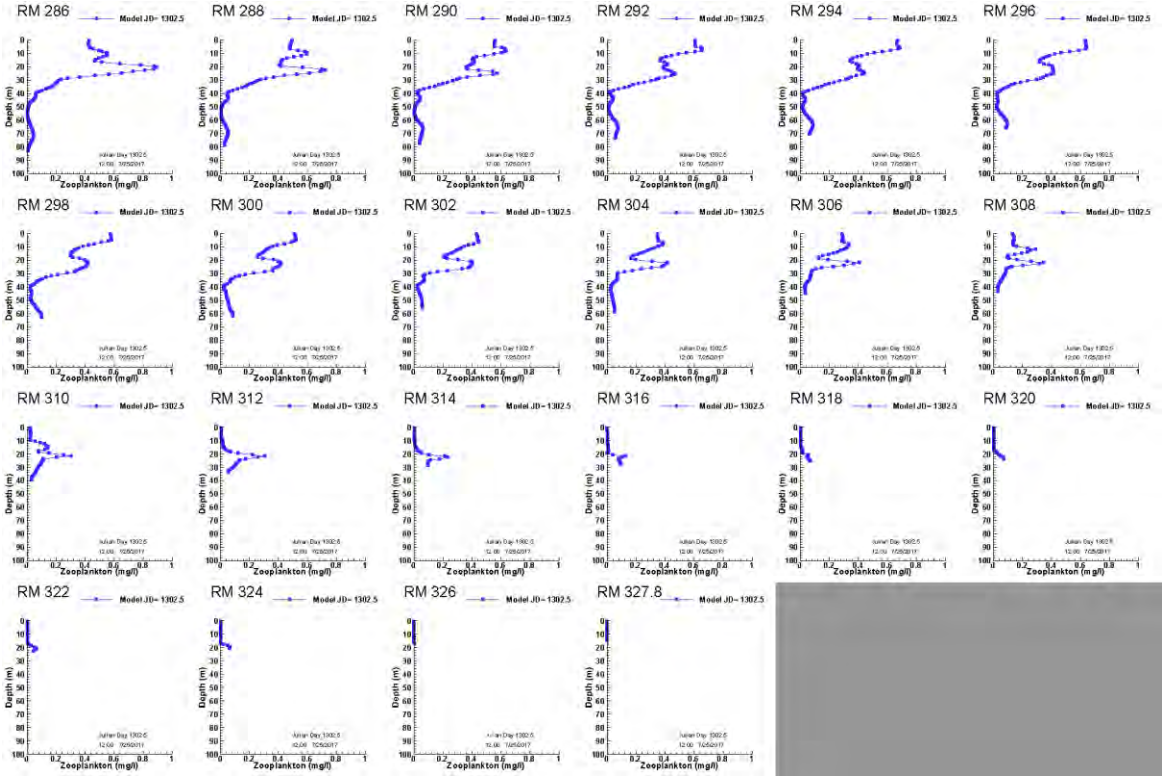


Figure 1394. Vertical profiles of zooplankton compared with data for 7/25/2017.

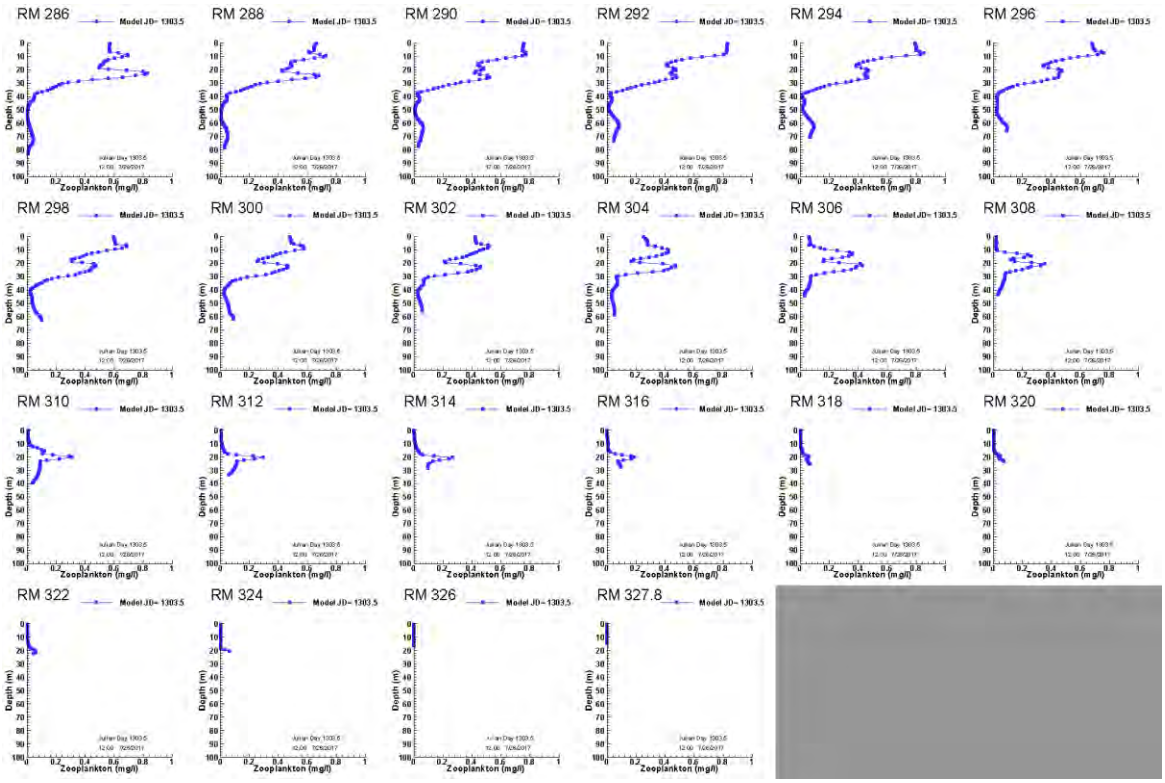


Figure 1395. Vertical profiles of zooplankton compared with data for 7/26/2017.

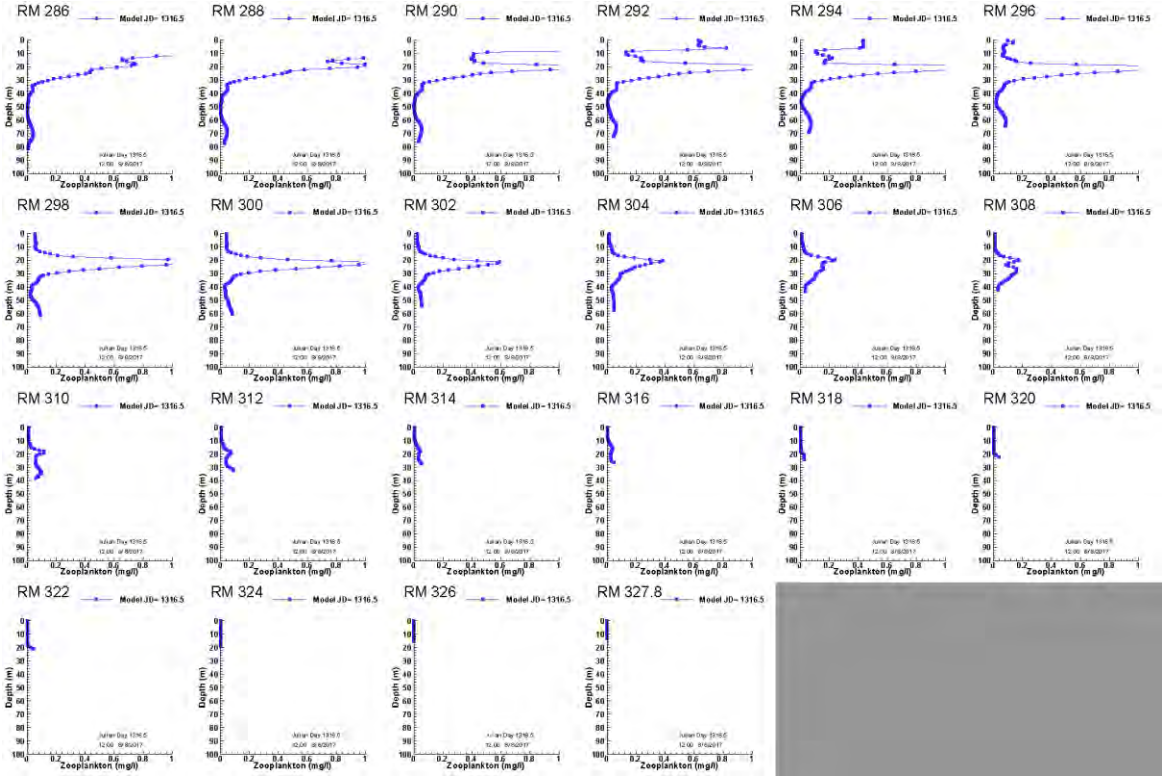


Figure 1396. Vertical profiles of zooplankton compared with data for 8/ 8/2017.

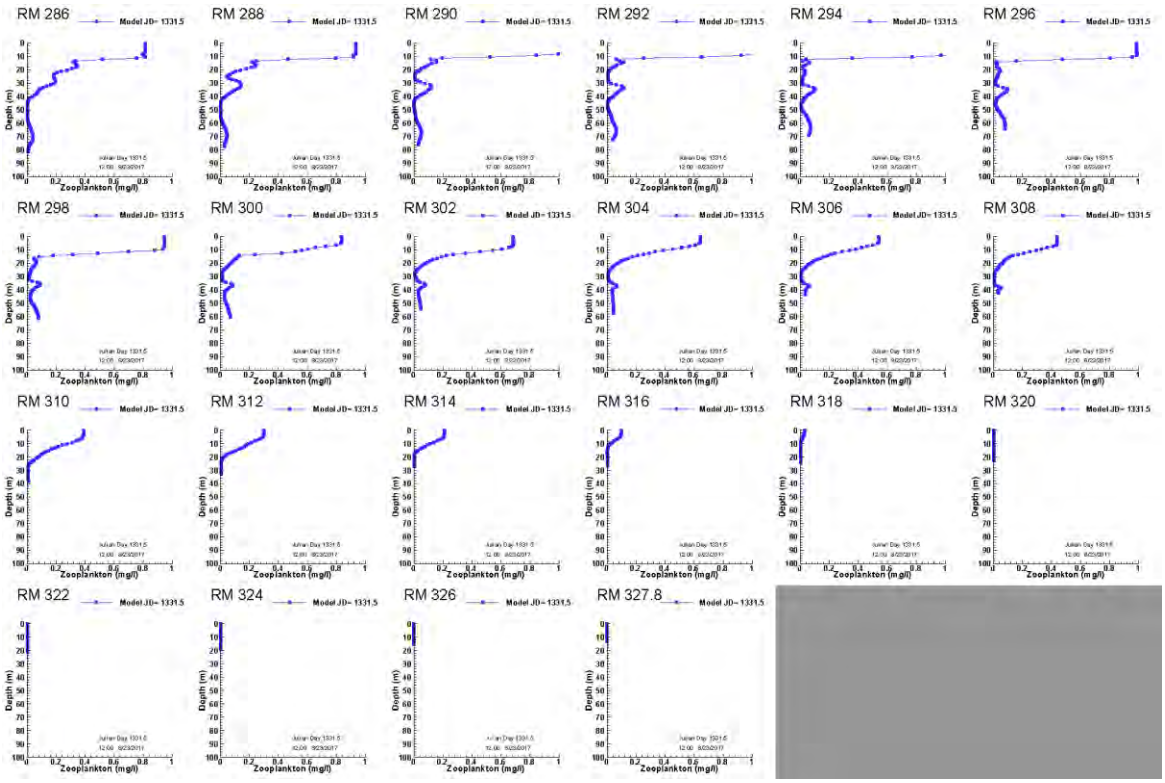


Figure 1397. Vertical profiles of zooplankton compared with data for 8/23/2017.

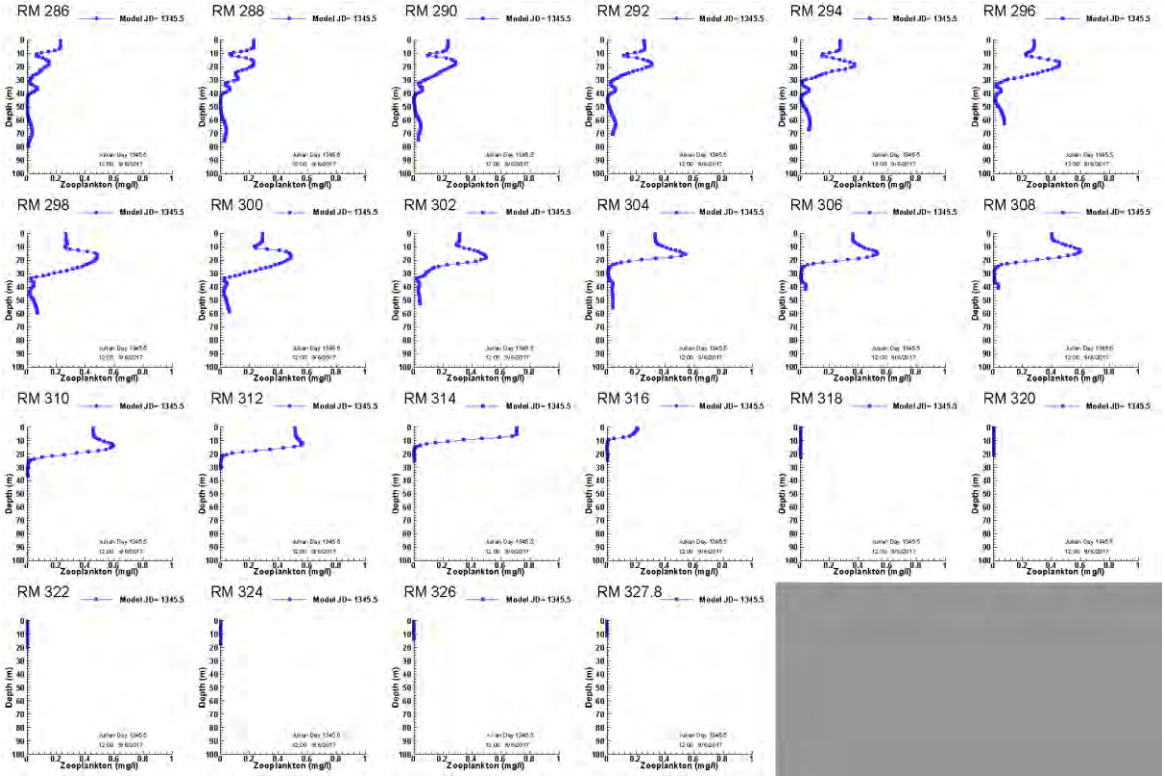


Figure 1398. Vertical profiles of zooplankton compared with data for 9/ 6/2017.

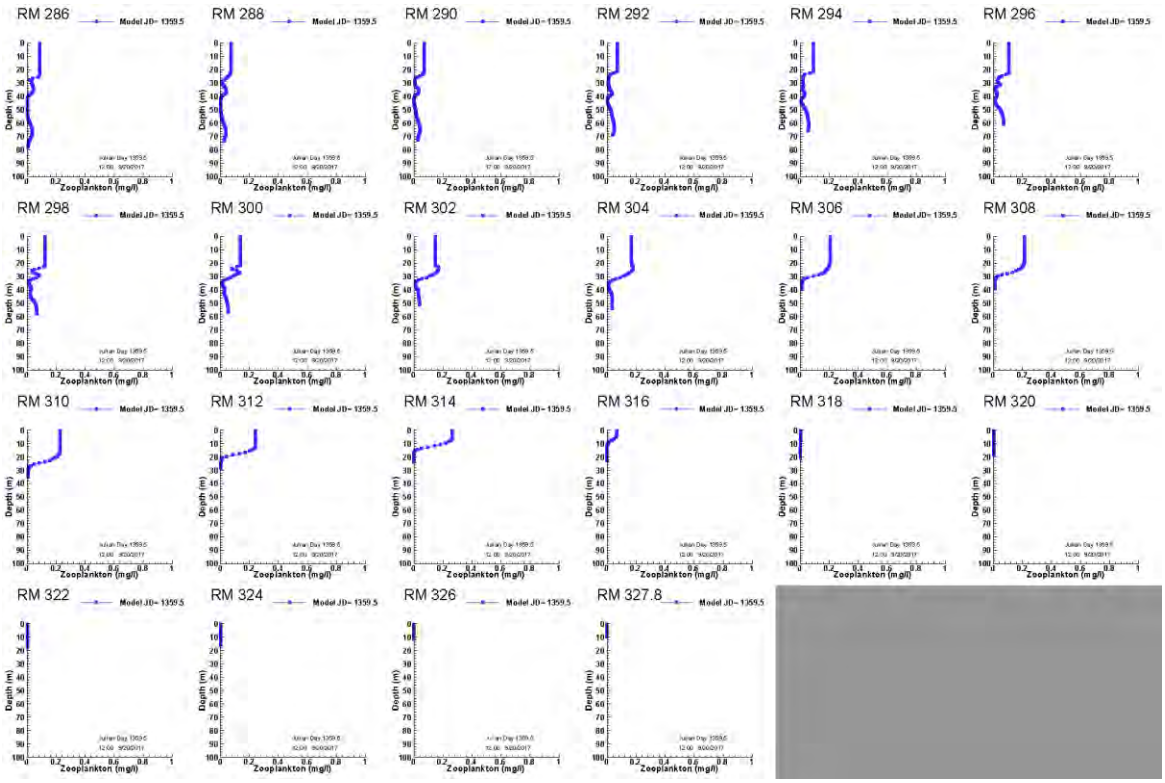


Figure 1399. Vertical profiles of zooplankton compared with data for 9/20/2017.

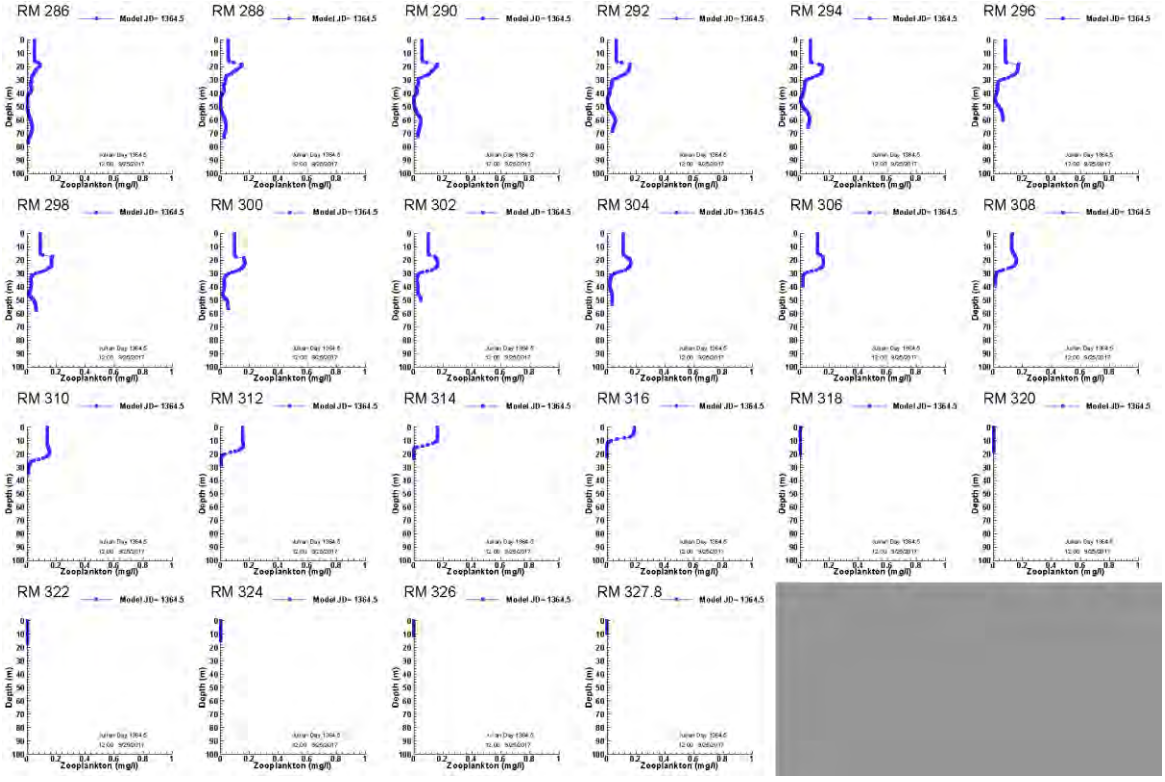


Figure 1400. Vertical profiles of zooplankton compared with data for 9/25/2017.

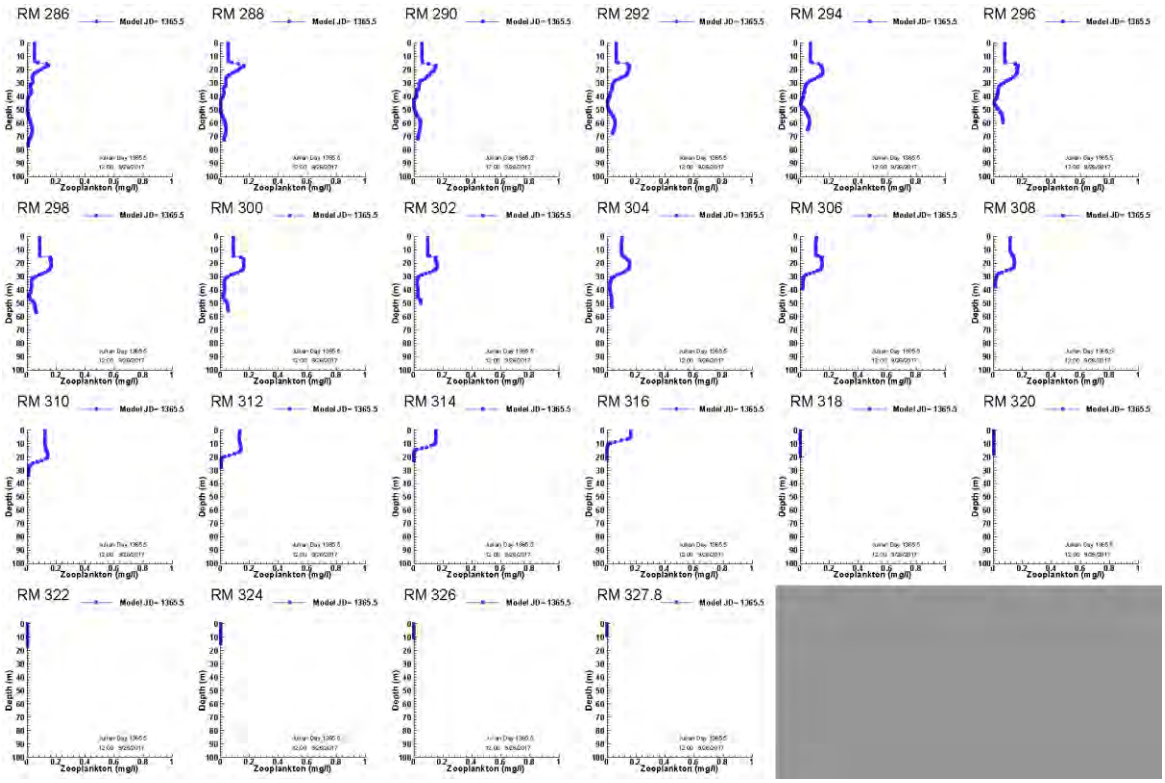


Figure 1401. Vertical profiles of zooplankton compared with data for 9/26/2017.

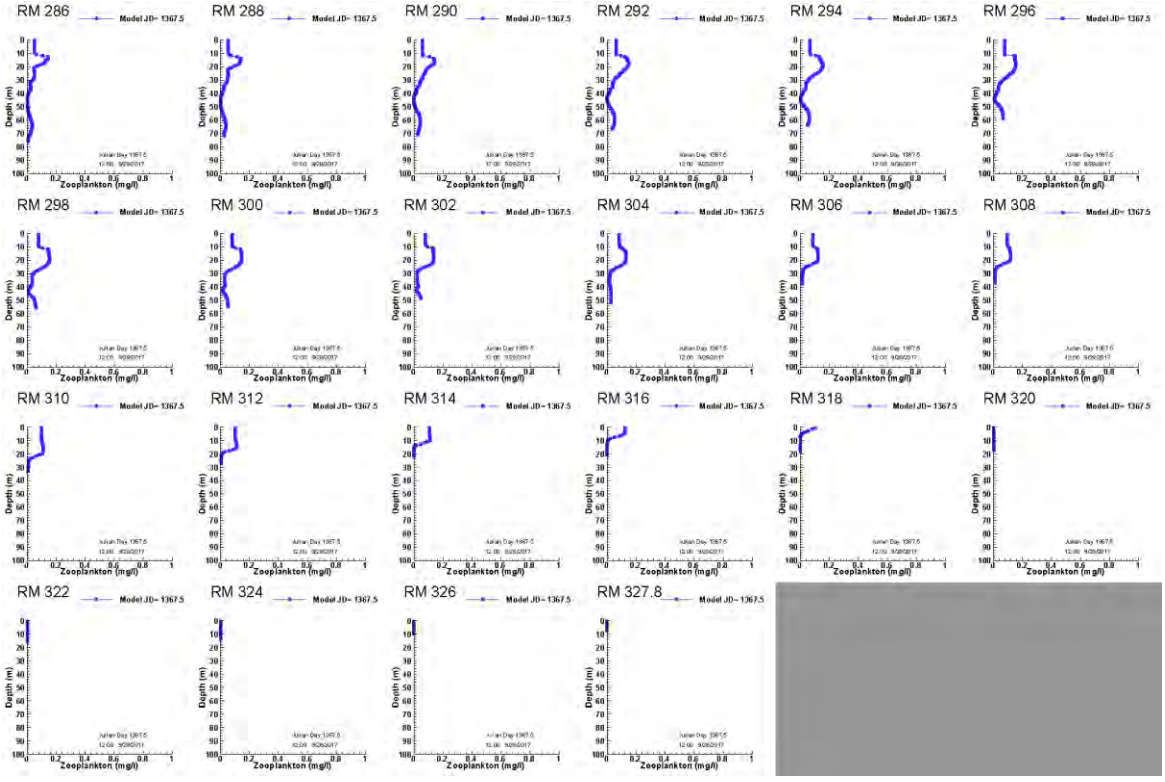


Figure 1402. Vertical profiles of zooplankton compared with data for 9/28/2017.

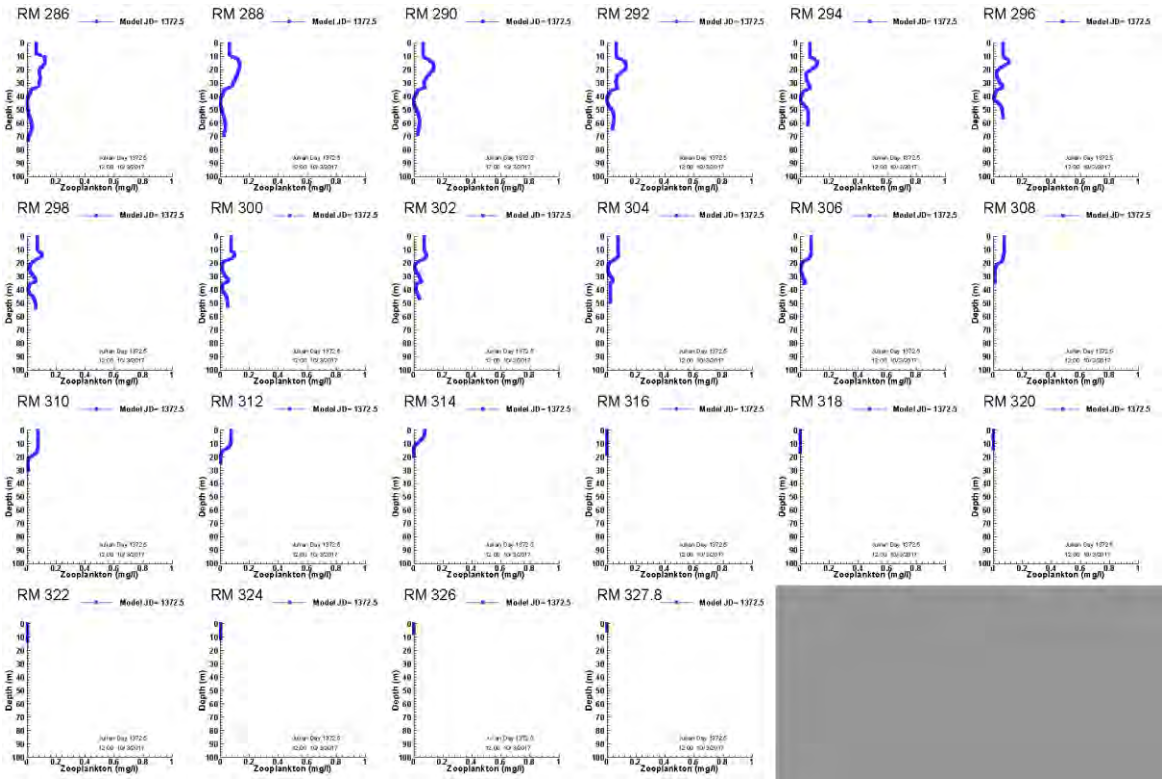


Figure 1403. Vertical profiles of zooplankton compared with data for 10/ 3/2017.

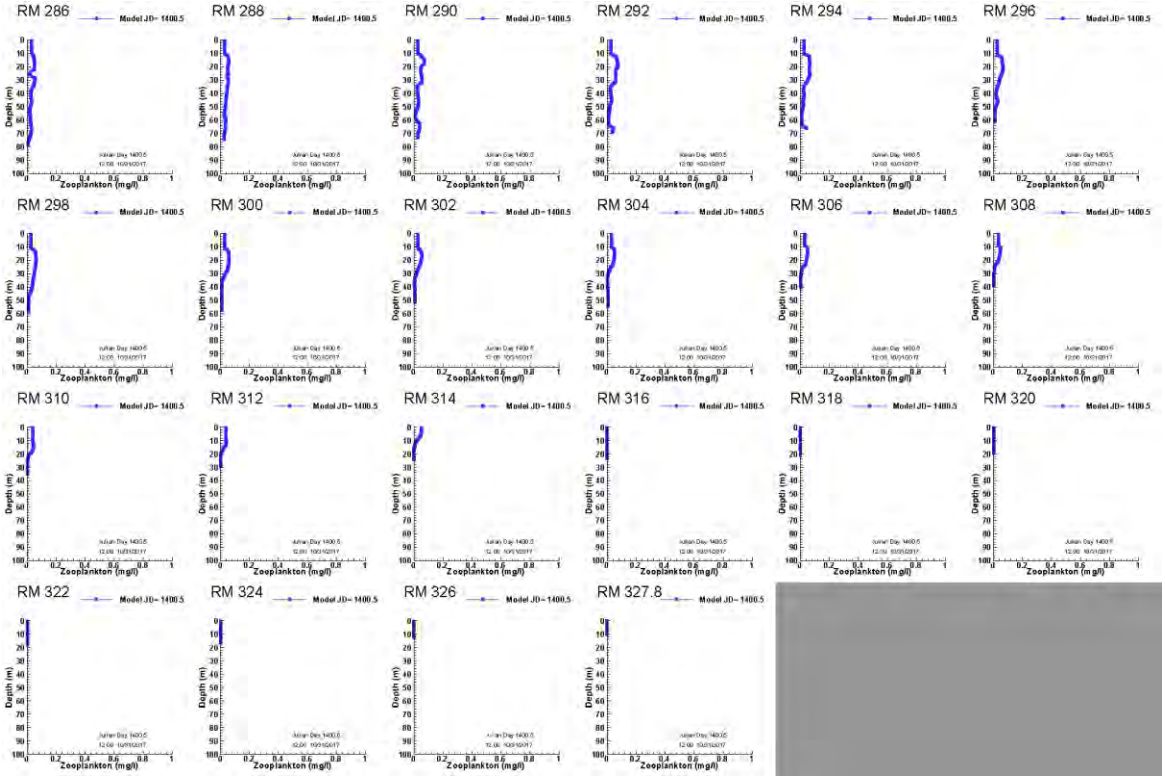


Figure 1404. Vertical profiles of zooplankton compared with data for 10/31/2017.

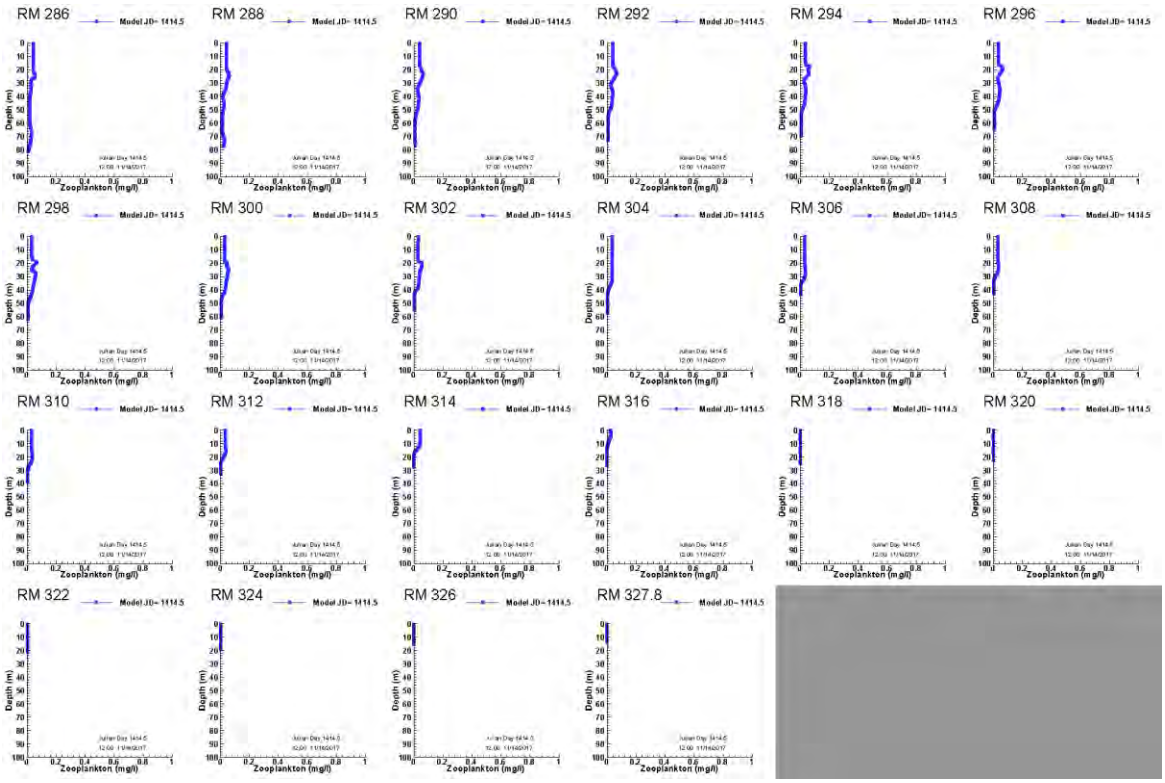


Figure 1405. Vertical profiles of zooplankton compared with data for 11/14/2017.

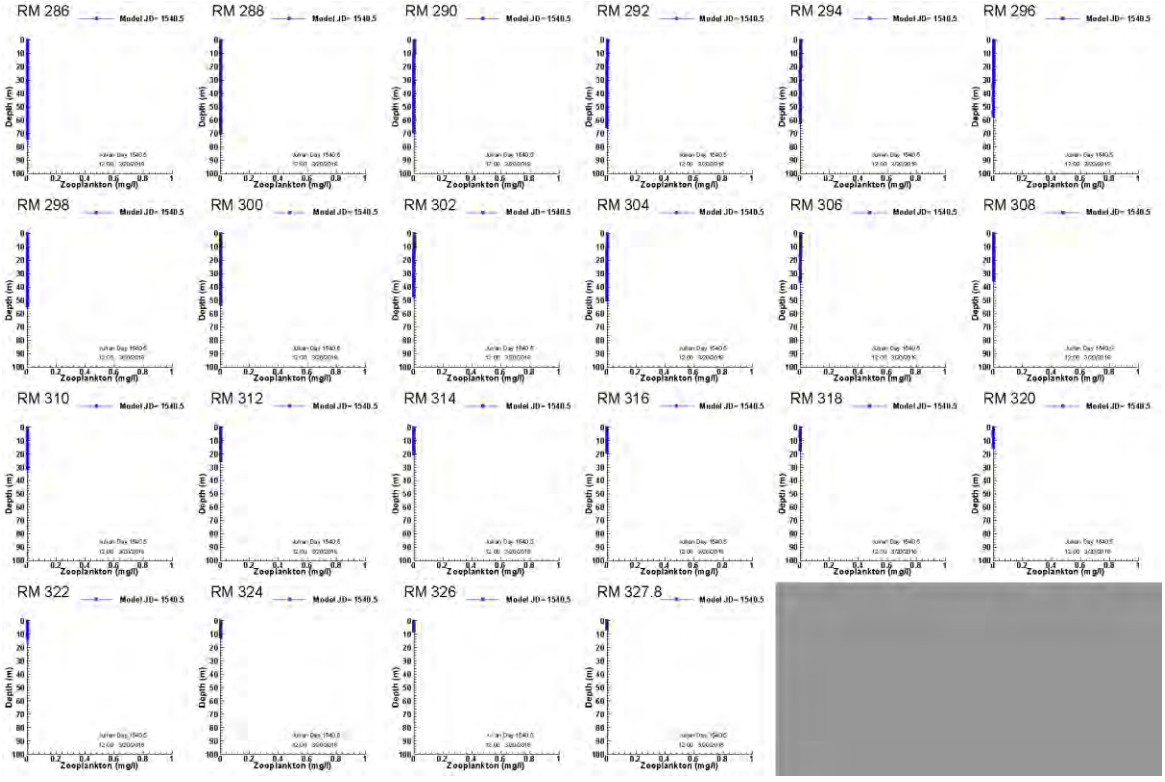


Figure 1406. Vertical profiles of zooplankton compared with data for 3/20/2018.

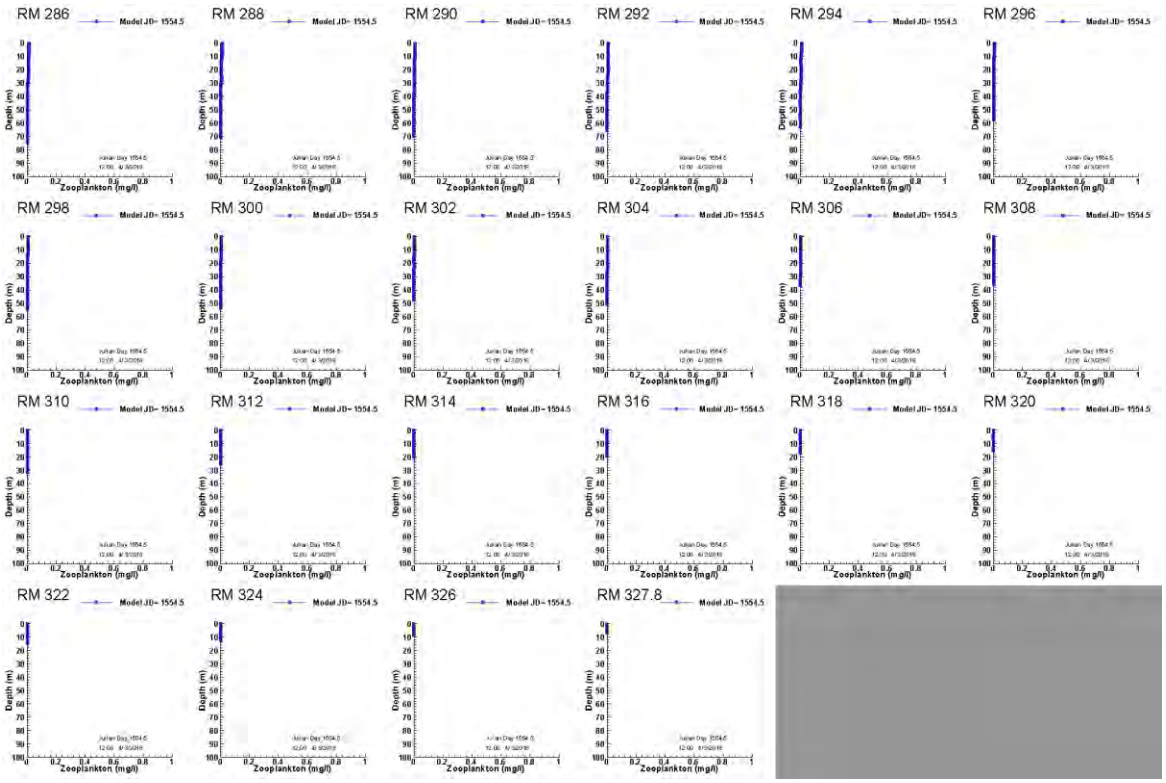


Figure 1407. Vertical profiles of zooplankton compared with data for 4/ 3/2018.

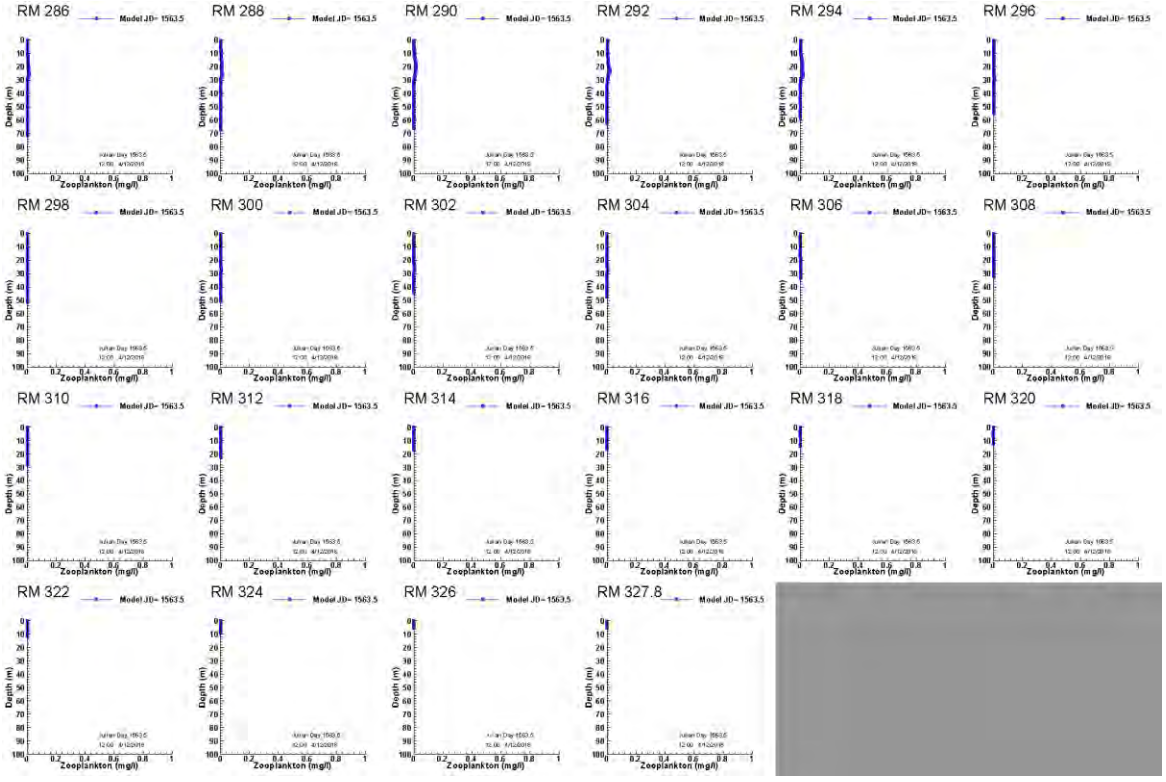


Figure 1408. Vertical profiles of zooplankton compared with data for 4/12/2018.

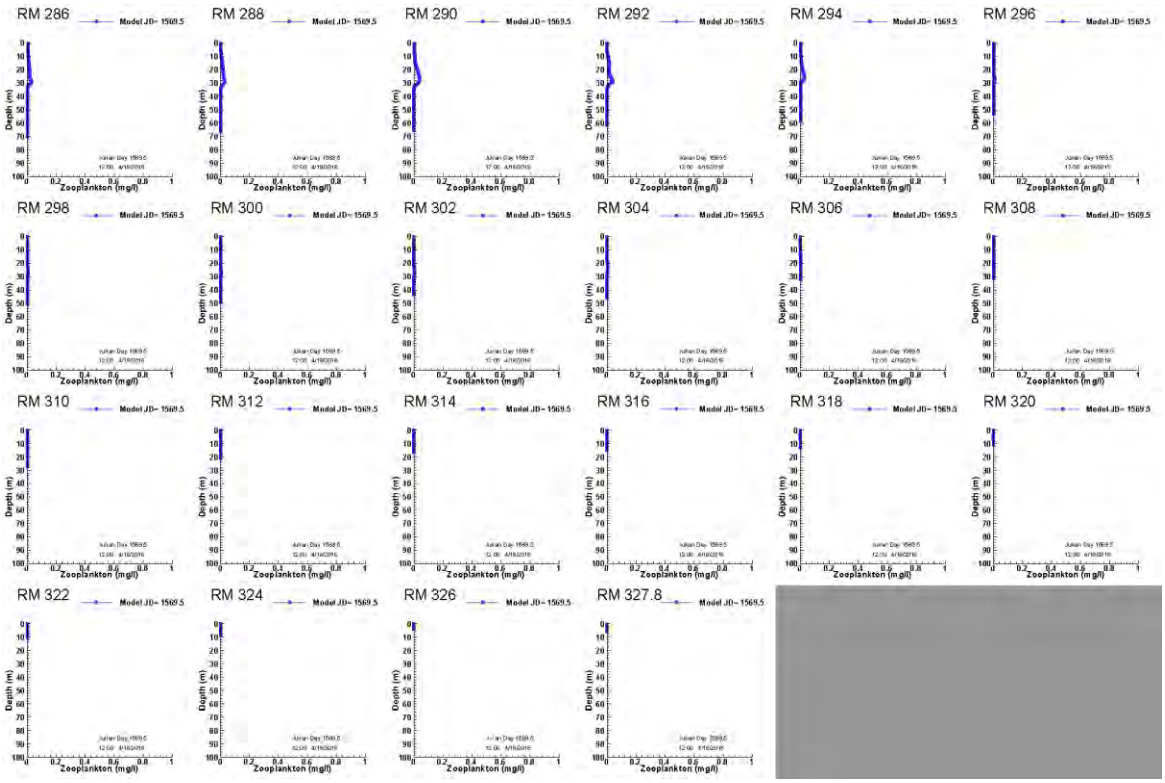


Figure 1409. Vertical profiles of zooplankton compared with data for 4/18/2018.

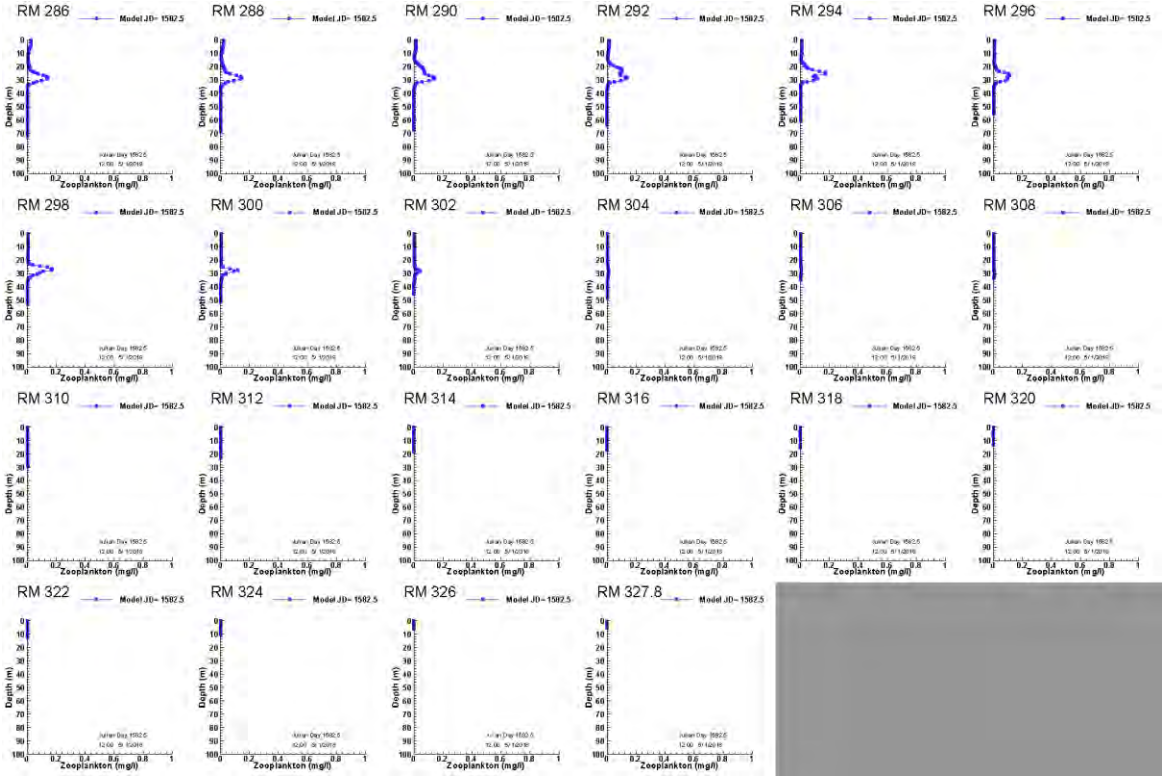


Figure 1410. Vertical profiles of zooplankton compared with data for 5/ 1/2018.

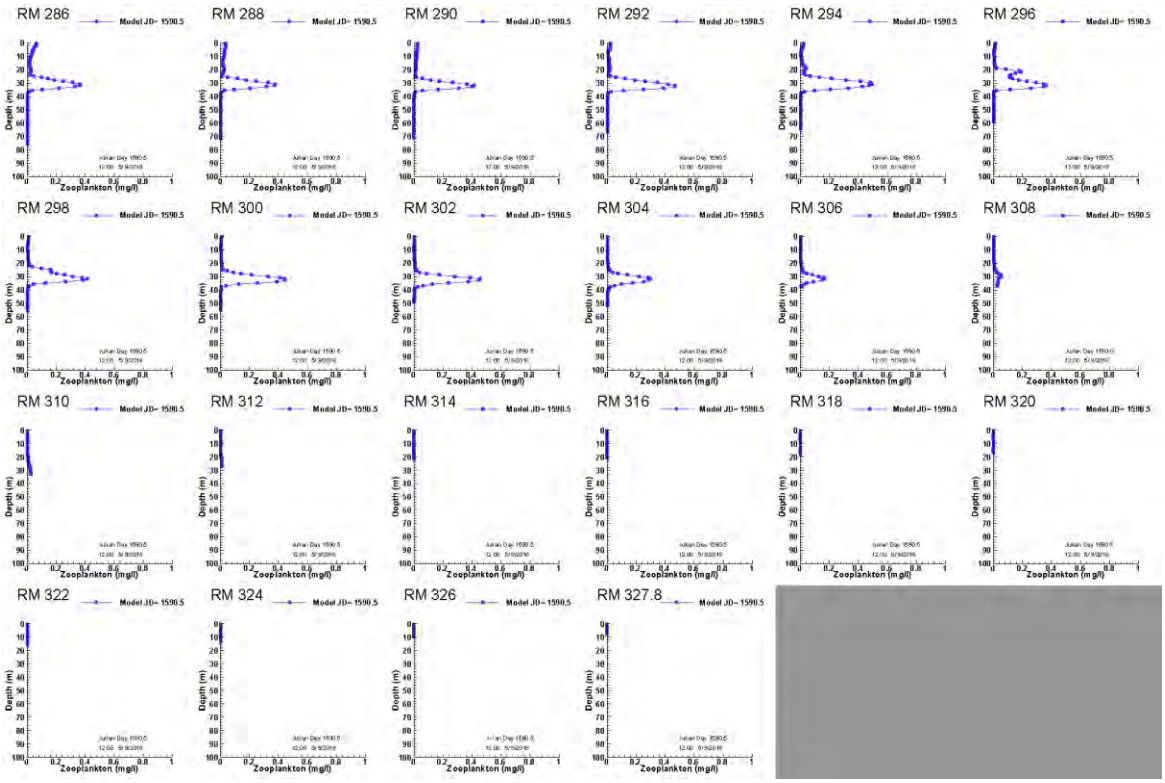


Figure 1411. Vertical profiles of zooplankton compared with data for 5/ 9/2018.

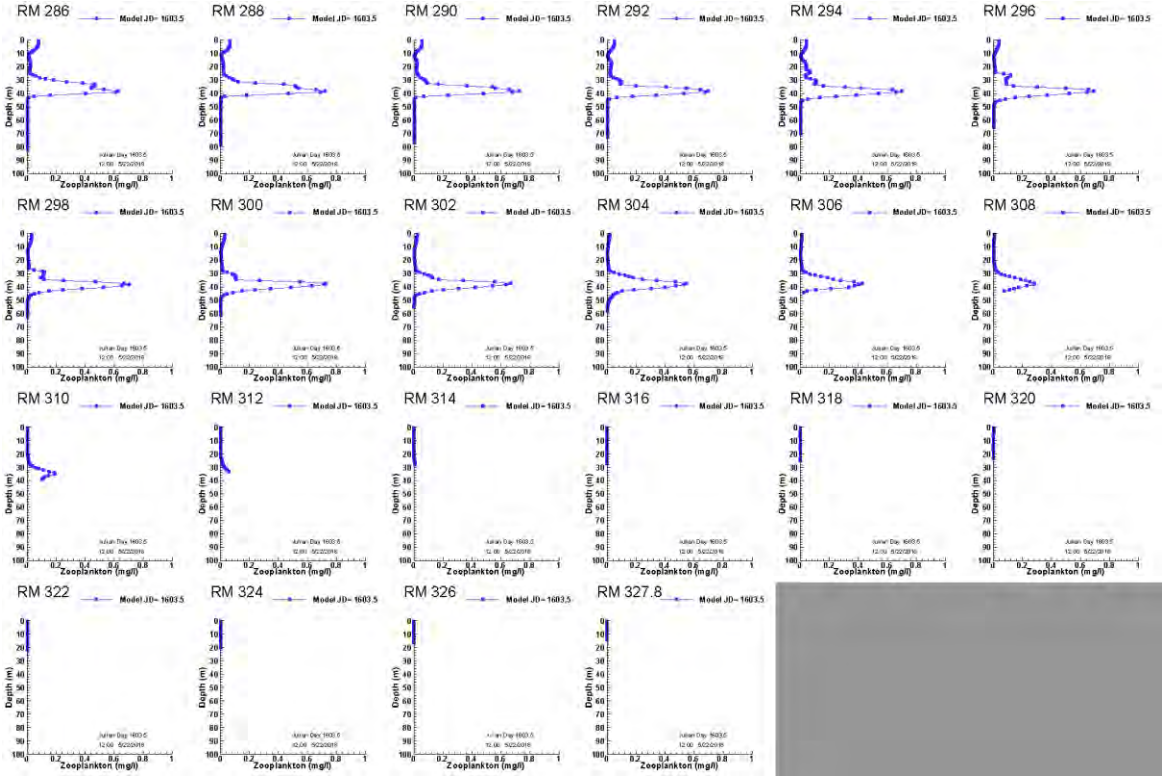


Figure 1412. Vertical profiles of zooplankton compared with data for 5/22/2018.

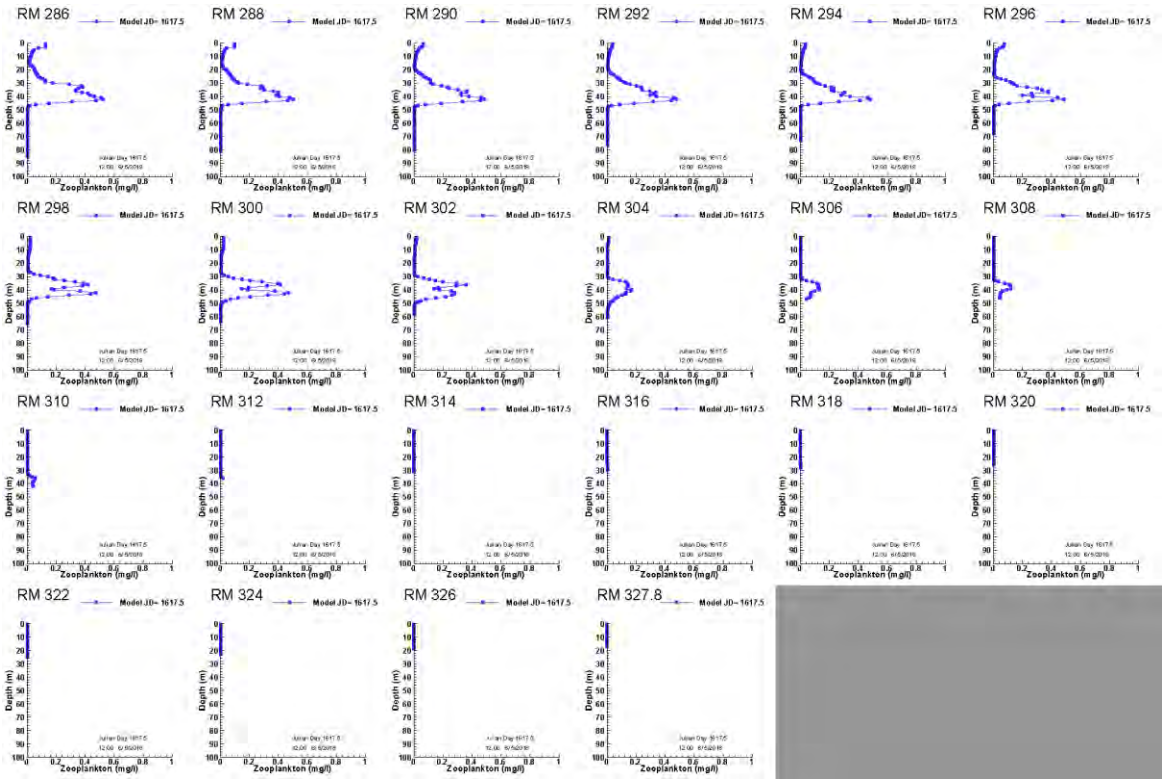


Figure 1413. Vertical profiles of zooplankton compared with data for 6/ 5/2018.

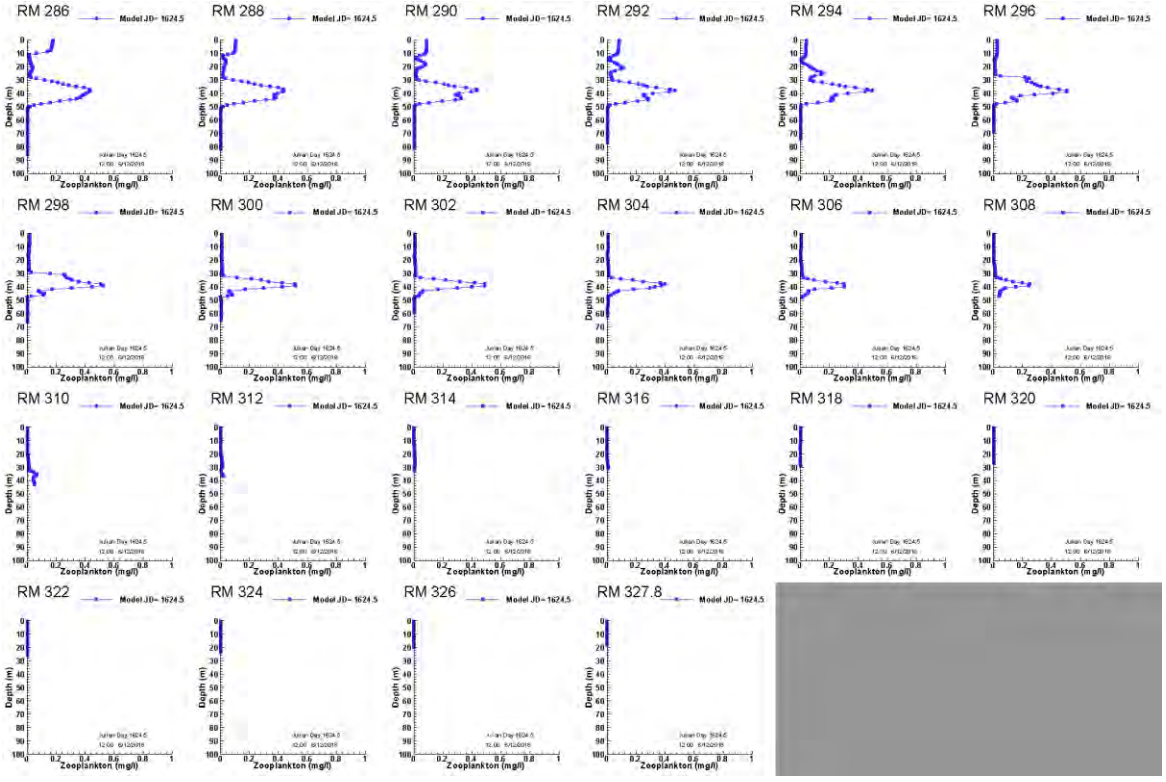


Figure 1414. Vertical profiles of zooplankton compared with data for 6/12/2018.

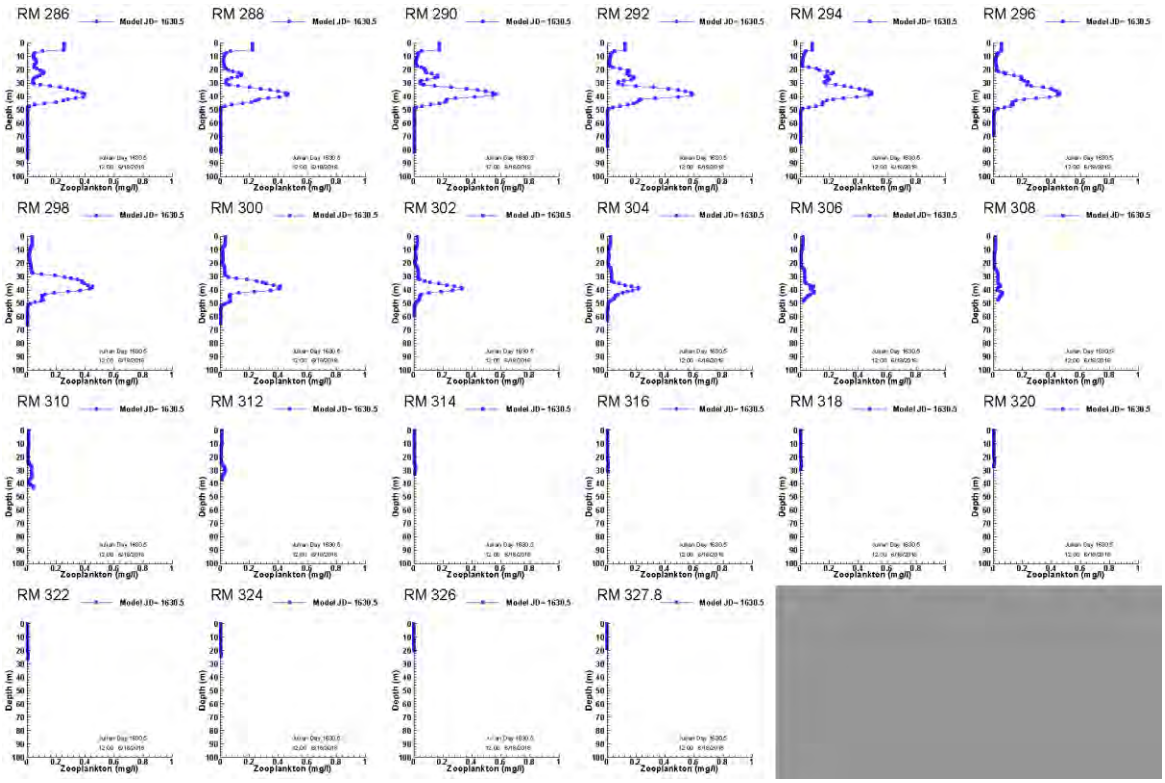


Figure 1415. Vertical profiles of zooplankton compared with data for 6/18/2018.

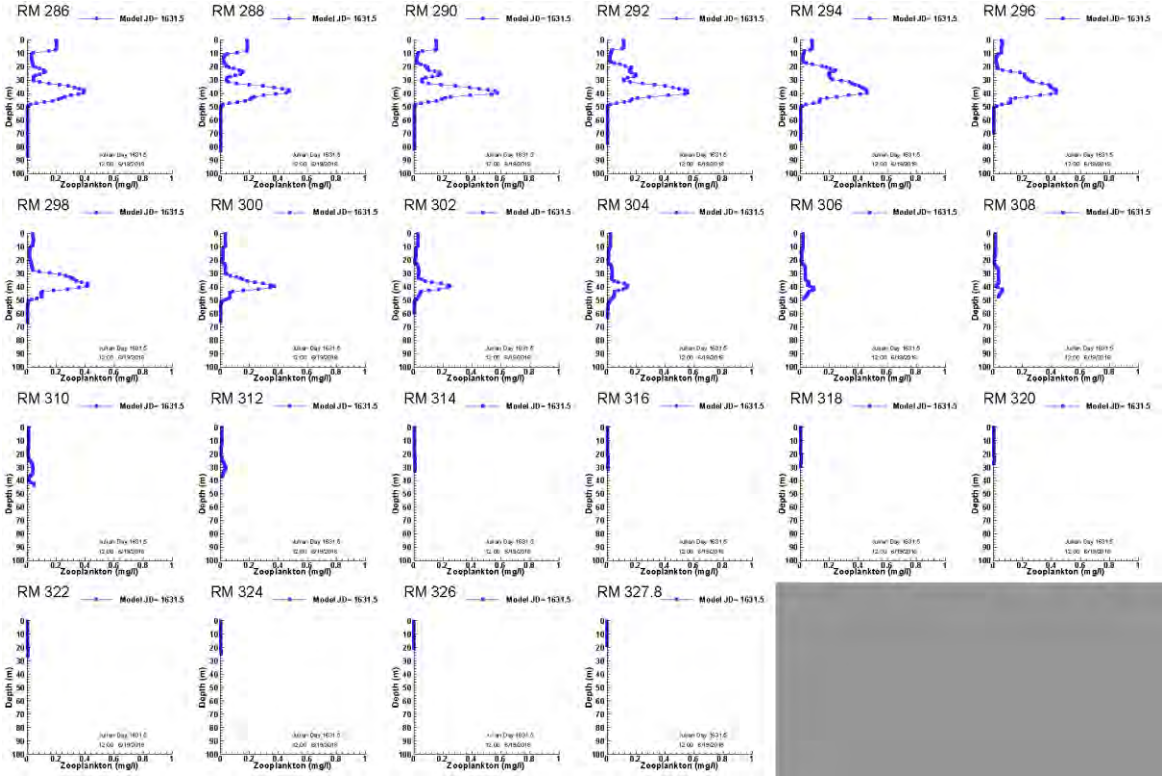


Figure 1416. Vertical profiles of zooplankton compared with data for 6/19/2018.

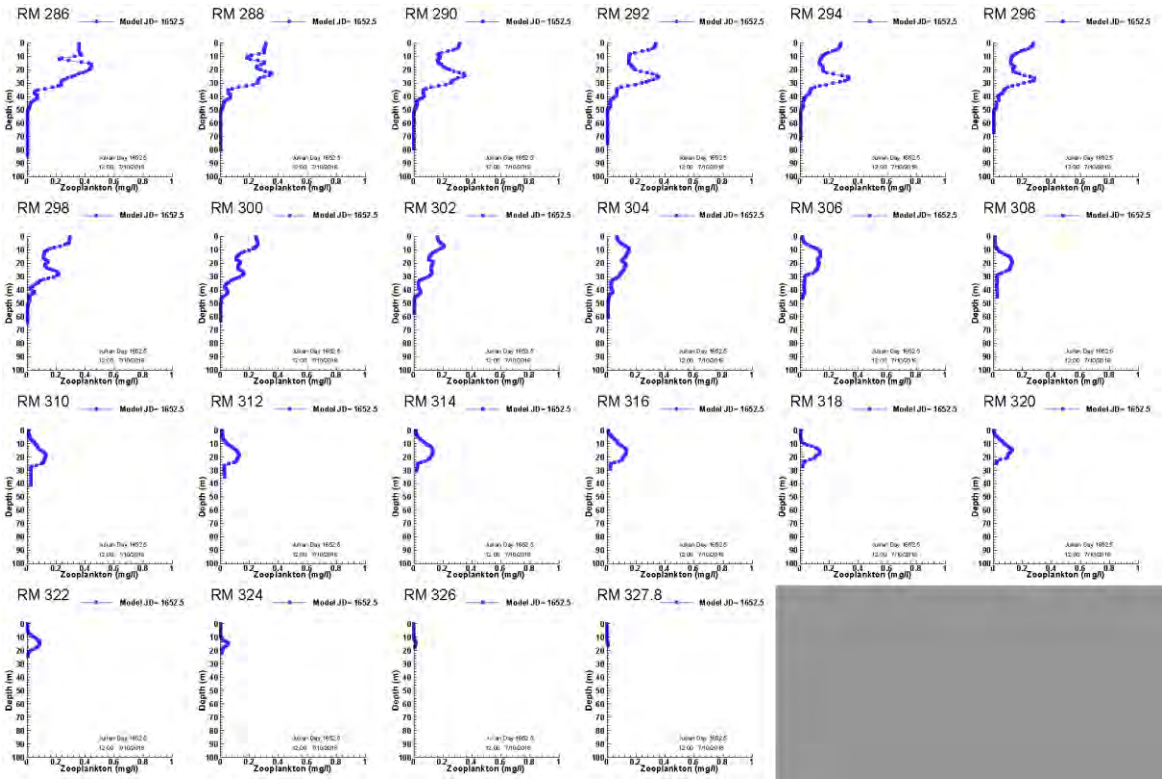


Figure 1417. Vertical profiles of zooplankton compared with data for 7/10/2018.

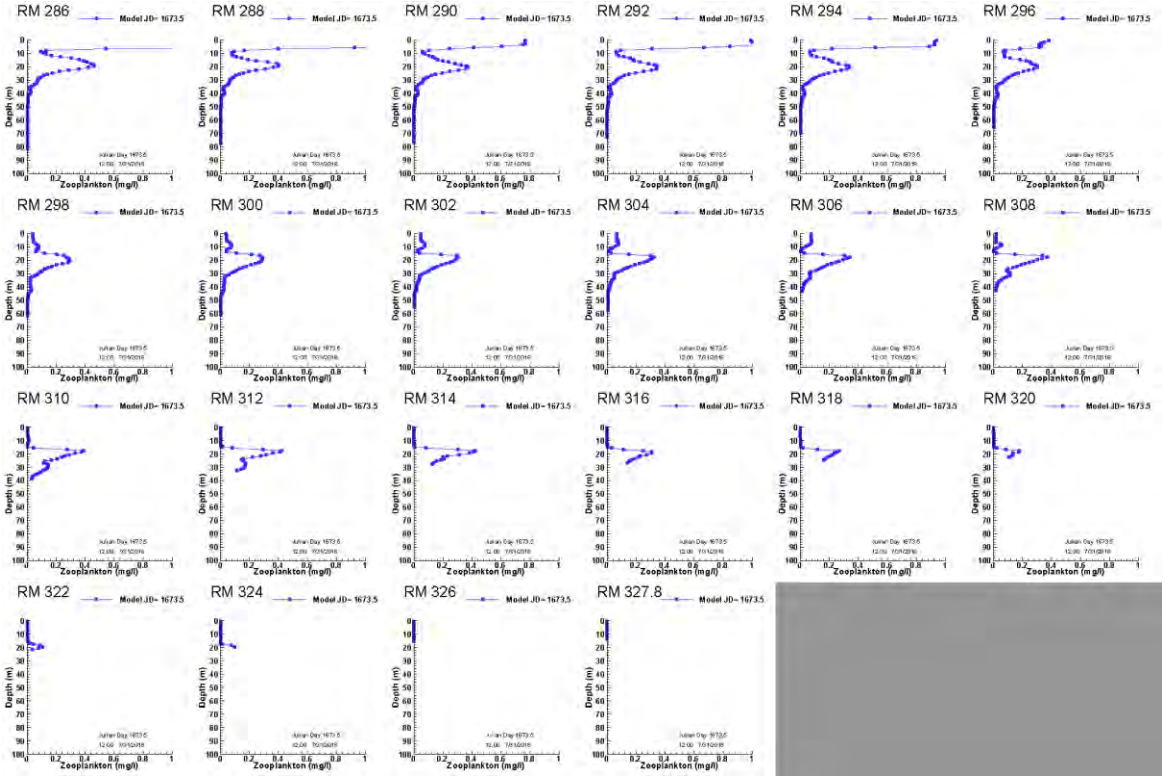


Figure 1418. Vertical profiles of zooplankton compared with data for 7/31/2018.

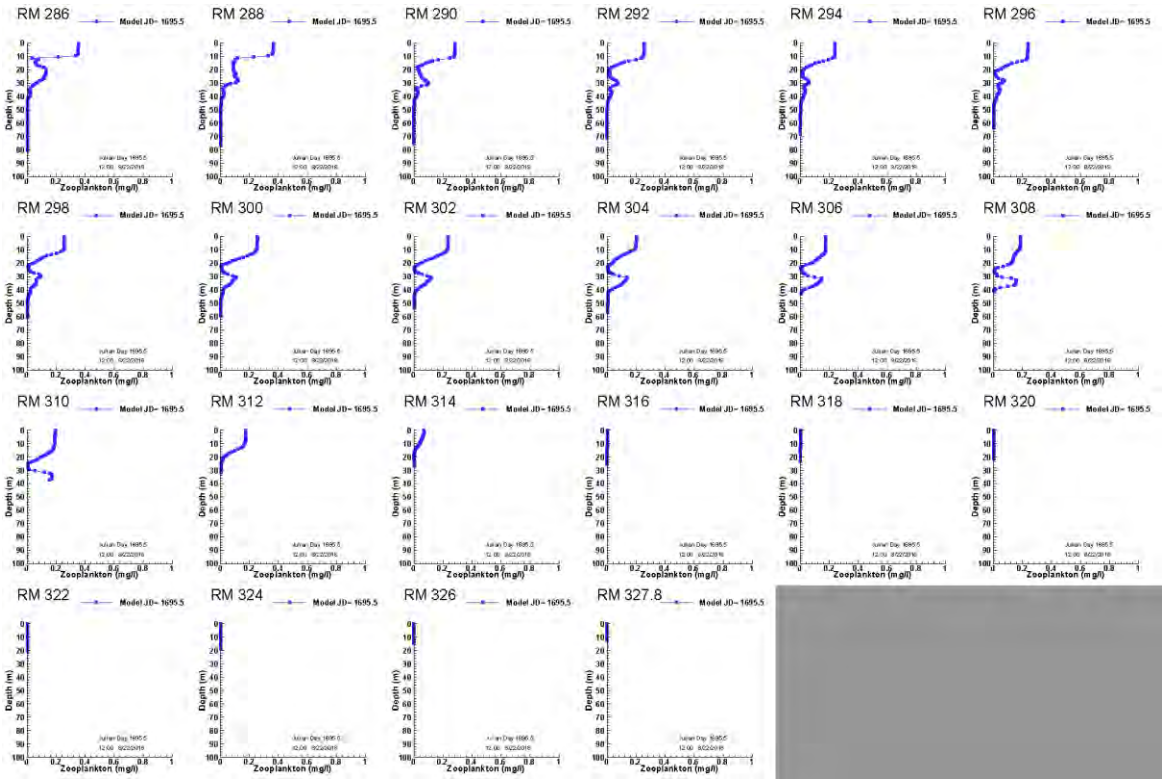


Figure 1419. Vertical profiles of zooplankton compared with data for 8/22/2018.

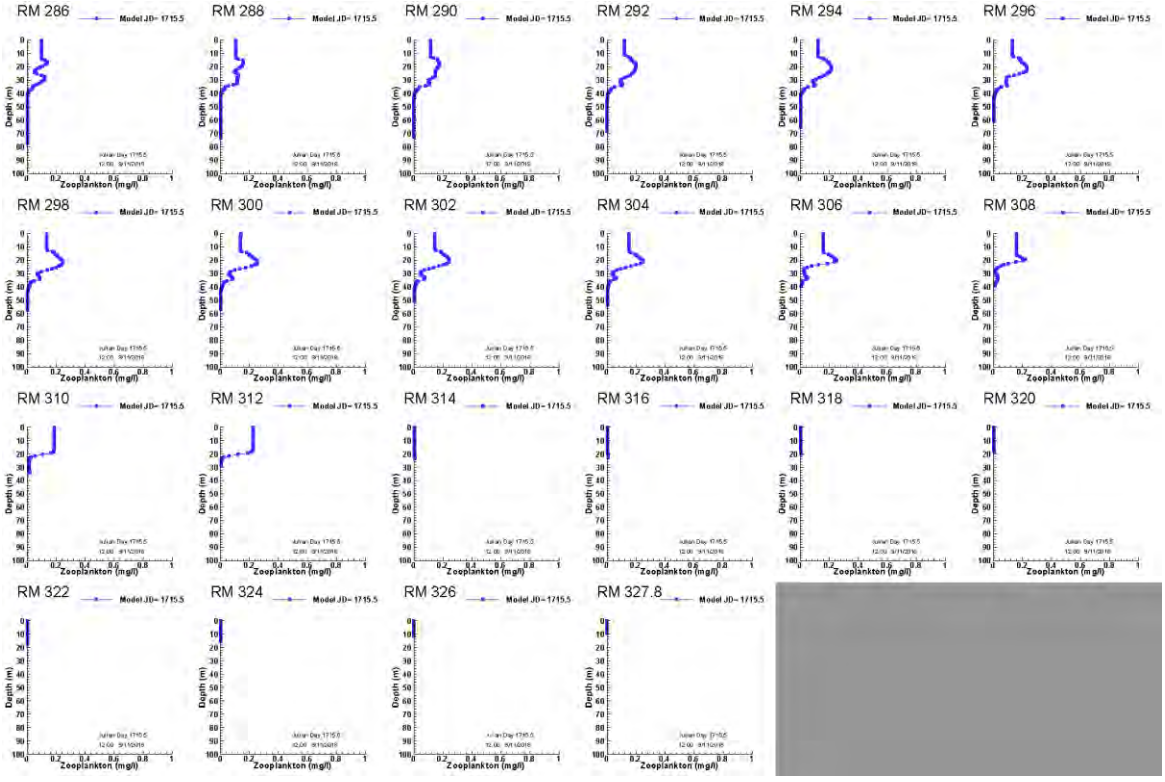


Figure 1420. Vertical profiles of zooplankton compared with data for 9/11/2018.

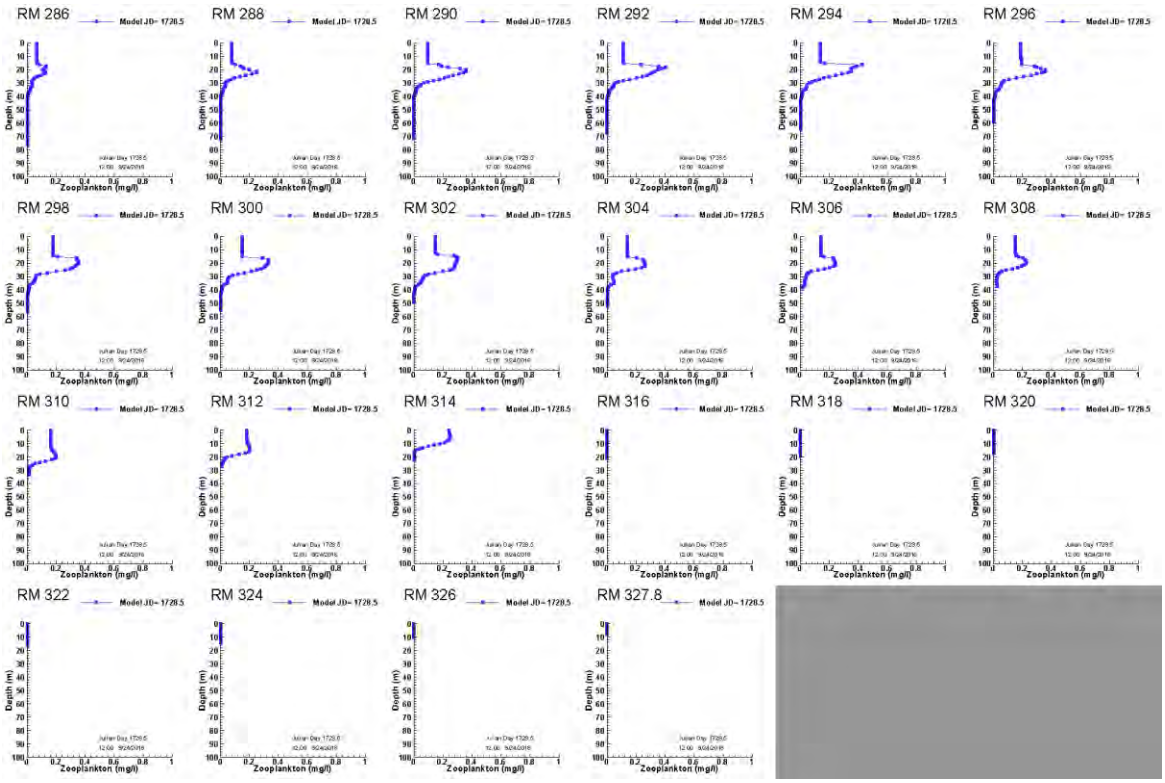


Figure 1421. Vertical profiles of zooplankton compared with data for 9/24/2018.

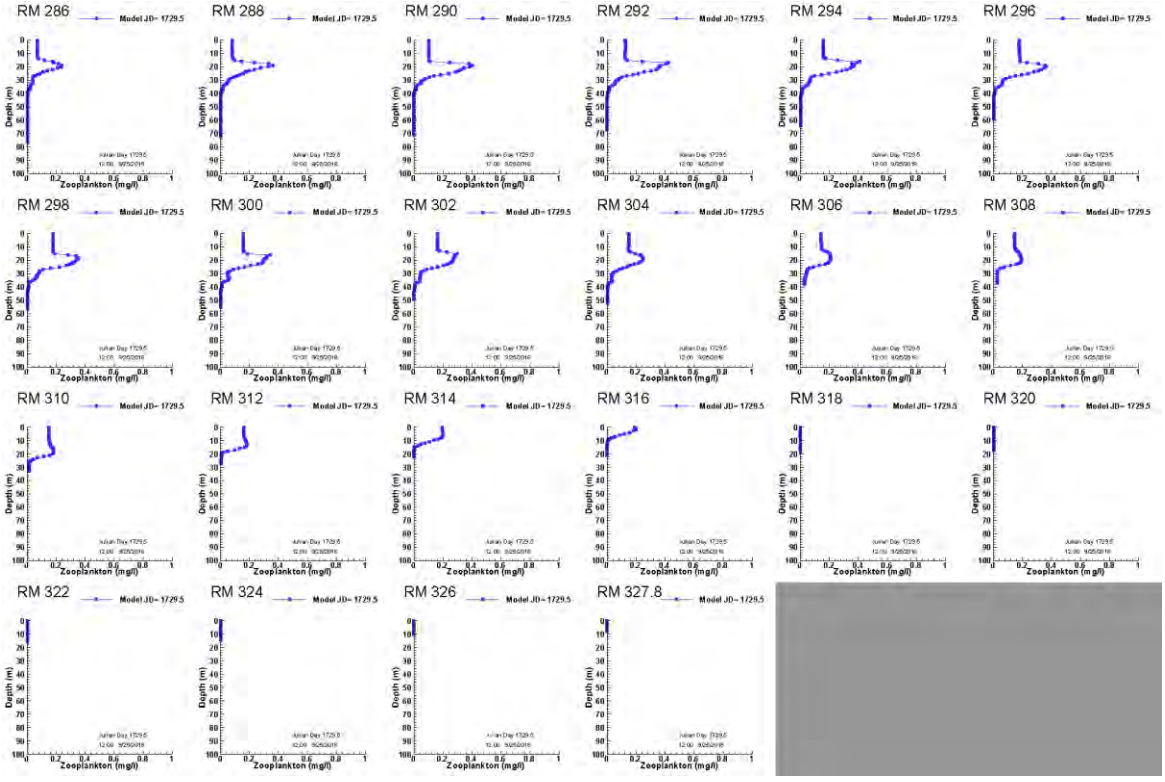


Figure 1422. Vertical profiles of zooplankton compared with data for 9/25/2018.

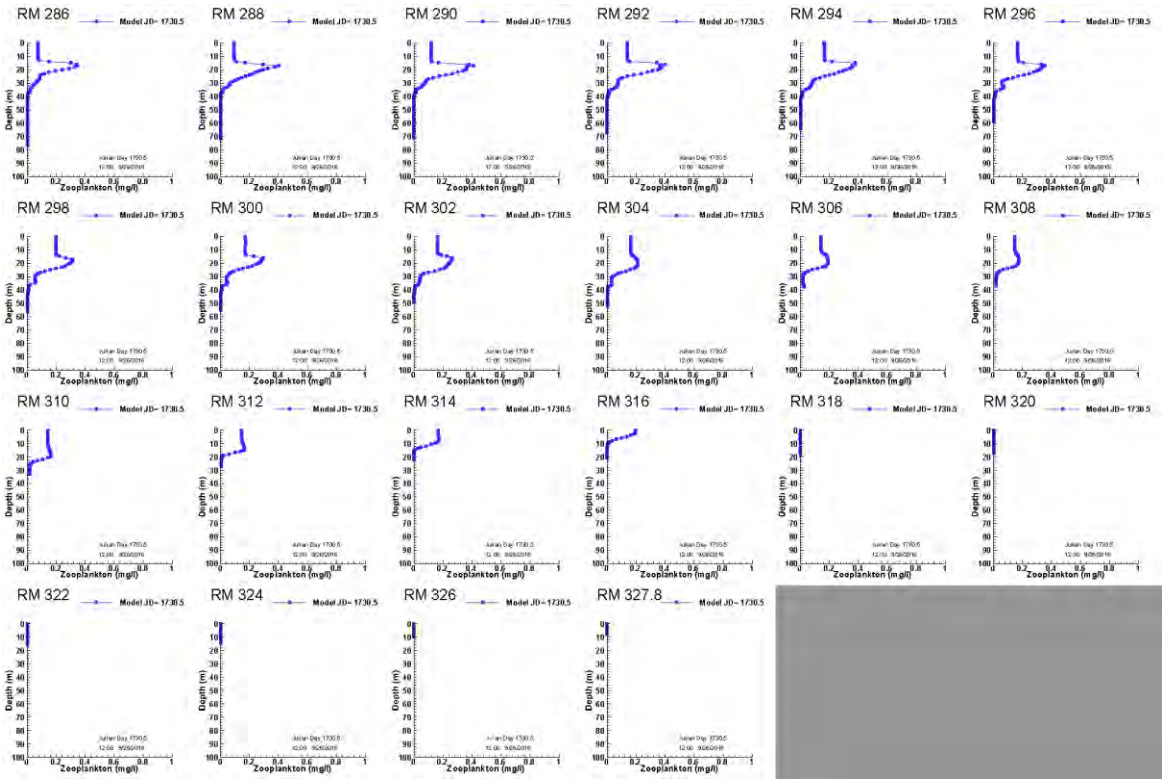


Figure 1423. Vertical profiles of zooplankton compared with data for 9/26/2018.

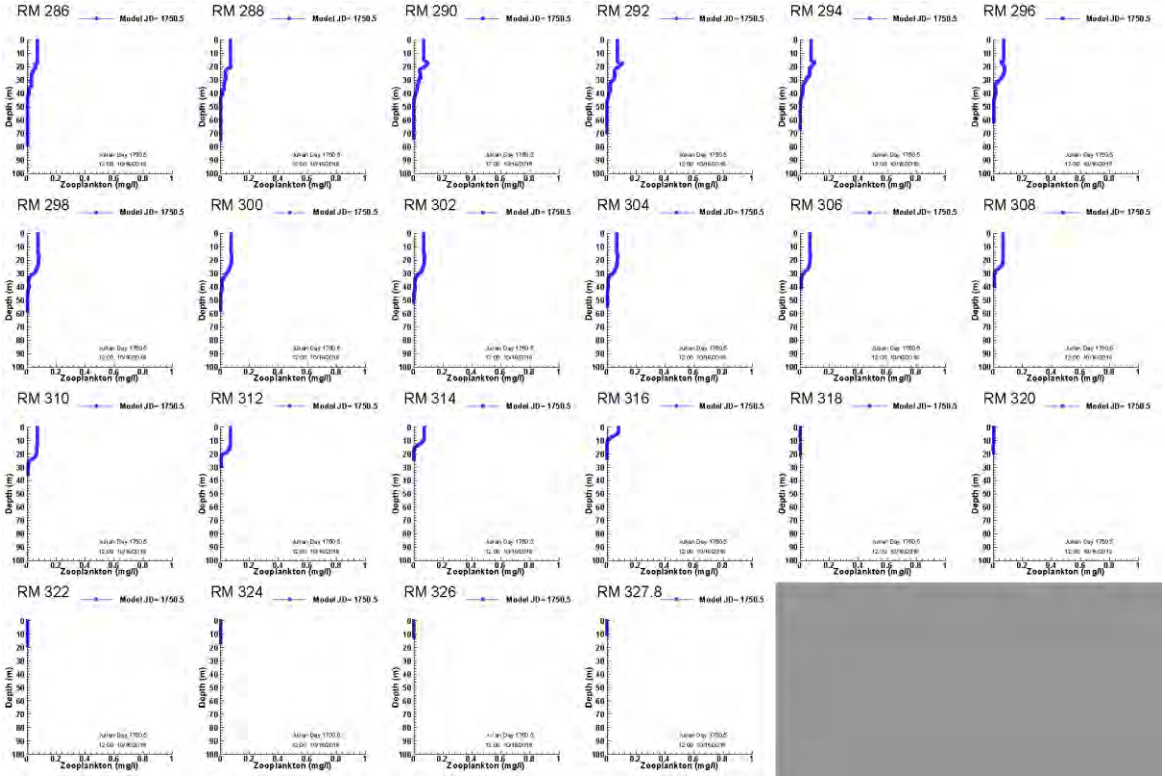


Figure 1424. Vertical profiles of zooplankton compared with data for 10/16/2018.

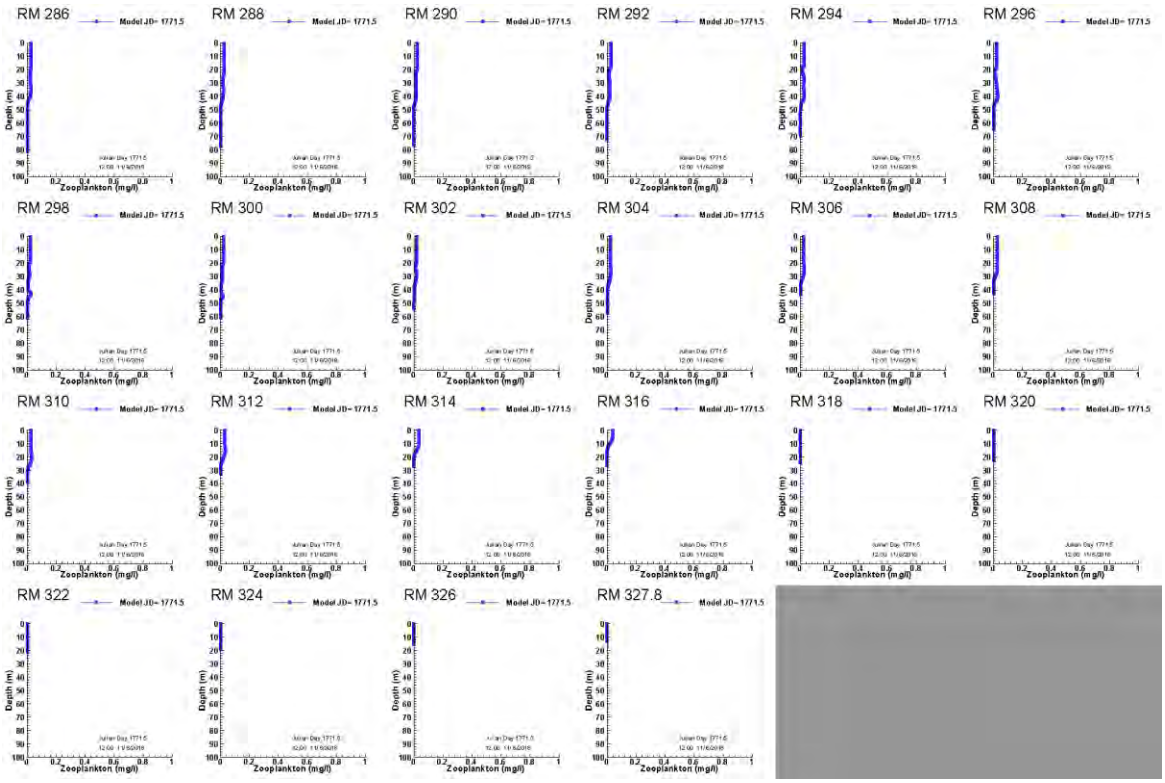


Figure 1425. Vertical profiles of zooplankton compared with data for 11/ 6/2018.

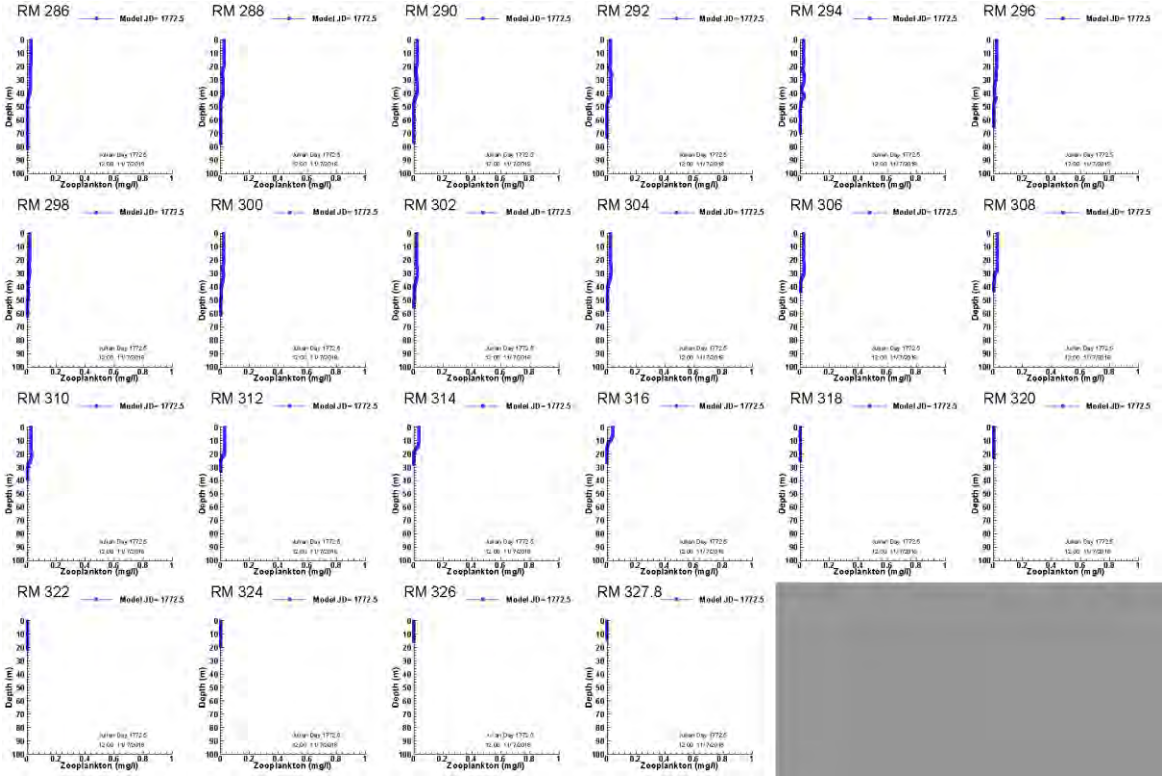


Figure 1426. Vertical profiles of zooplankton compared with data for 11/ 7/2018.

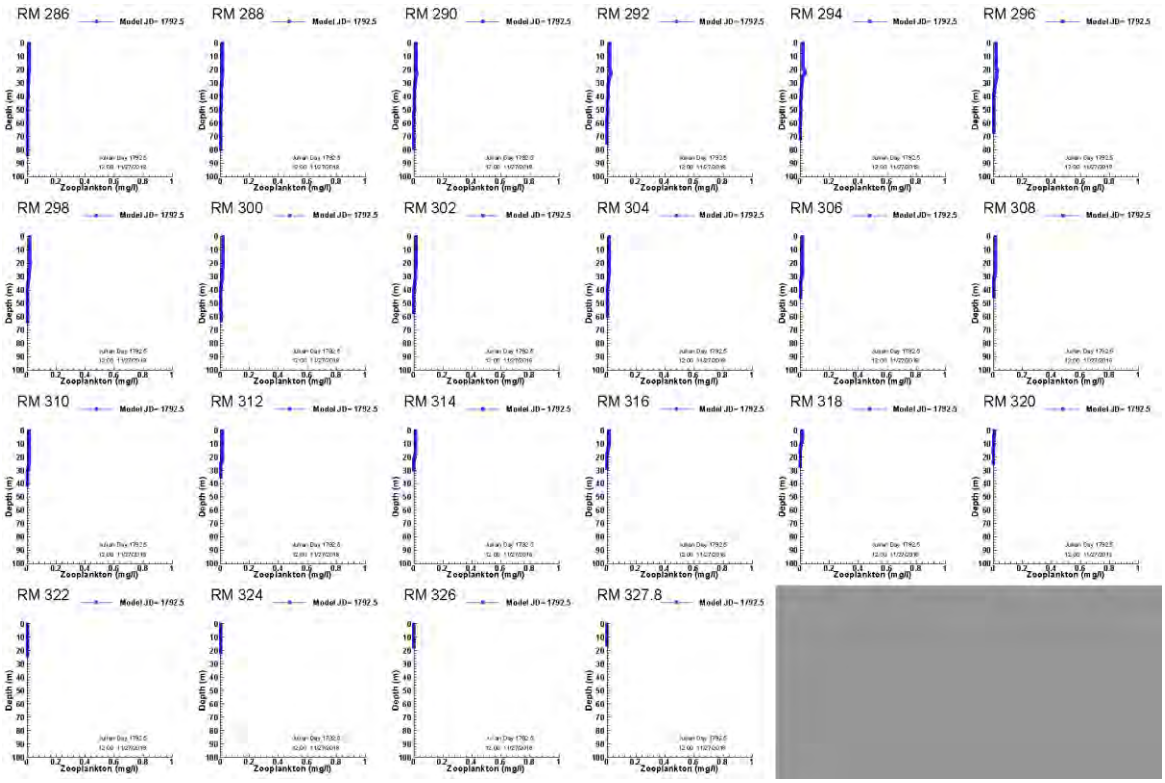


Figure 1427. Vertical profiles of zooplankton compared with data for 11/27/2018.

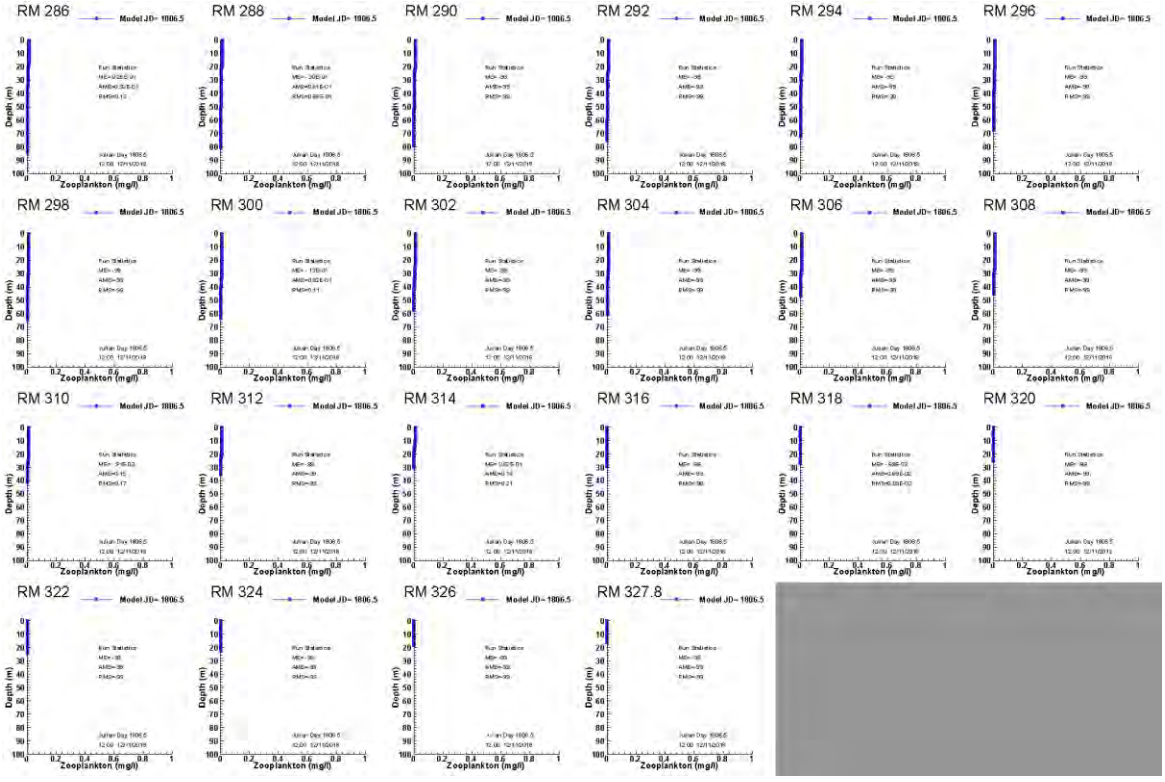


Figure 1428. Vertical profiles of zooplankton compared with data for 12/11/2018.

Dissolved Organic Carbon

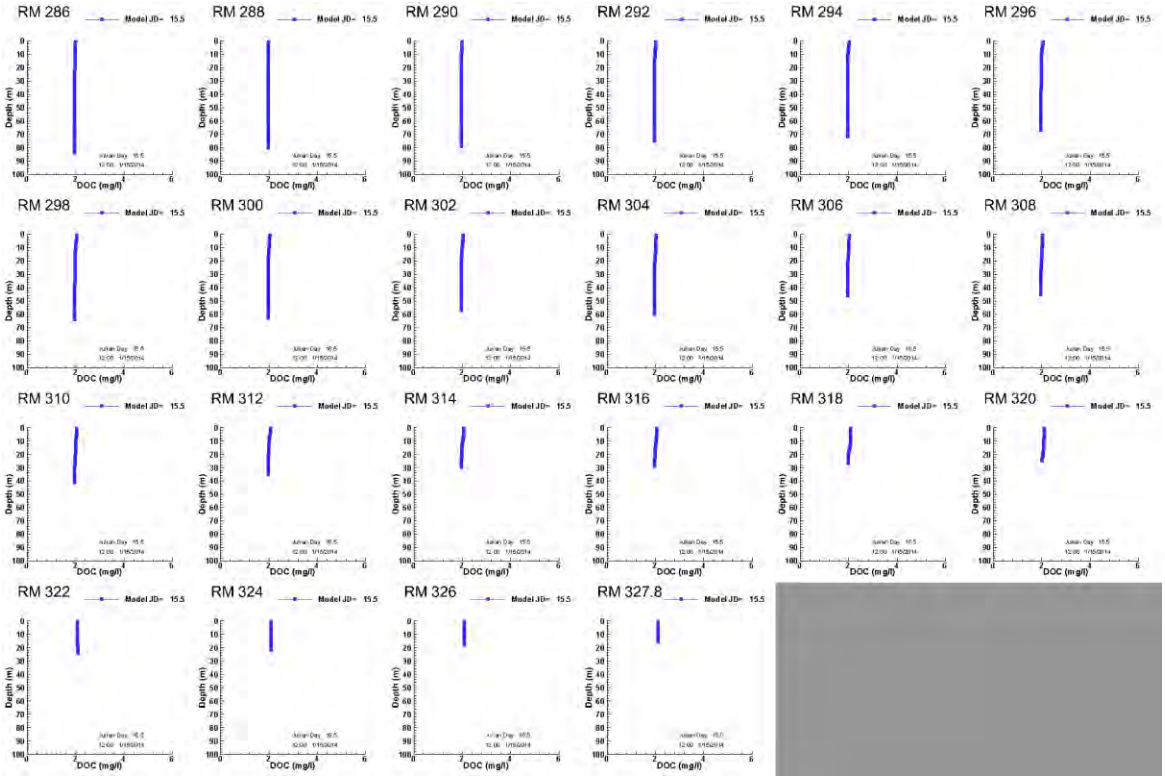


Figure 1429. Vertical profiles of DOC compared with data for 1/15/2014.

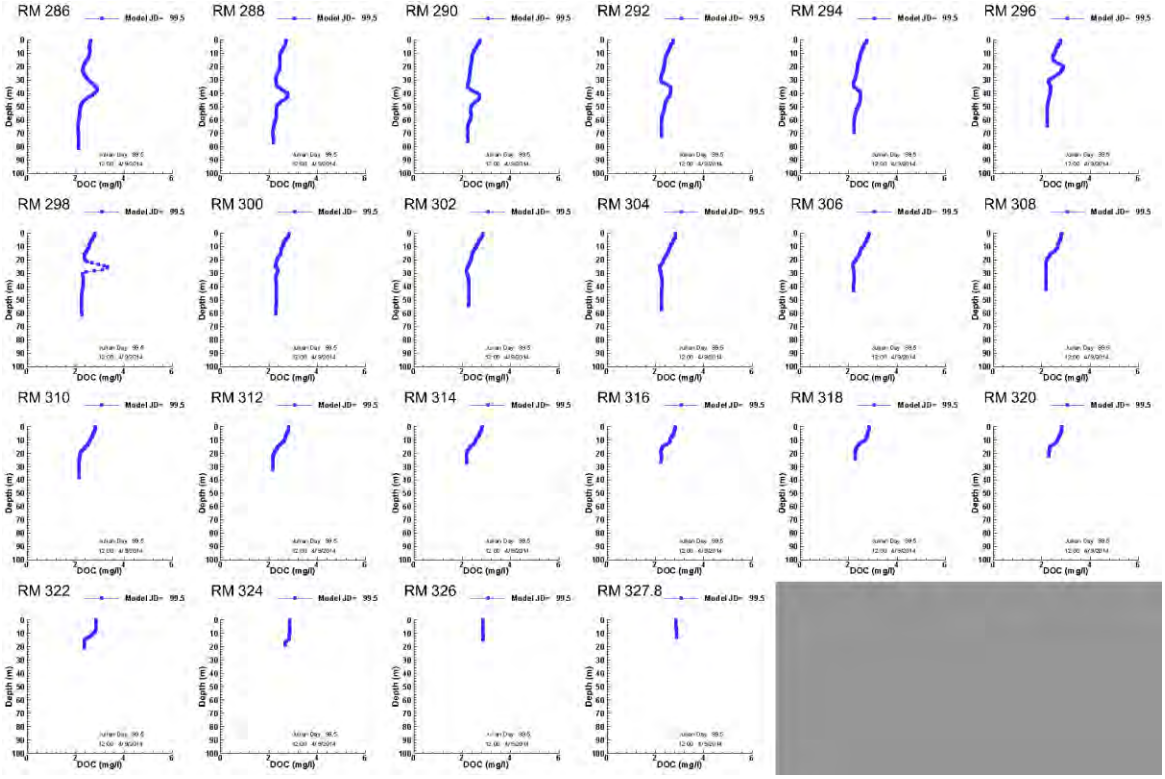


Figure 1430. Vertical profiles of DOC compared with data for 4/ 9/2014.

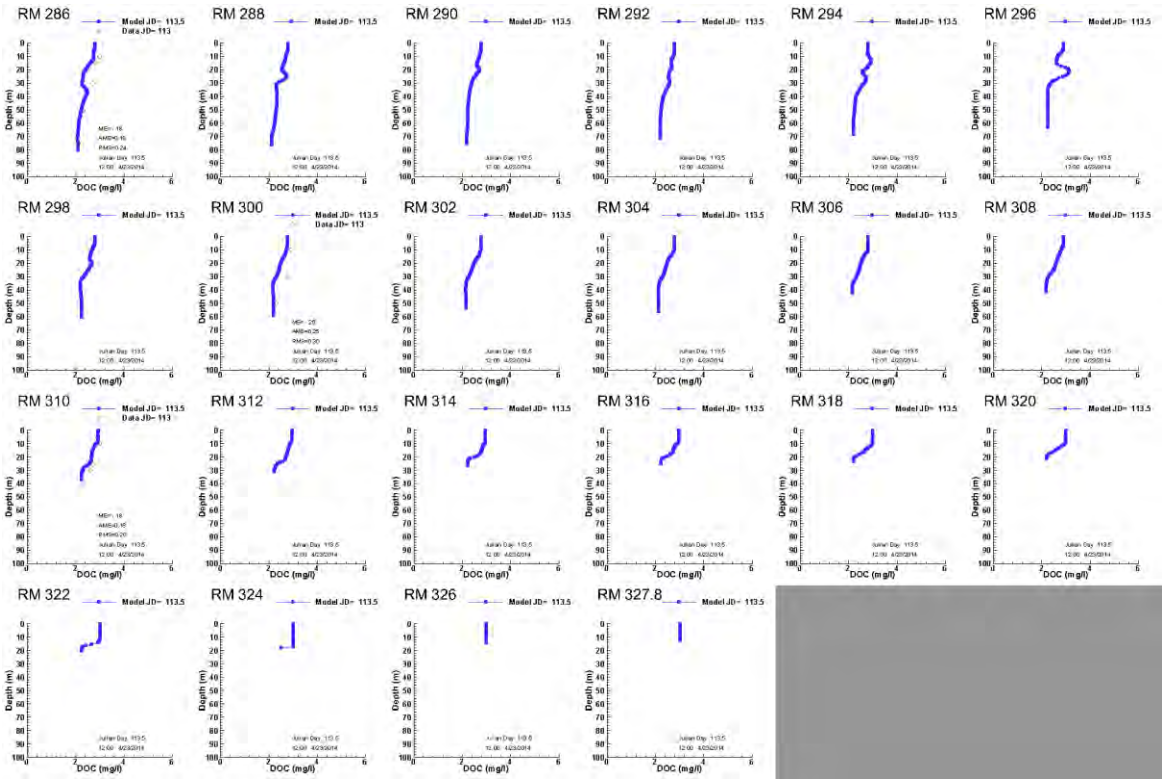


Figure 1431. Vertical profiles of DOC compared with data for 4/23/2014.

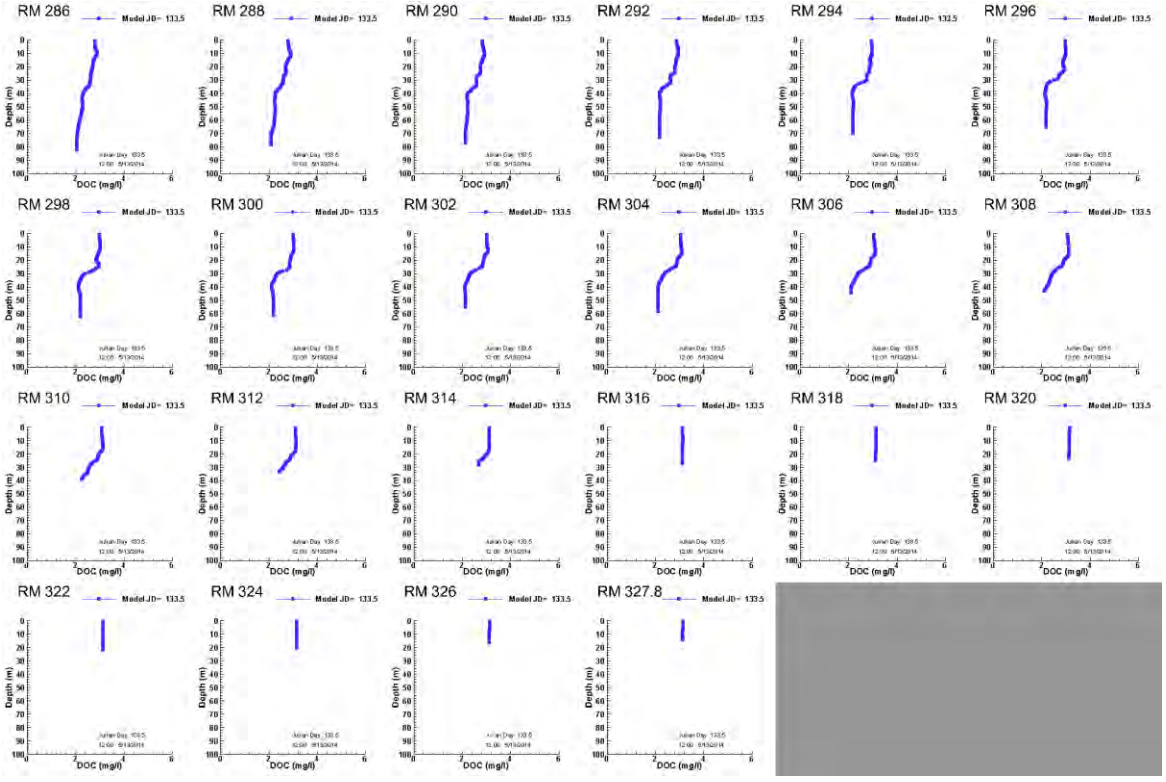


Figure 1432. Vertical profiles of DOC compared with data for 5/13/2014.

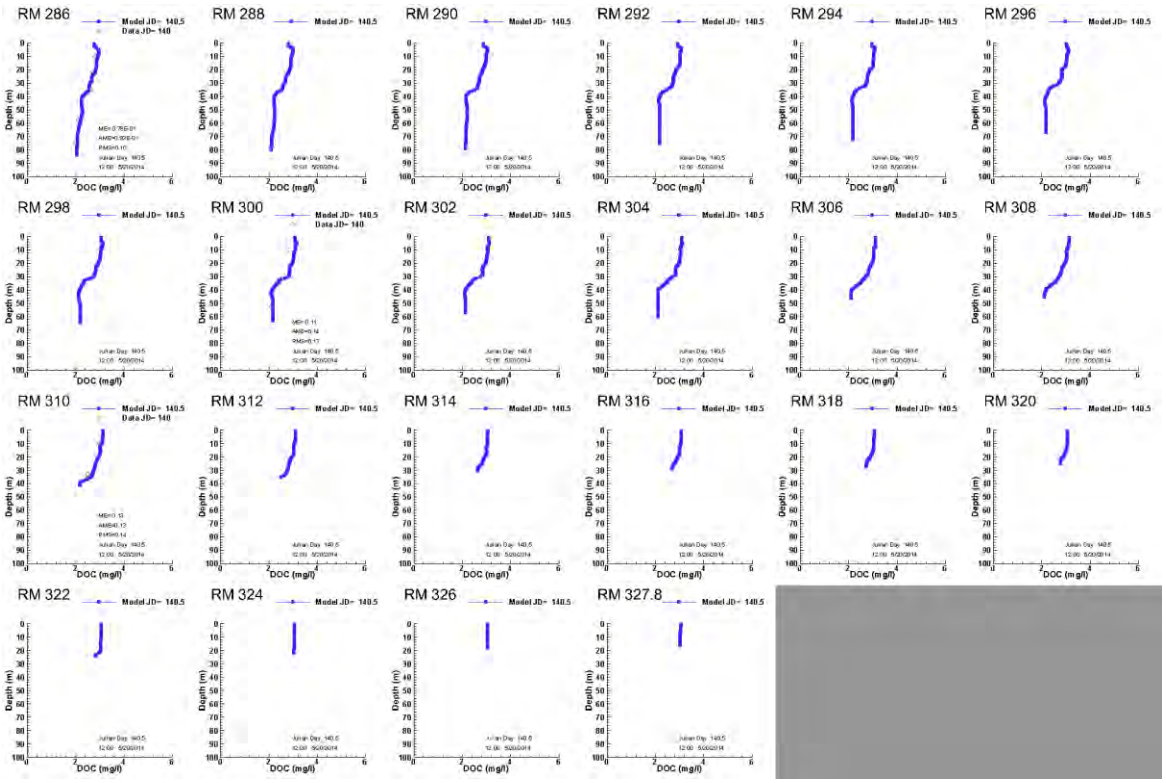


Figure 1433. Vertical profiles of DOC compared with data for 5/20/2014.

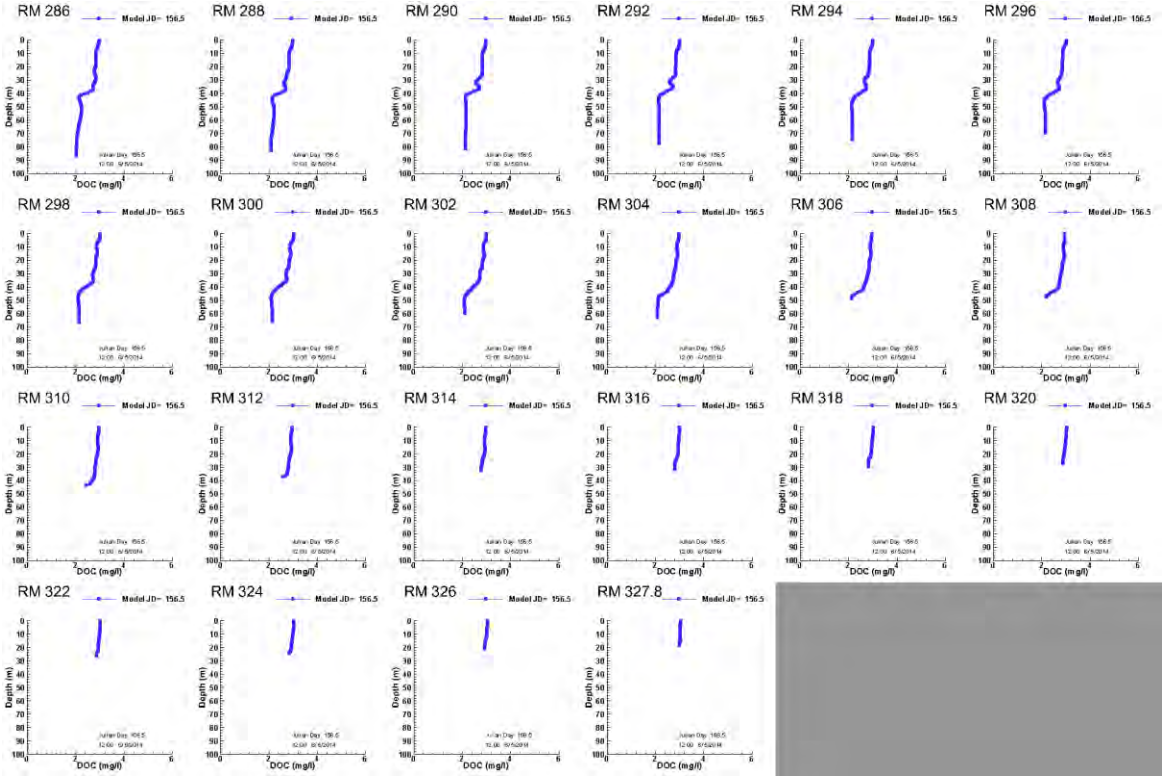


Figure 1434. Vertical profiles of DOC compared with data for 6/ 5/2014.

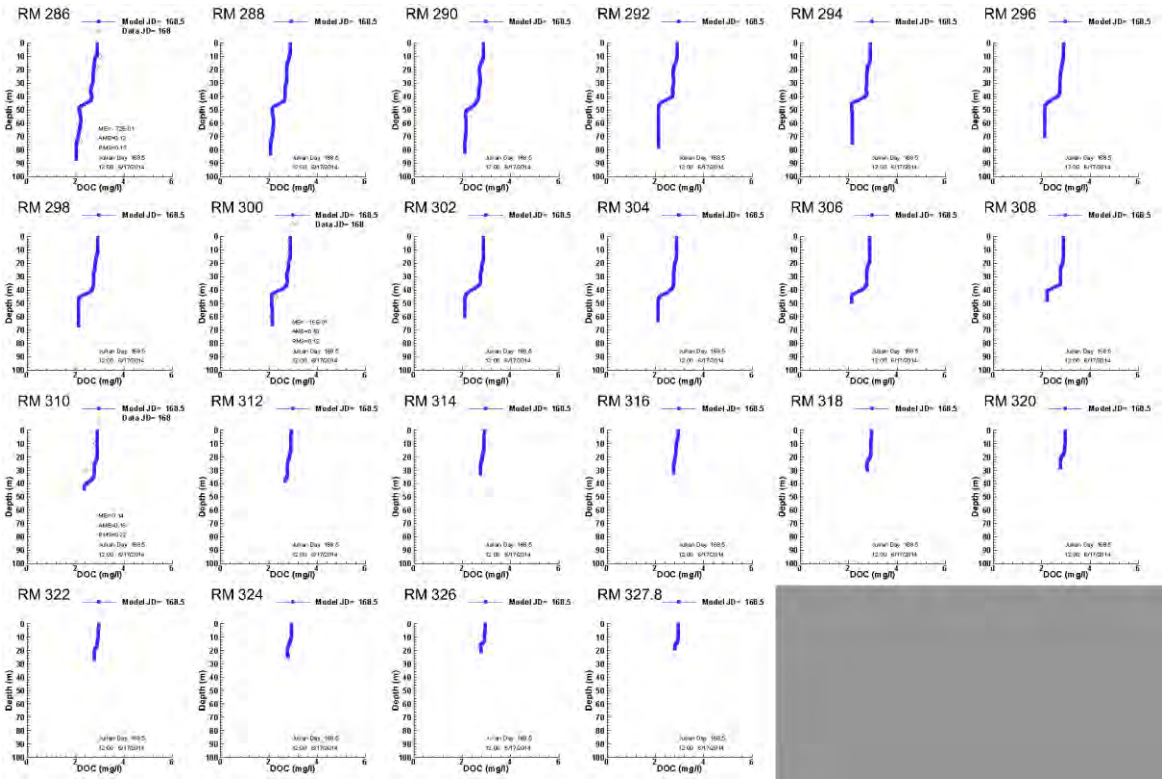


Figure 1435. Vertical profiles of DOC compared with data for 6/17/2014.

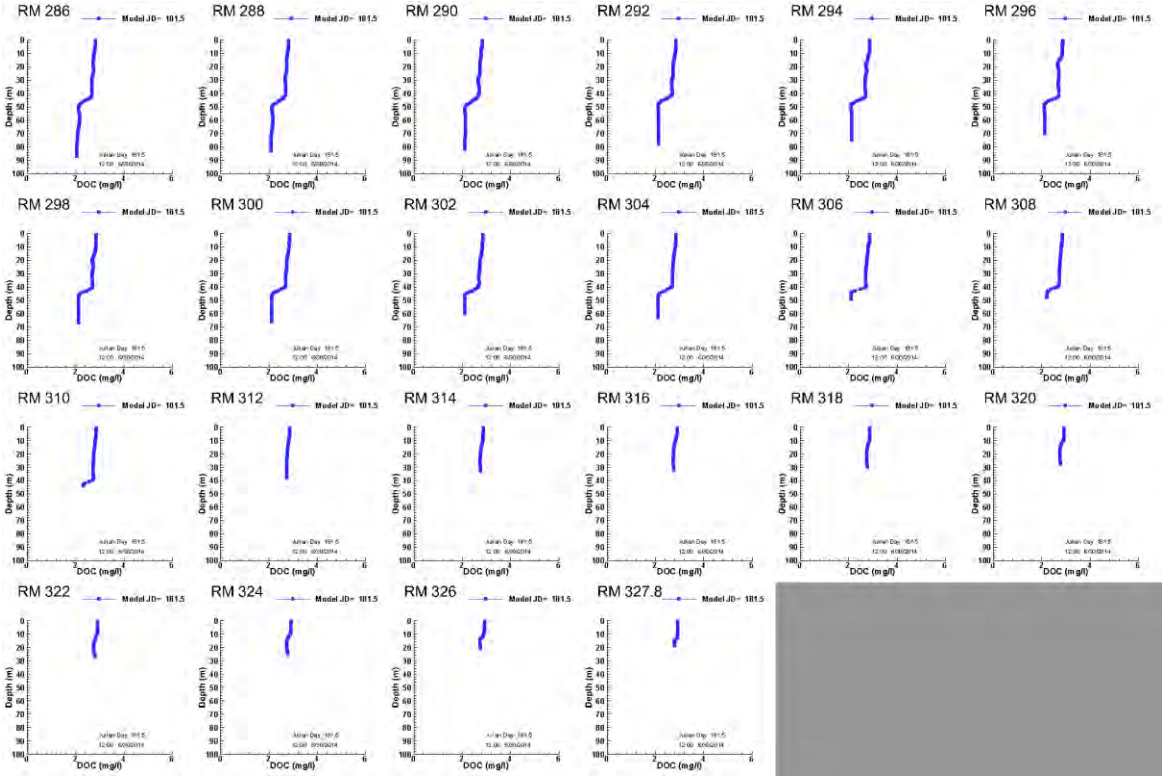


Figure 1436. Vertical profiles of DOC compared with data for 6/30/2014.

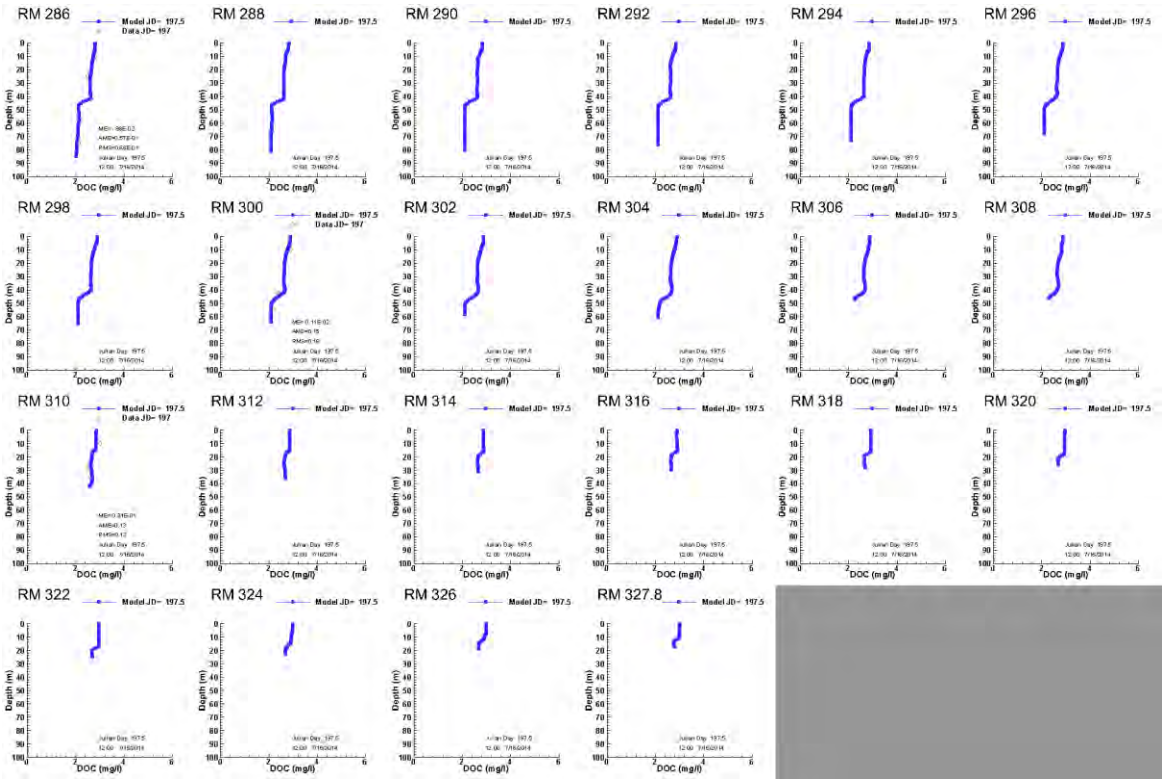


Figure 1437. Vertical profiles of DOC compared with data for 7/16/2014.

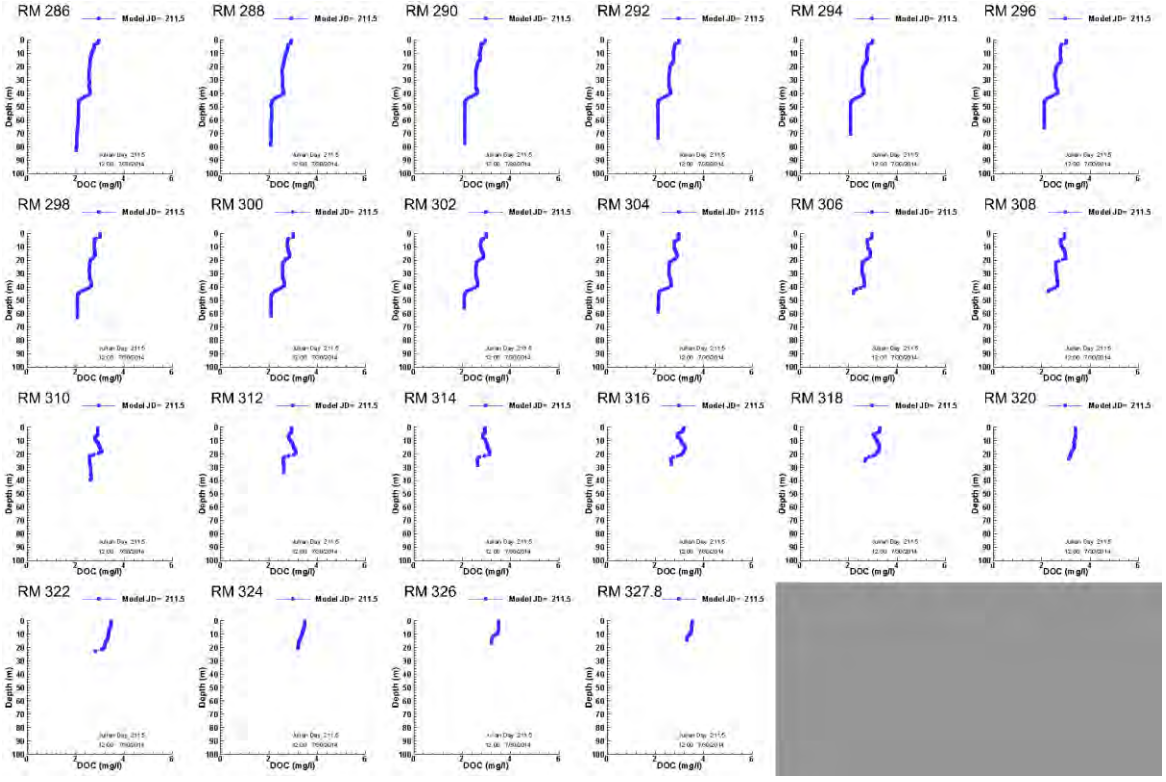


Figure 1438. Vertical profiles of DOC compared with data for 7/30/2014.

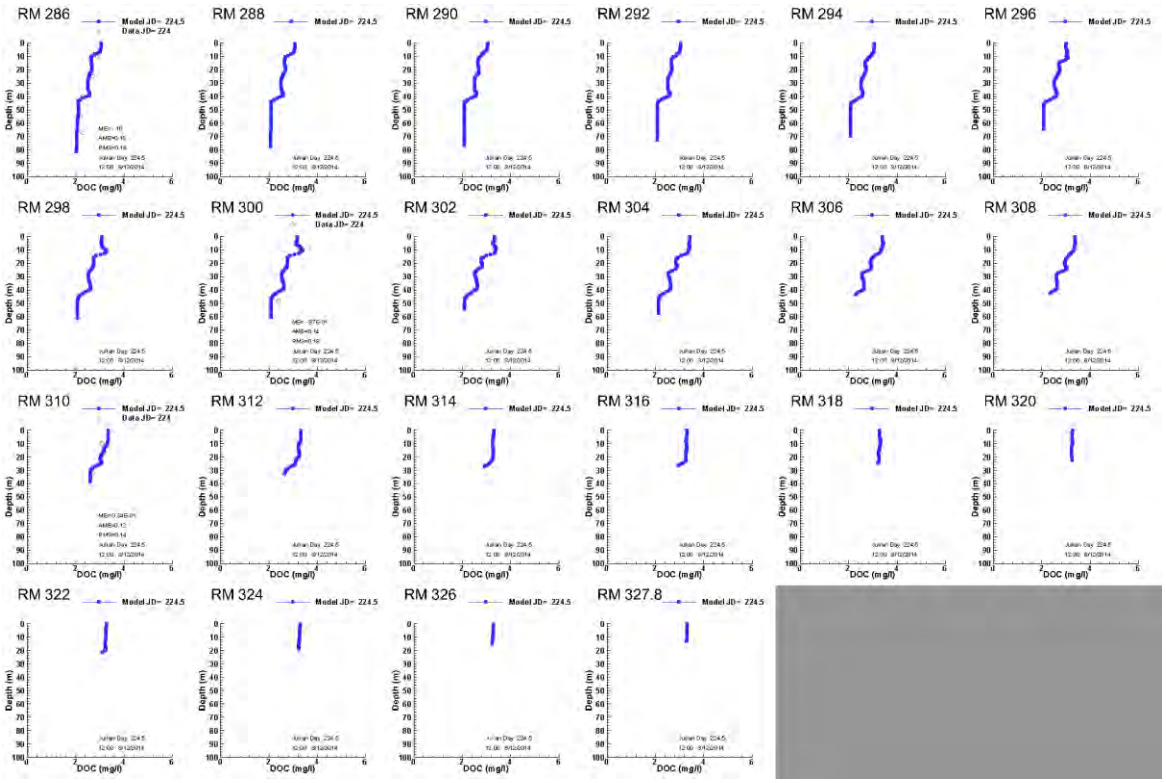


Figure 1439. Vertical profiles of DOC compared with data for 8/12/2014.

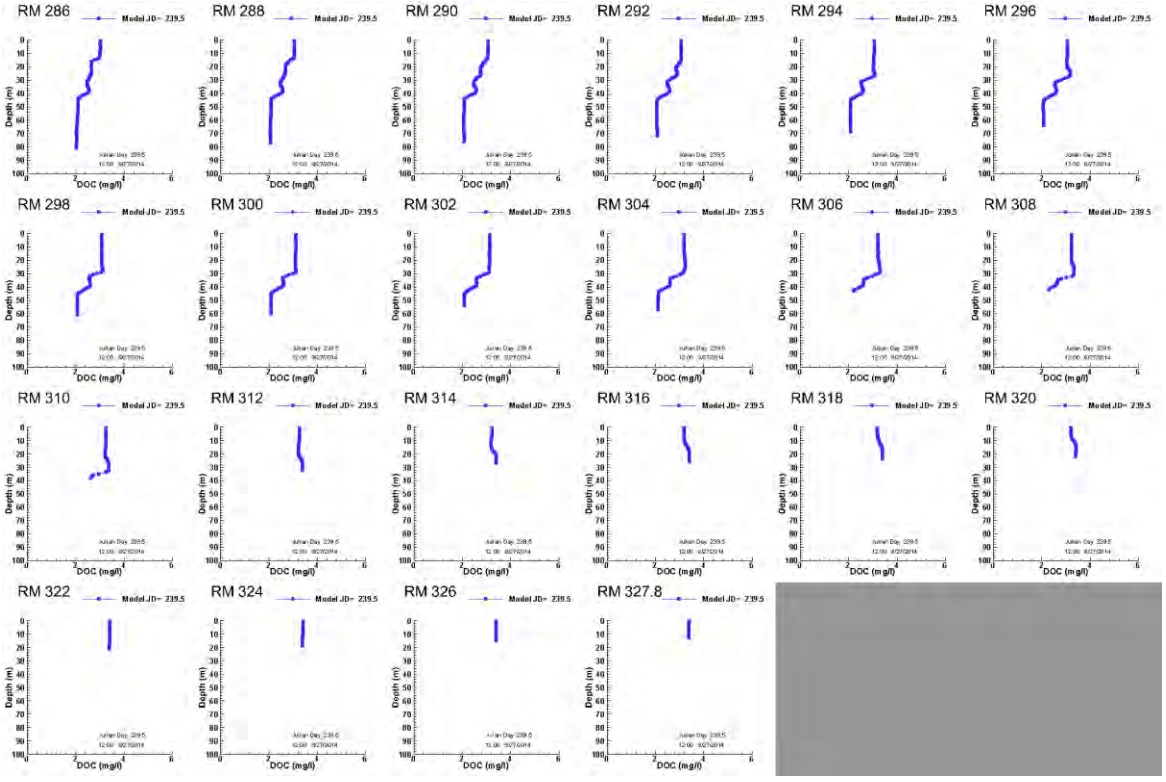


Figure 1440. Vertical profiles of DOC compared with data for 8/27/2014.

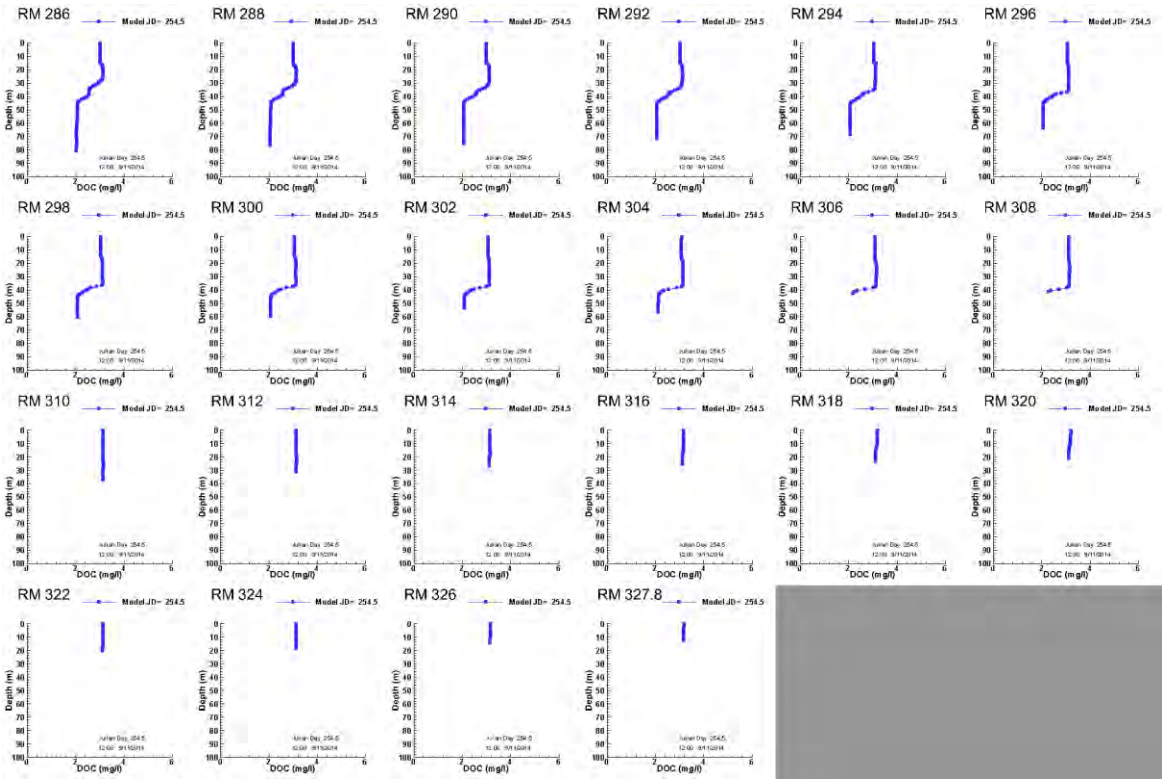


Figure 1441. Vertical profiles of DOC compared with data for 9/11/2014.

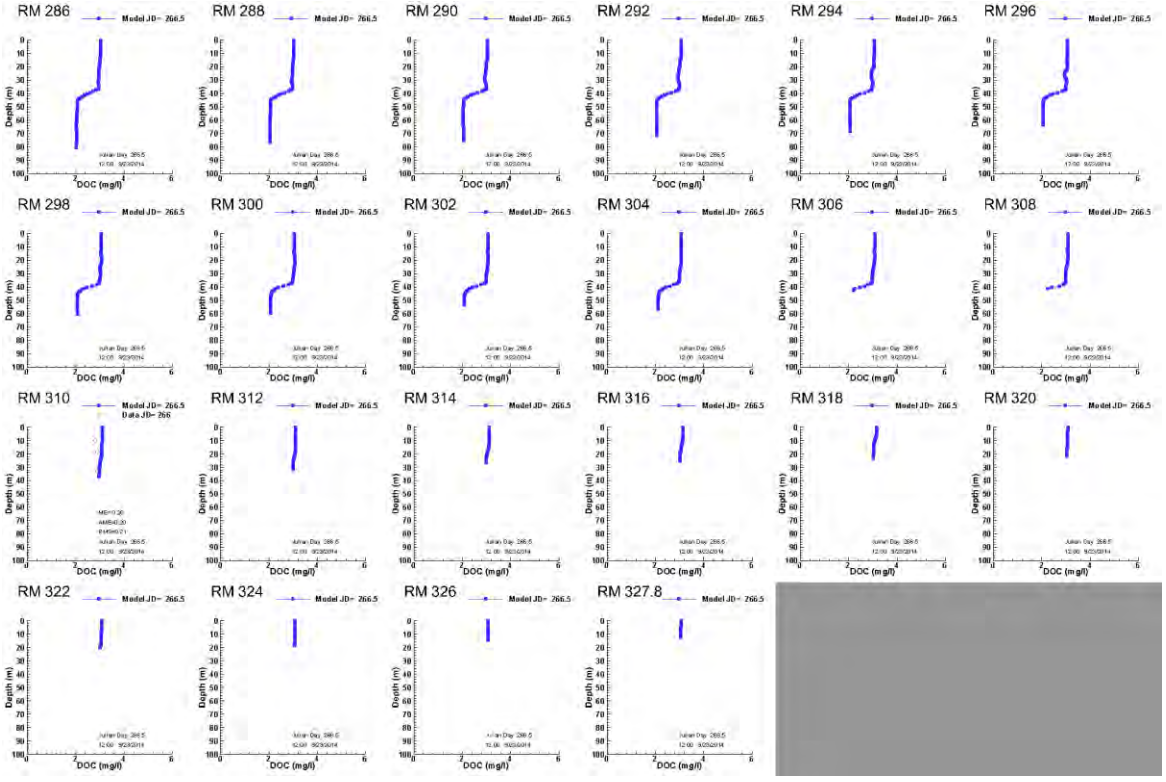


Figure 1442. Vertical profiles of DOC compared with data for 9/23/2014.

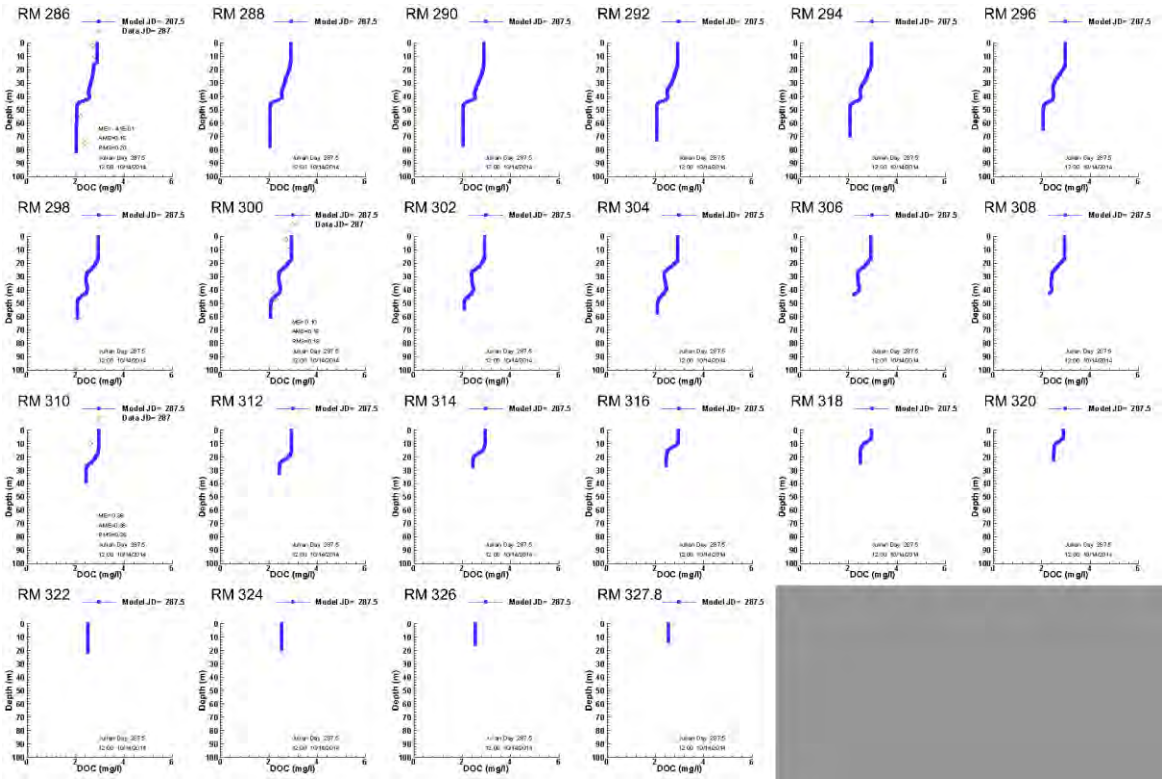


Figure 1443. Vertical profiles of DOC compared with data for 10/14/2014.

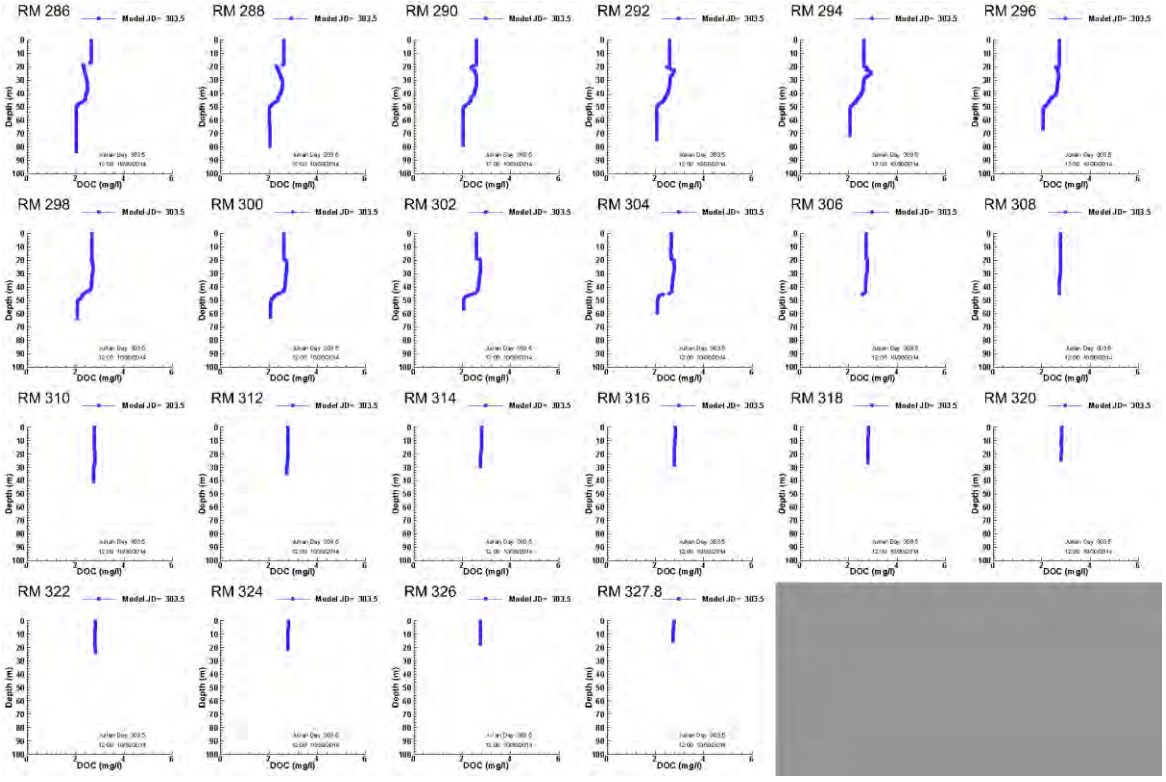


Figure 1444. Vertical profiles of DOC compared with data for 10/30/2014.

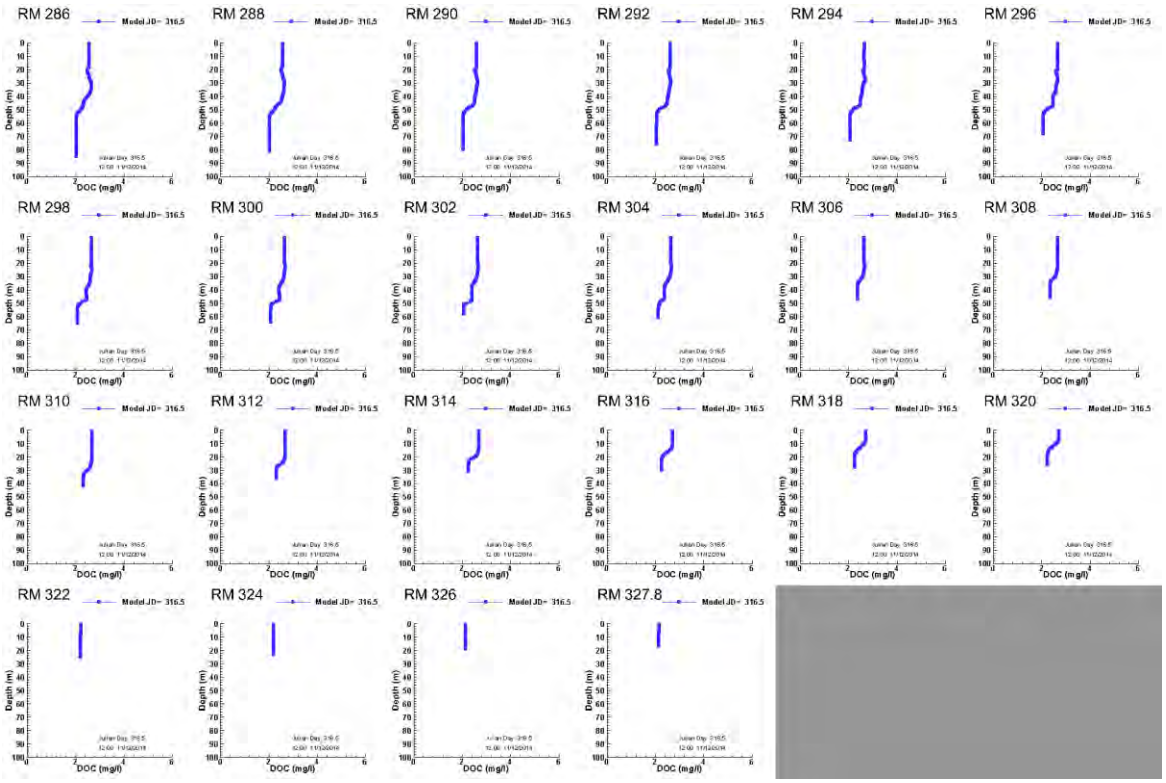


Figure 1445. Vertical profiles of DOC compared with data for 11/12/2014.

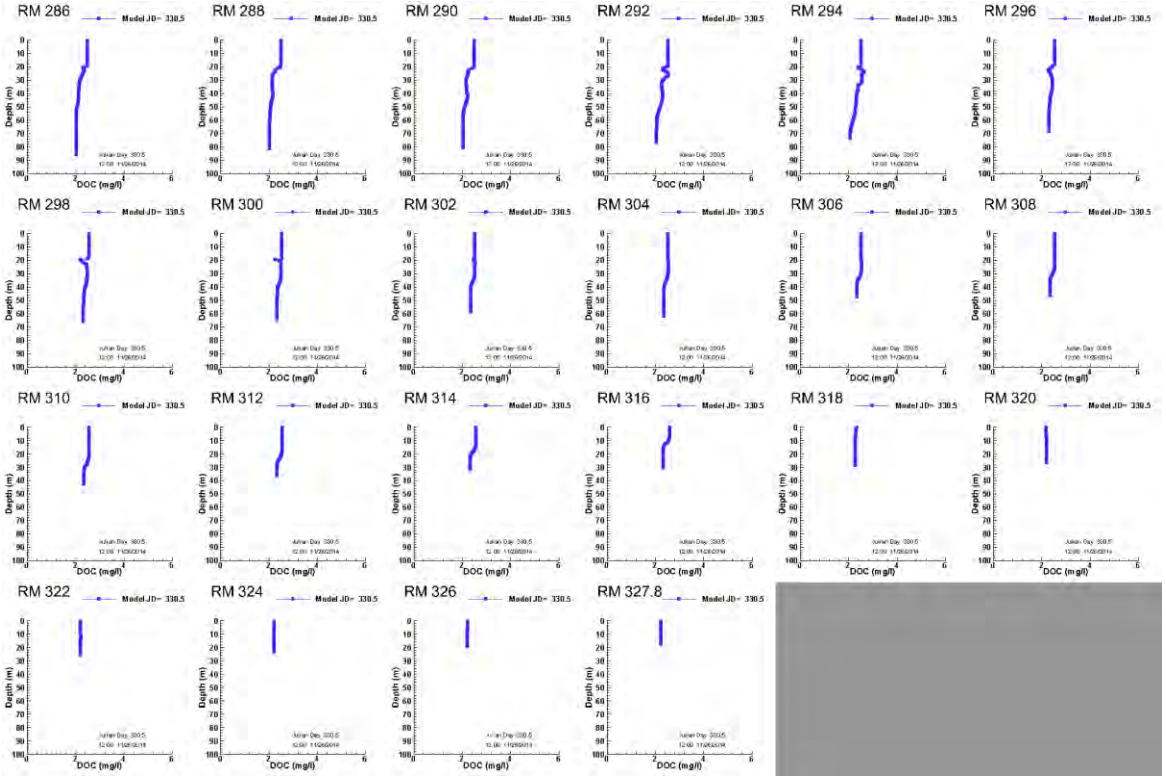


Figure 1446. Vertical profiles of DOC compared with data for 11/26/2014.

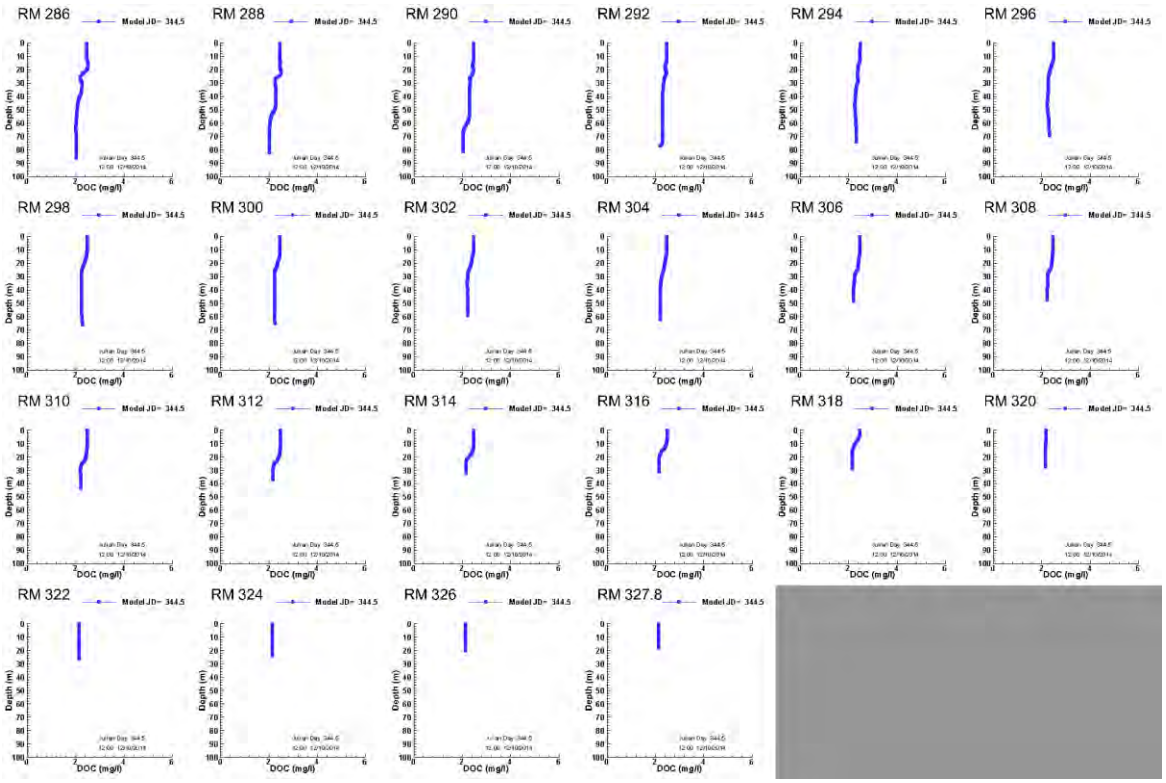


Figure 1447. Vertical profiles of DOC compared with data for 12/10/2014.

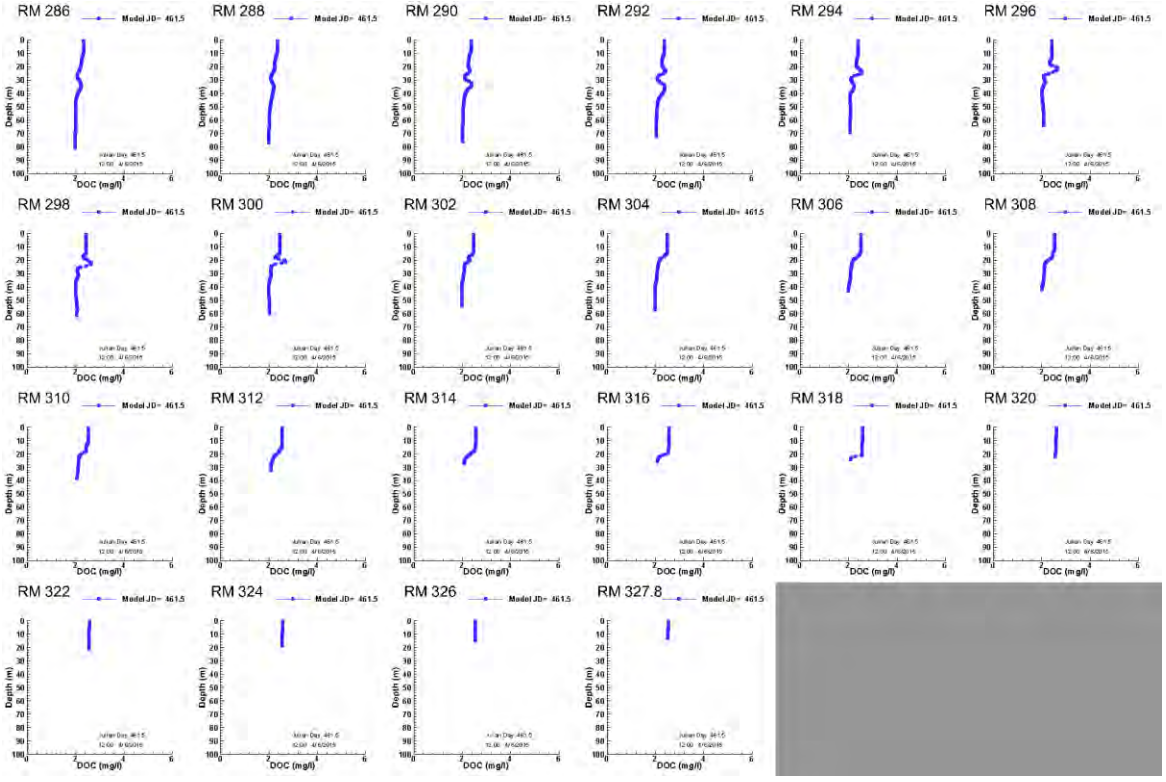


Figure 1448. Vertical profiles of DOC compared with data for 4/ 6/2015.

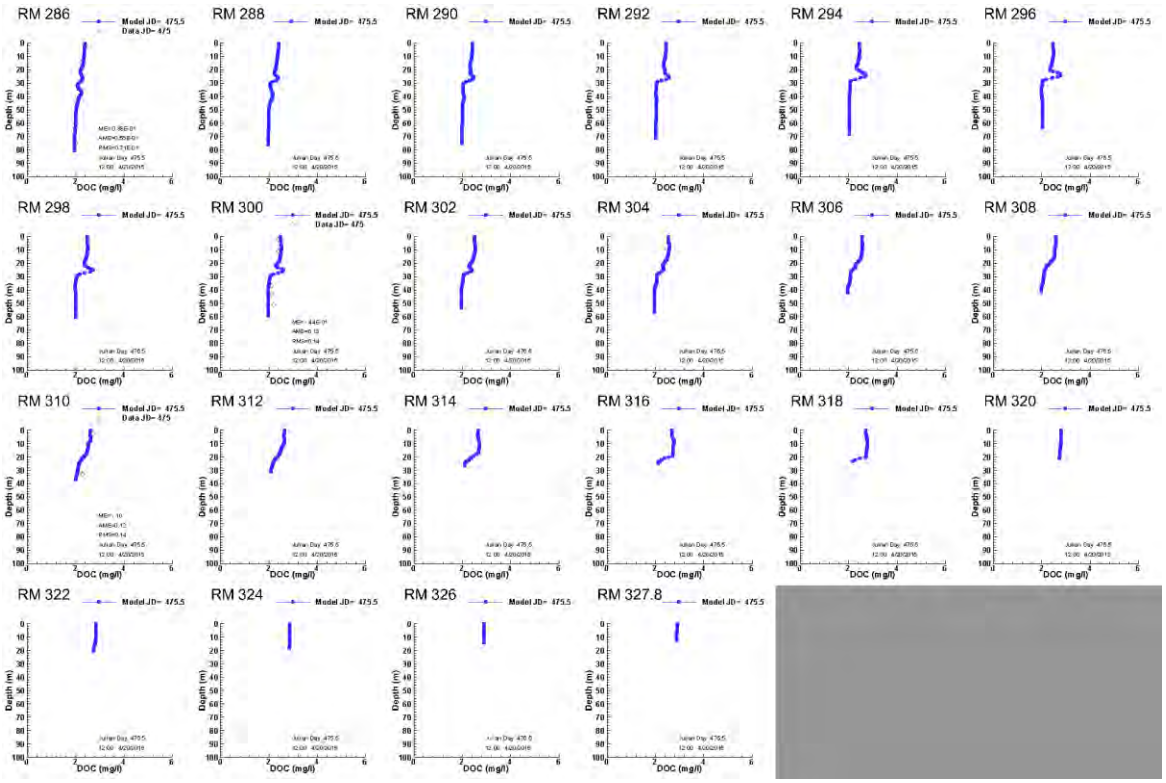


Figure 1449. Vertical profiles of DOC compared with data for 4/20/2015.

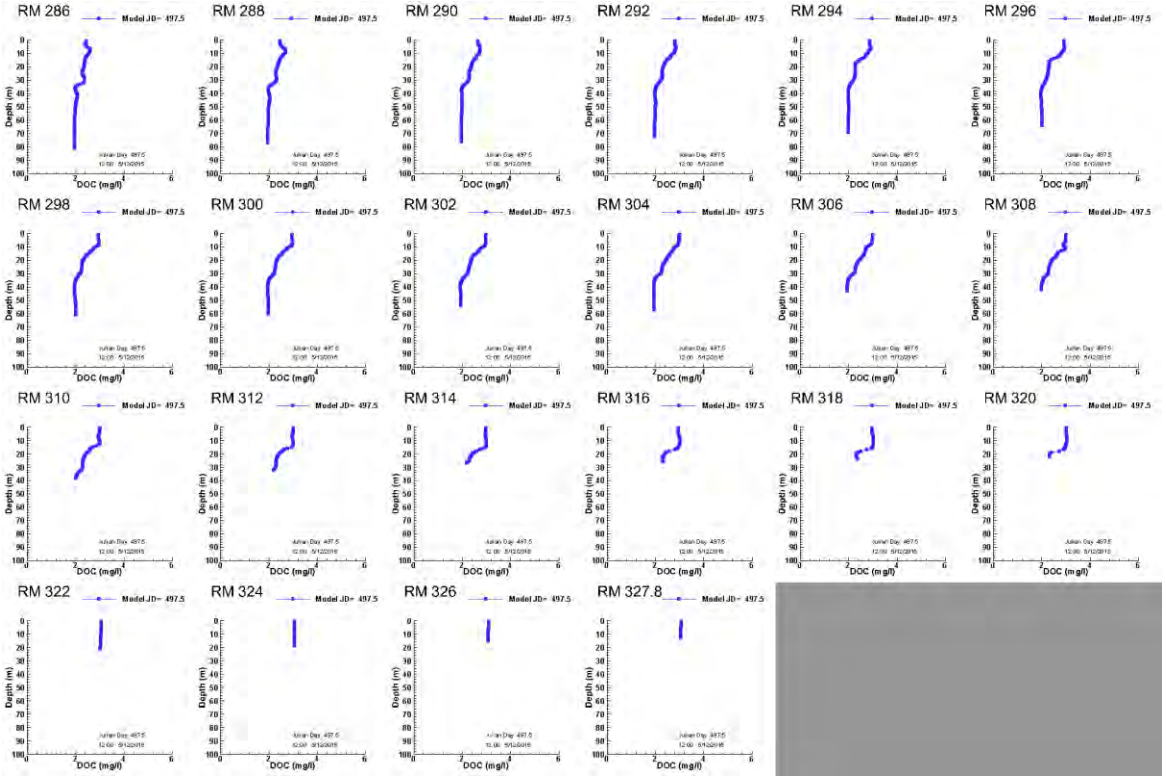


Figure 1450. Vertical profiles of DOC compared with data for 5/12/2015.

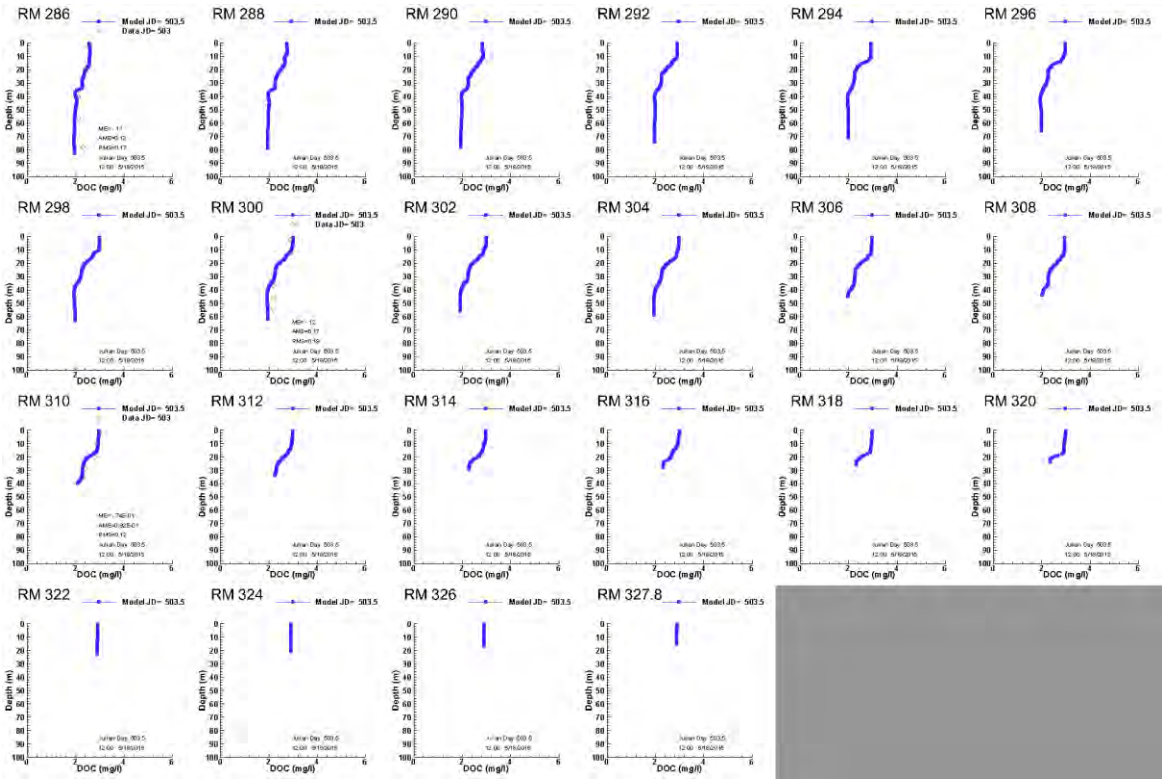


Figure 1451. Vertical profiles of DOC compared with data for 5/18/2015.

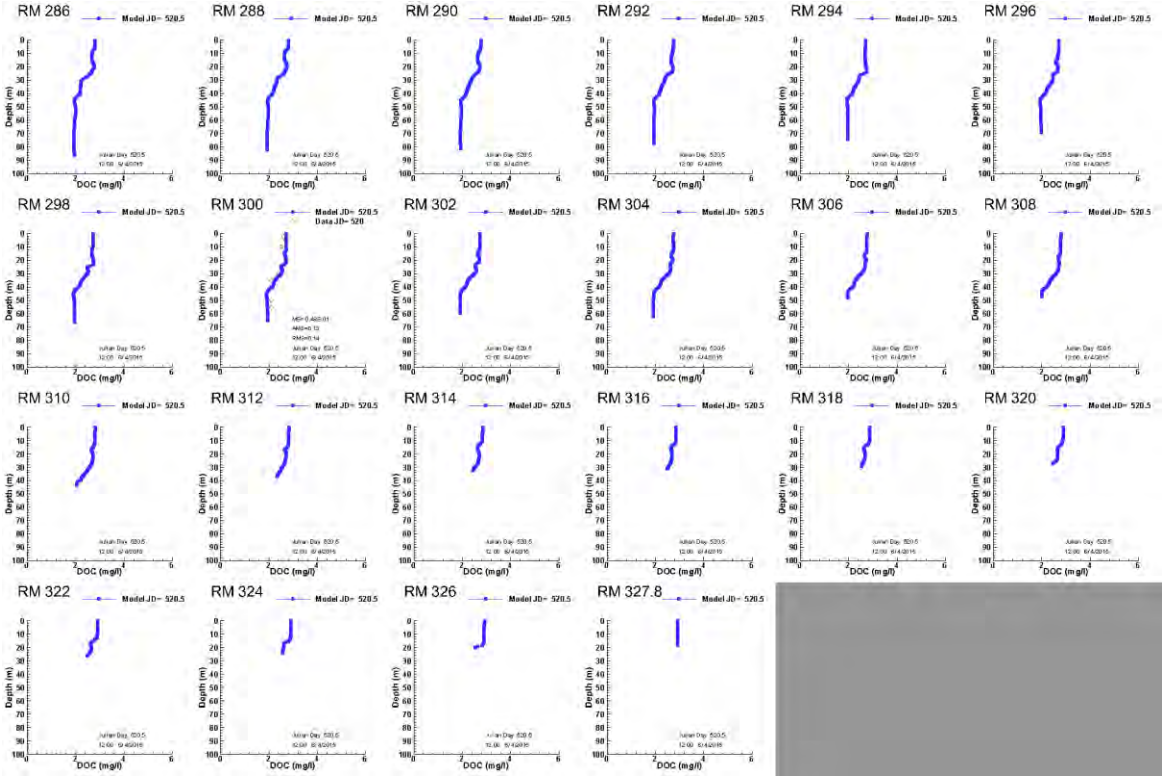


Figure 1452. Vertical profiles of DOC compared with data for 6/ 4/2015.

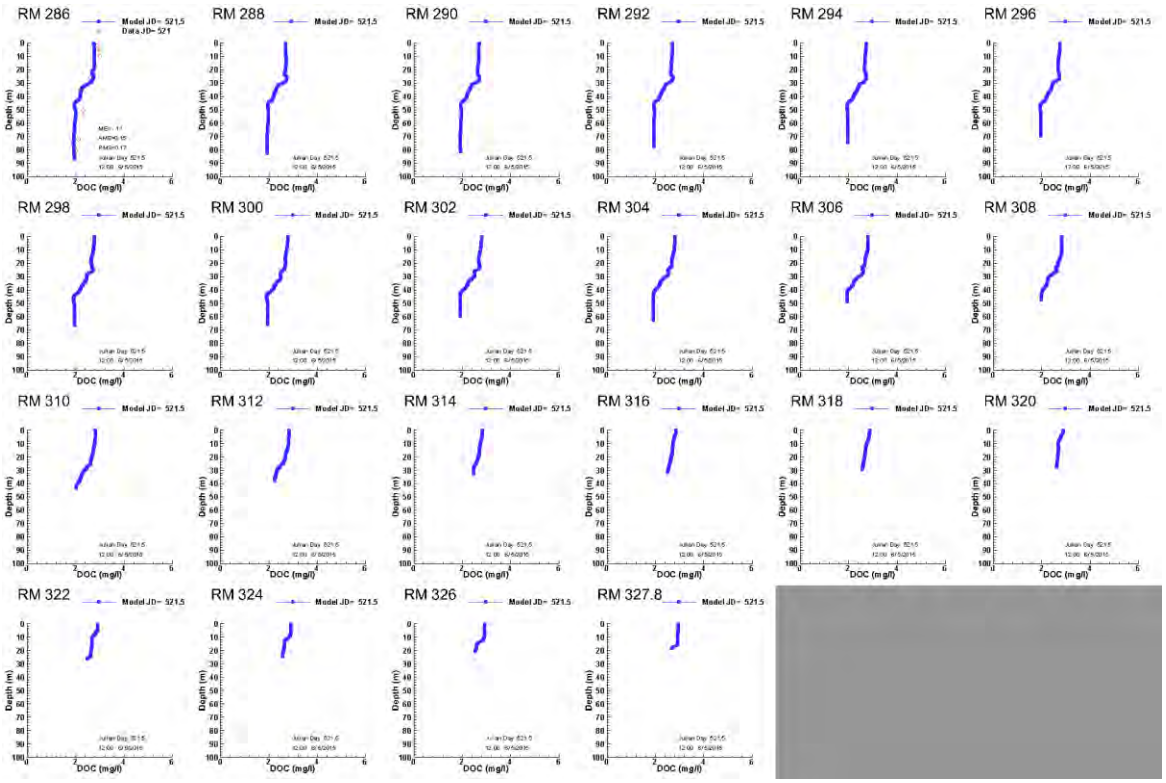


Figure 1453. Vertical profiles of DOC compared with data for 6/ 5/2015.

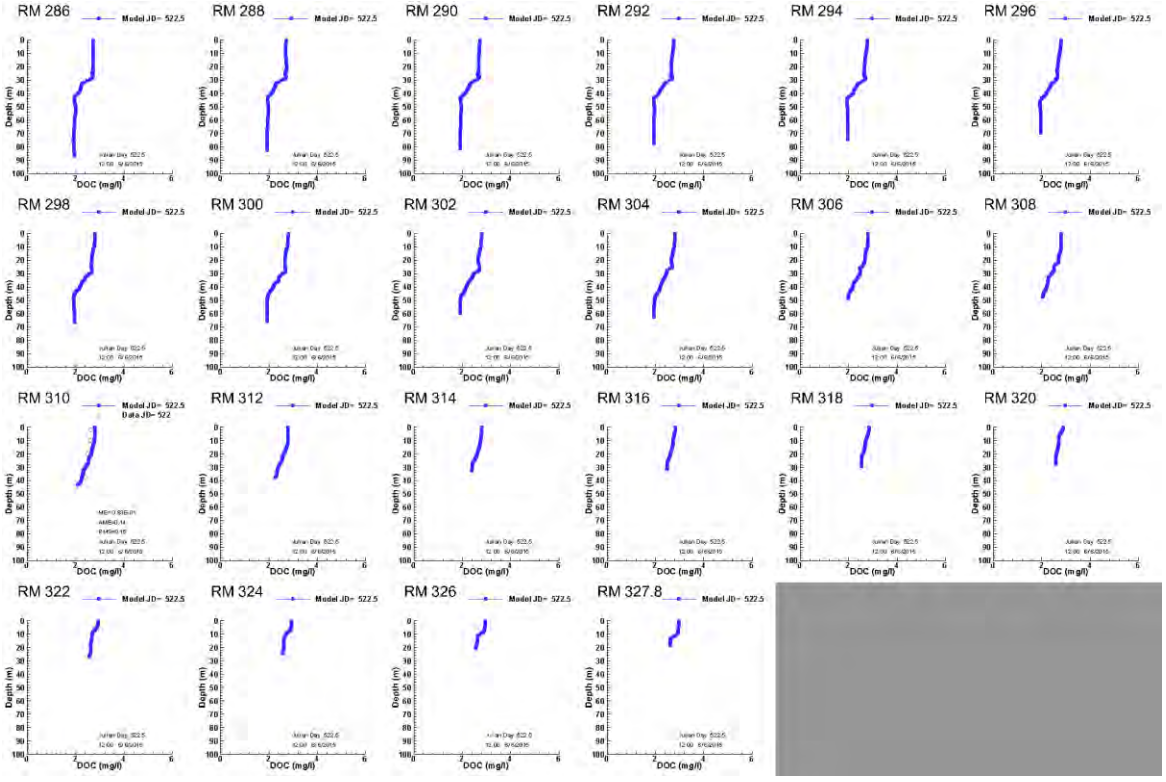


Figure 1454. Vertical profiles of DOC compared with data for 6/ 6/2015.

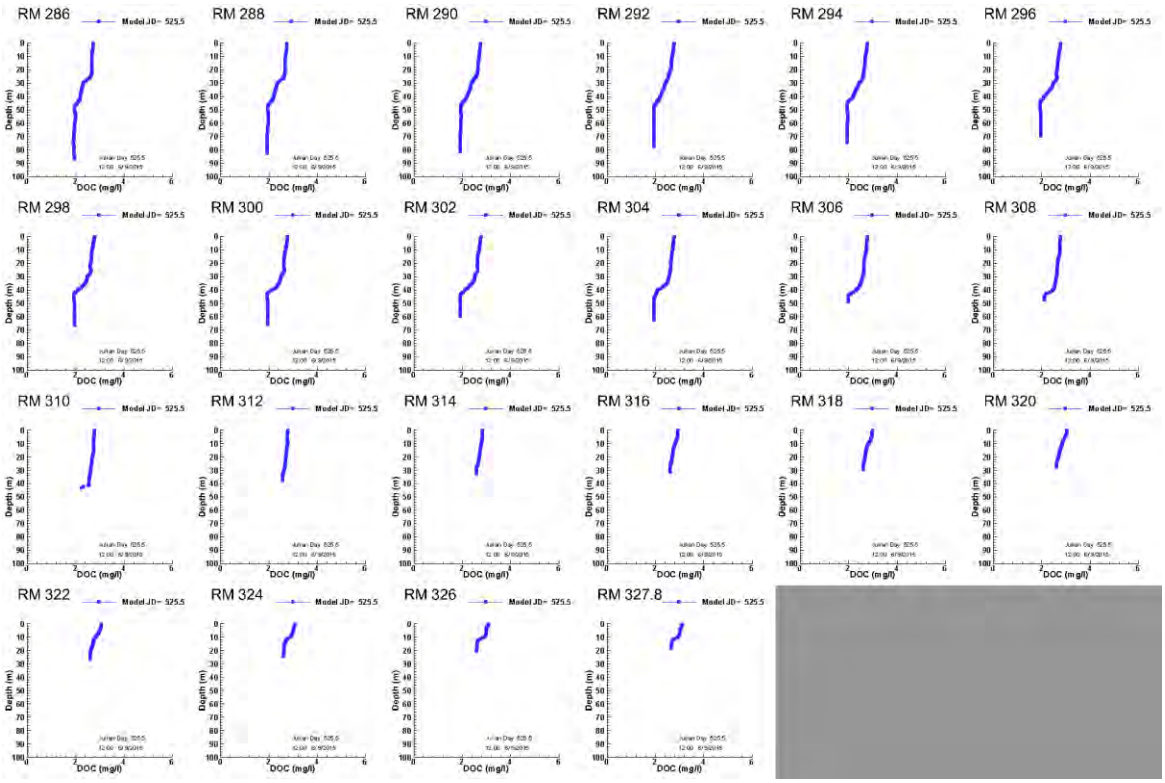


Figure 1455. Vertical profiles of DOC compared with data for 6/ 9/2015.

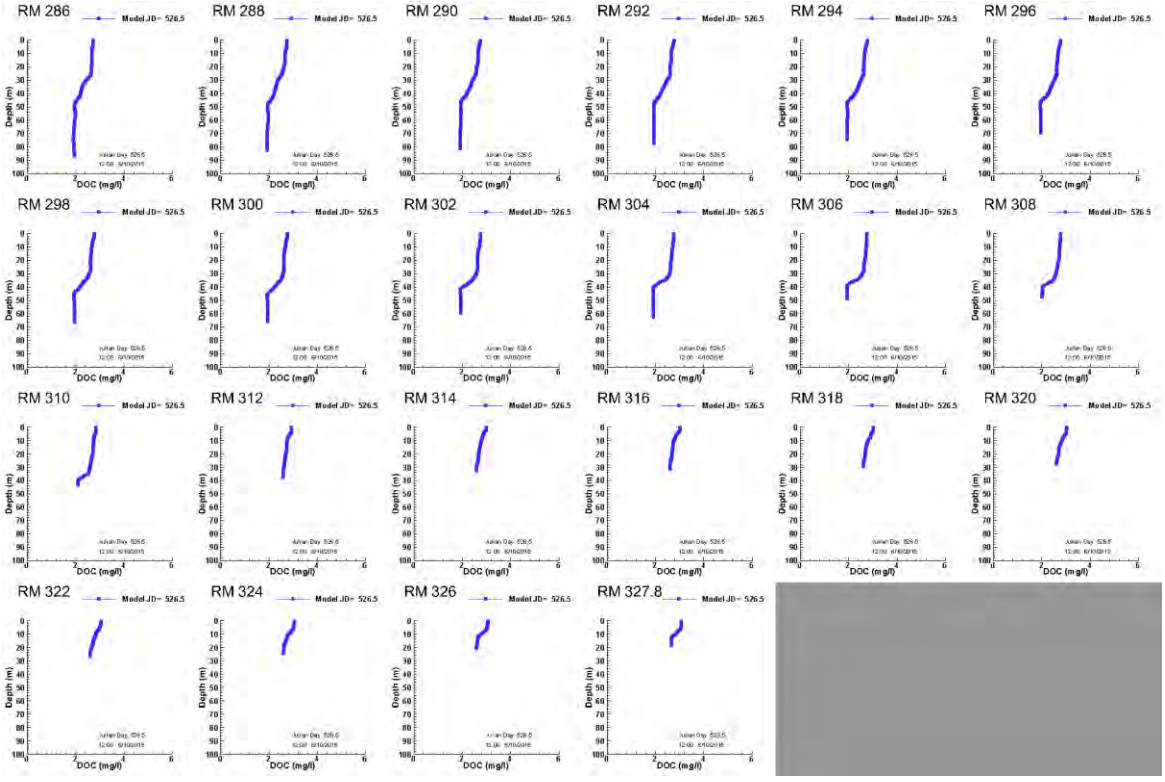


Figure 1456. Vertical profiles of DOC compared with data for 6/10/2015.

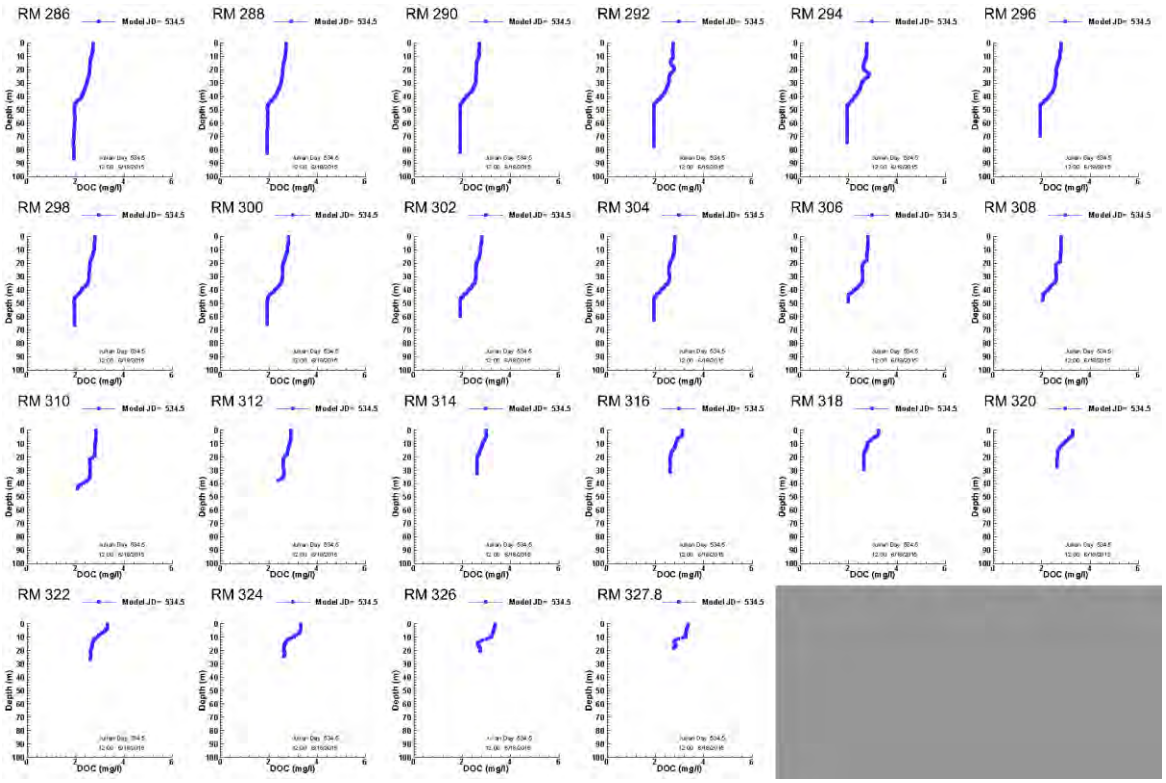


Figure 1457. Vertical profiles of DOC compared with data for 6/18/2015.

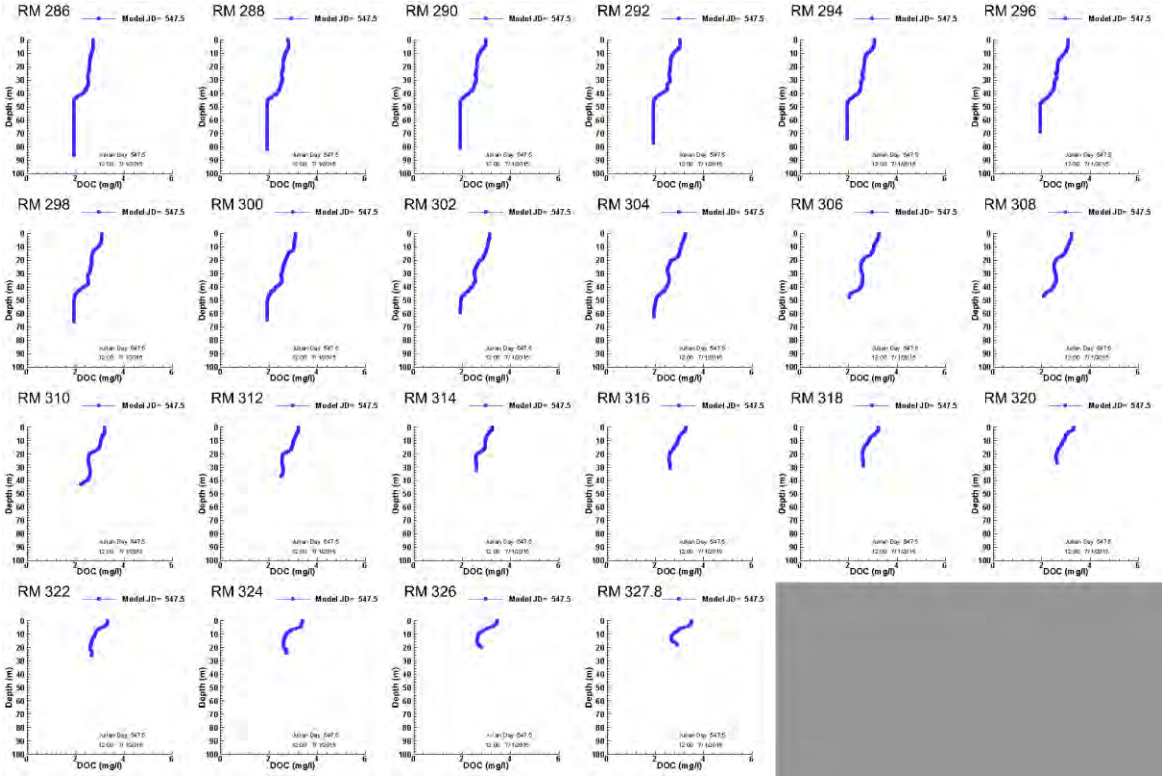


Figure 1458. Vertical profiles of DOC compared with data for 7/ 1/2015.

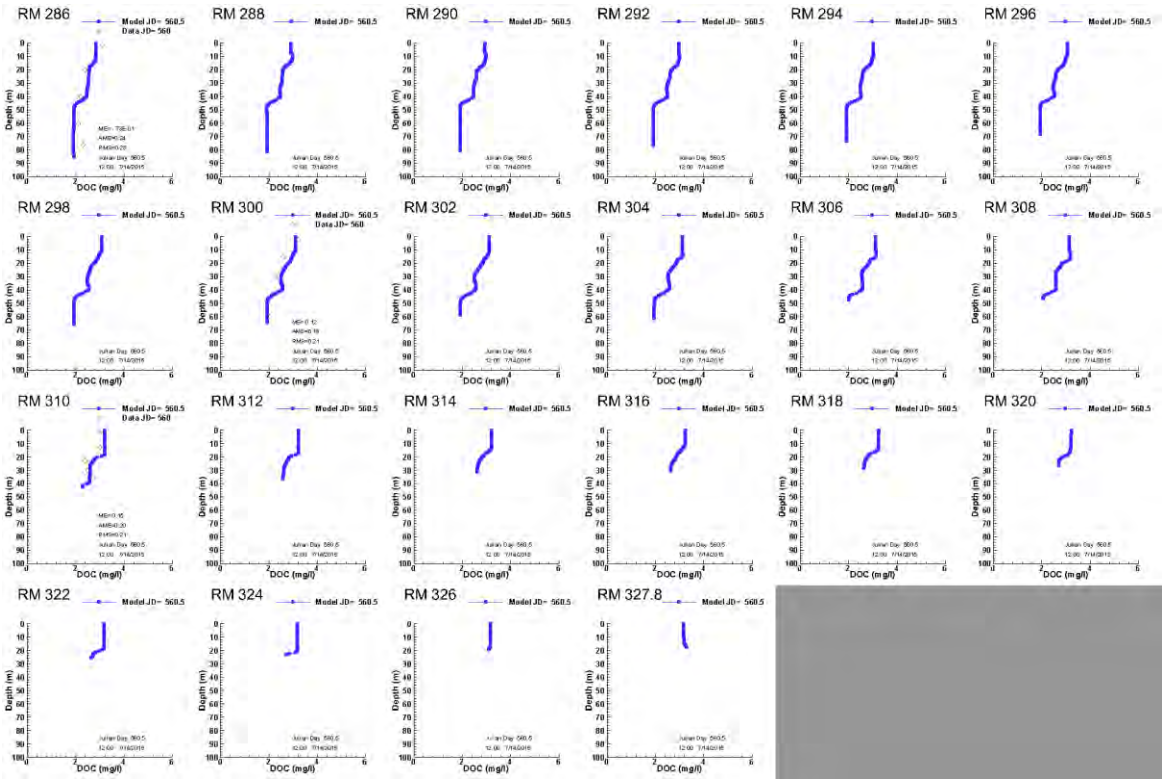


Figure 1459. Vertical profiles of DOC compared with data for 7/14/2015.

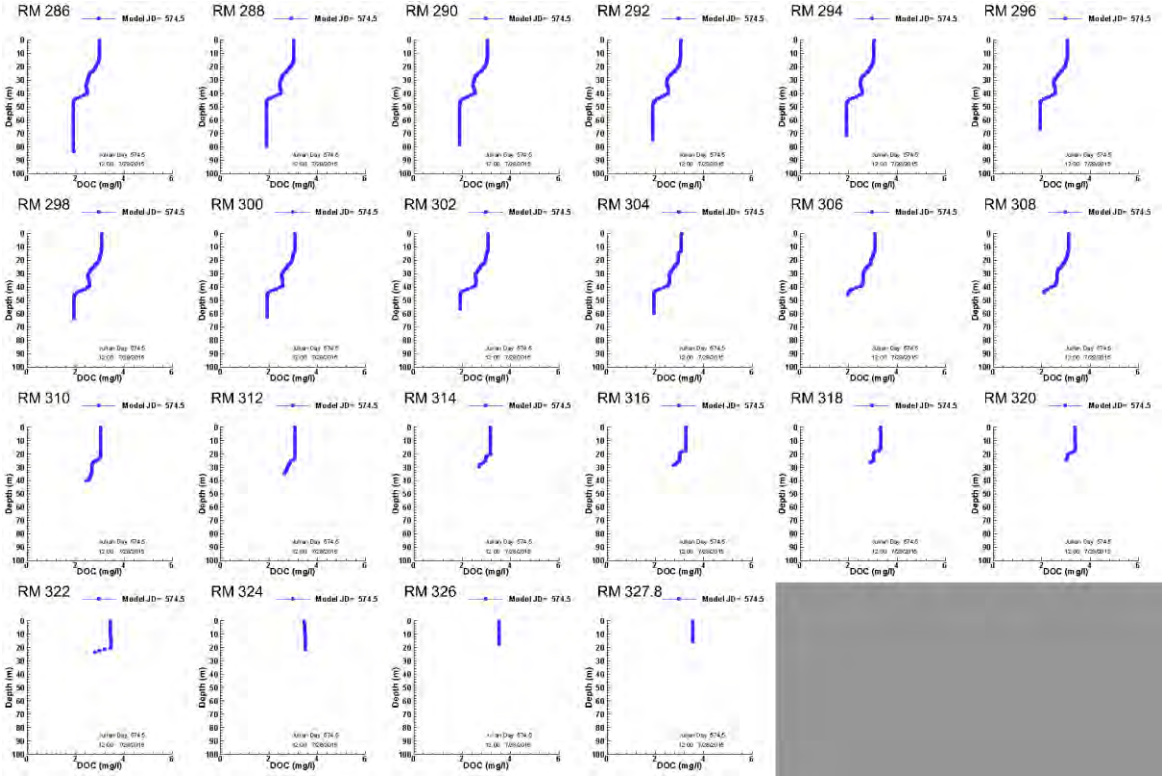


Figure 1460. Vertical profiles of DOC compared with data for 7/28/2015.

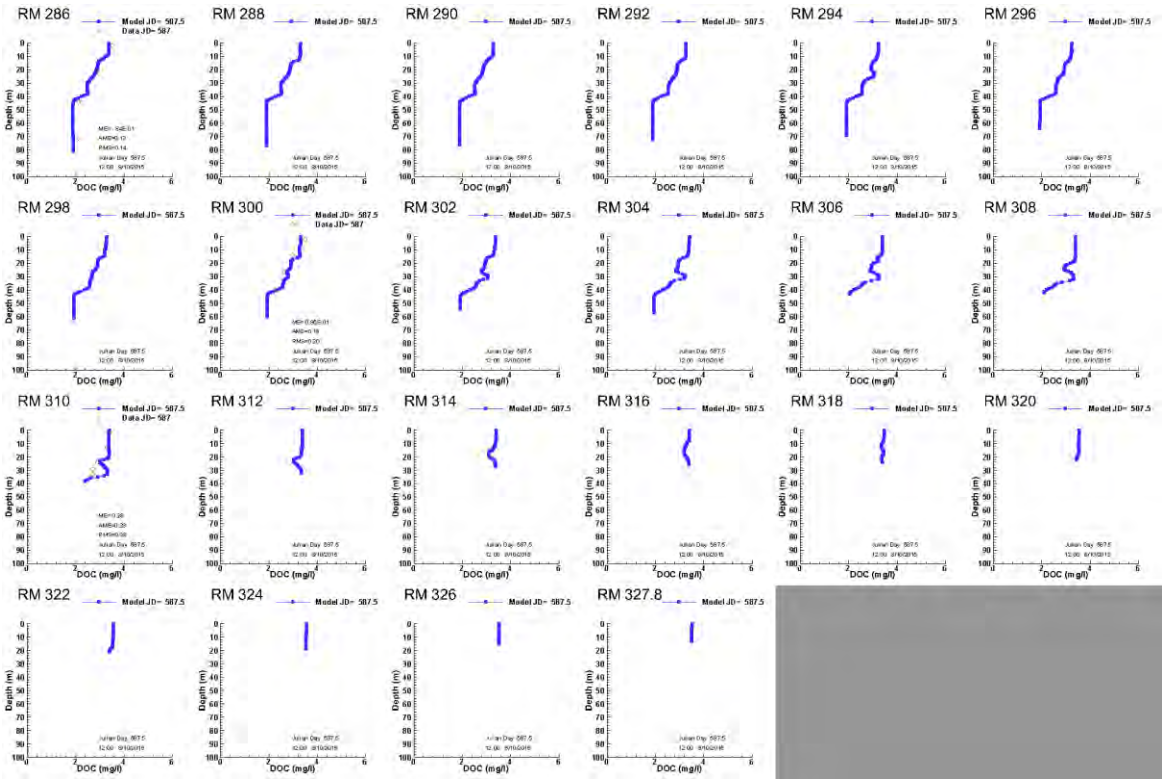


Figure 1461. Vertical profiles of DOC compared with data for 8/10/2015.

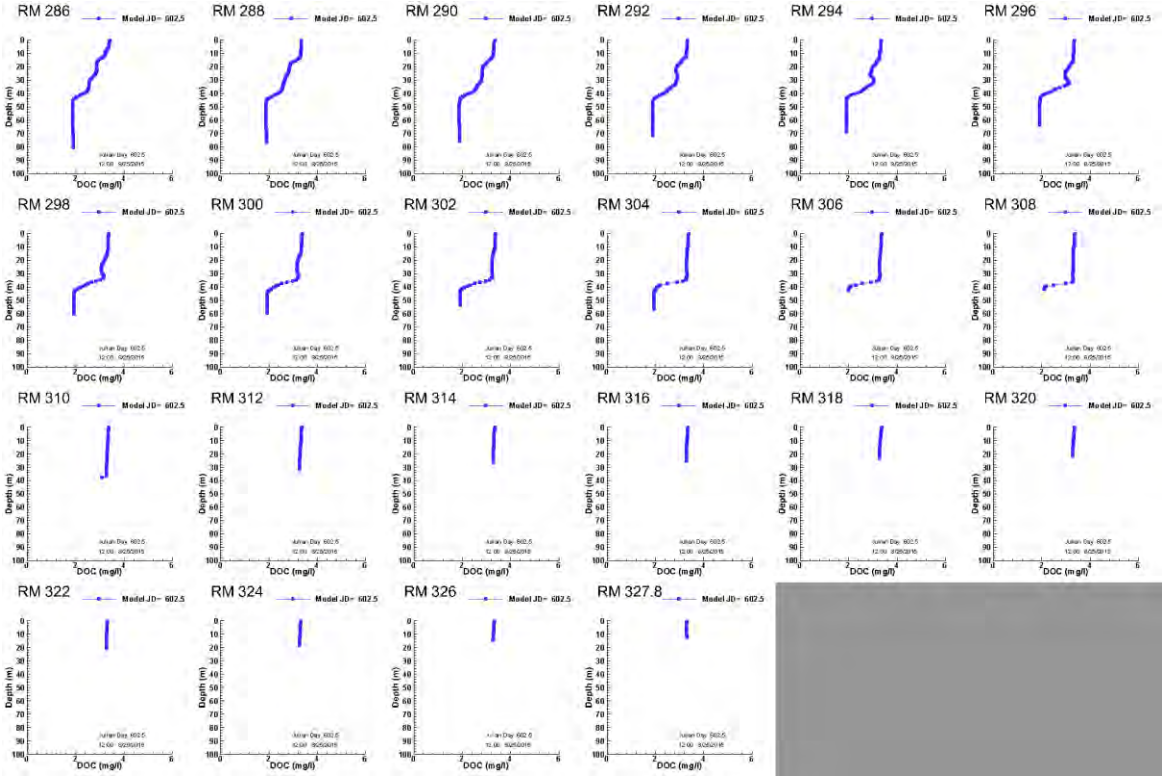


Figure 1462. Vertical profiles of DOC compared with data for 8/25/2015.

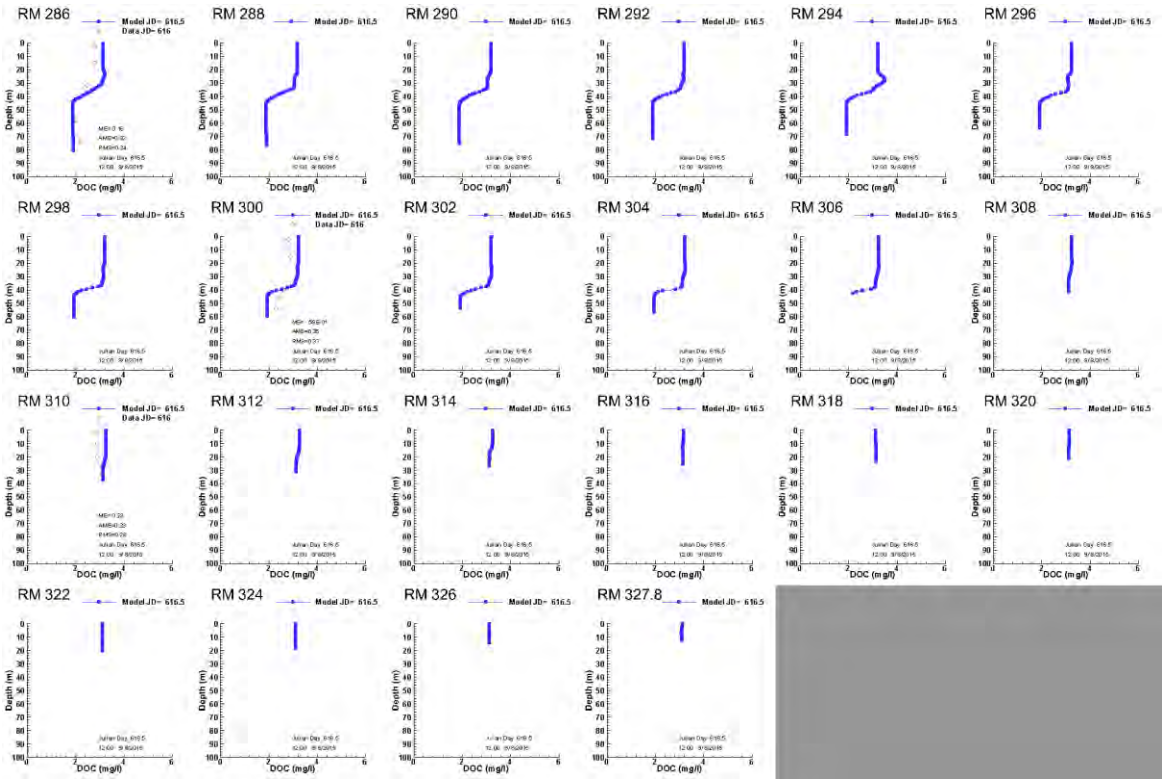


Figure 1463. Vertical profiles of DOC compared with data for 9/ 8/2015.

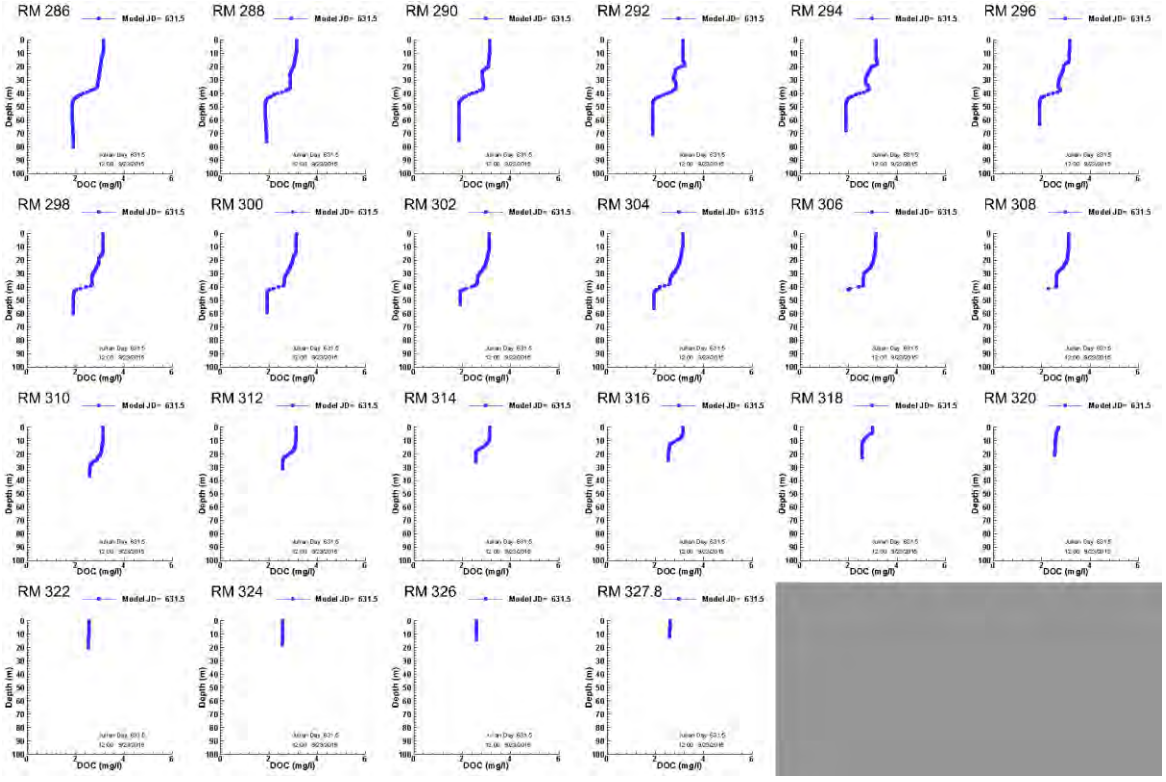


Figure 1464. Vertical profiles of DOC compared with data for 9/23/2015.

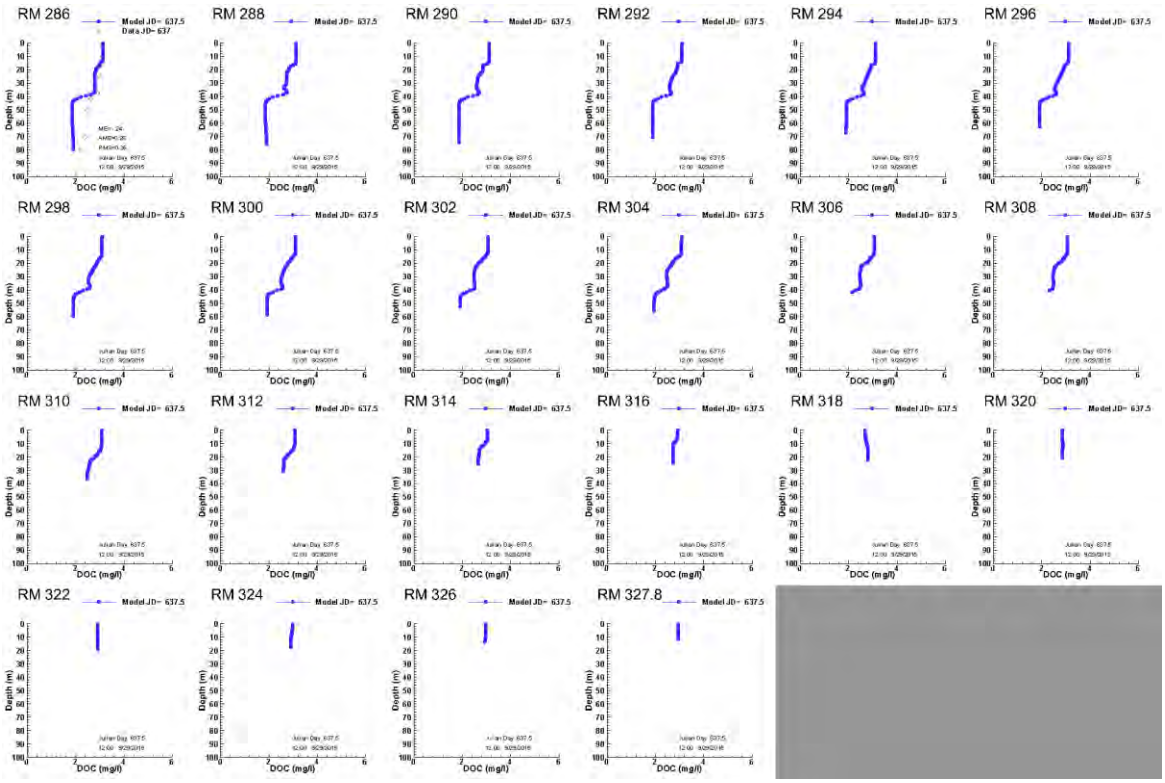


Figure 1465. Vertical profiles of DOC compared with data for 9/29/2015.

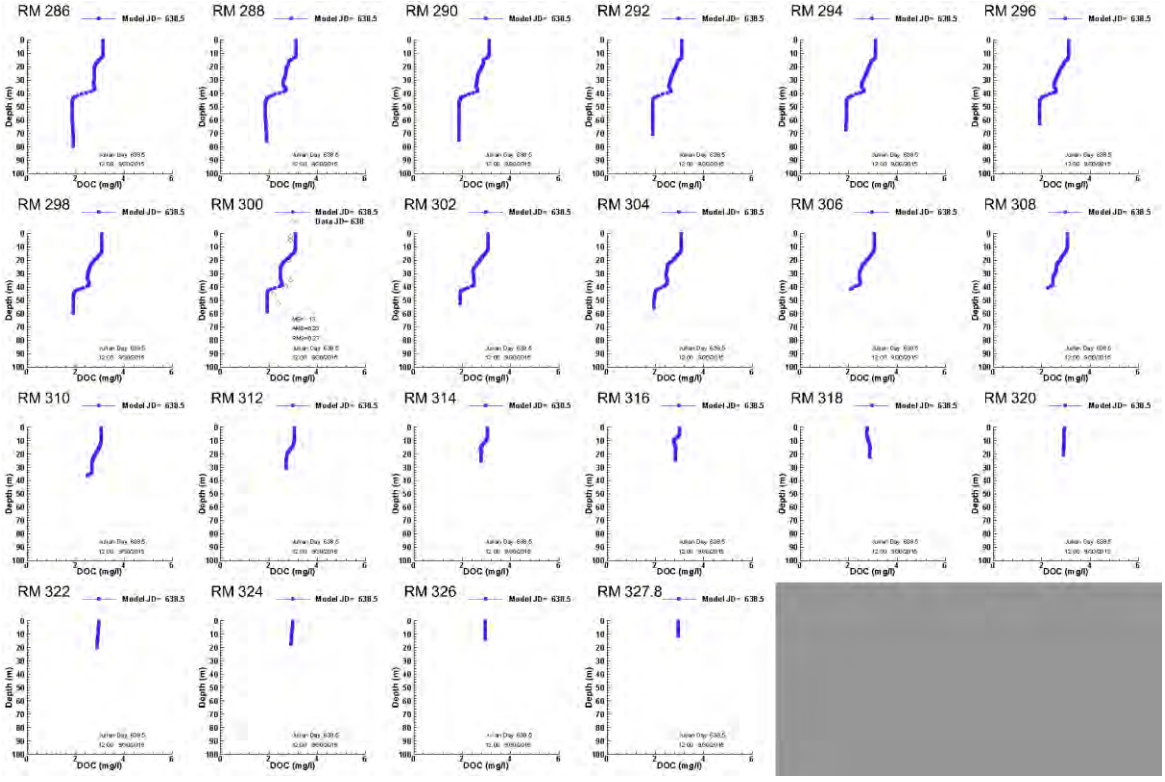


Figure 1466. Vertical profiles of DOC compared with data for 9/30/2015.

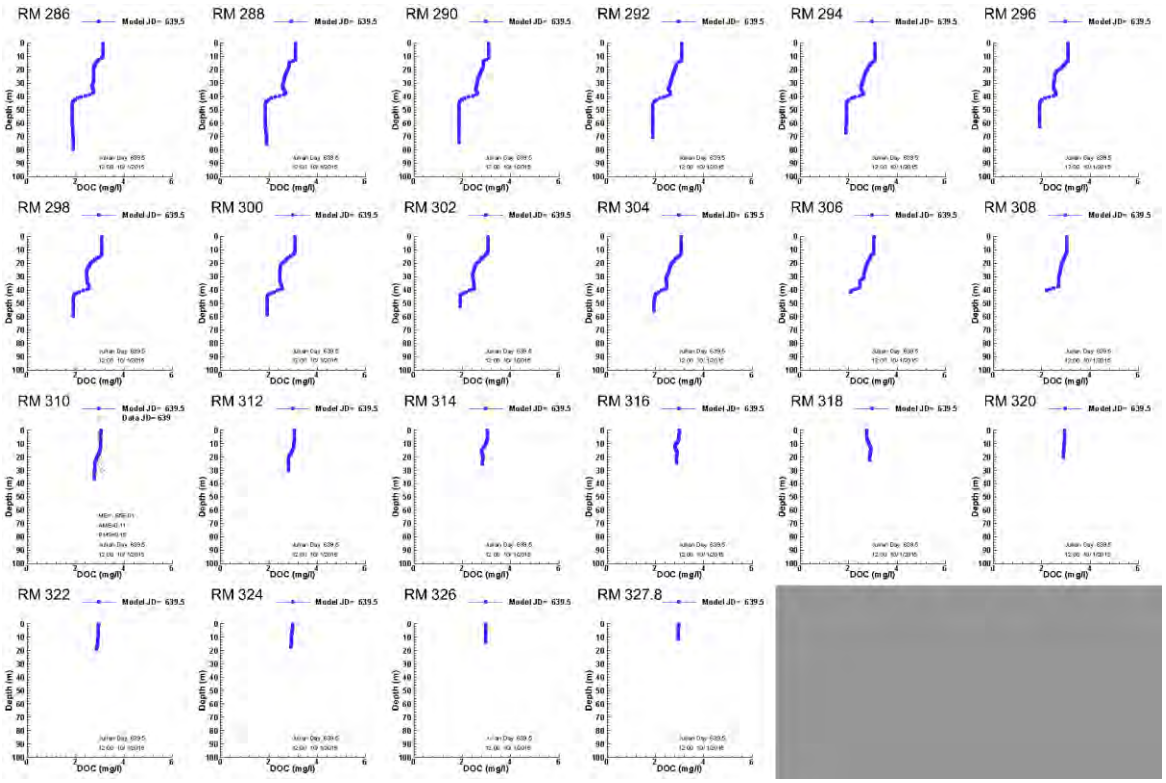


Figure 1467. Vertical profiles of DOC compared with data for 10/ 1/2015.

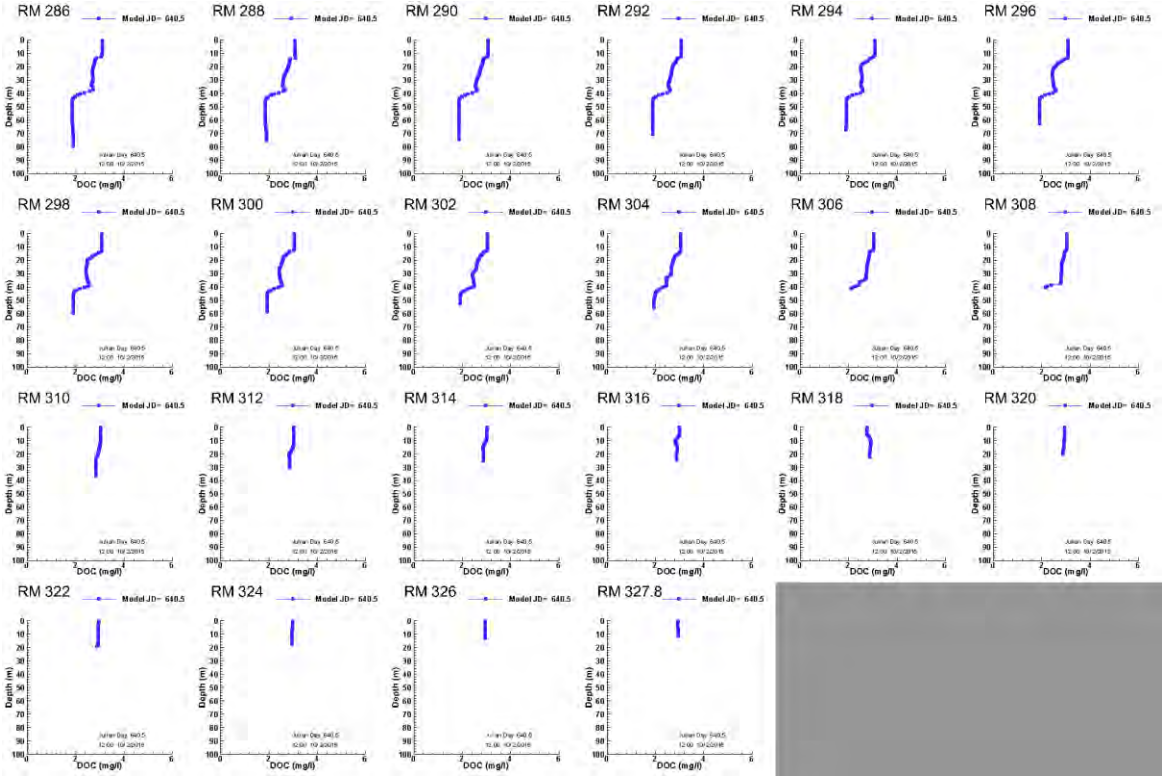


Figure 1468. Vertical profiles of DOC compared with data for 10/ 2/2015.

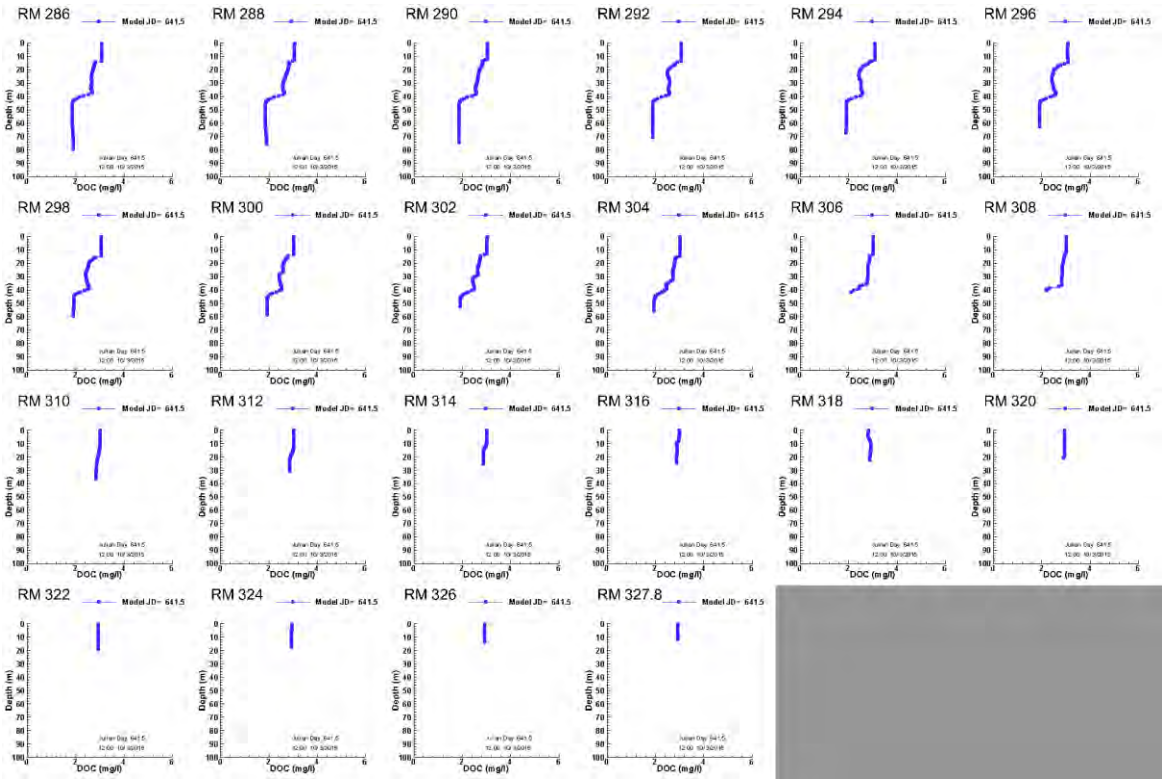


Figure 1469. Vertical profiles of DOC compared with data for 10/ 3/2015.

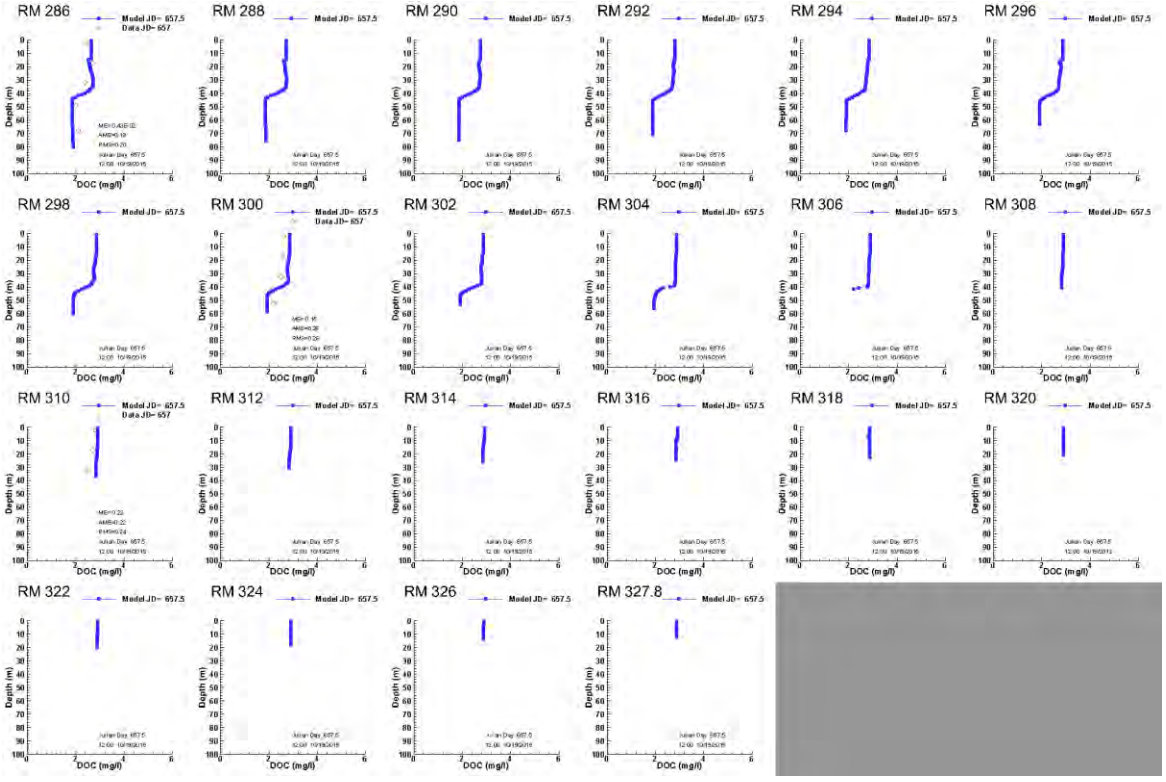


Figure 1470. Vertical profiles of DOC compared with data for 10/19/2015.

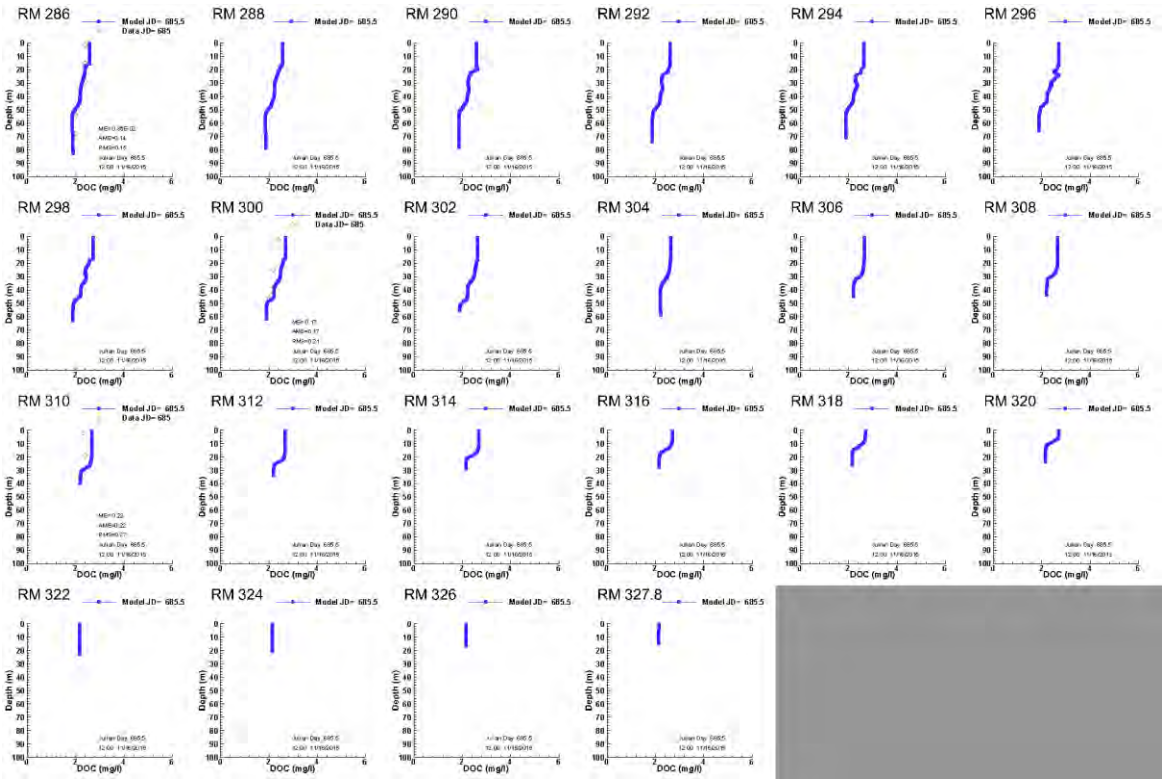


Figure 1471. Vertical profiles of DOC compared with data for 11/16/2015.

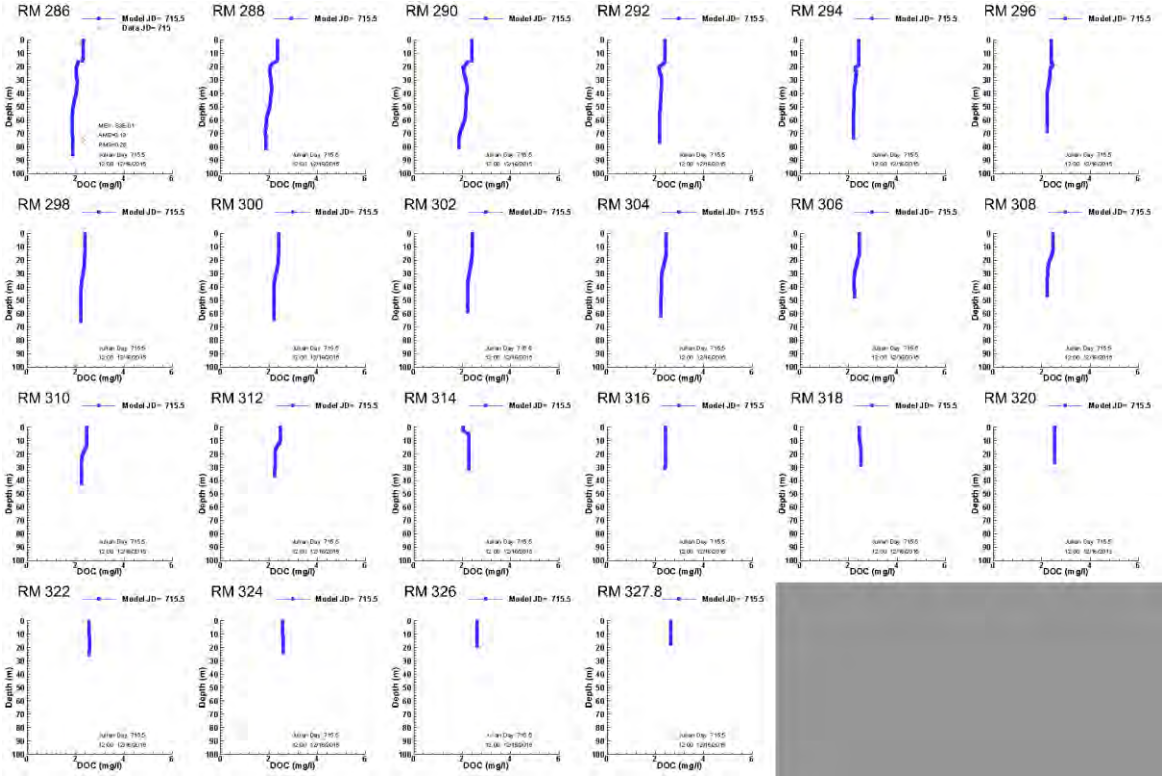


Figure 1472. Vertical profiles of DOC compared with data for 12/16/2015.

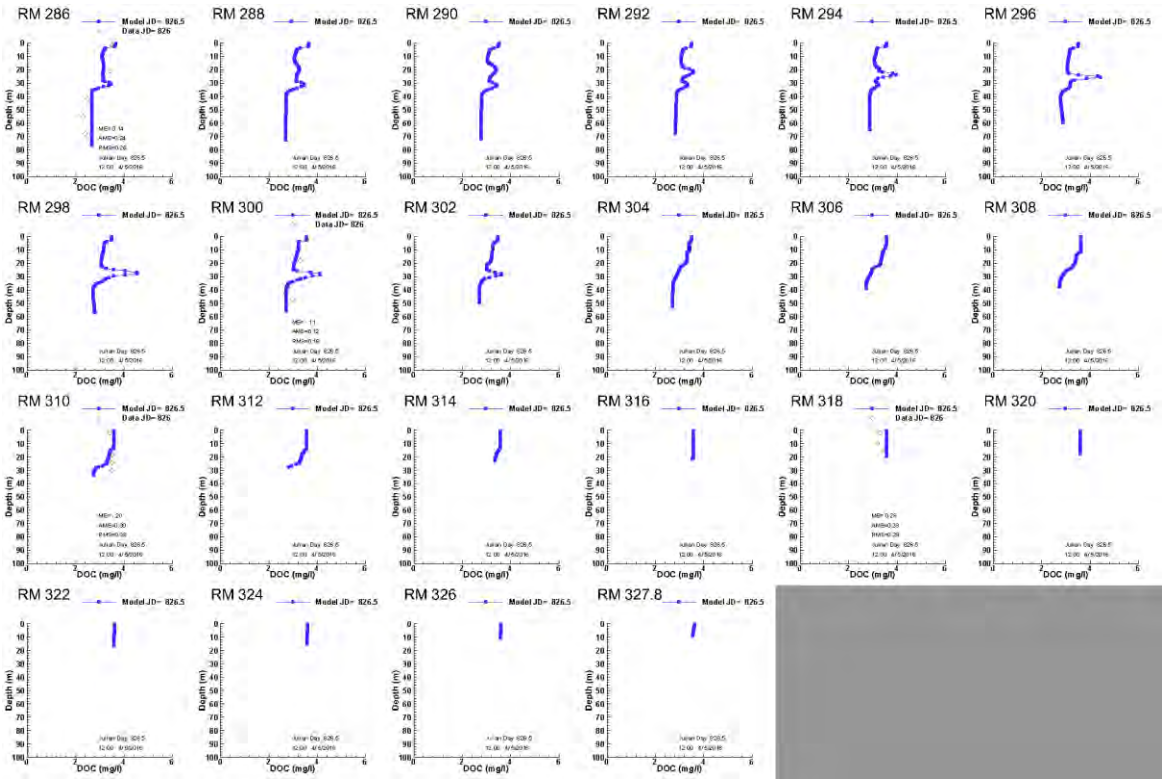


Figure 1473. Vertical profiles of DOC compared with data for 4/ 5/2016.

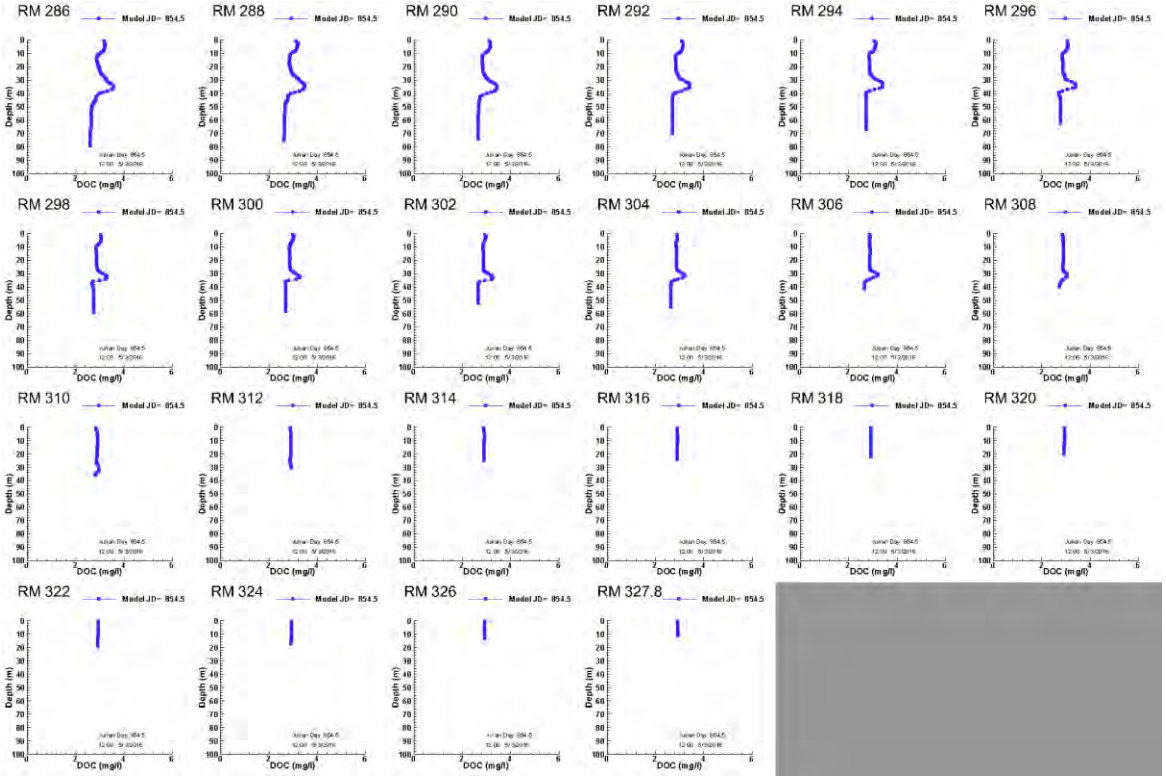


Figure 1474. Vertical profiles of DOC compared with data for 5/ 3/2016.

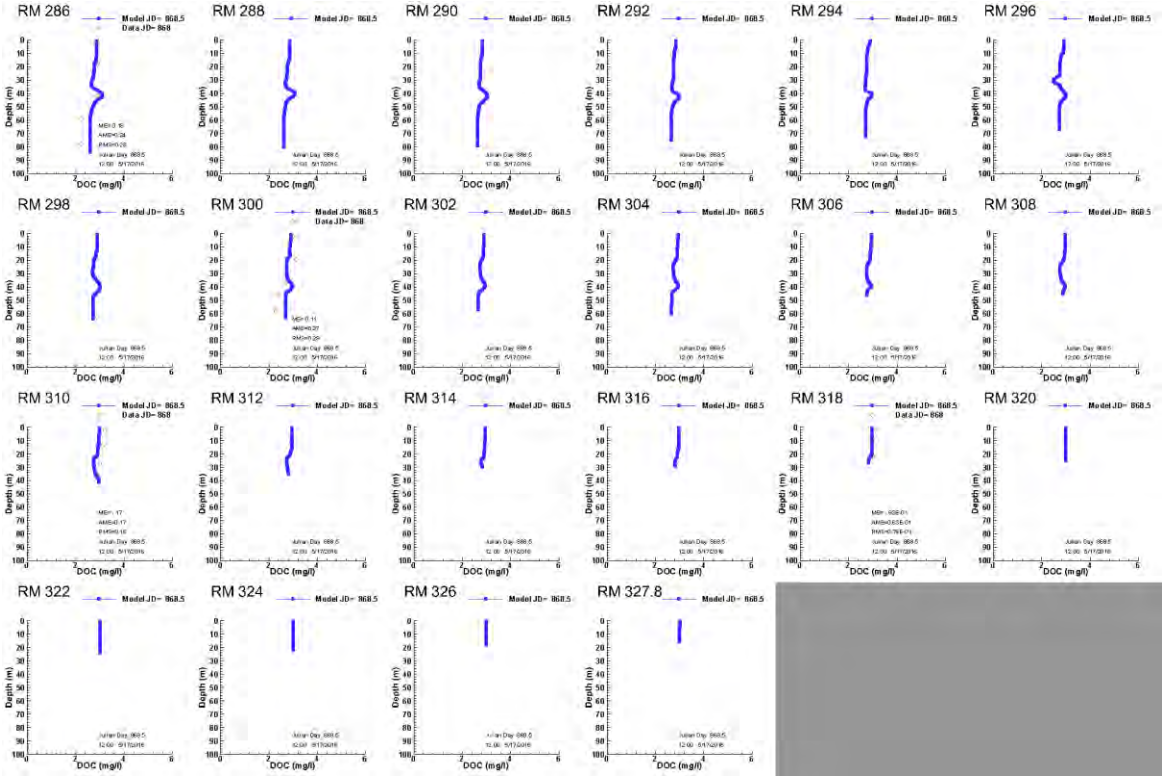


Figure 1475. Vertical profiles of DOC compared with data for 5/17/2016.

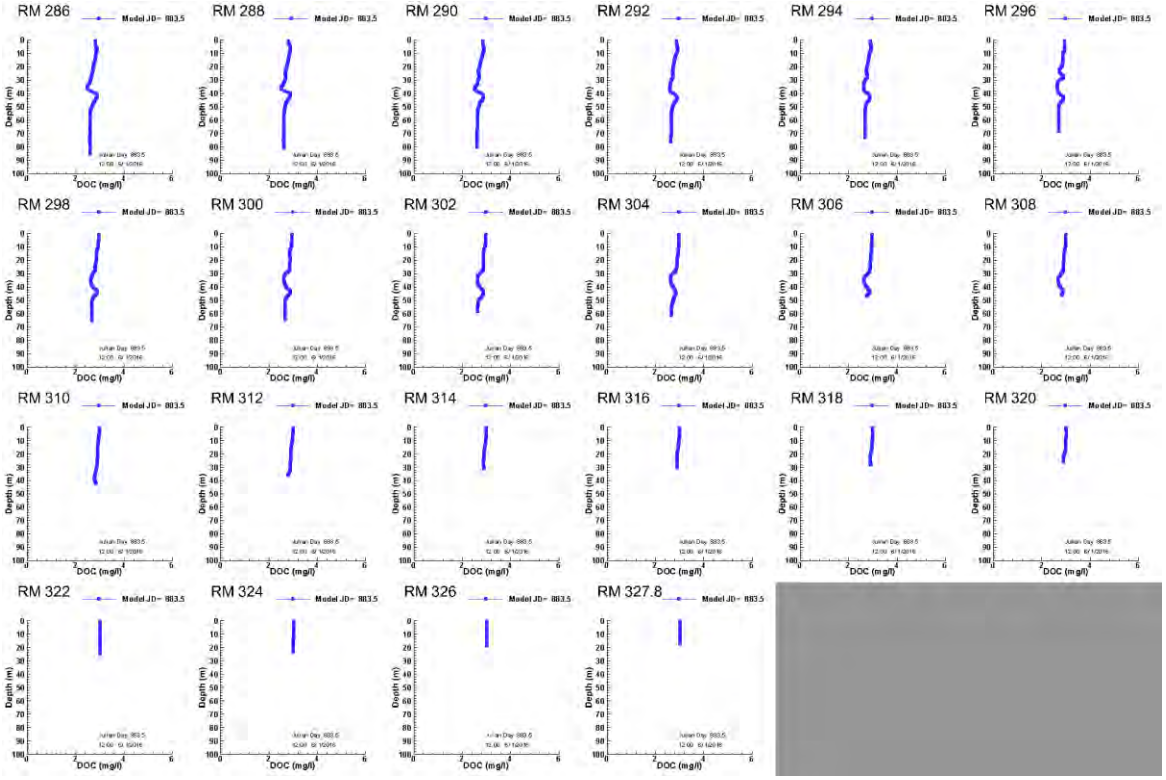


Figure 1476. Vertical profiles of DOC compared with data for 6/ 1/2016.

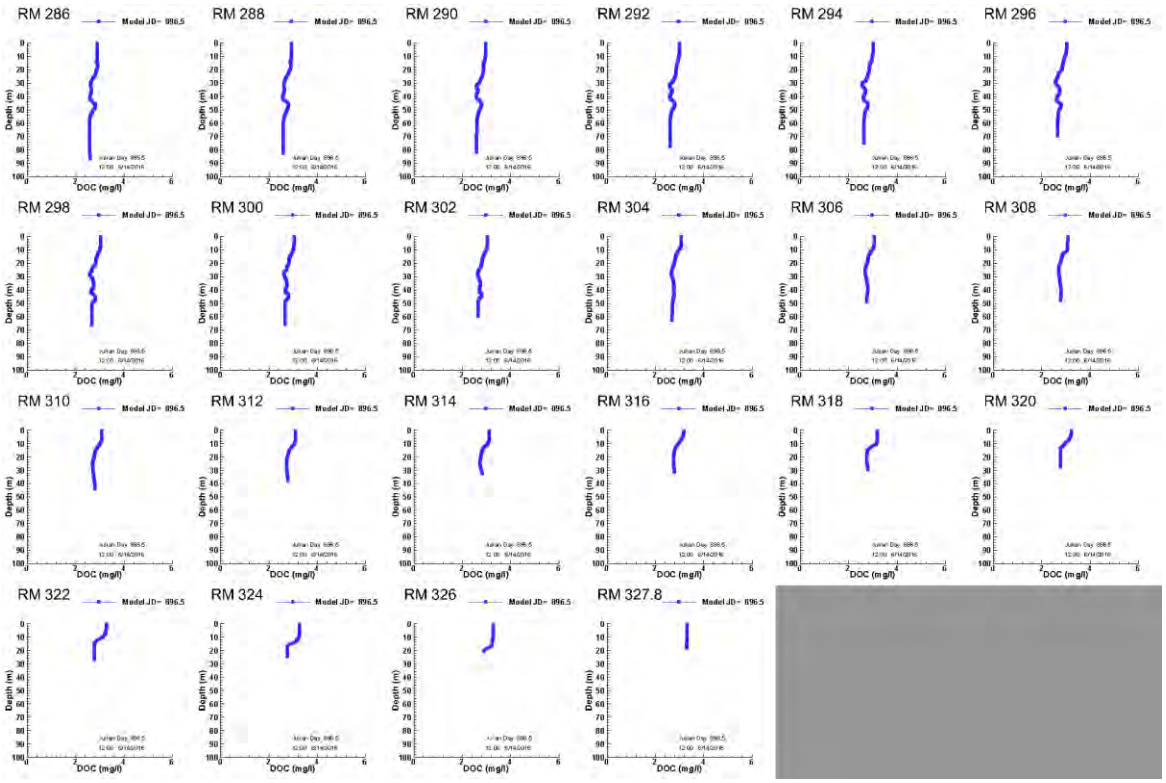


Figure 1477. Vertical profiles of DOC compared with data for 6/14/2016.

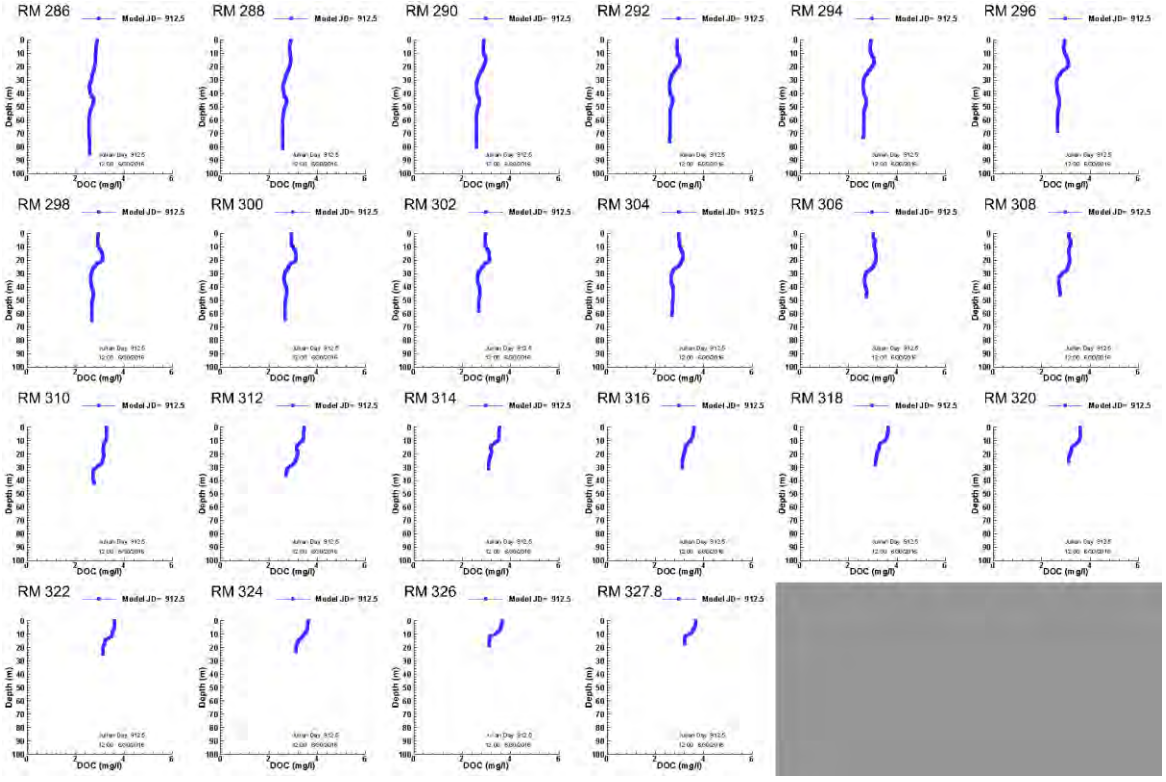


Figure 1478. Vertical profiles of DOC compared with data for 6/30/2016.

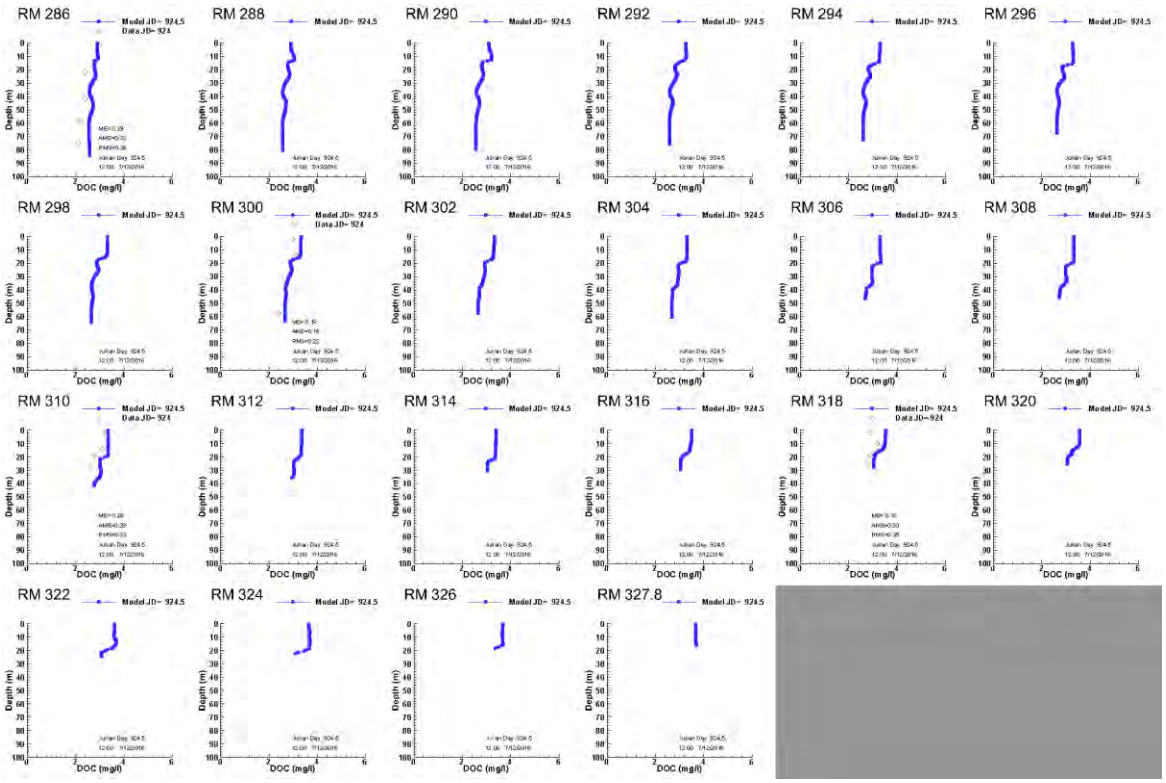


Figure 1479. Vertical profiles of DOC compared with data for 7/12/2016.

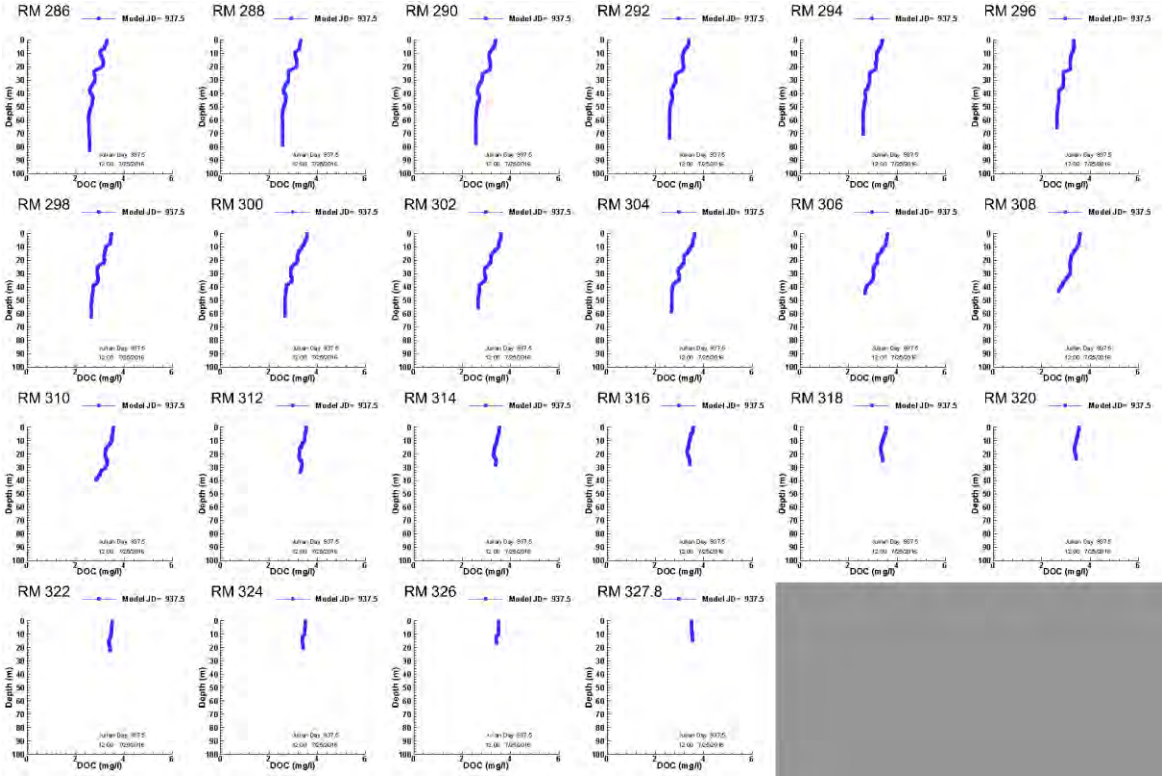


Figure 1480. Vertical profiles of DOC compared with data for 7/25/2016.

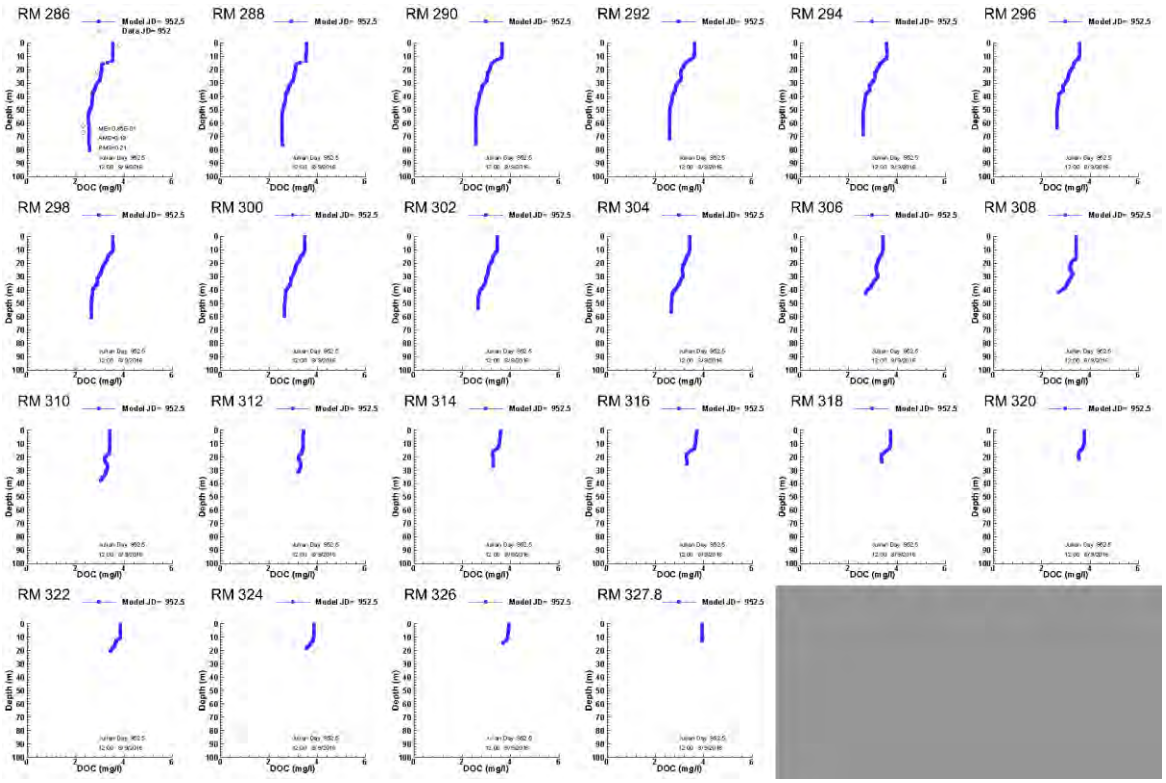


Figure 1481. Vertical profiles of DOC compared with data for 8/ 9/2016.

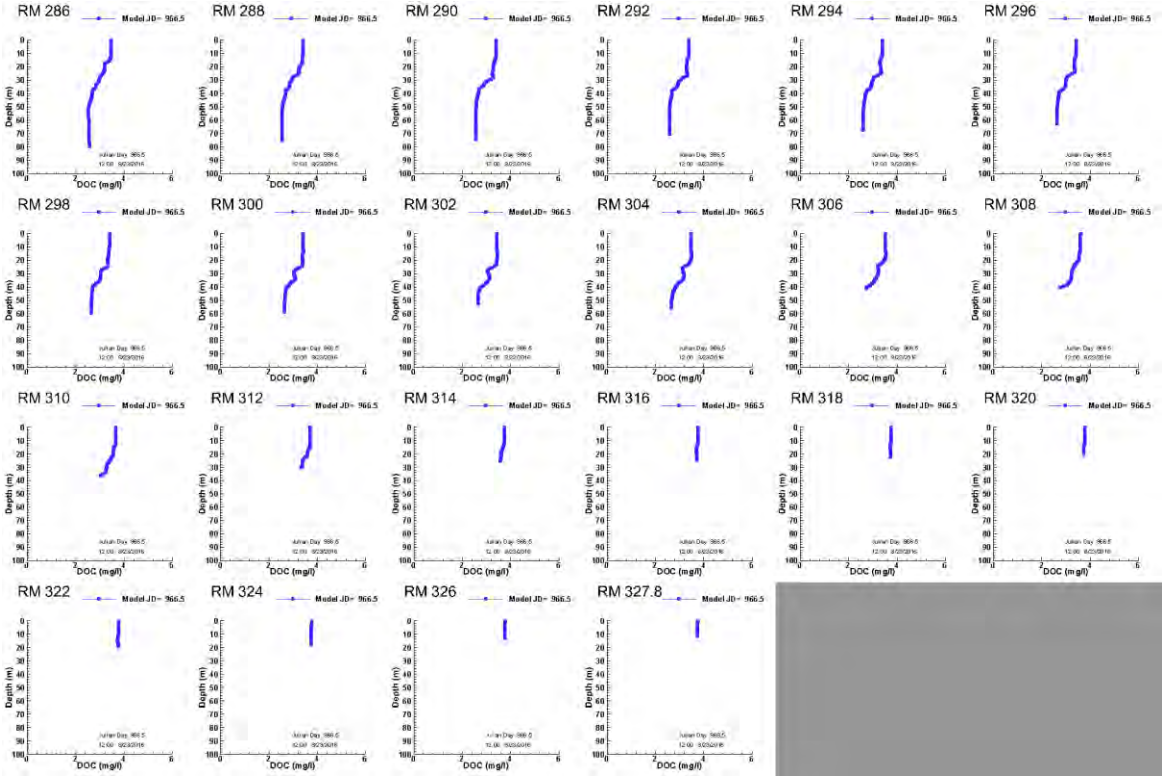


Figure 1482. Vertical profiles of DOC compared with data for 8/23/2016.

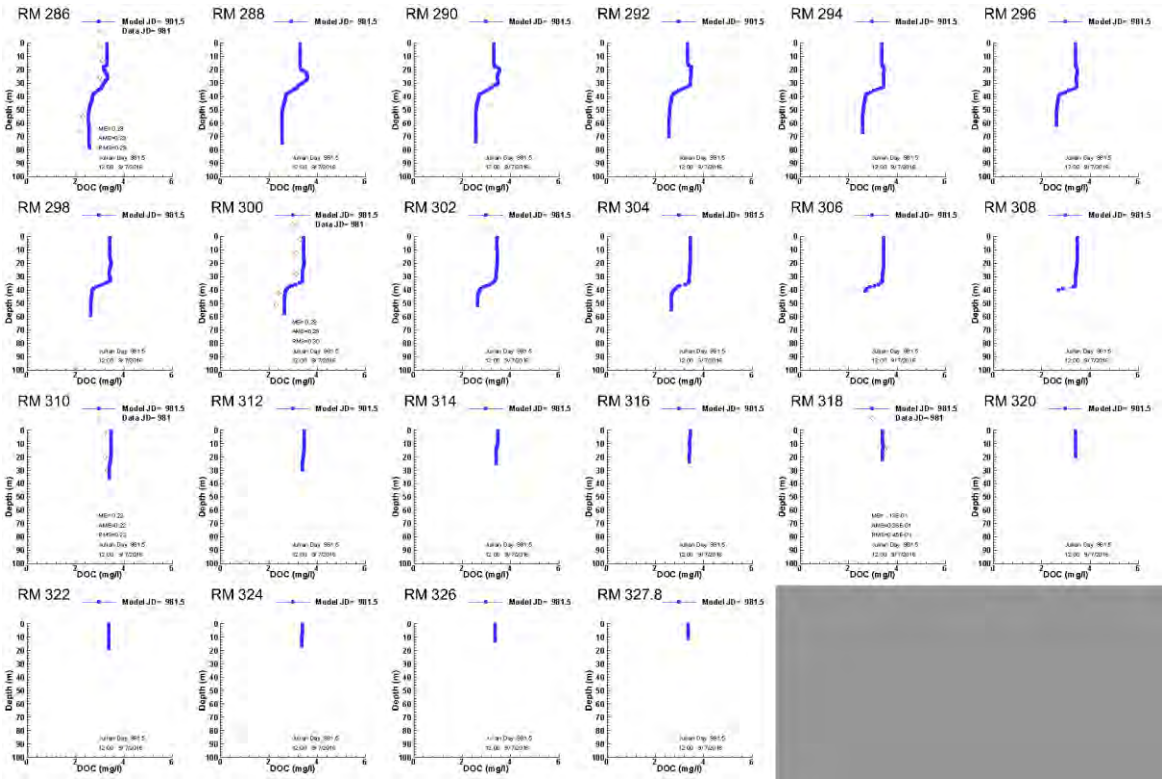


Figure 1483. Vertical profiles of DOC compared with data for 9/ 7/2016.

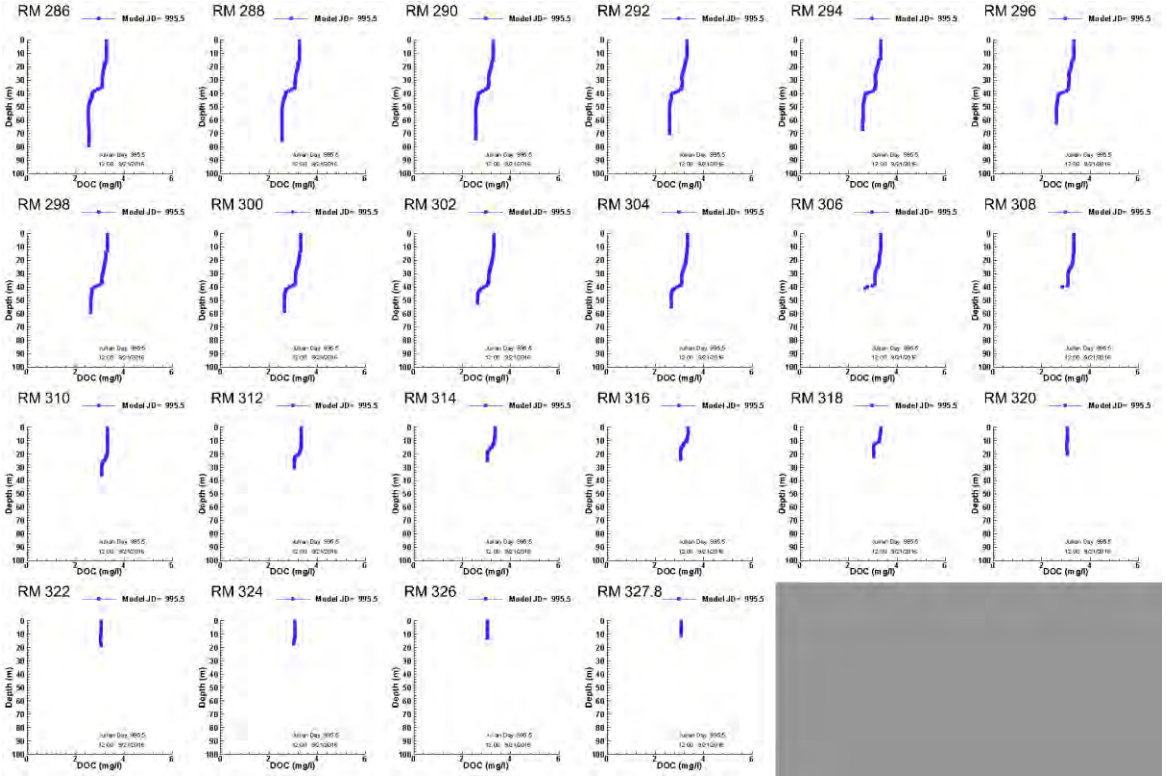


Figure 1484. Vertical profiles of DOC compared with data for 9/21/2016.

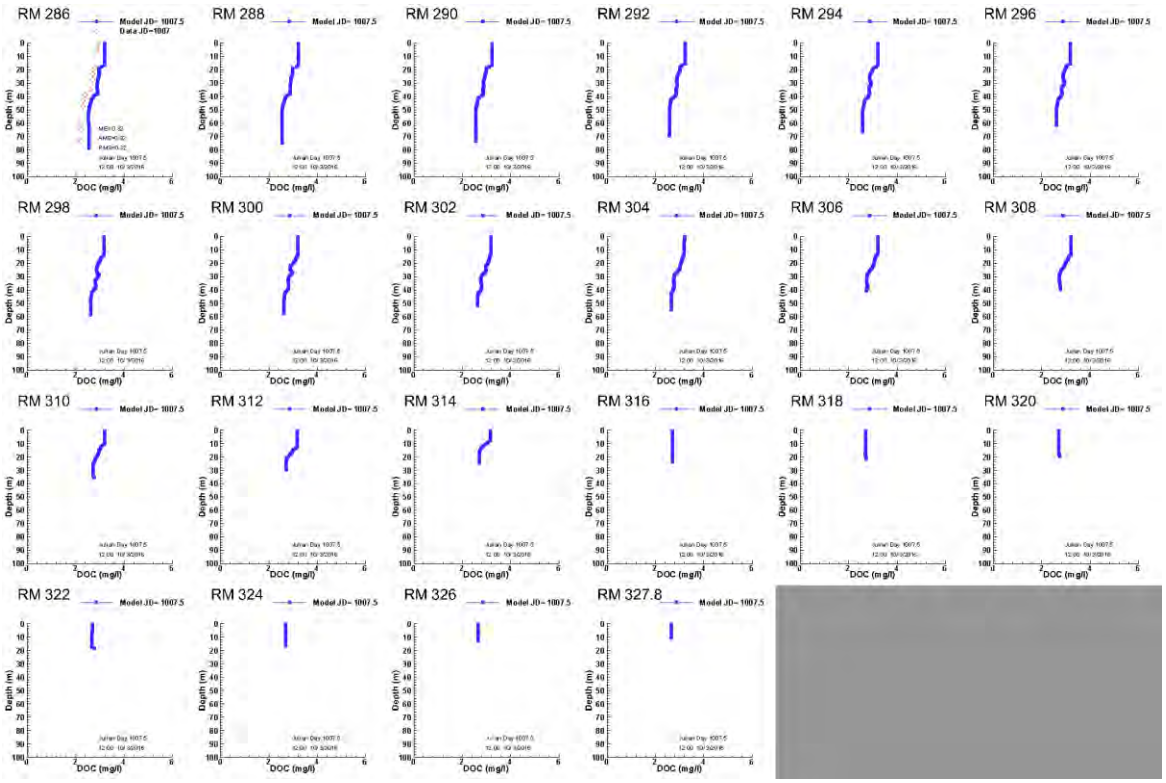


Figure 1485. Vertical profiles of DOC compared with data for 10/ 3/2016.

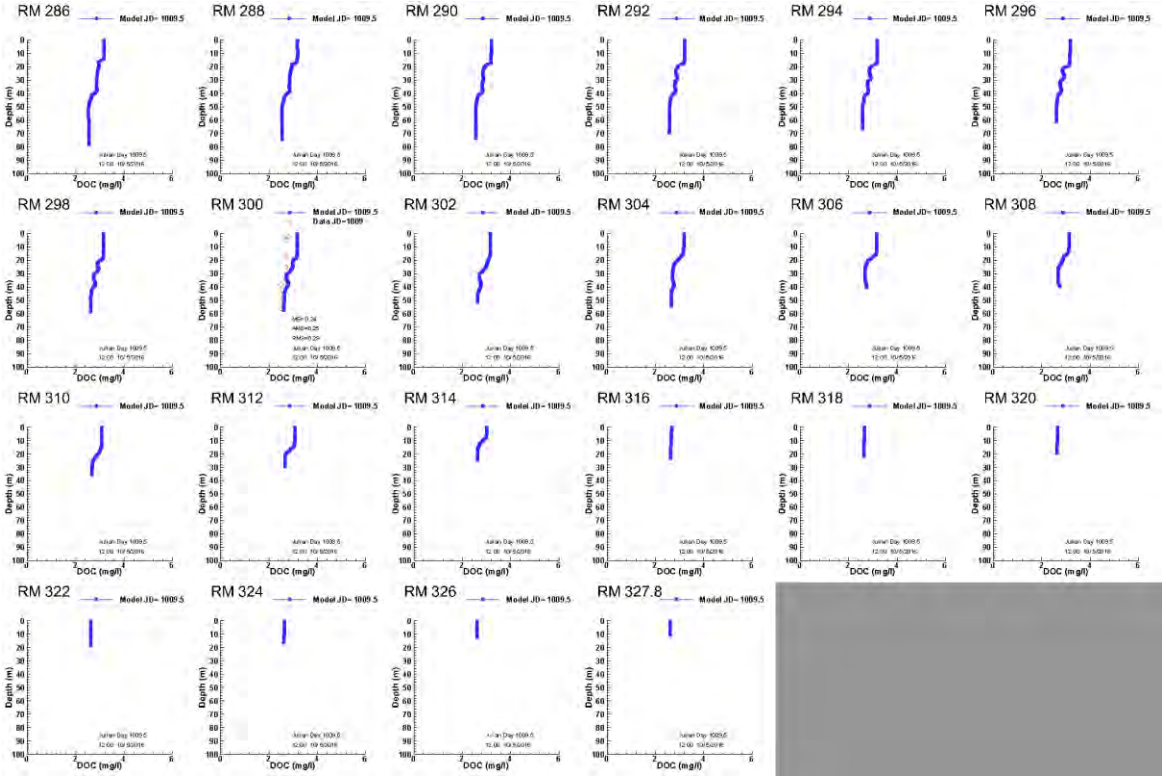


Figure 1486. Vertical profiles of DOC compared with data for 10/ 5/2016.

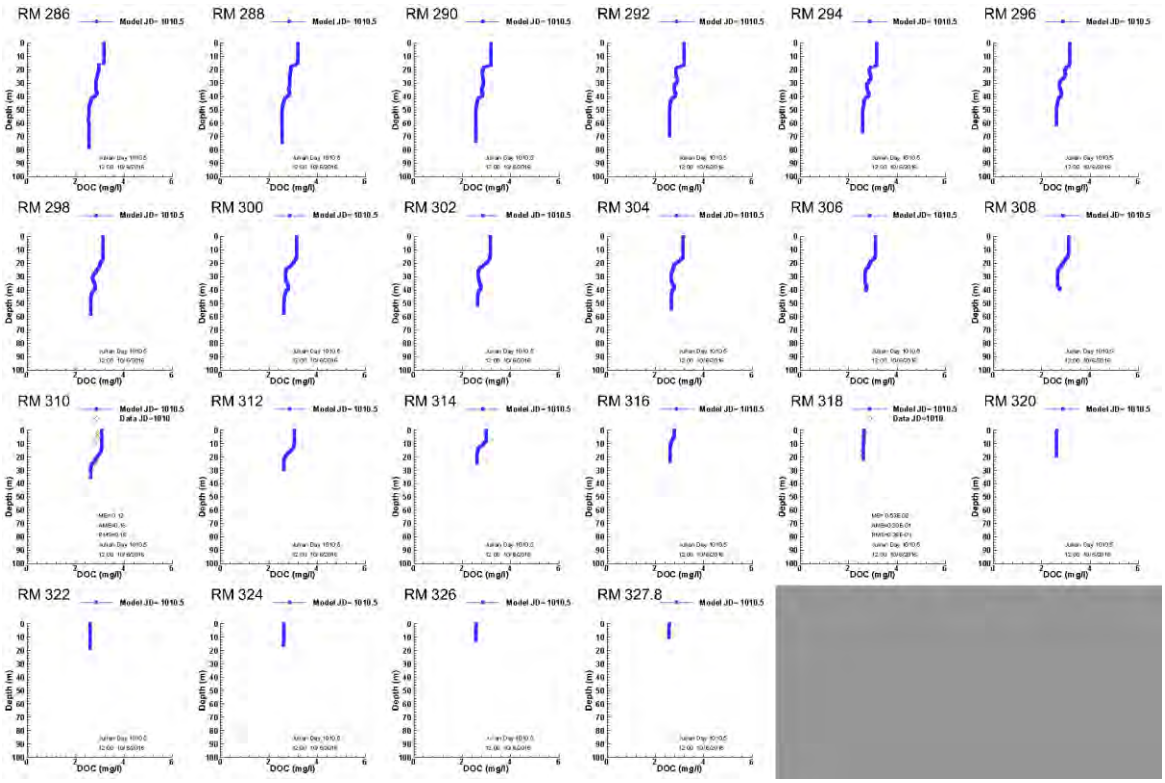


Figure 1487. Vertical profiles of DOC compared with data for 10/ 6/2016.

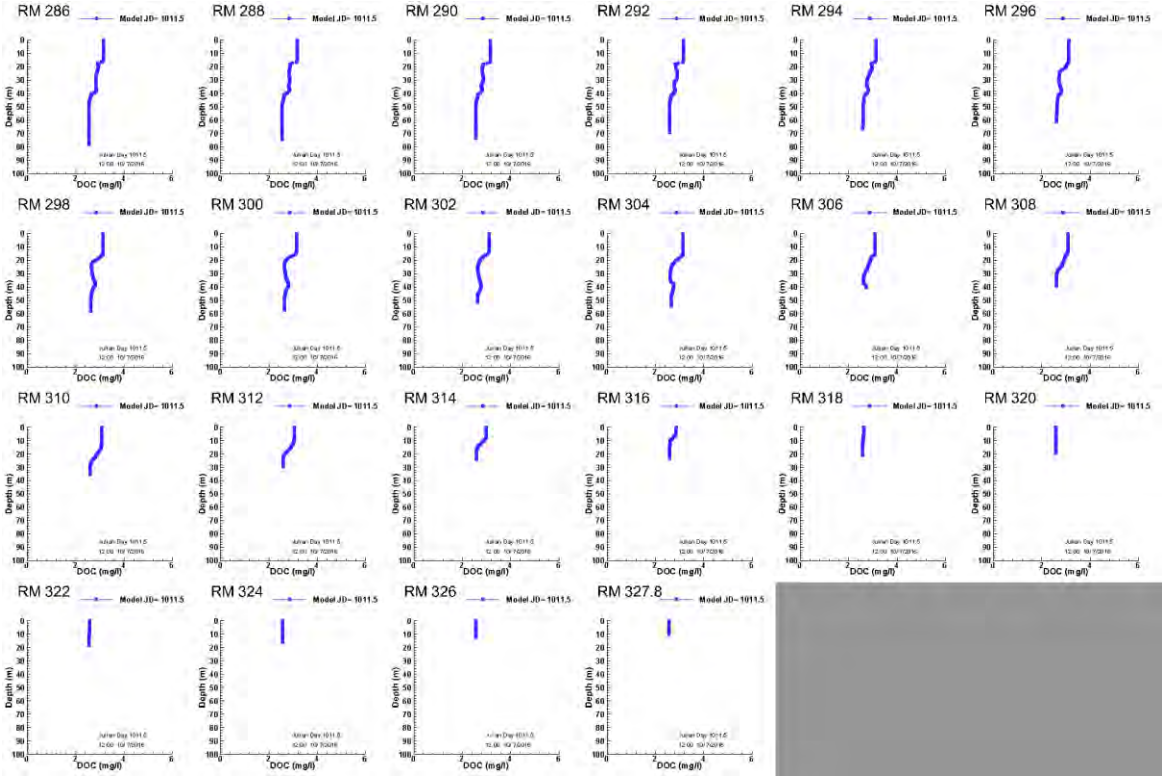


Figure 1488. Vertical profiles of DOC compared with data for 10/ 7/2016.

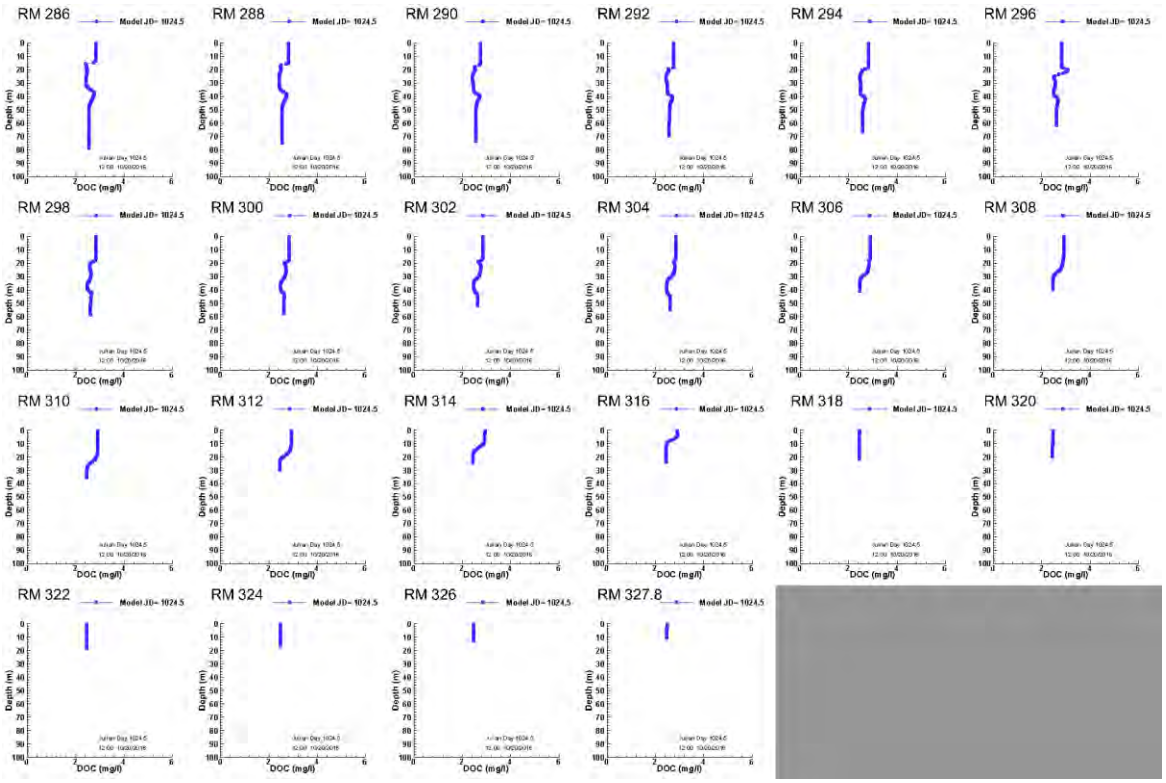


Figure 1489. Vertical profiles of DOC compared with data for 10/20/2016.

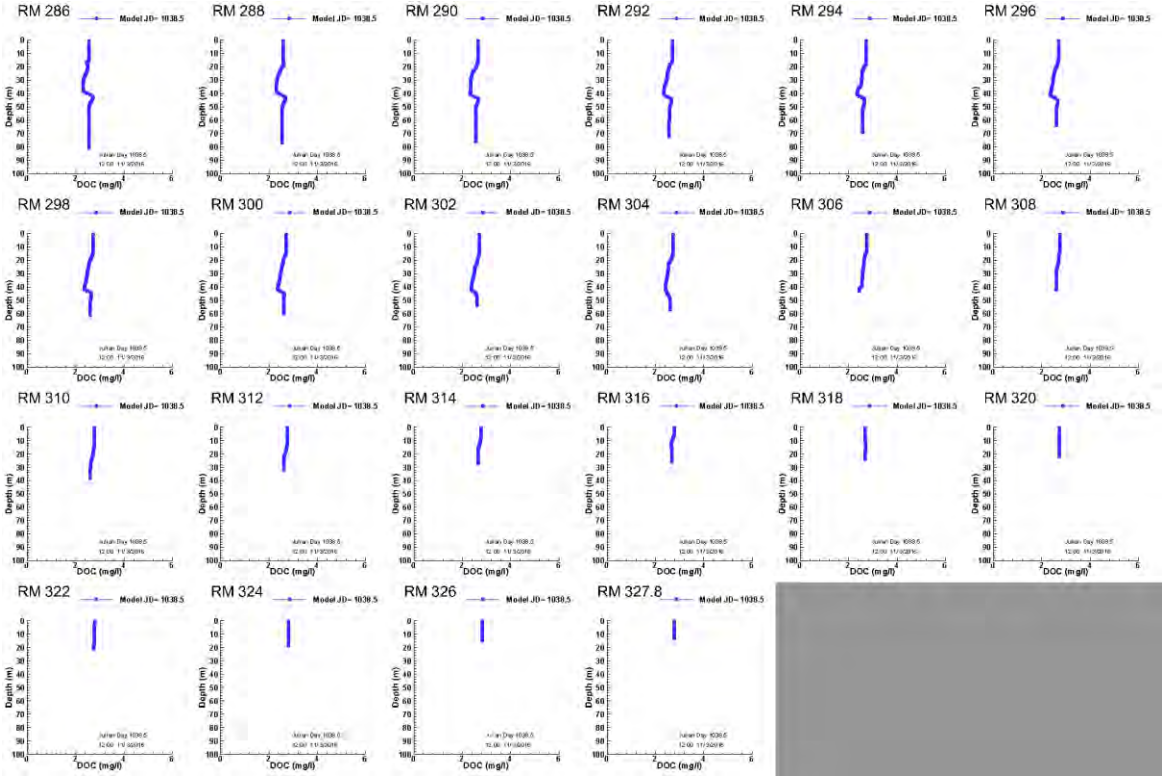


Figure 1490. Vertical profiles of DOC compared with data for 11/ 3/2016.

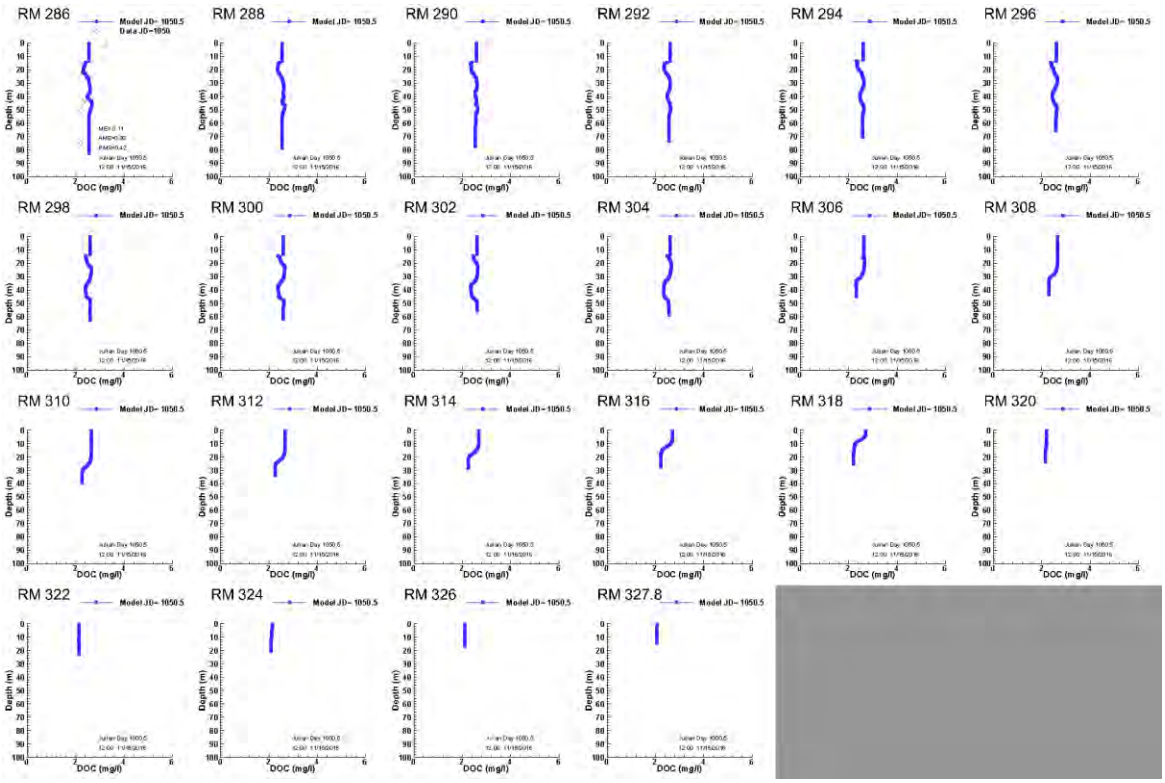


Figure 1491. Vertical profiles of DOC compared with data for 11/15/2016.

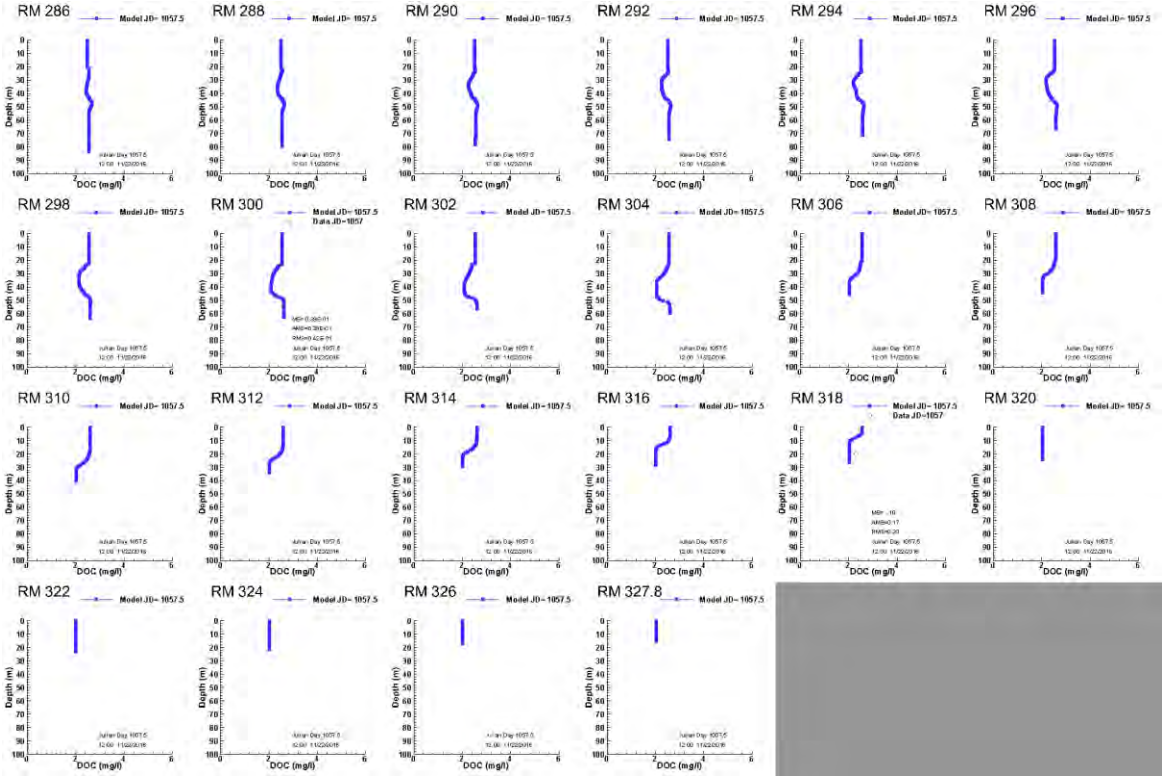


Figure 1492. Vertical profiles of DOC compared with data for 11/22/2016.

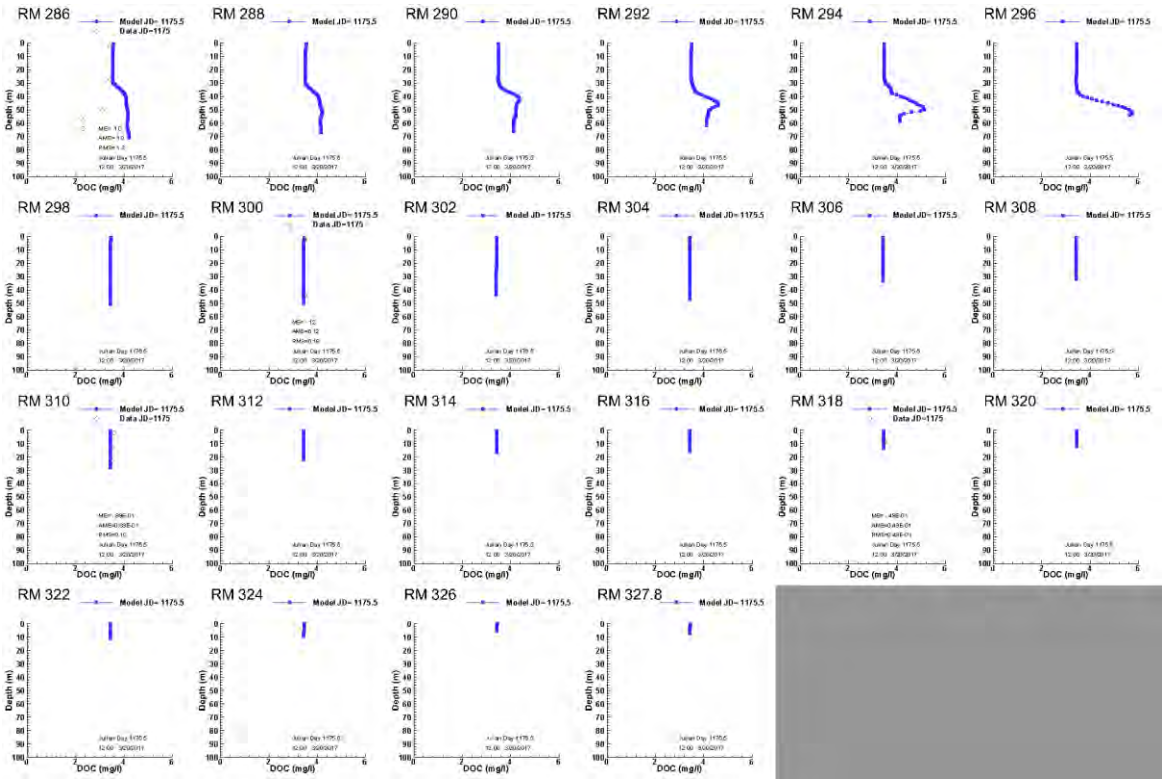


Figure 1493. Vertical profiles of DOC compared with data for 3/20/2017.

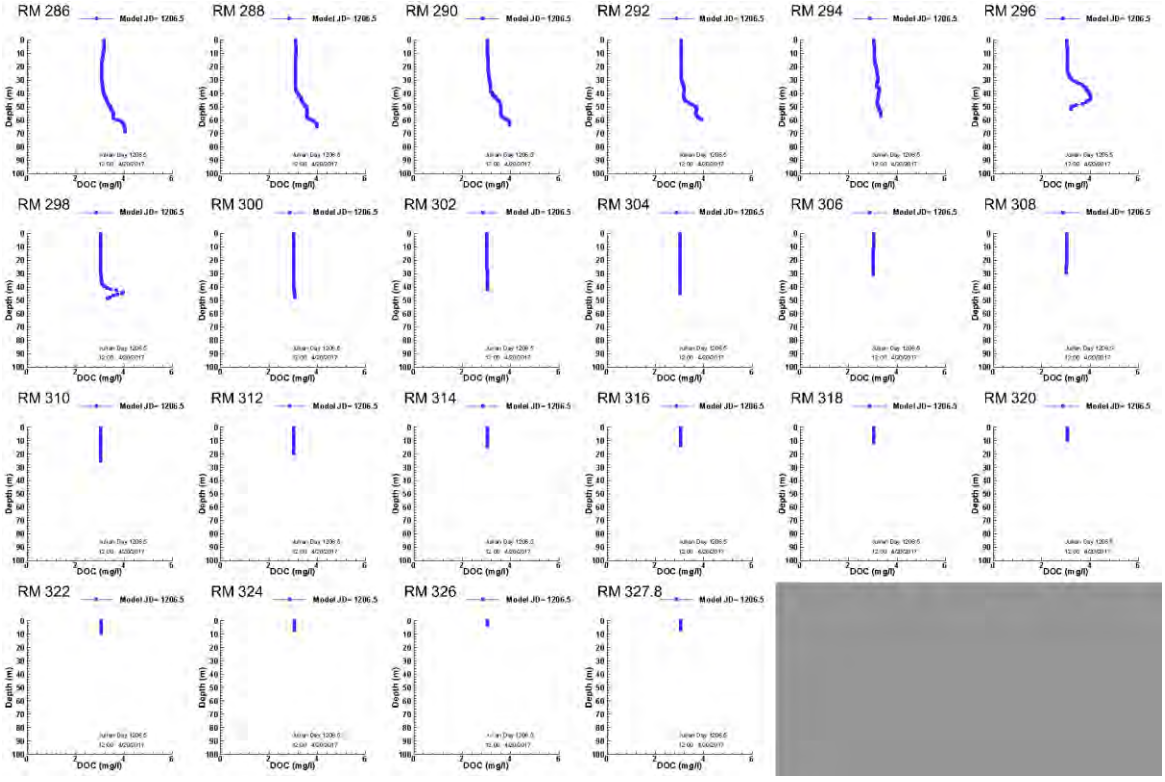


Figure 1494. Vertical profiles of DOC compared with data for 4/20/2017.

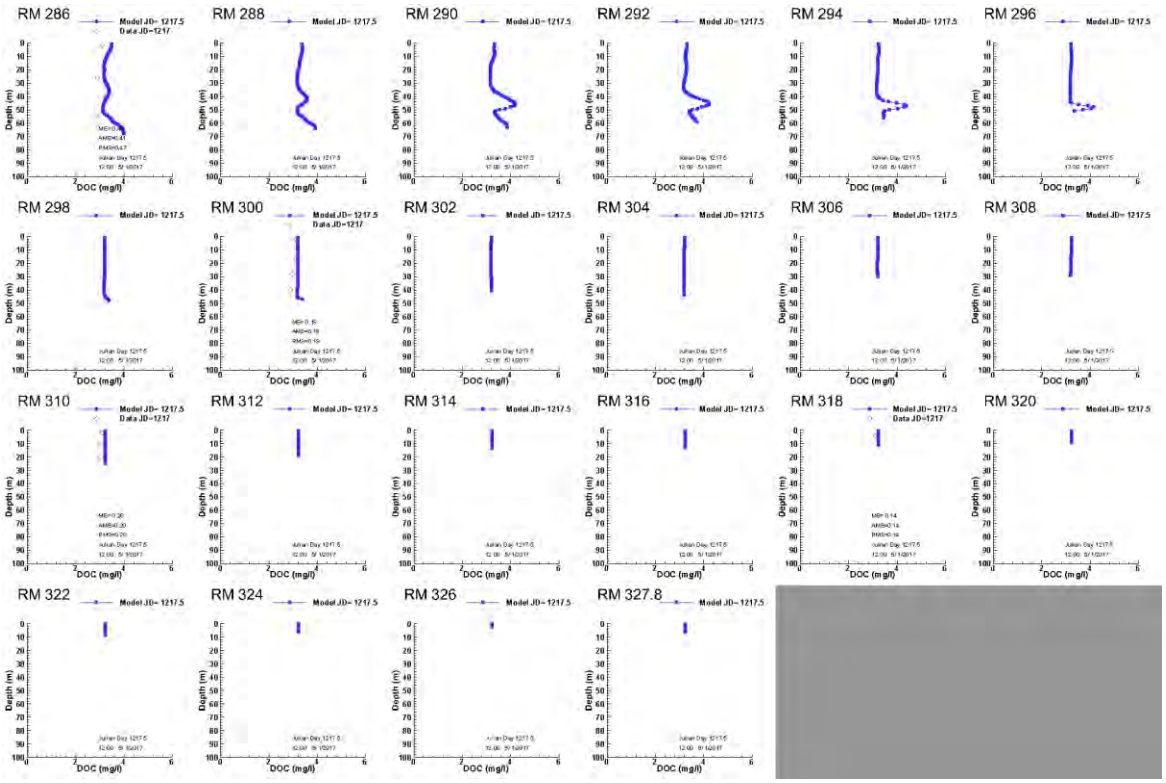


Figure 1495. Vertical profiles of DOC compared with data for 5/ 1/2017.

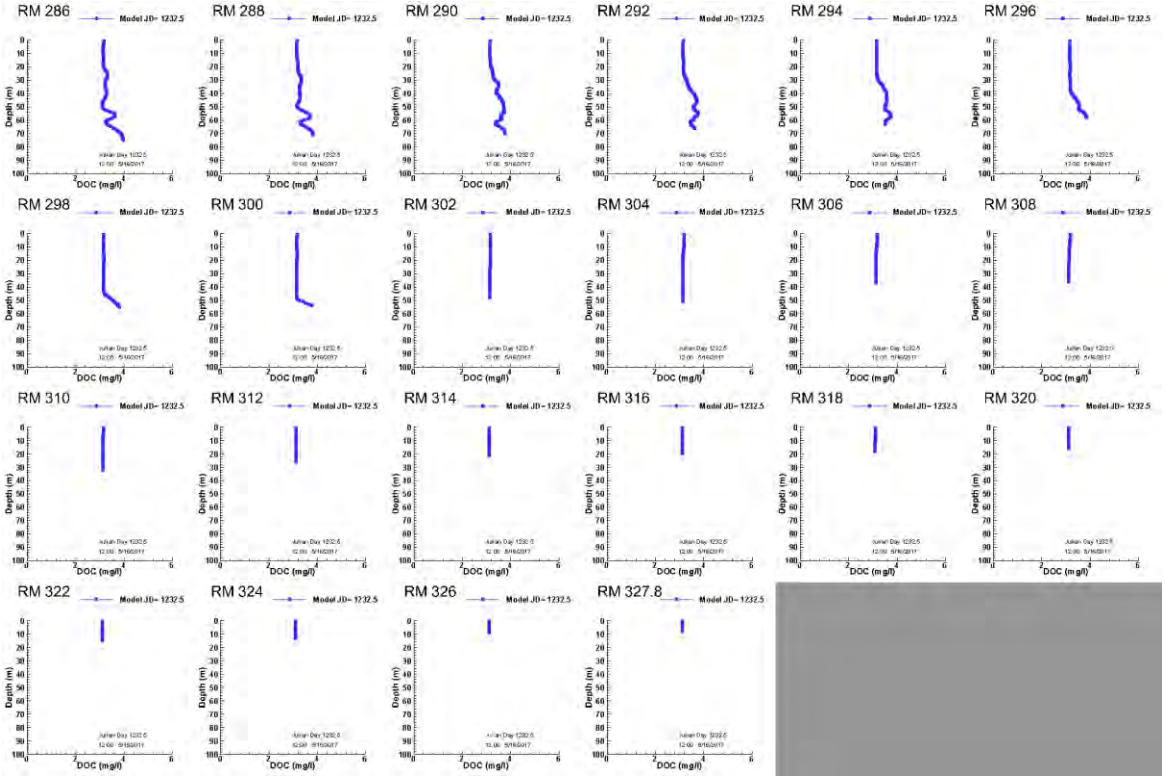


Figure 1496. Vertical profiles of DOC compared with data for 5/16/2017.

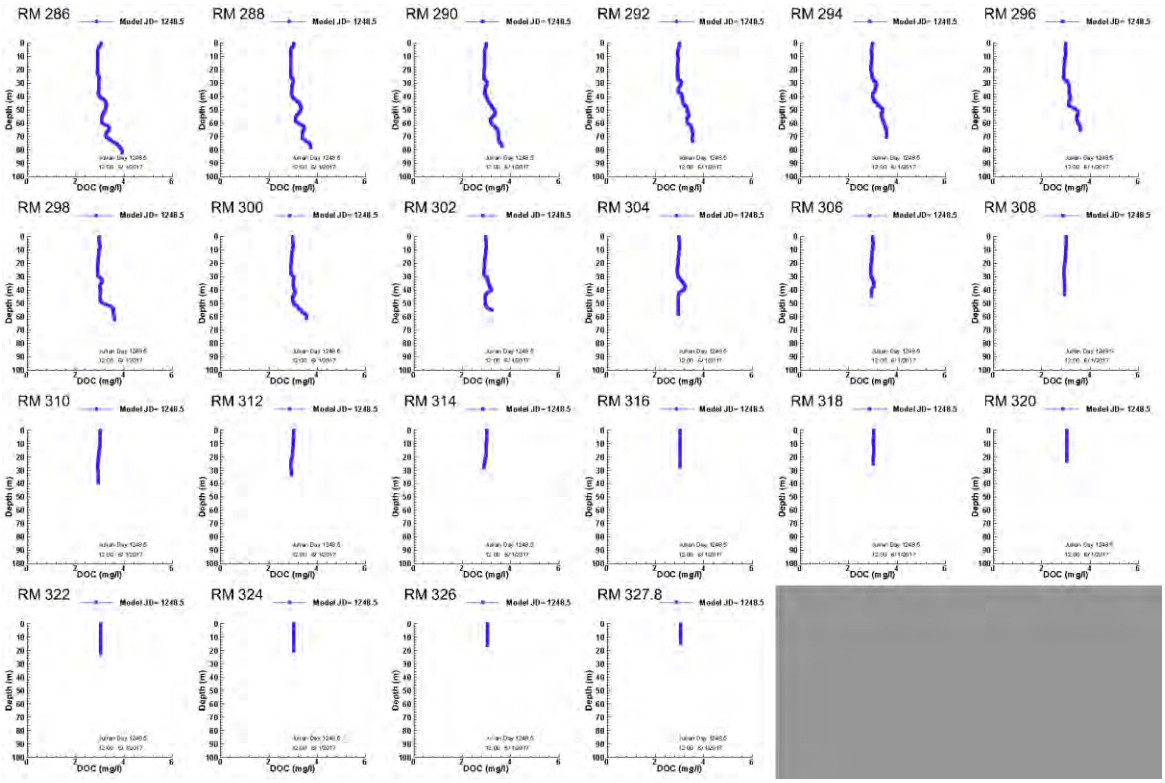


Figure 1497. Vertical profiles of DOC compared with data for 6/ 1/2017.

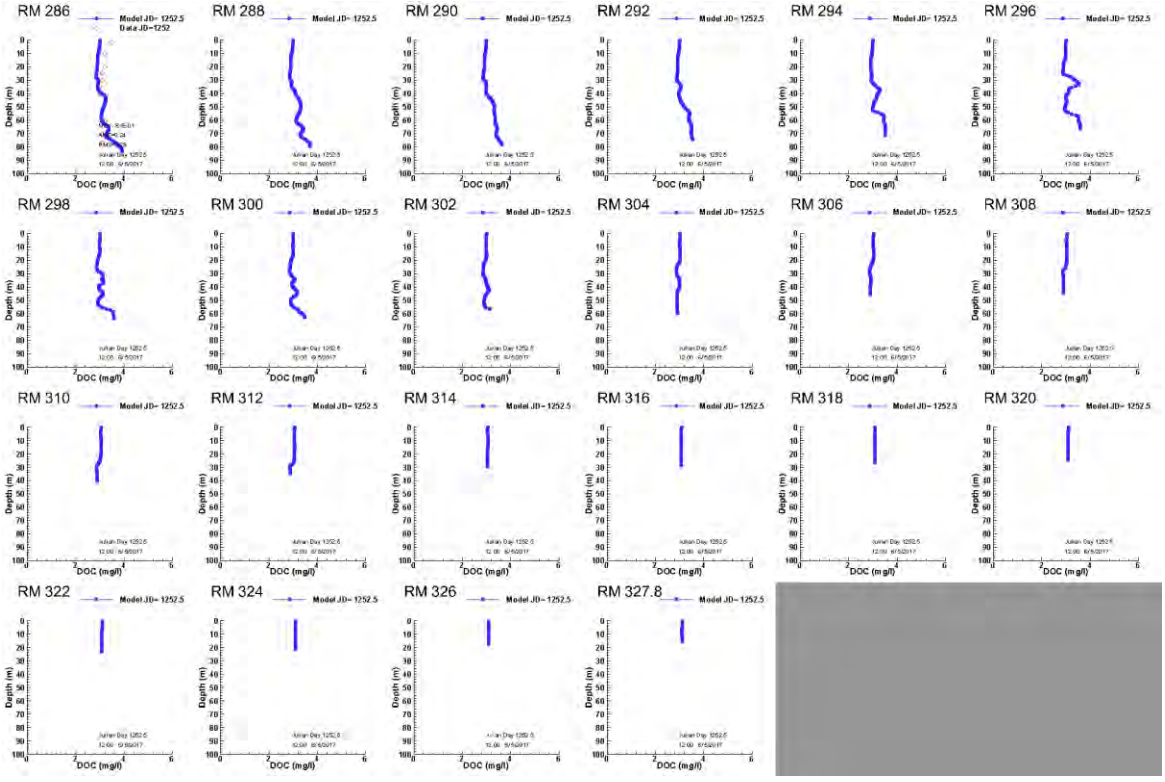


Figure 1498. Vertical profiles of DOC compared with data for 6/ 5/2017.

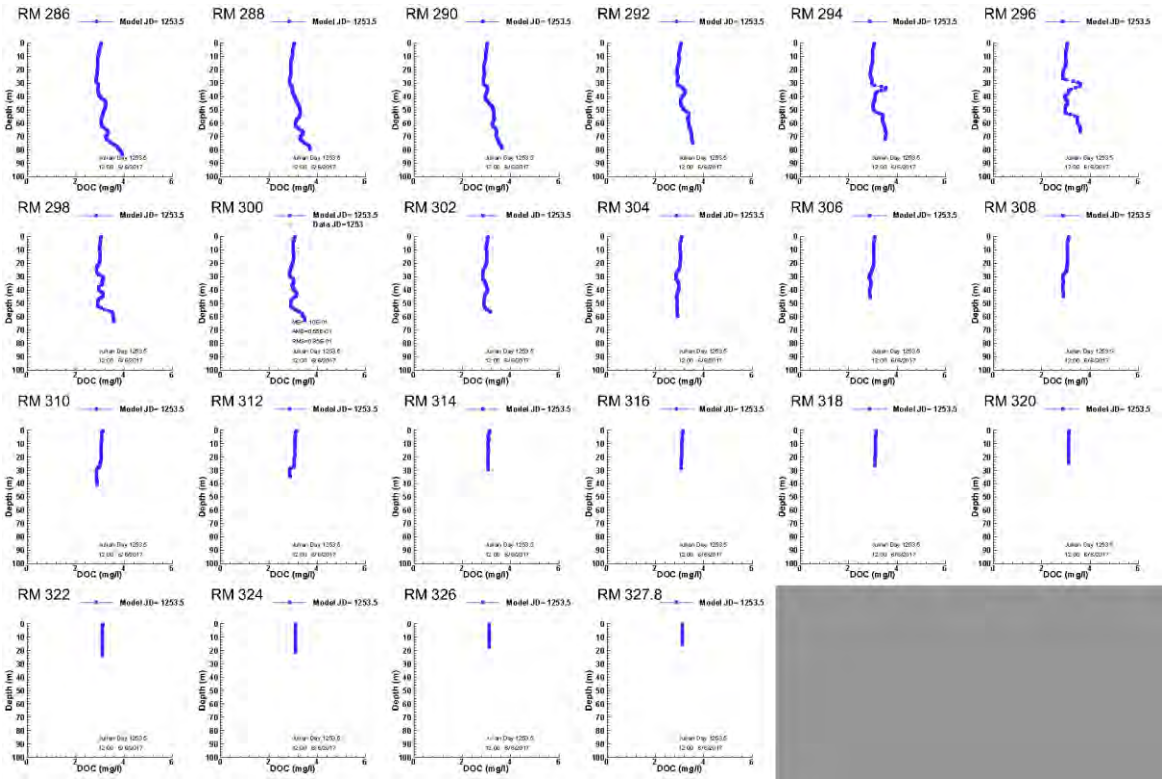


Figure 1499. Vertical profiles of DOC compared with data for 6/ 6/2017.

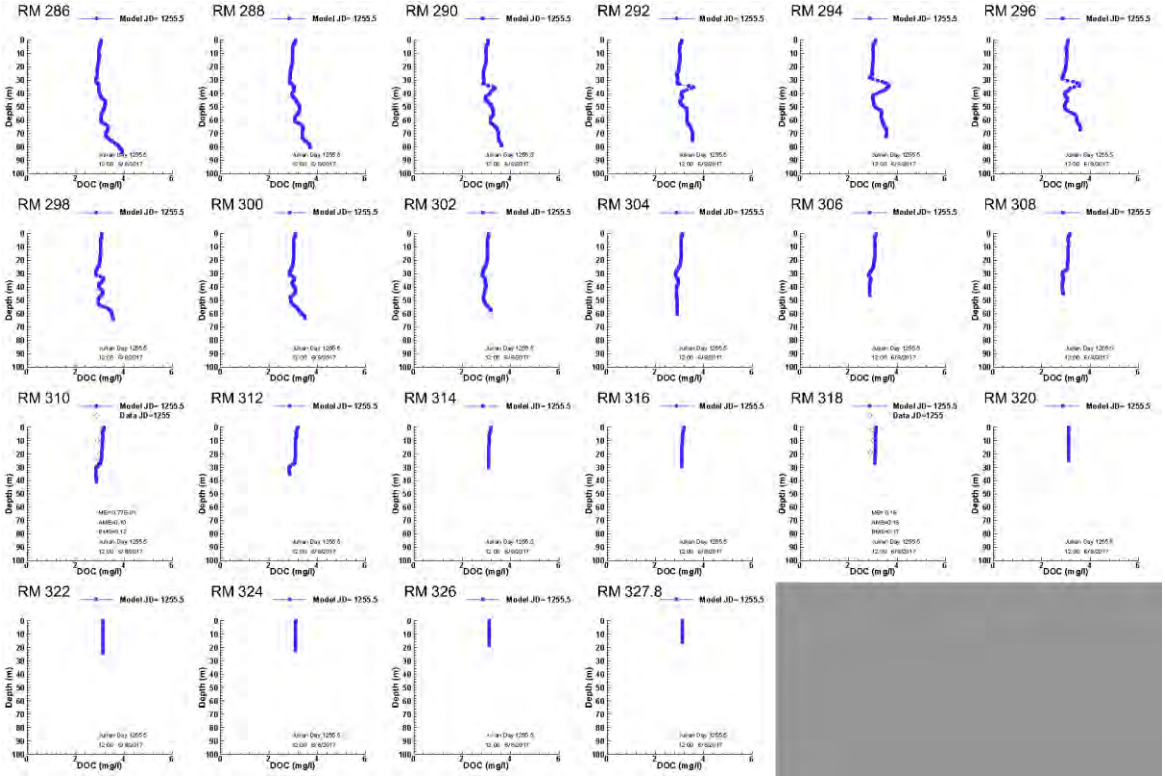


Figure 1500. Vertical profiles of DOC compared with data for 6/ 8/2017.

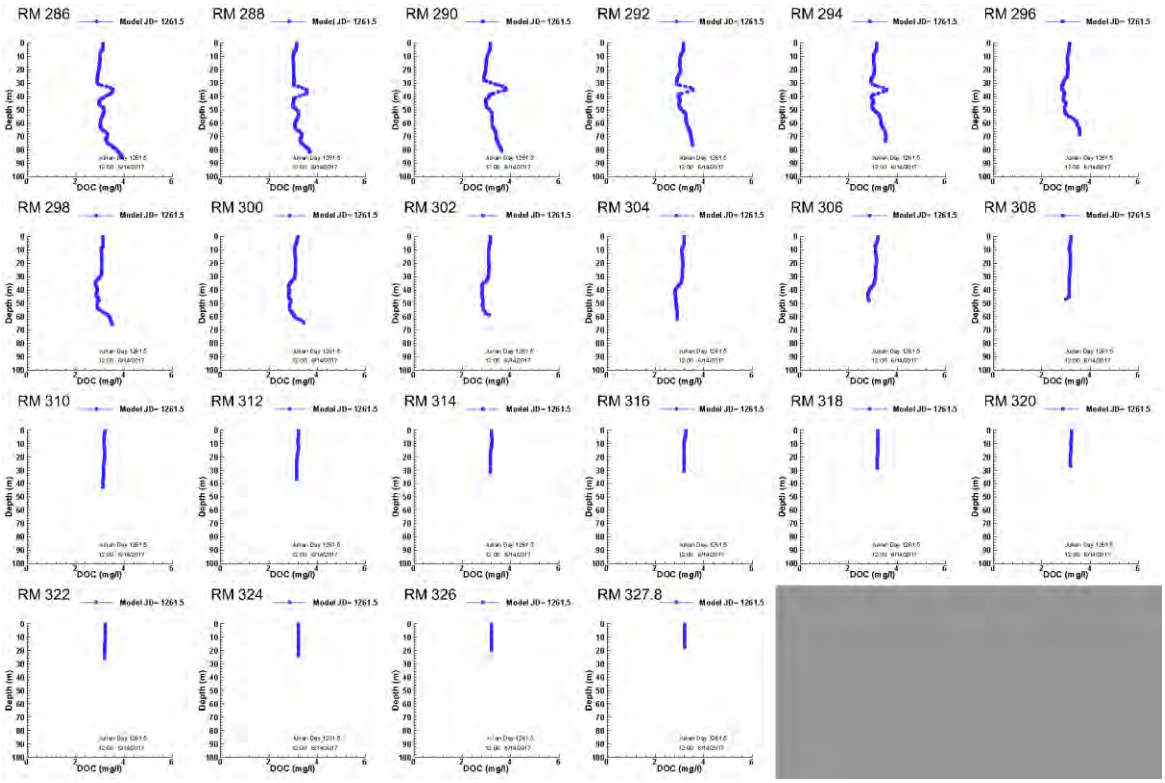


Figure 1501. Vertical profiles of DOC compared with data for 6/14/2017.

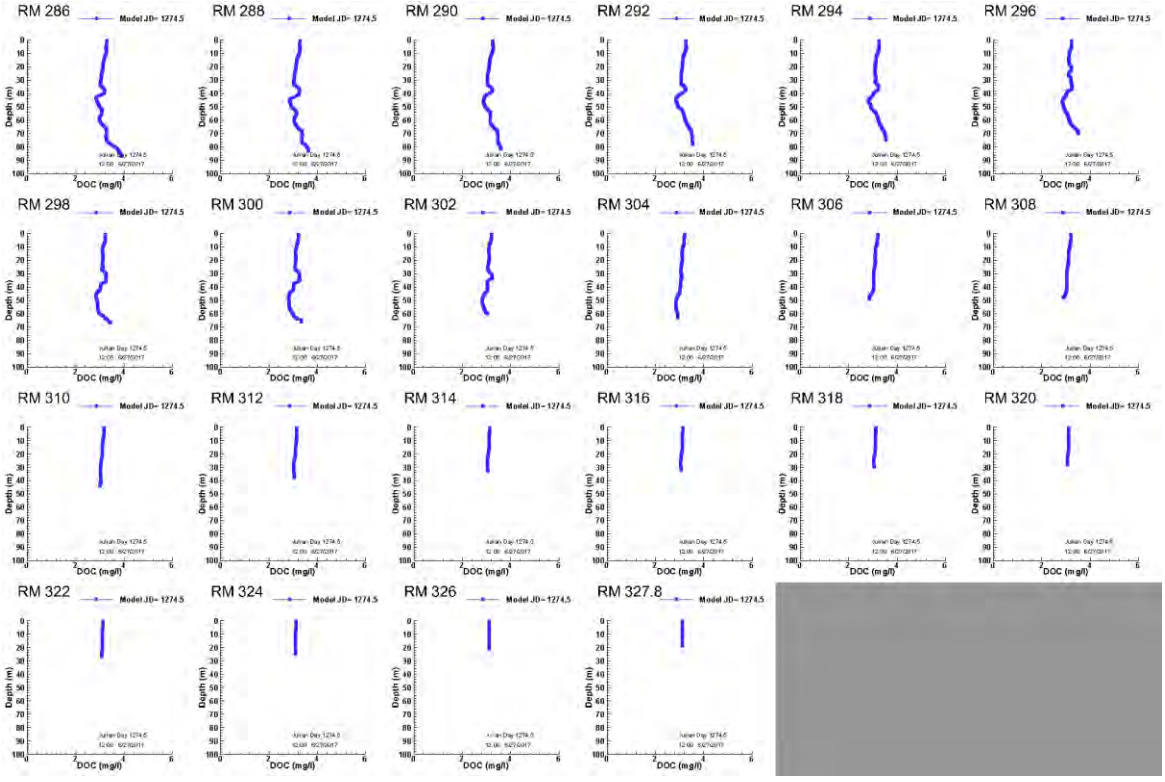


Figure 1502. Vertical profiles of DOC compared with data for 6/27/2017.

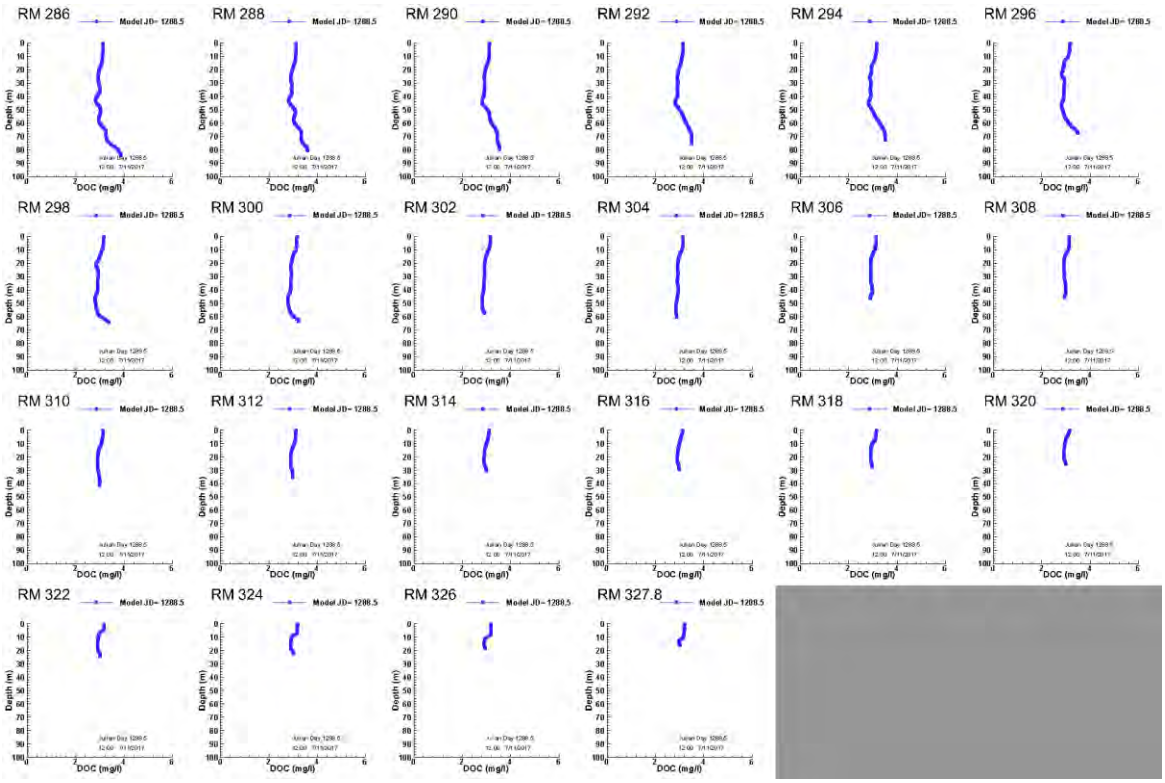


Figure 1503. Vertical profiles of DOC compared with data for 7/11/2017.

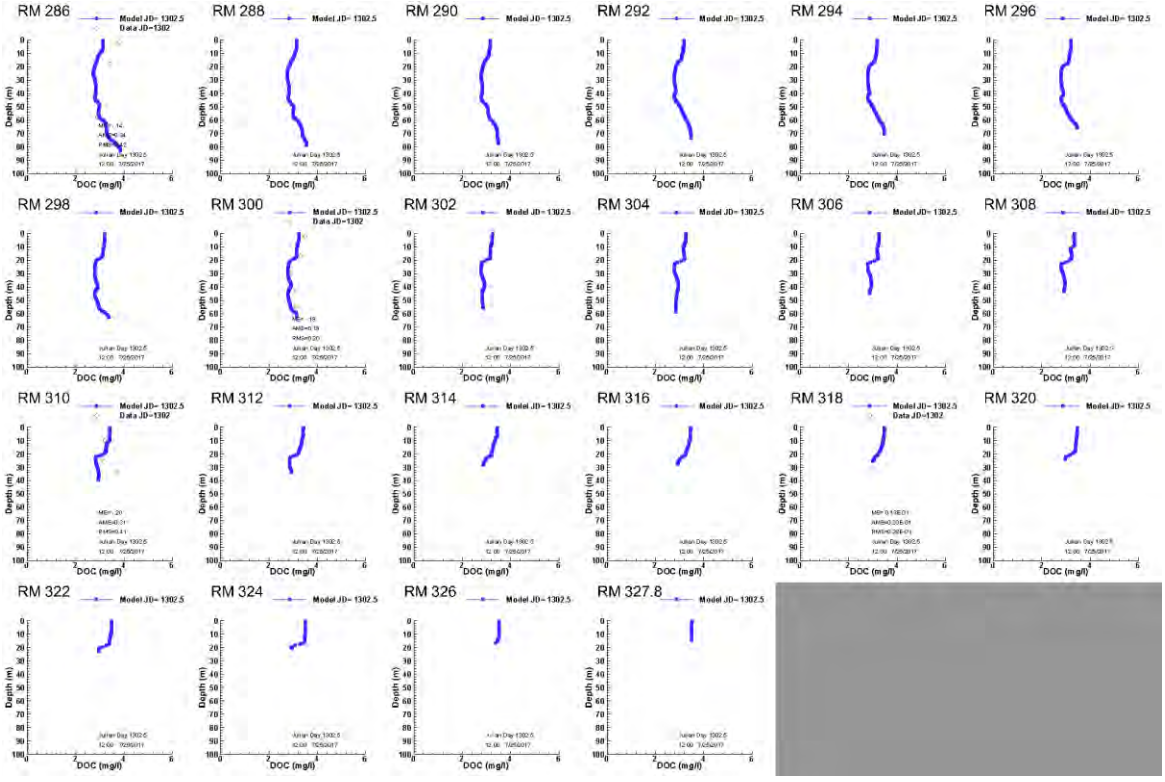


Figure 1504. Vertical profiles of DOC compared with data for 7/25/2017.

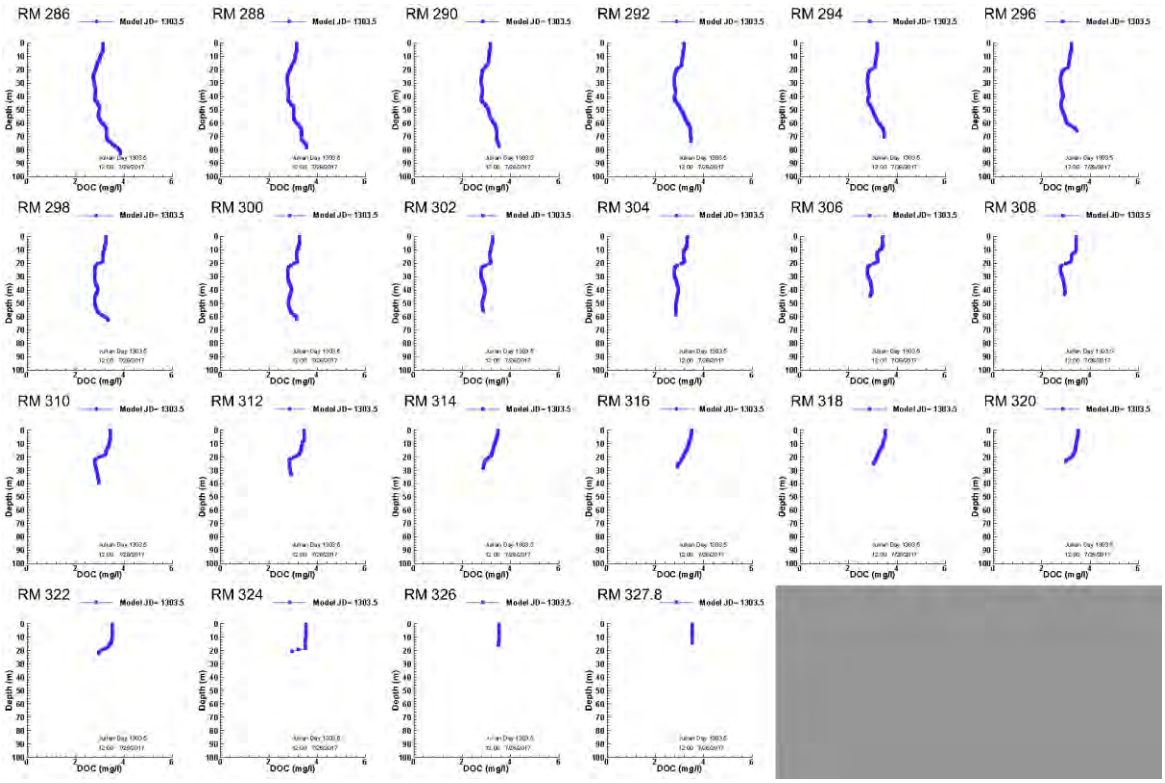


Figure 1505. Vertical profiles of DOC compared with data for 7/26/2017.

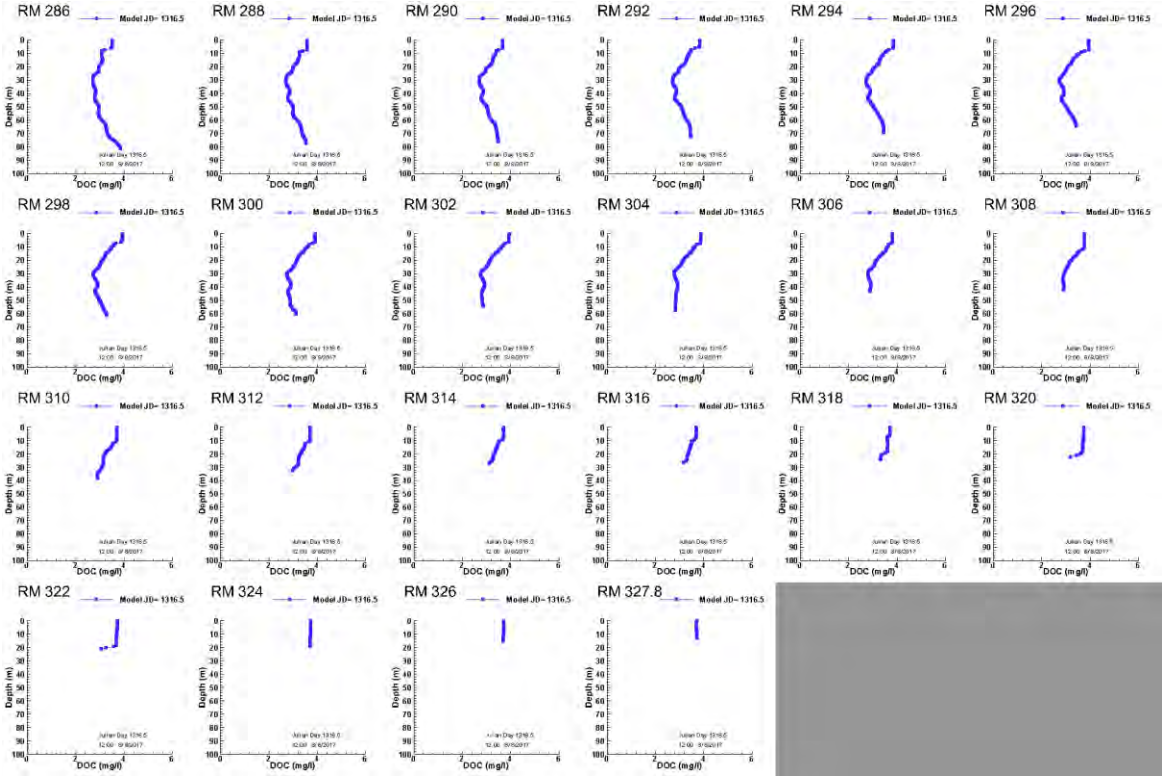


Figure 1506. Vertical profiles of DOC compared with data for 8/ 8/2017.

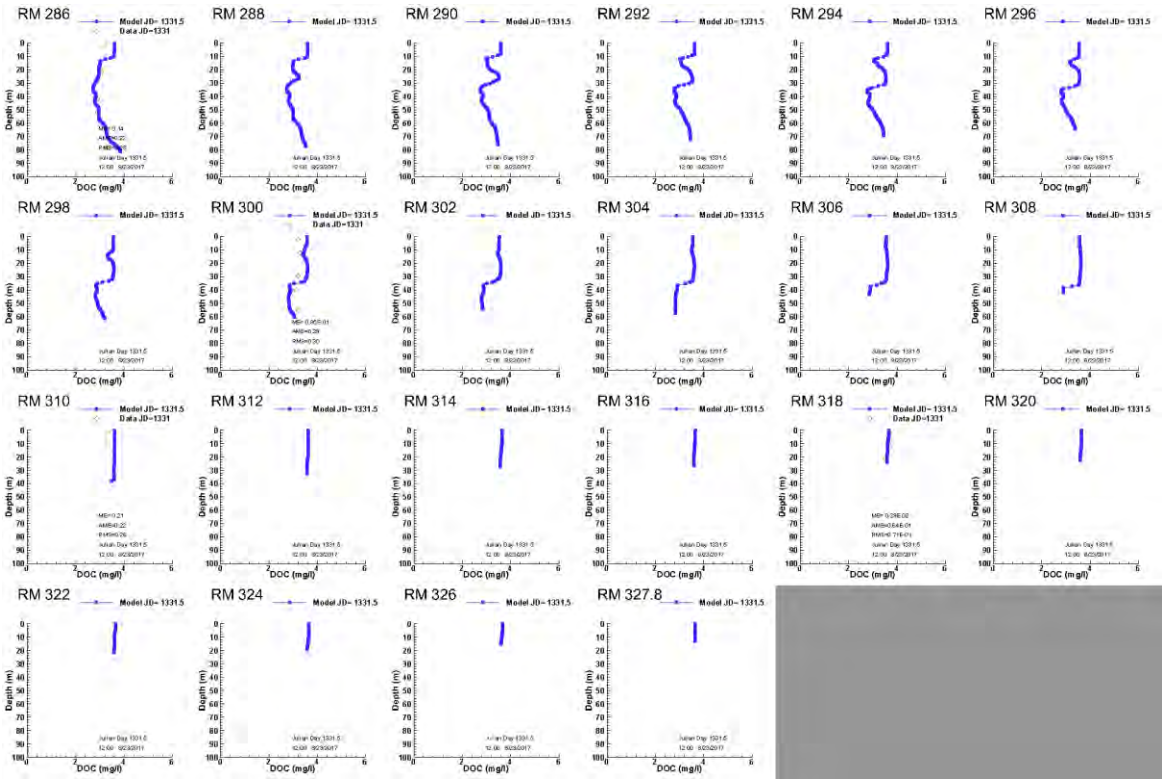


Figure 1507. Vertical profiles of DOC compared with data for 8/23/2017.

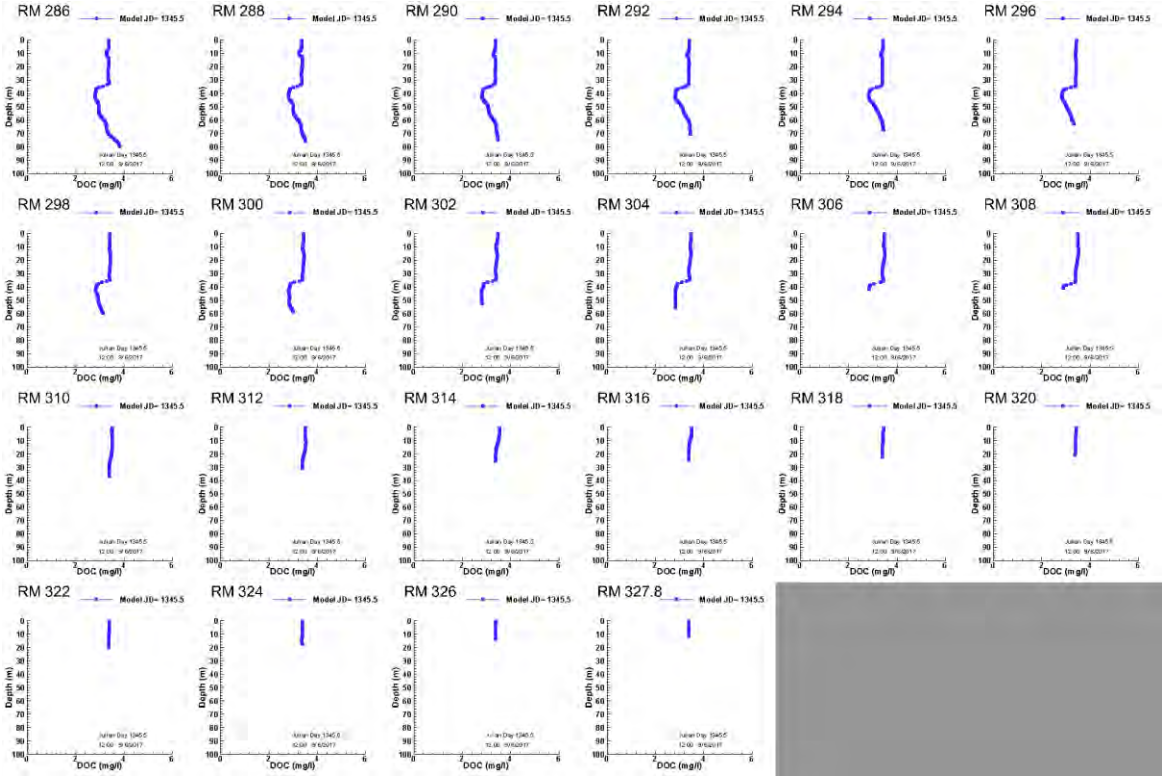


Figure 1508. Vertical profiles of DOC compared with data for 9/ 6/2017.

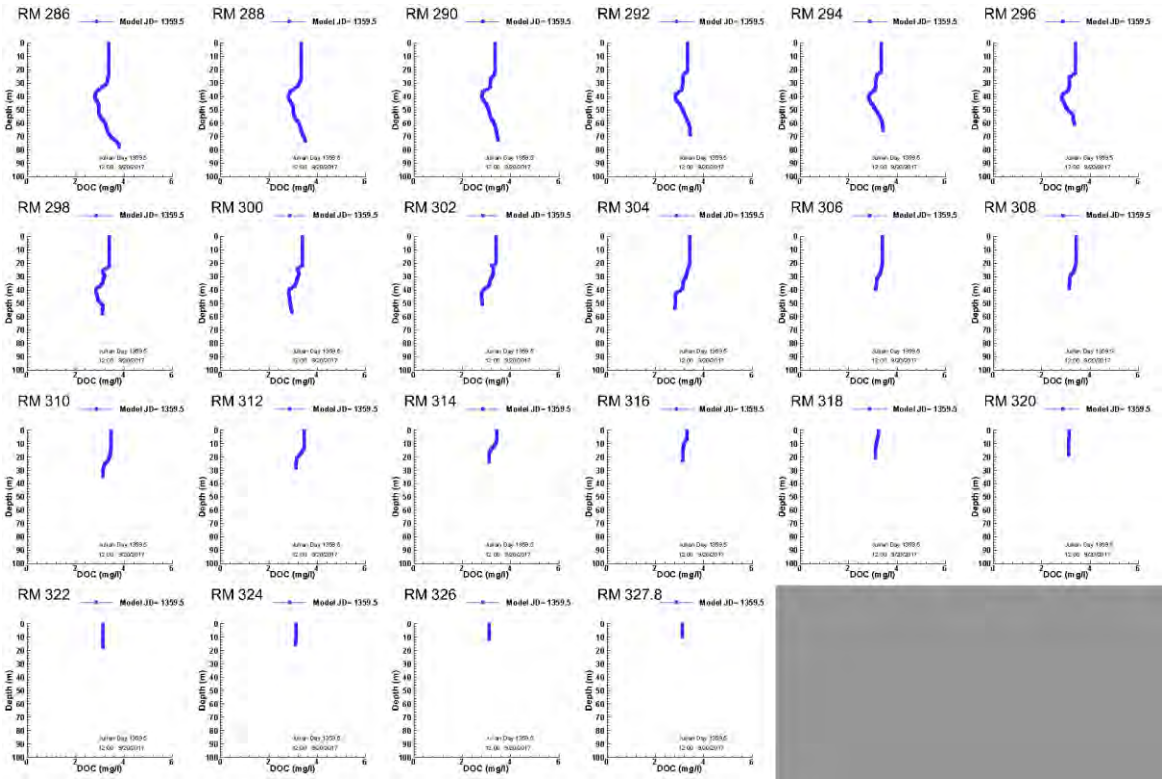


Figure 1509. Vertical profiles of DOC compared with data for 9/20/2017.

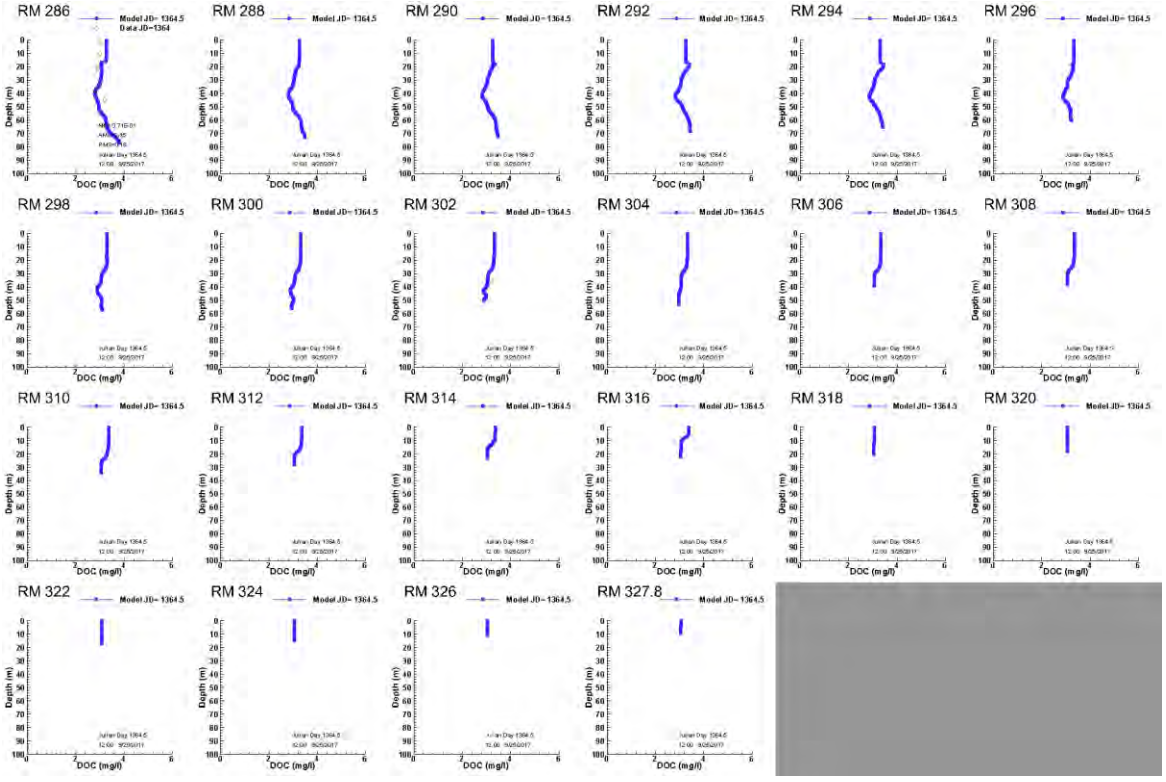


Figure 1510. Vertical profiles of DOC compared with data for 9/25/2017.

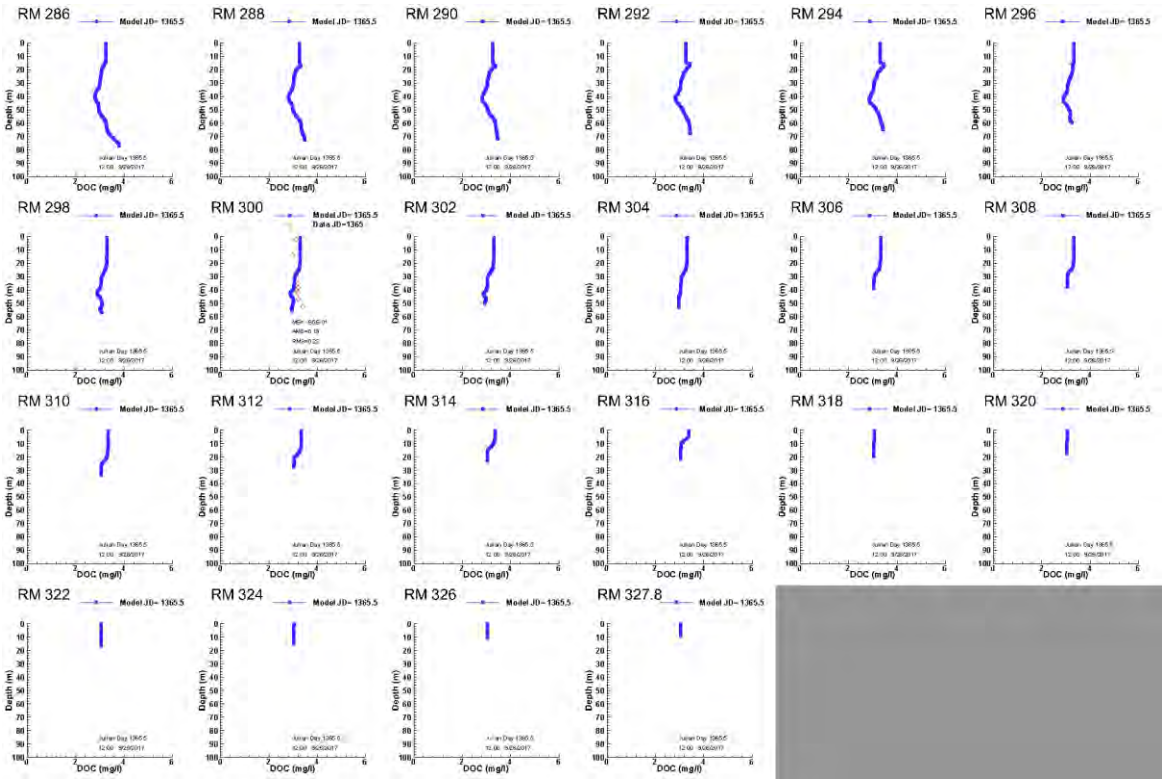


Figure 1511. Vertical profiles of DOC compared with data for 9/26/2017.

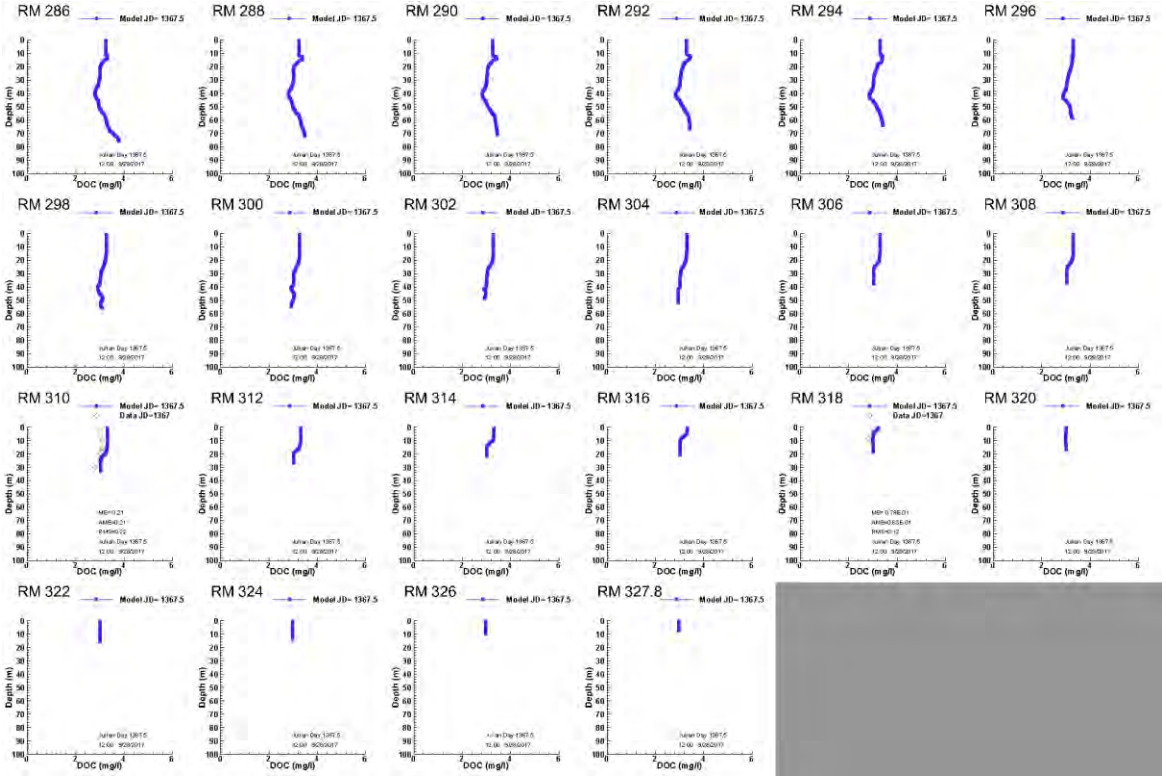


Figure 1512. Vertical profiles of DOC compared with data for 9/28/2017.

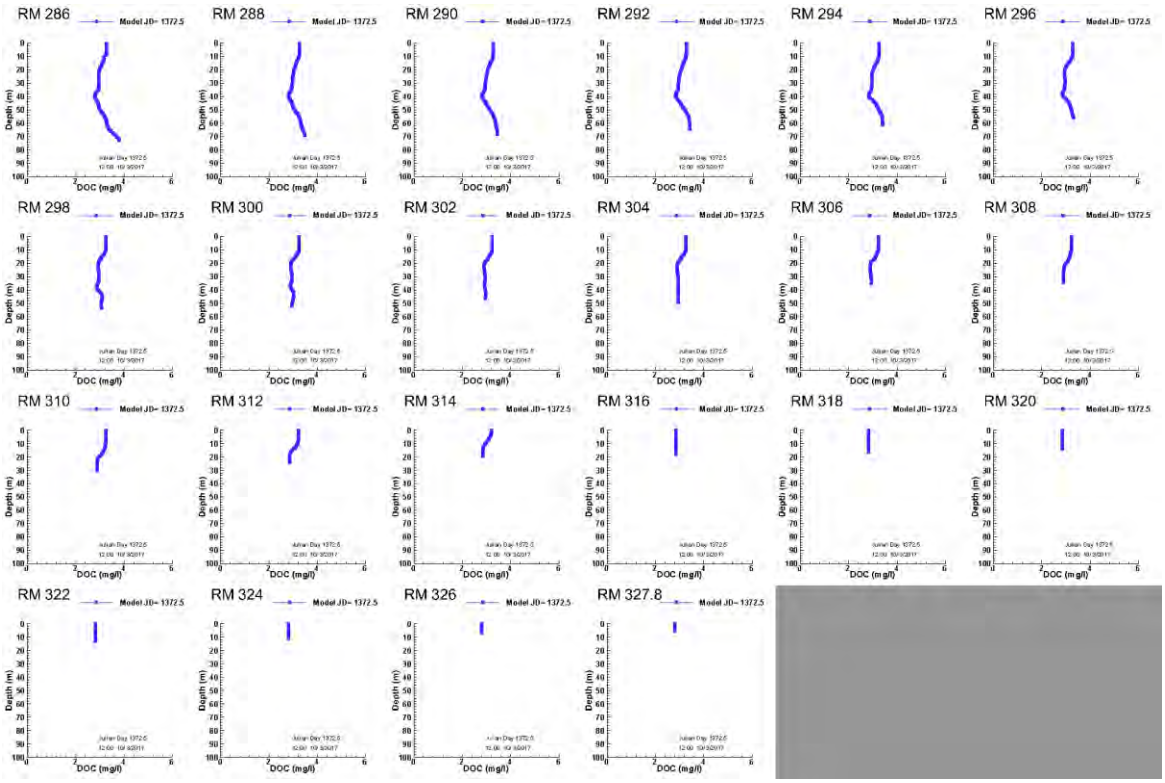


Figure 1513. Vertical profiles of DOC compared with data for 10/ 3/2017.

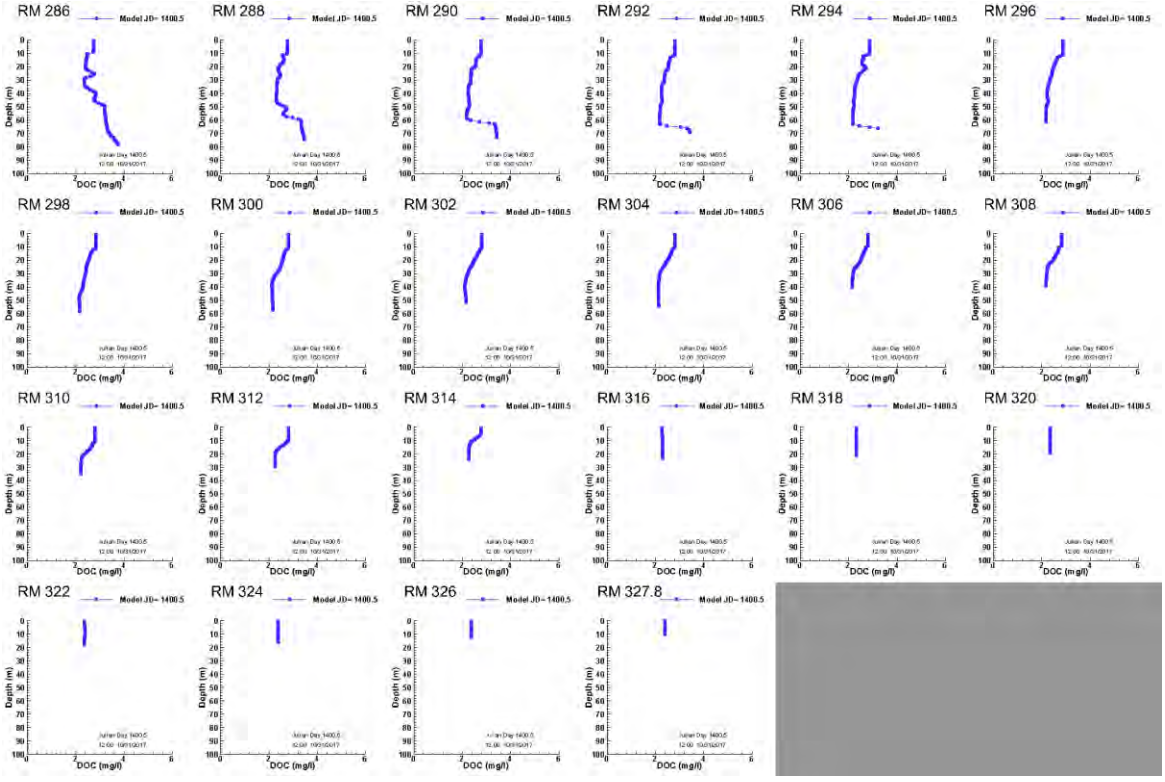


Figure 1514. Vertical profiles of DOC compared with data for 10/31/2017.

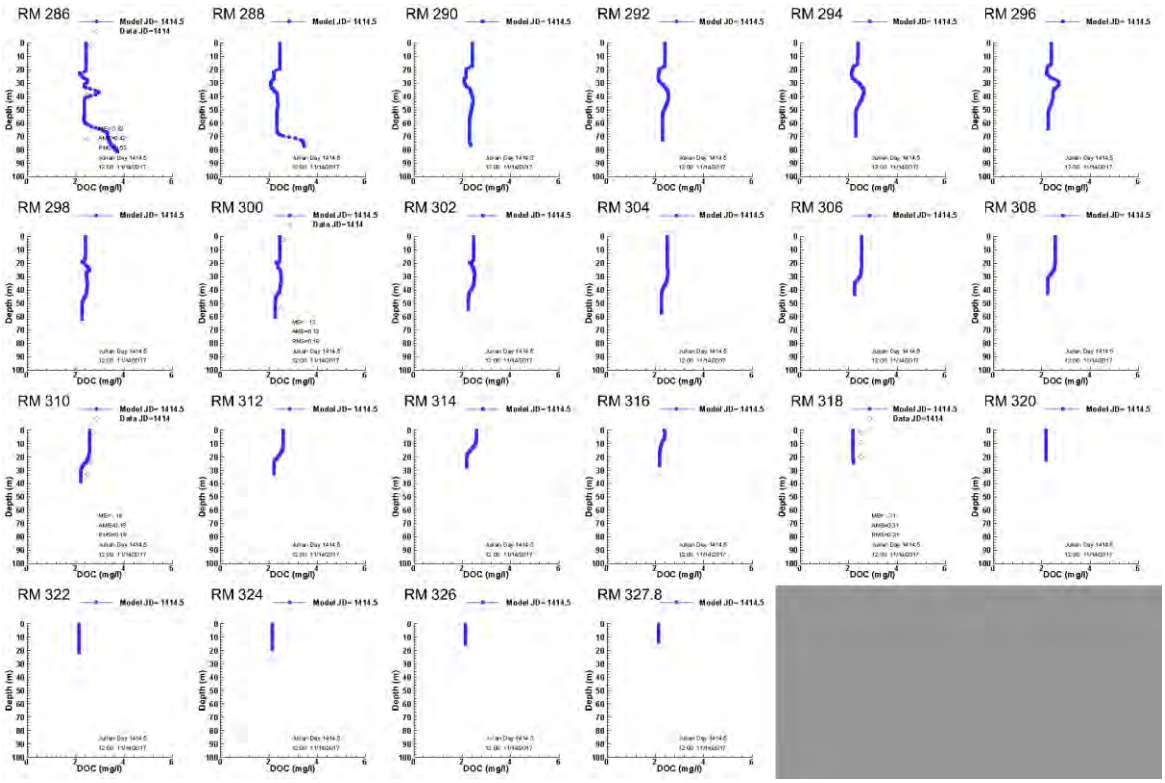


Figure 1515. Vertical profiles of DOC compared with data for 11/14/2017.

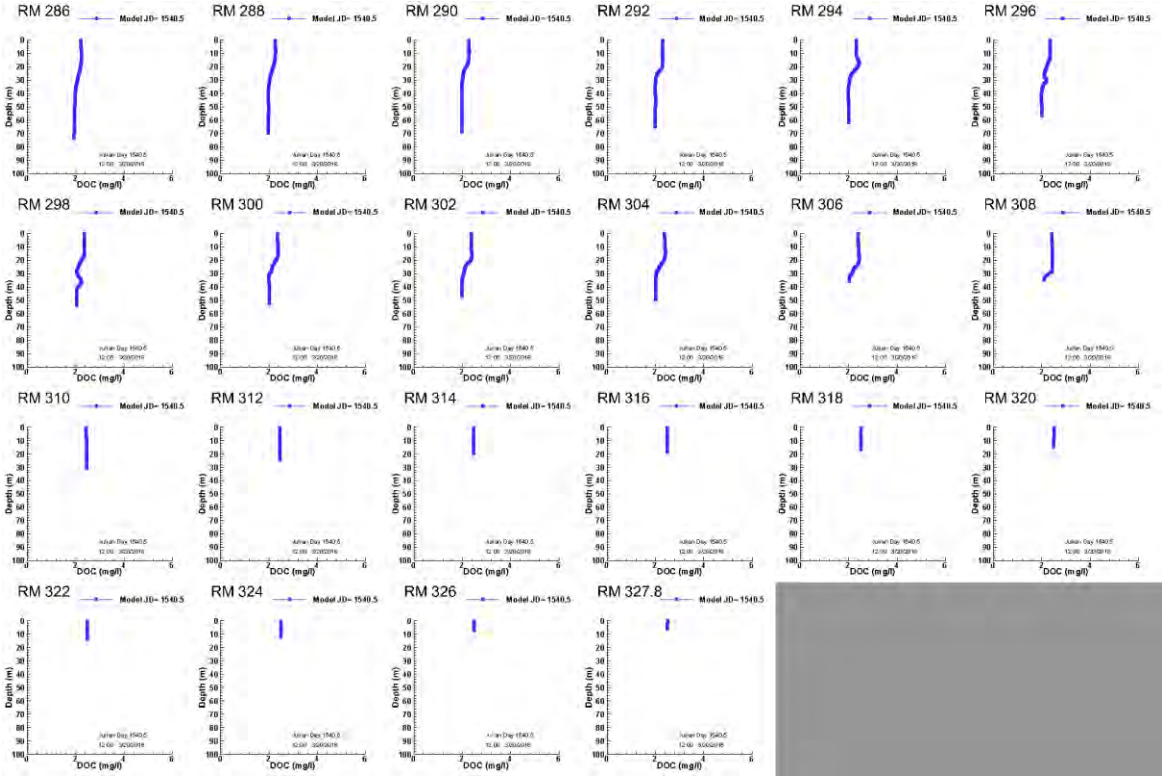


Figure 1516. Vertical profiles of DOC compared with data for 3/20/2018.

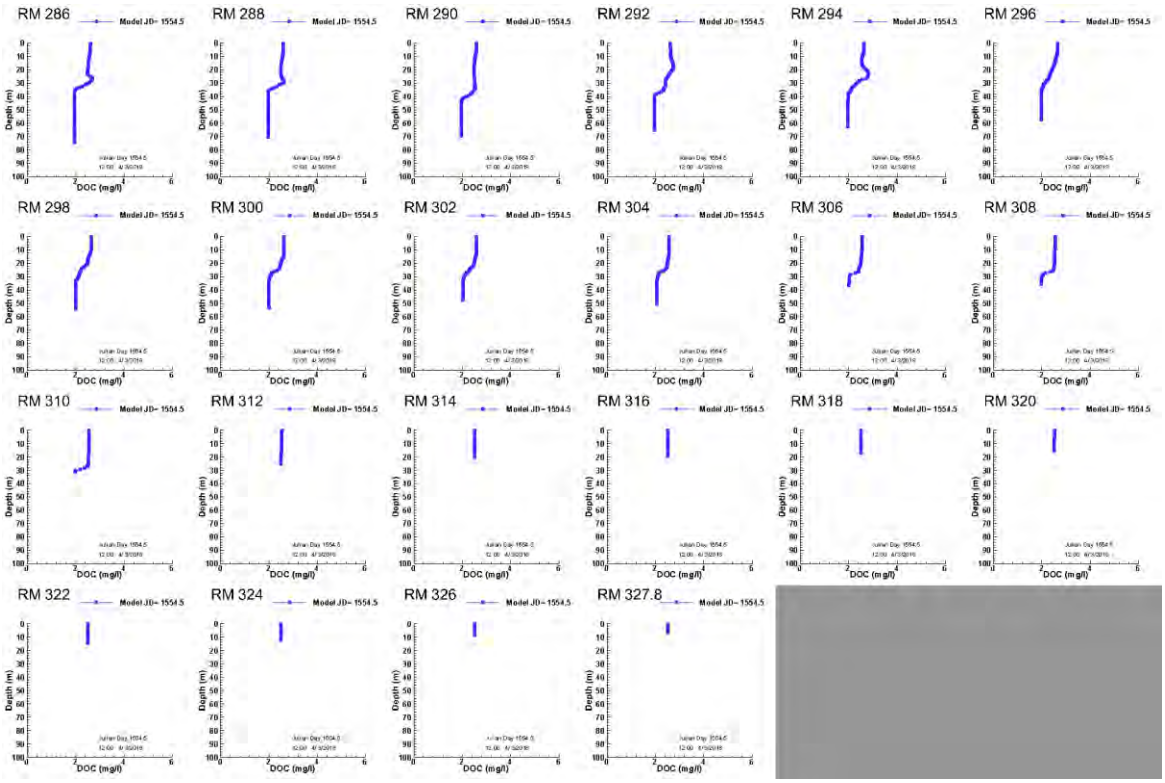


Figure 1517. Vertical profiles of DOC compared with data for 4/ 3/2018.

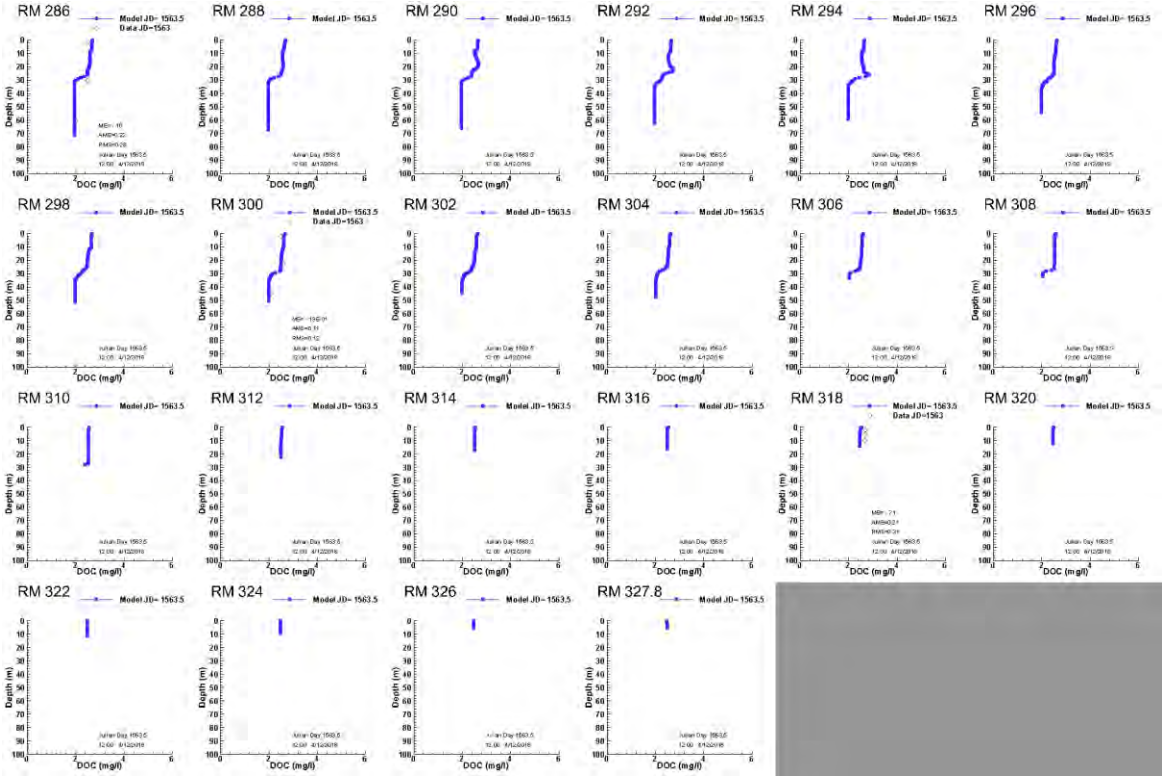


Figure 1518. Vertical profiles of DOC compared with data for 4/12/2018.

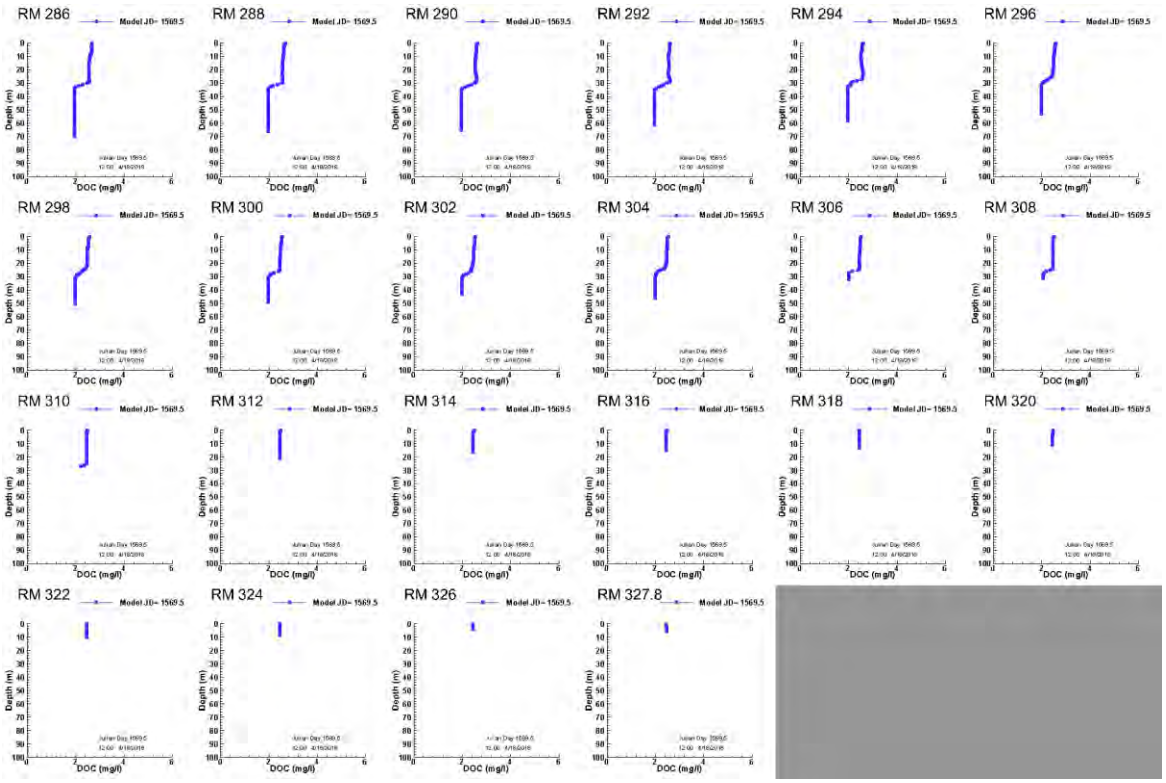


Figure 1519. Vertical profiles of DOC compared with data for 4/18/2018.

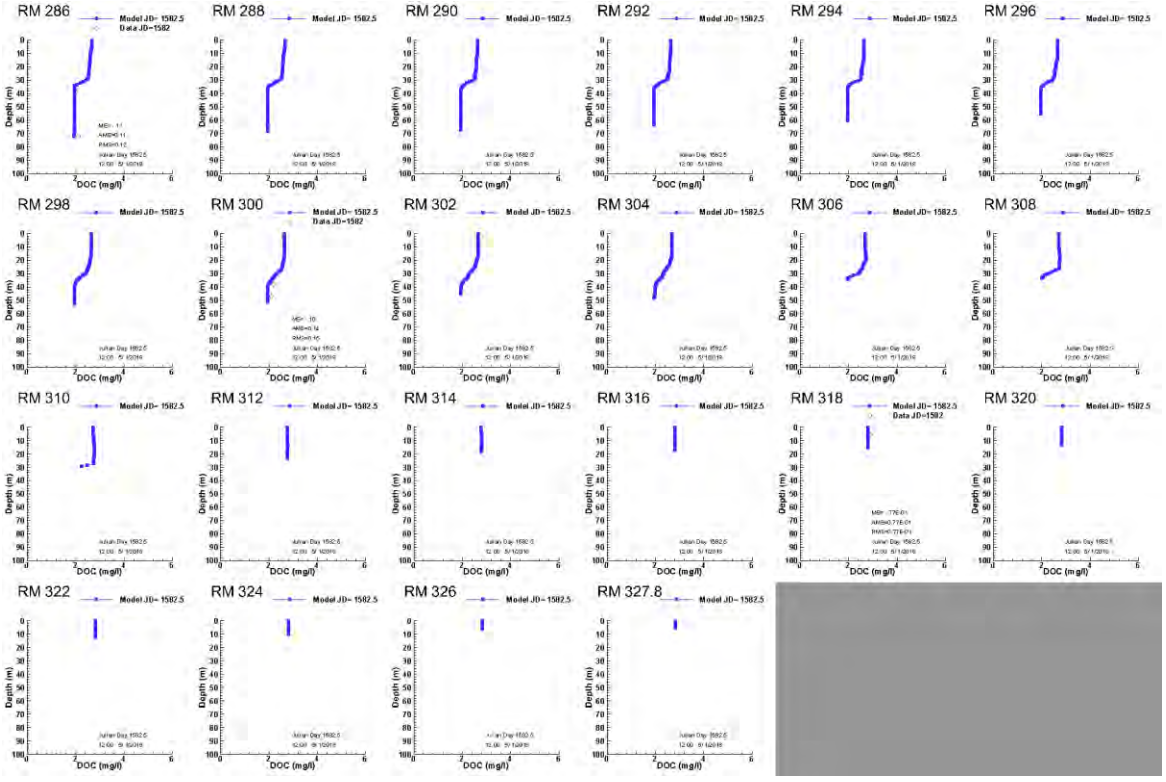


Figure 1520. Vertical profiles of DOC compared with data for 5/ 1/2018.

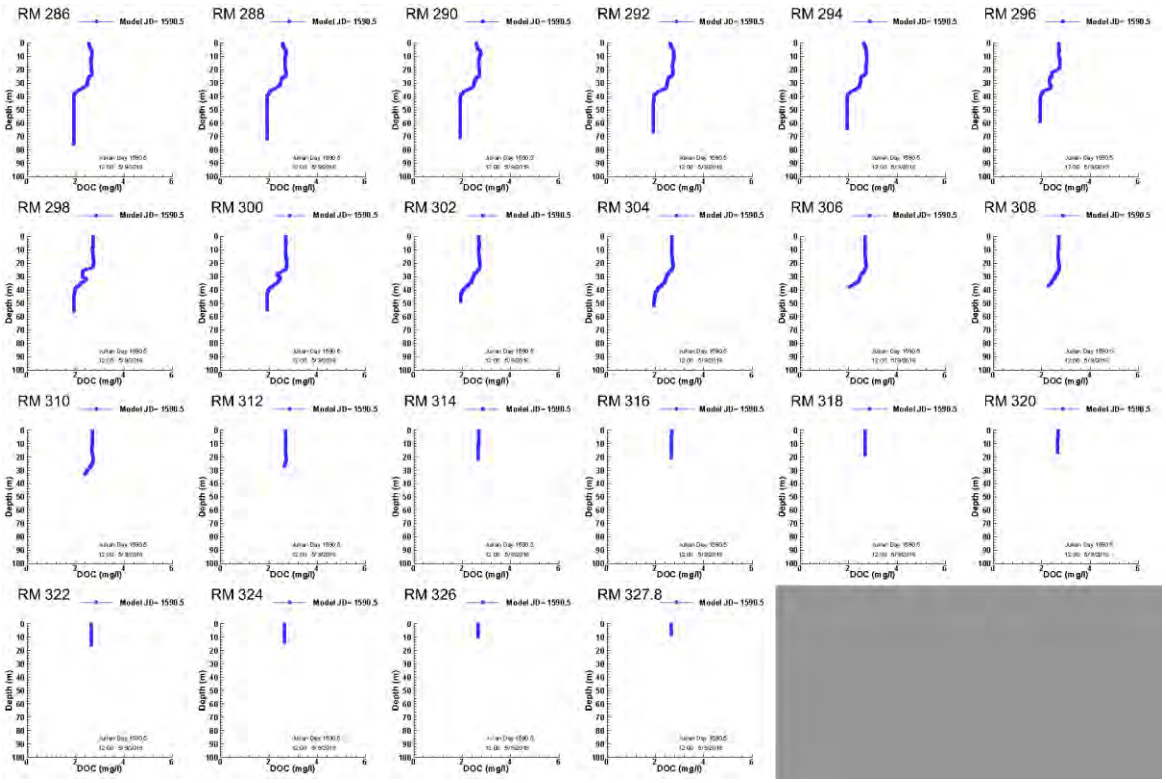


Figure 1521. Vertical profiles of DOC compared with data for 5/ 9/2018.

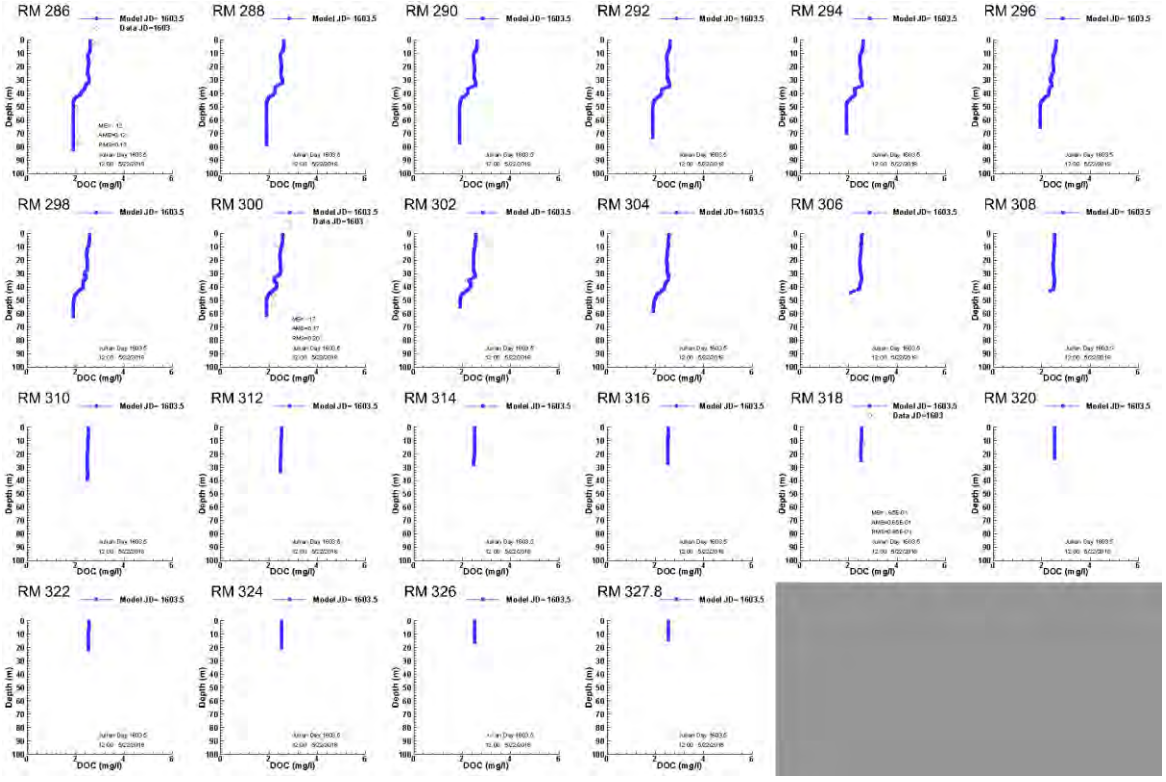


Figure 1522. Vertical profiles of DOC compared with data for 5/22/2018.

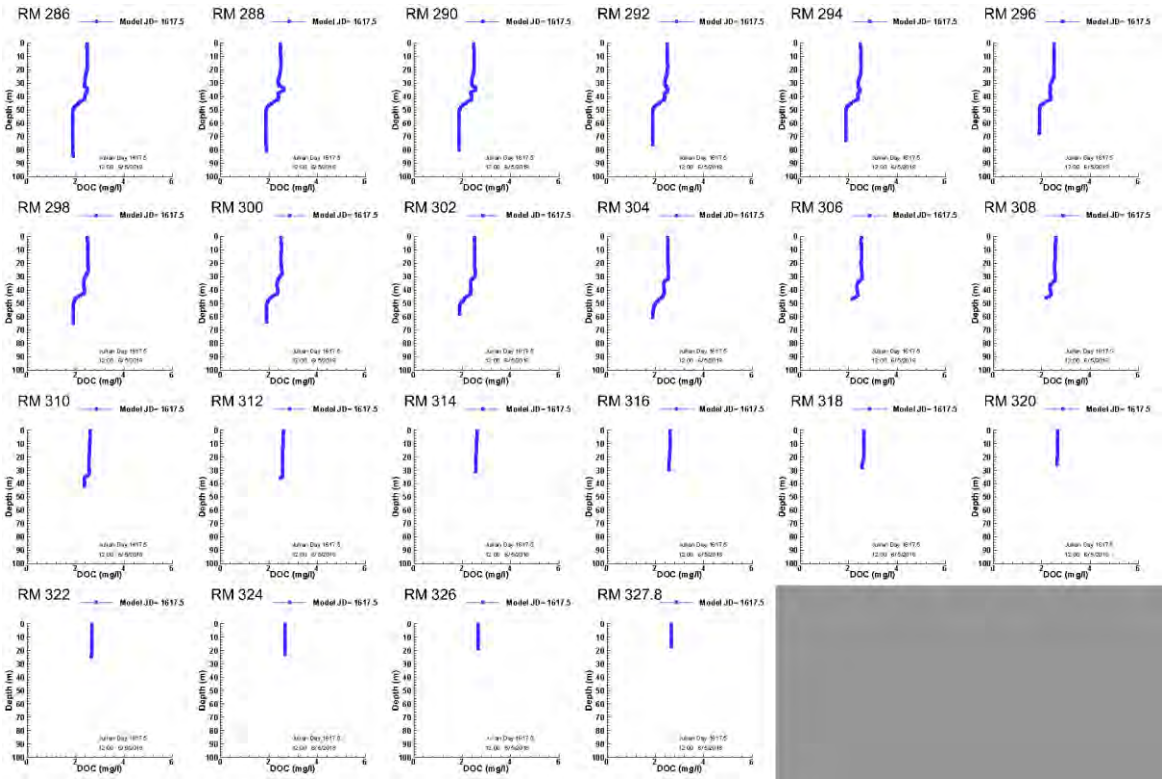


Figure 1523. Vertical profiles of DOC compared with data for 6/ 5/2018.

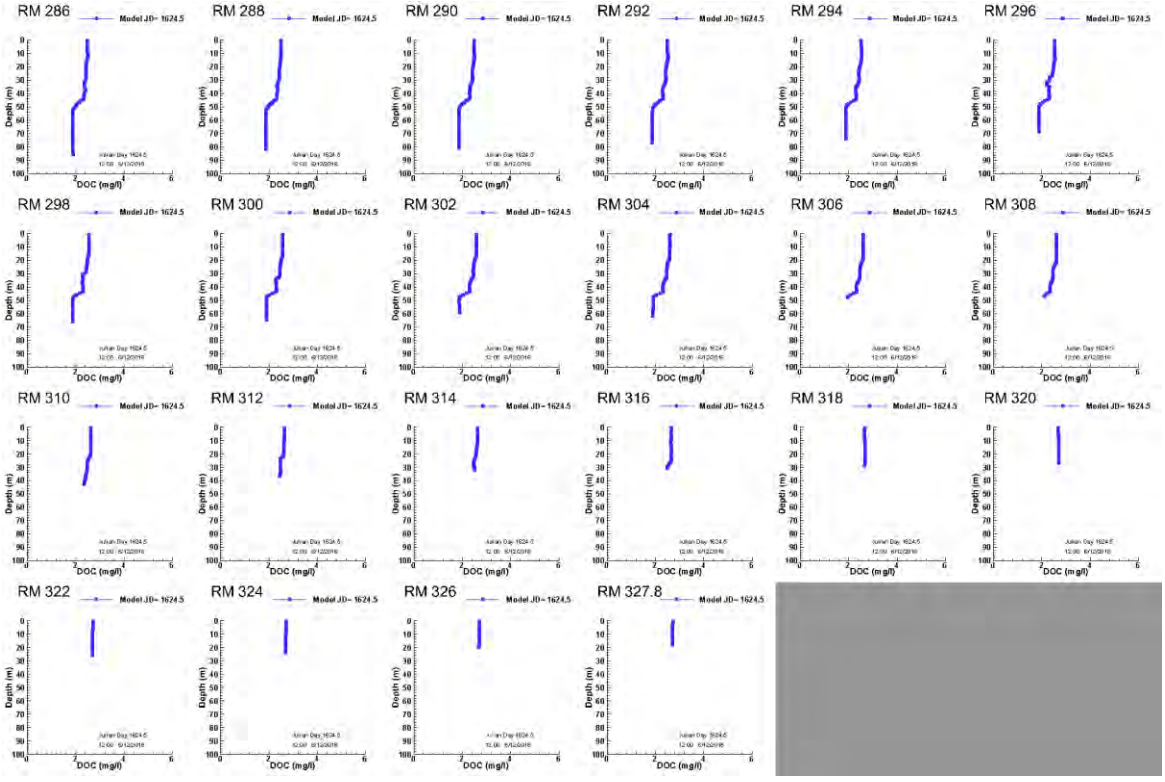


Figure 1524. Vertical profiles of DOC compared with data for 6/12/2018.

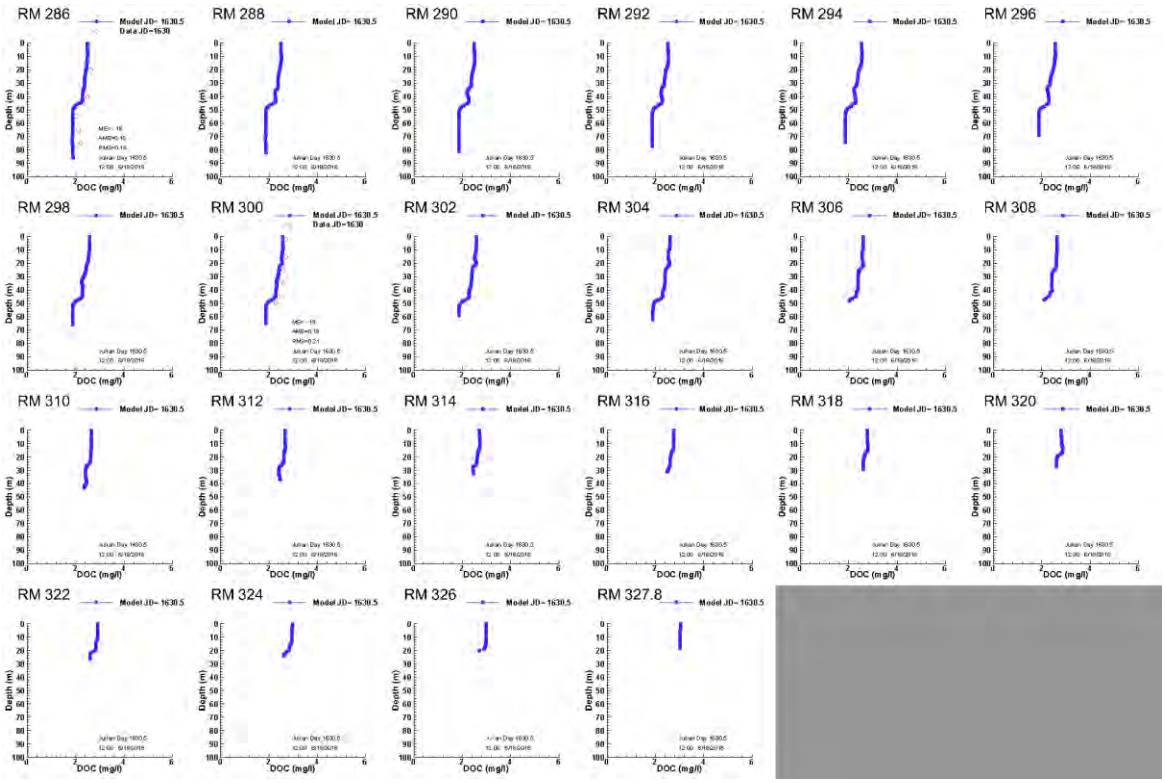


Figure 1525. Vertical profiles of DOC compared with data for 6/18/2018.

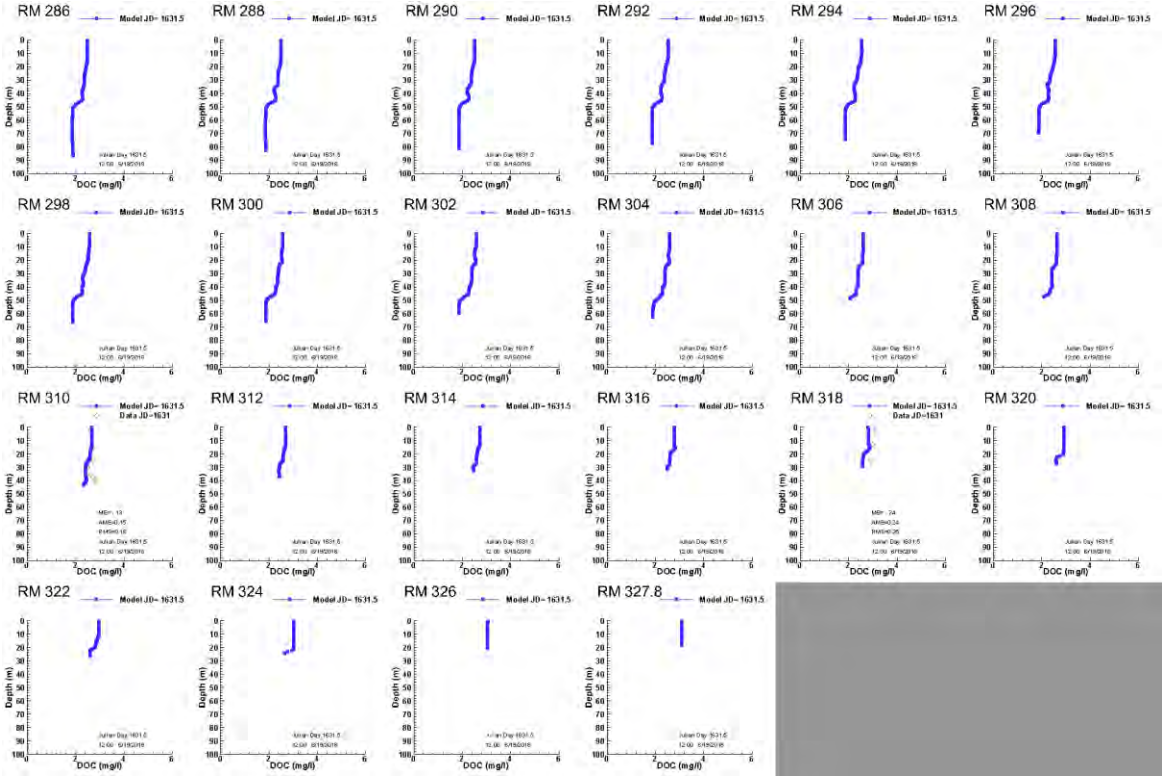


Figure 1526. Vertical profiles of DOC compared with data for 6/19/2018.

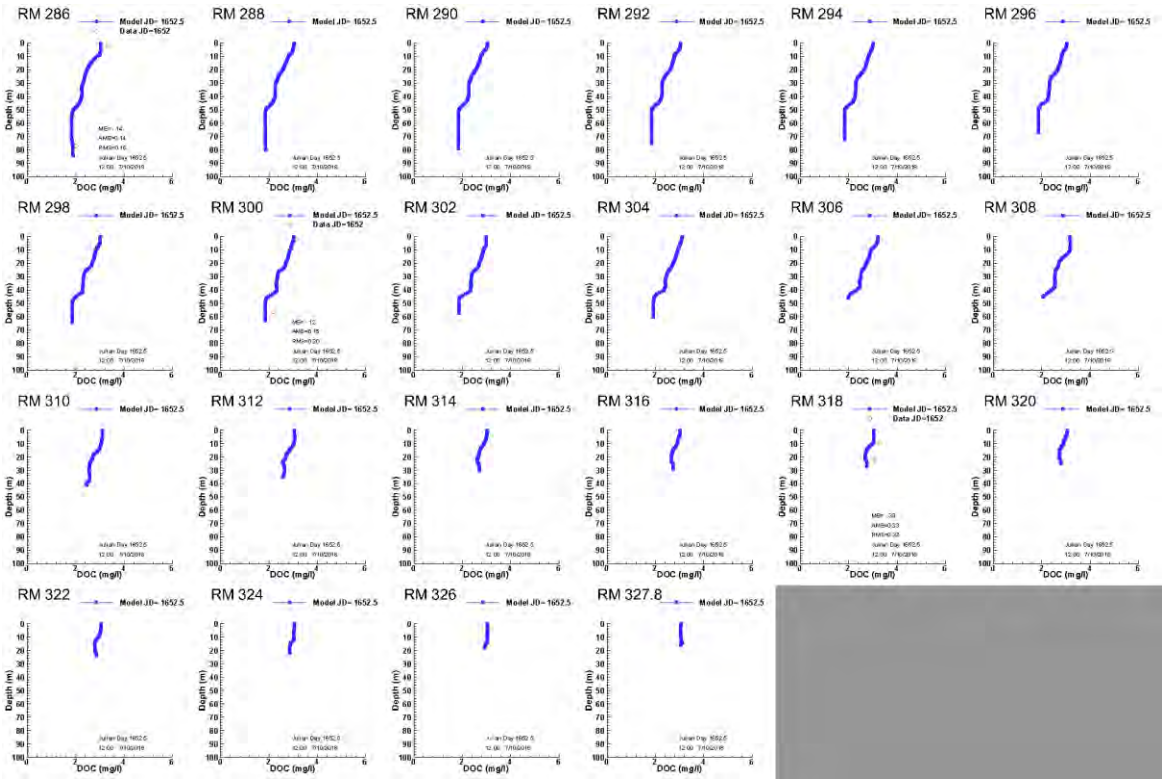


Figure 1527. Vertical profiles of DOC compared with data for 7/10/2018.

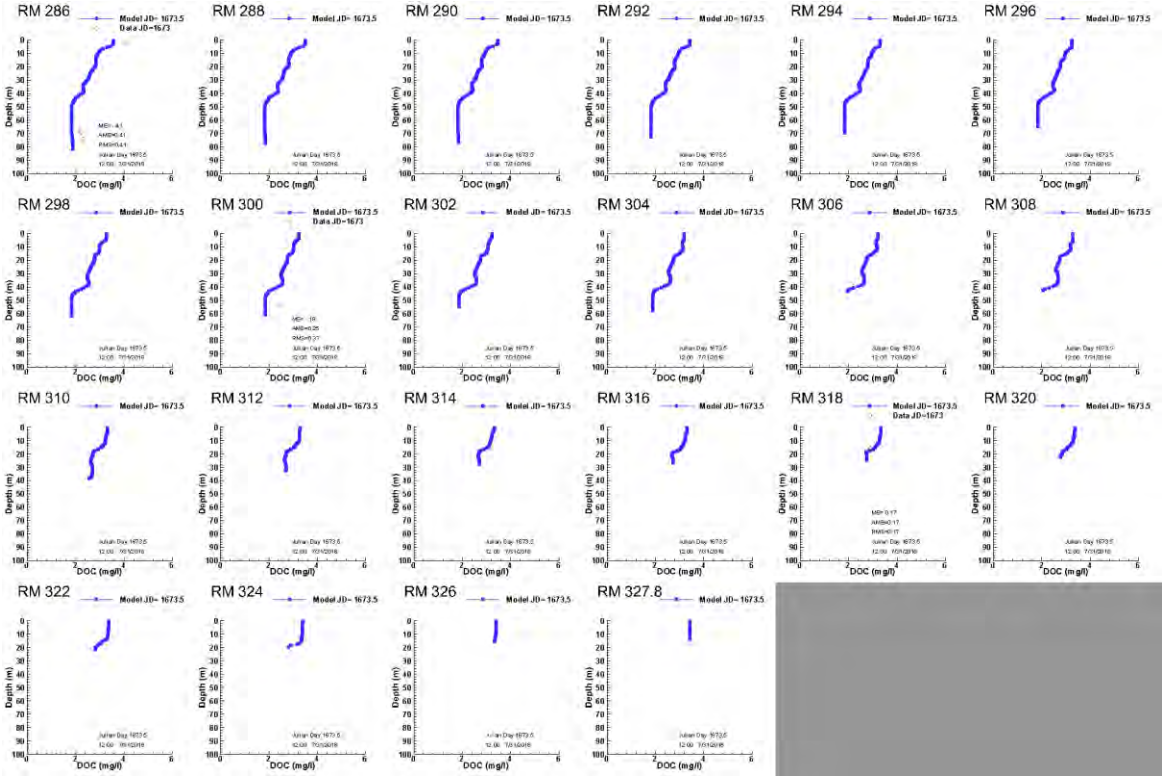


Figure 1528. Vertical profiles of DOC compared with data for 7/31/2018.

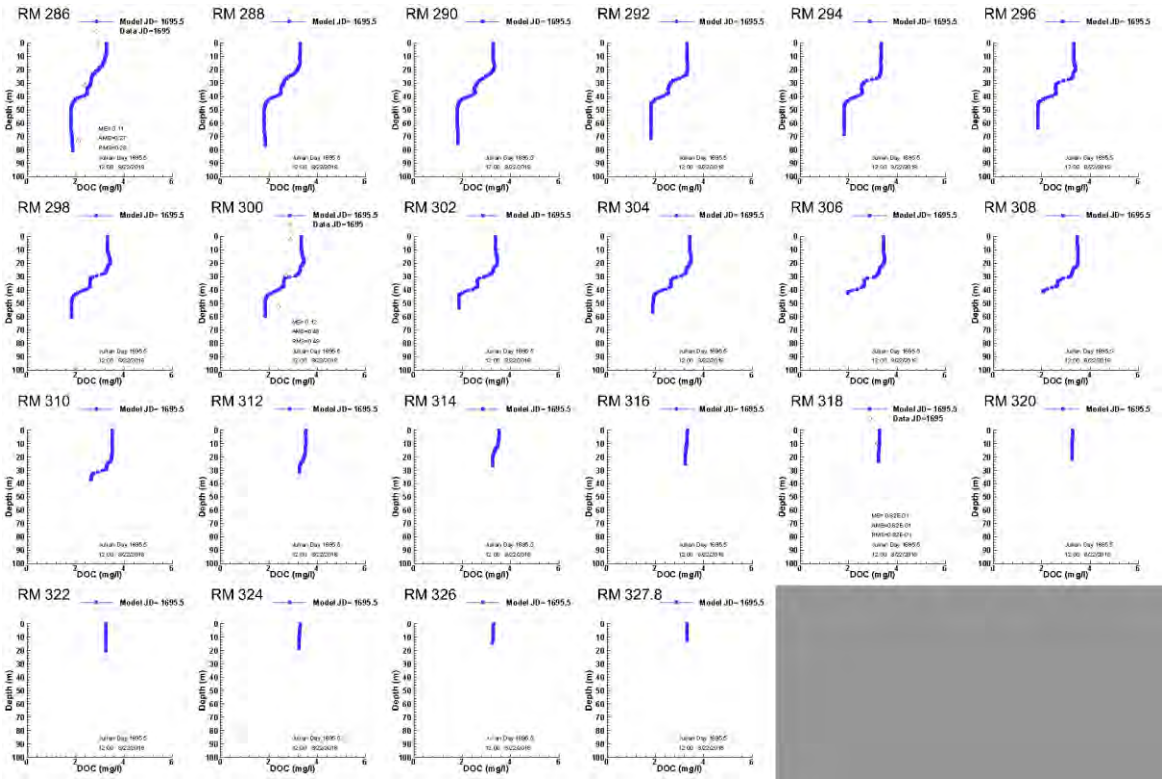


Figure 1529. Vertical profiles of DOC compared with data for 8/22/2018.

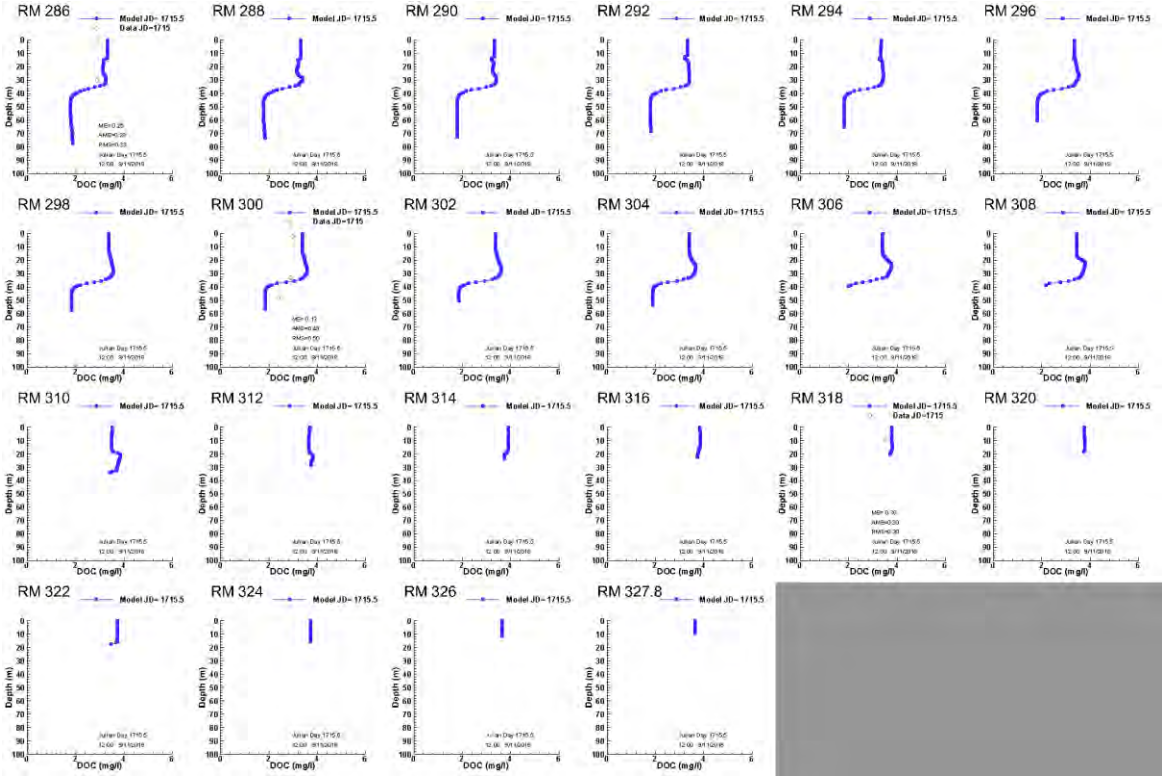


Figure 1530. Vertical profiles of DOC compared with data for 9/11/2018.

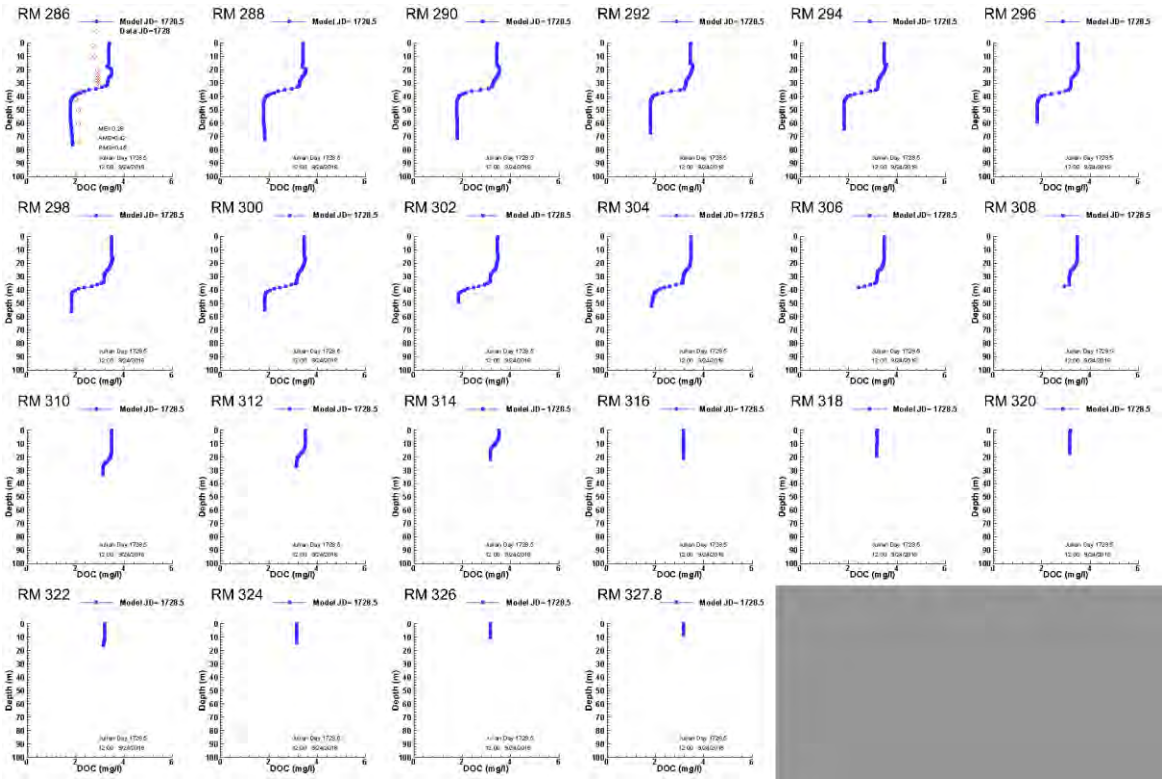


Figure 1531. Vertical profiles of DOC compared with data for 9/24/2018.

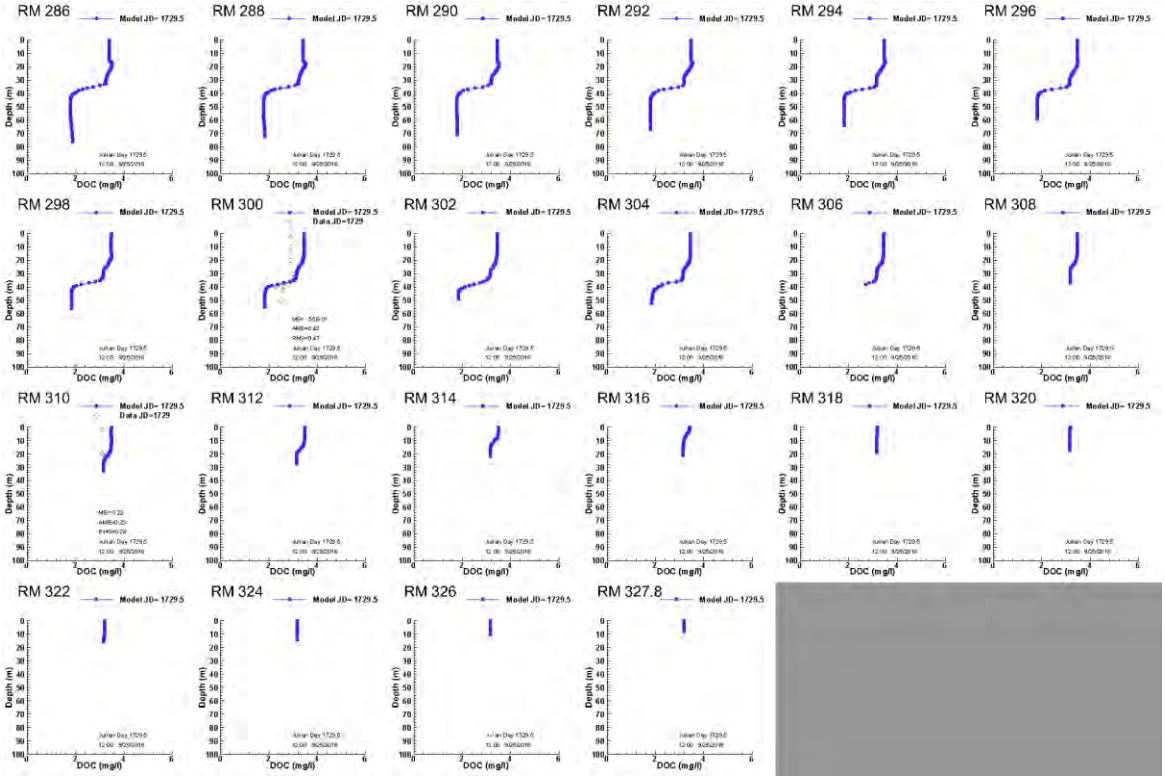


Figure 1532. Vertical profiles of DOC compared with data for 9/25/2018.

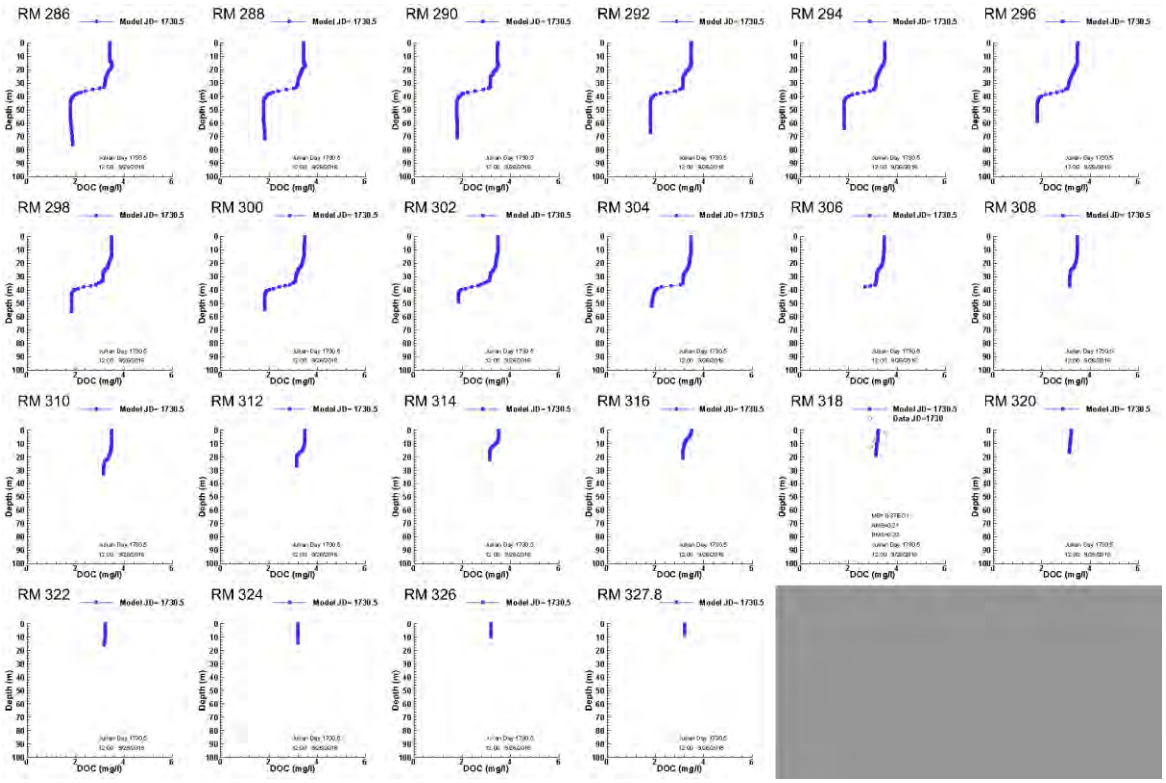


Figure 1533. Vertical profiles of DOC compared with data for 9/26/2018.

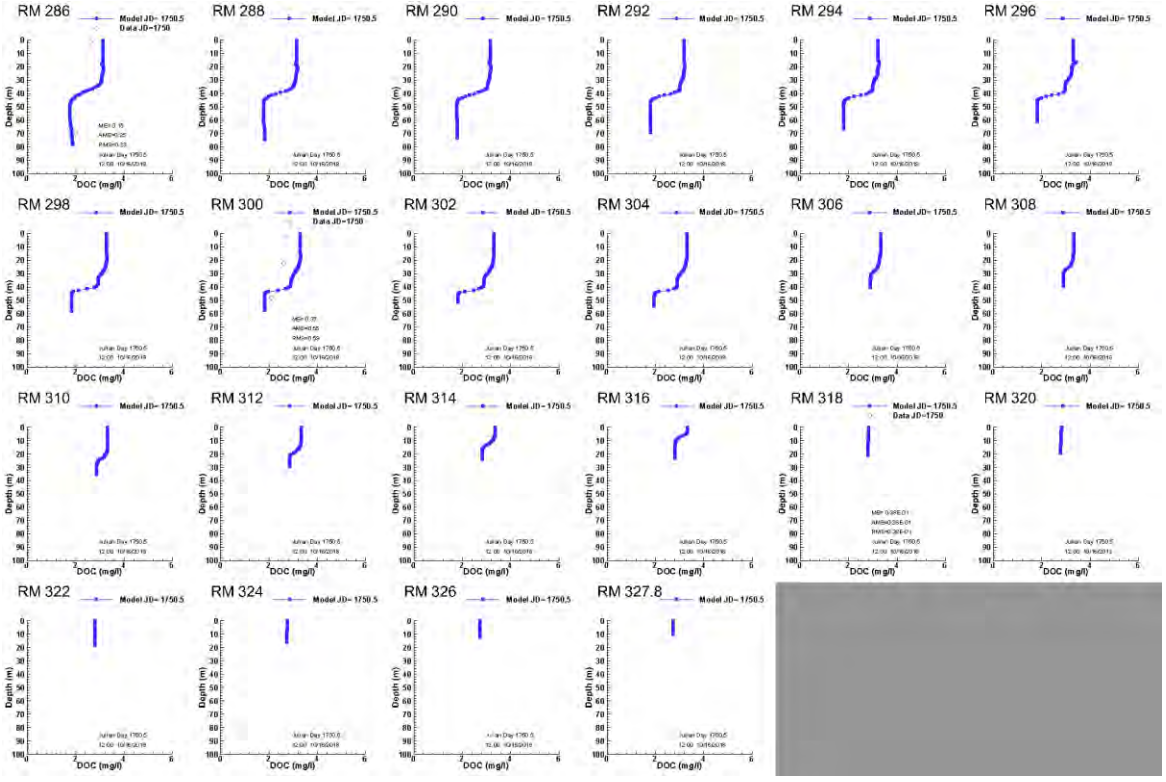


Figure 1534. Vertical profiles of DOC compared with data for 10/16/2018.

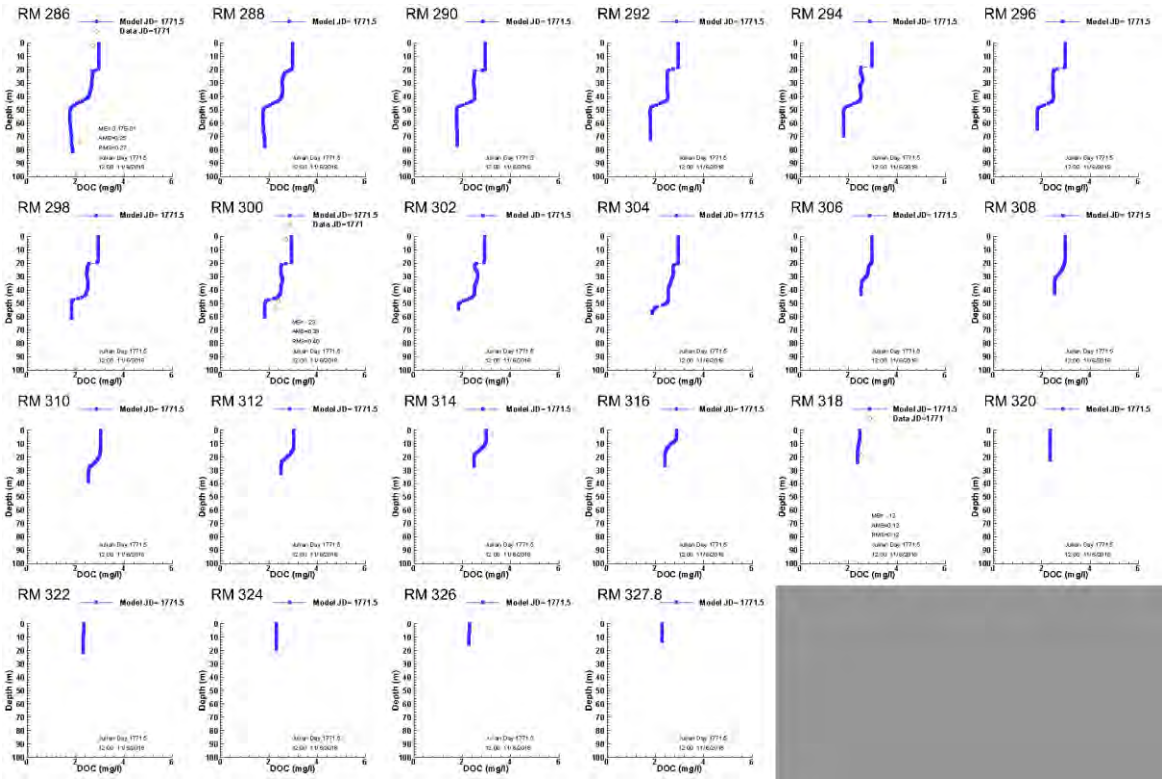


Figure 1535. Vertical profiles of DOC compared with data for 11/ 6/2018.

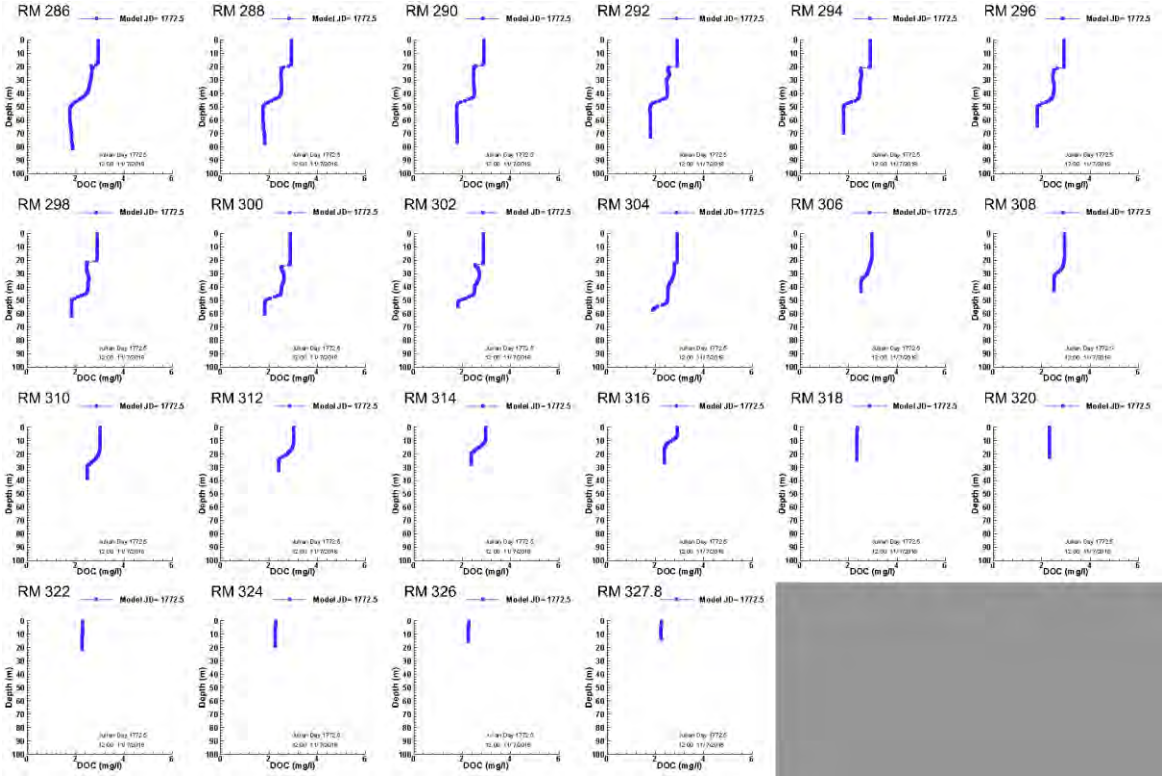


Figure 1536. Vertical profiles of DOC compared with data for 11/ 7/2018.

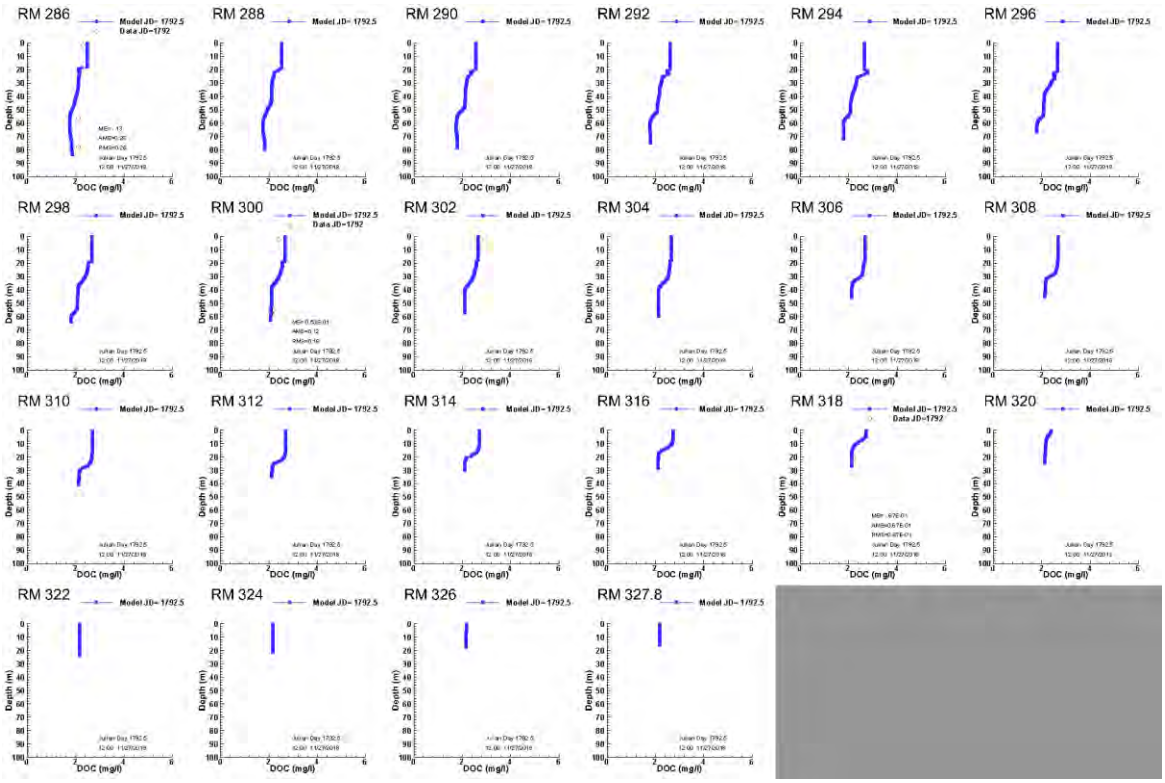


Figure 1537. Vertical profiles of DOC compared with data for 11/27/2018.

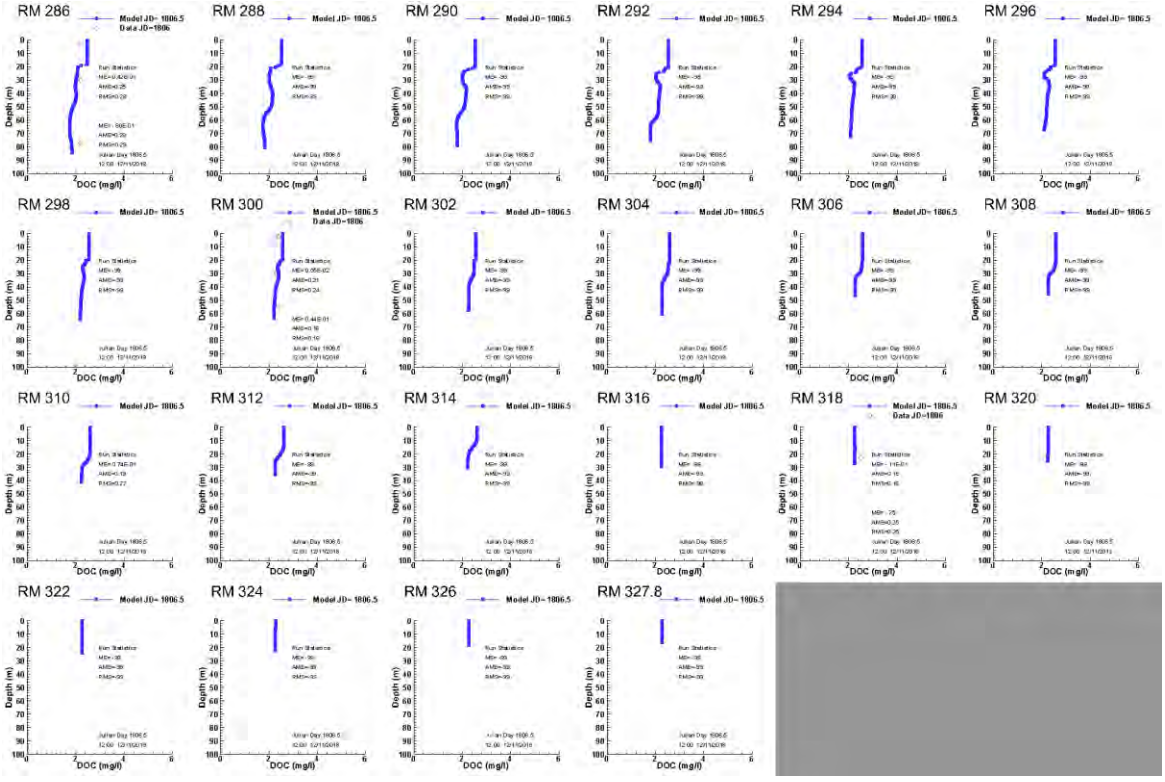


Figure 1538. Vertical profiles of DOC compared with data for 12/11/2018.

Particulate Organic Carbon

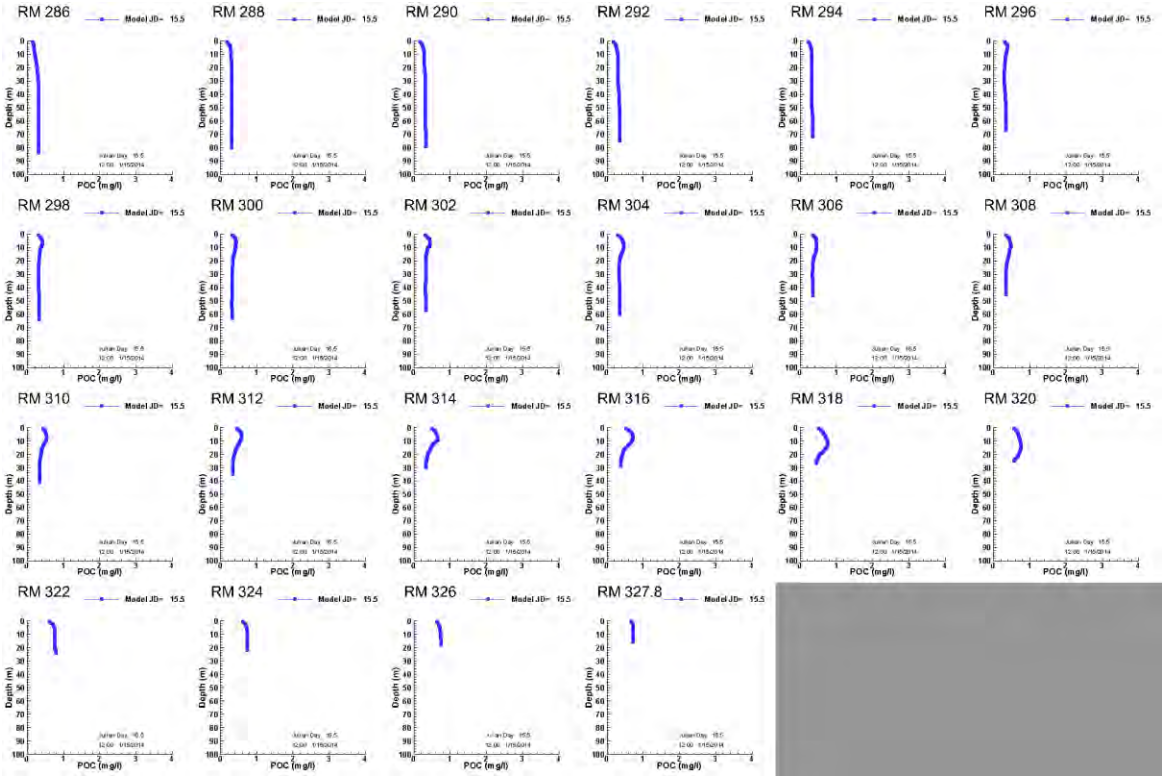


Figure 1539. Vertical profiles of POC compared with data for 1/15/2014.

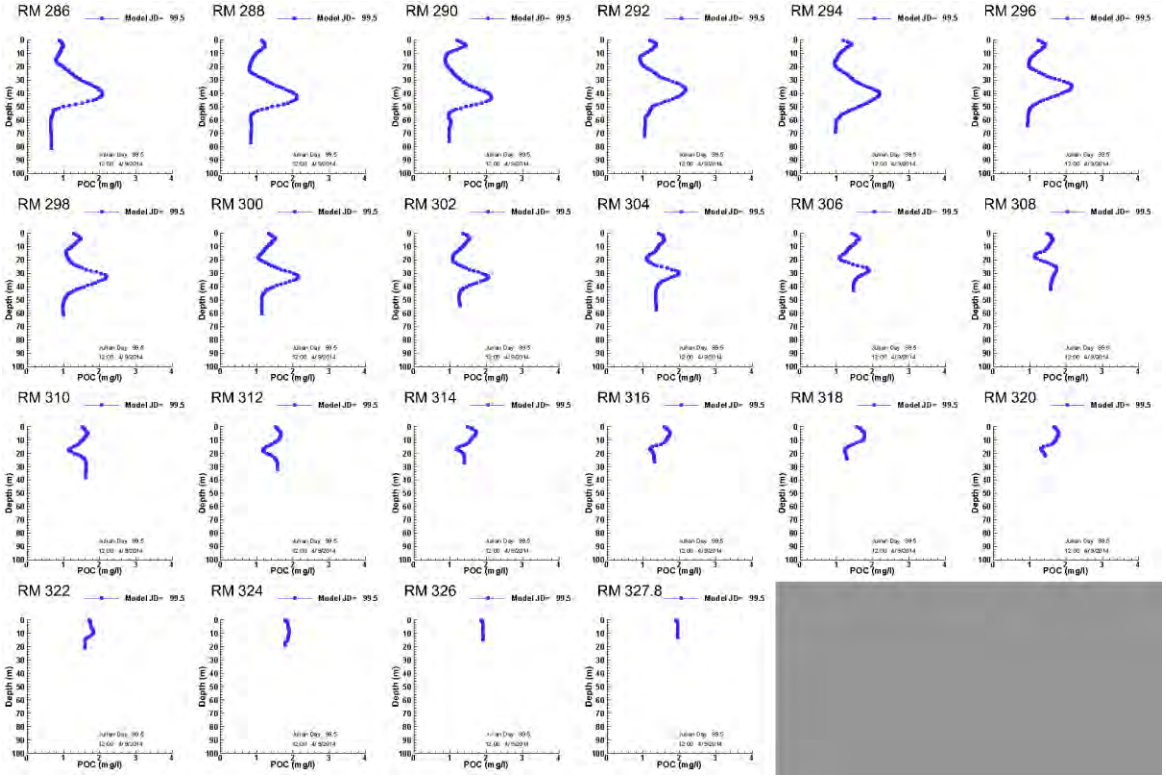


Figure 1540. Vertical profiles of POC compared with data for 4/ 9/2014.

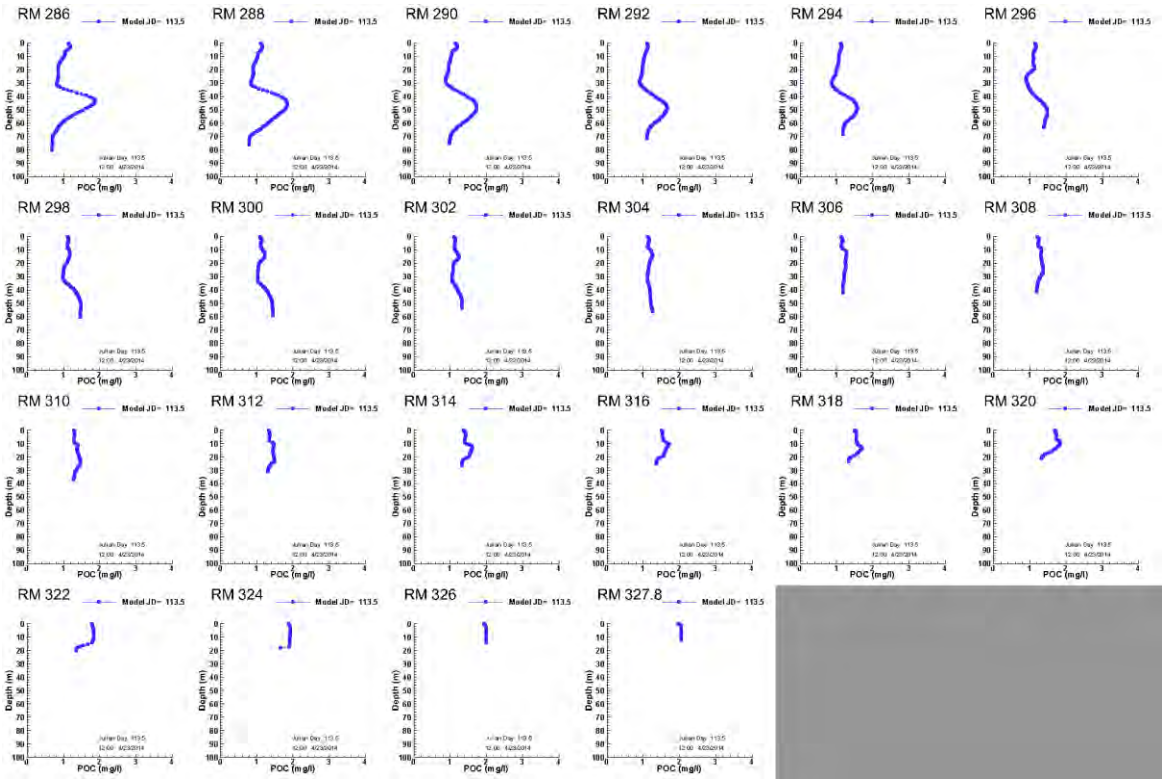


Figure 1541. Vertical profiles of POC compared with data for 4/23/2014.

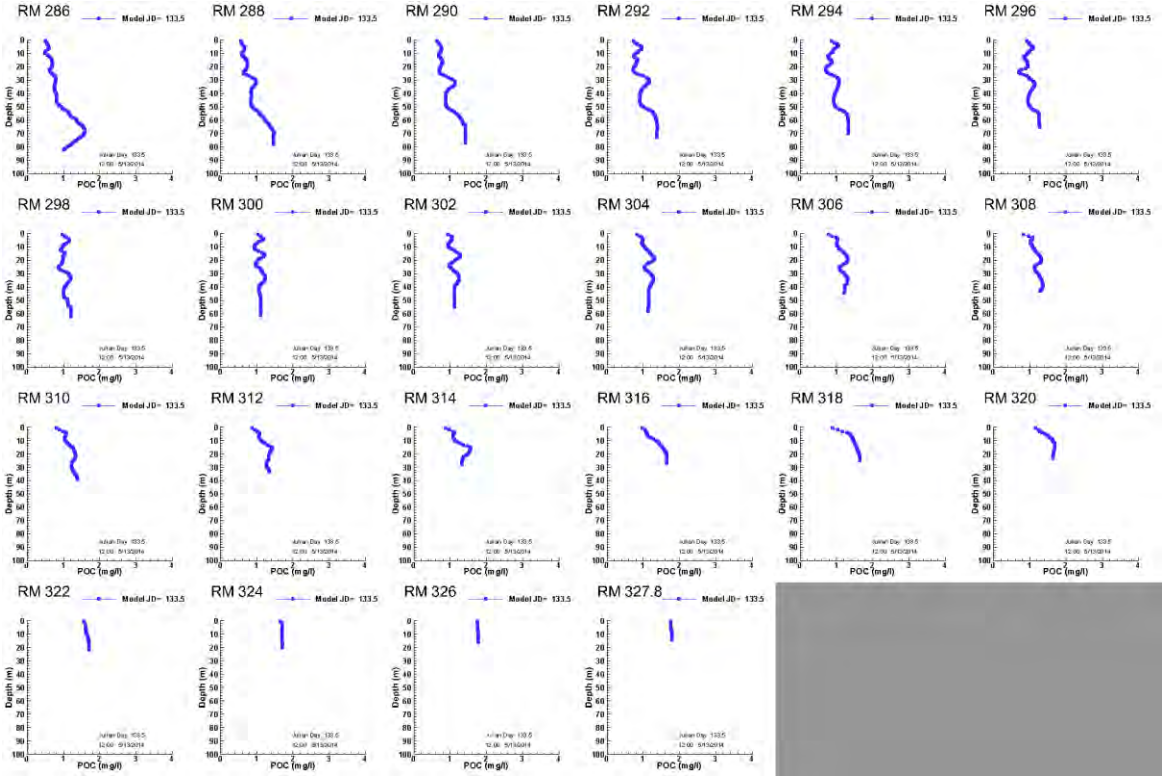


Figure 1542. Vertical profiles of POC compared with data for 5/13/2014.

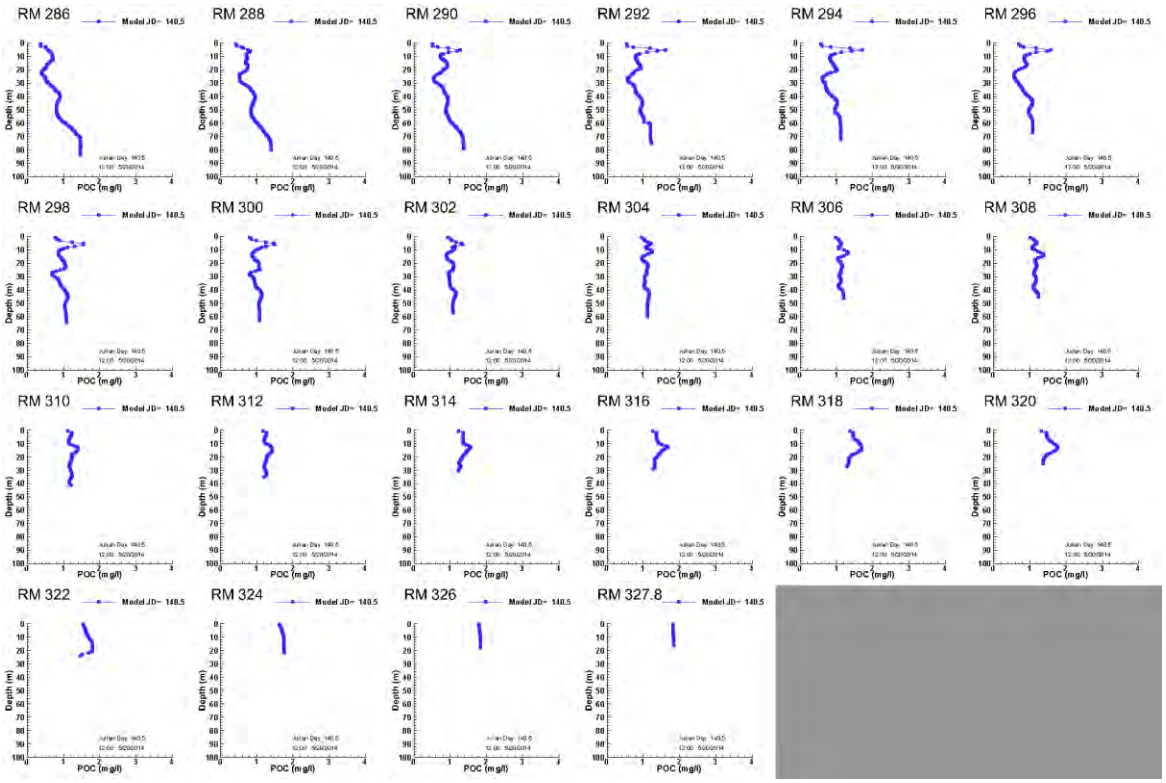


Figure 1543. Vertical profiles of POC compared with data for 5/20/2014.

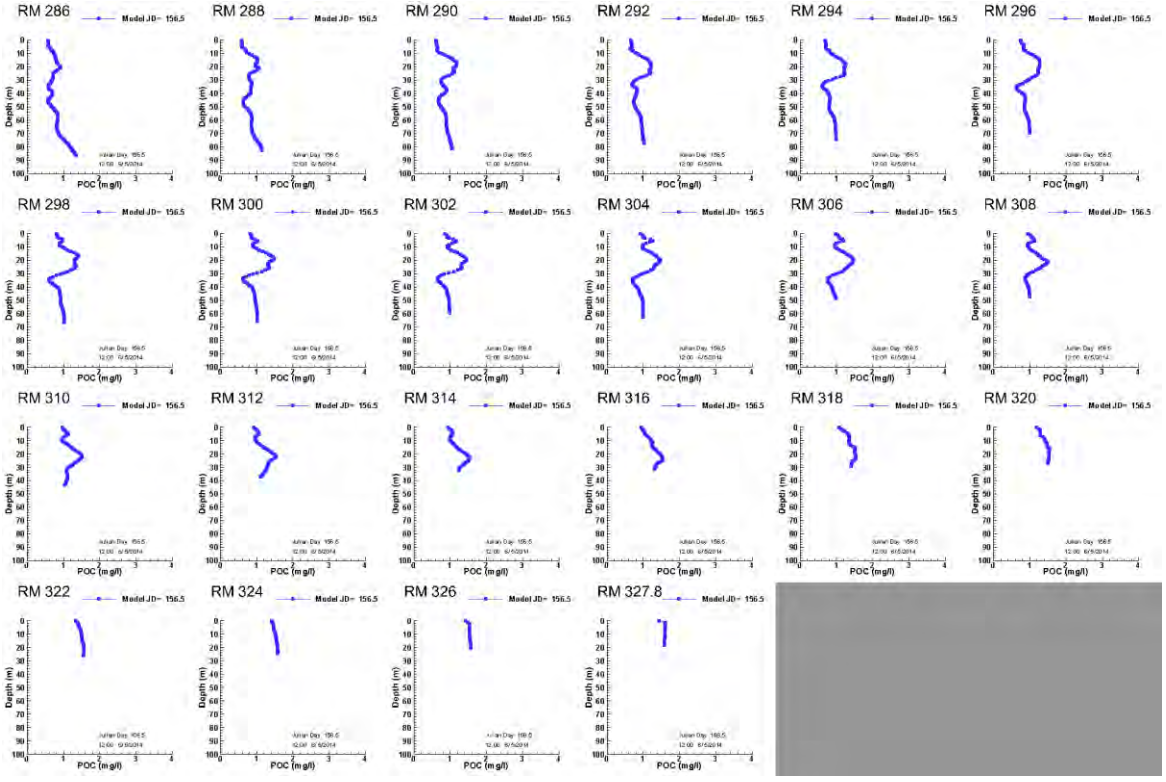


Figure 1544. Vertical profiles of POC compared with data for 6/ 5/2014.

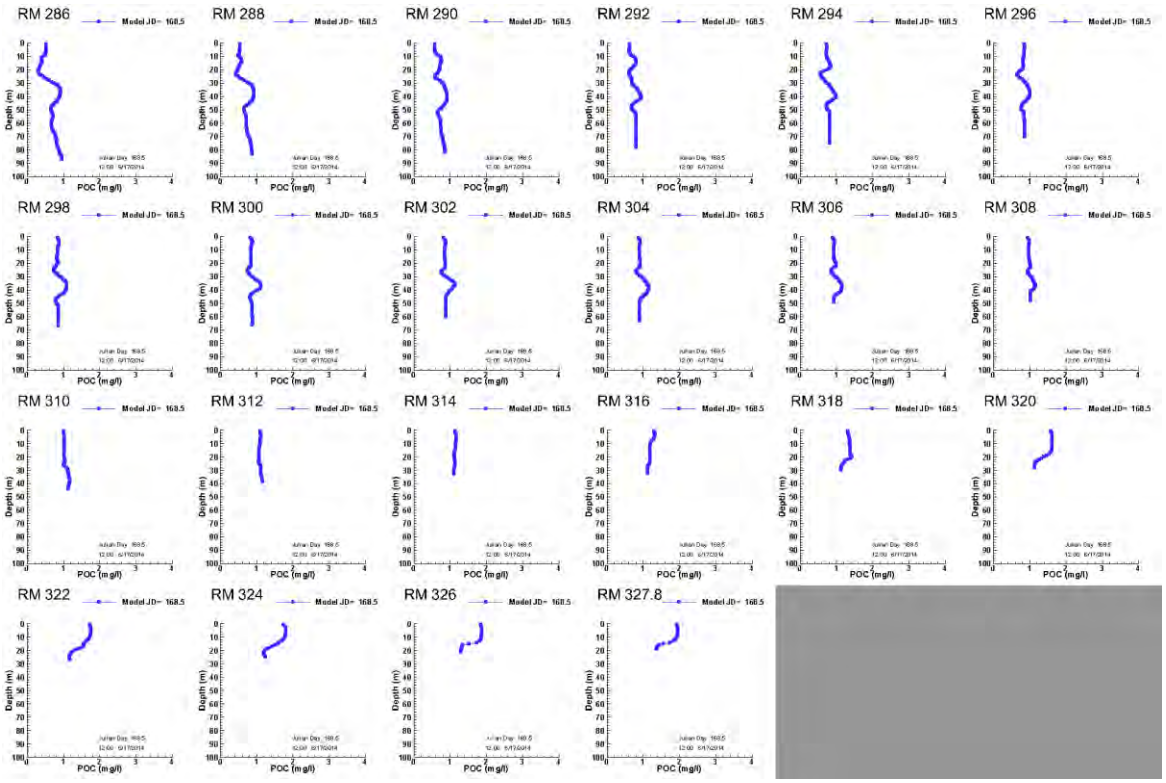


Figure 1545. Vertical profiles of POC compared with data for 6/17/2014.

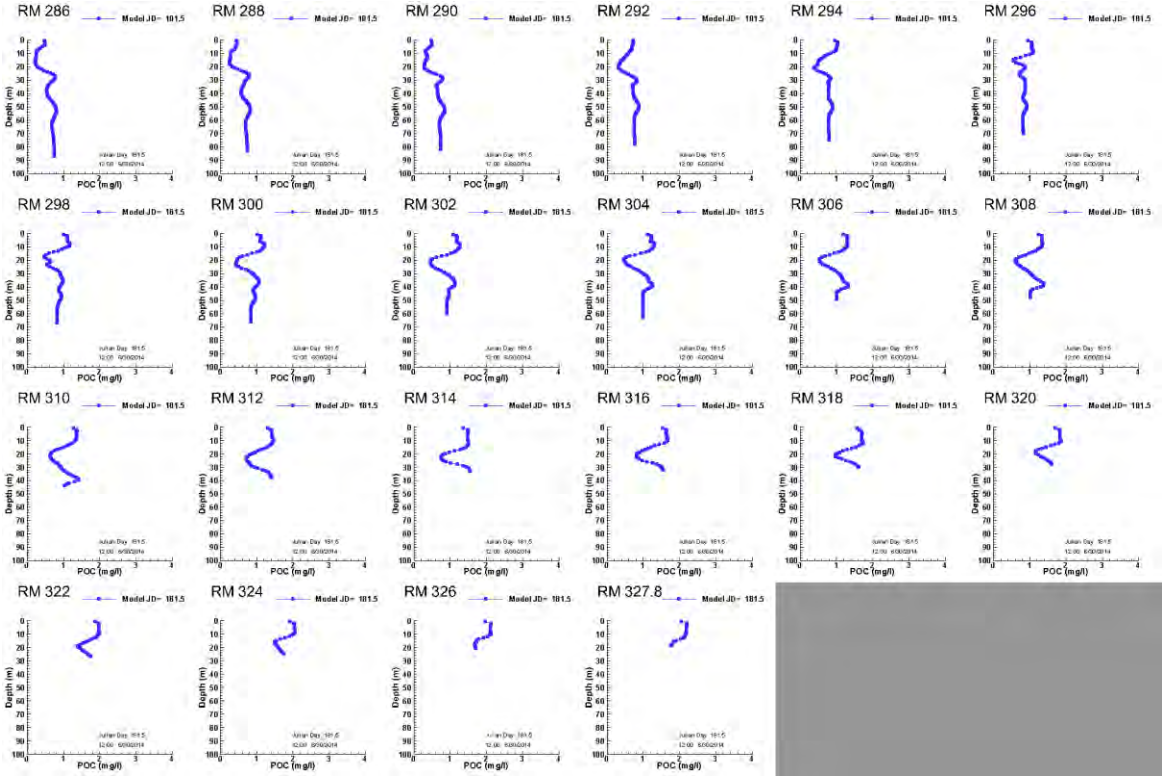


Figure 1546. Vertical profiles of POC compared with data for 6/30/2014.

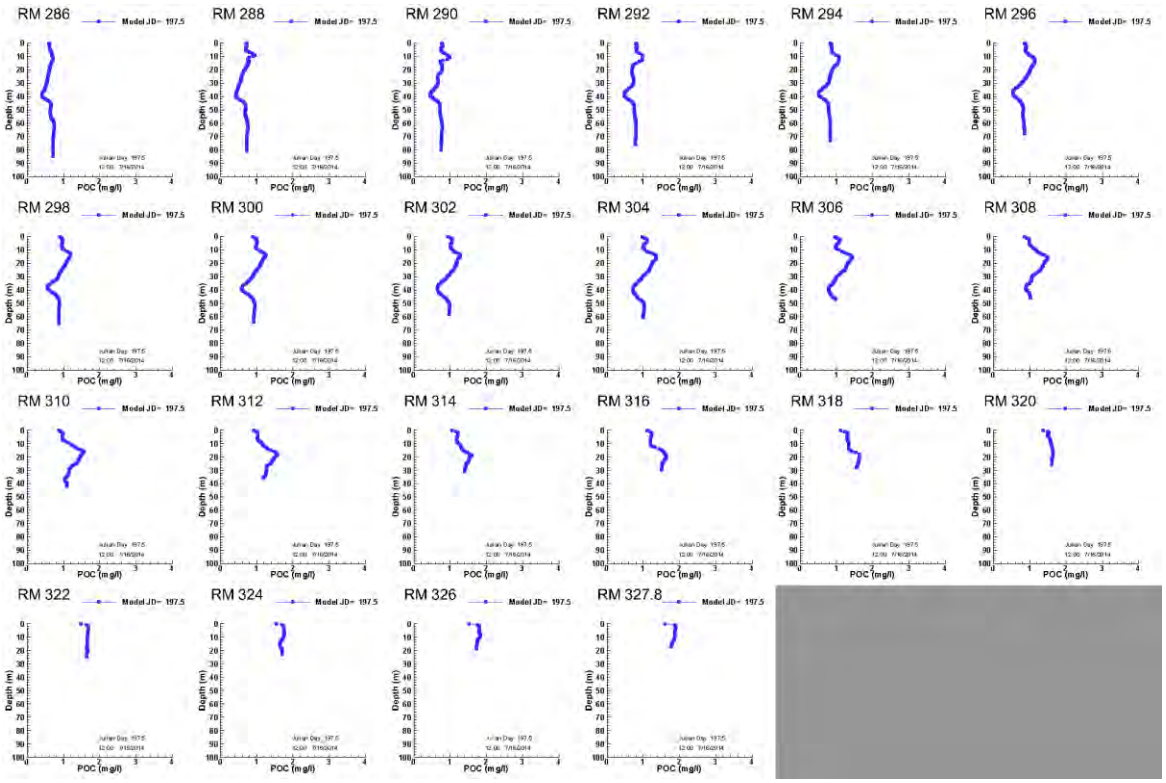


Figure 1547. Vertical profiles of POC compared with data for 7/16/2014.

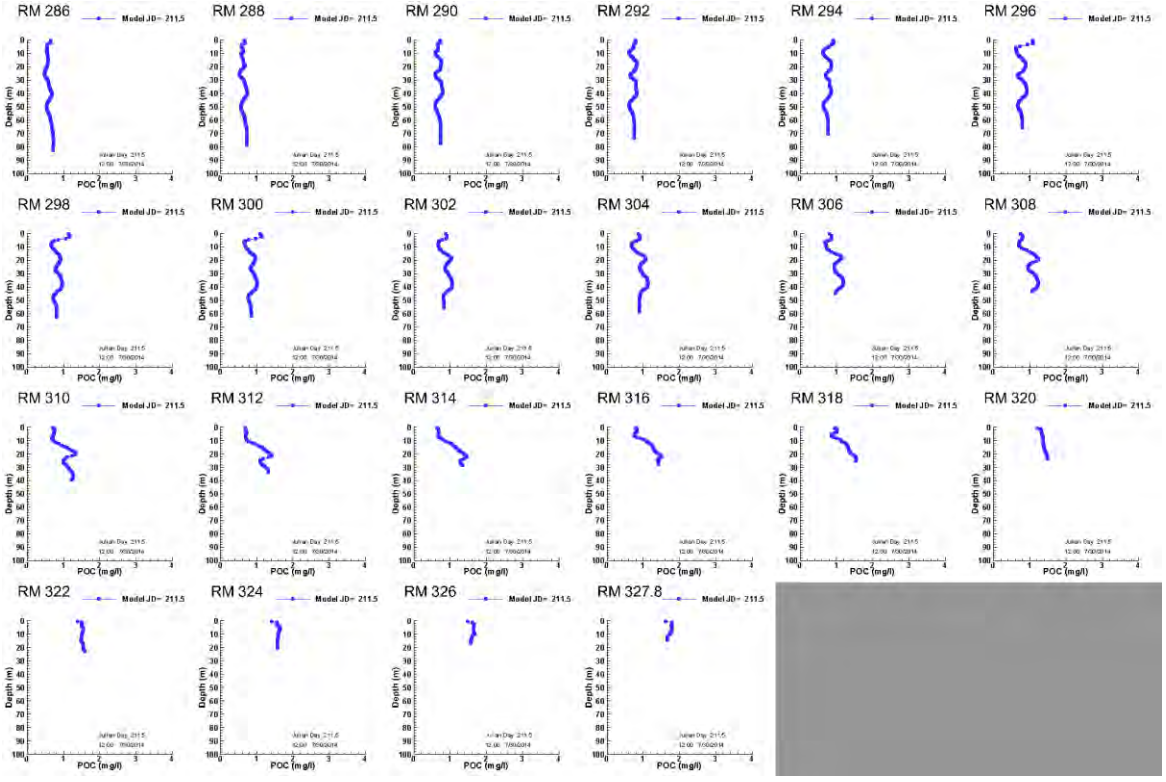


Figure 1548. Vertical profiles of POC compared with data for 7/30/2014.

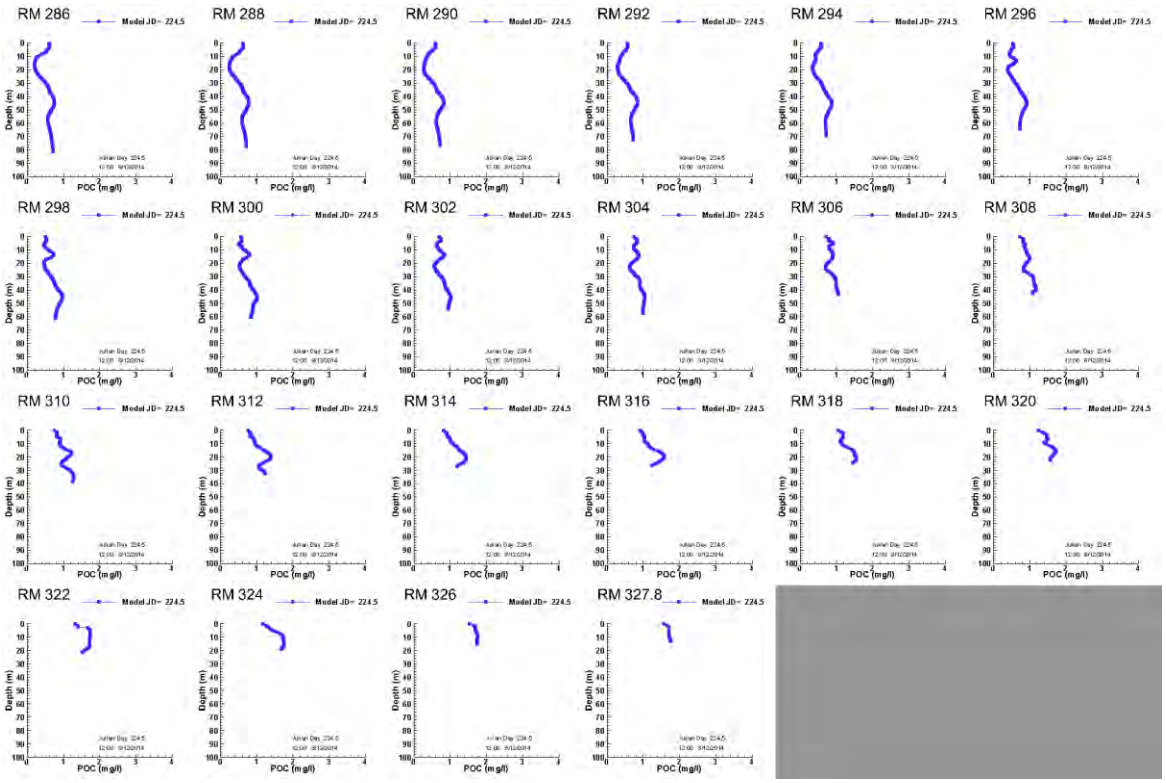


Figure 1549. Vertical profiles of POC compared with data for 8/12/2014.

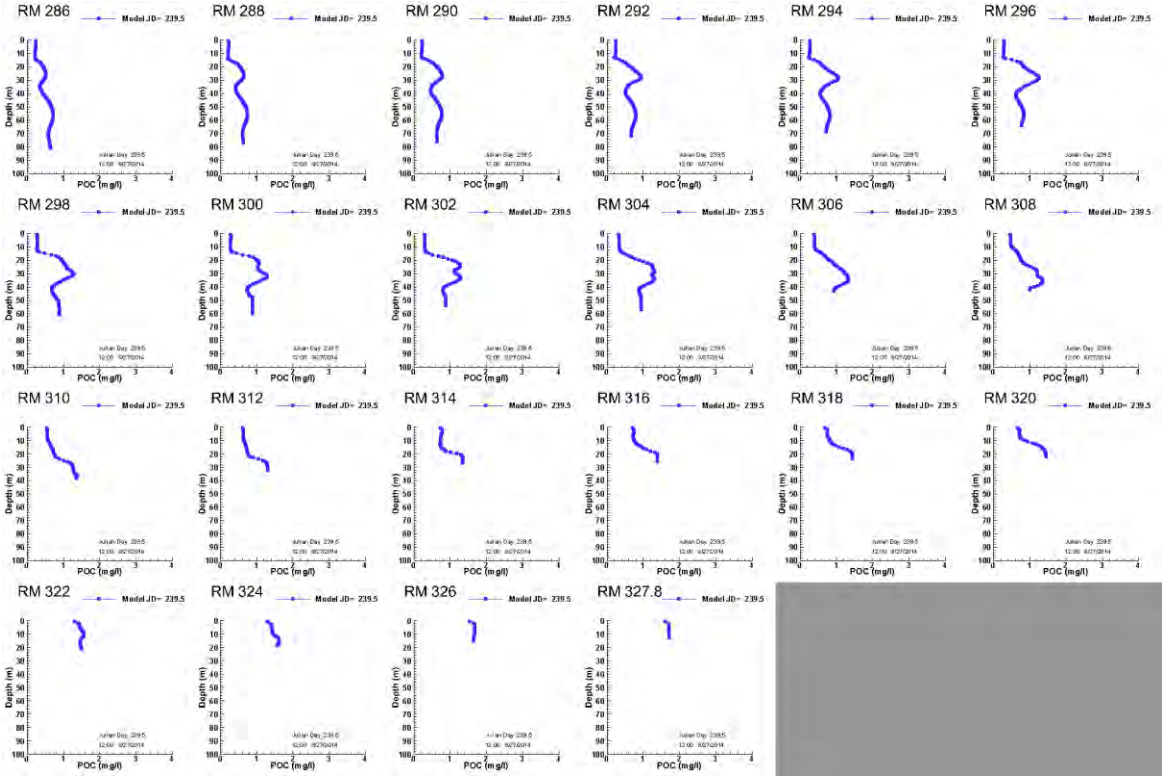


Figure 1550. Vertical profiles of POC compared with data for 8/27/2014.

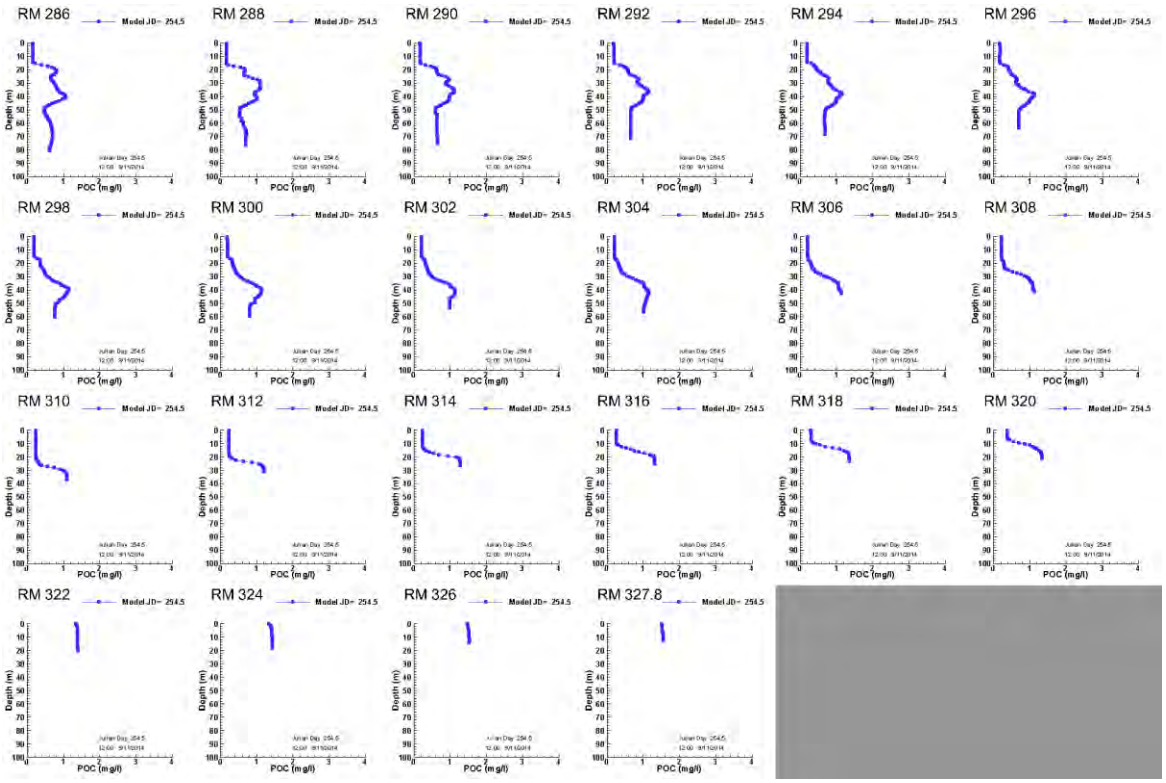


Figure 1551. Vertical profiles of POC compared with data for 9/11/2014.

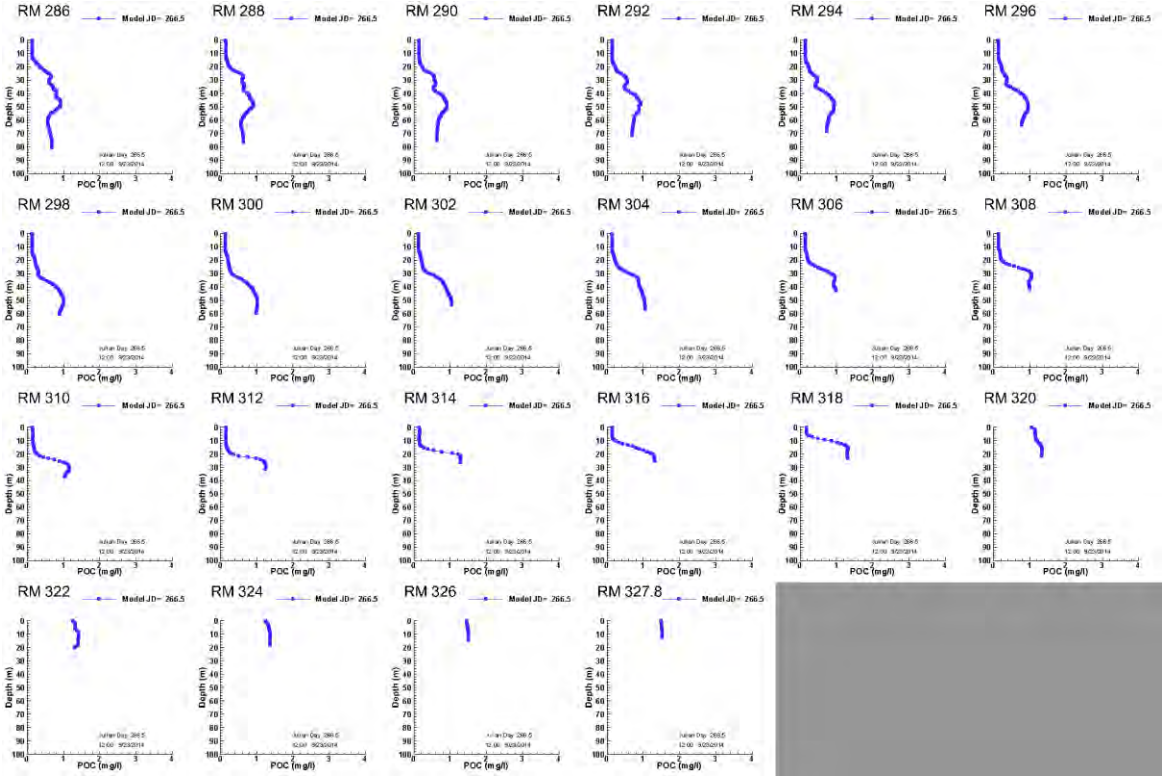


Figure 1552. Vertical profiles of POC compared with data for 9/23/2014.

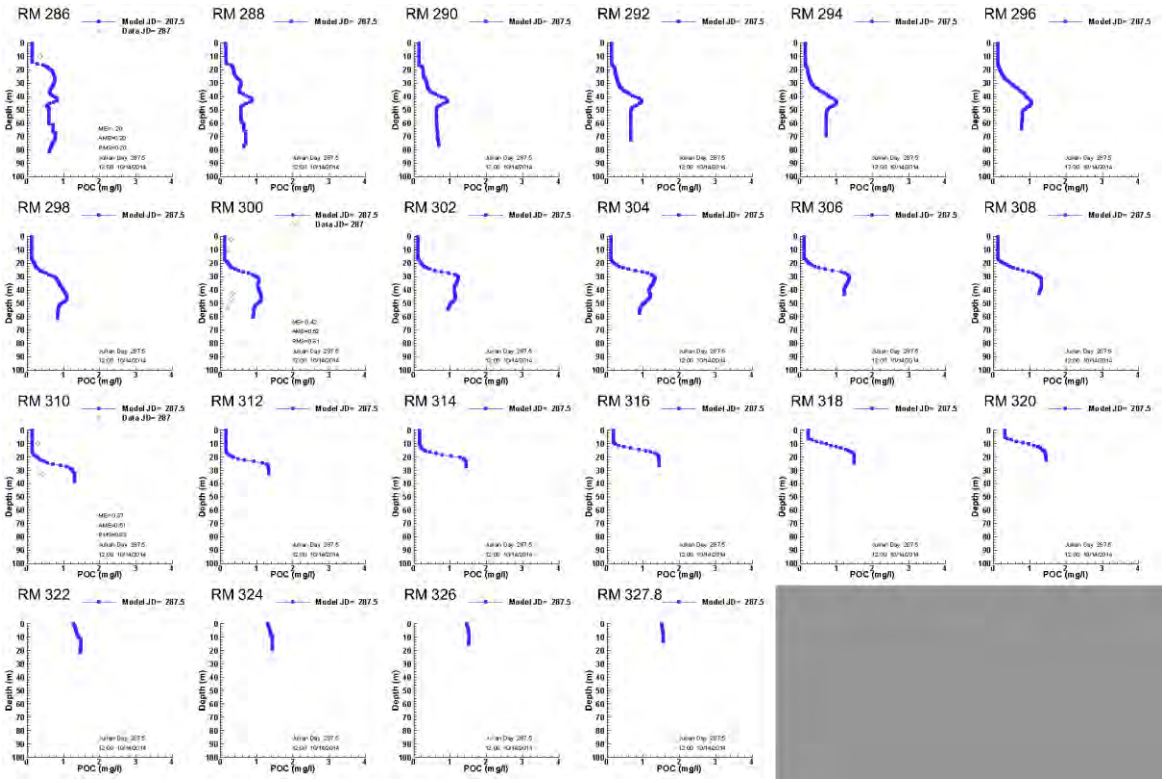


Figure 1553. Vertical profiles of POC compared with data for 10/14/2014.

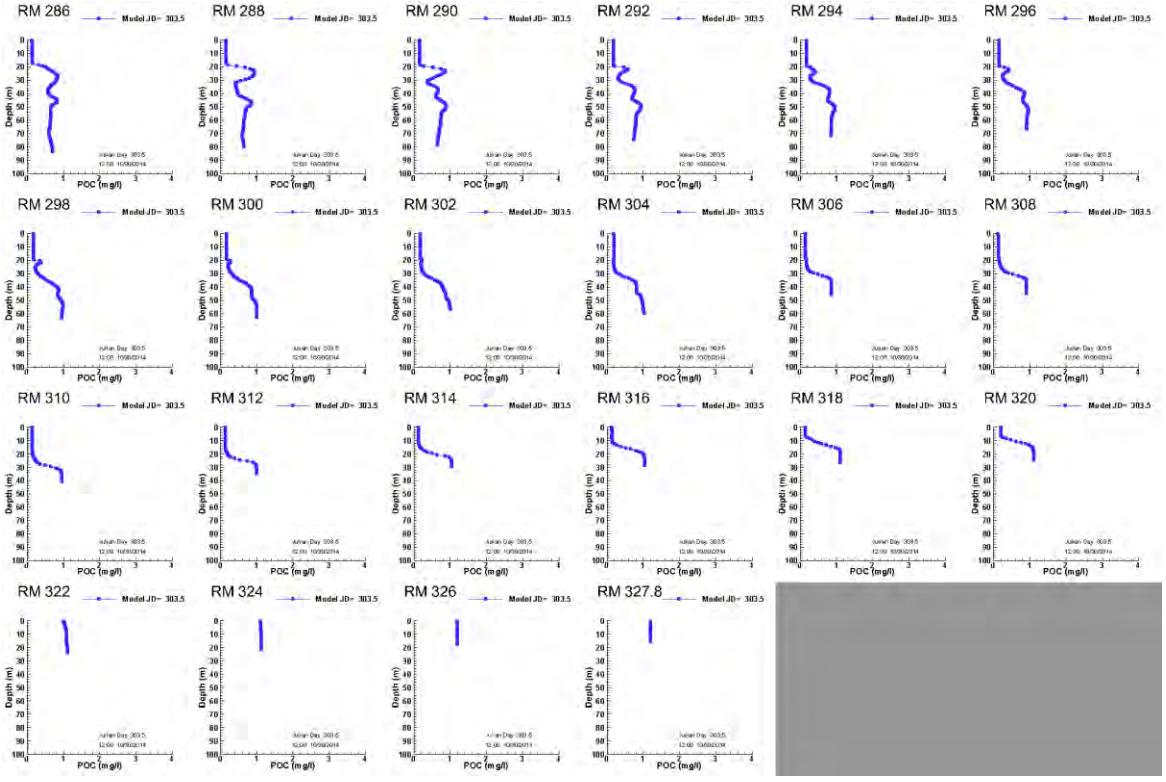


Figure 1554. Vertical profiles of POC compared with data for 10/30/2014.

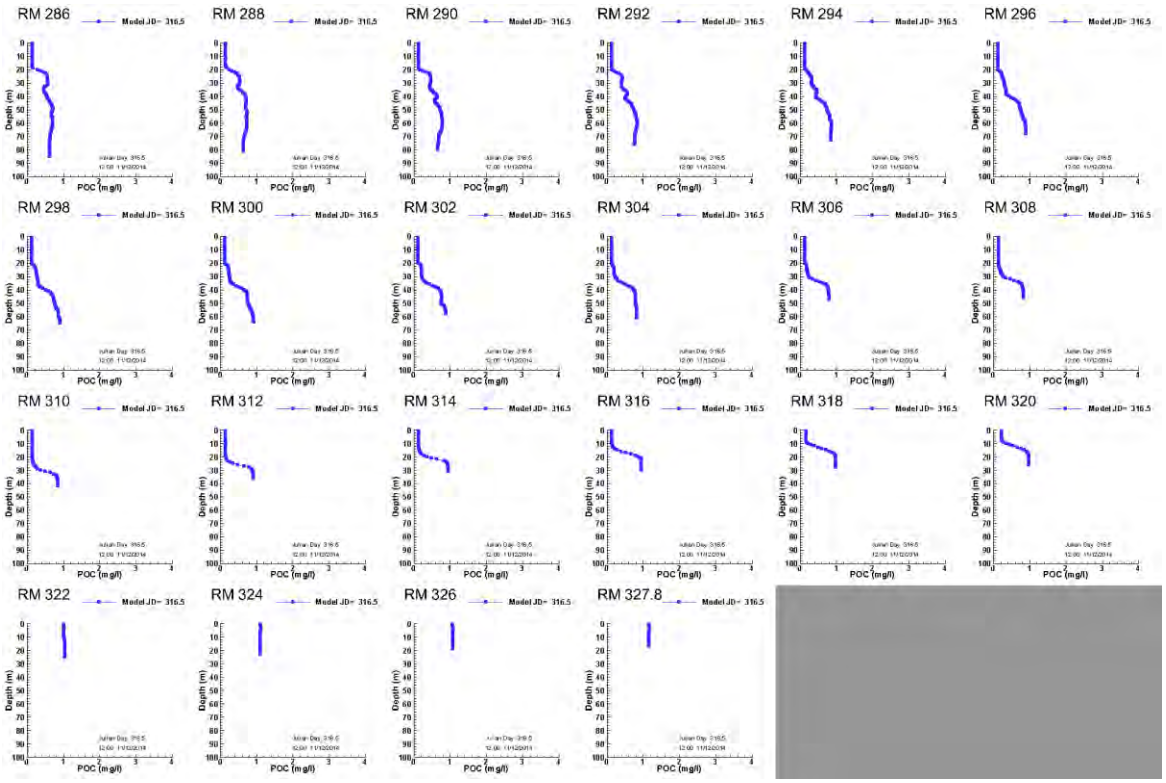


Figure 1555. Vertical profiles of POC compared with data for 11/12/2014.

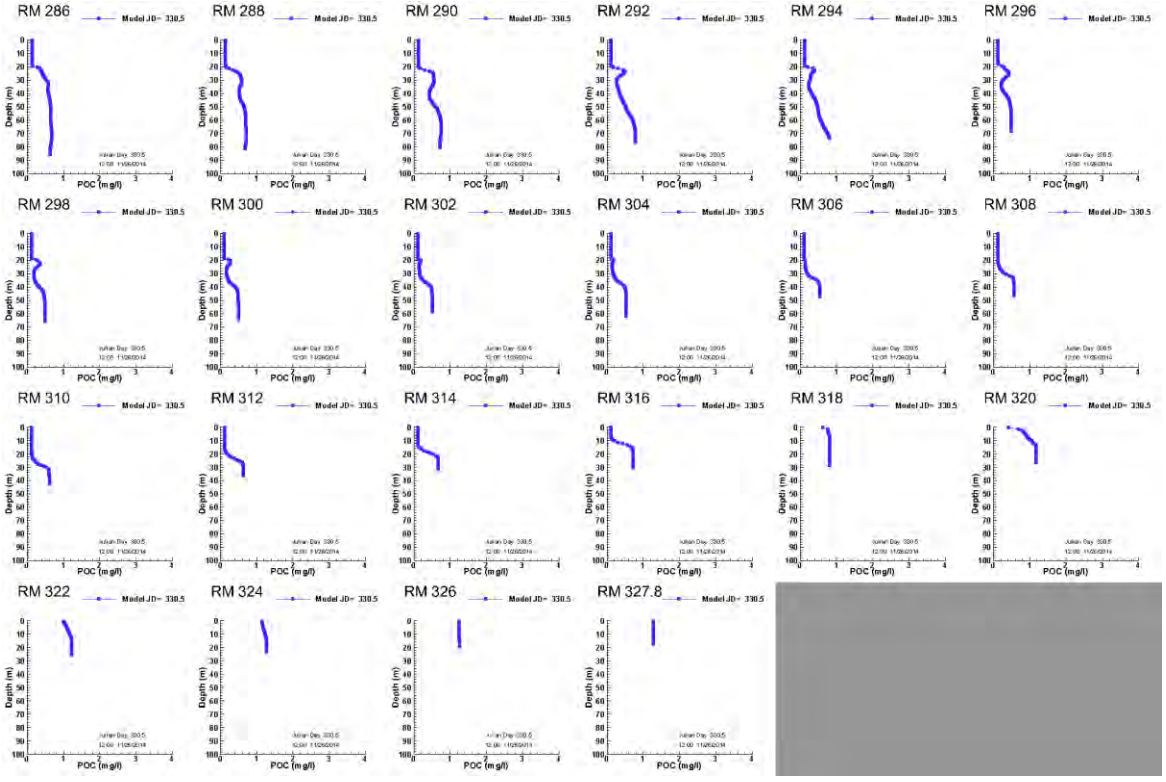


Figure 1556. Vertical profiles of POC compared with data for 11/26/2014.

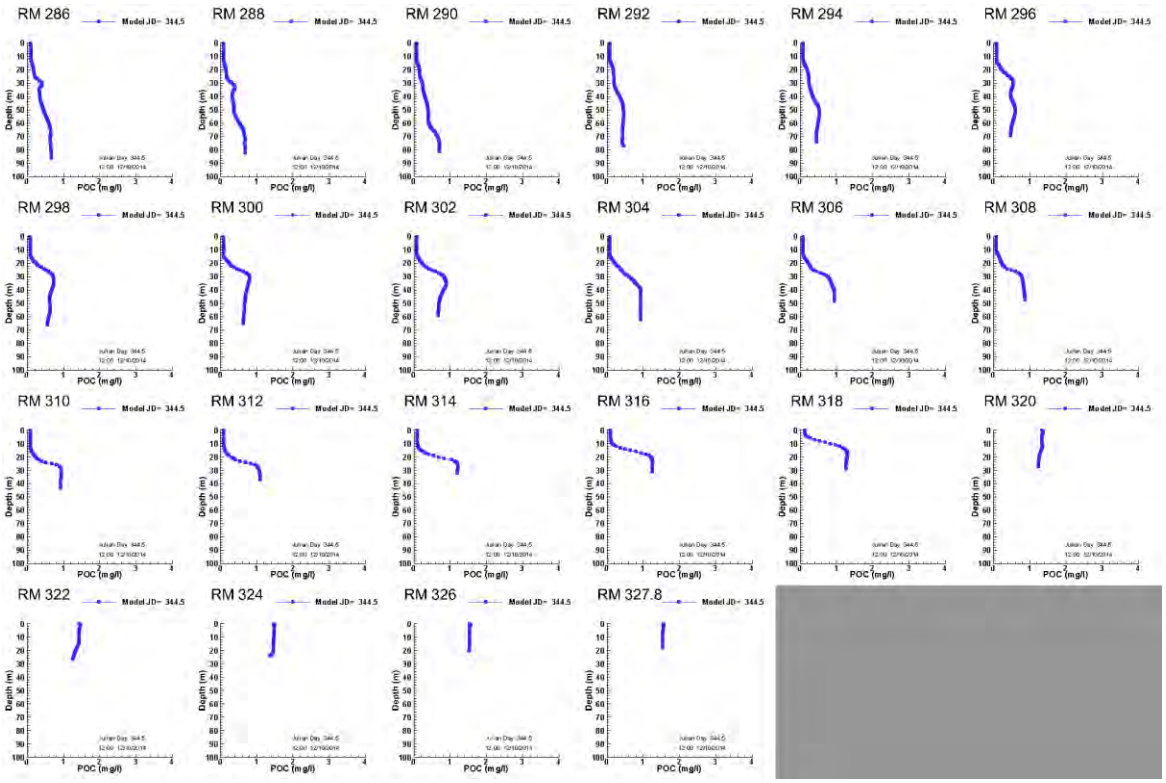


Figure 1557. Vertical profiles of POC compared with data for 12/10/2014.

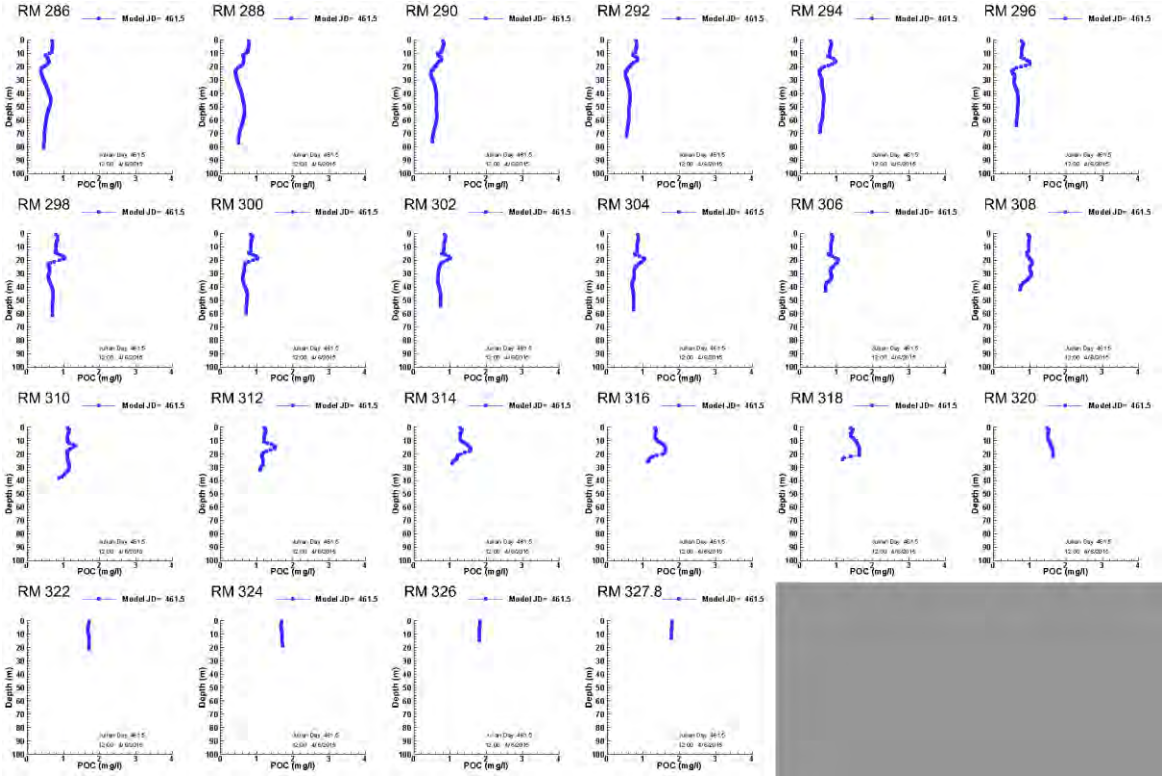


Figure 1558. Vertical profiles of POC compared with data for 4/ 6/2015.

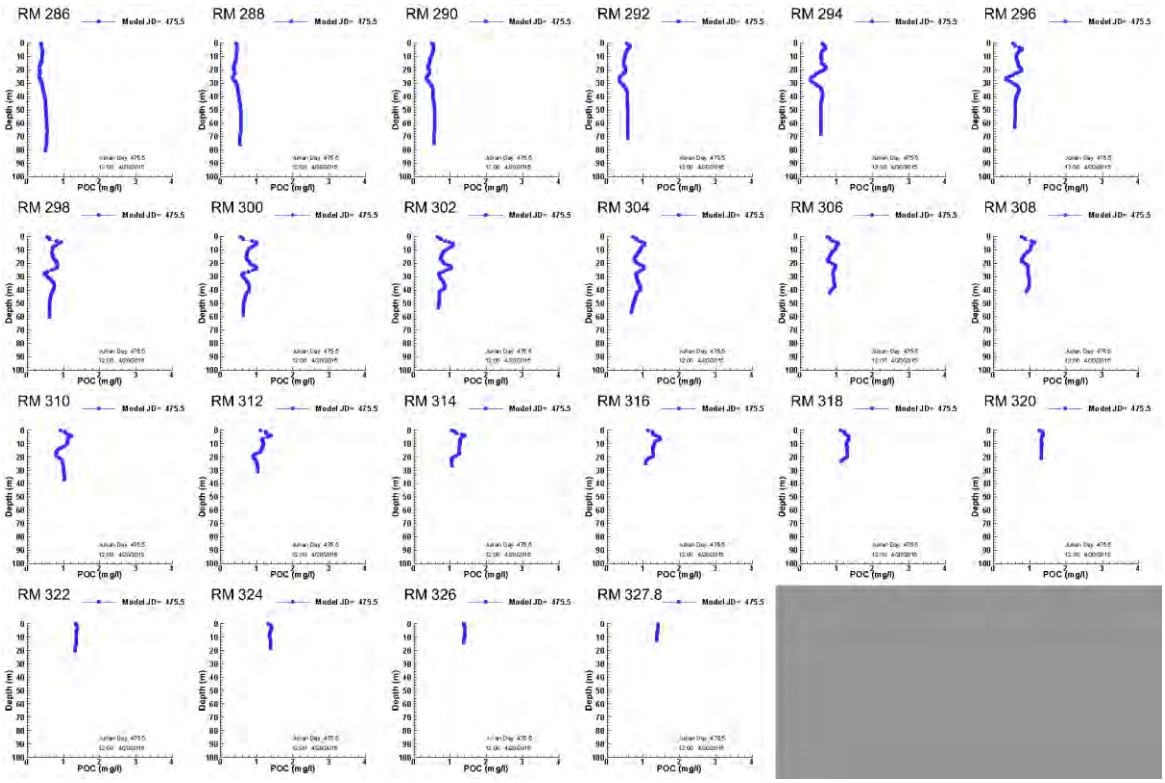


Figure 1559. Vertical profiles of POC compared with data for 4/20/2015.

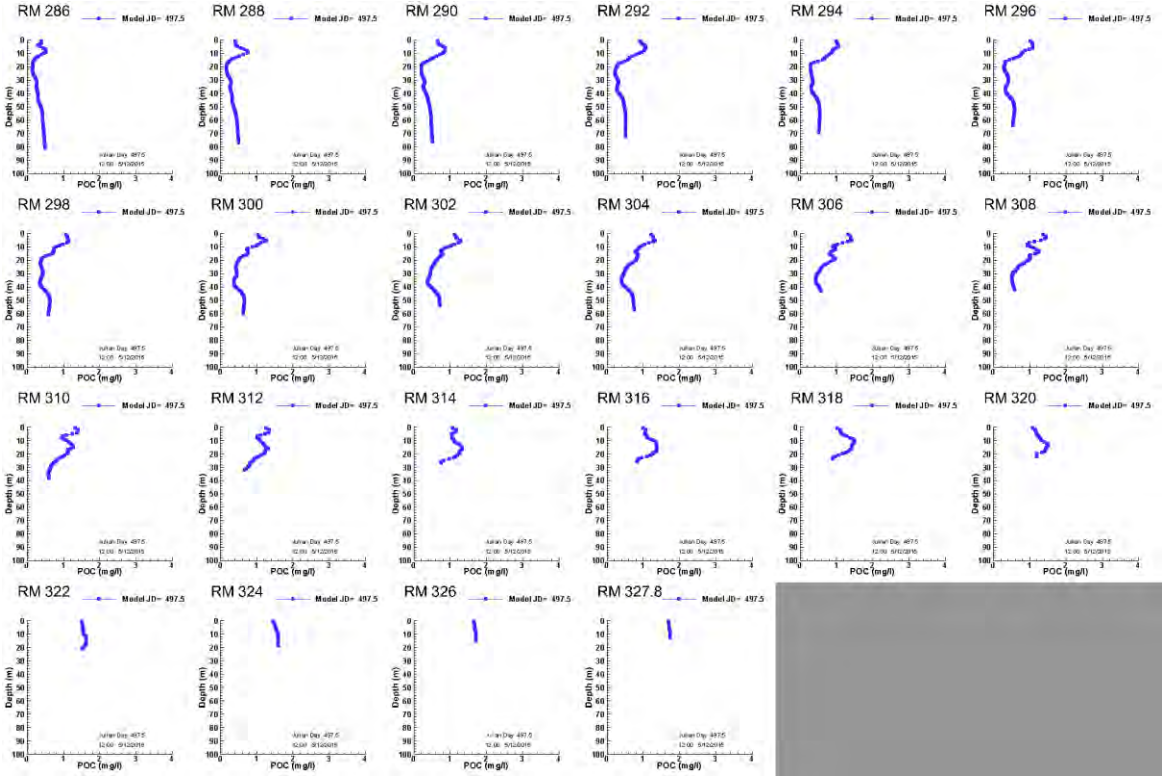


Figure 1560. Vertical profiles of POC compared with data for 5/12/2015.

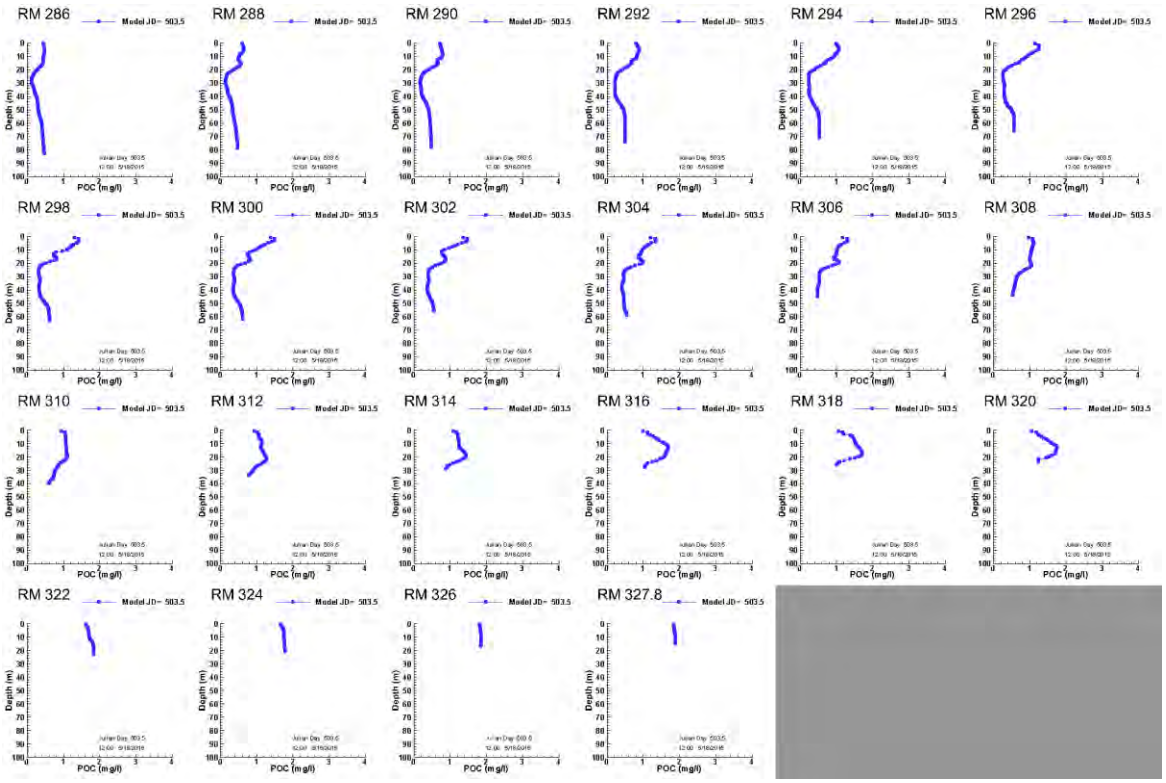


Figure 1561. Vertical profiles of POC compared with data for 5/18/2015.

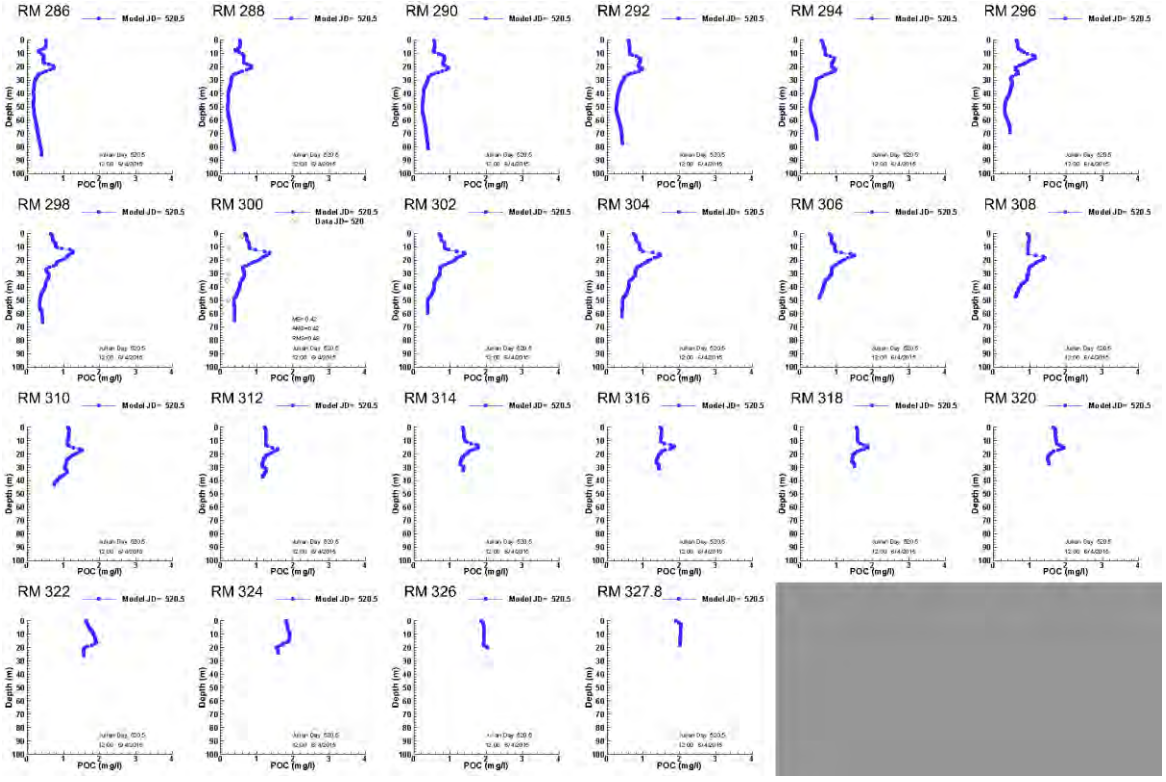


Figure 1562. Vertical profiles of POC compared with data for 6/ 4/2015.

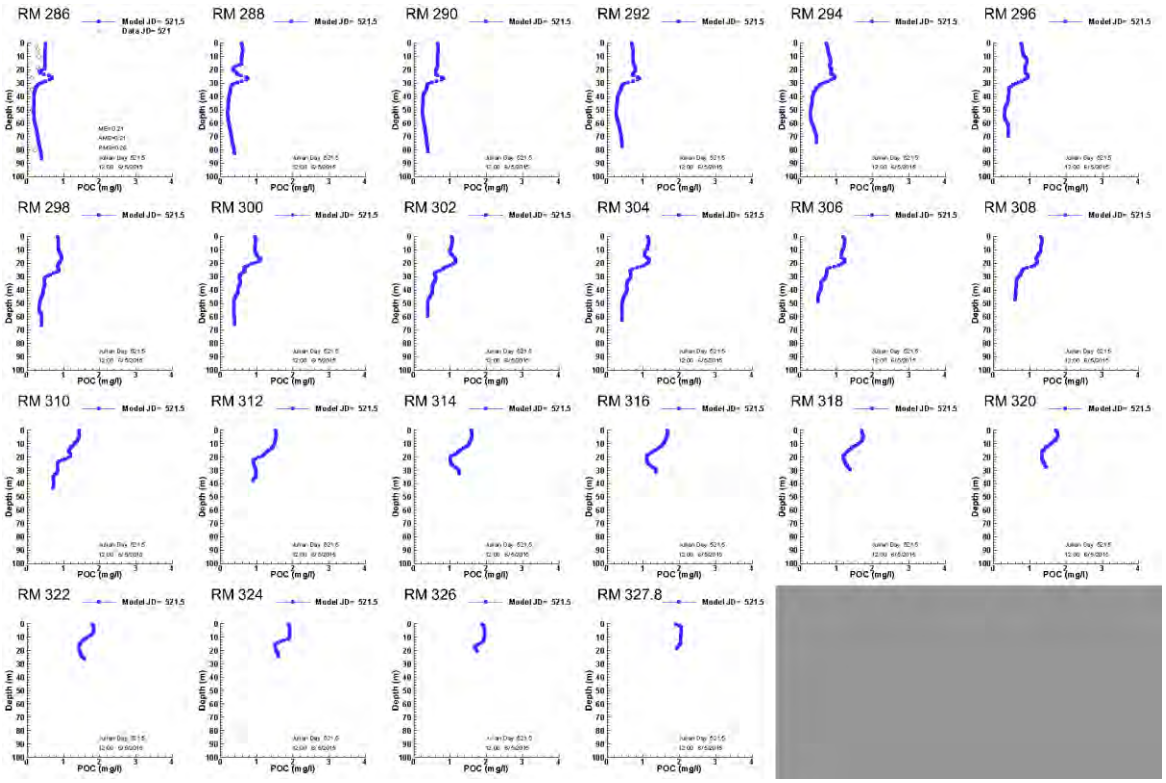


Figure 1563. Vertical profiles of POC compared with data for 6/ 5/2015.

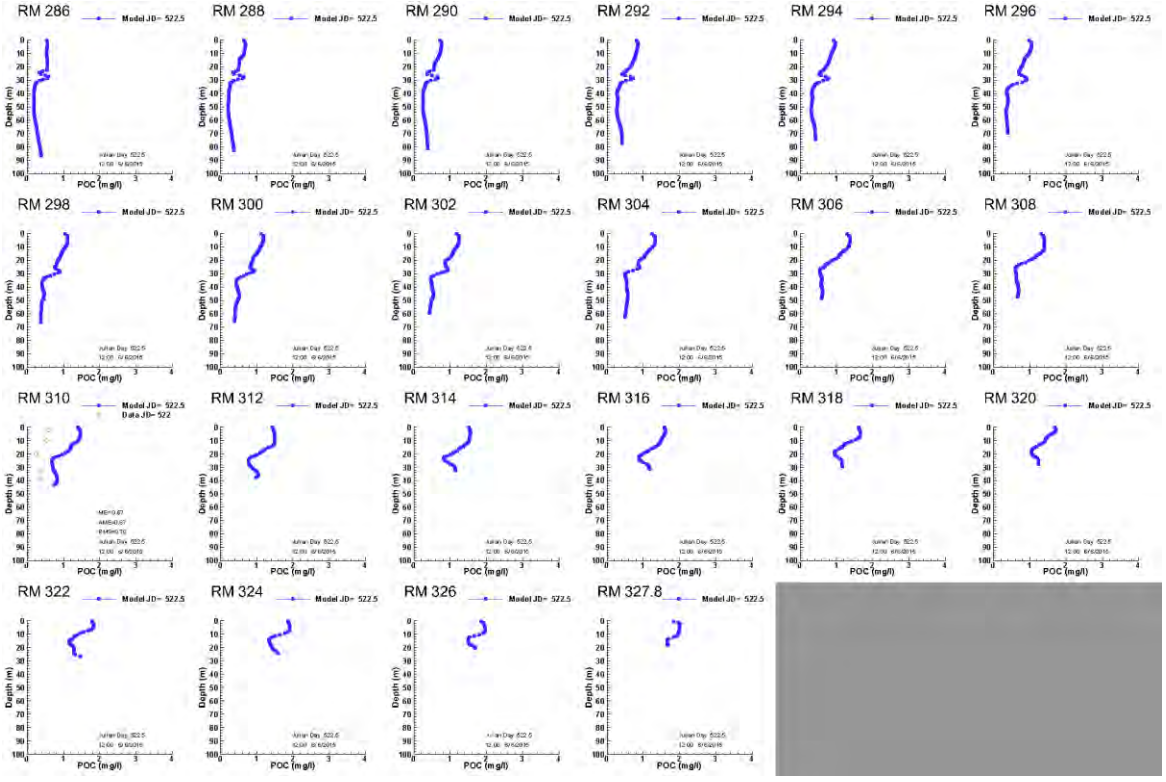


Figure 1564. Vertical profiles of POC compared with data for 6/ 6/2015.

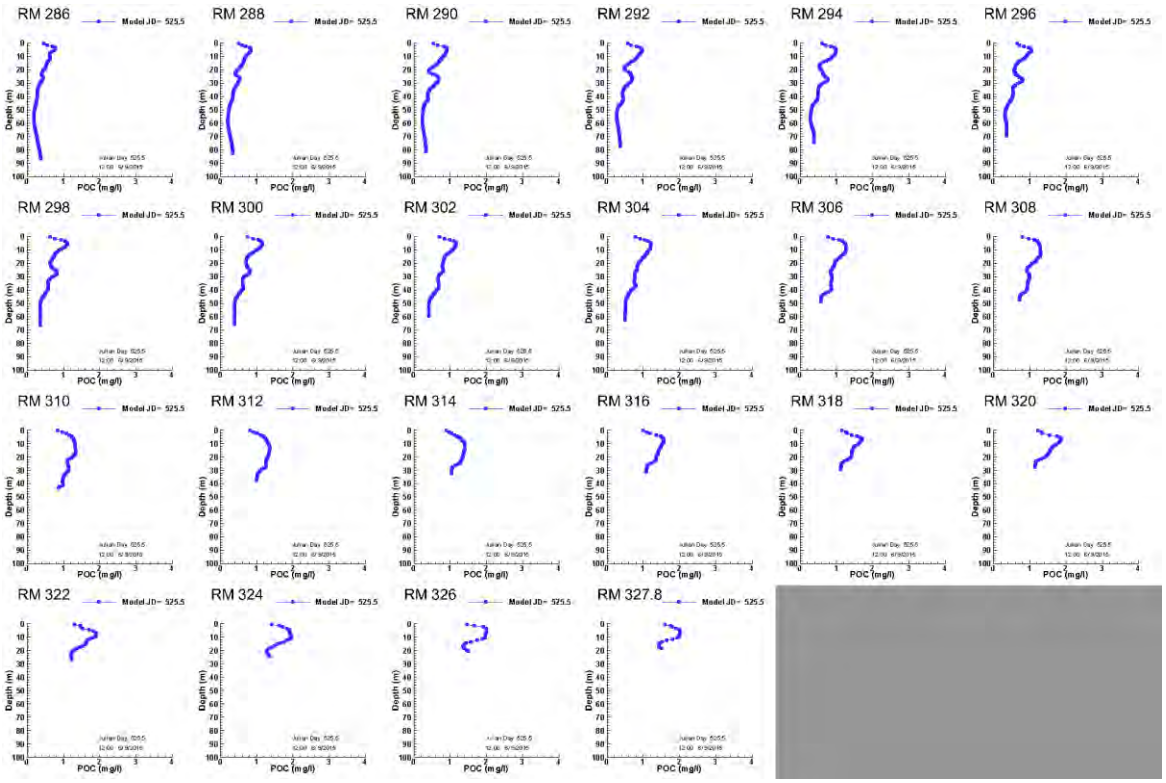


Figure 1565. Vertical profiles of POC compared with data for 6/ 9/2015.

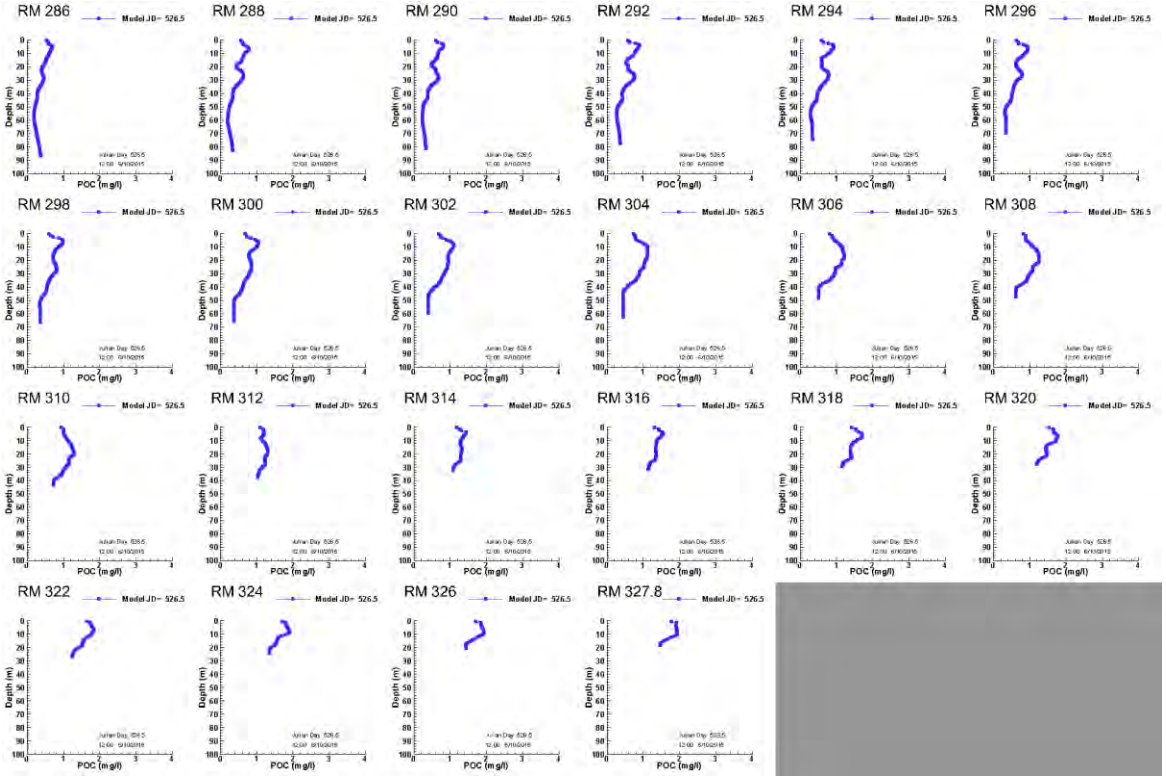


Figure 1566. Vertical profiles of POC compared with data for 6/10/2015.

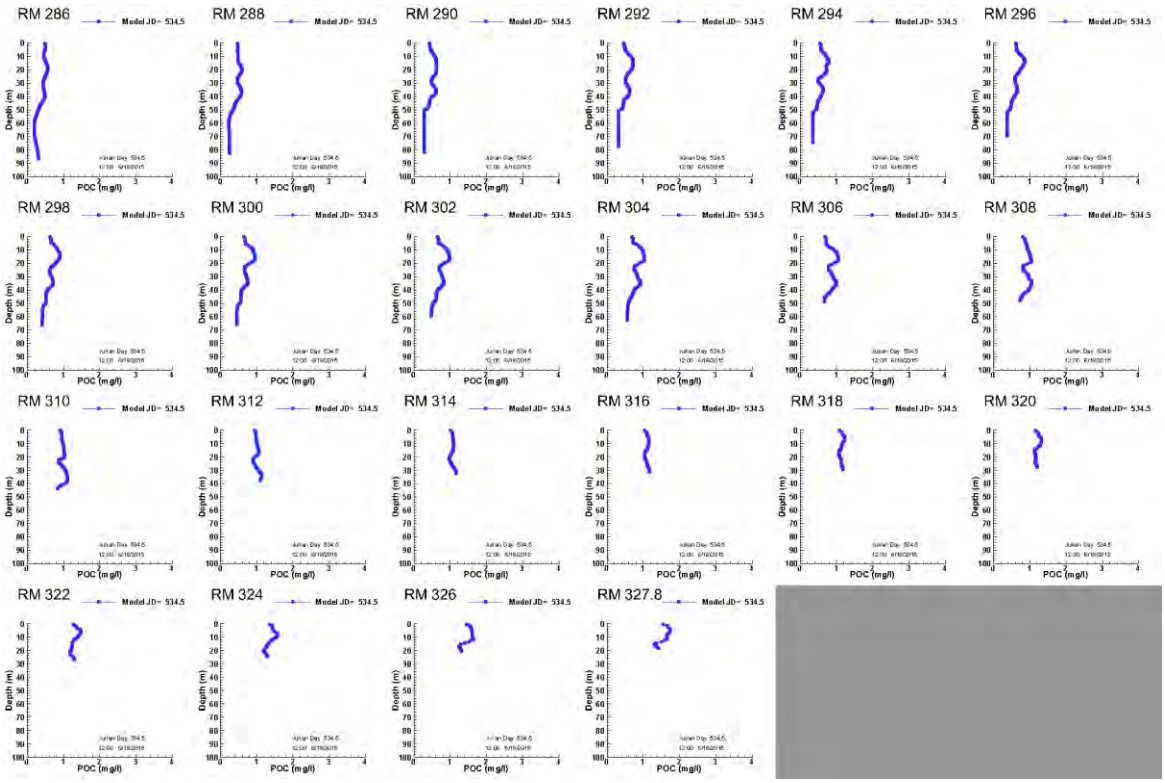


Figure 1567. Vertical profiles of POC compared with data for 6/18/2015.

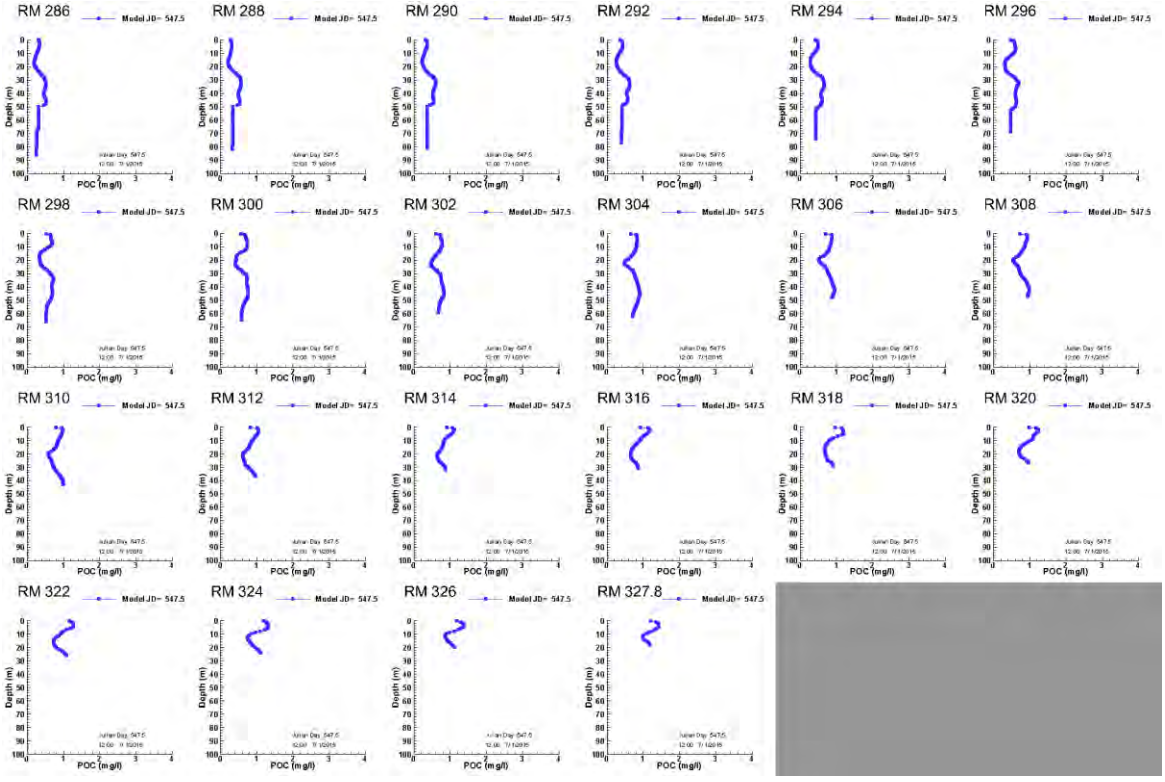


Figure 1568. Vertical profiles of POC compared with data for 7/ 1/2015.

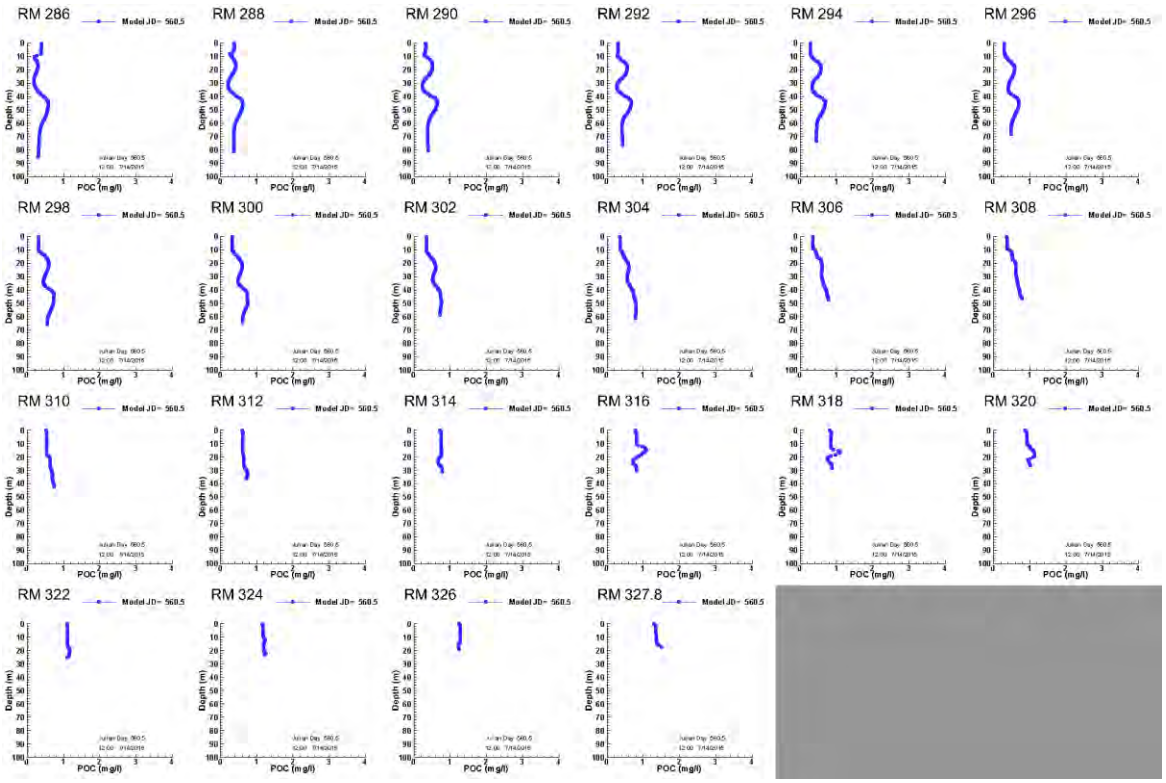


Figure 1569. Vertical profiles of POC compared with data for 7/14/2015.

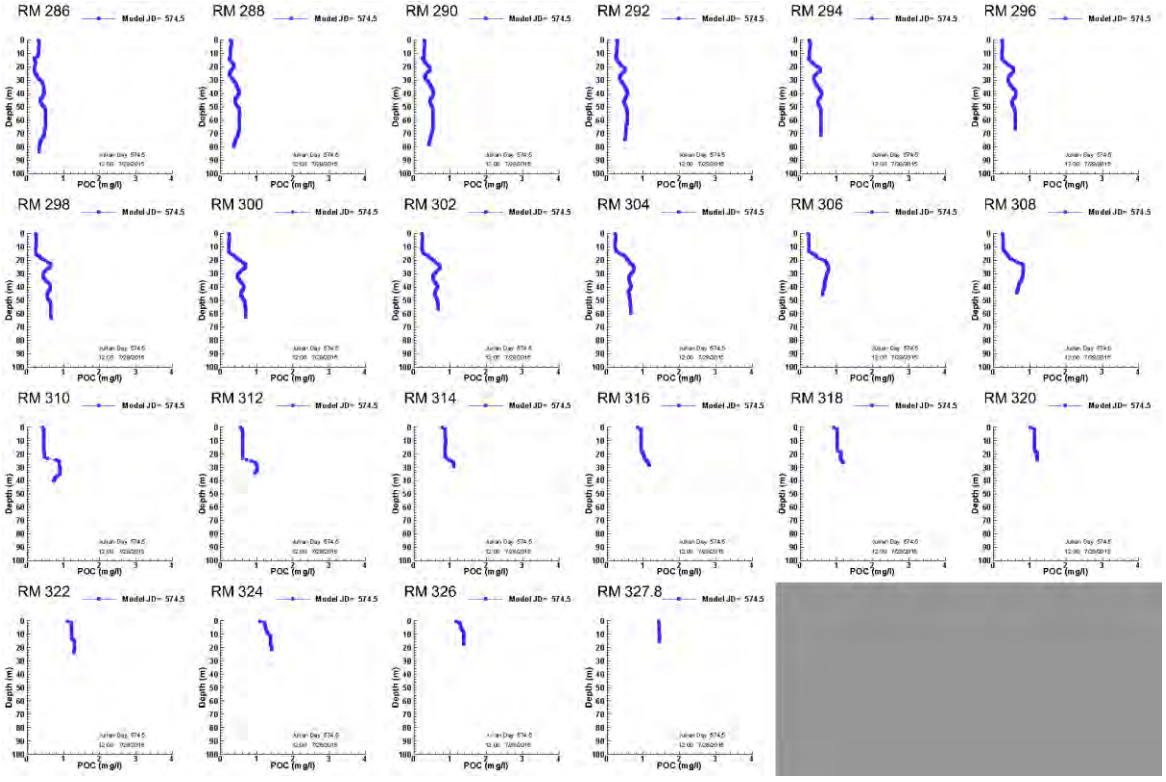


Figure 1570. Vertical profiles of POC compared with data for 7/28/2015.

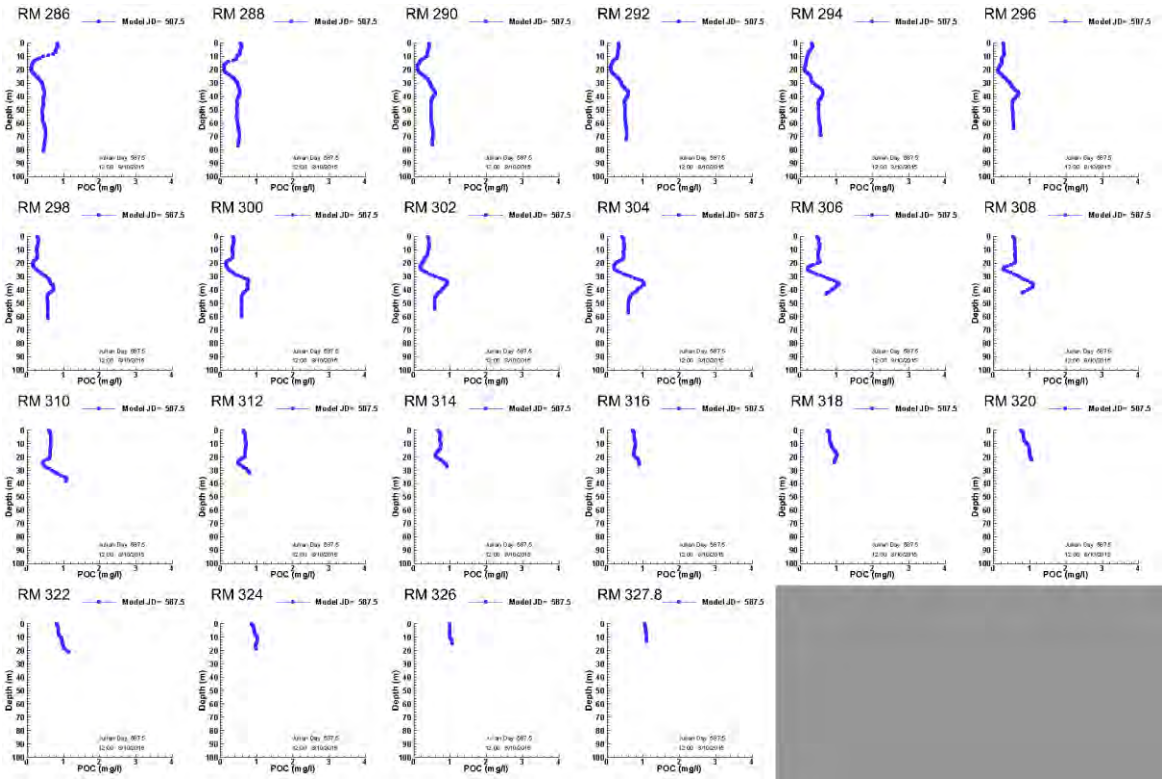


Figure 1571. Vertical profiles of POC compared with data for 8/10/2015.

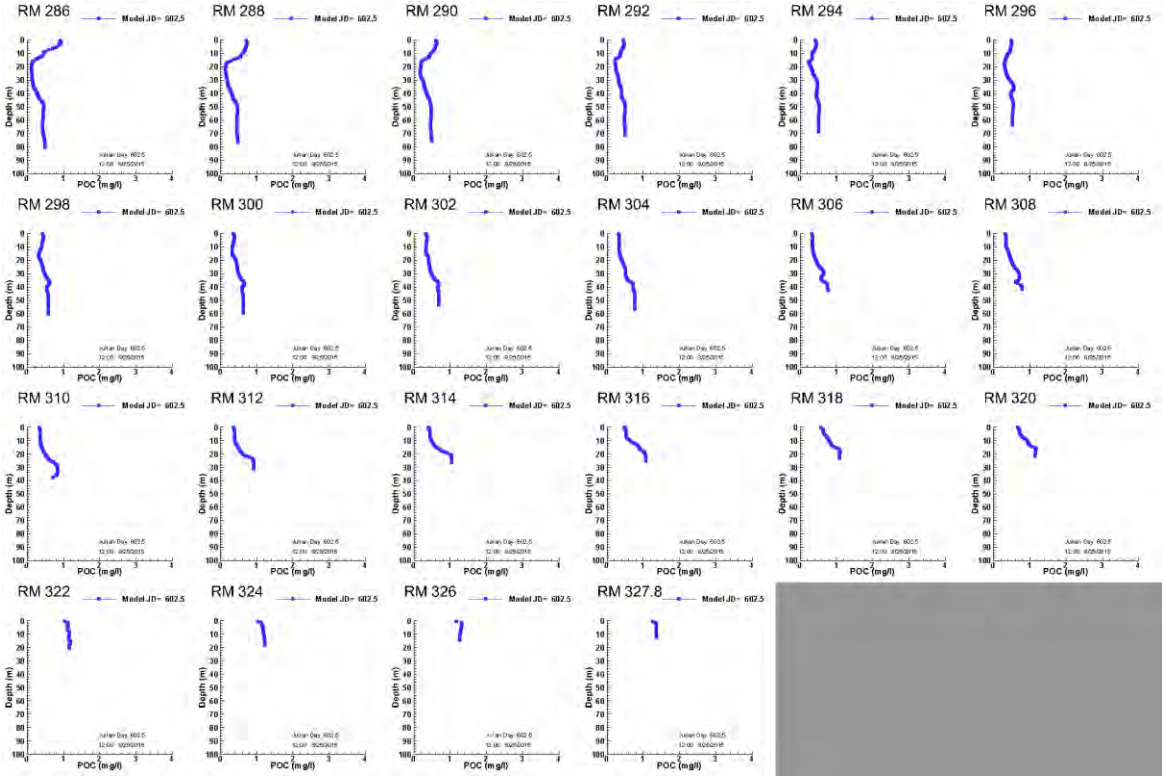


Figure 1572. Vertical profiles of POC compared with data for 8/25/2015.

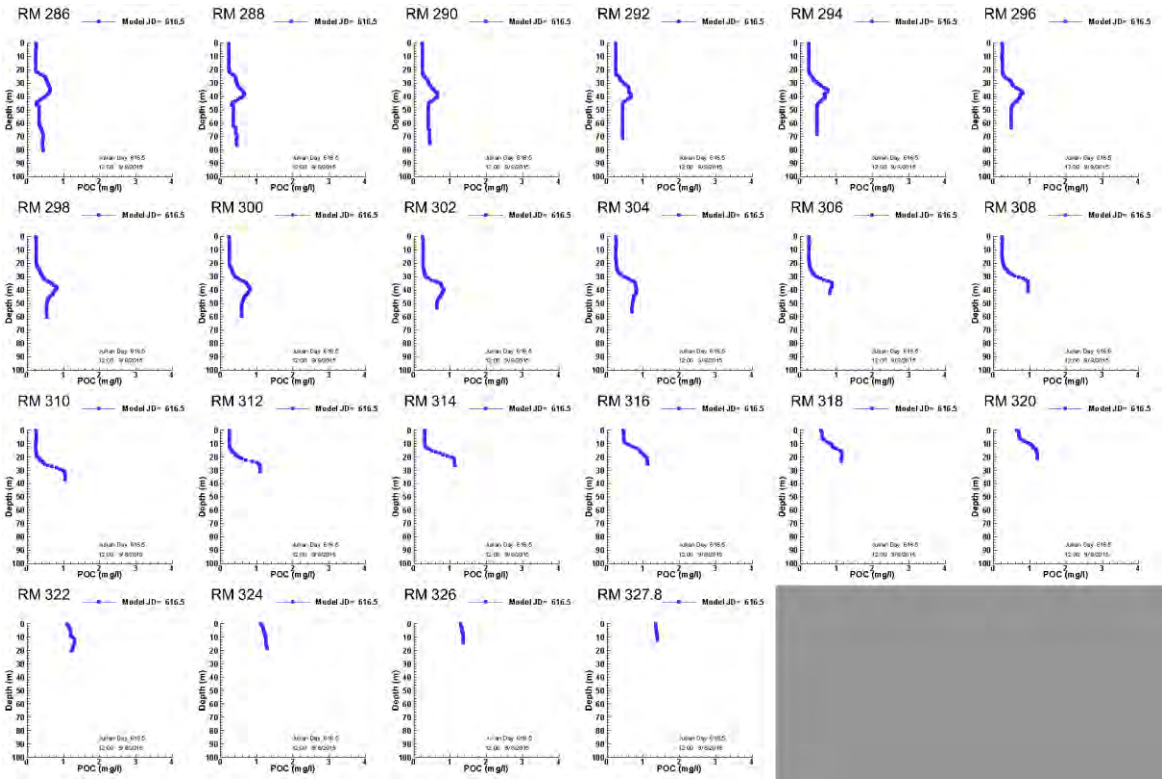


Figure 1573. Vertical profiles of POC compared with data for 9/ 8/2015.

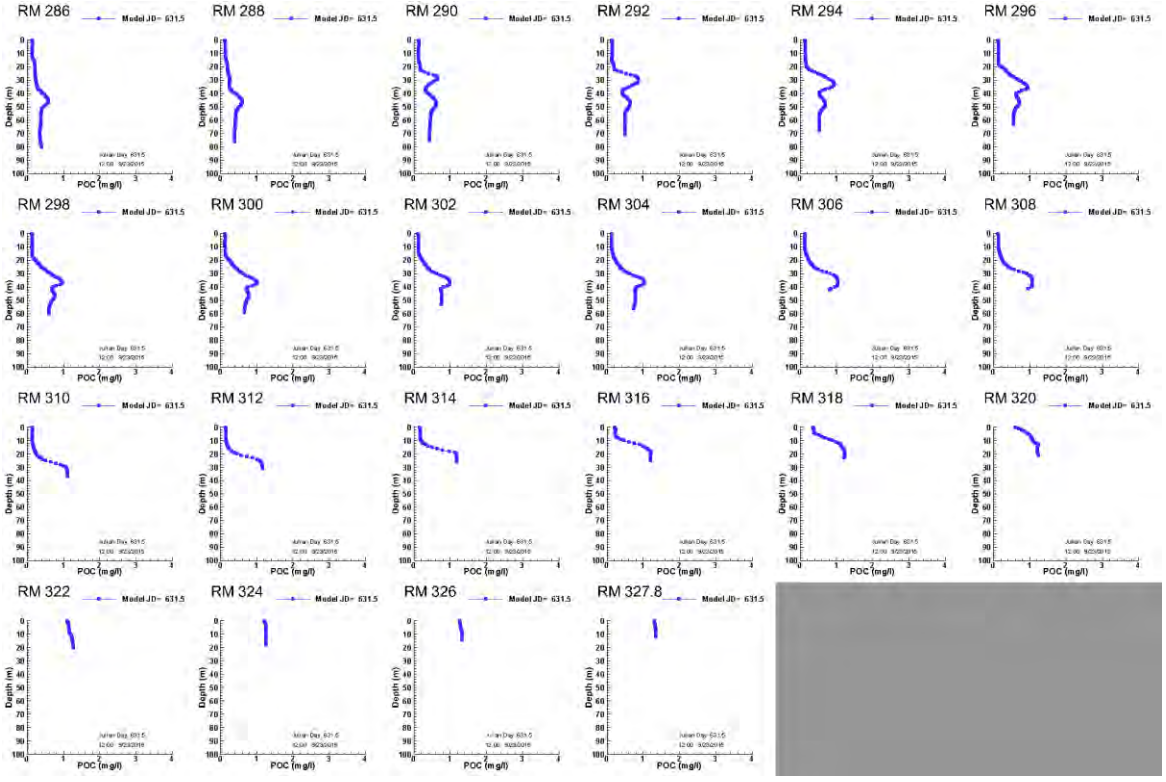


Figure 1574. Vertical profiles of POC compared with data for 9/23/2015.

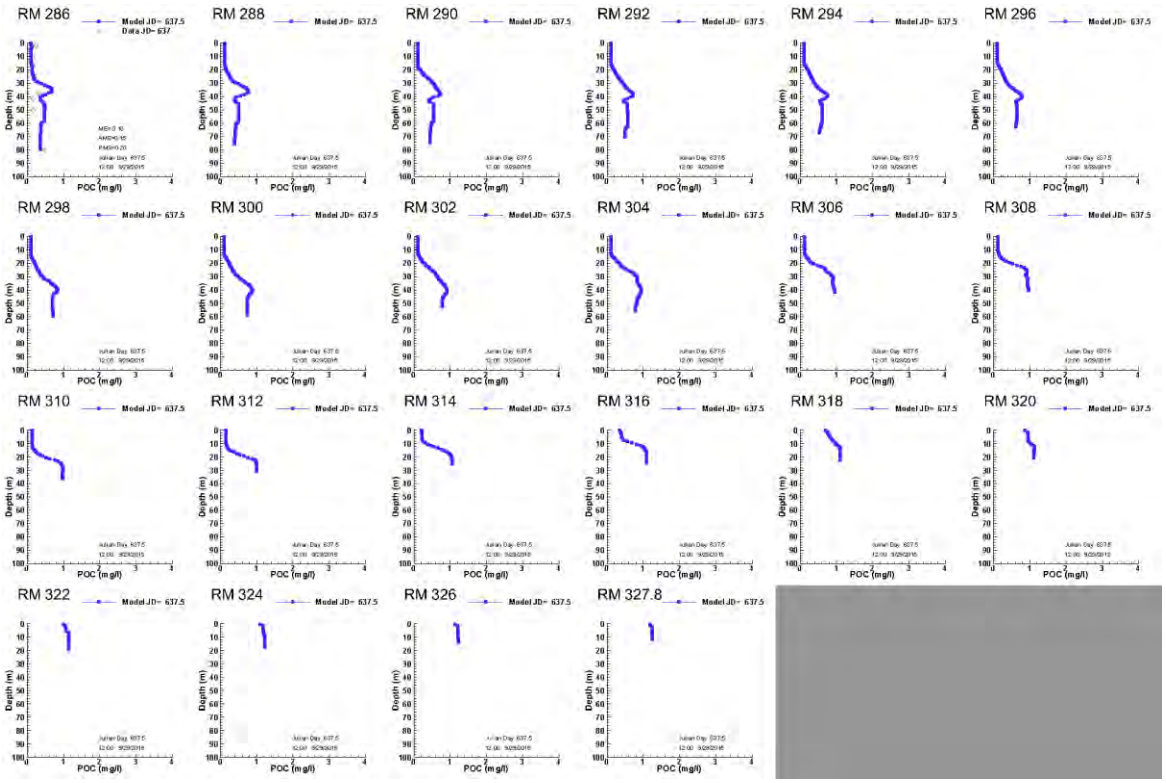


Figure 1575. Vertical profiles of POC compared with data for 9/29/2015.

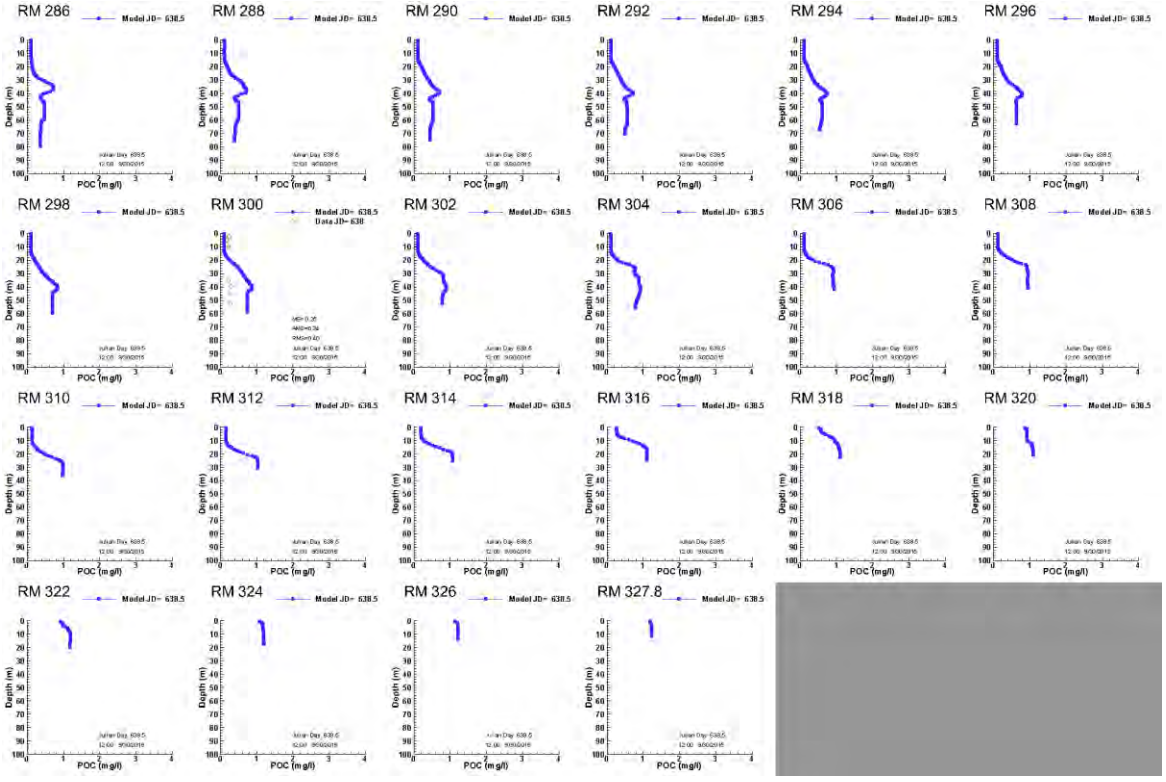


Figure 1576. Vertical profiles of POC compared with data for 9/30/2015.

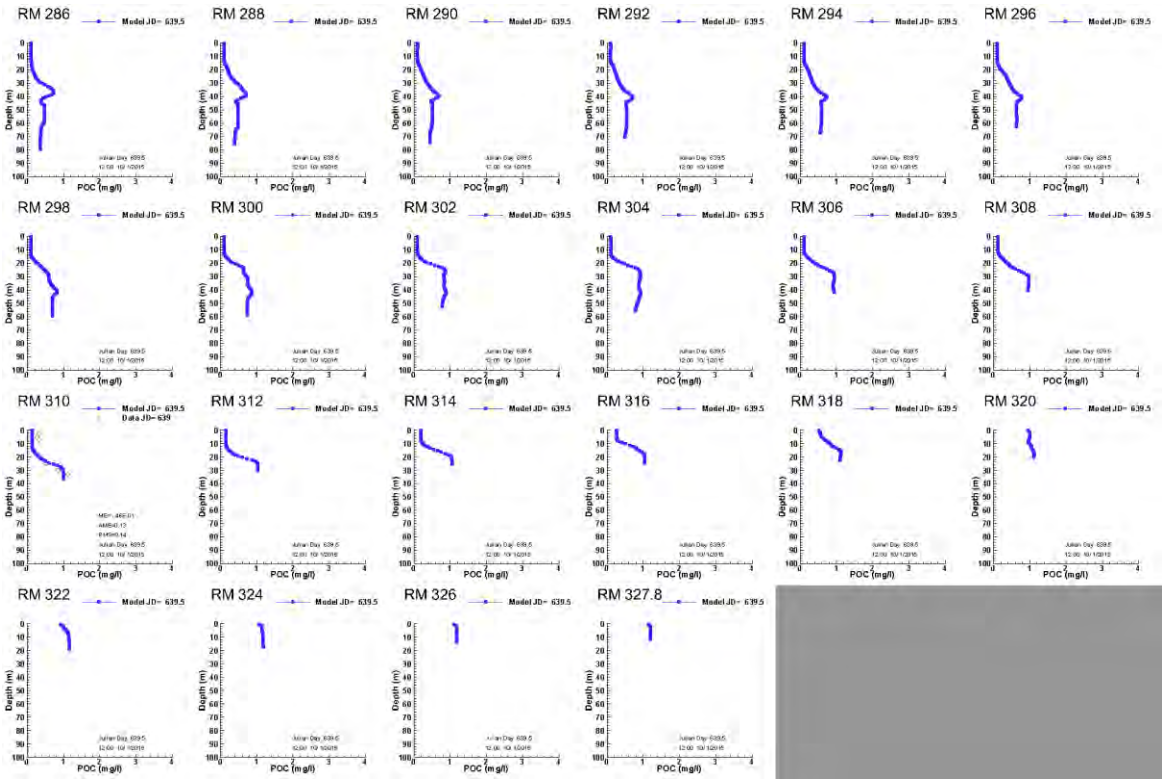


Figure 1577. Vertical profiles of POC compared with data for 10/ 1/2015.

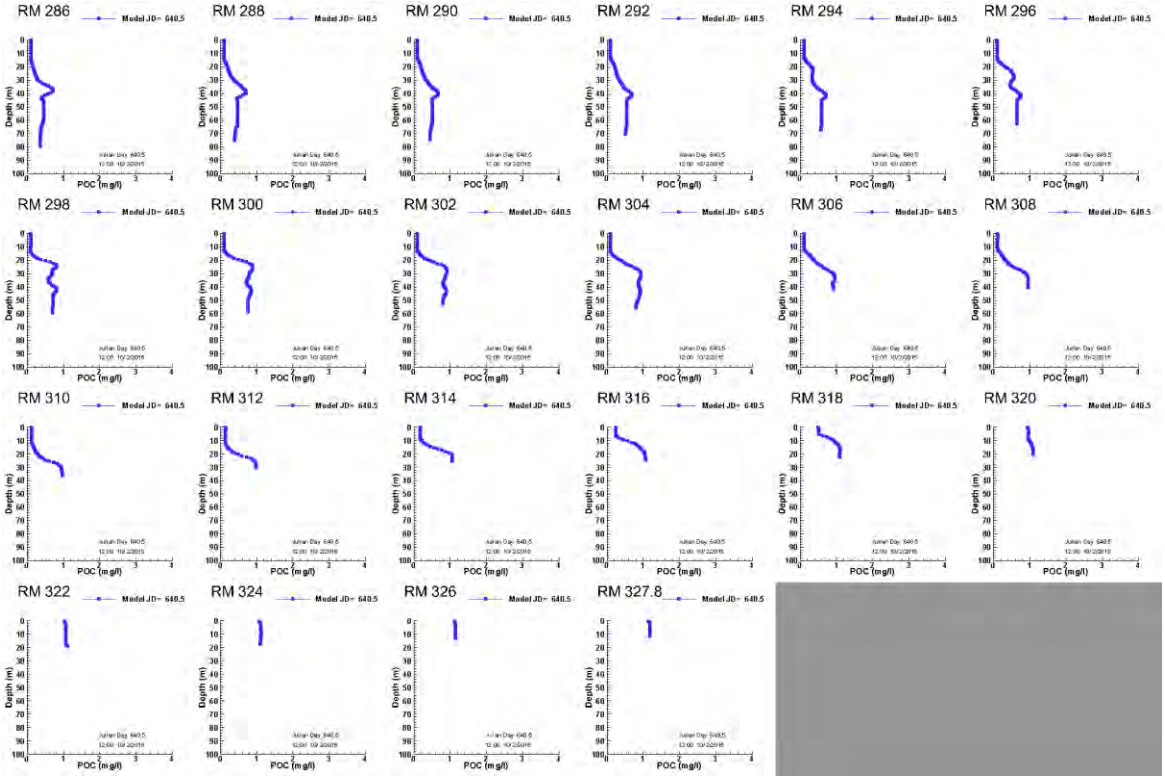


Figure 1578. Vertical profiles of POC compared with data for 10/ 2/2015.

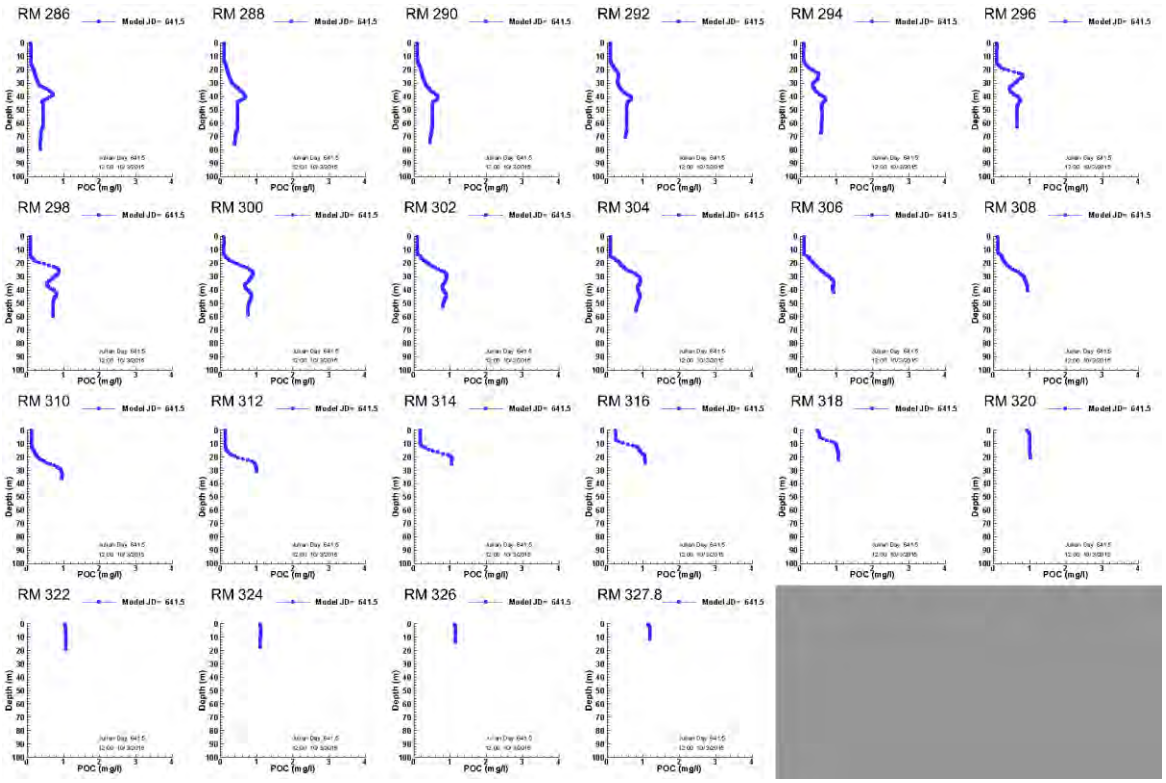


Figure 1579. Vertical profiles of POC compared with data for 10/ 3/2015.

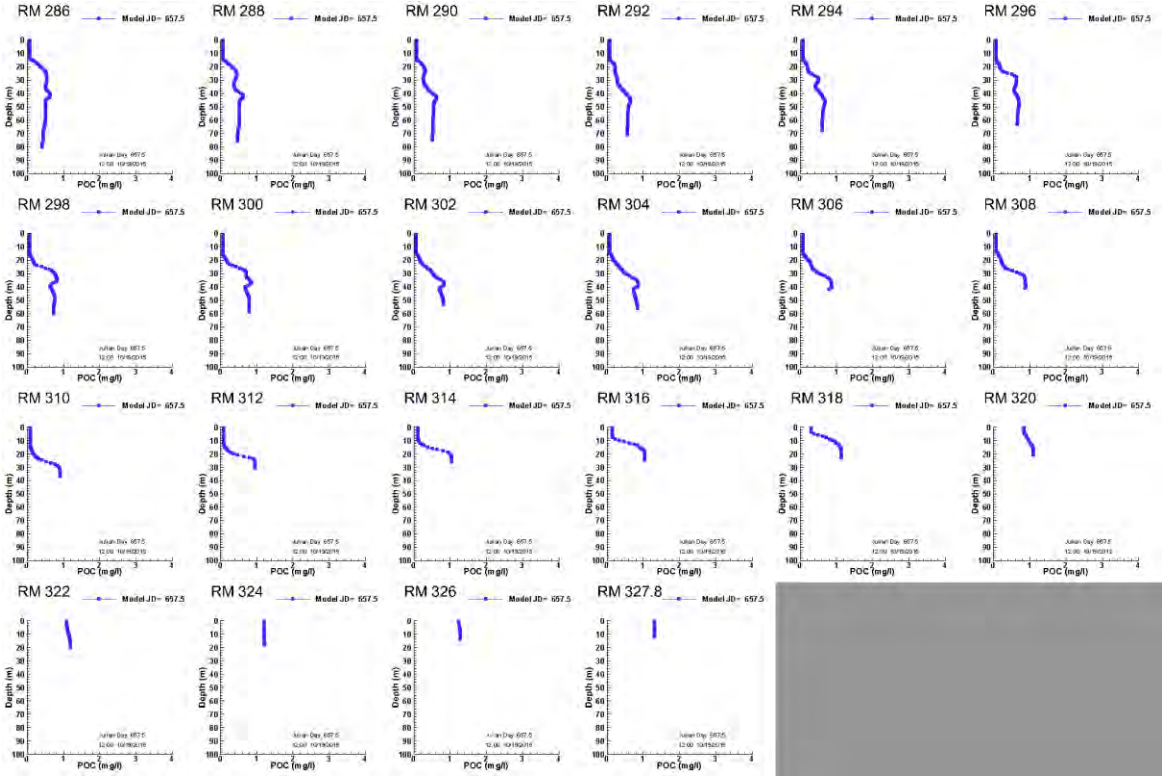


Figure 1580. Vertical profiles of POC compared with data for 10/19/2015.

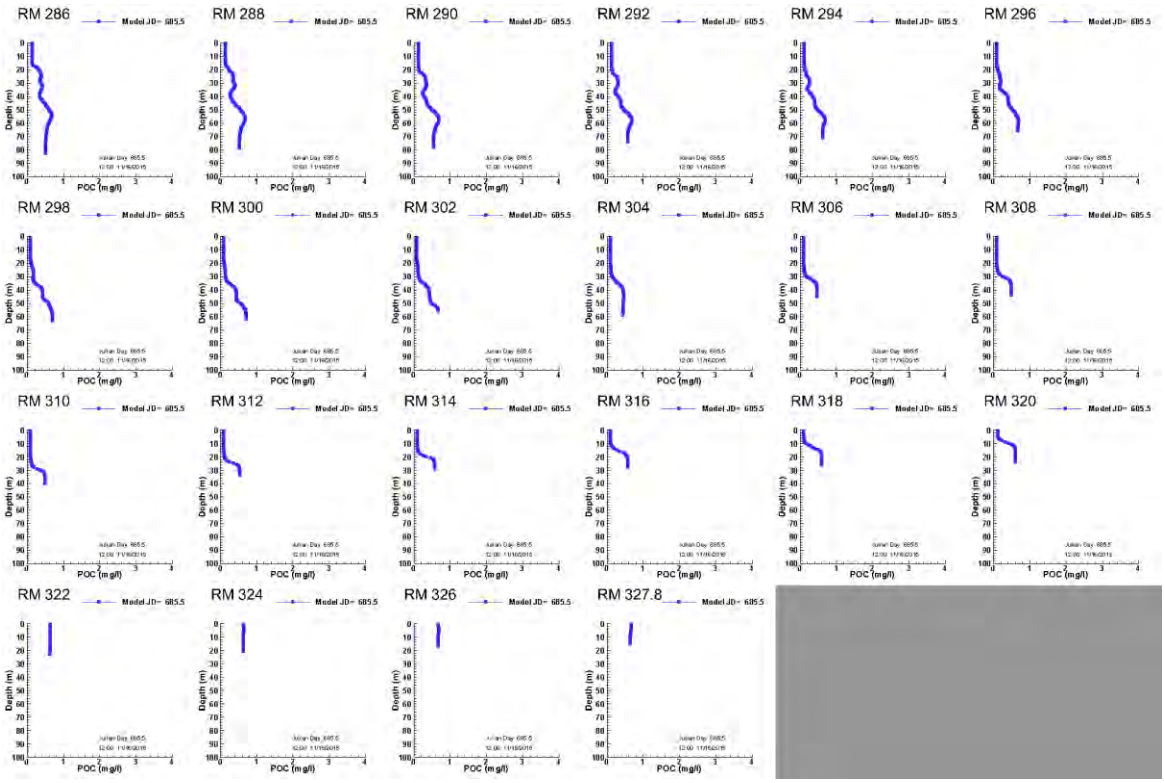


Figure 1581. Vertical profiles of POC compared with data for 11/16/2015.

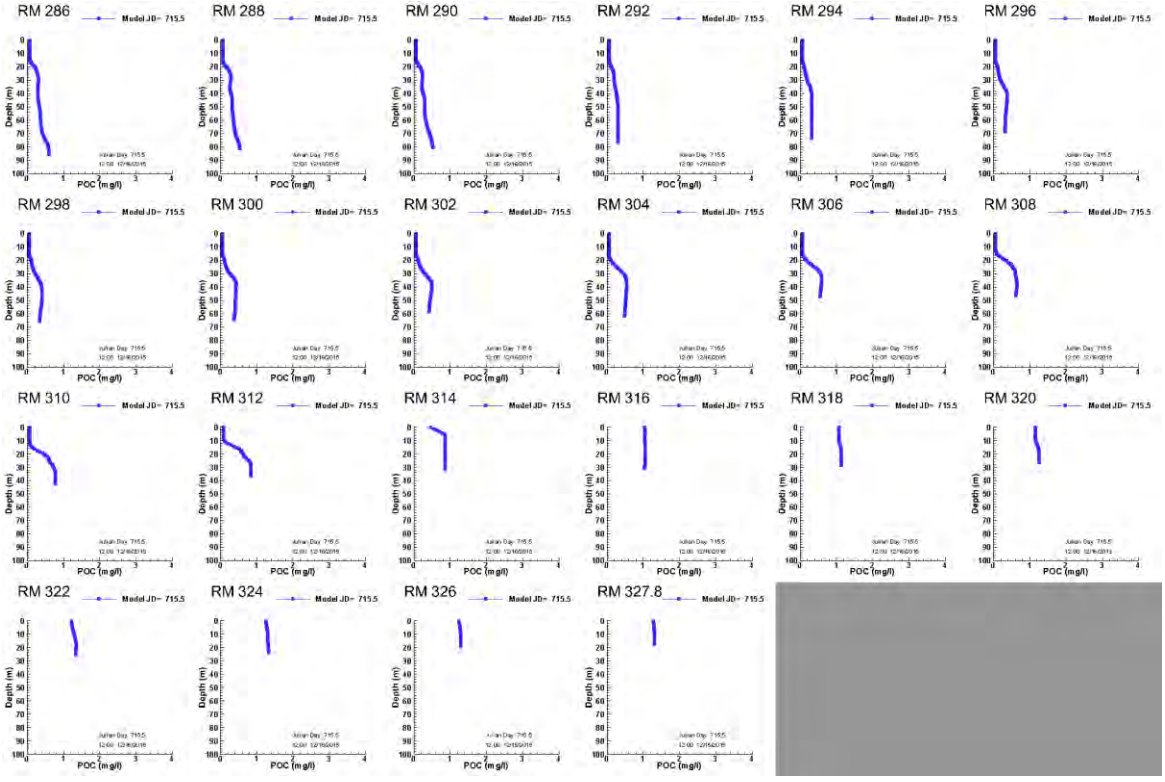


Figure 1582. Vertical profiles of POC compared with data for 12/16/2015.

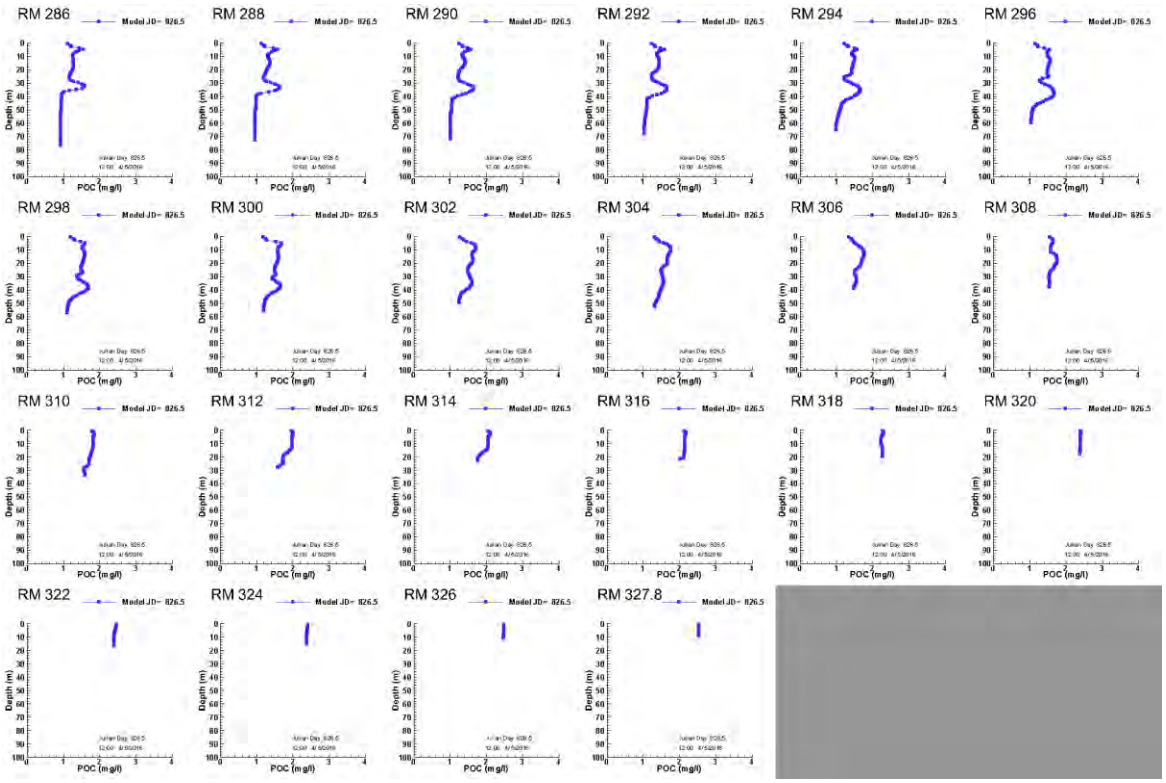


Figure 1583. Vertical profiles of POC compared with data for 4/ 5/2016.

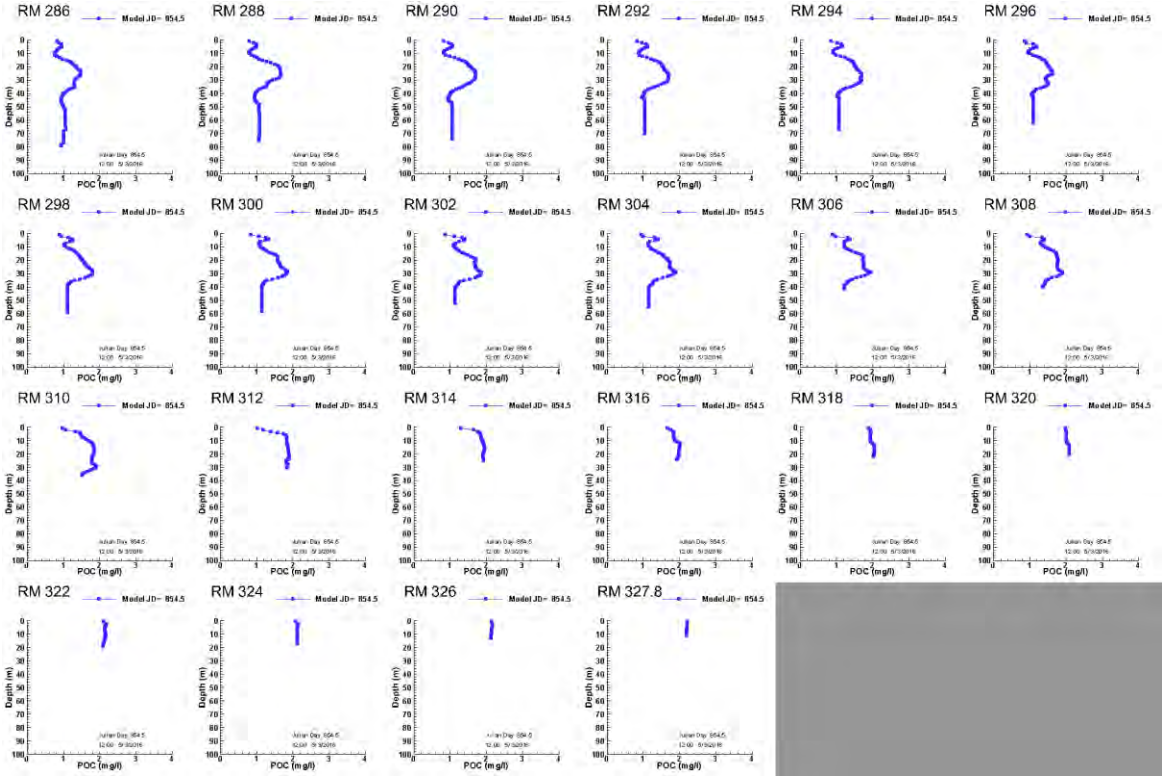


Figure 1584. Vertical profiles of POC compared with data for 5/ 3/2016.

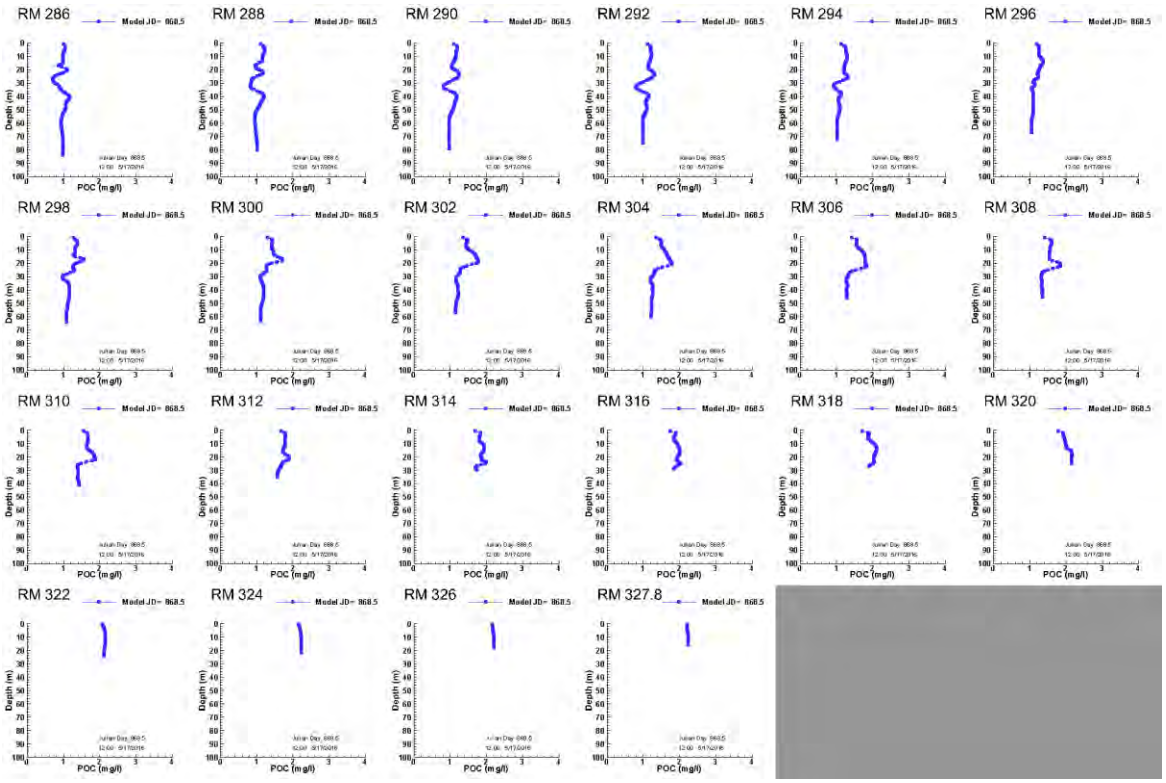


Figure 1585. Vertical profiles of POC compared with data for 5/17/2016.

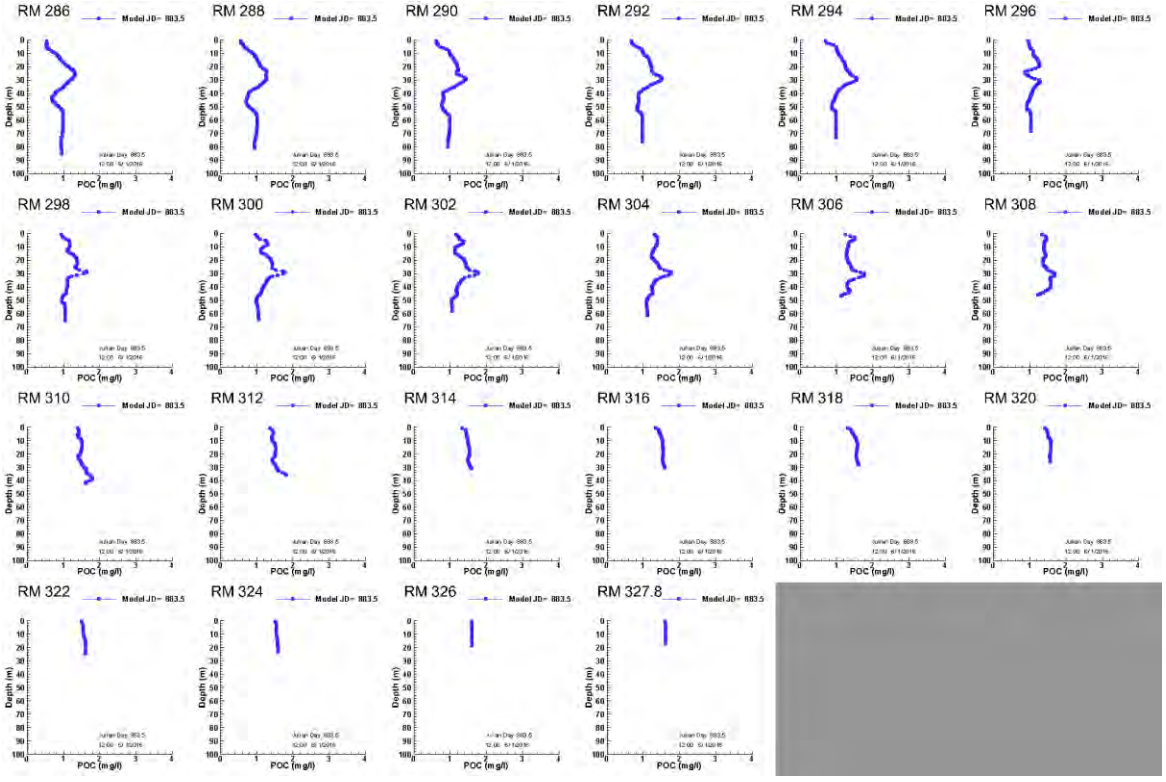


Figure 1586. Vertical profiles of POC compared with data for 6/ 1/2016.

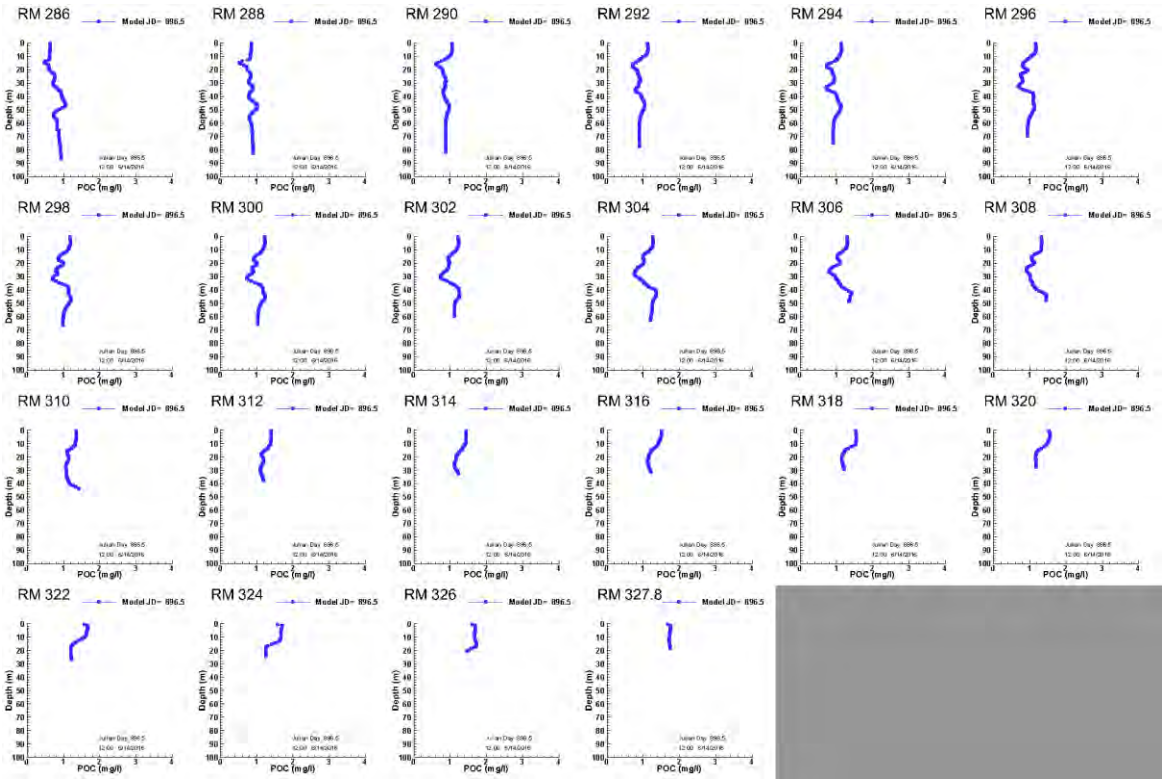


Figure 1587. Vertical profiles of POC compared with data for 6/14/2016.

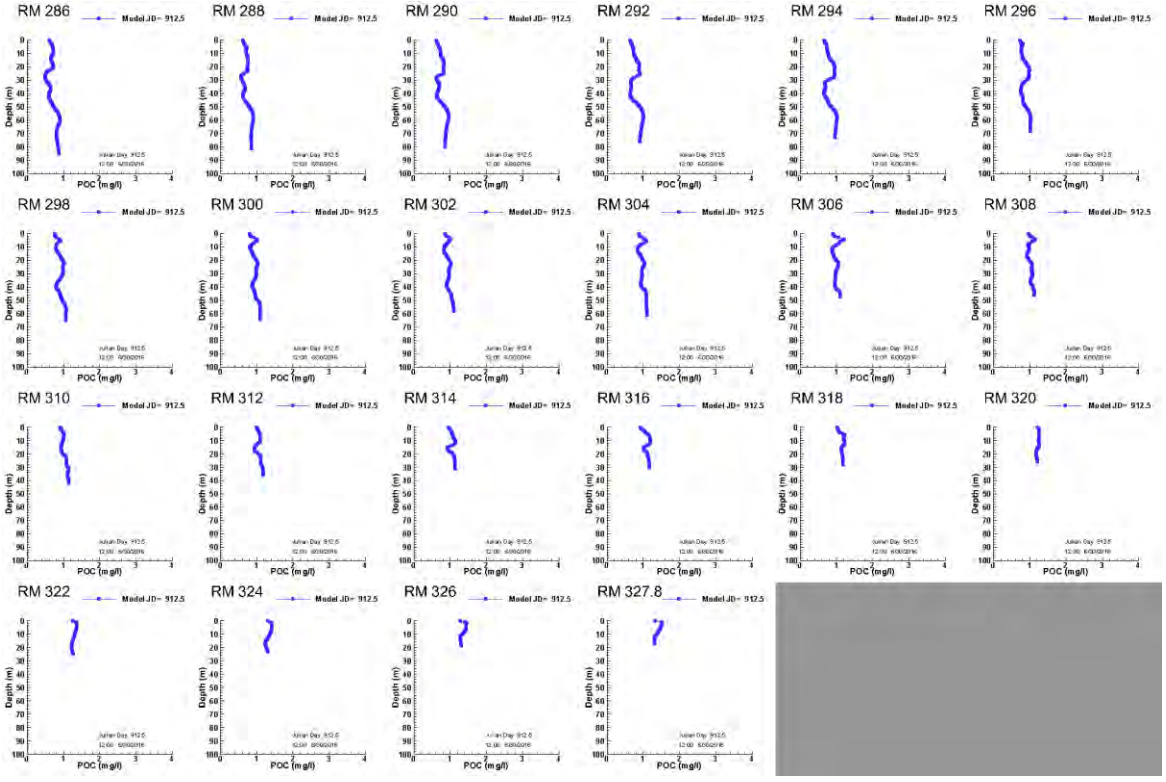


Figure 1588. Vertical profiles of POC compared with data for 6/30/2016.

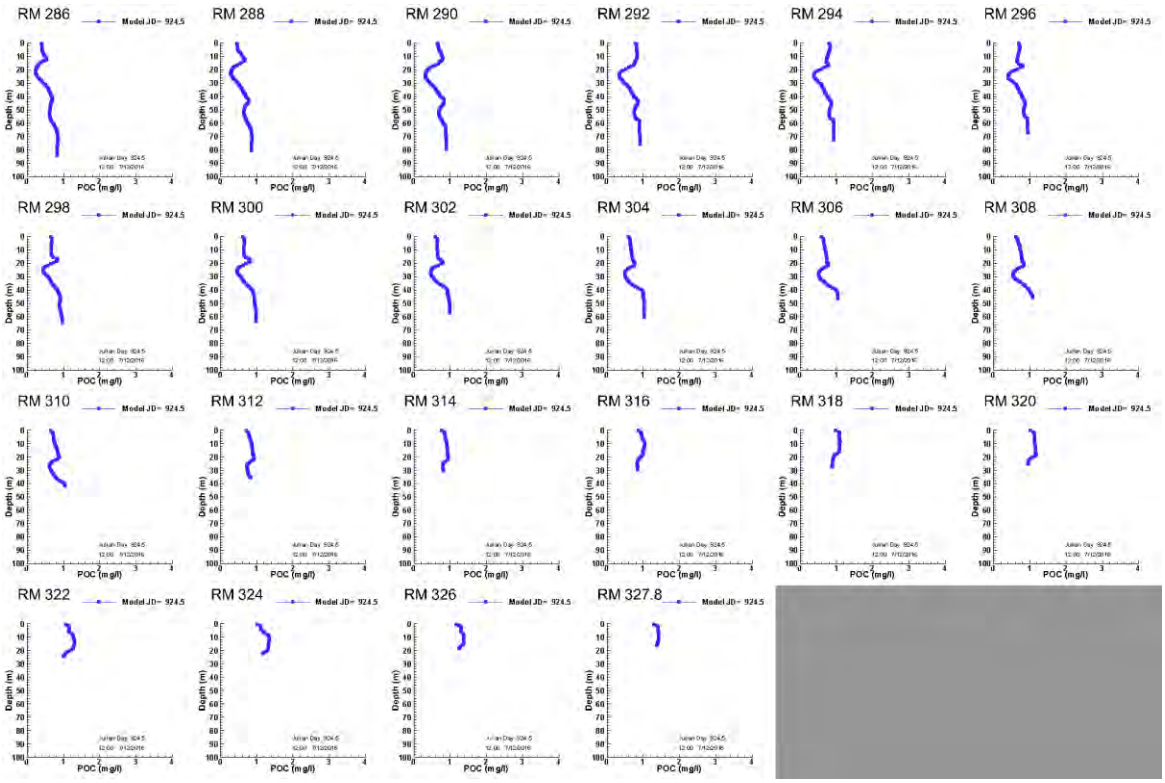


Figure 1589. Vertical profiles of POC compared with data for 7/12/2016.

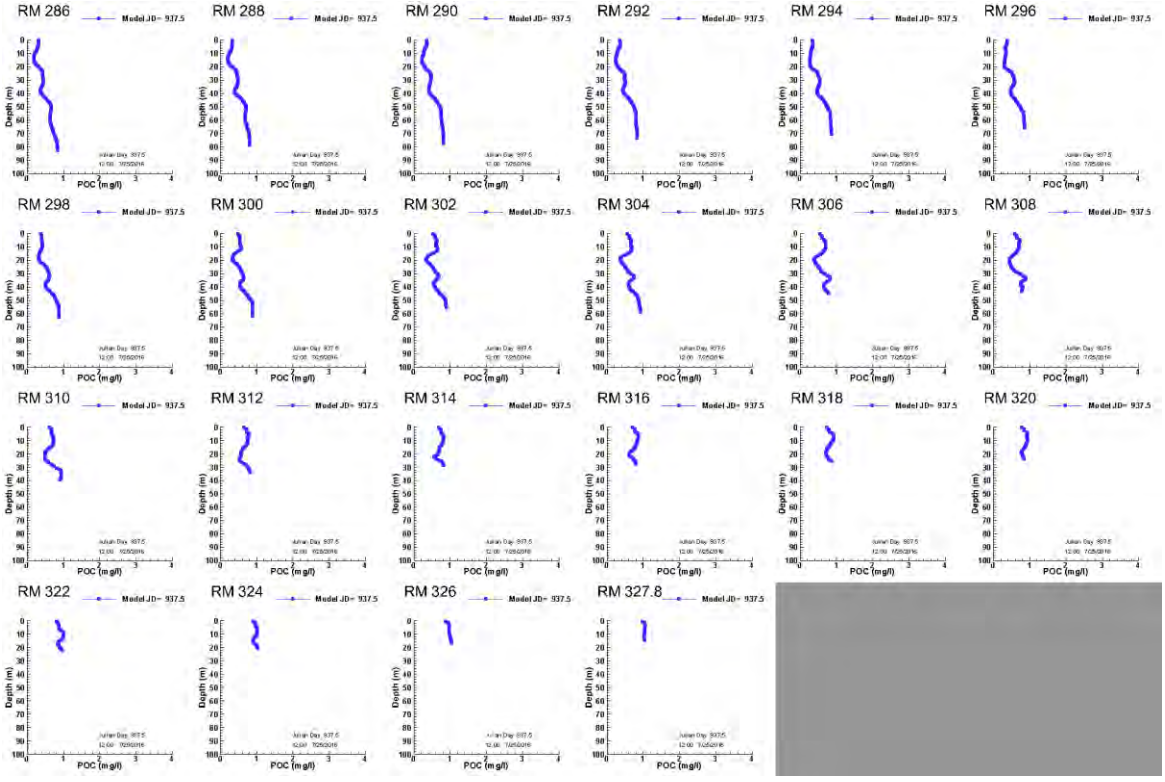


Figure 1590. Vertical profiles of POC compared with data for 7/25/2016.

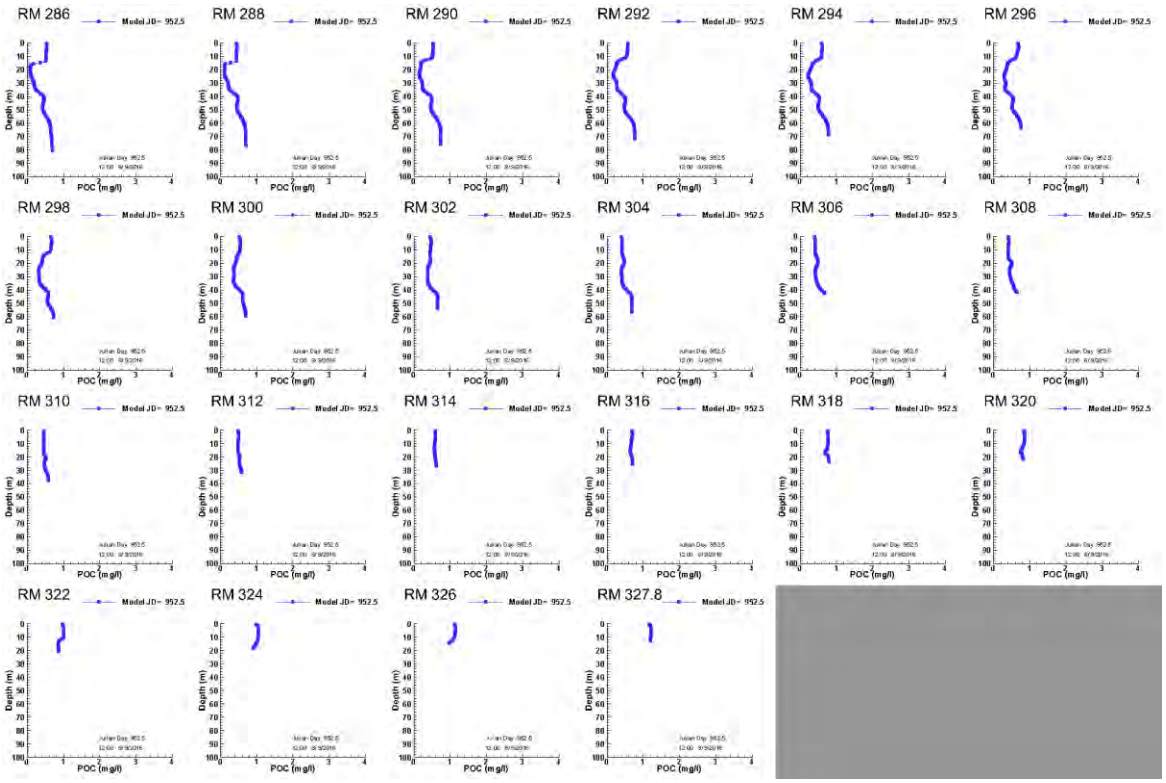


Figure 1591. Vertical profiles of POC compared with data for 8/ 9/2016.

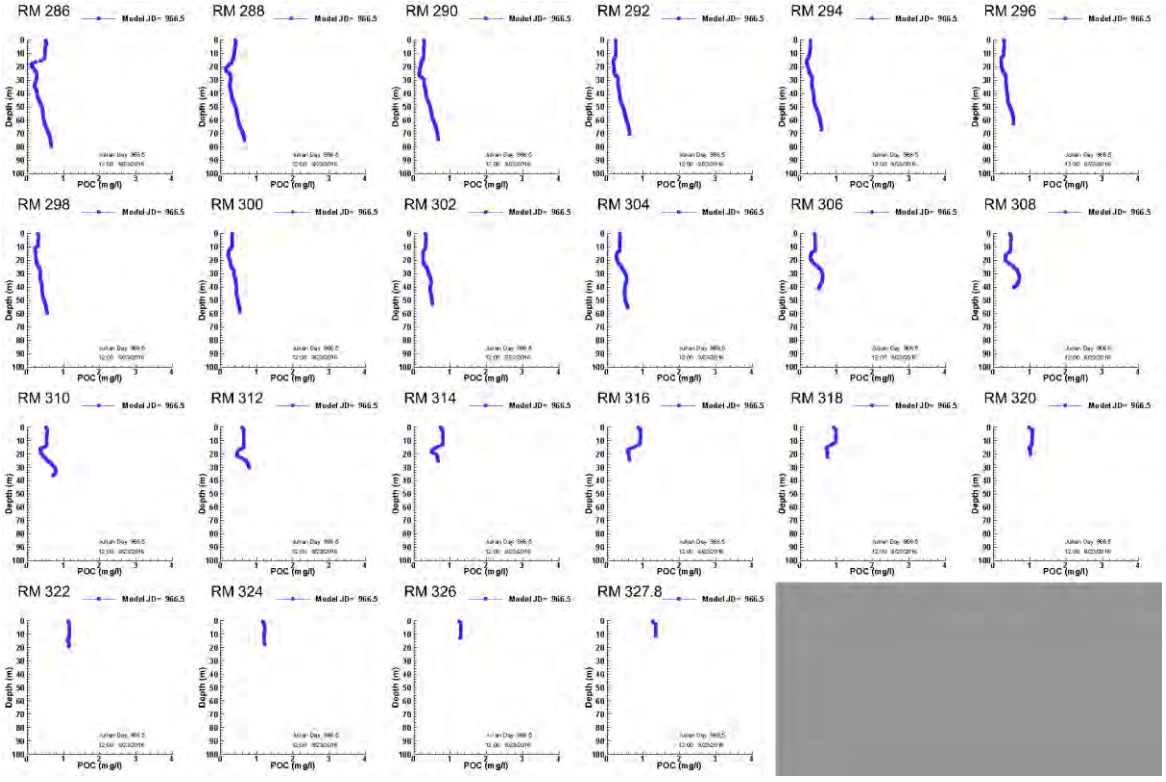


Figure 1592. Vertical profiles of POC compared with data for 8/23/2016.

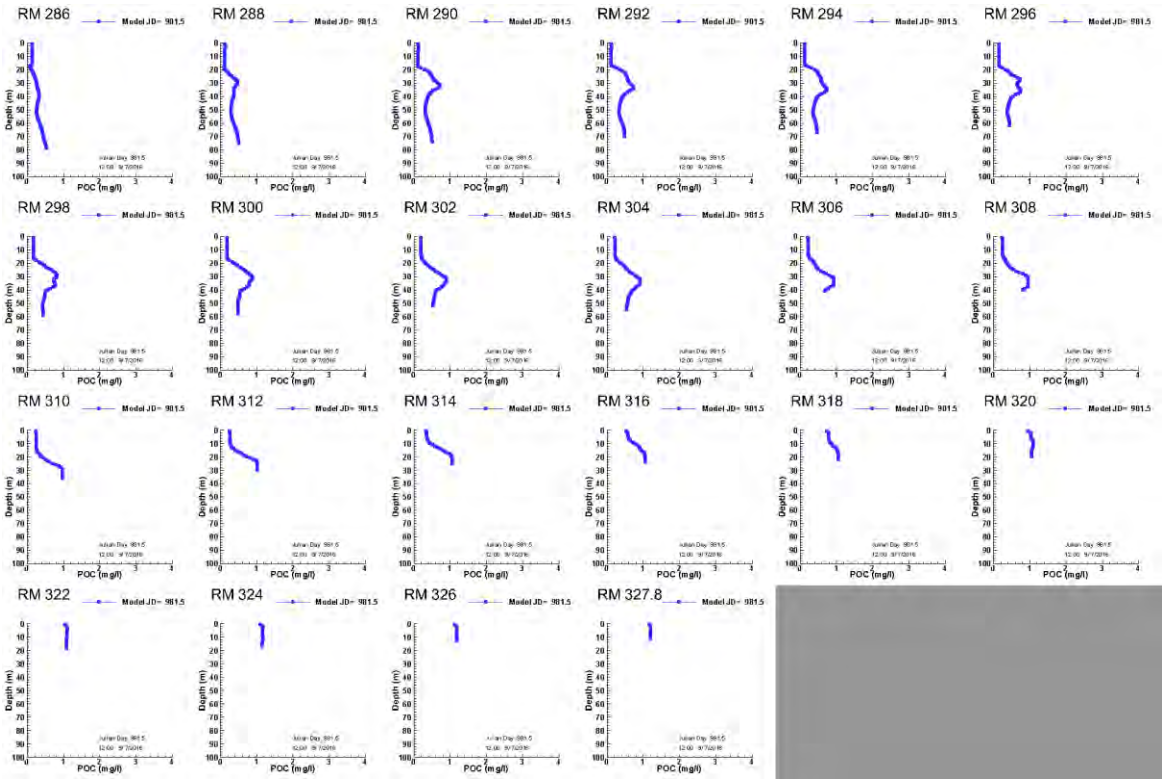


Figure 1593. Vertical profiles of POC compared with data for 9/ 7/2016.

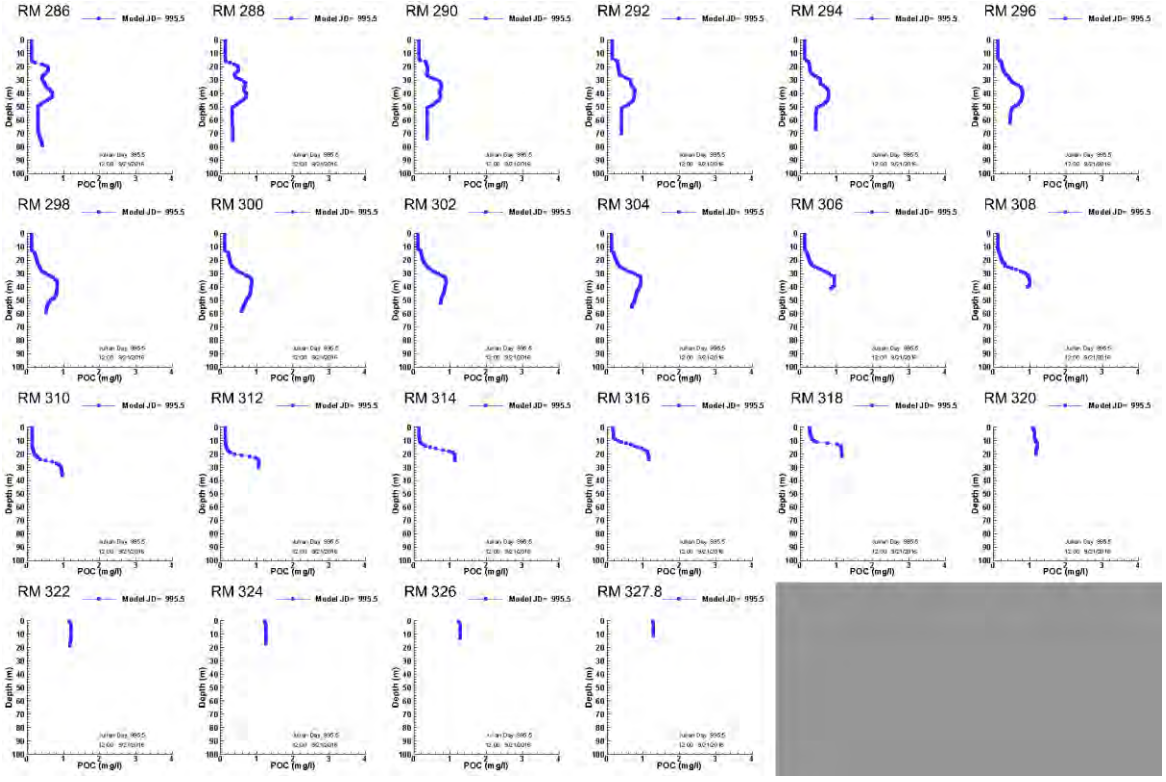


Figure 1594. Vertical profiles of POC compared with data for 9/21/2016.

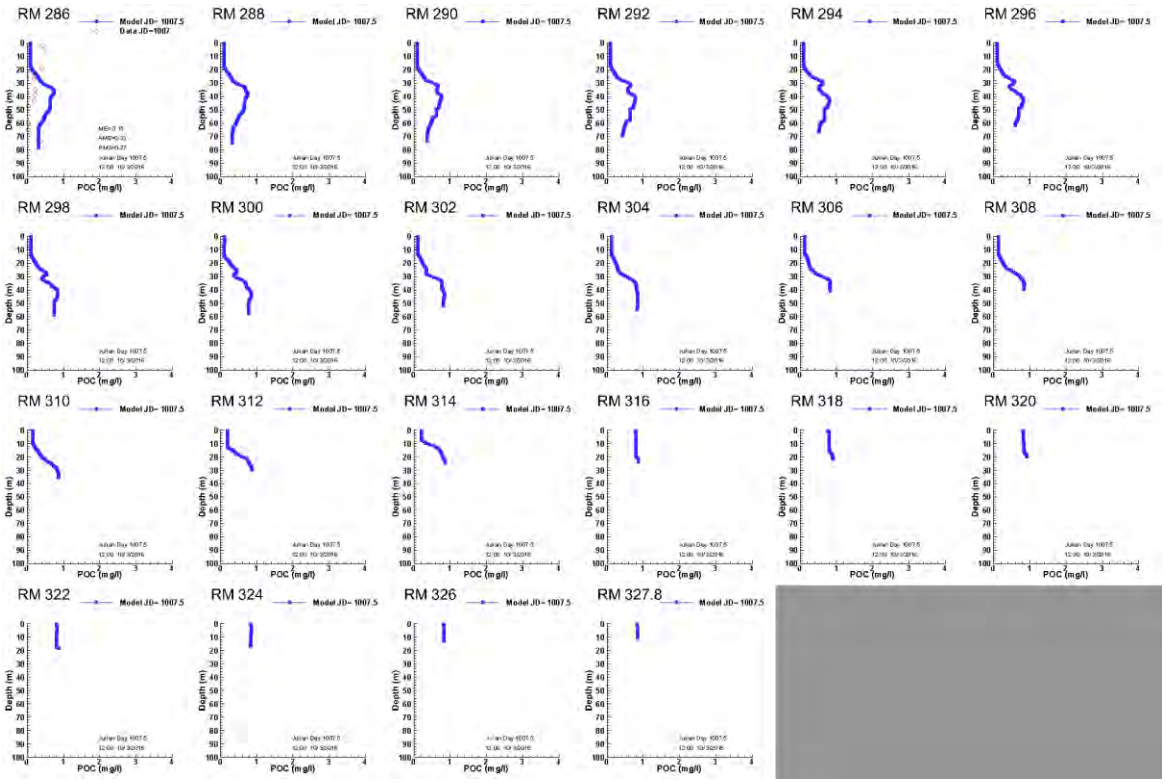


Figure 1595. Vertical profiles of POC compared with data for 10/ 3/2016.

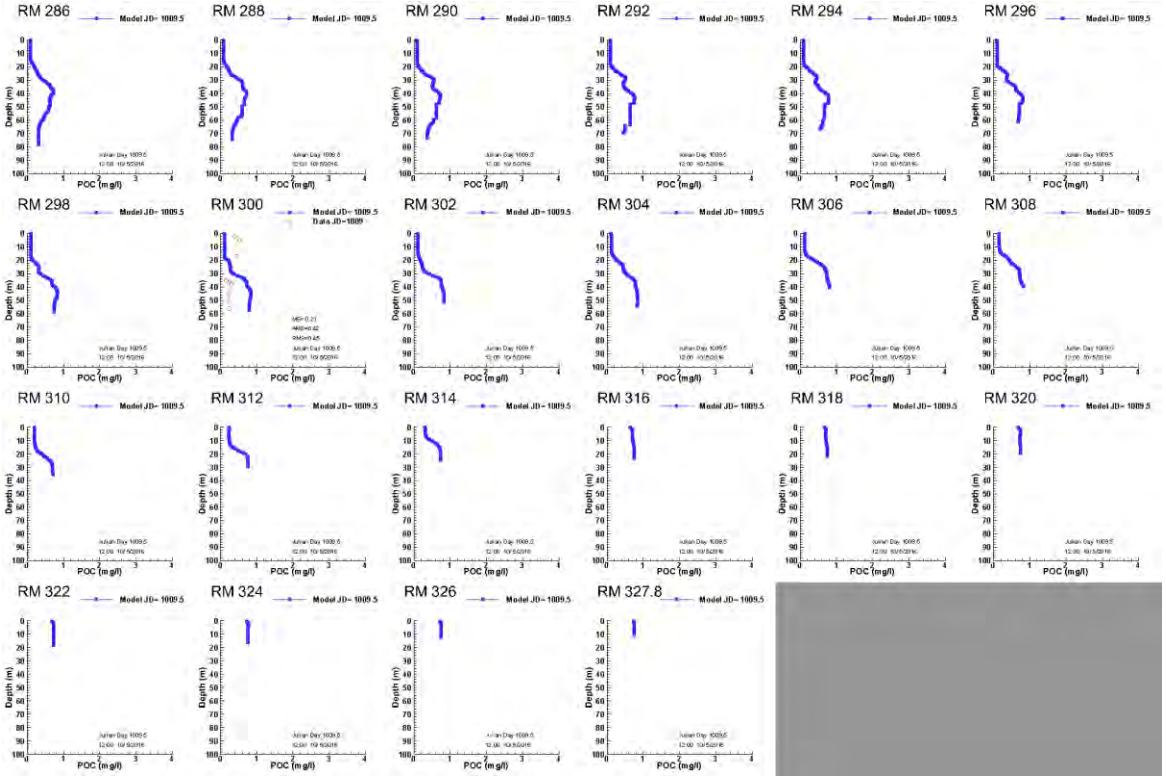


Figure 1596. Vertical profiles of POC compared with data for 10/ 5/2016.

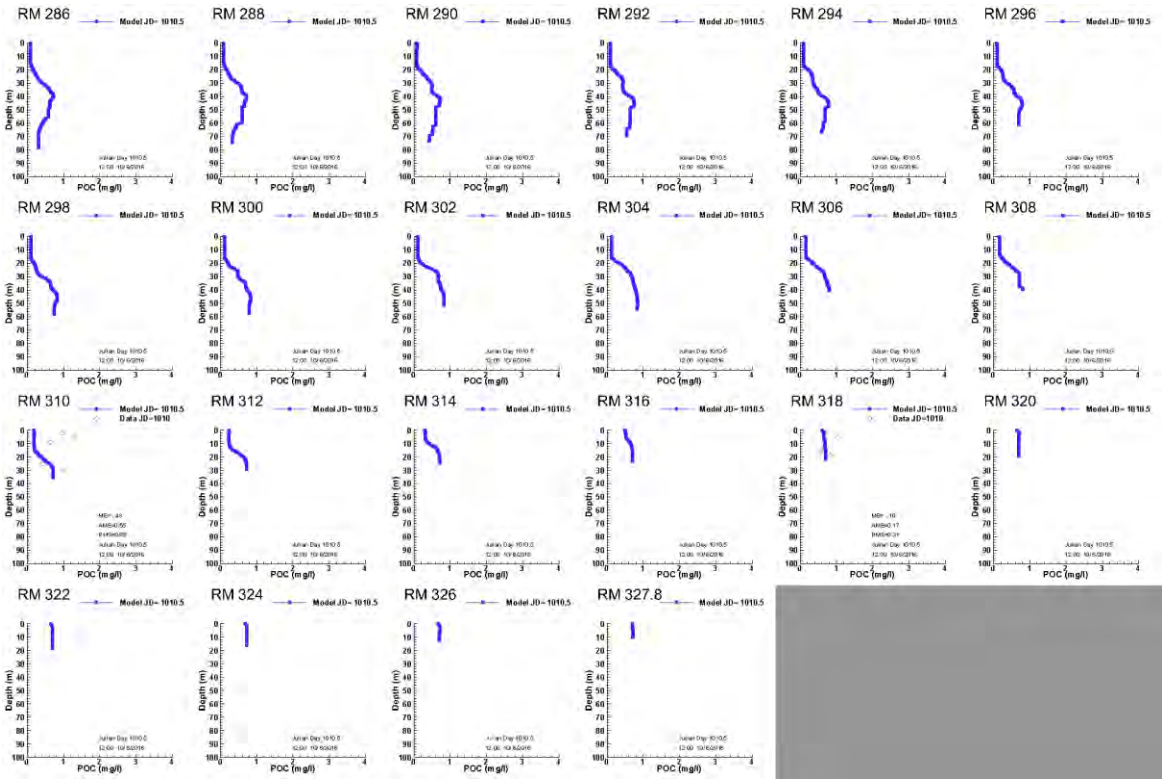


Figure 1597. Vertical profiles of POC compared with data for 10/ 6/2016.

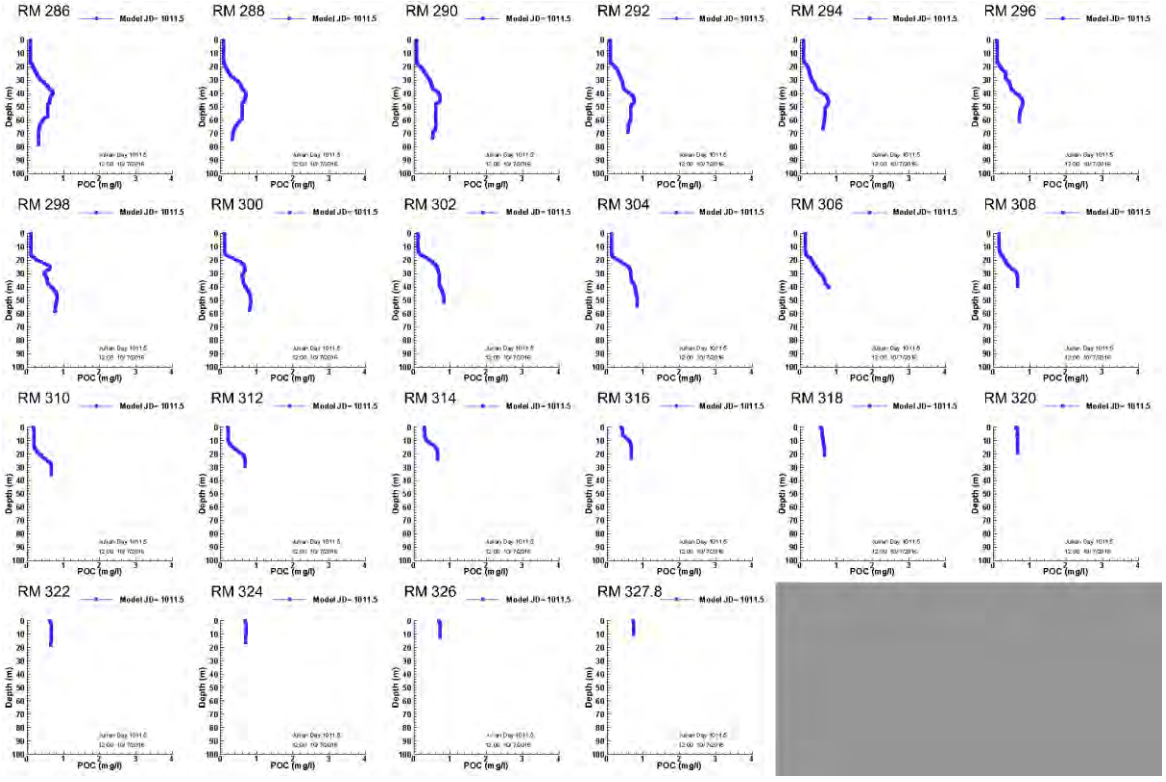


Figure 1598. Vertical profiles of POC compared with data for 10/ 7/2016.

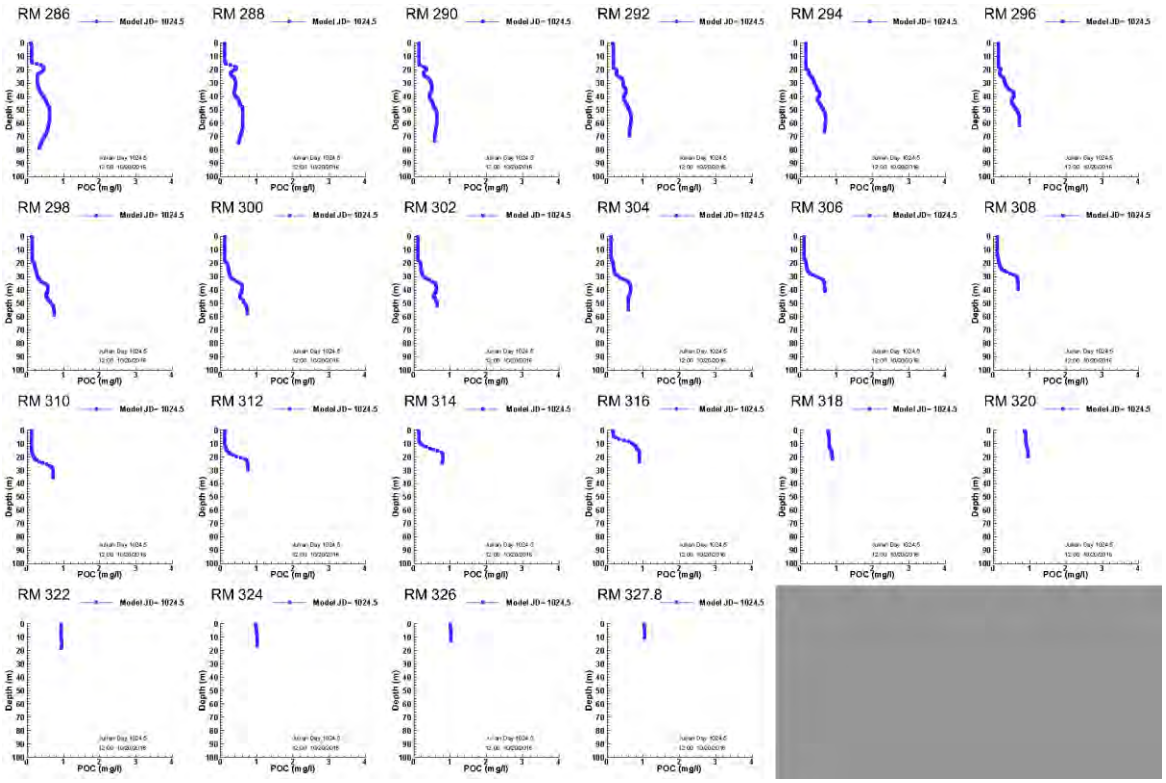


Figure 1599. Vertical profiles of POC compared with data for 10/20/2016.

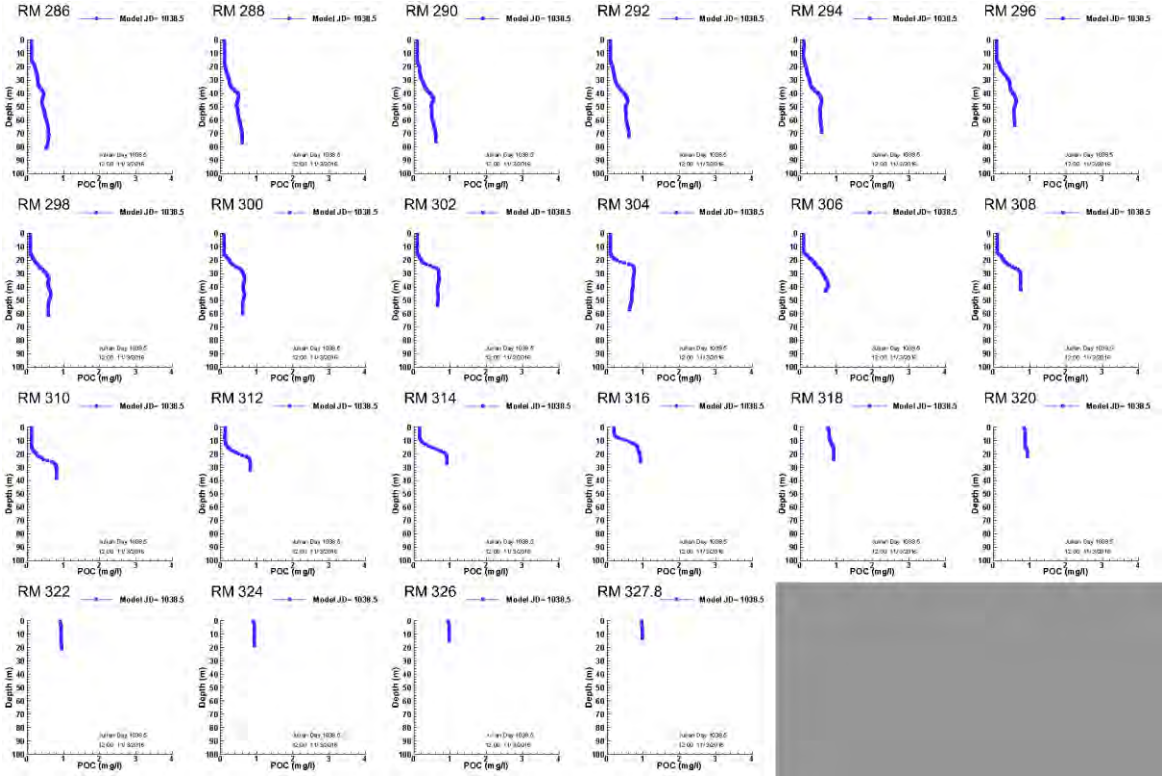


Figure 1600. Vertical profiles of POC compared with data for 11/ 3/2016.

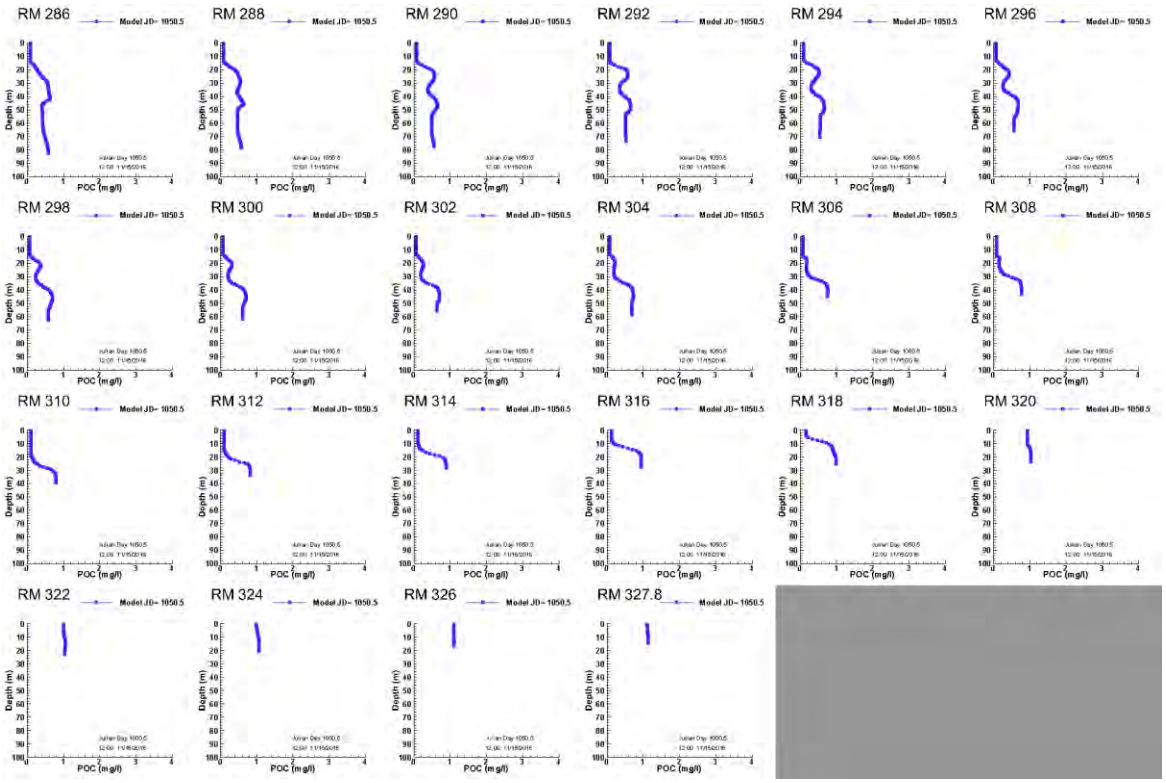


Figure 1601. Vertical profiles of POC compared with data for 11/15/2016.

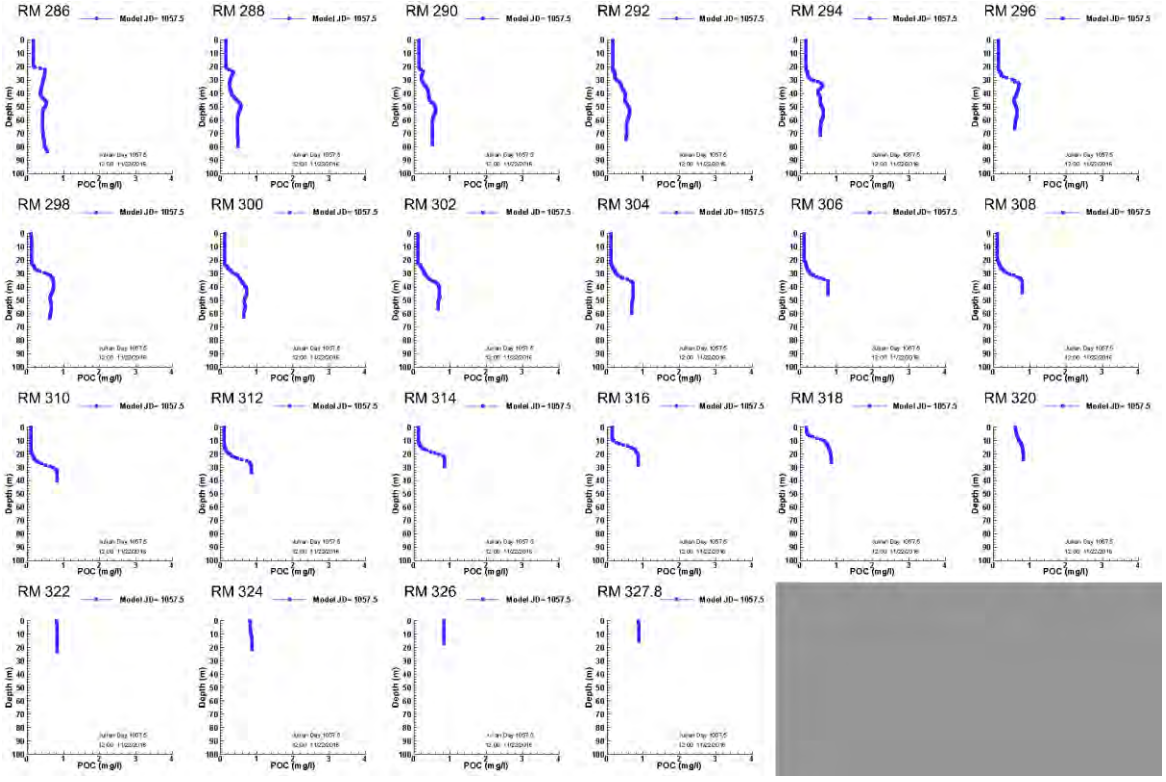


Figure 1602. Vertical profiles of POC compared with data for 11/22/2016.

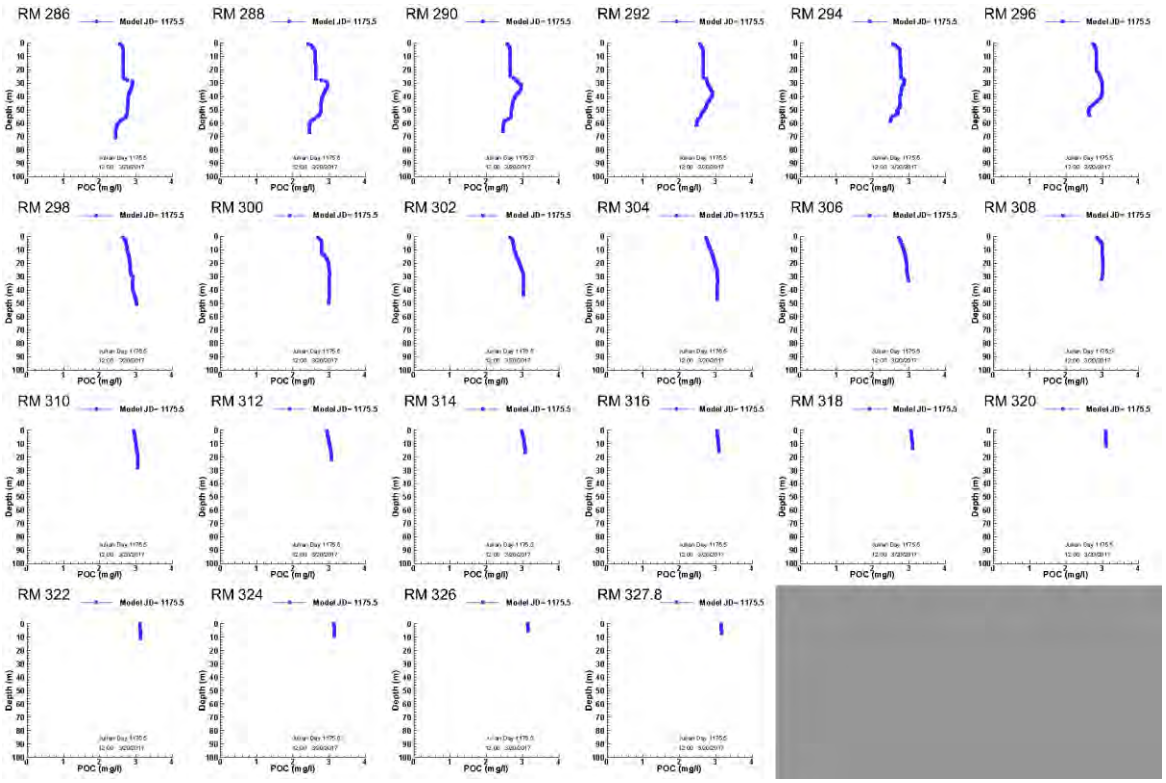


Figure 1603. Vertical profiles of POC compared with data for 3/20/2017.

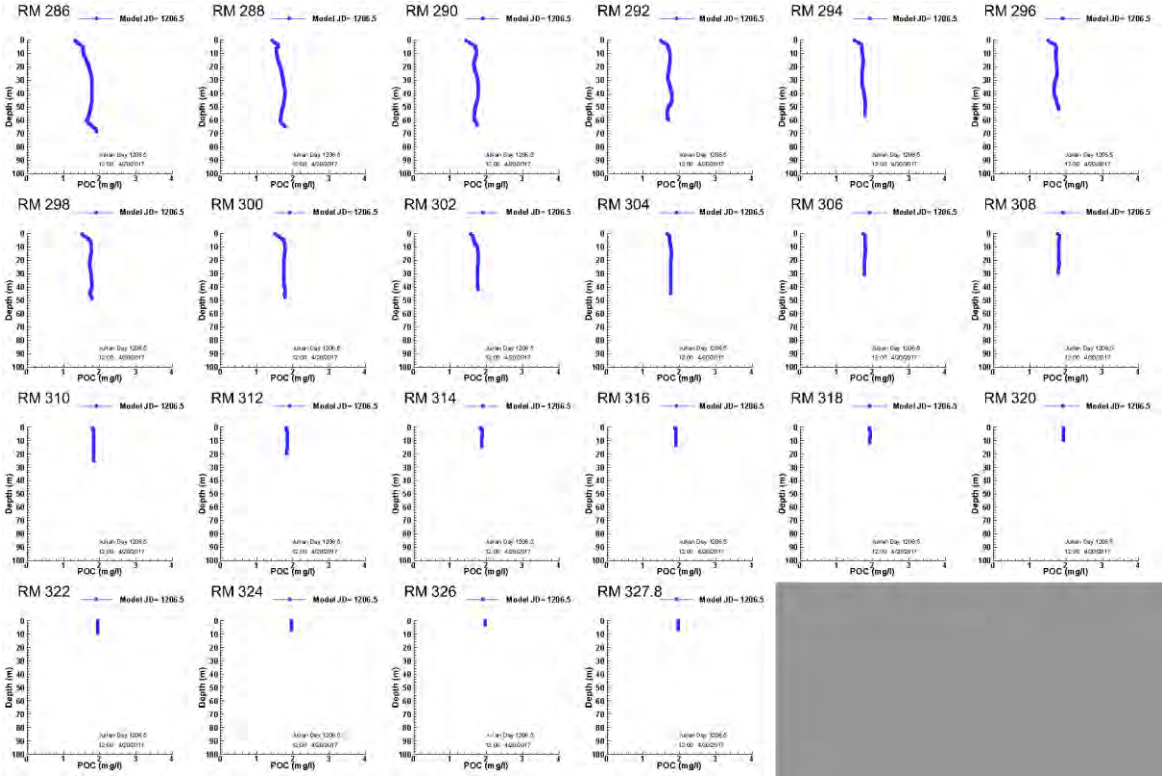


Figure 1604. Vertical profiles of POC compared with data for 4/20/2017.

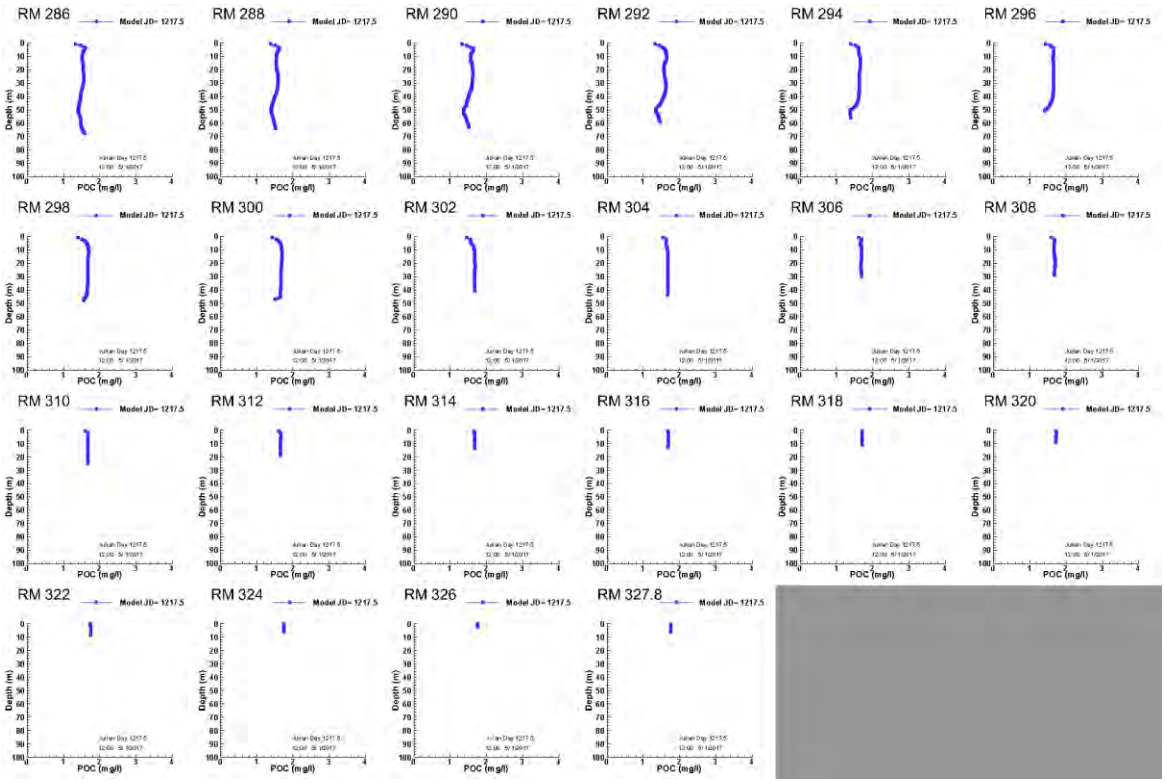


Figure 1605. Vertical profiles of POC compared with data for 5/ 1/2017.

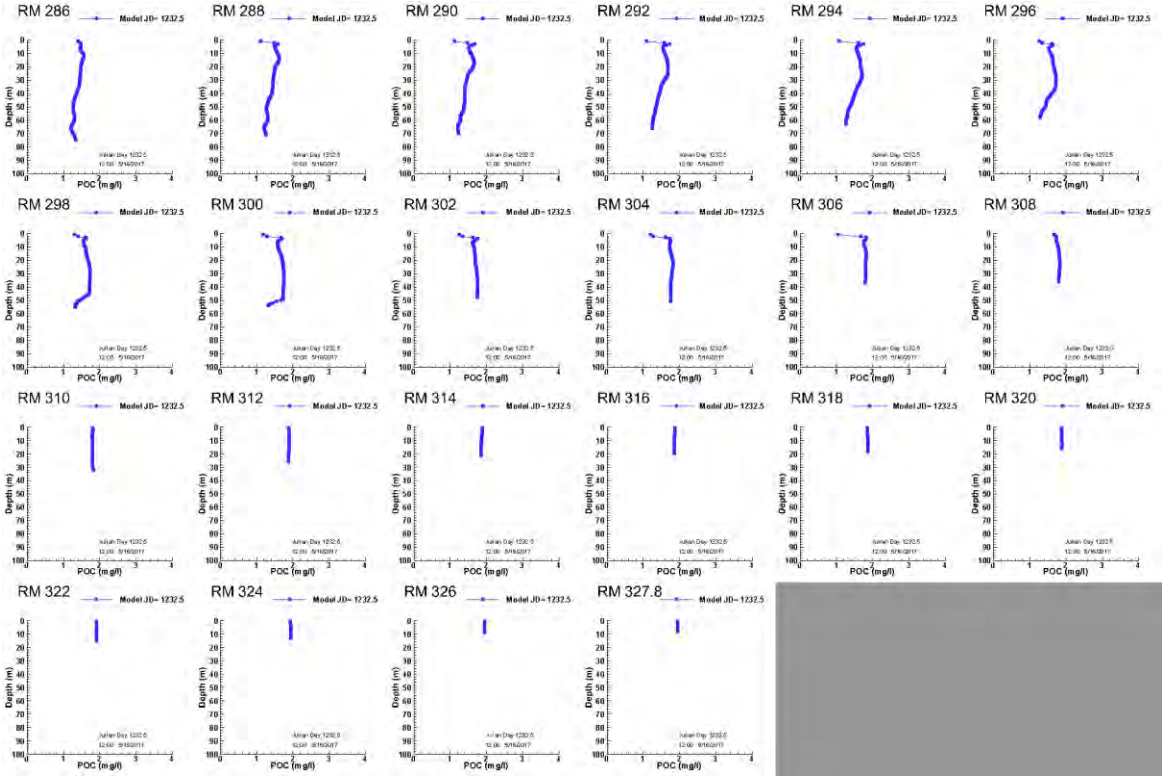


Figure 1606. Vertical profiles of POC compared with data for 5/16/2017.

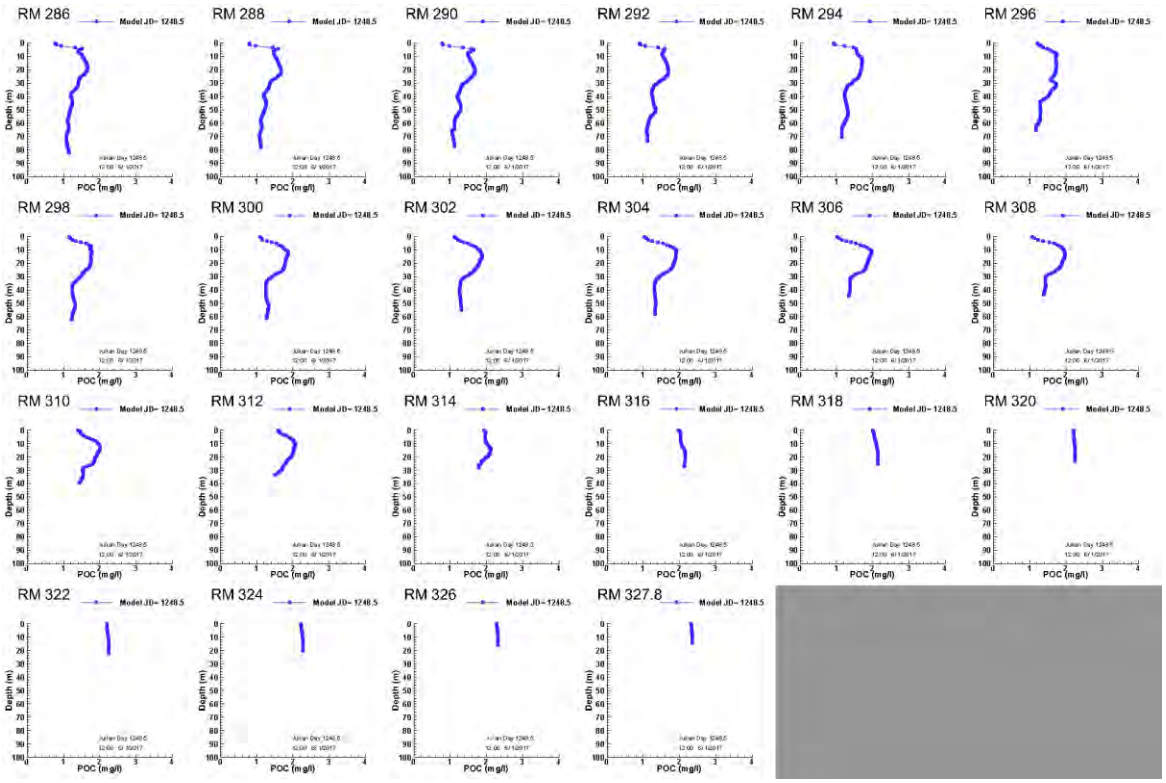


Figure 1607. Vertical profiles of POC compared with data for 6/ 1/2017.

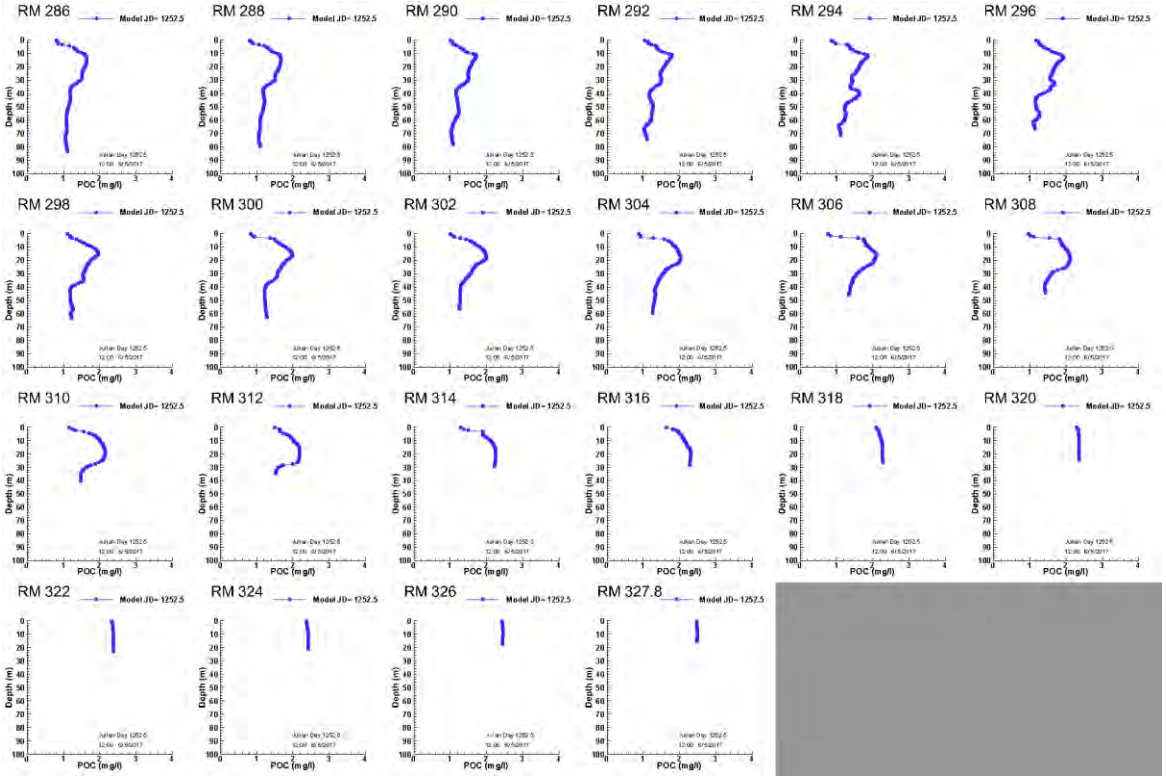


Figure 1608. Vertical profiles of POC compared with data for 6/ 5/2017.

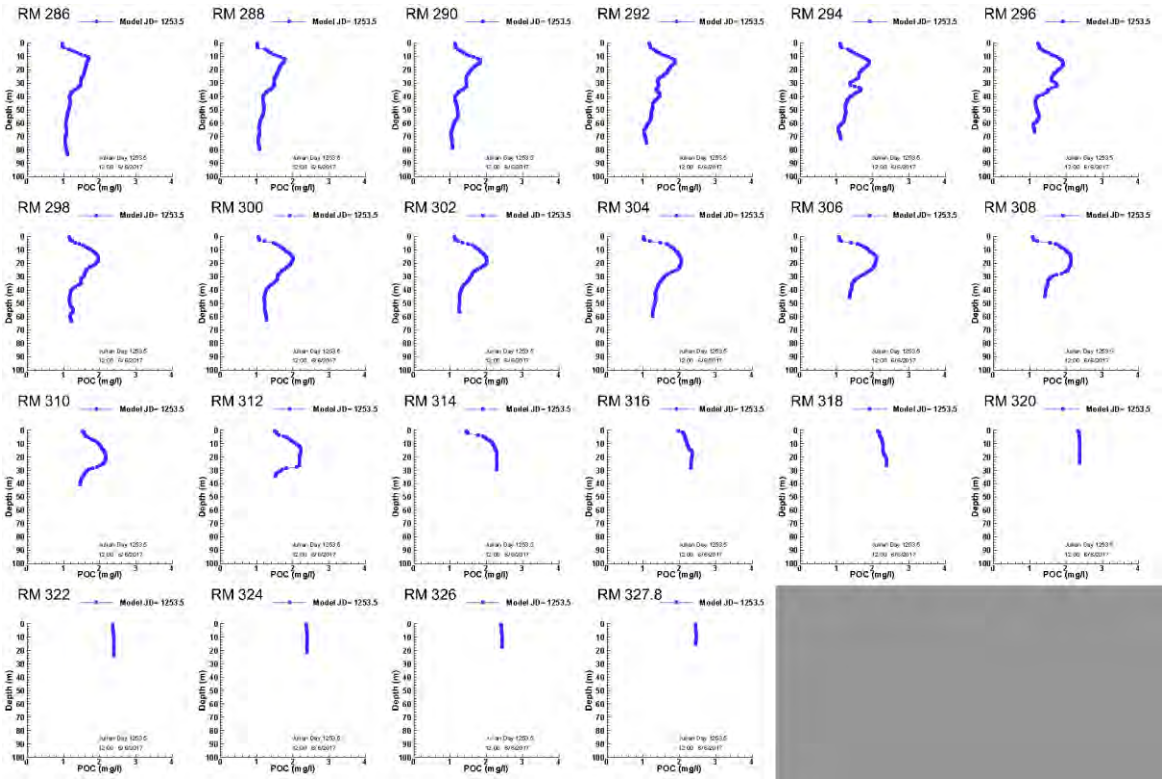


Figure 1609. Vertical profiles of POC compared with data for 6/ 6/2017.

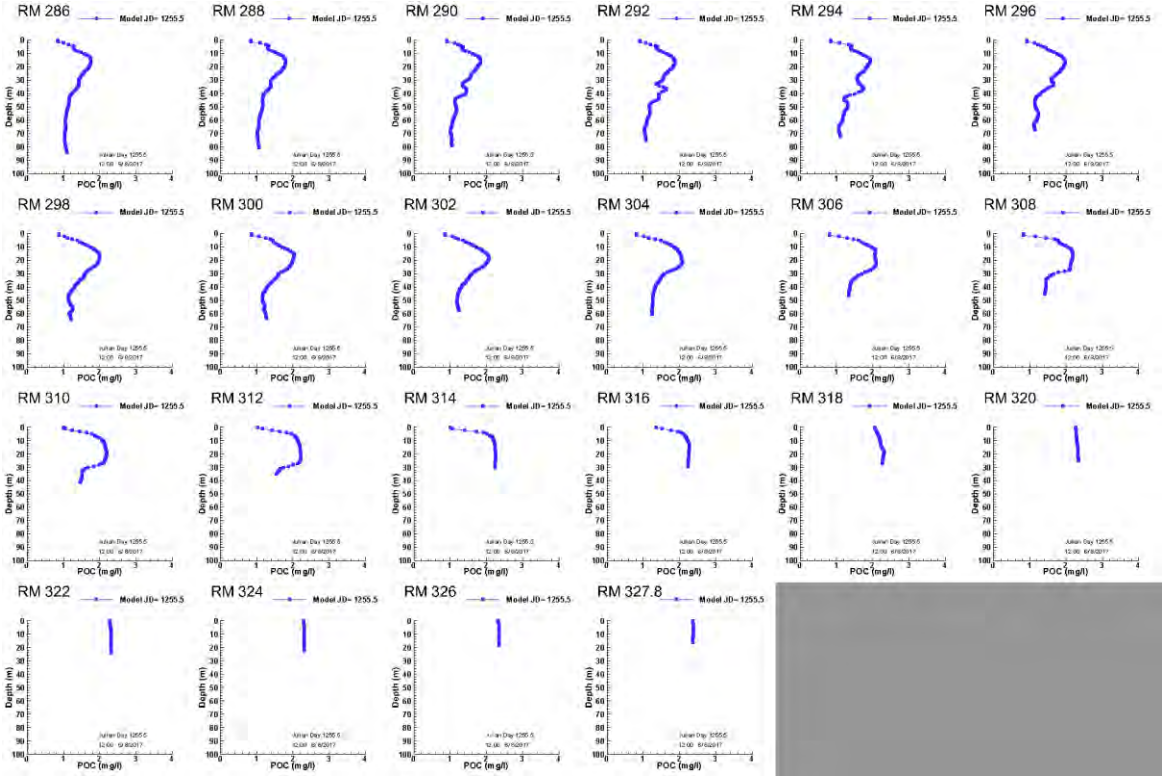


Figure 1610. Vertical profiles of POC compared with data for 6/ 8/2017.

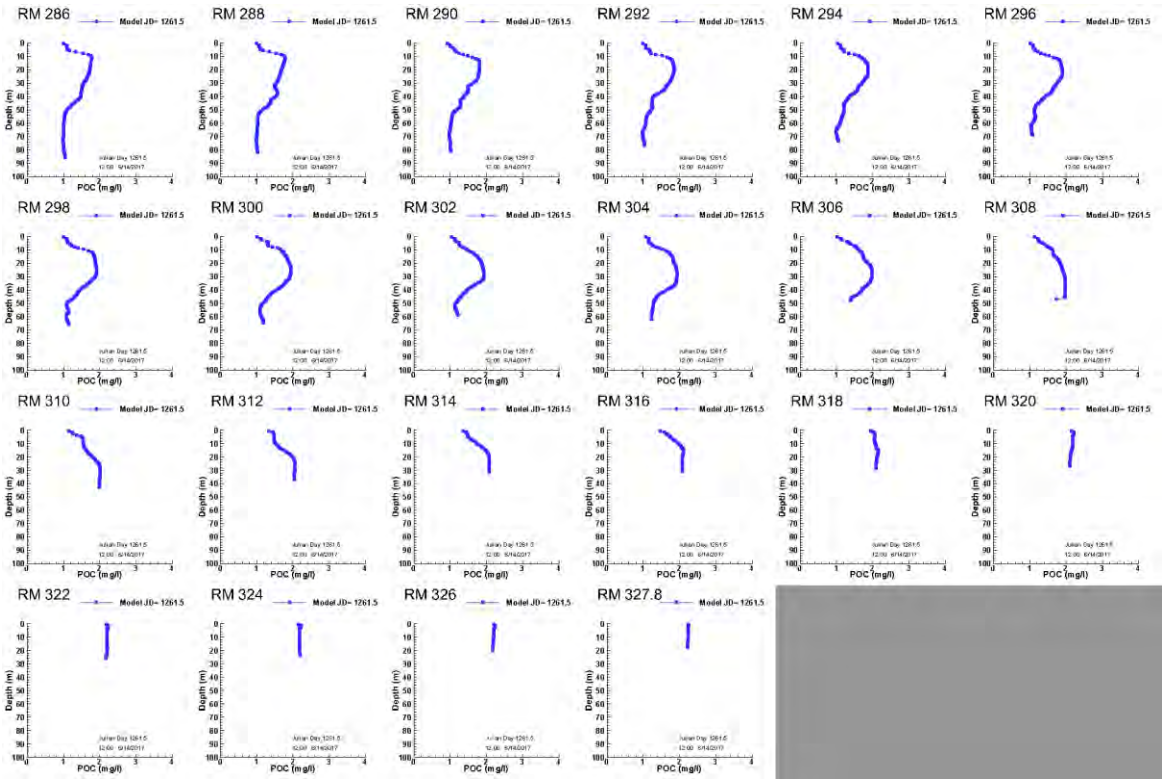


Figure 1611. Vertical profiles of POC compared with data for 6/14/2017.

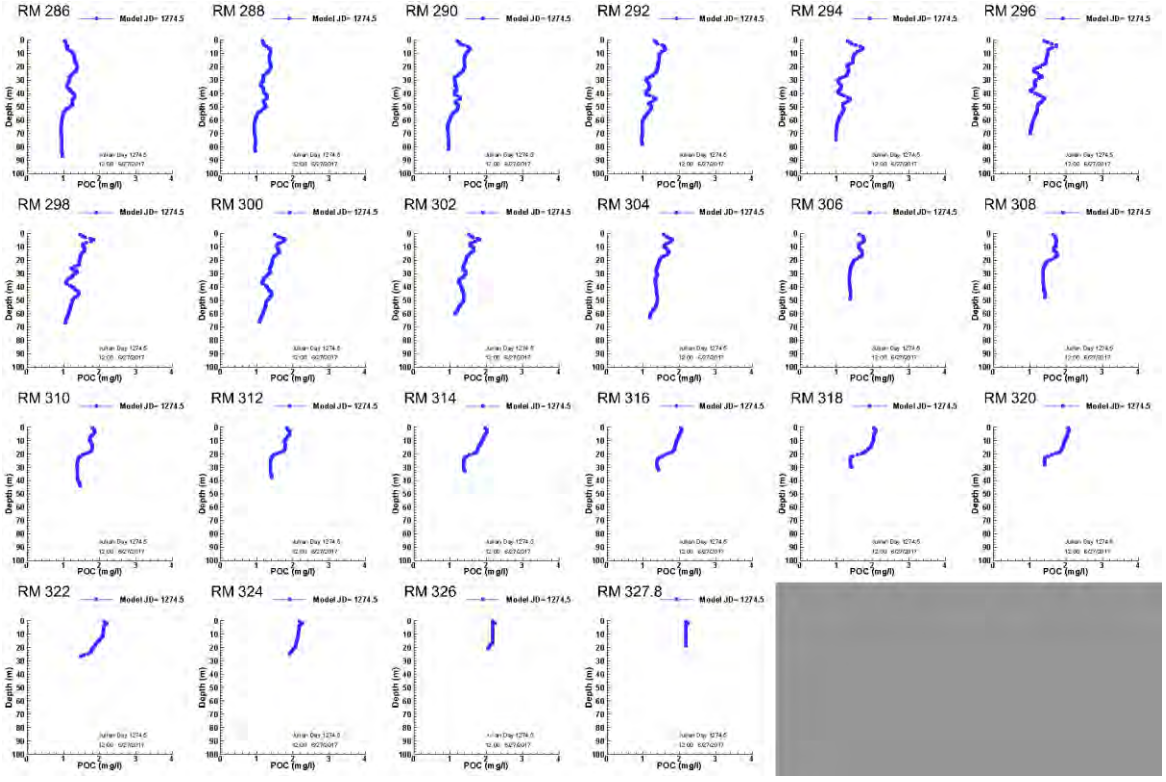


Figure 1612. Vertical profiles of POC compared with data for 6/27/2017.

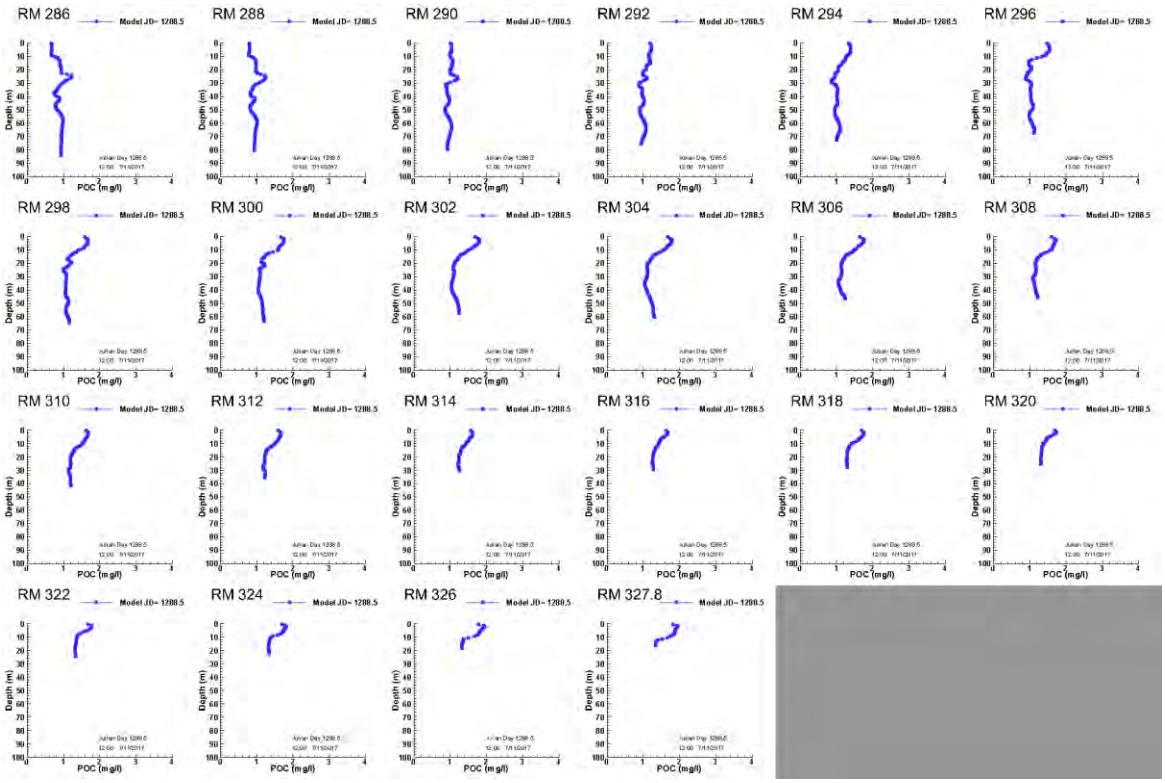


Figure 1613. Vertical profiles of POC compared with data for 7/11/2017.

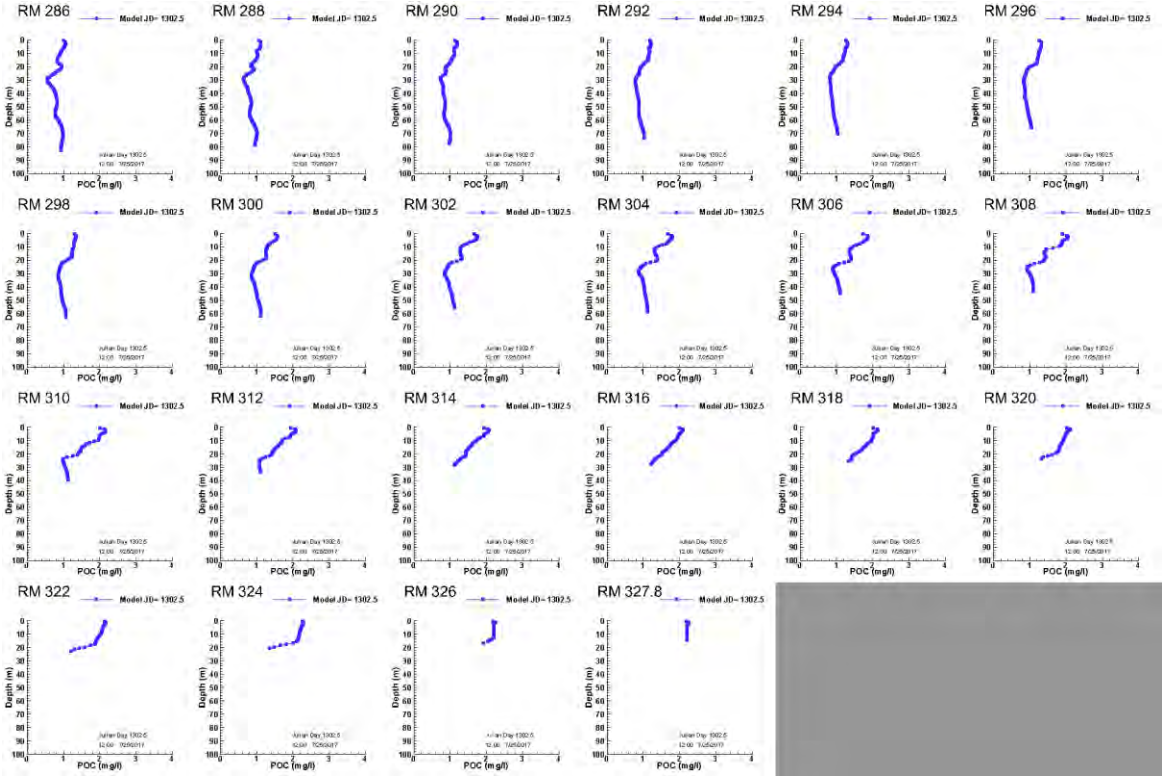


Figure 1614. Vertical profiles of POC compared with data for 7/25/2017.

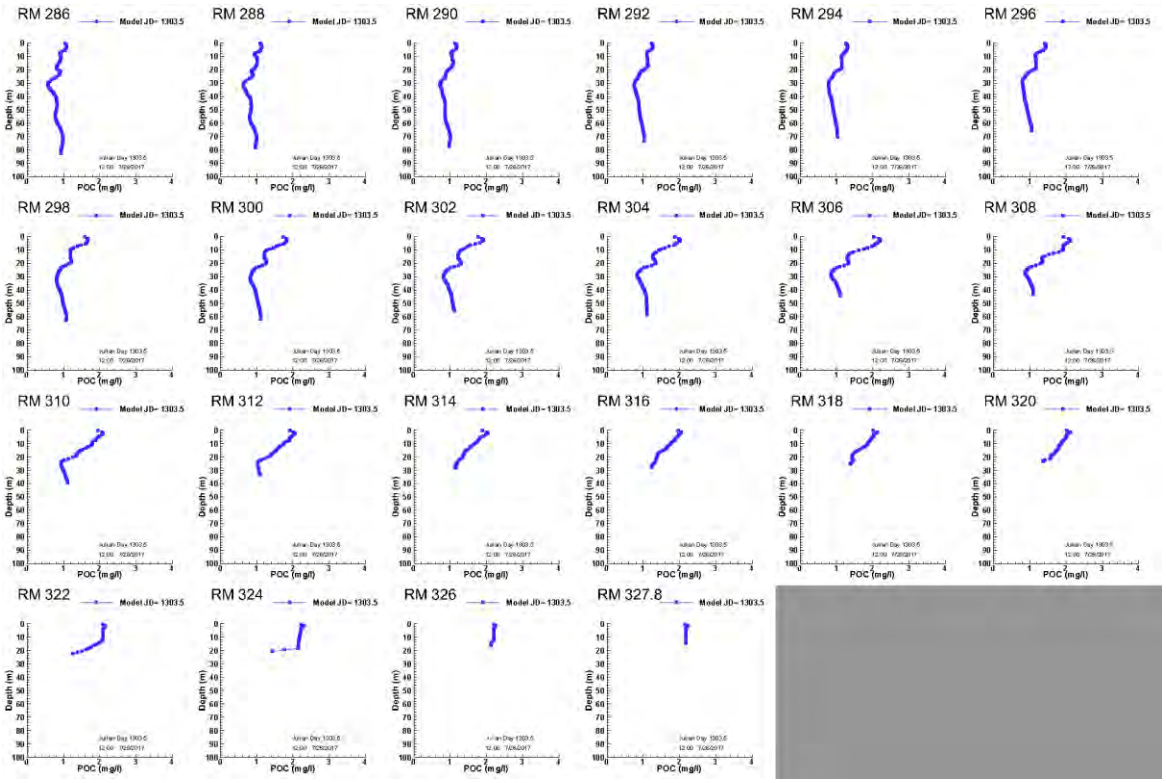


Figure 1615. Vertical profiles of POC compared with data for 7/26/2017.

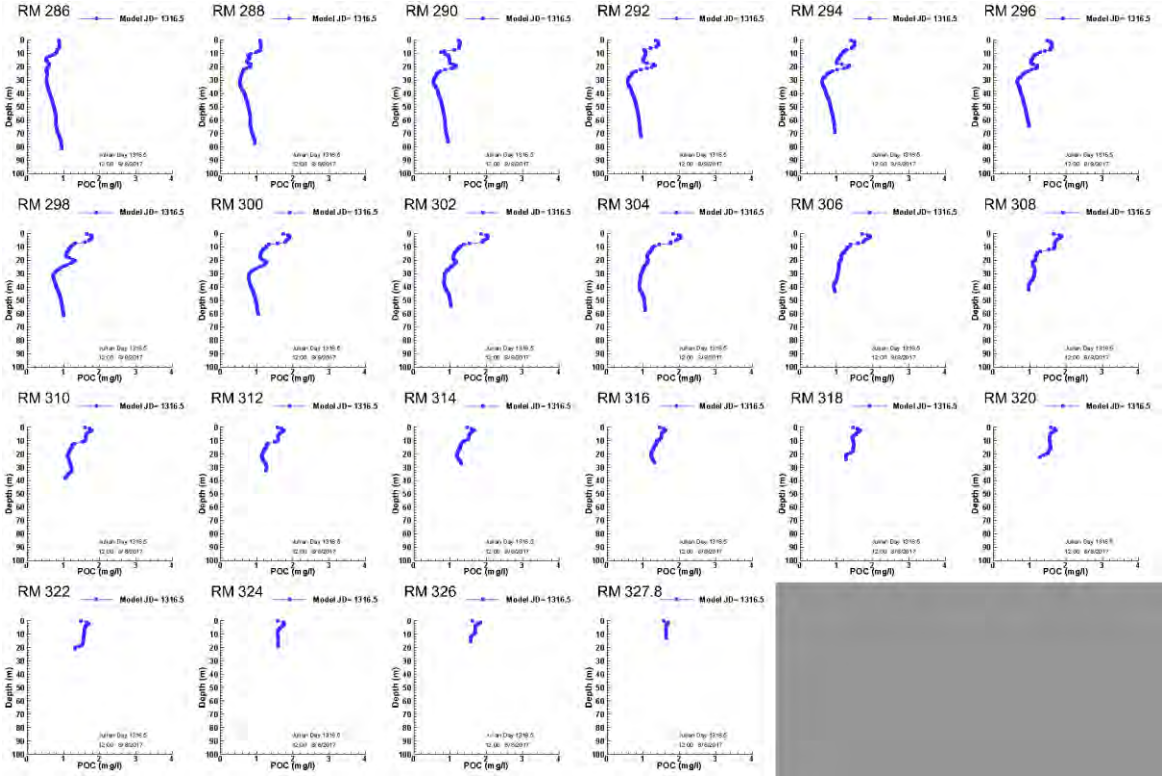


Figure 1616. Vertical profiles of POC compared with data for 8/ 8/2017.

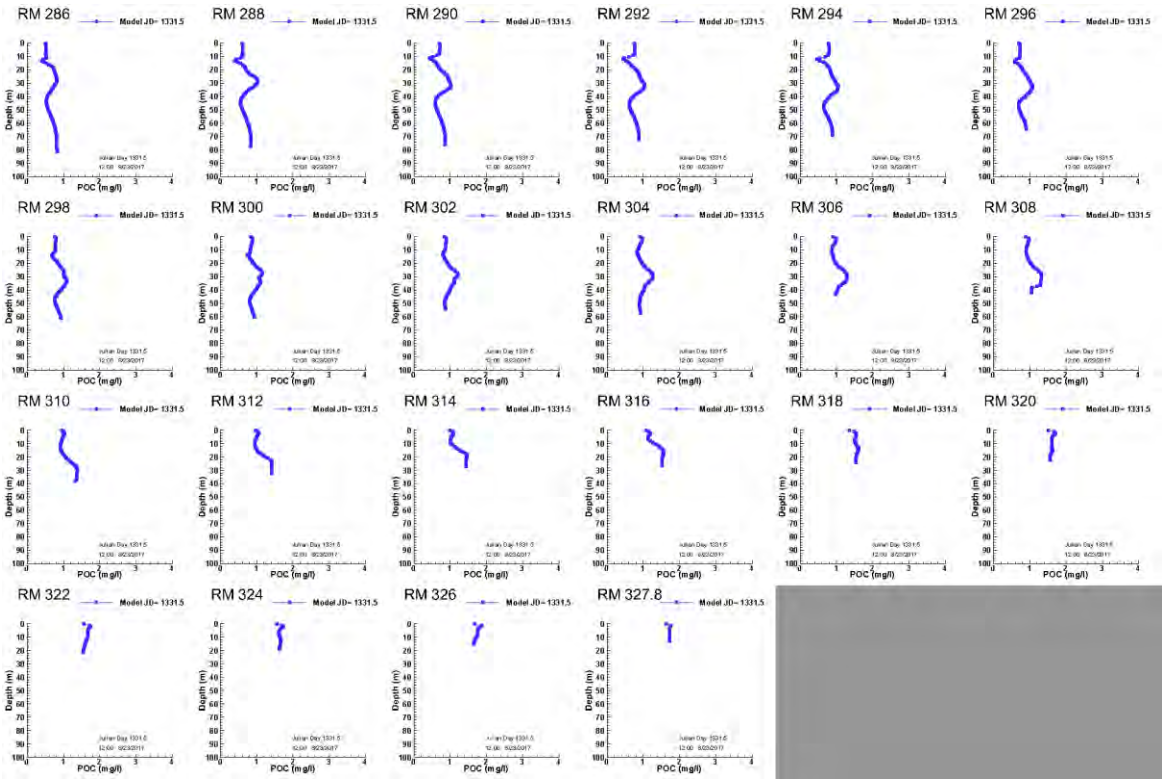


Figure 1617. Vertical profiles of POC compared with data for 8/23/2017.

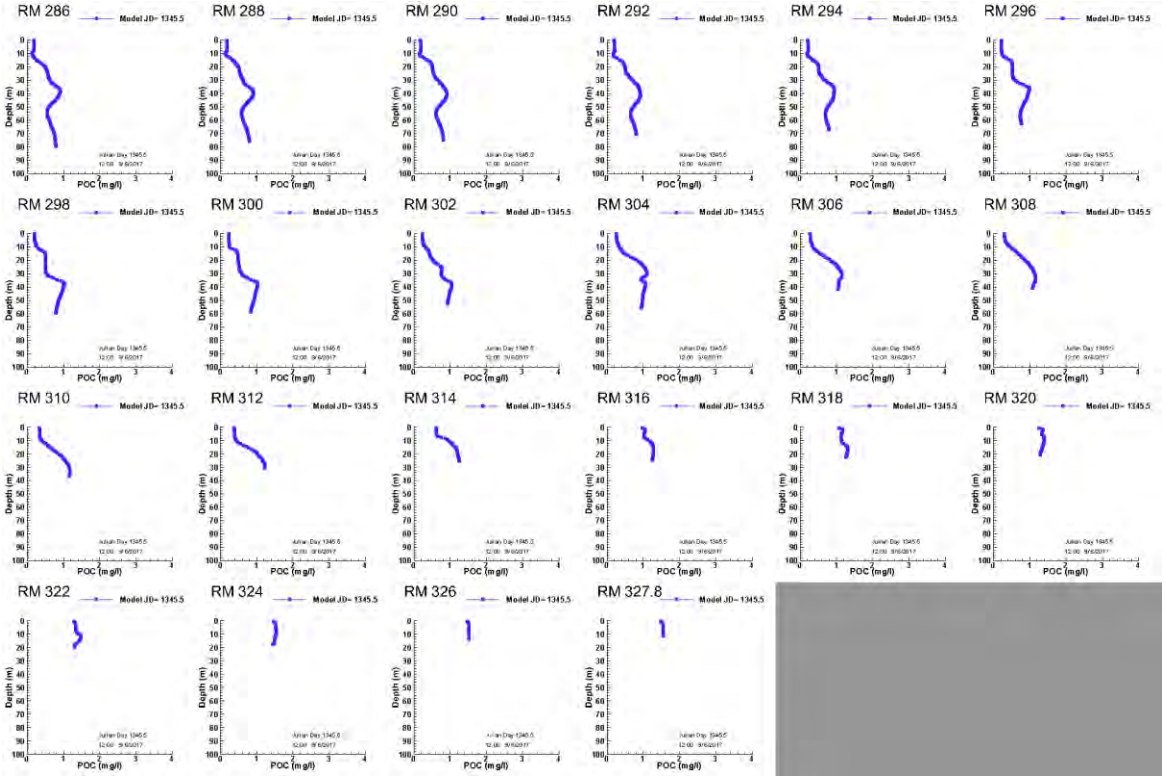


Figure 1618. Vertical profiles of POC compared with data for 9/ 6/2017.

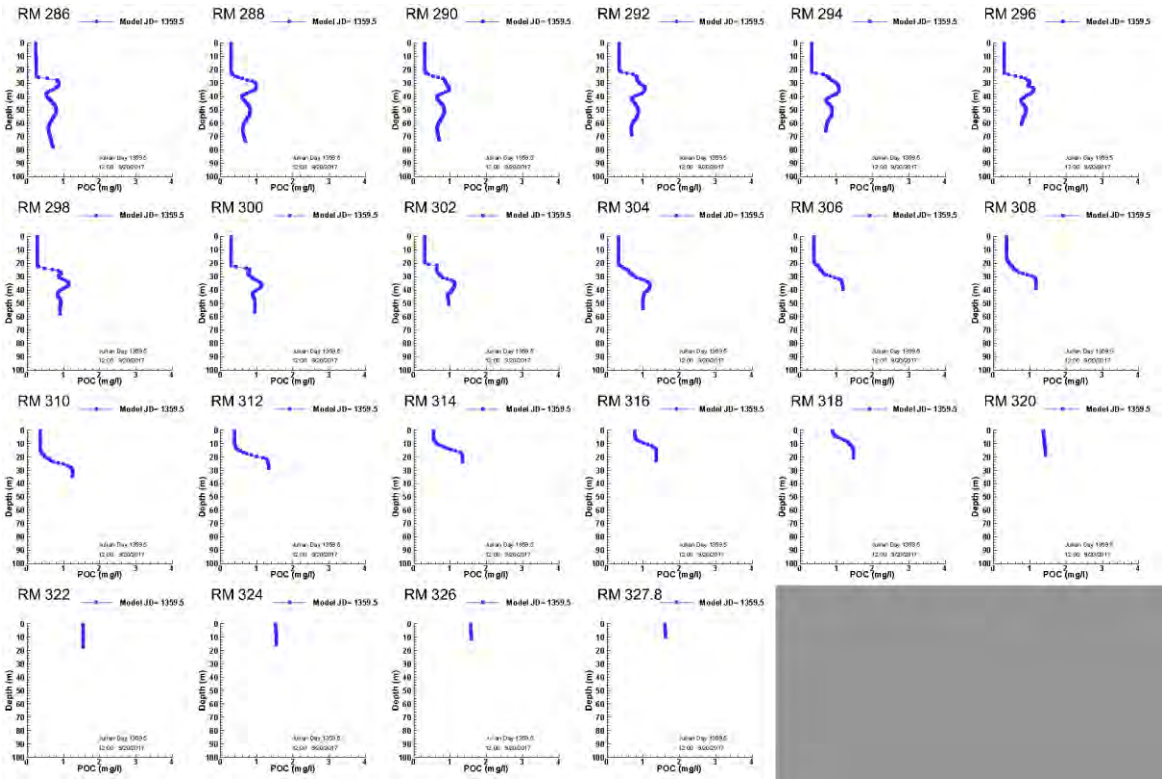


Figure 1619. Vertical profiles of POC compared with data for 9/20/2017.

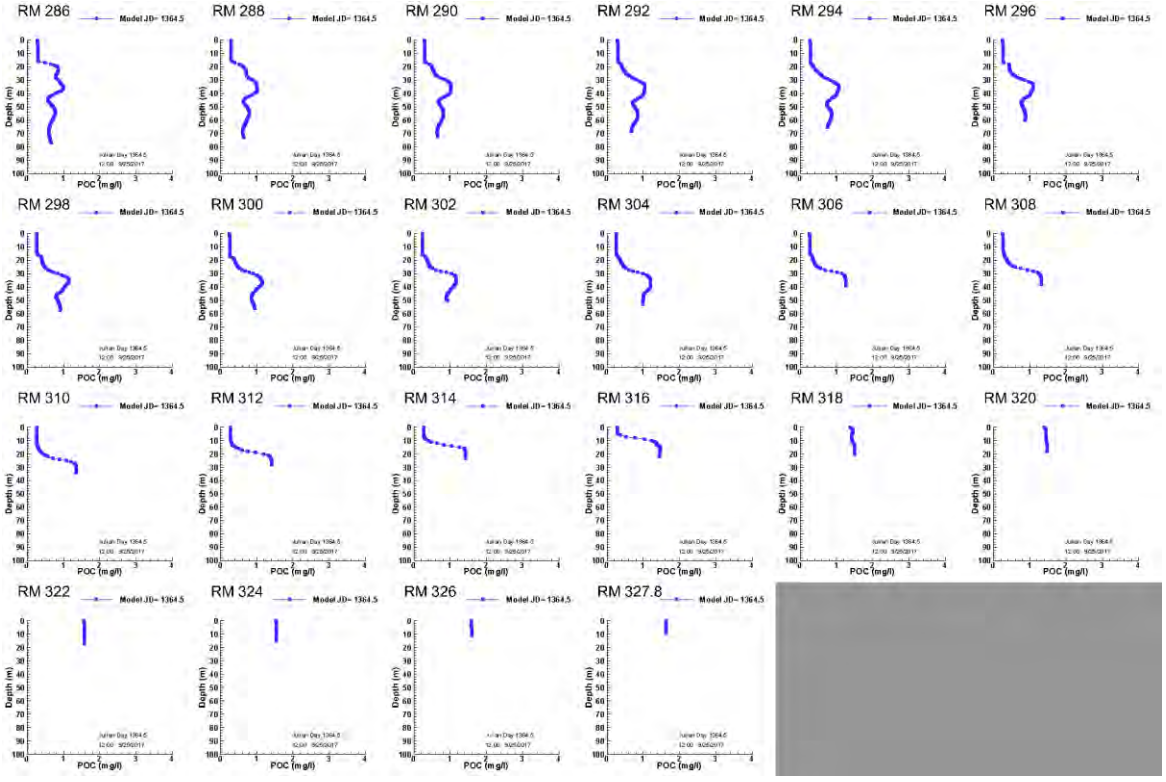


Figure 1620. Vertical profiles of POC compared with data for 9/25/2017.

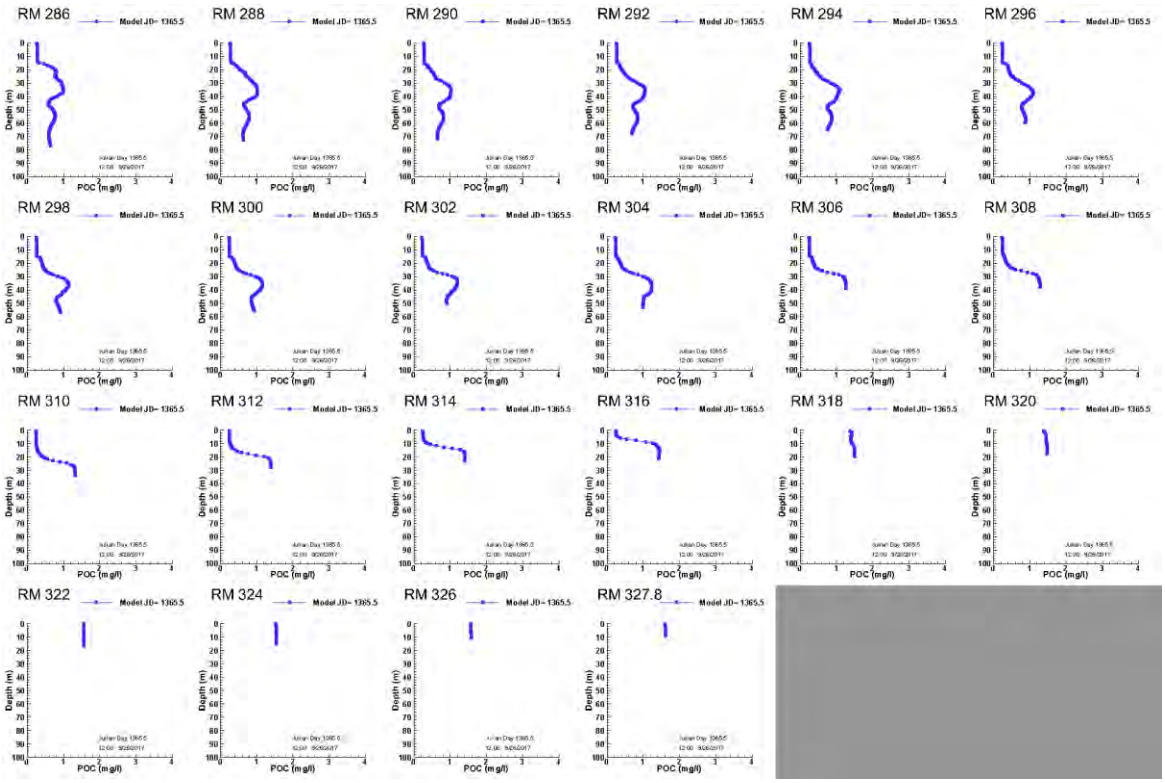


Figure 1621. Vertical profiles of POC compared with data for 9/26/2017.

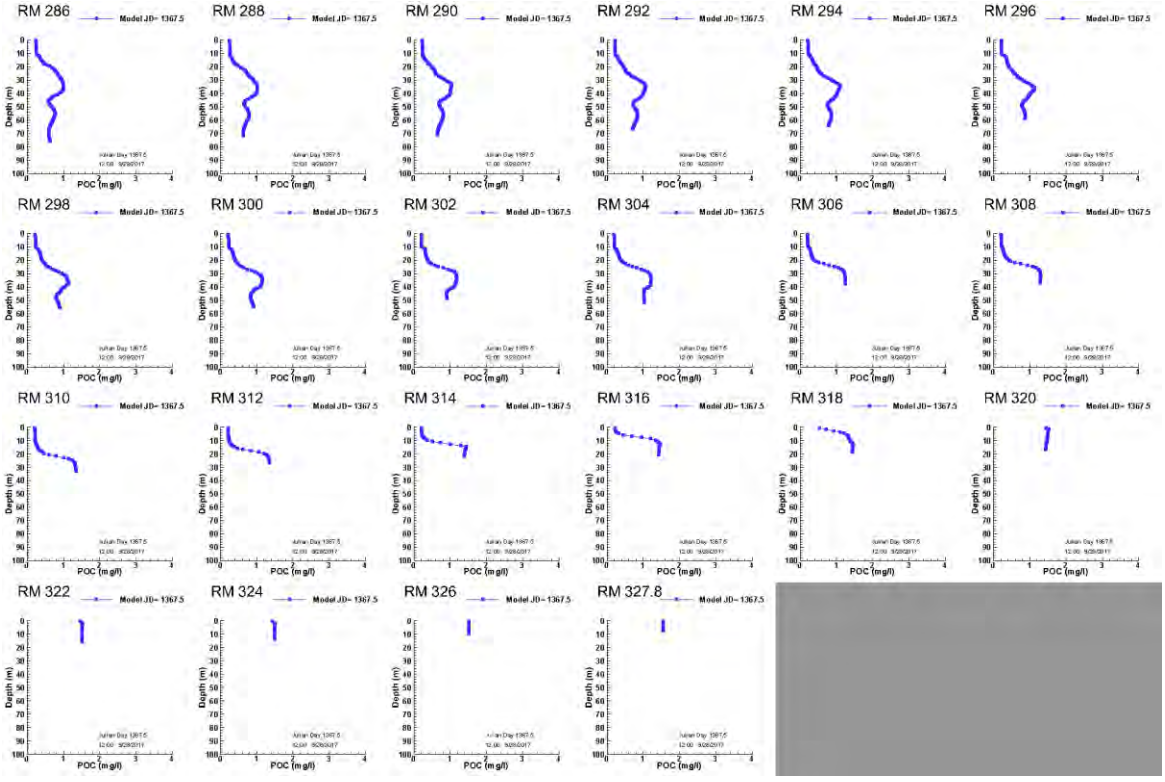


Figure 1622. Vertical profiles of POC compared with data for 9/28/2017.

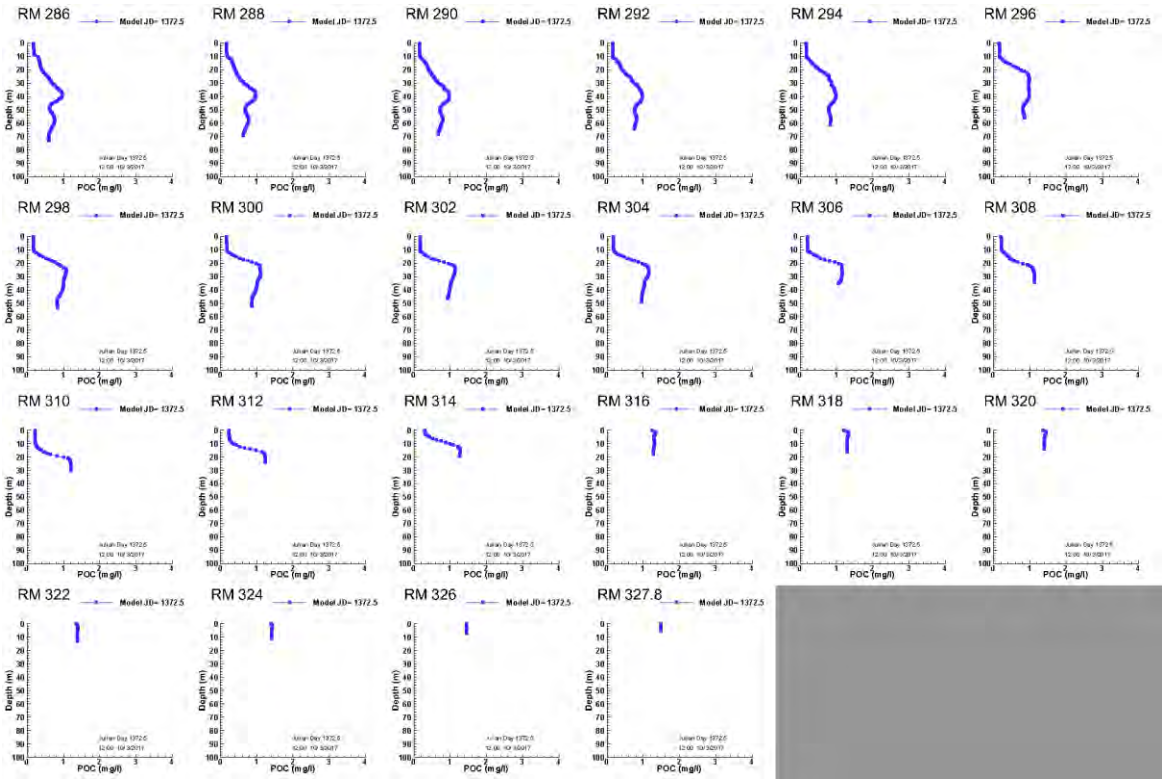


Figure 1623. Vertical profiles of POC compared with data for 10/ 3/2017.

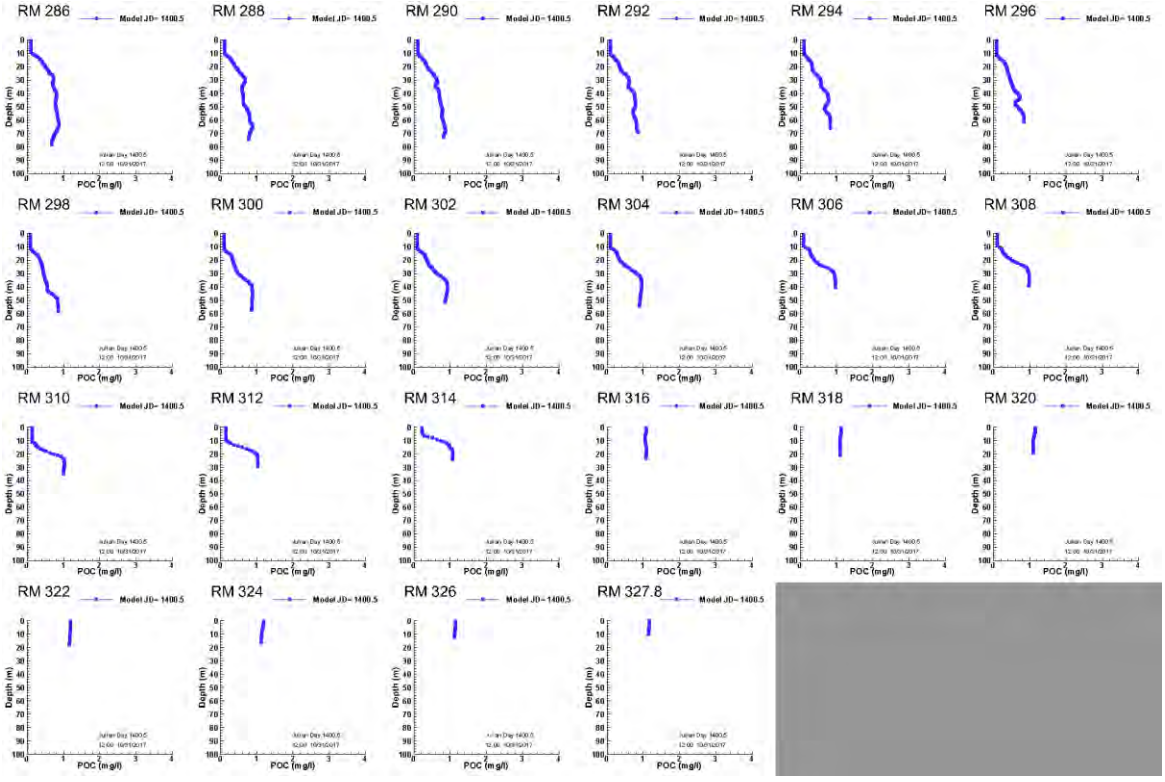


Figure 1624. Vertical profiles of POC compared with data for 10/31/2017.

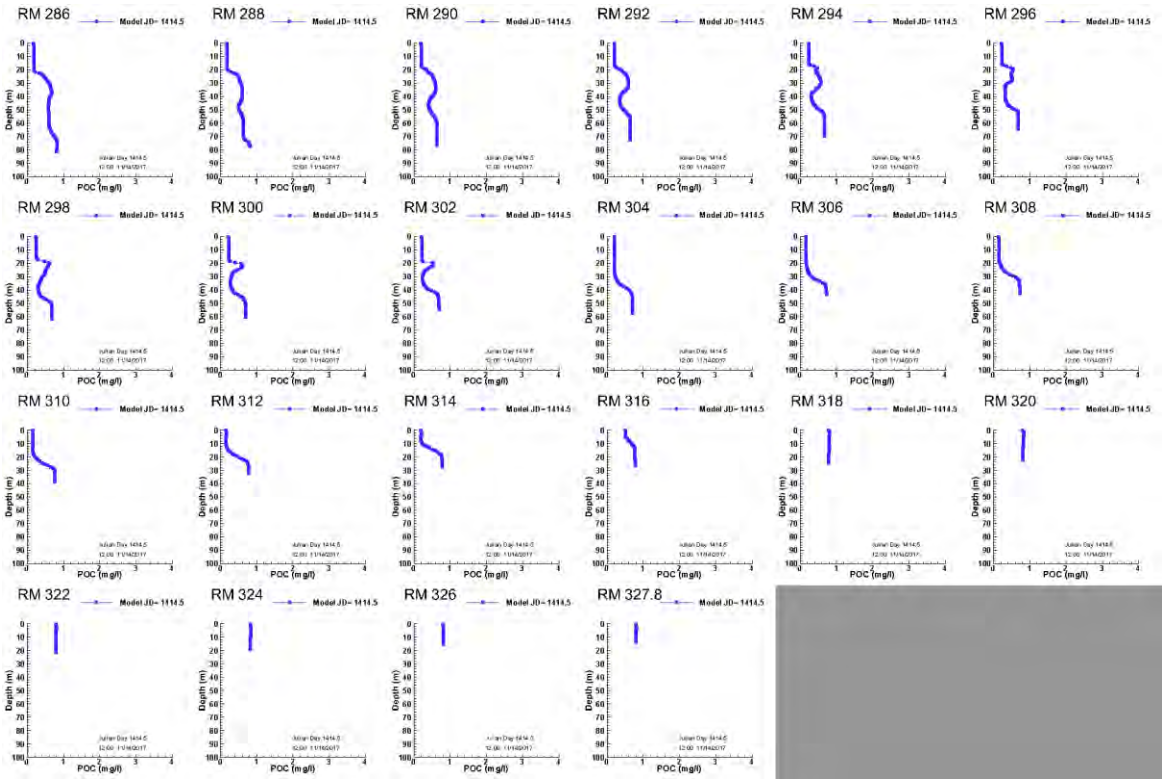


Figure 1625. Vertical profiles of POC compared with data for 11/14/2017.

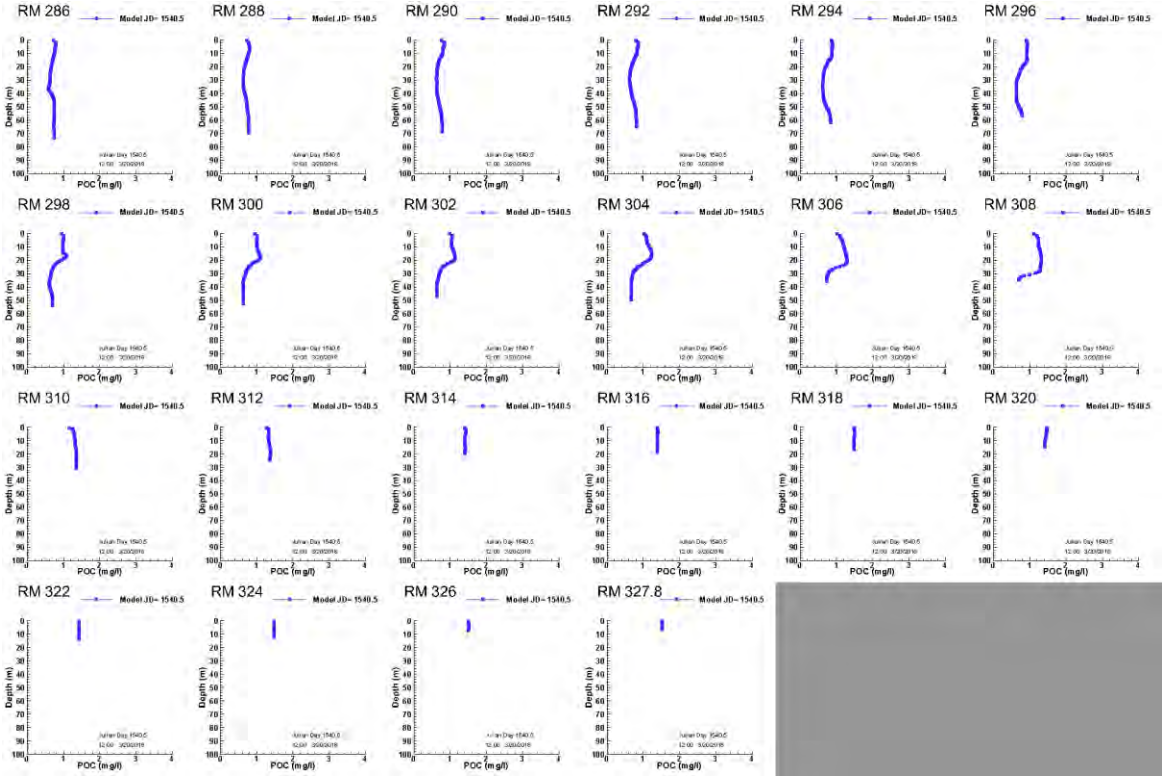


Figure 1626. Vertical profiles of POC compared with data for 3/20/2018.

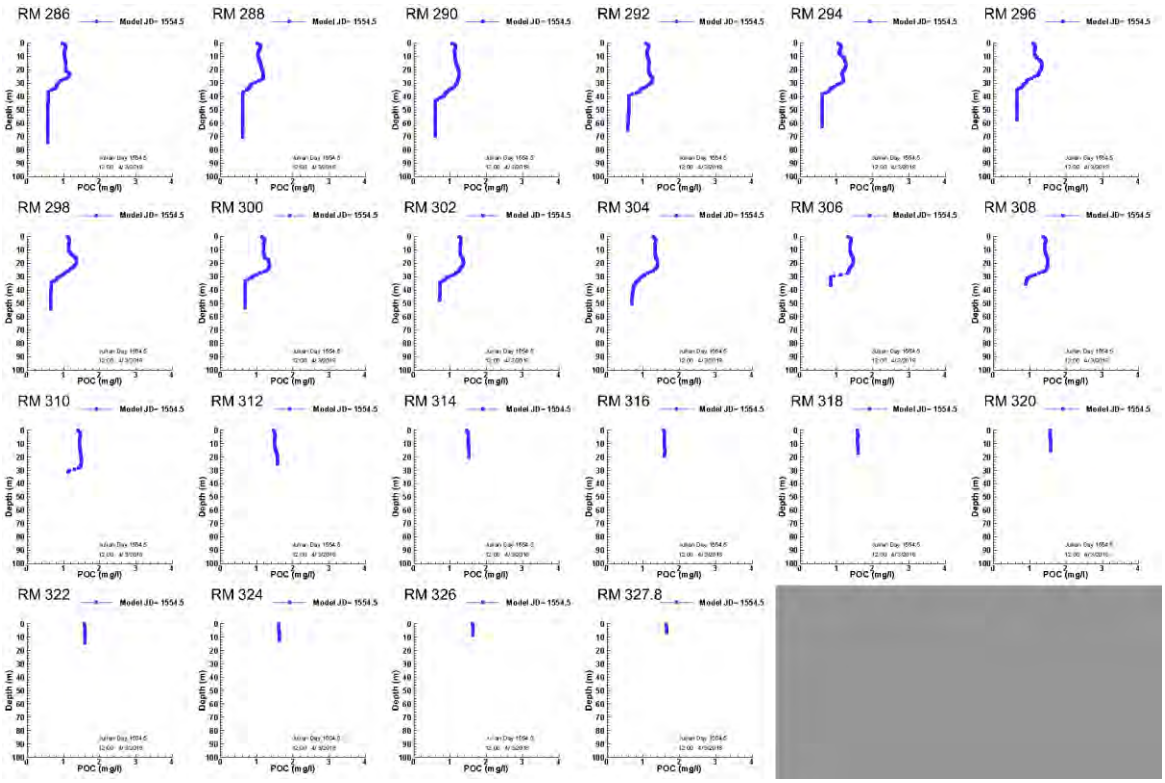


Figure 1627. Vertical profiles of POC compared with data for 4/ 3/2018.

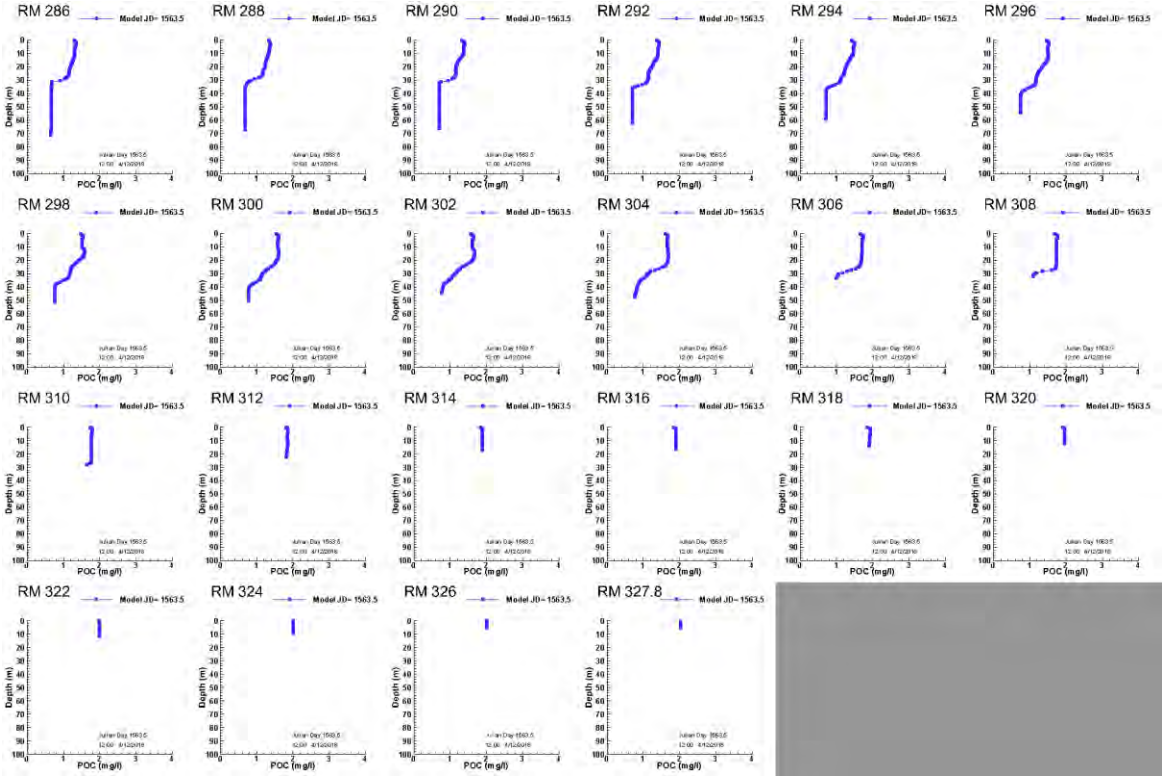


Figure 1628. Vertical profiles of POC compared with data for 4/12/2018.

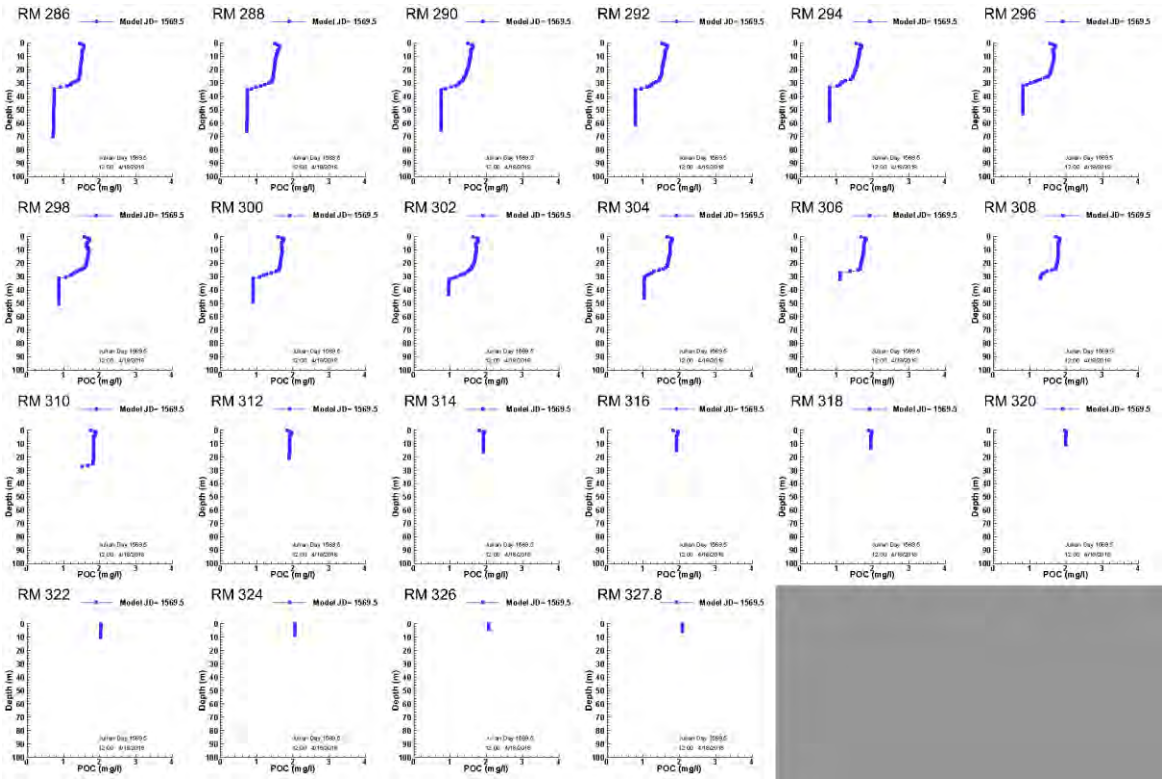


Figure 1629. Vertical profiles of POC compared with data for 4/18/2018.

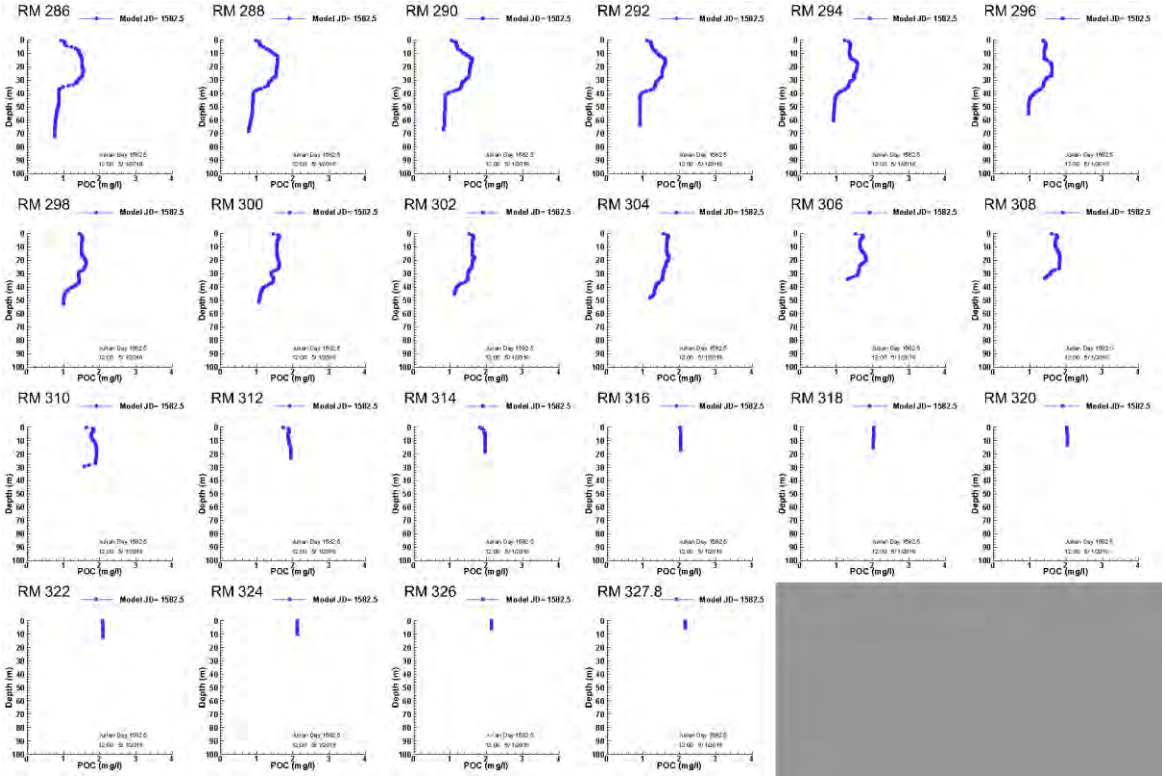


Figure 1630. Vertical profiles of POC compared with data for 5/ 1/2018.

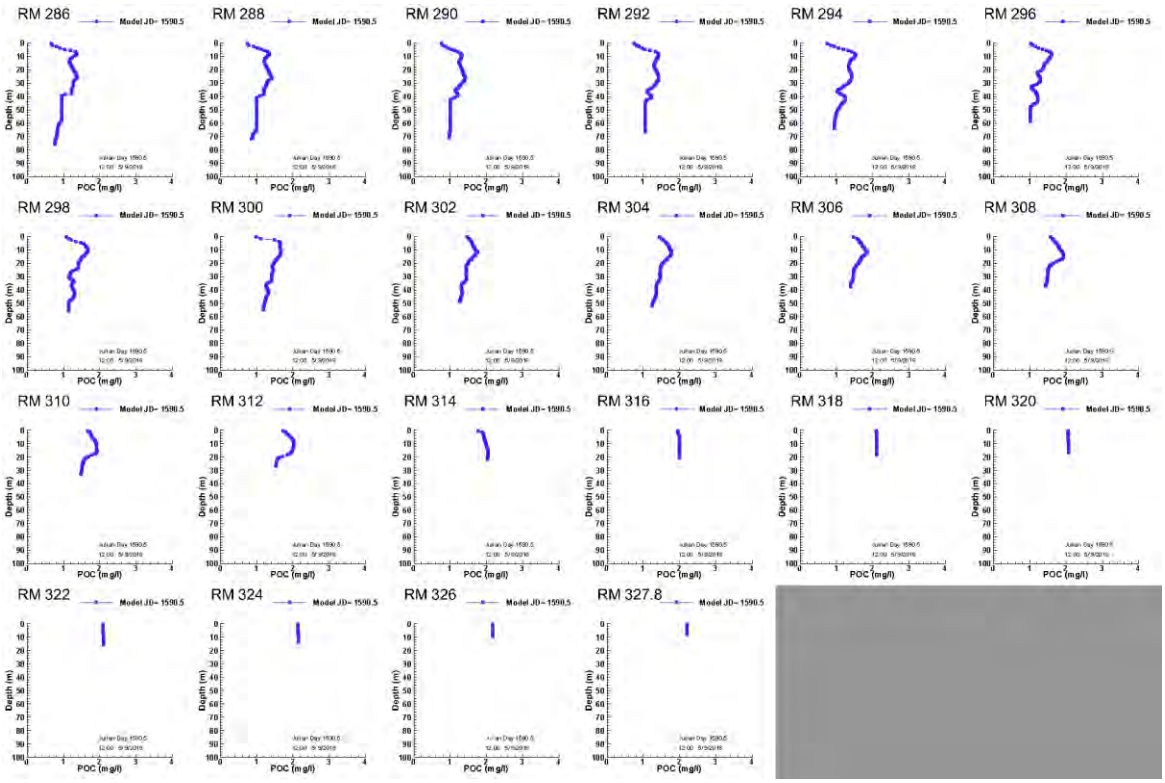


Figure 1631. Vertical profiles of POC compared with data for 5/ 9/2018.

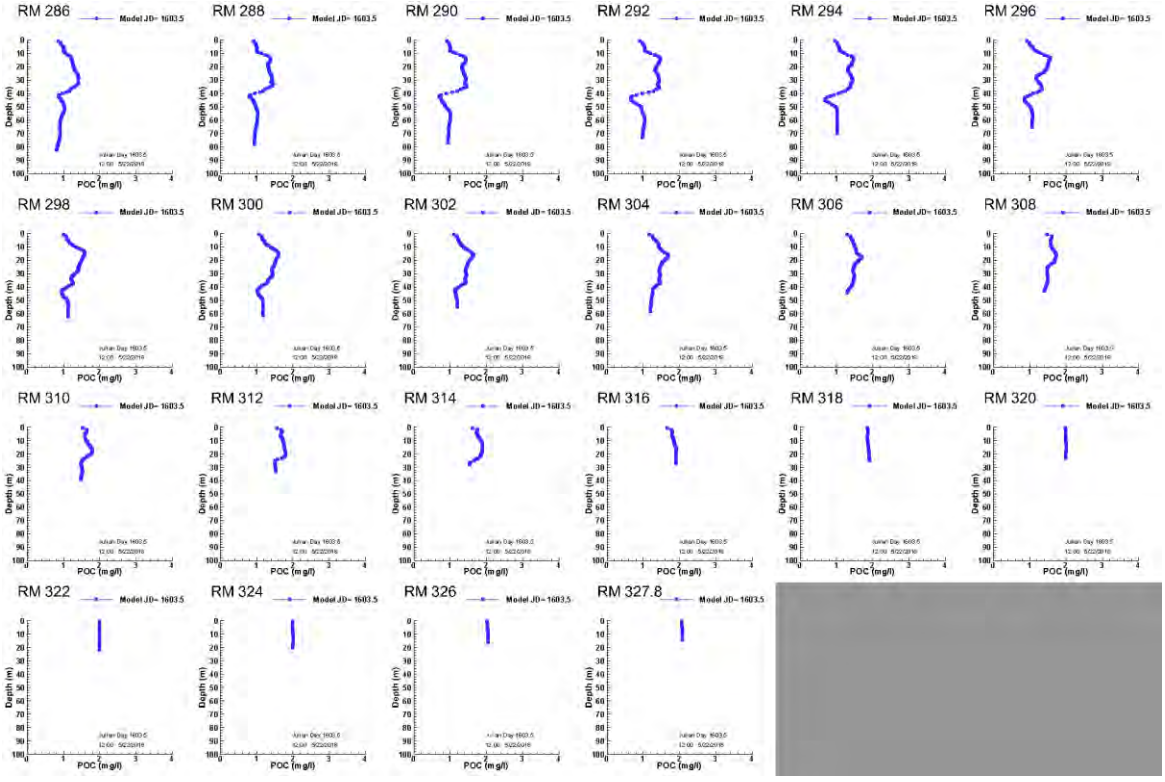


Figure 1632. Vertical profiles of POC compared with data for 5/22/2018.

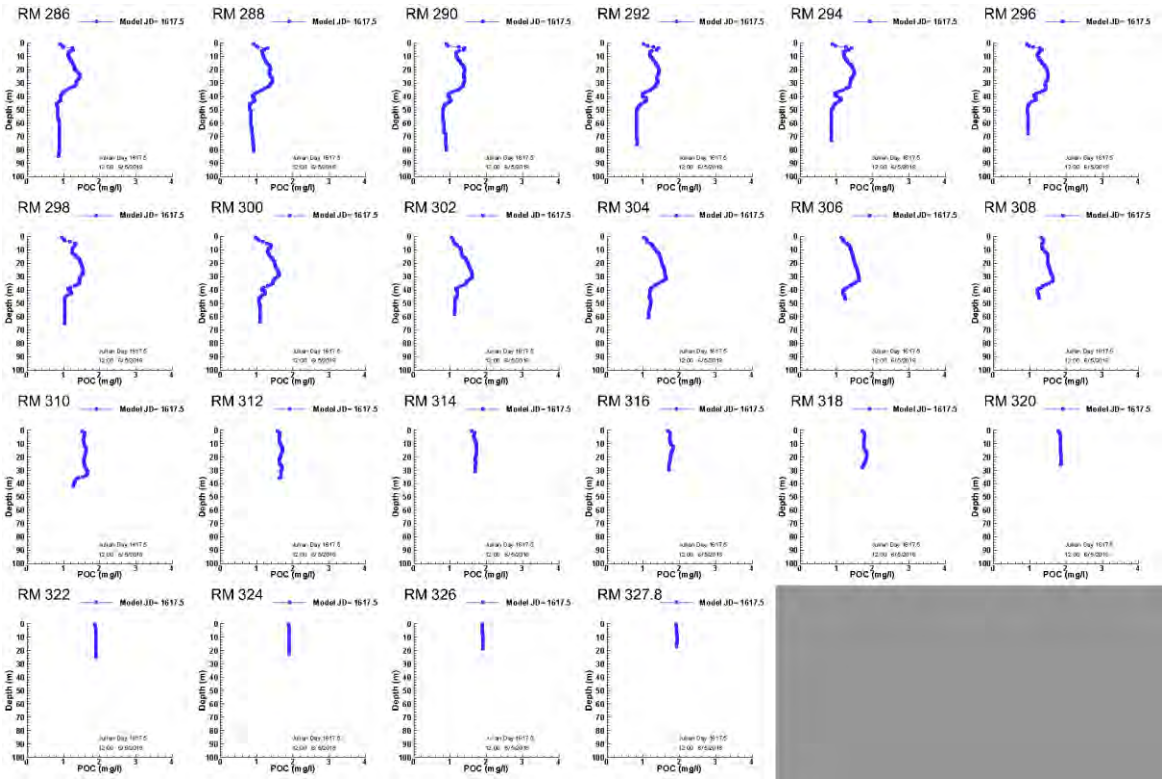


Figure 1633. Vertical profiles of POC compared with data for 6/ 5/2018.

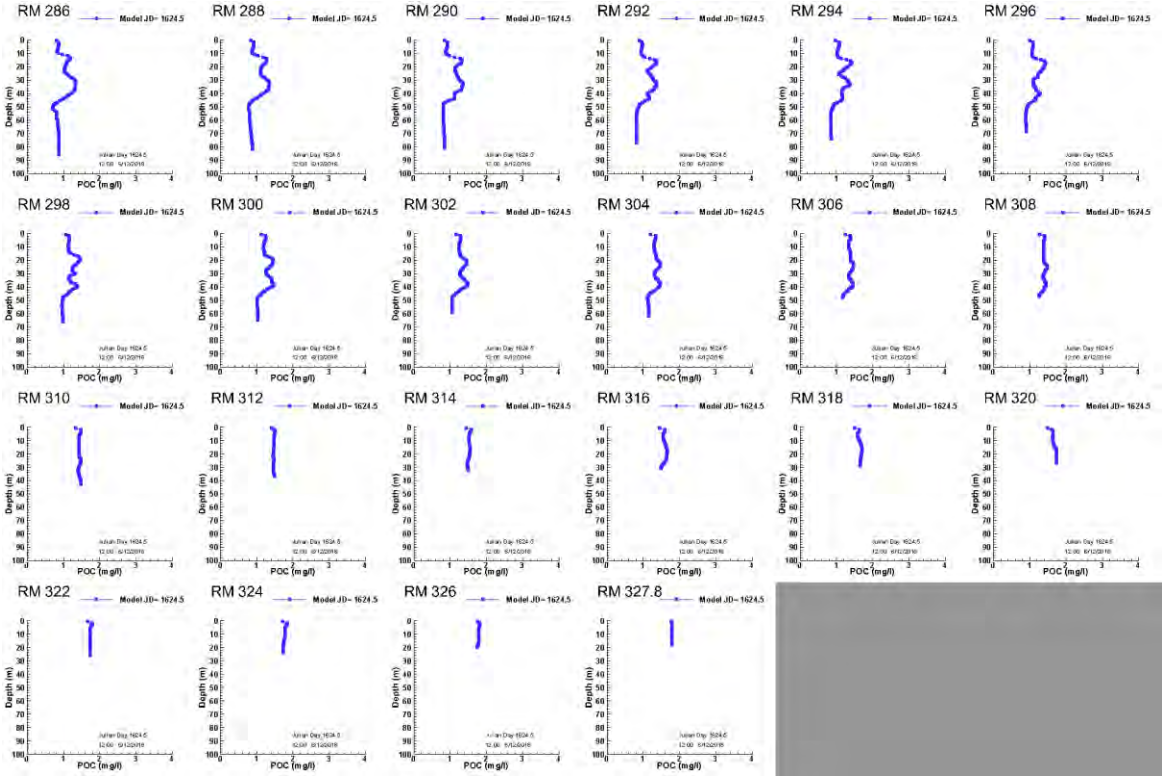


Figure 1634. Vertical profiles of POC compared with data for 6/12/2018.

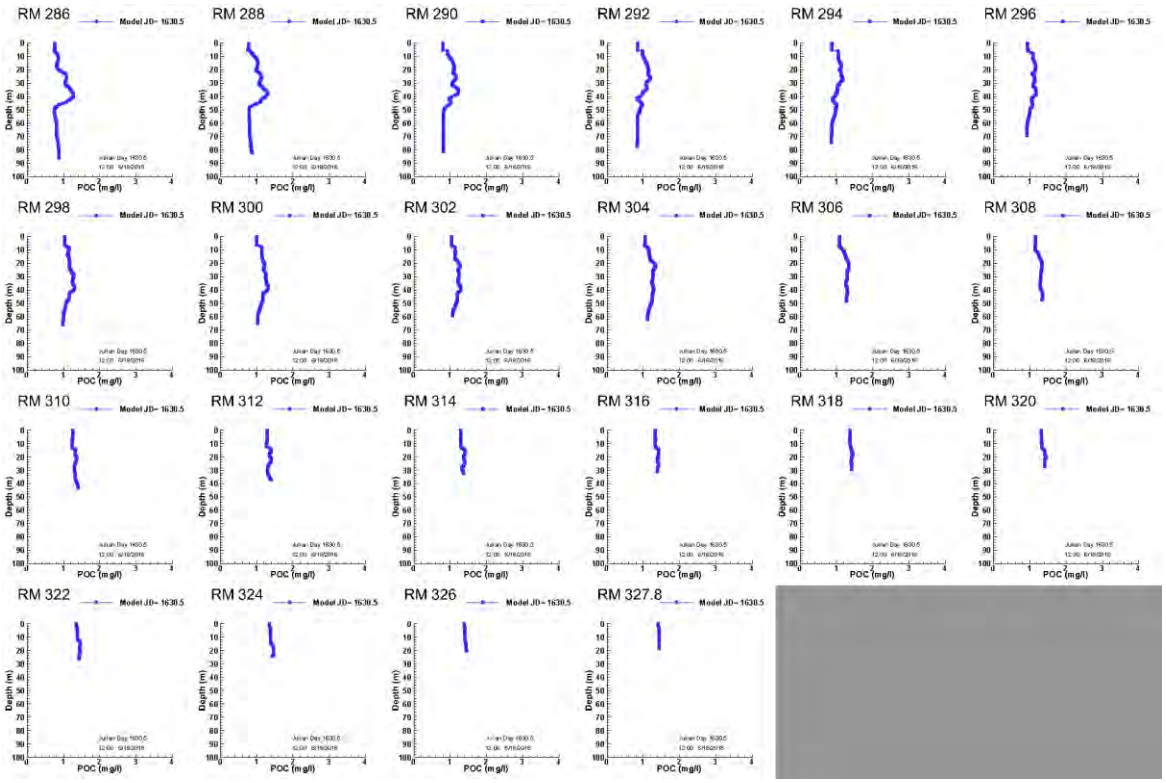


Figure 1635. Vertical profiles of POC compared with data for 6/18/2018.

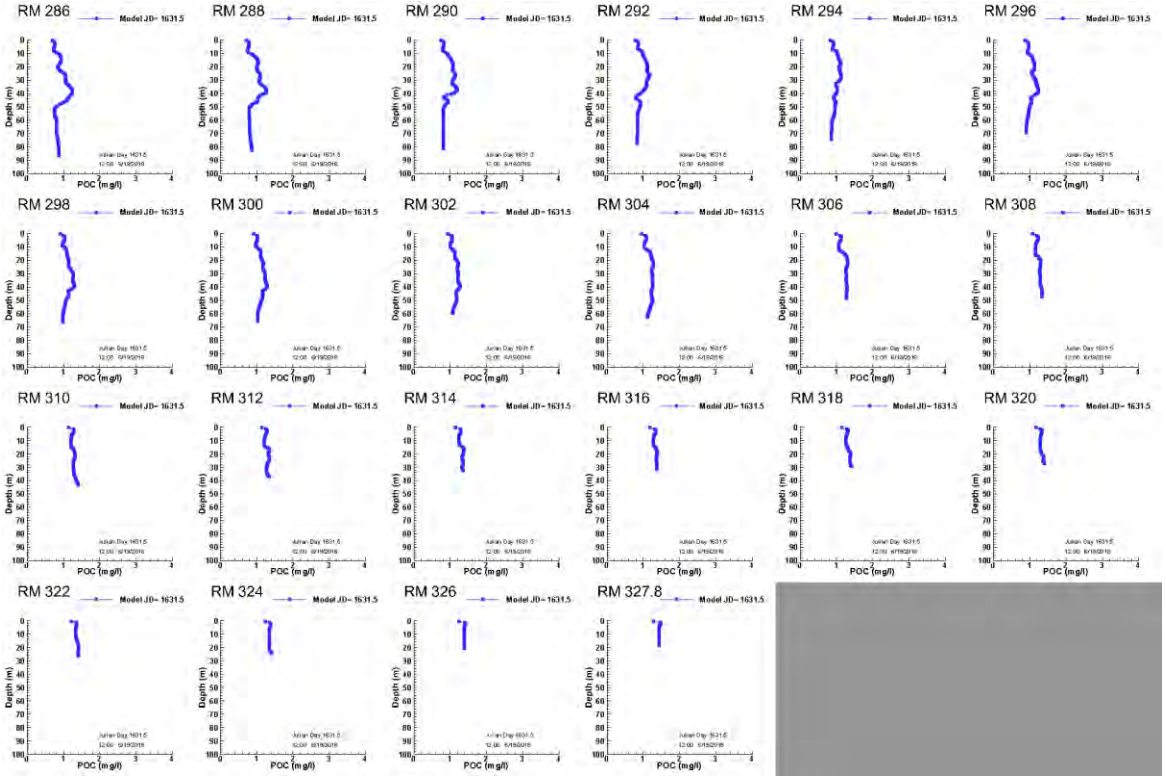


Figure 1636. Vertical profiles of POC compared with data for 6/19/2018.

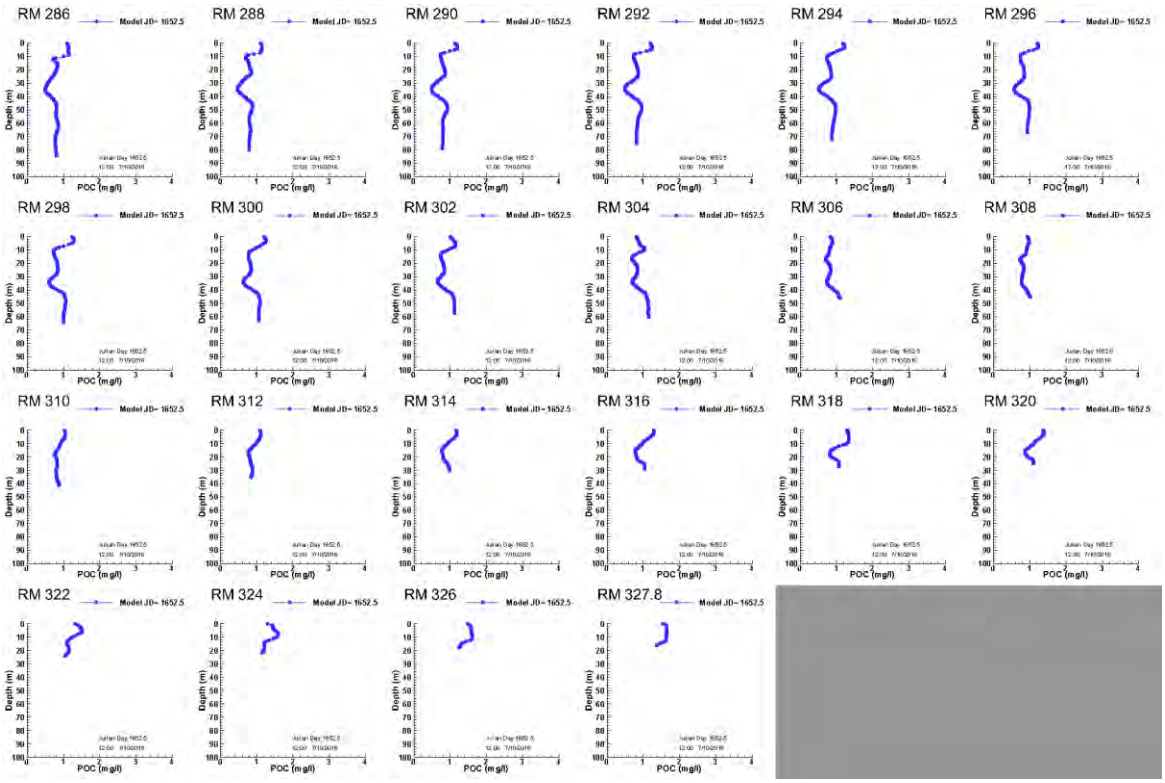


Figure 1637. Vertical profiles of POC compared with data for 7/10/2018.

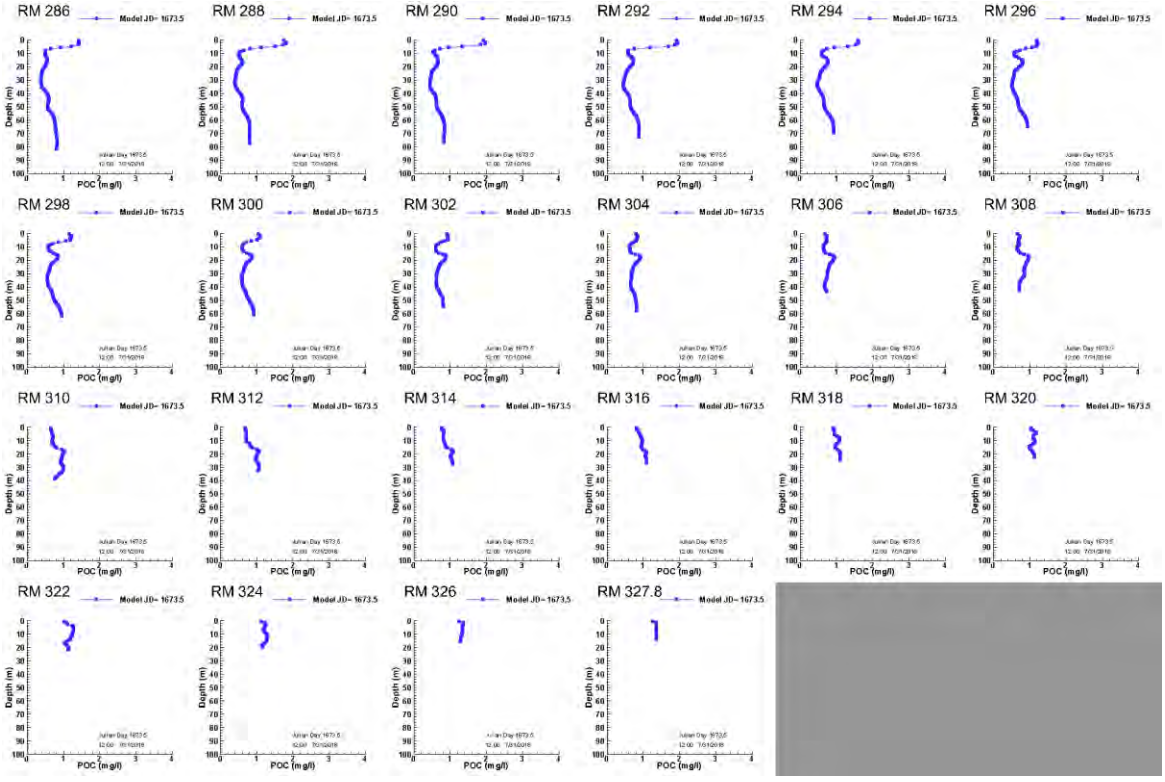


Figure 1638. Vertical profiles of POC compared with data for 7/31/2018.

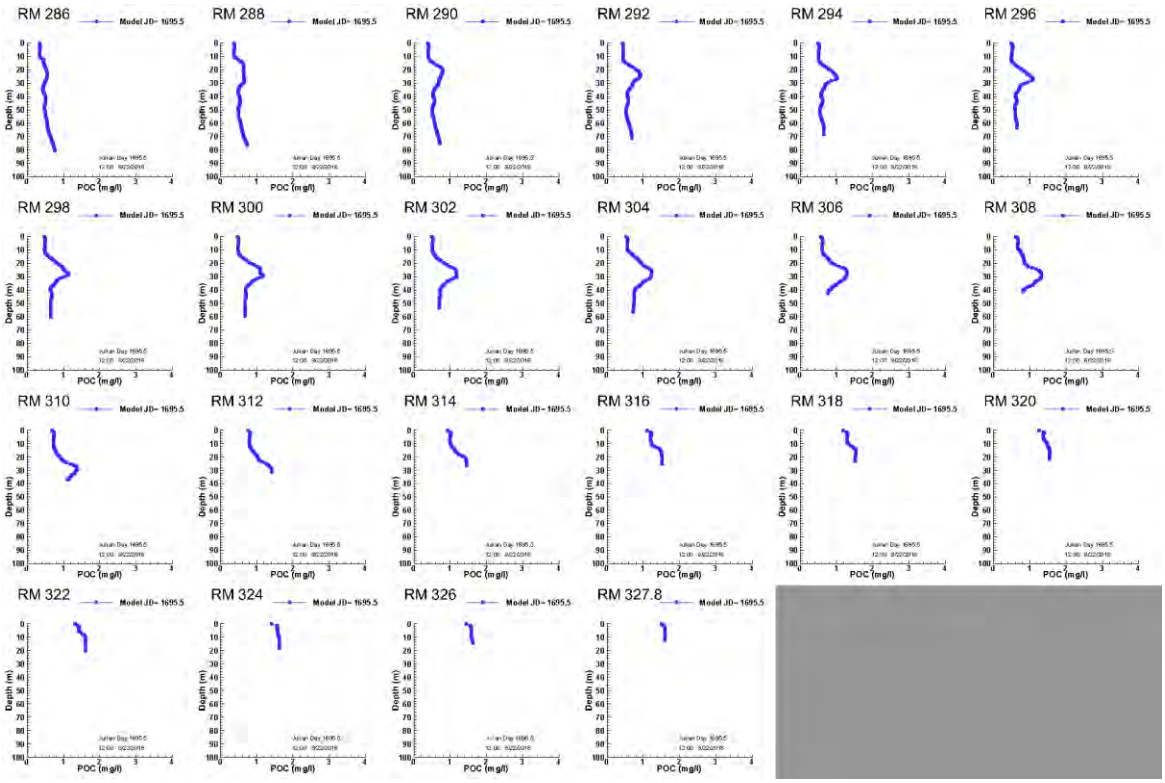


Figure 1639. Vertical profiles of POC compared with data for 8/22/2018.

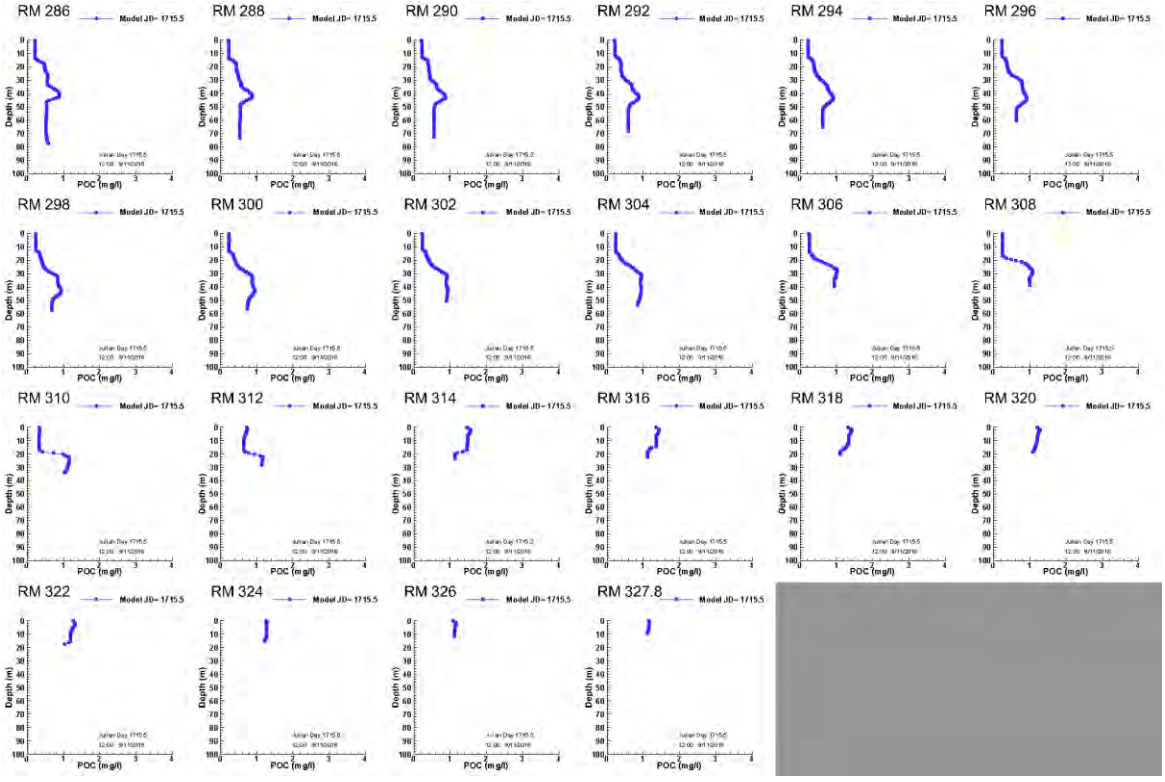


Figure 1640. Vertical profiles of POC compared with data for 9/11/2018.

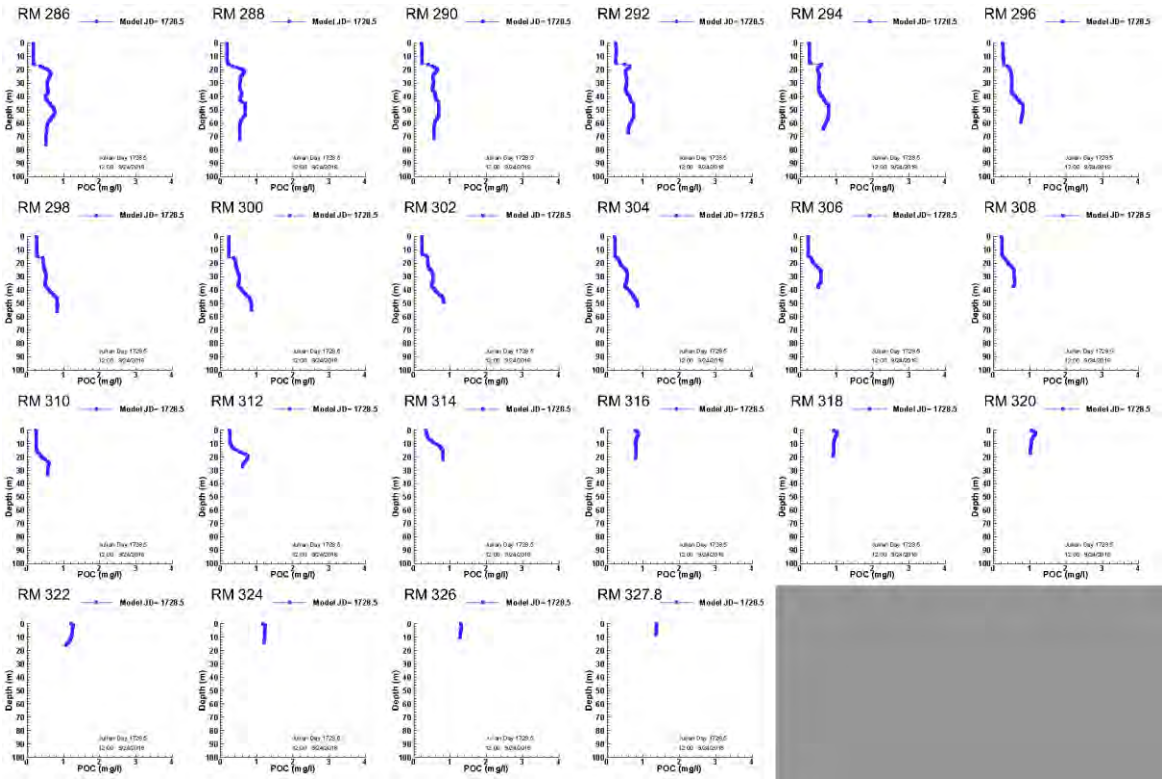


Figure 1641. Vertical profiles of POC compared with data for 9/24/2018.

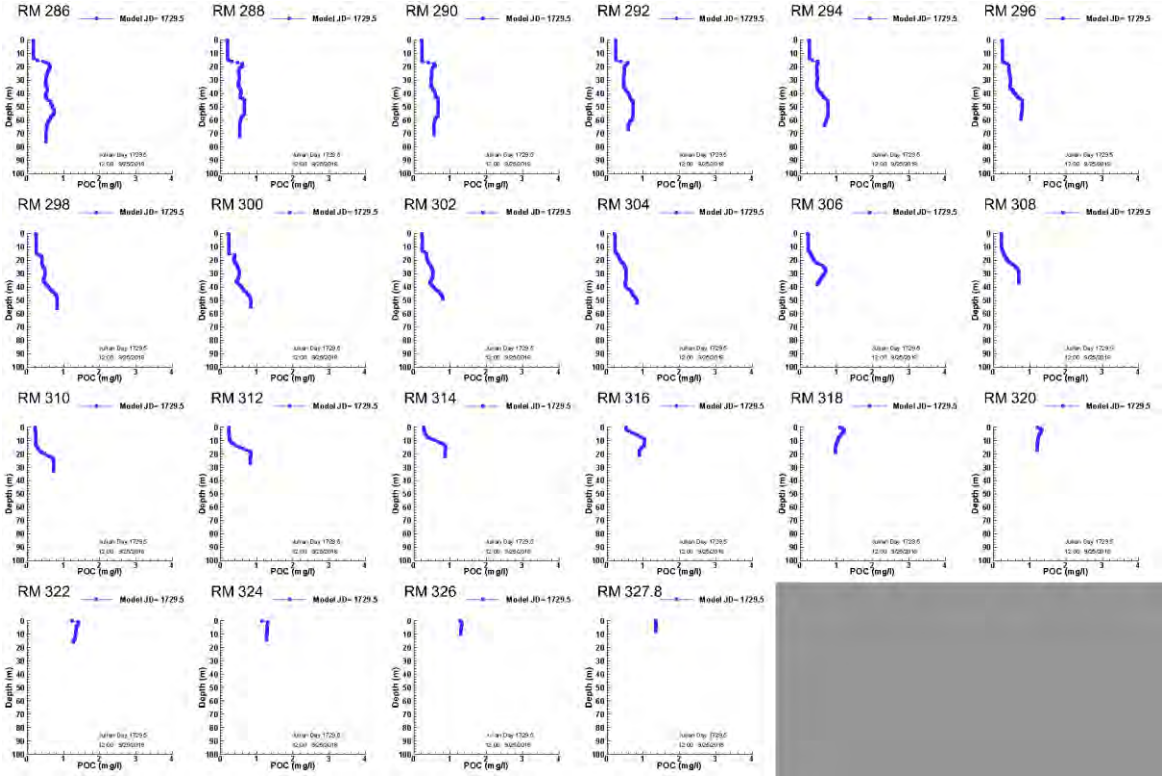


Figure 1642. Vertical profiles of POC compared with data for 9/25/2018.

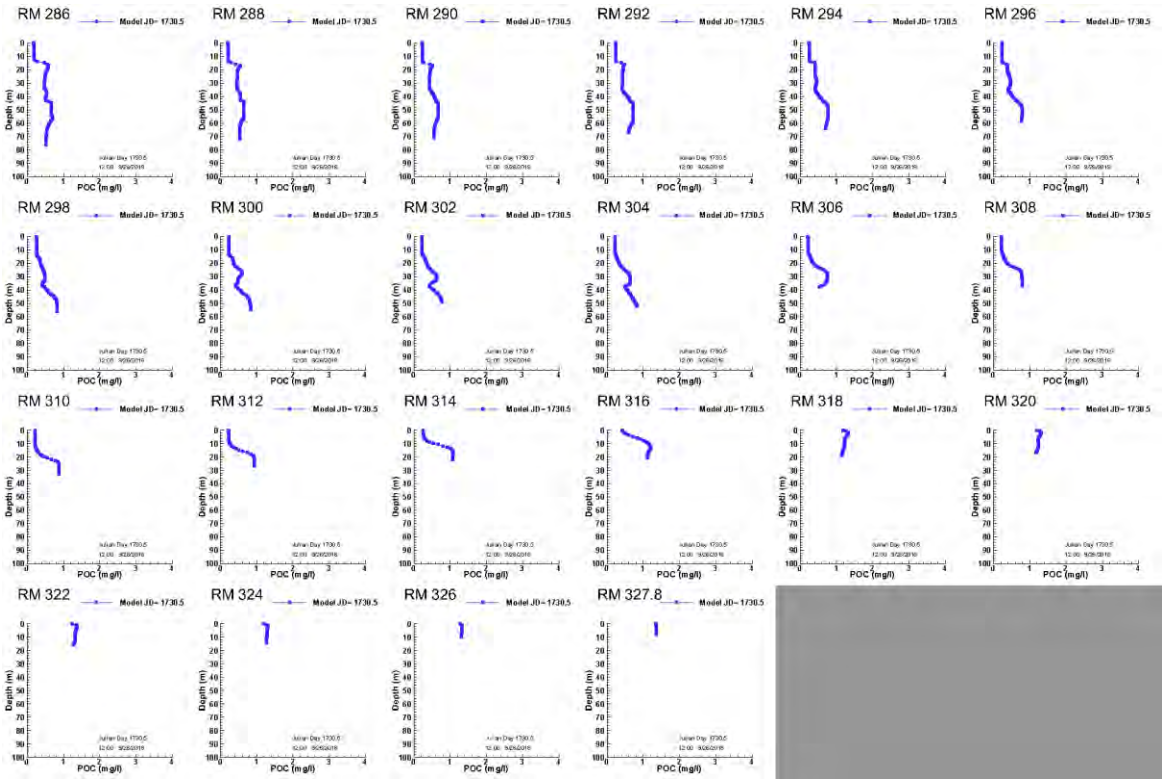


Figure 1643. Vertical profiles of POC compared with data for 9/26/2018.

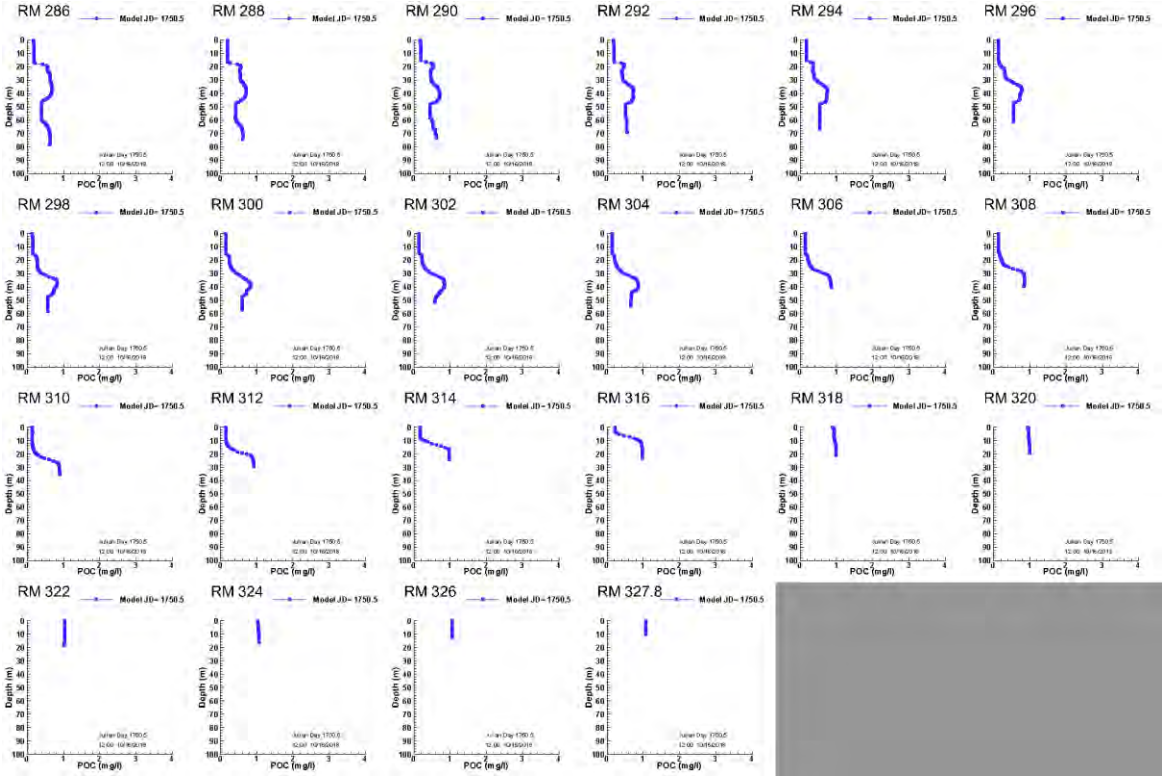


Figure 1644. Vertical profiles of POC compared with data for 10/16/2018.

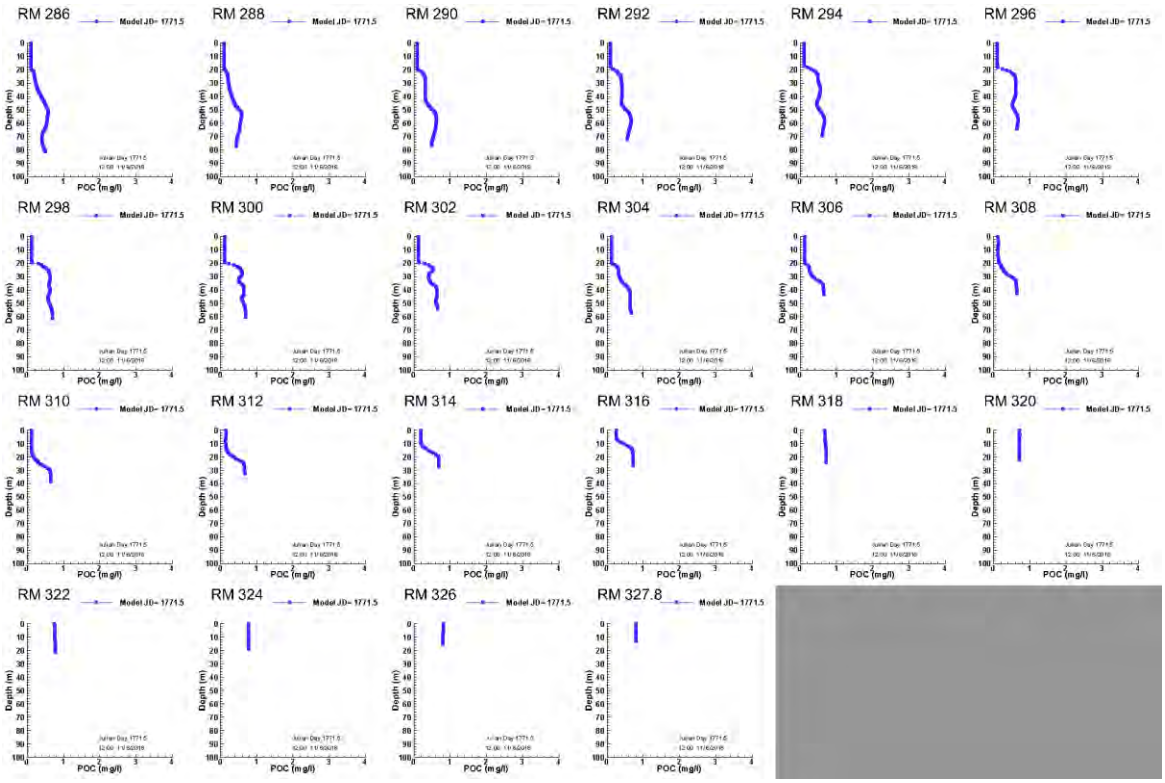


Figure 1645. Vertical profiles of POC compared with data for 11/ 6/2018.

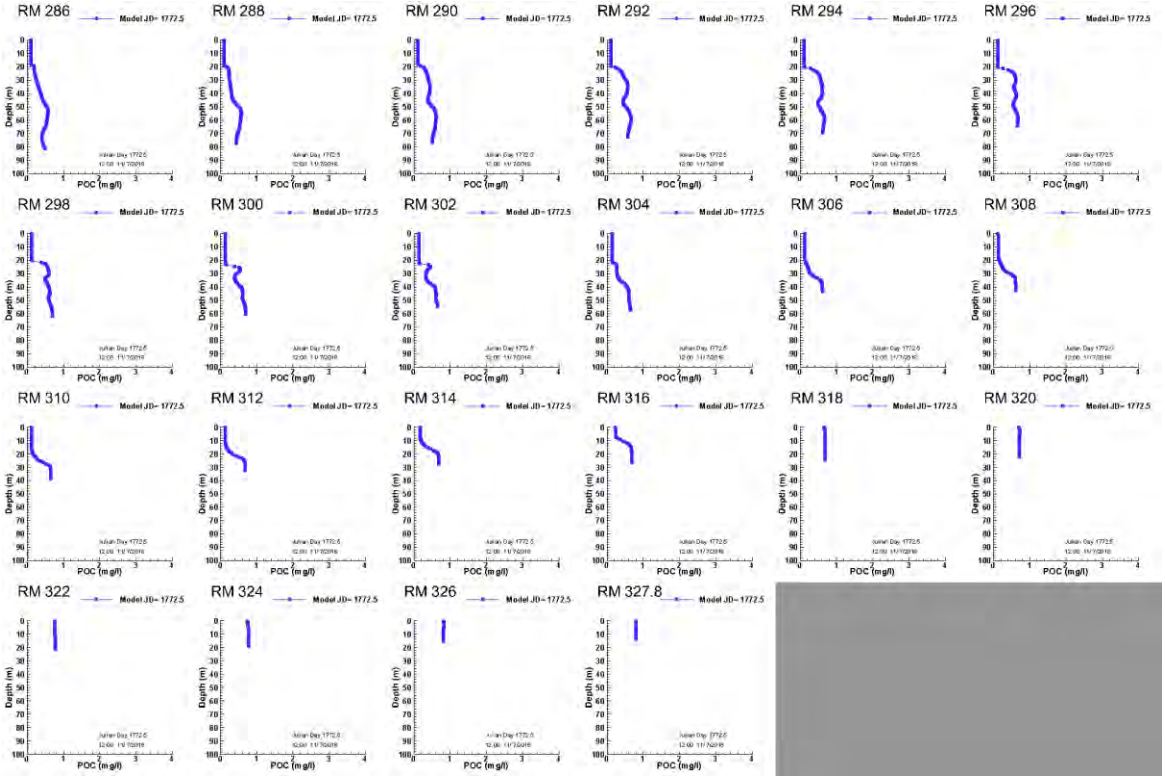


Figure 1646. Vertical profiles of POC compared with data for 11/ 7/2018.

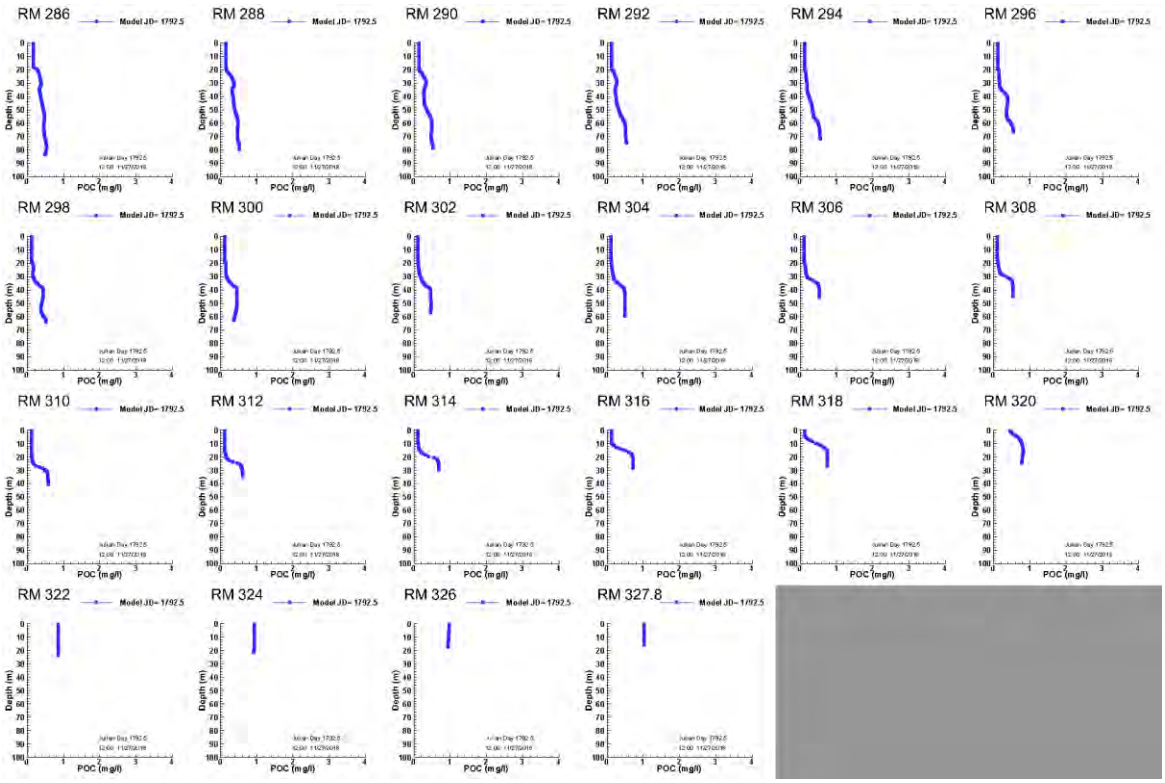


Figure 1647. Vertical profiles of POC compared with data for 11/27/2018.

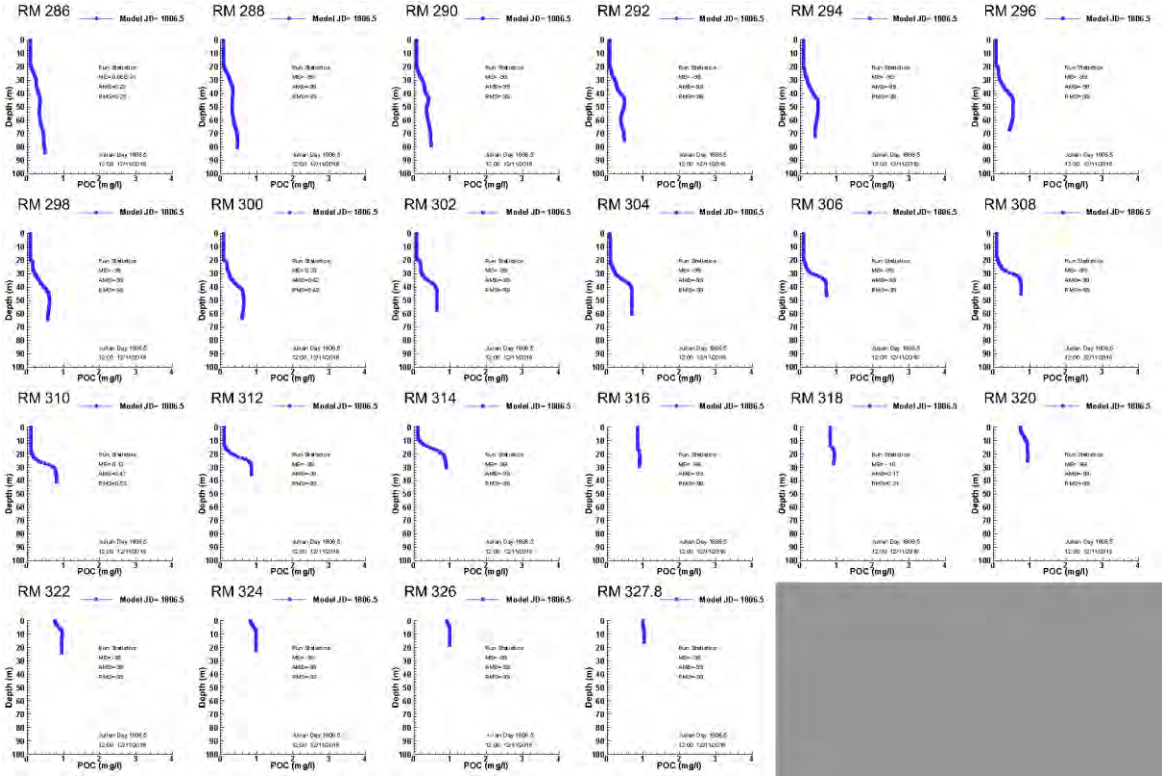


Figure 1648. Vertical profiles of POC compared with data for 12/11/2018.

Particulate Organic Nitrogen

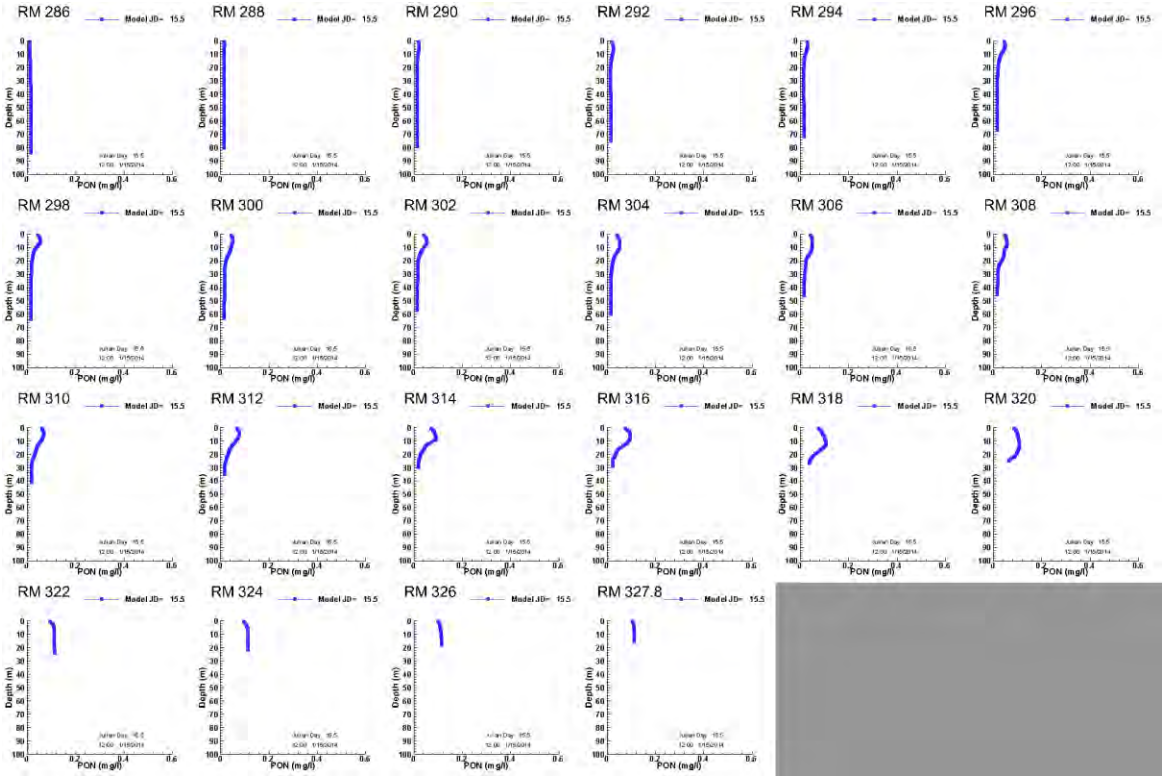


Figure 1649. Vertical profiles of PON compared with data for 1/15/2014.

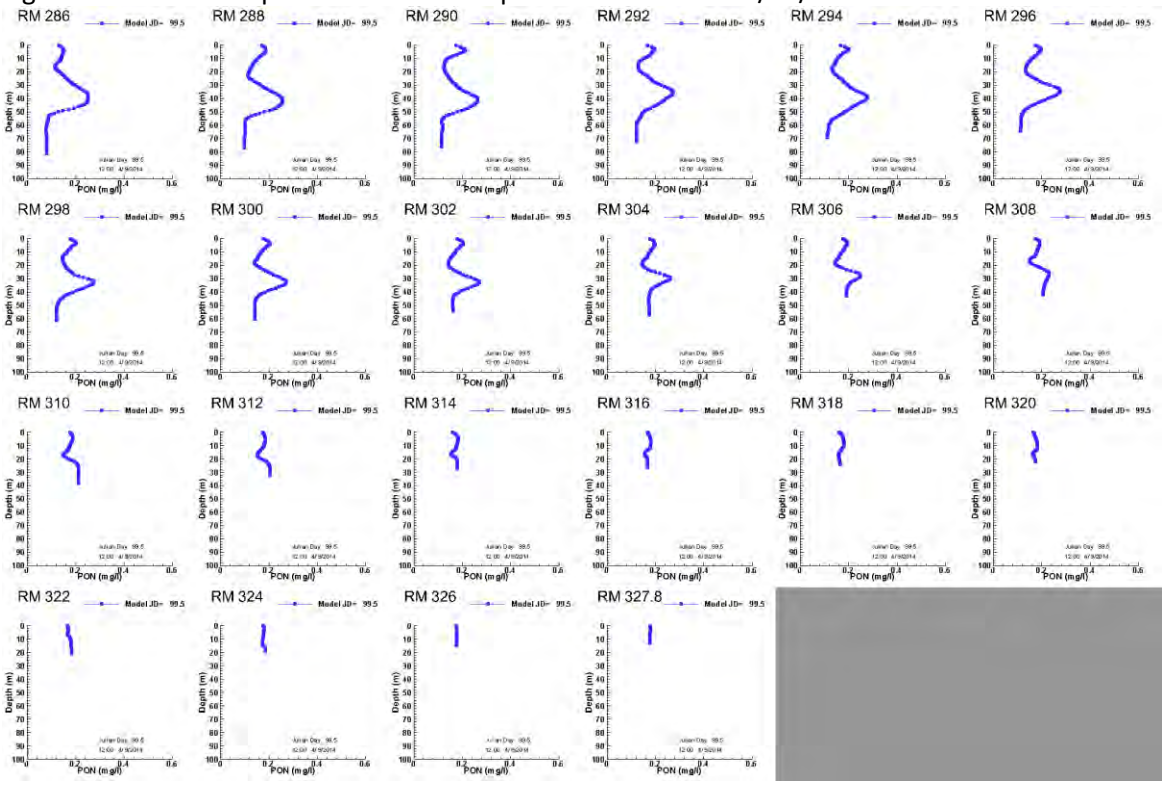


Figure 1650. Vertical profiles of PON compared with data for 4/ 9/2014.

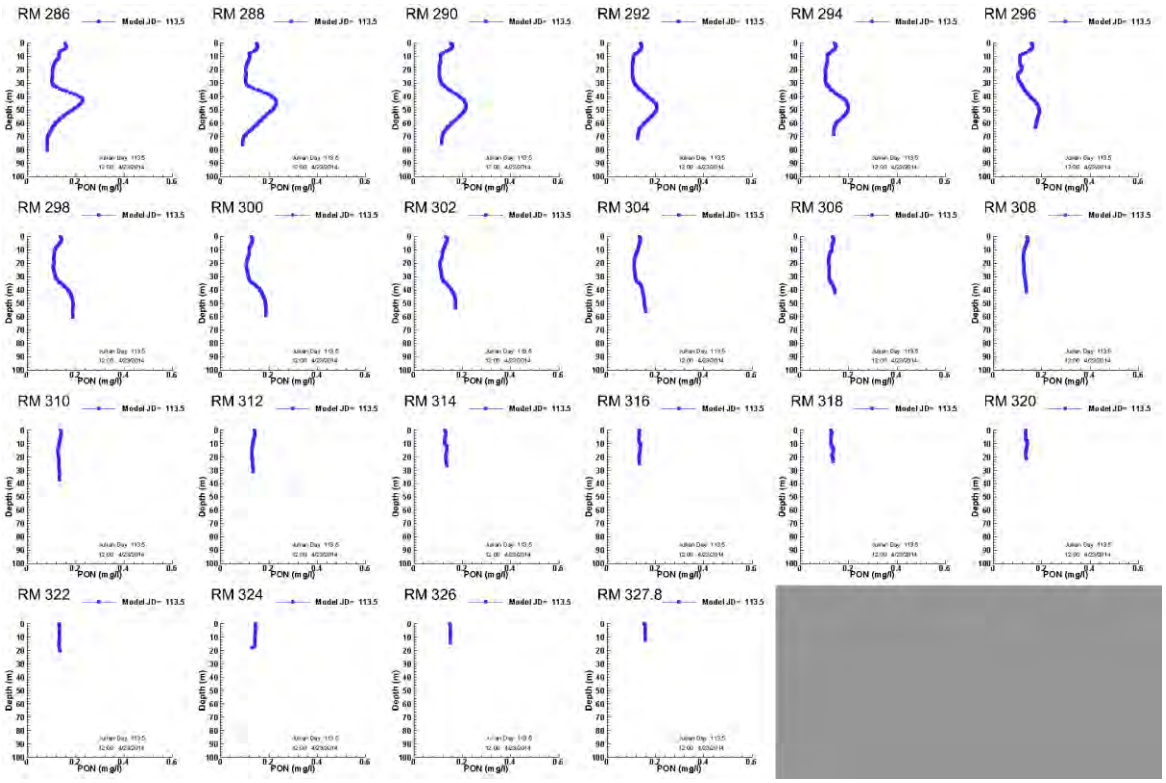


Figure 1651. Vertical profiles of PON compared with data for 4/23/2014.

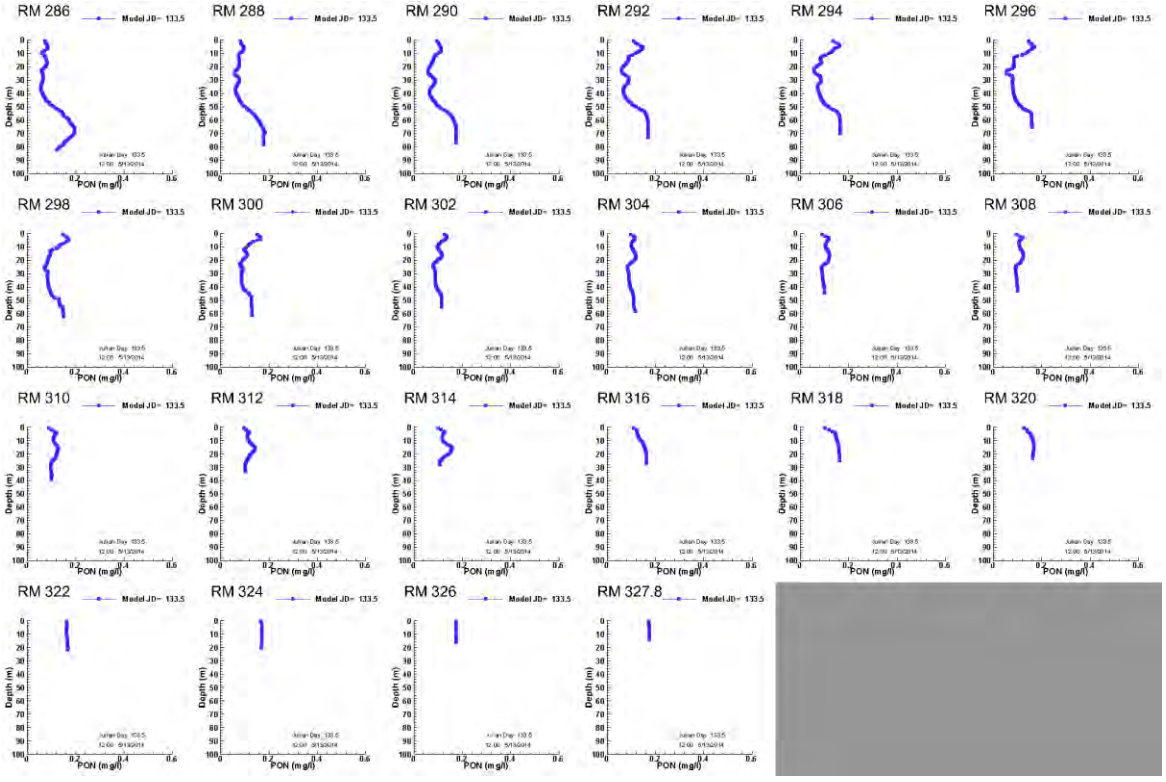


Figure 1652. Vertical profiles of PON compared with data for 5/13/2014.

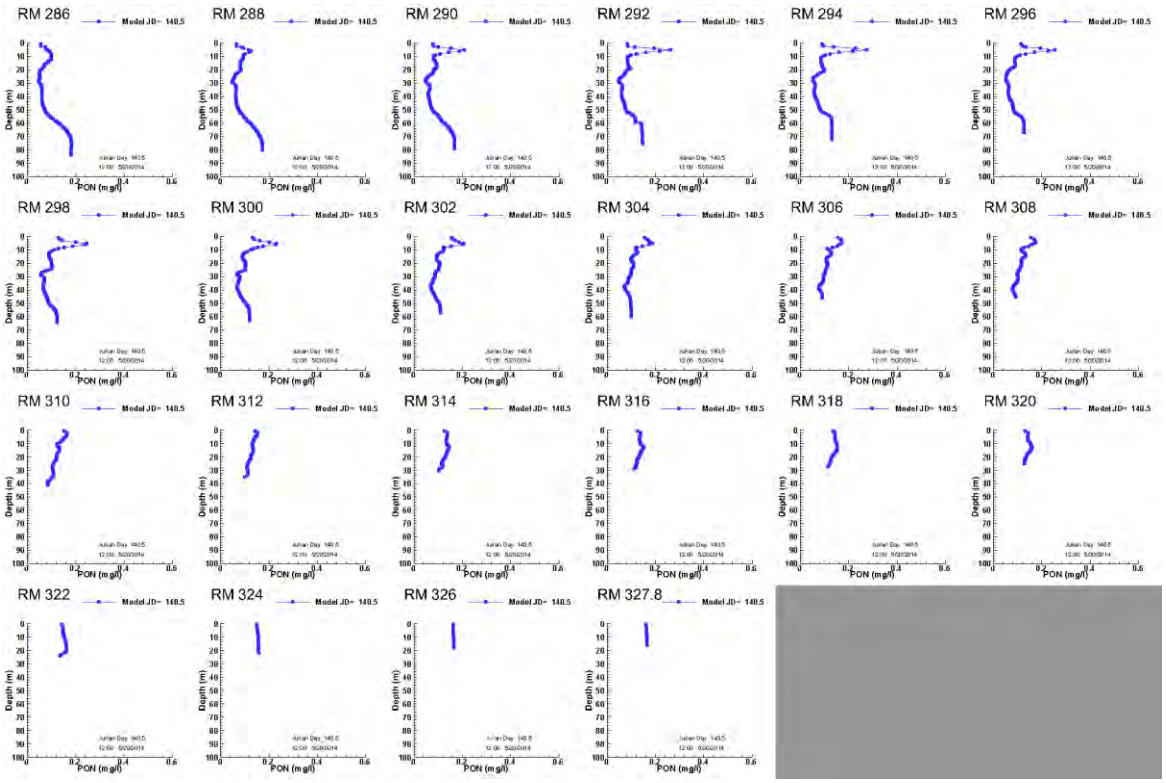


Figure 1653. Vertical profiles of PON compared with data for 5/20/2014.

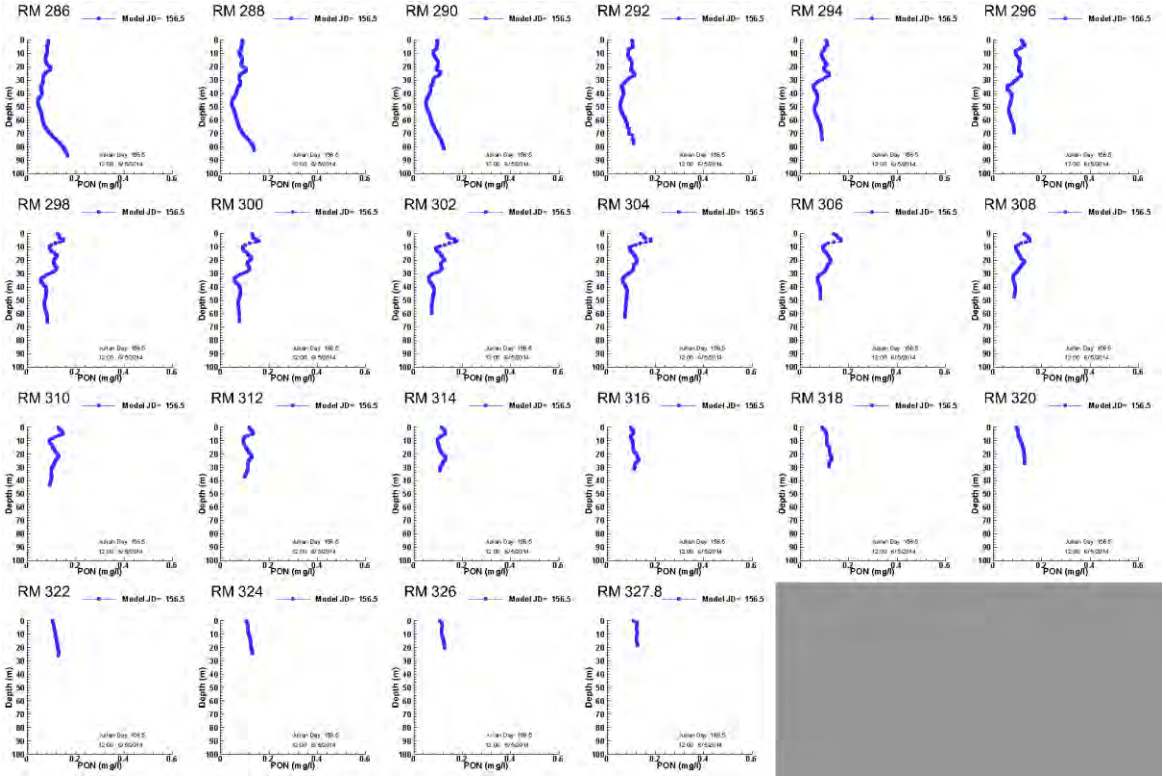


Figure 1654. Vertical profiles of PON compared with data for 6/ 5/2014.

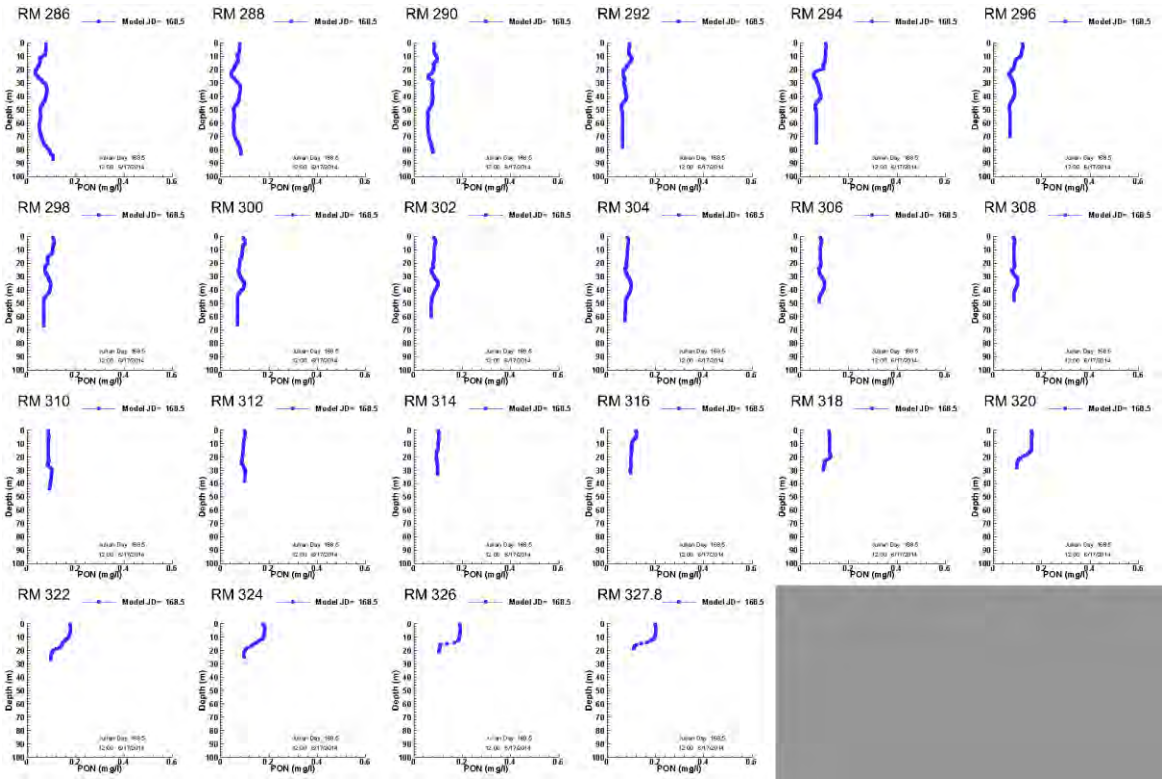


Figure 1655. Vertical profiles of PON compared with data for 6/17/2014.

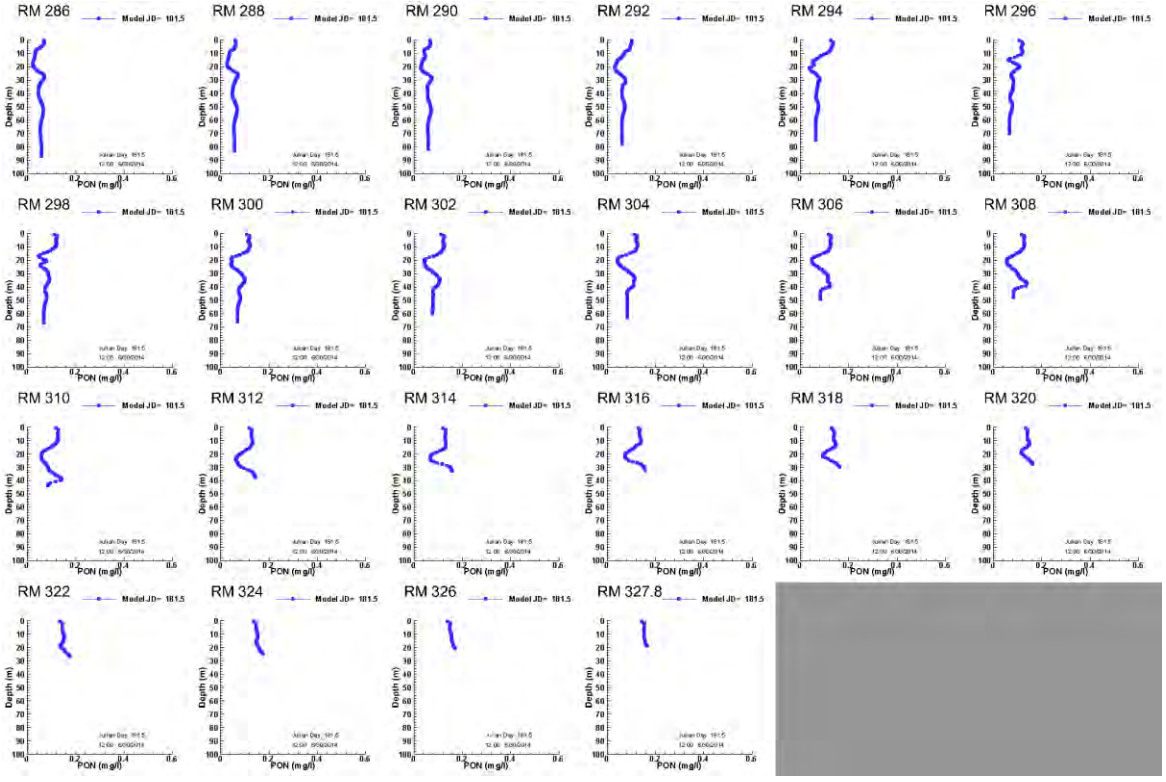


Figure 1656. Vertical profiles of PON compared with data for 6/30/2014.

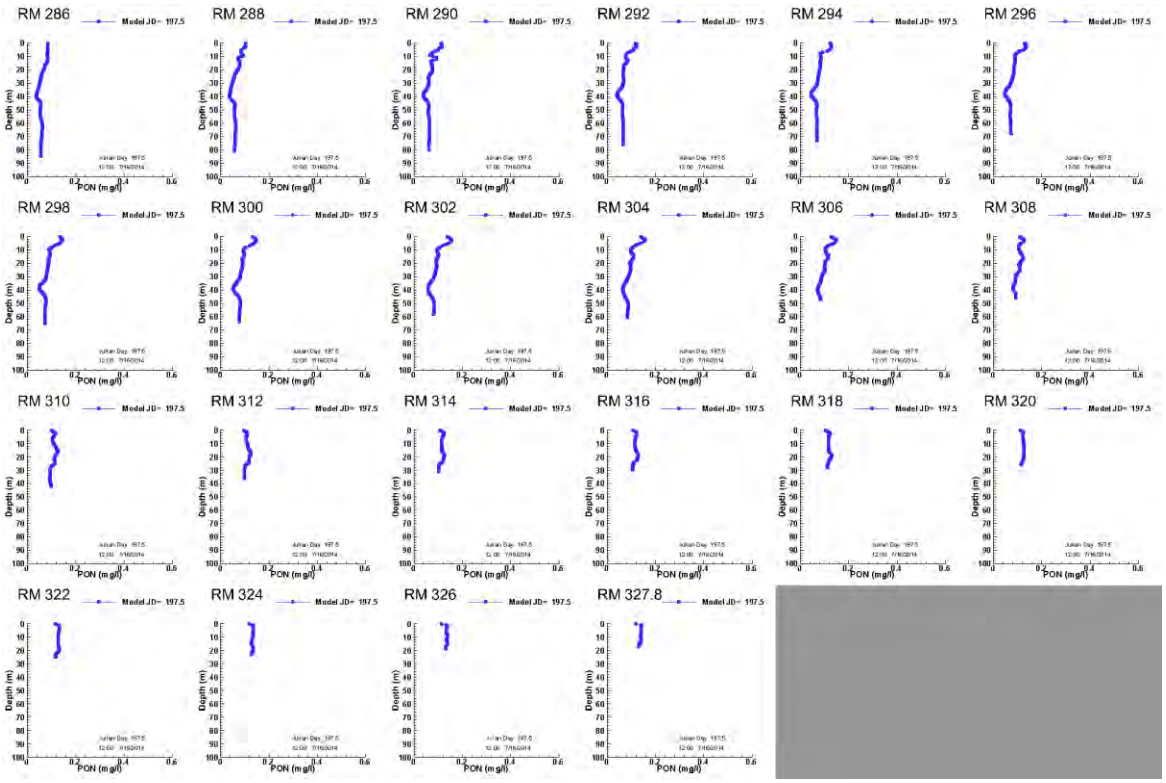


Figure 1657. Vertical profiles of PON compared with data for 7/16/2014.

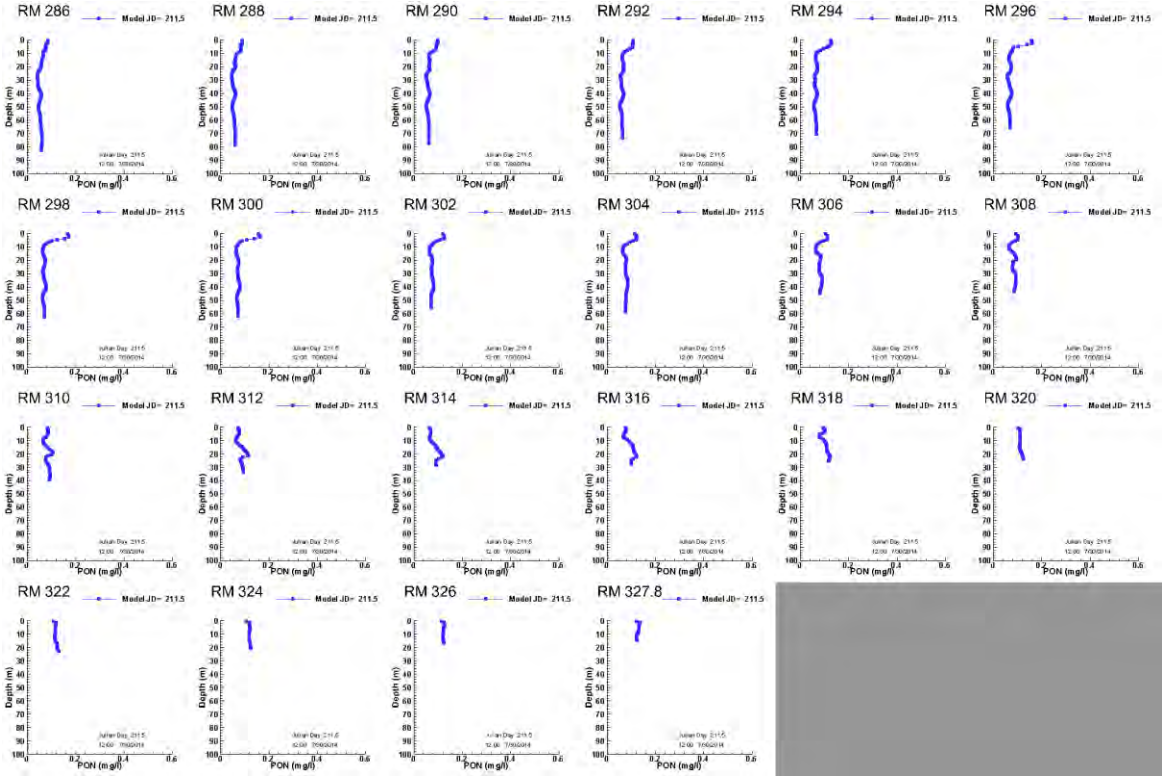


Figure 1658. Vertical profiles of PON compared with data for 7/30/2014.

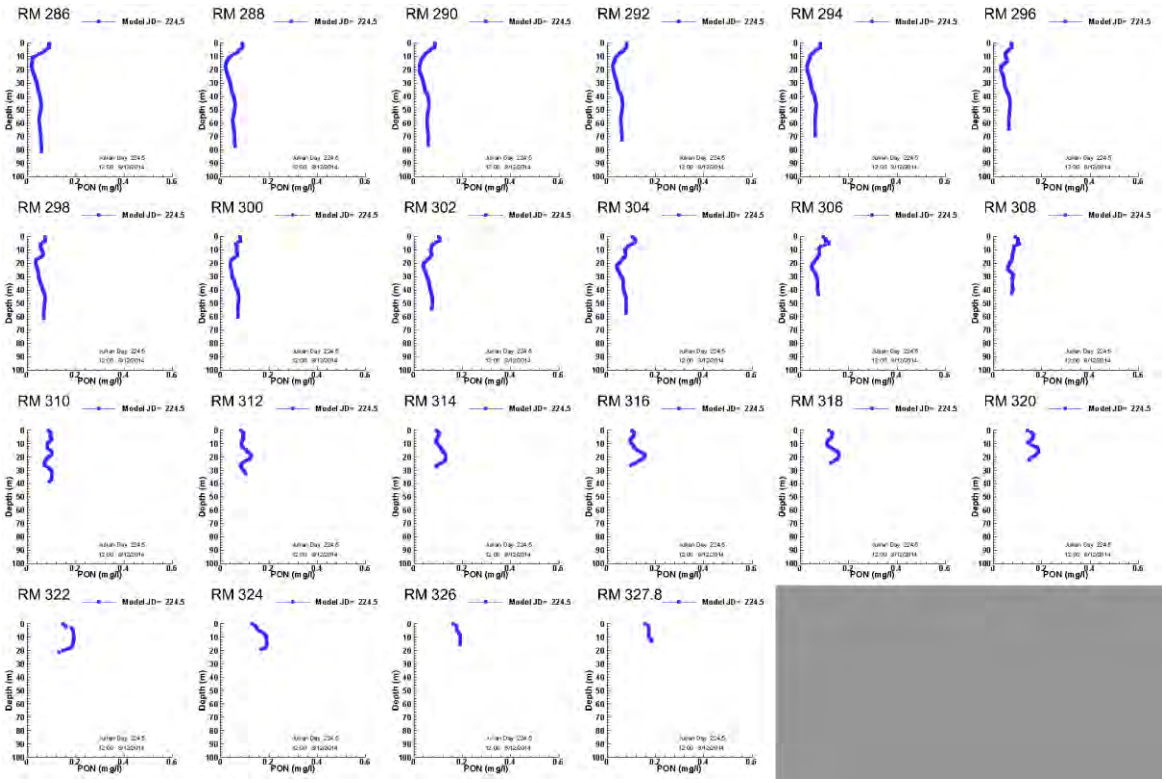


Figure 1659. Vertical profiles of PON compared with data for 8/12/2014.

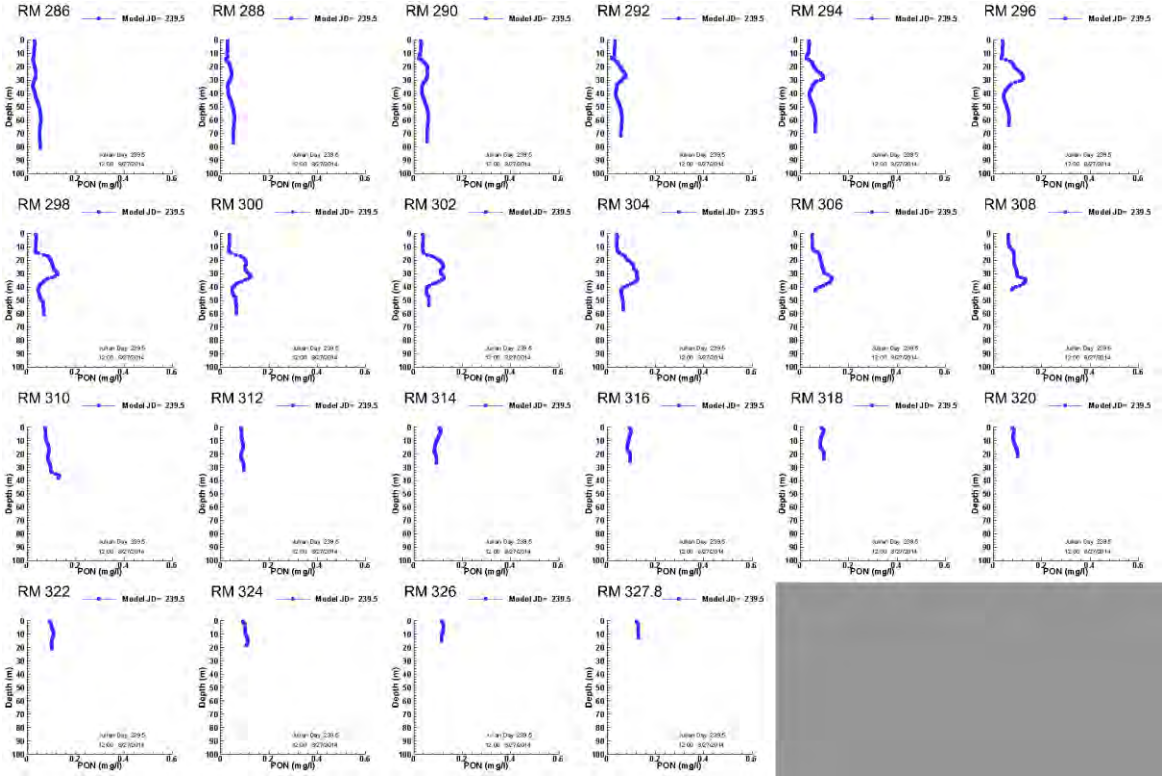


Figure 1660. Vertical profiles of PON compared with data for 8/27/2014.

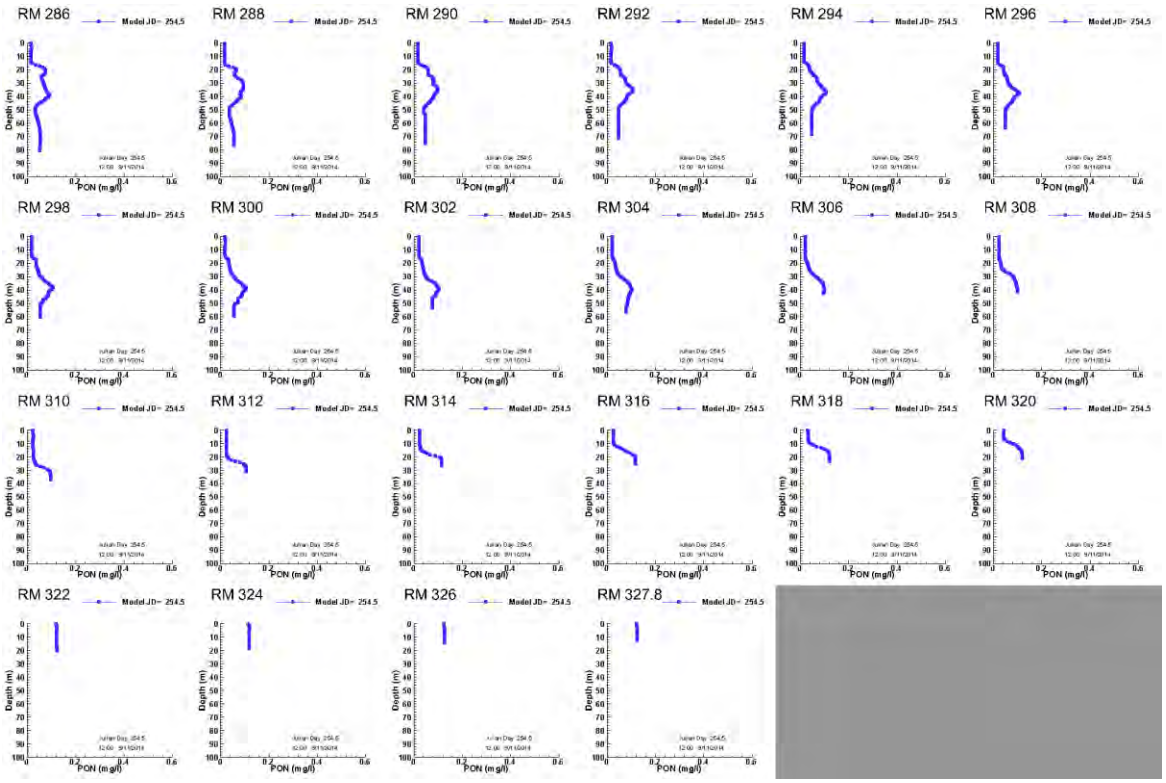


Figure 1661. Vertical profiles of PON compared with data for 9/11/2014.

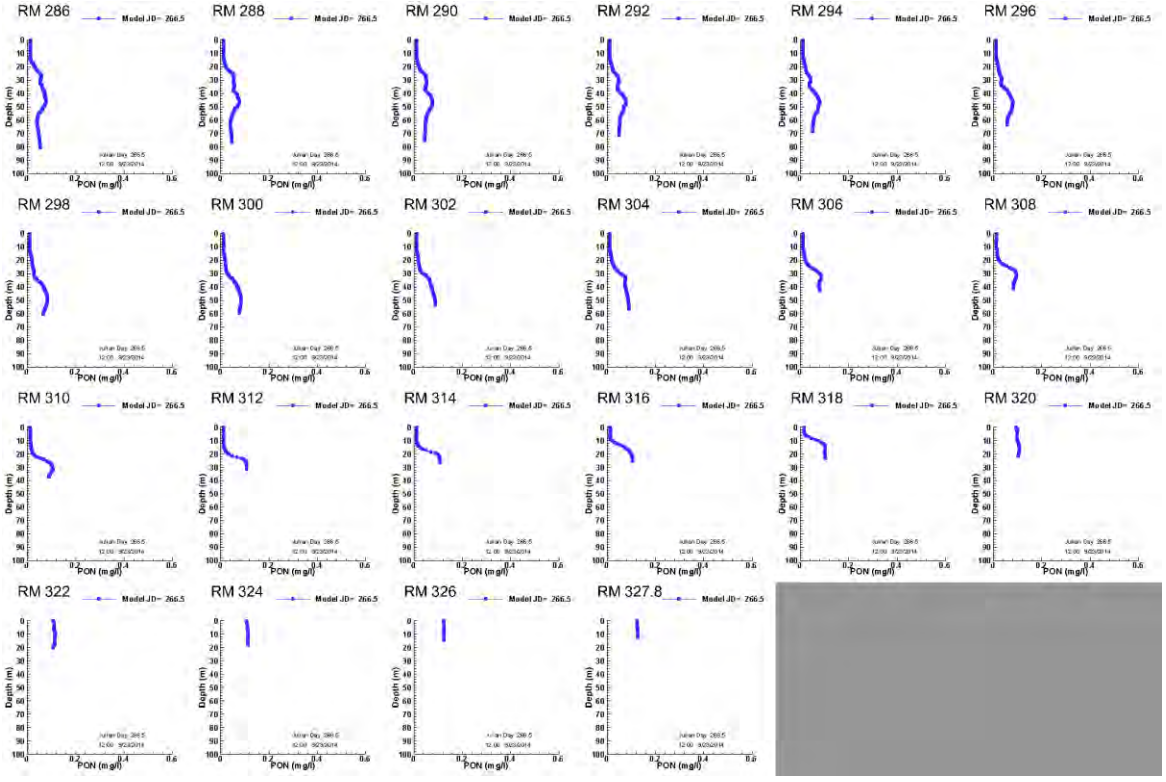


Figure 1662. Vertical profiles of PON compared with data for 9/23/2014.

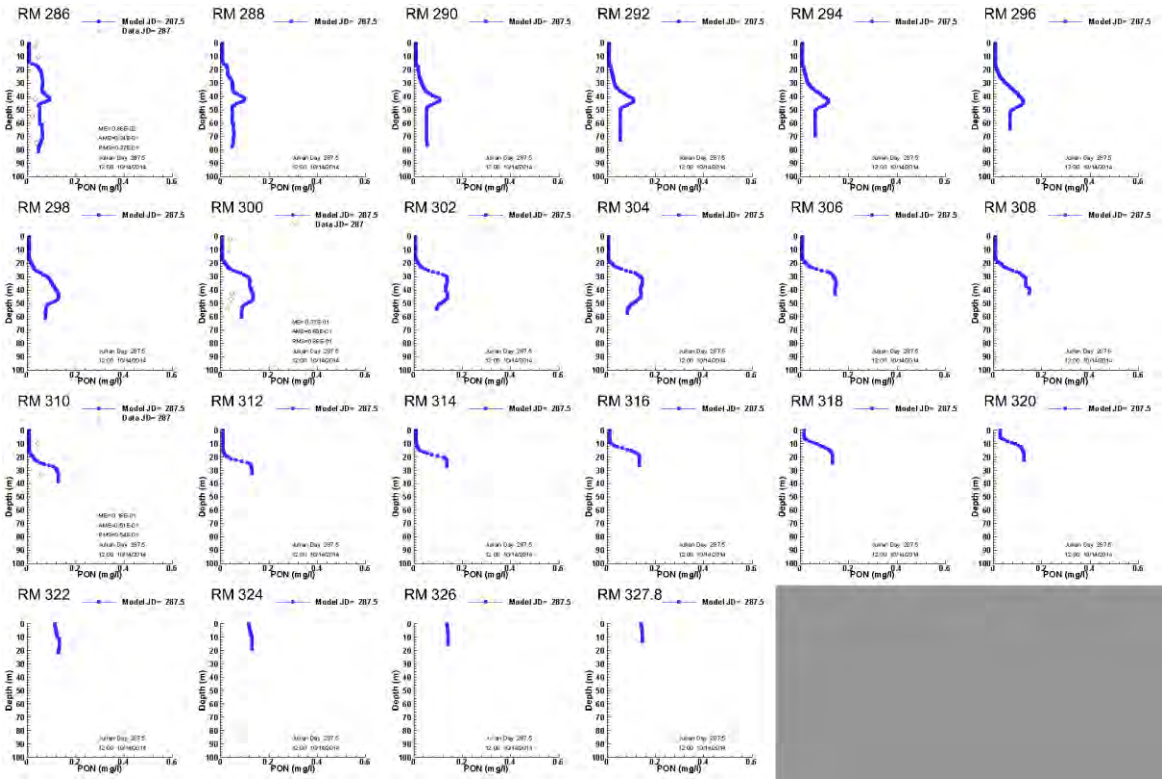


Figure 1663. Vertical profiles of PON compared with data for 10/14/2014.

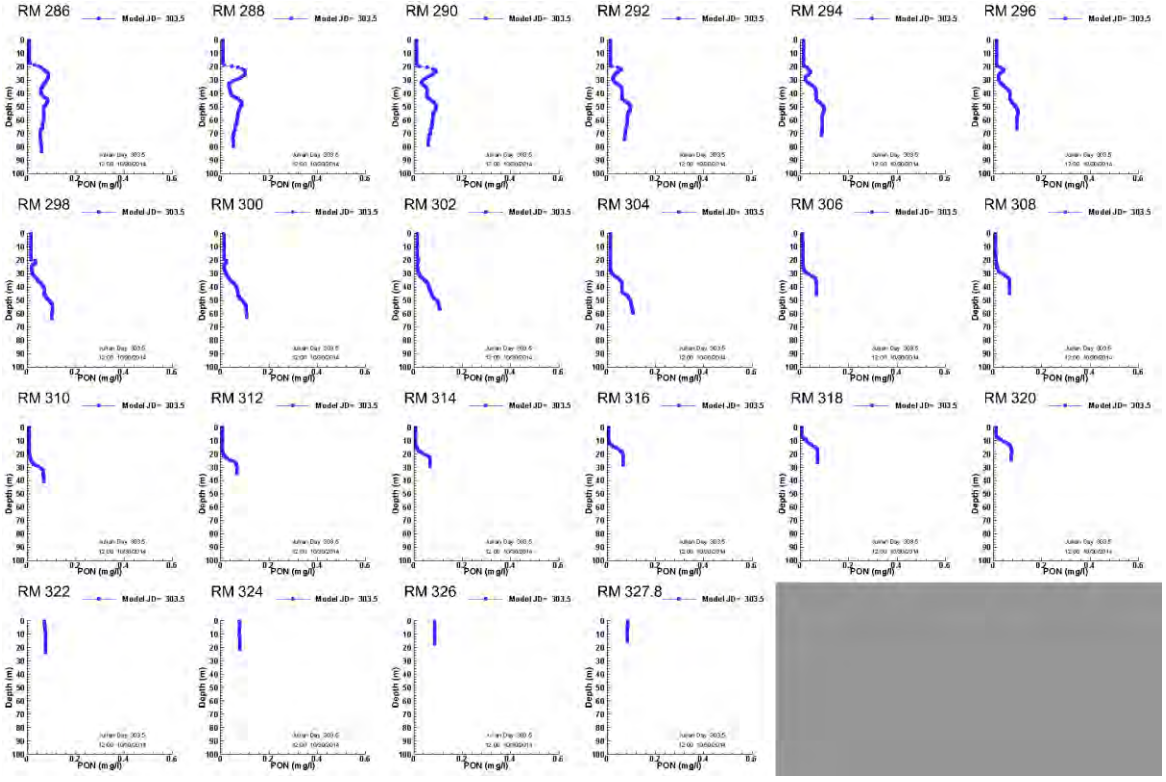


Figure 1664. Vertical profiles of PON compared with data for 10/30/2014.

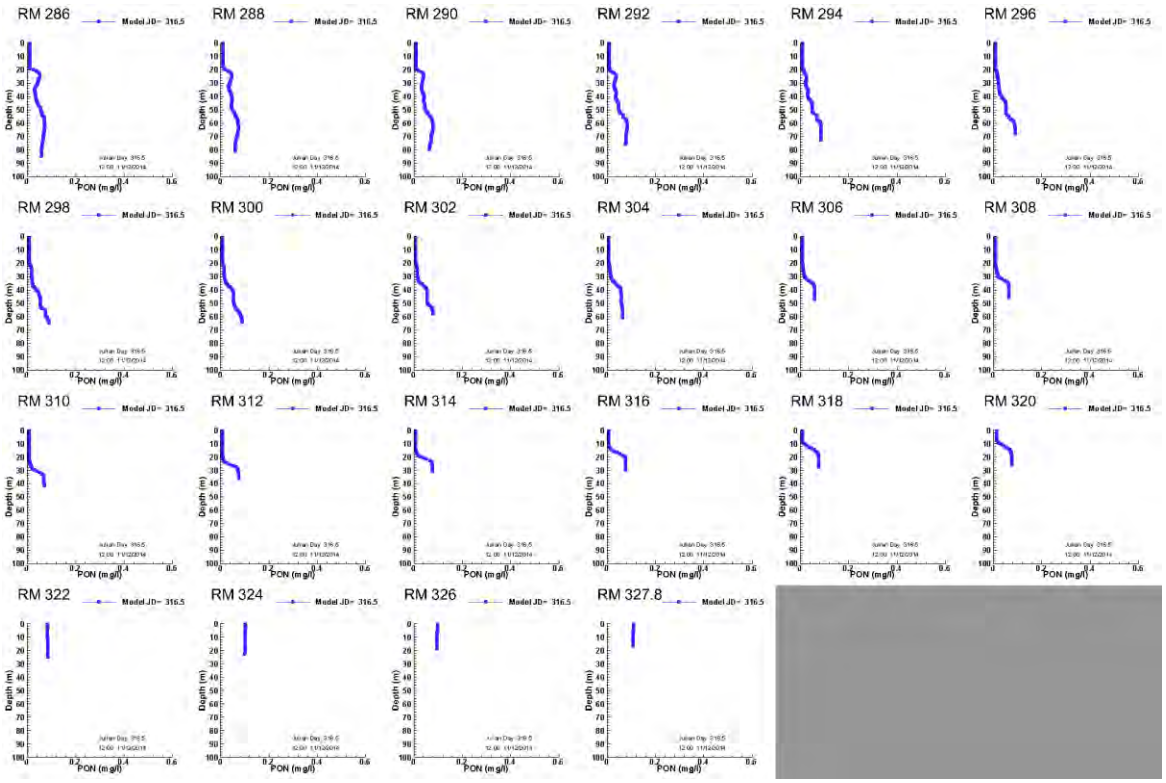


Figure 1665. Vertical profiles of PON compared with data for 11/12/2014.

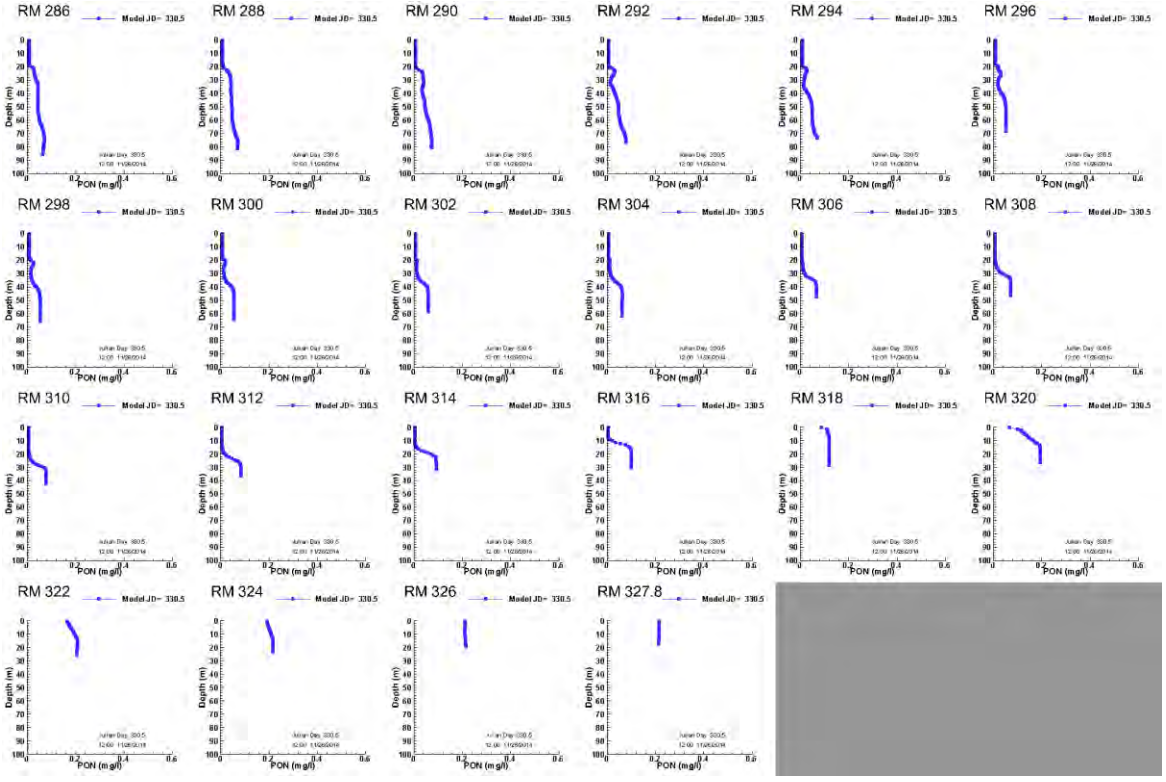


Figure 1666. Vertical profiles of PON compared with data for 11/26/2014.

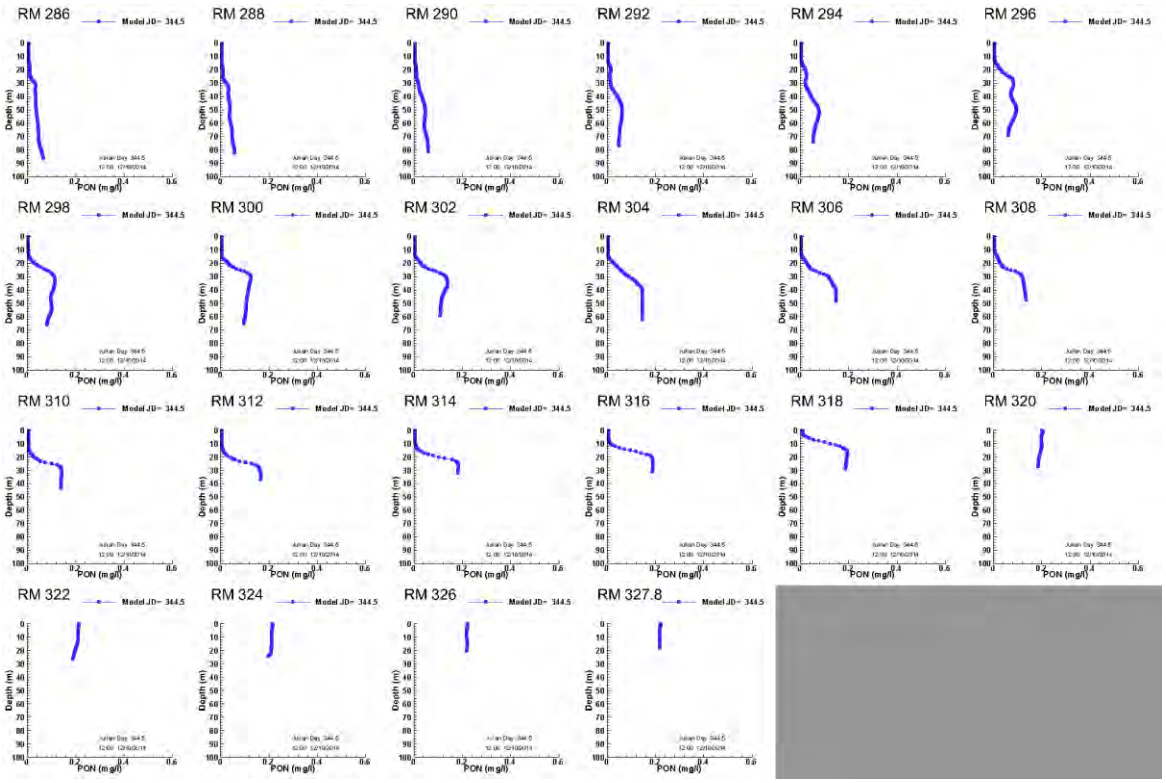


Figure 1667. Vertical profiles of PON compared with data for 12/10/2014.

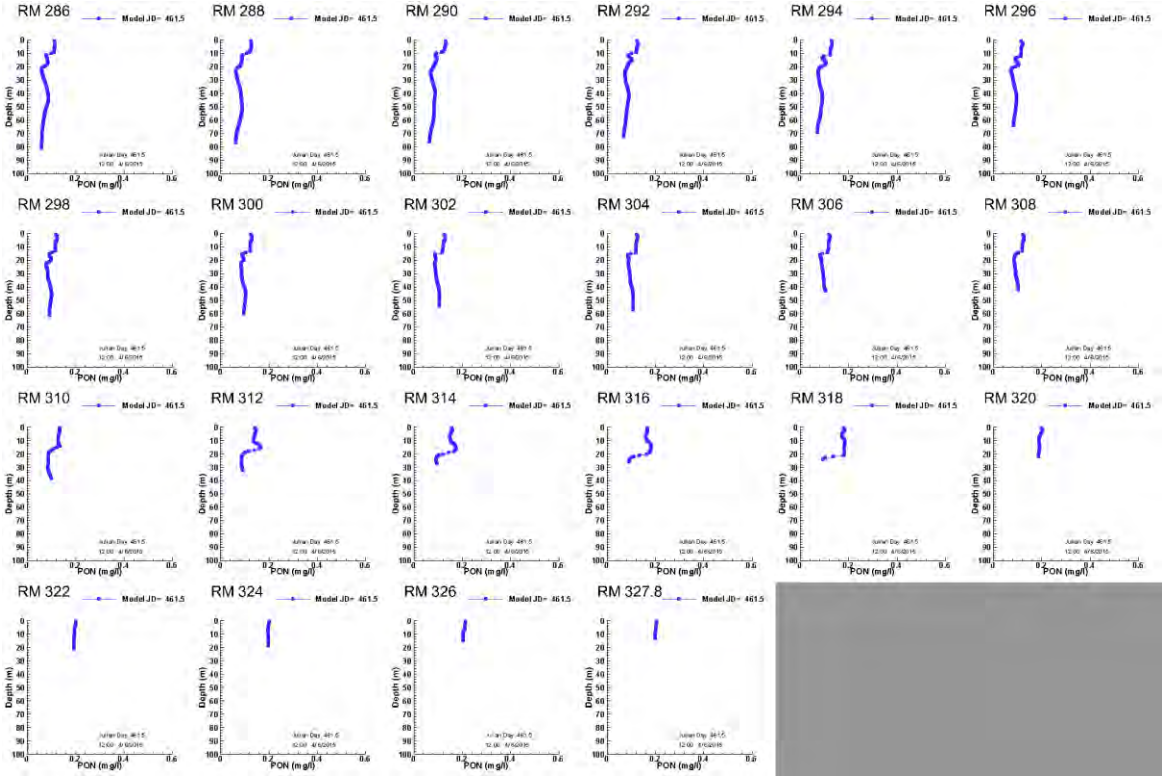


Figure 1668. Vertical profiles of PON compared with data for 4/ 6/2015.

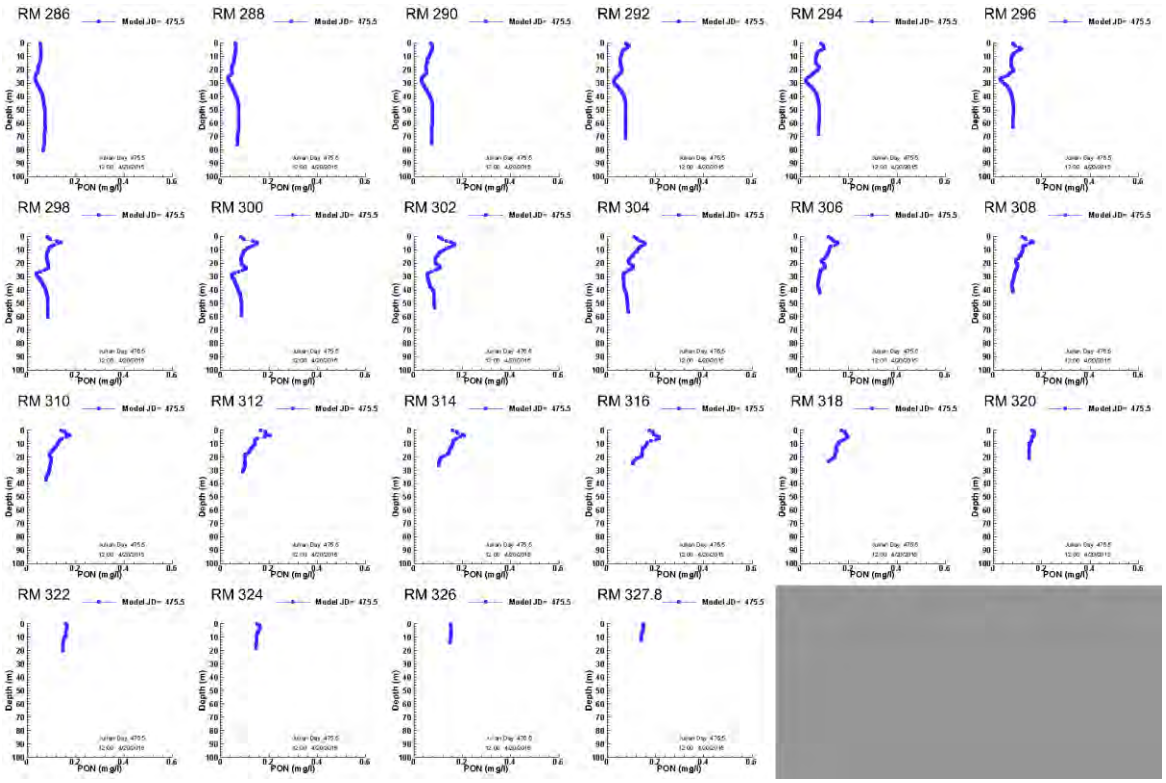


Figure 1669. Vertical profiles of PON compared with data for 4/20/2015.

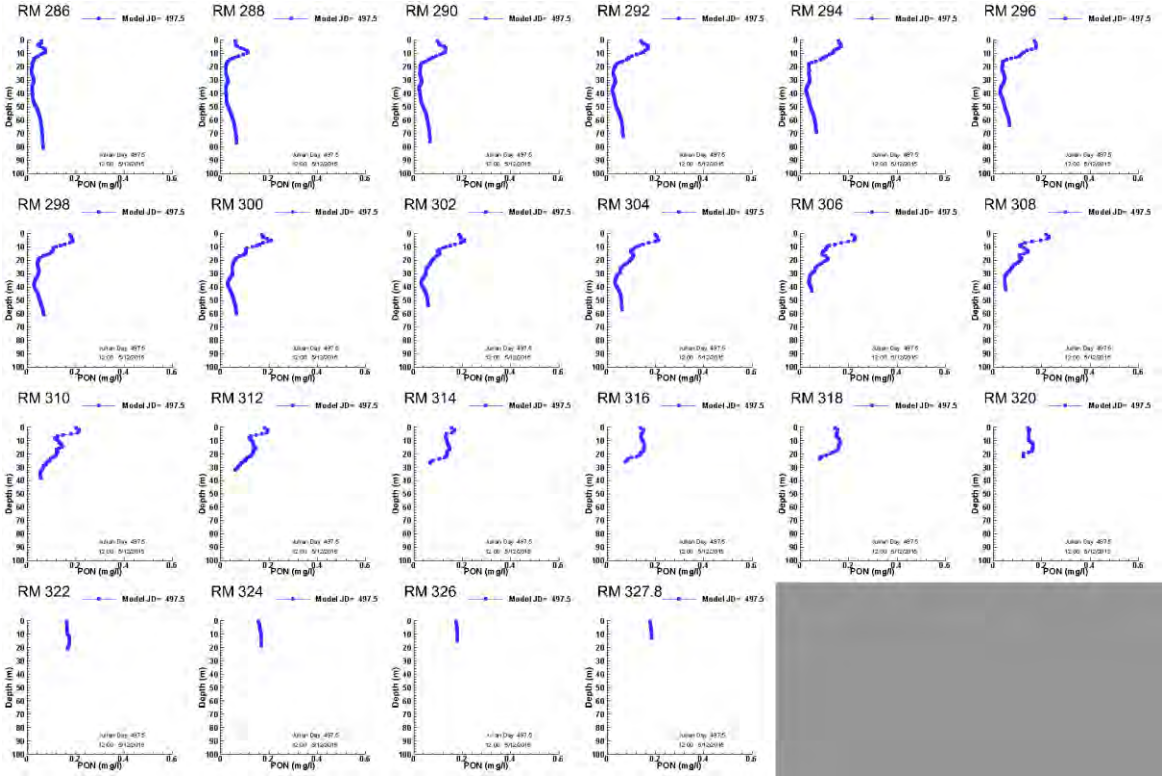


Figure 1670. Vertical profiles of PON compared with data for 5/12/2015.

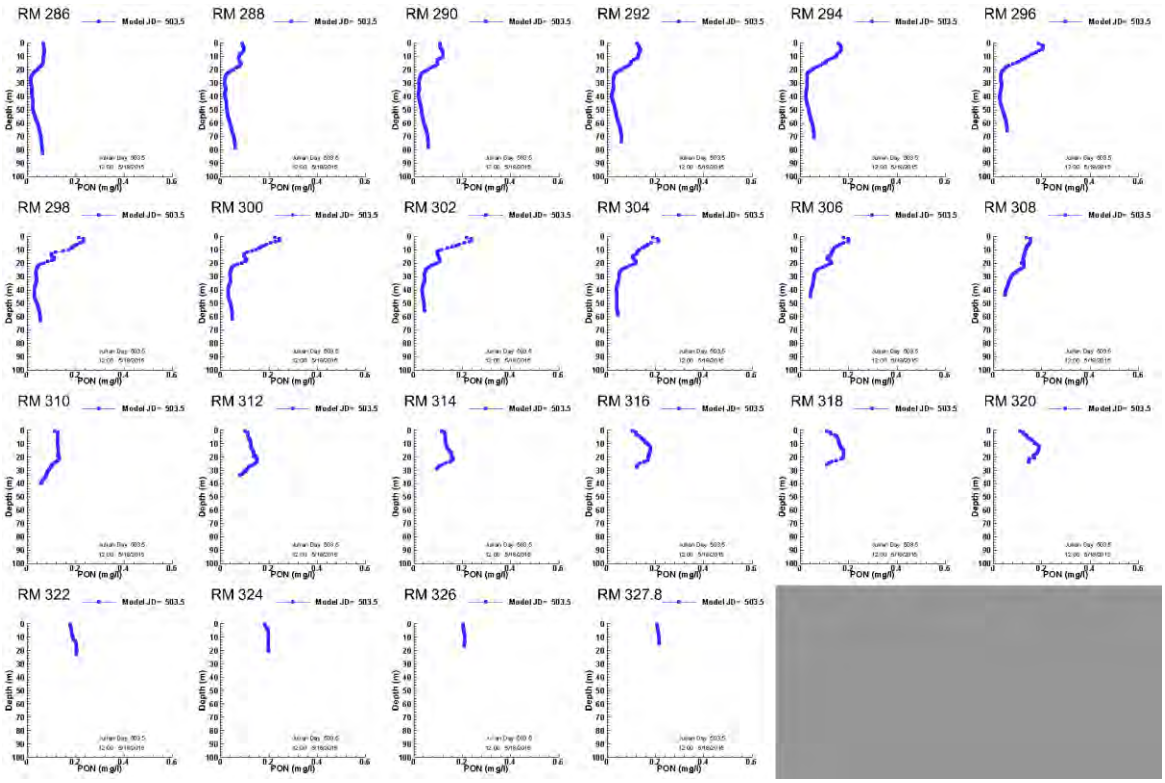


Figure 1671. Vertical profiles of PON compared with data for 5/18/2015.

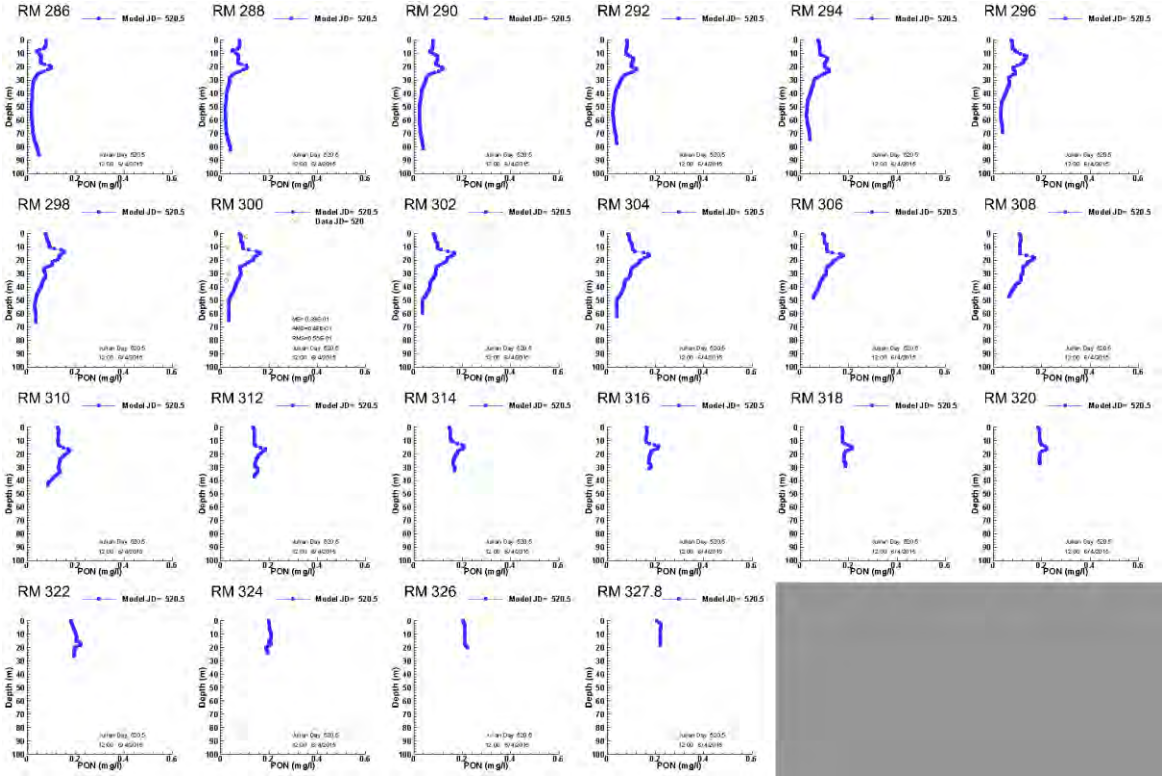


Figure 1672. Vertical profiles of PON compared with data for 6/ 4/2015.

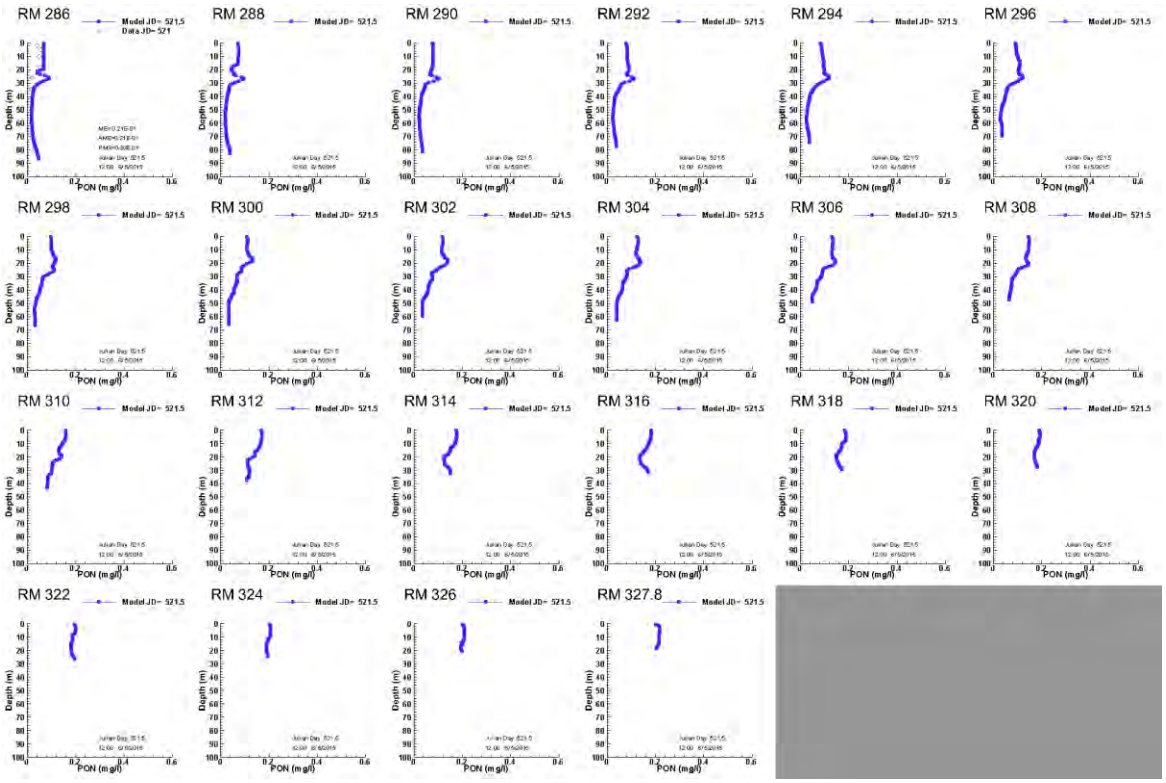


Figure 1673. Vertical profiles of PON compared with data for 6/ 5/2015.

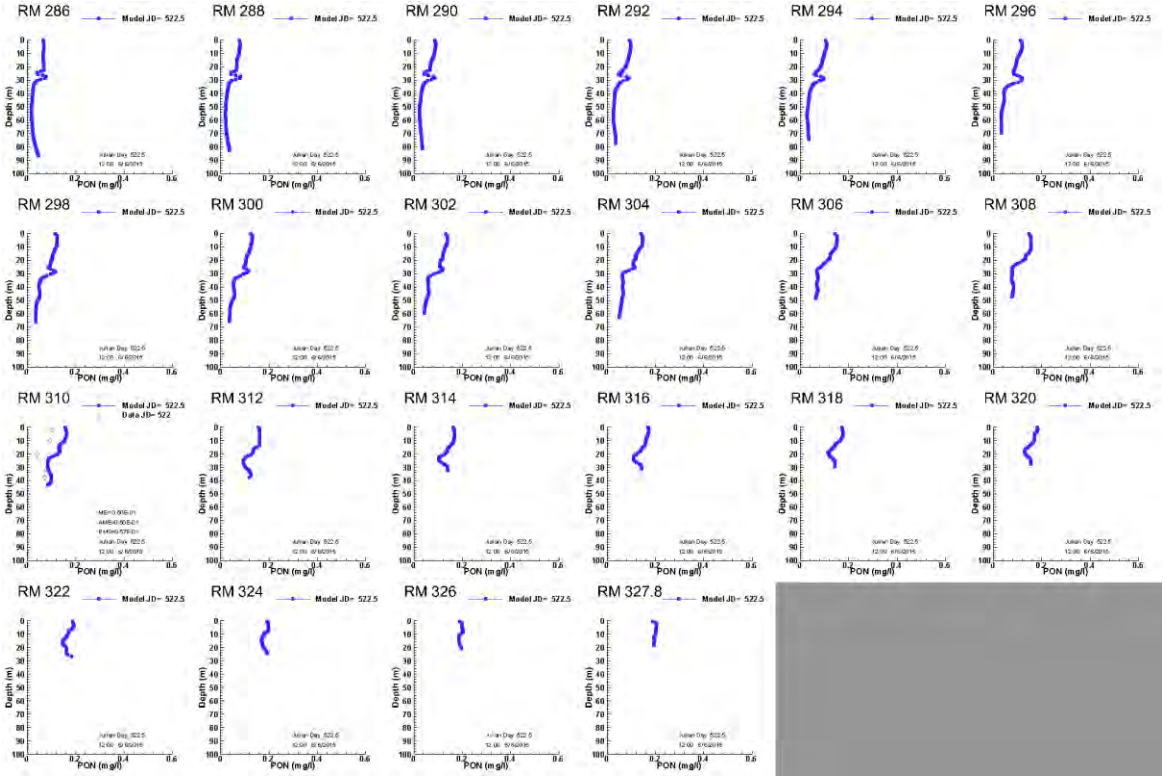


Figure 1674. Vertical profiles of PON compared with data for 6/ 6/2015.

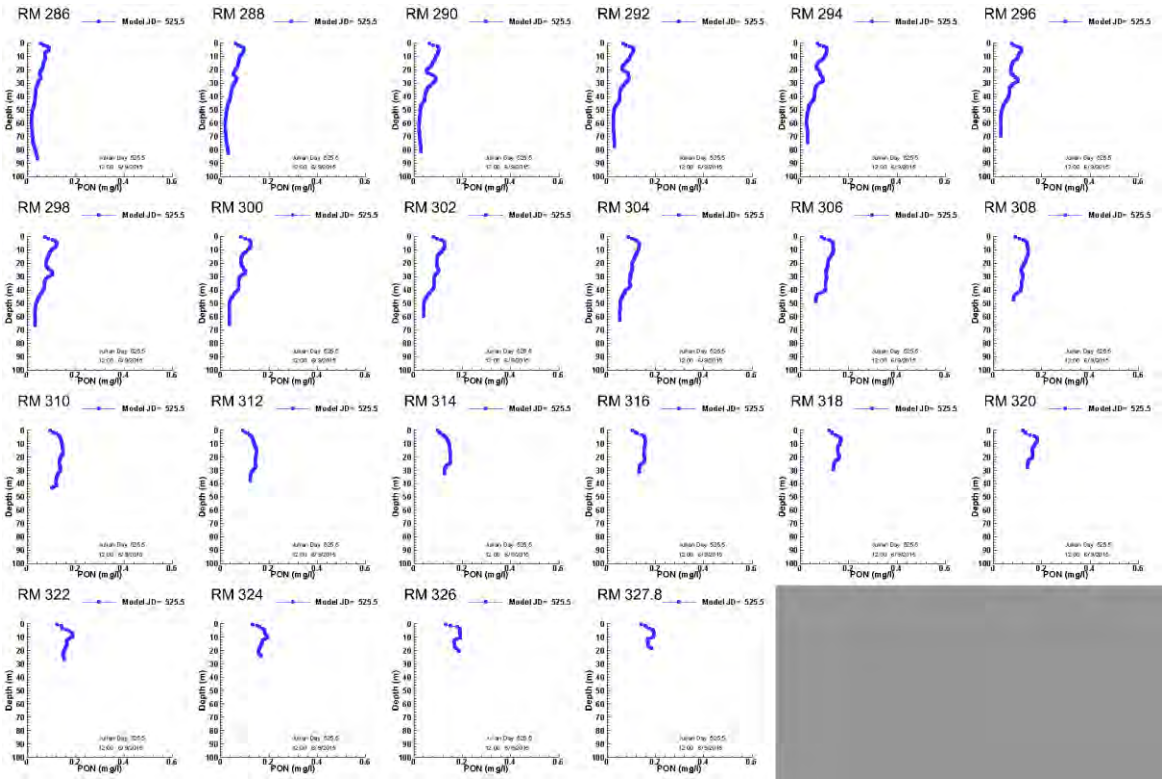


Figure 1675. Vertical profiles of PON compared with data for 6/ 9/2015.

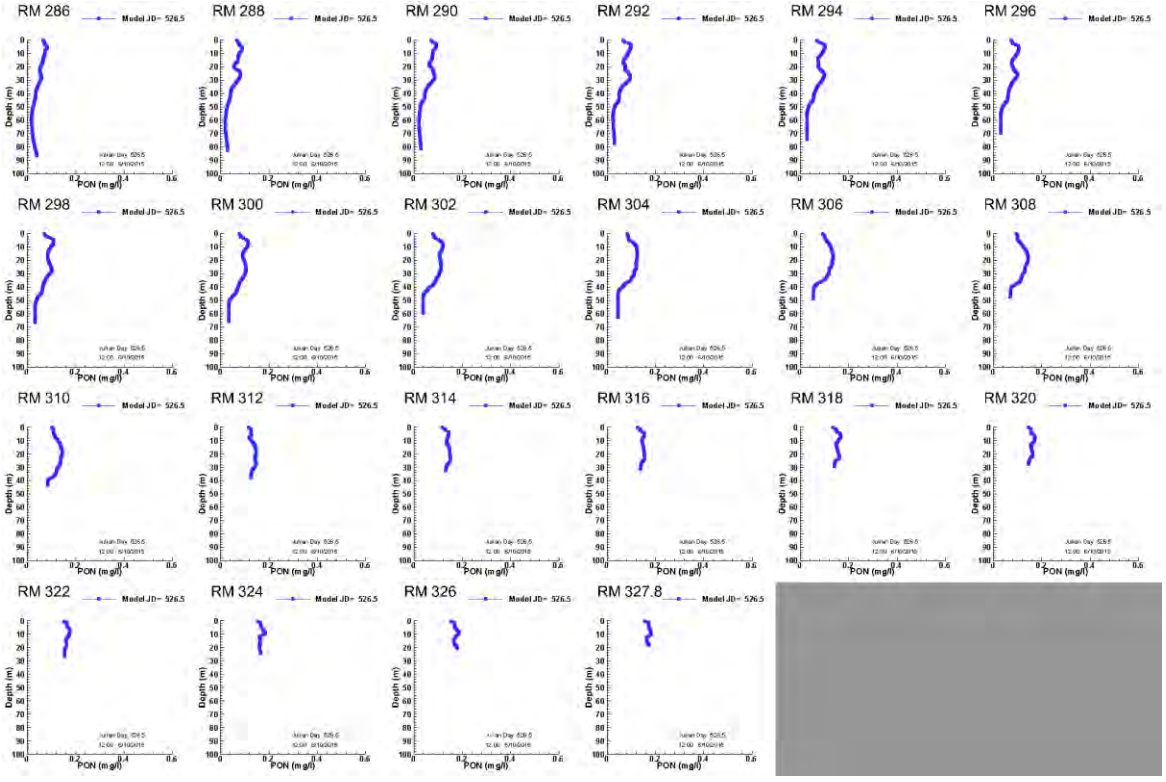


Figure 1676. Vertical profiles of PON compared with data for 6/10/2015.

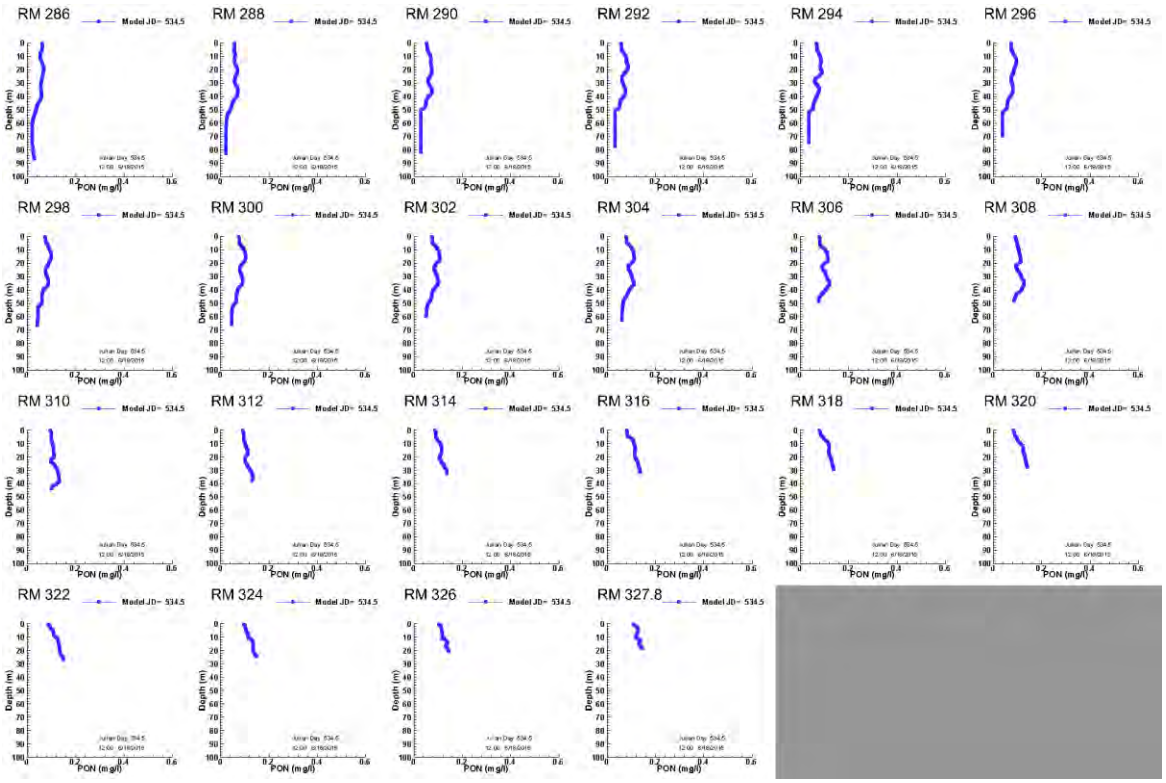


Figure 1677. Vertical profiles of PON compared with data for 6/18/2015.

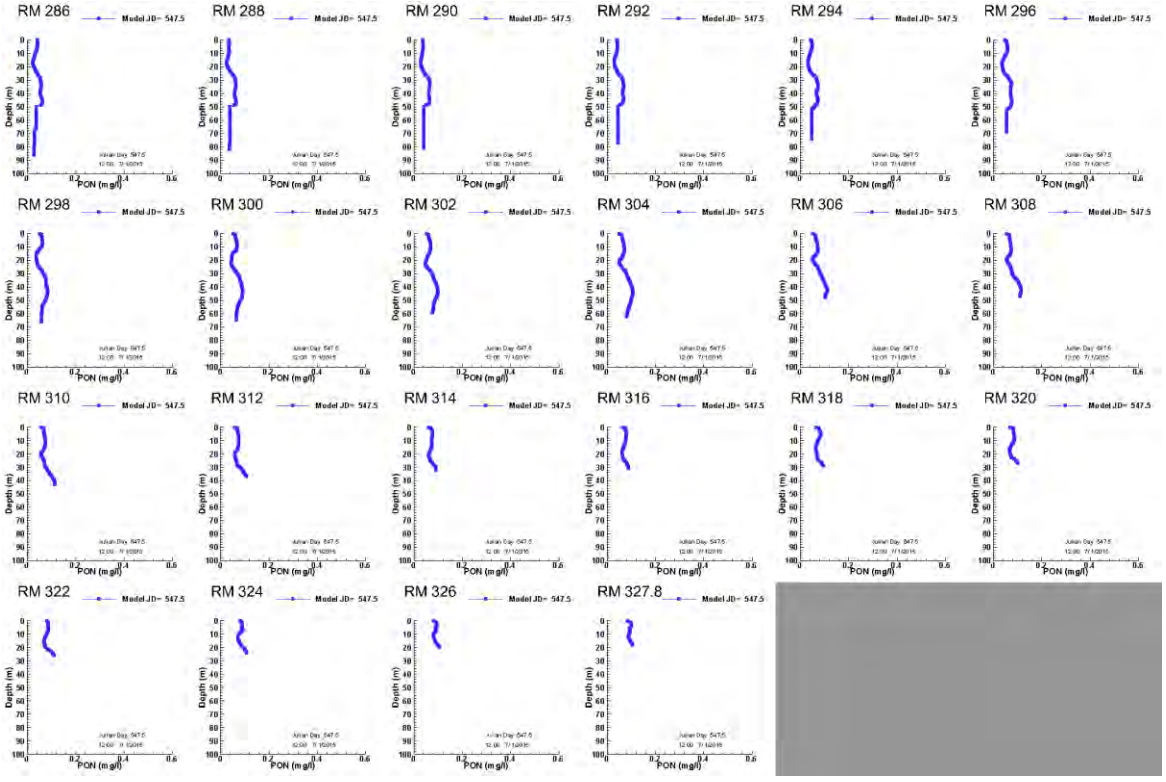


Figure 1678. Vertical profiles of PON compared with data for 7/ 1/2015.

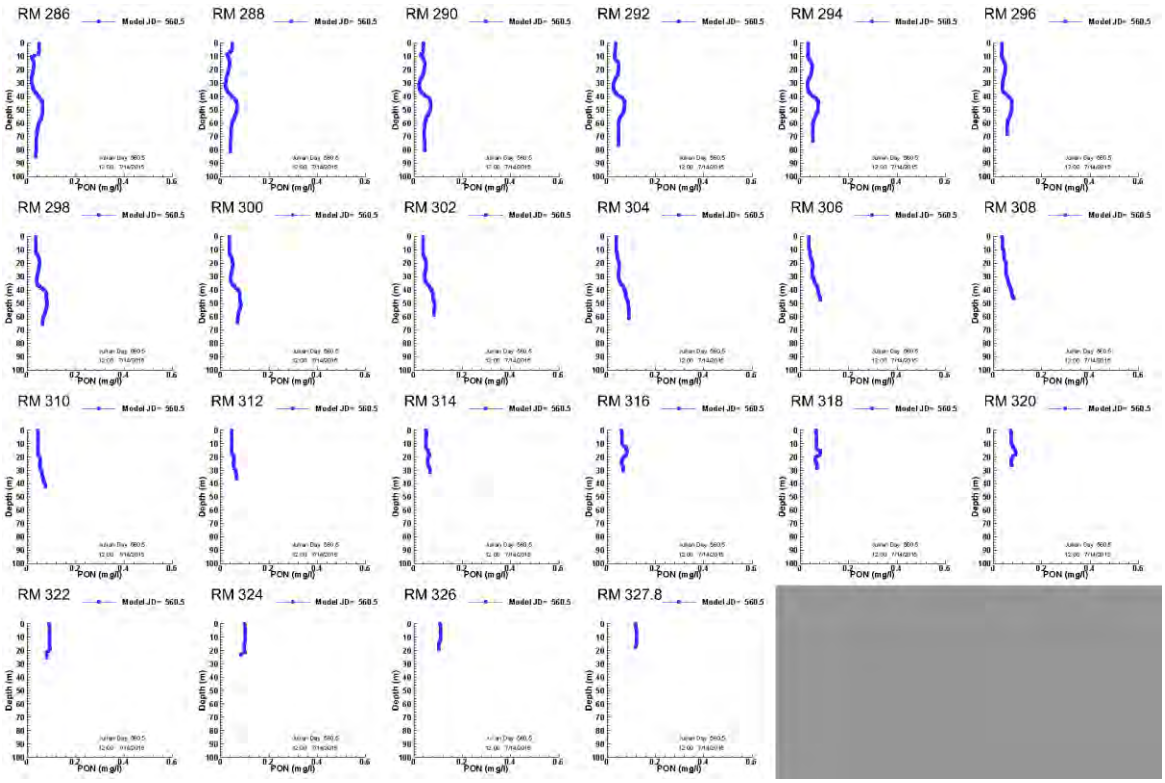


Figure 1679. Vertical profiles of PON compared with data for 7/14/2015.

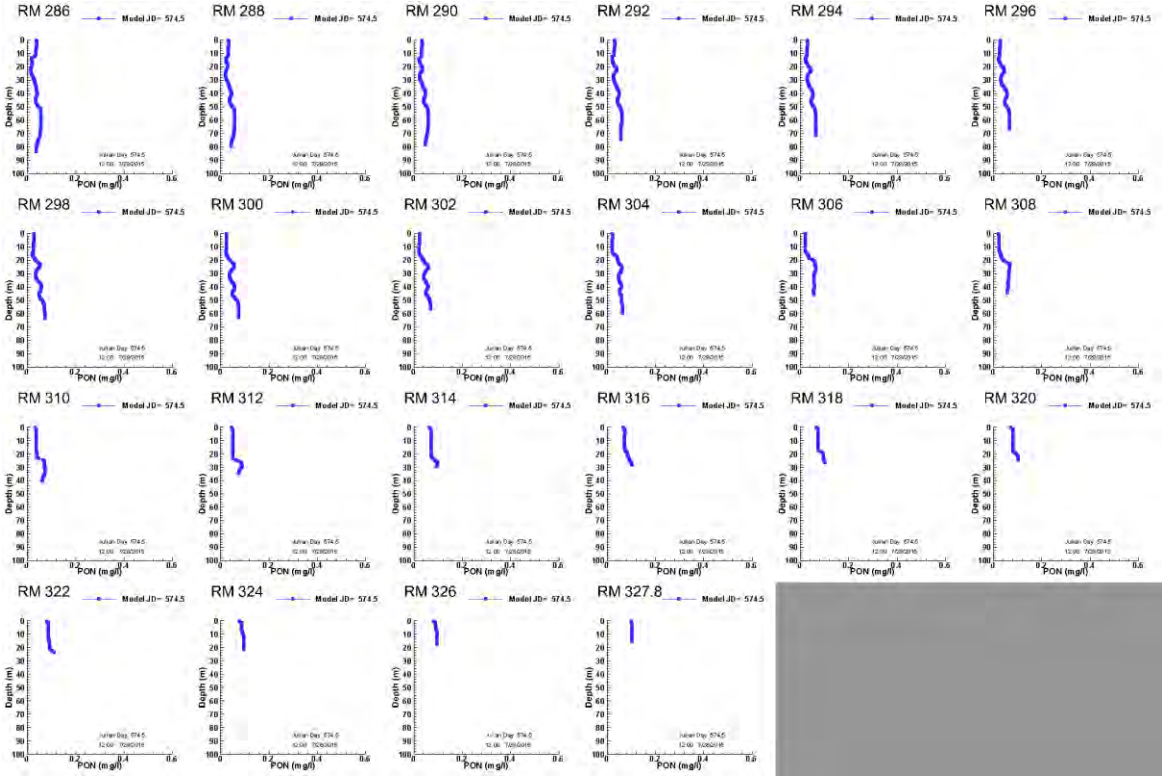


Figure 1680. Vertical profiles of PON compared with data for 7/28/2015.

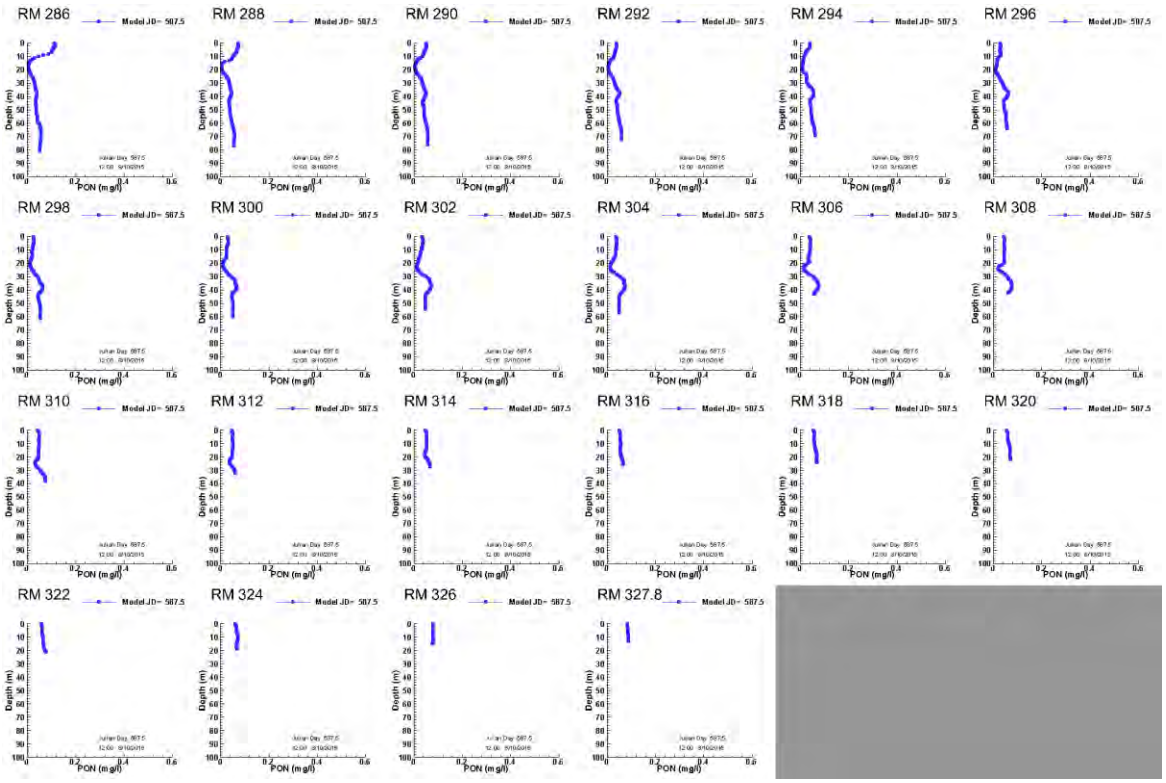


Figure 1681. Vertical profiles of PON compared with data for 8/10/2015.

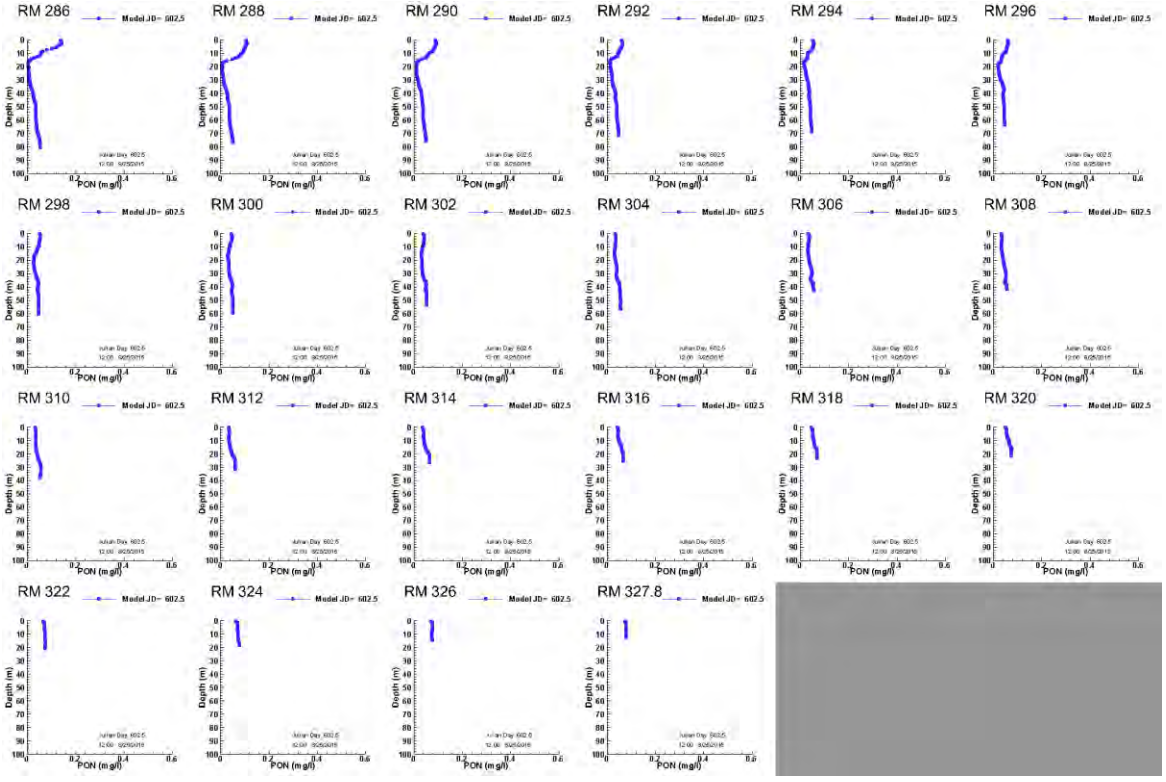


Figure 1682. Vertical profiles of PON compared with data for 8/25/2015.

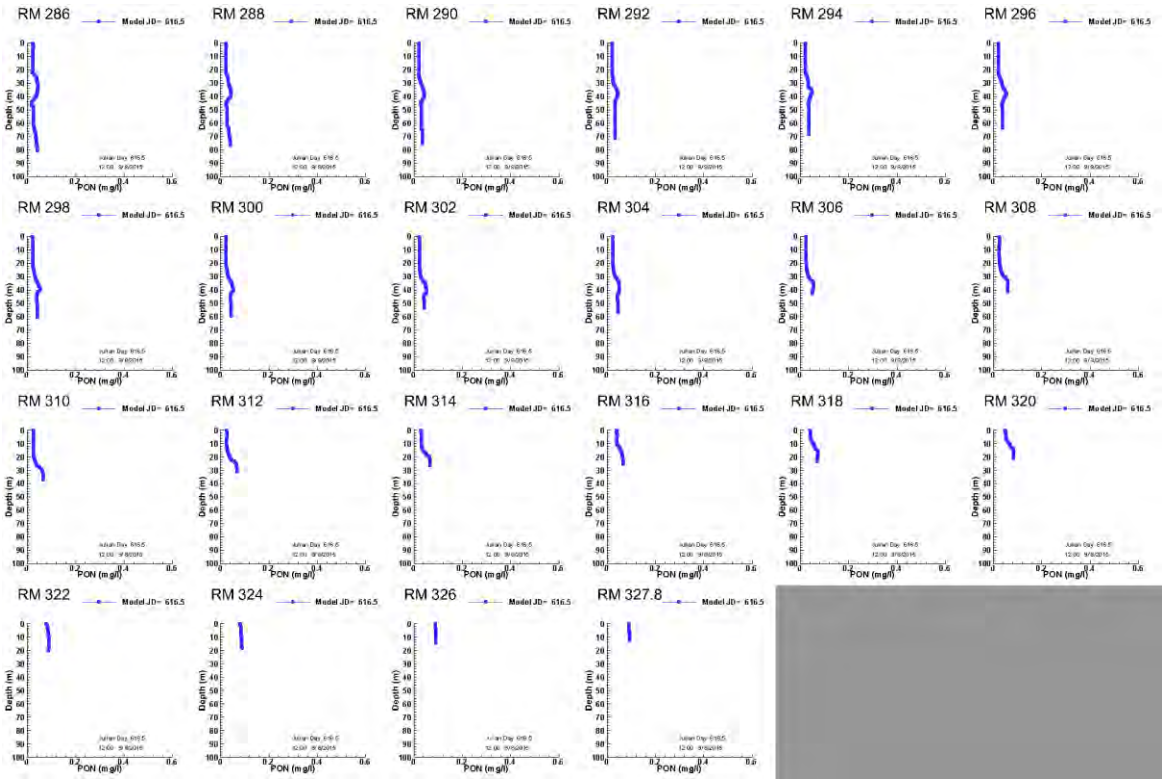


Figure 1683. Vertical profiles of PON compared with data for 9/ 8/2015.

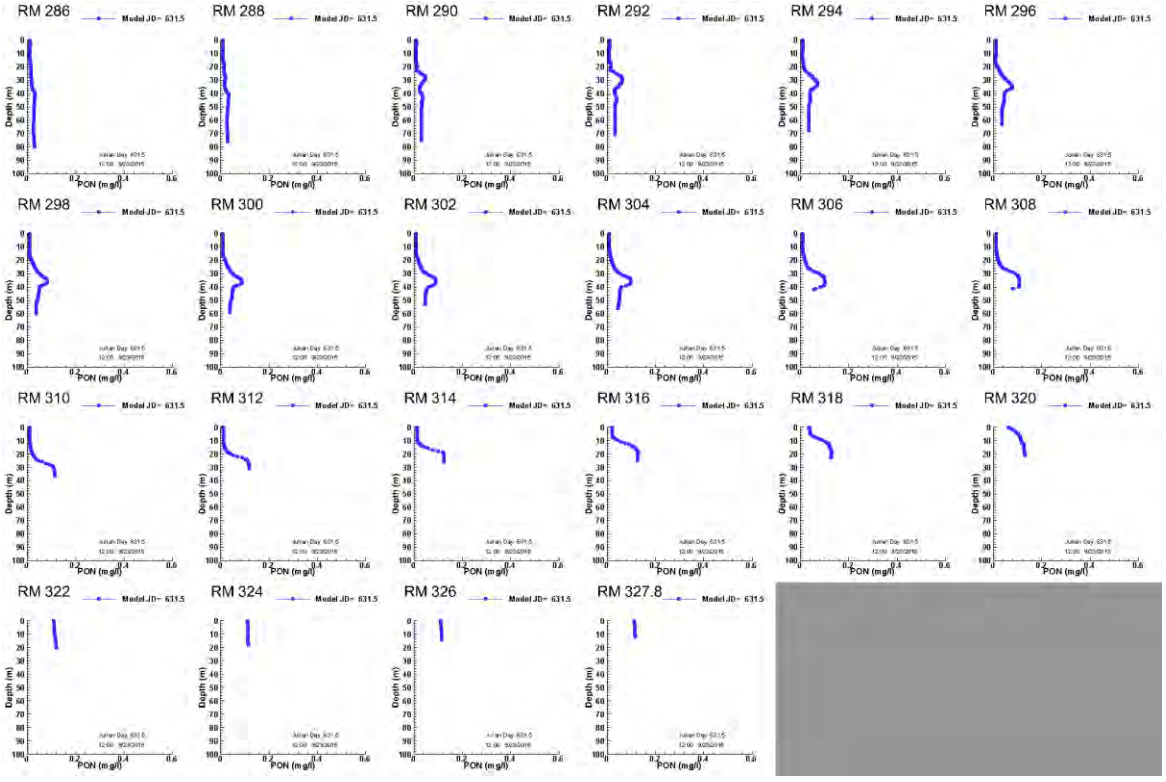


Figure 1684. Vertical profiles of PON compared with data for 9/23/2015.

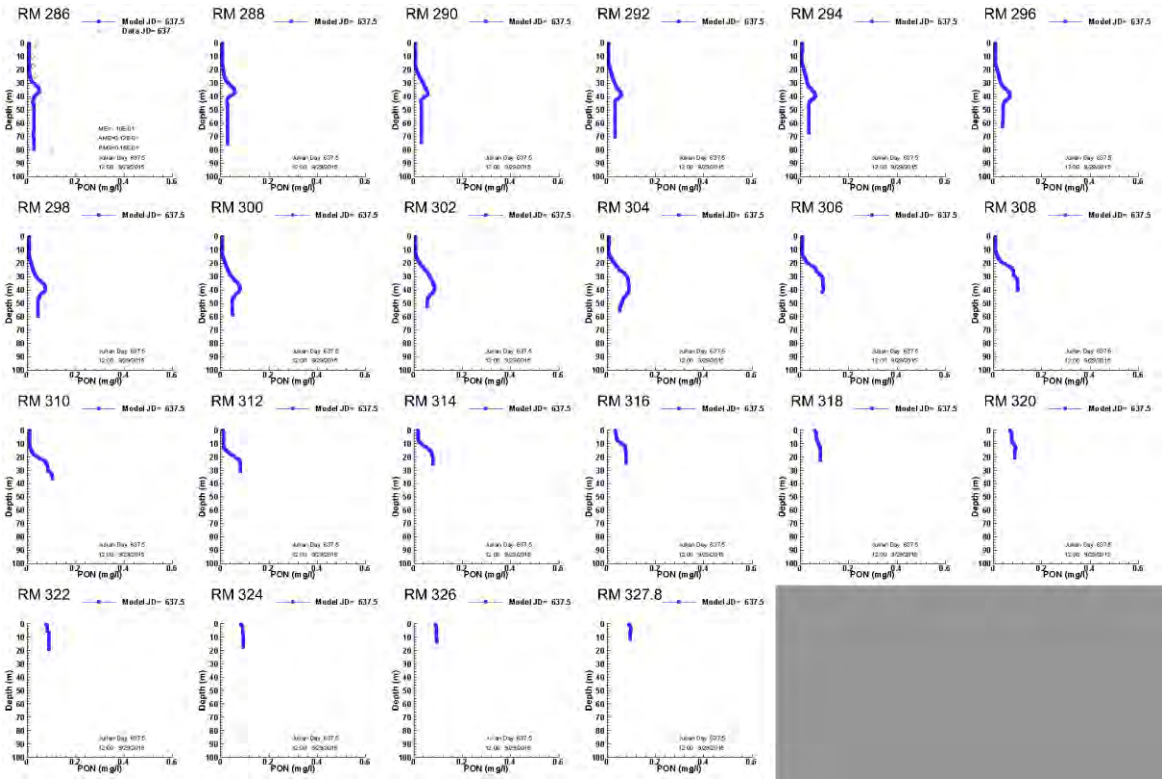


Figure 1685. Vertical profiles of PON compared with data for 9/29/2015.

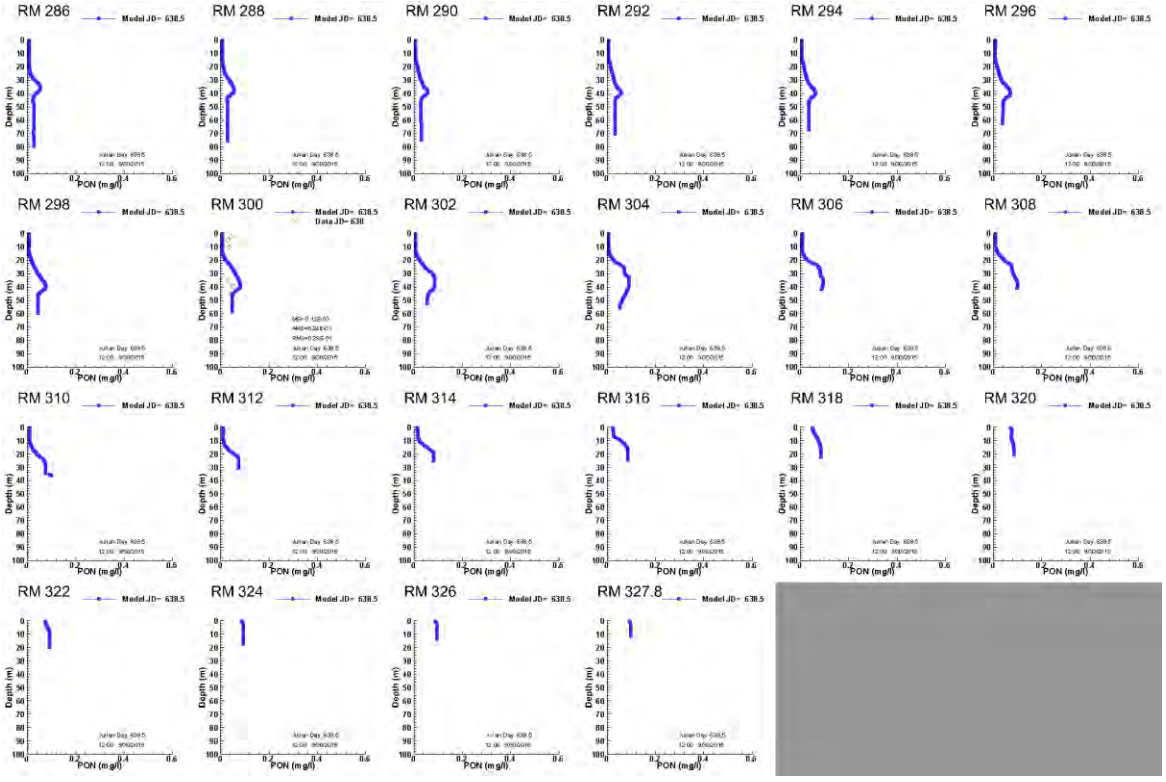


Figure 1686. Vertical profiles of PON compared with data for 9/30/2015.

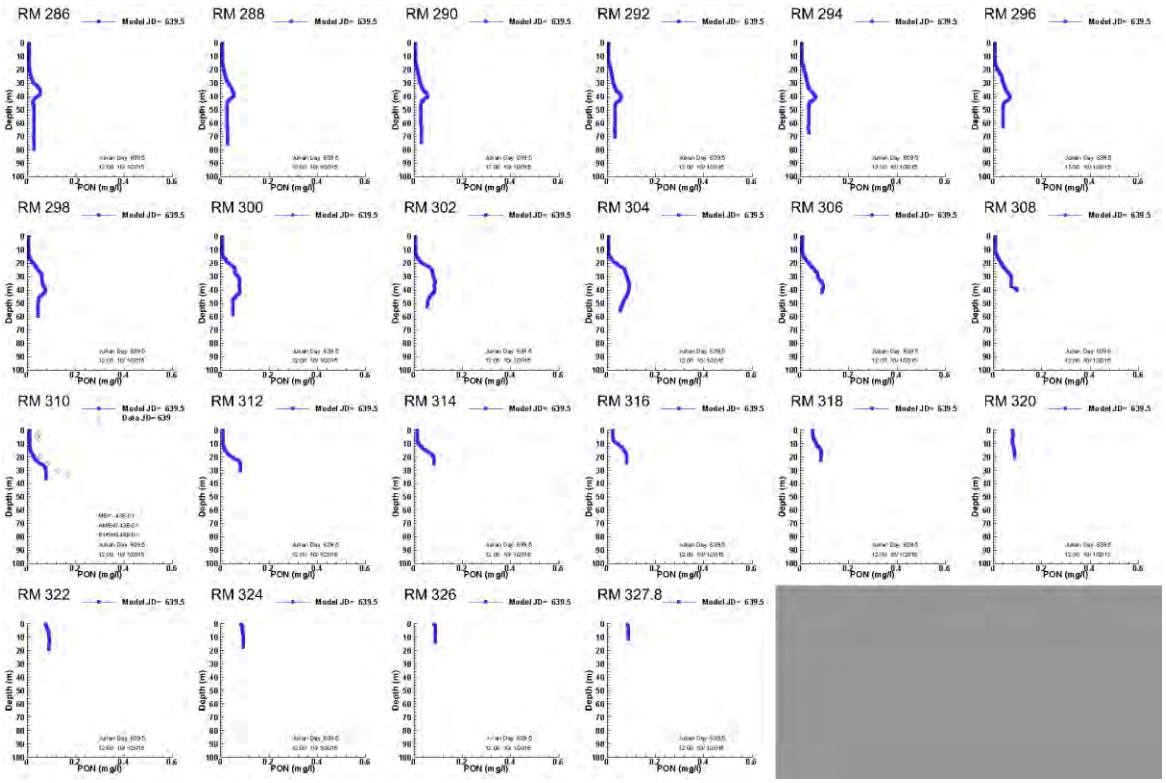


Figure 1687. Vertical profiles of PON compared with data for 10/ 1/2015.

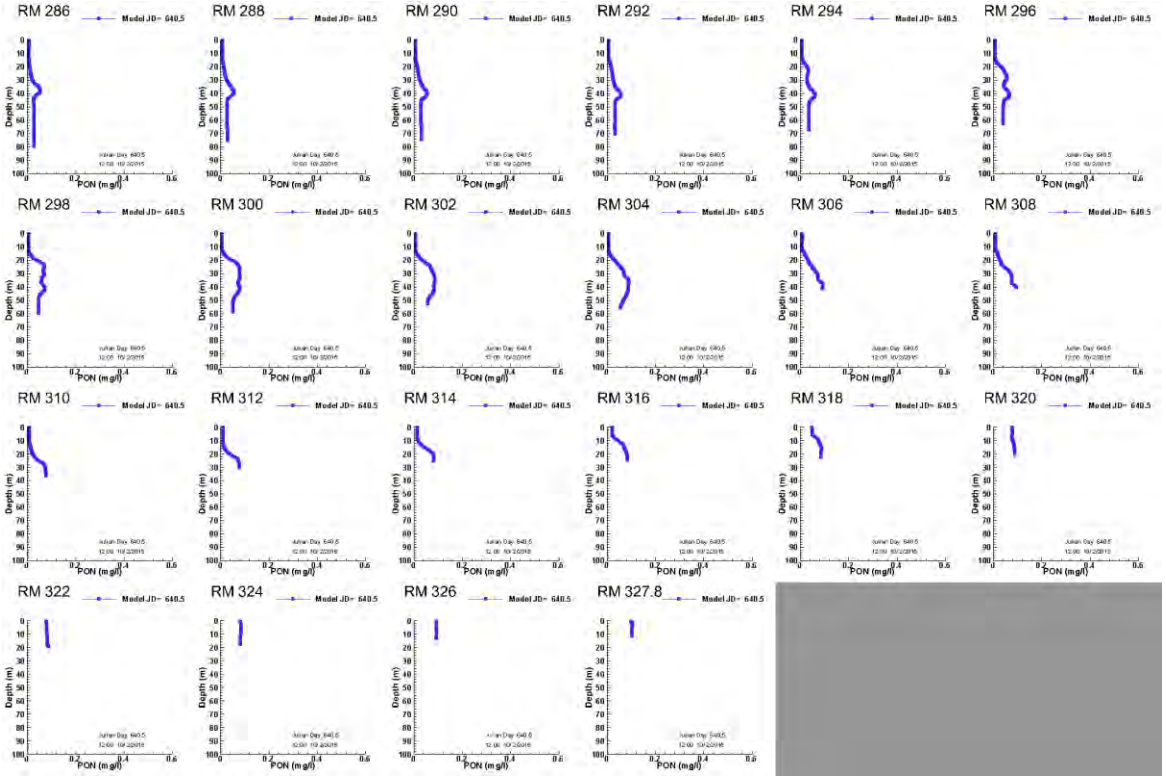


Figure 1688. Vertical profiles of PON compared with data for 10/ 2/2015.

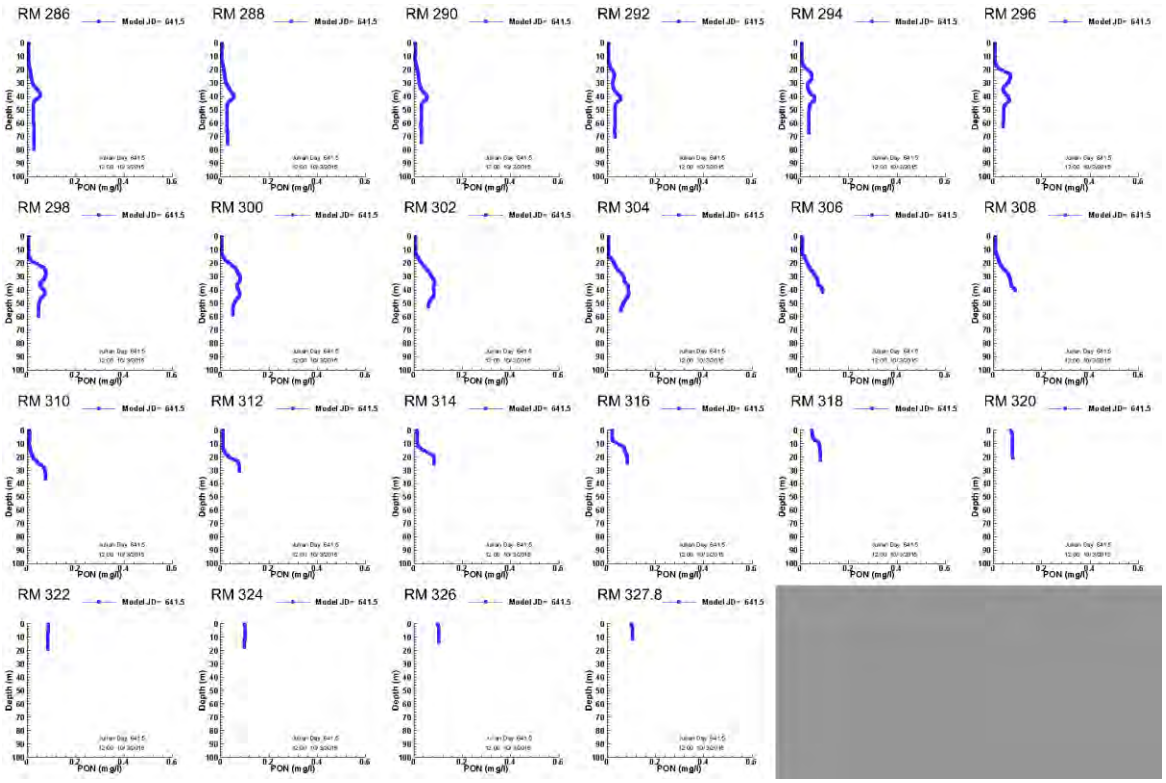


Figure 1689. Vertical profiles of PON compared with data for 10/ 3/2015.

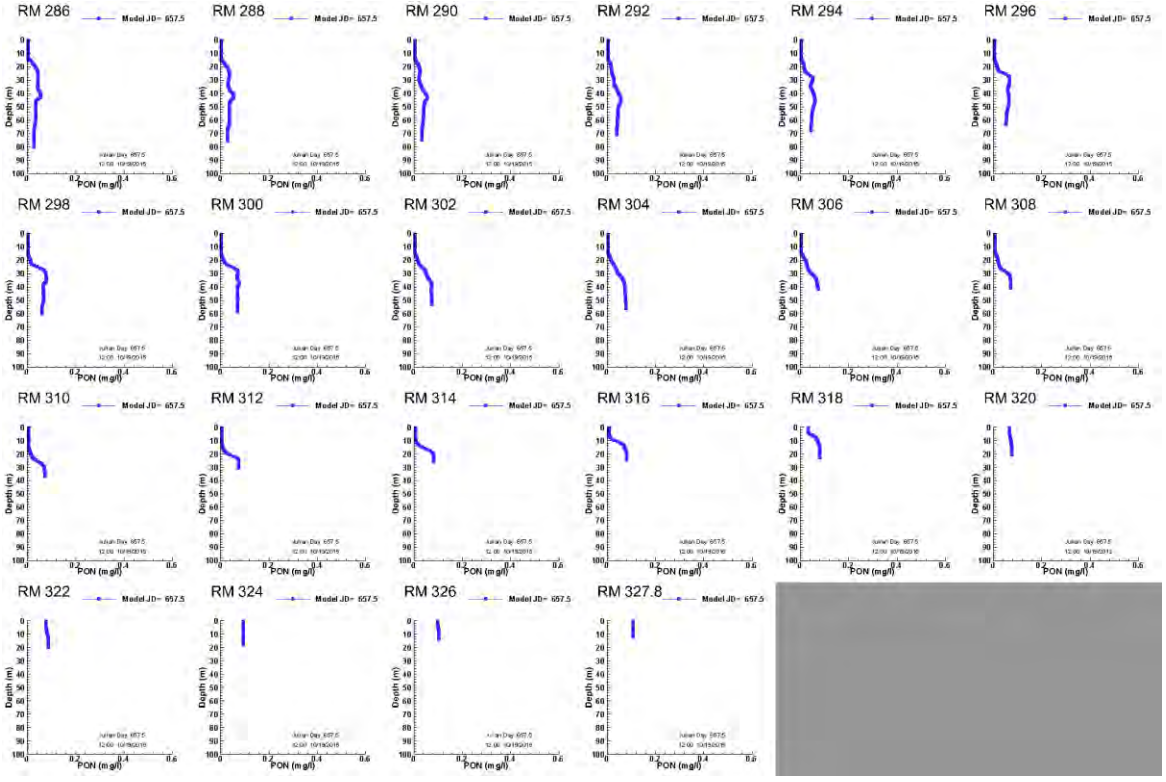


Figure 1690. Vertical profiles of PON compared with data for 10/19/2015.

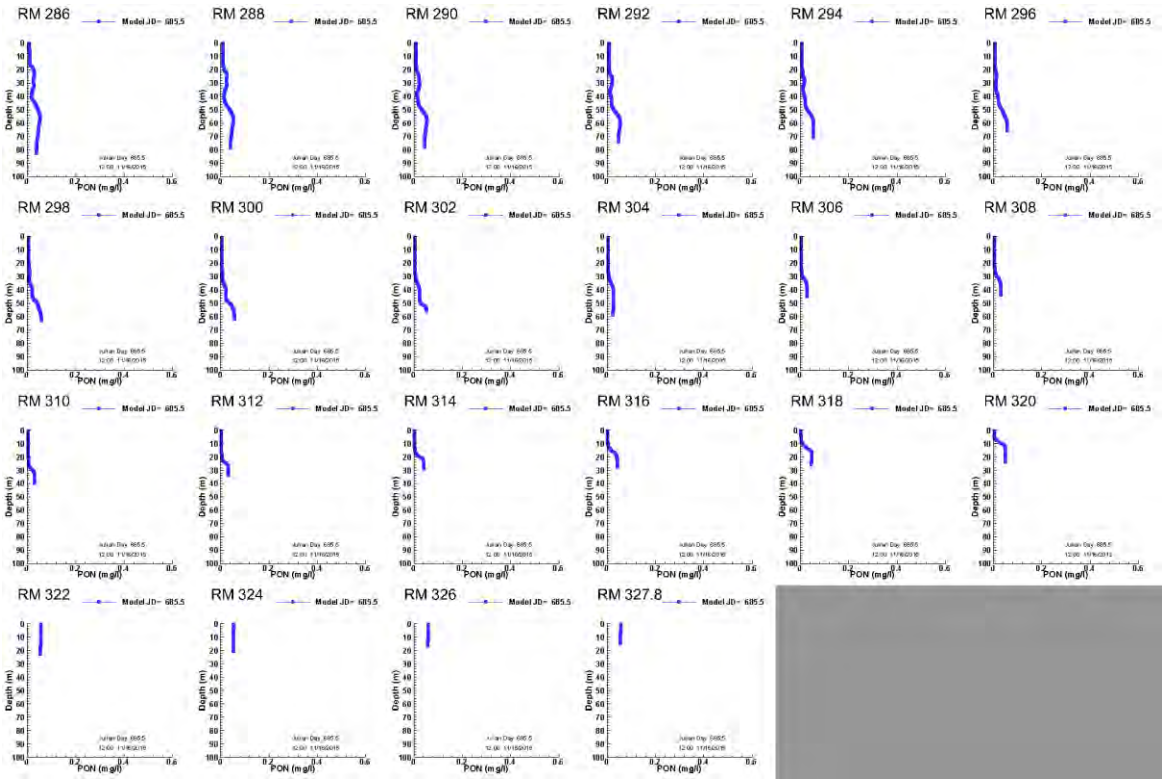


Figure 1691. Vertical profiles of PON compared with data for 11/16/2015.

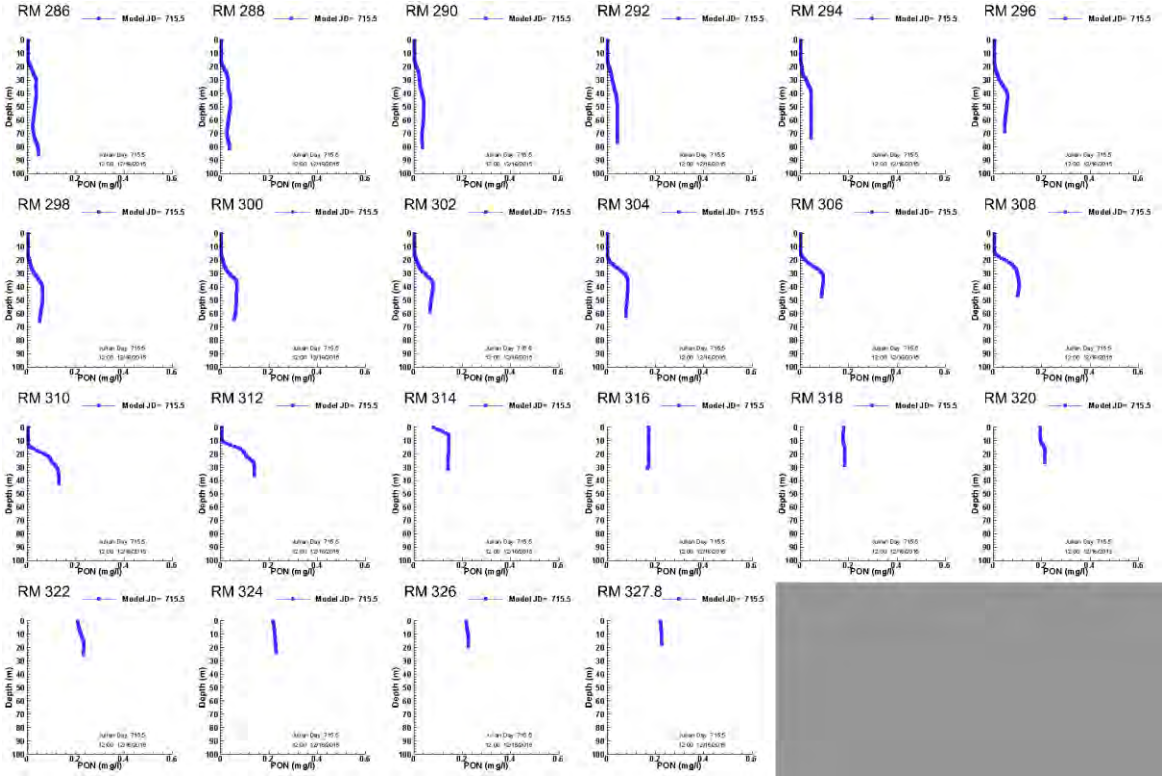


Figure 1692. Vertical profiles of PON compared with data for 12/16/2015.

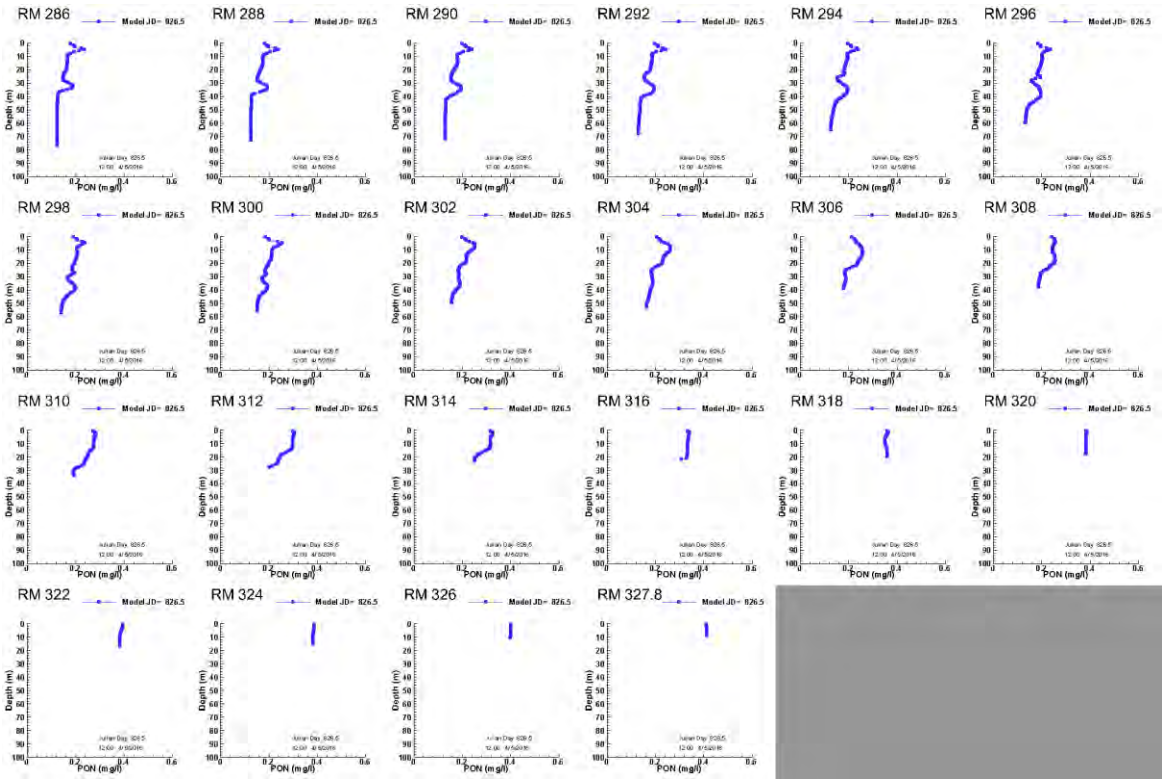


Figure 1693. Vertical profiles of PON compared with data for 4/ 5/2016.

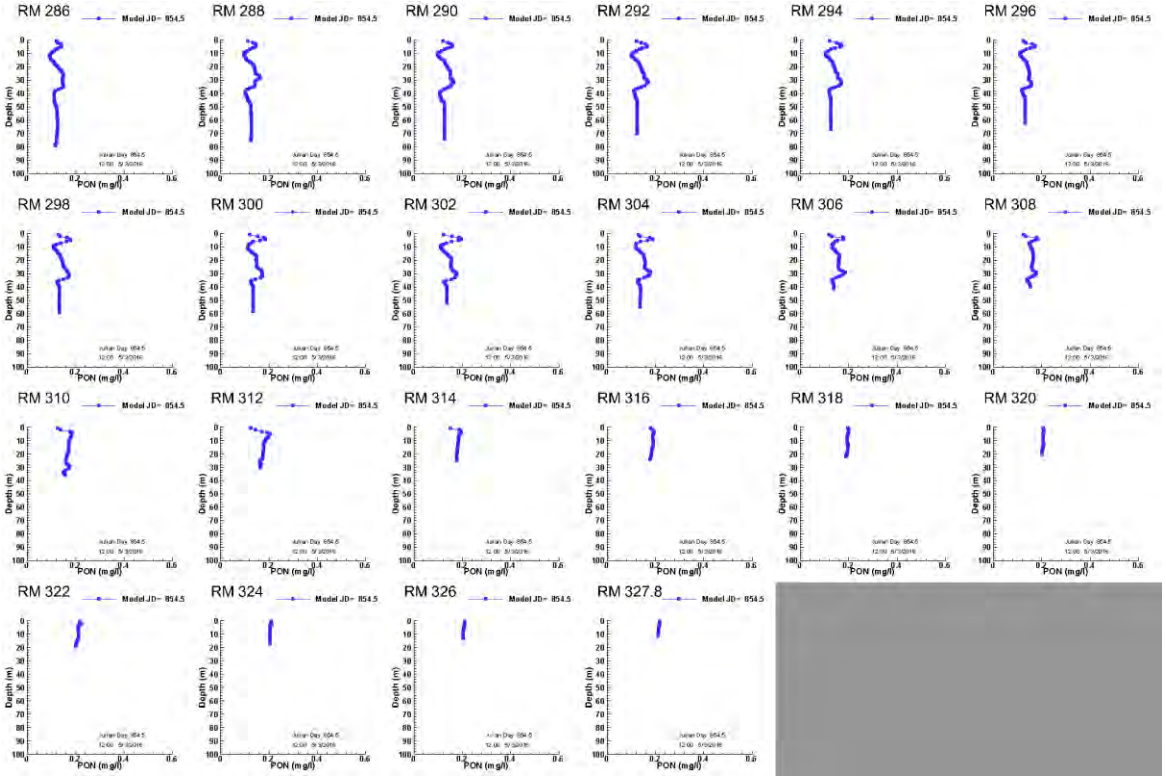


Figure 1694. Vertical profiles of PON compared with data for 5/ 3/2016.

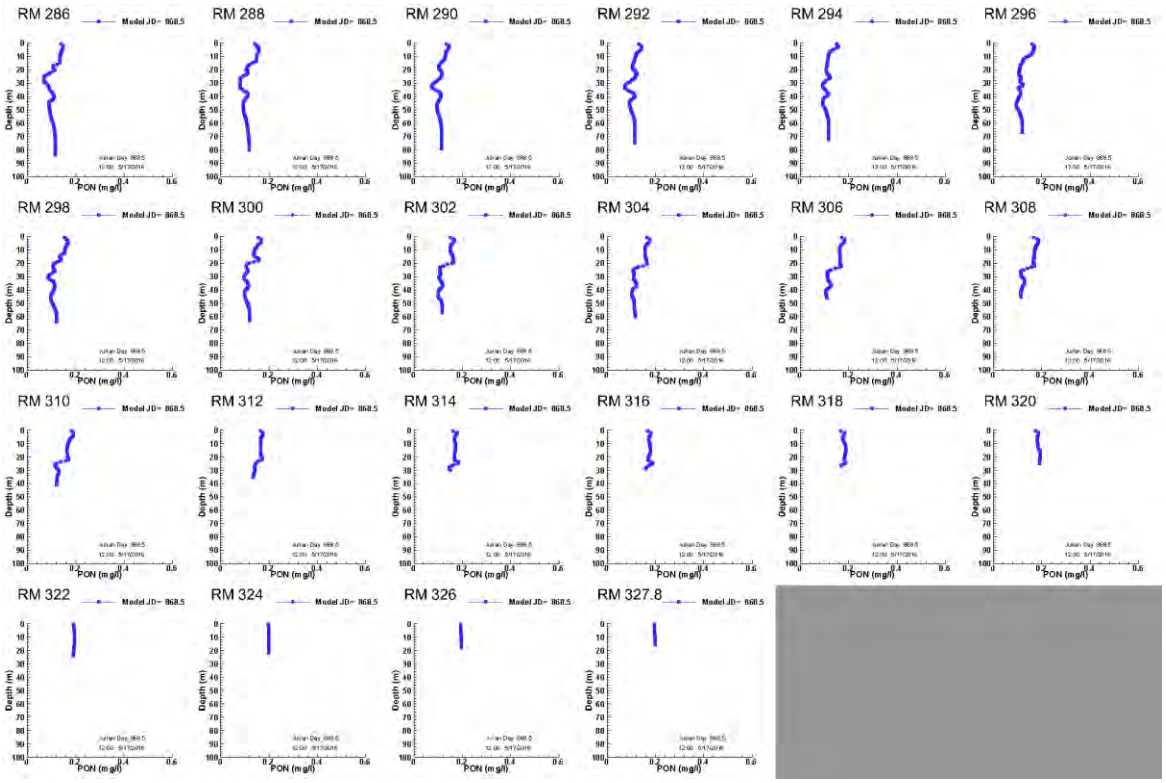


Figure 1695. Vertical profiles of PON compared with data for 5/17/2016.

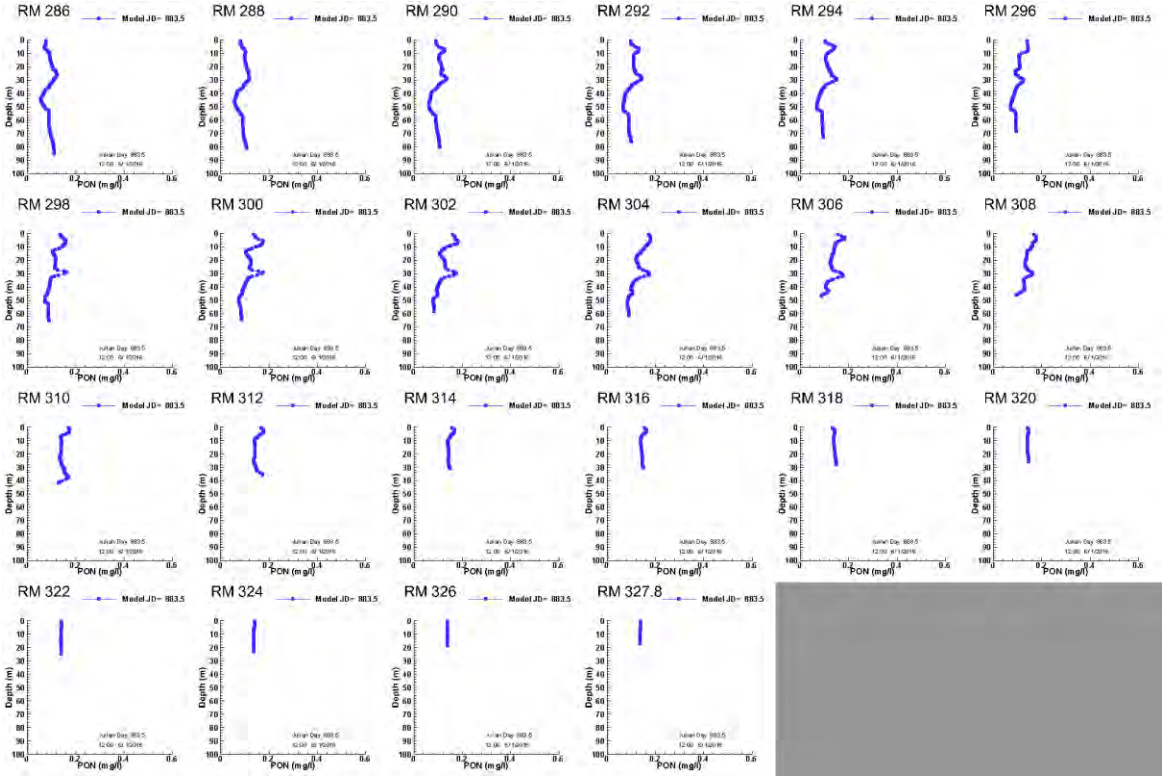


Figure 1696. Vertical profiles of PON compared with data for 6/ 1/2016.

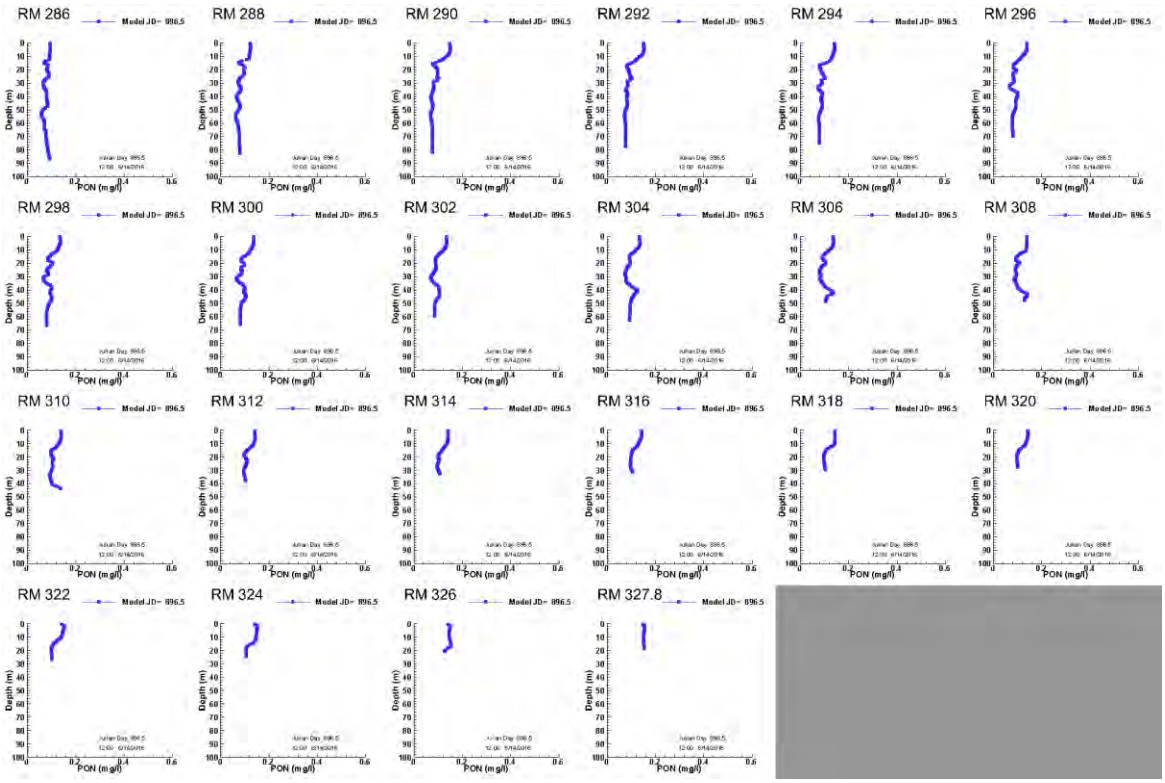


Figure 1697. Vertical profiles of PON compared with data for 6/14/2016.

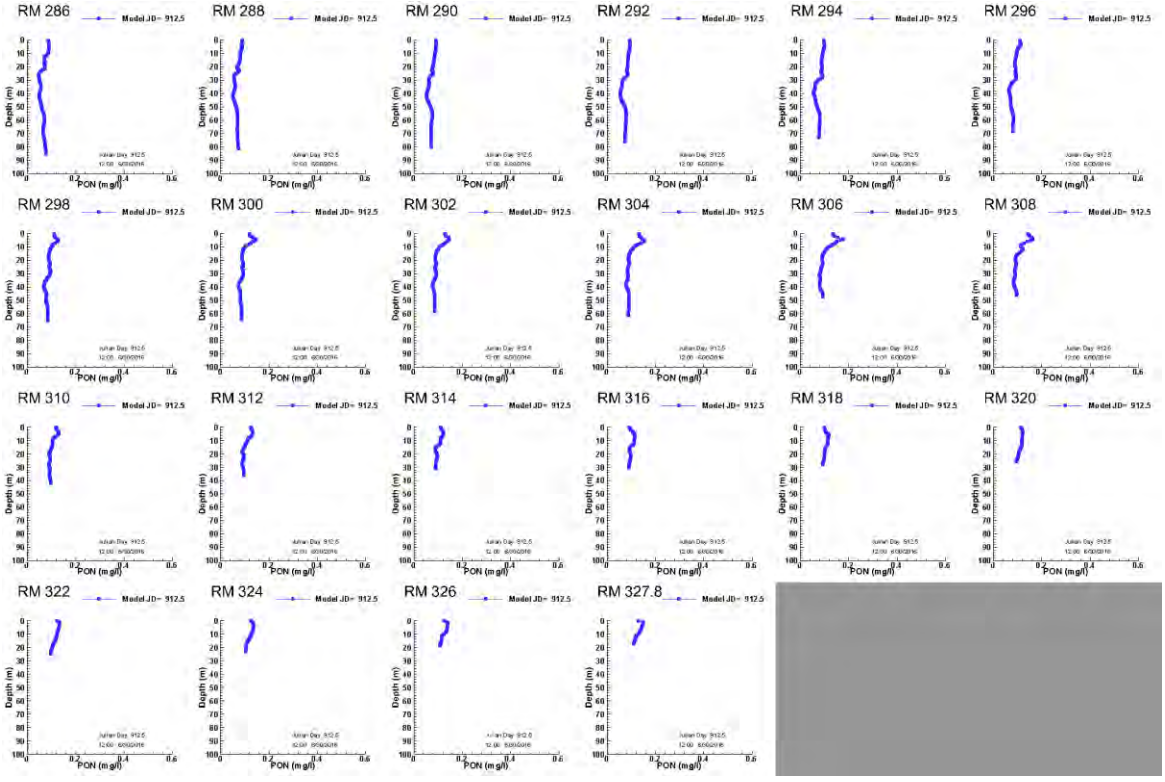


Figure 1698. Vertical profiles of PON compared with data for 6/30/2016.

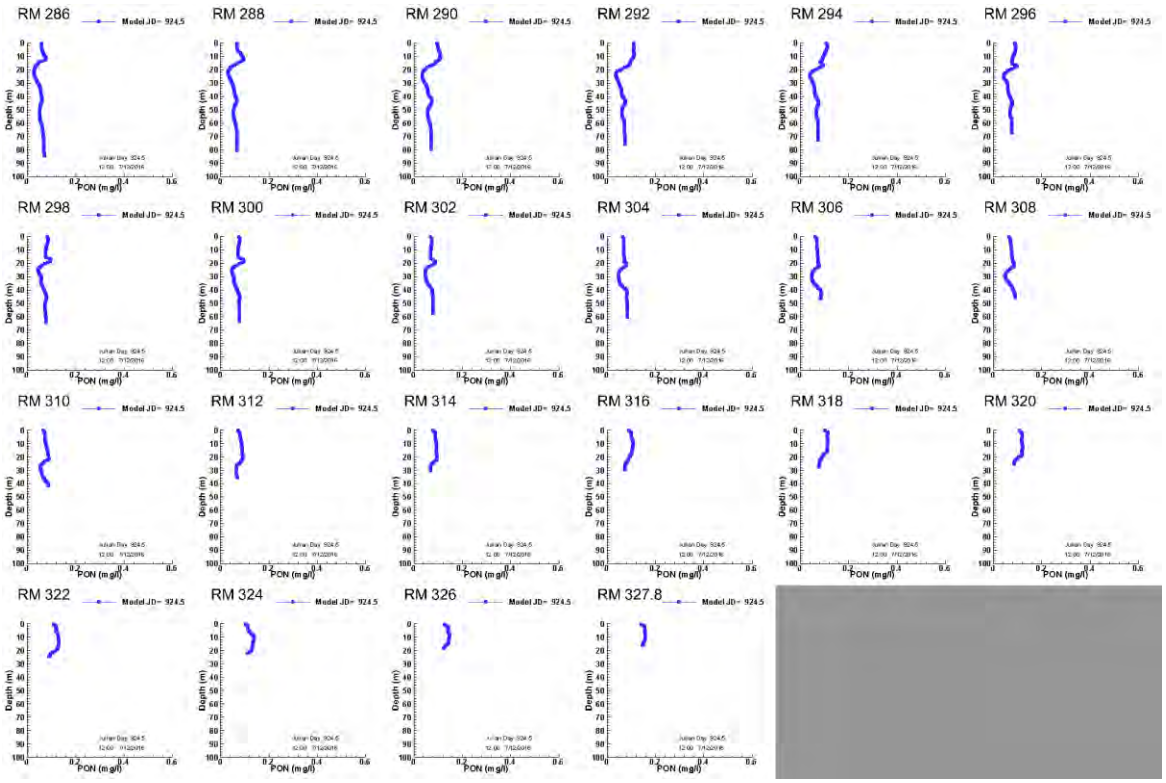


Figure 1699. Vertical profiles of PON compared with data for 7/12/2016.

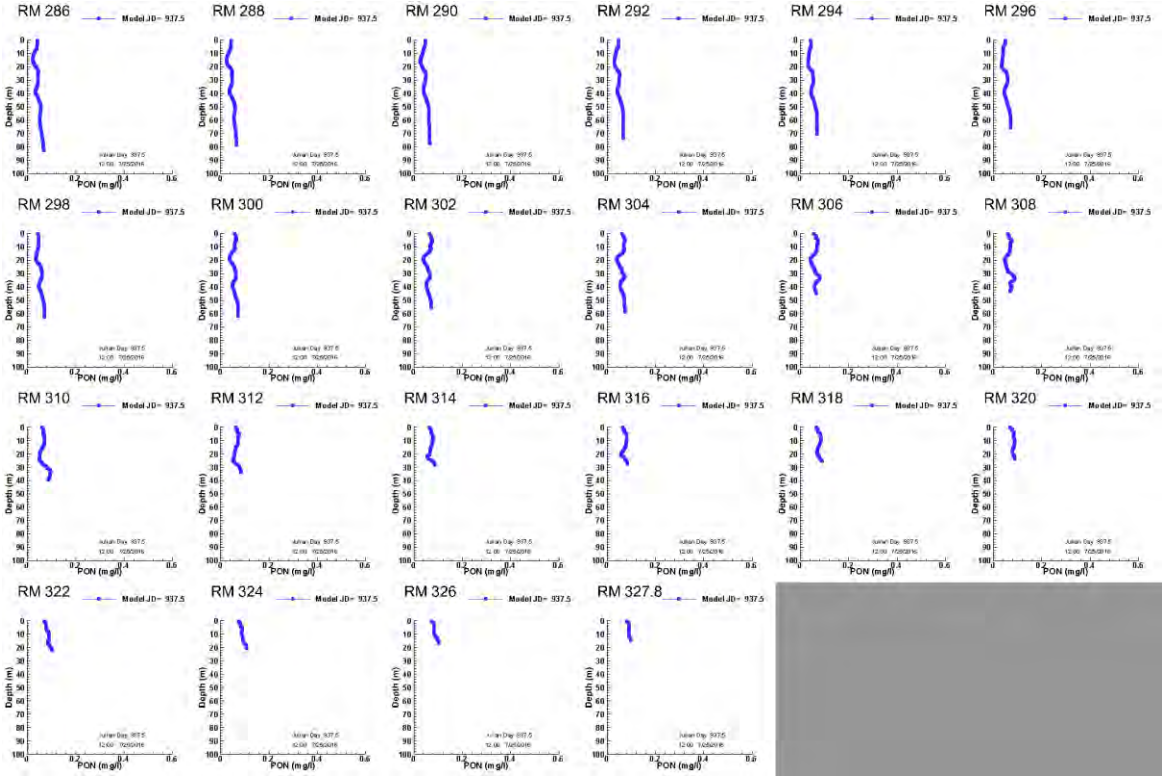


Figure 1700. Vertical profiles of PON compared with data for 7/25/2016.

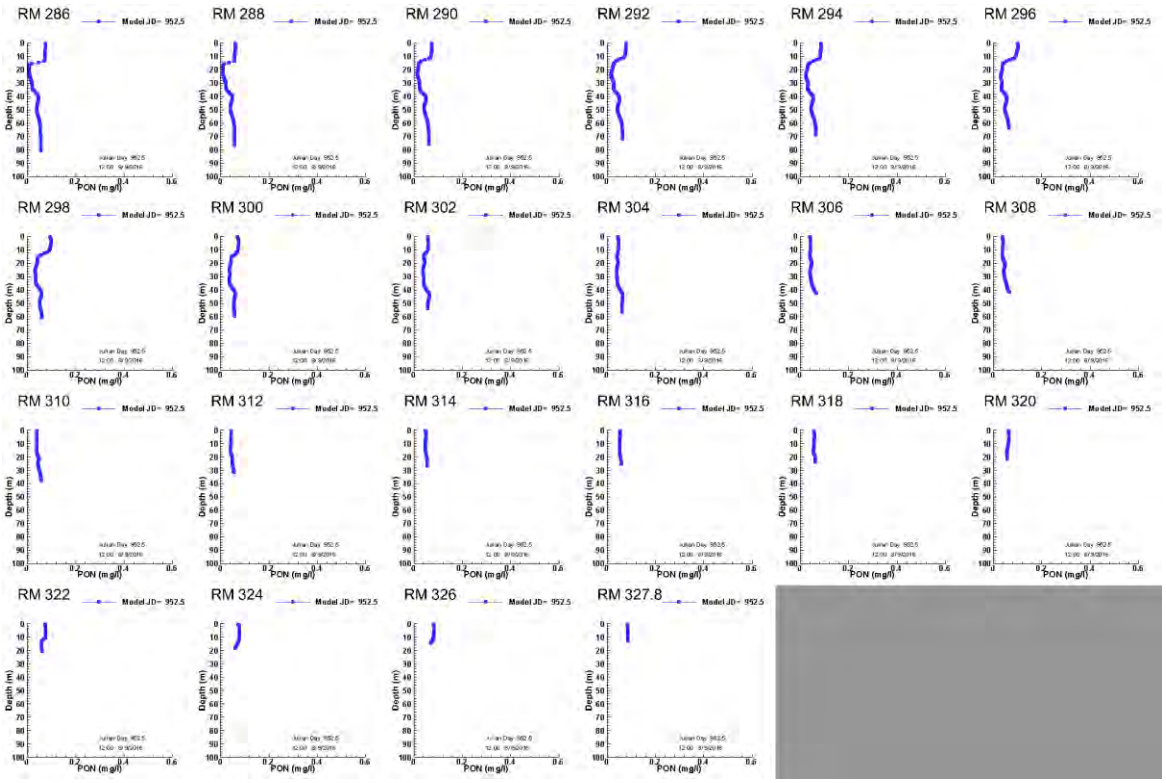


Figure 1701. Vertical profiles of PON compared with data for 8/ 9/2016.

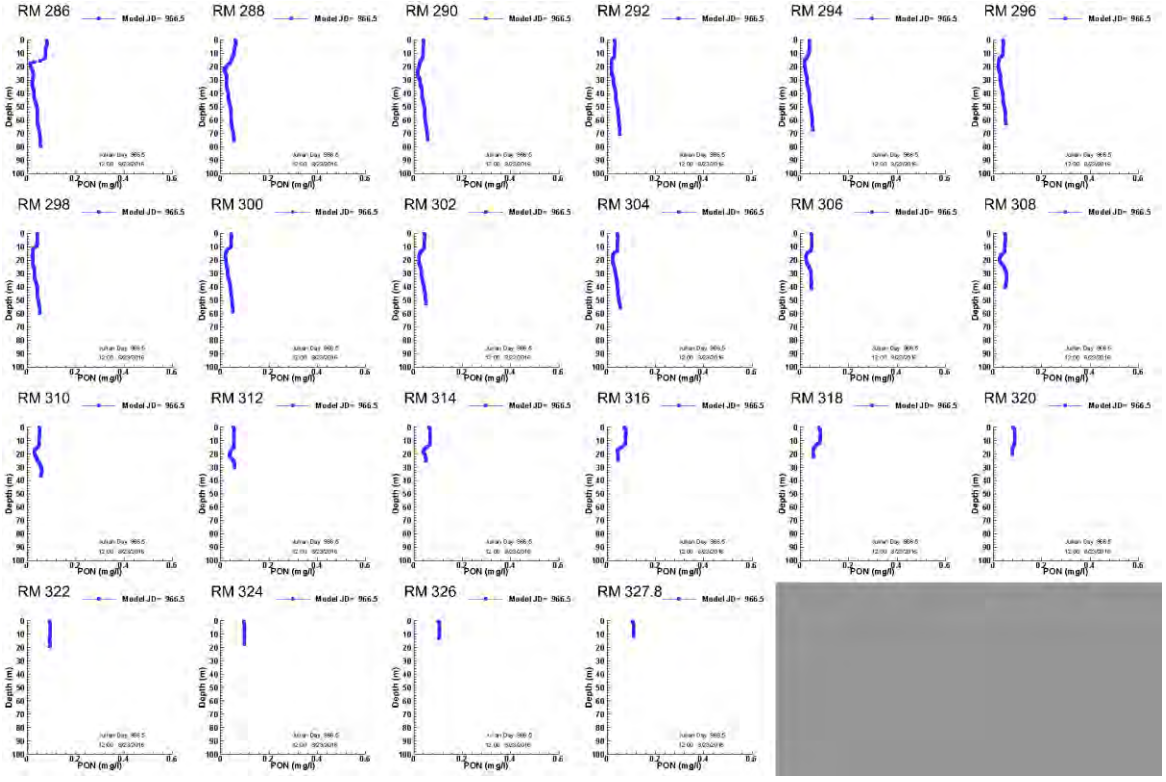


Figure 1702. Vertical profiles of PON compared with data for 8/23/2016.

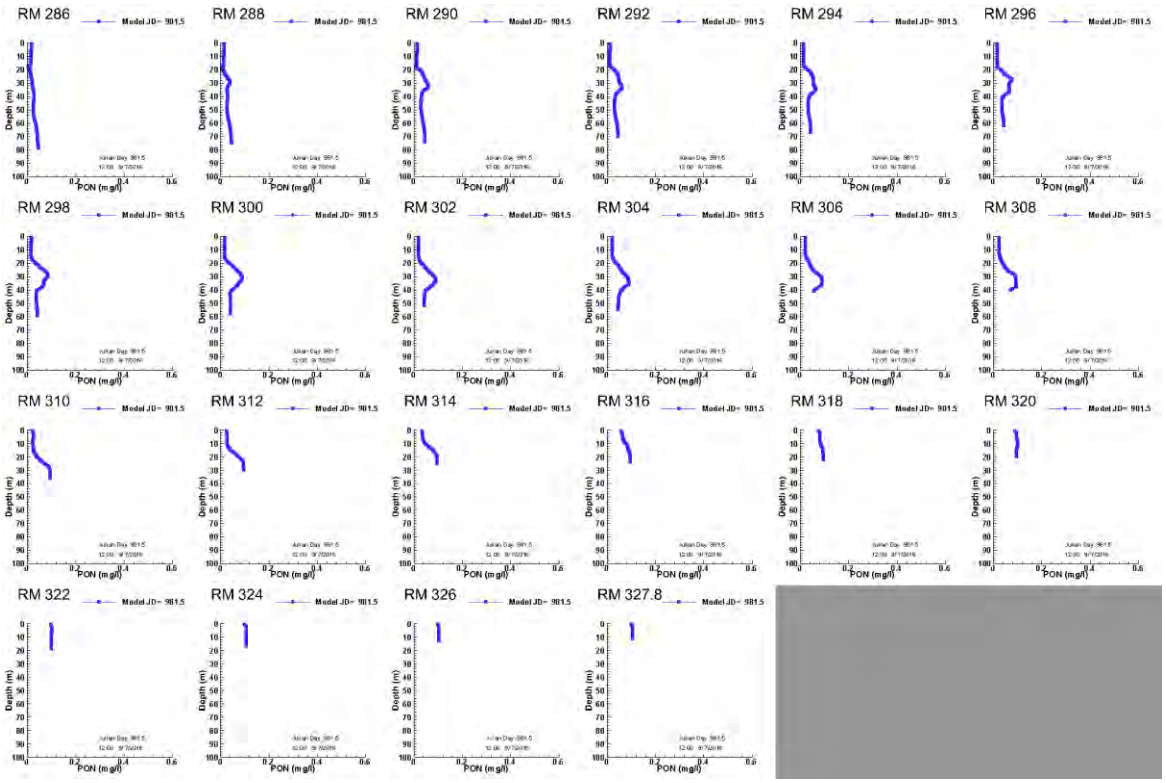


Figure 1703. Vertical profiles of PON compared with data for 9/ 7/2016.

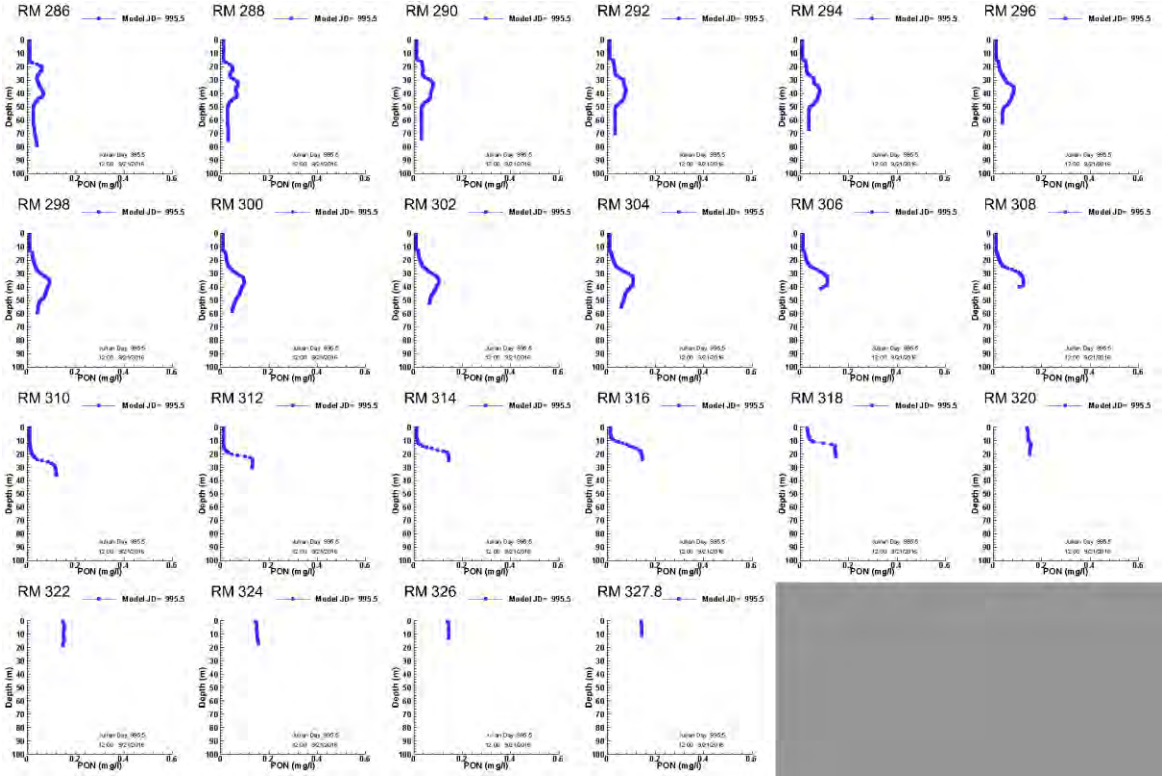


Figure 1704. Vertical profiles of PON compared with data for 9/21/2016.

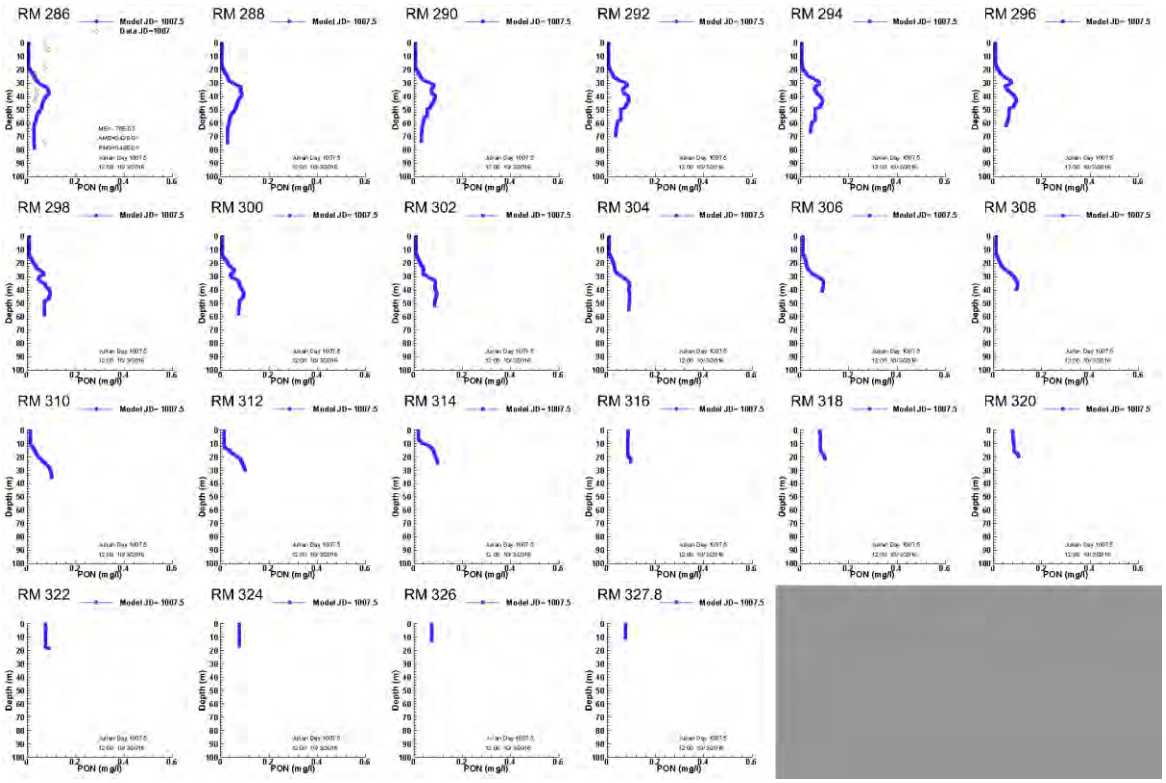


Figure 1705. Vertical profiles of PON compared with data for 10/ 3/2016.

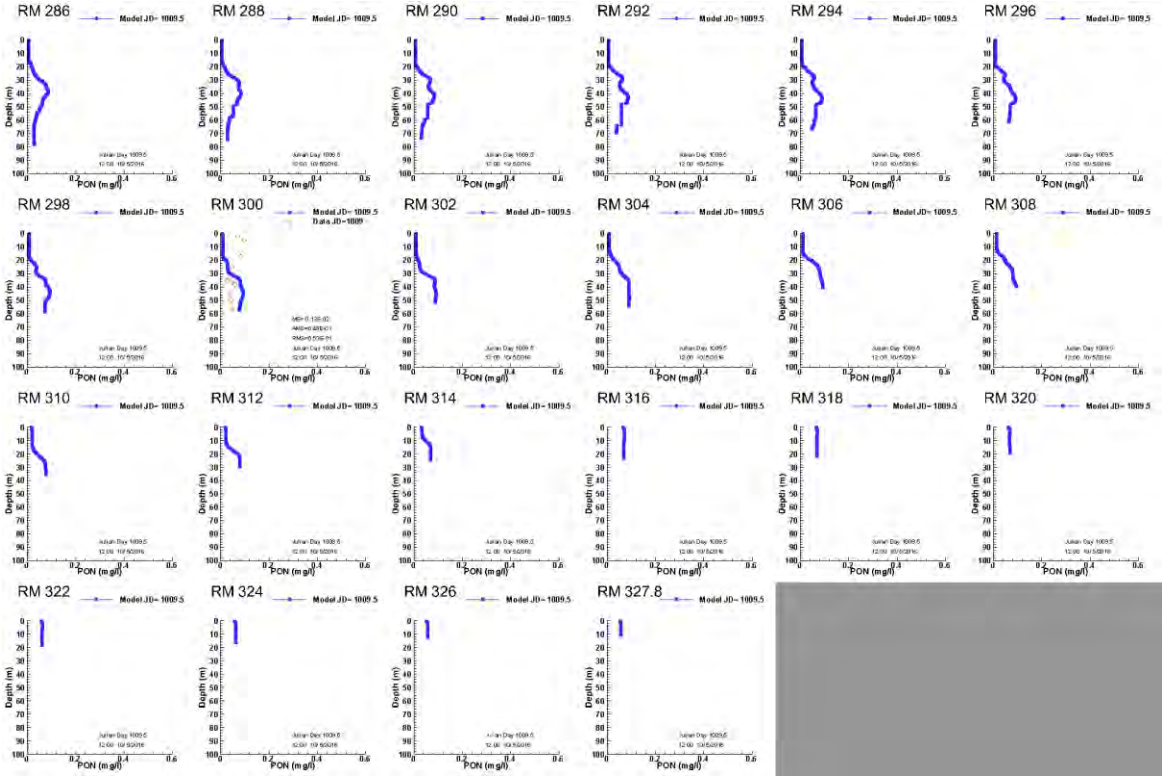


Figure 1706. Vertical profiles of PON compared with data for 10/ 5/2016.

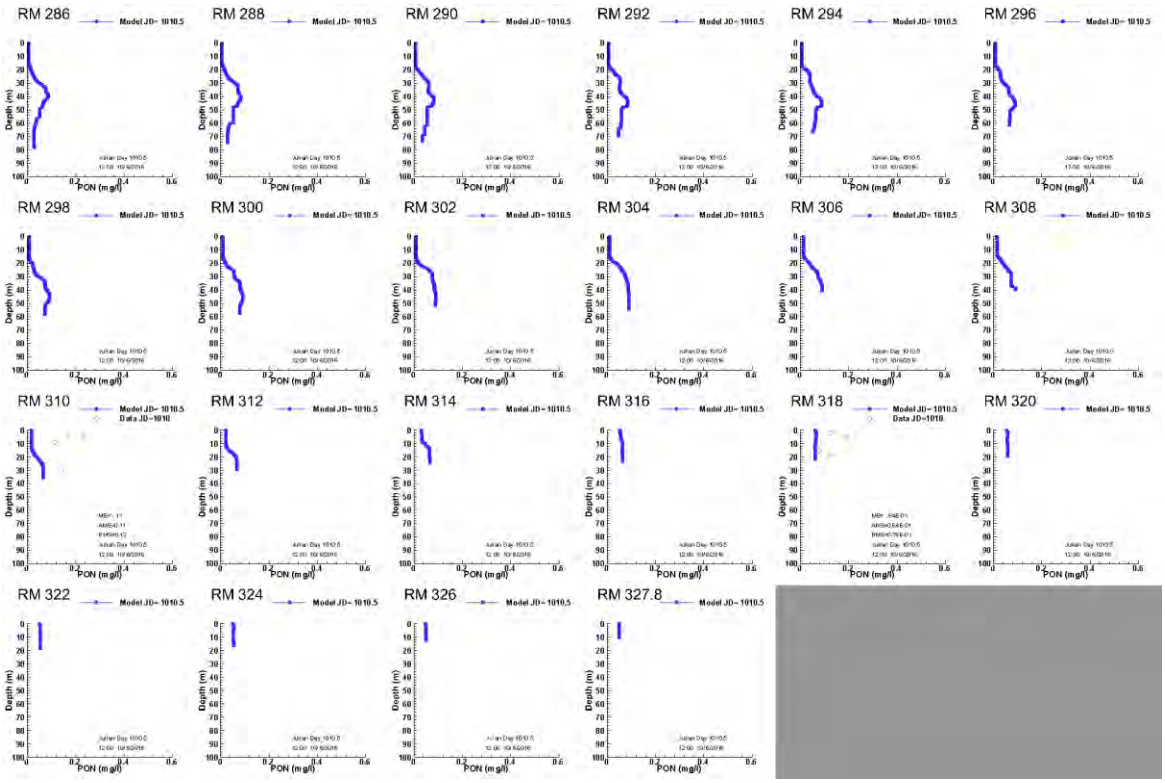


Figure 1707. Vertical profiles of PON compared with data for 10/ 6/2016.

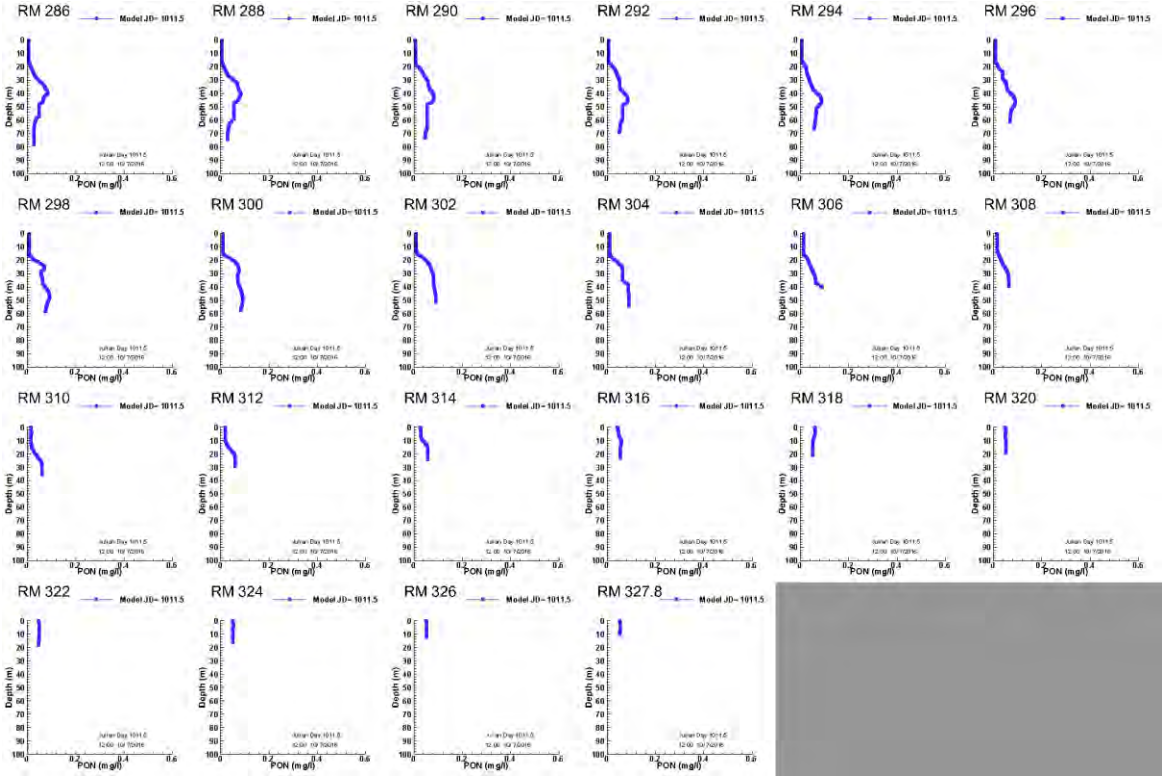


Figure 1708. Vertical profiles of PON compared with data for 10/ 7/2016.

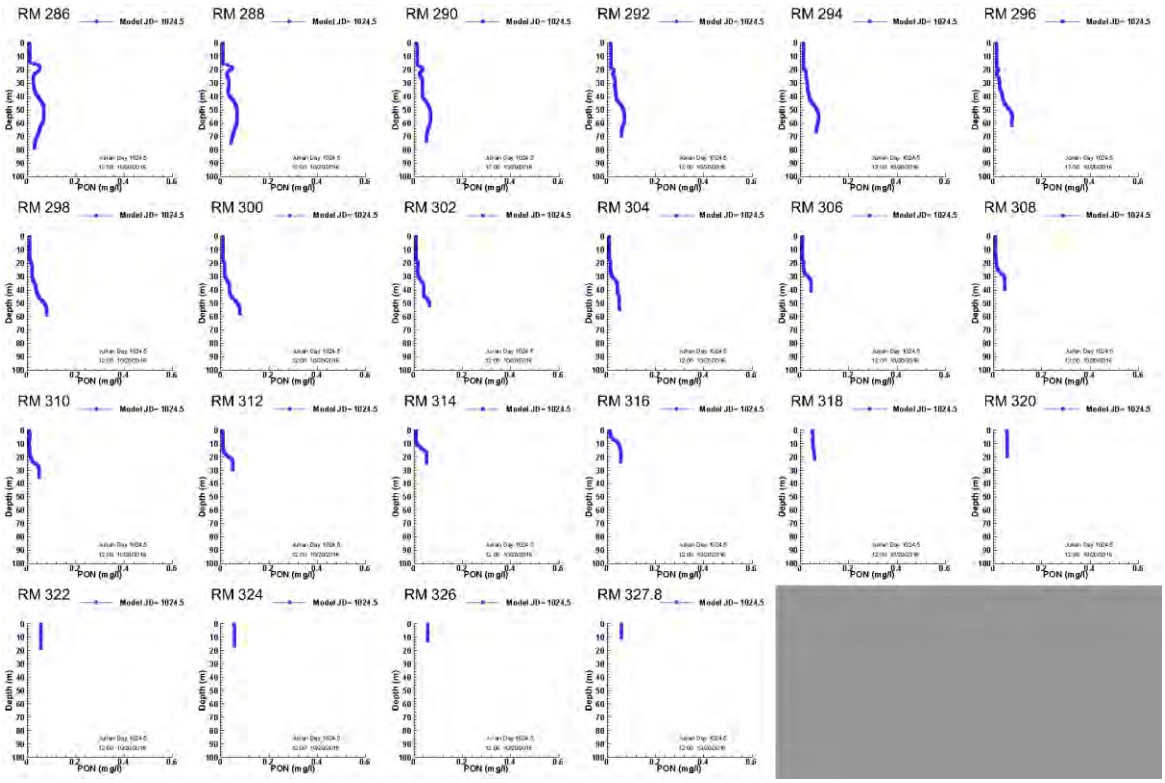


Figure 1709. Vertical profiles of PON compared with data for 10/20/2016.

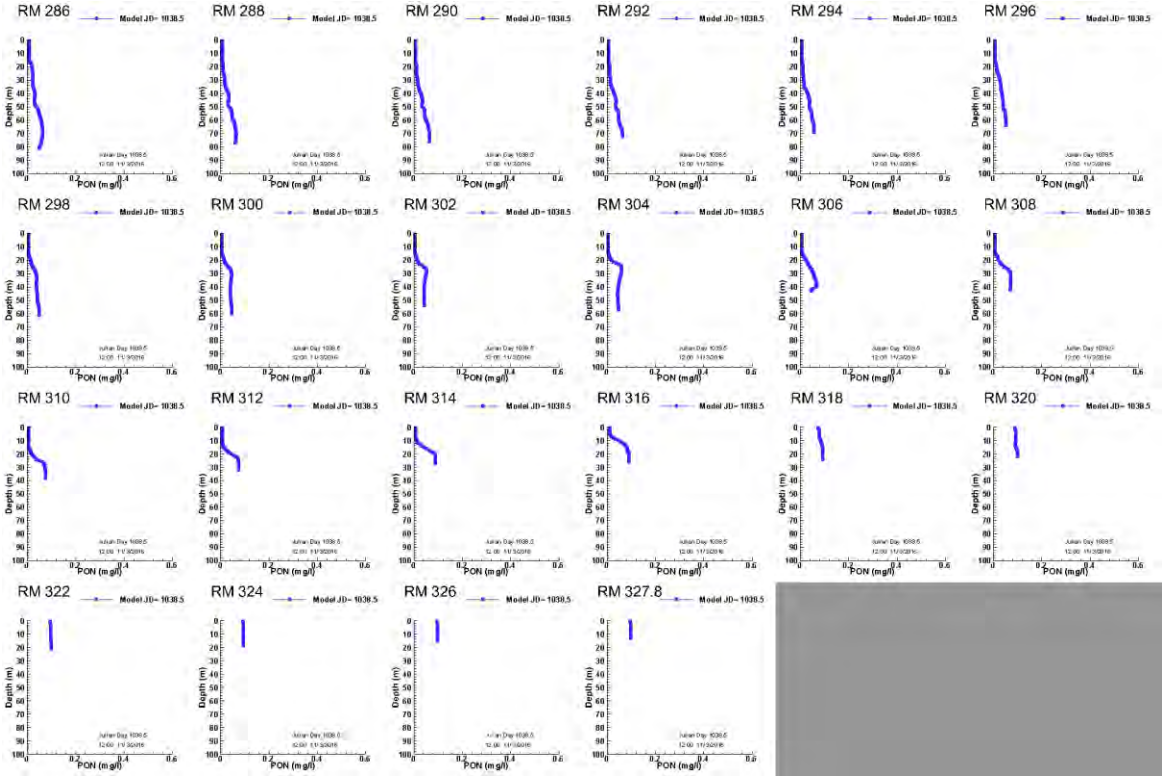


Figure 1710. Vertical profiles of PON compared with data for 11/ 3/2016.

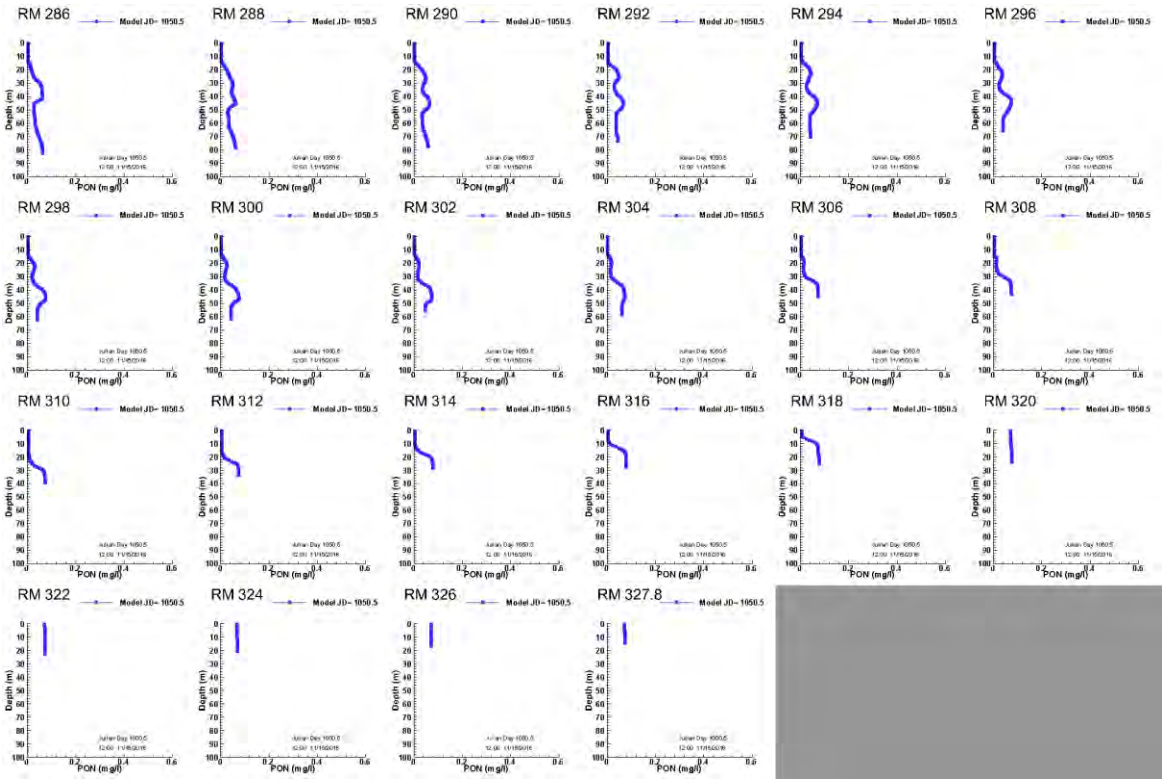


Figure 1711. Vertical profiles of PON compared with data for 11/15/2016.

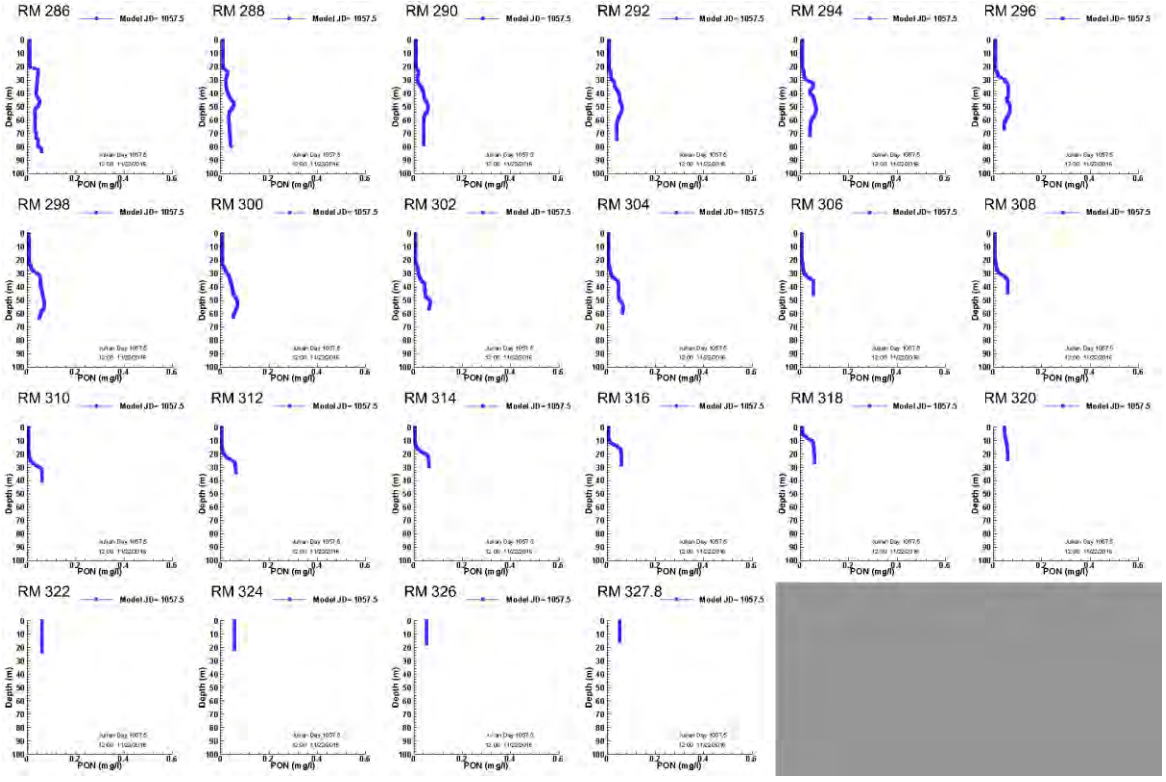


Figure 1712. Vertical profiles of PON compared with data for 11/22/2016.

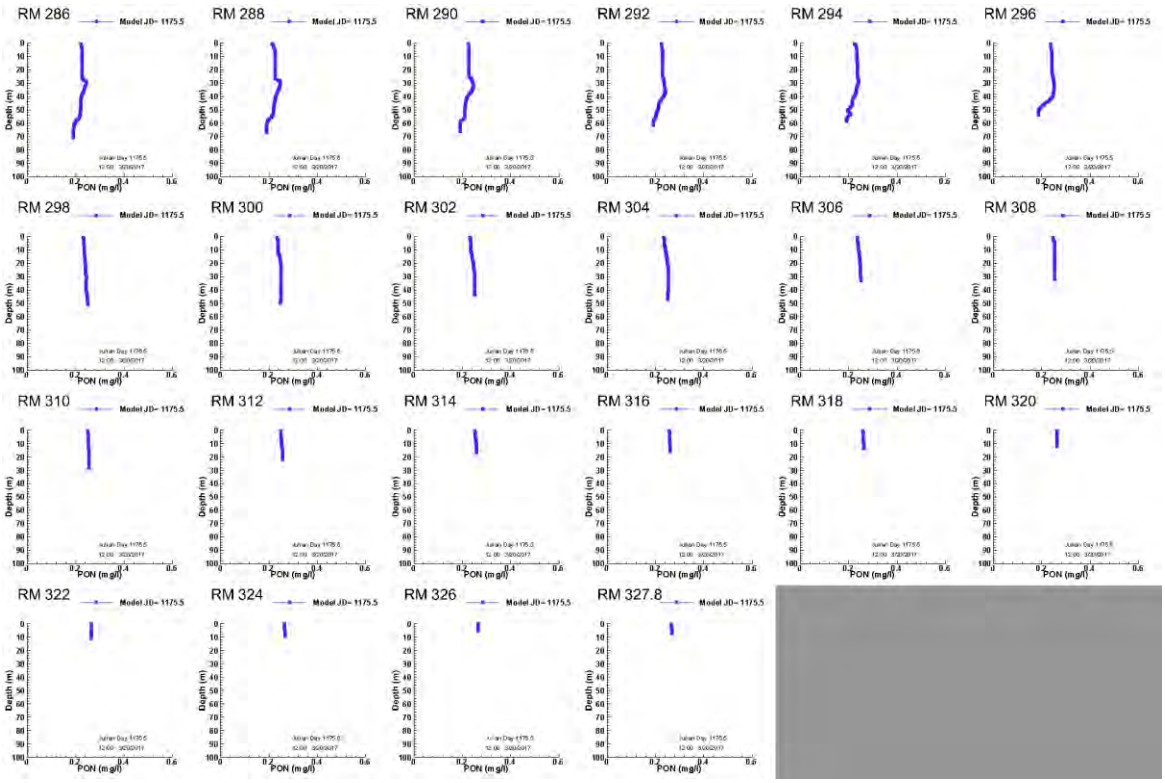


Figure 1713. Vertical profiles of PON compared with data for 3/20/2017.

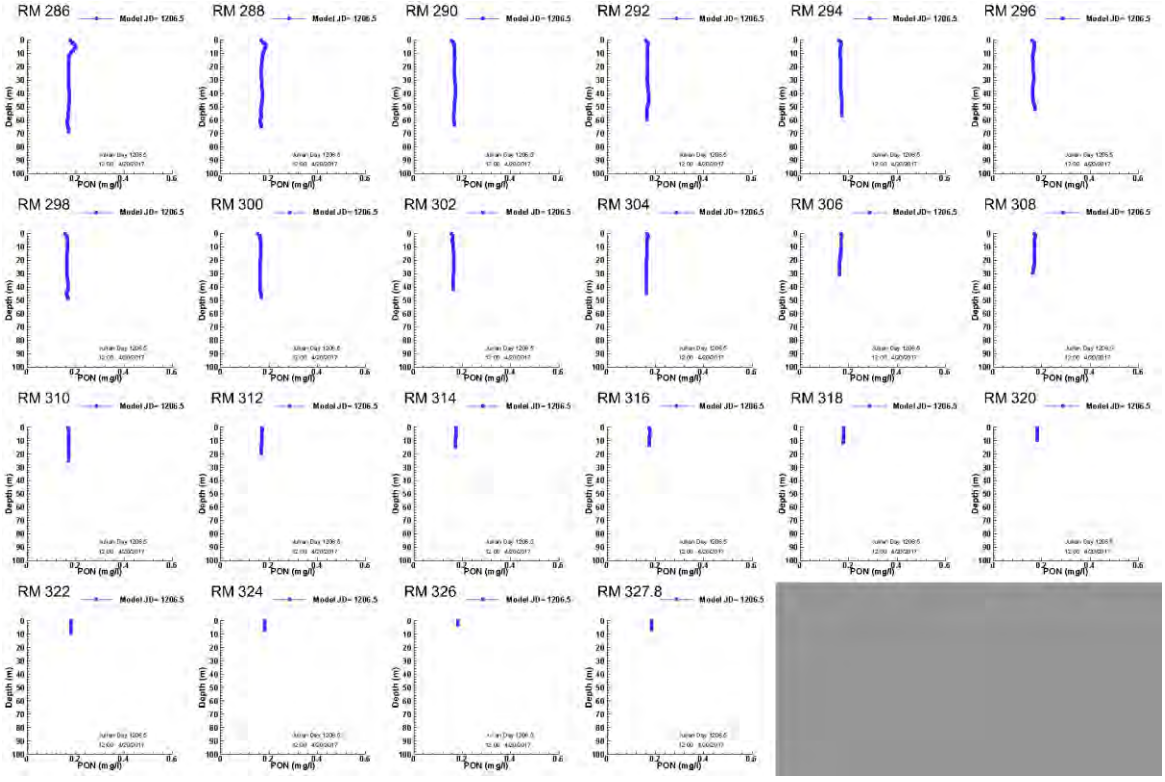


Figure 1714. Vertical profiles of PON compared with data for 4/20/2017.

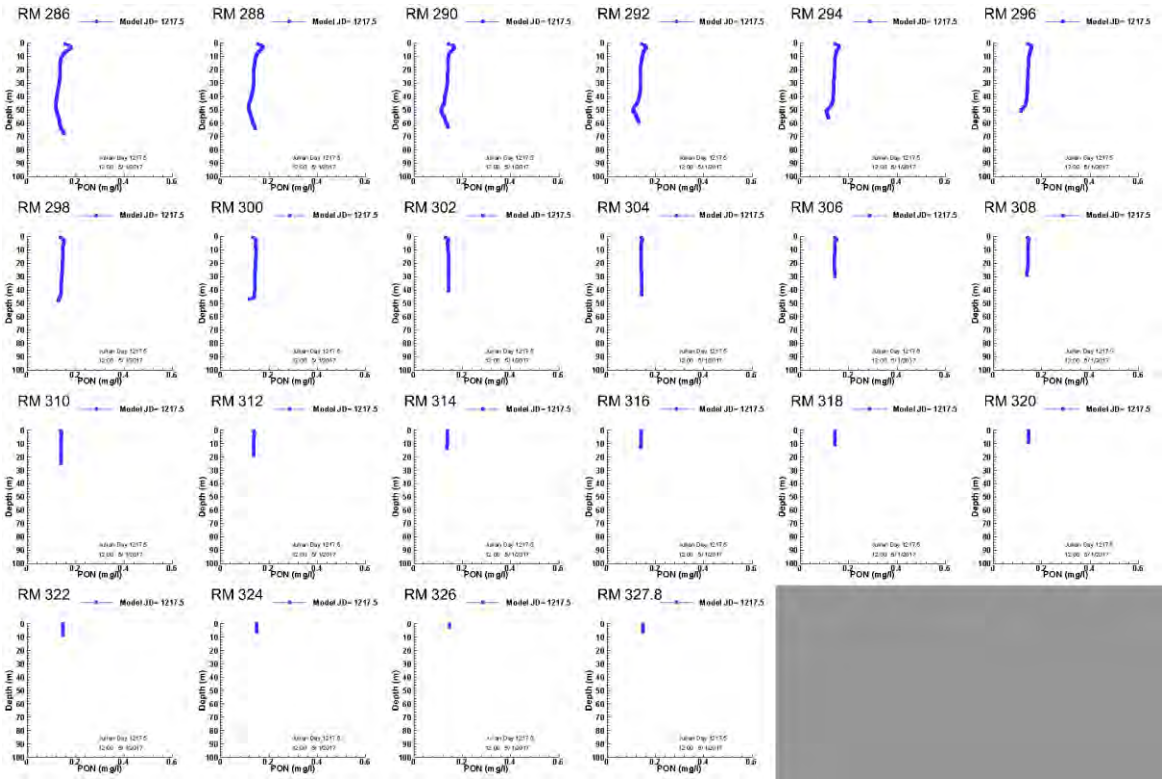


Figure 1715. Vertical profiles of PON compared with data for 5/ 1/2017.

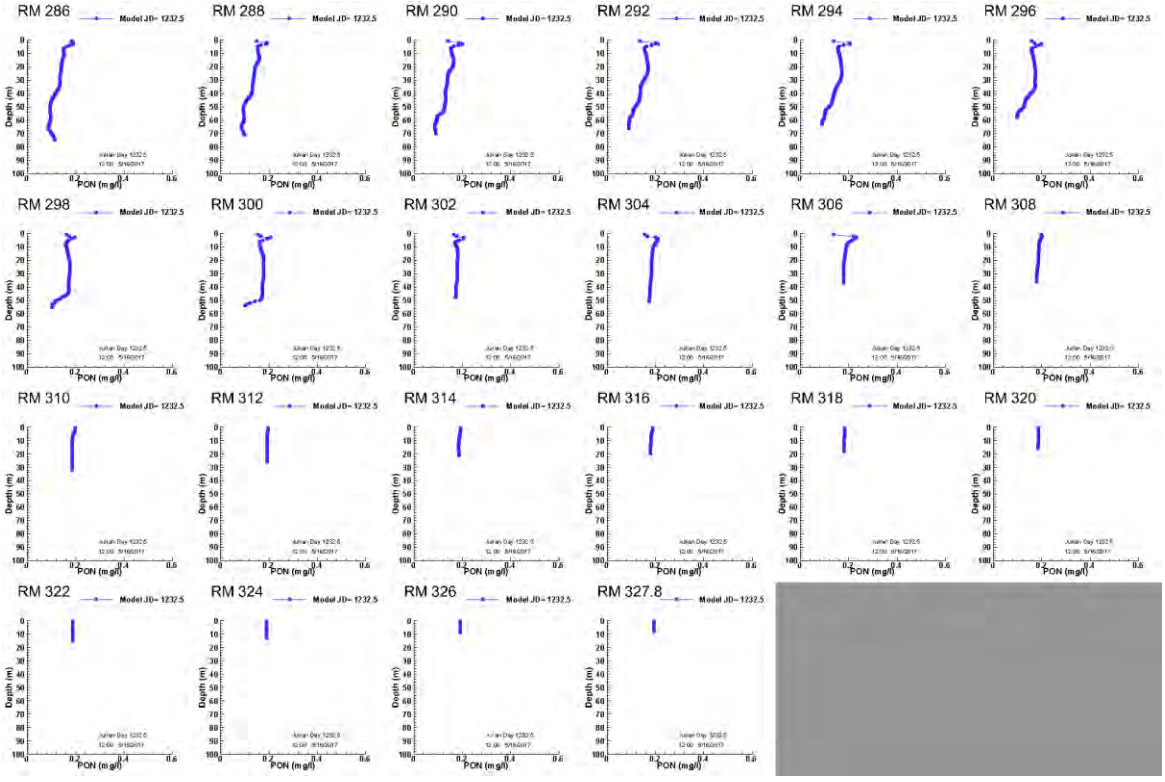


Figure 1716. Vertical profiles of PON compared with data for 5/16/2017.

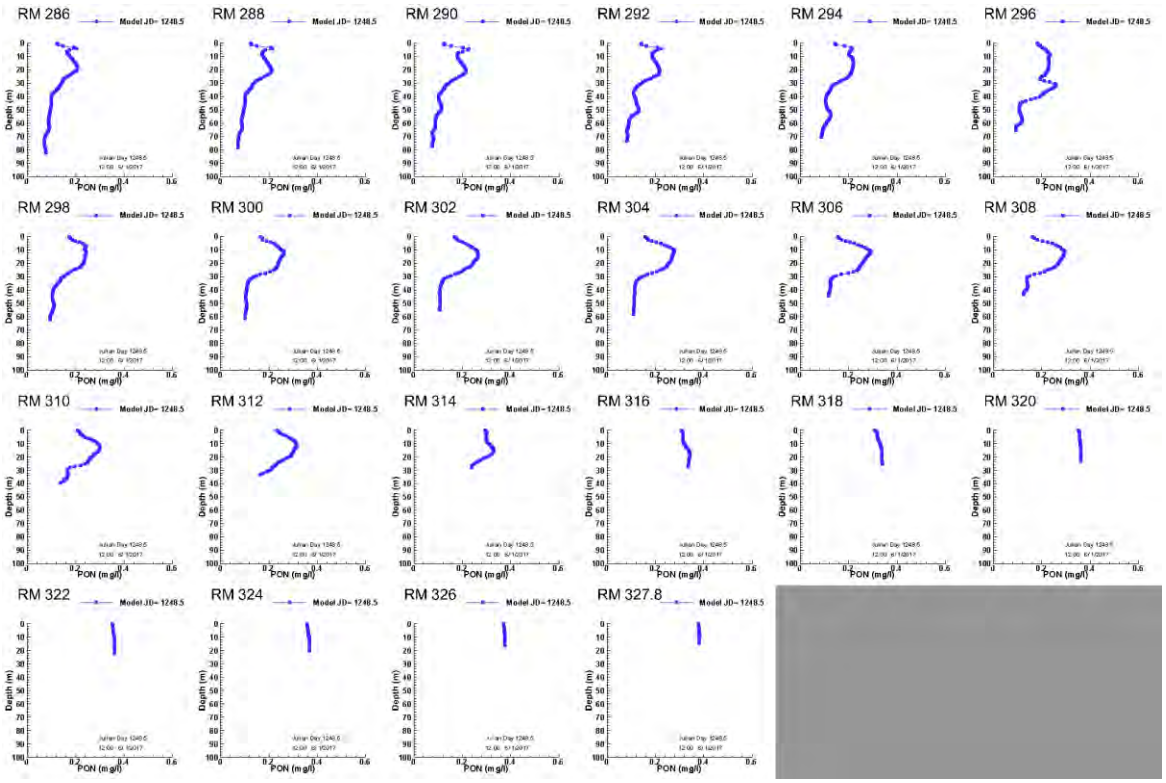


Figure 1717. Vertical profiles of PON compared with data for 6/ 1/2017.

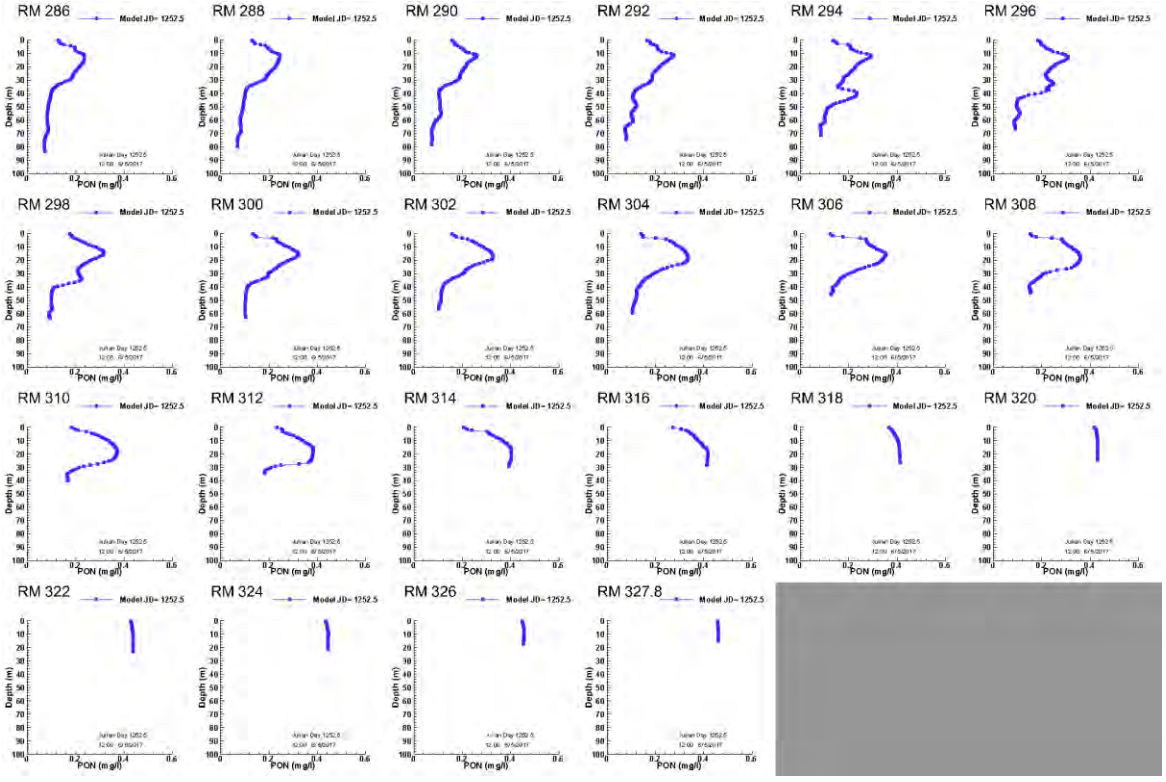


Figure 1718. Vertical profiles of PON compared with data for 6/ 5/2017.

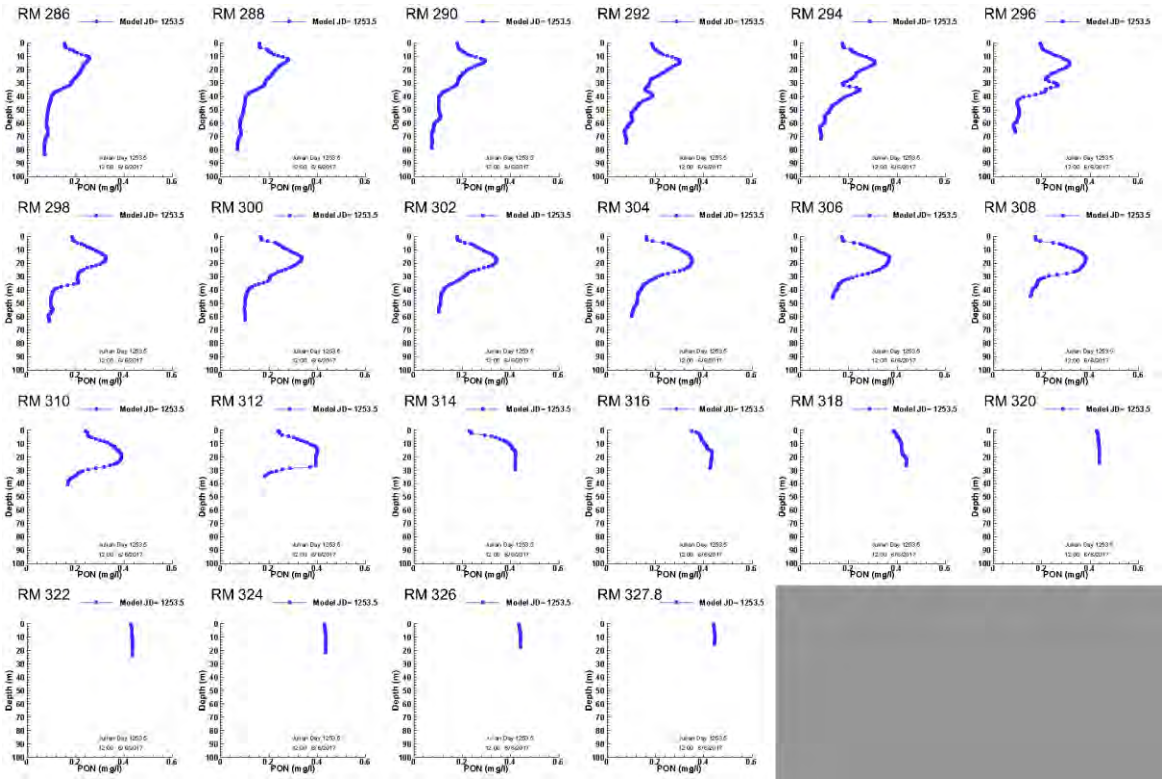


Figure 1719. Vertical profiles of PON compared with data for 6/ 6/2017.

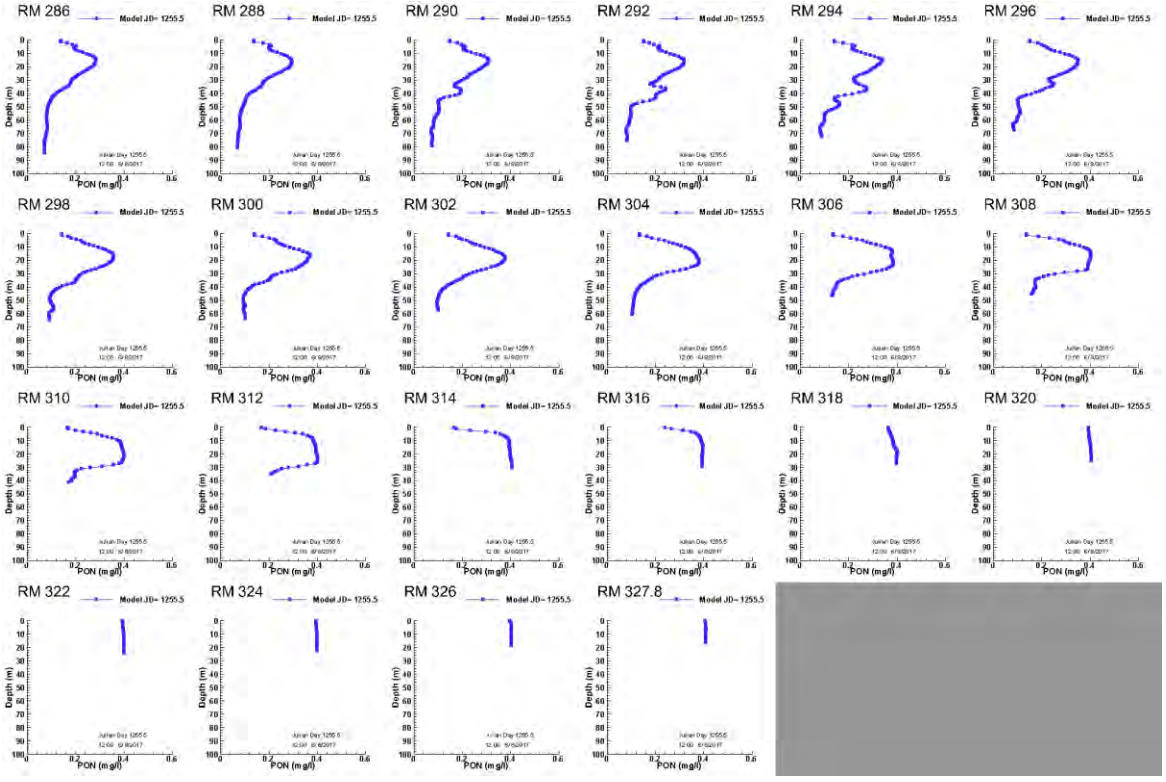


Figure 1720. Vertical profiles of PON compared with data for 6/ 8/2017.

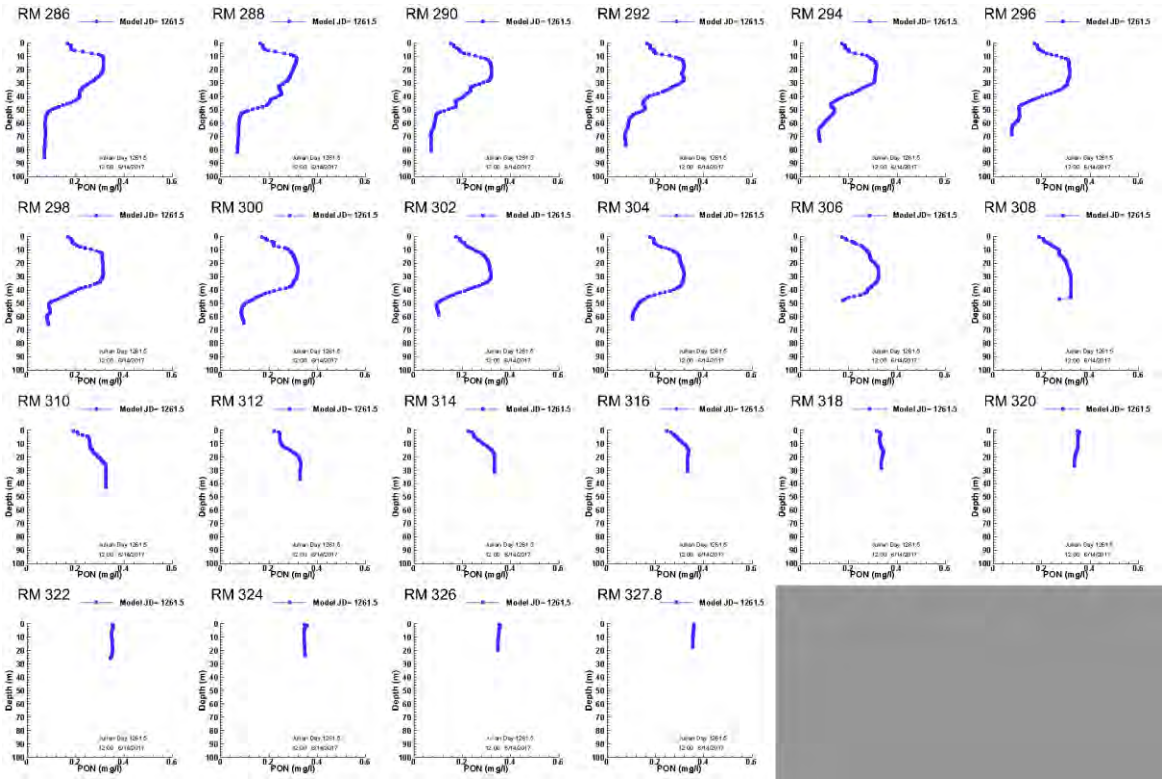


Figure 1721. Vertical profiles of PON compared with data for 6/14/2017.

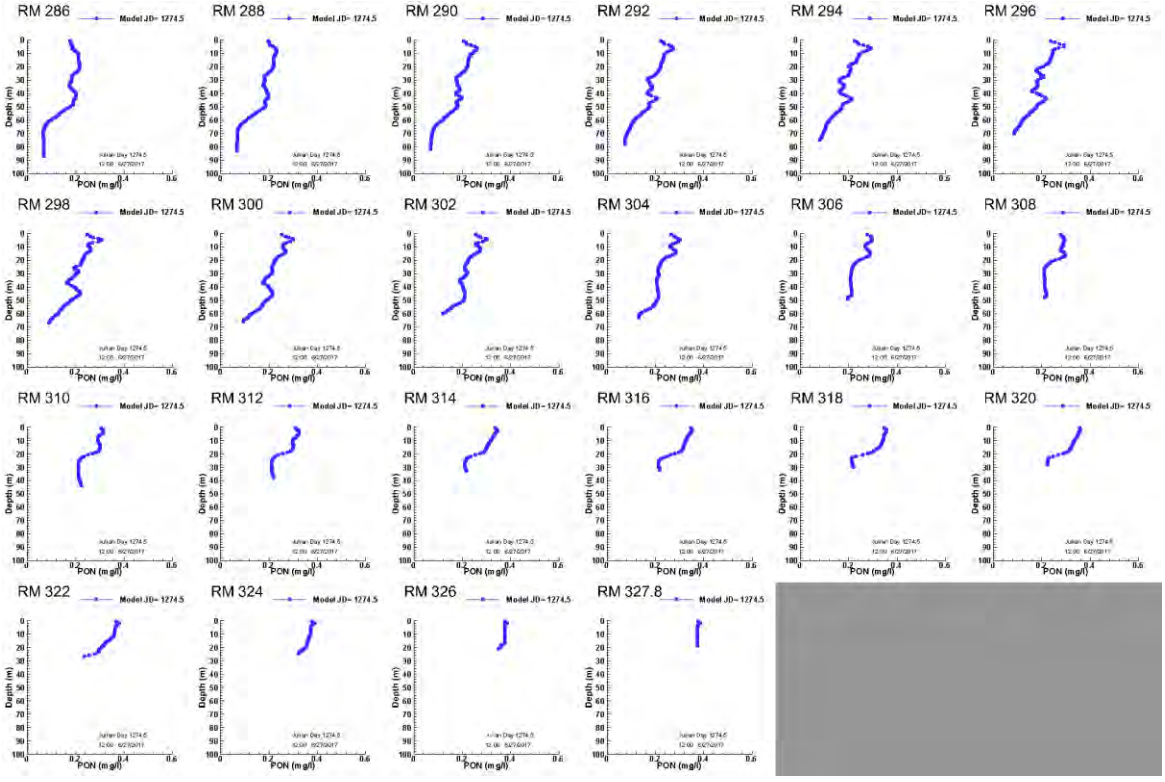


Figure 1722. Vertical profiles of PON compared with data for 6/27/2017.

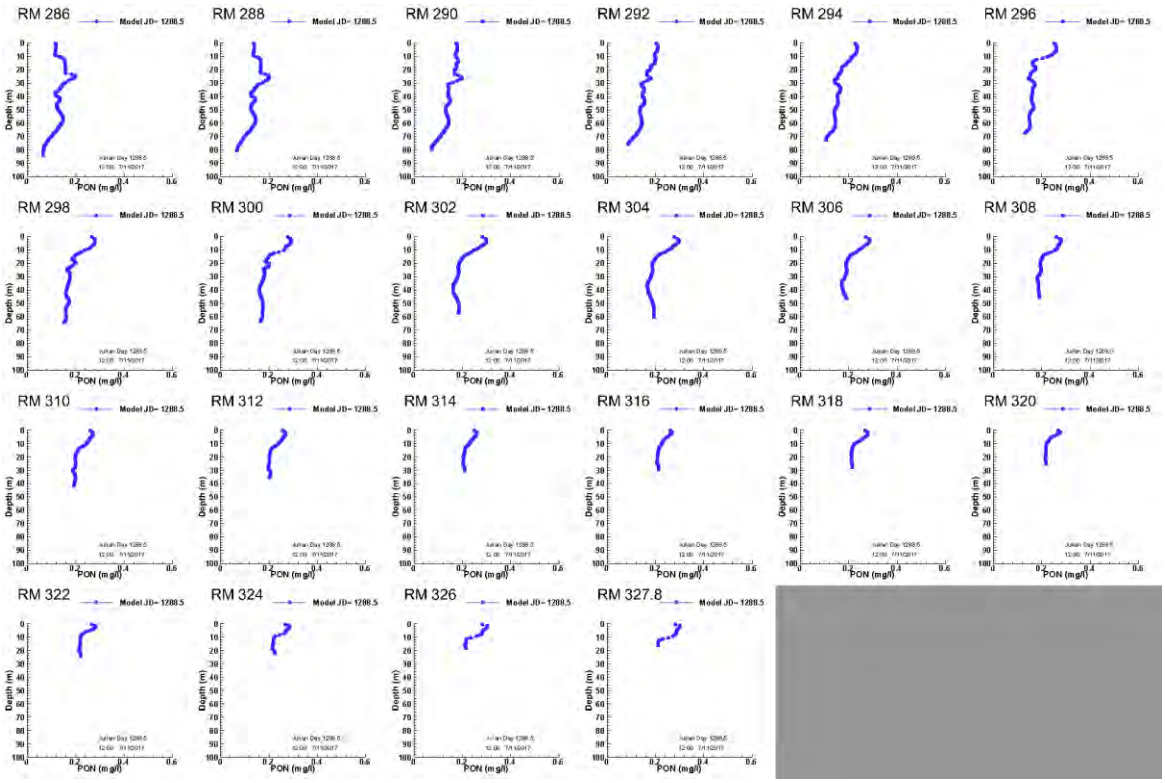


Figure 1723. Vertical profiles of PON compared with data for 7/11/2017.

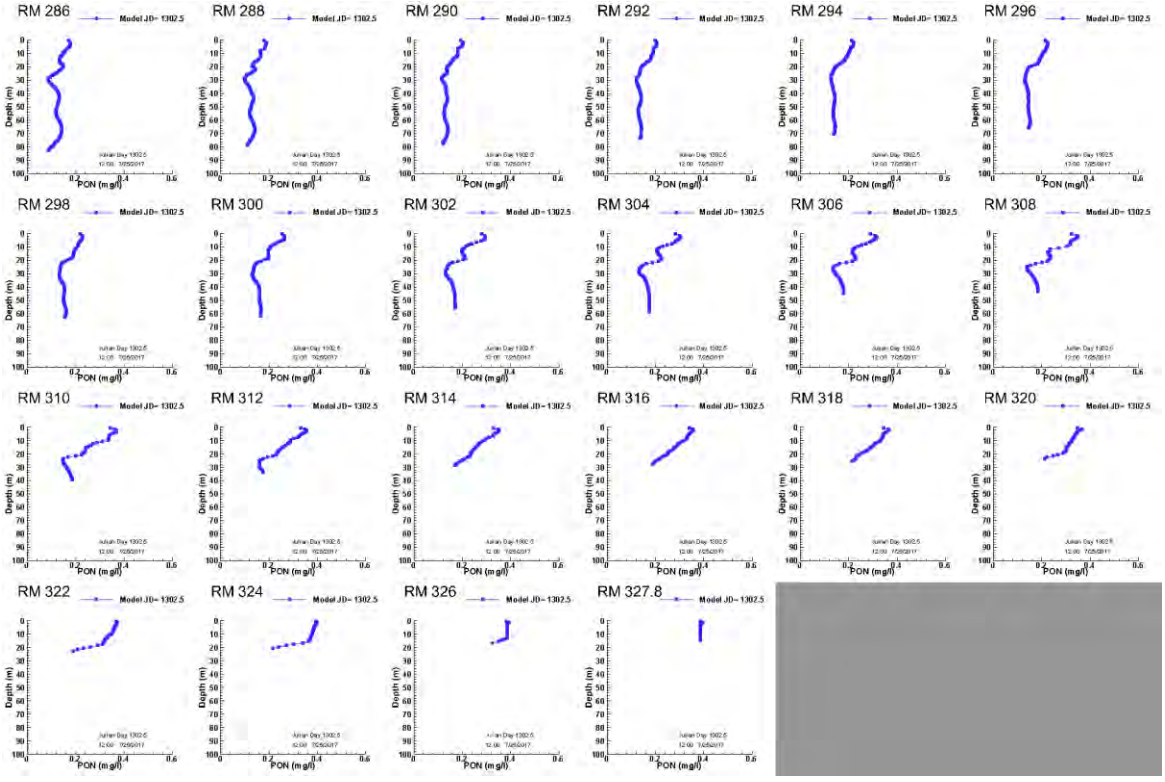


Figure 1724. Vertical profiles of PON compared with data for 7/25/2017.

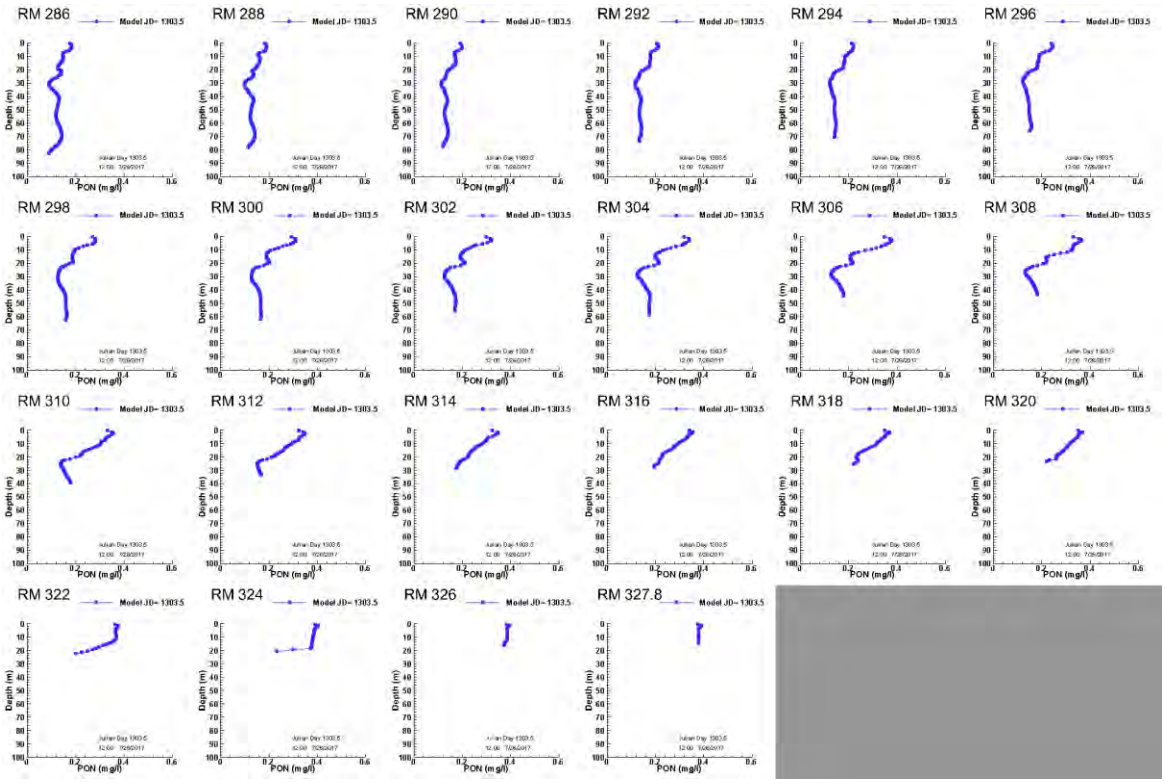


Figure 1725. Vertical profiles of PON compared with data for 7/26/2017.

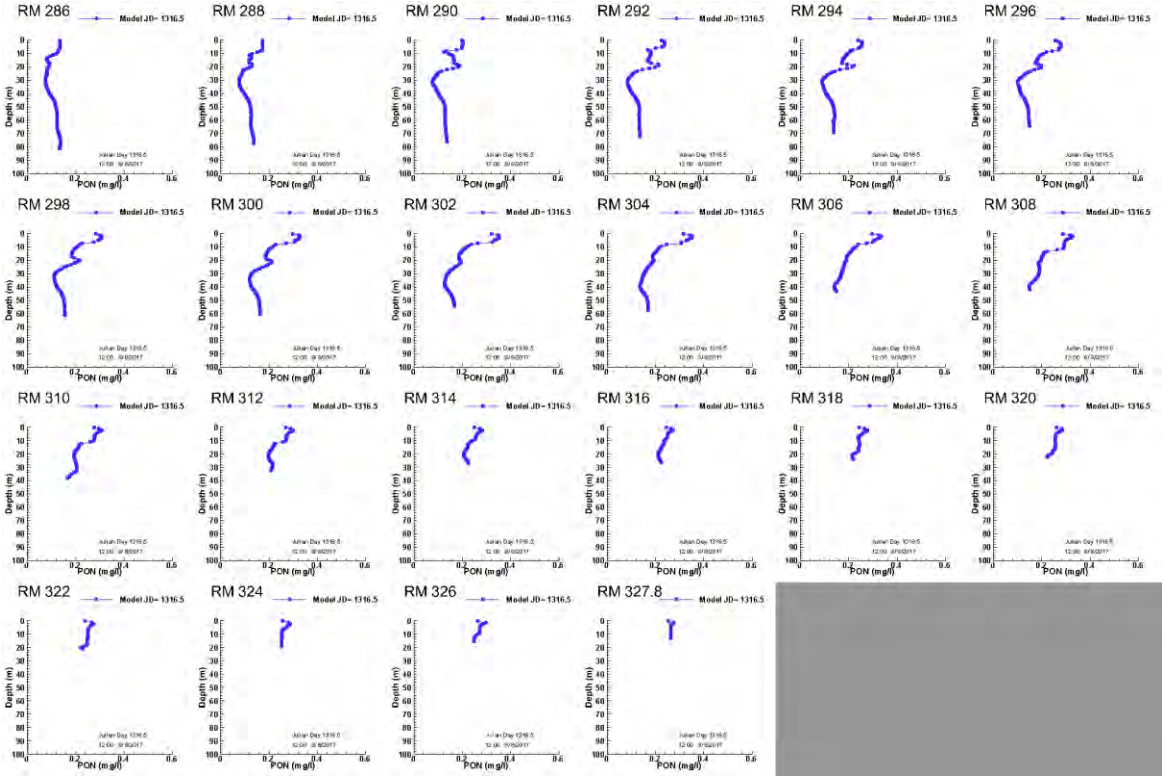


Figure 1726. Vertical profiles of PON compared with data for 8/ 8/2017.

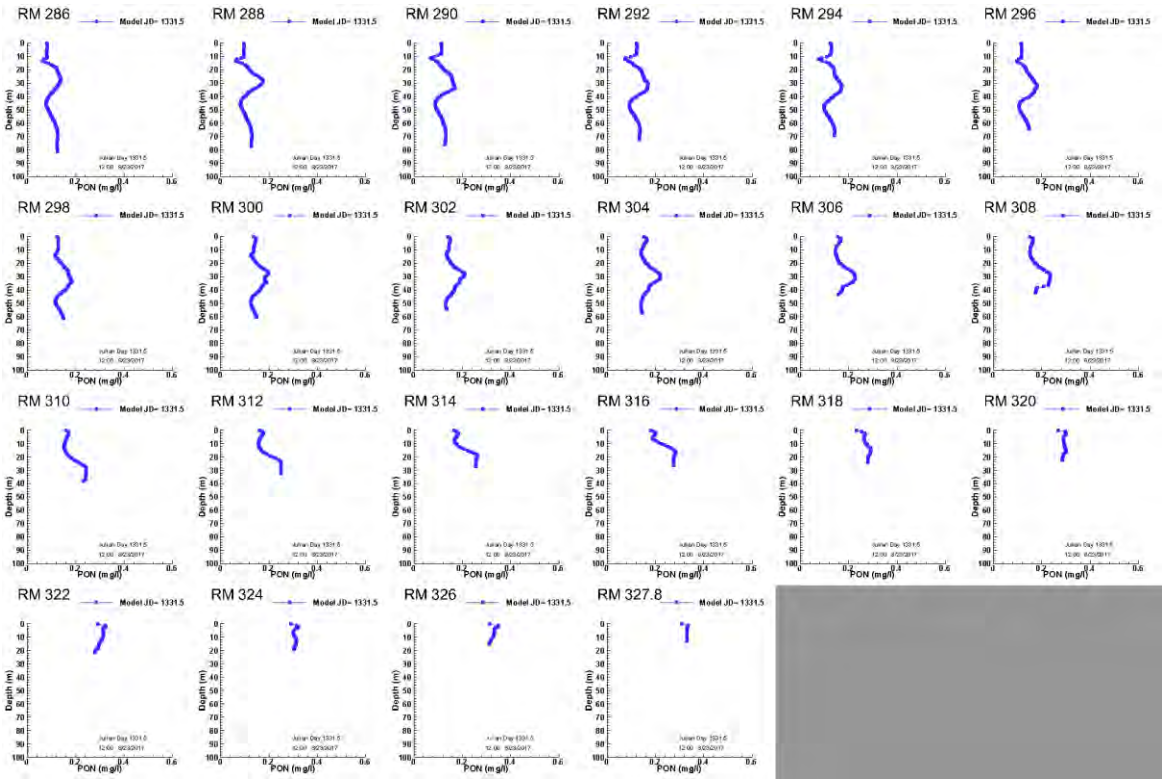


Figure 1727. Vertical profiles of PON compared with data for 8/23/2017.

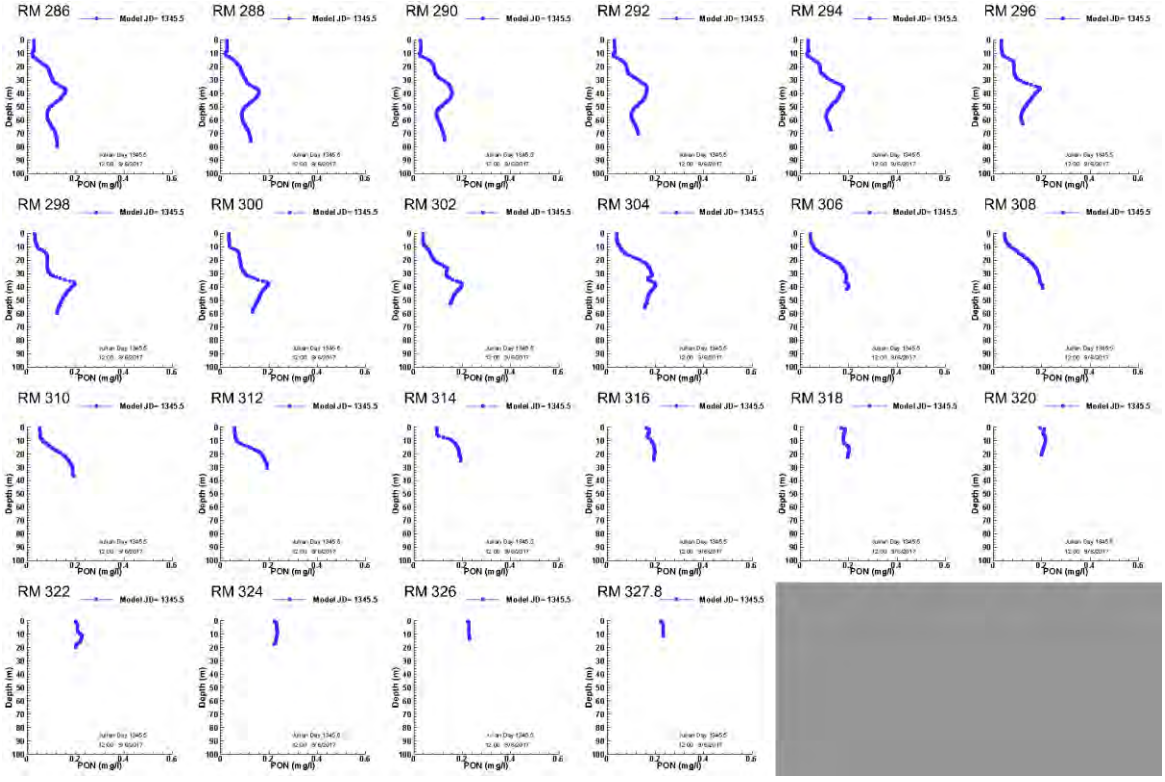


Figure 1728. Vertical profiles of PON compared with data for 9/ 6/2017.

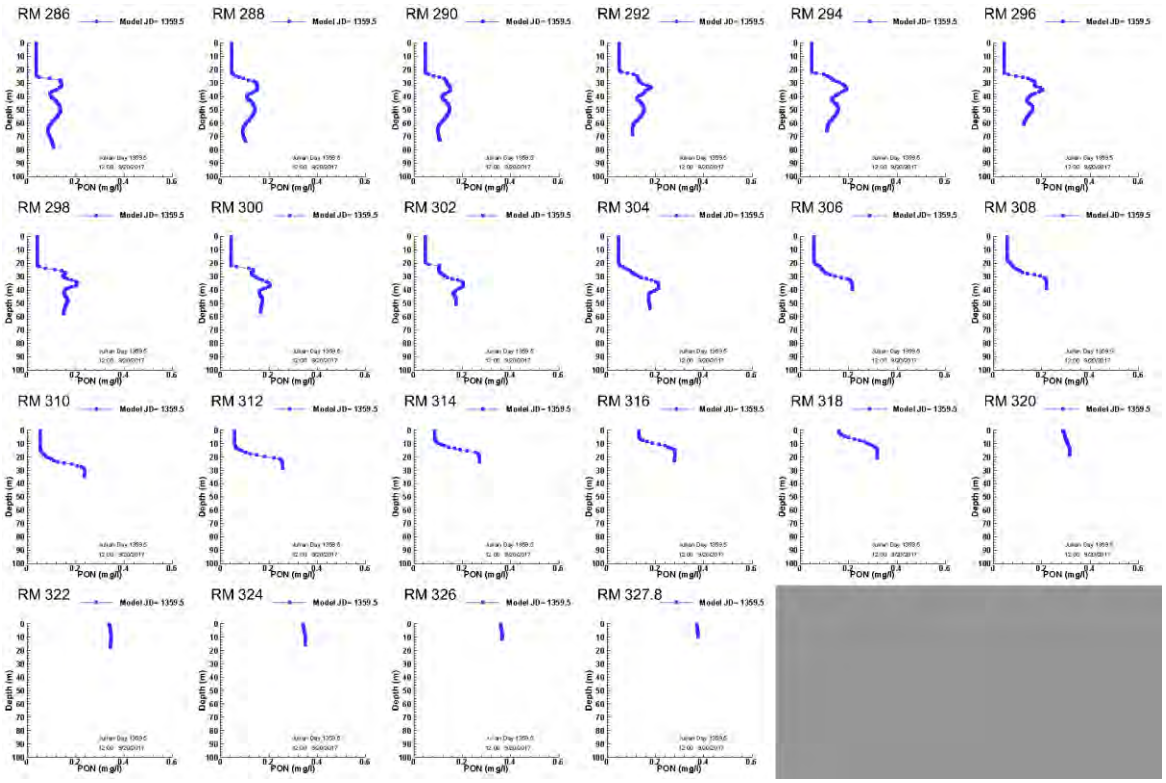


Figure 1729. Vertical profiles of PON compared with data for 9/20/2017.

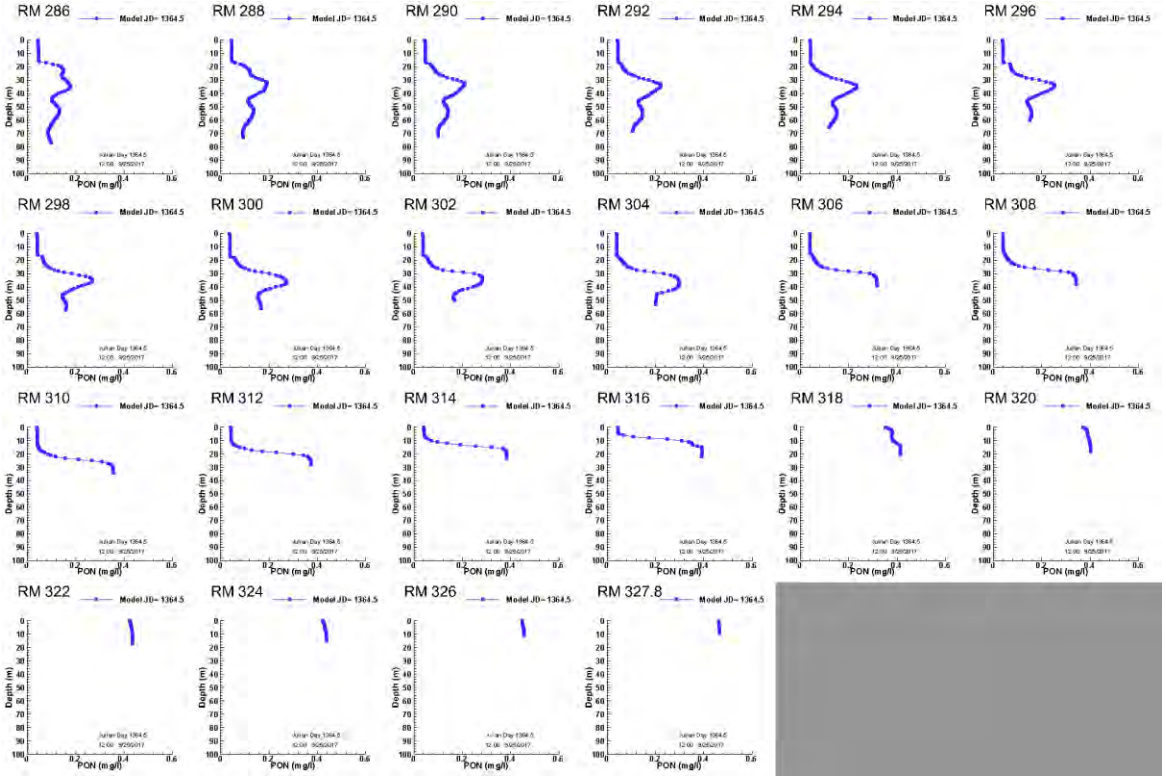


Figure 1730. Vertical profiles of PON compared with data for 9/25/2017.

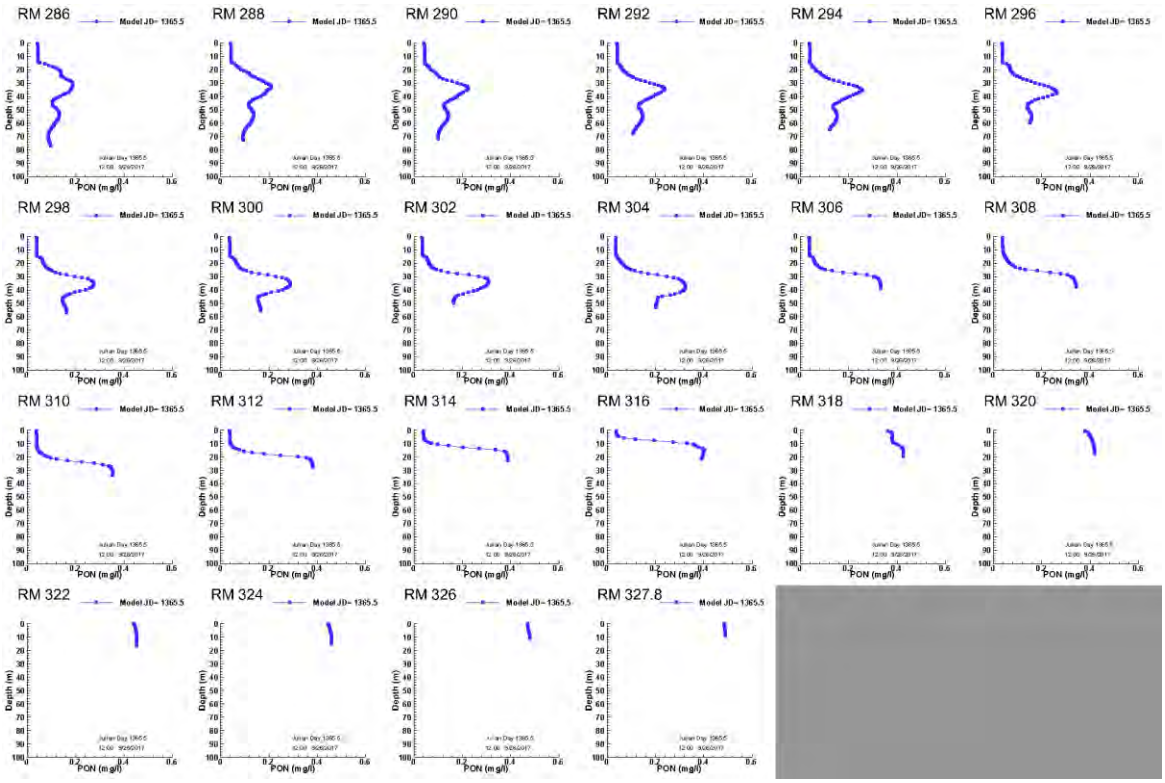


Figure 1731. Vertical profiles of PON compared with data for 9/26/2017.

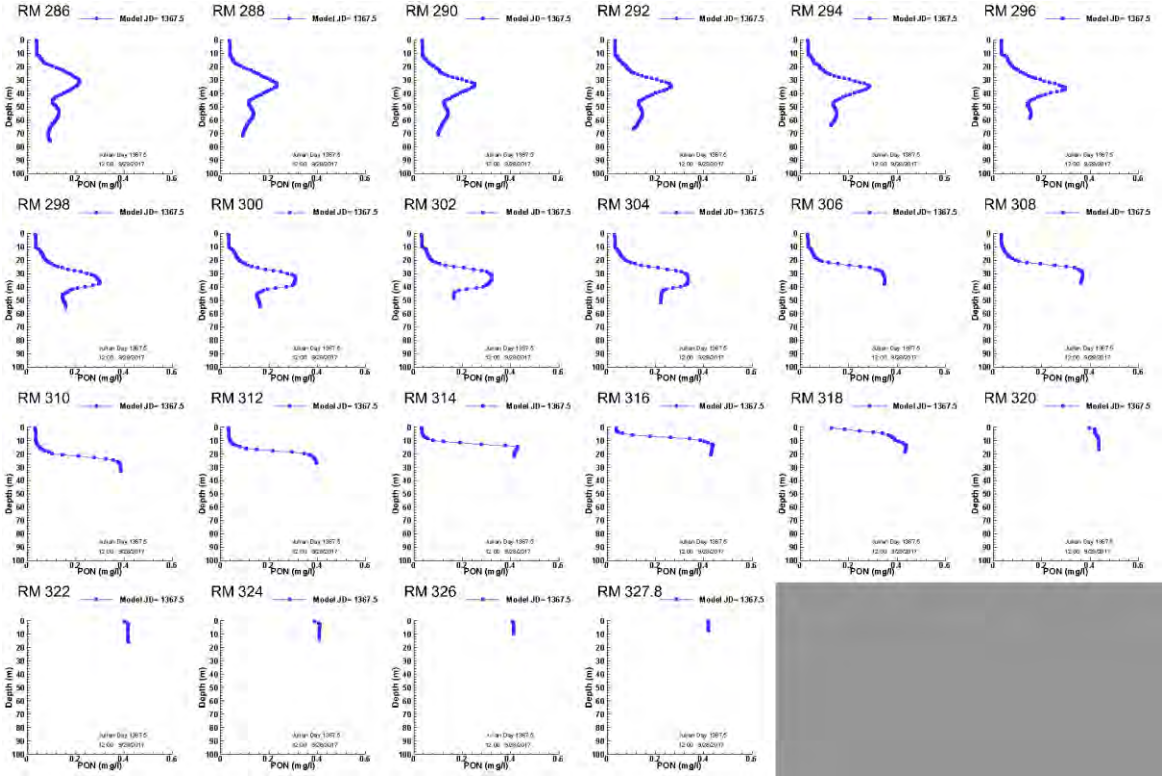


Figure 1732. Vertical profiles of PON compared with data for 9/28/2017.

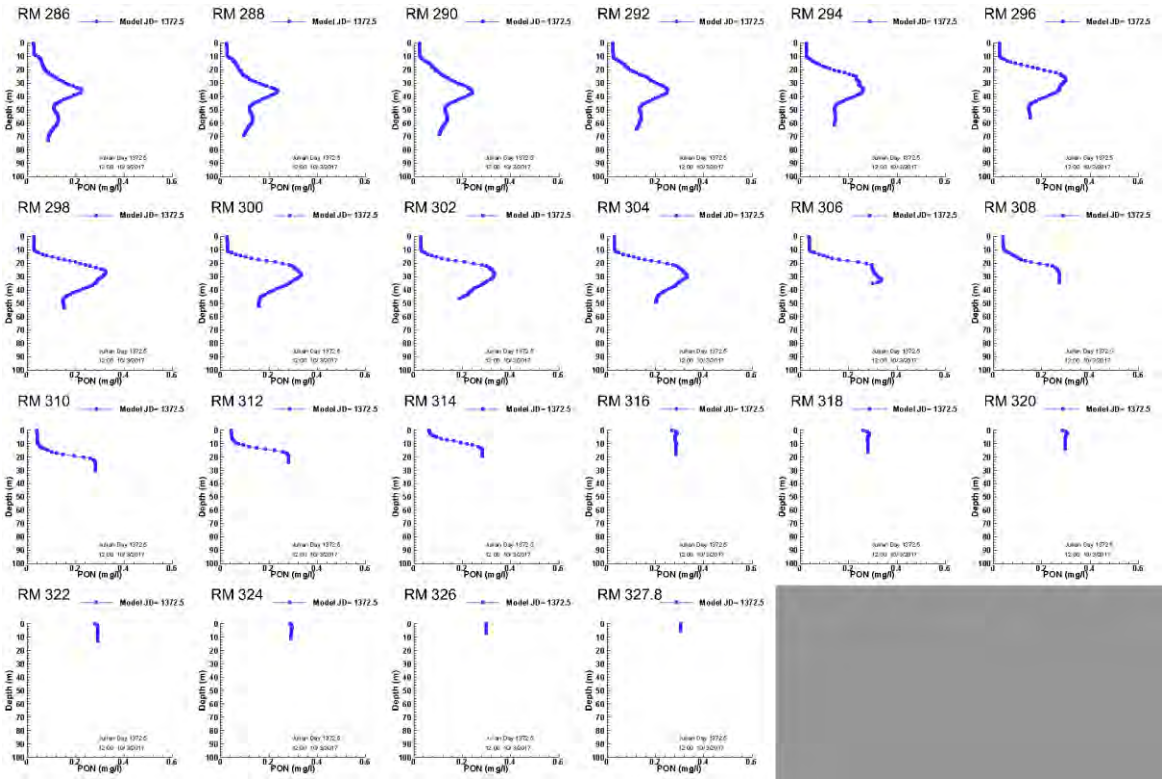


Figure 1733. Vertical profiles of PON compared with data for 10/ 3/2017.

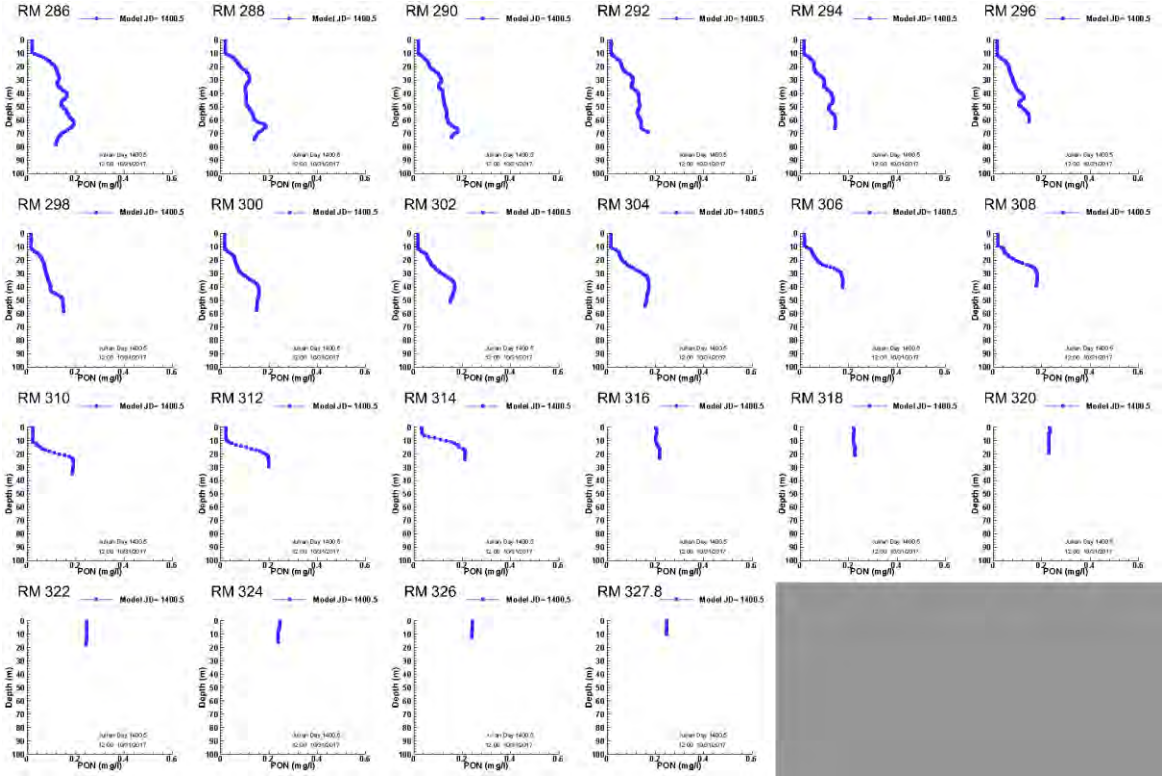


Figure 1734. Vertical profiles of PON compared with data for 10/31/2017.

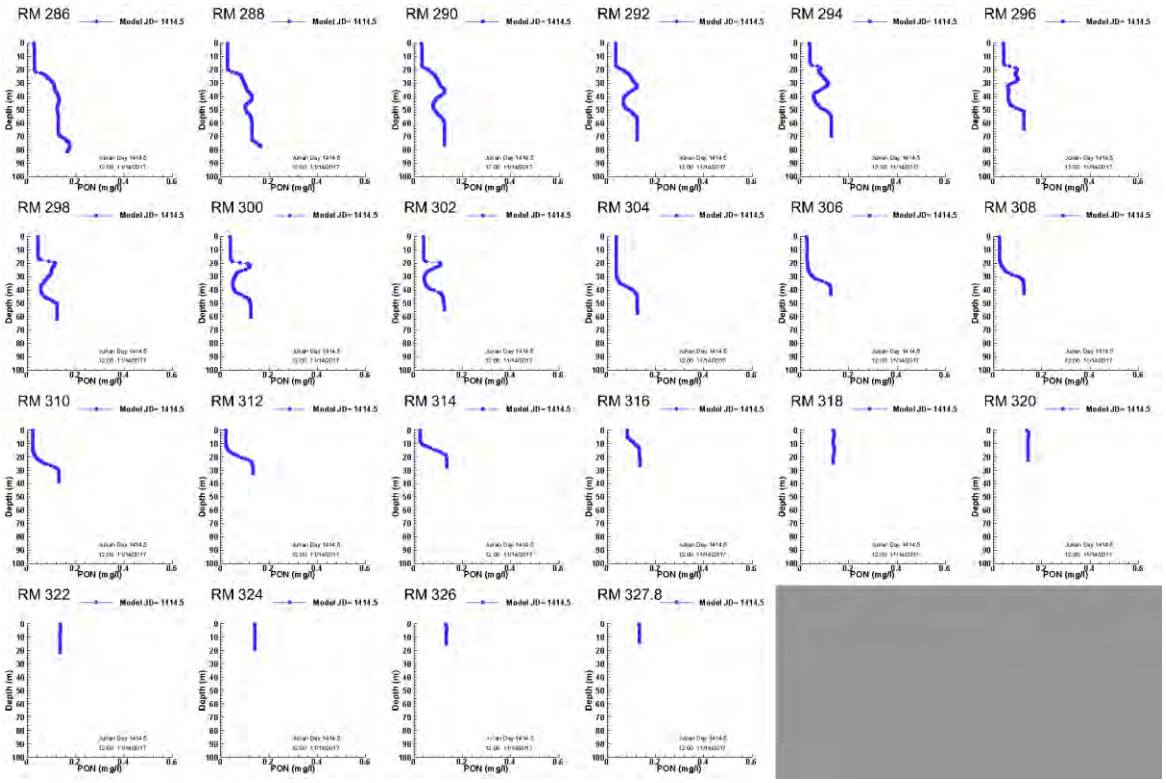


Figure 1735. Vertical profiles of PON compared with data for 11/14/2017.

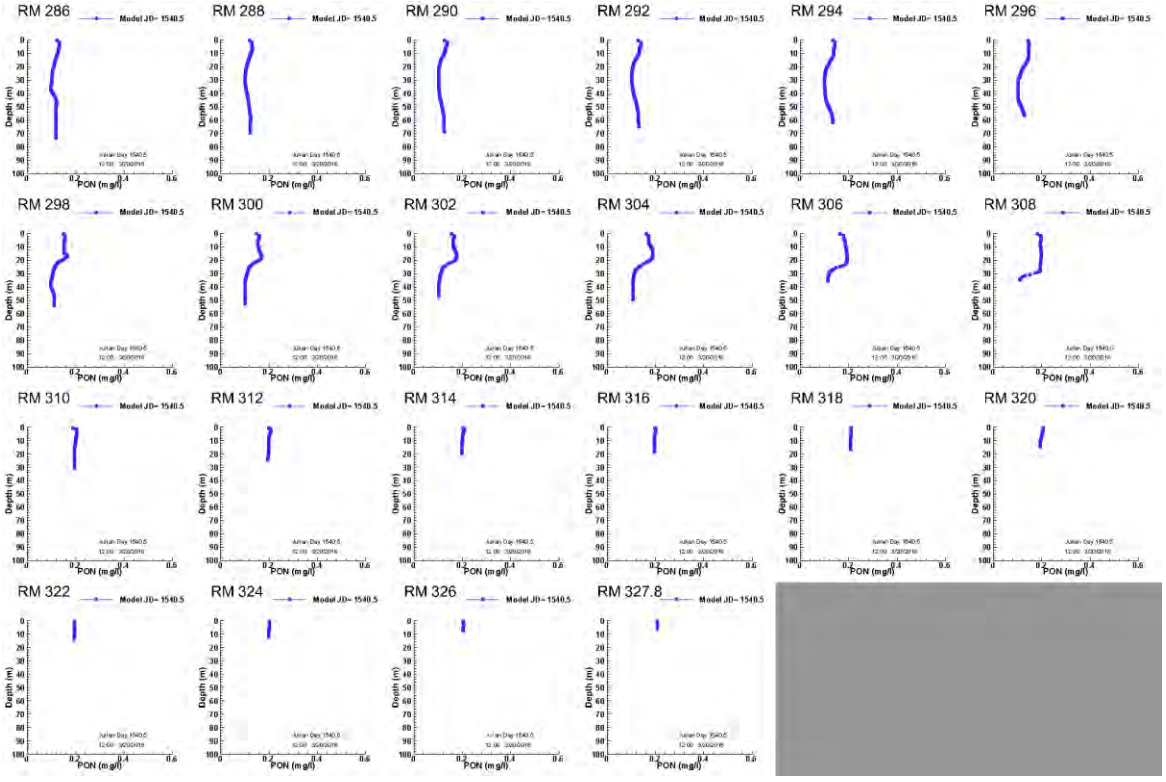


Figure 1736. Vertical profiles of PON compared with data for 3/20/2018.

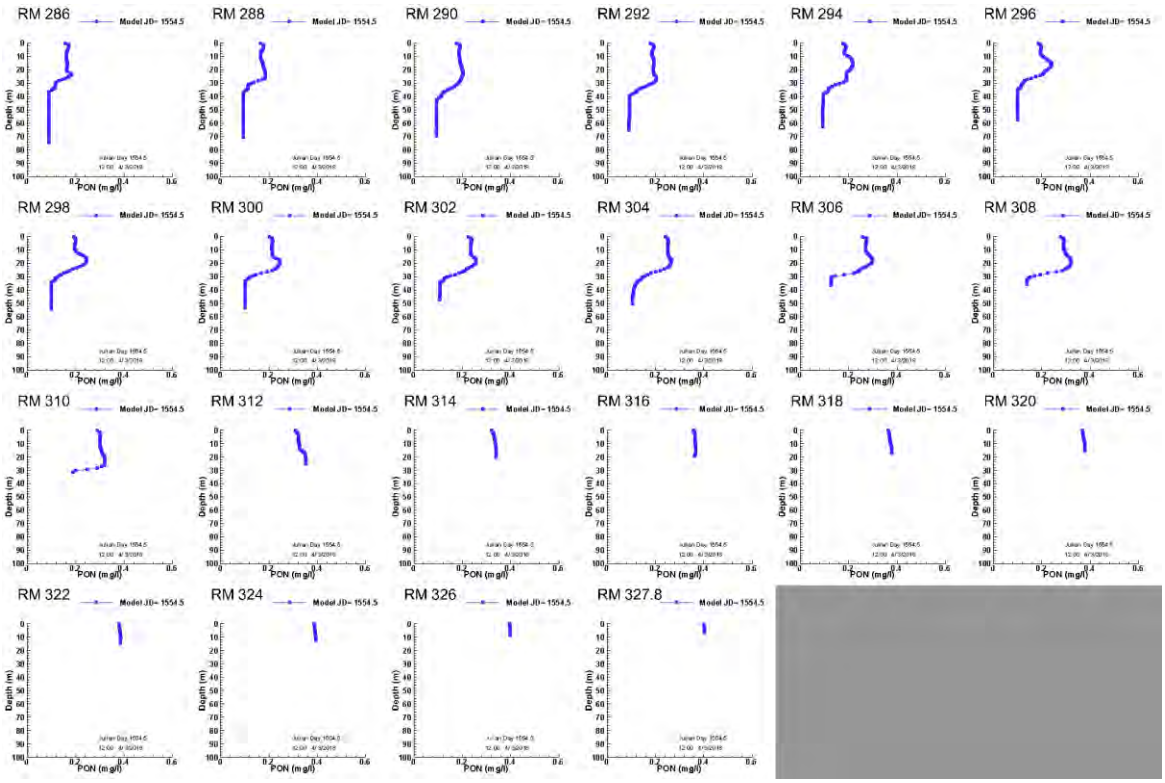


Figure 1737. Vertical profiles of PON compared with data for 4/ 3/2018.

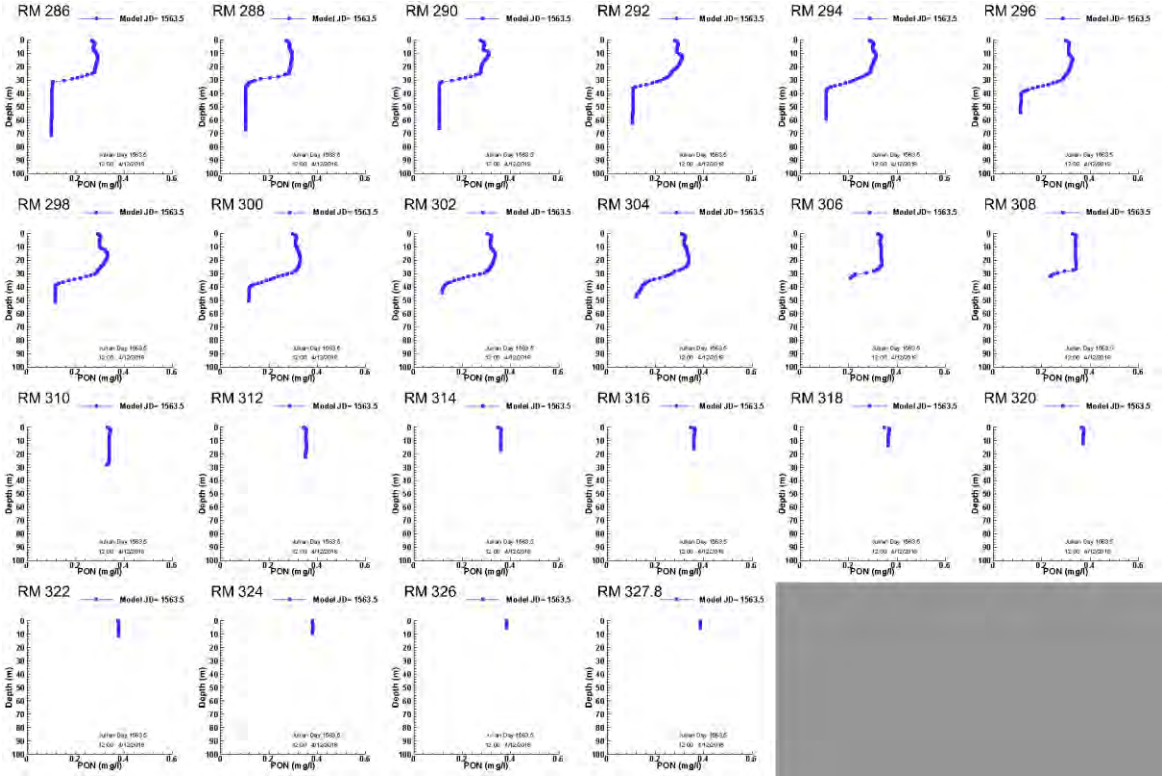


Figure 1738. Vertical profiles of PON compared with data for 4/12/2018.

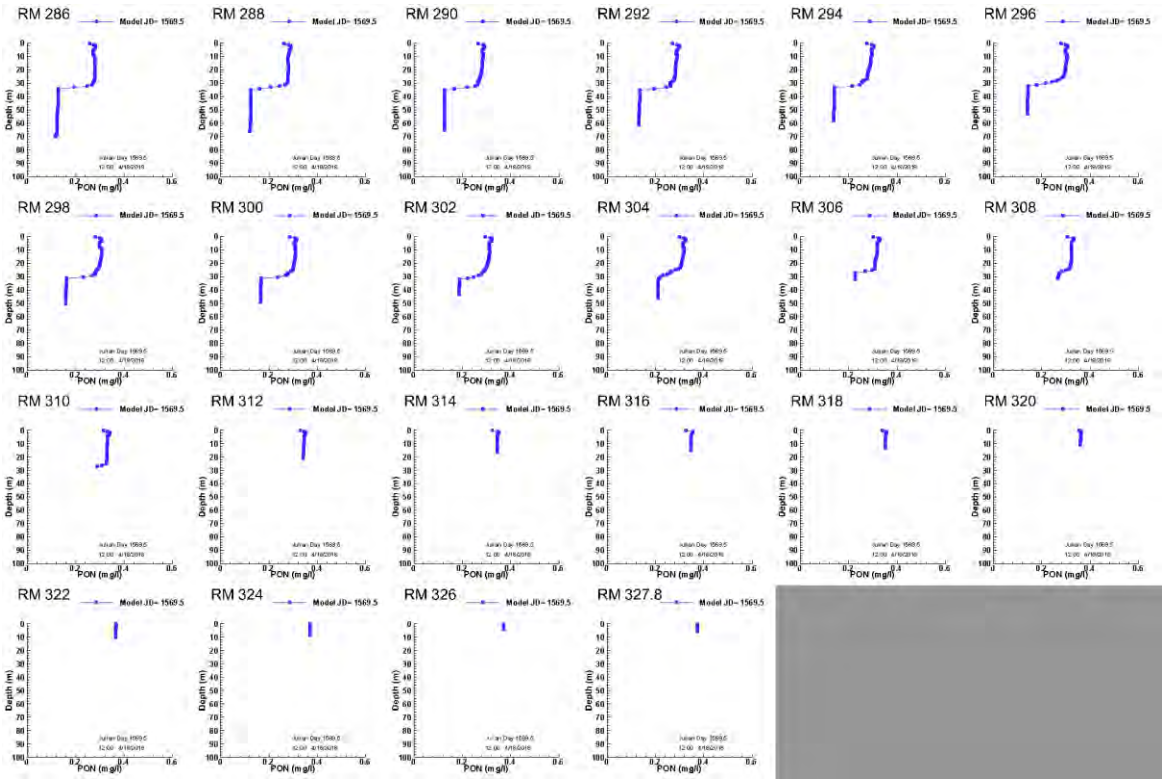


Figure 1739. Vertical profiles of PON compared with data for 4/18/2018.

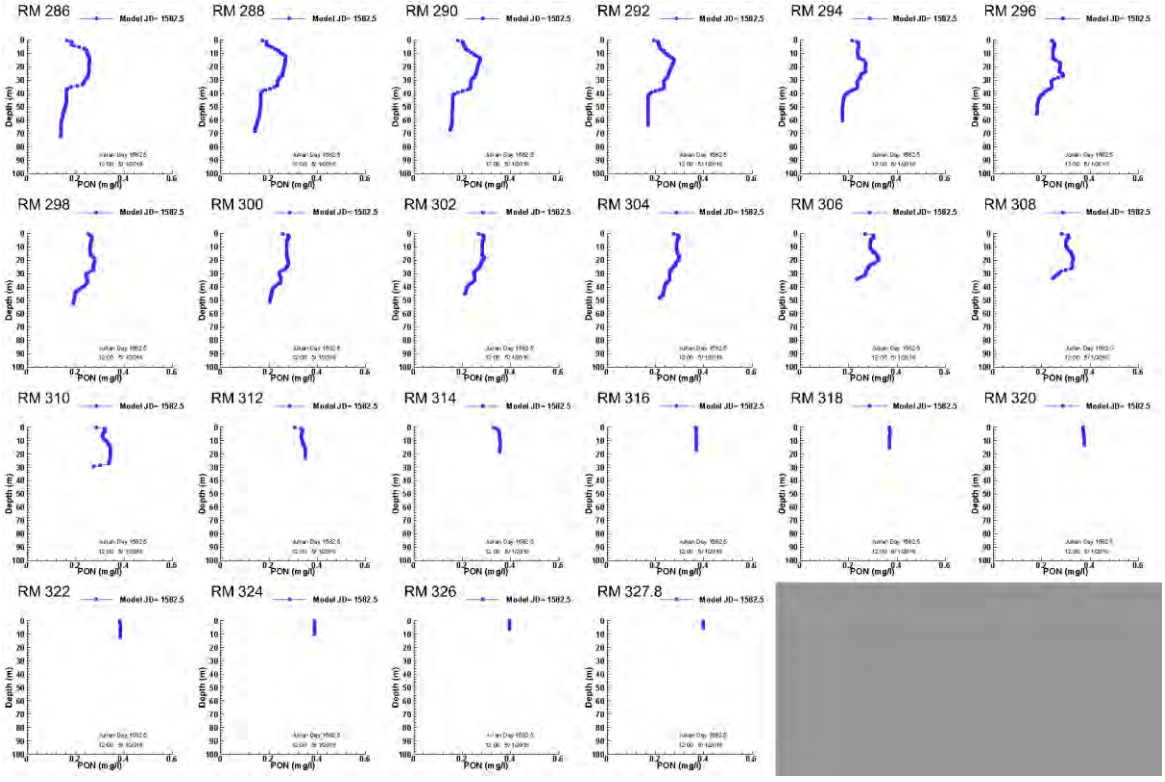


Figure 1740. Vertical profiles of PON compared with data for 5/ 1/2018.

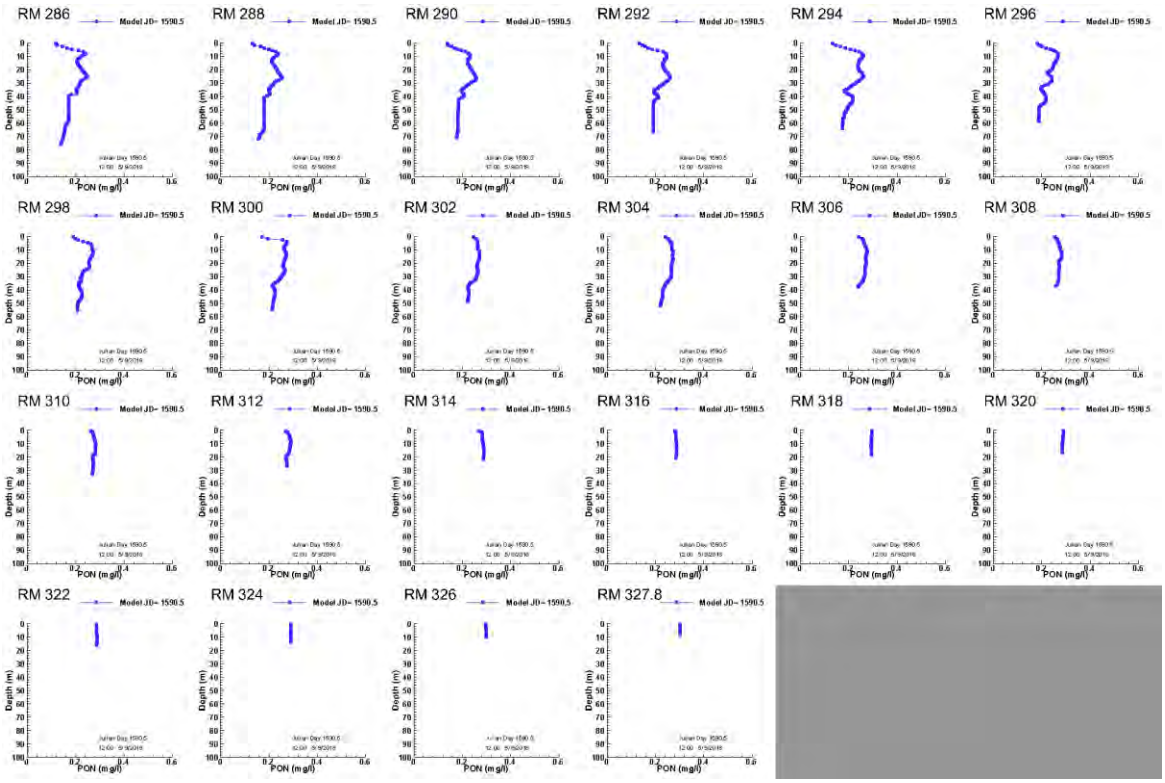


Figure 1741. Vertical profiles of PON compared with data for 5/ 9/2018.

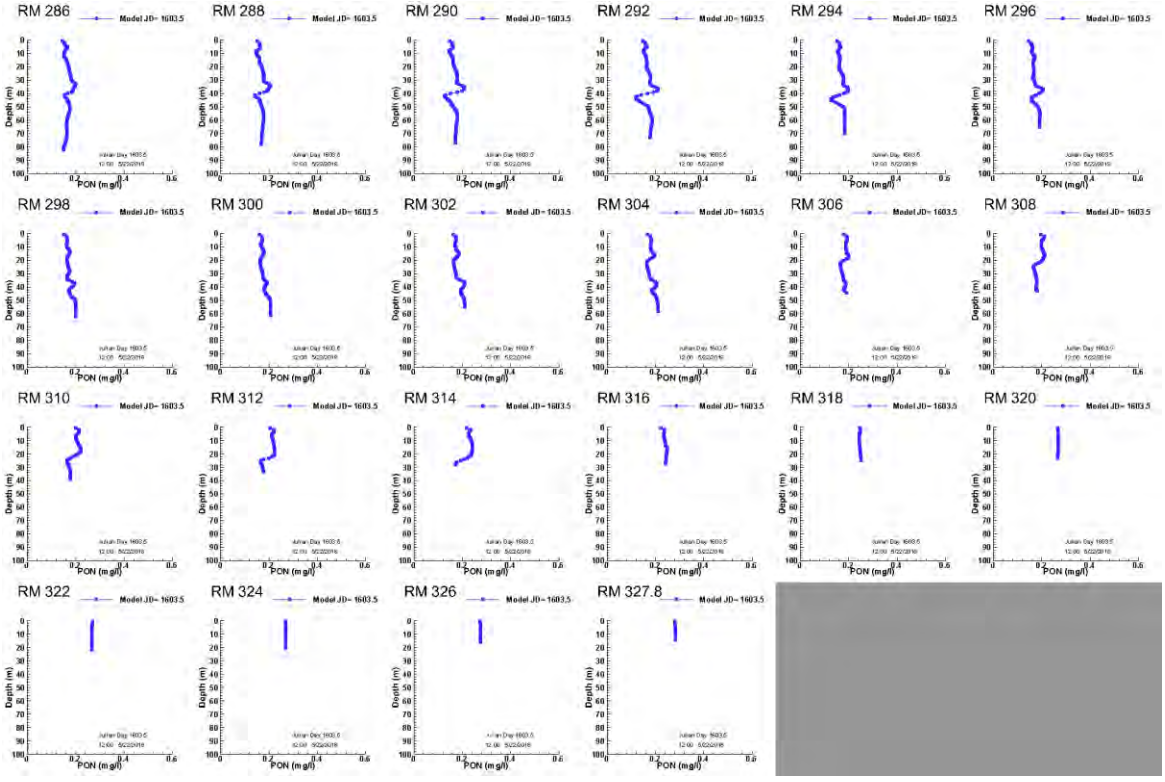


Figure 1742. Vertical profiles of PON compared with data for 5/22/2018.

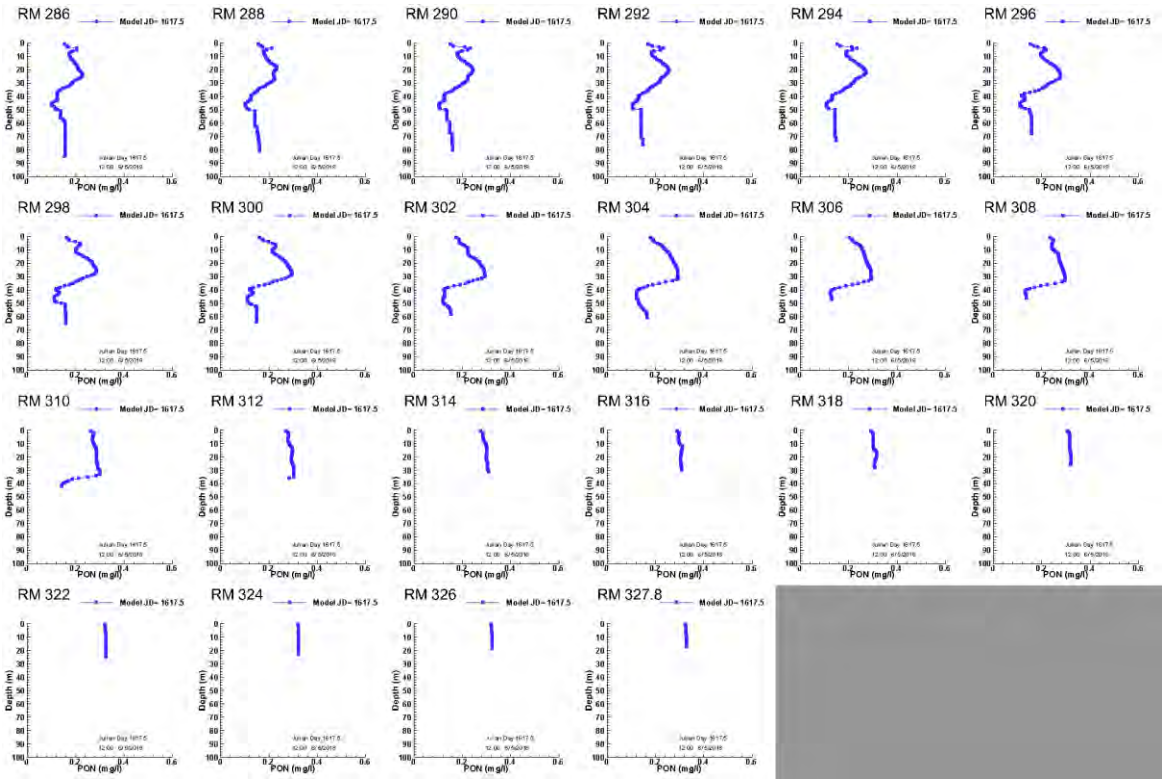


Figure 1743. Vertical profiles of PON compared with data for 6/ 5/2018.

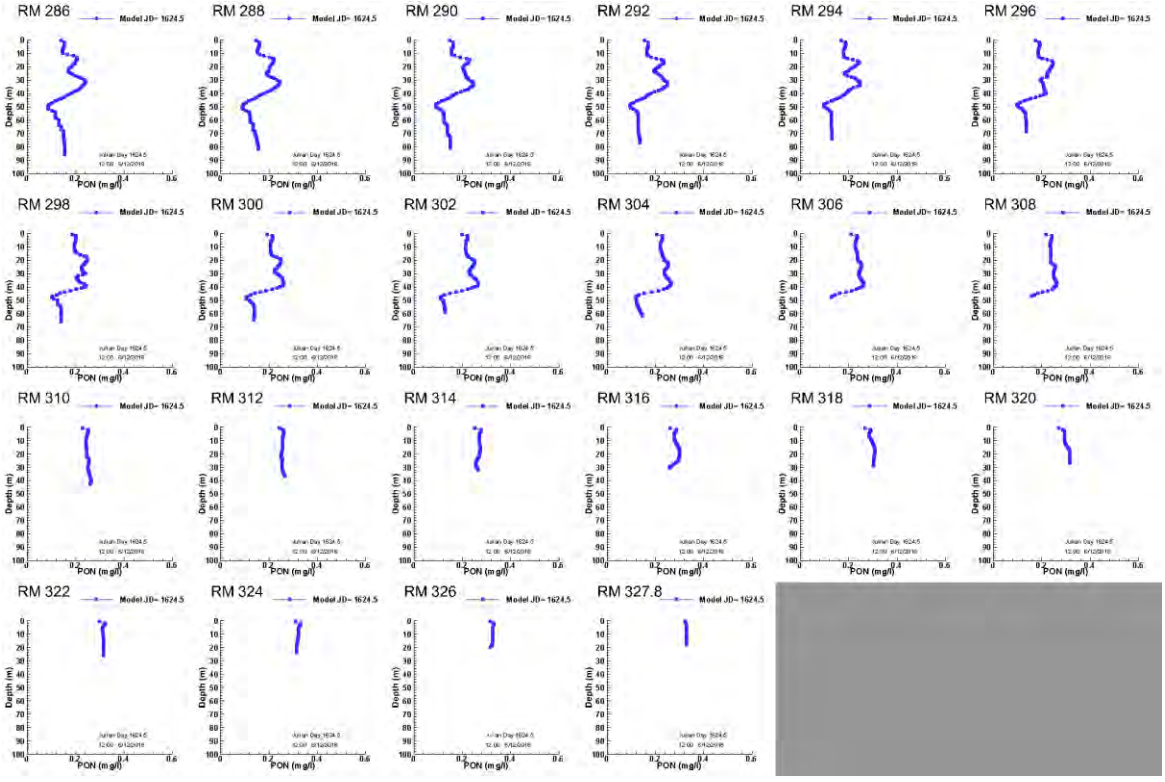


Figure 1744. Vertical profiles of PON compared with data for 6/12/2018.

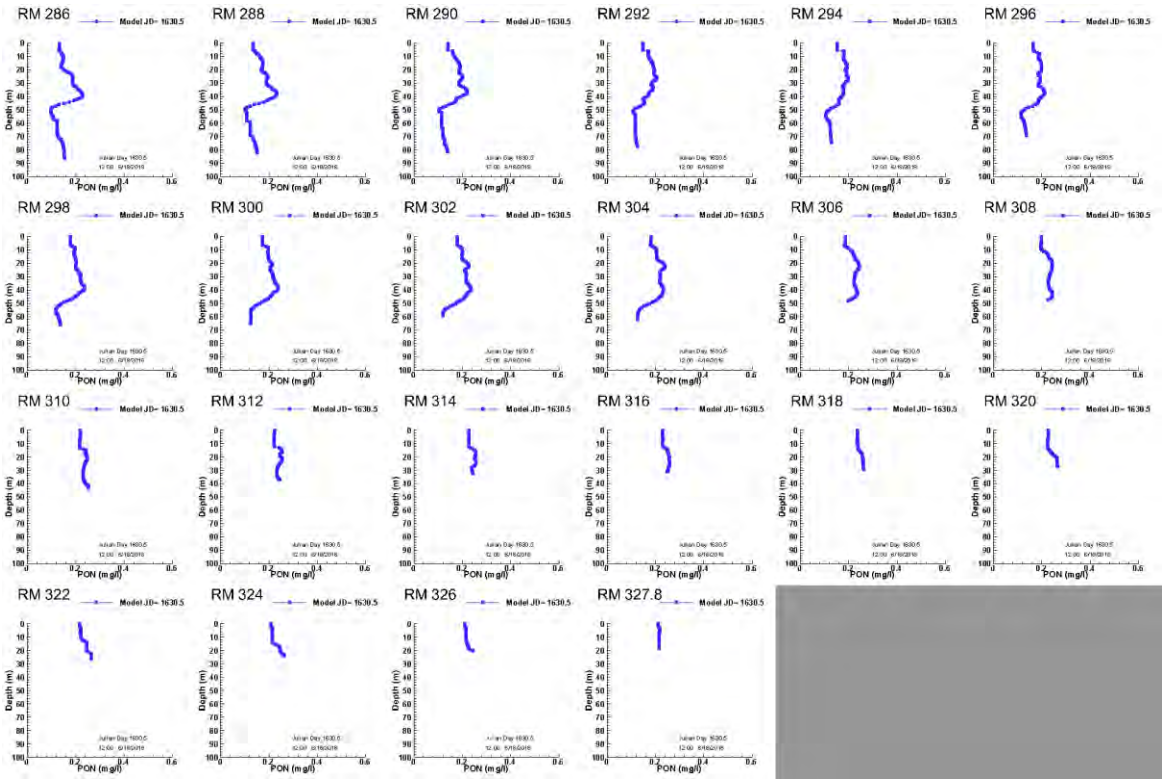


Figure 1745. Vertical profiles of PON compared with data for 6/18/2018.

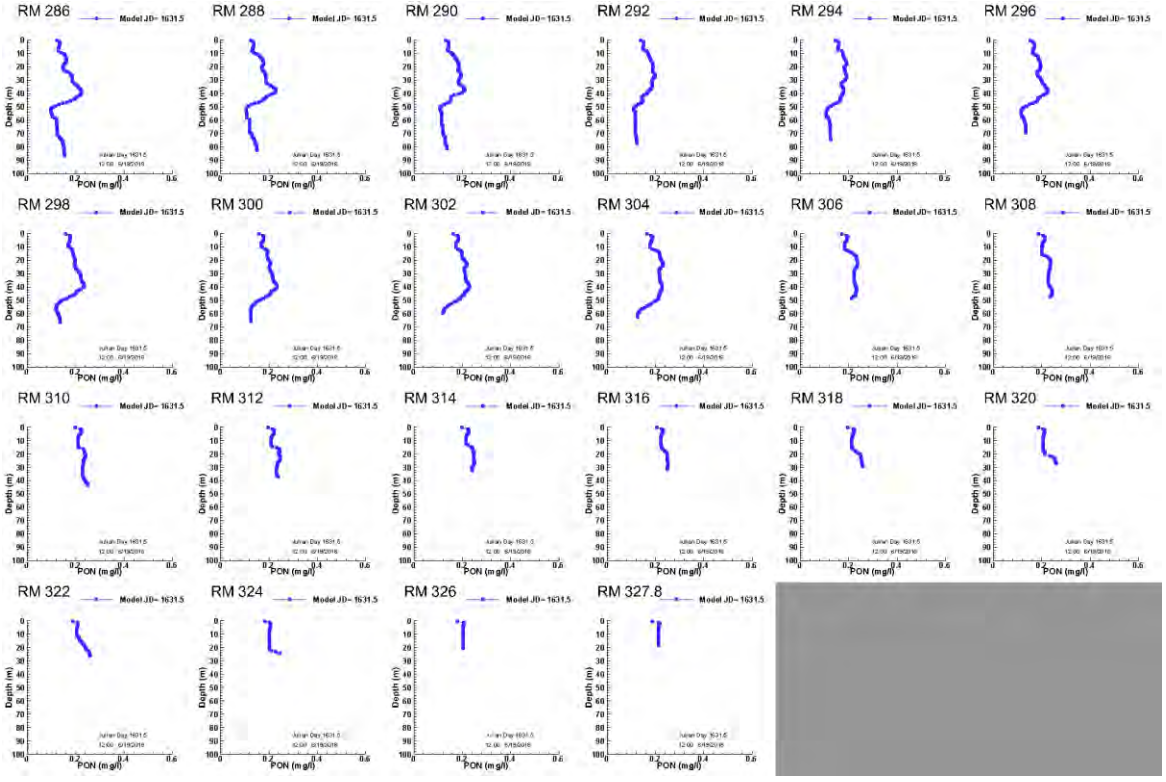


Figure 1746. Vertical profiles of PON compared with data for 6/19/2018.

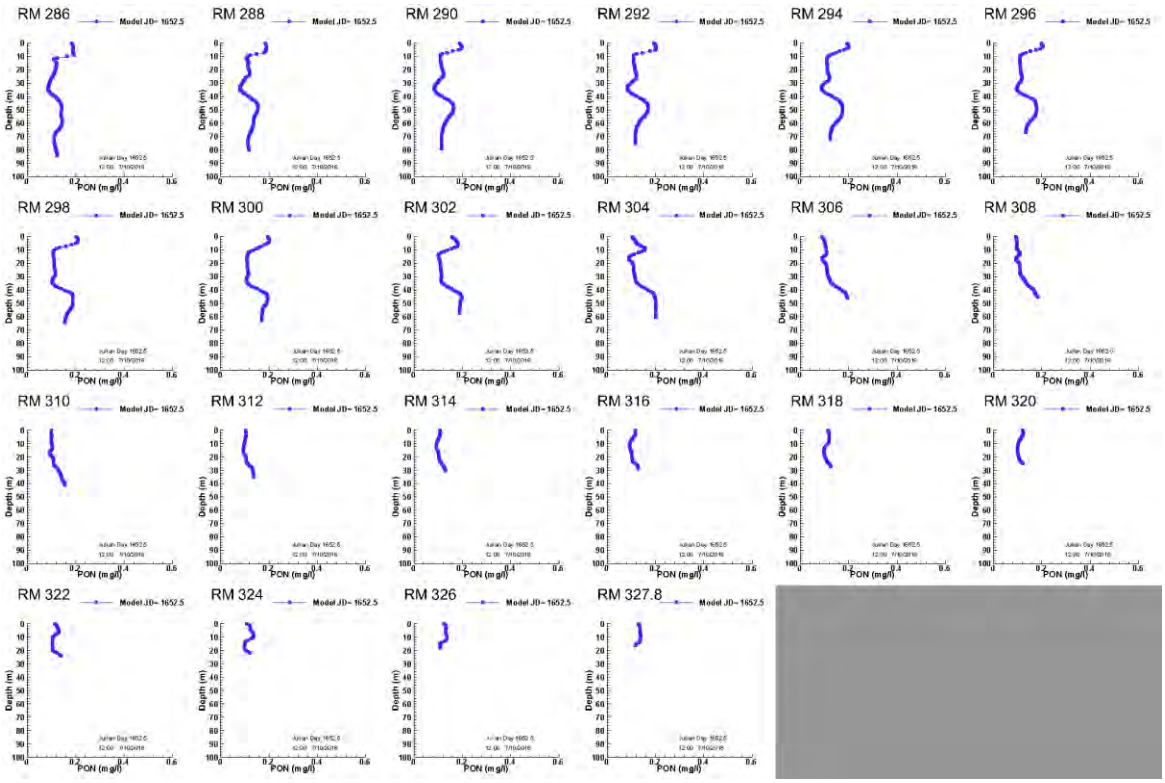


Figure 1747. Vertical profiles of PON compared with data for 7/10/2018.

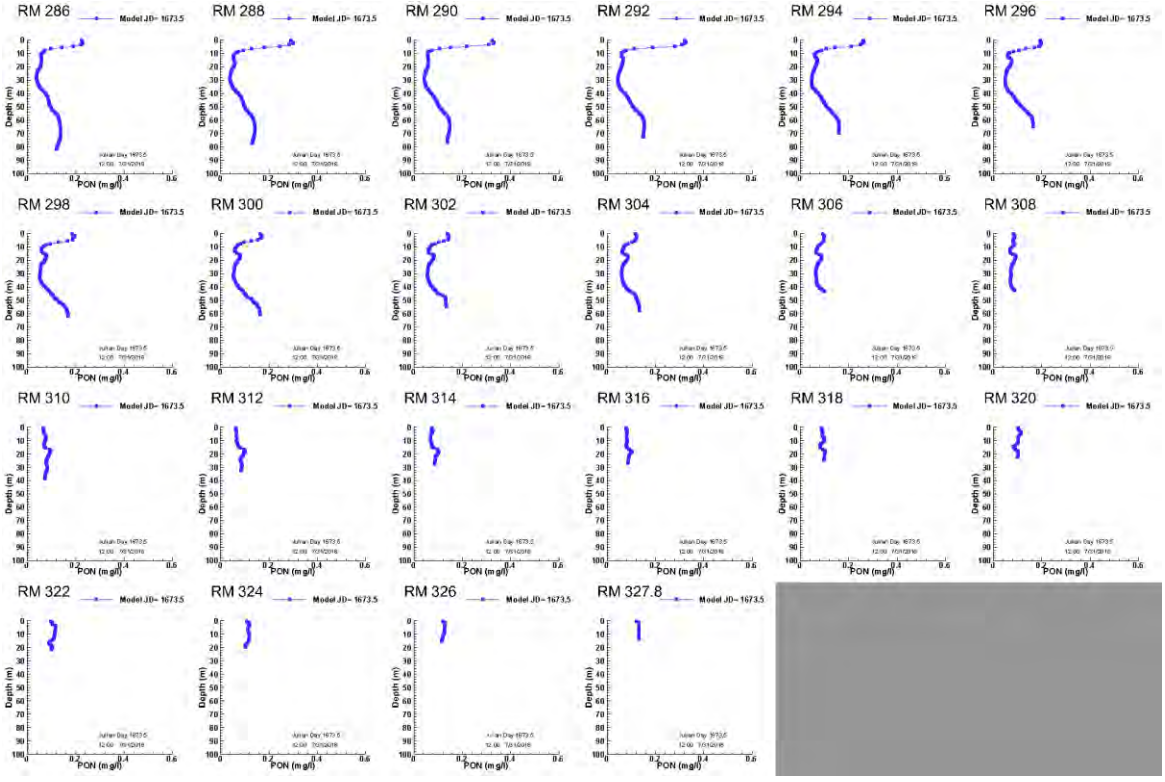


Figure 1748. Vertical profiles of PON compared with data for 7/31/2018.

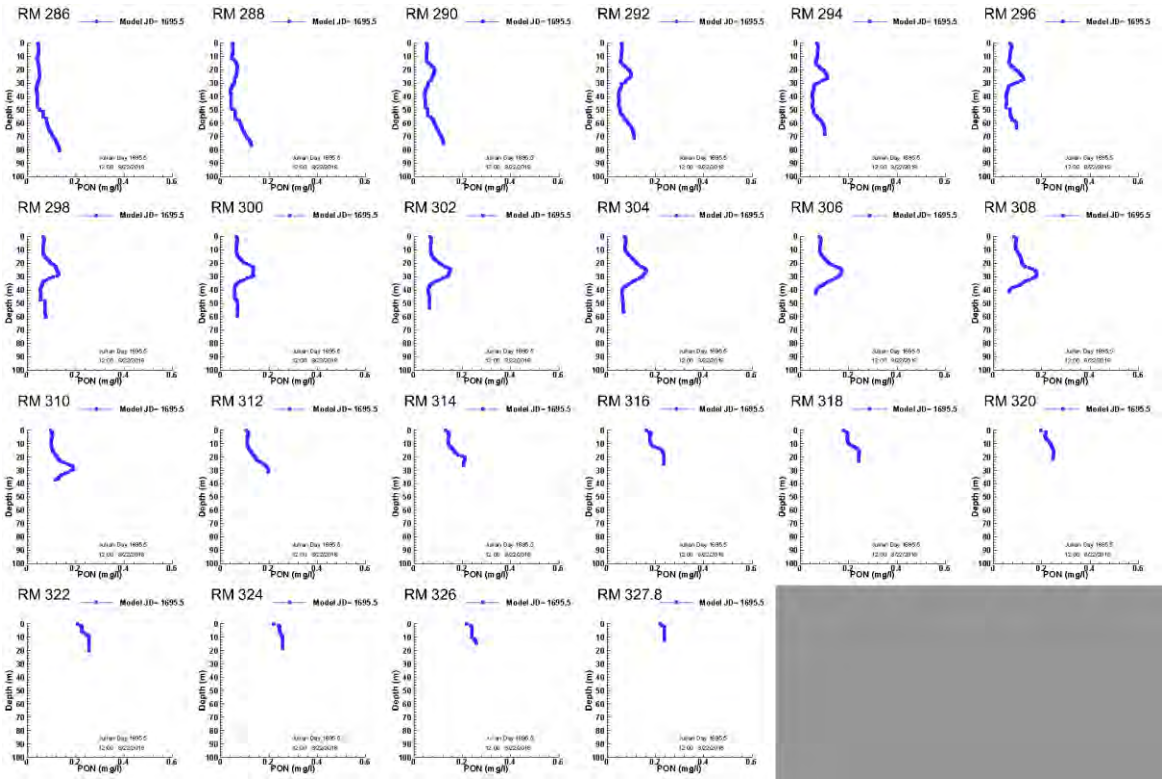


Figure 1749. Vertical profiles of PON compared with data for 8/22/2018.

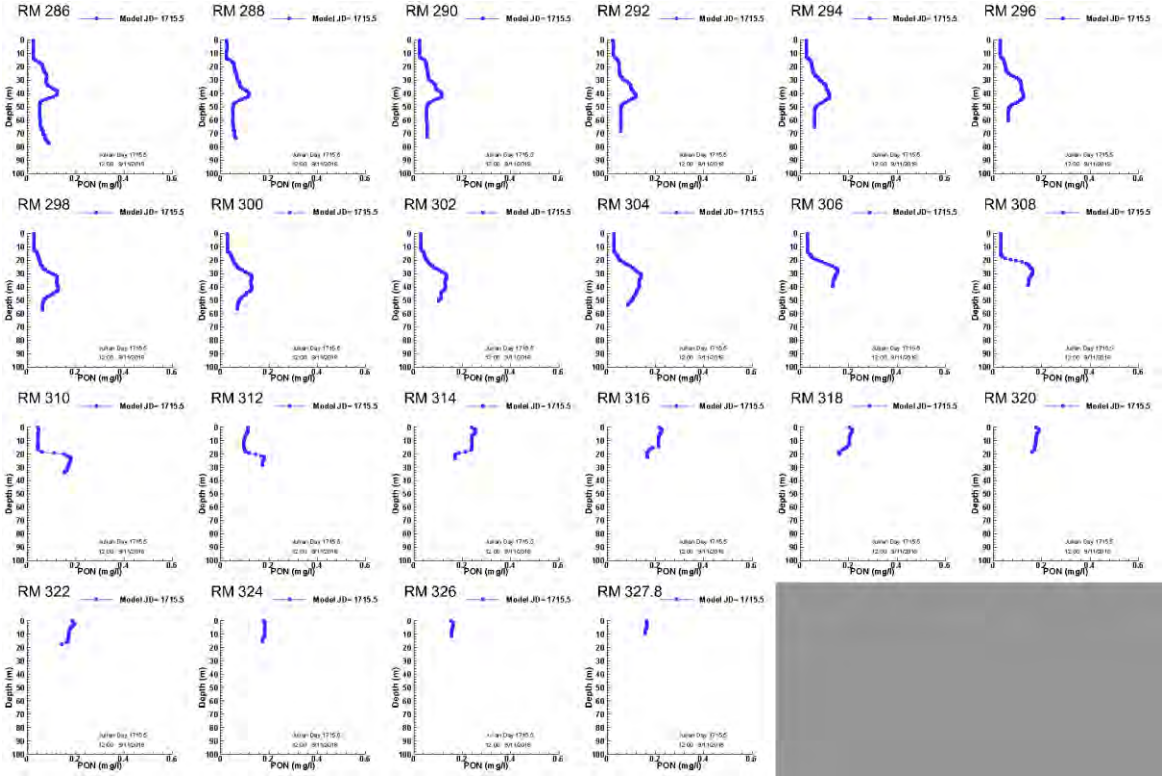


Figure 1750. Vertical profiles of PON compared with data for 9/11/2018.

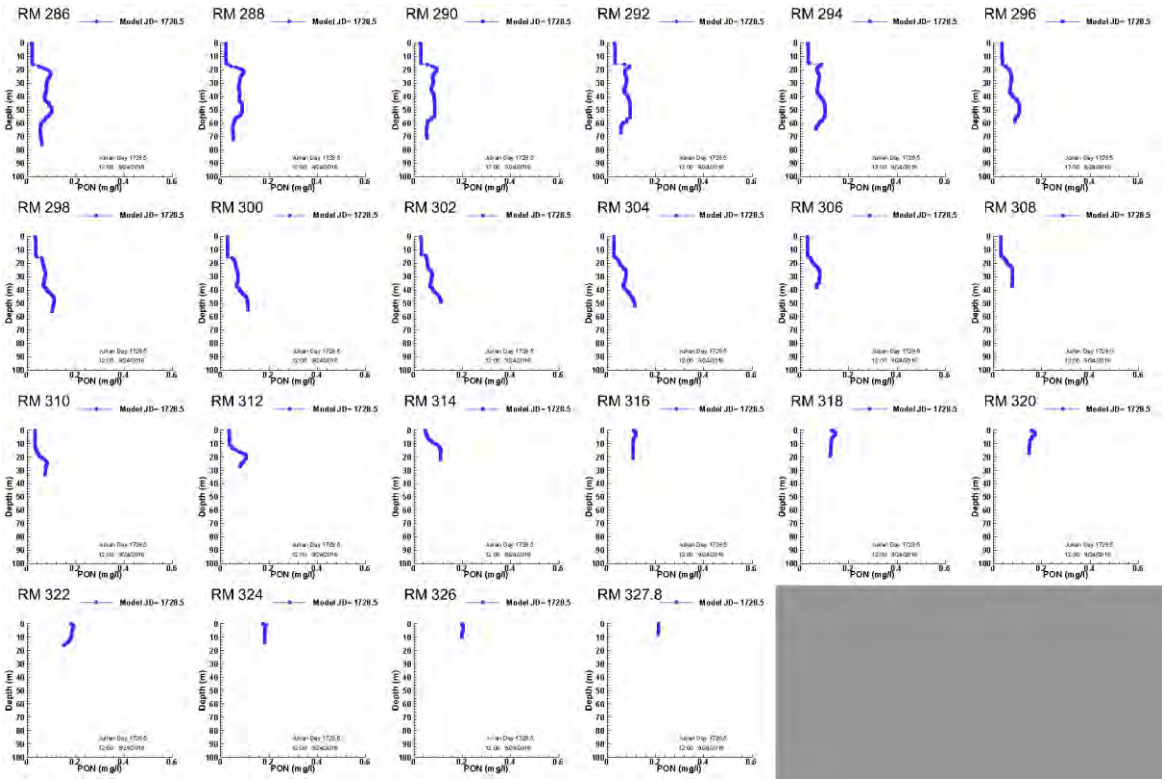


Figure 1751. Vertical profiles of PON compared with data for 9/24/2018.

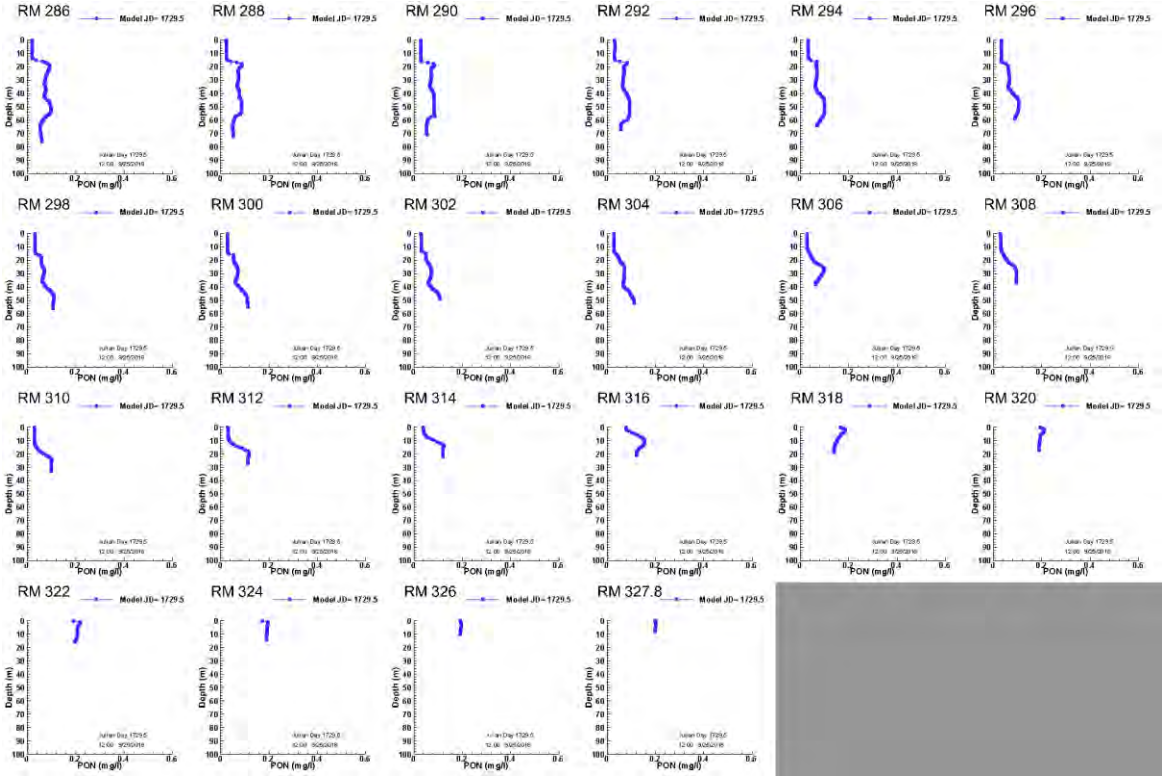


Figure 1752. Vertical profiles of PON compared with data for 9/25/2018.

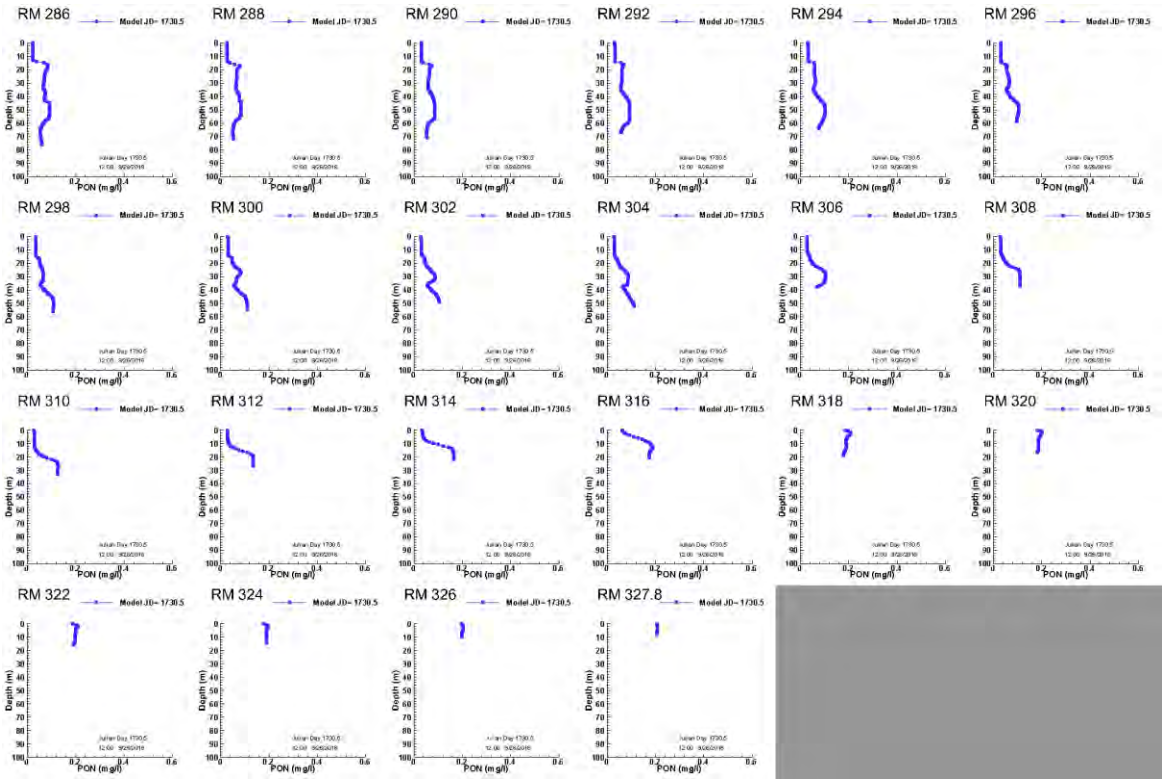


Figure 1753. Vertical profiles of PON compared with data for 9/26/2018.

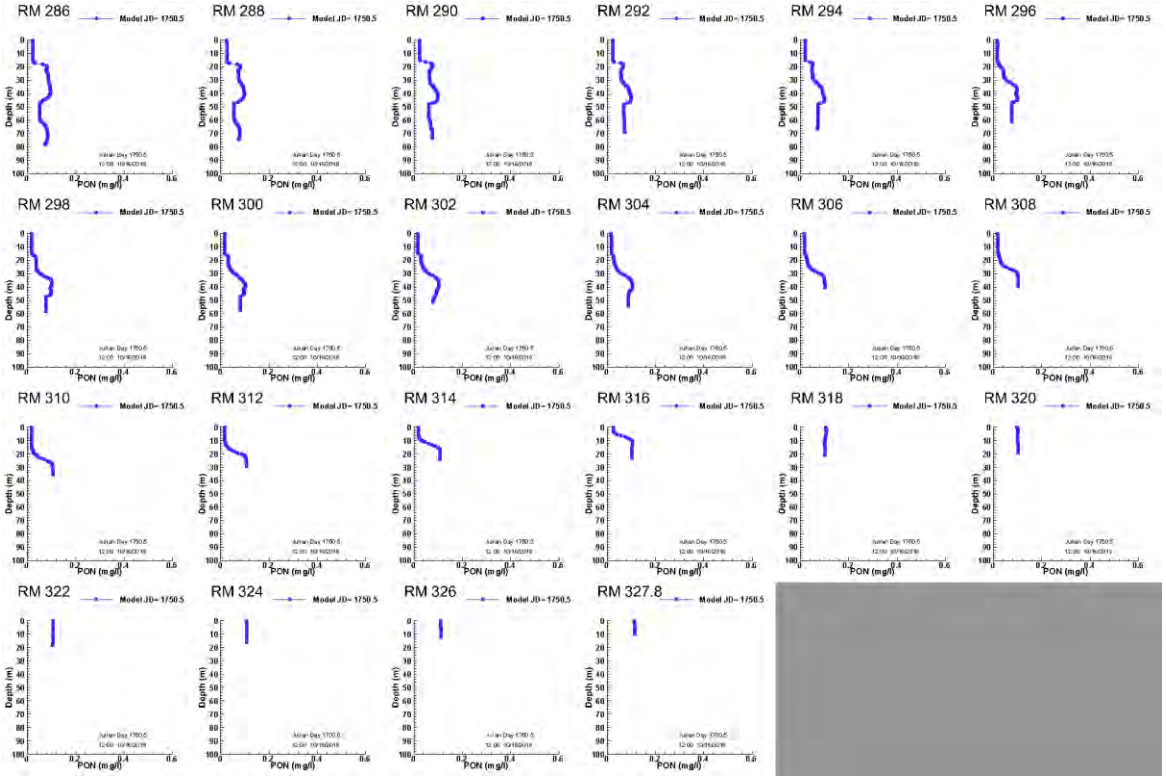


Figure 1754. Vertical profiles of PON compared with data for 10/16/2018.

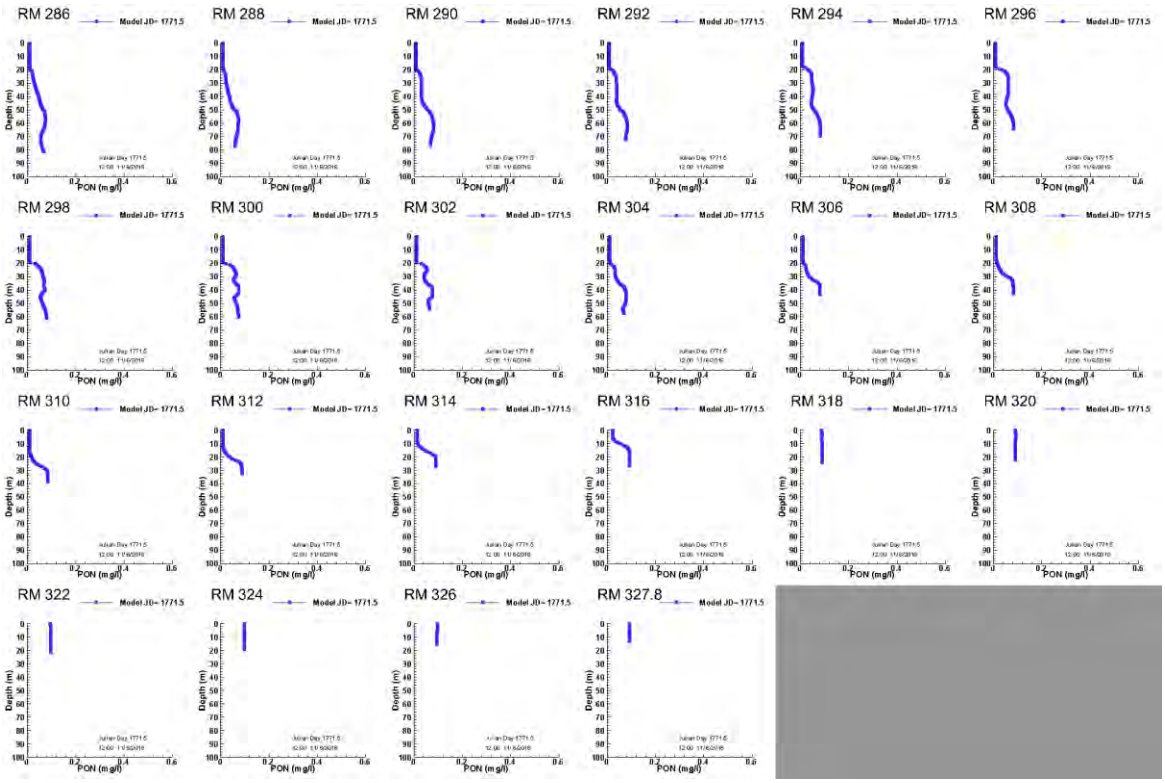


Figure 1755. Vertical profiles of PON compared with data for 11/ 6/2018.

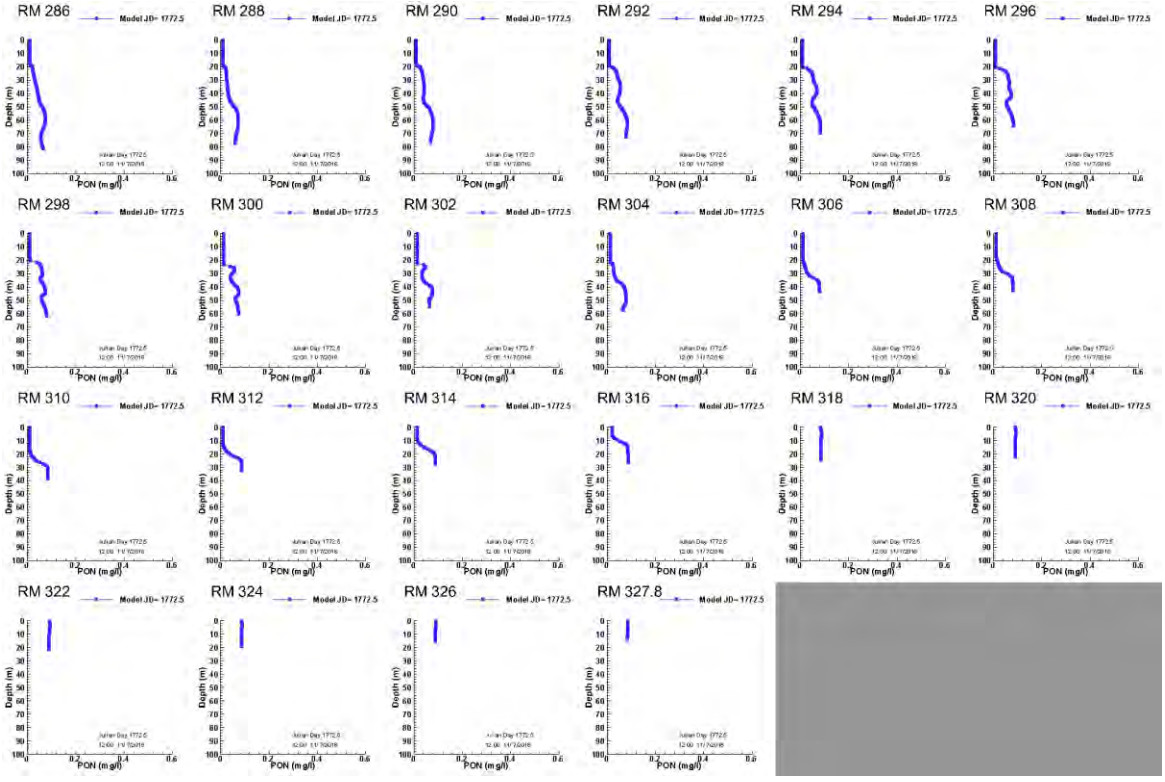


Figure 1756. Vertical profiles of PON compared with data for 11/ 7/2018.

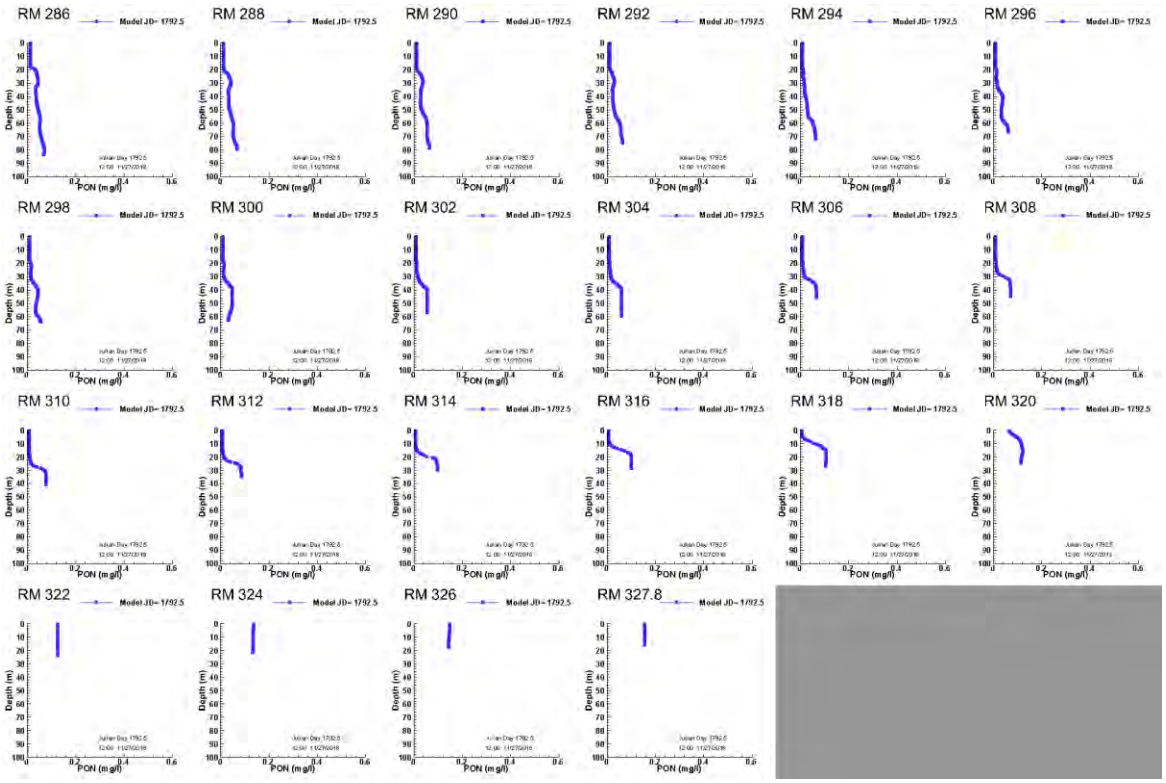


Figure 1757. Vertical profiles of PON compared with data for 11/27/2018.

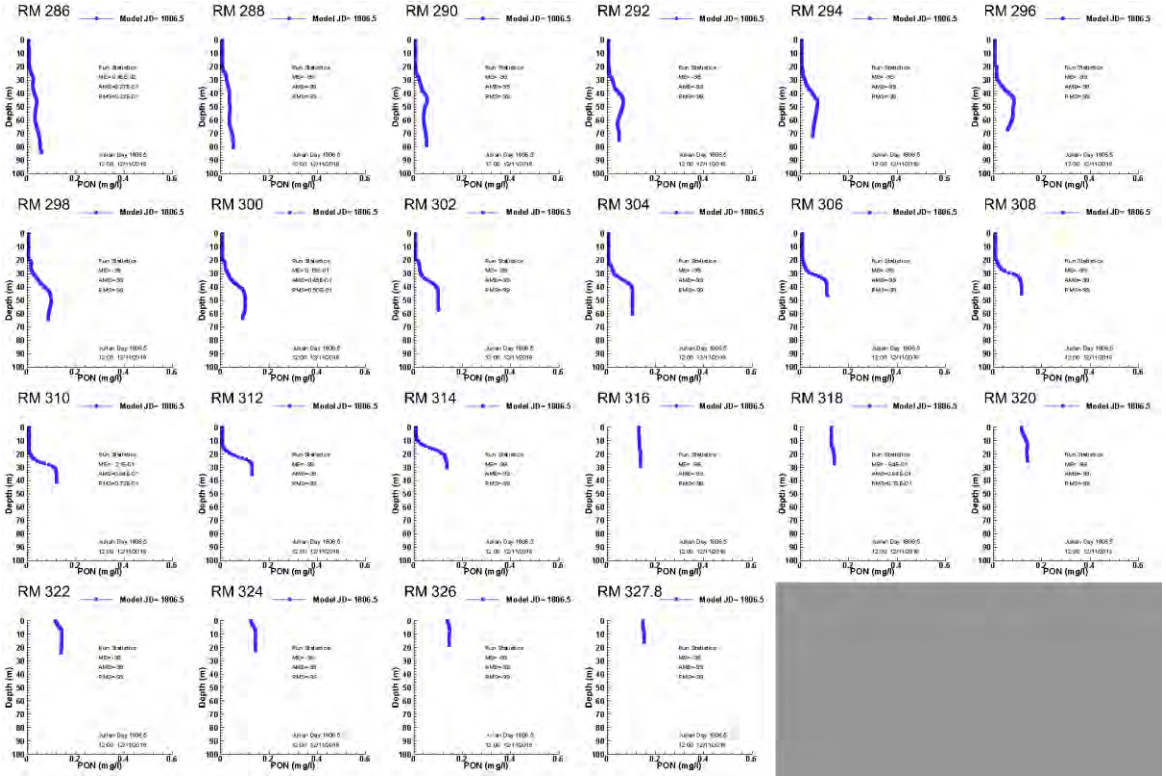


Figure 1758. Vertical profiles of PON compared with data for 12/11/2018.

TKN

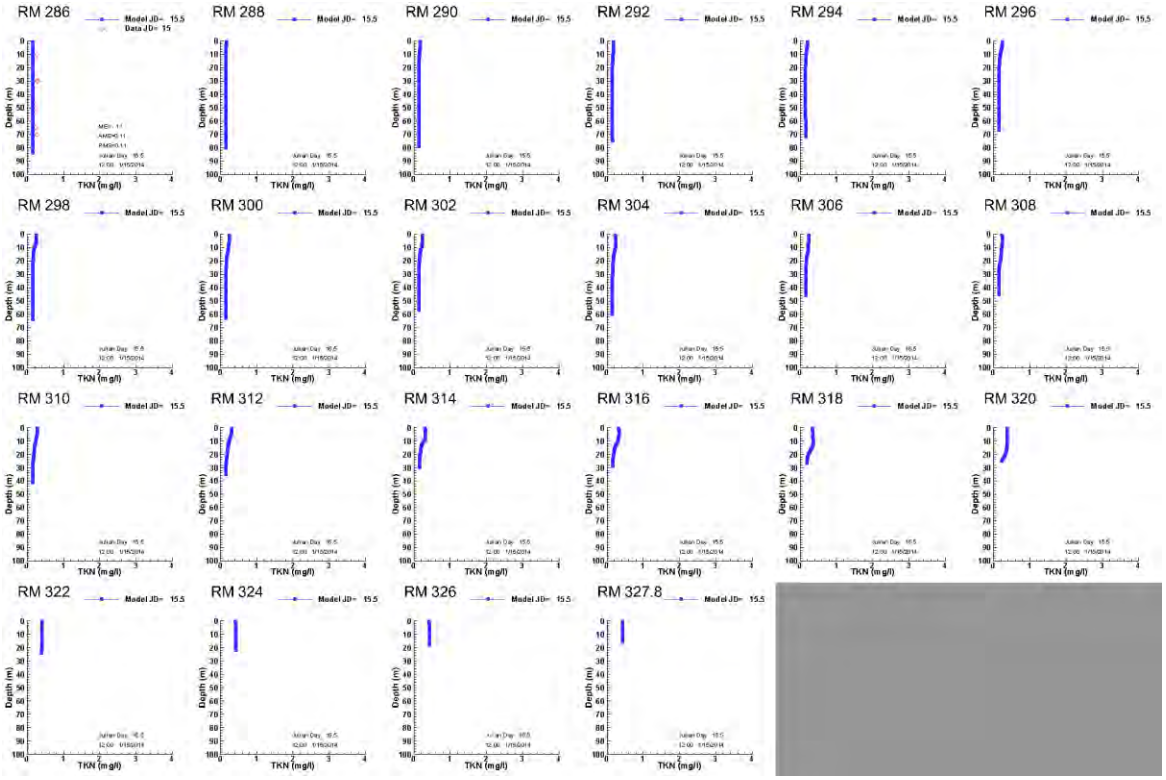


Figure 1759. Vertical profiles of TKN compared with data for 1/15/2014.

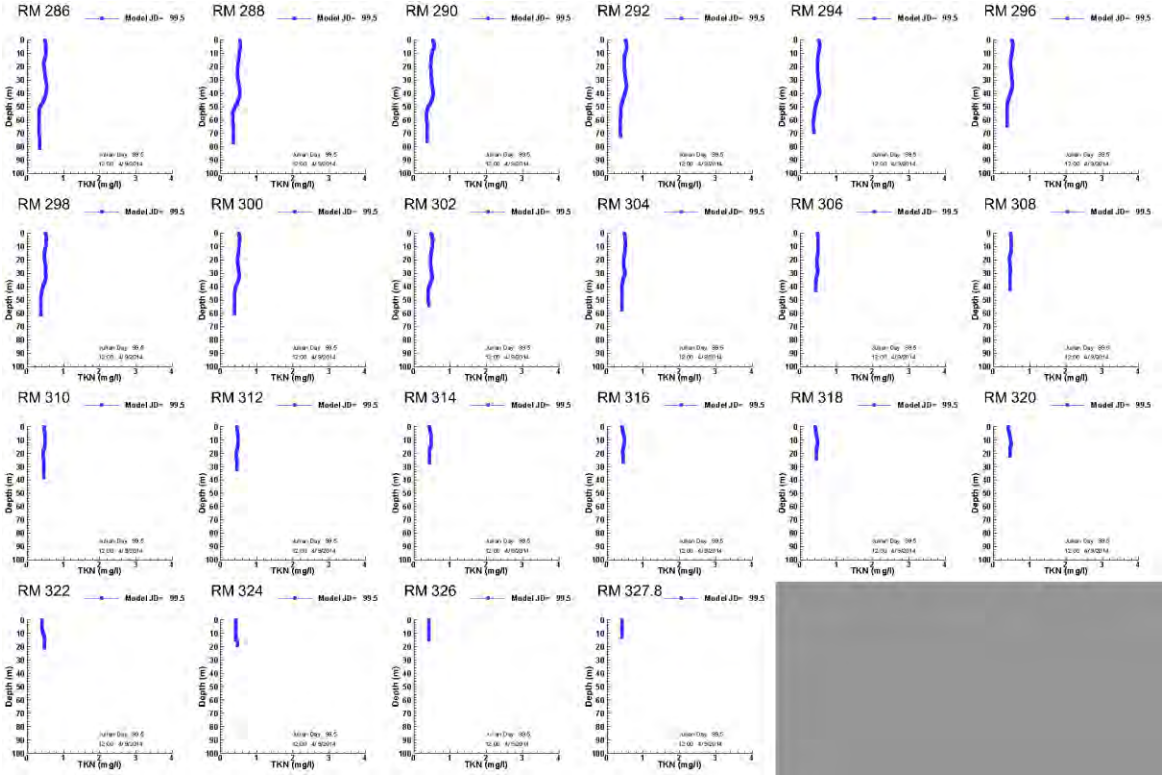


Figure 1760. Vertical profiles of TKN compared with data for 4/ 9/2014.

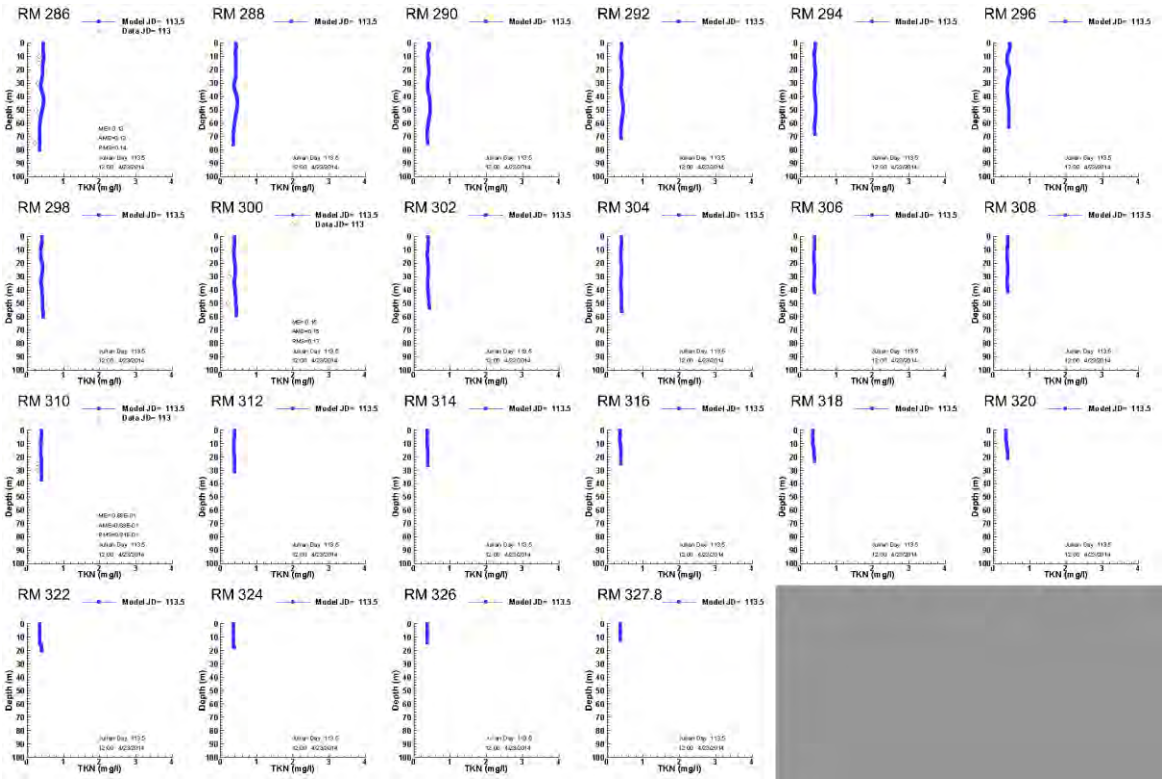


Figure 1761. Vertical profiles of TKN compared with data for 4/23/2014.

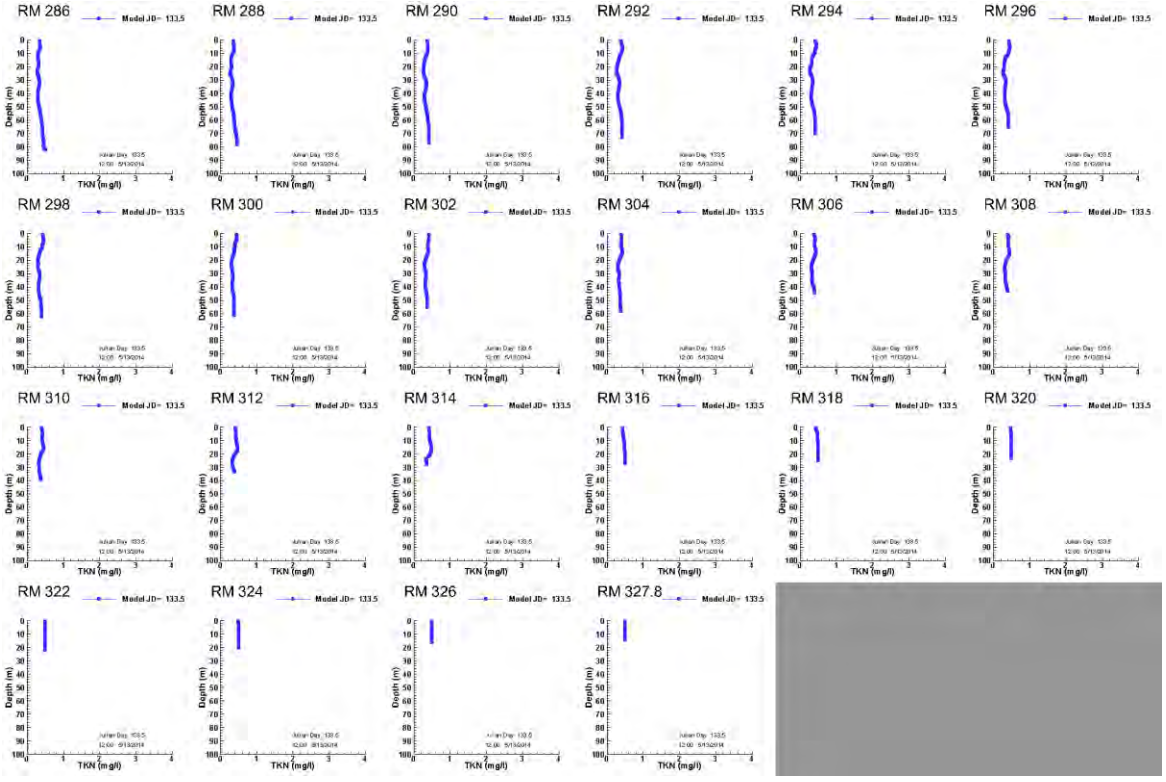


Figure 1762. Vertical profiles of TKN compared with data for 5/13/2014.

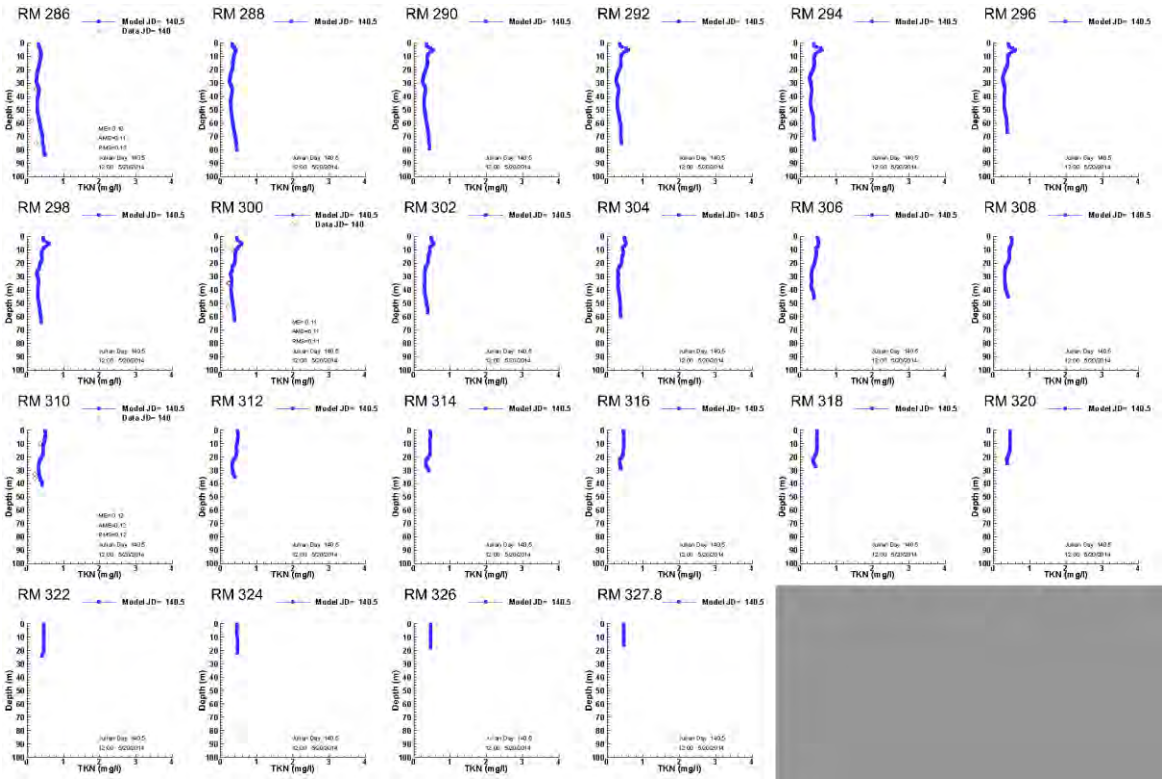


Figure 1763. Vertical profiles of TKN compared with data for 5/20/2014.

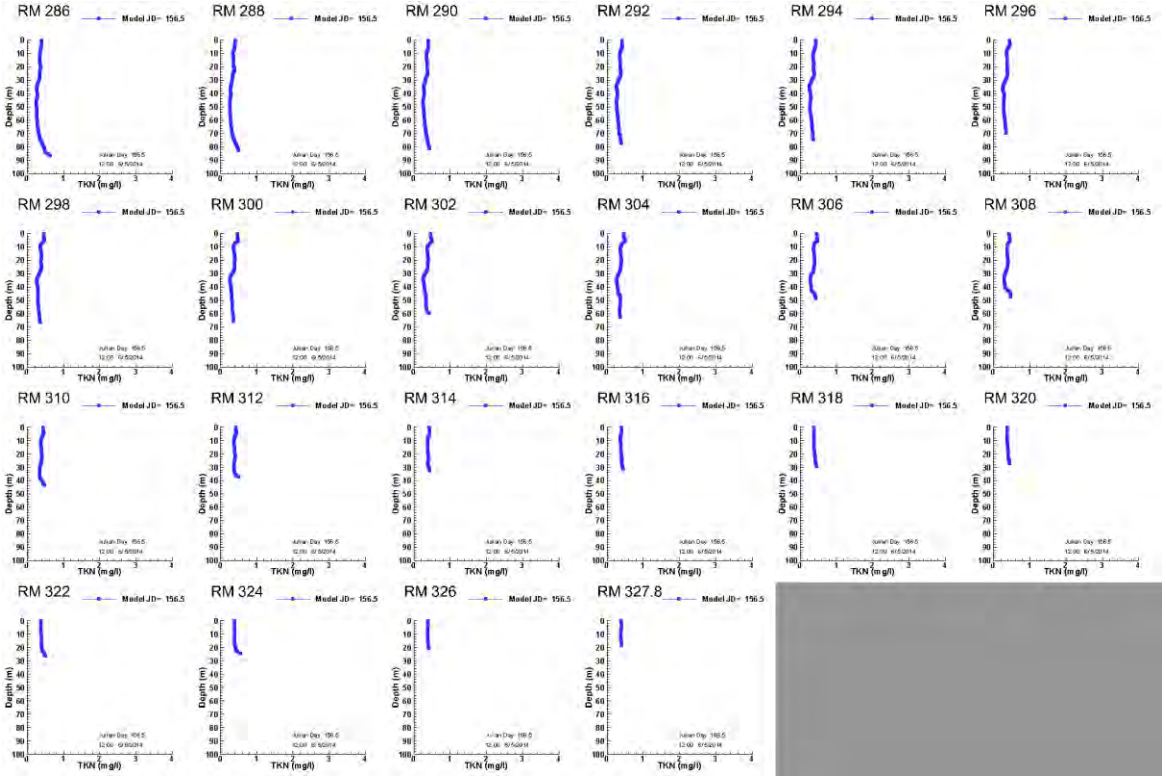


Figure 1764. Vertical profiles of TKN compared with data for 6/ 5/2014.

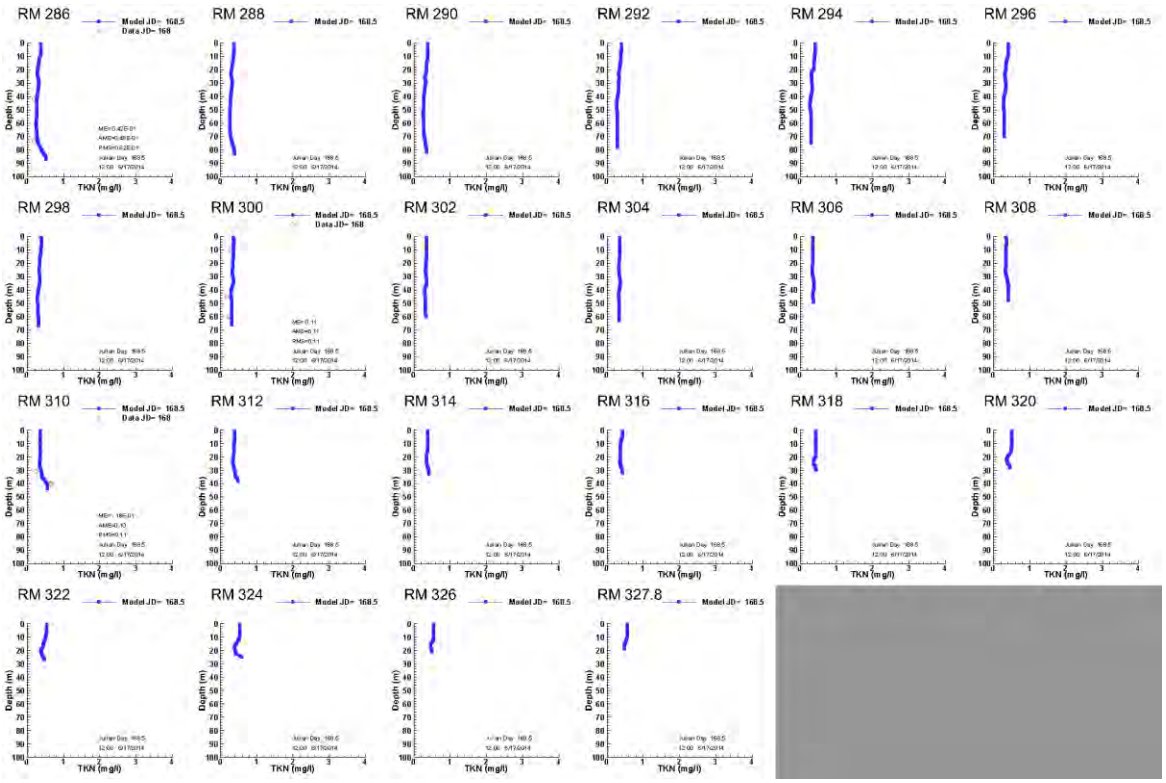


Figure 1765. Vertical profiles of TKN compared with data for 6/17/2014.

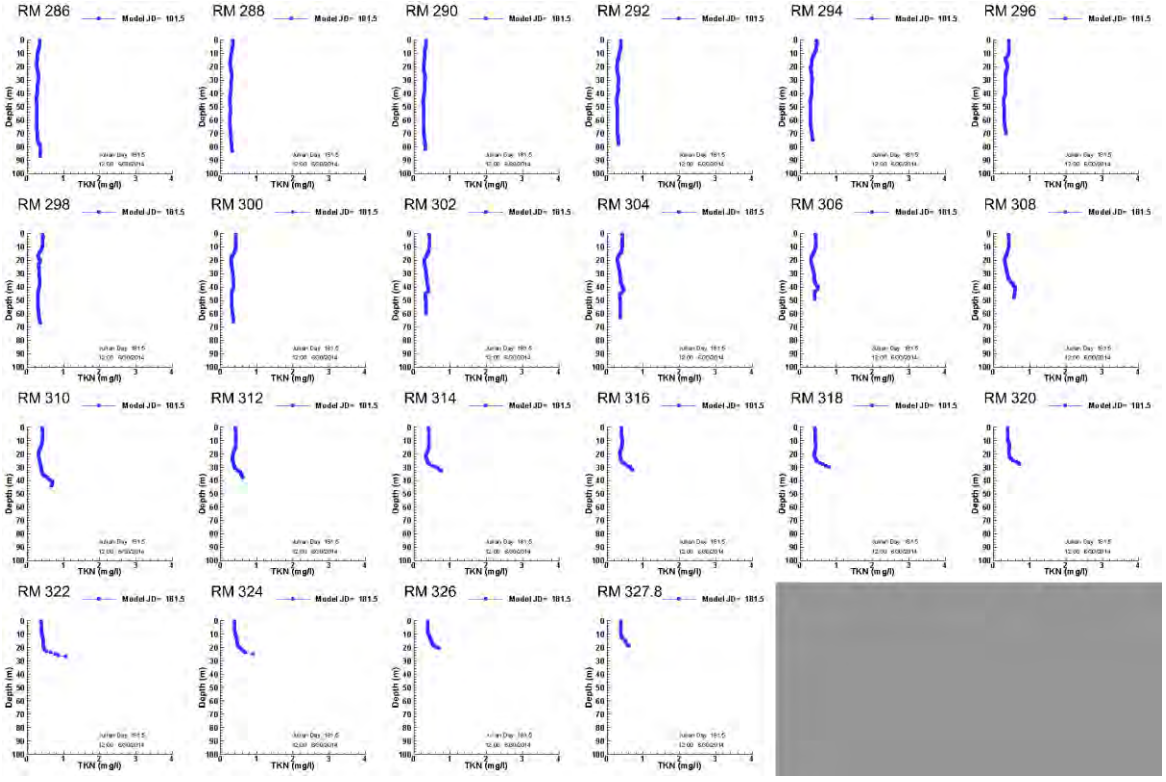


Figure 1766. Vertical profiles of TKN compared with data for 6/30/2014.

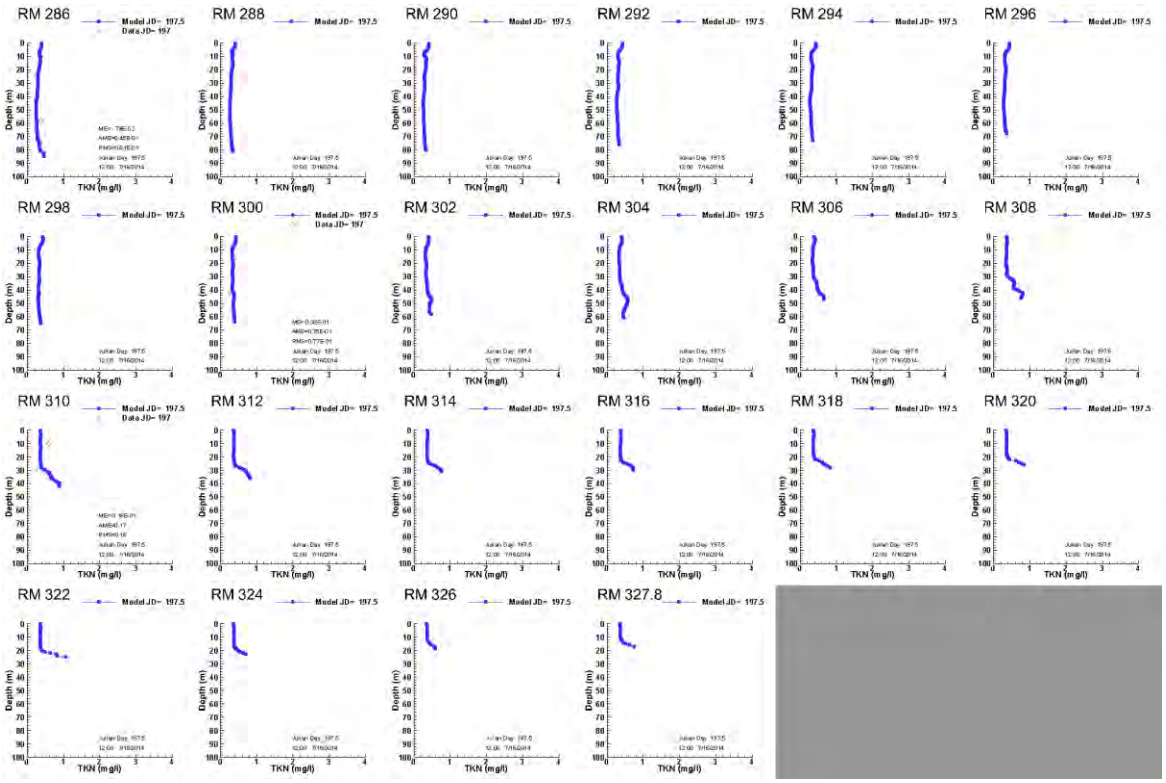


Figure 1767. Vertical profiles of TKN compared with data for 7/16/2014.

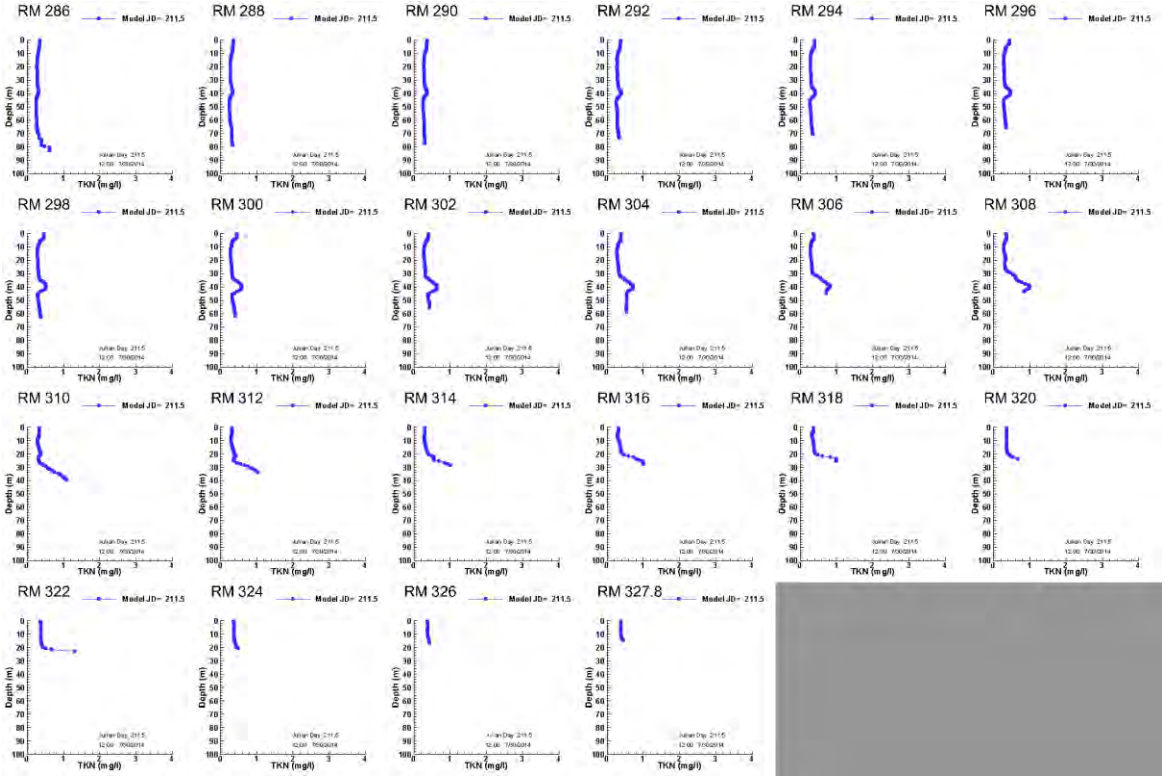


Figure 1768. Vertical profiles of TKN compared with data for 7/30/2014.

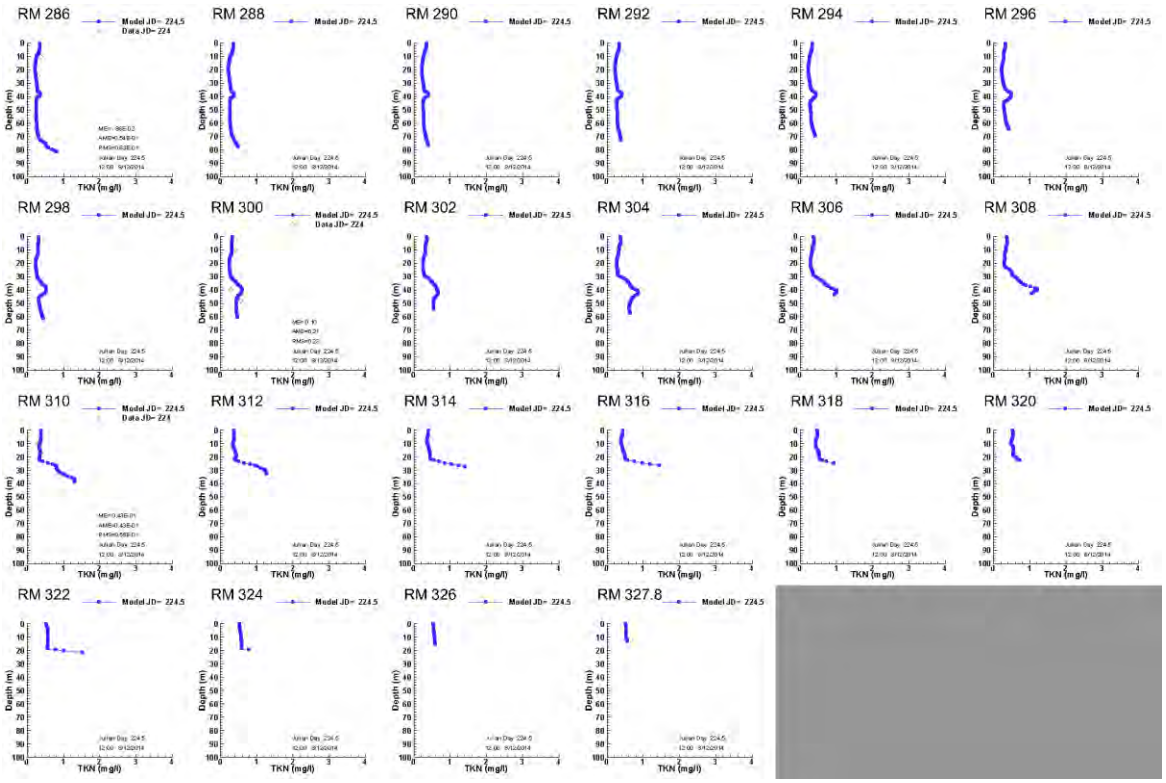


Figure 1769. Vertical profiles of TKN compared with data for 8/12/2014.

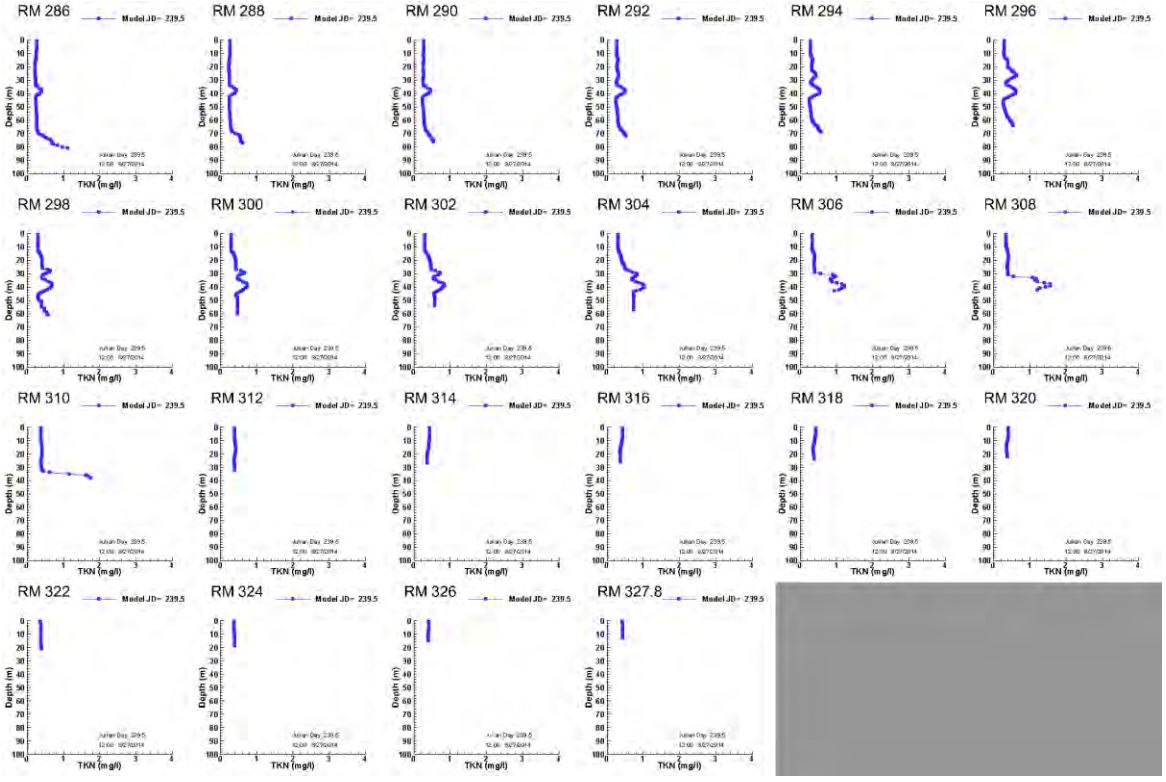


Figure 1770. Vertical profiles of TKN compared with data for 8/27/2014.

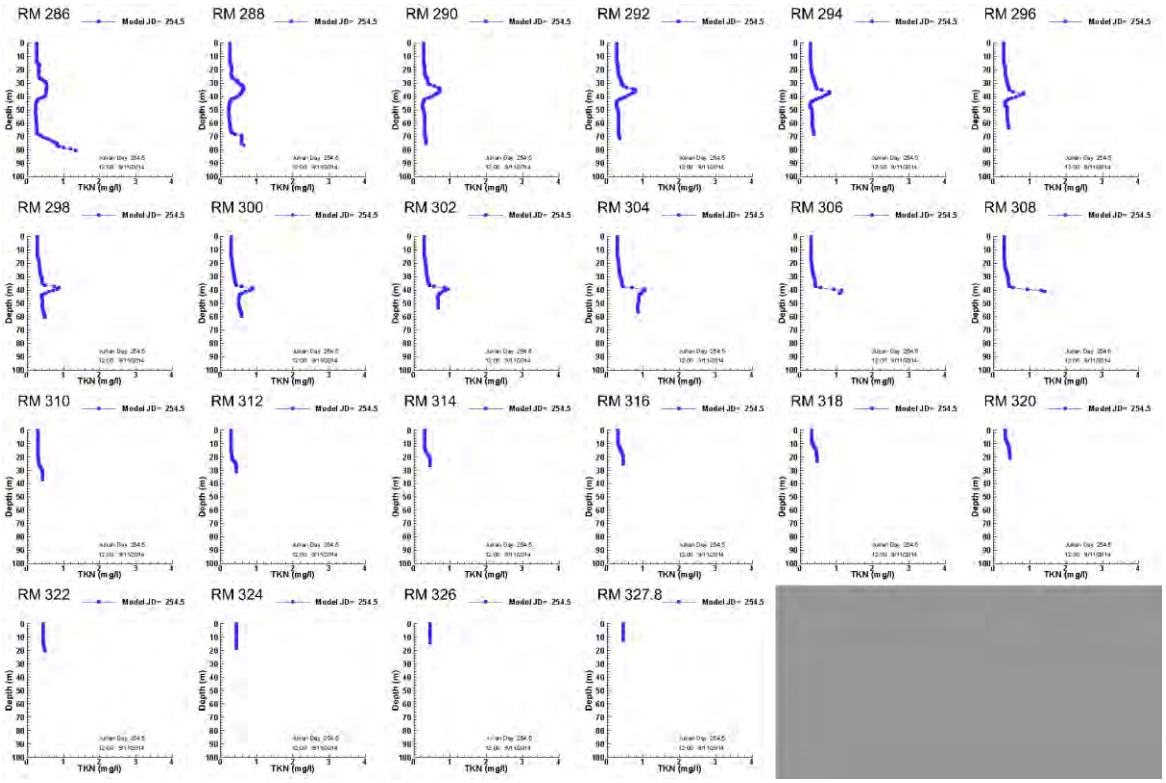


Figure 1771. Vertical profiles of TKN compared with data for 9/11/2014.

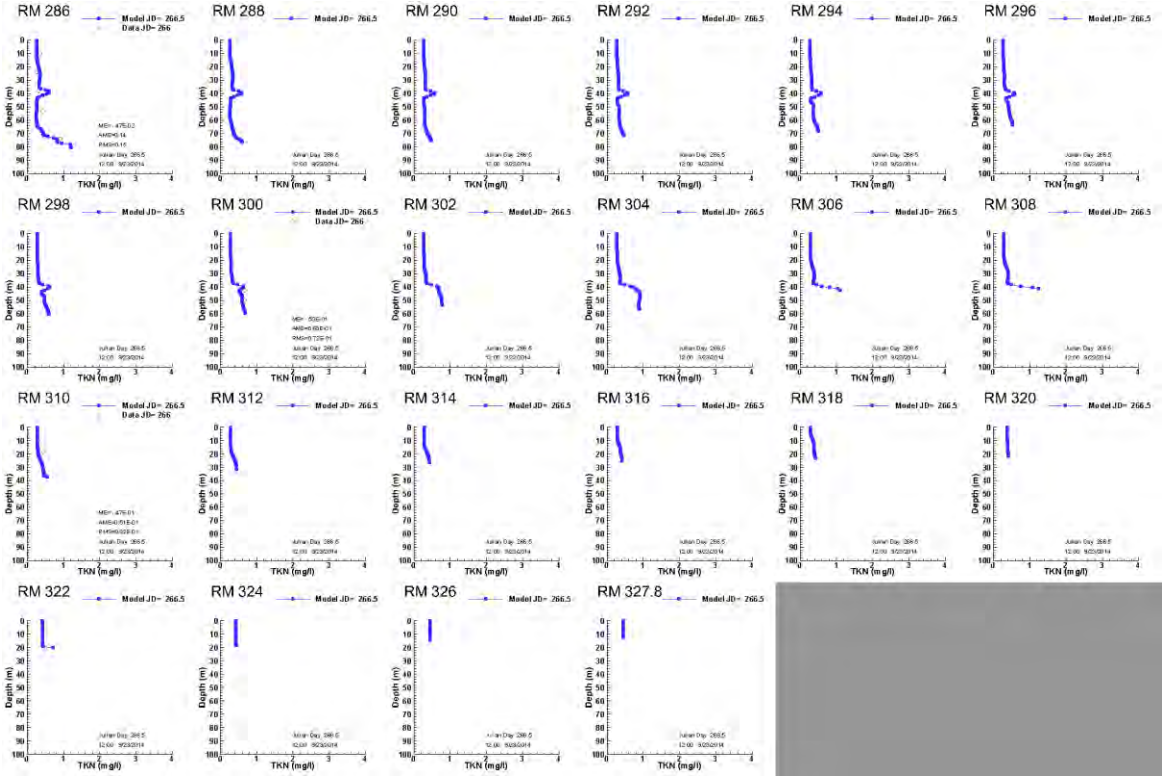


Figure 1772. Vertical profiles of TKN compared with data for 9/23/2014.

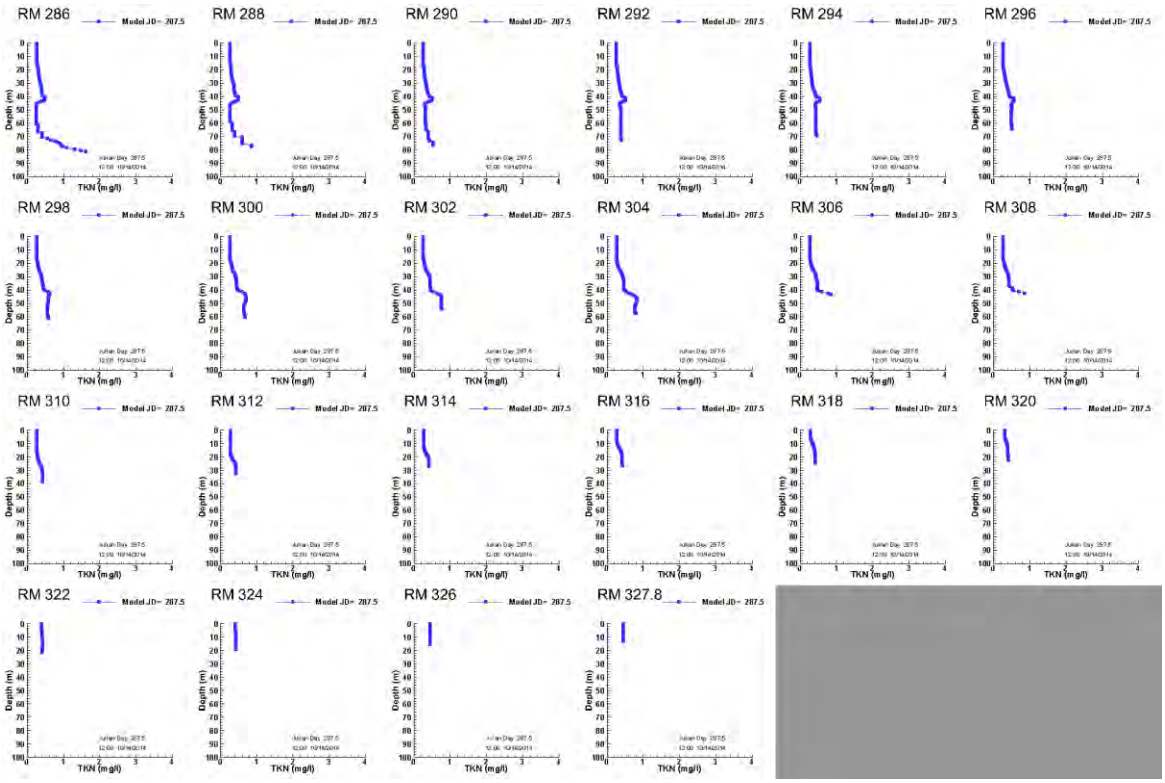


Figure 1773. Vertical profiles of TKN compared with data for 10/14/2014.

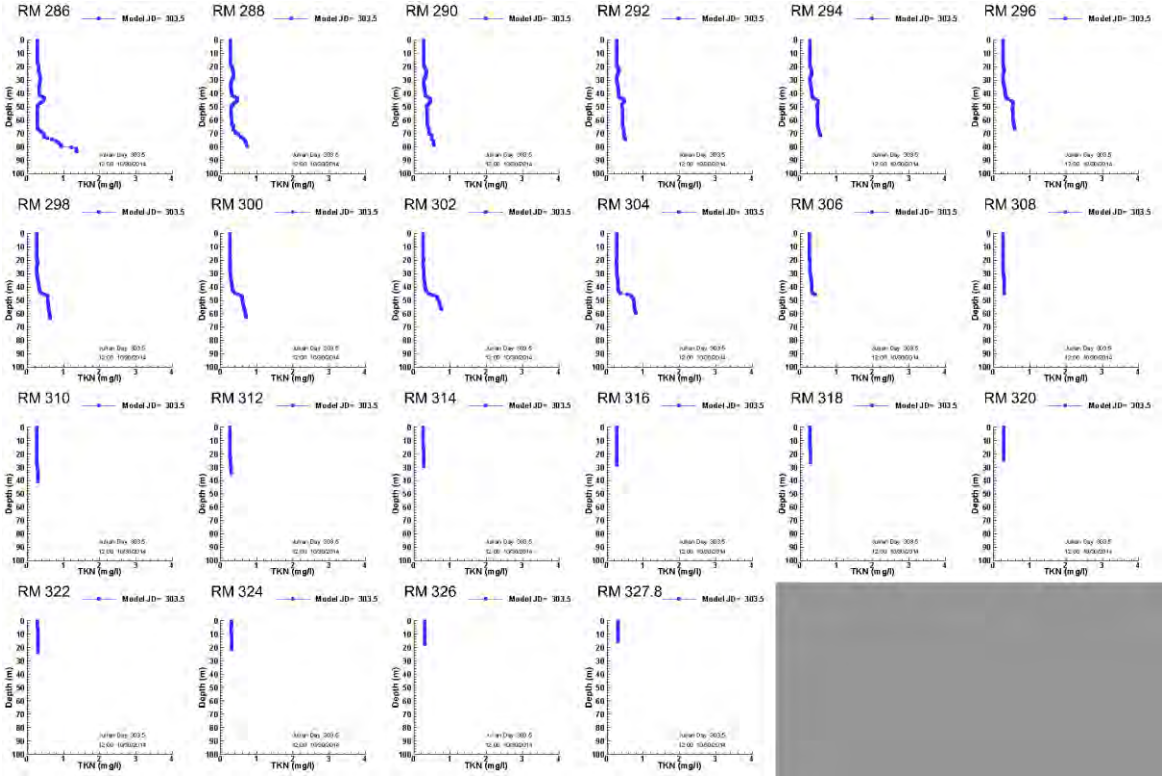


Figure 1774. Vertical profiles of TKN compared with data for 10/30/2014.

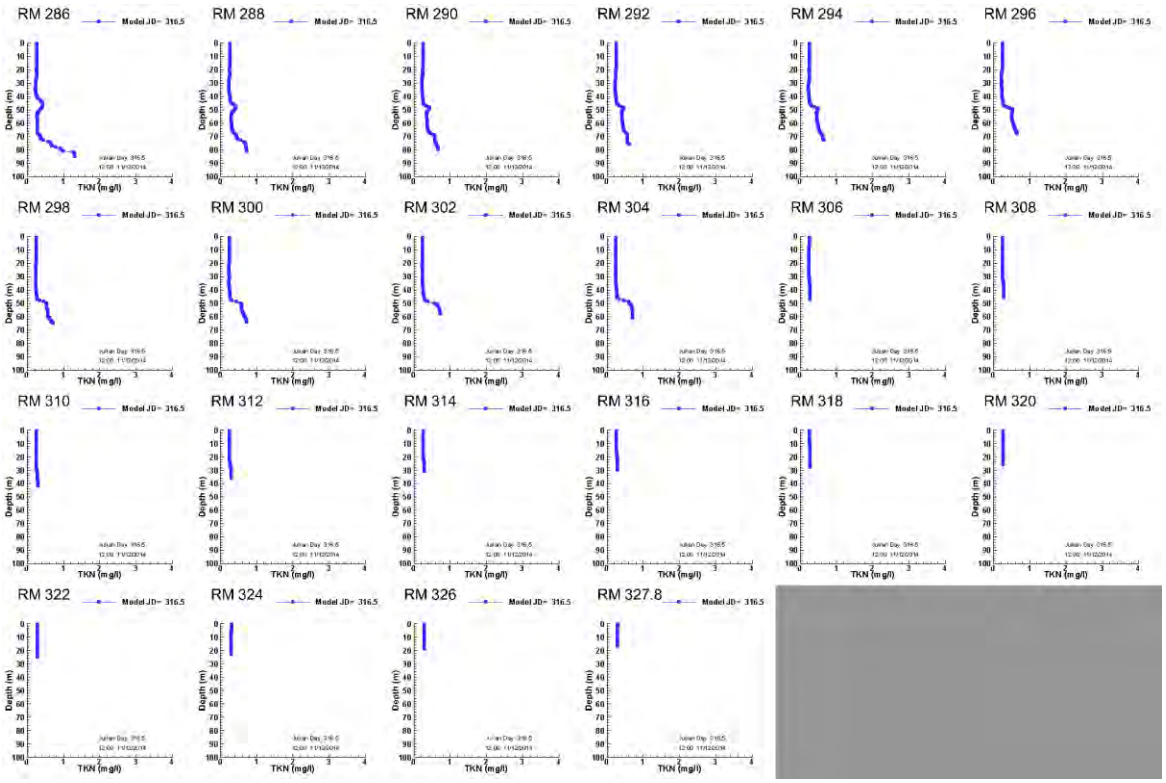


Figure 1775. Vertical profiles of TKN compared with data for 11/12/2014.

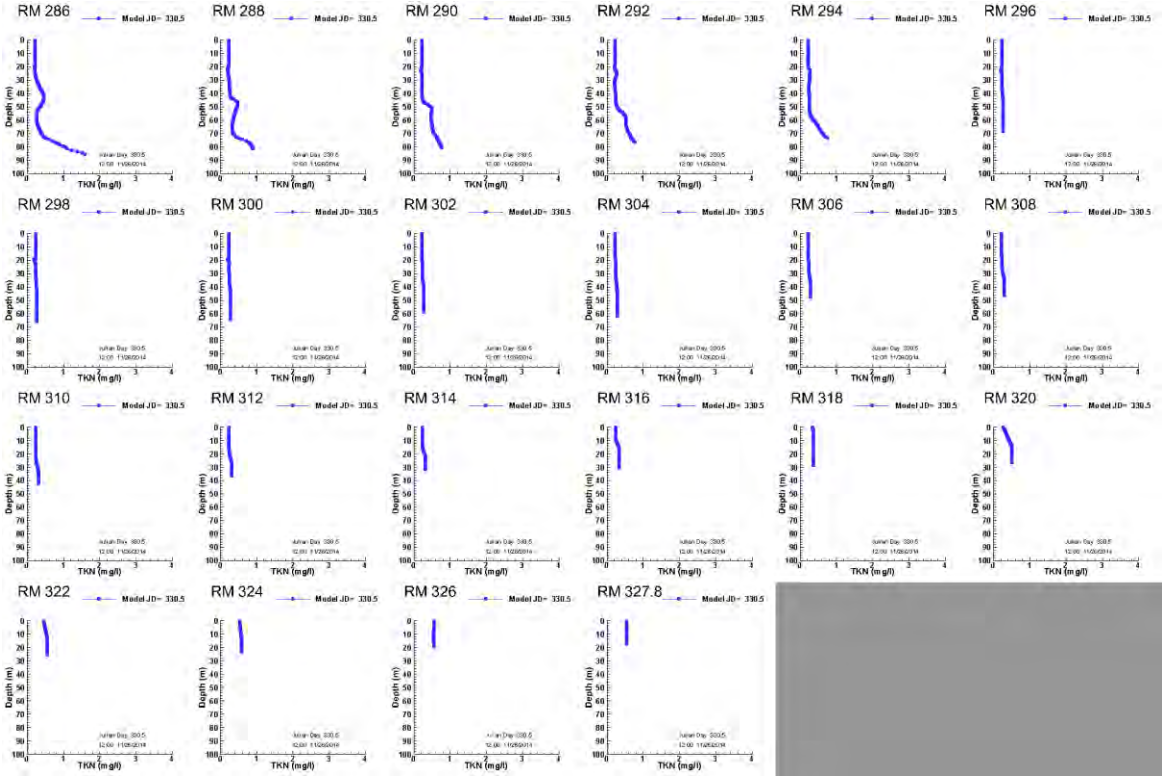


Figure 1776. Vertical profiles of TKN compared with data for 11/26/2014.

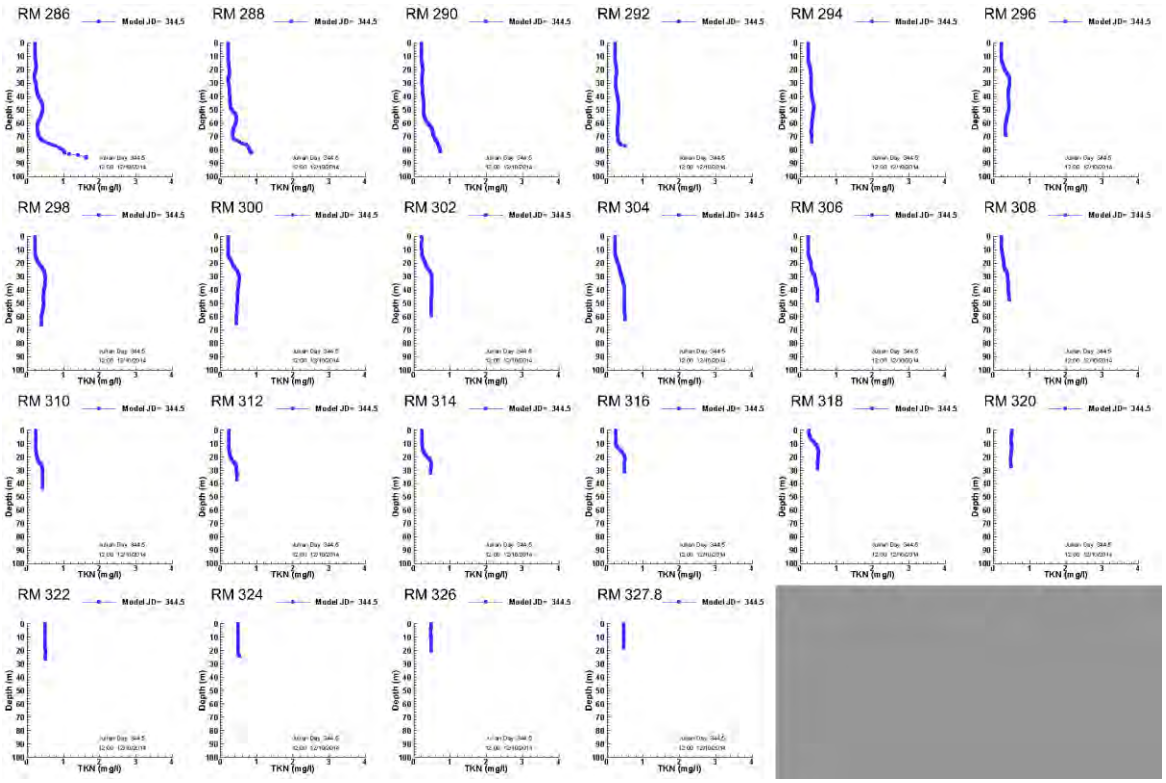


Figure 1777. Vertical profiles of TKN compared with data for 12/10/2014.

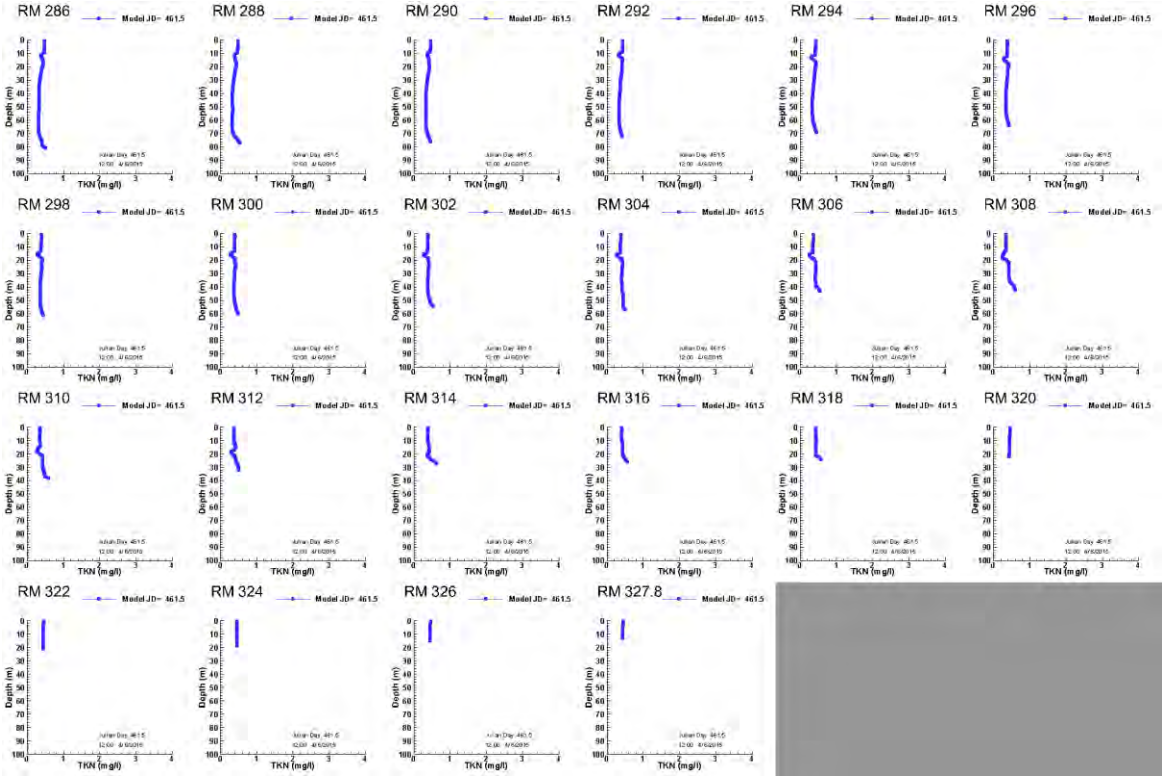


Figure 1778. Vertical profiles of TKN compared with data for 4/ 6/2015.

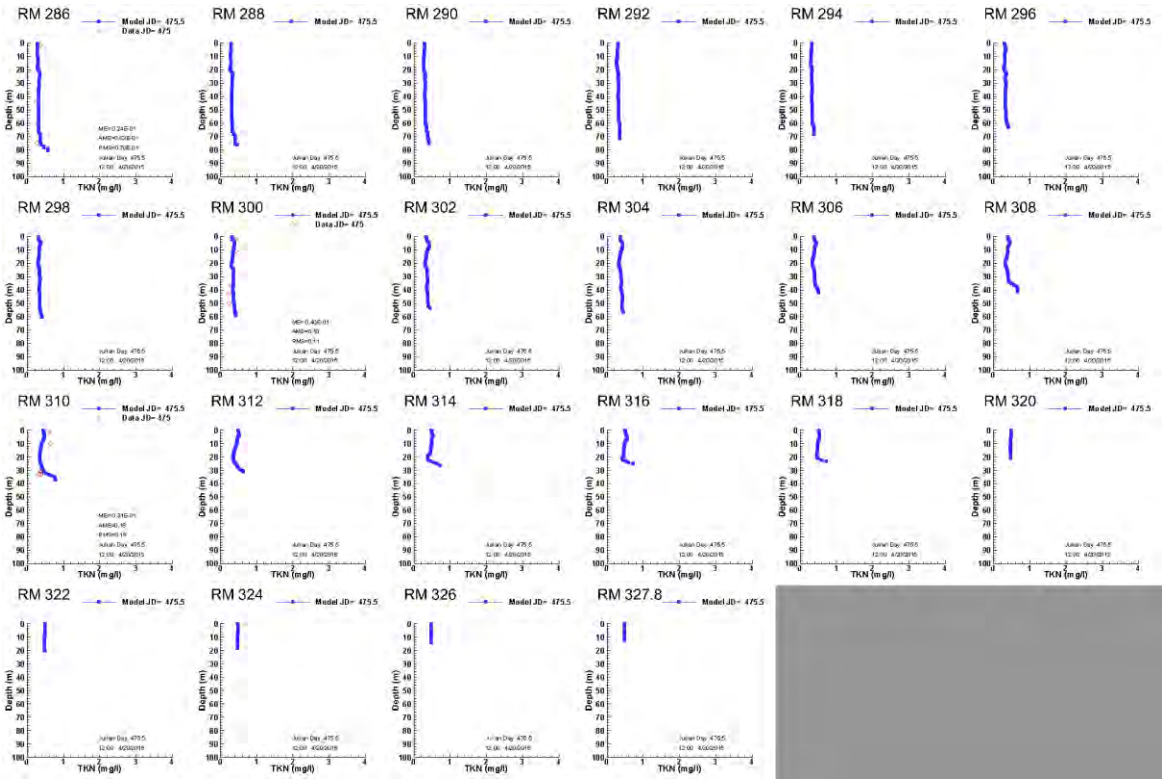


Figure 1779. Vertical profiles of TKN compared with data for 4/20/2015.

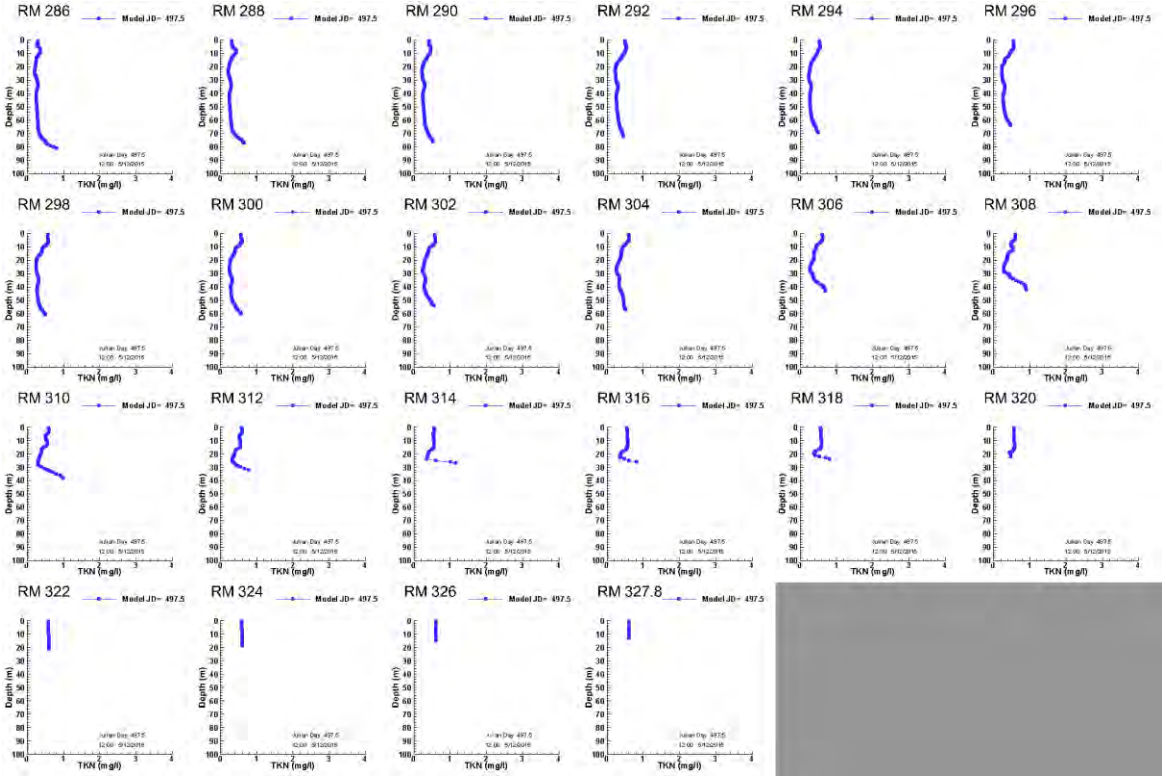


Figure 1780. Vertical profiles of TKN compared with data for 5/12/2015.

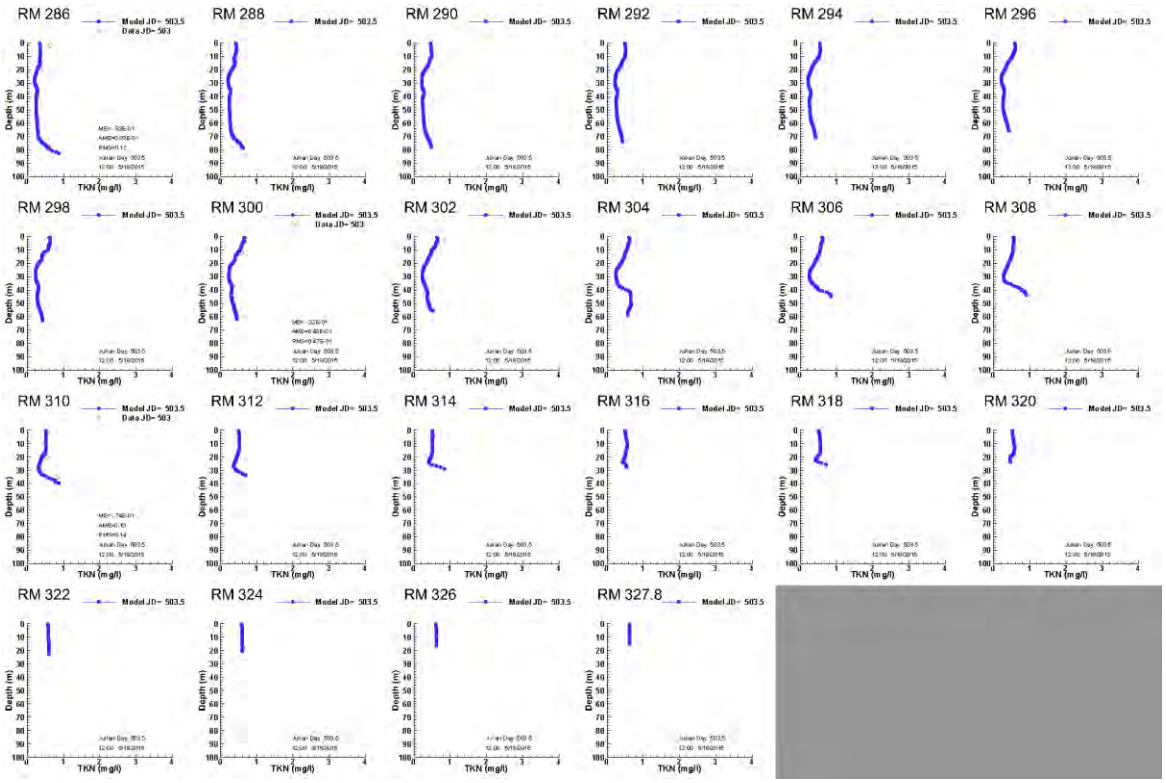


Figure 1781. Vertical profiles of TKN compared with data for 5/18/2015.

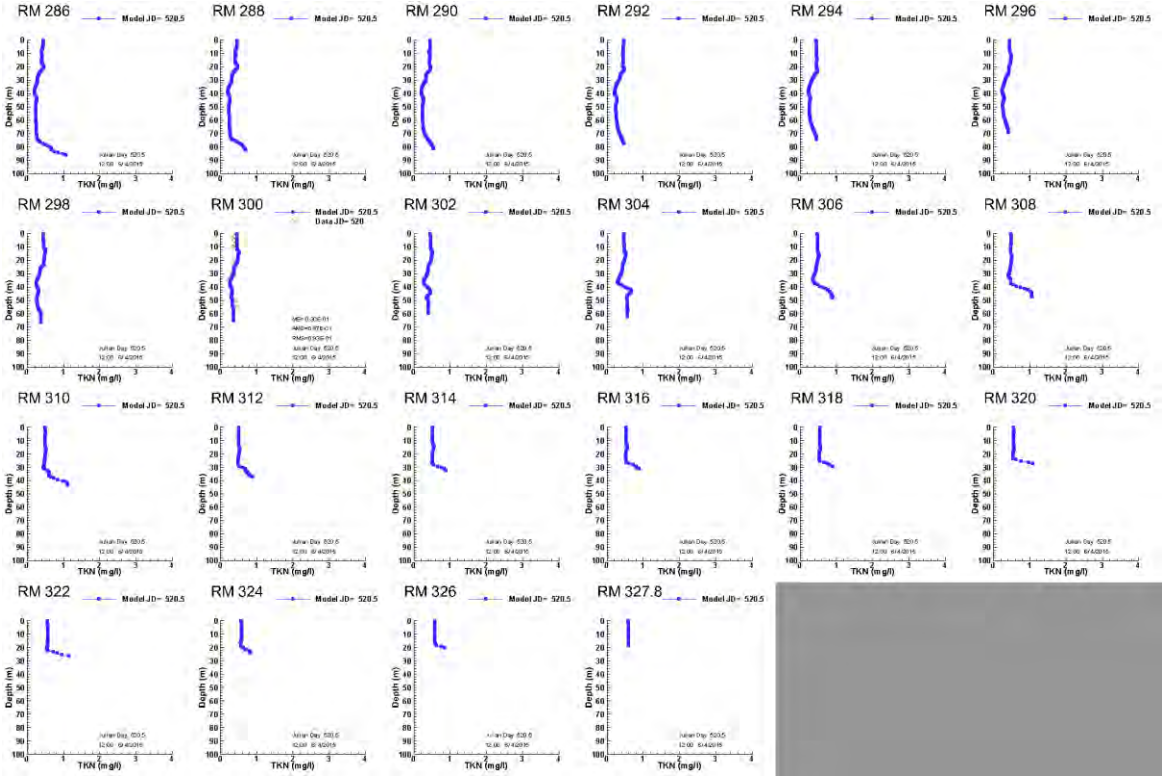


Figure 1782. Vertical profiles of TKN compared with data for 6/ 4/2015.

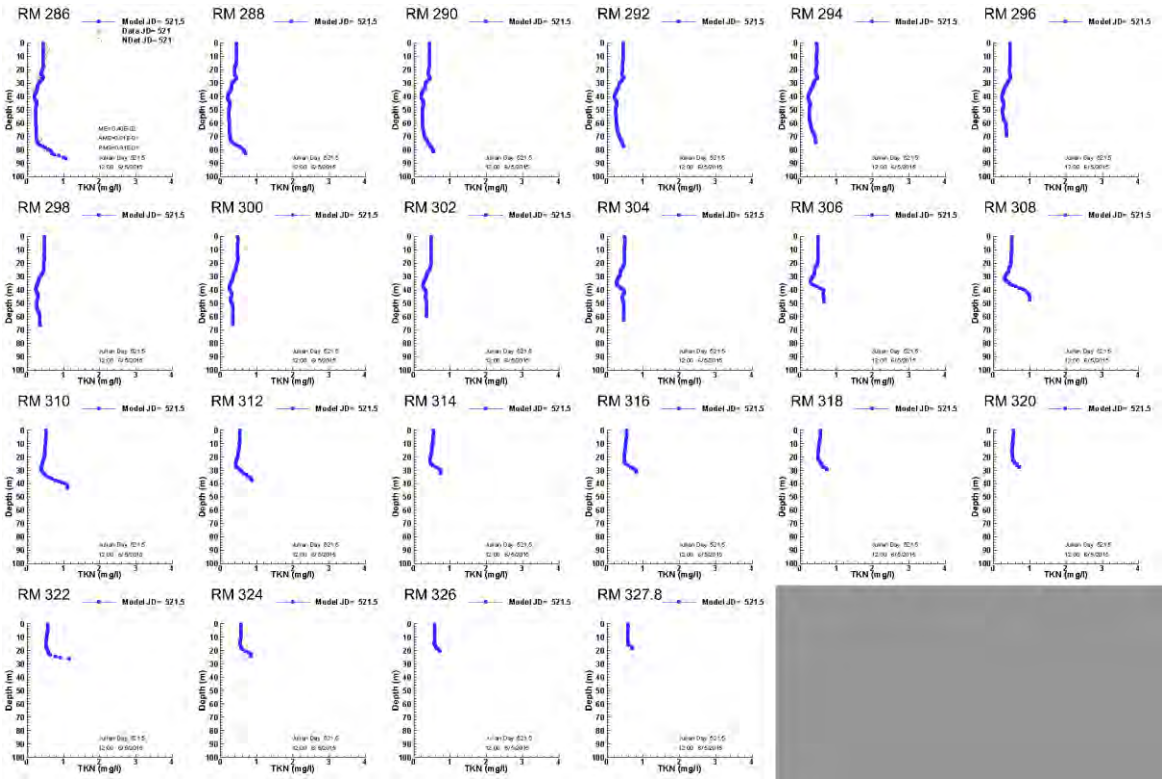


Figure 1783. Vertical profiles of TKN compared with data for 6/ 5/2015.

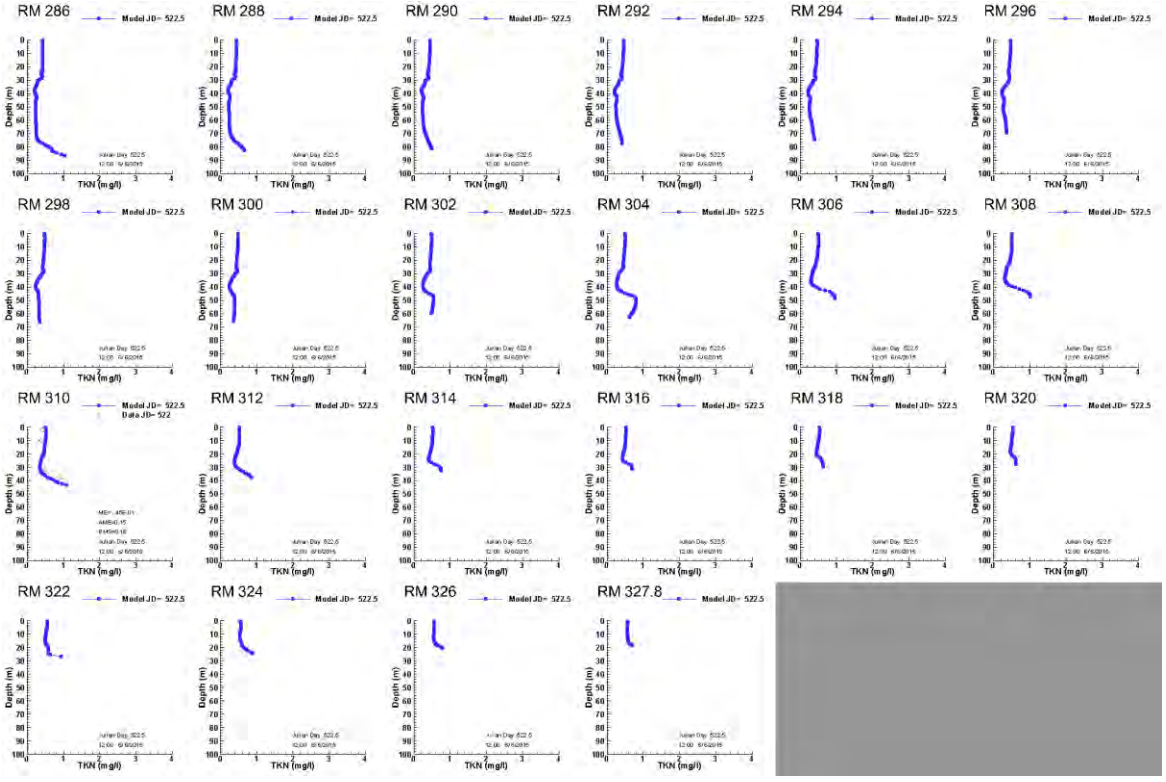


Figure 1784. Vertical profiles of TKN compared with data for 6/ 6/2015.

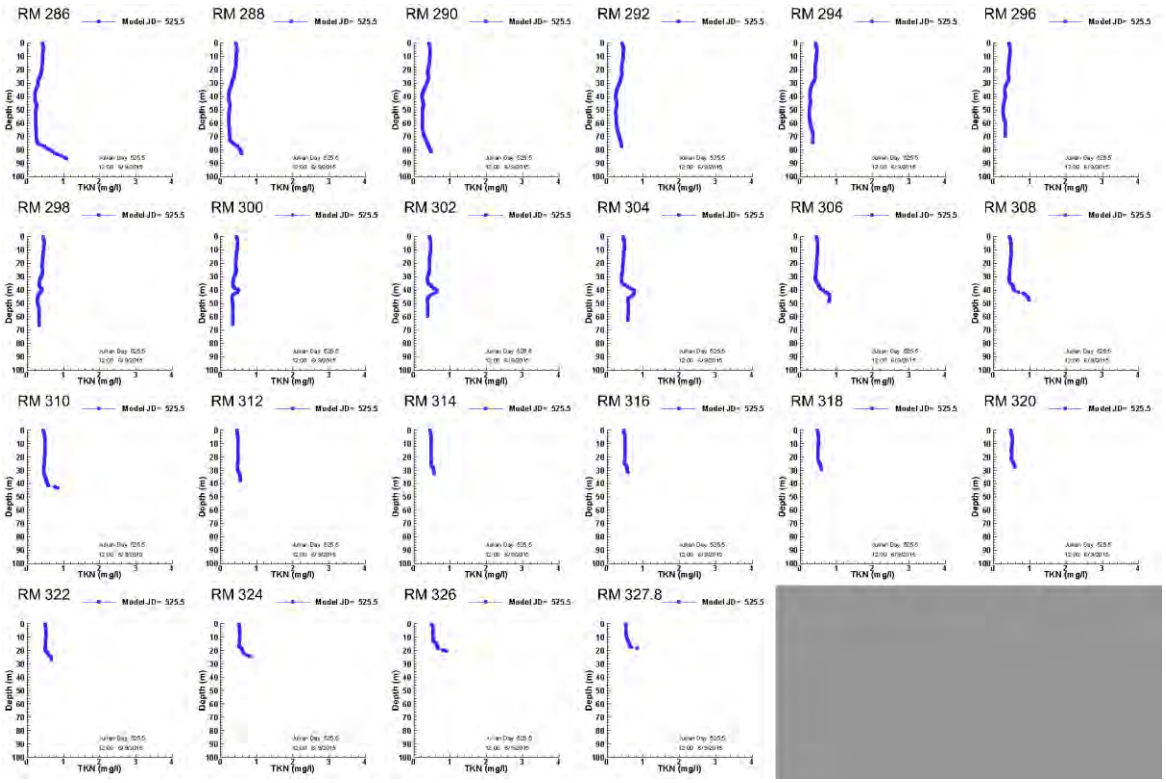


Figure 1785. Vertical profiles of TKN compared with data for 6/ 9/2015.

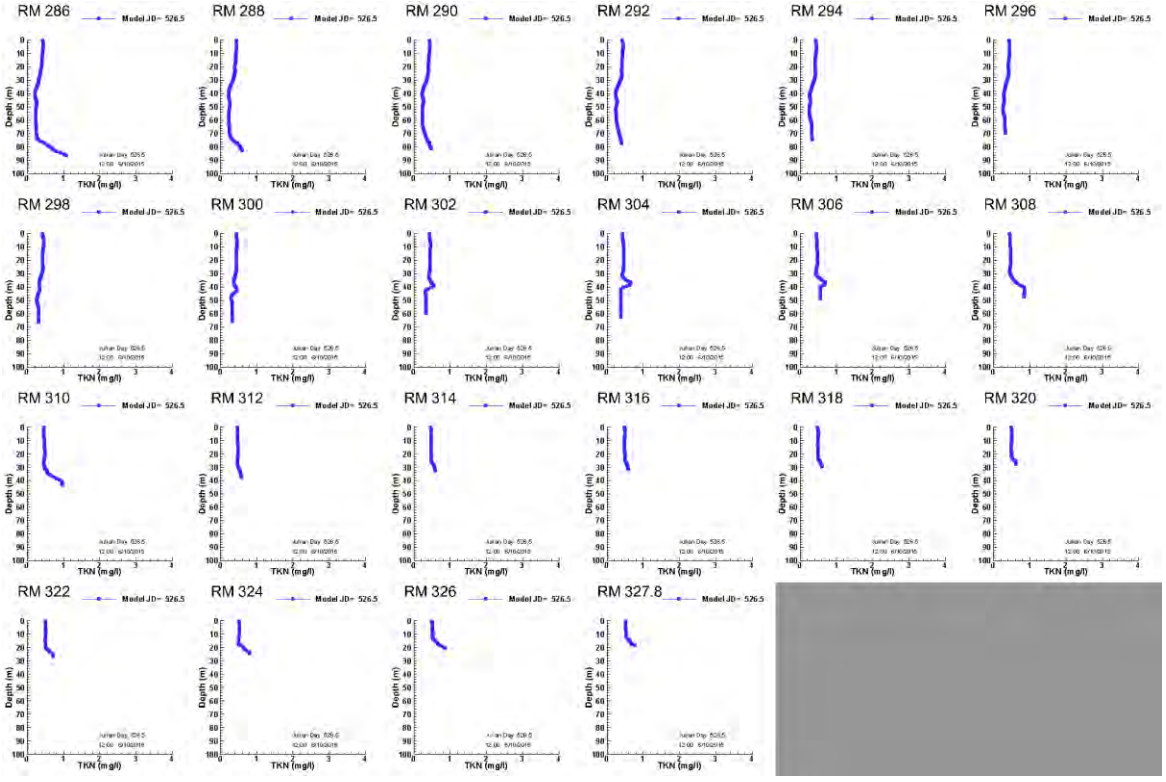


Figure 1786. Vertical profiles of TKN compared with data for 6/10/2015.

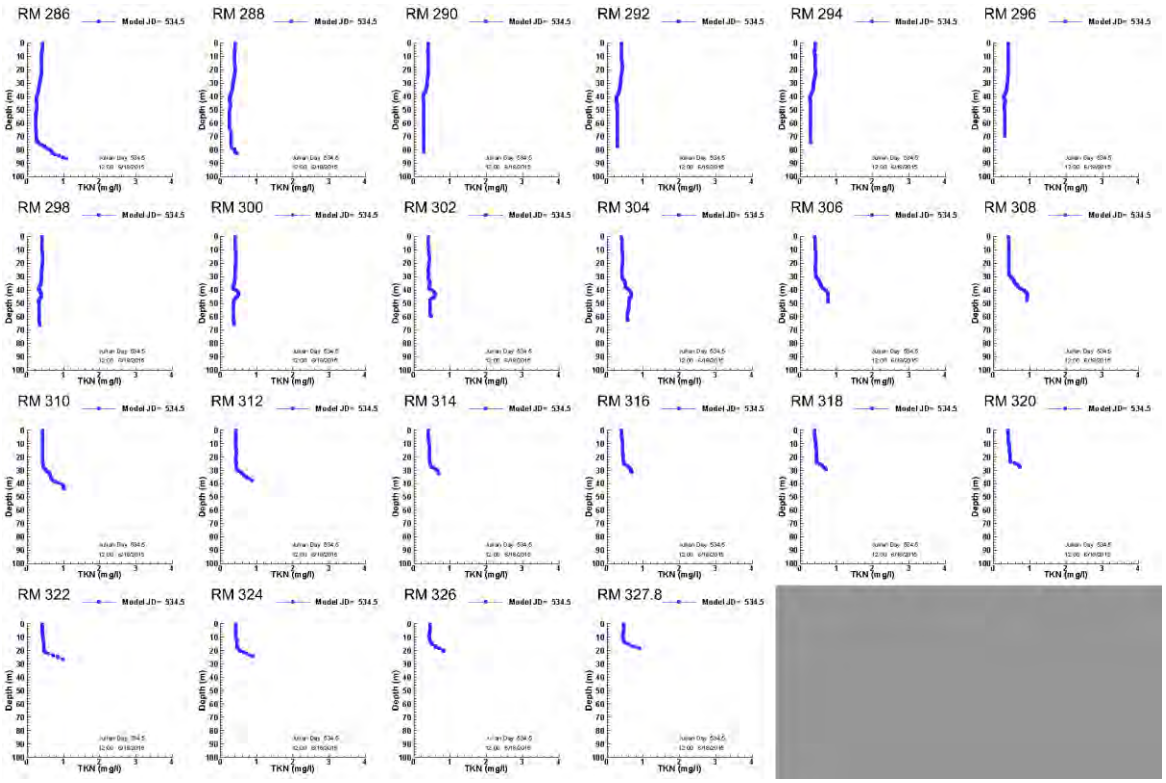


Figure 1787. Vertical profiles of TKN compared with data for 6/18/2015.

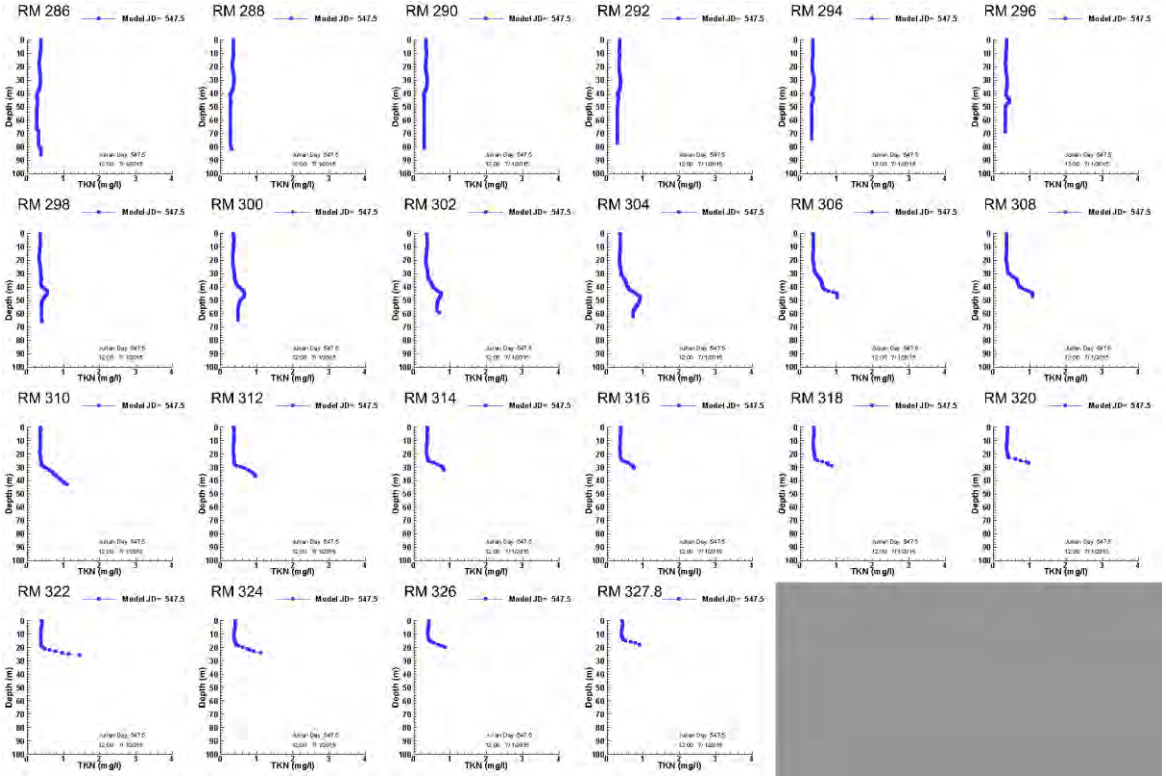


Figure 1788. Vertical profiles of TKN compared with data for 7/ 1/2015.

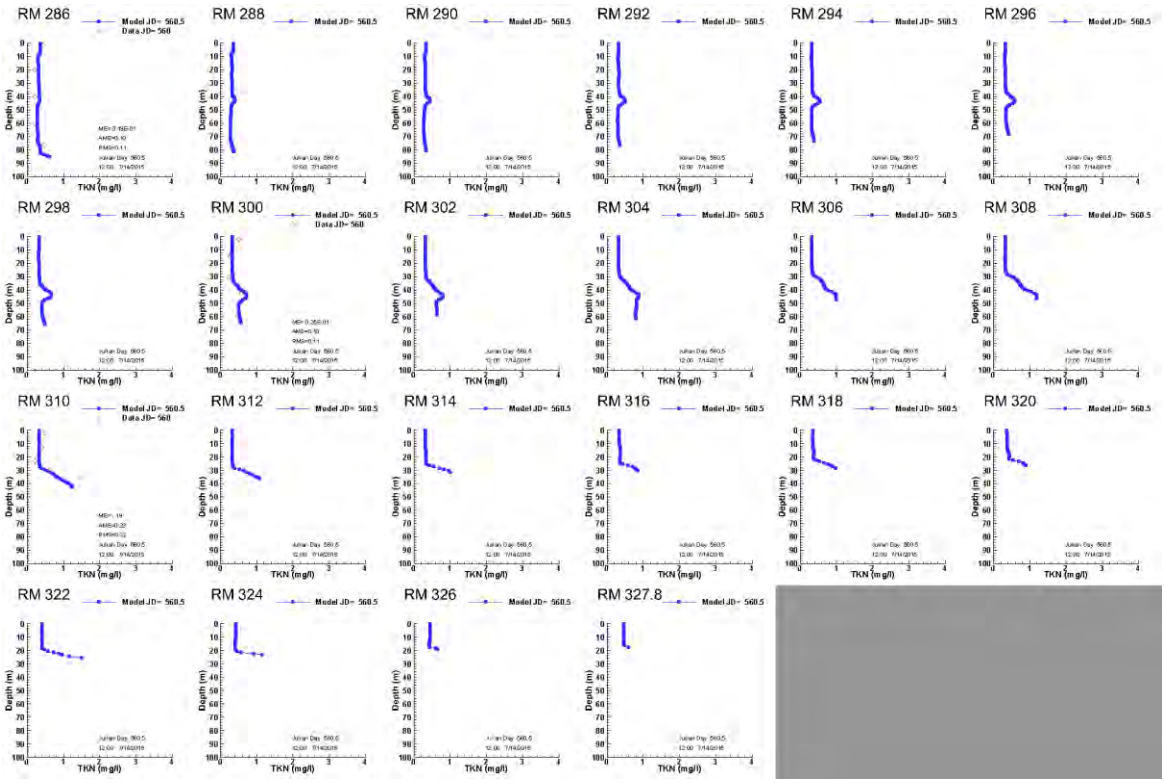


Figure 1789. Vertical profiles of TKN compared with data for 7/14/2015.

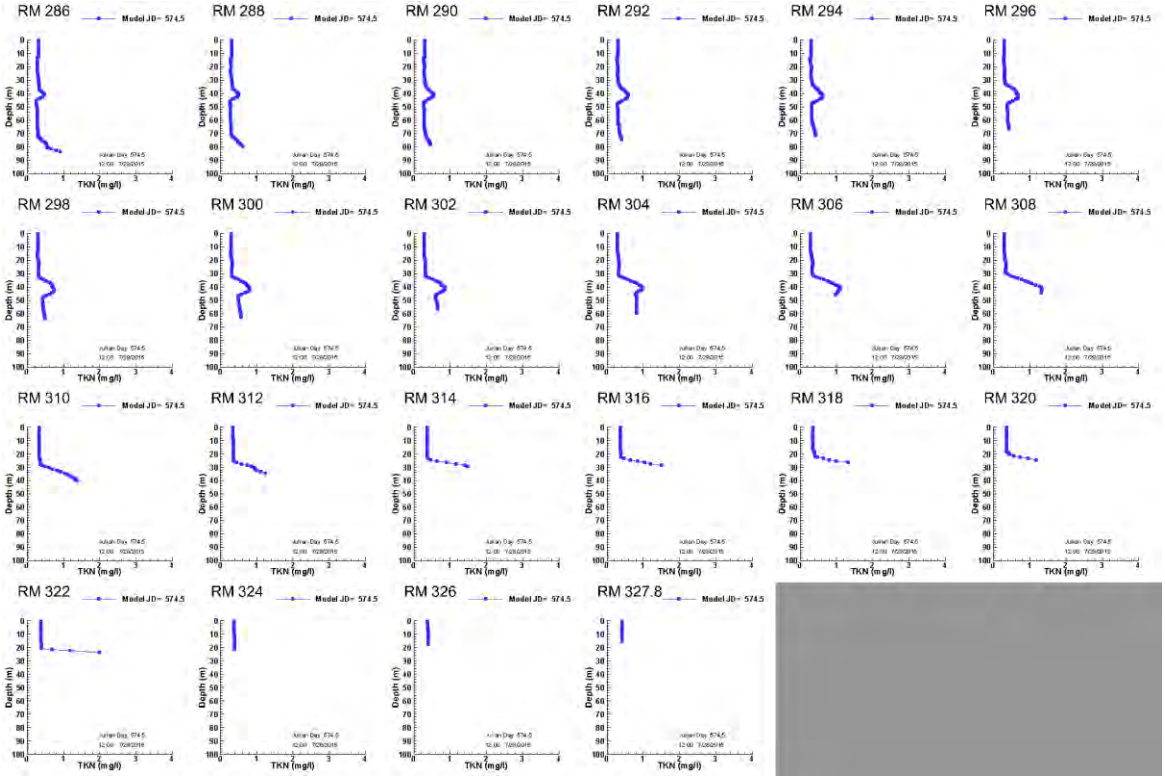


Figure 1790. Vertical profiles of TKN compared with data for 7/28/2015.

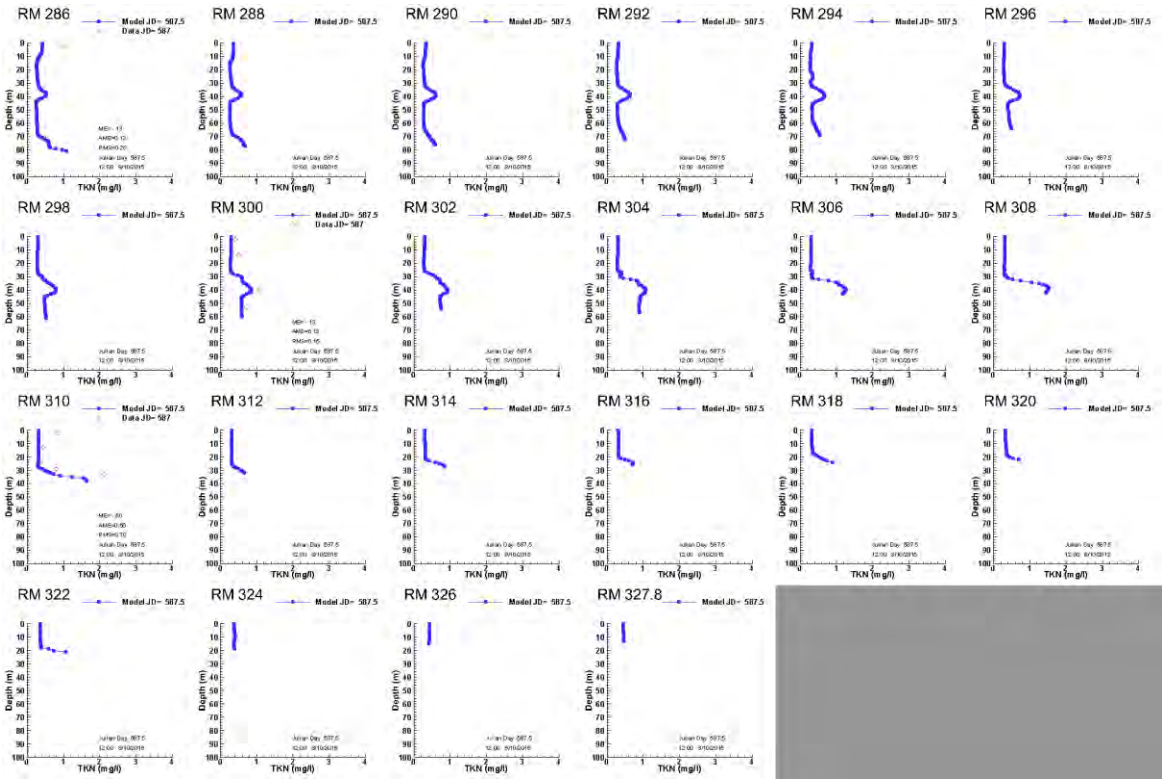


Figure 1791. Vertical profiles of TKN compared with data for 8/10/2015.

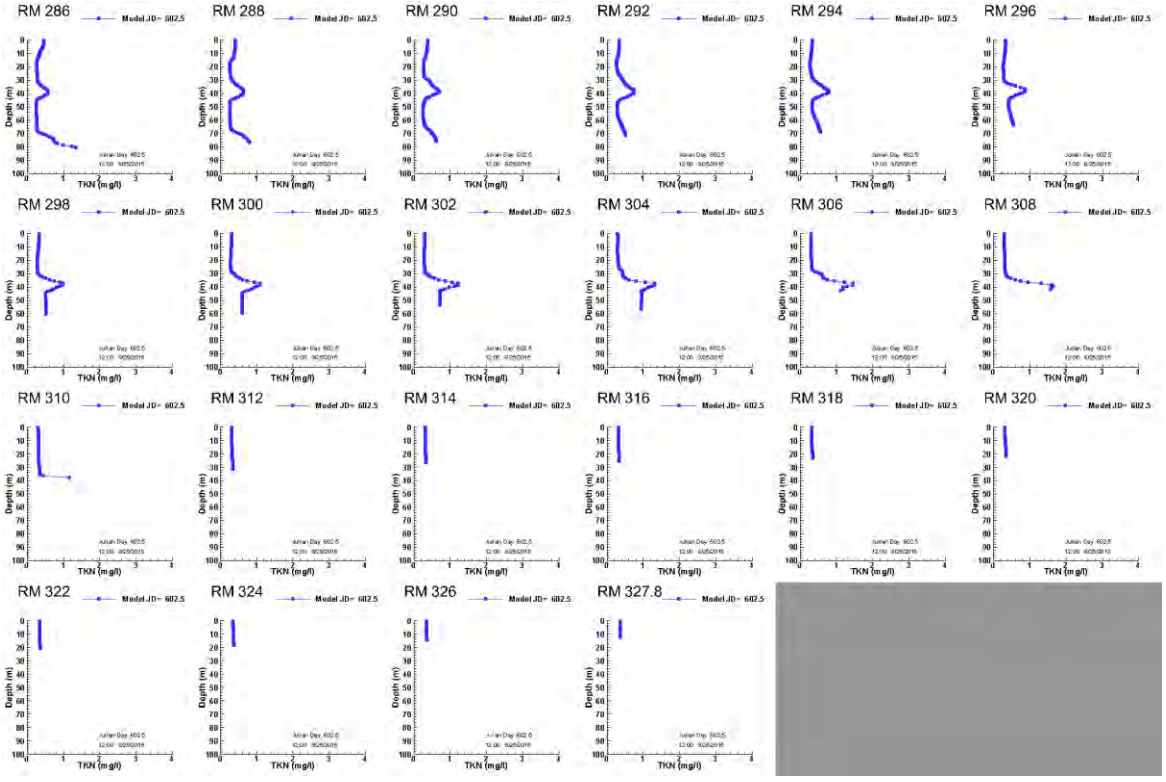


Figure 1792. Vertical profiles of TKN compared with data for 8/25/2015.

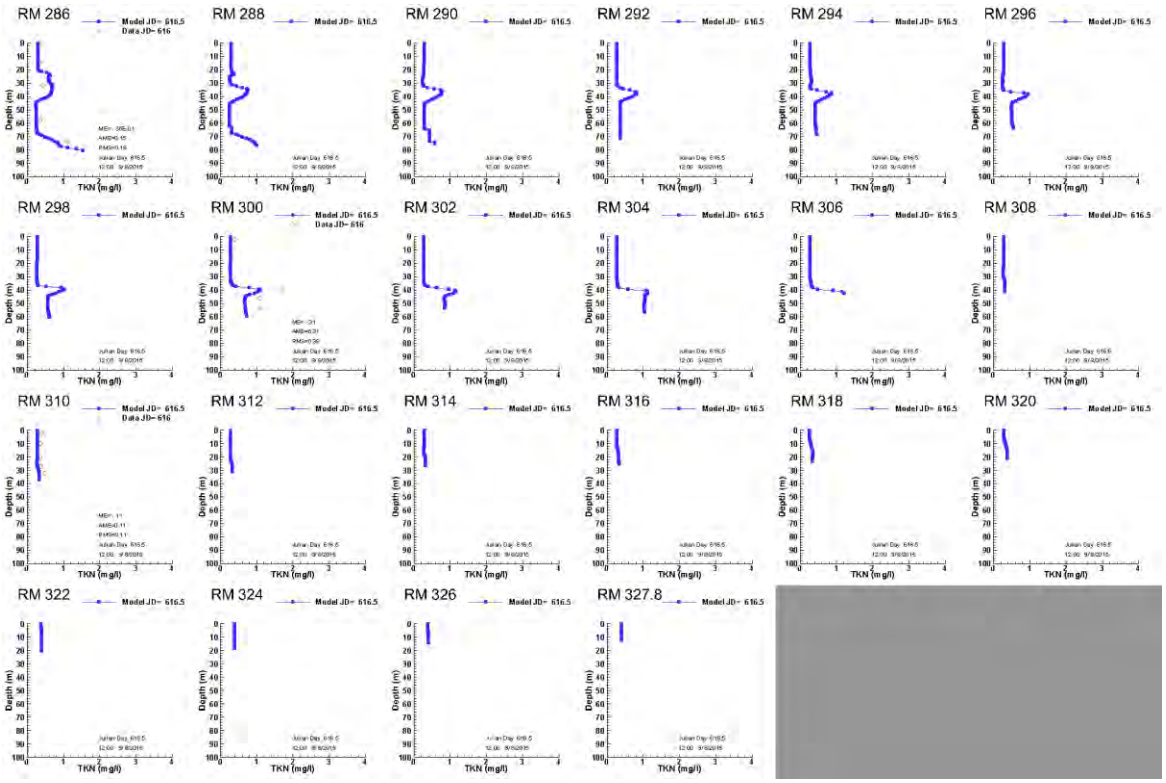


Figure 1793. Vertical profiles of TKN compared with data for 9/ 8/2015.

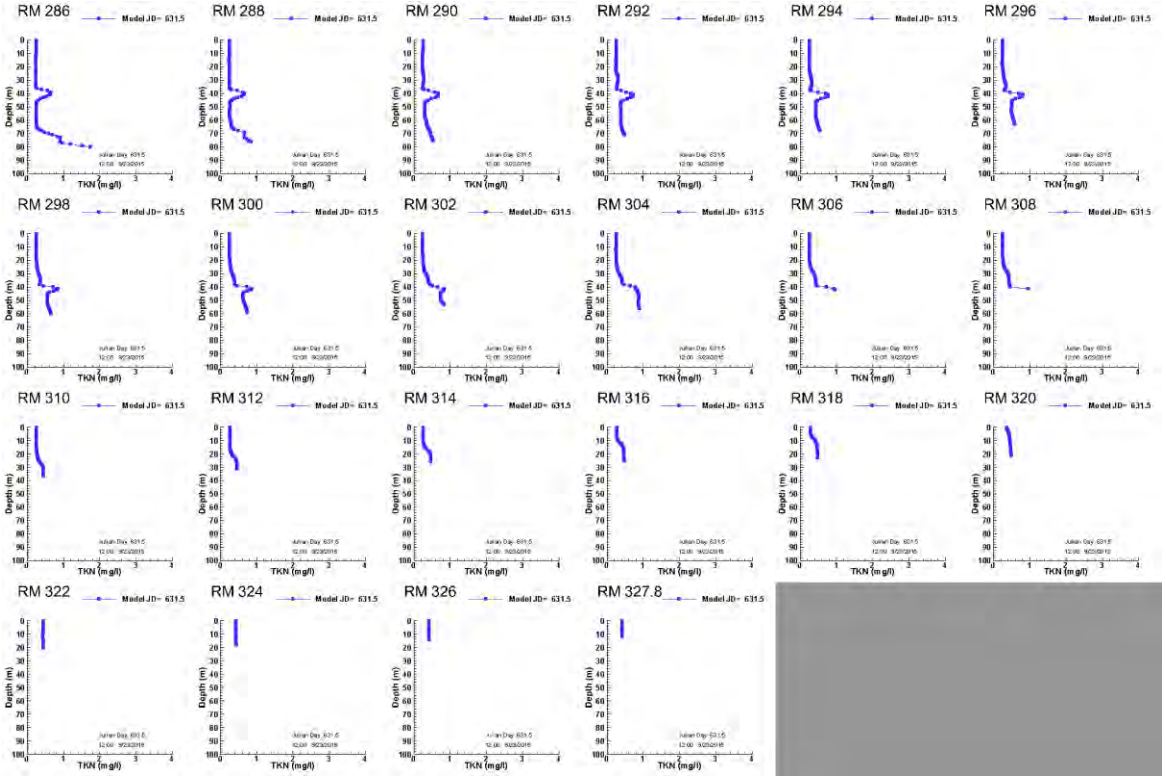


Figure 1794. Vertical profiles of TKN compared with data for 9/23/2015.

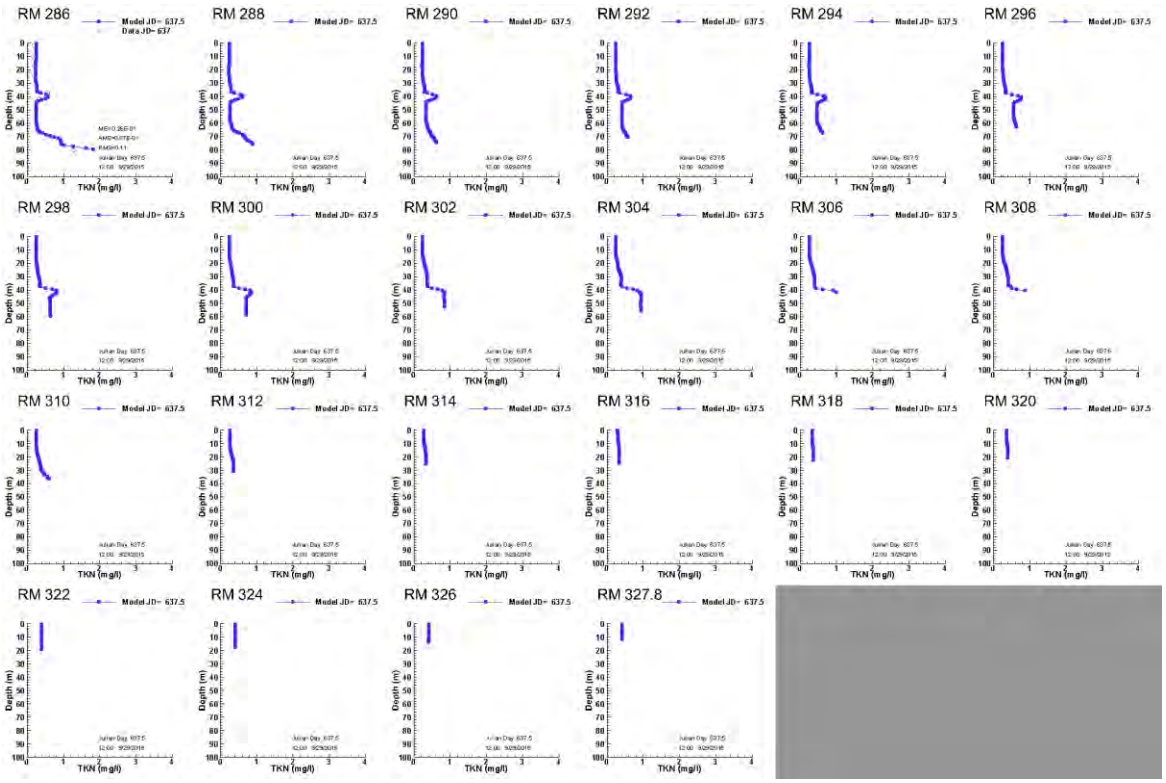


Figure 1795. Vertical profiles of TKN compared with data for 9/29/2015.

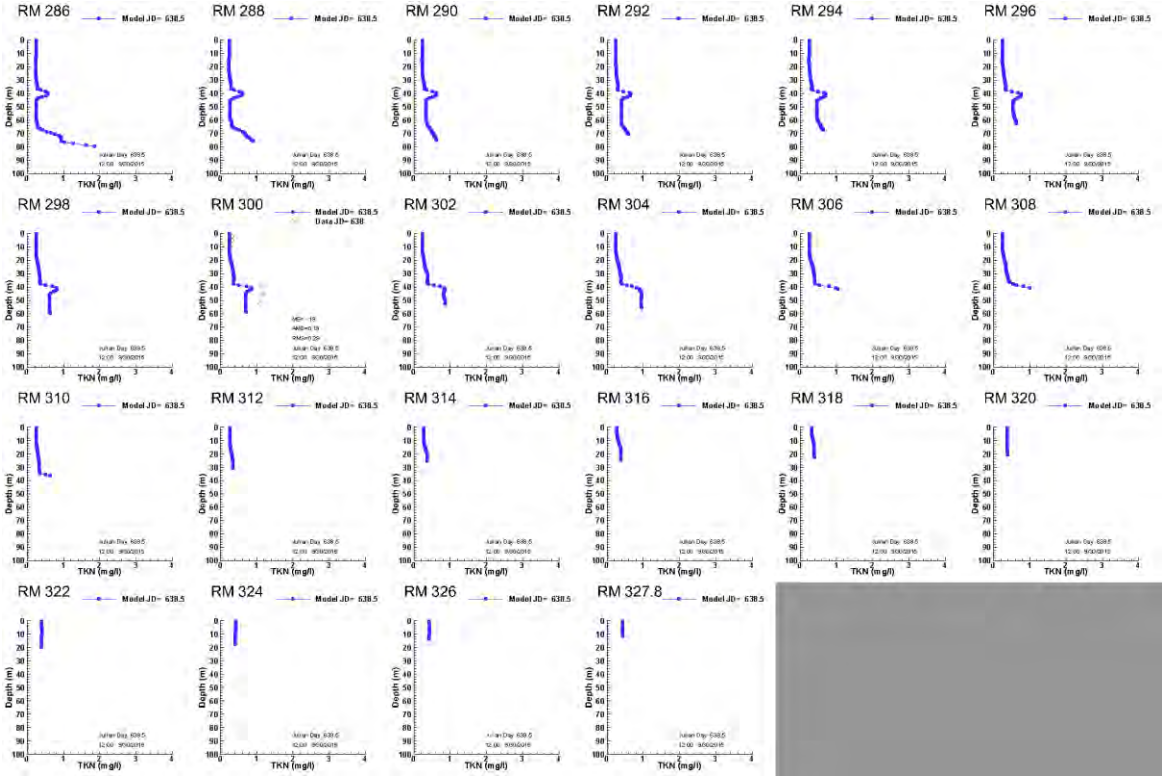


Figure 1796. Vertical profiles of TKN compared with data for 9/30/2015.

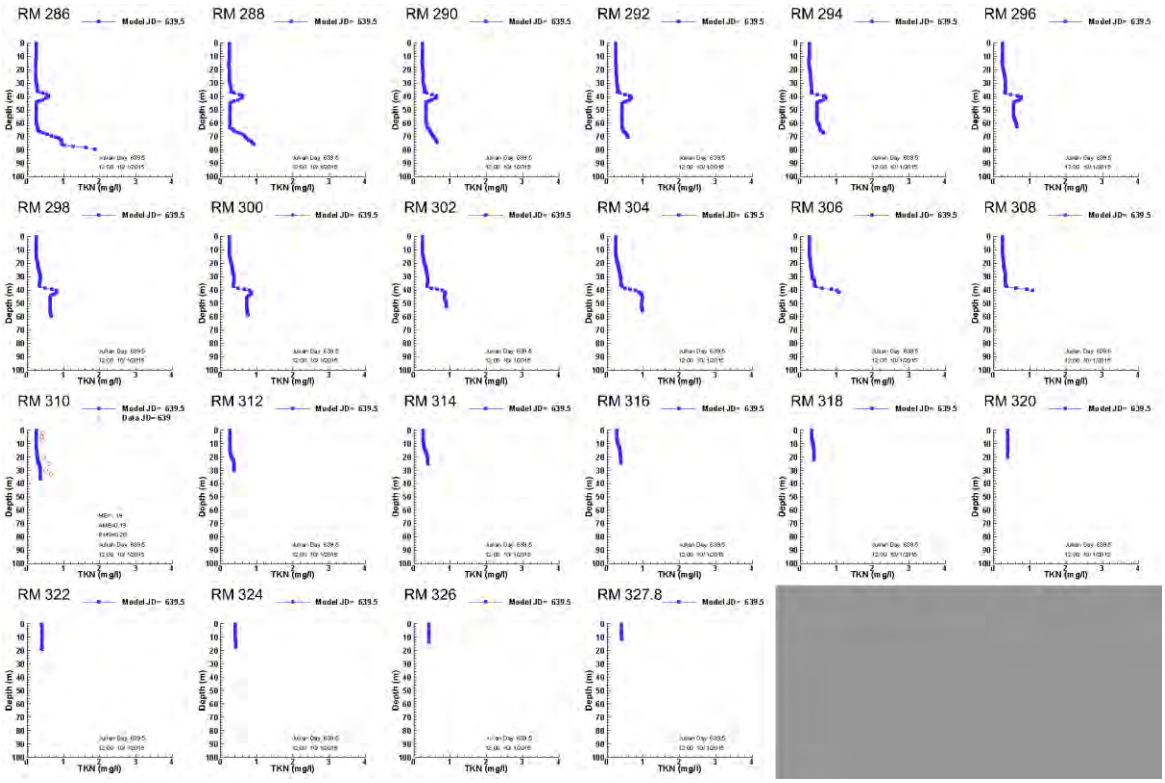


Figure 1797. Vertical profiles of TKN compared with data for 10/ 1/2015.

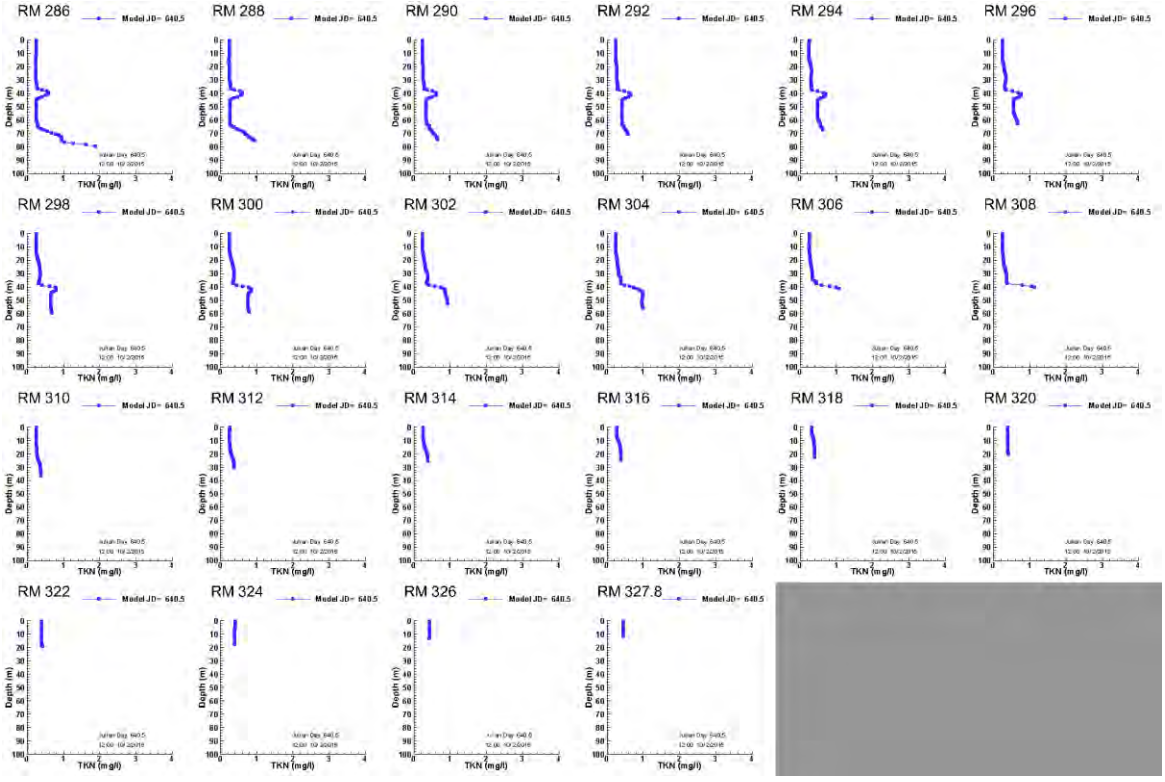


Figure 1798. Vertical profiles of TKN compared with data for 10/ 2/2015.

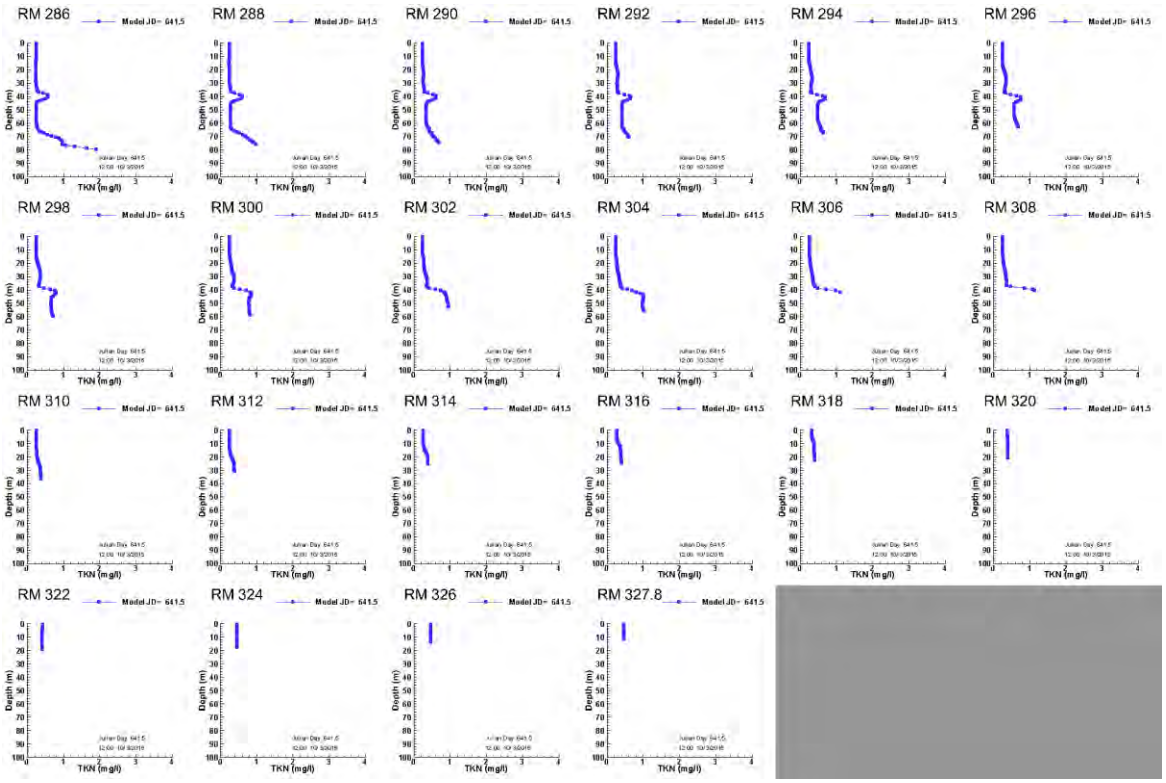


Figure 1799. Vertical profiles of TKN compared with data for 10/ 3/2015.

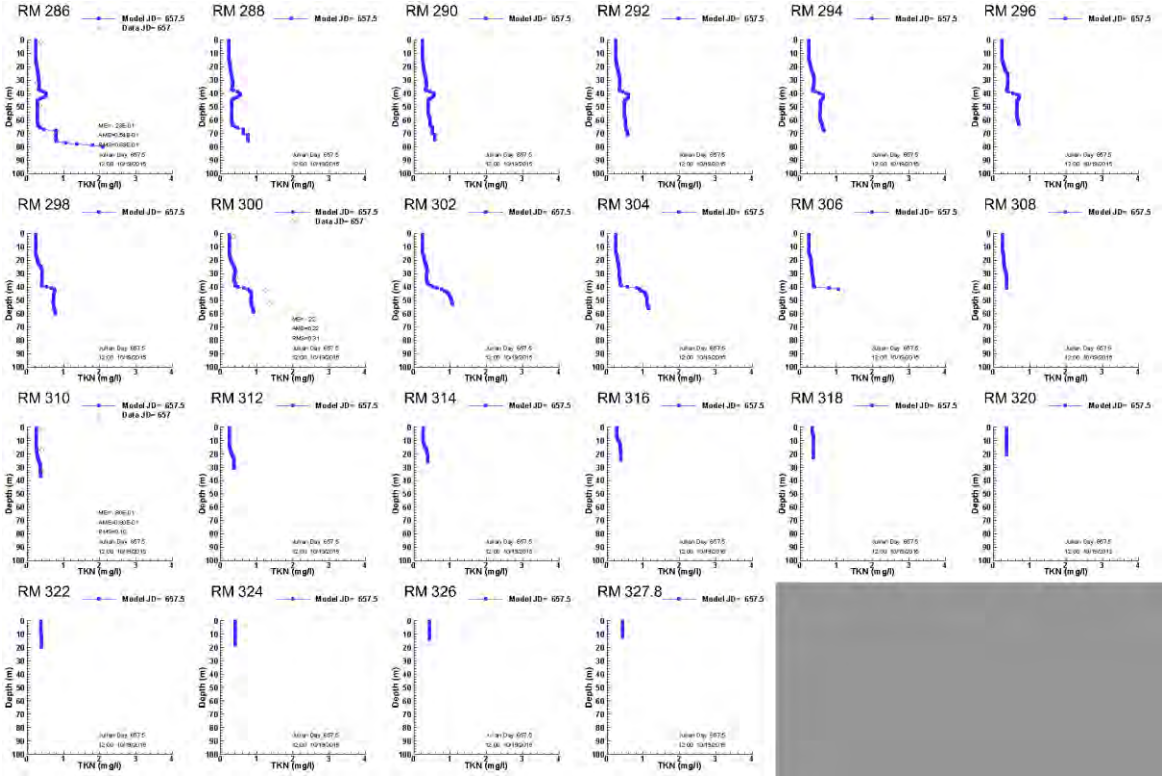


Figure 1800. Vertical profiles of TKN compared with data for 10/19/2015.

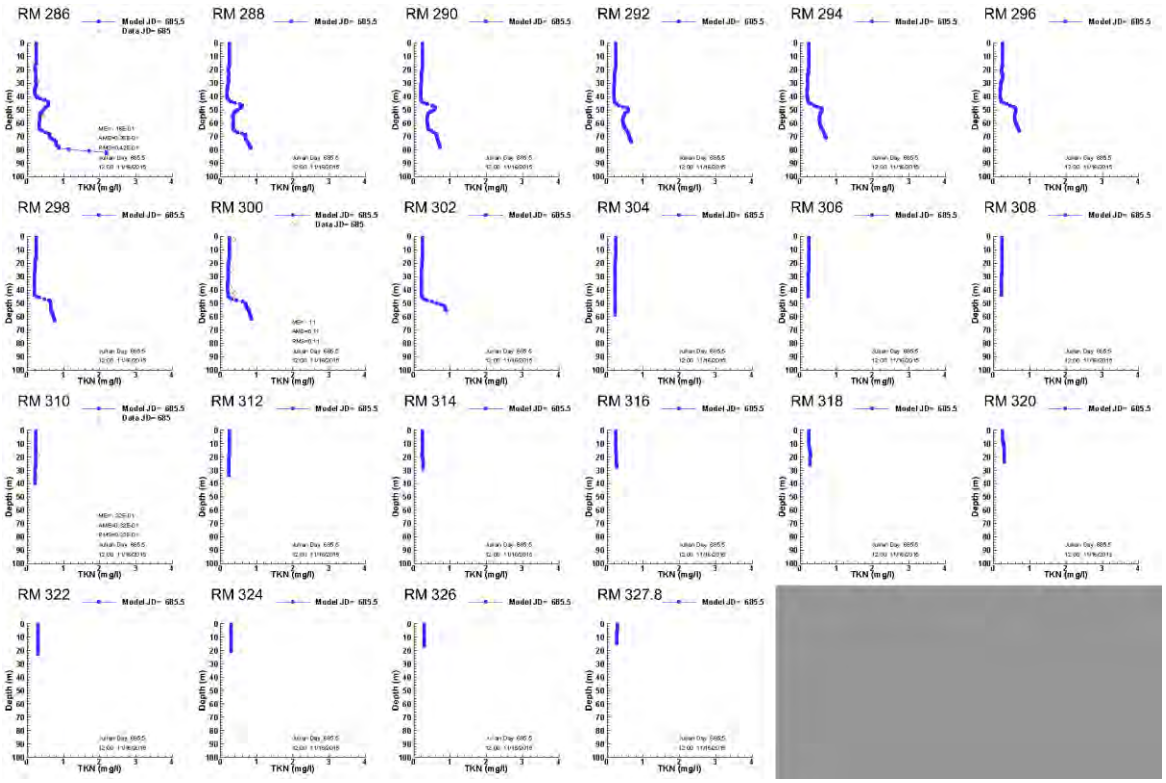


Figure 1801. Vertical profiles of TKN compared with data for 11/16/2015.

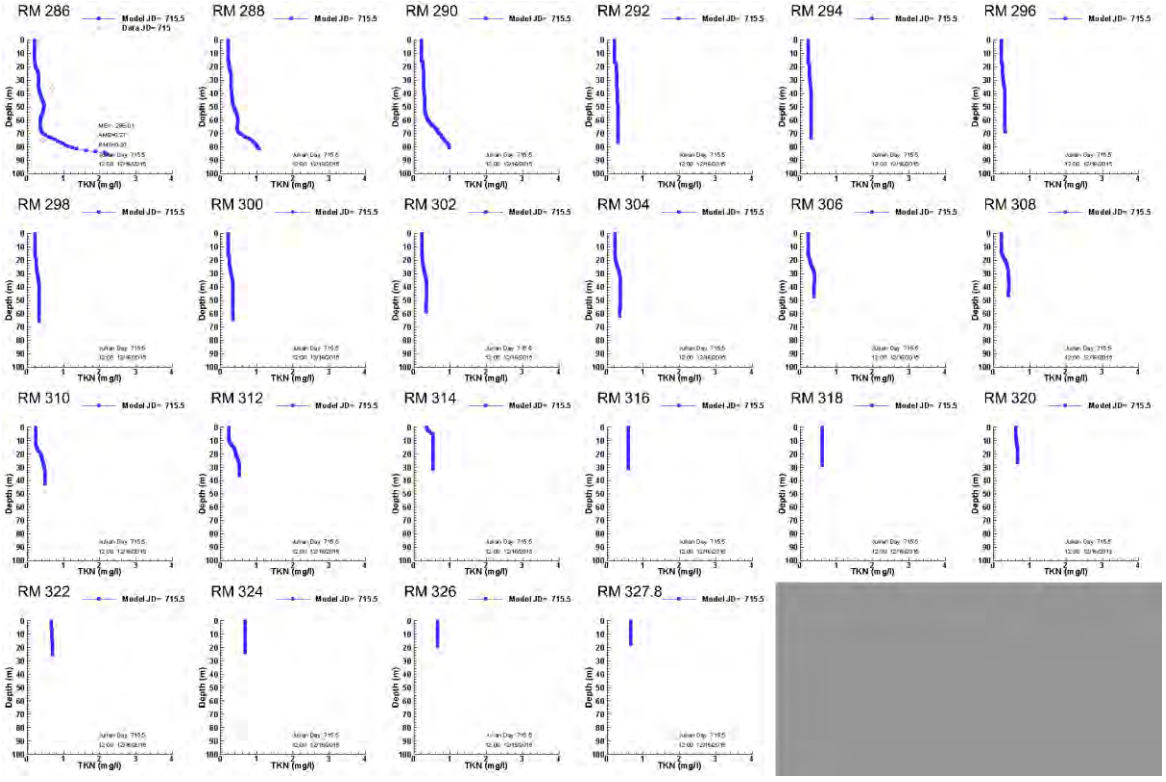


Figure 1802. Vertical profiles of TKN compared with data for 12/16/2015.

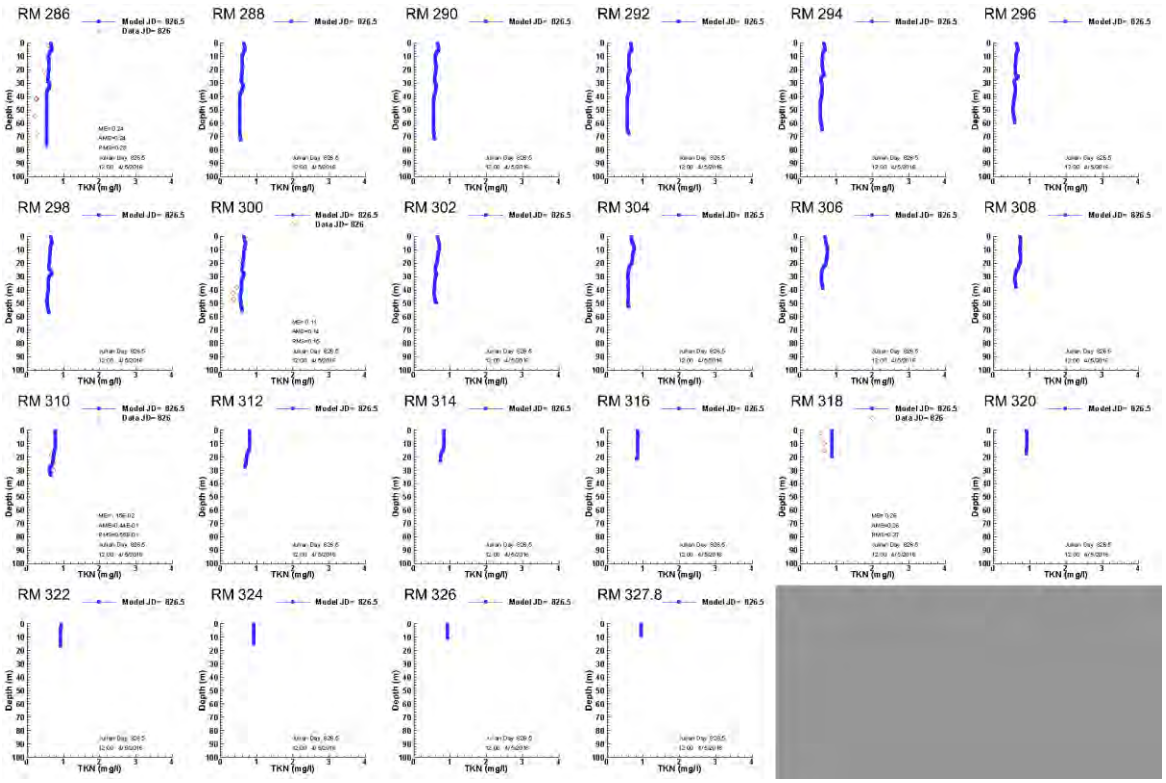


Figure 1803. Vertical profiles of TKN compared with data for 4/ 5/2016.

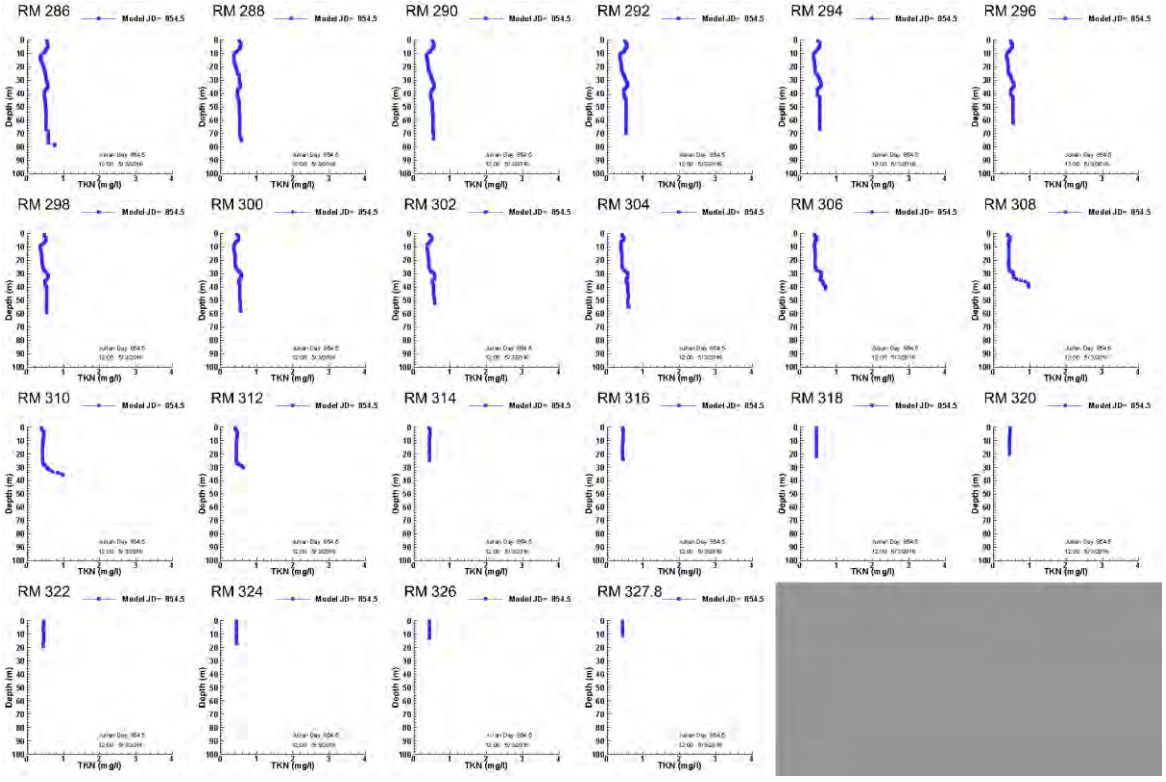


Figure 1804. Vertical profiles of TKN compared with data for 5/ 3/2016.

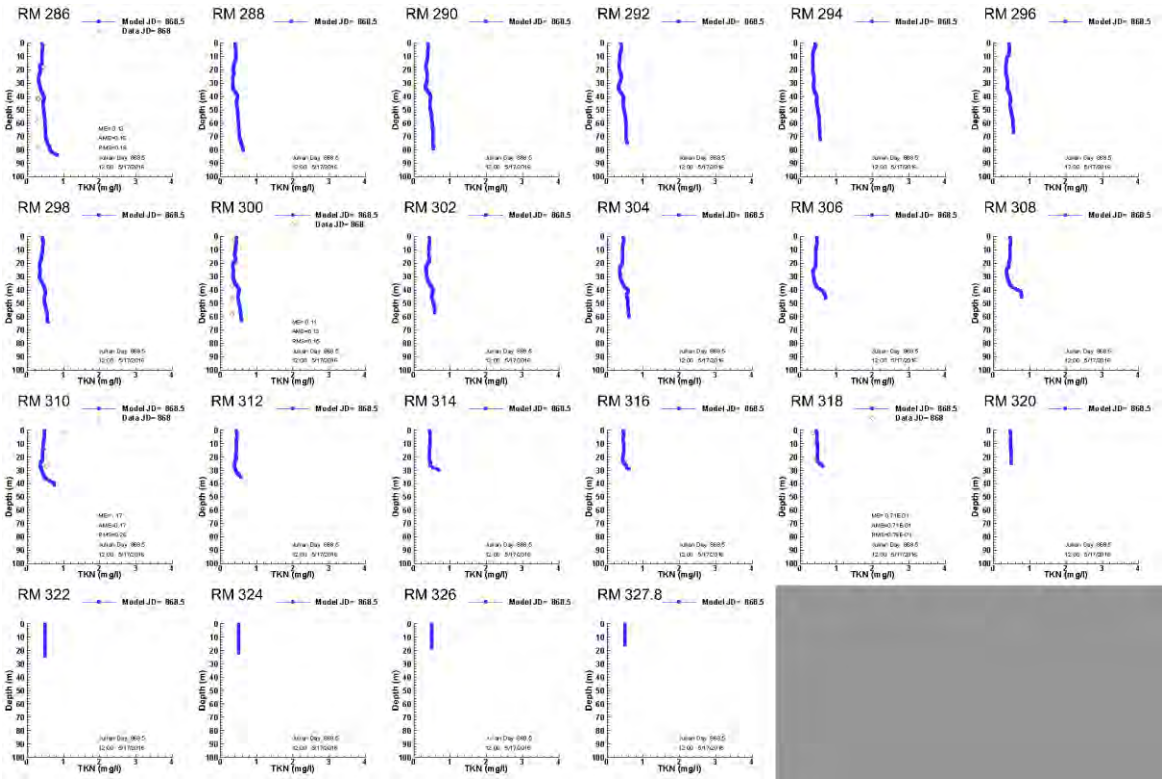


Figure 1805. Vertical profiles of TKN compared with data for 5/17/2016.

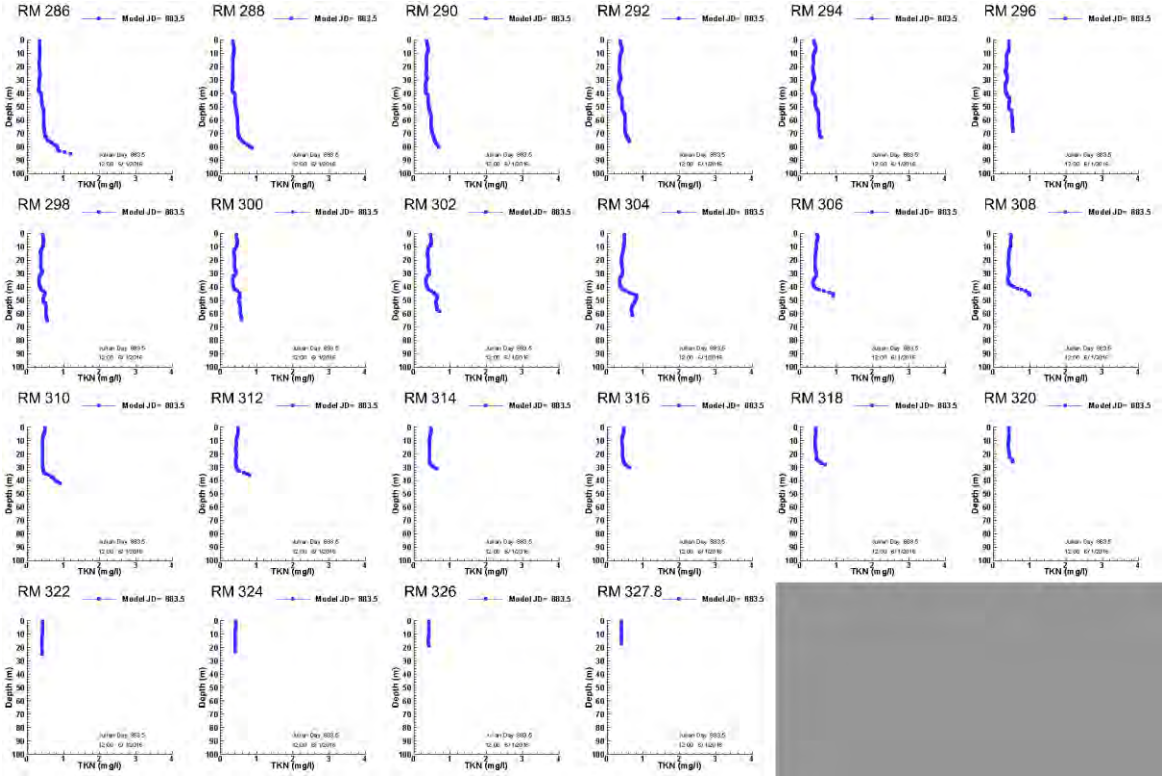


Figure 1806. Vertical profiles of TKN compared with data for 6/ 1/2016.

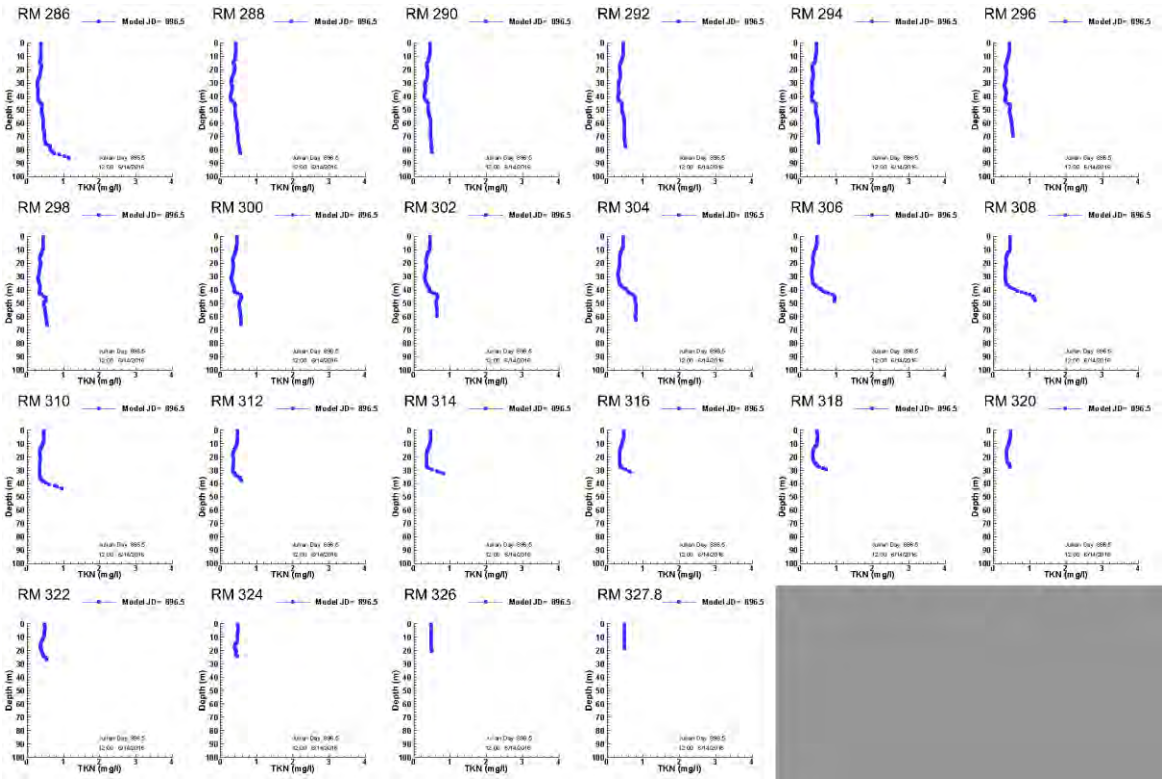


Figure 1807. Vertical profiles of TKN compared with data for 6/14/2016.

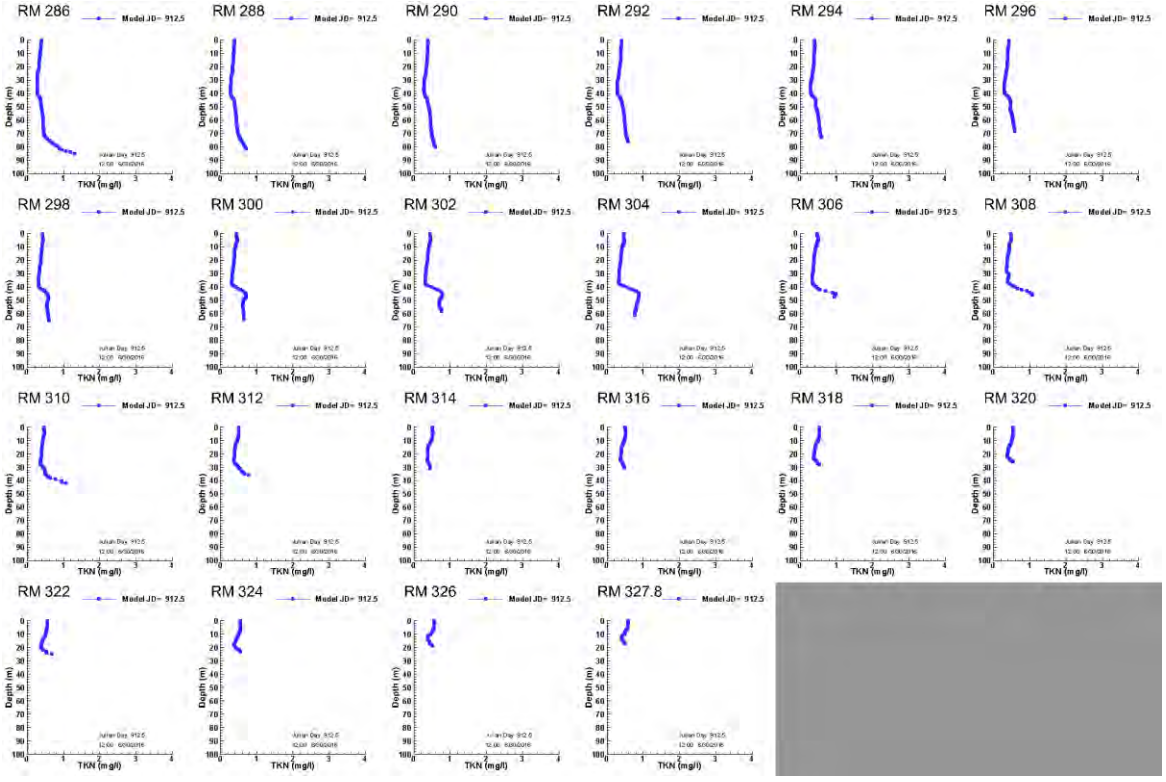


Figure 1808. Vertical profiles of TKN compared with data for 6/30/2016.

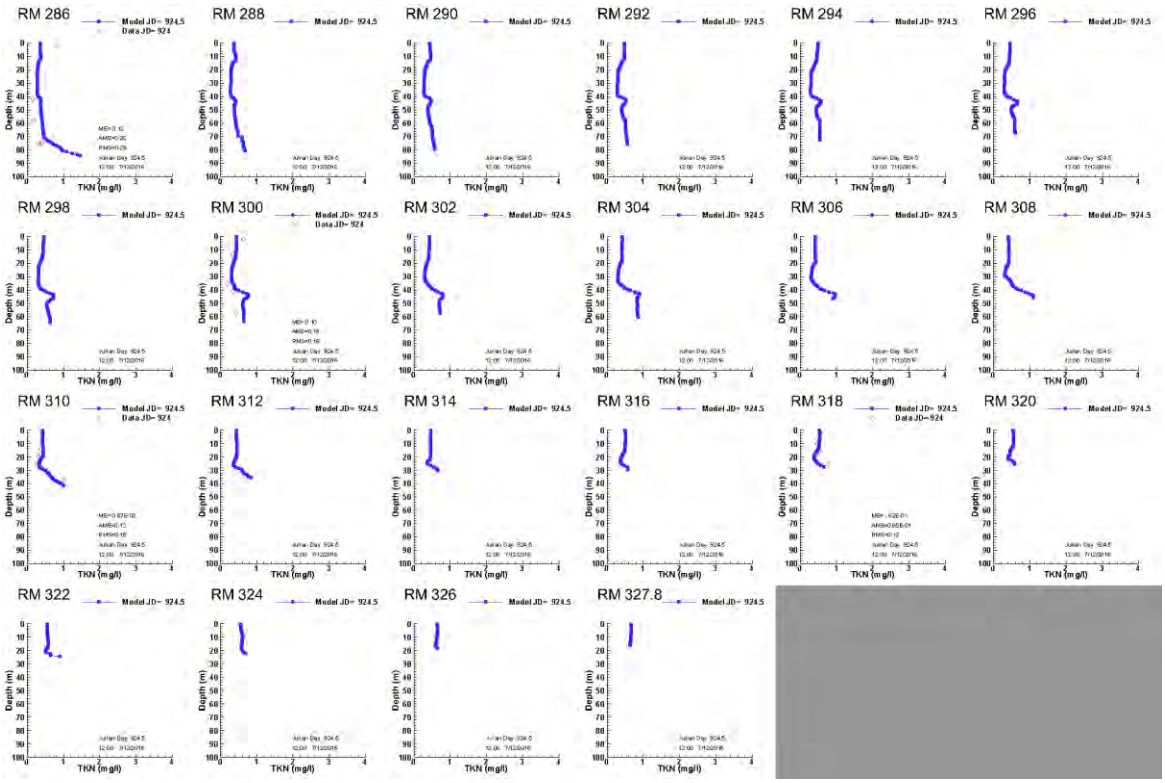


Figure 1809. Vertical profiles of TKN compared with data for 7/12/2016.

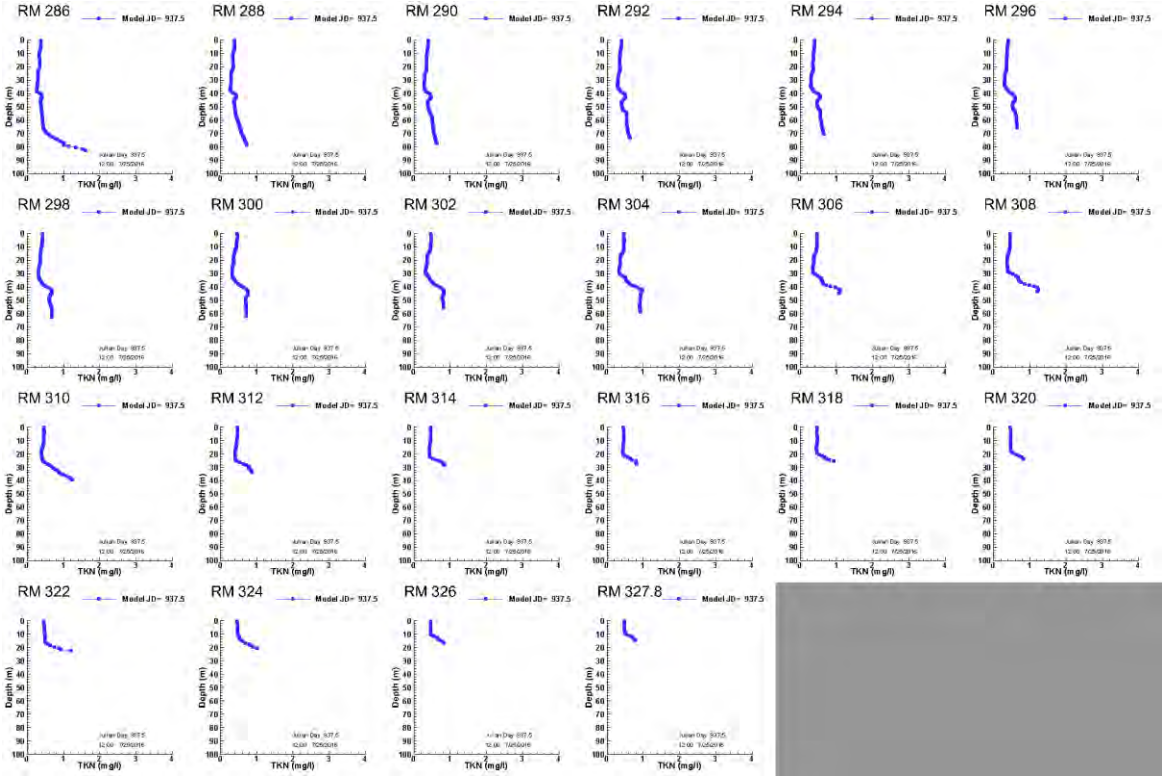


Figure 1810. Vertical profiles of TKN compared with data for 7/25/2016.

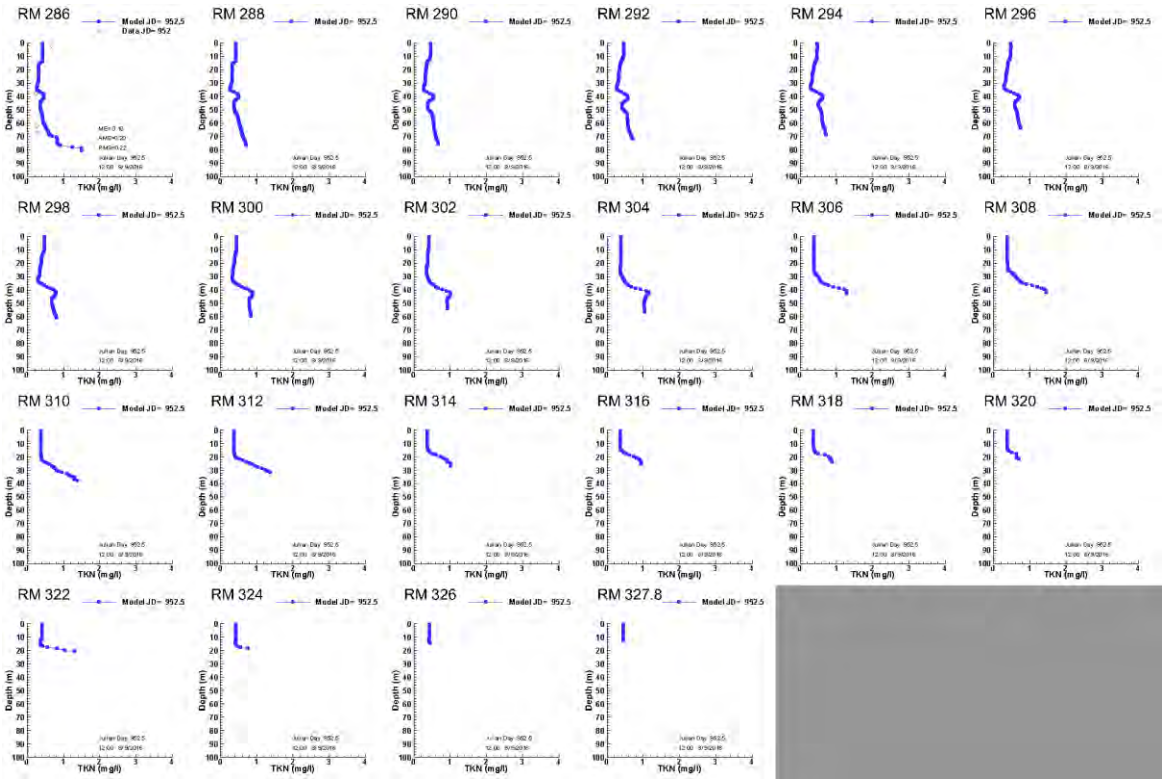


Figure 1811. Vertical profiles of TKN compared with data for 8/ 9/2016.

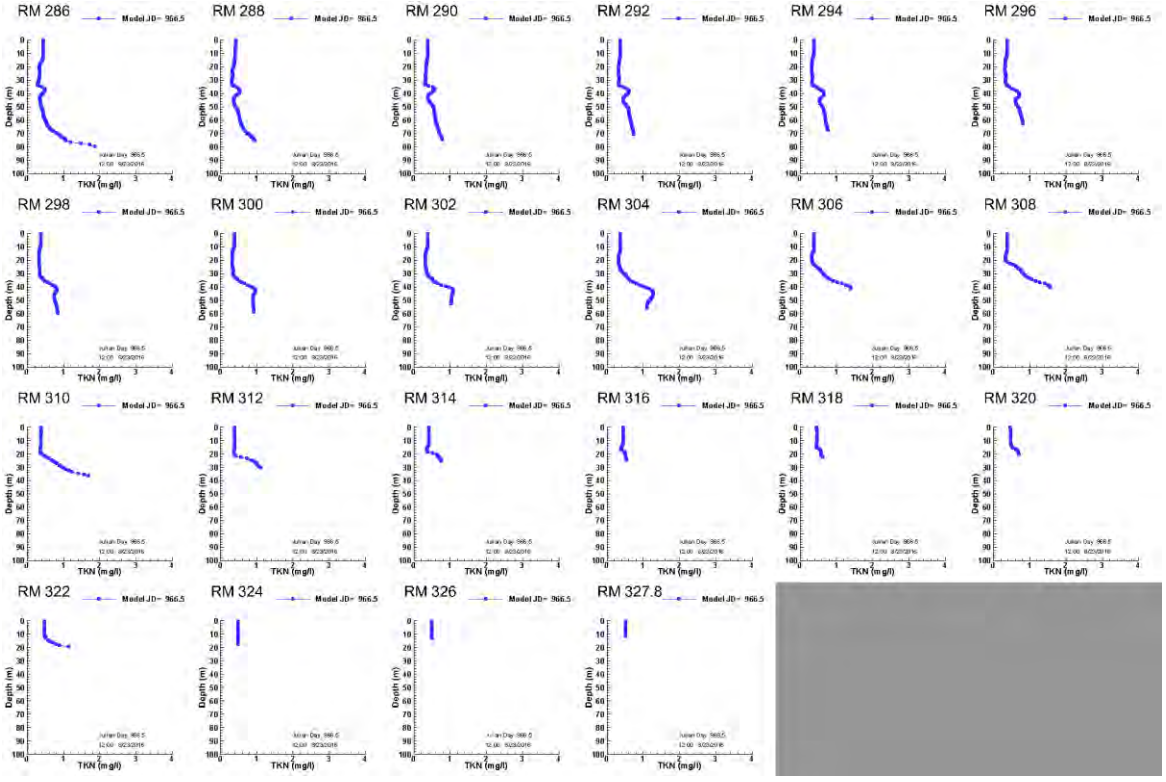


Figure 1812. Vertical profiles of TKN compared with data for 8/23/2016.

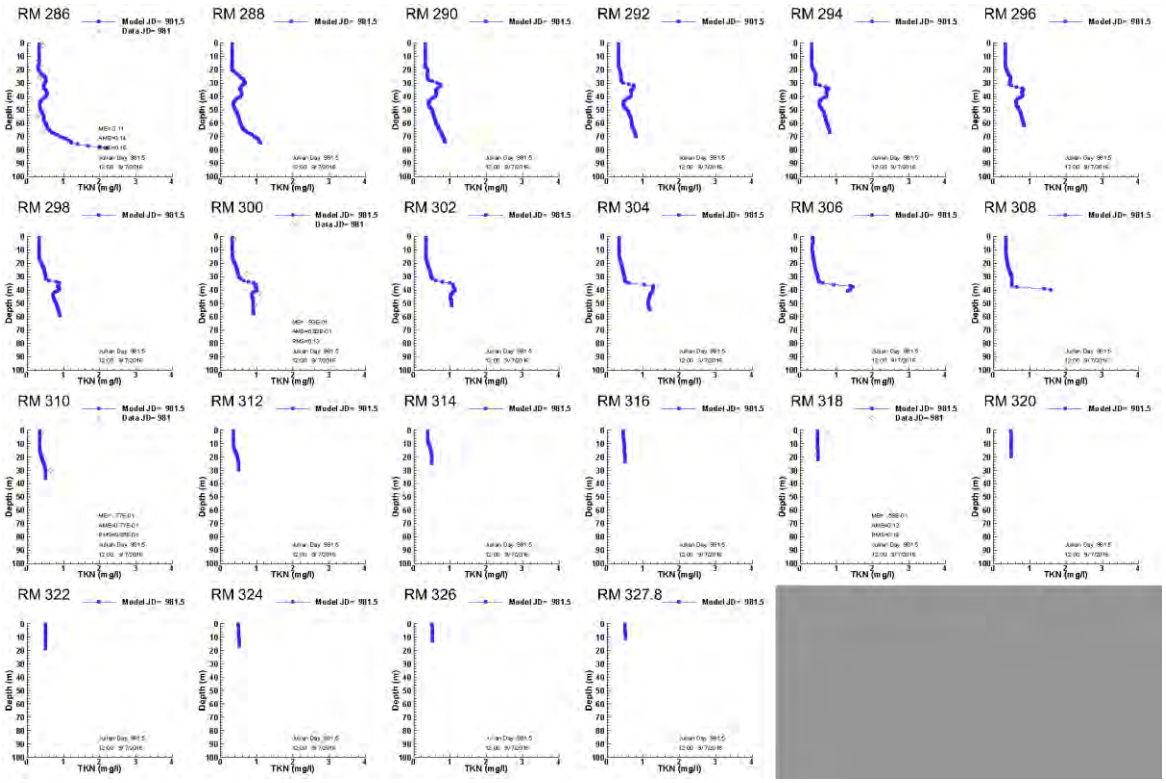


Figure 1813. Vertical profiles of TKN compared with data for 9/ 7/2016.

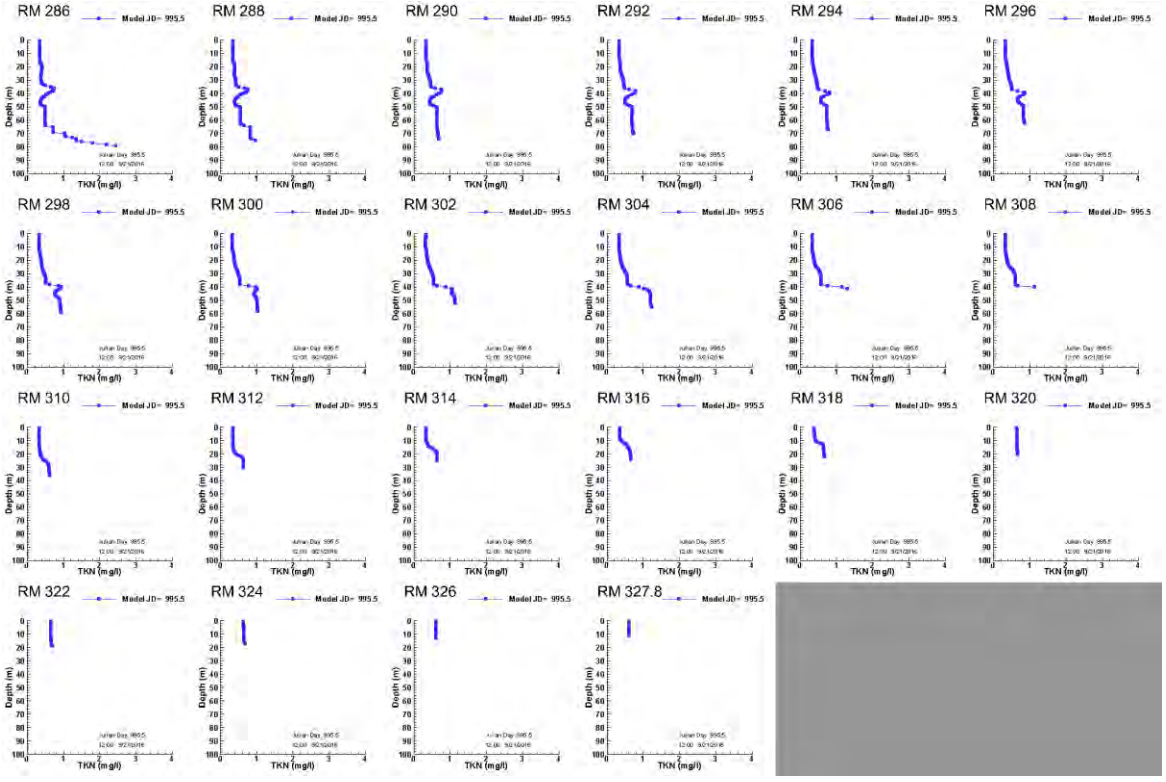


Figure 1814. Vertical profiles of TKN compared with data for 9/21/2016.

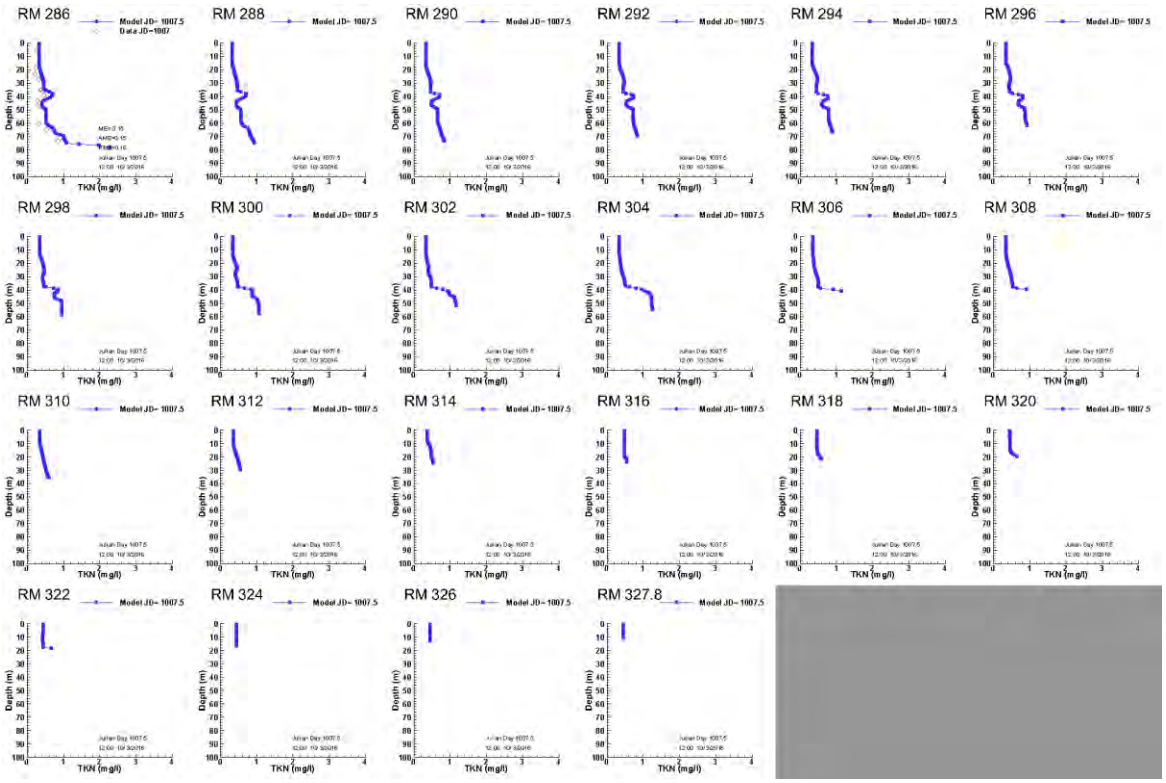


Figure 1815. Vertical profiles of TKN compared with data for 10/ 3/2016.

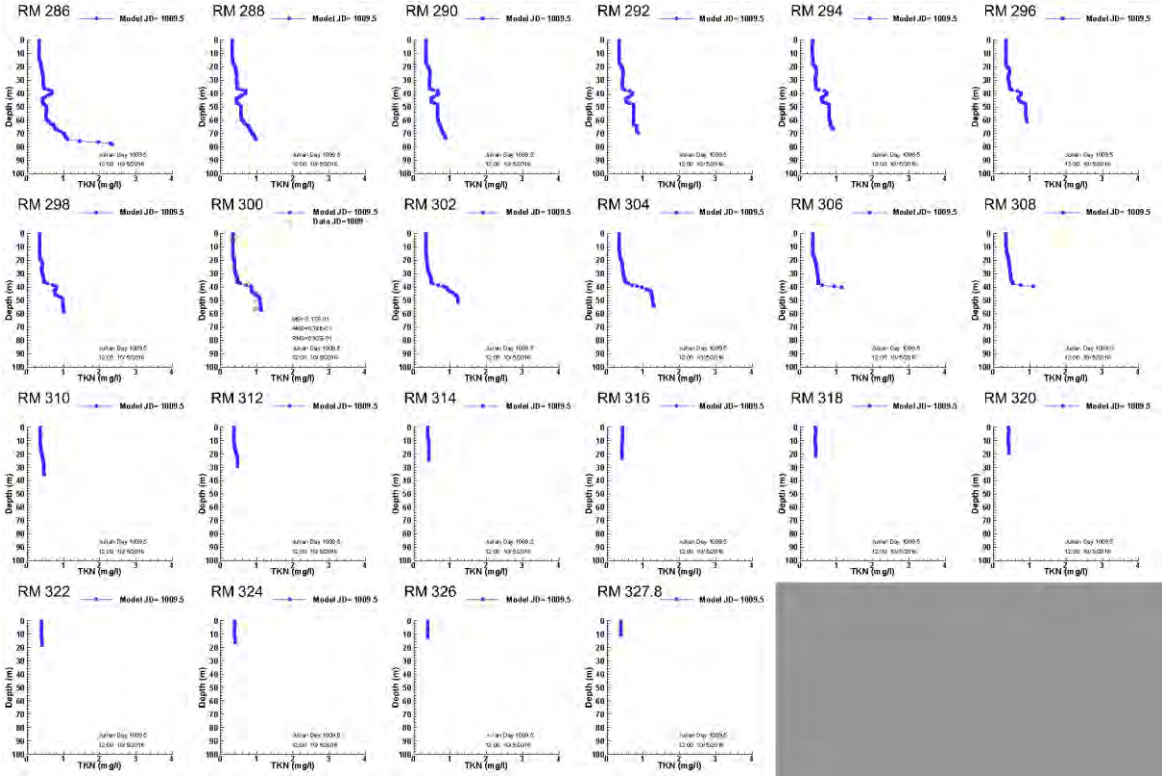


Figure 1816. Vertical profiles of TKN compared with data for 10/ 5/2016.

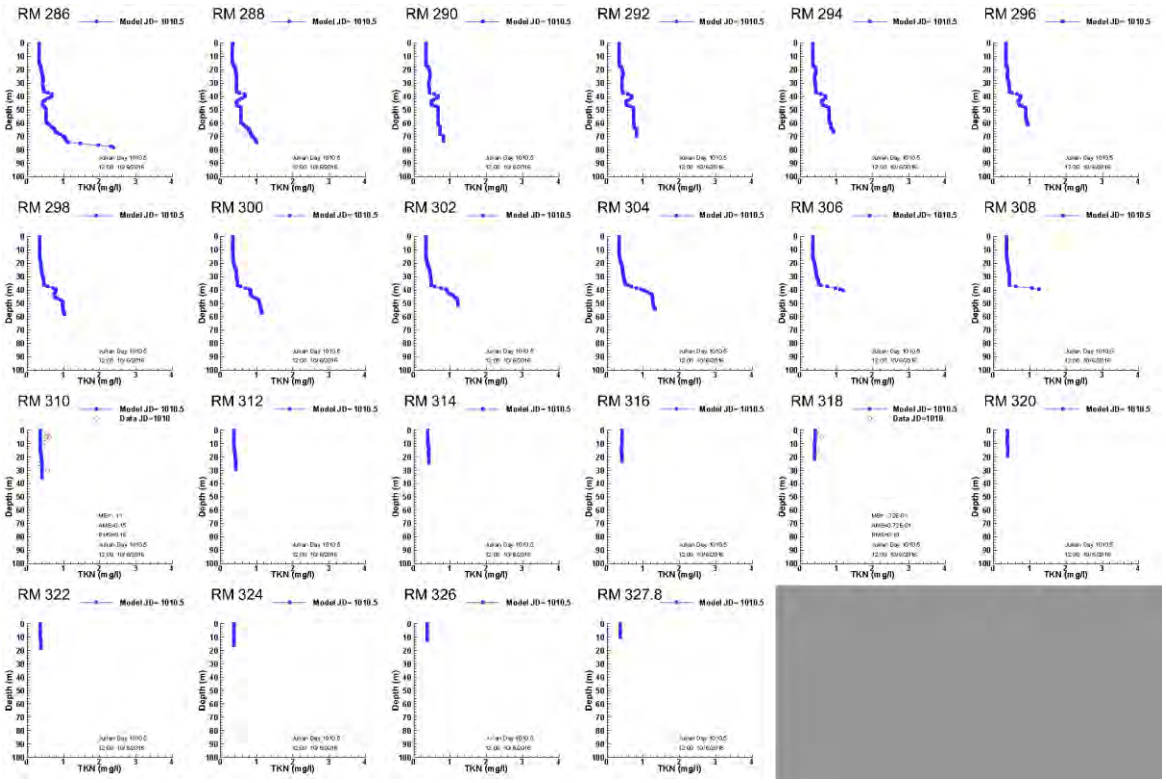


Figure 1817. Vertical profiles of TKN compared with data for 10/ 6/2016.

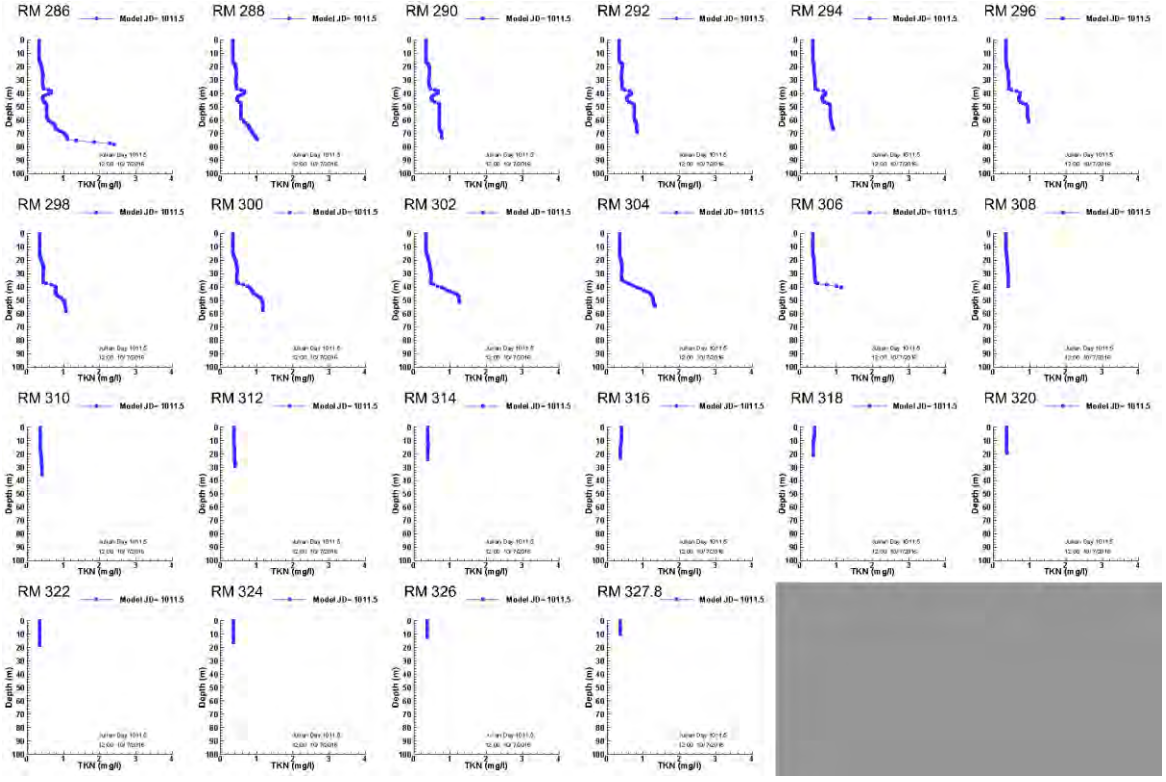


Figure 1818. Vertical profiles of TKN compared with data for 10/ 7/2016.

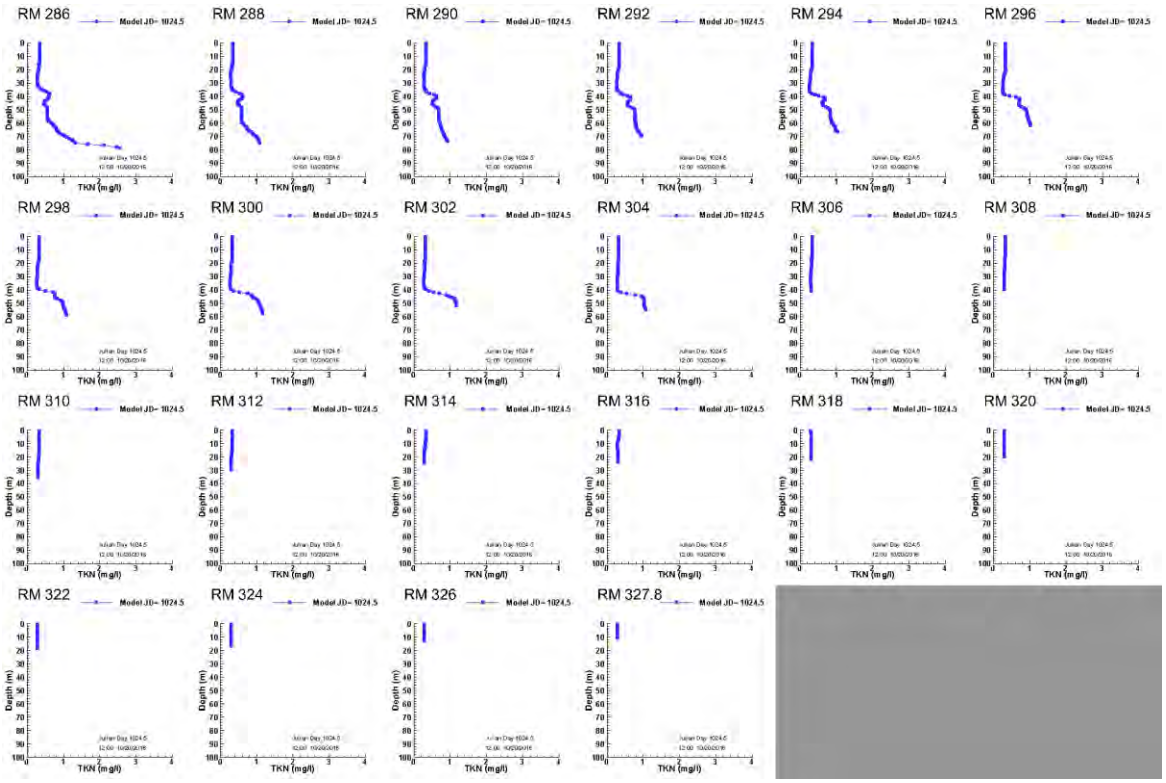


Figure 1819. Vertical profiles of TKN compared with data for 10/20/2016.

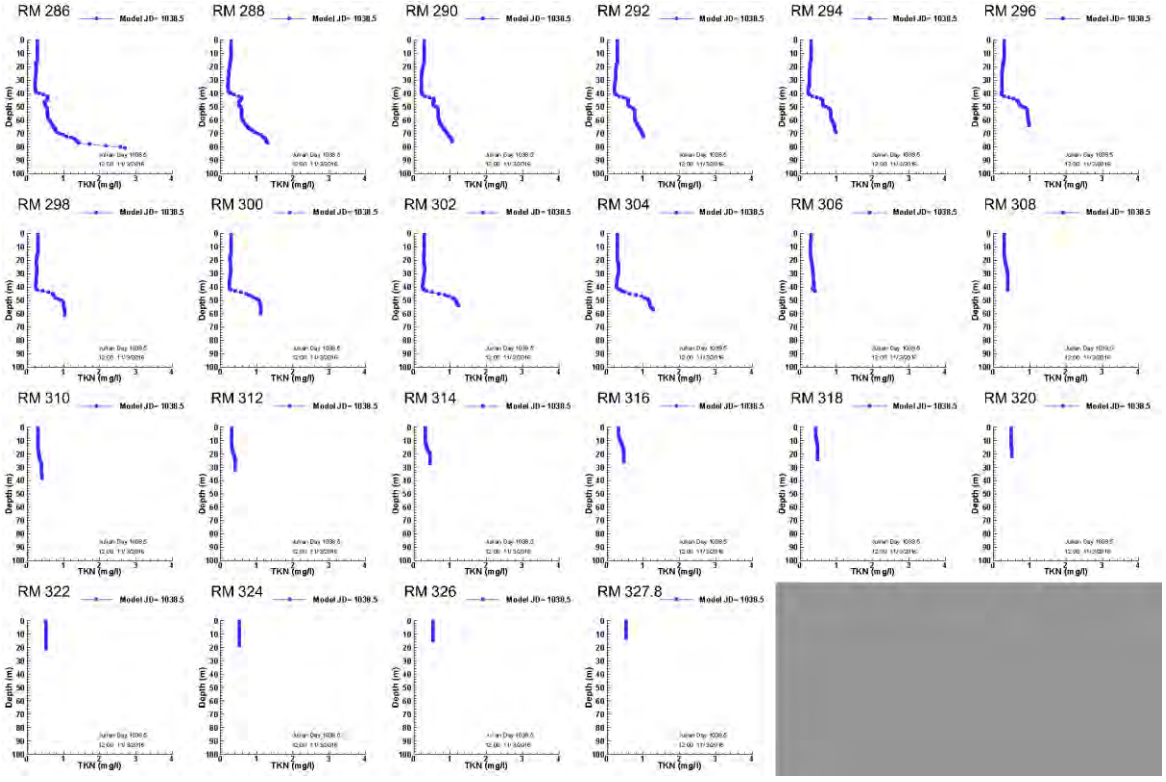


Figure 1820. Vertical profiles of TKN compared with data for 11/ 3/2016.

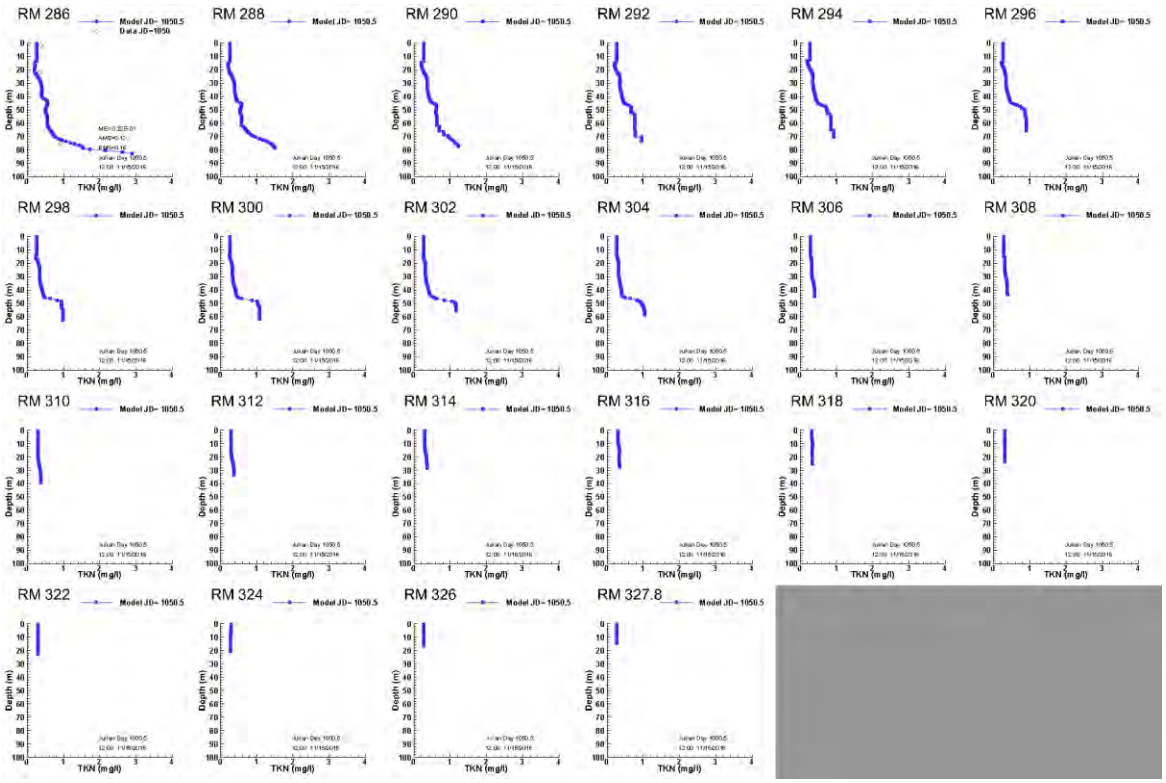


Figure 1821. Vertical profiles of TKN compared with data for 11/15/2016.

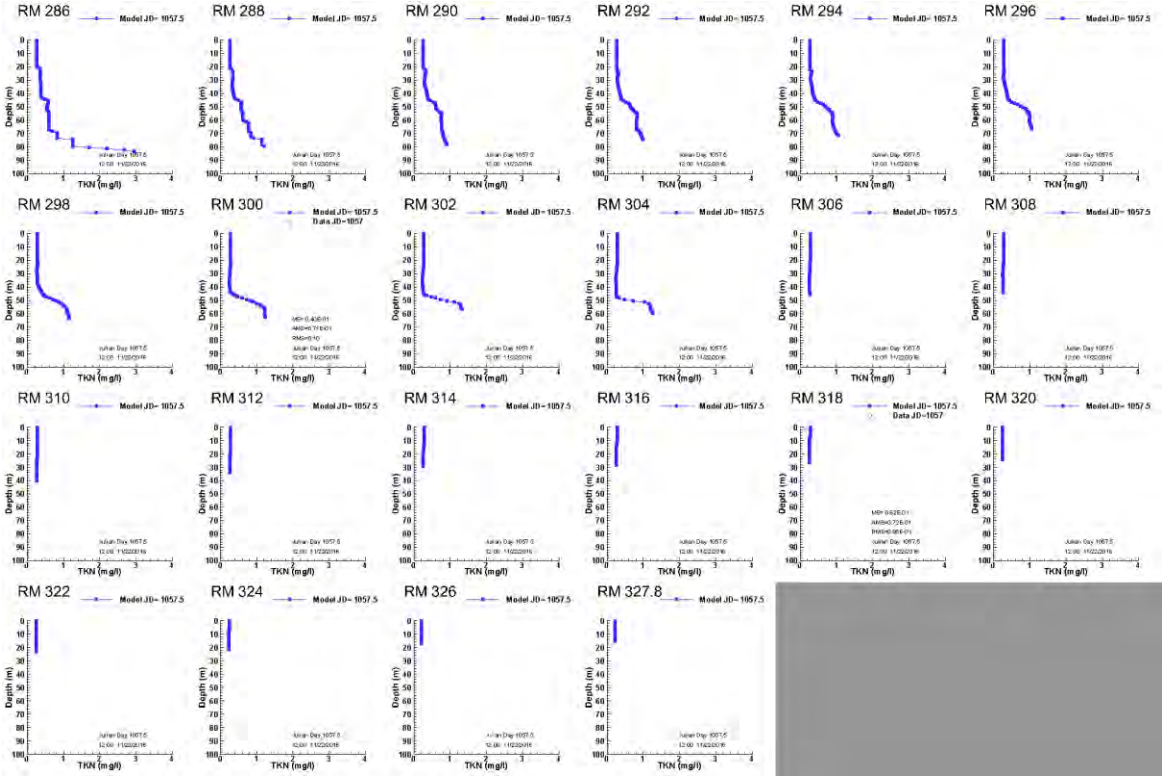


Figure 1822. Vertical profiles of TKN compared with data for 11/22/2016.

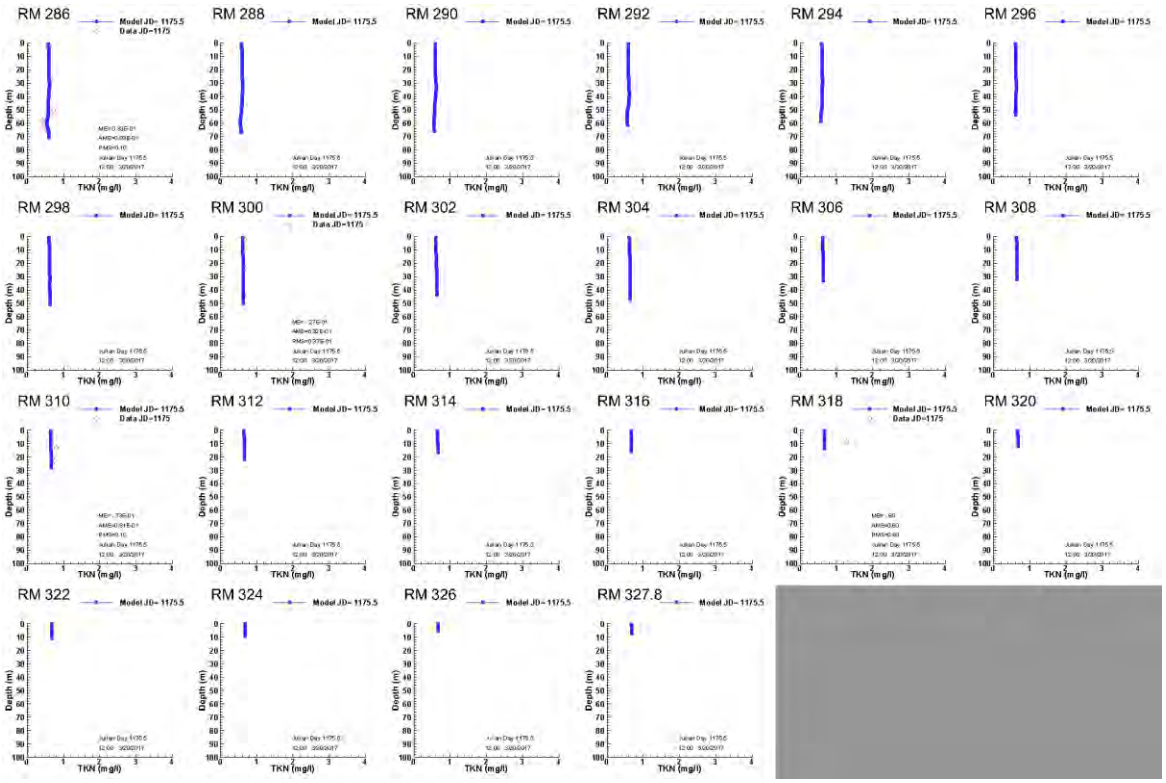


Figure 1823. Vertical profiles of TKN compared with data for 3/20/2017.

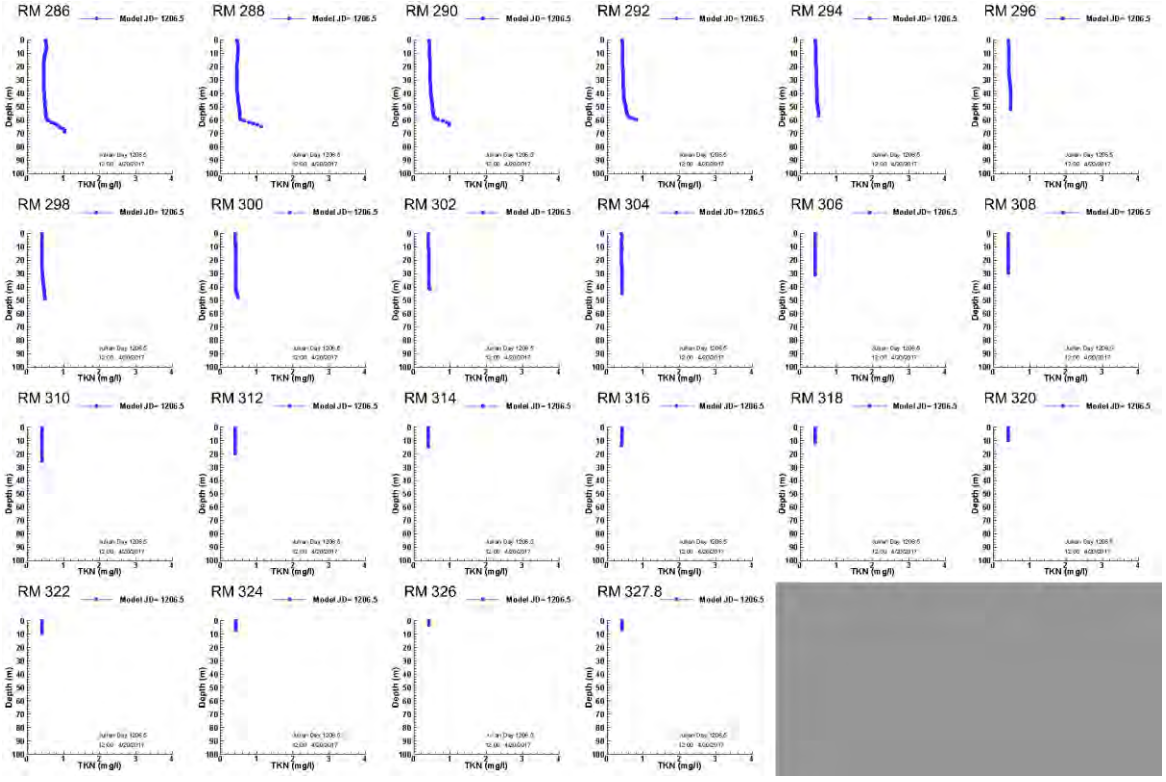


Figure 1824. Vertical profiles of TKN compared with data for 4/20/2017.

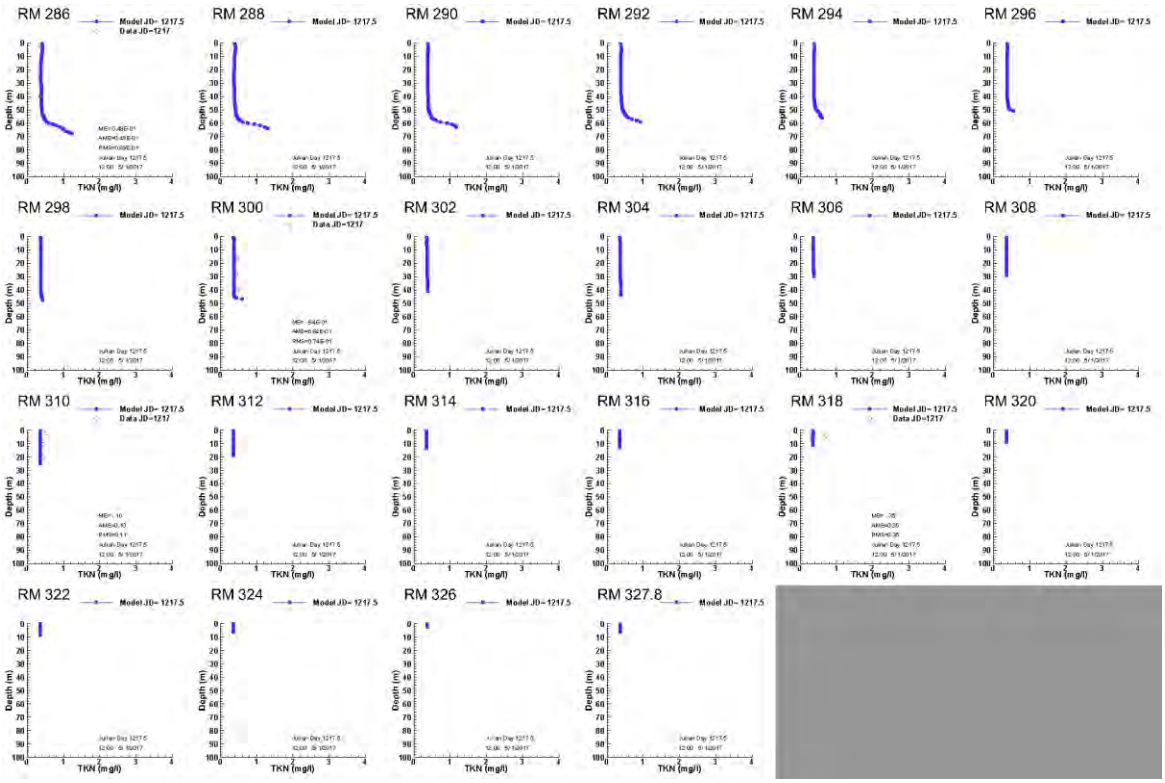


Figure 1825. Vertical profiles of TKN compared with data for 5/ 1/2017.

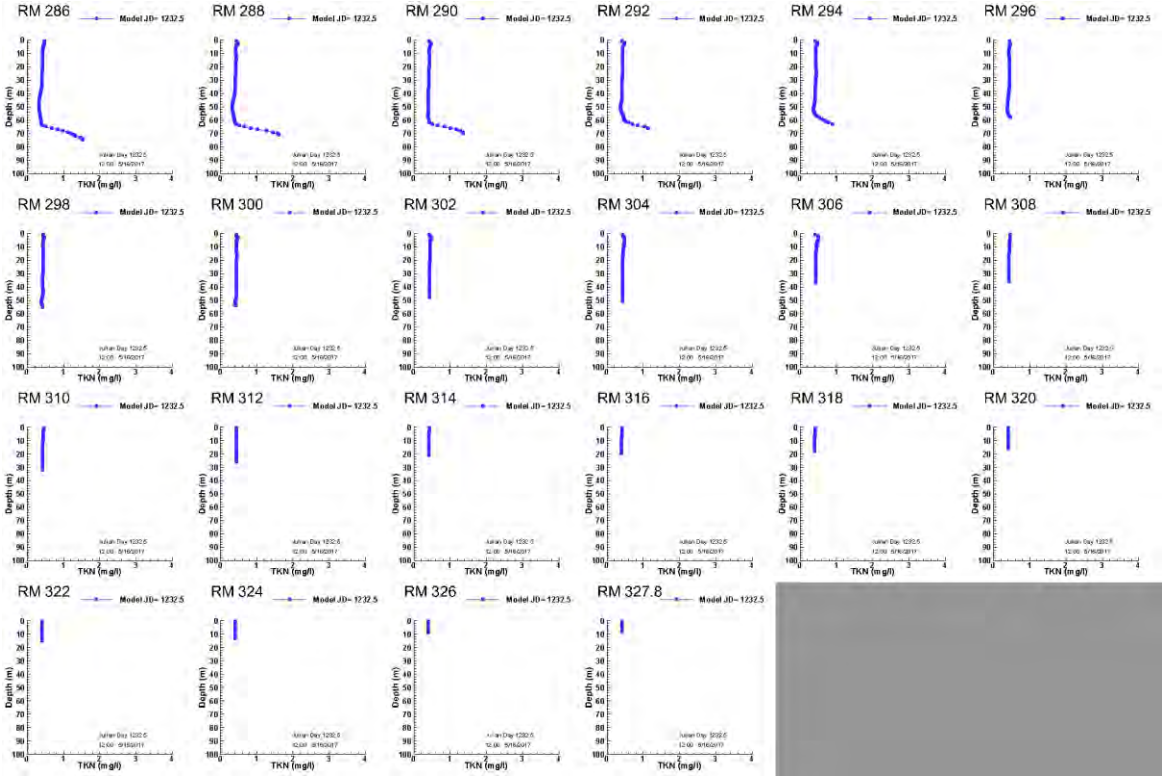


Figure 1826. Vertical profiles of TKN compared with data for 5/16/2017.

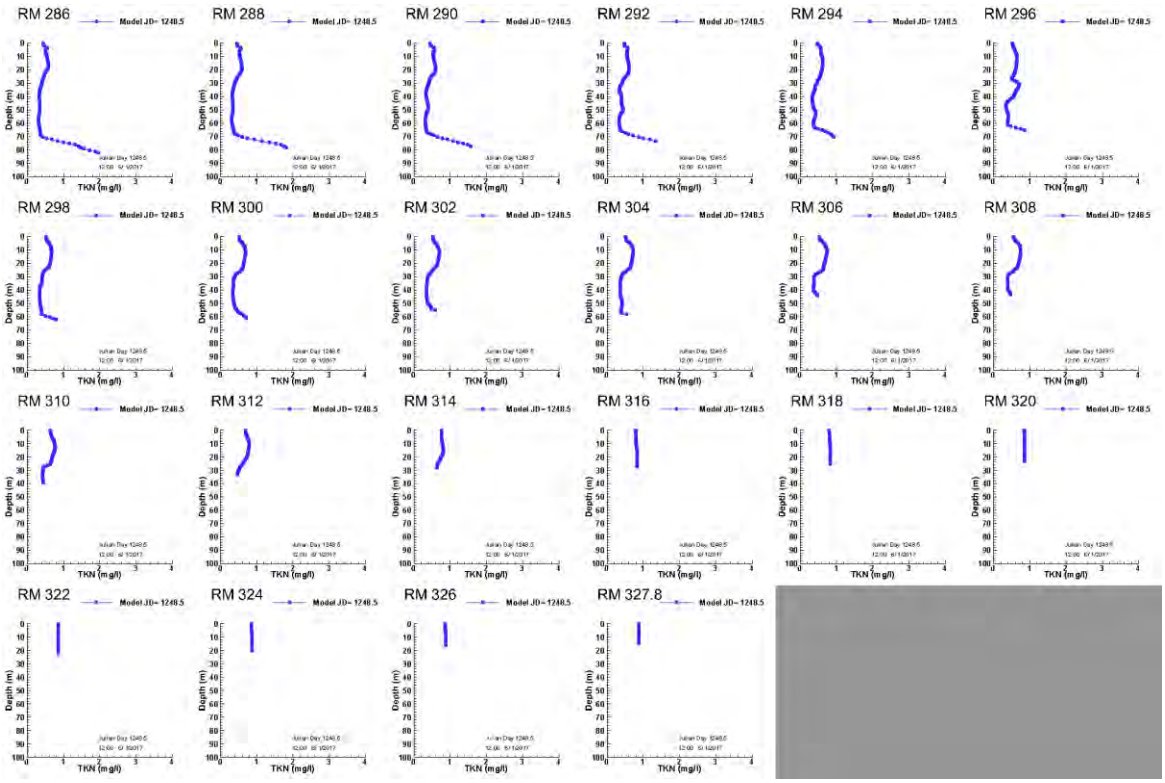


Figure 1827. Vertical profiles of TKN compared with data for 6/ 1/2017.

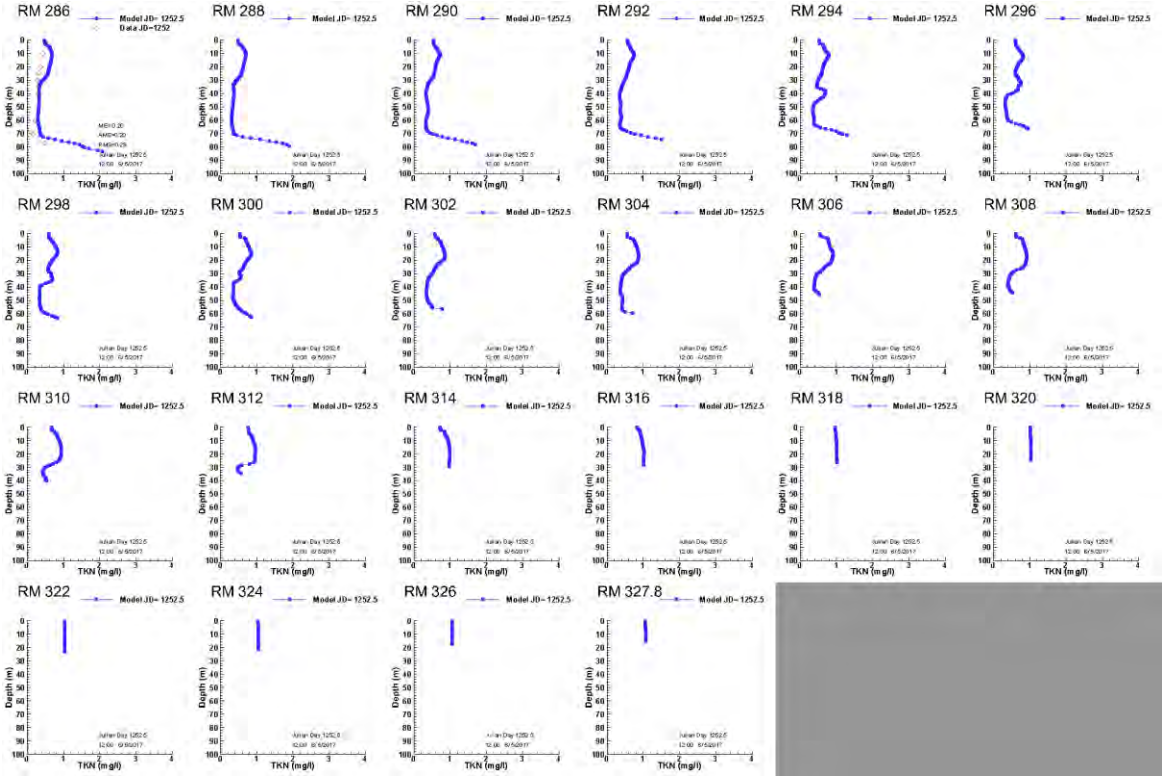


Figure 1828. Vertical profiles of TKN compared with data for 6/ 5/2017.

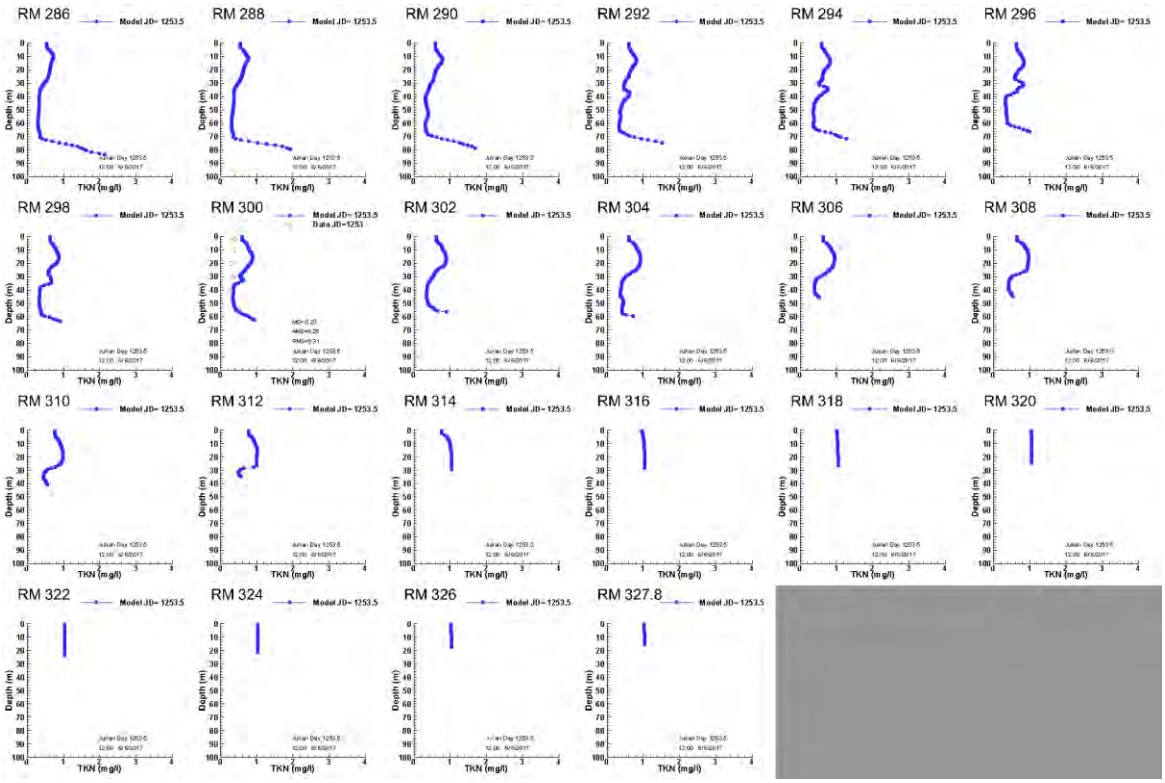


Figure 1829. Vertical profiles of TKN compared with data for 6/ 6/2017.

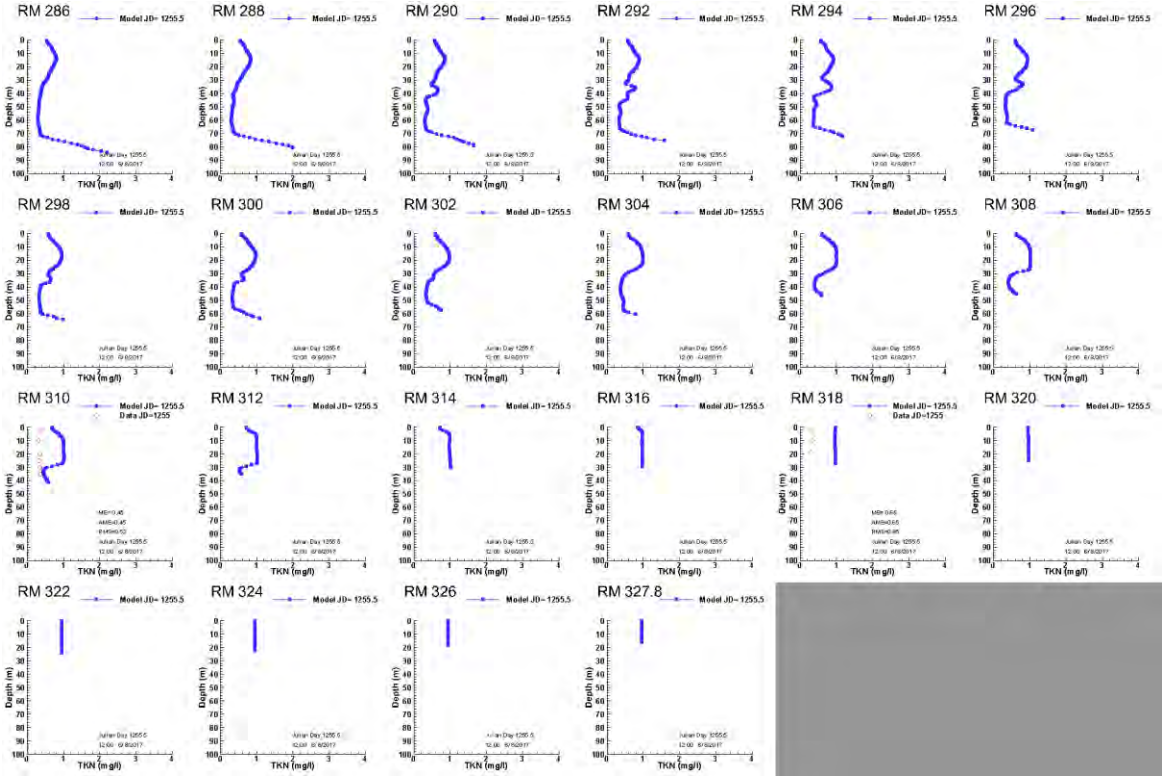


Figure 1830. Vertical profiles of TKN compared with data for 6/ 8/2017.

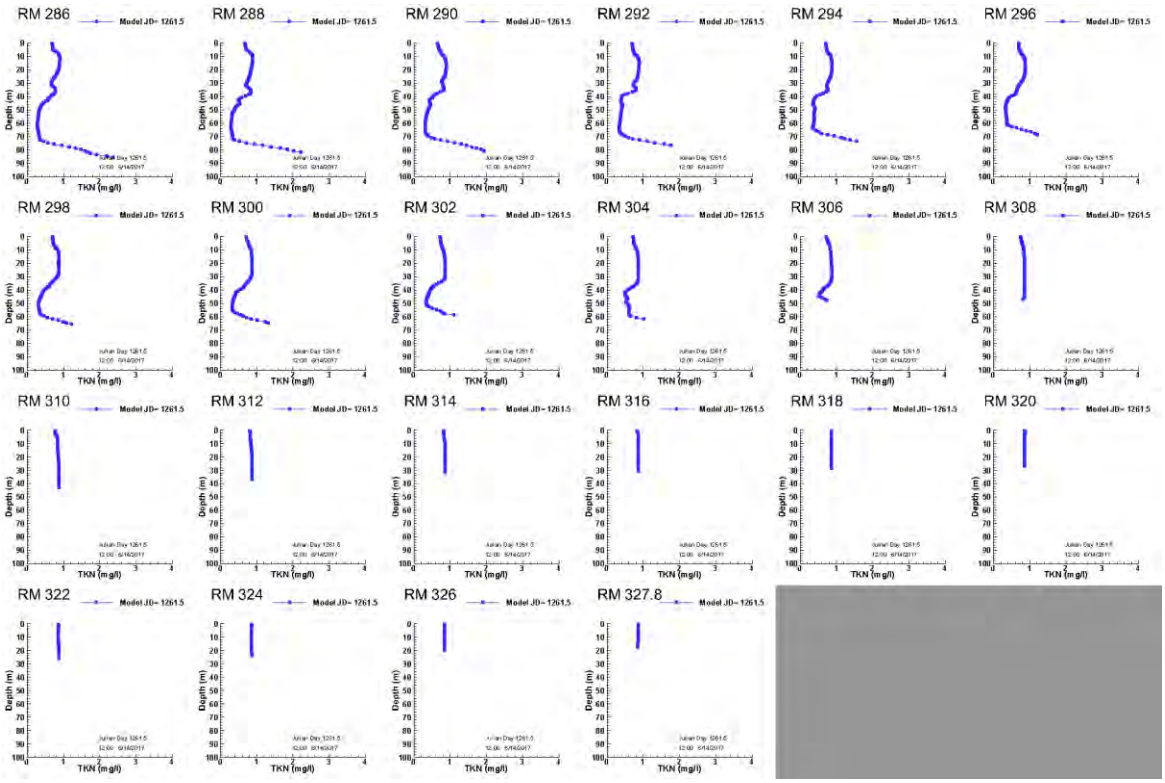


Figure 1831. Vertical profiles of TKN compared with data for 6/14/2017.

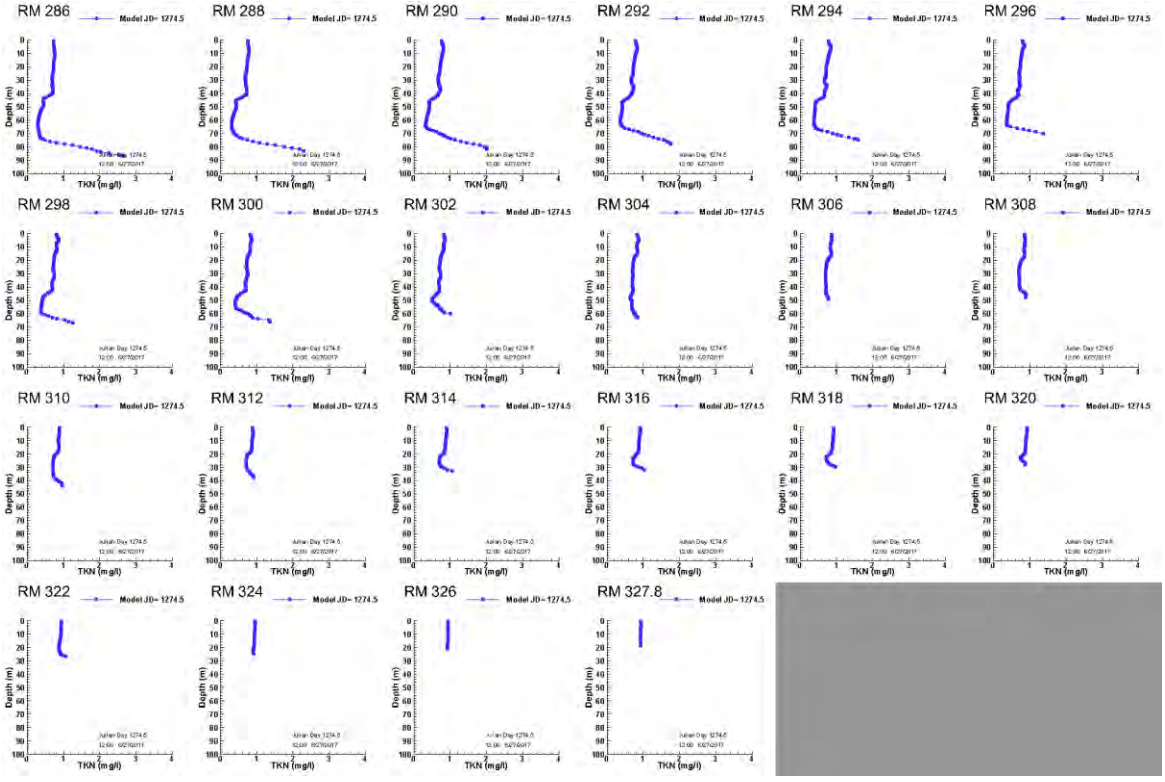


Figure 1832. Vertical profiles of TKN compared with data for 6/27/2017.

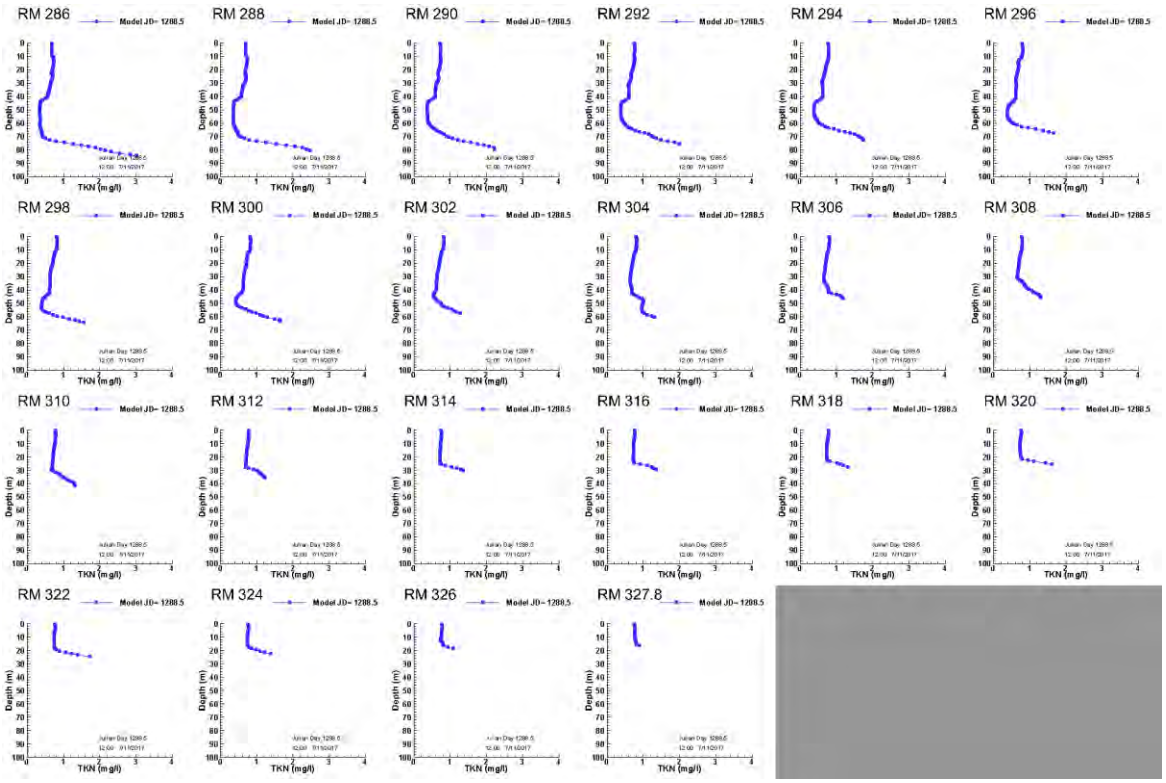


Figure 1833. Vertical profiles of TKN compared with data for 7/11/2017.

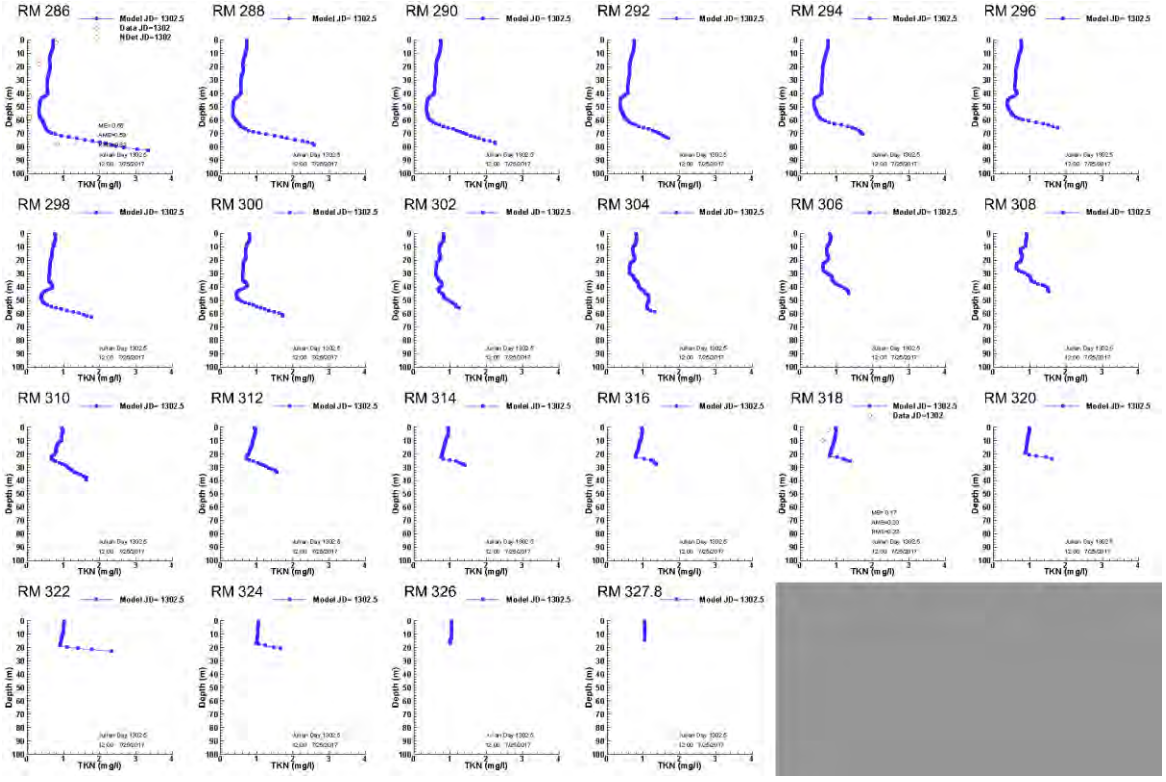


Figure 1834. Vertical profiles of TKN compared with data for 7/25/2017.

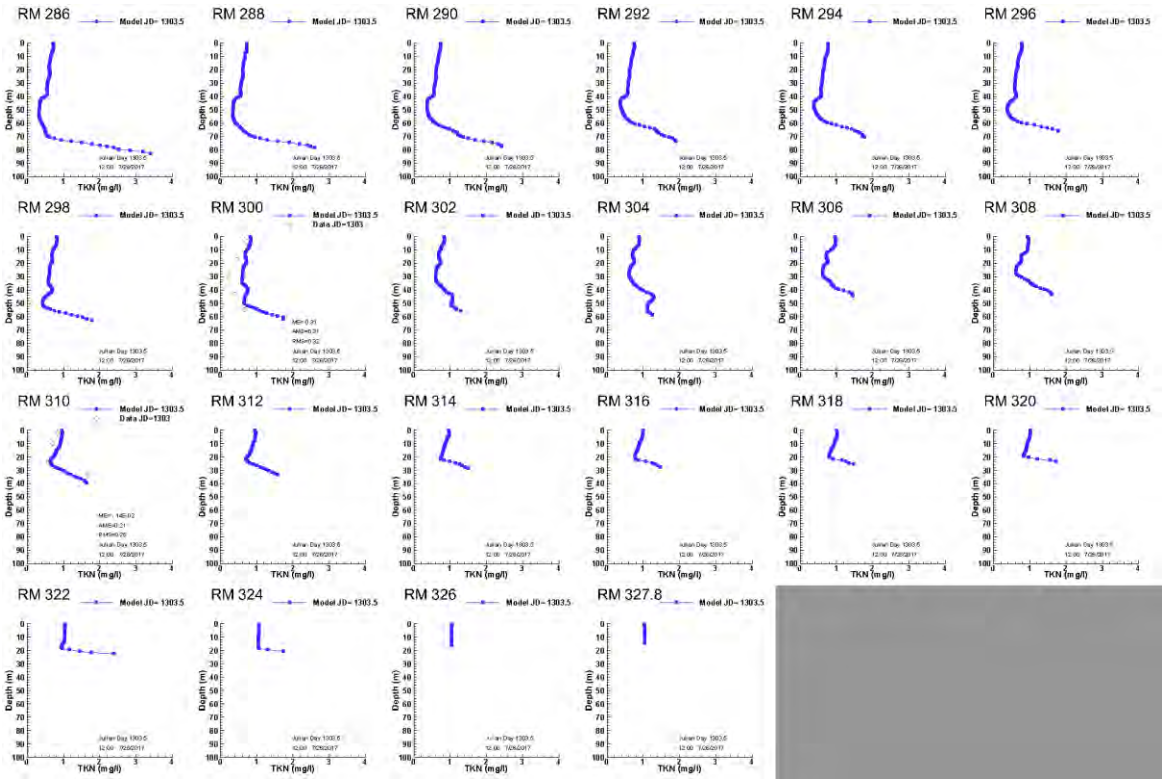


Figure 1835. Vertical profiles of TKN compared with data for 7/26/2017.

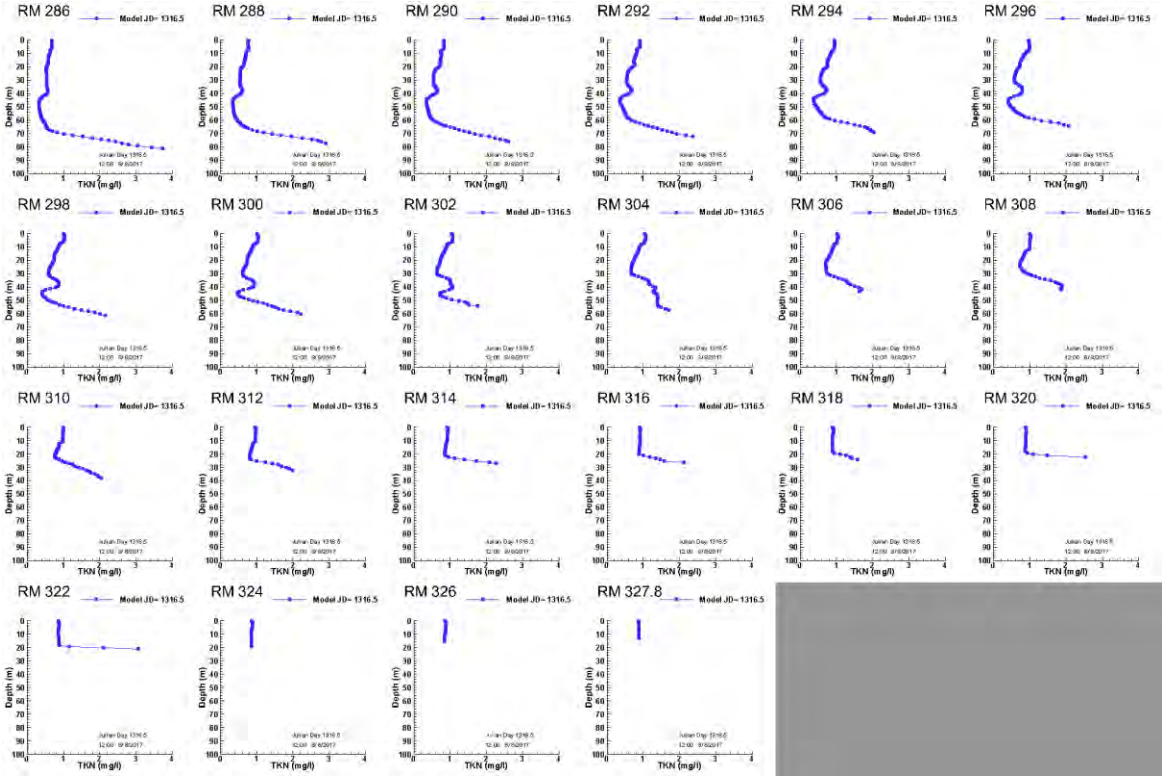


Figure 1836. Vertical profiles of TKN compared with data for 8/ 8/2017.

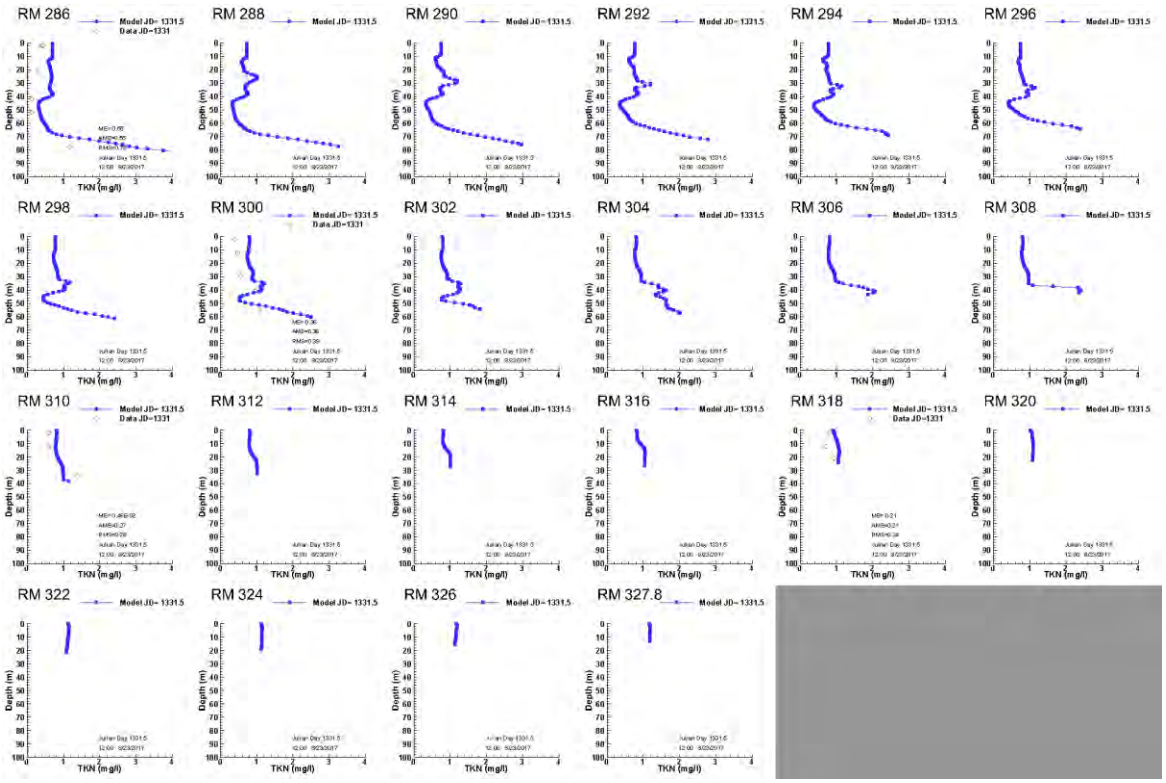


Figure 1837. Vertical profiles of TKN compared with data for 8/23/2017.

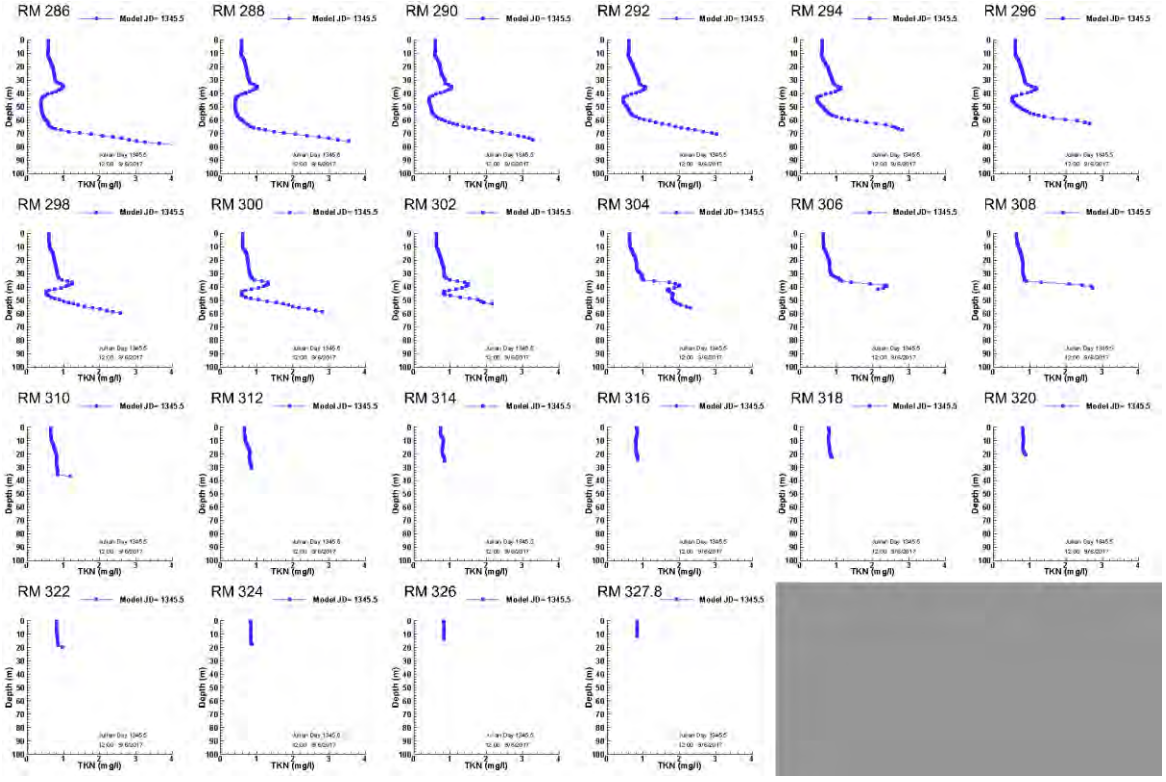


Figure 1838. Vertical profiles of TKN compared with data for 9/ 6/2017.

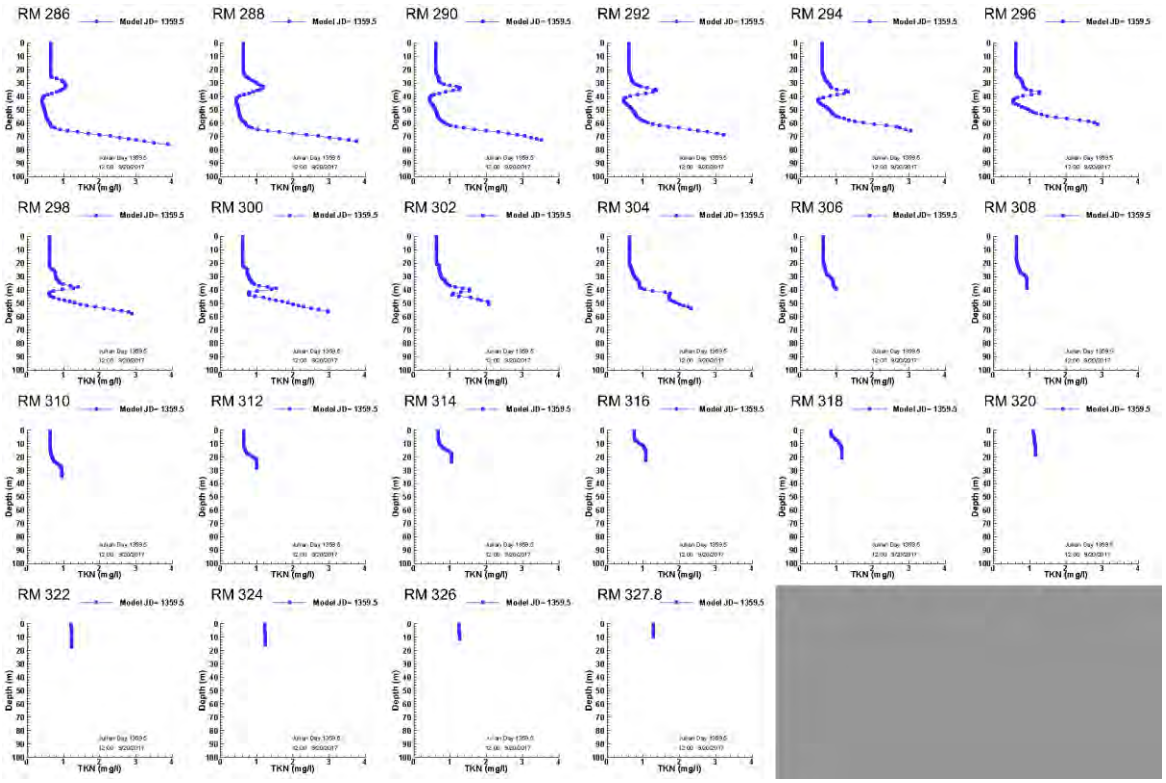


Figure 1839. Vertical profiles of TKN compared with data for 9/20/2017.

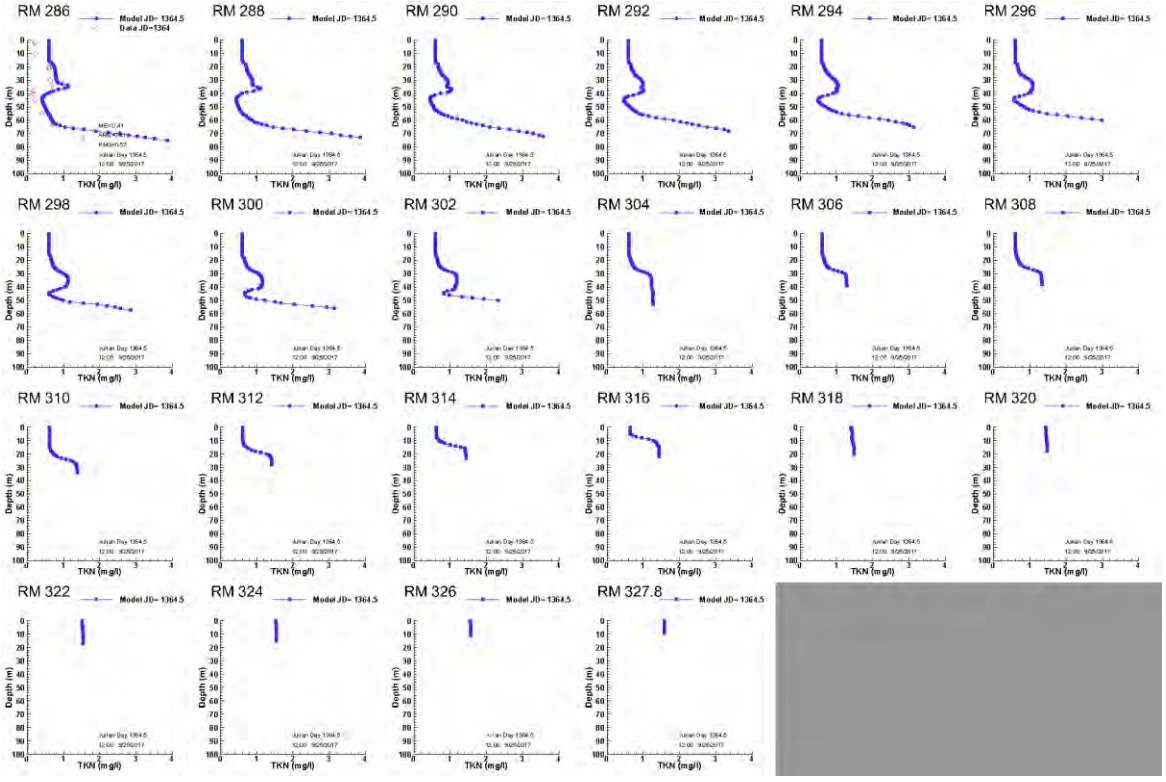


Figure 1840. Vertical profiles of TKN compared with data for 9/25/2017.

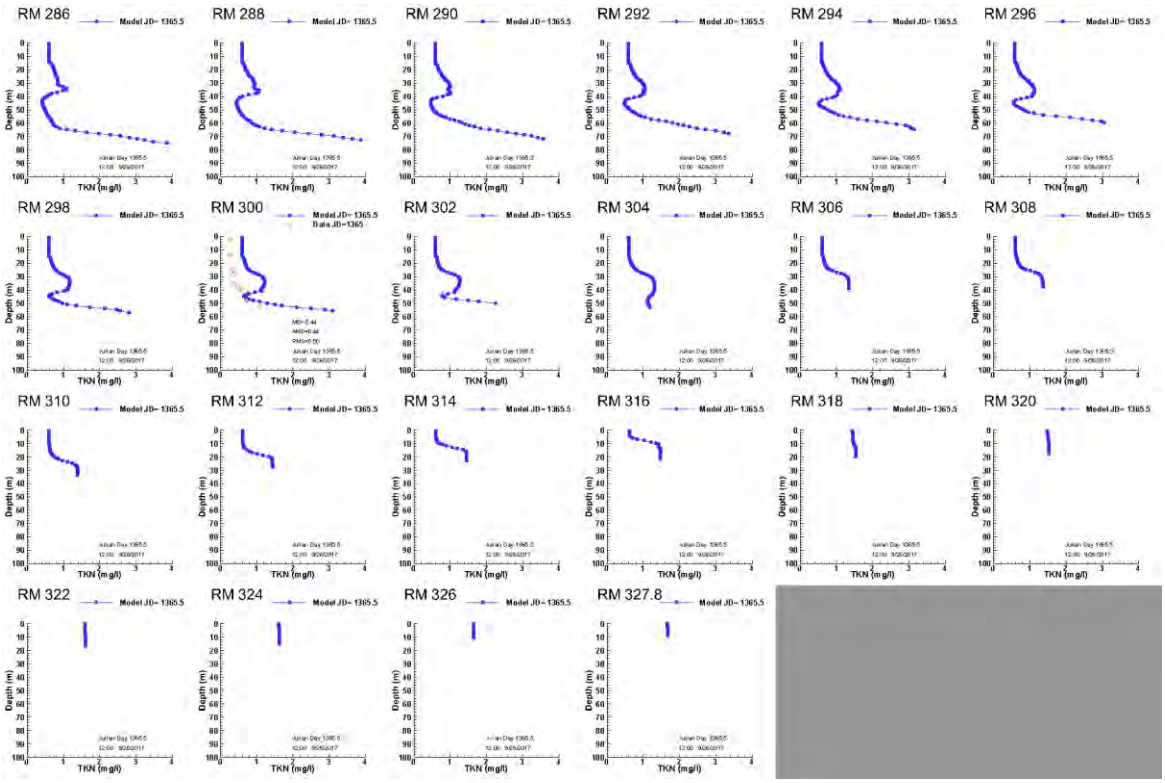


Figure 1841. Vertical profiles of TKN compared with data for 9/26/2017.

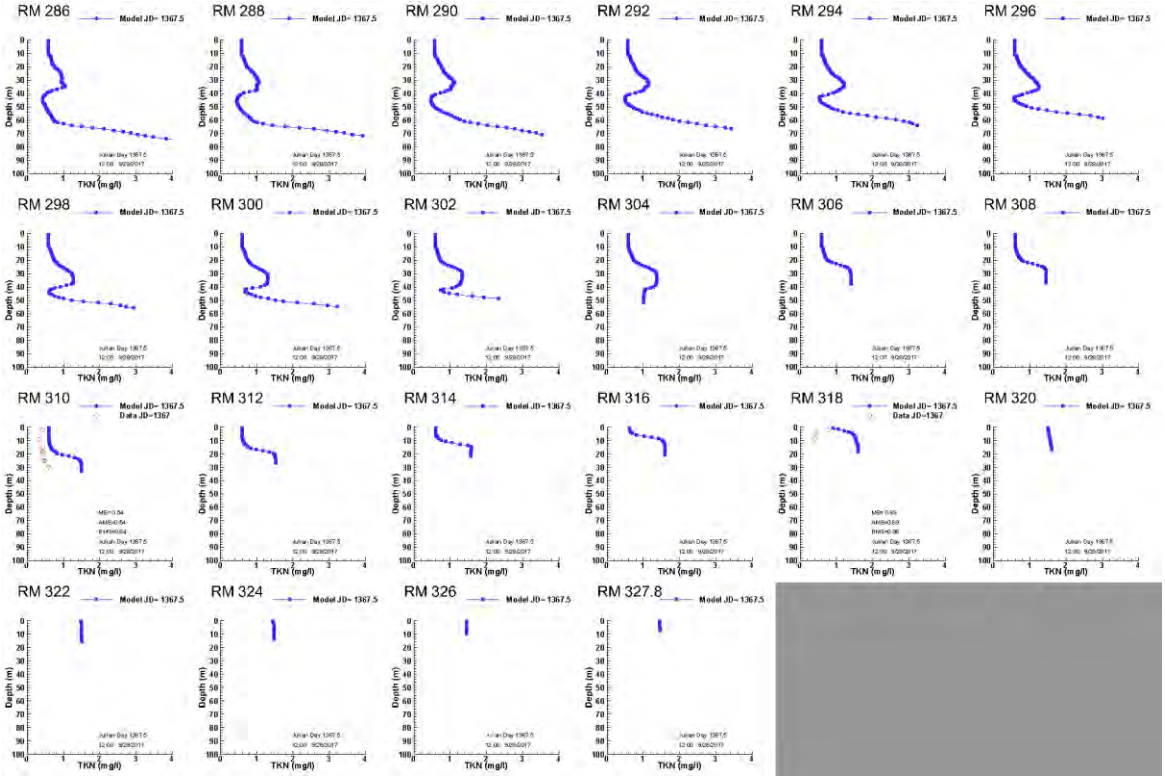


Figure 1842. Vertical profiles of TKN compared with data for 9/28/2017.

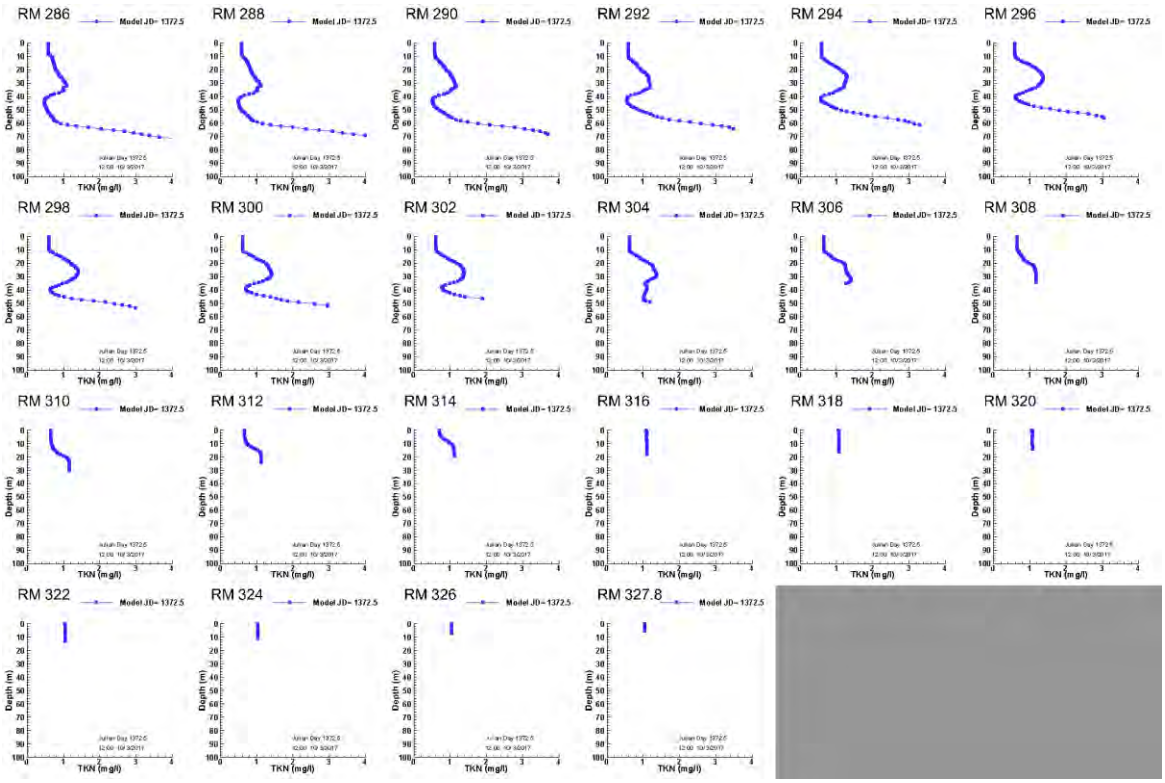


Figure 1843. Vertical profiles of TKN compared with data for 10/ 3/2017.

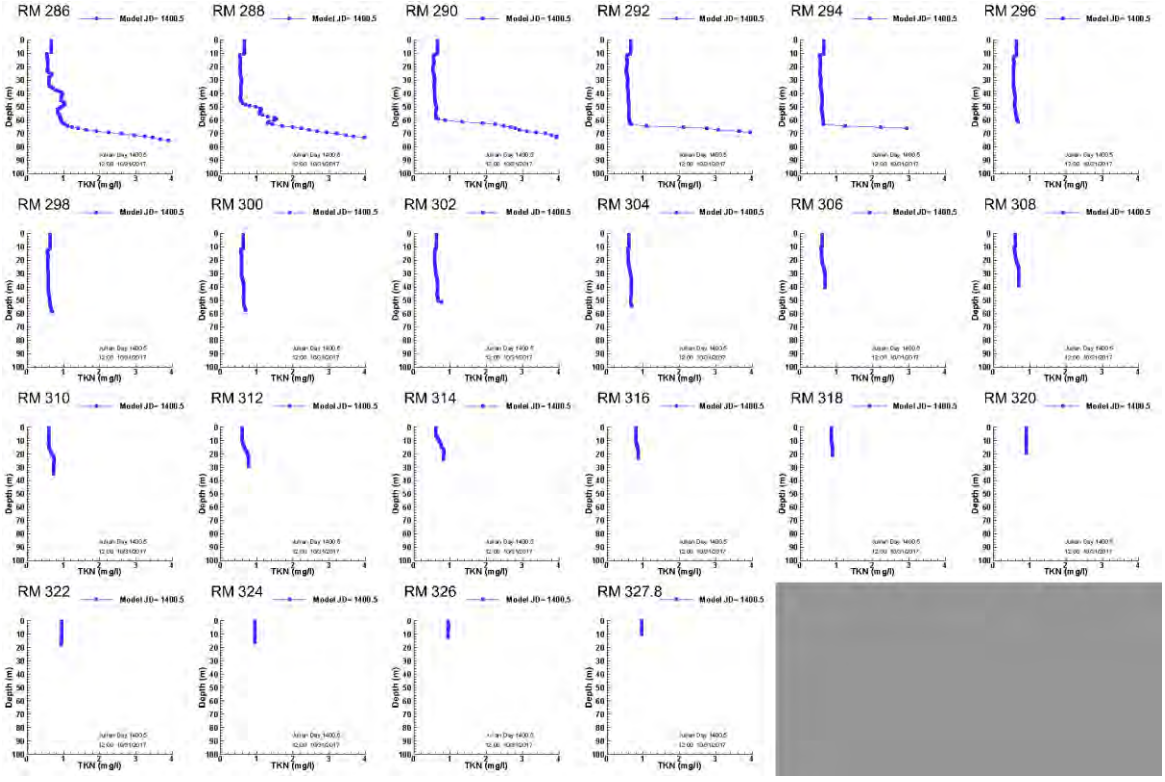


Figure 1844. Vertical profiles of TKN compared with data for 10/31/2017.

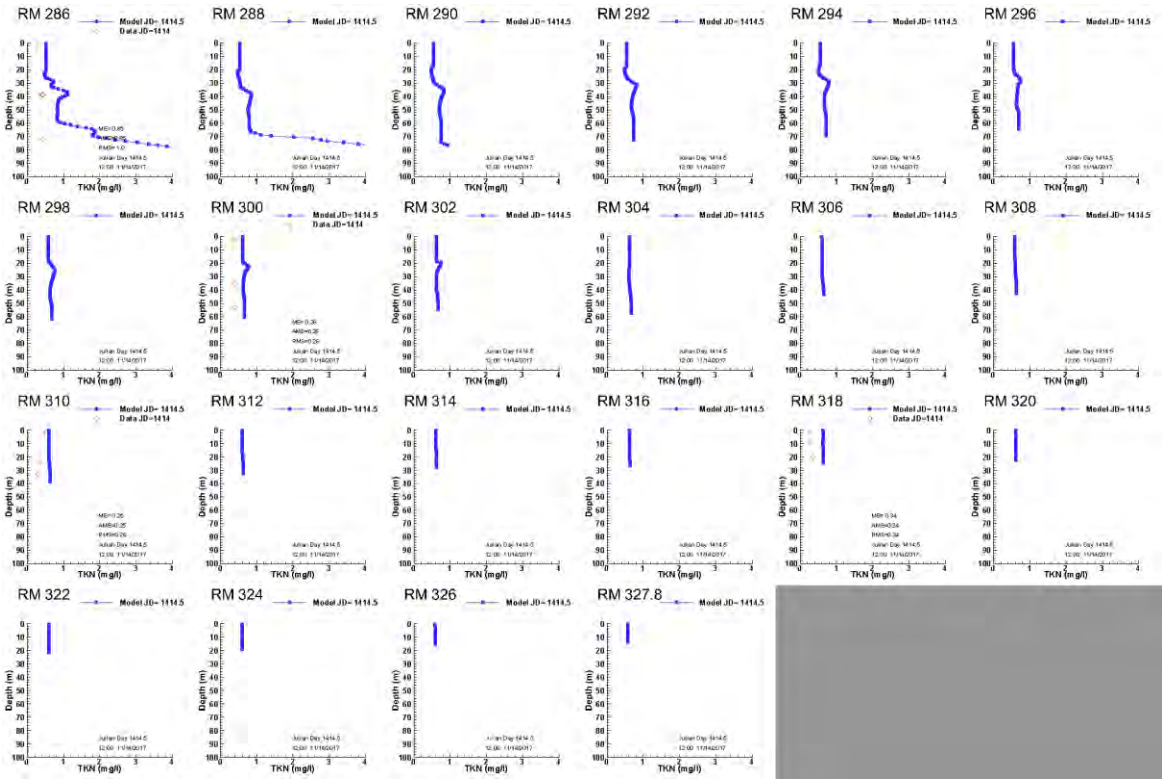


Figure 1845. Vertical profiles of TKN compared with data for 11/14/2017.

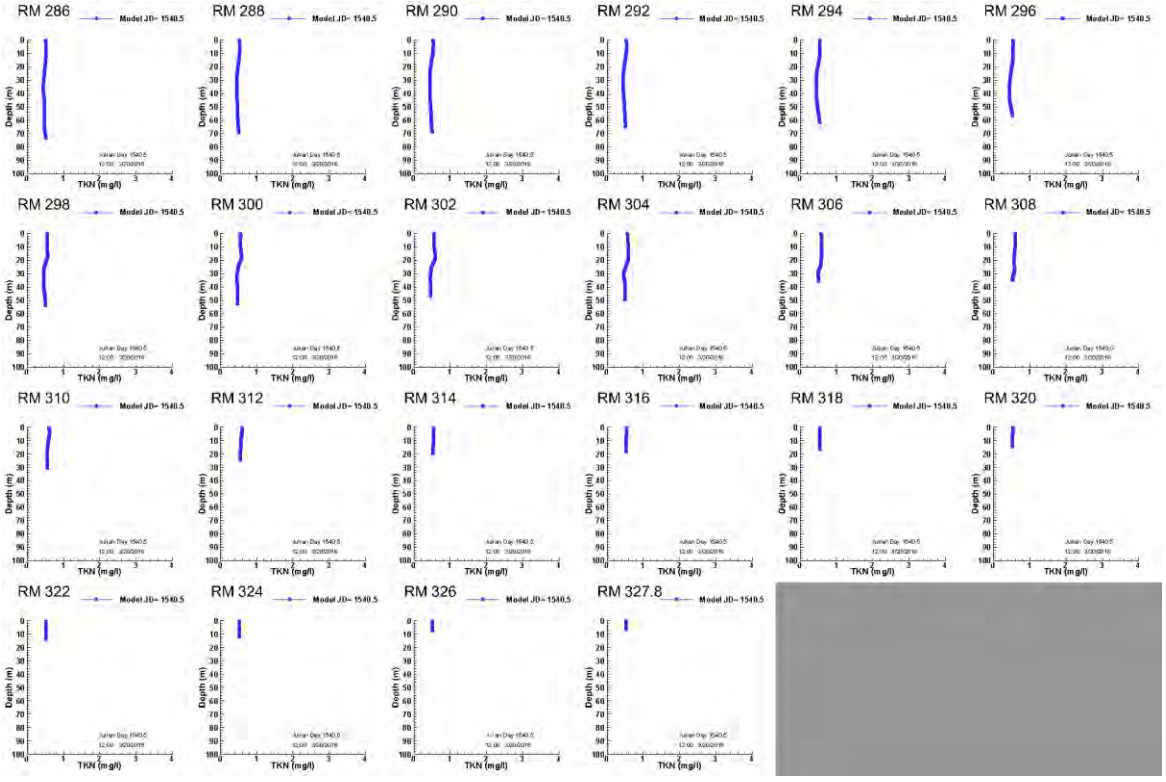


Figure 1846. Vertical profiles of TKN compared with data for 3/20/2018.

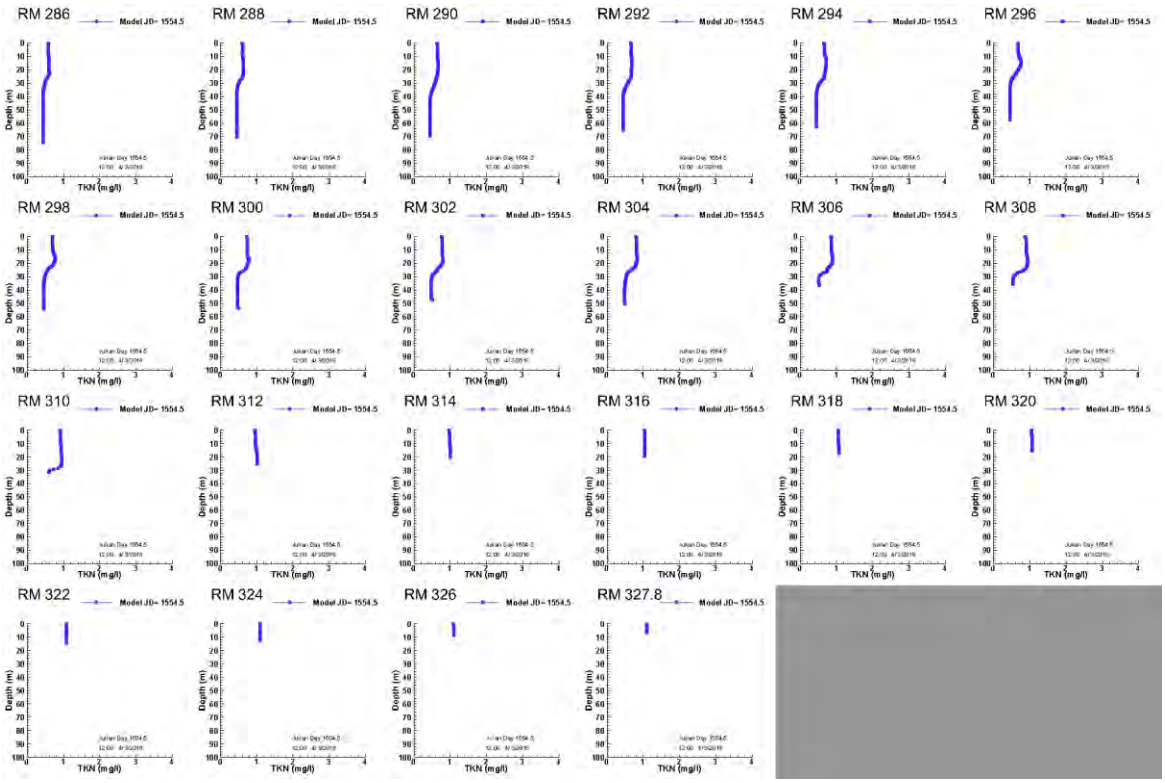


Figure 1847. Vertical profiles of TKN compared with data for 4/ 3/2018.

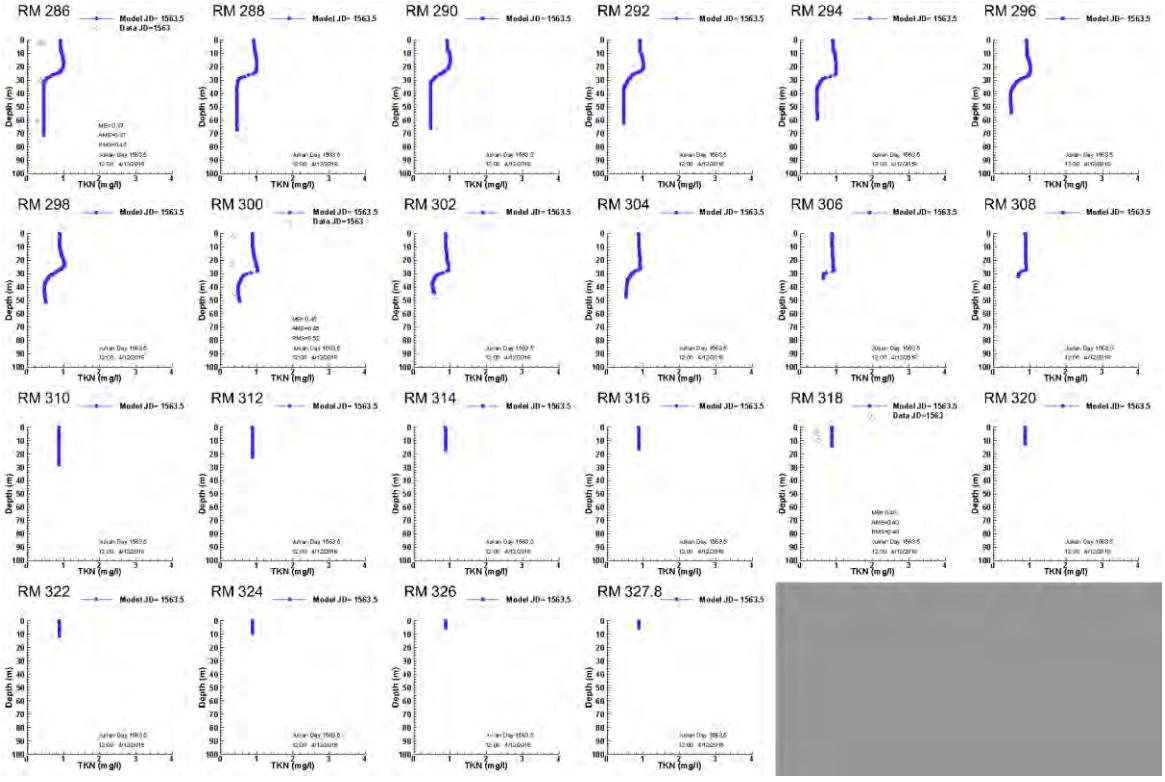


Figure 1848. Vertical profiles of TKN compared with data for 4/12/2018.

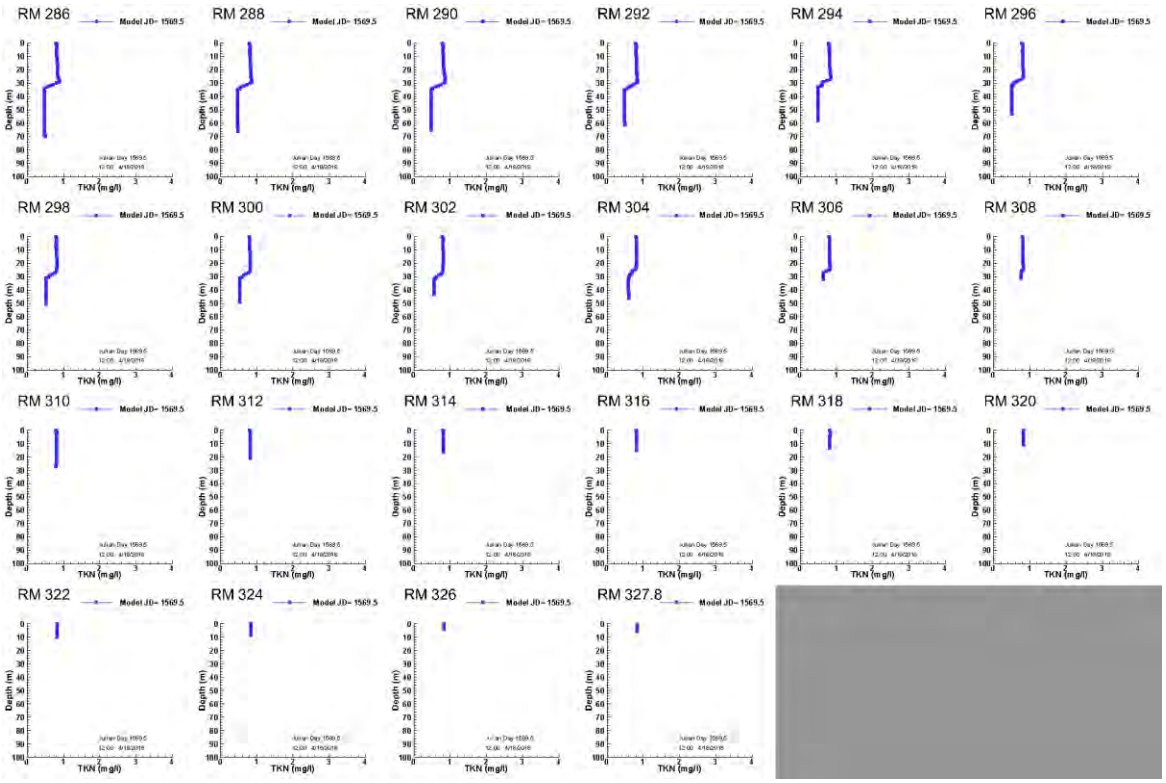


Figure 1849. Vertical profiles of TKN compared with data for 4/18/2018.

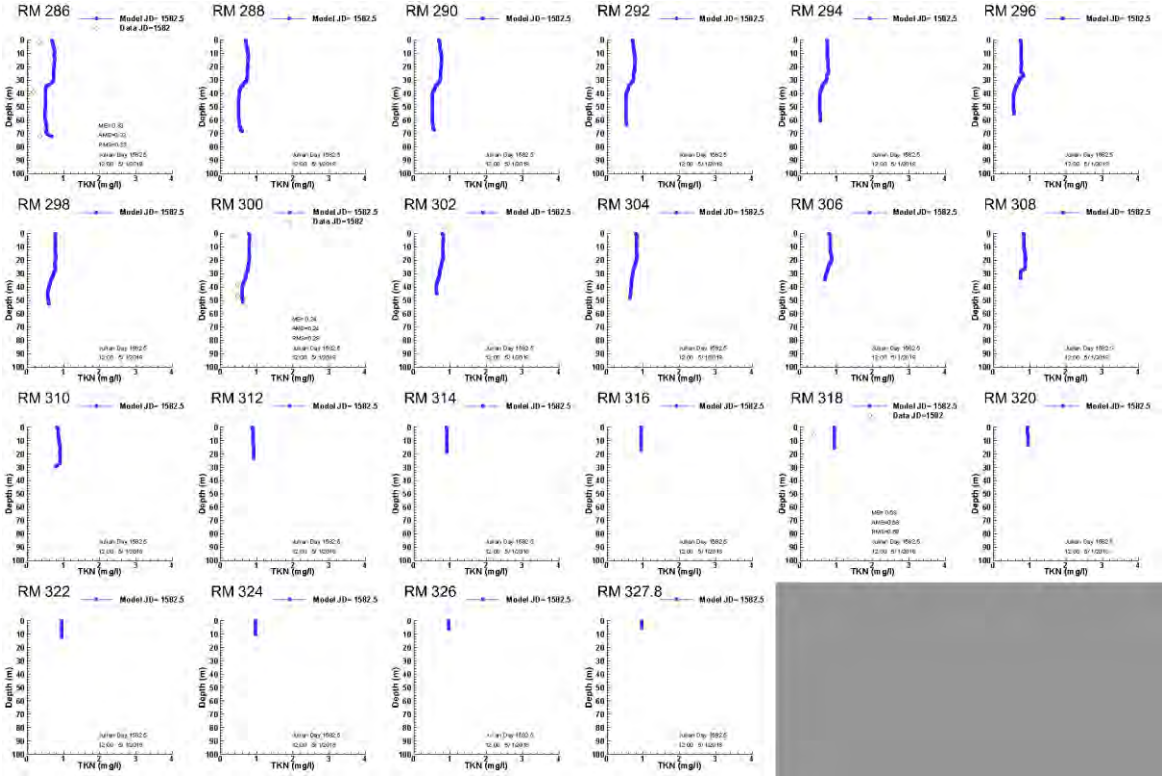


Figure 1850. Vertical profiles of TKN compared with data for 5/ 1/2018.

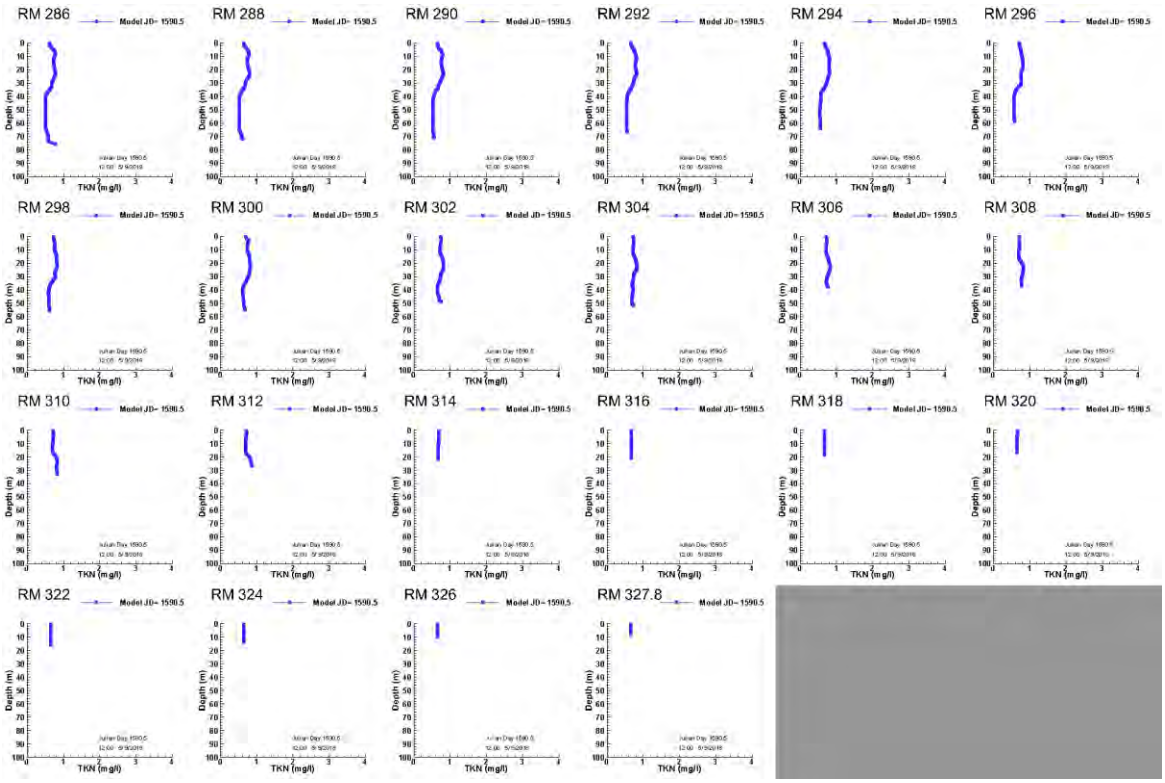


Figure 1851. Vertical profiles of TKN compared with data for 5/ 9/2018.

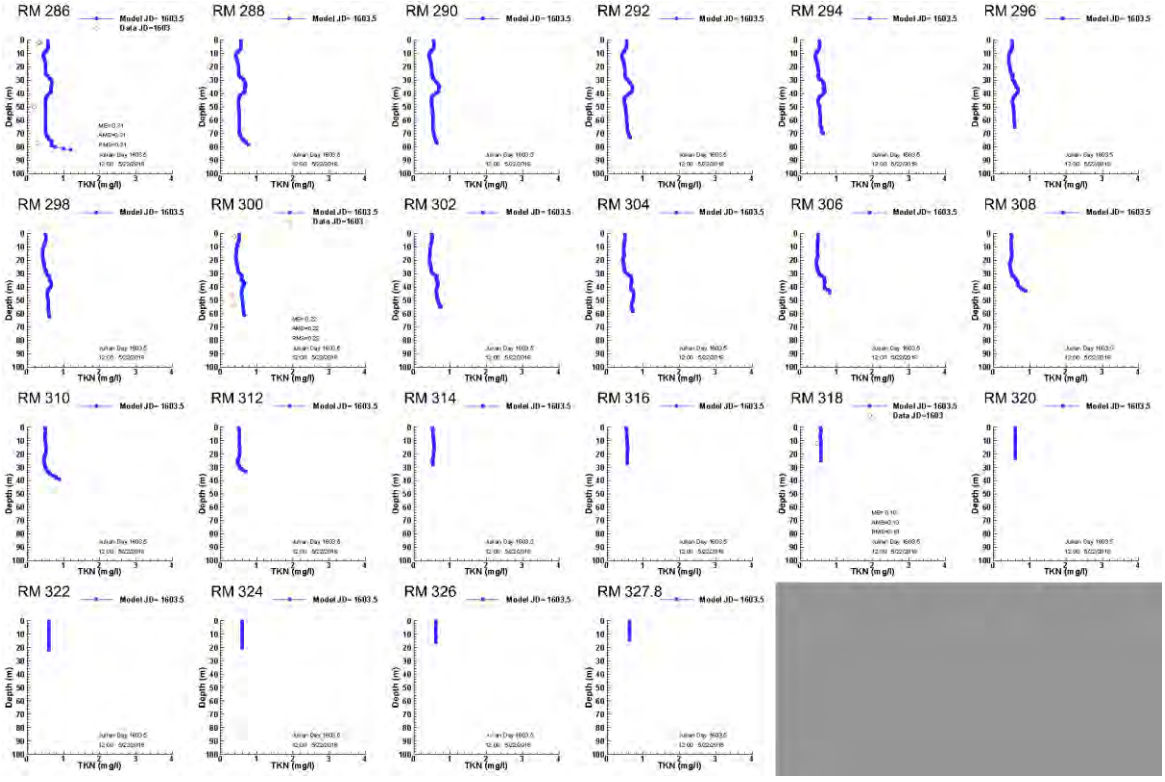


Figure 1852. Vertical profiles of TKN compared with data for 5/22/2018.

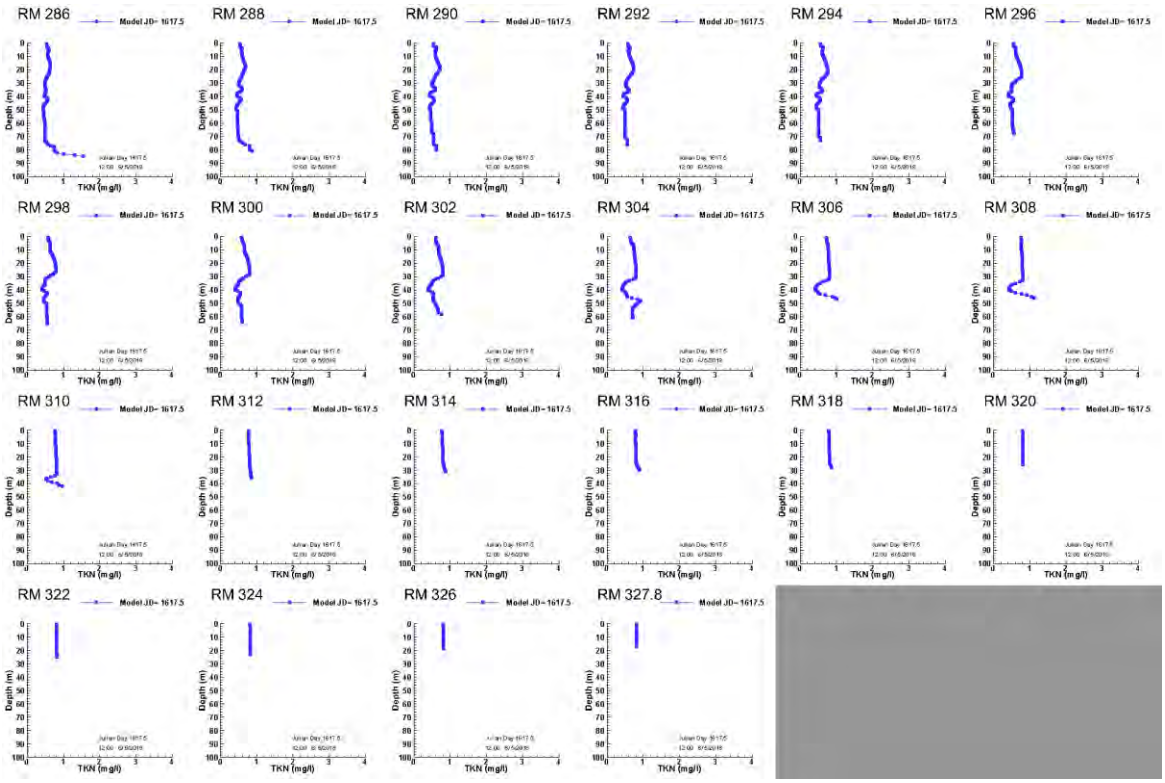


Figure 1853. Vertical profiles of TKN compared with data for 6/ 5/2018.

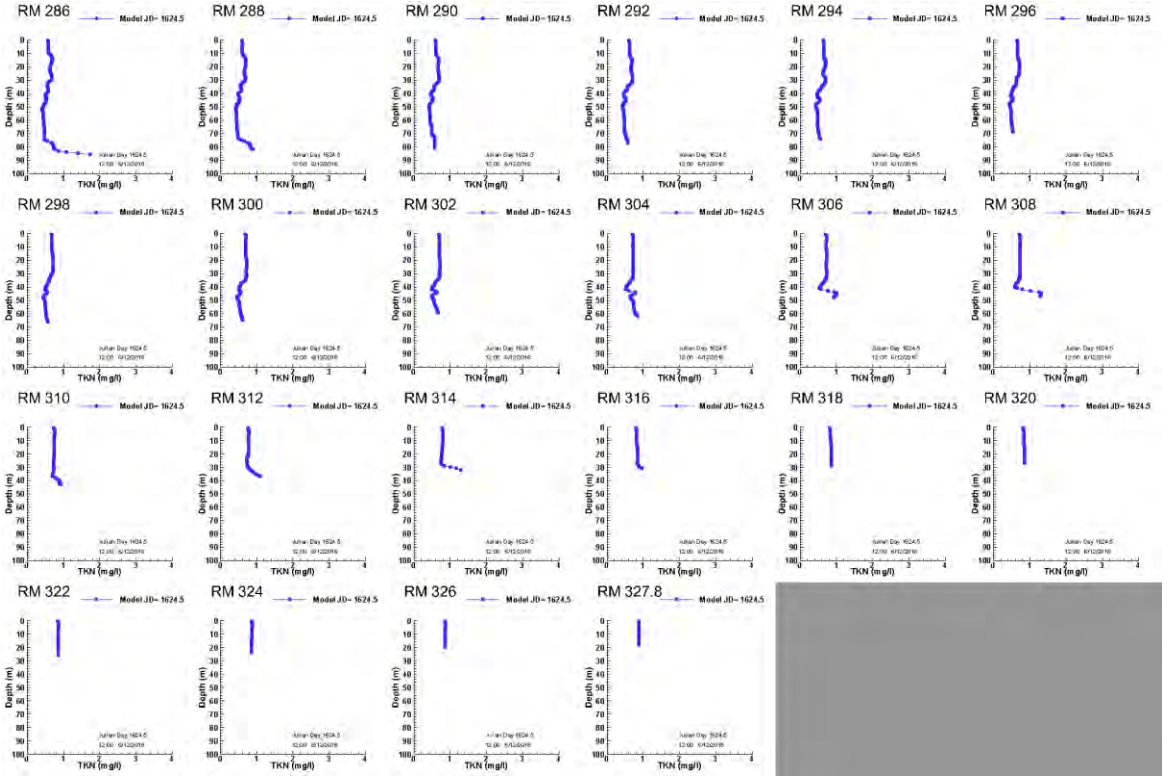


Figure 1854. Vertical profiles of TKN compared with data for 6/12/2018.

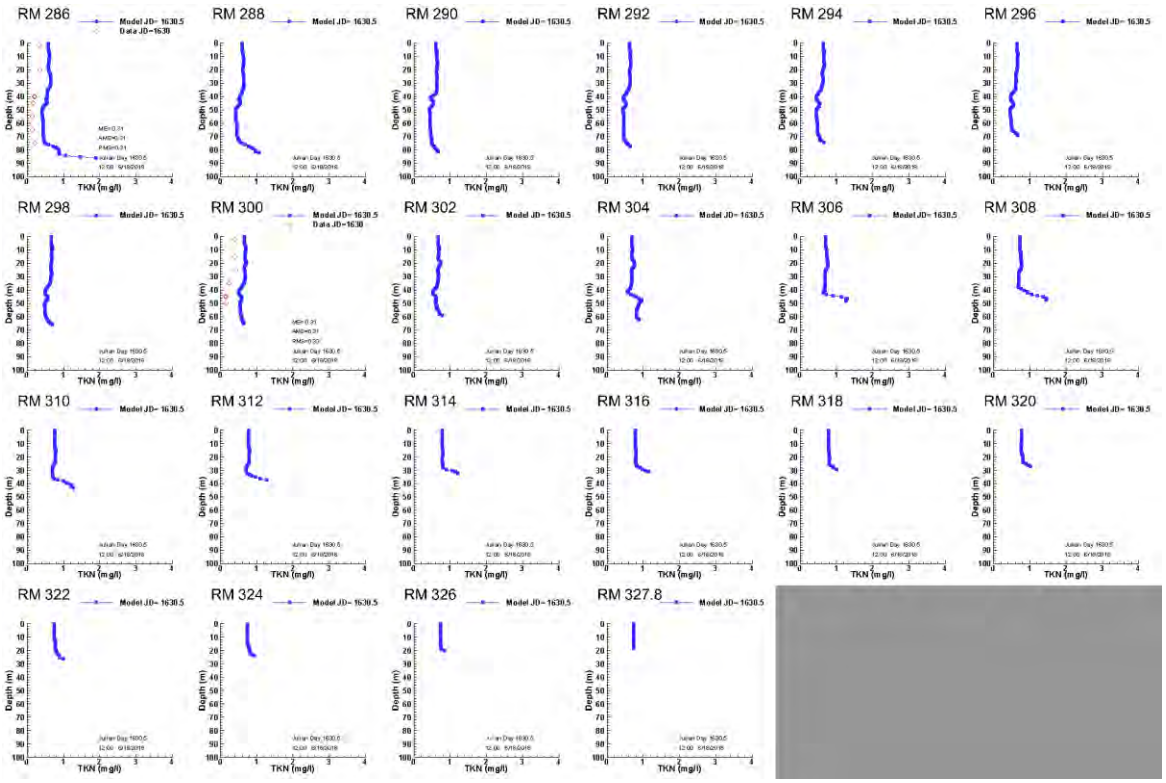


Figure 1855. Vertical profiles of TKN compared with data for 6/18/2018.

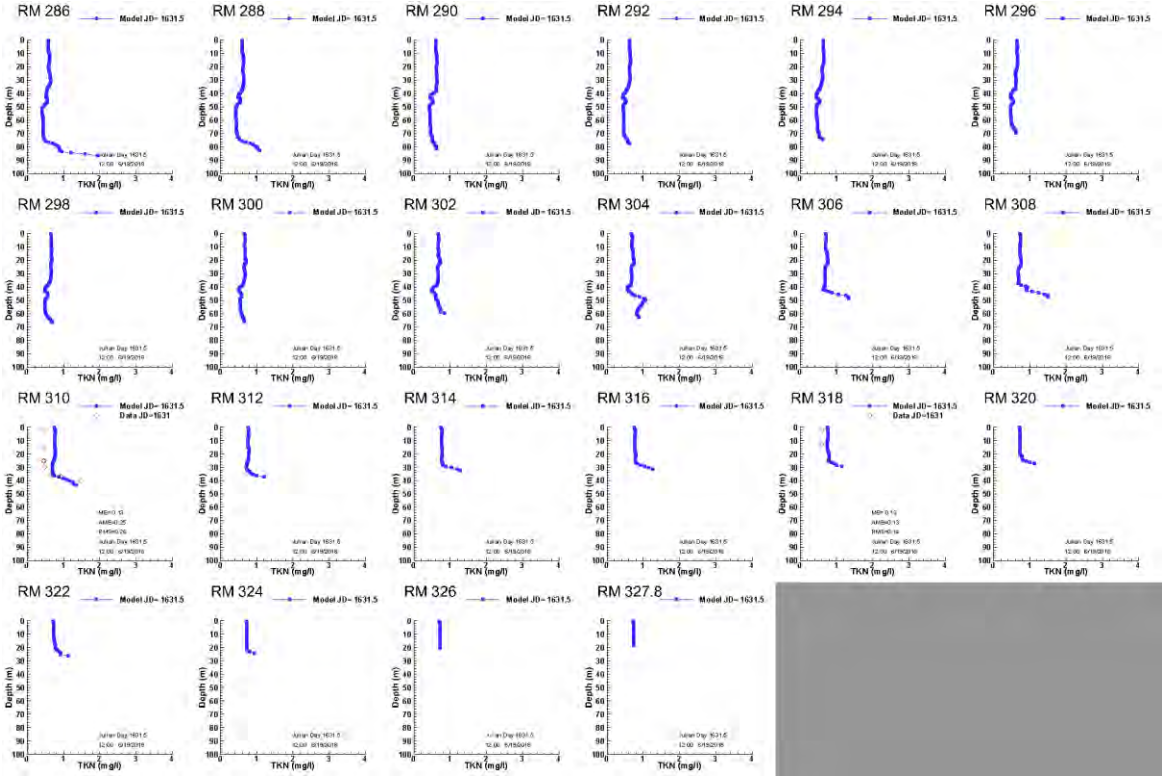


Figure 1856. Vertical profiles of TKN compared with data for 6/19/2018.

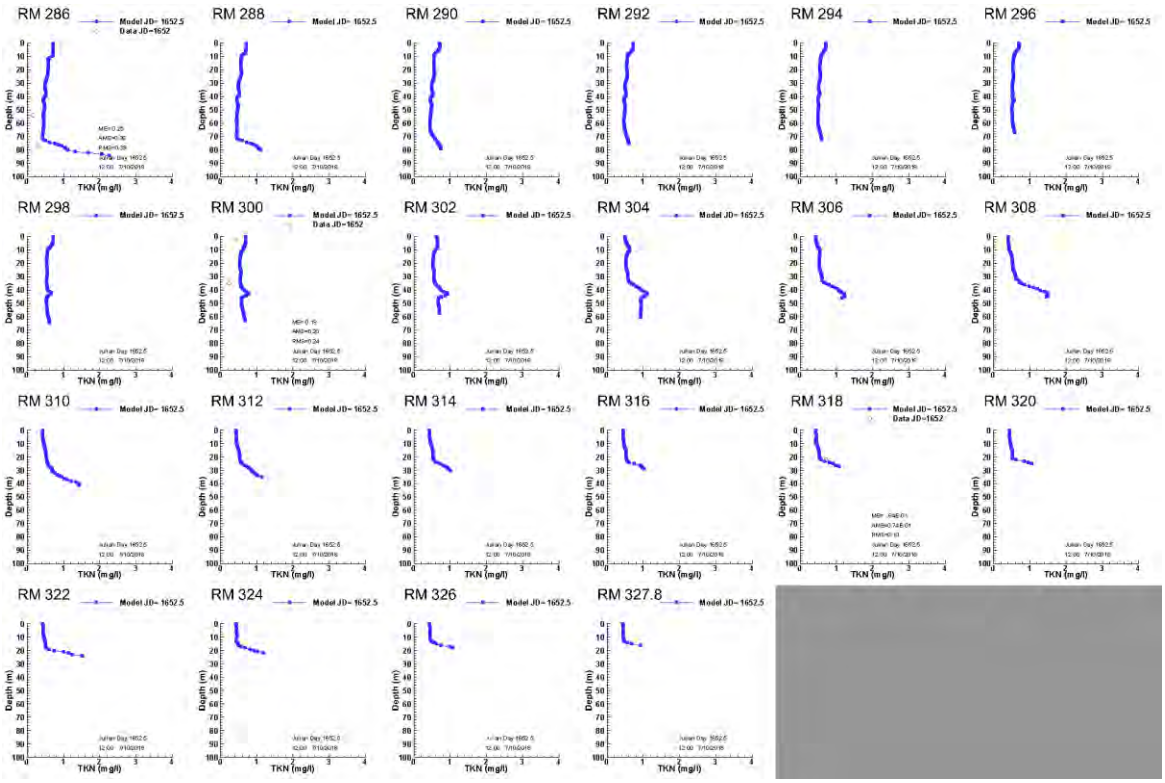


Figure 1857. Vertical profiles of TKN compared with data for 7/10/2018.

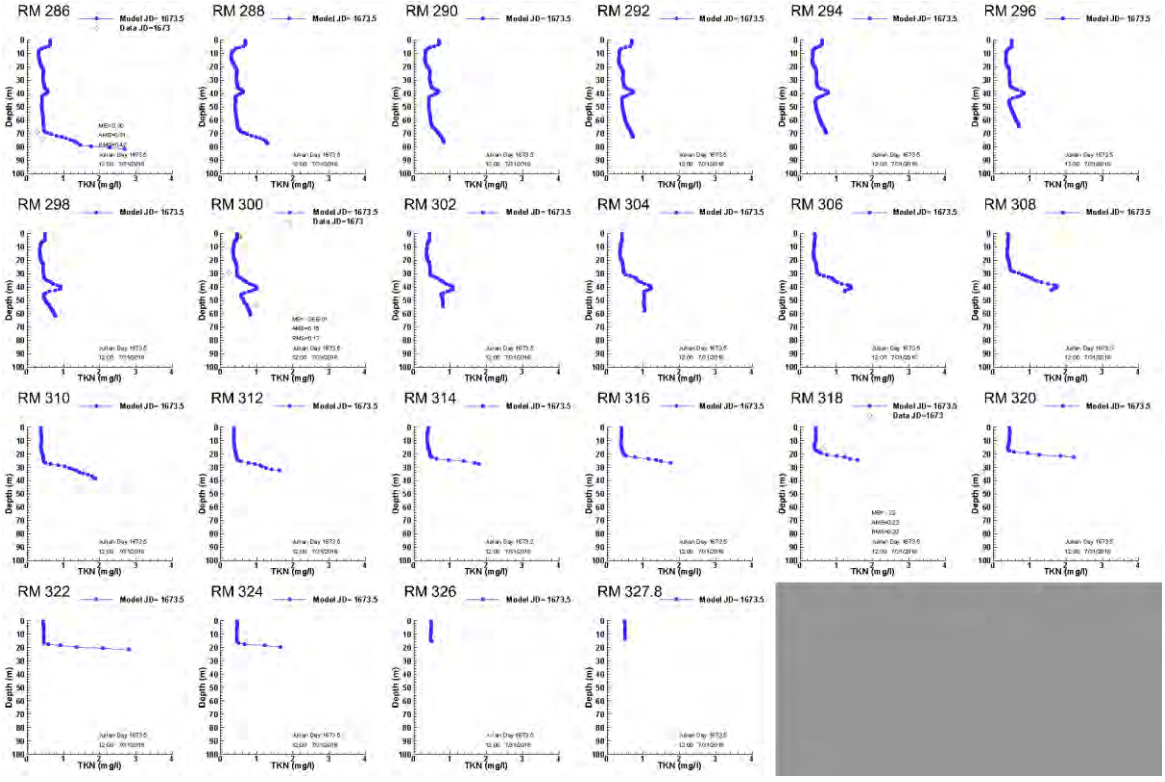


Figure 1858. Vertical profiles of TKN compared with data for 7/31/2018.

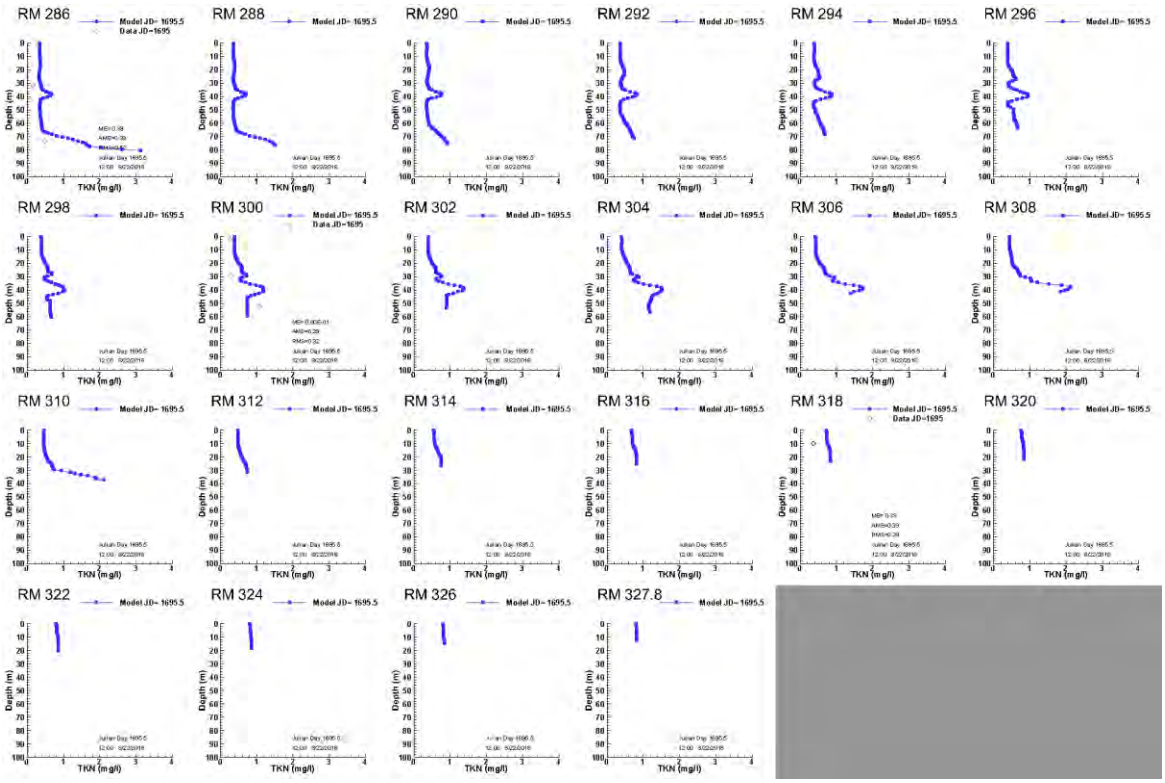


Figure 1859. Vertical profiles of TKN compared with data for 8/22/2018.

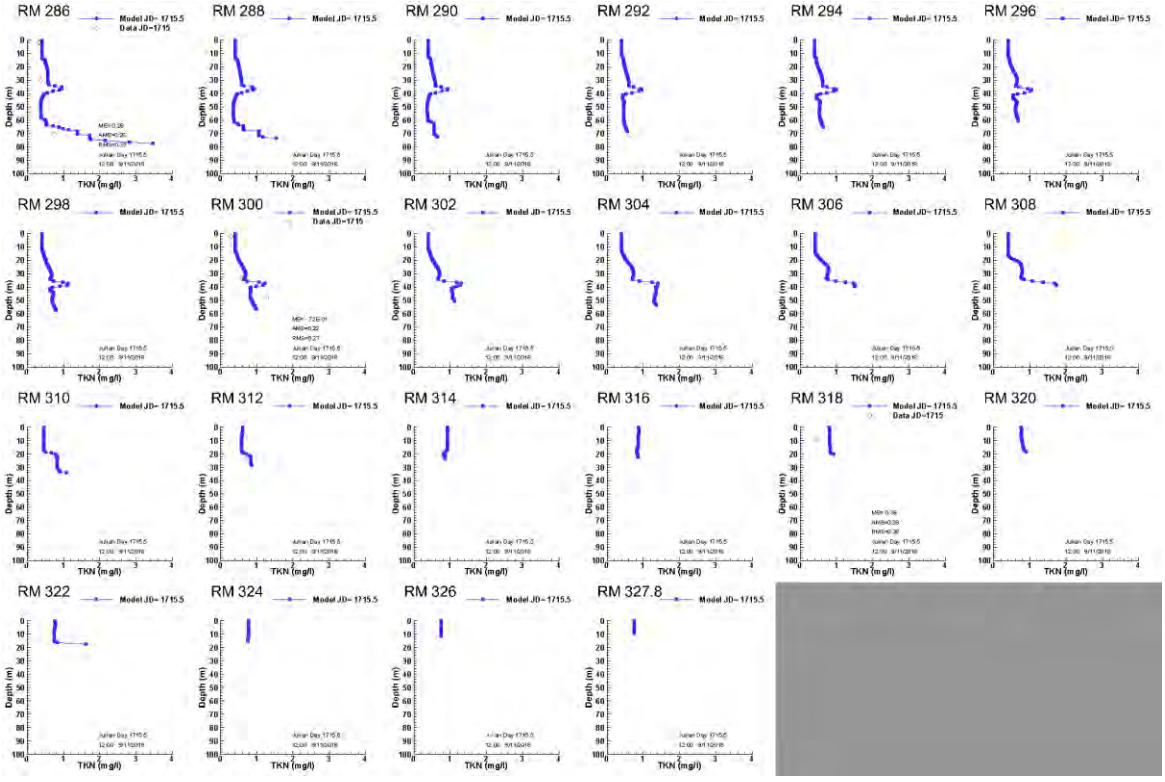


Figure 1860. Vertical profiles of TKN compared with data for 9/11/2018.

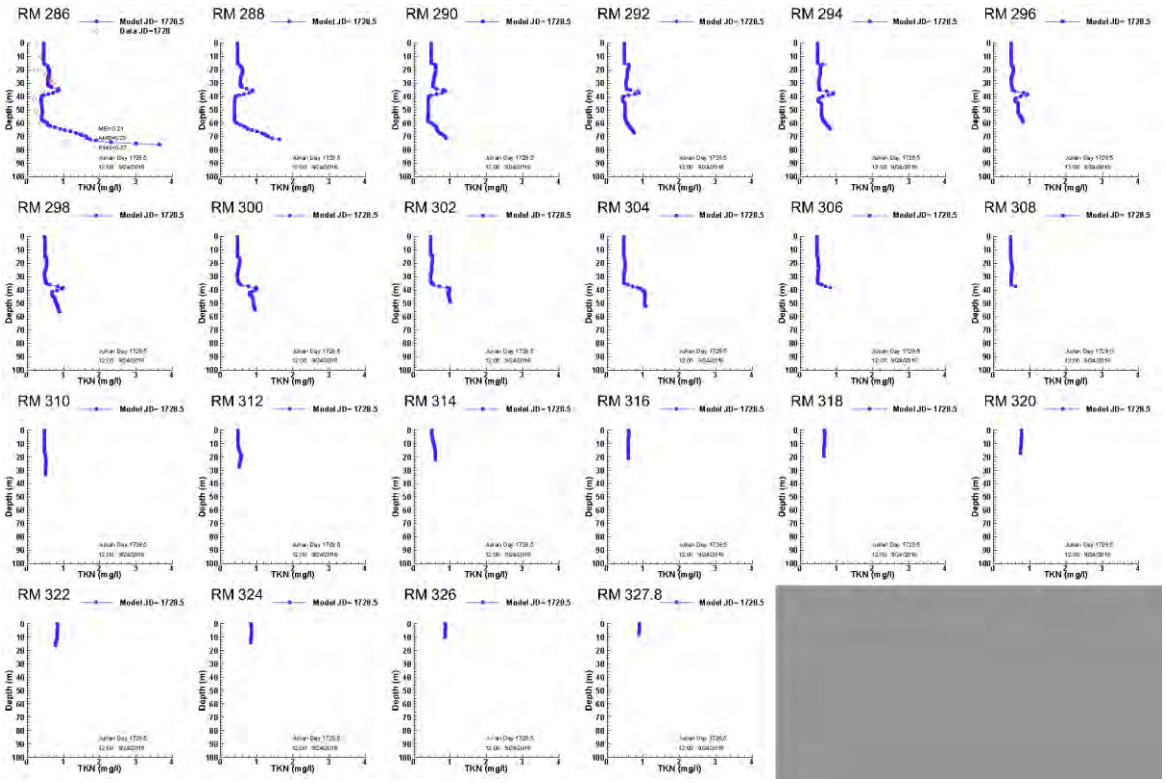


Figure 1861. Vertical profiles of TKN compared with data for 9/24/2018.

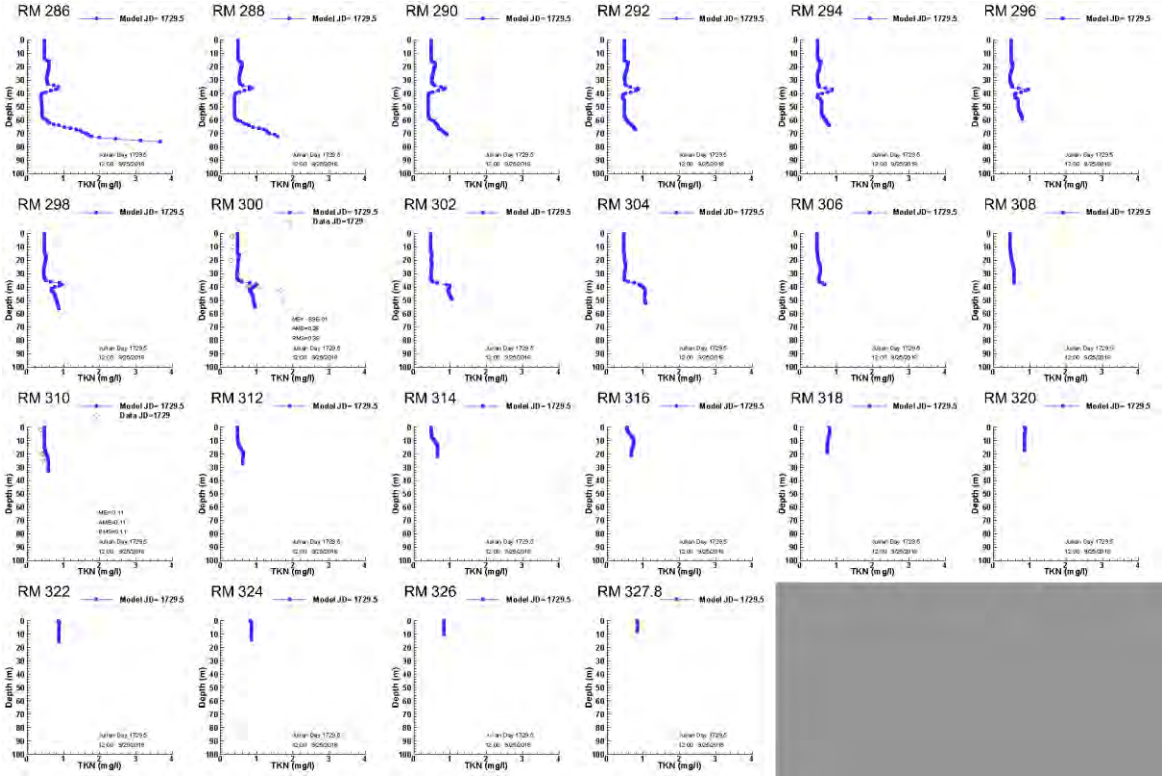


Figure 1862. Vertical profiles of TKN compared with data for 9/25/2018.

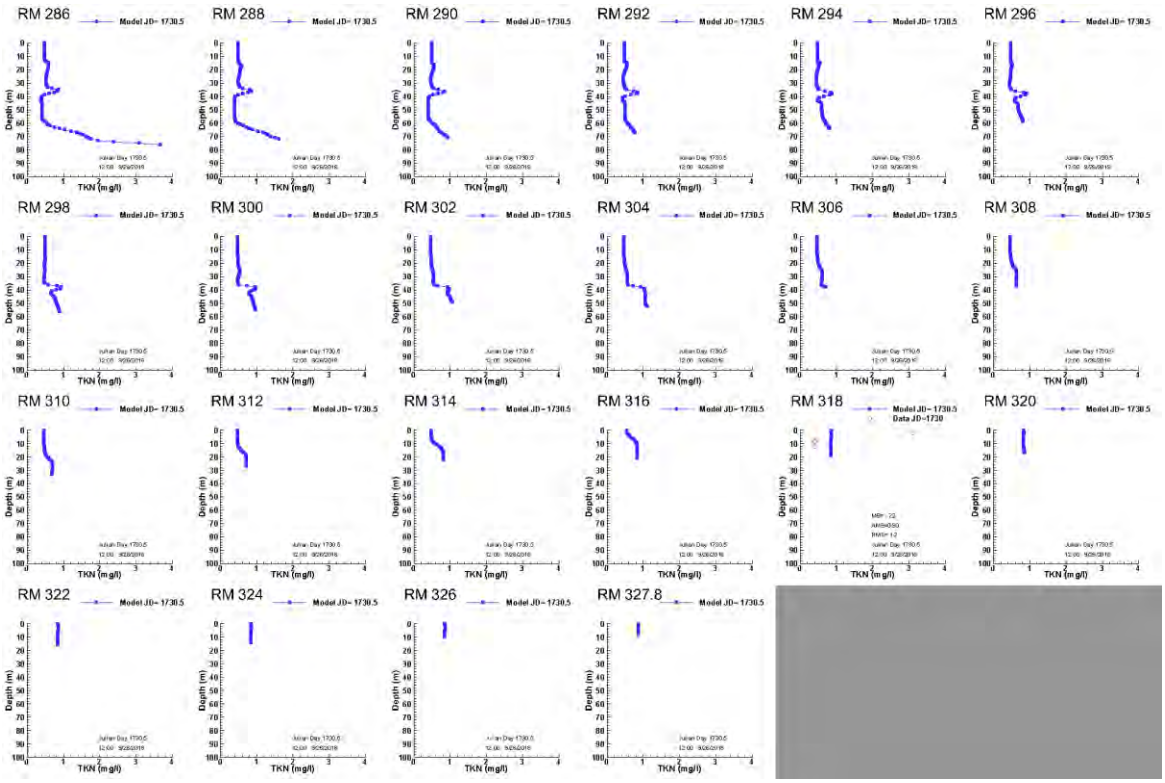


Figure 1863. Vertical profiles of TKN compared with data for 9/26/2018.

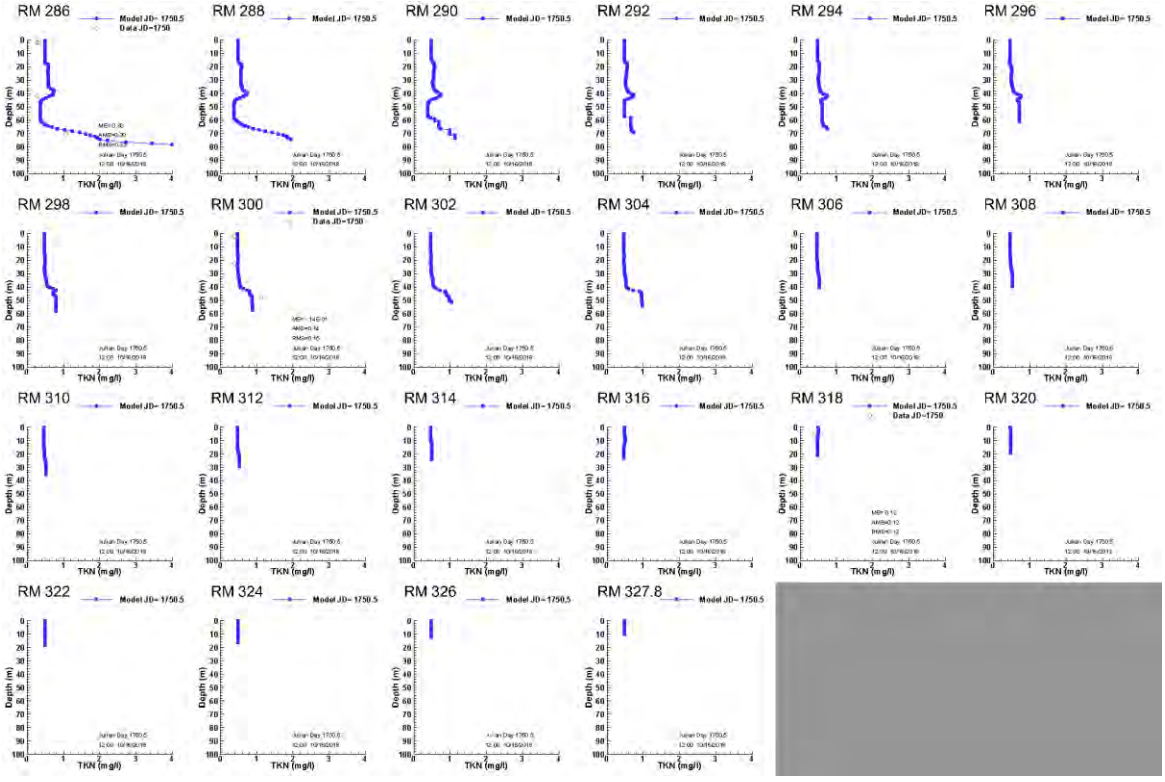


Figure 1864. Vertical profiles of TKN compared with data for 10/16/2018.

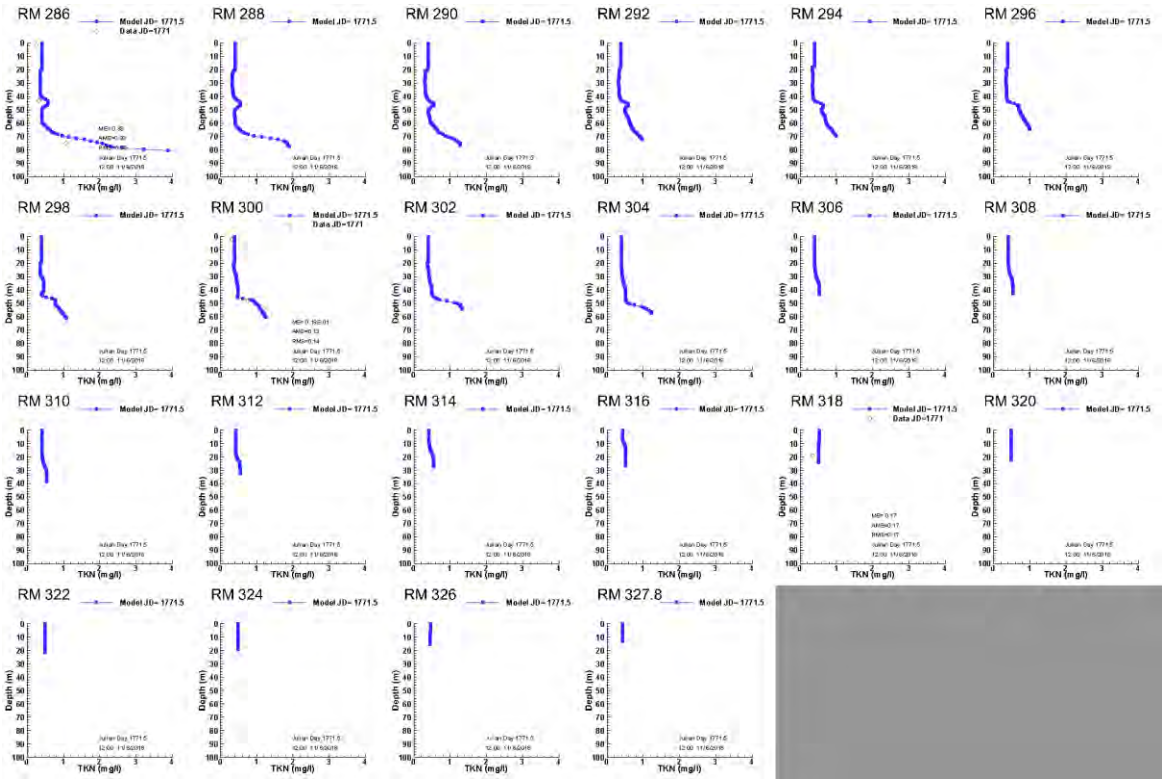


Figure 1865. Vertical profiles of TKN compared with data for 11/ 6/2018.

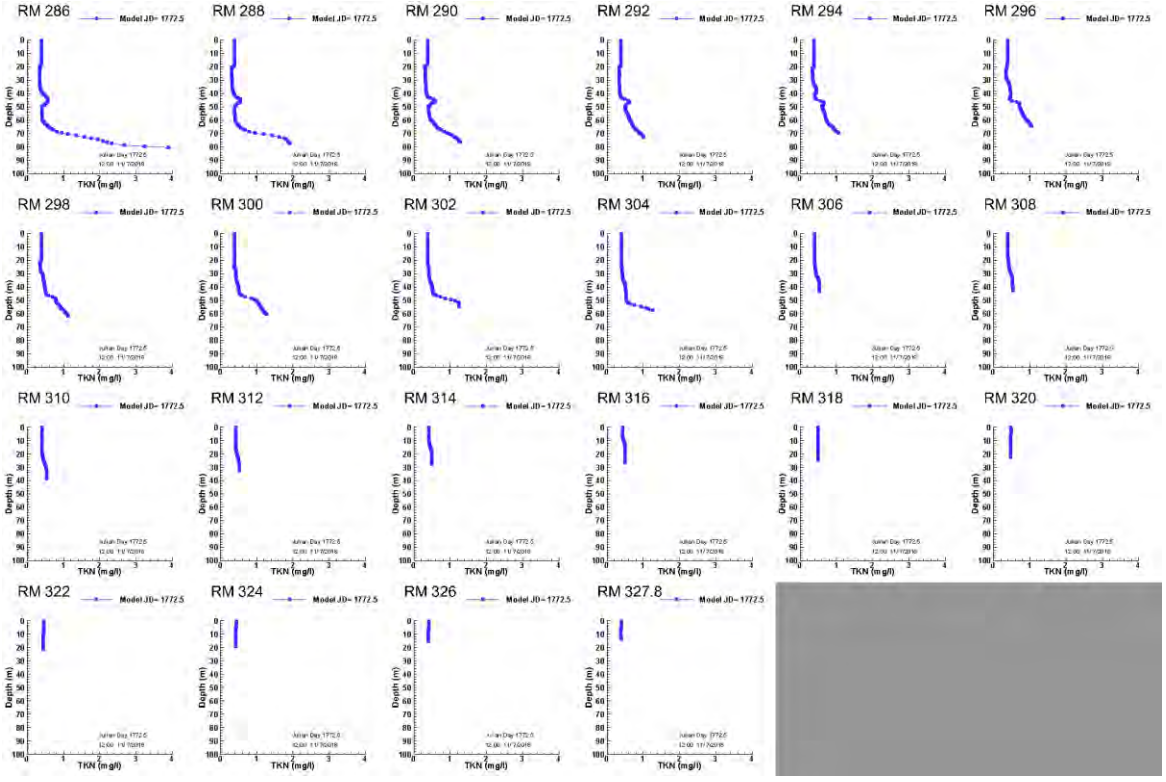


Figure 1866. Vertical profiles of TKN compared with data for 11/ 7/2018.

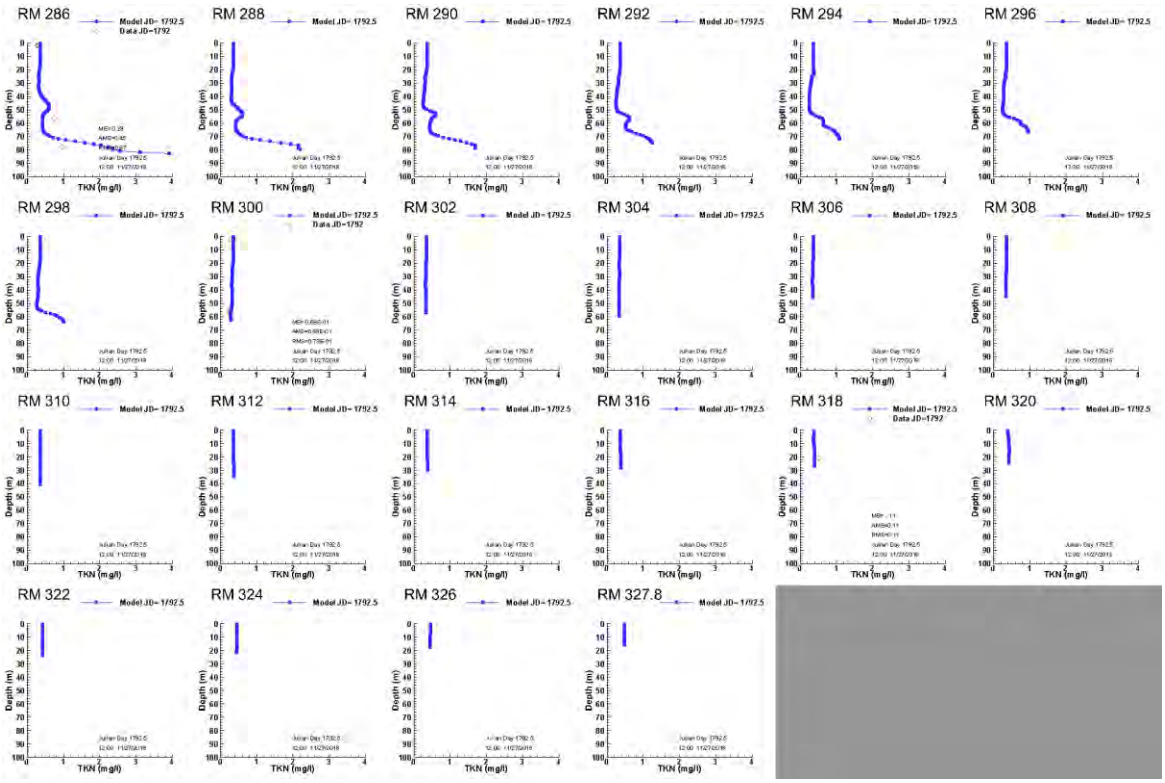


Figure 1867. Vertical profiles of TKN compared with data for 11/27/2018.

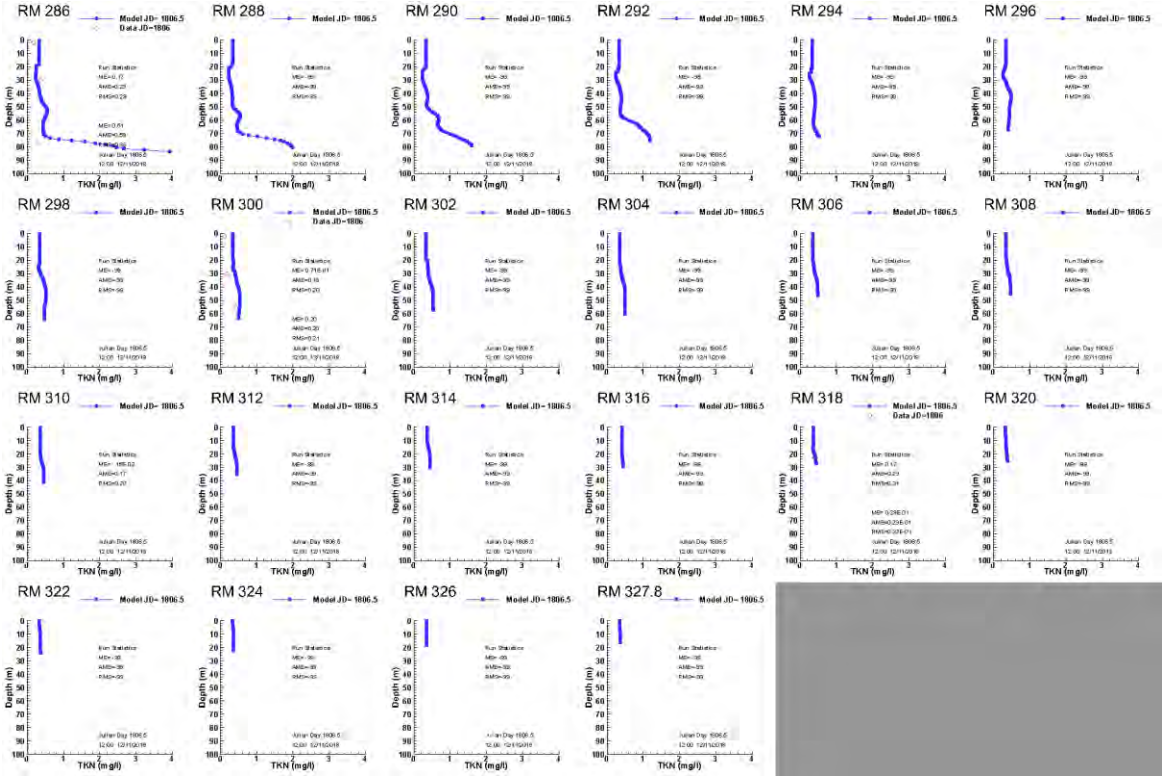


Figure 1868. Vertical profiles of TKN compared with data for 12/11/2018.

Total Phosphorus

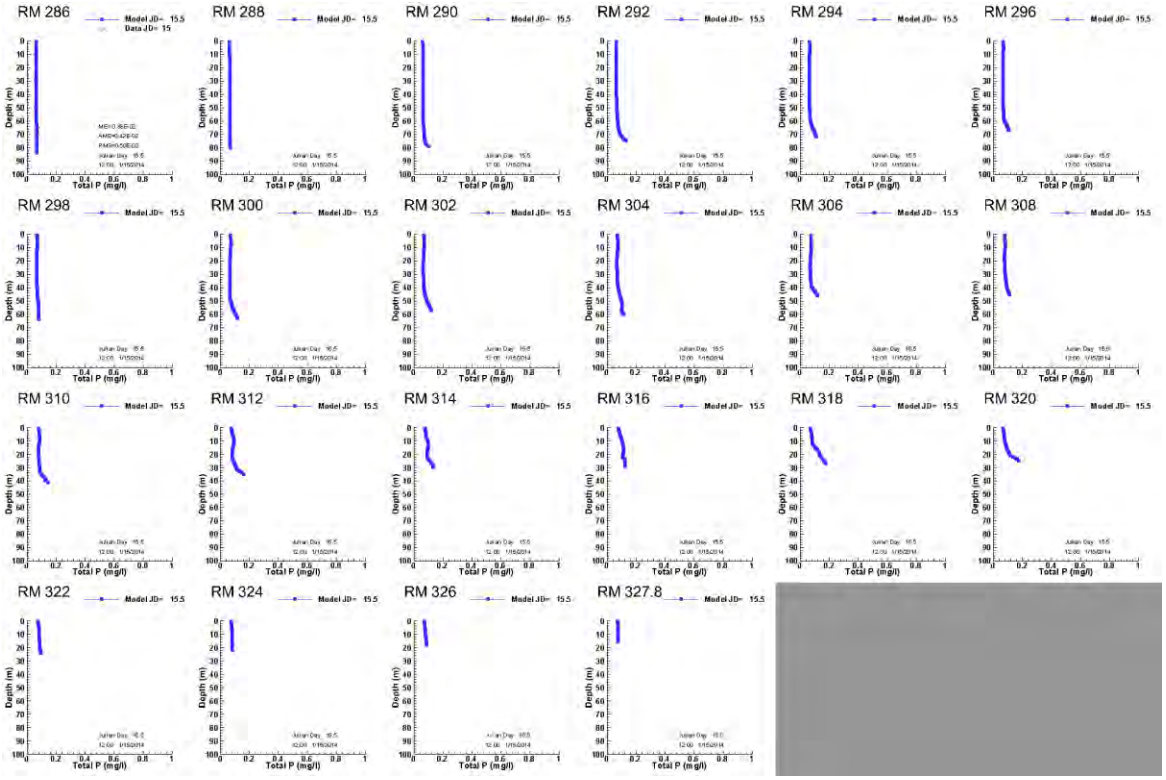


Figure 1869. Vertical profiles of TP compared with data for 1/15/2014.

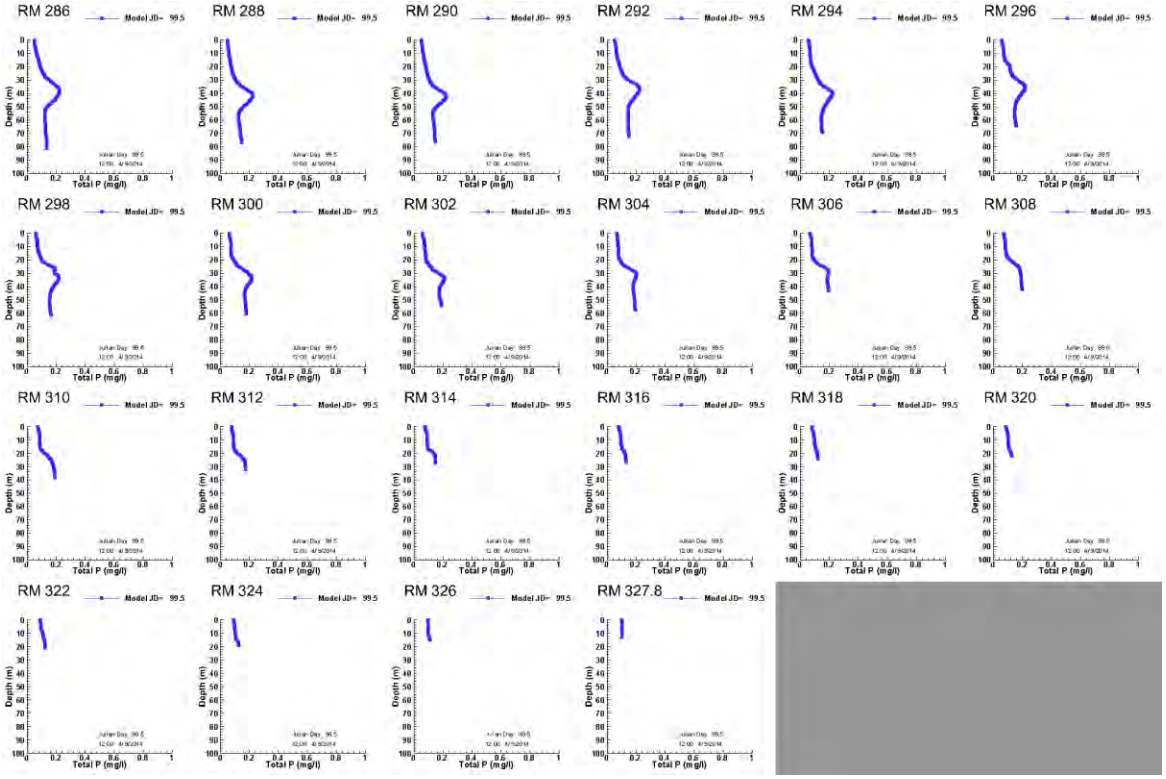


Figure 1870. Vertical profiles of TP compared with data for 4/ 9/2014.

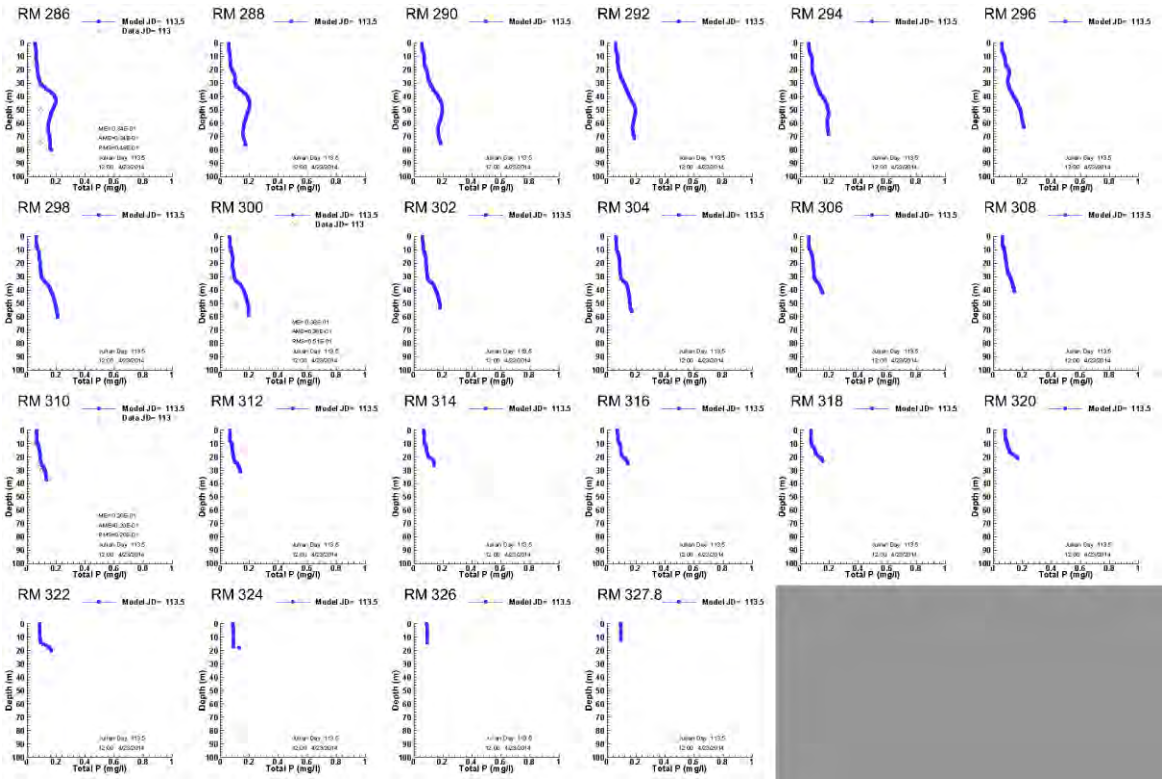


Figure 1871. Vertical profiles of TP compared with data for 4/23/2014.

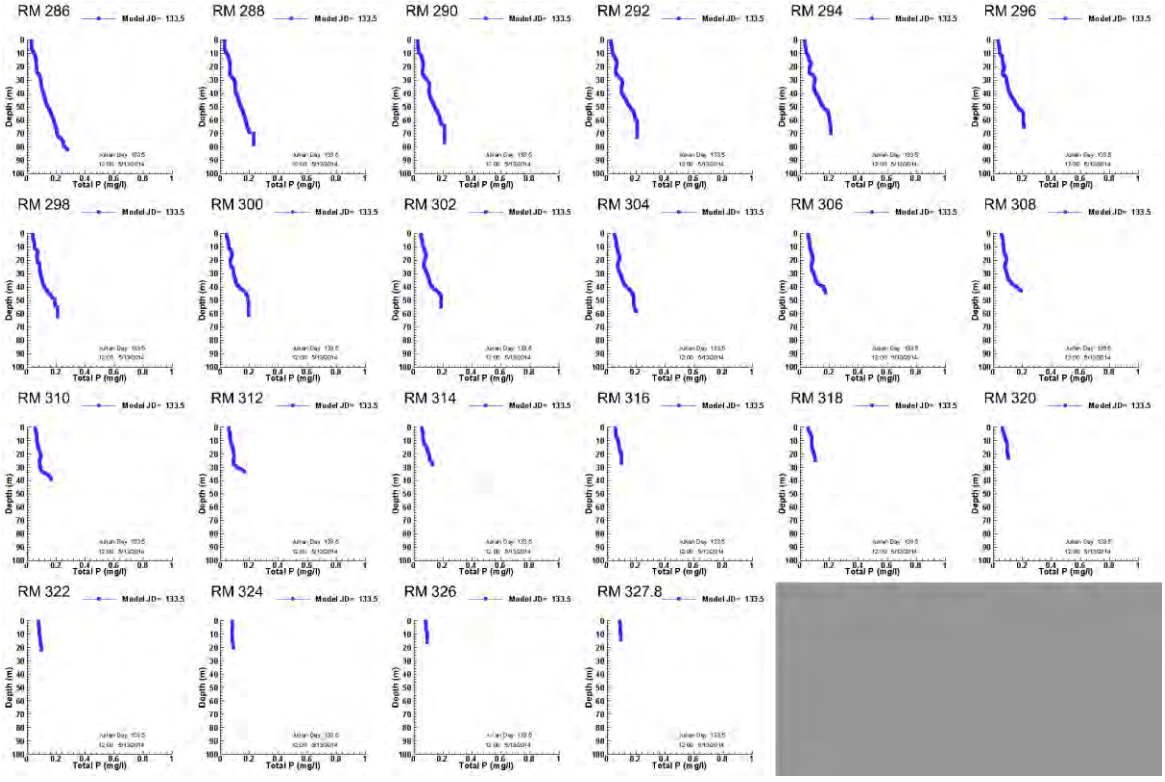


Figure 1872. Vertical profiles of TP compared with data for 5/13/2014.

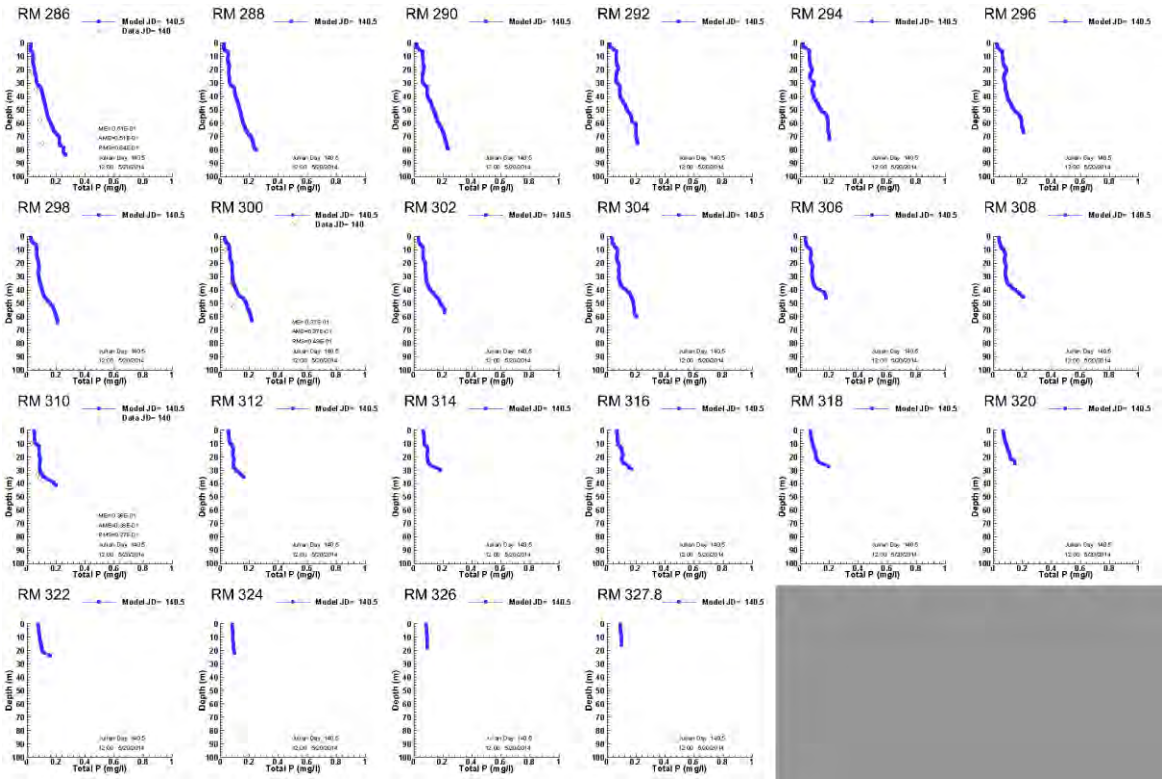


Figure 1873. Vertical profiles of TP compared with data for 5/20/2014.

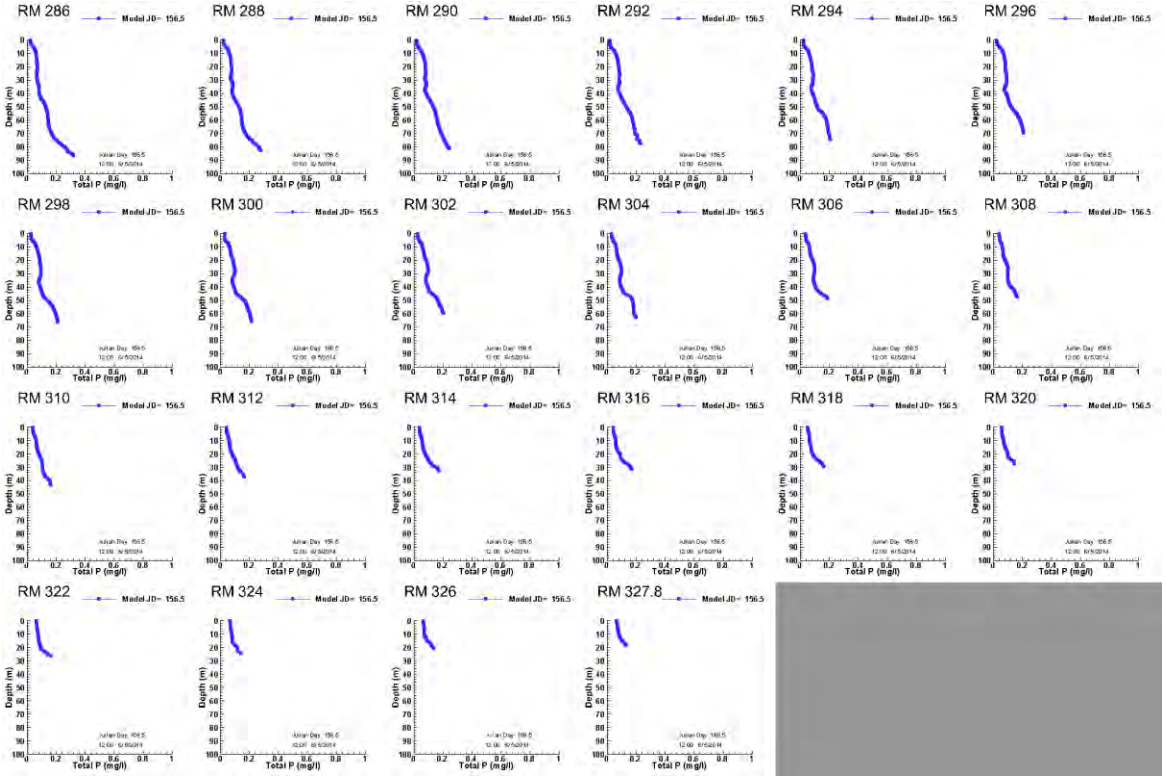


Figure 1874. Vertical profiles of TP compared with data for 6/ 5/2014.

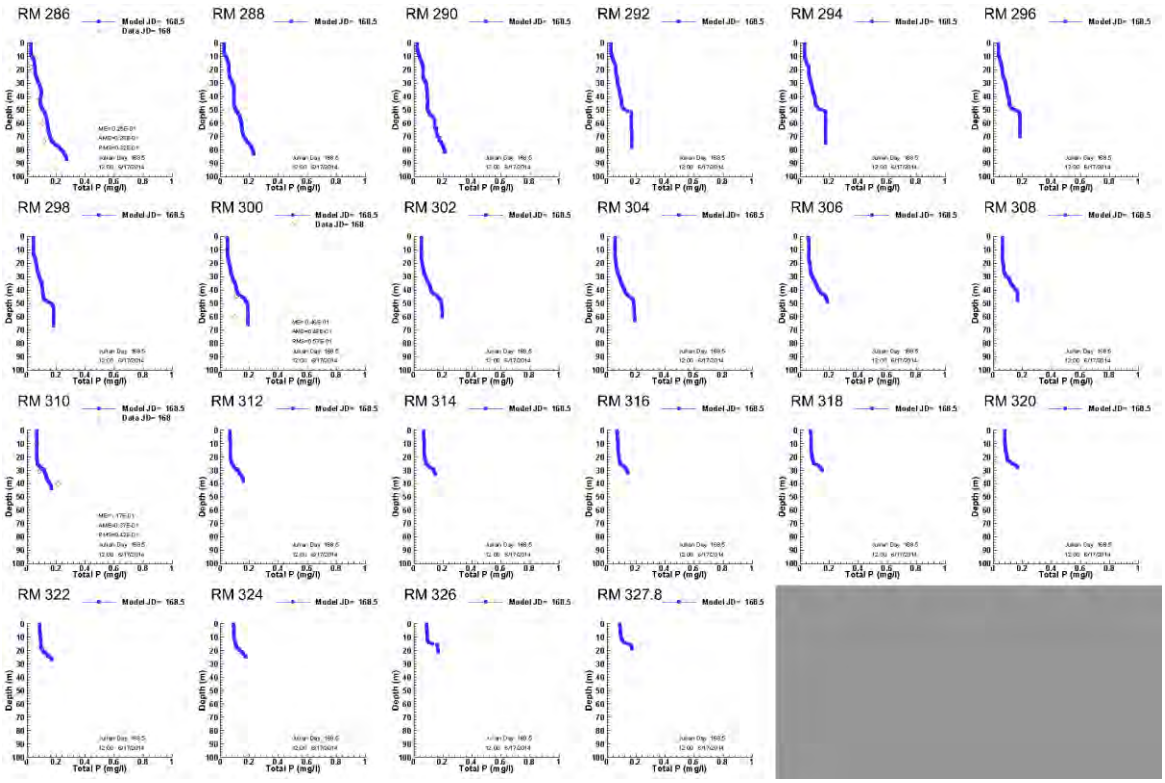


Figure 1875. Vertical profiles of TP compared with data for 6/17/2014.

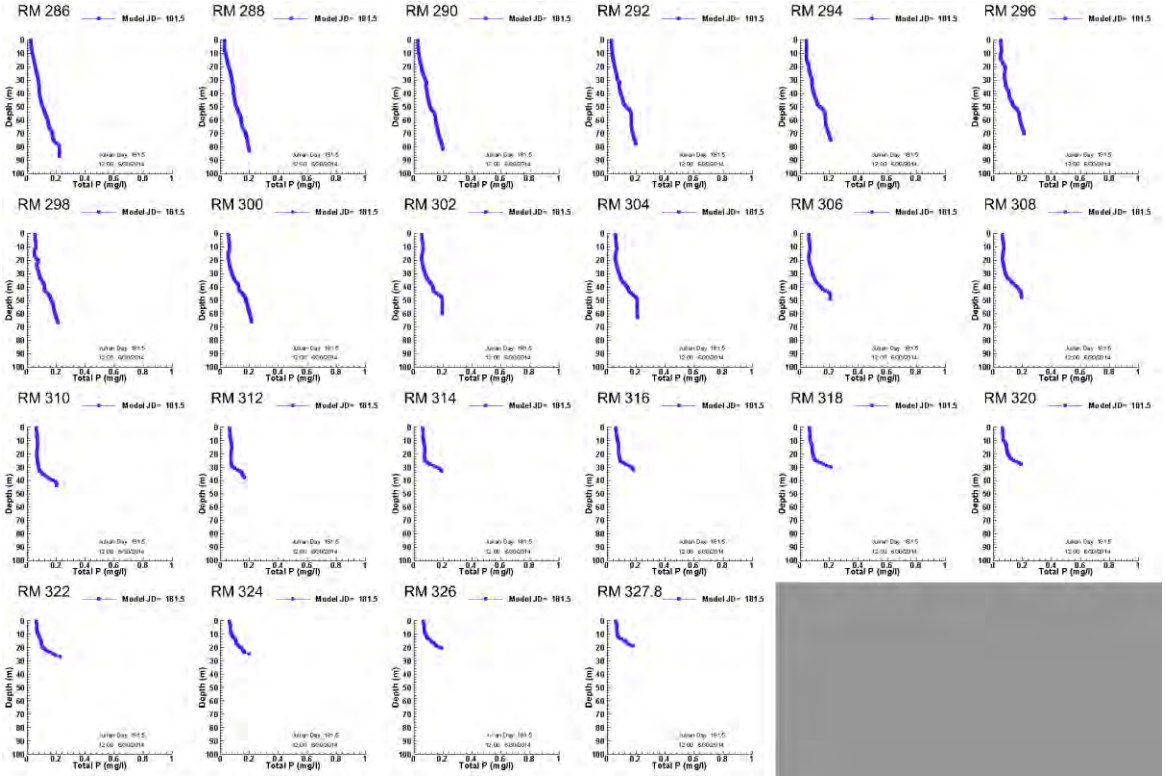


Figure 1876. Vertical profiles of TP compared with data for 6/30/2014.

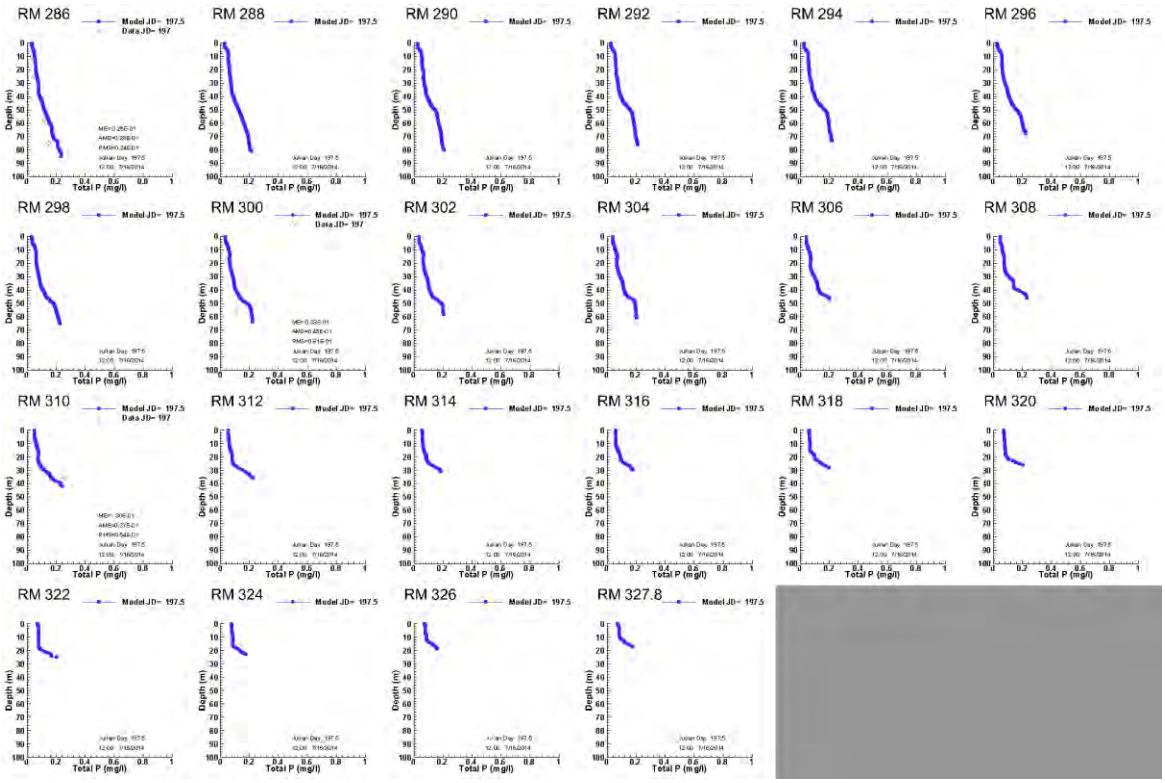


Figure 1877. Vertical profiles of TP compared with data for 7/16/2014.

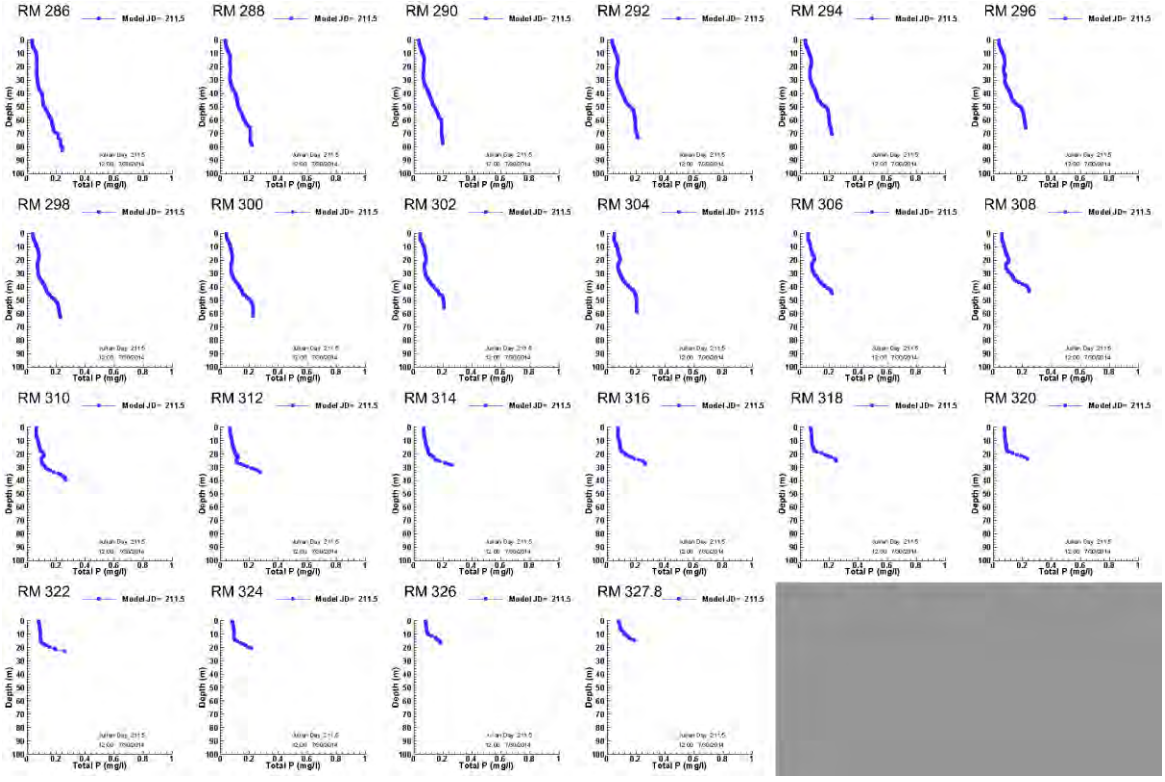


Figure 1878. Vertical profiles of TP compared with data for 7/30/2014.

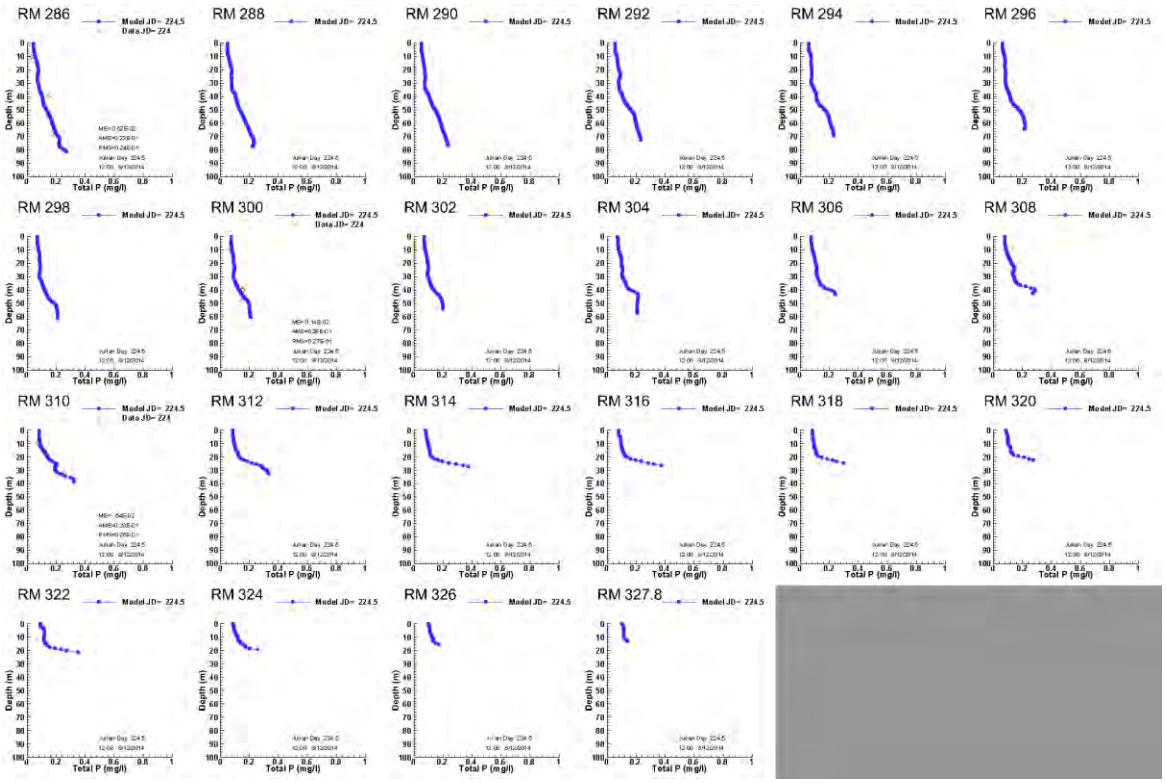


Figure 1879. Vertical profiles of TP compared with data for 8/12/2014.

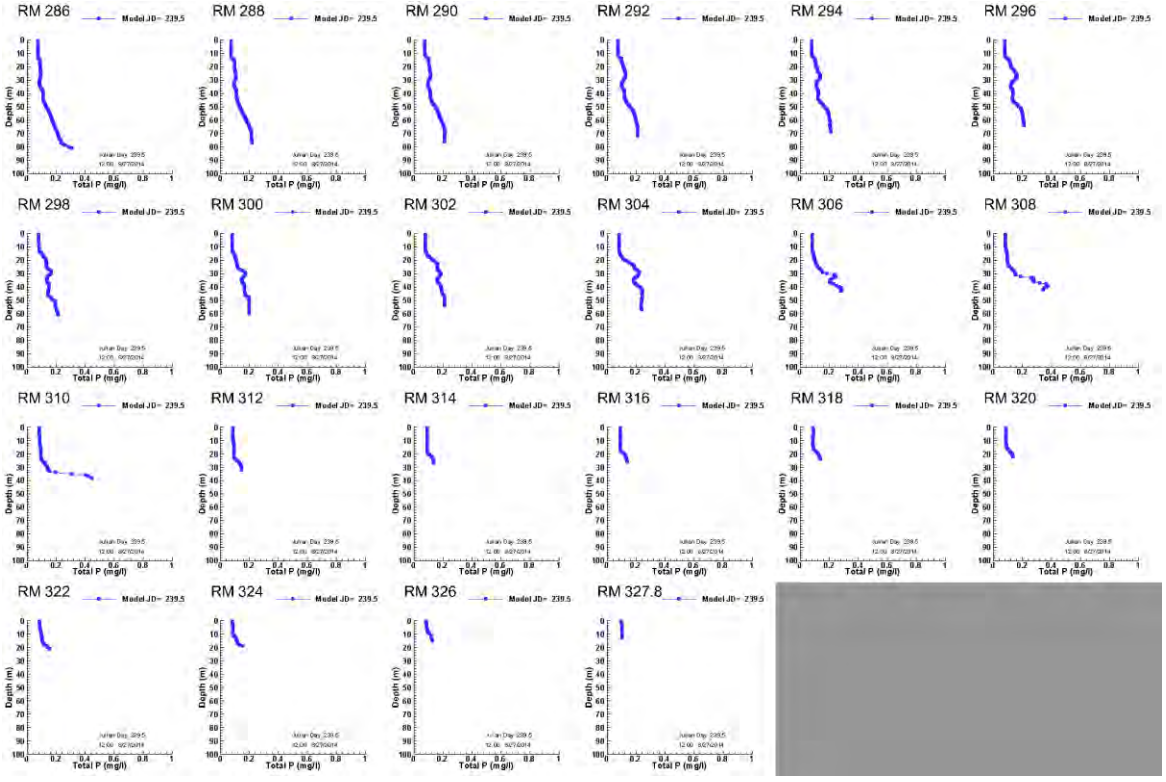


Figure 1880. Vertical profiles of TP compared with data for 8/27/2014.

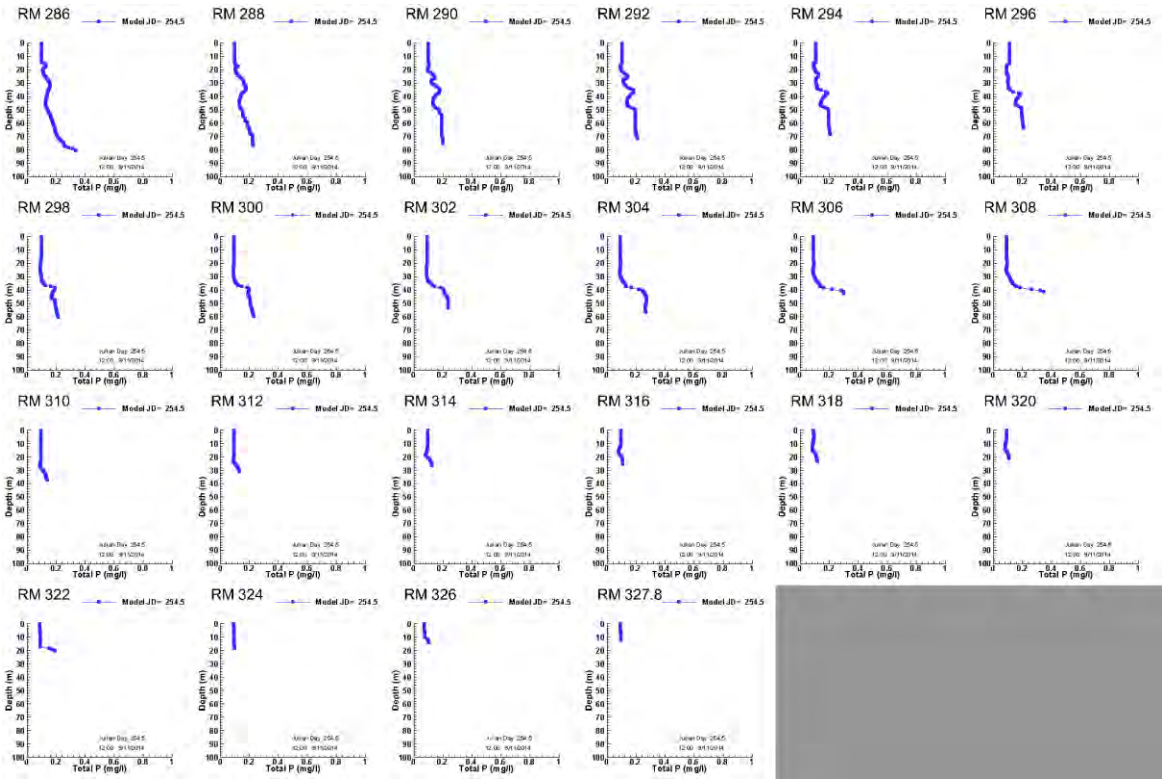


Figure 1881. Vertical profiles of TP compared with data for 9/11/2014.

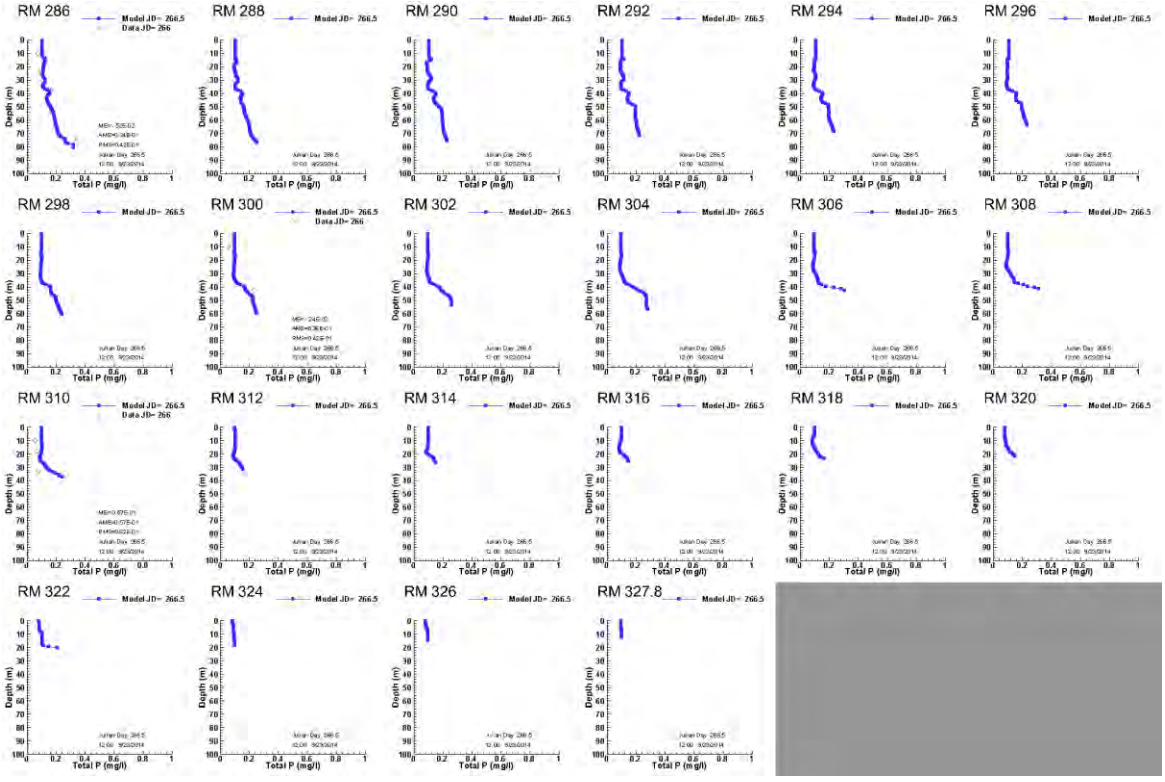


Figure 1882. Vertical profiles of TP compared with data for 9/23/2014.

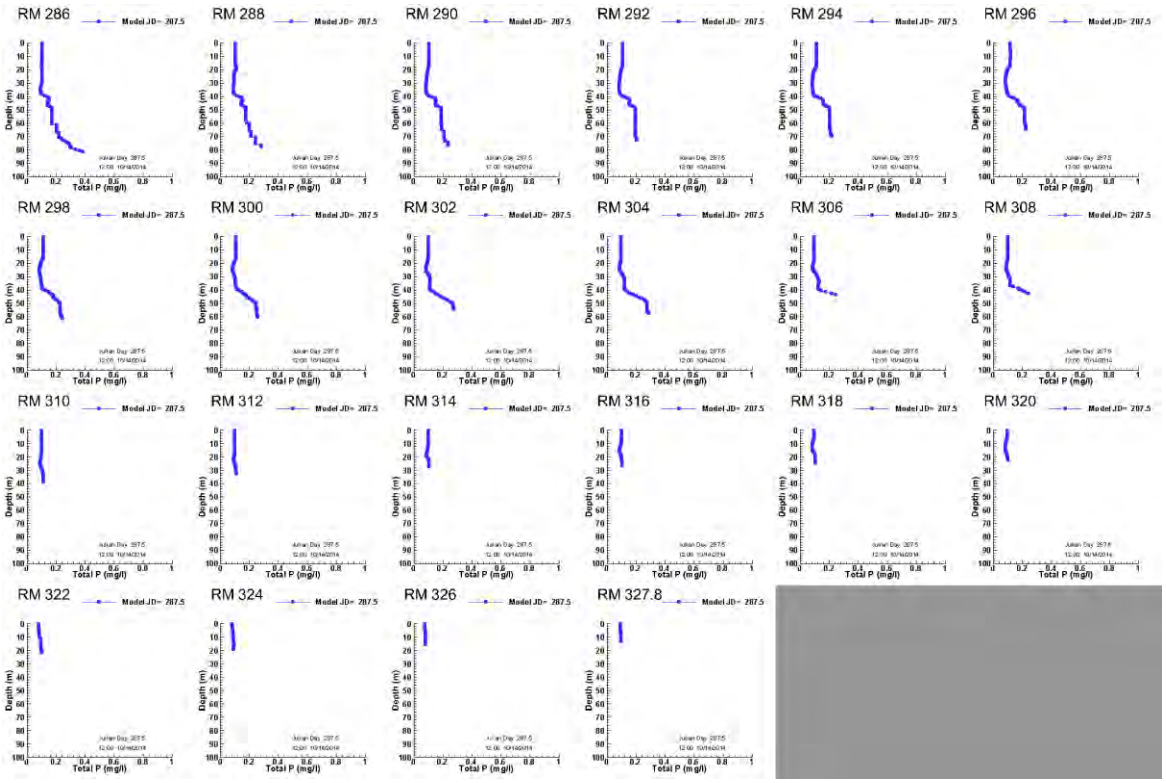


Figure 1883. Vertical profiles of TP compared with data for 10/14/2014.

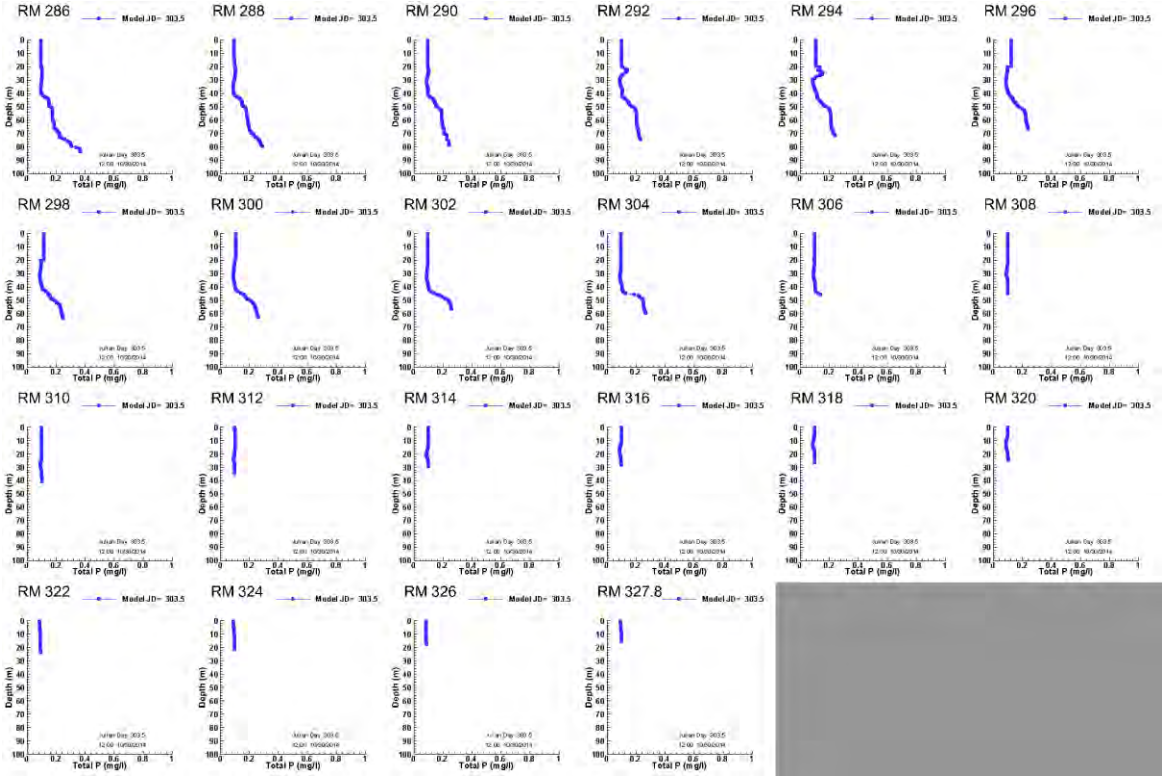


Figure 1884. Vertical profiles of TP compared with data for 10/30/2014.

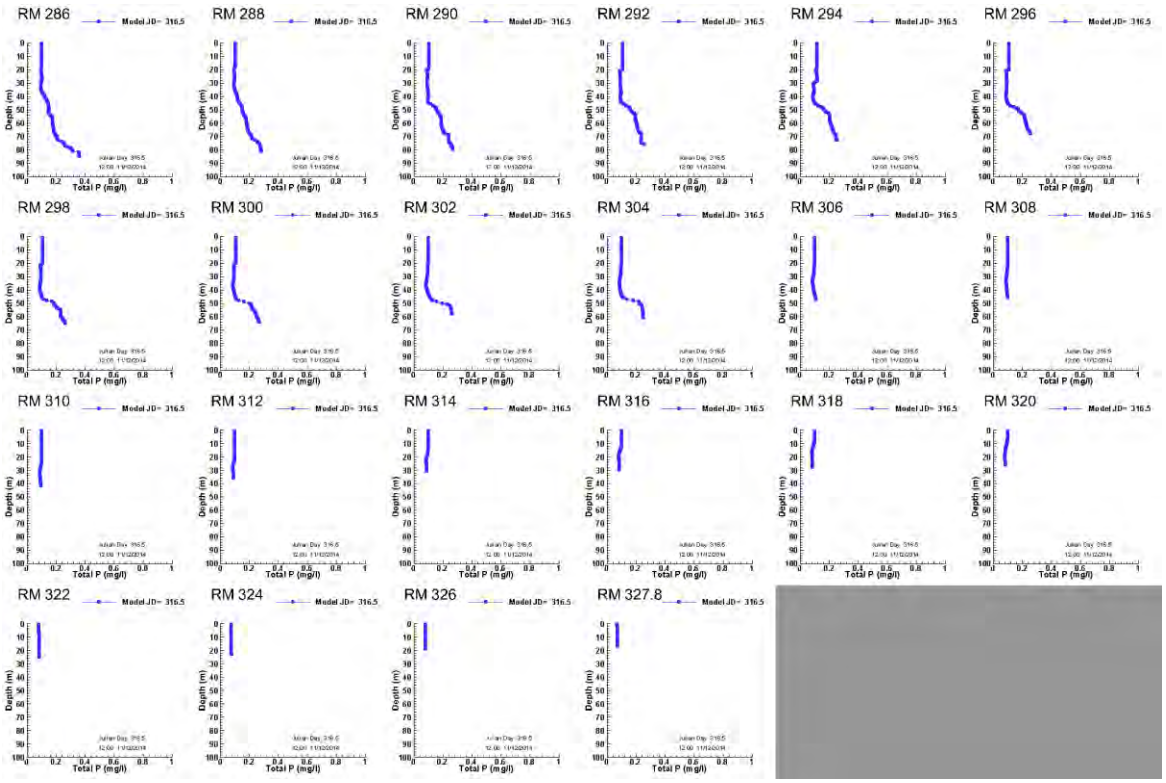


Figure 1885. Vertical profiles of TP compared with data for 11/12/2014.

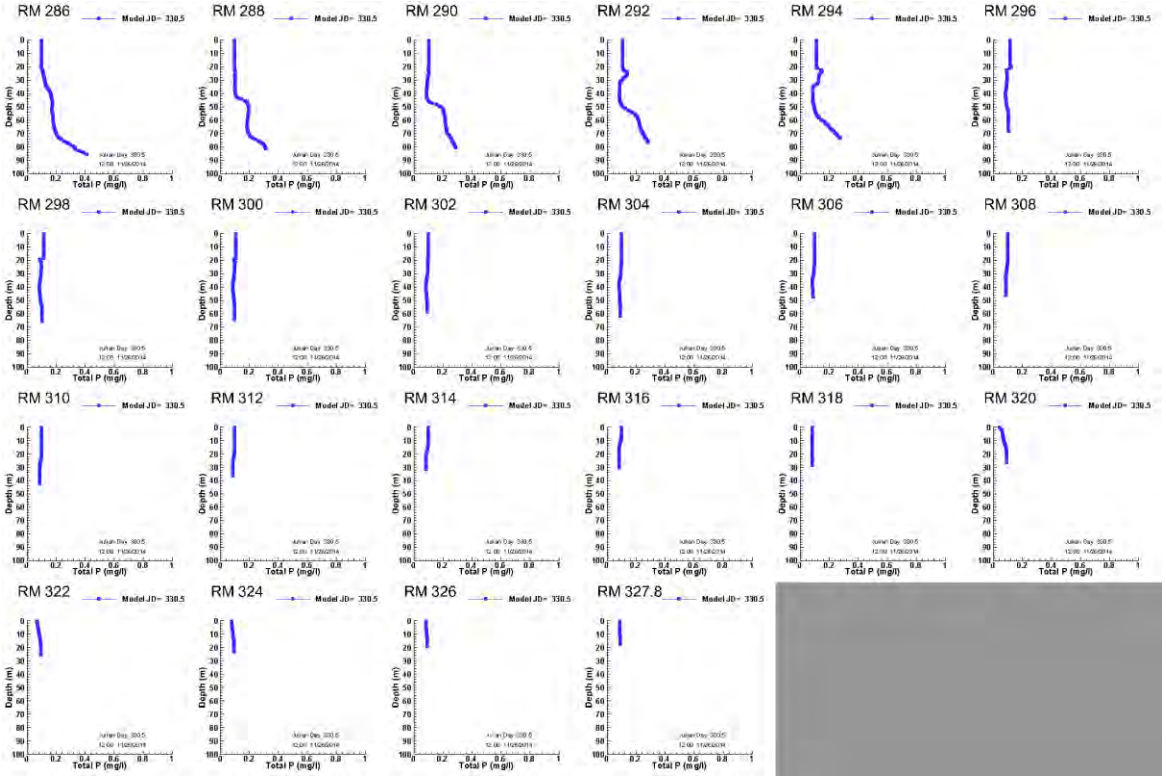


Figure 1886. Vertical profiles of TP compared with data for 11/26/2014.

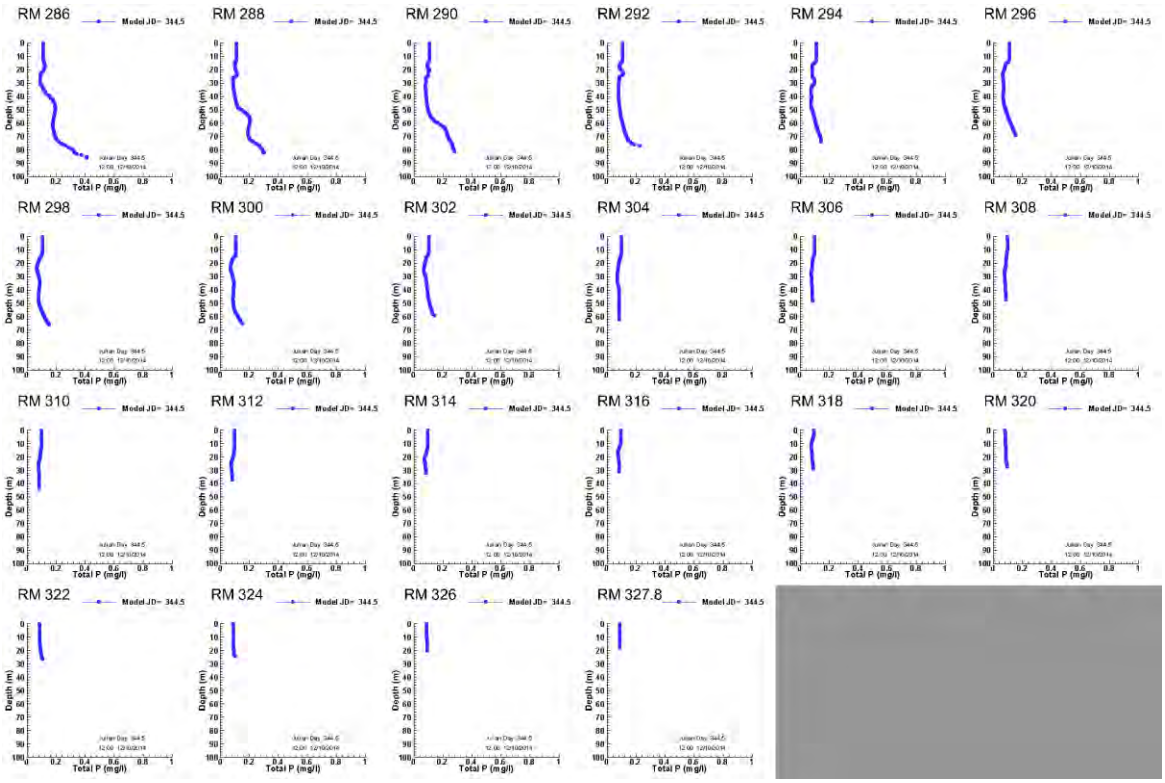


Figure 1887. Vertical profiles of TP compared with data for 12/10/2014.

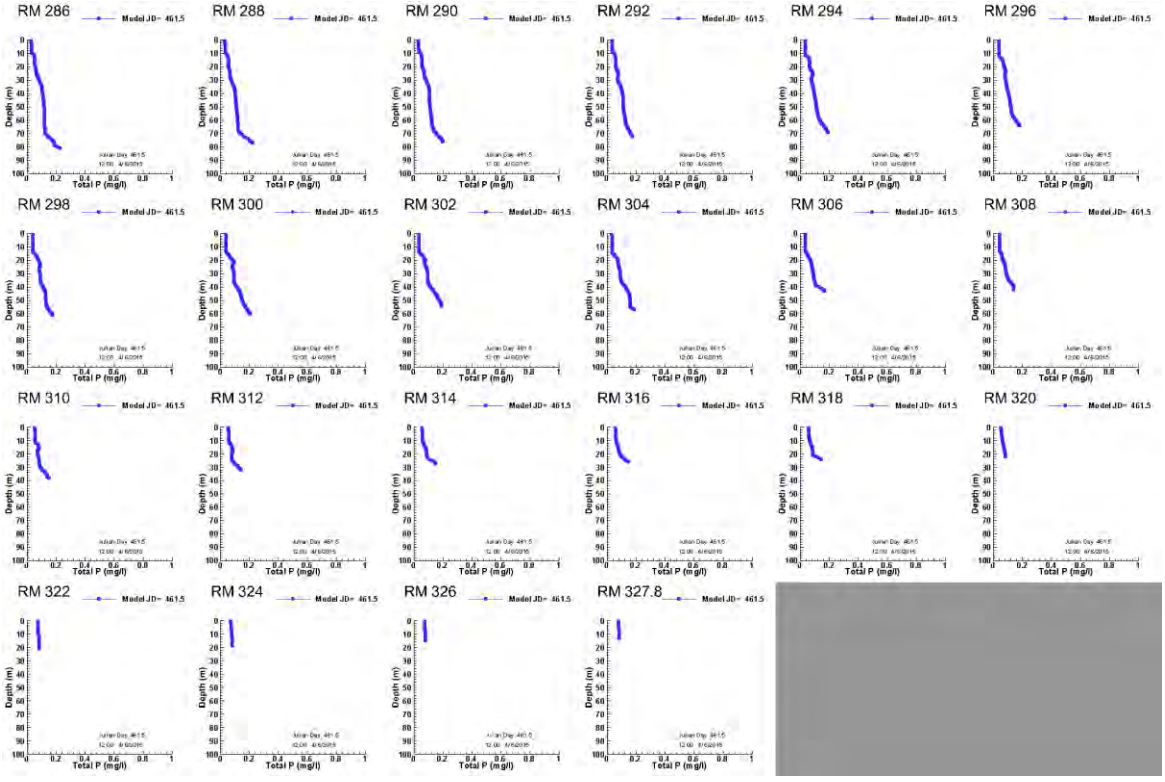


Figure 1888. Vertical profiles of TP compared with data for 4/ 6/2015.

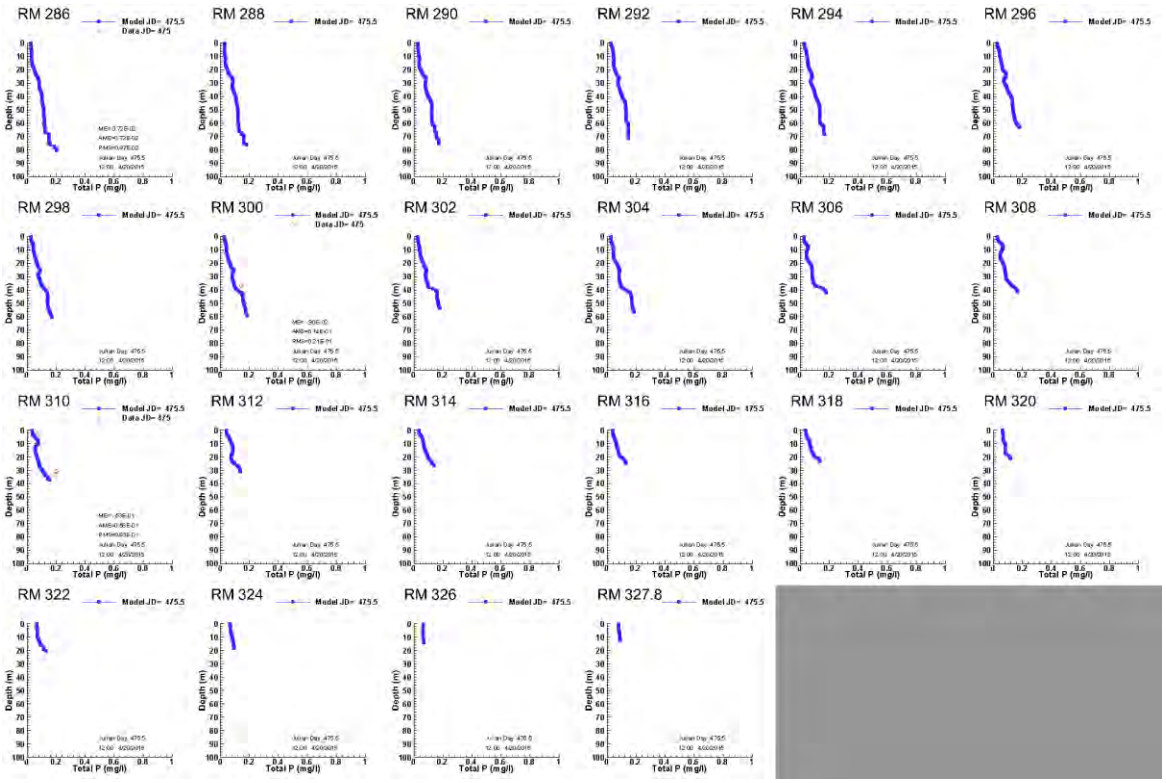


Figure 1889. Vertical profiles of TP compared with data for 4/20/2015.

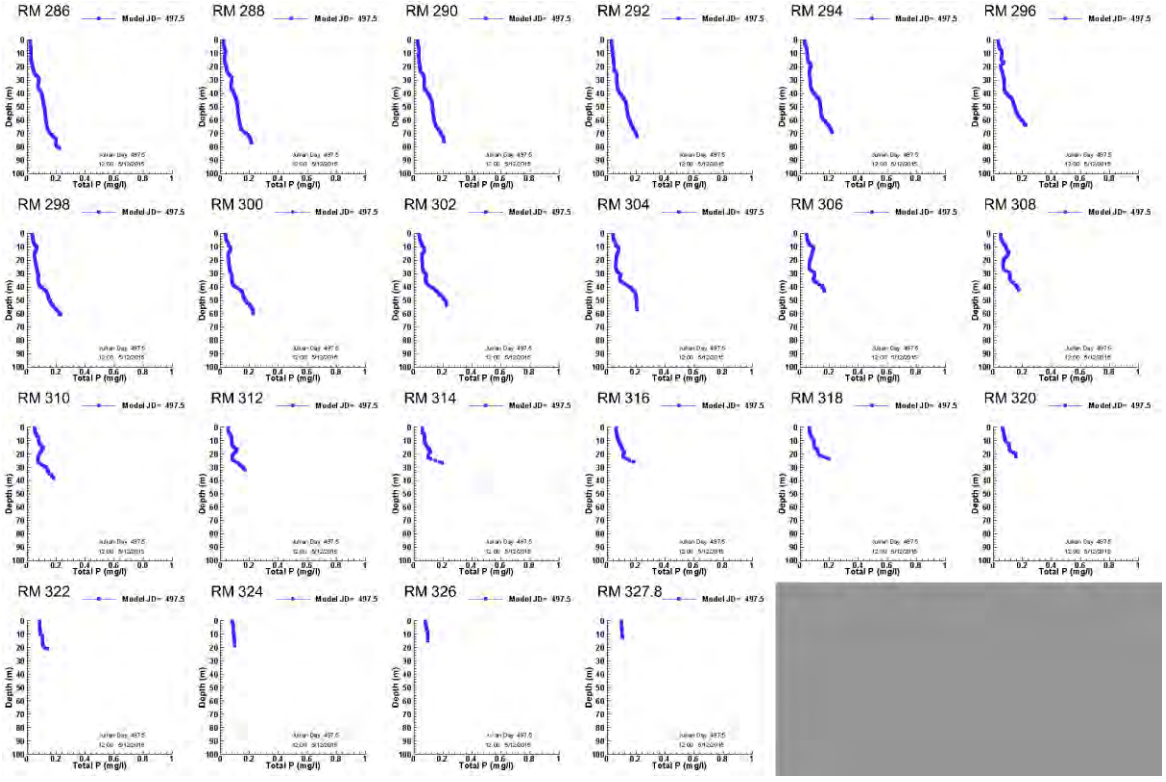


Figure 1890. Vertical profiles of TP compared with data for 5/12/2015.

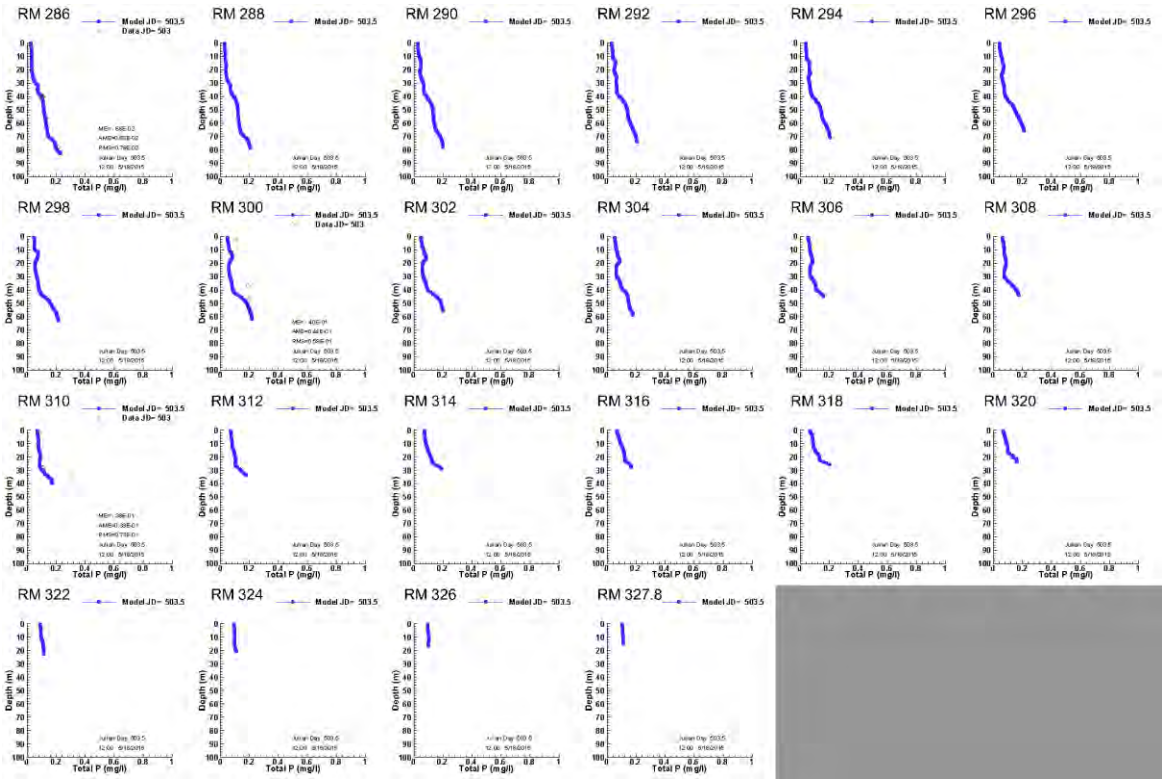


Figure 1891. Vertical profiles of TP compared with data for 5/18/2015.

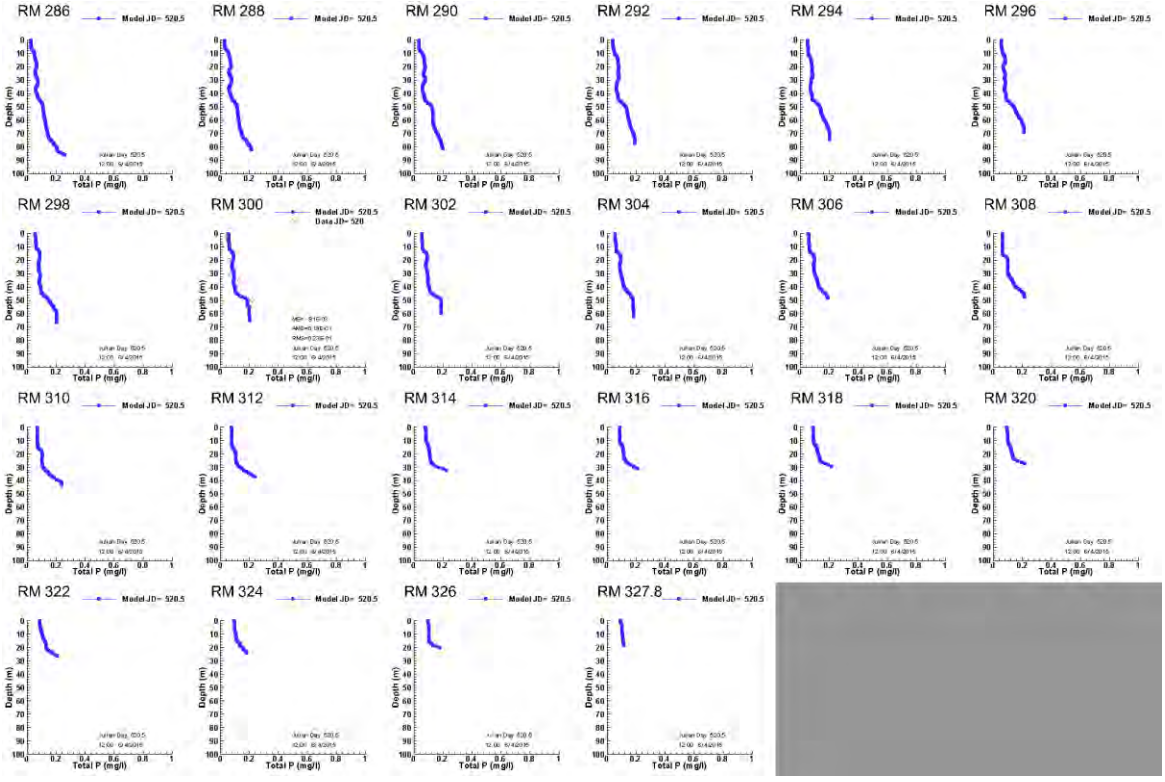


Figure 1892. Vertical profiles of TP compared with data for 6/ 4/2015.

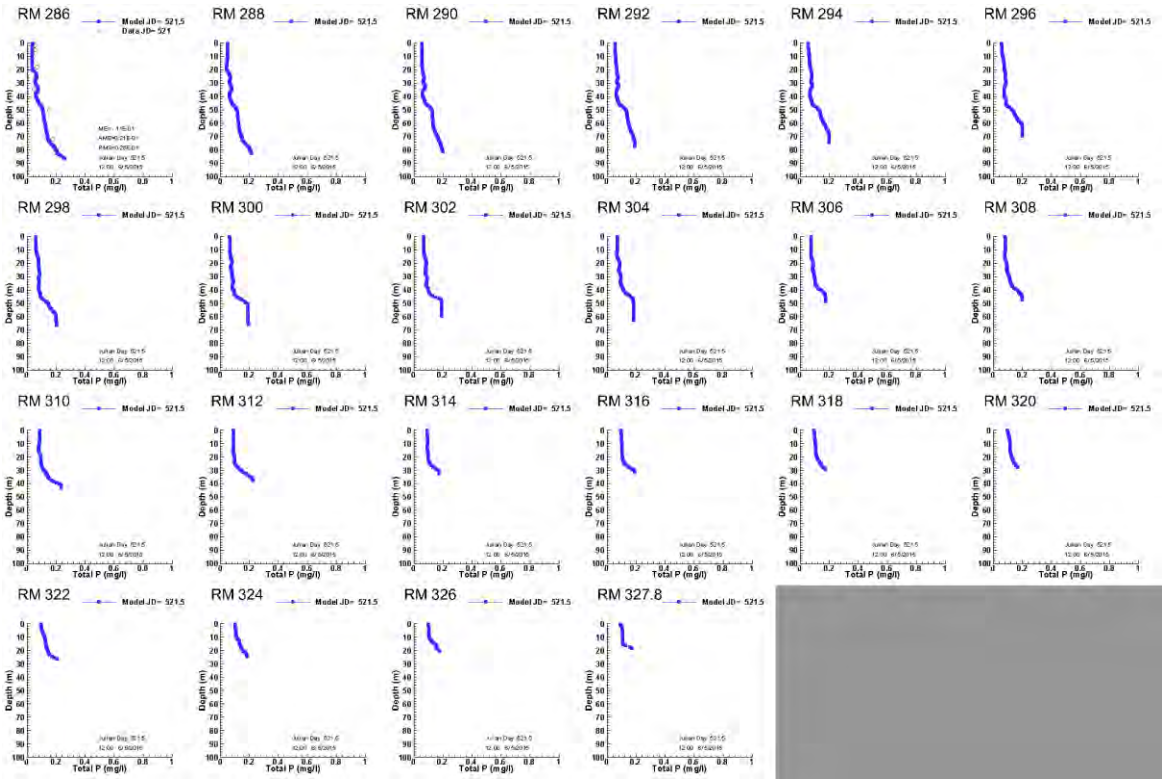


Figure 1893. Vertical profiles of TP compared with data for 6/ 5/2015.

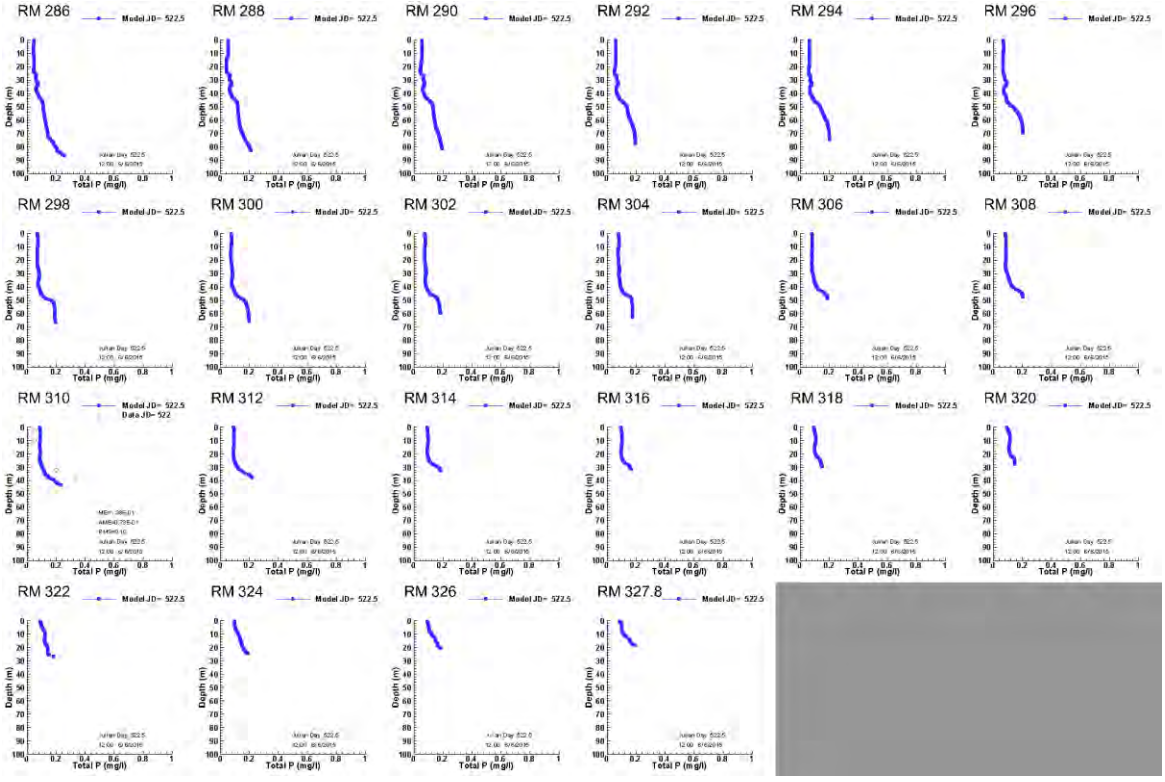


Figure 1894. Vertical profiles of TP compared with data for 6/ 6/2015.

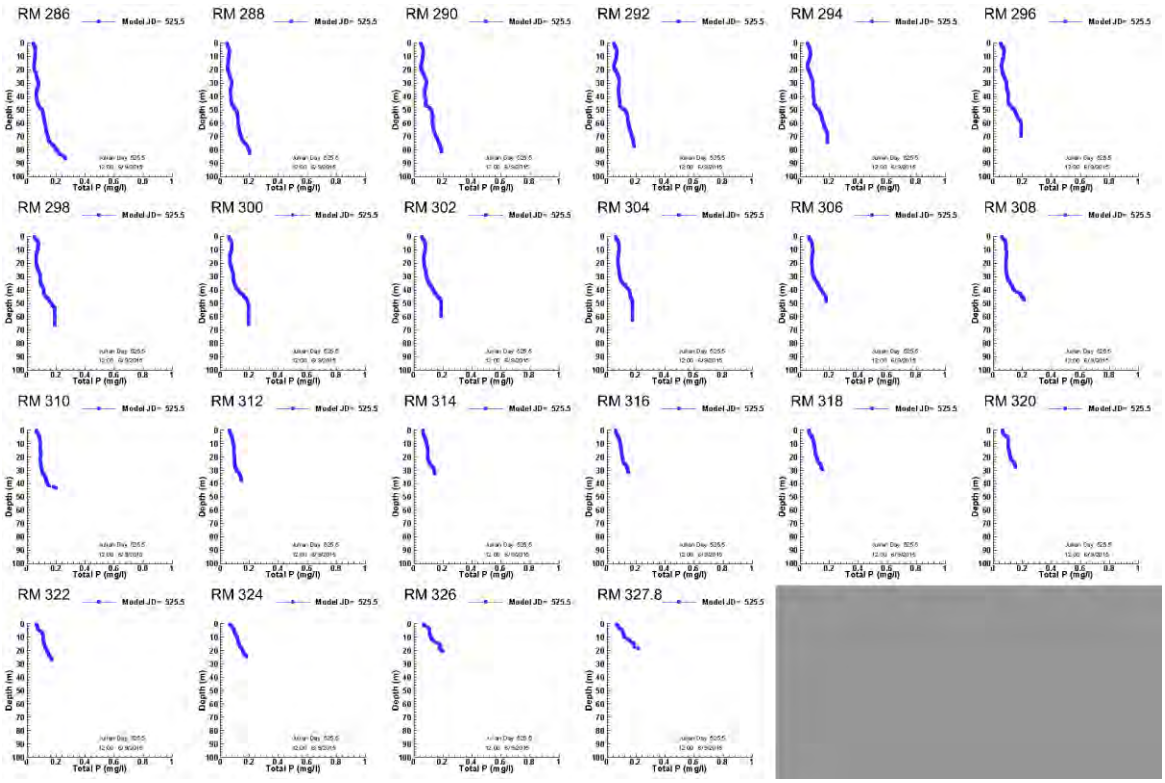


Figure 1895. Vertical profiles of TP compared with data for 6/ 9/2015.

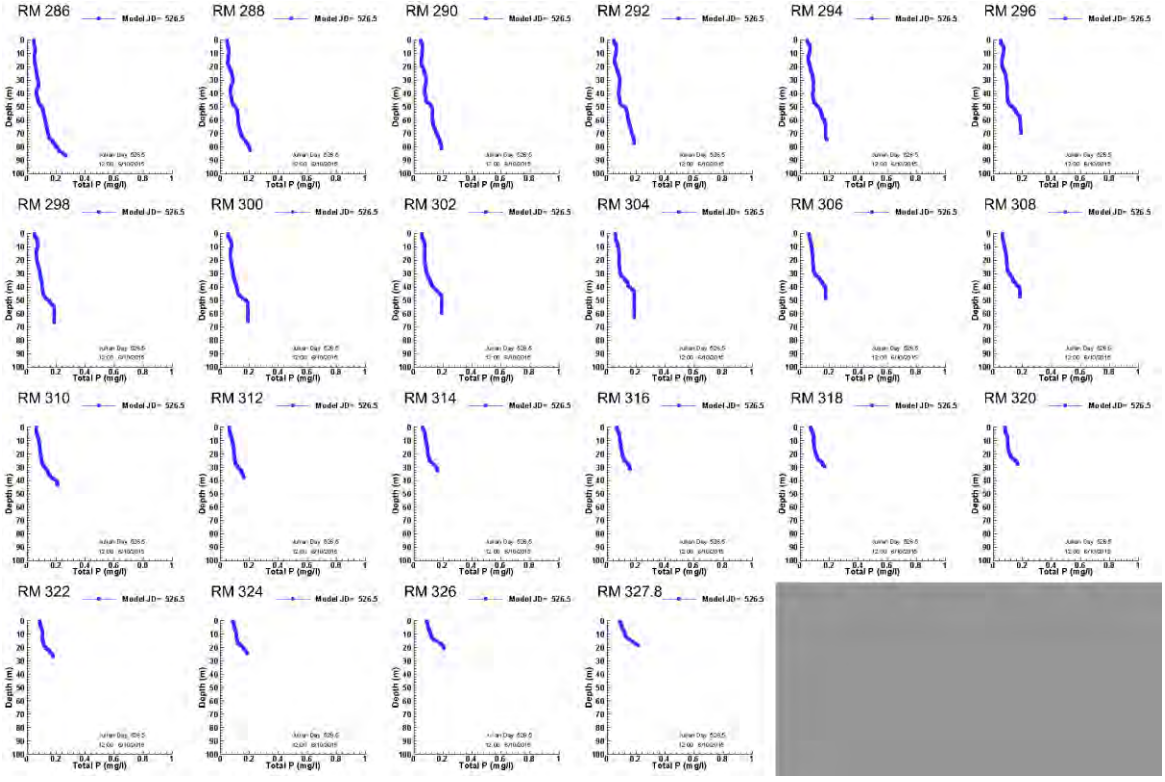


Figure 1896. Vertical profiles of TP compared with data for 6/10/2015.

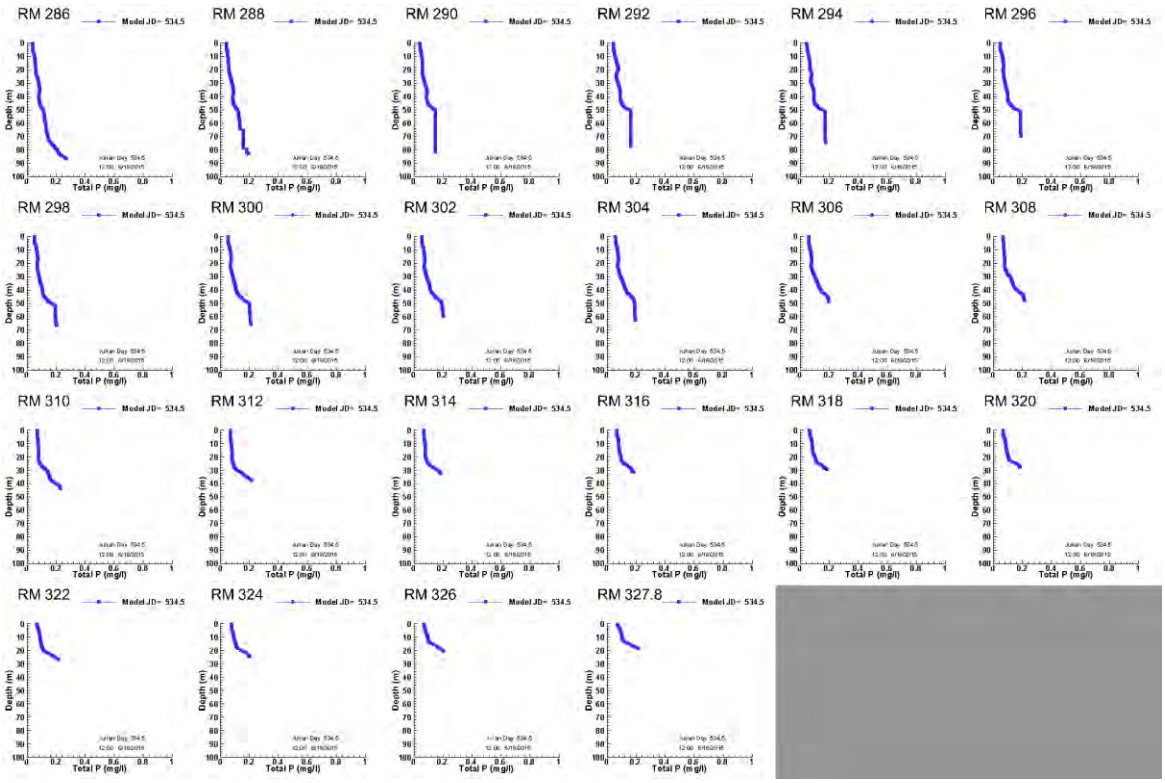


Figure 1897. Vertical profiles of TP compared with data for 6/18/2015.

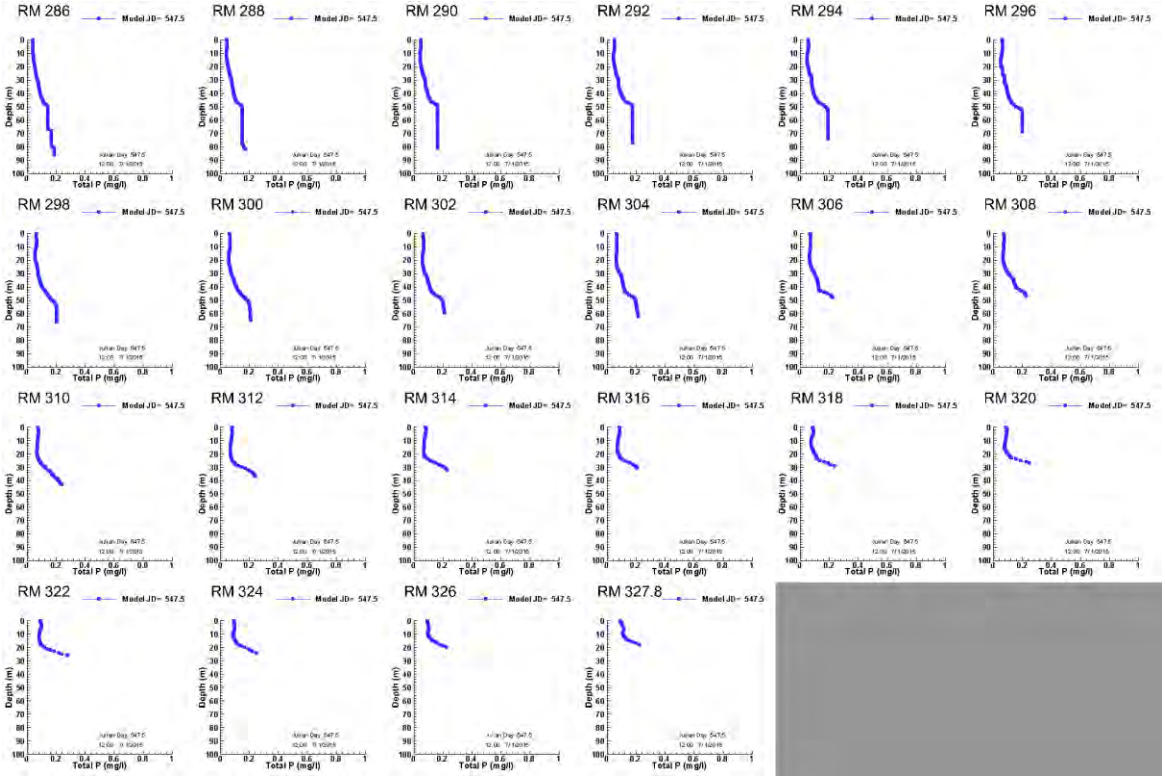


Figure 1898. Vertical profiles of TP compared with data for 7/ 1/2015.

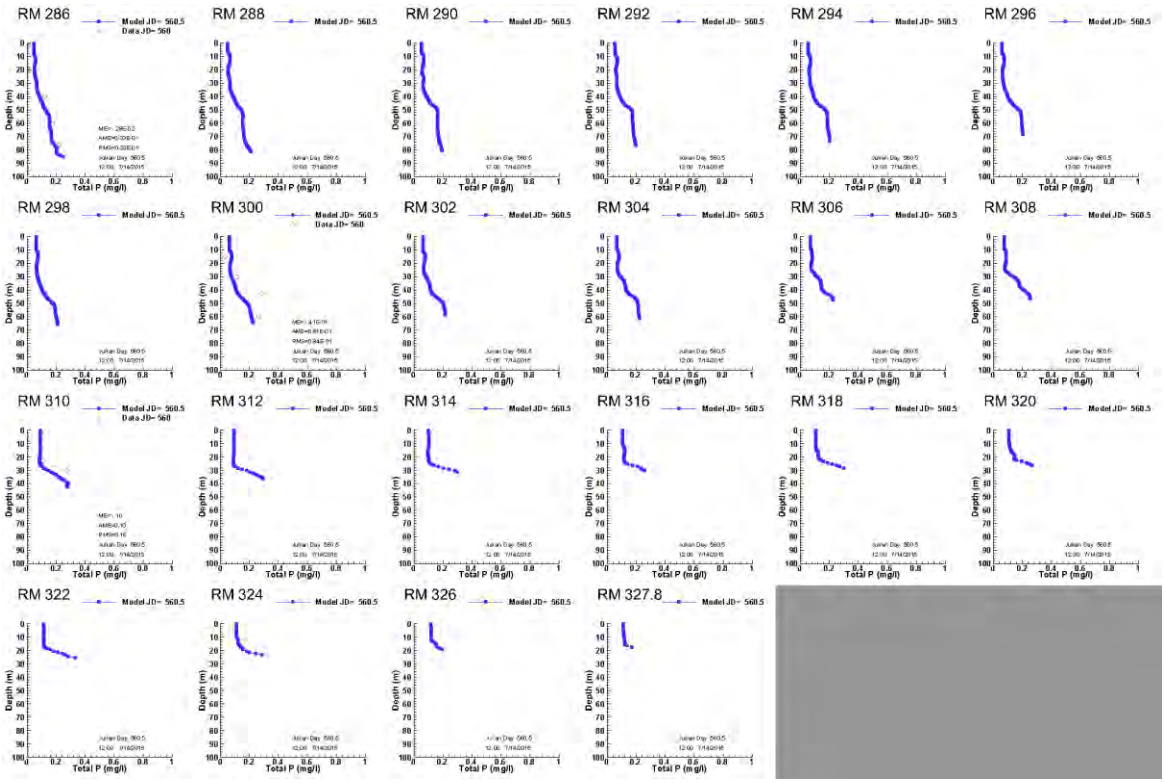


Figure 1899. Vertical profiles of TP compared with data for 7/14/2015.

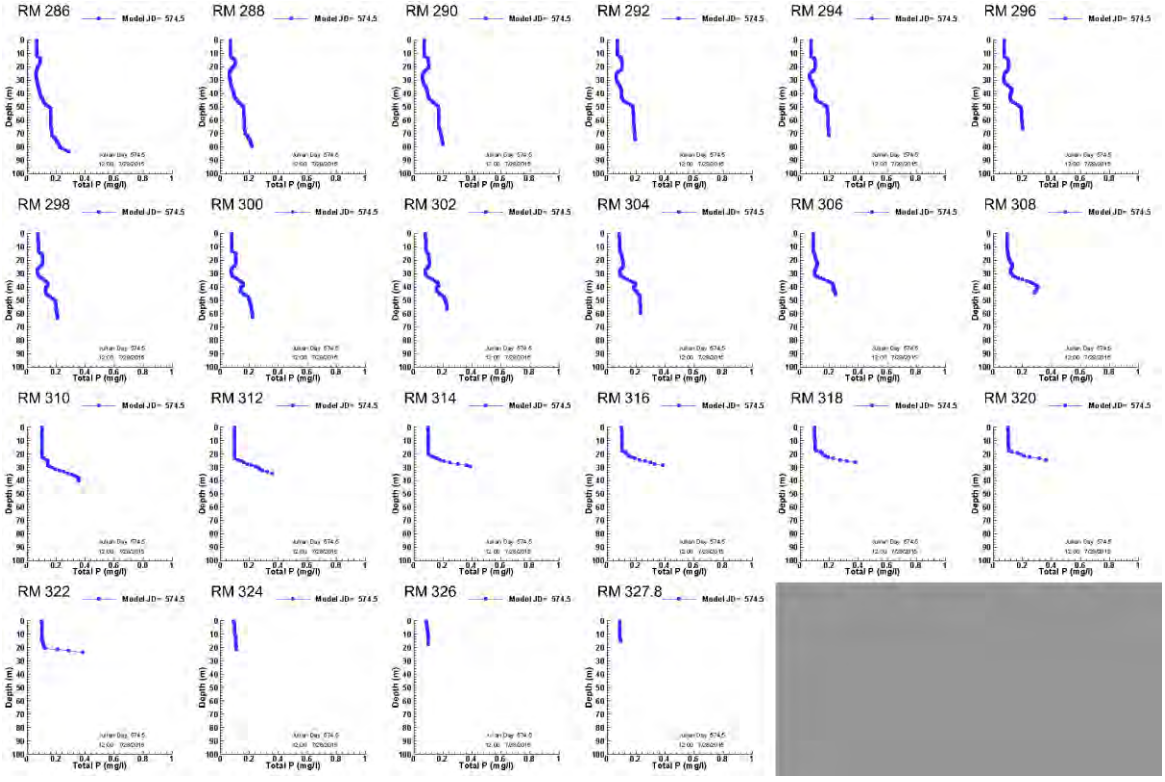


Figure 1900. Vertical profiles of TP compared with data for 7/28/2015.

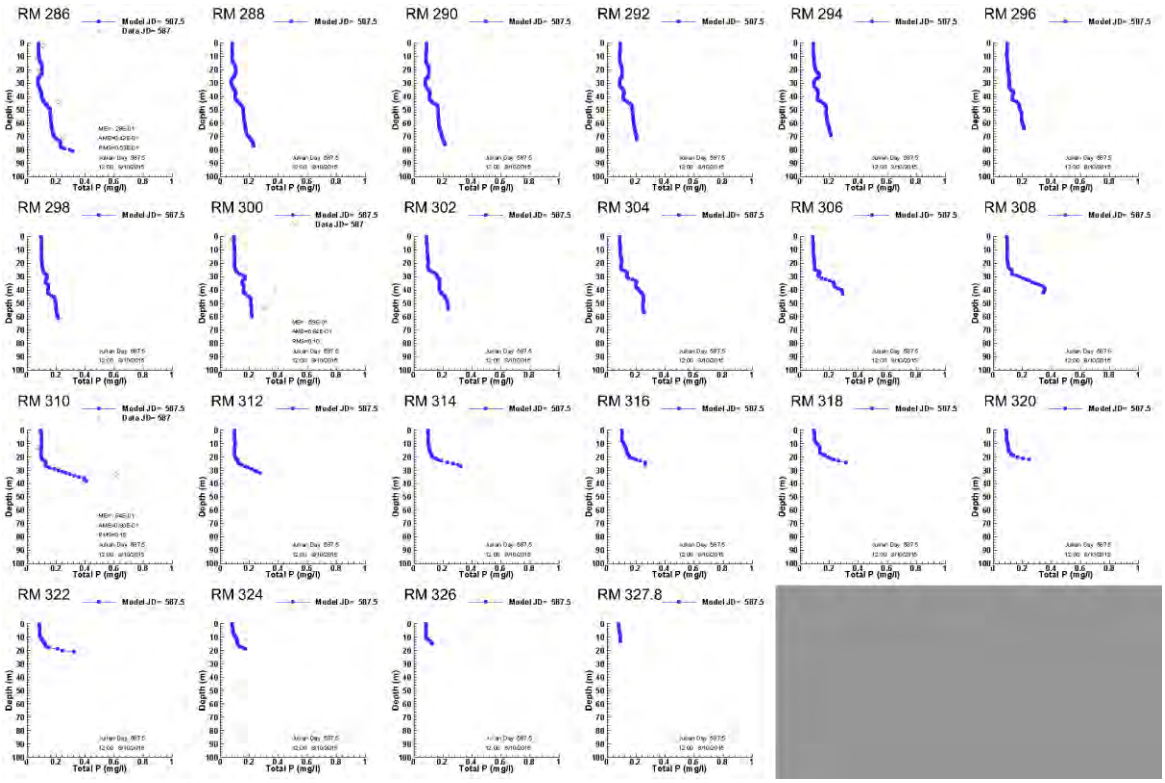


Figure 1901. Vertical profiles of TP compared with data for 8/10/2015.

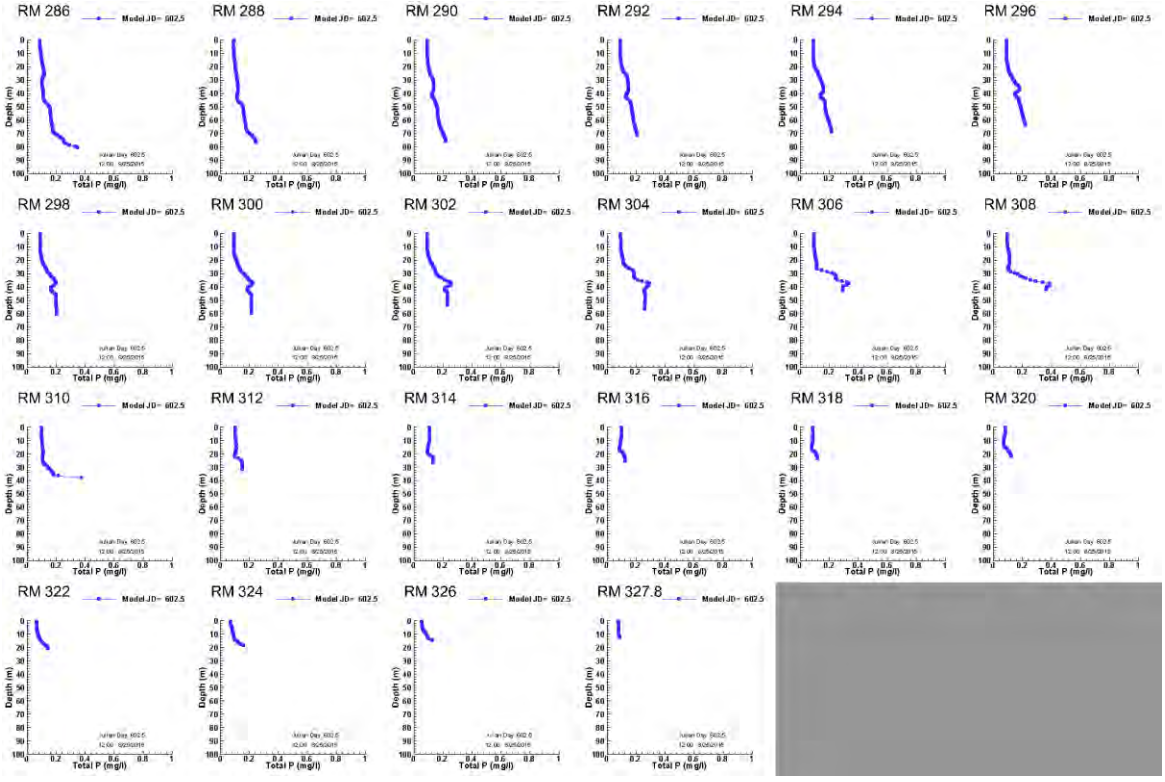


Figure 1902. Vertical profiles of TP compared with data for 8/25/2015.

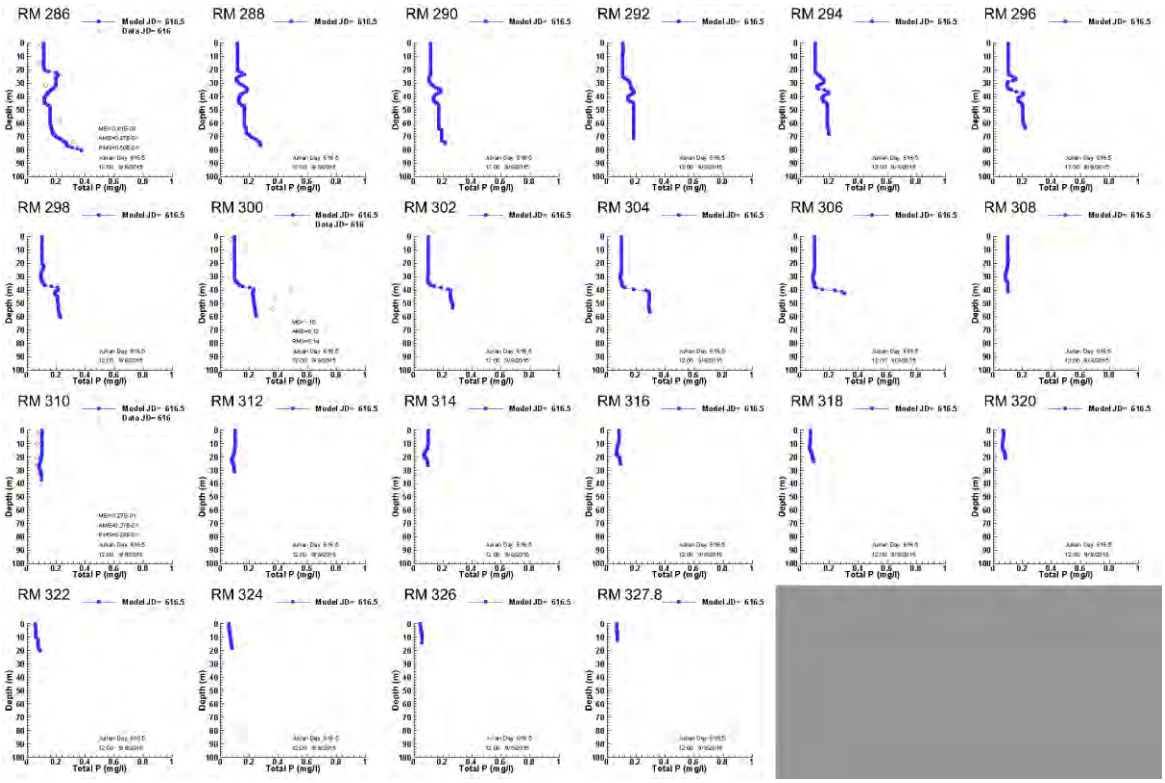


Figure 1903. Vertical profiles of TP compared with data for 9/ 8/2015.

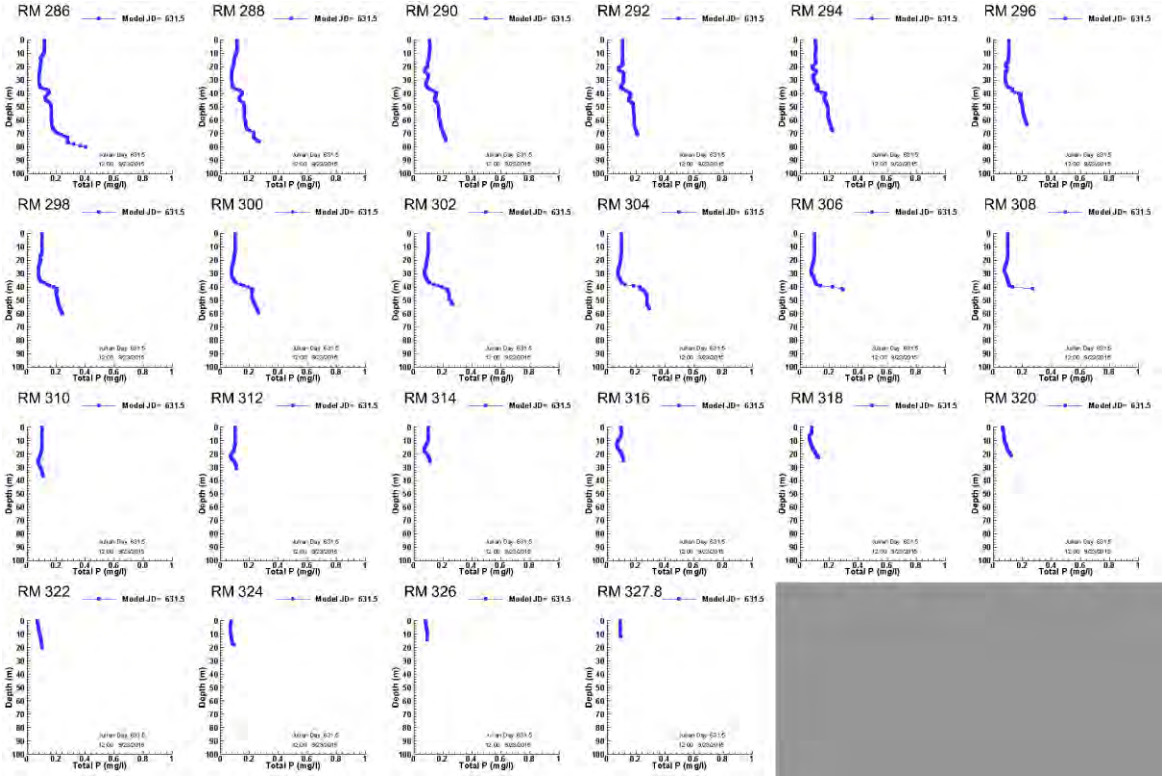


Figure 1904. Vertical profiles of TP compared with data for 9/23/2015.

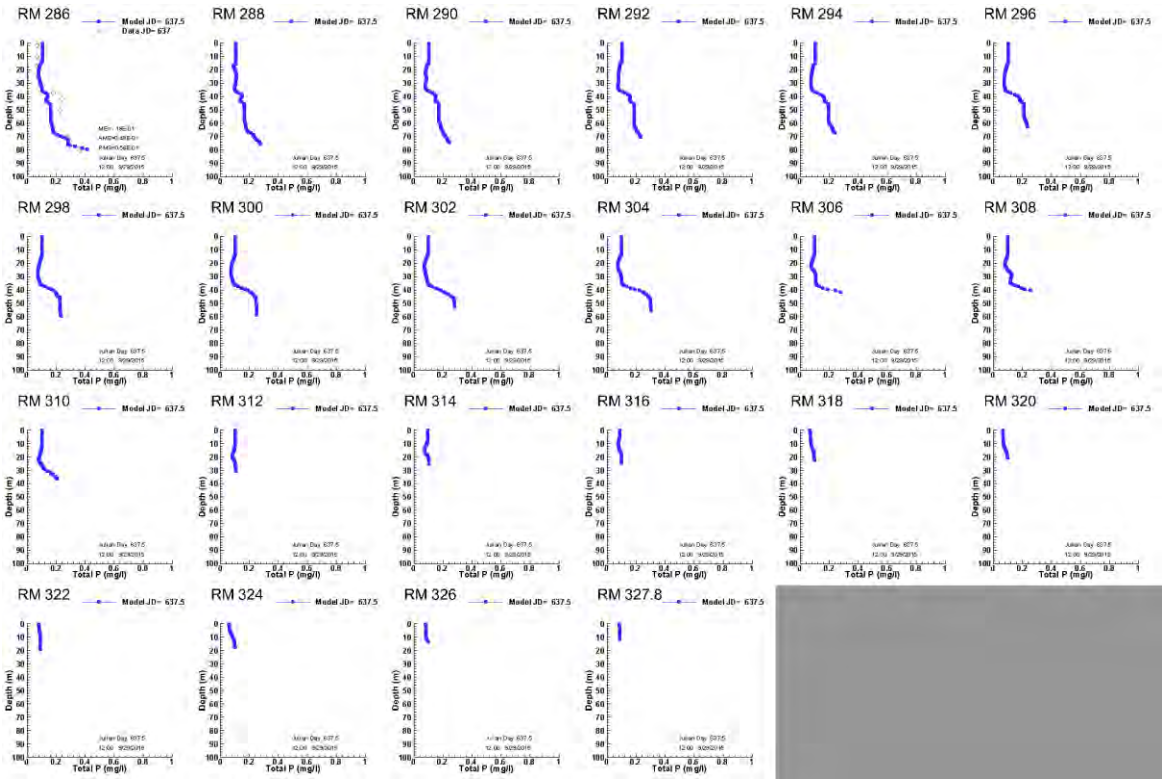


Figure 1905. Vertical profiles of TP compared with data for 9/29/2015.

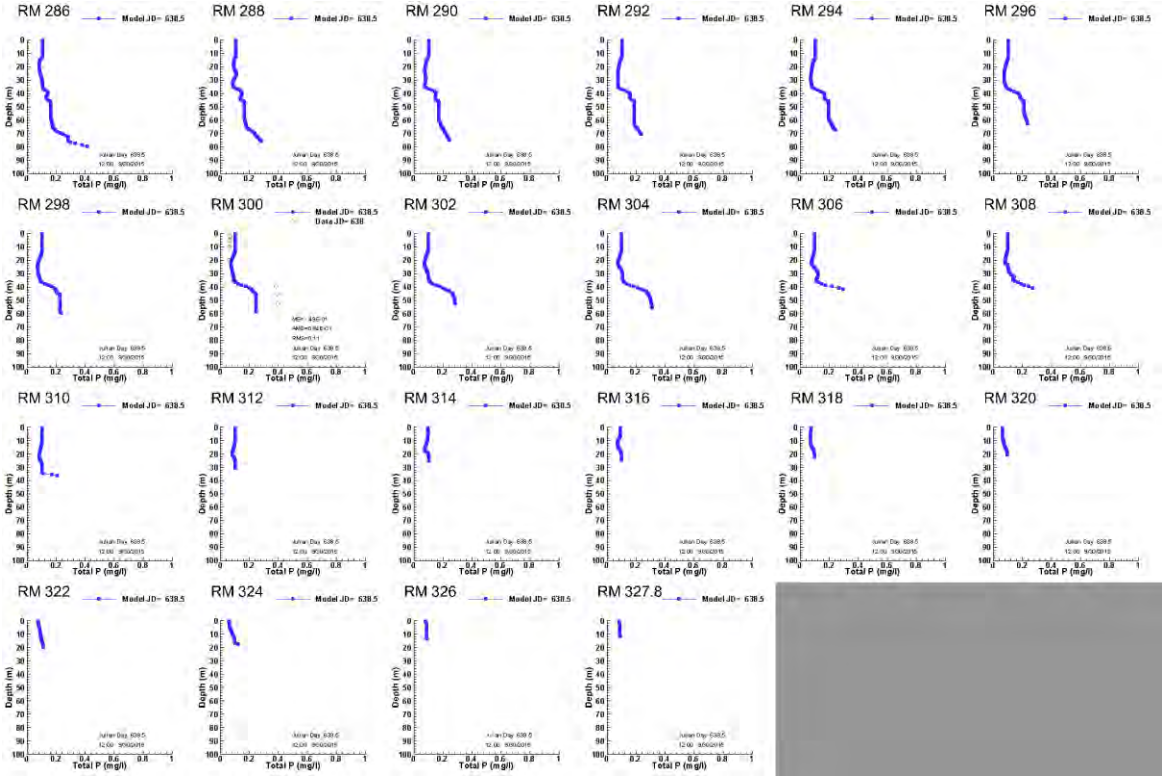


Figure 1906. Vertical profiles of TP compared with data for 9/30/2015.

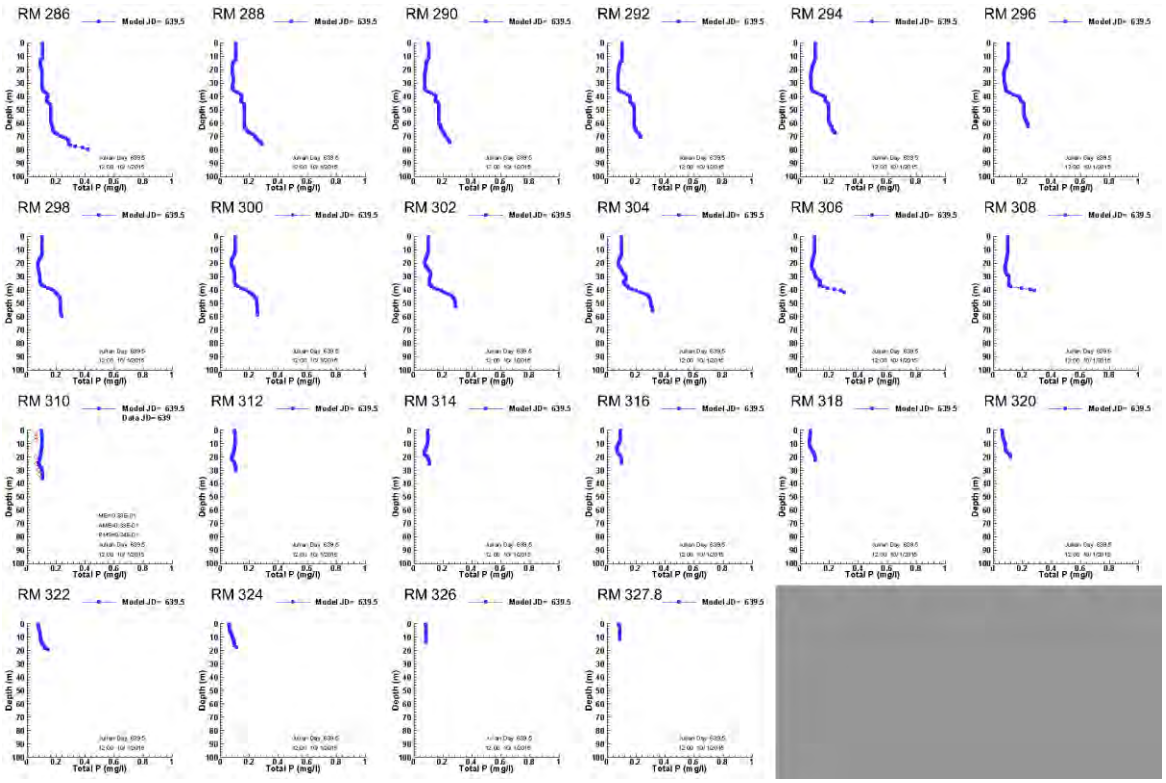


Figure 1907. Vertical profiles of TP compared with data for 10/ 1/2015.

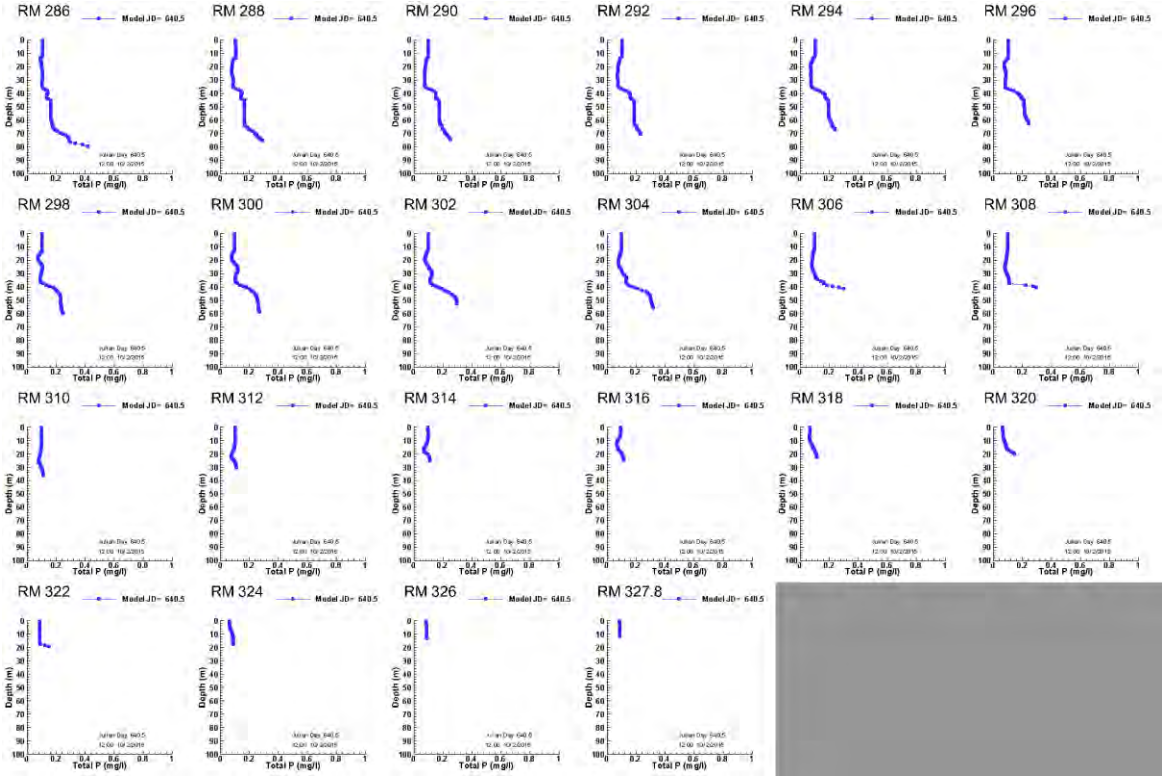


Figure 1908. Vertical profiles of TP compared with data for 10/ 2/2015.

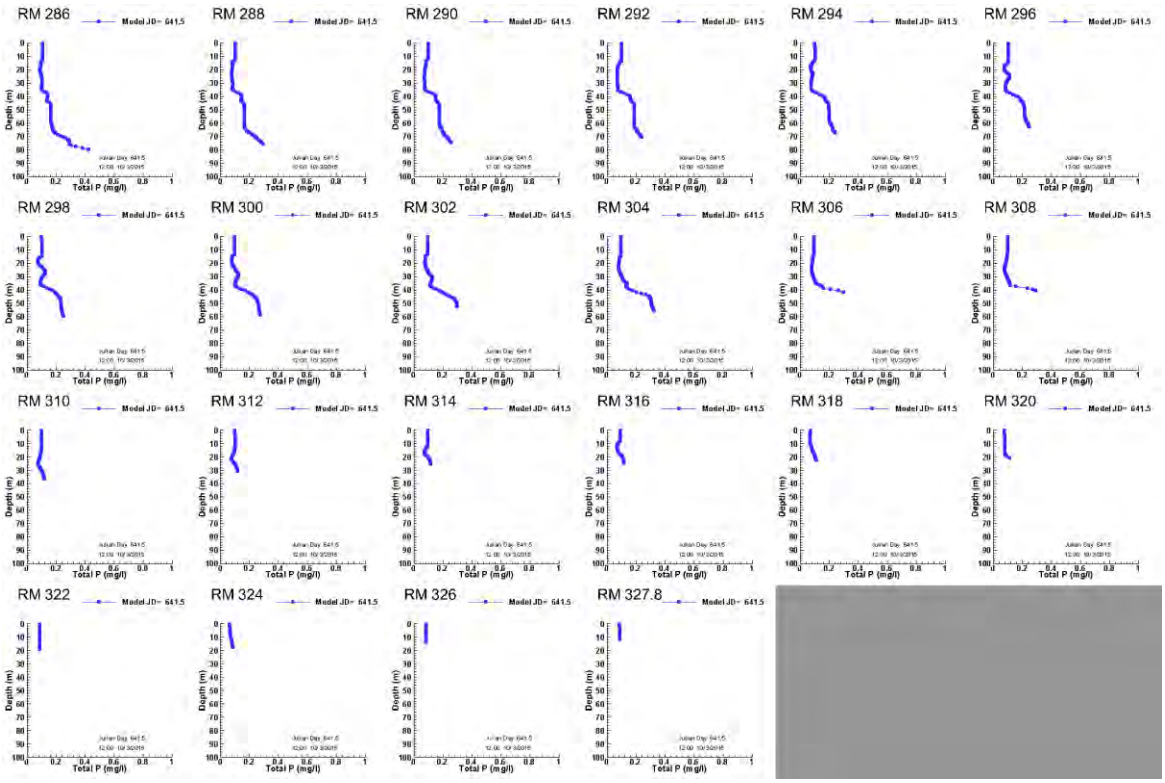


Figure 1909. Vertical profiles of TP compared with data for 10/ 3/2015.

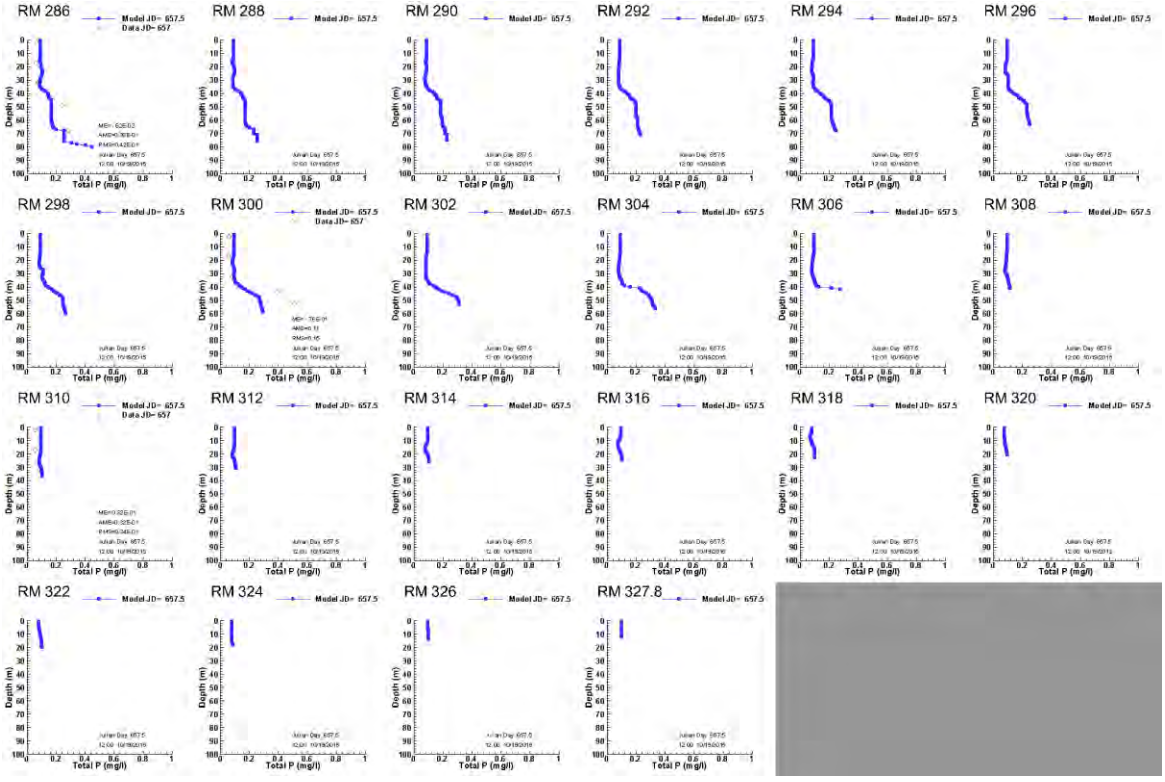


Figure 1910. Vertical profiles of TP compared with data for 10/19/2015.

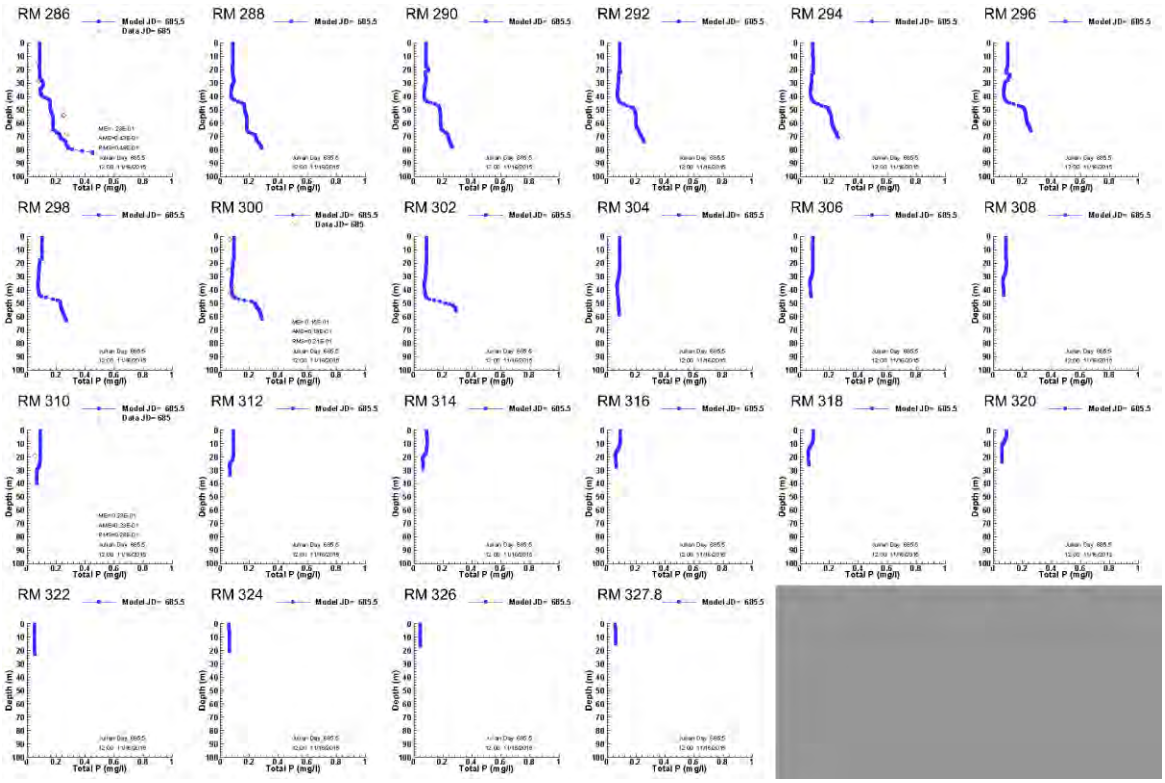


Figure 1911. Vertical profiles of TP compared with data for 11/16/2015.

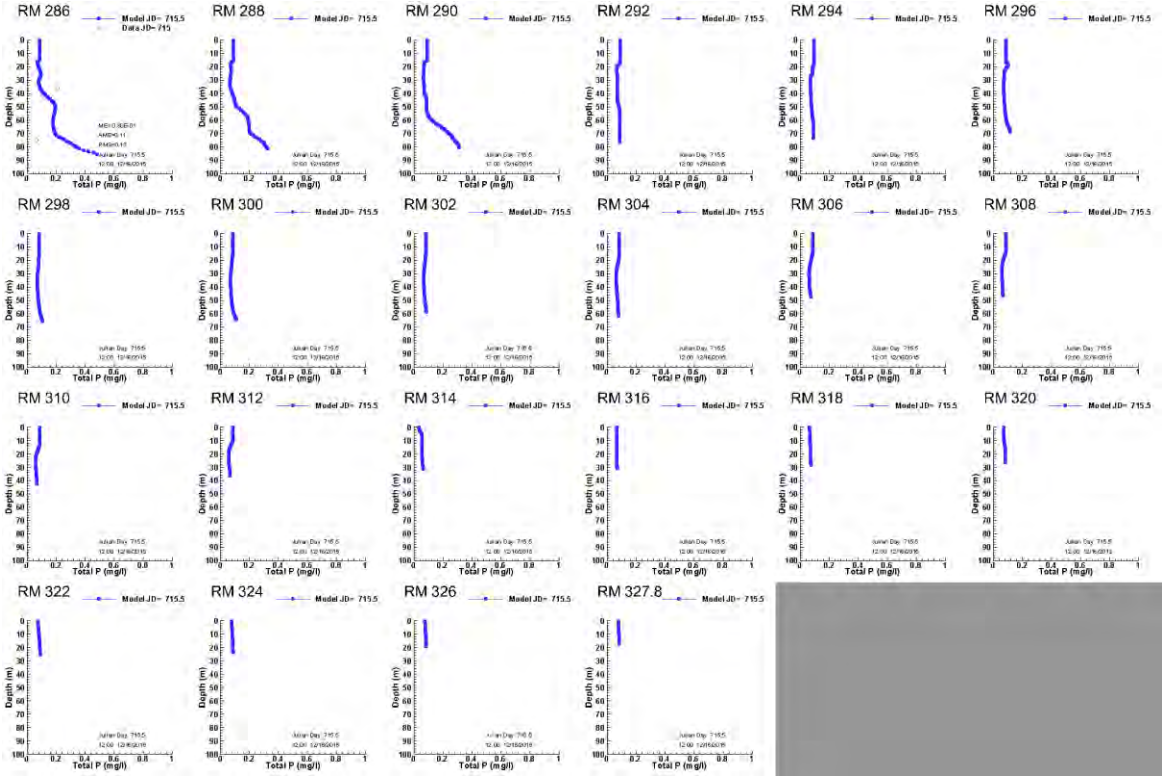


Figure 1912. Vertical profiles of TP compared with data for 12/16/2015.

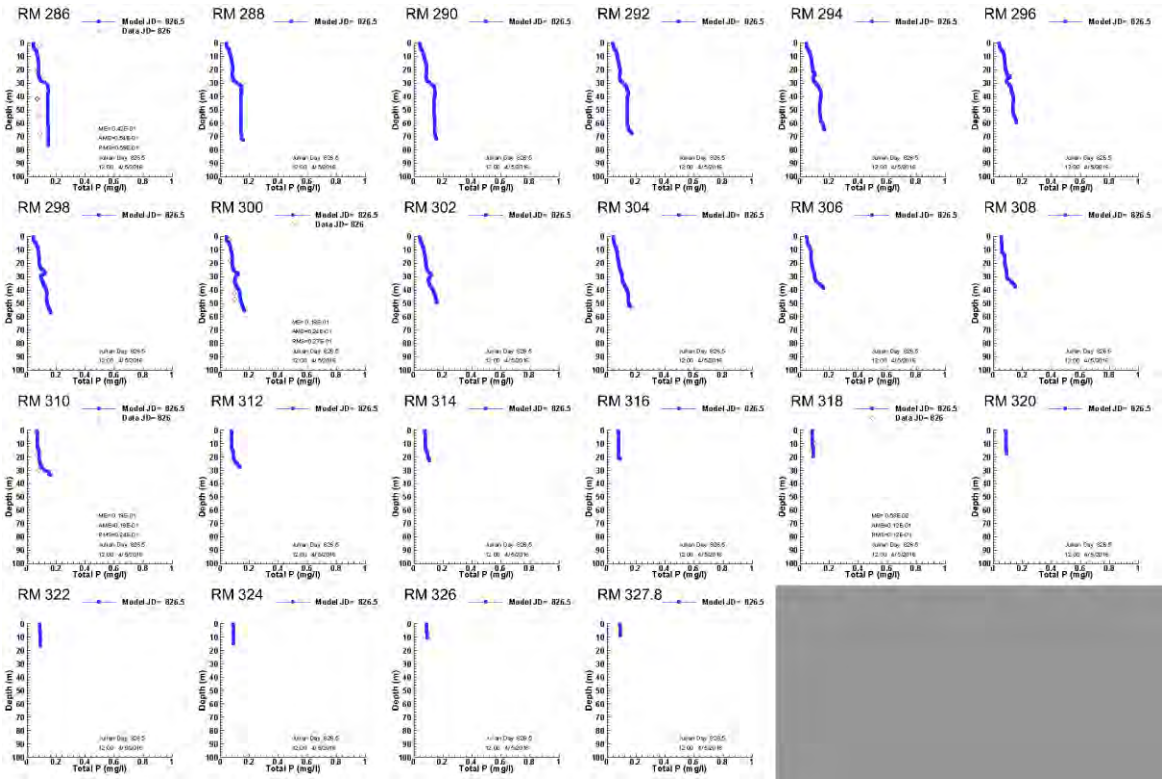


Figure 1913. Vertical profiles of TP compared with data for 4/ 5/2016.

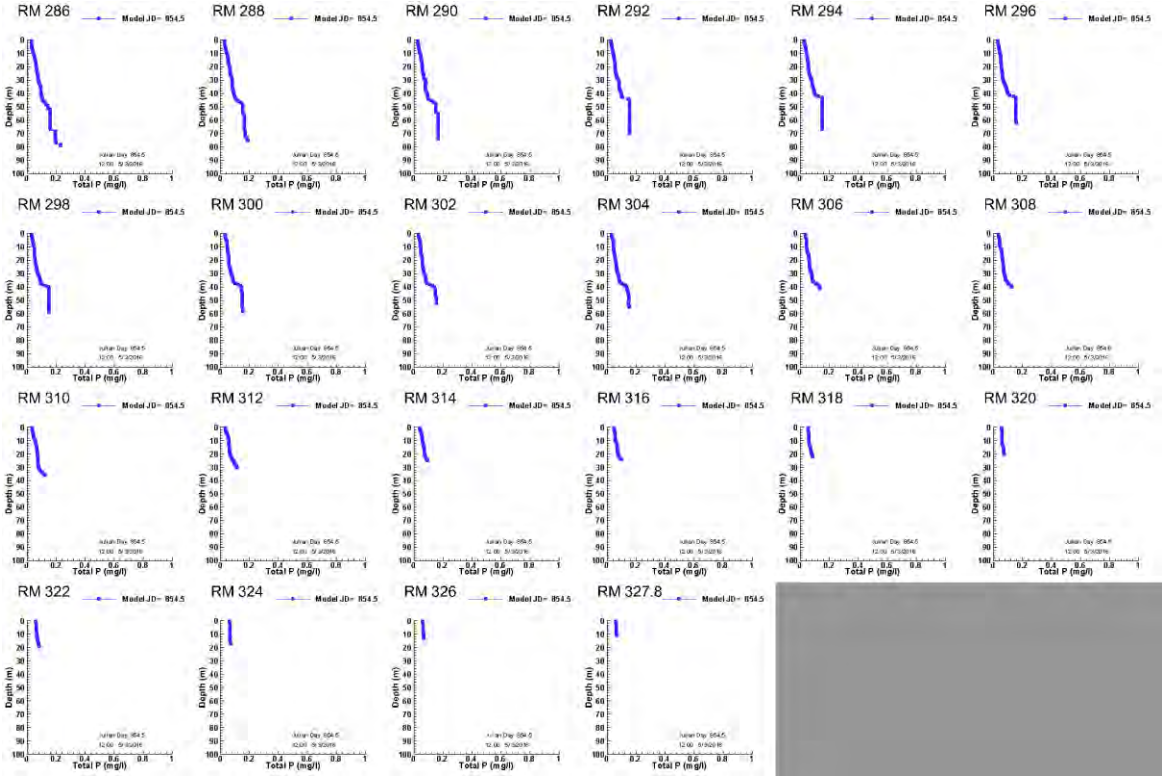


Figure 1914. Vertical profiles of TP compared with data for 5/ 3/2016.

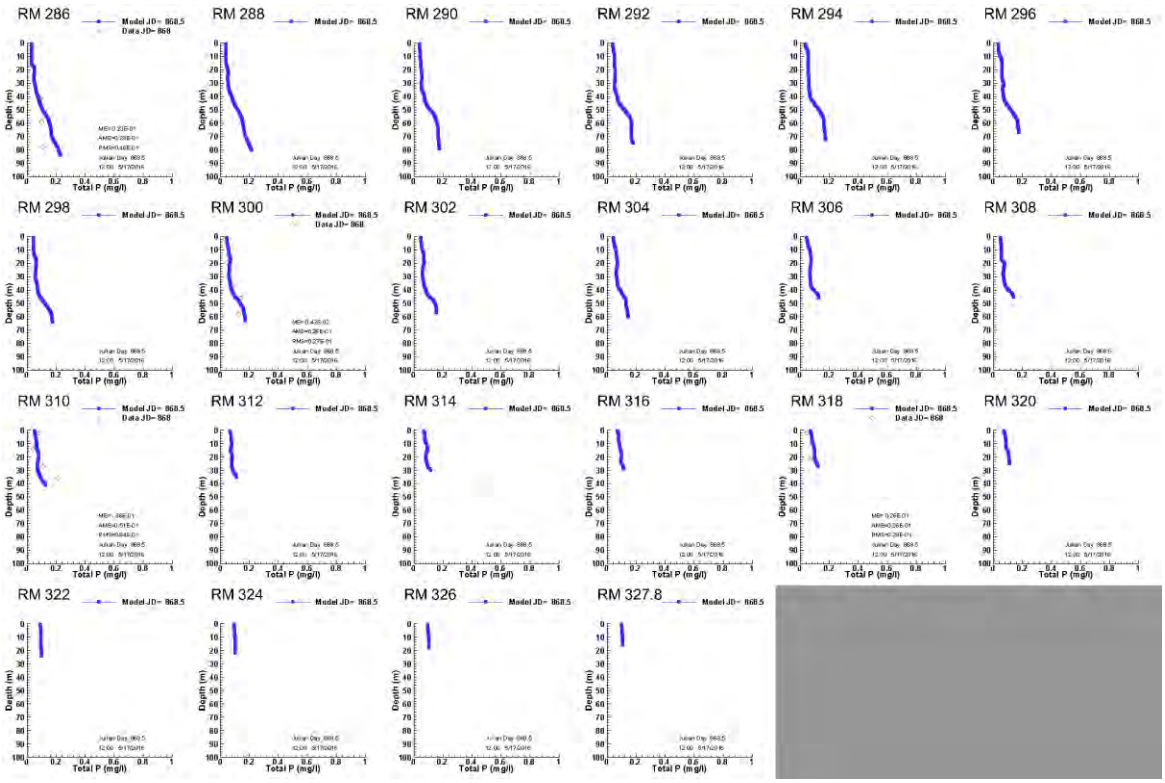


Figure 1915. Vertical profiles of TP compared with data for 5/17/2016.

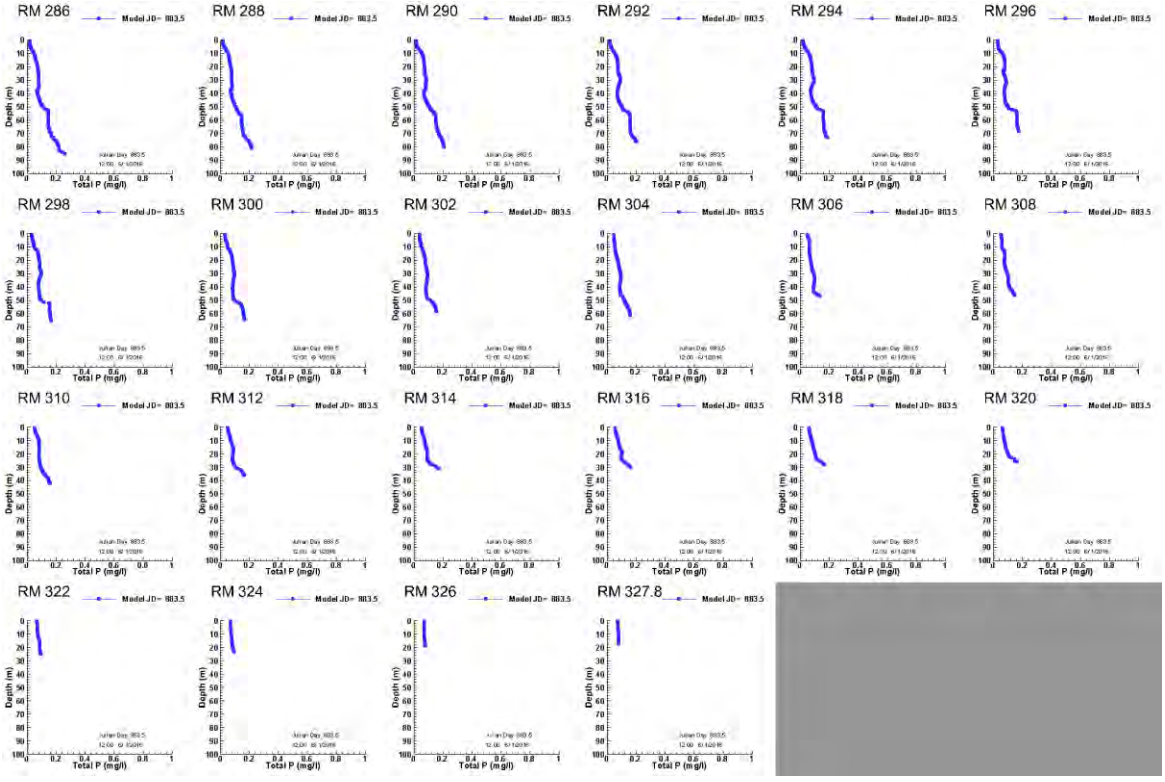


Figure 1916. Vertical profiles of TP compared with data for 6/ 1/2016.

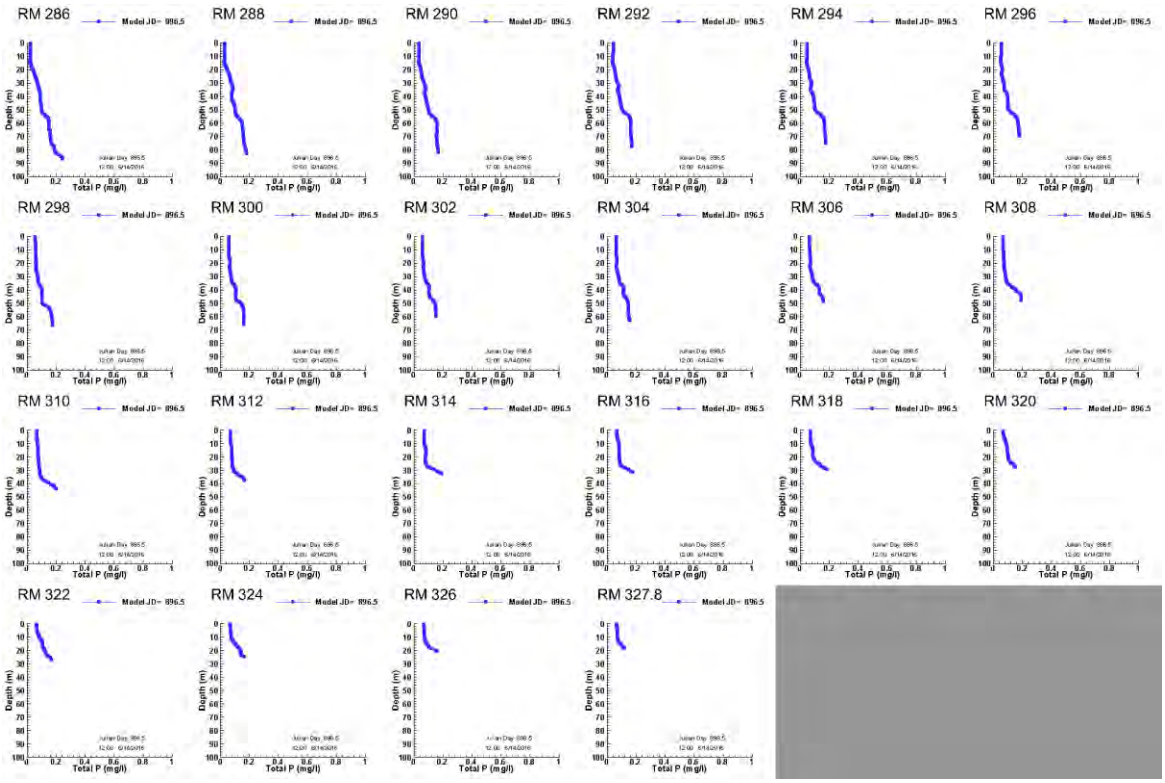


Figure 1917. Vertical profiles of TP compared with data for 6/14/2016.

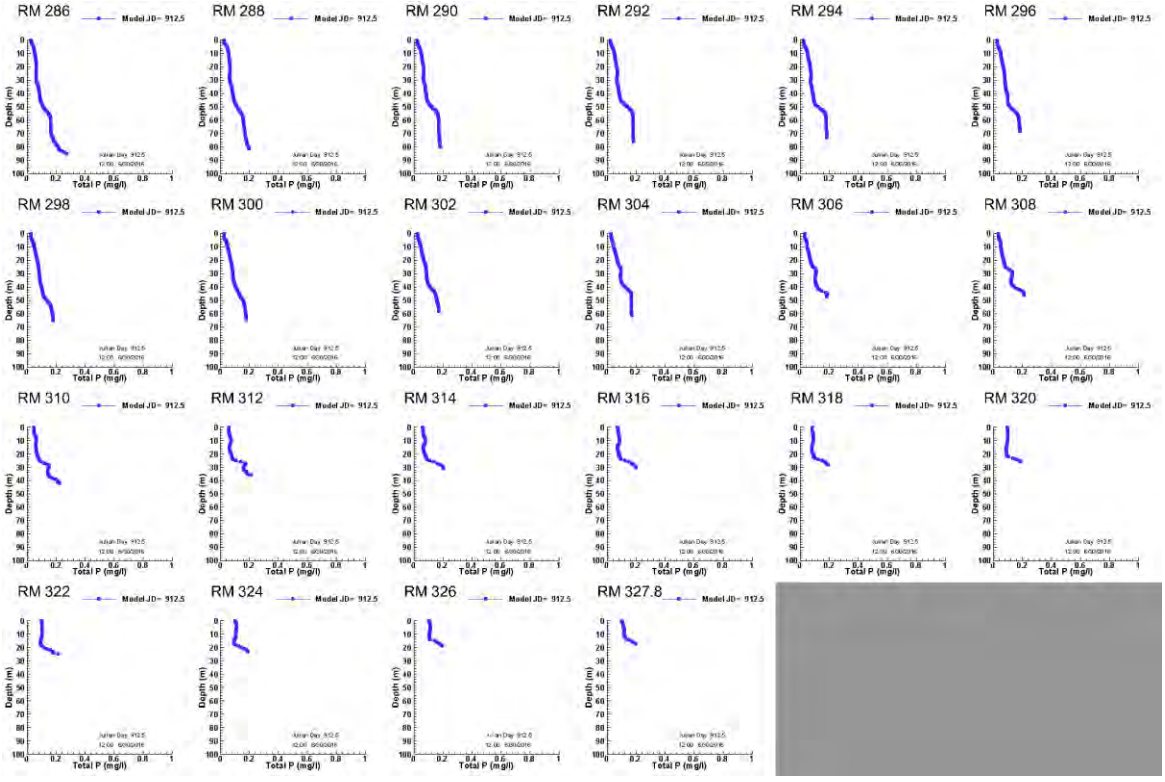


Figure 1918. Vertical profiles of TP compared with data for 6/30/2016.

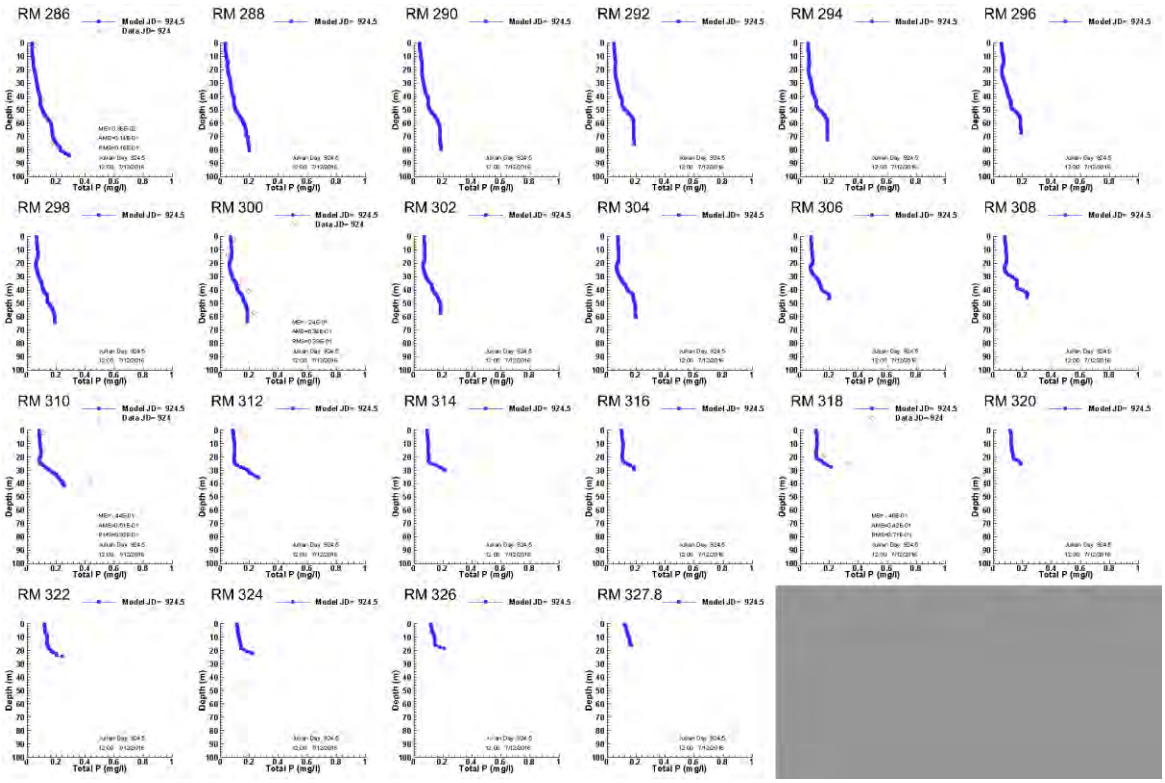


Figure 1919. Vertical profiles of TP compared with data for 7/12/2016.

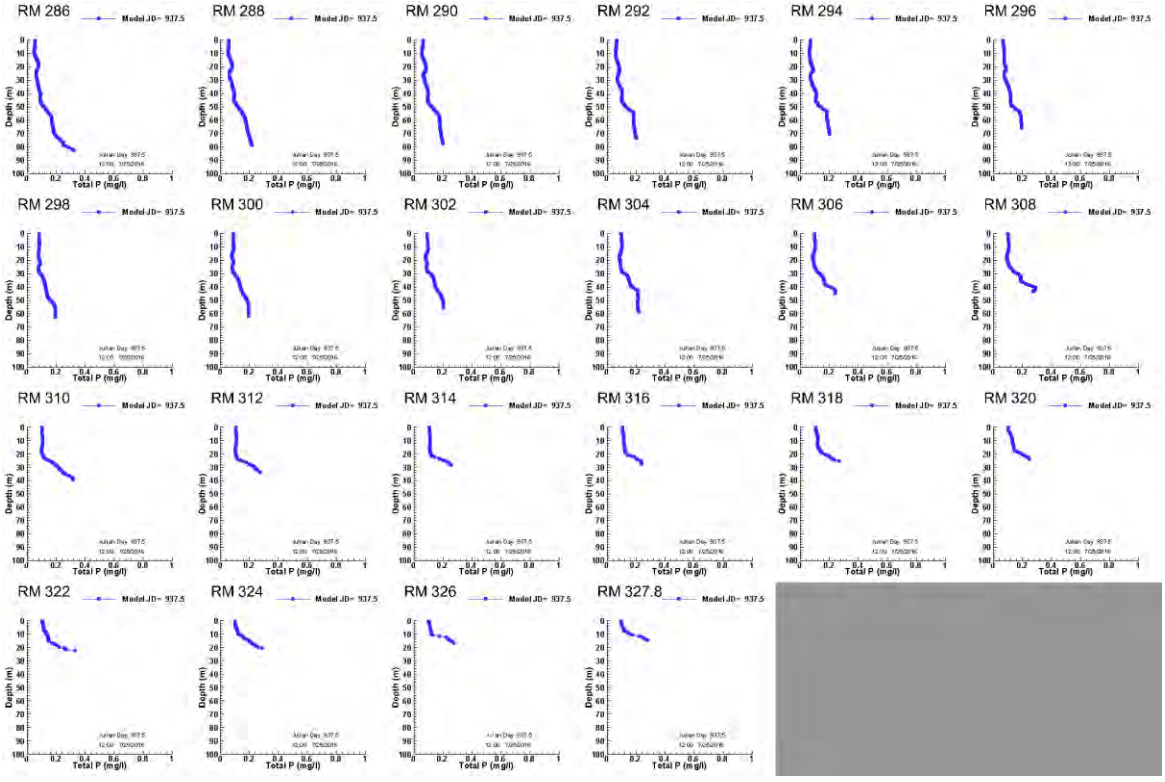


Figure 1920. Vertical profiles of TP compared with data for 7/25/2016.

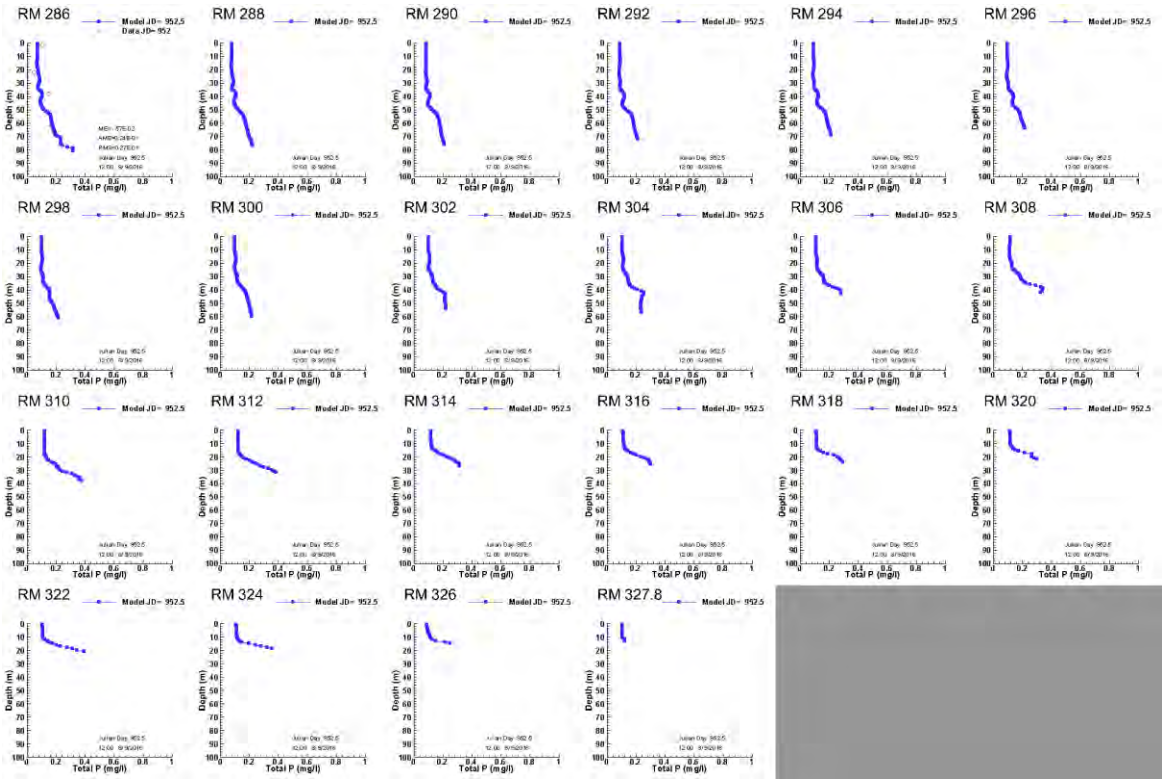


Figure 1921. Vertical profiles of TP compared with data for 8/ 9/2016.

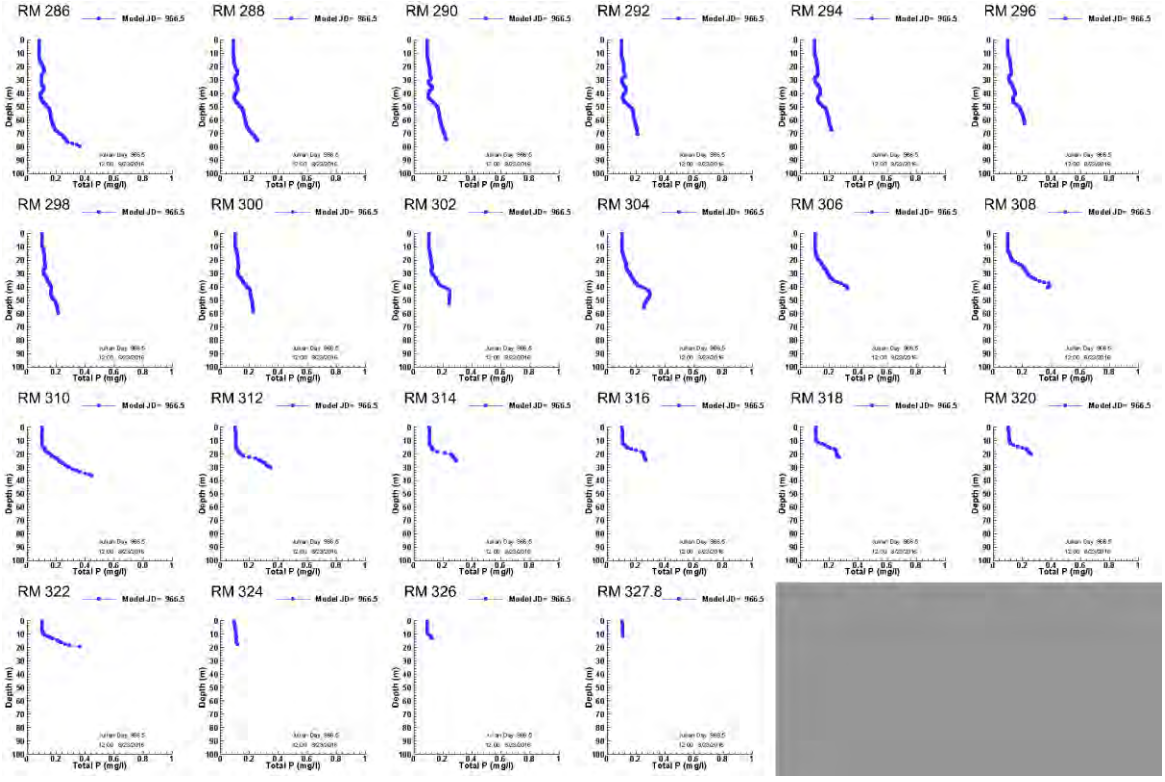


Figure 1922. Vertical profiles of TP compared with data for 8/23/2016.

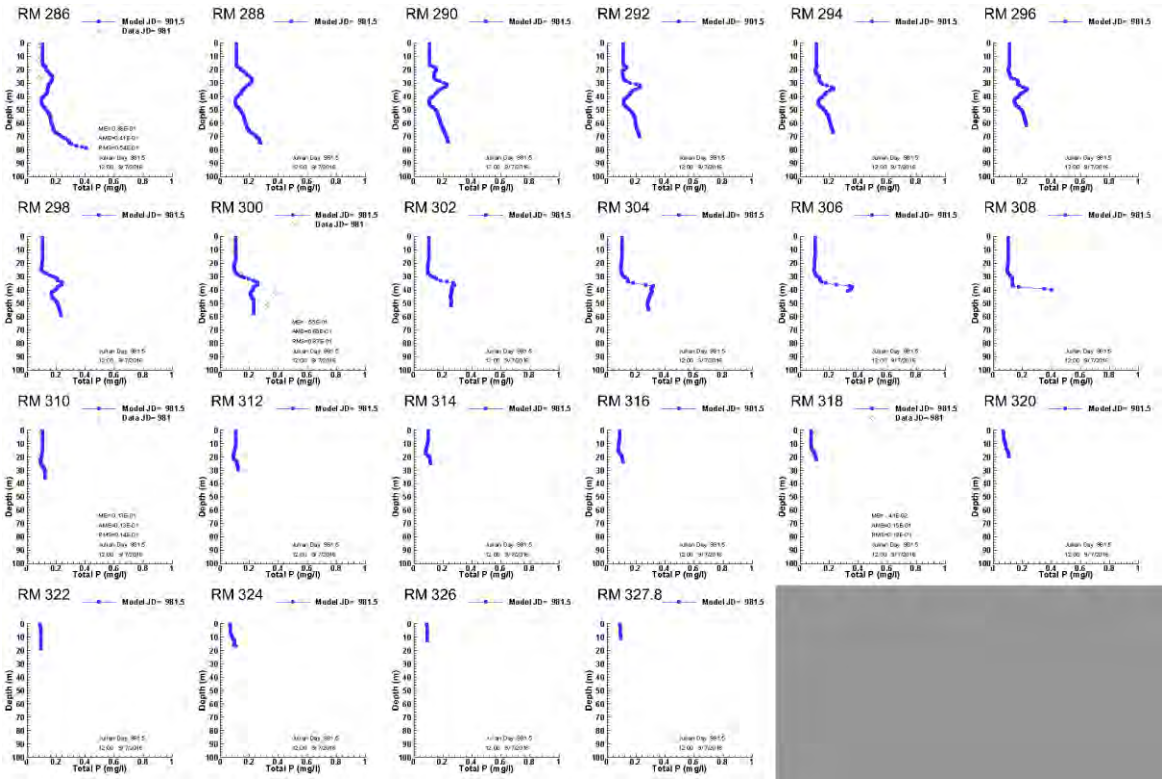


Figure 1923. Vertical profiles of TP compared with data for 9/ 7/2016.

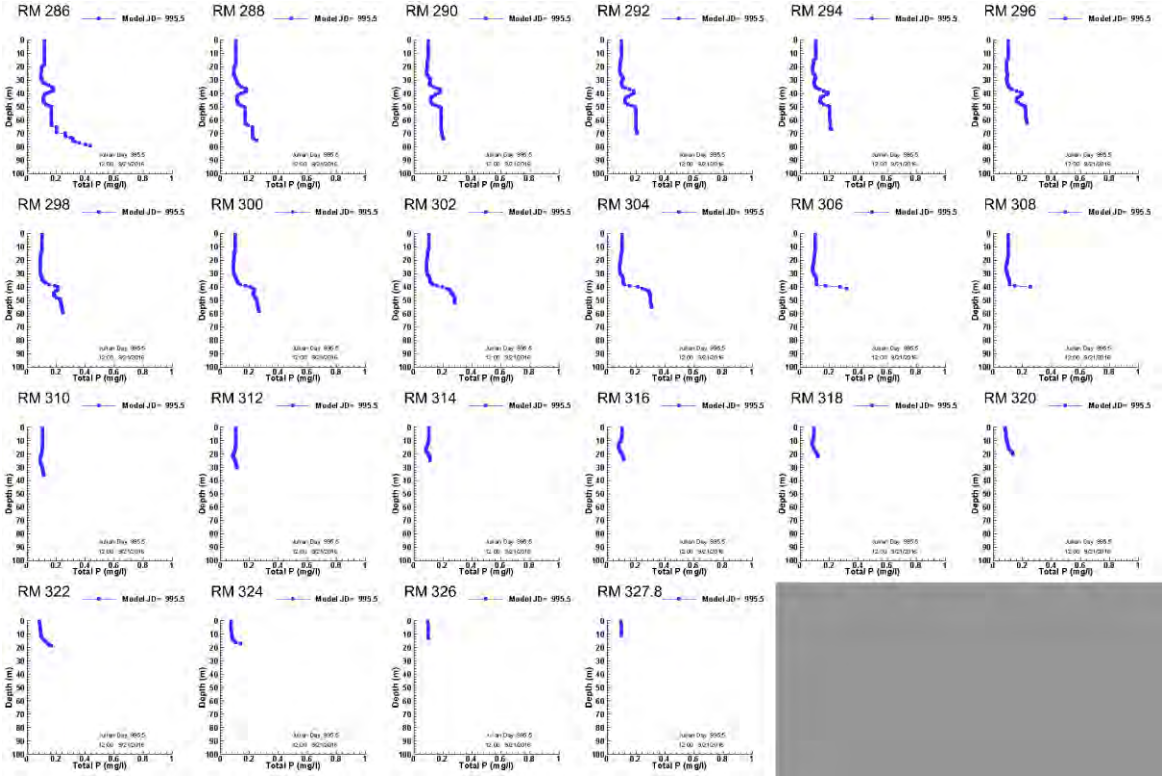


Figure 1924. Vertical profiles of TP compared with data for 9/21/2016.

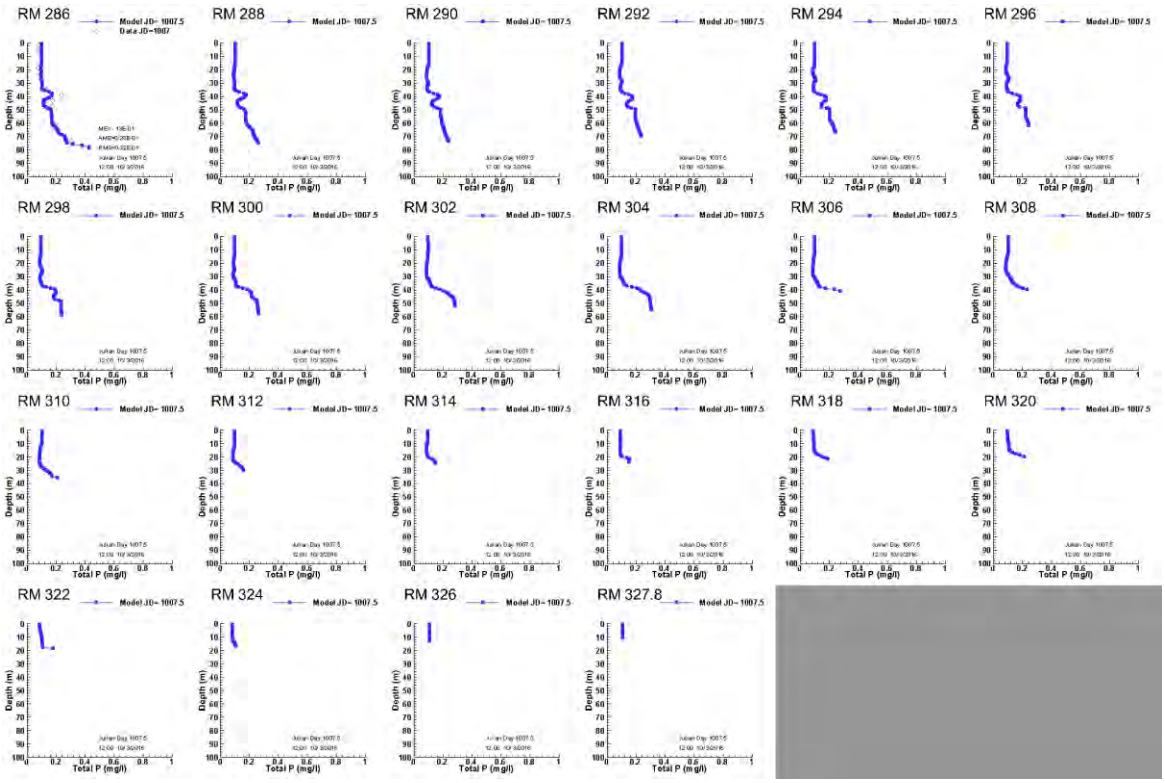


Figure 1925. Vertical profiles of TP compared with data for 10/ 3/2016.

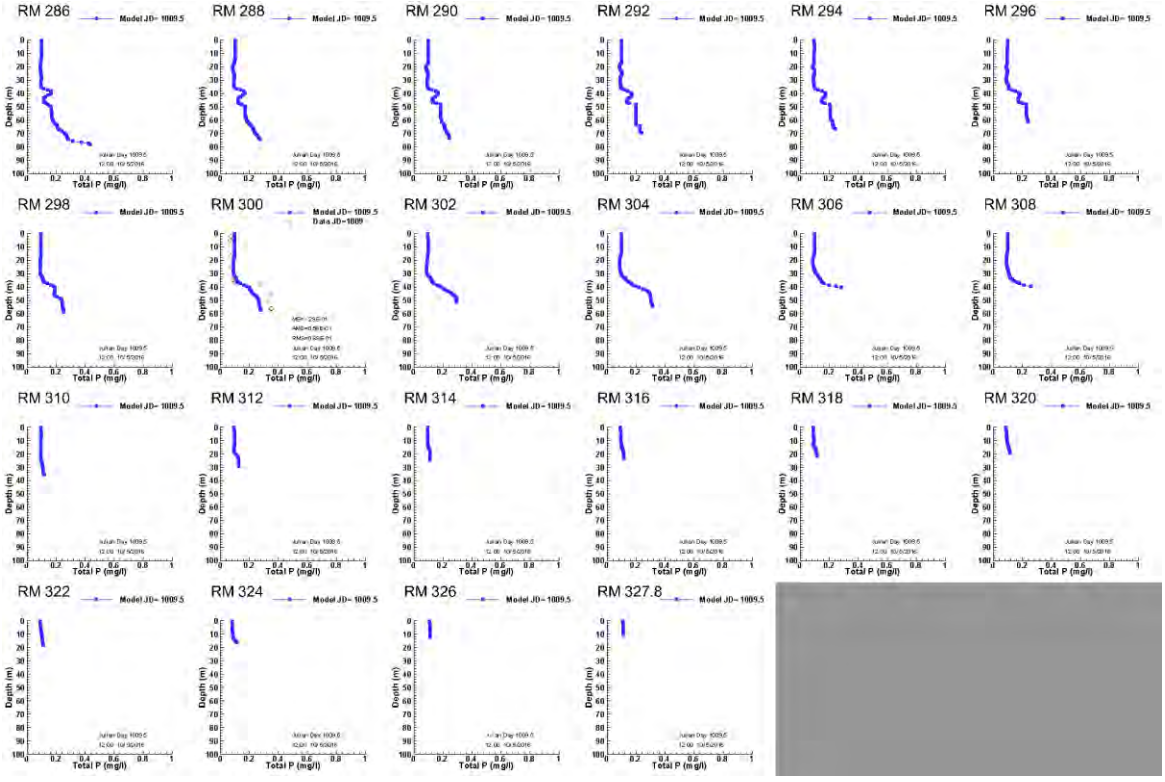


Figure 1926. Vertical profiles of TP compared with data for 10/ 5/2016.

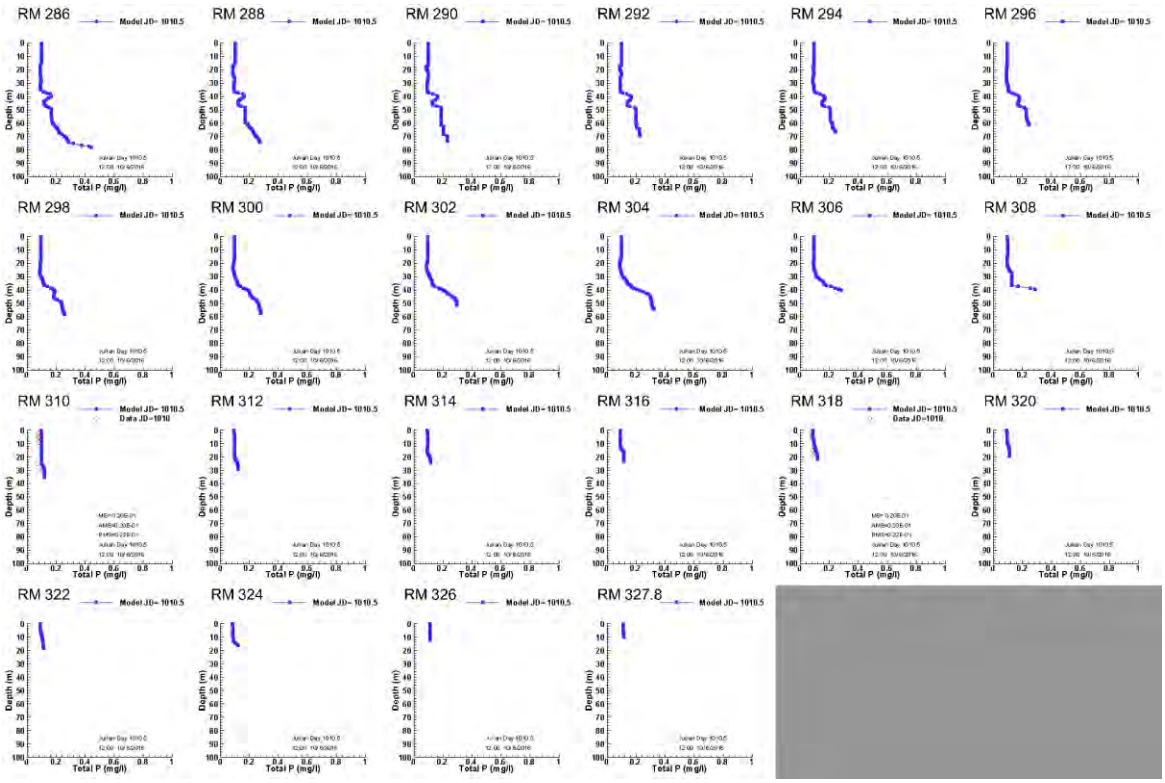


Figure 1927. Vertical profiles of TP compared with data for 10/ 6/2016.

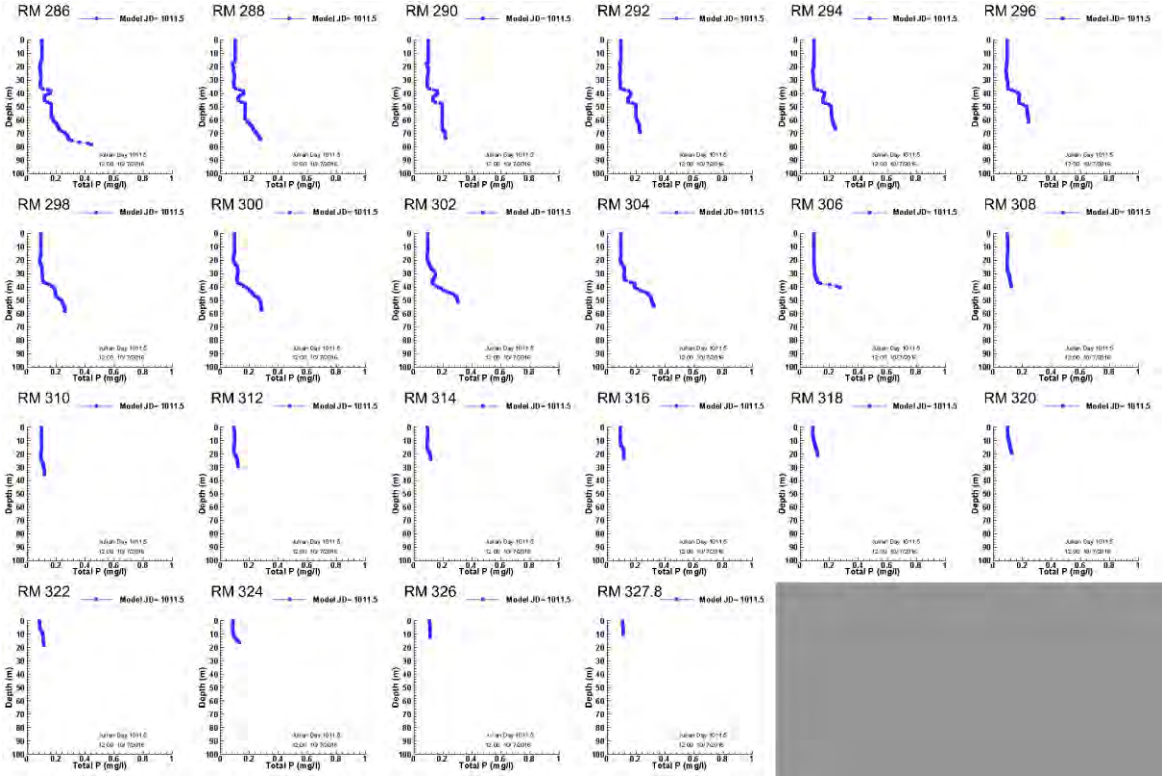


Figure 1928. Vertical profiles of TP compared with data for 10/ 7/2016.

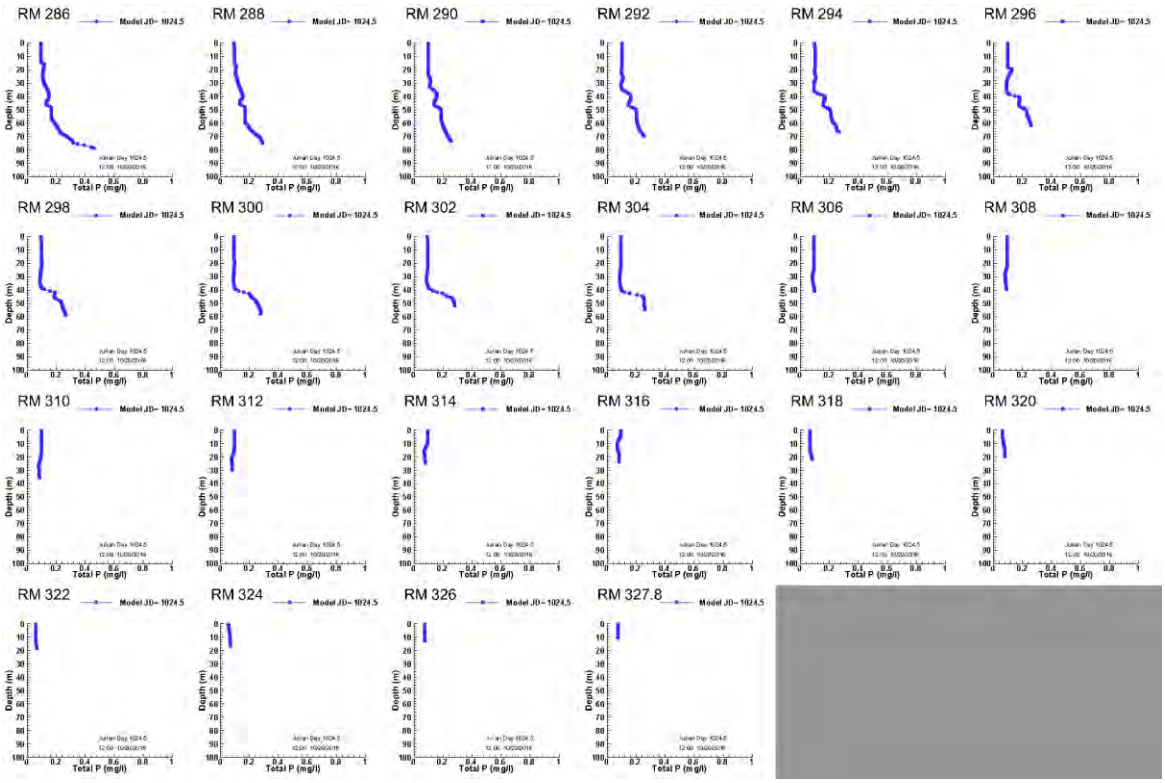


Figure 1929. Vertical profiles of TP compared with data for 10/20/2016.

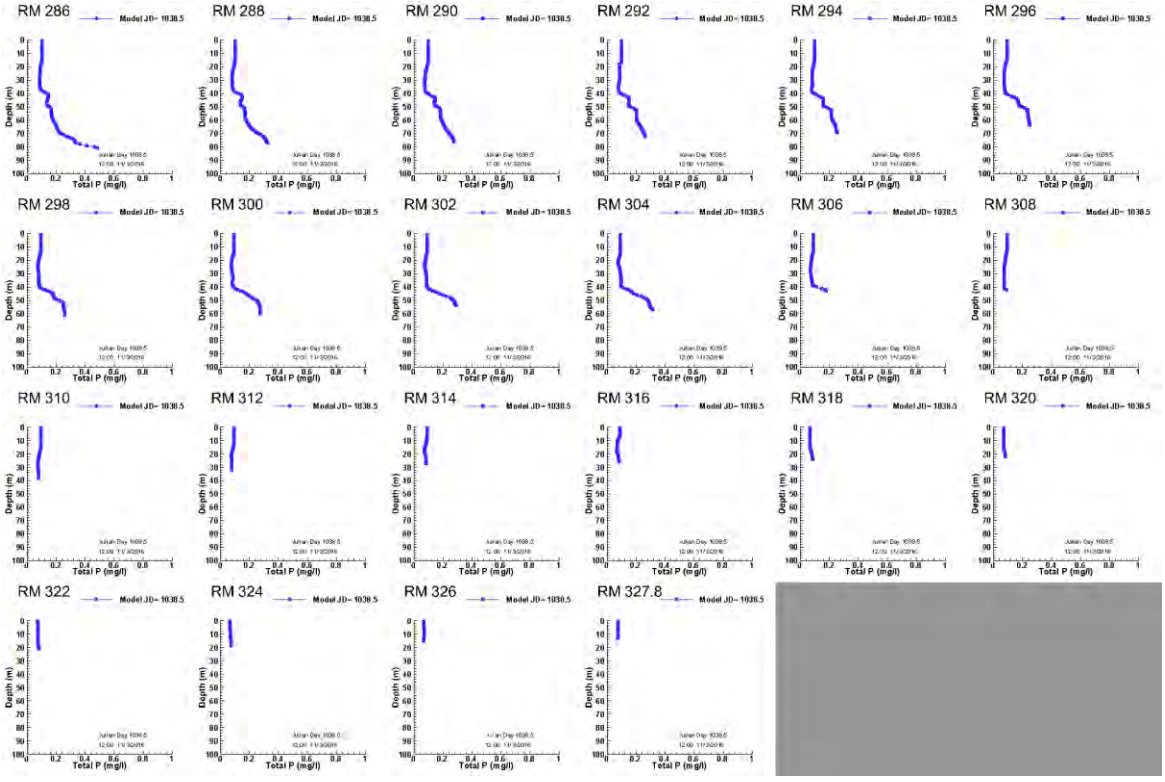


Figure 1930. Vertical profiles of TP compared with data for 11/ 3/2016.

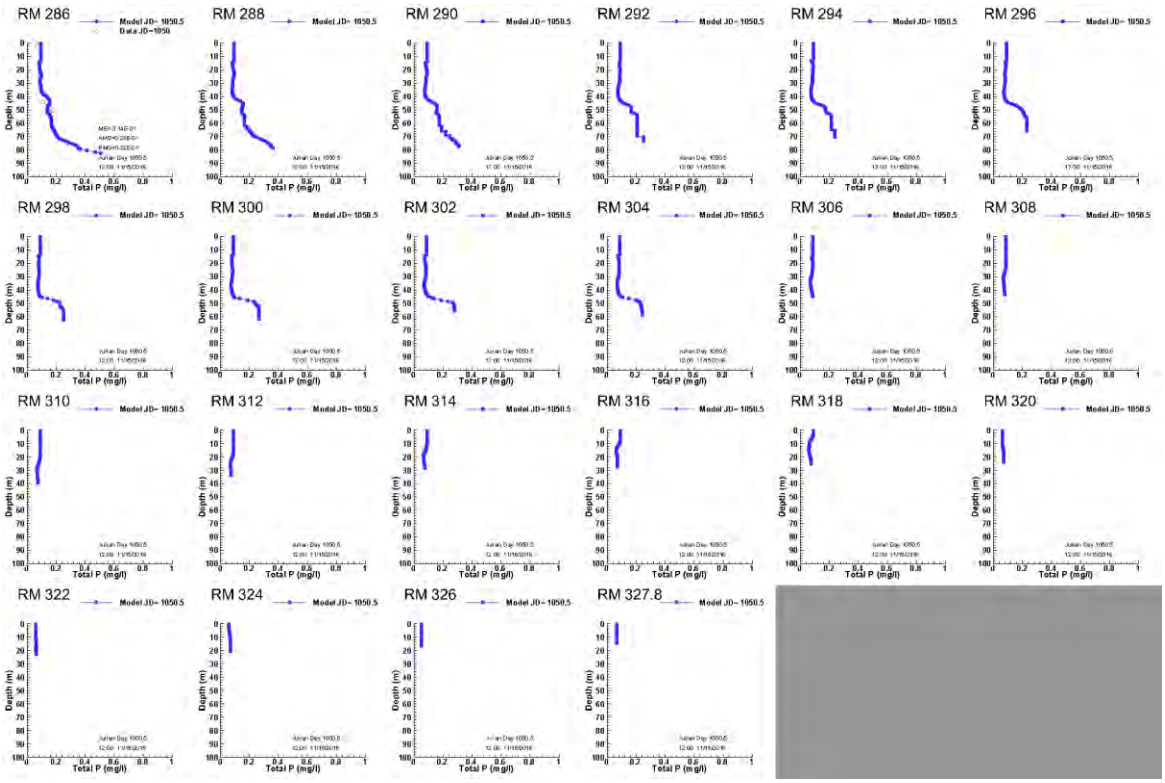


Figure 1931. Vertical profiles of TP compared with data for 11/15/2016.

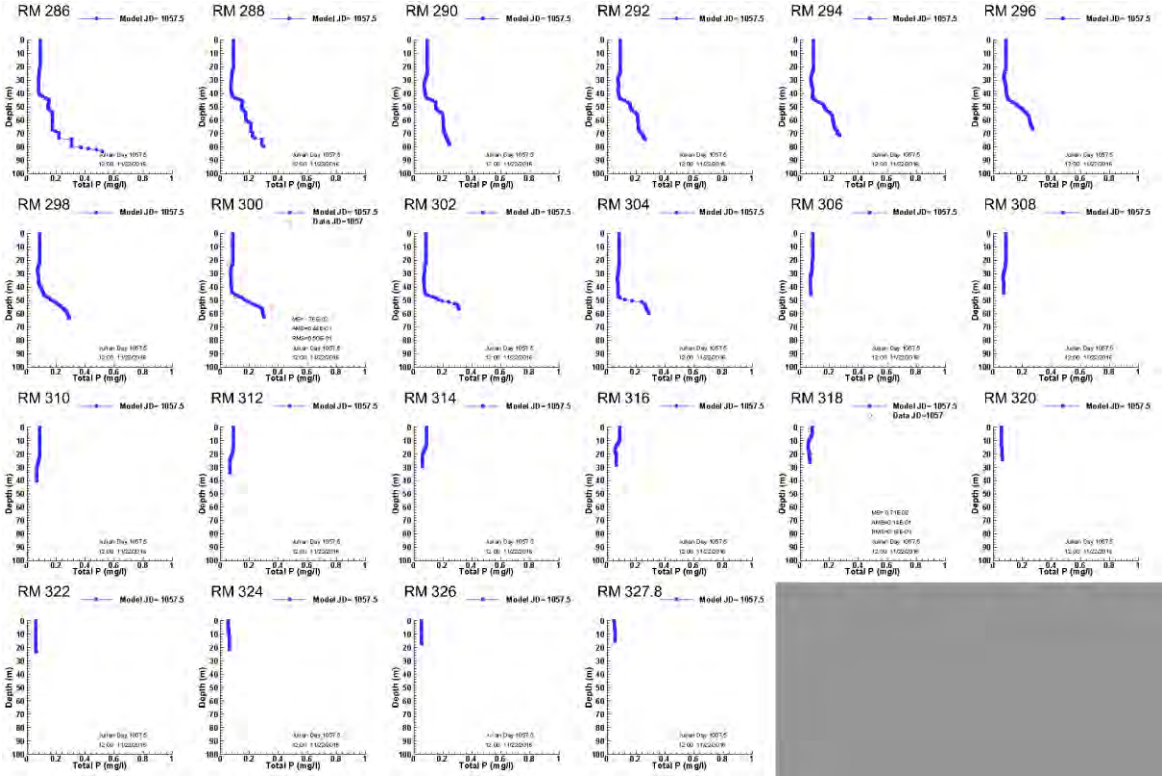


Figure 1932. Vertical profiles of TP compared with data for 11/22/2016.

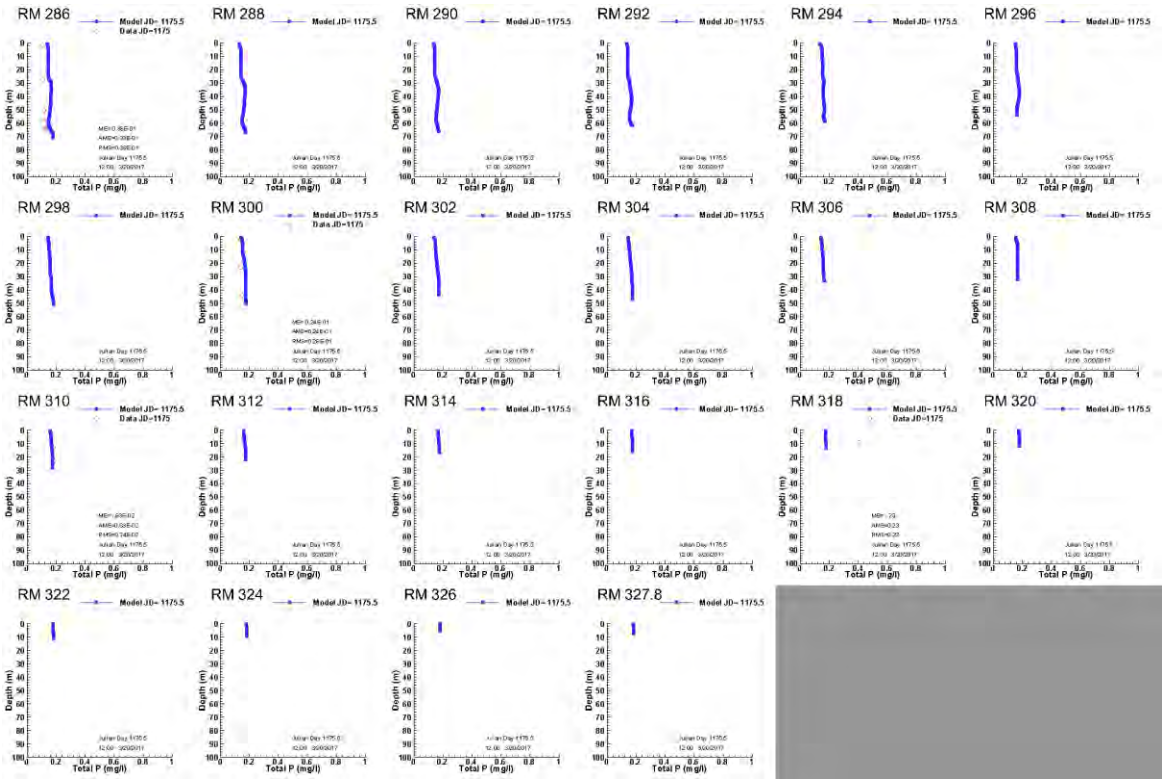


Figure 1933. Vertical profiles of TP compared with data for 3/20/2017.

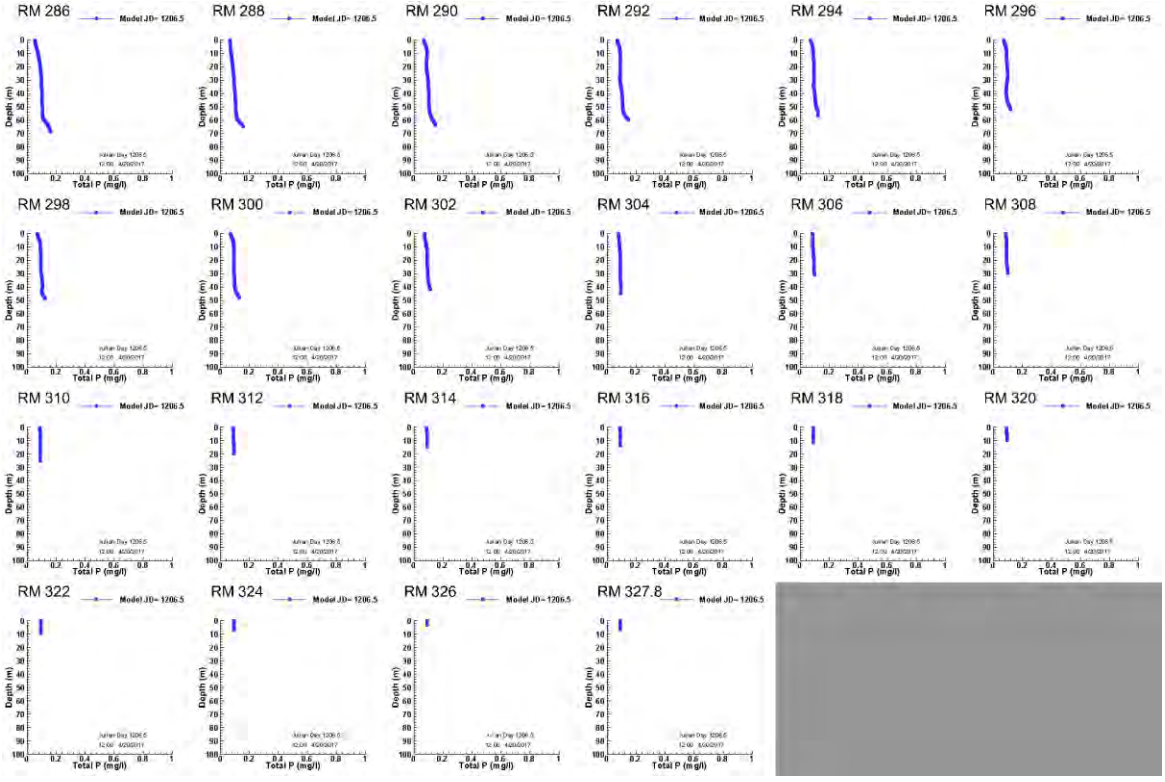


Figure 1934. Vertical profiles of TP compared with data for 4/20/2017.

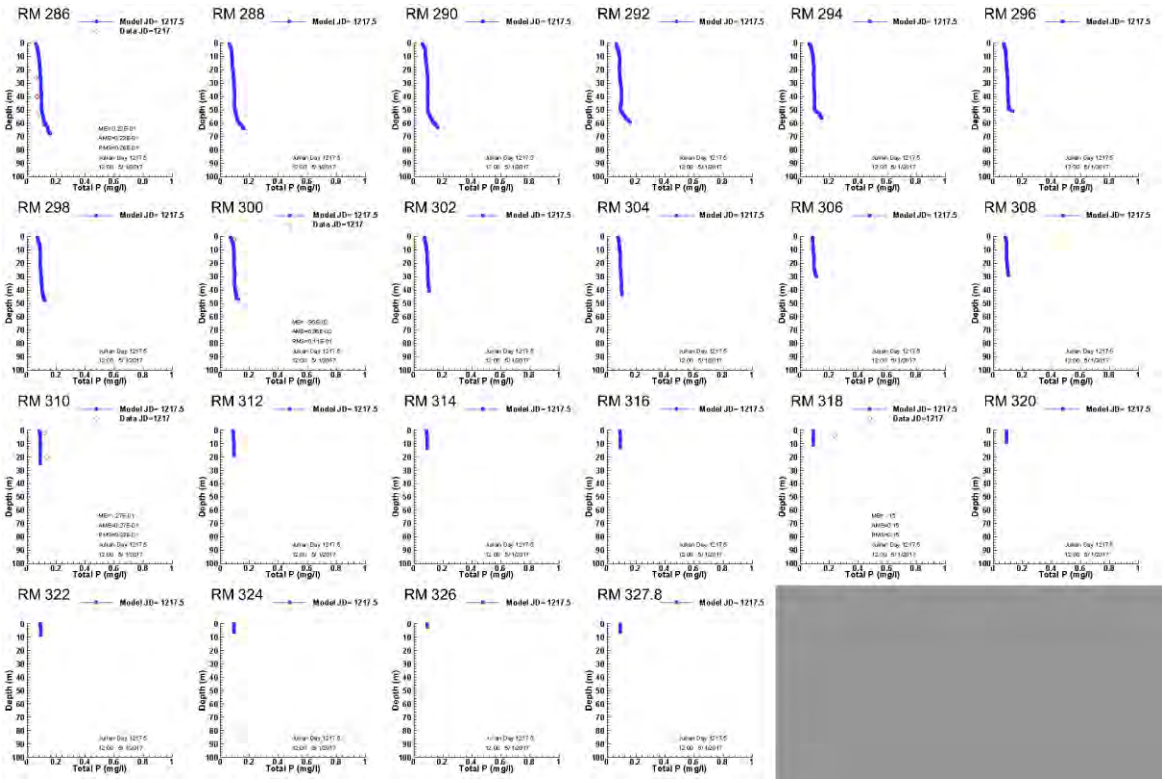


Figure 1935. Vertical profiles of TP compared with data for 5/ 1/2017.

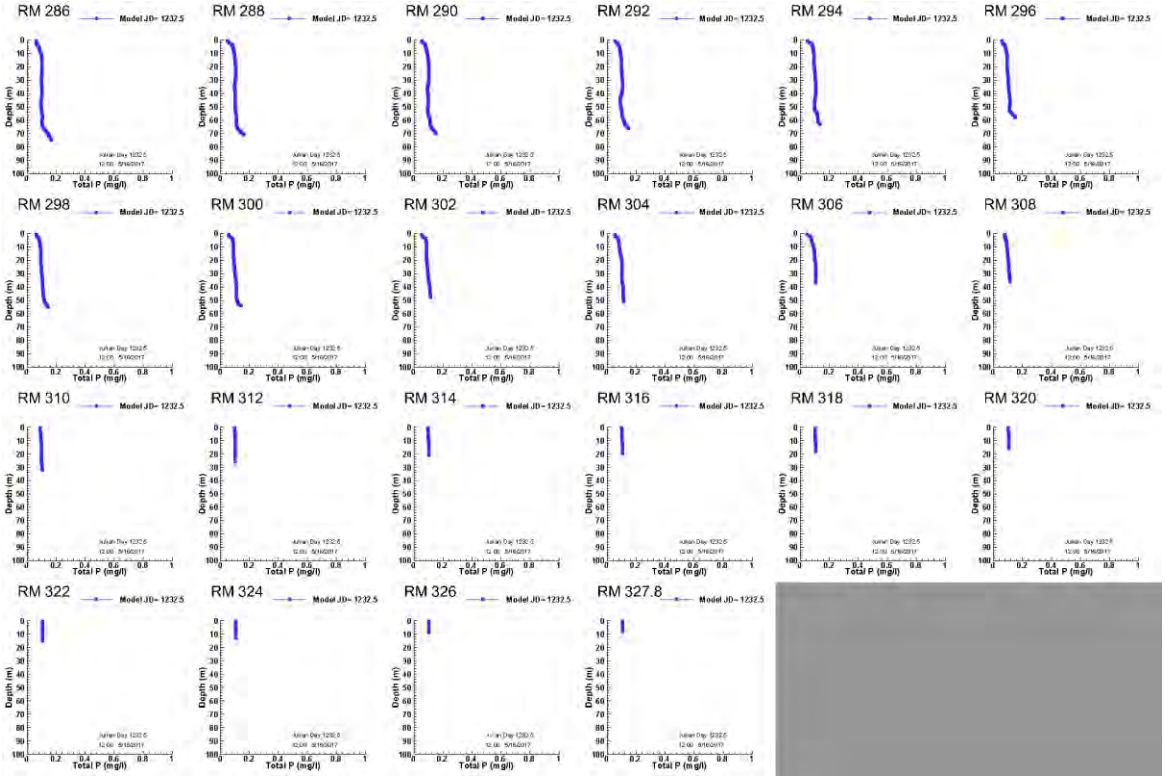


Figure 1936. Vertical profiles of TP compared with data for 5/16/2017.

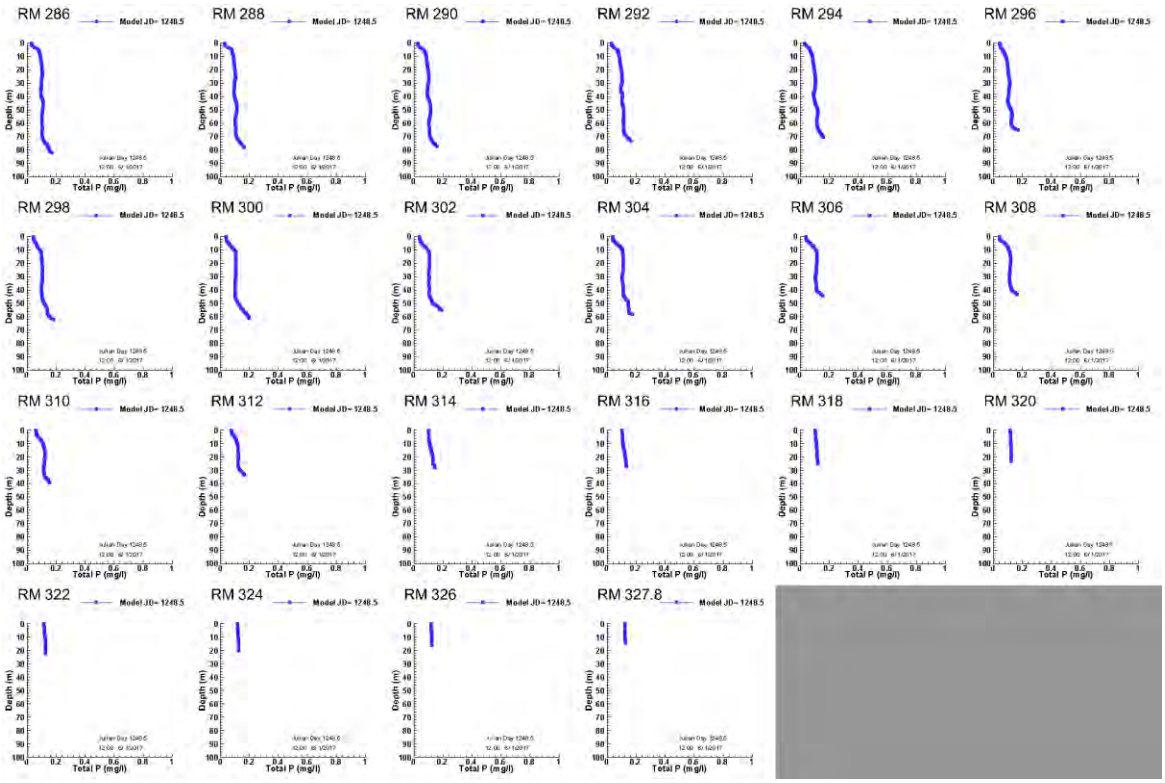


Figure 1937. Vertical profiles of TP compared with data for 6/ 1/2017.

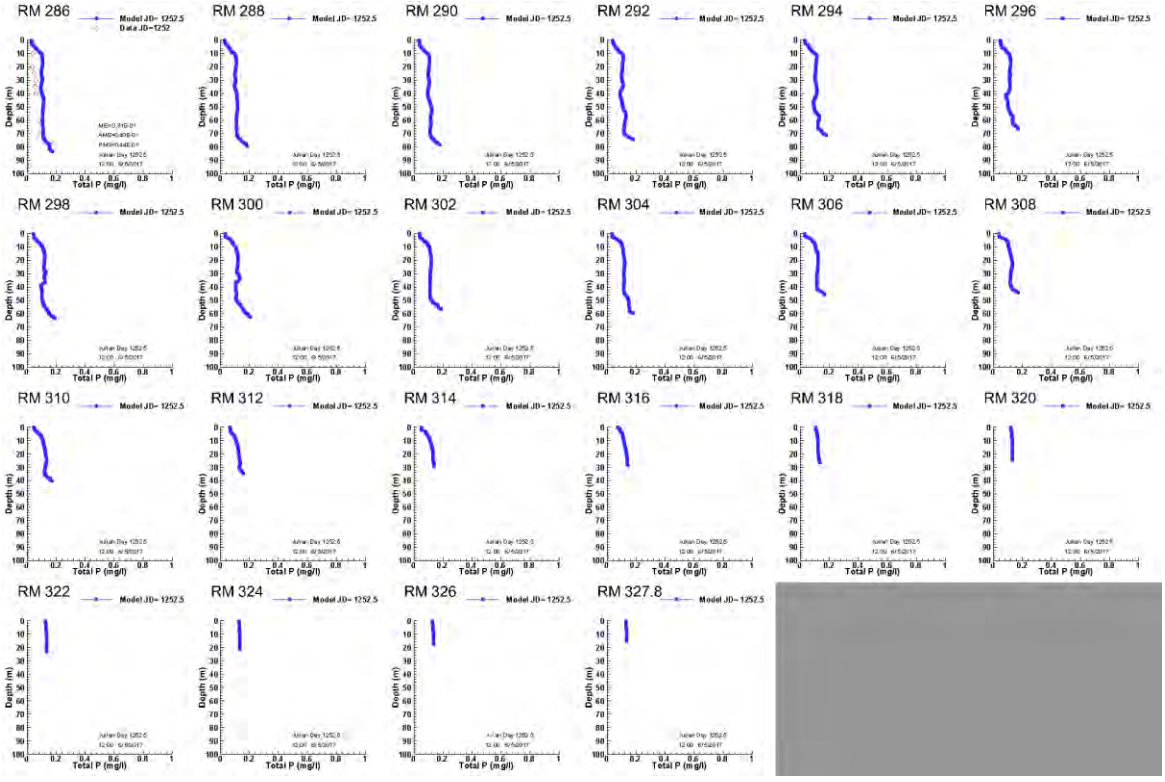


Figure 1938. Vertical profiles of TP compared with data for 6/ 5/2017.

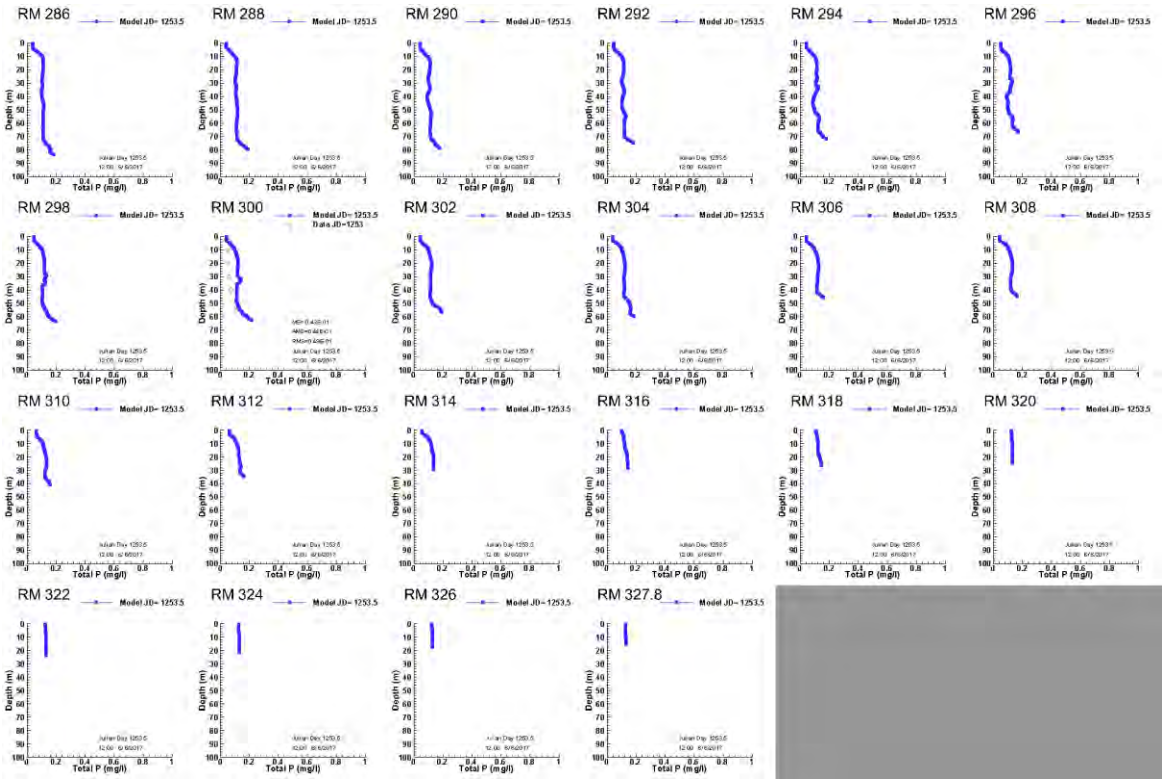


Figure 1939. Vertical profiles of TP compared with data for 6/ 6/2017.

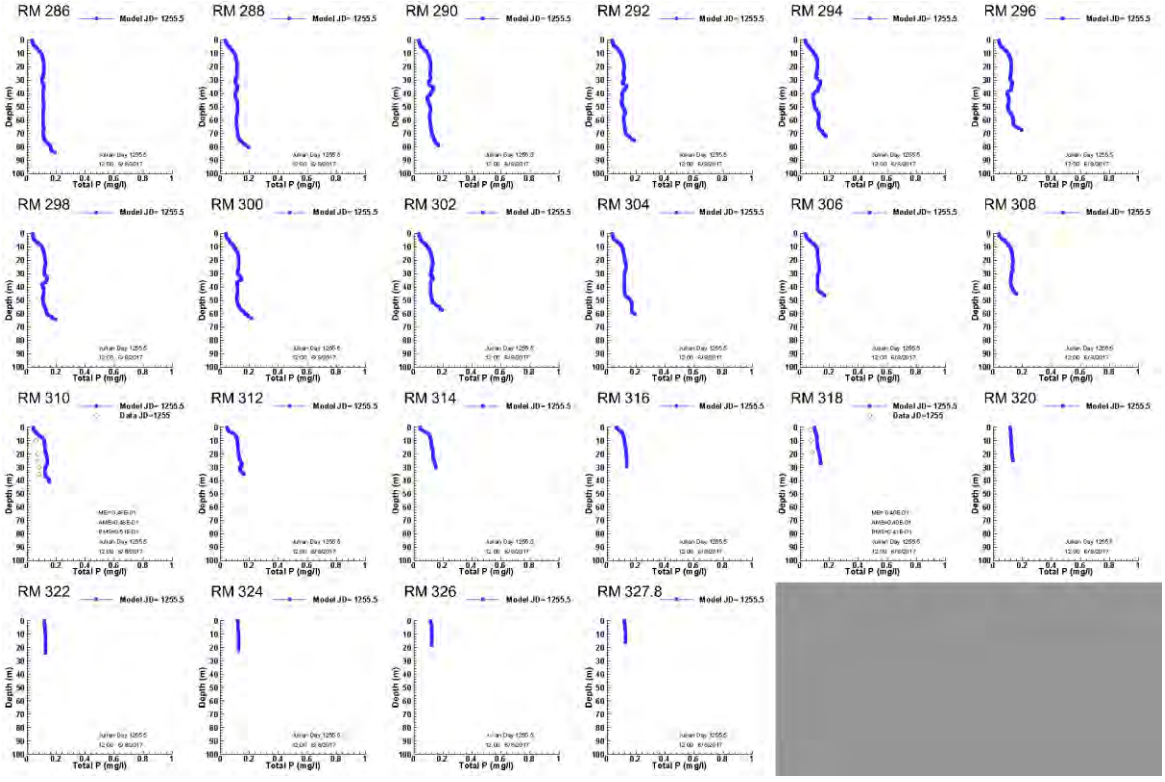


Figure 1940. Vertical profiles of TP compared with data for 6/ 8/2017.

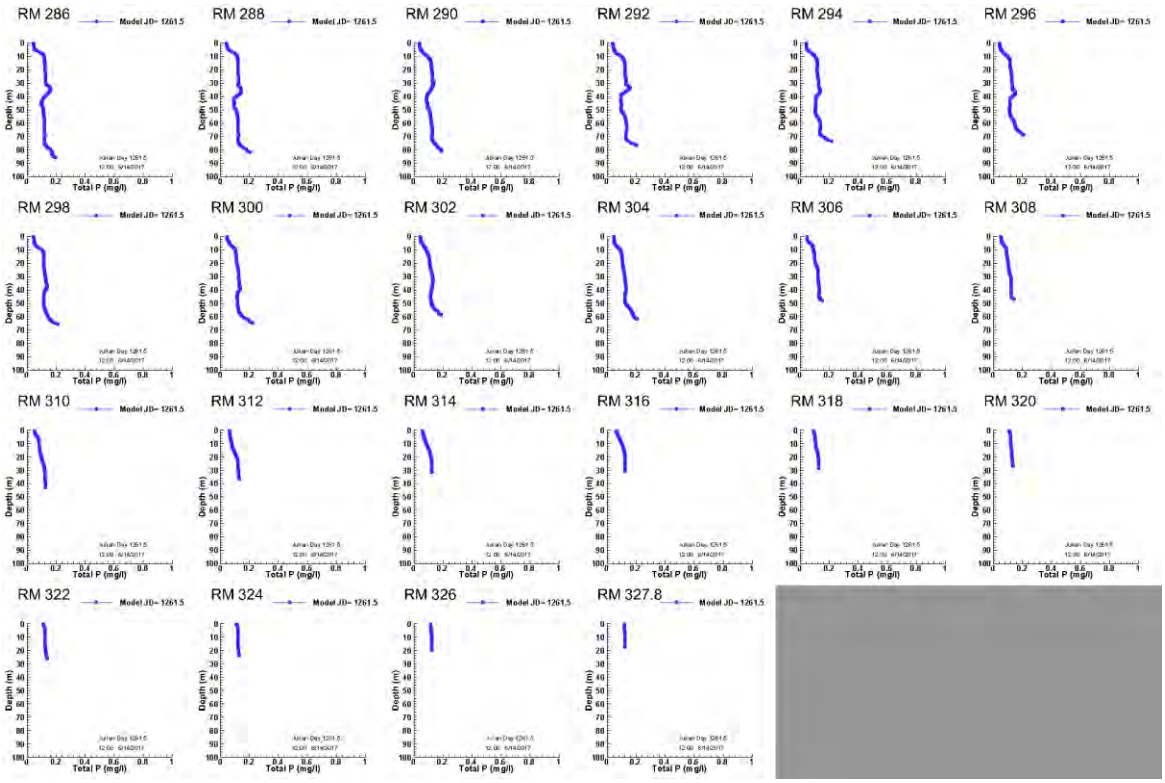


Figure 1941. Vertical profiles of TP compared with data for 6/14/2017.

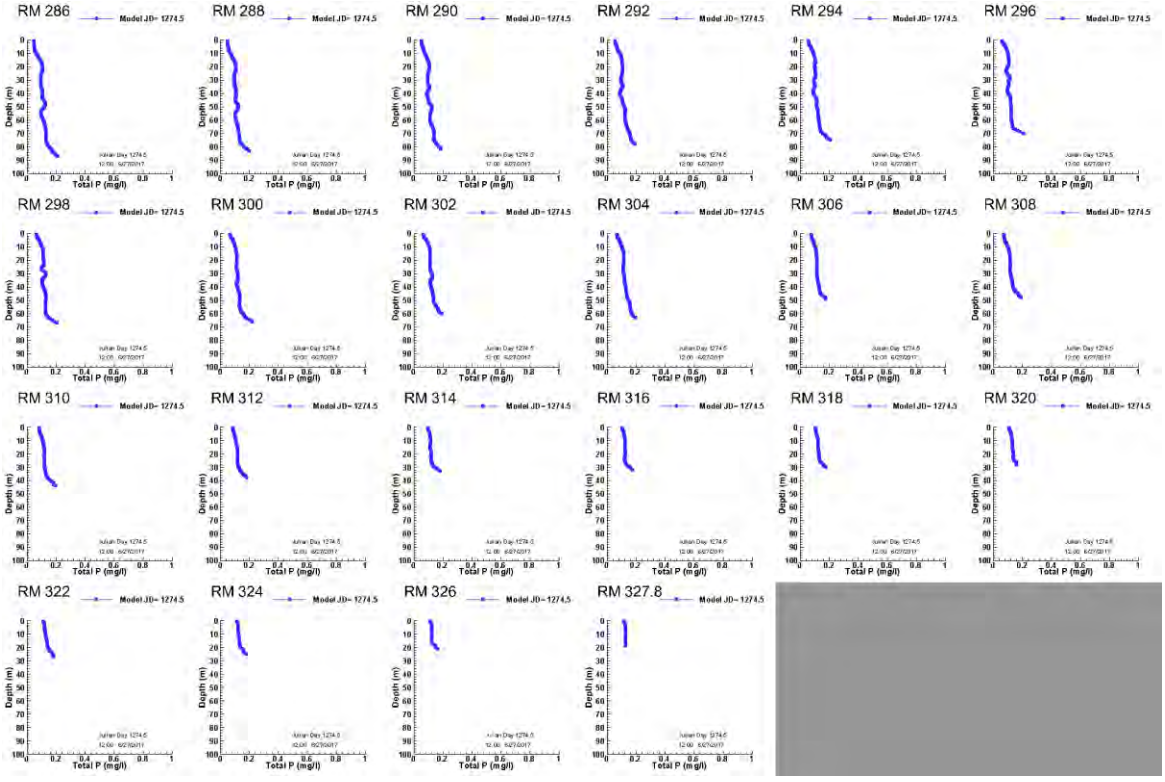


Figure 1942. Vertical profiles of TP compared with data for 6/27/2017.

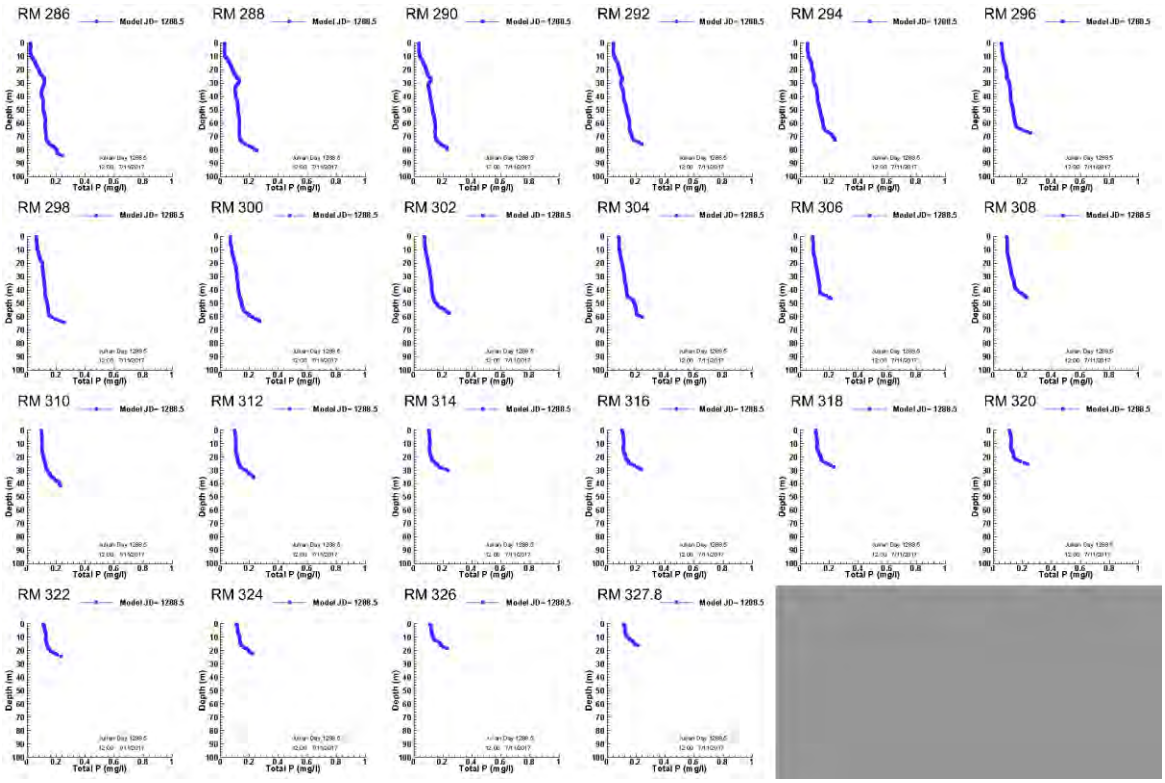


Figure 1943. Vertical profiles of TP compared with data for 7/11/2017.

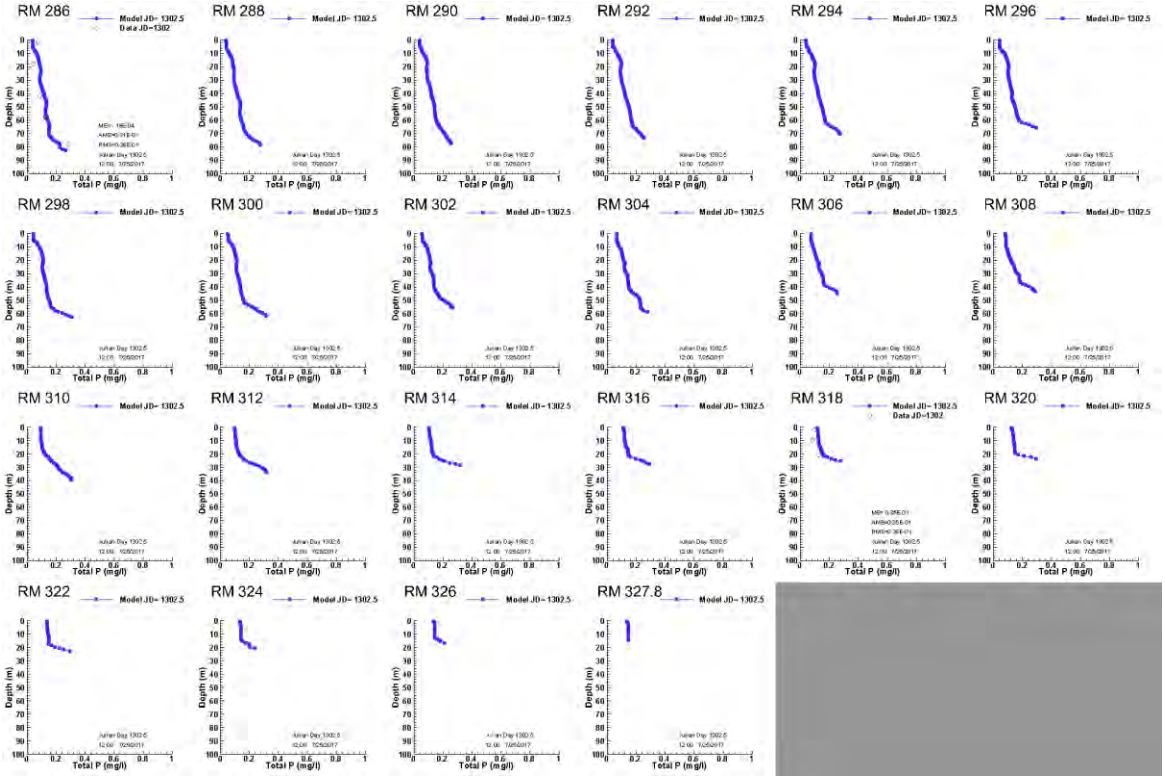


Figure 1944. Vertical profiles of TP compared with data for 7/25/2017.

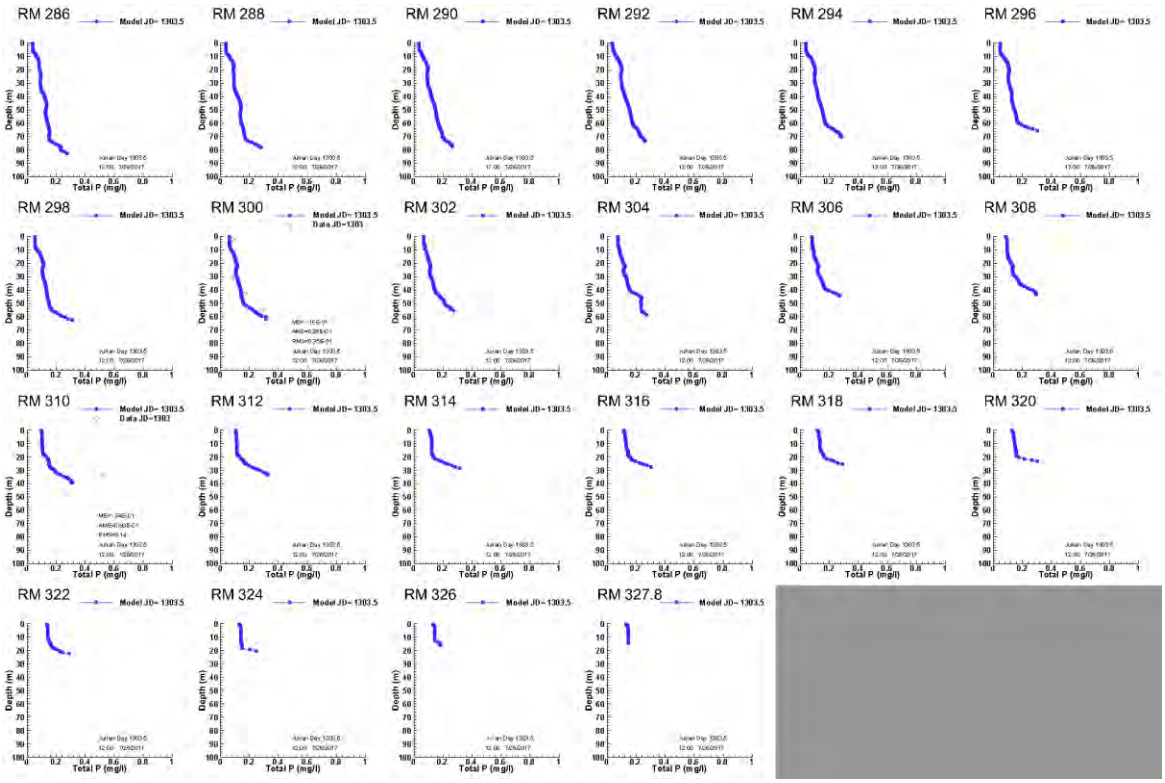


Figure 1945. Vertical profiles of TP compared with data for 7/26/2017.

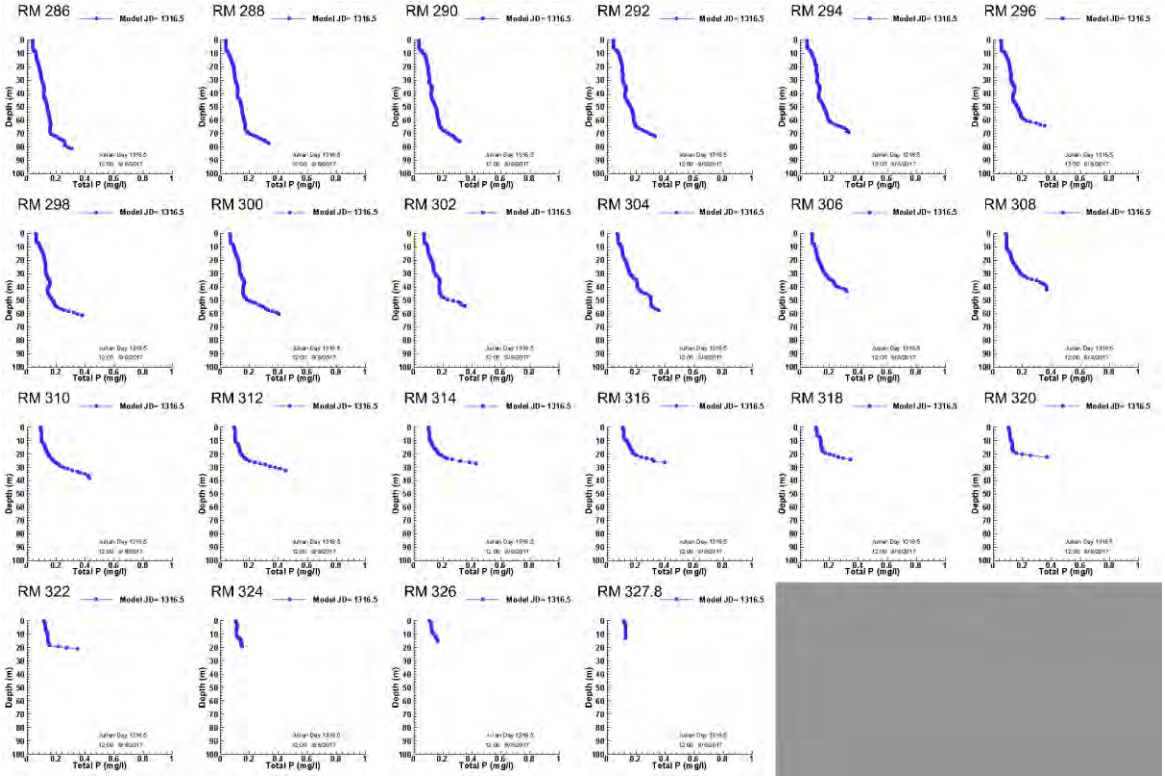


Figure 1946. Vertical profiles of TP compared with data for 8/ 8/2017.

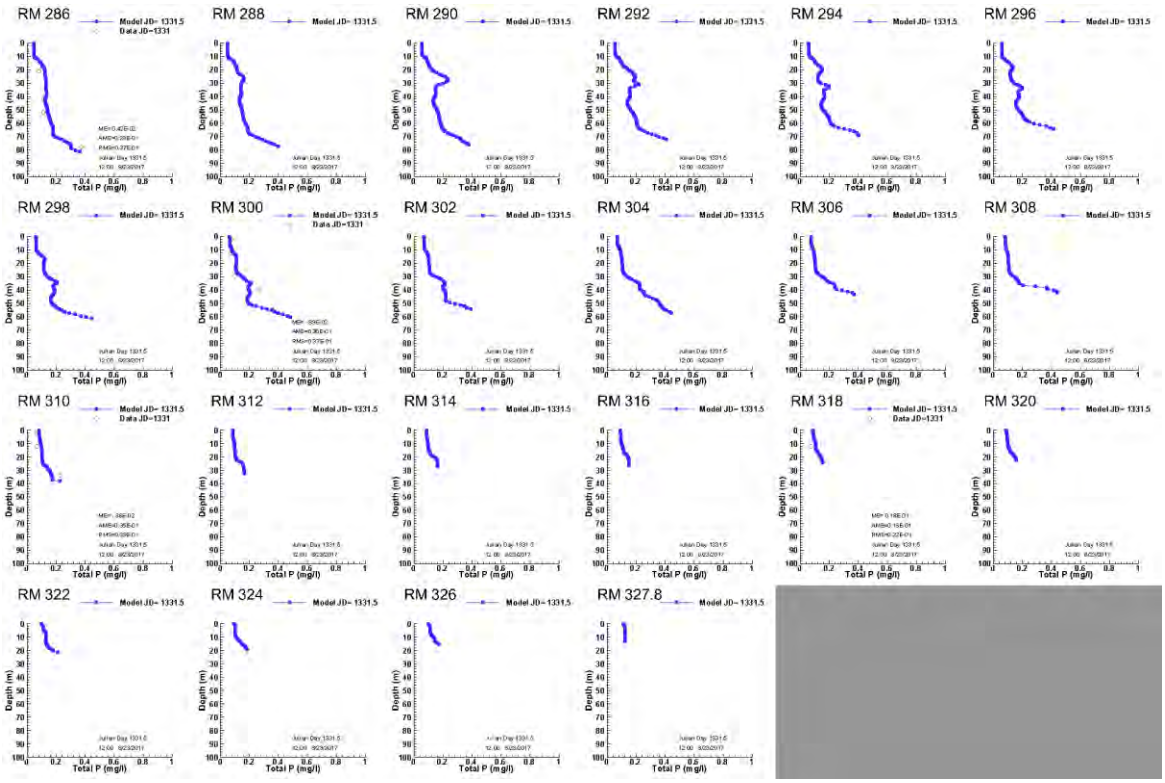


Figure 1947. Vertical profiles of TP compared with data for 8/23/2017.

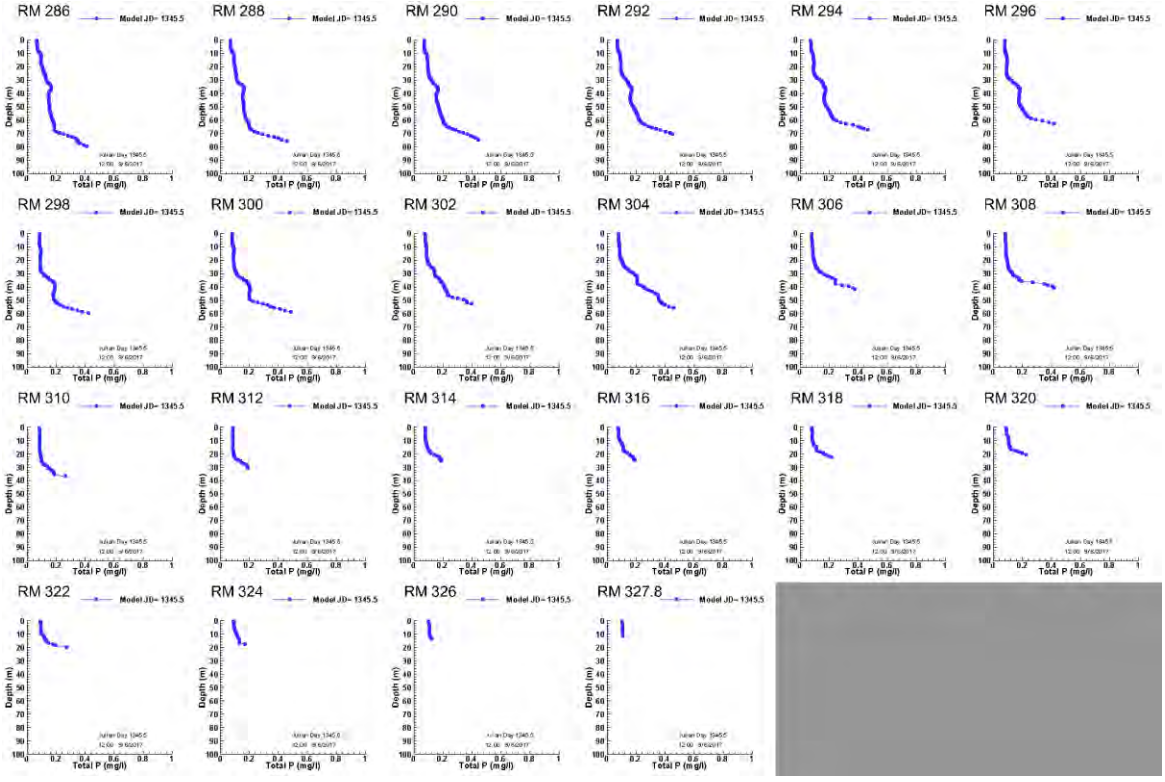


Figure 1948. Vertical profiles of TP compared with data for 9/ 6/2017.

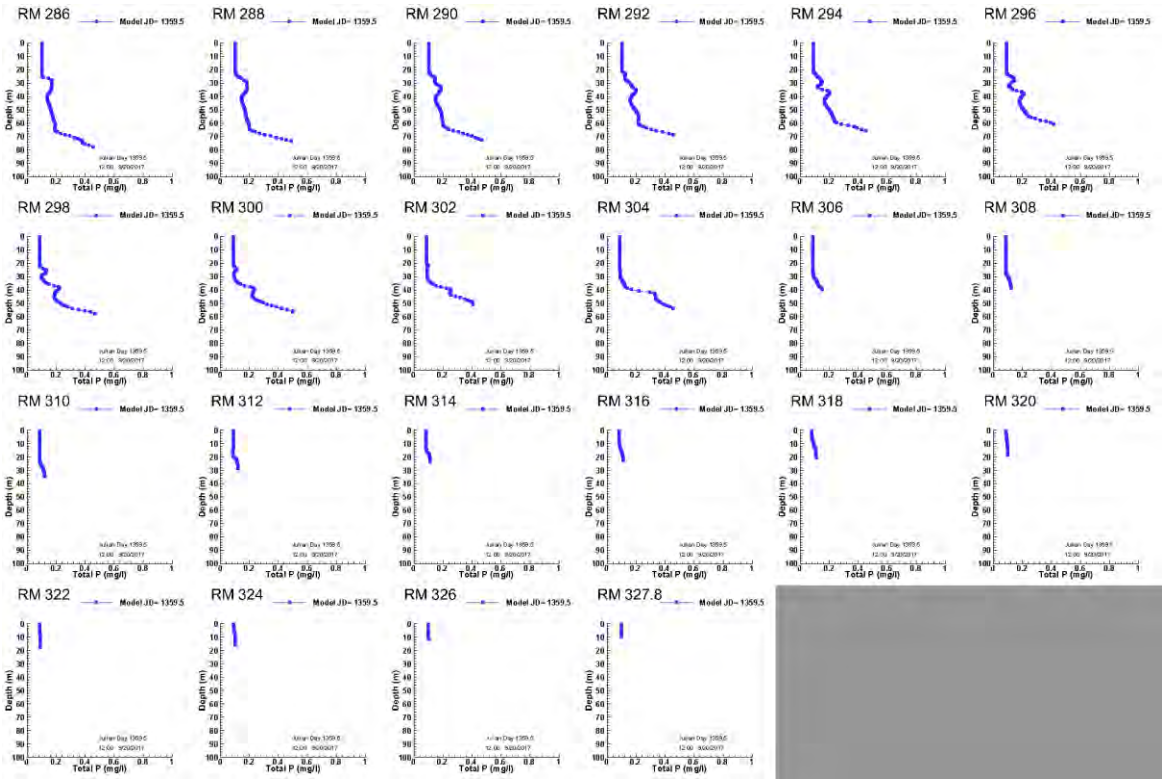


Figure 1949. Vertical profiles of TP compared with data for 9/20/2017.

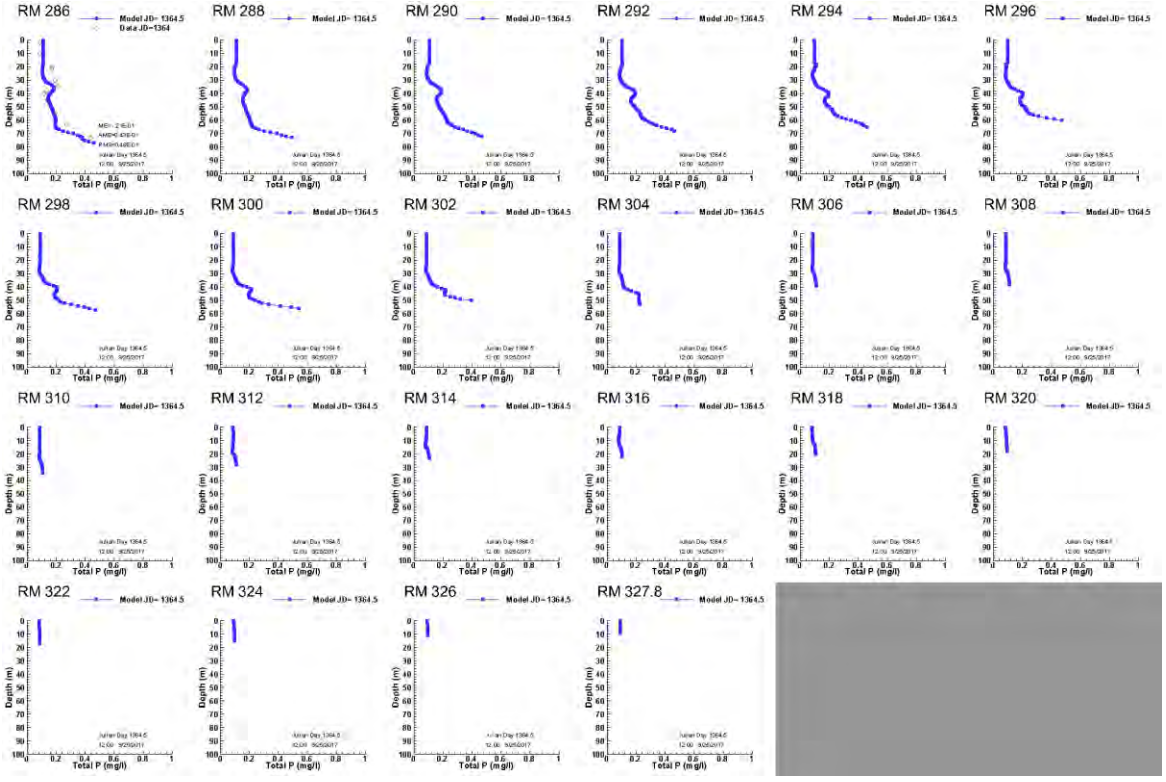


Figure 1950. Vertical profiles of TP compared with data for 9/25/2017.

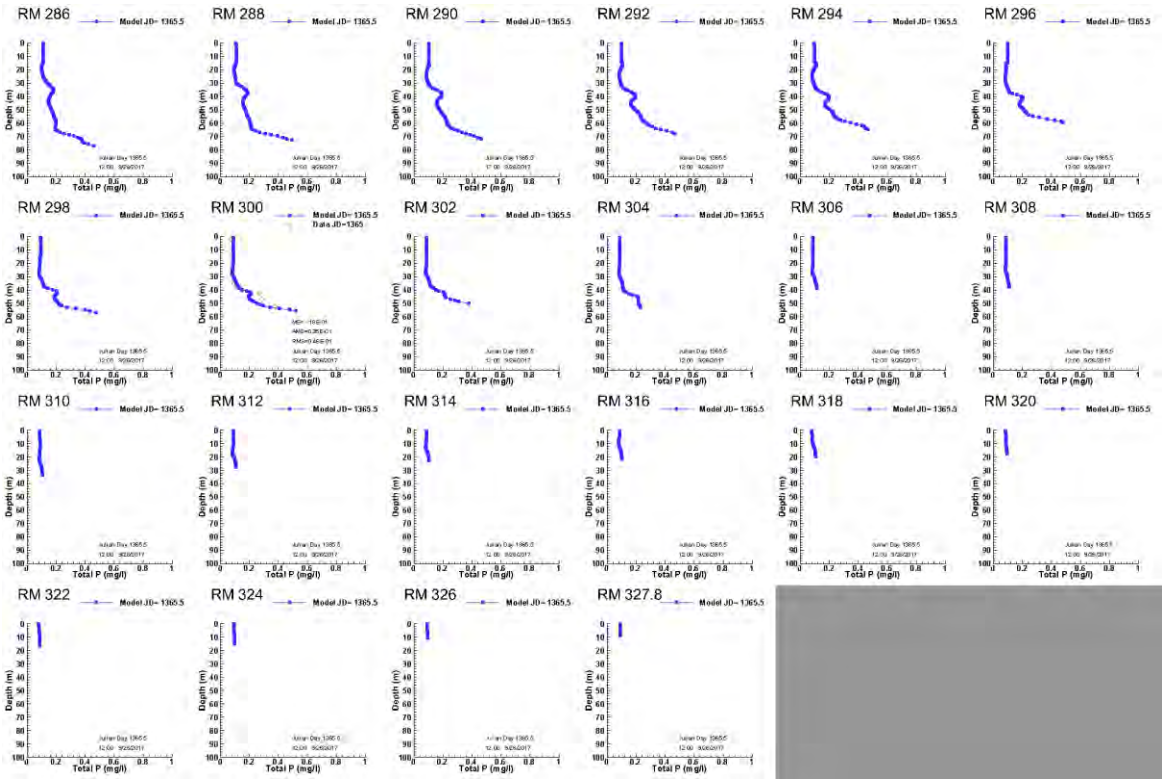


Figure 1951. Vertical profiles of TP compared with data for 9/26/2017.

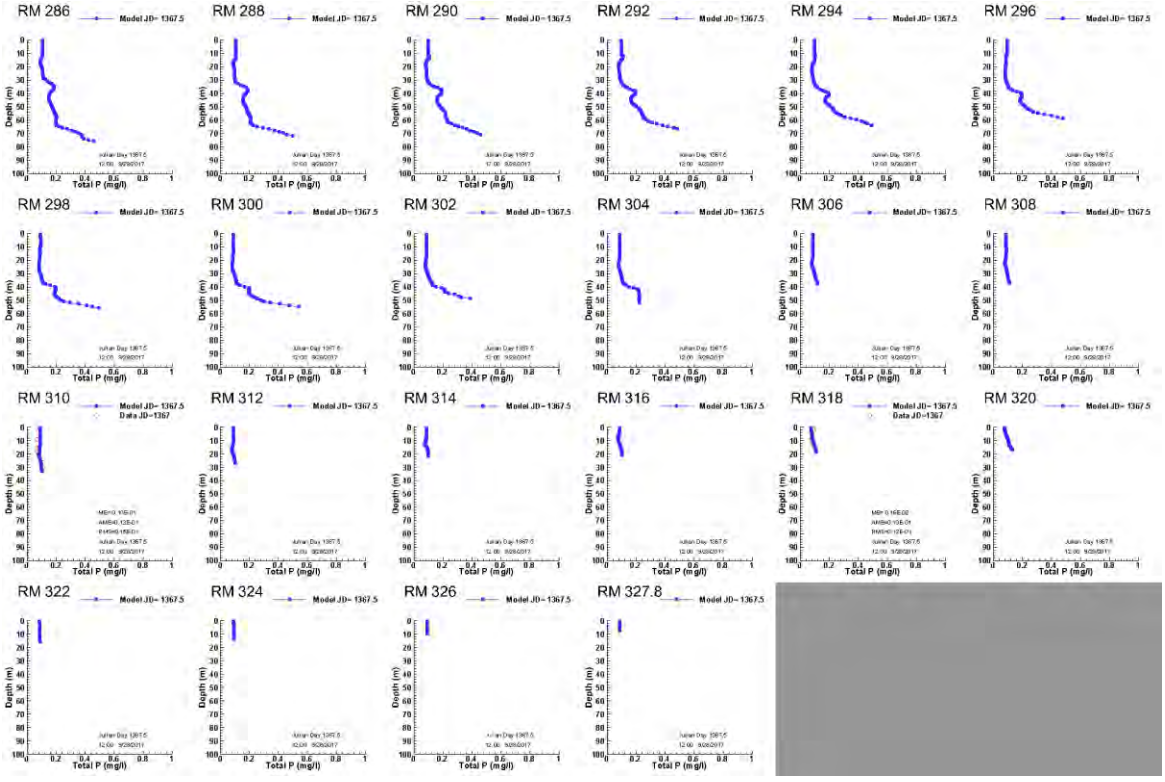


Figure 1952. Vertical profiles of TP compared with data for 9/28/2017.

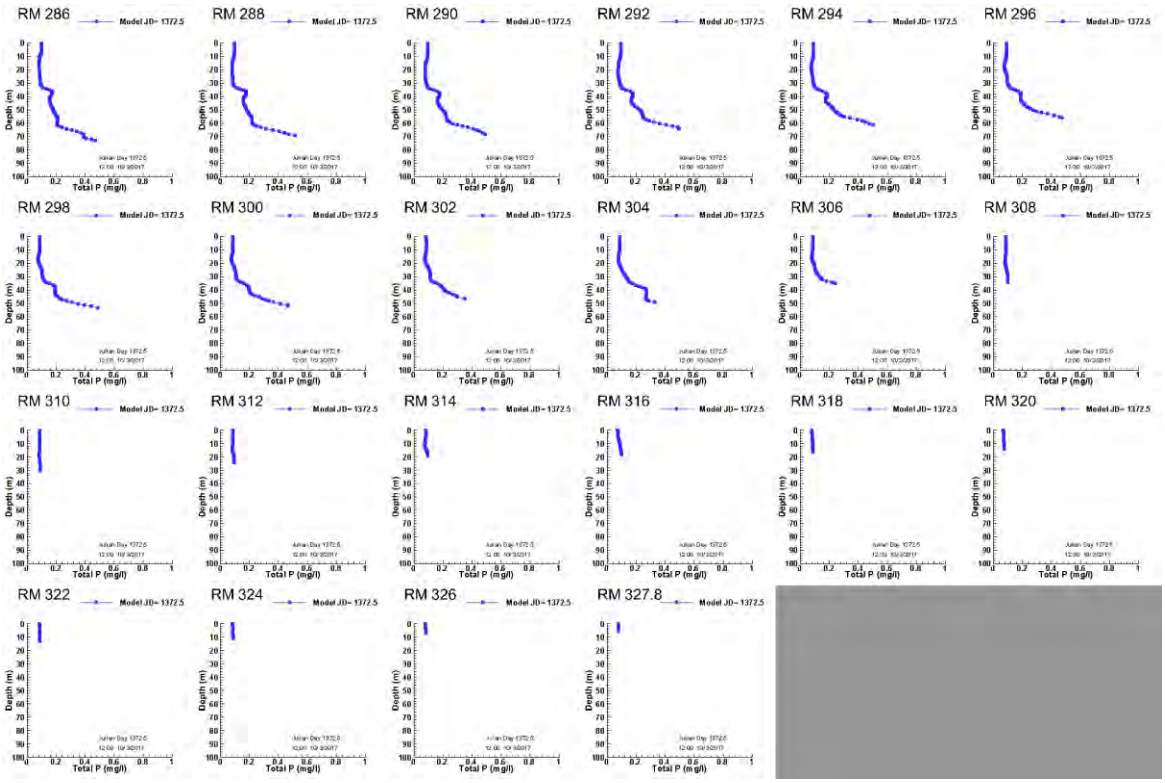


Figure 1953. Vertical profiles of TP compared with data for 10/ 3/2017.

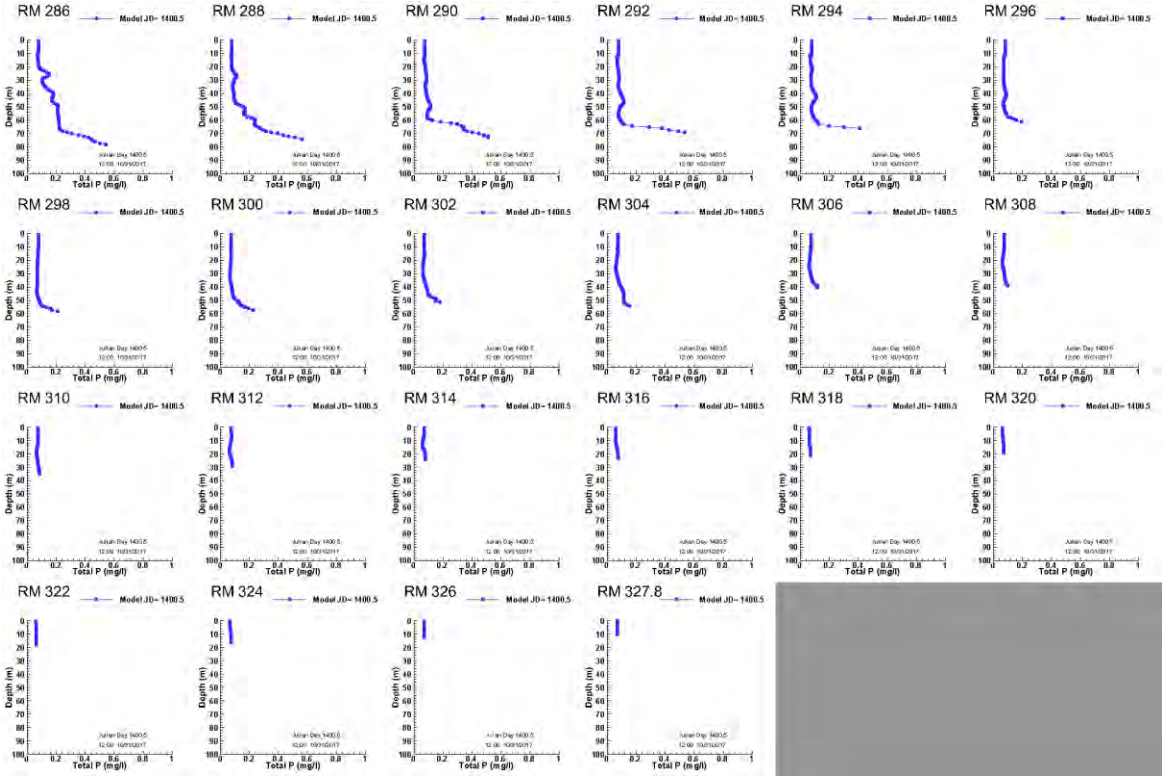


Figure 1954. Vertical profiles of TP compared with data for 10/31/2017.

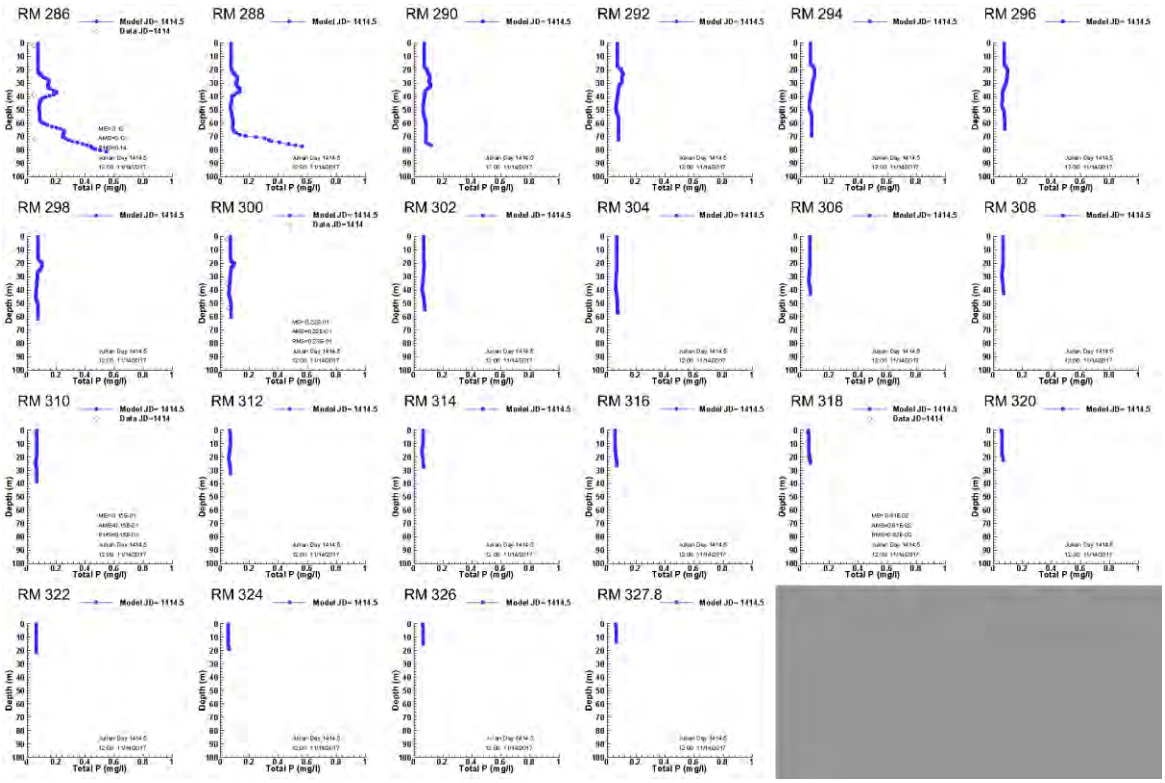


Figure 1955. Vertical profiles of TP compared with data for 11/14/2017.

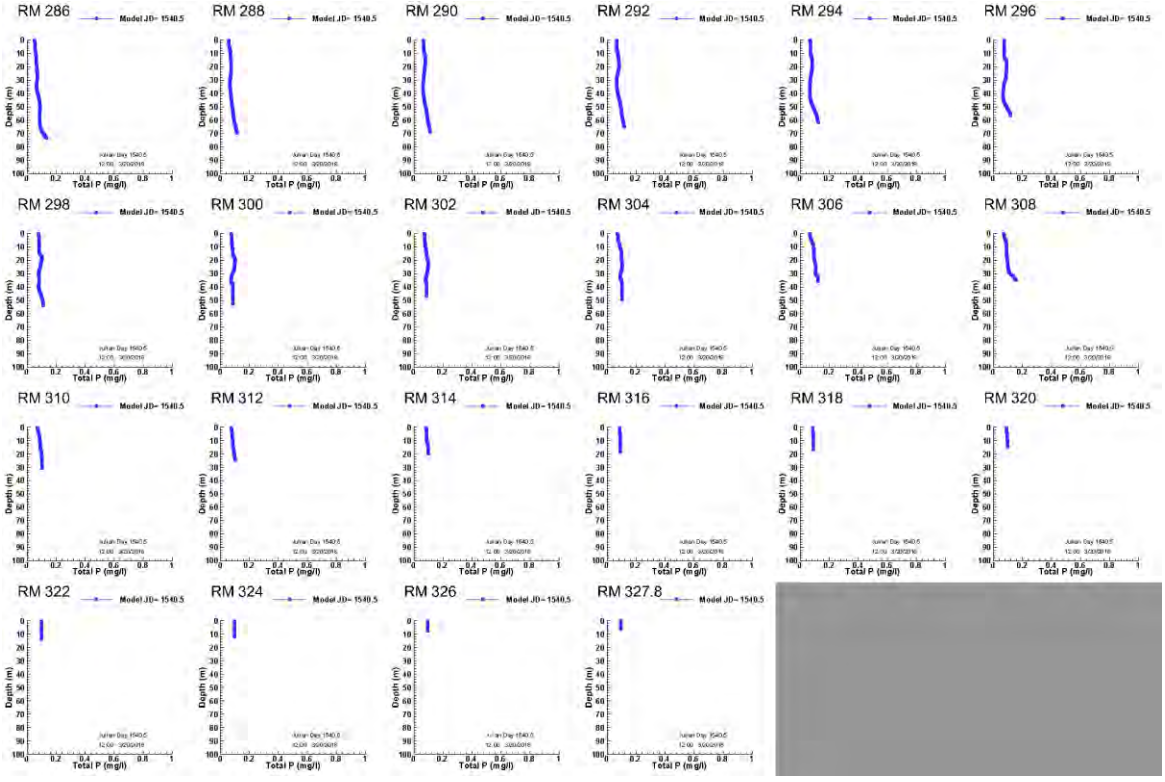


Figure 1956. Vertical profiles of TP compared with data for 3/20/2018.

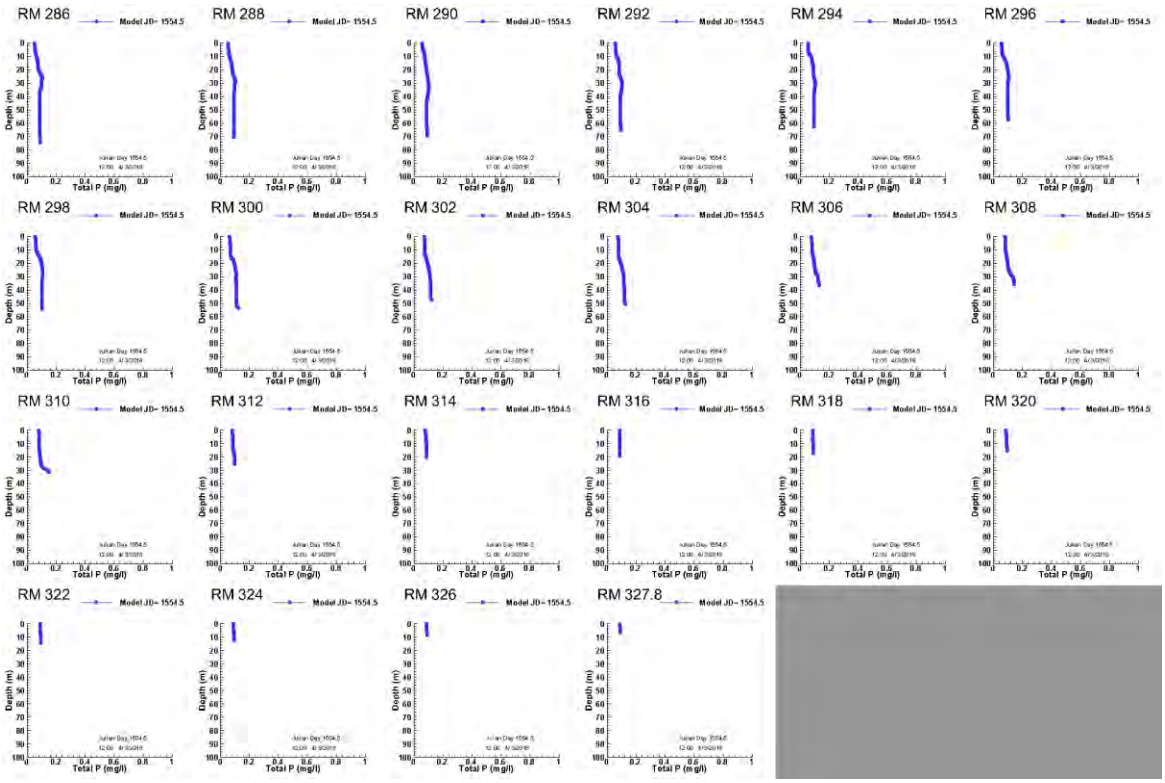


Figure 1957. Vertical profiles of TP compared with data for 4/ 3/2018.

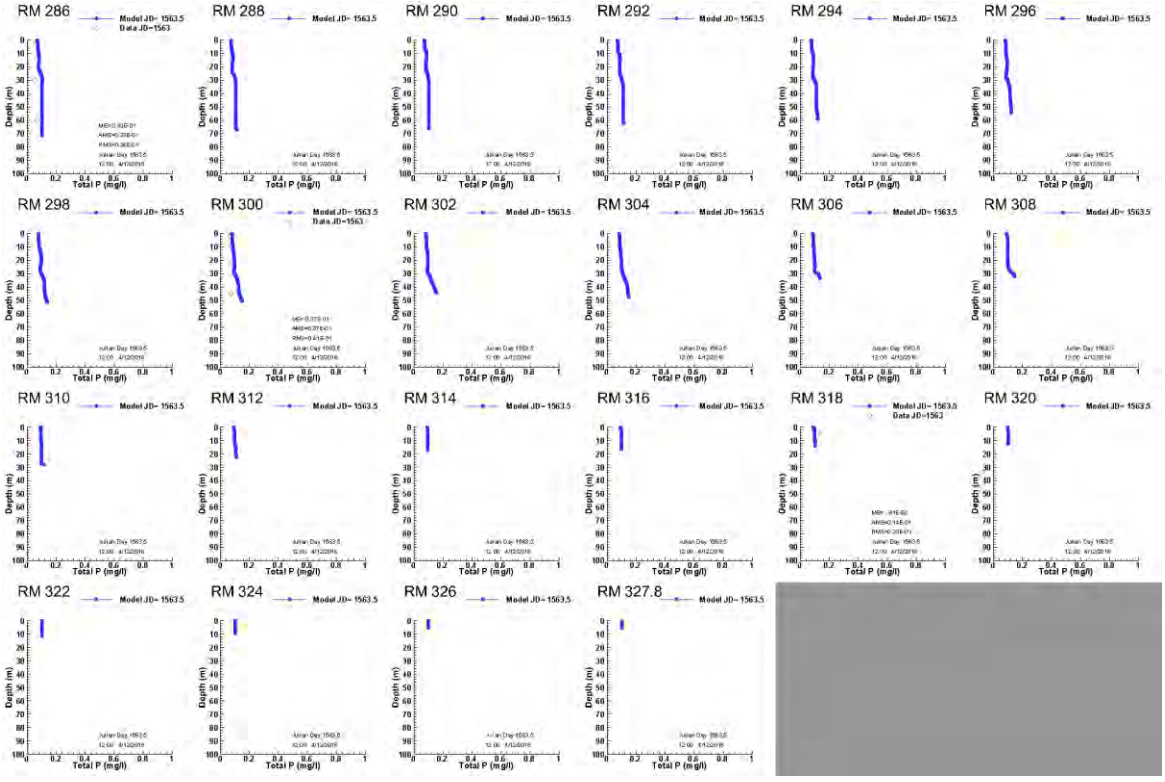


Figure 1958. Vertical profiles of TP compared with data for 4/12/2018.

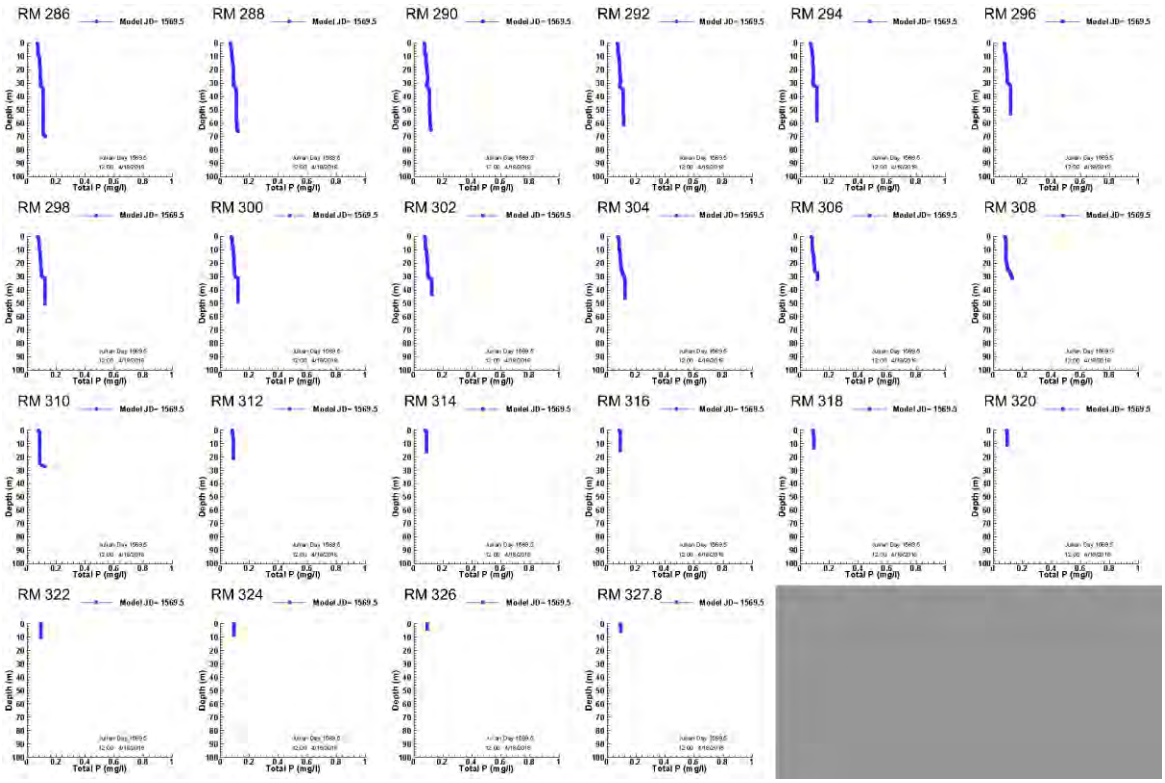


Figure 1959. Vertical profiles of TP compared with data for 4/18/2018.

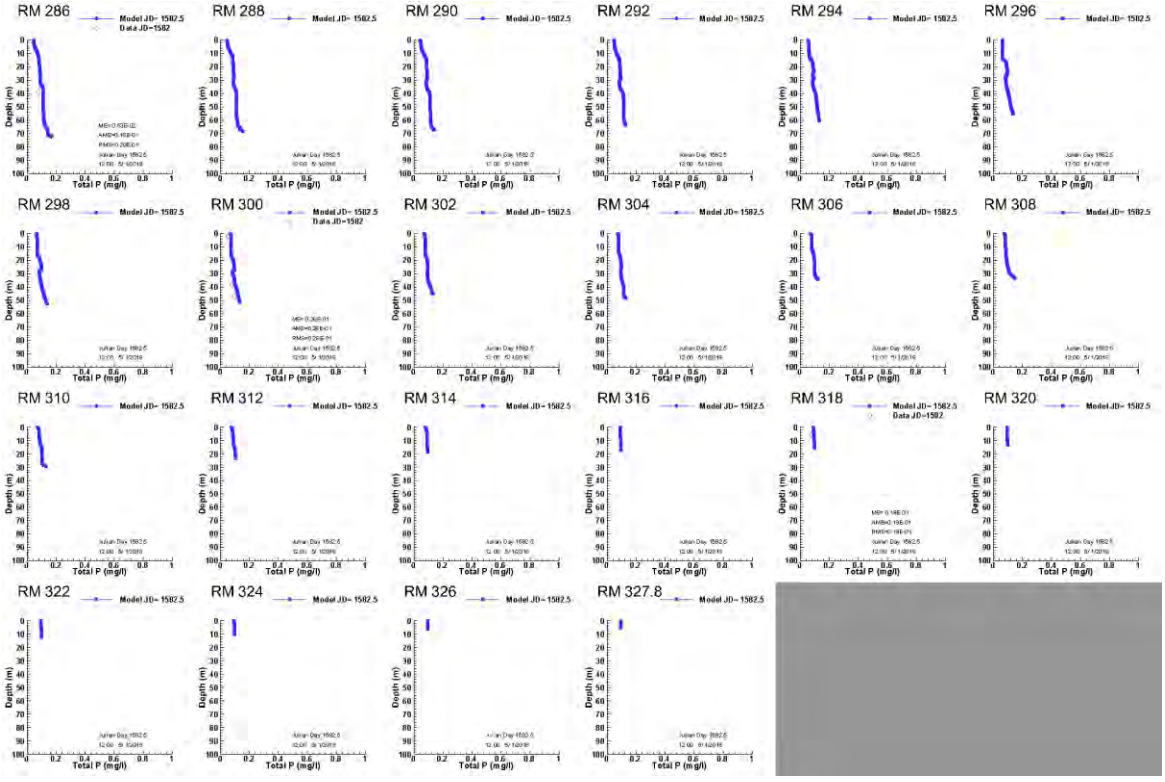


Figure 1960. Vertical profiles of TP compared with data for 5/ 1/2018.

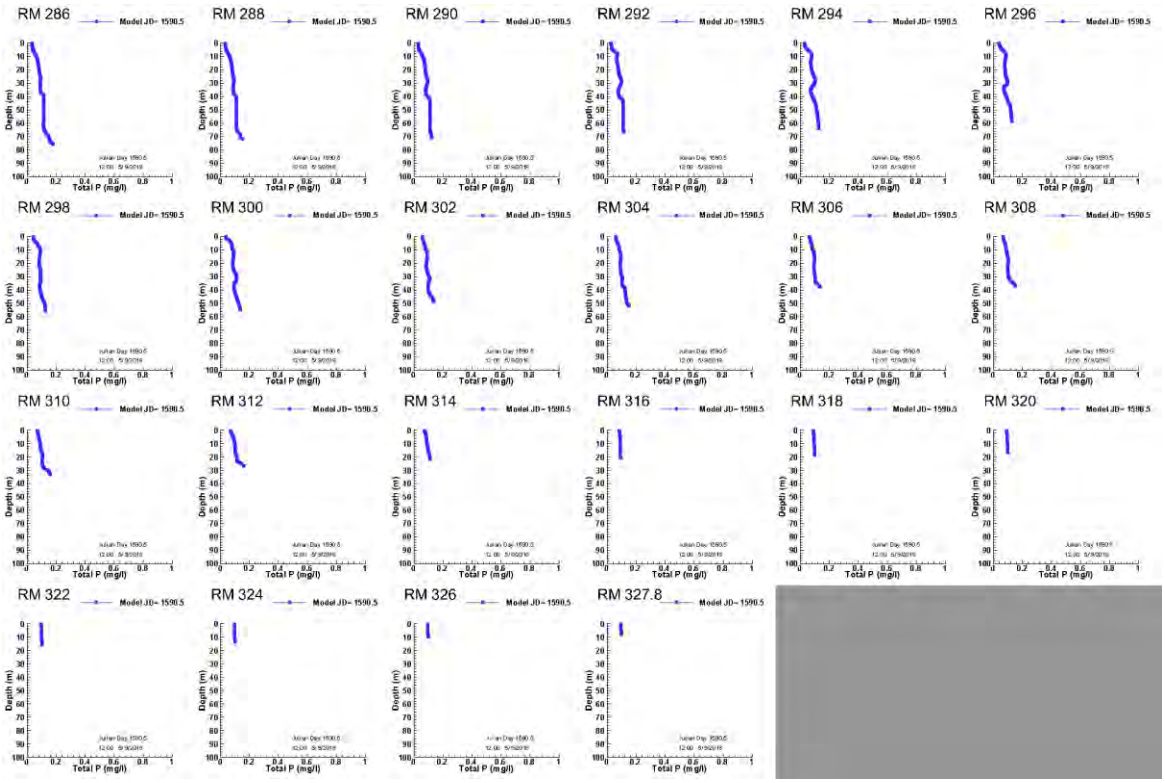


Figure 1961. Vertical profiles of TP compared with data for 5/ 9/2018.

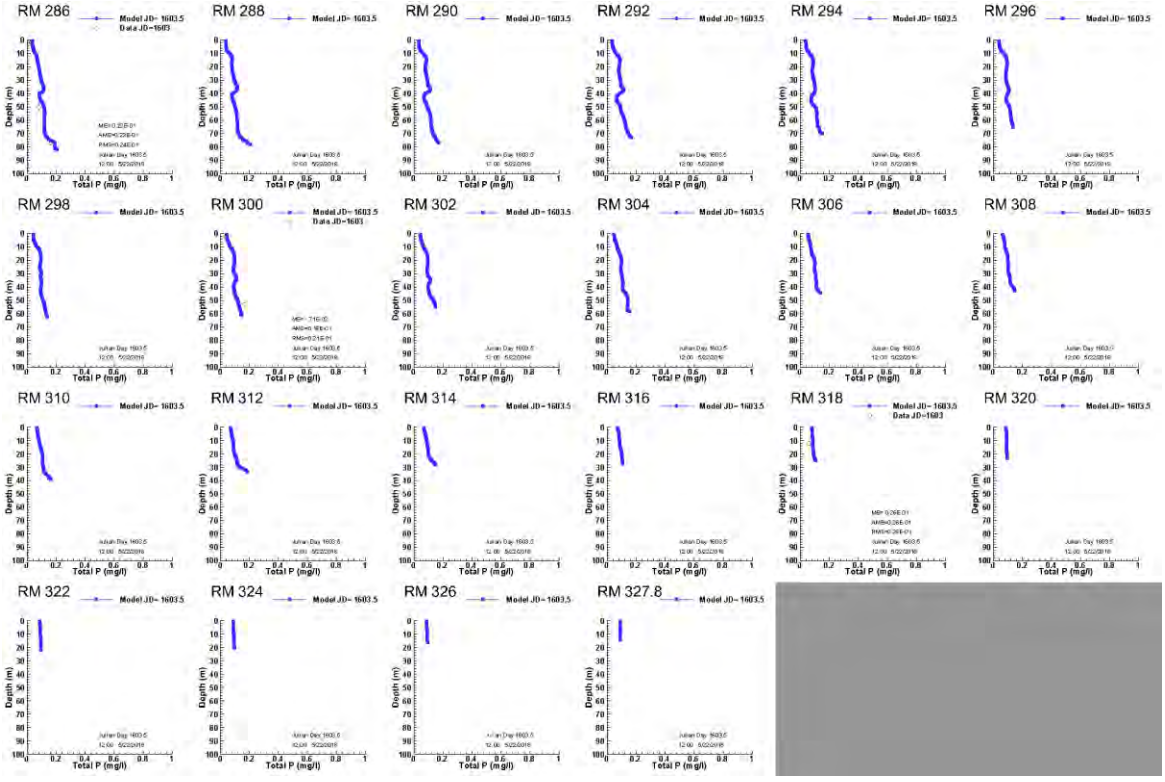


Figure 1962. Vertical profiles of TP compared with data for 5/22/2018.

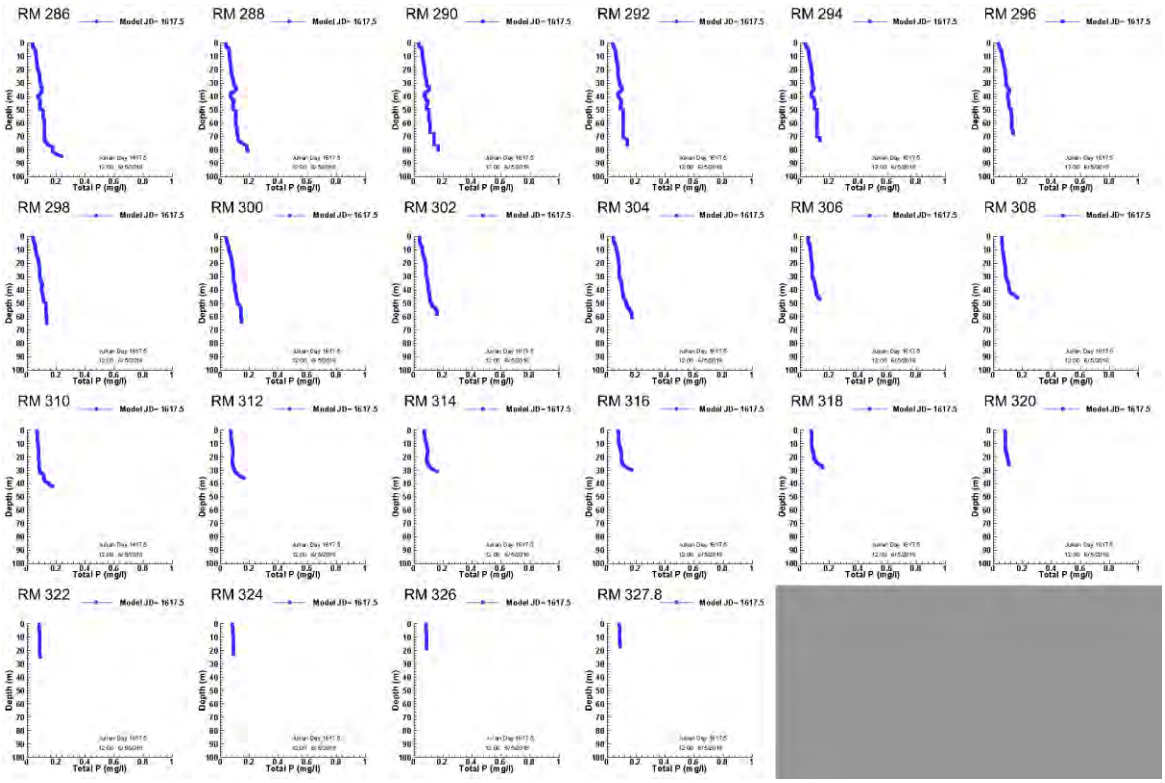


Figure 1963. Vertical profiles of TP compared with data for 6/ 5/2018.

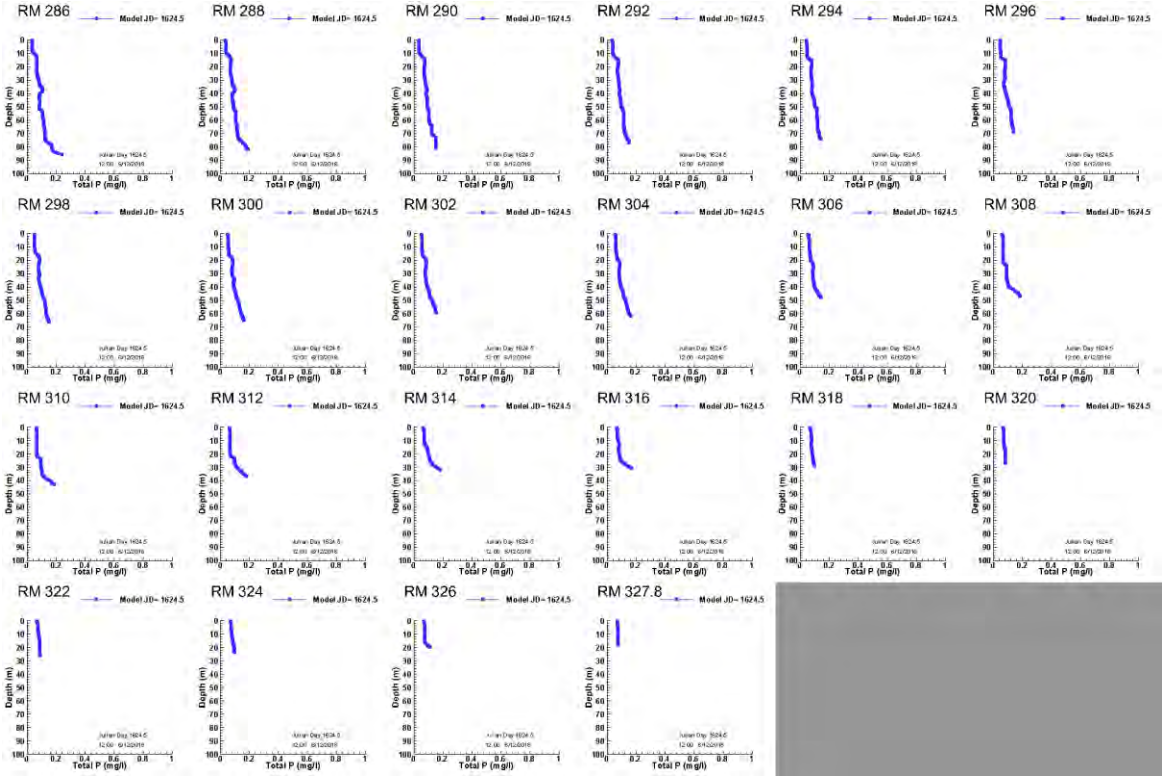


Figure 1964. Vertical profiles of TP compared with data for 6/12/2018.

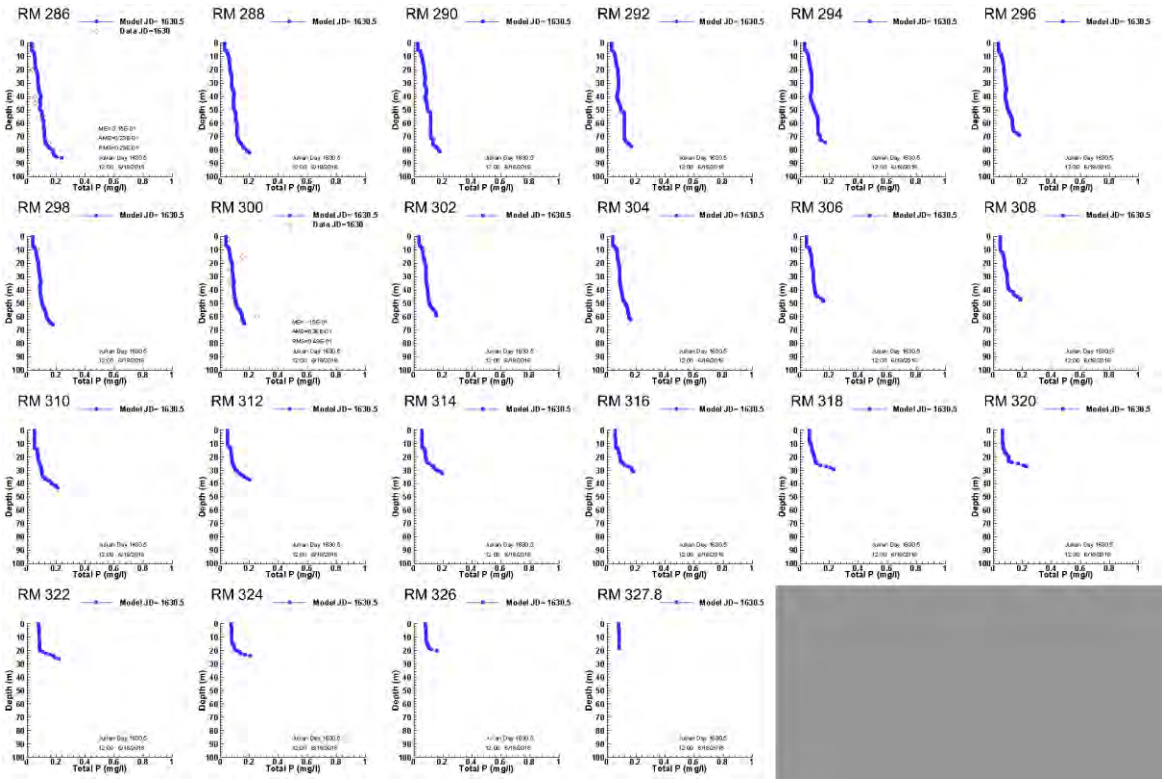


Figure 1965. Vertical profiles of TP compared with data for 6/18/2018.

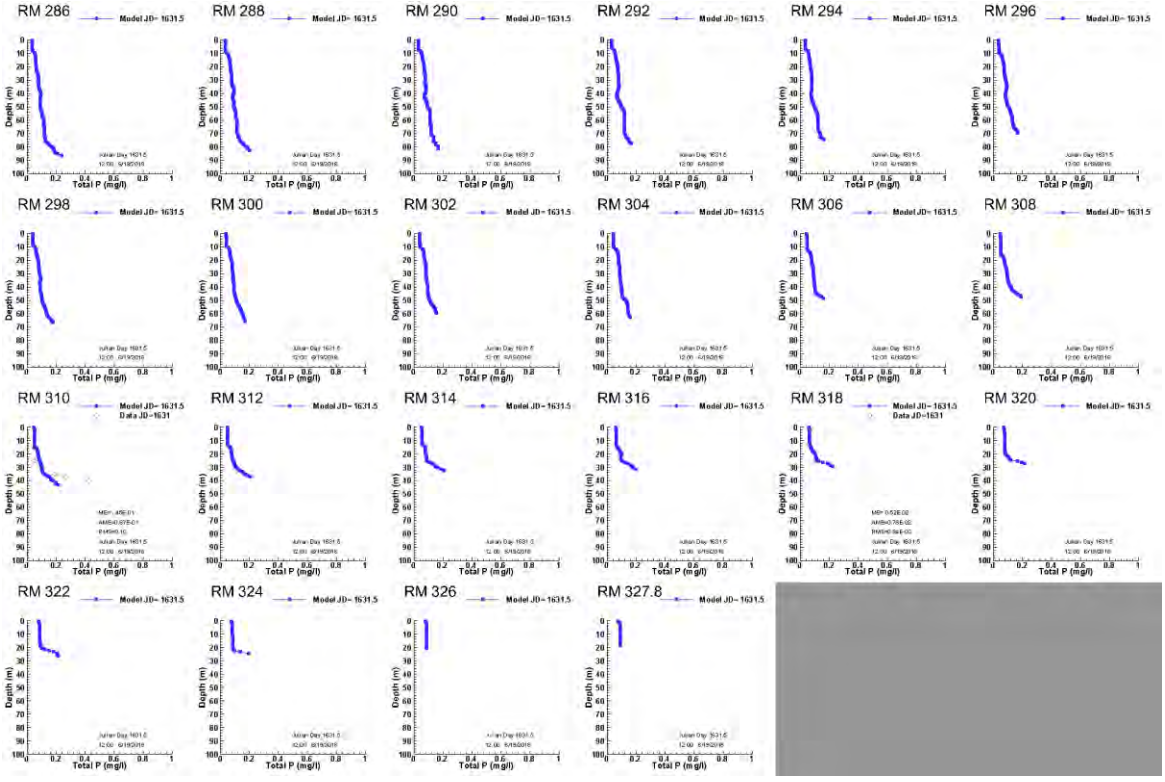


Figure 1966. Vertical profiles of TP compared with data for 6/19/2018.

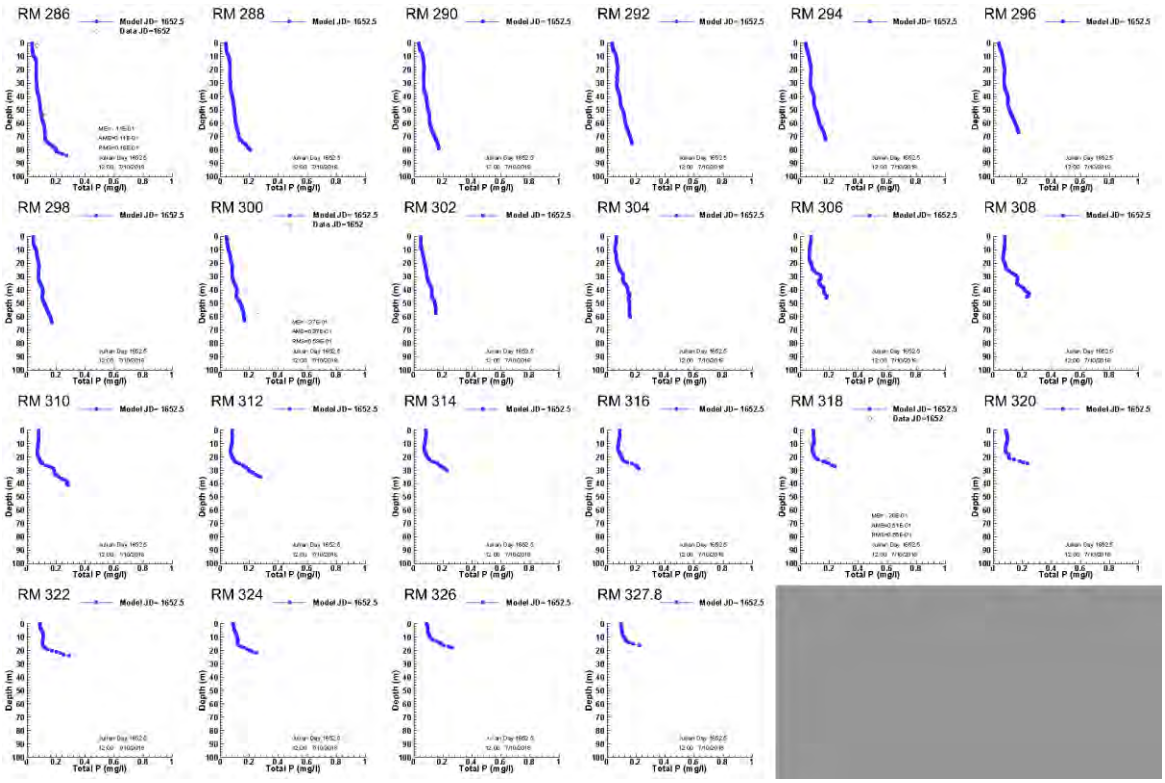


Figure 1967. Vertical profiles of TP compared with data for 7/10/2018.

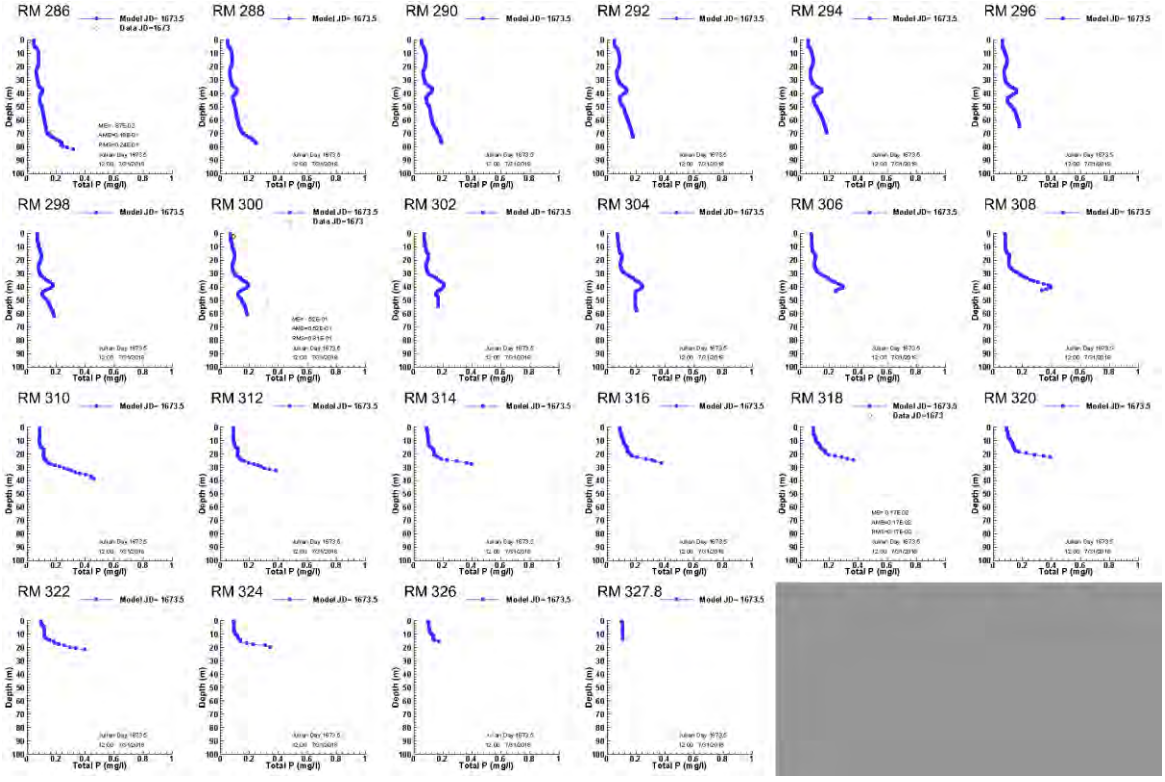


Figure 1968. Vertical profiles of TP compared with data for 7/31/2018.

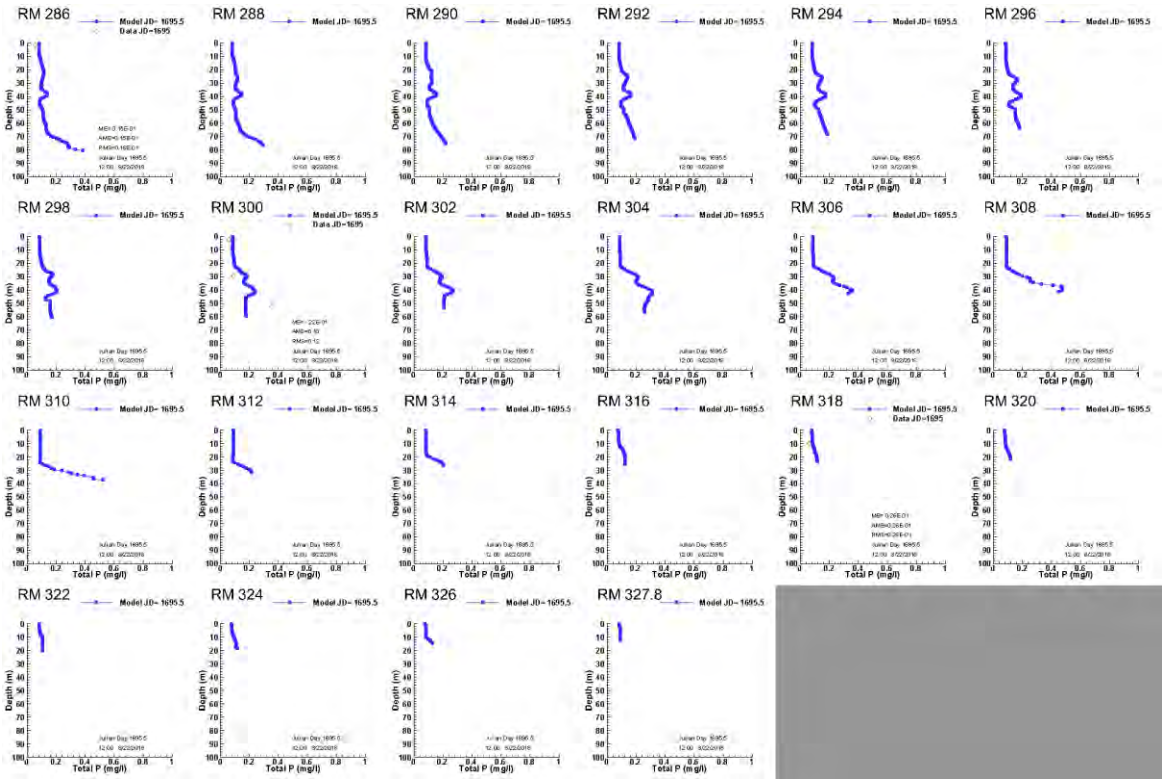


Figure 1969. Vertical profiles of TP compared with data for 8/22/2018.

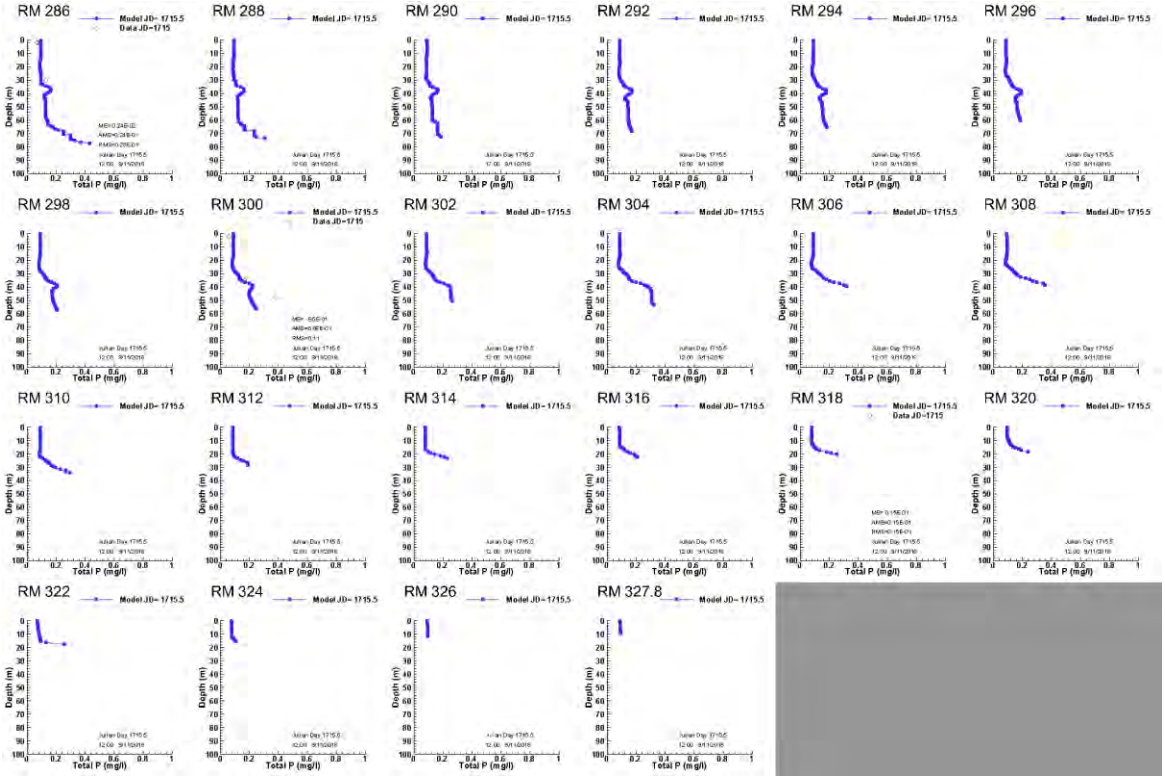


Figure 1970. Vertical profiles of TP compared with data for 9/11/2018.

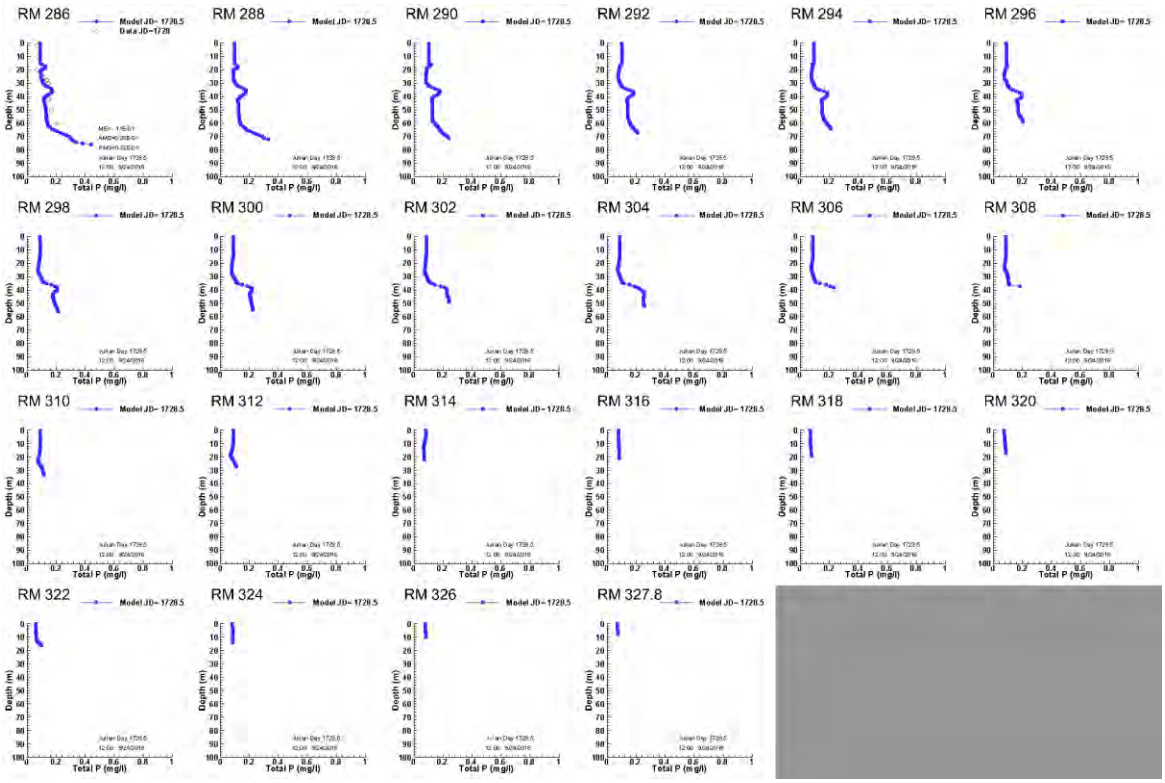


Figure 1971. Vertical profiles of TP compared with data for 9/24/2018.

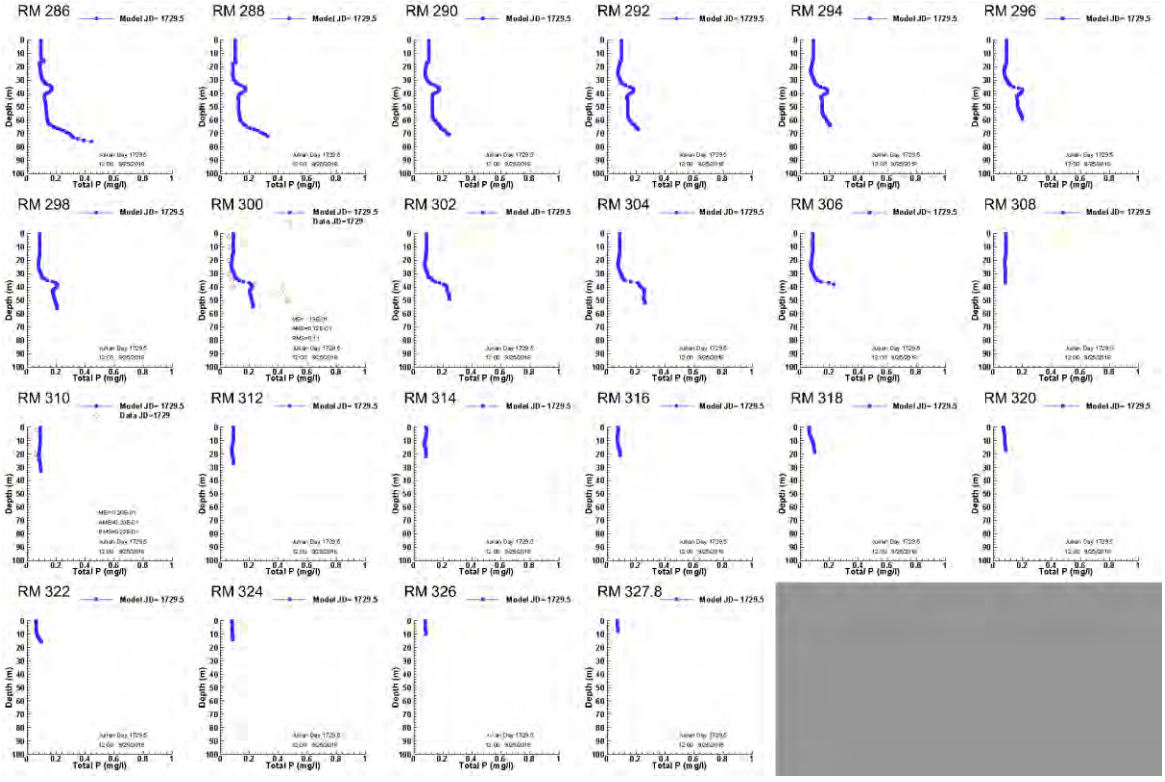


Figure 1972. Vertical profiles of TP compared with data for 9/25/2018.

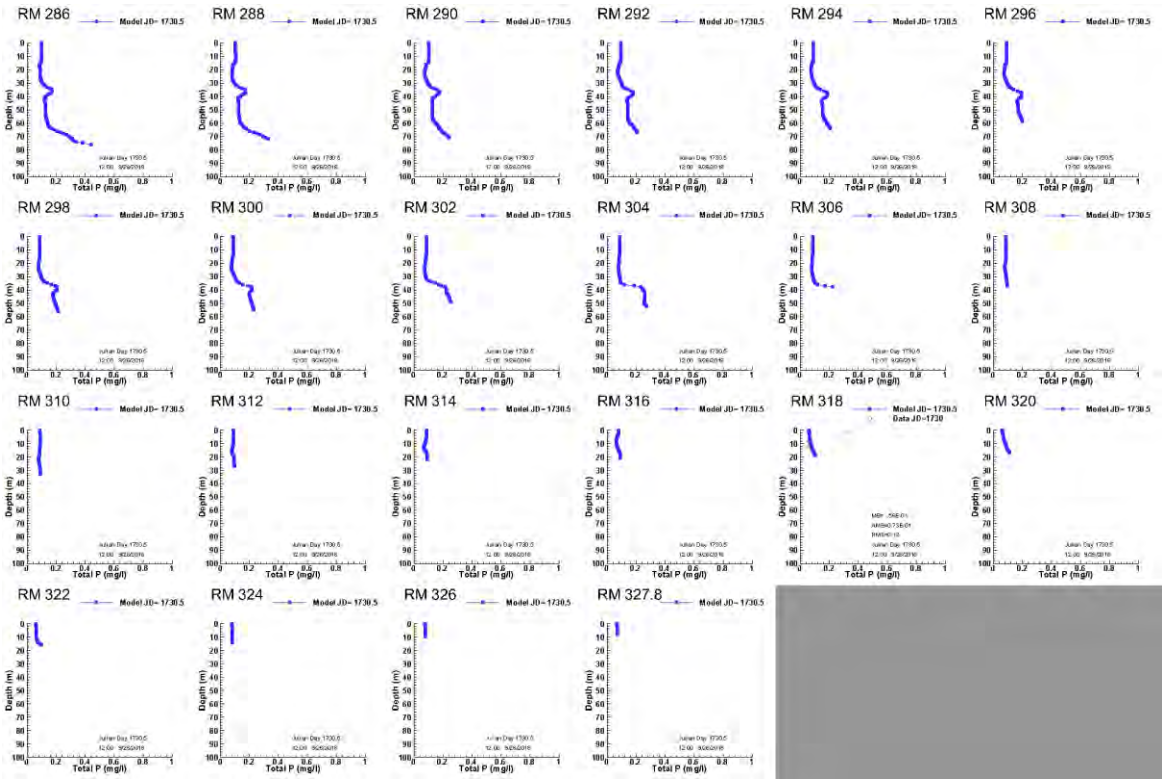


Figure 1973. Vertical profiles of TP compared with data for 9/26/2018.

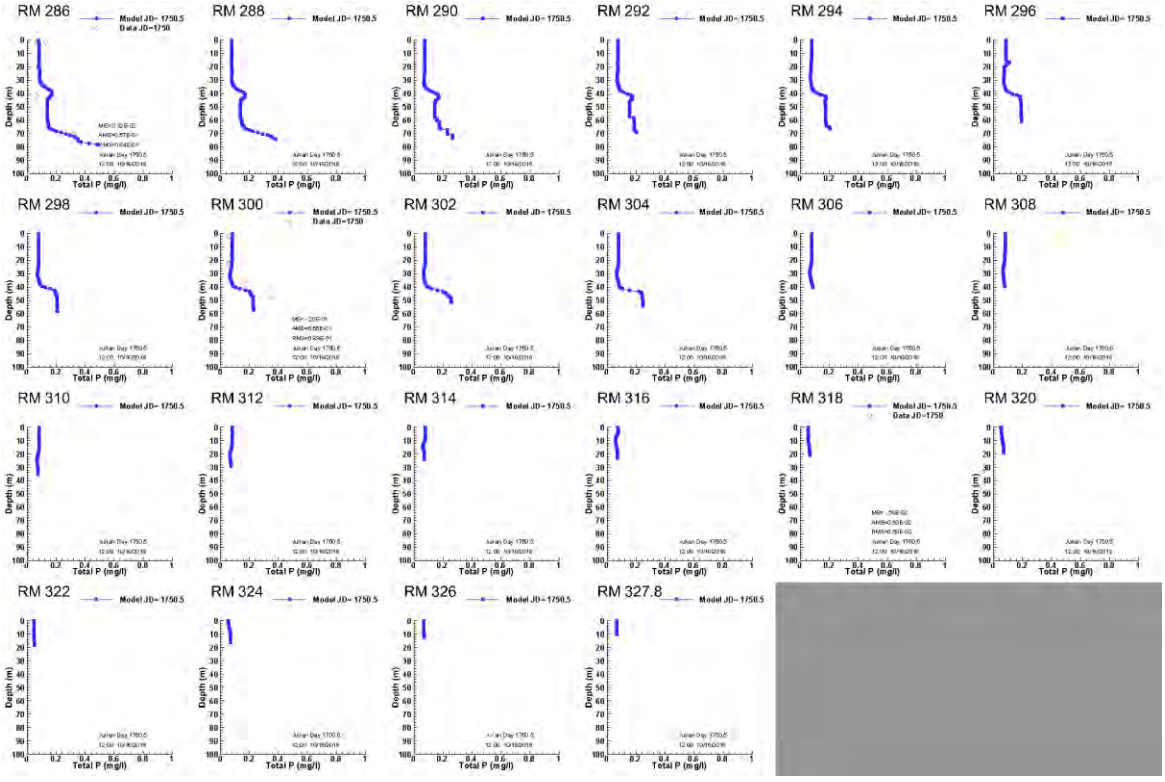


Figure 1974. Vertical profiles of TP compared with data for 10/16/2018.

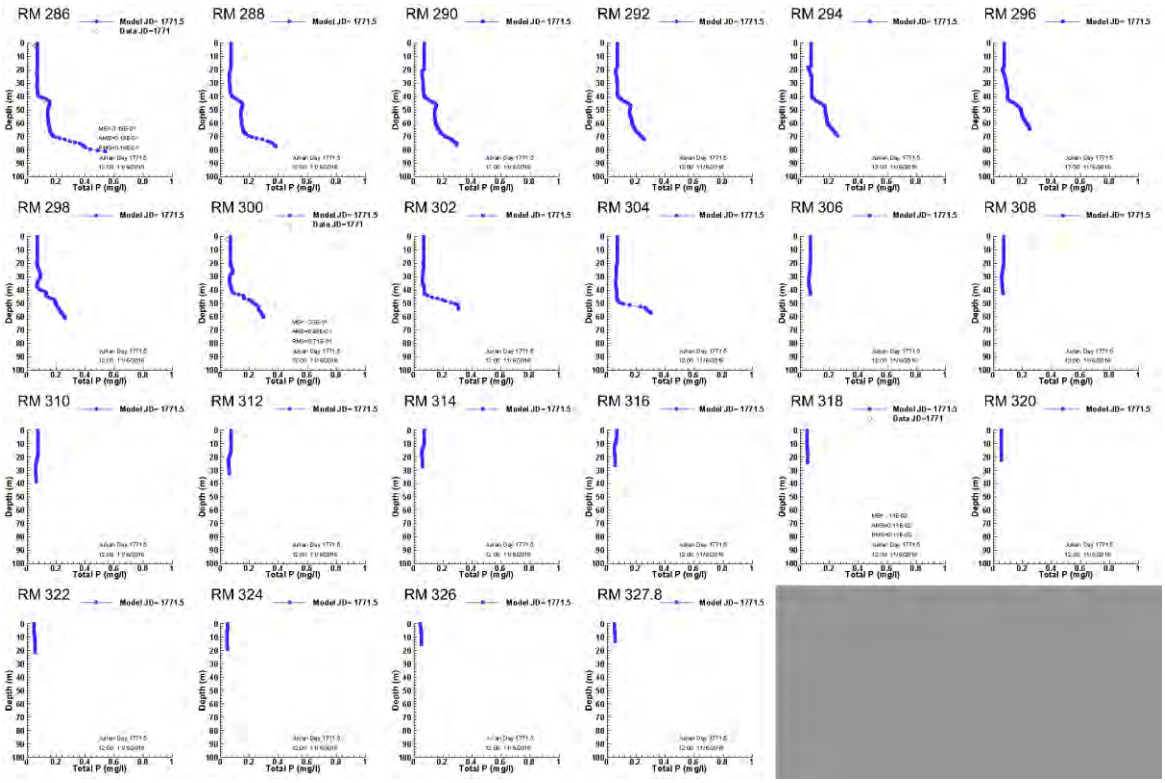


Figure 1975. Vertical profiles of TP compared with data for 11/ 6/2018.

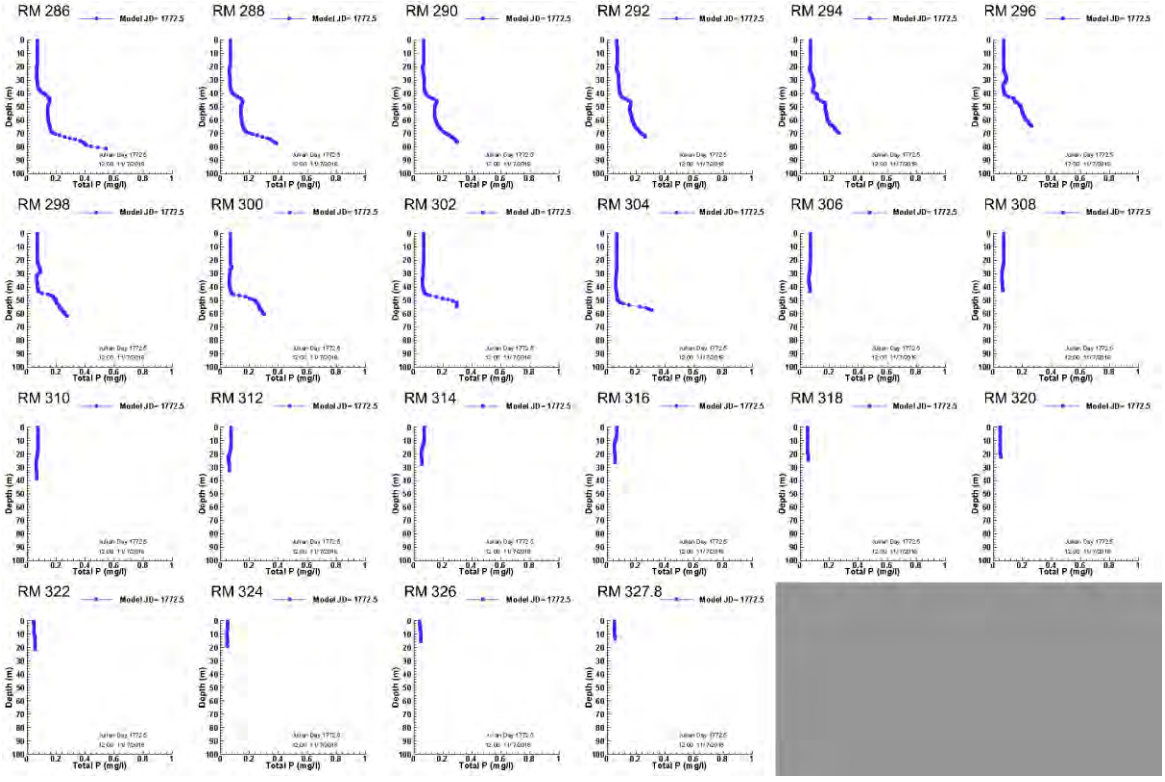


Figure 1976. Vertical profiles of TP compared with data for 11/ 7/2018.

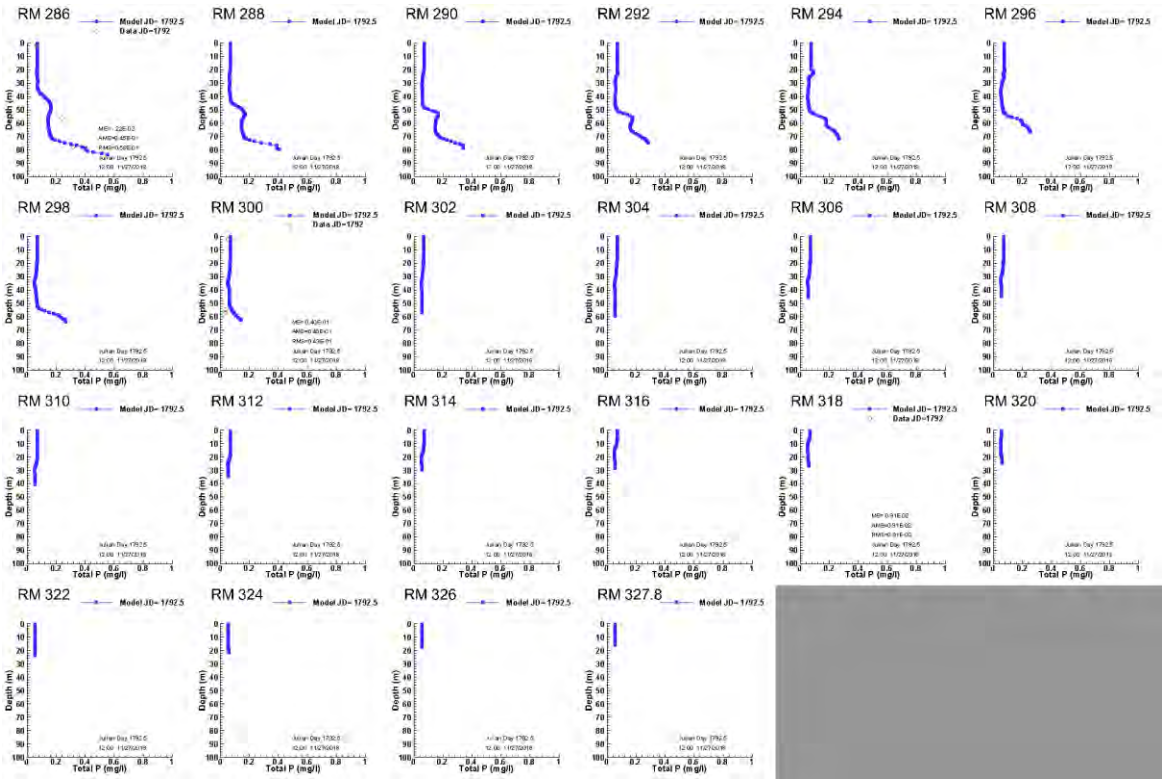


Figure 1977. Vertical profiles of TP compared with data for 11/27/2018.

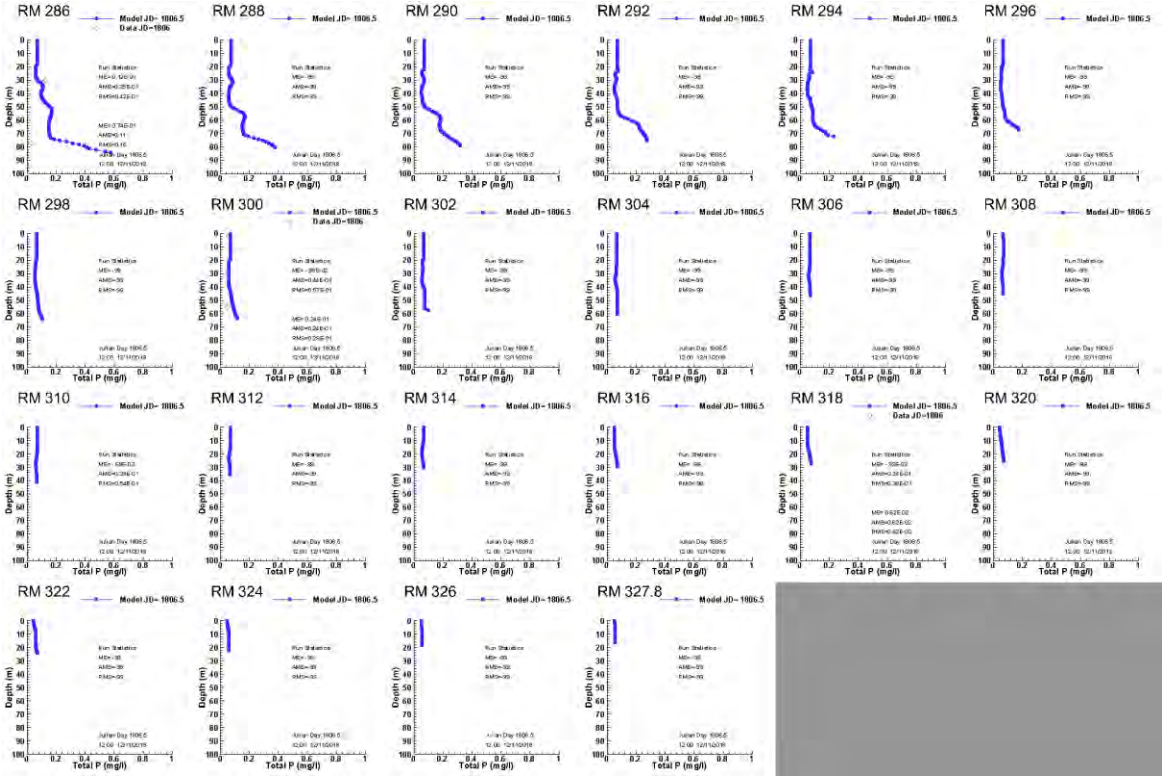


Figure 1978. Vertical profiles of TP compared with data for 12/11/2018.

Chlorophyll *a*

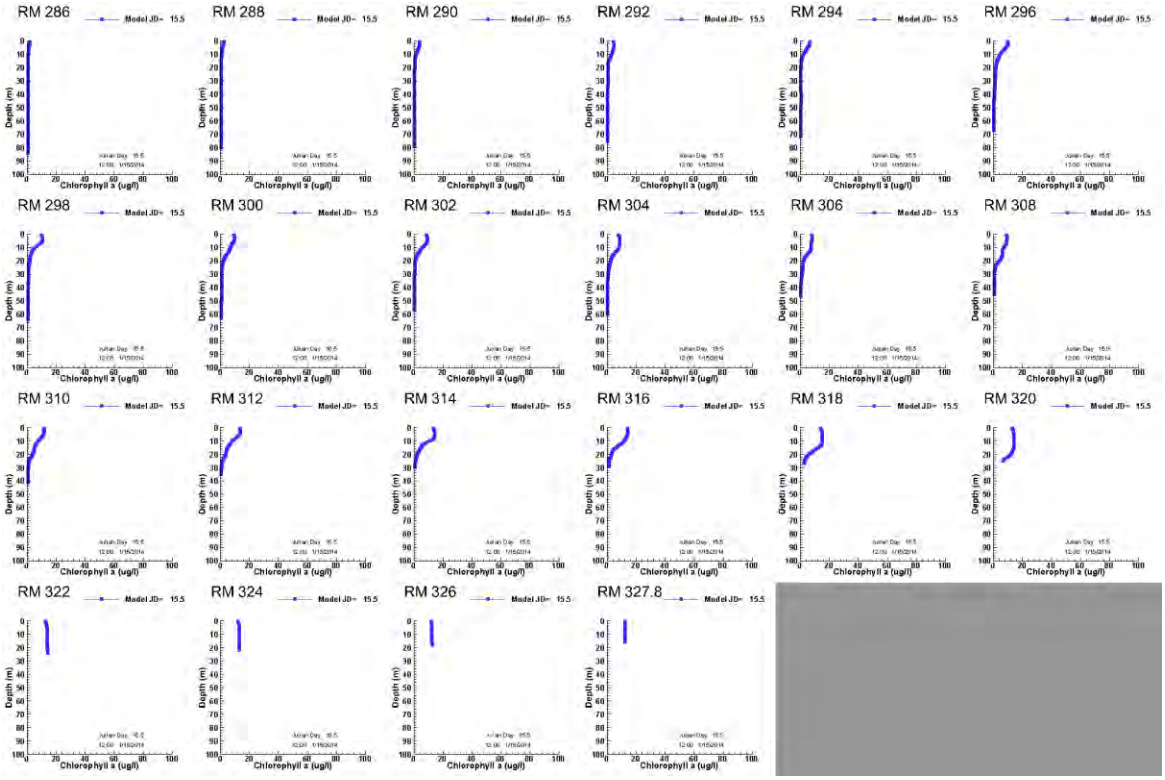


Figure 1979. Vertical profiles of chlorophyll a compared with data for 1/15/2014.

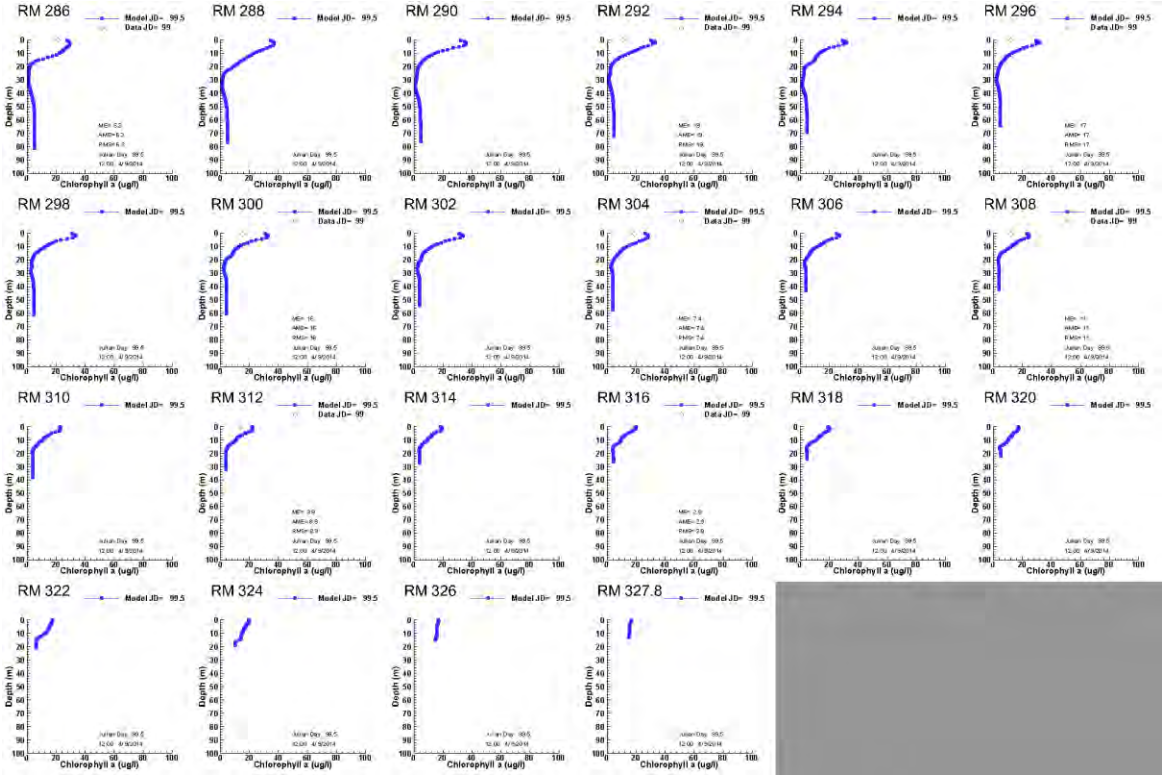


Figure 1980. Vertical profiles of chlorophyll a compared with data for 4/ 9/2014.

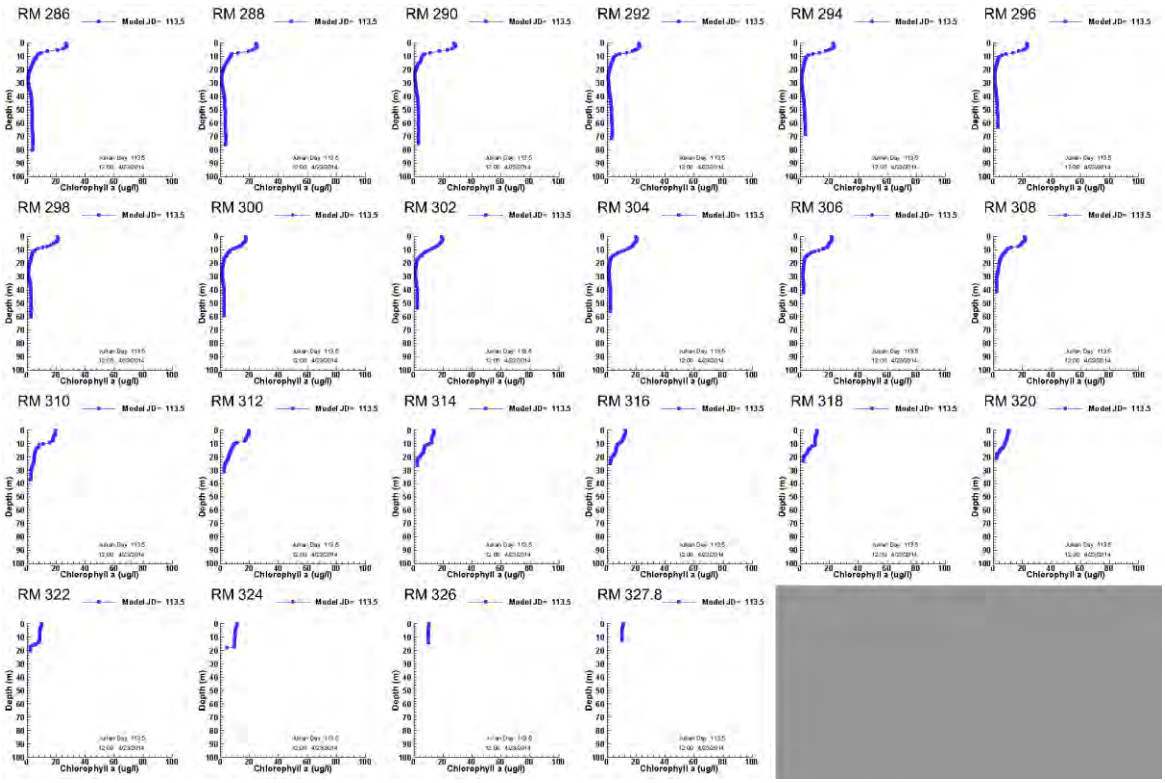


Figure 1981. Vertical profiles of chlorophyll a compared with data for 4/23/2014.

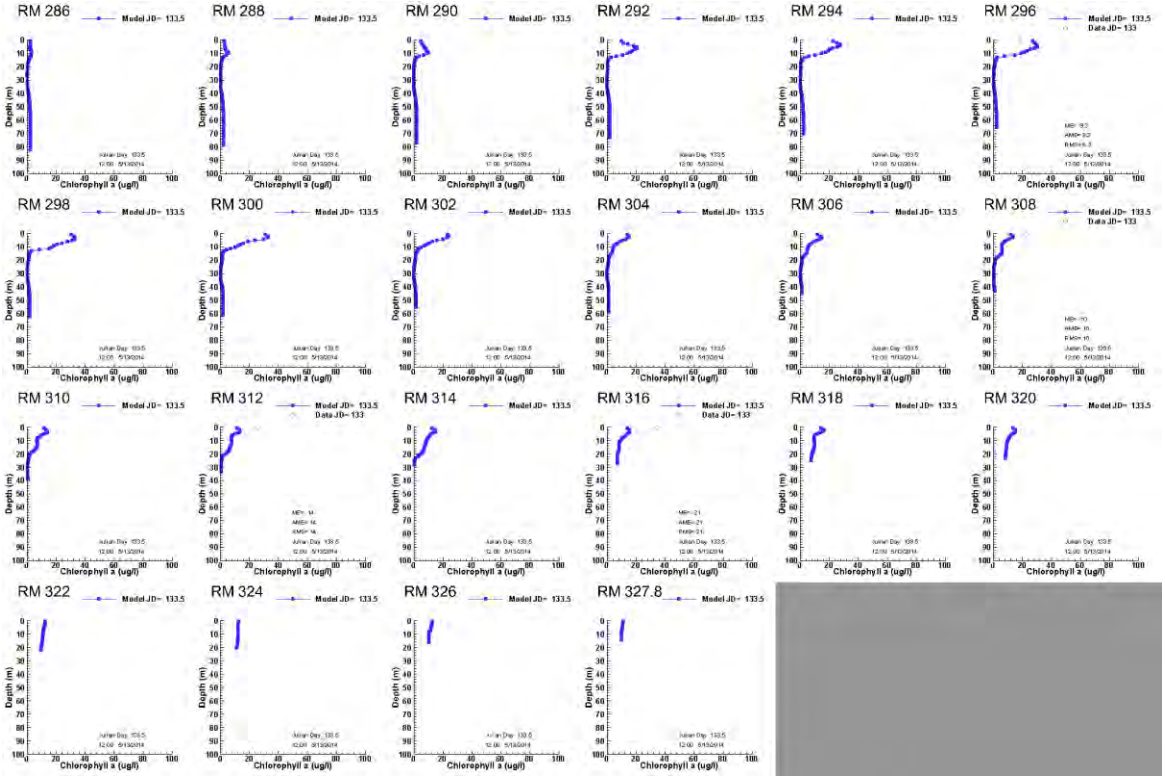


Figure 1982. Vertical profiles of chlorophyll a compared with data for 5/13/2014.

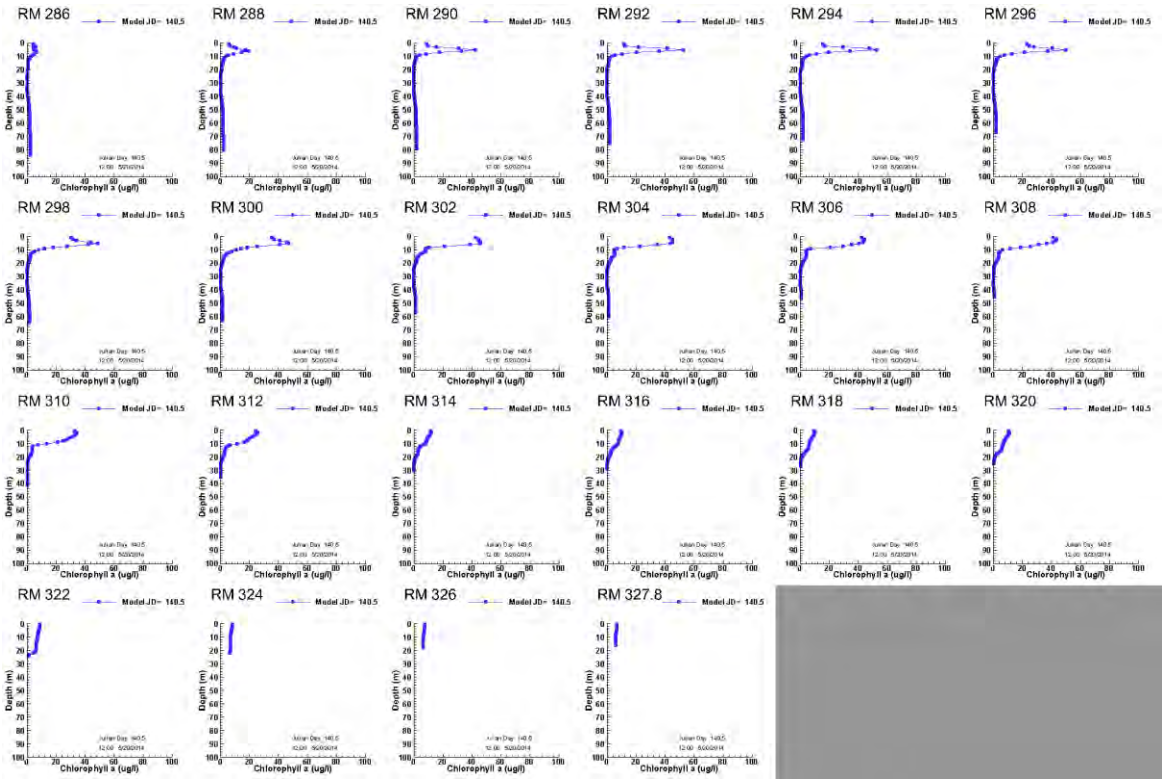


Figure 1983. Vertical profiles of chlorophyll a compared with data for 5/20/2014.

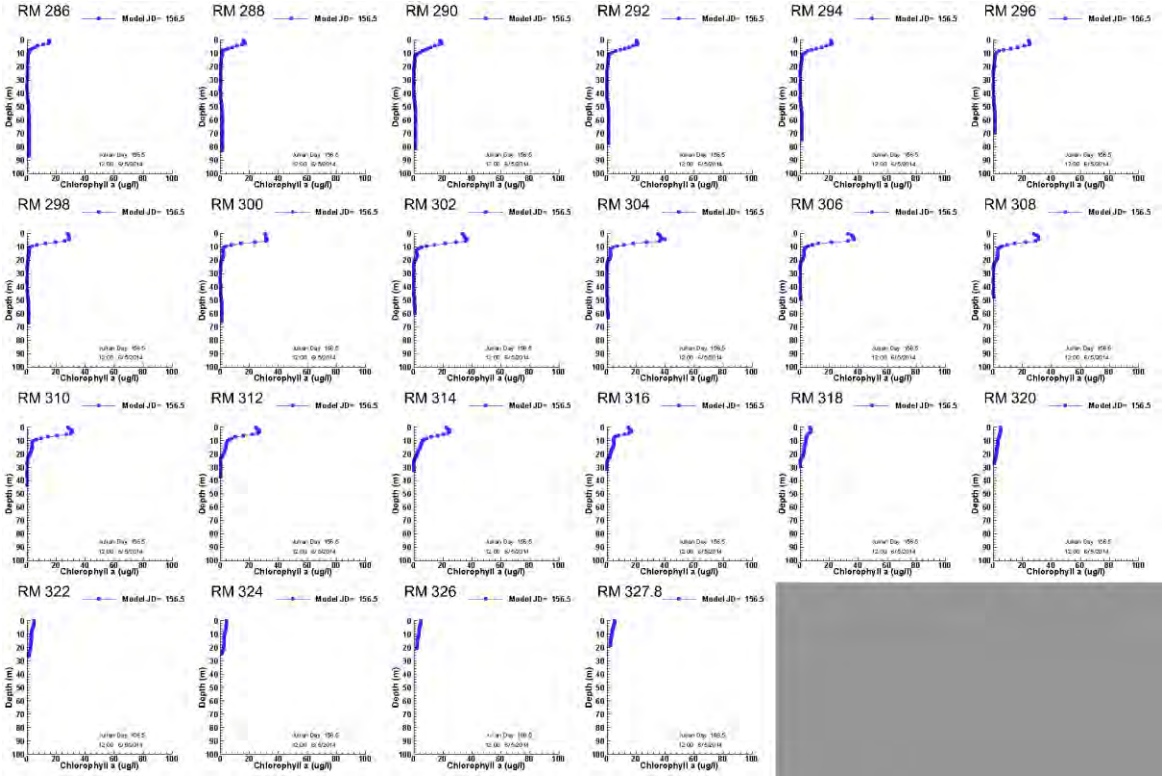


Figure 1984. Vertical profiles of chlorophyll a compared with data for 6/ 5/2014.

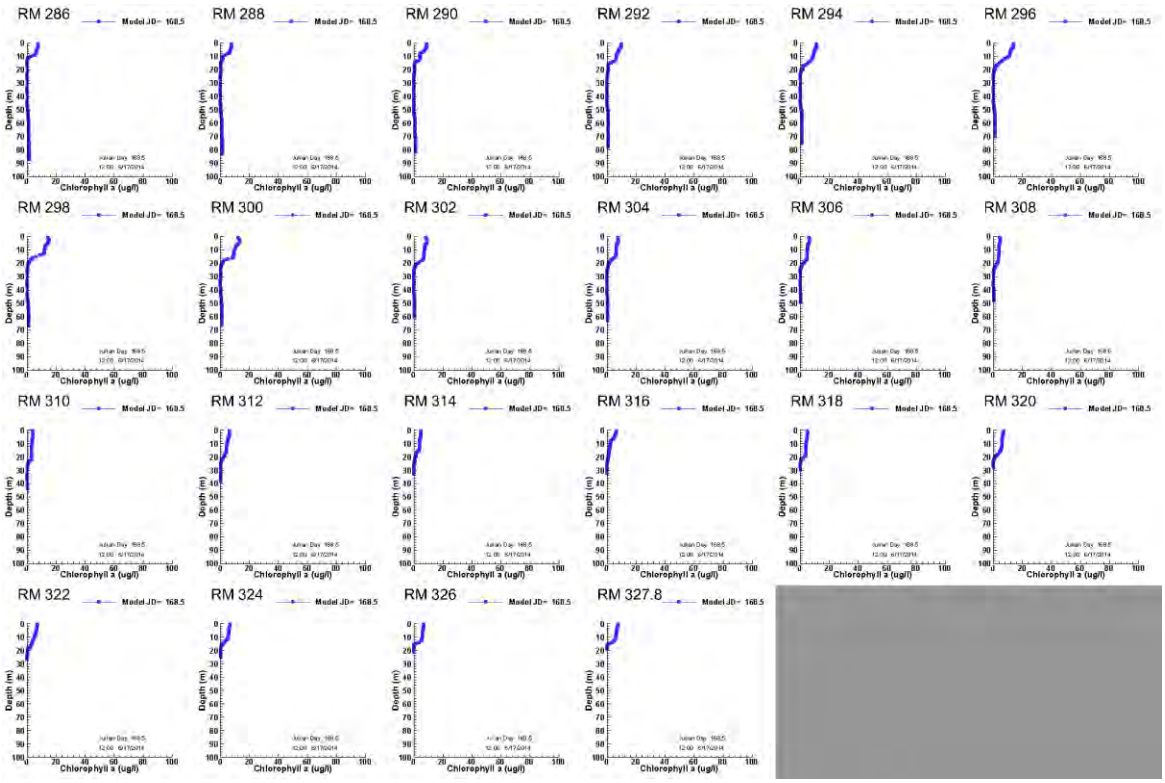


Figure 1985. Vertical profiles of chlorophyll a compared with data for 6/17/2014.

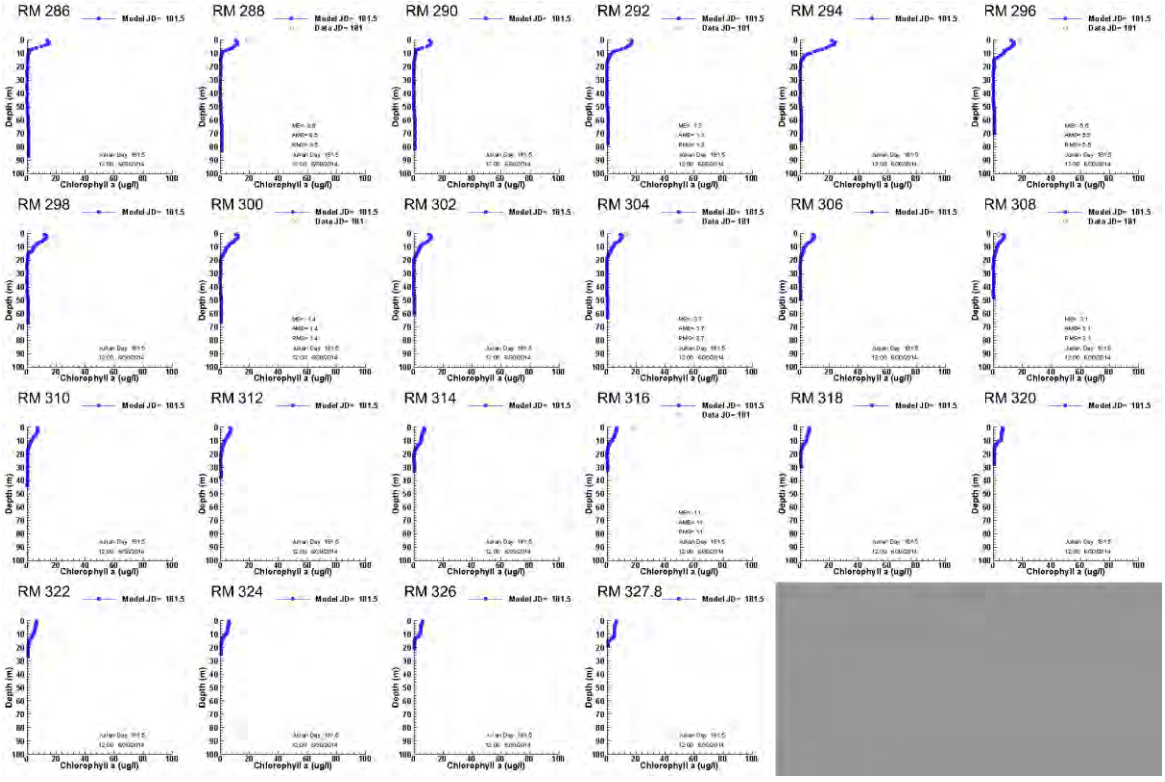


Figure 1986. Vertical profiles of chlorophyll a compared with data for 6/30/2014.

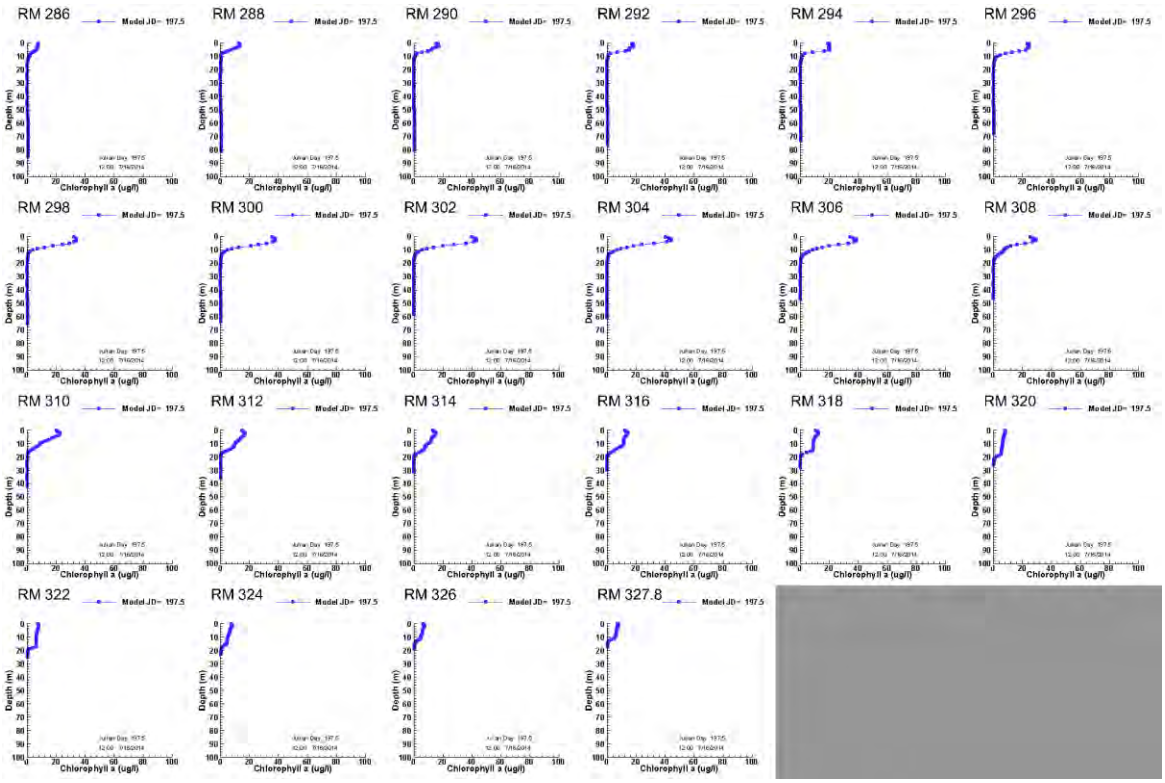


Figure 1987. Vertical profiles of chlorophyll a compared with data for 7/16/2014.

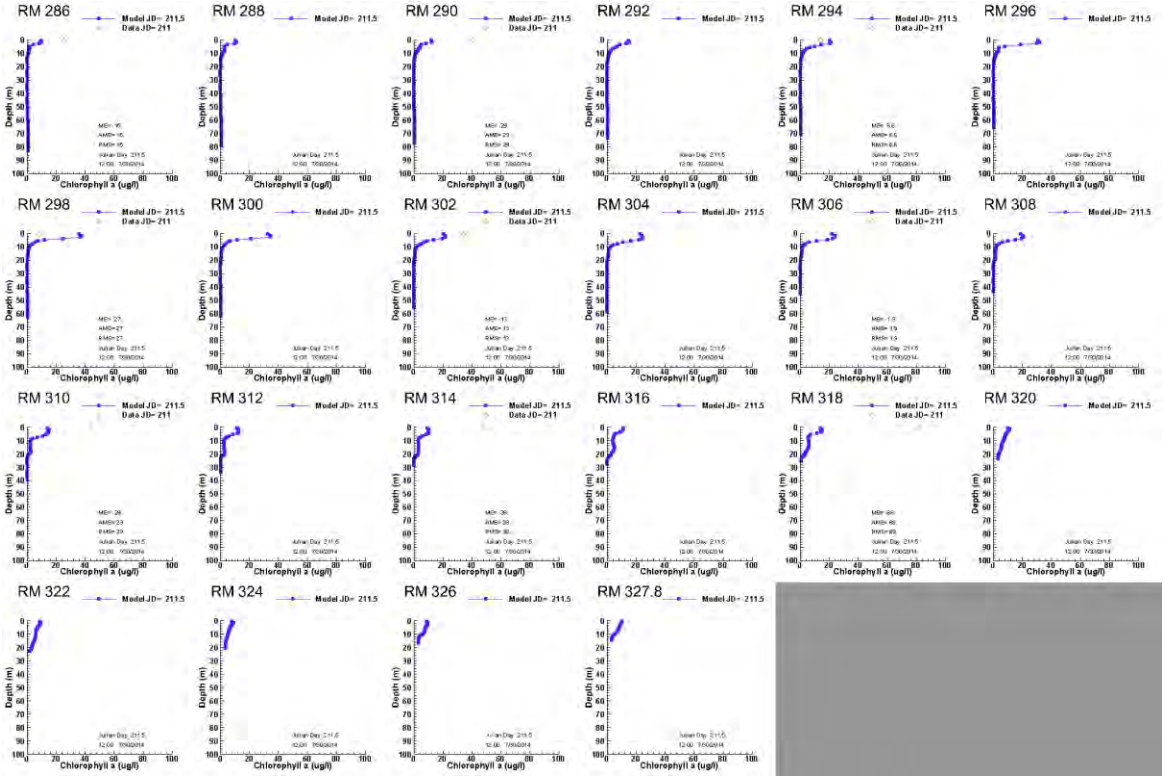


Figure 1988. Vertical profiles of chlorophyll a compared with data for 7/30/2014.

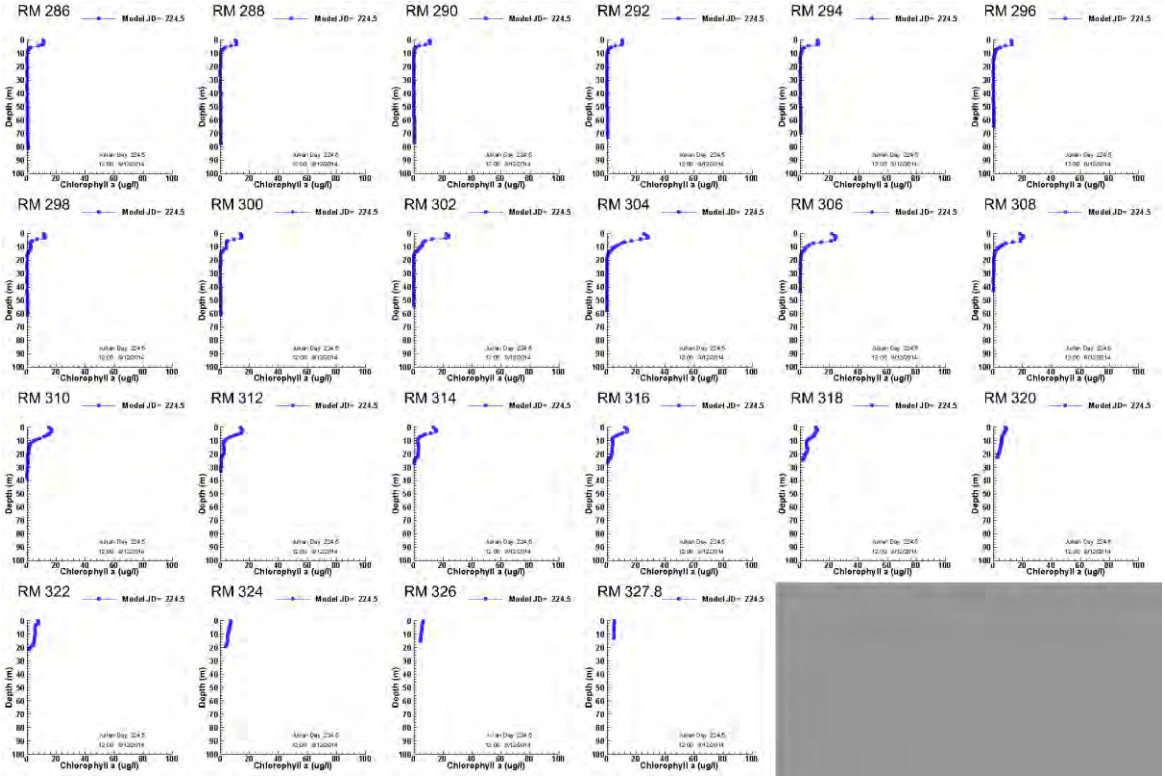


Figure 1989. Vertical profiles of chlorophyll a compared with data for 8/12/2014.

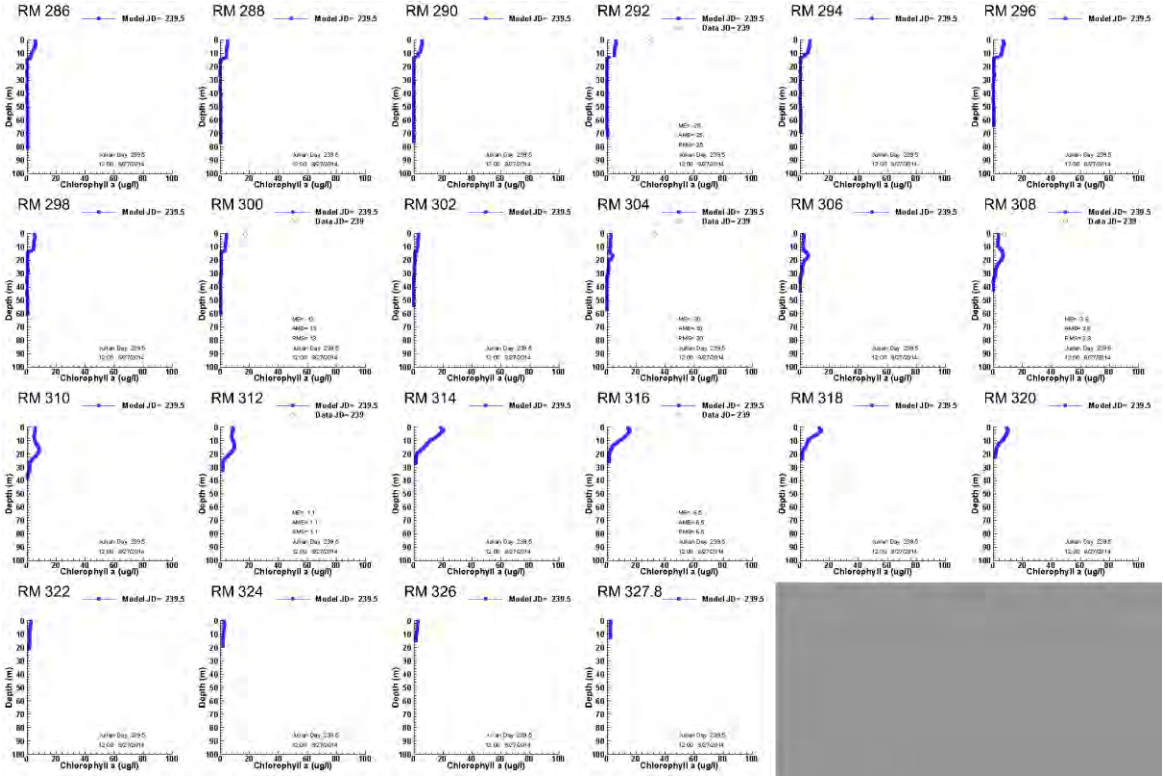


Figure 1990. Vertical profiles of chlorophyll a compared with data for 8/27/2014.

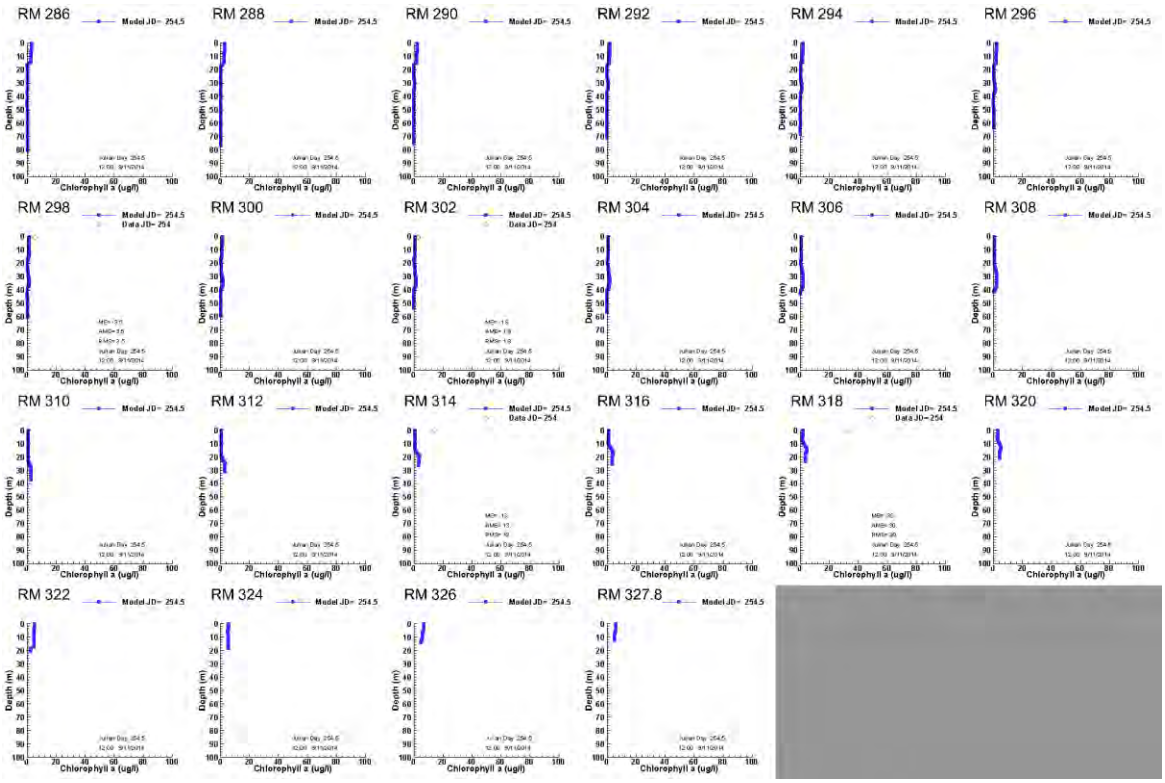


Figure 1991. Vertical profiles of chlorophyll a compared with data for 9/11/2014.

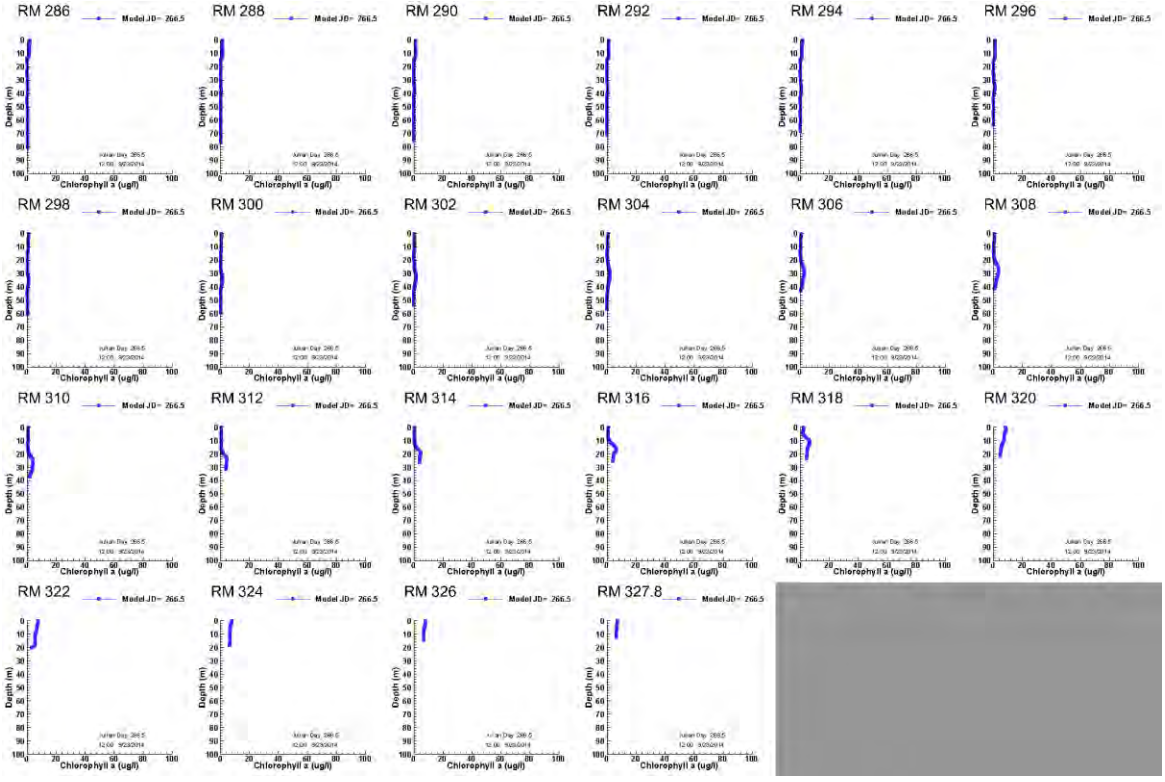


Figure 1992. Vertical profiles of chlorophyll a compared with data for 9/23/2014.

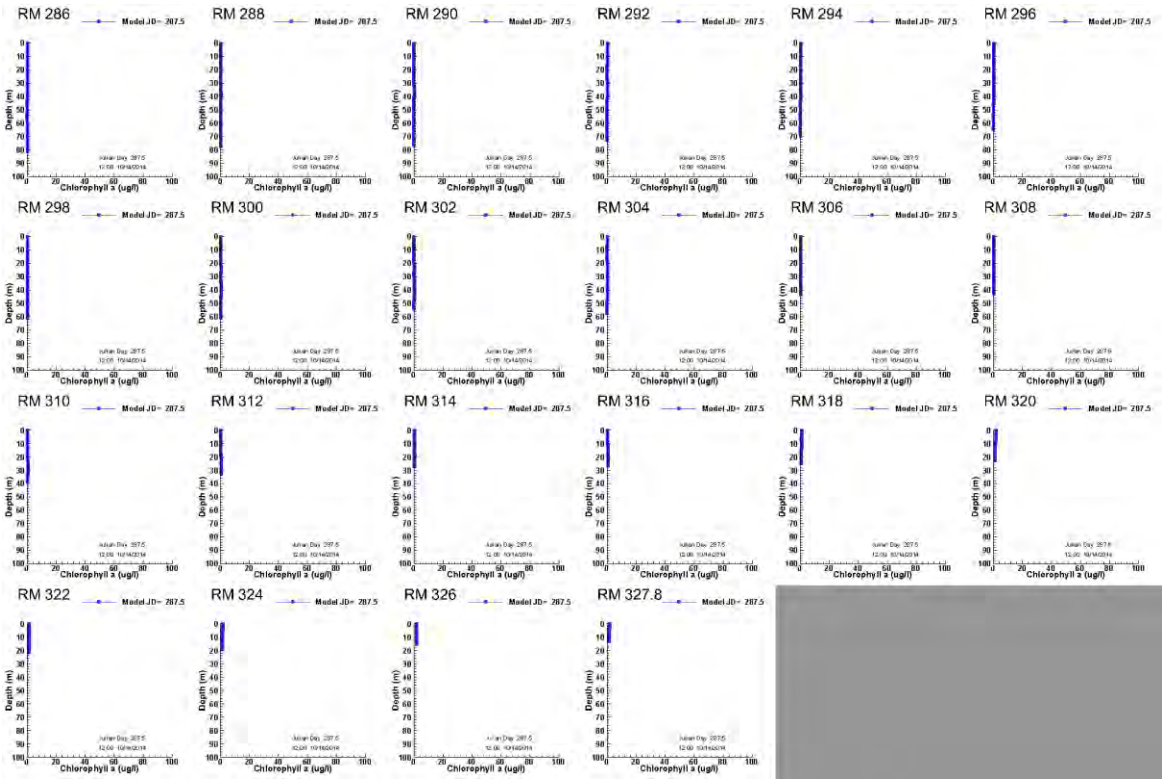


Figure 1993. Vertical profiles of chlorophyll a compared with data for 10/14/2014.

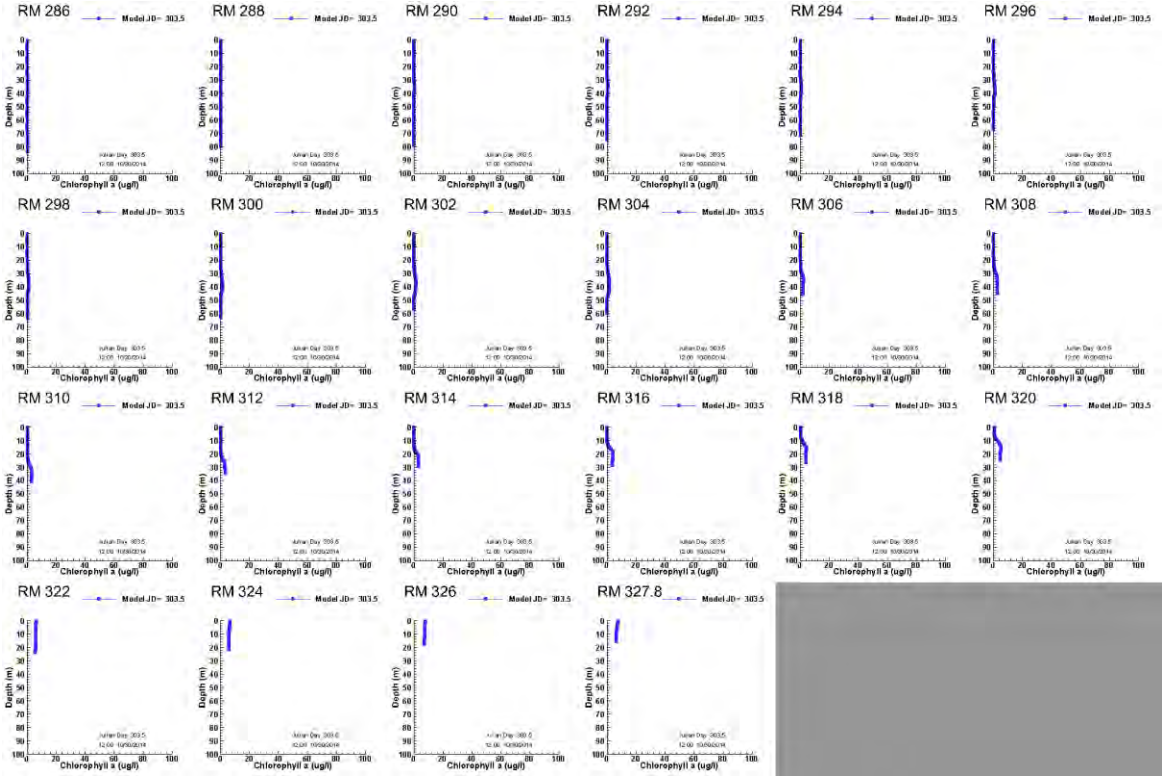


Figure 1994. Vertical profiles of chlorophyll a compared with data for 10/30/2014.

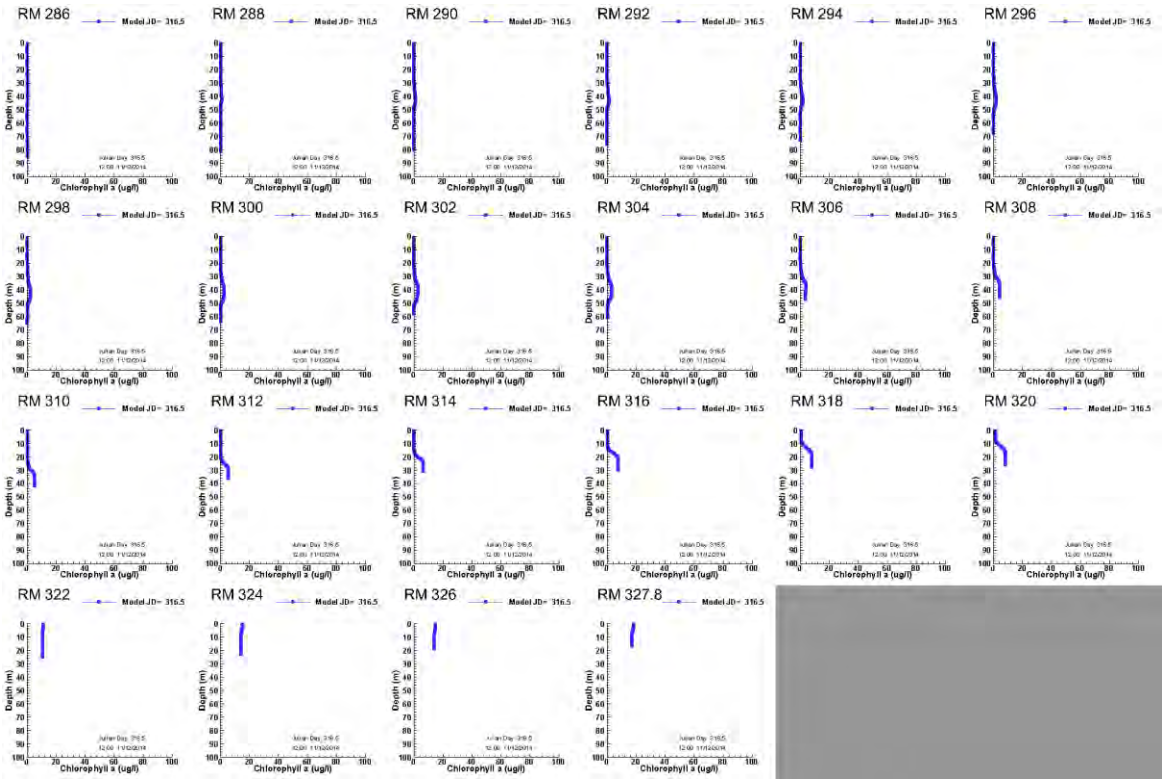


Figure 1995. Vertical profiles of chlorophyll a compared with data for 11/12/2014.

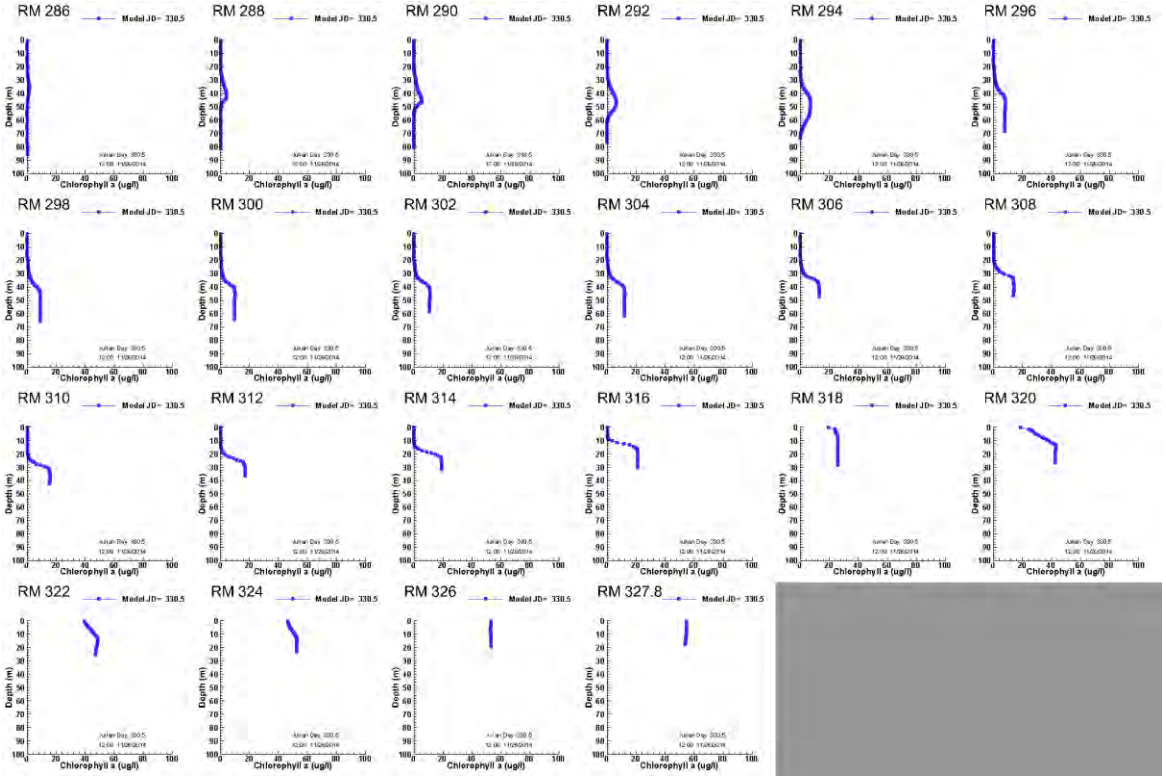


Figure 1996. Vertical profiles of chlorophyll a compared with data for 11/26/2014.

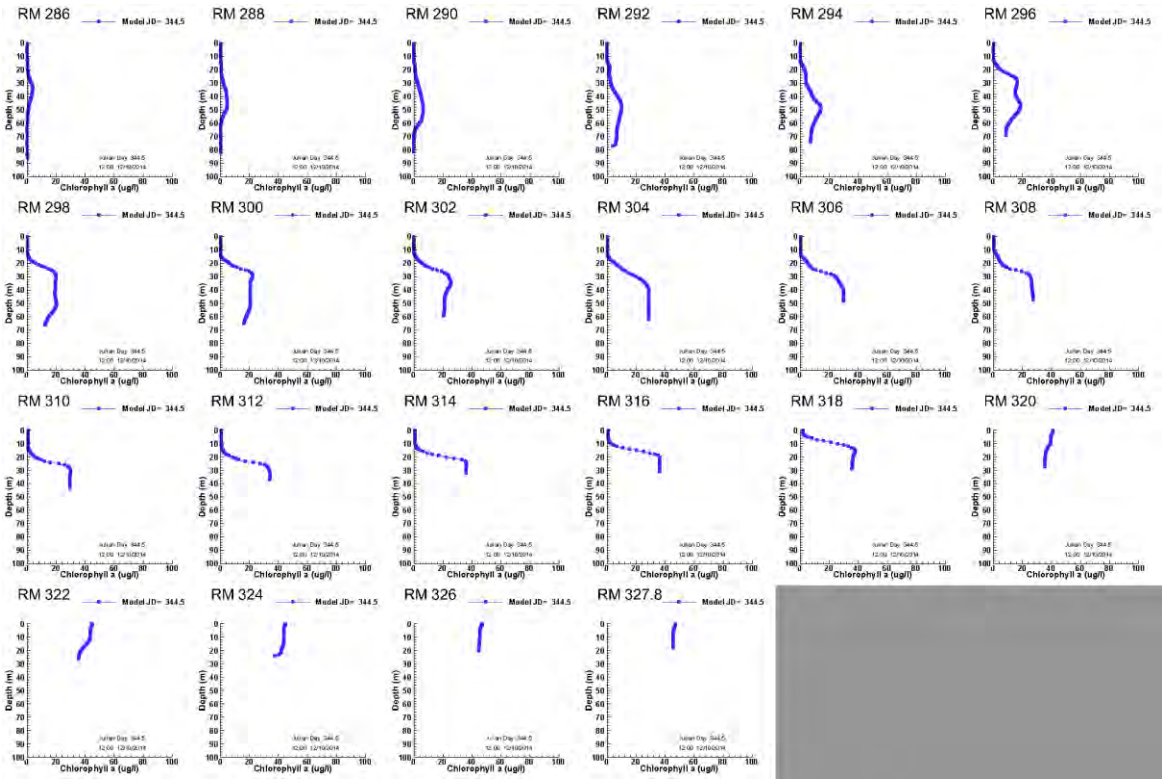


Figure 1997. Vertical profiles of chlorophyll a compared with data for 12/10/2014.

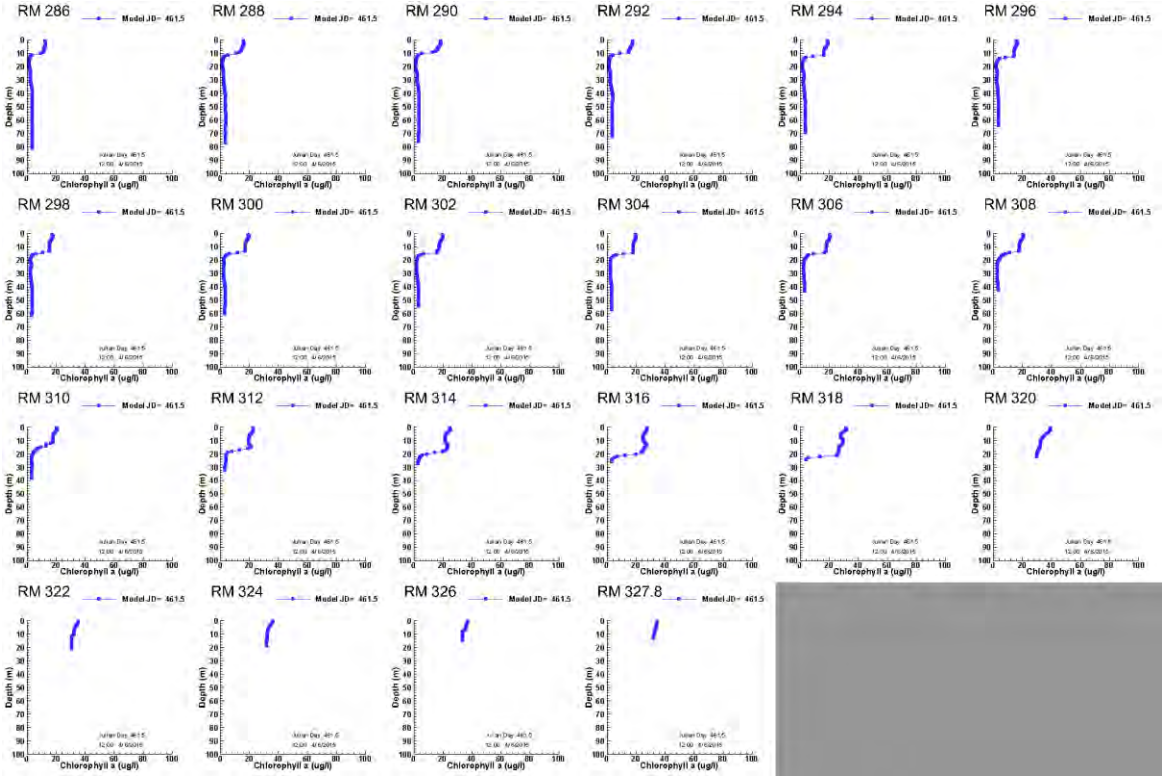


Figure 1998. Vertical profiles of chlorophyll a compared with data for 4/ 6/2015.

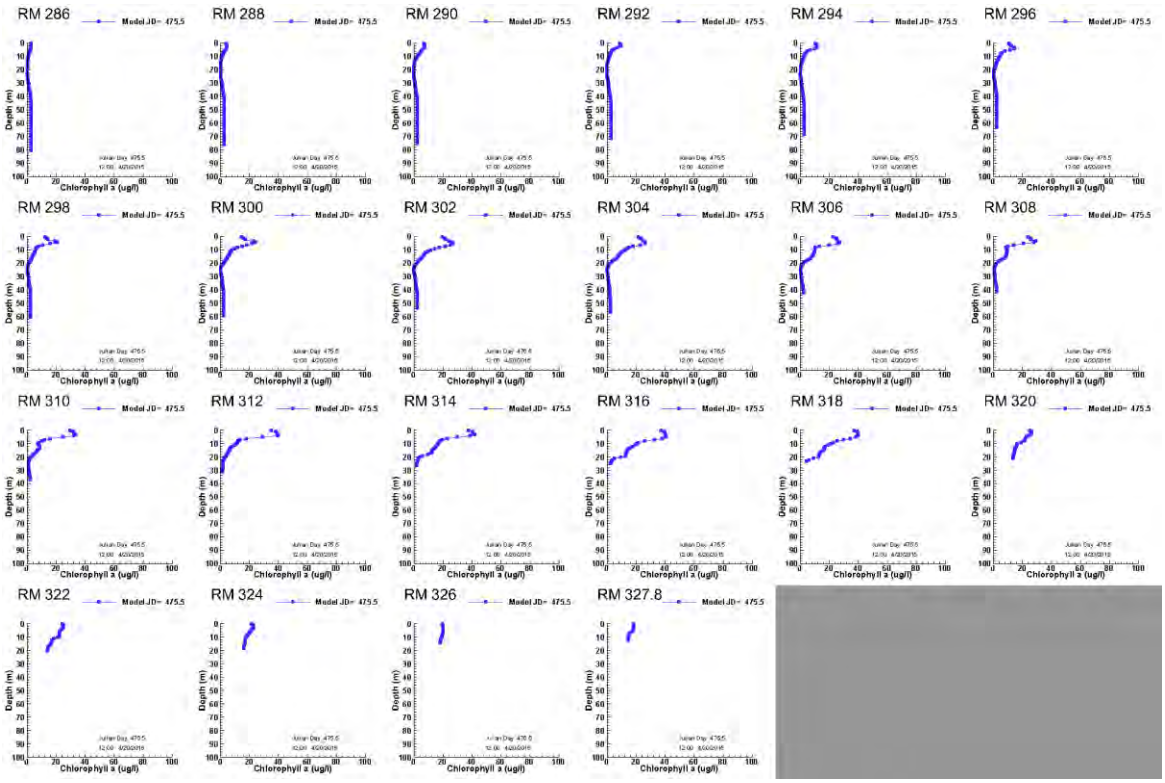


Figure 1999. Vertical profiles of chlorophyll a compared with data for 4/20/2015.

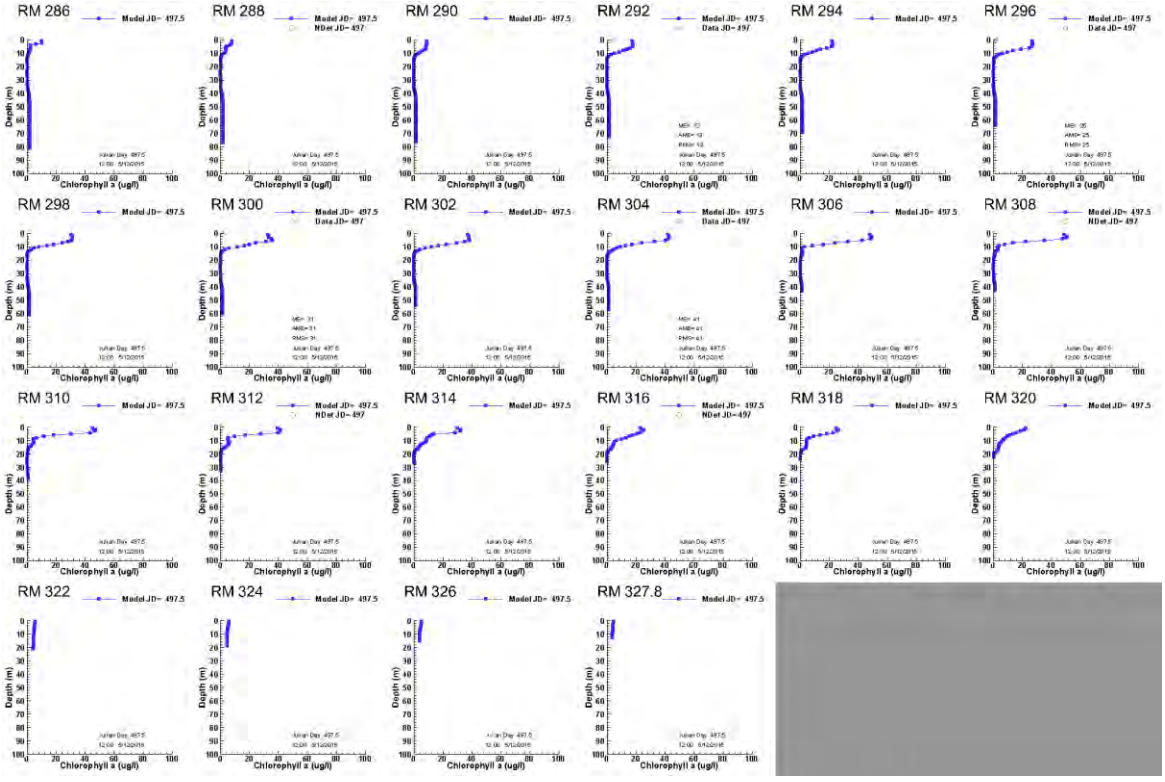


Figure 2000. Vertical profiles of chlorophyll a compared with data for 5/12/2015.

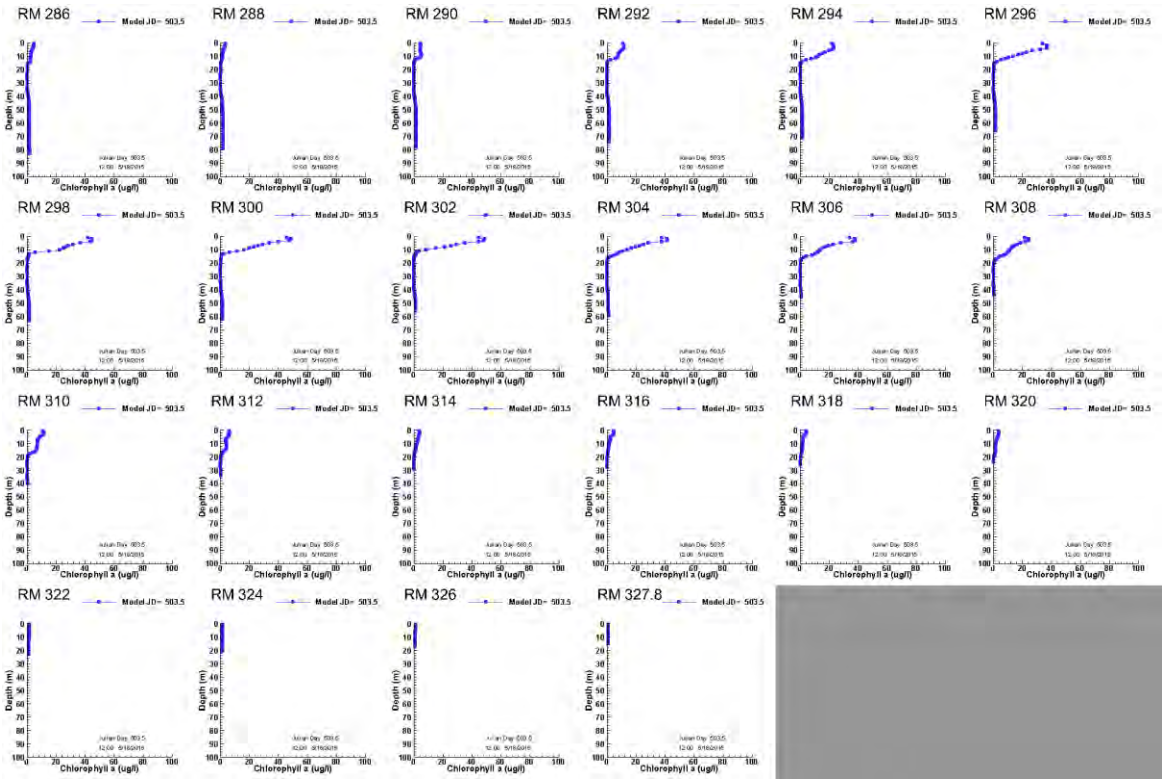


Figure 2001. Vertical profiles of chlorophyll a compared with data for 5/18/2015.

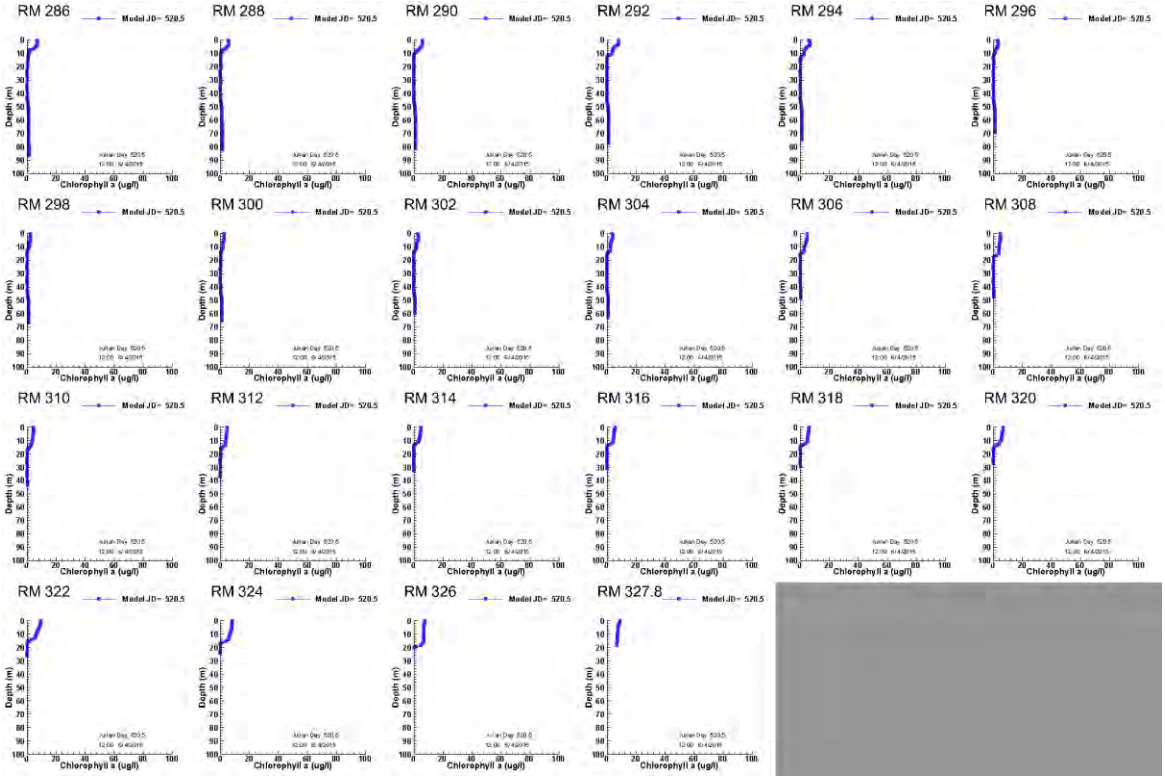


Figure 2002. Vertical profiles of chlorophyll a compared with data for 6/ 4/2015.

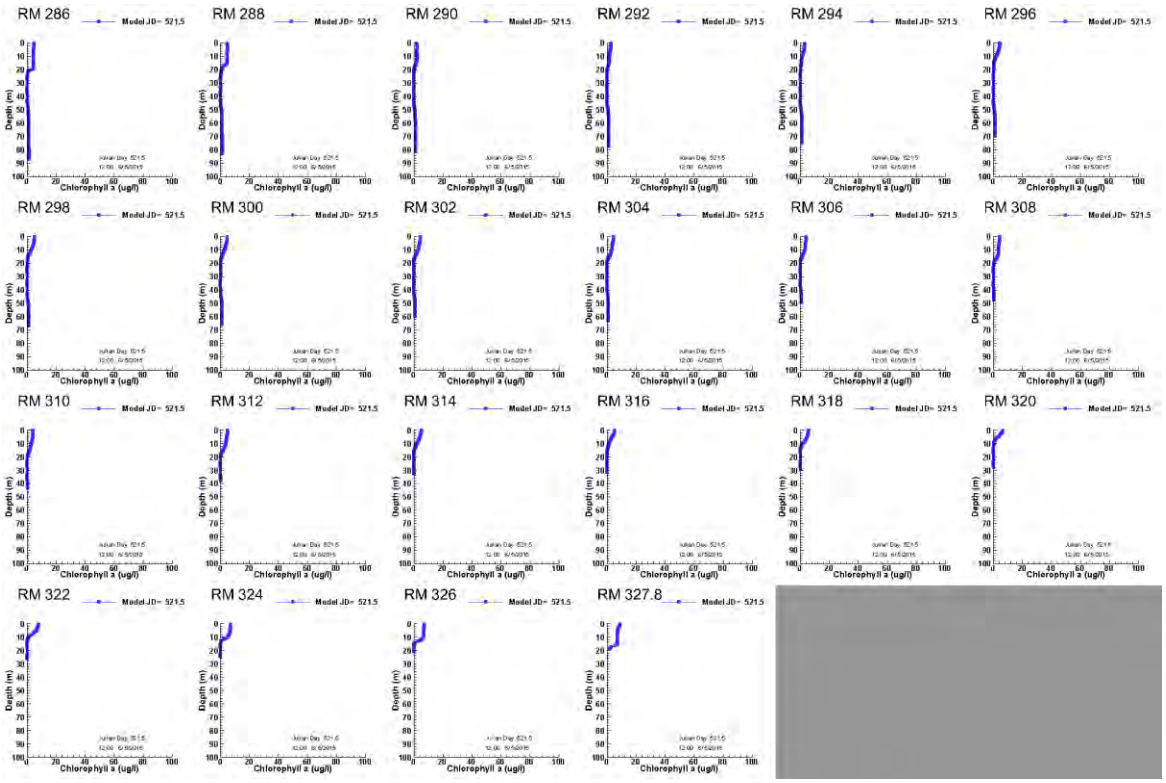


Figure 2003. Vertical profiles of chlorophyll a compared with data for 6/ 5/2015.

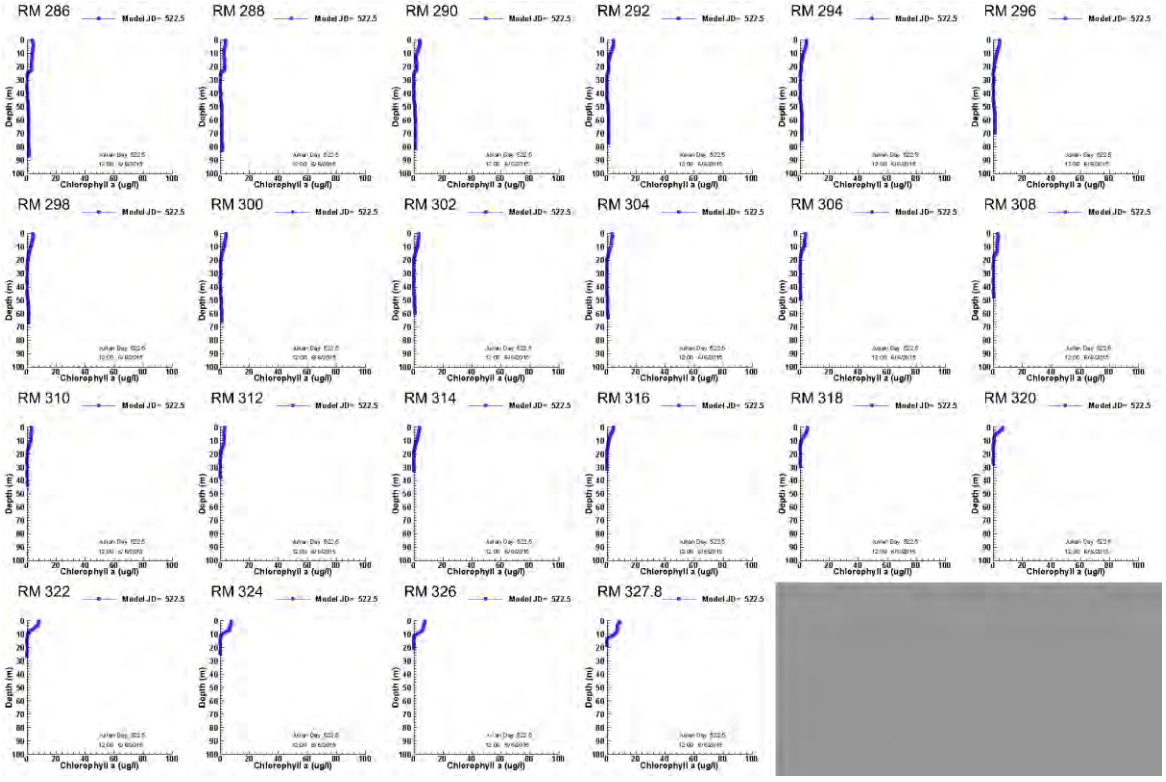


Figure 2004. Vertical profiles of chlorophyll a compared with data for 6/ 6/2015.

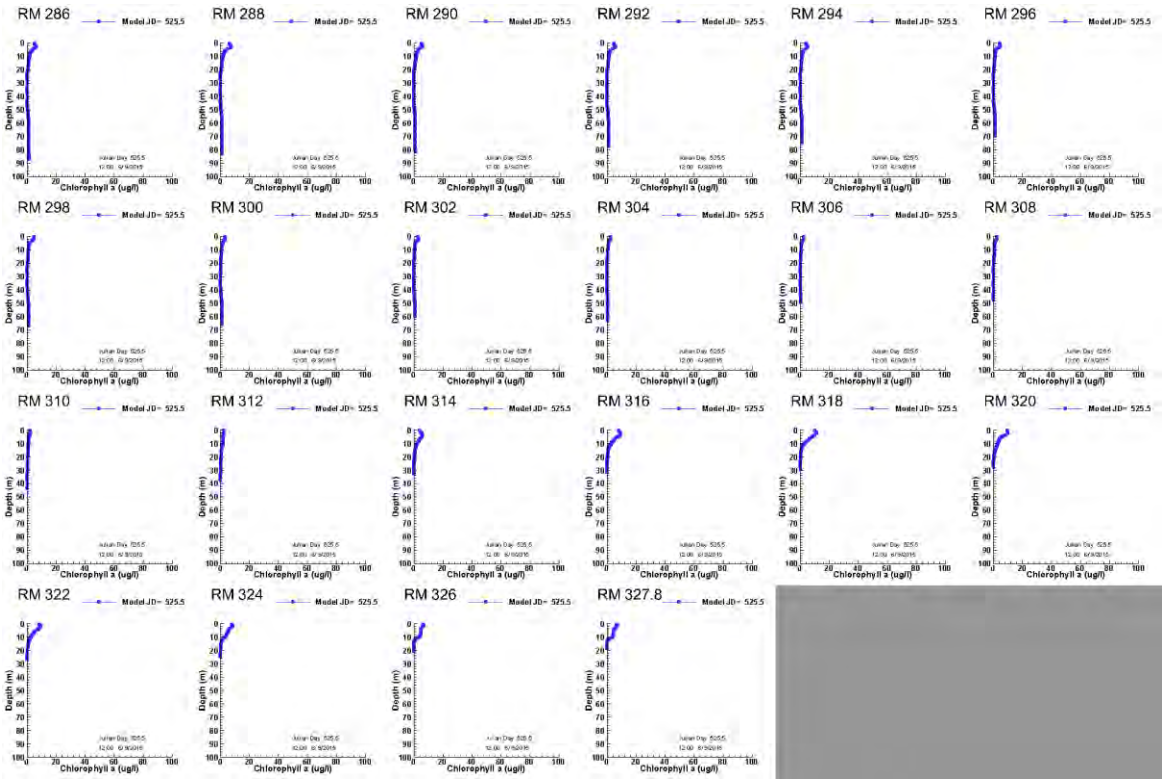


Figure 2005. Vertical profiles of chlorophyll a compared with data for 6/ 9/2015.

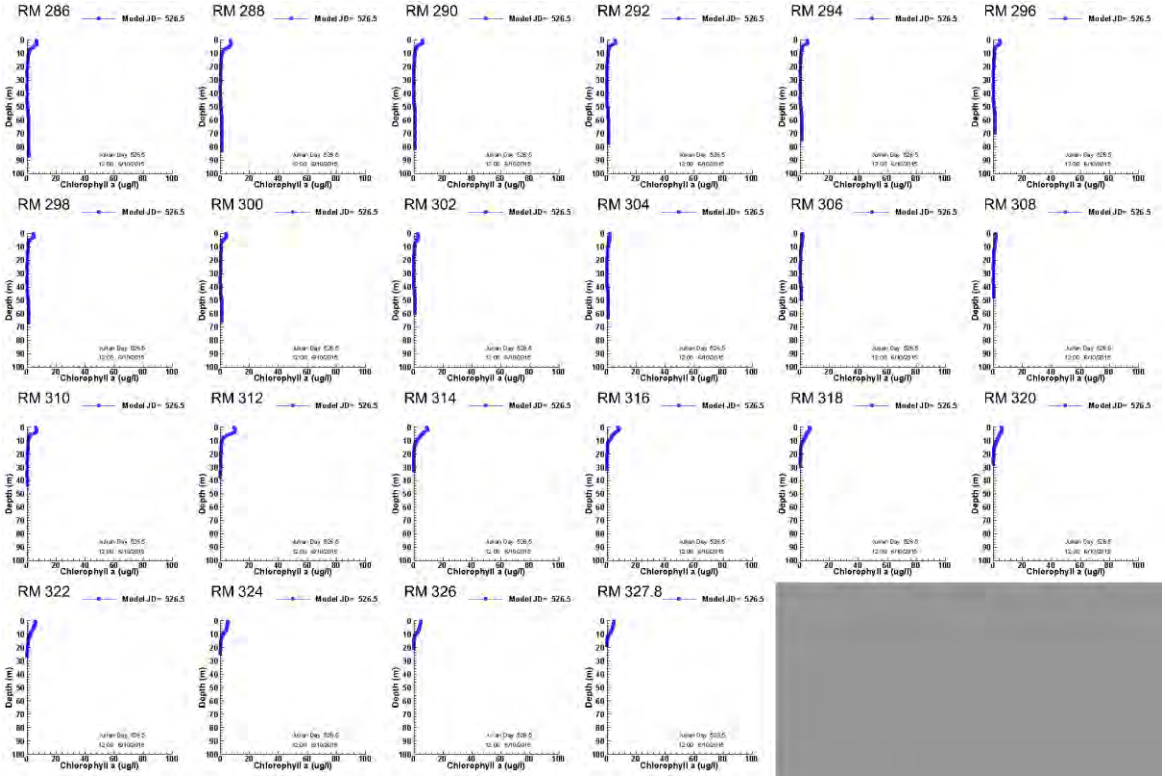


Figure 2006. Vertical profiles of chlorophyll a compared with data for 6/10/2015.

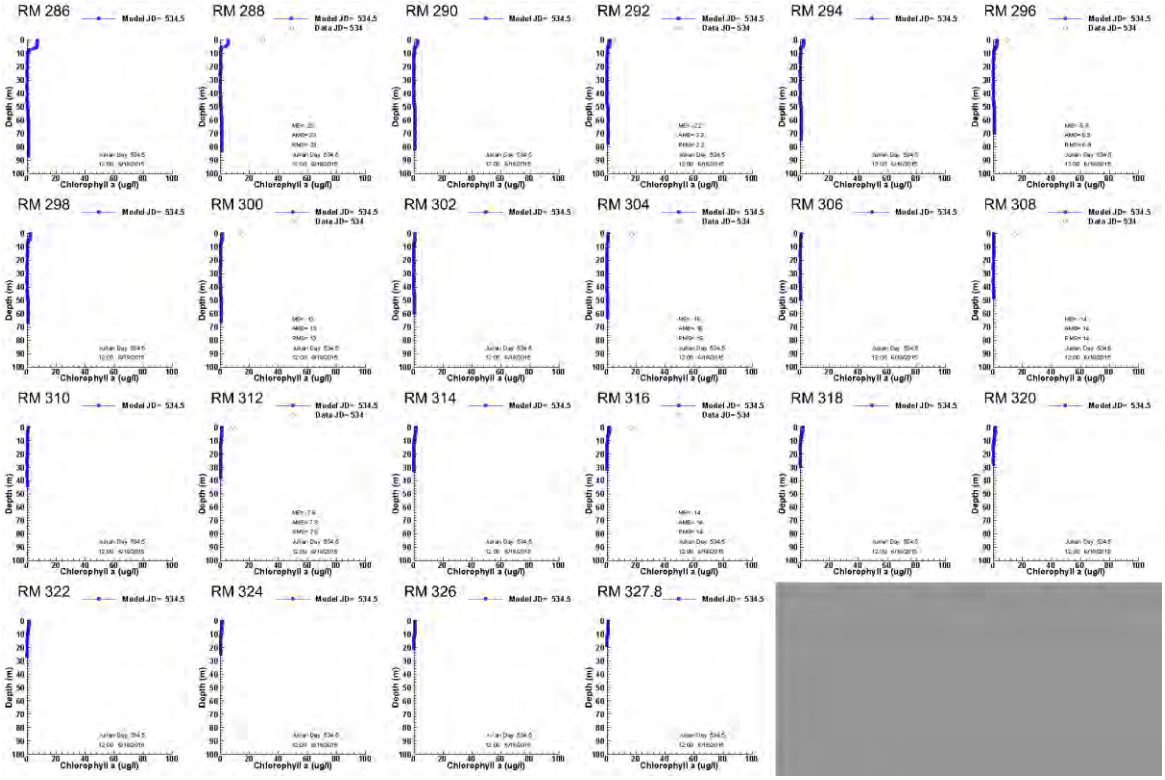


Figure 2007. Vertical profiles of chlorophyll a compared with data for 6/18/2015.

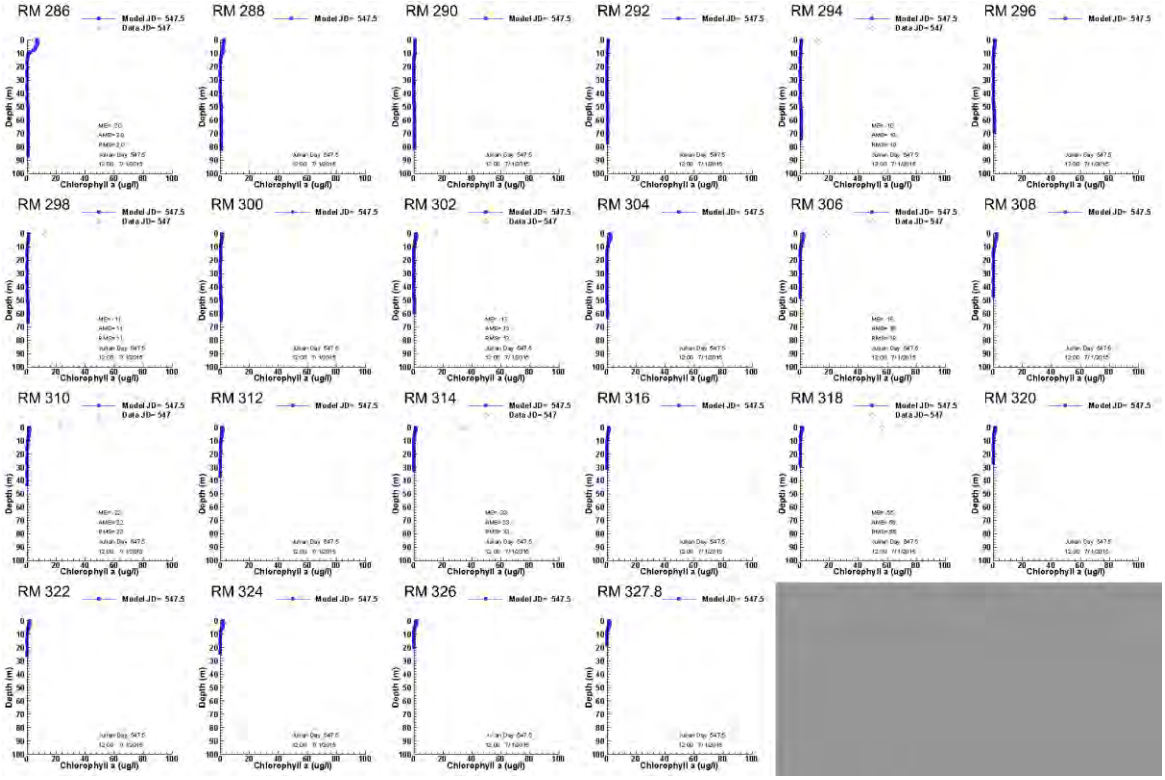


Figure 2008. Vertical profiles of chlorophyll a compared with data for 7/ 1/2015.

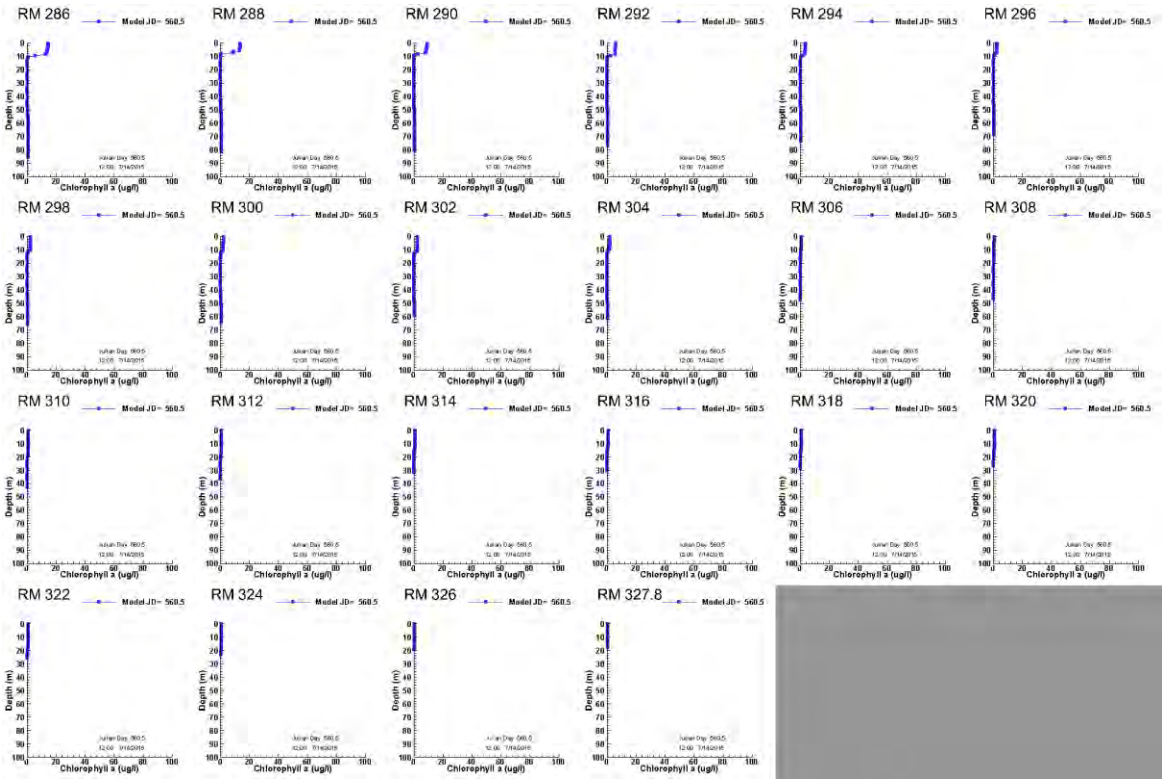


Figure 2009. Vertical profiles of chlorophyll a compared with data for 7/14/2015.

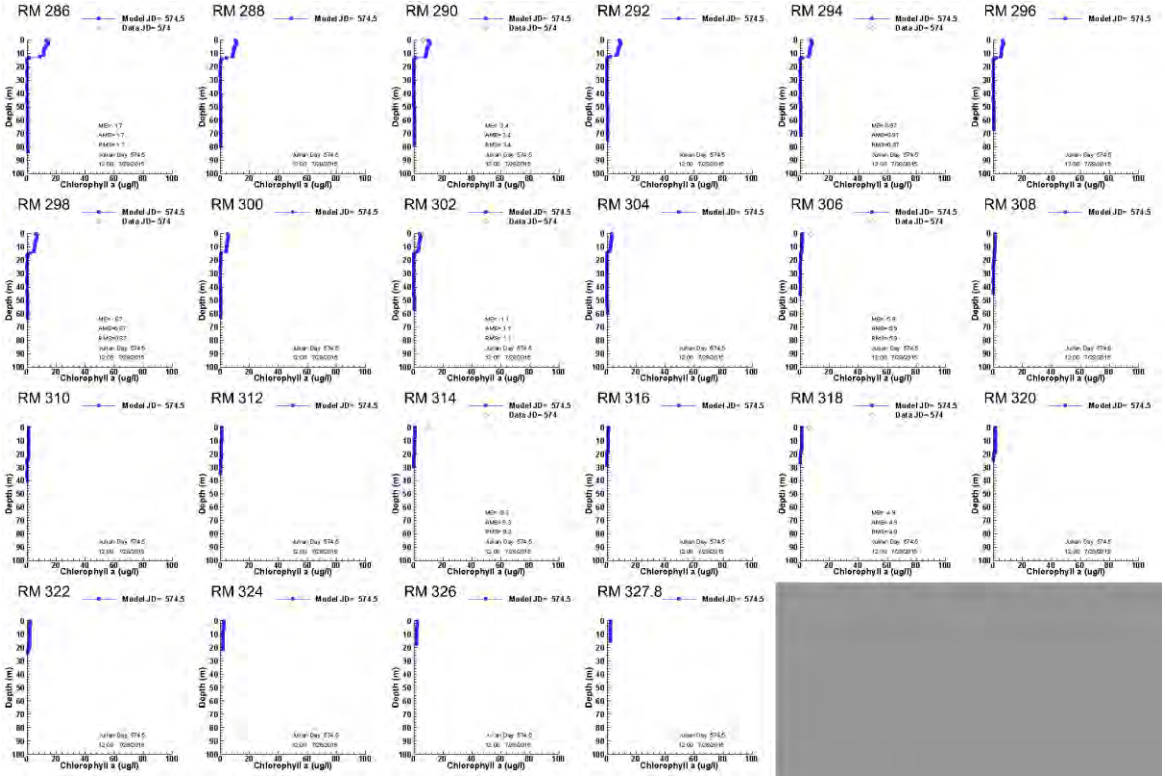


Figure 2010. Vertical profiles of chlorophyll a compared with data for 7/28/2015.

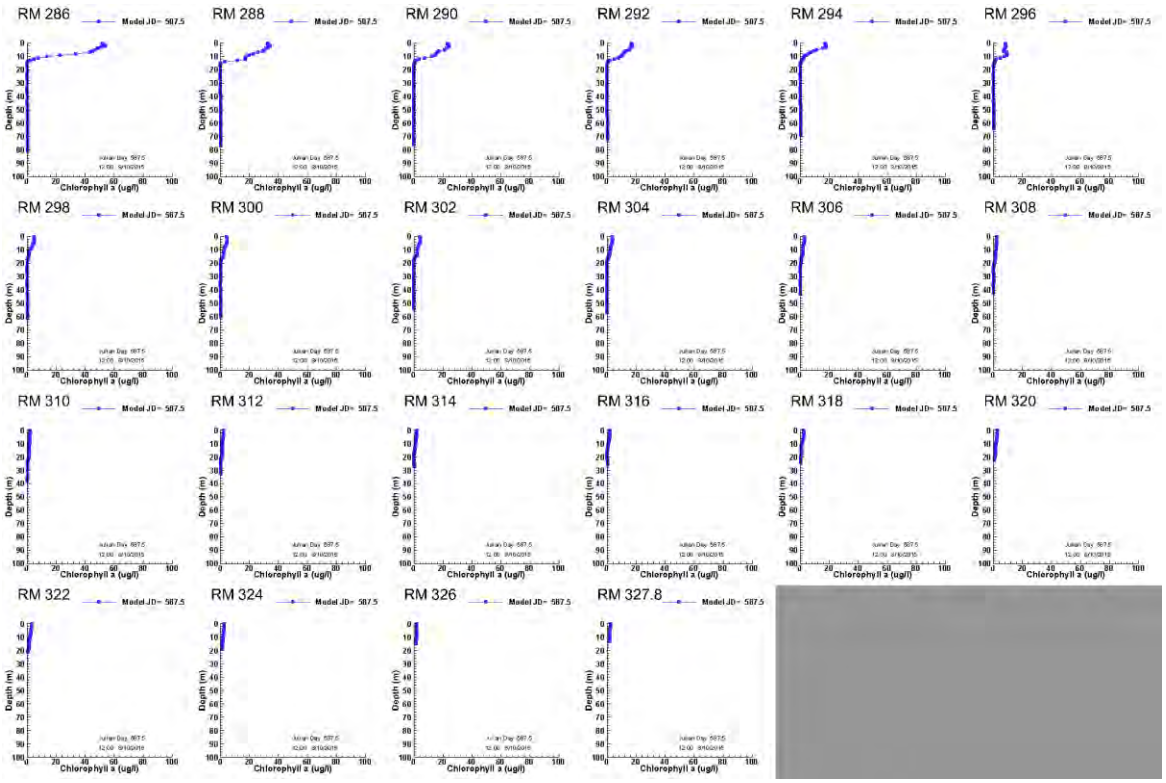


Figure 2011. Vertical profiles of chlorophyll a compared with data for 8/10/2015.

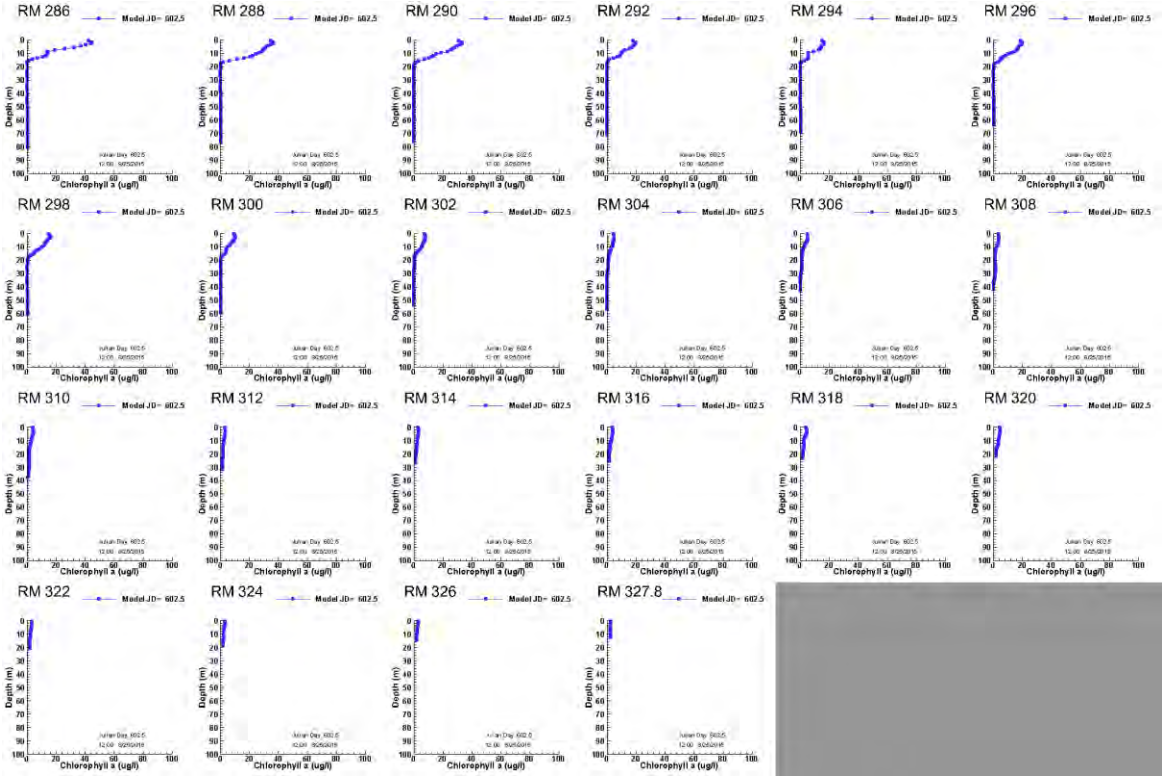


Figure 2012. Vertical profiles of chlorophyll a compared with data for 8/25/2015.

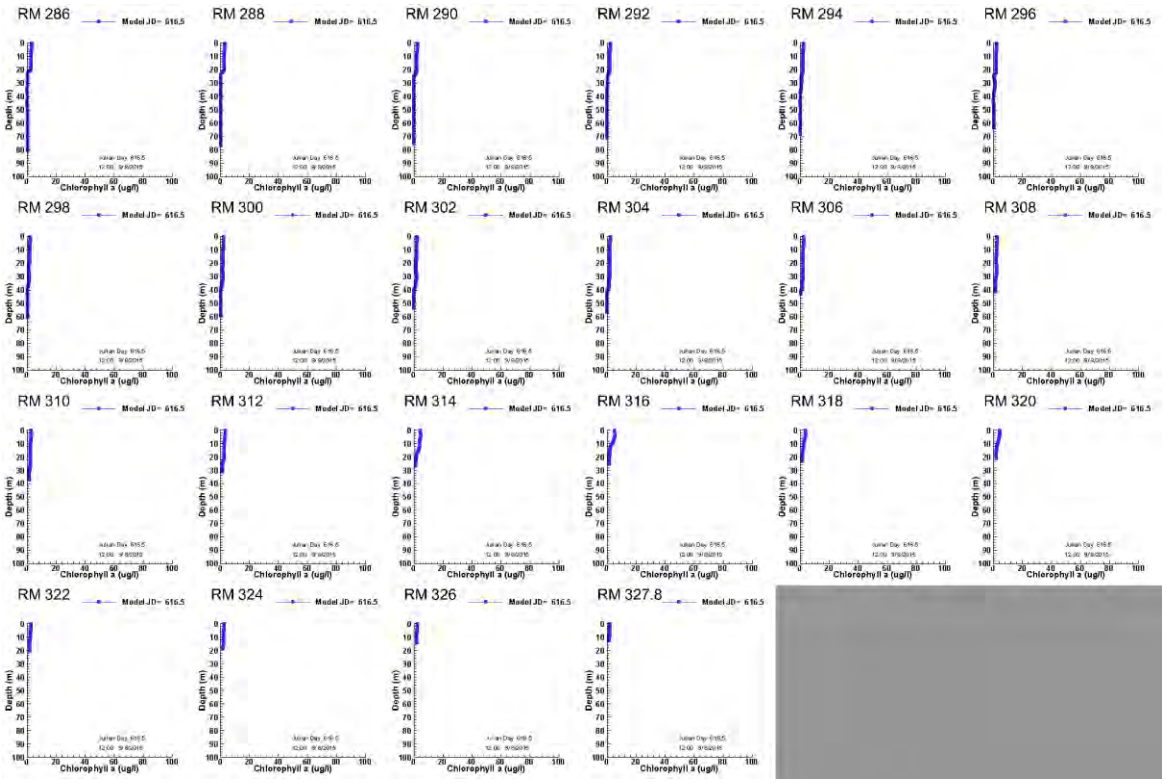


Figure 2013. Vertical profiles of chlorophyll a compared with data for 9/ 8/2015.

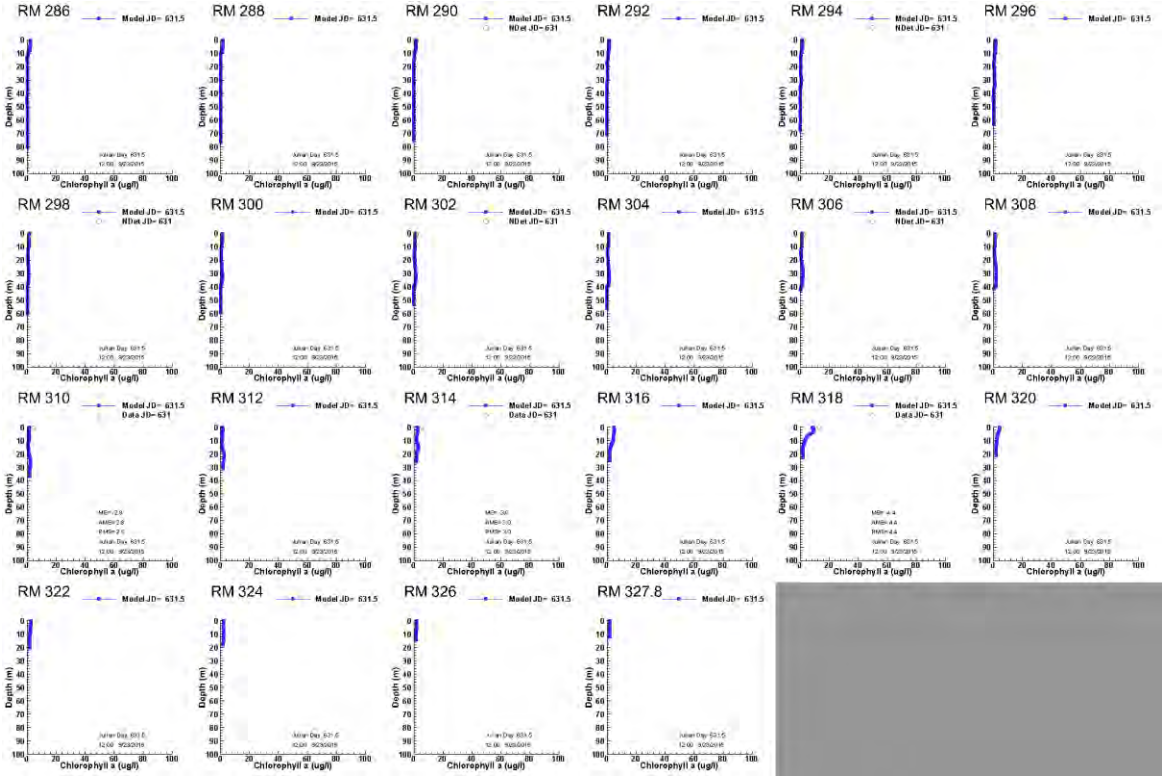


Figure 2014. Vertical profiles of chlorophyll a compared with data for 9/23/2015.

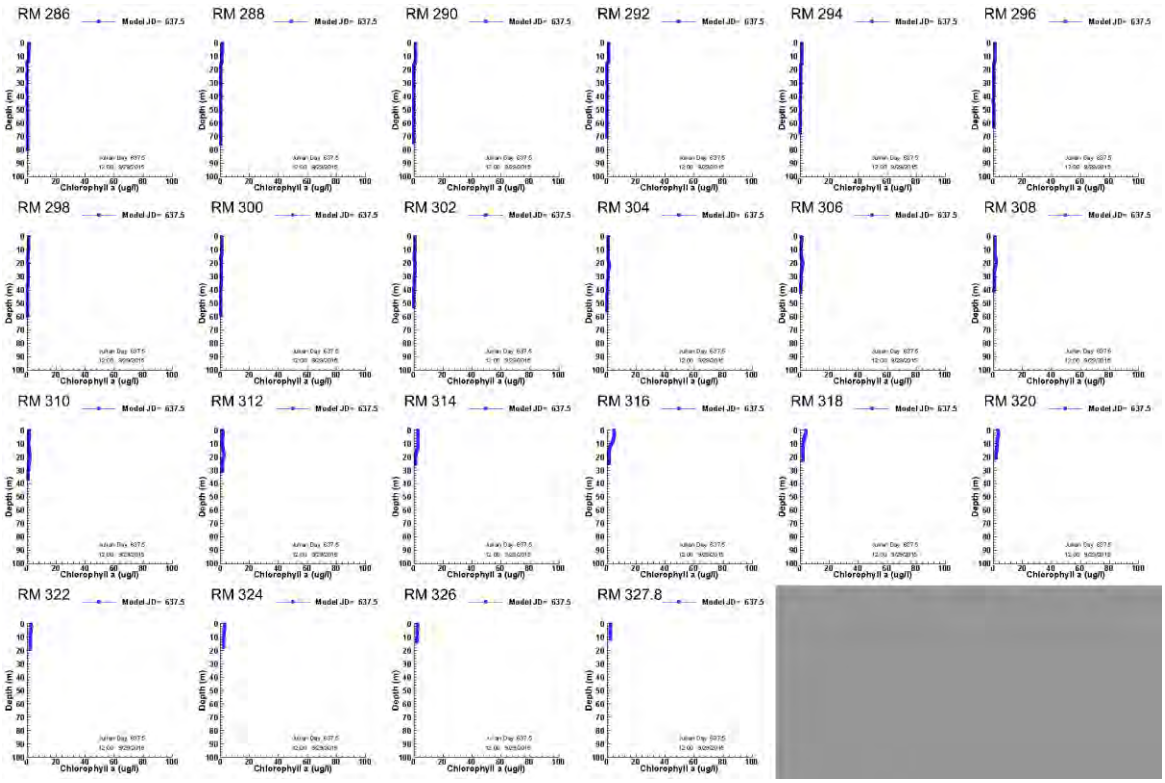


Figure 2015. Vertical profiles of chlorophyll a compared with data for 9/29/2015.

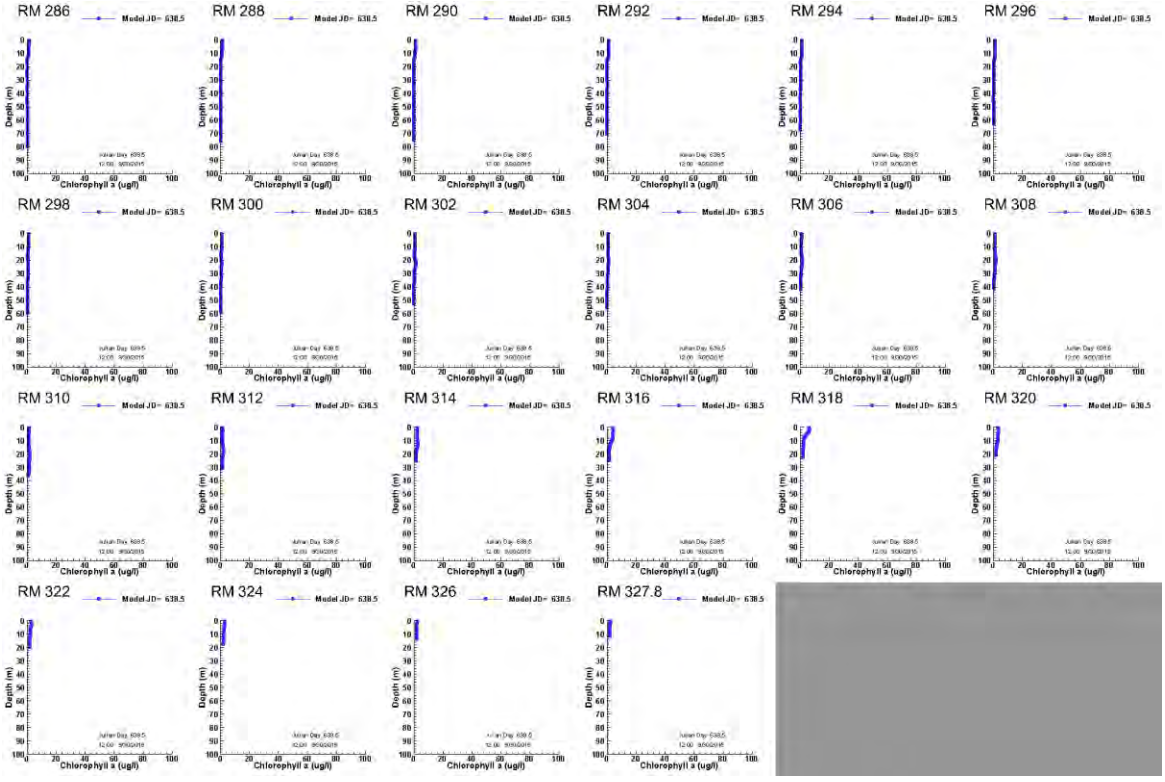


Figure 2016. Vertical profiles of chlorophyll a compared with data for 9/30/2015.

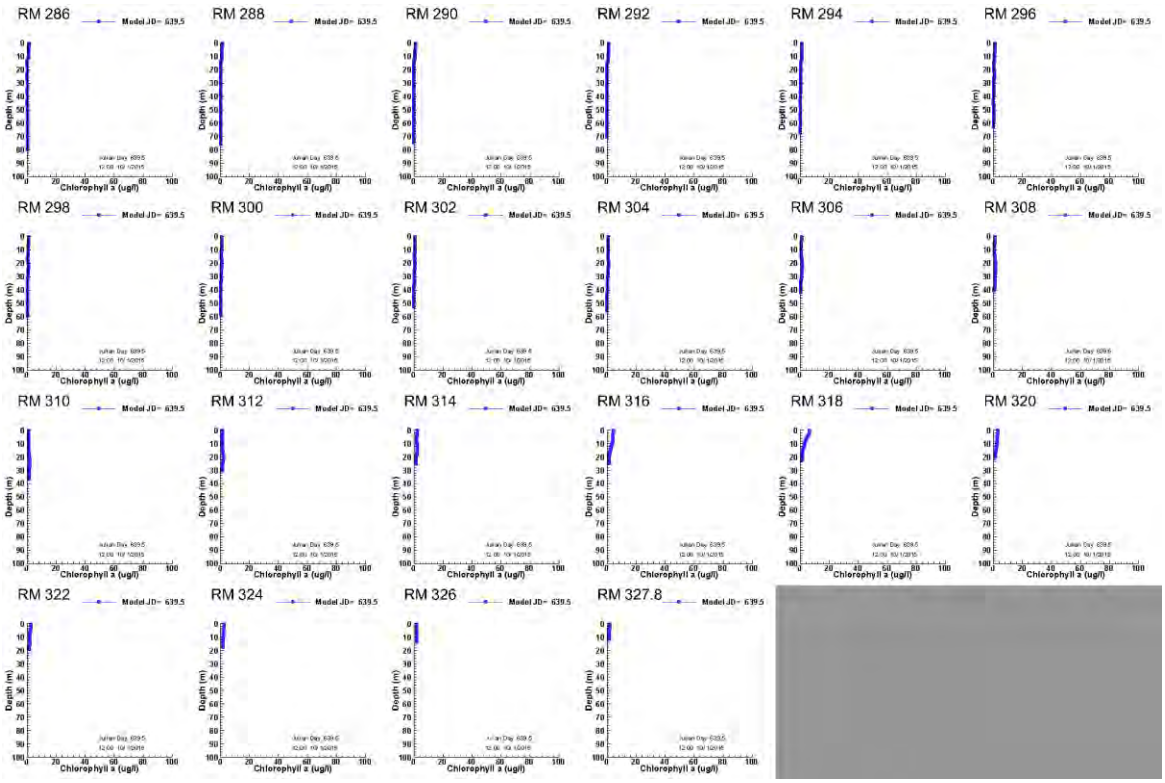


Figure 2017. Vertical profiles of chlorophyll a compared with data for 10/ 1/2015.

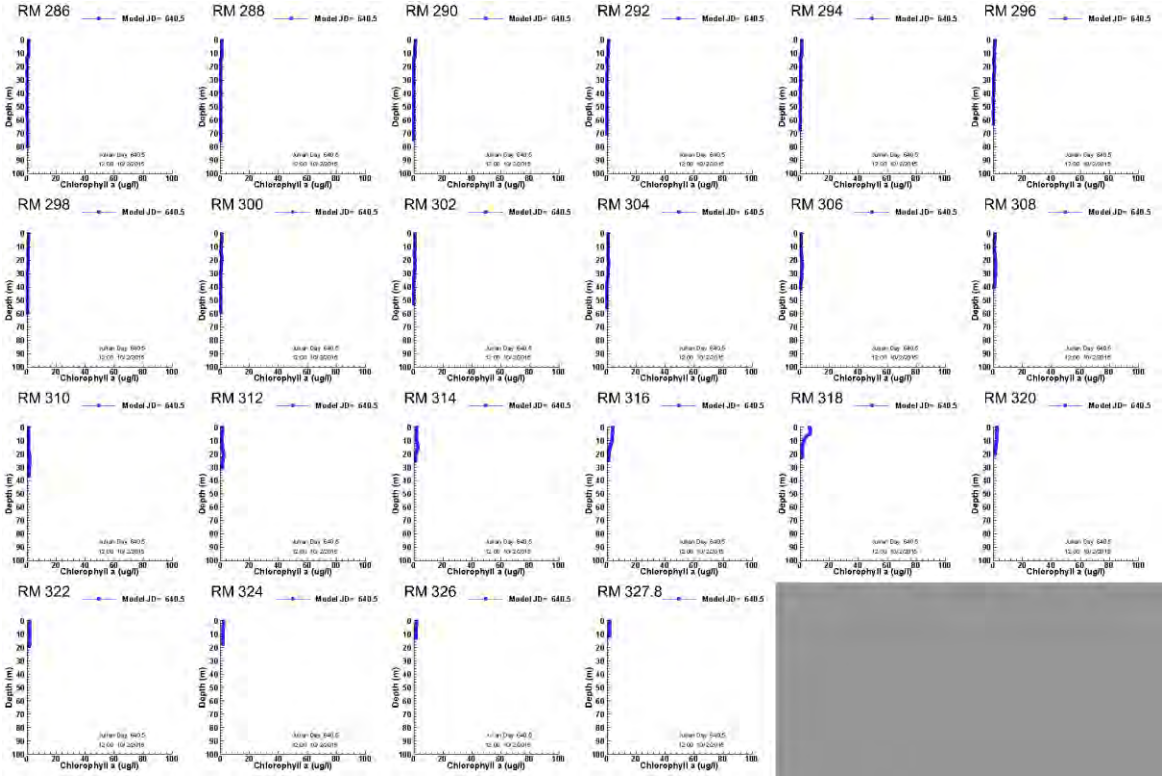


Figure 2018. Vertical profiles of chlorophyll a compared with data for 10/ 2/2015.

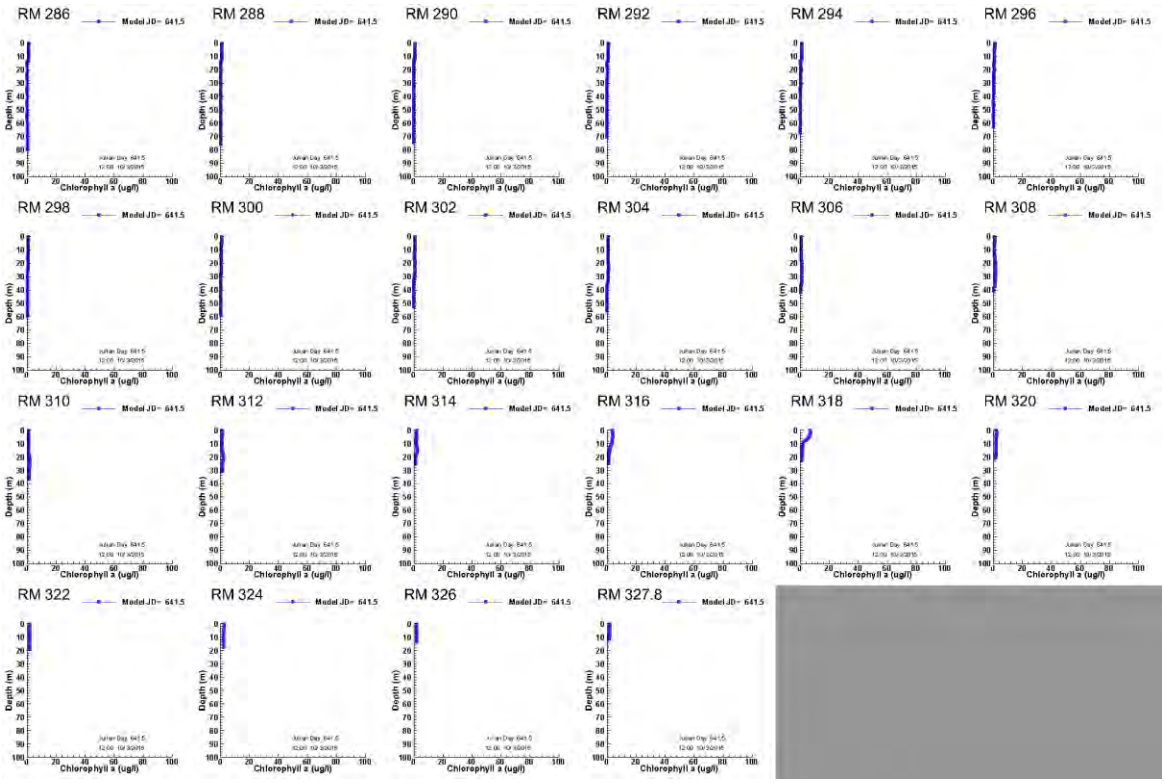


Figure 2019. Vertical profiles of chlorophyll a compared with data for 10/ 3/2015.

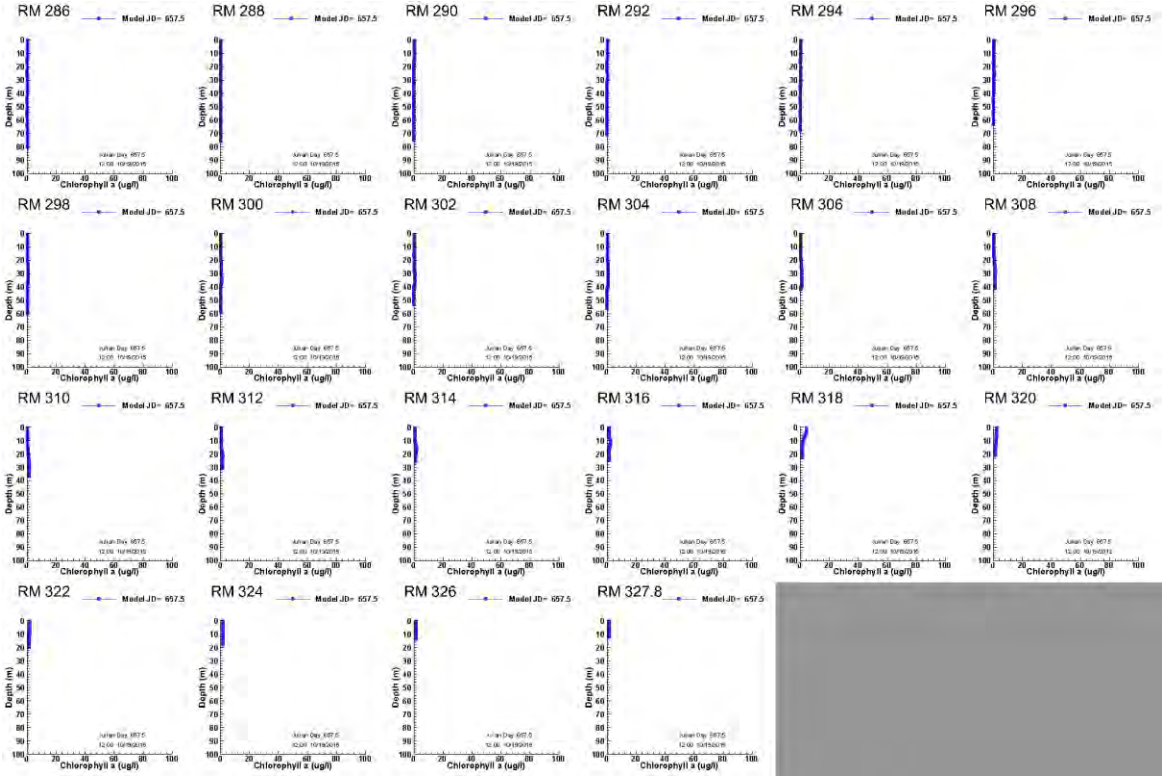


Figure 2020. Vertical profiles of chlorophyll a compared with data for 10/19/2015.

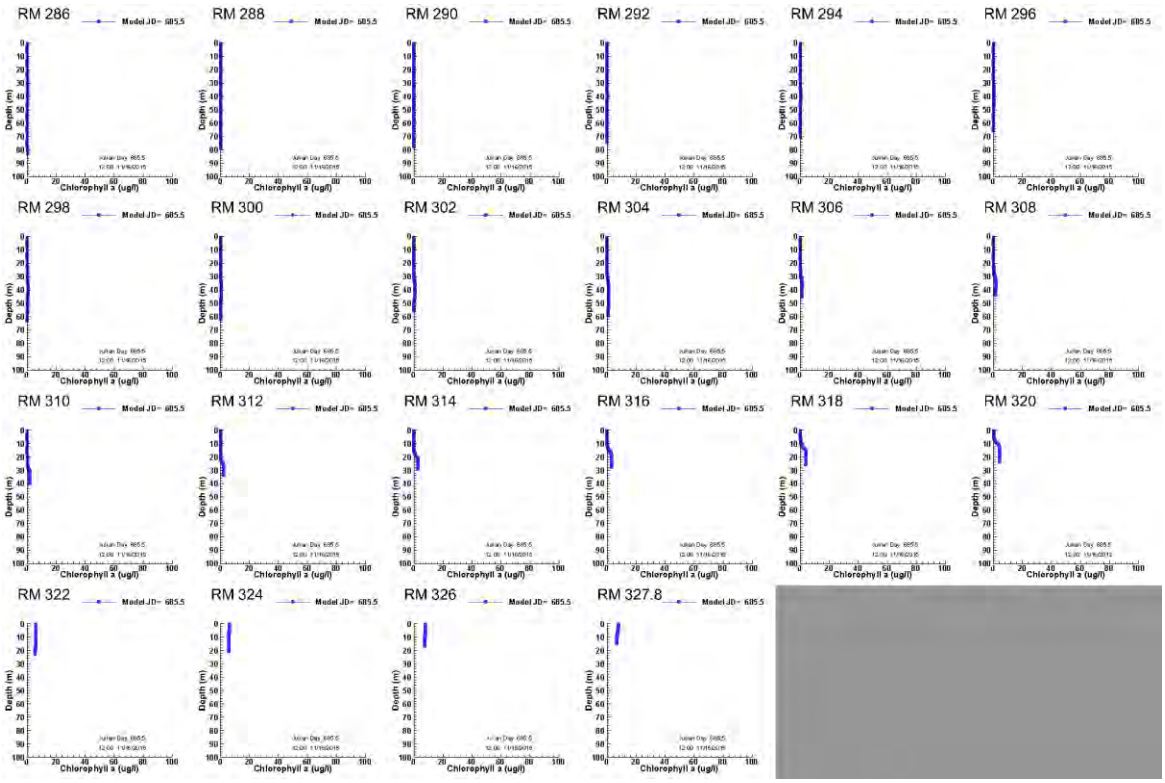


Figure 2021. Vertical profiles of chlorophyll a compared with data for 11/16/2015.

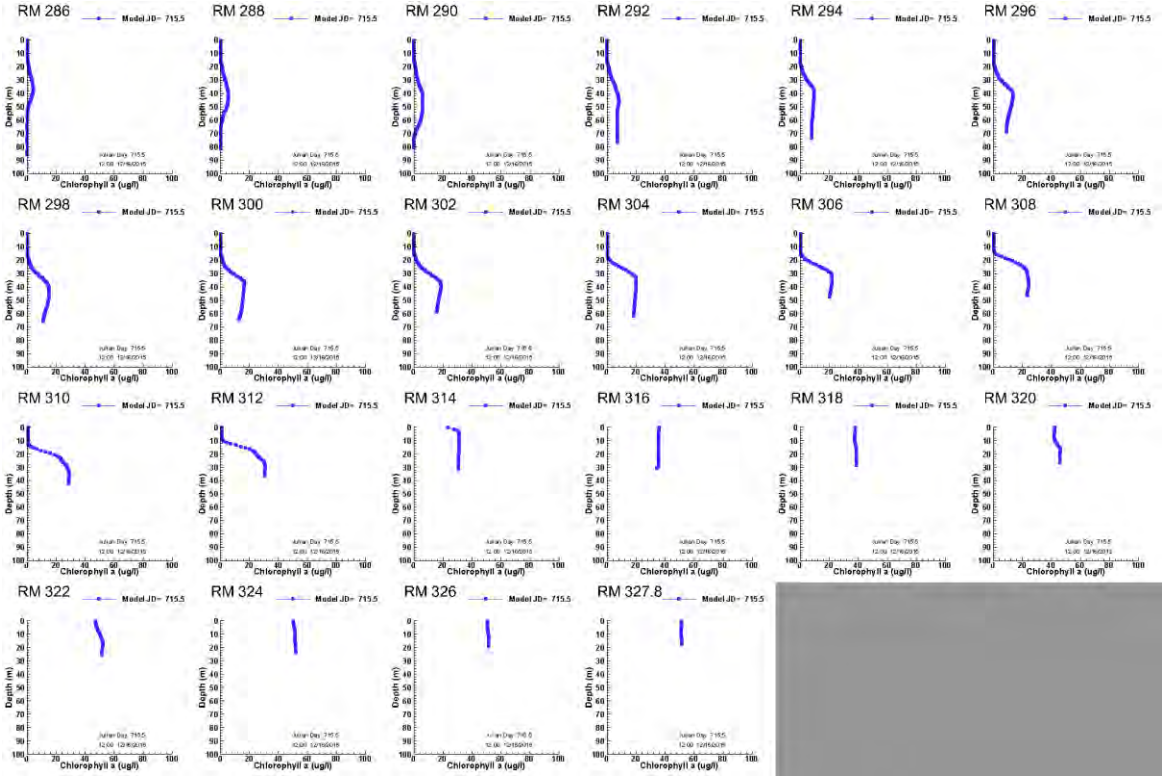


Figure 2022. Vertical profiles of chlorophyll a compared with data for 12/16/2015.

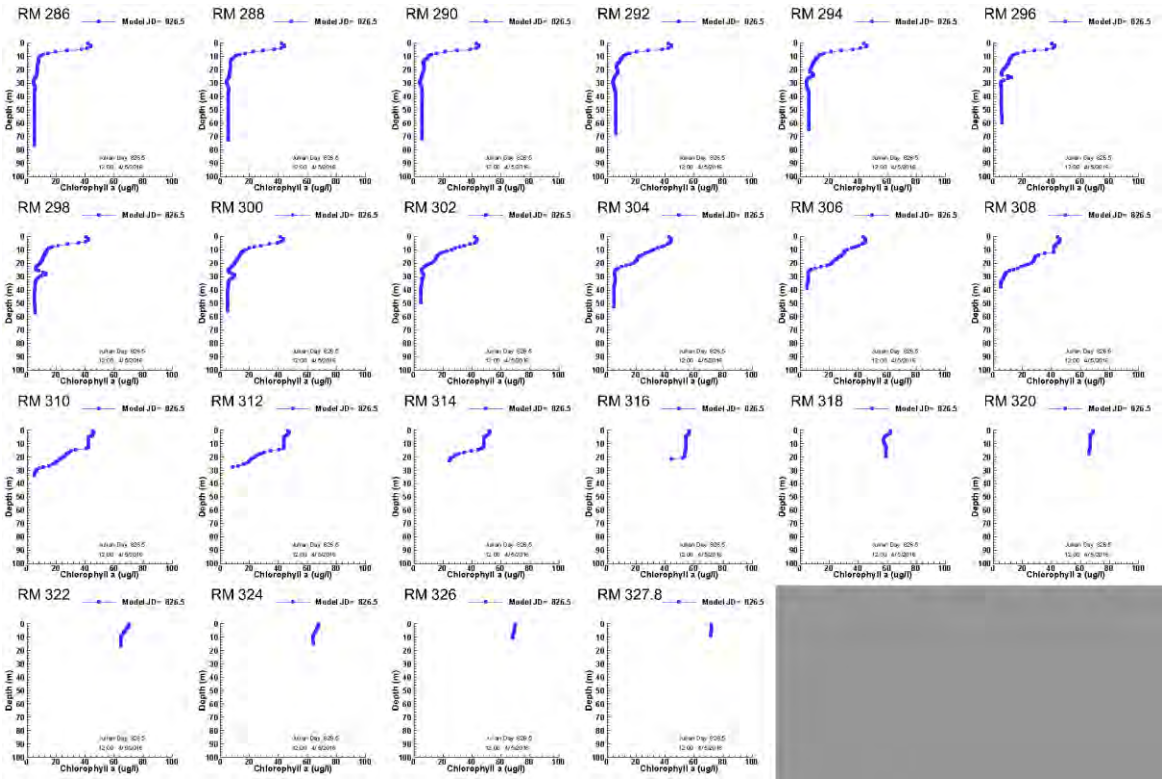


Figure 2023. Vertical profiles of chlorophyll a compared with data for 4/ 5/2016.

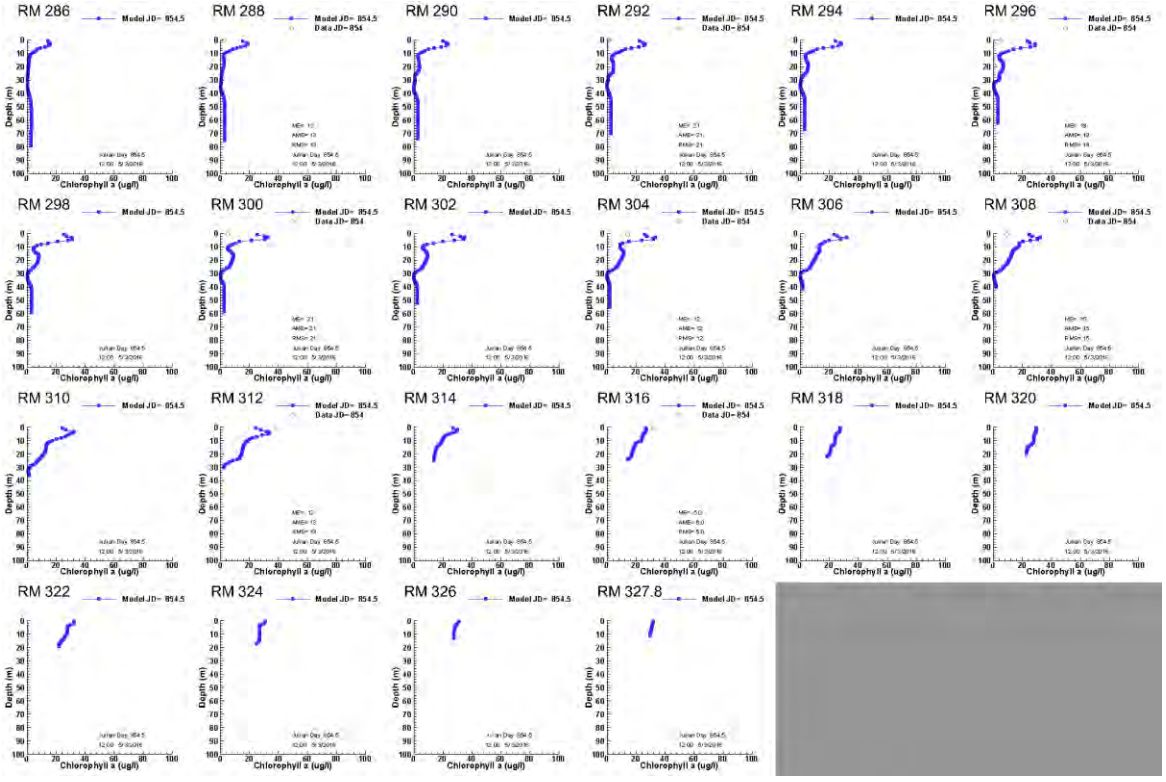


Figure 2024. Vertical profiles of chlorophyll a compared with data for 5/ 3/2016.

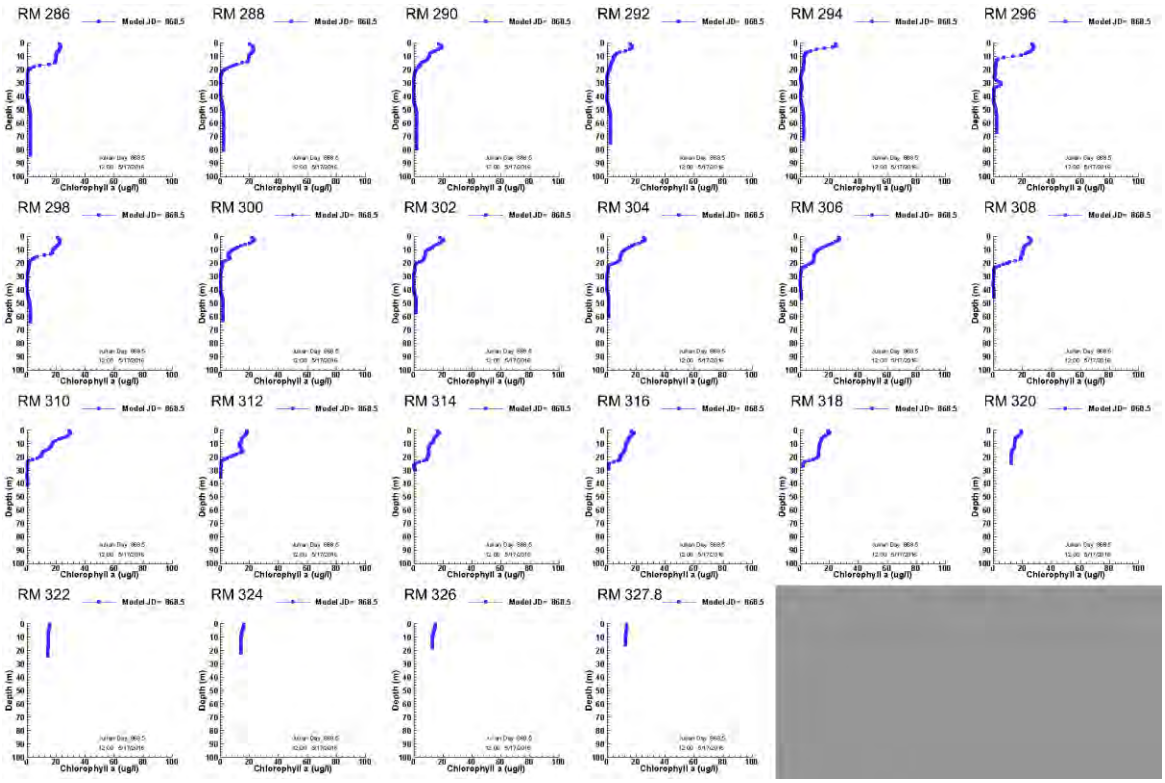


Figure 2025. Vertical profiles of chlorophyll a compared with data for 5/17/2016.

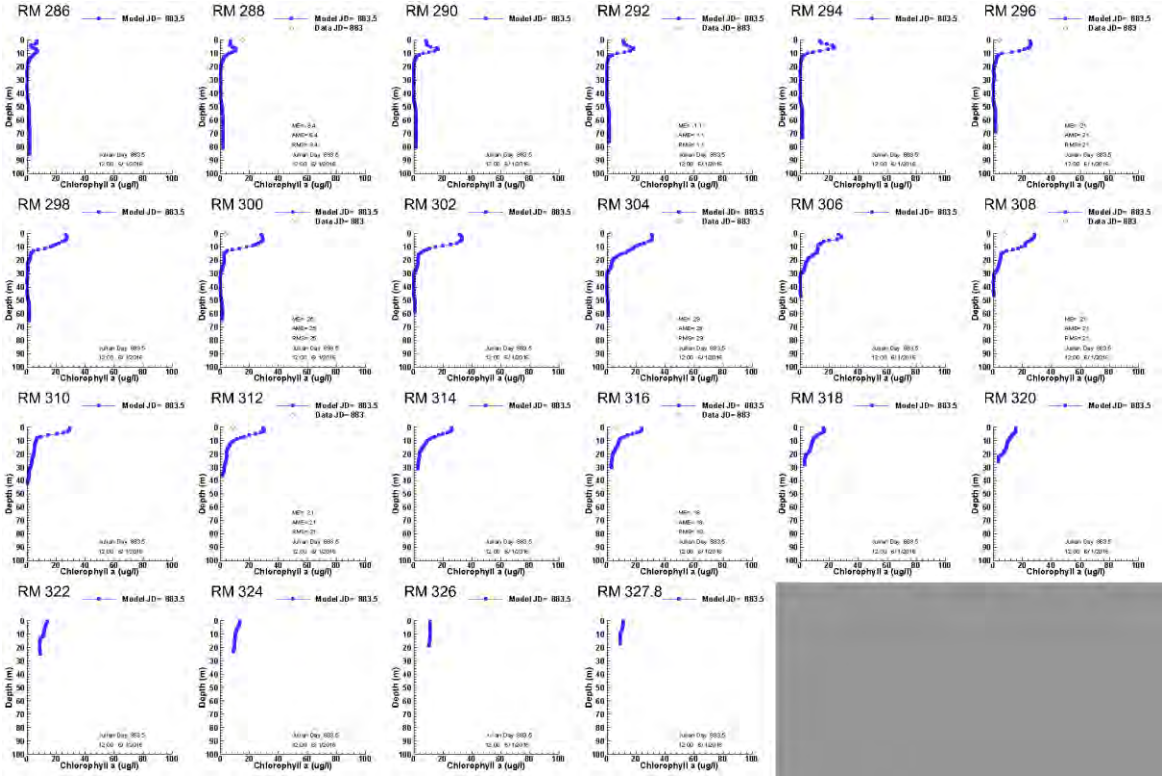


Figure 2026. Vertical profiles of chlorophyll a compared with data for 6/ 1/2016.

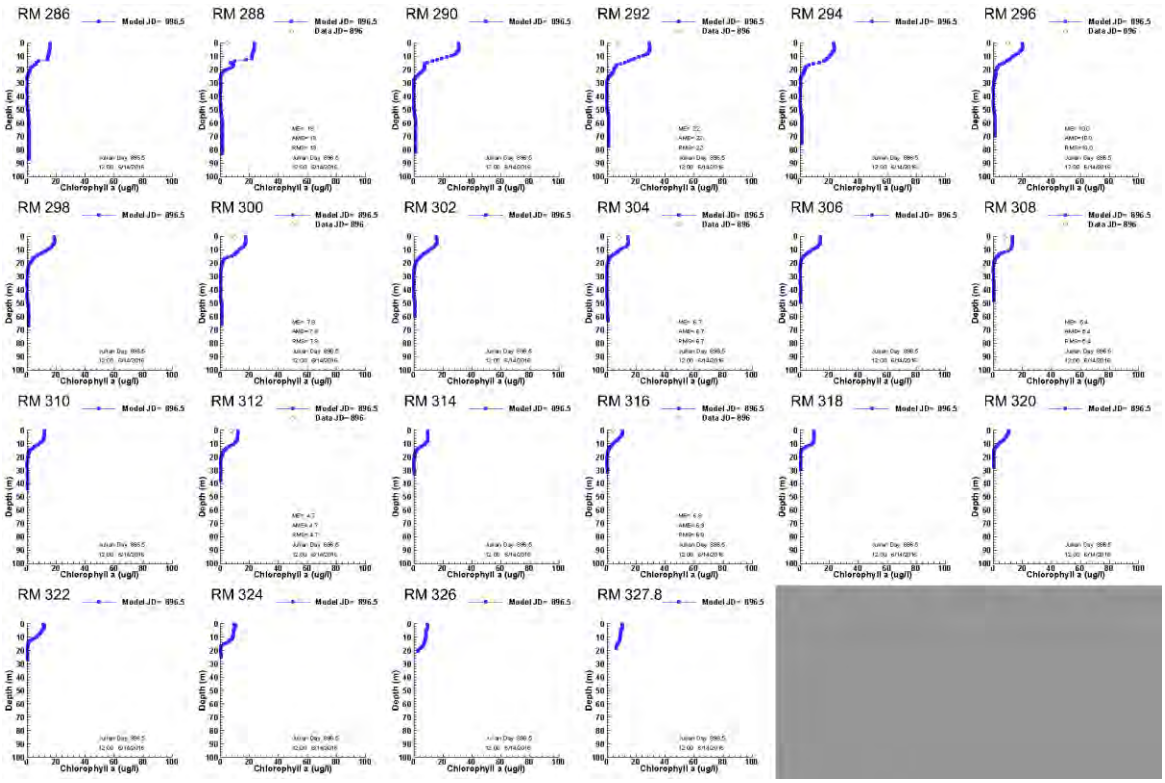


Figure 2027. Vertical profiles of chlorophyll a compared with data for 6/14/2016.

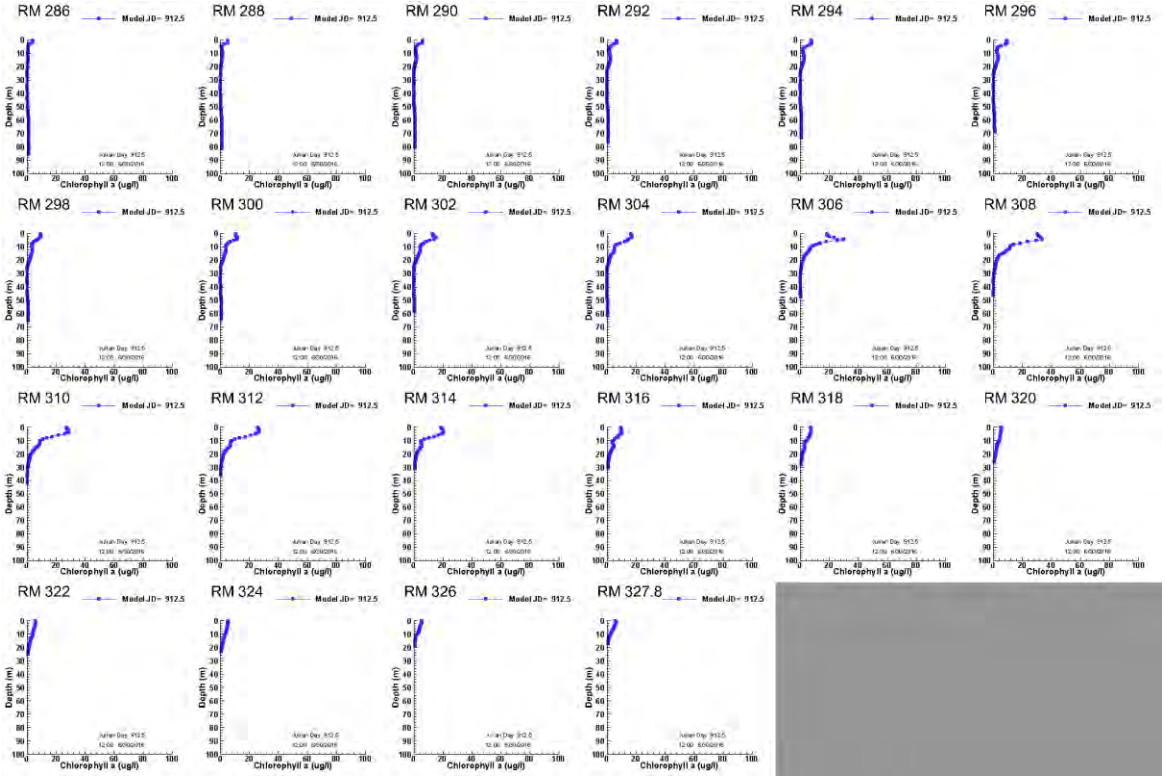


Figure 2028. Vertical profiles of chlorophyll a compared with data for 6/30/2016.

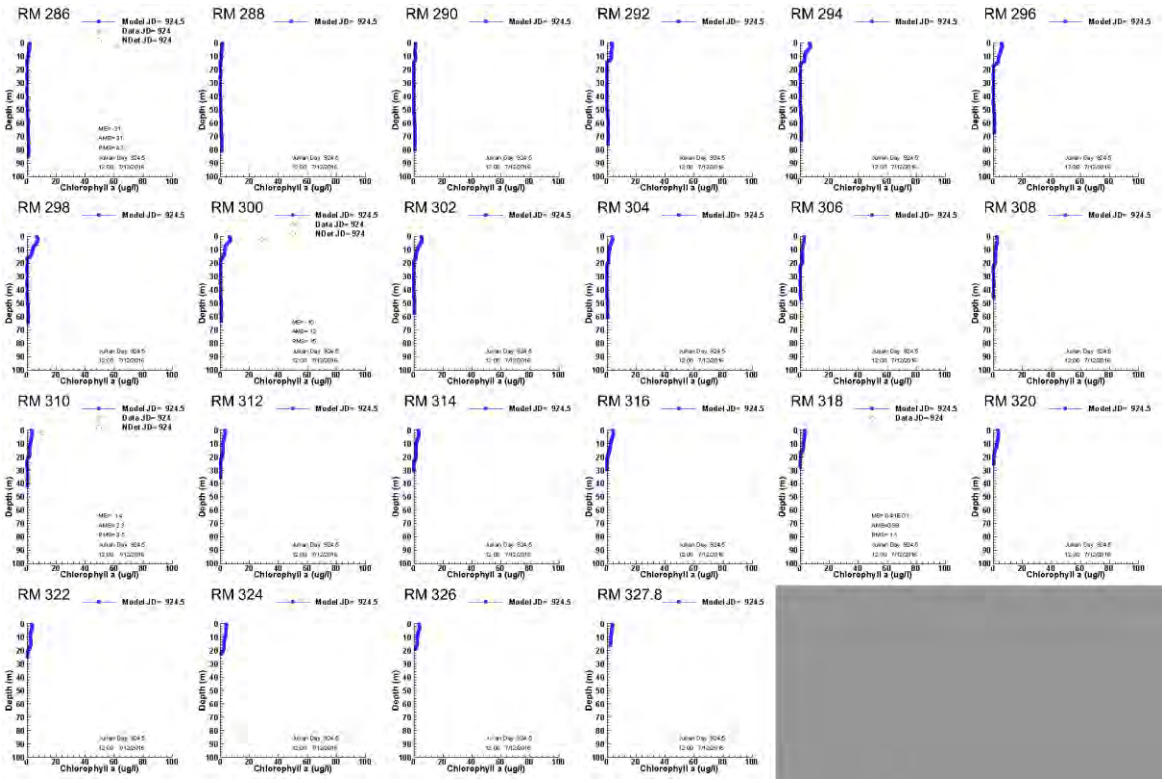


Figure 2029. Vertical profiles of chlorophyll a compared with data for 7/12/2016.

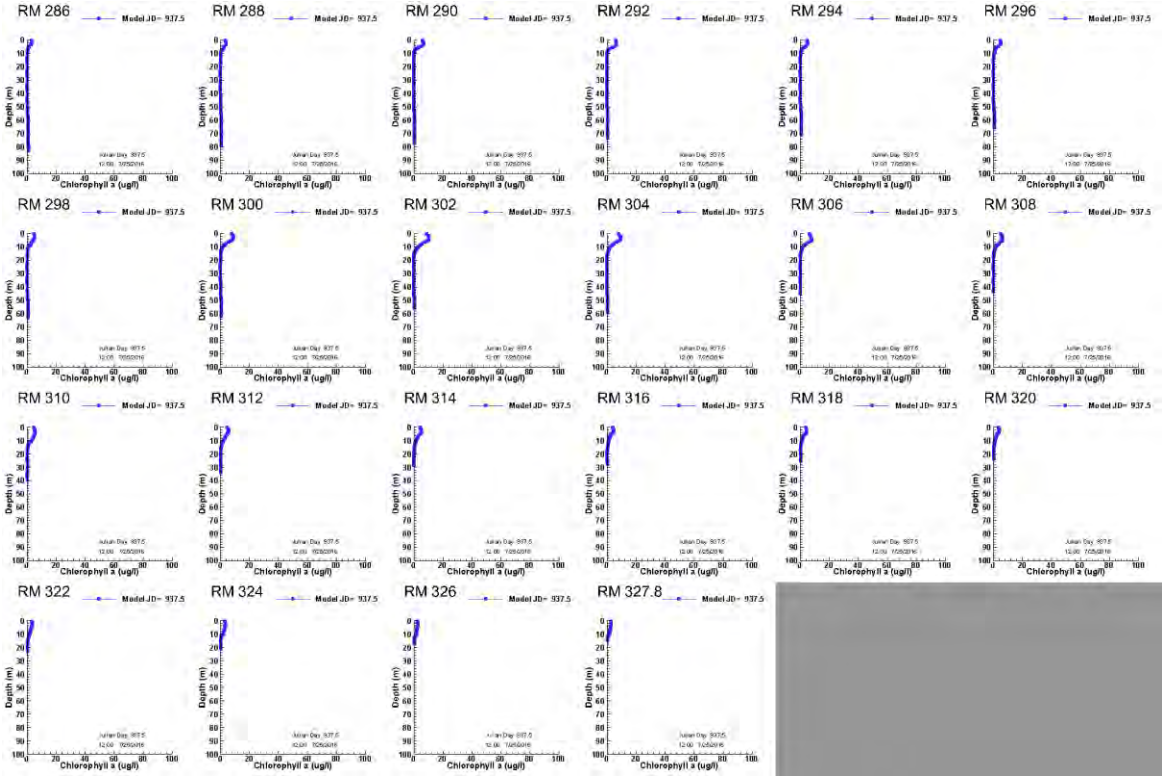


Figure 2030. Vertical profiles of chlorophyll a compared with data for 7/25/2016.

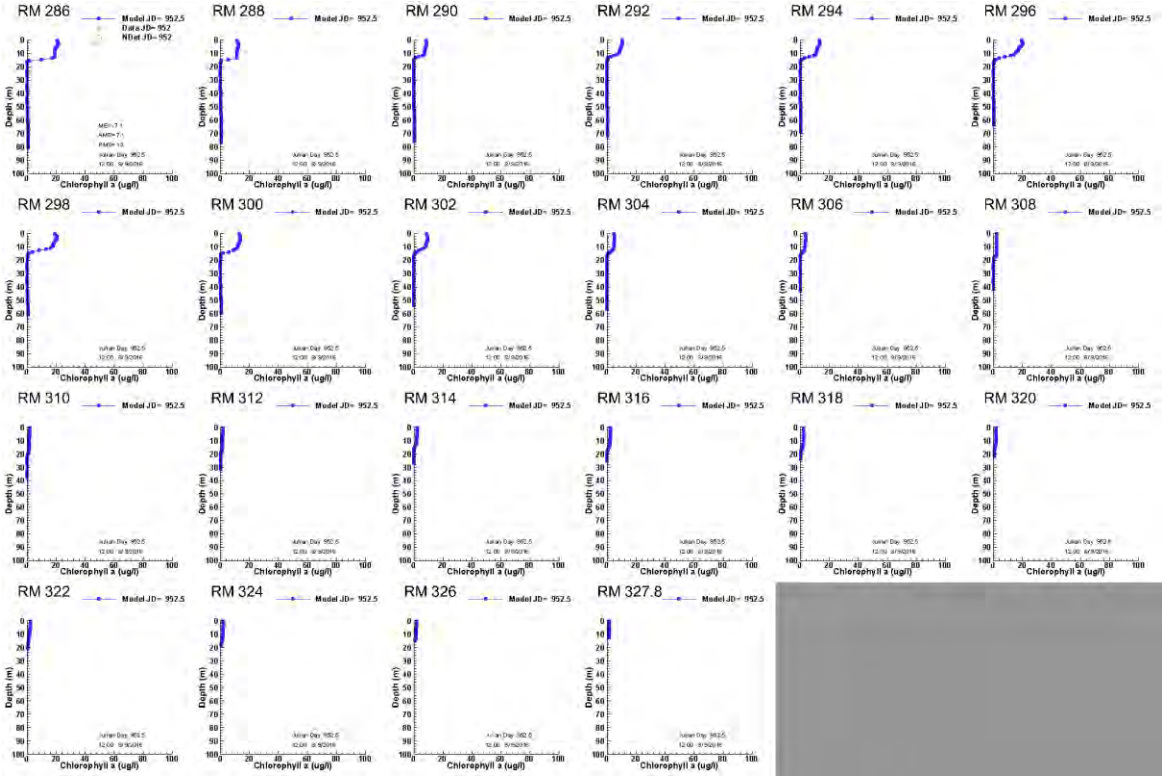


Figure 2031. Vertical profiles of chlorophyll a compared with data for 8/ 9/2016.

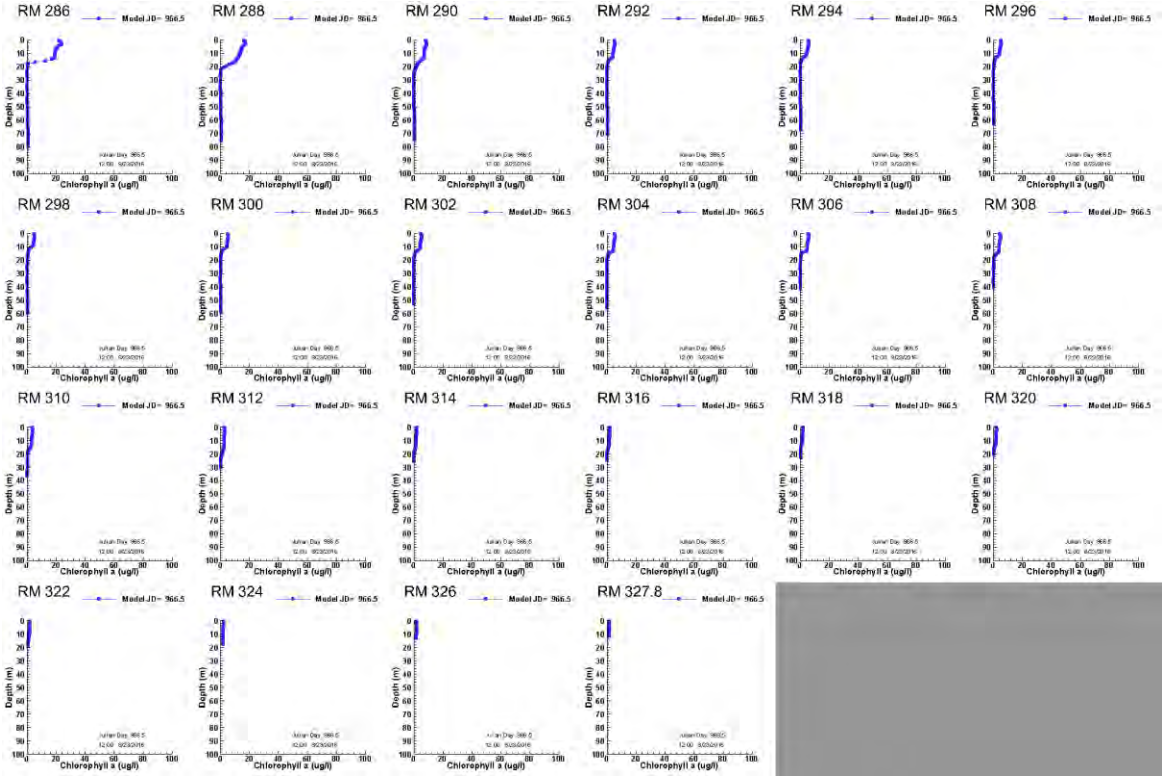


Figure 2032. Vertical profiles of chlorophyll a compared with data for 8/23/2016.

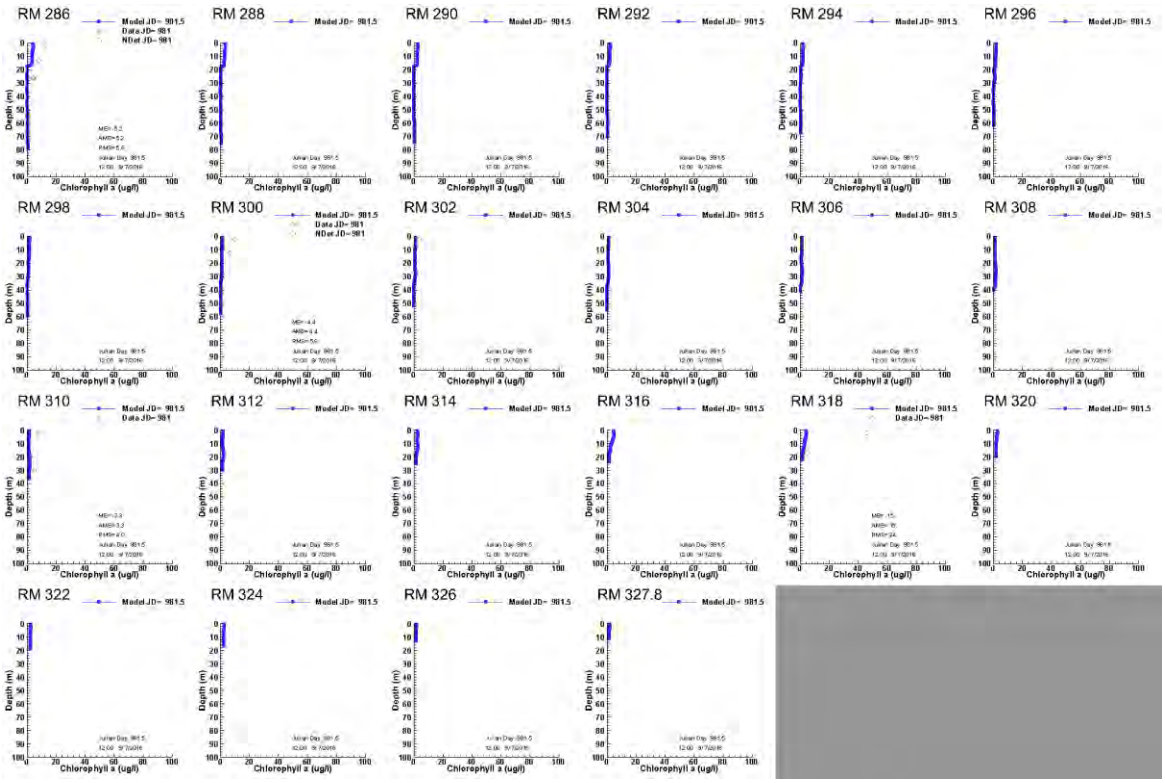


Figure 2033. Vertical profiles of chlorophyll a compared with data for 9/ 7/2016.

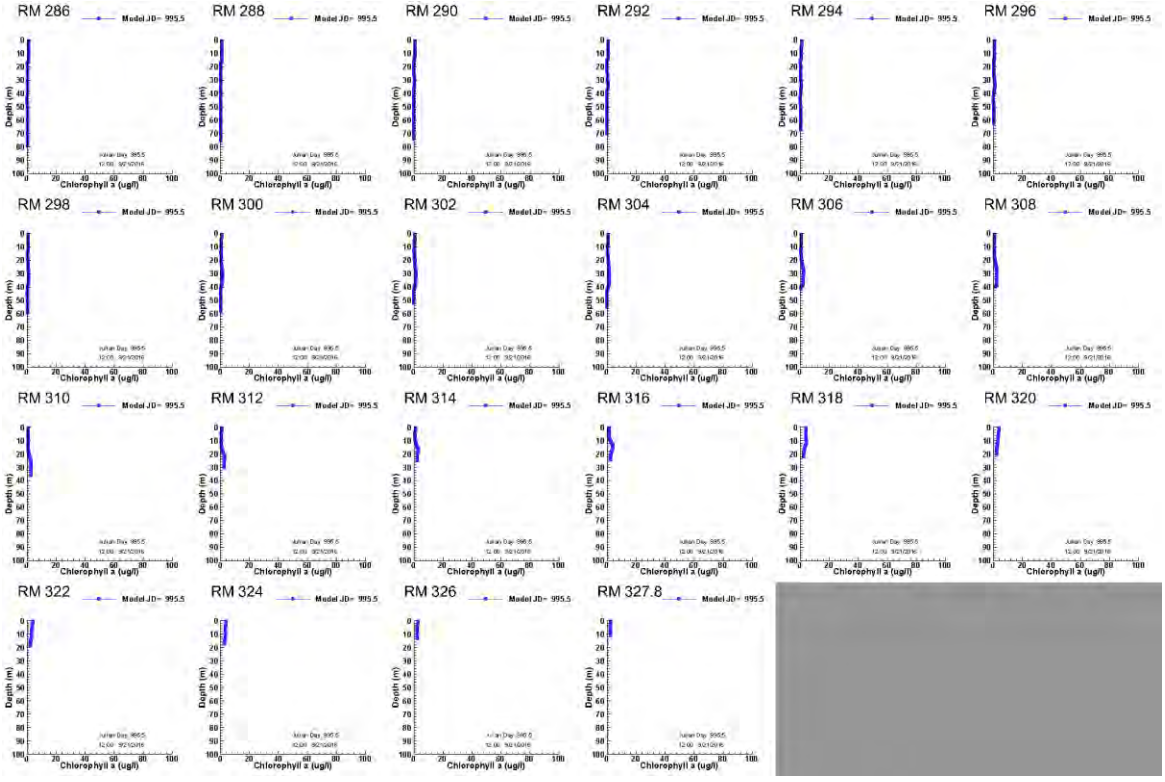


Figure 2034. Vertical profiles of chlorophyll a compared with data for 9/21/2016.

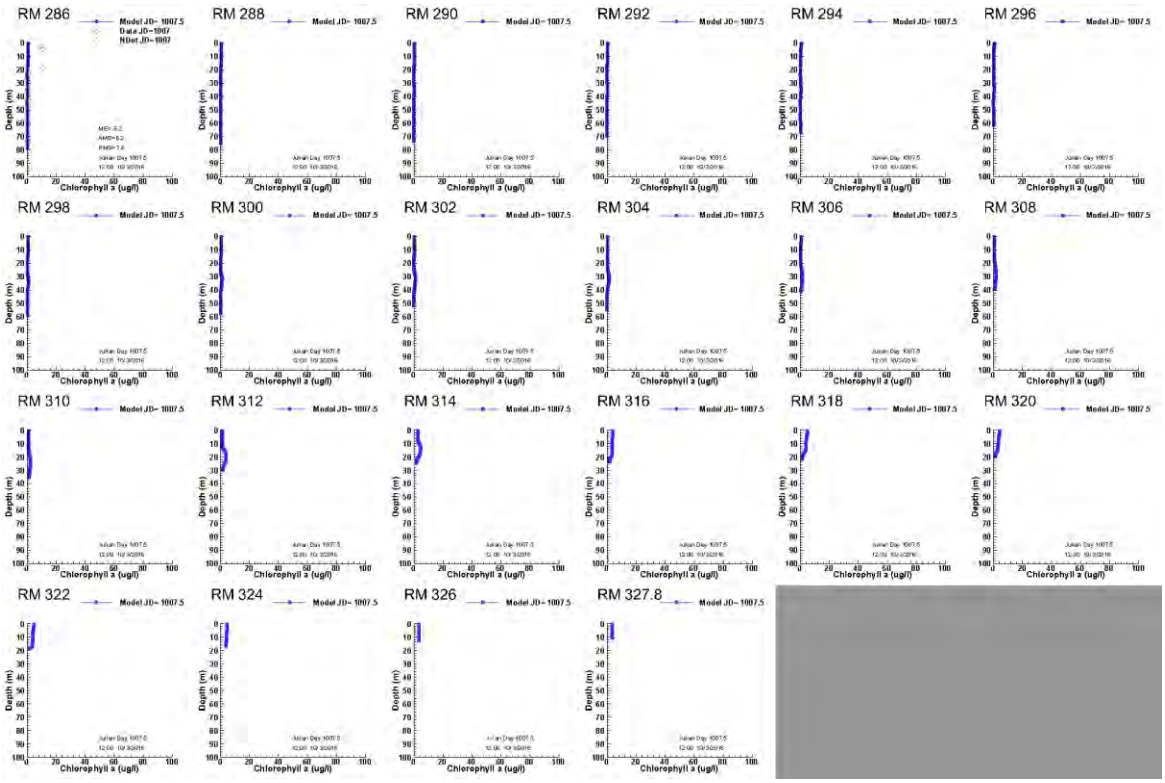


Figure 2035. Vertical profiles of chlorophyll a compared with data for 10/ 3/2016.

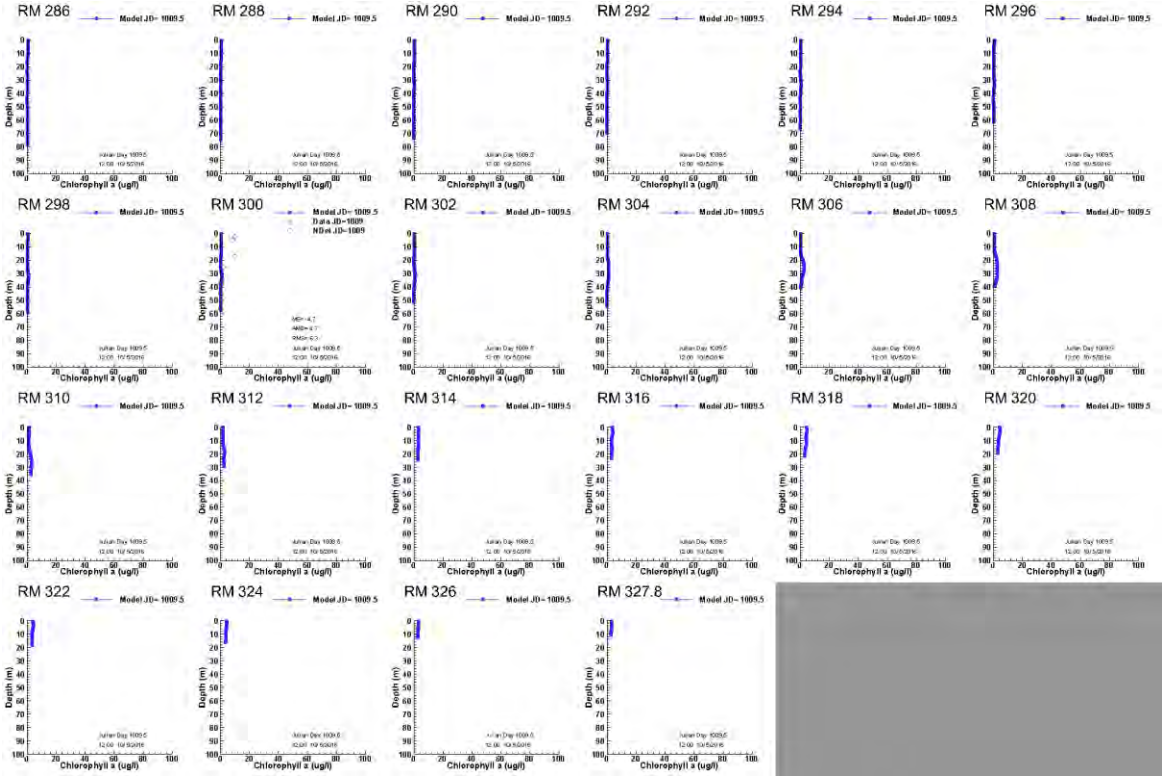


Figure 2036. Vertical profiles of chlorophyll a compared with data for 10/ 5/2016.

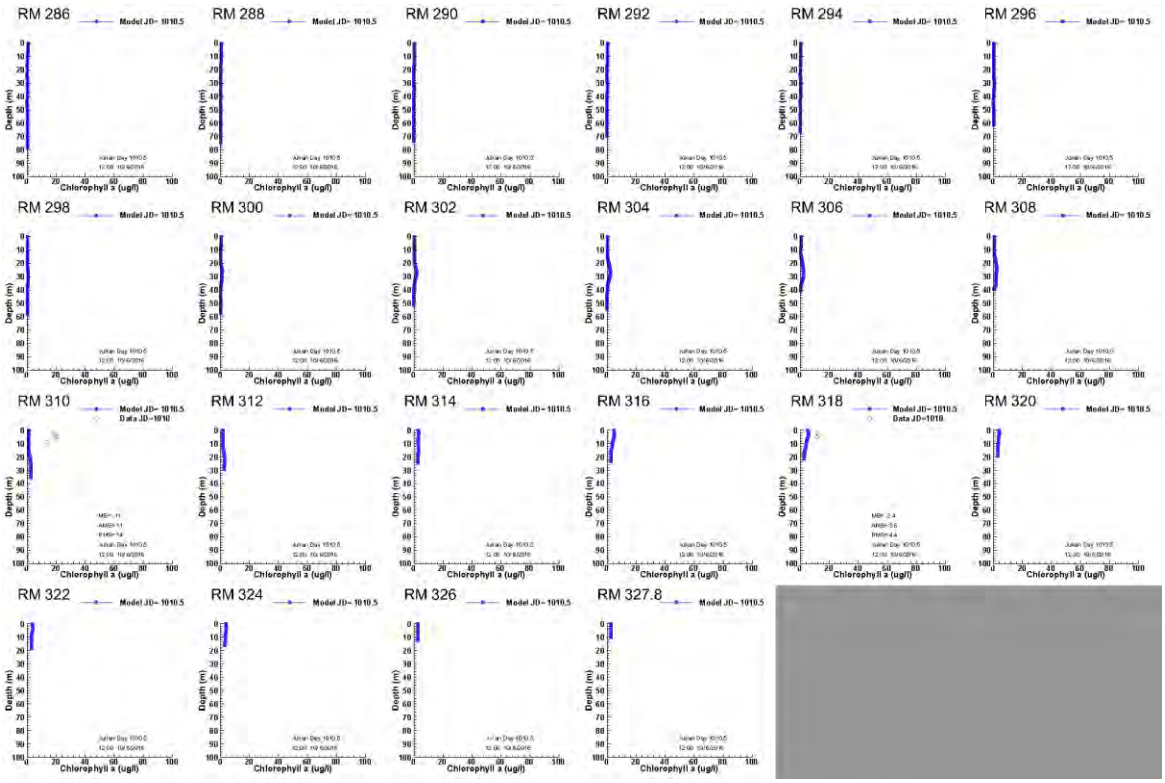


Figure 2037. Vertical profiles of chlorophyll a compared with data for 10/ 6/2016.

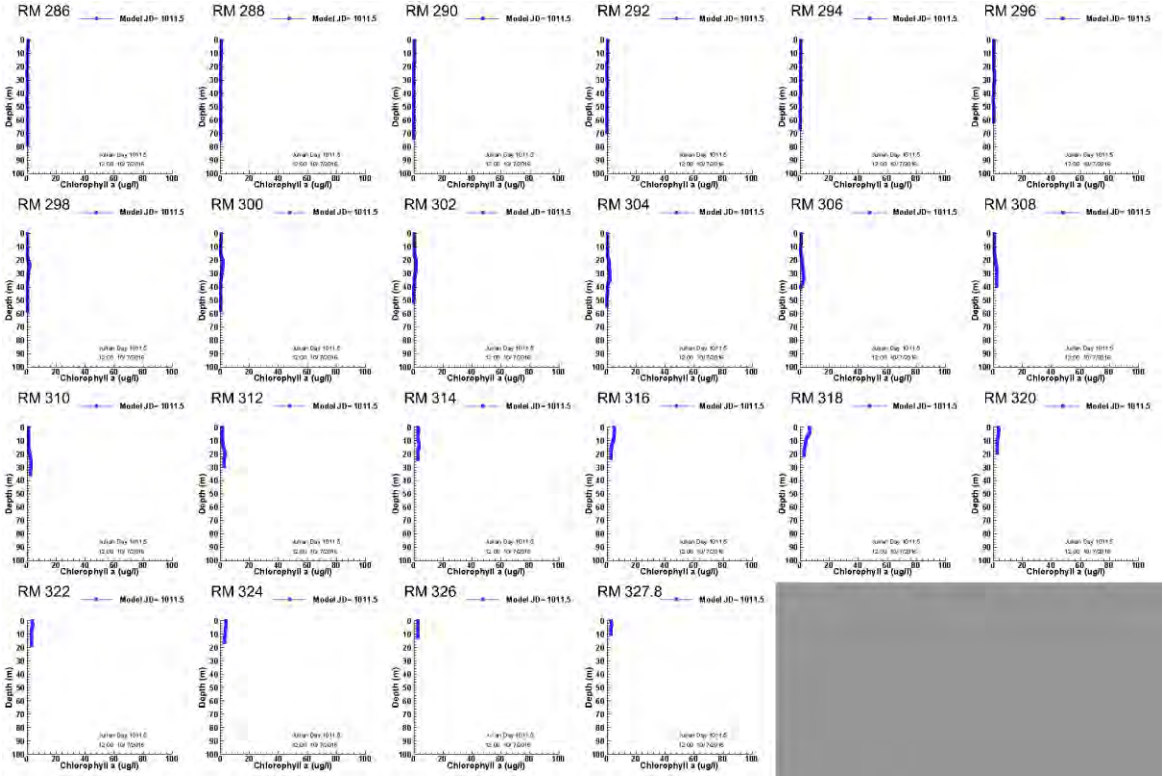


Figure 2038. Vertical profiles of chlorophyll a compared with data for 10/ 7/2016.

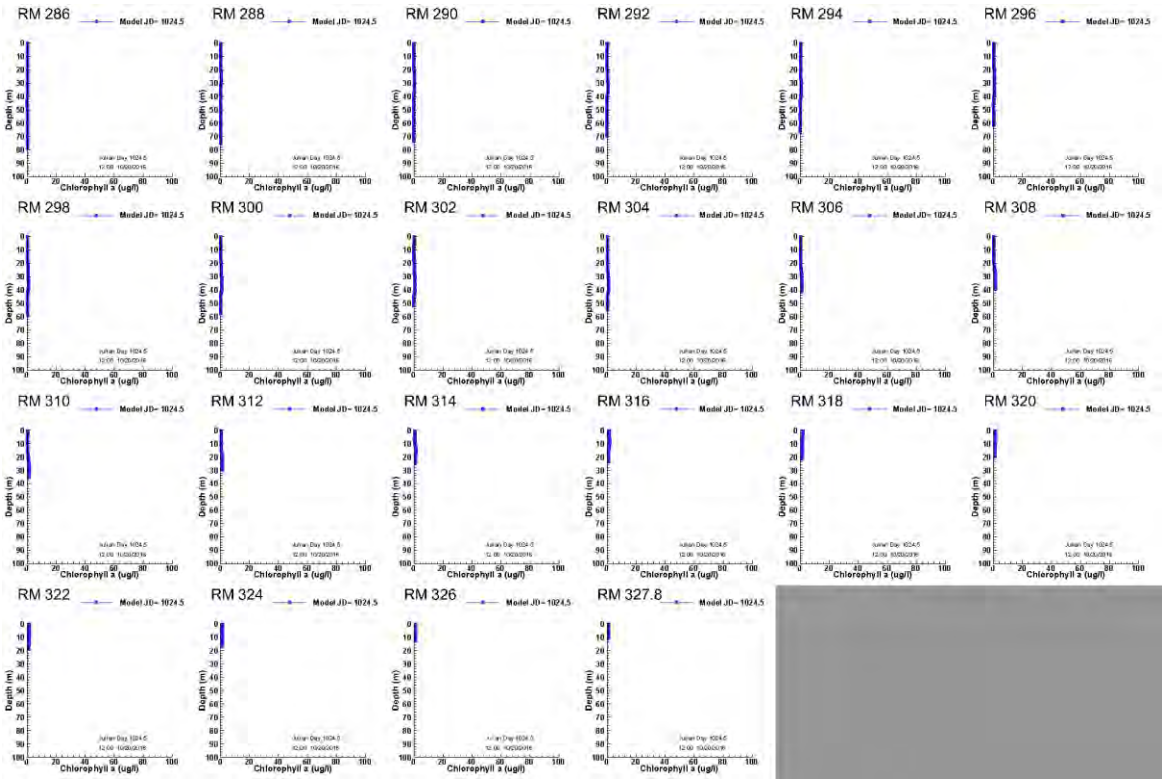


Figure 2039. Vertical profiles of chlorophyll a compared with data for 10/20/2016.

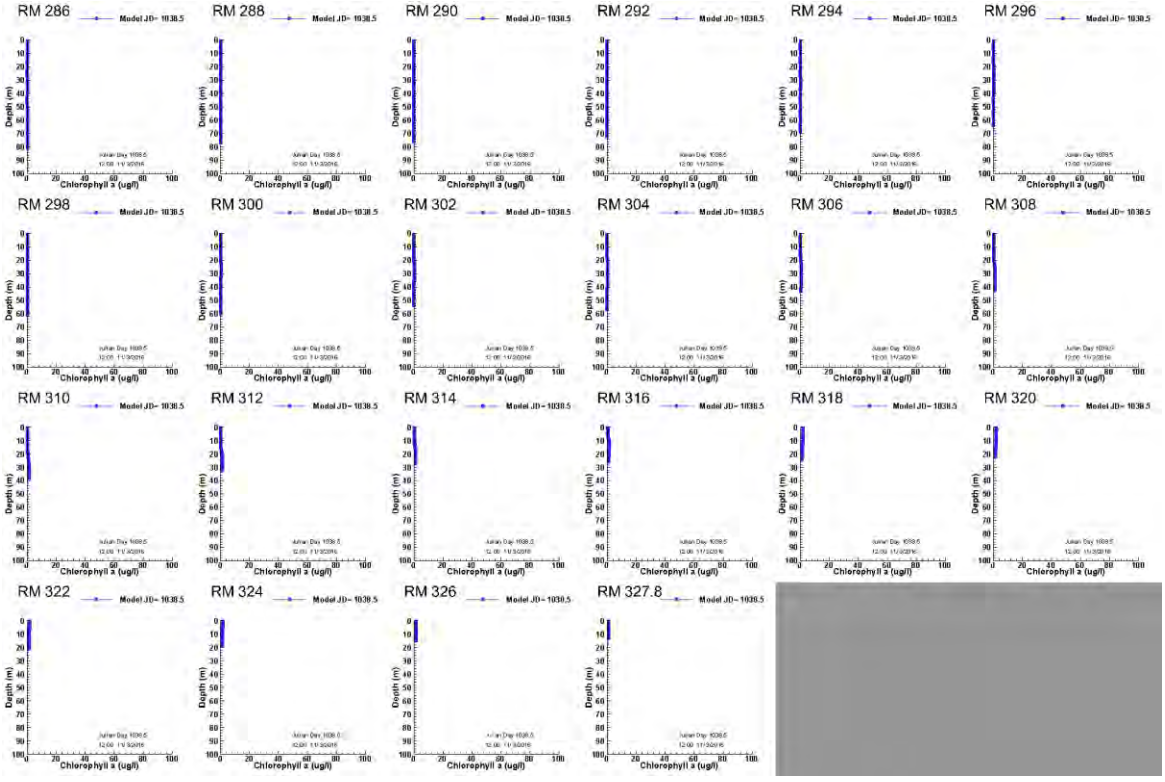


Figure 2040. Vertical profiles of chlorophyll a compared with data for 11/ 3/2016.

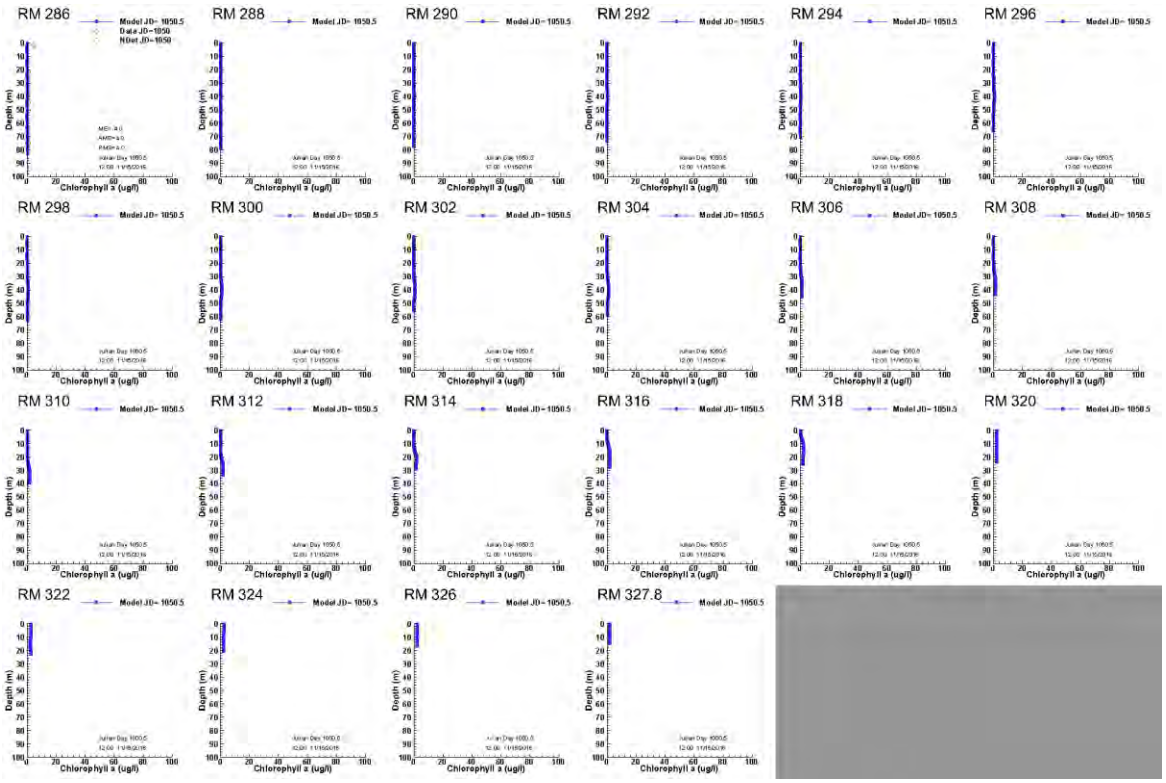


Figure 2041. Vertical profiles of chlorophyll a compared with data for 11/15/2016.

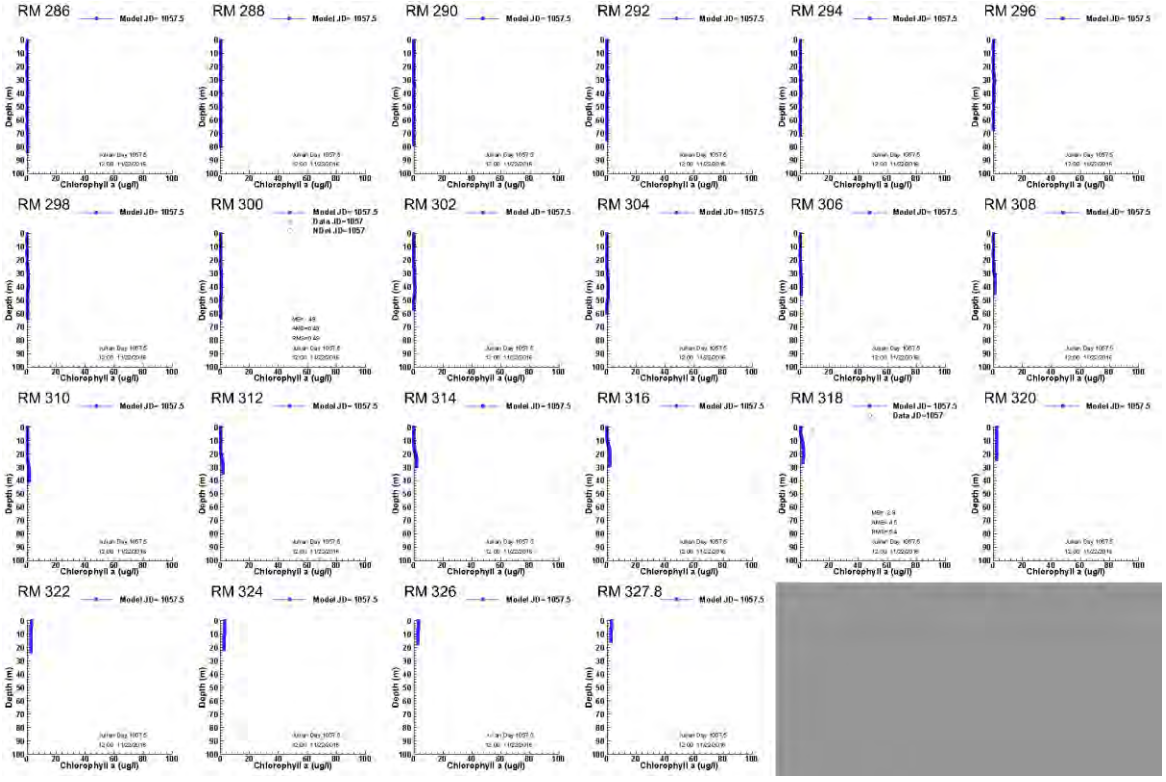


Figure 2042. Vertical profiles of chlorophyll a compared with data for 11/22/2016.

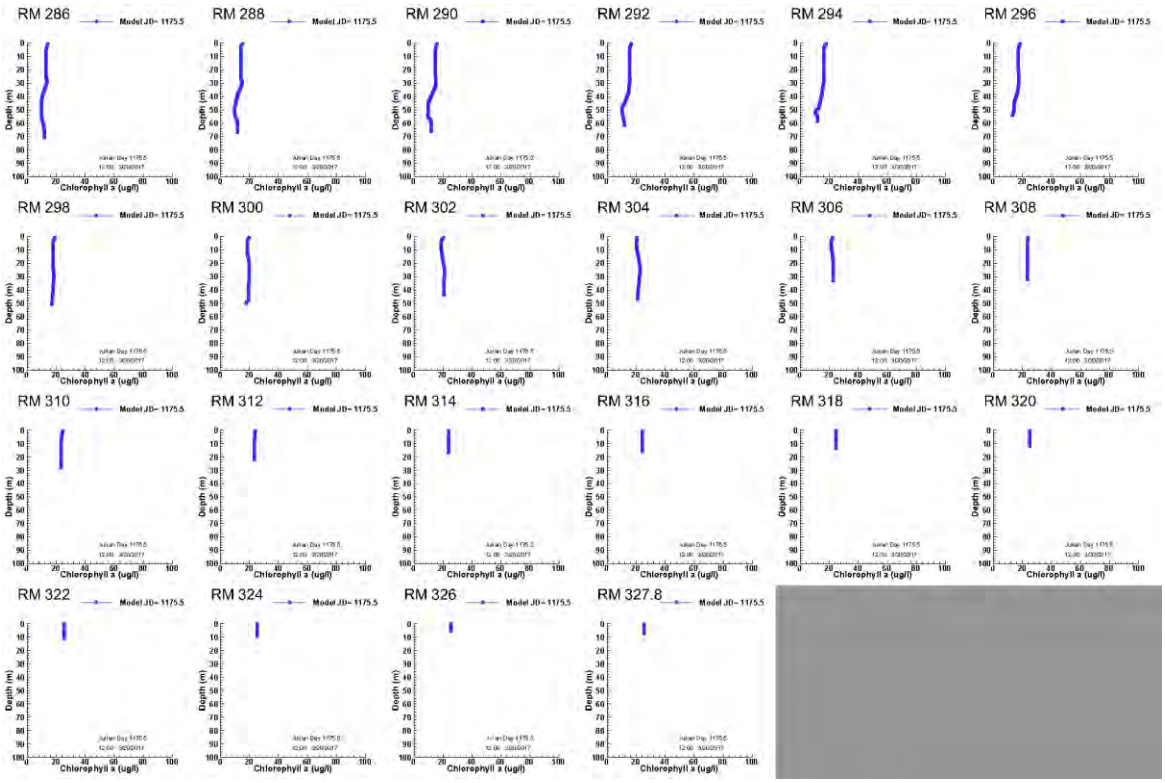


Figure 2043. Vertical profiles of chlorophyll a compared with data for 3/20/2017.

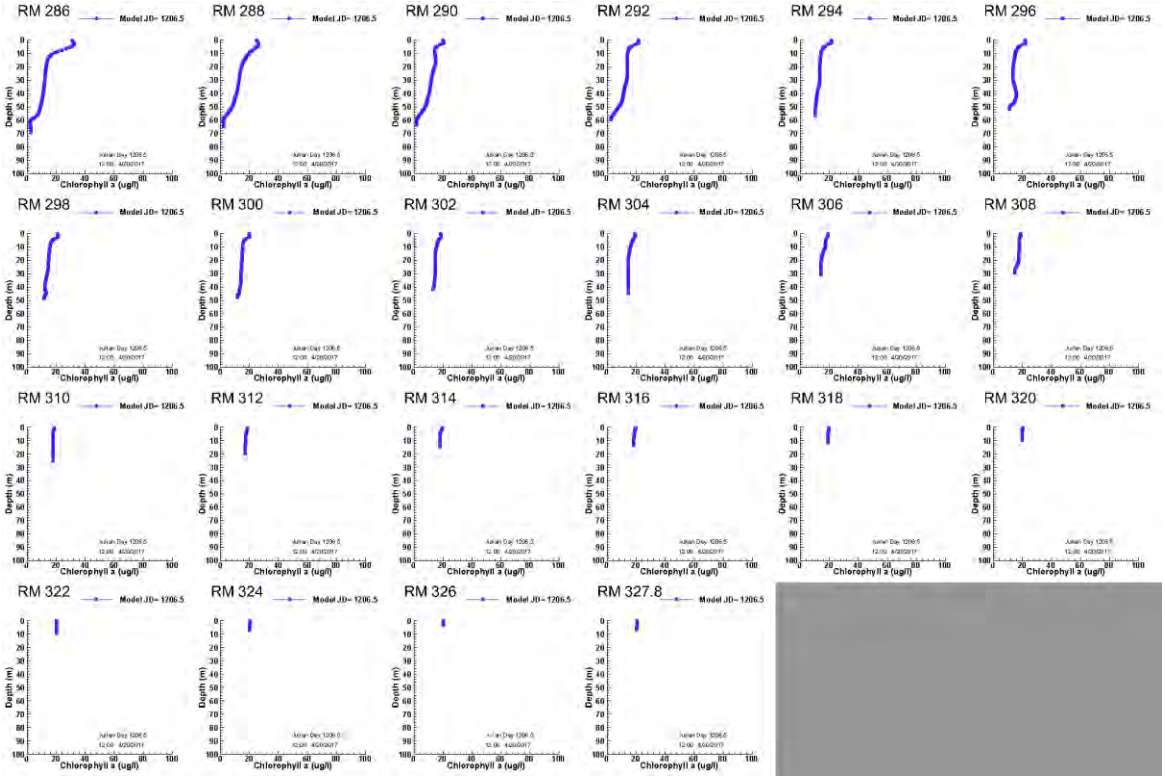


Figure 2044. Vertical profiles of chlorophyll a compared with data for 4/20/2017.

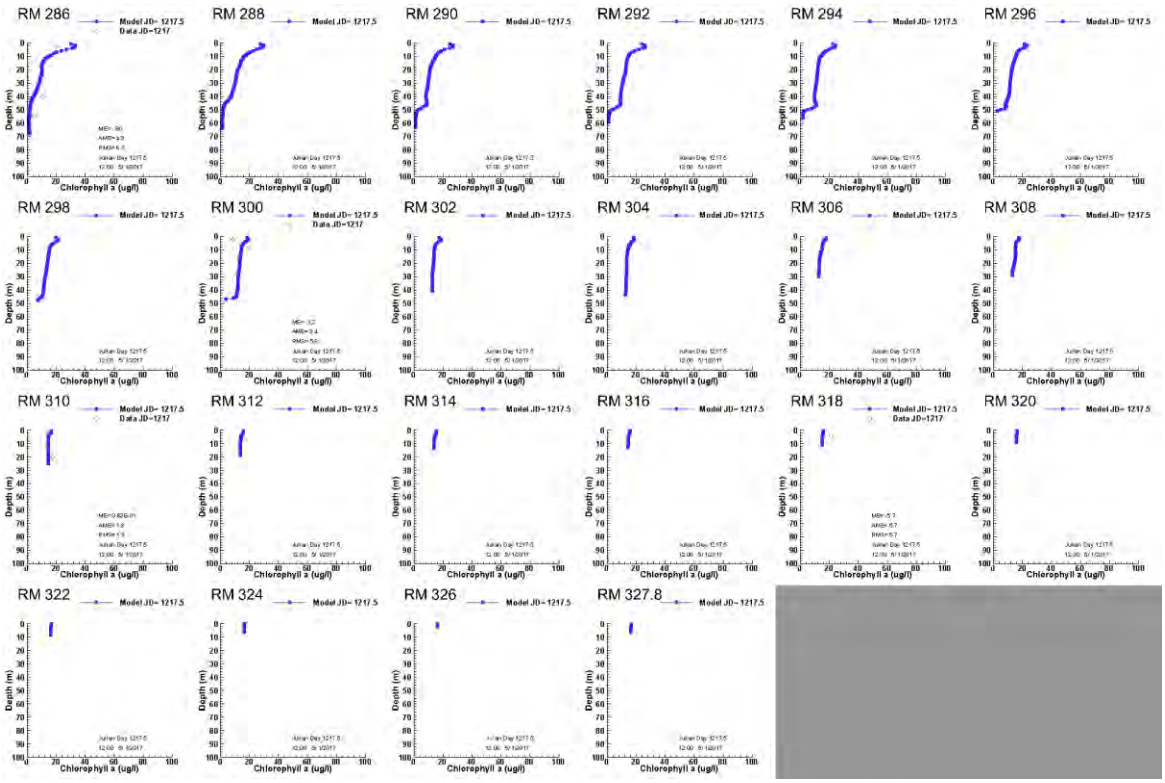


Figure 2045. Vertical profiles of chlorophyll a compared with data for 5/ 1/2017.

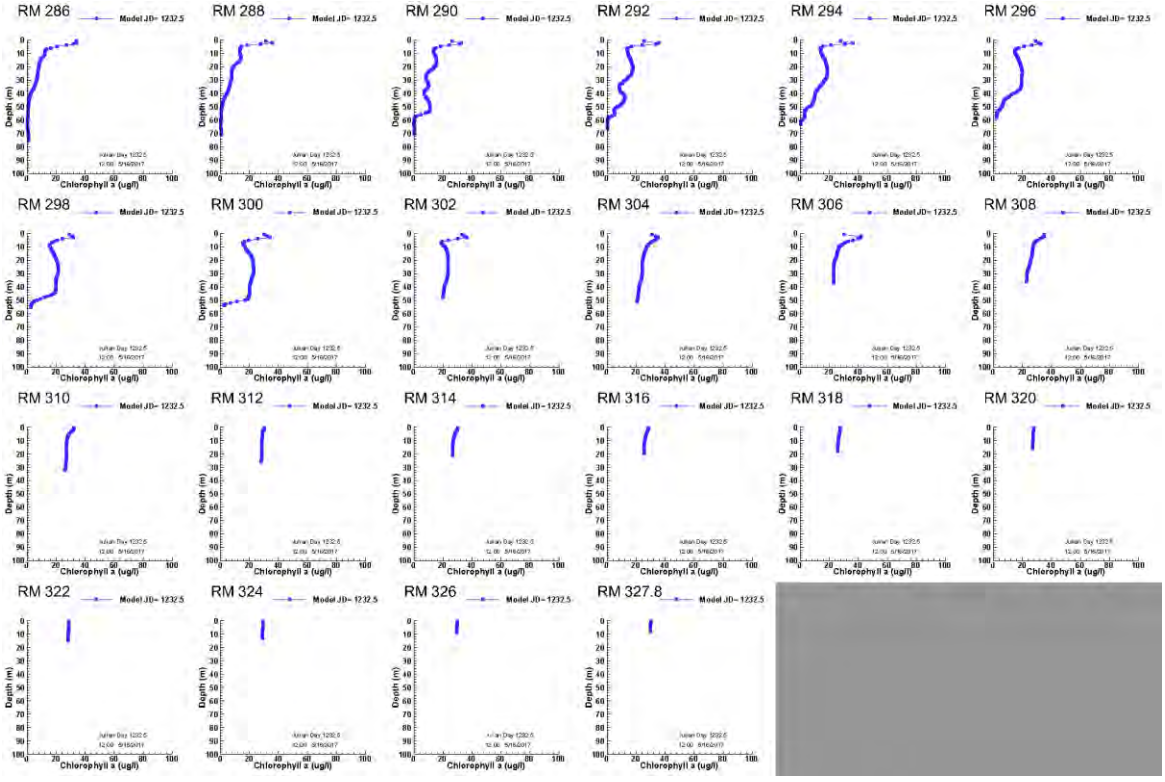


Figure 2046. Vertical profiles of chlorophyll a compared with data for 5/16/2017.

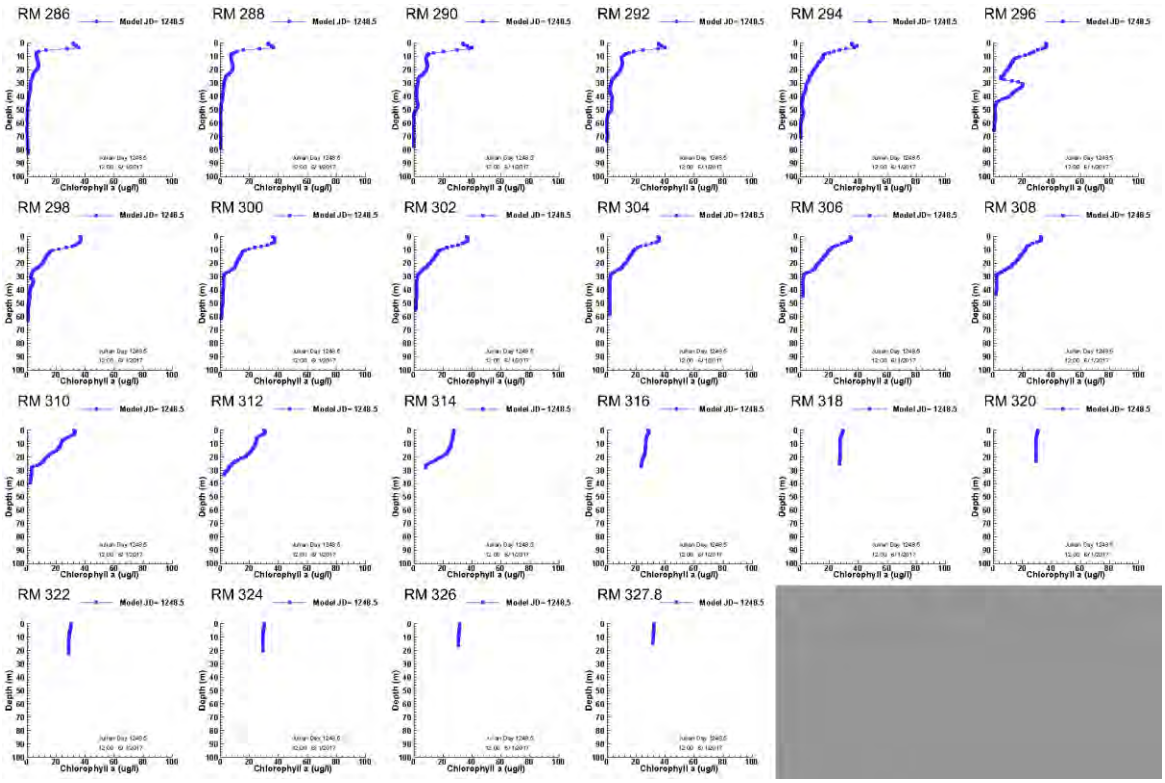


Figure 2047. Vertical profiles of chlorophyll a compared with data for 6/ 1/2017.

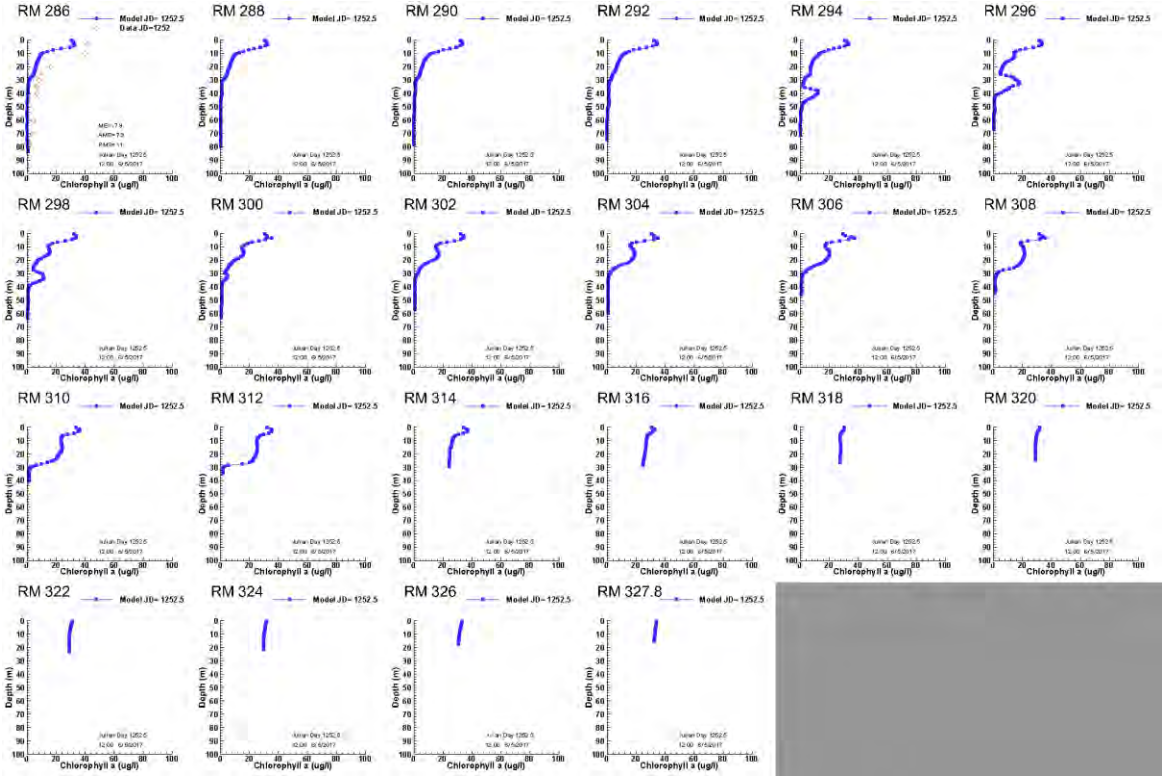


Figure 2048. Vertical profiles of chlorophyll a compared with data for 6/ 5/2017.

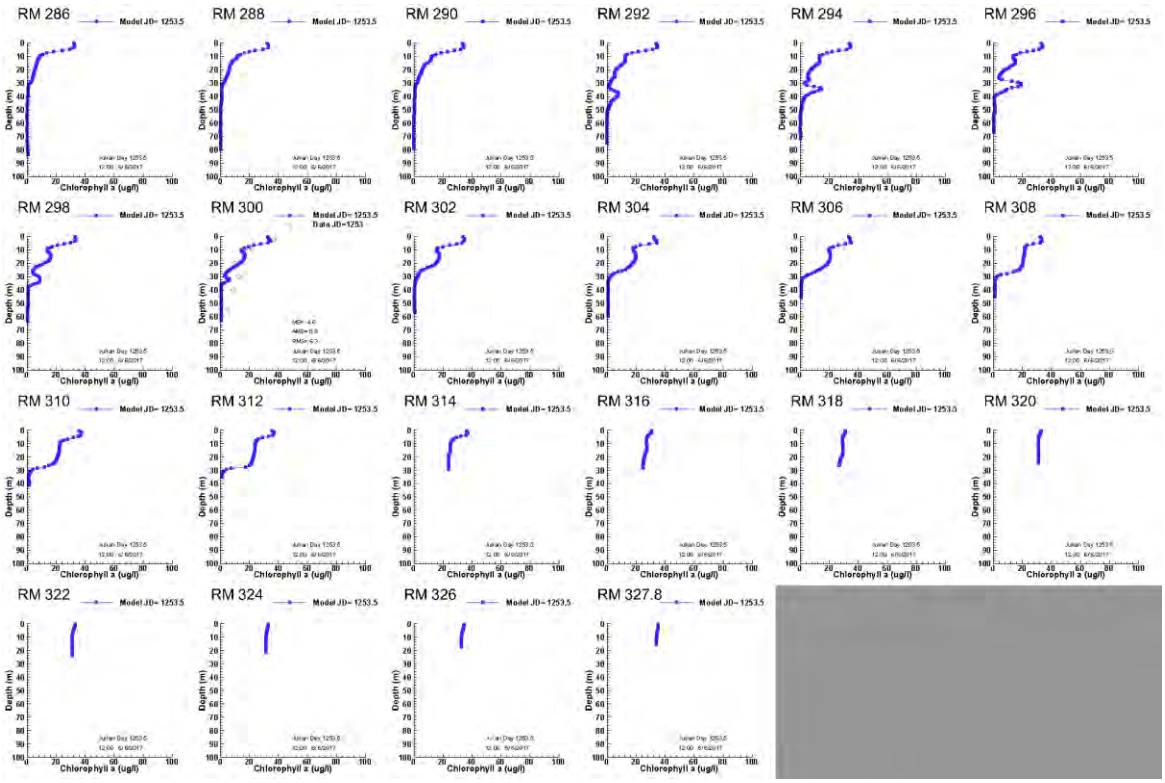


Figure 2049. Vertical profiles of chlorophyll a compared with data for 6/ 6/2017.

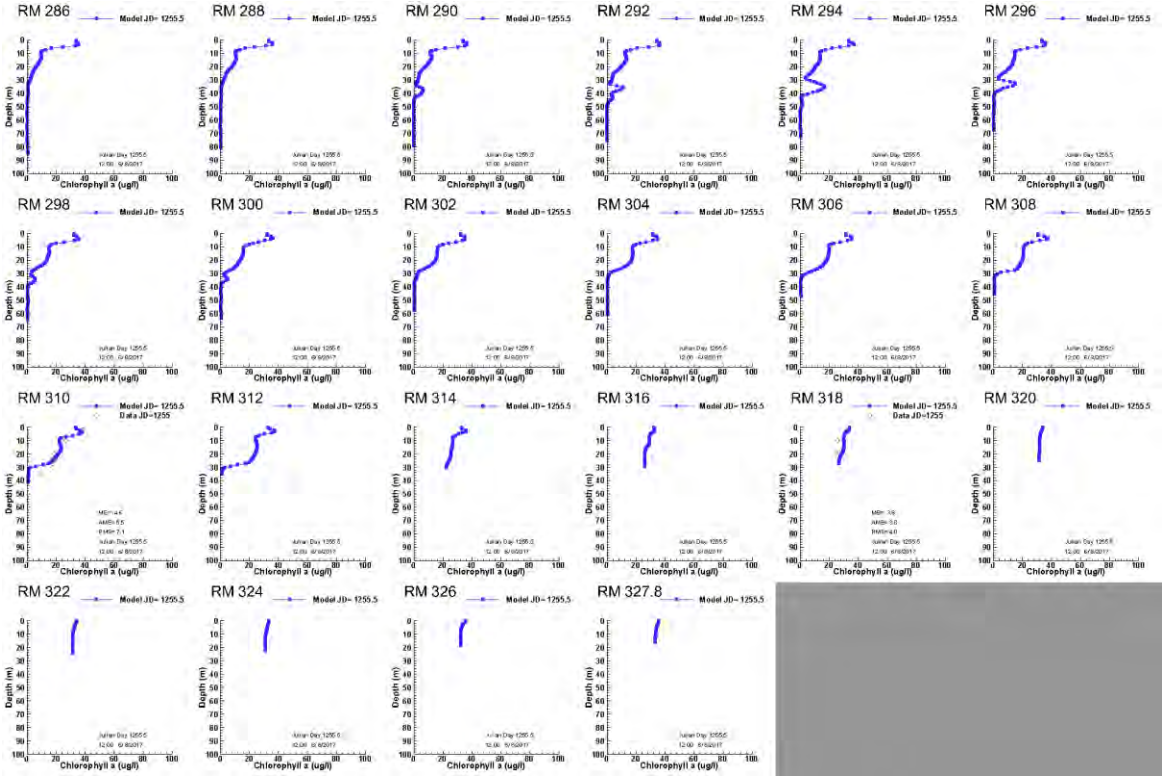


Figure 2050. Vertical profiles of chlorophyll a compared with data for 6/ 8/2017.

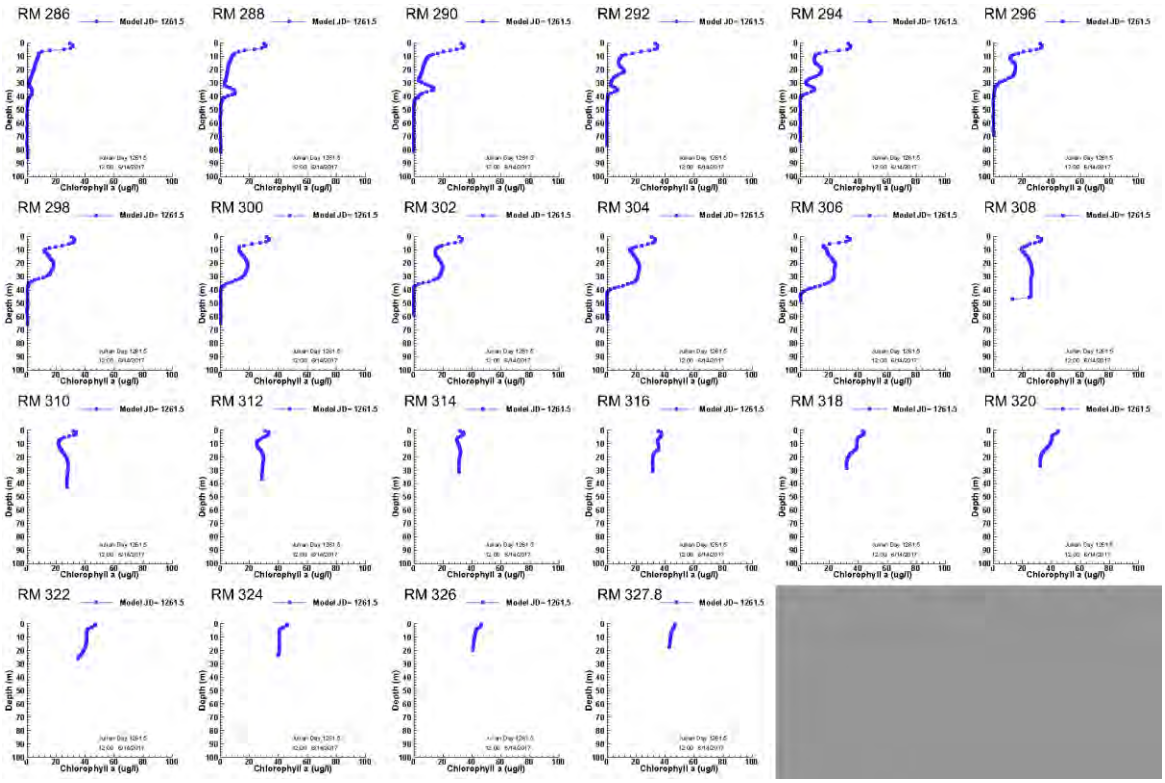


Figure 2051. Vertical profiles of chlorophyll a compared with data for 6/14/2017.

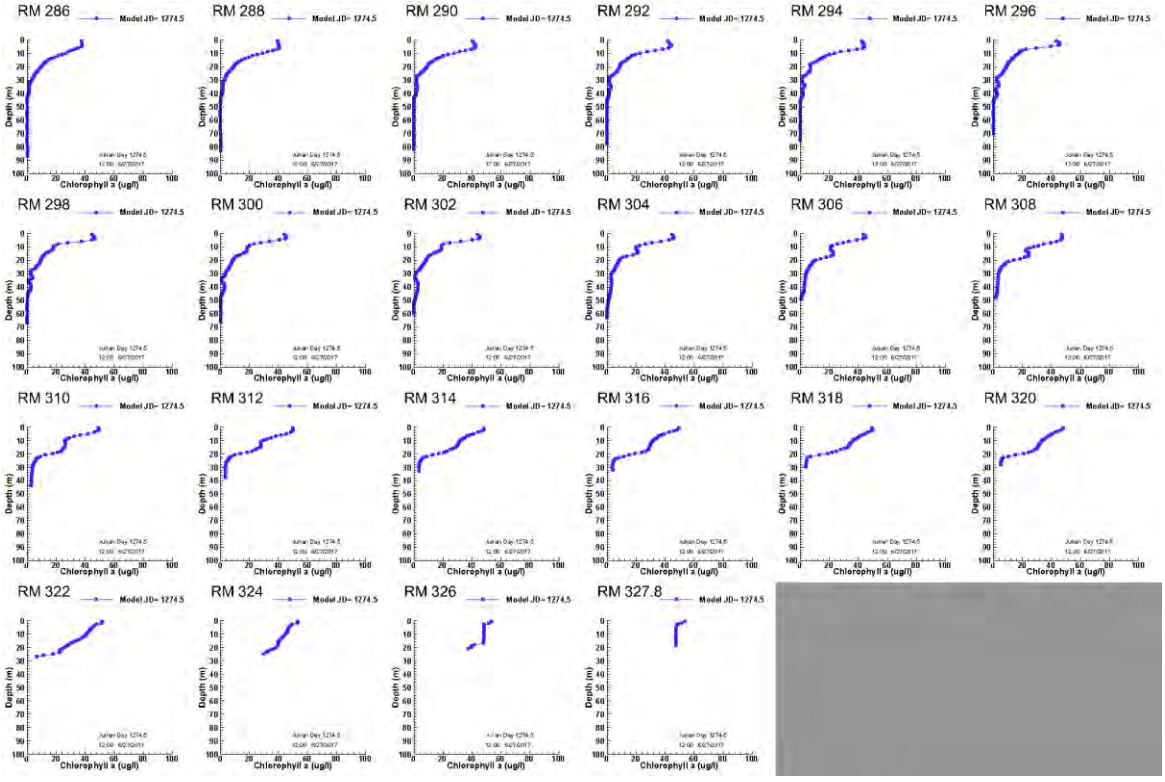


Figure 2052. Vertical profiles of chlorophyll a compared with data for 6/27/2017.

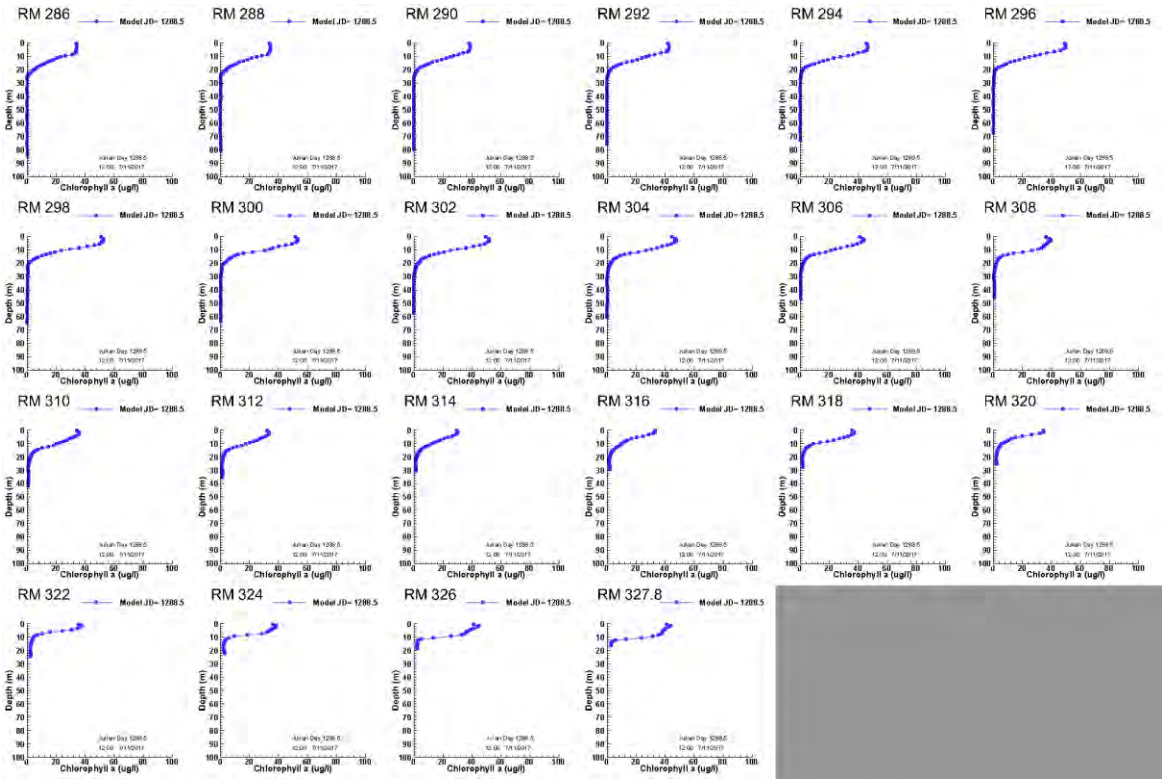


Figure 2053. Vertical profiles of chlorophyll a compared with data for 7/11/2017.

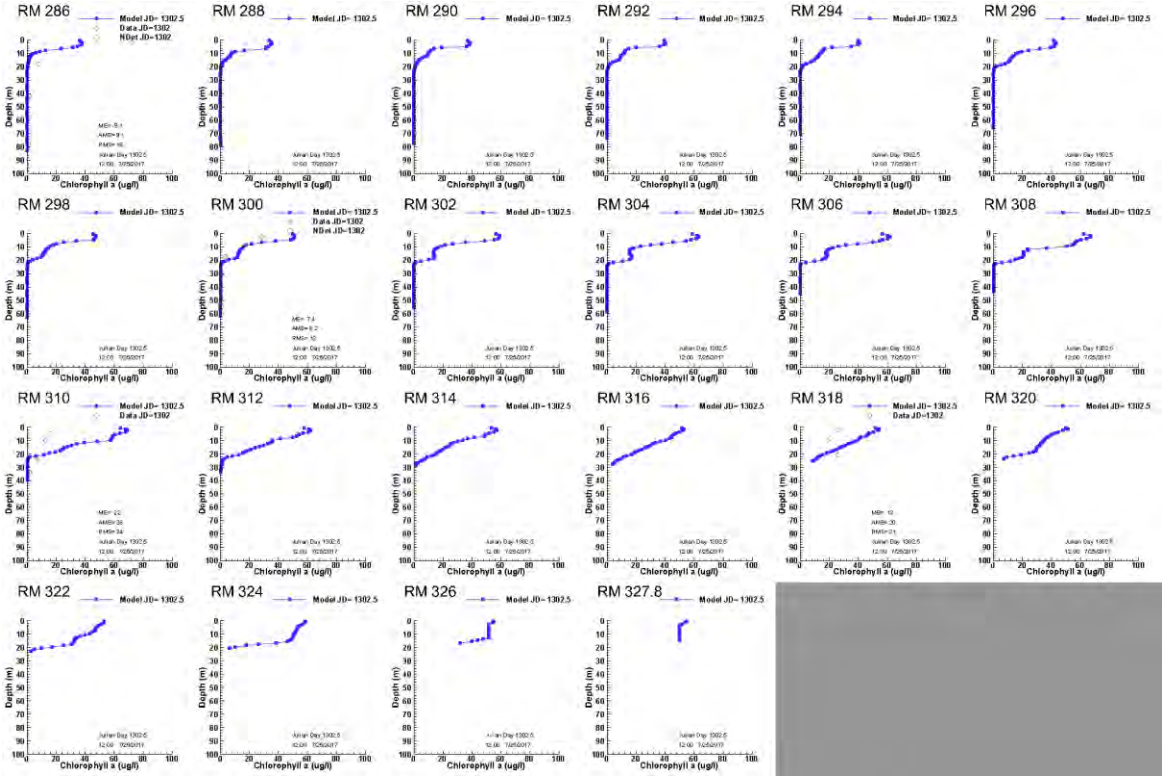


Figure 2054. Vertical profiles of chlorophyll a compared with data for 7/25/2017.

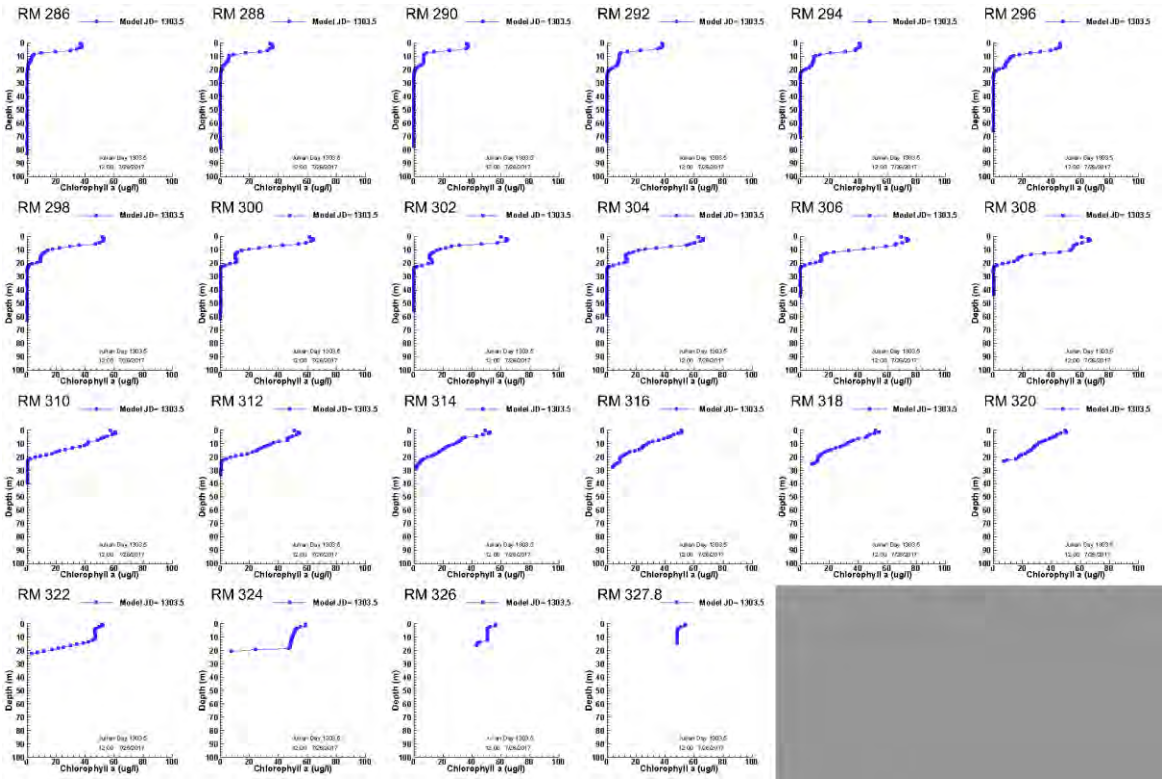


Figure 2055. Vertical profiles of chlorophyll a compared with data for 7/26/2017.

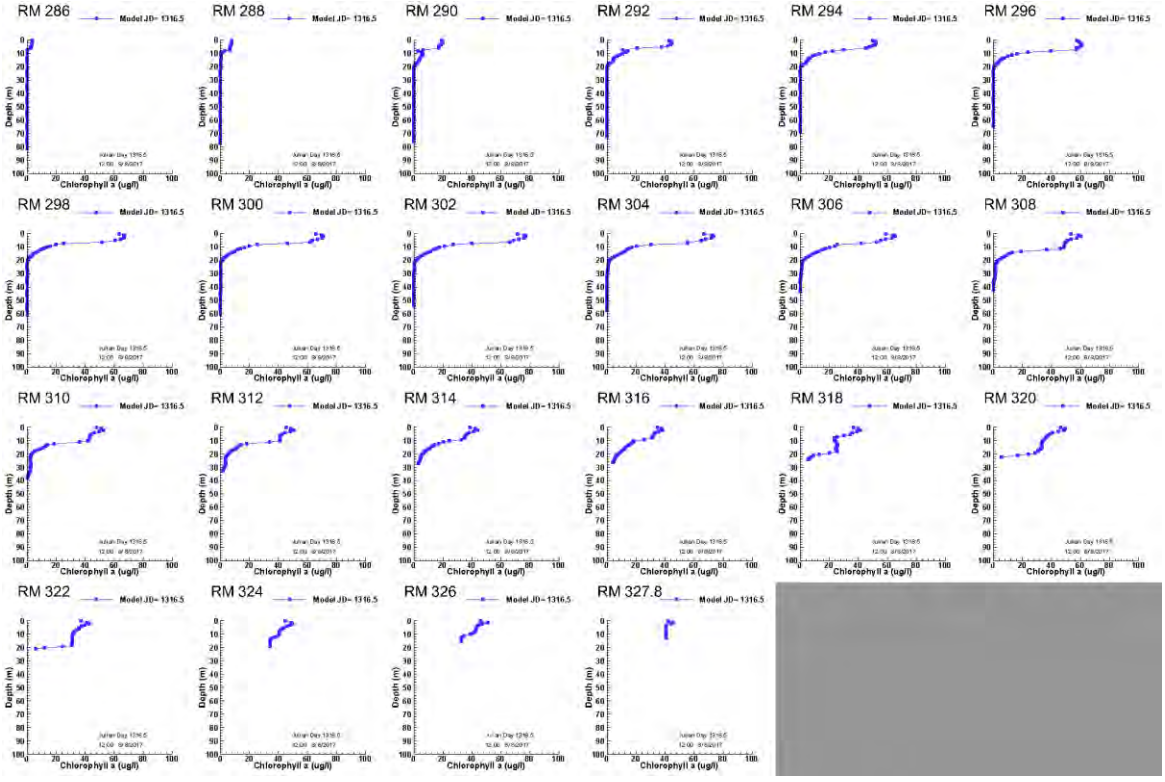


Figure 2056. Vertical profiles of chlorophyll a compared with data for 8/ 8/2017.

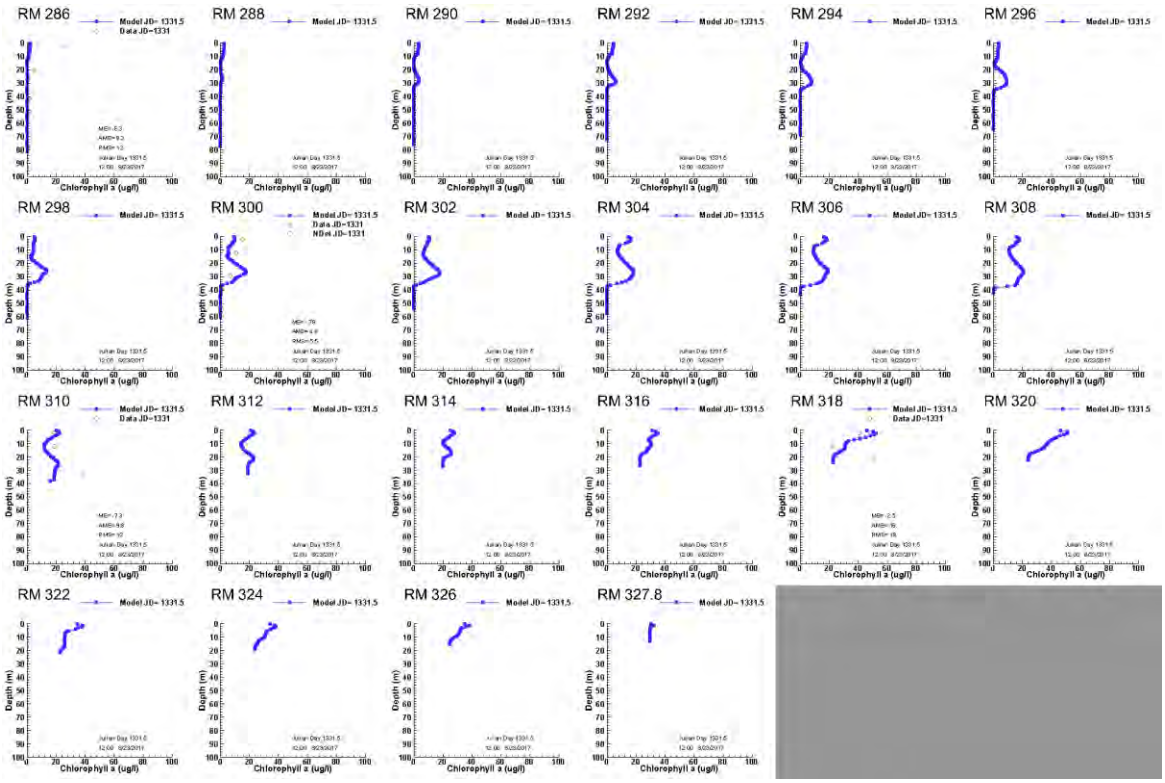


Figure 2057. Vertical profiles of chlorophyll a compared with data for 8/23/2017.

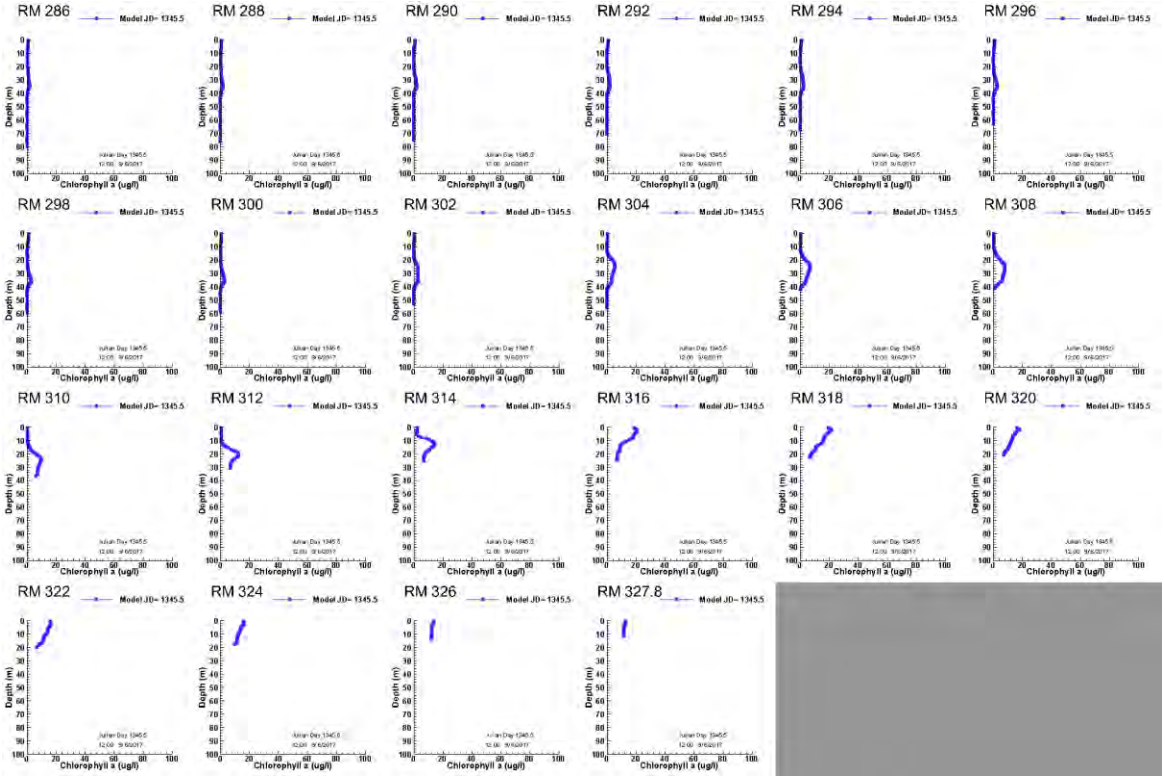


Figure 2058. Vertical profiles of chlorophyll a compared with data for 9/ 6/2017.

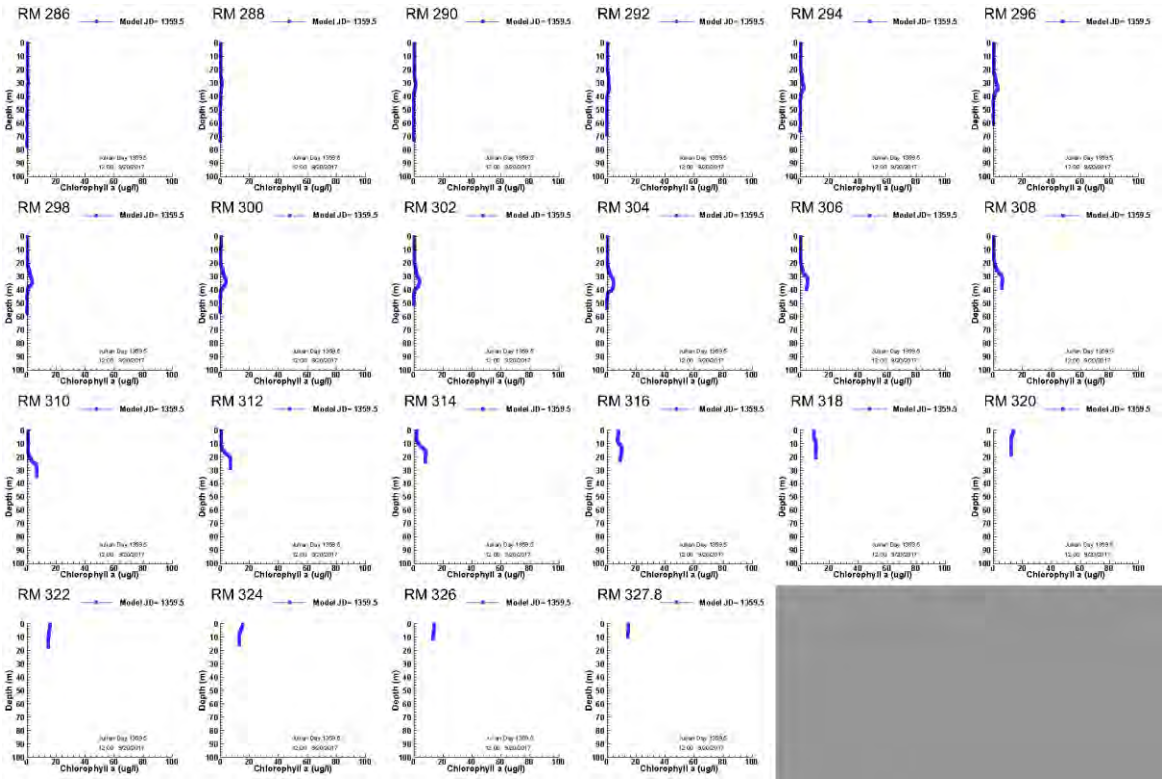


Figure 2059. Vertical profiles of chlorophyll a compared with data for 9/20/2017.

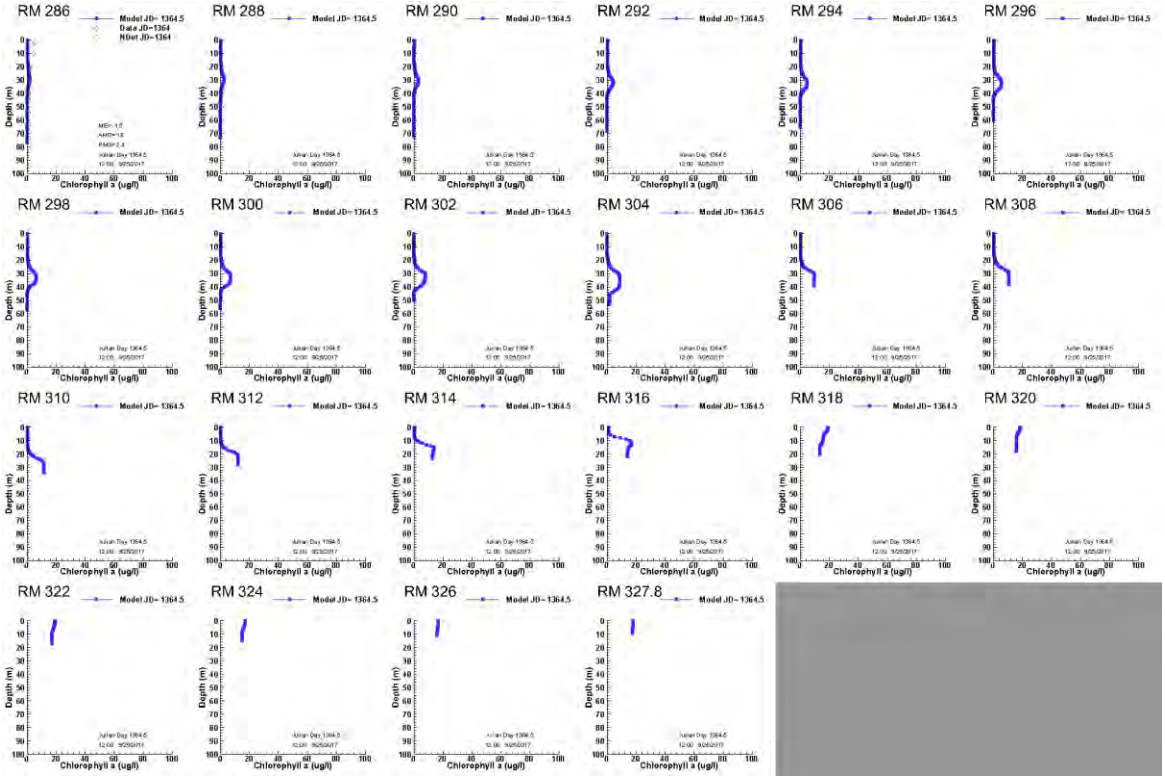


Figure 2060. Vertical profiles of chlorophyll a compared with data for 9/25/2017.

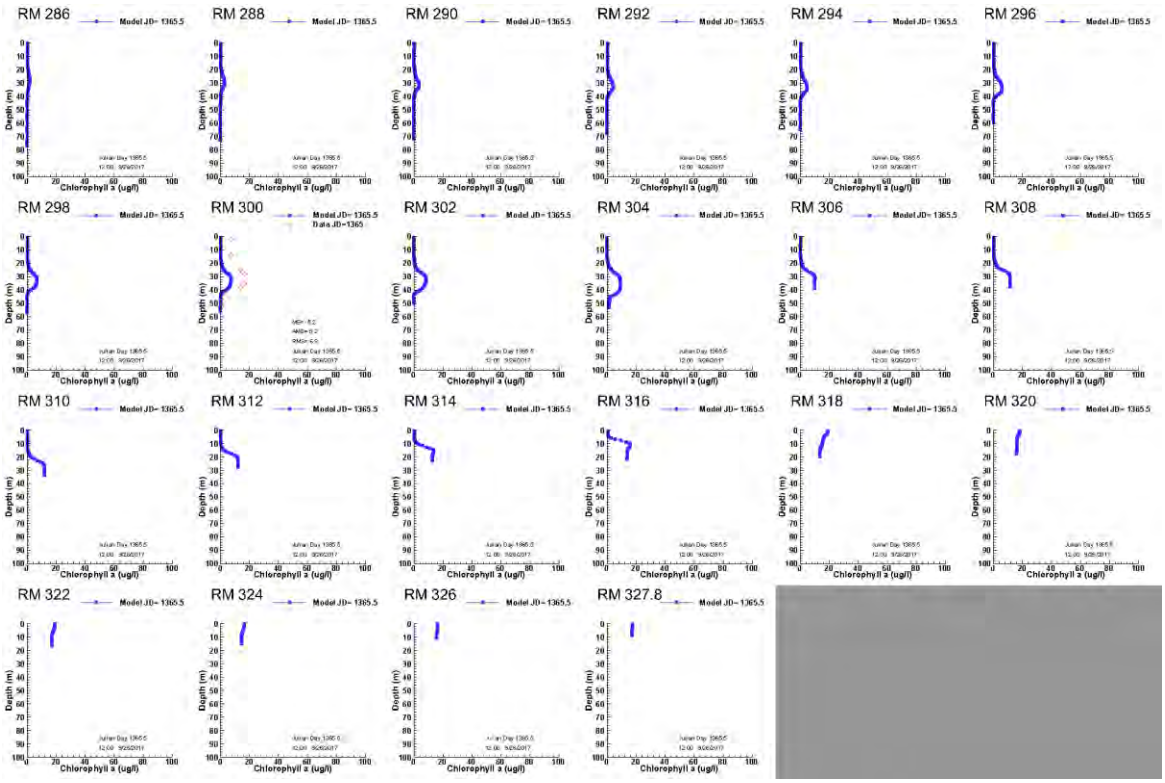


Figure 2061. Vertical profiles of chlorophyll a compared with data for 9/26/2017.

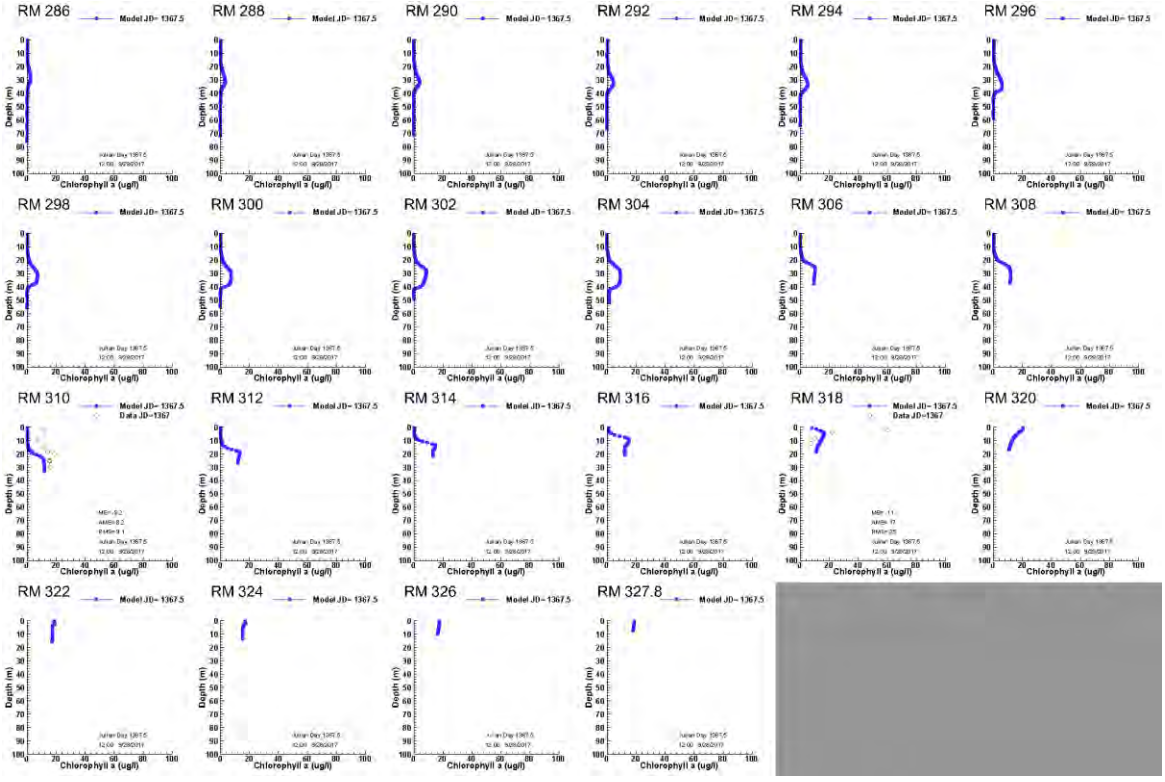


Figure 2062. Vertical profiles of chlorophyll a compared with data for 9/28/2017.

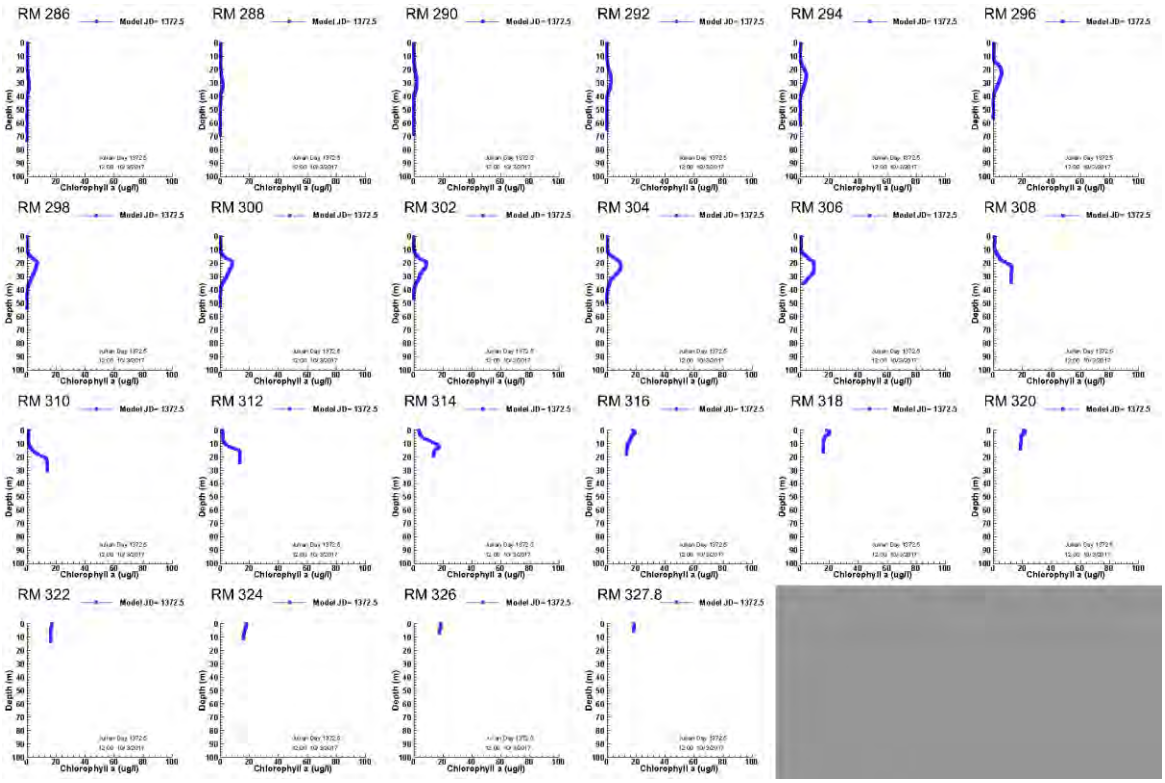


Figure 2063. Vertical profiles of chlorophyll a compared with data for 10/ 3/2017.

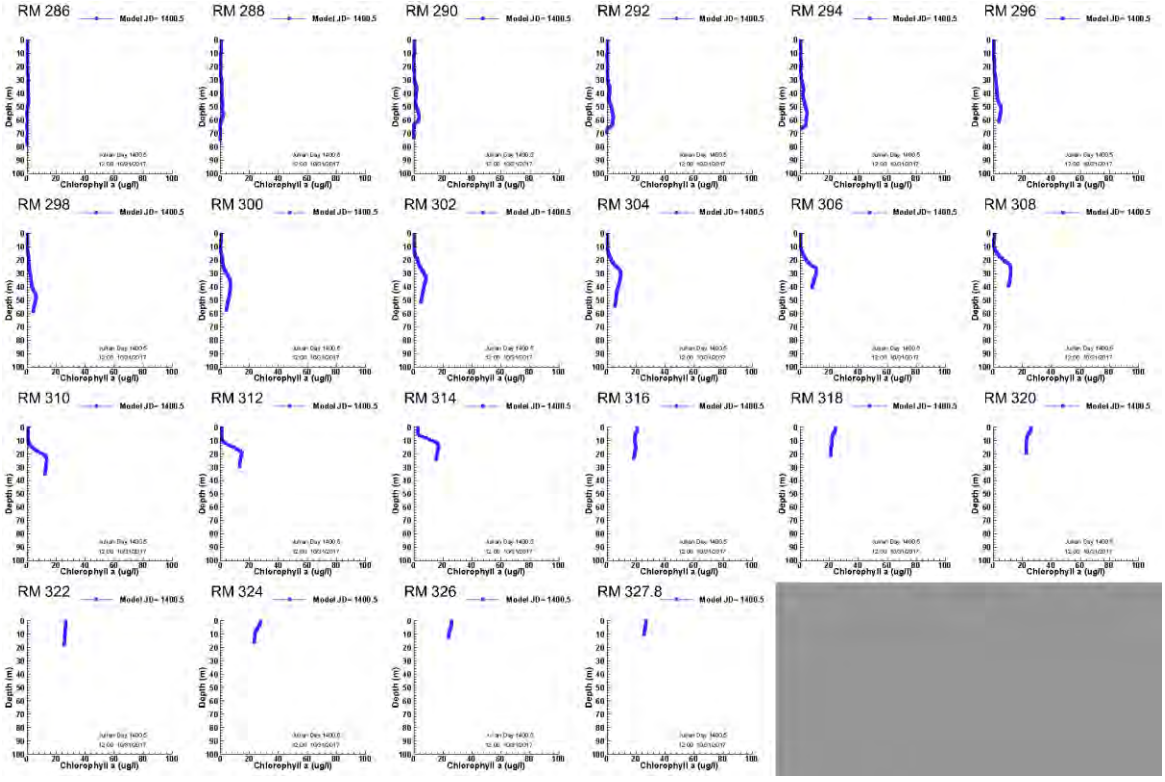


Figure 2064. Vertical profiles of chlorophyll a compared with data for 10/31/2017.

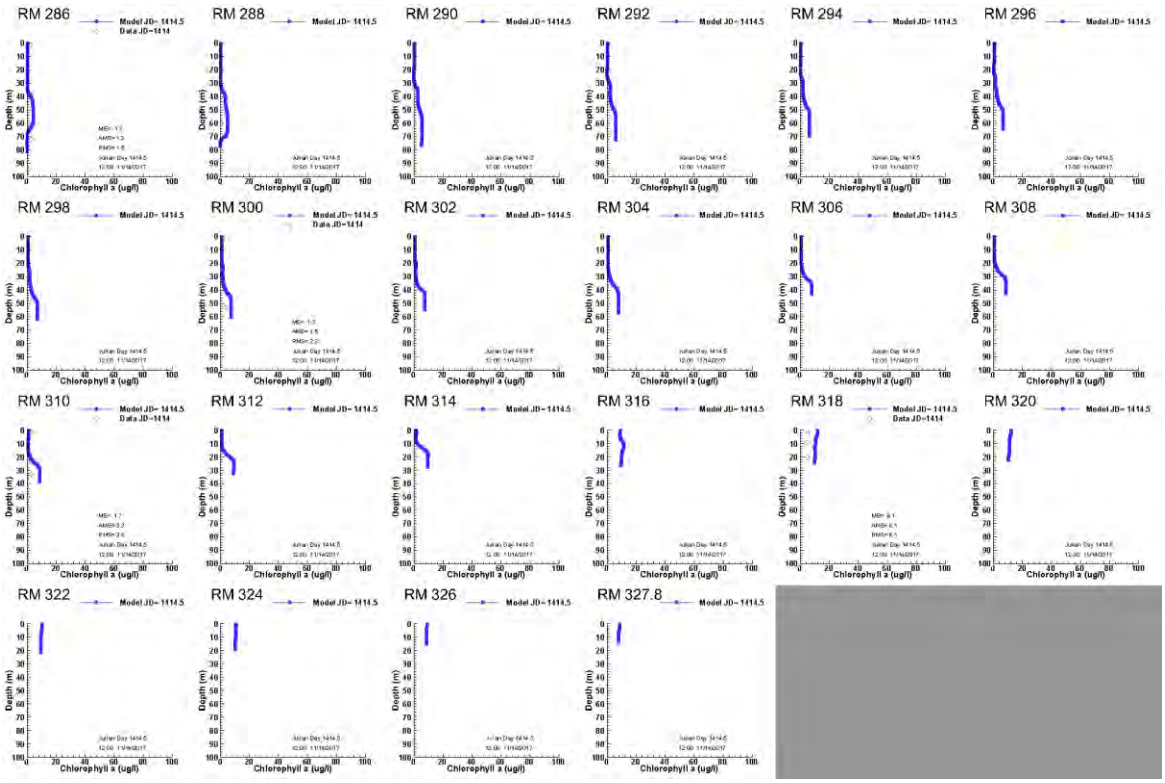


Figure 2065. Vertical profiles of chlorophyll a compared with data for 11/14/2017.

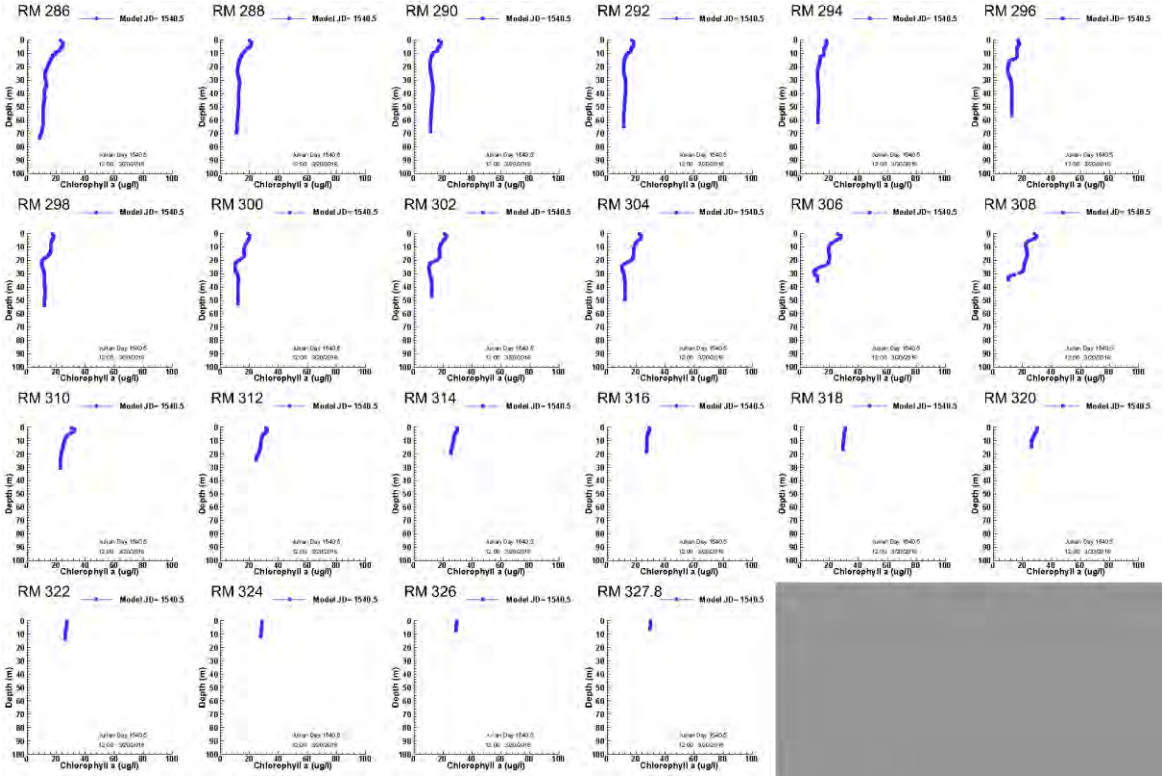


Figure 2066. Vertical profiles of chlorophyll a compared with data for 3/20/2018.

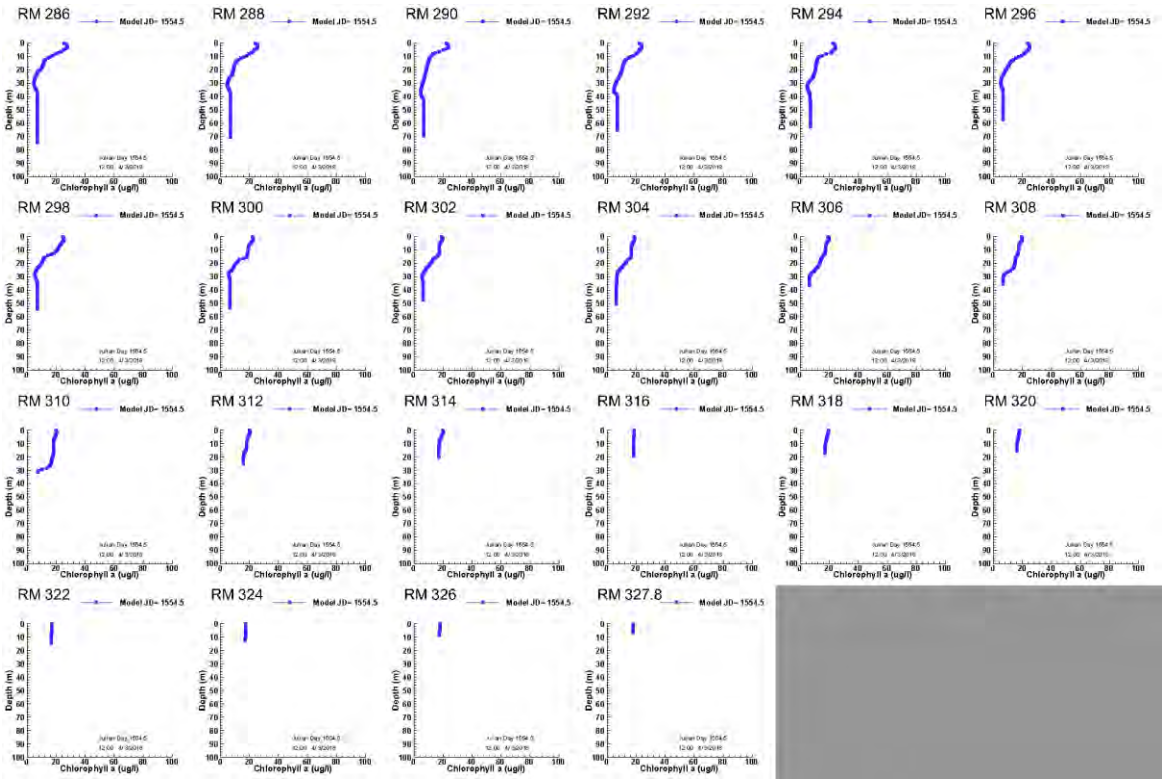


Figure 2067. Vertical profiles of chlorophyll a compared with data for 4/ 3/2018.

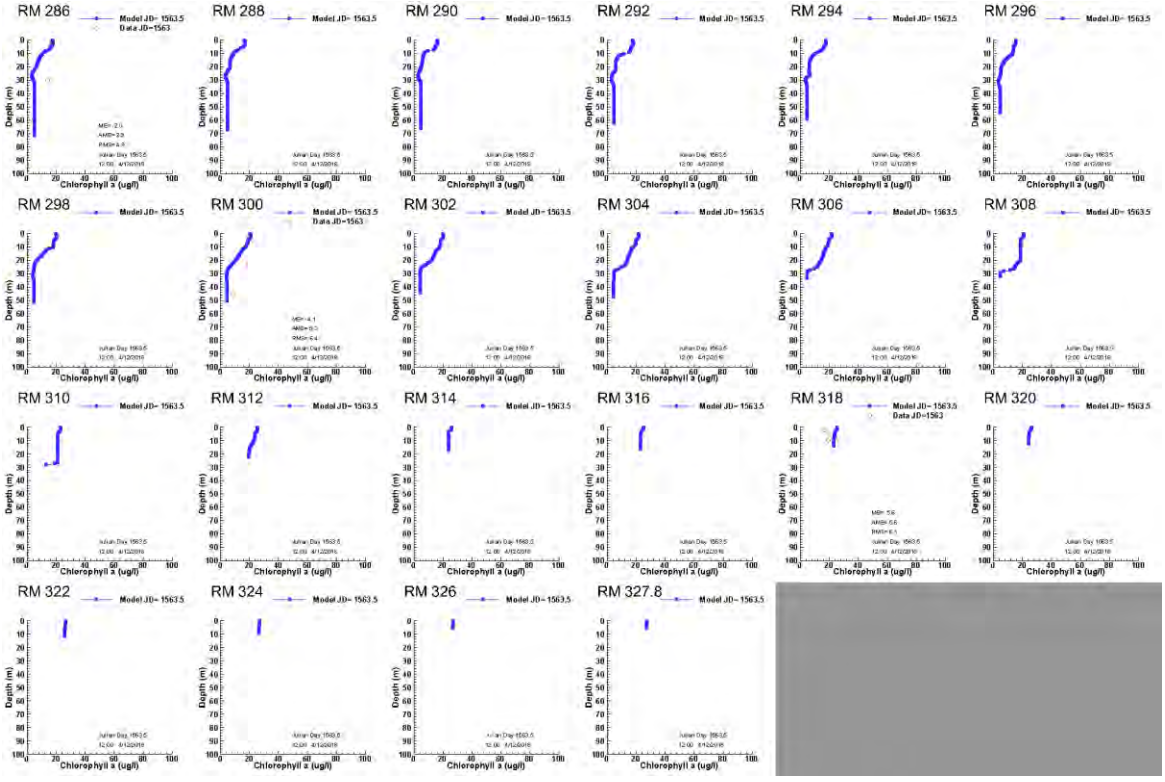


Figure 2068. Vertical profiles of chlorophyll a compared with data for 4/12/2018.

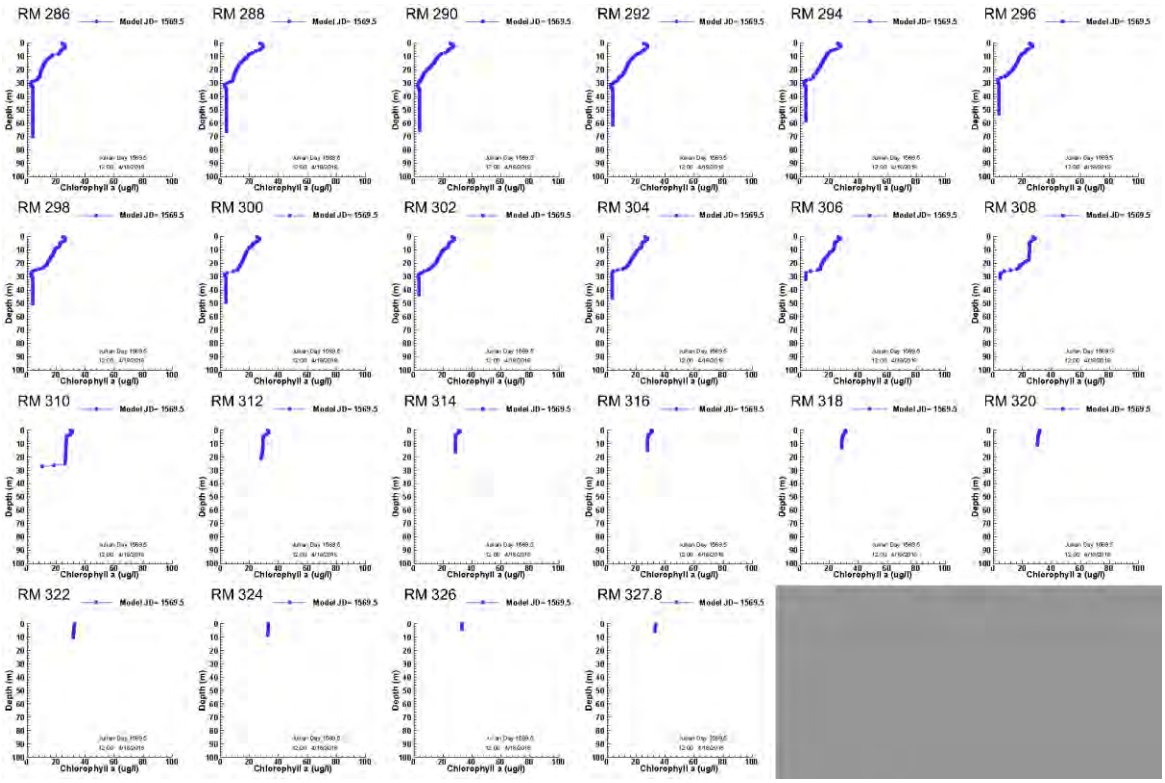


Figure 2069. Vertical profiles of chlorophyll a compared with data for 4/18/2018.

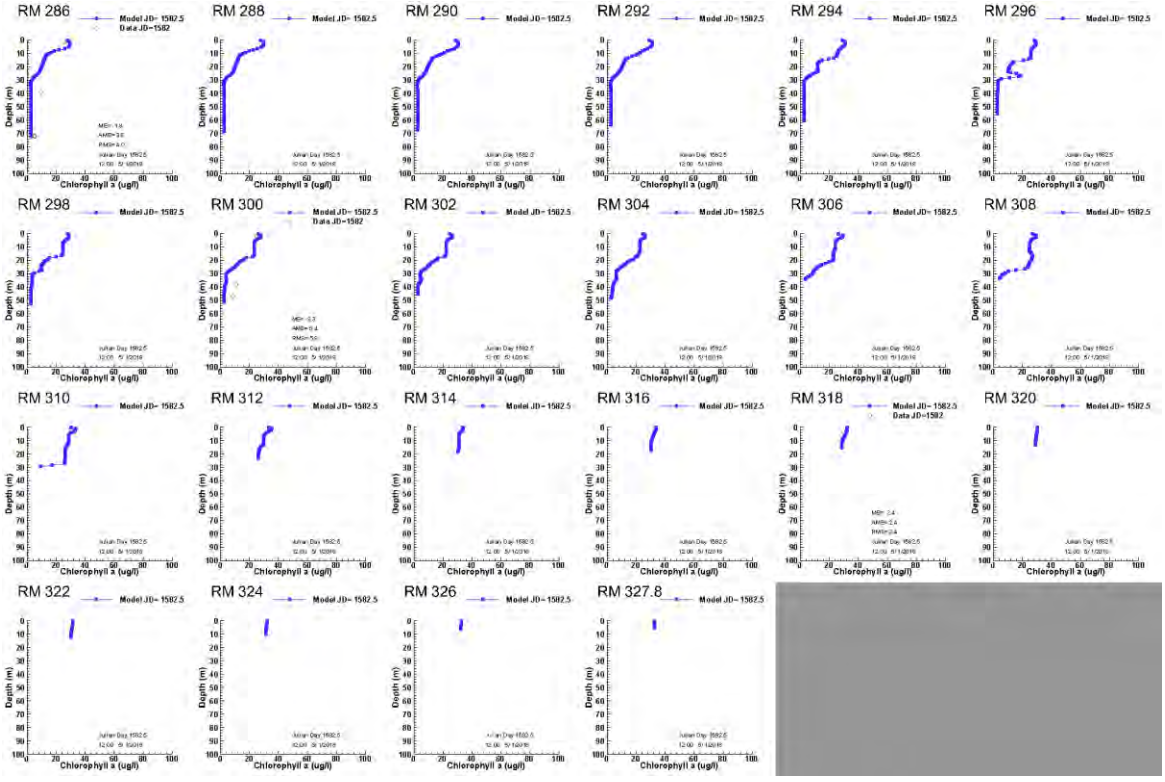


Figure 2070. Vertical profiles of chlorophyll a compared with data for 5/ 1/2018.

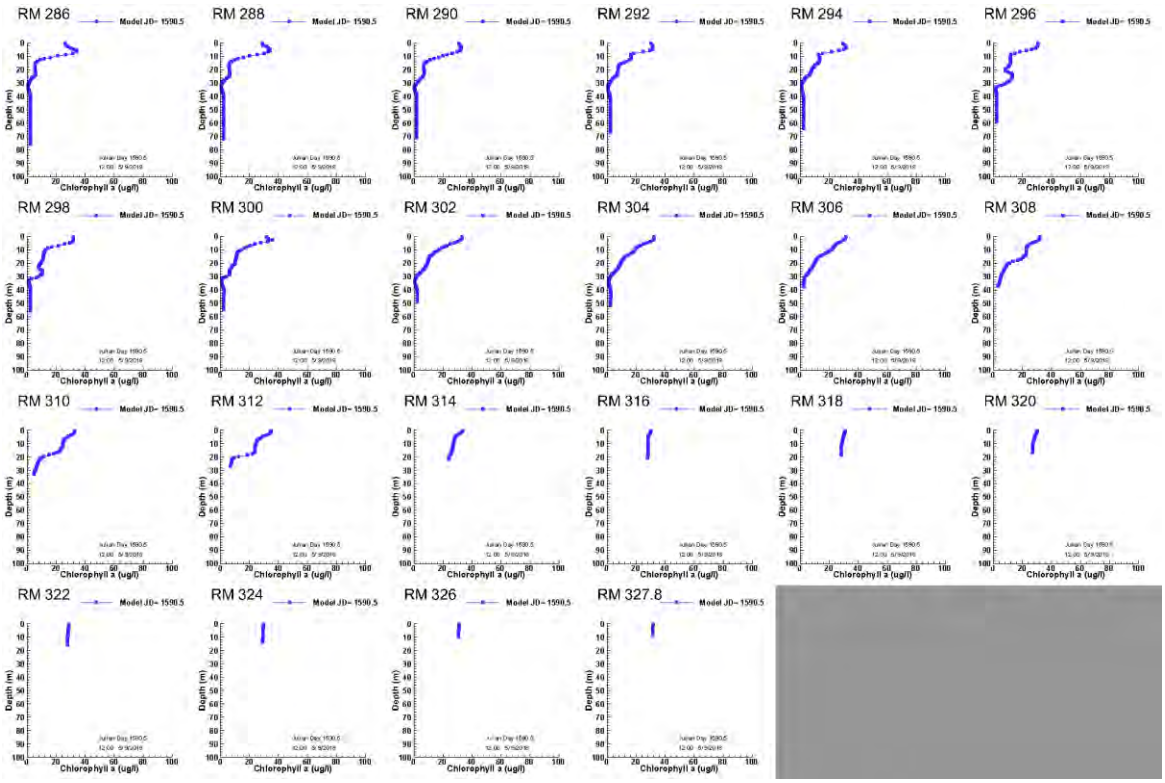


Figure 2071. Vertical profiles of chlorophyll a compared with data for 5/ 9/2018.

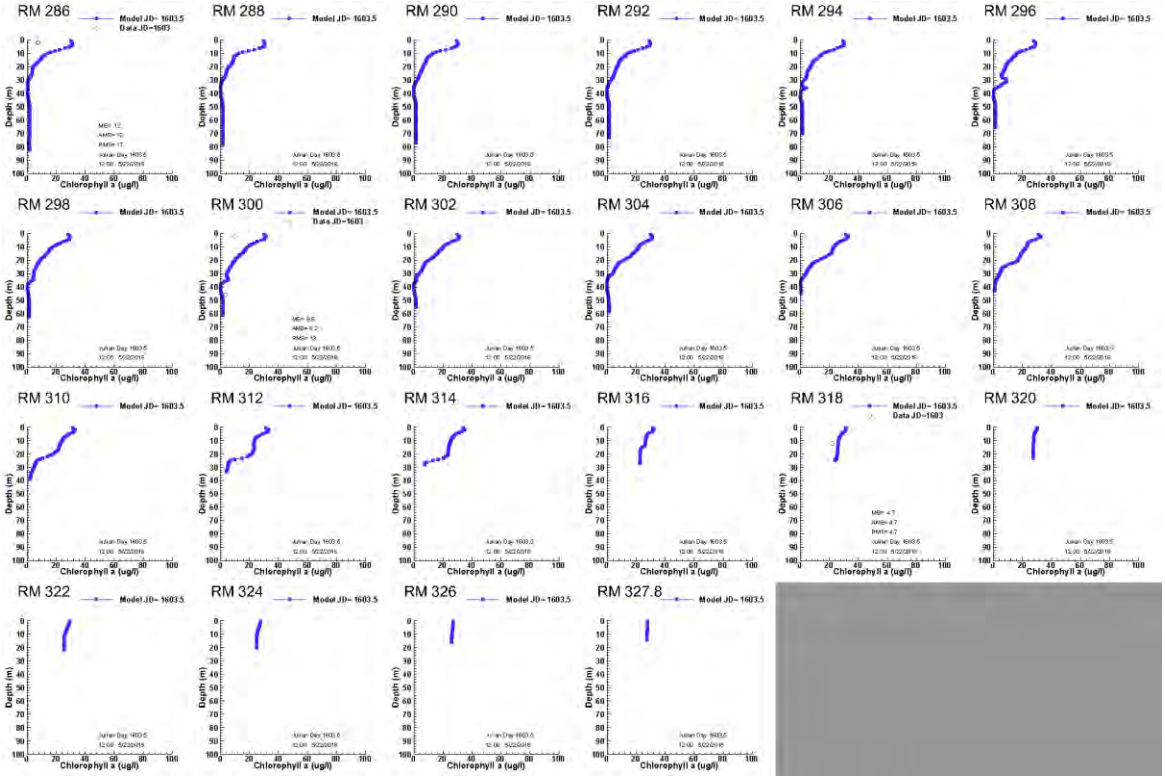


Figure 2072. Vertical profiles of chlorophyll a compared with data for 5/22/2018.

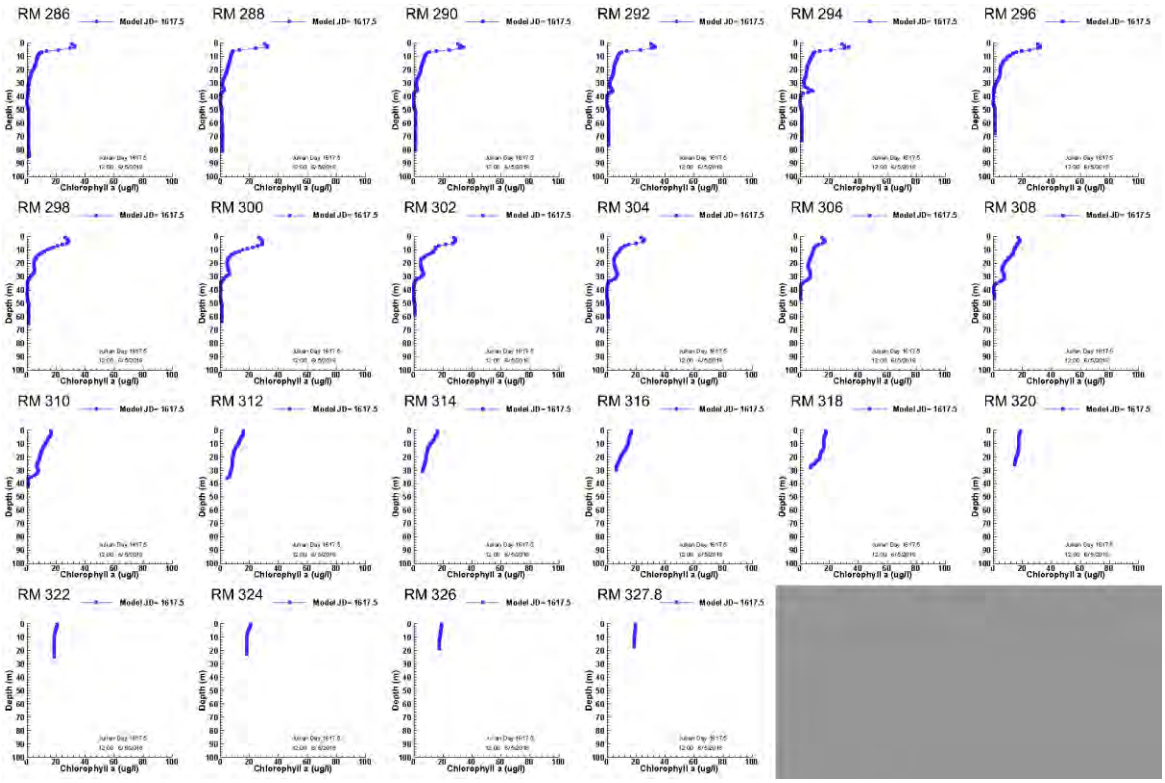


Figure 2073. Vertical profiles of chlorophyll a compared with data for 6/ 5/2018.

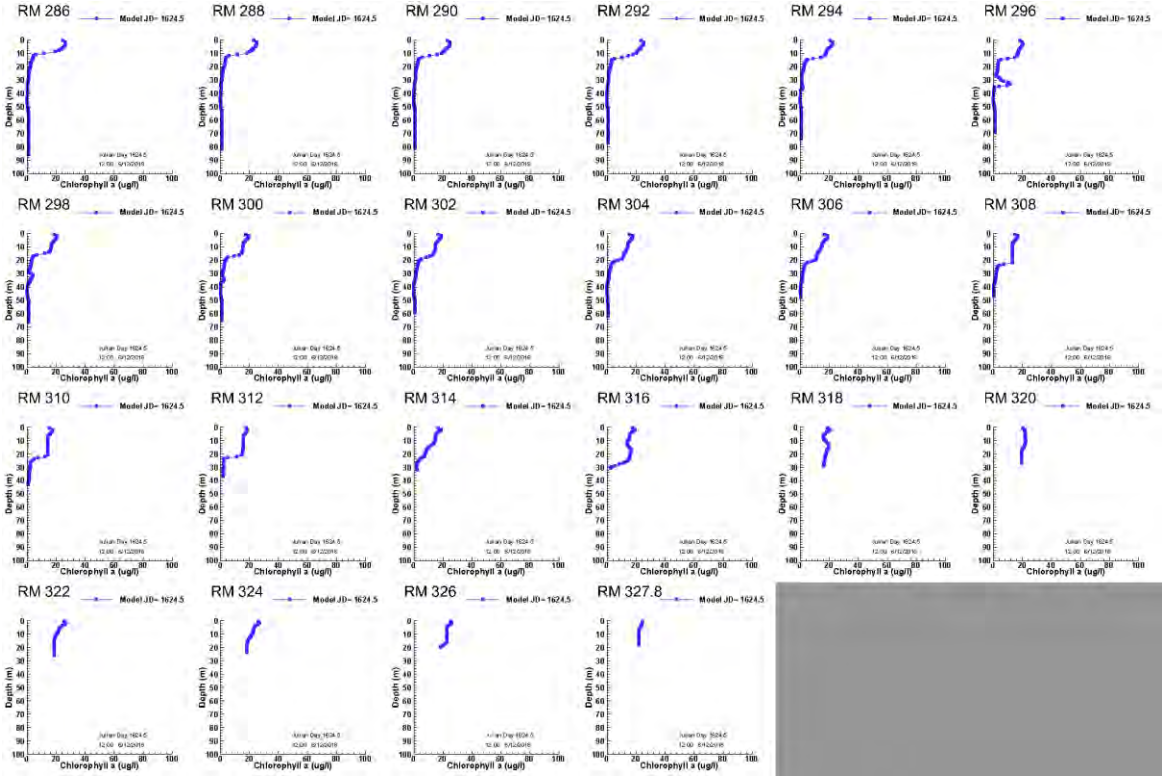


Figure 2074. Vertical profiles of chlorophyll a compared with data for 6/12/2018.

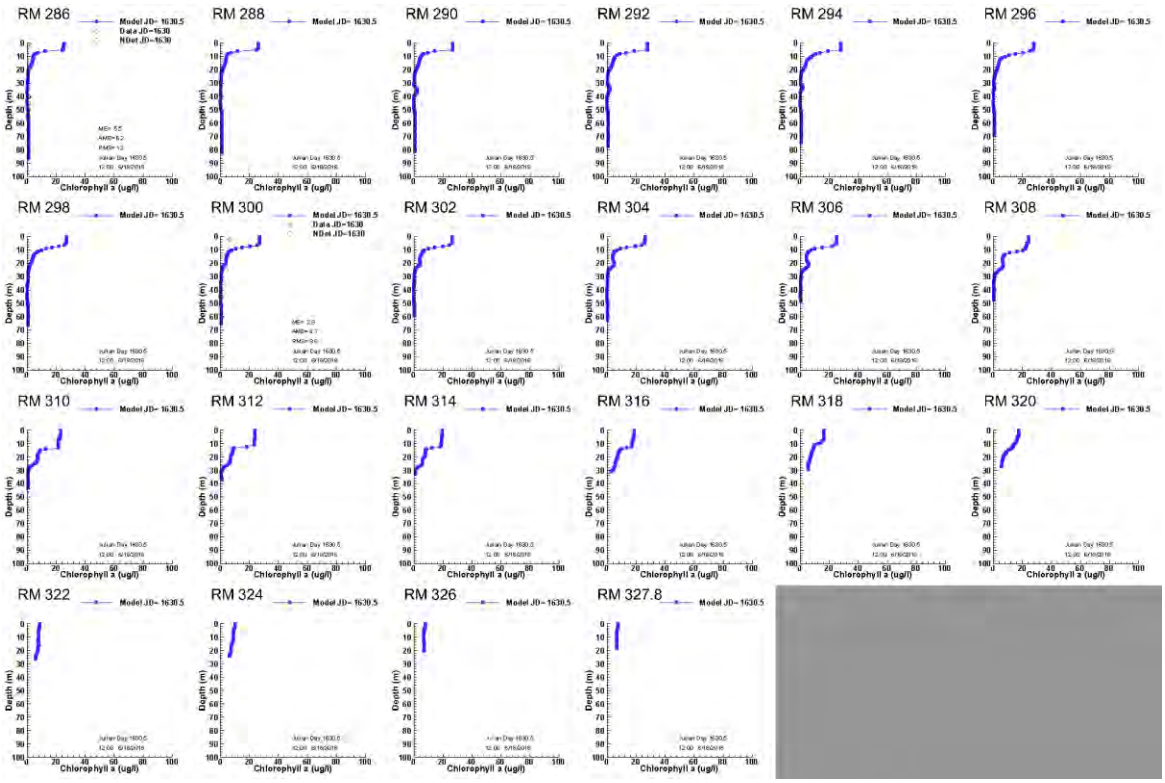


Figure 2075. Vertical profiles of chlorophyll a compared with data for 6/18/2018.

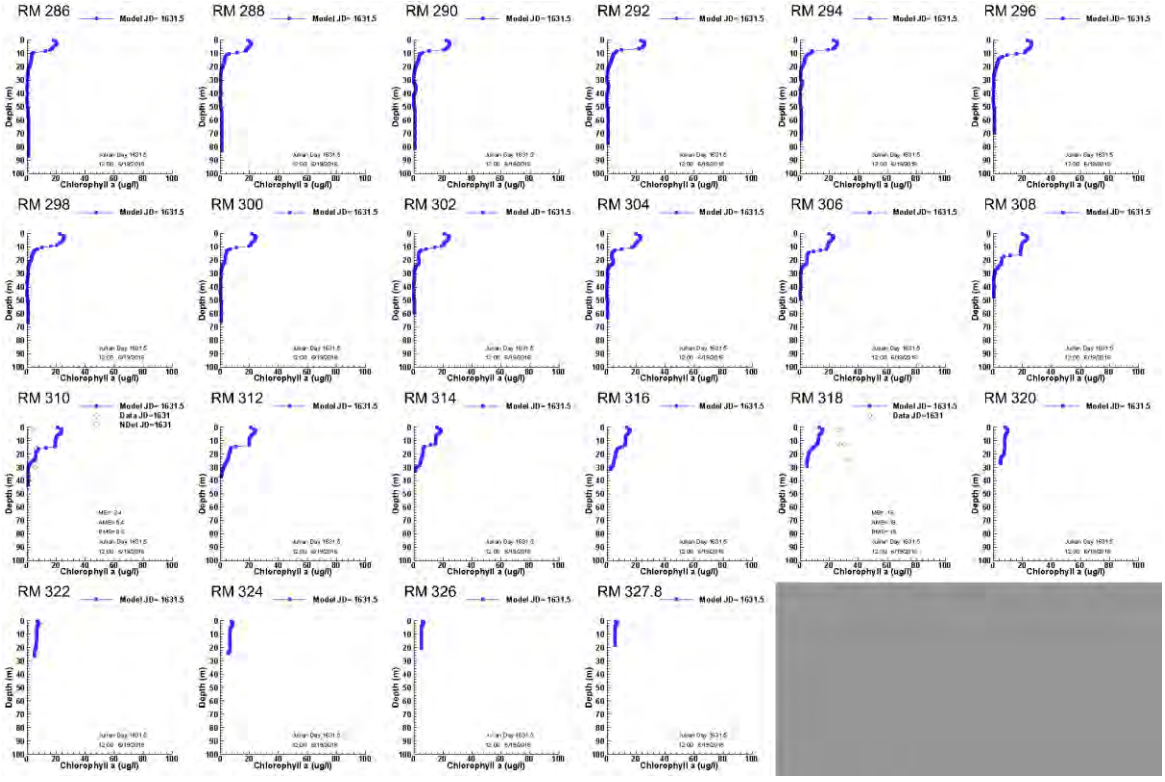


Figure 2076. Vertical profiles of chlorophyll a compared with data for 6/19/2018.

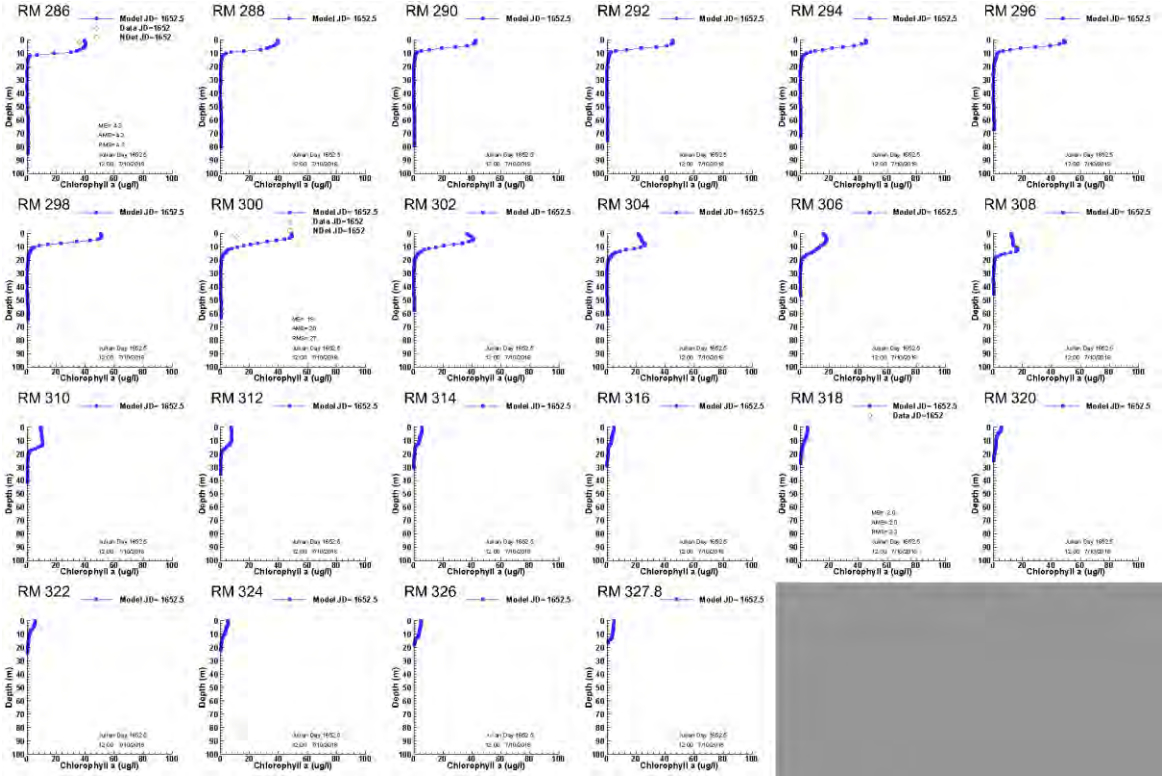


Figure 2077. Vertical profiles of chlorophyll a compared with data for 7/10/2018.

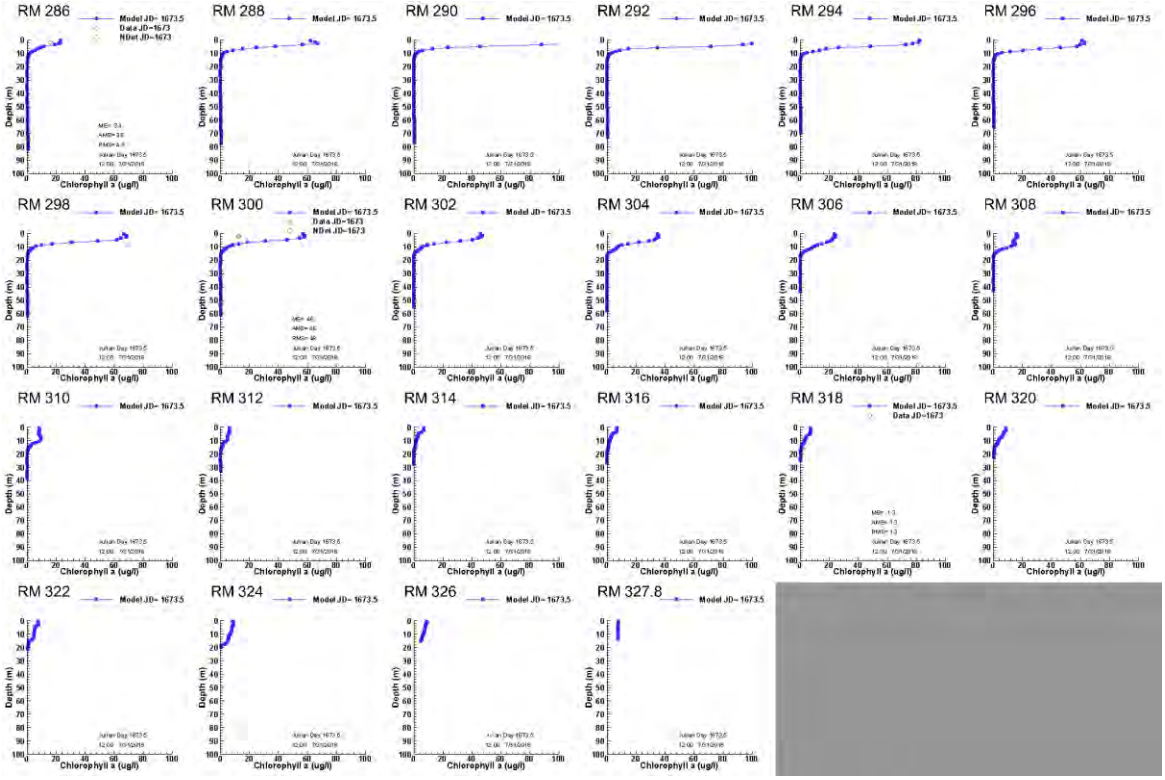


Figure 2078. Vertical profiles of chlorophyll a compared with data for 7/31/2018.

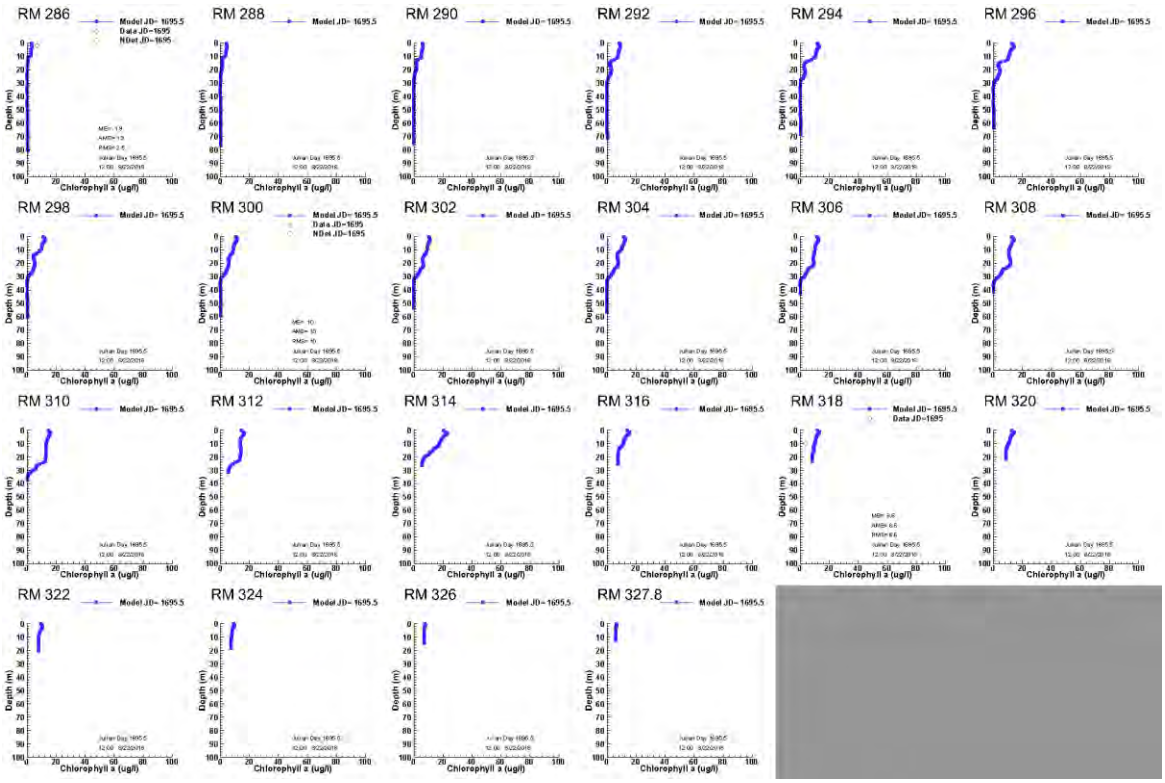


Figure 2079. Vertical profiles of chlorophyll a compared with data for 8/22/2018.

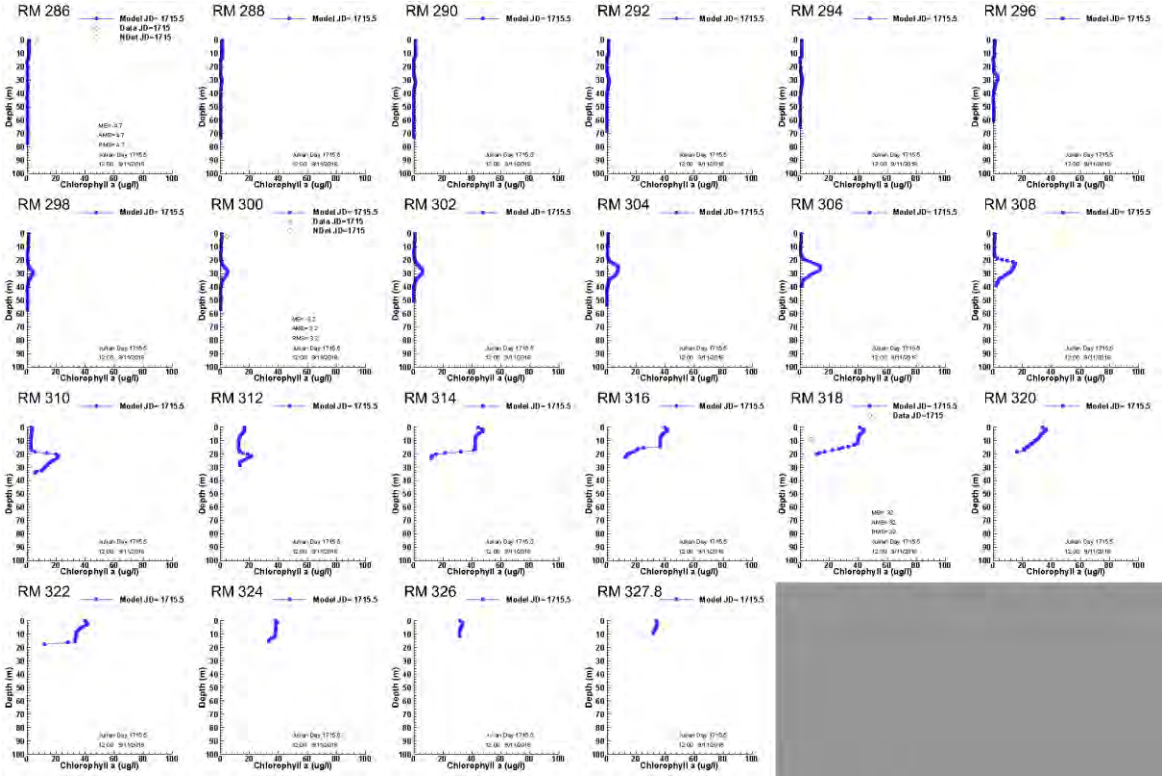


Figure 2080. Vertical profiles of chlorophyll a compared with data for 9/11/2018.

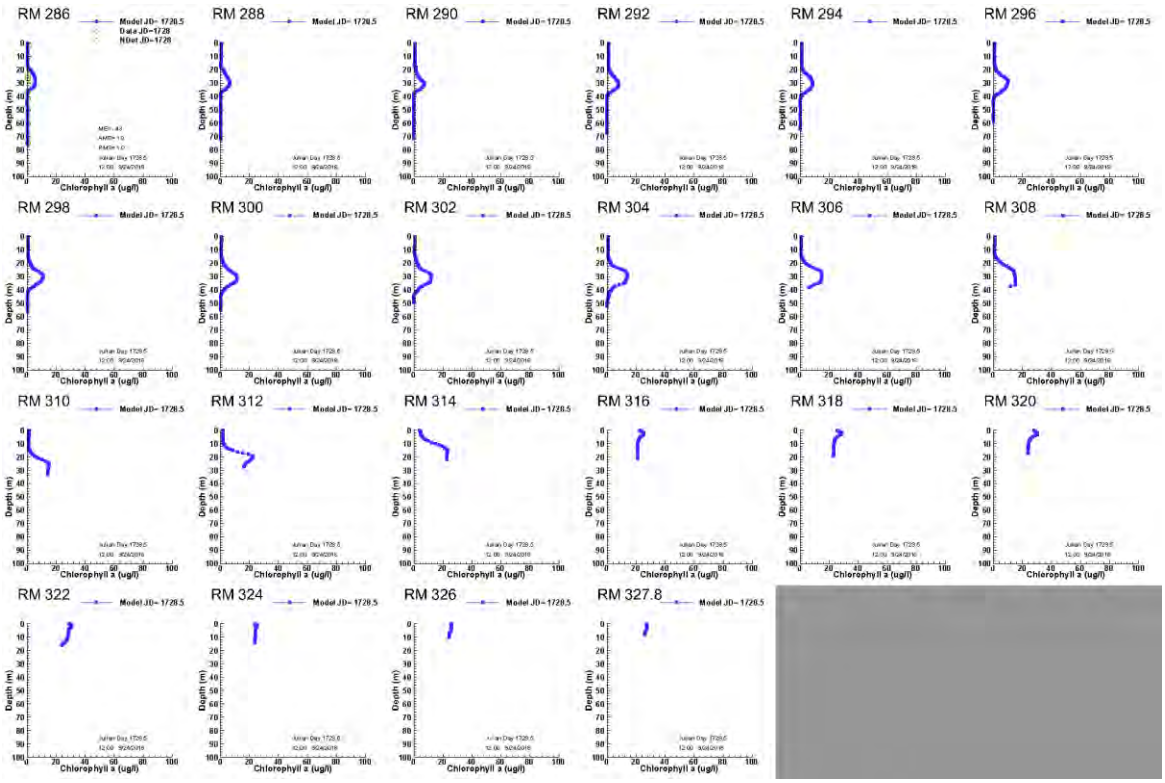


Figure 2081. Vertical profiles of chlorophyll a compared with data for 9/24/2018.

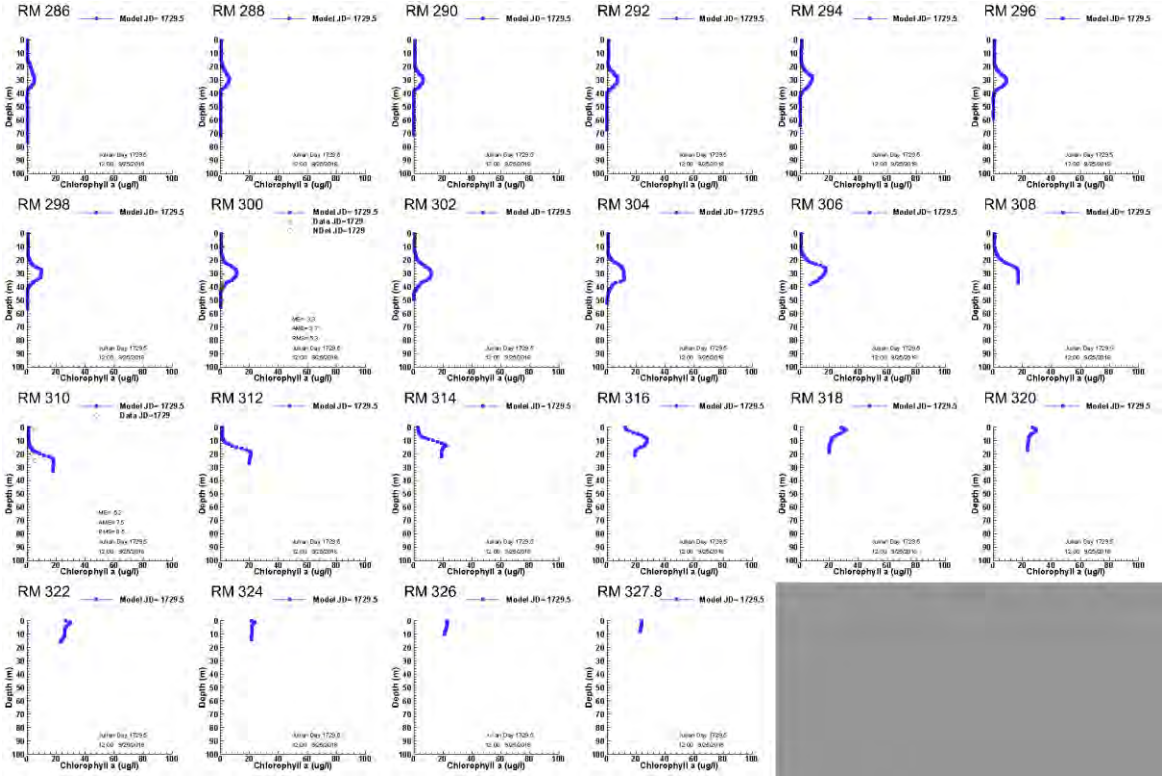


Figure 2082. Vertical profiles of chlorophyll a compared with data for 9/25/2018.

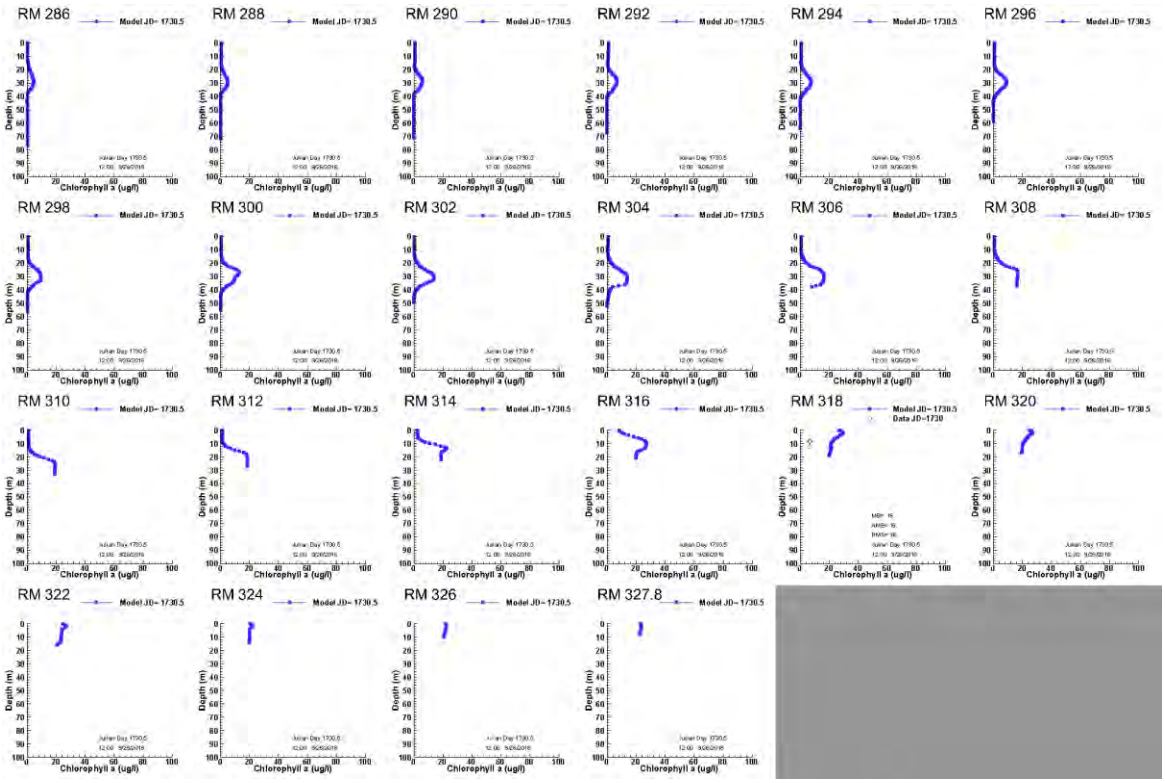


Figure 2083. Vertical profiles of chlorophyll a compared with data for 9/26/2018.

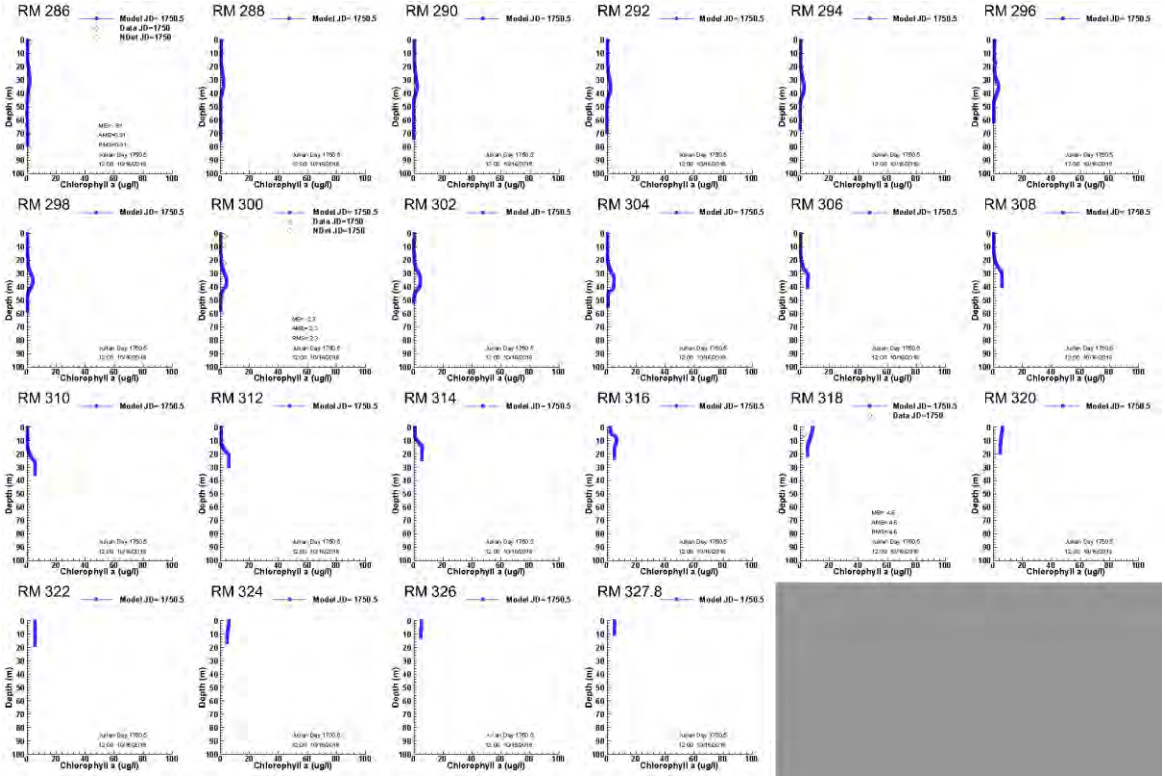


Figure 2084. Vertical profiles of chlorophyll a compared with data for 10/16/2018.

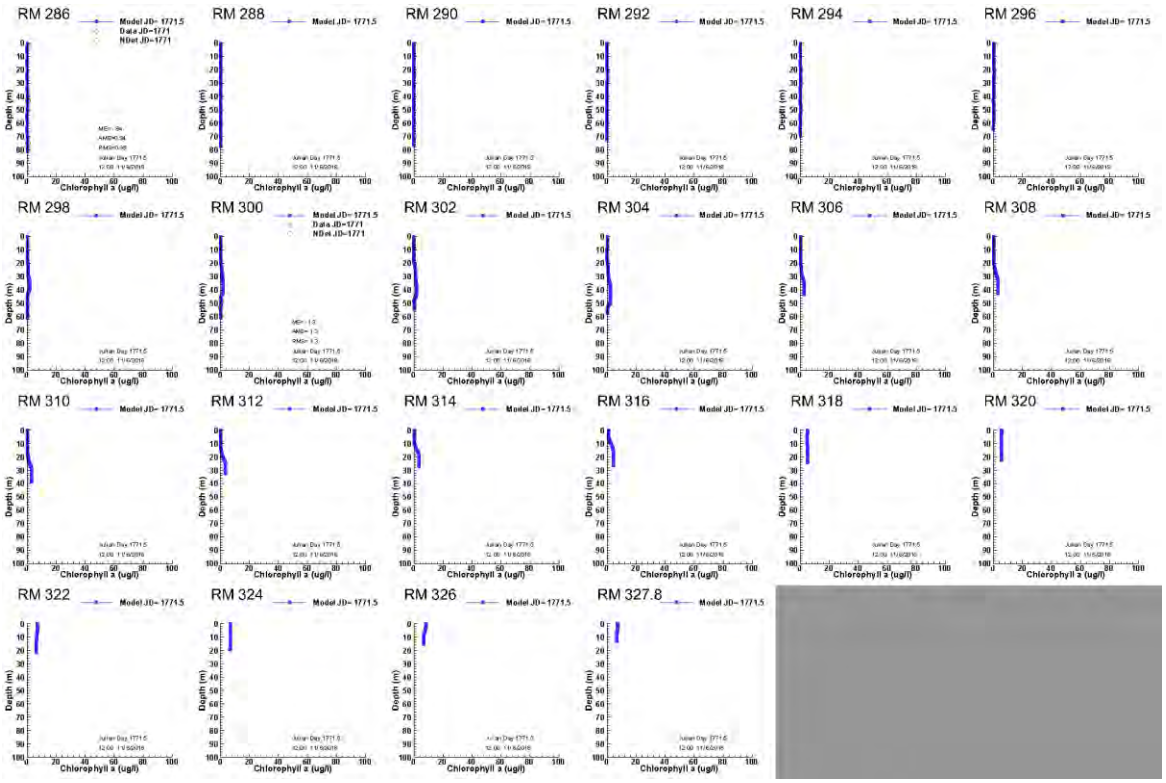


Figure 2085. Vertical profiles of chlorophyll a compared with data for 11/ 6/2018.

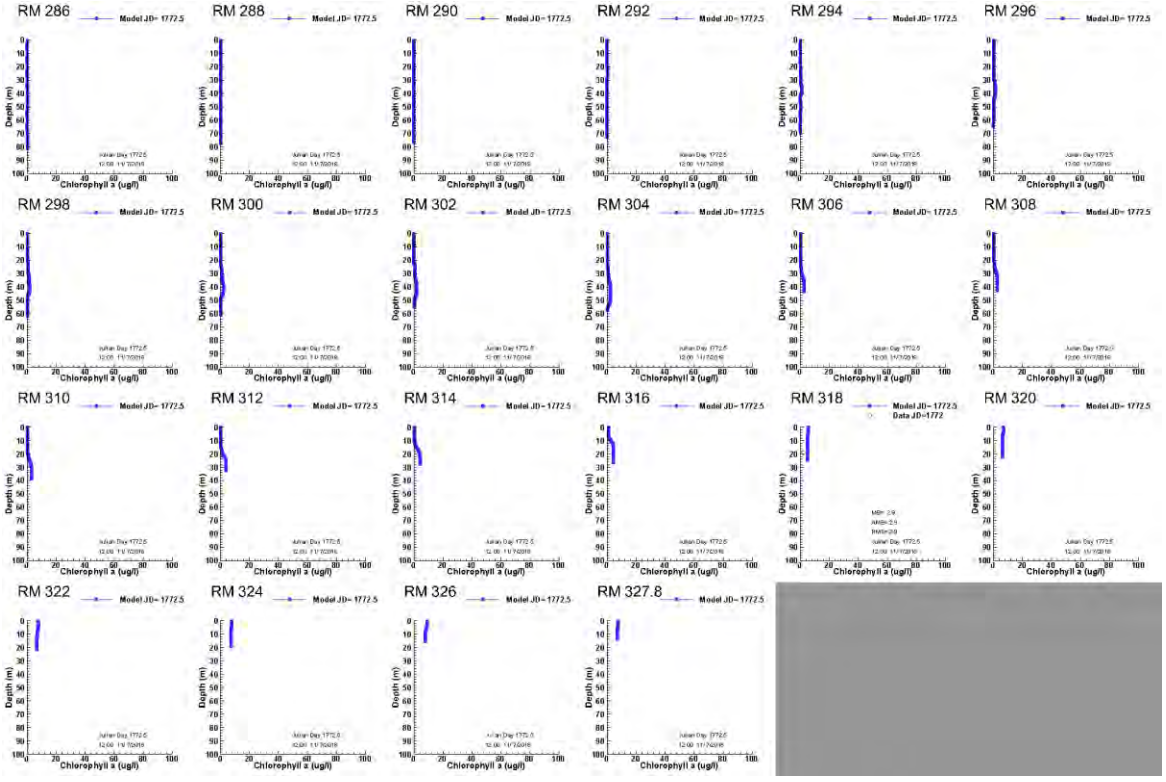


Figure 2086. Vertical profiles of chlorophyll a compared with data for 11/ 7/2018.

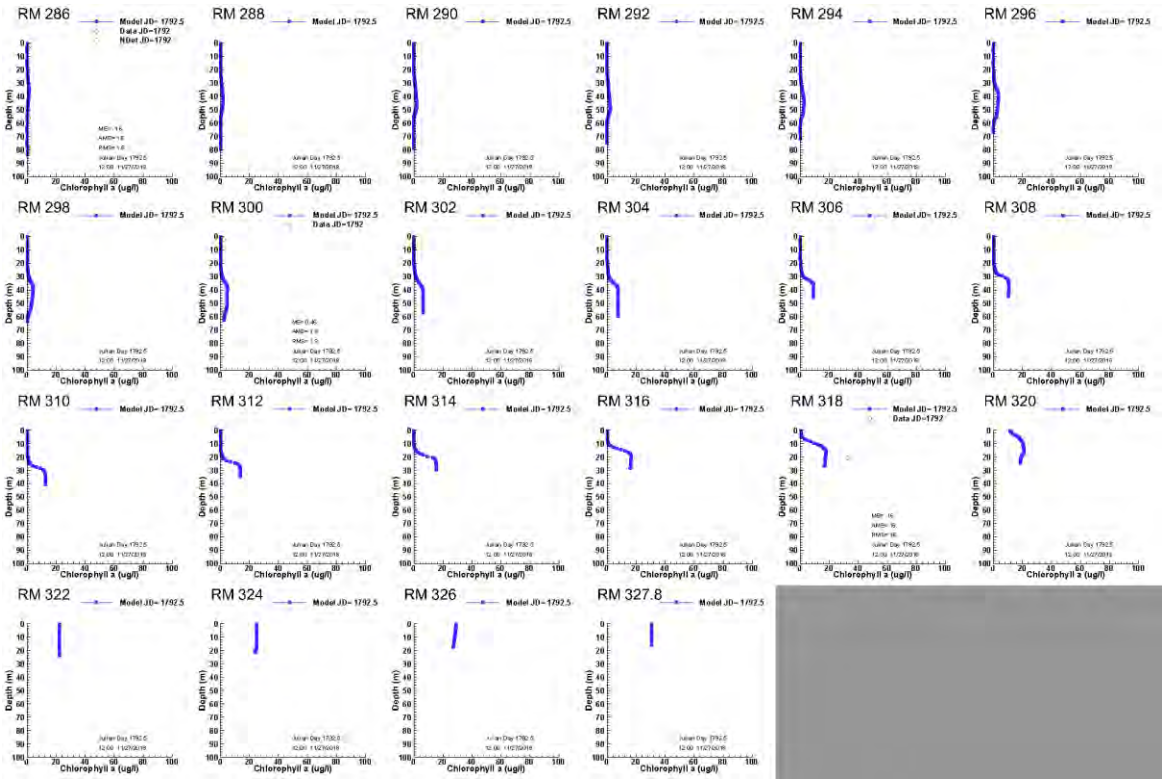


Figure 2087. Vertical profiles of chlorophyll a compared with data for 11/27/2018.

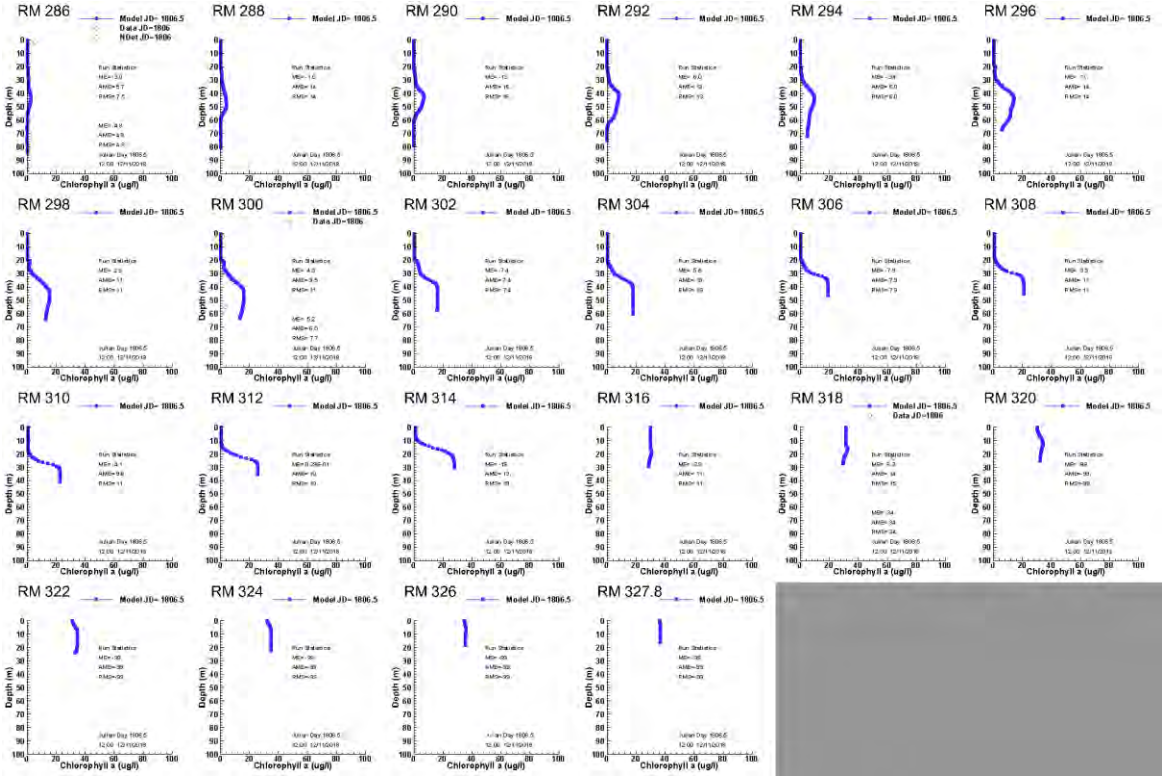


Figure 2088. Vertical profiles of chlorophyll a compared with data for 12/11/2018.

Total Suspended Solids

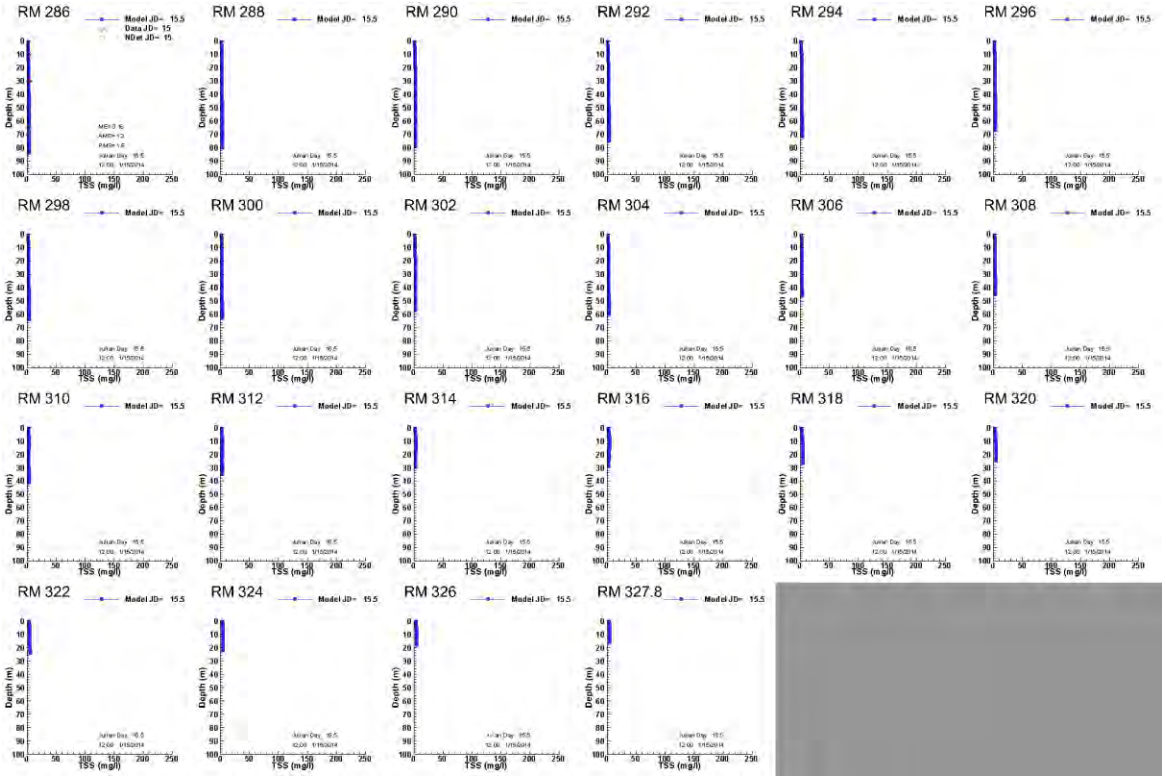


Figure 2089. Vertical profiles of TSS compared with data for 1/15/2014.

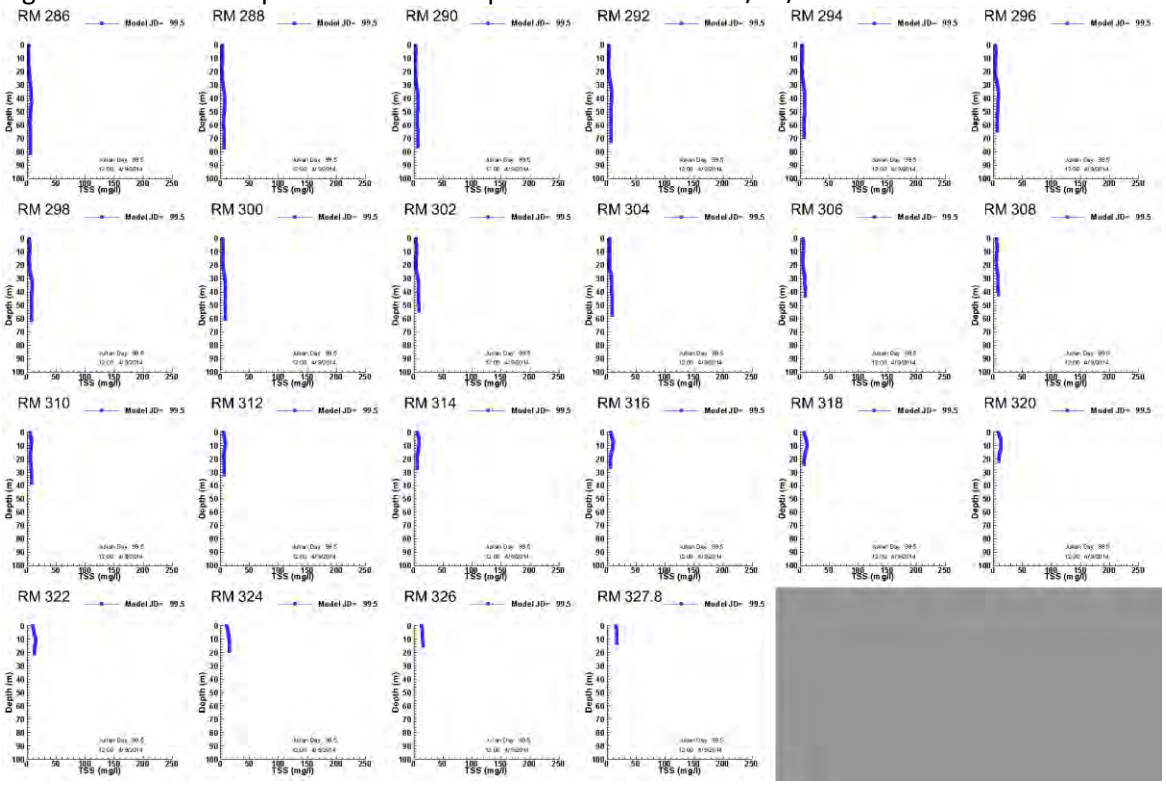


Figure 2090. Vertical profiles of TSS compared with data for 4/ 9/2014.

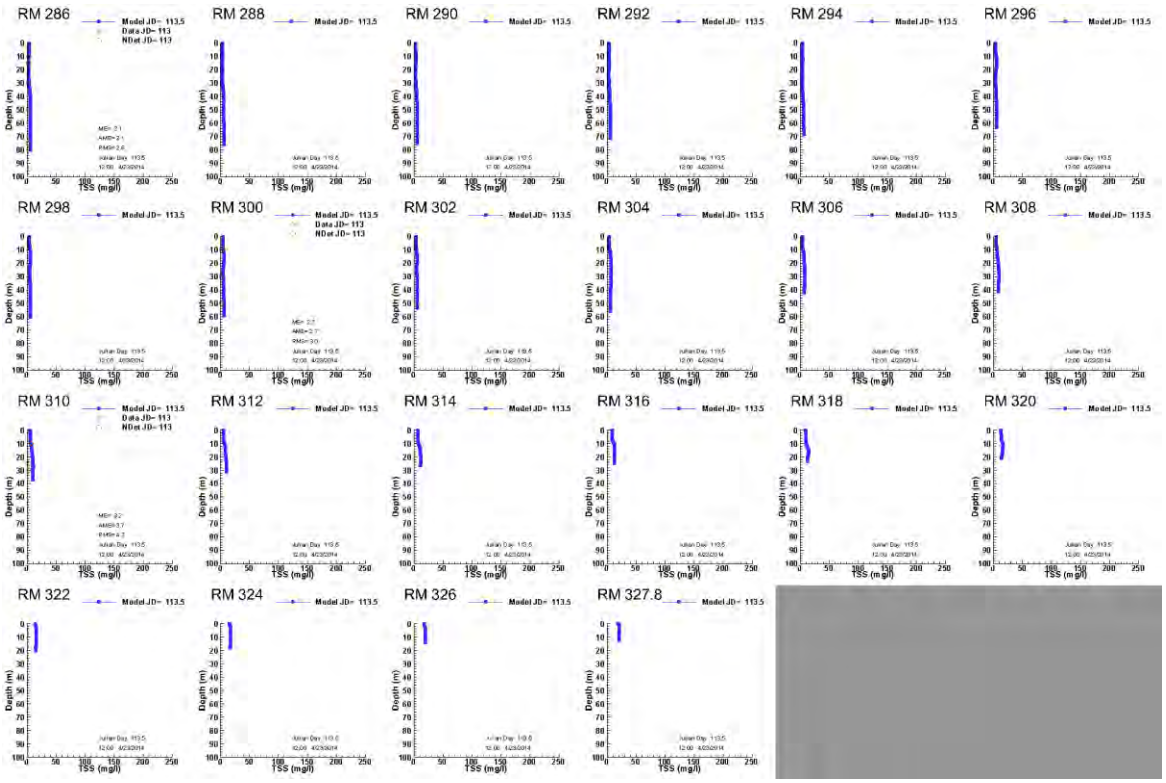


Figure 2091. Vertical profiles of TSS compared with data for 4/23/2014.

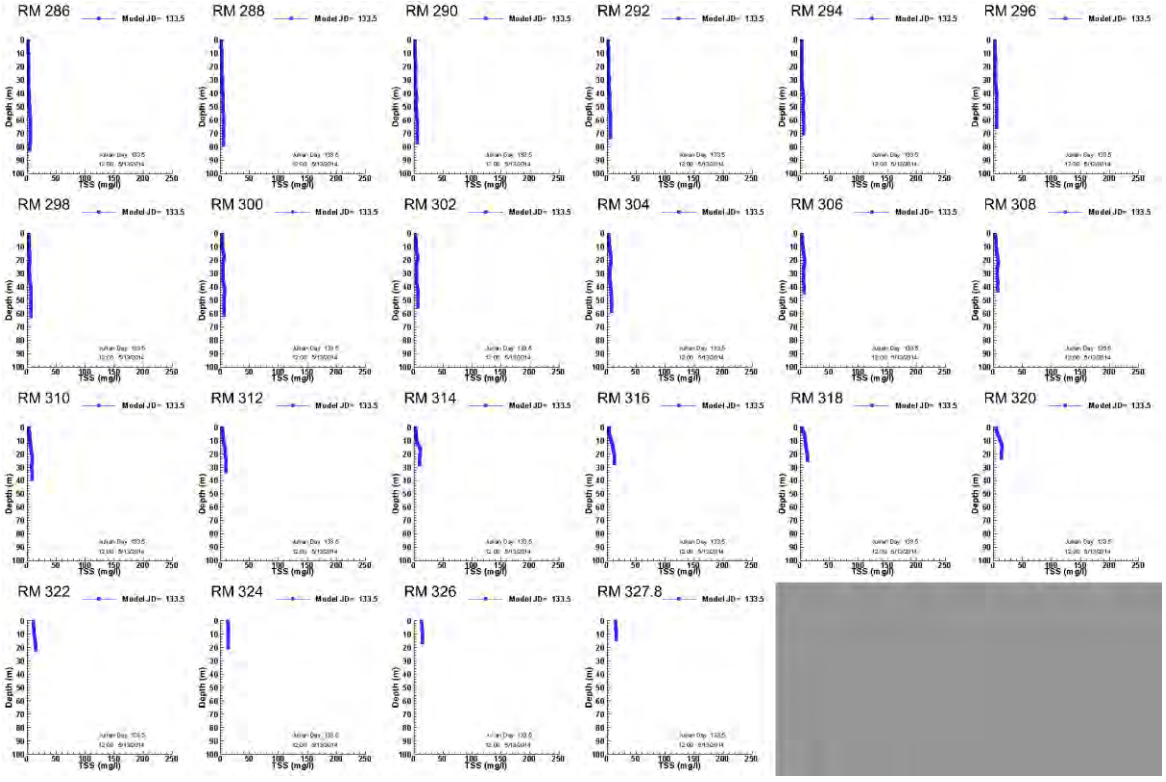


Figure 2092. Vertical profiles of TSS compared with data for 5/13/2014.

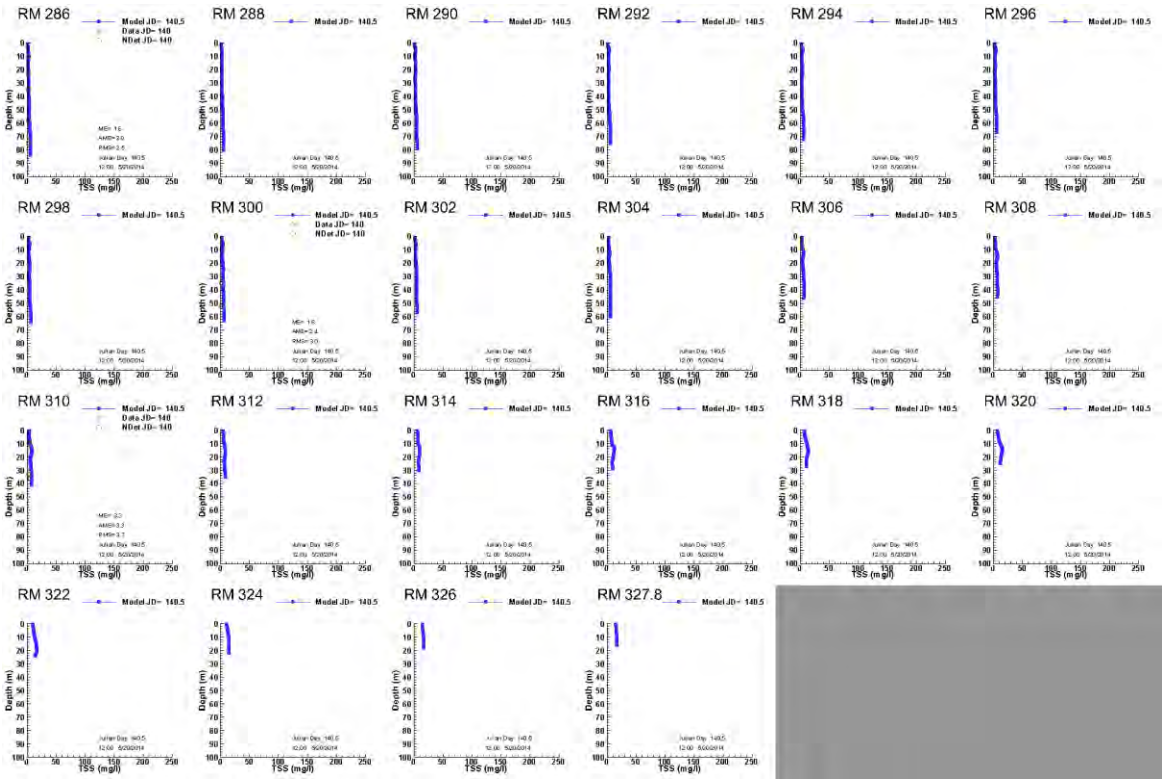


Figure 2093. Vertical profiles of TSS compared with data for 5/20/2014.

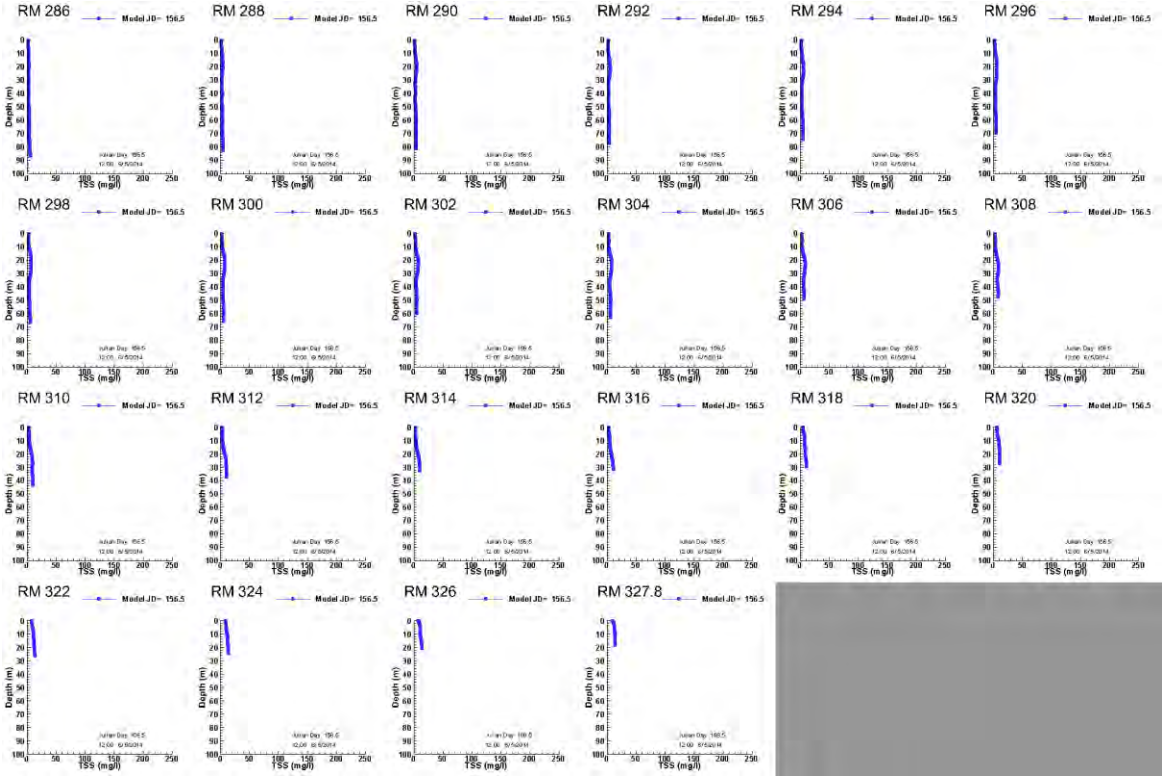


Figure 2094. Vertical profiles of TSS compared with data for 6/ 5/2014.

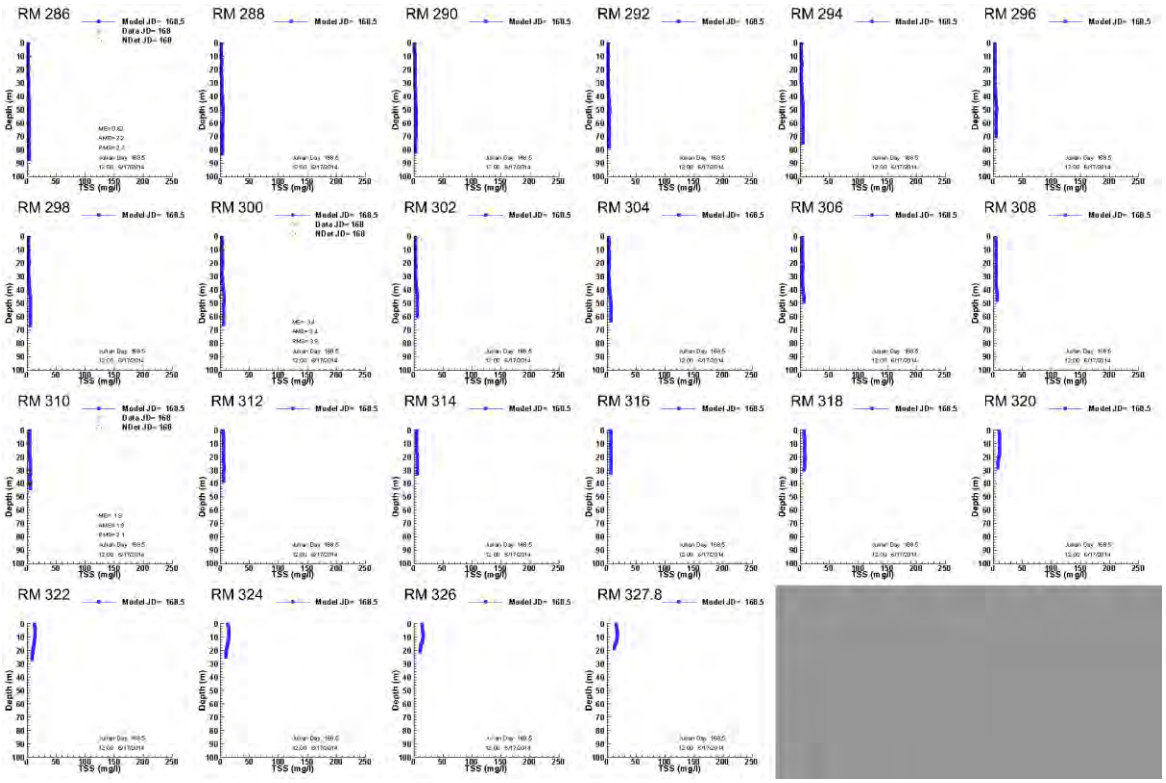


Figure 2095. Vertical profiles of TSS compared with data for 6/17/2014.

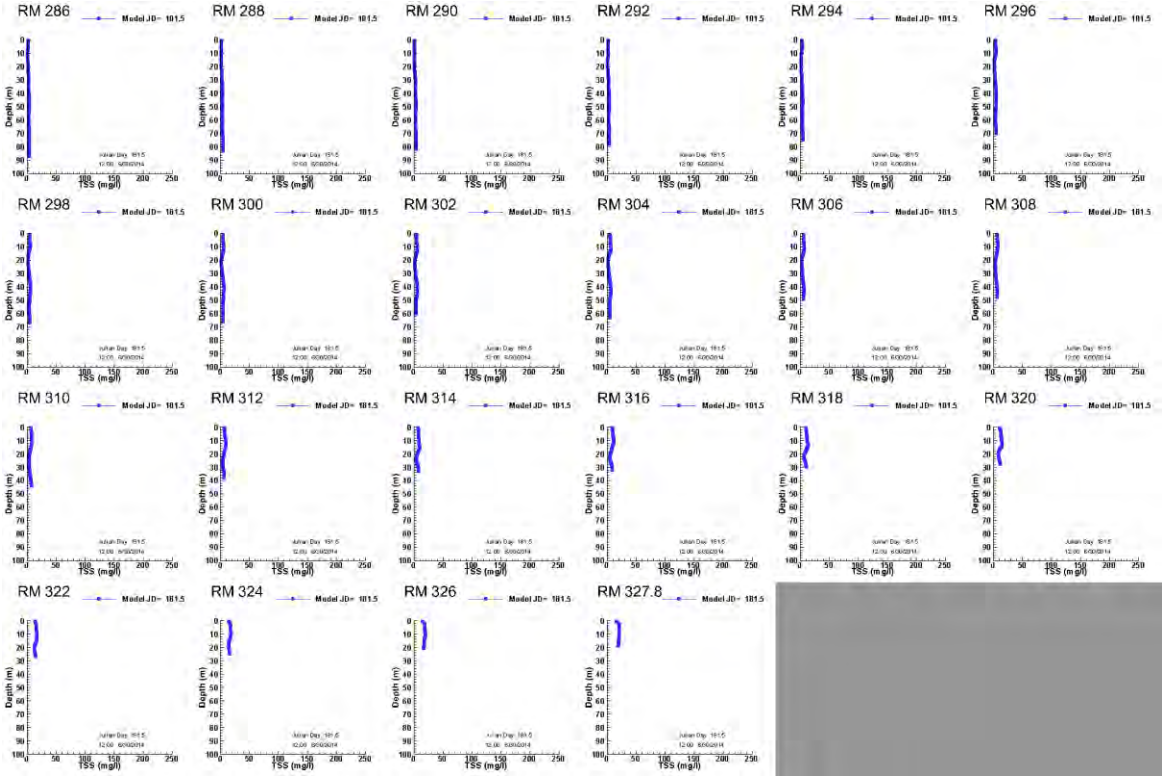


Figure 2096. Vertical profiles of TSS compared with data for 6/30/2014.

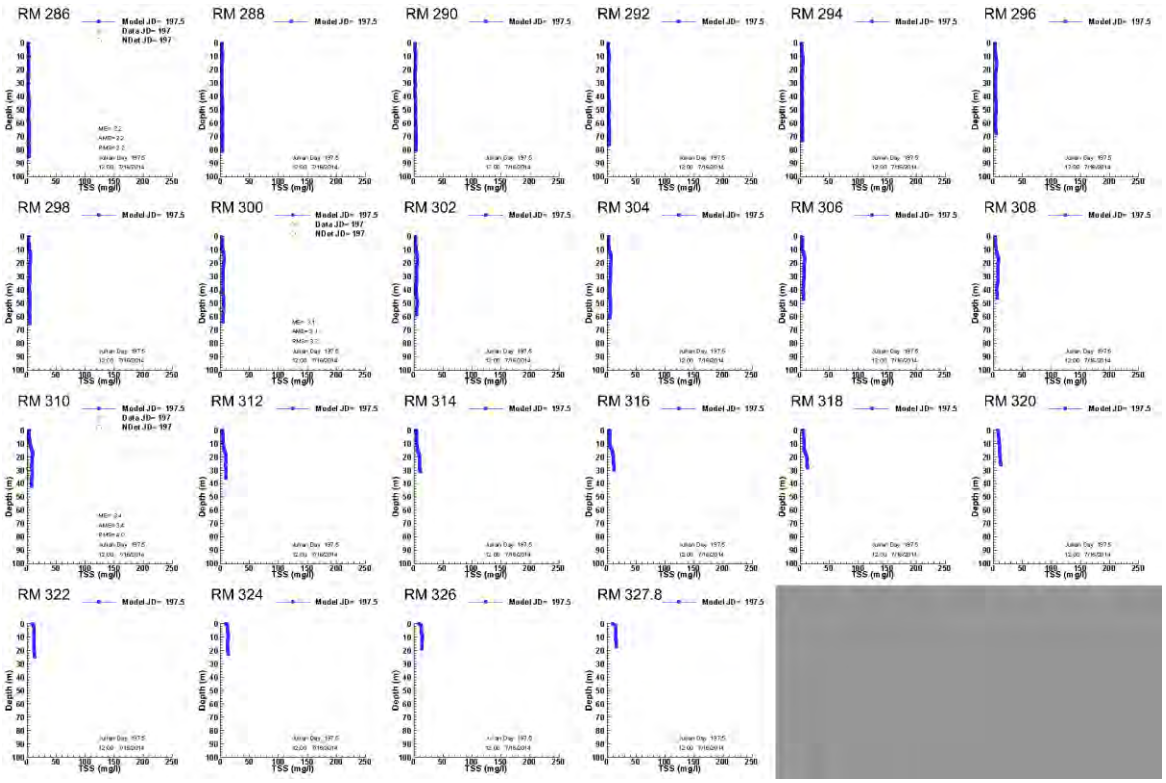


Figure 2097. Vertical profiles of TSS compared with data for 7/16/2014.

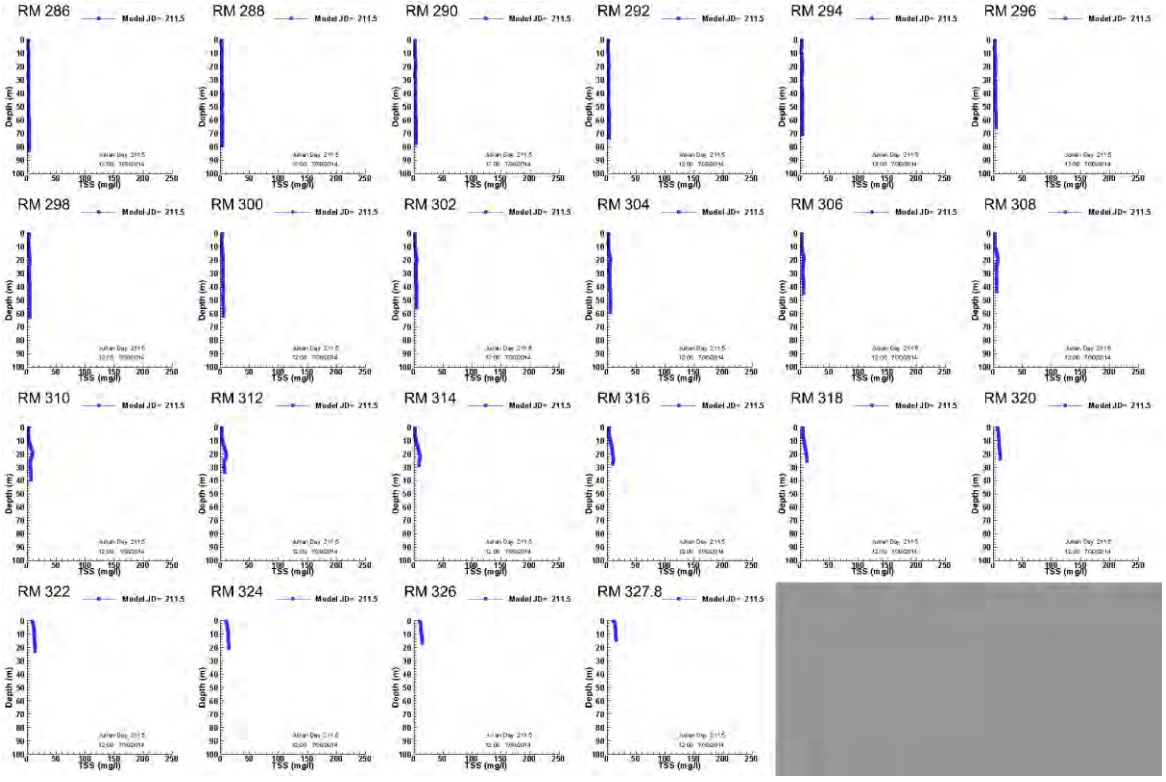


Figure 2098. Vertical profiles of TSS compared with data for 7/30/2014.

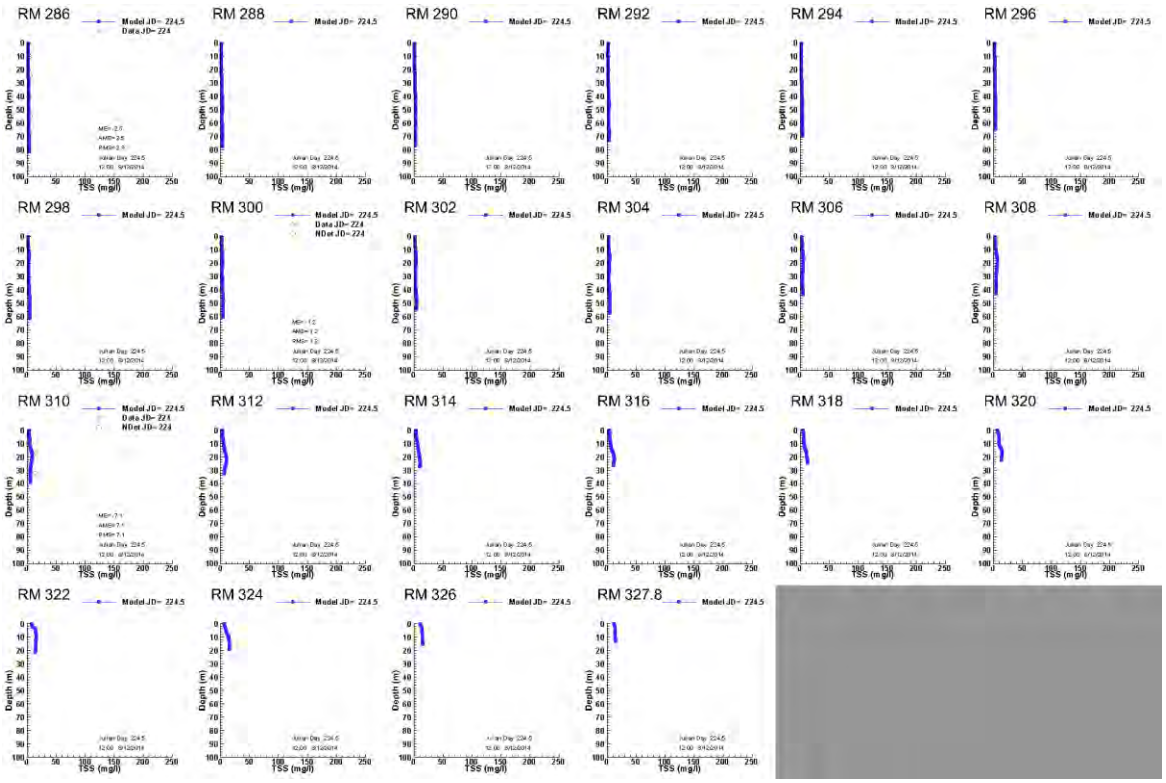


Figure 2099. Vertical profiles of TSS compared with data for 8/12/2014.

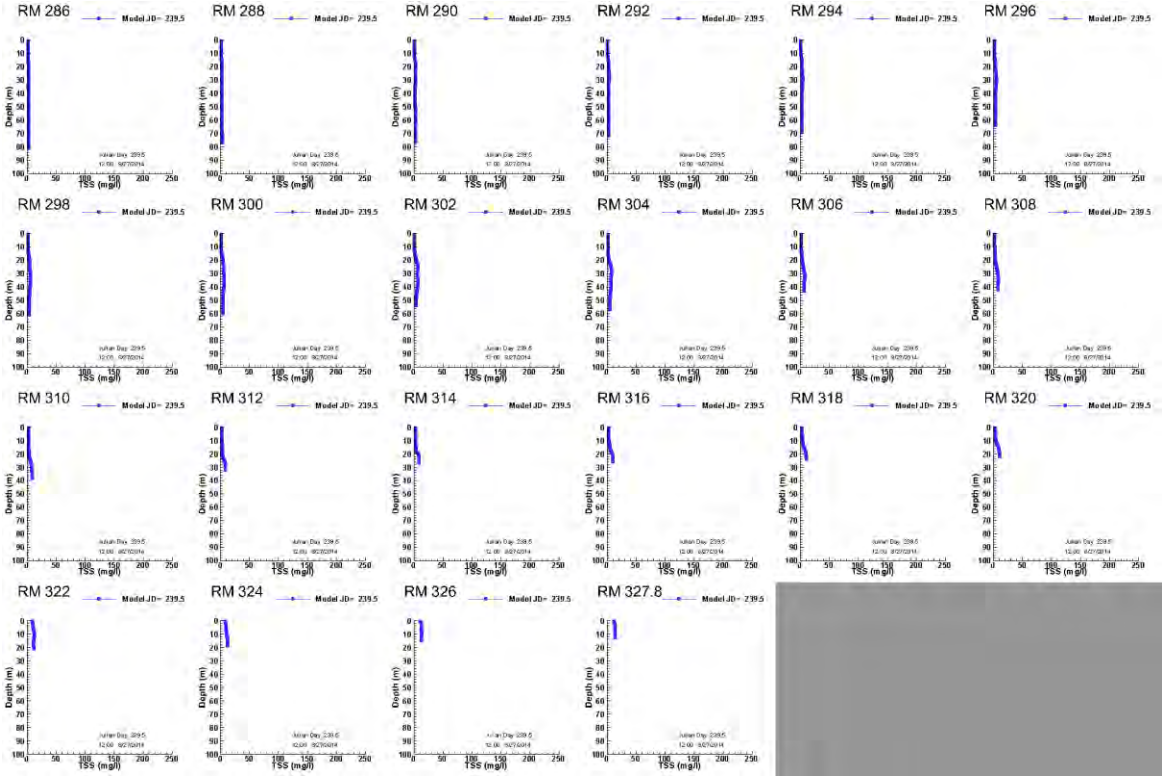


Figure 2100. Vertical profiles of TSS compared with data for 8/27/2014.

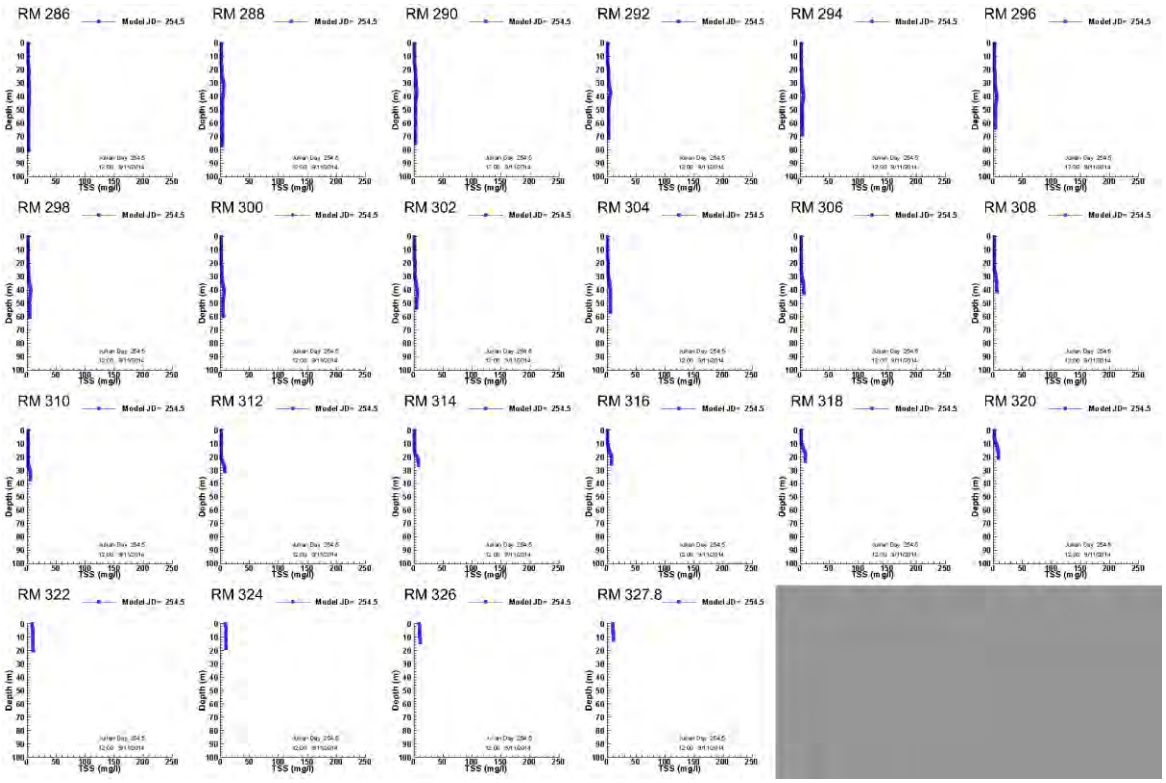


Figure 2101. Vertical profiles of TSS compared with data for 9/11/2014.

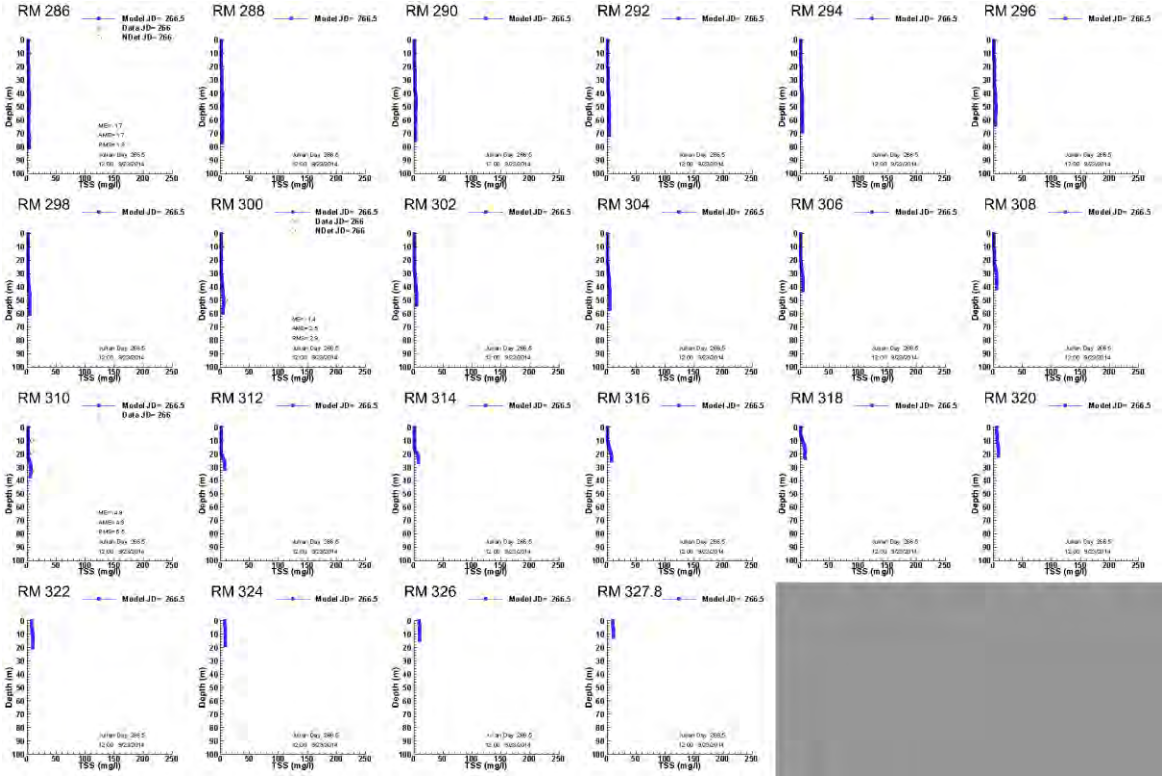


Figure 2102. Vertical profiles of TSS compared with data for 9/23/2014.

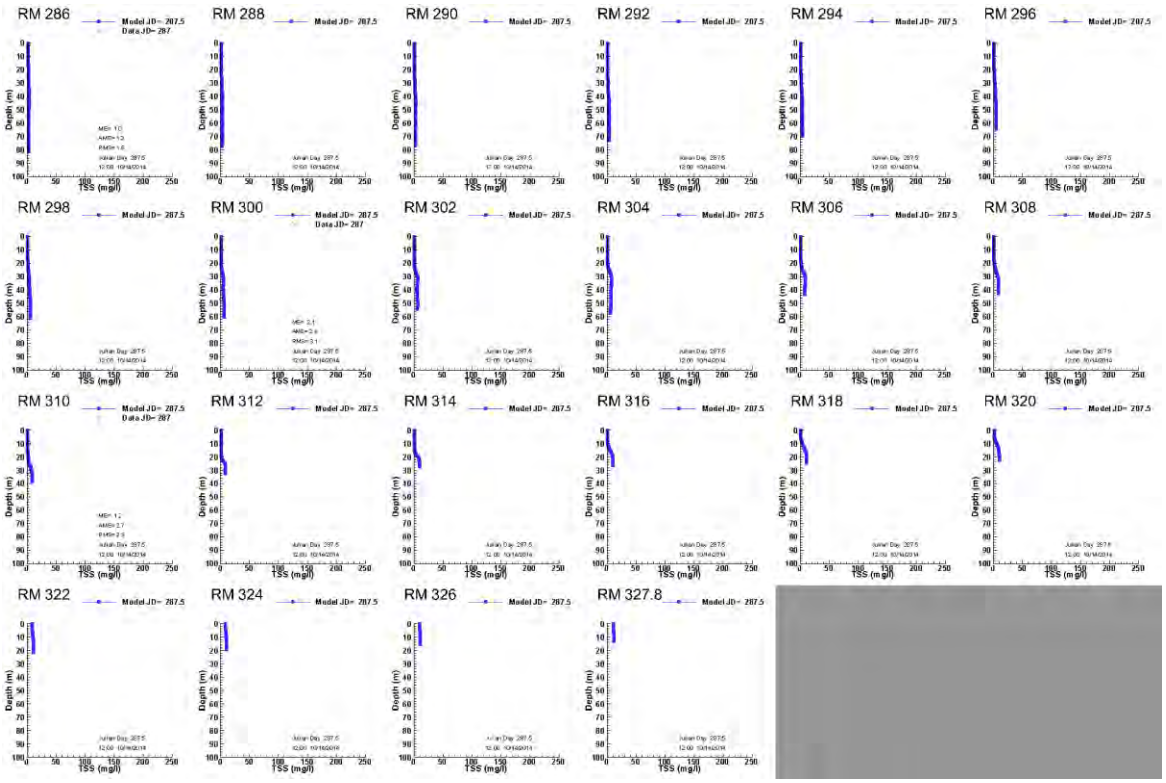


Figure 2103. Vertical profiles of TSS compared with data for 10/14/2014.

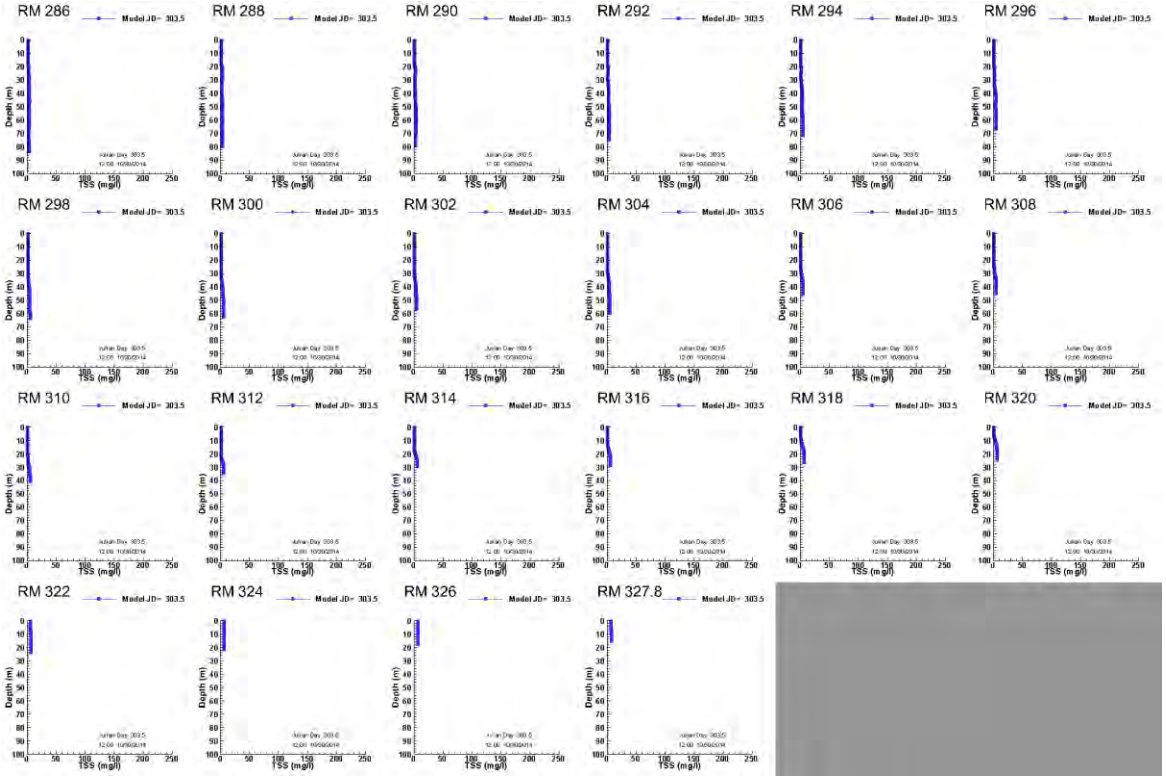


Figure 2104. Vertical profiles of TSS compared with data for 10/30/2014.

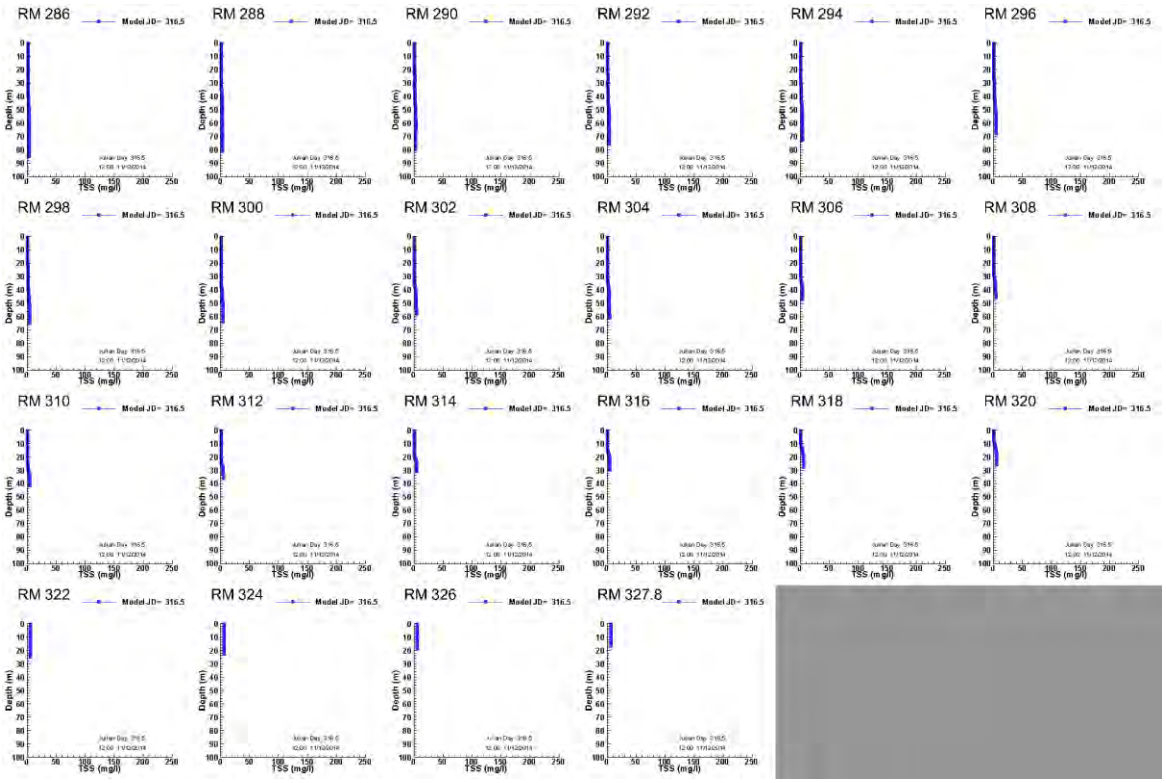


Figure 2105. Vertical profiles of TSS compared with data for 11/12/2014.

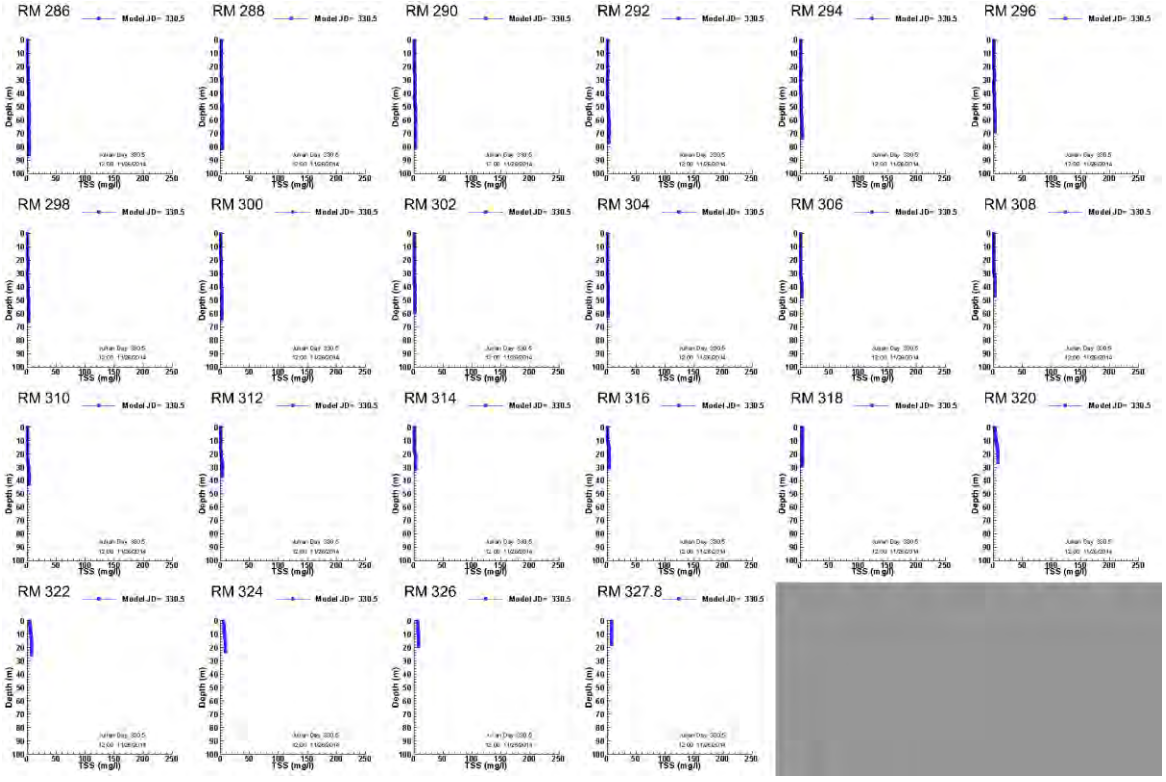


Figure 2106. Vertical profiles of TSS compared with data for 11/26/2014.

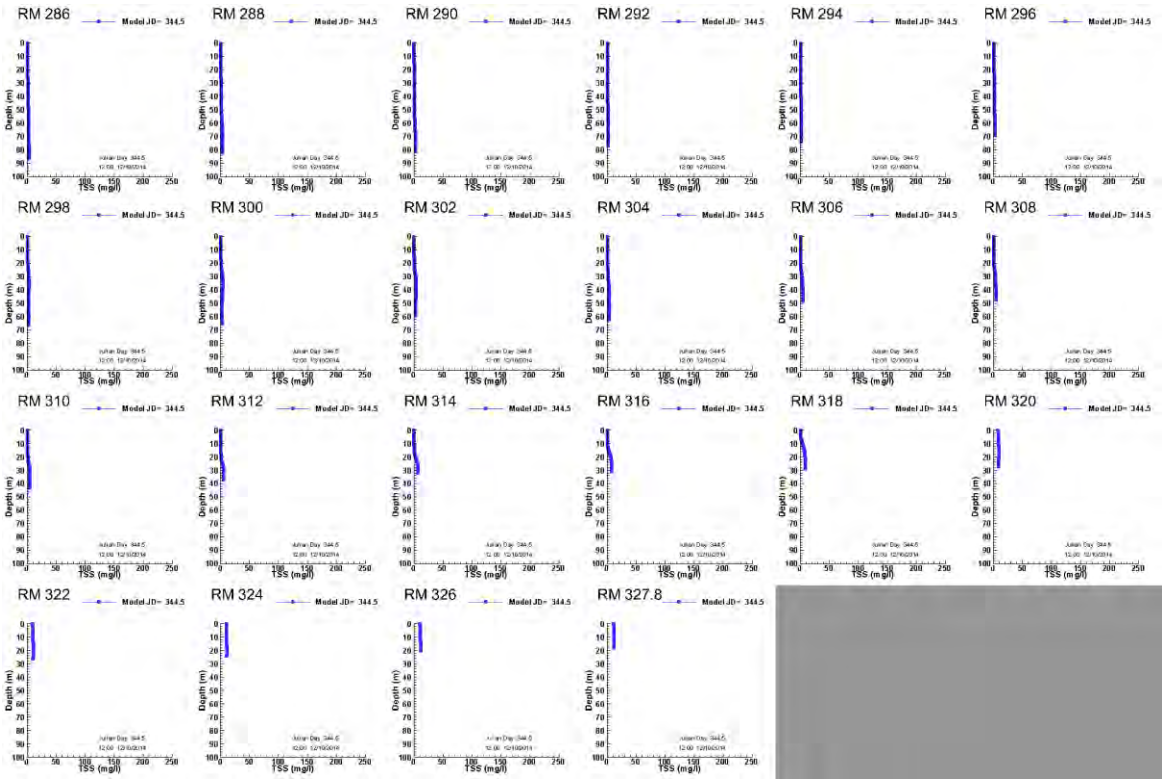


Figure 2107. Vertical profiles of TSS compared with data for 12/10/2014.

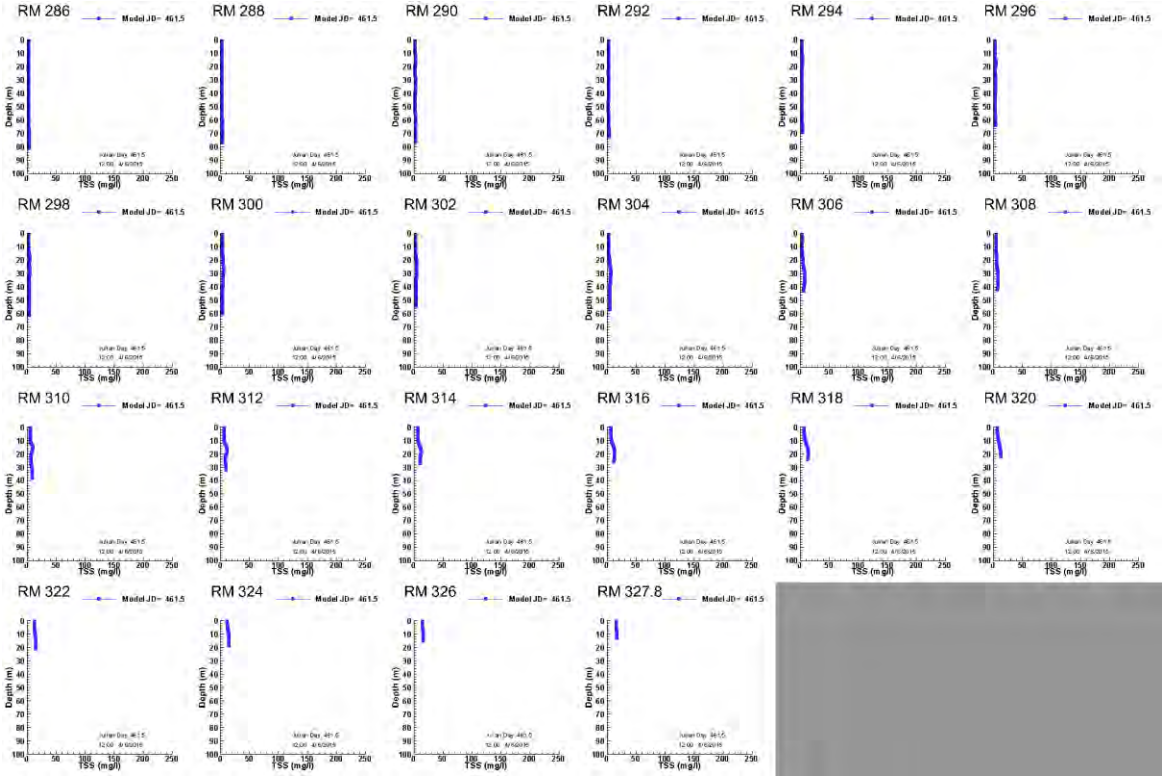


Figure 2108. Vertical profiles of TSS compared with data for 4/ 6/2015.

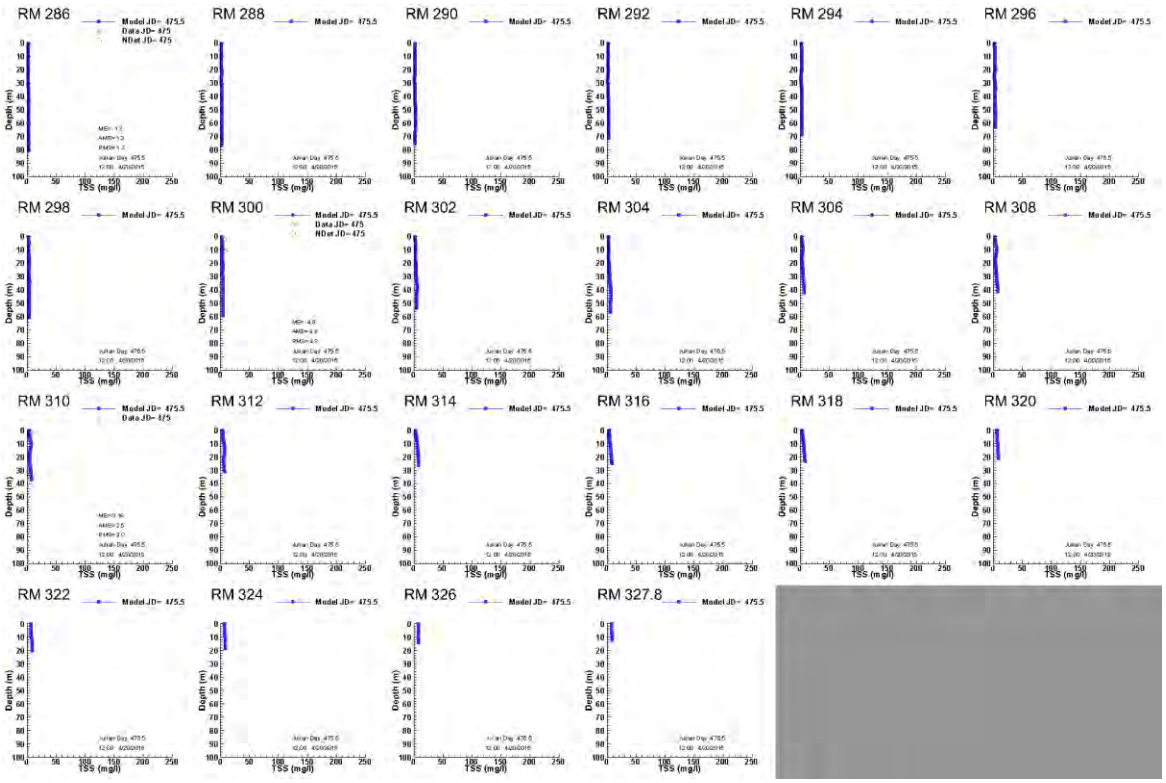


Figure 2109. Vertical profiles of TSS compared with data for 4/20/2015.

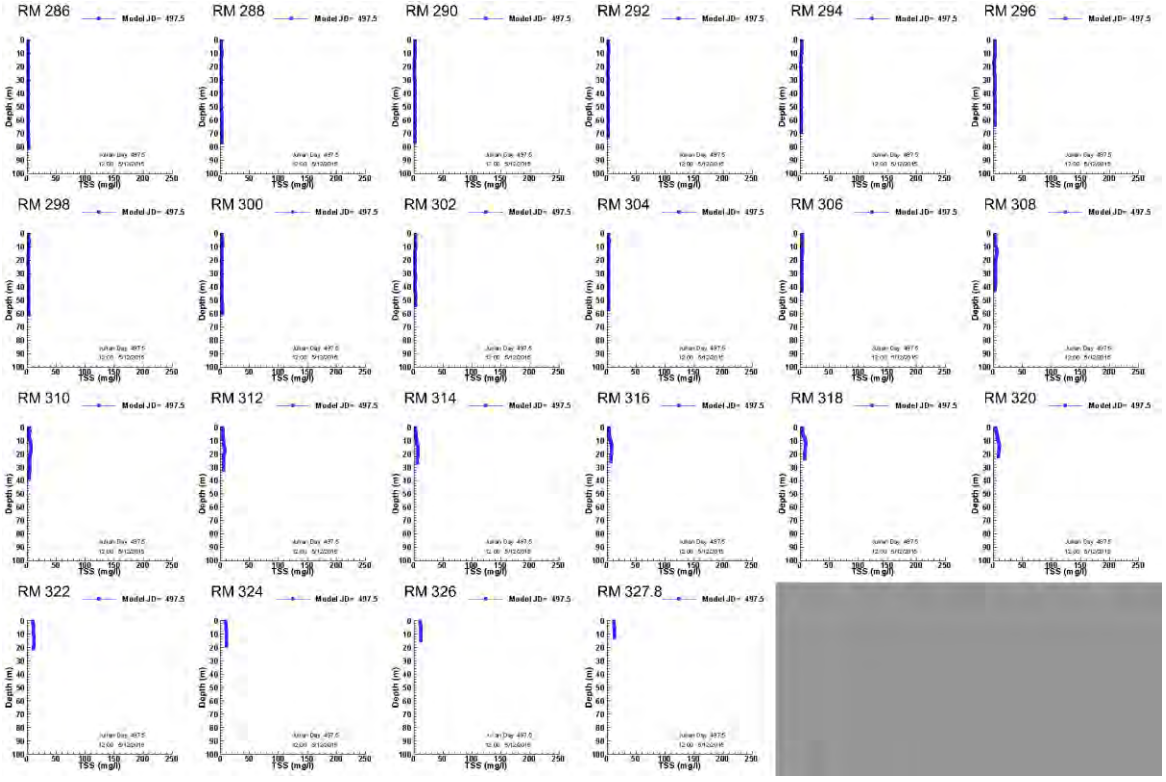


Figure 2110. Vertical profiles of TSS compared with data for 5/12/2015.

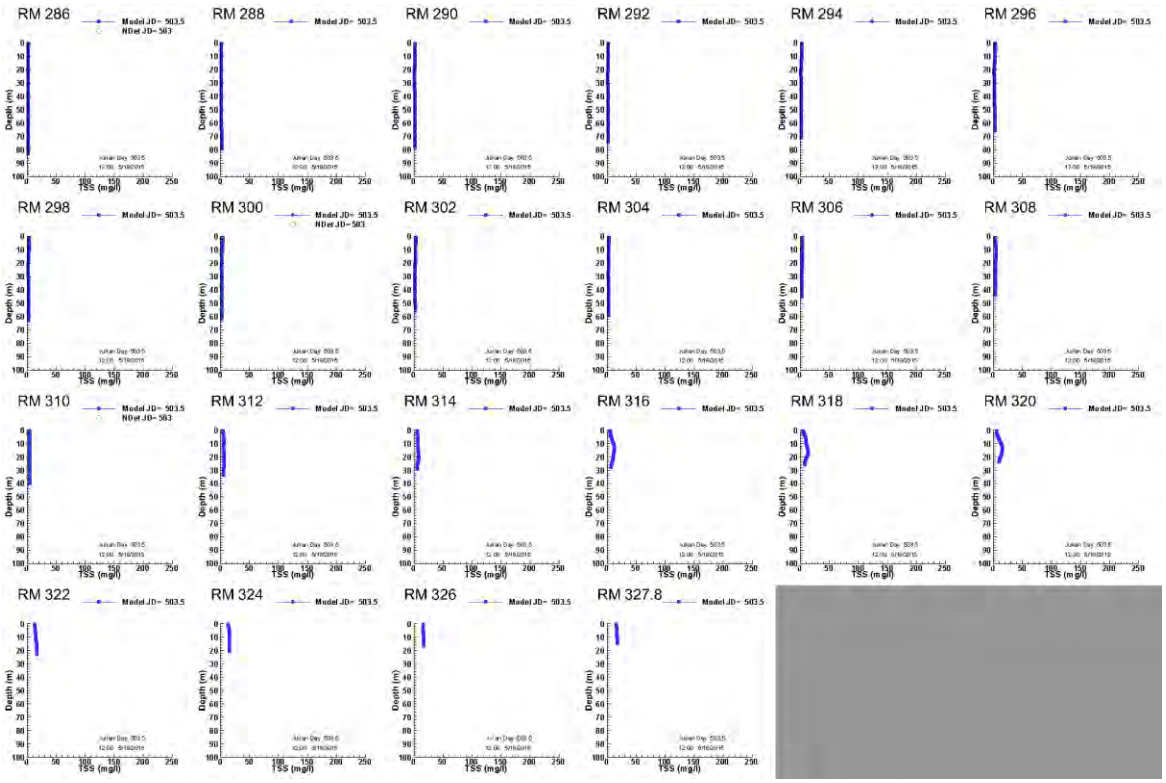


Figure 2111. Vertical profiles of TSS compared with data for 5/18/2015.

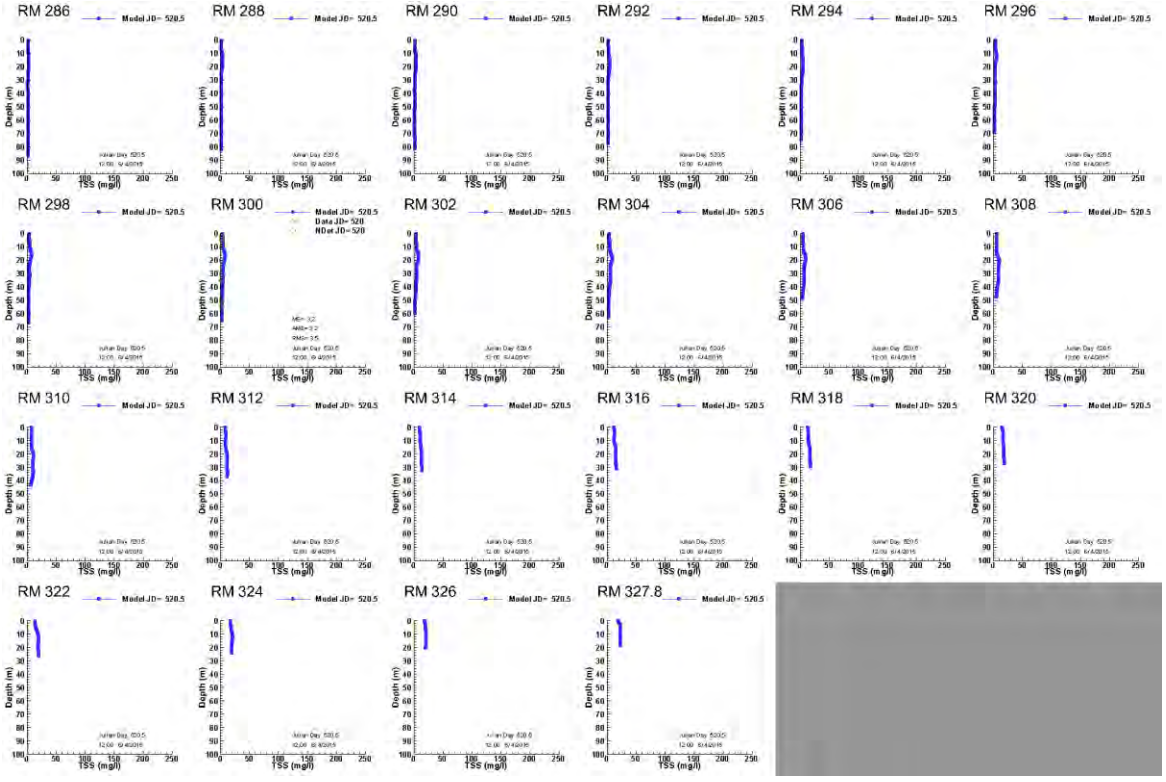


Figure 2112. Vertical profiles of TSS compared with data for 6/ 4/2015.

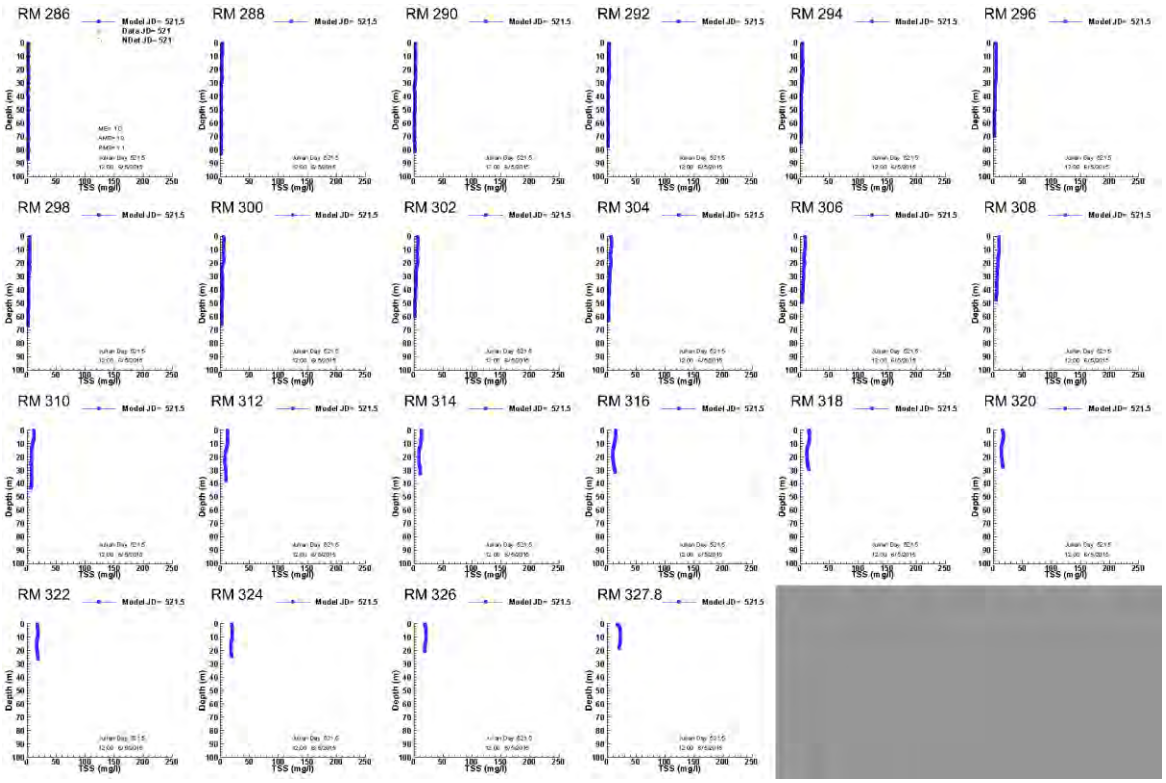


Figure 2113. Vertical profiles of TSS compared with data for 6/ 5/2015.

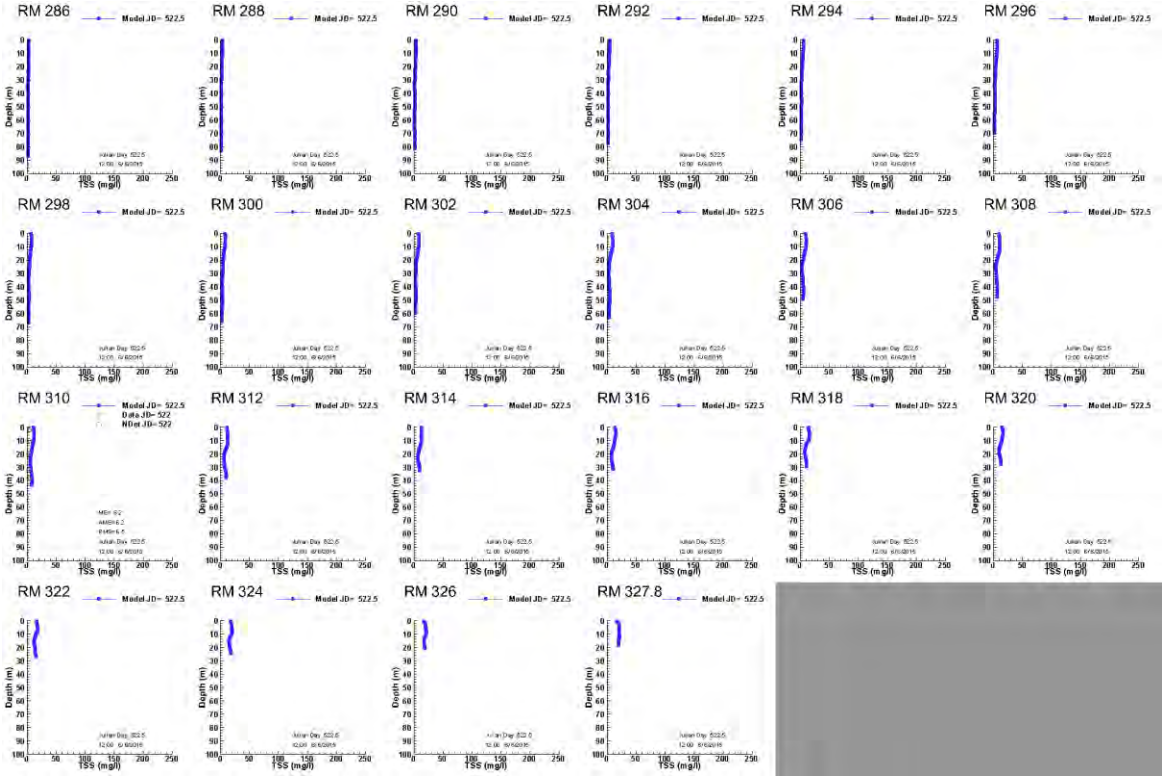


Figure 2114. Vertical profiles of TSS compared with data for 6/ 6/2015.

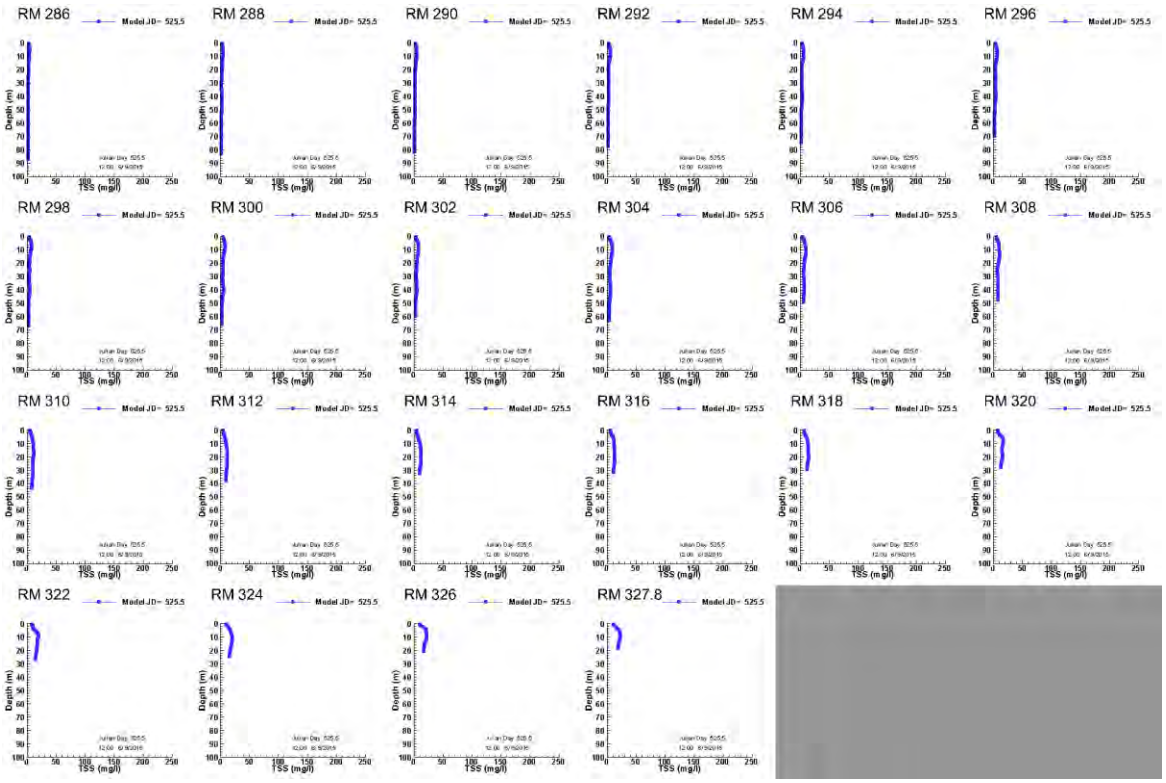


Figure 2115. Vertical profiles of TSS compared with data for 6/ 9/2015.

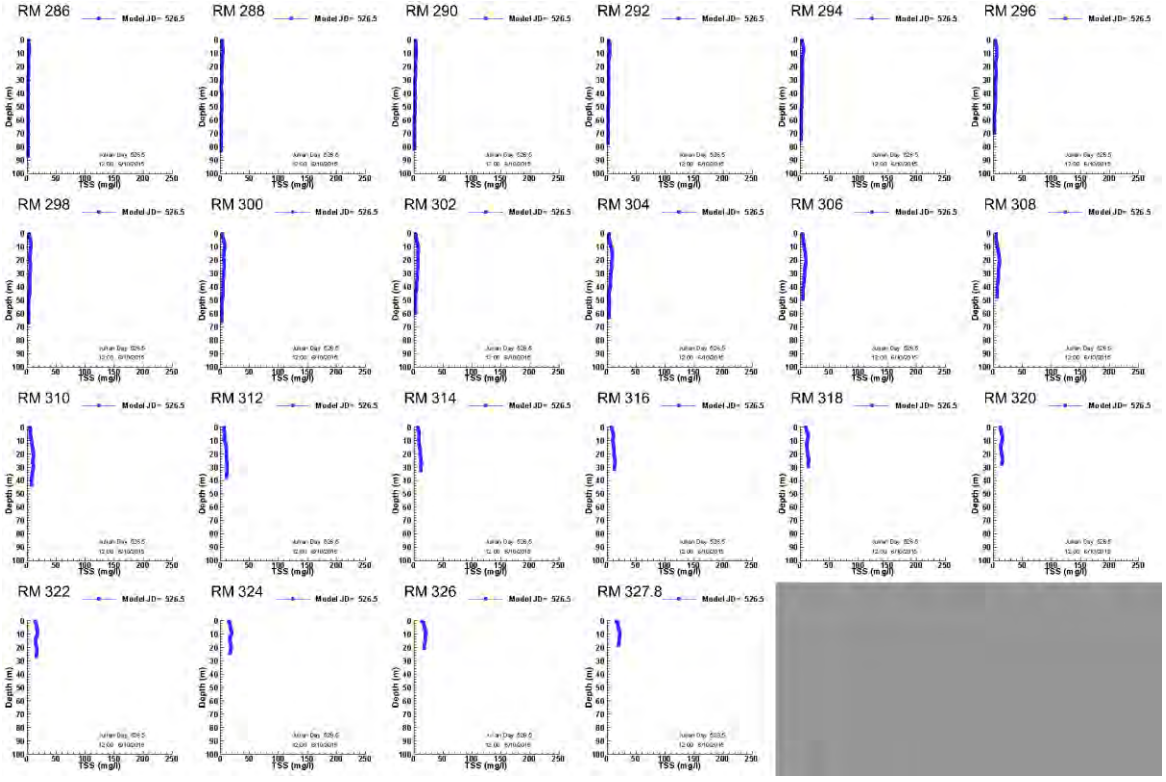


Figure 2116. Vertical profiles of TSS compared with data for 6/10/2015.

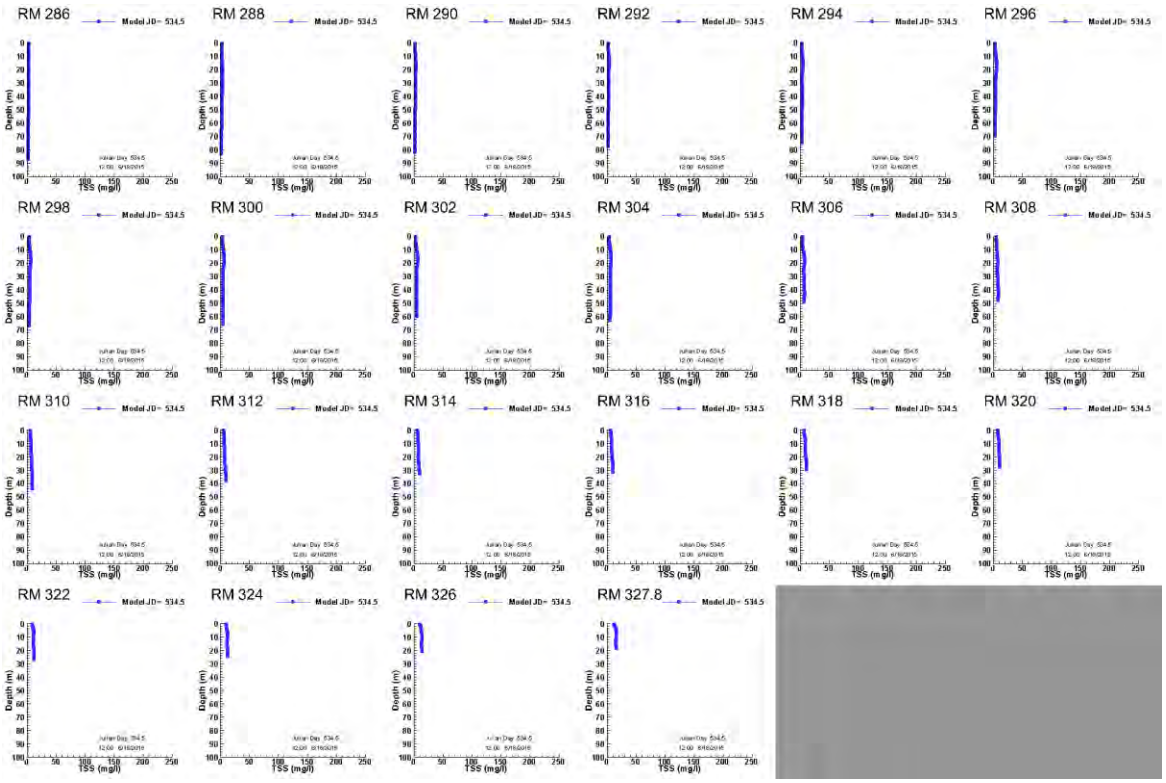


Figure 2117. Vertical profiles of TSS compared with data for 6/18/2015.

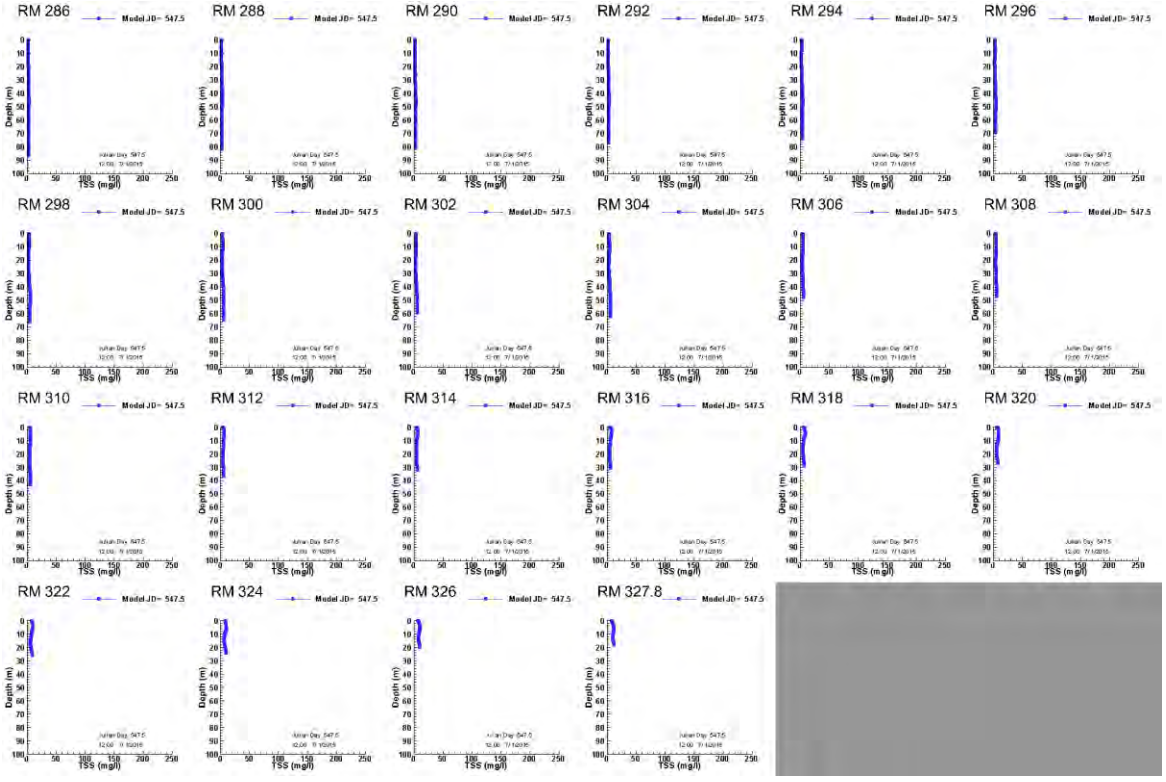


Figure 2118. Vertical profiles of TSS compared with data for 7/ 1/2015.

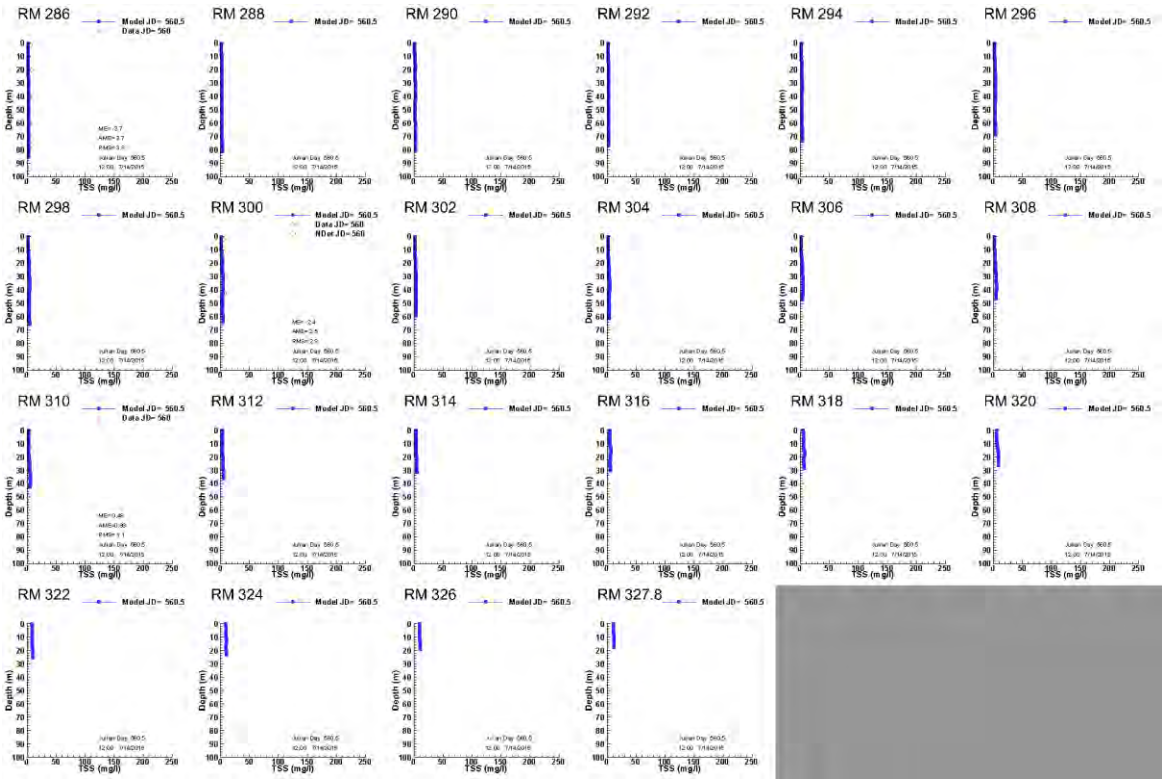


Figure 2119. Vertical profiles of TSS compared with data for 7/14/2015.

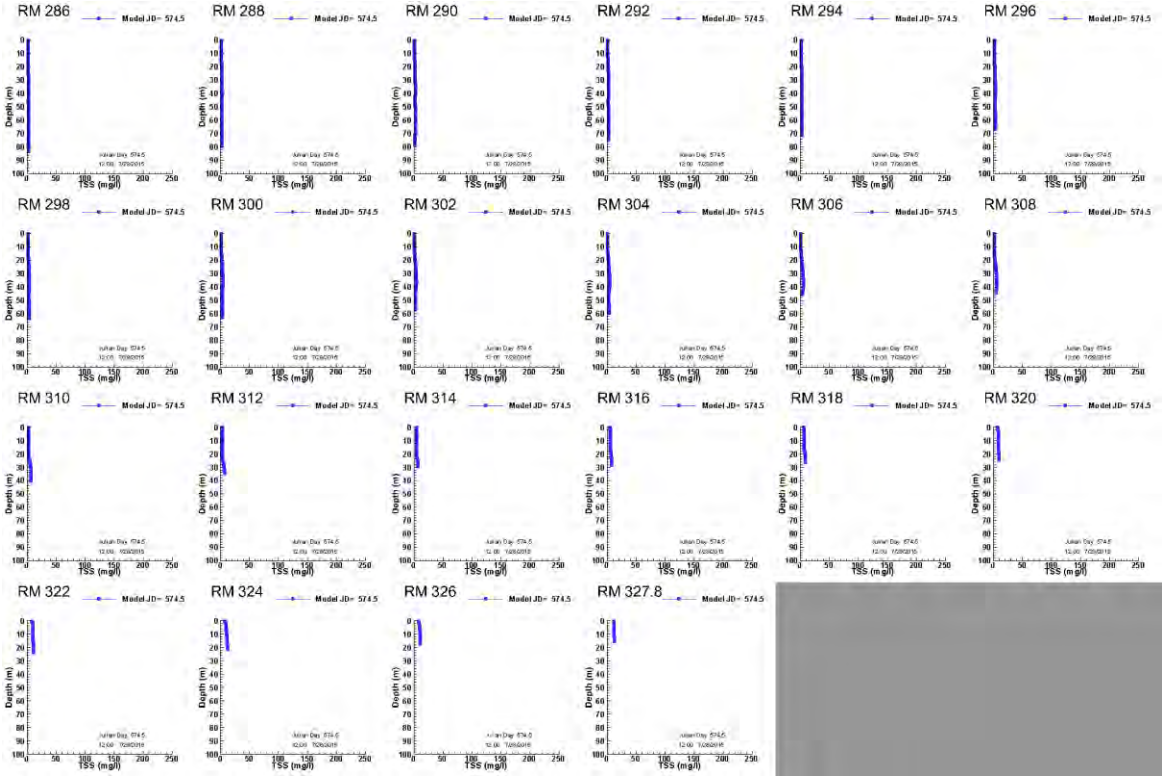


Figure 2120. Vertical profiles of TSS compared with data for 7/28/2015.

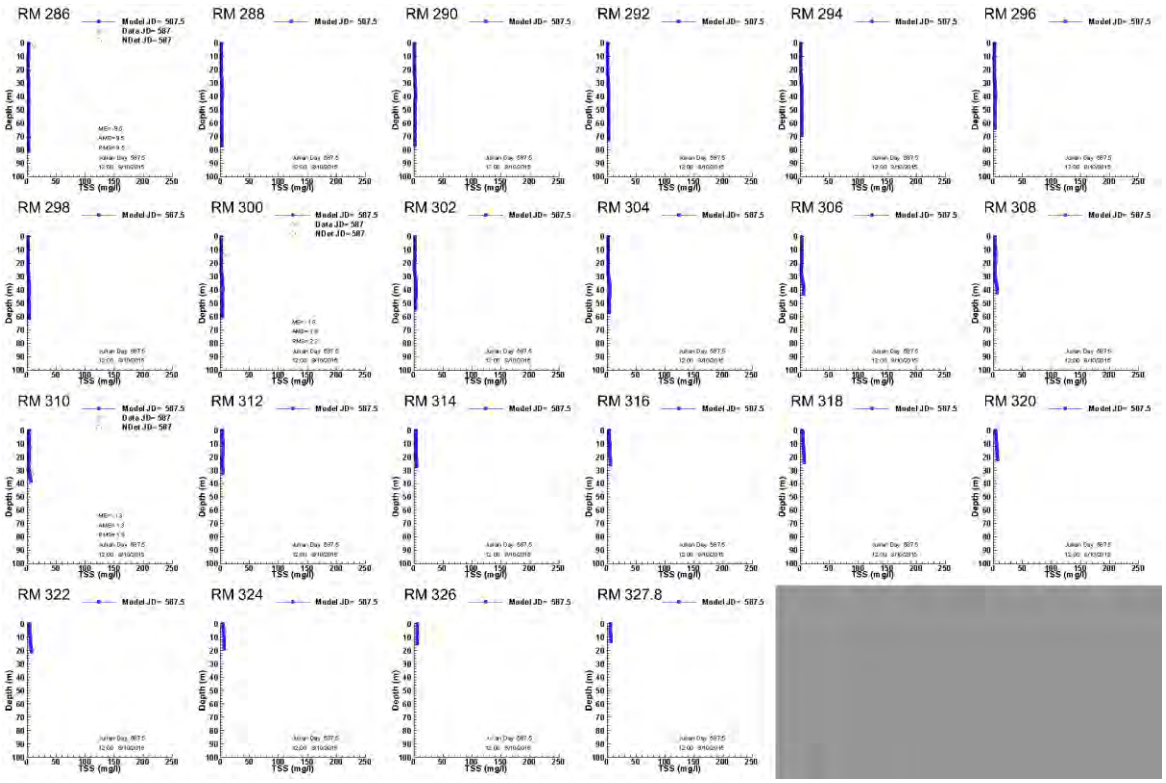


Figure 2121. Vertical profiles of TSS compared with data for 8/10/2015.

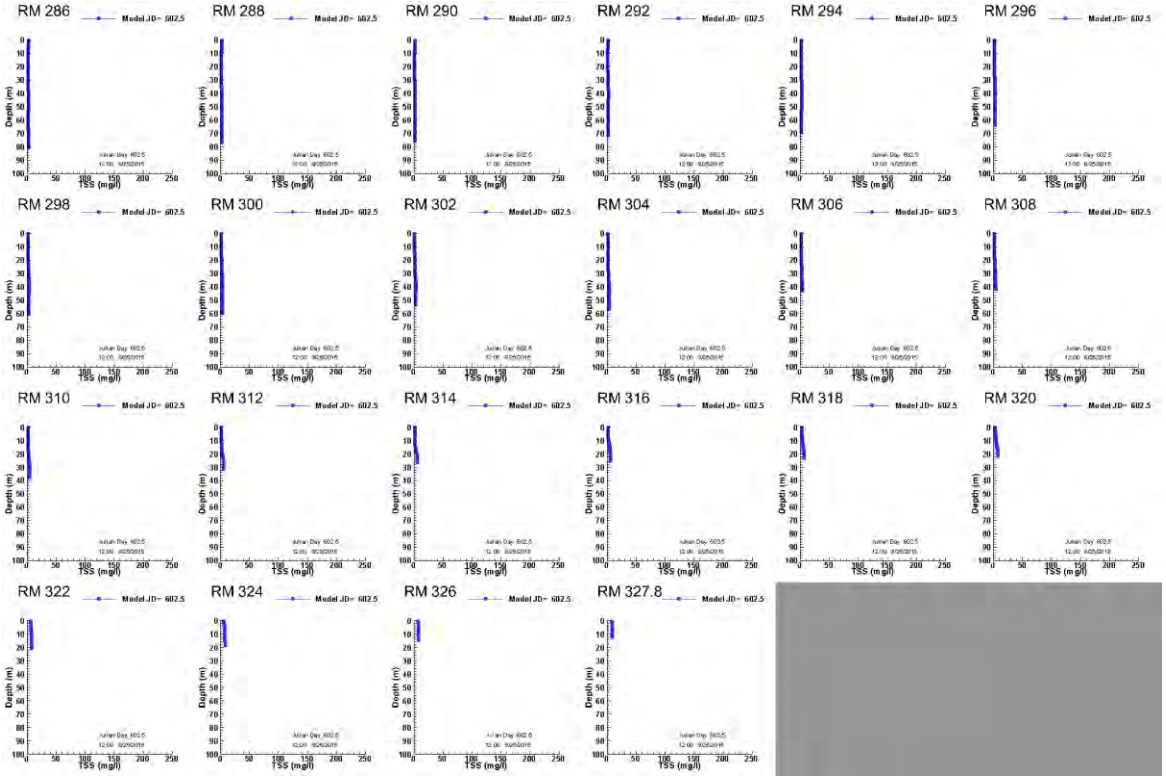


Figure 2122. Vertical profiles of TSS compared with data for 8/25/2015.

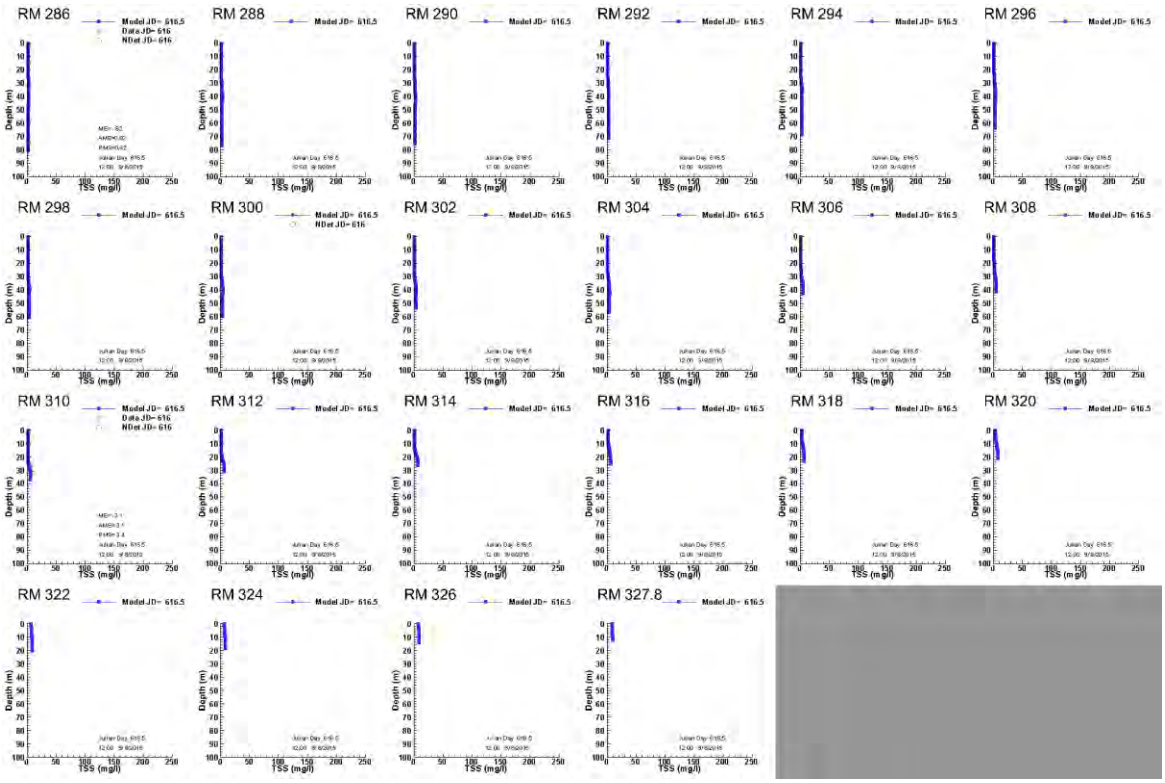


Figure 2123. Vertical profiles of TSS compared with data for 9/ 8/2015.

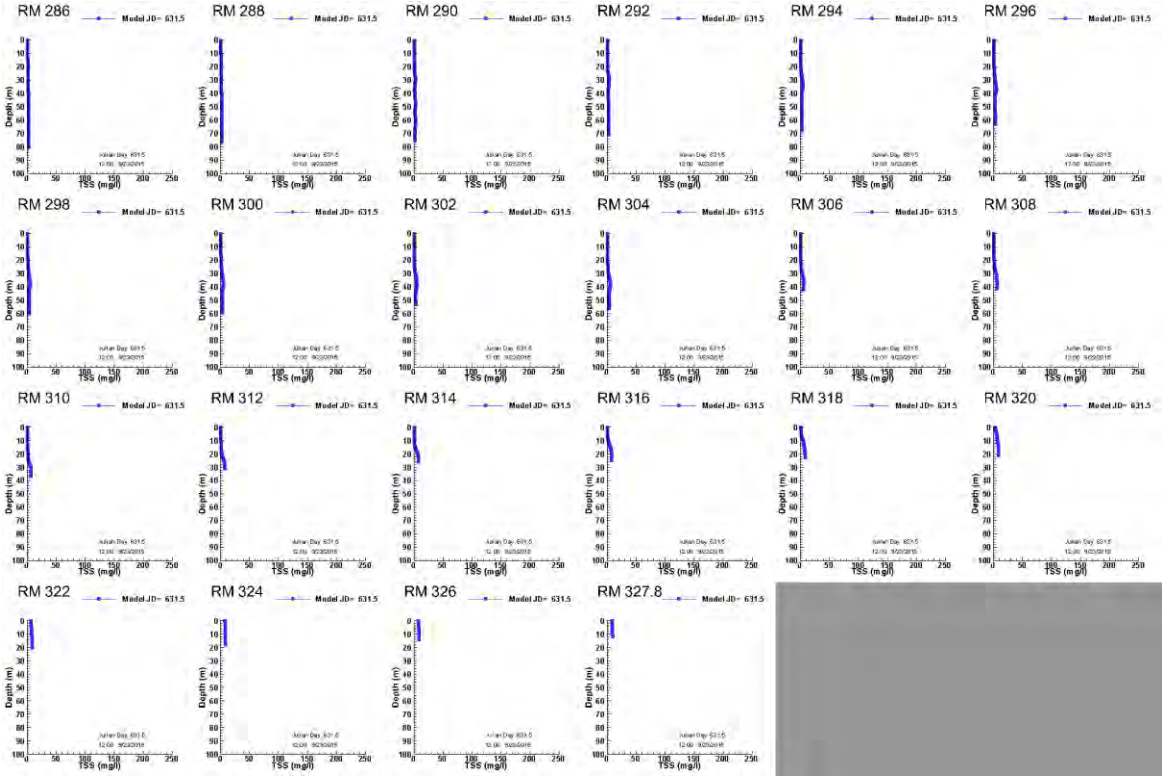


Figure 2124. Vertical profiles of TSS compared with data for 9/23/2015.

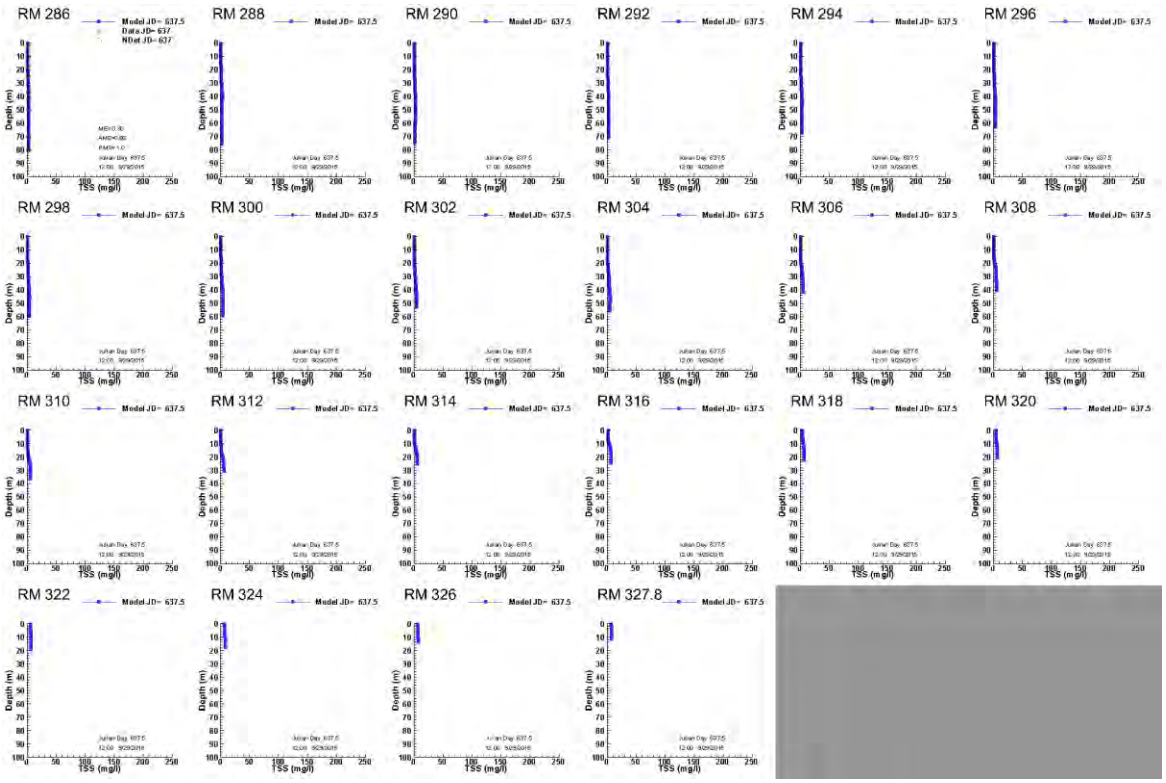


Figure 2125. Vertical profiles of TSS compared with data for 9/29/2015.

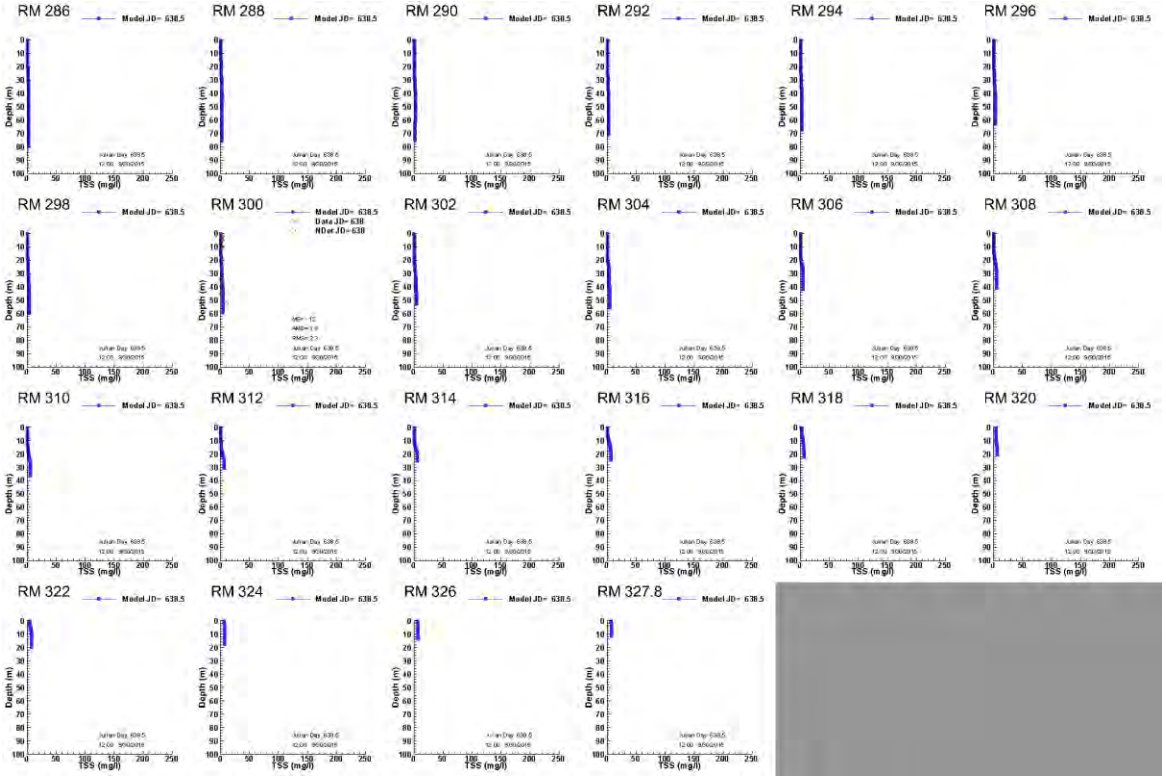


Figure 2126. Vertical profiles of TSS compared with data for 9/30/2015.

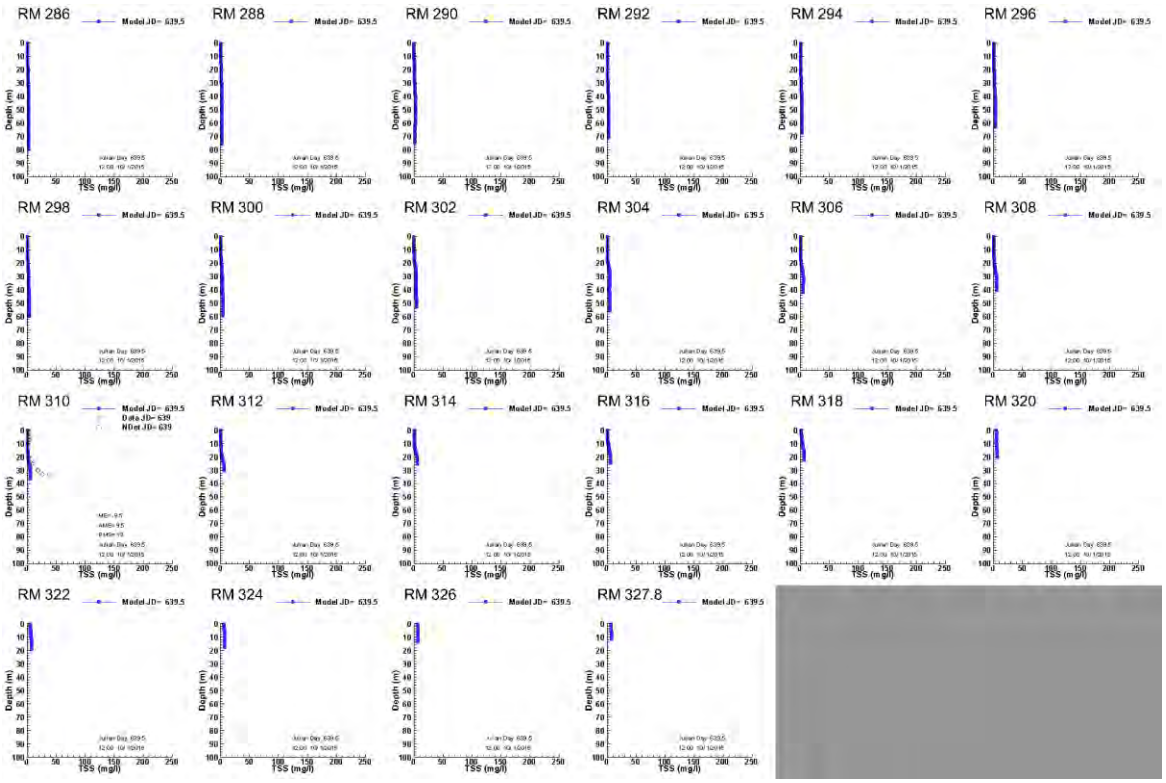


Figure 2127. Vertical profiles of TSS compared with data for 10/ 1/2015.

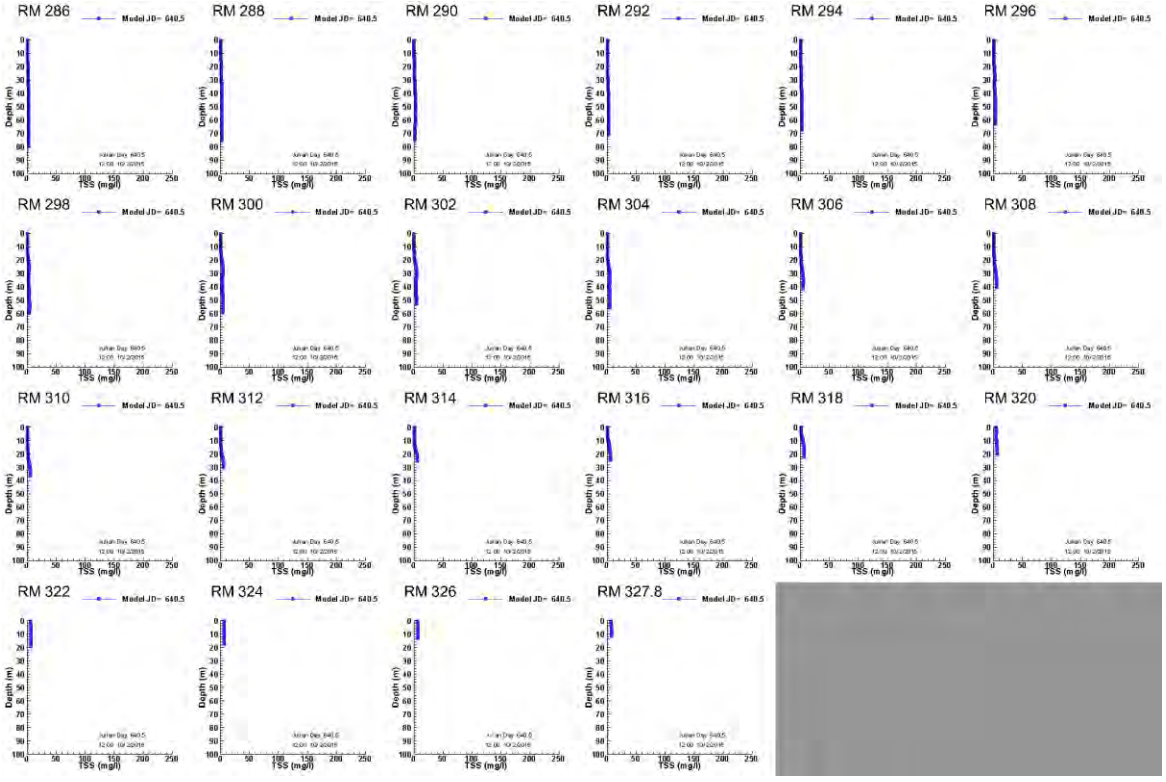


Figure 2128. Vertical profiles of TSS compared with data for 10/ 2/2015.

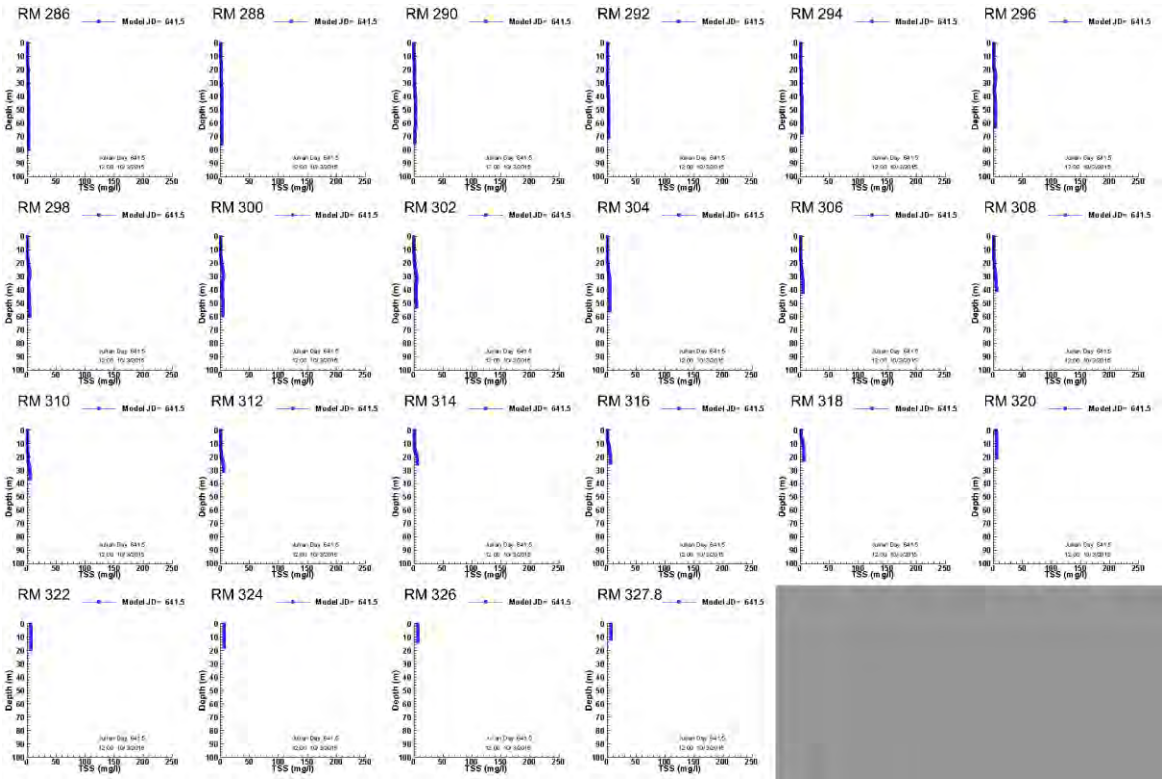


Figure 2129. Vertical profiles of TSS compared with data for 10/ 3/2015.

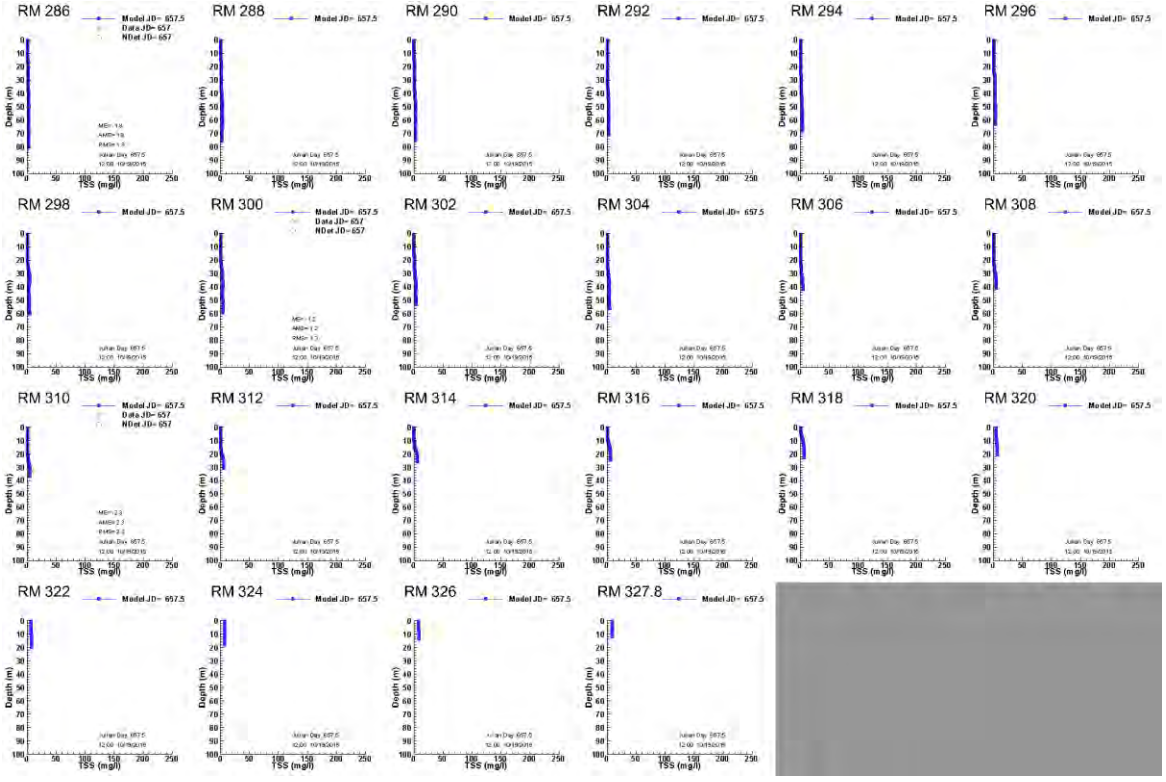


Figure 2130. Vertical profiles of TSS compared with data for 10/19/2015.

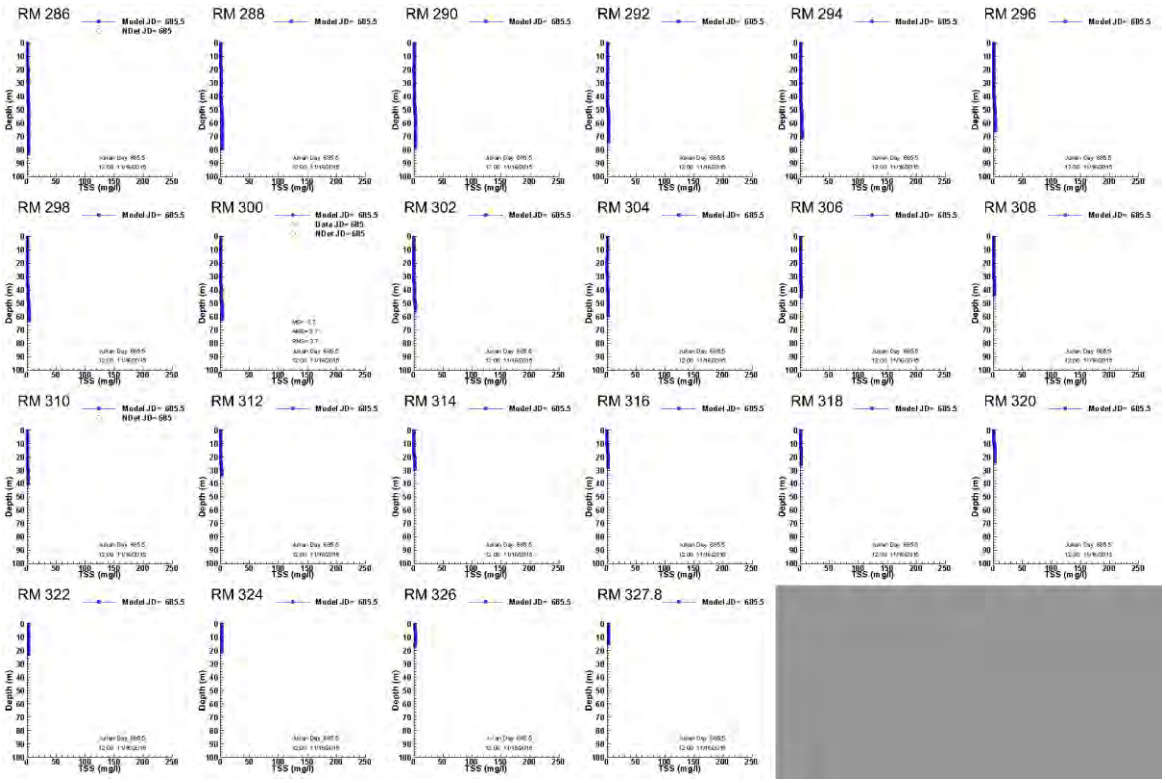


Figure 2131. Vertical profiles of TSS compared with data for 11/16/2015.

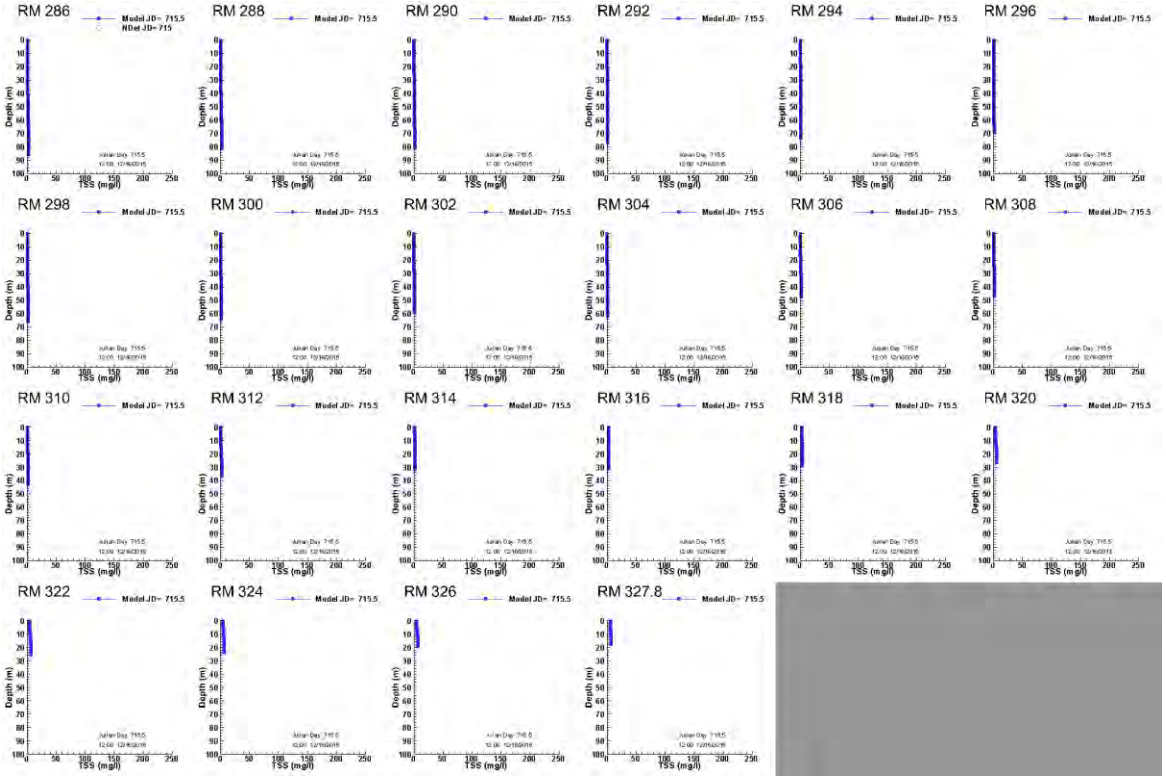


Figure 2132. Vertical profiles of TSS compared with data for 12/16/2015.

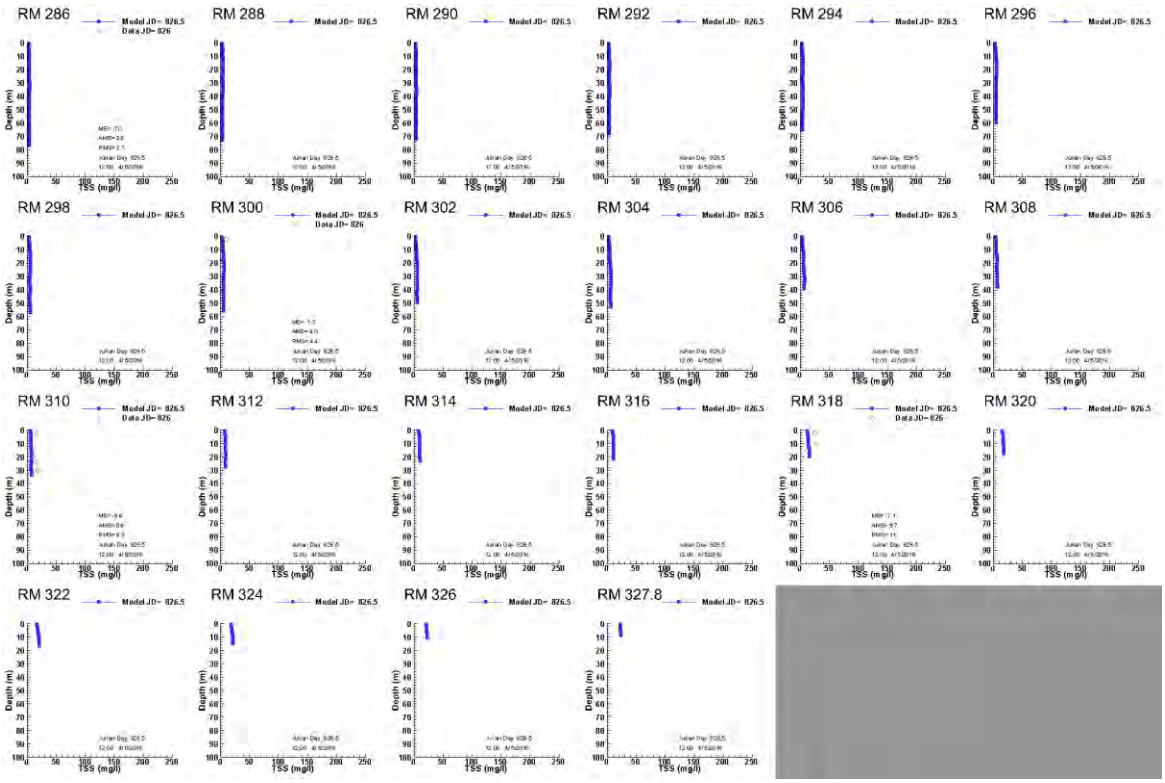


Figure 2133. Vertical profiles of TSS compared with data for 4/ 5/2016.

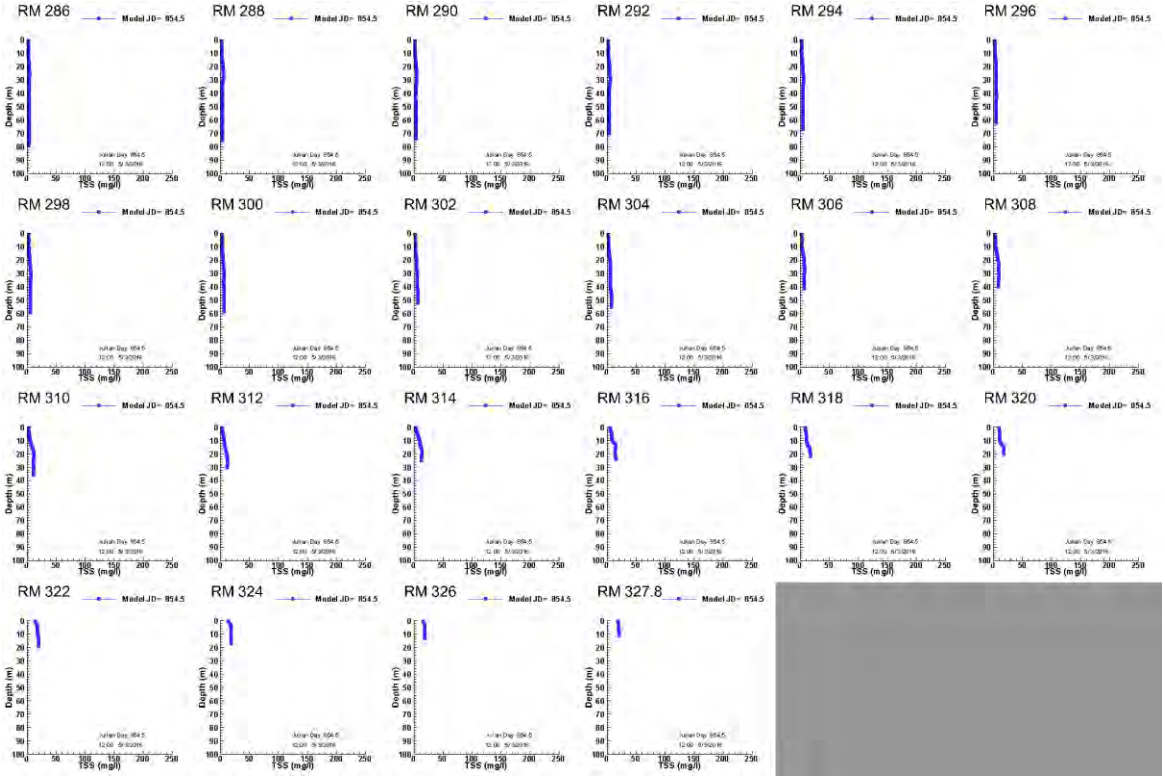


Figure 2134. Vertical profiles of TSS compared with data for 5/ 3/2016.

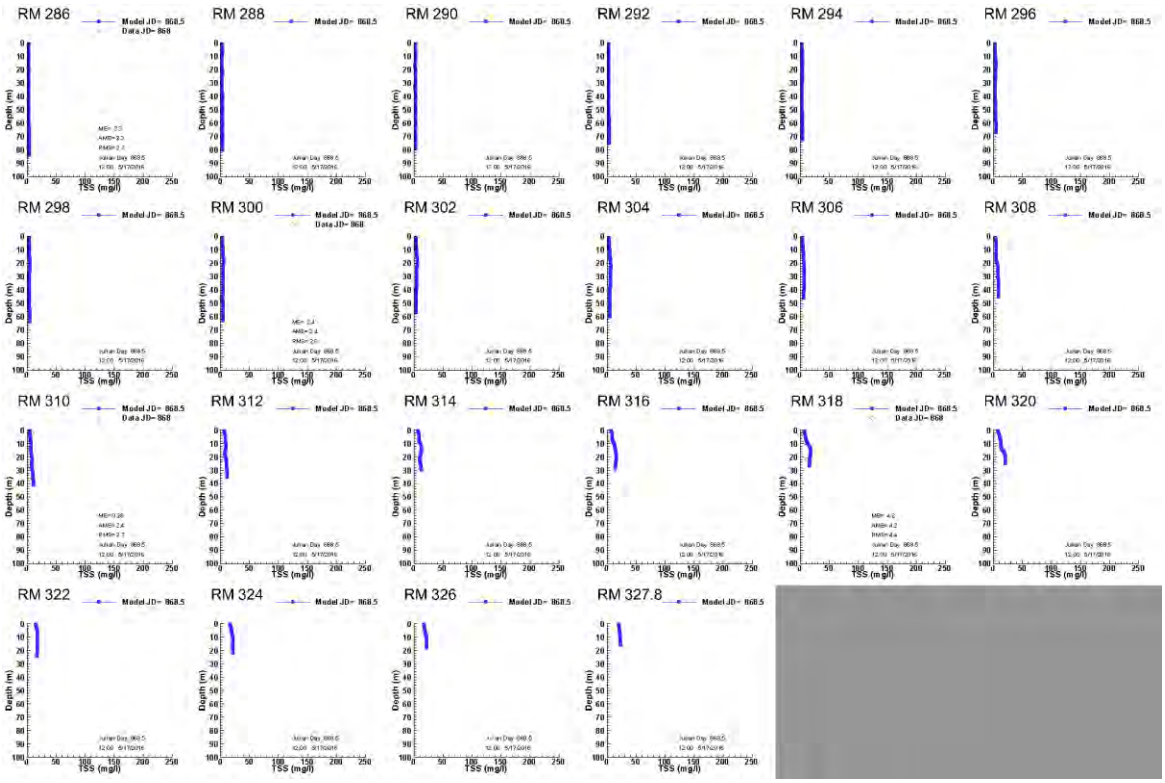


Figure 2135. Vertical profiles of TSS compared with data for 5/17/2016.

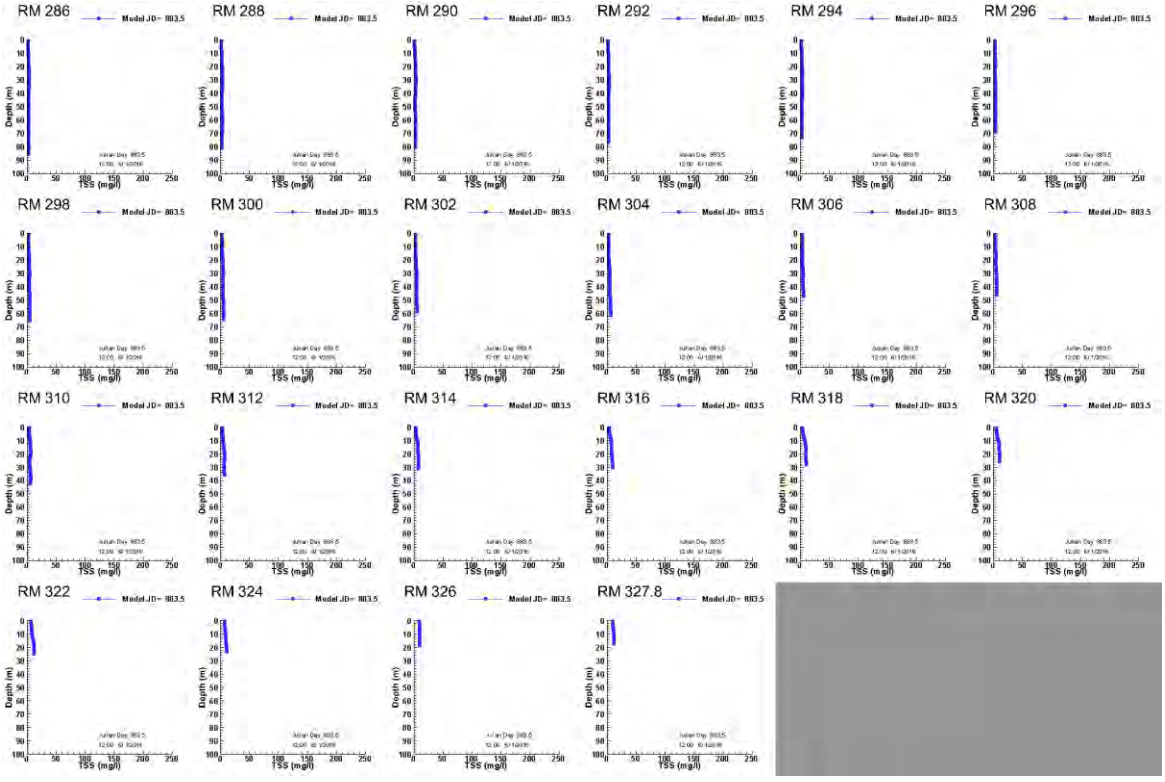


Figure 2136. Vertical profiles of TSS compared with data for 6/ 1/2016.

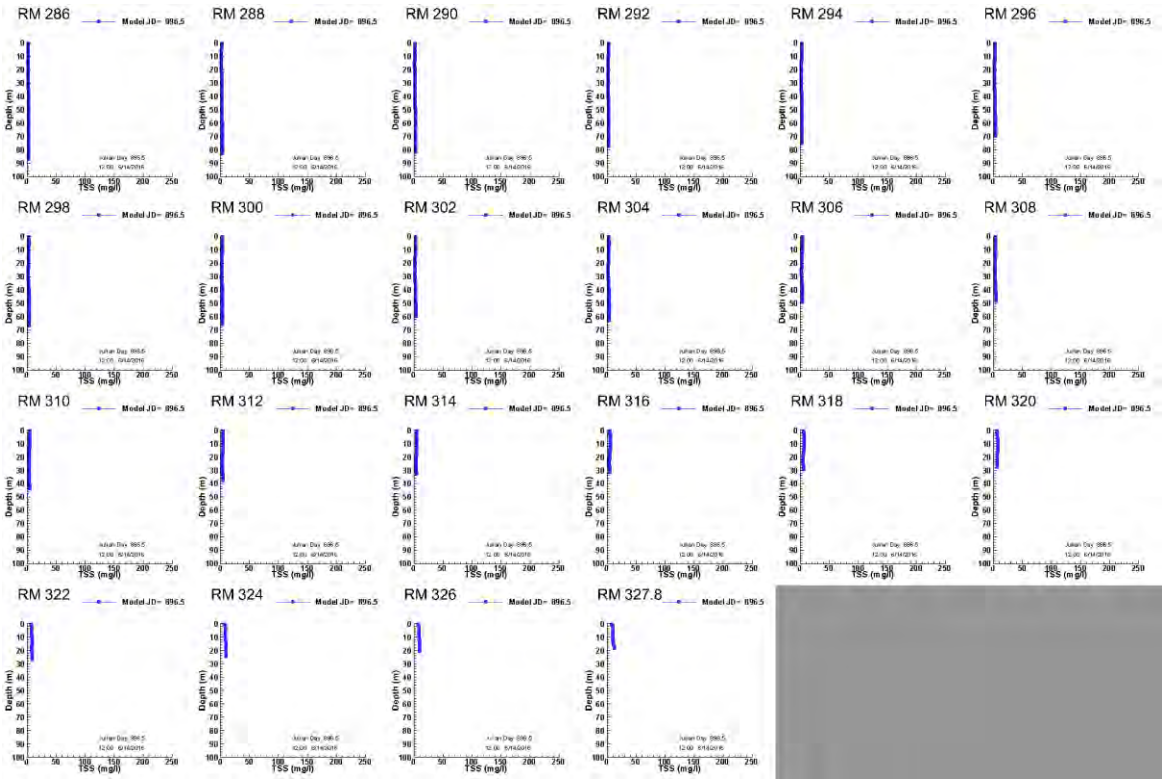


Figure 2137. Vertical profiles of TSS compared with data for 6/14/2016.

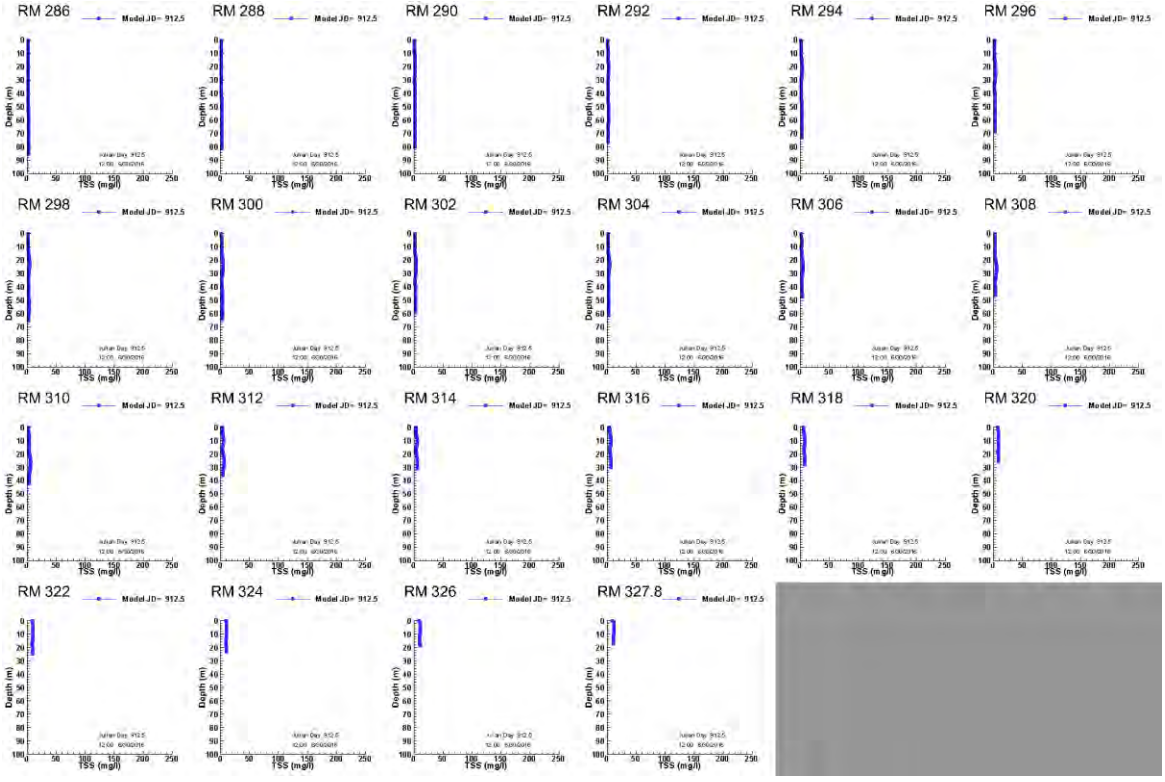


Figure 2138. Vertical profiles of TSS compared with data for 6/30/2016.

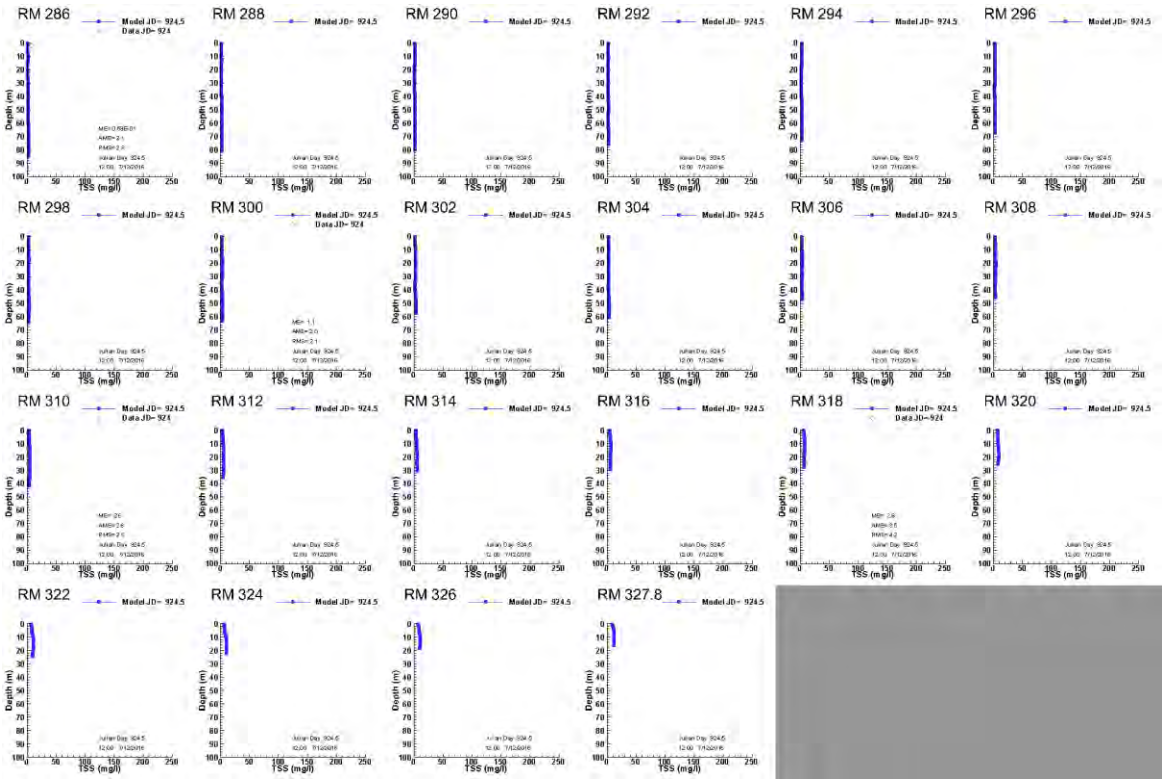


Figure 2139. Vertical profiles of TSS compared with data for 7/12/2016.

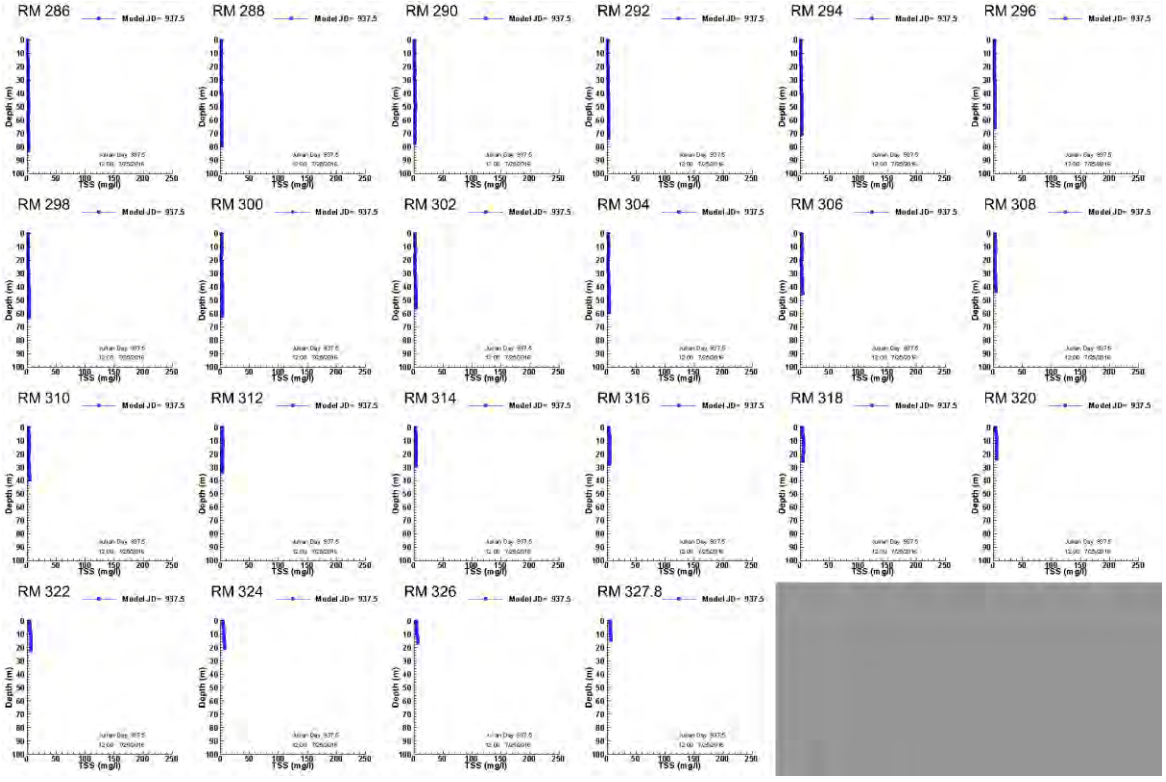


Figure 2140. Vertical profiles of TSS compared with data for 7/25/2016.

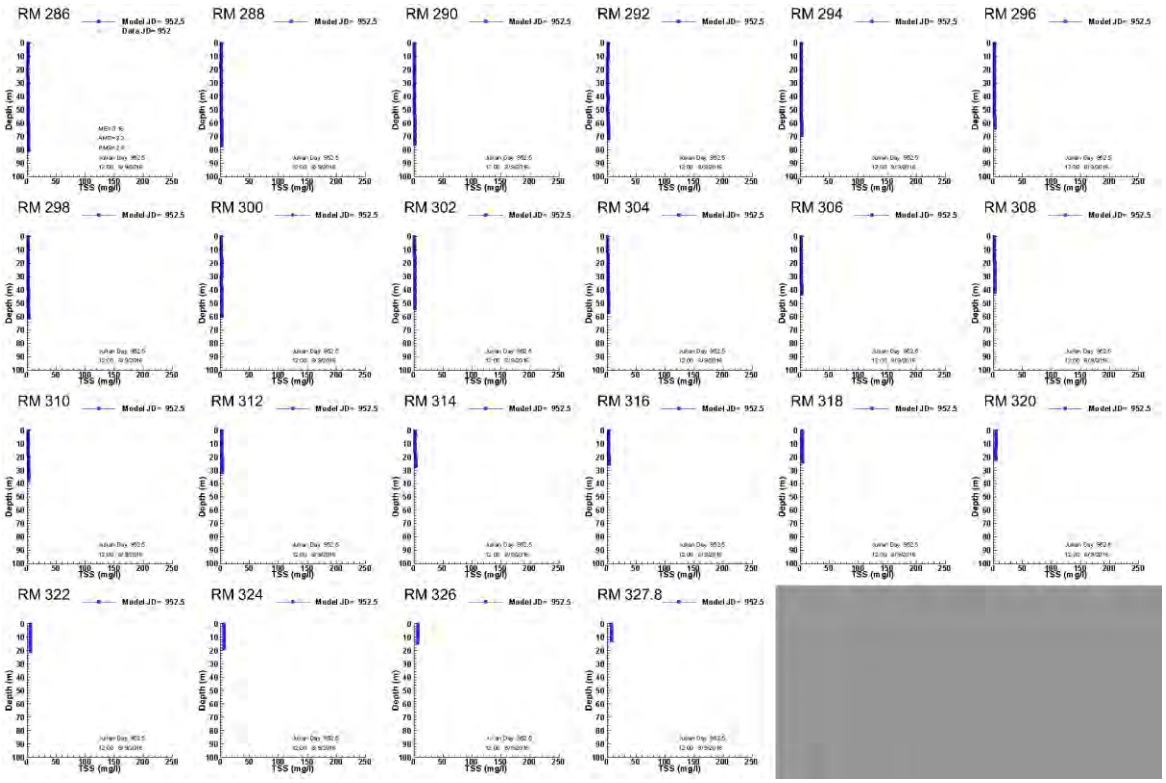


Figure 2141. Vertical profiles of TSS compared with data for 8/ 9/2016.

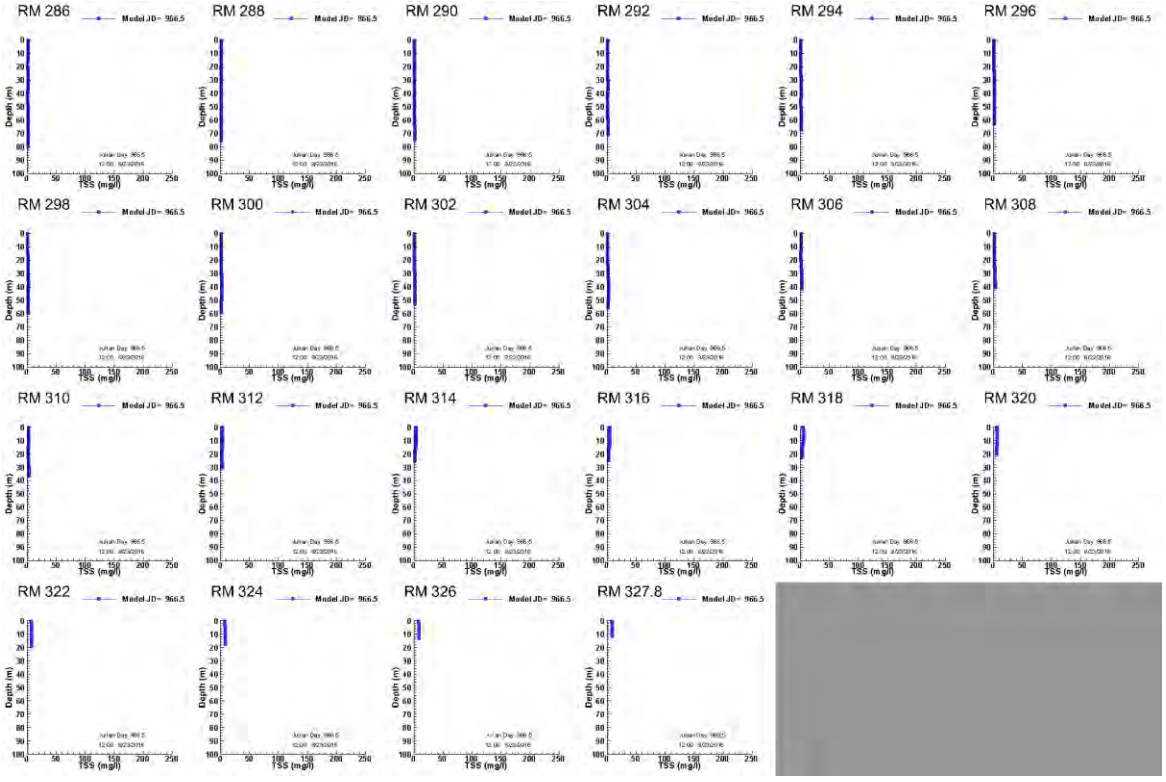


Figure 2142. Vertical profiles of TSS compared with data for 8/23/2016.

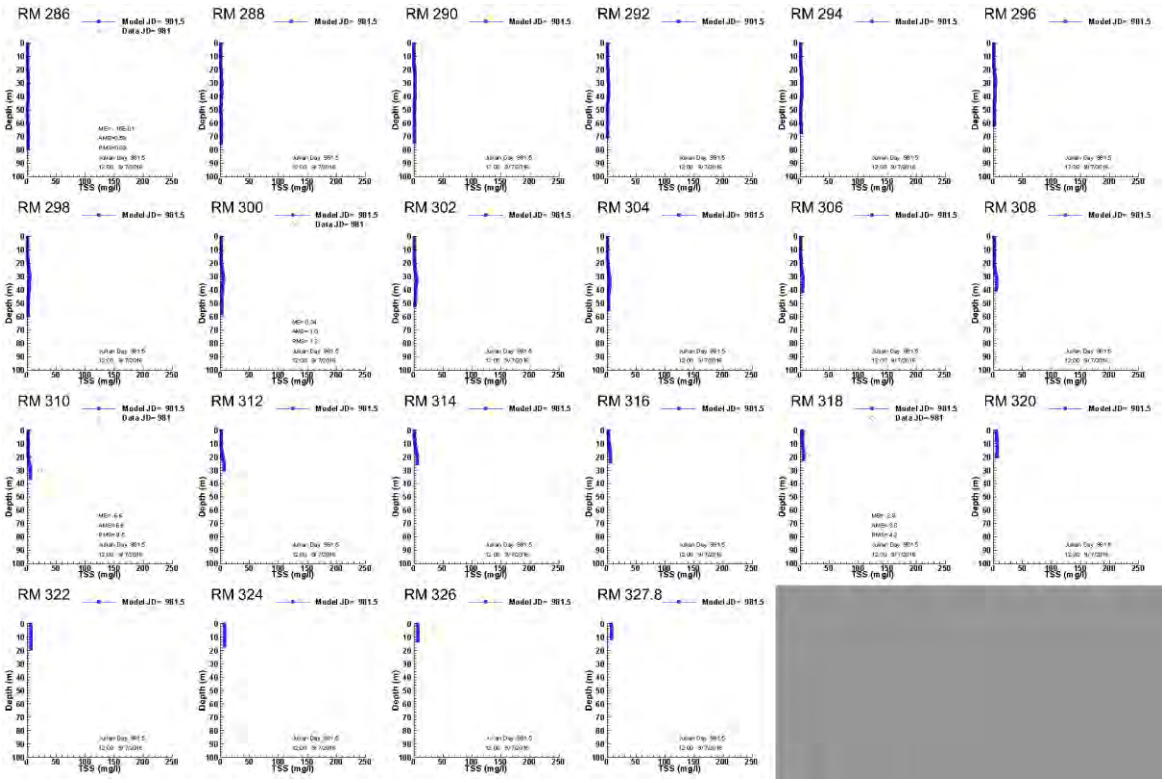


Figure 2143. Vertical profiles of TSS compared with data for 9/ 7/2016.

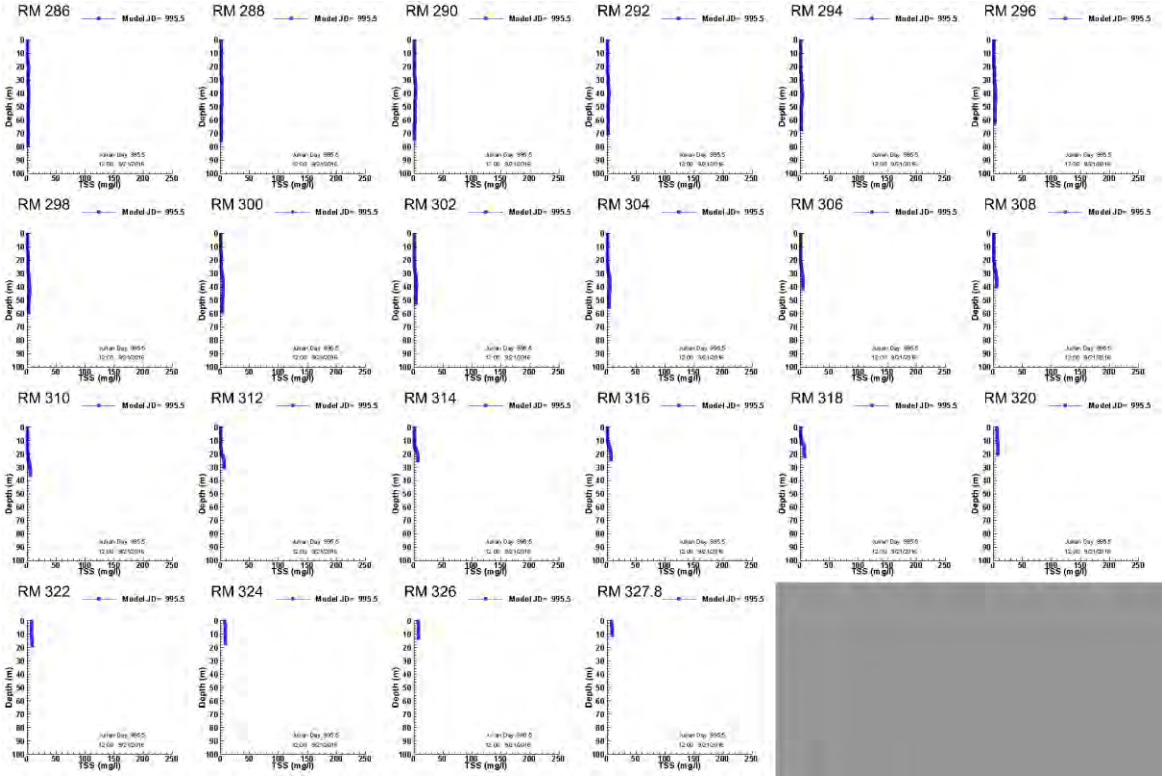


Figure 2144. Vertical profiles of TSS compared with data for 9/21/2016.

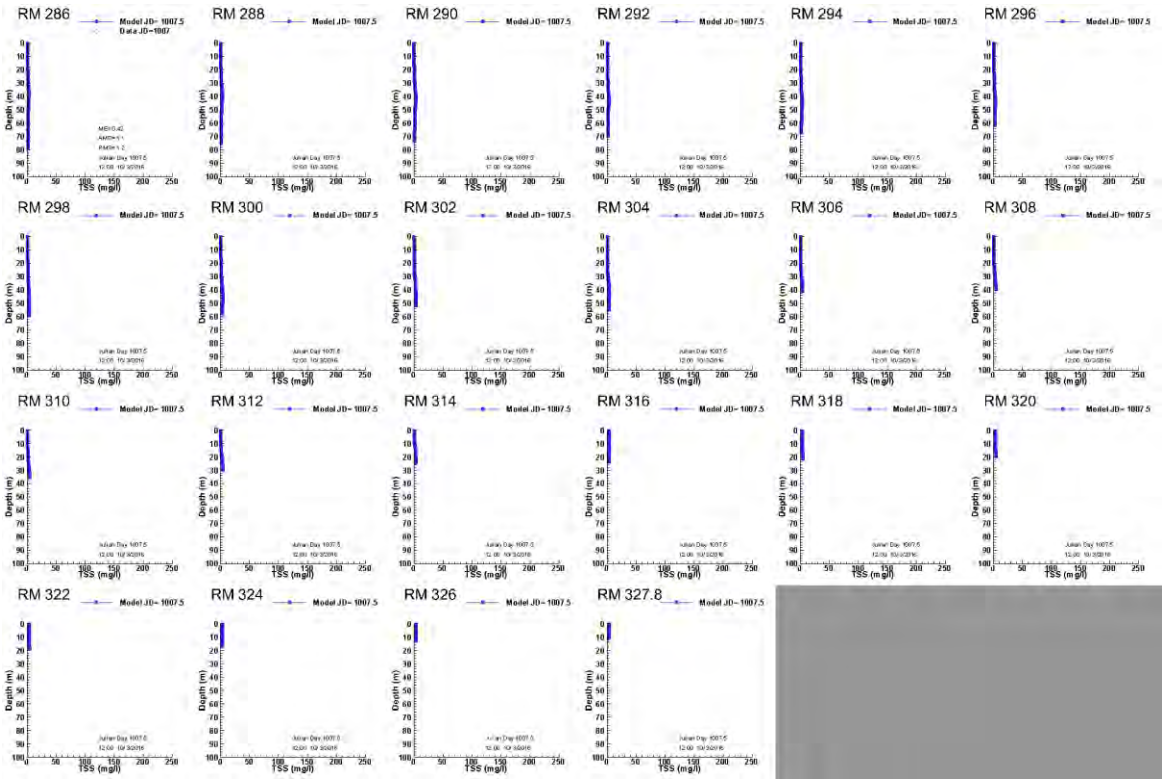


Figure 2145. Vertical profiles of TSS compared with data for 10/ 3/2016.

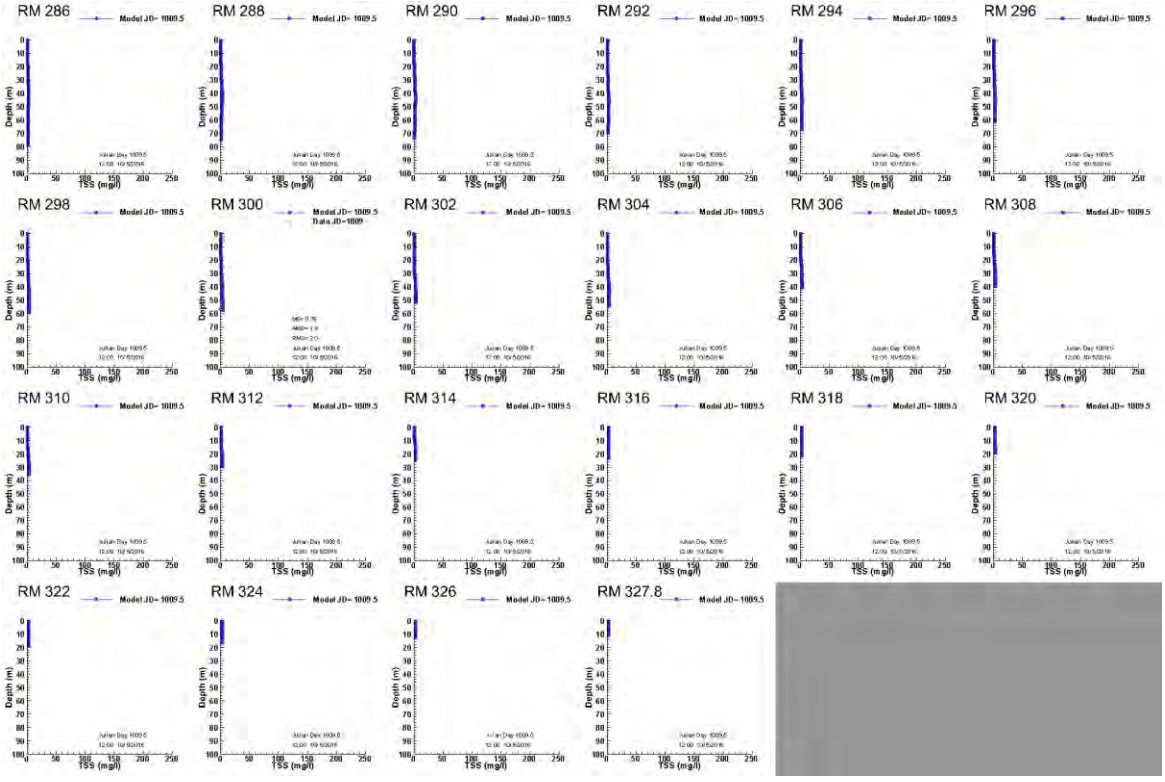


Figure 2146. Vertical profiles of TSS compared with data for 10/ 5/2016.

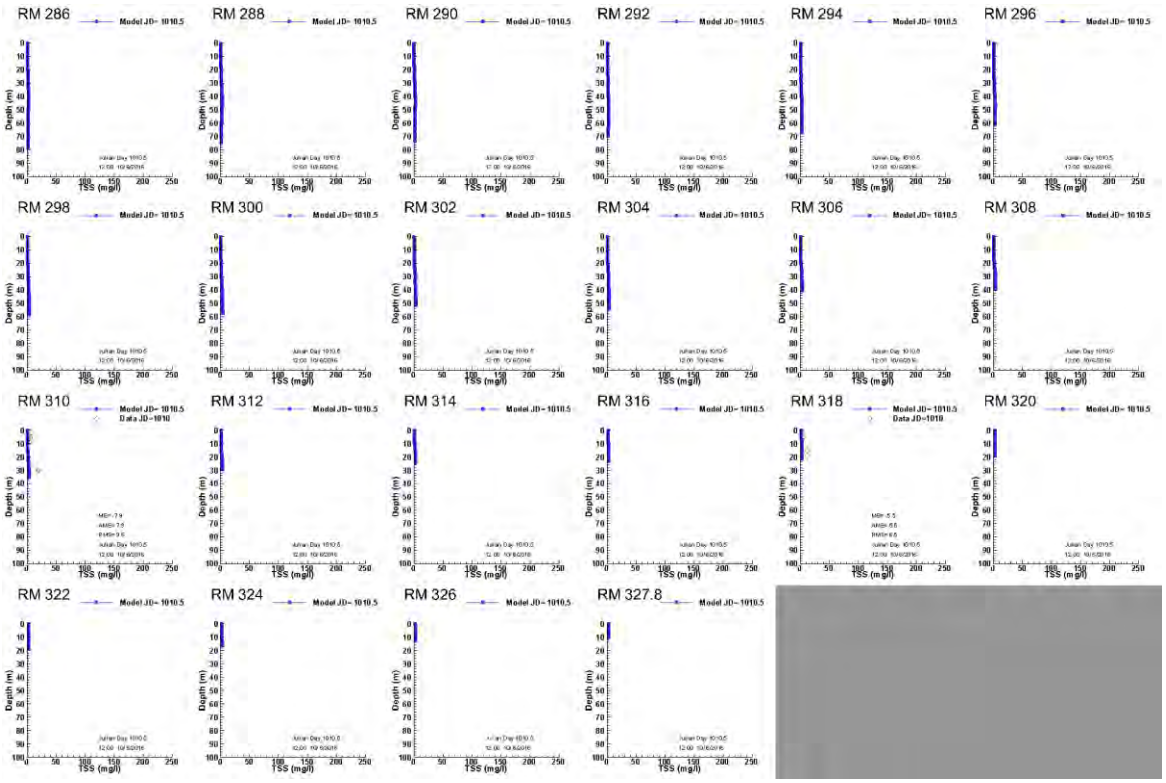


Figure 2147. Vertical profiles of TSS compared with data for 10/ 6/2016.

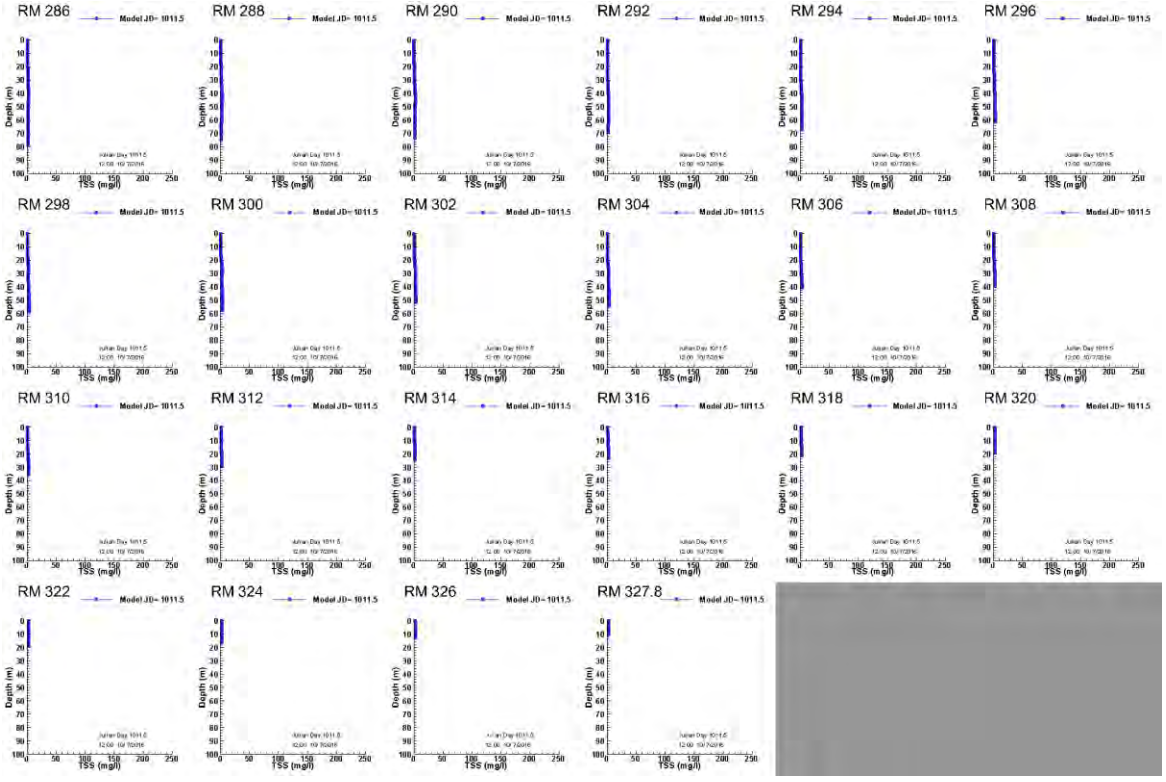


Figure 2148. Vertical profiles of TSS compared with data for 10/ 7/2016.

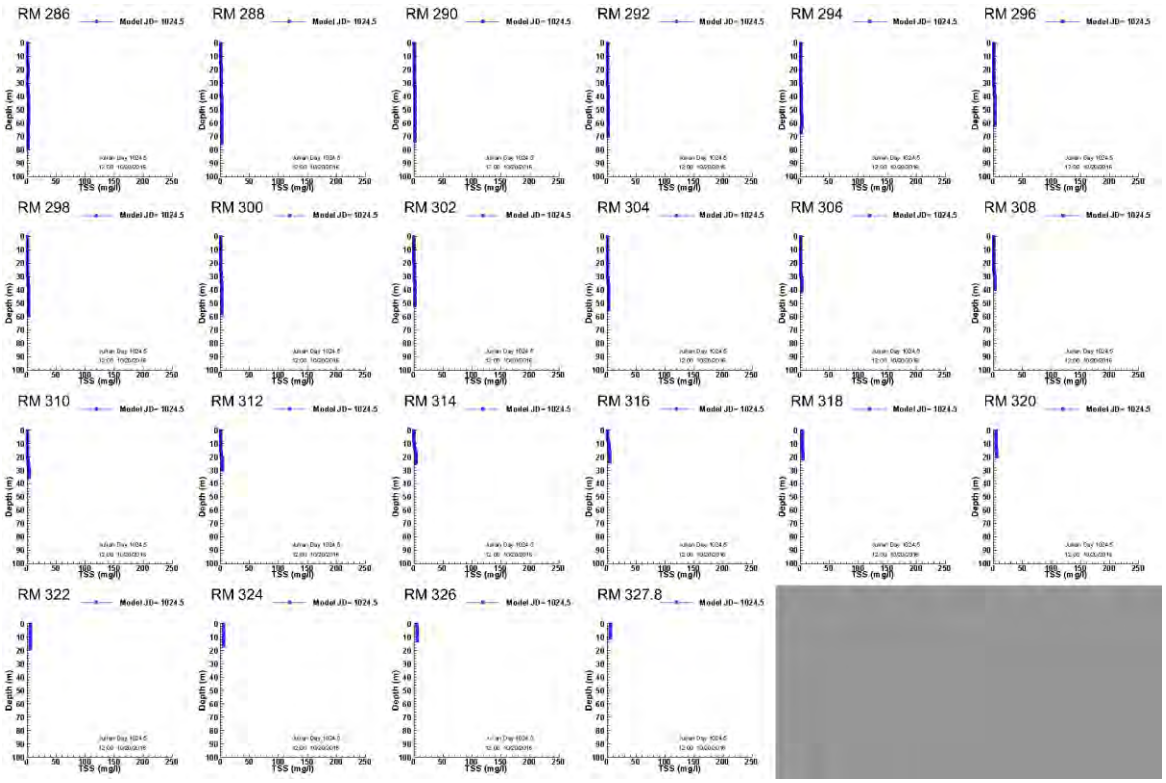


Figure 2149. Vertical profiles of TSS compared with data for 10/20/2016.

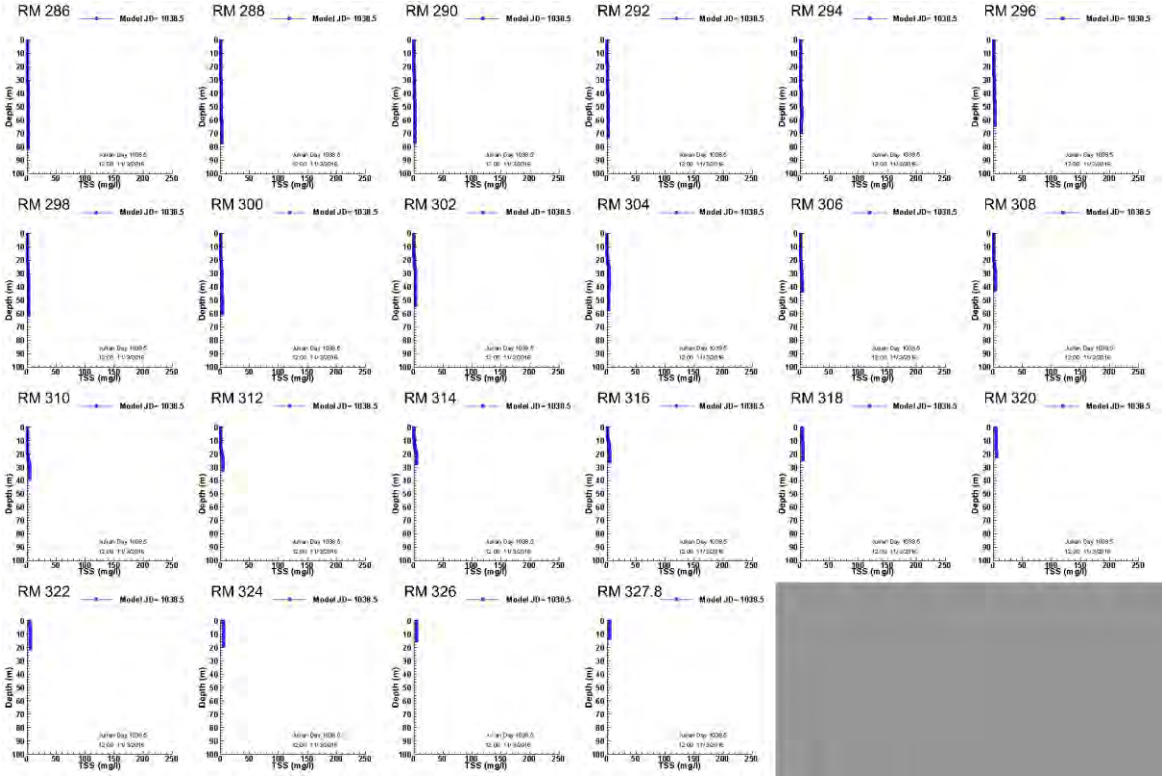


Figure 2150. Vertical profiles of TSS compared with data for 11/ 3/2016.

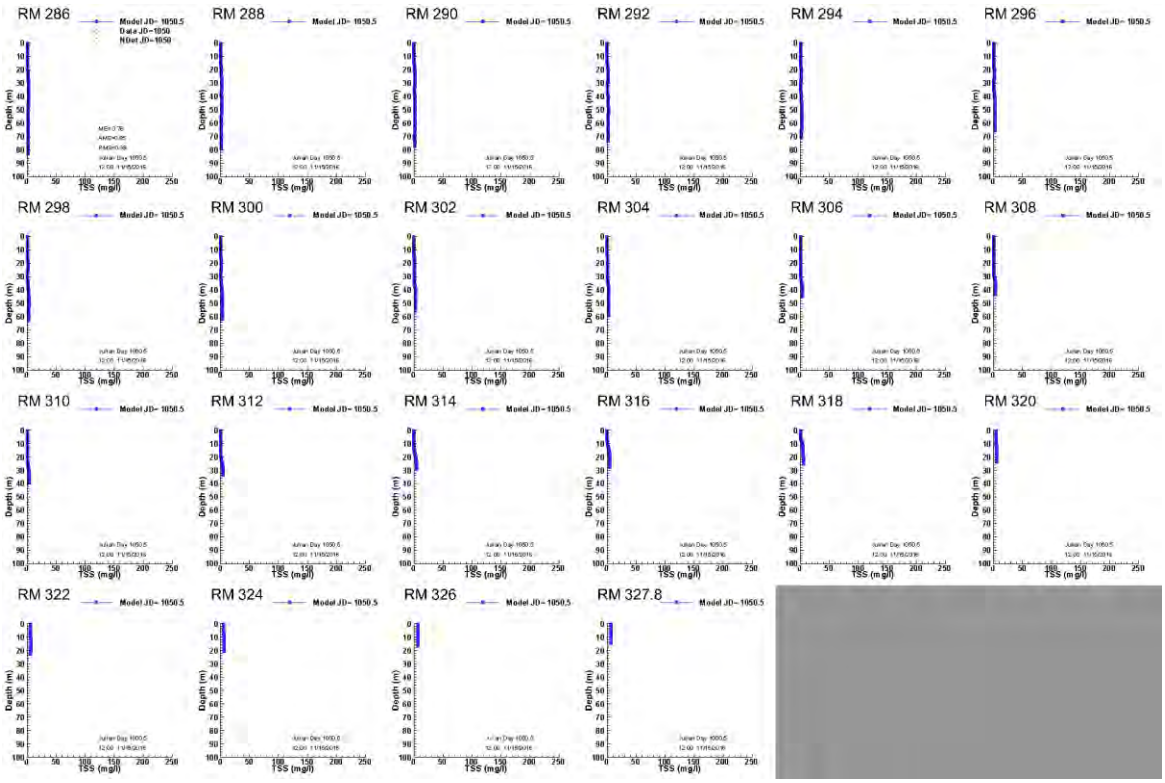


Figure 2151. Vertical profiles of TSS compared with data for 11/15/2016.

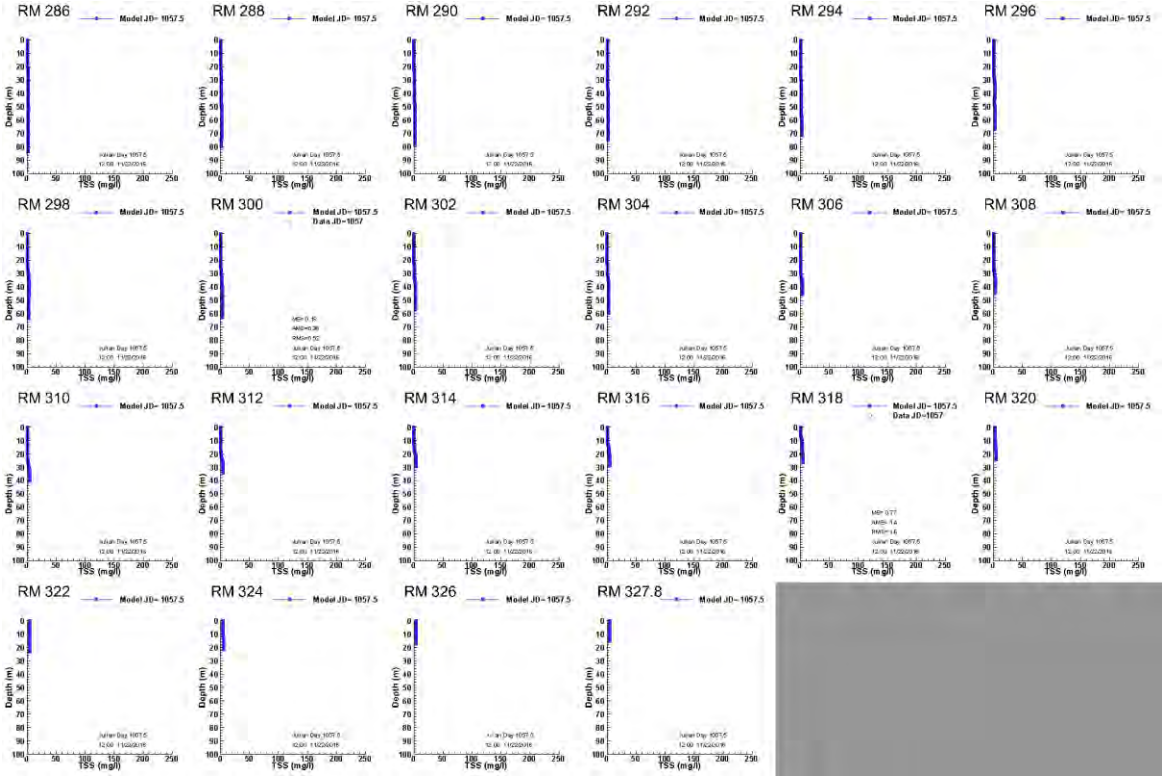


Figure 2152. Vertical profiles of TSS compared with data for 11/22/2016.

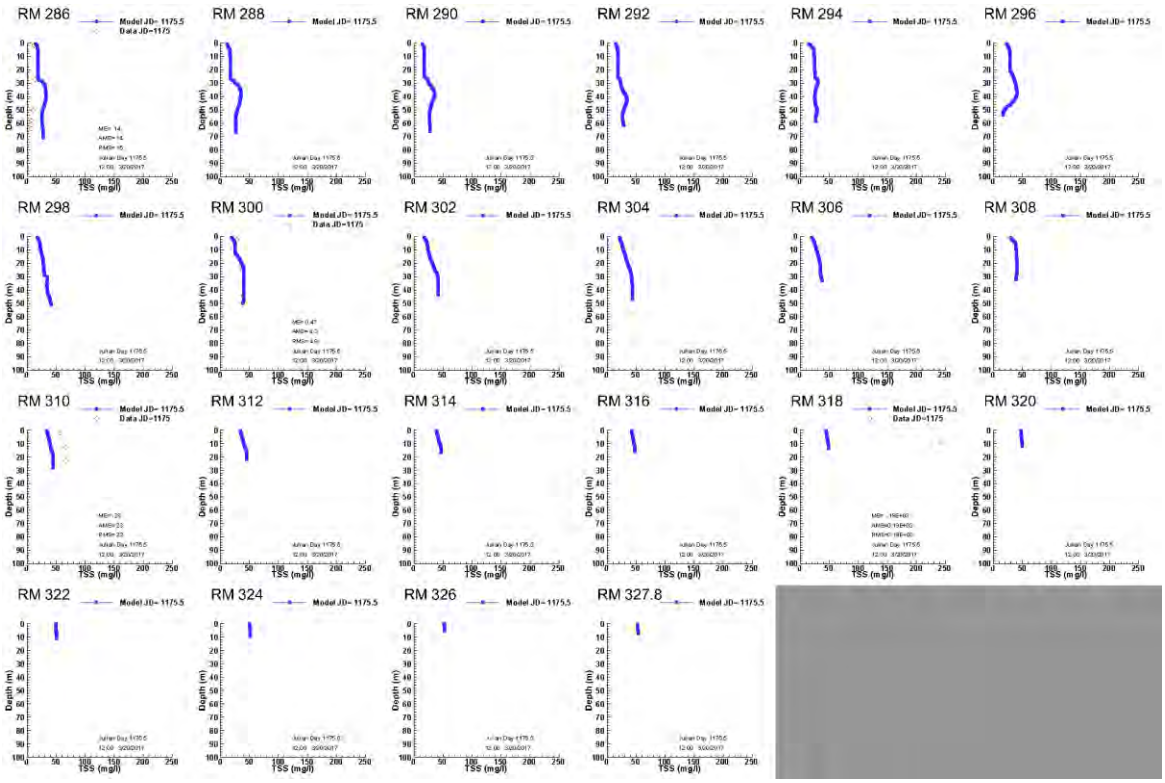


Figure 2153. Vertical profiles of TSS compared with data for 3/20/2017.

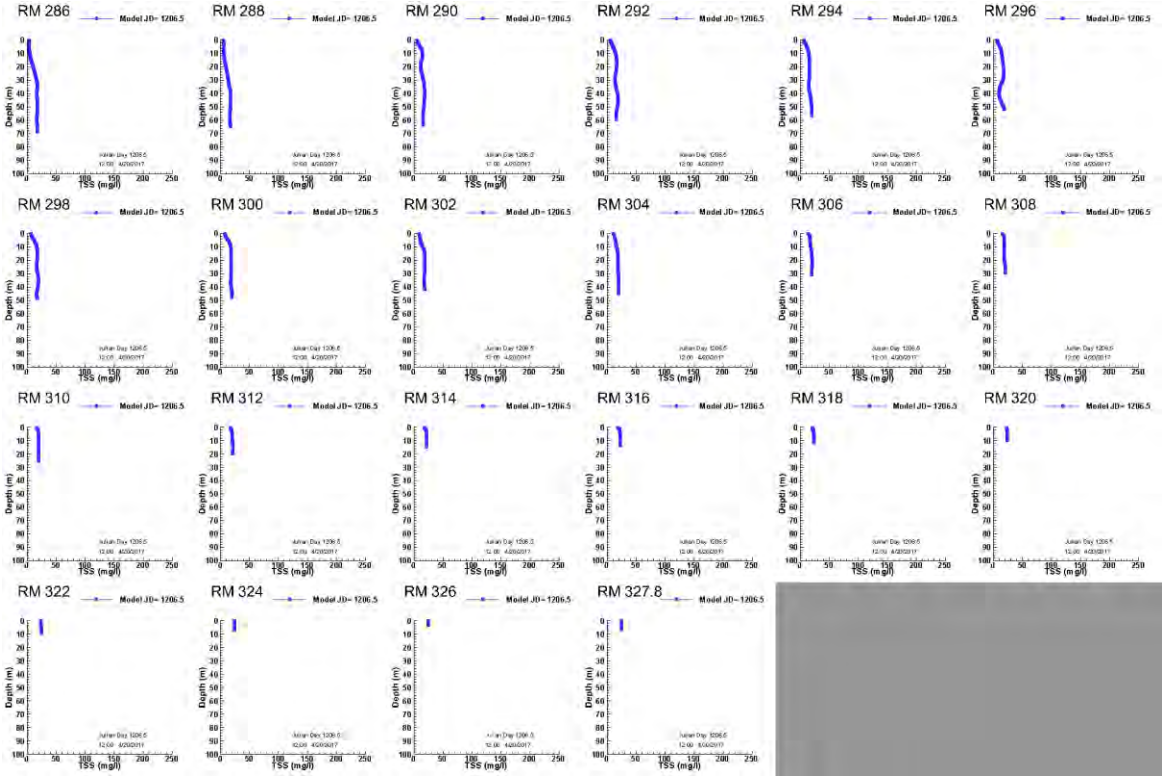


Figure 2154. Vertical profiles of TSS compared with data for 4/20/2017.

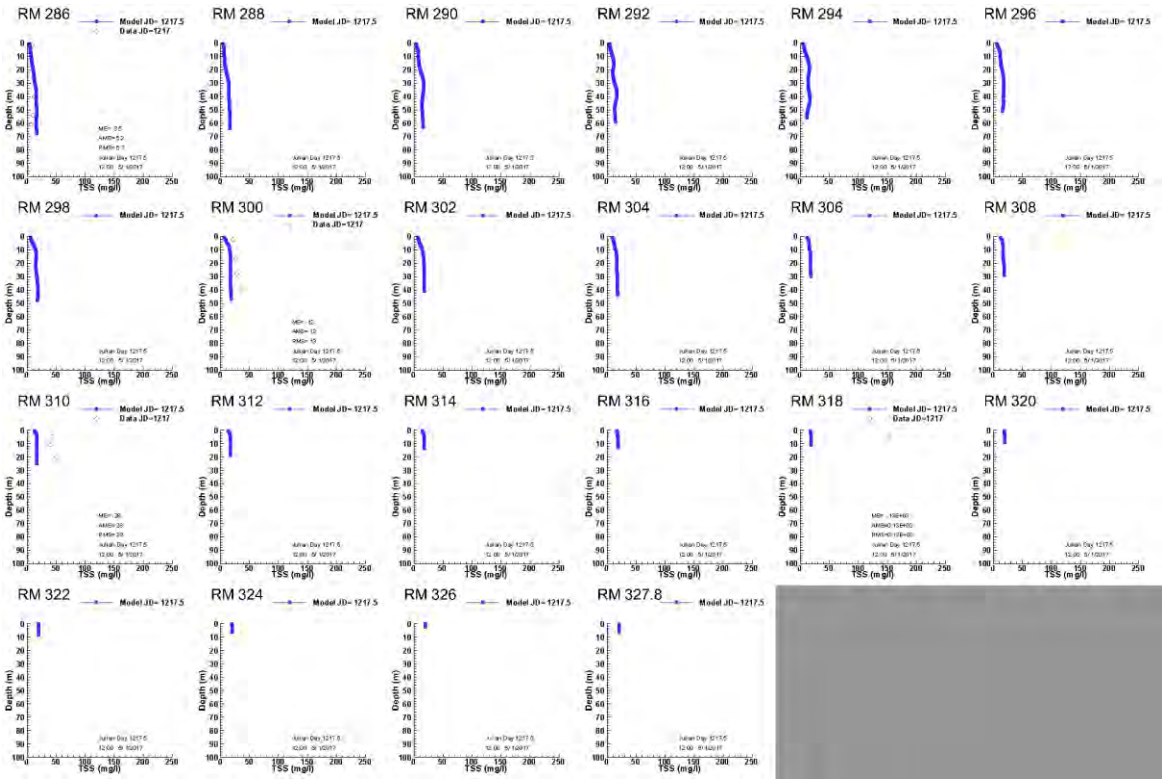


Figure 2155. Vertical profiles of TSS compared with data for 5/ 1/2017.

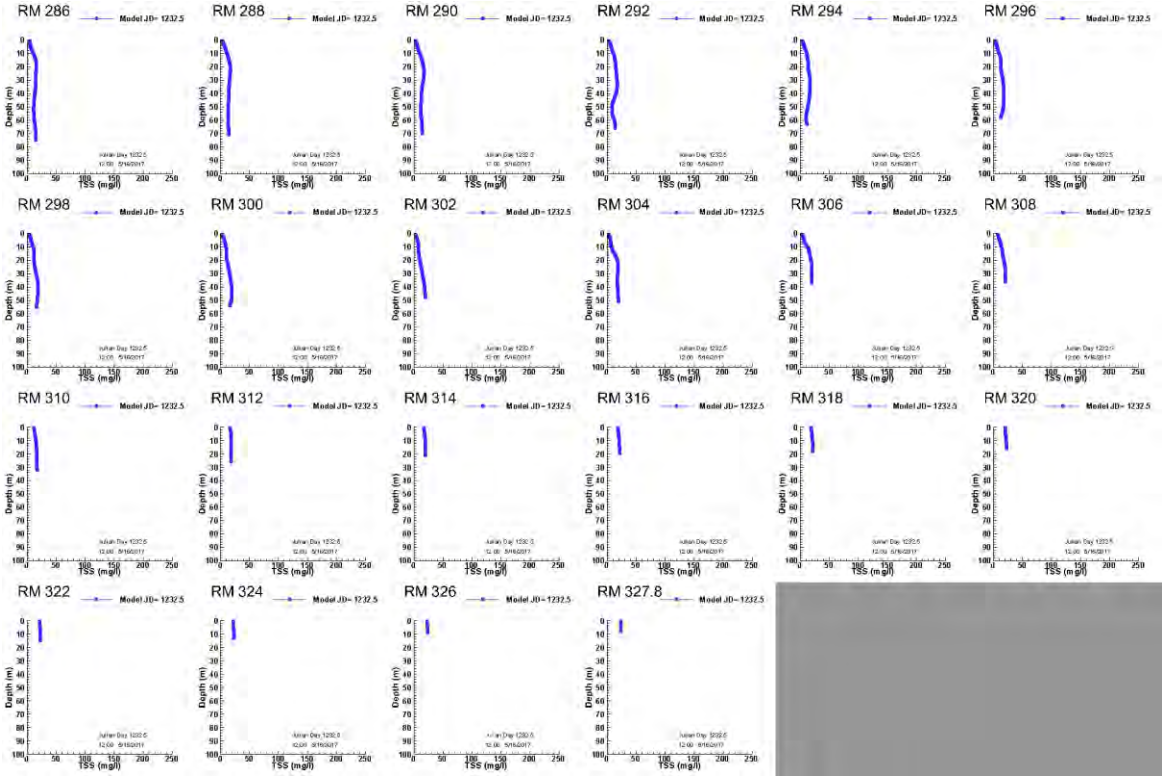


Figure 2156. Vertical profiles of TSS compared with data for 5/16/2017.

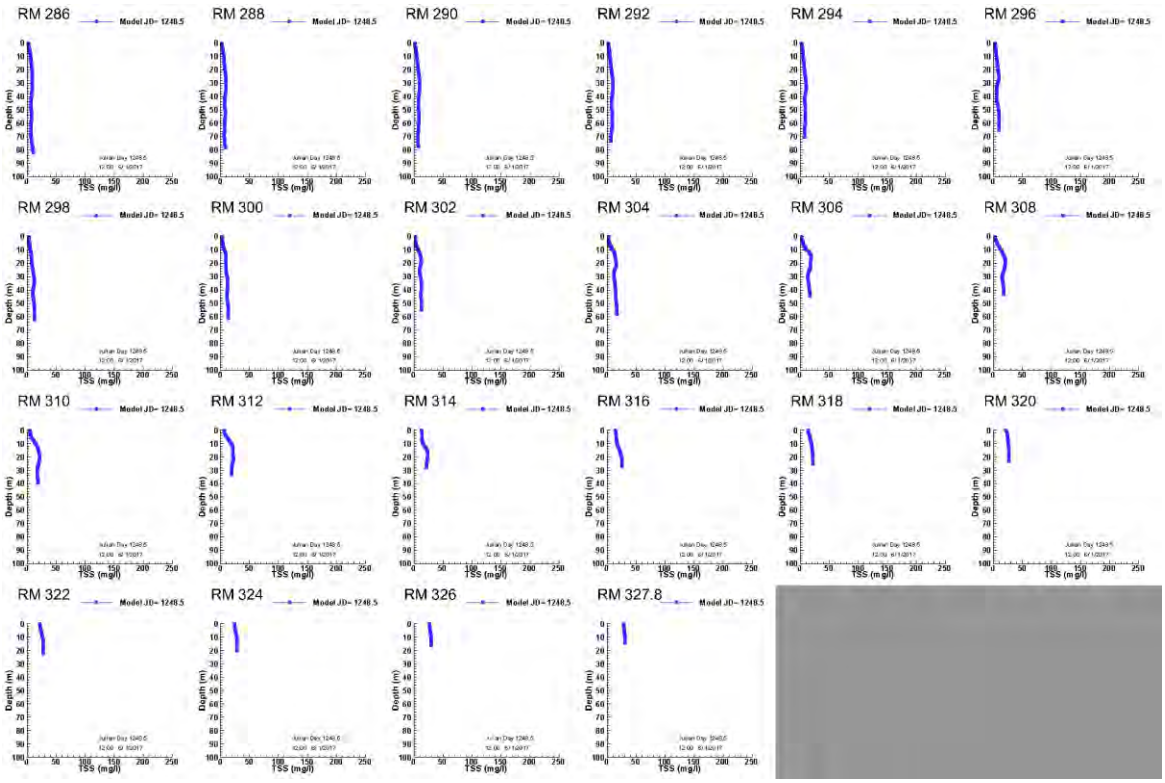


Figure 2157. Vertical profiles of TSS compared with data for 6/ 1/2017.

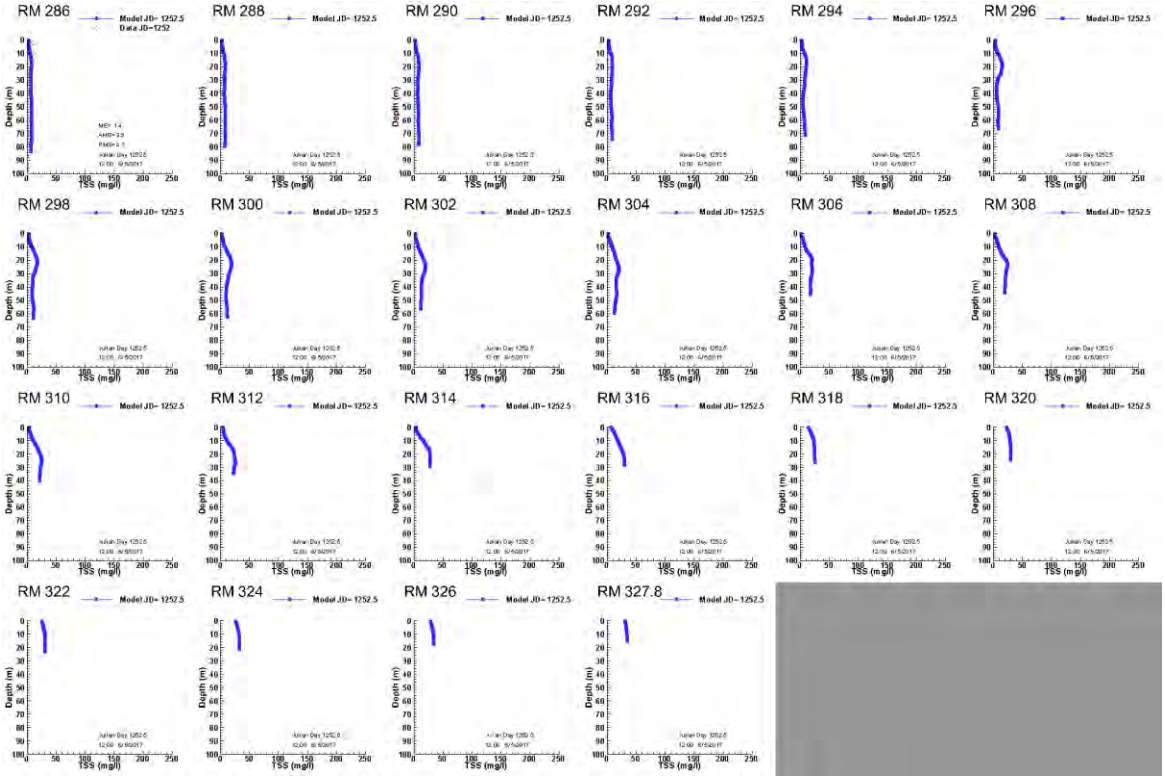


Figure 2158. Vertical profiles of TSS compared with data for 6/ 5/2017.

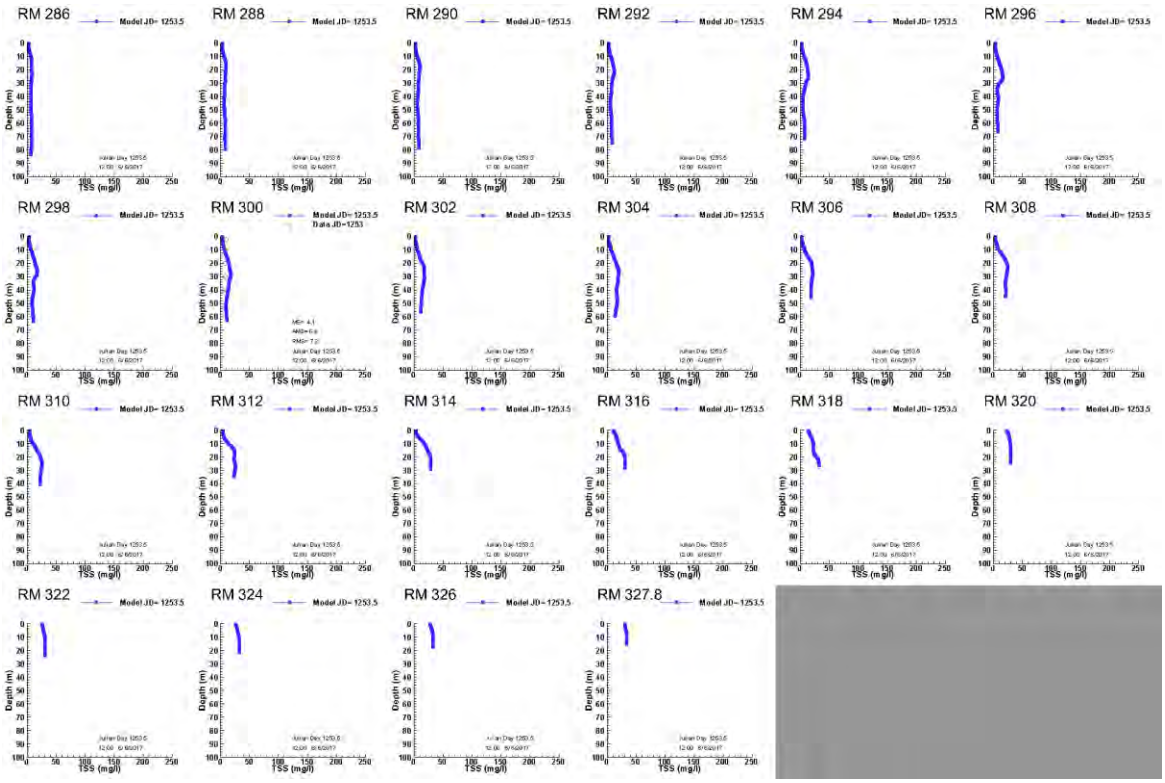


Figure 2159. Vertical profiles of TSS compared with data for 6/ 6/2017.

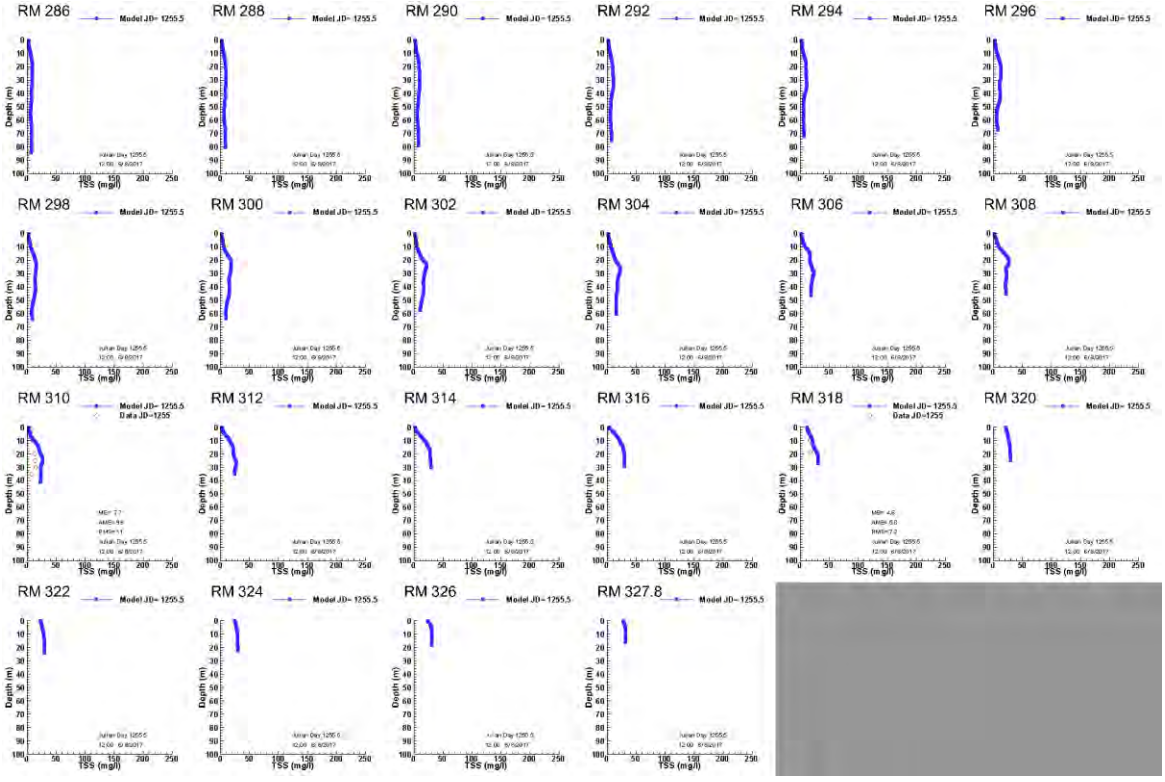


Figure 2160. Vertical profiles of TSS compared with data for 6/ 8/2017.

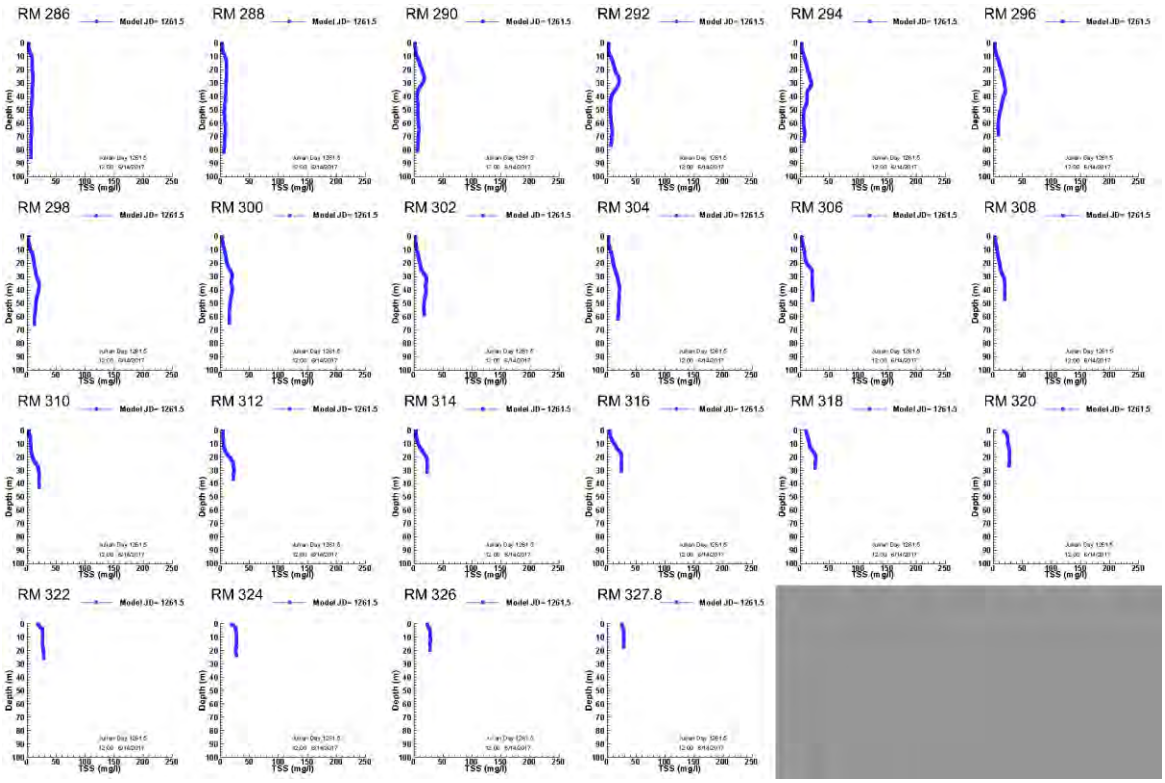


Figure 2161. Vertical profiles of TSS compared with data for 6/14/2017.

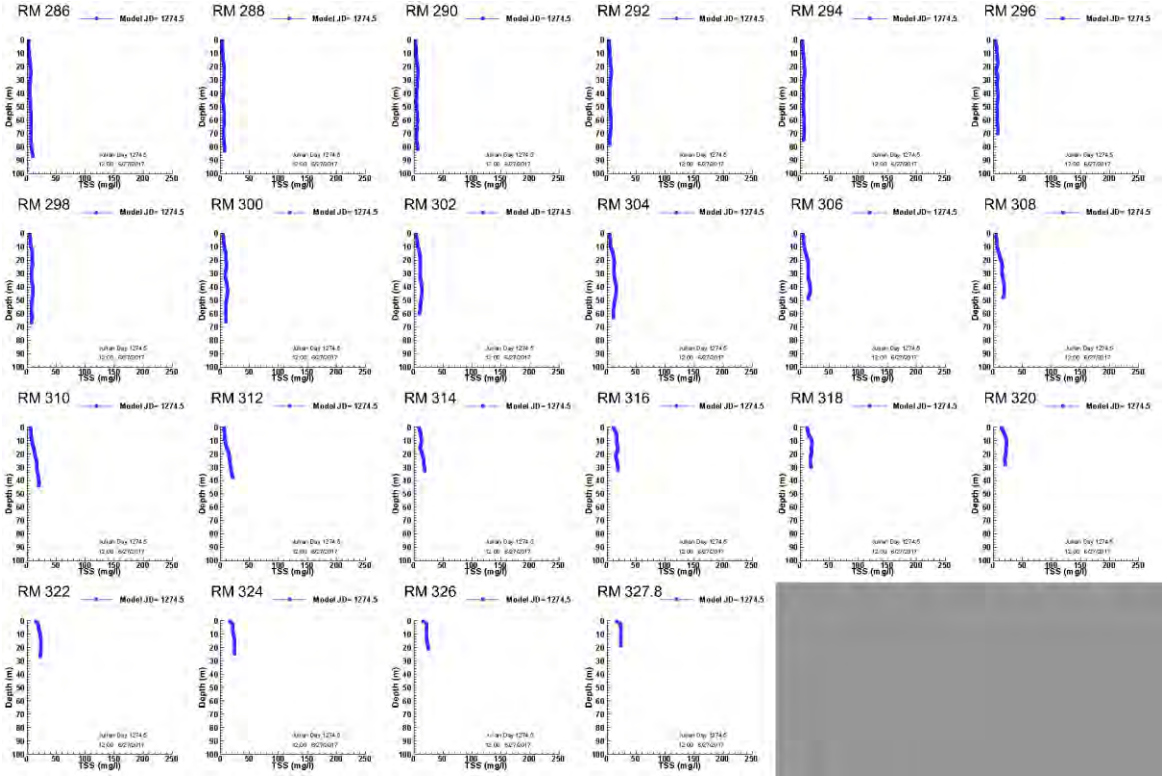


Figure 2162. Vertical profiles of TSS compared with data for 6/27/2017.

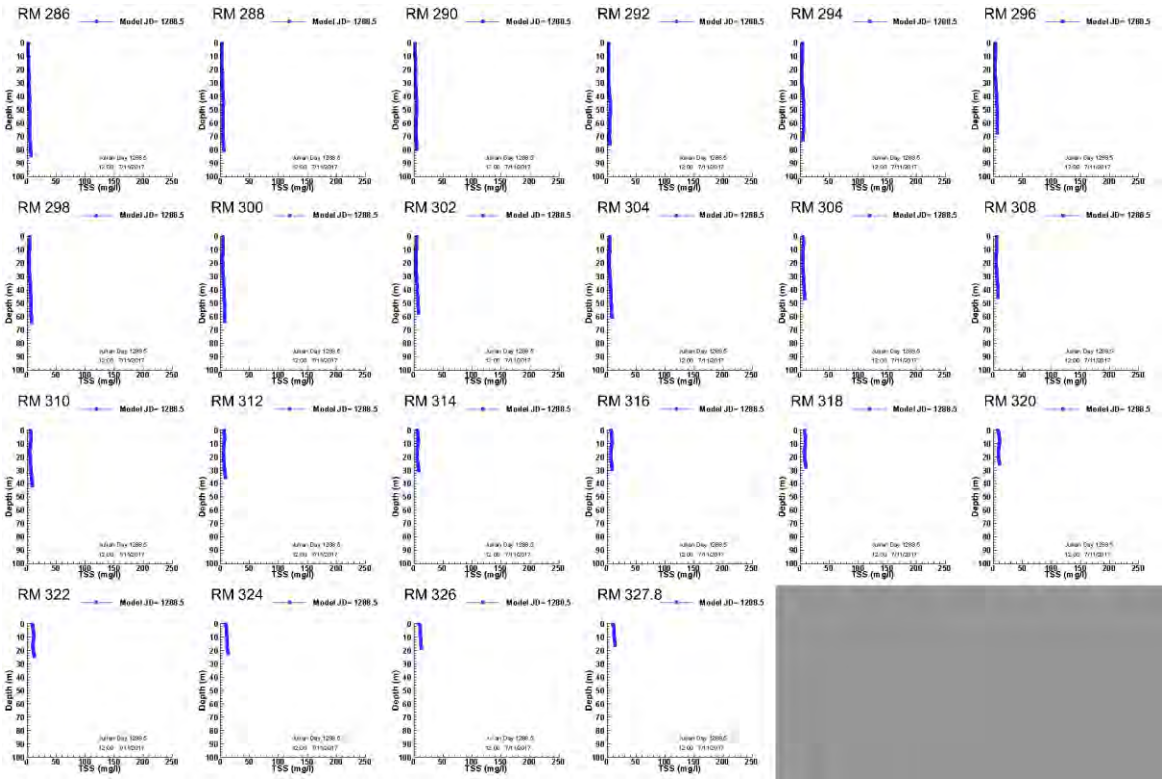


Figure 2163. Vertical profiles of TSS compared with data for 7/11/2017.

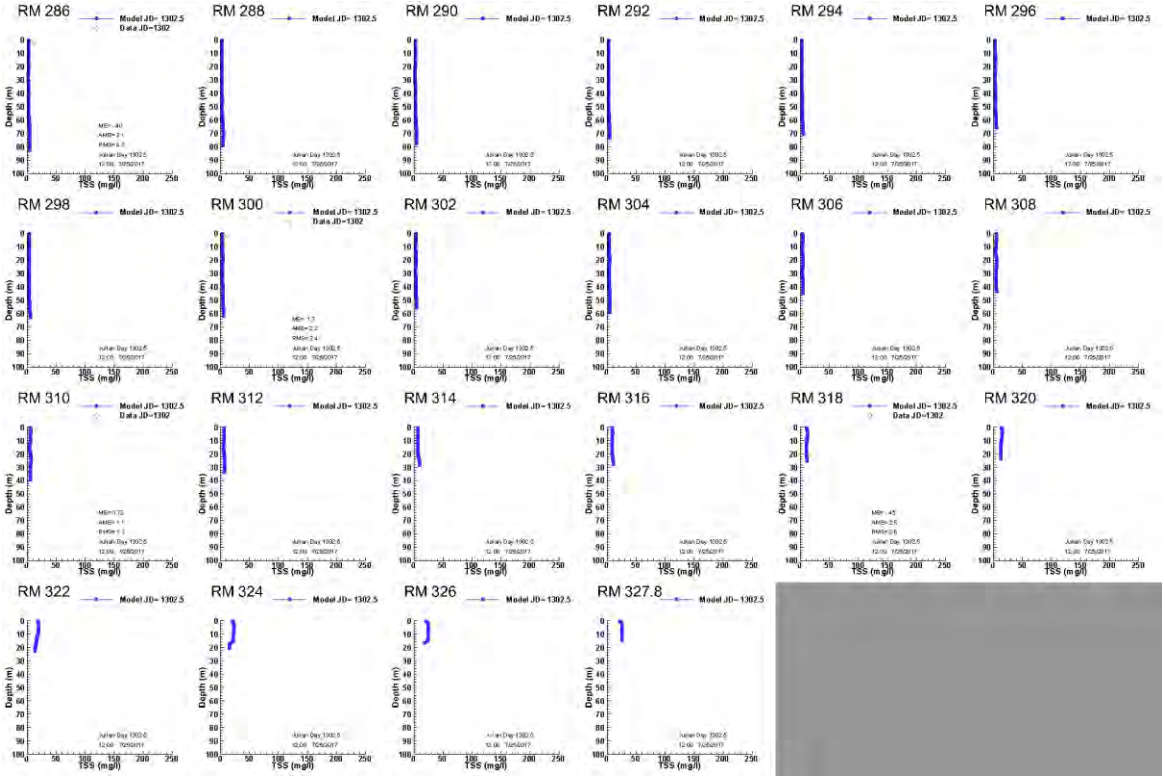


Figure 2164. Vertical profiles of TSS compared with data for 7/25/2017.

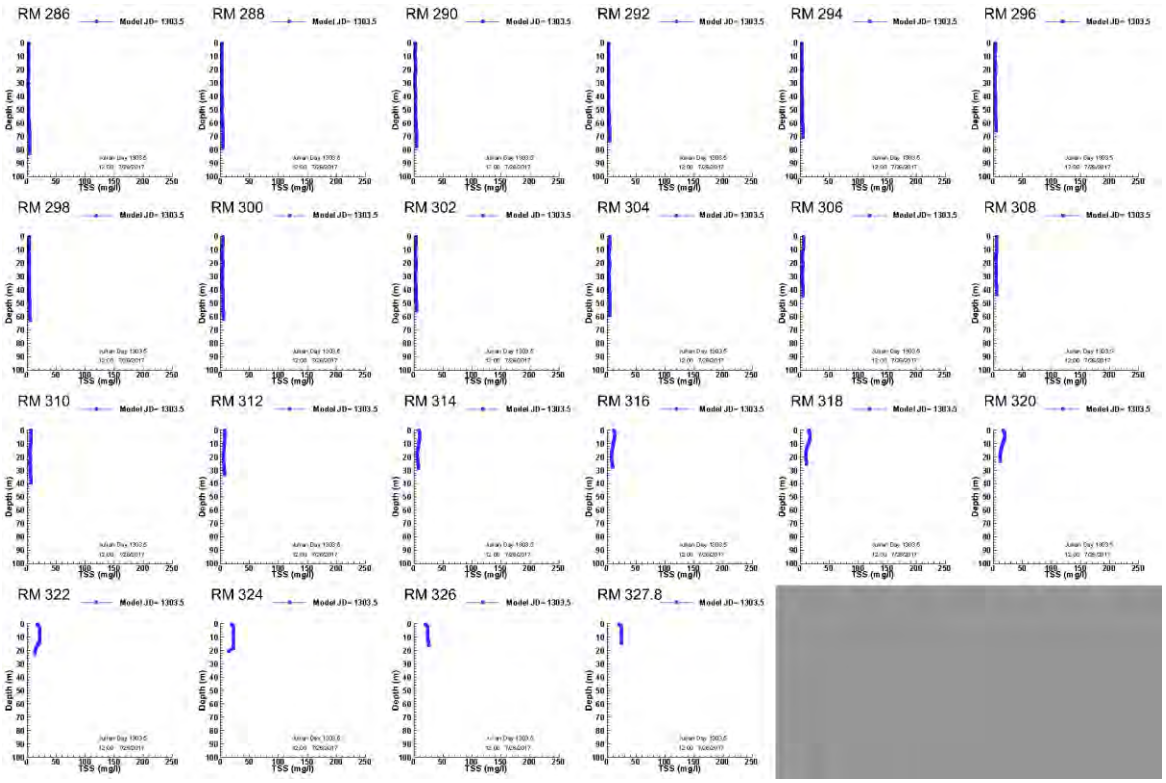


Figure 2165. Vertical profiles of TSS compared with data for 7/26/2017.

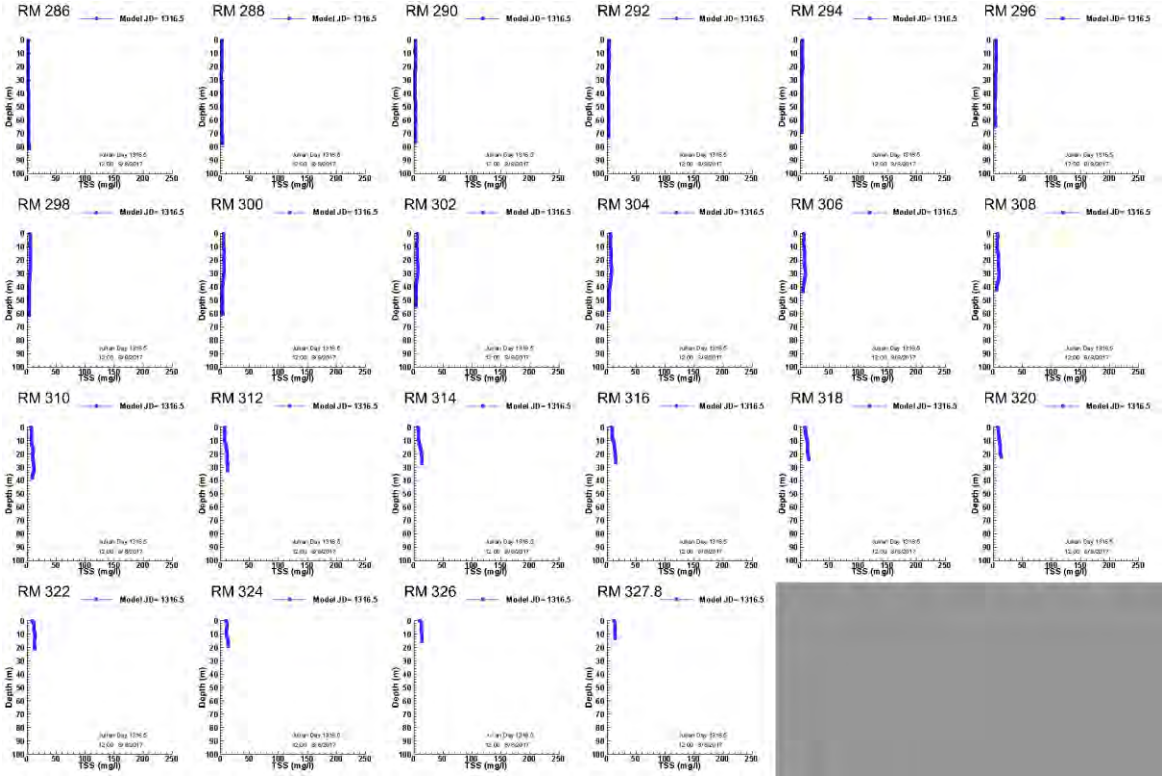


Figure 2166. Vertical profiles of TSS compared with data for 8/ 8/2017.

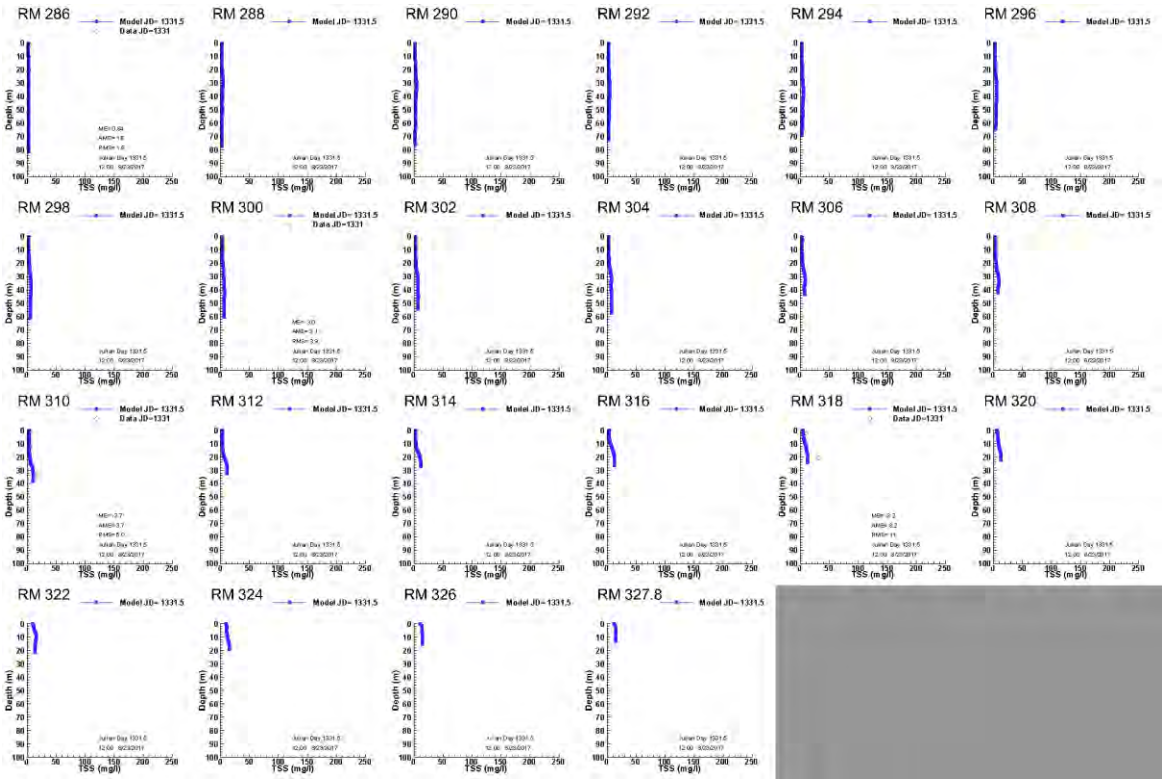


Figure 2167. Vertical profiles of TSS compared with data for 8/23/2017.

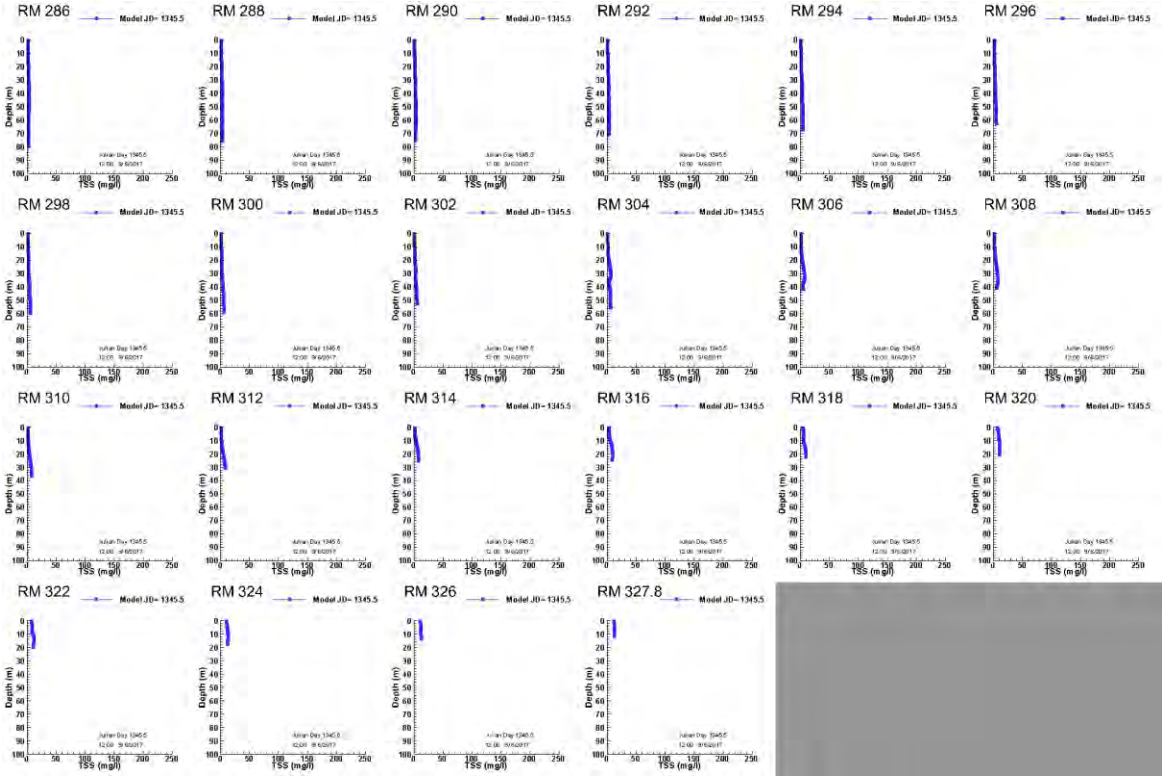


Figure 2168. Vertical profiles of TSS compared with data for 9/ 6/2017.

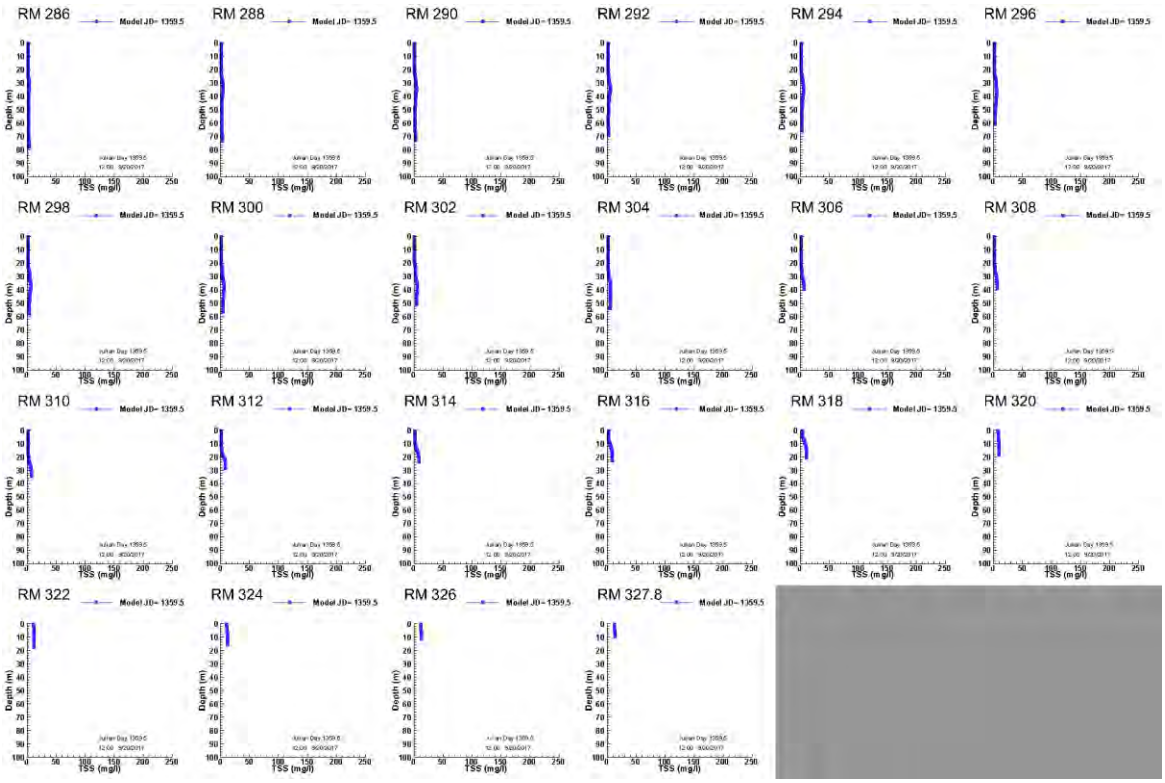


Figure 2169. Vertical profiles of TSS compared with data for 9/20/2017.

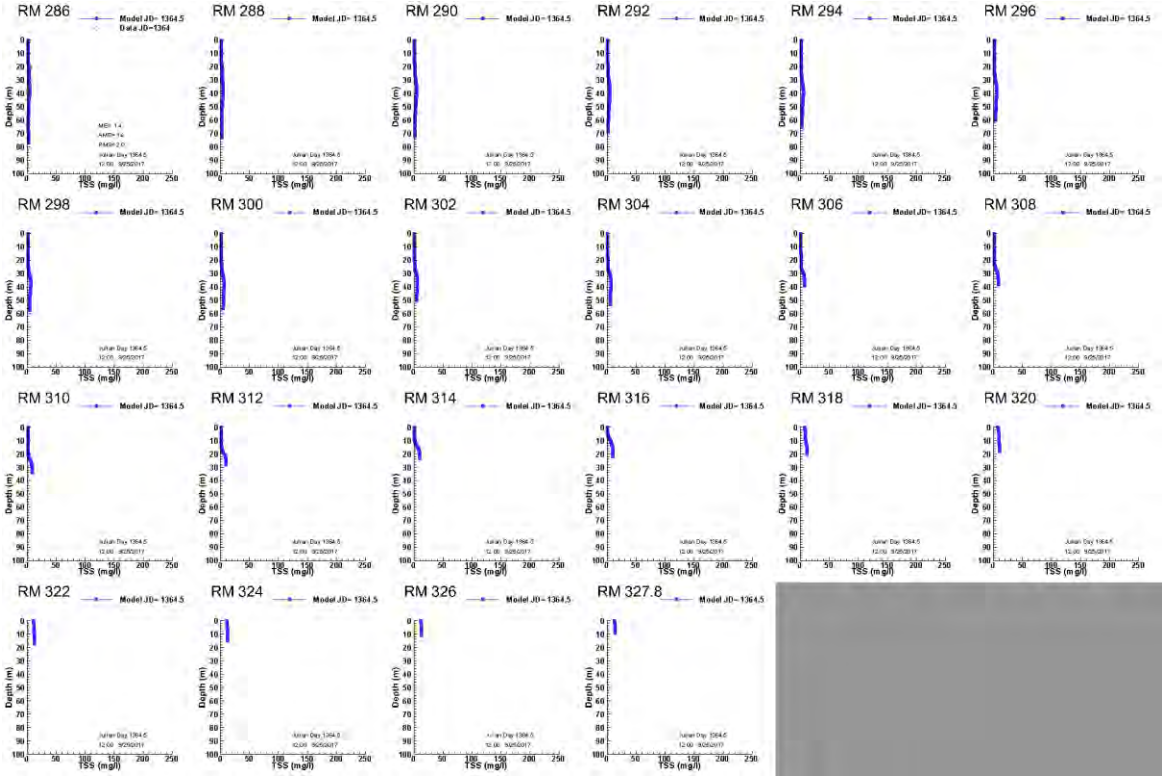


Figure 2170. Vertical profiles of TSS compared with data for 9/25/2017.

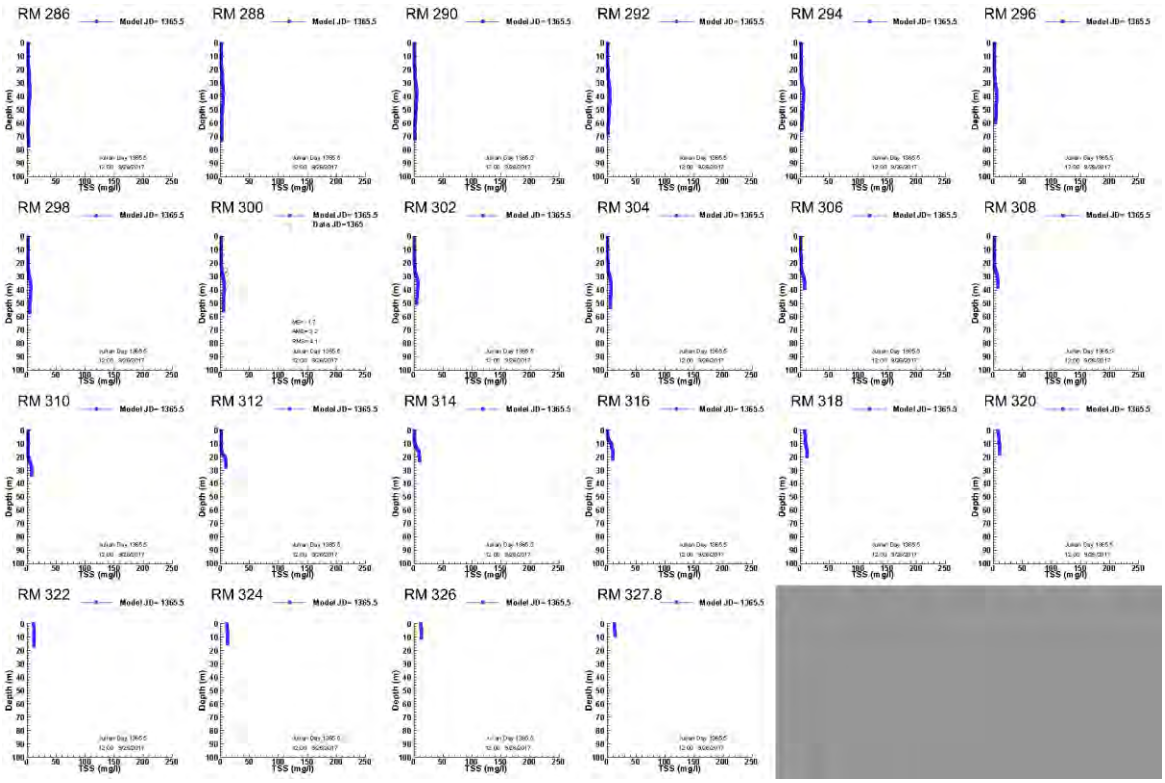


Figure 2171. Vertical profiles of TSS compared with data for 9/26/2017.

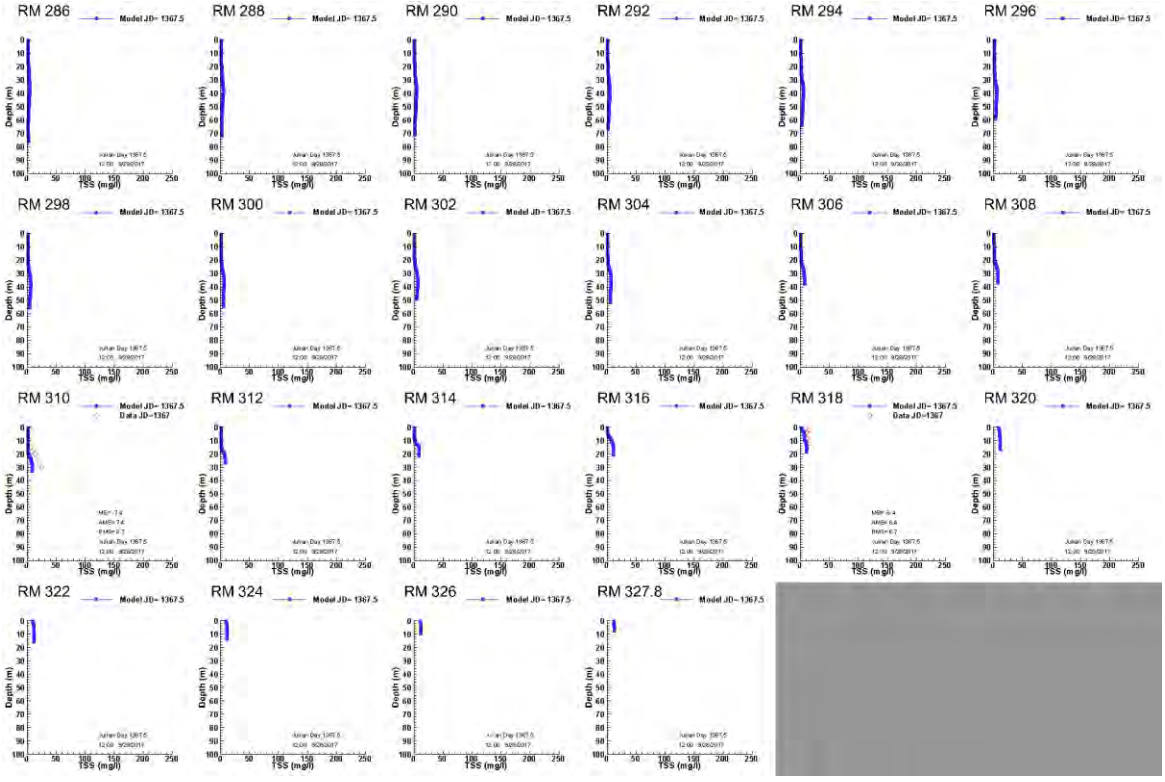


Figure 2172. Vertical profiles of TSS compared with data for 9/28/2017.

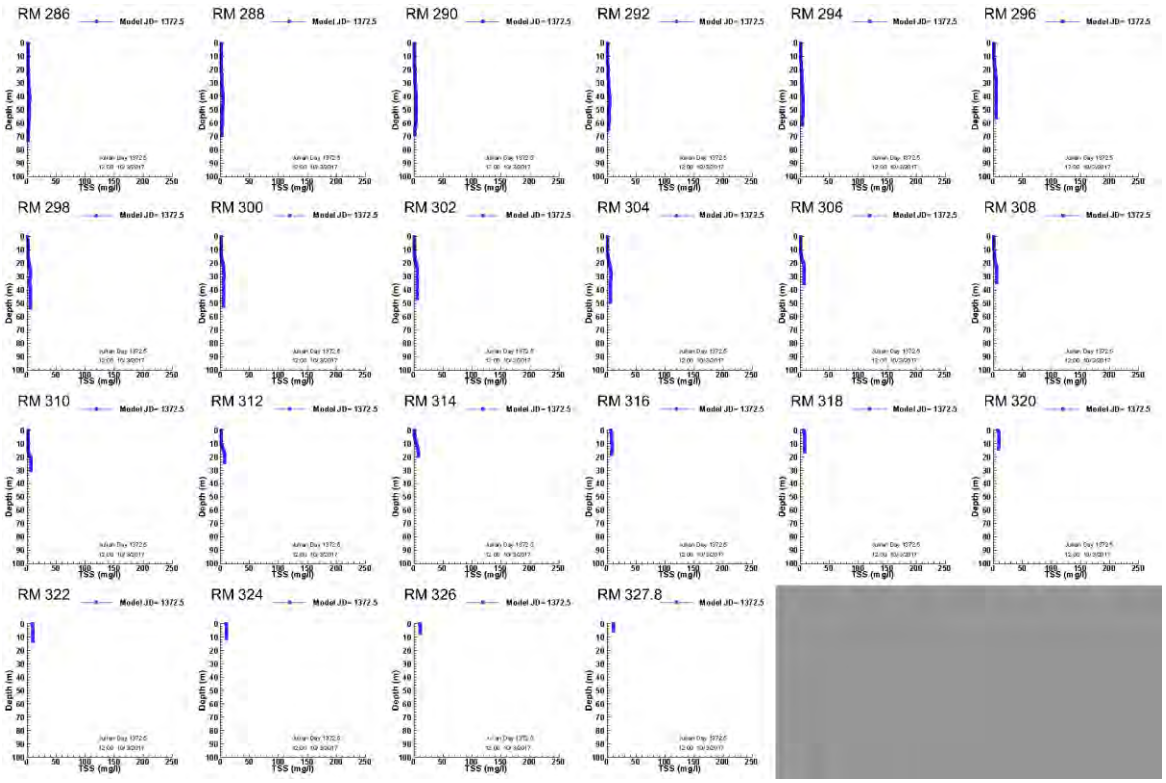


Figure 2173. Vertical profiles of TSS compared with data for 10/ 3/2017.

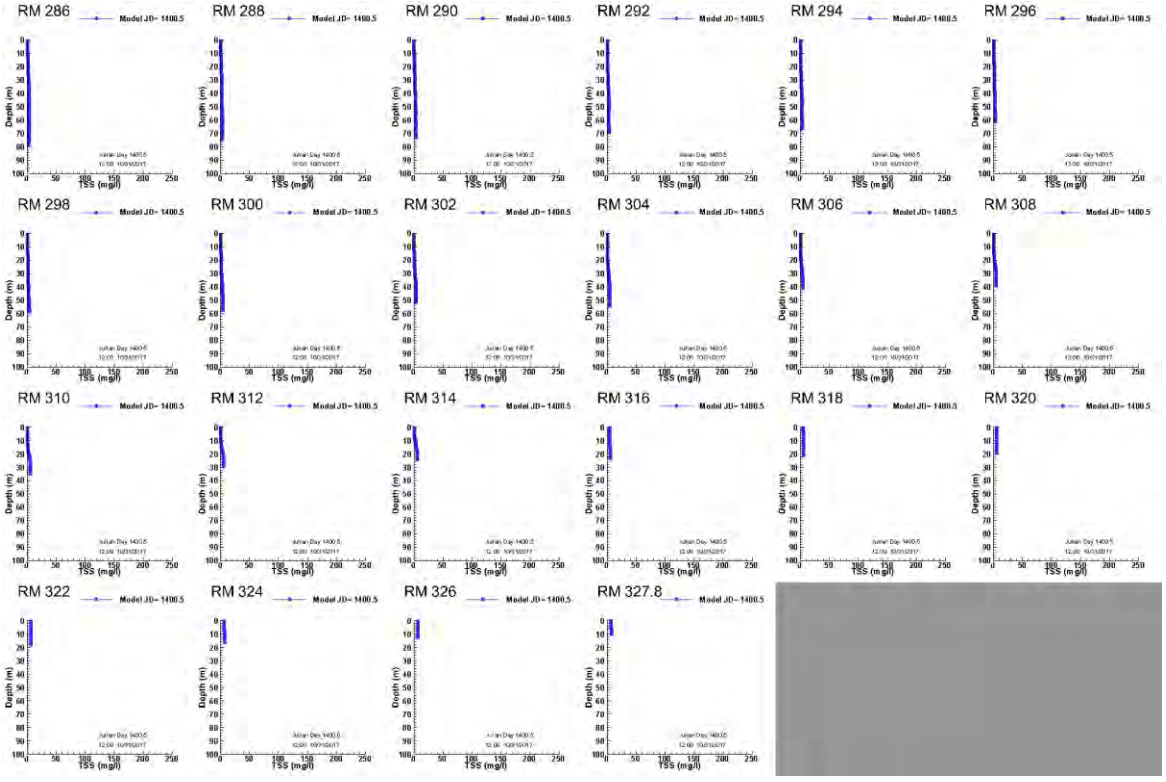


Figure 2174. Vertical profiles of TSS compared with data for 10/31/2017.

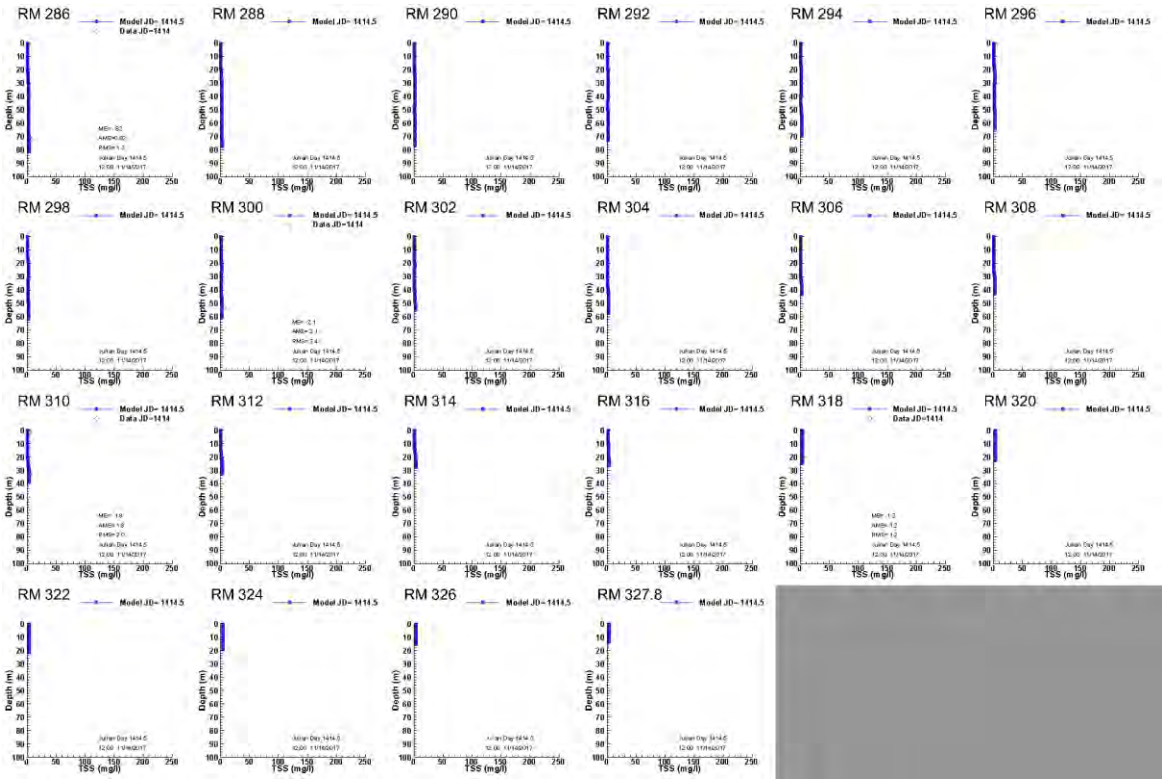


Figure 2175. Vertical profiles of TSS compared with data for 11/14/2017.

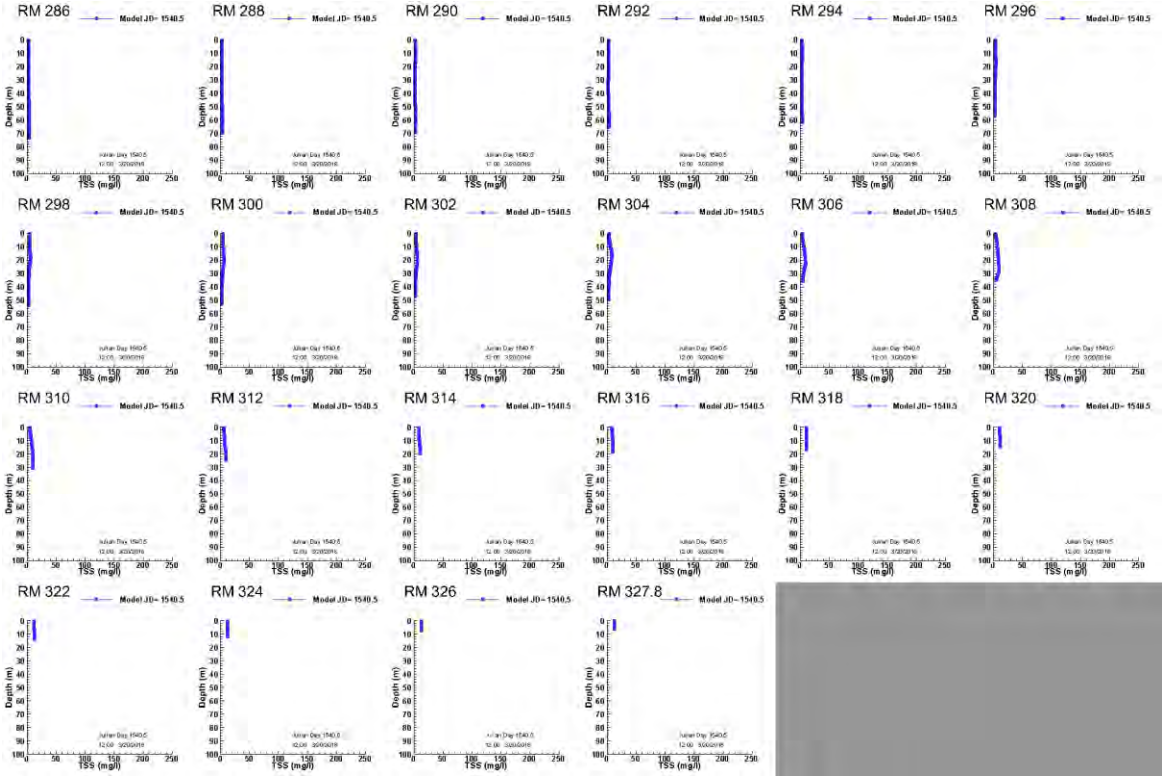


Figure 2176. Vertical profiles of TSS compared with data for 3/20/2018.

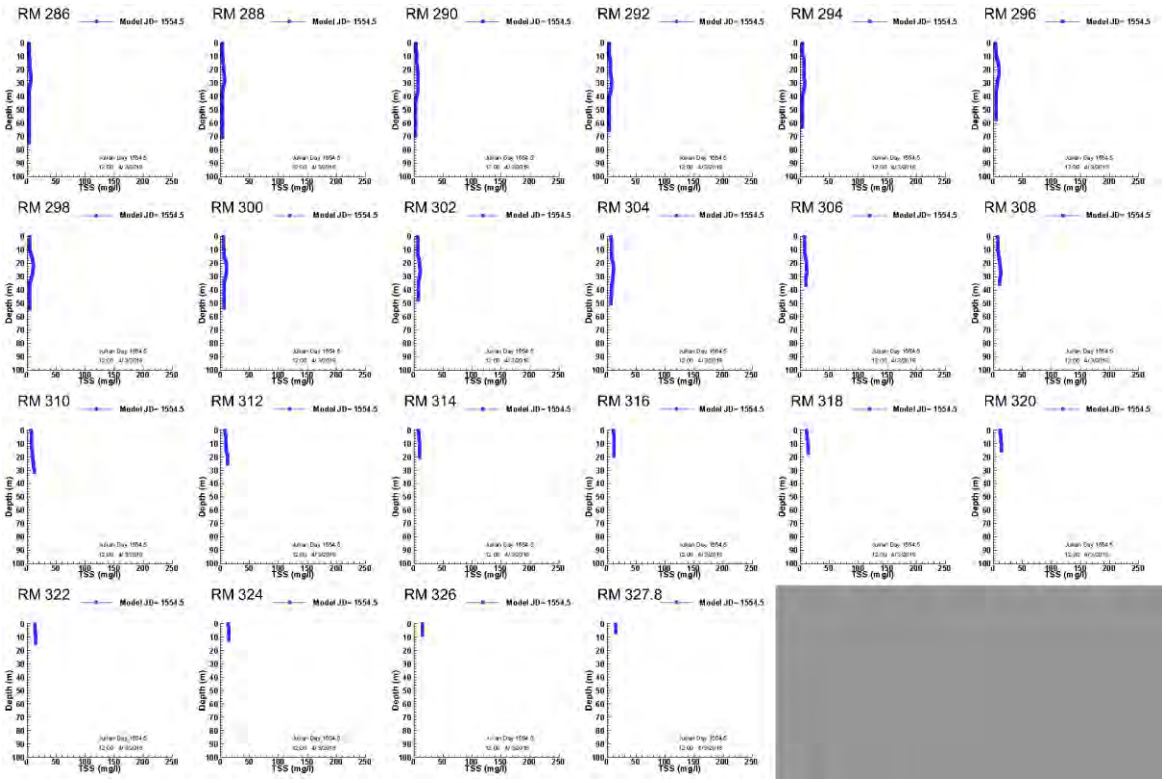


Figure 2177. Vertical profiles of TSS compared with data for 4/ 3/2018.

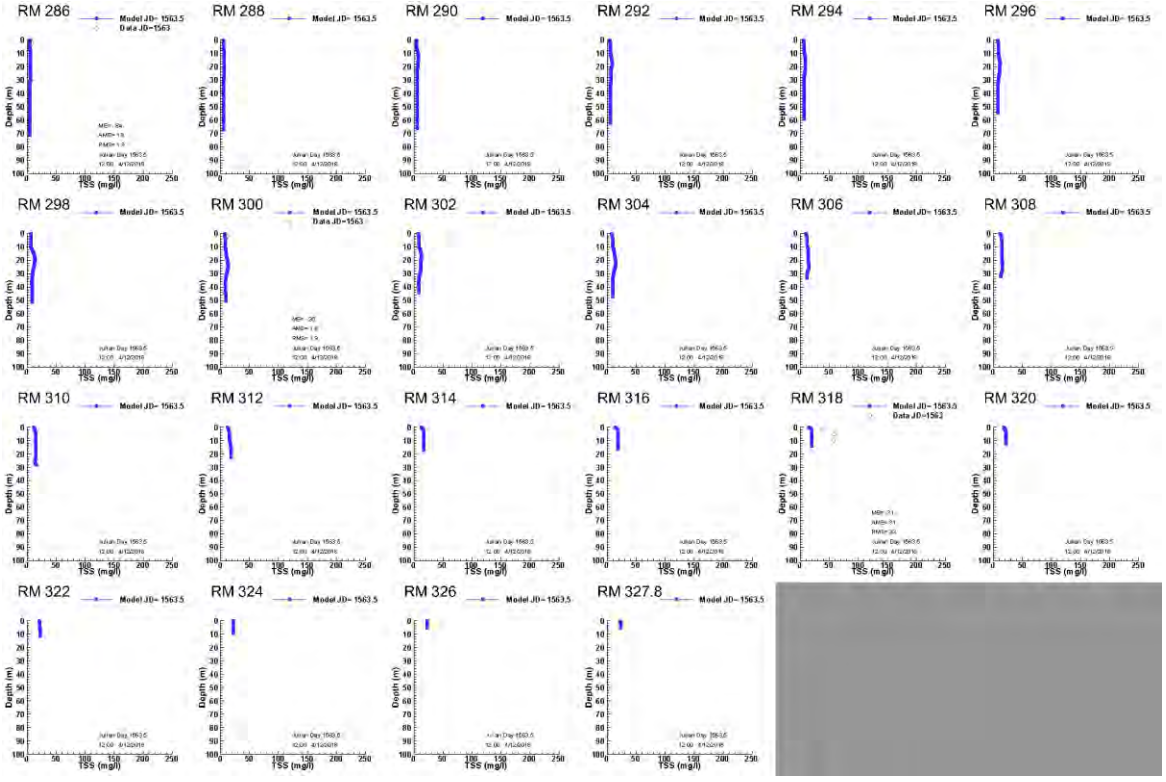


Figure 2178. Vertical profiles of TSS compared with data for 4/12/2018.

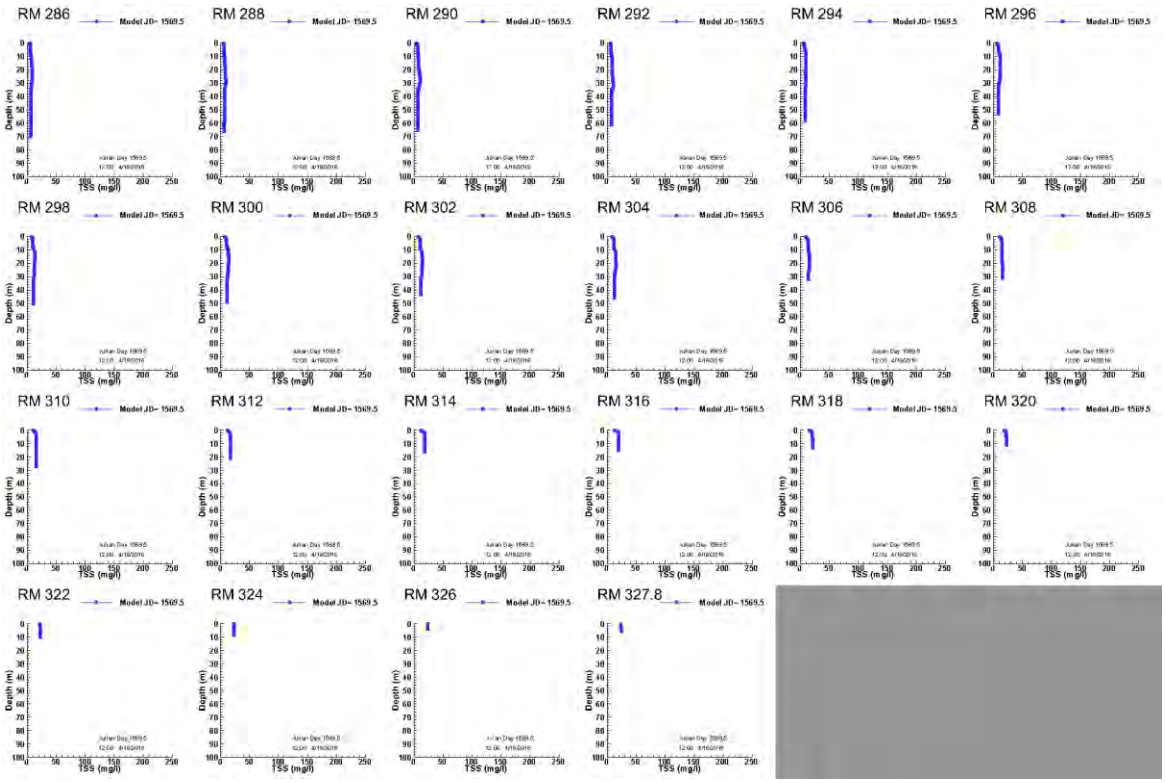


Figure 2179. Vertical profiles of TSS compared with data for 4/18/2018.

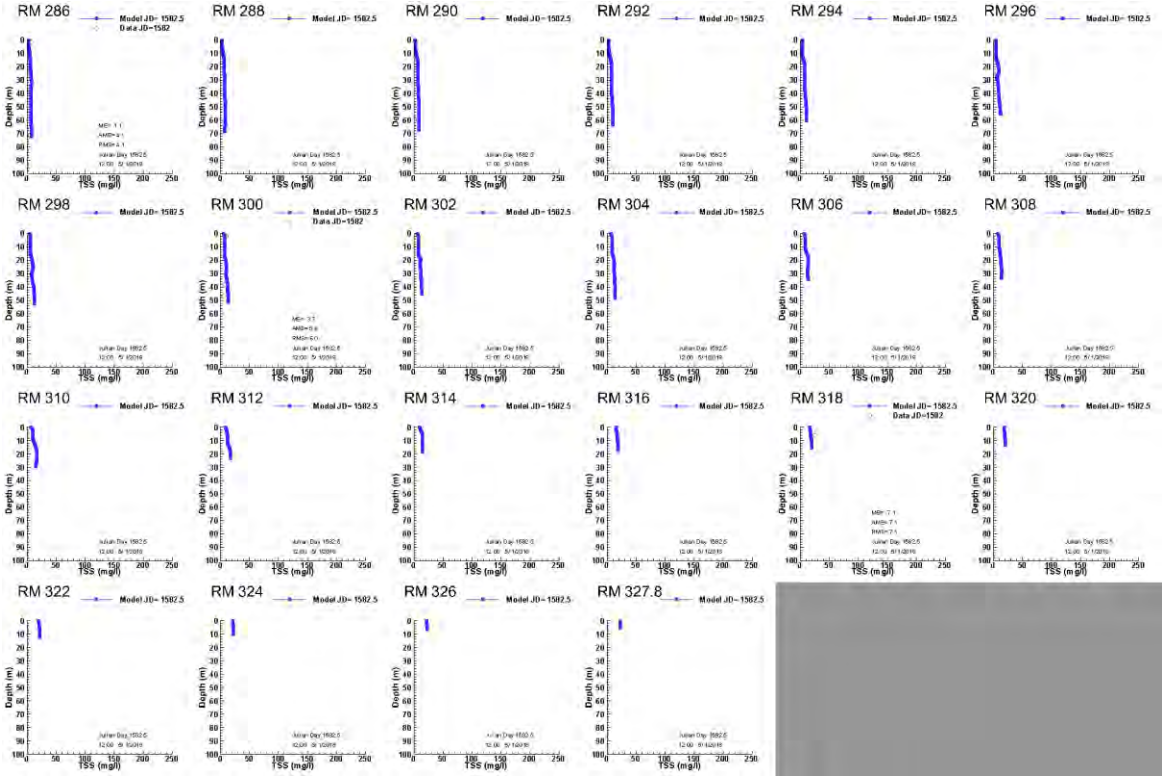


Figure 2180. Vertical profiles of TSS compared with data for 5/ 1/2018.

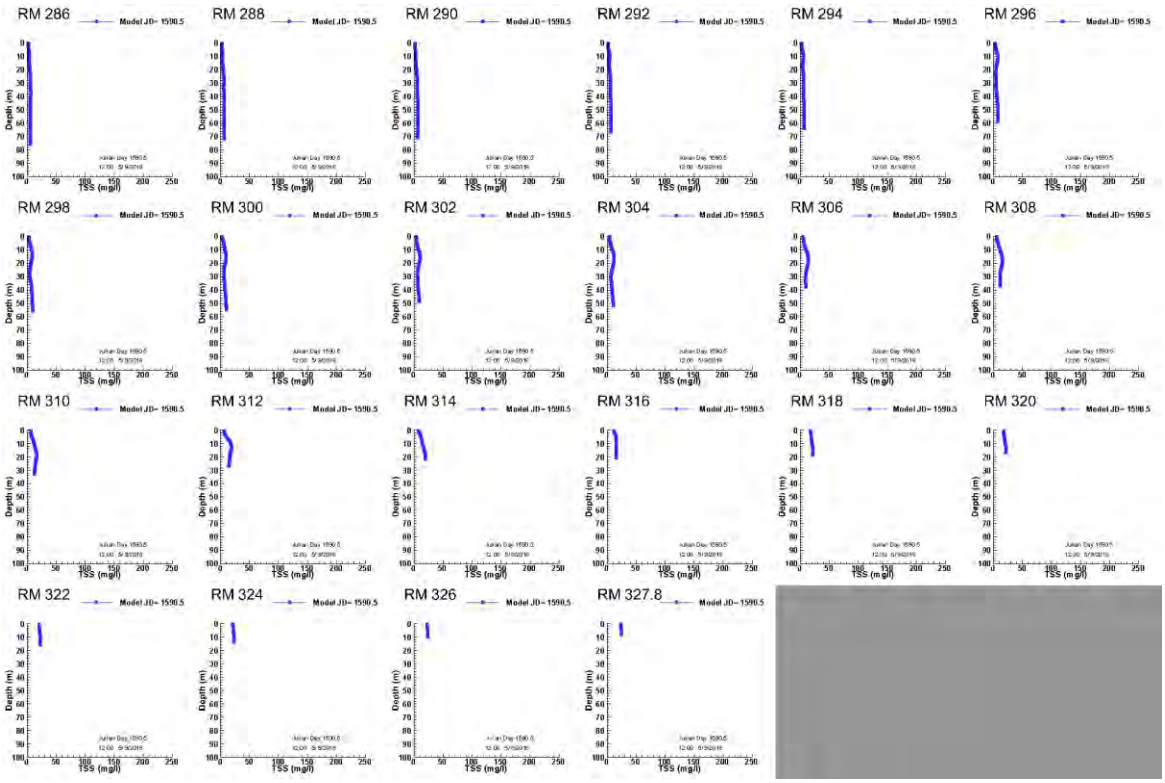


Figure 2181. Vertical profiles of TSS compared with data for 5/ 9/2018.

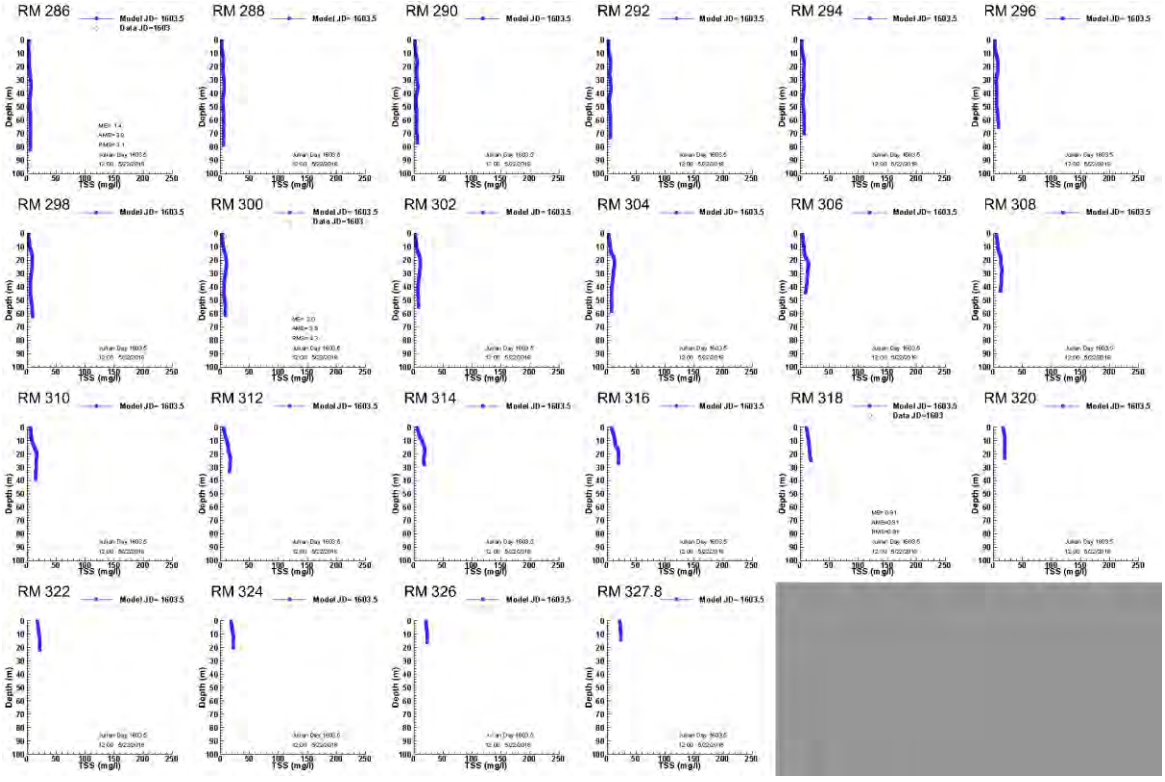


Figure 2182. Vertical profiles of TSS compared with data for 5/22/2018.

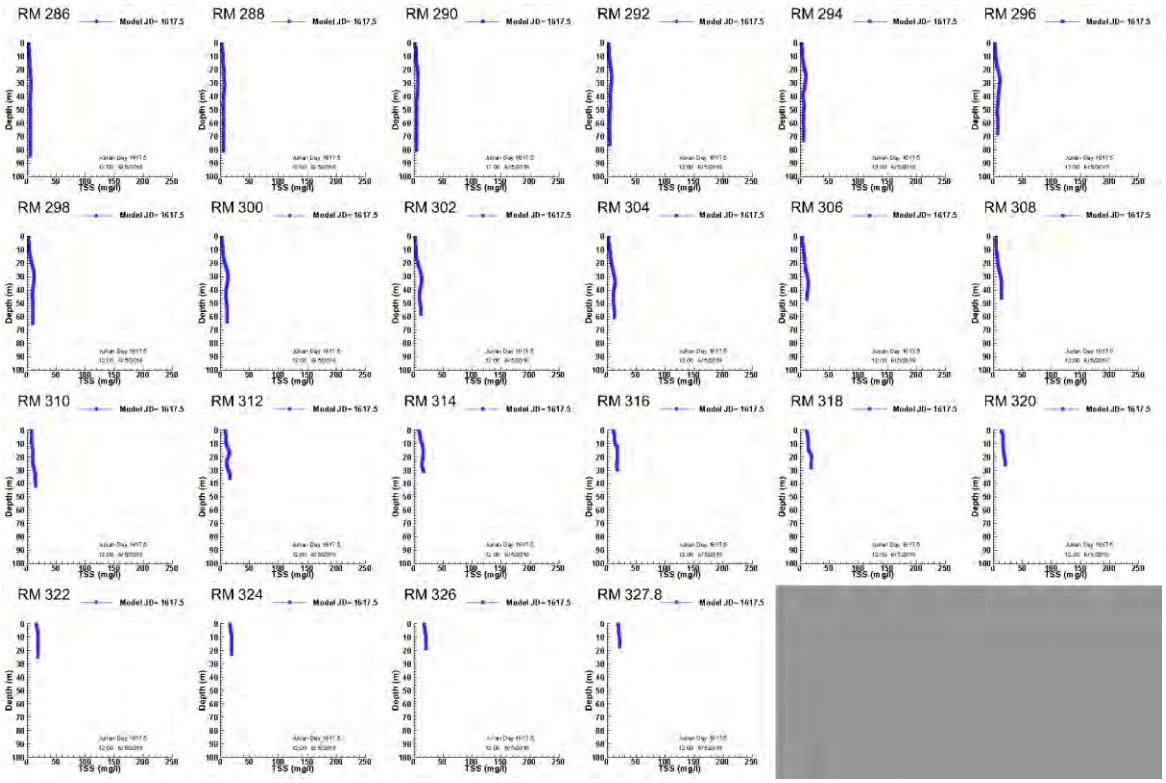


Figure 2183. Vertical profiles of TSS compared with data for 6/ 5/2018.

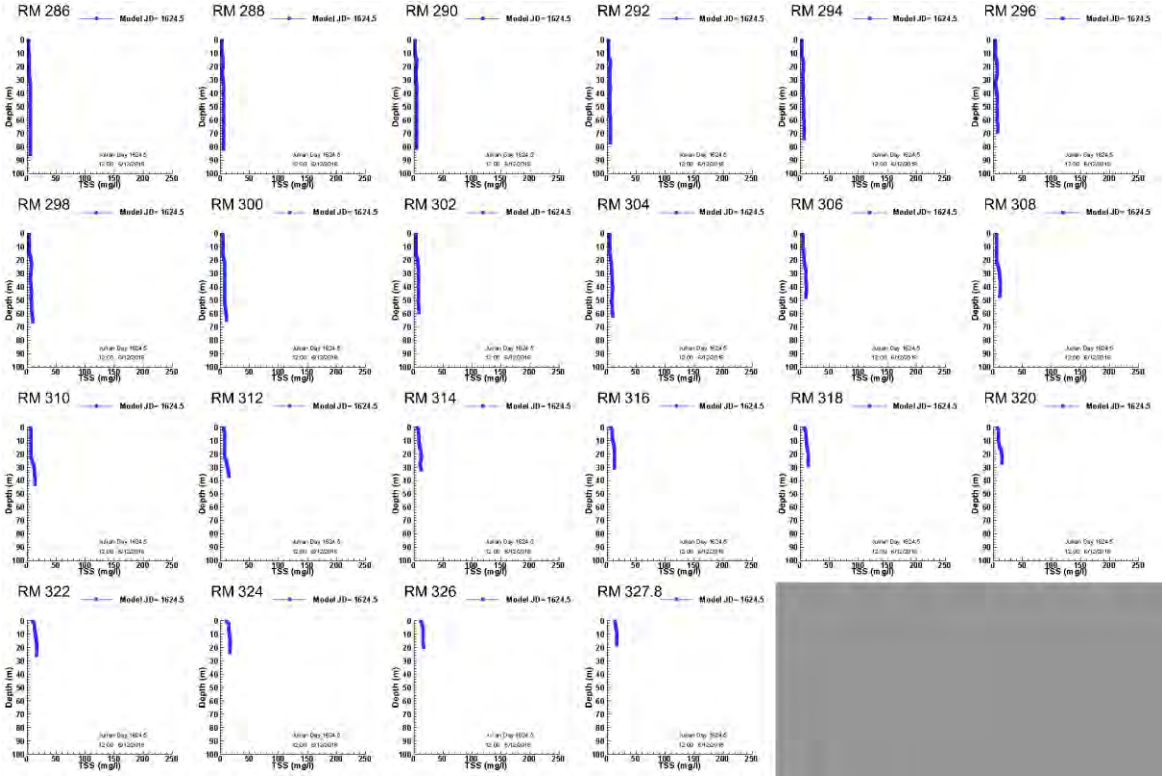


Figure 2184. Vertical profiles of TSS compared with data for 6/12/2018.

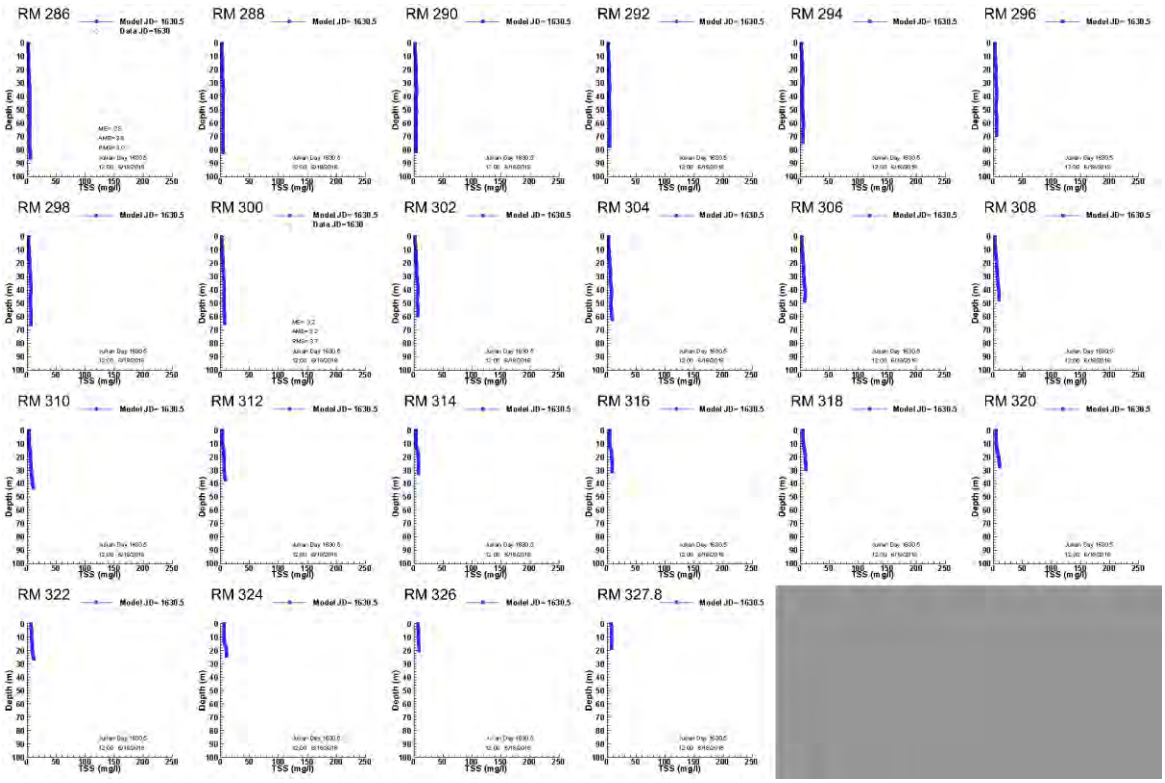


Figure 2185. Vertical profiles of TSS compared with data for 6/18/2018.

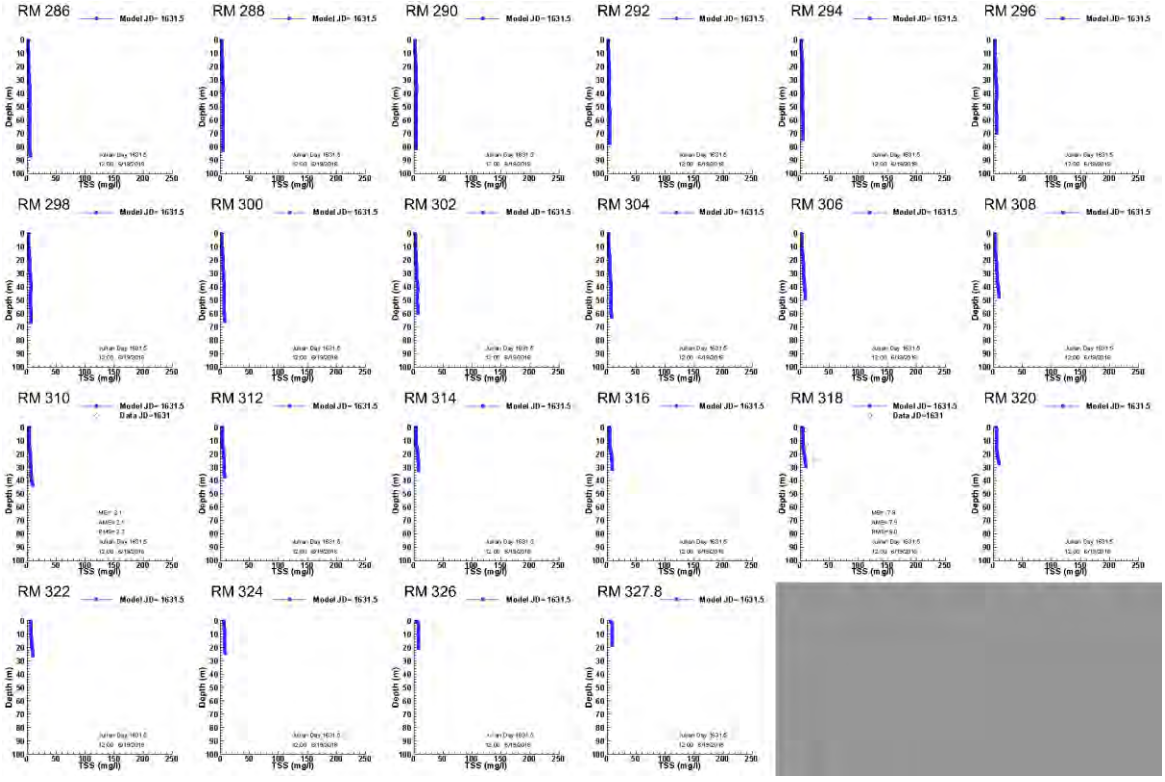


Figure 2186. Vertical profiles of TSS compared with data for 6/19/2018.

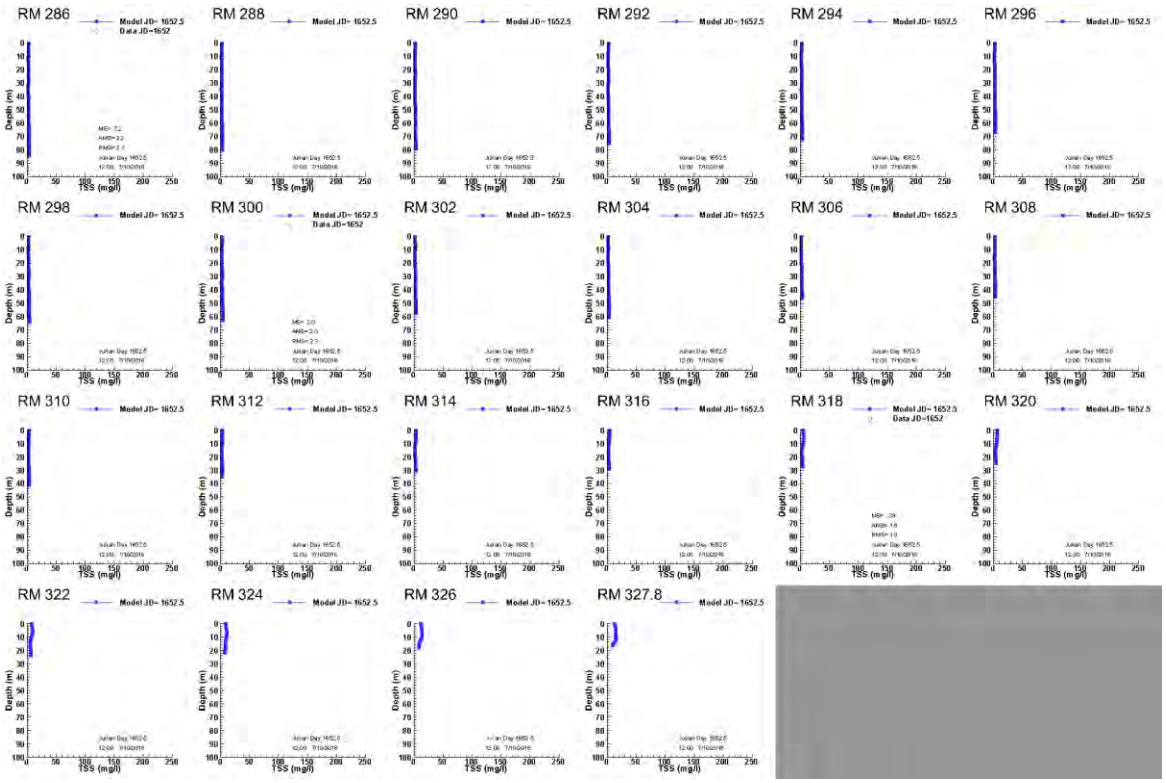


Figure 2187. Vertical profiles of TSS compared with data for 7/10/2018.

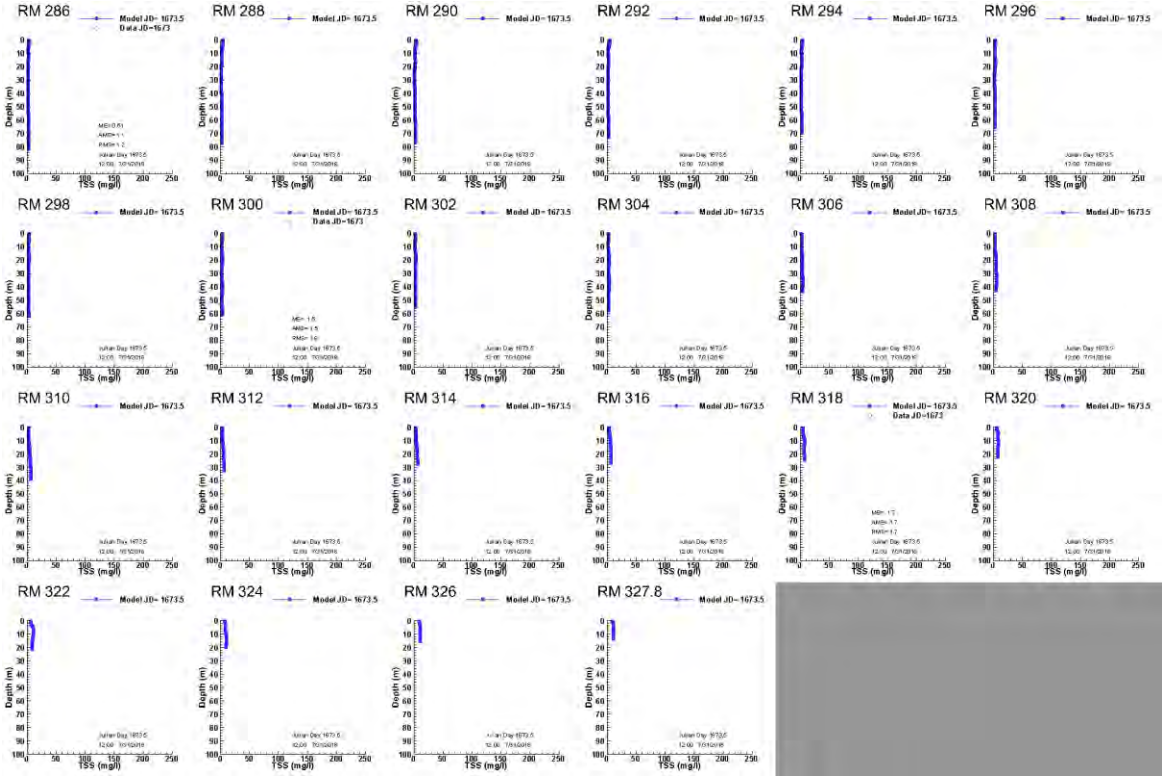


Figure 2188. Vertical profiles of TSS compared with data for 7/31/2018.

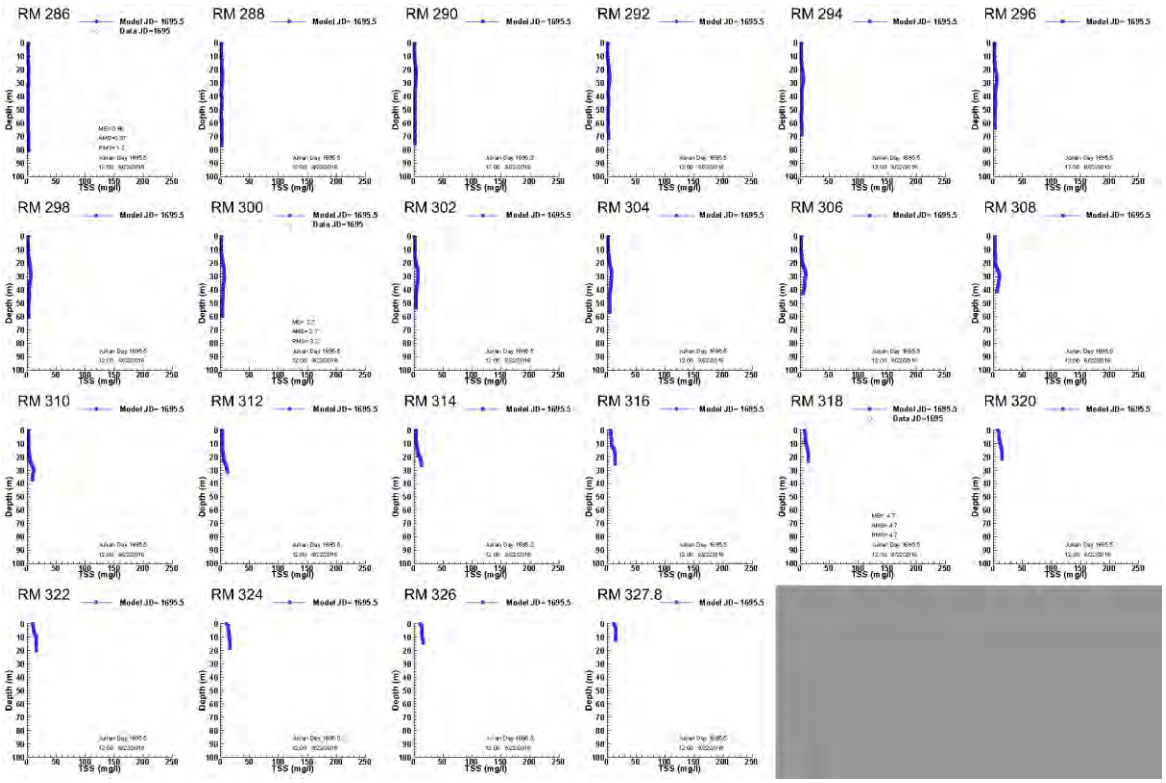


Figure 2189. Vertical profiles of TSS compared with data for 8/22/2018.

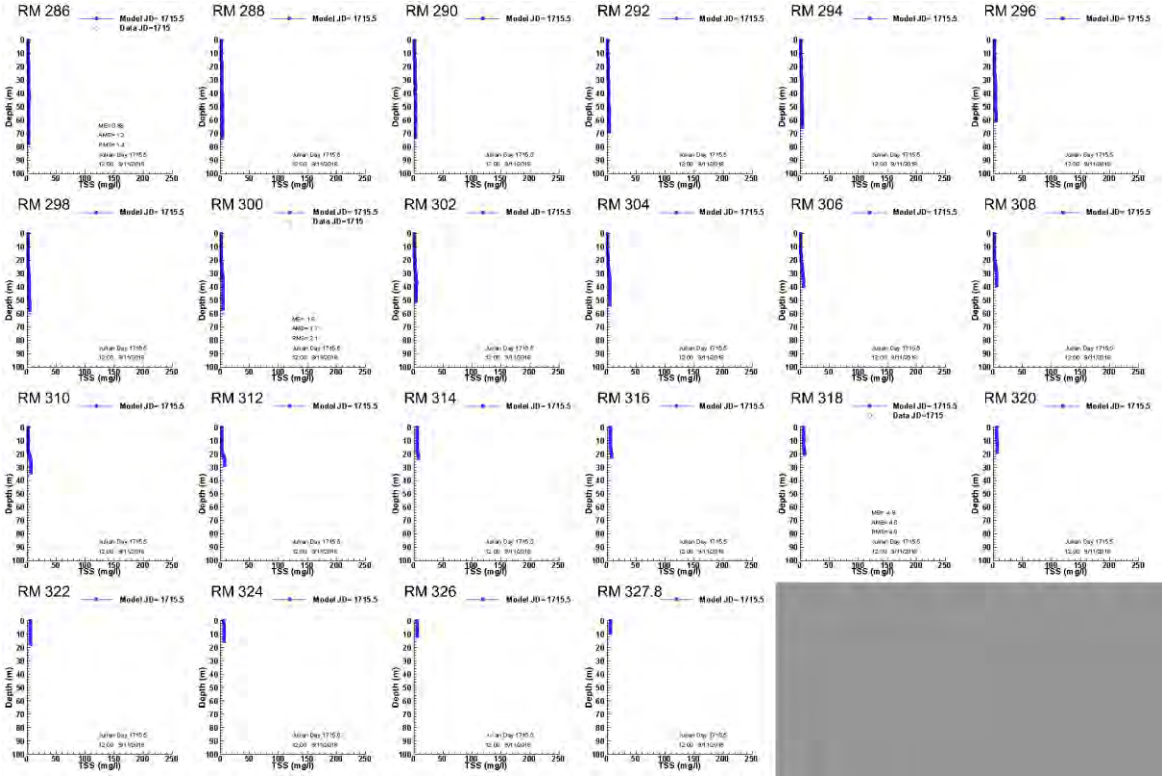


Figure 2190. Vertical profiles of TSS compared with data for 9/11/2018.

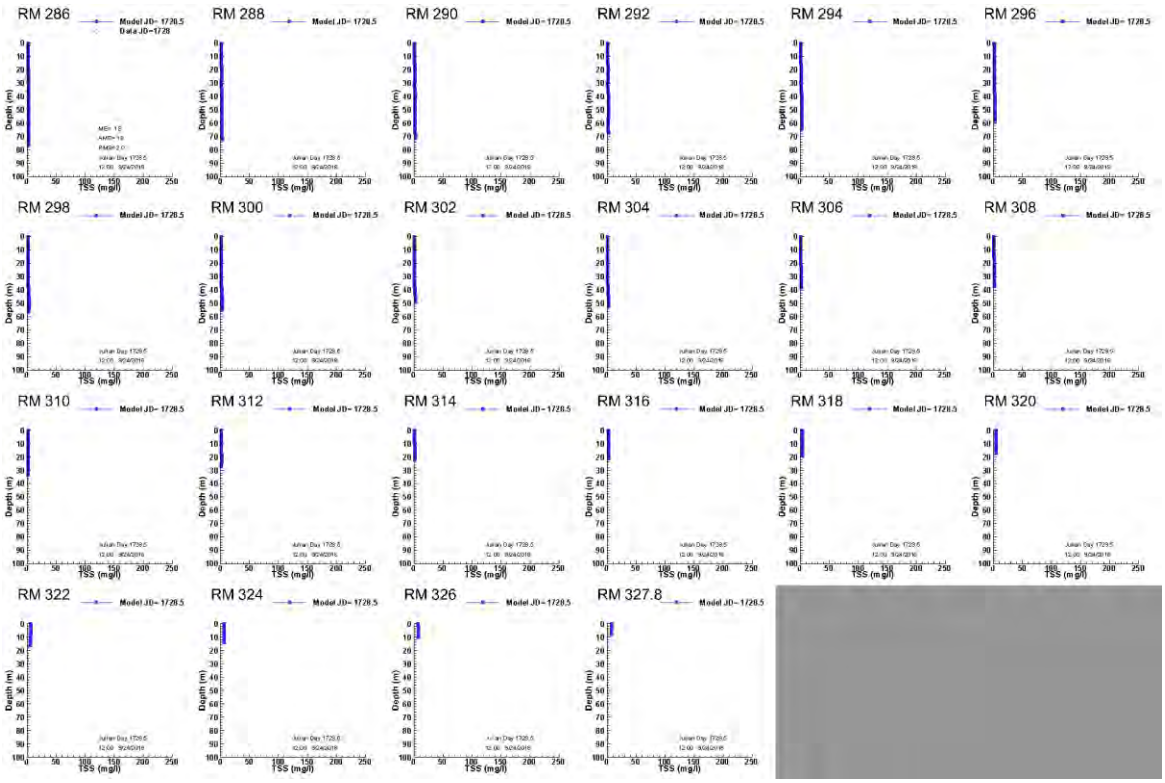


Figure 2191. Vertical profiles of TSS compared with data for 9/24/2018.

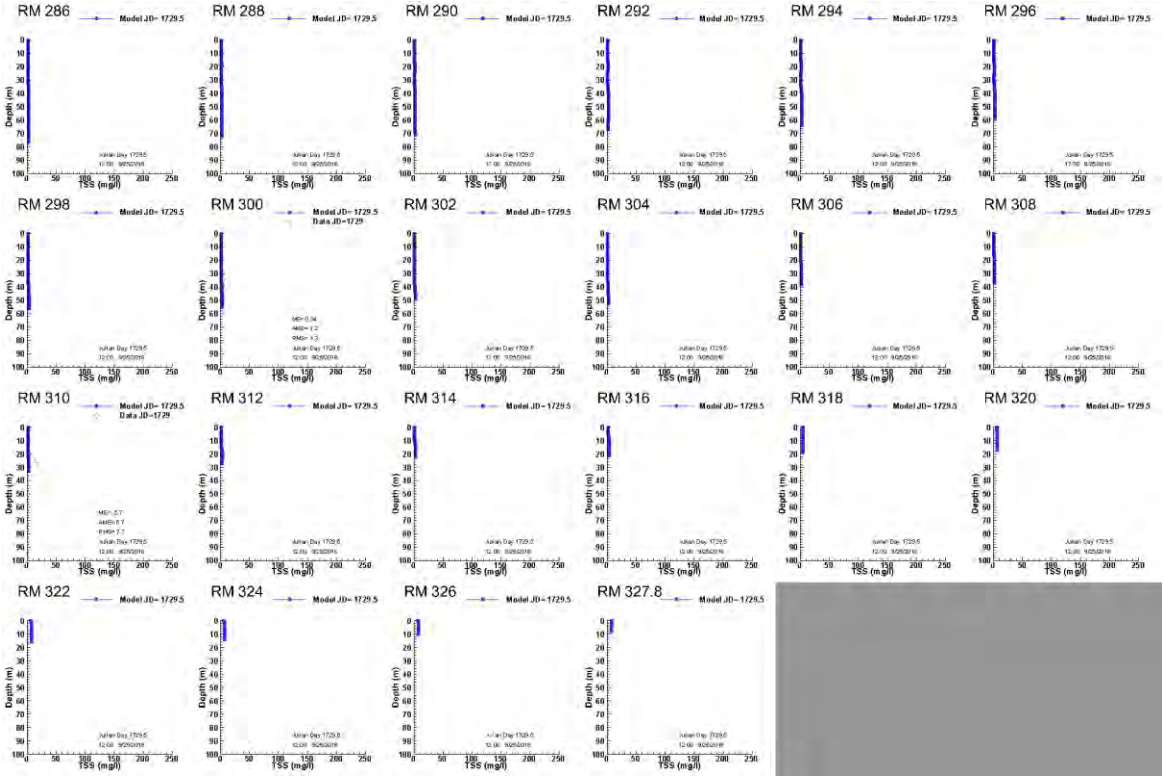


Figure 2192. Vertical profiles of TSS compared with data for 9/25/2018.

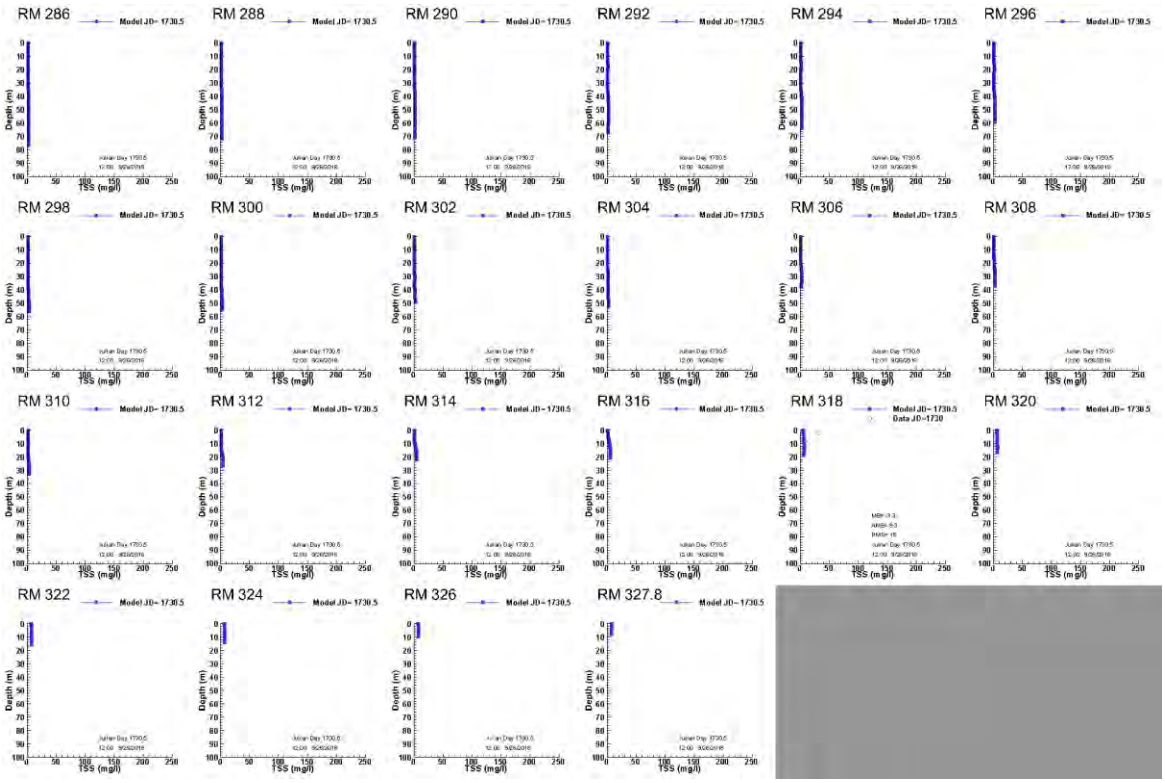


Figure 2193. Vertical profiles of TSS compared with data for 9/26/2018.

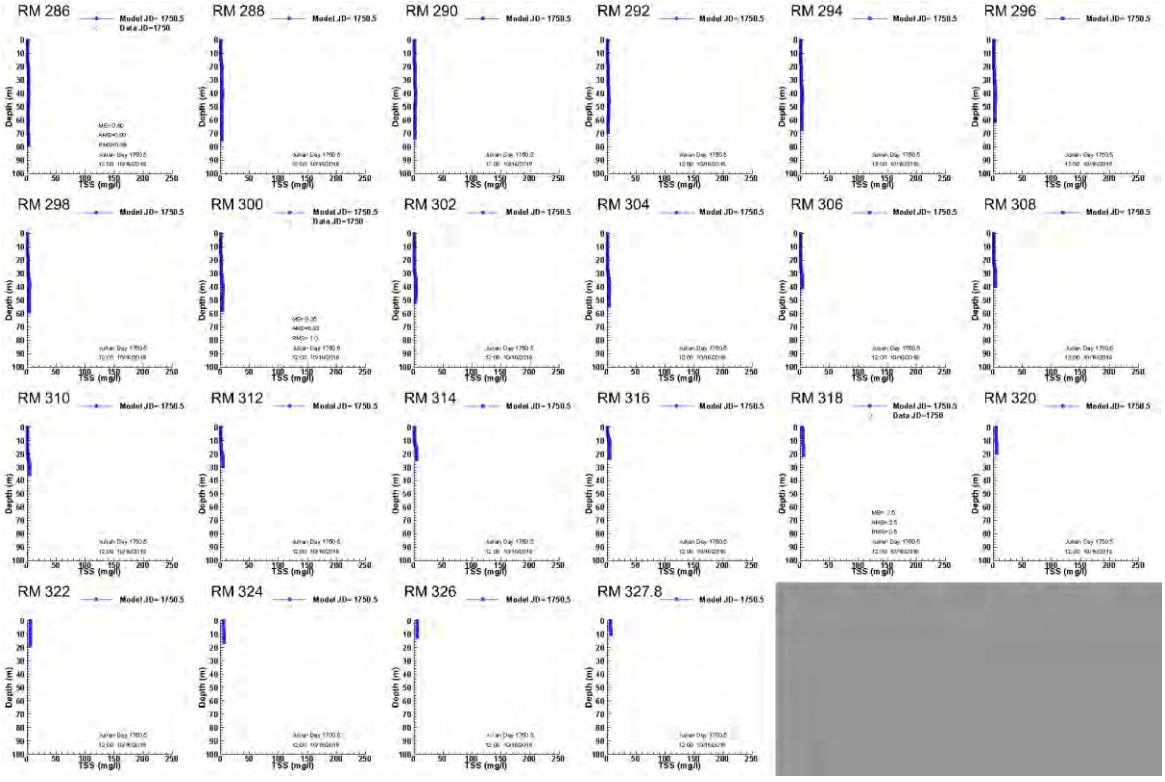


Figure 2194. Vertical profiles of TSS compared with data for 10/16/2018.

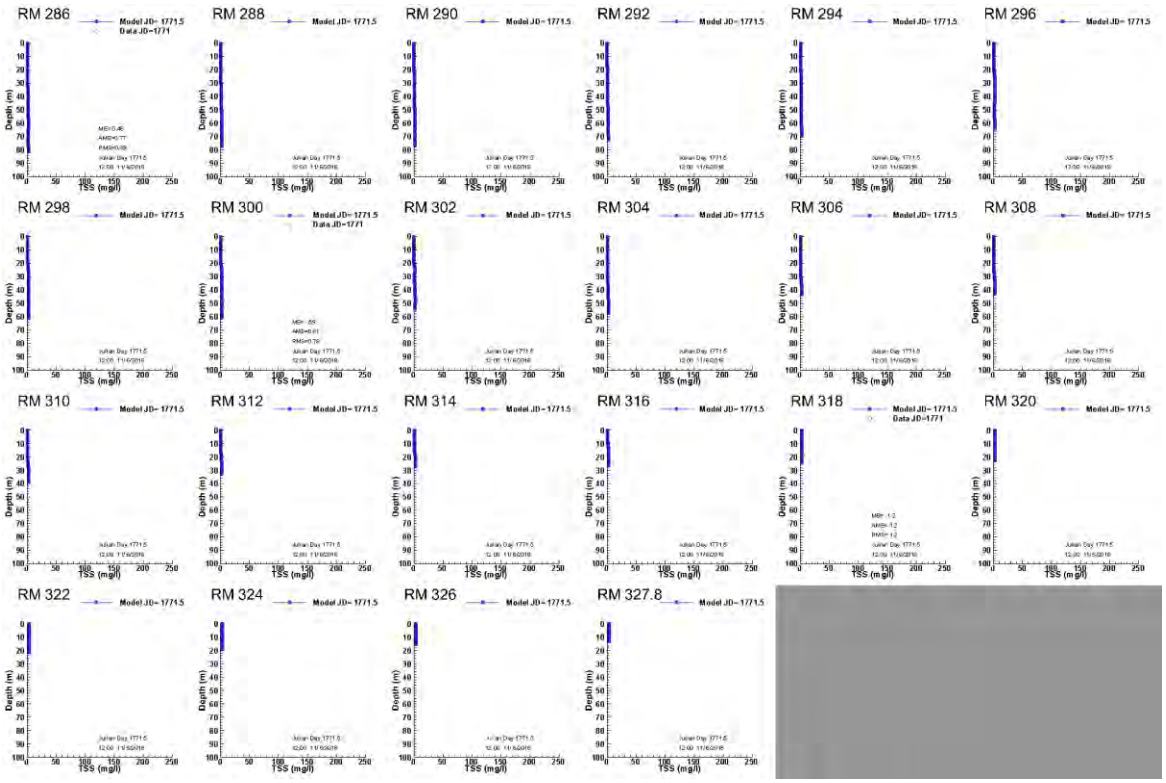


Figure 2195. Vertical profiles of TSS compared with data for 11/ 6/2018.

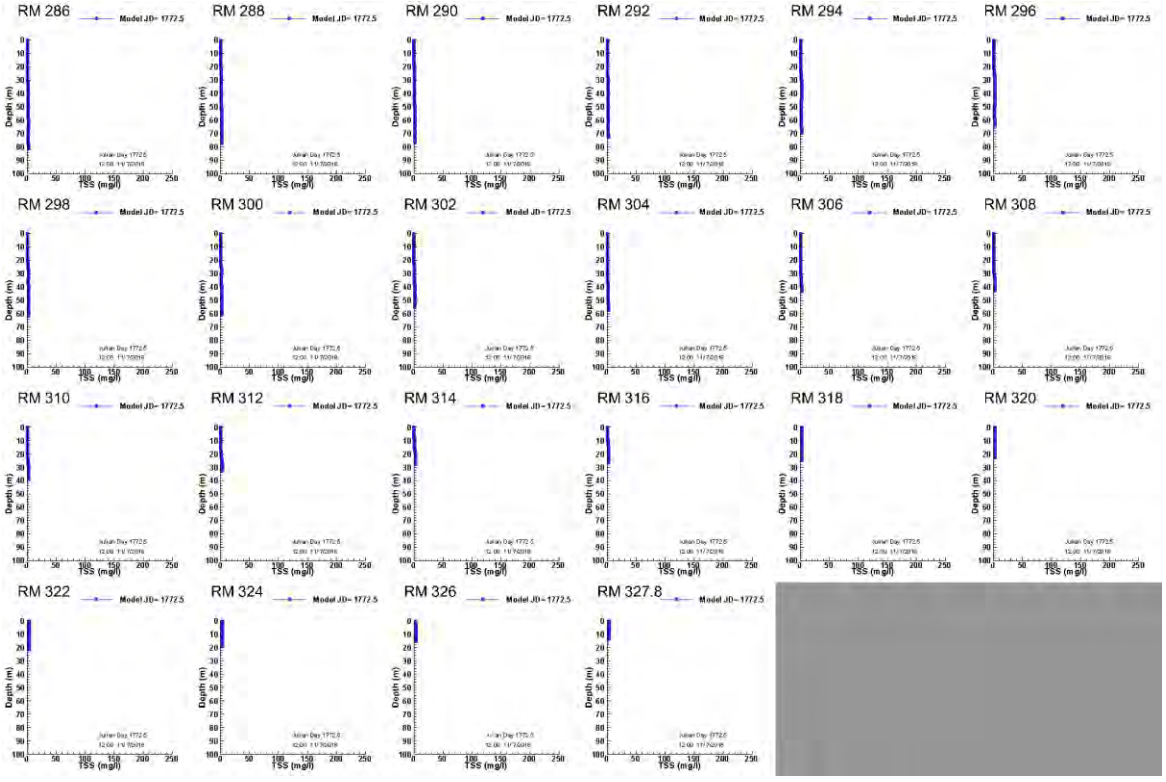


Figure 2196. Vertical profiles of TSS compared with data for 11/ 7/2018.

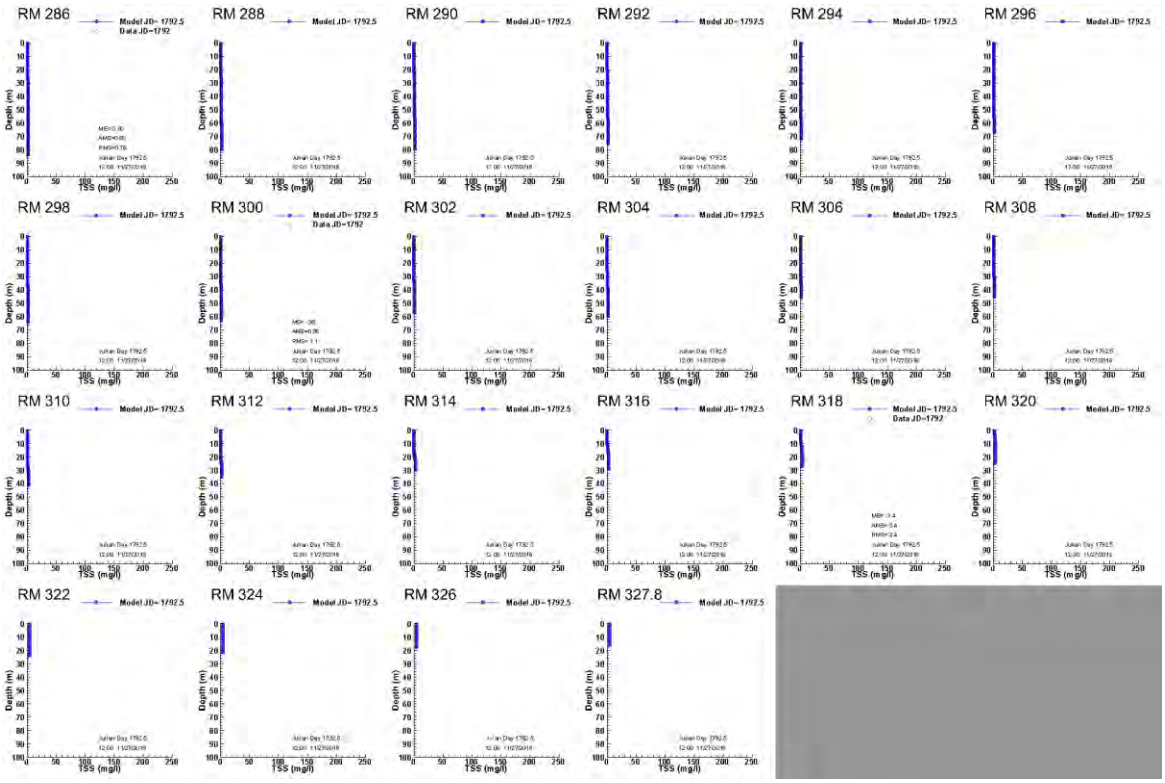


Figure 2197. Vertical profiles of TSS compared with data for 11/27/2018.

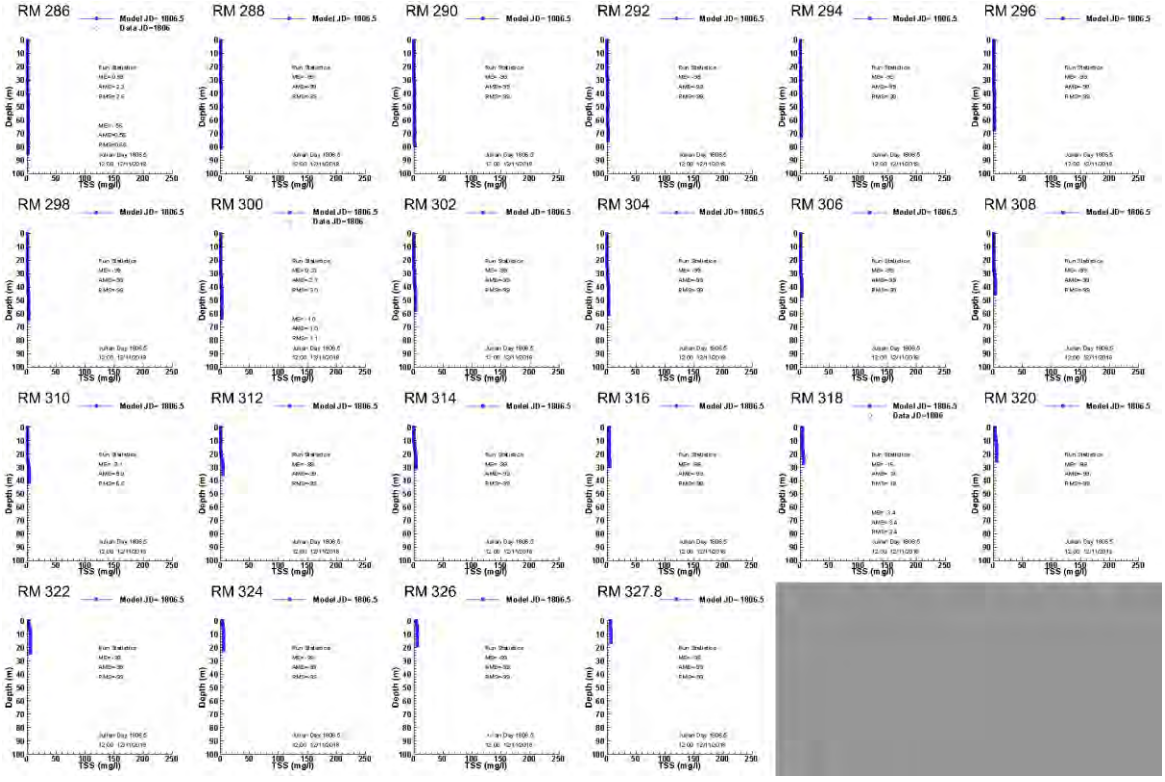


Figure 2198. Vertical profiles of TSS compared with data for 12/11/2018.

pH

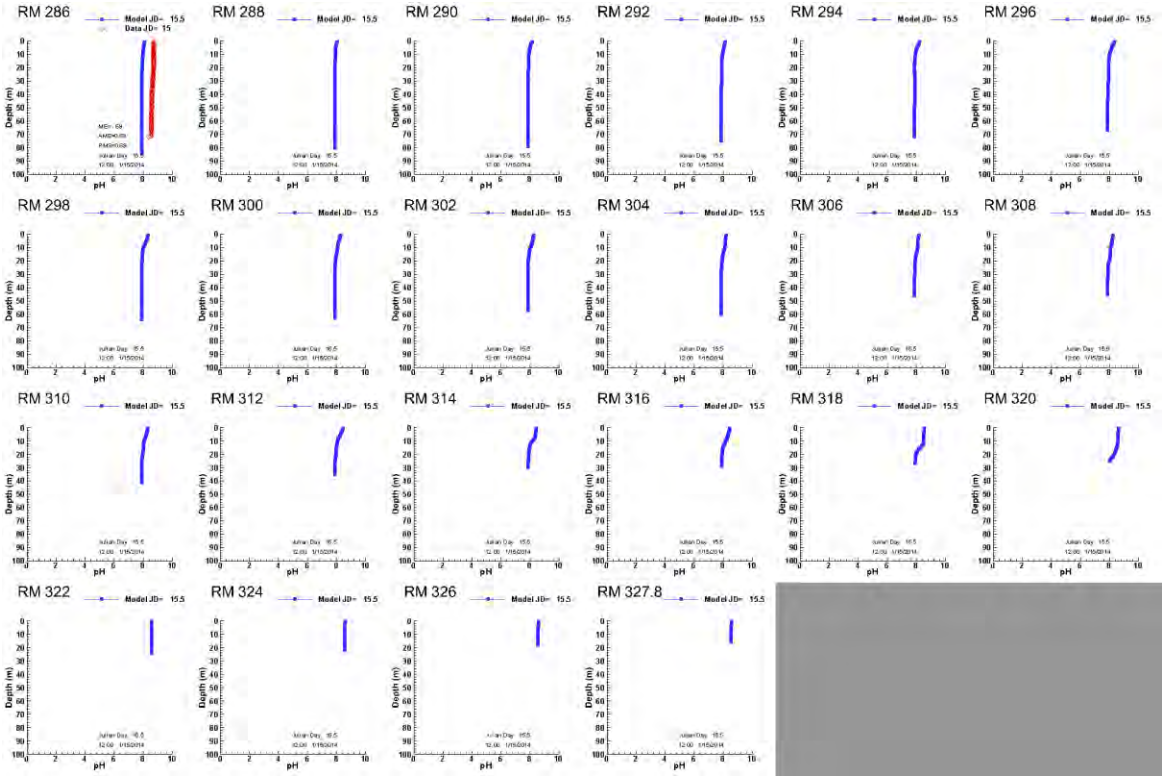


Figure 2199. Vertical profiles of pH compared with data for 1/15/2014.

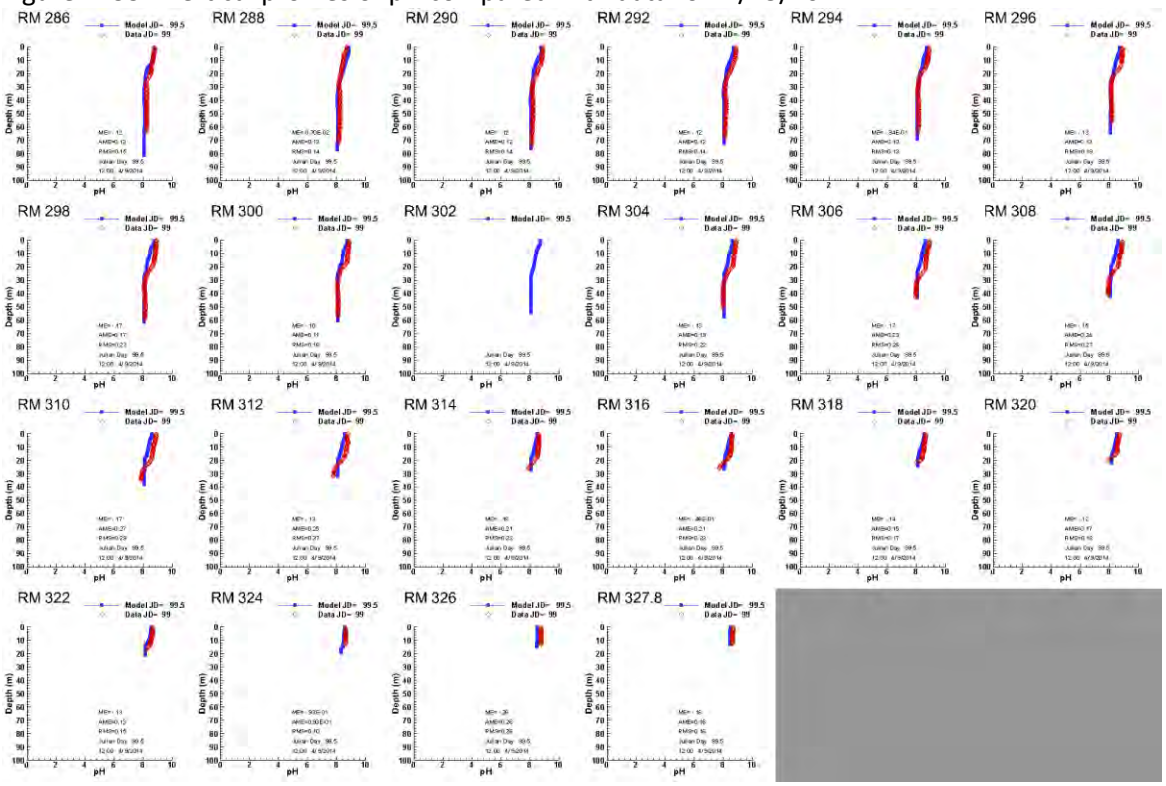


Figure 2200. Vertical profiles of pH compared with data for 4/ 9/2014.

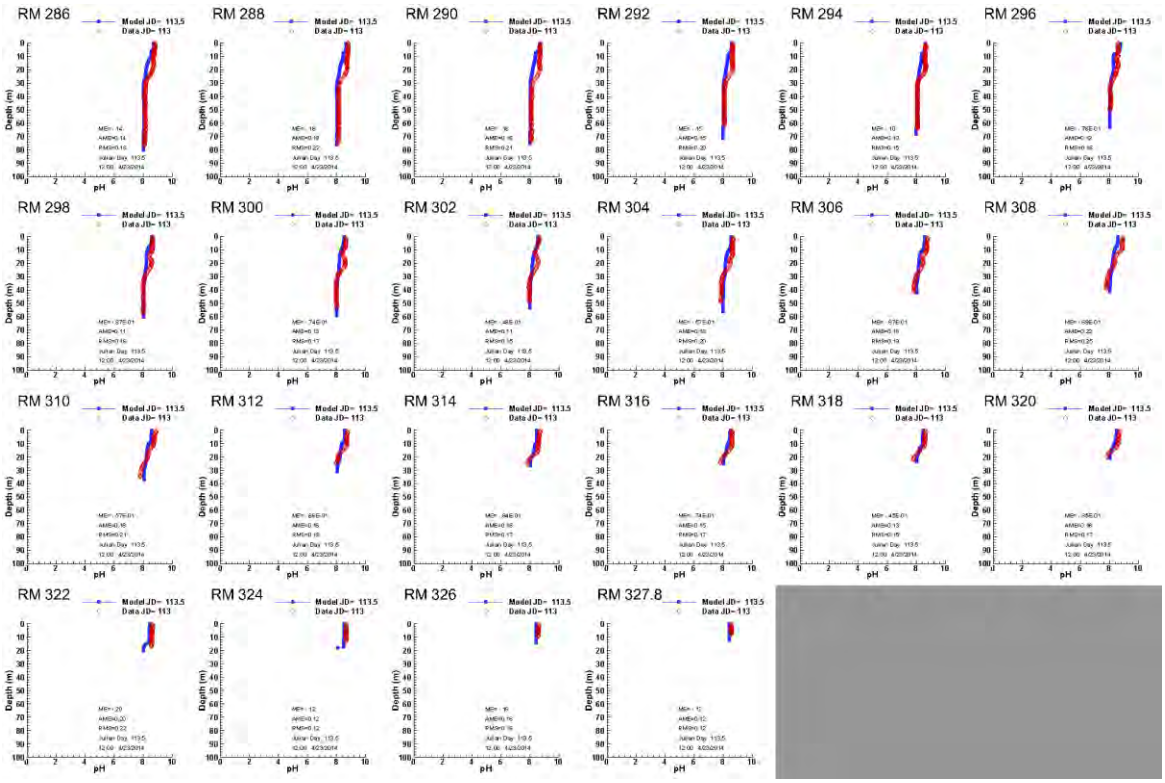


Figure 2201. Vertical profiles of pH compared with data for 4/23/2014.

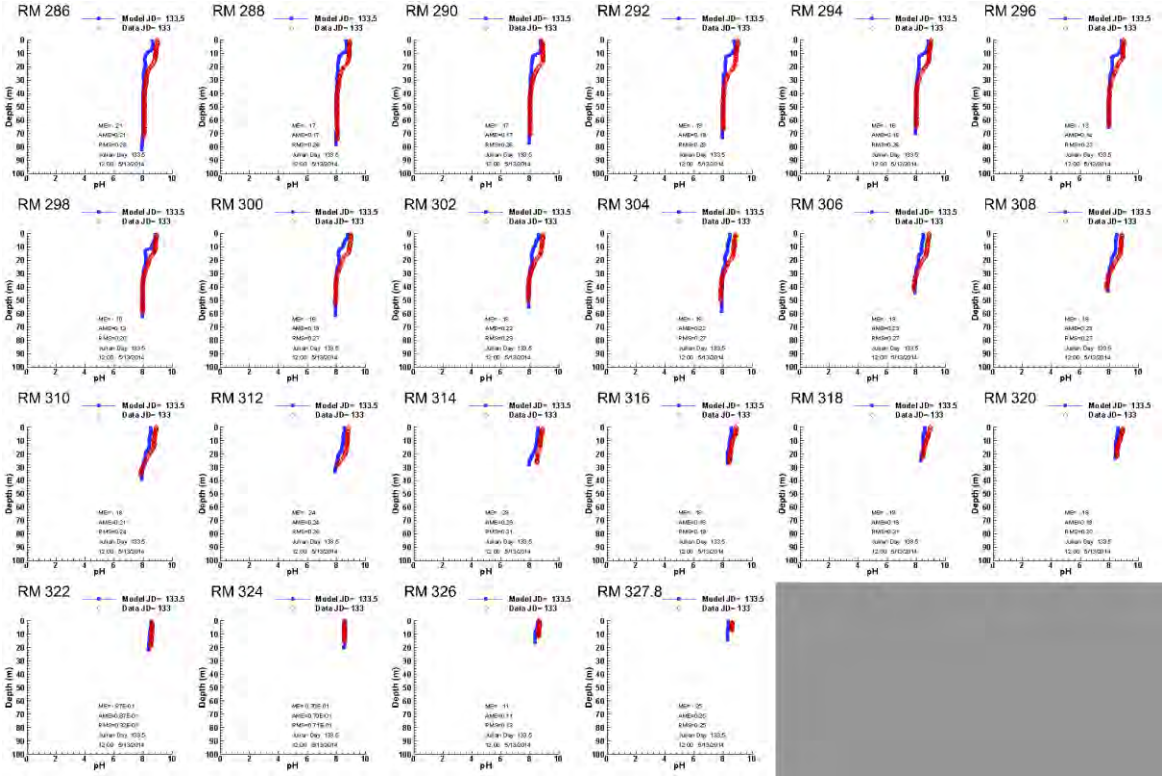


Figure 2202. Vertical profiles of pH compared with data for 5/13/2014.

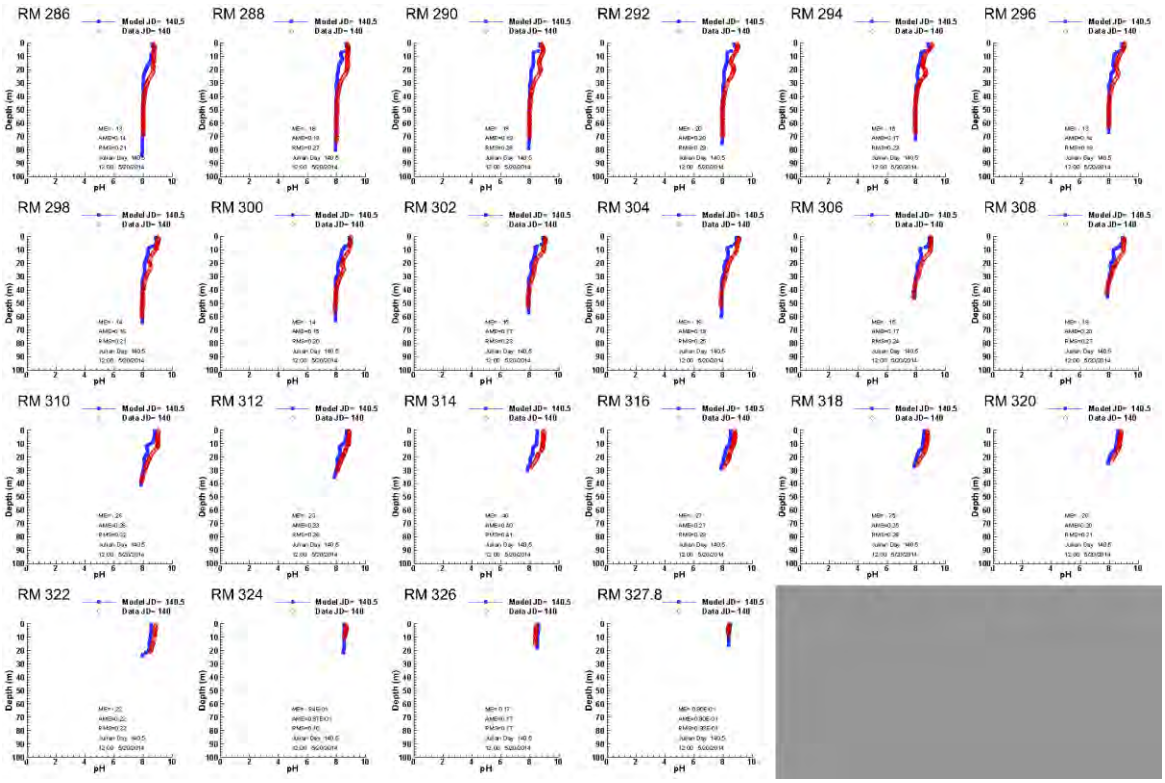


Figure 2203. Vertical profiles of pH compared with data for 5/20/2014.

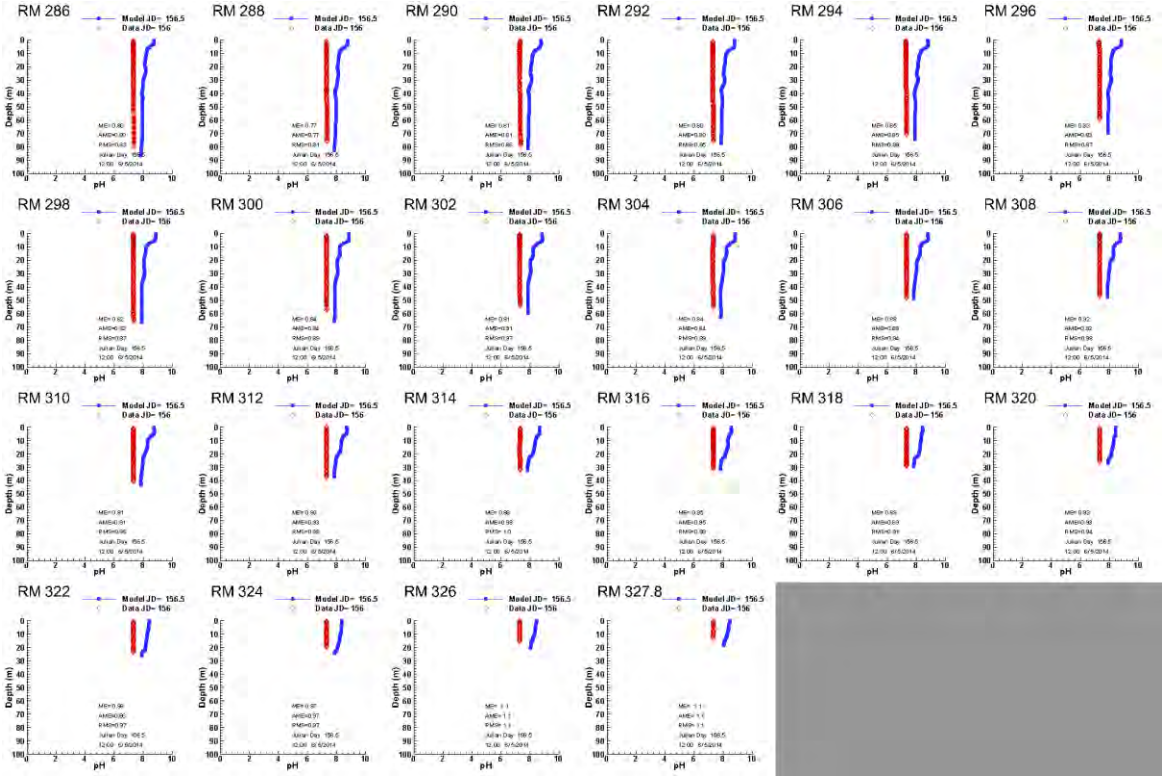


Figure 2204. Vertical profiles of pH compared with data for 6/ 5/2014.

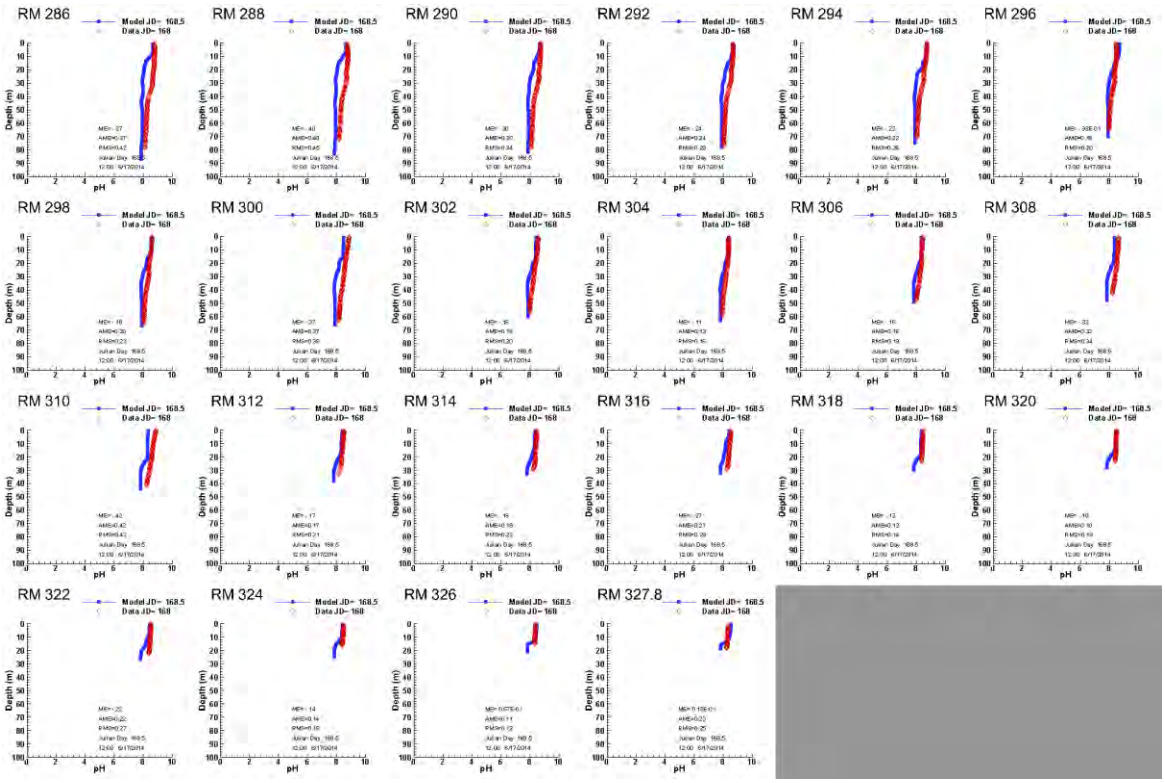


Figure 2205. Vertical profiles of pH compared with data for 6/17/2014.

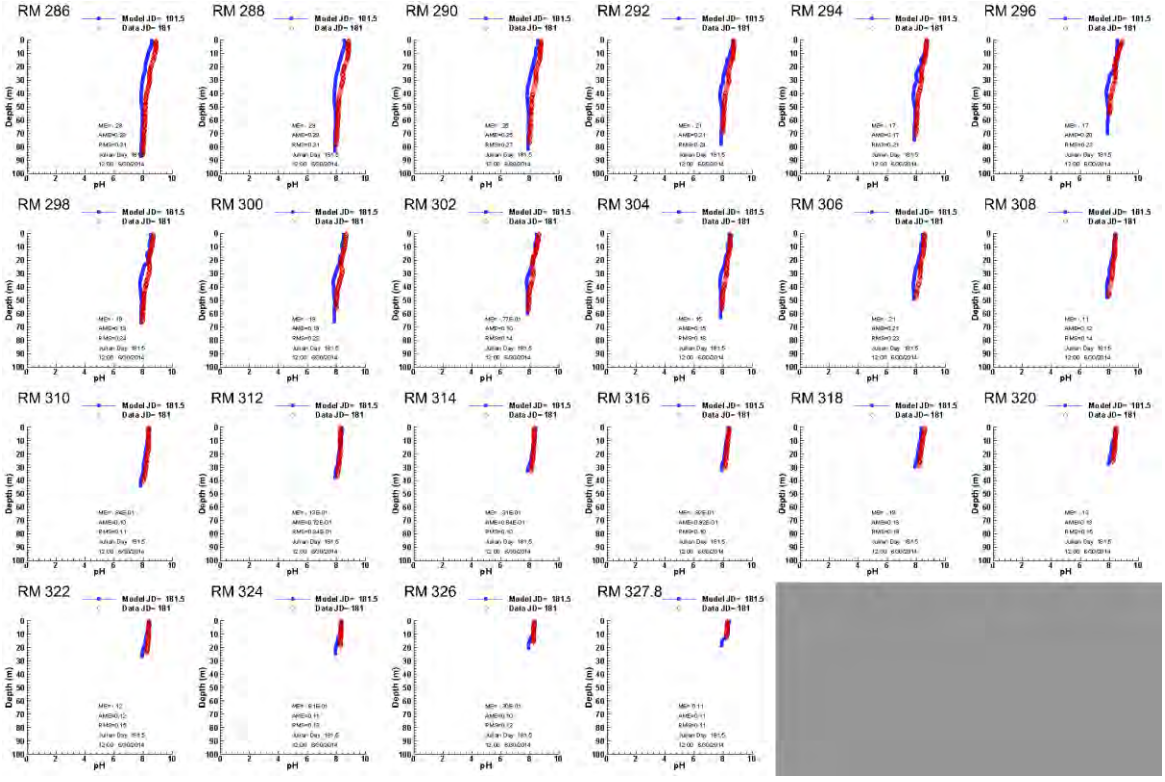


Figure 2206. Vertical profiles of pH compared with data for 6/30/2014.

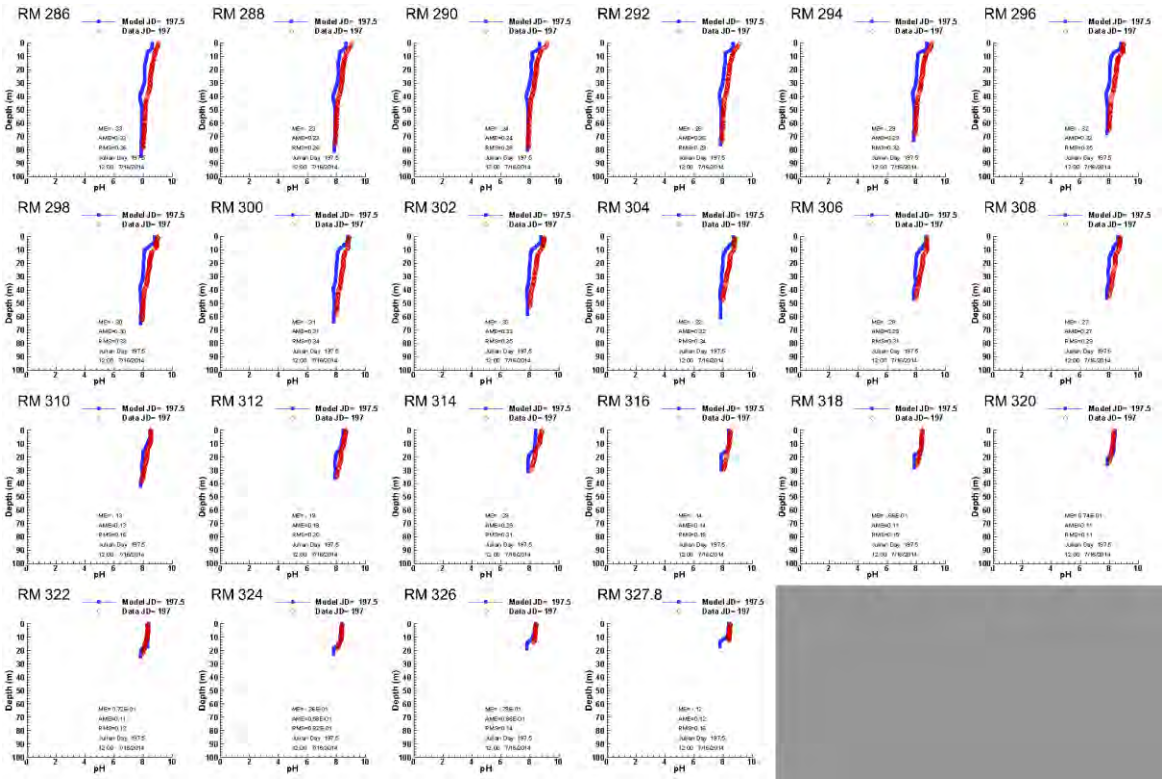


Figure 2207. Vertical profiles of pH compared with data for 7/16/2014.

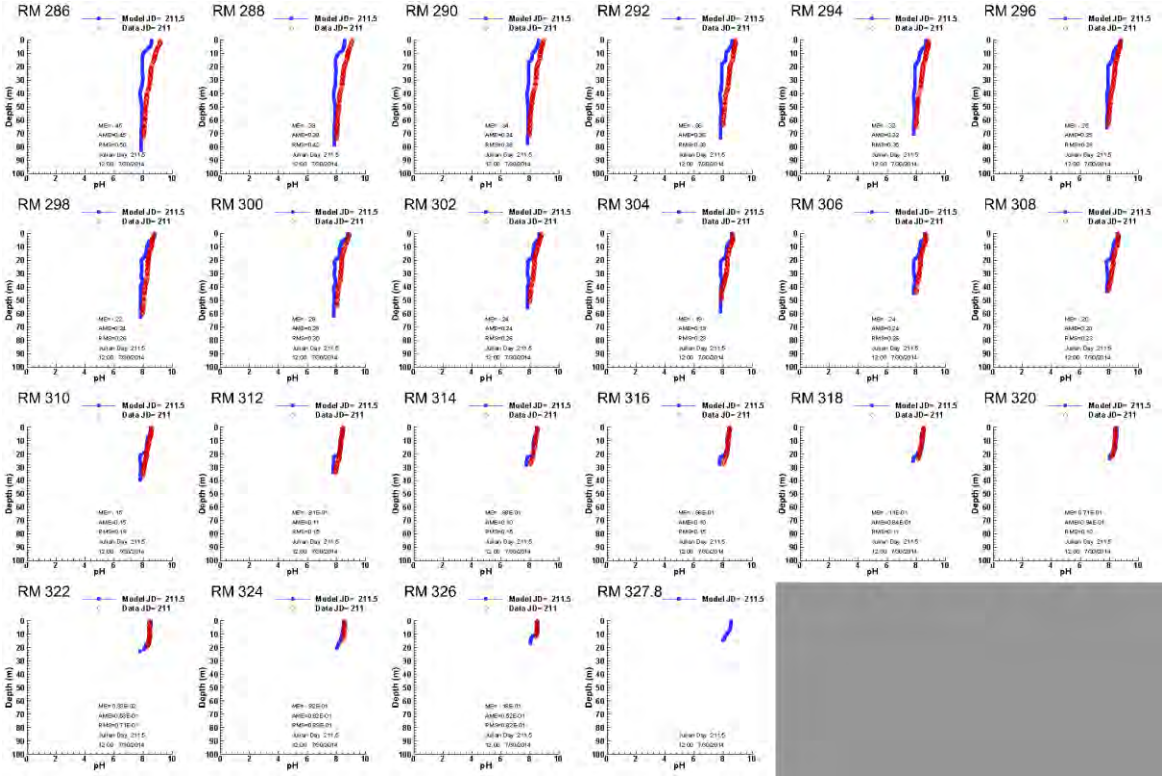


Figure 2208. Vertical profiles of pH compared with data for 7/30/2014.

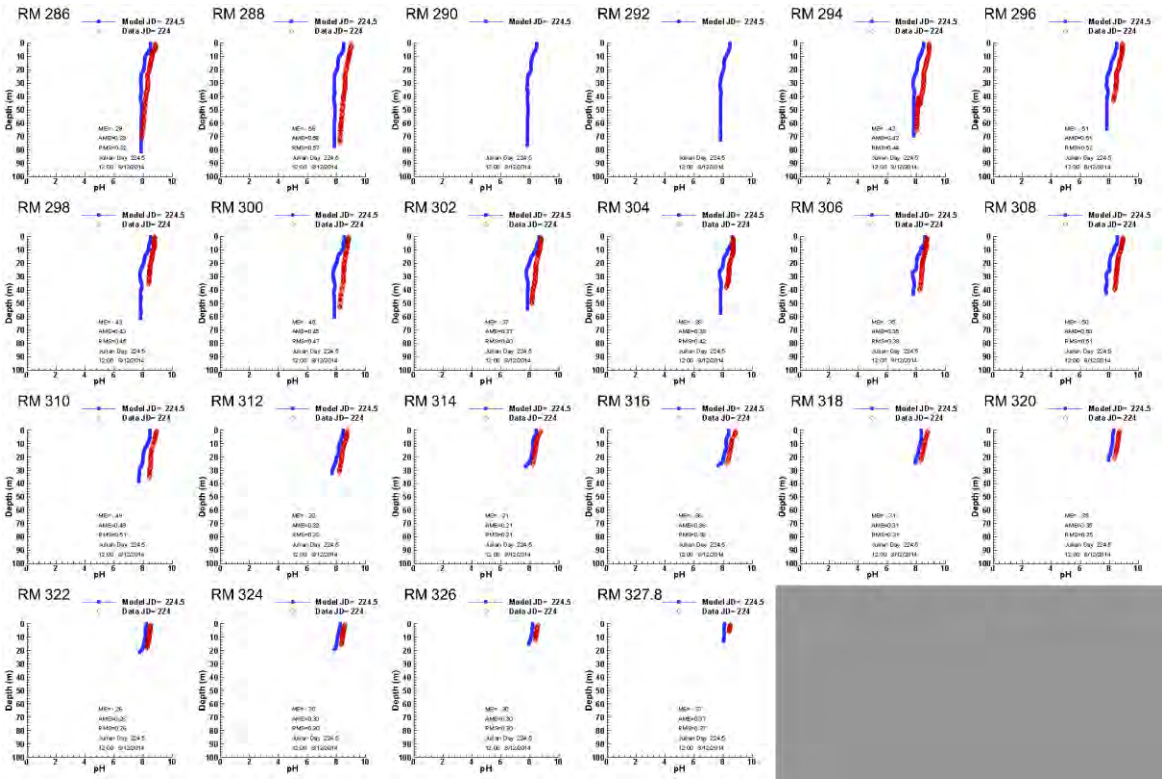


Figure 2209. Vertical profiles of pH compared with data for 8/12/2014.

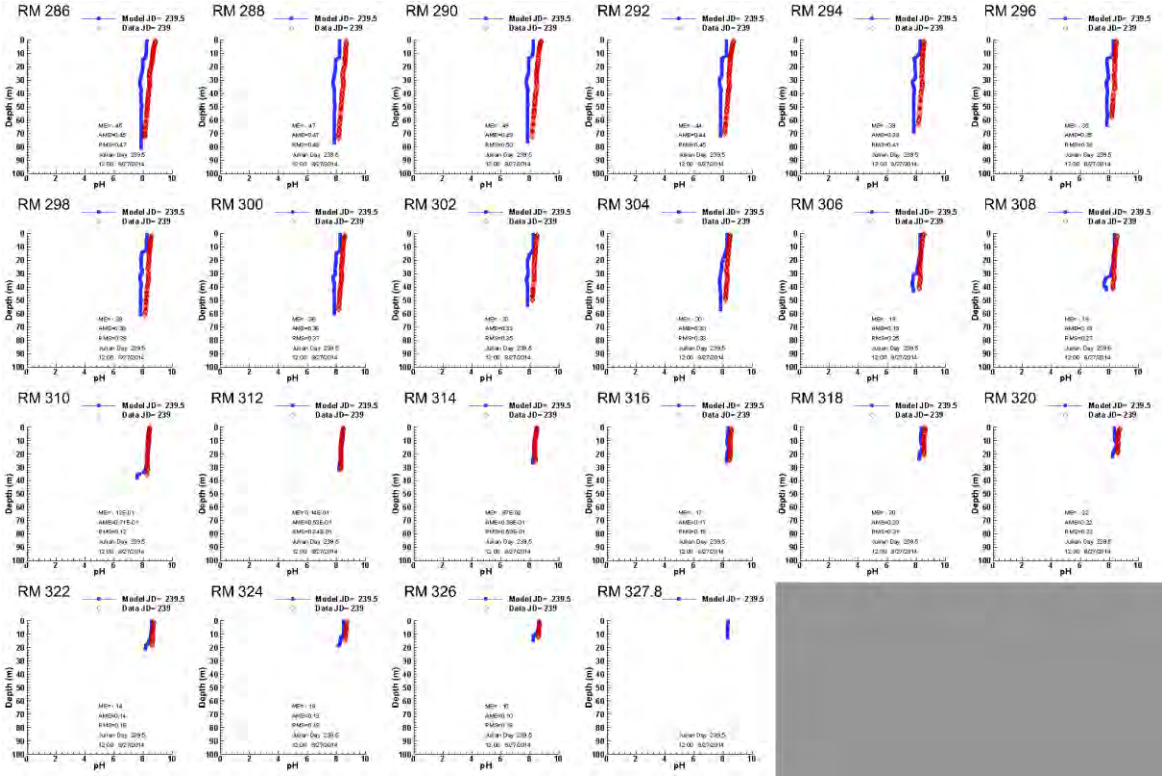


Figure 2210. Vertical profiles of pH compared with data for 8/27/2014.

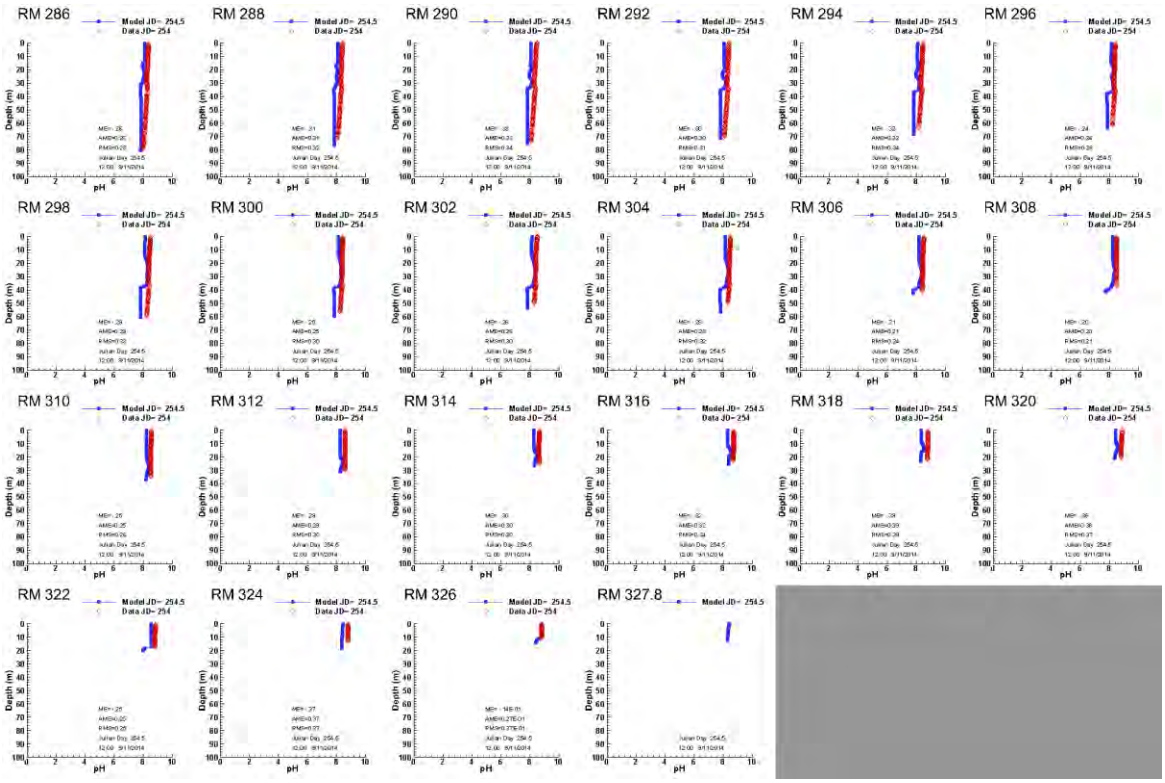


Figure 2211. Vertical profiles of pH compared with data for 9/11/2014.

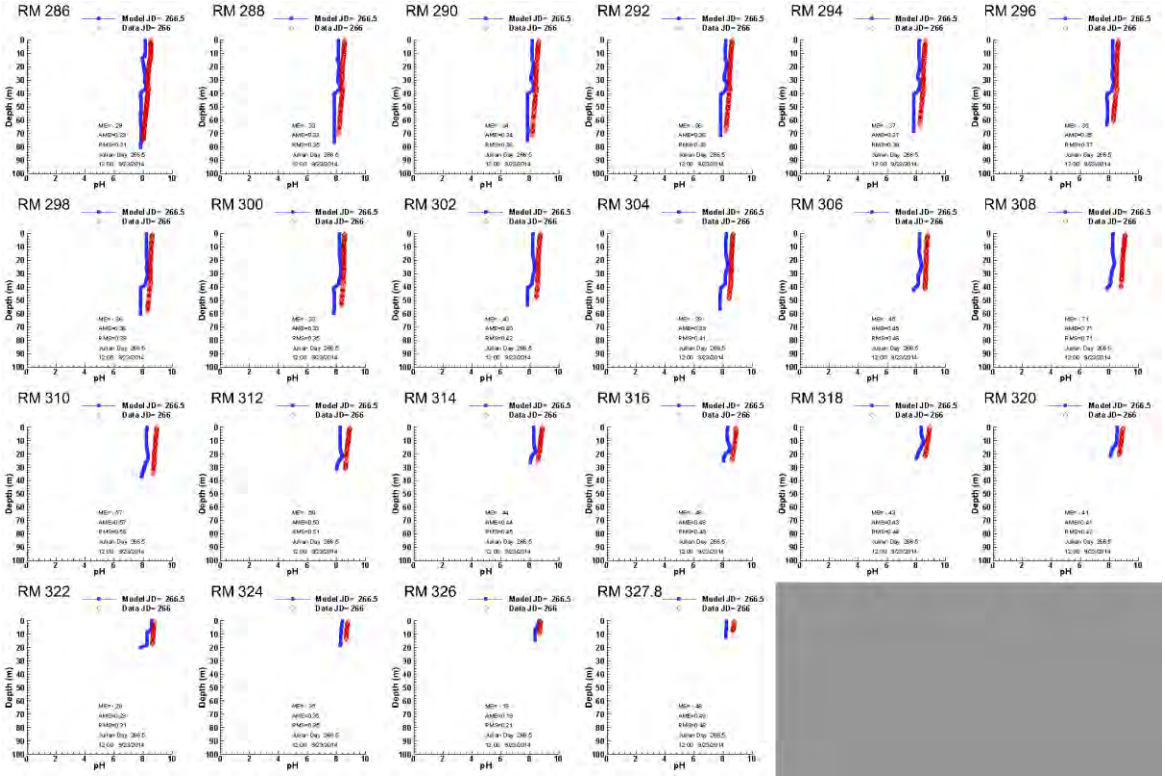


Figure 2212. Vertical profiles of pH compared with data for 9/23/2014.

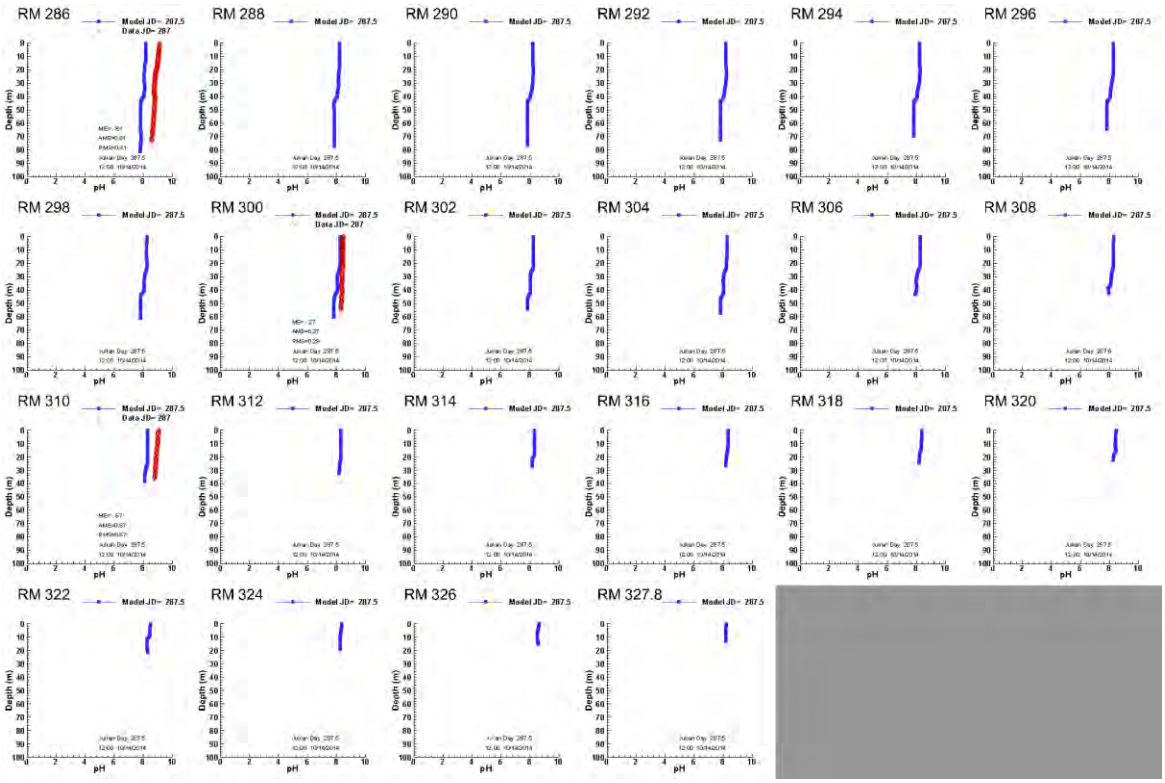


Figure 2213. Vertical profiles of pH compared with data for 10/14/2014.

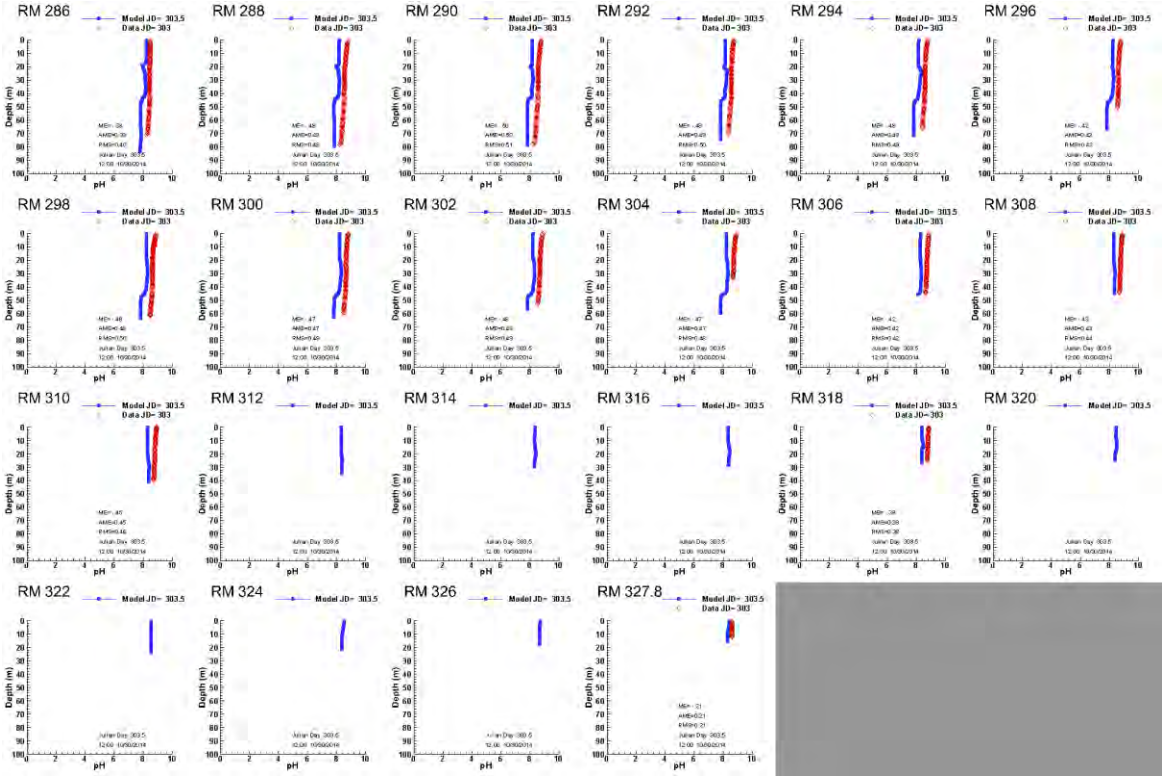


Figure 2214. Vertical profiles of pH compared with data for 10/30/2014.

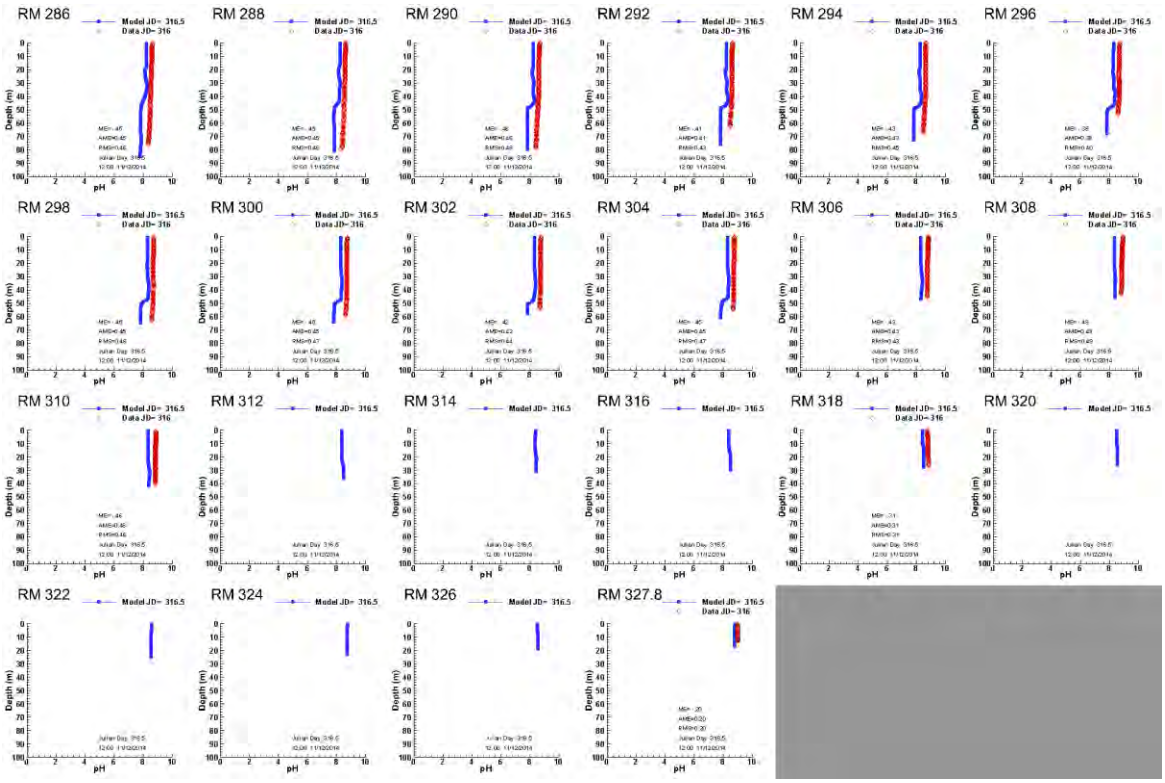


Figure 2215. Vertical profiles of pH compared with data for 11/12/2014.

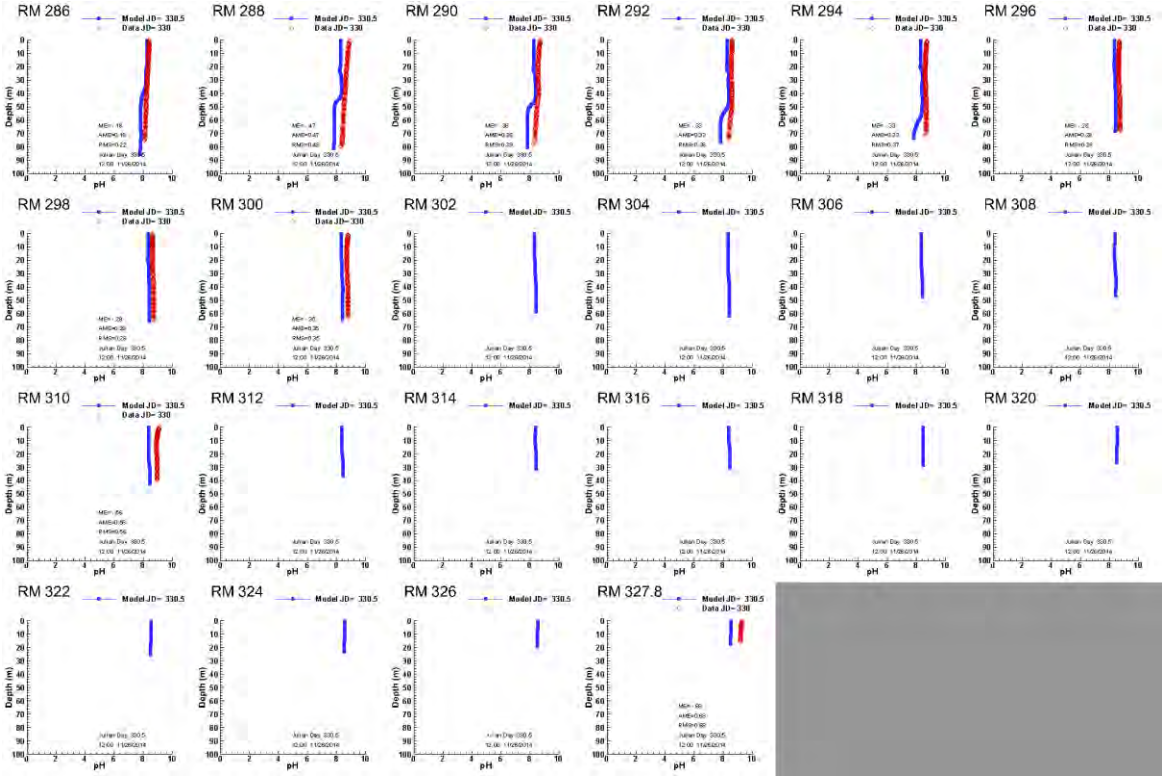


Figure 2216. Vertical profiles of pH compared with data for 11/26/2014.

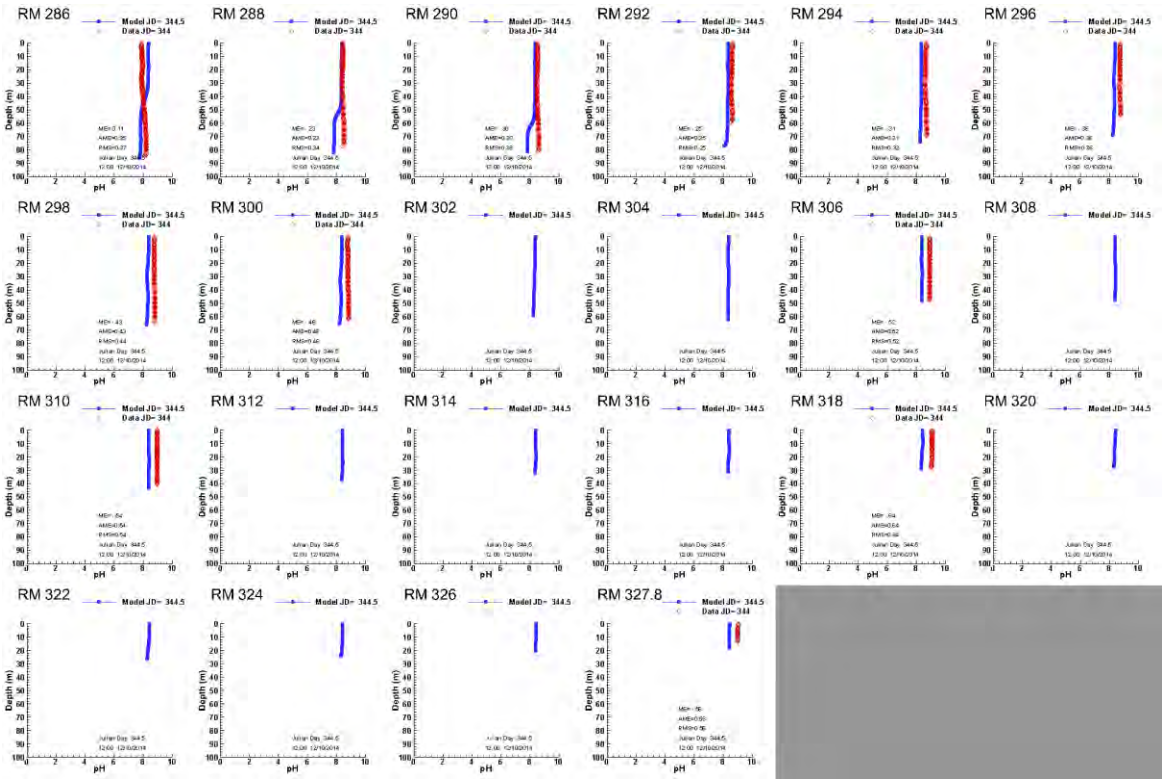


Figure 2217. Vertical profiles of pH compared with data for 12/10/2014.

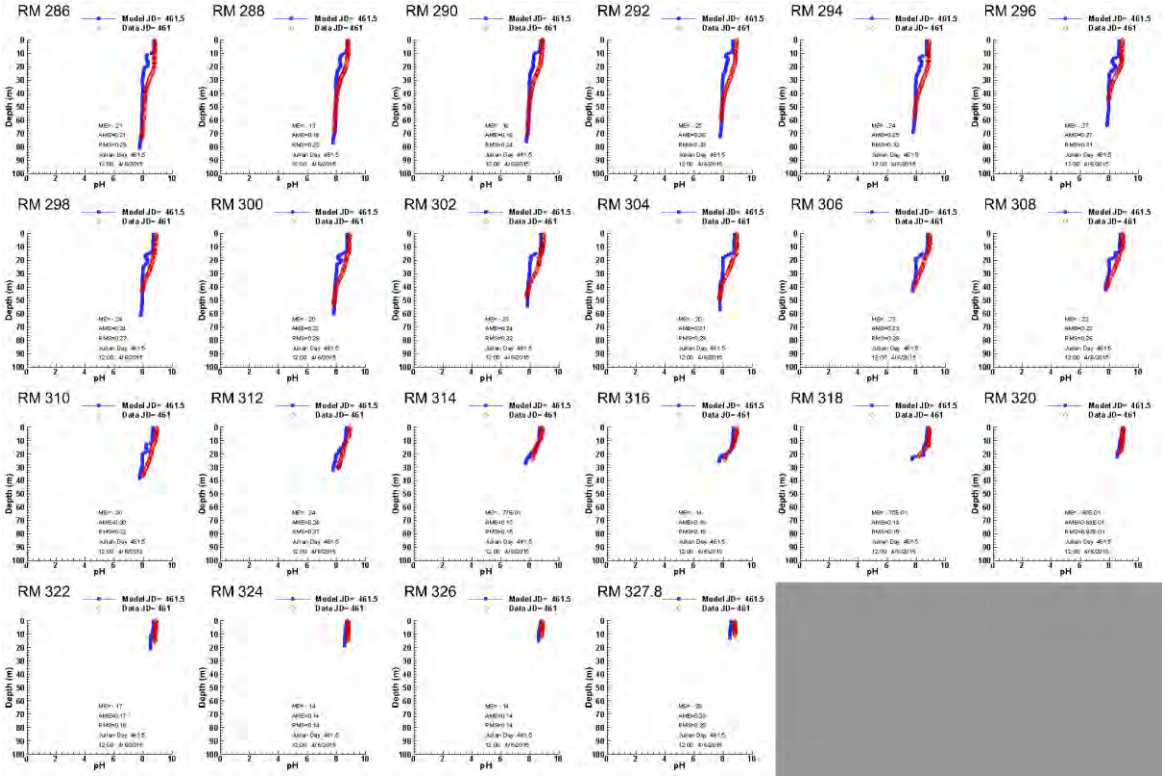


Figure 2218. Vertical profiles of pH compared with data for 4/ 6/2015.

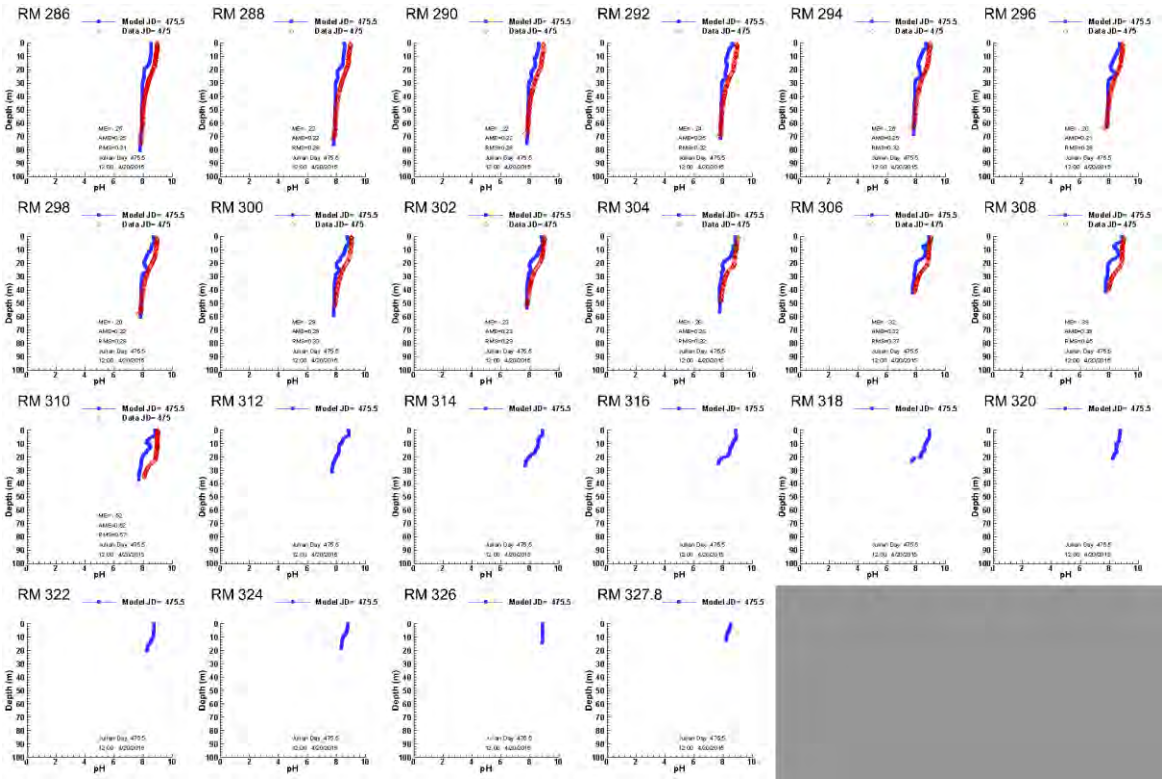


Figure 2219. Vertical profiles of pH compared with data for 4/20/2015.

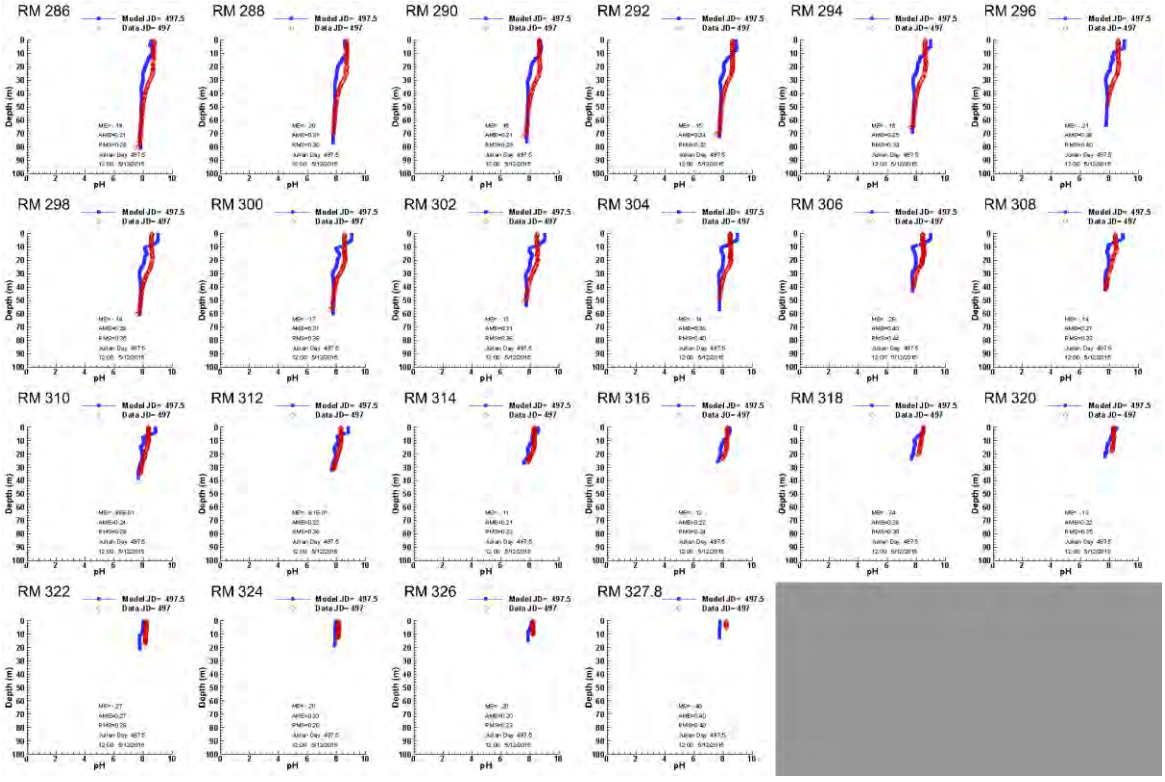


Figure 2220. Vertical profiles of pH compared with data for 5/12/2015.

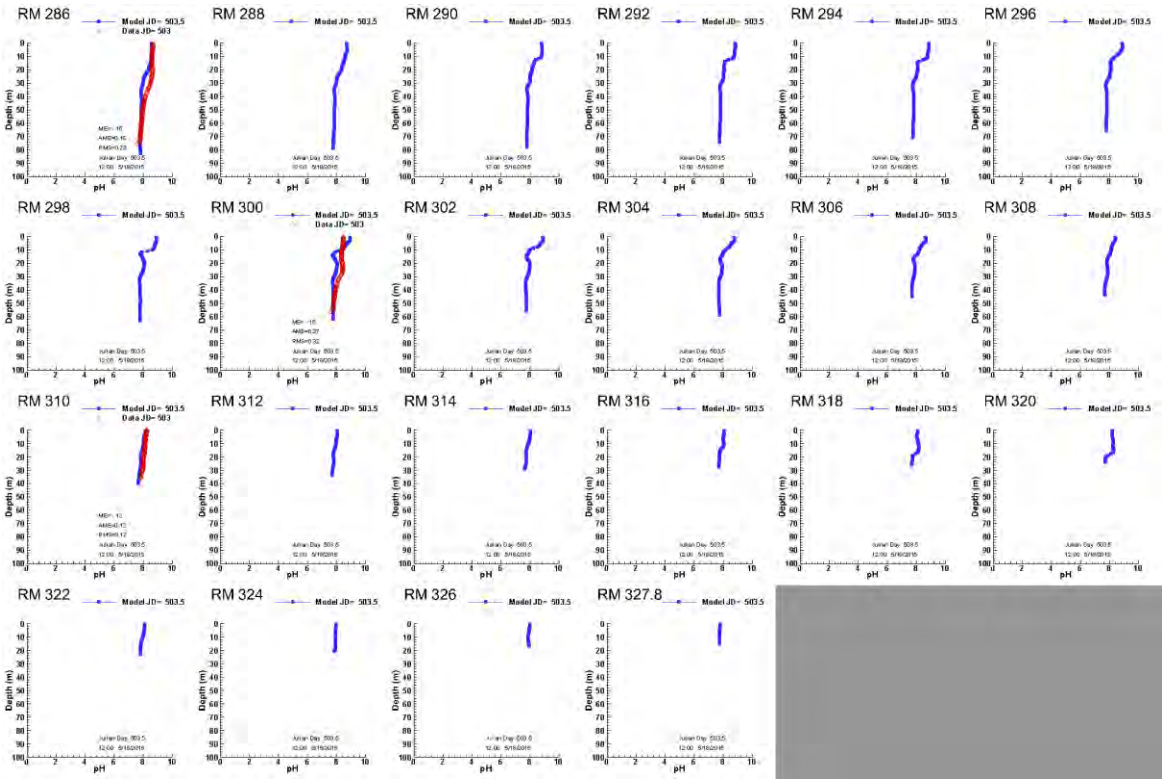


Figure 2221. Vertical profiles of pH compared with data for 5/18/2015.

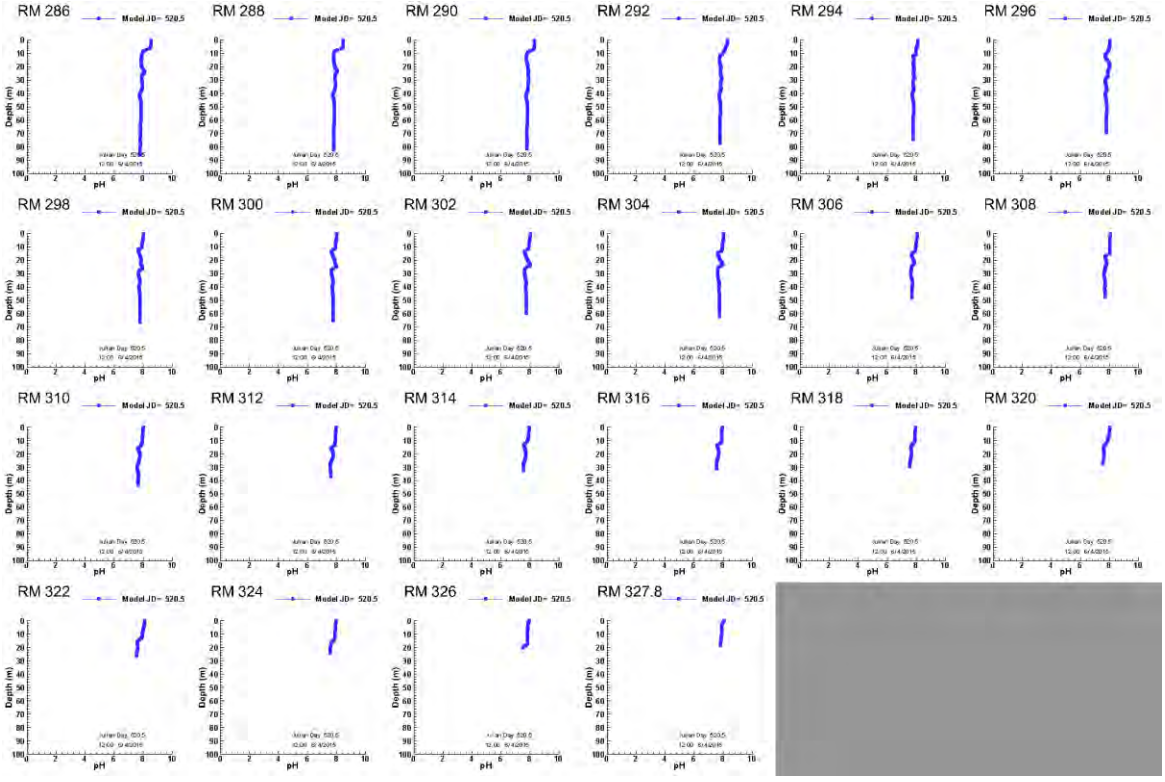


Figure 2222. Vertical profiles of pH compared with data for 6/ 4/2015.

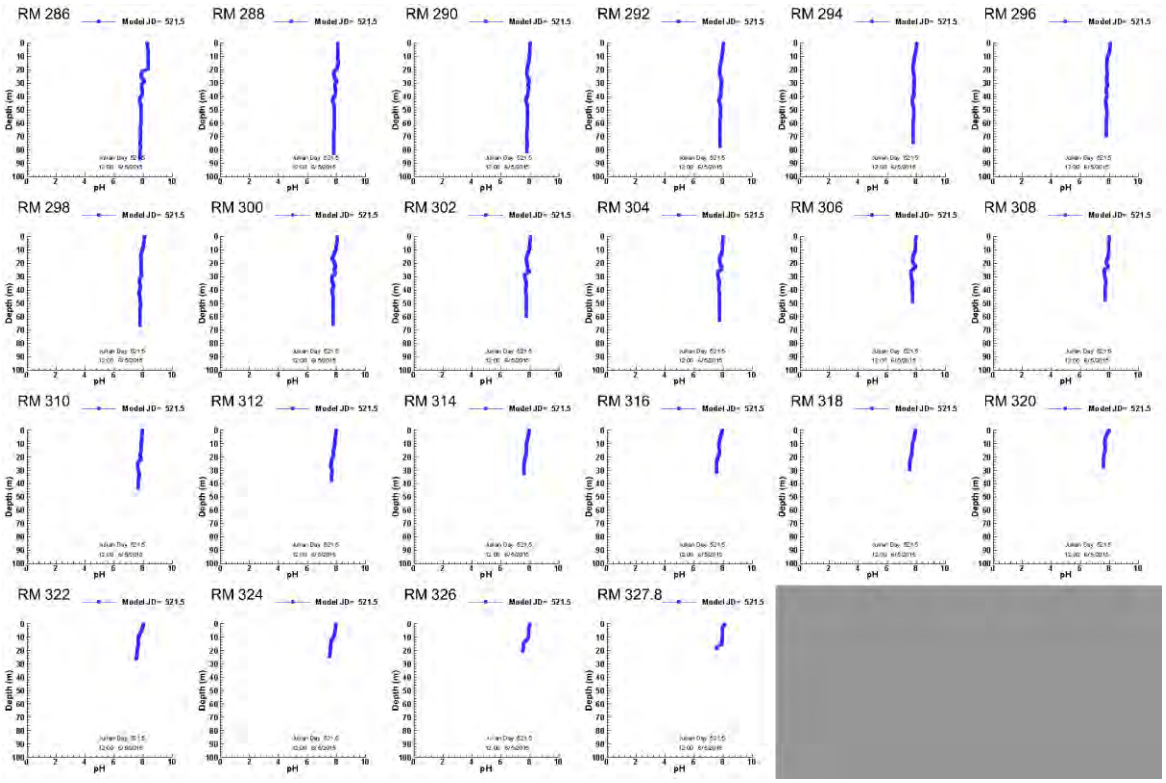


Figure 2223. Vertical profiles of pH compared with data for 6/ 5/2015.

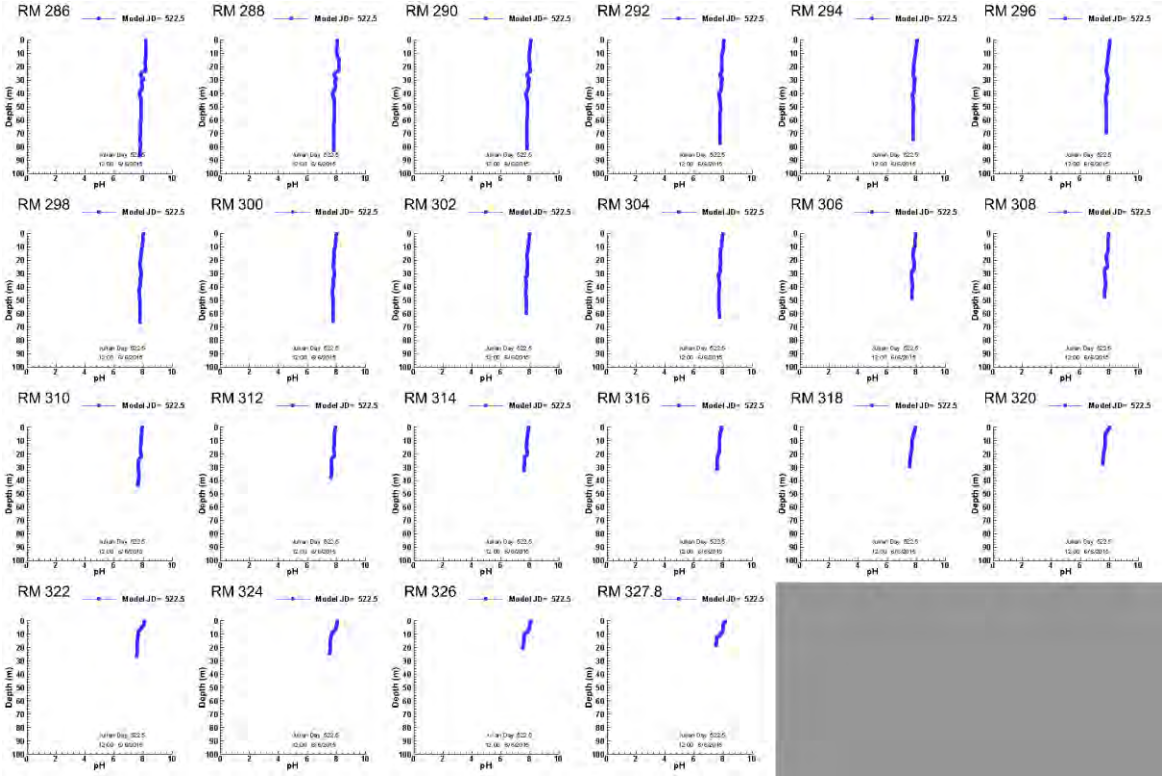


Figure 2224. Vertical profiles of pH compared with data for 6/ 6/2015.

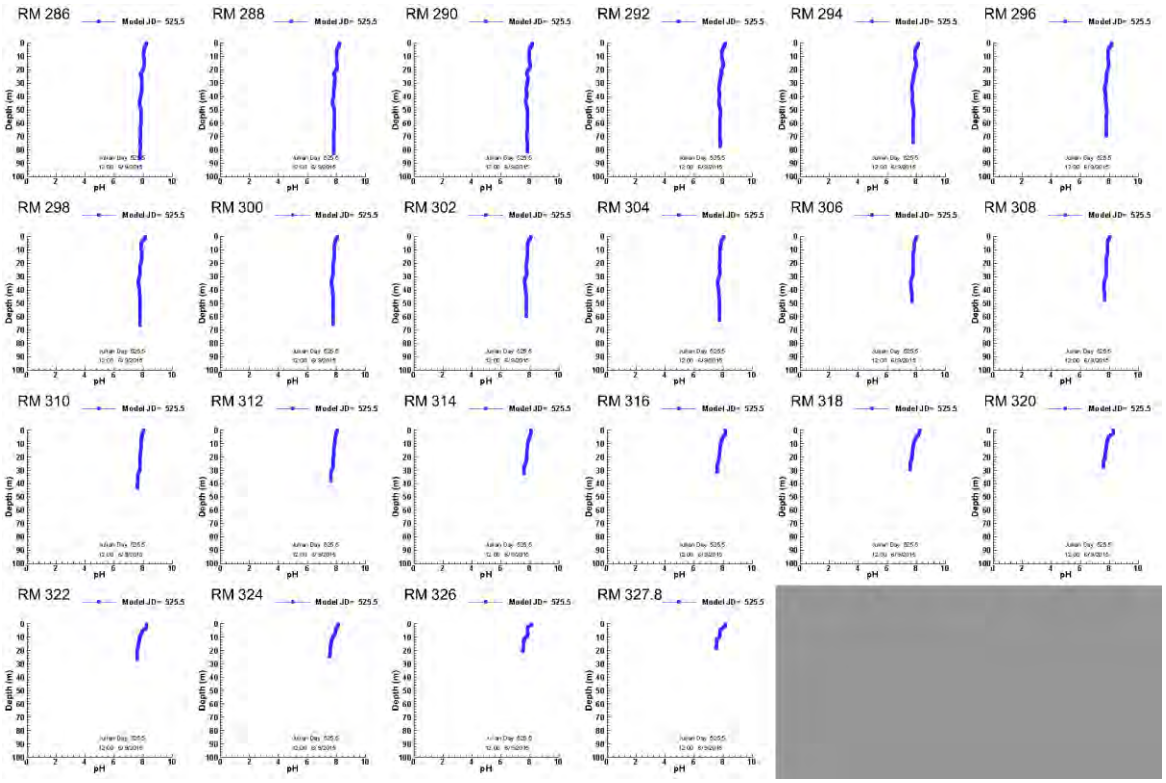


Figure 2225. Vertical profiles of pH compared with data for 6/ 9/2015.

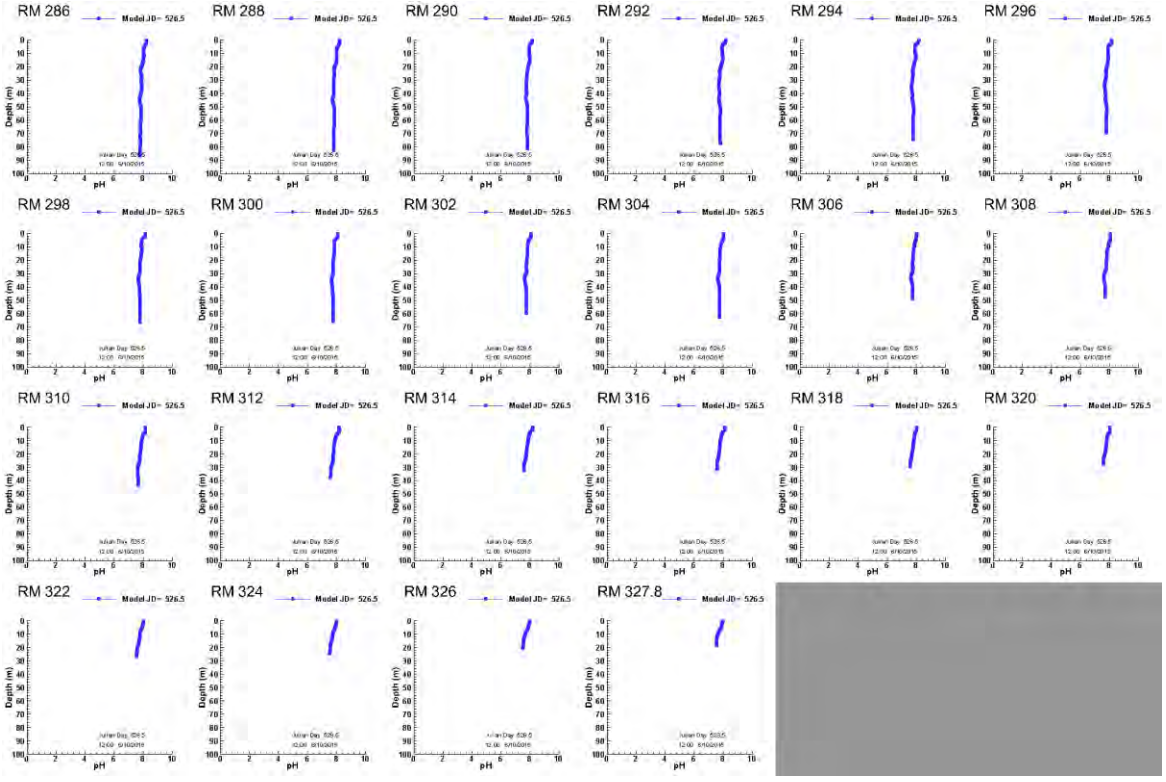


Figure 2226. Vertical profiles of pH compared with data for 6/10/2015.

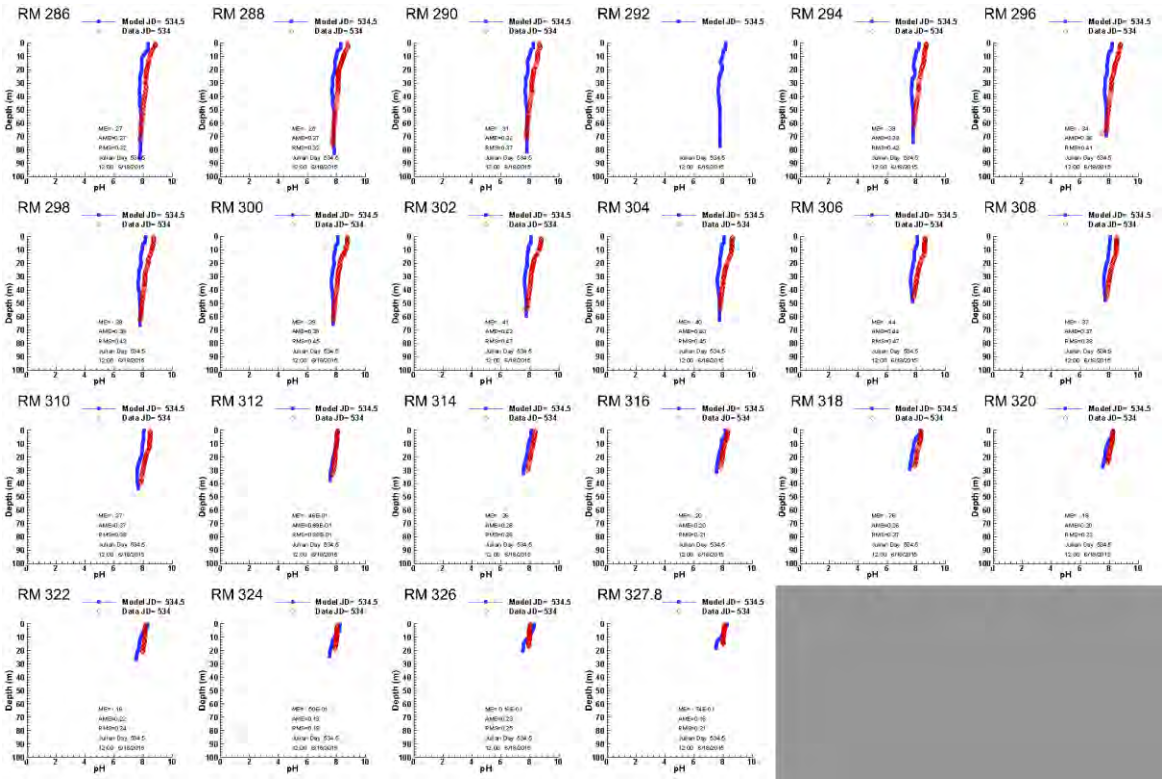


Figure 2227. Vertical profiles of pH compared with data for 6/18/2015.

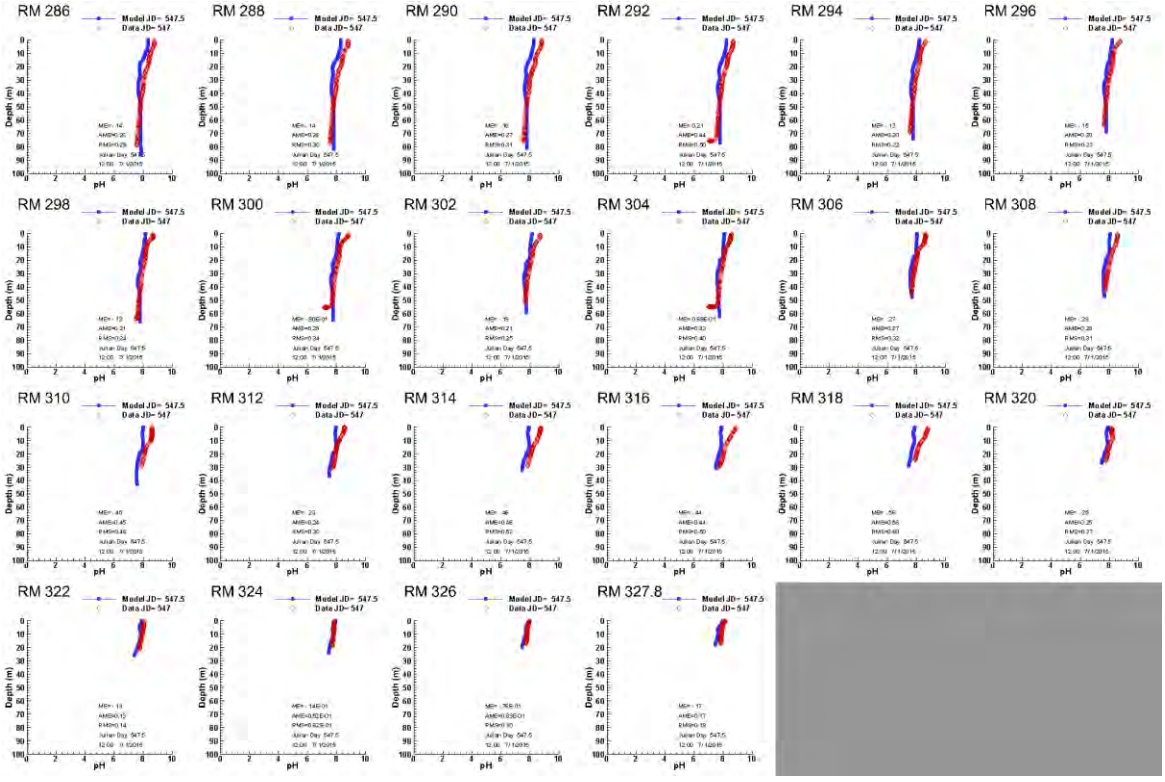


Figure 2228. Vertical profiles of pH compared with data for 7/ 1/2015.

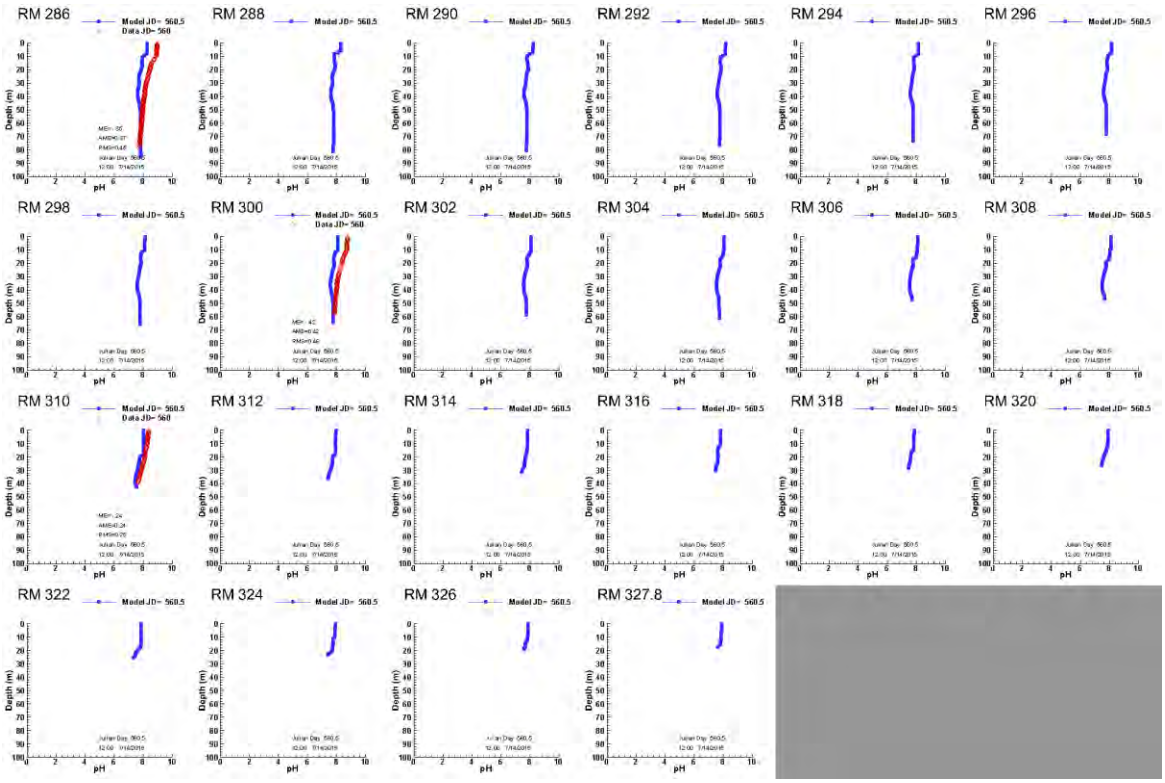


Figure 2229. Vertical profiles of pH compared with data for 7/14/2015.

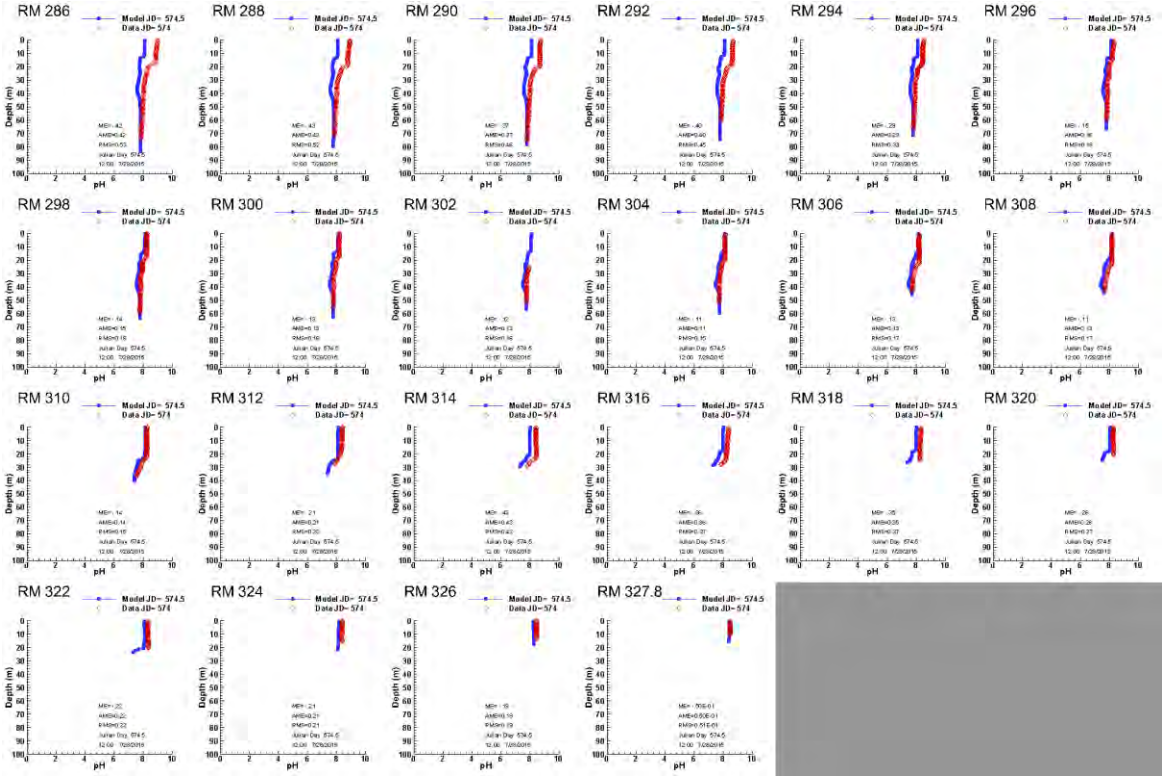


Figure 2230. Vertical profiles of pH compared with data for 7/28/2015.

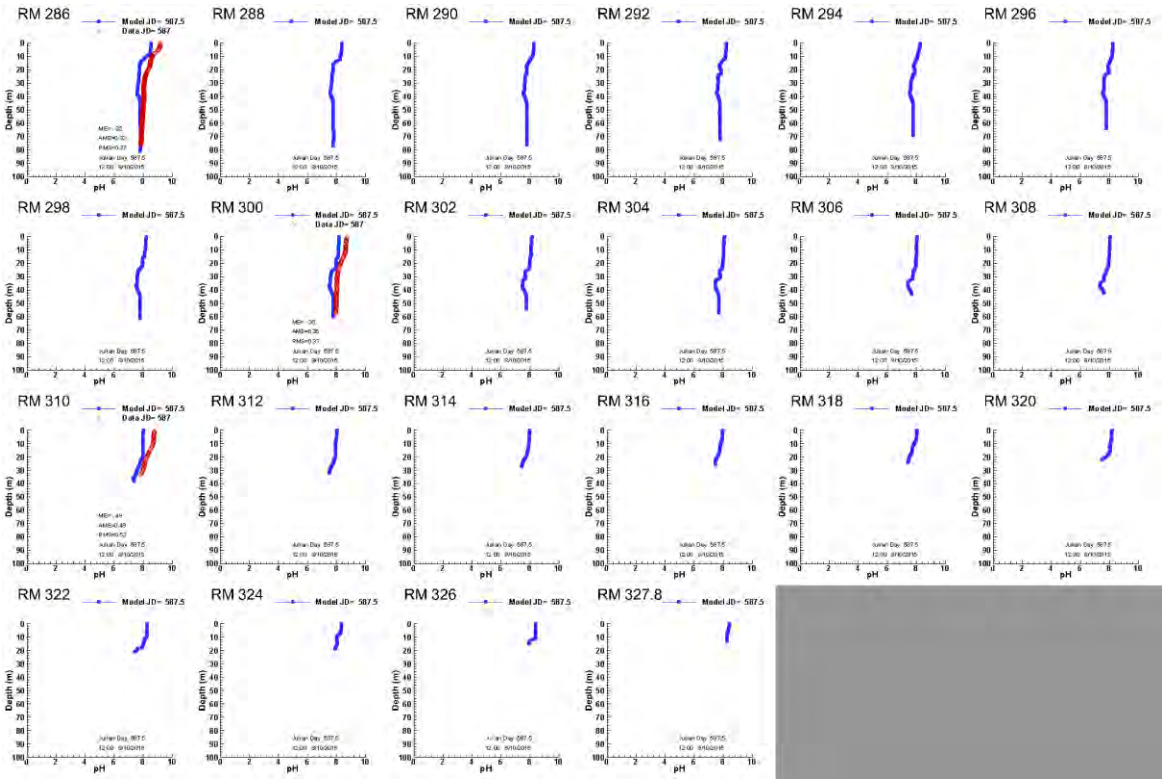


Figure 2231. Vertical profiles of pH compared with data for 8/10/2015.

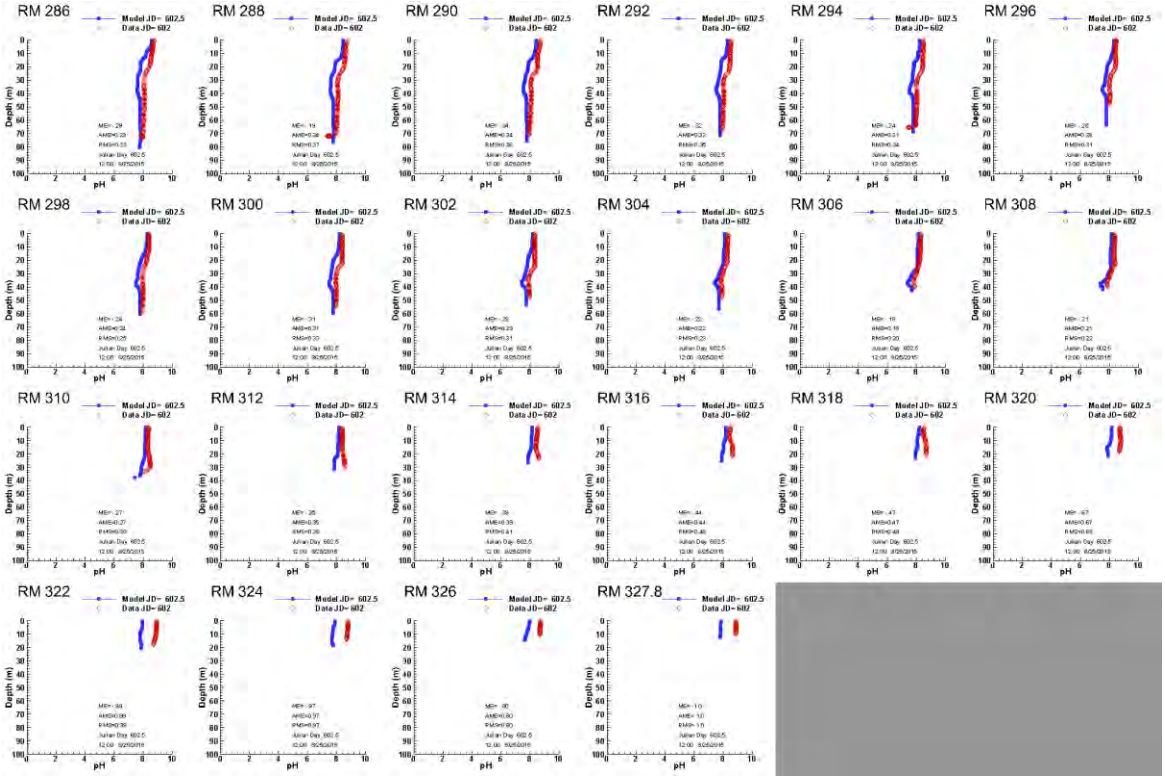


Figure 2232. Vertical profiles of pH compared with data for 8/25/2015.

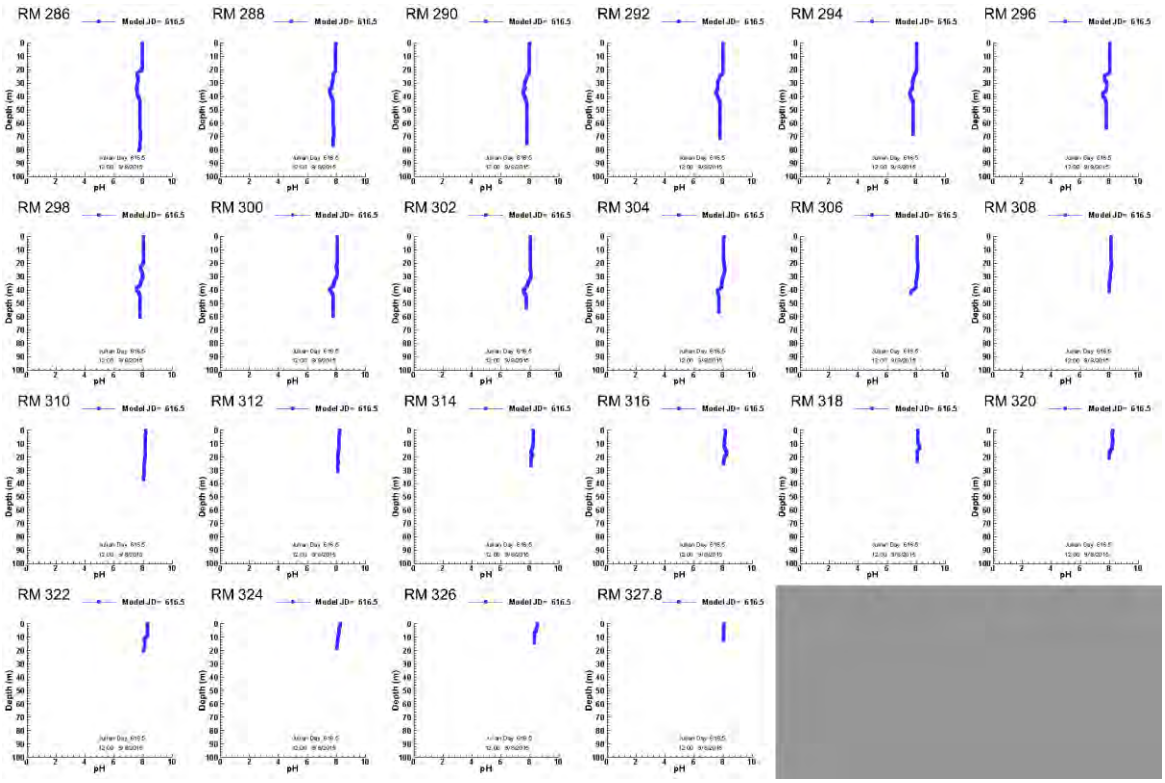


Figure 2233. Vertical profiles of pH compared with data for 9/ 8/2015.

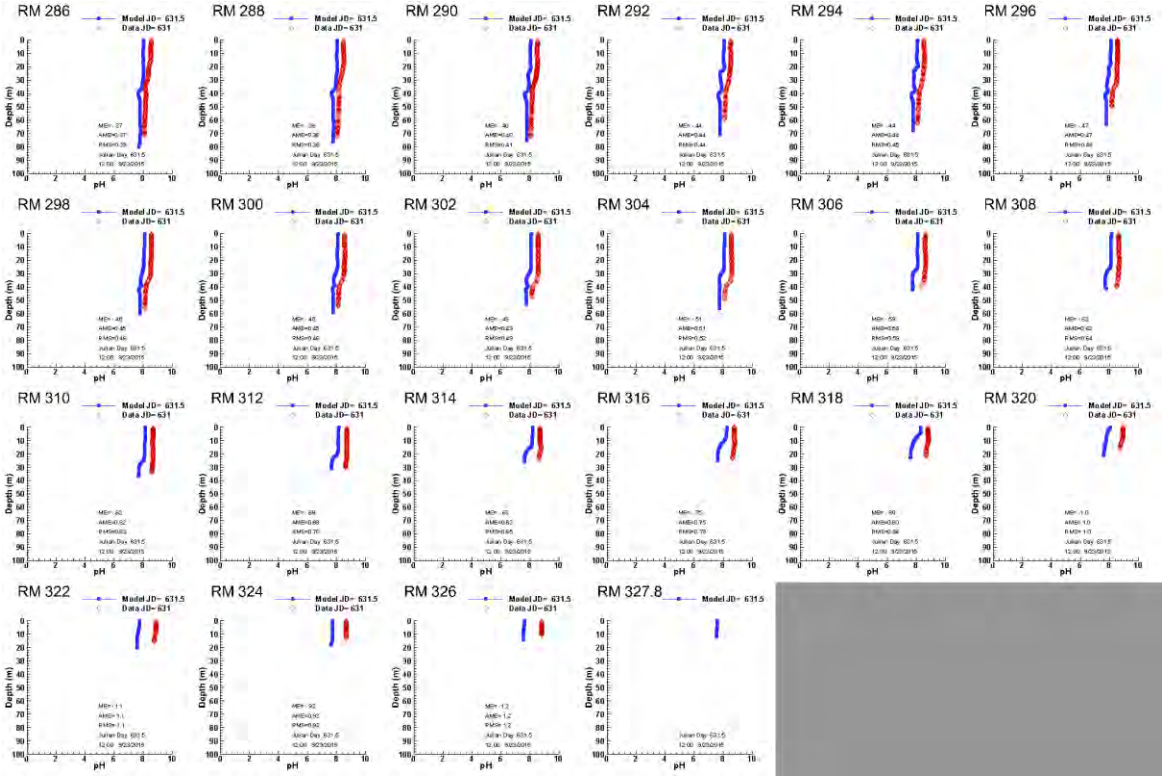


Figure 2234. Vertical profiles of pH compared with data for 9/23/2015.

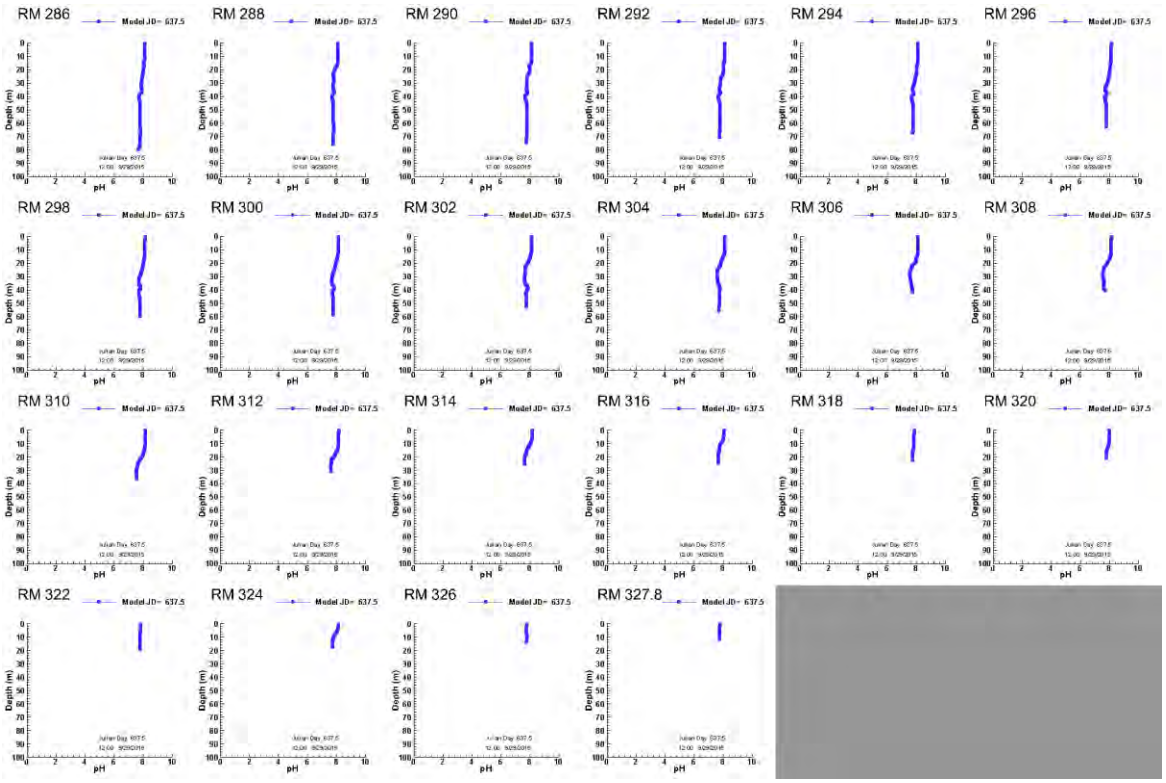


Figure 2235. Vertical profiles of pH compared with data for 9/29/2015.

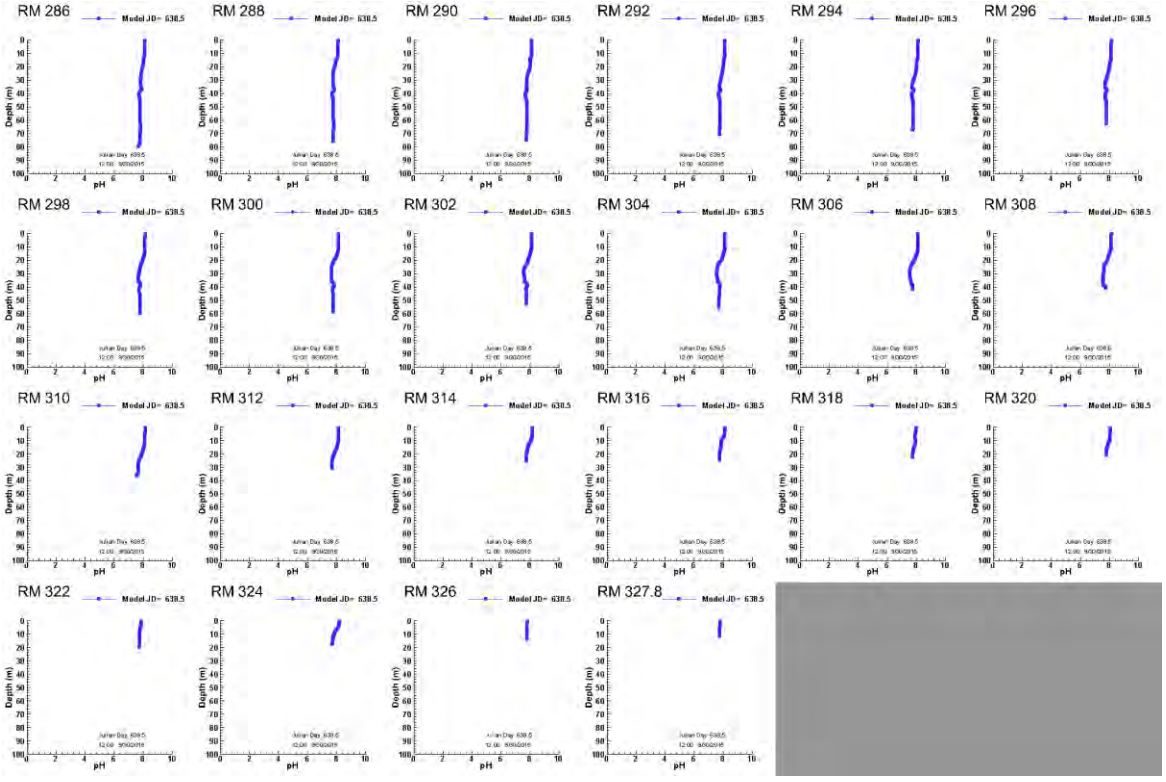


Figure 2236. Vertical profiles of pH compared with data for 9/30/2015.

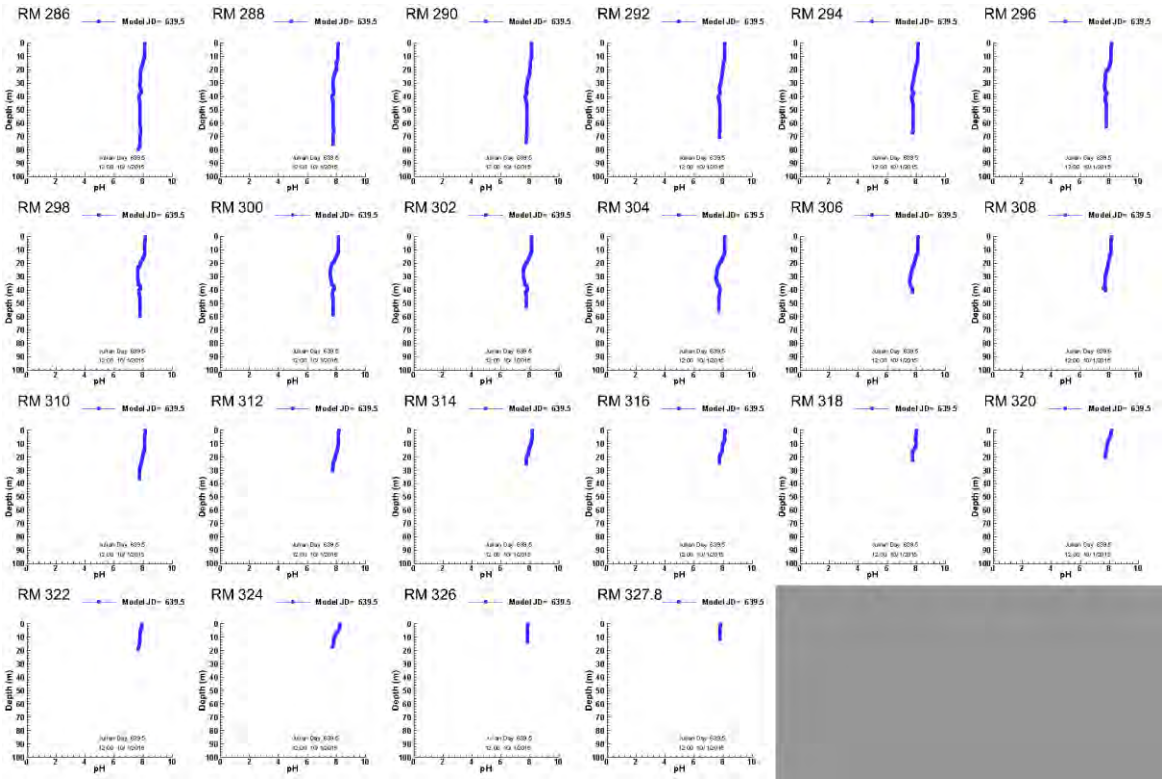


Figure 2237. Vertical profiles of pH compared with data for 10/ 1/2015.

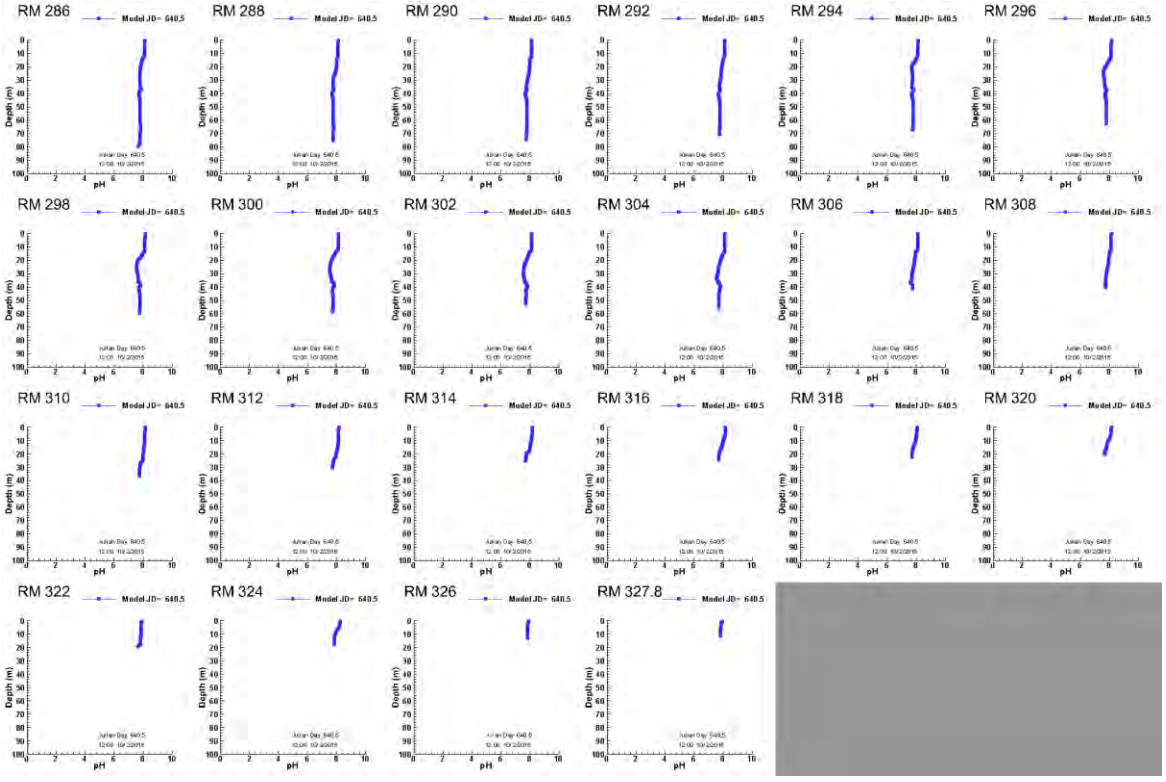


Figure 2238. Vertical profiles of pH compared with data for 10/ 2/2015.

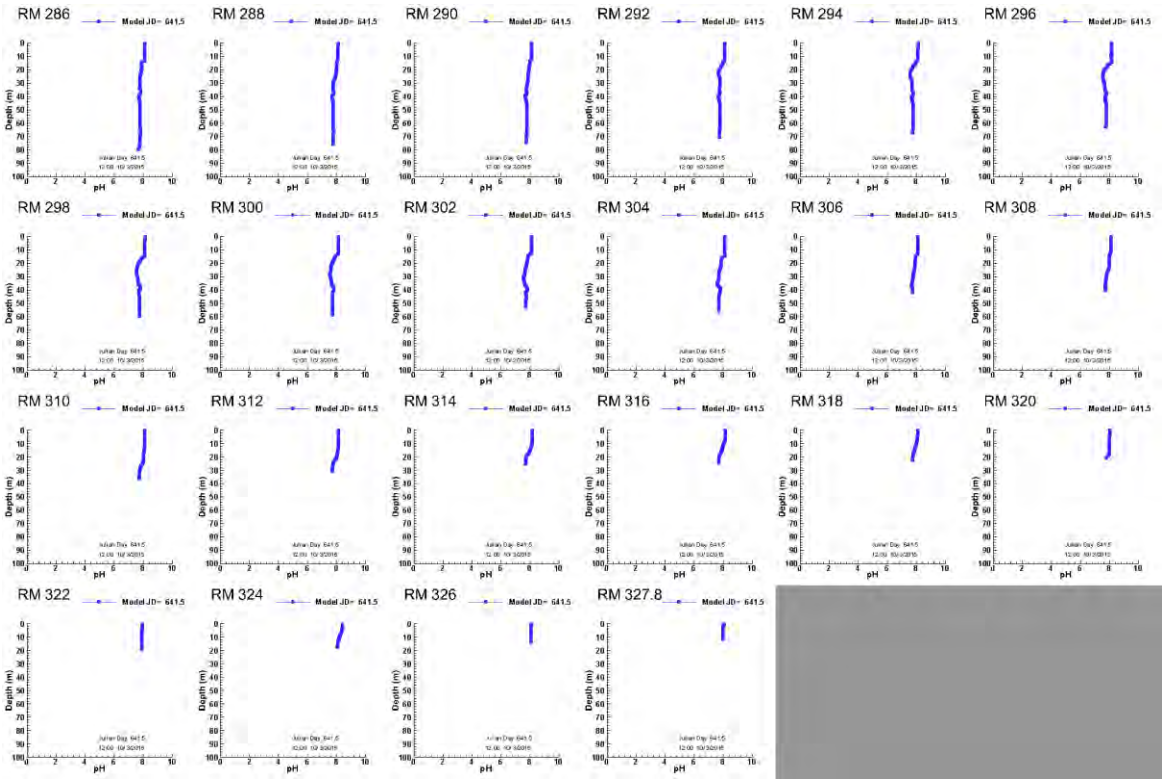


Figure 2239. Vertical profiles of pH compared with data for 10/ 3/2015.

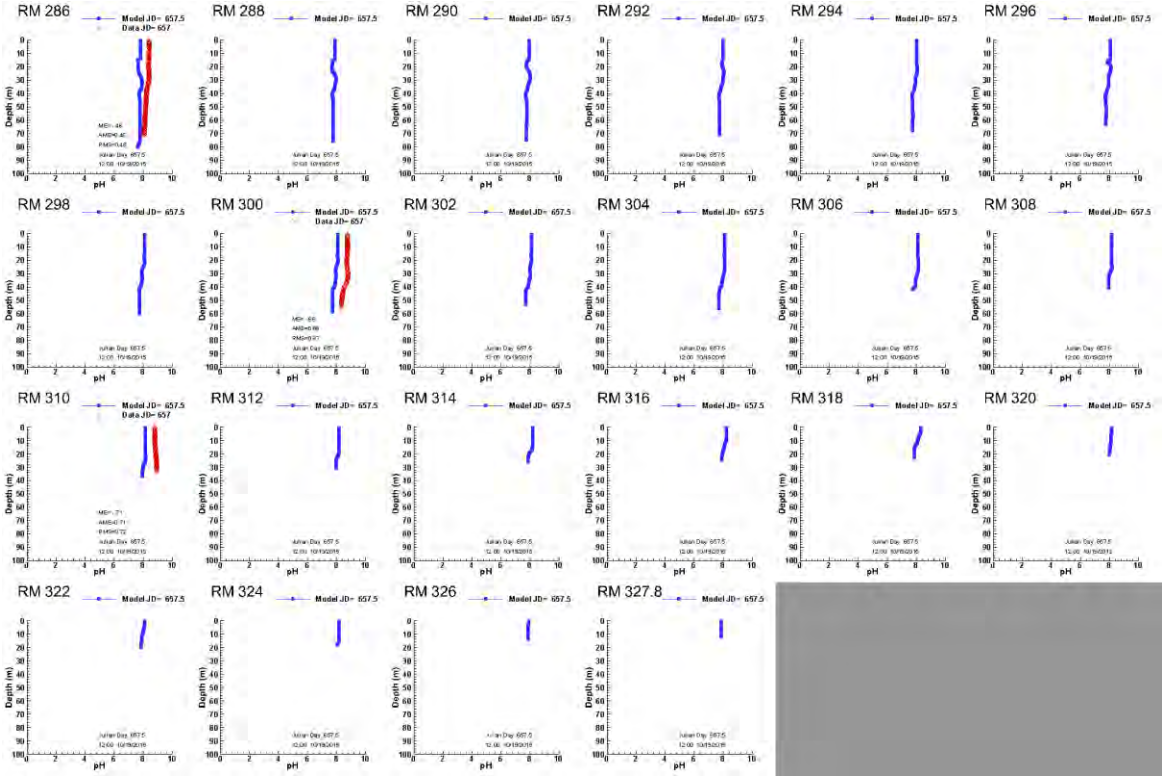


Figure 2240. Vertical profiles of pH compared with data for 10/19/2015.

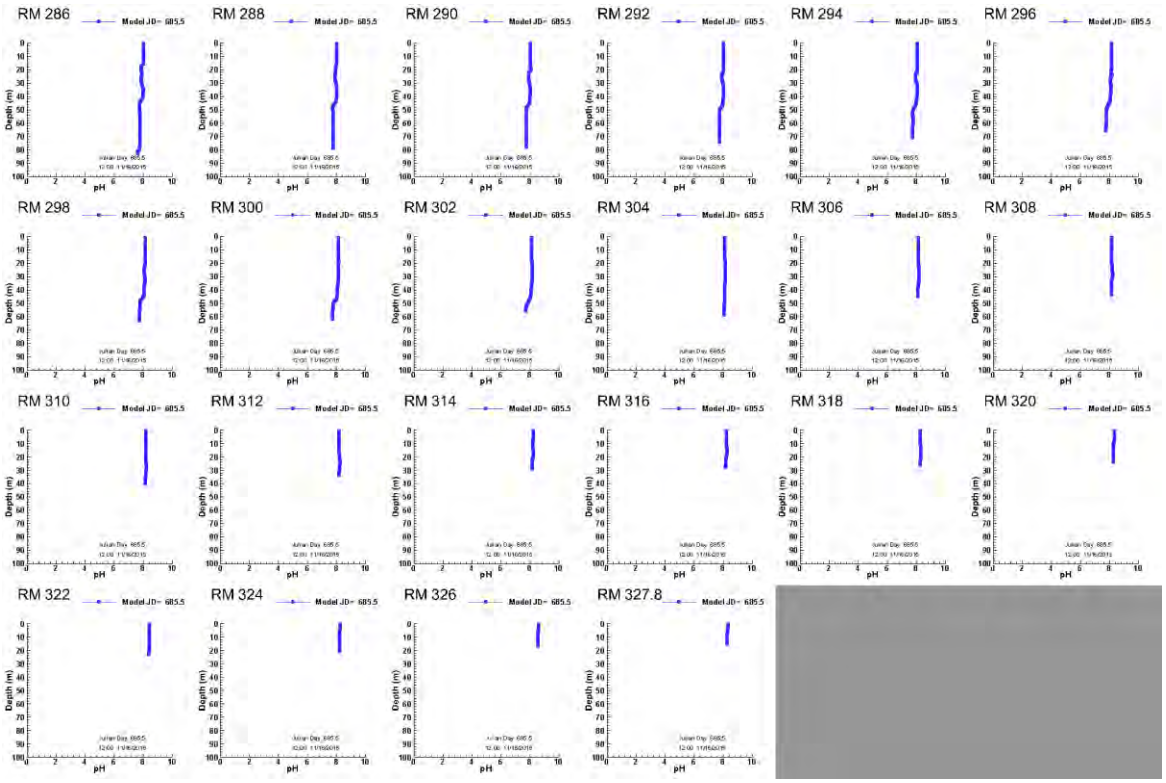


Figure 2241. Vertical profiles of pH compared with data for 11/16/2015.

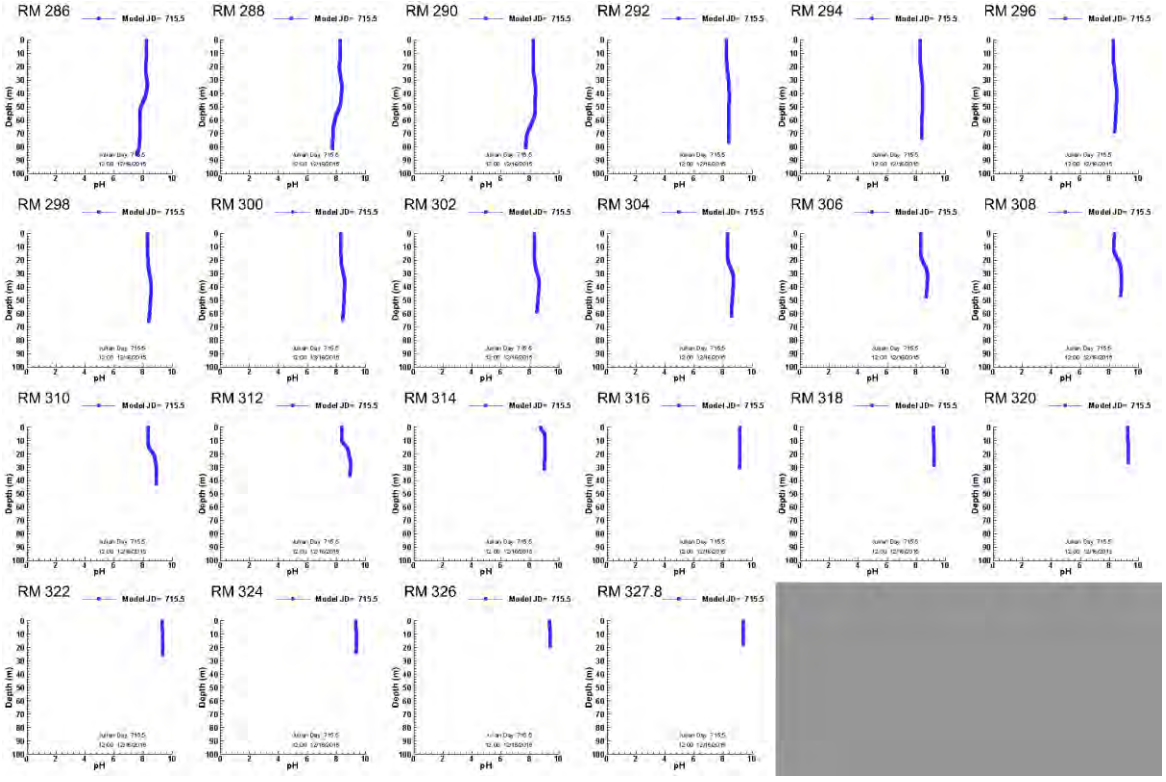


Figure 2242. Vertical profiles of pH compared with data for 12/16/2015.

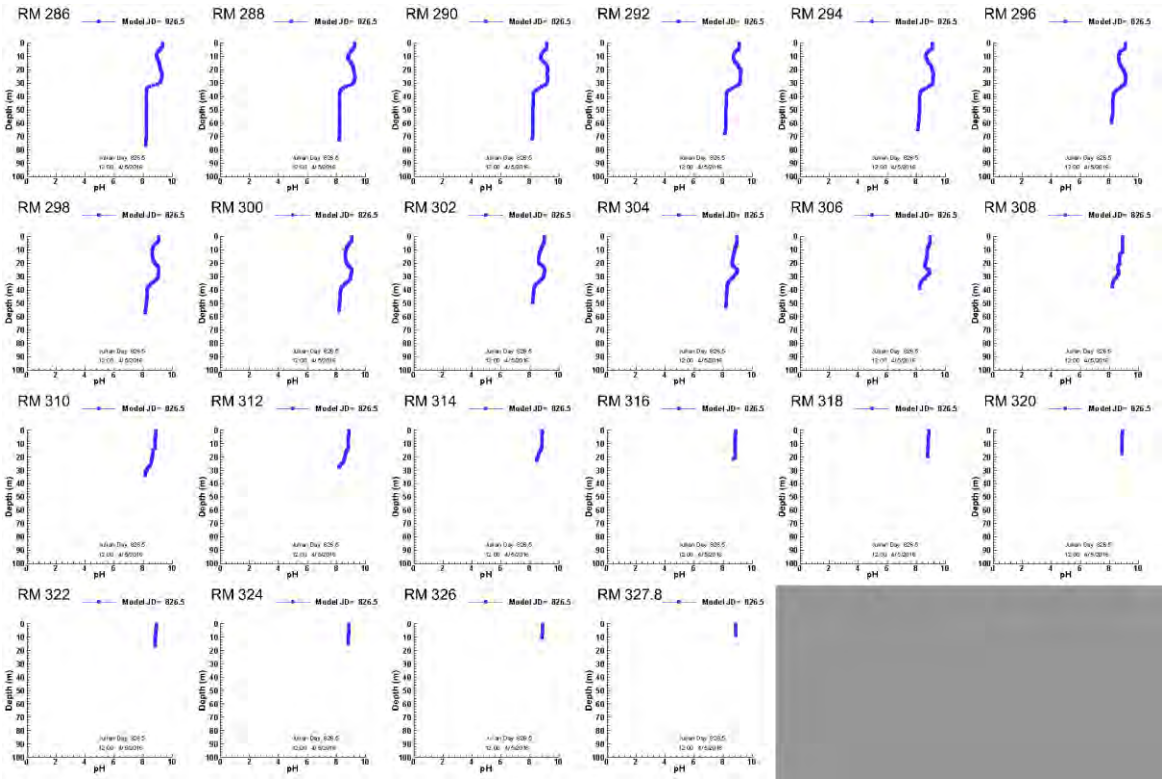


Figure 2243. Vertical profiles of pH compared with data for 4/ 5/2016.

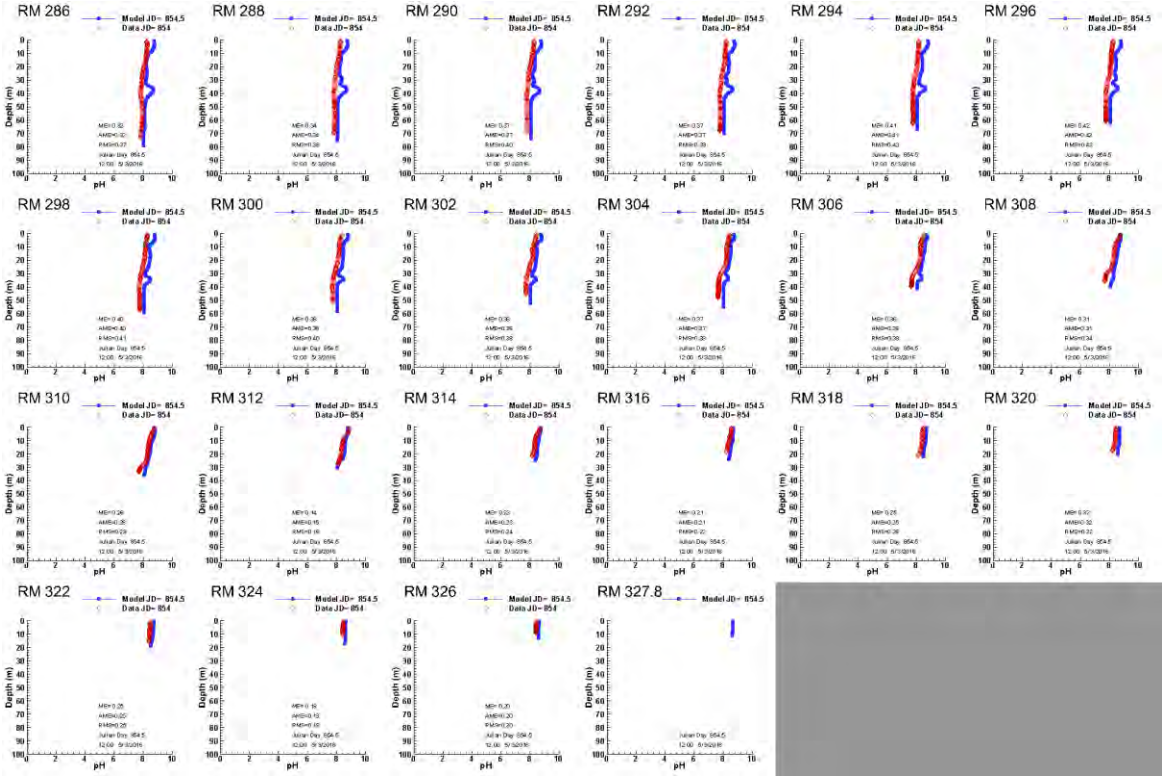


Figure 2244. Vertical profiles of pH compared with data for 5/ 3/2016.

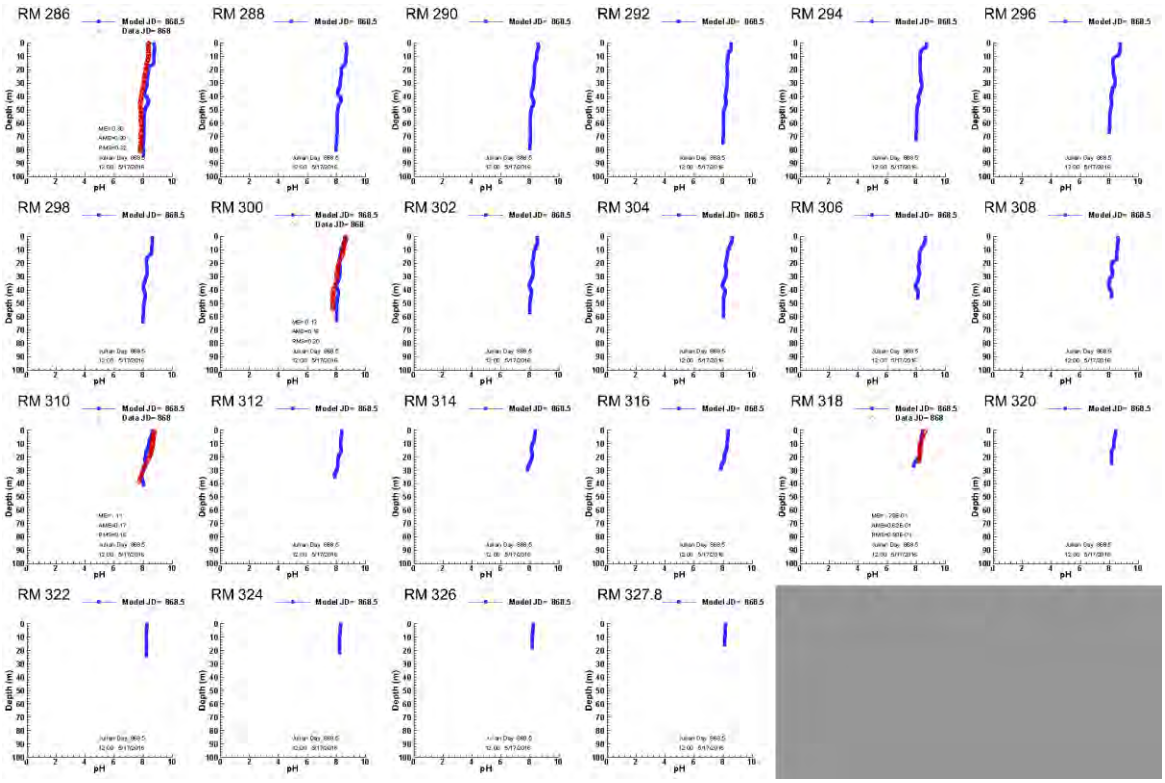


Figure 2245. Vertical profiles of pH compared with data for 5/17/2016.

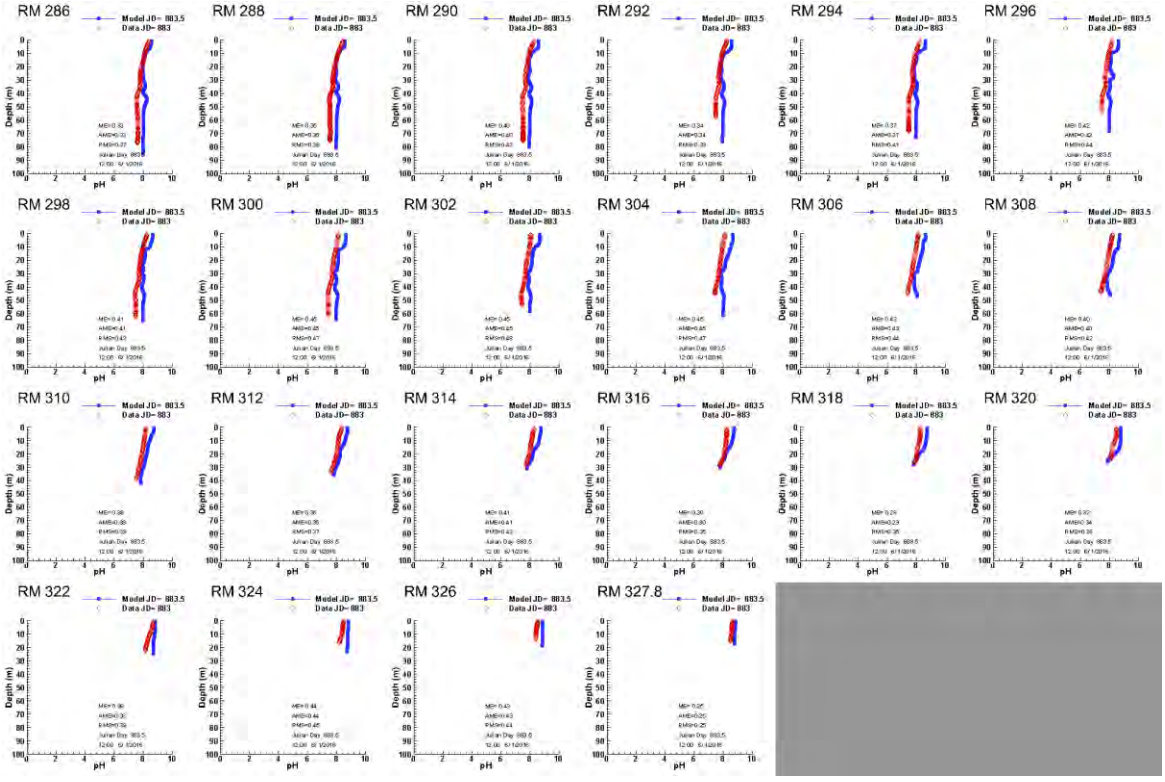


Figure 2246. Vertical profiles of pH compared with data for 6/ 1/2016.

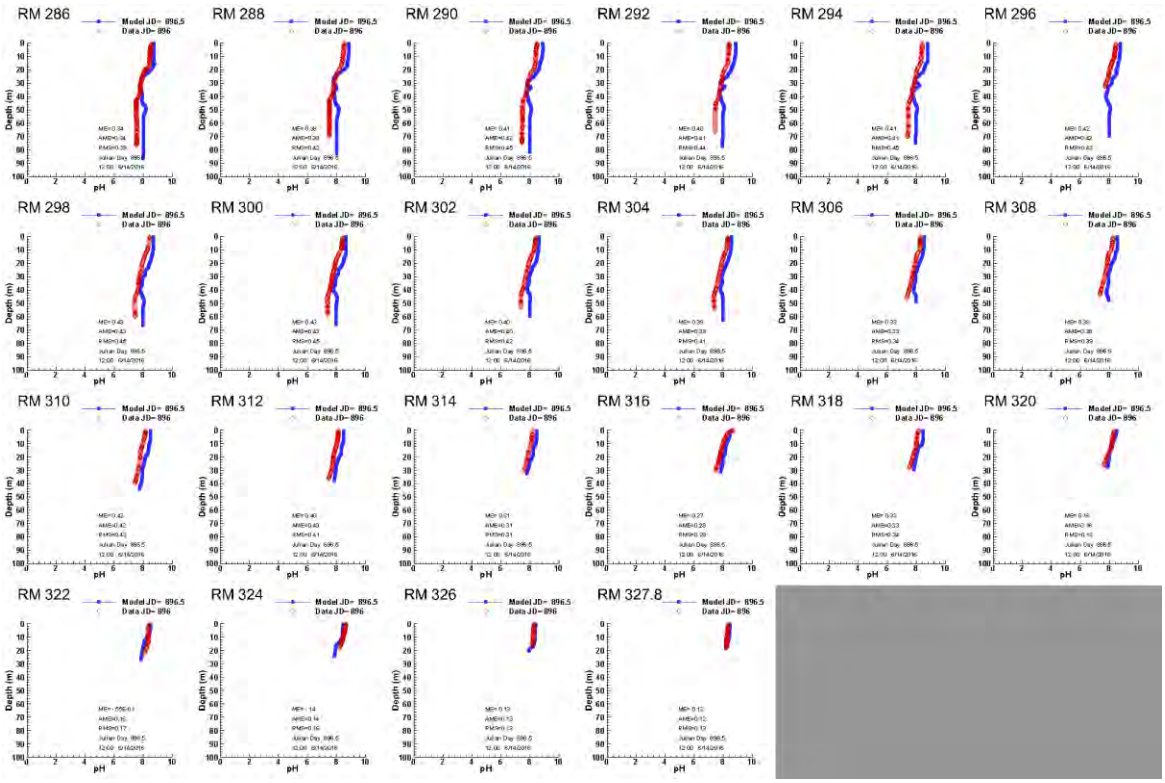


Figure 2247. Vertical profiles of pH compared with data for 6/14/2016.

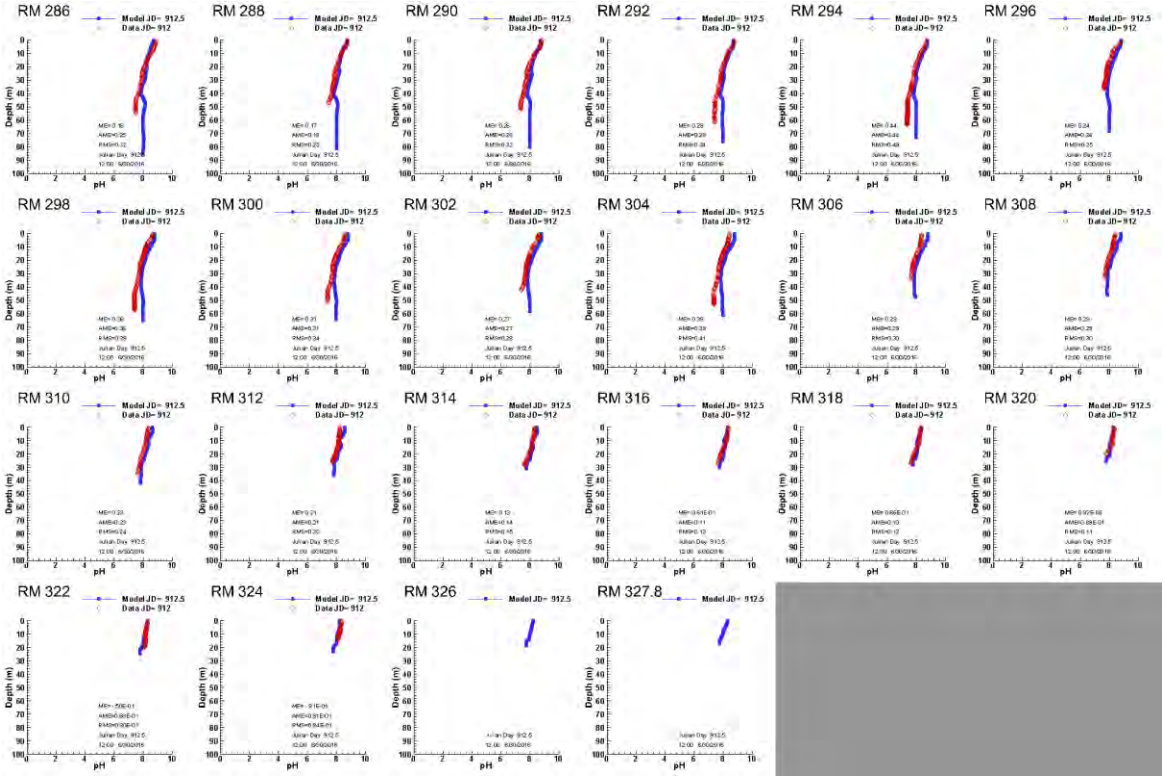


Figure 2248. Vertical profiles of pH compared with data for 6/30/2016.

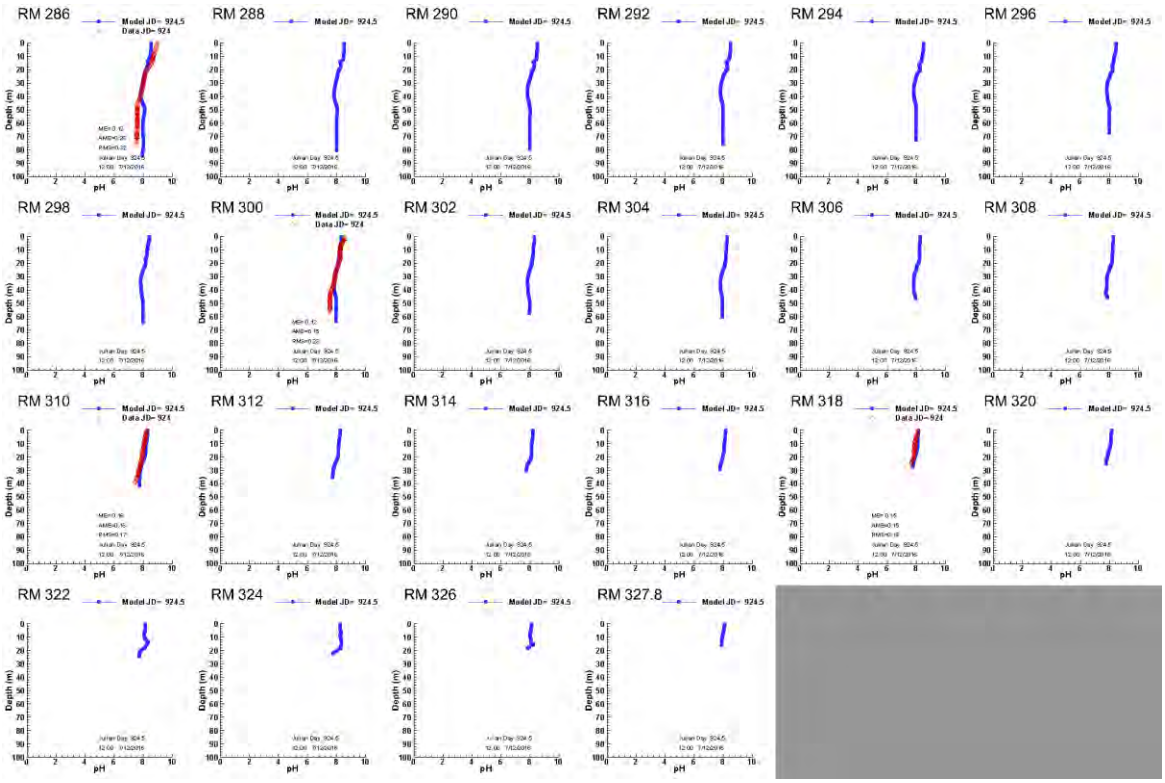


Figure 2249. Vertical profiles of pH compared with data for 7/12/2016.

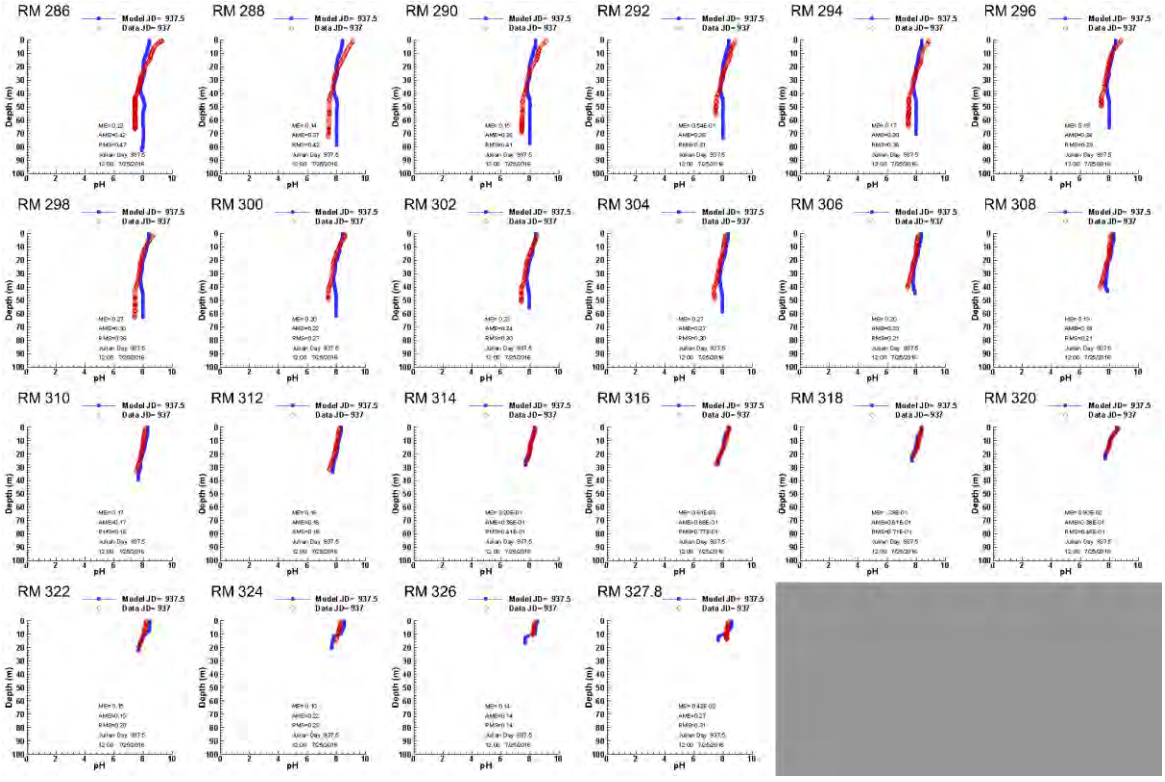


Figure 2250. Vertical profiles of pH compared with data for 7/25/2016.

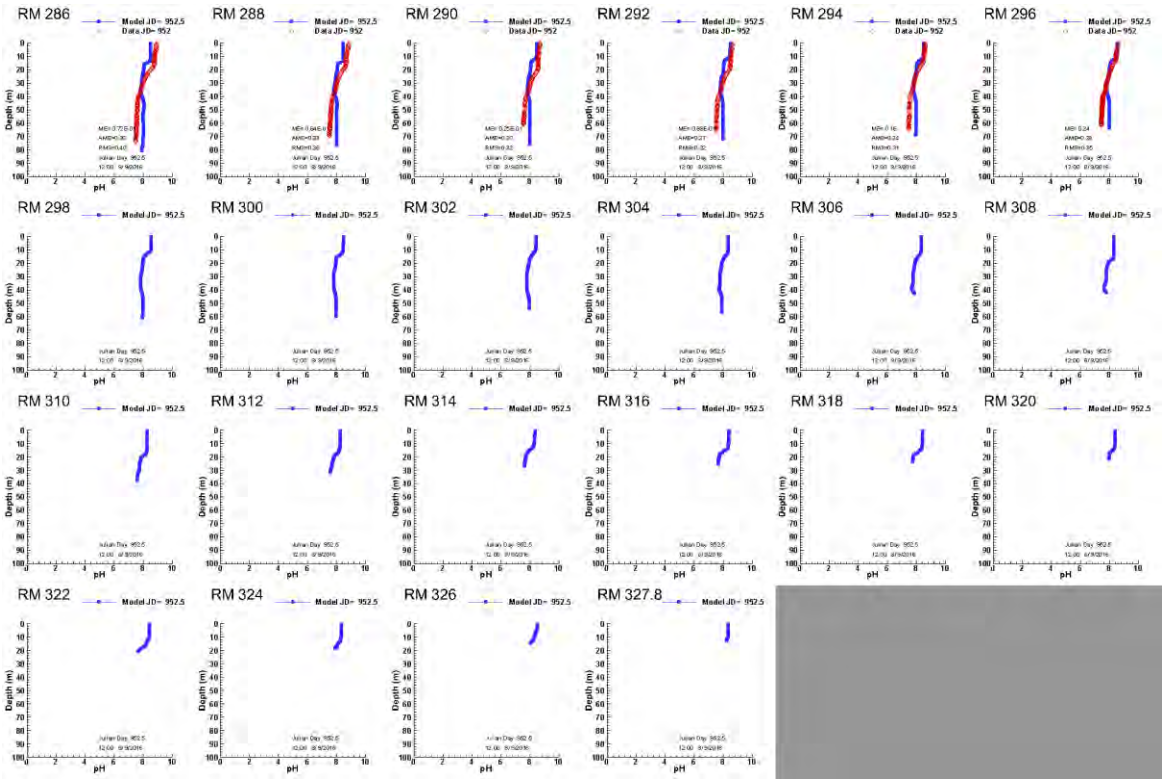


Figure 2251. Vertical profiles of pH compared with data for 8/ 9/2016.

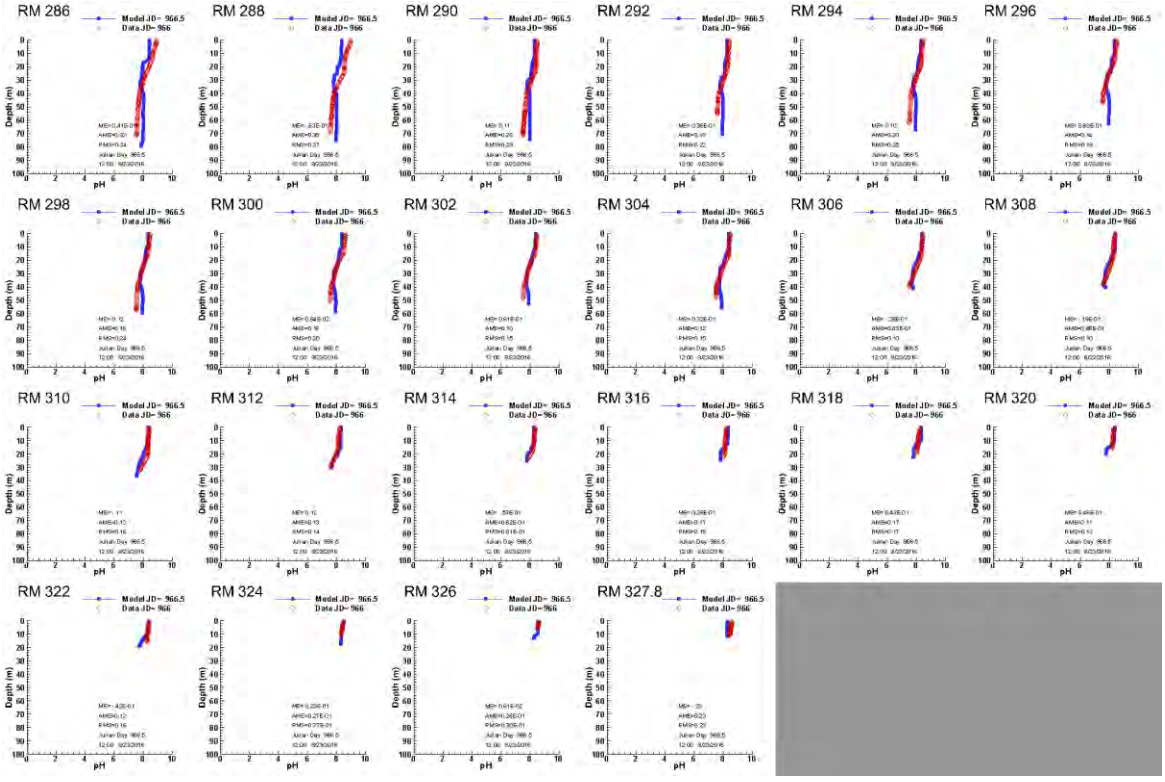


Figure 2252. Vertical profiles of pH compared with data for 8/23/2016.

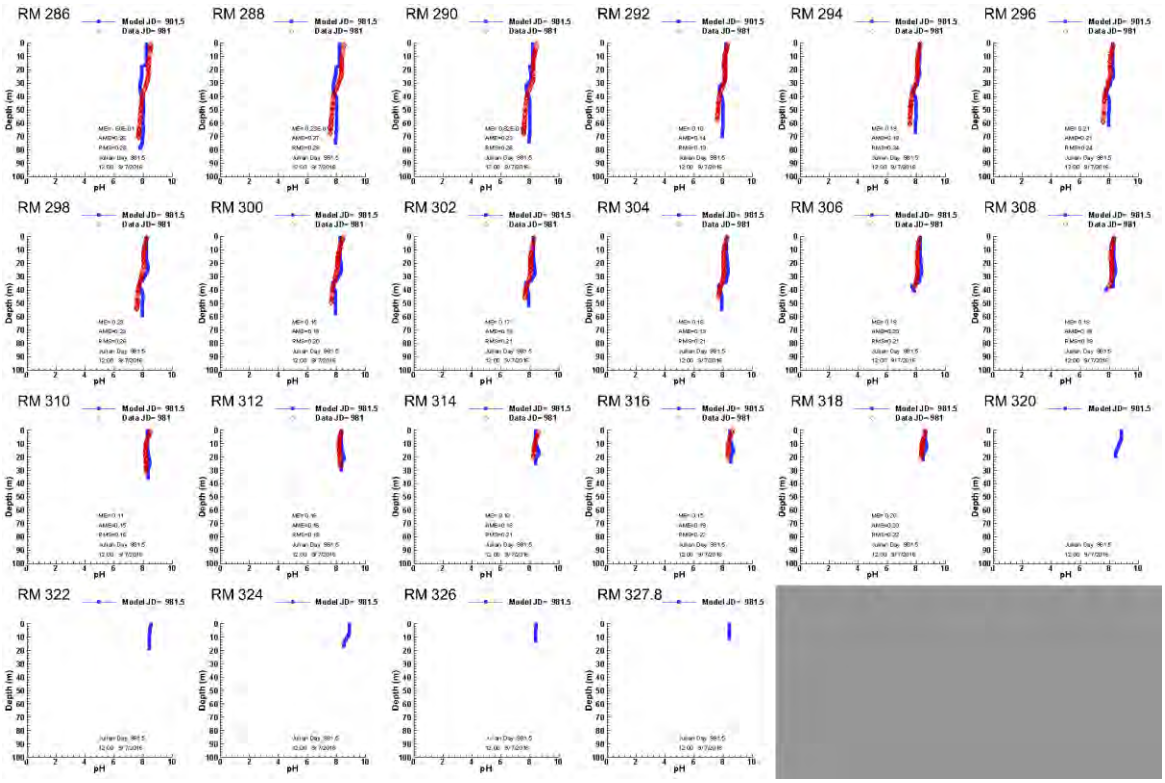


Figure 2253. Vertical profiles of pH compared with data for 9/ 7/2016.

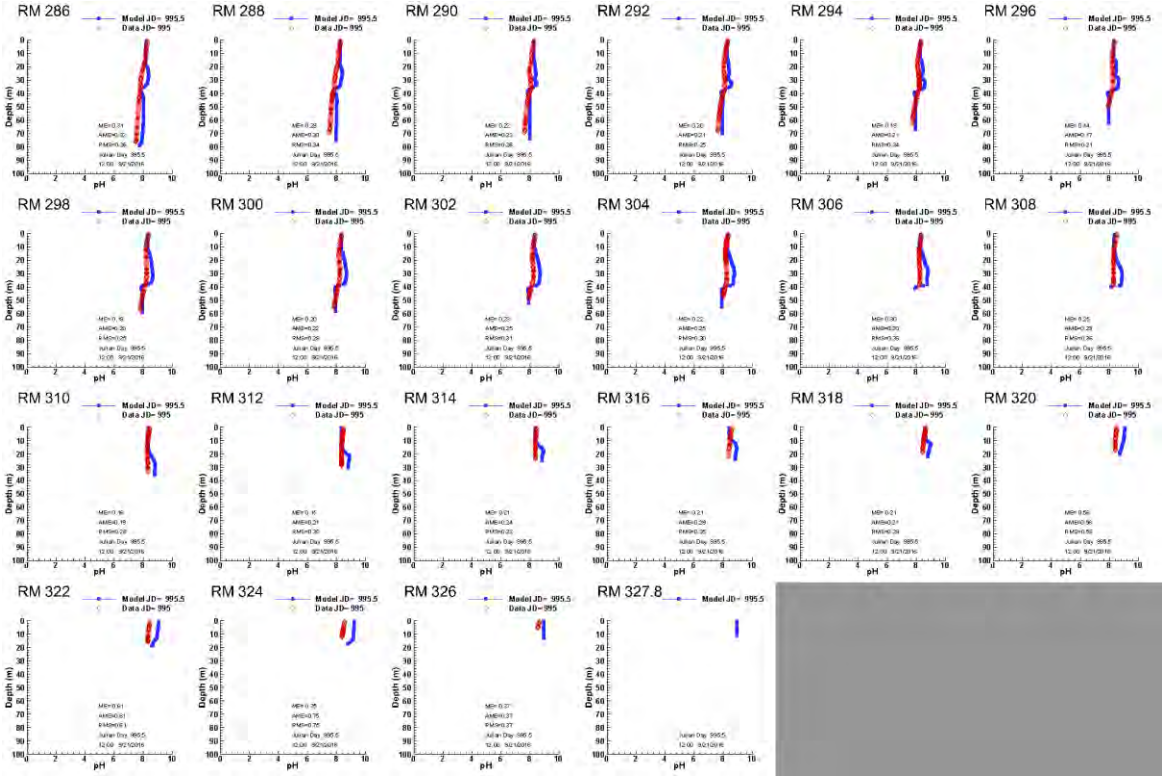


Figure 2254. Vertical profiles of pH compared with data for 9/21/2016.

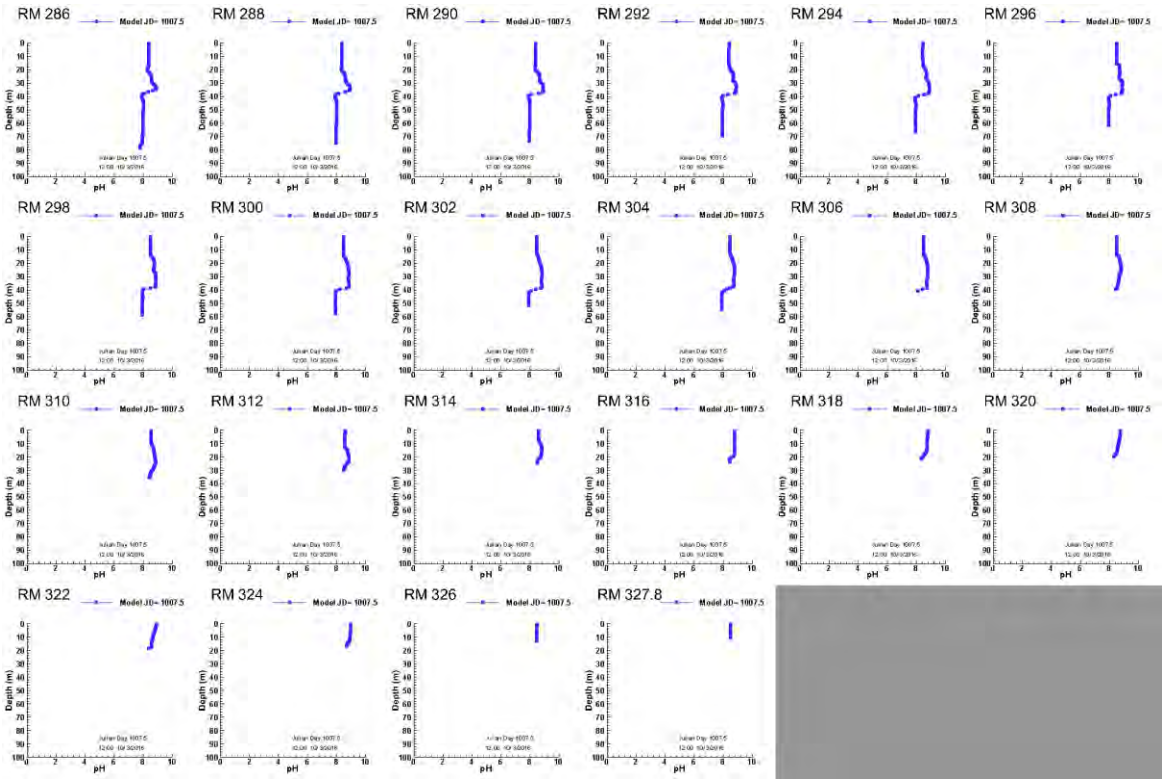


Figure 2255. Vertical profiles of pH compared with data for 10/ 3/2016.

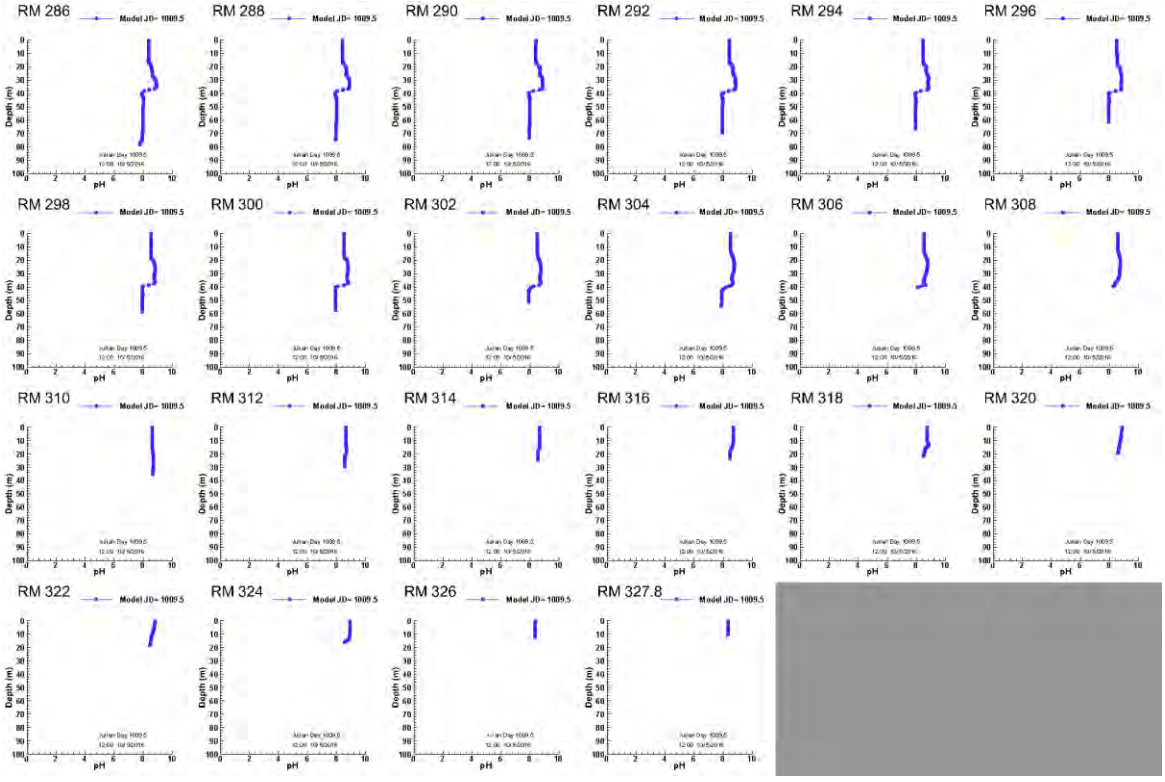


Figure 2256. Vertical profiles of pH compared with data for 10/ 5/2016.

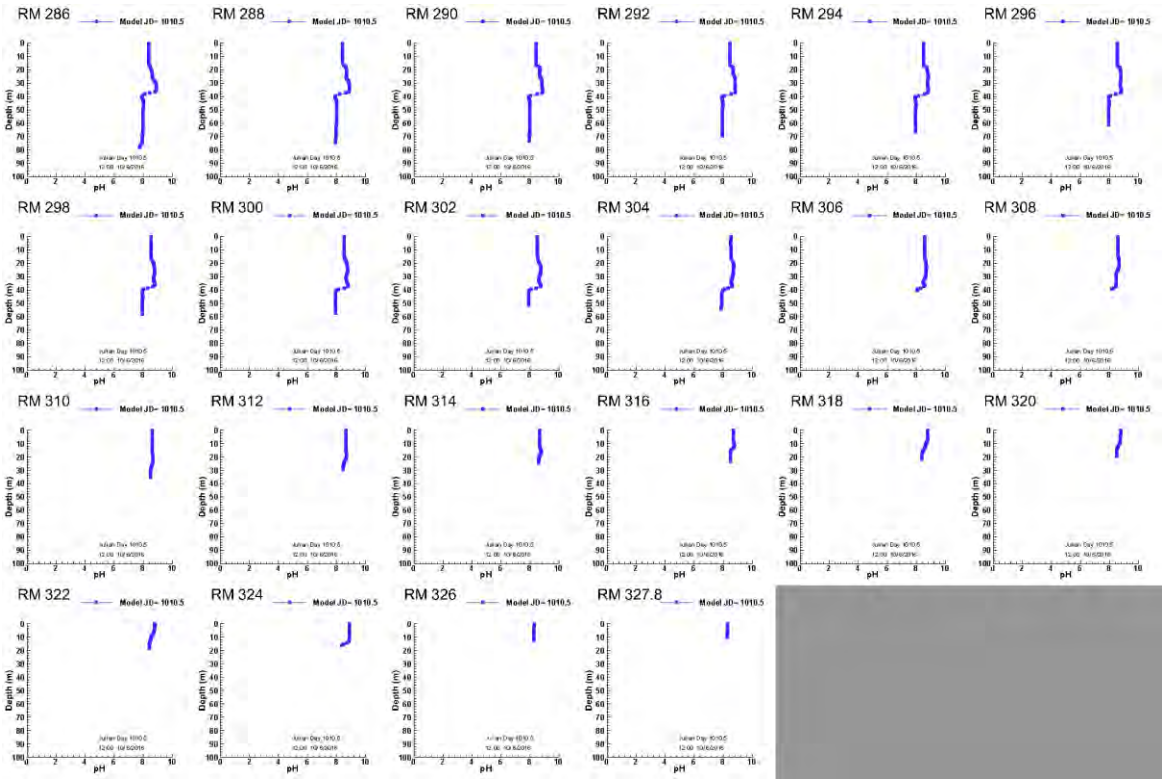


Figure 2257. Vertical profiles of pH compared with data for 10/ 6/2016.

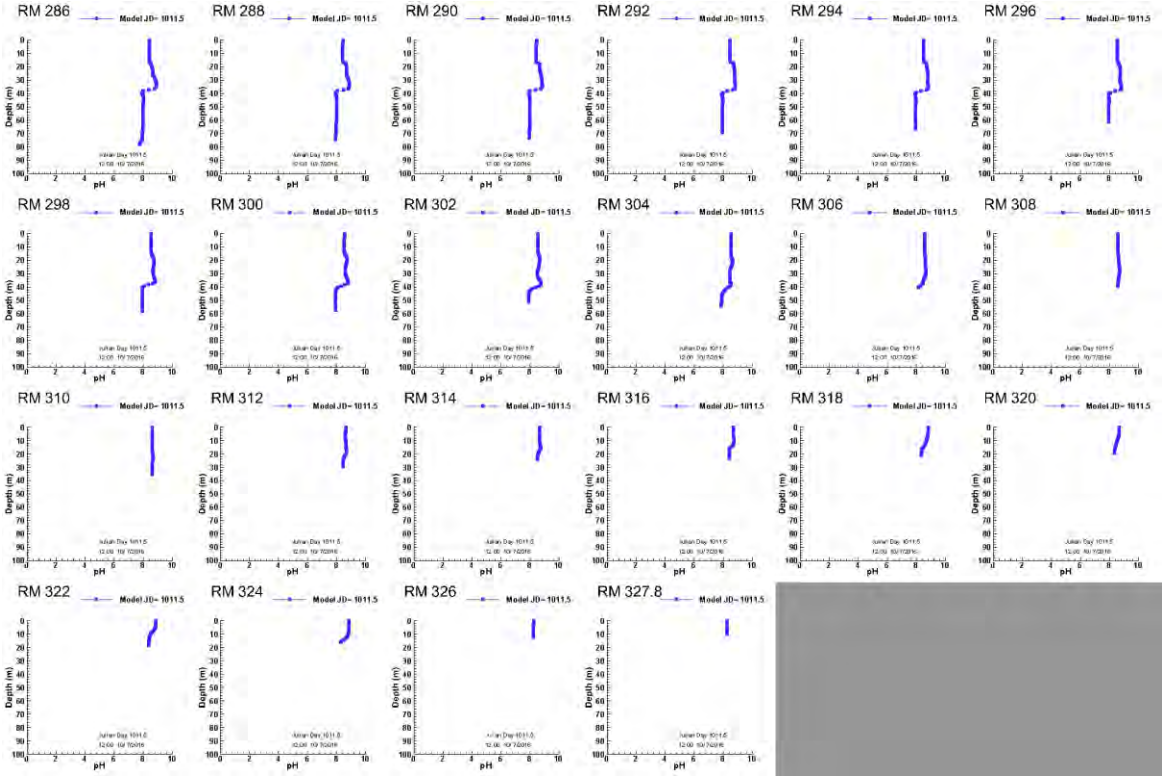


Figure 2258. Vertical profiles of pH compared with data for 10/ 7/2016.

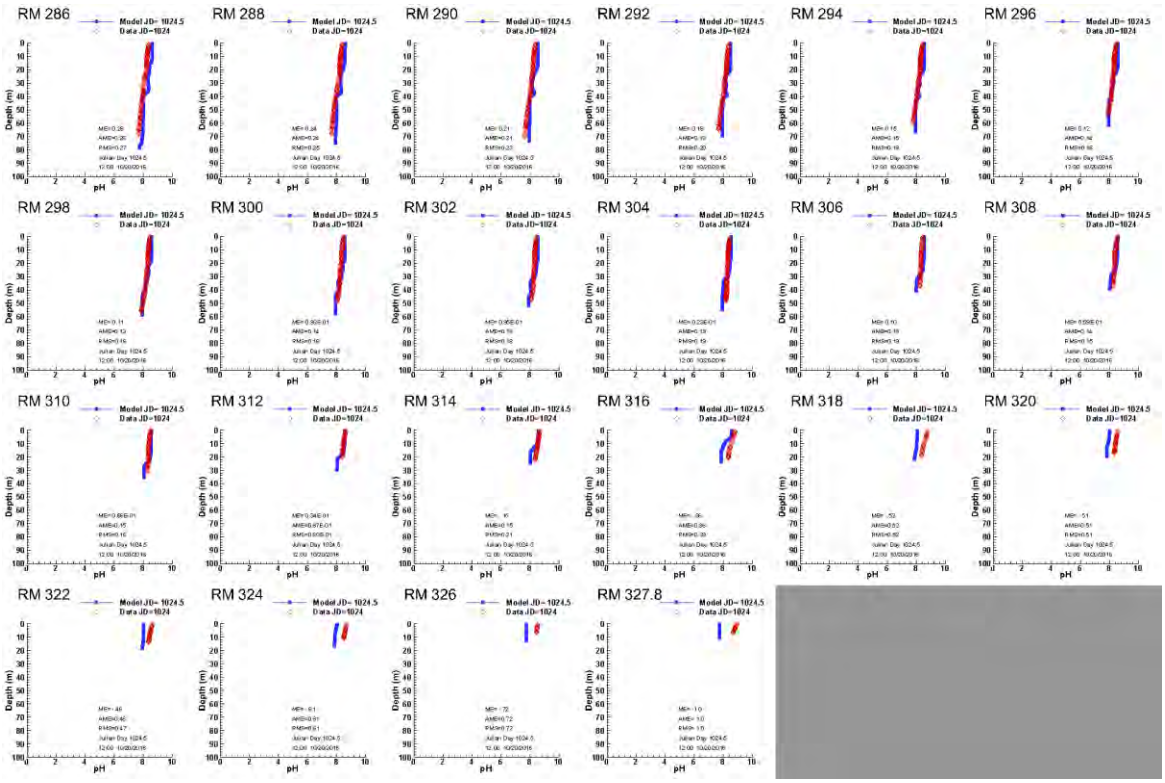


Figure 2259. Vertical profiles of pH compared with data for 10/20/2016.

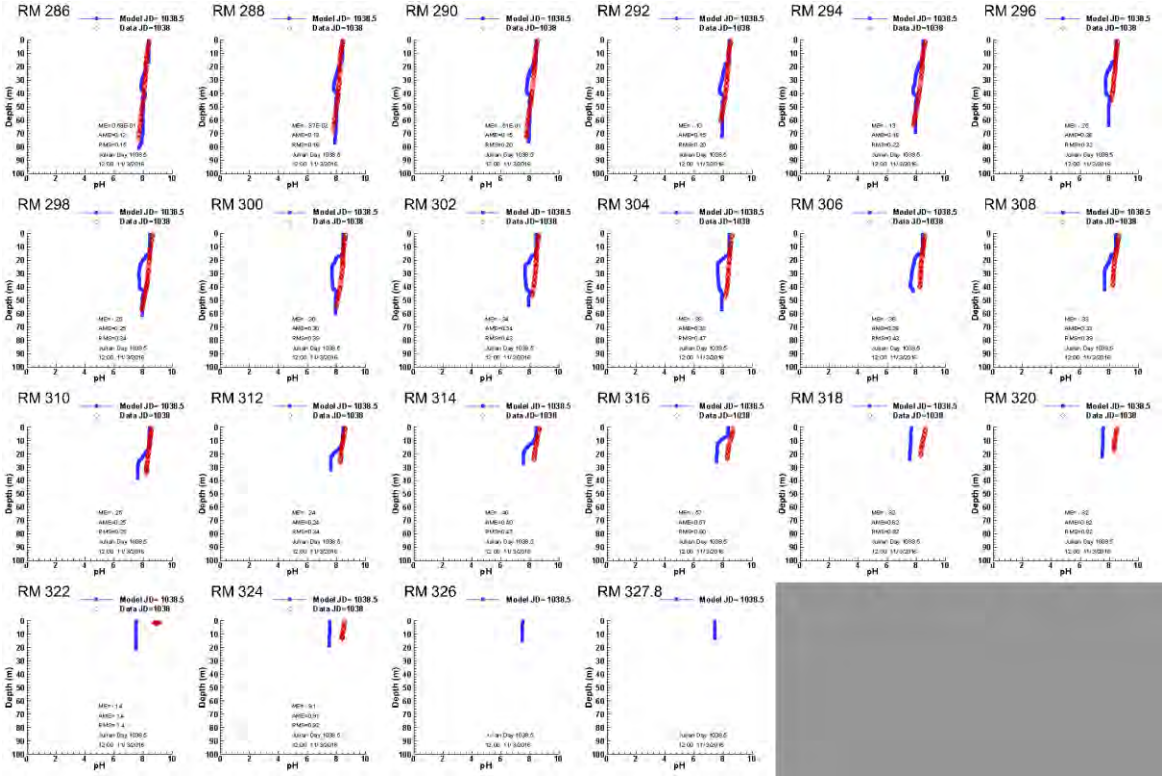


Figure 2260. Vertical profiles of pH compared with data for 11/ 3/2016.

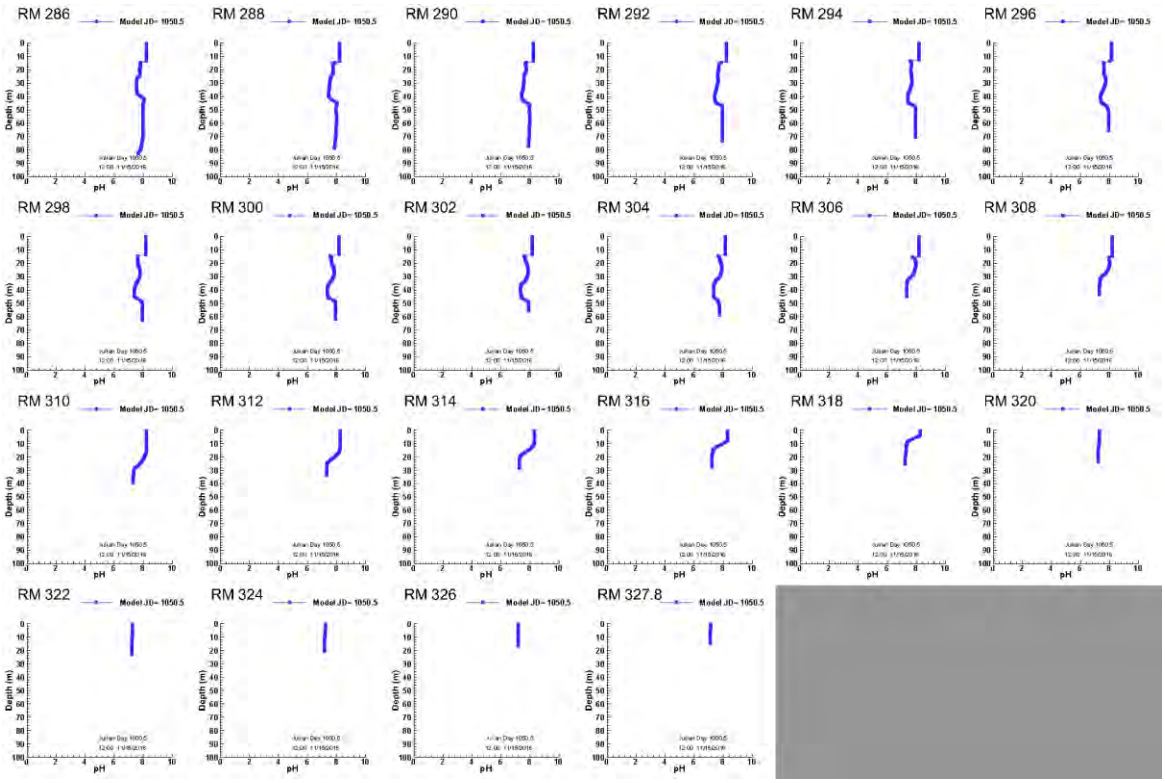


Figure 2261. Vertical profiles of pH compared with data for 11/15/2016.

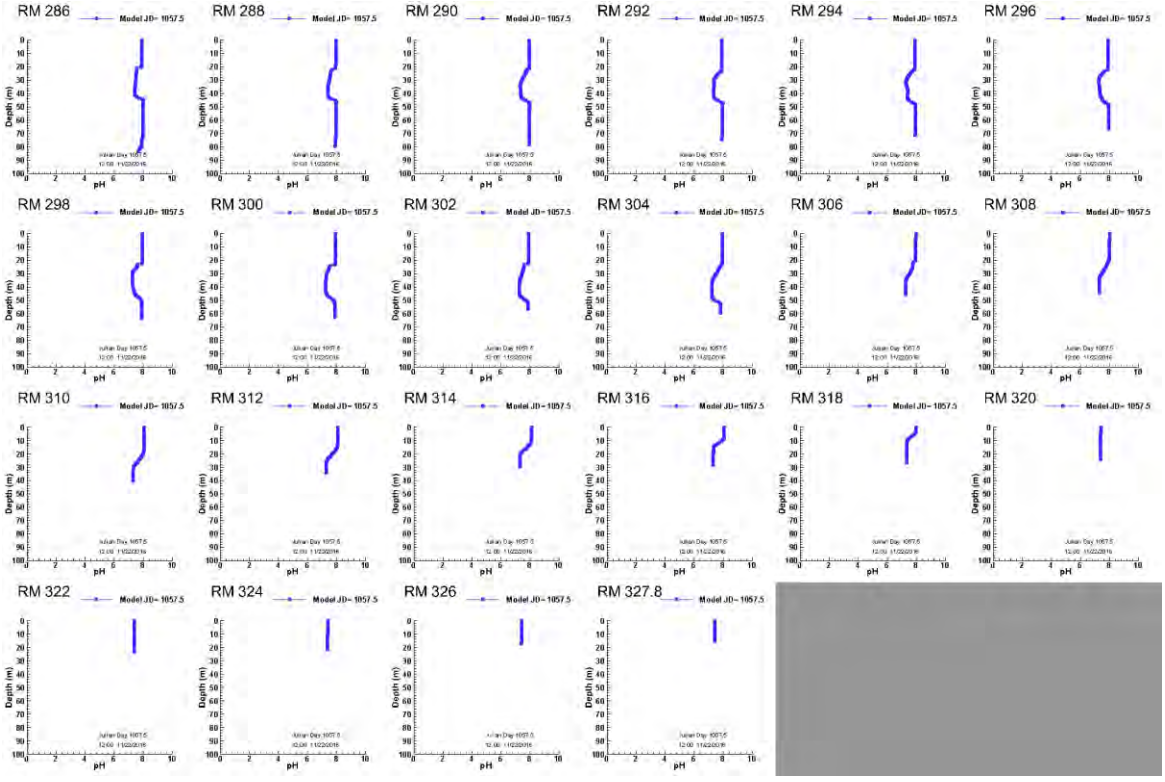


Figure 2262. Vertical profiles of pH compared with data for 11/22/2016.

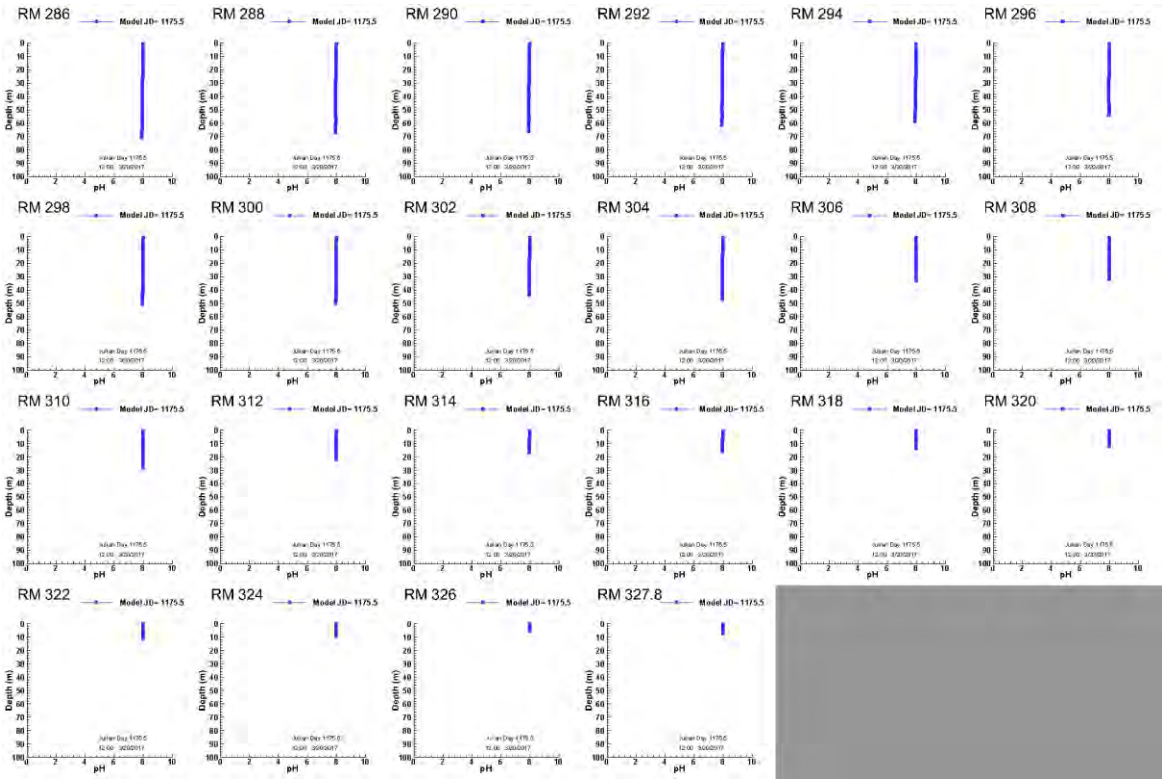


Figure 2263. Vertical profiles of pH compared with data for 3/20/2017.

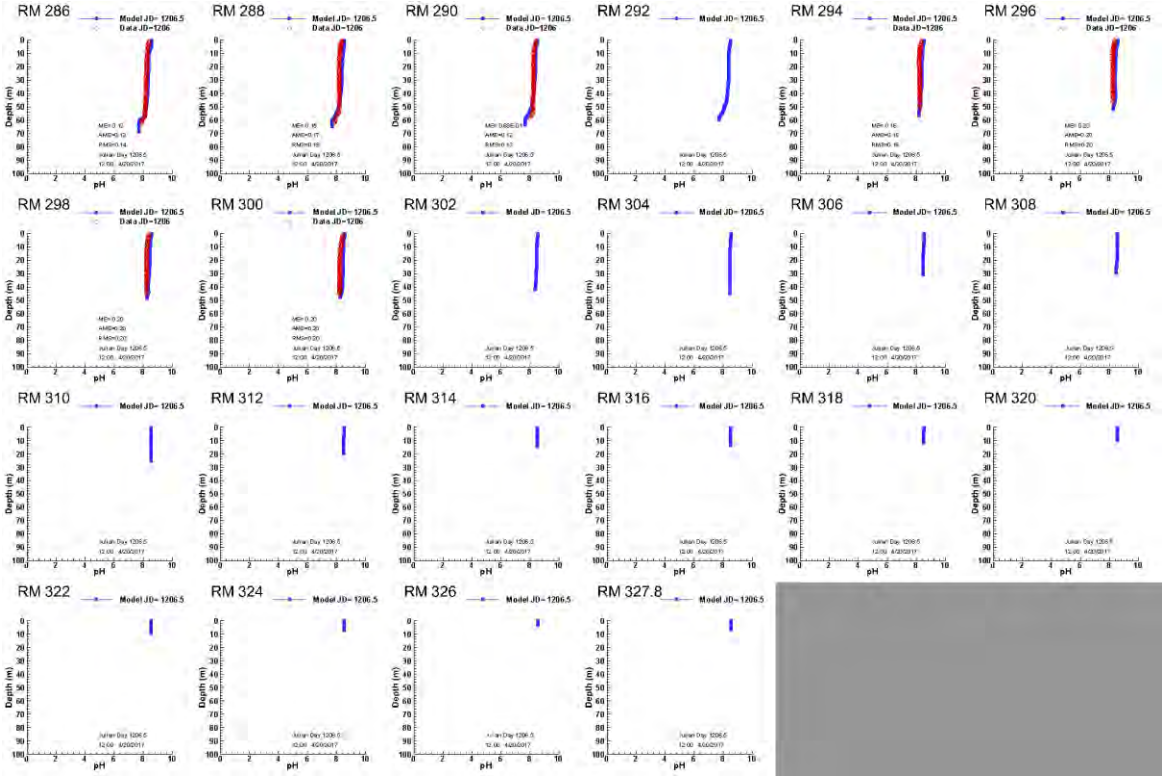


Figure 2264. Vertical profiles of pH compared with data for 4/20/2017.

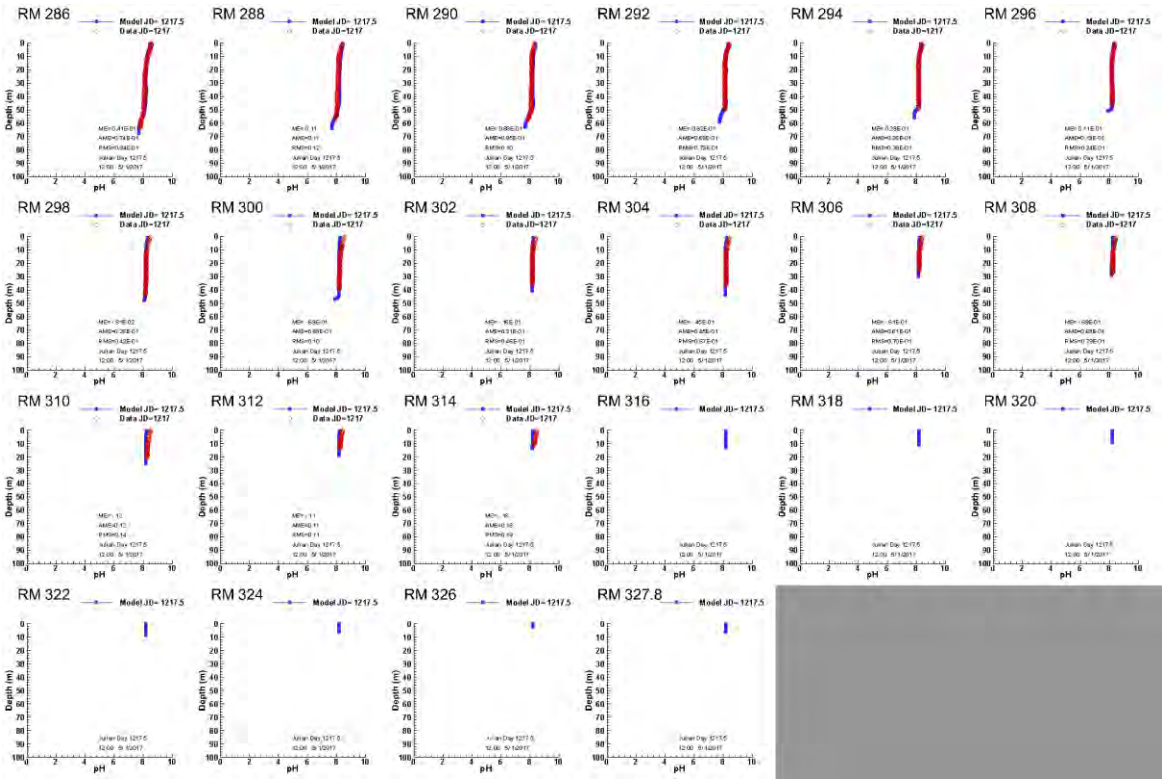


Figure 2265. Vertical profiles of pH compared with data for 5/ 1/2017.

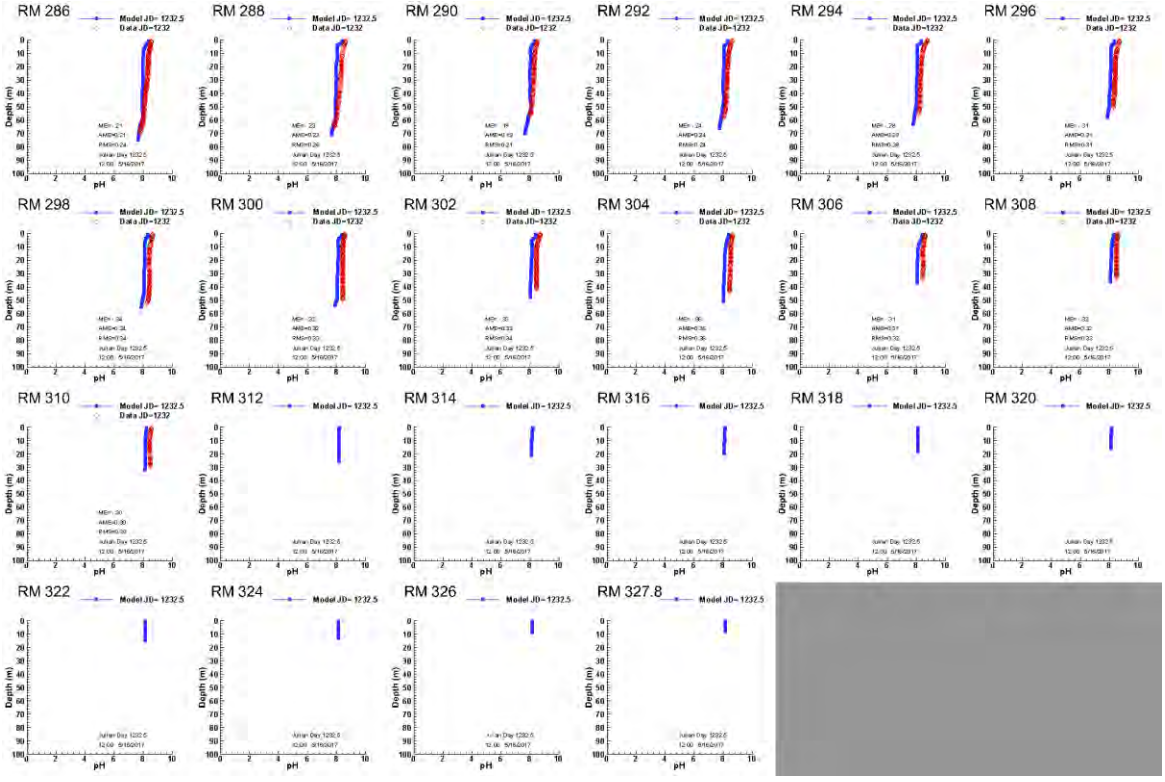


Figure 2266. Vertical profiles of pH compared with data for 5/16/2017.

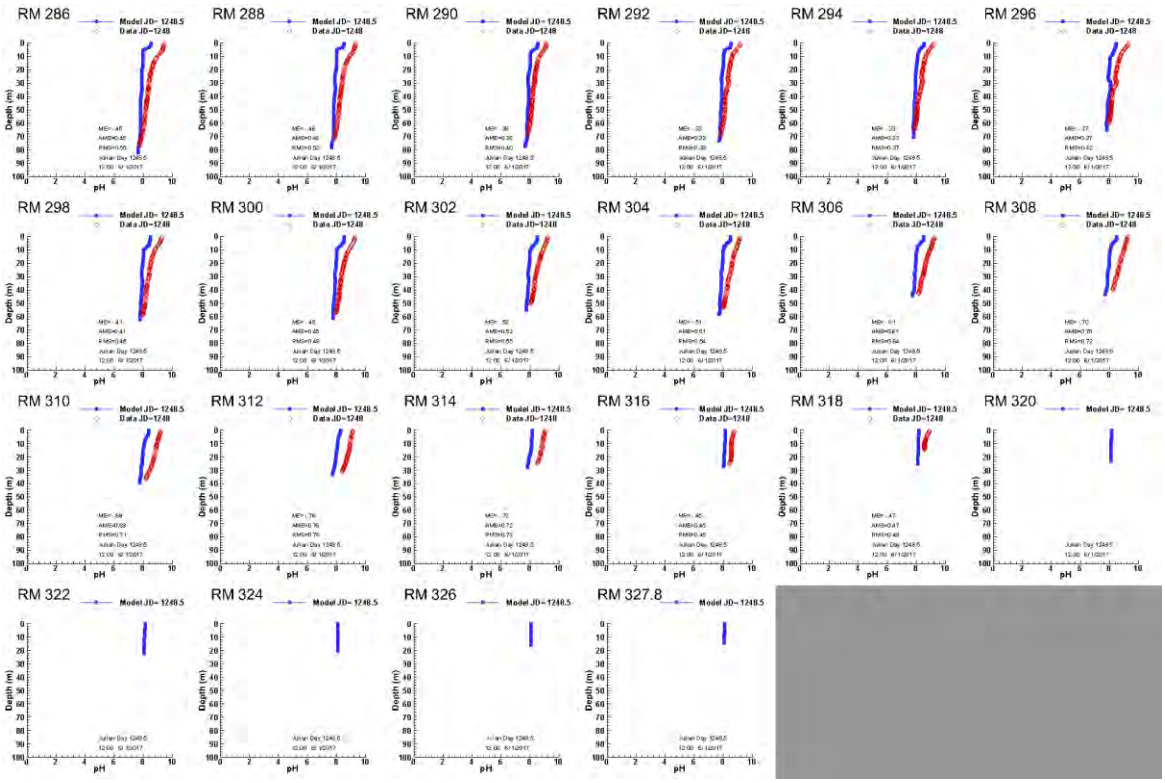


Figure 2267. Vertical profiles of pH compared with data for 6/ 1/2017.

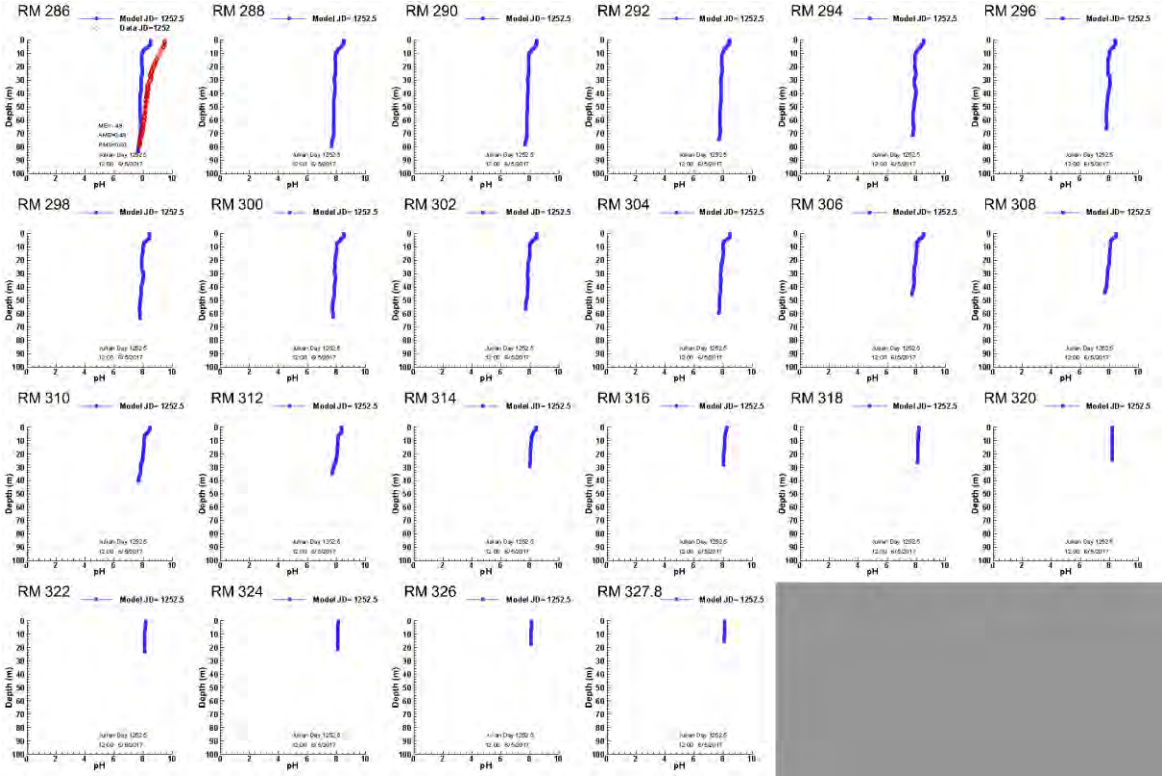


Figure 2268. Vertical profiles of pH compared with data for 6/ 5/2017.

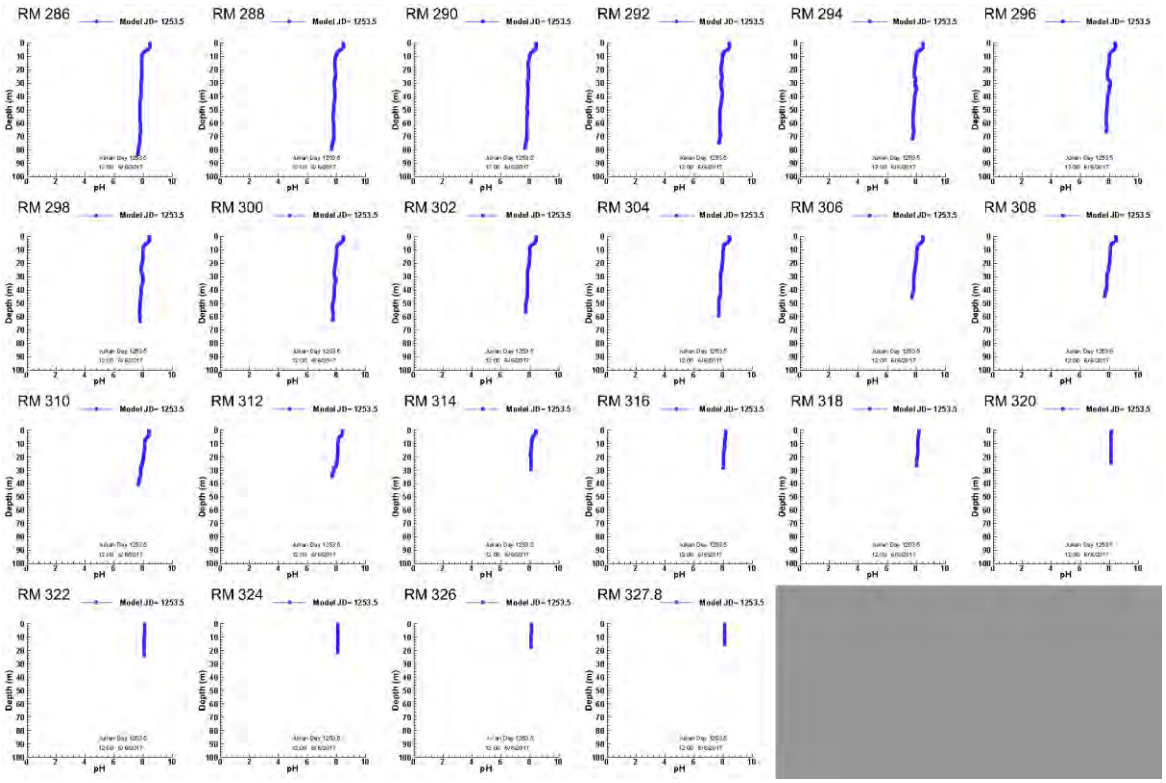


Figure 2269. Vertical profiles of pH compared with data for 6/ 6/2017.

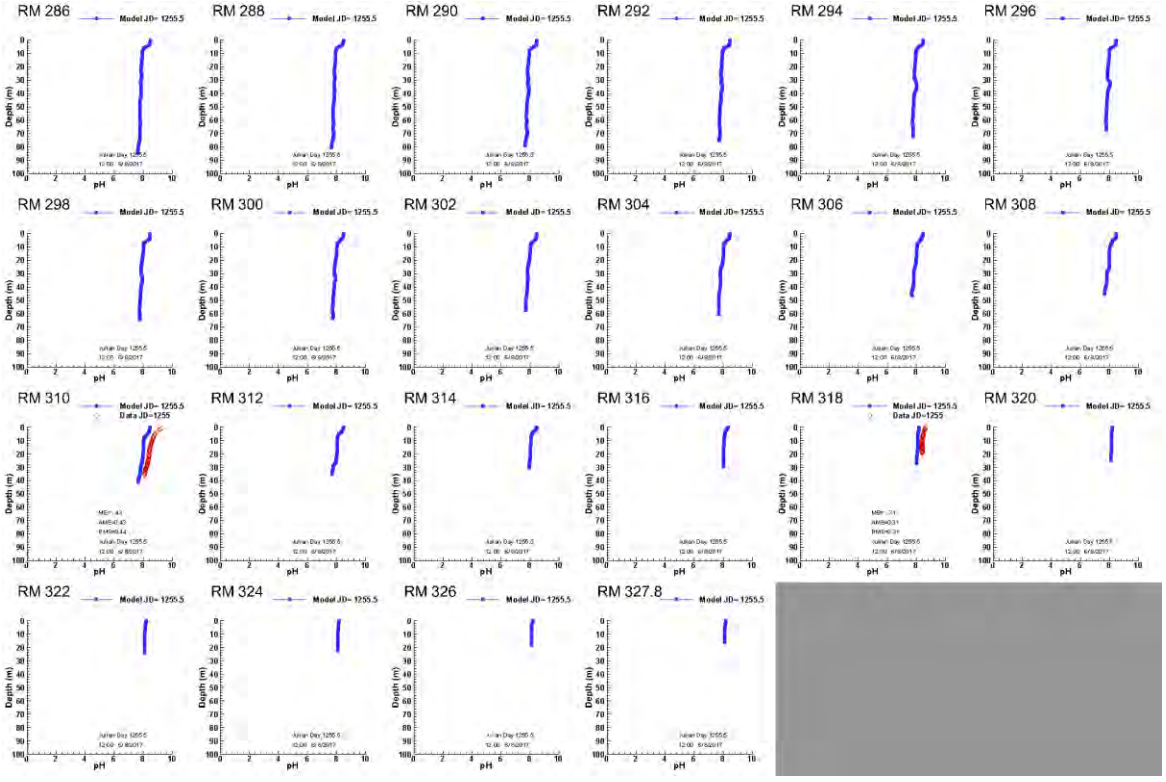


Figure 2270. Vertical profiles of pH compared with data for 6/ 8/2017.

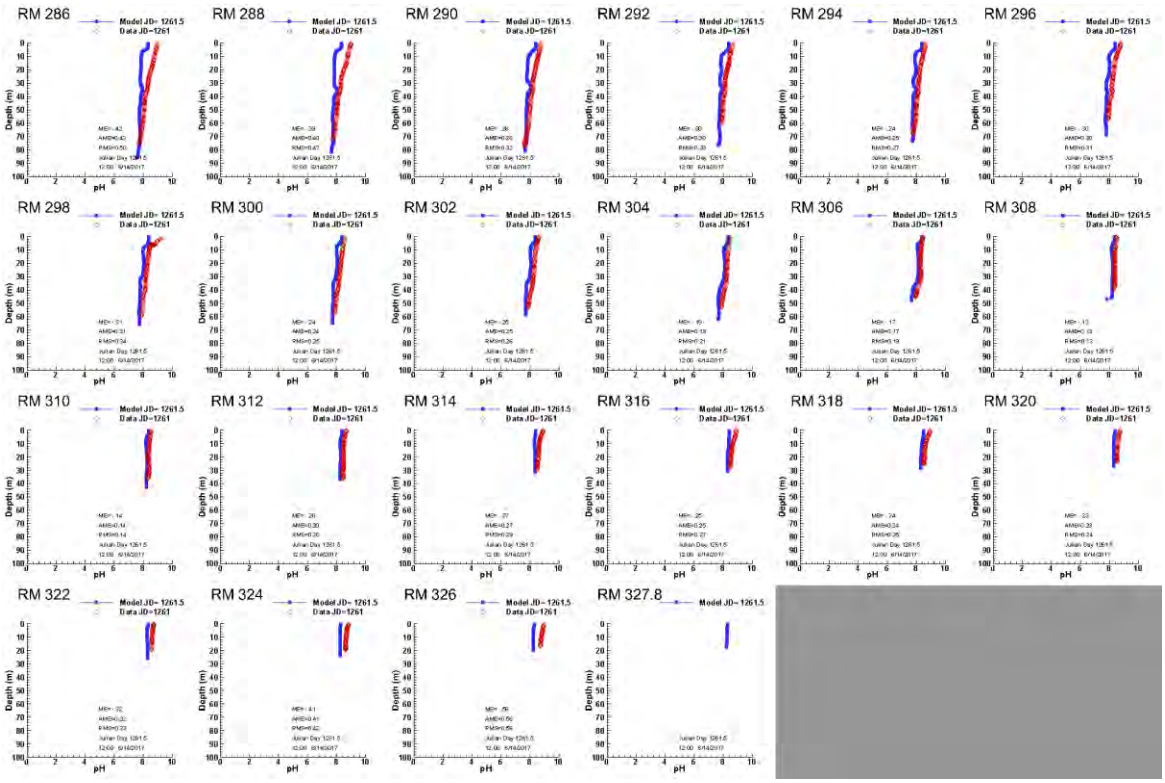


Figure 2271. Vertical profiles of pH compared with data for 6/14/2017.

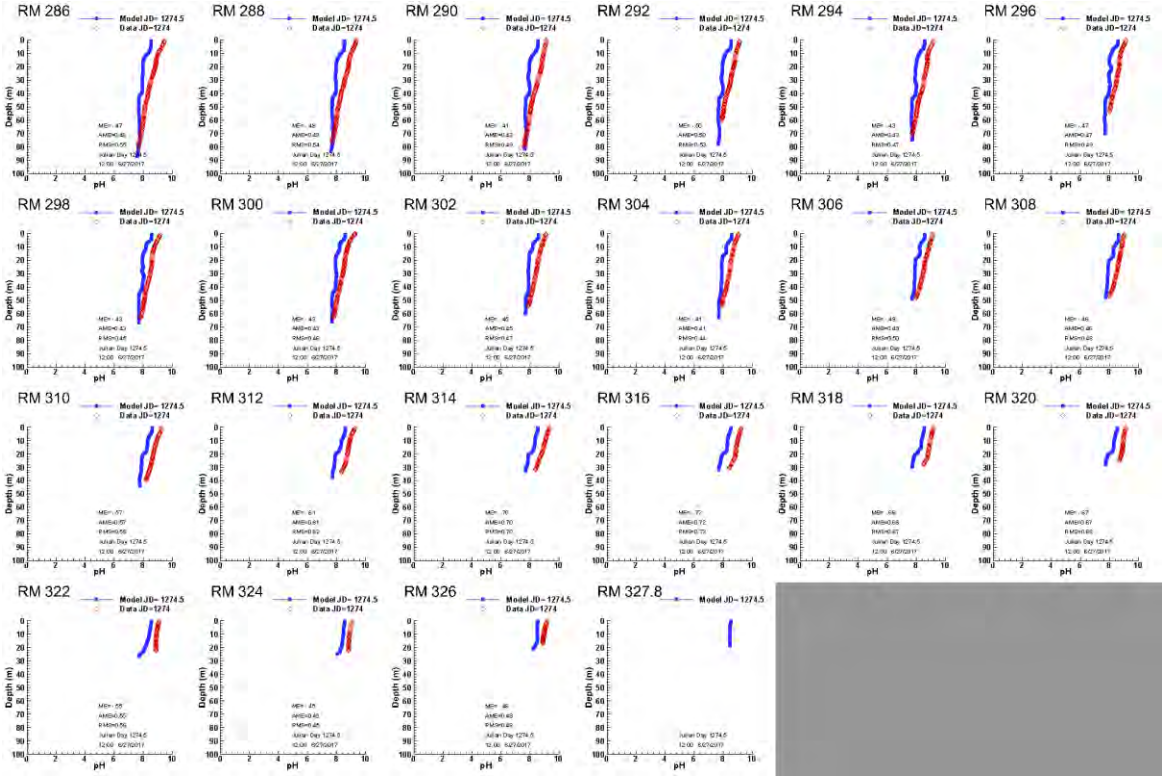


Figure 2272. Vertical profiles of pH compared with data for 6/27/2017.

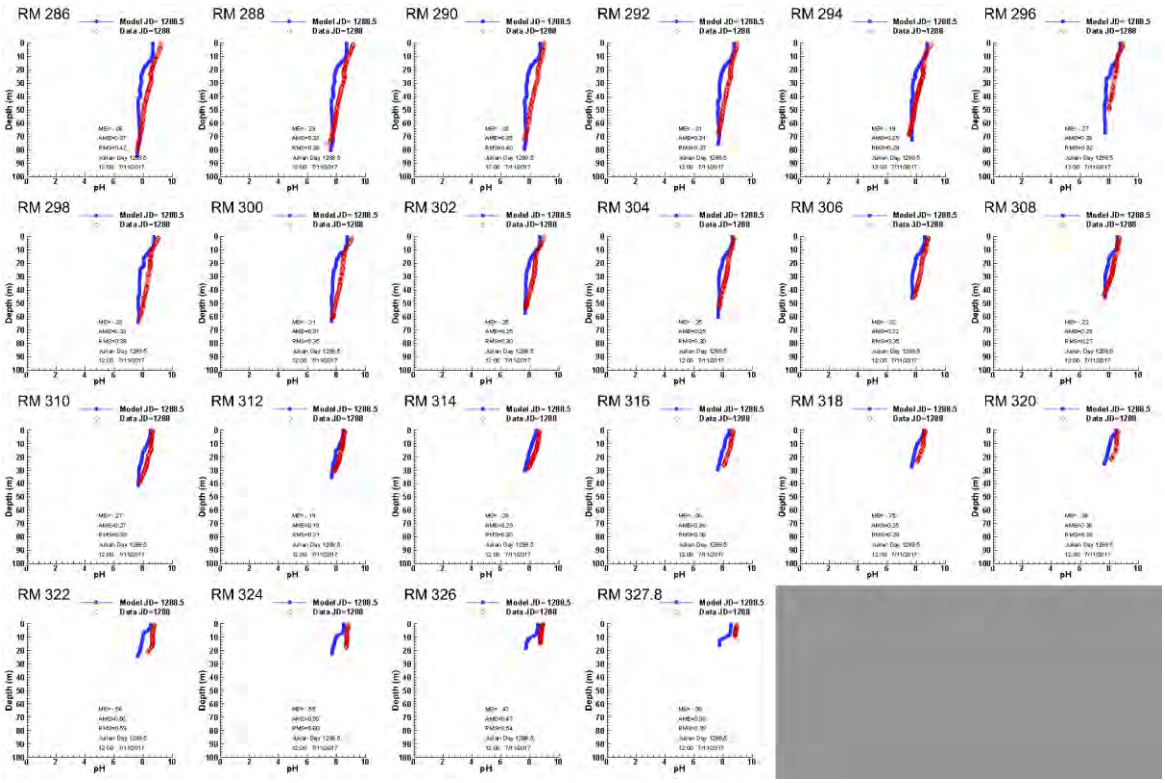


Figure 2273. Vertical profiles of pH compared with data for 7/11/2017.

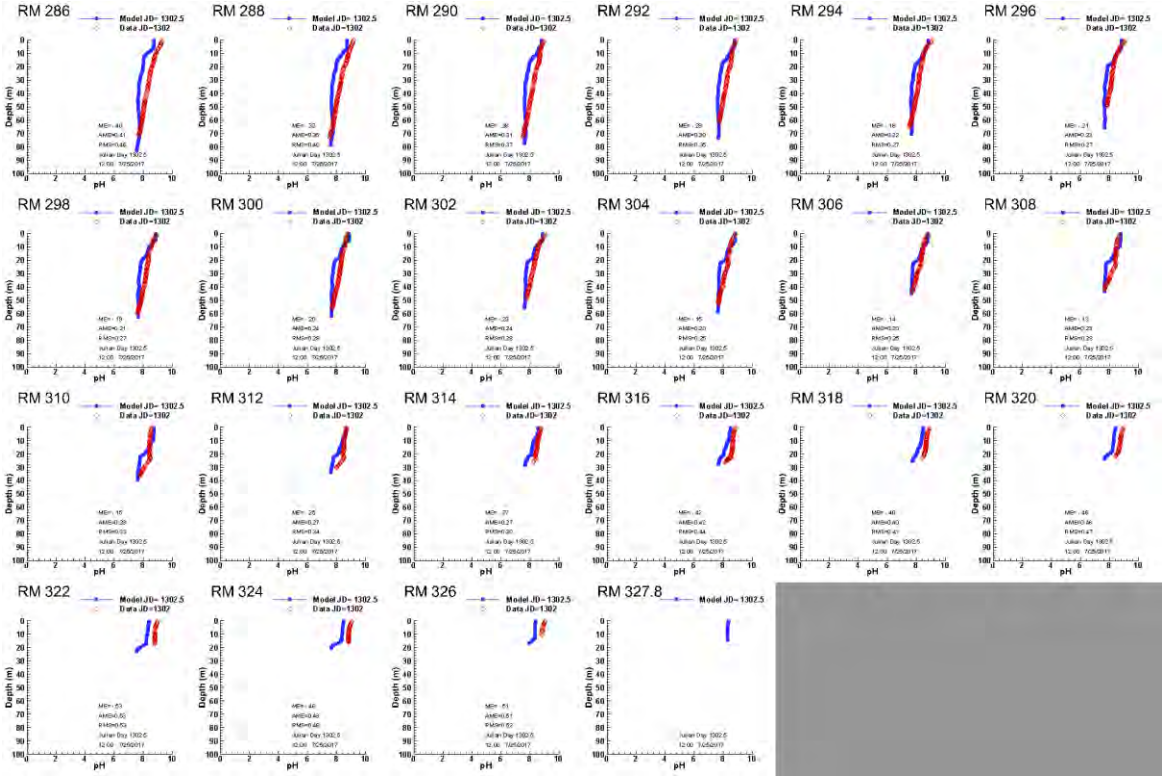


Figure 2274. Vertical profiles of pH compared with data for 7/25/2017.

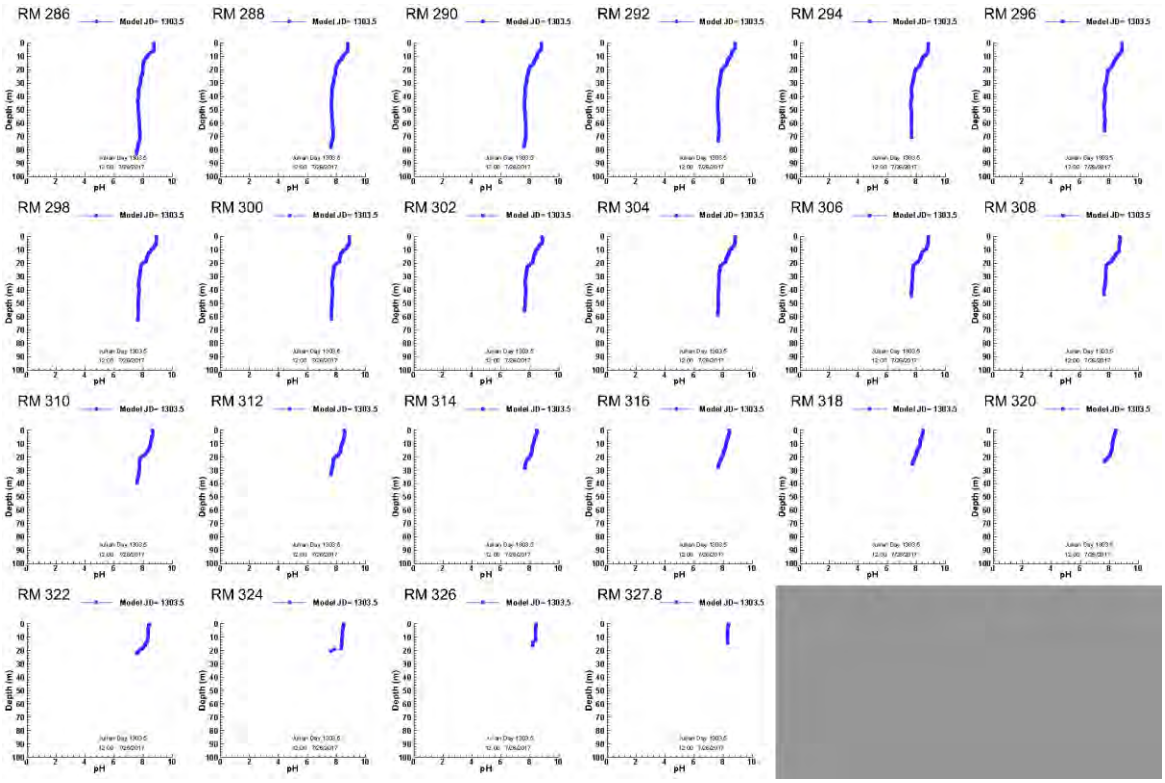


Figure 2275. Vertical profiles of pH compared with data for 7/26/2017.

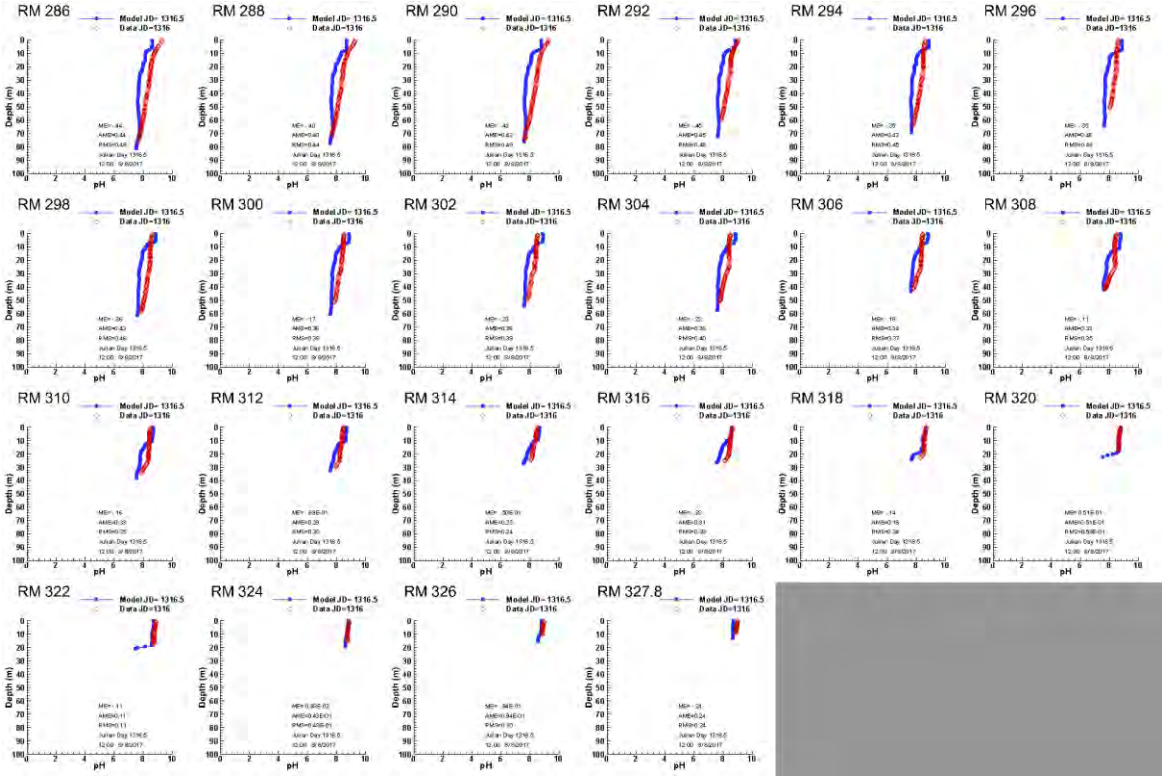


Figure 2276. Vertical profiles of pH compared with data for 8/ 8/2017.

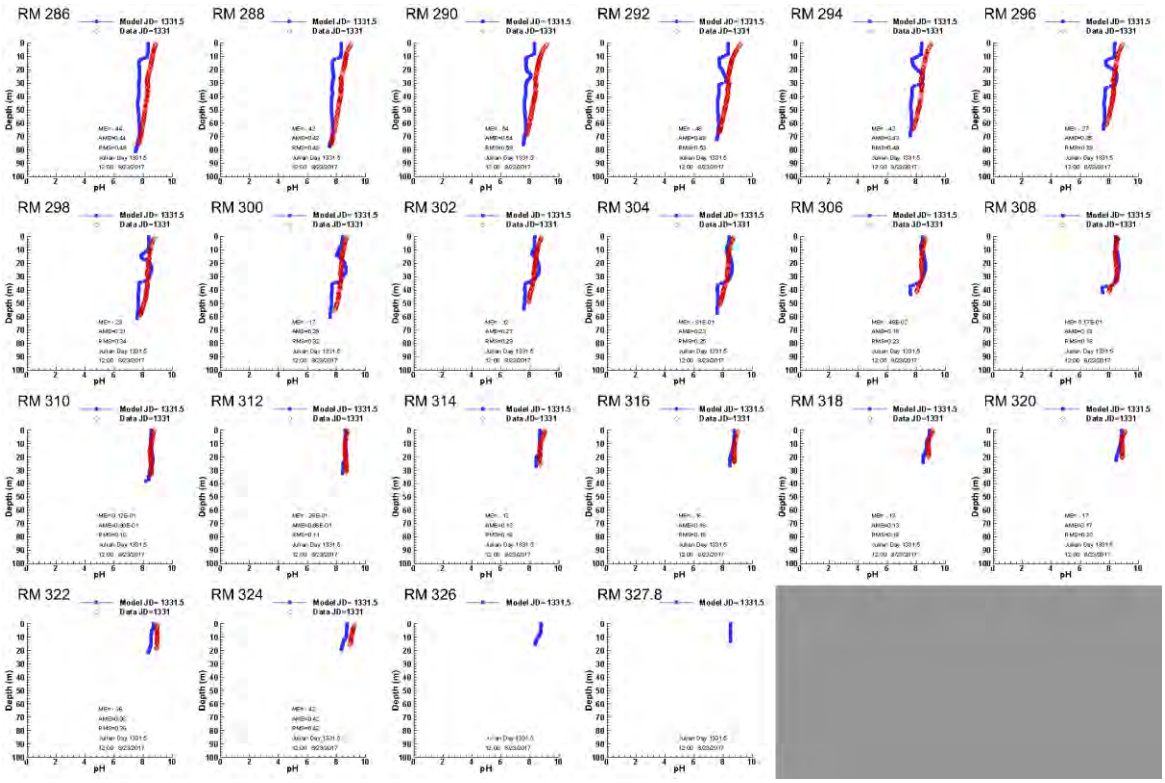


Figure 2277. Vertical profiles of pH compared with data for 8/23/2017.

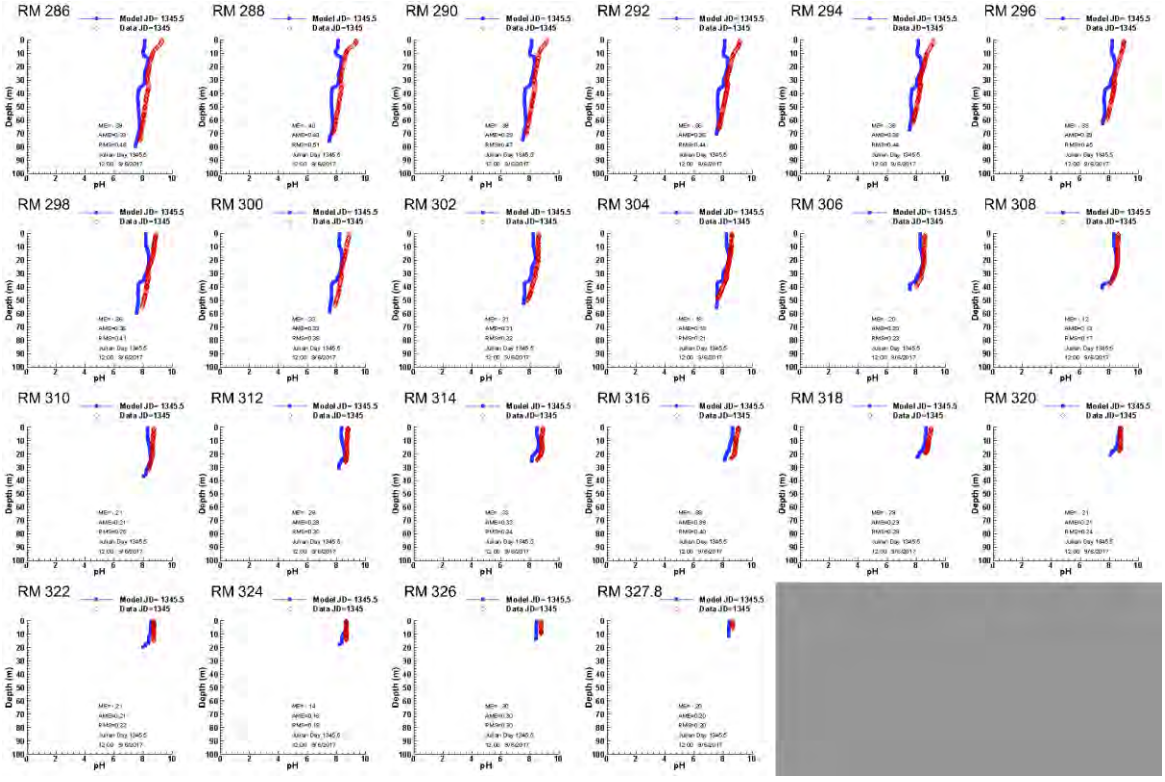


Figure 2278. Vertical profiles of pH compared with data for 9/ 6/2017.

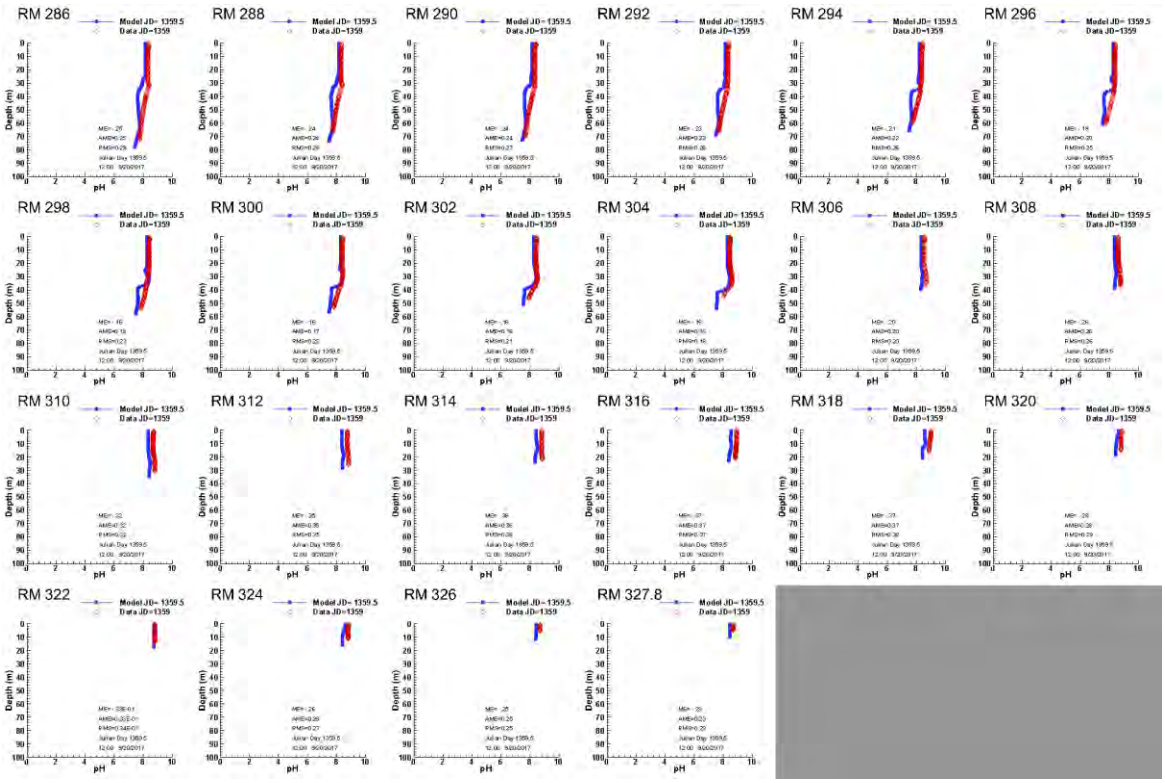


Figure 2279. Vertical profiles of pH compared with data for 9/20/2017.

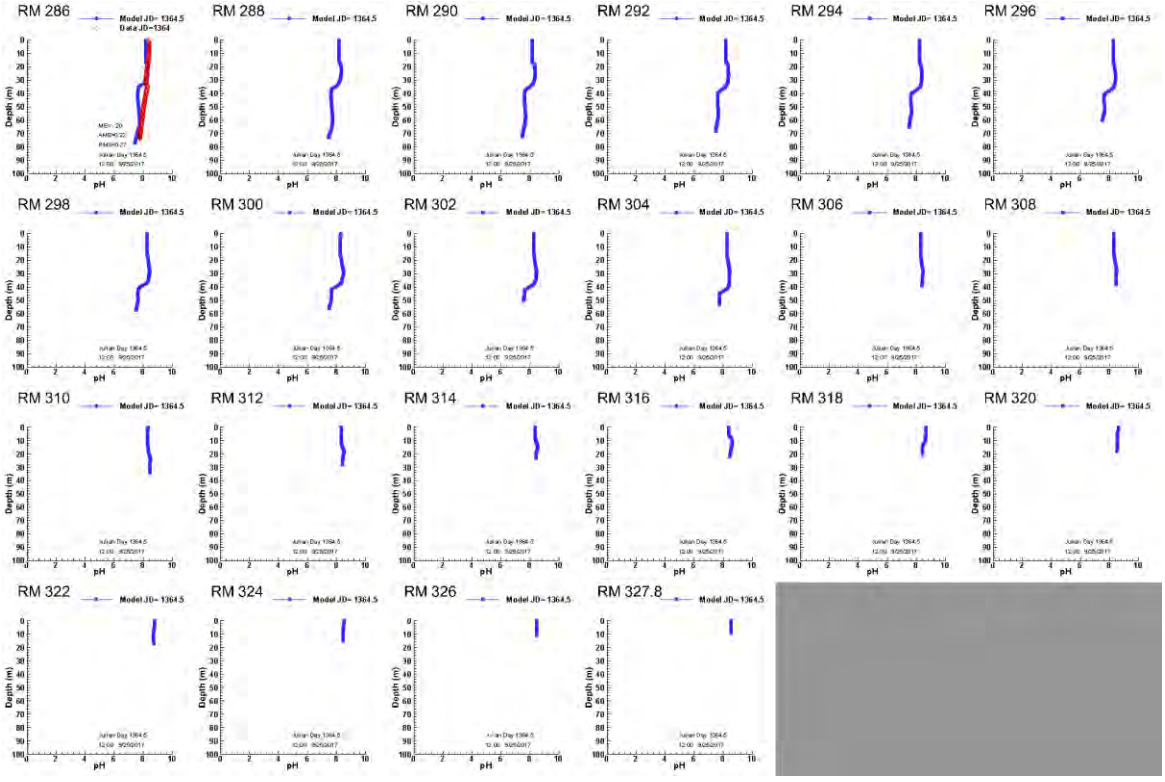


Figure 2280. Vertical profiles of pH compared with data for 9/25/2017.

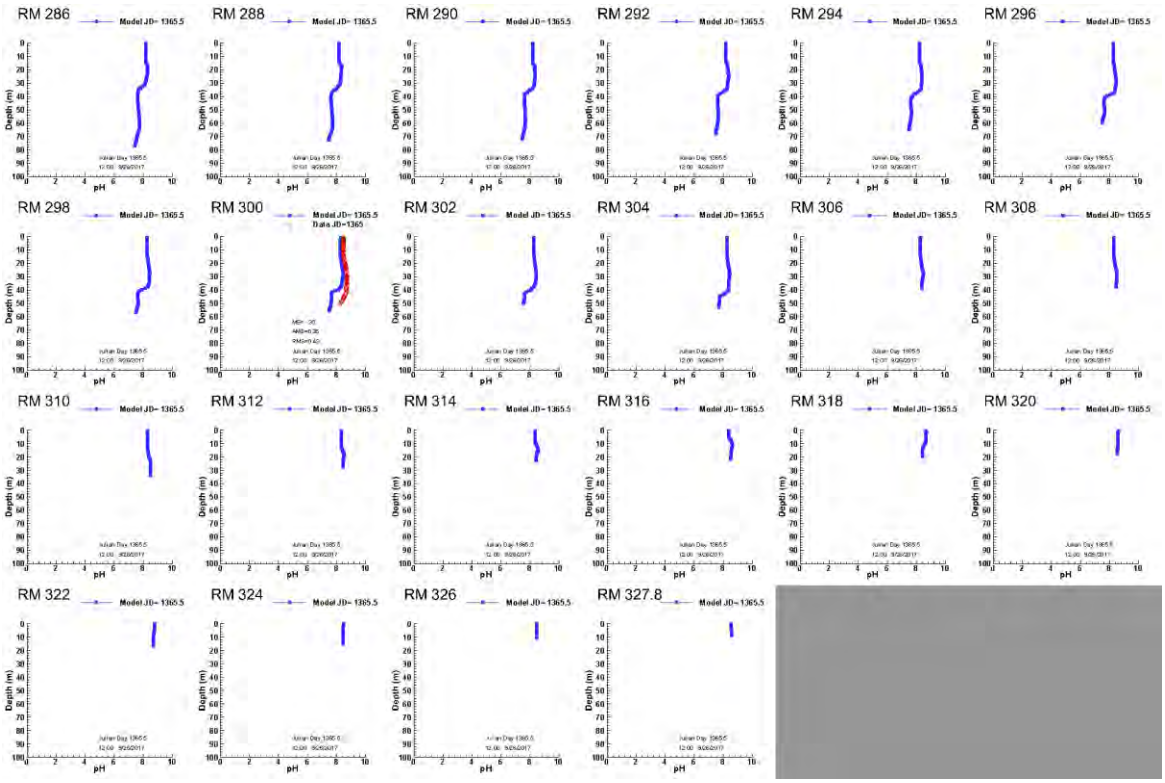


Figure 2281. Vertical profiles of pH compared with data for 9/26/2017.

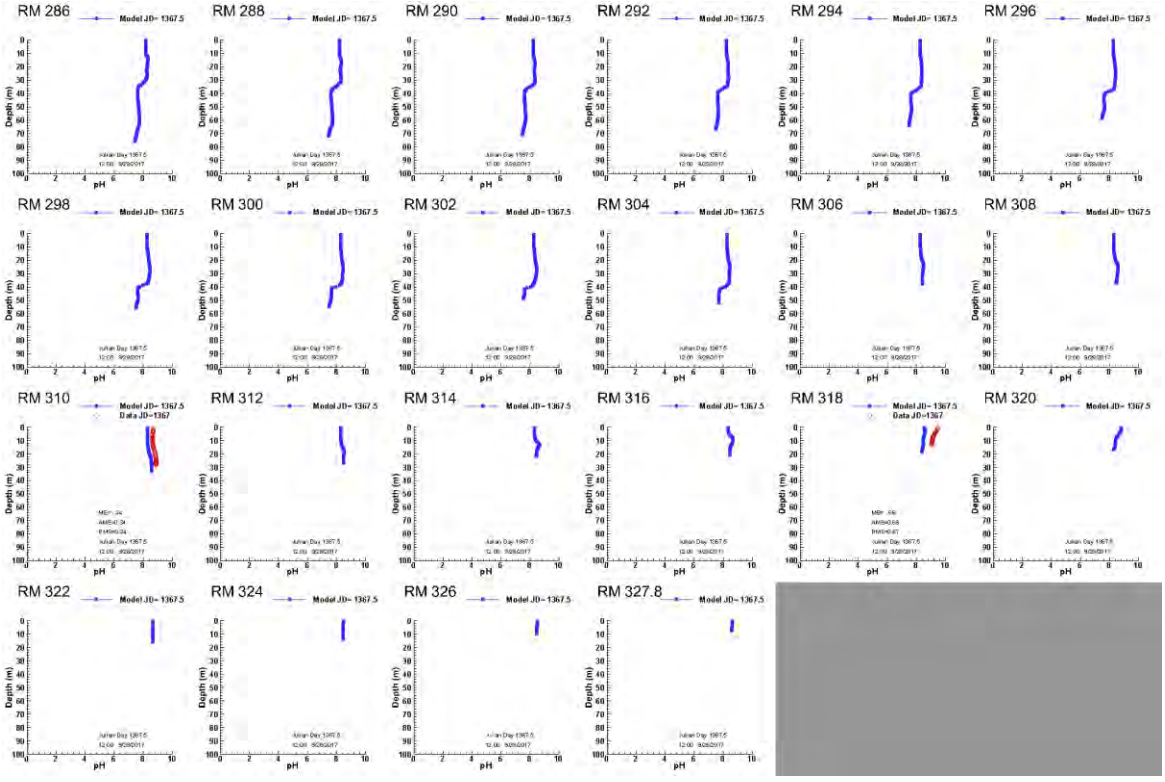


Figure 2282. Vertical profiles of pH compared with data for 9/28/2017.

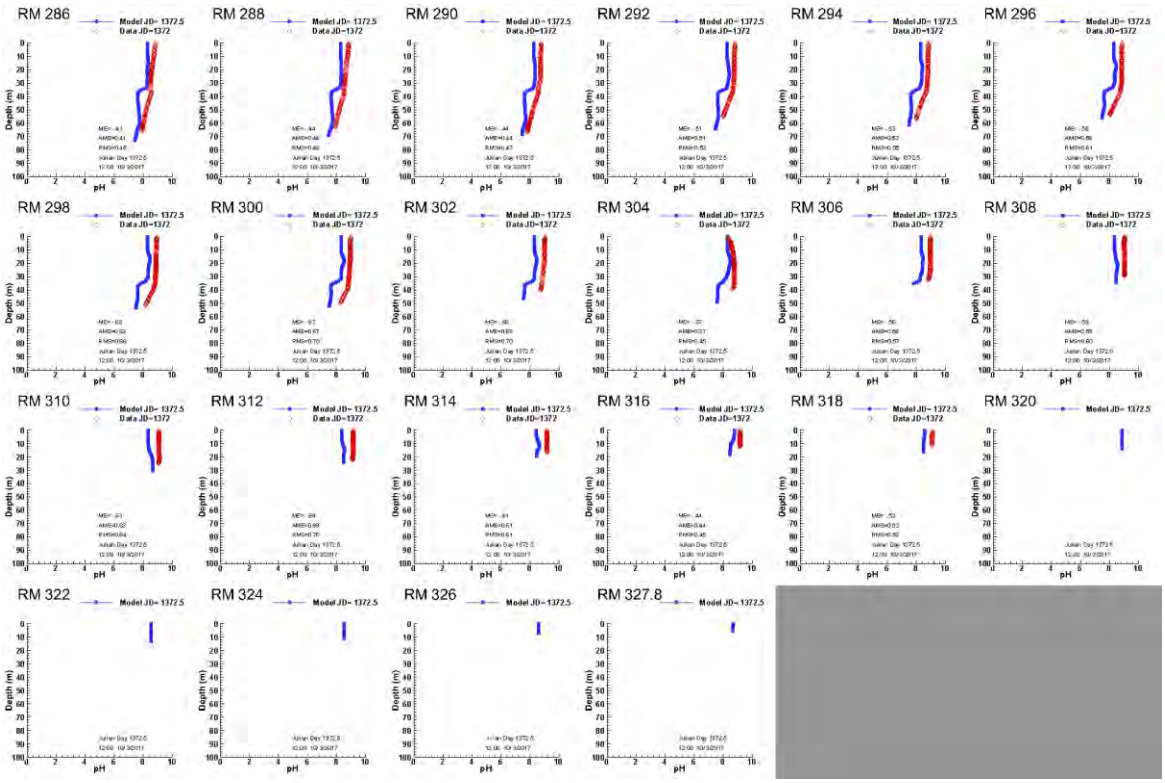


Figure 2283. Vertical profiles of pH compared with data for 10/ 3/2017.

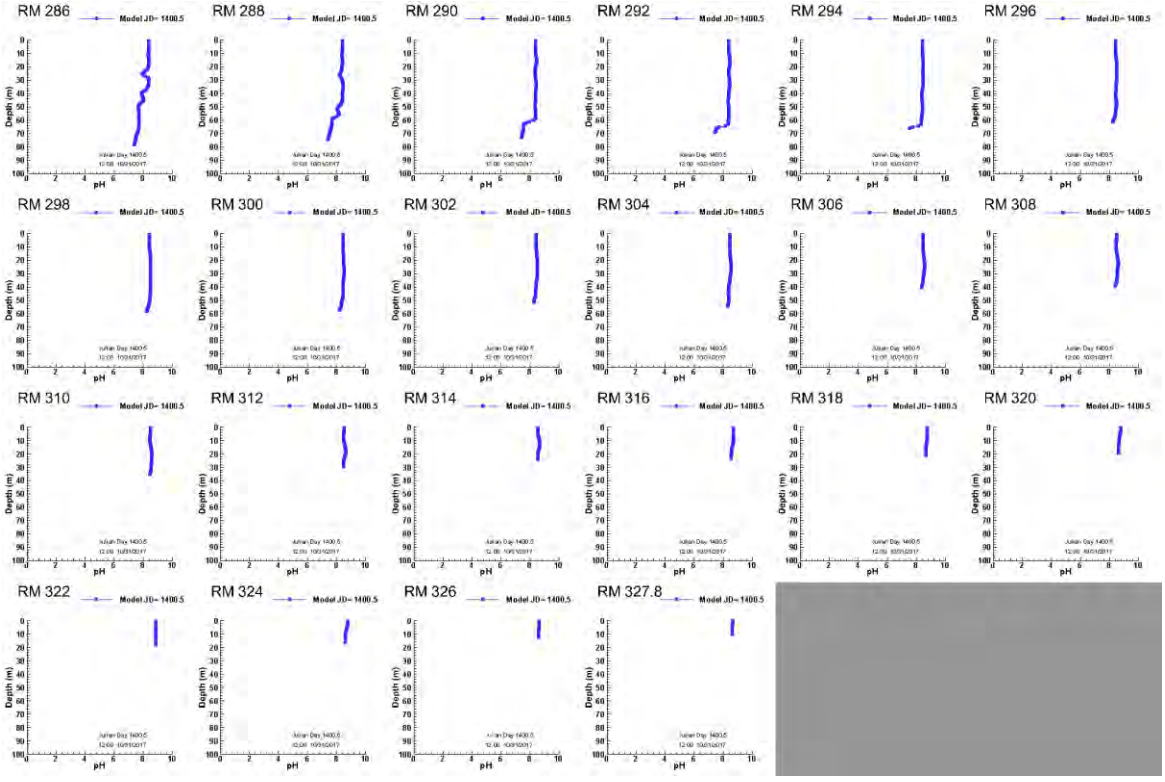


Figure 2284. Vertical profiles of pH compared with data for 10/31/2017.

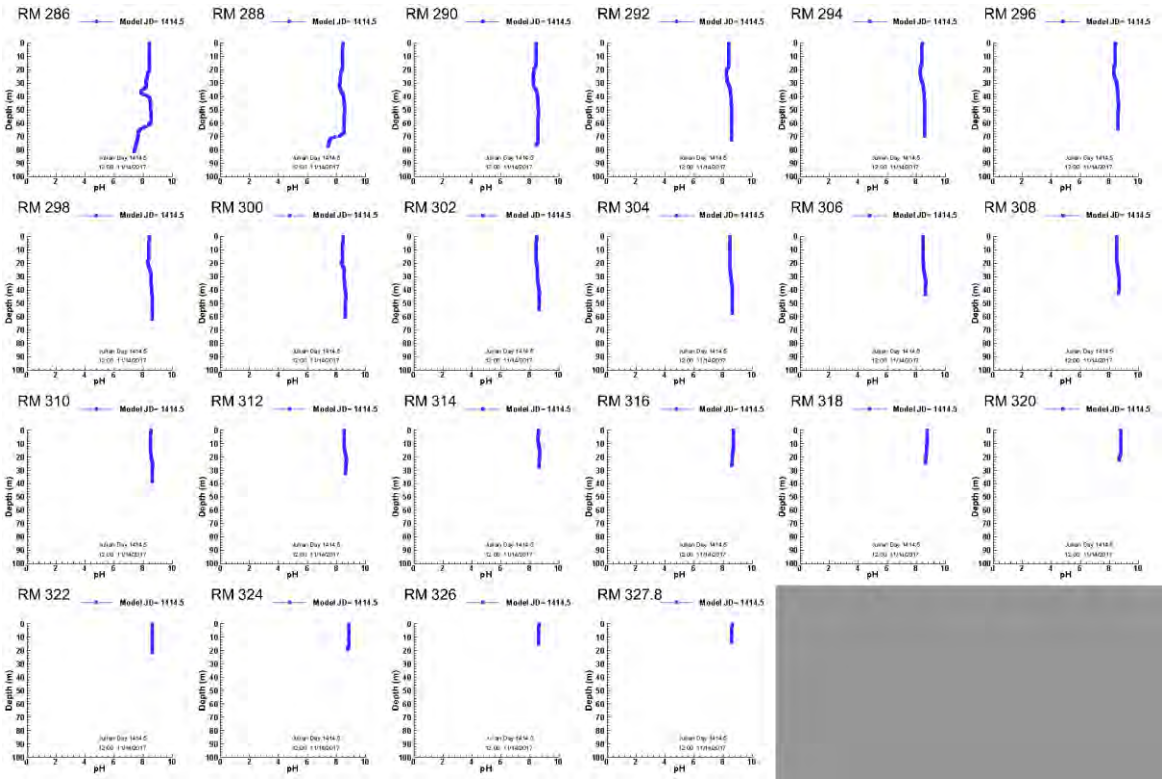


Figure 2285. Vertical profiles of pH compared with data for 11/14/2017.

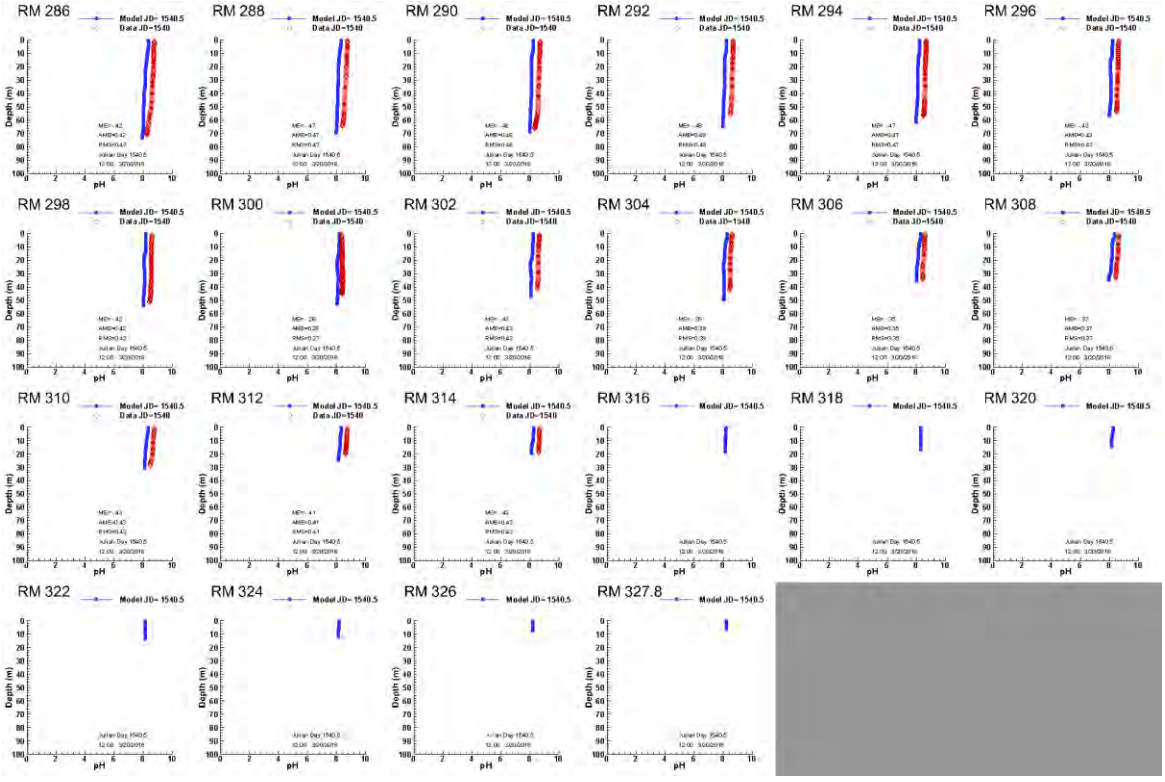


Figure 2286. Vertical profiles of pH compared with data for 3/20/2018.

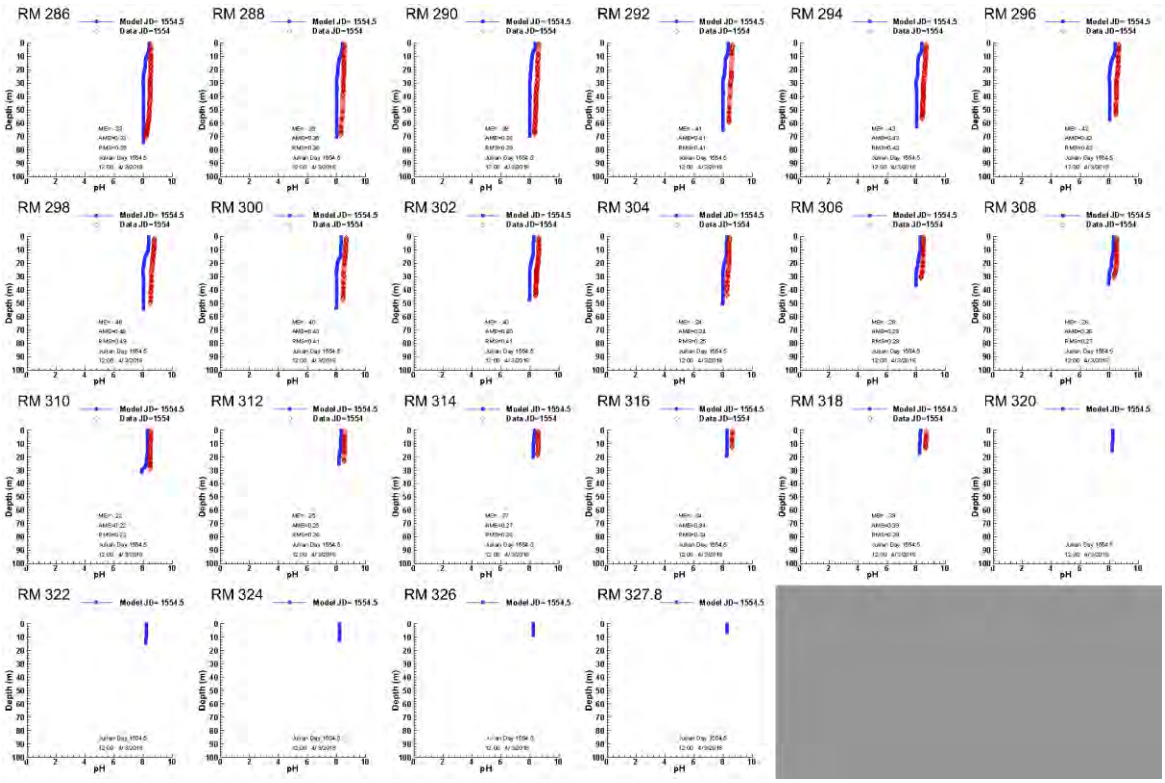


Figure 2287. Vertical profiles of pH compared with data for 4/ 3/2018.

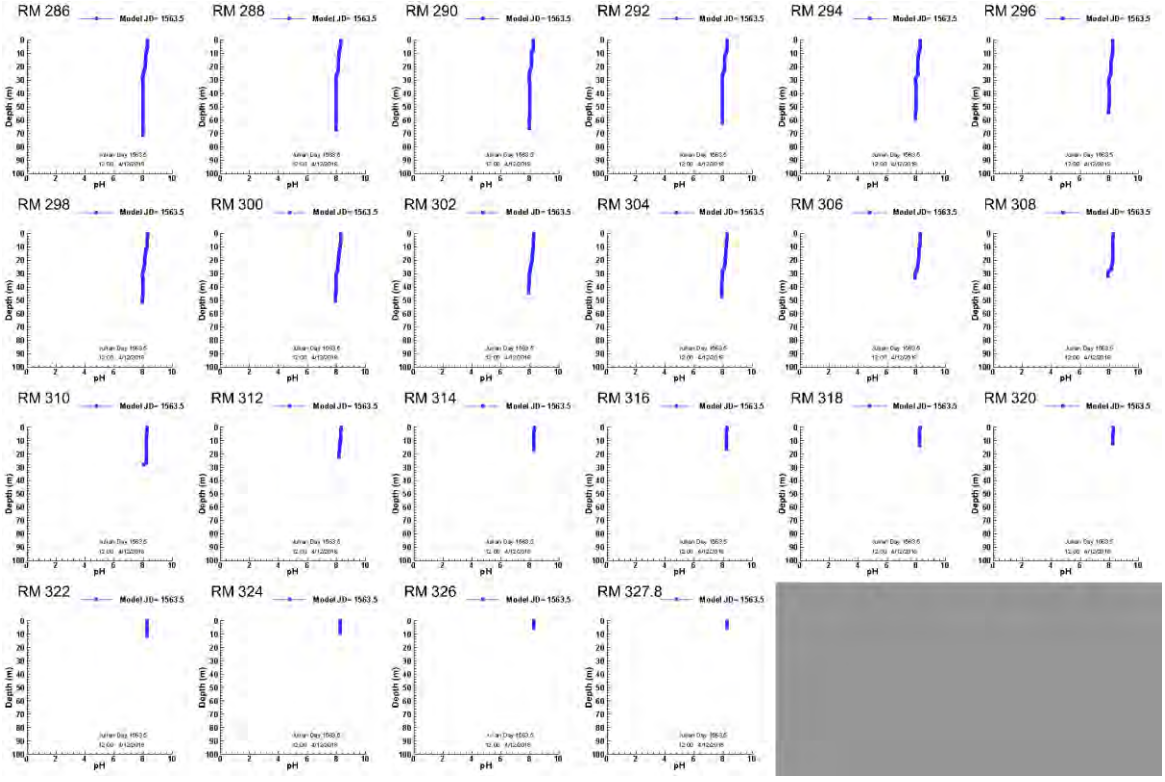


Figure 2288. Vertical profiles of pH compared with data for 4/12/2018.

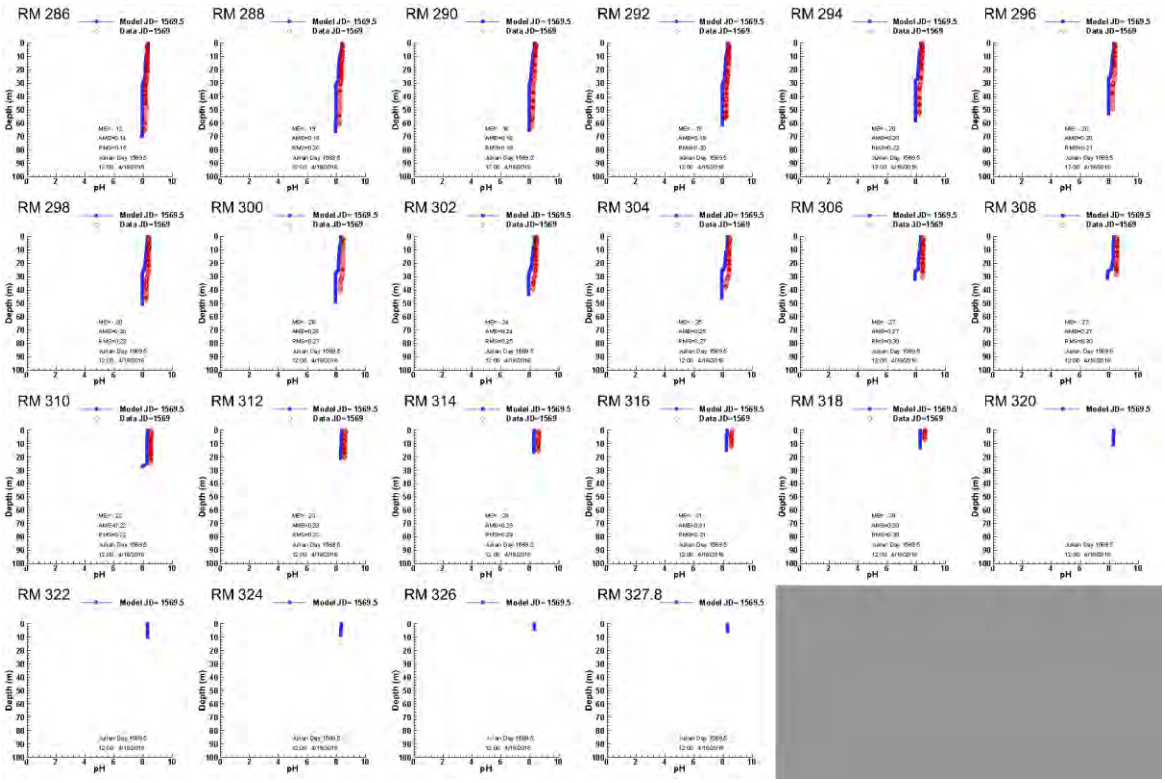


Figure 2289. Vertical profiles of pH compared with data for 4/18/2018.

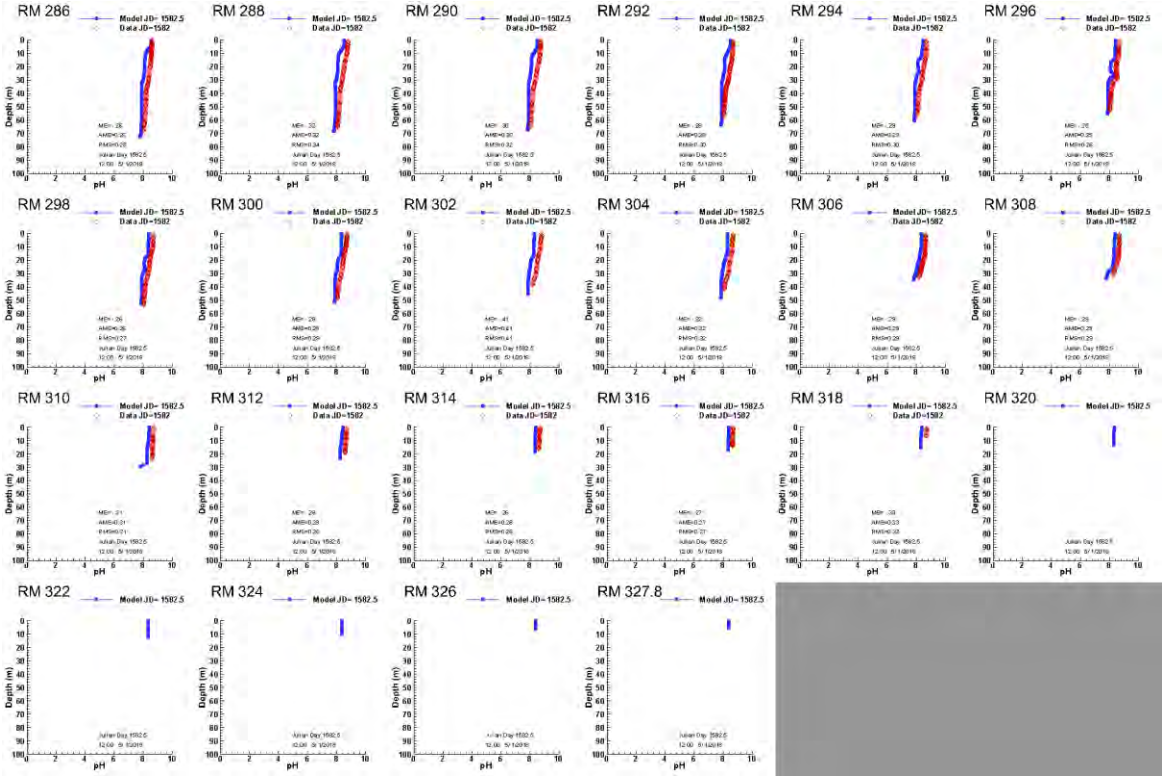


Figure 2290. Vertical profiles of pH compared with data for 5/ 1/2018.

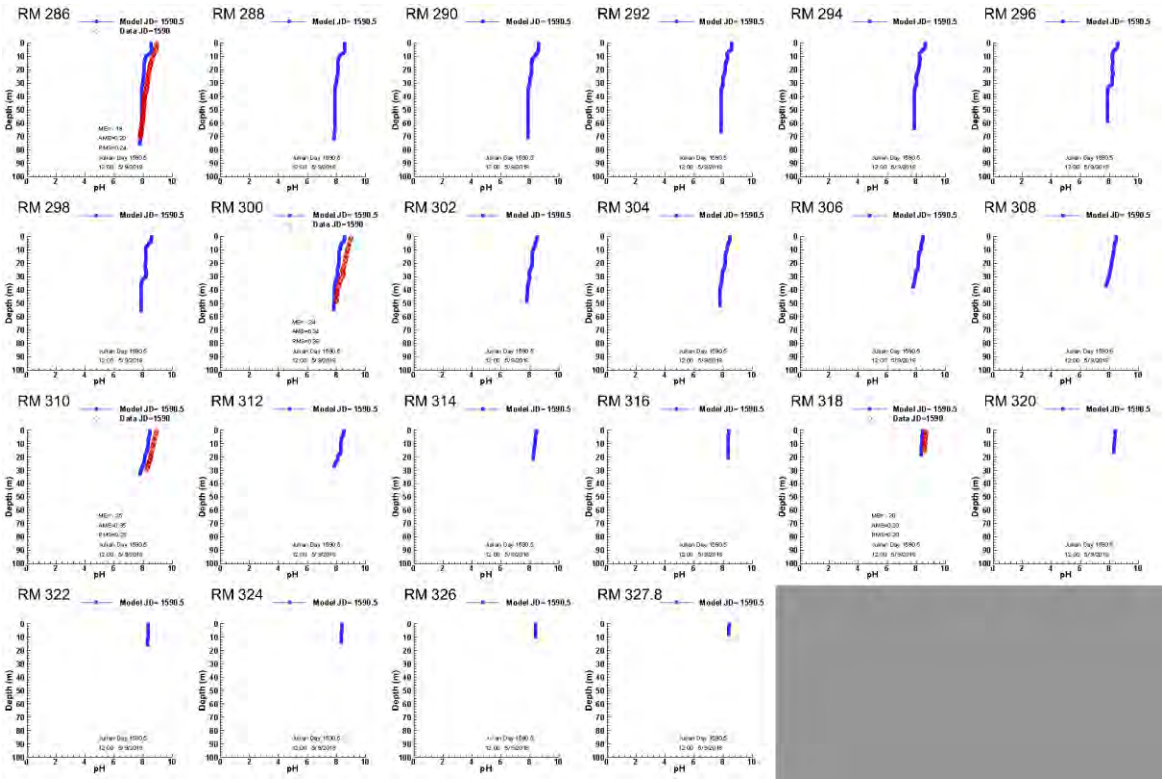


Figure 2291. Vertical profiles of pH compared with data for 5/ 9/2018.

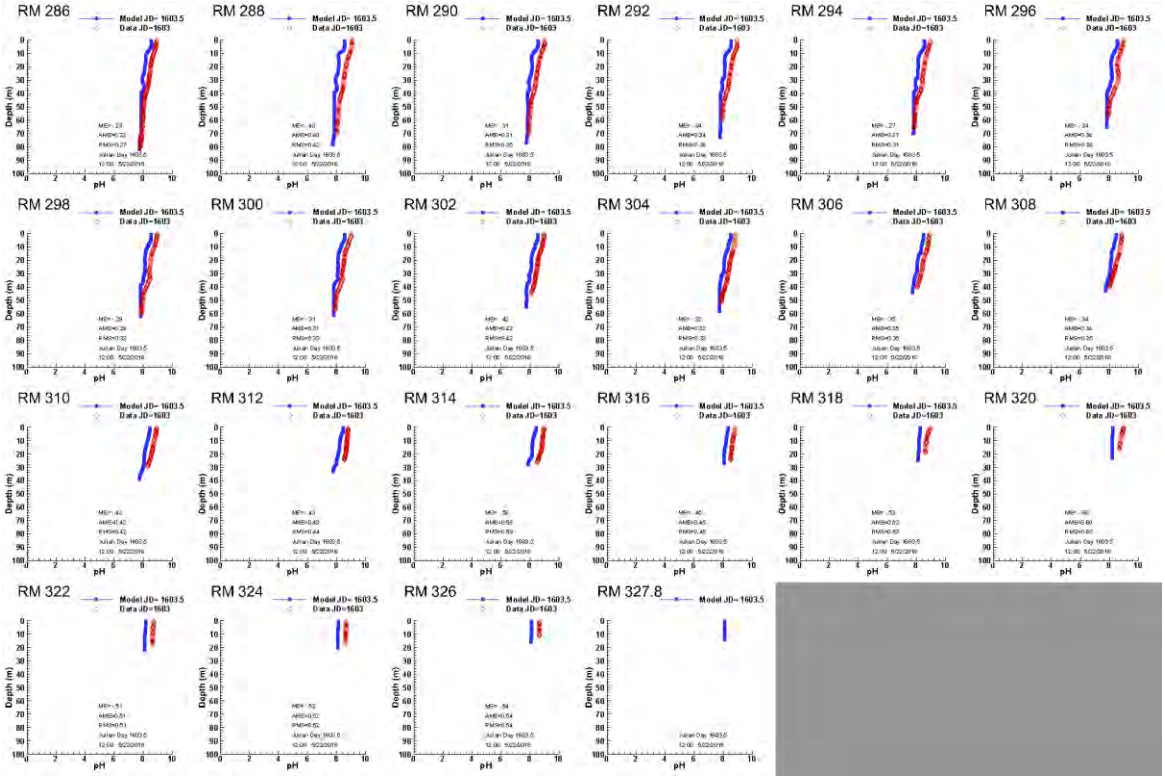


Figure 2292. Vertical profiles of pH compared with data for 5/22/2018.

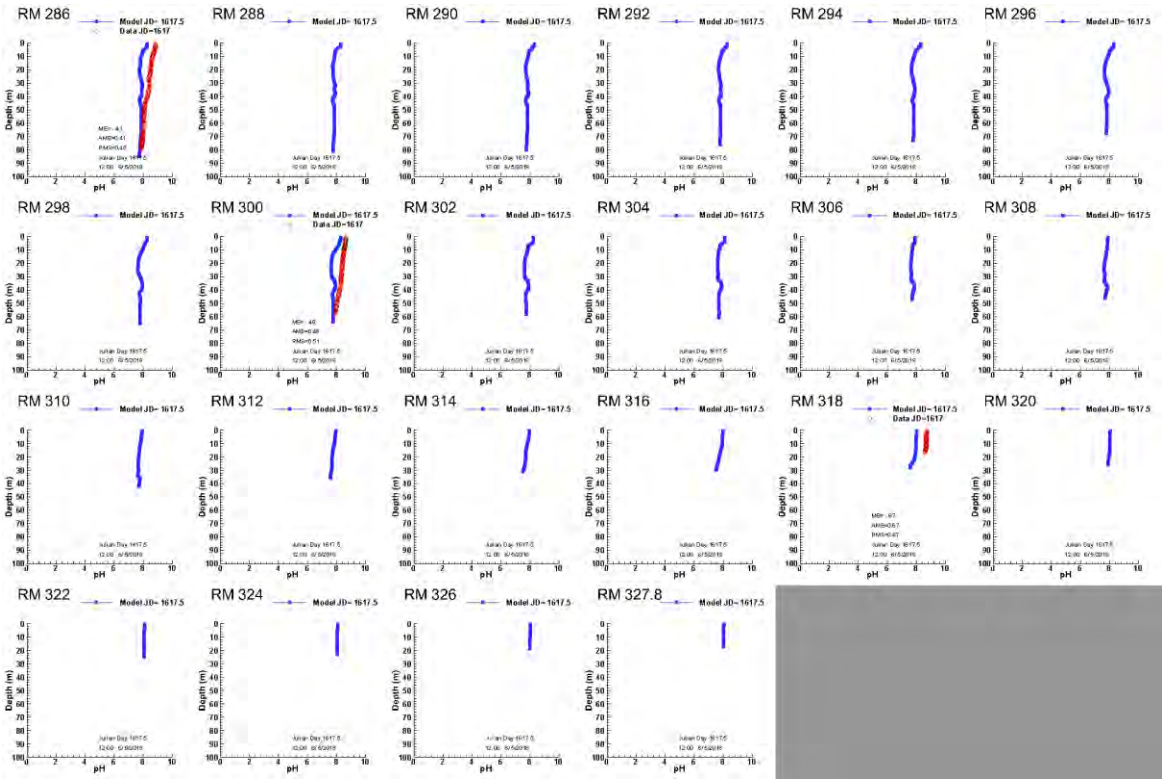


Figure 2293. Vertical profiles of pH compared with data for 6/ 5/2018.

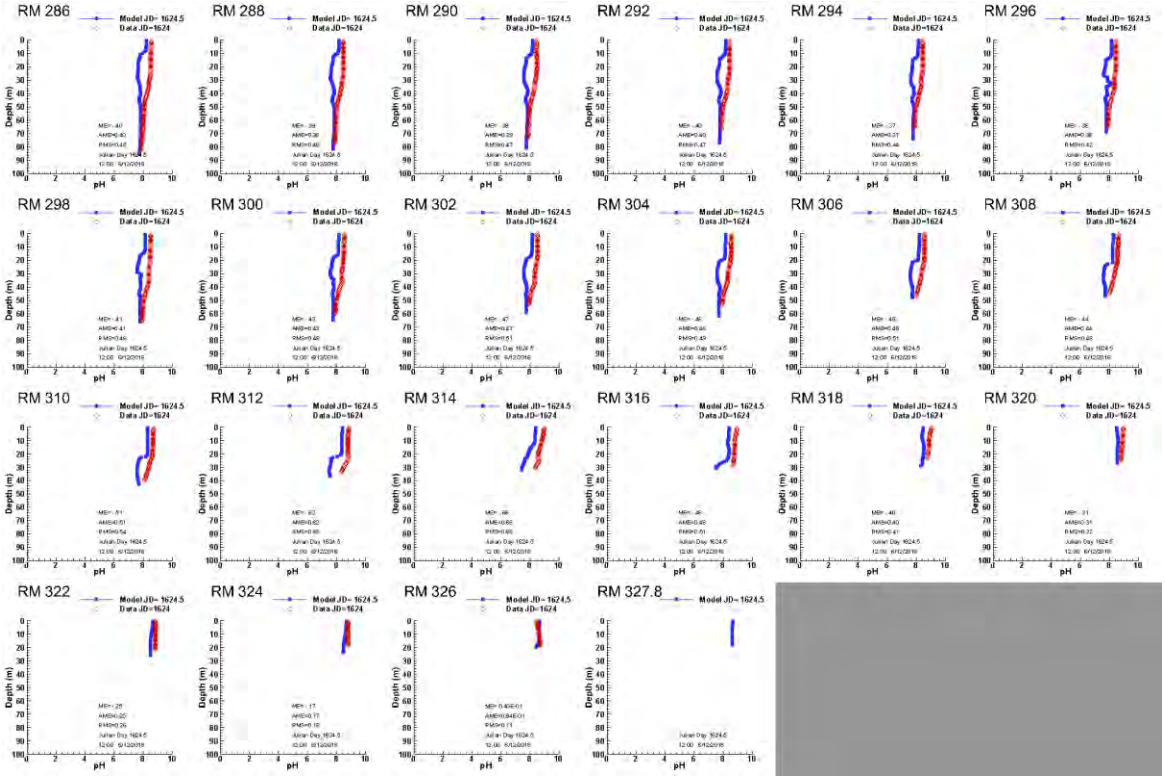


Figure 2294. Vertical profiles of pH compared with data for 6/12/2018.

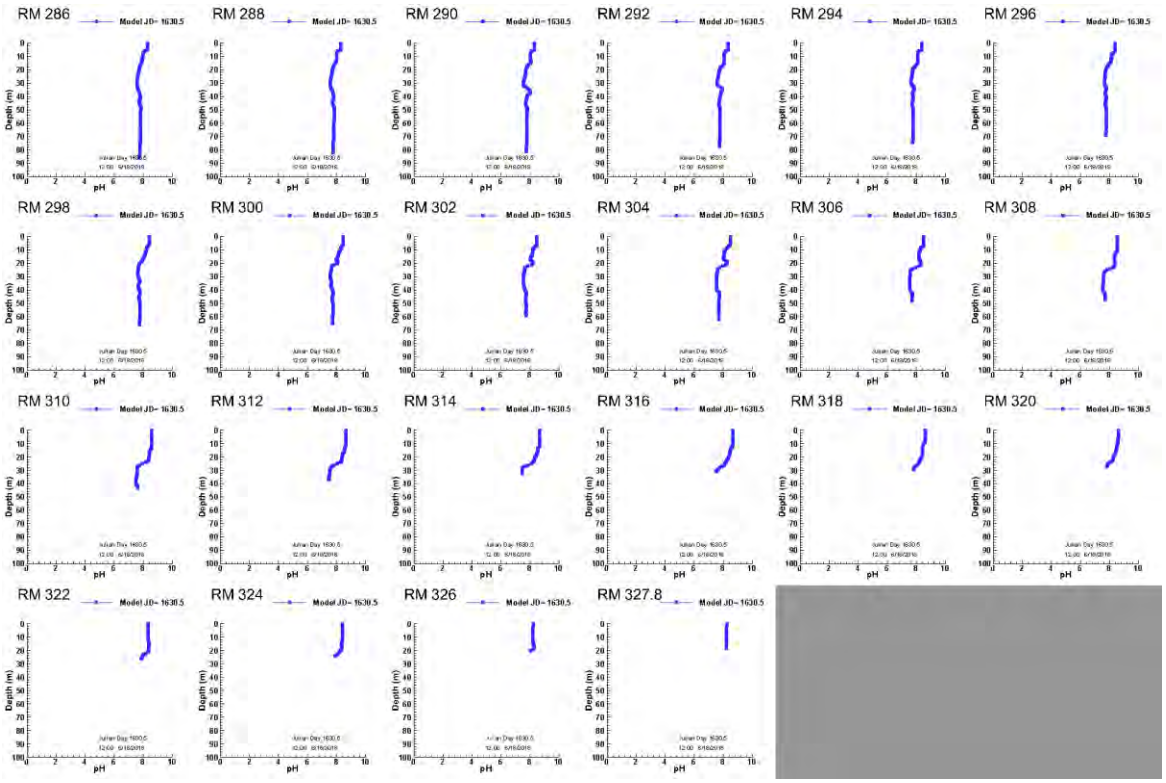


Figure 2295. Vertical profiles of pH compared with data for 6/18/2018.

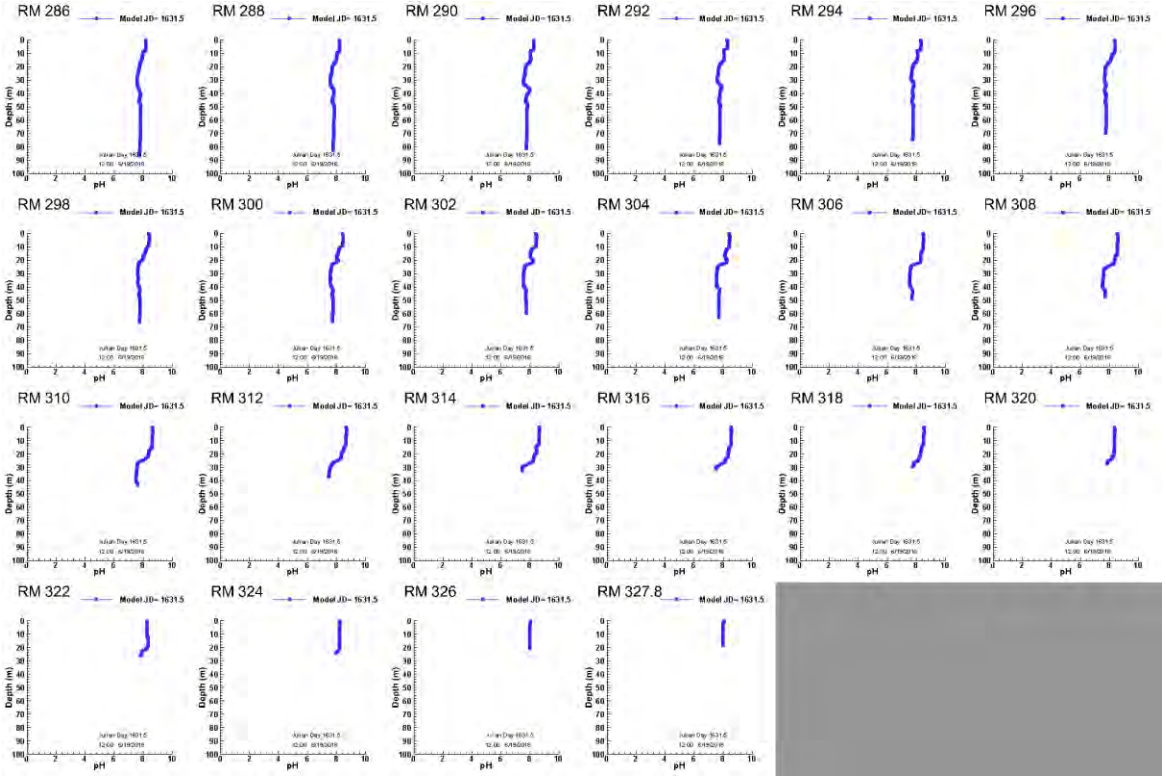


Figure 2296. Vertical profiles of pH compared with data for 6/19/2018.

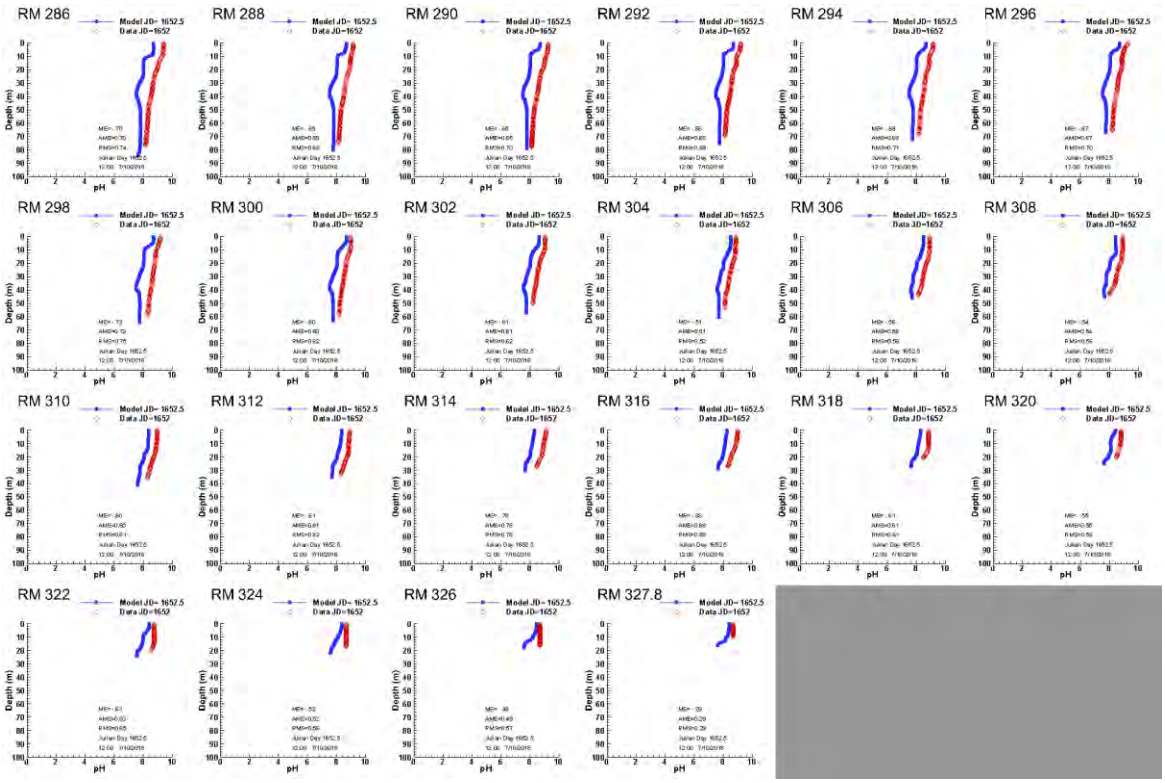


Figure 2297. Vertical profiles of pH compared with data for 7/10/2018.

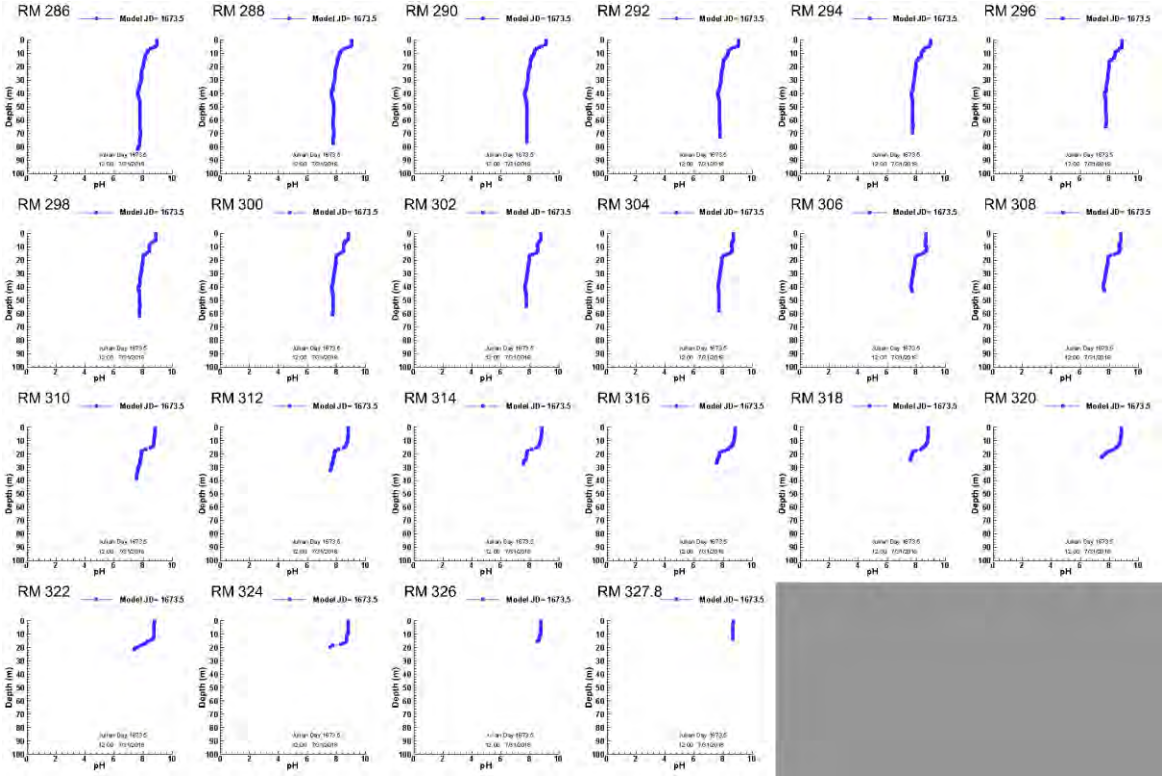


Figure 2298. Vertical profiles of pH compared with data for 7/31/2018.

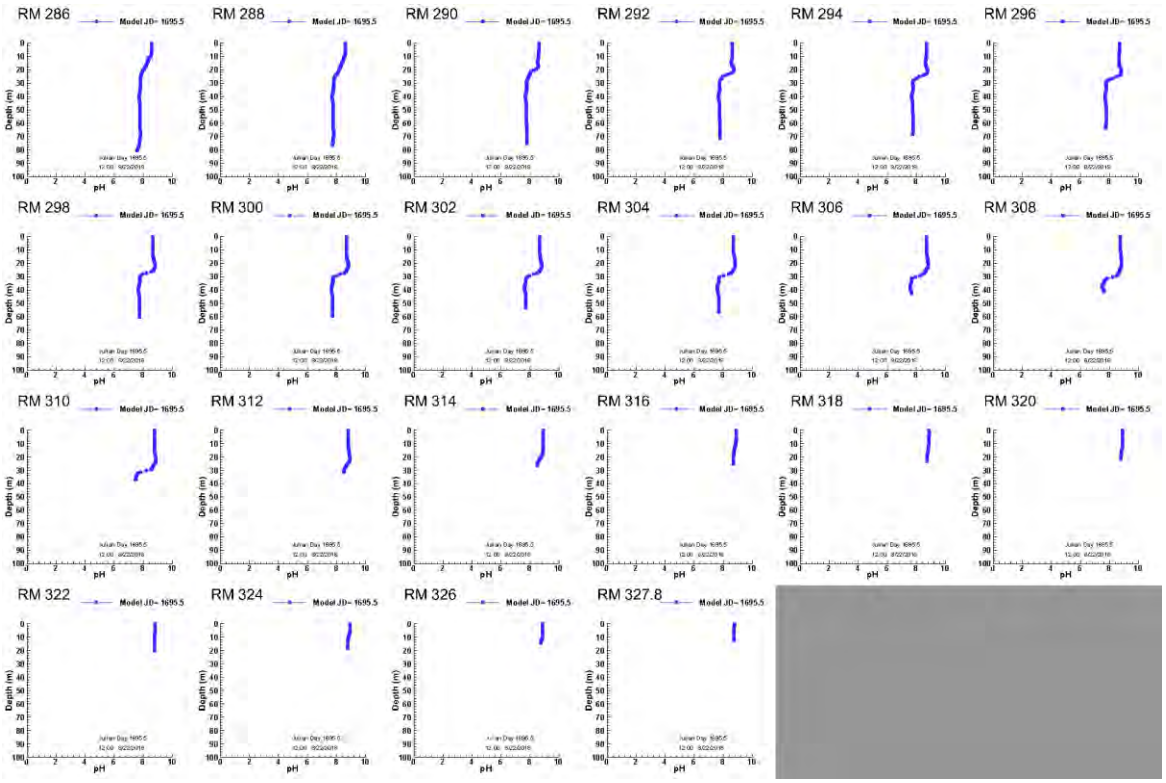


Figure 2299. Vertical profiles of pH compared with data for 8/22/2018.

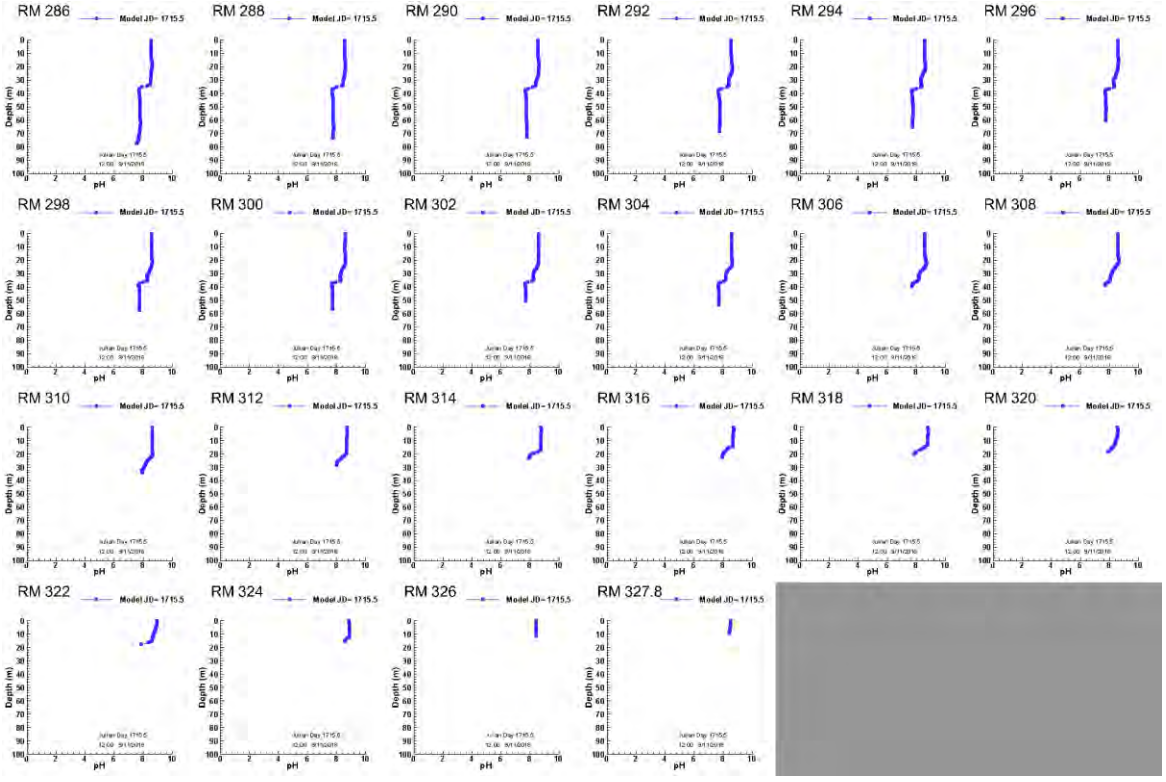


Figure 2300. Vertical profiles of pH compared with data for 9/11/2018.

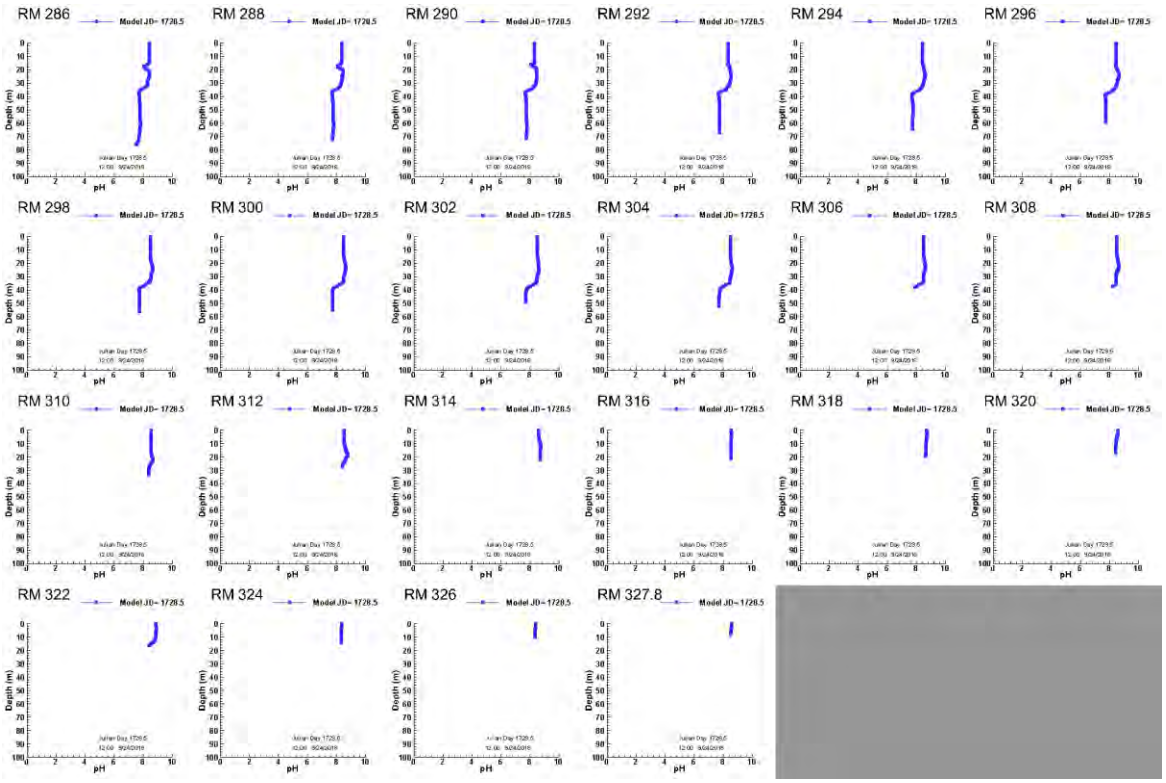


Figure 2301. Vertical profiles of pH compared with data for 9/24/2018.

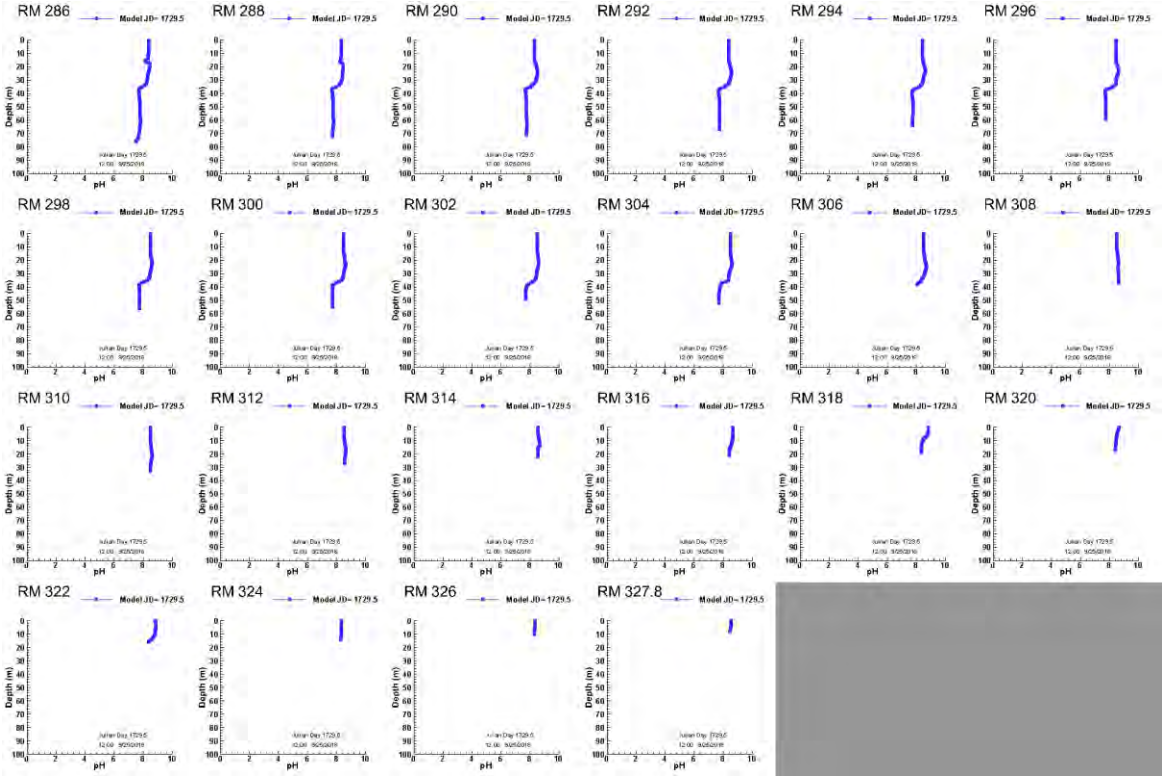


Figure 2302. Vertical profiles of pH compared with data for 9/25/2018.

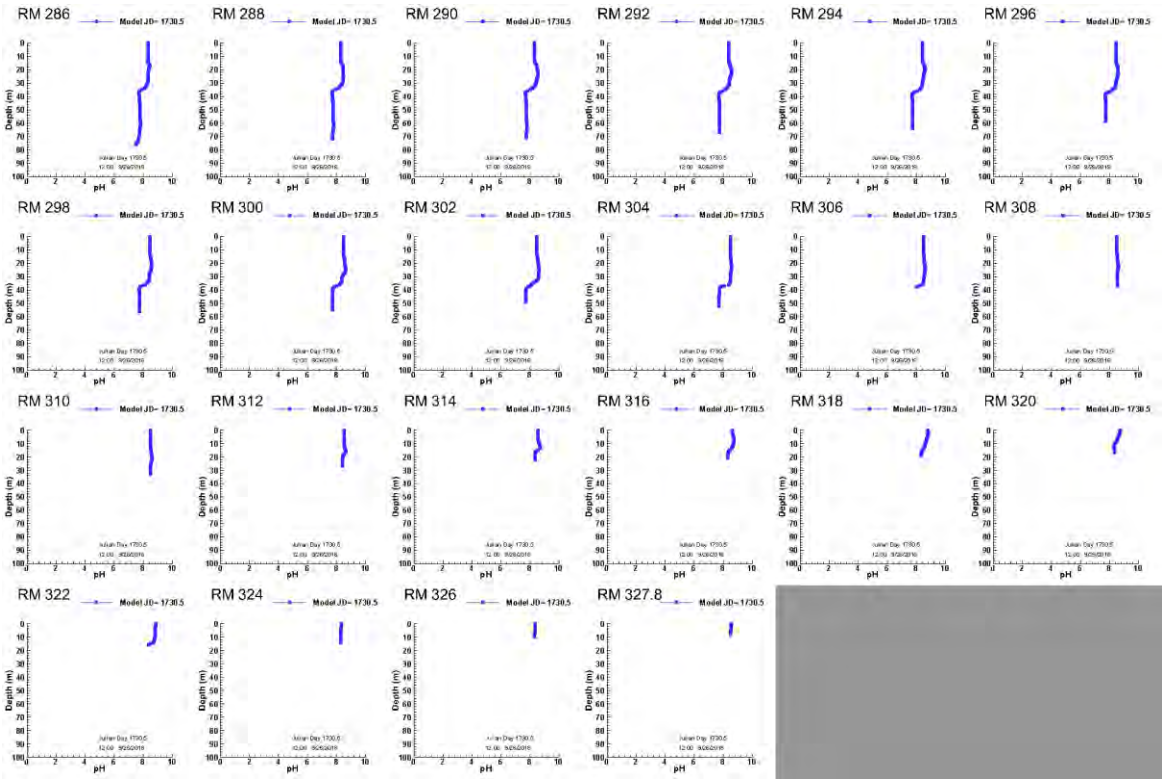


Figure 2303. Vertical profiles of pH compared with data for 9/26/2018.

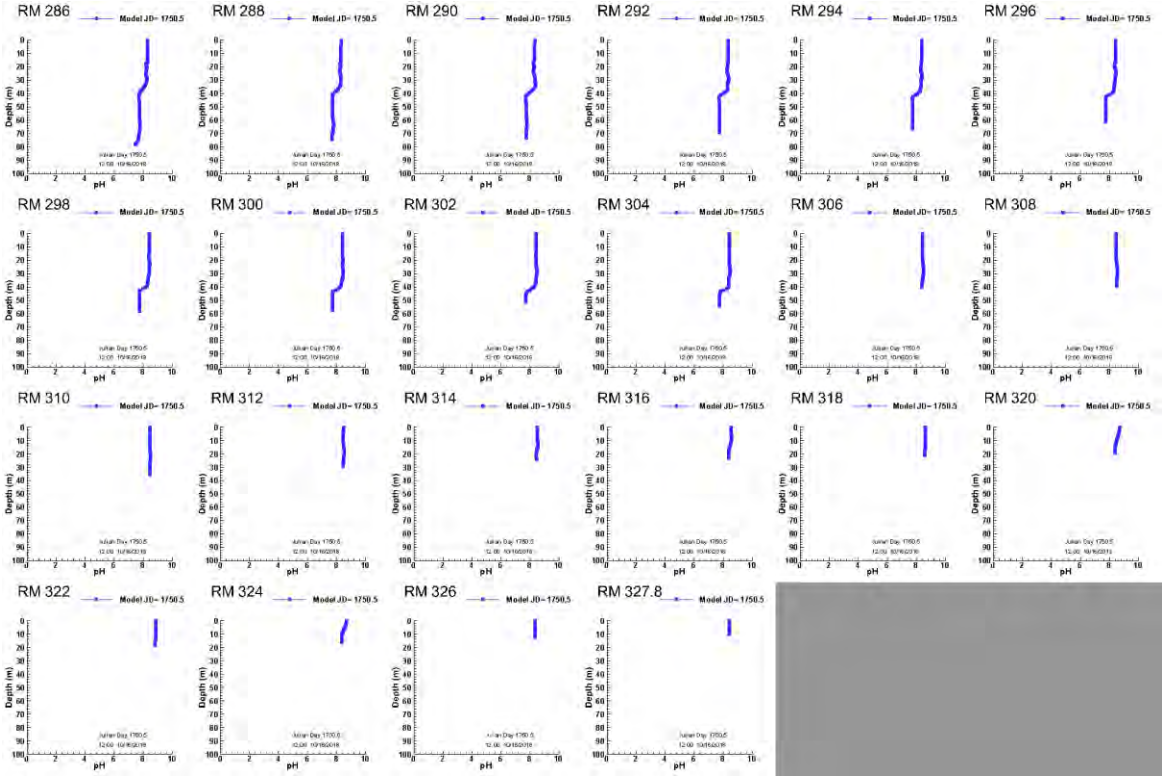


Figure 2304. Vertical profiles of pH compared with data for 10/16/2018.

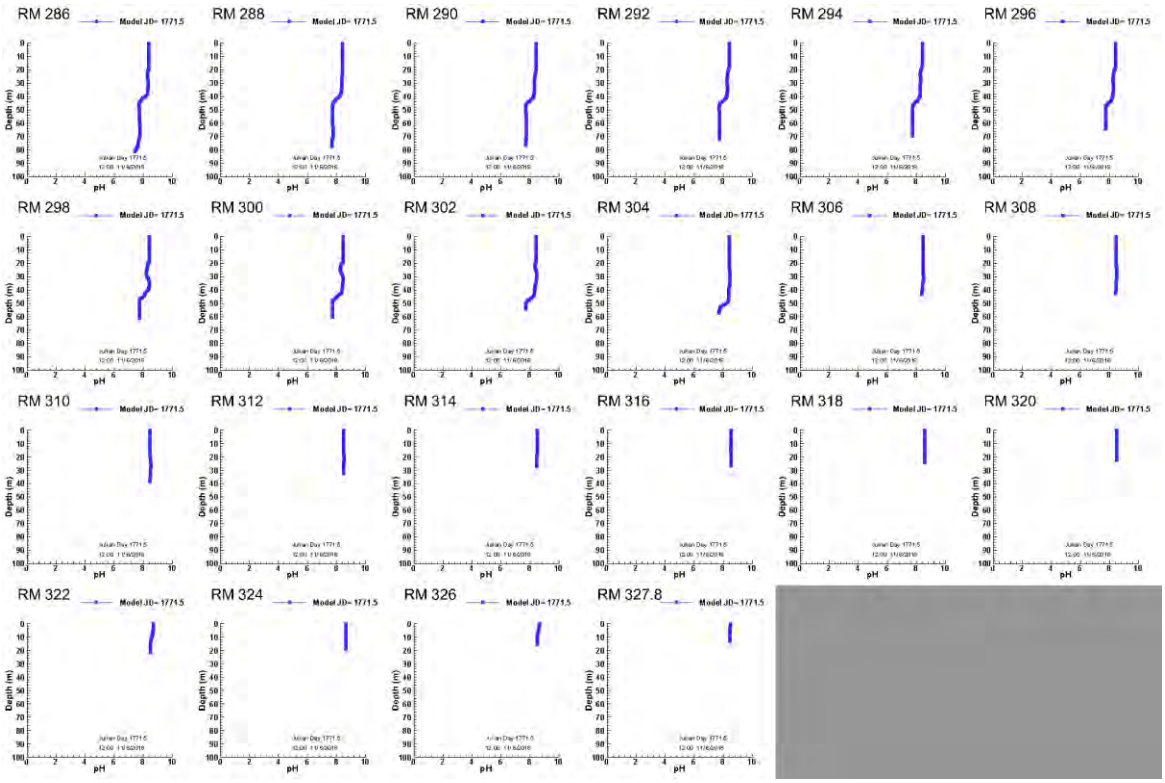


Figure 2305. Vertical profiles of pH compared with data for 11/ 6/2018.

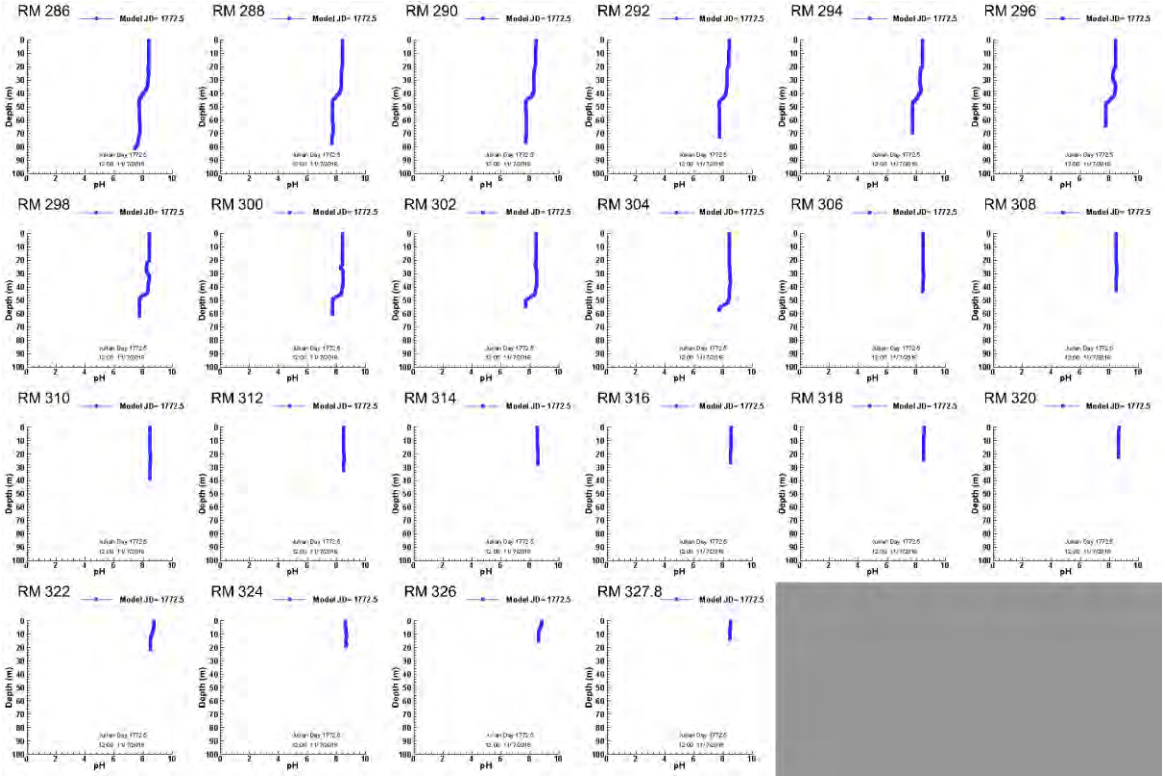


Figure 2306. Vertical profiles of pH compared with data for 11/ 7/2018.

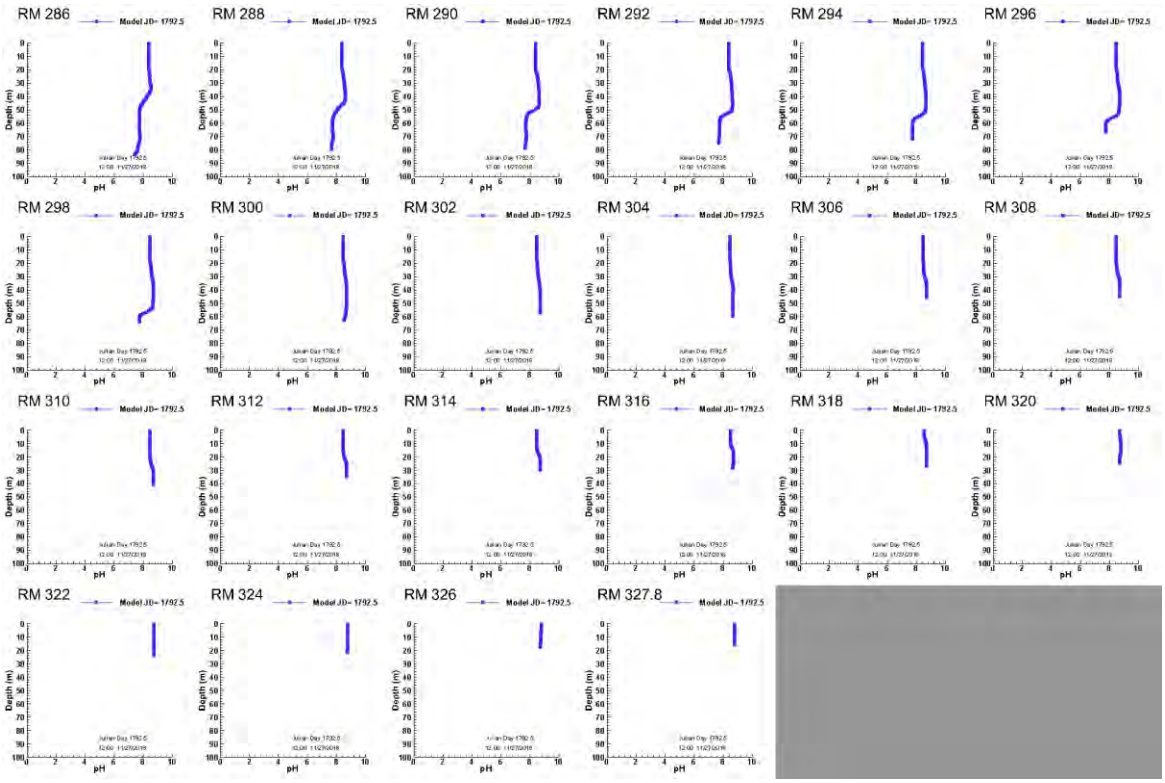


Figure 2307. Vertical profiles of pH compared with data for 11/27/2018.

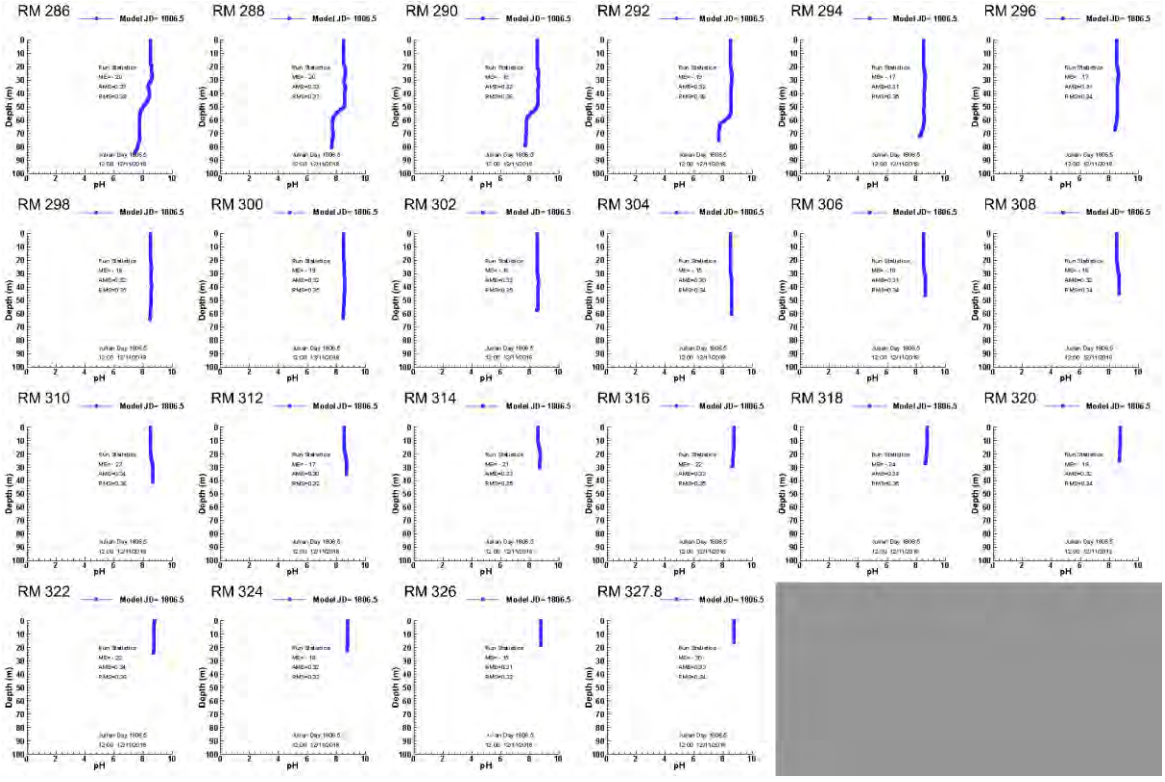


Figure 2308. Vertical profiles of pH compared with data for 12/11/2018.

Temperature

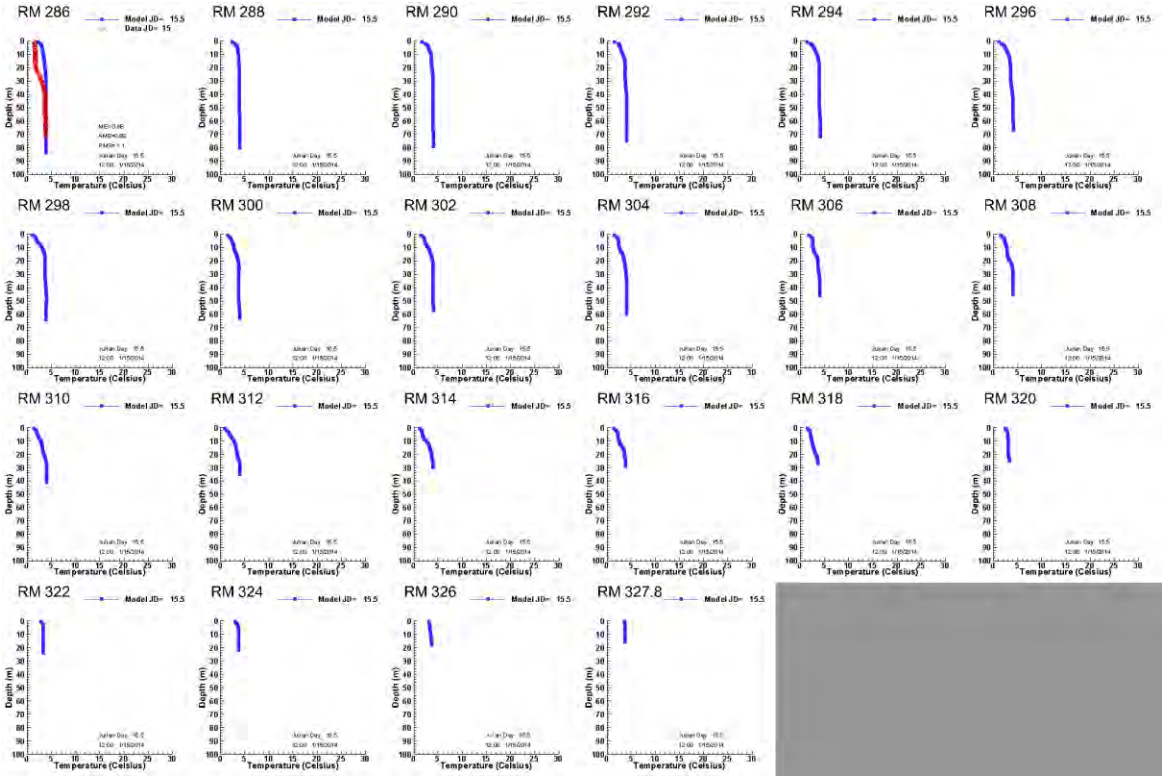


Figure 2309. Vertical profiles of temperature compared with data for 1/15/2014.

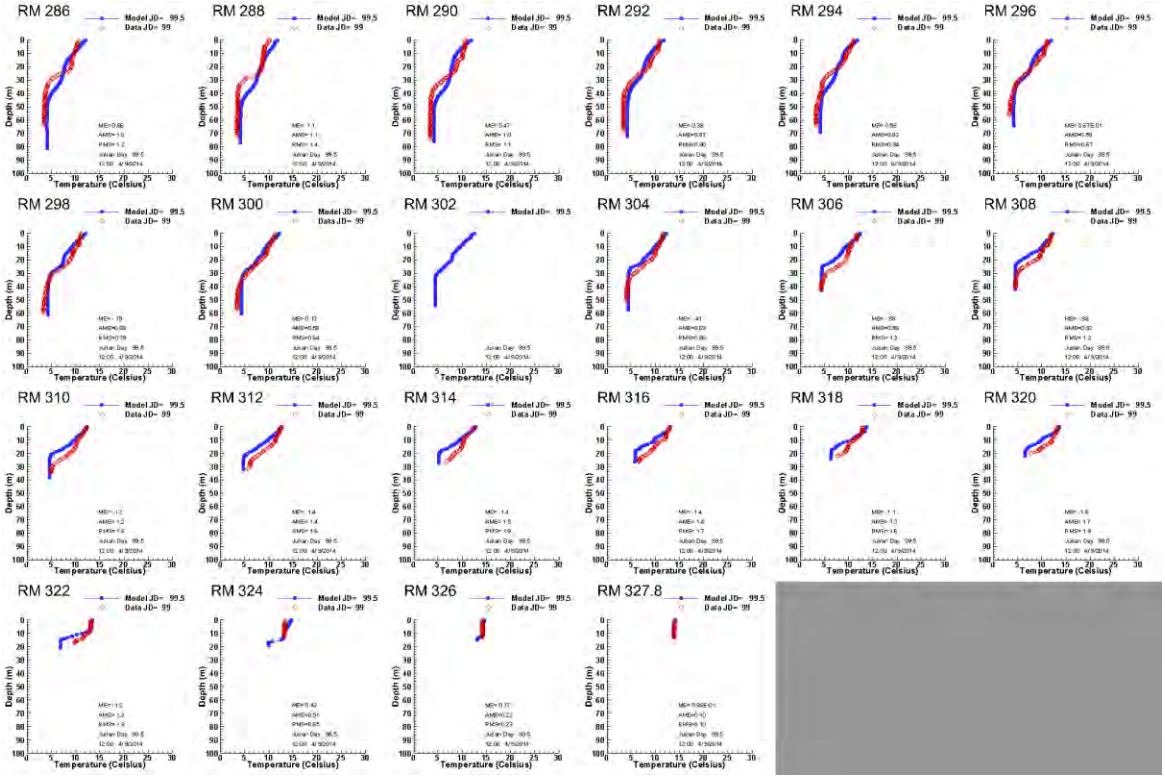


Figure 2310. Vertical profiles of temperature compared with data for 4/ 9/2014.

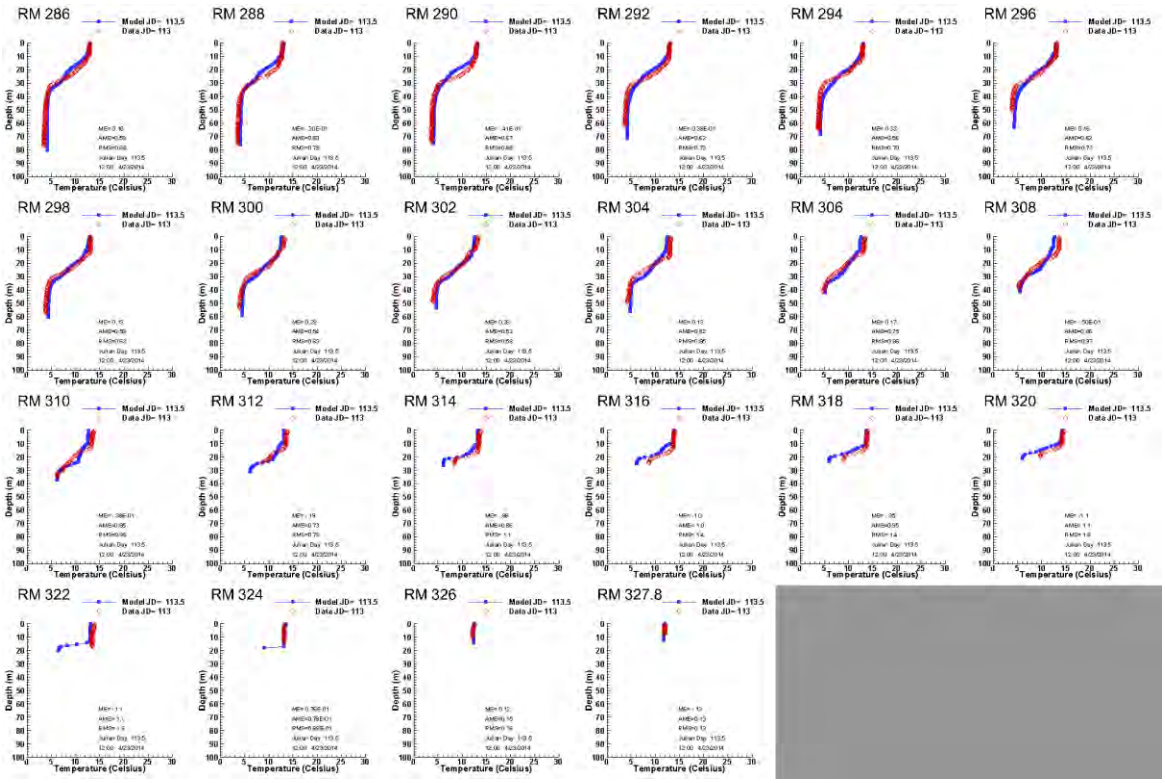


Figure 2311. Vertical profiles of temperature compared with data for 4/23/2014.

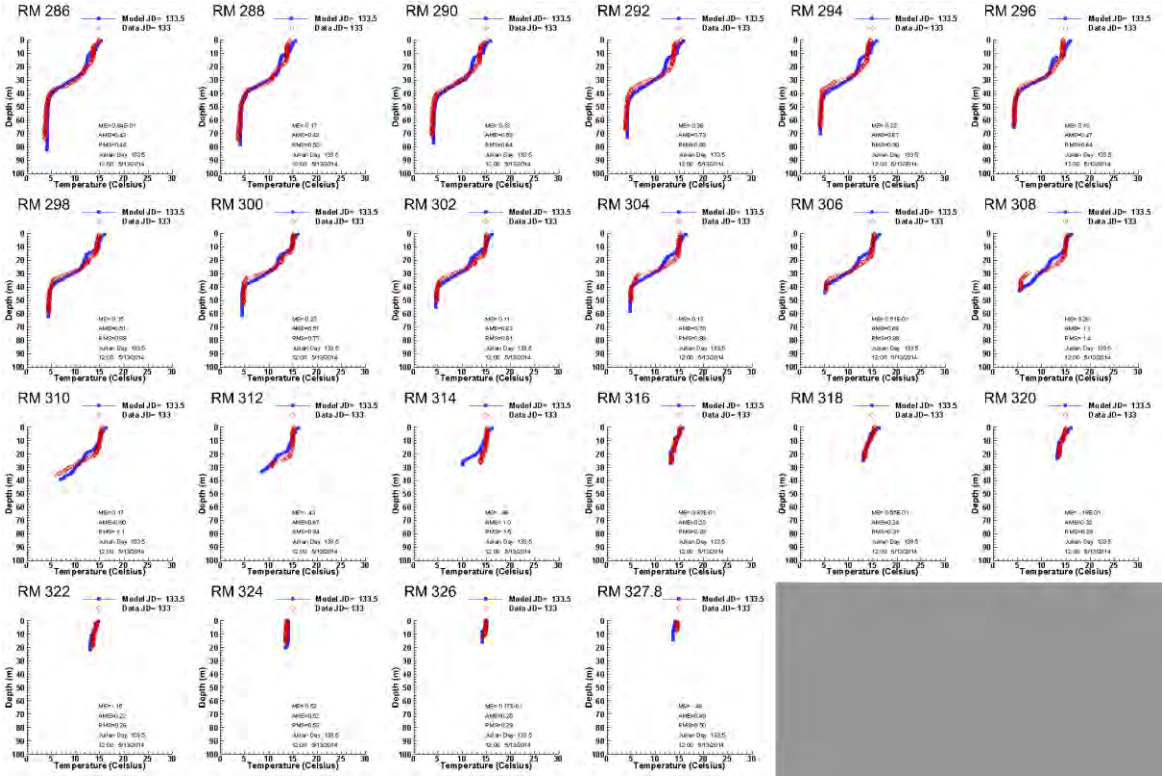


Figure 2312. Vertical profiles of temperature compared with data for 5/13/2014.

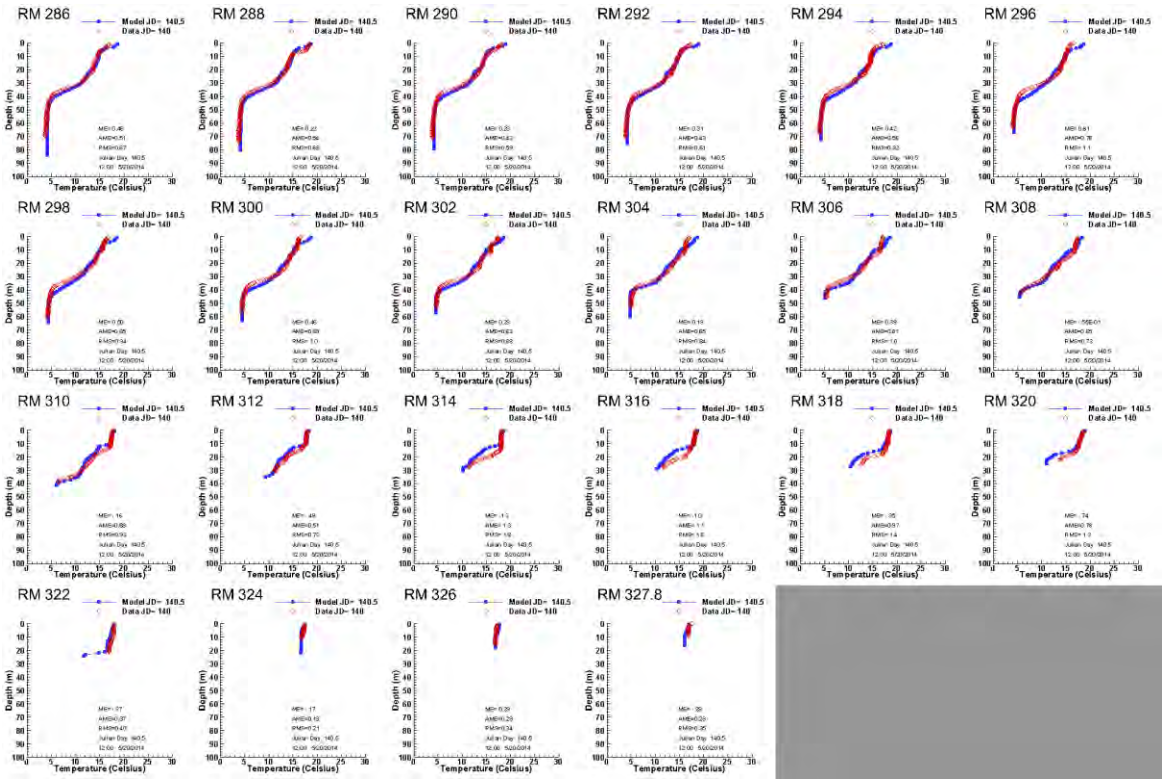


Figure 2313. Vertical profiles of temperature compared with data for 5/20/2014.

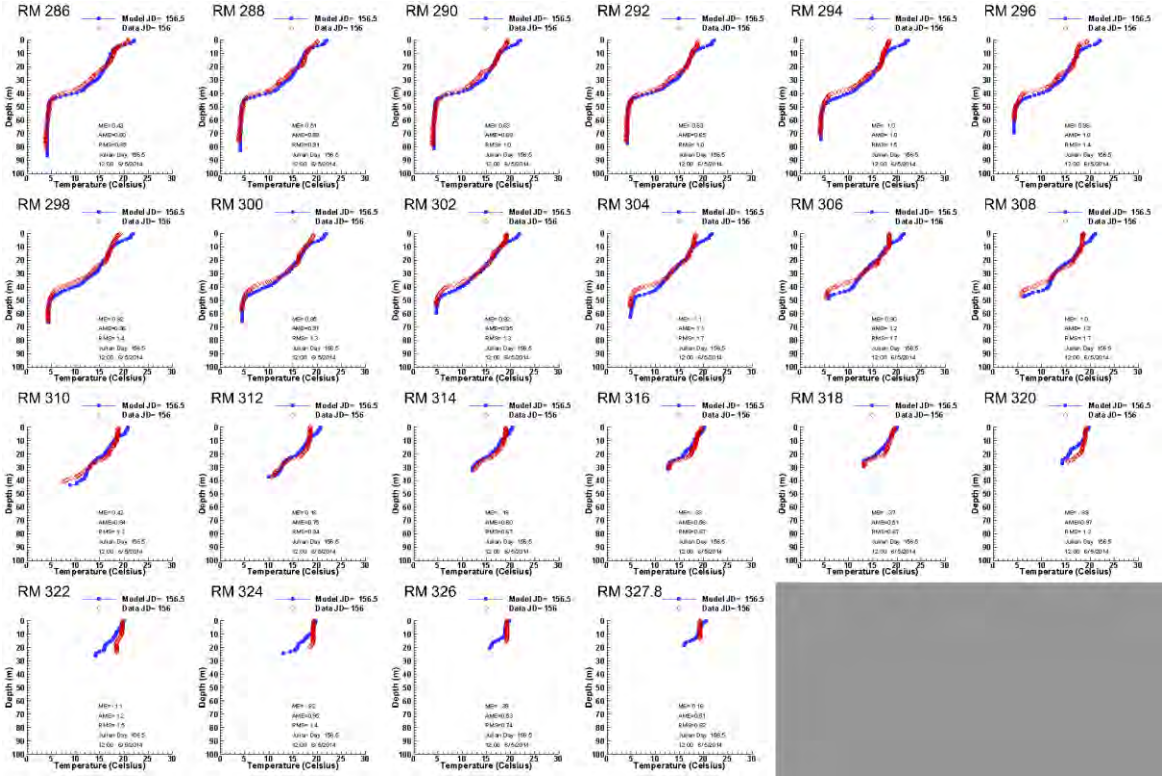


Figure 2314. Vertical profiles of temperature compared with data for 6/ 5/2014.

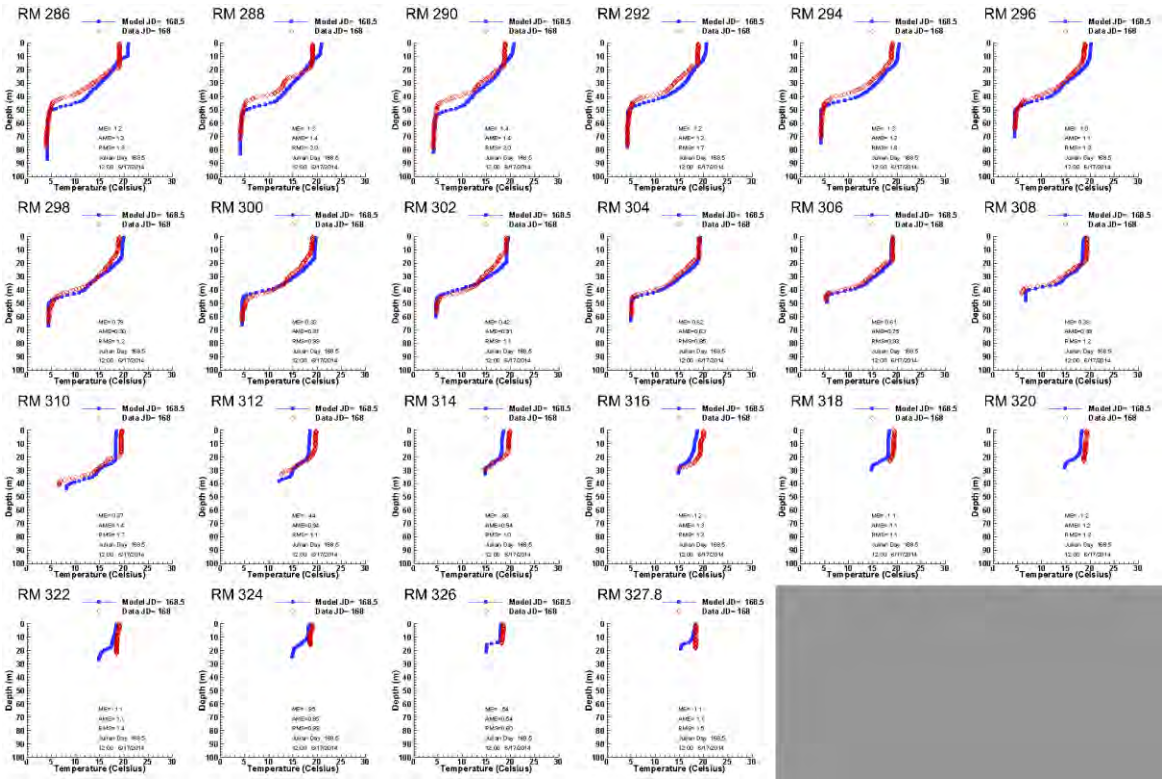


Figure 2315. Vertical profiles of temperature compared with data for 6/17/2014.

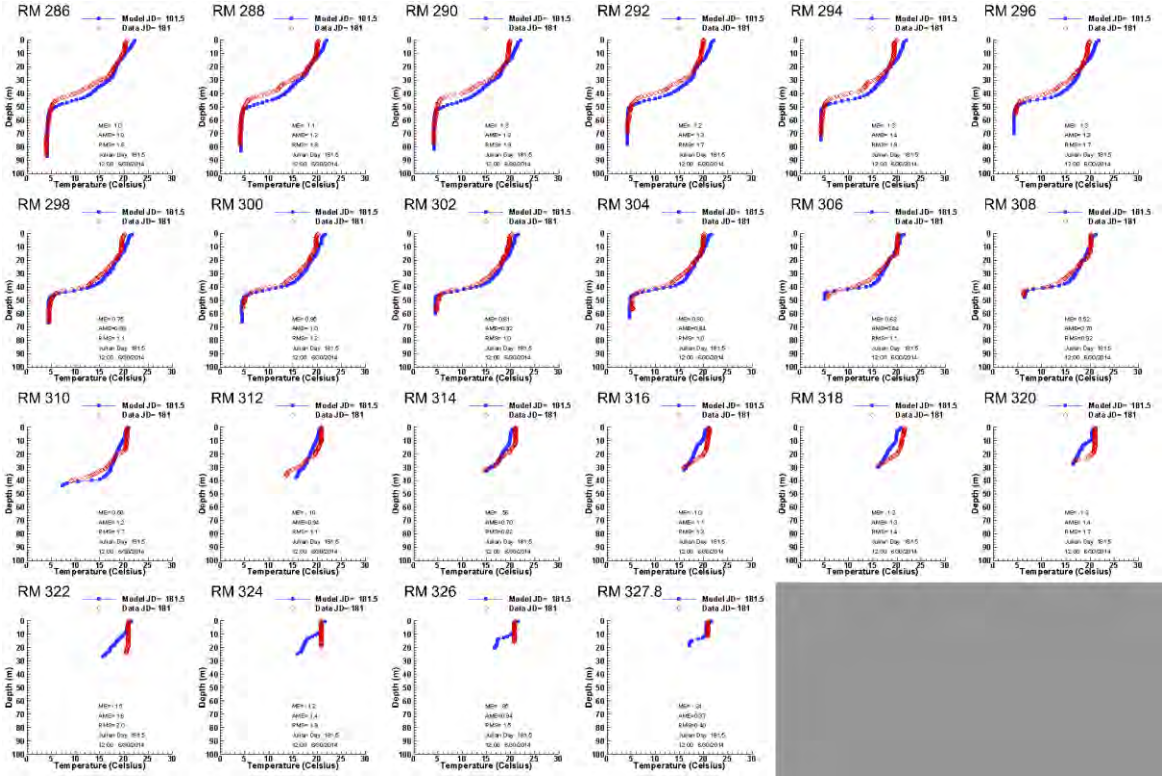


Figure 2316. Vertical profiles of temperature compared with data for 6/30/2014.

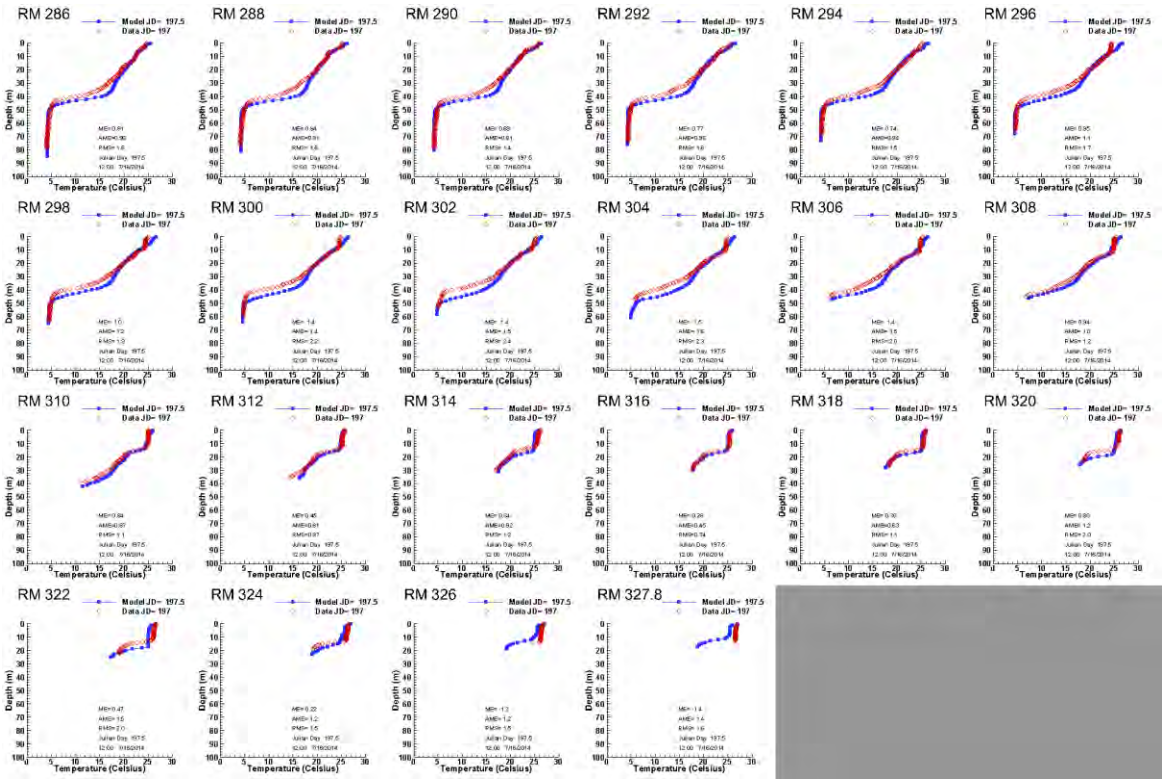


Figure 2317. Vertical profiles of temperature compared with data for 7/16/2014.

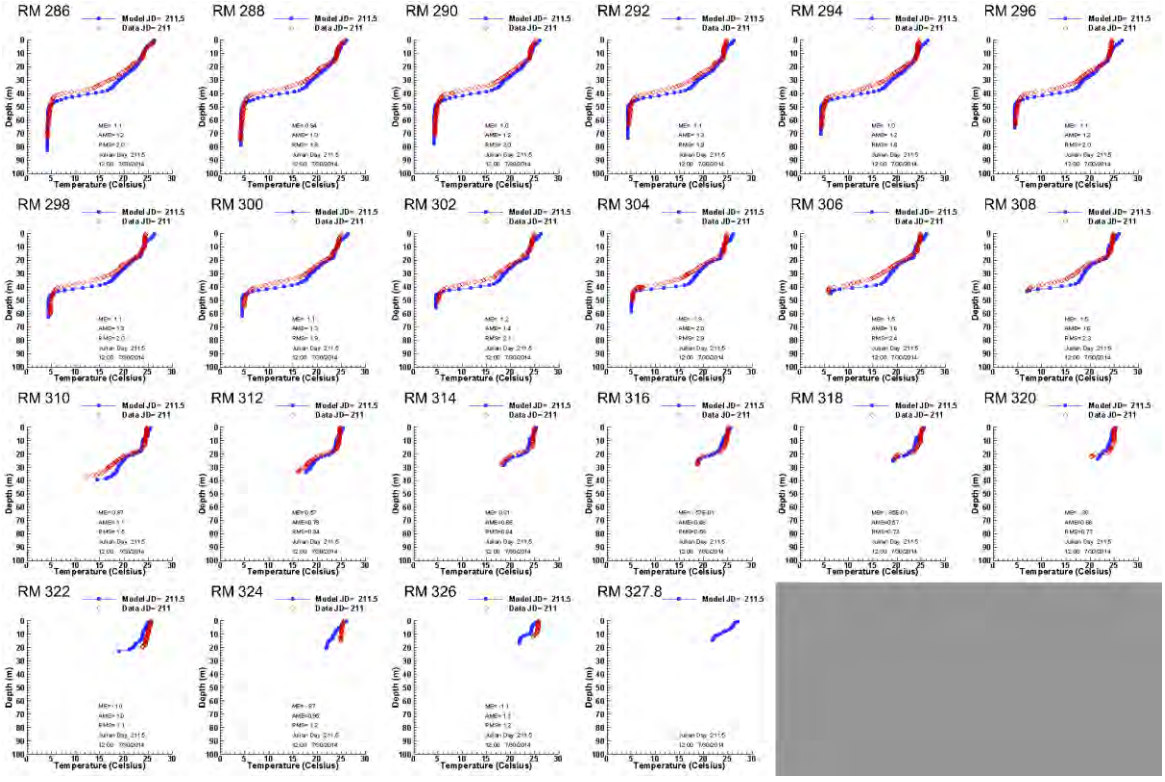


Figure 2318. Vertical profiles of temperature compared with data for 7/30/2014.

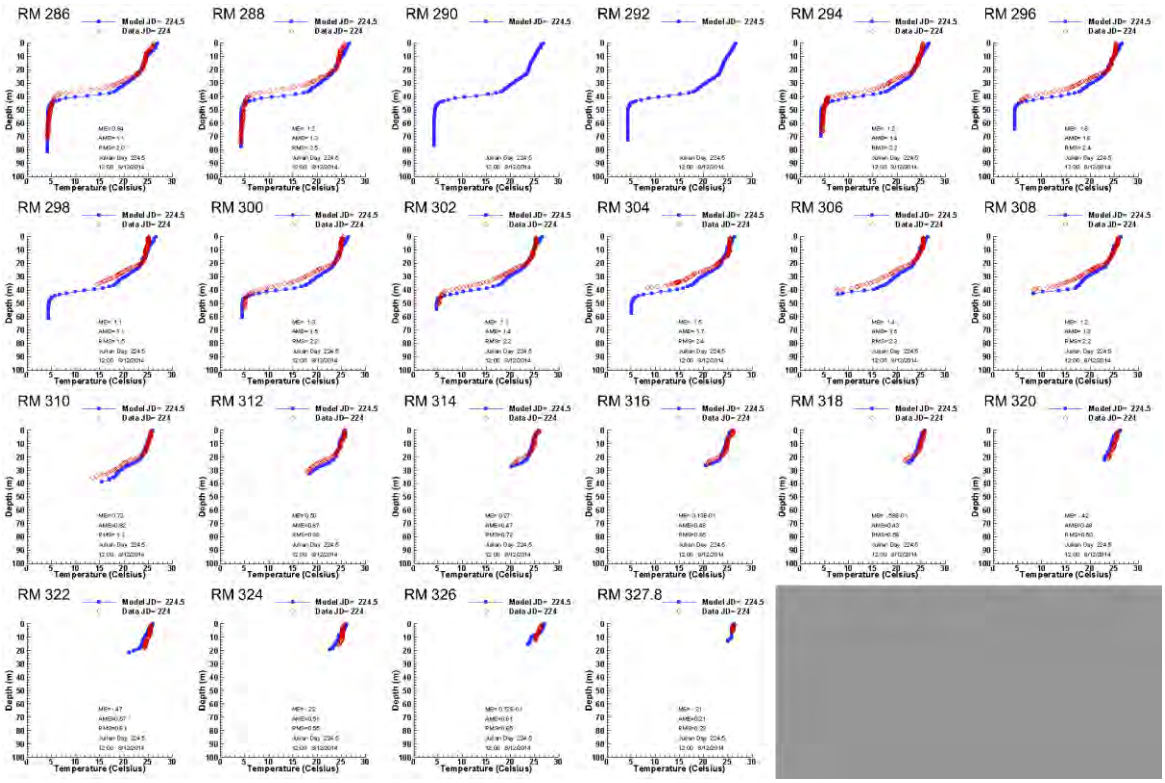


Figure 2319. Vertical profiles of temperature compared with data for 8/12/2014.

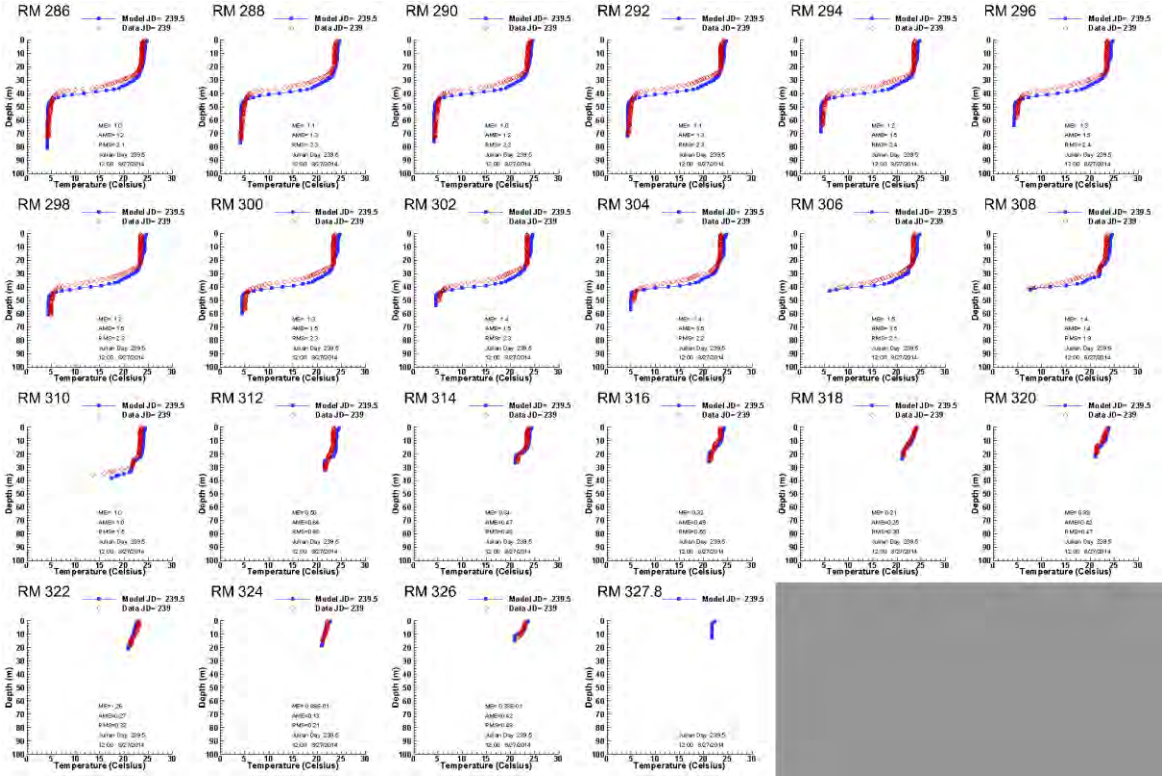


Figure 2320. Vertical profiles of temperature compared with data for 8/27/2014.

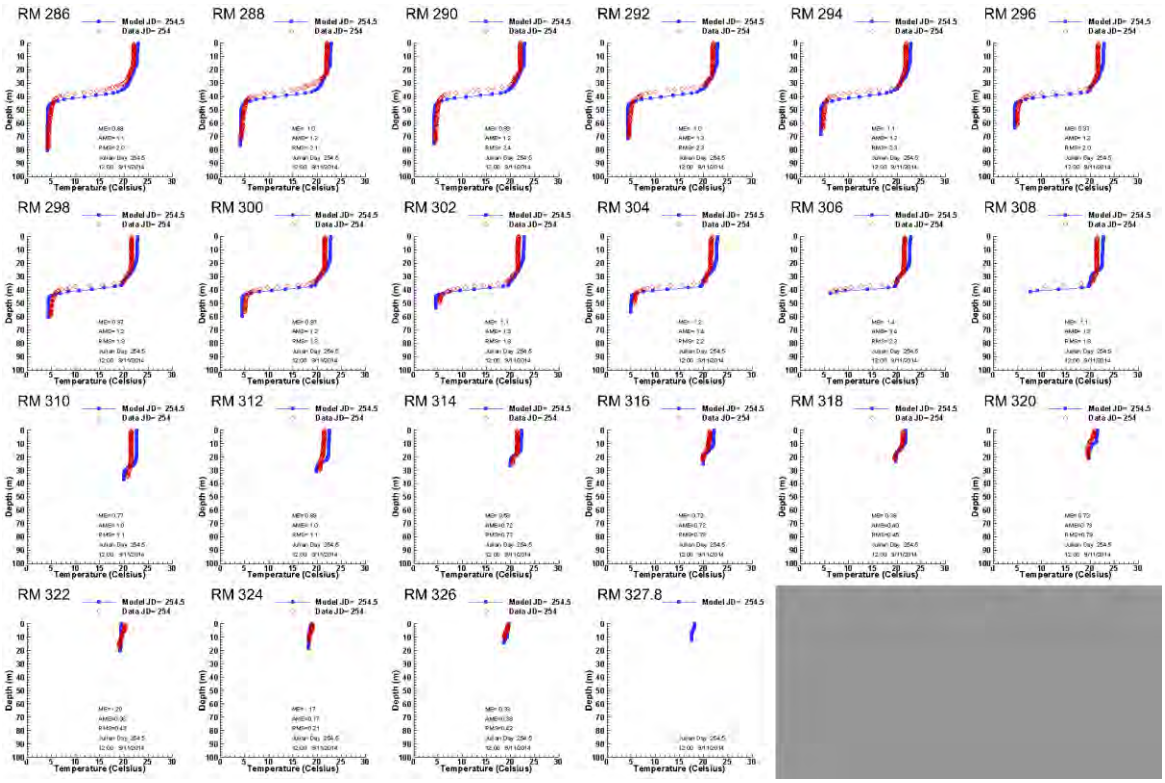


Figure 2321. Vertical profiles of temperature compared with data for 9/11/2014.

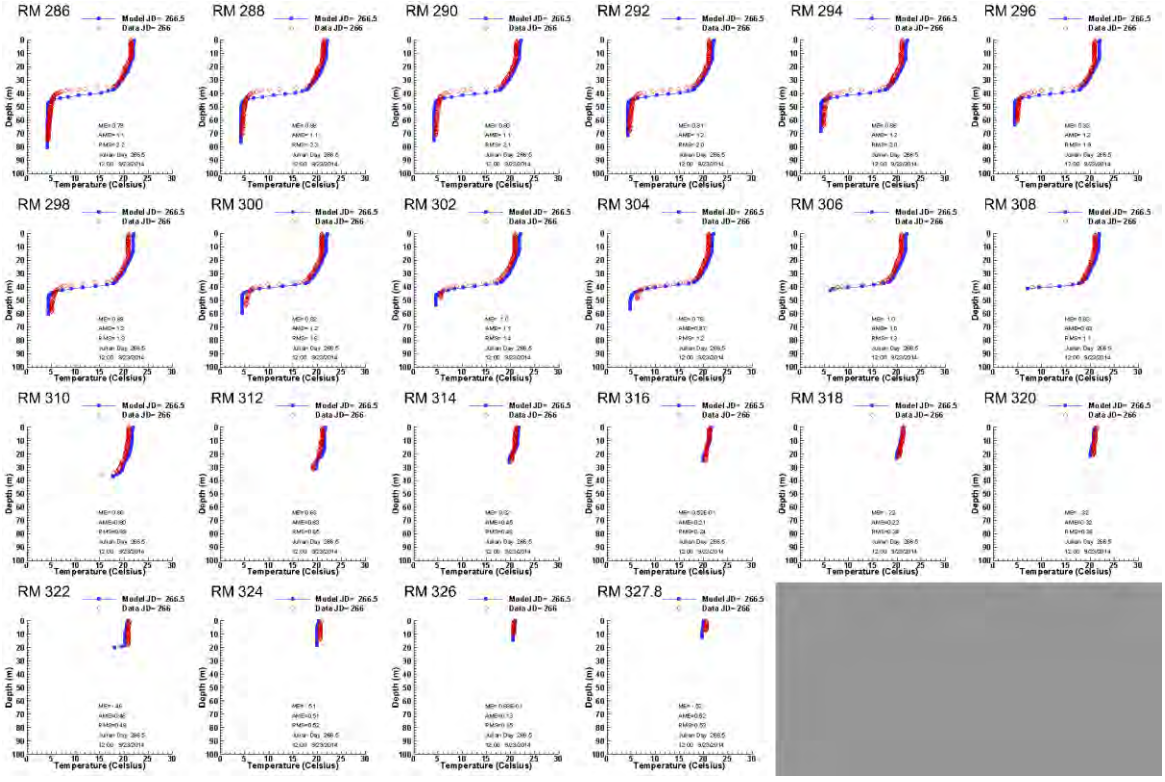


Figure 2322. Vertical profiles of temperature compared with data for 9/23/2014.

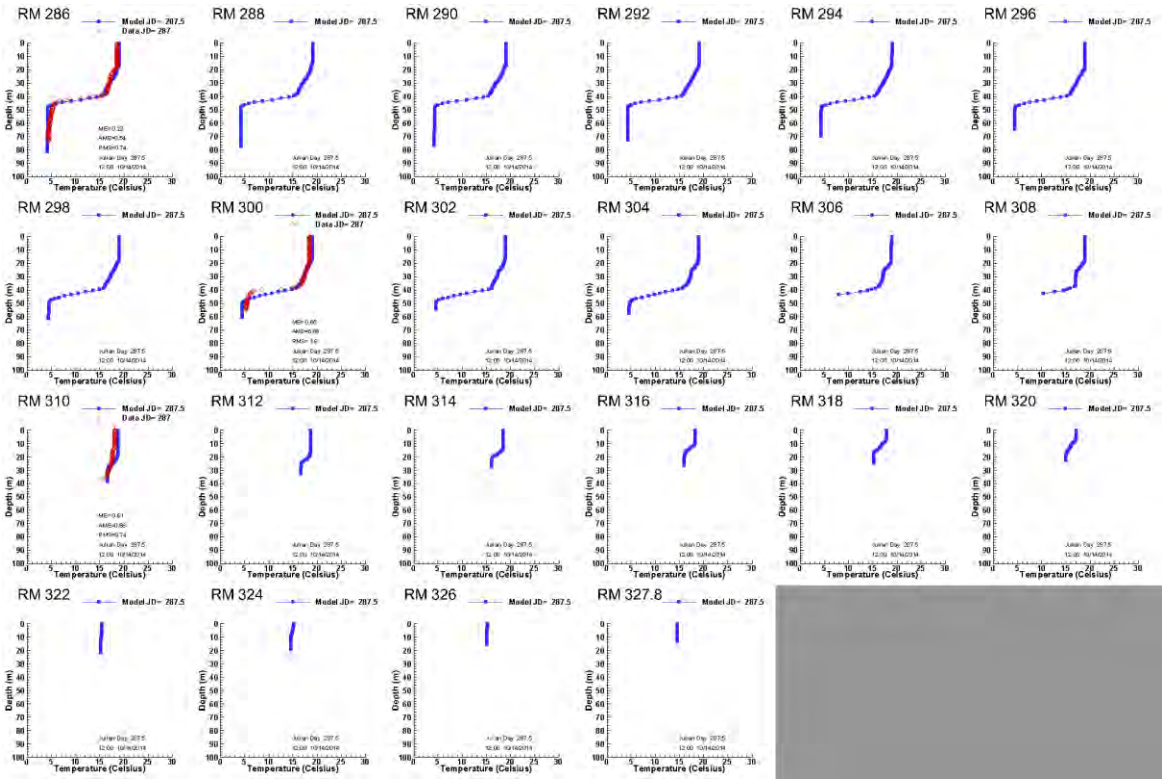


Figure 2323. Vertical profiles of temperature compared with data for 10/14/2014.

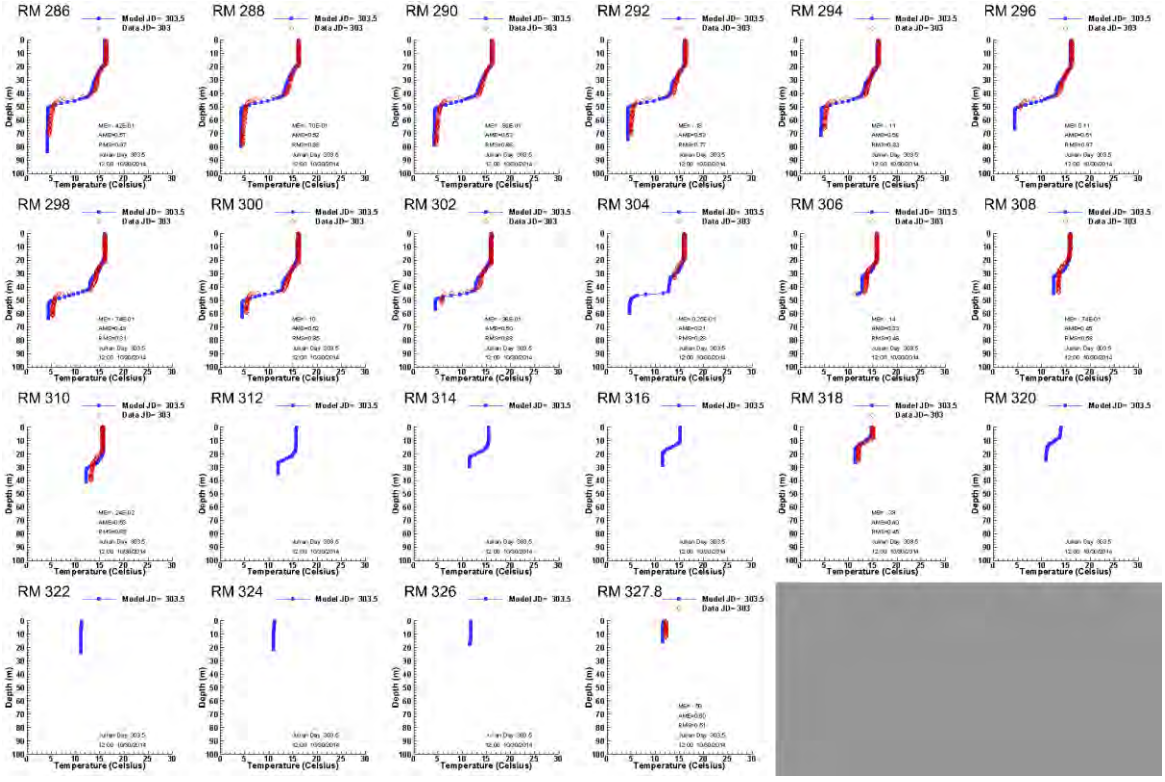


Figure 2324. Vertical profiles of temperature compared with data for 10/30/2014.

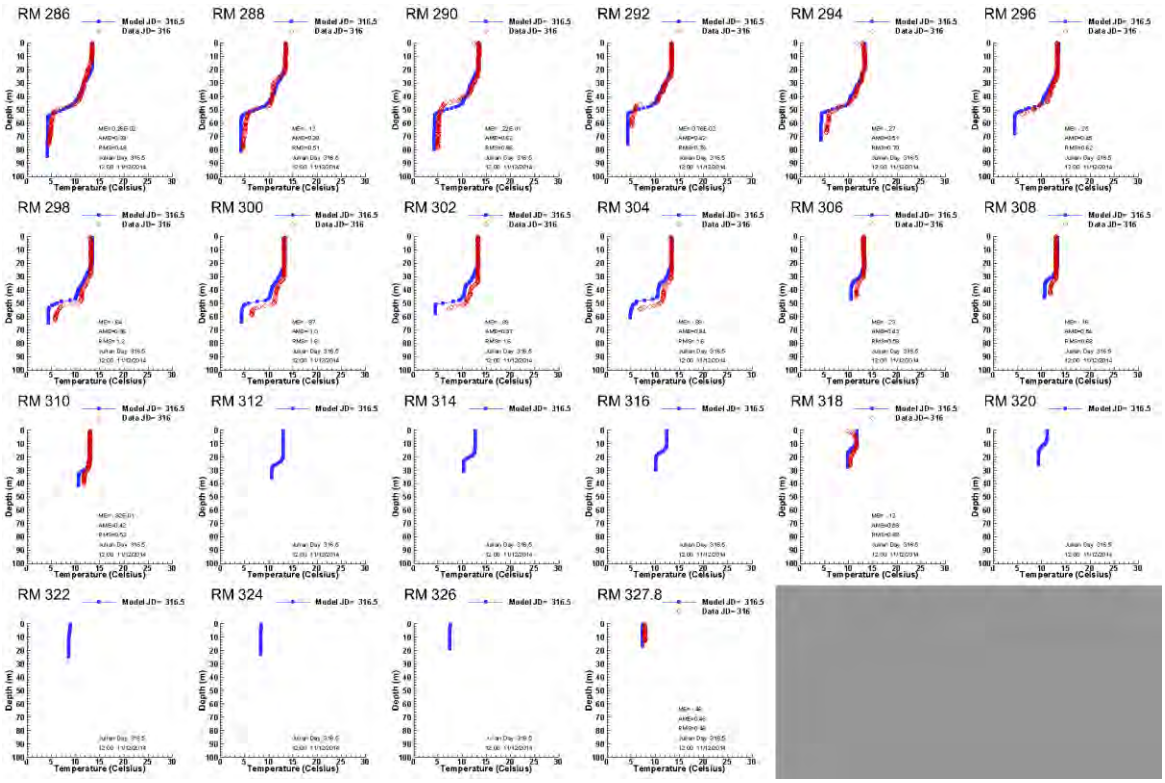


Figure 2325. Vertical profiles of temperature compared with data for 11/12/2014.

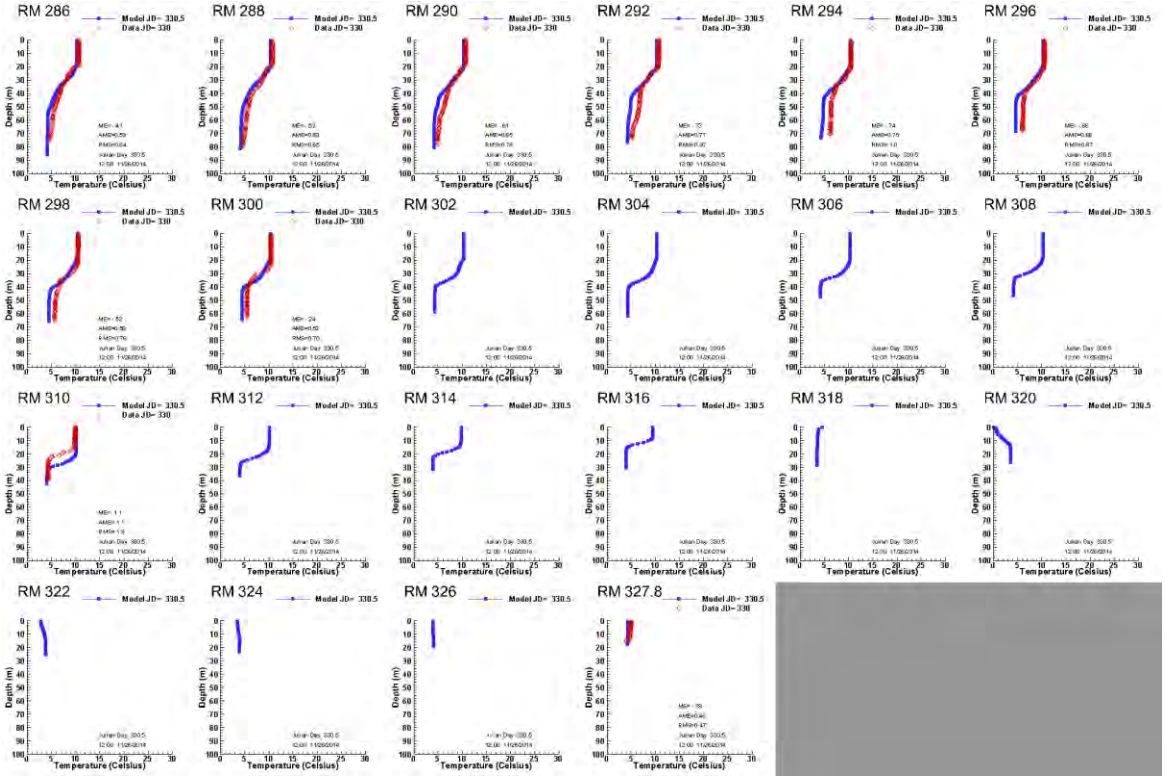


Figure 2326. Vertical profiles of temperature compared with data for 11/26/2014.

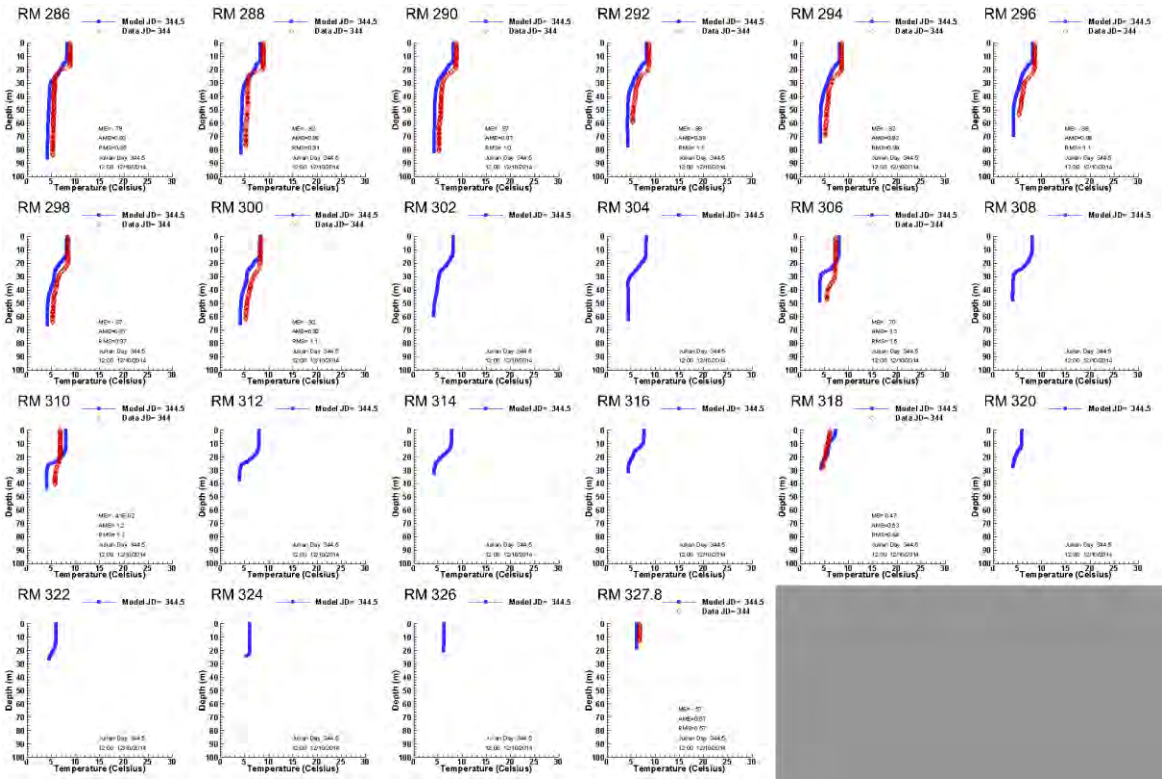


Figure 2327. Vertical profiles of temperature compared with data for 12/10/2014.

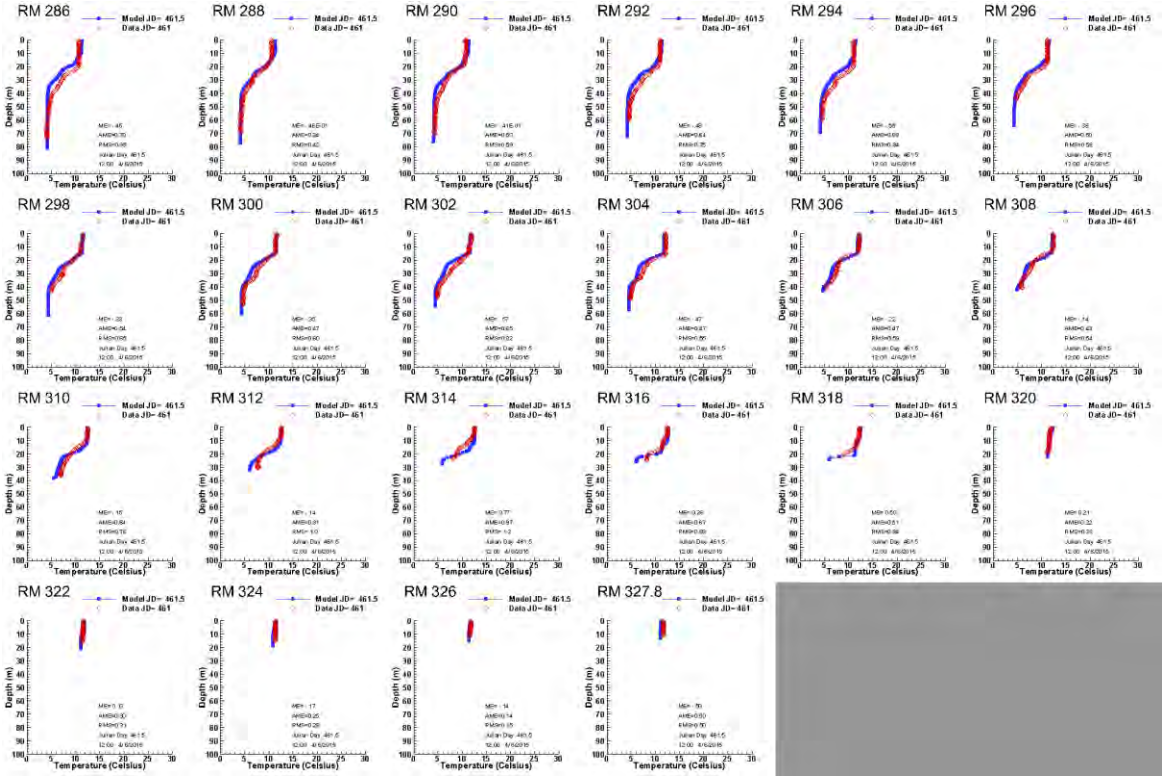


Figure 2328. Vertical profiles of temperature compared with data for 4/ 6/2015.

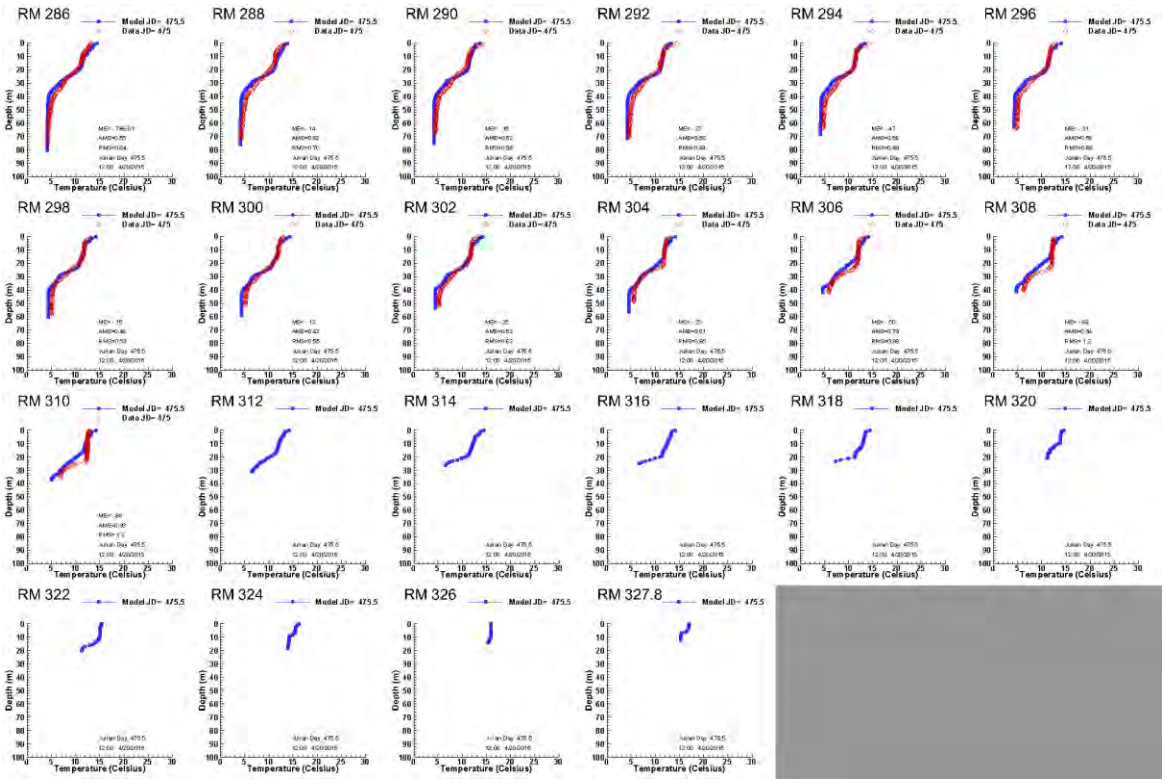


Figure 2329. Vertical profiles of temperature compared with data for 4/20/2015.

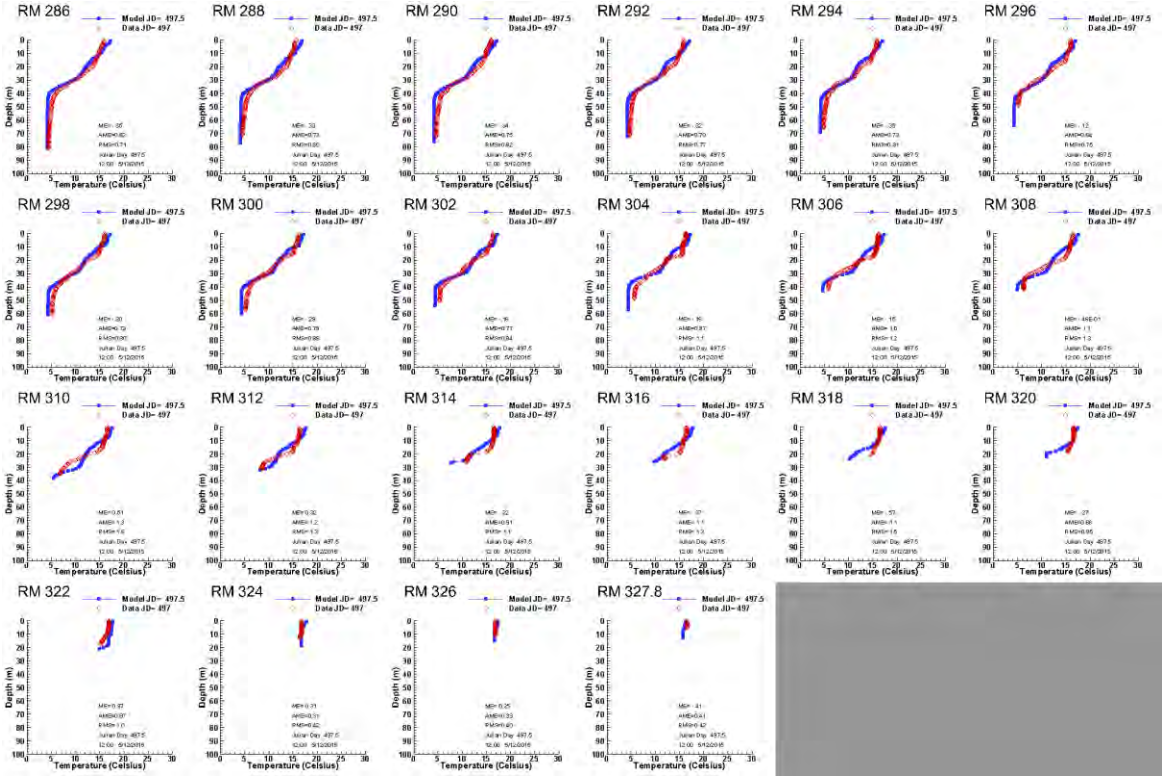


Figure 2330. Vertical profiles of temperature compared with data for 5/12/2015.

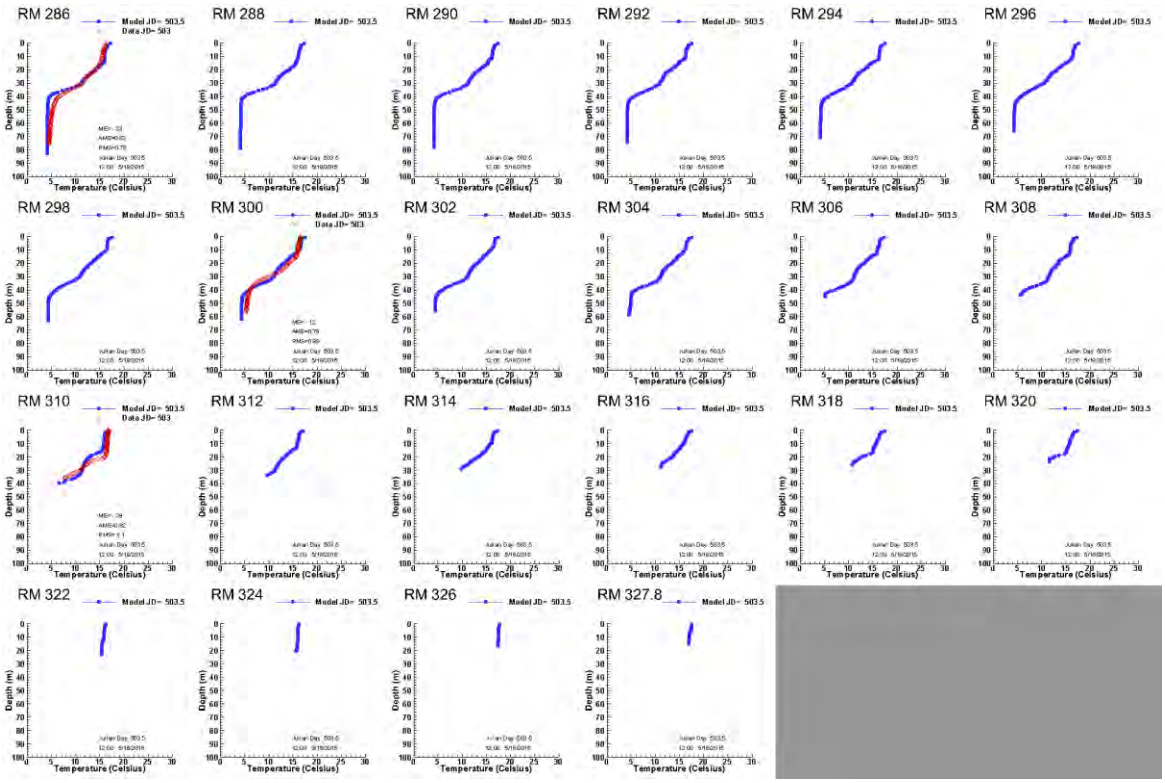


Figure 2331. Vertical profiles of temperature compared with data for 5/18/2015.

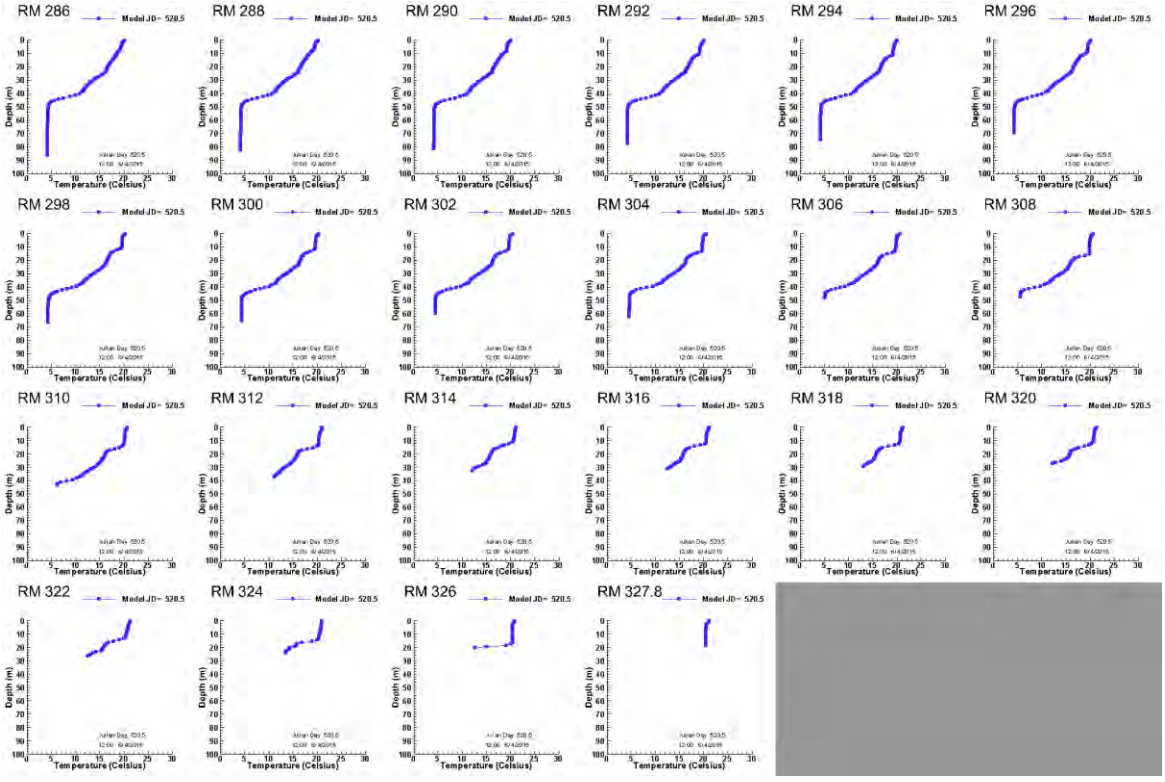


Figure 2332. Vertical profiles of temperature compared with data for 6/ 4/2015.

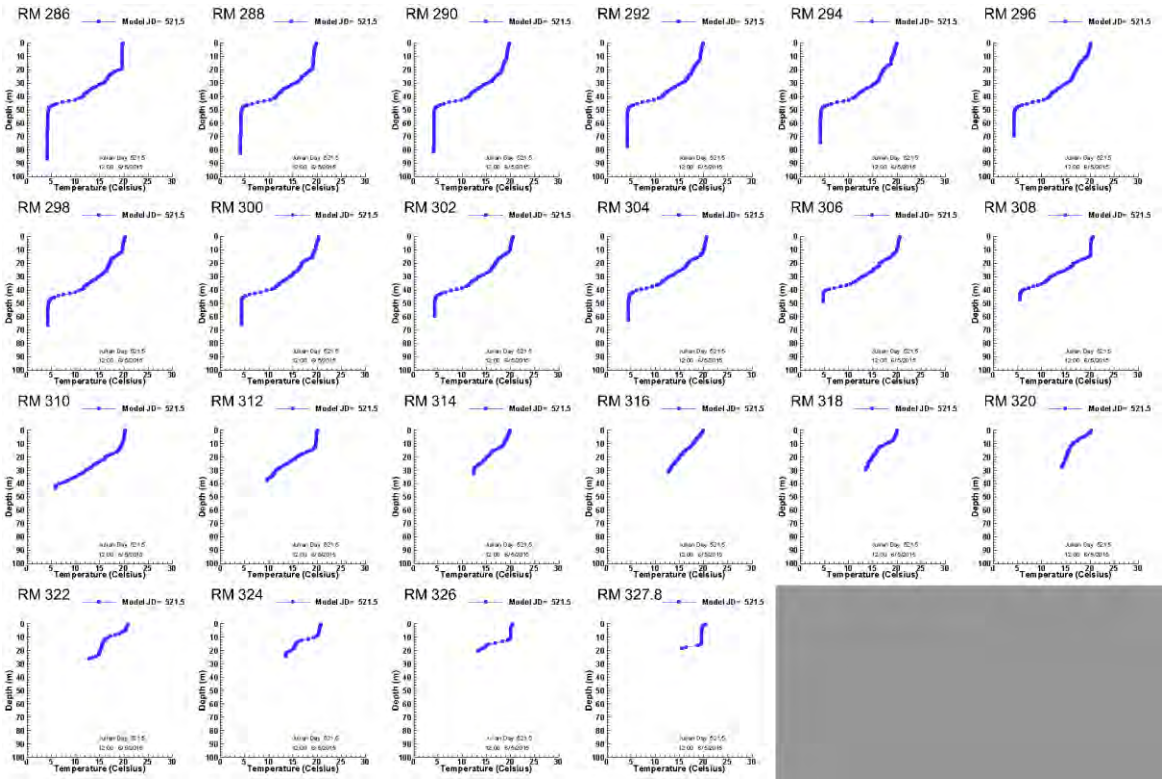


Figure 2333. Vertical profiles of temperature compared with data for 6/ 5/2015.

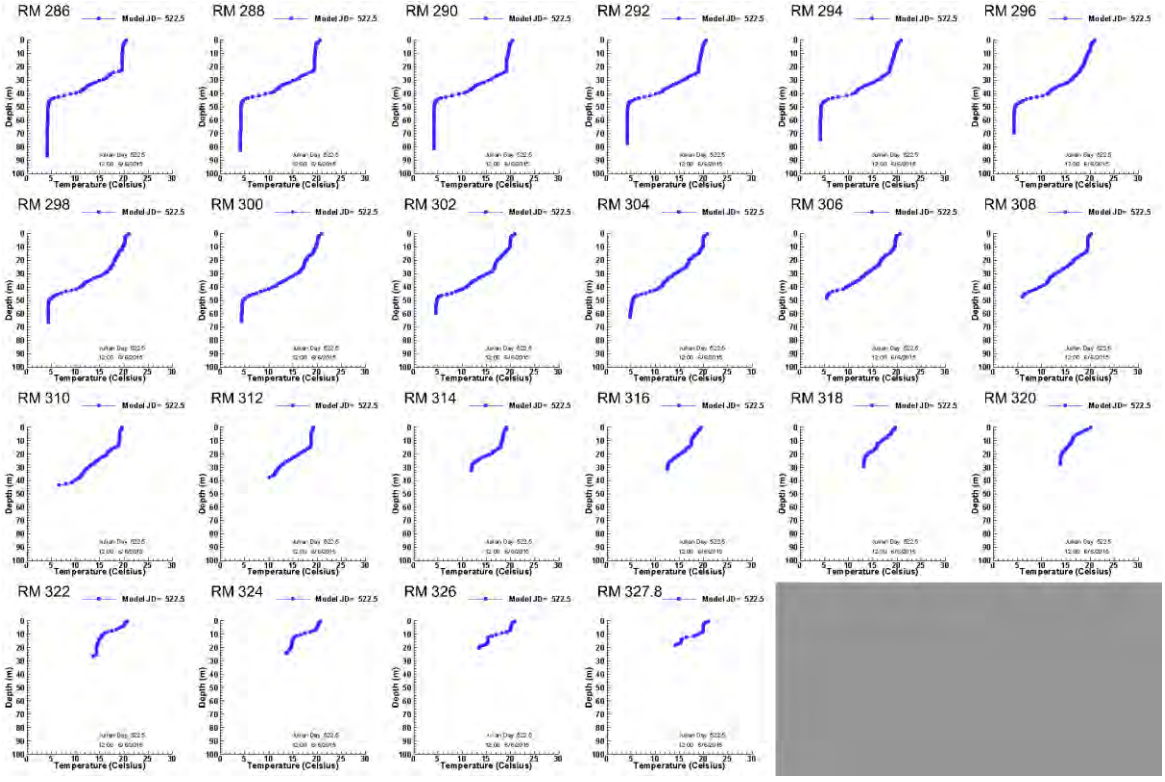


Figure 2334. Vertical profiles of temperature compared with data for 6/ 6/2015.

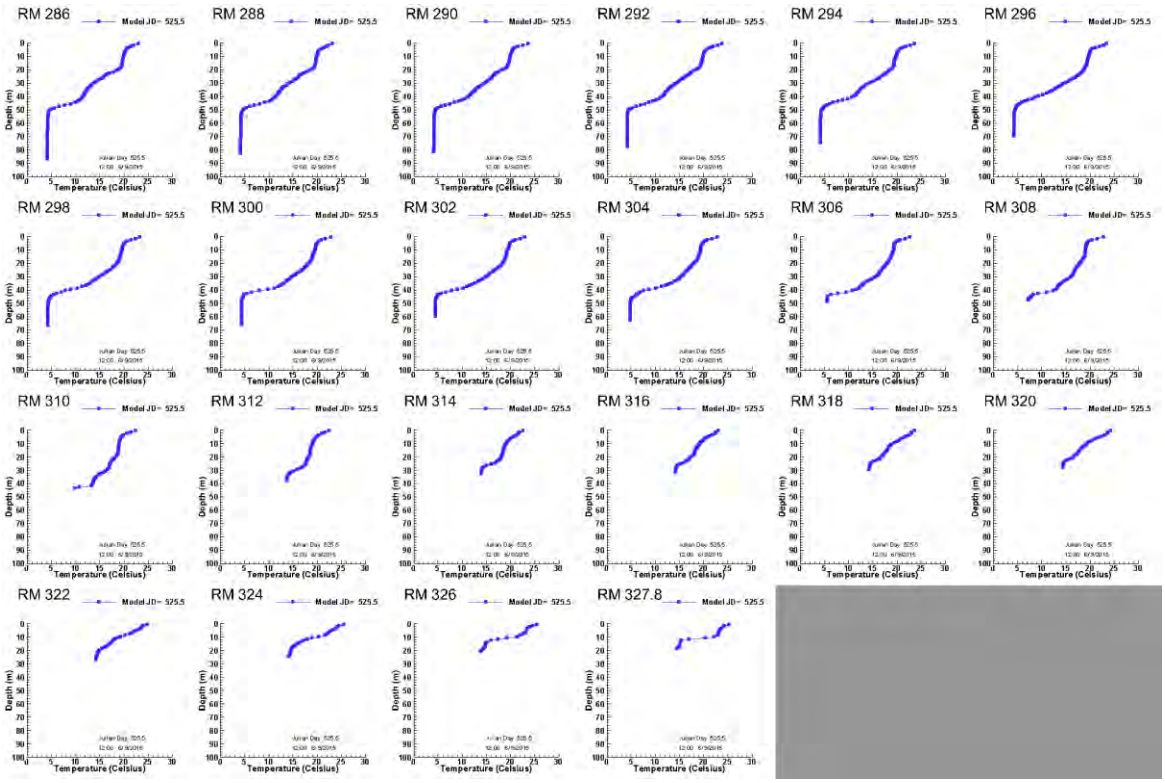


Figure 2335. Vertical profiles of temperature compared with data for 6/ 9/2015.

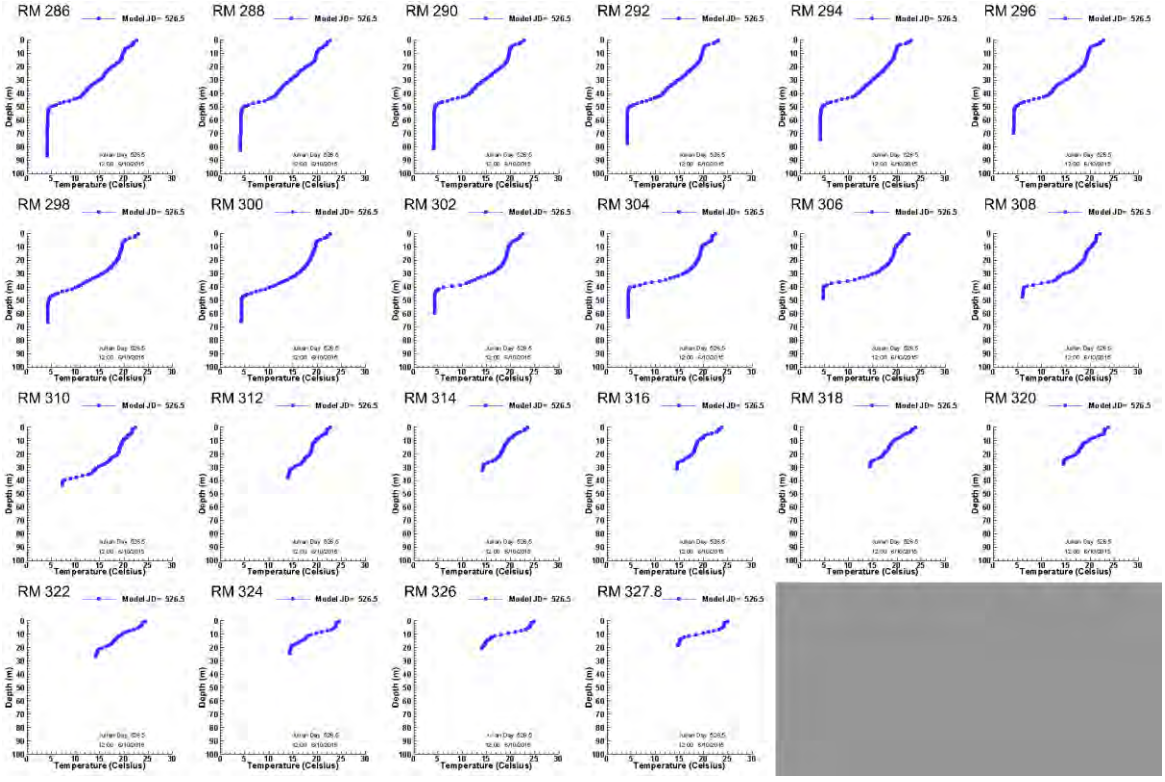


Figure 2336. Vertical profiles of temperature compared with data for 6/10/2015.

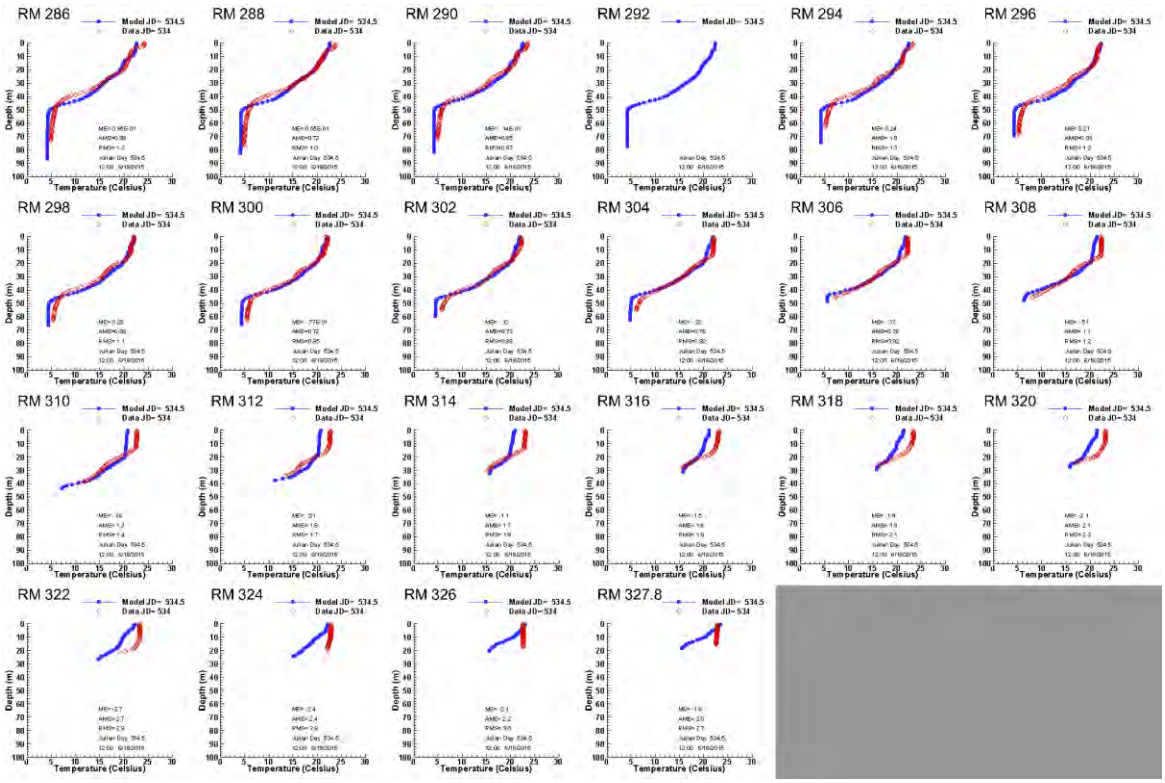


Figure 2337. Vertical profiles of temperature compared with data for 6/18/2015.

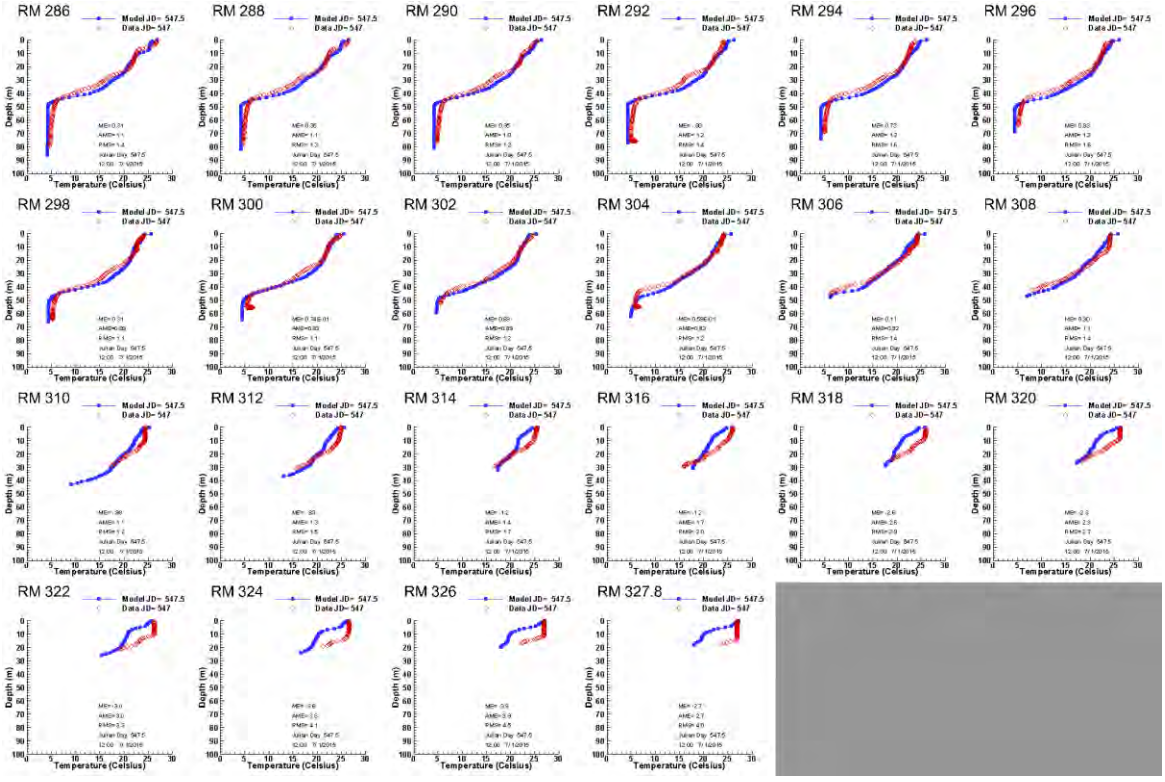


Figure 2338. Vertical profiles of temperature compared with data for 7/ 1/2015.

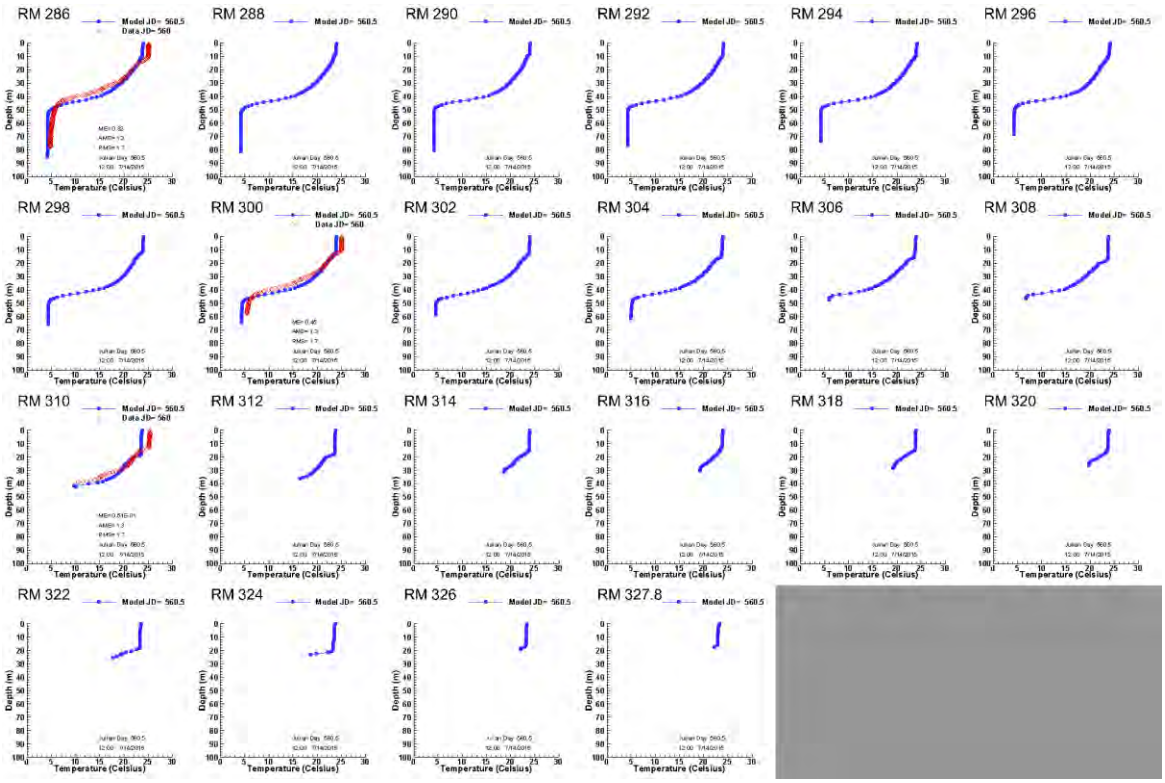


Figure 2339. Vertical profiles of temperature compared with data for 7/14/2015.

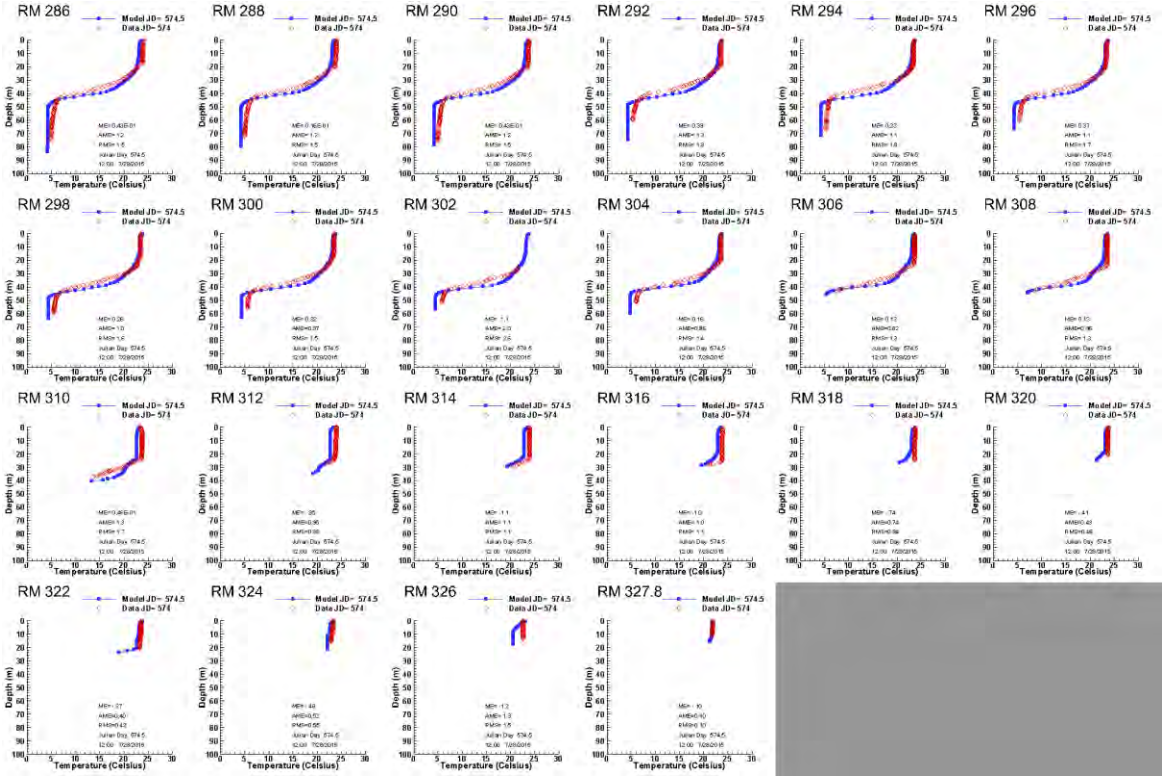


Figure 2340. Vertical profiles of temperature compared with data for 7/28/2015.

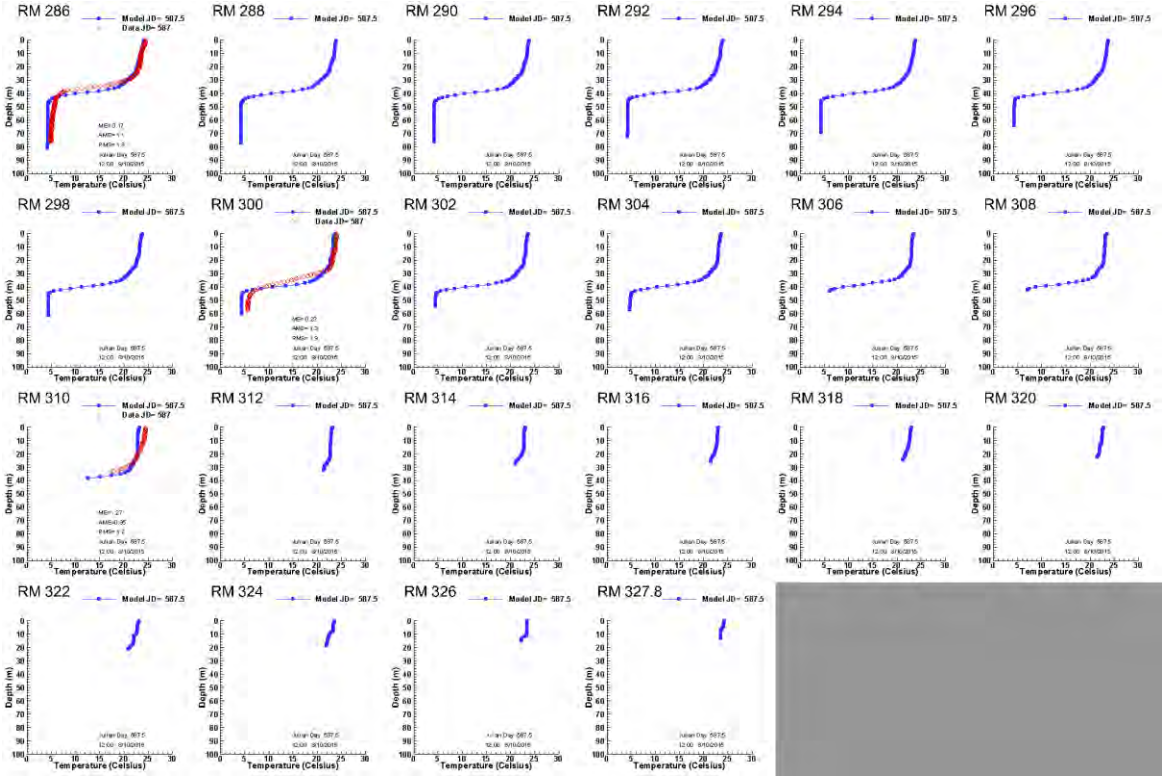


Figure 2341. Vertical profiles of temperature compared with data for 8/10/2015.

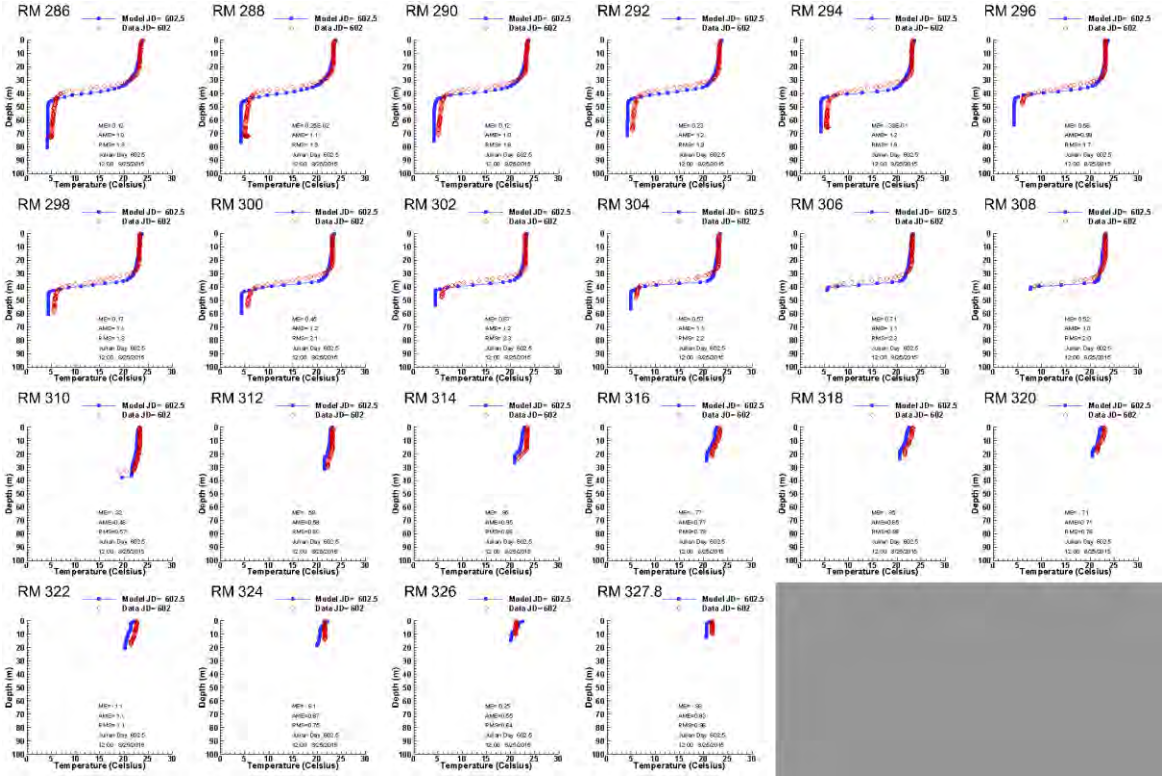


Figure 2342. Vertical profiles of temperature compared with data for 8/25/2015.

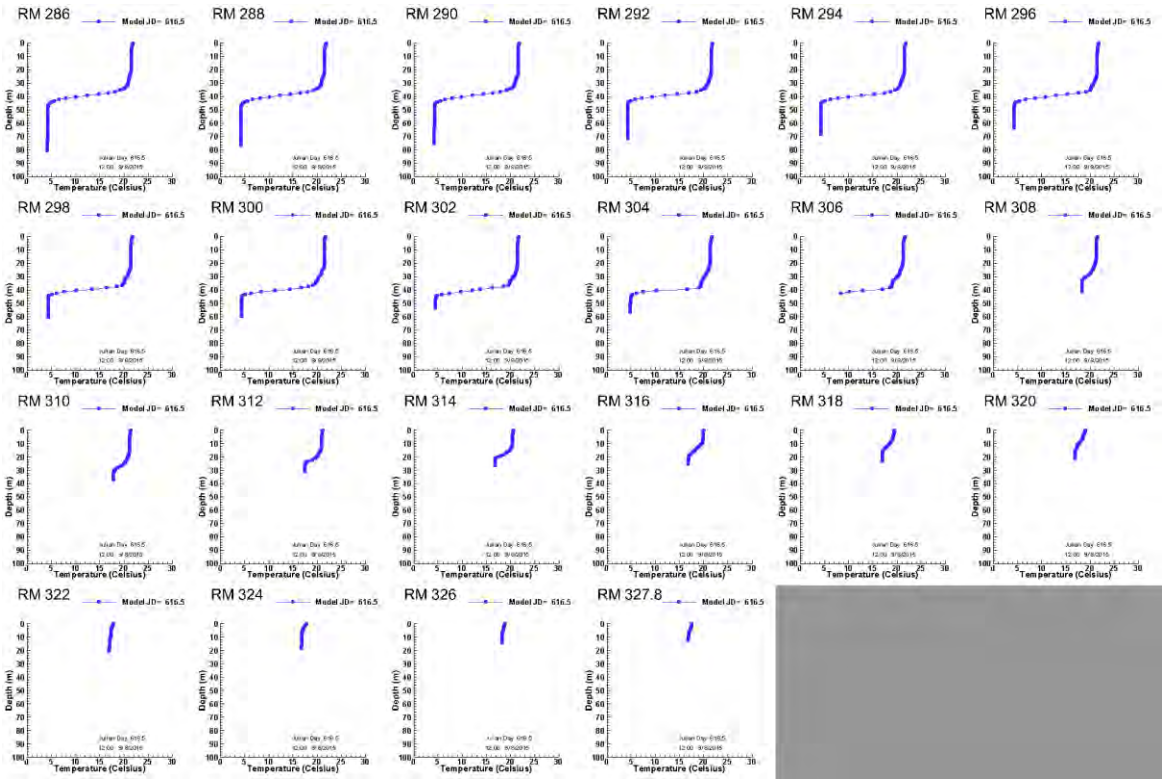


Figure 2343. Vertical profiles of temperature compared with data for 9/ 8/2015.

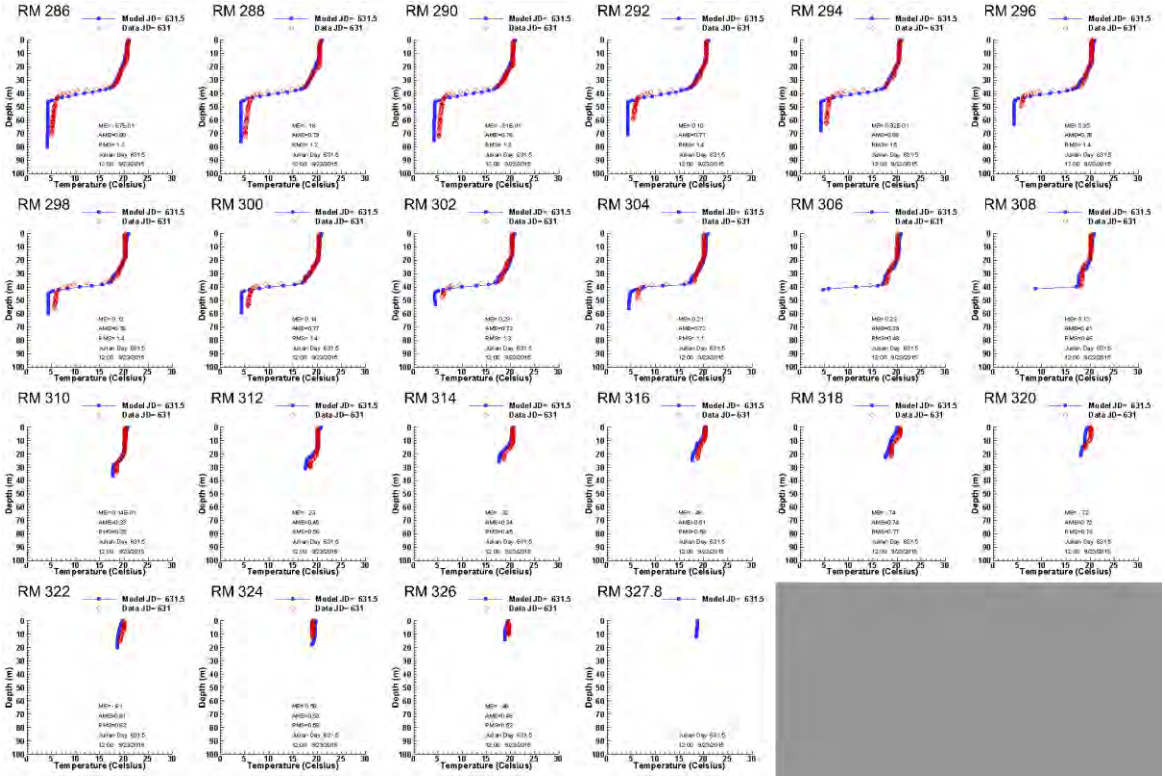


Figure 2344. Vertical profiles of temperature compared with data for 9/23/2015.

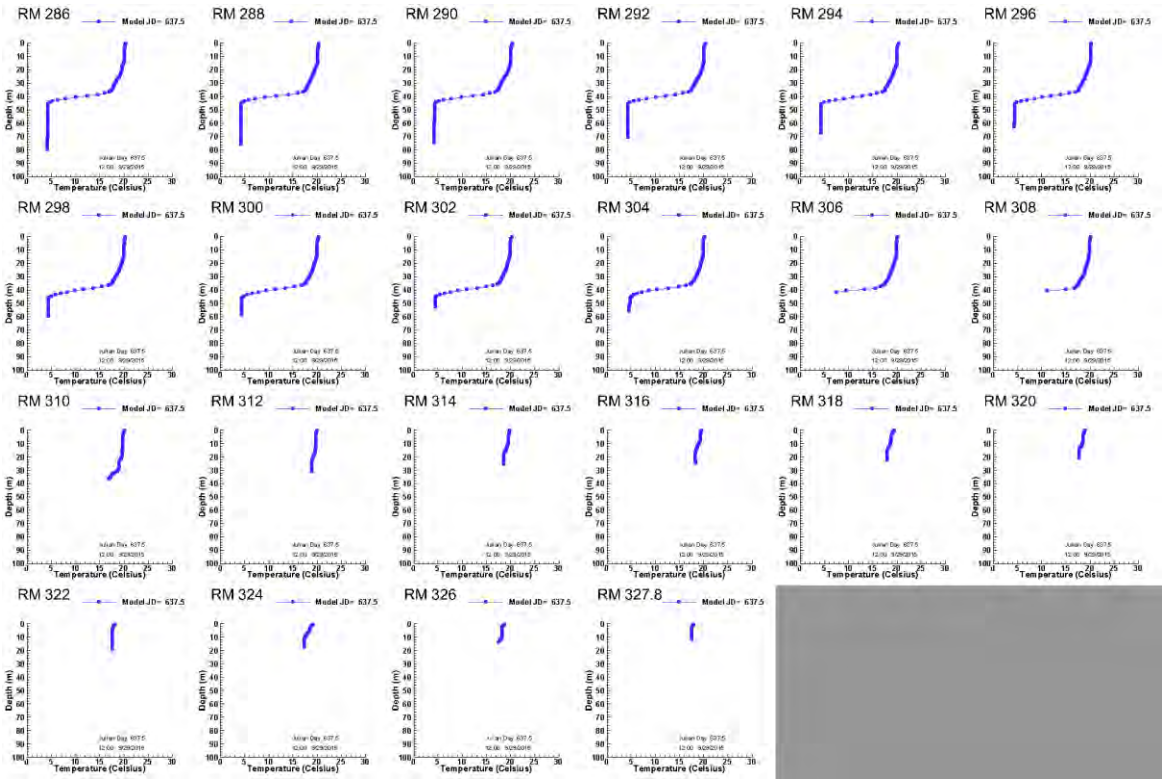


Figure 2345. Vertical profiles of temperature compared with data for 9/29/2015.

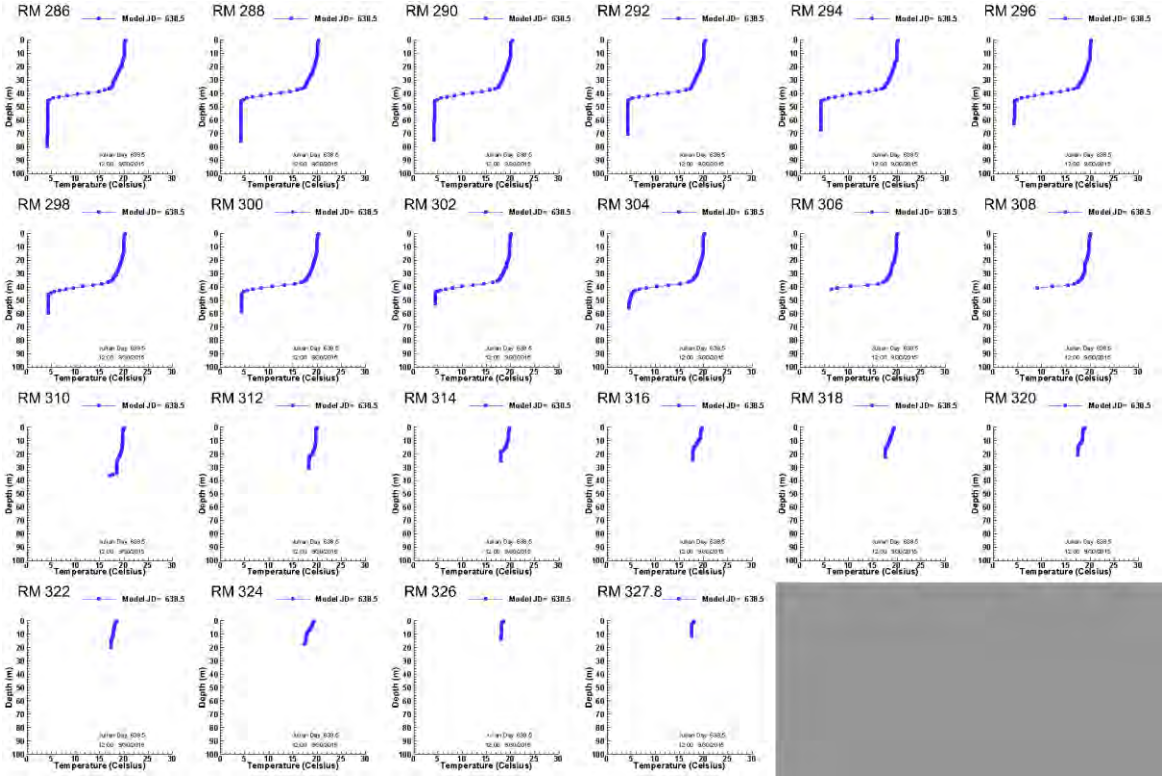


Figure 2346. Vertical profiles of temperature compared with data for 9/30/2015.

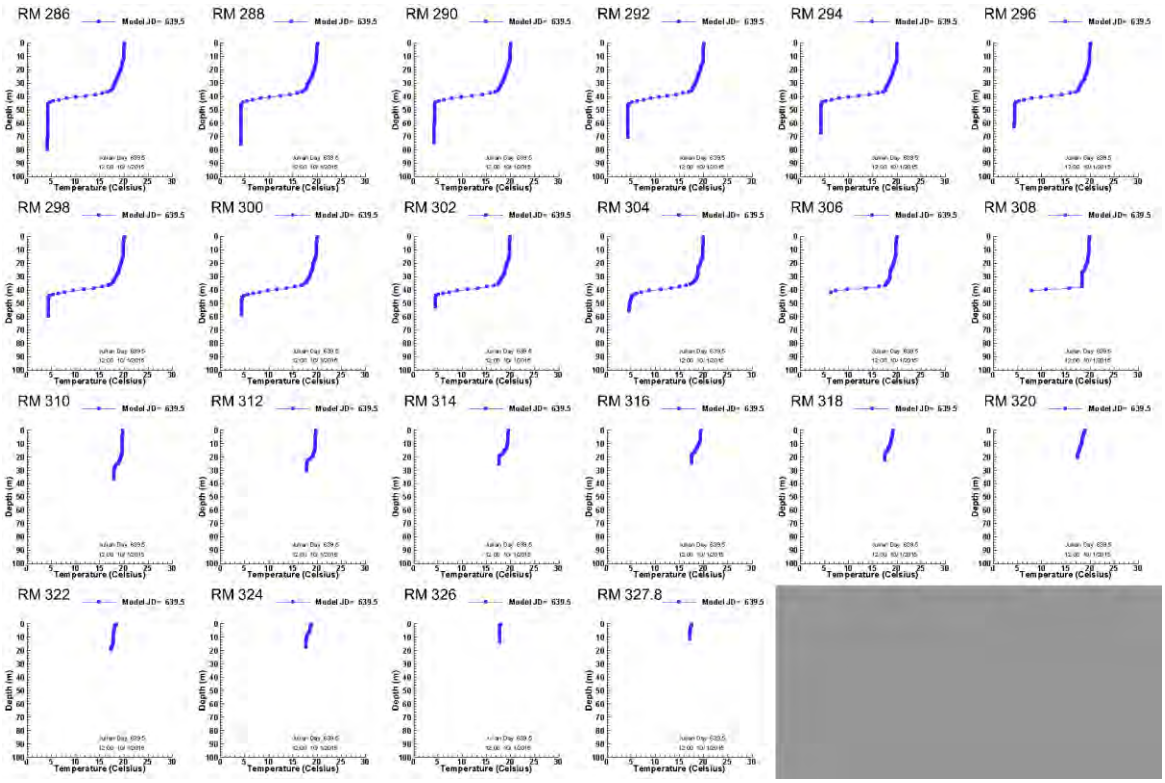


Figure 2347. Vertical profiles of temperature compared with data for 10/ 1/2015.

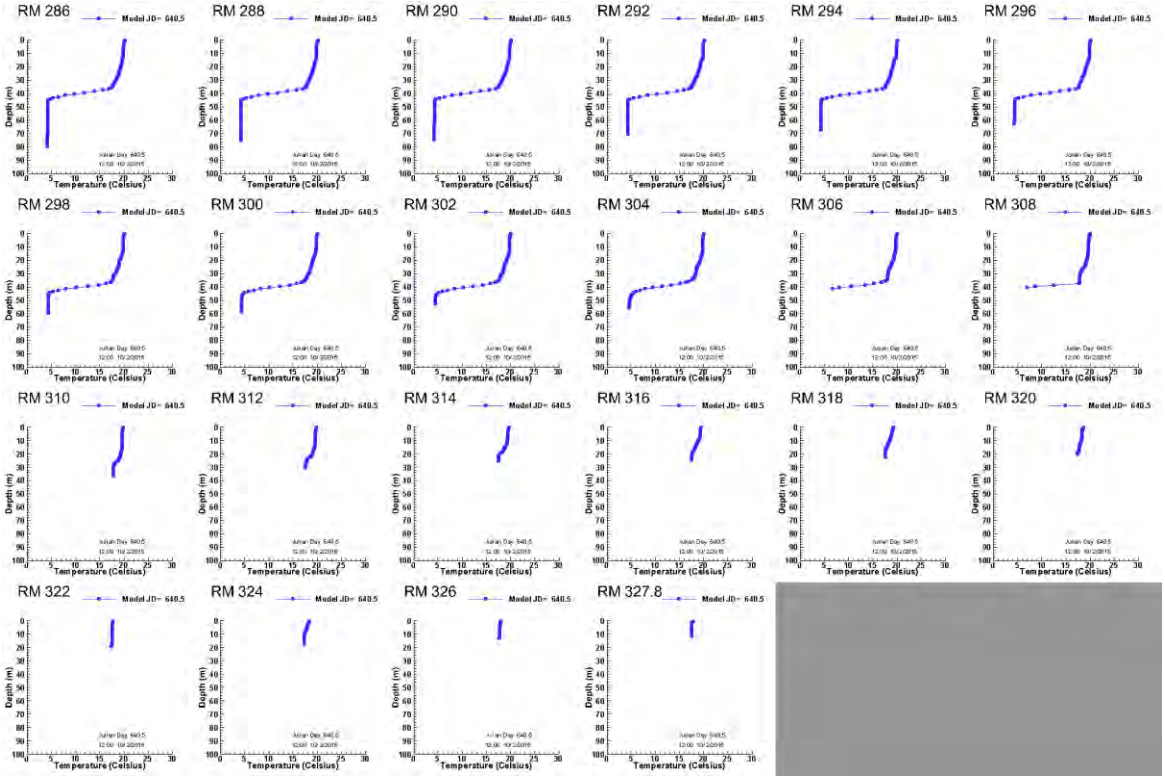


Figure 2348. Vertical profiles of temperature compared with data for 10/ 2/2015.

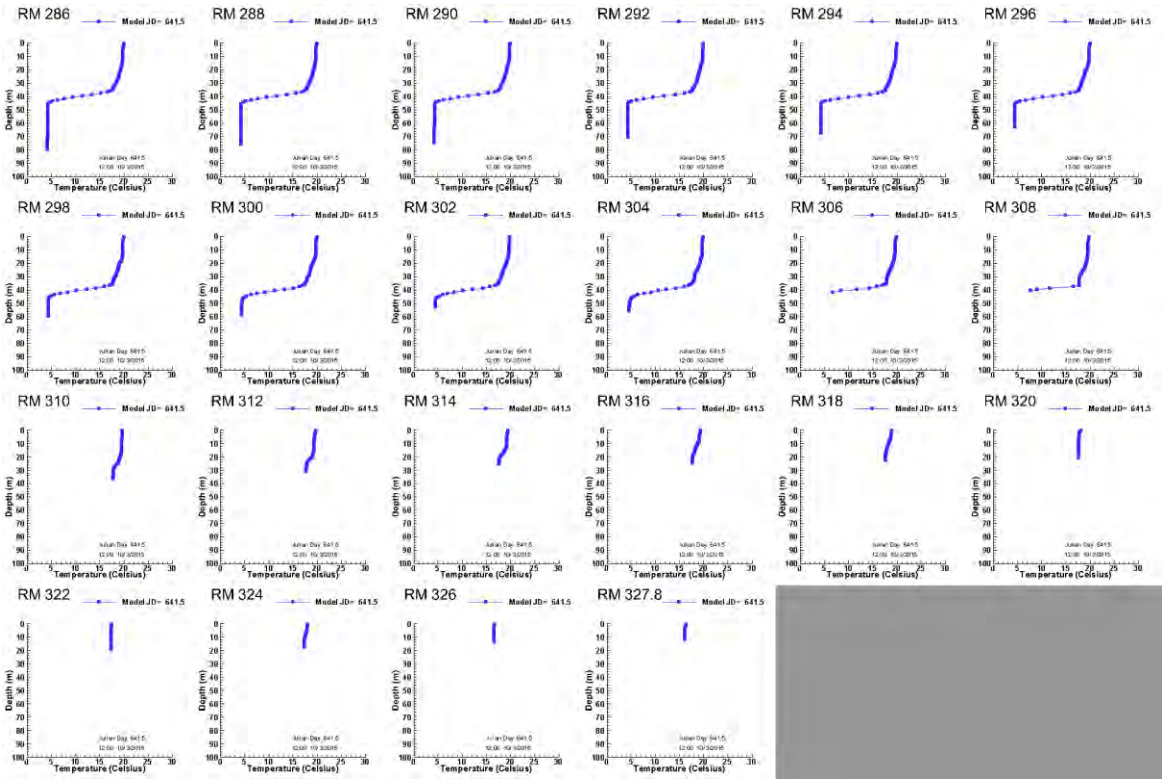


Figure 2349. Vertical profiles of temperature compared with data for 10/ 3/2015.

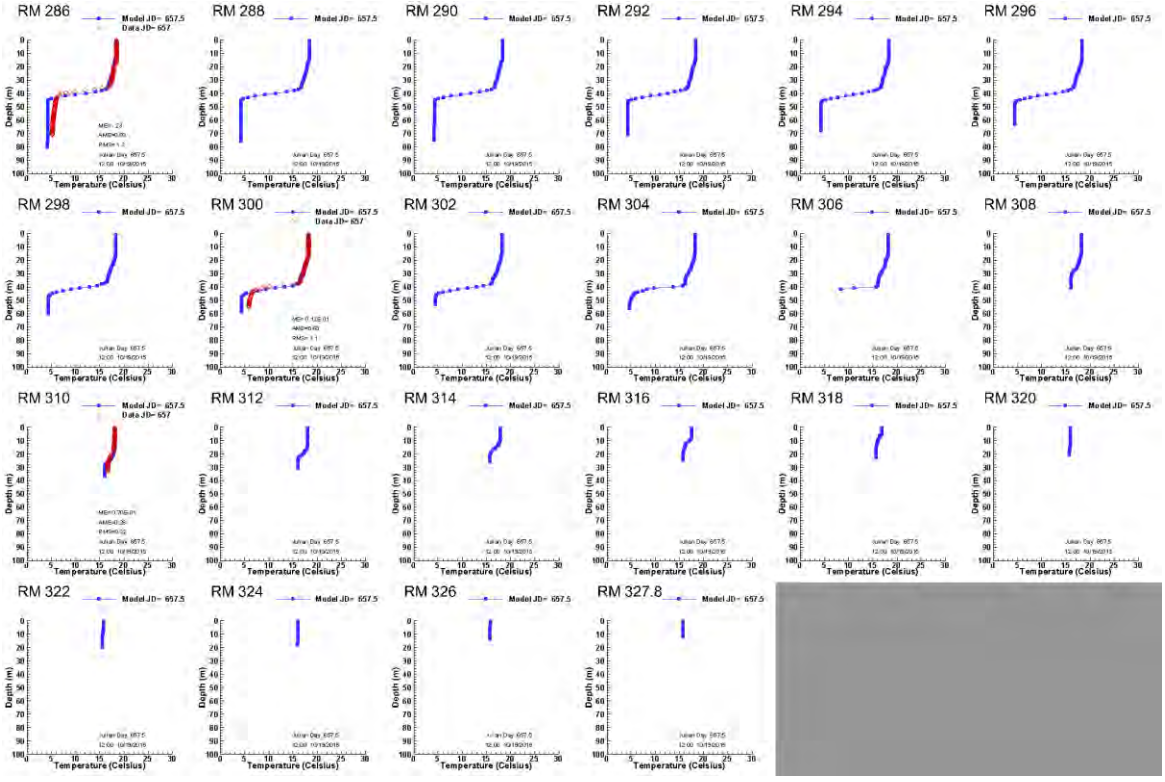


Figure 2350. Vertical profiles of temperature compared with data for 10/19/2015.

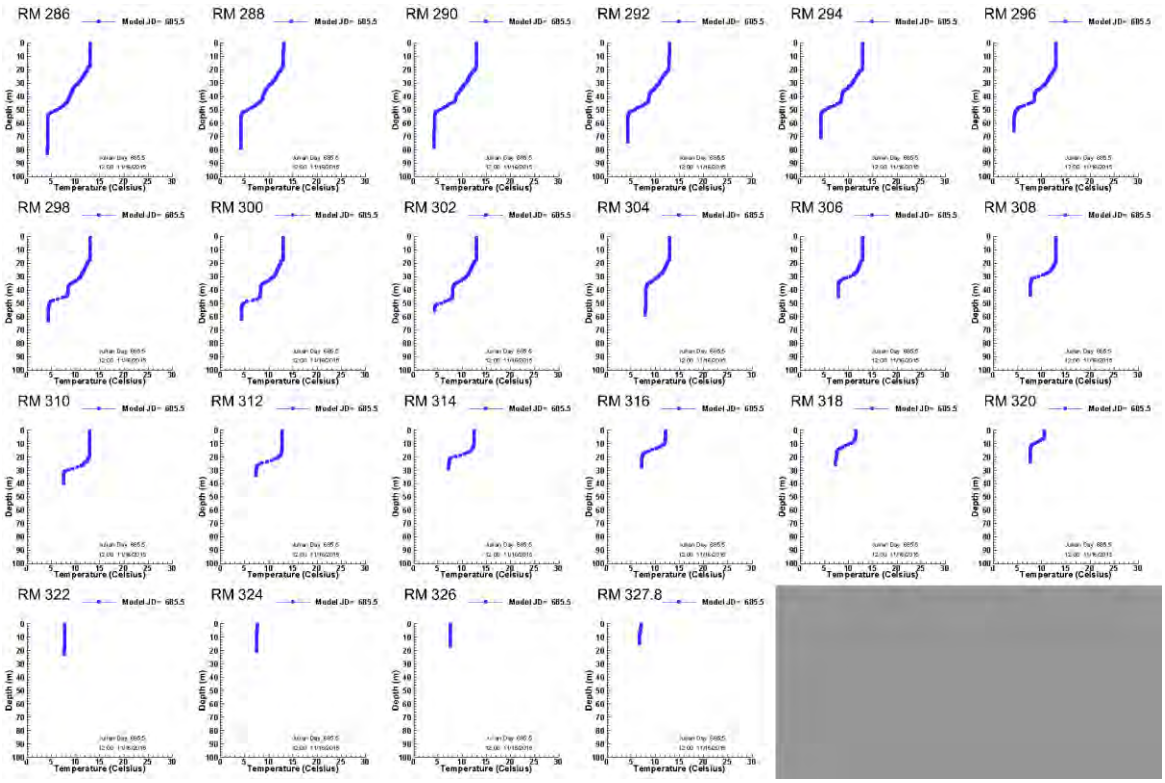


Figure 2351. Vertical profiles of temperature compared with data for 11/16/2015.

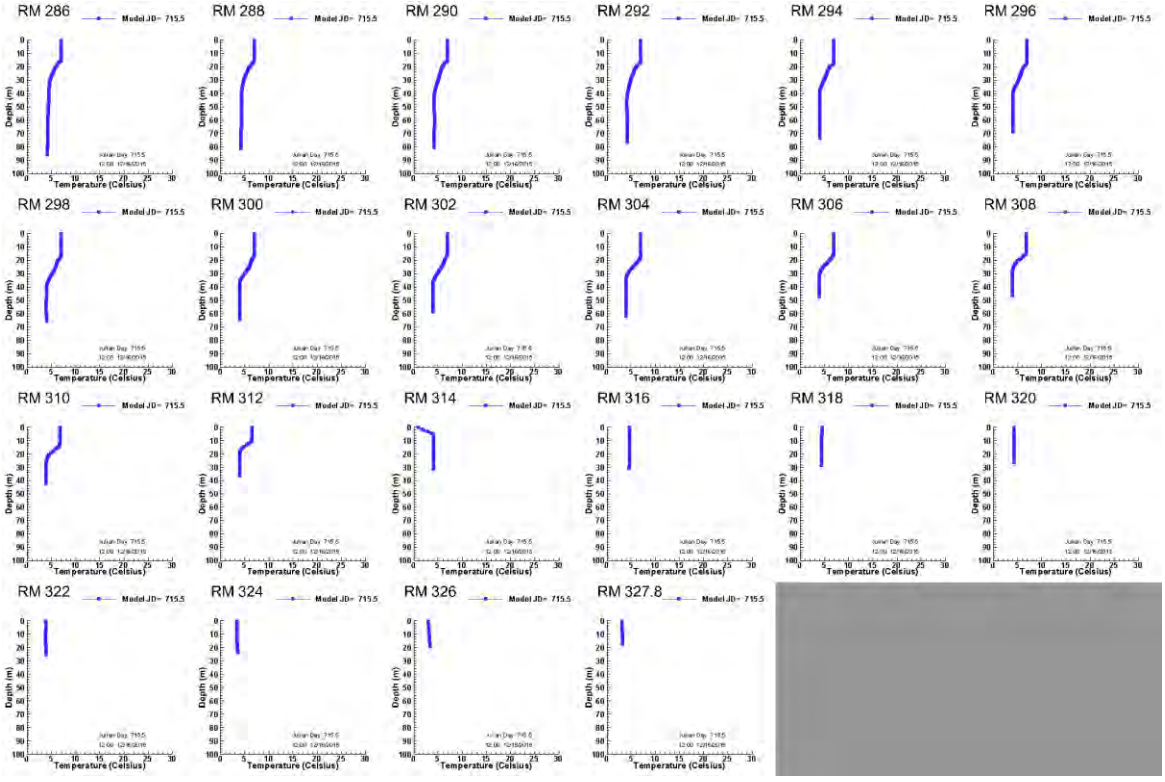


Figure 2352. Vertical profiles of temperature compared with data for 12/16/2015.

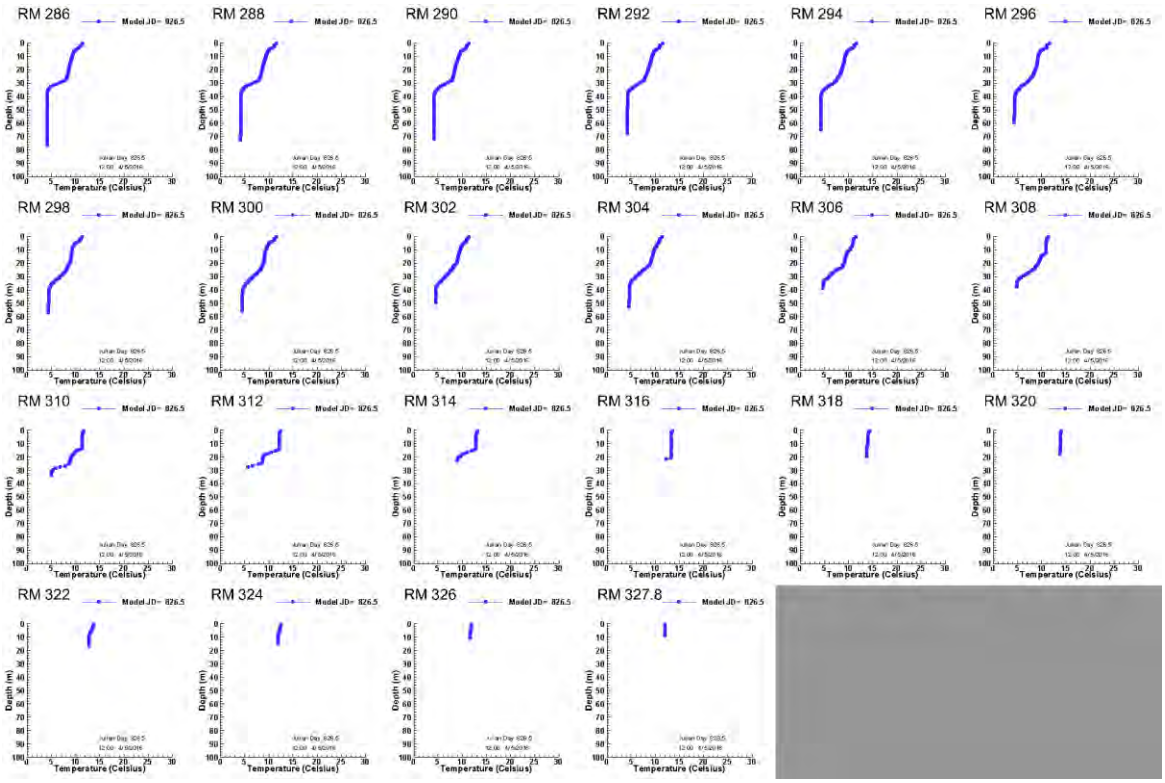


Figure 2353. Vertical profiles of temperature compared with data for 4/ 5/2016.

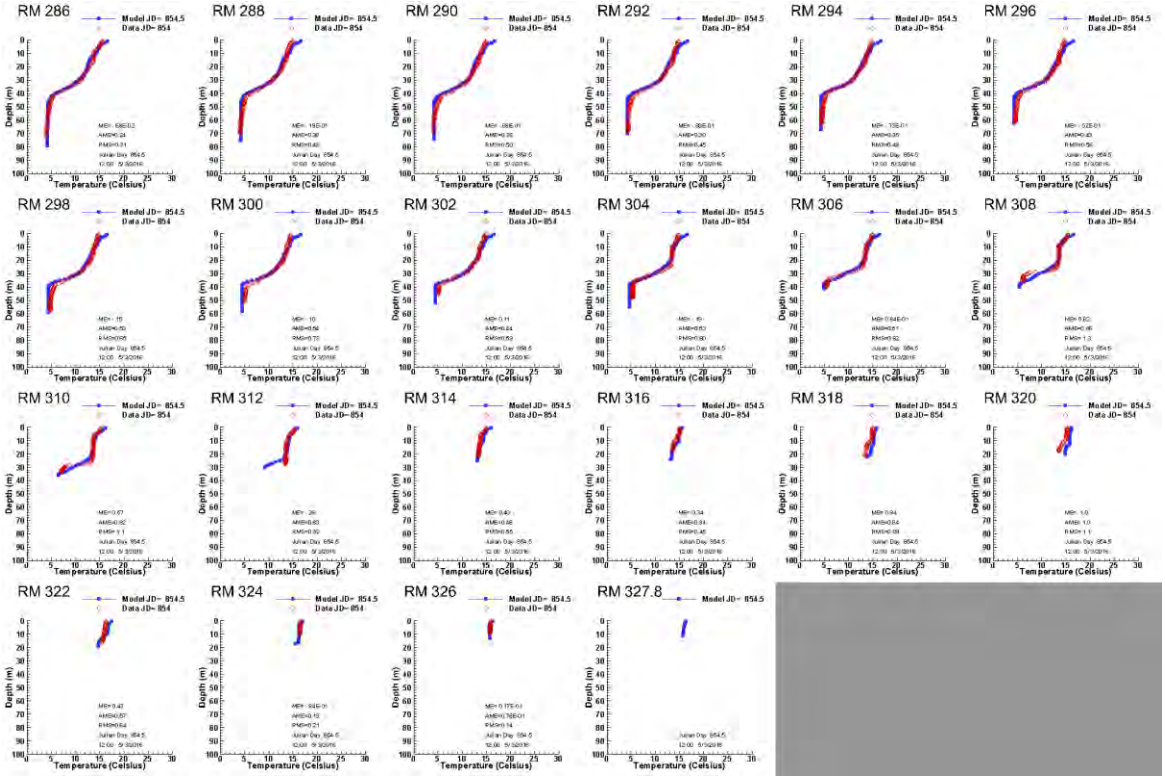


Figure 2354. Vertical profiles of temperature compared with data for 5/ 3/2016.

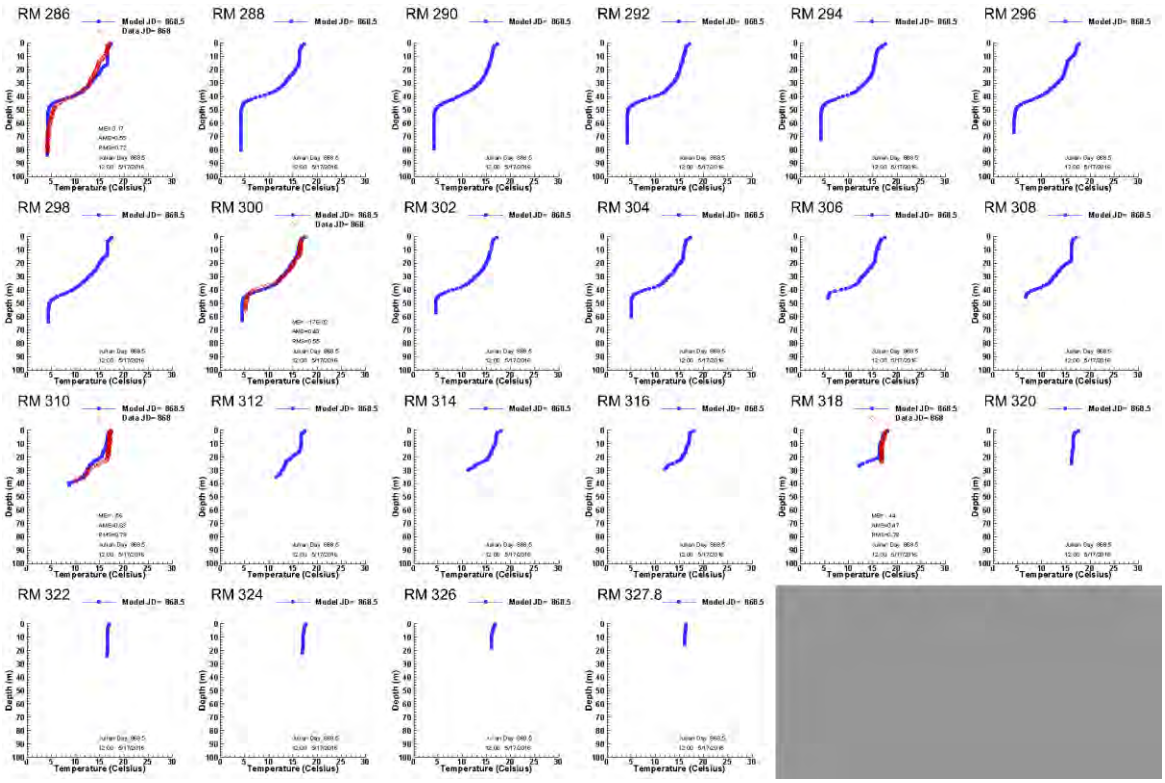


Figure 2355. Vertical profiles of temperature compared with data for 5/17/2016.

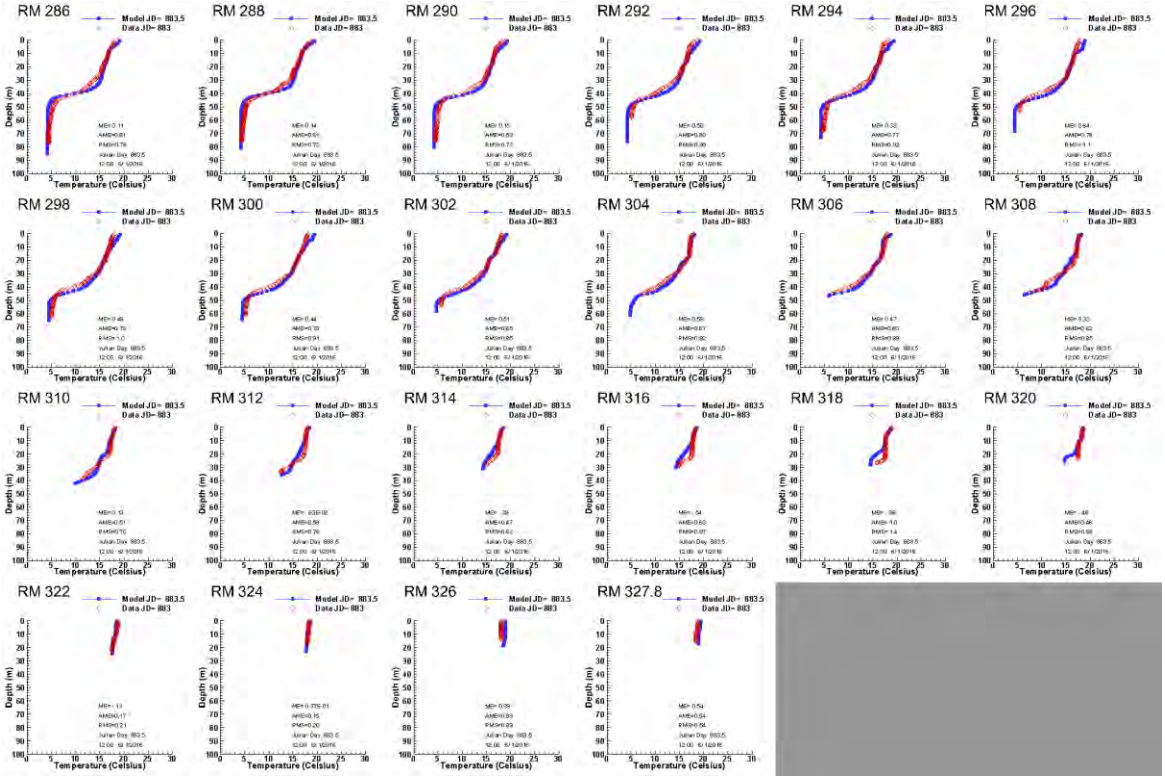


Figure 2356. Vertical profiles of temperature compared with data for 6/ 1/2016.

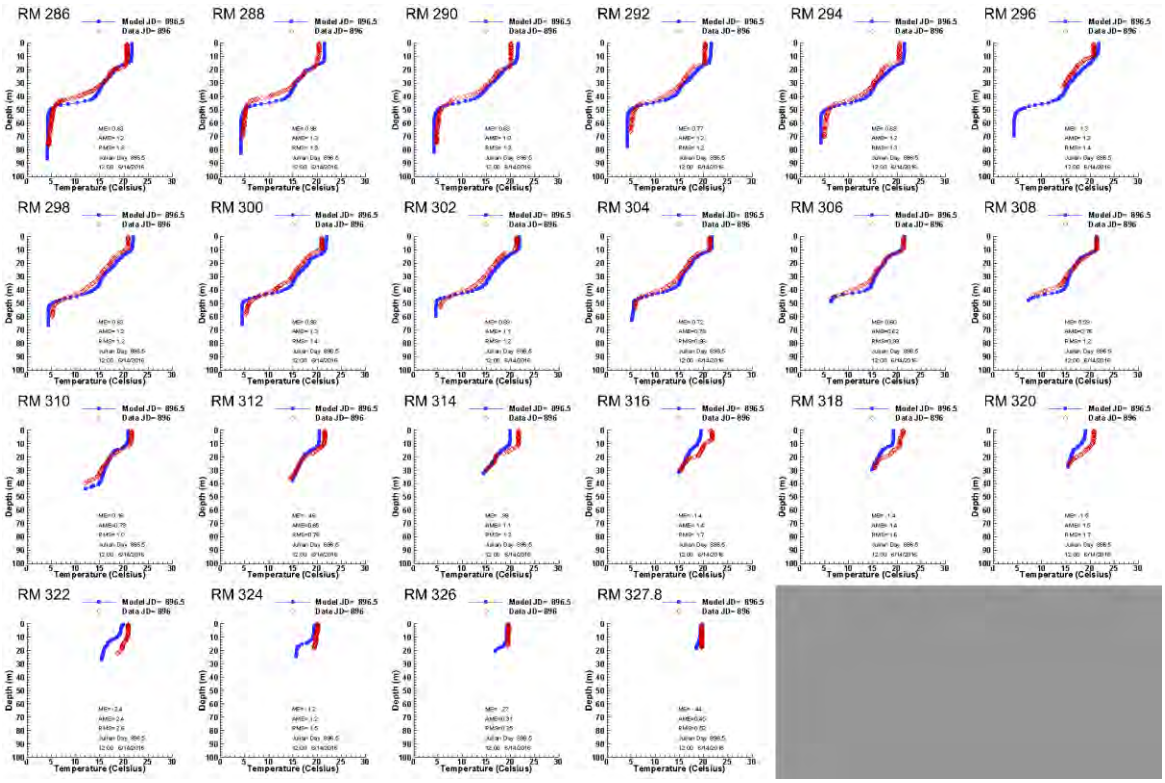


Figure 2357. Vertical profiles of temperature compared with data for 6/14/2016.

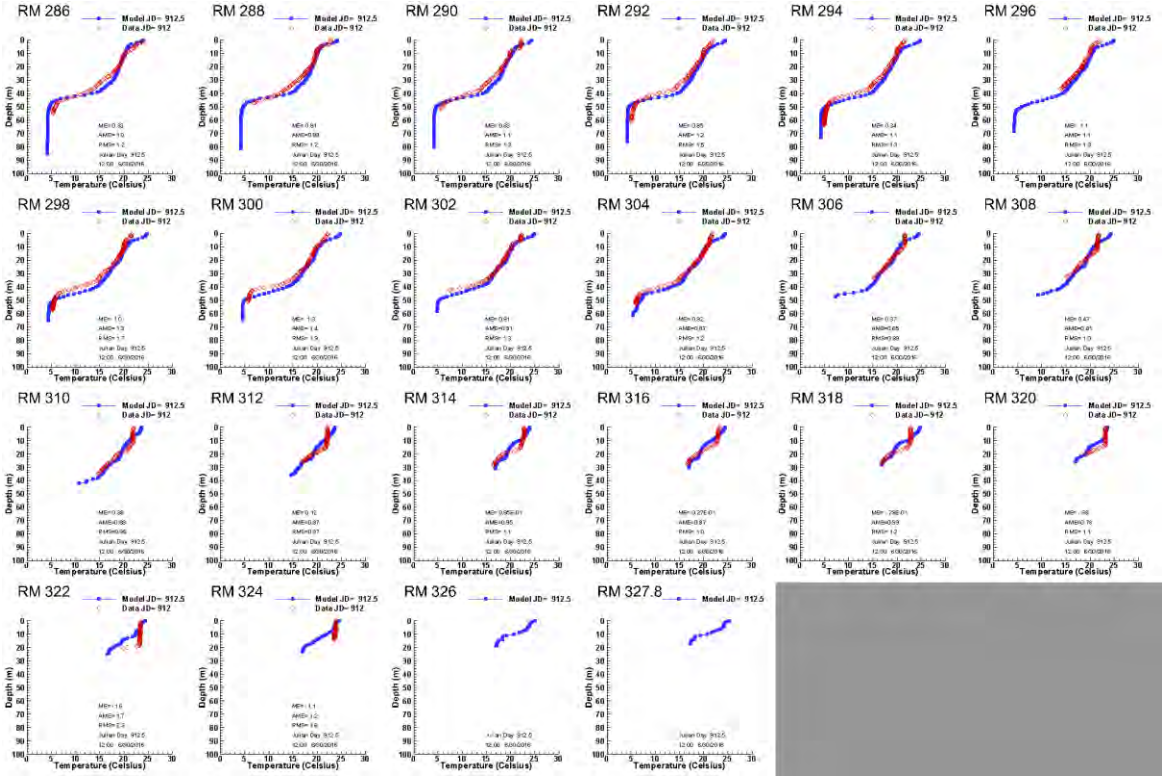


Figure 2358. Vertical profiles of temperature compared with data for 6/30/2016.

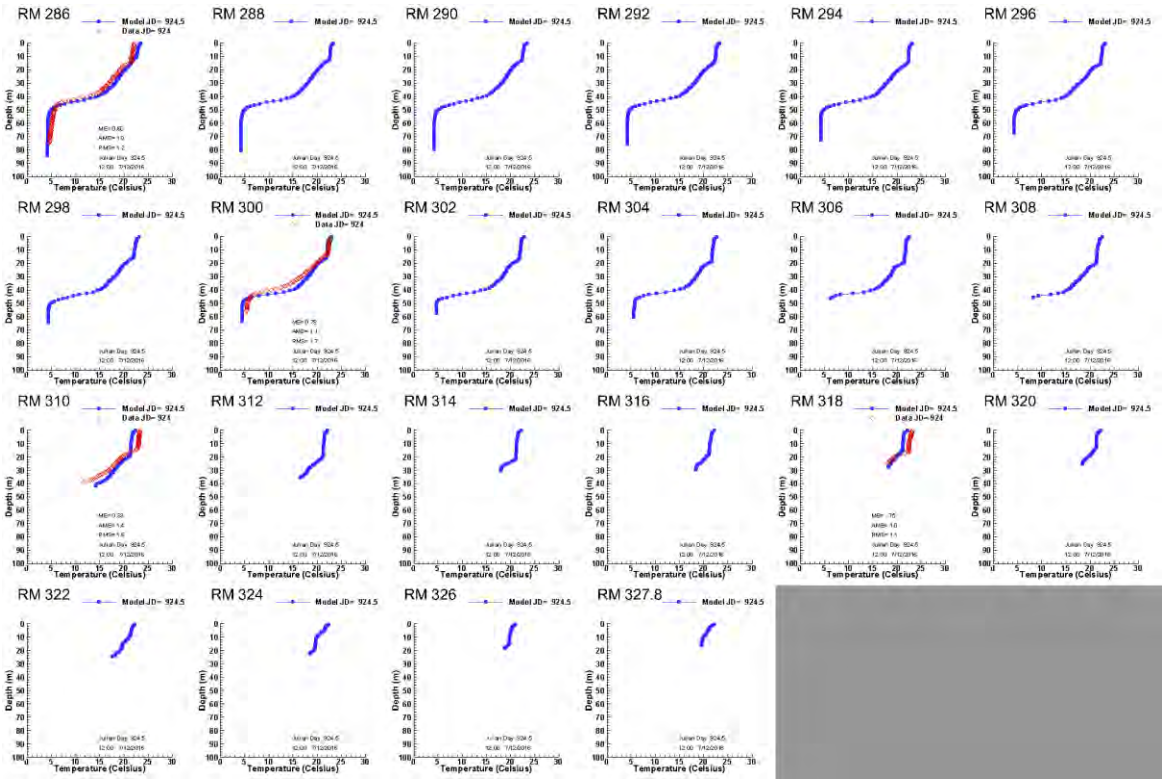


Figure 2359. Vertical profiles of temperature compared with data for 7/12/2016.

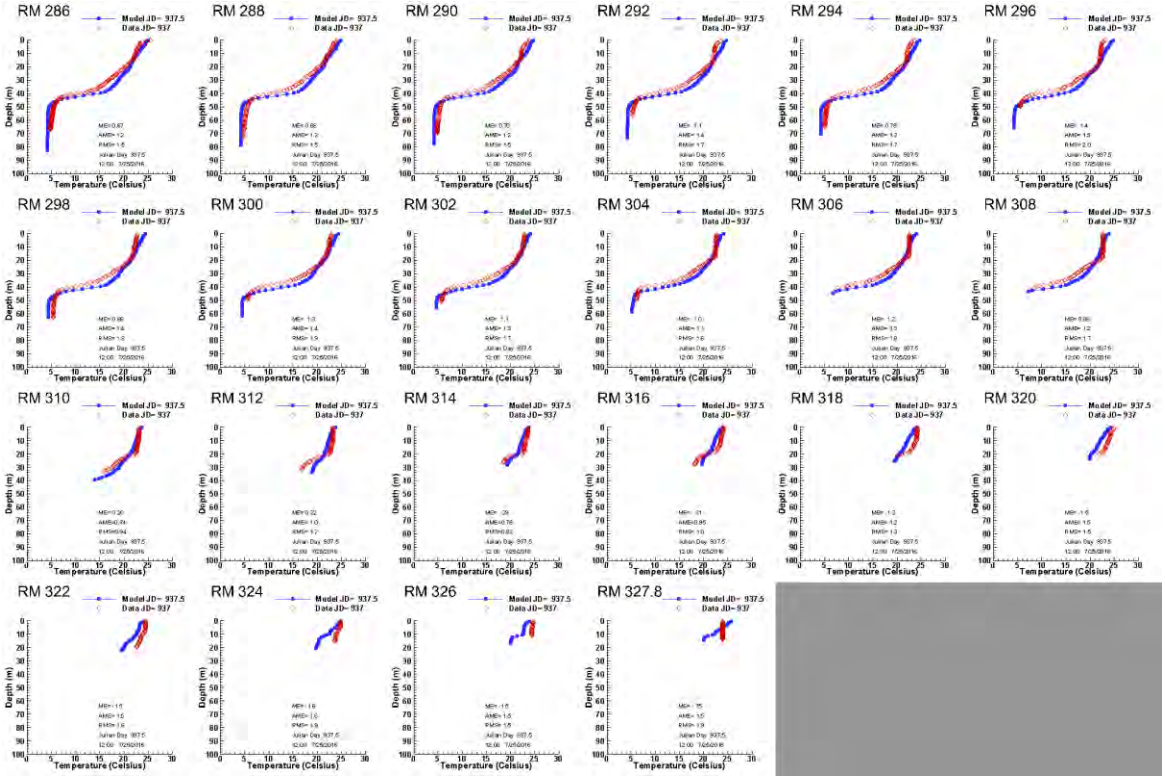


Figure 2360. Vertical profiles of temperature compared with data for 7/25/2016.

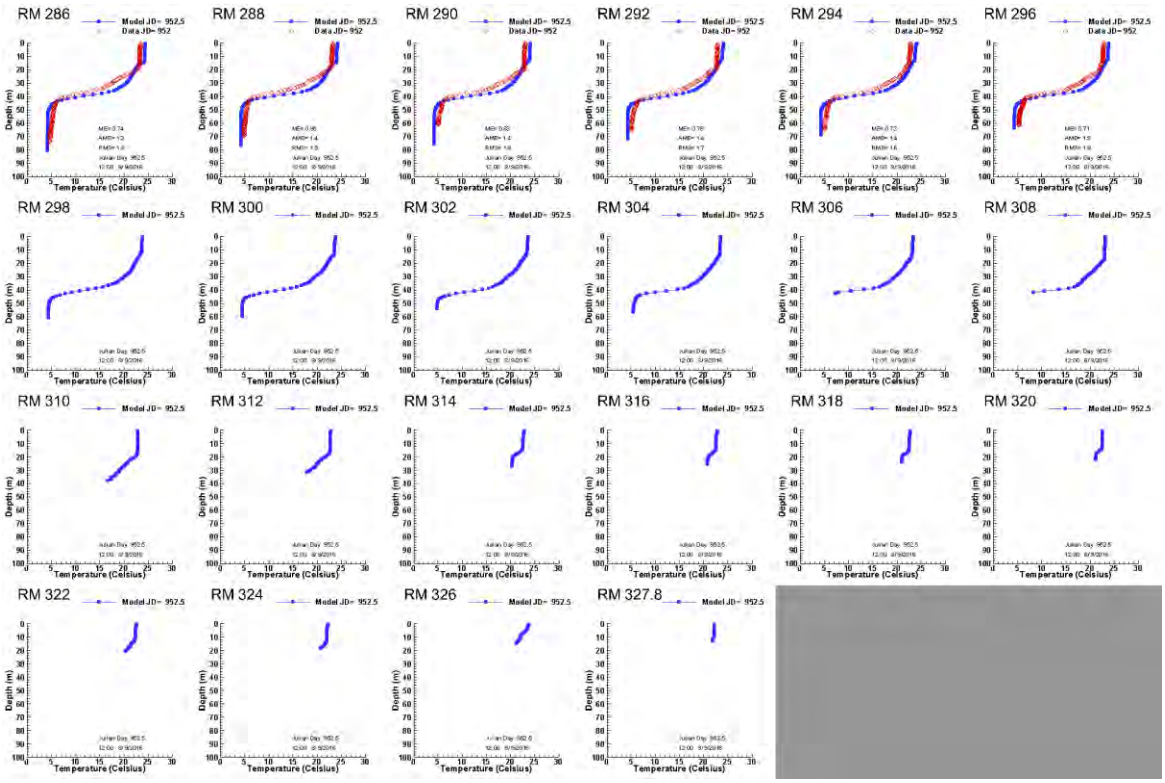


Figure 2361. Vertical profiles of temperature compared with data for 8/ 9/2016.

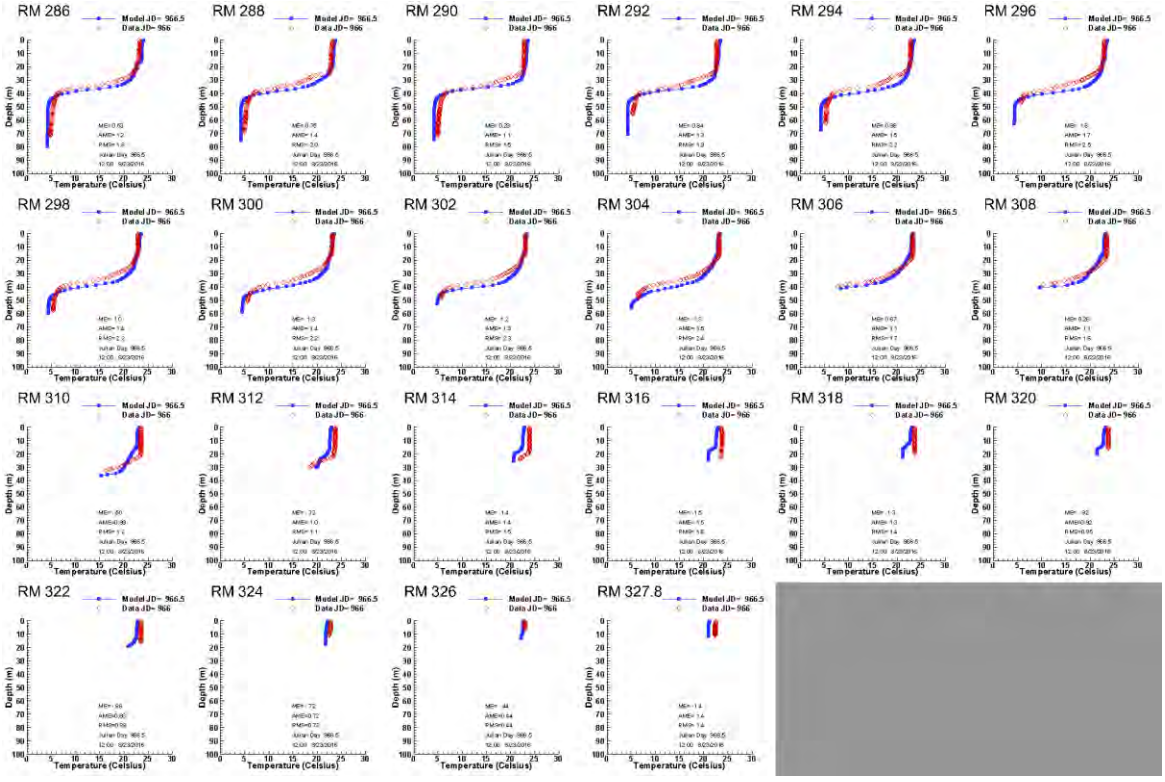


Figure 2362. Vertical profiles of temperature compared with data for 8/23/2016.

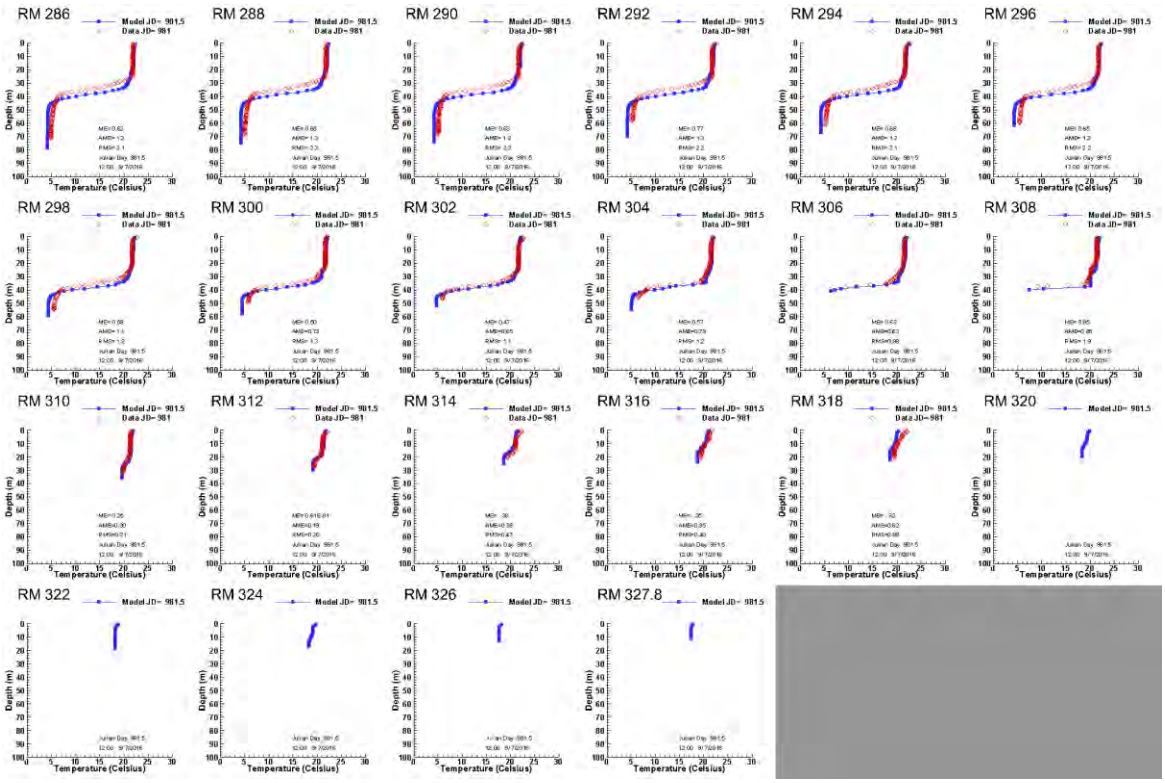


Figure 2363. Vertical profiles of temperature compared with data for 9/ 7/2016.

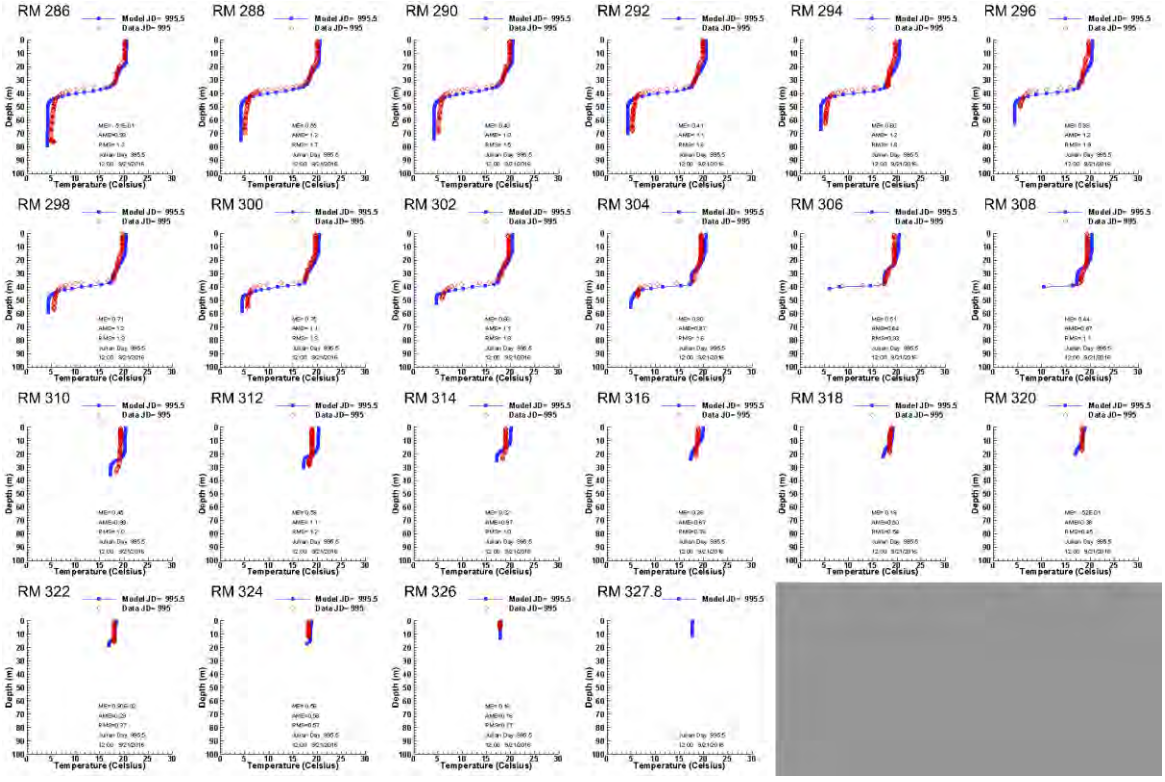


Figure 2364. Vertical profiles of temperature compared with data for 9/21/2016.

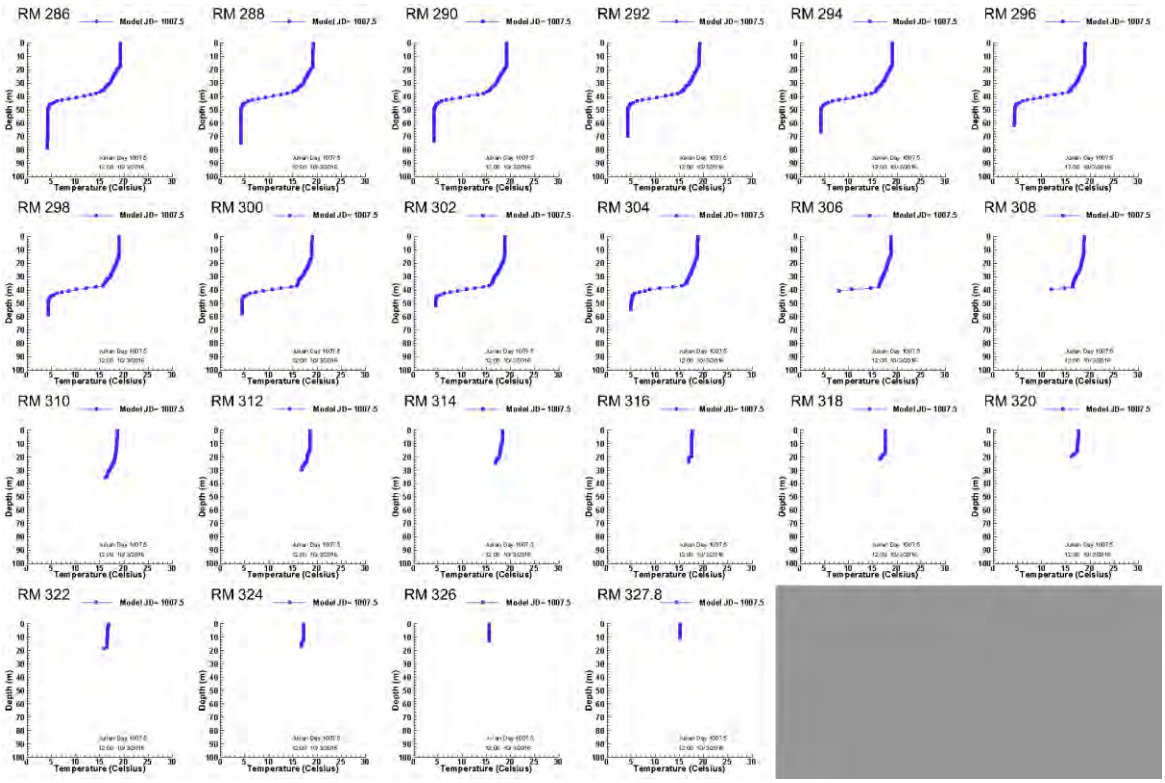


Figure 2365. Vertical profiles of temperature compared with data for 10/ 3/2016.

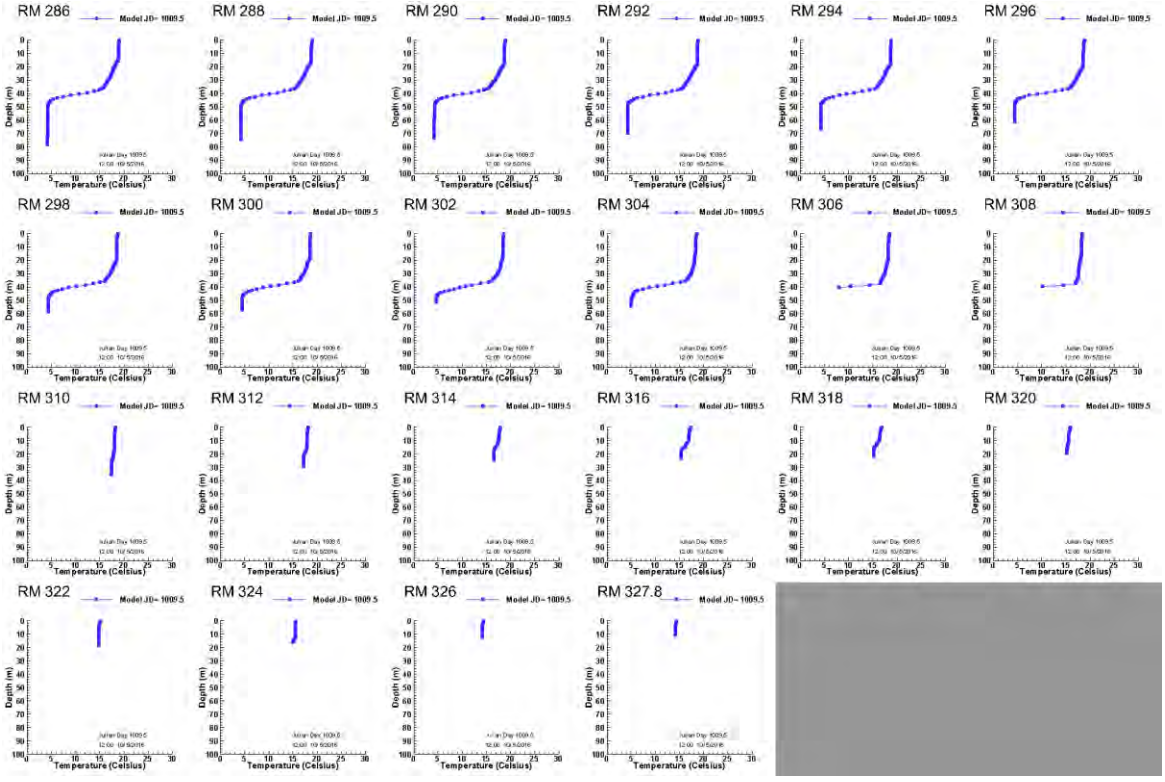


Figure 2366. Vertical profiles of temperature compared with data for 10/ 5/2016.

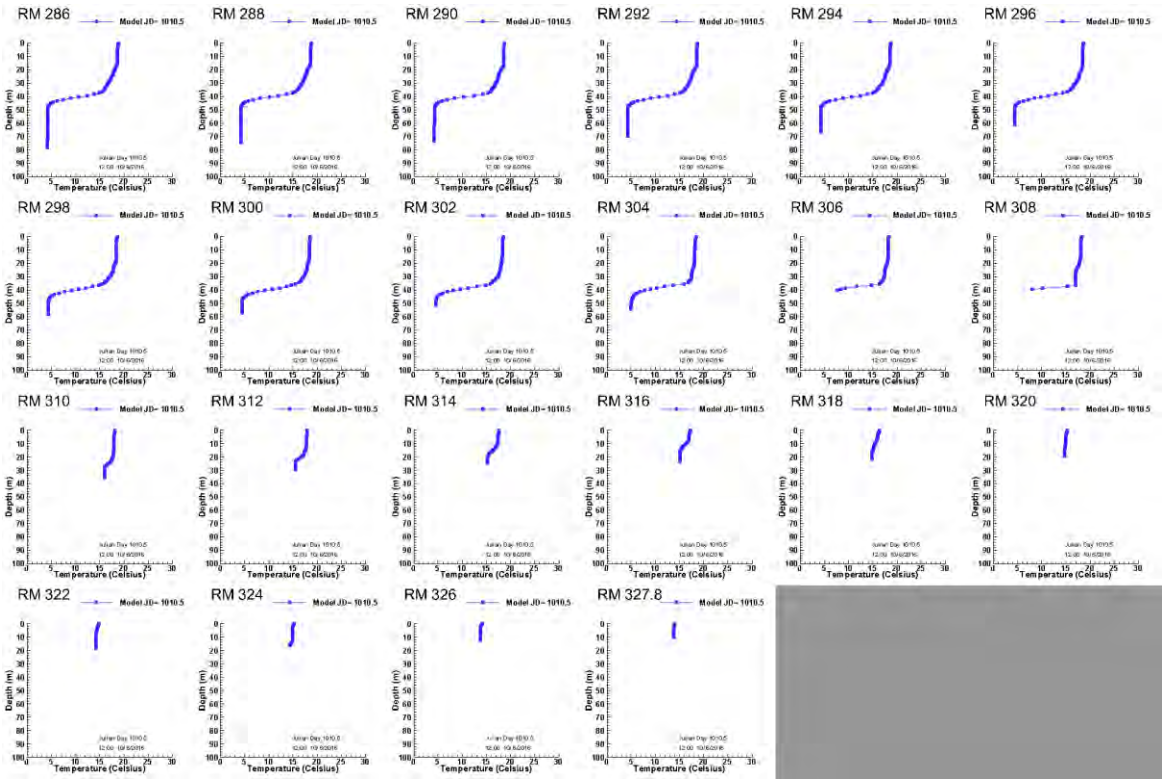


Figure 2367. Vertical profiles of temperature compared with data for 10/ 6/2016.

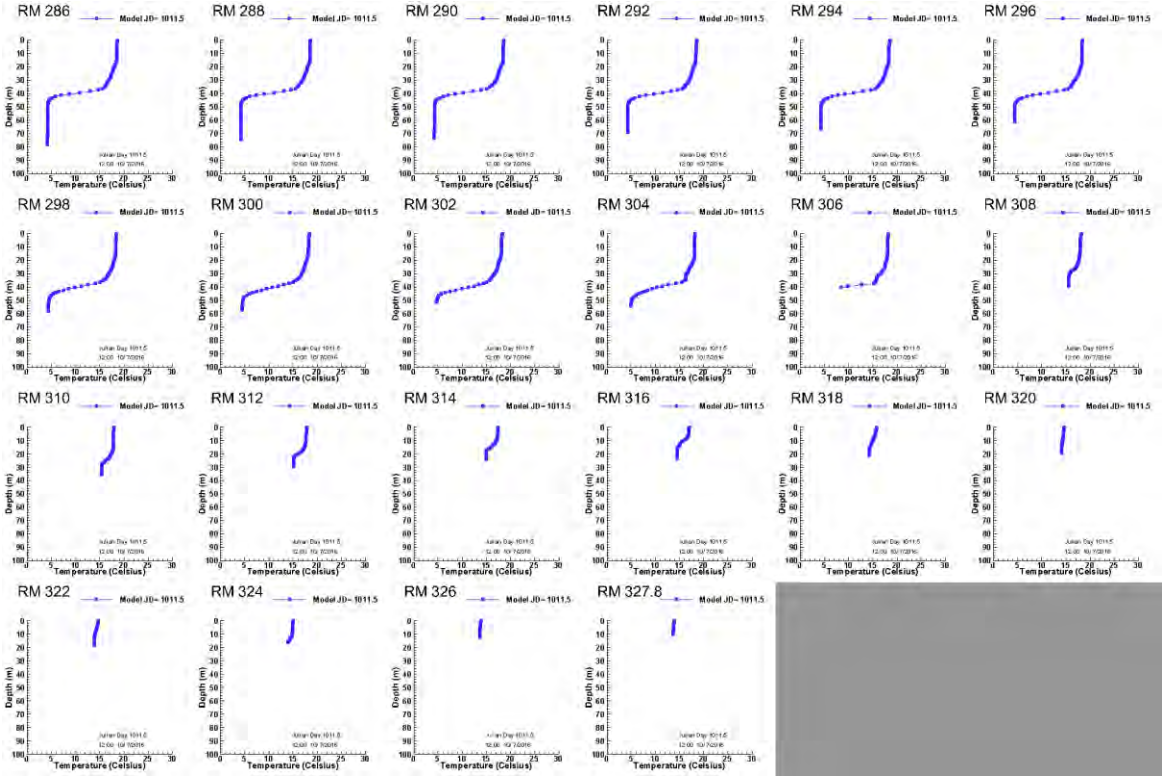


Figure 2368. Vertical profiles of temperature compared with data for 10/ 7/2016.

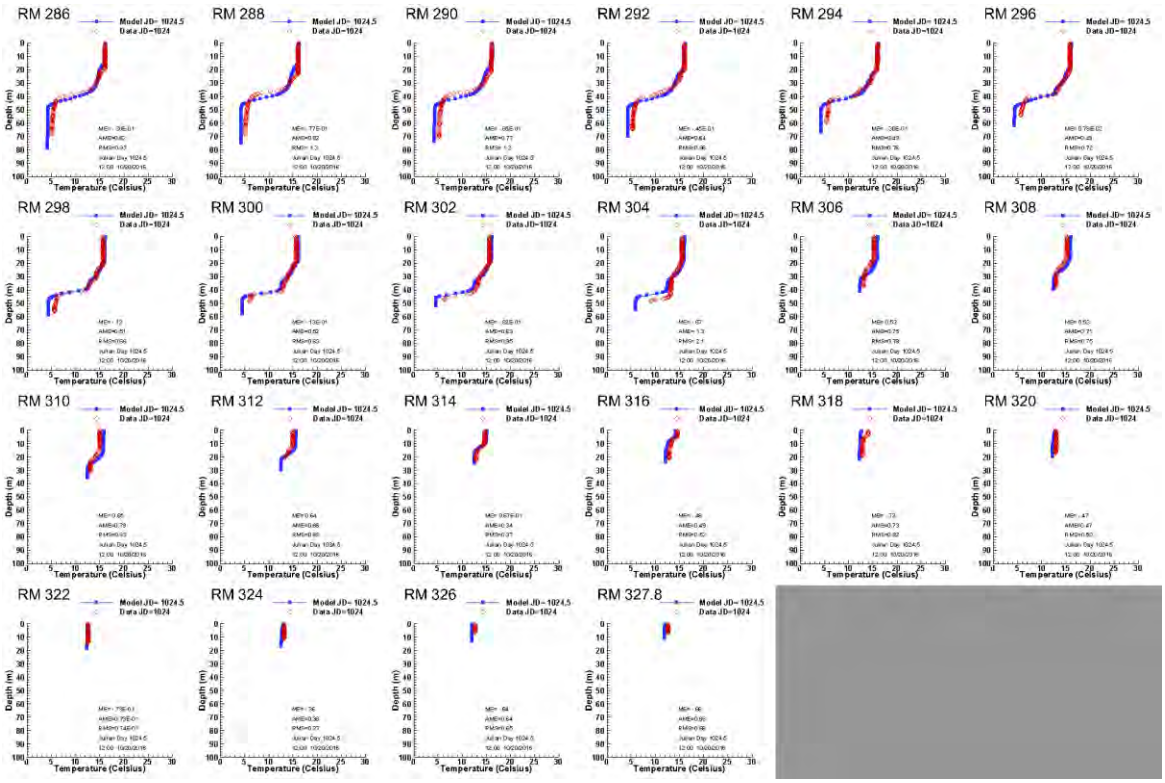


Figure 2369. Vertical profiles of temperature compared with data for 10/20/2016.

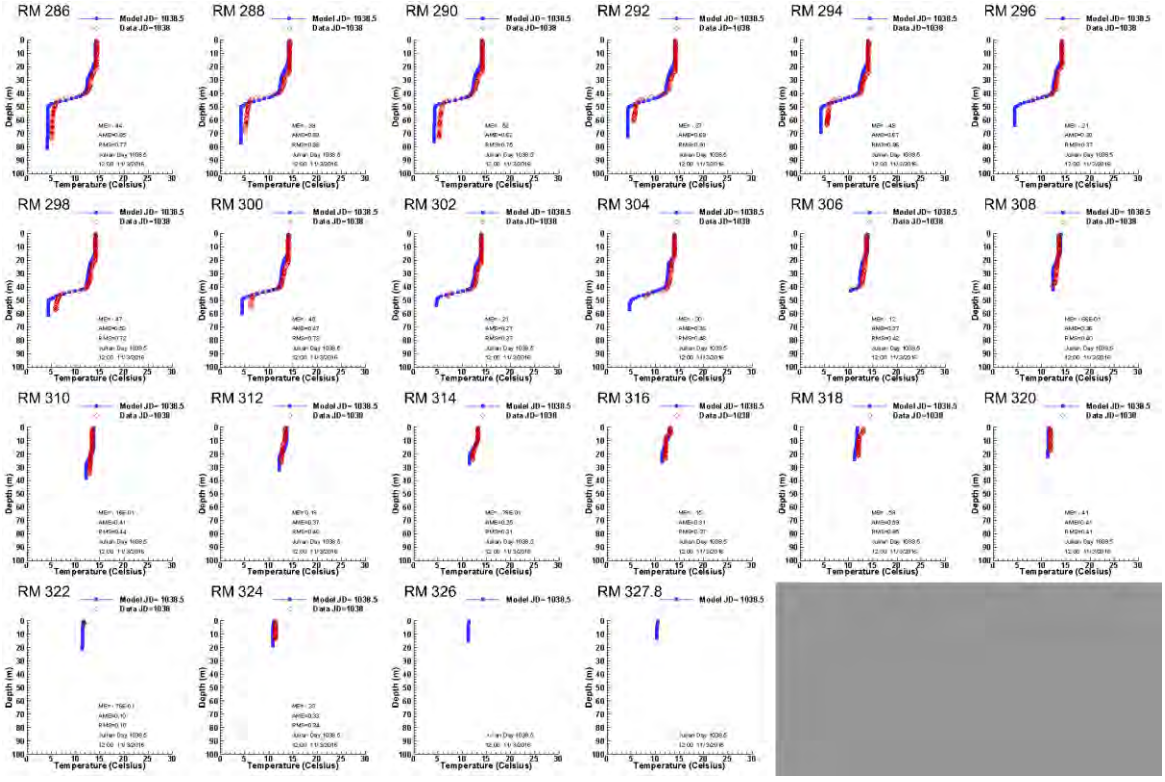


Figure 2370. Vertical profiles of temperature compared with data for 11/ 3/2016.

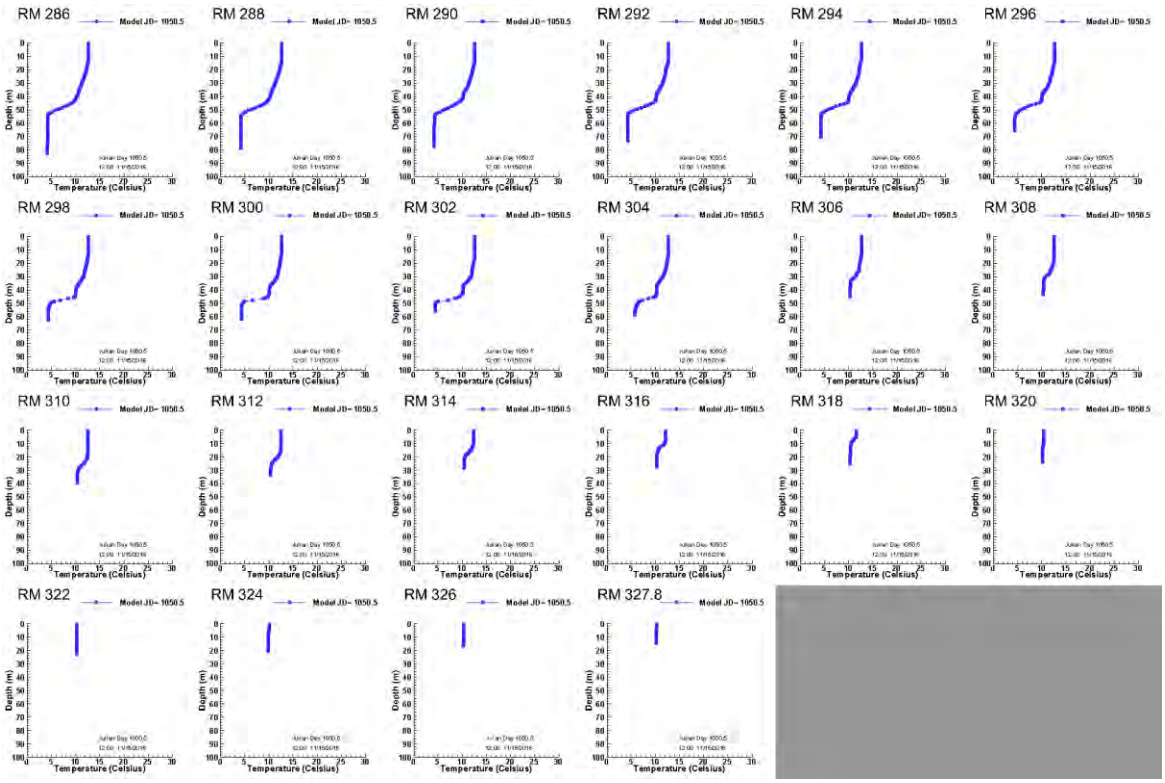


Figure 2371. Vertical profiles of temperature compared with data for 11/15/2016.

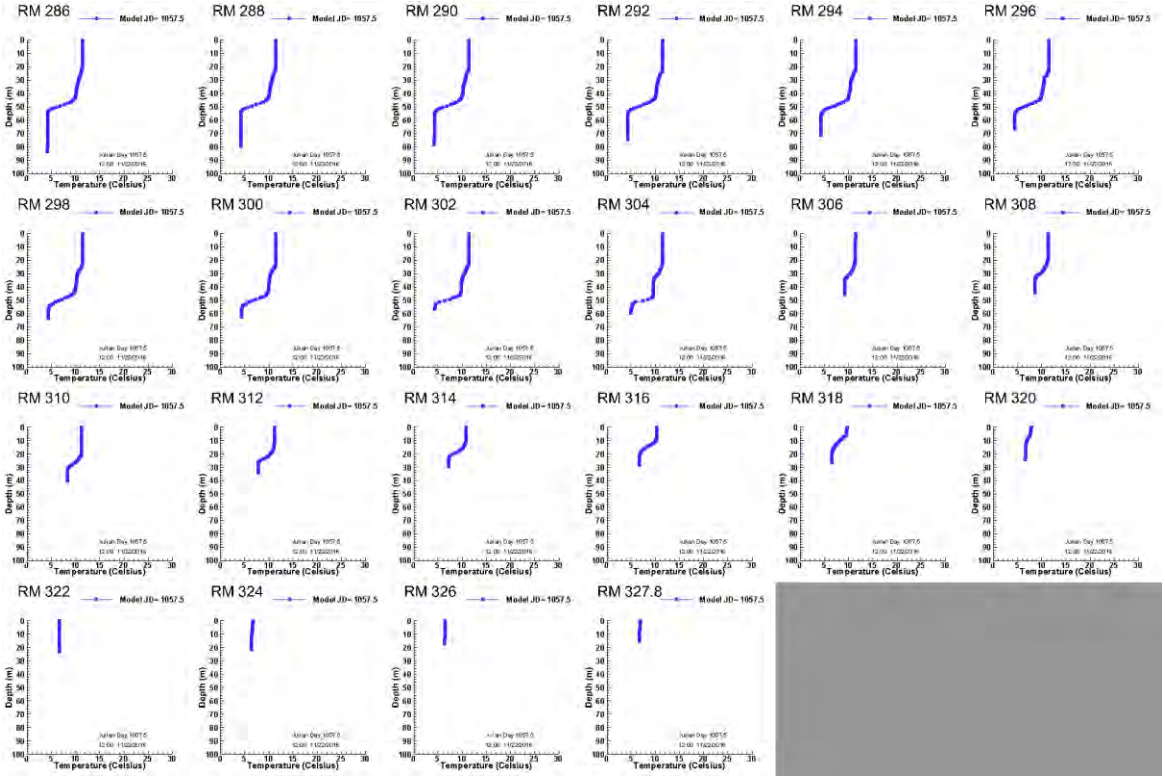


Figure 2372. Vertical profiles of temperature compared with data for 11/22/2016.

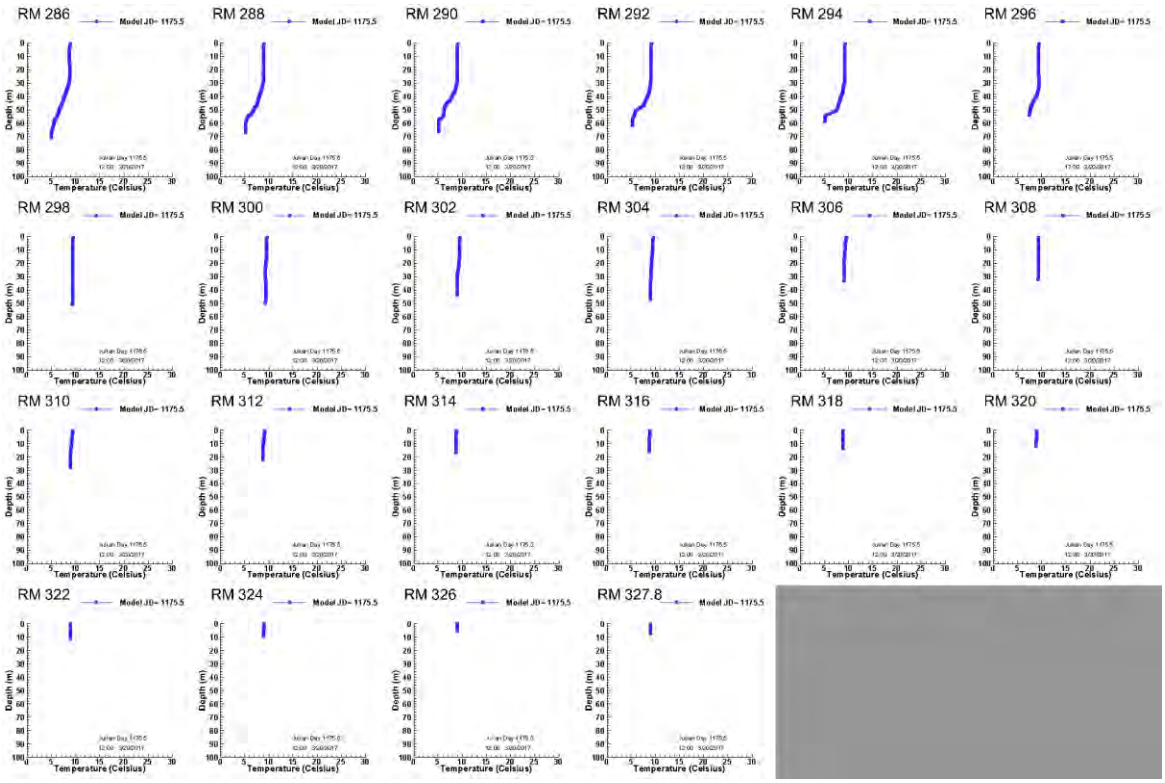


Figure 2373. Vertical profiles of temperature compared with data for 3/20/2017.

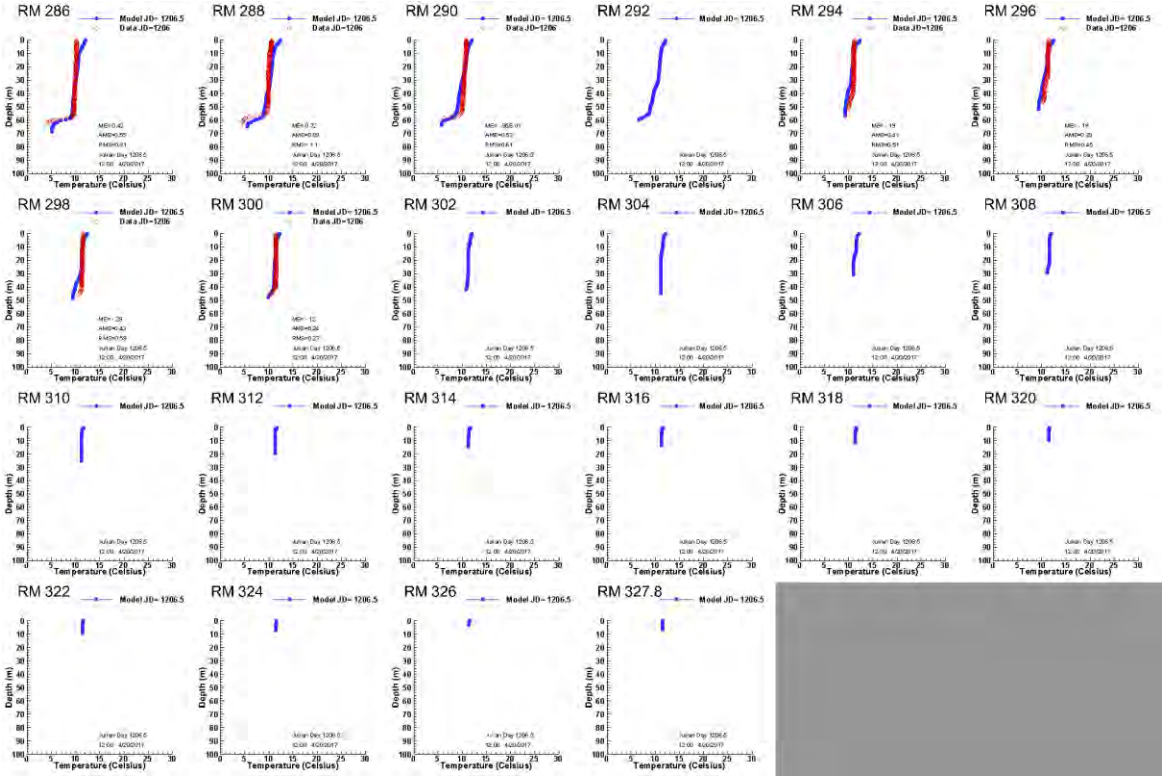


Figure 2374. Vertical profiles of temperature compared with data for 4/20/2017.

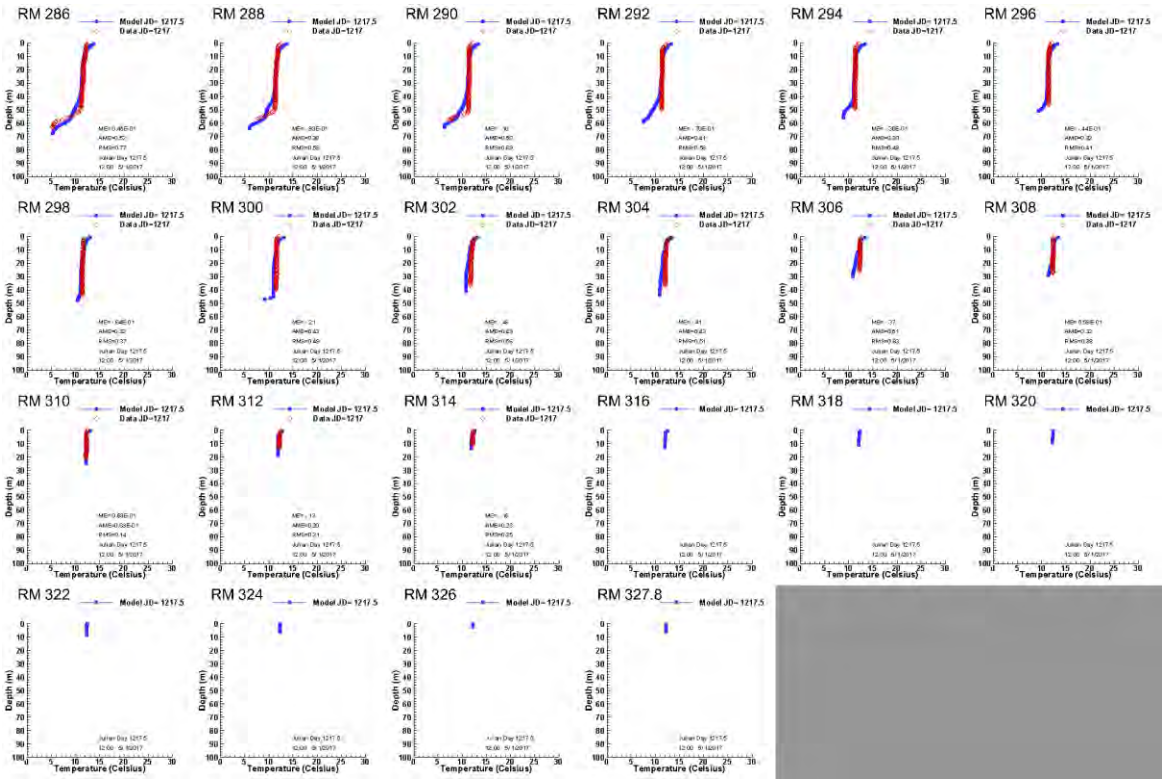


Figure 2375. Vertical profiles of temperature compared with data for 5/ 1/2017.

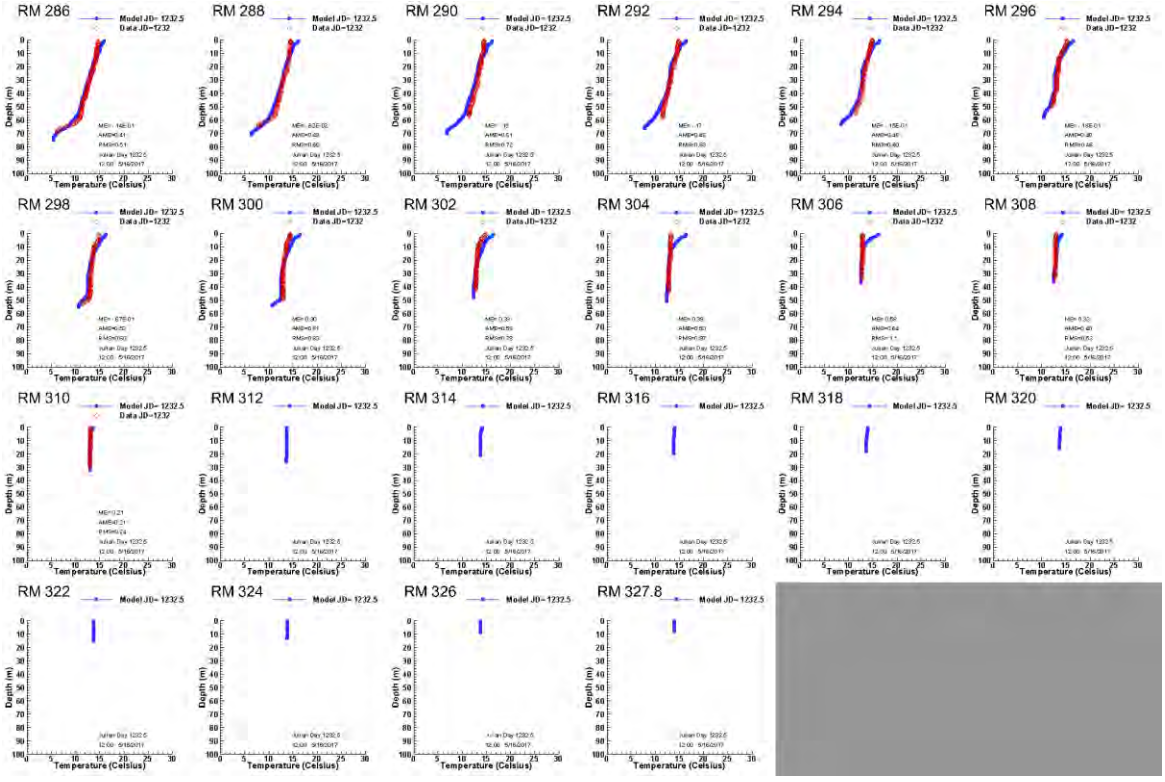


Figure 2376. Vertical profiles of temperature compared with data for 5/16/2017.

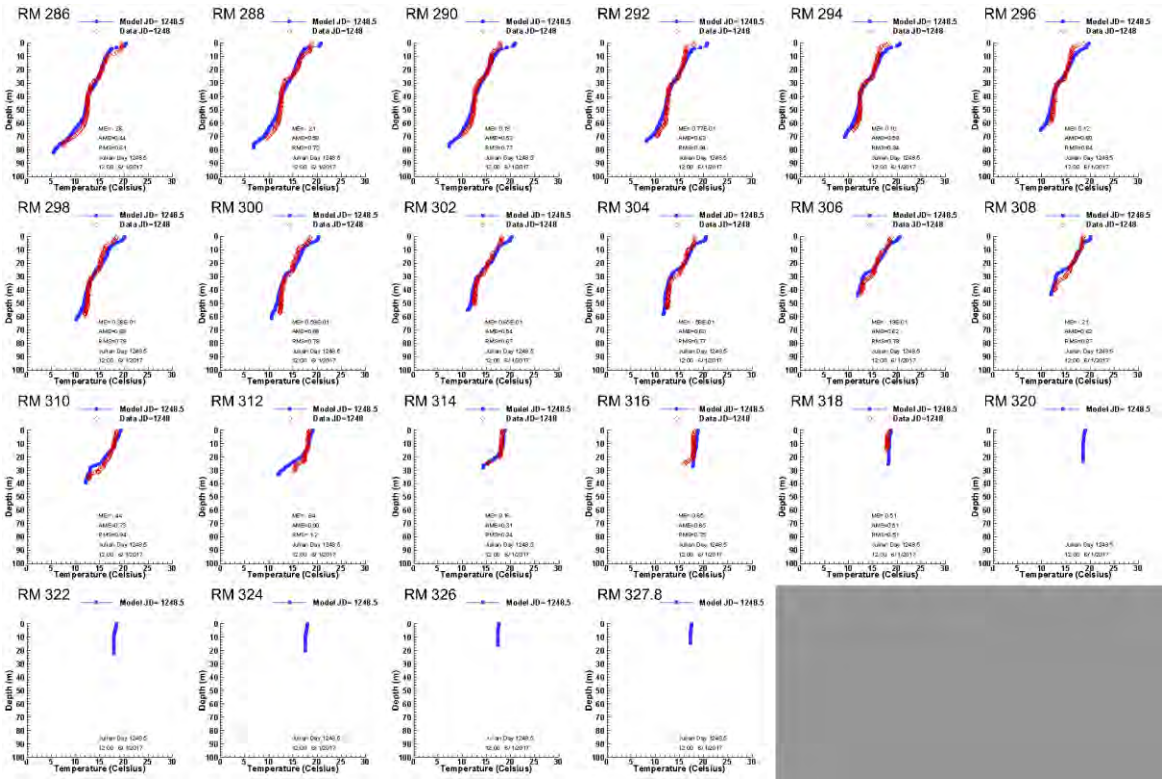


Figure 2377. Vertical profiles of temperature compared with data for 6/ 1/2017.

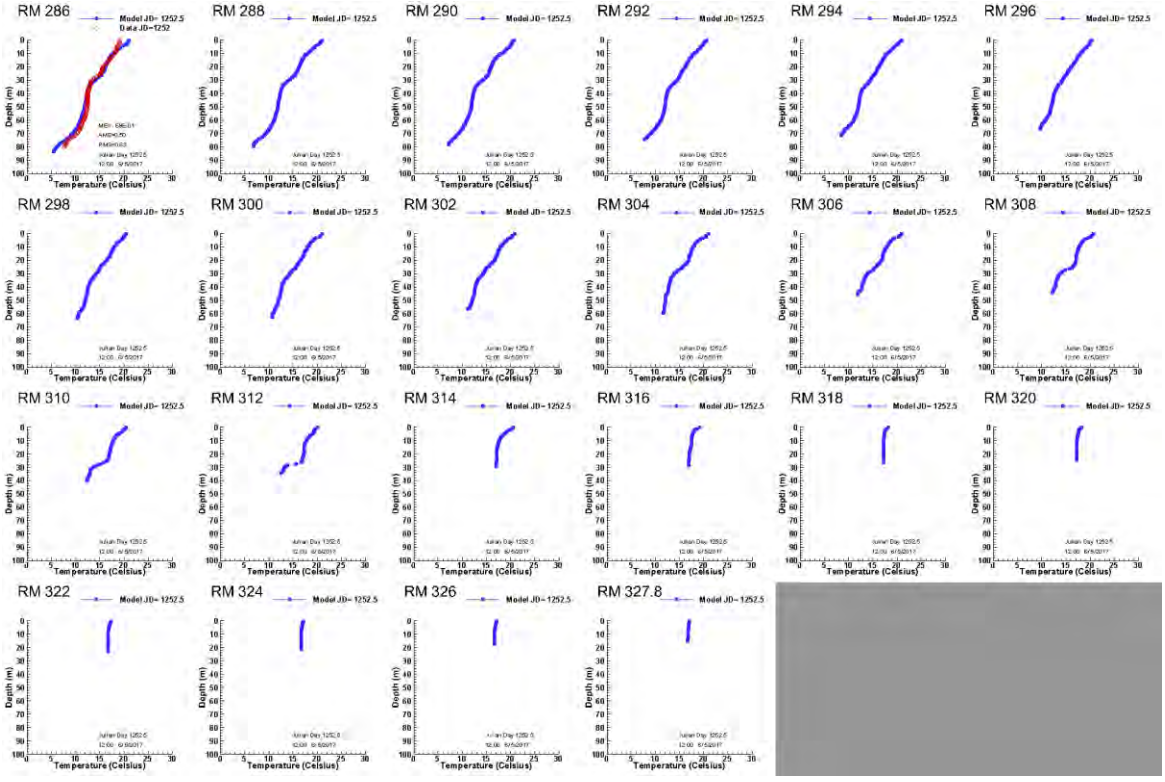


Figure 2378. Vertical profiles of temperature compared with data for 6/ 5/2017.

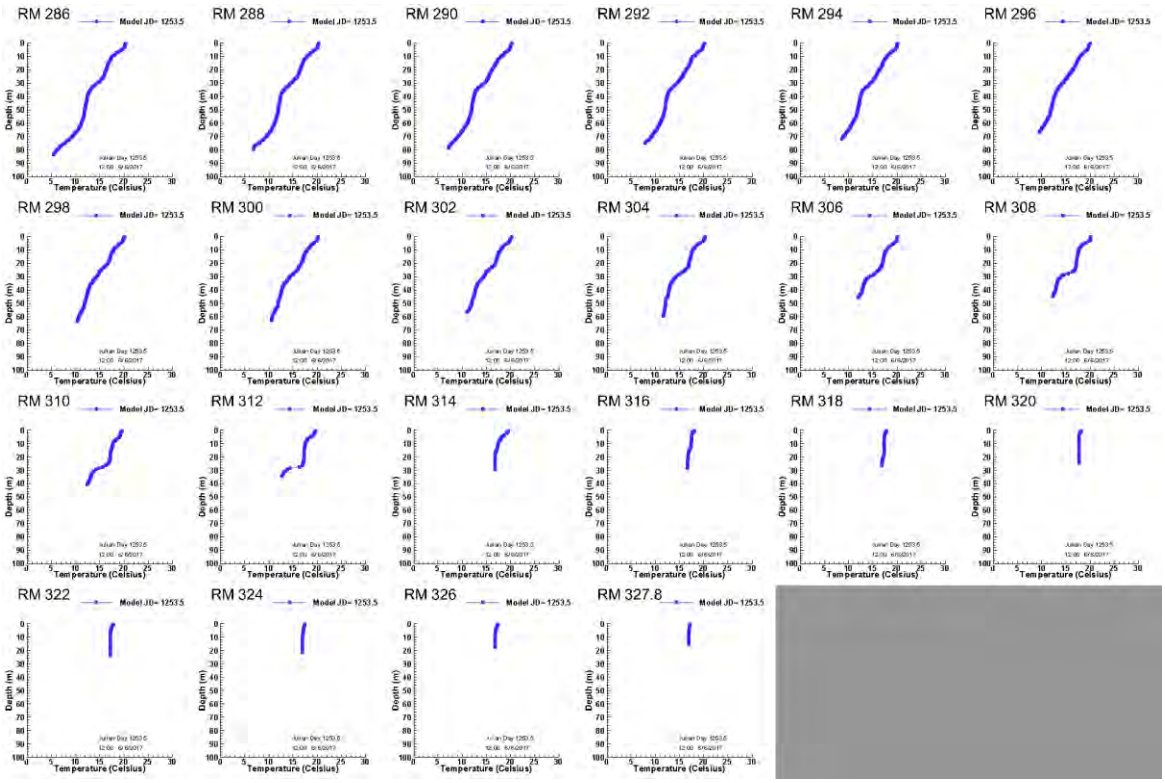


Figure 2379. Vertical profiles of temperature compared with data for 6/ 6/2017.

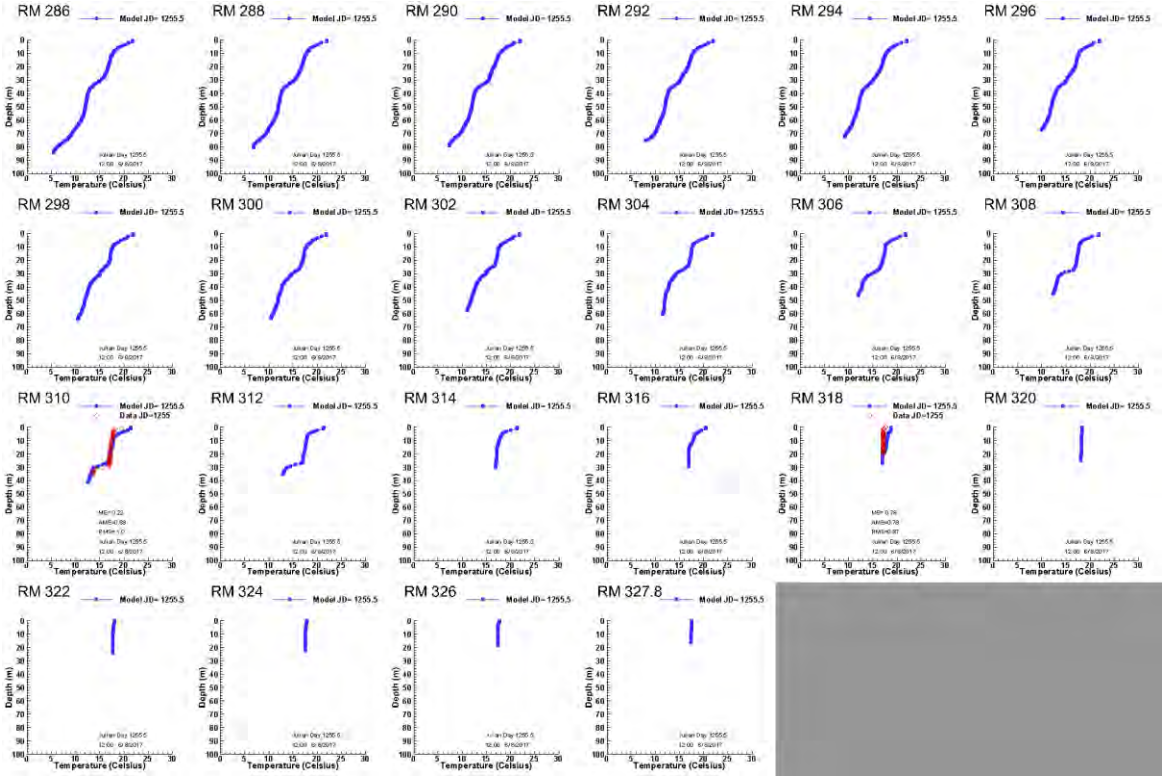


Figure 2380. Vertical profiles of temperature compared with data for 6/ 8/2017.

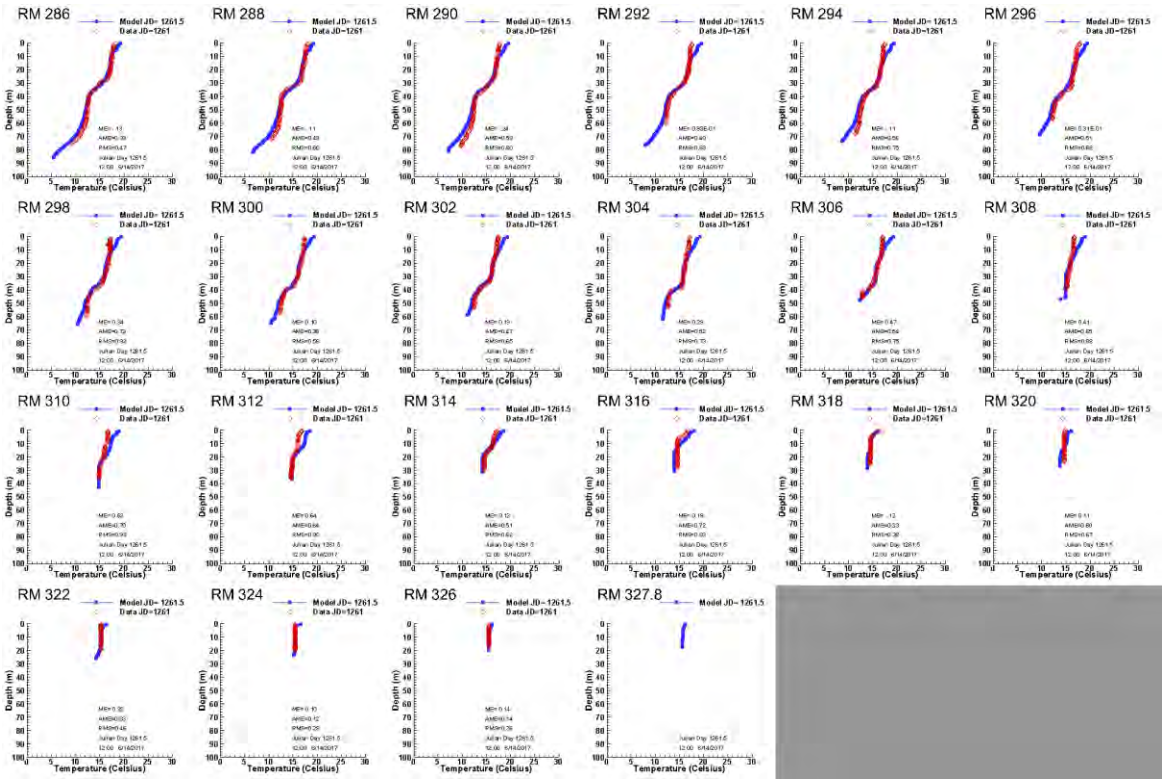


Figure 2381. Vertical profiles of temperature compared with data for 6/14/2017.

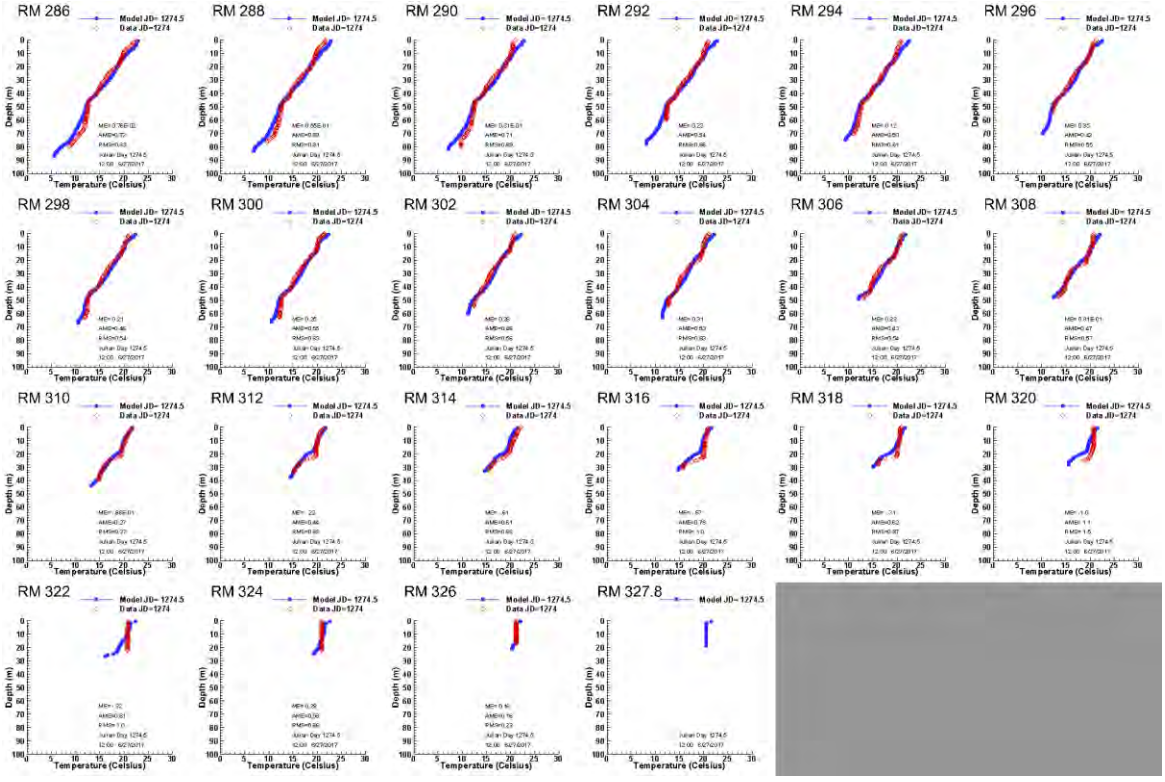


Figure 2382. Vertical profiles of temperature compared with data for 6/27/2017.

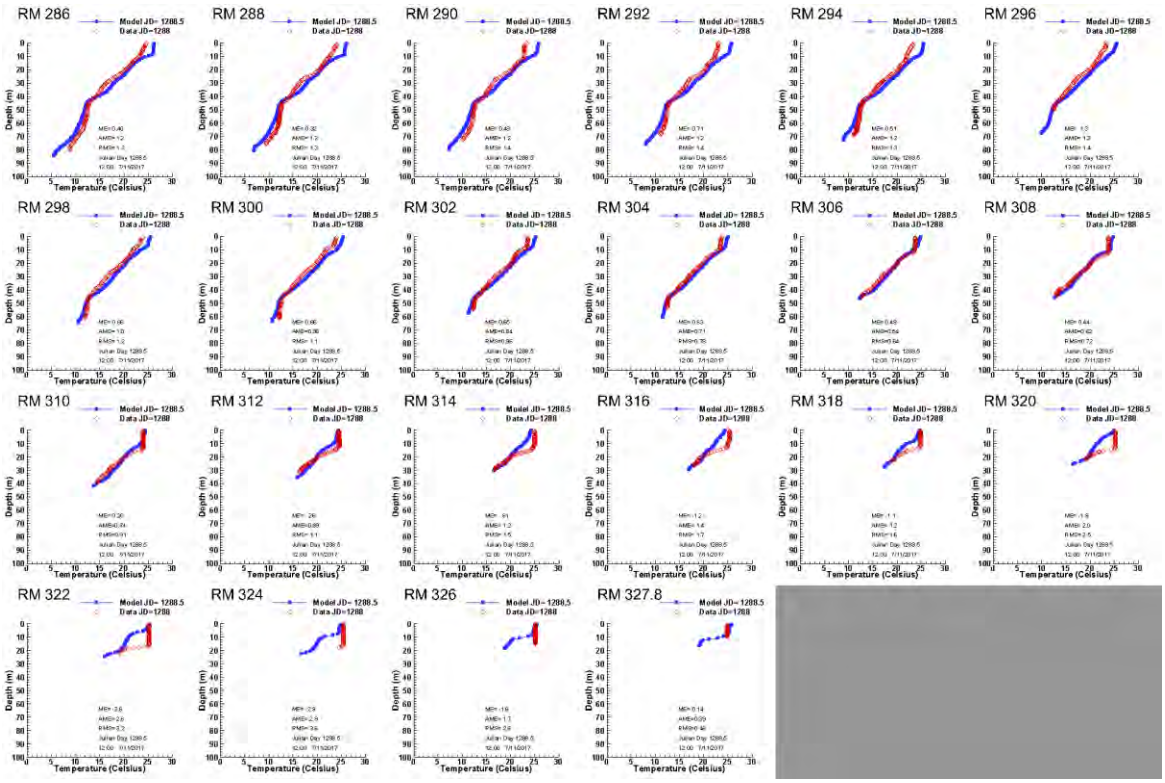


Figure 2383. Vertical profiles of temperature compared with data for 7/11/2017.

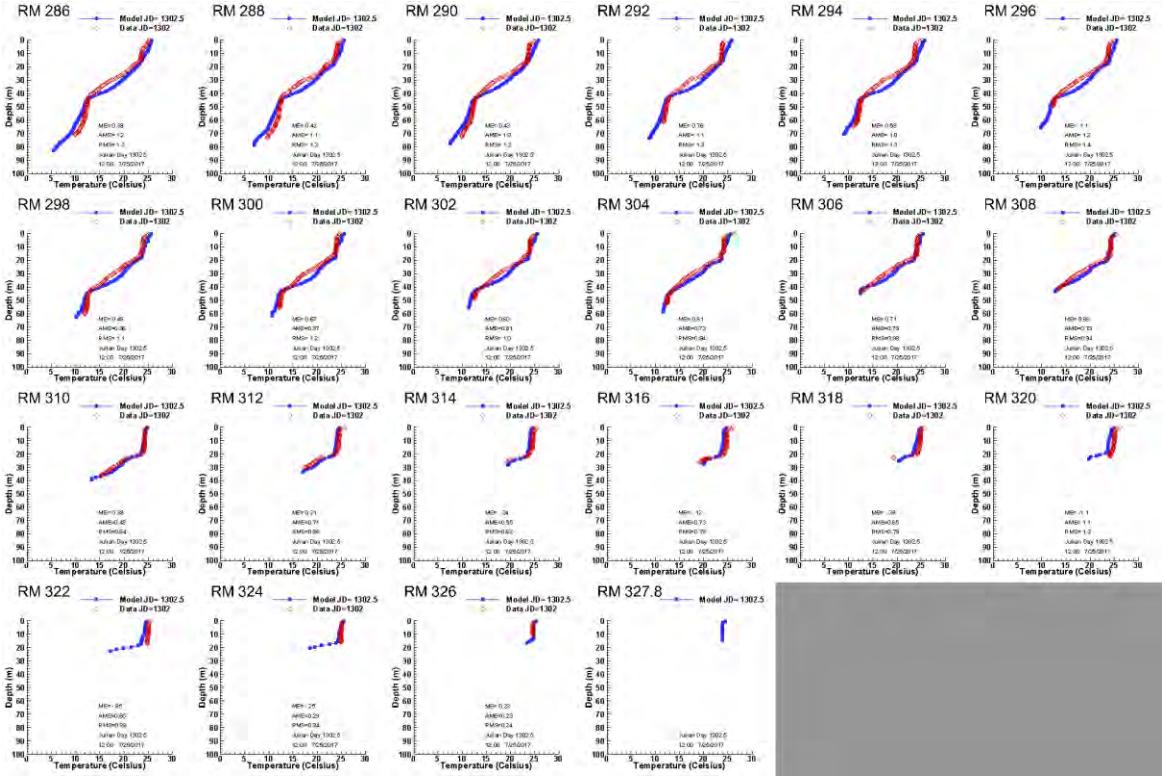


Figure 2384. Vertical profiles of temperature compared with data for 7/25/2017.

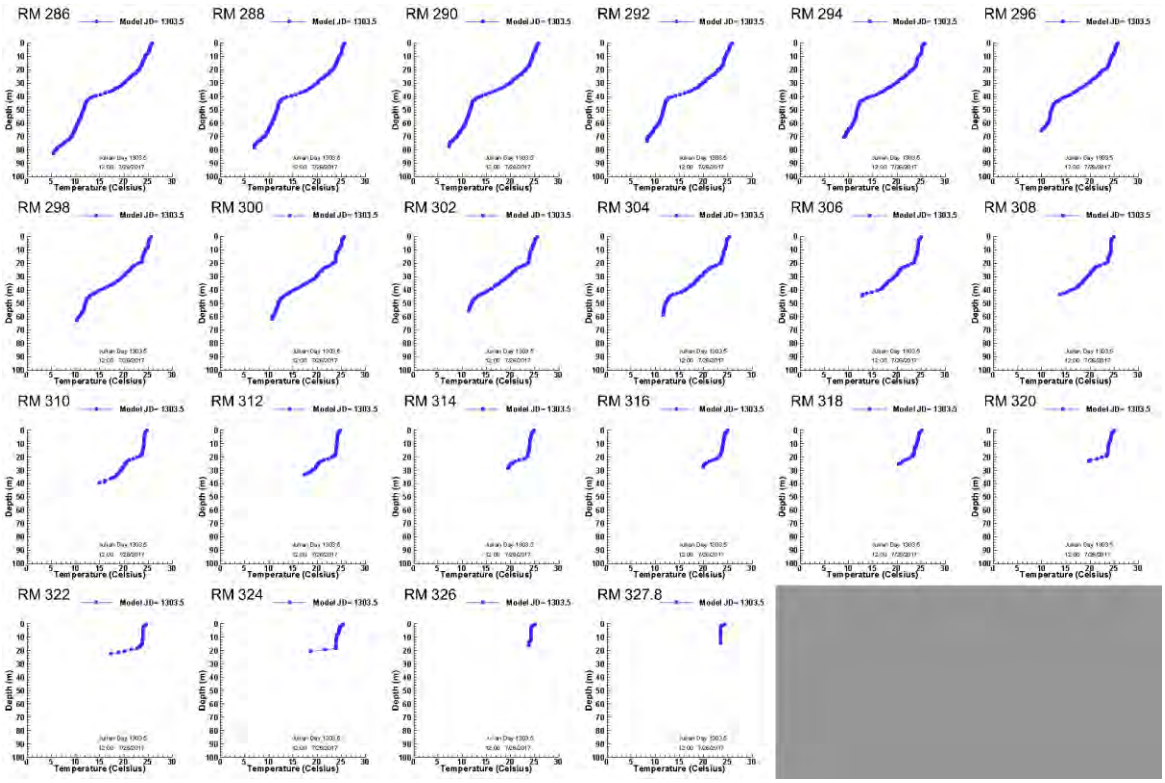


Figure 2385. Vertical profiles of temperature compared with data for 7/26/2017.

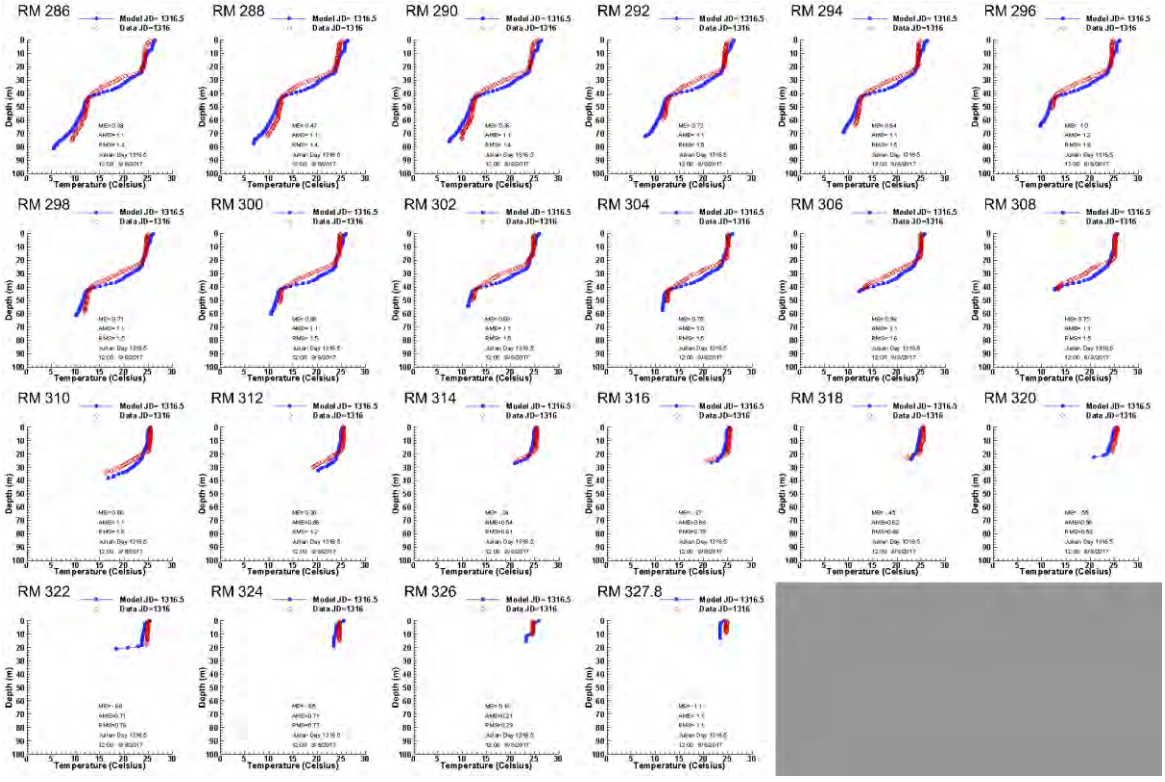


Figure 2386. Vertical profiles of temperature compared with data for 8/ 8/2017.

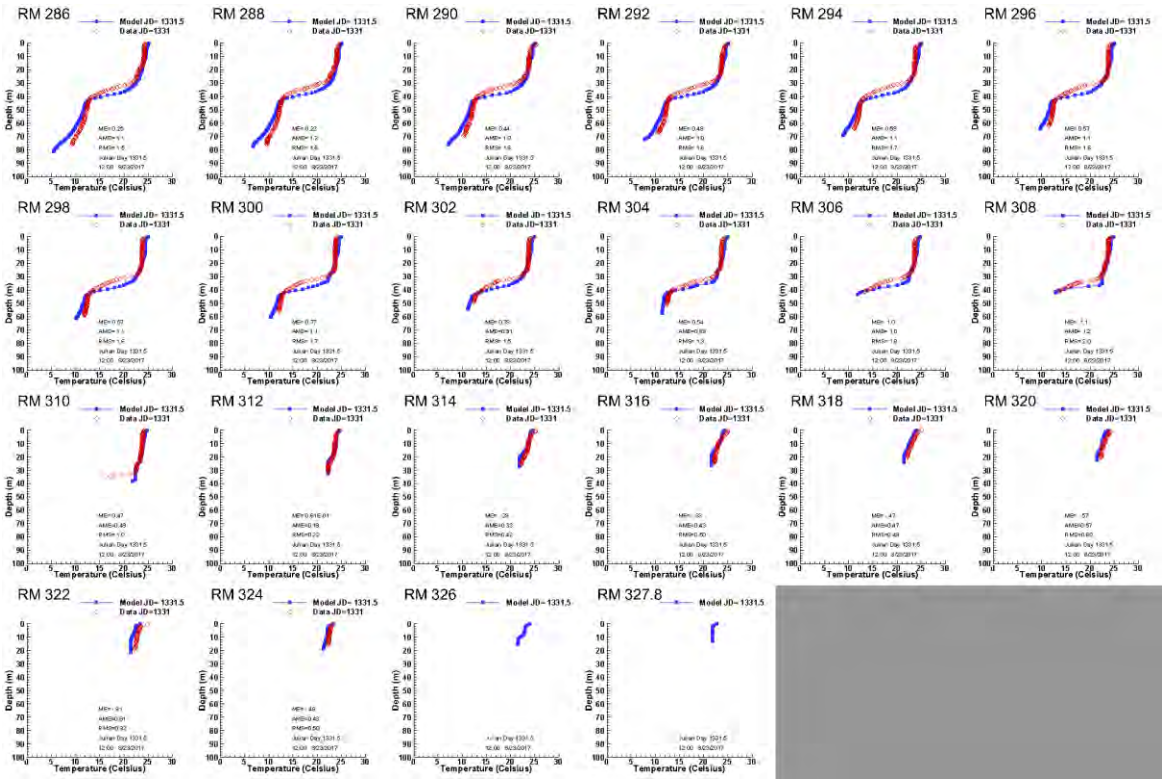


Figure 2387. Vertical profiles of temperature compared with data for 8/23/2017.

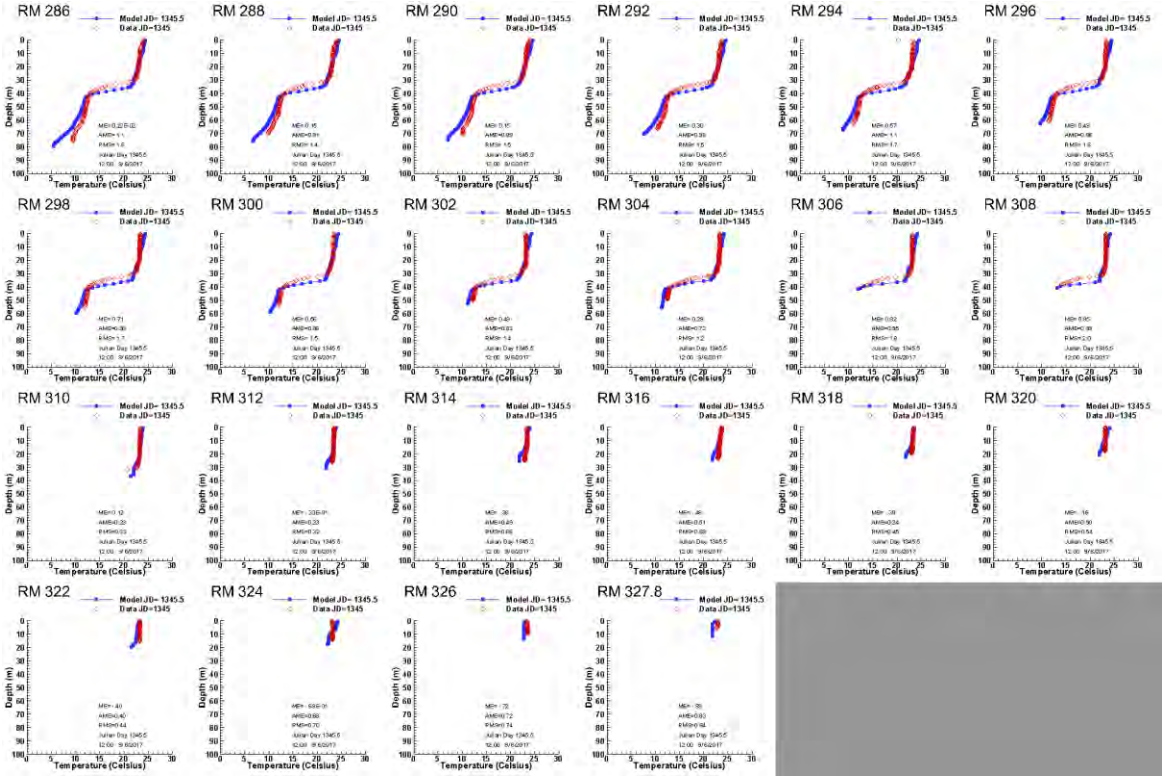


Figure 2388. Vertical profiles of temperature compared with data for 9/ 6/2017.

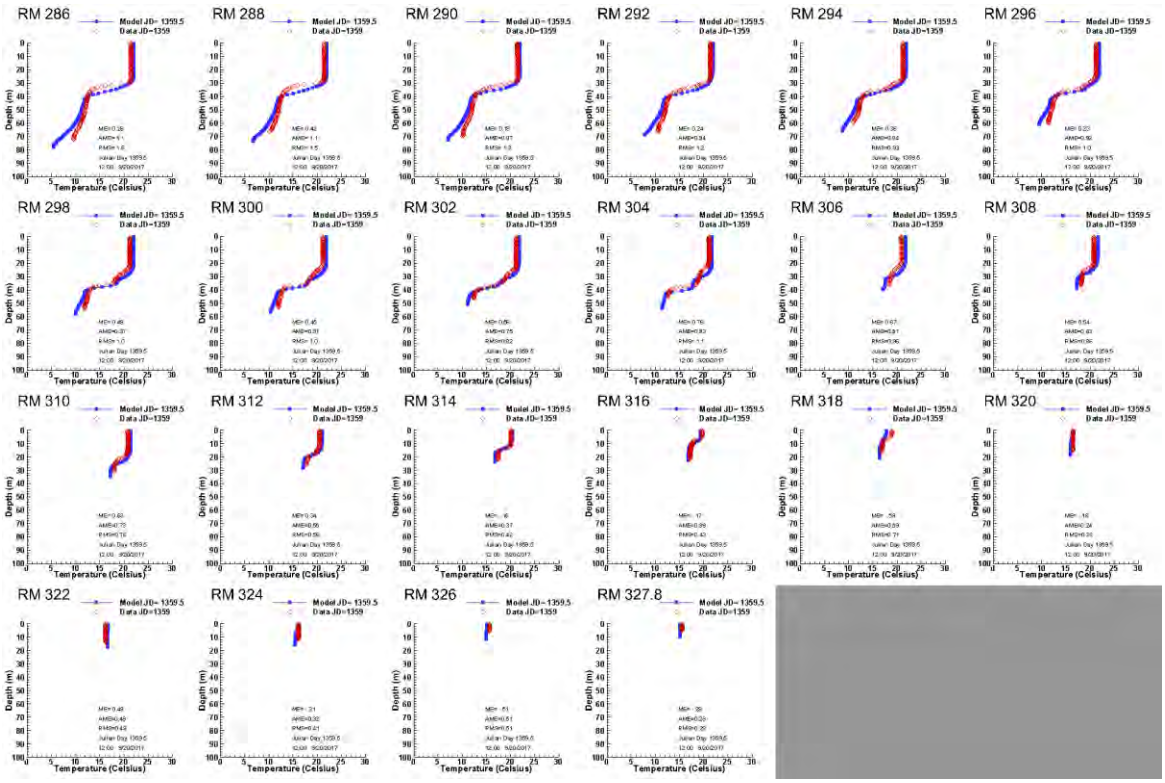


Figure 2389. Vertical profiles of temperature compared with data for 9/20/2017.

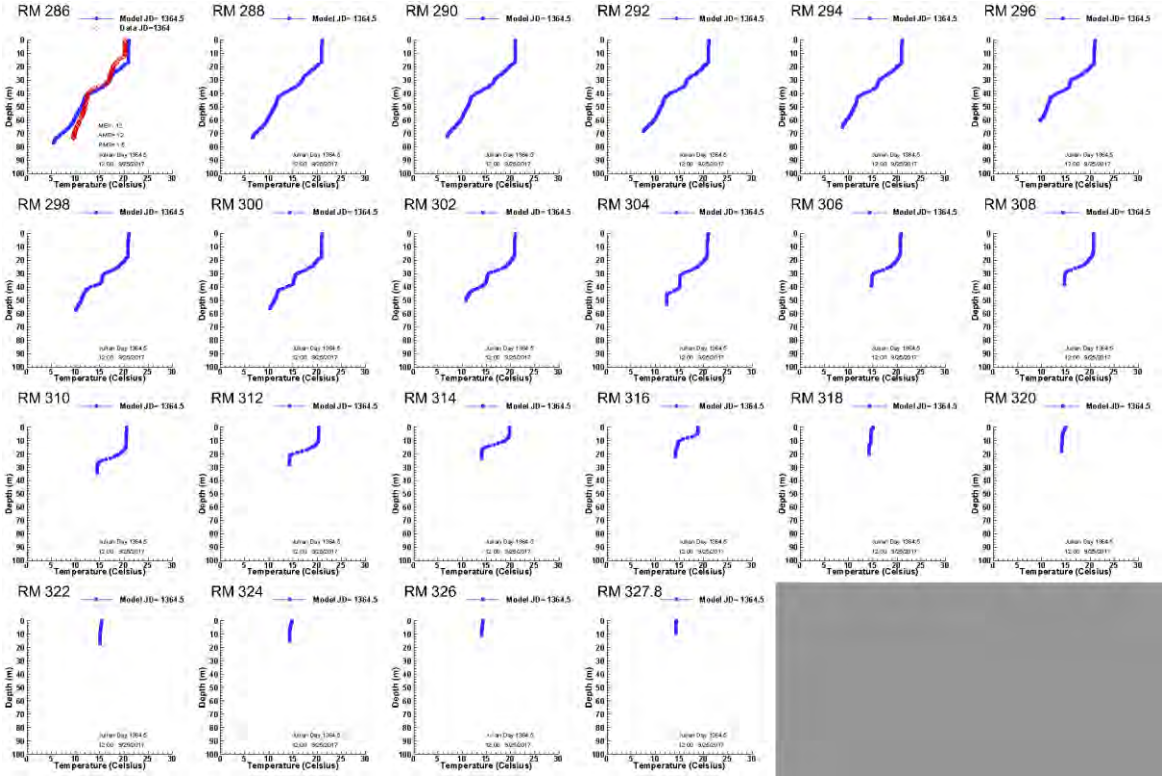


Figure 2390. Vertical profiles of temperature compared with data for 9/25/2017.

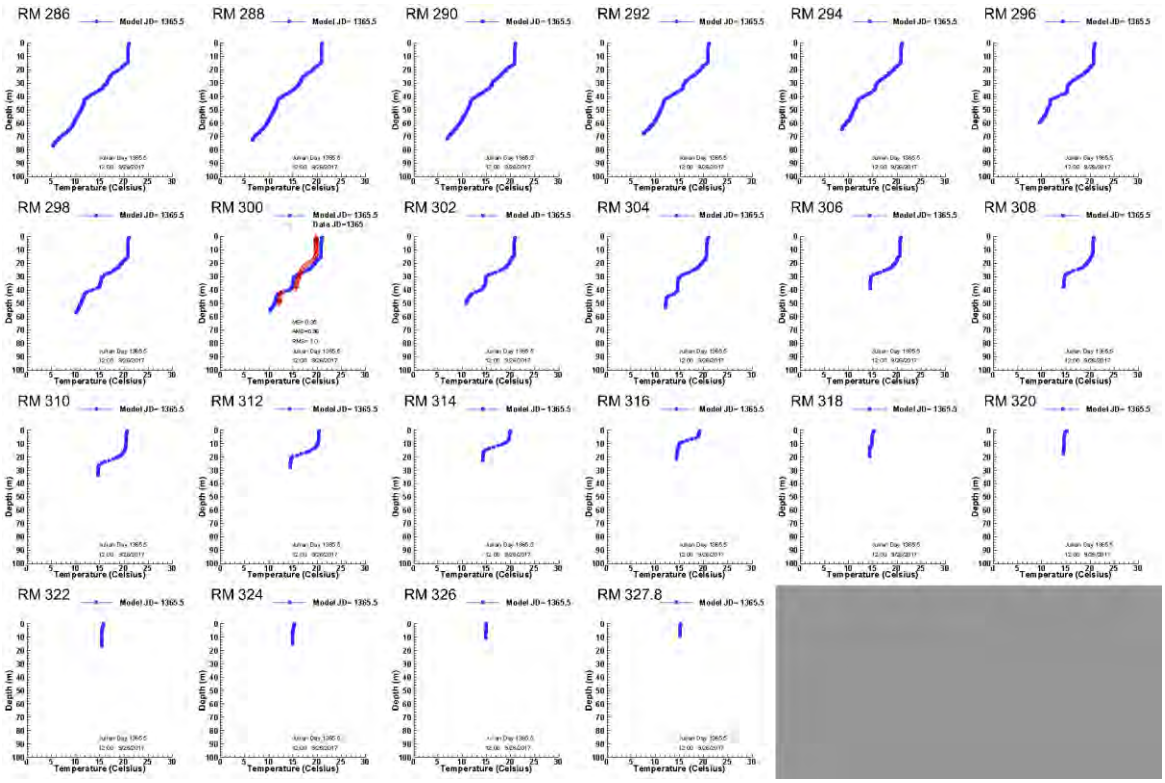


Figure 2391. Vertical profiles of temperature compared with data for 9/26/2017.

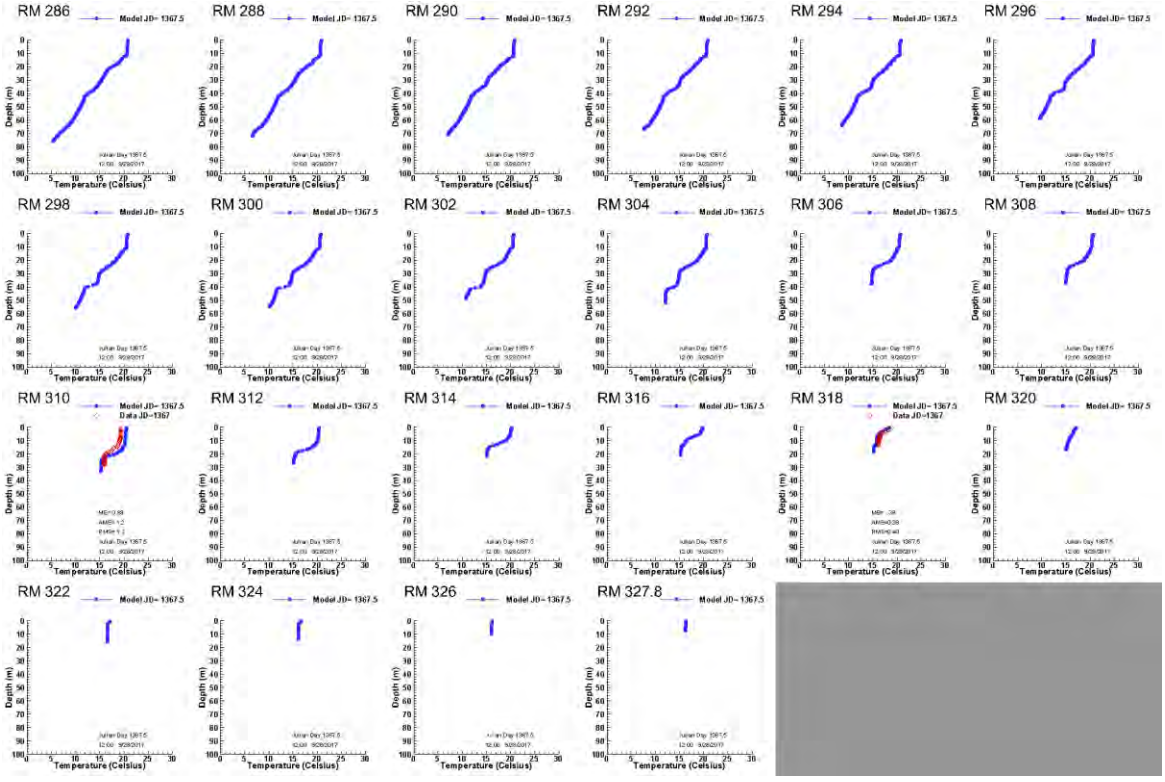


Figure 2392. Vertical profiles of temperature compared with data for 9/28/2017.

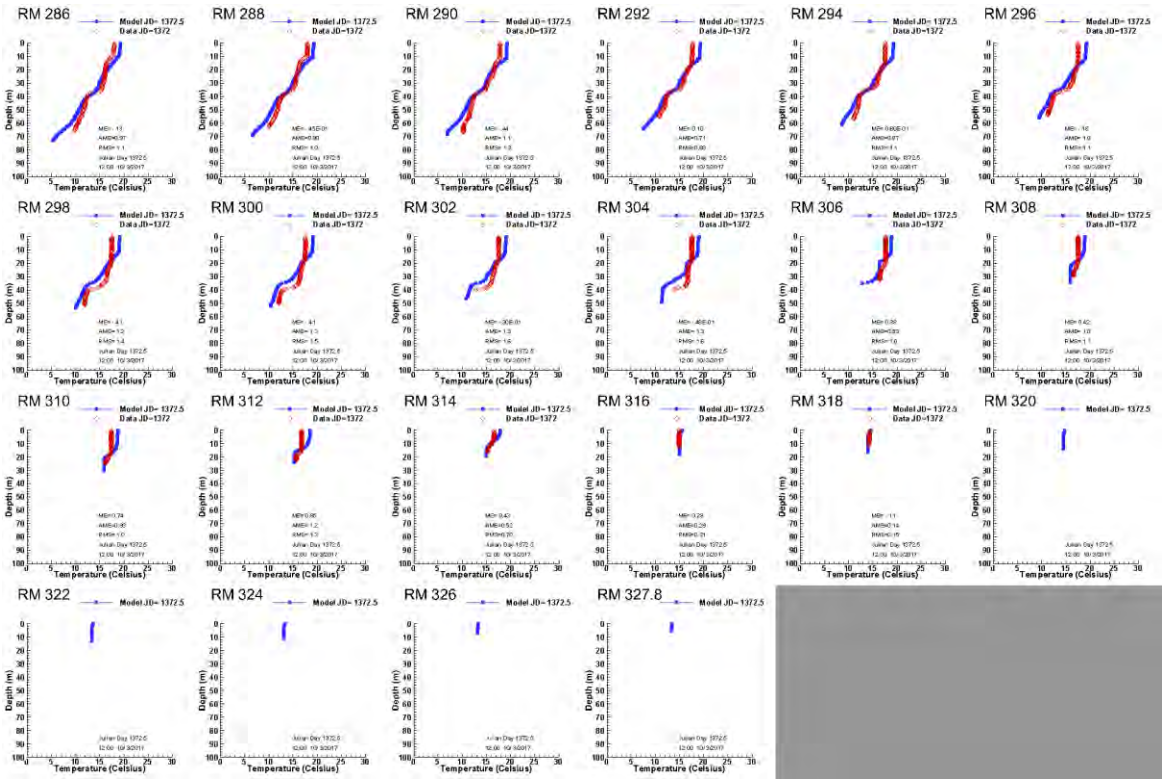


Figure 2393. Vertical profiles of temperature compared with data for 10/ 3/2017.

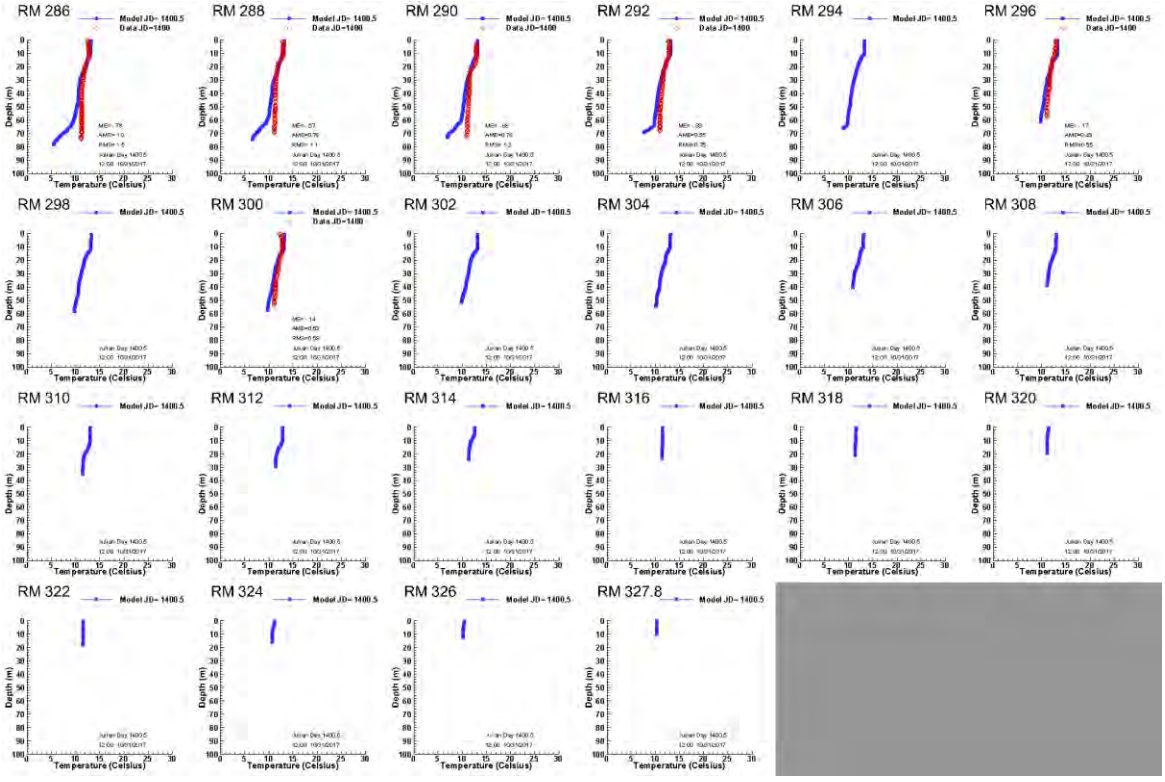


Figure 2394. Vertical profiles of temperature compared with data for 10/31/2017.

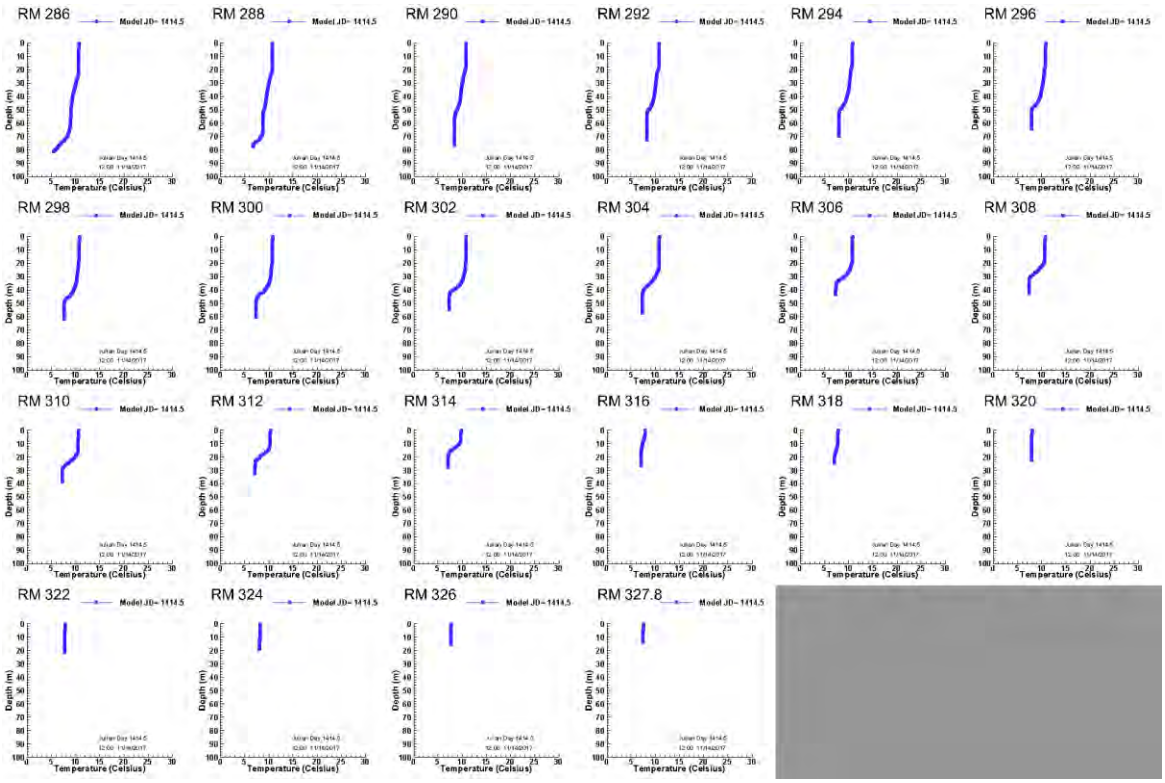


Figure 2395. Vertical profiles of temperature compared with data for 11/14/2017.

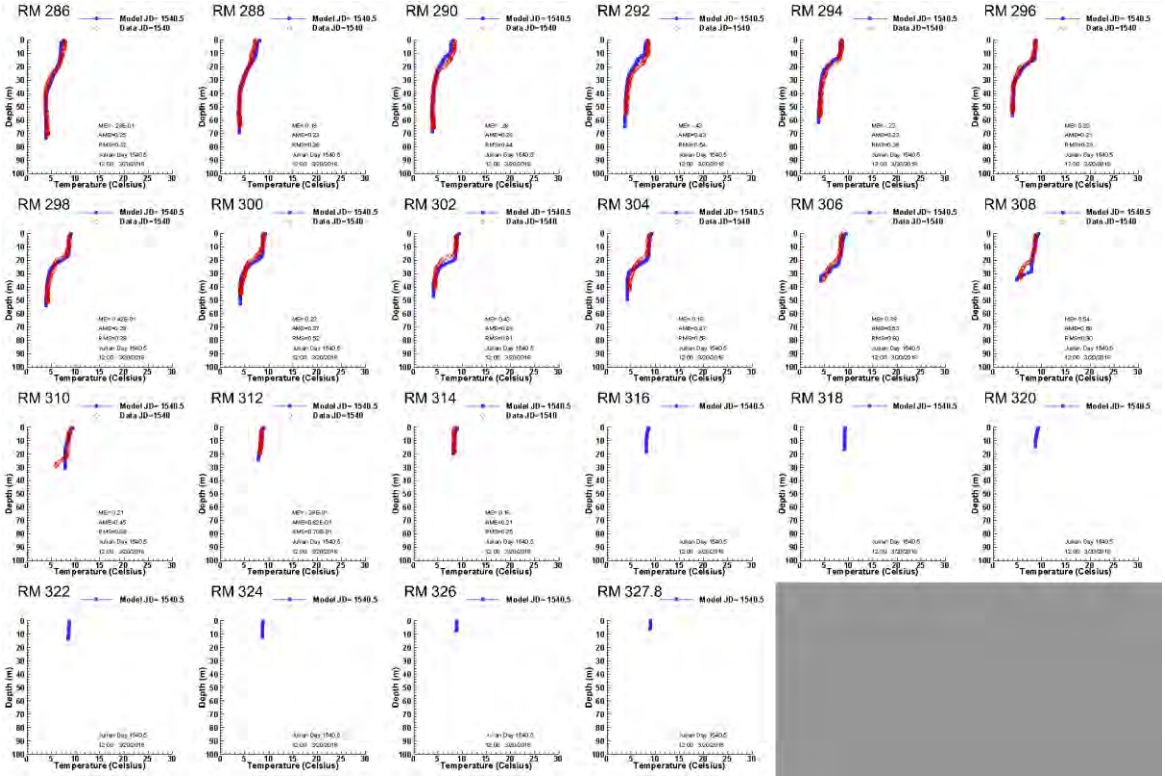


Figure 2396. Vertical profiles of temperature compared with data for 3/20/2018.

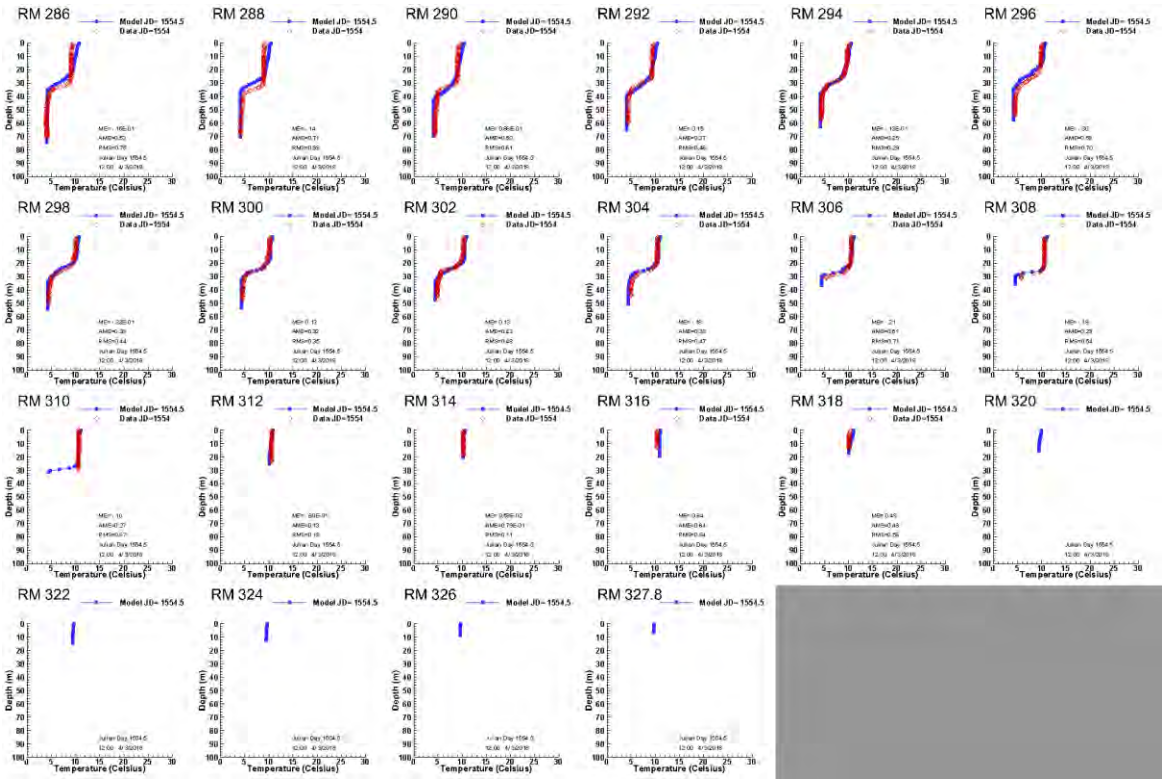


Figure 2397. Vertical profiles of temperature compared with data for 4/ 3/2018.

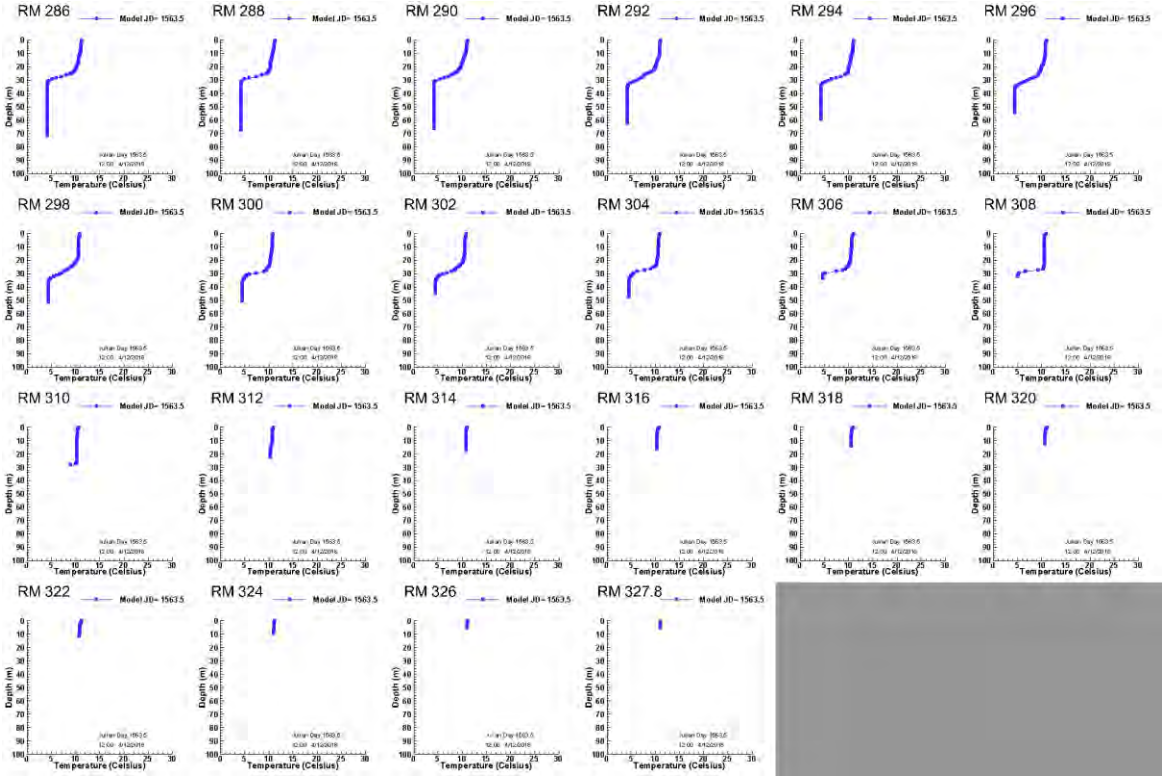


Figure 2398. Vertical profiles of temperature compared with data for 4/12/2018.

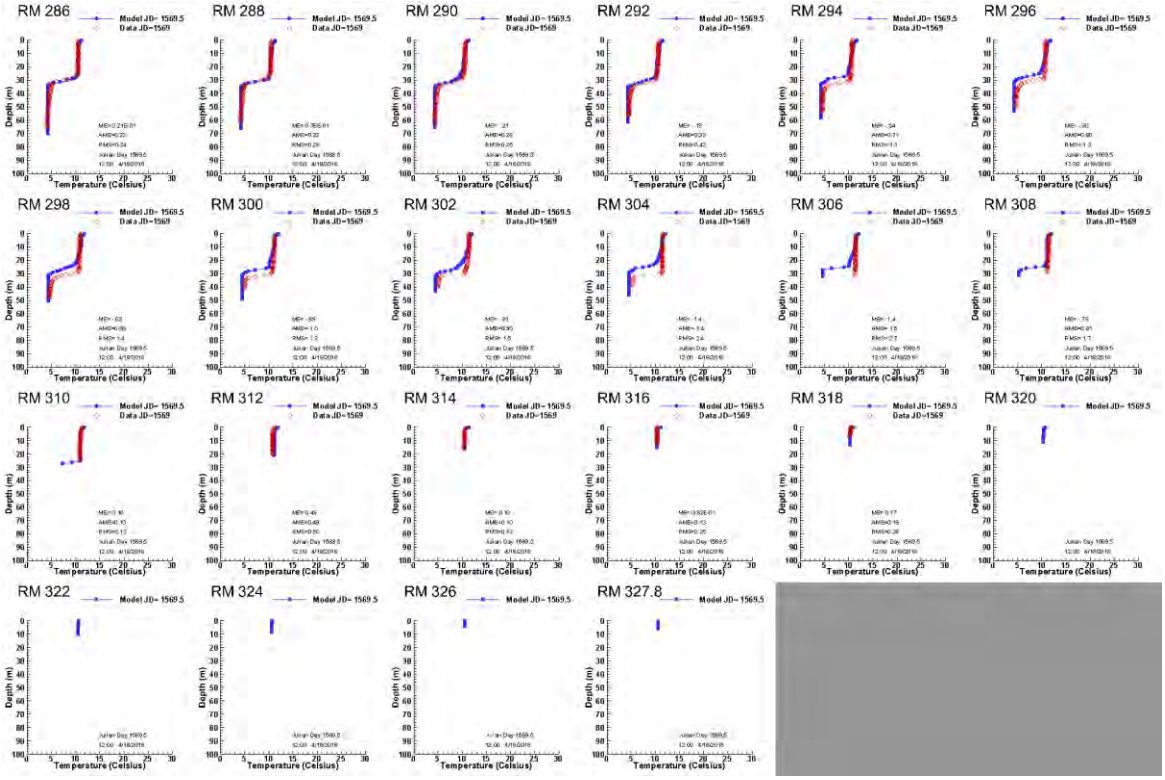


Figure 2399. Vertical profiles of temperature compared with data for 4/18/2018.

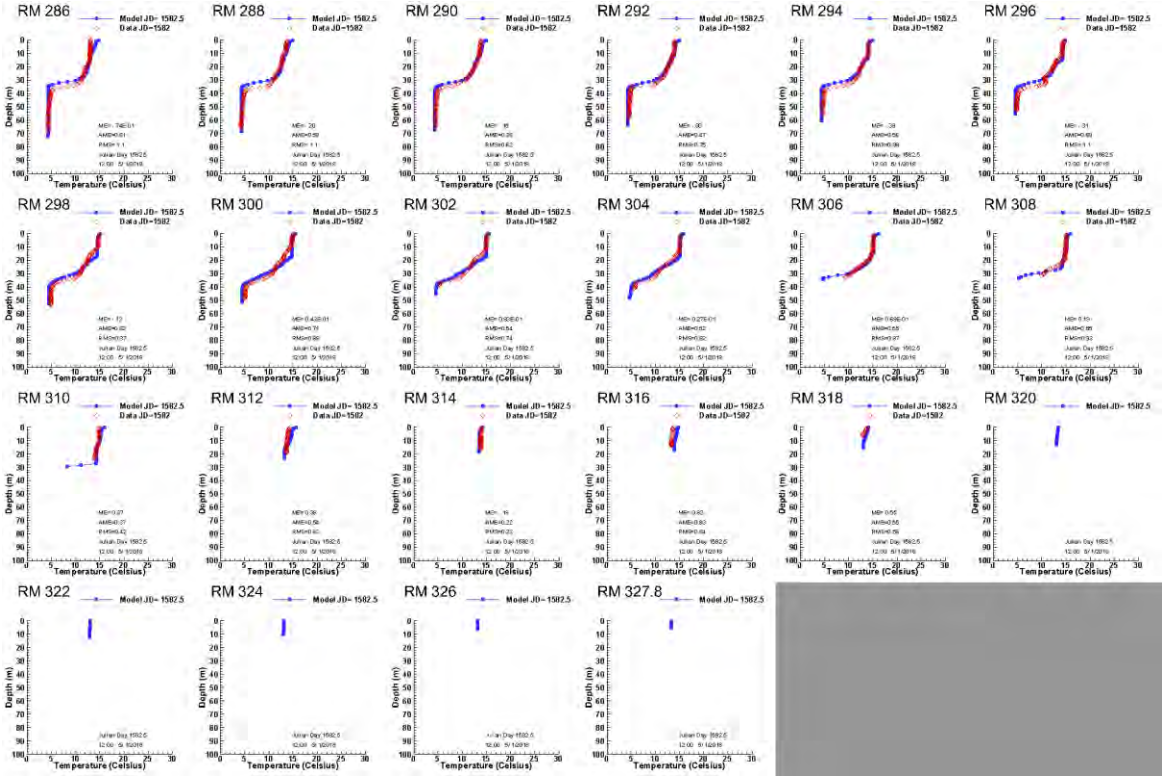


Figure 2400. Vertical profiles of temperature compared with data for 5/ 1/2018.

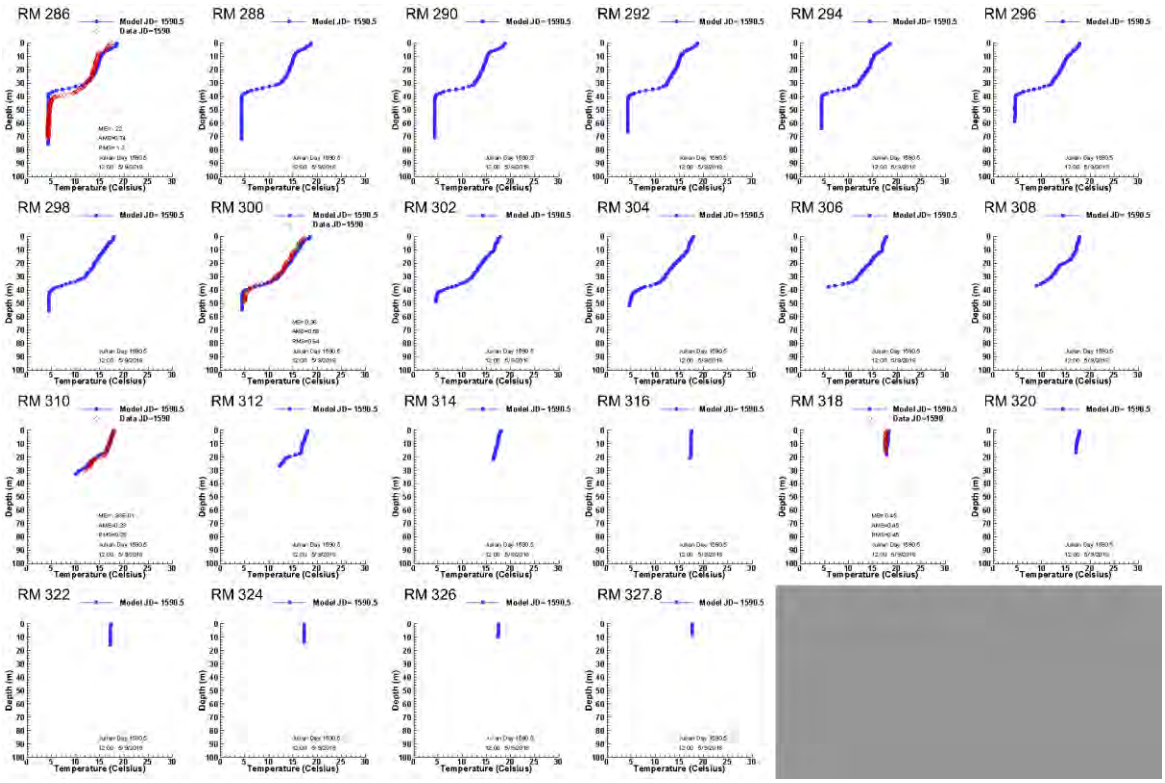


Figure 2401. Vertical profiles of temperature compared with data for 5/ 9/2018.

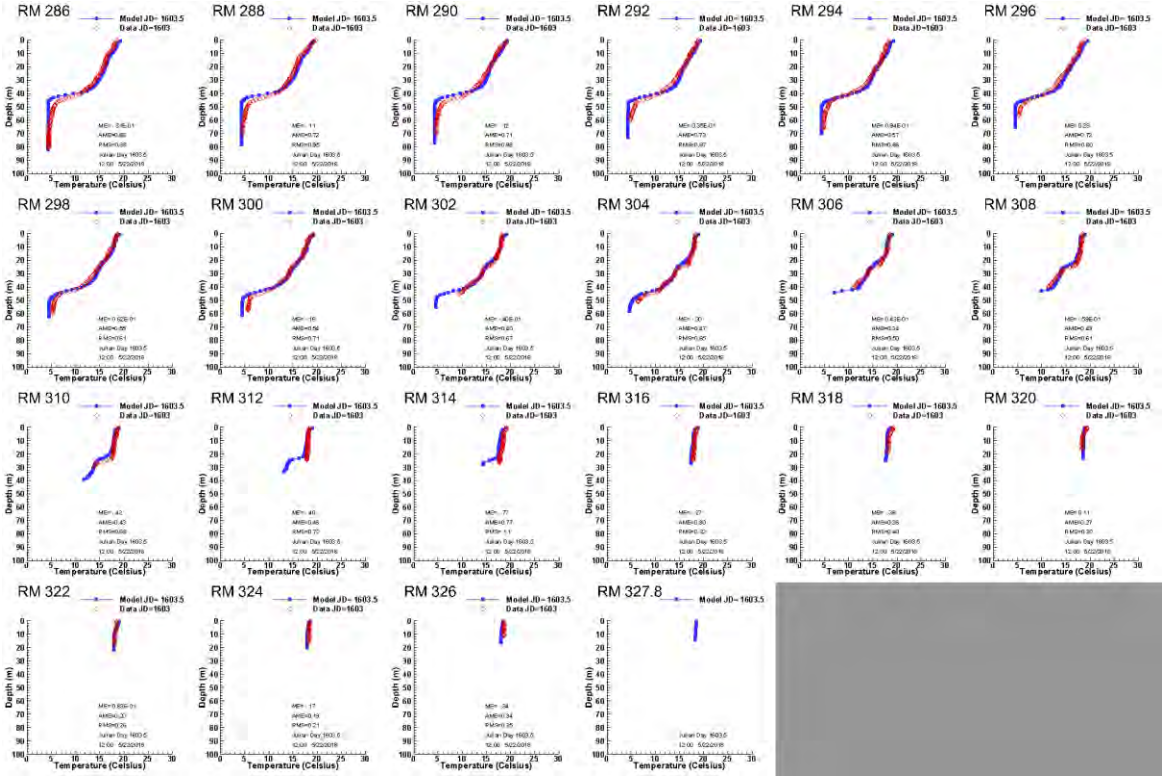


Figure 2402. Vertical profiles of temperature compared with data for 5/22/2018.

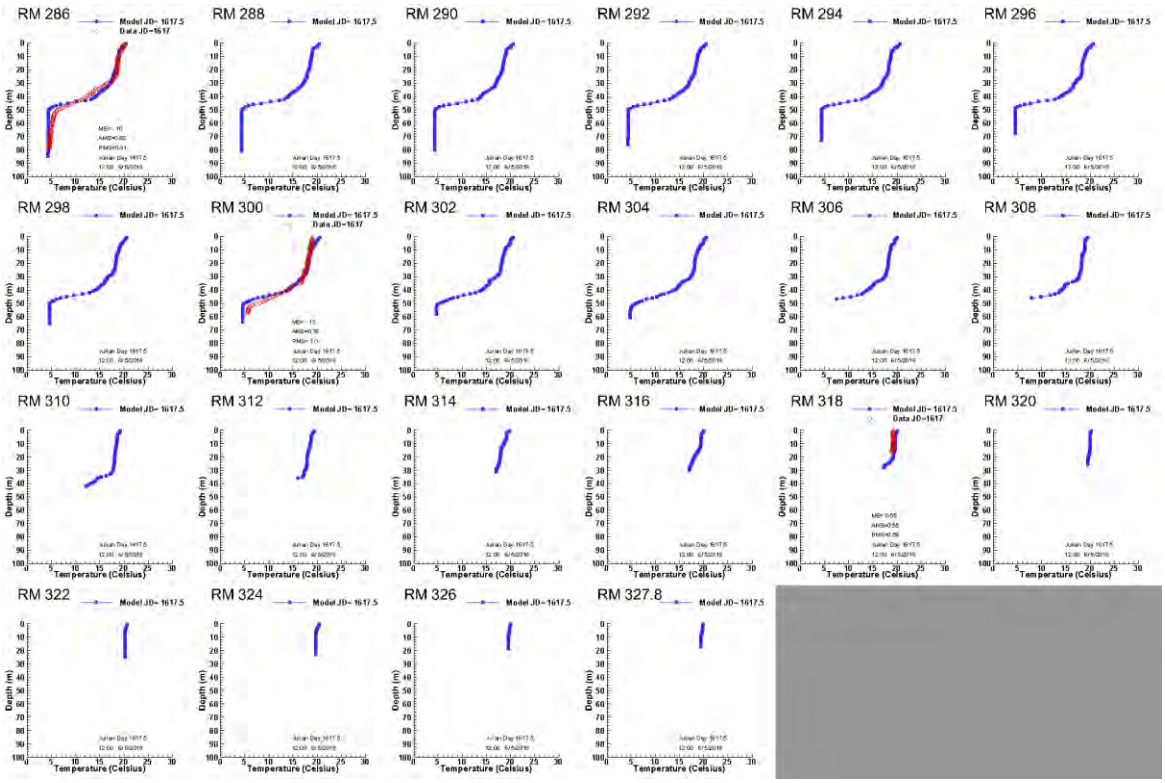


Figure 2403. Vertical profiles of temperature compared with data for 6/ 5/2018.

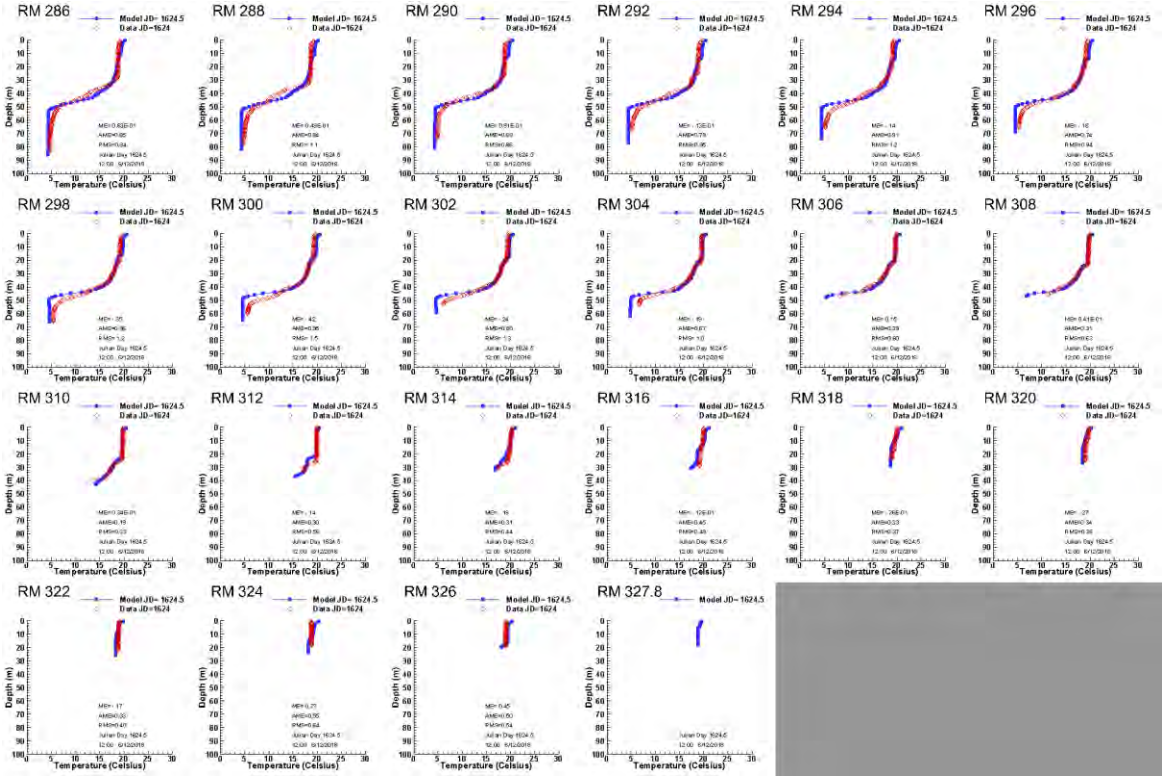


Figure 2404. Vertical profiles of temperature compared with data for 6/12/2018.

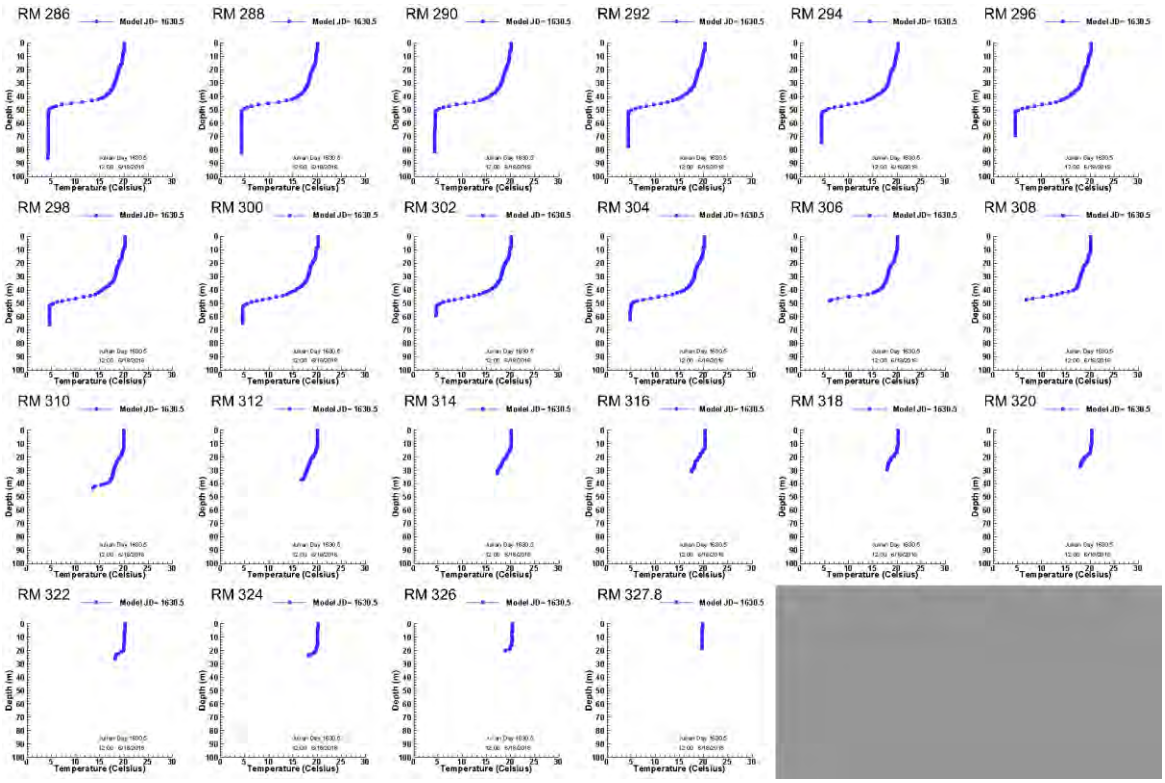


Figure 2405. Vertical profiles of temperature compared with data for 6/18/2018.

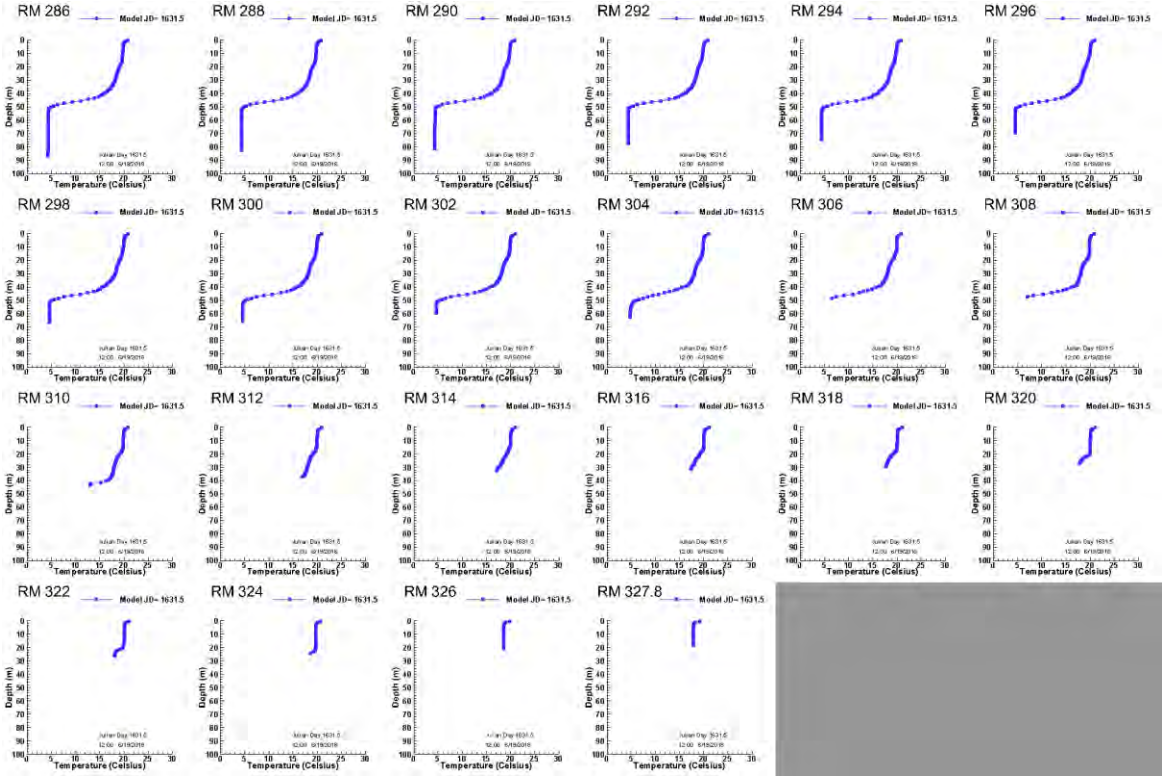


Figure 2406. Vertical profiles of temperature compared with data for 6/19/2018.

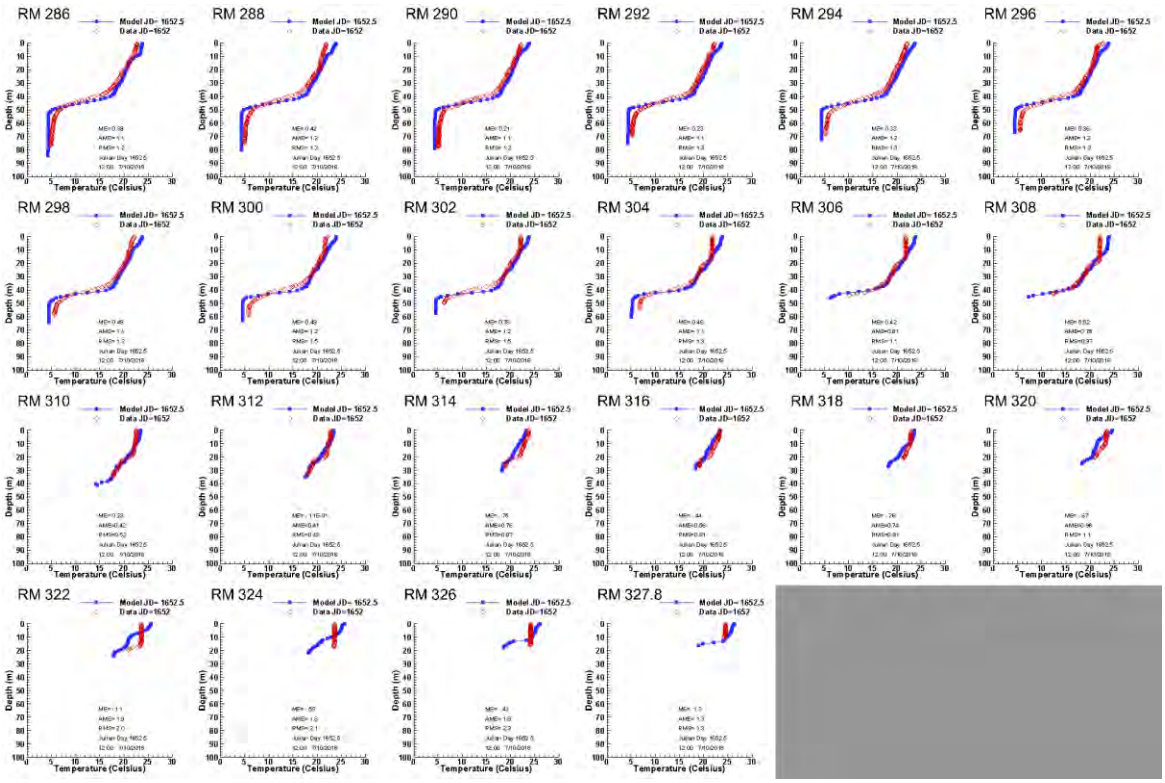


Figure 2407. Vertical profiles of temperature compared with data for 7/10/2018.

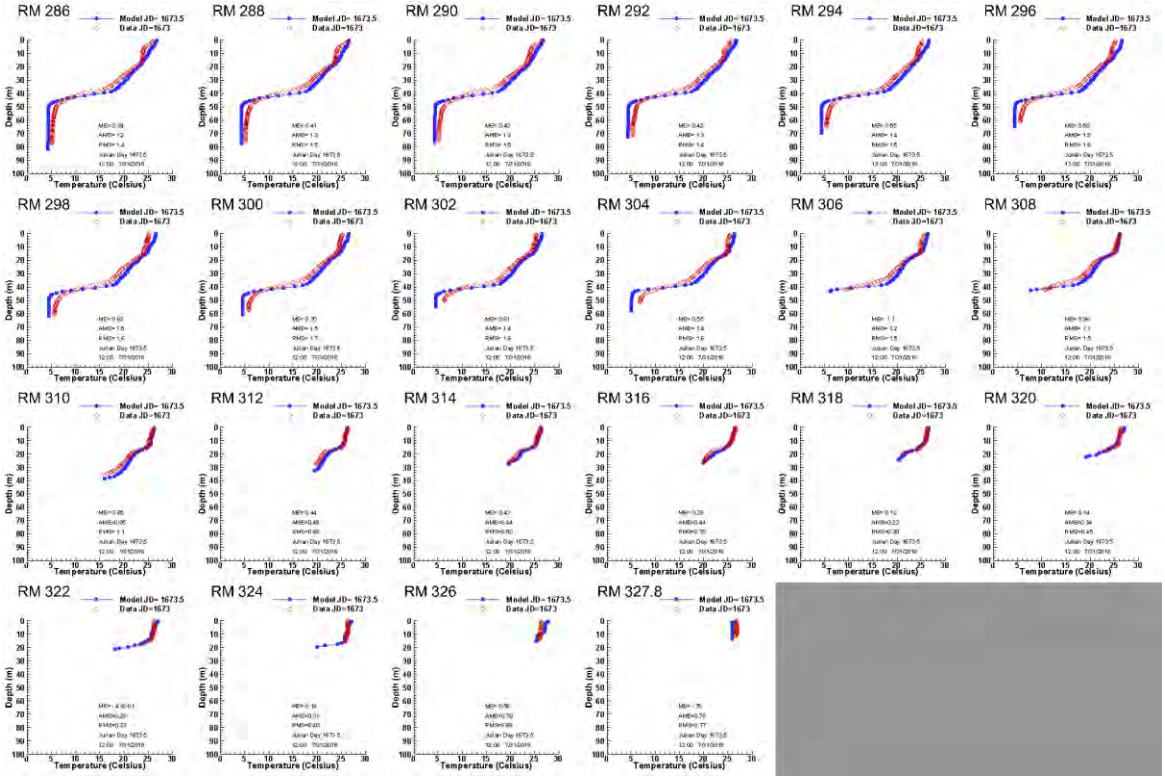


Figure 2408. Vertical profiles of temperature compared with data for 7/31/2018.

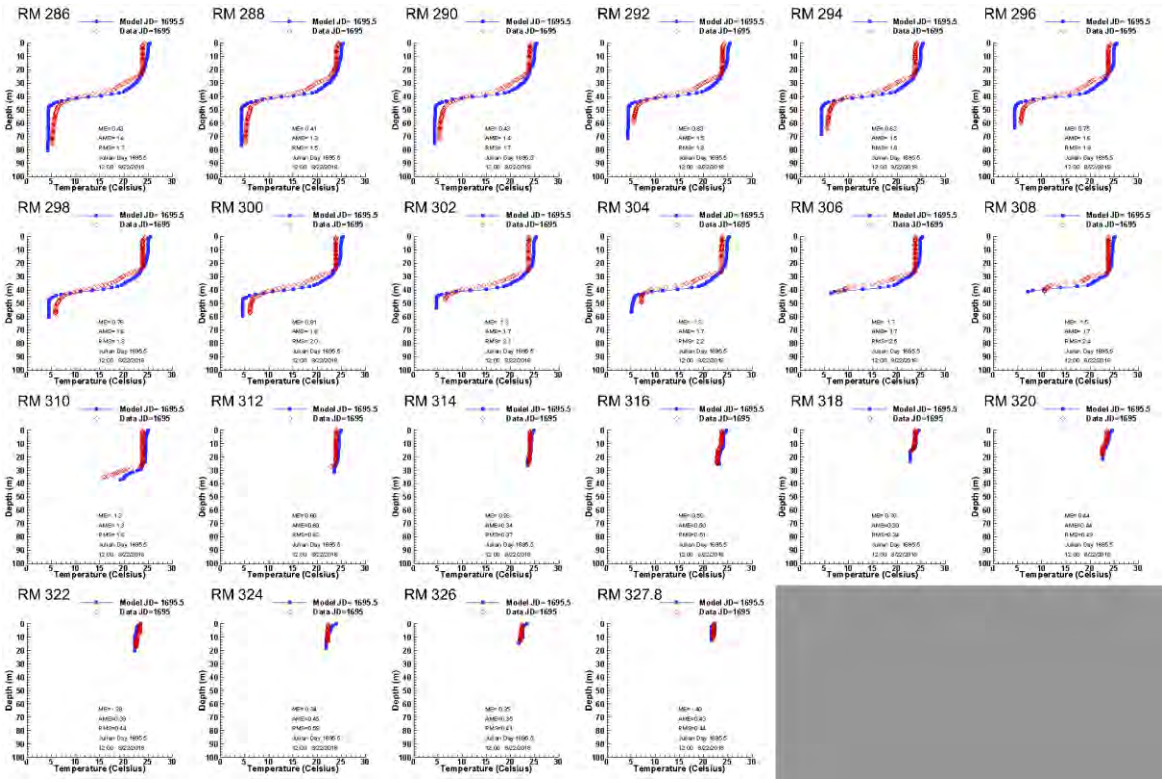


Figure 2409. Vertical profiles of temperature compared with data for 8/22/2018.

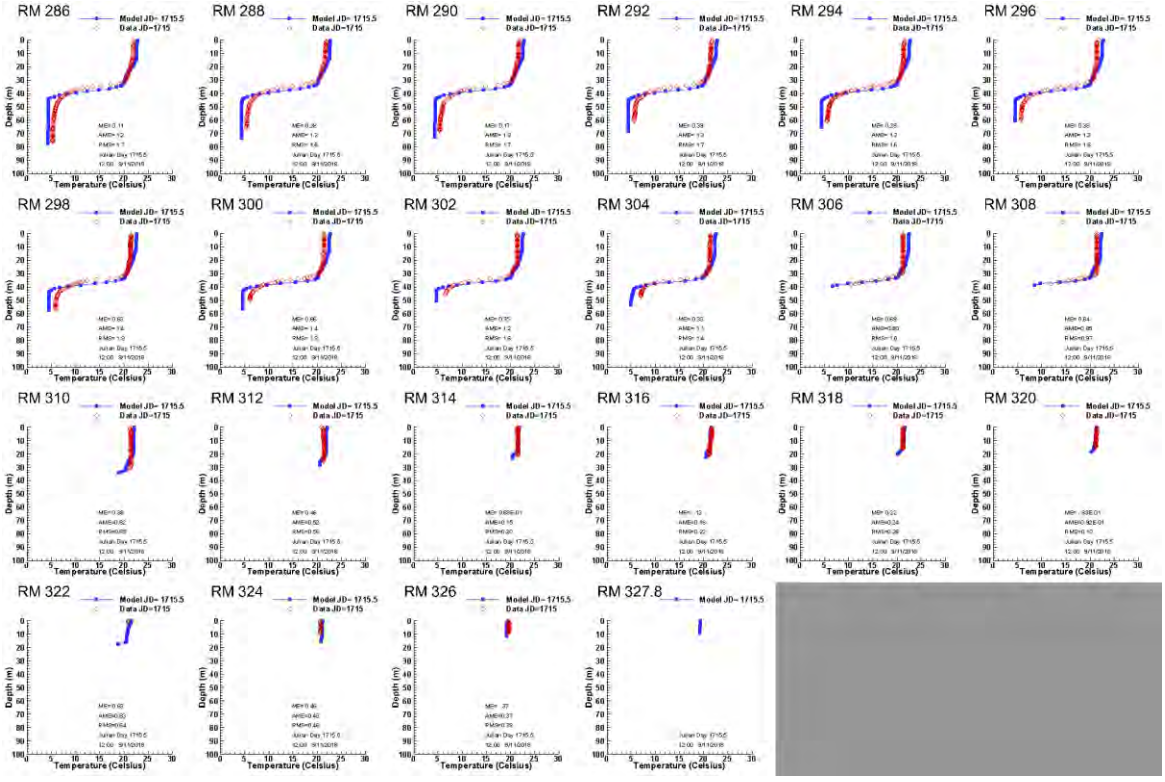


Figure 2410. Vertical profiles of temperature compared with data for 9/11/2018.

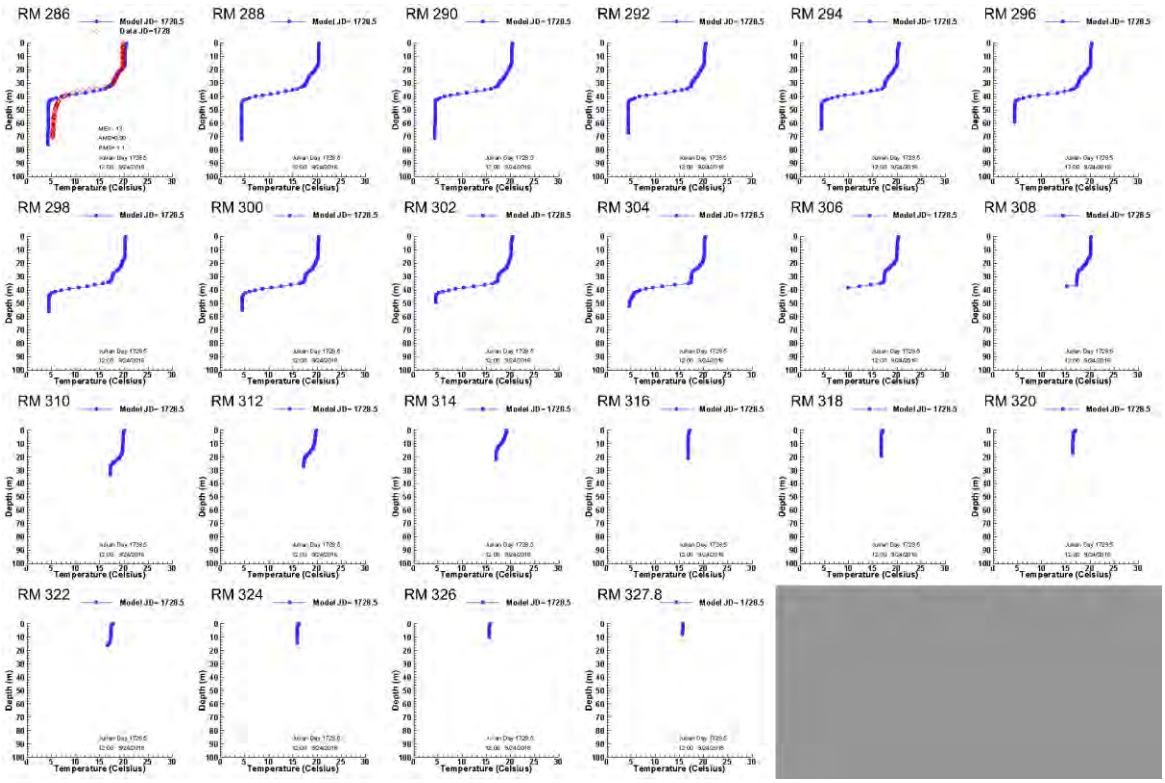


Figure 2411. Vertical profiles of temperature compared with data for 9/24/2018.

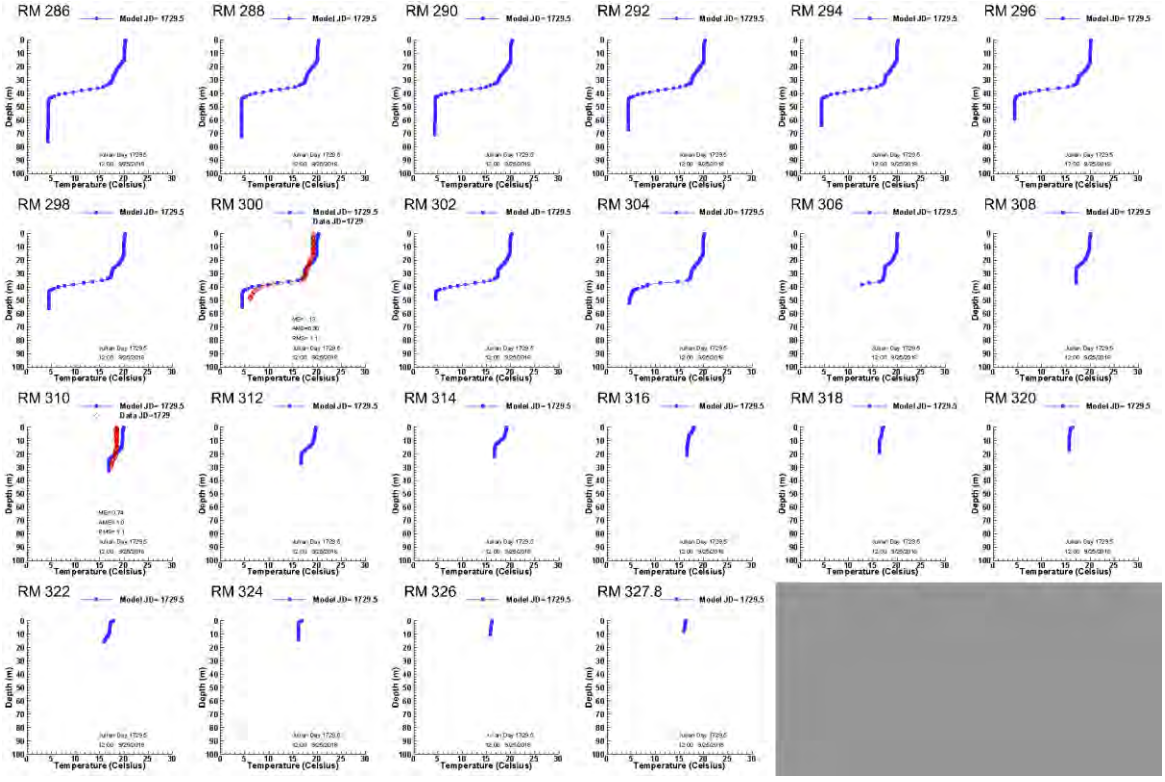


Figure 2412. Vertical profiles of temperature compared with data for 9/25/2018.

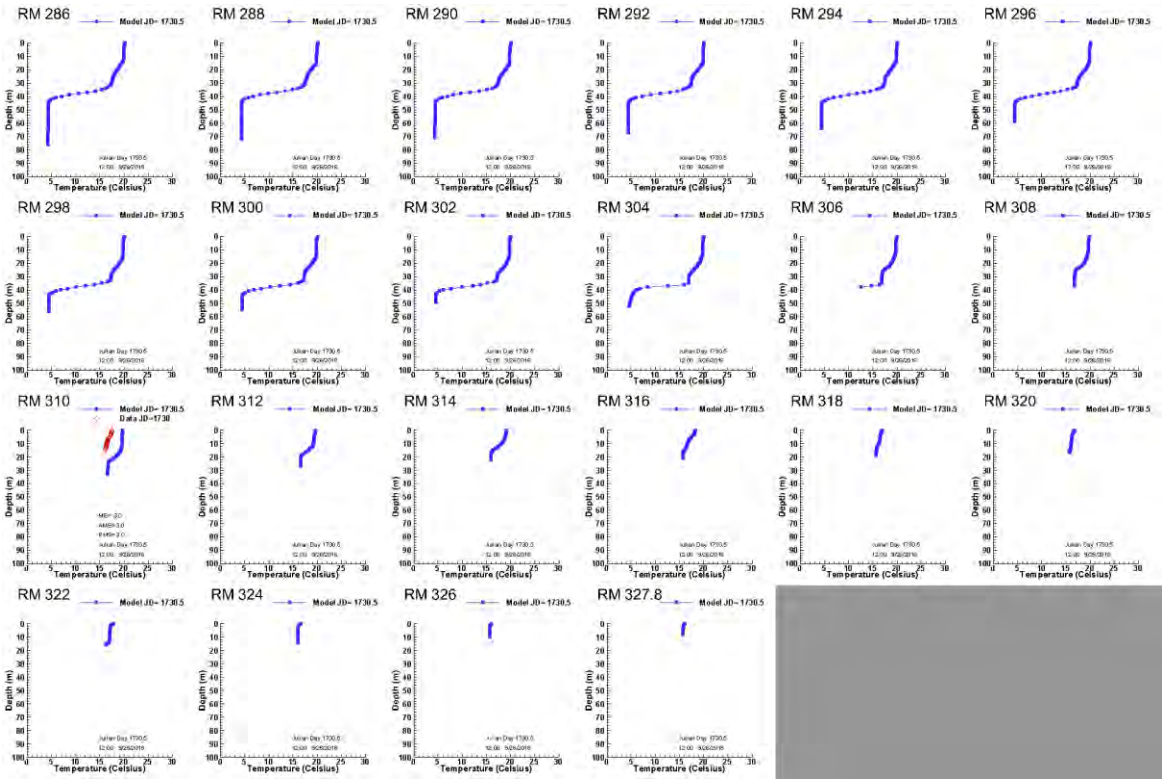


Figure 2413. Vertical profiles of temperature compared with data for 9/26/2018.

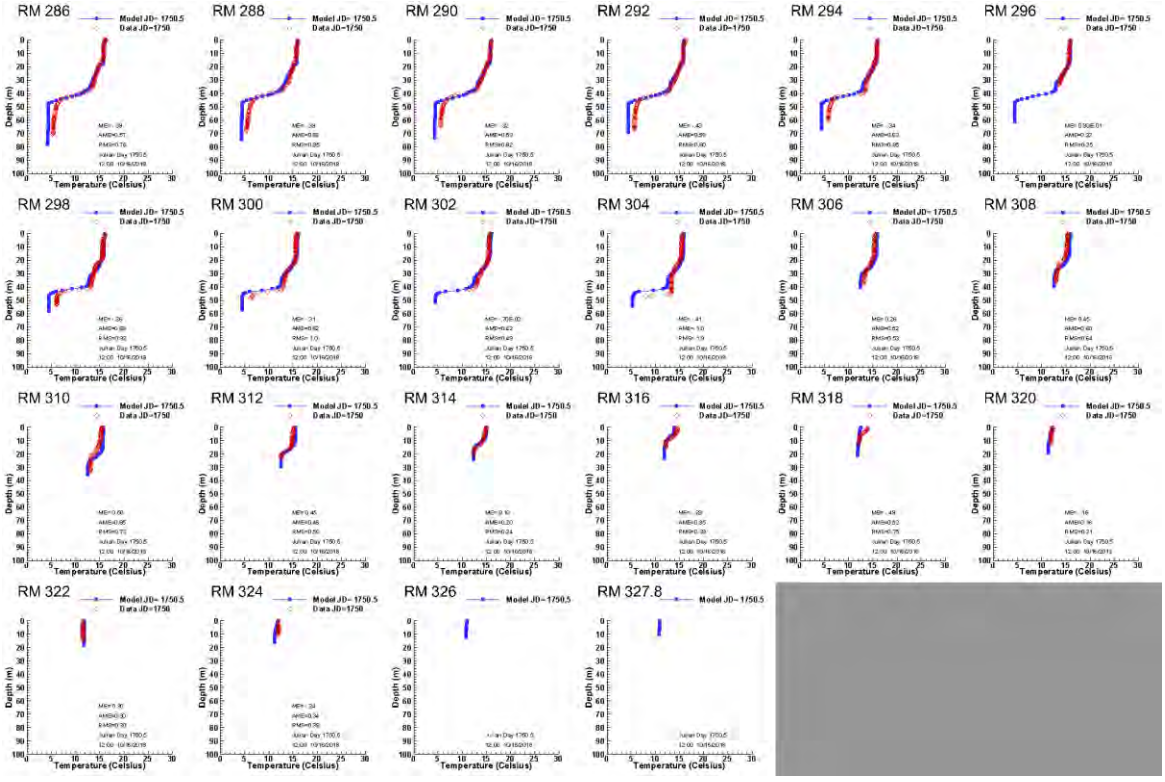


Figure 2414. Vertical profiles of temperature compared with data for 10/16/2018.

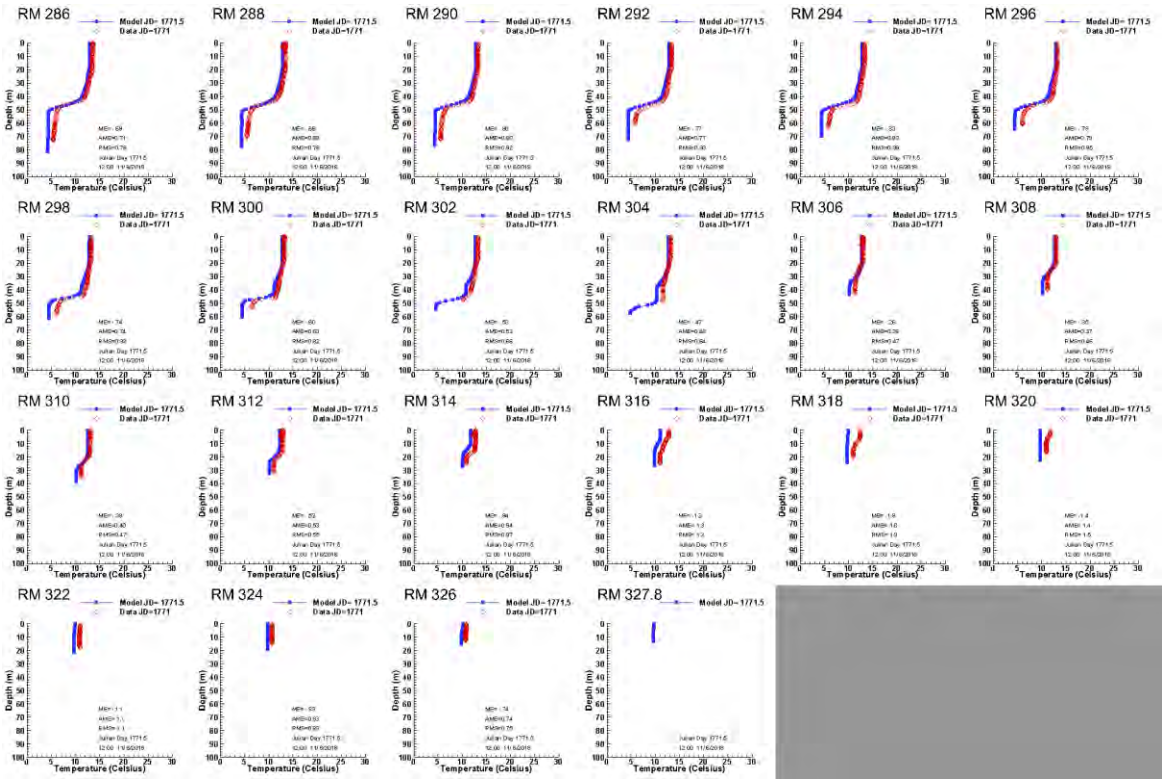


Figure 2415. Vertical profiles of temperature compared with data for 11/ 6/2018.

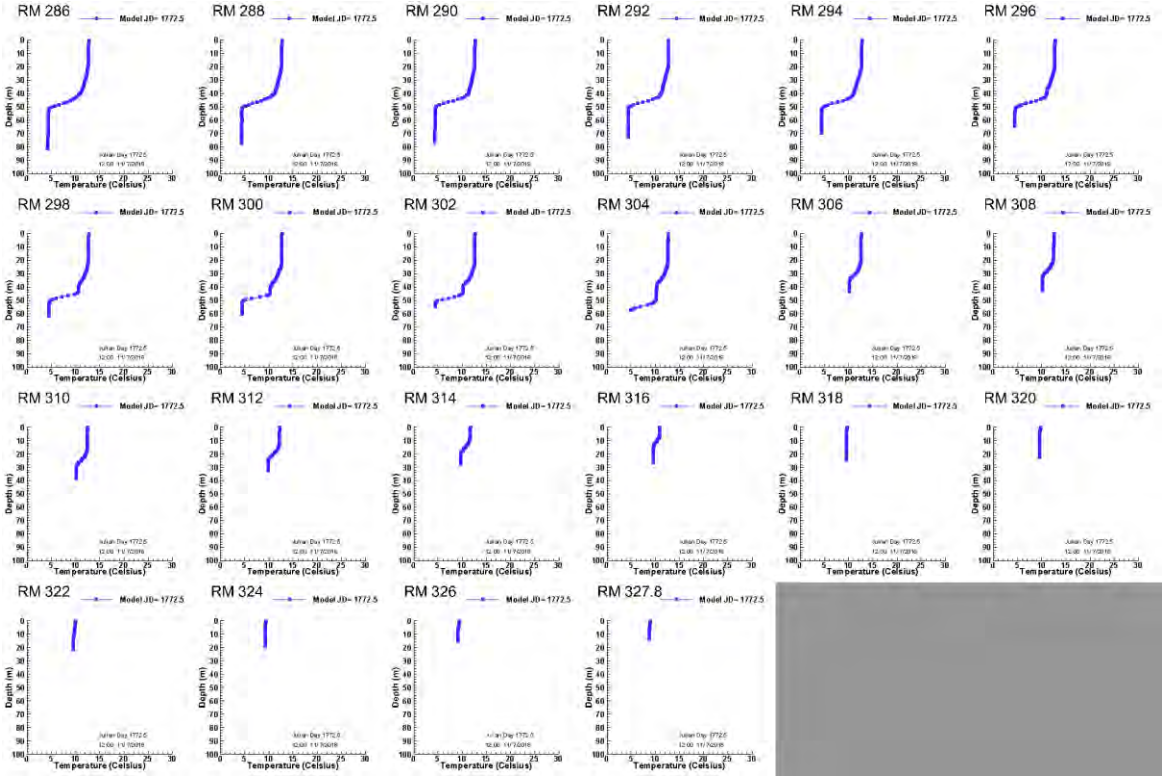


Figure 2416. Vertical profiles of temperature compared with data for 11/ 7/2018.

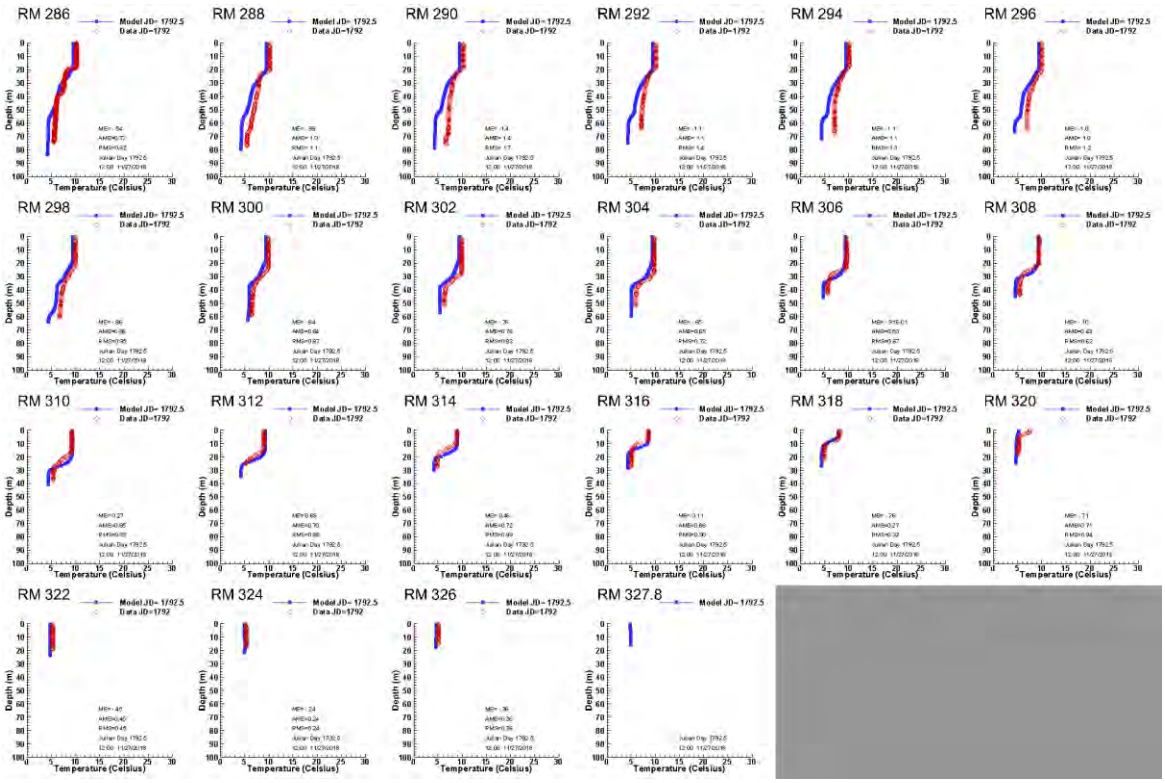


Figure 2417. Vertical profiles of temperature compared with data for 11/27/2018.

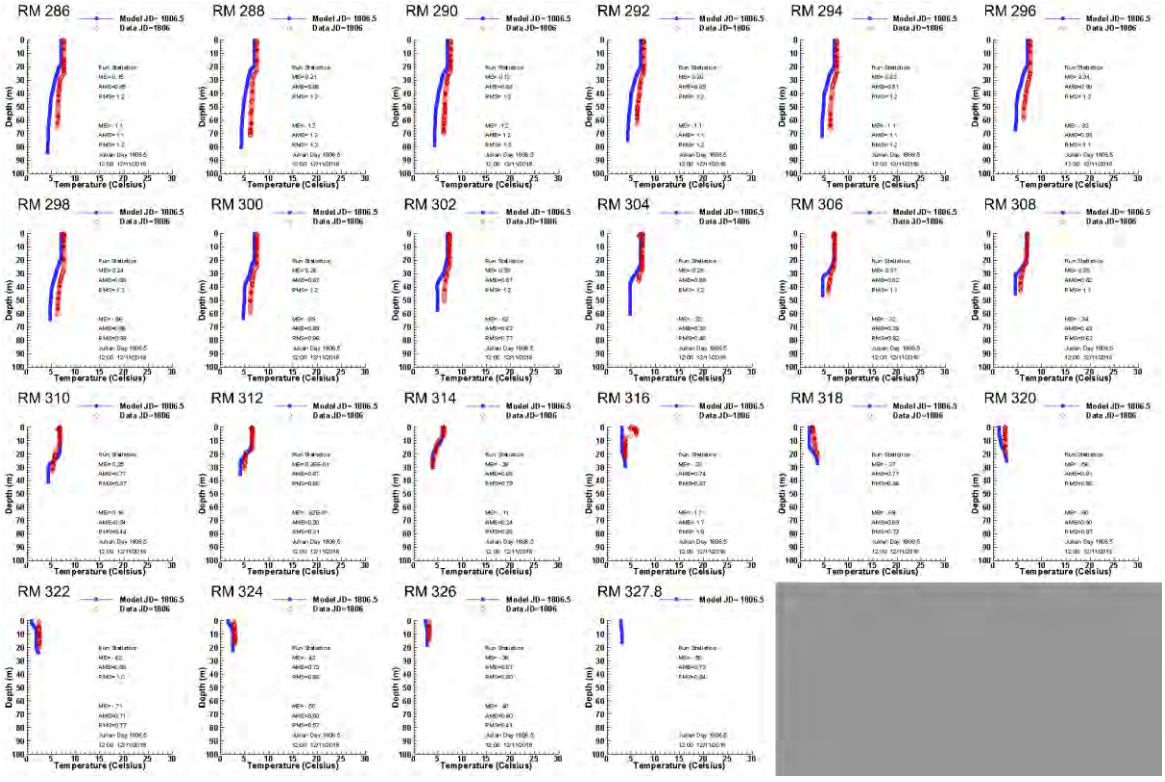


Figure 2418. Vertical profiles of temperature compared with data for 12/11/2018.

Appendix A5 Oxbow Reservoir Vertical Profiles

Chloride

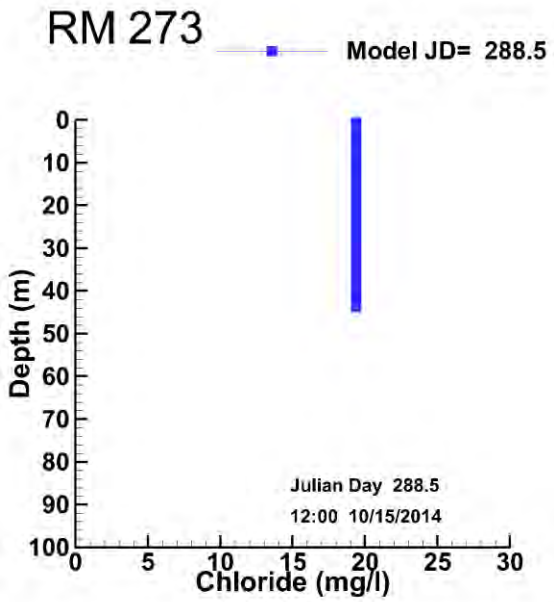


Figure 1. Vertical profiles of chloride compared with data for 10/15/2014.

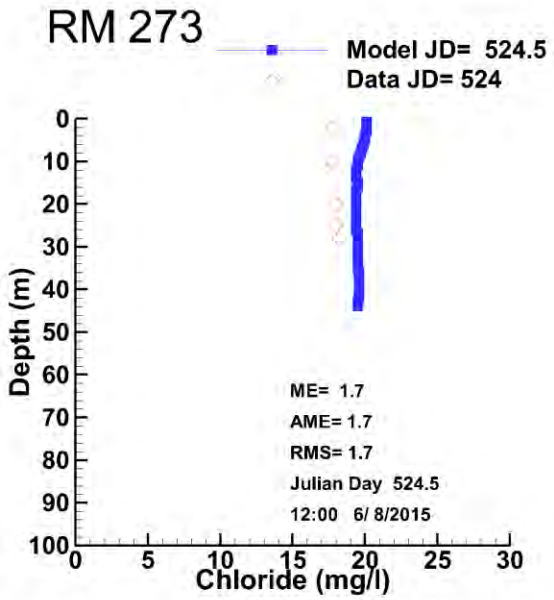


Figure 2. Vertical profiles of chloride compared with data for 6/ 8/2015.

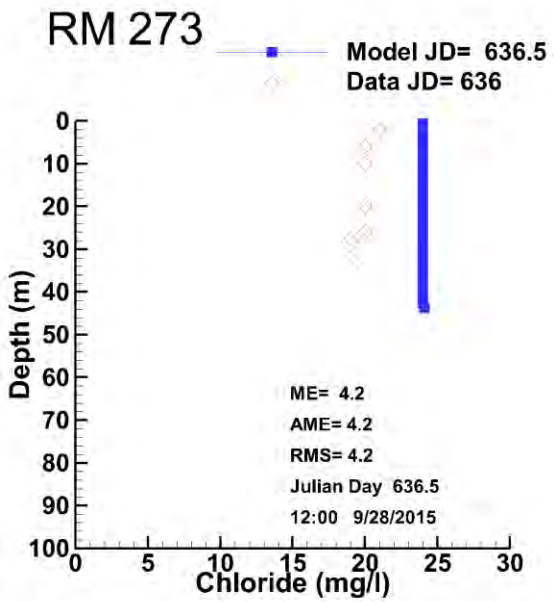


Figure 3. Vertical profiles of chloride compared with data for 9/28/2015.

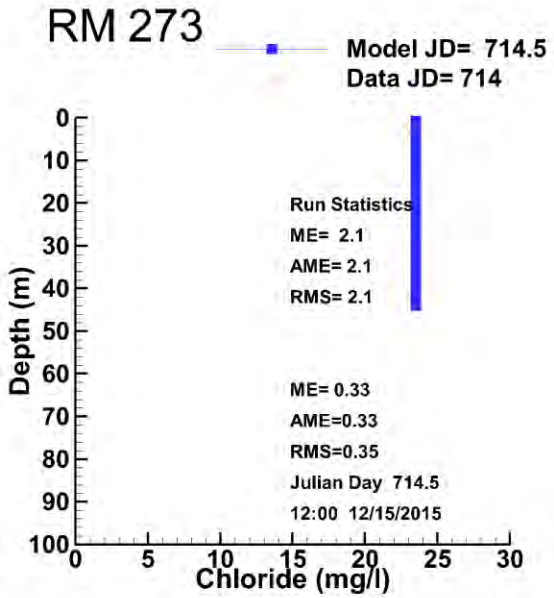


Figure 4. Vertical profiles of chloride compared with data for 12/15/2015.

Sulfate

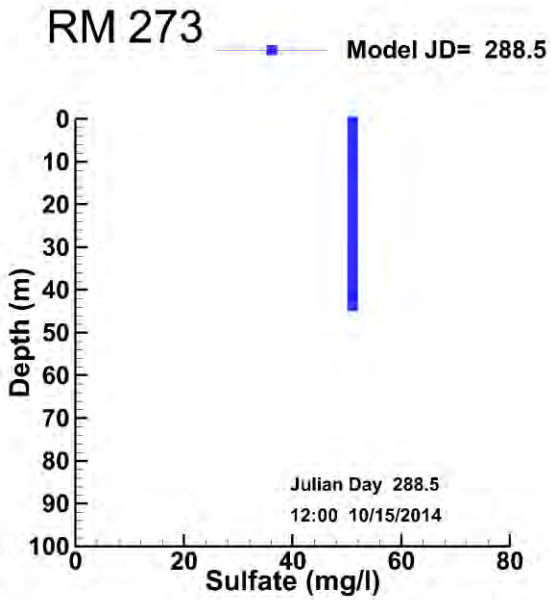


Figure 5. Vertical profiles of SULFATE compared with data for 10/15/2014.

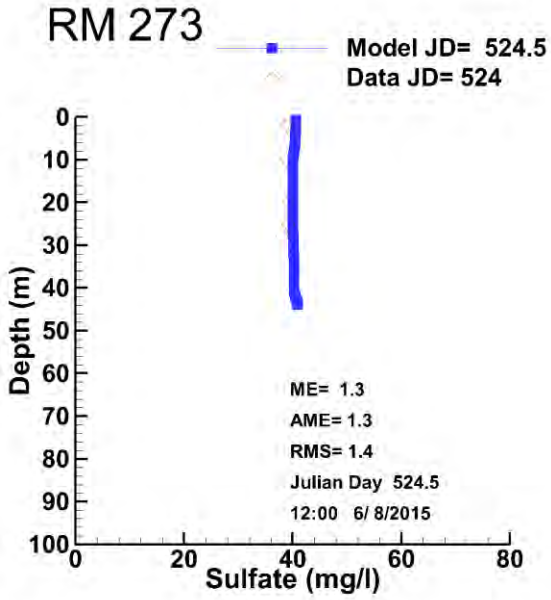


Figure 6. Vertical profiles of SULFATE compared with data for 6/ 8/2015.

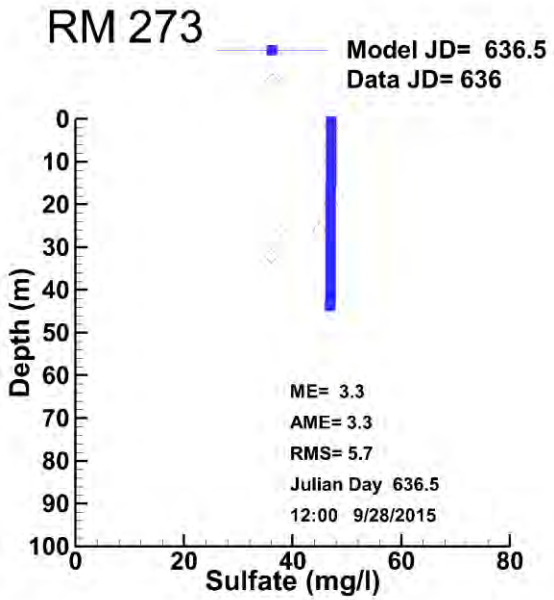


Figure 7. Vertical profiles of SULFATE compared with data for 9/28/2015.

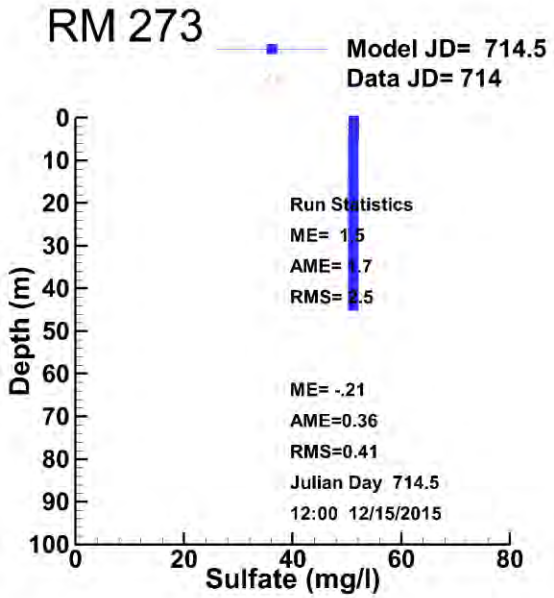


Figure 8. Vertical profiles of SULFATE compared with data for 12/15/2015.

Fe(II)

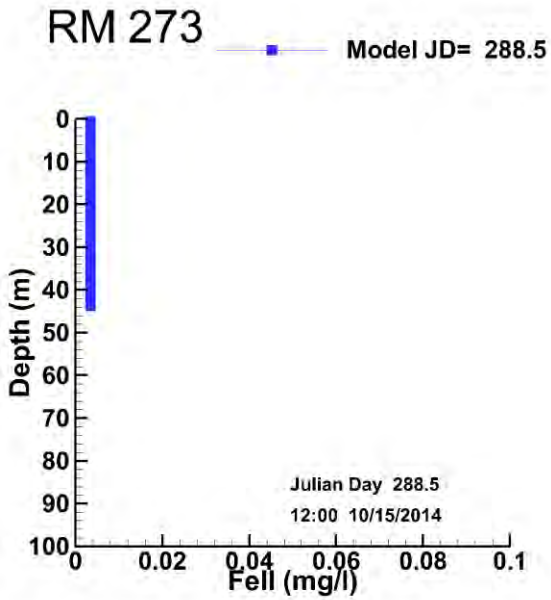


Figure 9. Vertical profiles of FE(II) compared with data for 10/15/2014.

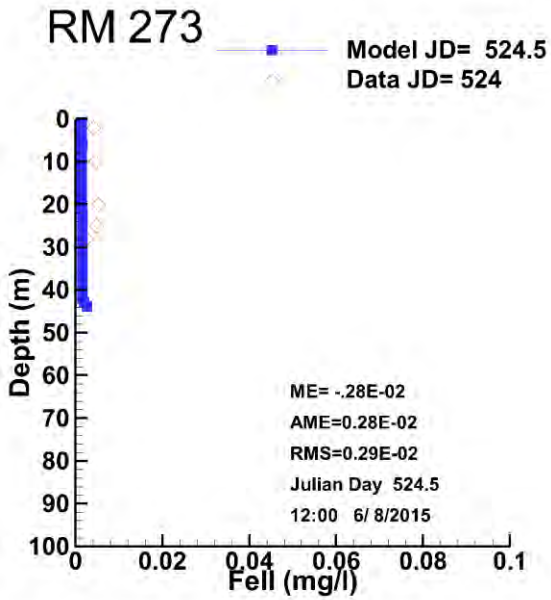


Figure 10. Vertical profiles of FE(II) compared with data for 6/ 8/2015.

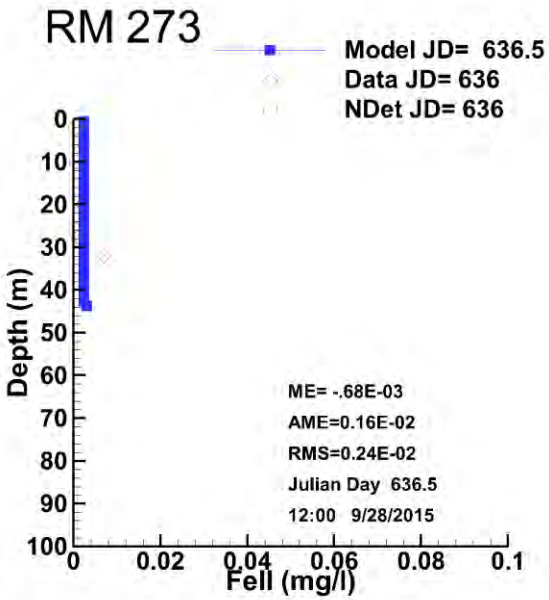


Figure 11. Vertical profiles of FE(II) compared with data for 9/28/2015.

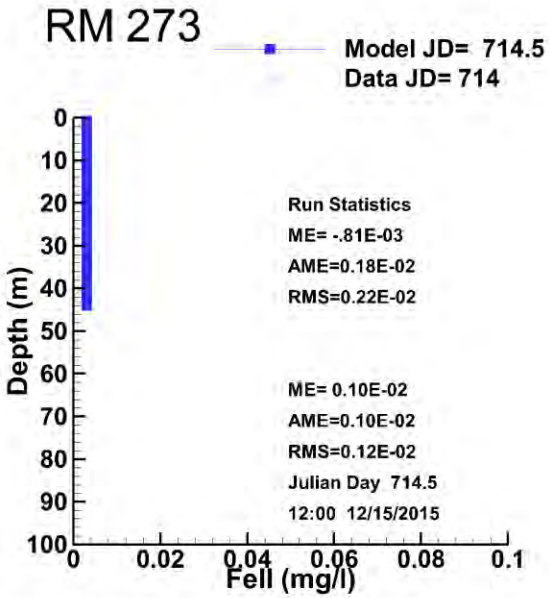


Figure 12. Vertical profiles of FE(II) compared with data for 12/15/2015.

Mn(II)

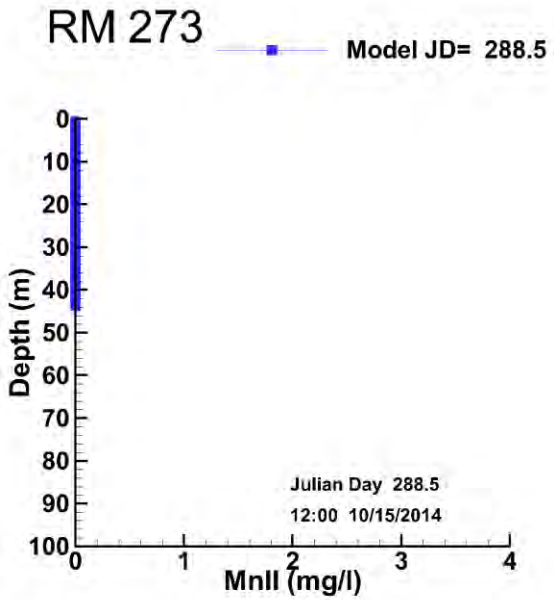


Figure 13. Vertical profiles of Mn(II) compared with data for 10/15/2014.

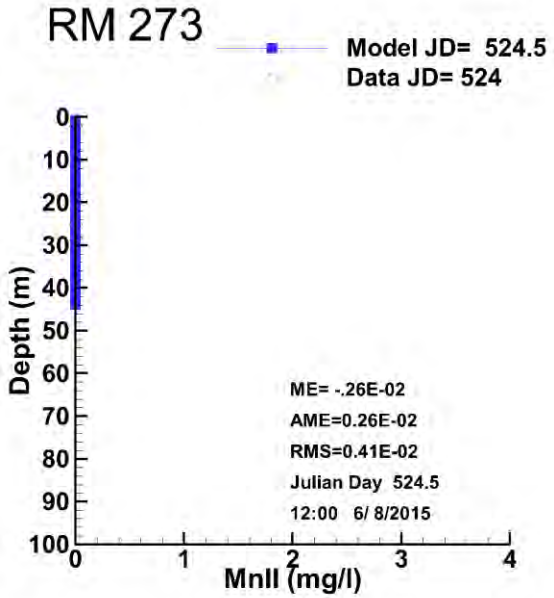


Figure 14. Vertical profiles of Mn(II) compared with data for 6/ 8/2015.

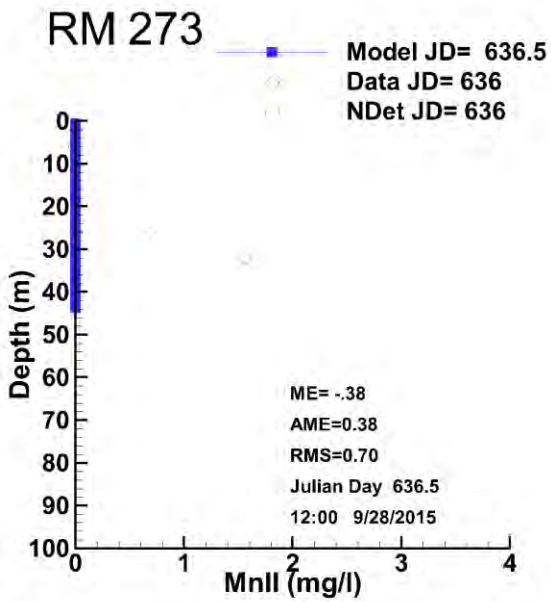


Figure 15. Vertical profiles of Mn(II) compared with data for 9/28/2015.

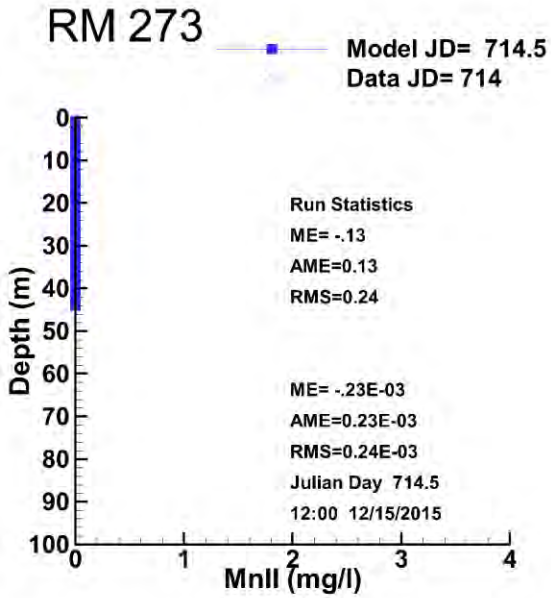


Figure 16. Vertical profiles of Mn(II) compared with data for 12/15/2015.

Orthophosphate

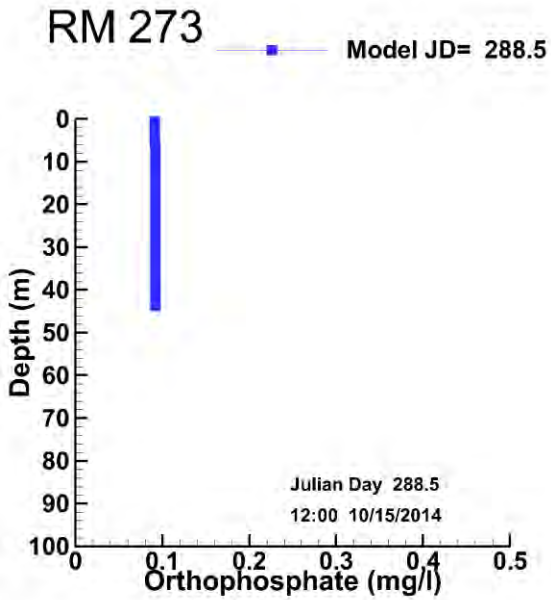


Figure 17. Vertical profiles of orthophosphate compared with data for 10/15/2014.

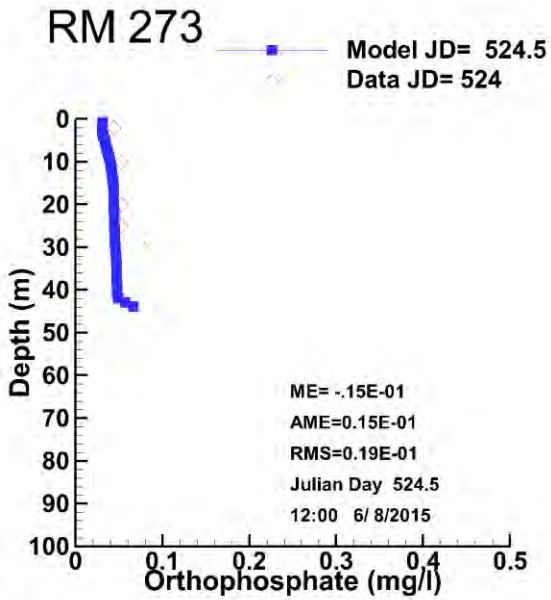


Figure 18. Vertical profiles of orthophosphate compared with data for 6/ 8/2015.

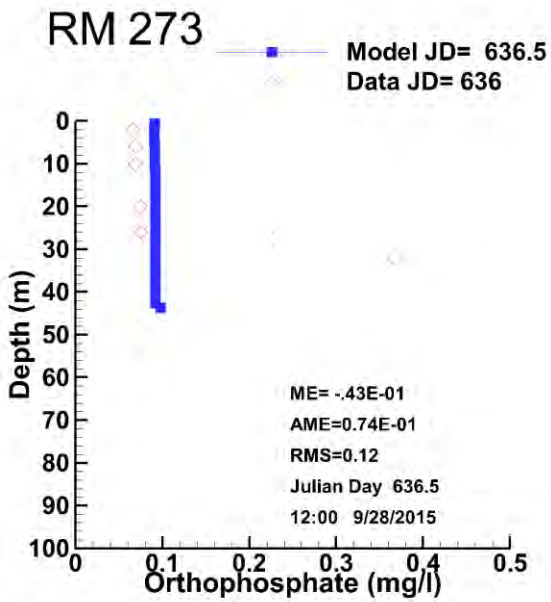


Figure 19. Vertical profiles of orthophosphate compared with data for 9/28/2015.

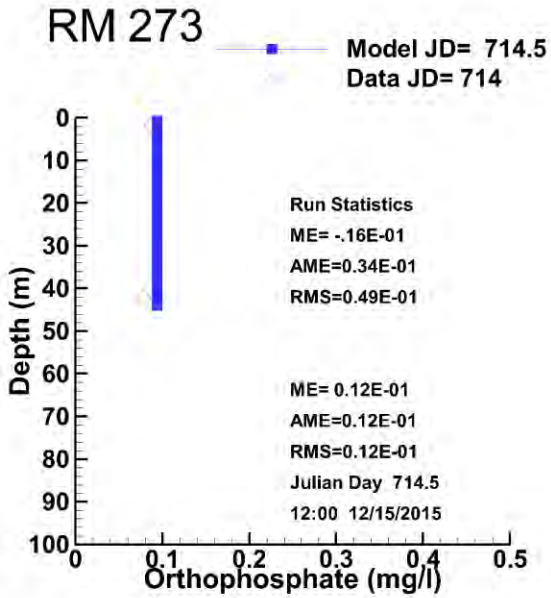


Figure 20. Vertical profiles of orthophosphate compared with data for 12/15/2015.

Nitrate Nitrogen

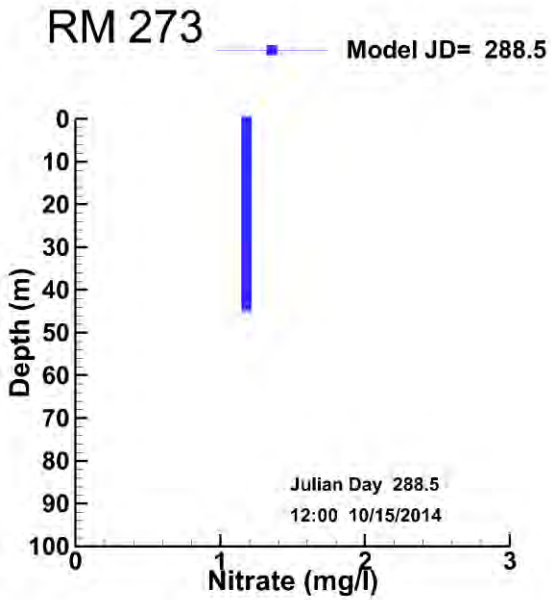


Figure 21. Vertical profiles of nitrate nitrogen compared with data for 10/15/2014.

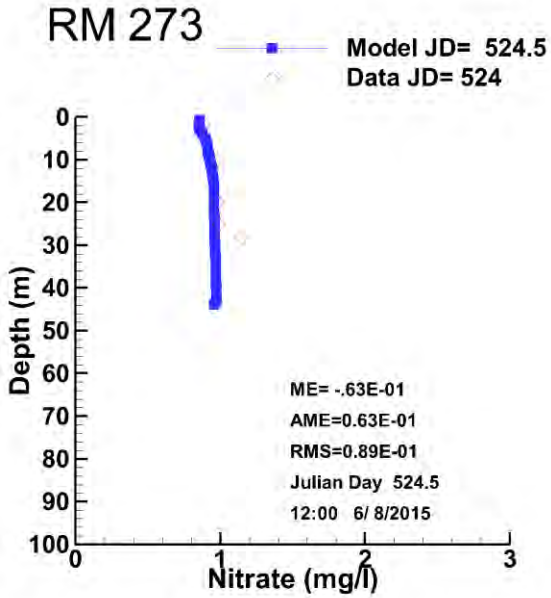


Figure 22. Vertical profiles of nitrate nitrogen compared with data for 6/ 8/2015.

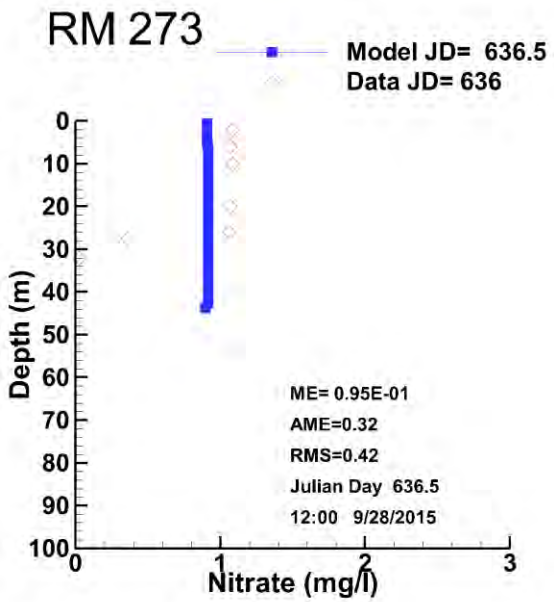


Figure 23. Vertical profiles of nitrate nitrogen compared with data for 9/28/2015.

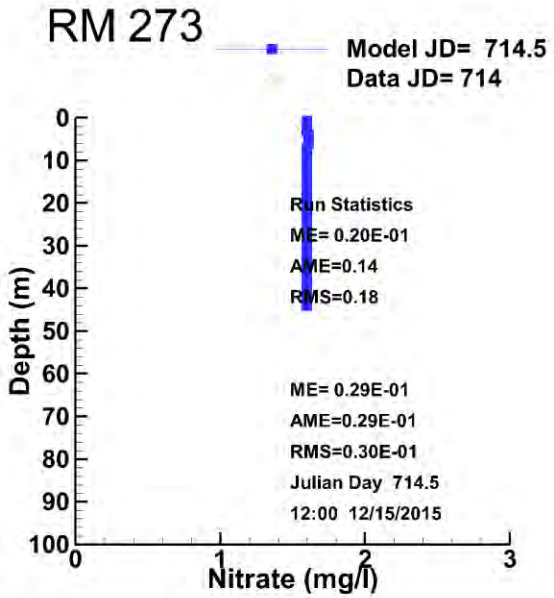


Figure 24. Vertical profiles of nitrate nitrogen compared with data for 12/15/2015.

Total Inorganic Carbon

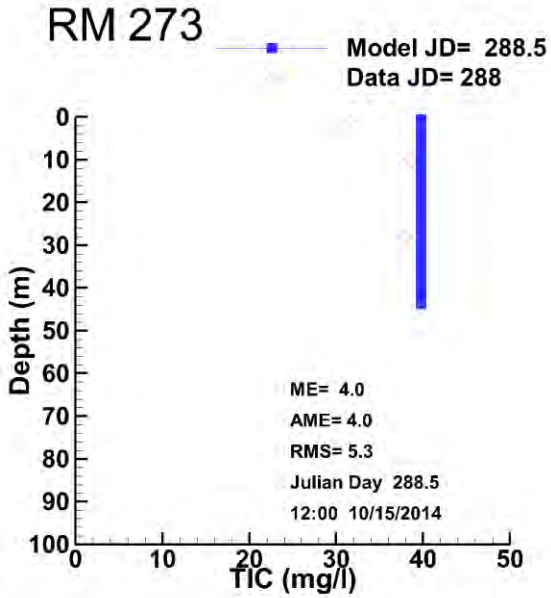


Figure 25. Vertical profiles of total inorganic carbon compared with data for 10/15/2014.

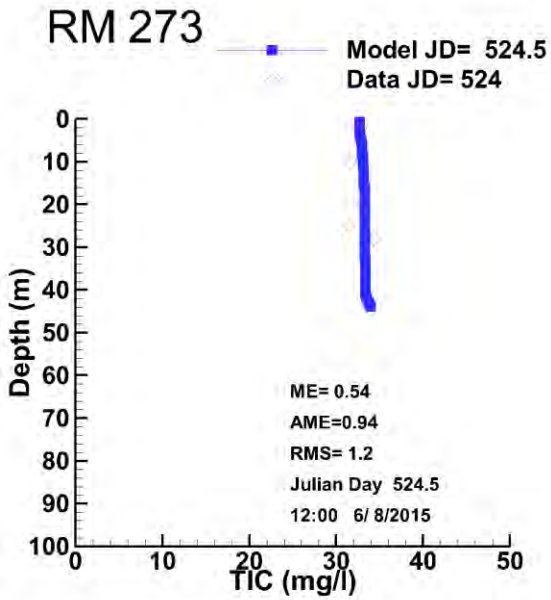


Figure 26. Vertical profiles of total inorganic carbon compared with data for 6/ 8/2015.

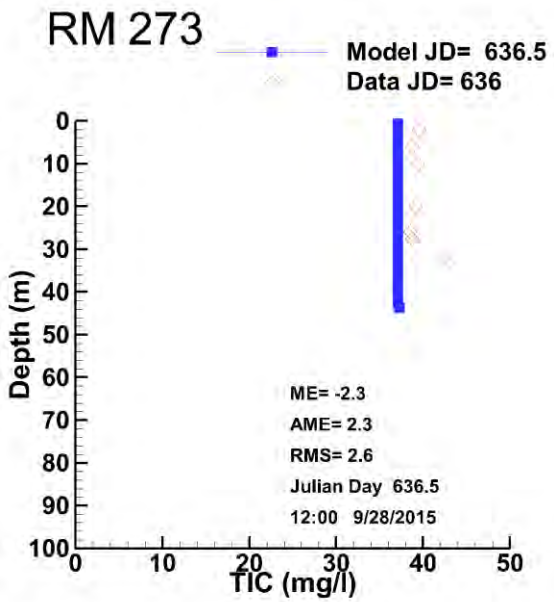


Figure 27. Vertical profiles of total inorganic carbon compared with data for 9/28/2015.

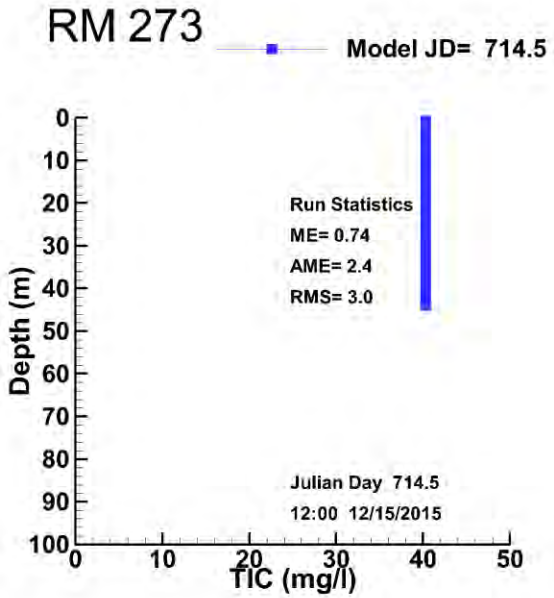


Figure 28. Vertical profiles of total inorganic carbon compared with data for 12/15/2015.

Dissolved Organic Carbon

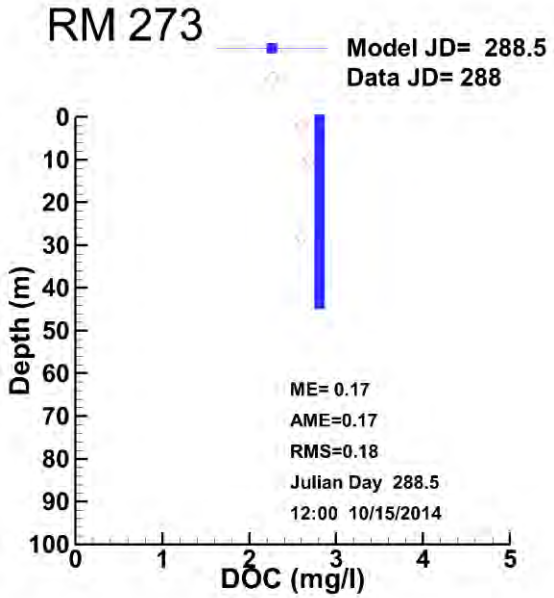


Figure 29. Vertical profiles of DOC compared with data for 10/15/2014.

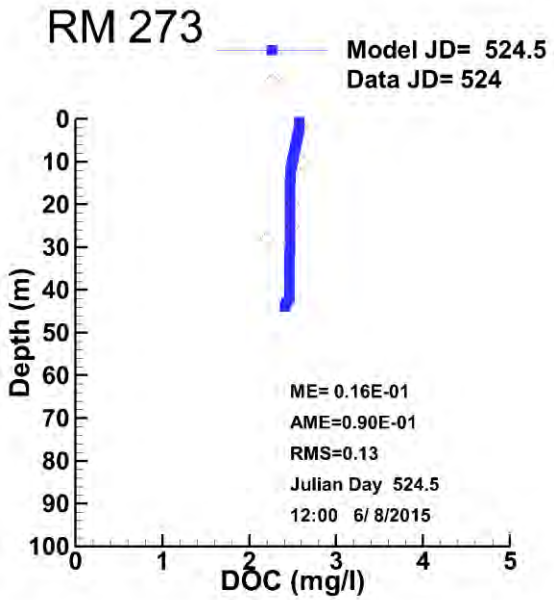


Figure 30. Vertical profiles of DOC compared with data for 6/ 8/2015.

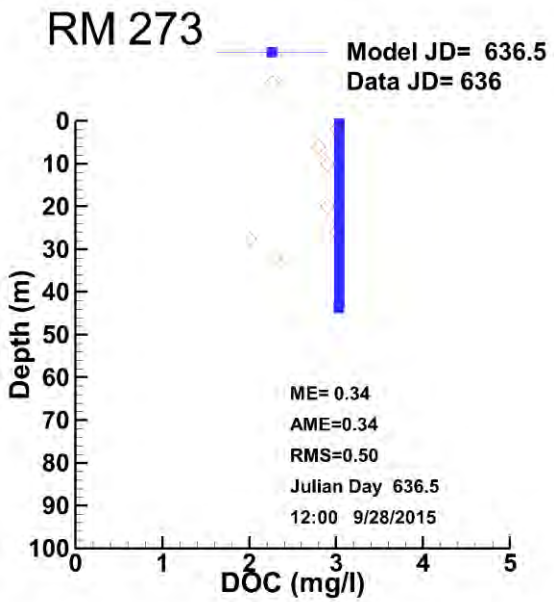


Figure 31. Vertical profiles of DOC compared with data for 9/28/2015.

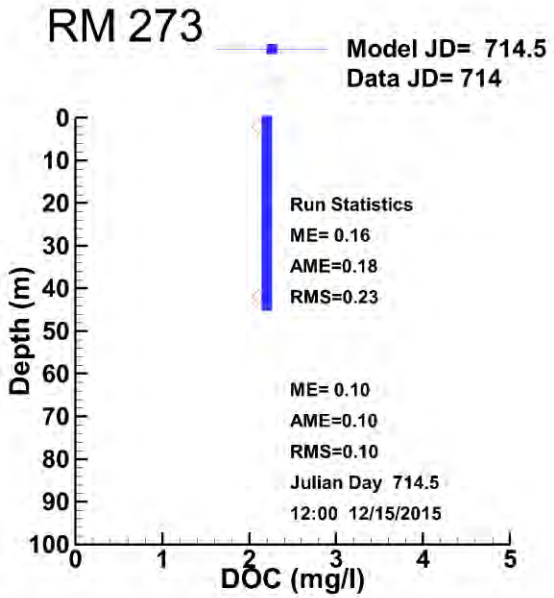


Figure 32. Vertical profiles of DOC compared with data for 12/15/2015.

Particulate Organic Carbon

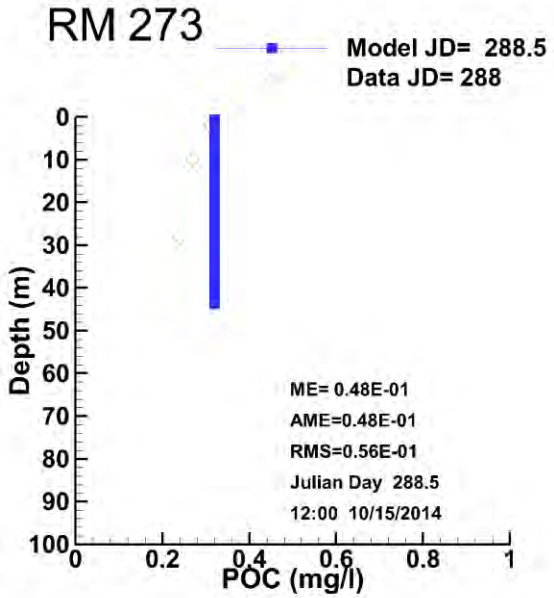


Figure 33. Vertical profiles of POC compared with data for 10/15/2014.

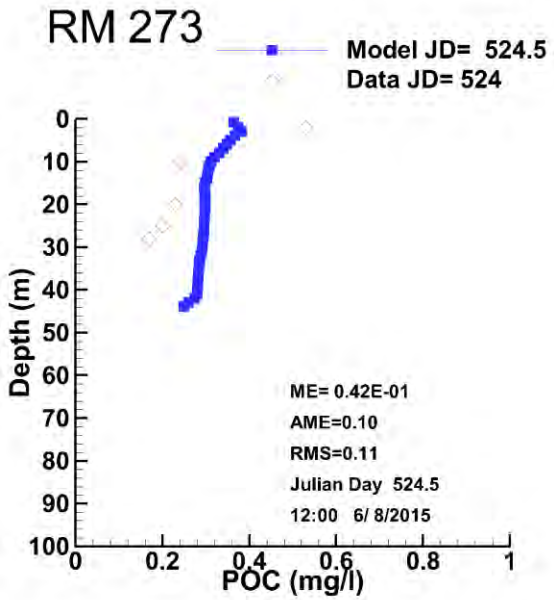


Figure 34. Vertical profiles of POC compared with data for 6/ 8/2015.

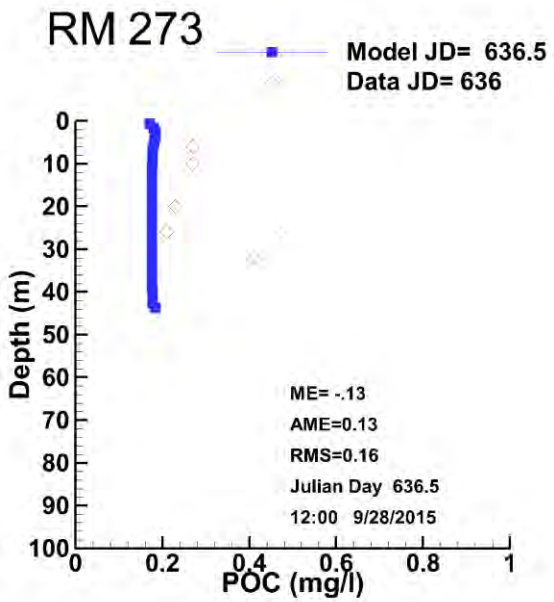


Figure 35. Vertical profiles of POC compared with data for 9/28/2015.

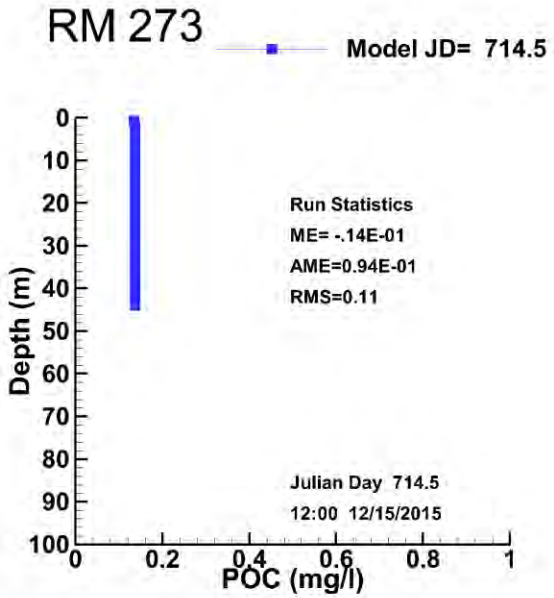


Figure 36. Vertical profiles of POC compared with data for 12/15/2015.

Particulate Organic Nitrogen

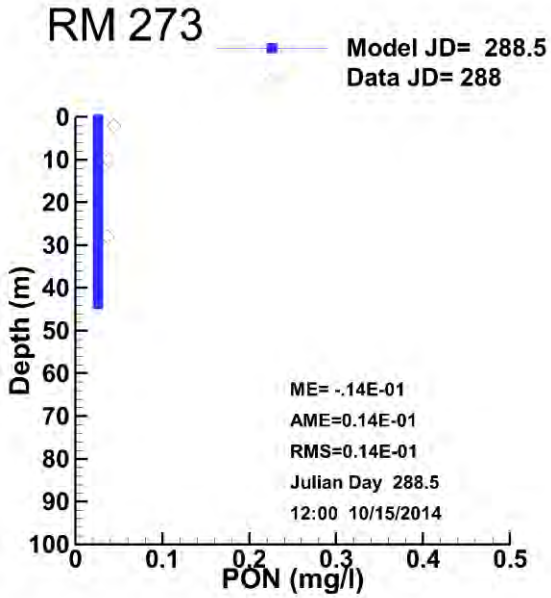


Figure 37. Vertical profiles of PON compared with data for 10/15/2014.

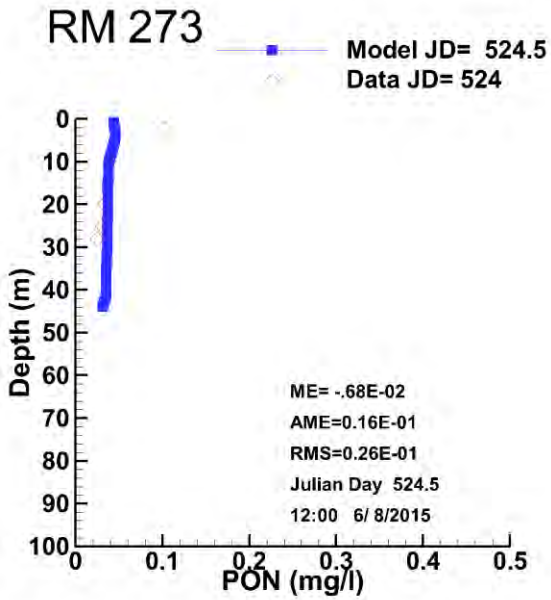


Figure 38. Vertical profiles of PON compared with data for 6/ 8/2015.

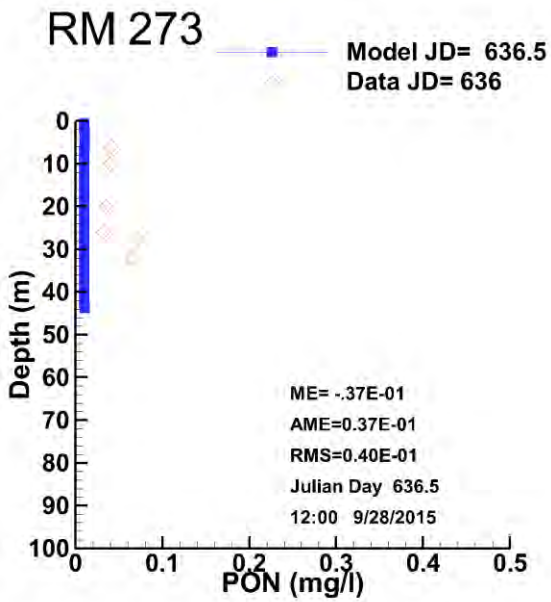


Figure 39. Vertical profiles of PON compared with data for 9/28/2015.

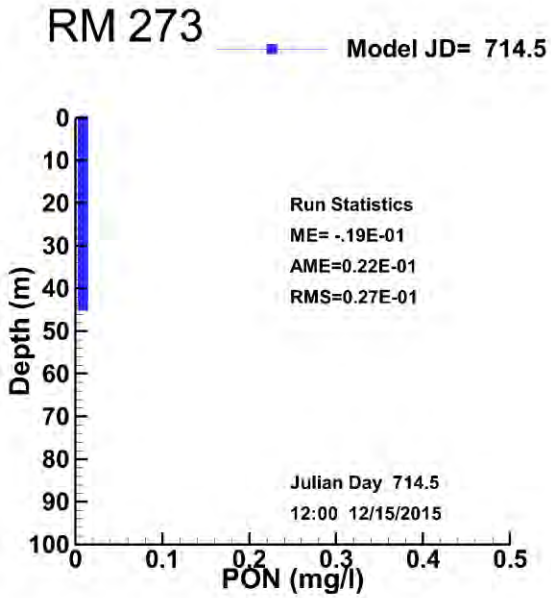


Figure 40. Vertical profiles of PON compared with data for 12/15/2015.

Total Suspended Solids

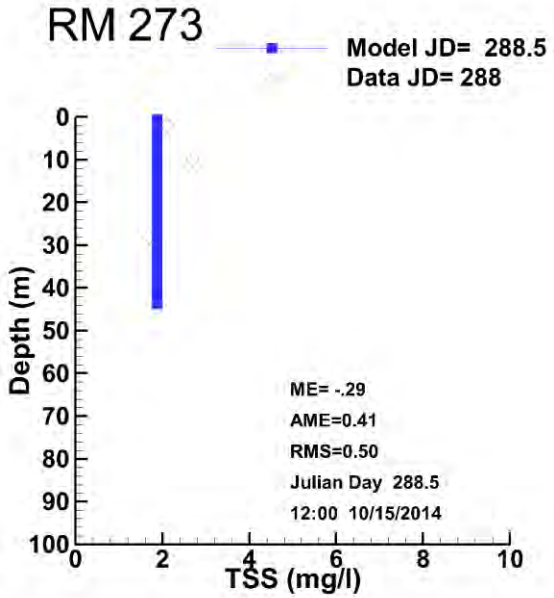


Figure 41. Vertical profiles of TSS compared with data for 10/15/2014.

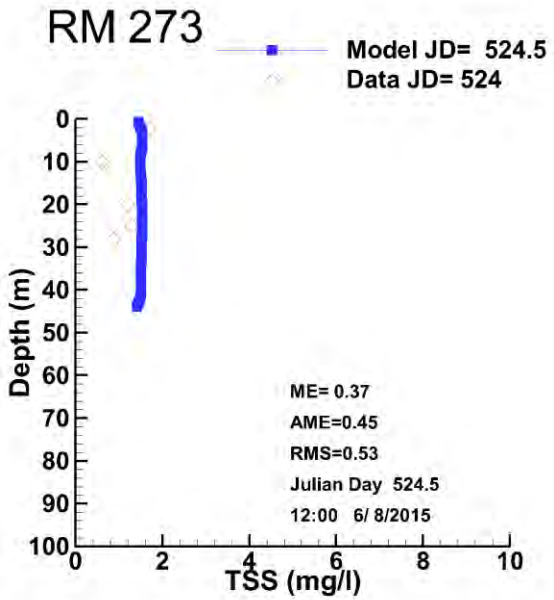


Figure 42. Vertical profiles of TSS compared with data for 6/ 8/2015.

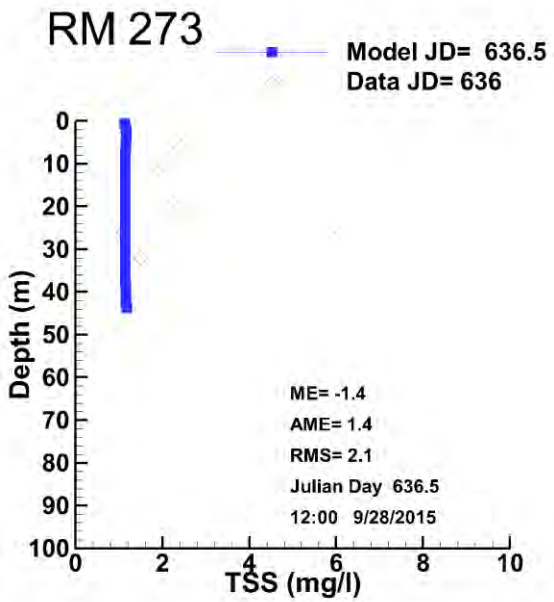


Figure 43. Vertical profiles of TSS compared with data for 9/28/2015.

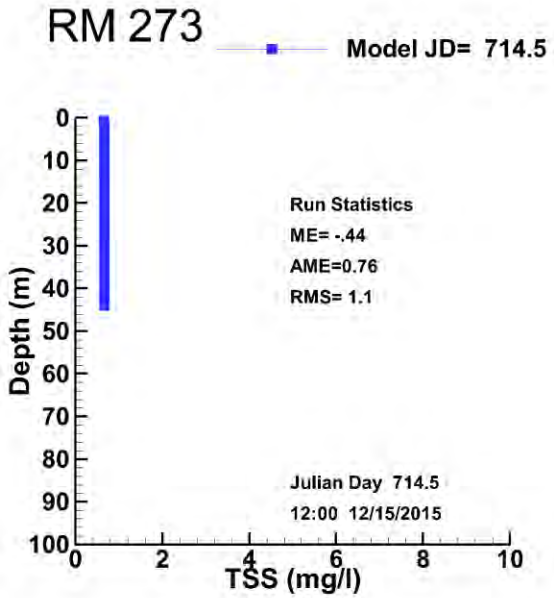


Figure 44. Vertical profiles of TSS compared with data for 12/15/2015.

Zooplankton

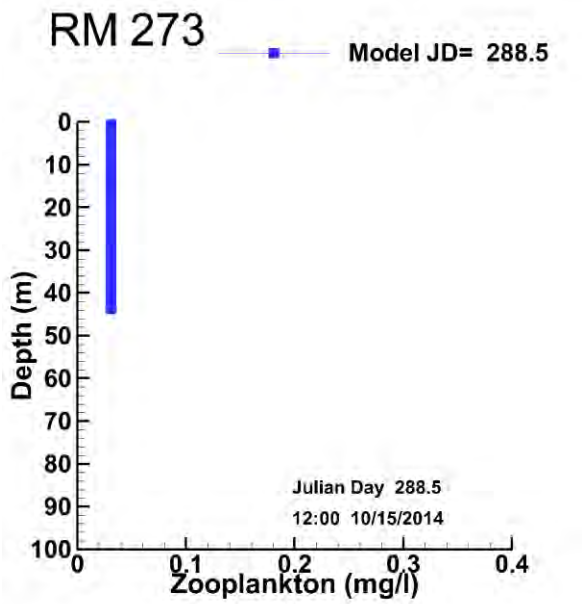


Figure 45. Vertical profiles of ZOO_ compared with data for 10/15/2014.

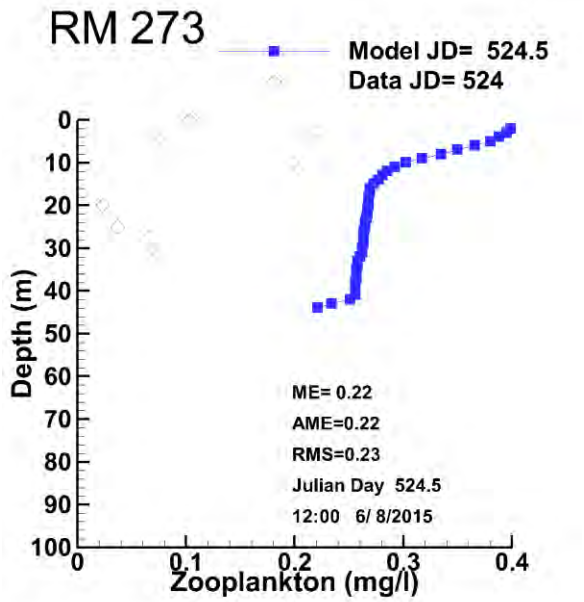


Figure 46. Vertical profiles of ZOO_ compared with data for 6/ 8/2015.

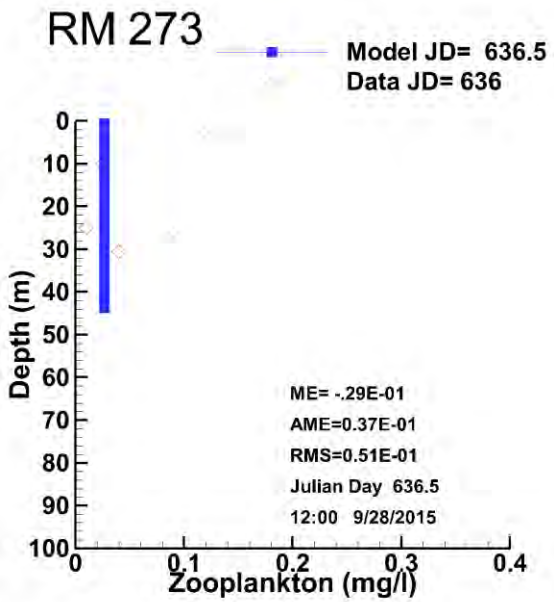


Figure 47. Vertical profiles of ZOO_ compared with data for 9/28/2015.

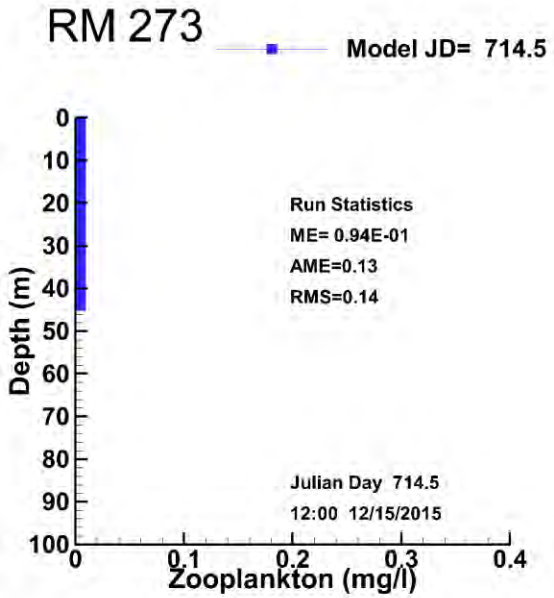


Figure 48. Vertical profiles of ZOO_ compared with data for 12/15/2015.

Appendix A6 Hells Canyon Reservoir Vertical Profiles

Chloride

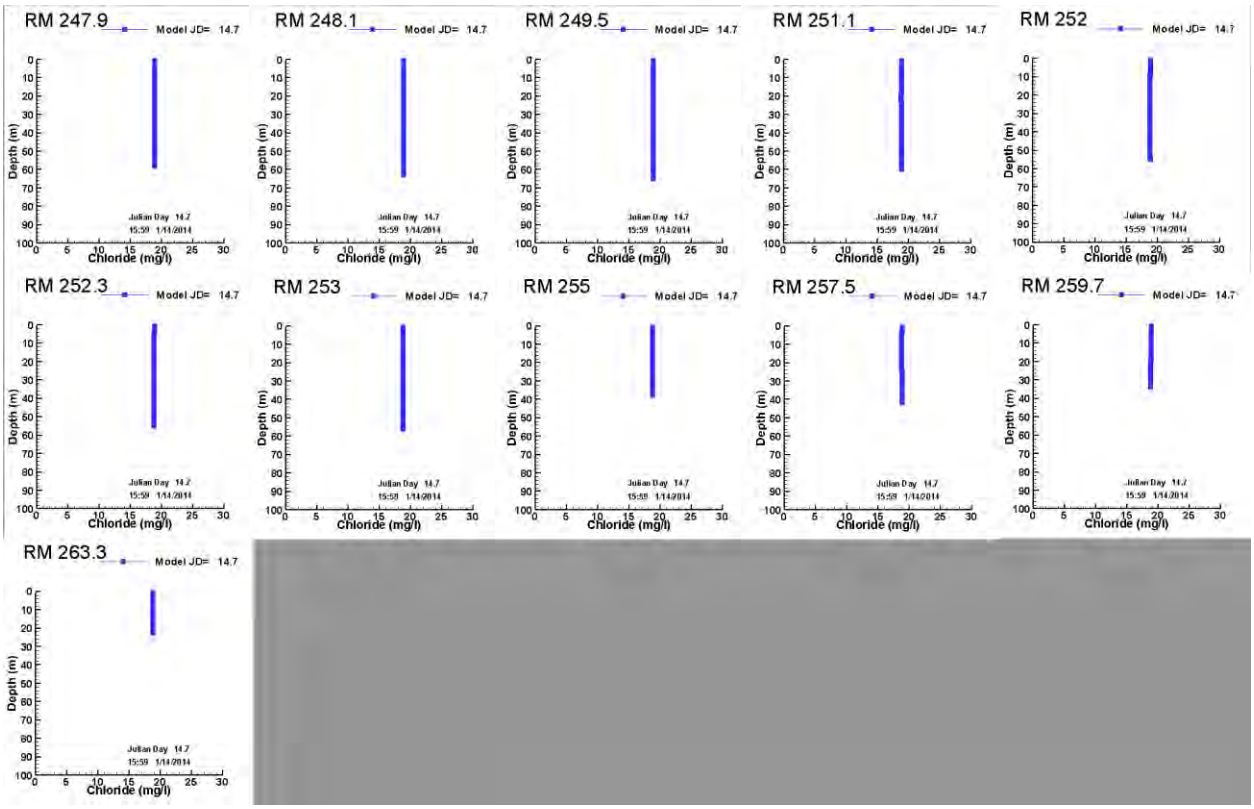


Figure 1. Vertical profiles of chloride compared with data for 1/14/2014.

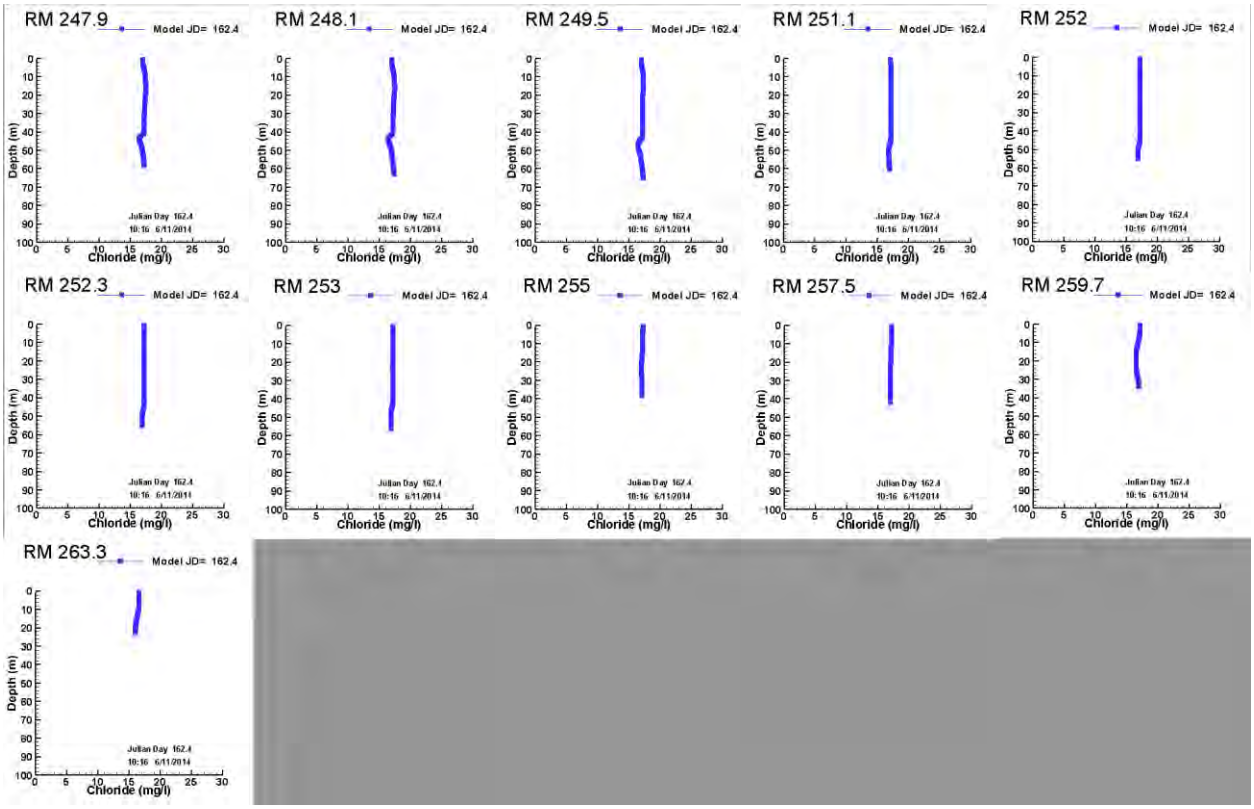


Figure 2. Vertical profiles of chloride compared with data for 6/11/2014.

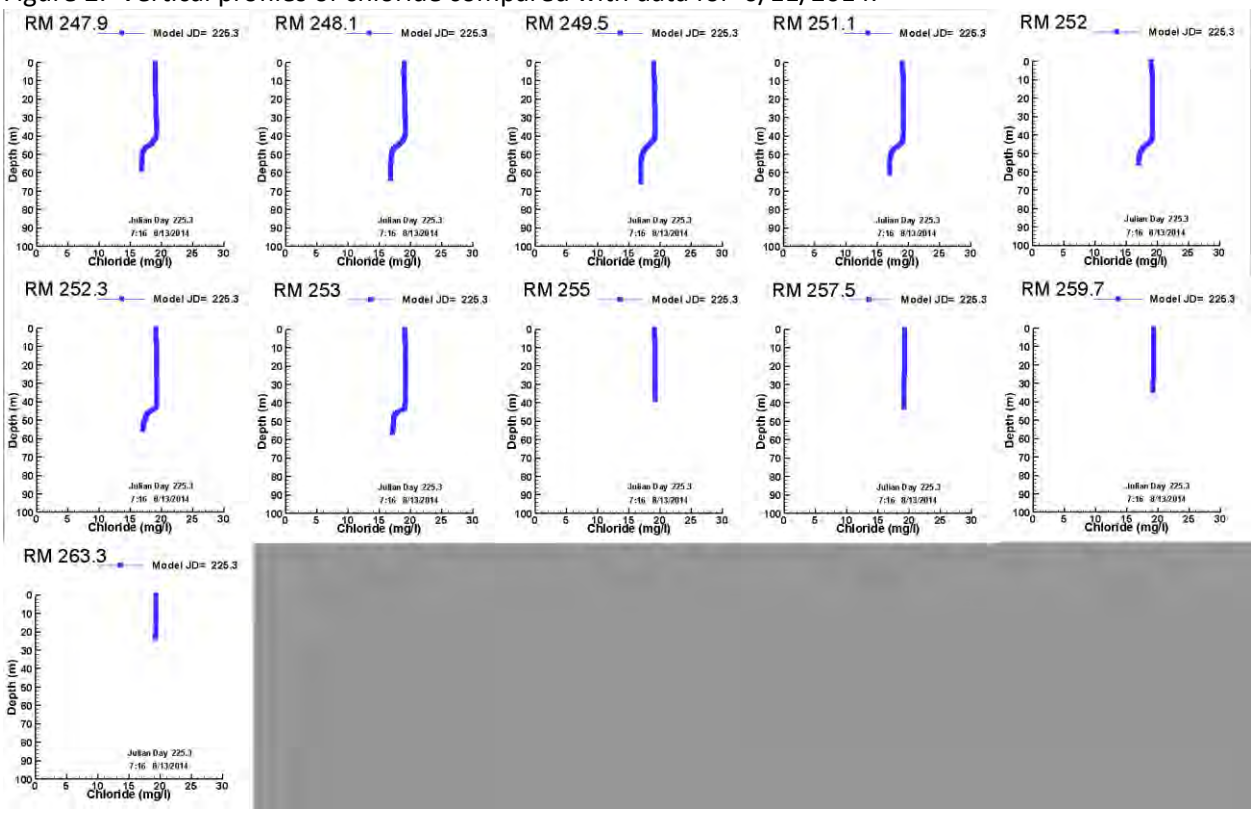


Figure 3. Vertical profiles of chloride compared with data for 8/13/2014.

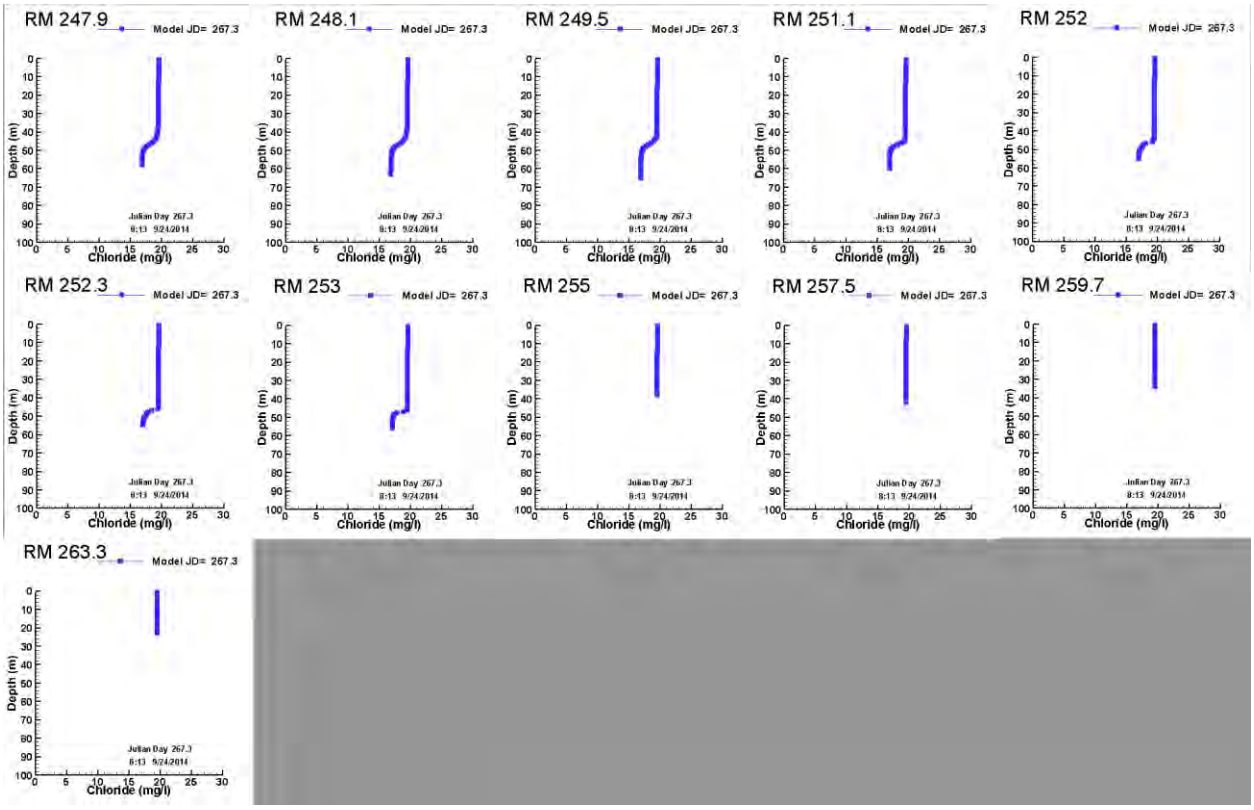


Figure 4. Vertical profiles of chloride compared with data for 9/24/2014.

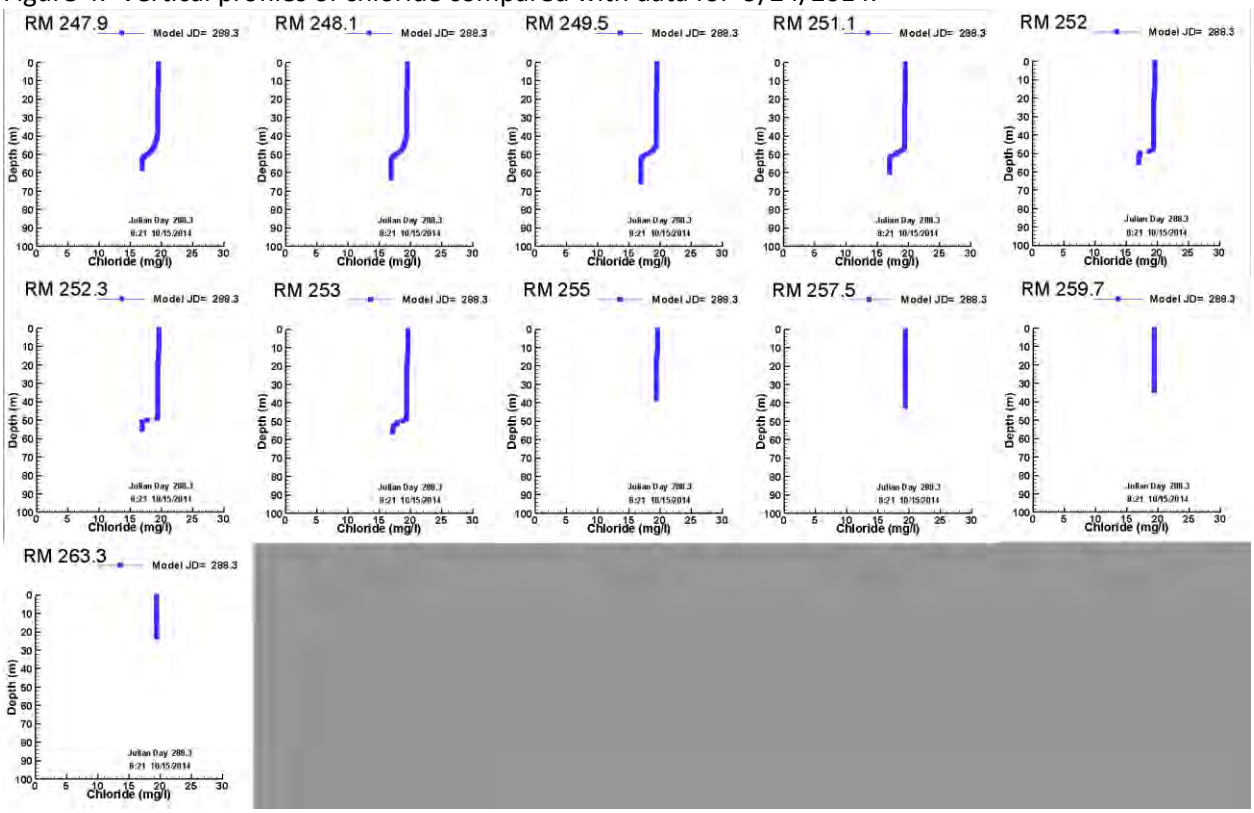


Figure 5. Vertical profiles of chloride compared with data for 10/15/2014.

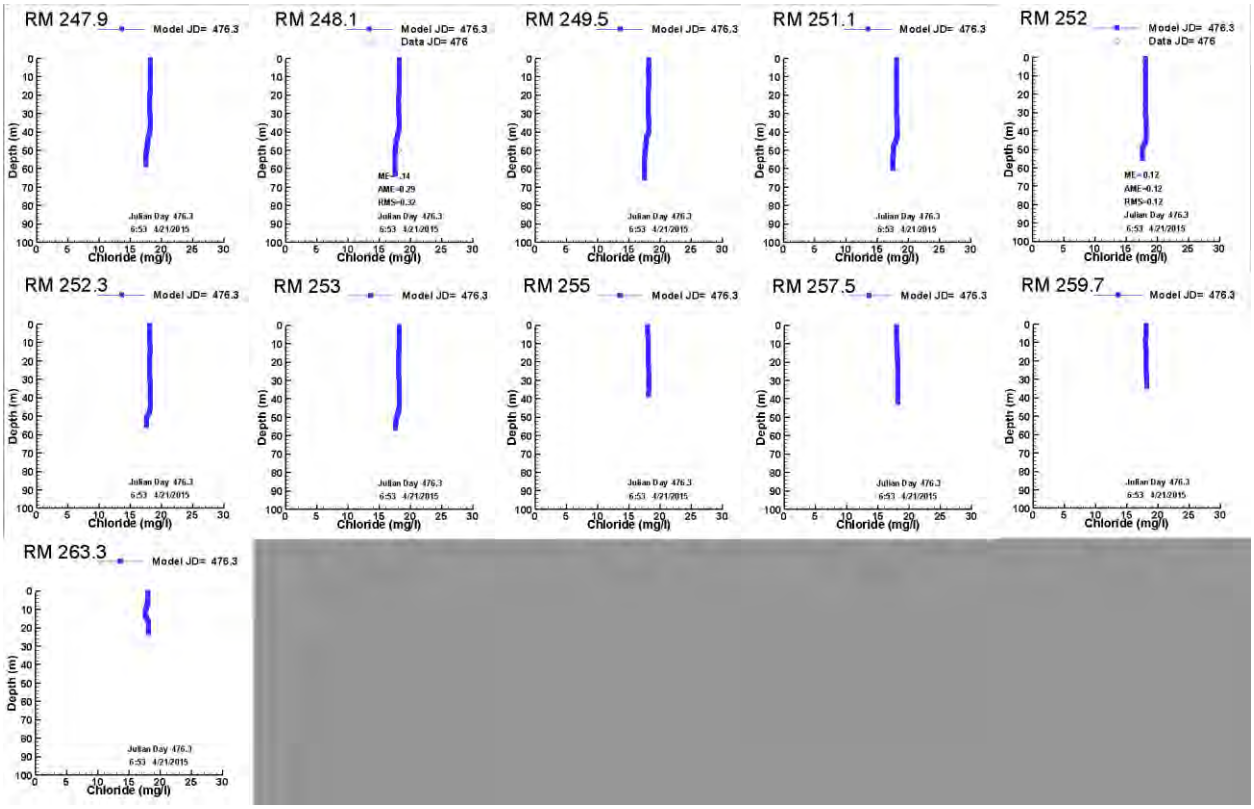


Figure 6. Vertical profiles of chloride compared with data for 4/21/2015.

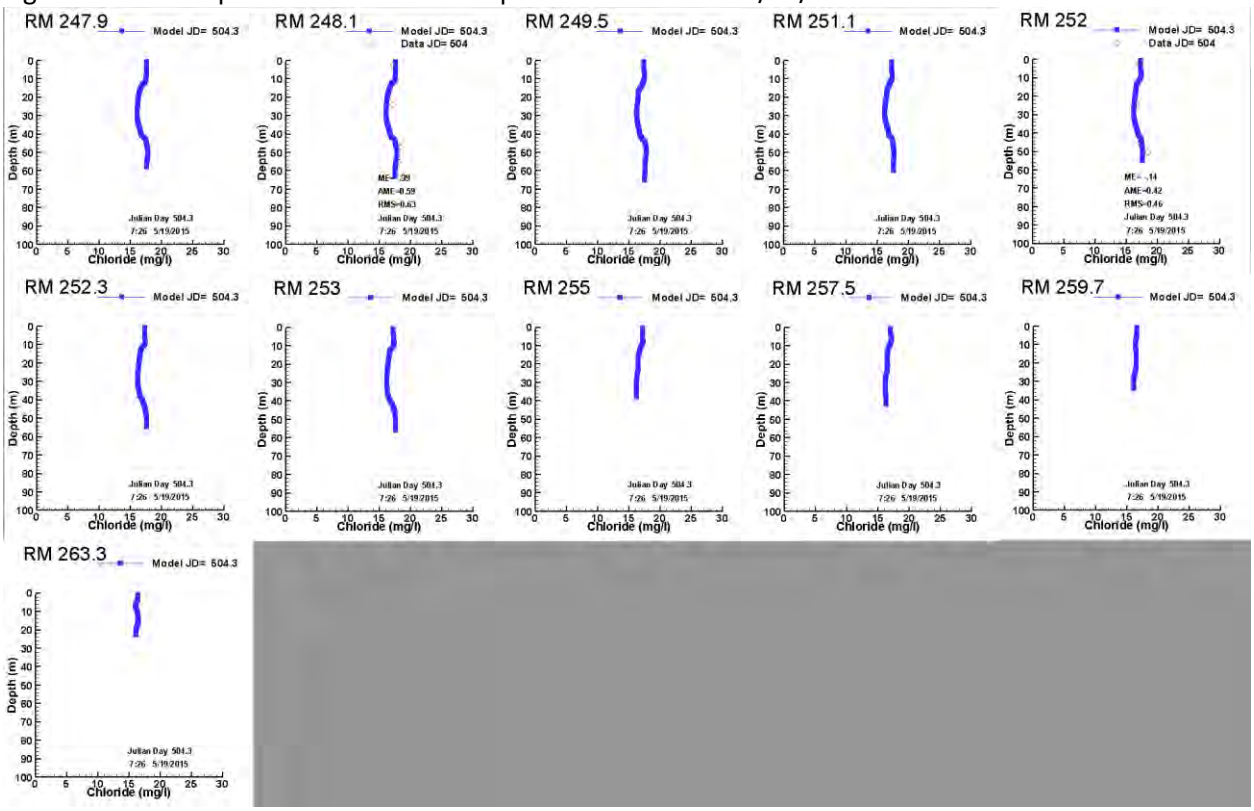


Figure 7. Vertical profiles of chloride compared with data for 5/19/2015.

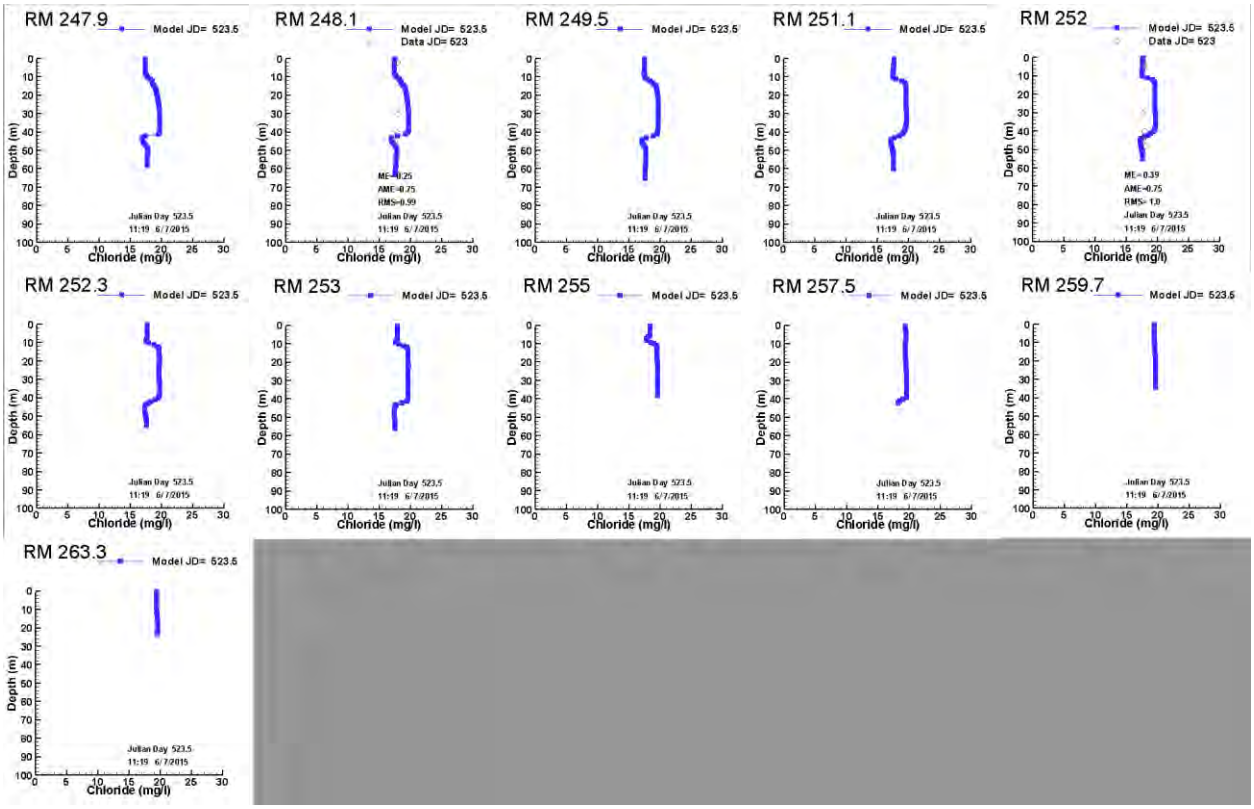


Figure 8. Vertical profiles of chloride compared with data for 6/ 7/2015.

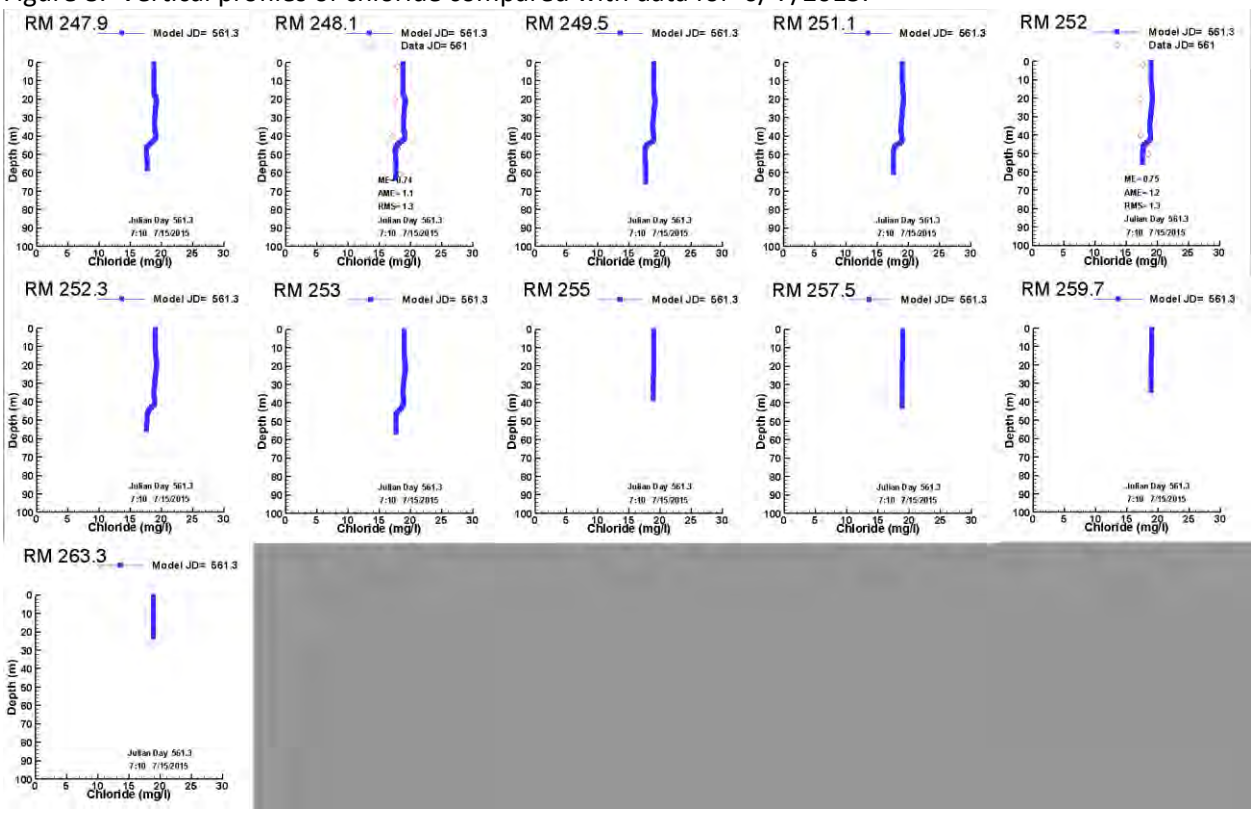


Figure 9. Vertical profiles of chloride compared with data for 7/15/2015.

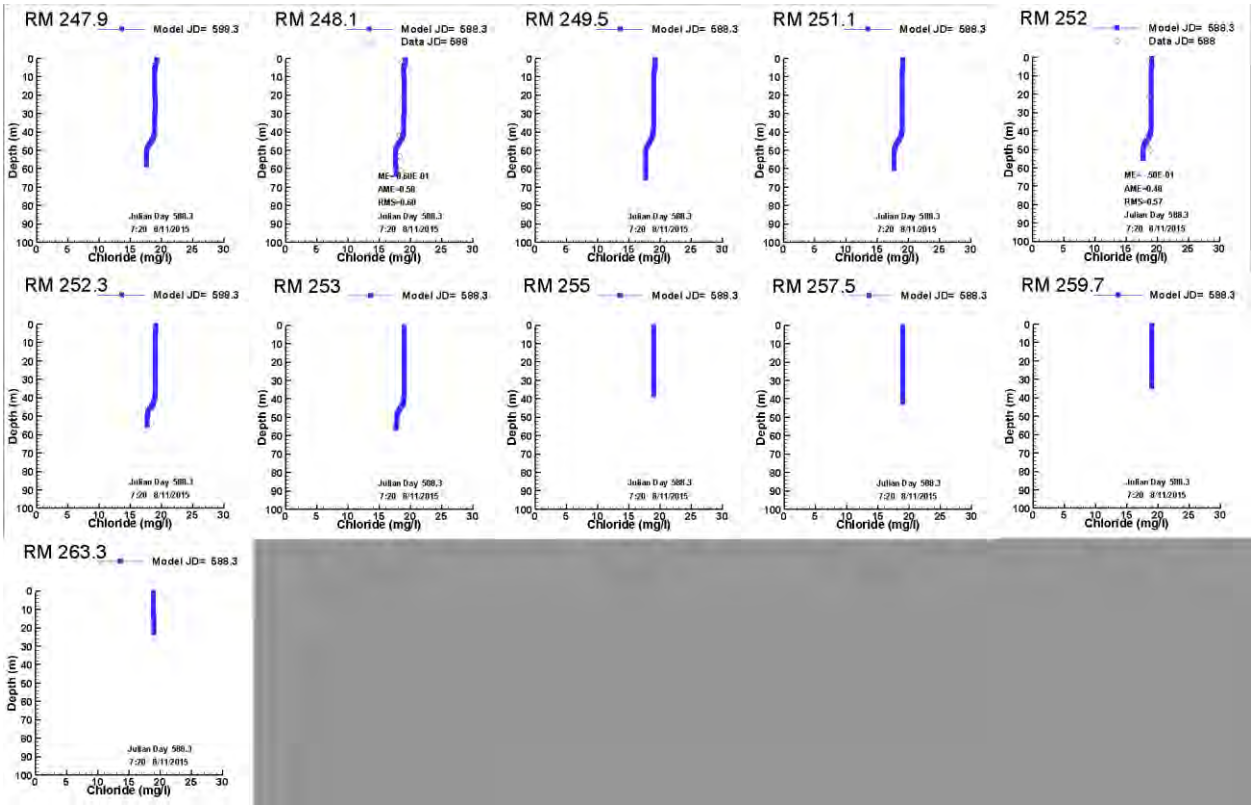


Figure 10. Vertical profiles of chloride compared with data for 8/11/2015.

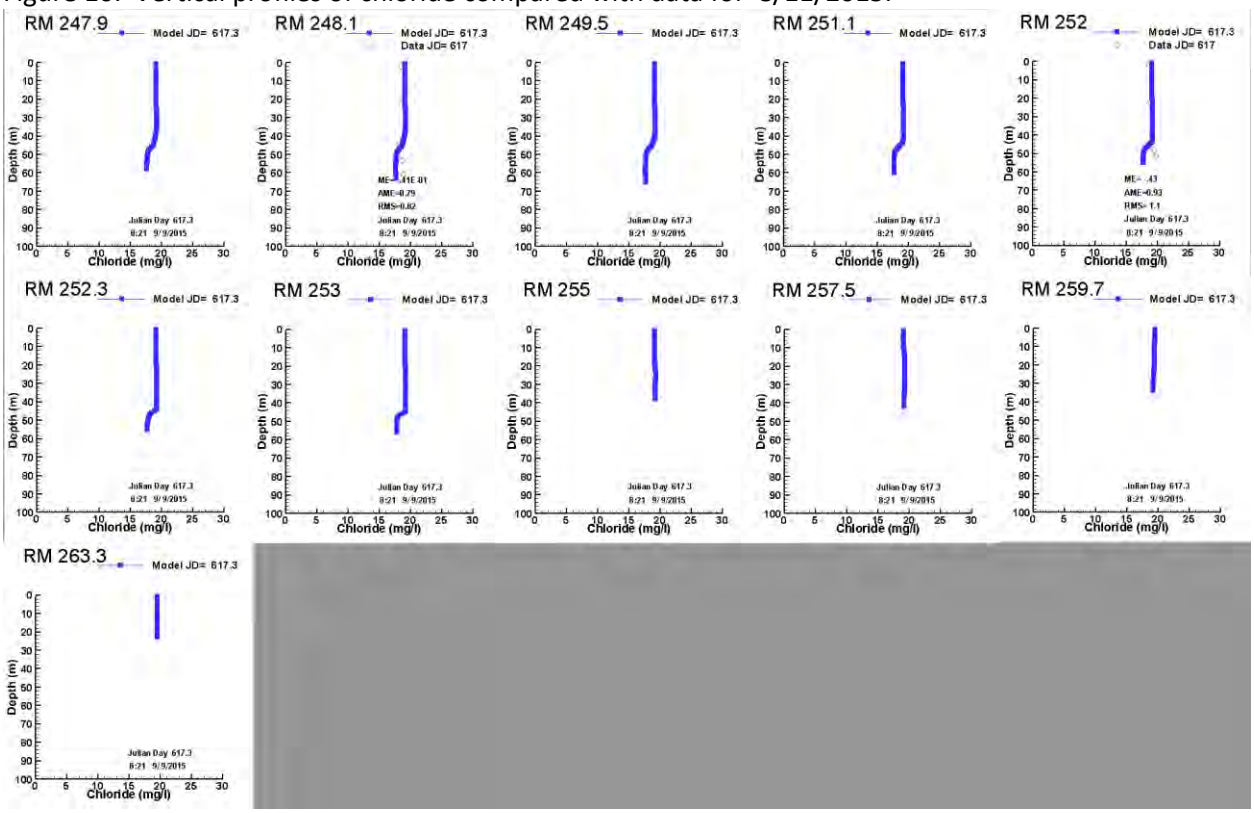


Figure 11. Vertical profiles of chloride compared with data for 9/ 9/2015.

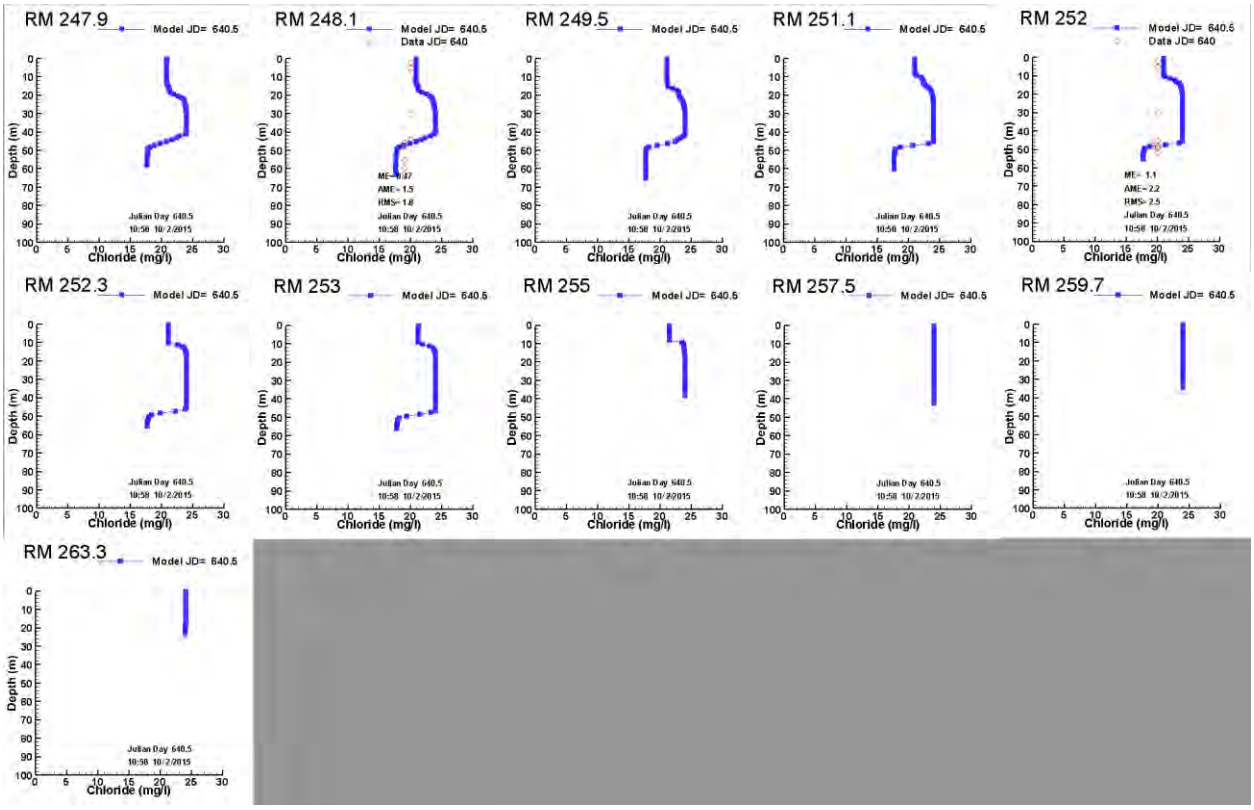


Figure 12. Vertical profiles of chloride compared with data for 10/ 2/2015.

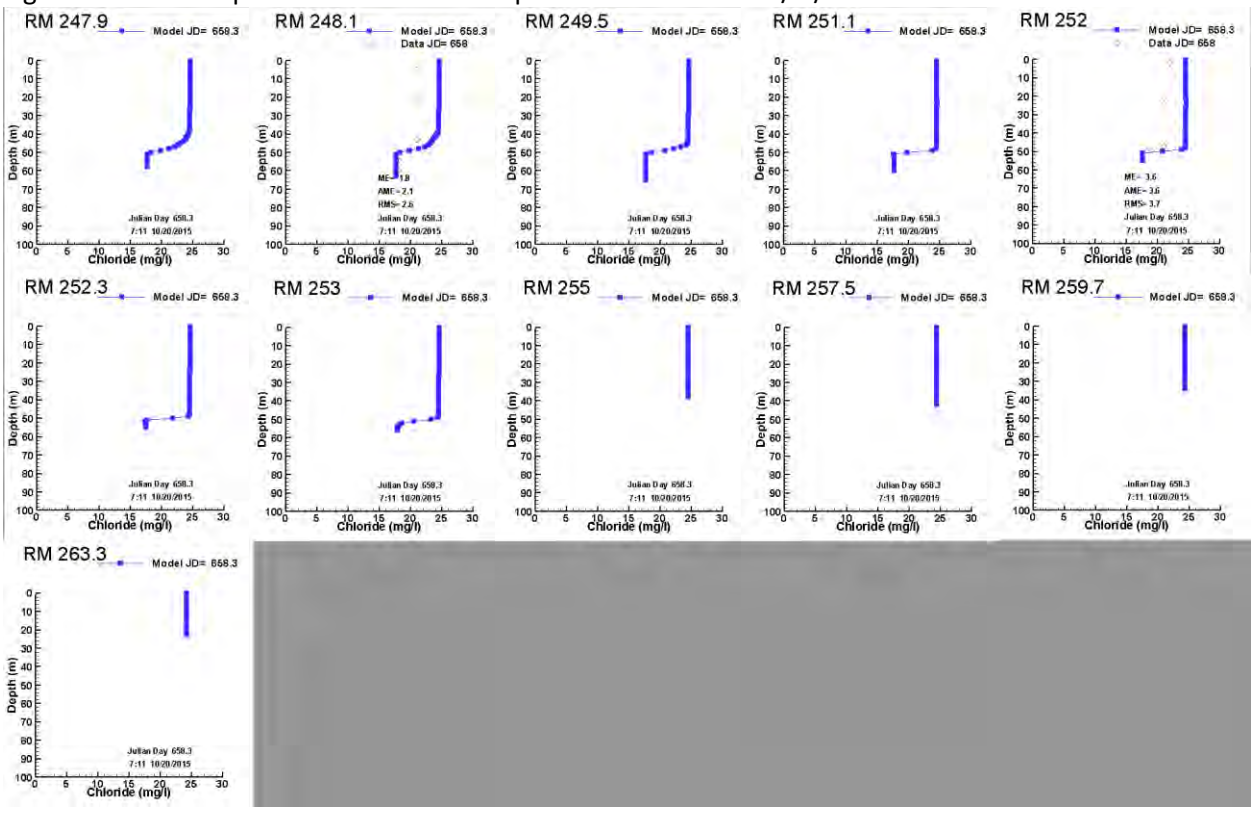


Figure 13. Vertical profiles of chloride compared with data for 10/20/2015.

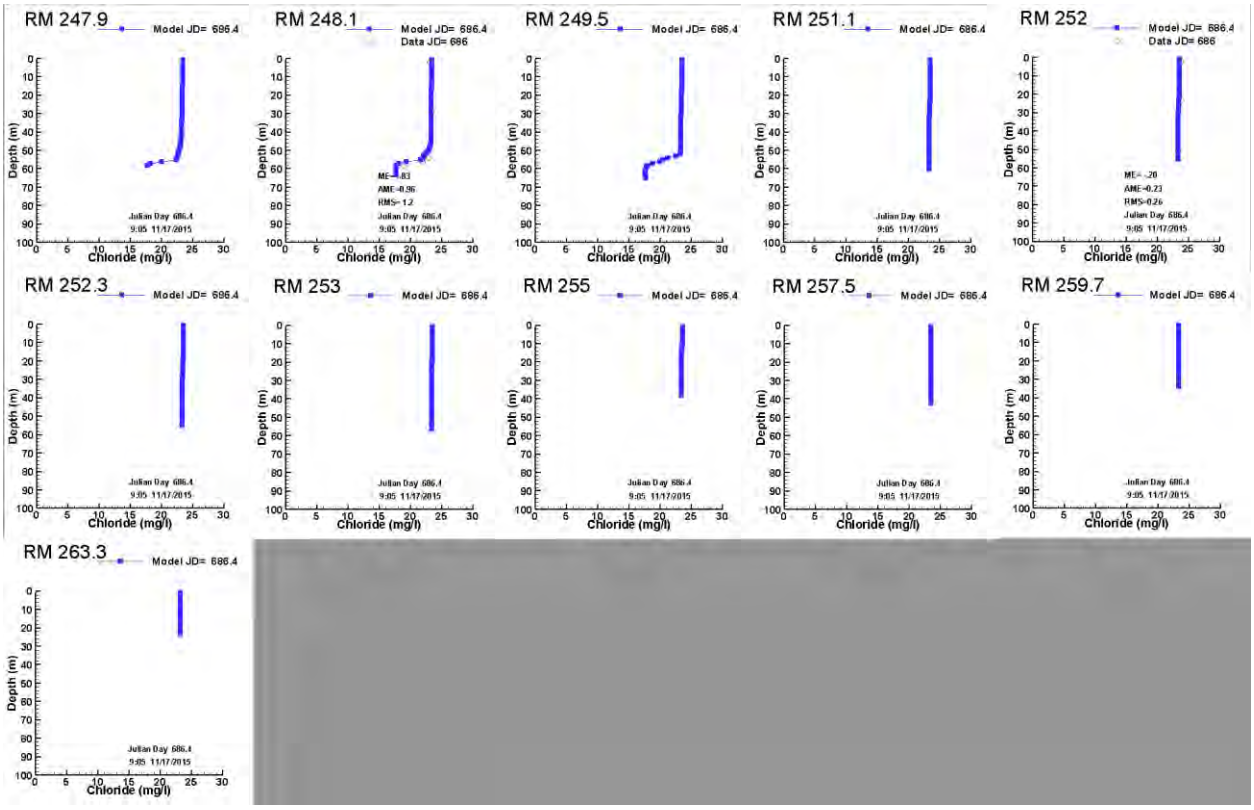


Figure 14. Vertical profiles of chloride compared with data for 11/17/2015.

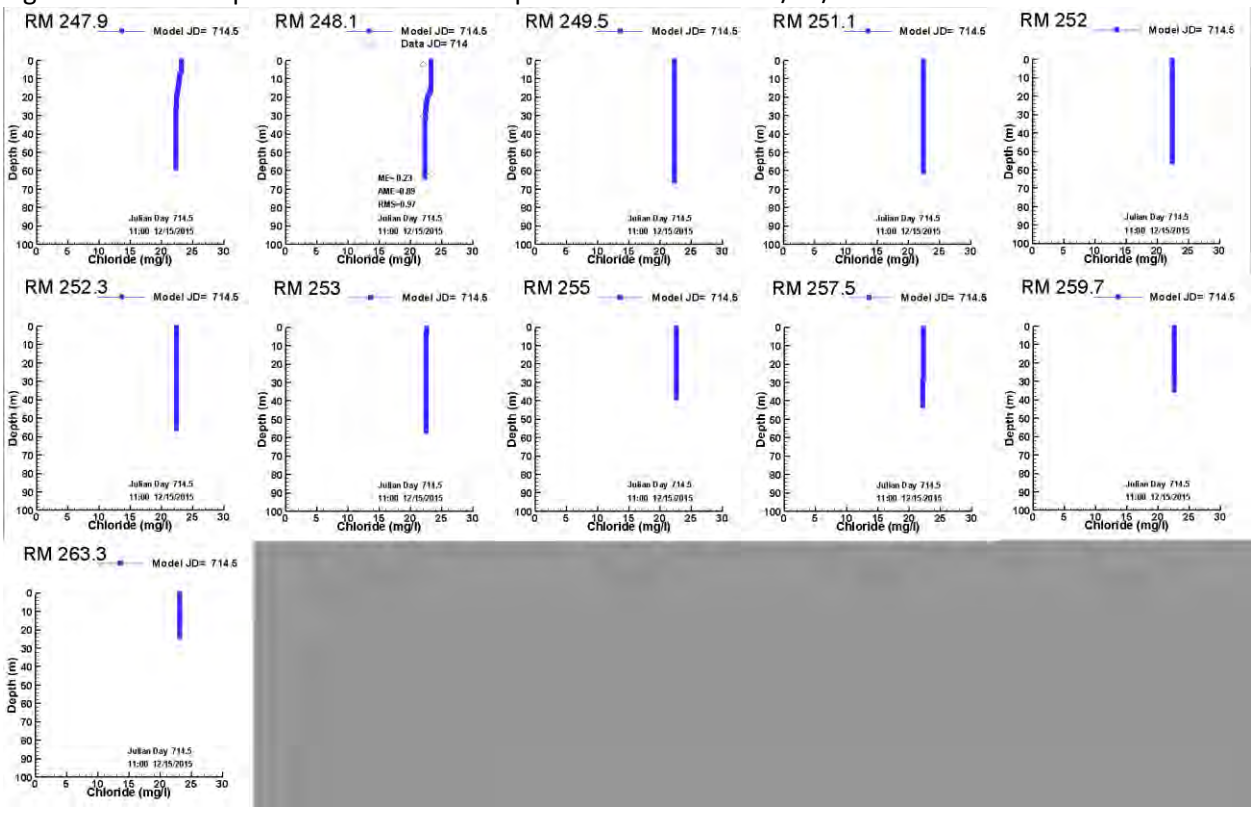


Figure 15. Vertical profiles of chloride compared with data for 12/15/2015.

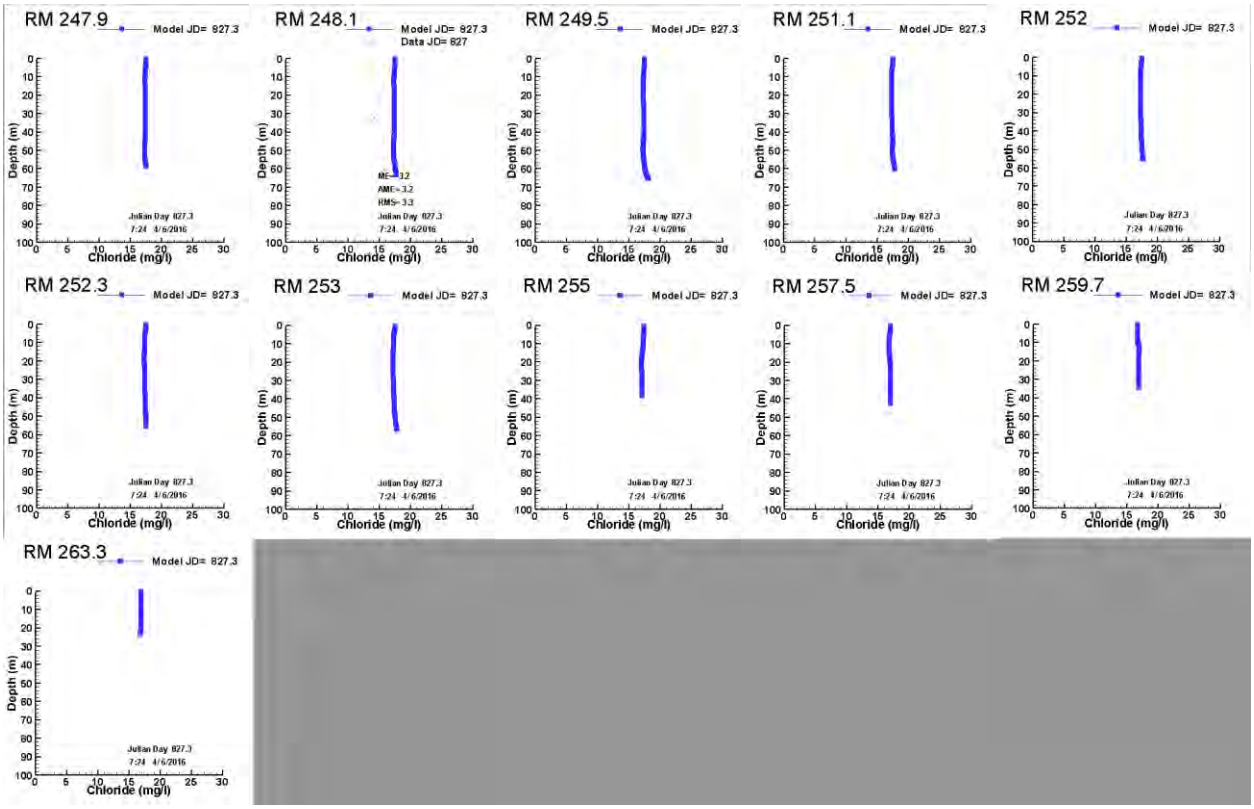


Figure 16. Vertical profiles of chloride compared with data for 4/ 6/2016.

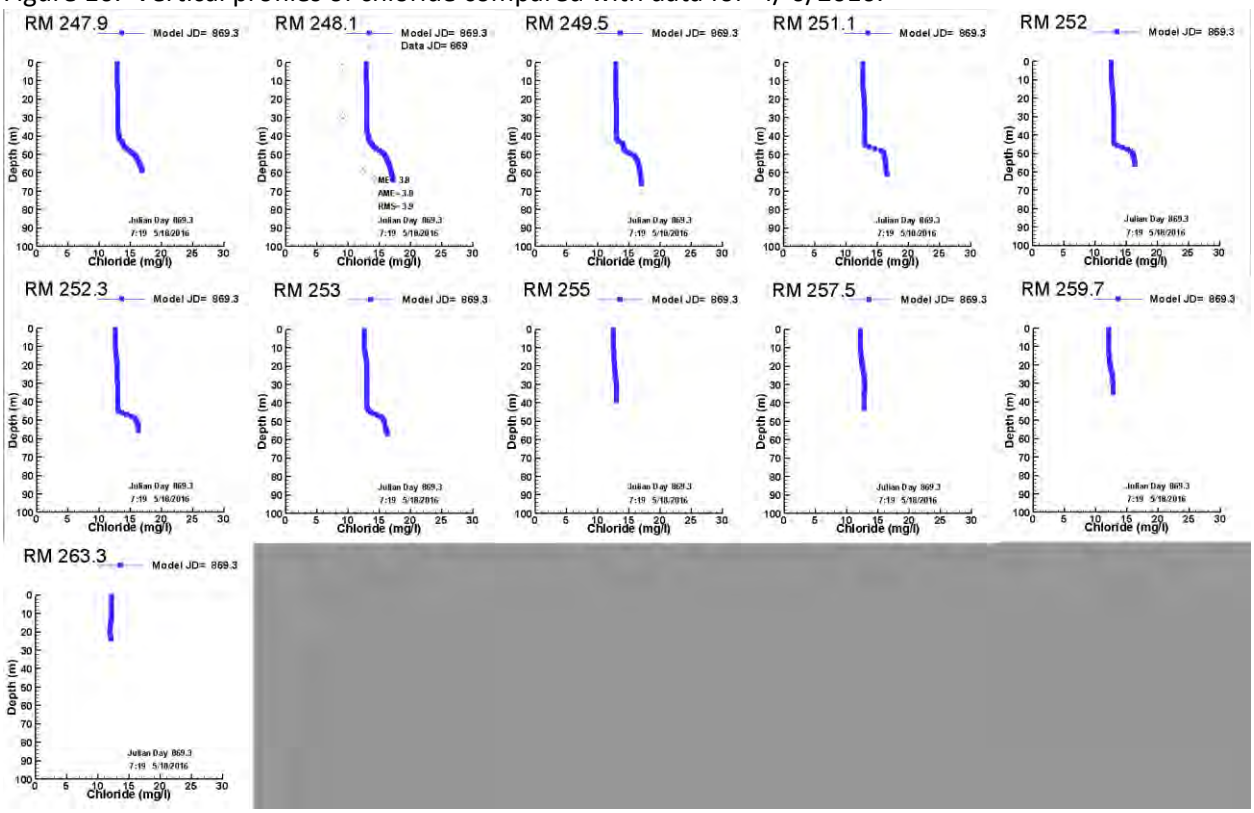


Figure 17. Vertical profiles of chloride compared with data for 5/18/2016.

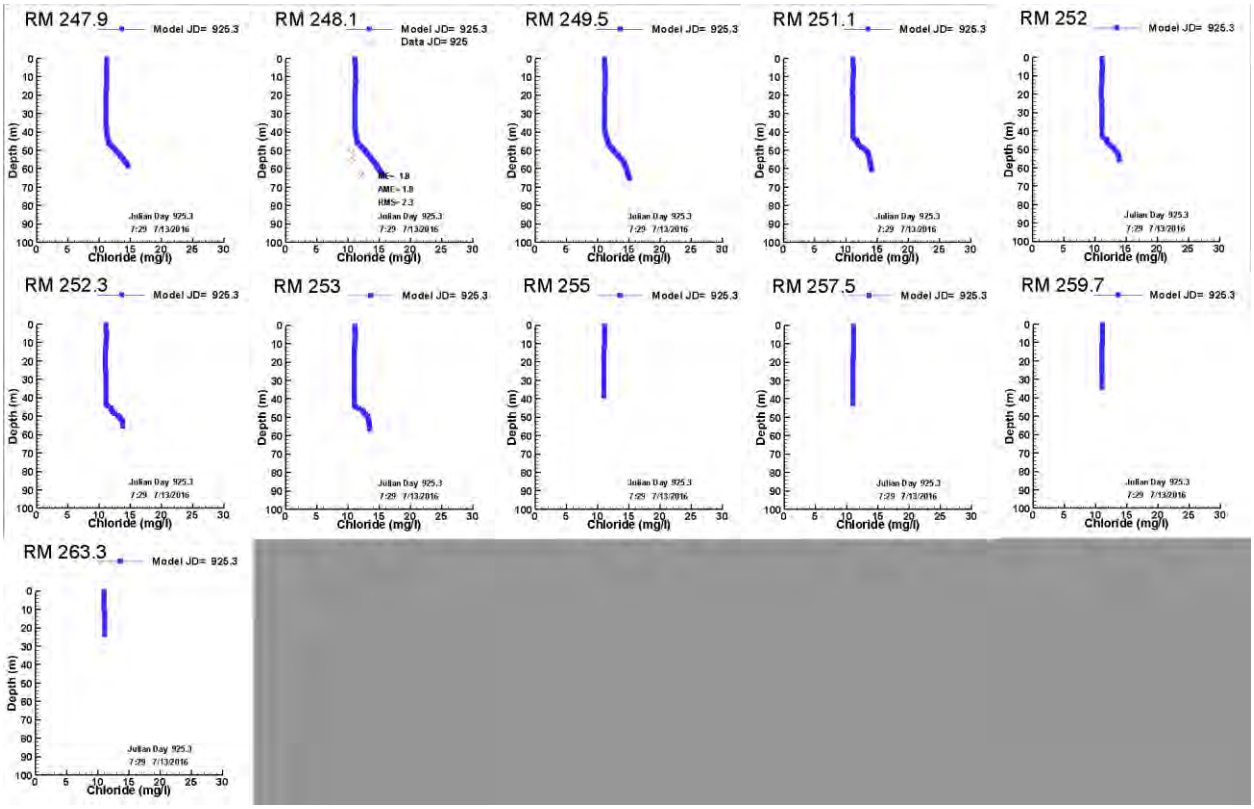


Figure 18. Vertical profiles of chloride compared with data for 7/13/2016.

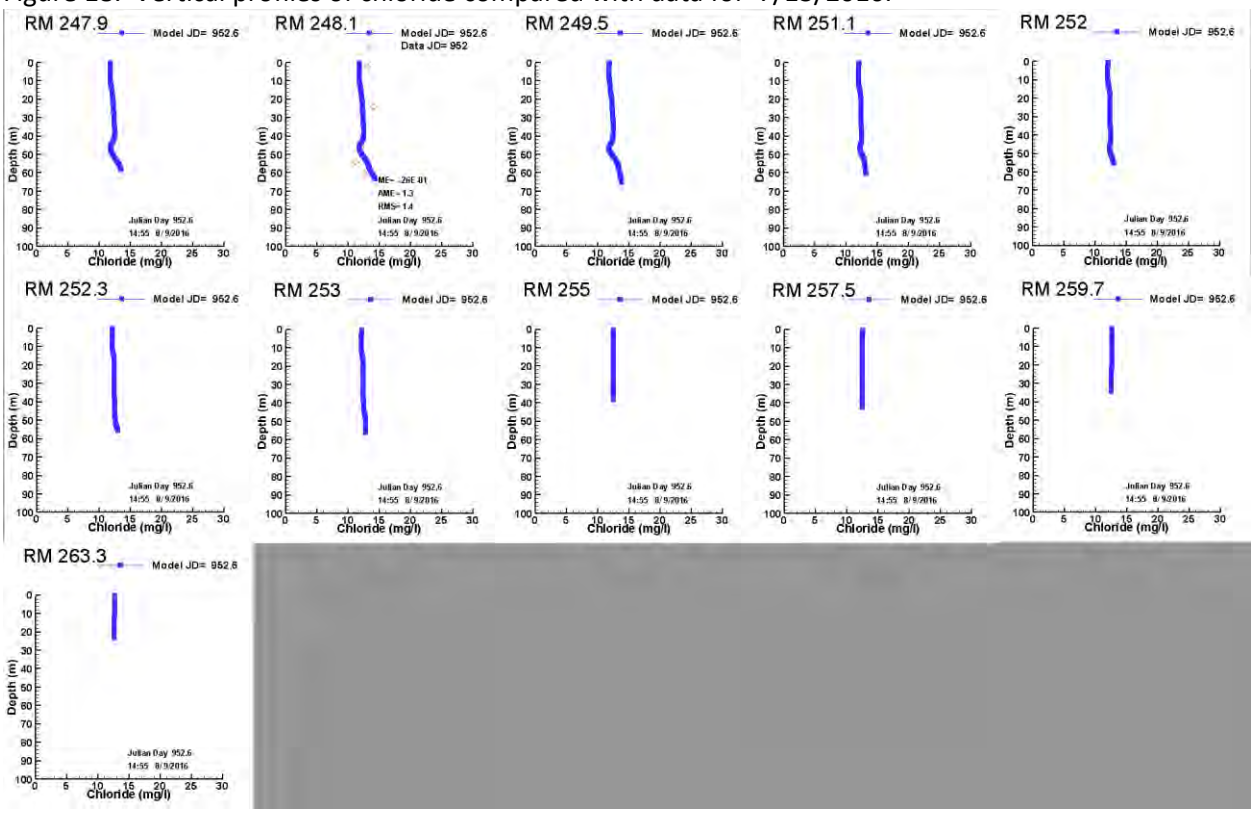


Figure 19. Vertical profiles of chloride compared with data for 8/ 9/2016.

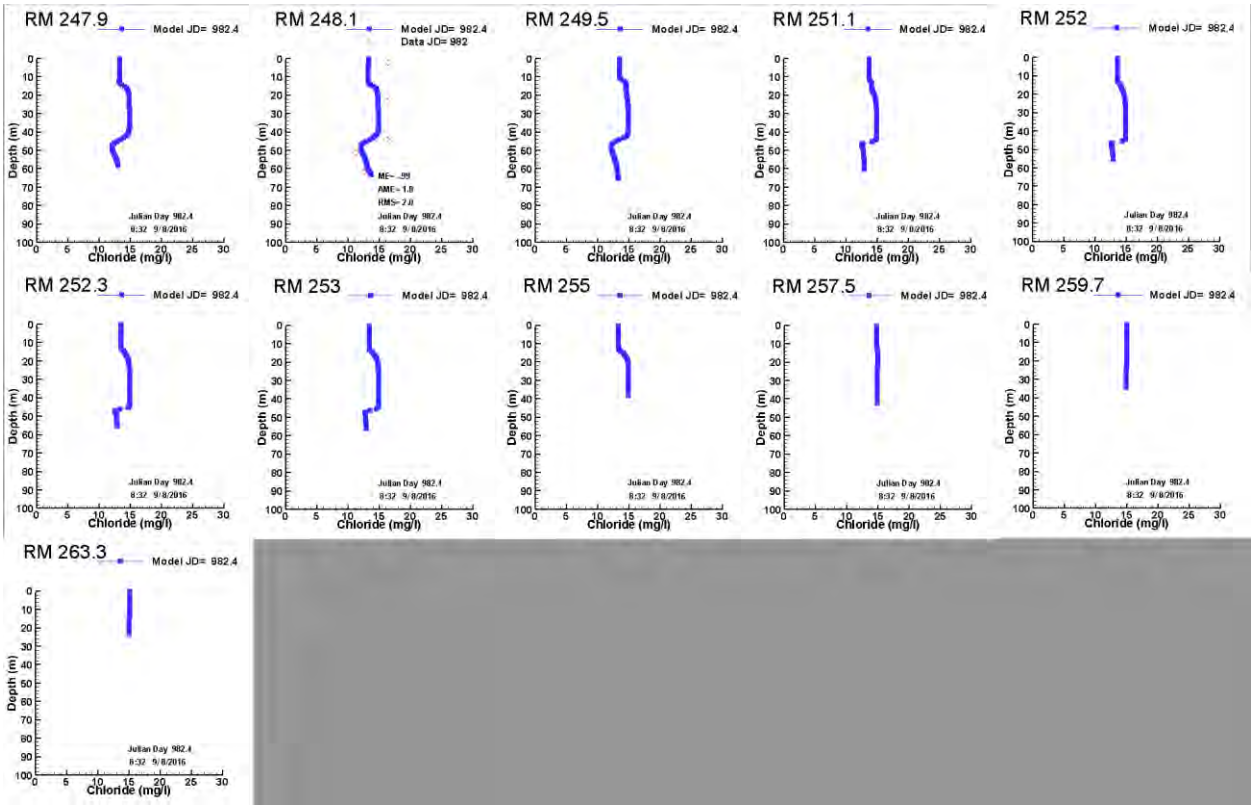


Figure 20. Vertical profiles of chloride compared with data for 9/ 8/2016.

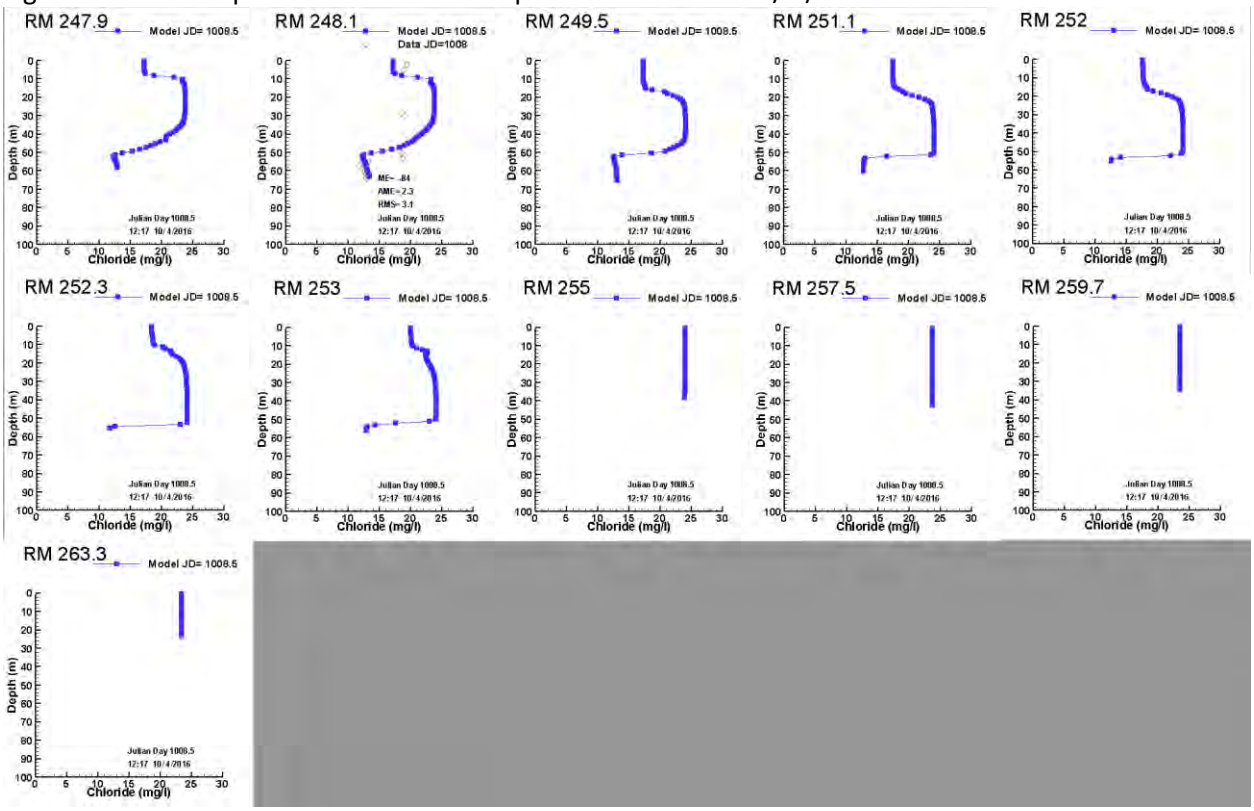


Figure 21. Vertical profiles of chloride compared with data for 10/ 4/2016.

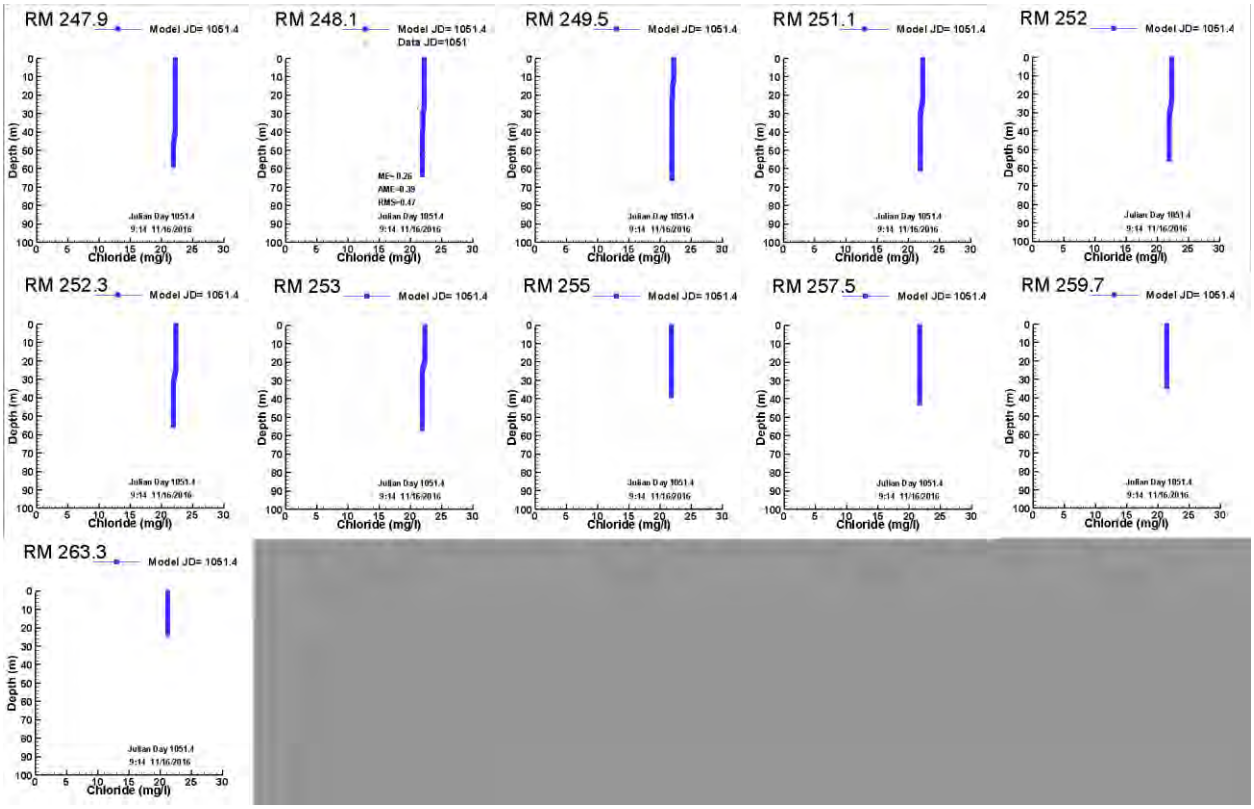


Figure 22. Vertical profiles of chloride compared with data for 11/16/2016.

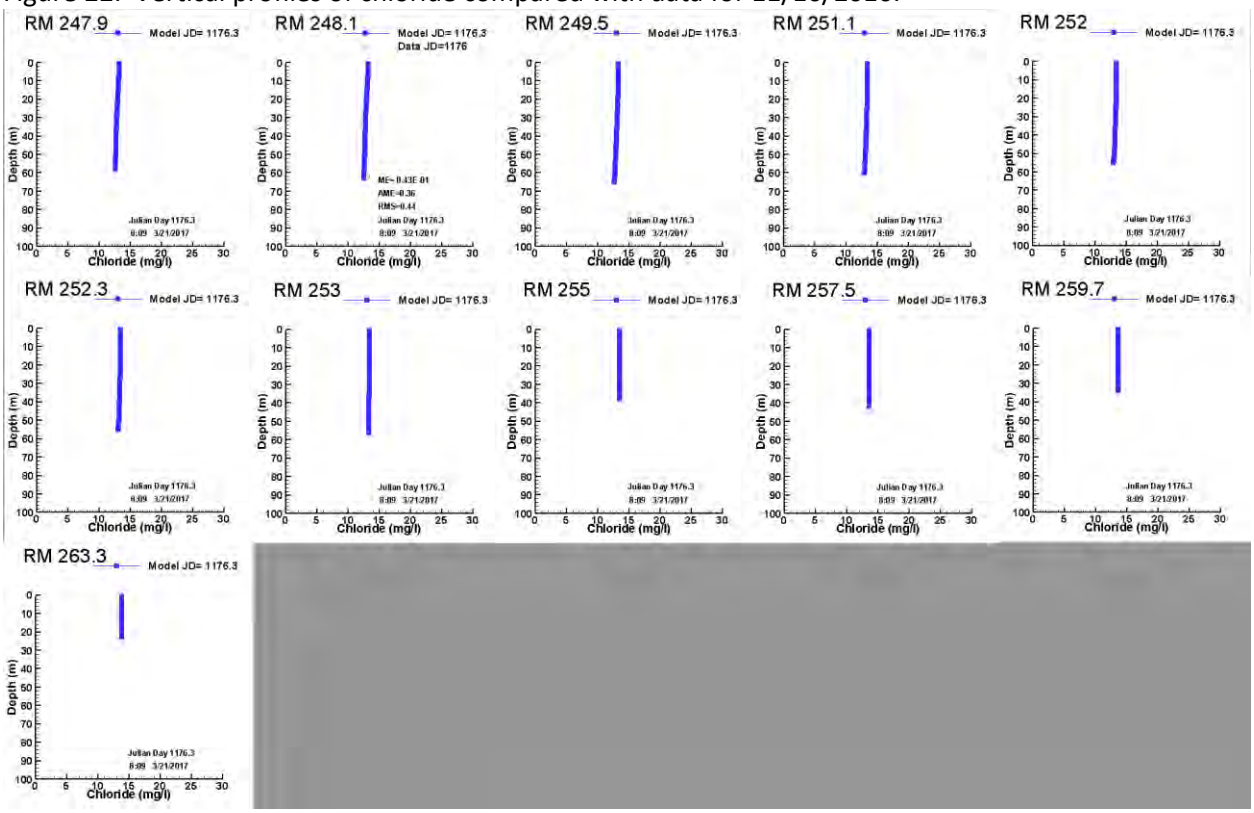


Figure 23. Vertical profiles of chloride compared with data for 3/21/2017.

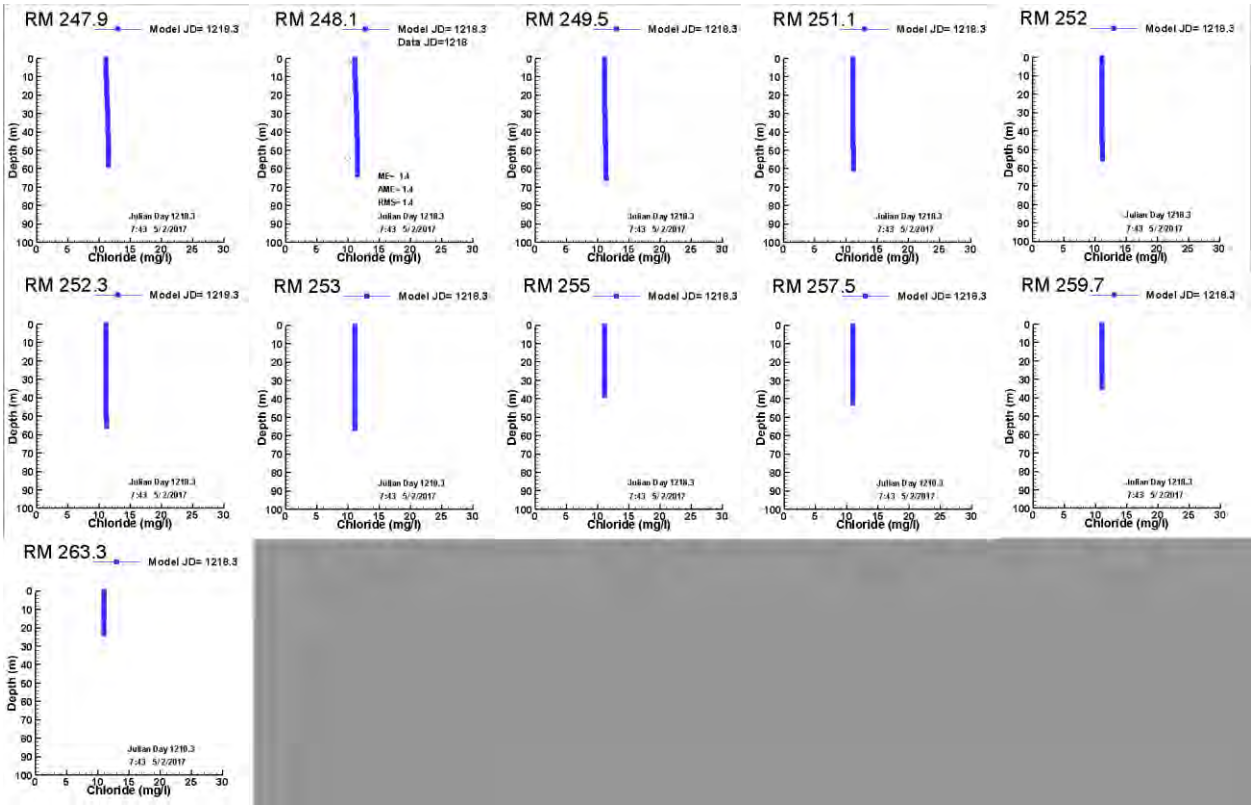


Figure 24. Vertical profiles of chloride compared with data for 5/ 2/2017.

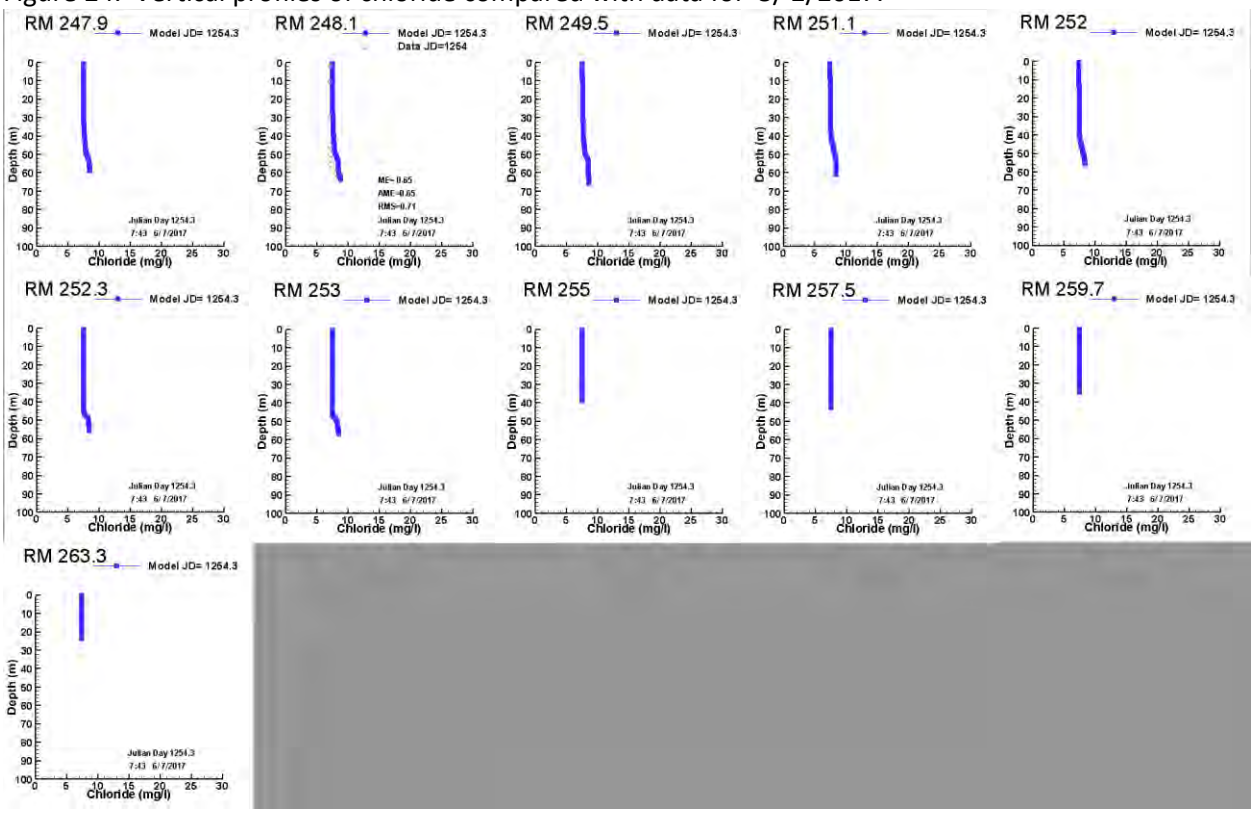


Figure 25. Vertical profiles of chloride compared with data for 6/ 7/2017.

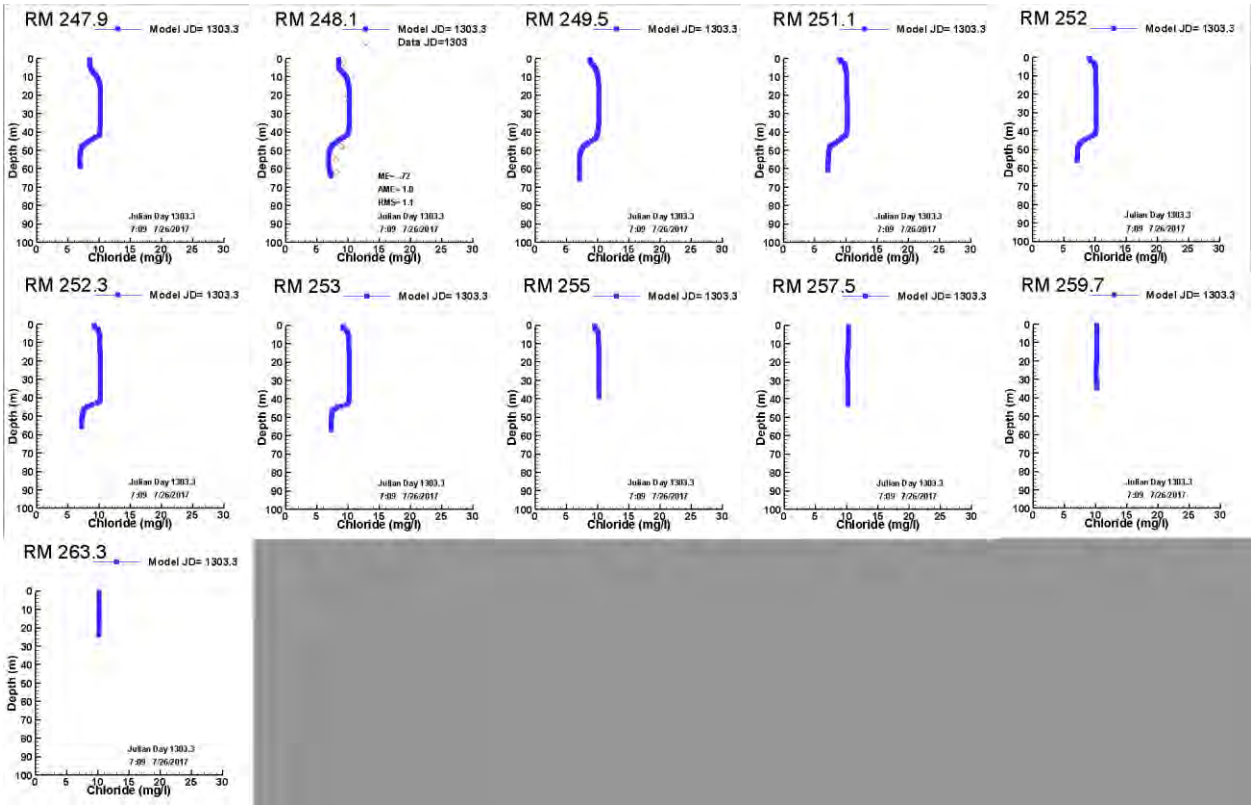


Figure 26. Vertical profiles of chloride compared with data for 7/26/2017.

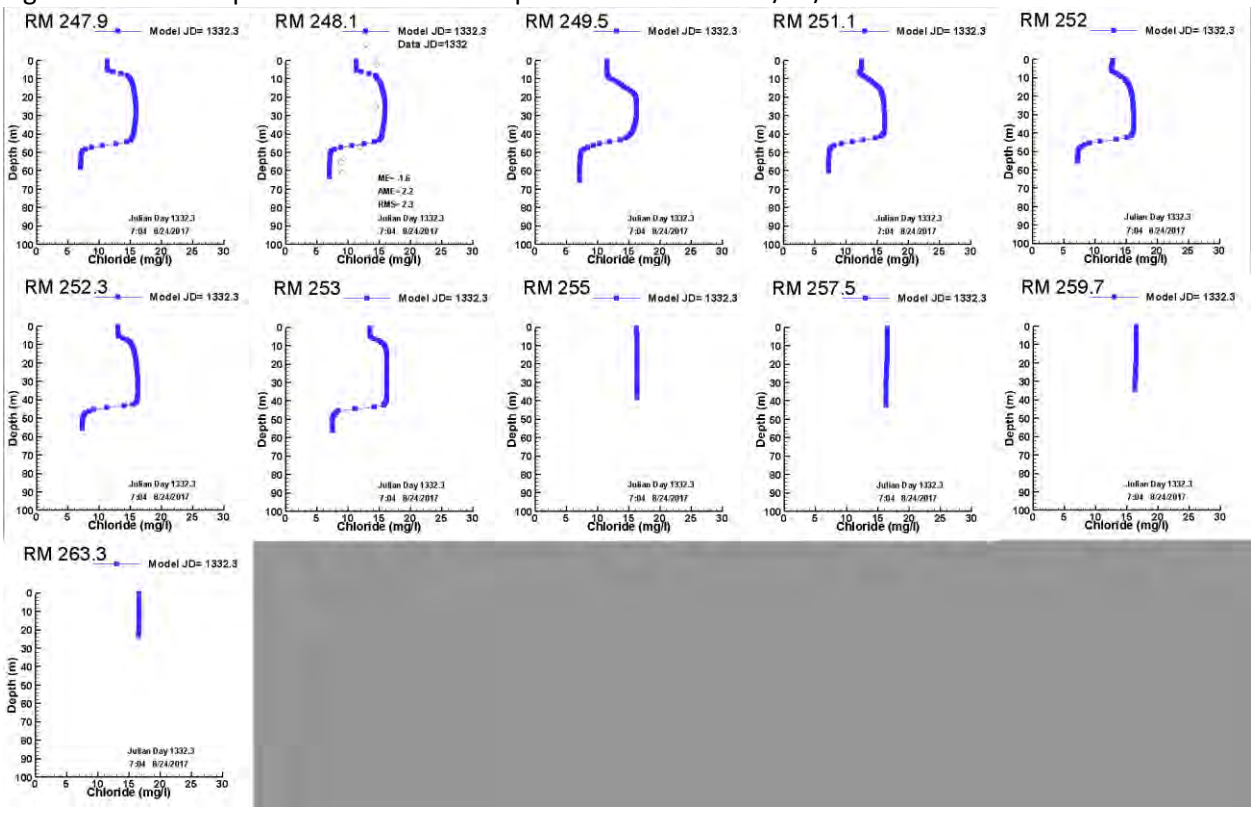


Figure 27. Vertical profiles of chloride compared with data for 8/24/2017.

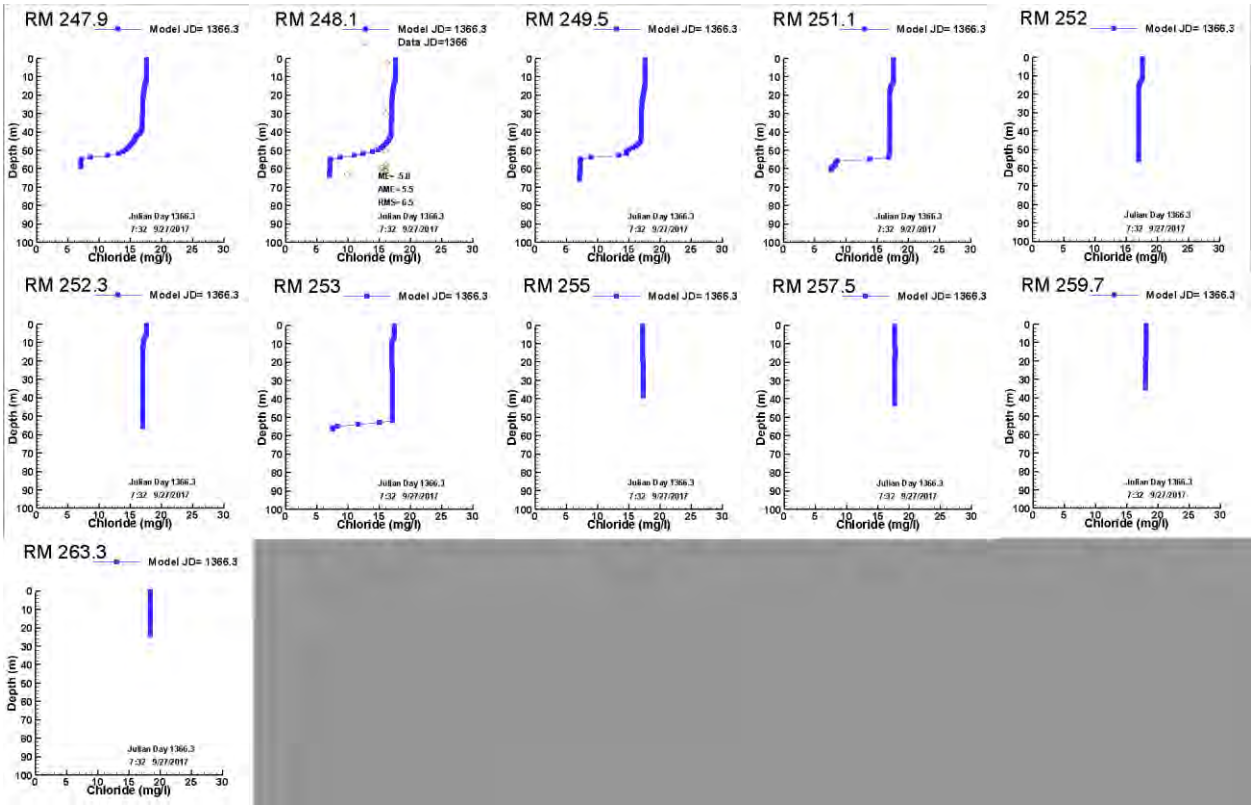


Figure 28. Vertical profiles of chloride compared with data for 9/27/2017.

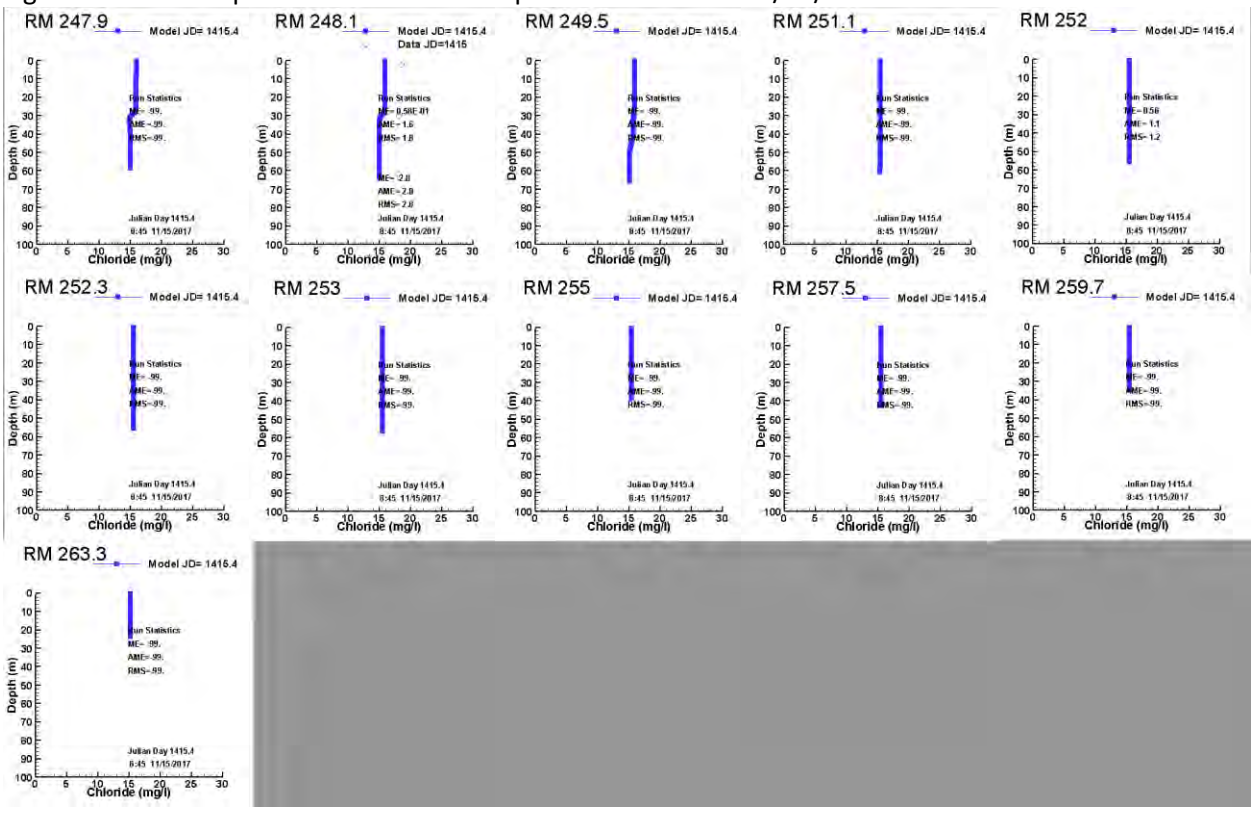


Figure 29. Vertical profiles of chloride compared with data for 11/15/2017.

Hydrogen Sulfide

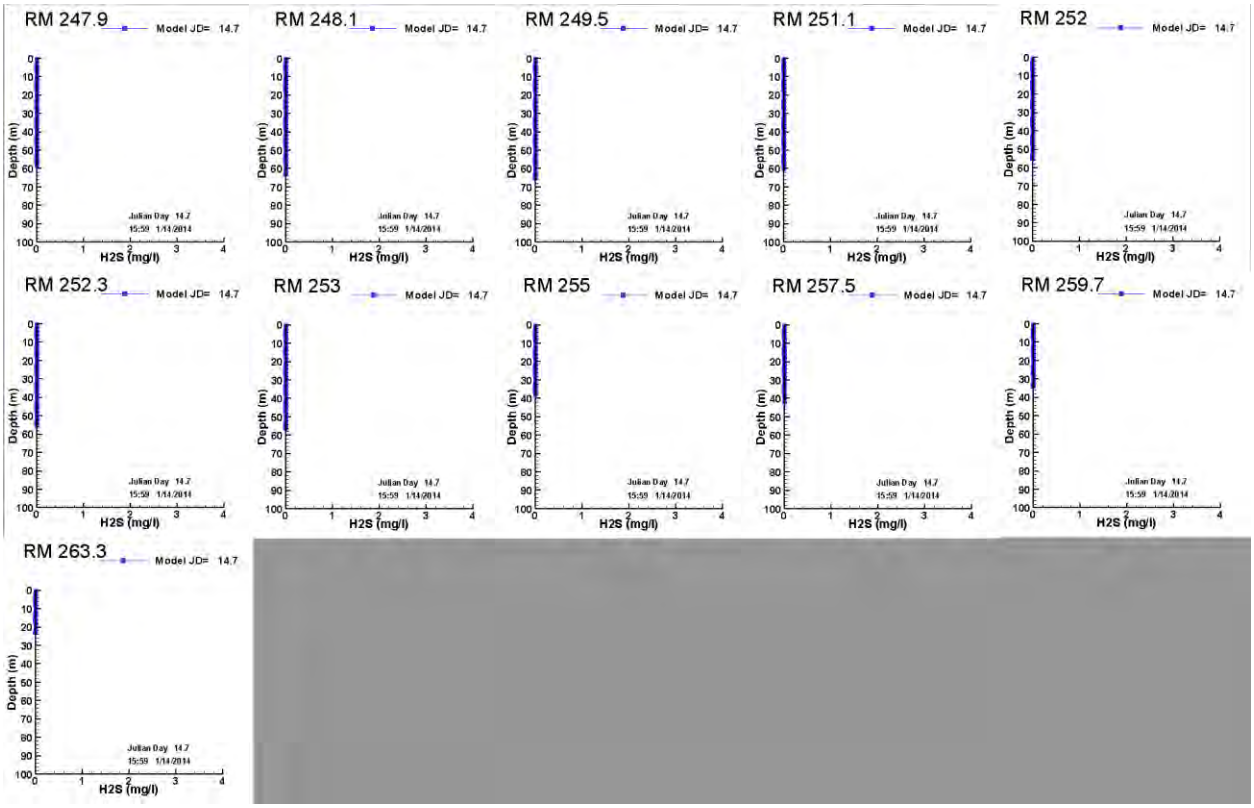


Figure 30. Vertical profiles of hydrogen sulfide compared with data for 1/14/2014.

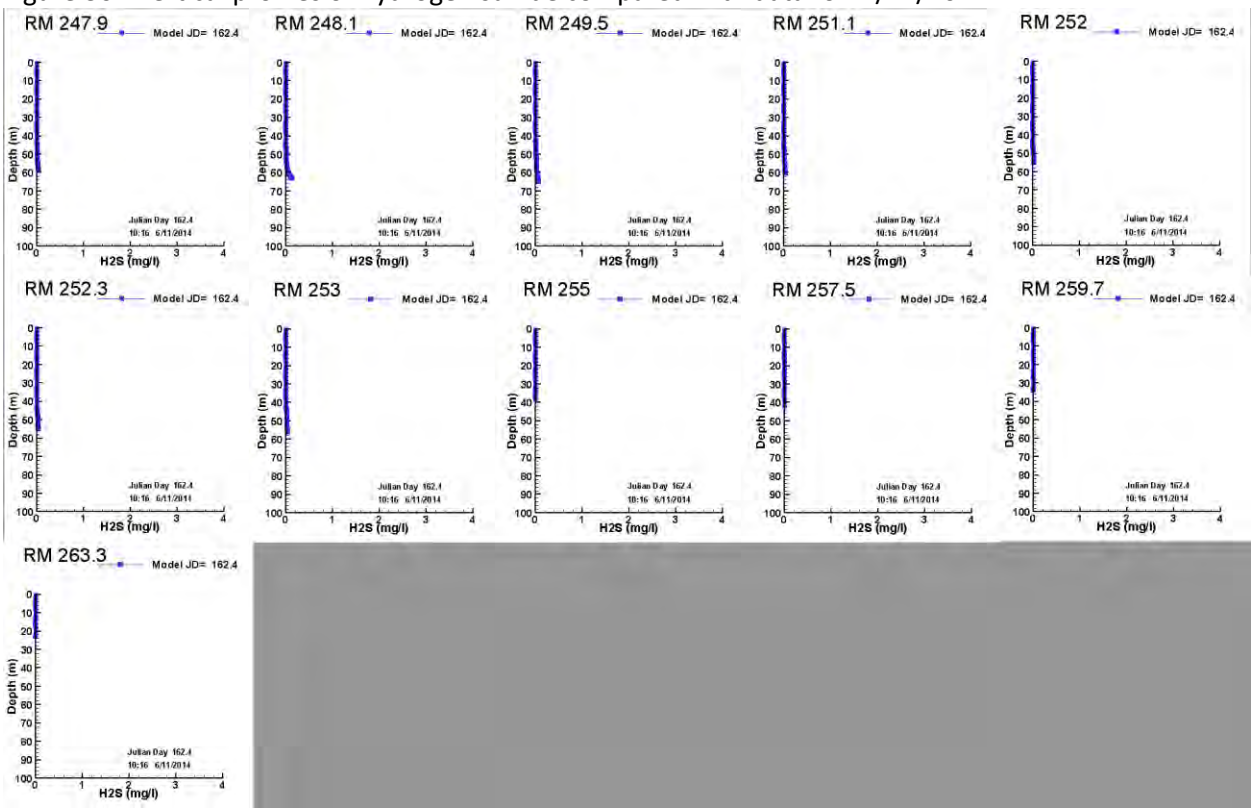


Figure 31. Vertical profiles of hydrogen sulfide compared with data for 6/11/2014.

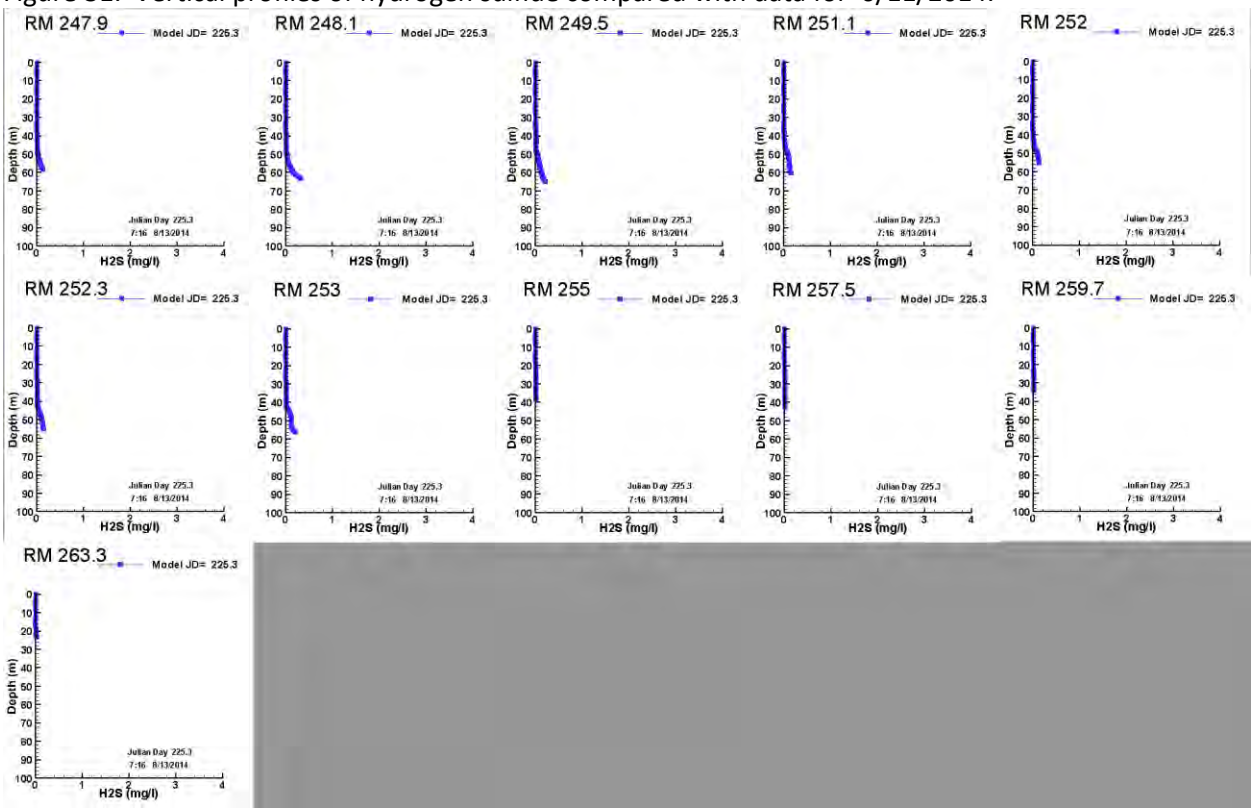


Figure 32. Vertical profiles of hydrogen sulfide compared with data for 8/13/2014.

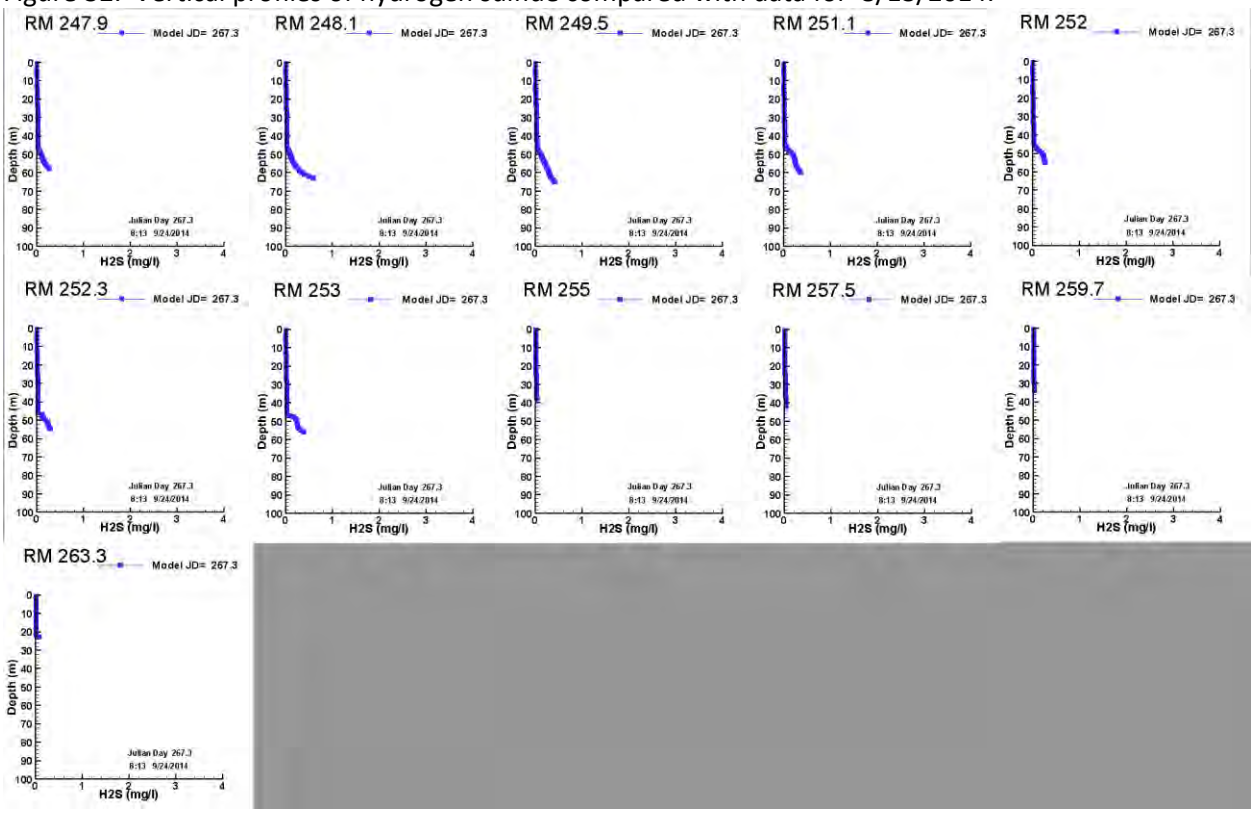


Figure 33. Vertical profiles of hydrogen sulfide compared with data for 9/24/2014.

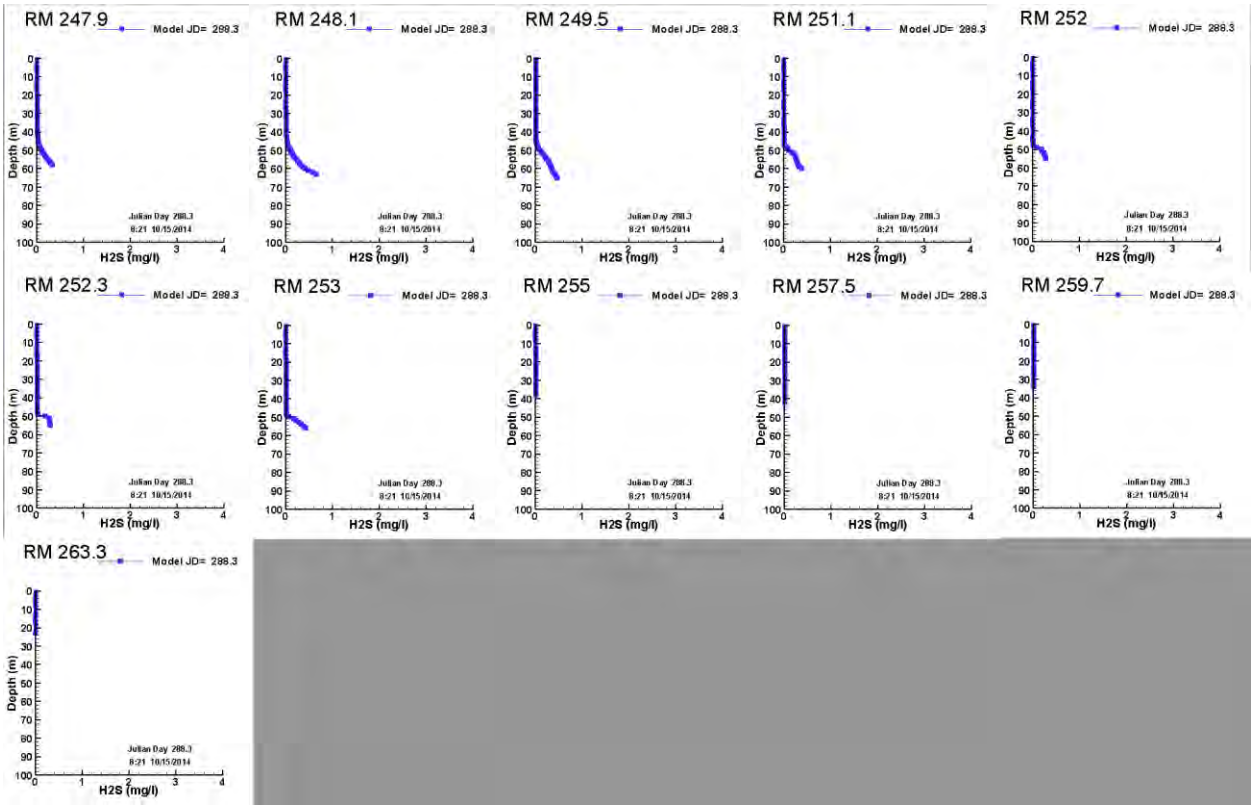


Figure 34. Vertical profiles of hydrogen sulfide compared with data for 10/15/2014.

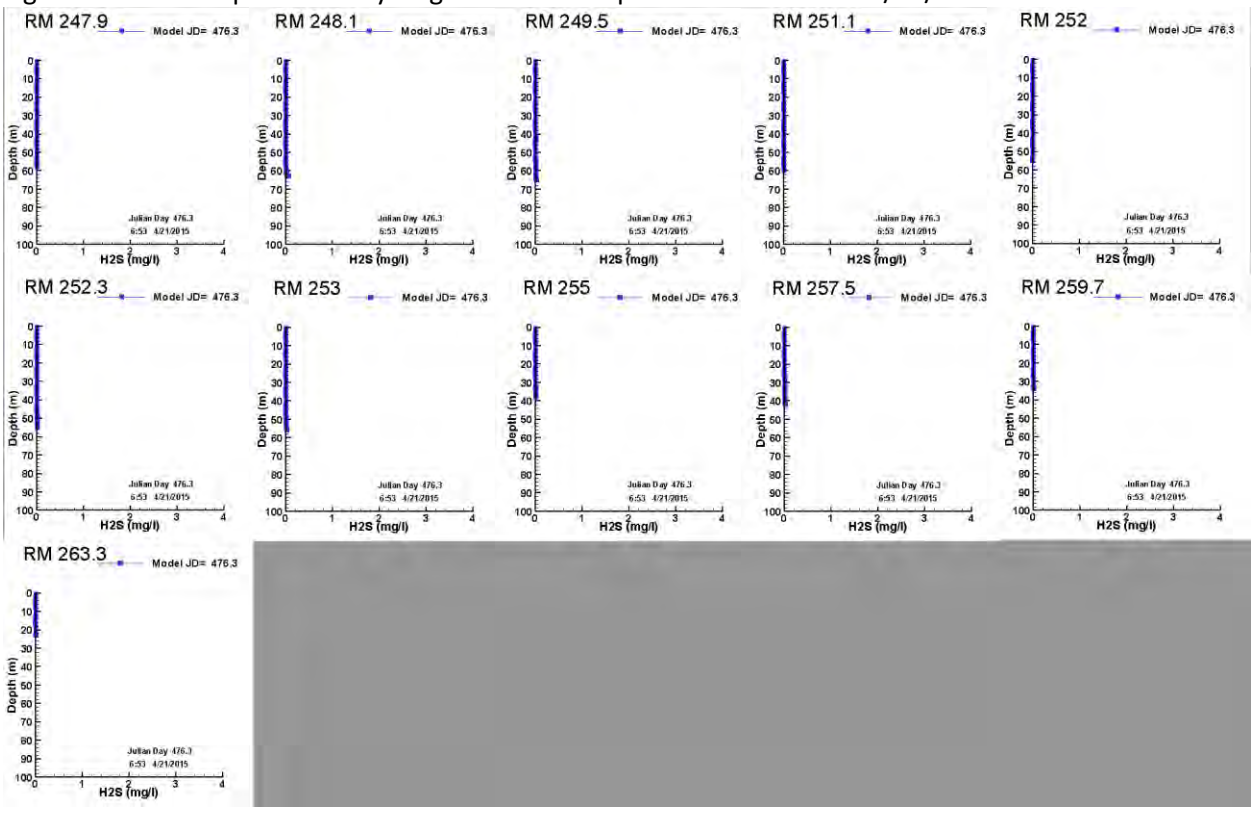


Figure 35. Vertical profiles of hydrogen sulfide compared with data for 4/21/2015.

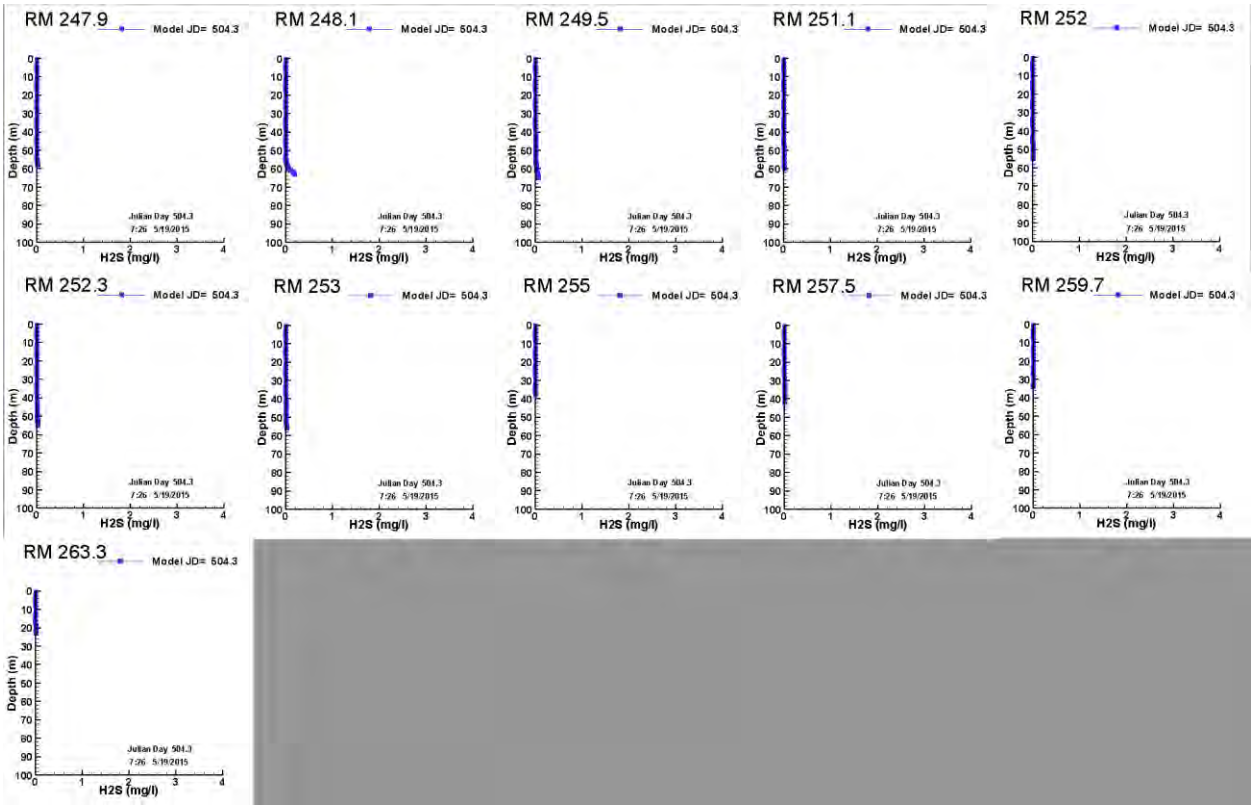


Figure 36. Vertical profiles of hydrogen sulfide compared with data for 5/19/2015.

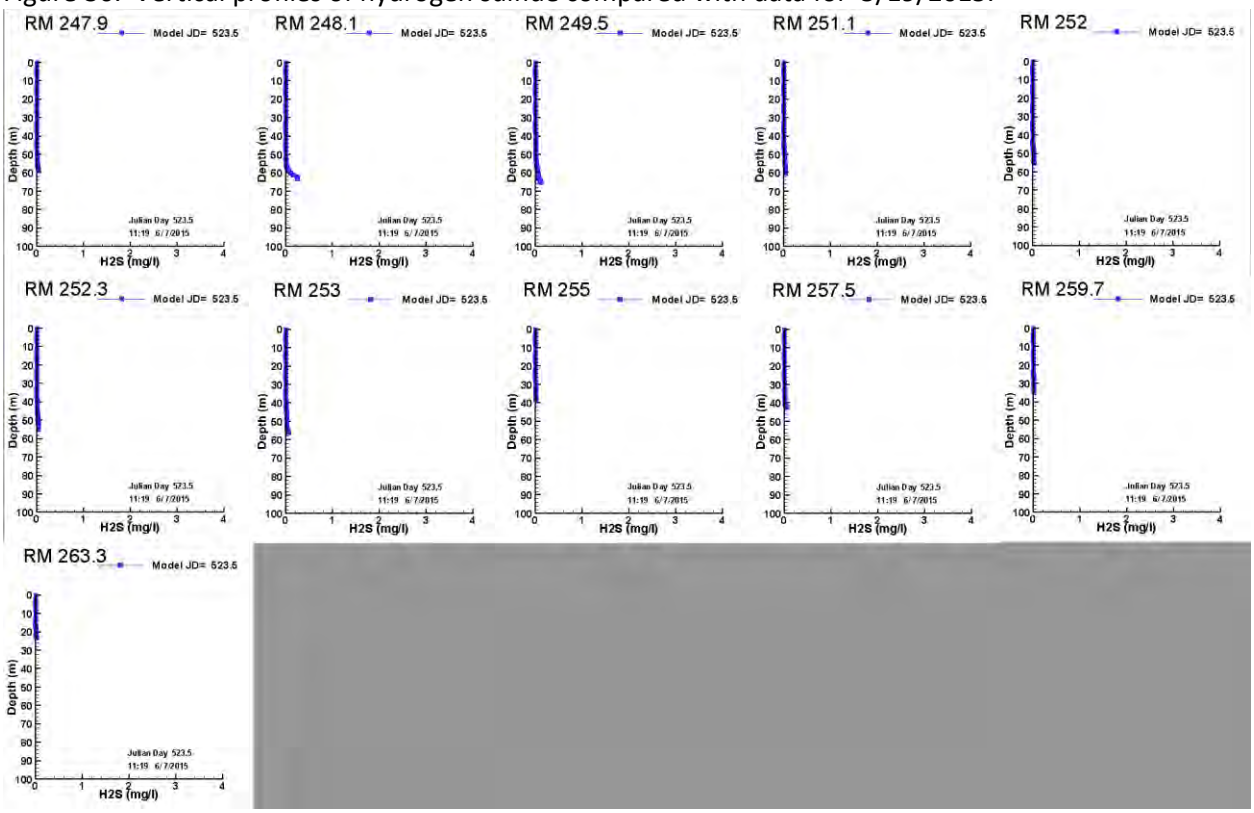


Figure 37. Vertical profiles of hydrogen sulfide compared with data for 6/ 7/2015.

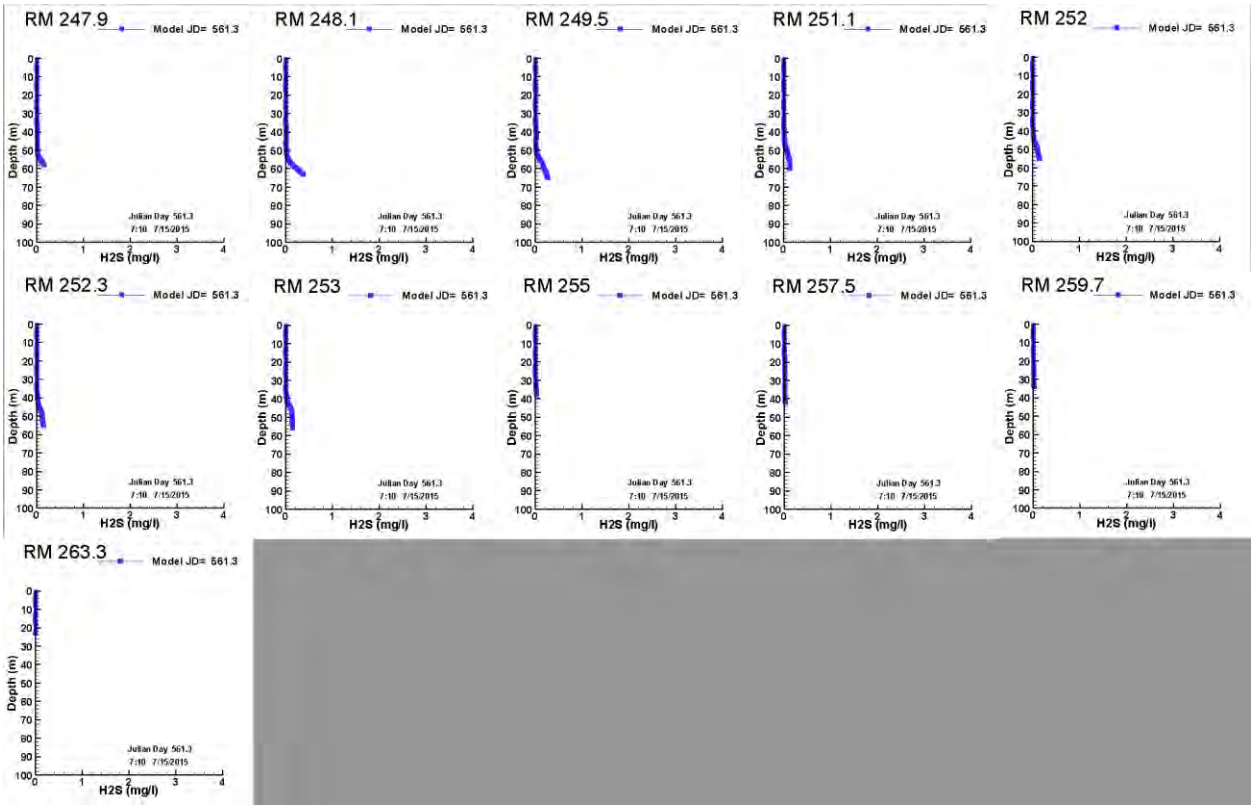


Figure 38. Vertical profiles of hydrogen sulfide compared with data for 7/15/2015.

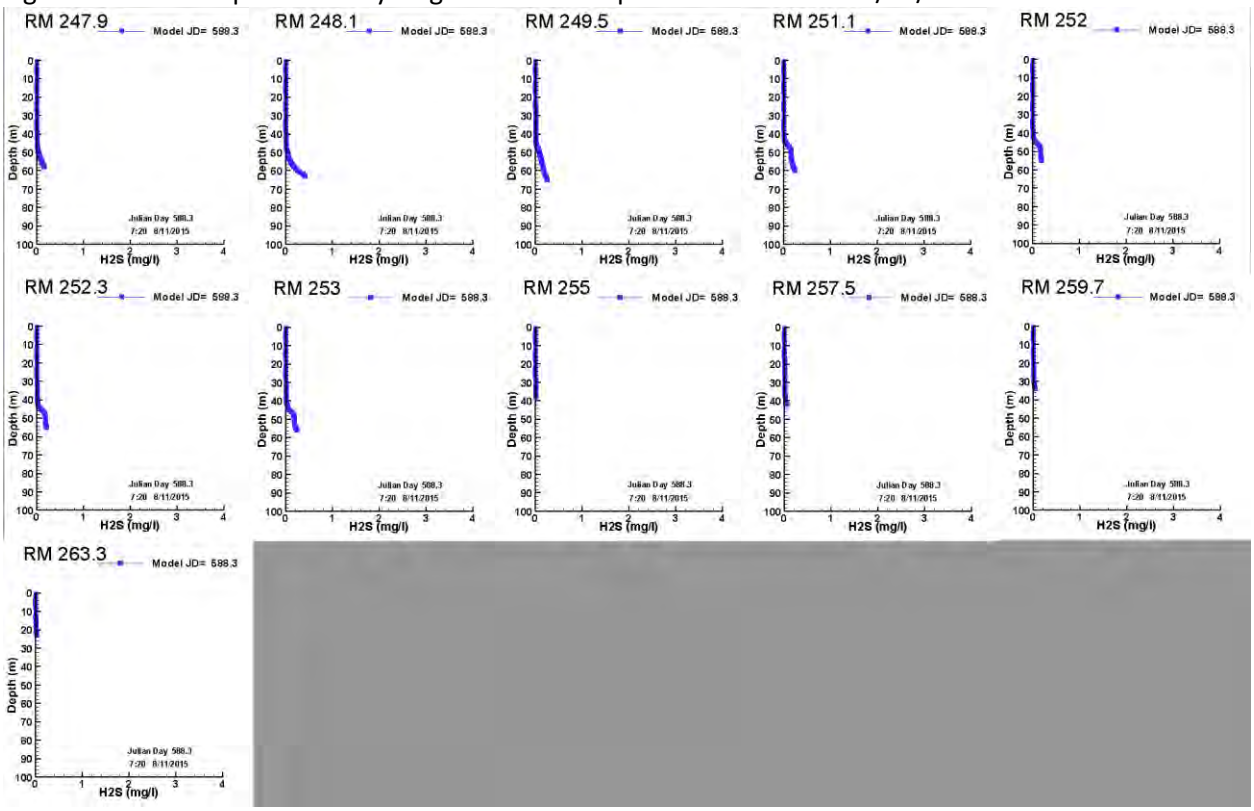


Figure 39. Vertical profiles of hydrogen sulfide compared with data for 8/11/2015.

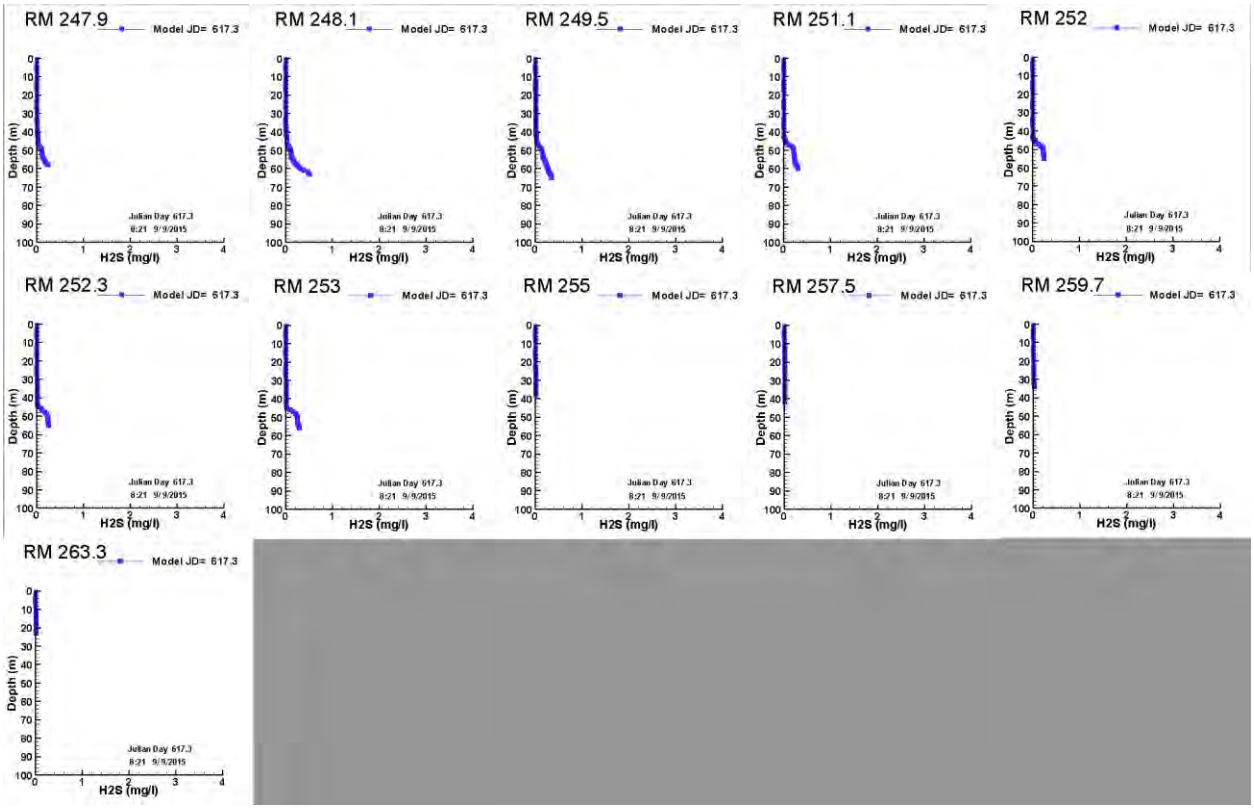


Figure 40. Vertical profiles of hydrogen sulfide compared with data for 9/ 9/2015.

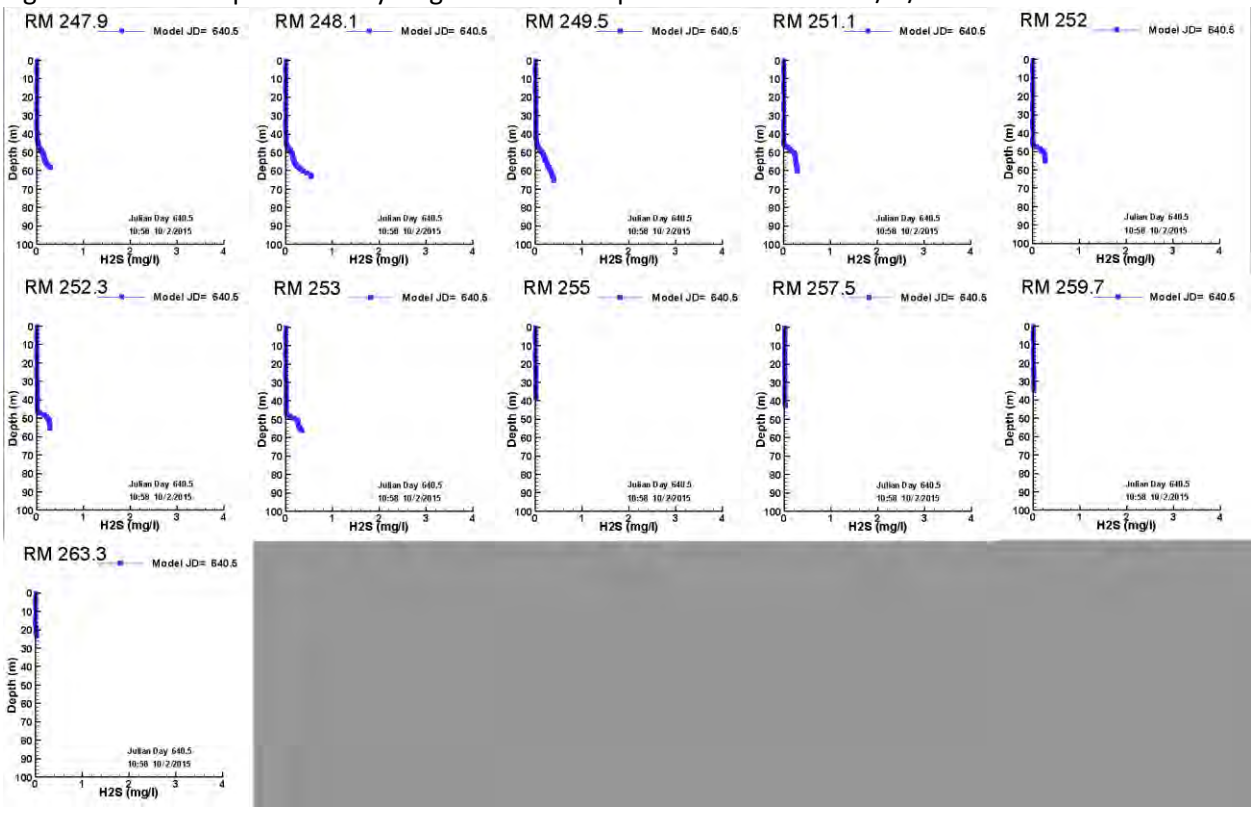


Figure 41. Vertical profiles of hydrogen sulfide compared with data for 10/ 2/2015.

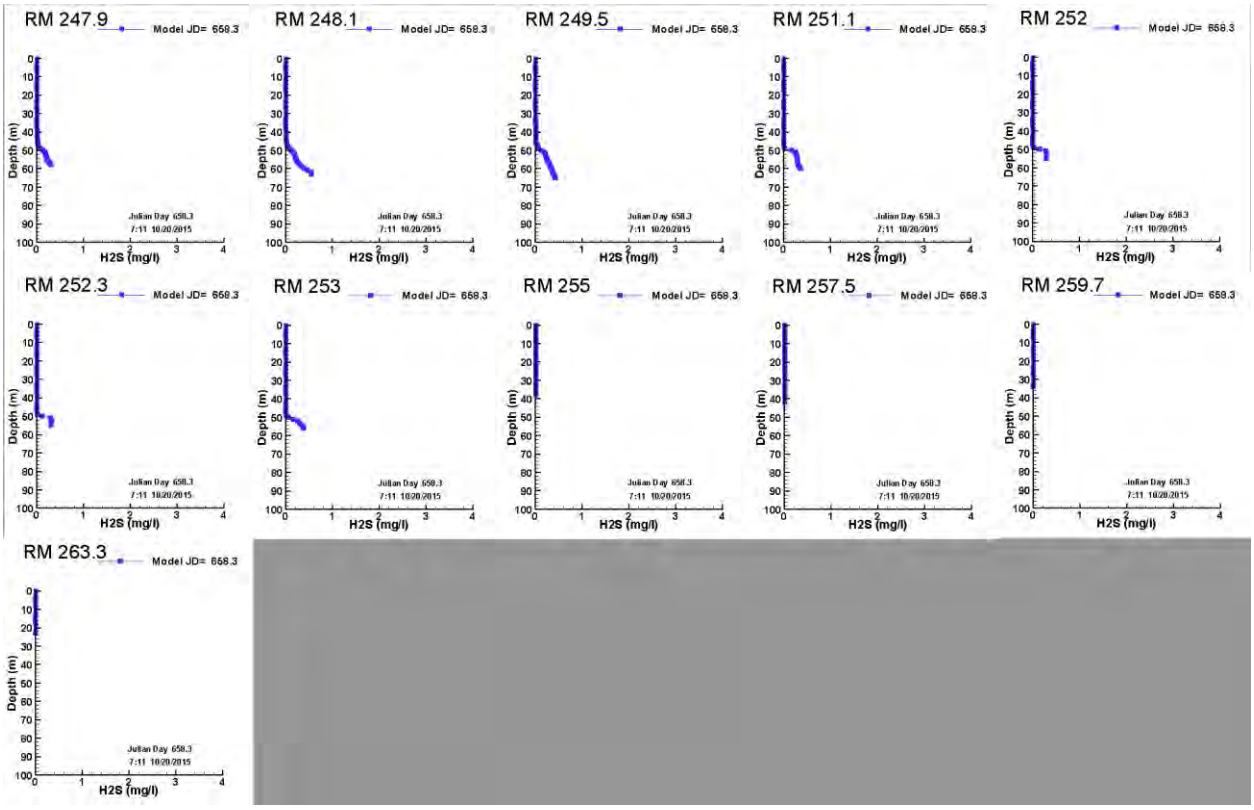


Figure 42. Vertical profiles of hydrogen sulfide compared with data for 10/20/2015.

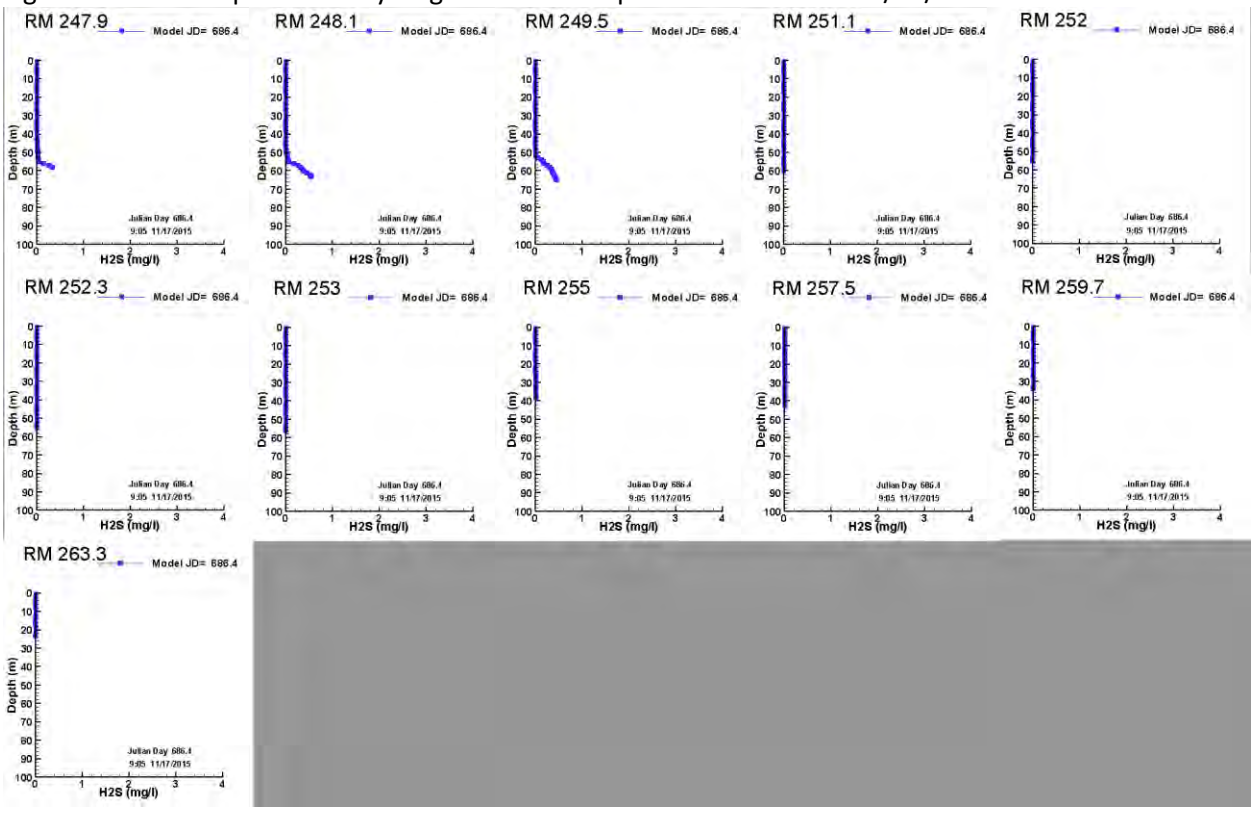


Figure 43. Vertical profiles of hydrogen sulfide compared with data for 11/17/2015.

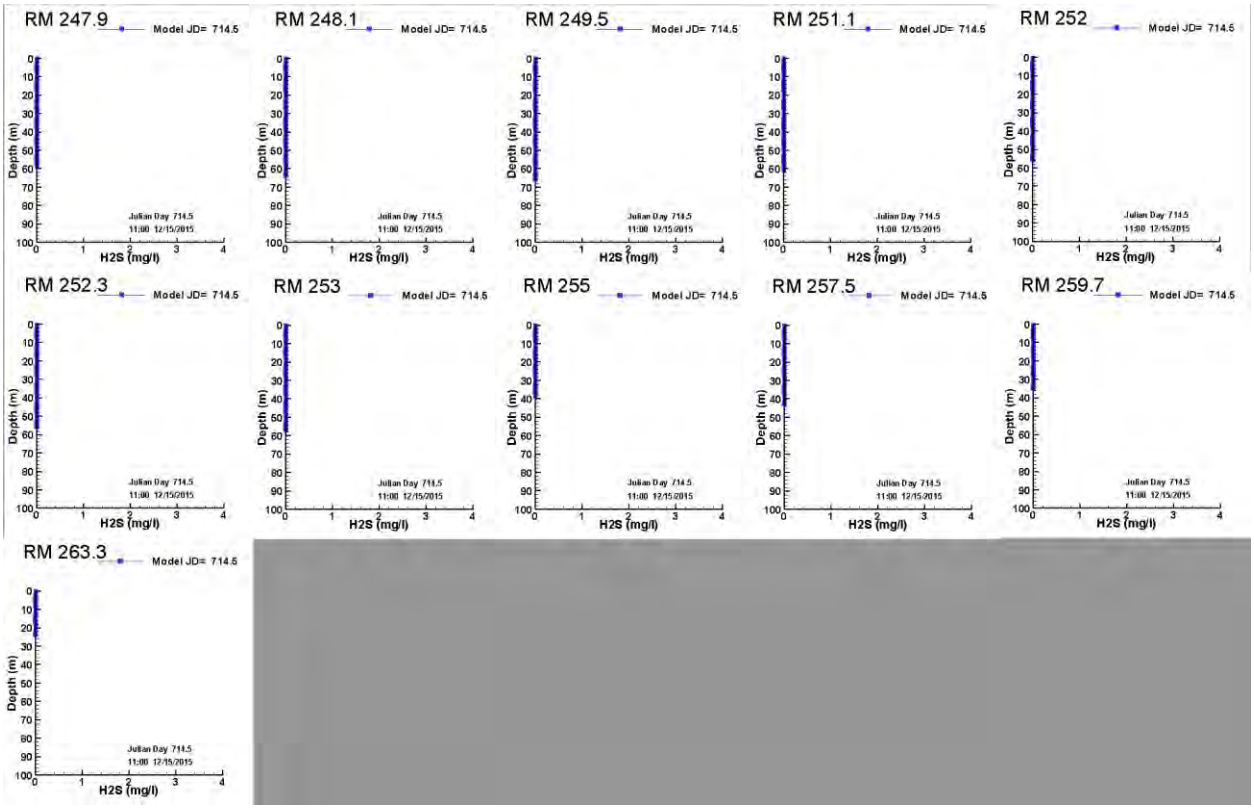


Figure 44. Vertical profiles of hydrogen sulfide compared with data for 12/15/2015.

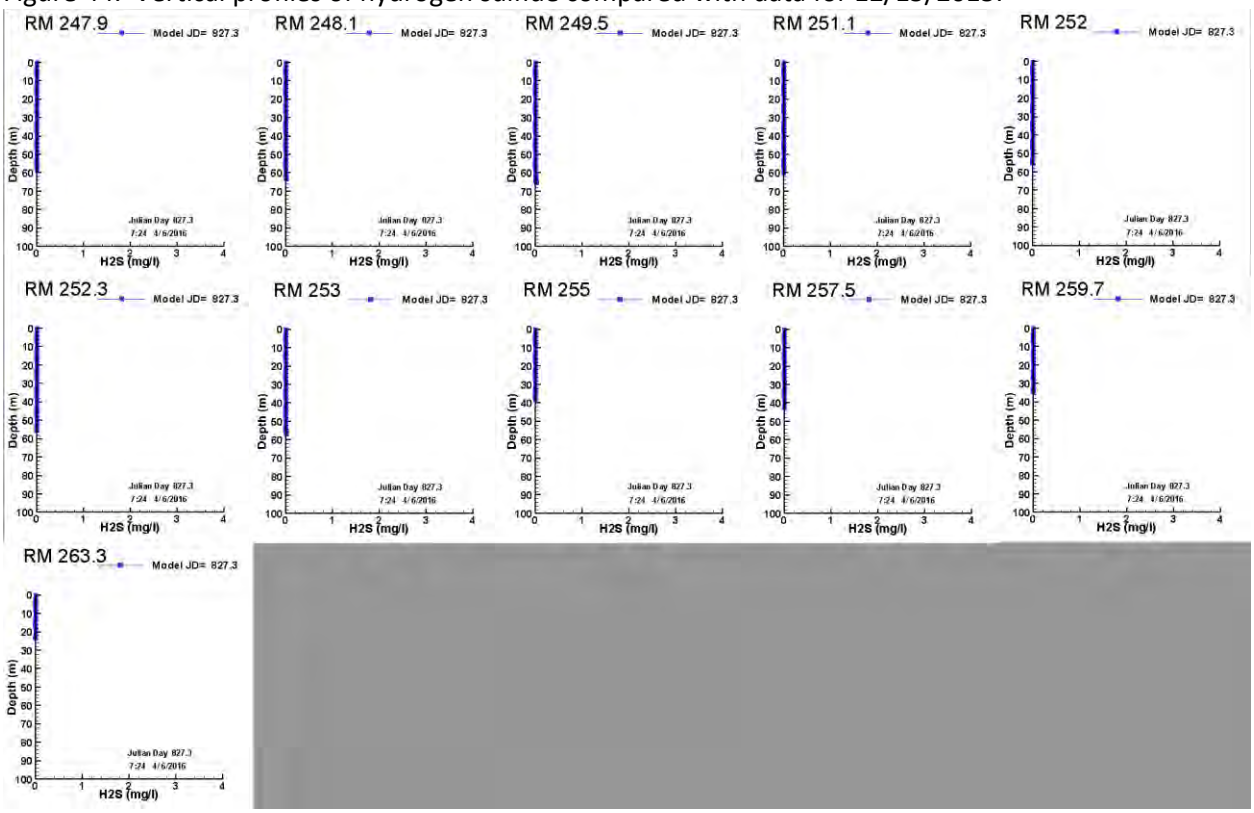


Figure 45. Vertical profiles of hydrogen sulfide compared with data for 4/ 6/2016.

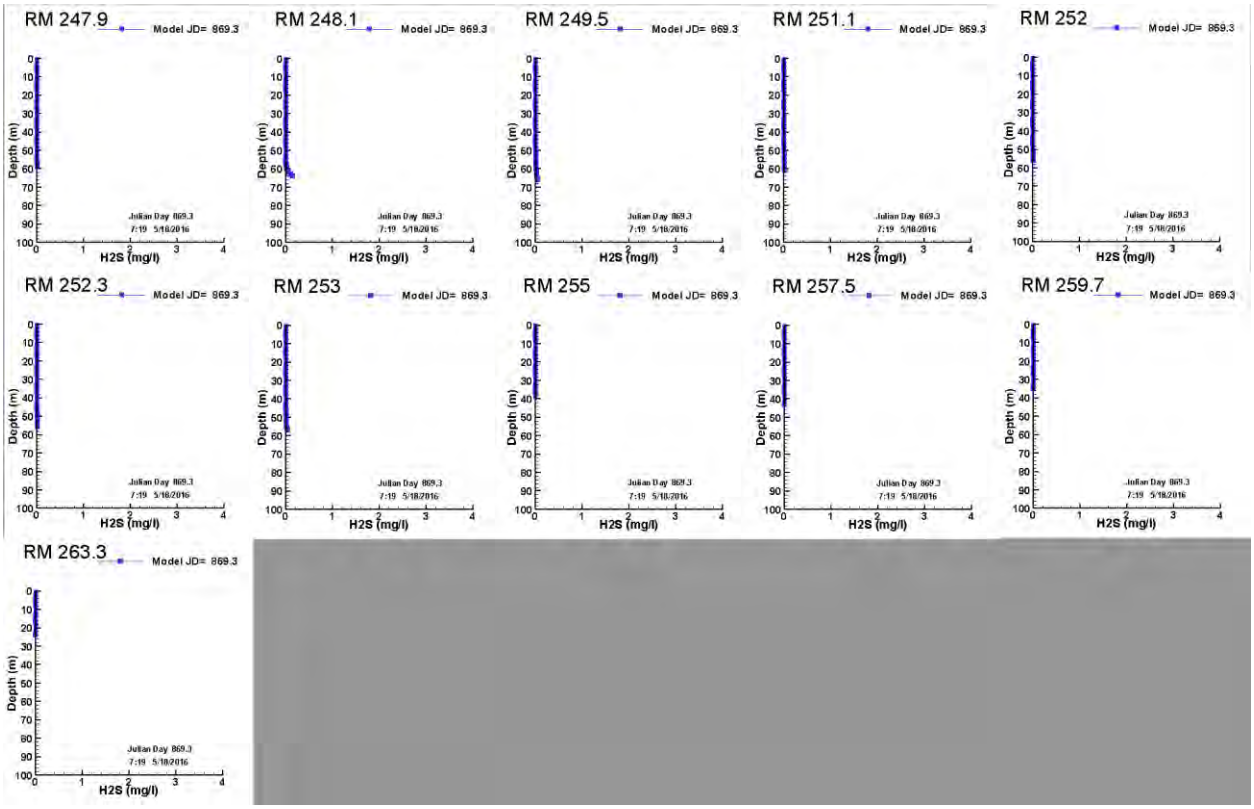


Figure 46. Vertical profiles of hydrogen sulfide compared with data for 5/18/2016.

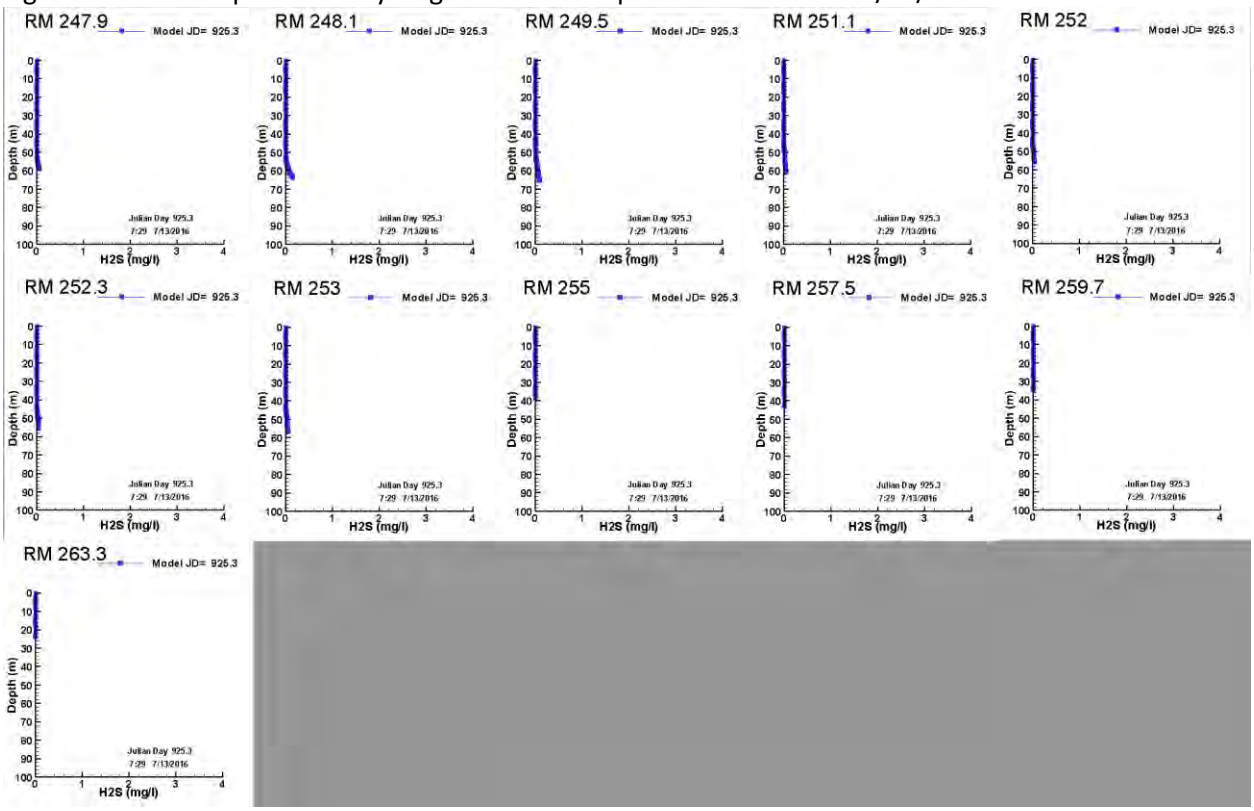


Figure 47. Vertical profiles of hydrogen sulfide compared with data for 7/13/2016.

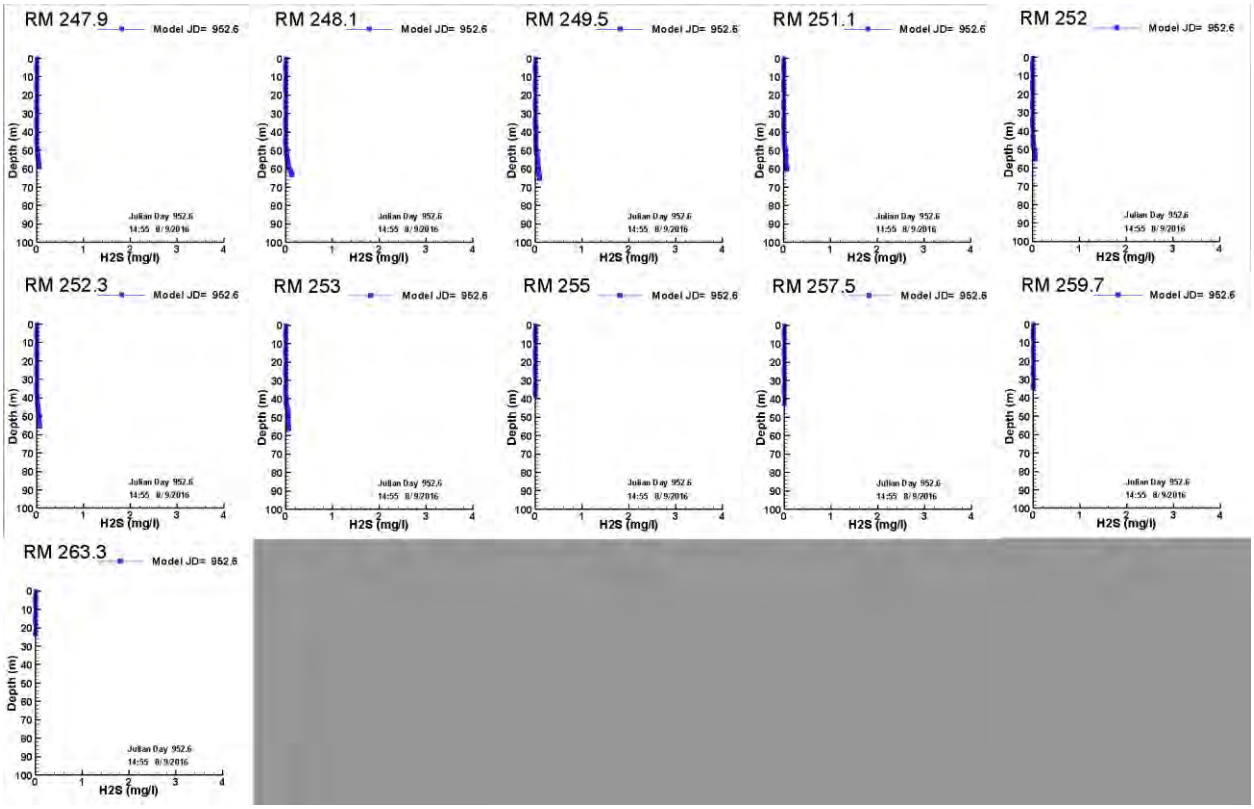


Figure 48. Vertical profiles of hydrogen sulfide compared with data for 8/ 9/2016.

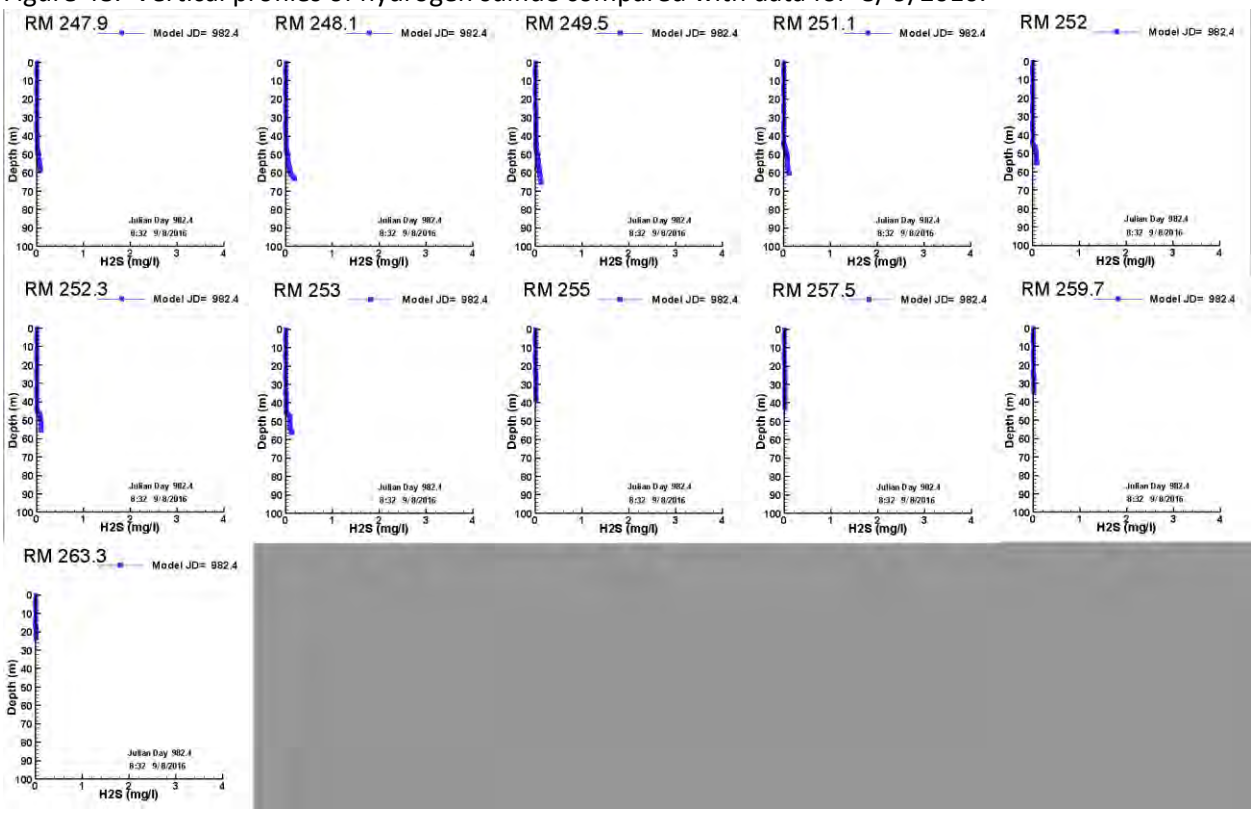


Figure 49. Vertical profiles of hydrogen sulfide compared with data for 9/ 8/2016.

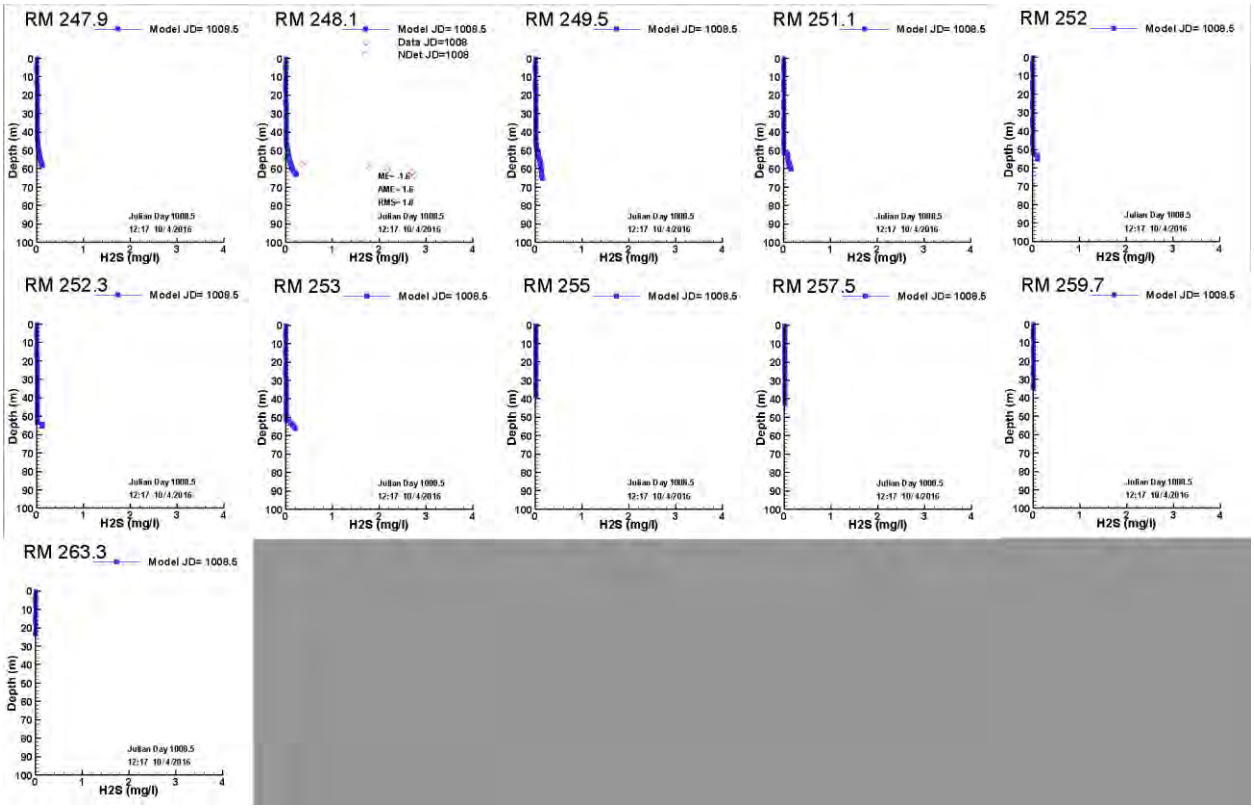


Figure 50. Vertical profiles of hydrogen sulfide compared with data for 10/ 4/2016.

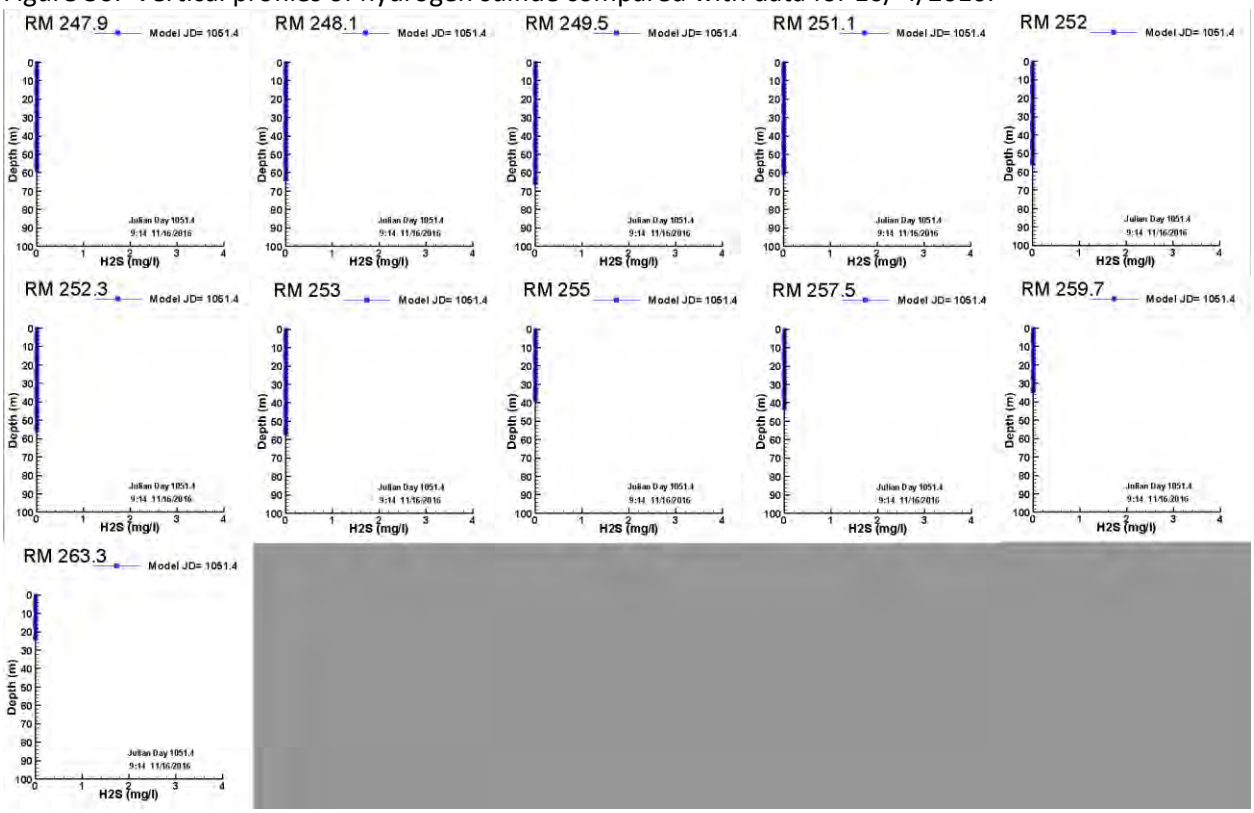


Figure 51. Vertical profiles of hydrogen sulfide compared with data for 11/16/2016.

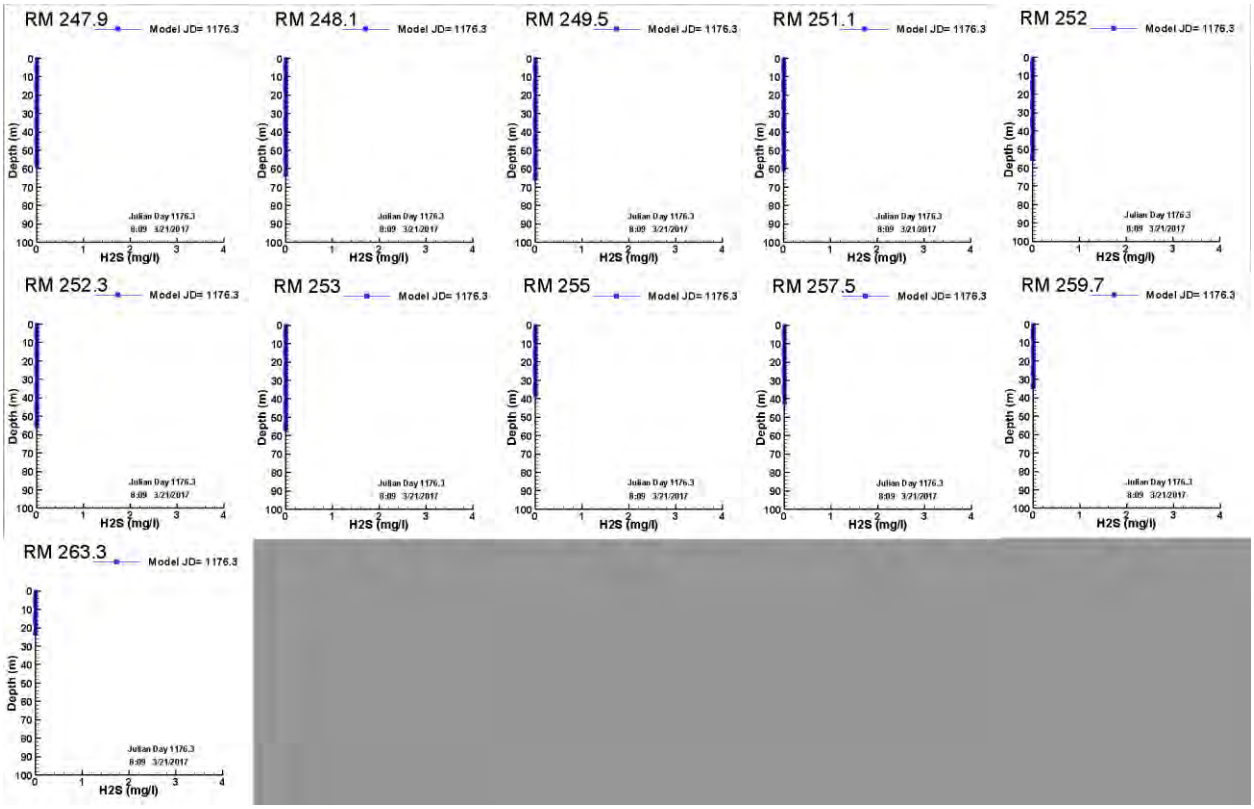


Figure 52. Vertical profiles of hydrogen sulfide compared with data for 3/21/2017.

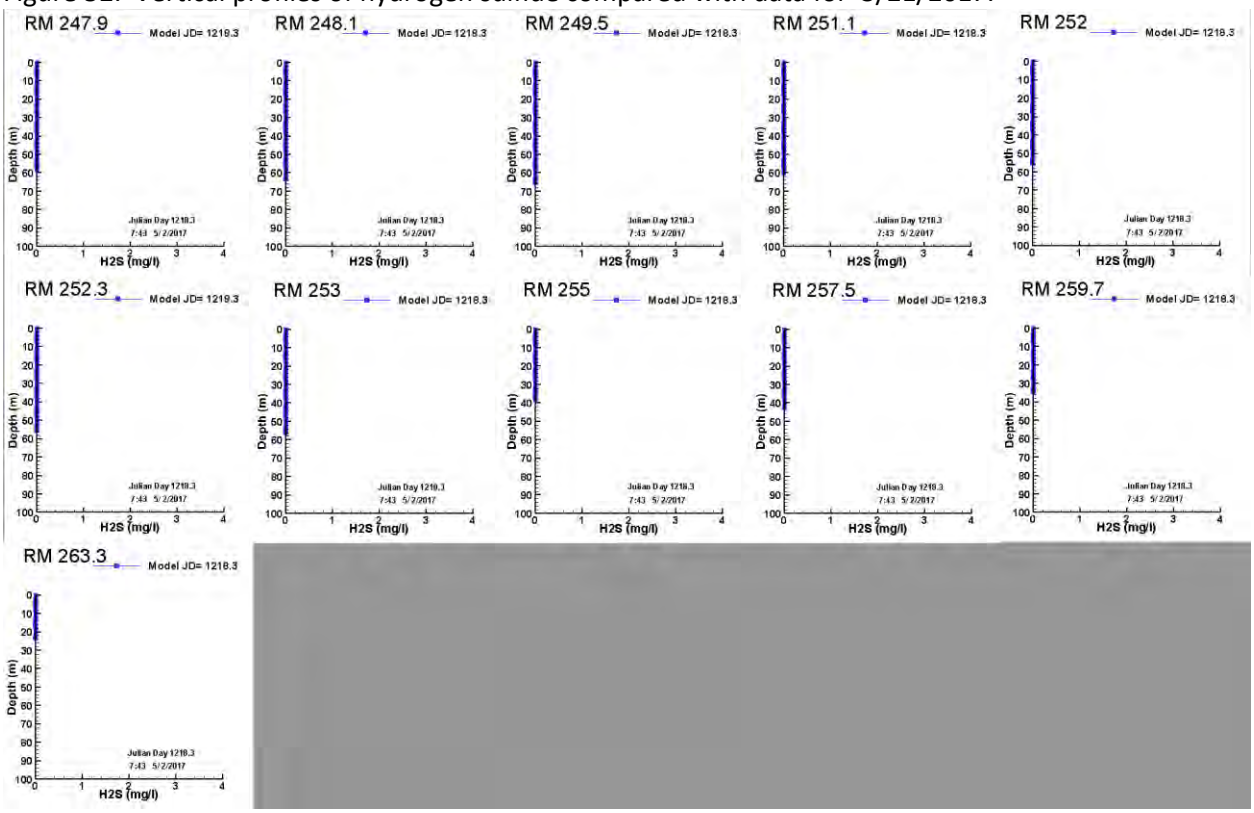


Figure 53. Vertical profiles of hydrogen sulfide compared with data for 5/ 2/2017.

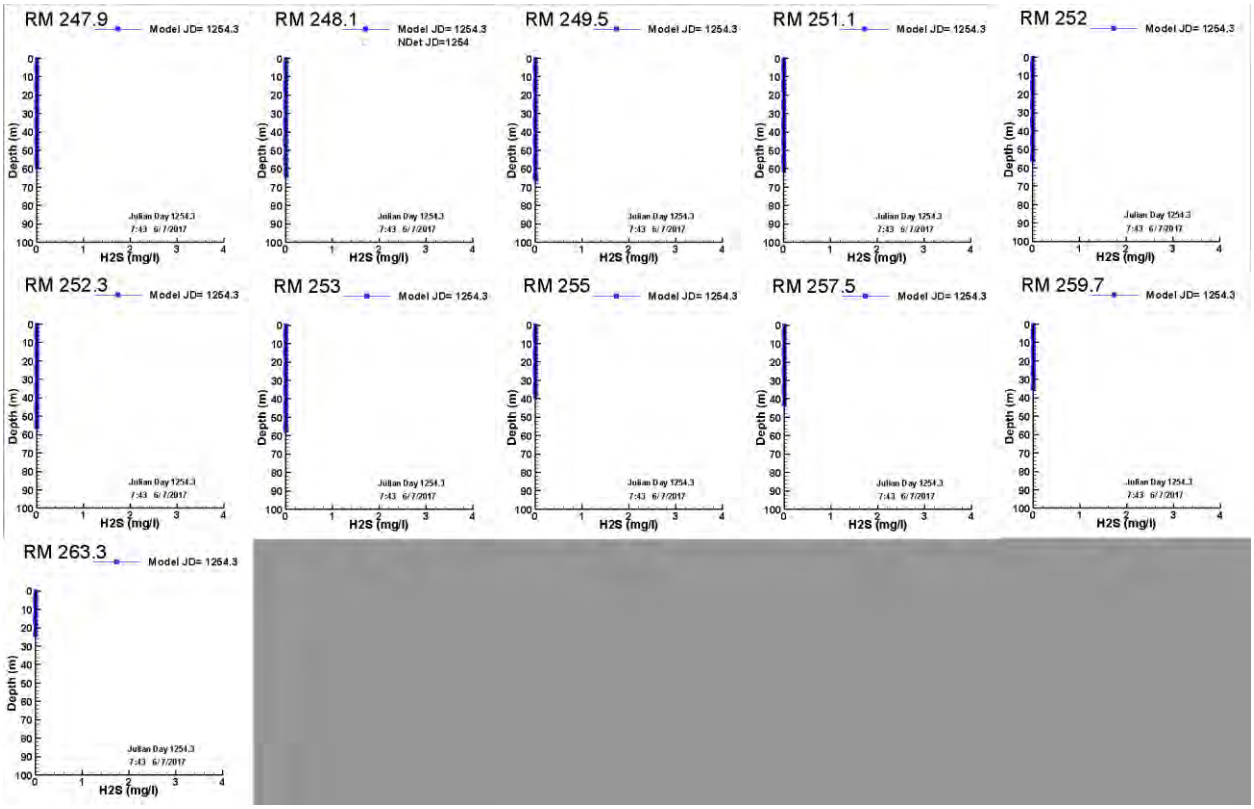


Figure 54. Vertical profiles of hydrogen sulfide compared with data for 6/ 7/2017.

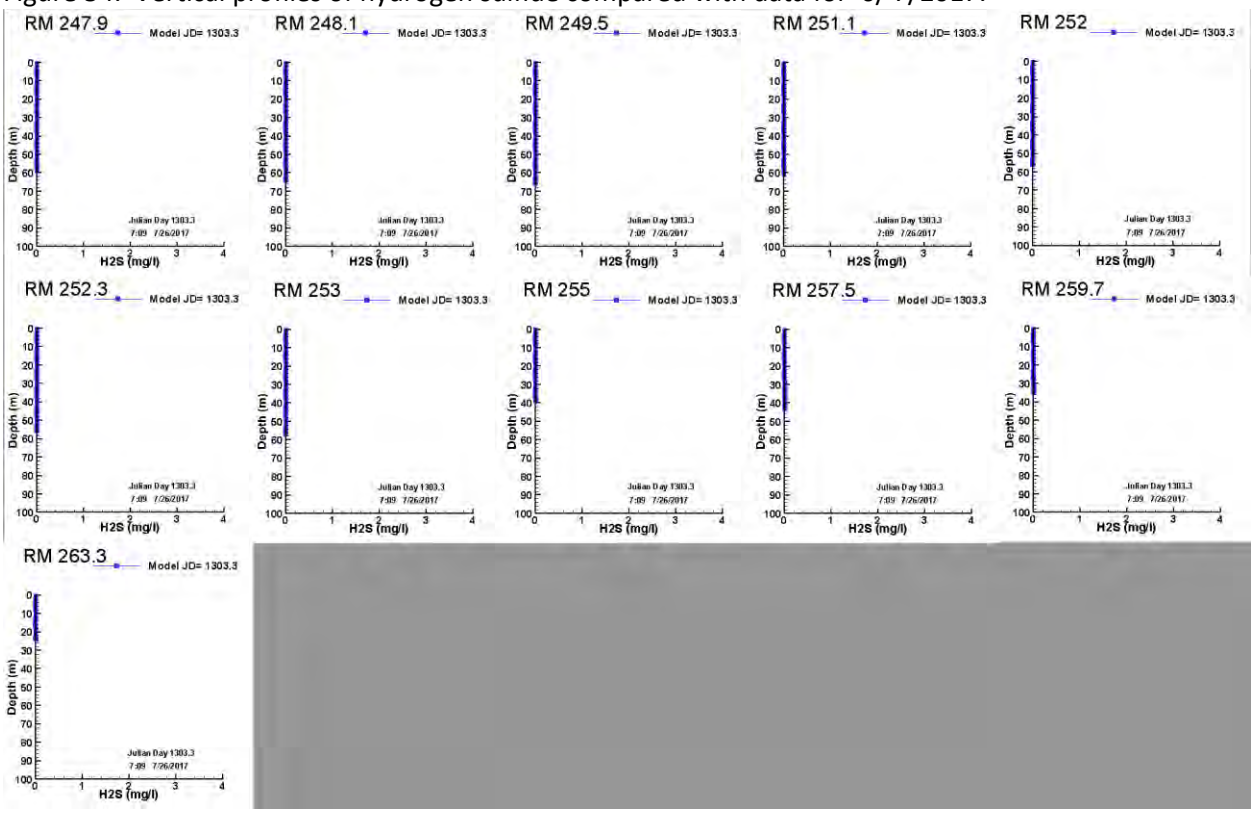


Figure 55. Vertical profiles of hydrogen sulfide compared with data for 7/26/2017.

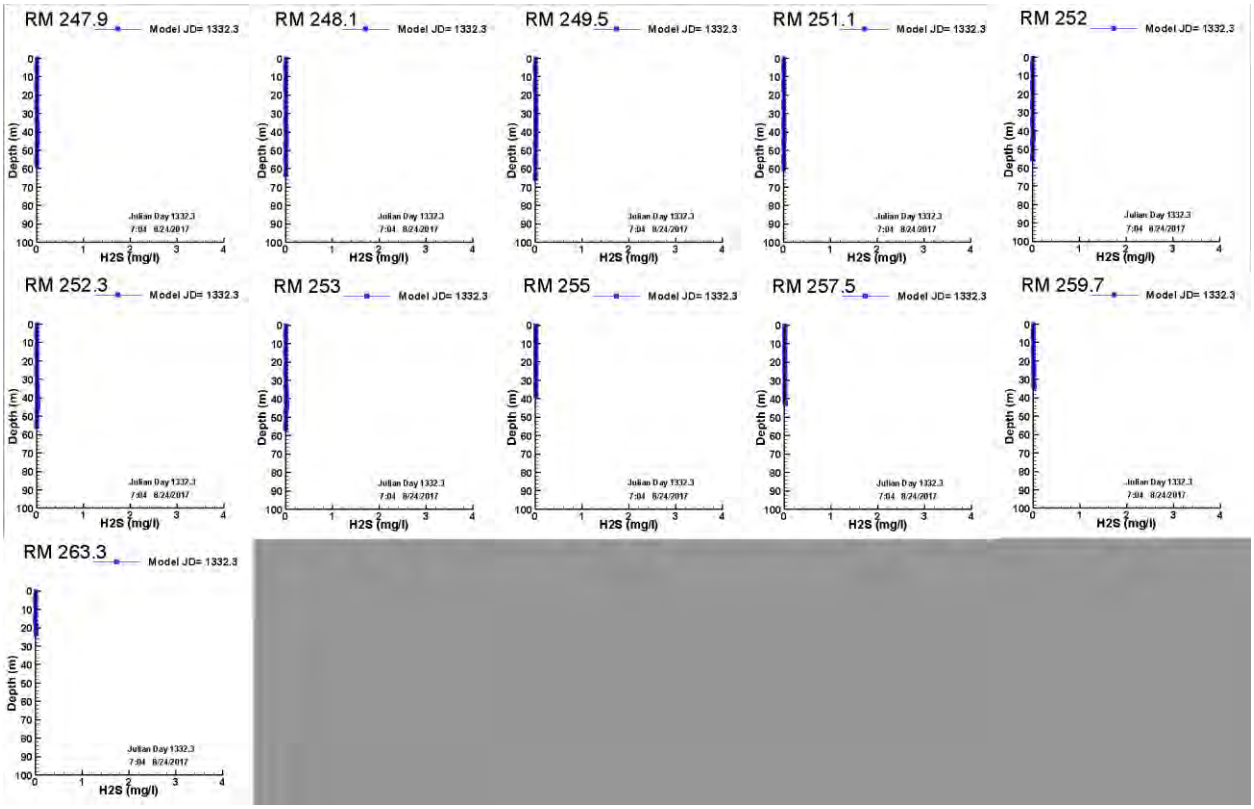


Figure 56. Vertical profiles of hydrogen sulfide compared with data for 8/24/2017.

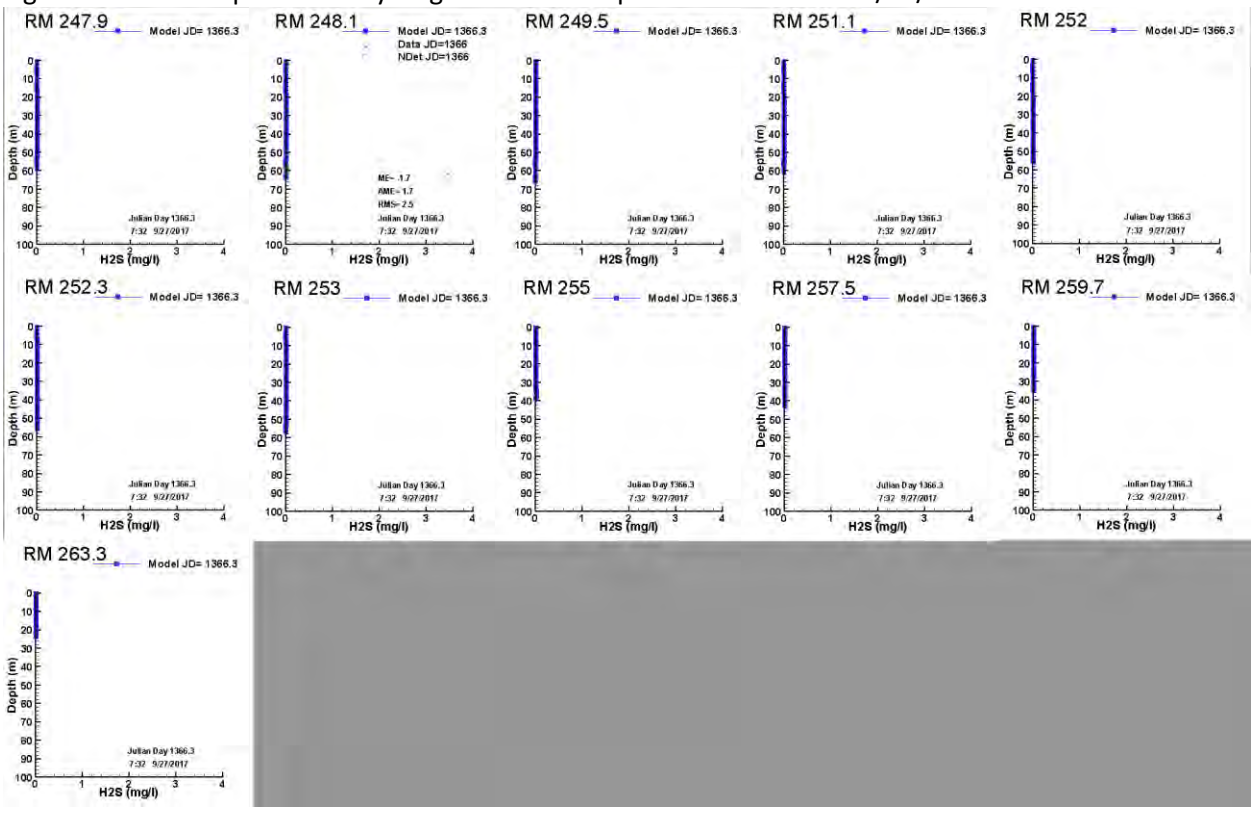


Figure 57. Vertical profiles of hydrogen sulfide compared with data for 9/27/2017.

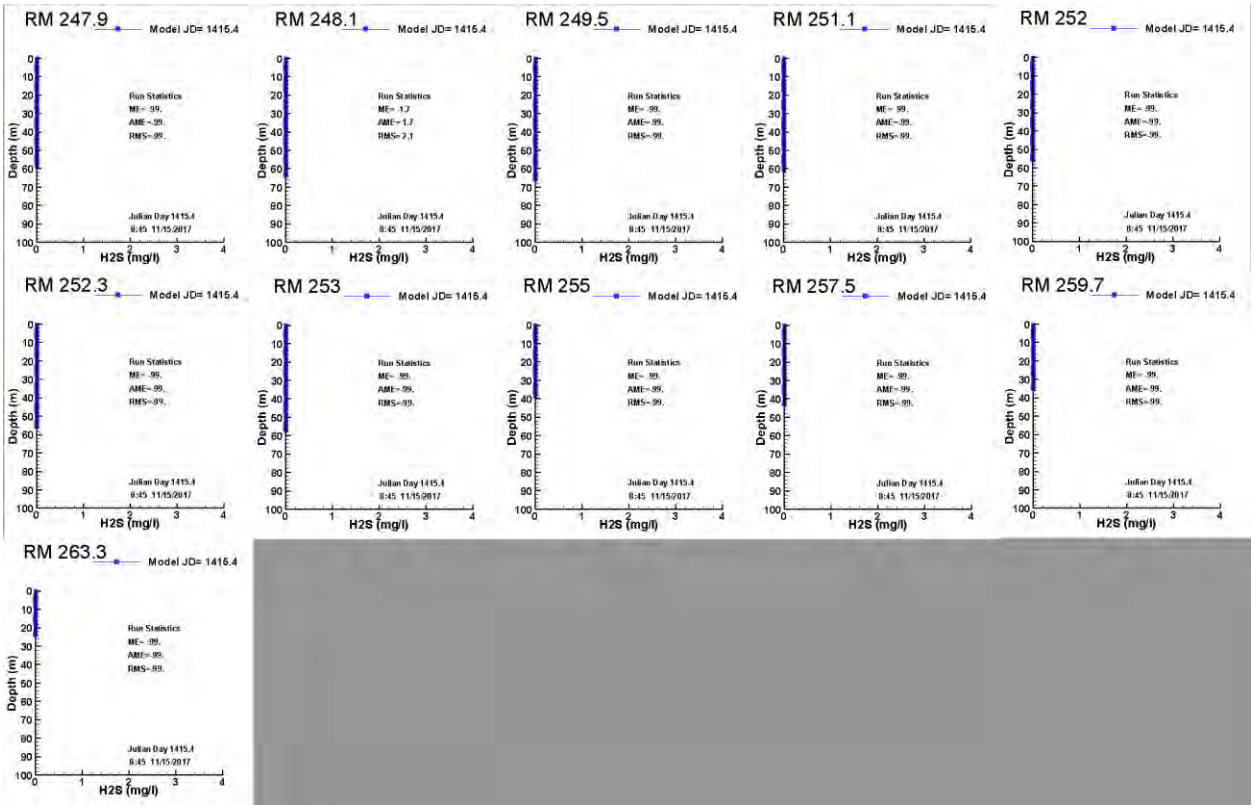


Figure 58. Vertical profiles of hydrogen sulfide compared with data for 11/15/2017.

Sulfate

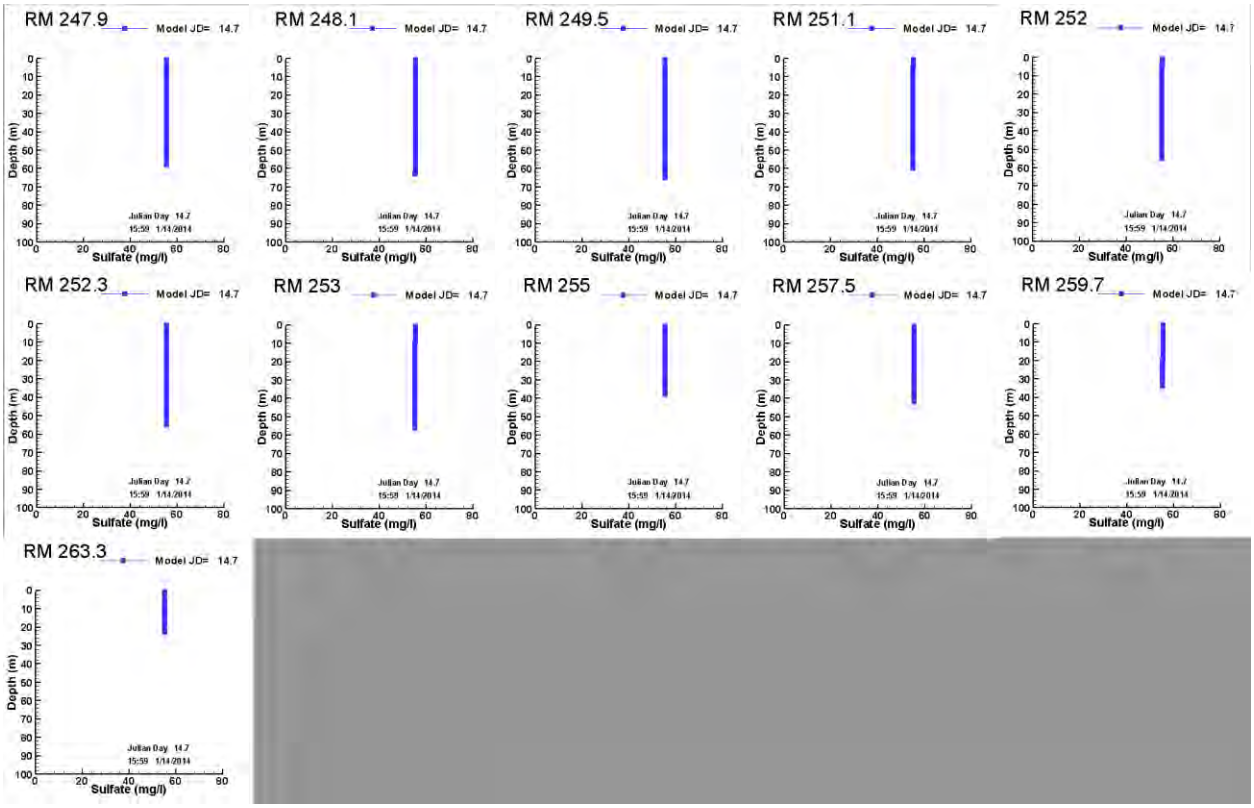


Figure 59. Vertical profiles of sulfate compared with data for 1/14/2014.

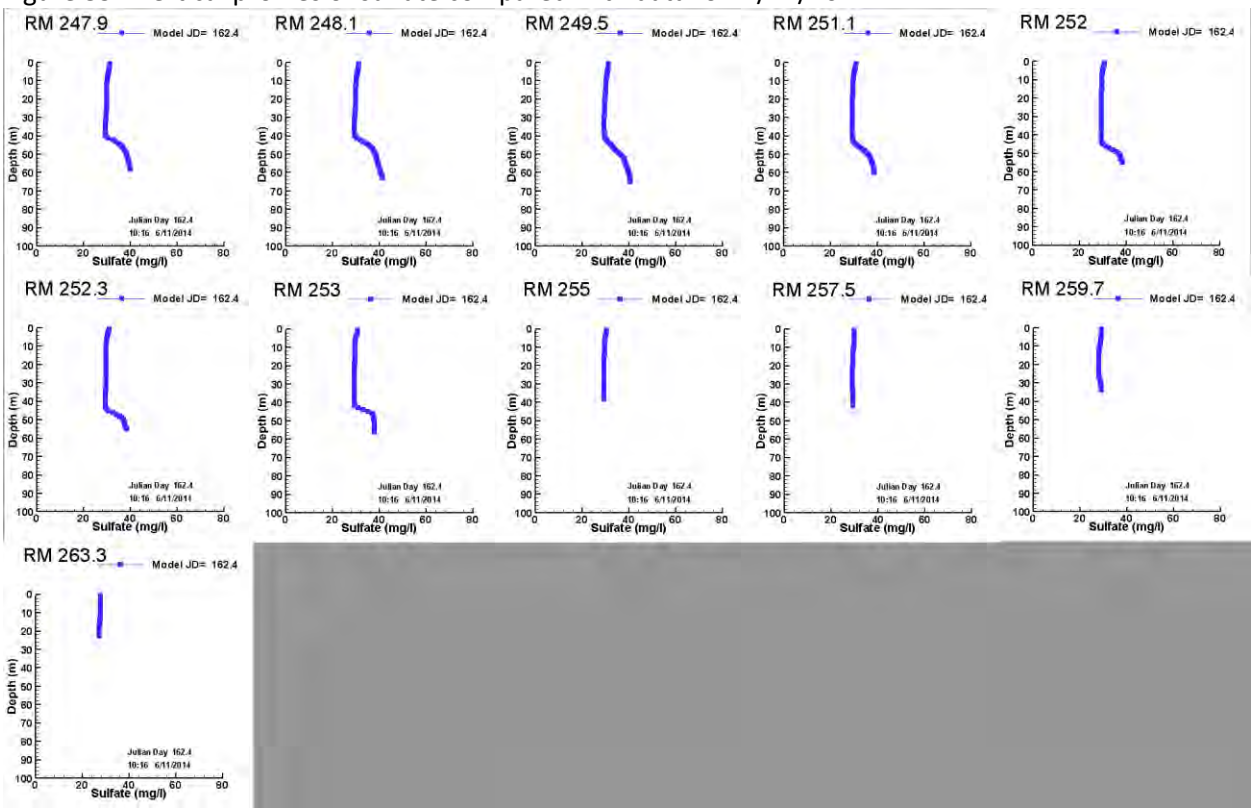


Figure 60. Vertical profiles of sulfate compared with data for 6/11/2014.

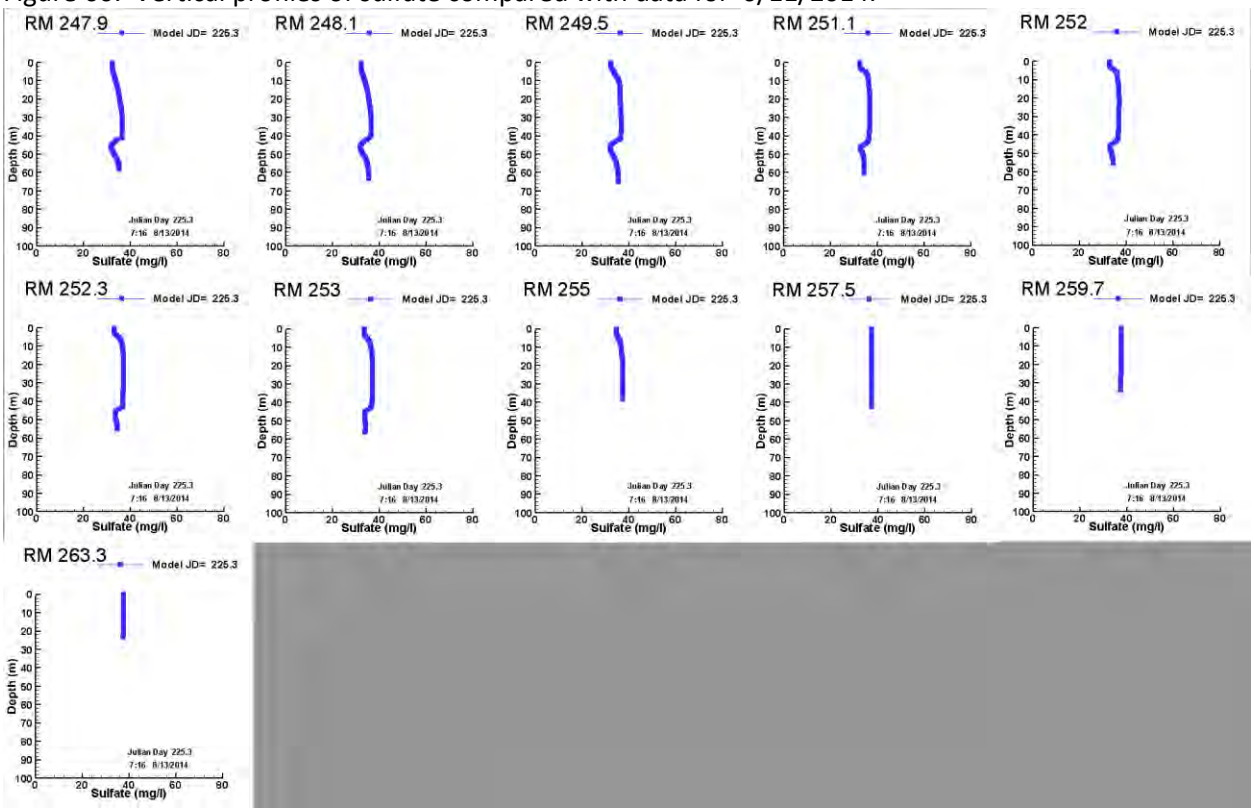


Figure 61. Vertical profiles of sulfate compared with data for 8/13/2014.

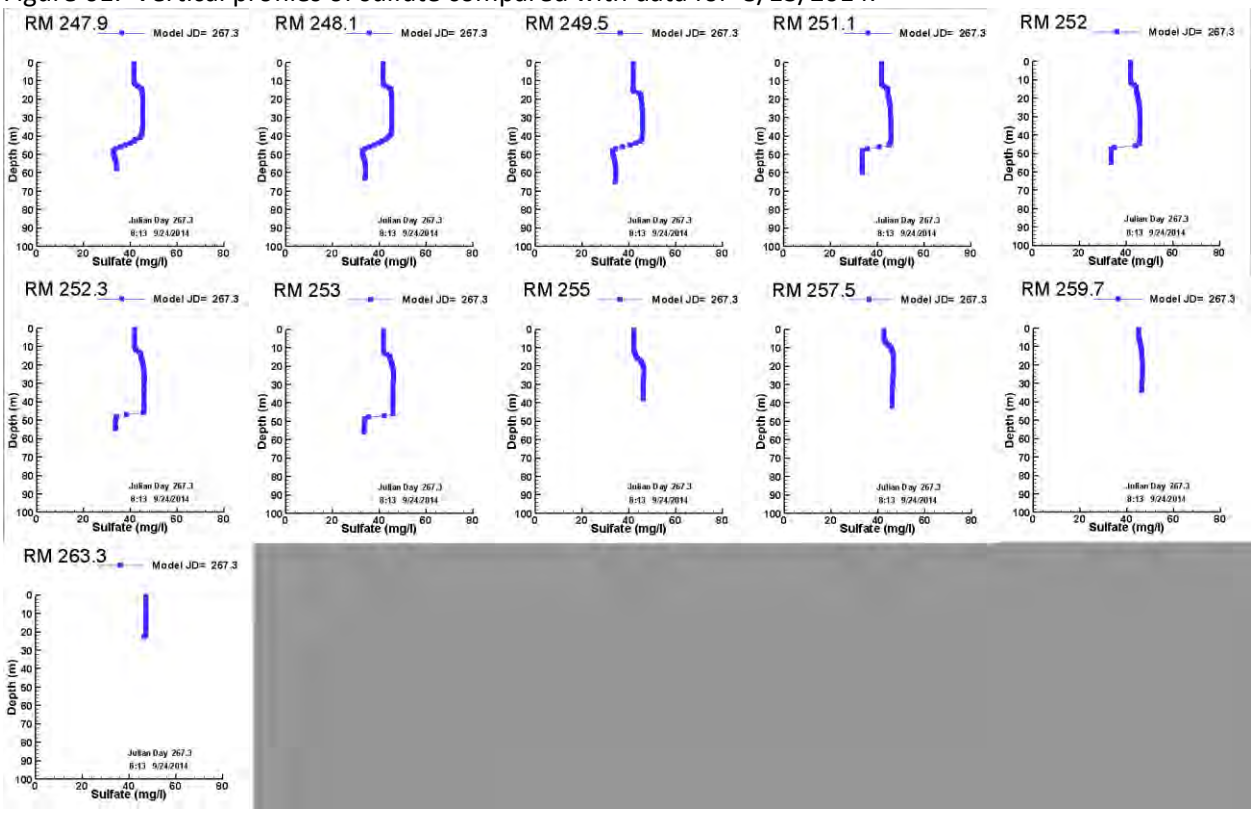


Figure 62. Vertical profiles of sulfate compared with data for 9/24/2014.

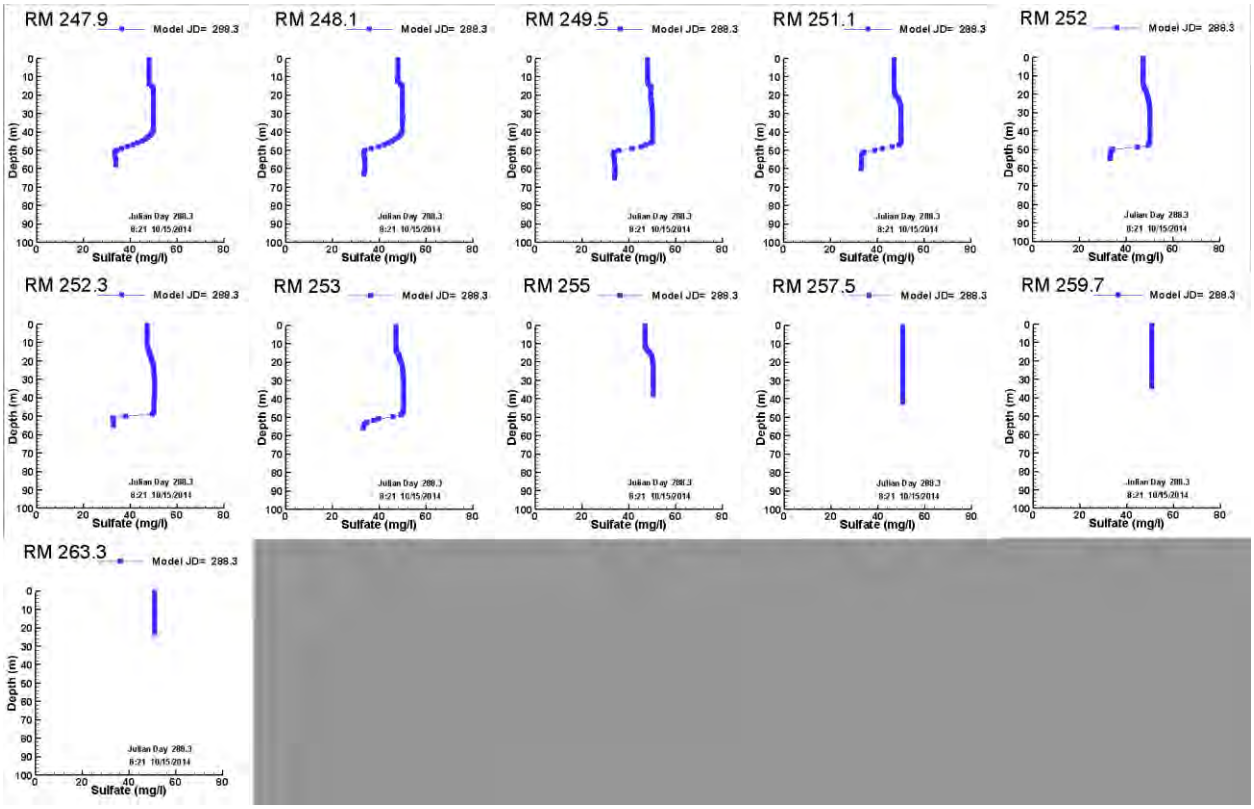


Figure 63. Vertical profiles of sulfate compared with data for 10/15/2014.

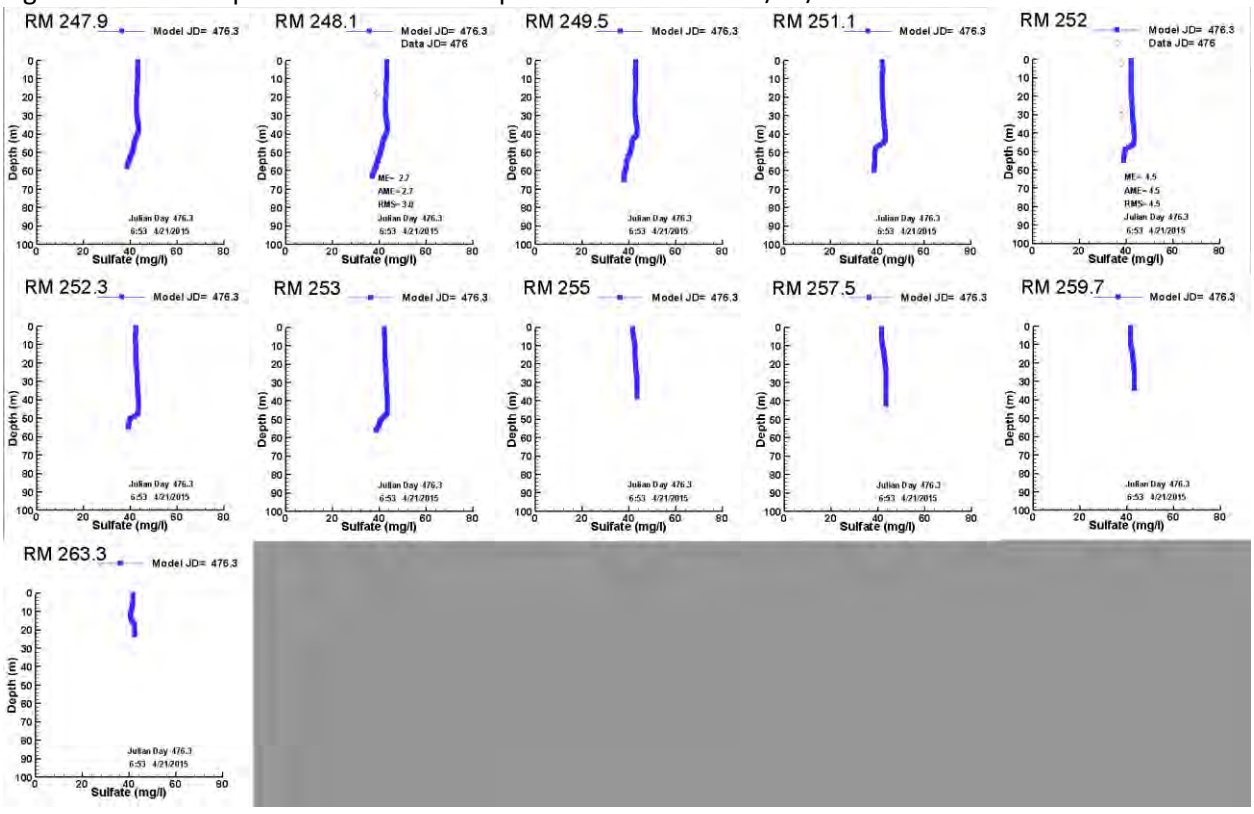


Figure 64. Vertical profiles of sulfate compared with data for 4/21/2015.

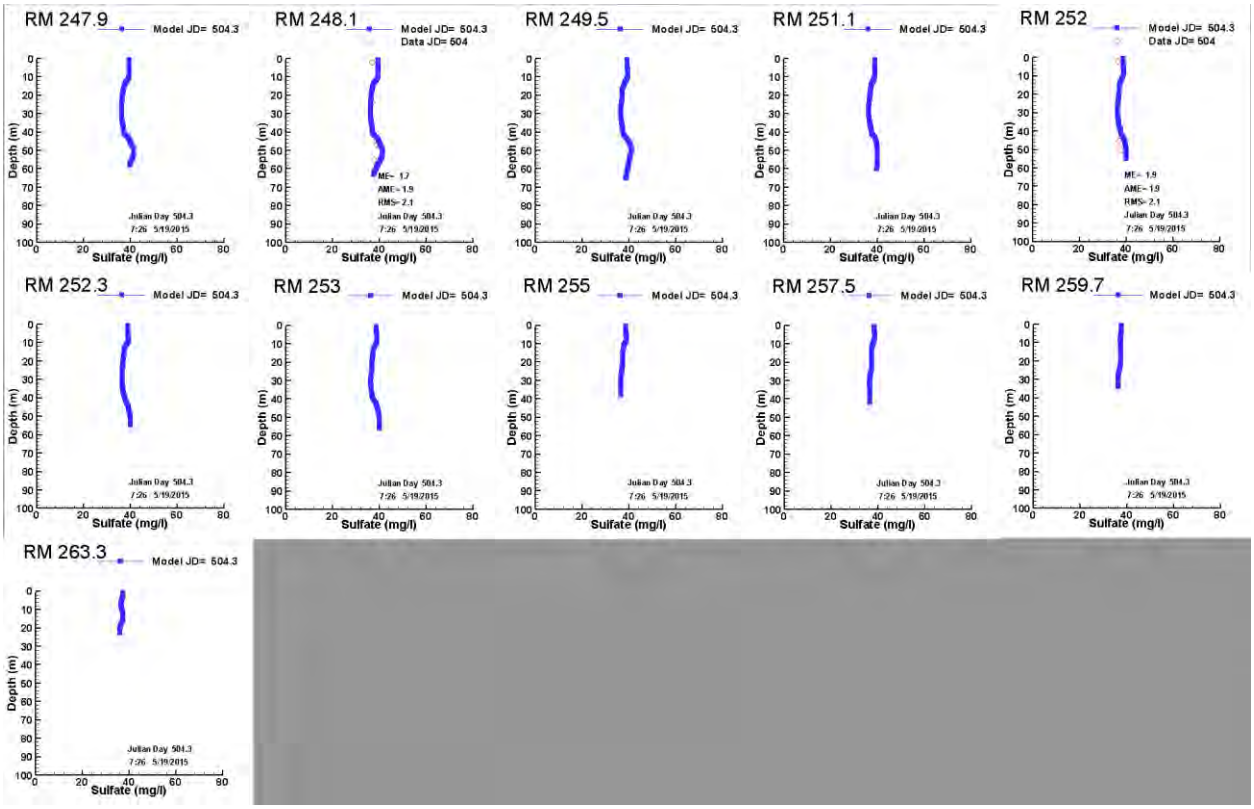


Figure 65. Vertical profiles of sulfate compared with data for 5/19/2015.

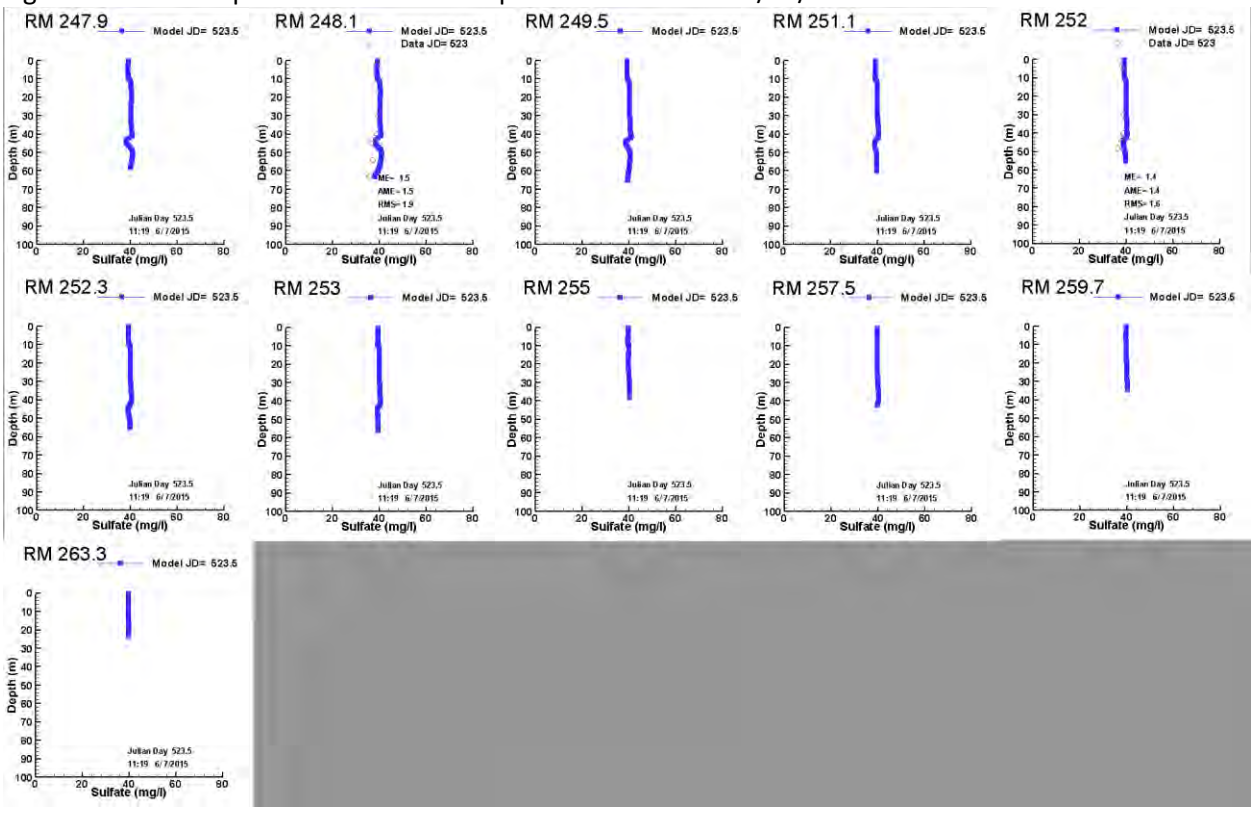


Figure 66. Vertical profiles of sulfate compared with data for 6/ 7/2015.

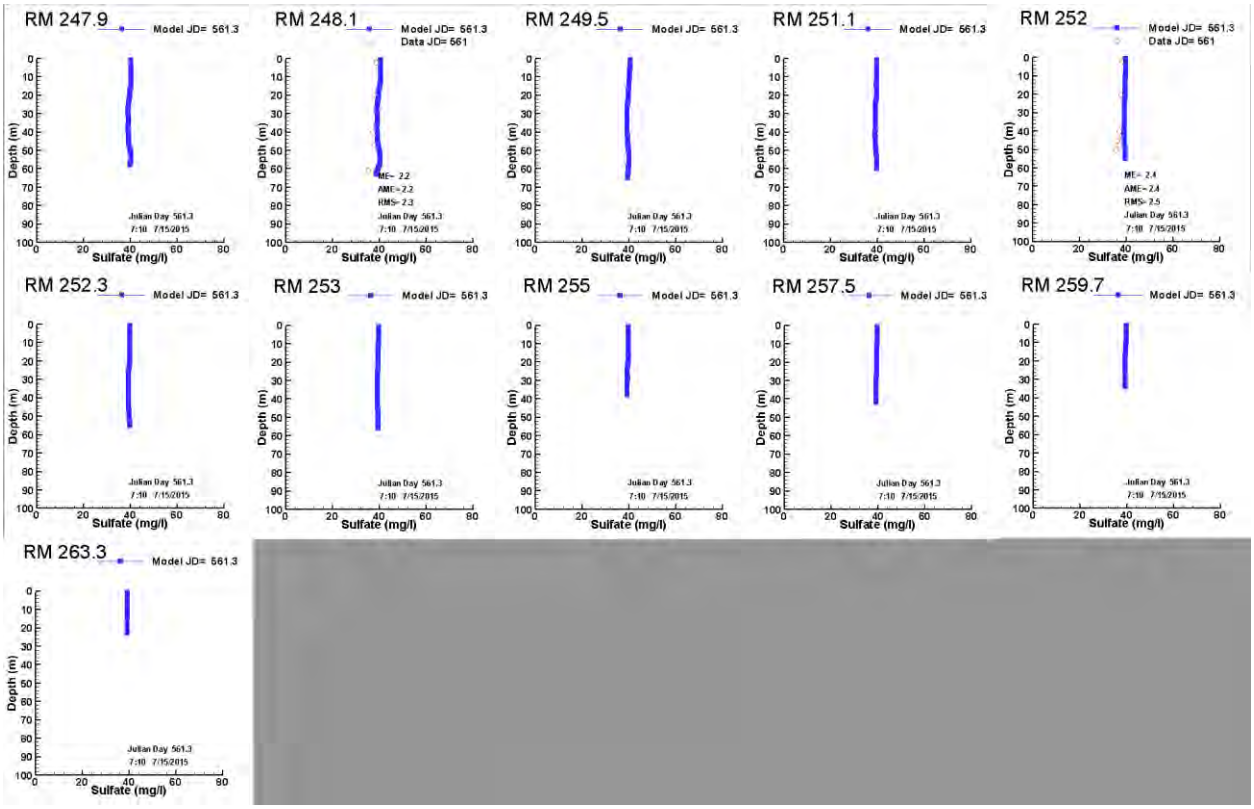


Figure 67. Vertical profiles of sulfate compared with data for 7/15/2015.

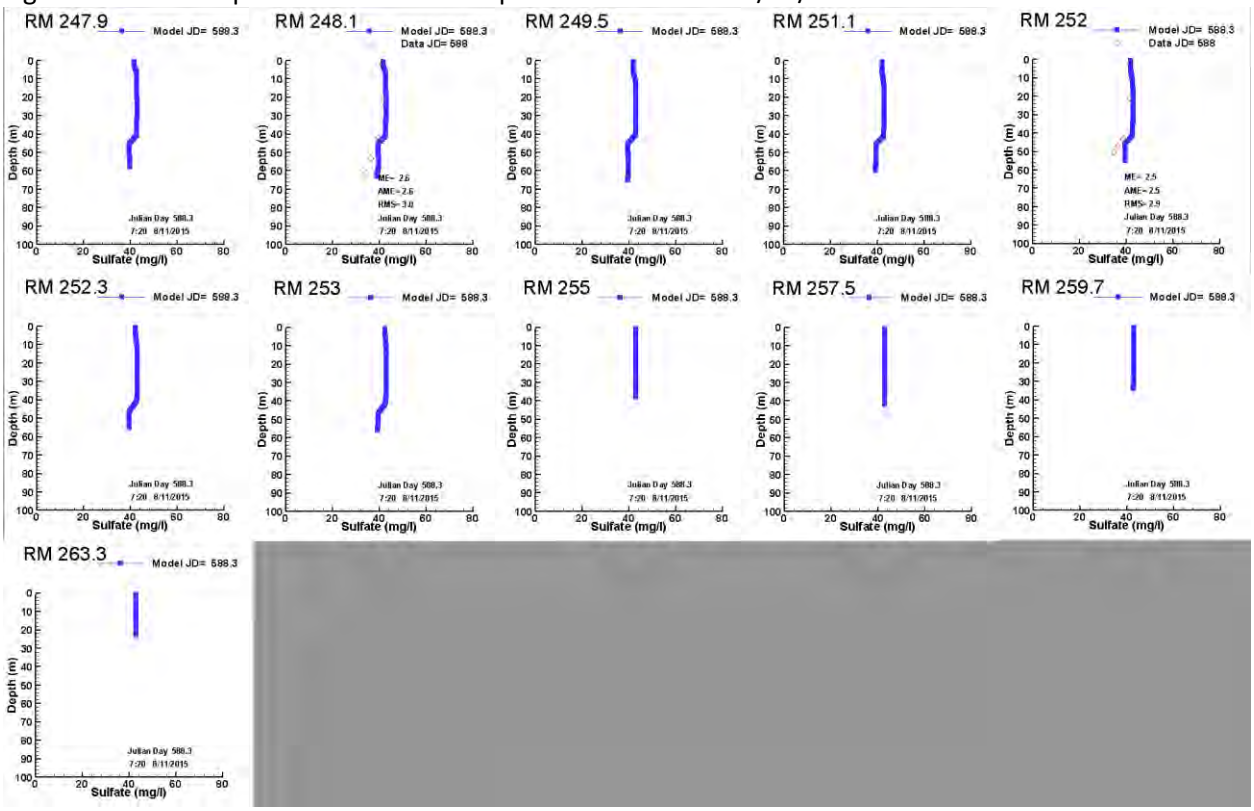


Figure 68. Vertical profiles of sulfate compared with data for 8/11/2015.

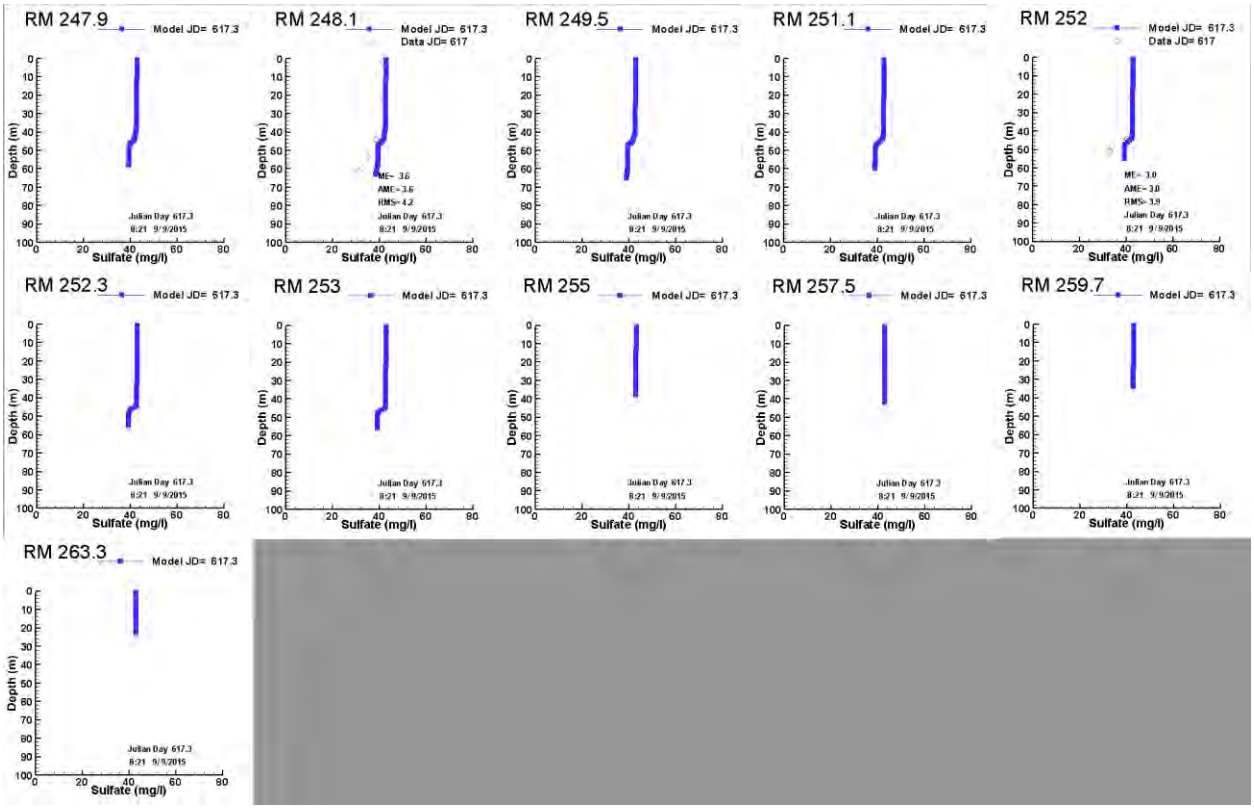


Figure 69. Vertical profiles of sulfate compared with data for 9/ 9/2015.

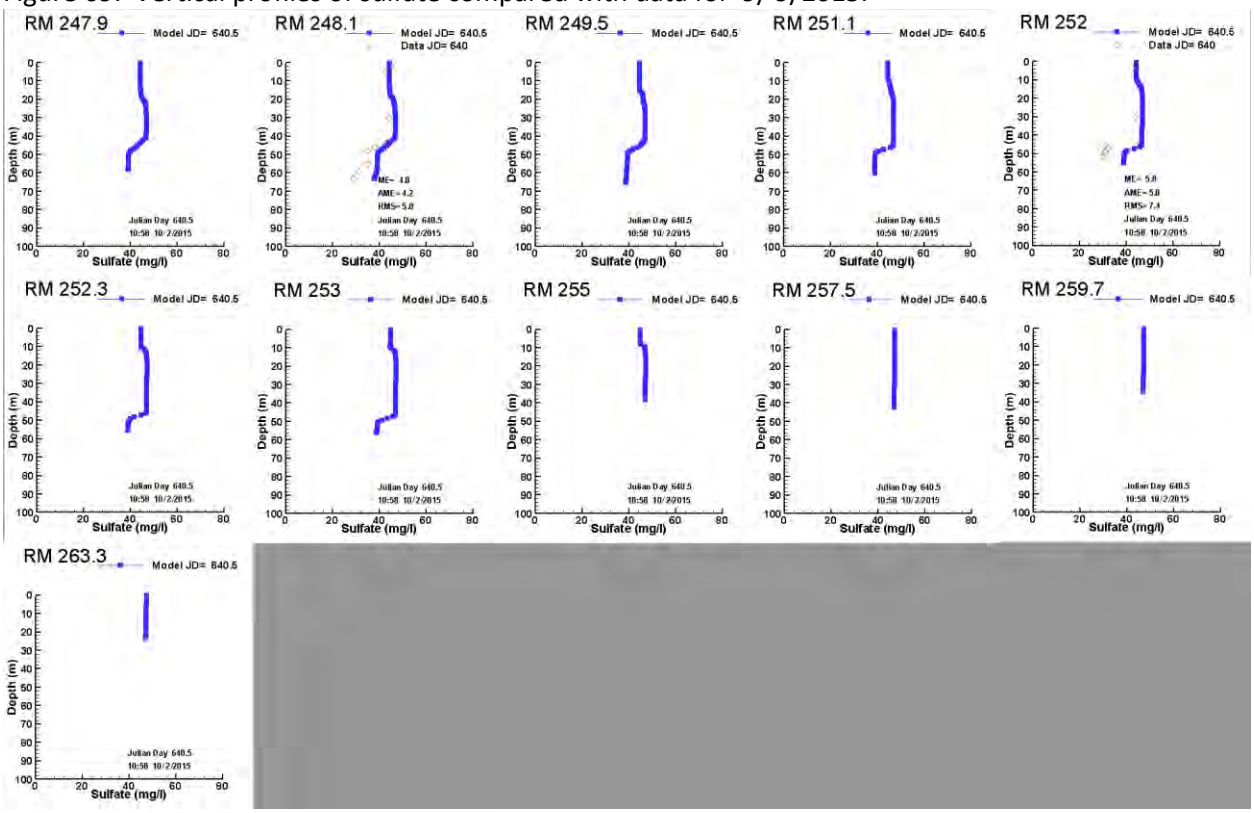


Figure 70. Vertical profiles of sulfate compared with data for 10/ 2/2015.

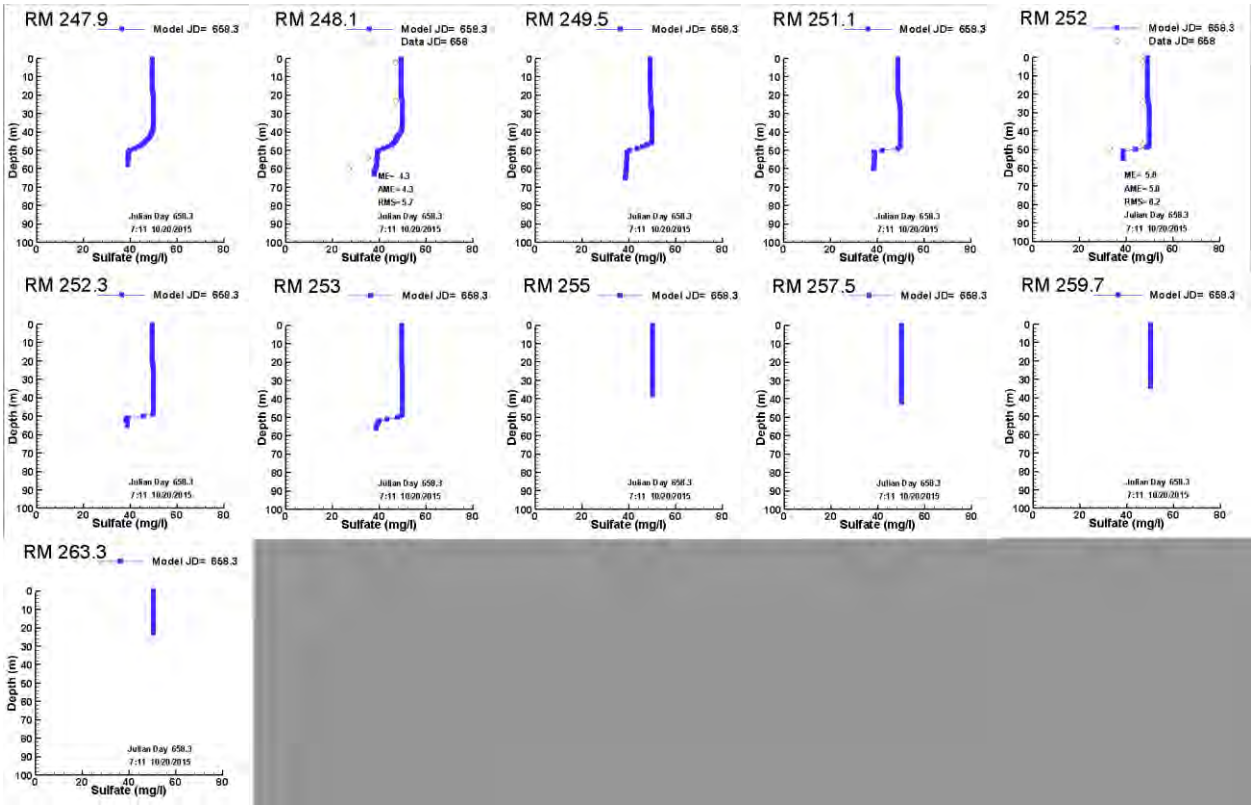


Figure 71. Vertical profiles of sulfate compared with data for 10/20/2015.

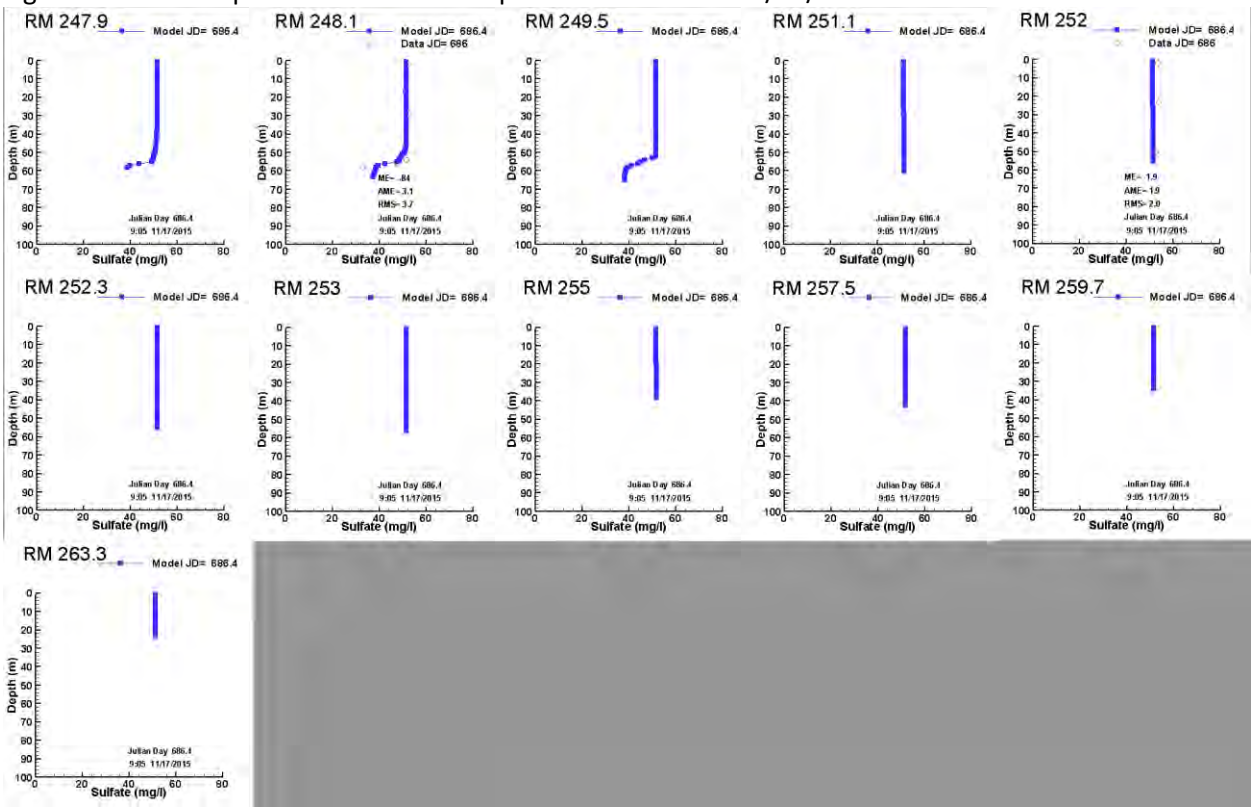


Figure 72. Vertical profiles of sulfate compared with data for 11/17/2015.

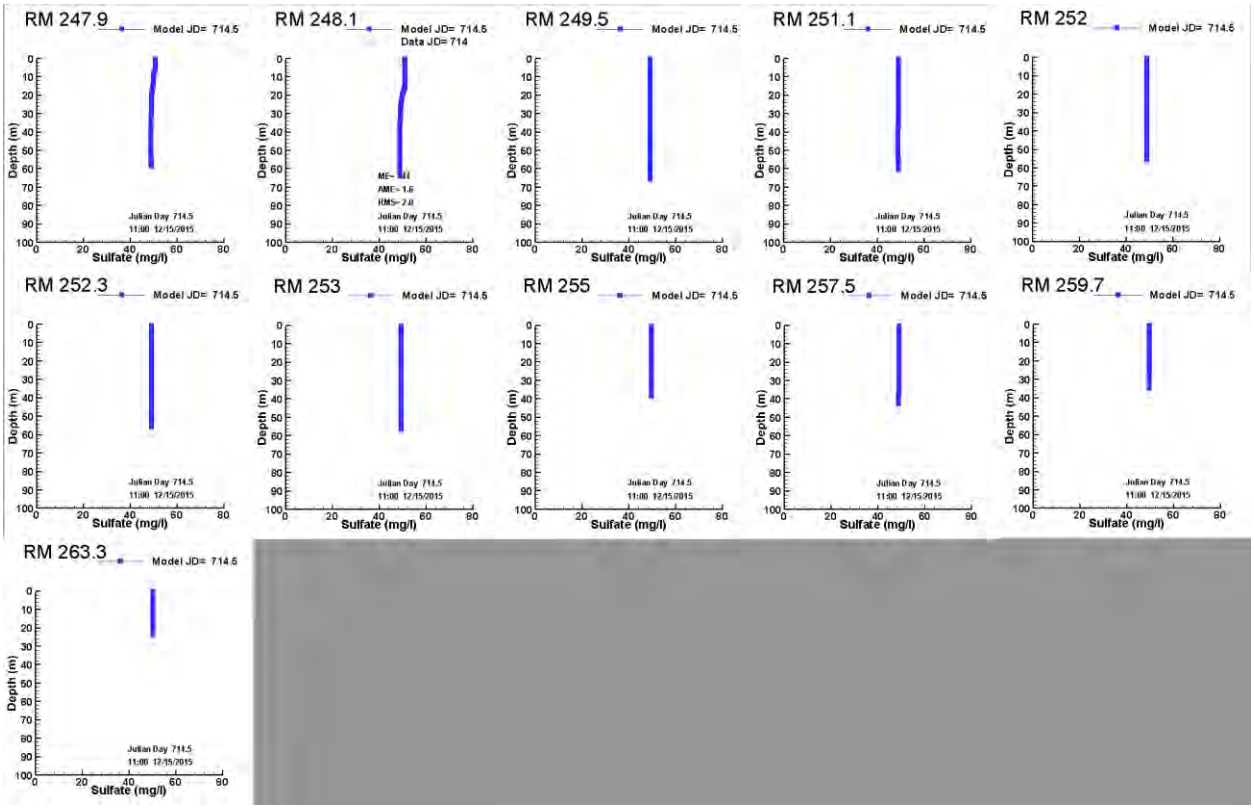


Figure 73. Vertical profiles of sulfate compared with data for 12/15/2015.

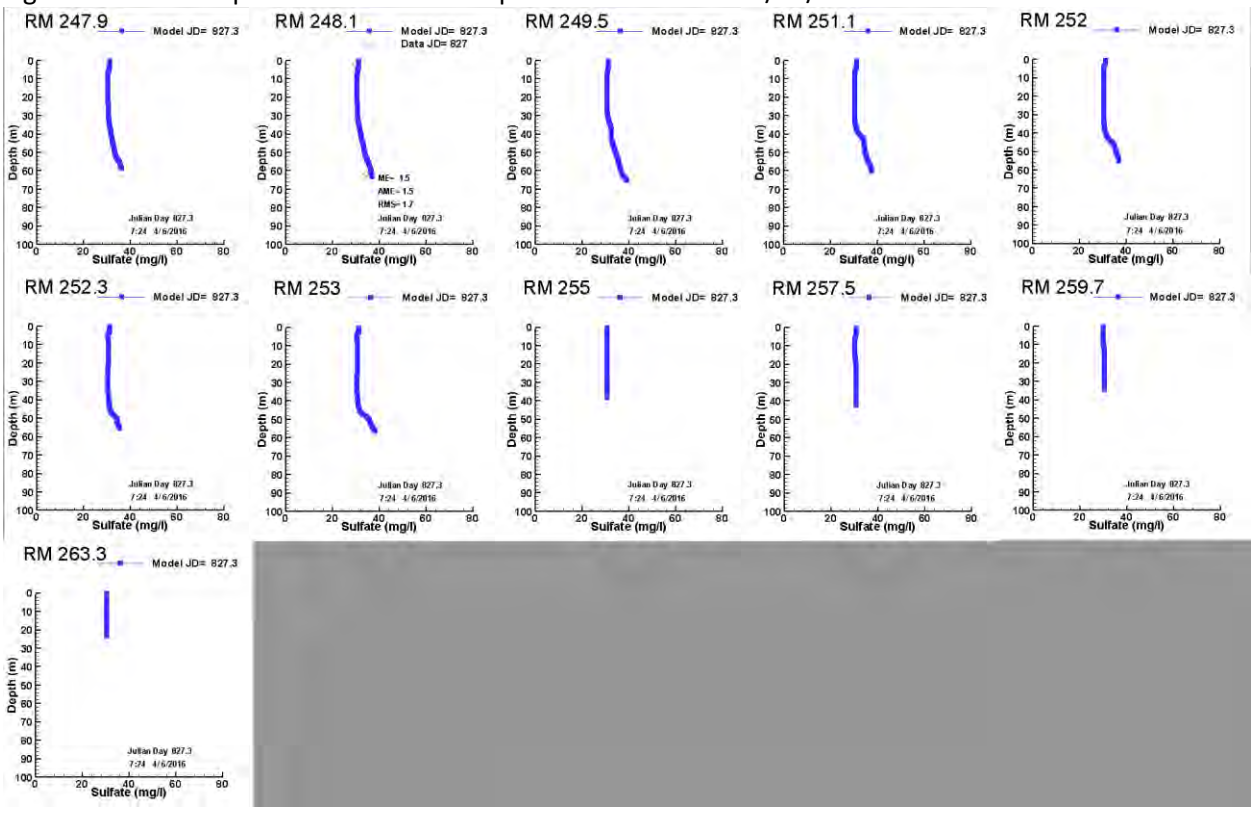


Figure 74. Vertical profiles of sulfate compared with data for 4/ 6/2016.

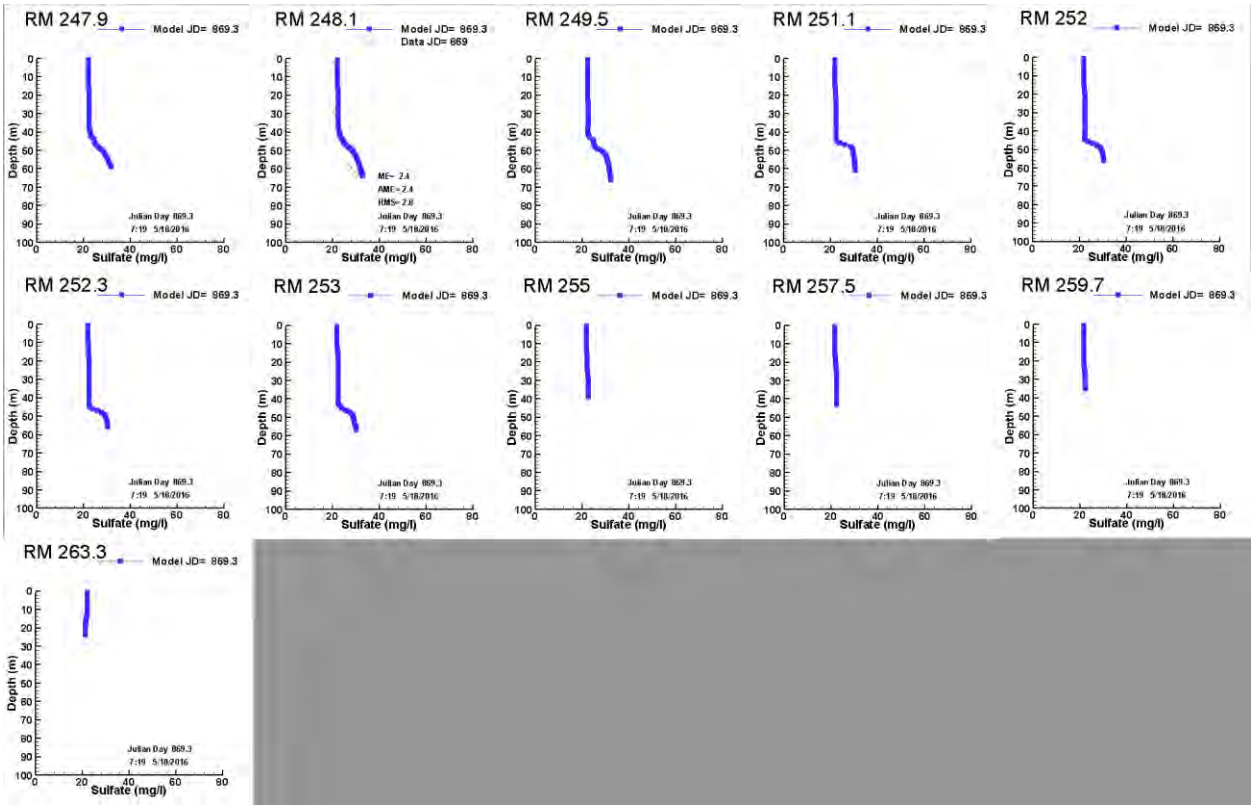


Figure 75. Vertical profiles of sulfate compared with data for 5/18/2016.

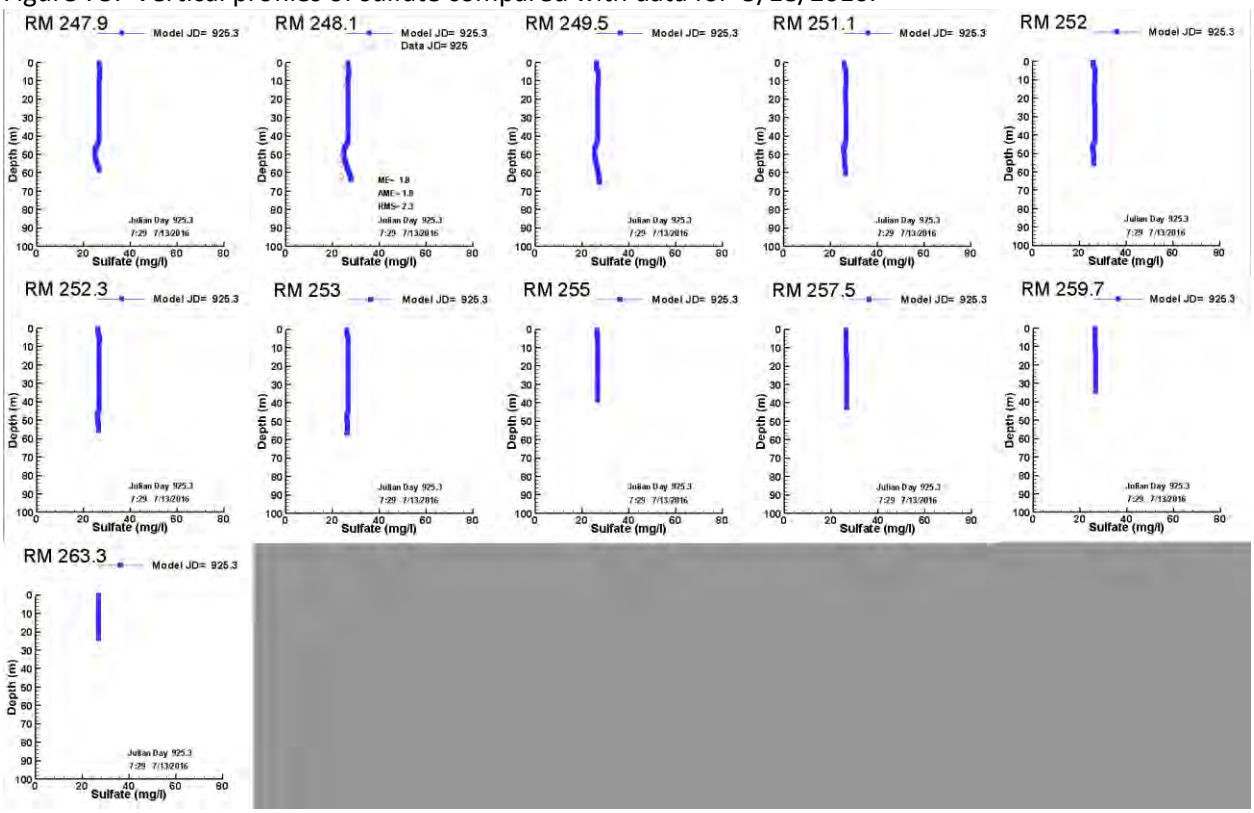


Figure 76. Vertical profiles of sulfate compared with data for 7/13/2016.

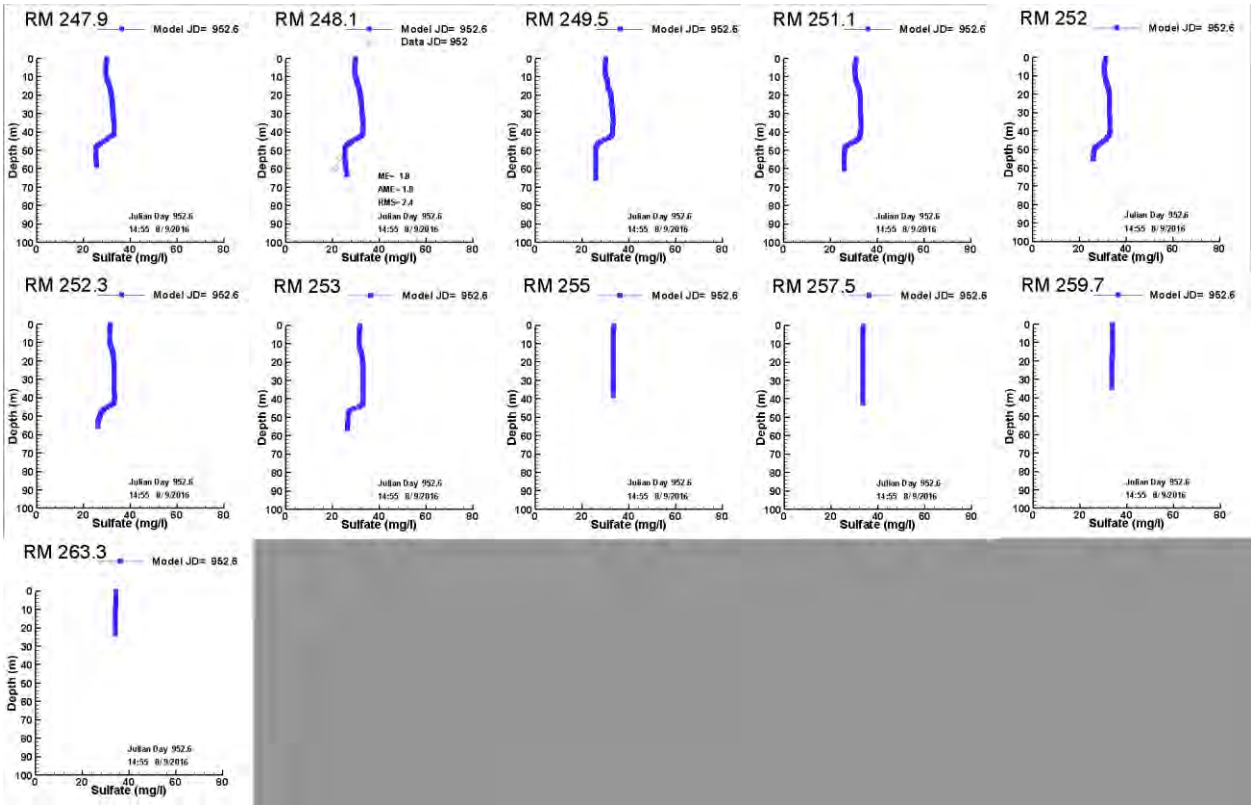


Figure 77. Vertical profiles of sulfate compared with data for 8/ 9/2016.

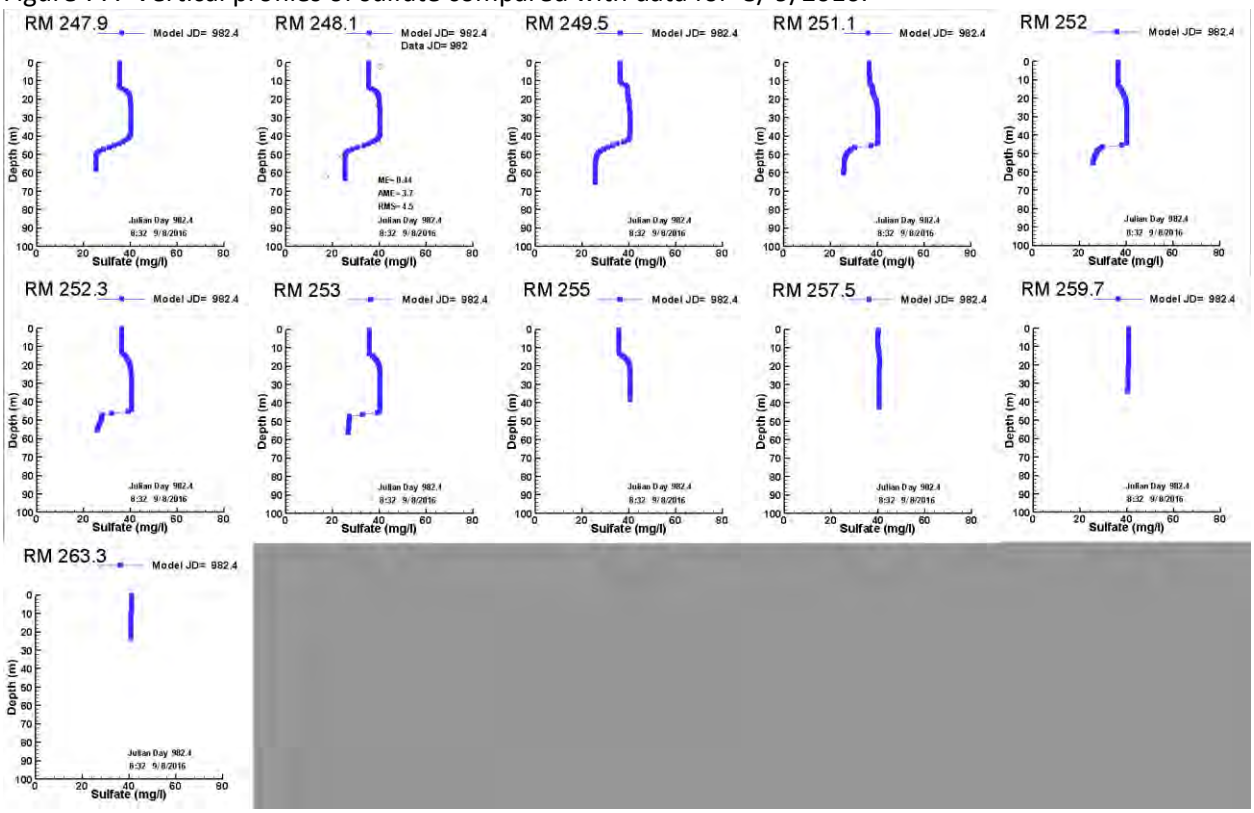


Figure 78. Vertical profiles of sulfate compared with data for 9/ 8/2016.

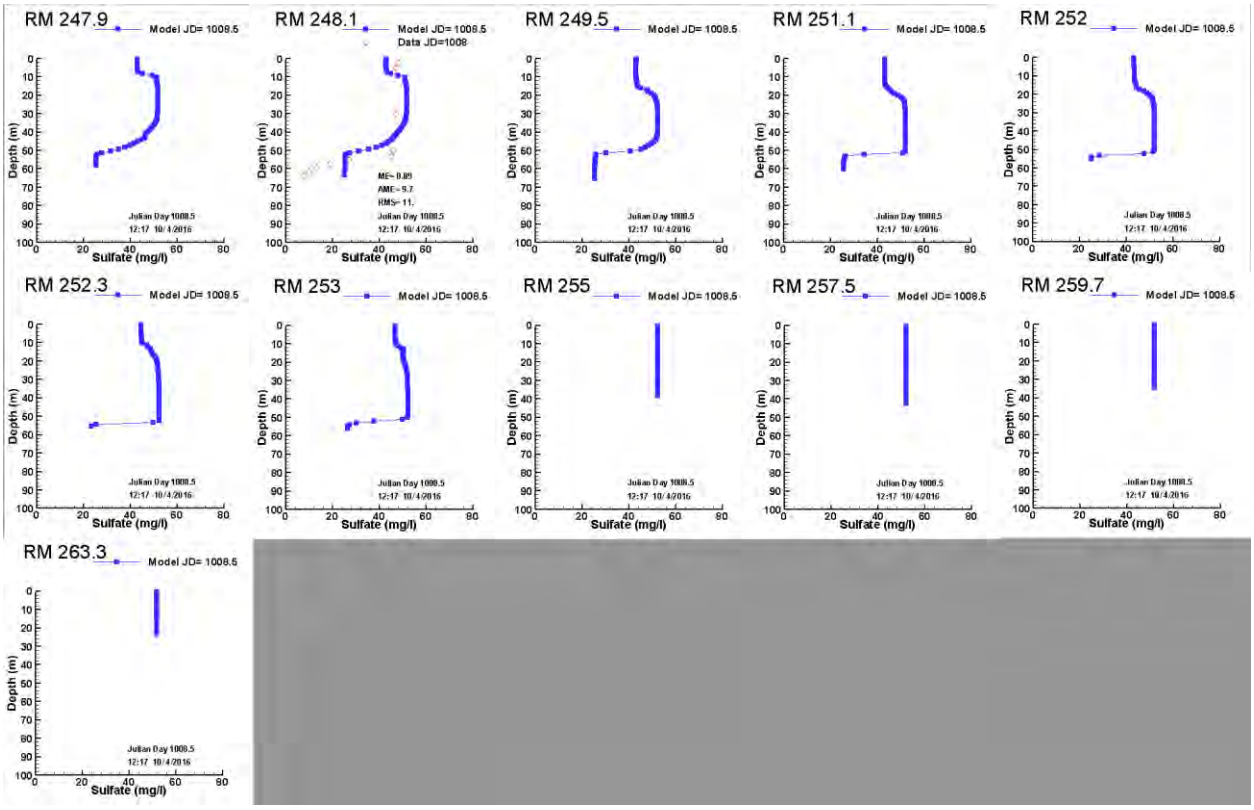


Figure 79. Vertical profiles of sulfate compared with data for 10/ 4/2016.

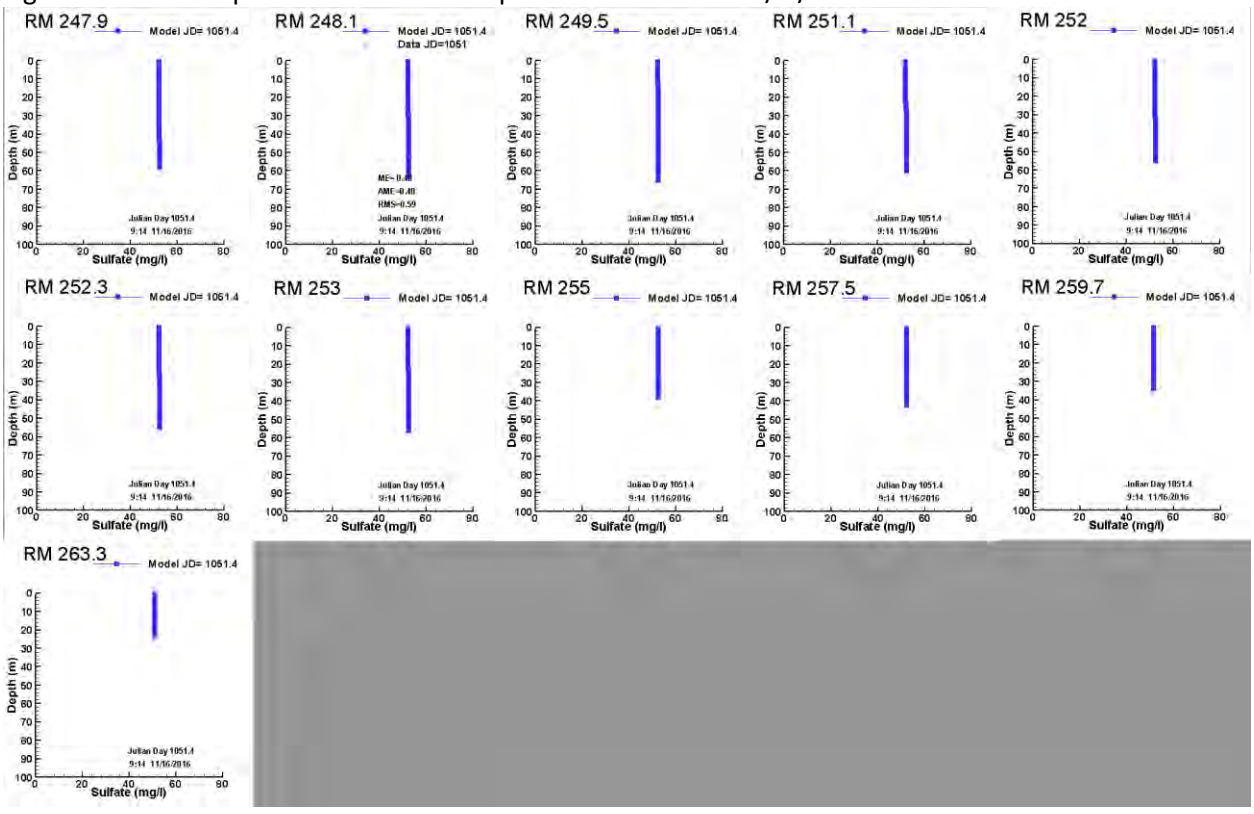


Figure 80. Vertical profiles of sulfate compared with data for 11/16/2016.

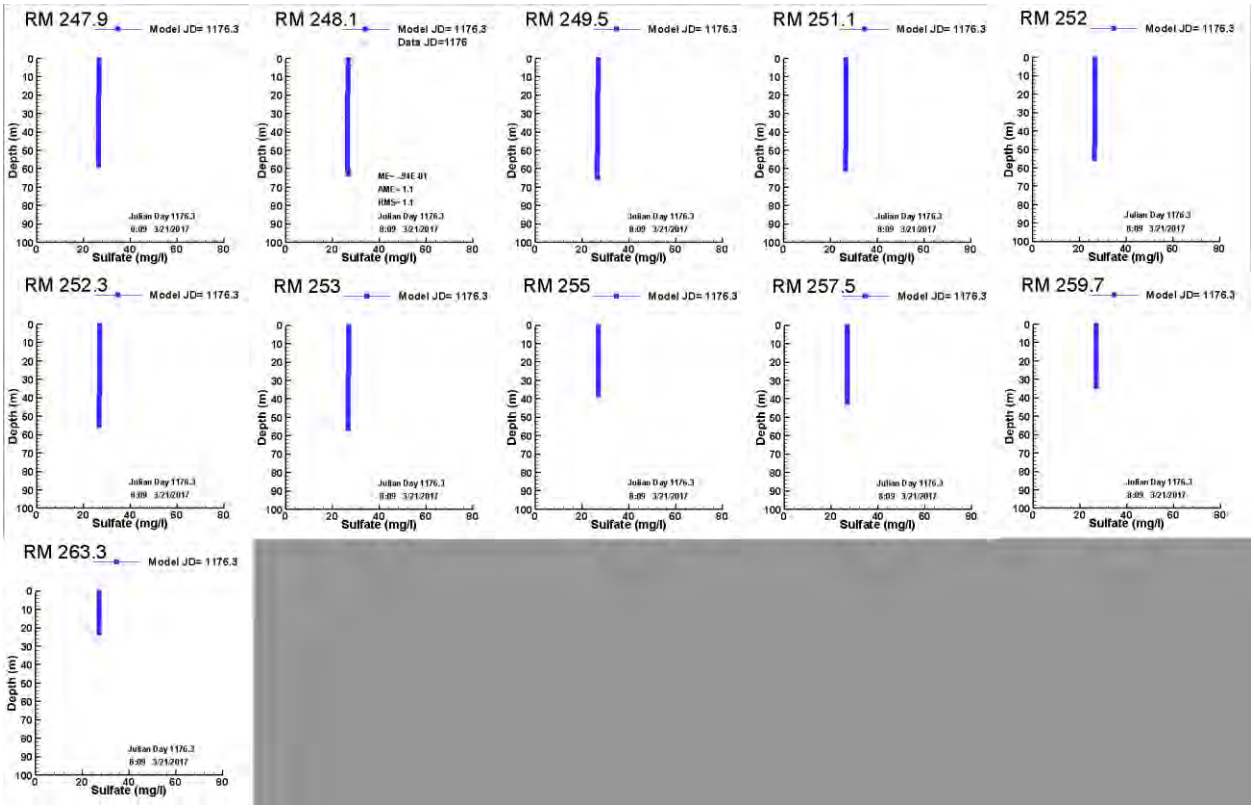


Figure 81. Vertical profiles of sulfate compared with data for 3/21/2017.

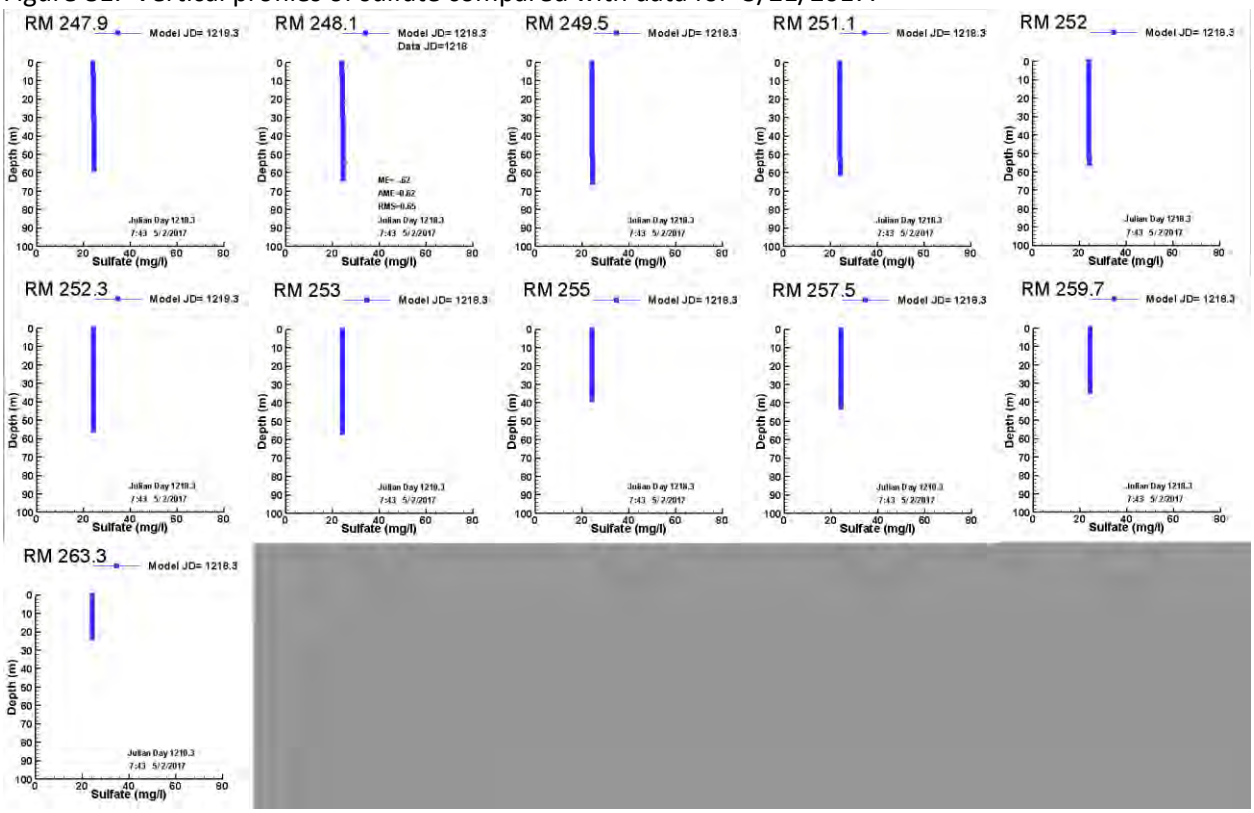


Figure 82. Vertical profiles of sulfate compared with data for 5/ 2/2017.

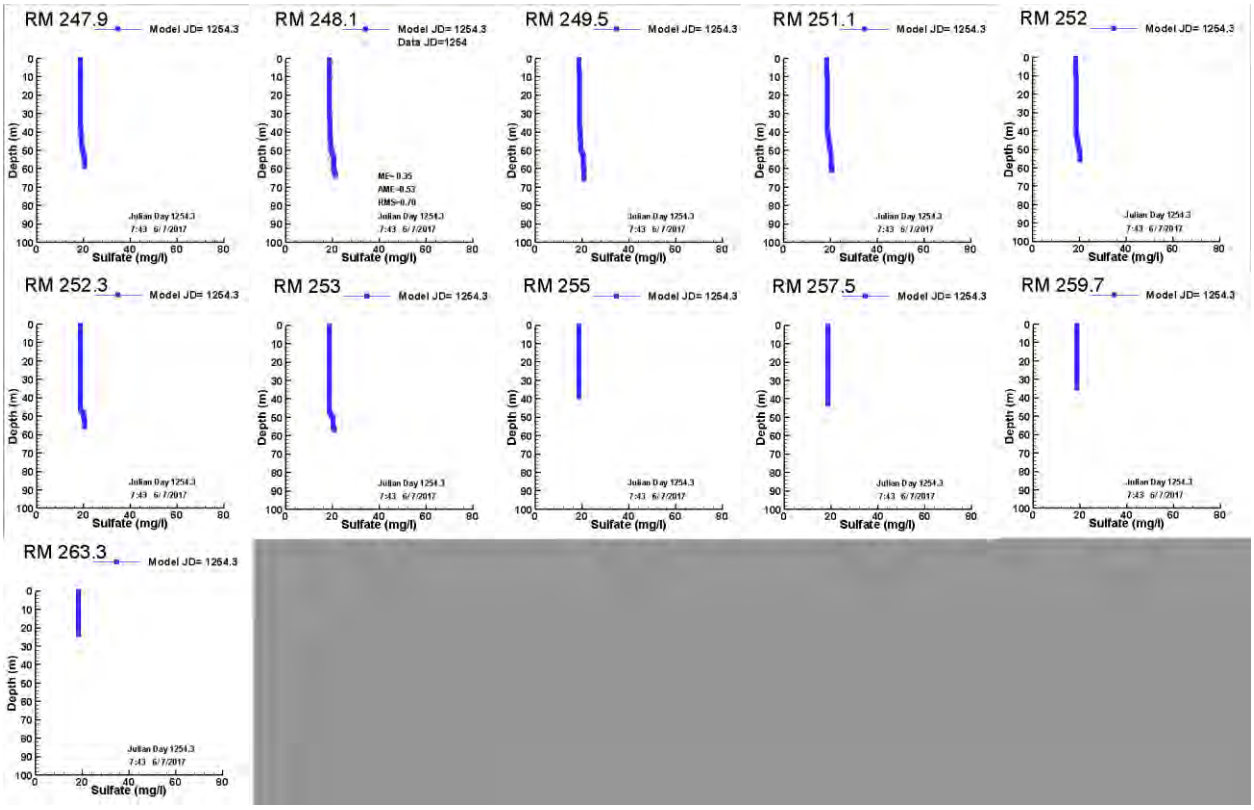


Figure 83. Vertical profiles of sulfate compared with data for 6/ 7/2017.

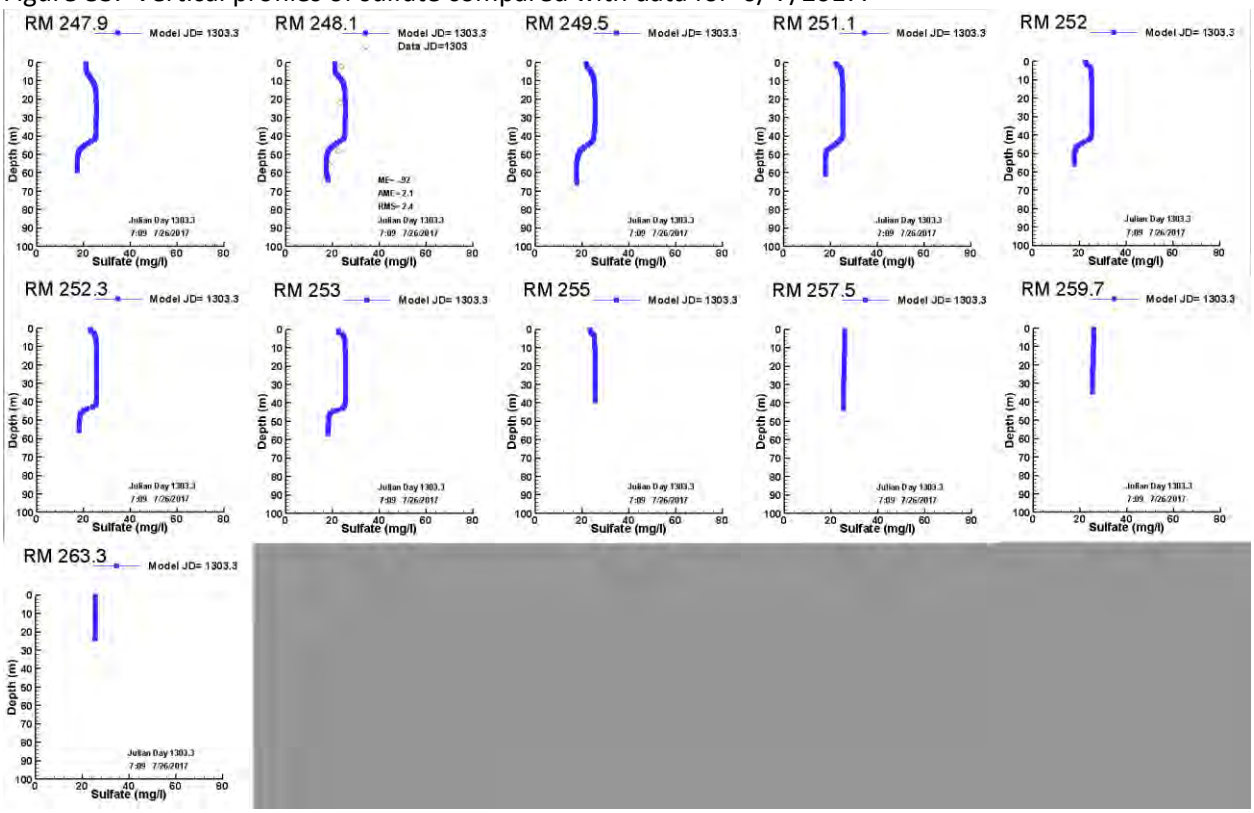


Figure 84. Vertical profiles of sulfate compared with data for 7/26/2017.

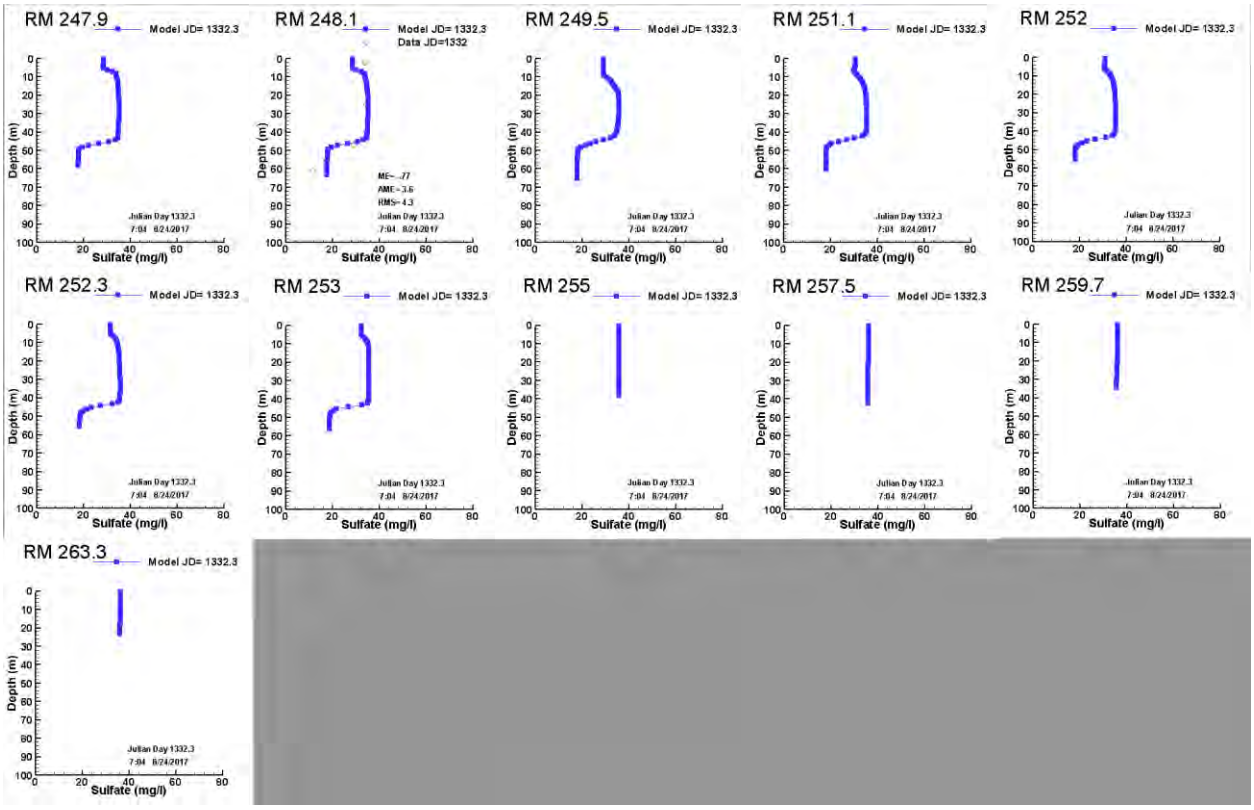


Figure 85. Vertical profiles of sulfate compared with data for 8/24/2017.

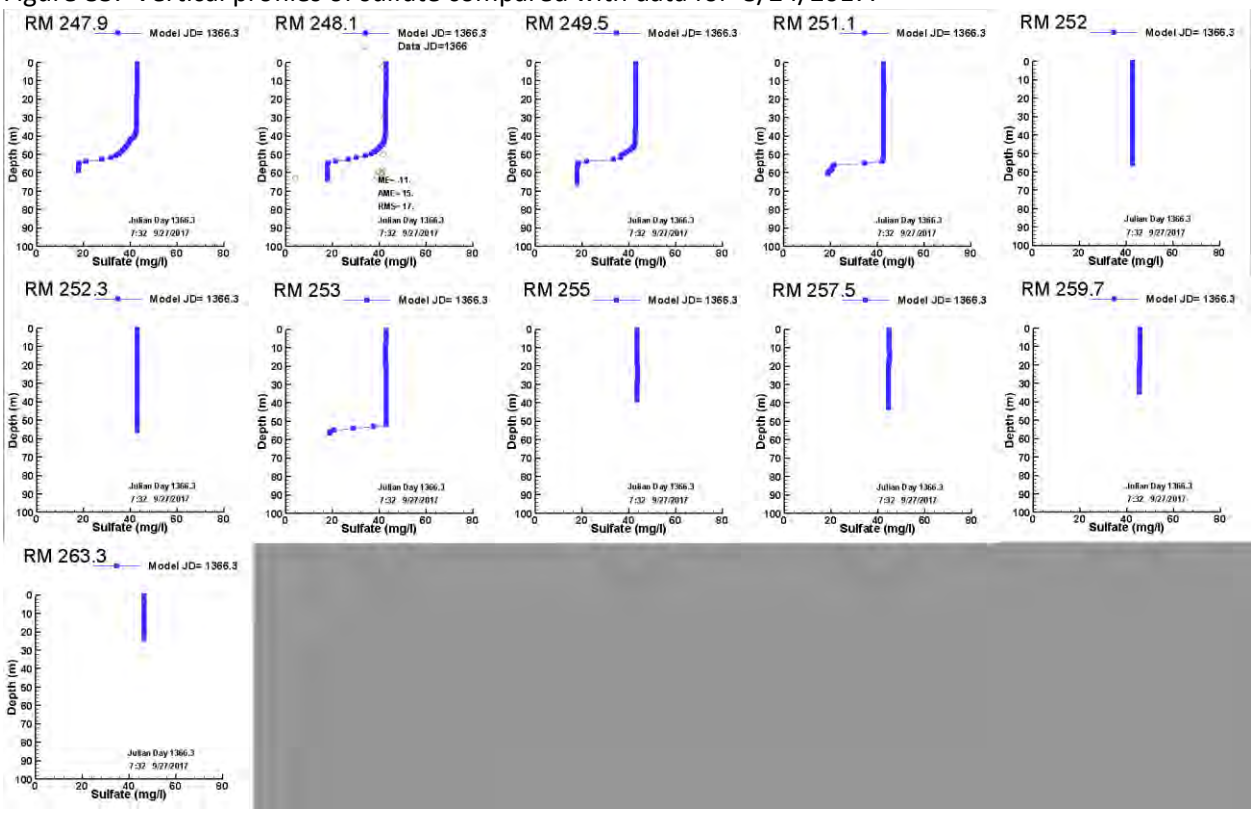


Figure 86. Vertical profiles of sulfate compared with data for 9/27/2017.

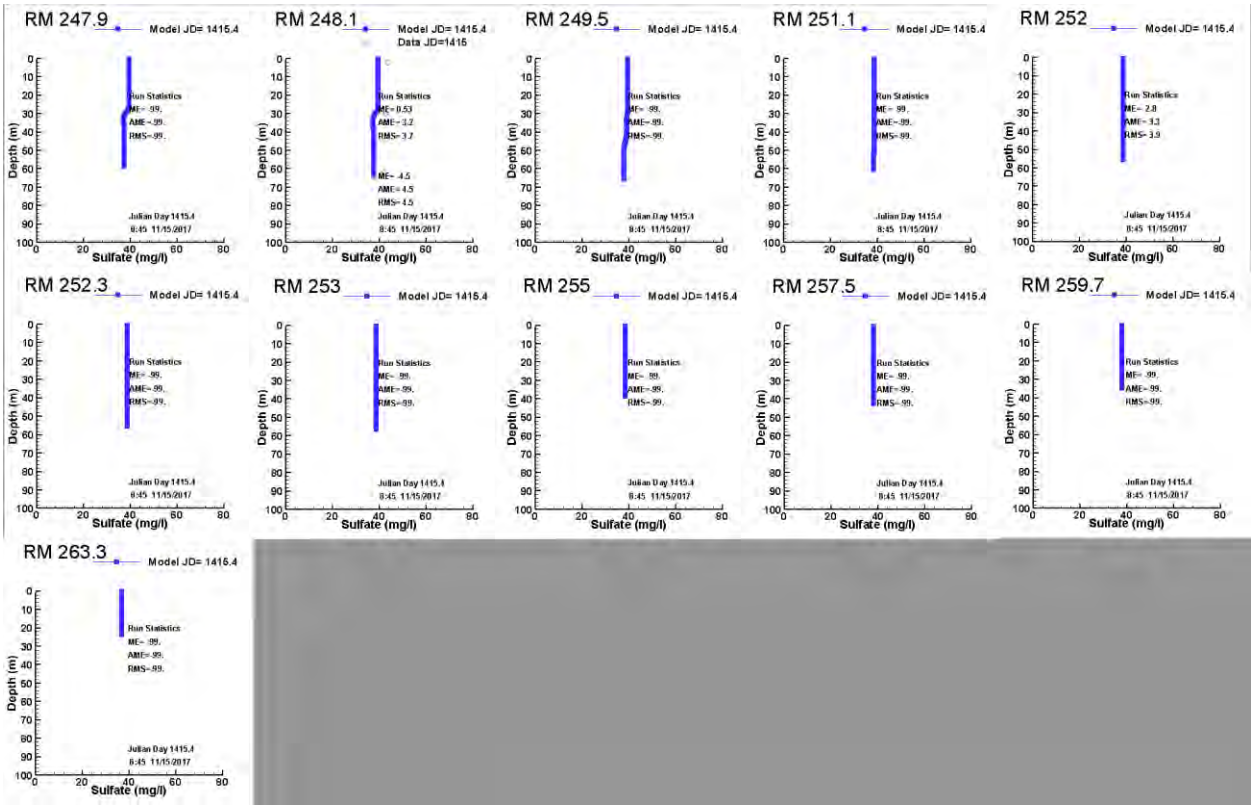


Figure 87. Vertical profiles of sulfate compared with data for 11/15/2017.

Fe(II)

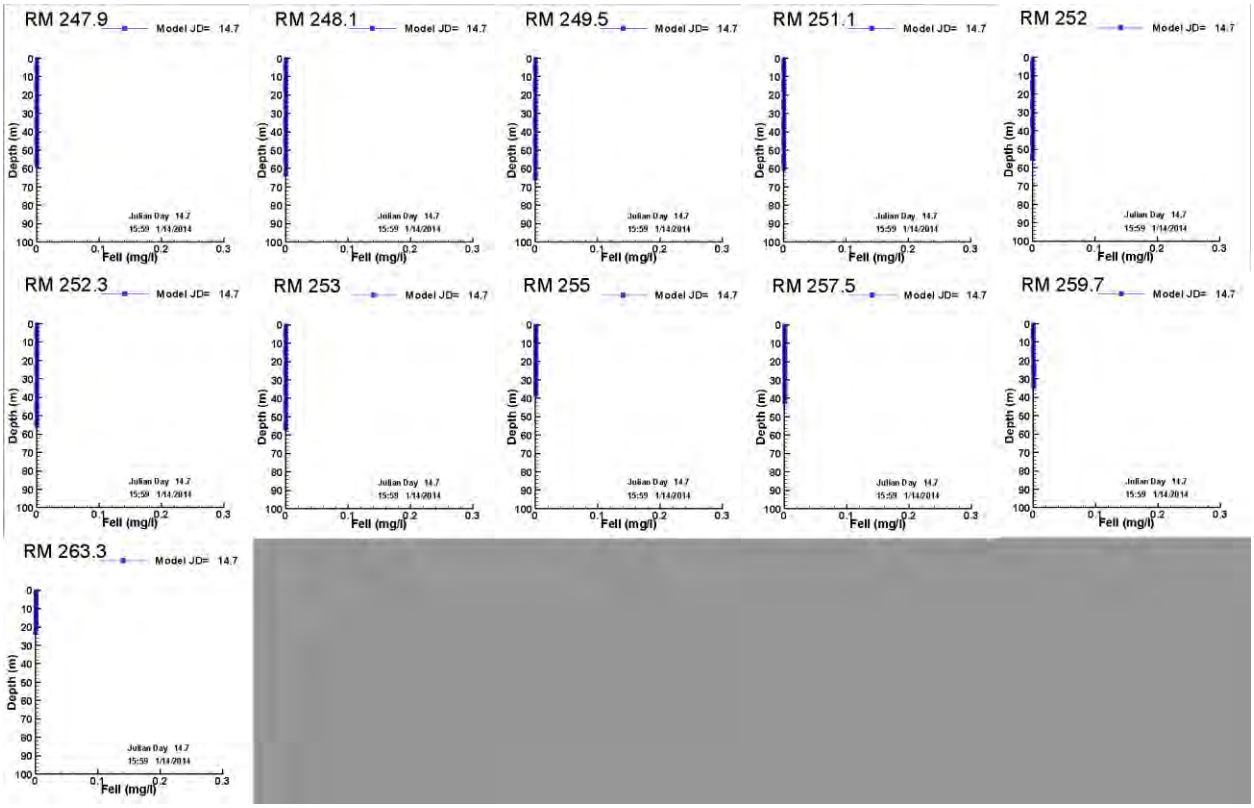


Figure 88. Vertical profiles of Fe(II) compared with data for 1/14/2014.

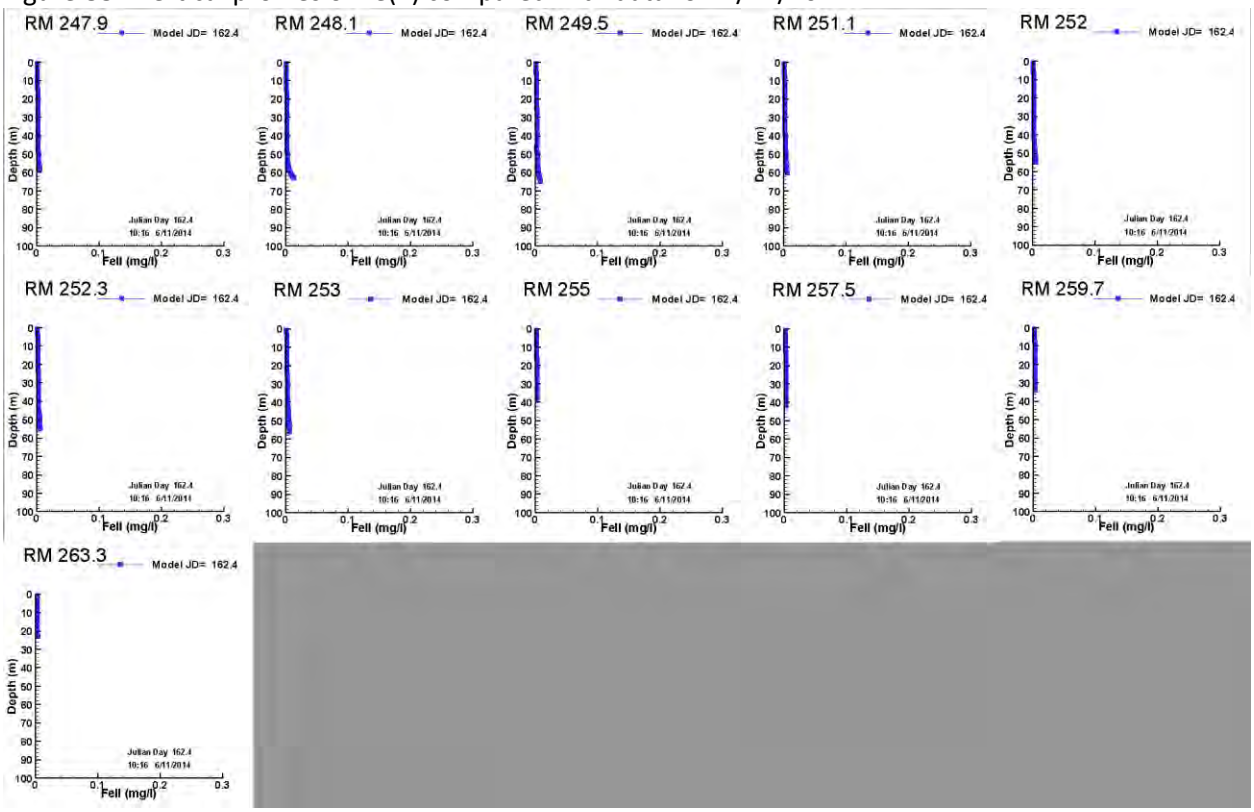


Figure 89. Vertical profiles of Fe(II) compared with data for 6/11/2014.

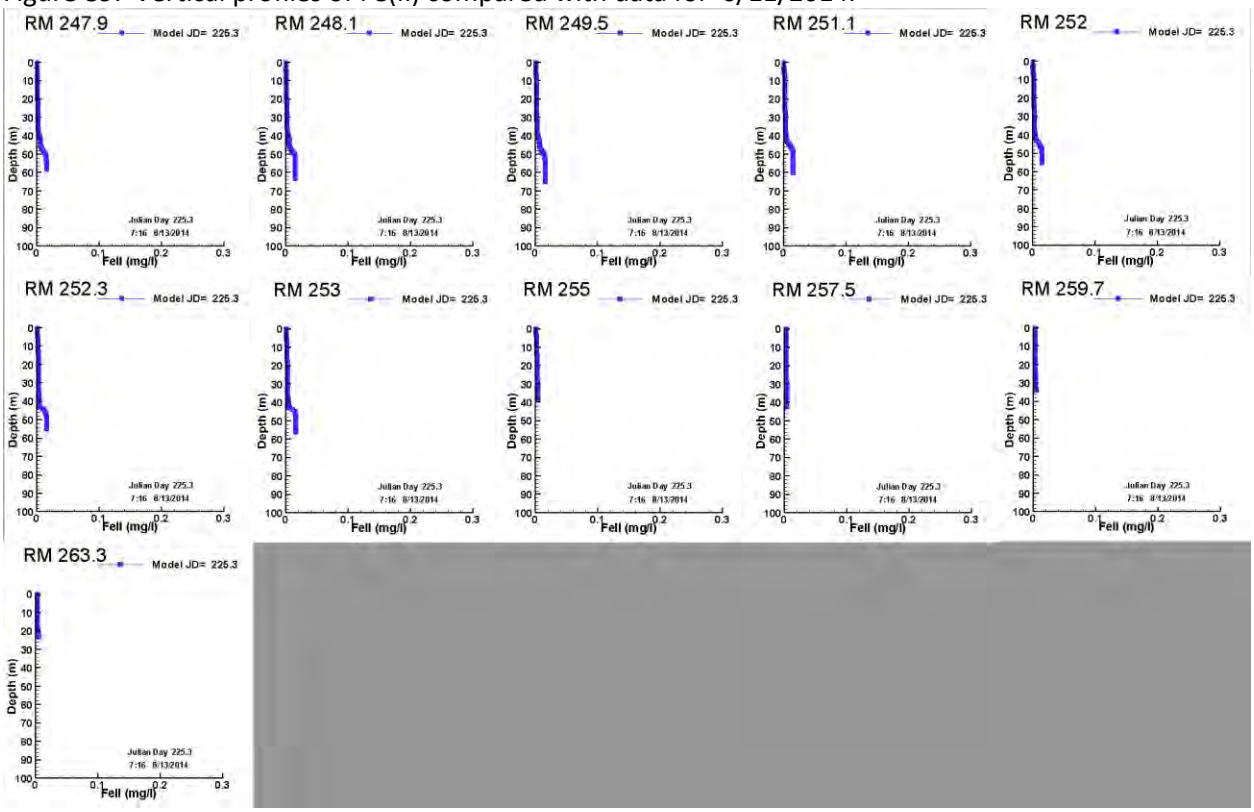


Figure 90. Vertical profiles of Fe(II) compared with data for 8/13/2014.

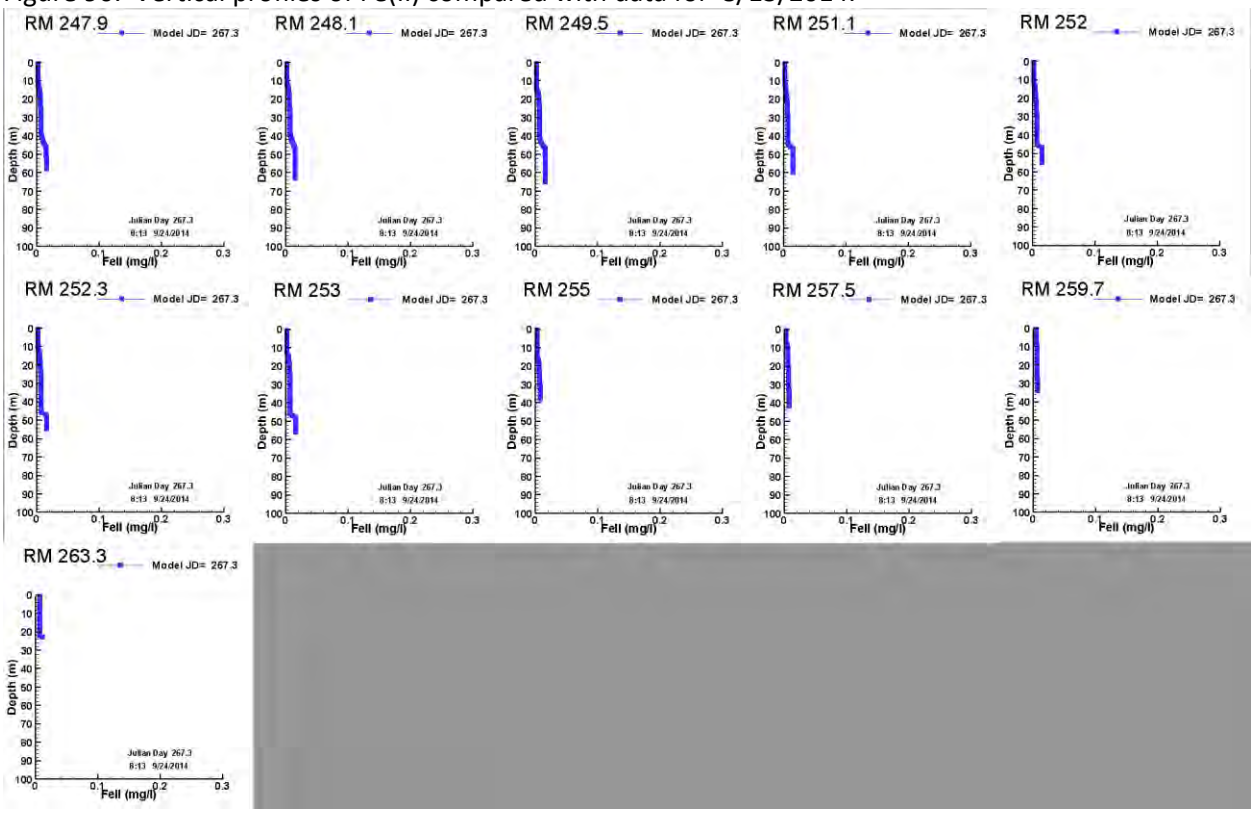


Figure 91. Vertical profiles of Fe(II) compared with data for 9/24/2014.

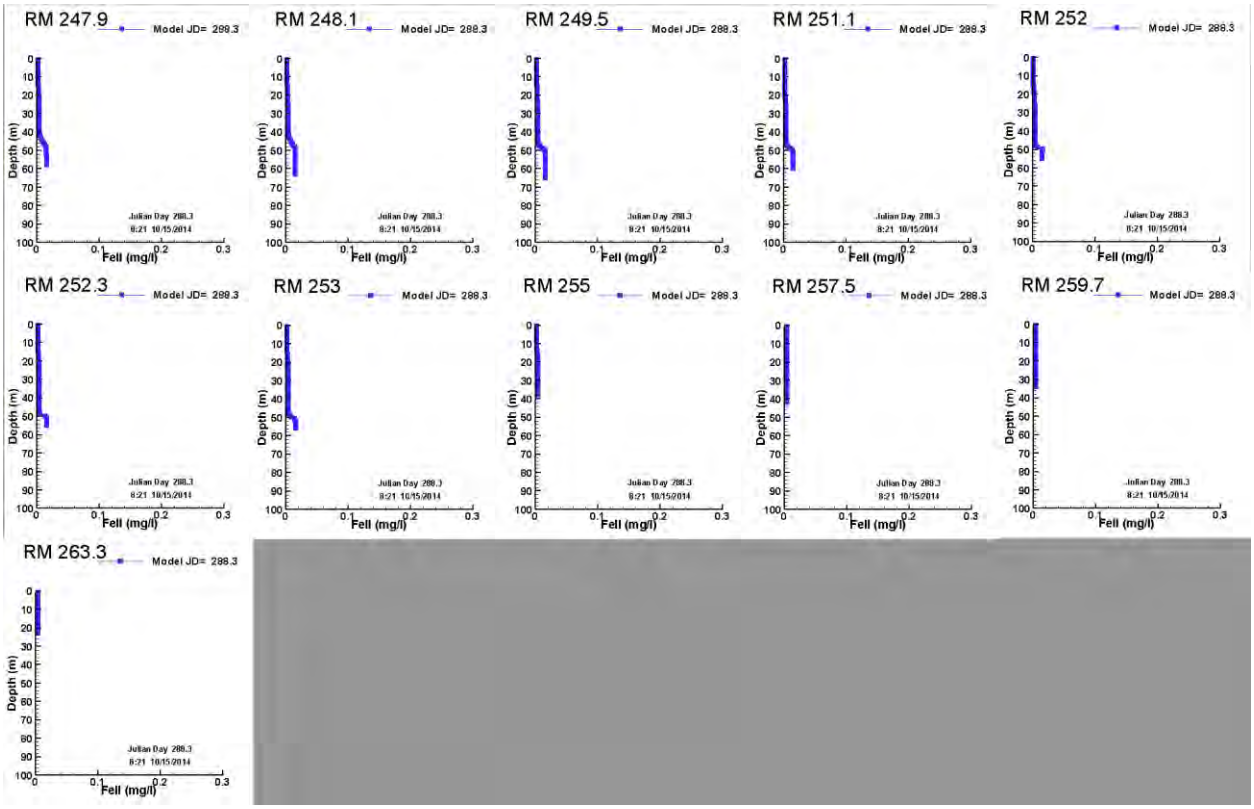


Figure 92. Vertical profiles of Fe(II) compared with data for 10/15/2014.

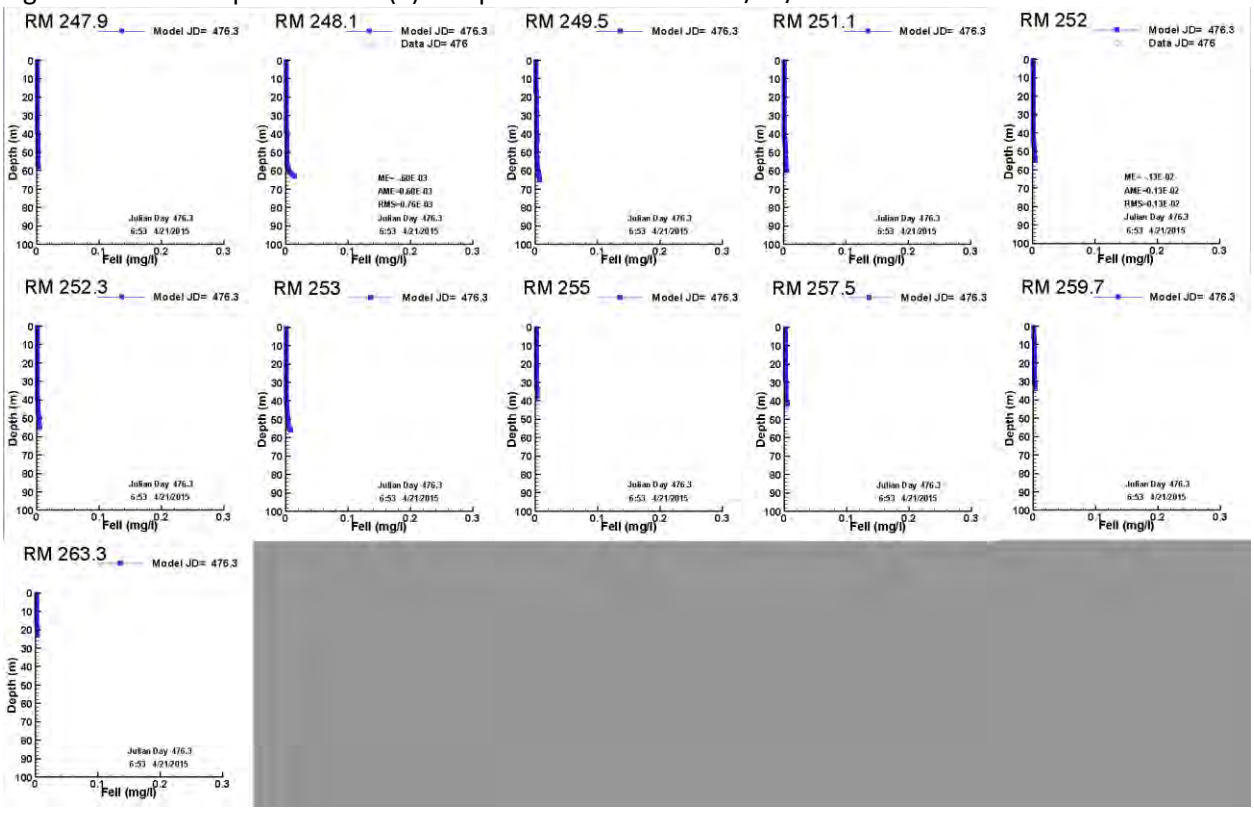


Figure 93. Vertical profiles of Fe(II) compared with data for 4/21/2015.

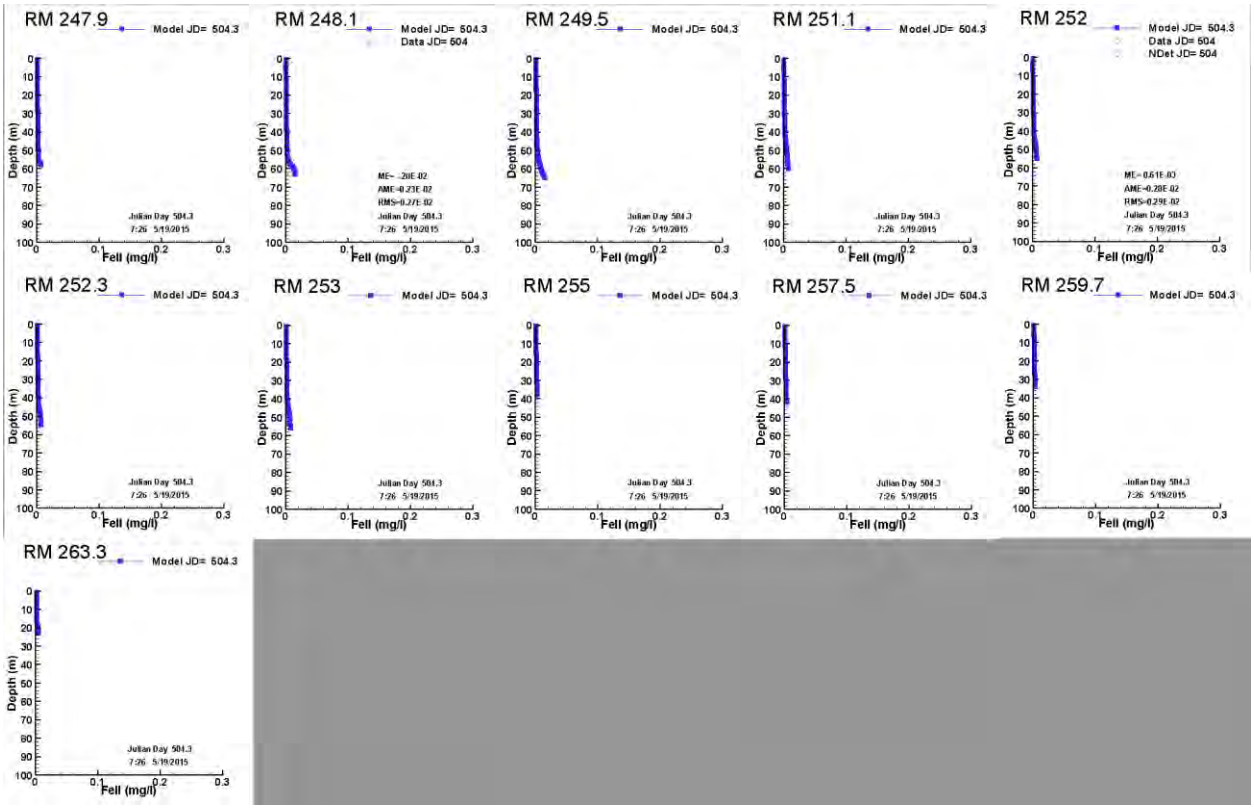


Figure 94. Vertical profiles of Fe(II) compared with data for 5/19/2015.

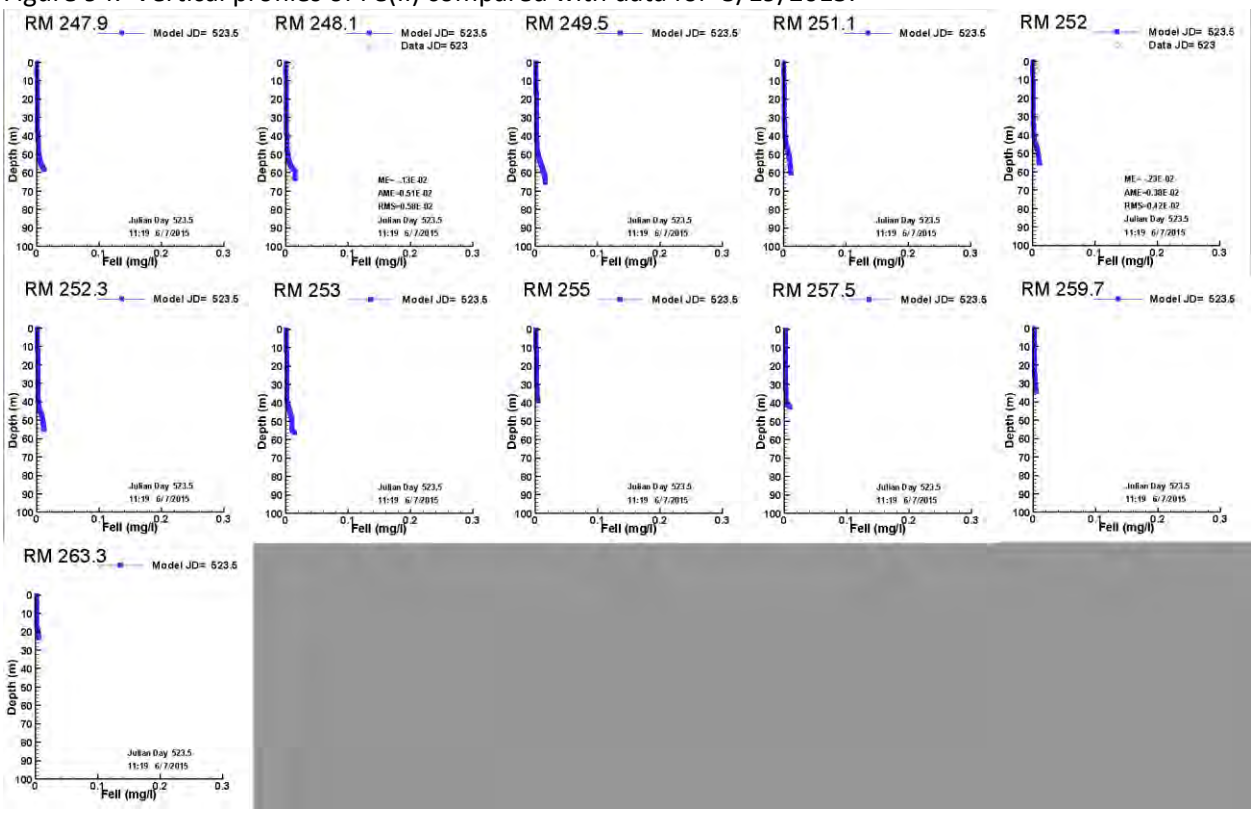


Figure 95. Vertical profiles of Fe(II) compared with data for 6/ 7/2015.

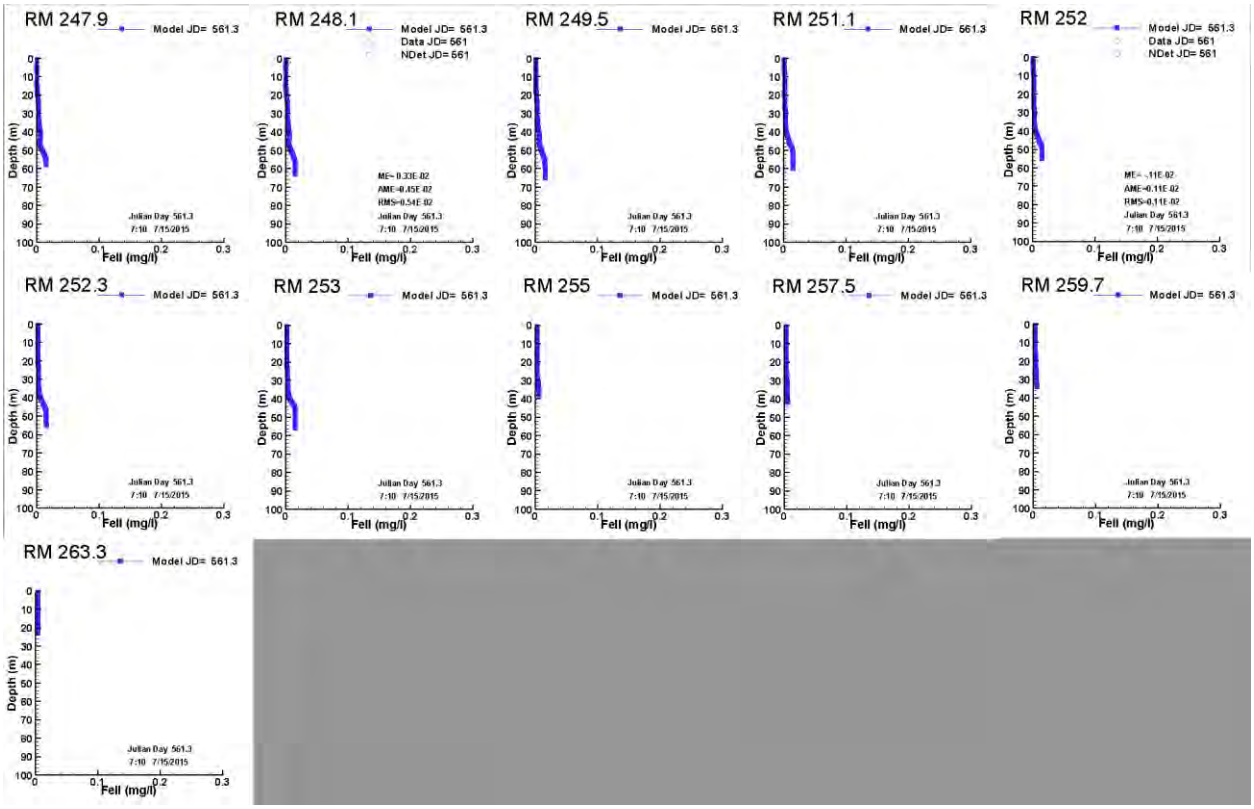


Figure 96. Vertical profiles of Fe(II) compared with data for 7/15/2015.

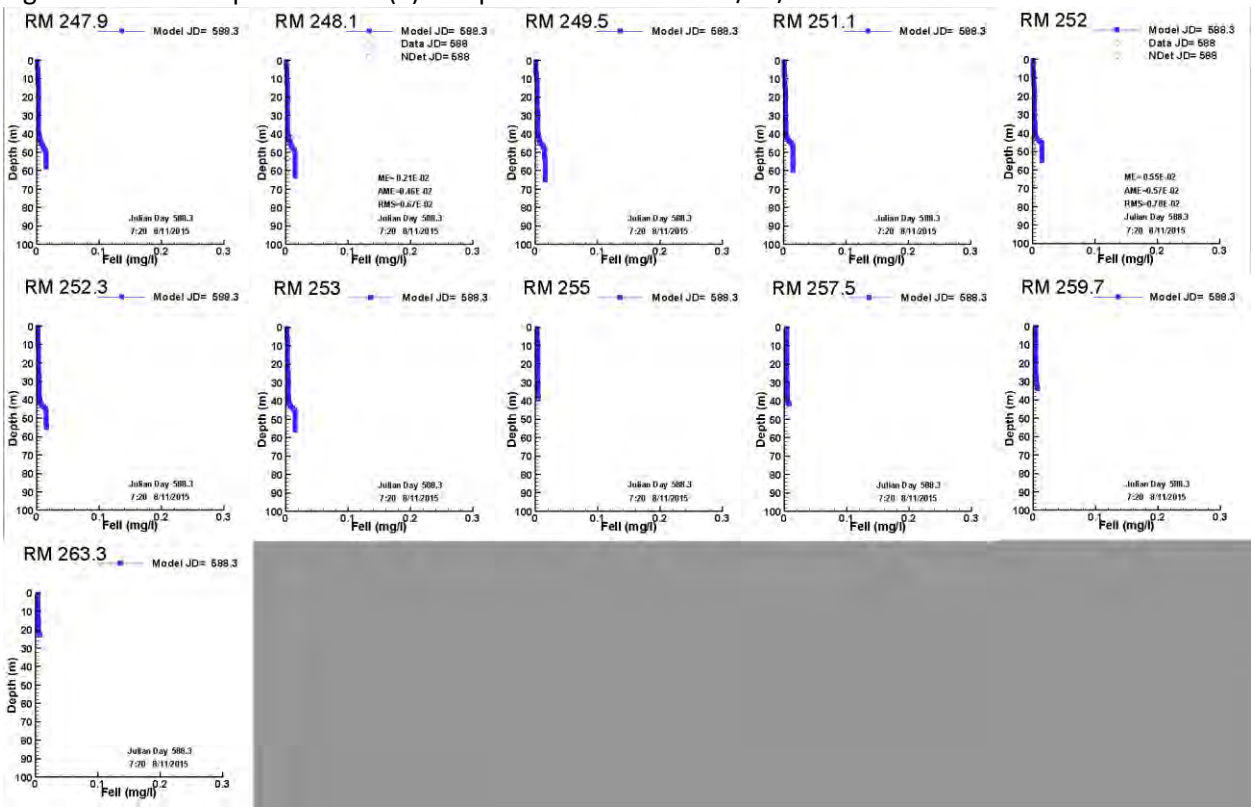


Figure 97. Vertical profiles of Fe(II) compared with data for 8/11/2015.

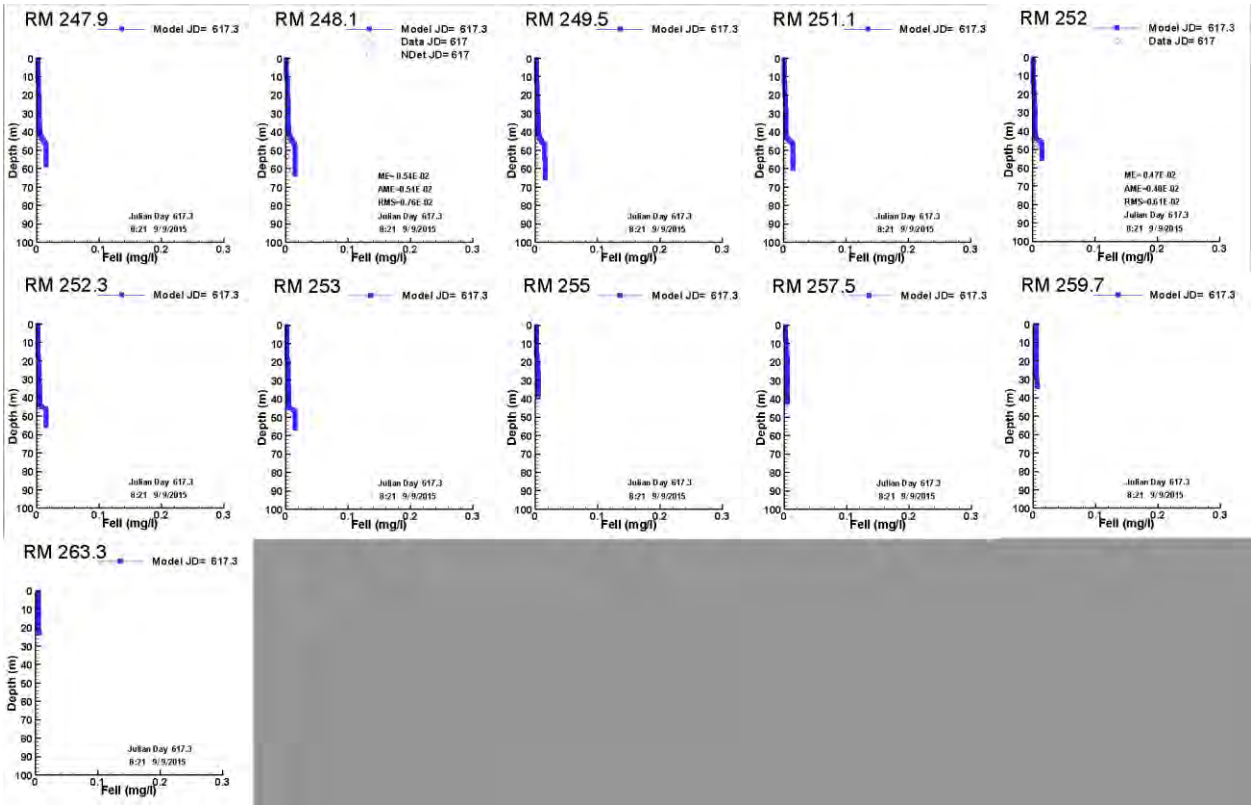


Figure 98. Vertical profiles of Fe(II) compared with data for 9/ 9/2015.

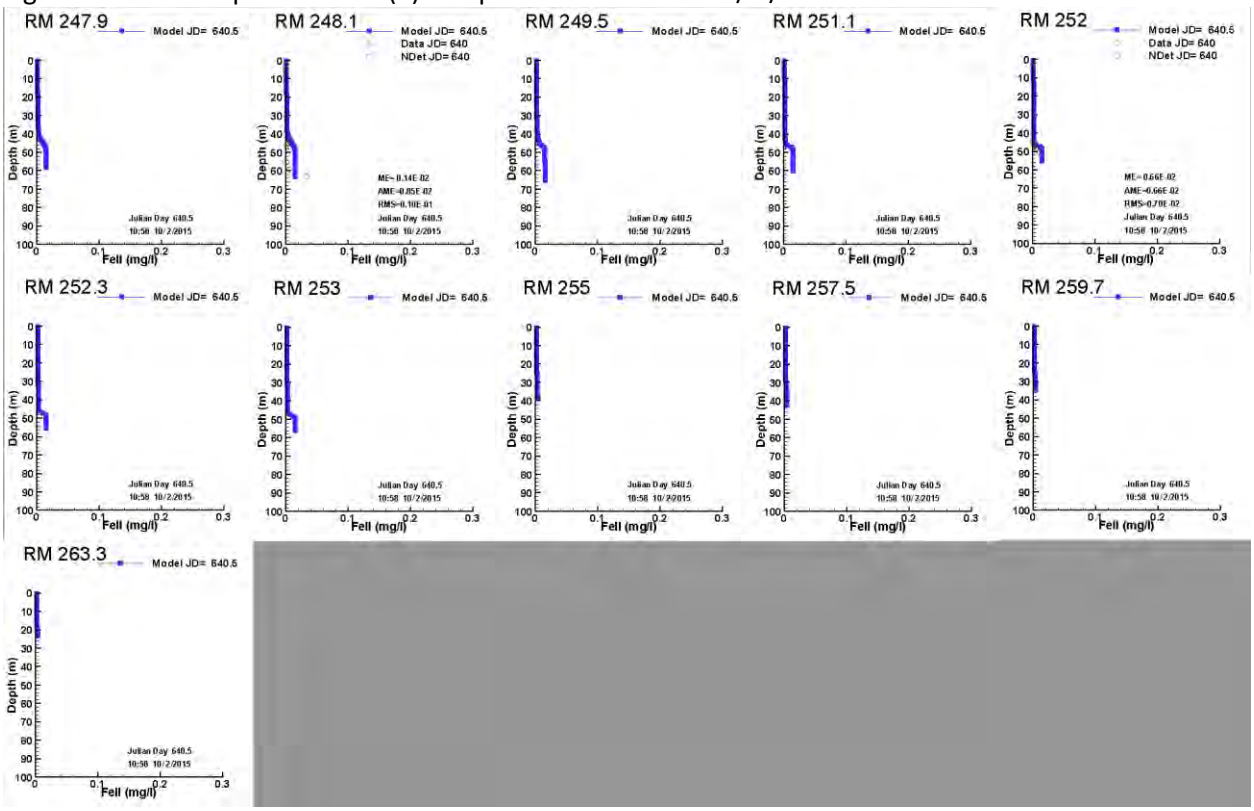


Figure 99. Vertical profiles of Fe(II) compared with data for 10/ 2/2015.

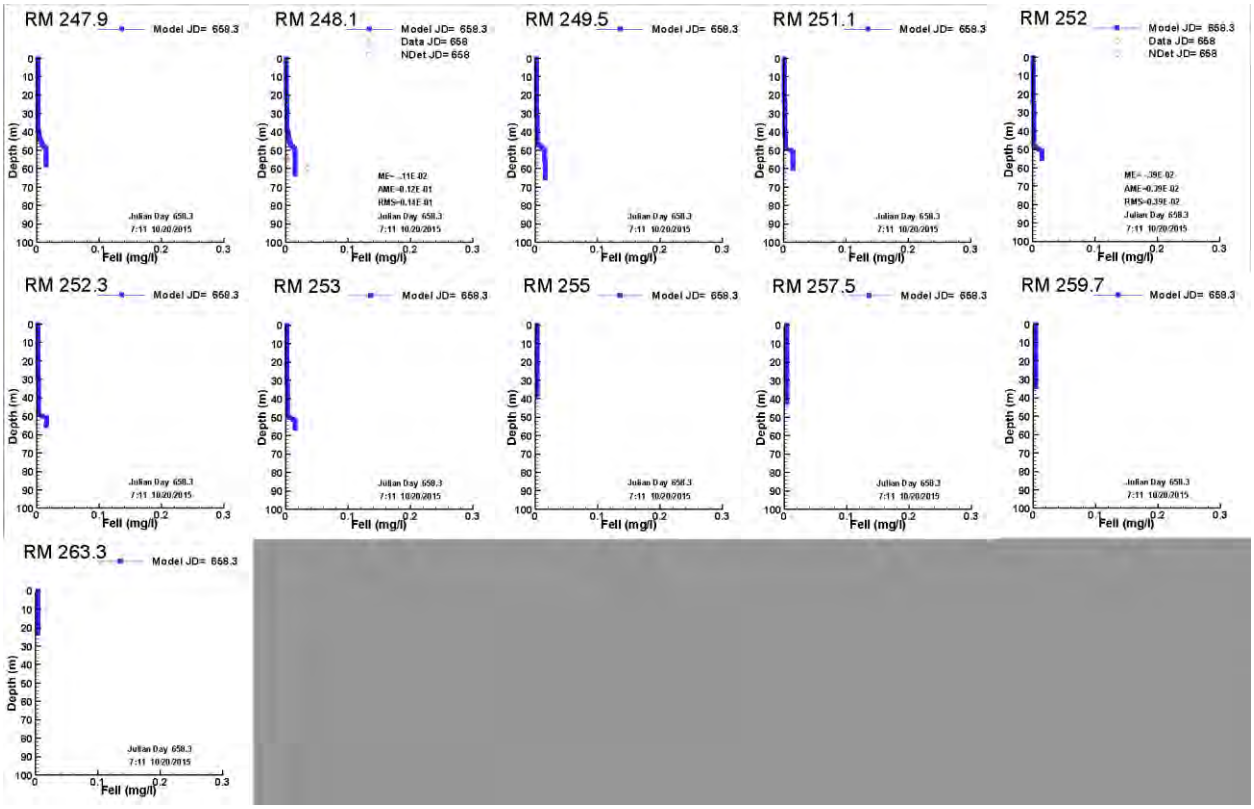


Figure 100. Vertical profiles of Fe(II) compared with data for 10/20/2015.

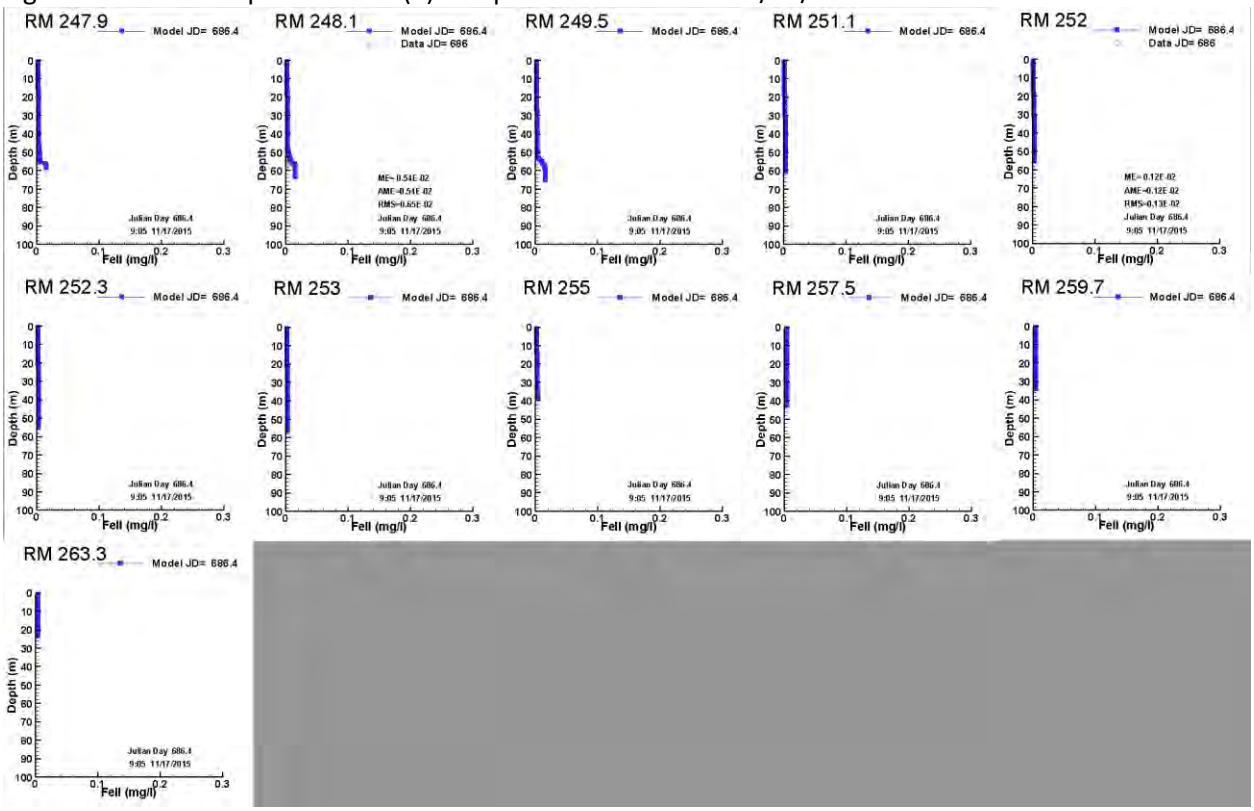


Figure 101. Vertical profiles of Fe(II) compared with data for 11/17/2015.

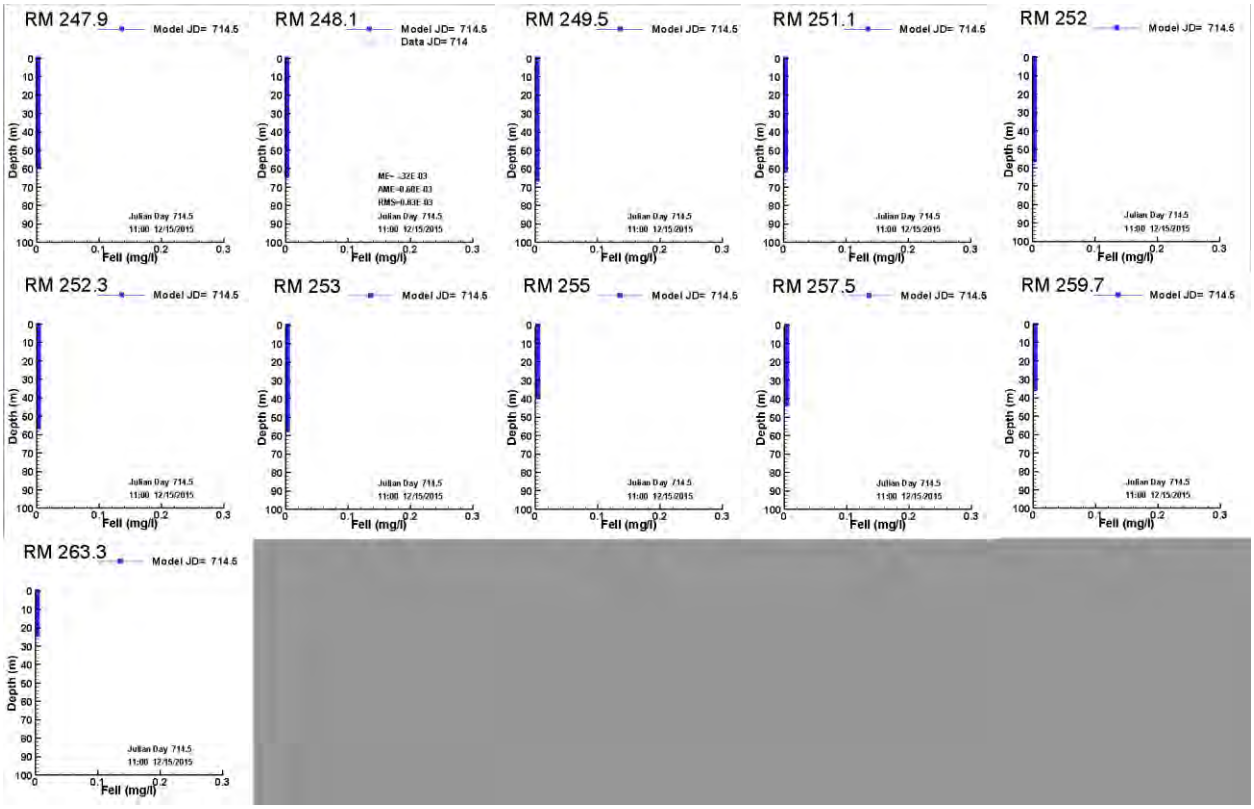


Figure 102. Vertical profiles of Fe(II) compared with data for 12/15/2015.

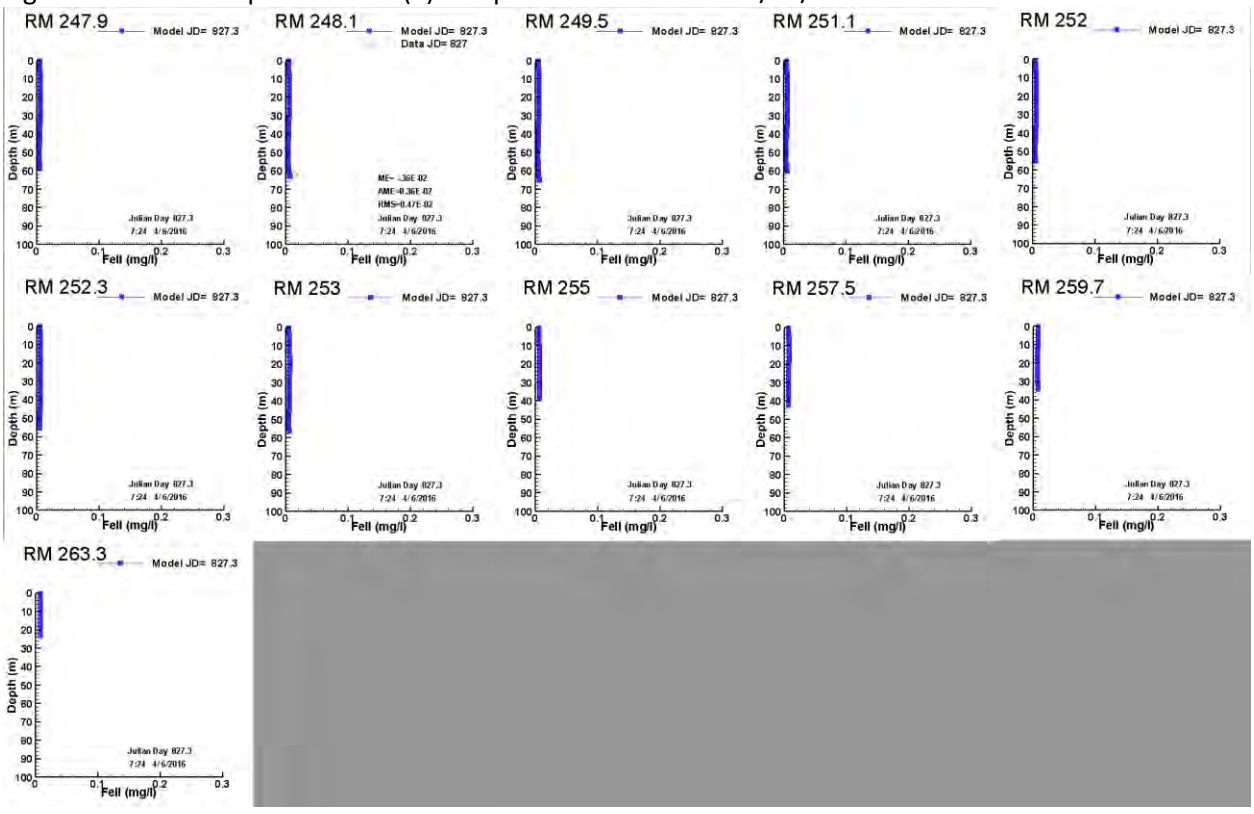


Figure 103. Vertical profiles of Fe(II) compared with data for 4/ 6/2016.

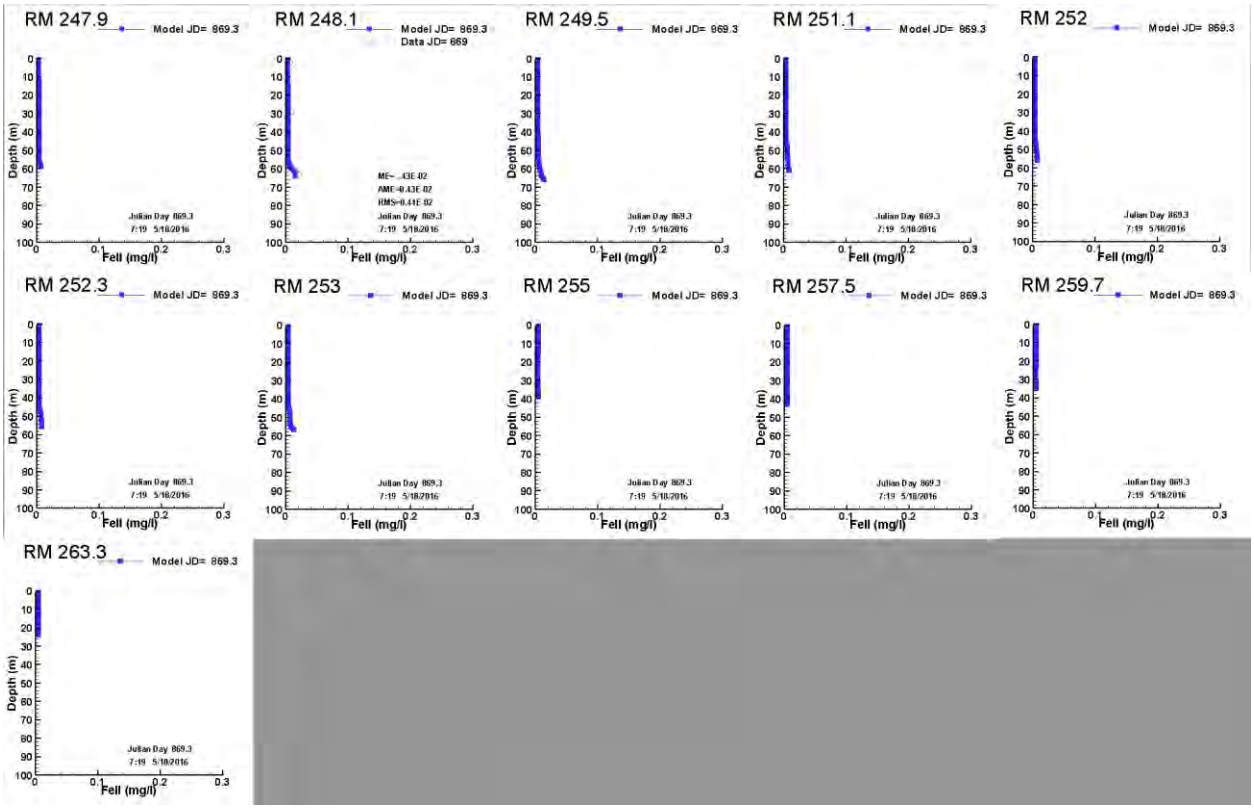


Figure 104. Vertical profiles of Fe(II) compared with data for 5/18/2016.

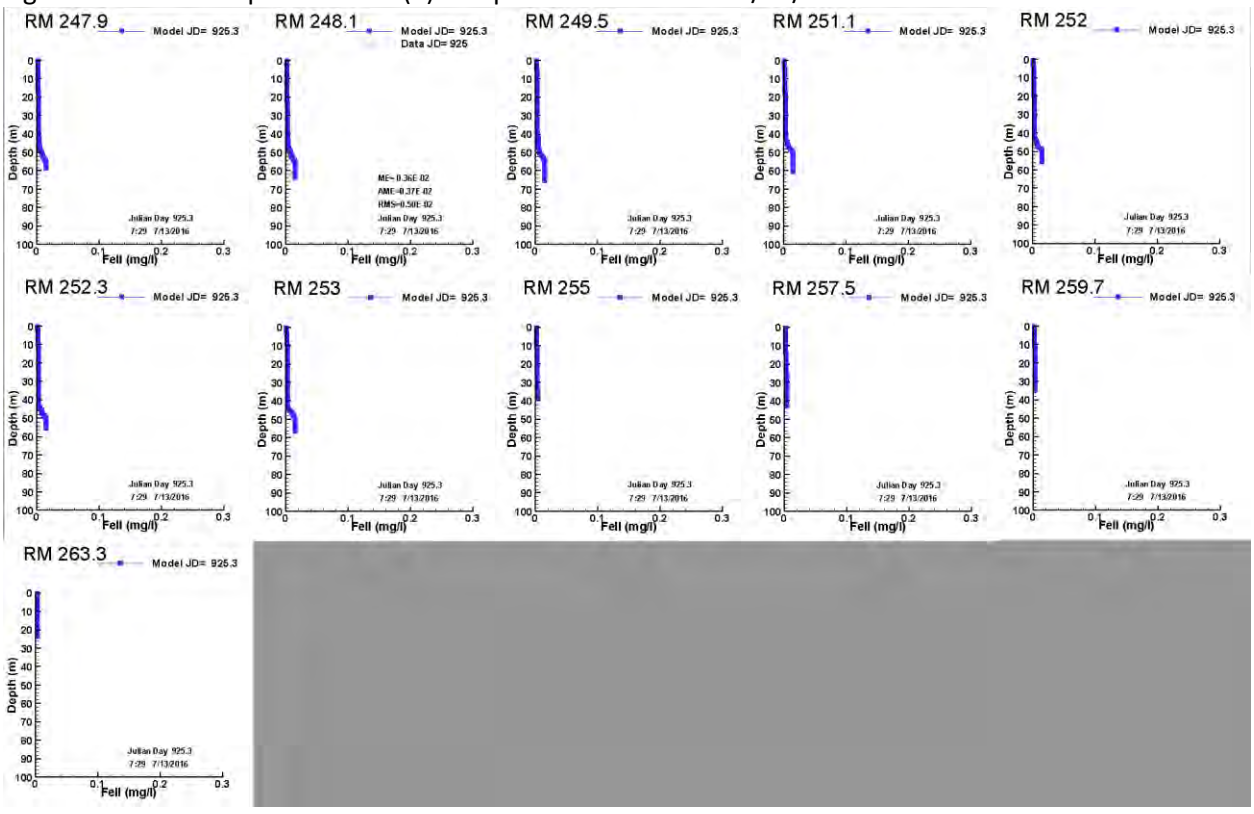


Figure 105. Vertical profiles of Fe(II) compared with data for 7/13/2016.

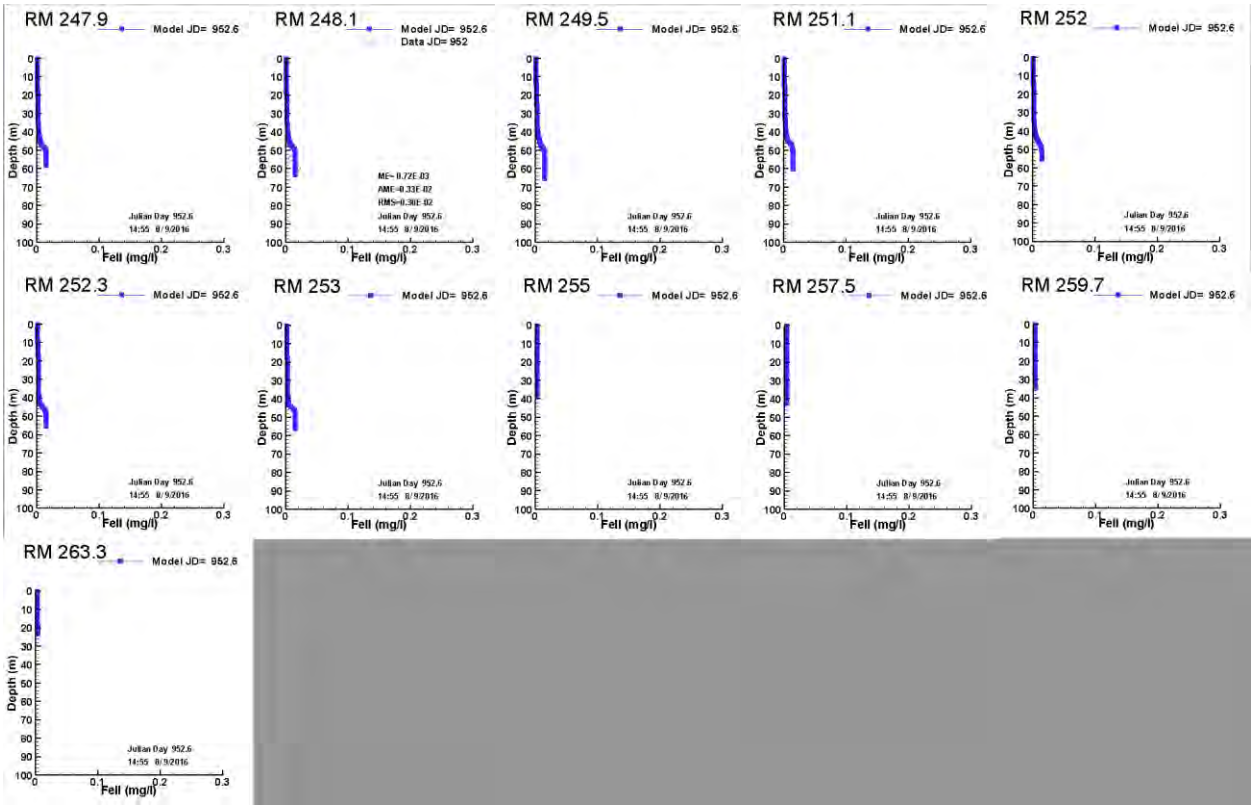


Figure 106. Vertical profiles of Fe(II) compared with data for 8/ 9/2016.

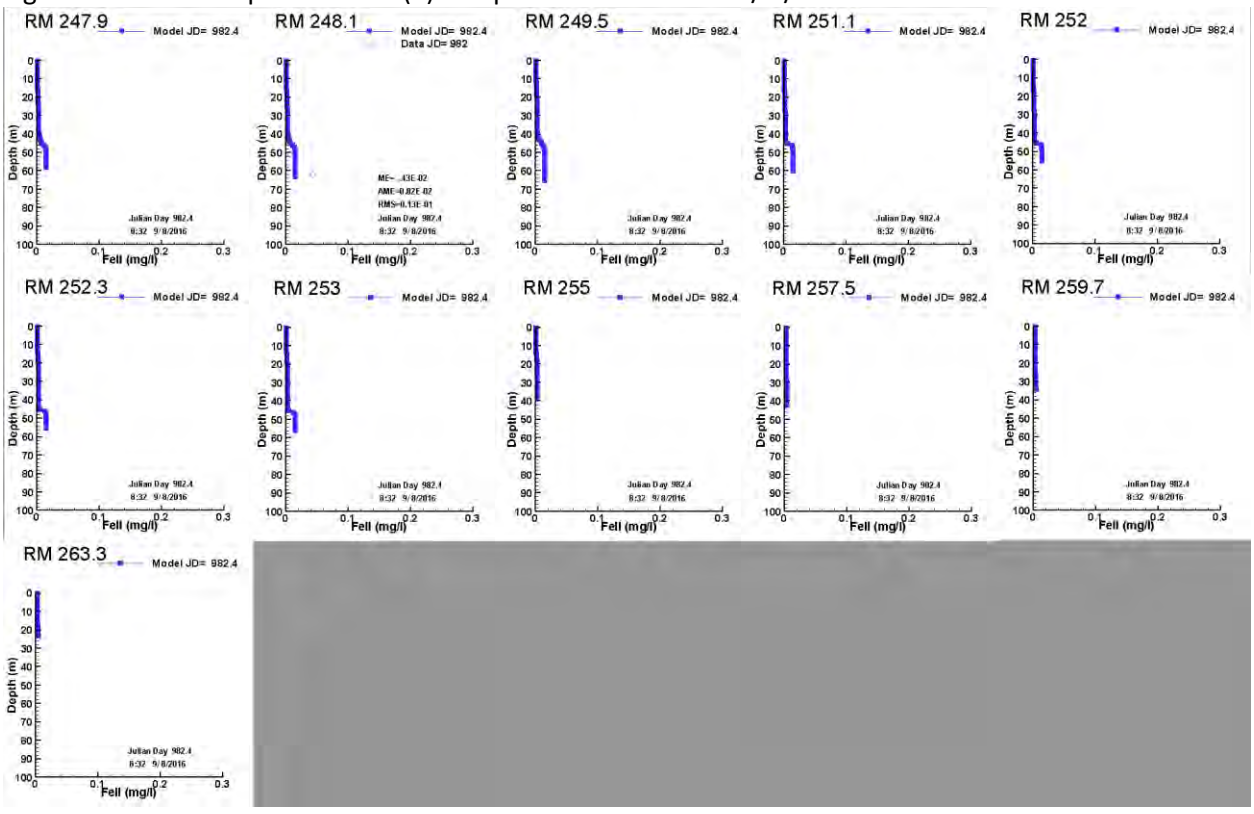


Figure 107. Vertical profiles of Fe(II) compared with data for 9/ 8/2016.

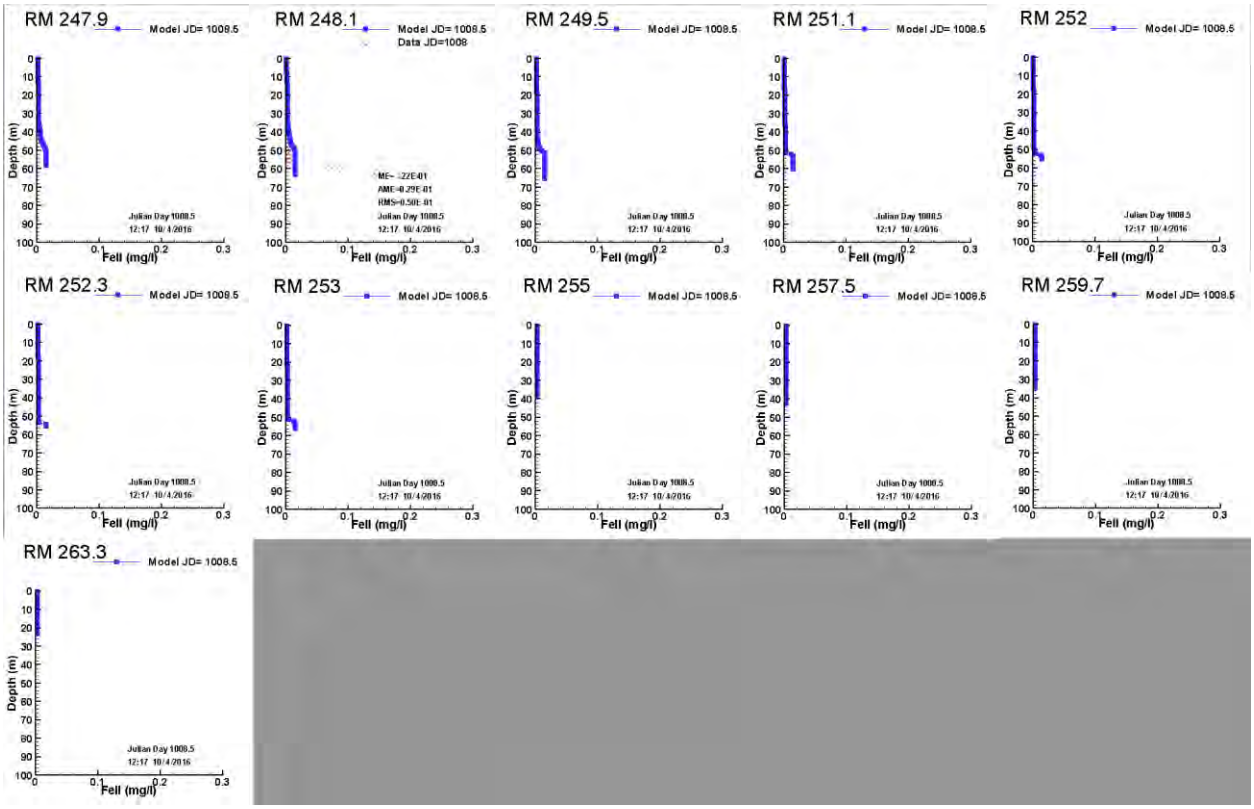


Figure 108. Vertical profiles of Fe(II) compared with data for 10/ 4/2016.

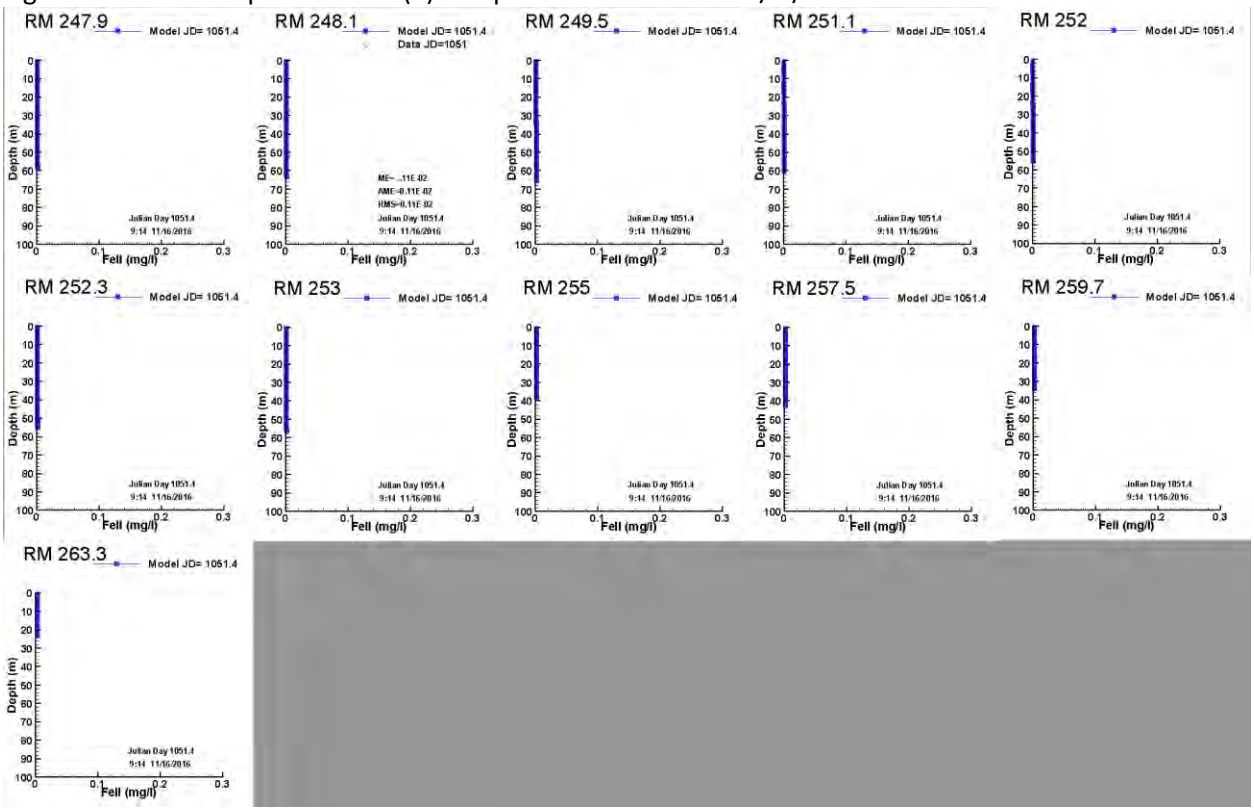


Figure 109. Vertical profiles of Fe(II) compared with data for 11/16/2016.

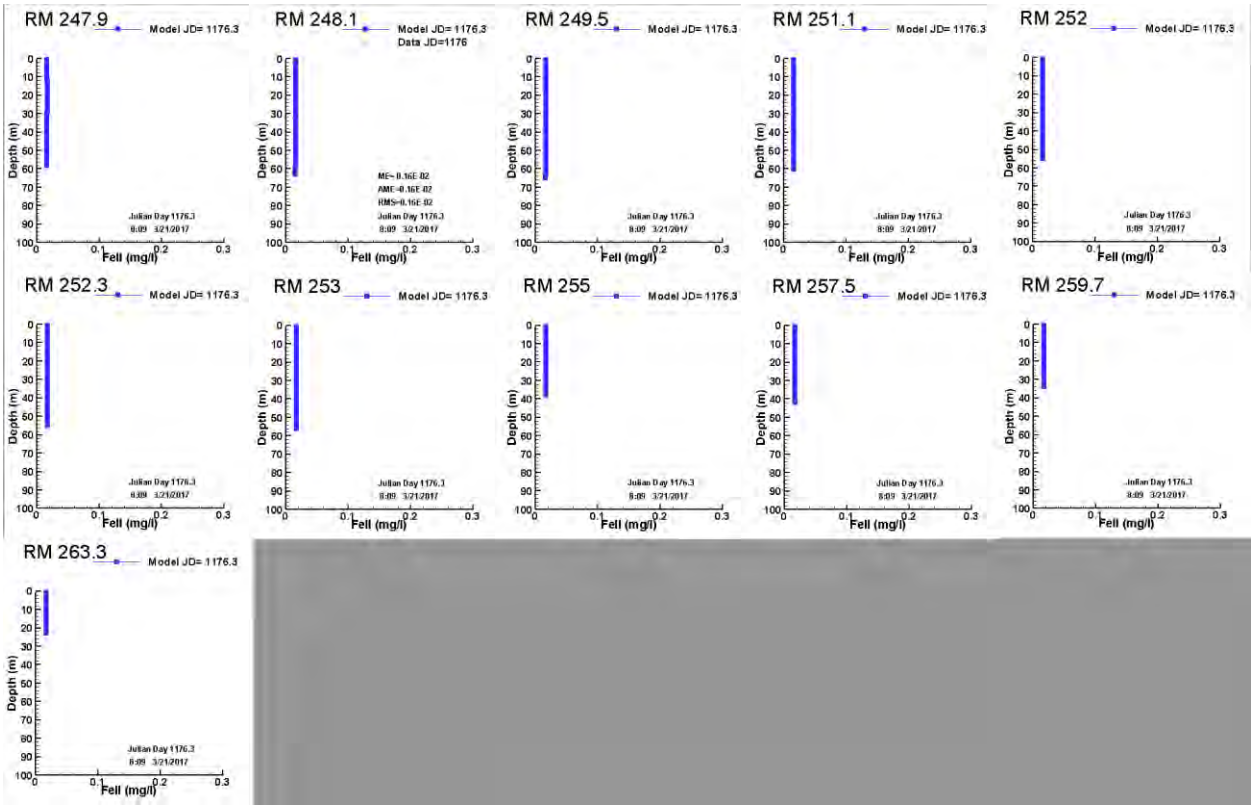


Figure 110. Vertical profiles of Fe(II) compared with data for 3/21/2017.

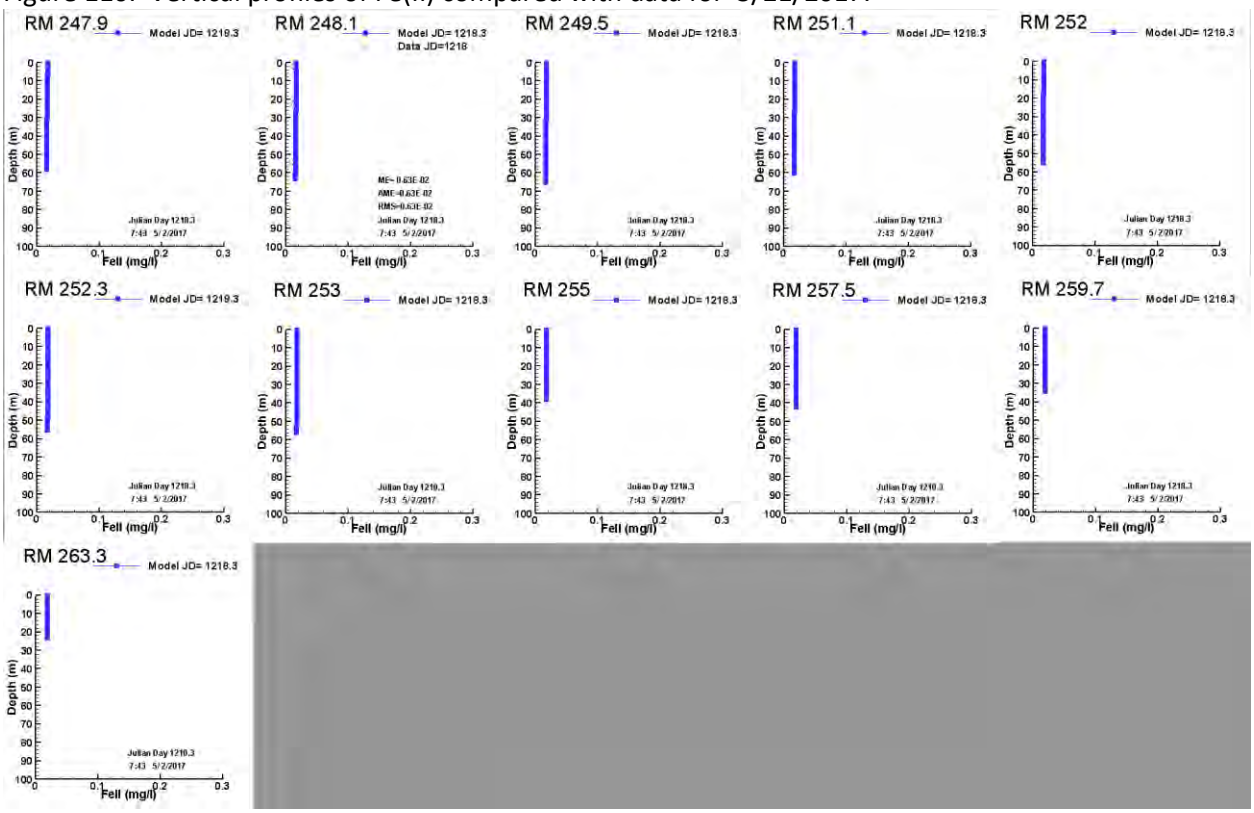


Figure 111. Vertical profiles of Fe(II) compared with data for 5/ 2/2017.

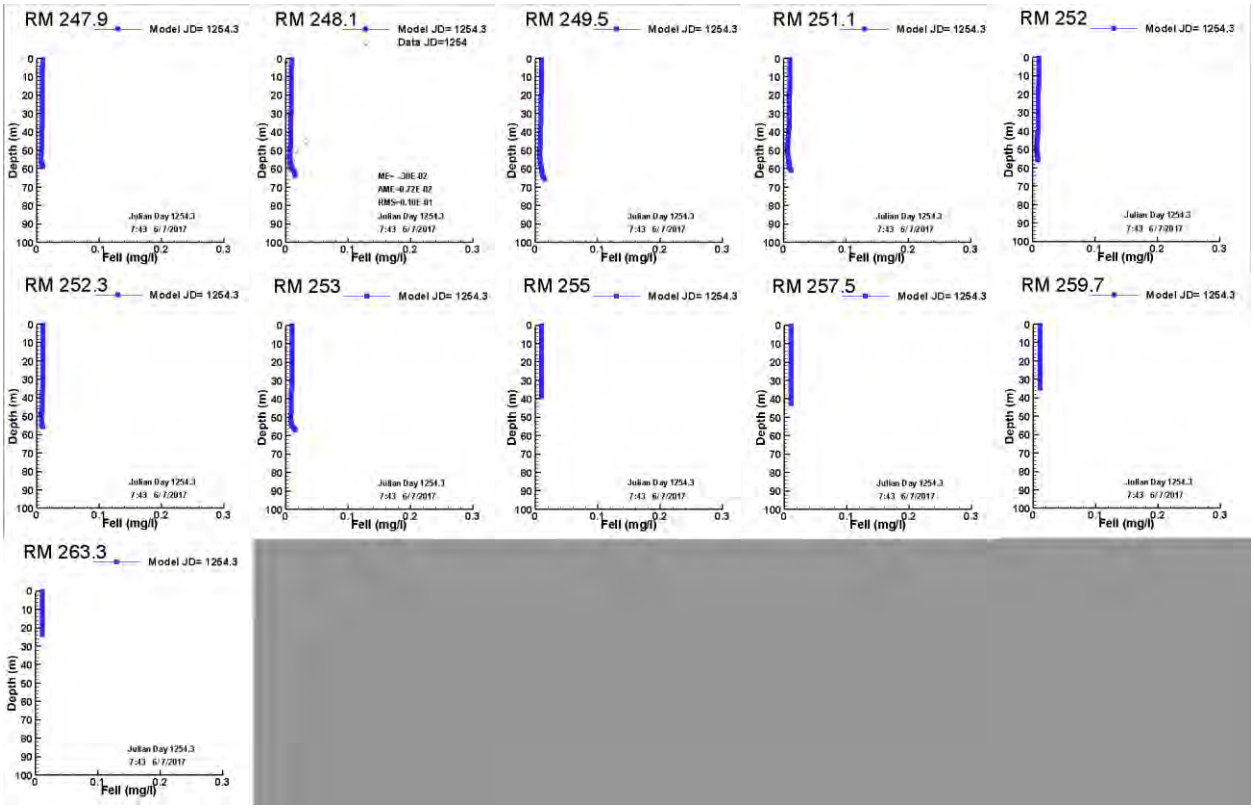


Figure 112. Vertical profiles of Fe(II) compared with data for 6/ 7/2017.

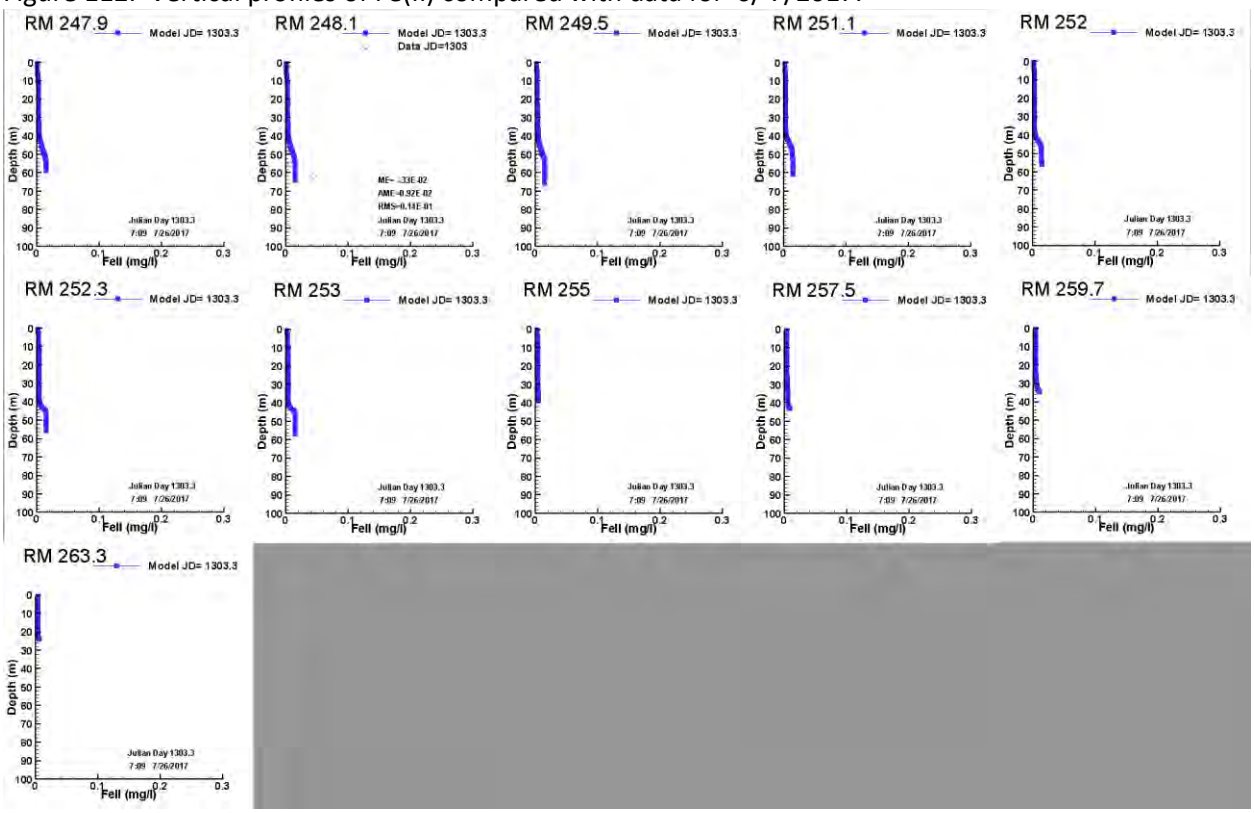


Figure 113. Vertical profiles of Fe(II) compared with data for 7/26/2017.

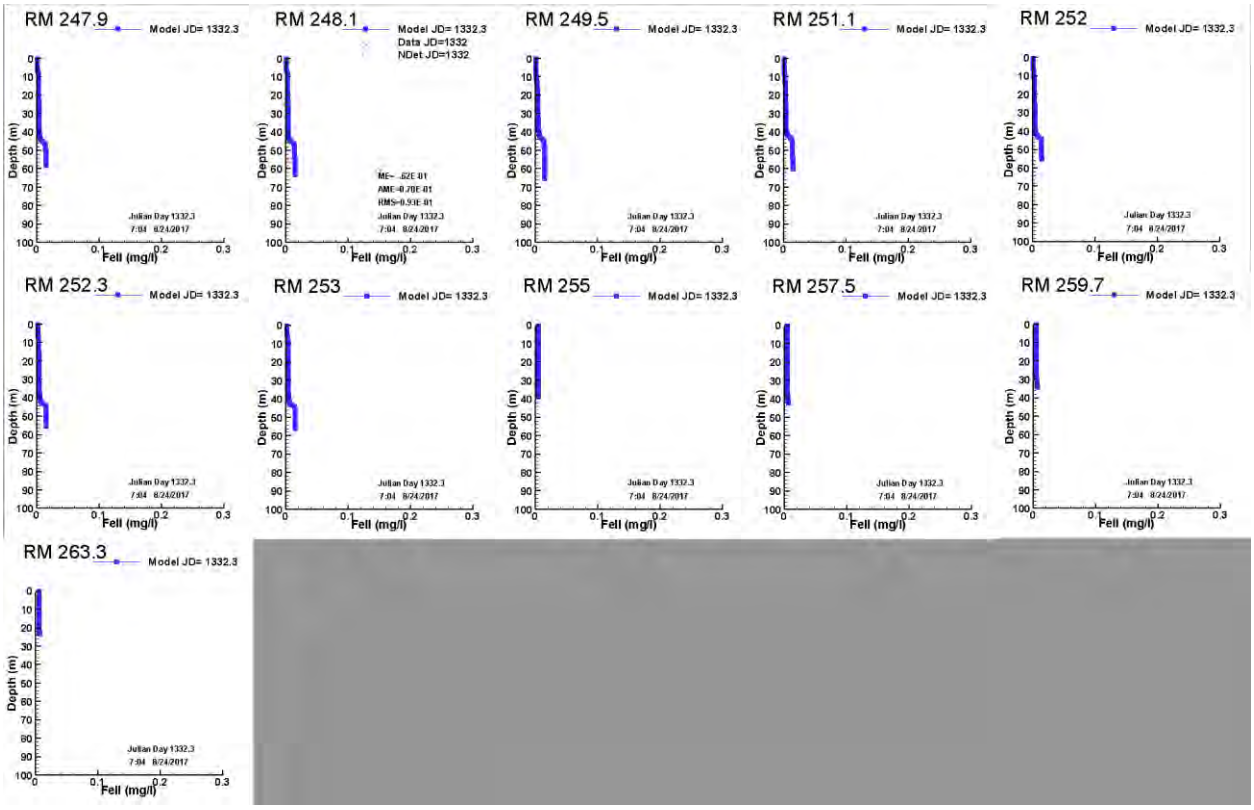


Figure 114. Vertical profiles of Fe(II) compared with data for 8/24/2017.

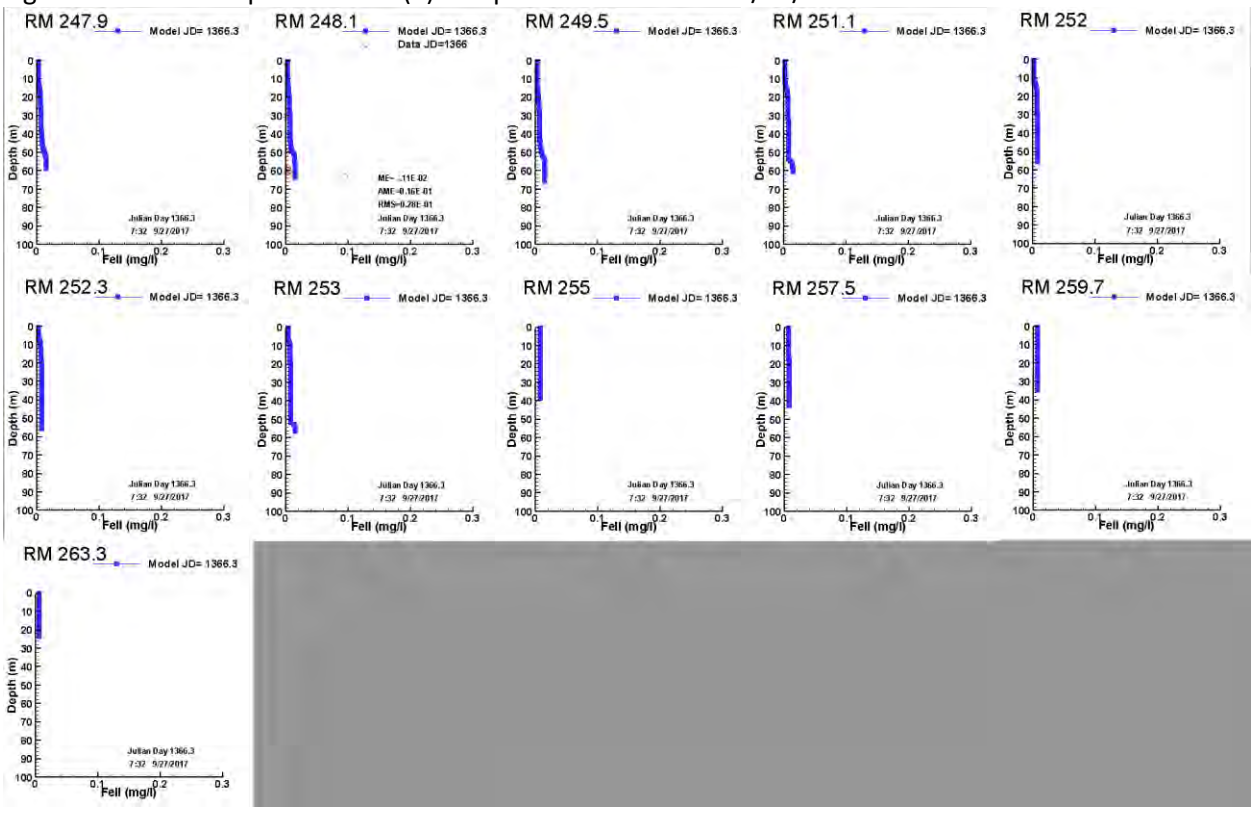


Figure 115. Vertical profiles of Fe(II) compared with data for 9/27/2017.

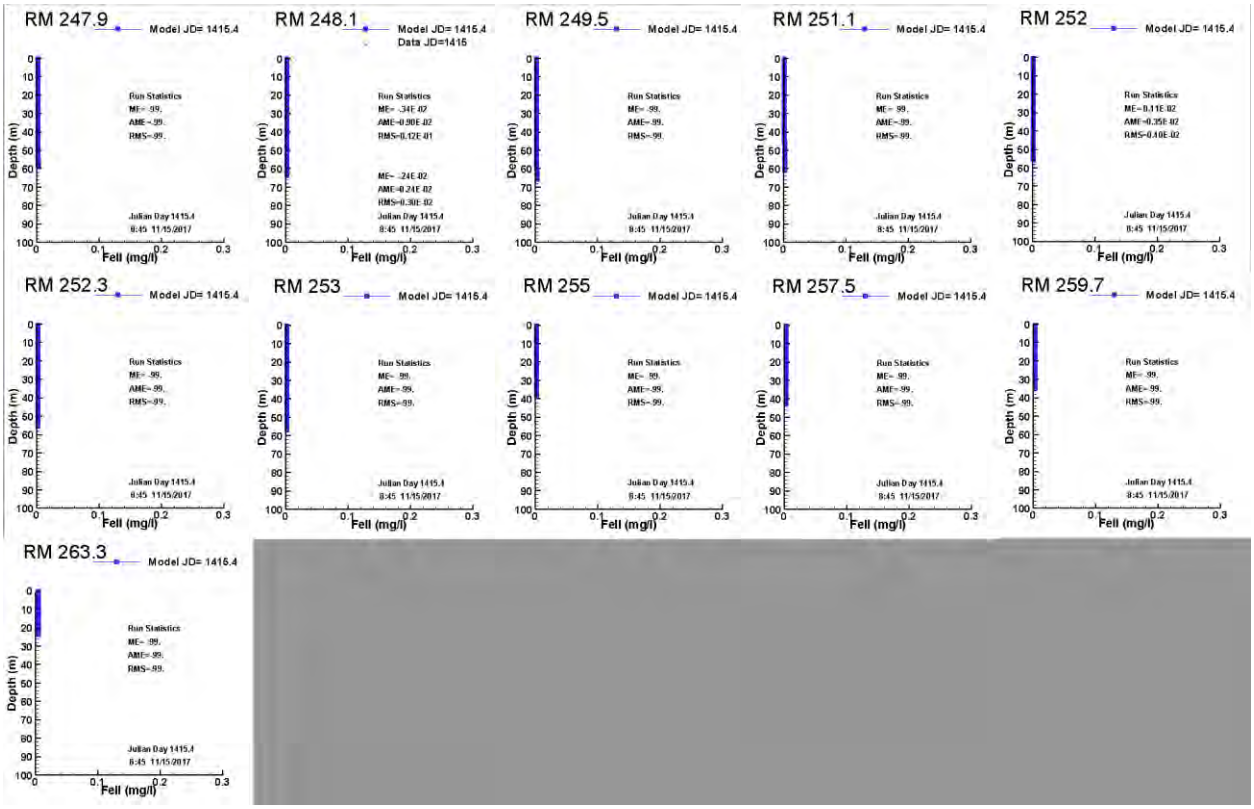


Figure 116. Vertical profiles of Fe(II) compared with data for 11/15/2017.

FeOOH

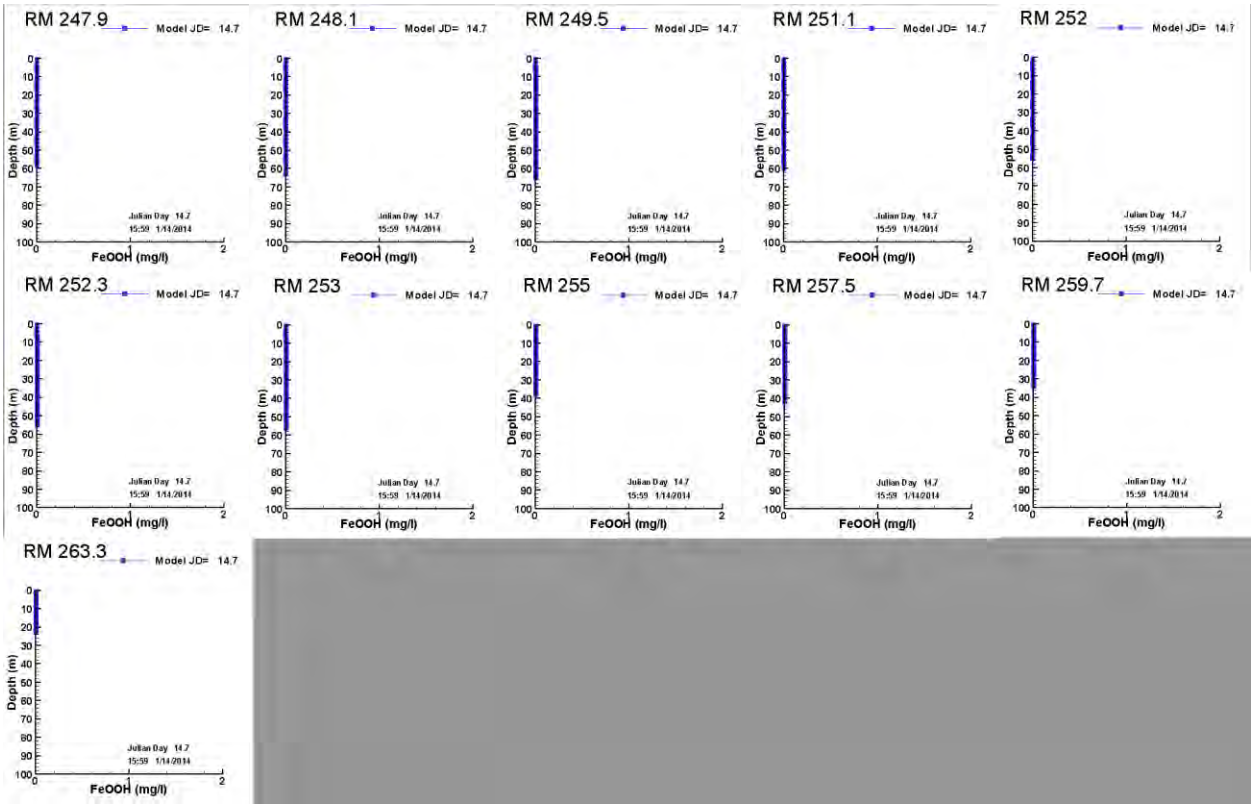


Figure 117. Vertical profiles of FeOOH compared with data for 1/14/2014.

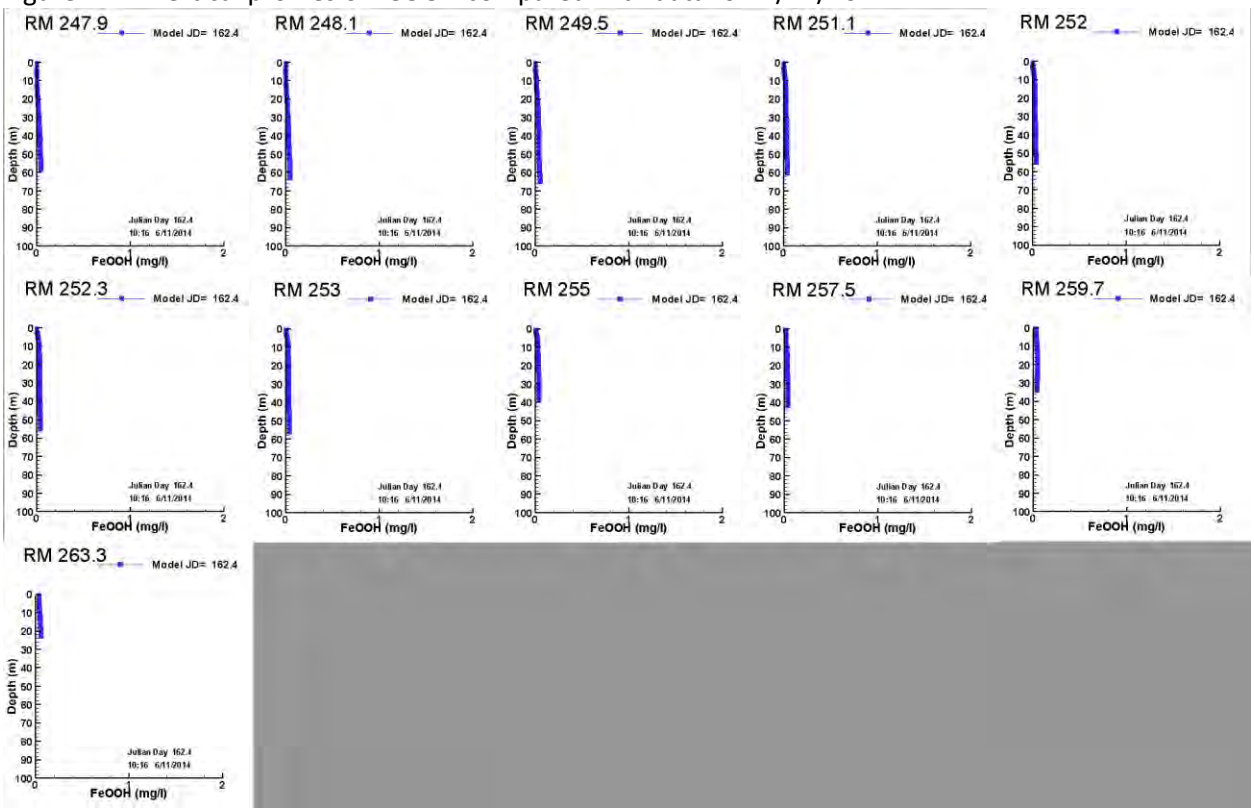


Figure 118. Vertical profiles of FeOOH compared with data for 6/11/2014.

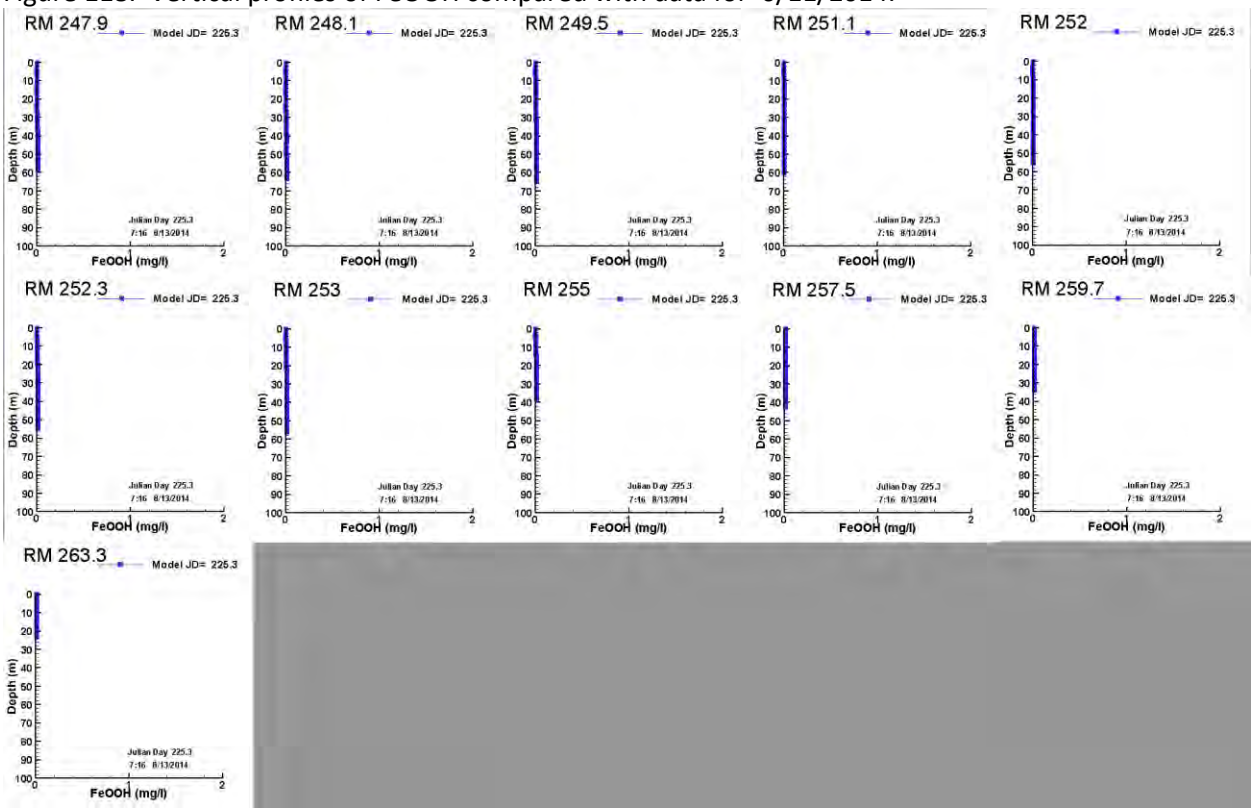


Figure 119. Vertical profiles of FeOOH compared with data for 8/13/2014.

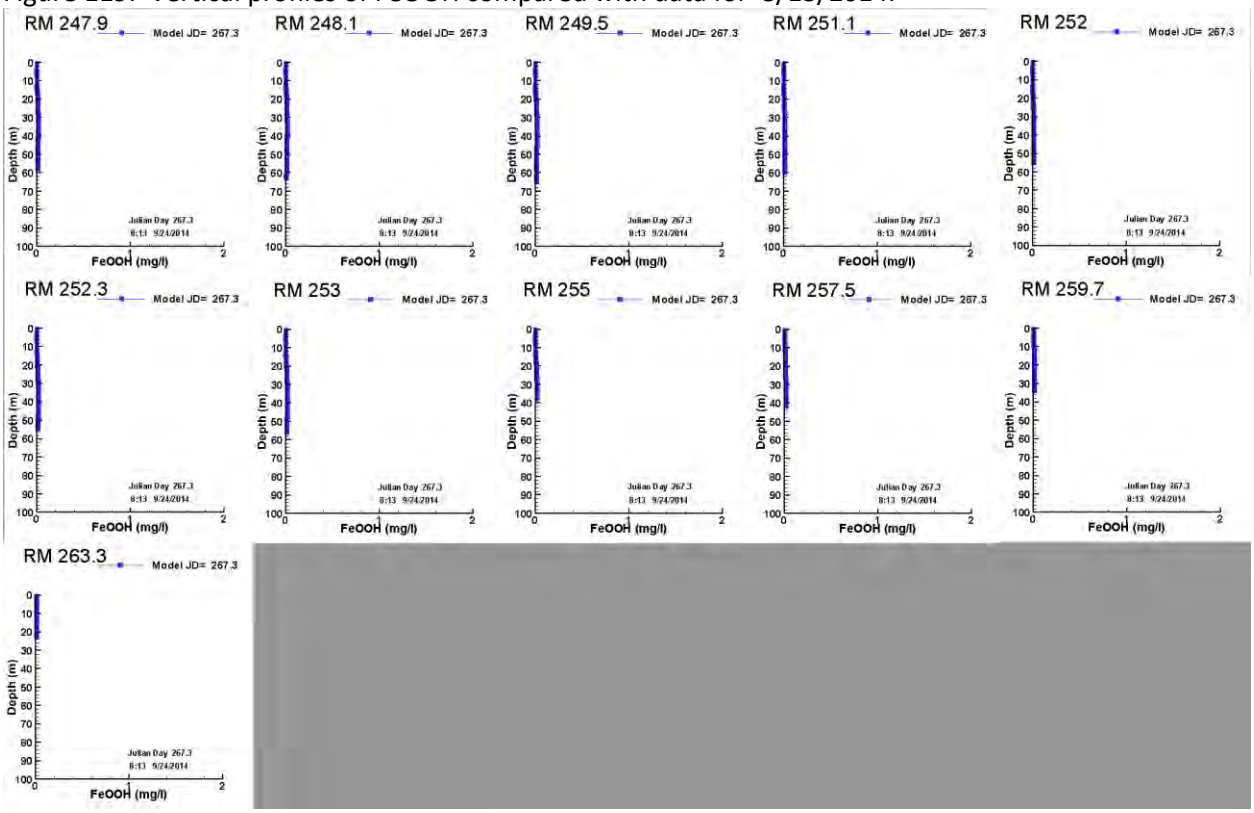


Figure 120. Vertical profiles of FeOOH compared with data for 9/24/2014.

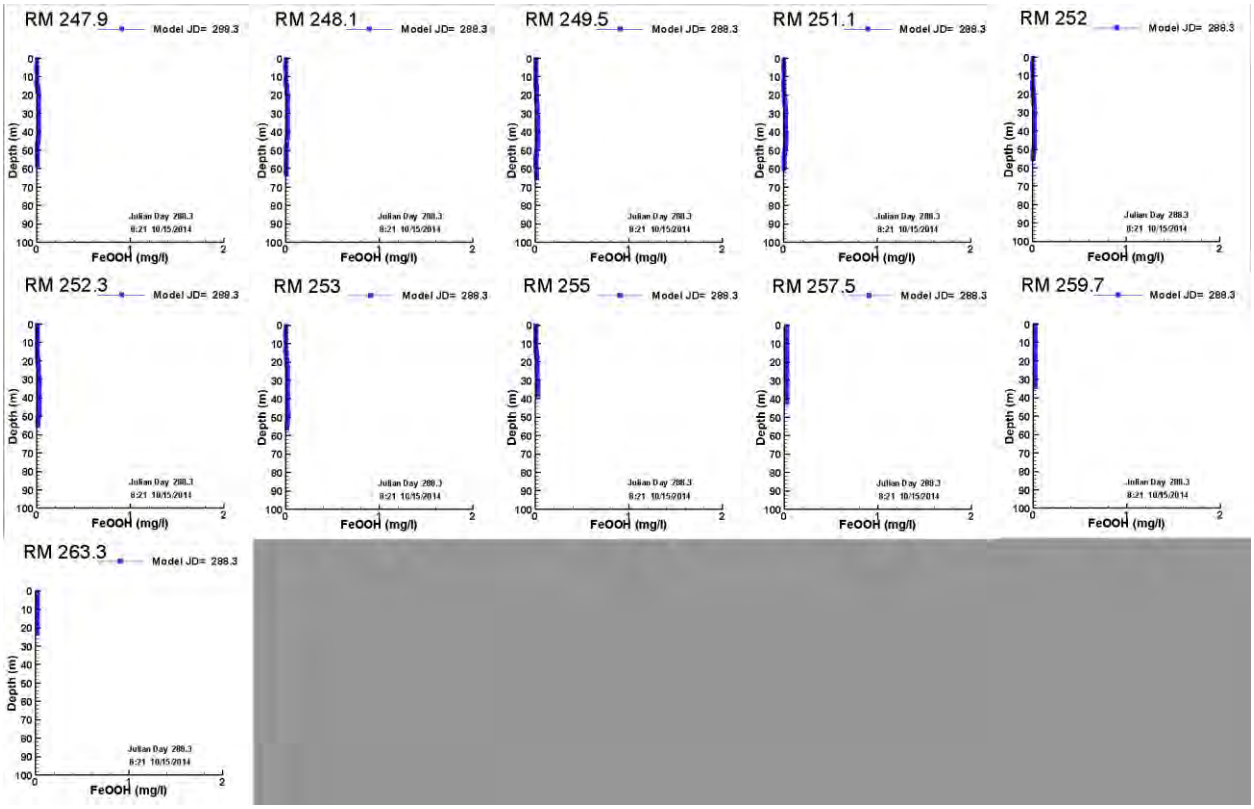


Figure 121. Vertical profiles of FeOOH compared with data for 10/15/2014.

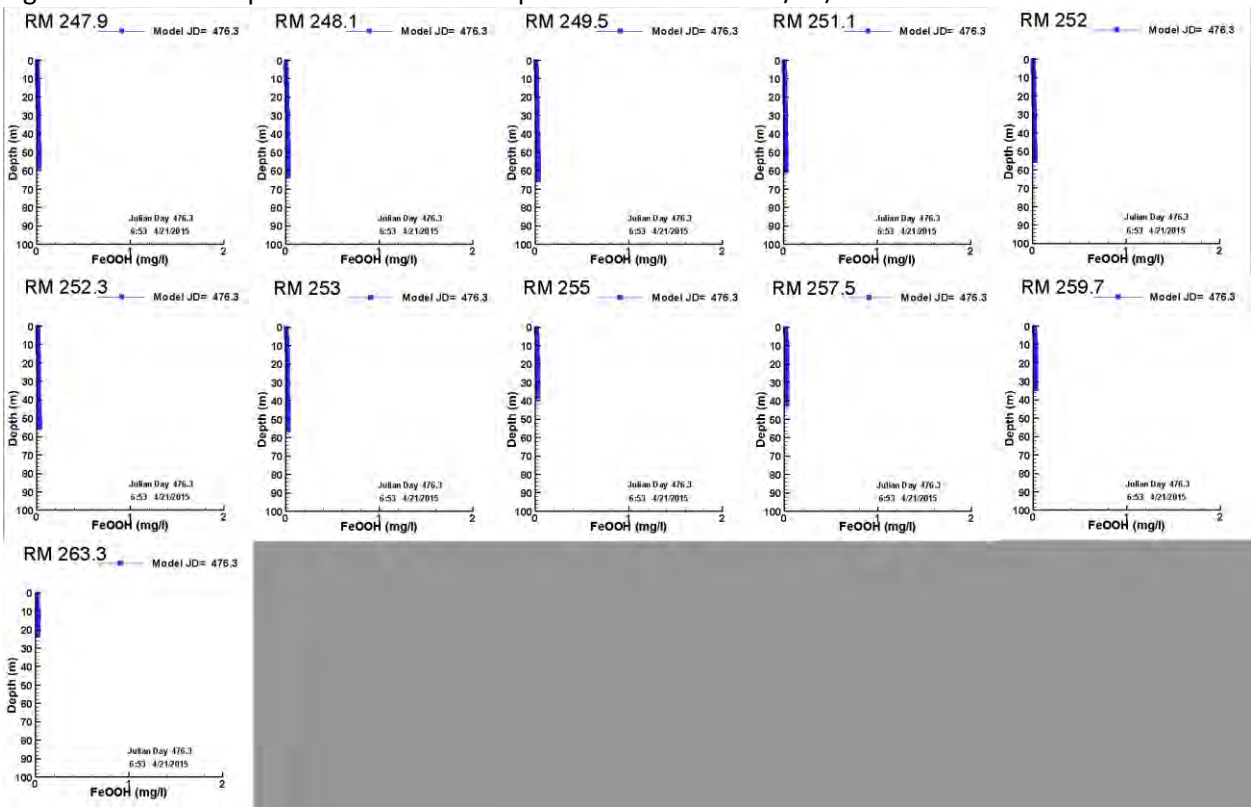


Figure 122. Vertical profiles of FeOOH compared with data for 4/21/2015.

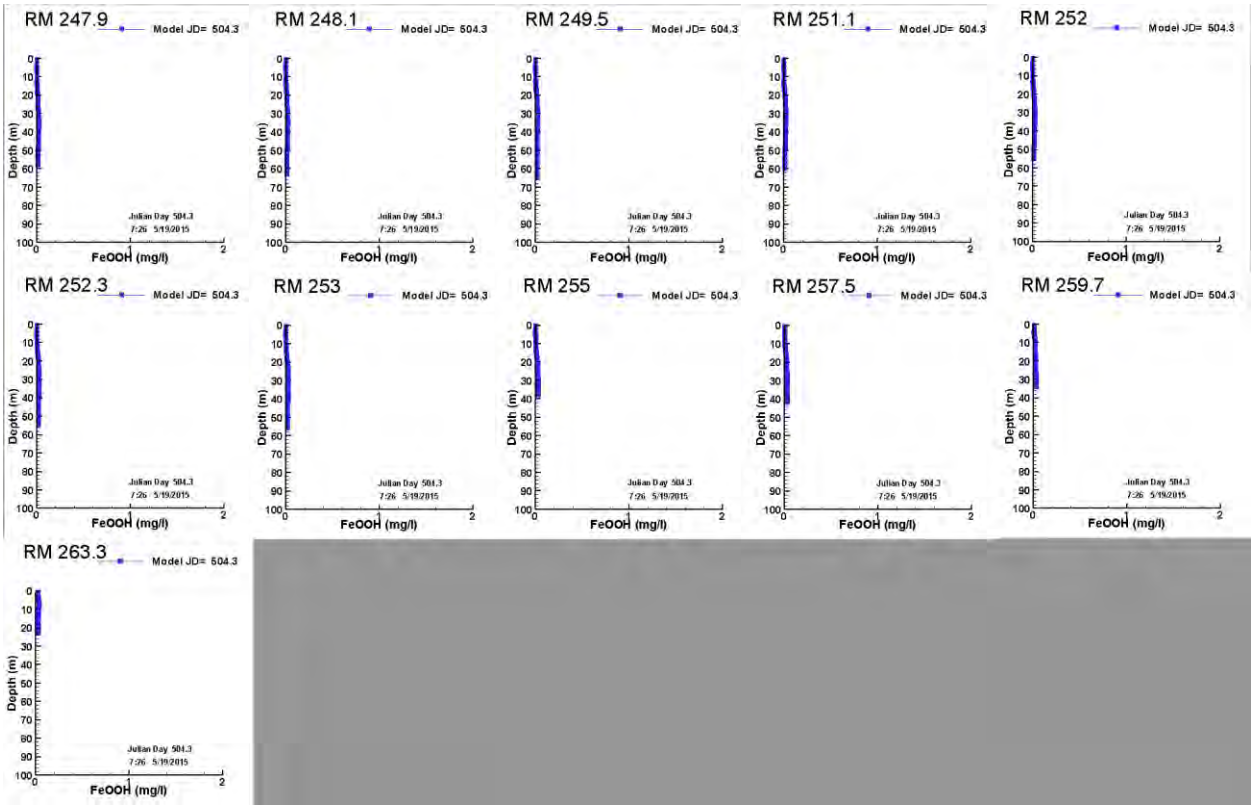


Figure 123. Vertical profiles of FeOOH compared with data for 5/19/2015.

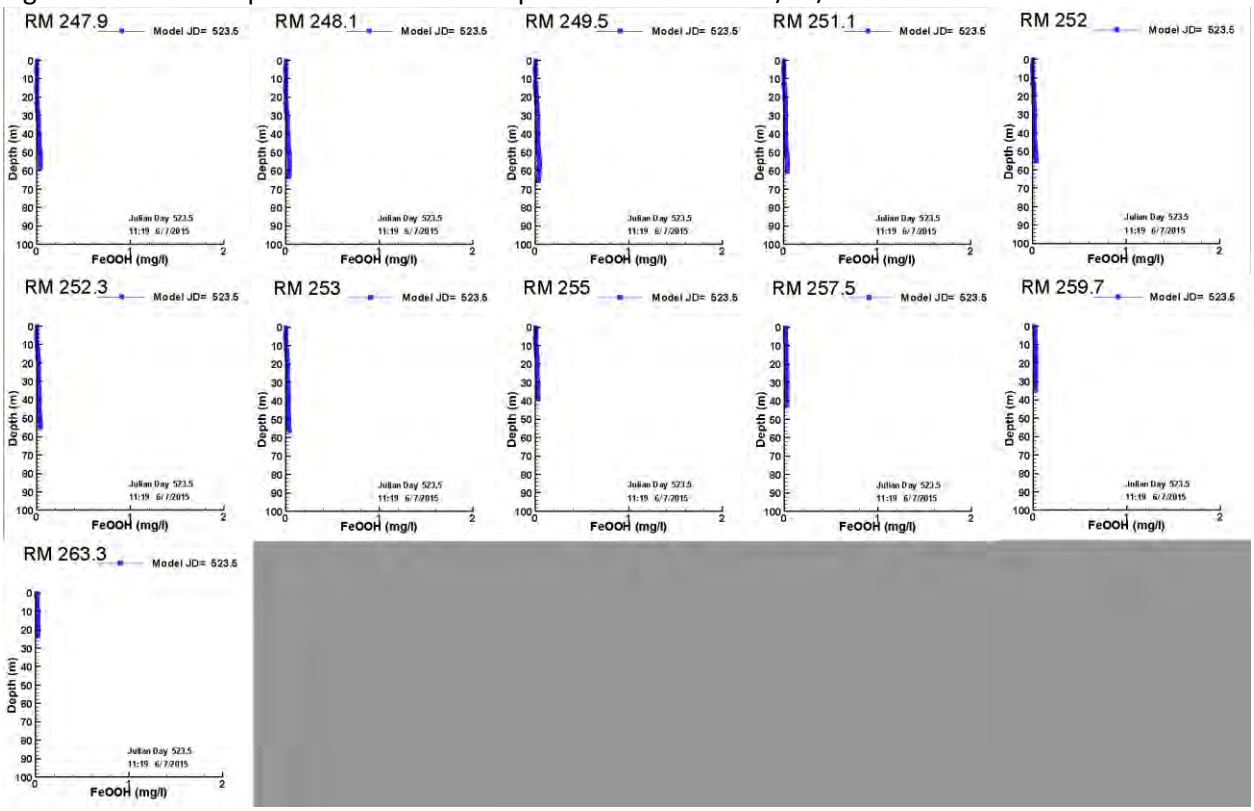


Figure 124. Vertical profiles of FeOOH compared with data for 6/ 7/2015.

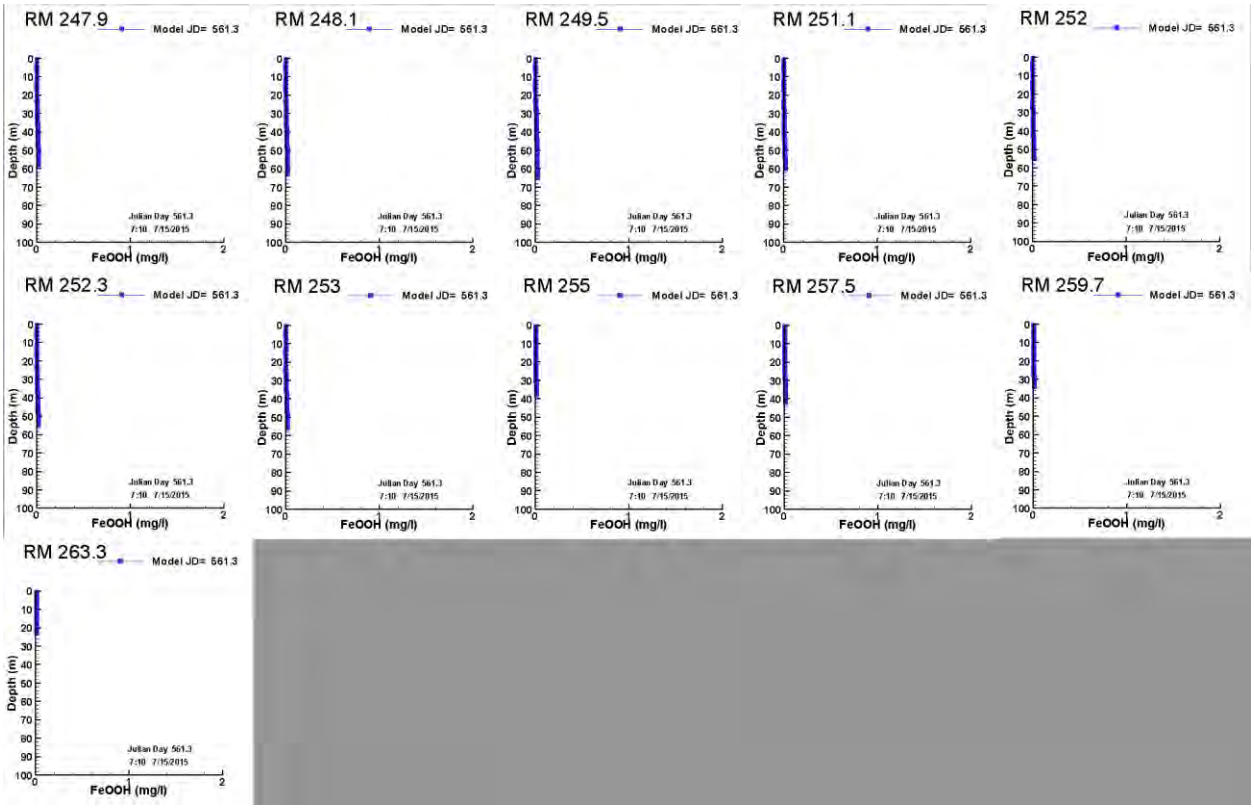


Figure 125. Vertical profiles of FeOOH compared with data for 7/15/2015.

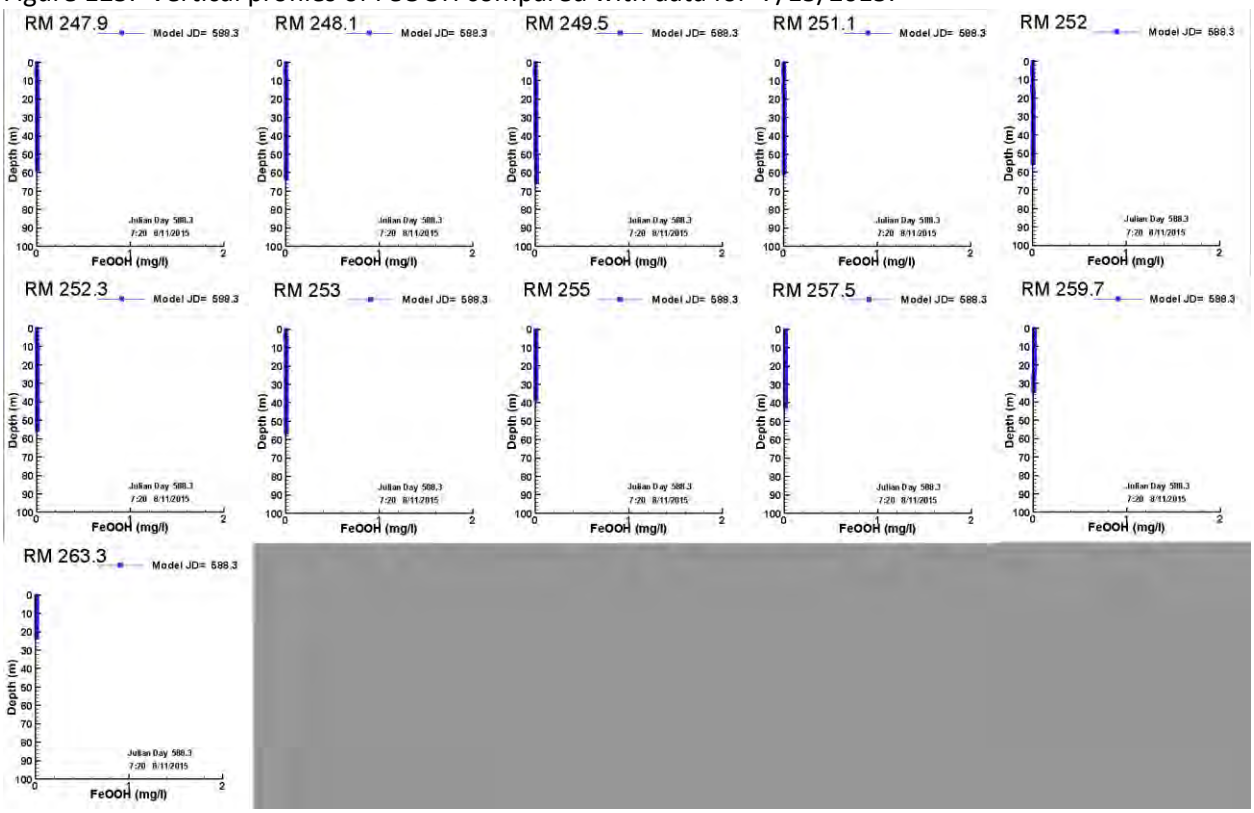


Figure 126. Vertical profiles of FeOOH compared with data for 8/11/2015.

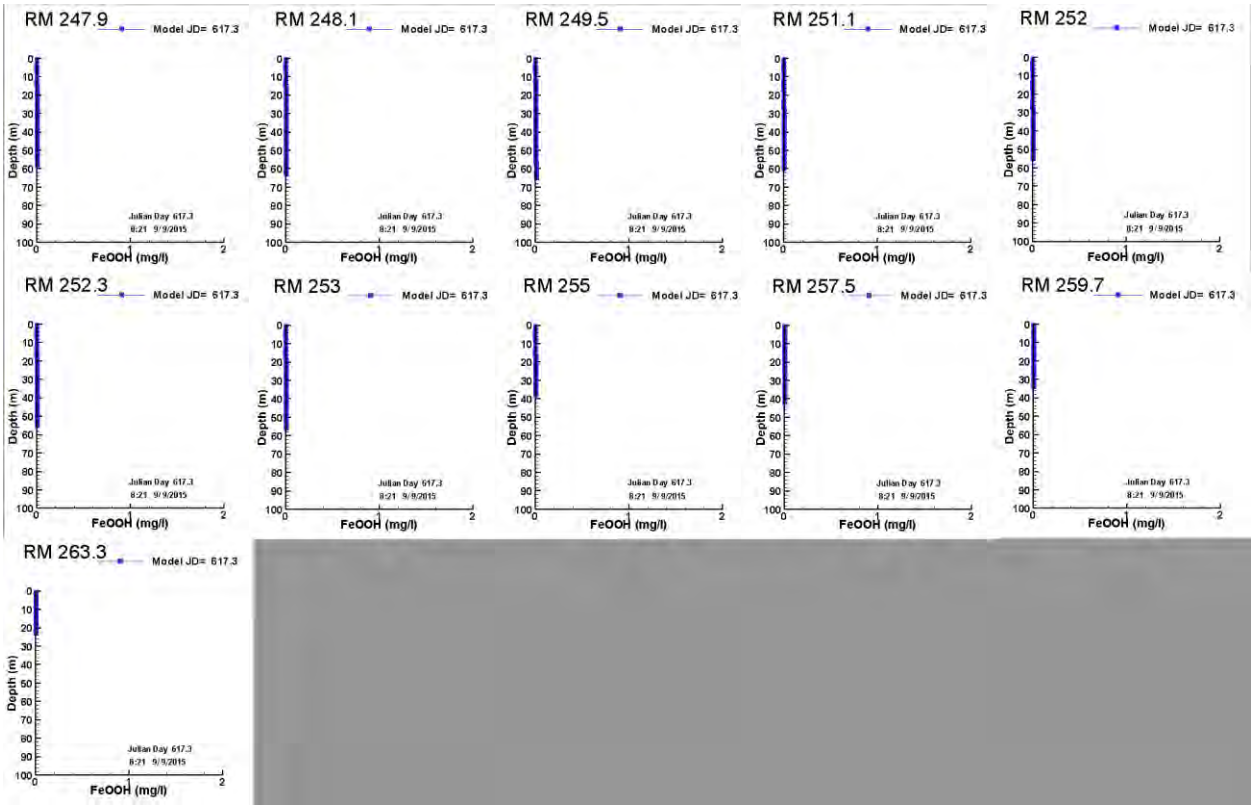


Figure 127. Vertical profiles of FeOOH compared with data for 9/ 9/2015.

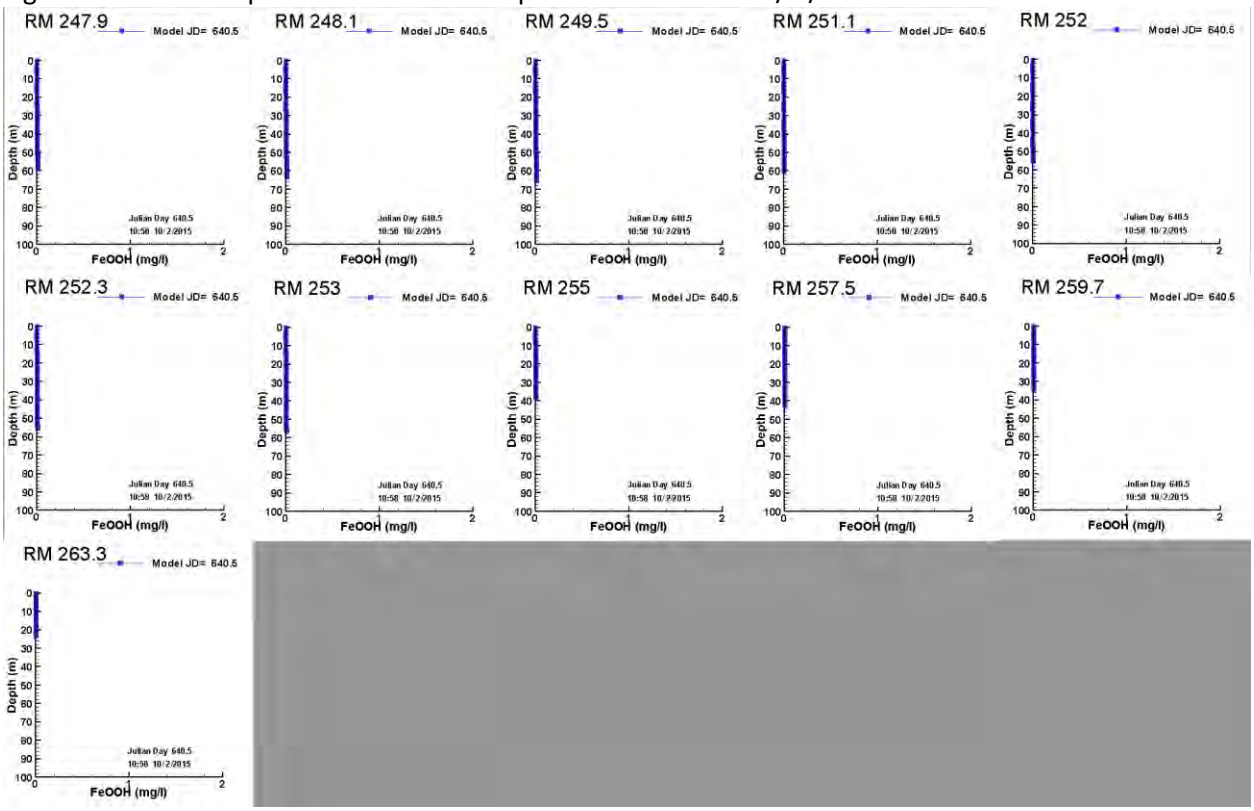


Figure 128. Vertical profiles of FeOOH compared with data for 10/ 2/2015.

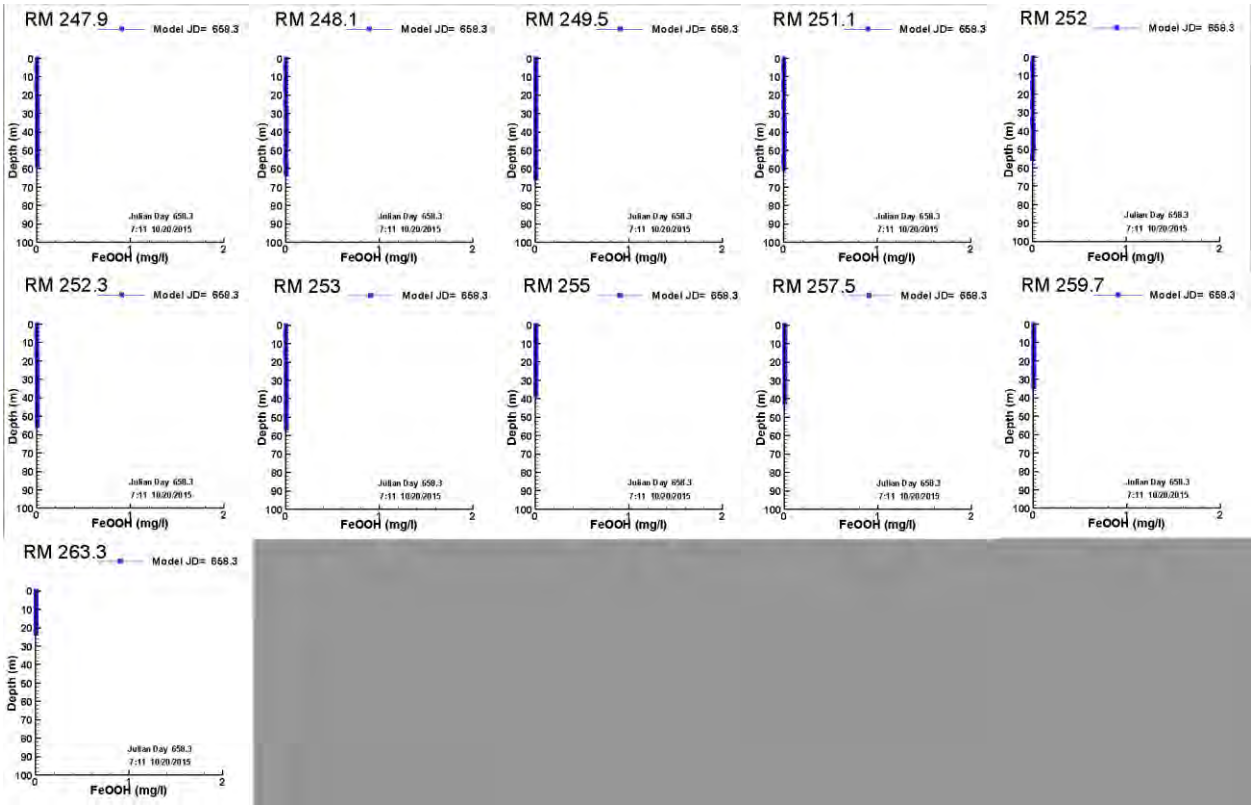


Figure 129. Vertical profiles of FeOOH compared with data for 10/20/2015.

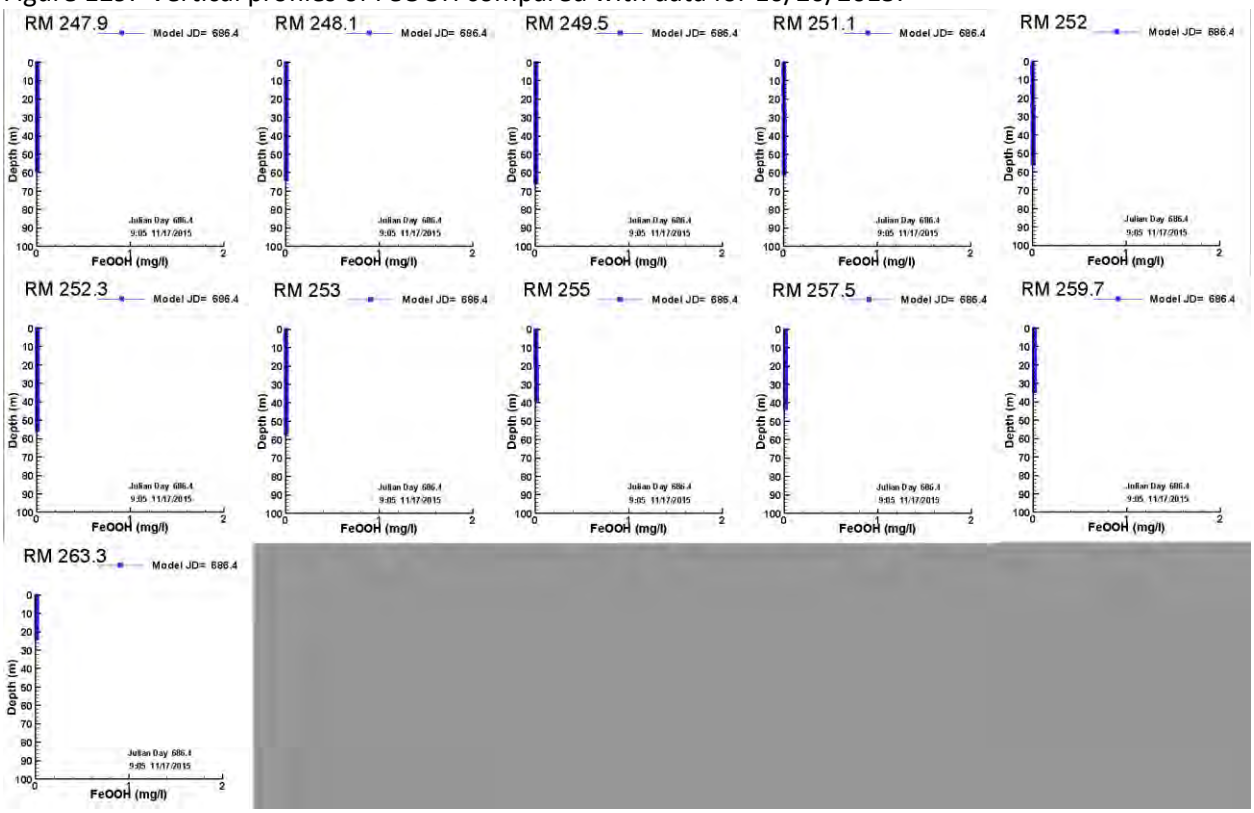


Figure 130. Vertical profiles of FeOOH compared with data for 11/17/2015.

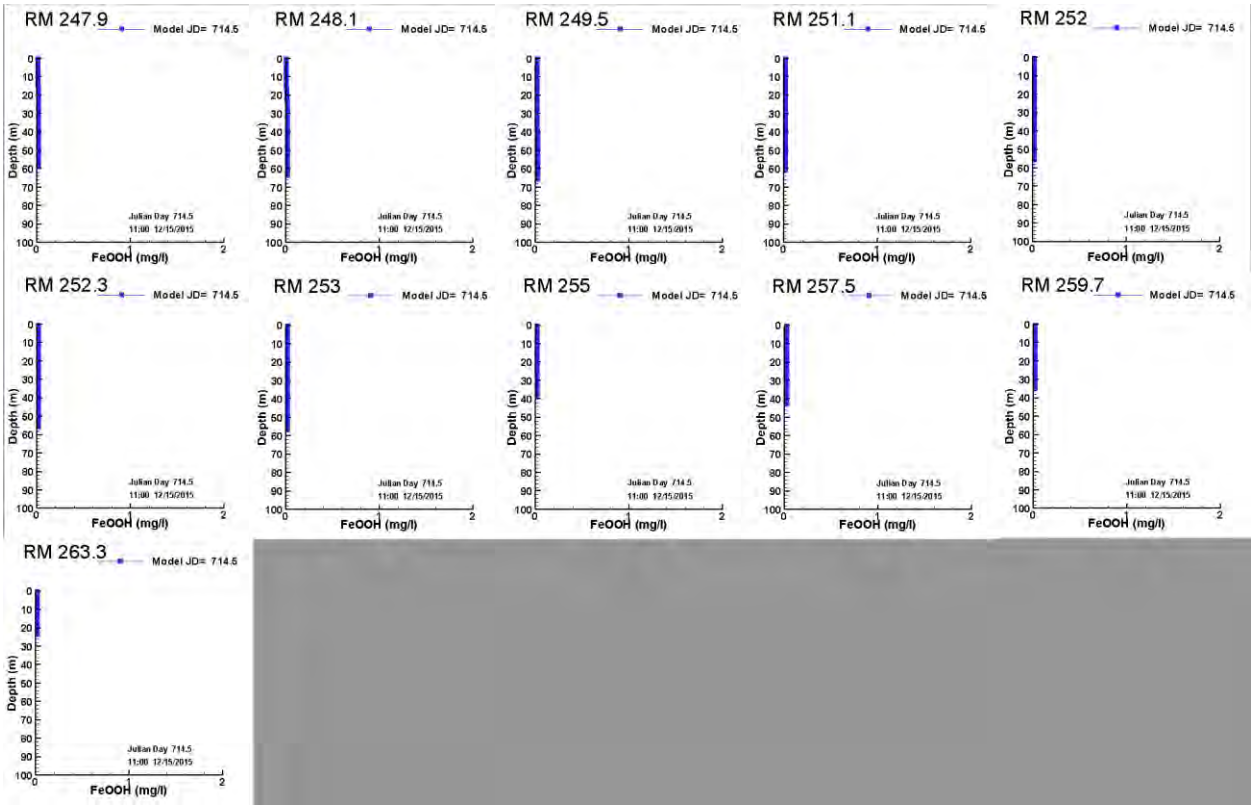


Figure 131. Vertical profiles of FeOOH compared with data for 12/15/2015.

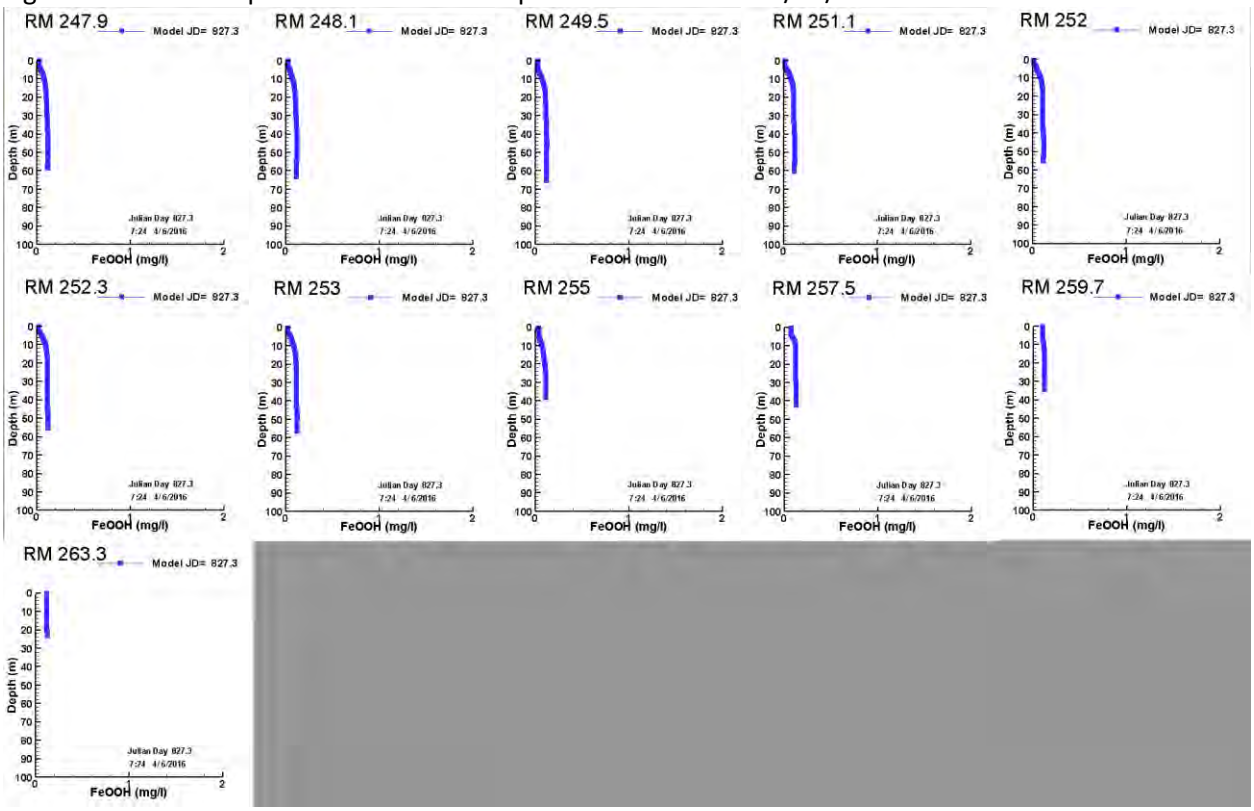


Figure 132. Vertical profiles of FeOOH compared with data for 4/ 6/2016.

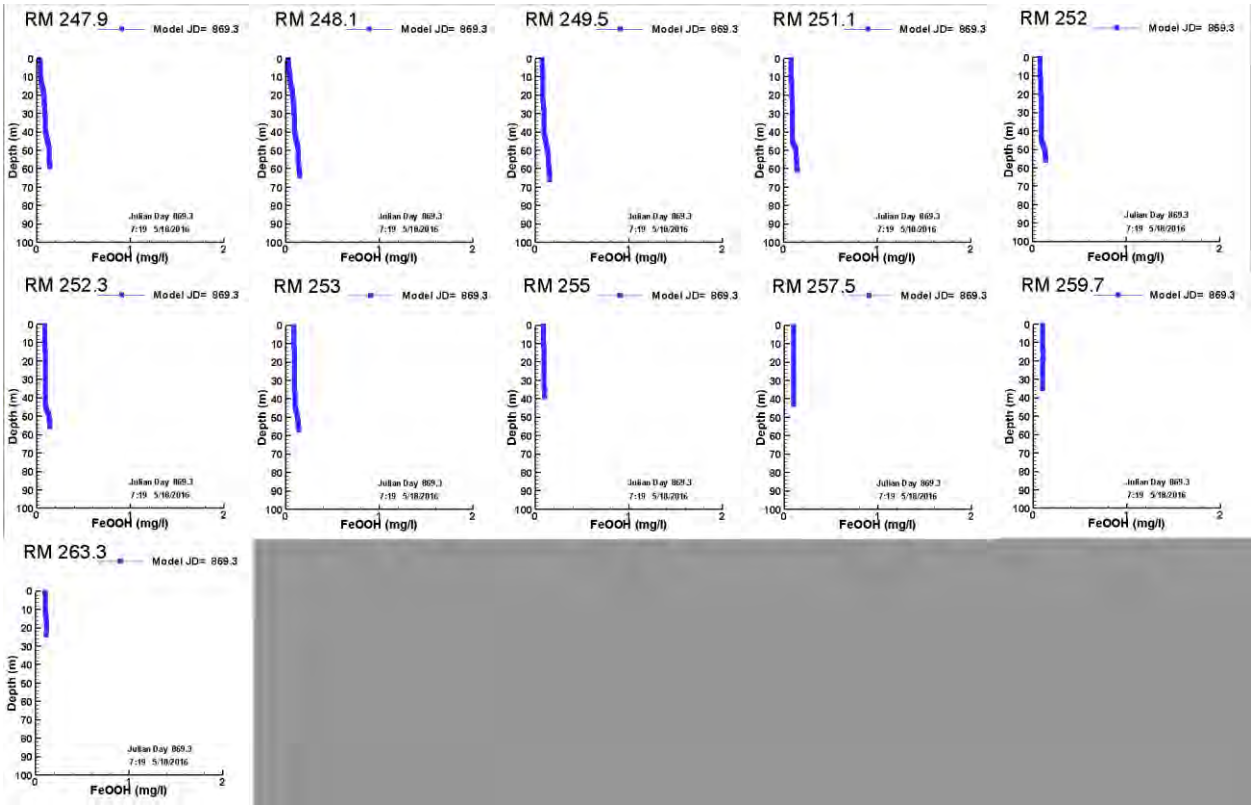


Figure 133. Vertical profiles of FeOOH compared with data for 5/18/2016.

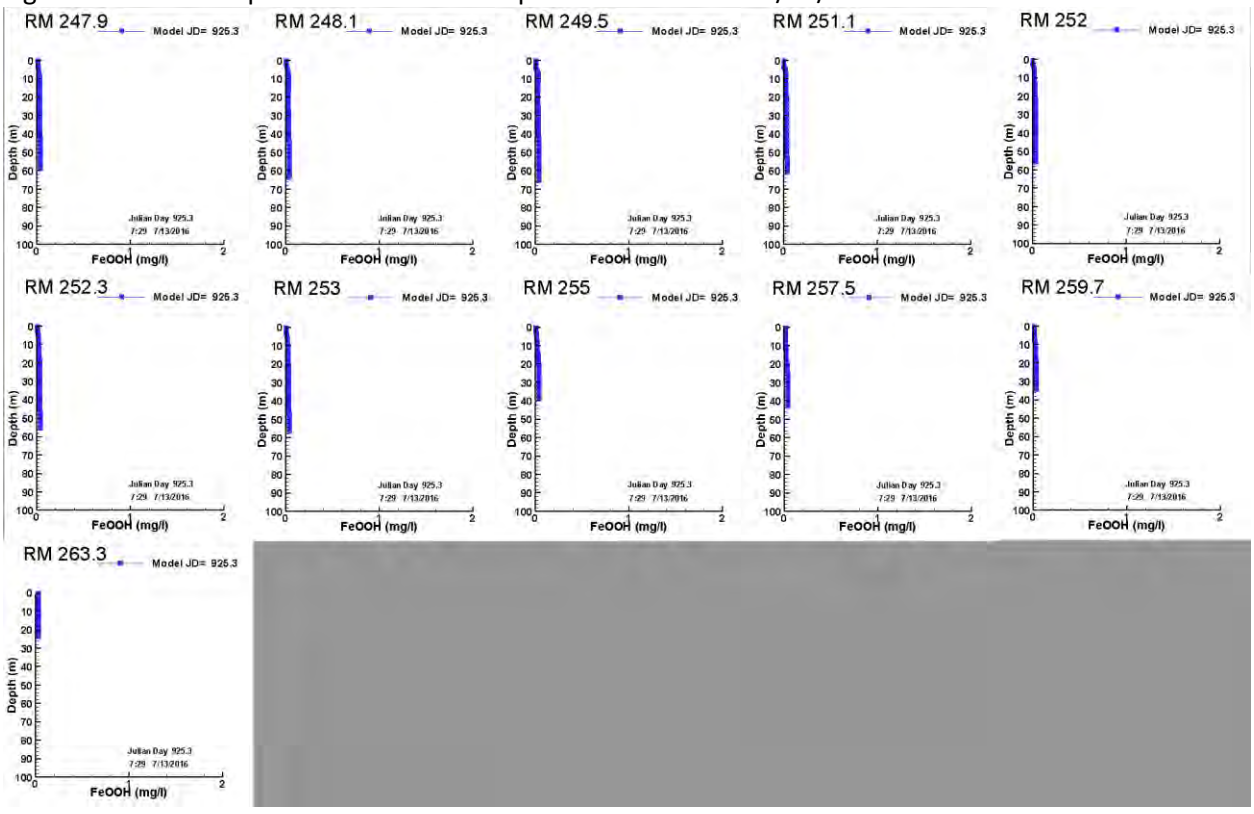


Figure 134. Vertical profiles of FeOOH compared with data for 7/13/2016.

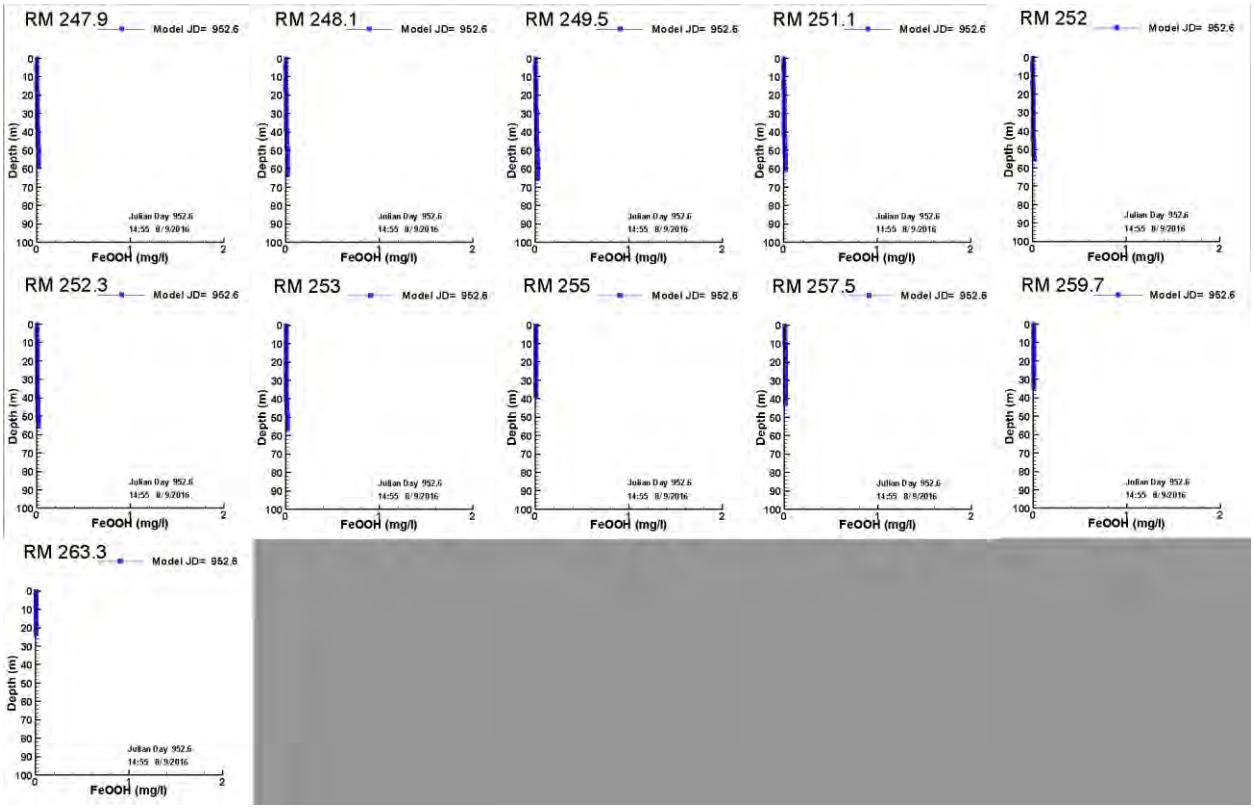


Figure 135. Vertical profiles of FeOOH compared with data for 8/ 9/2016.

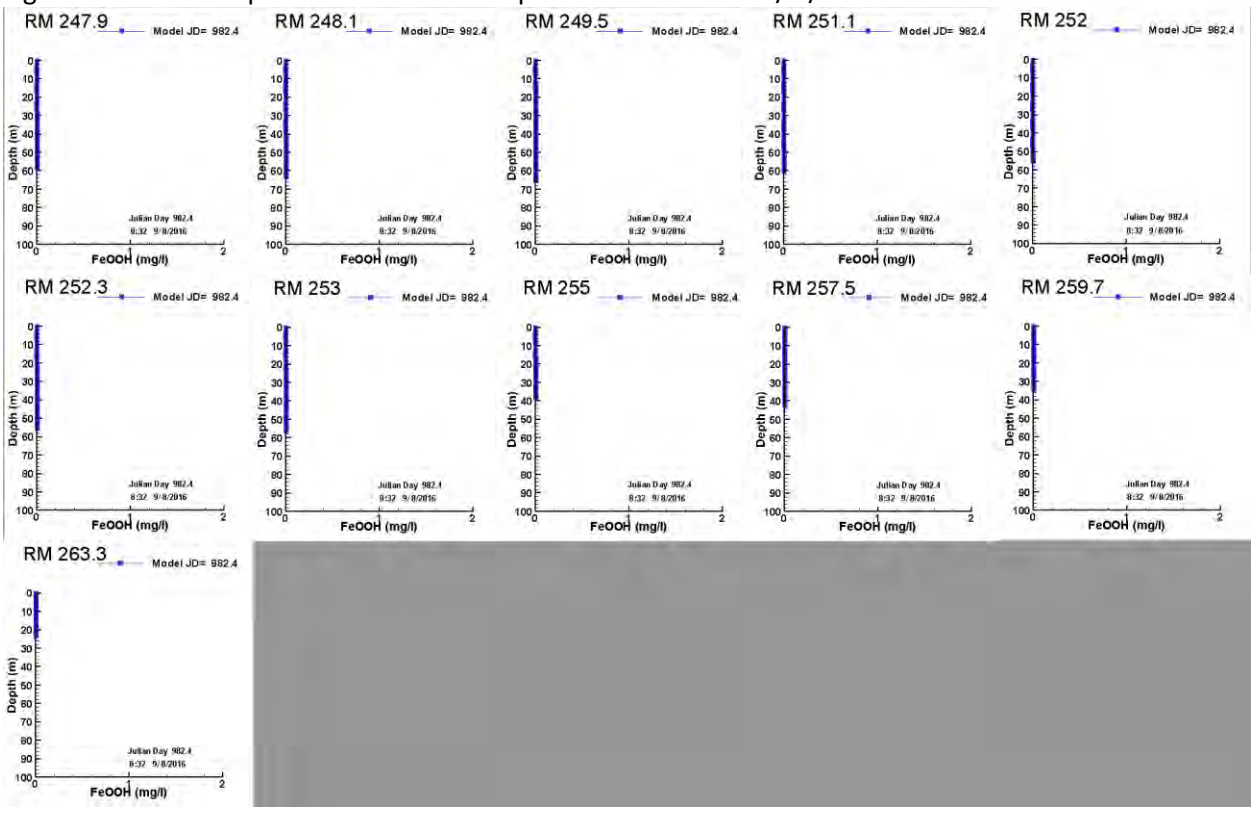


Figure 136. Vertical profiles of FeOOH compared with data for 9/ 8/2016.

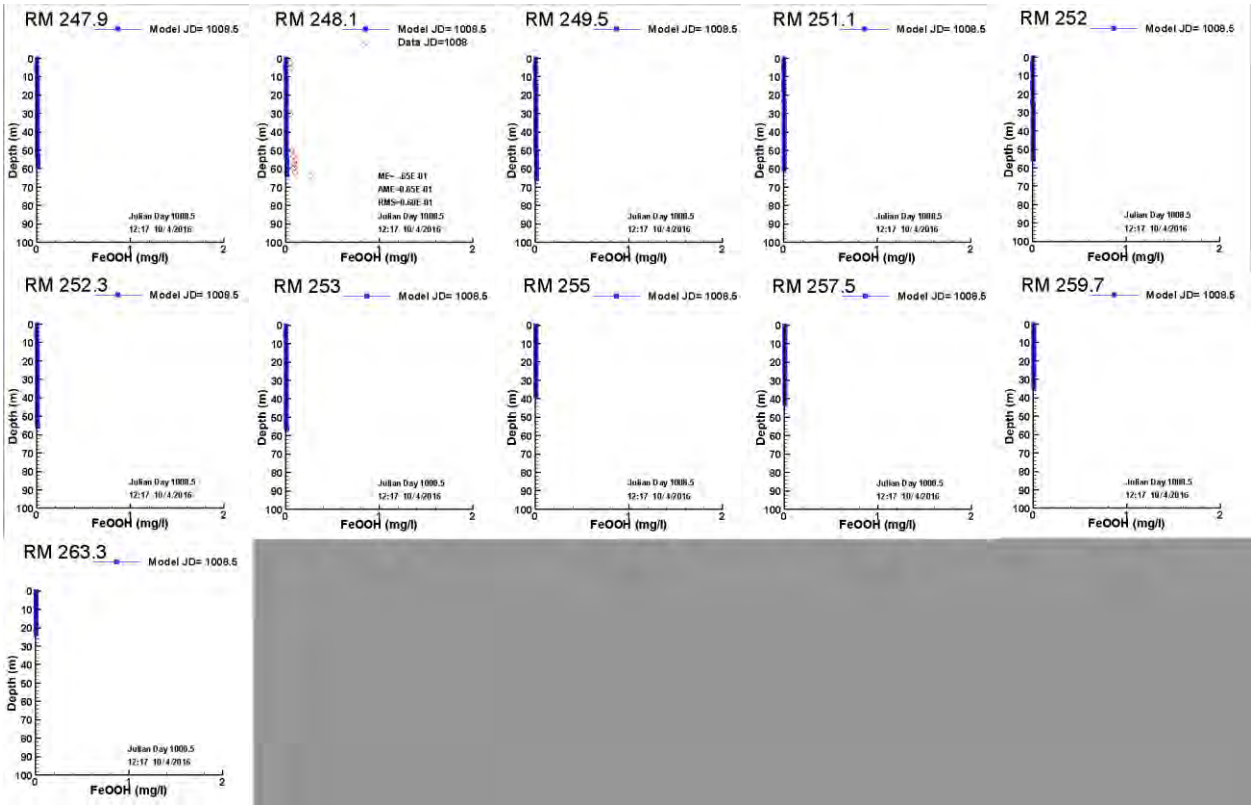


Figure 137. Vertical profiles of FeOOH compared with data for 10/ 4/2016.

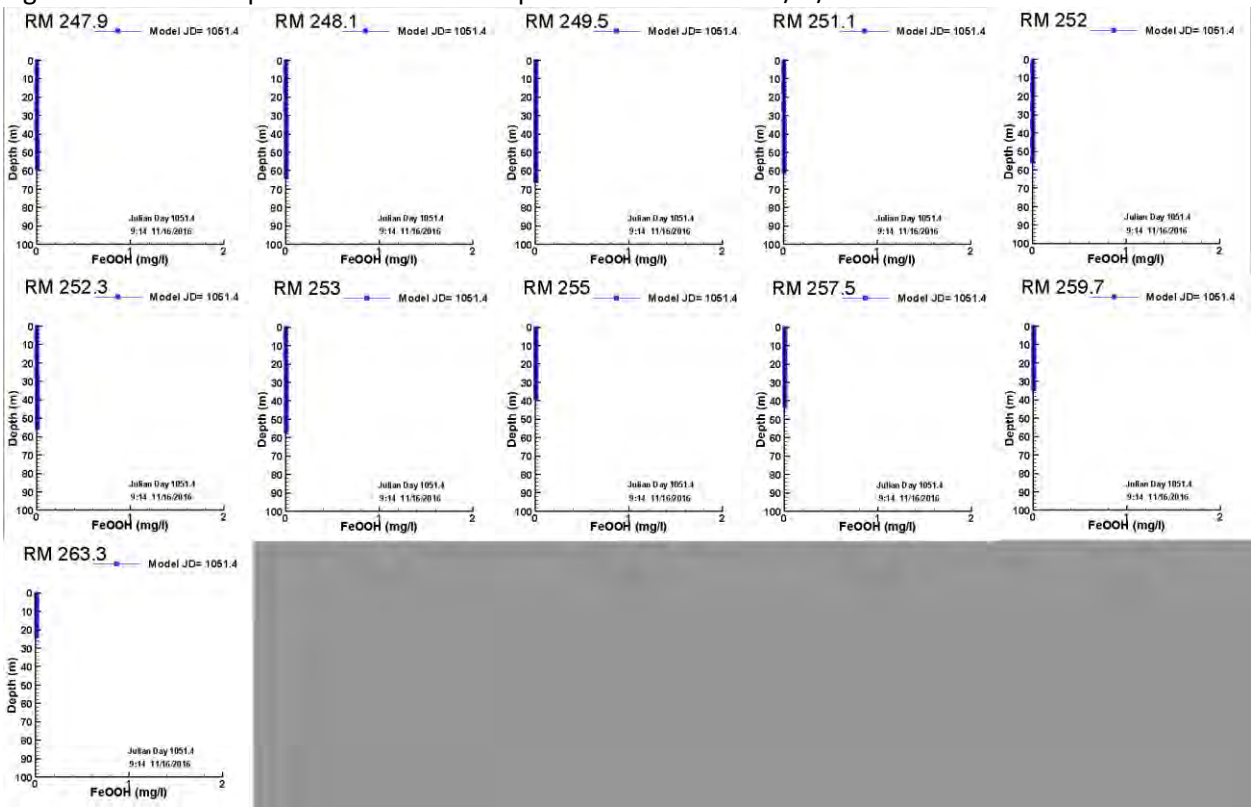


Figure 138. Vertical profiles of FeOOH compared with data for 11/16/2016.

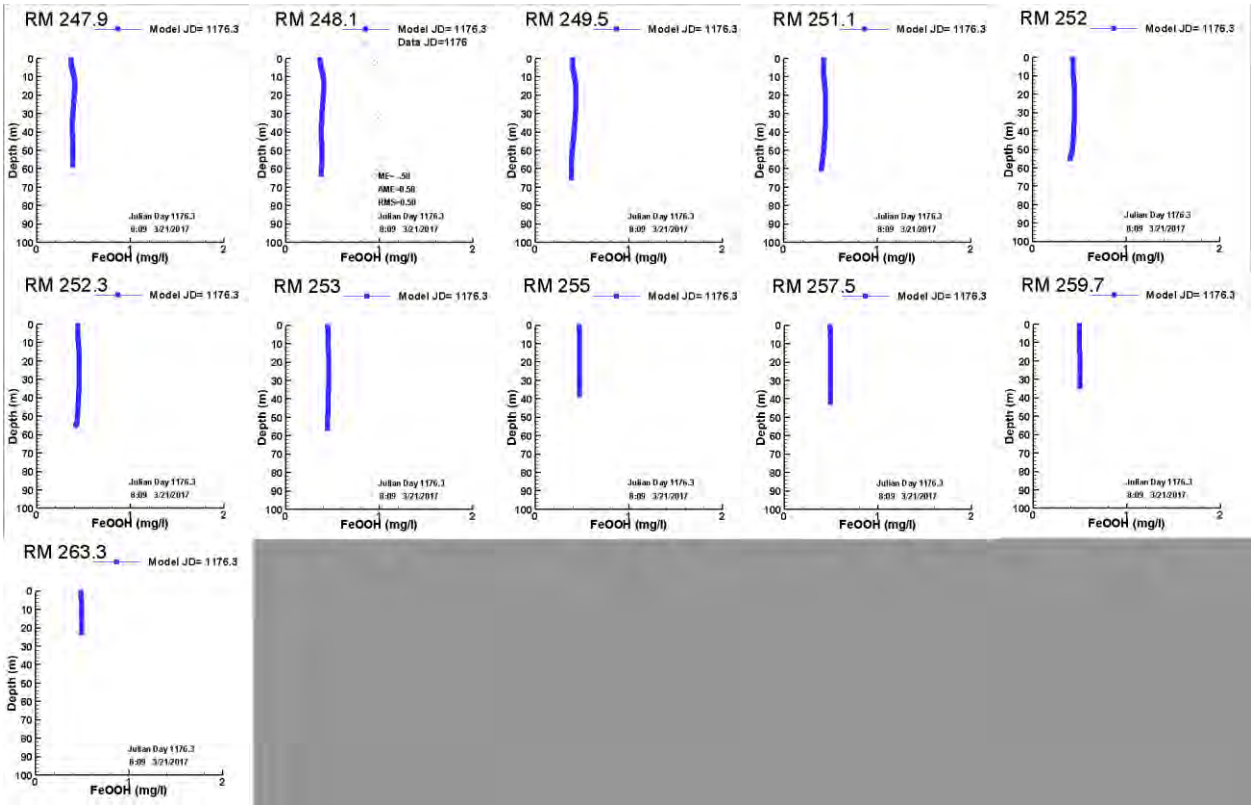


Figure 139. Vertical profiles of FeOOH compared with data for 3/21/2017.

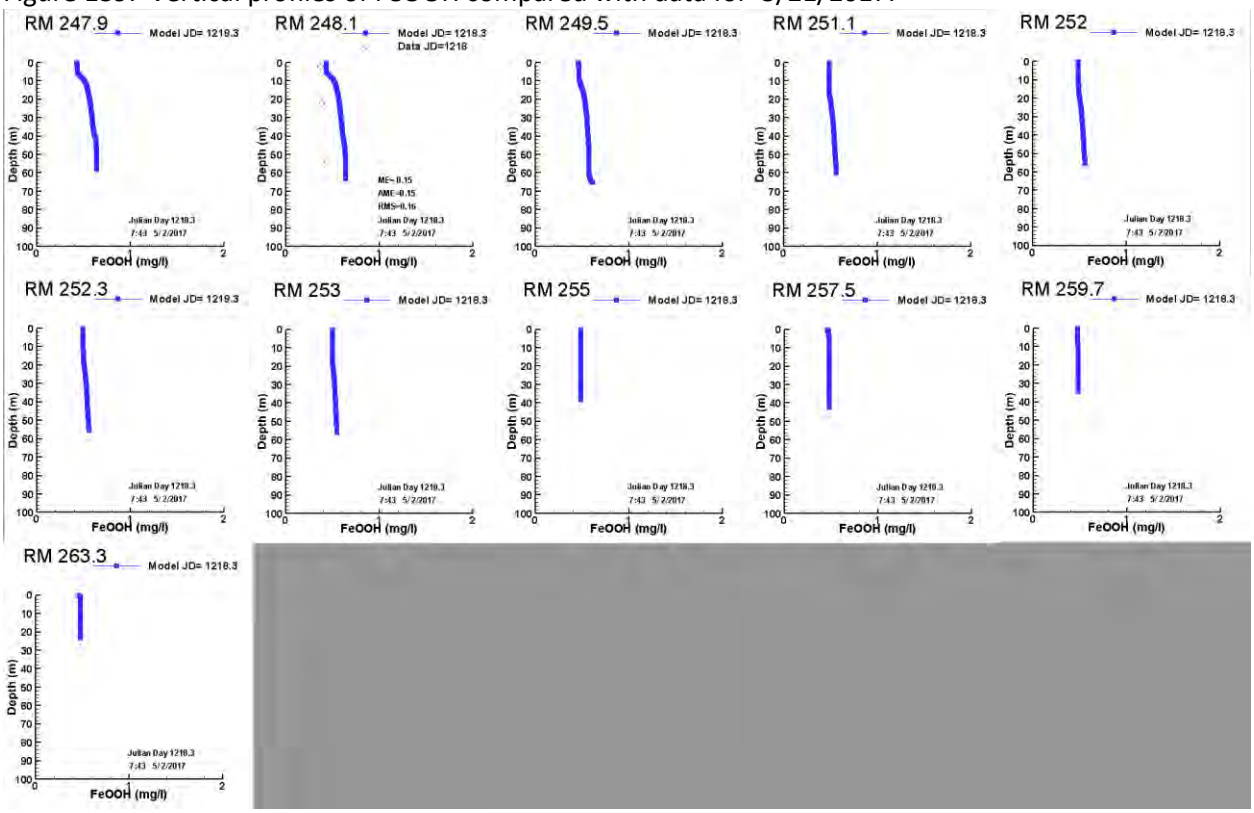


Figure 140. Vertical profiles of FeOOH compared with data for 5/ 2/2017.

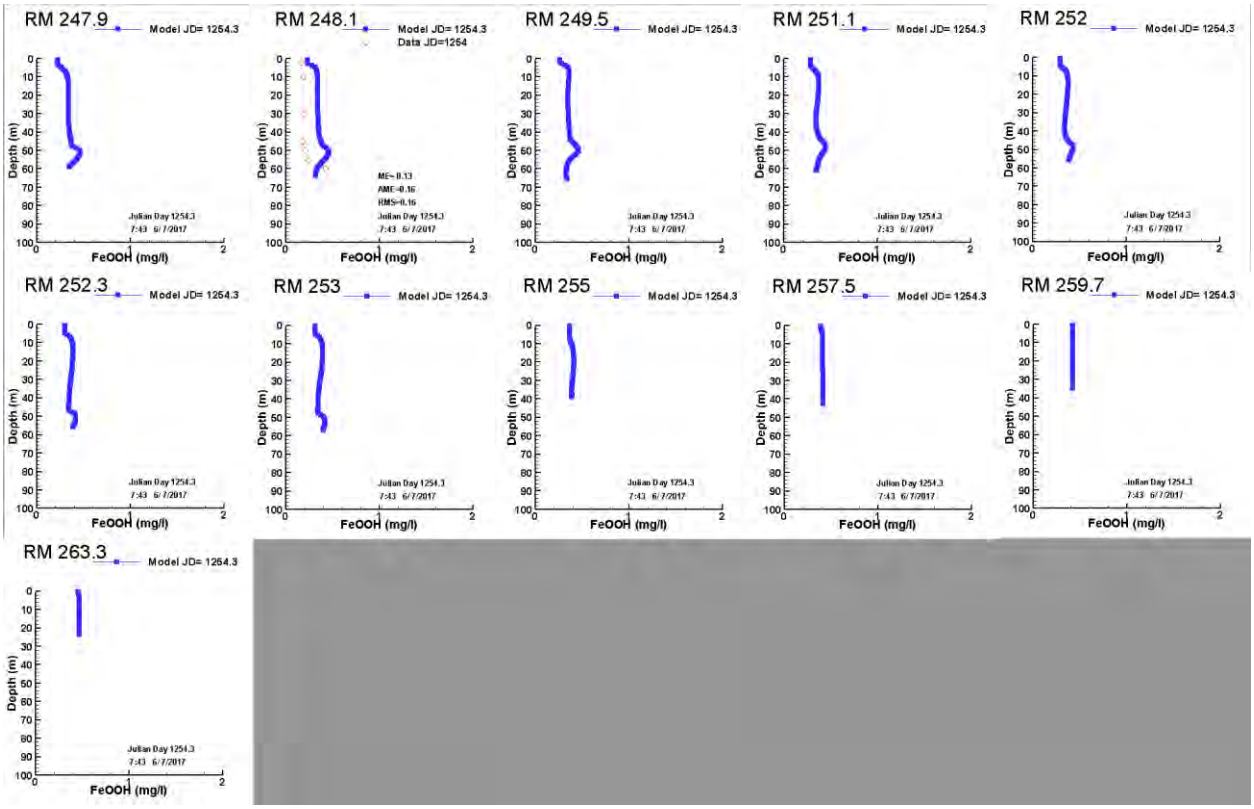


Figure 141. Vertical profiles of FeOOH compared with data for 6/ 7/2017.

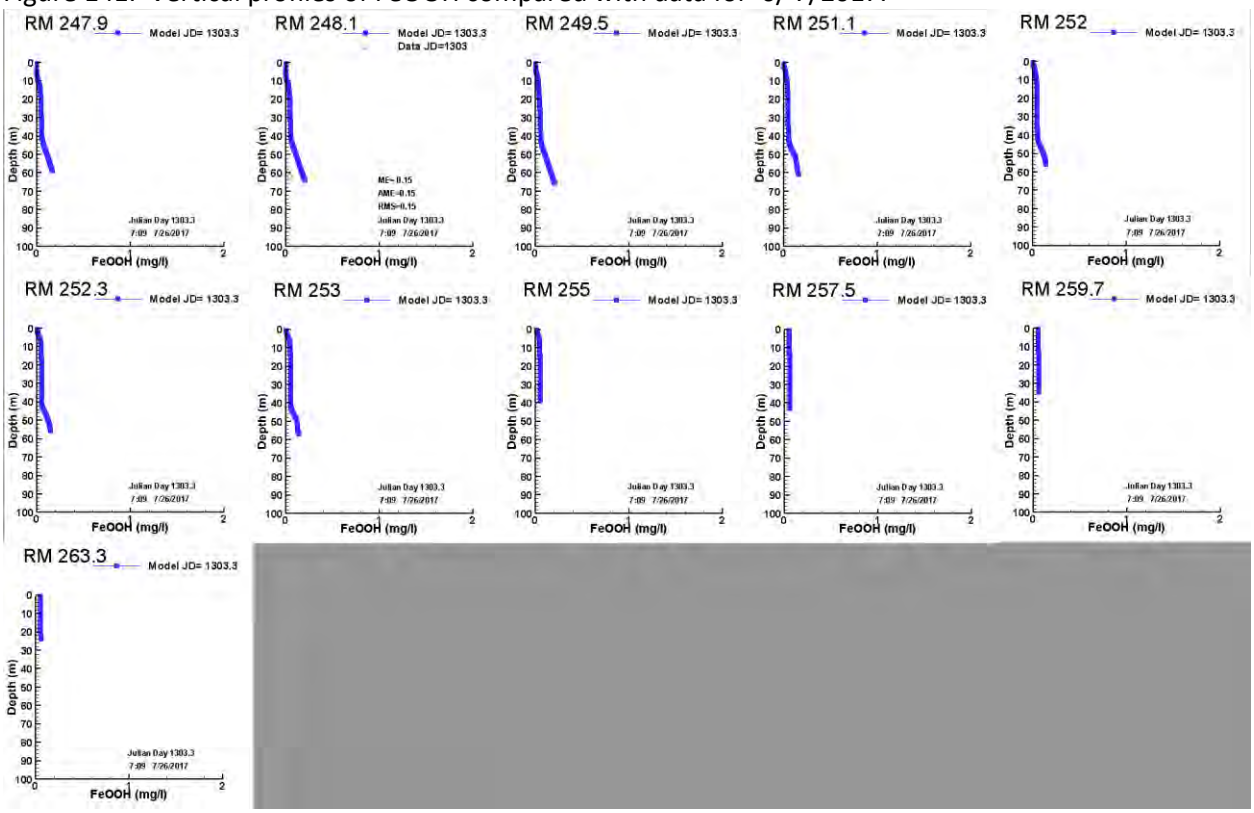


Figure 142. Vertical profiles of FeOOH compared with data for 7/26/2017.

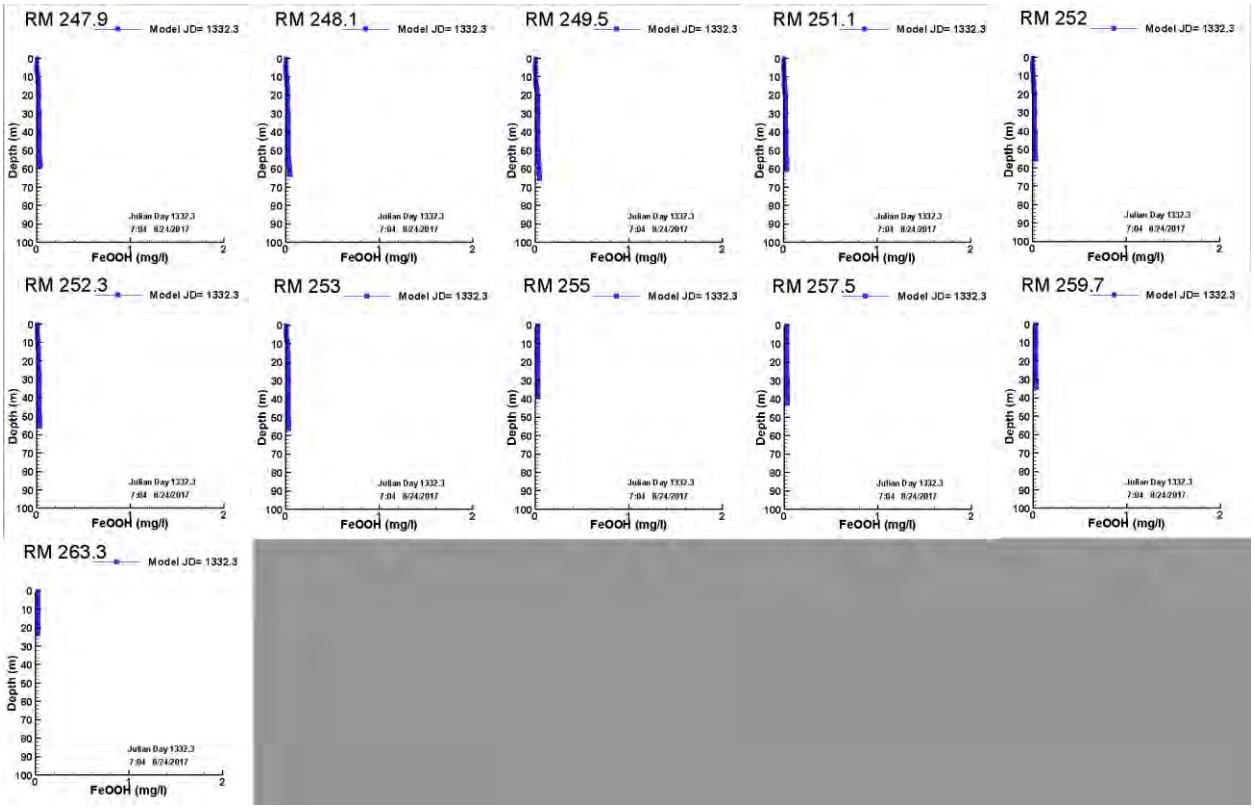


Figure 143. Vertical profiles of FeOOH compared with data for 8/24/2017.

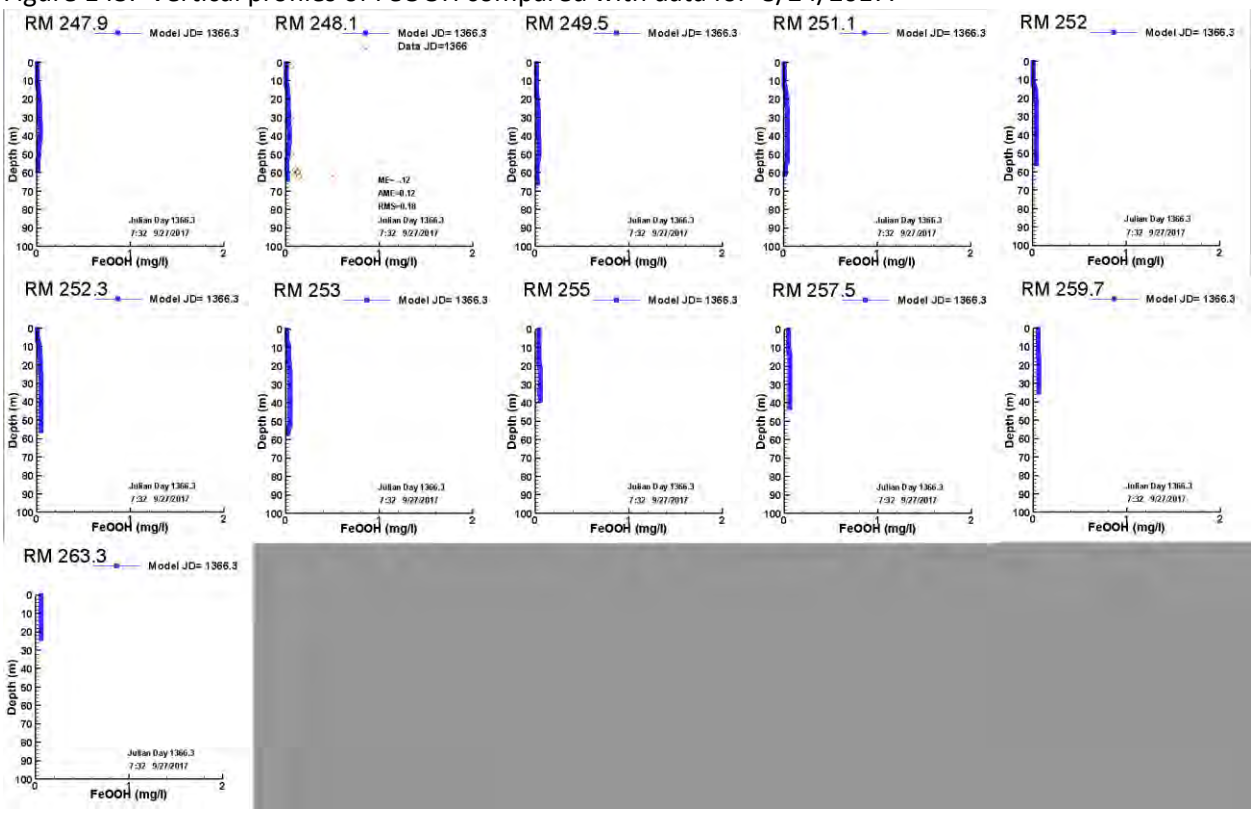


Figure 144. Vertical profiles of FeOOH compared with data for 9/27/2017.

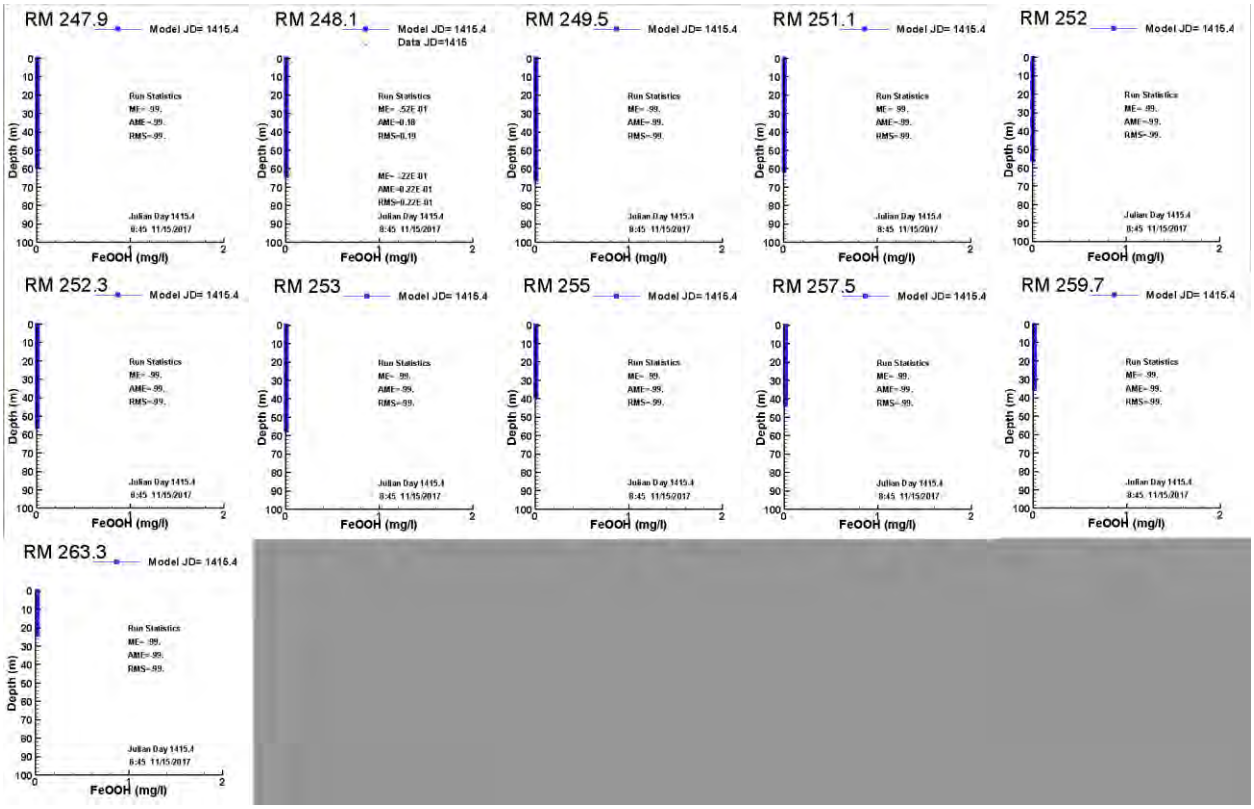


Figure 145. Vertical profiles of FeOOH compared with data for 11/15/2017.

Mn(II)

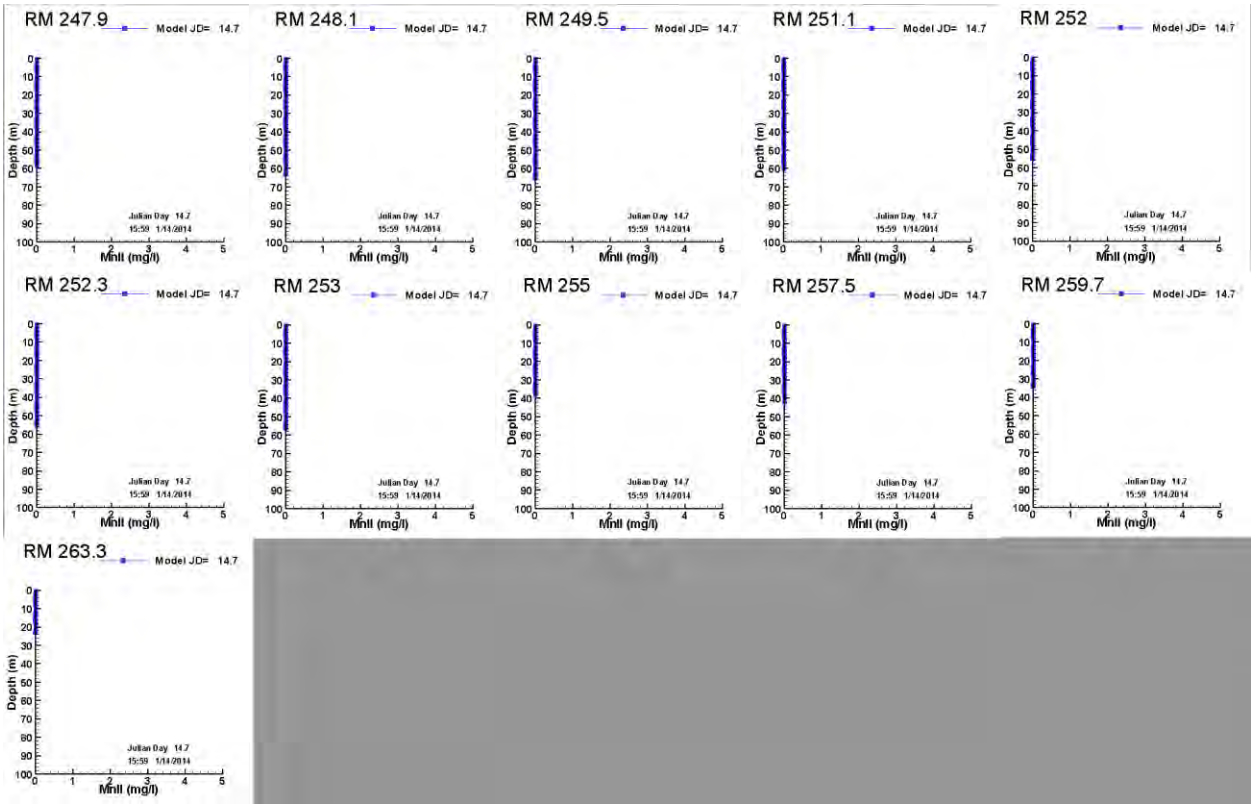


Figure 146. Vertical profiles of MNII compared with data for 1/14/2014.

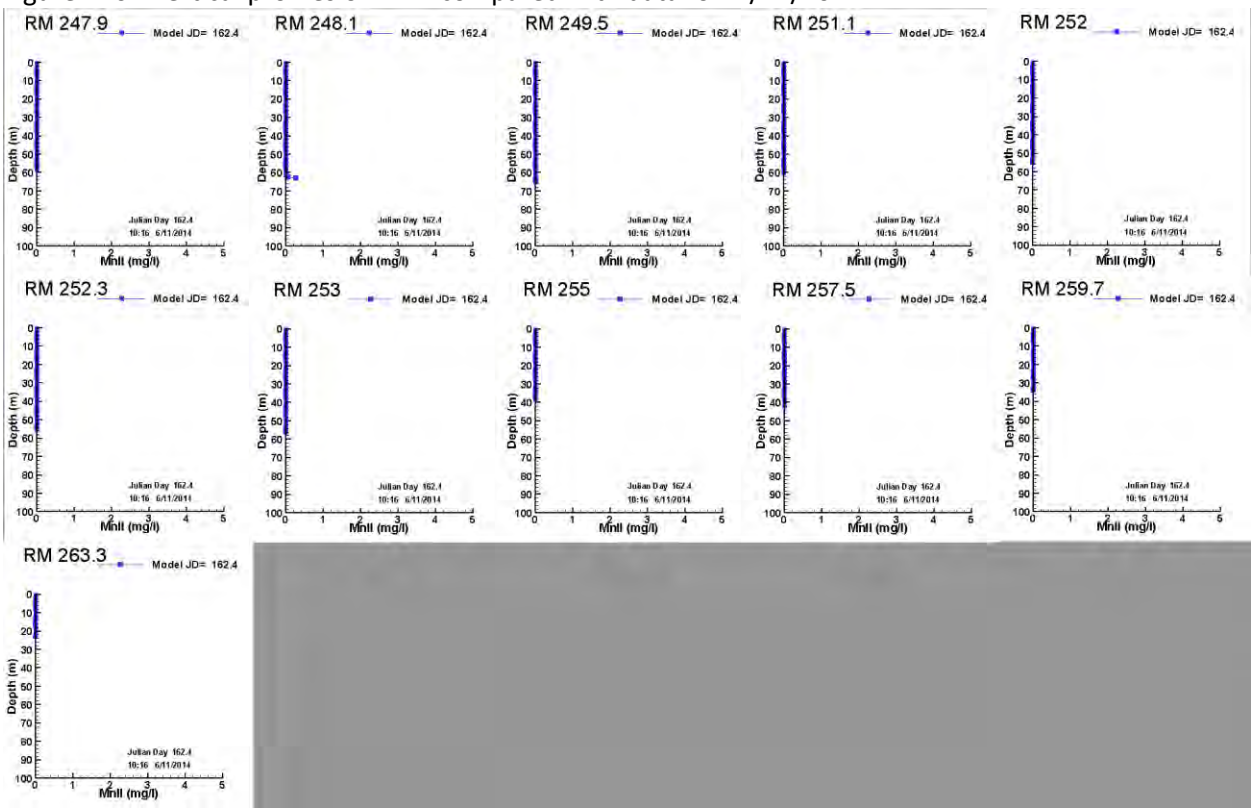


Figure 147. Vertical profiles of MNII compared with data for 6/11/2014.

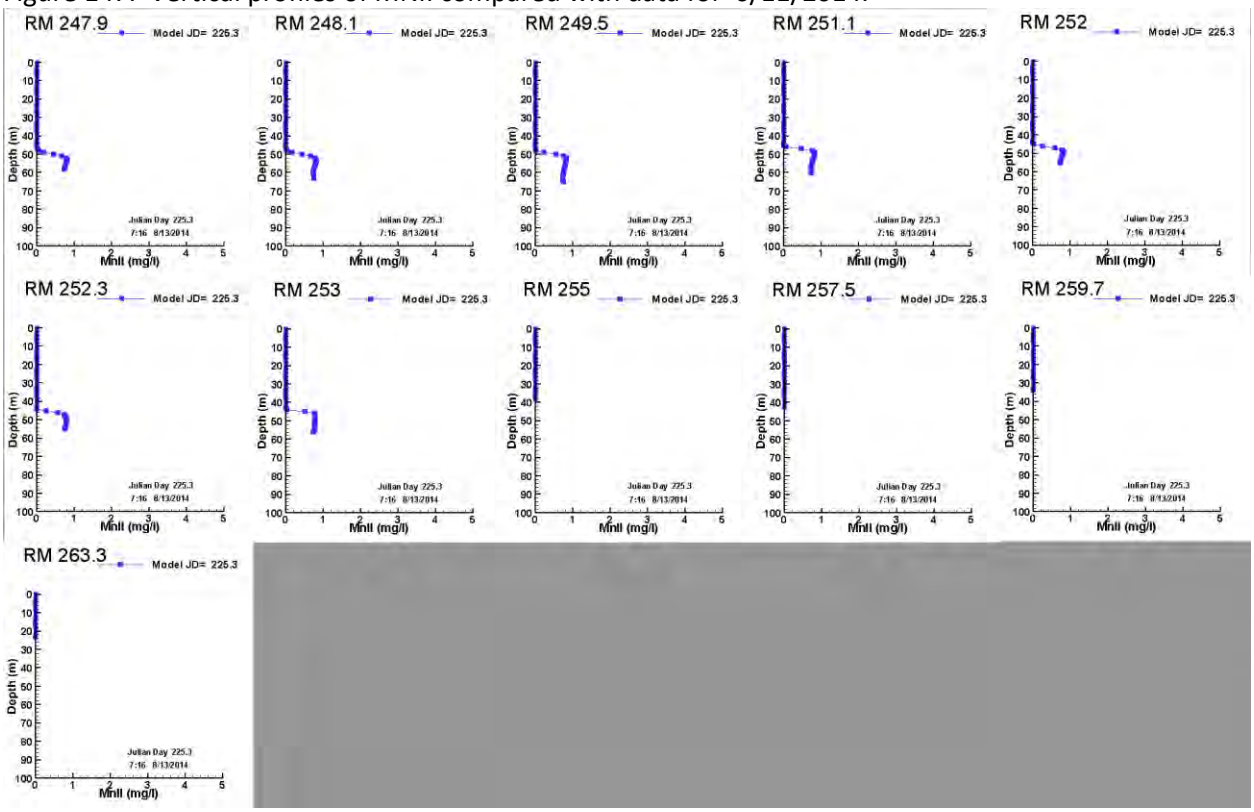


Figure 148. Vertical profiles of MNII compared with data for 8/13/2014.

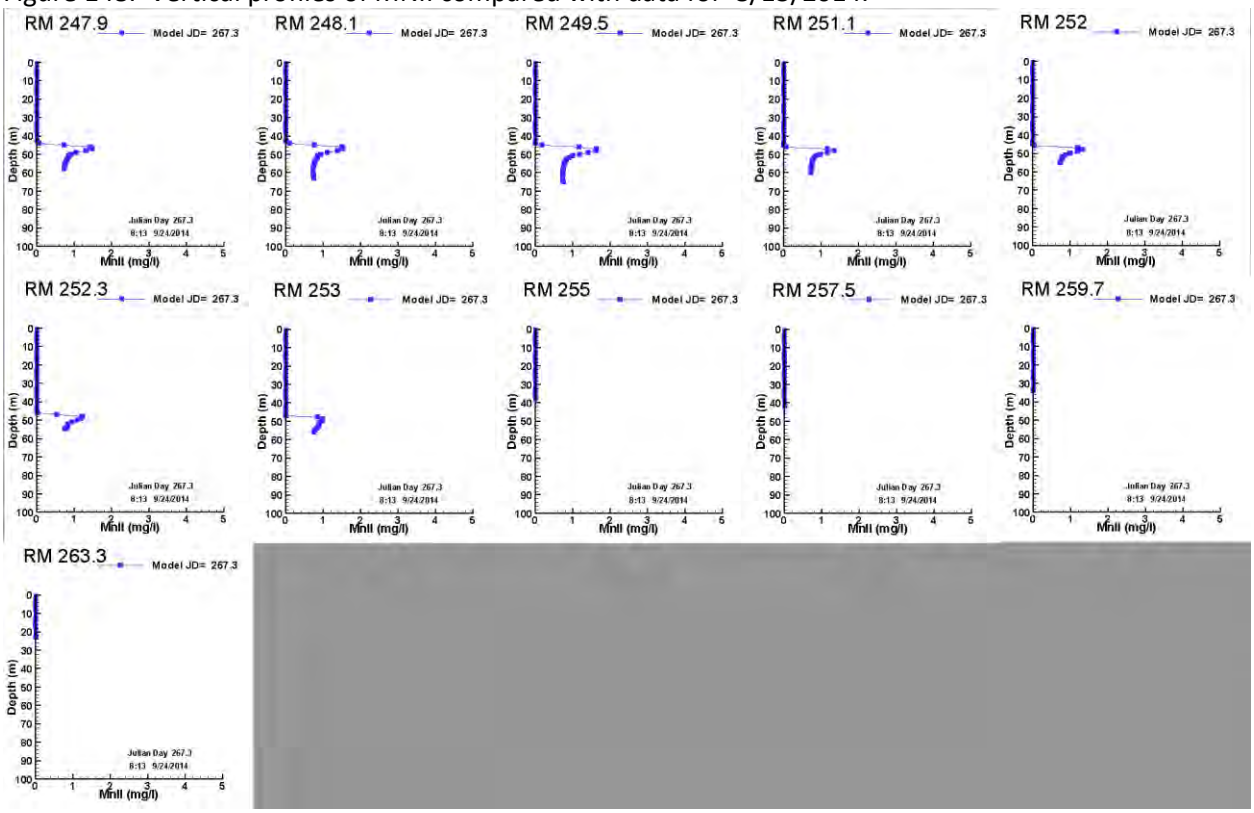


Figure 149. Vertical profiles of MNII compared with data for 9/24/2014.

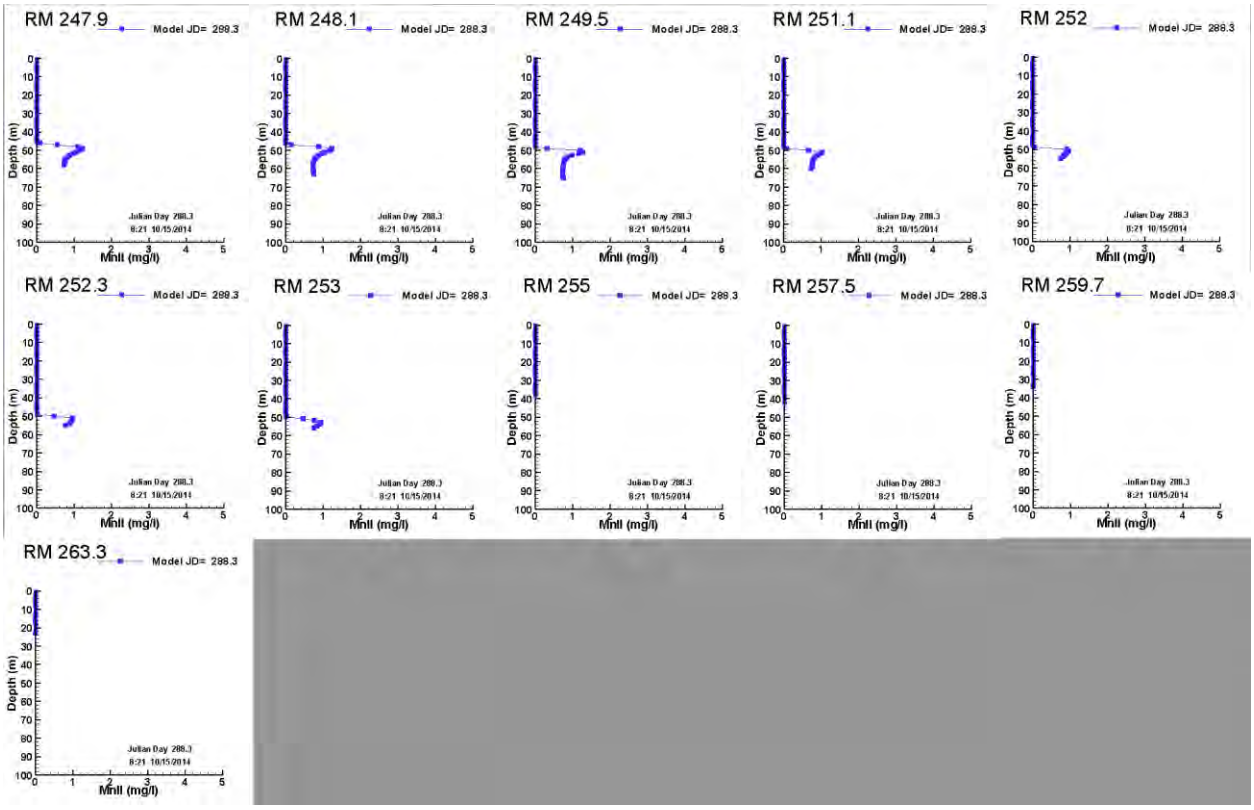


Figure 150. Vertical profiles of MNII compared with data for 10/15/2014.

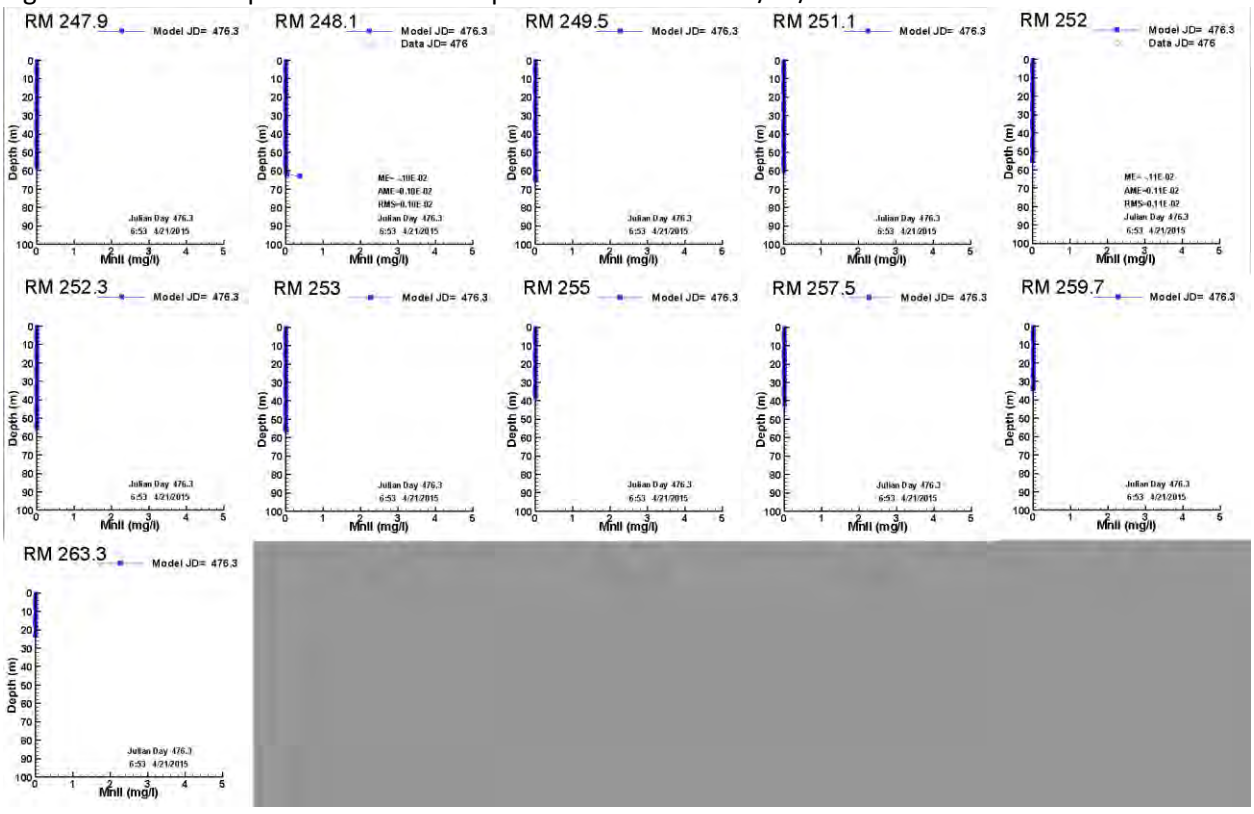


Figure 151. Vertical profiles of MNII compared with data for 4/21/2015.

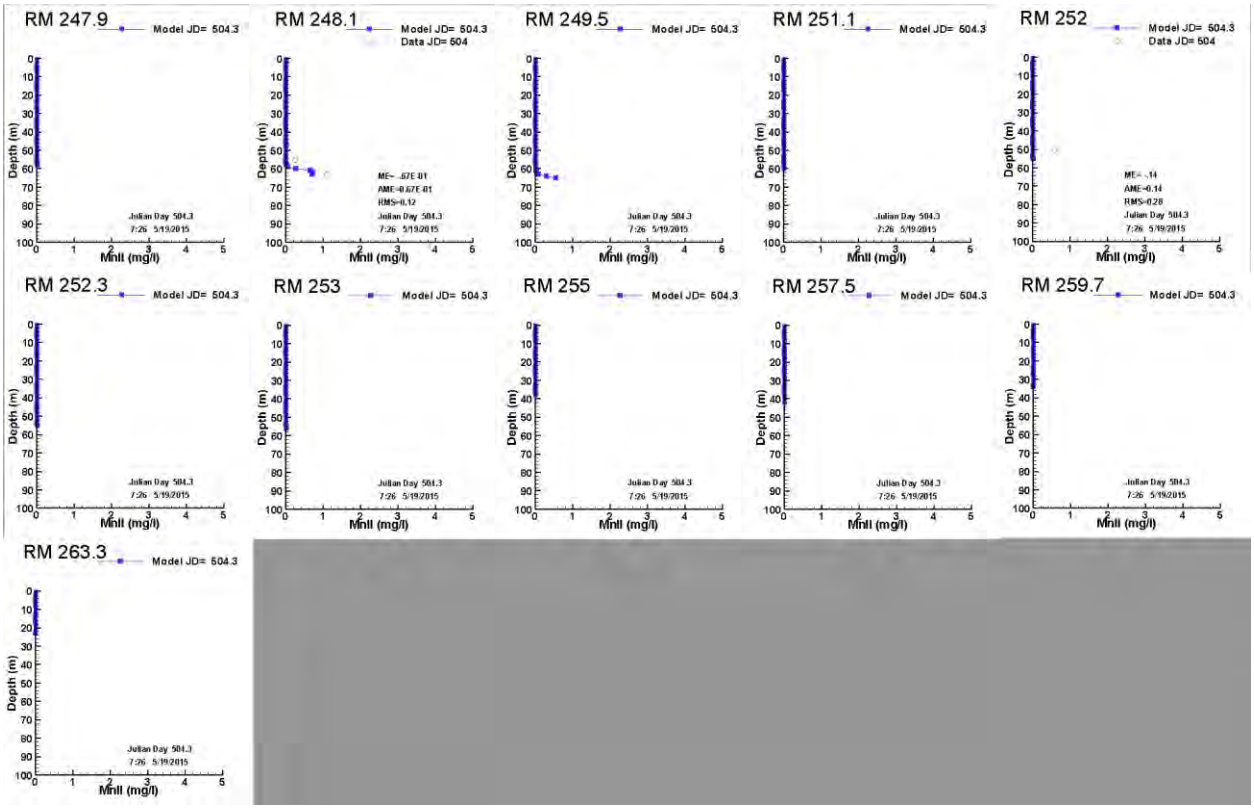


Figure 152. Vertical profiles of MNII compared with data for 5/19/2015.

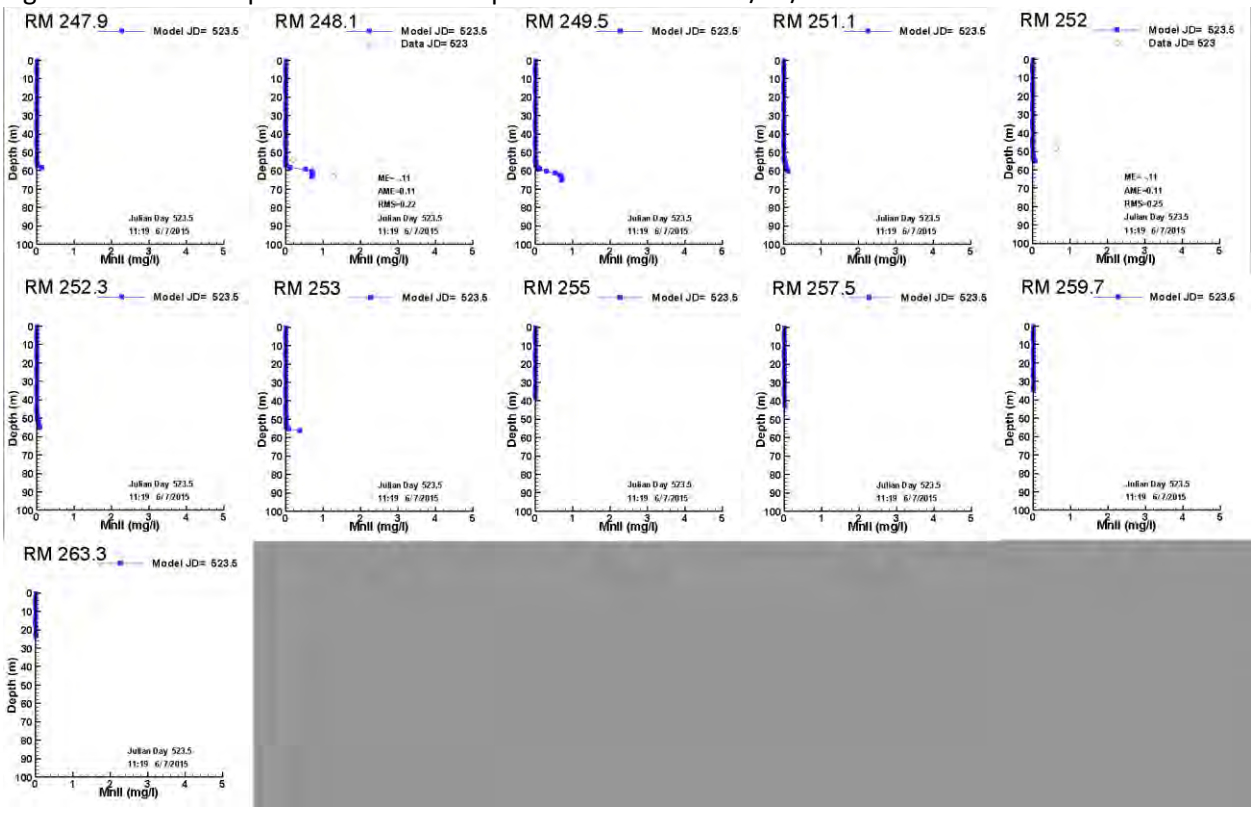


Figure 153. Vertical profiles of MNII compared with data for 6/ 7/2015.

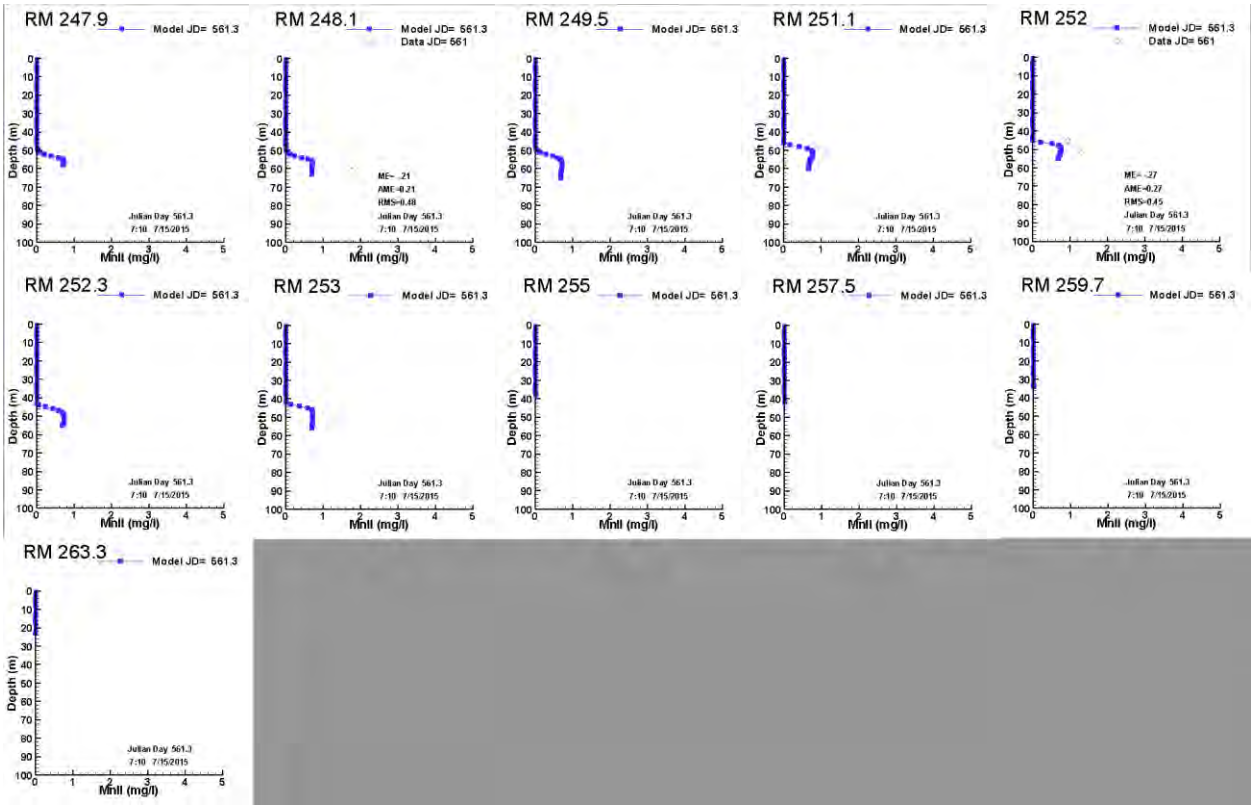


Figure 154. Vertical profiles of MNII compared with data for 7/15/2015.

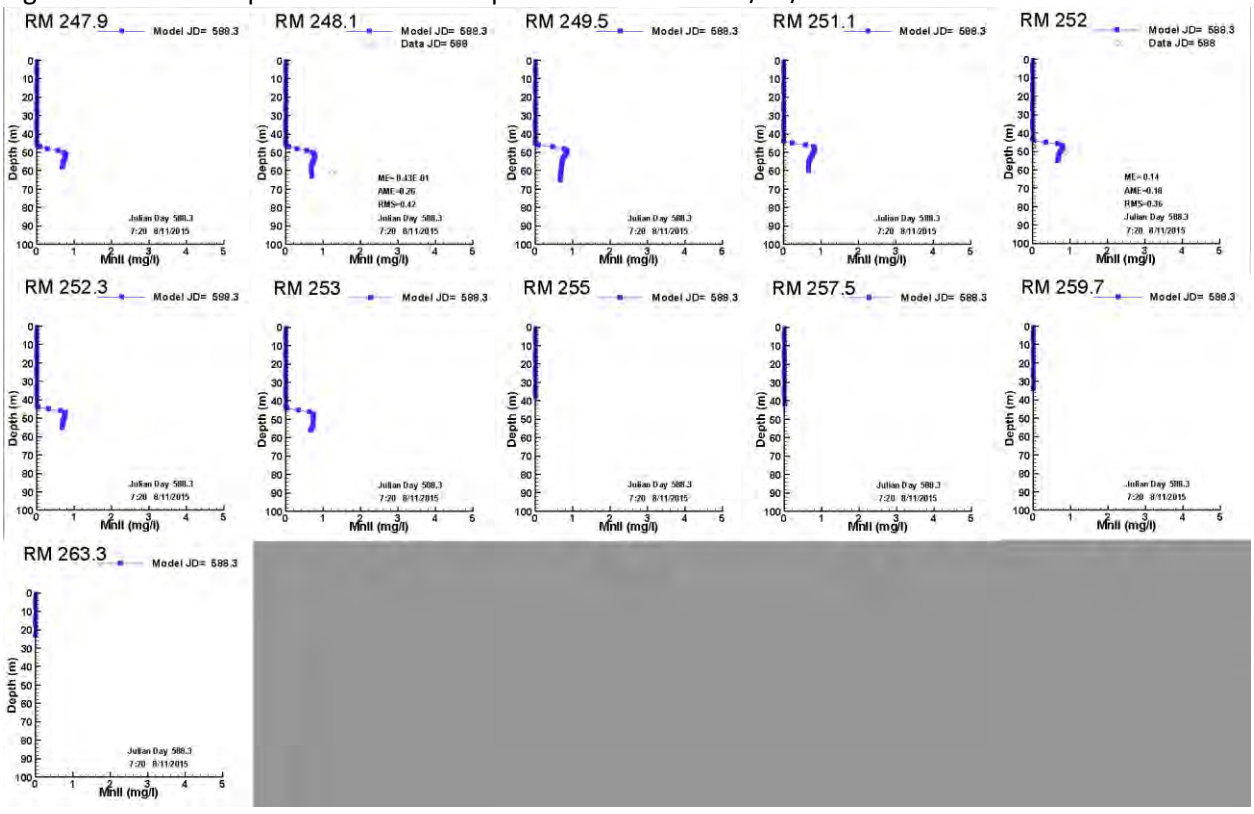


Figure 155. Vertical profiles of MNII compared with data for 8/11/2015.

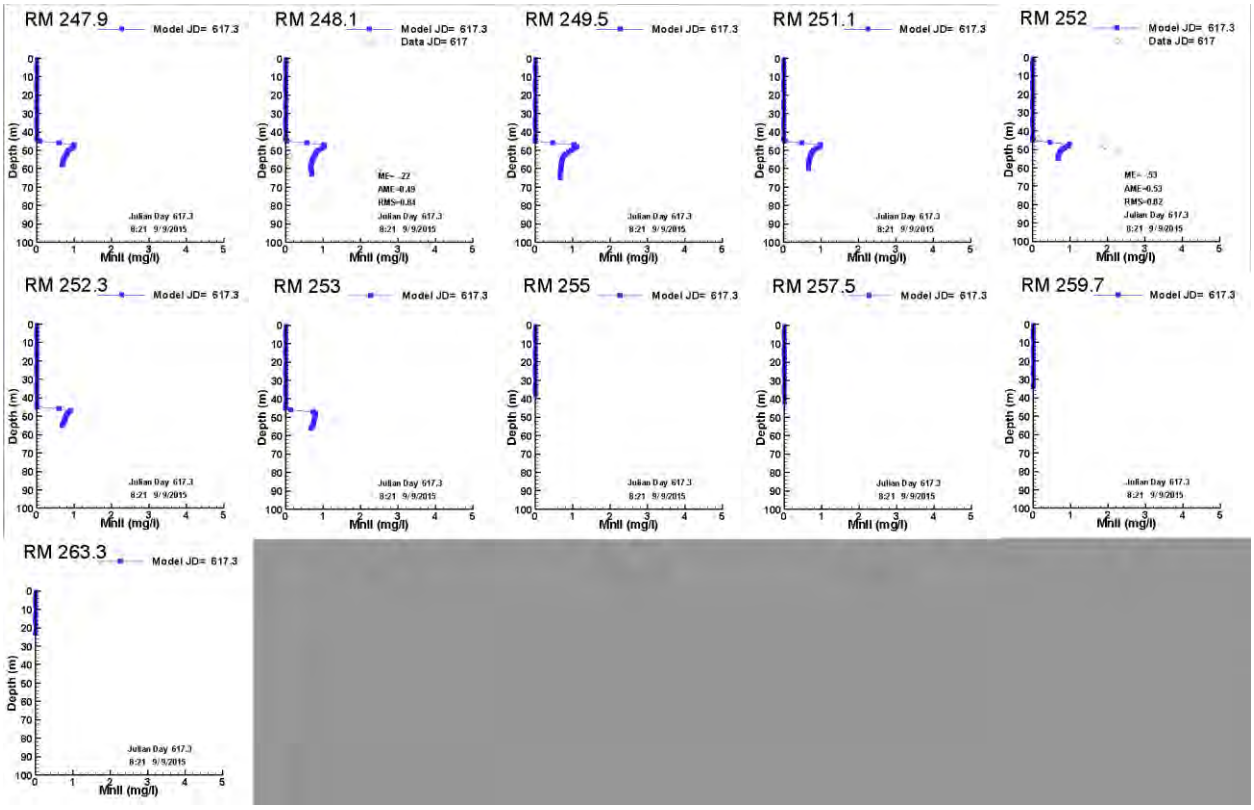


Figure 156. Vertical profiles of MNII compared with data for 9/ 9/2015.

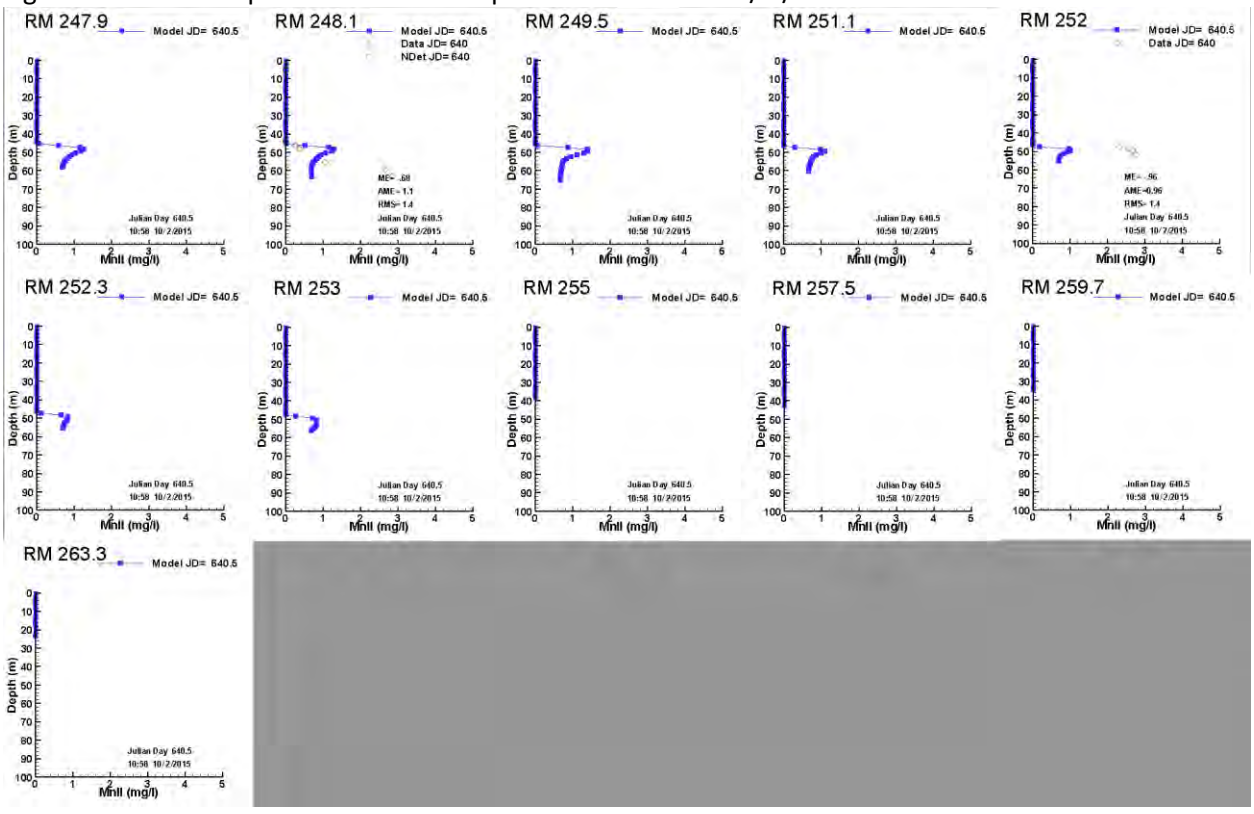


Figure 157. Vertical profiles of MNII compared with data for 10/ 2/2015.

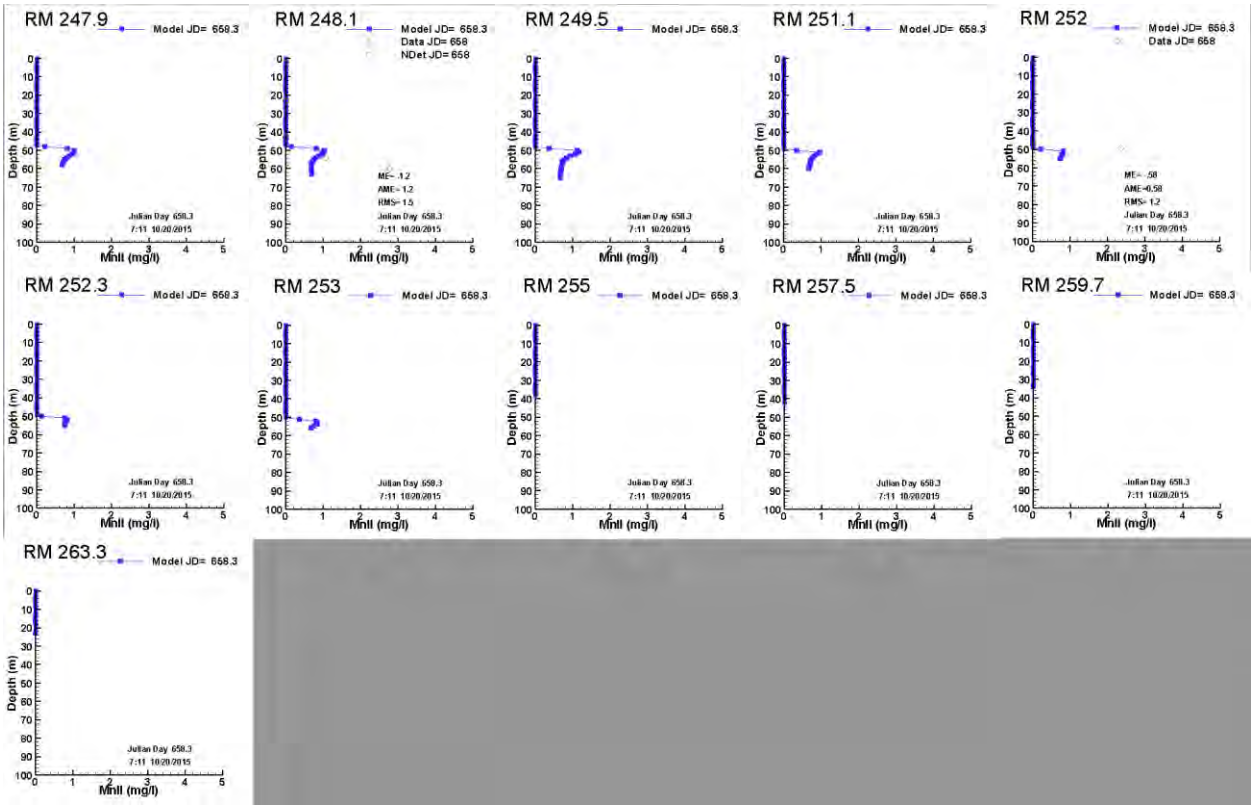


Figure 158. Vertical profiles of MNII compared with data for 10/20/2015.

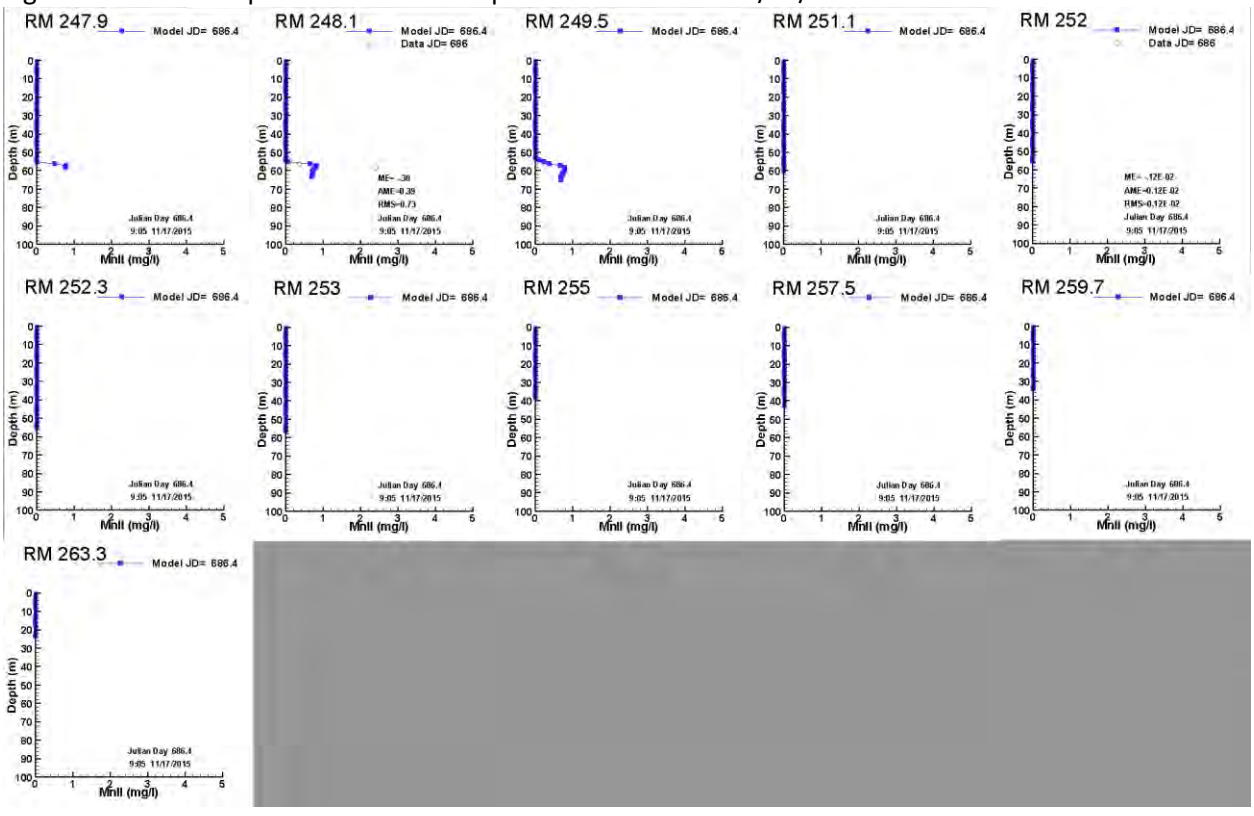


Figure 159. Vertical profiles of MNII compared with data for 11/17/2015.

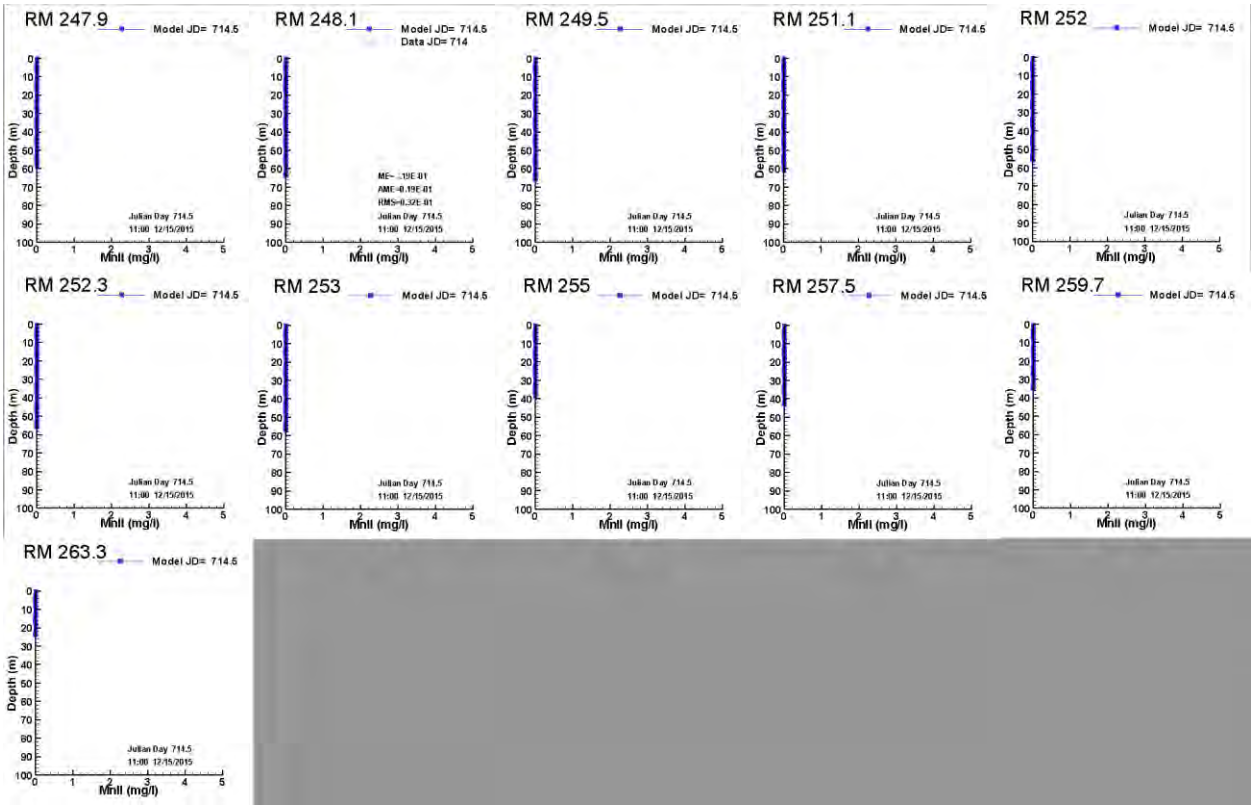


Figure 160. Vertical profiles of MNII compared with data for 12/15/2015.

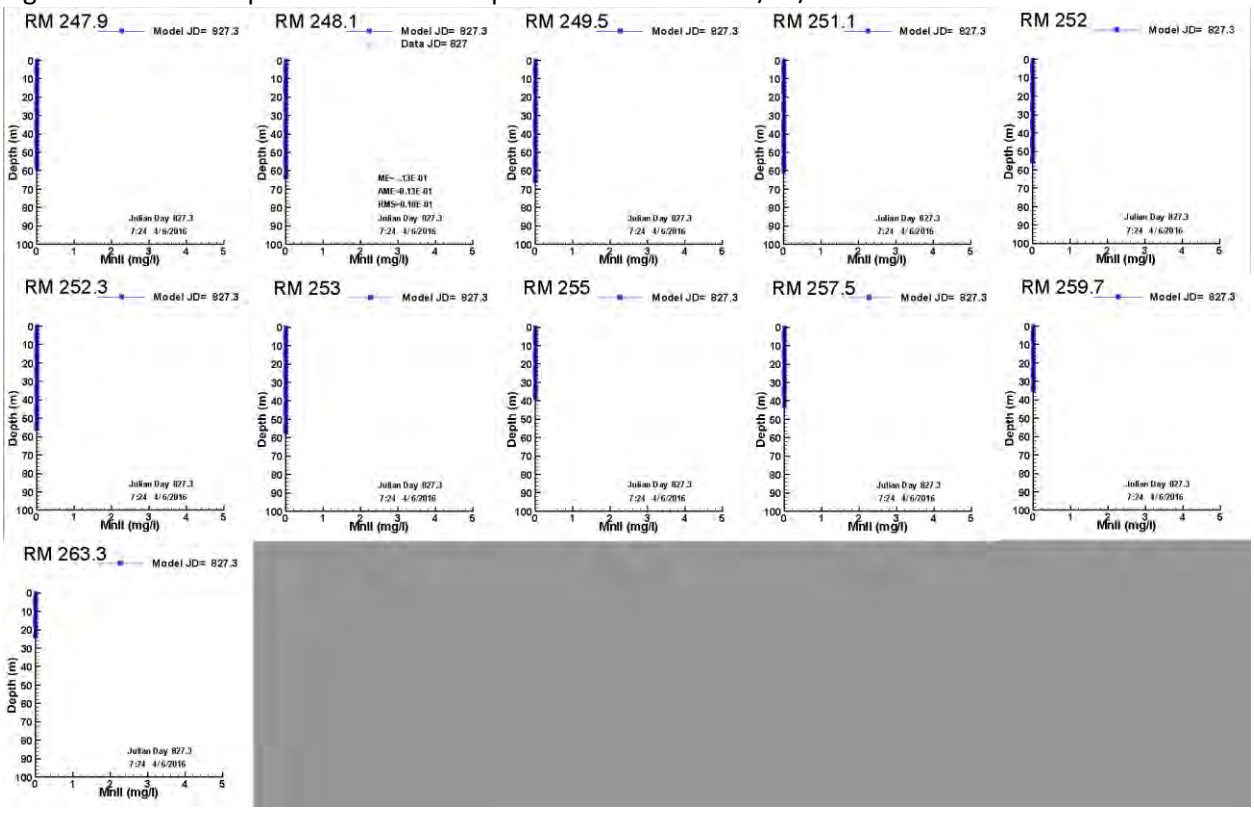


Figure 161. Vertical profiles of MNII compared with data for 4/ 6/2016.

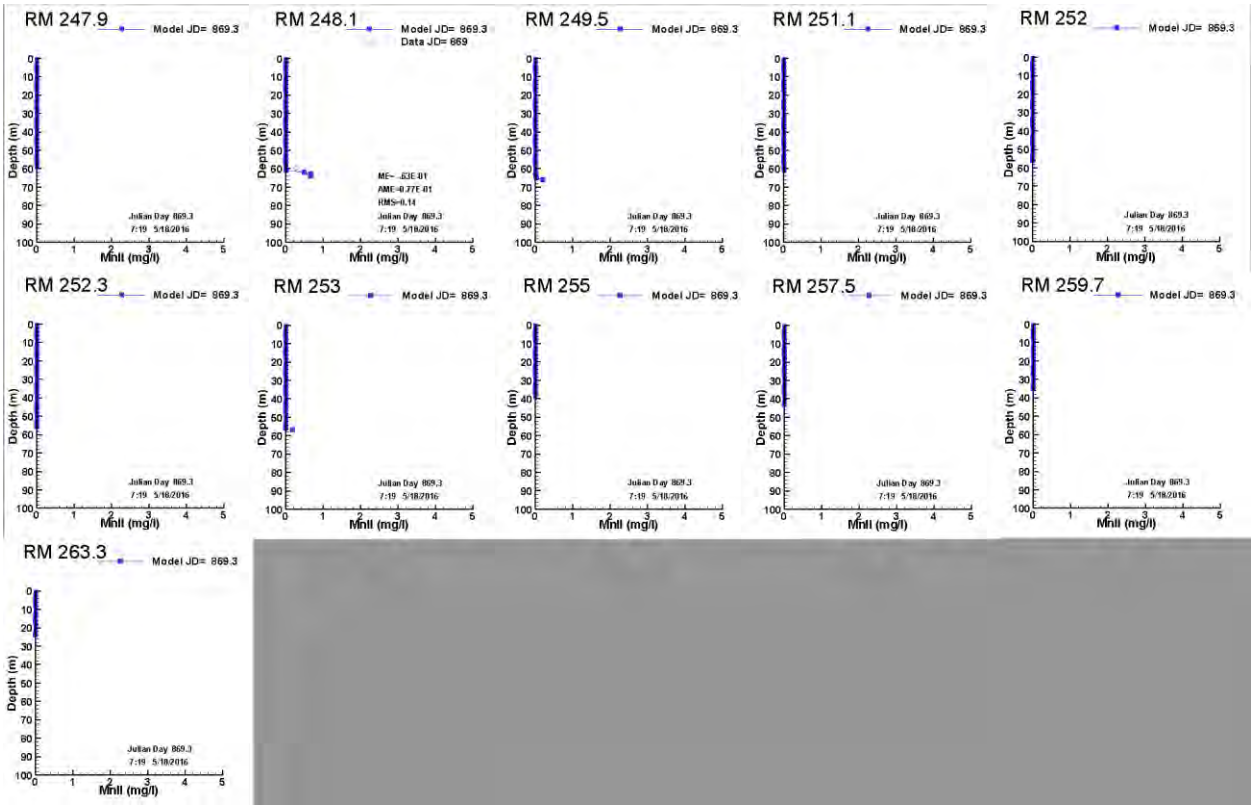


Figure 162. Vertical profiles of MNII compared with data for 5/18/2016.

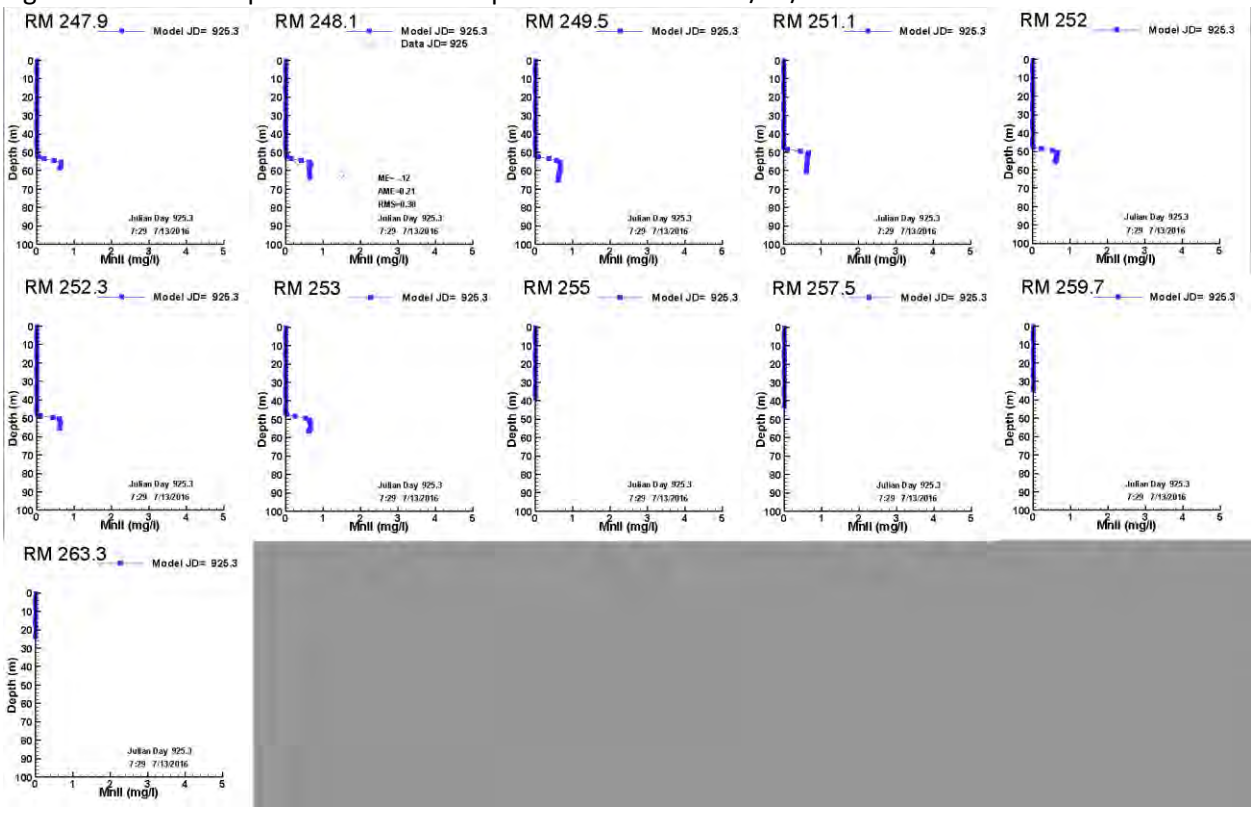


Figure 163. Vertical profiles of MNII compared with data for 7/13/2016.

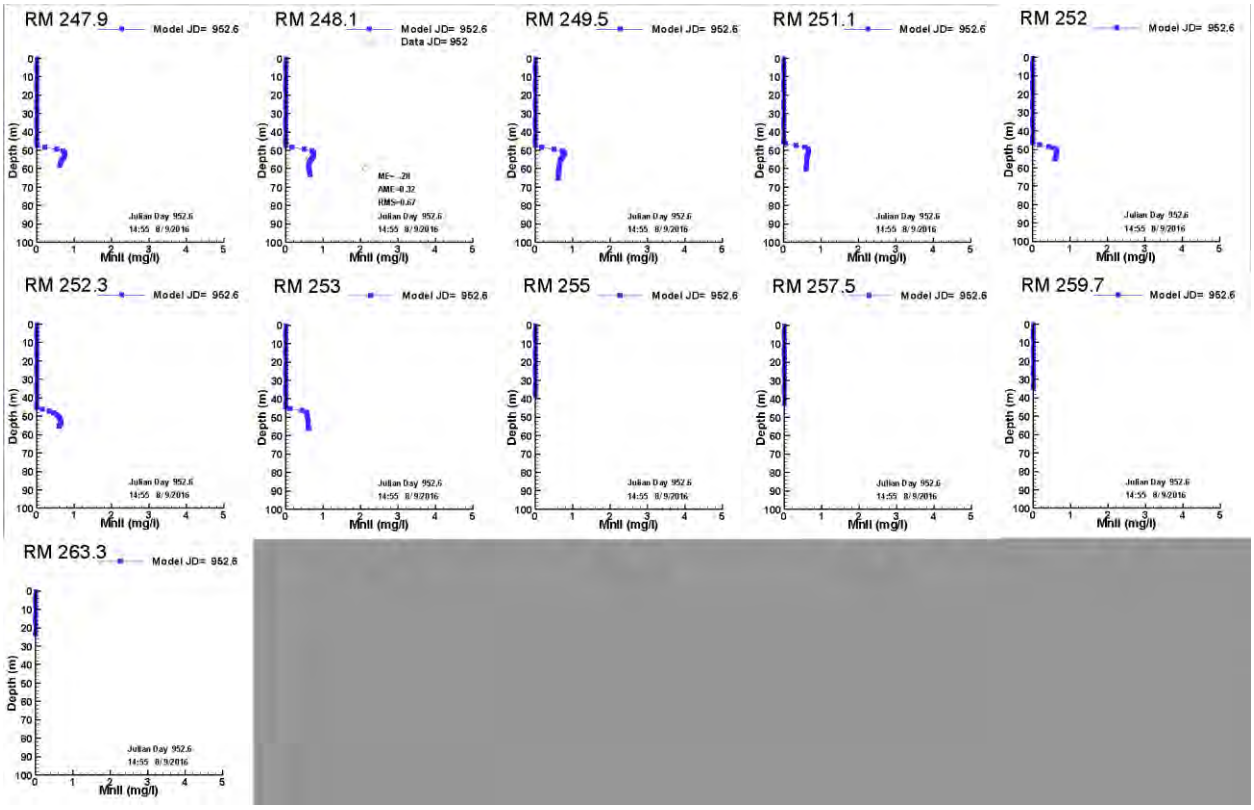


Figure 164. Vertical profiles of MNII compared with data for 8/ 9/2016.

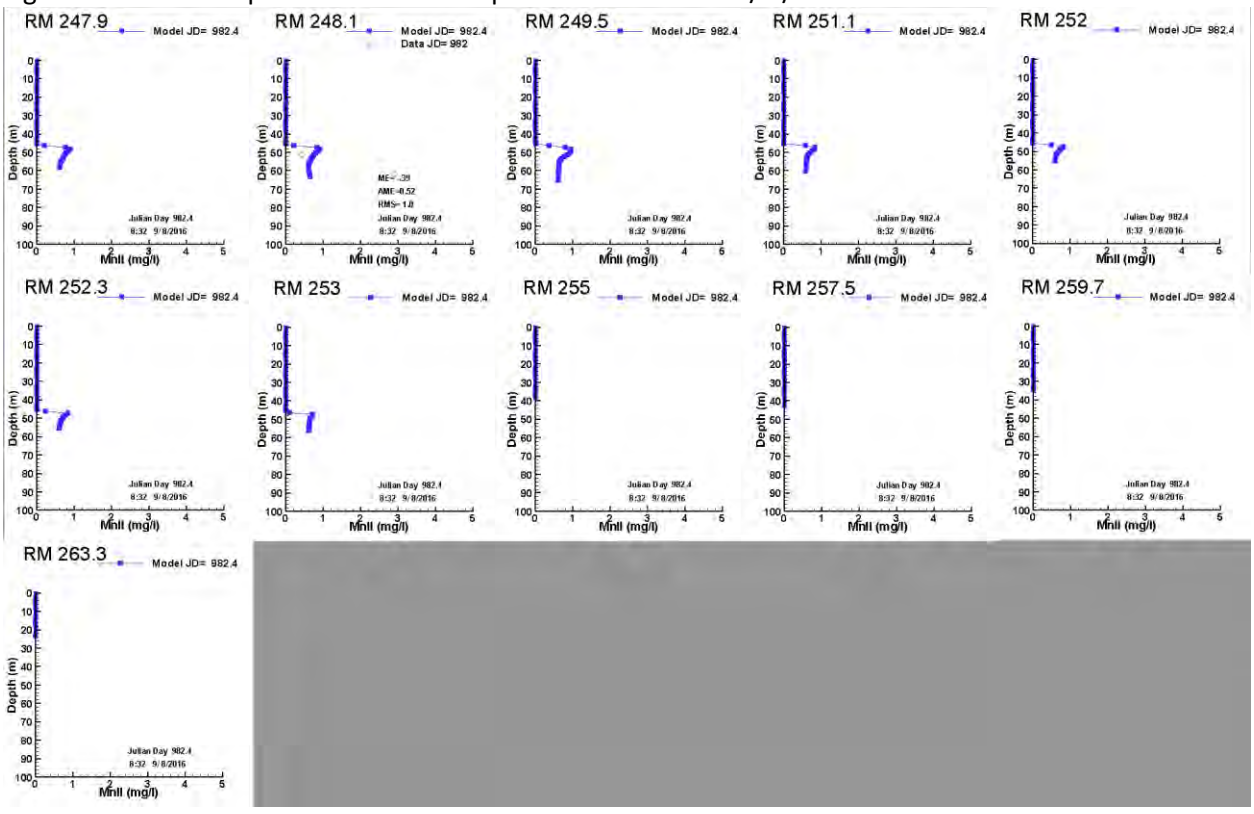


Figure 165. Vertical profiles of MNII compared with data for 9/ 8/2016.

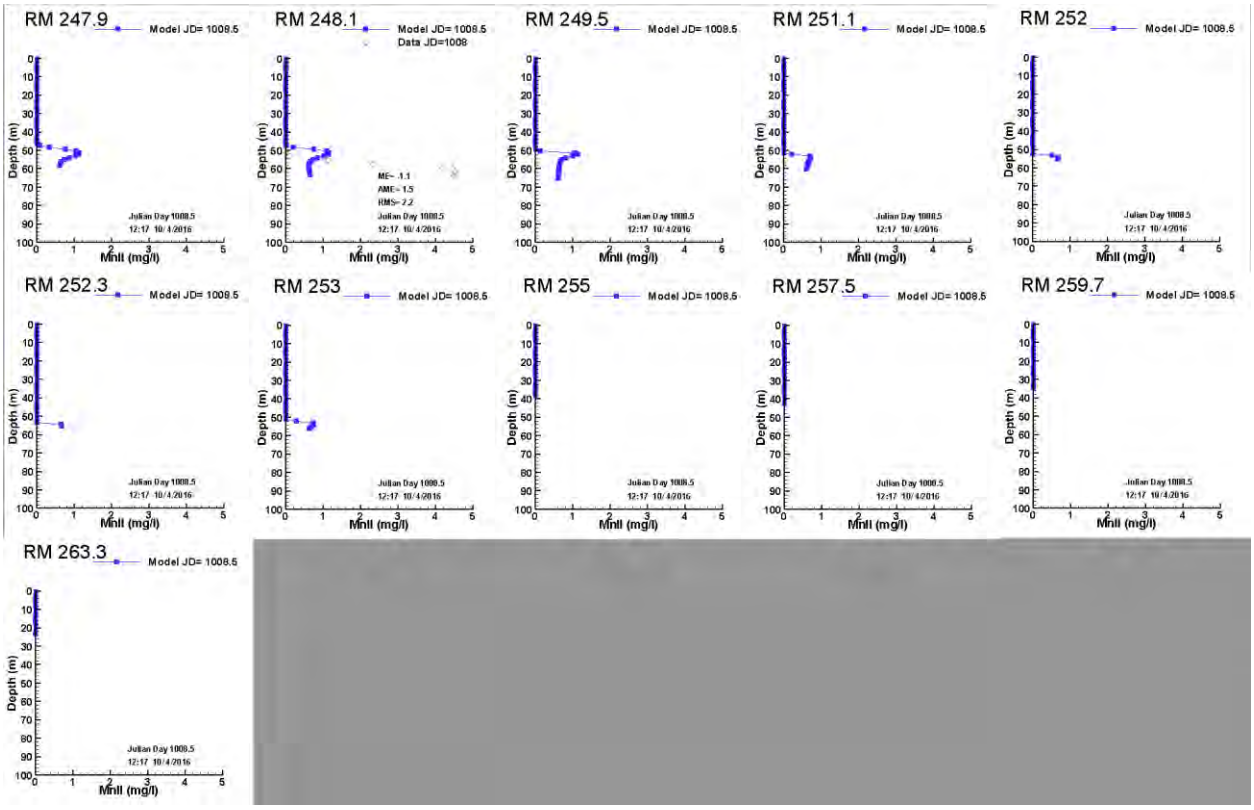


Figure 166. Vertical profiles of MNII compared with data for 10/ 4/2016.

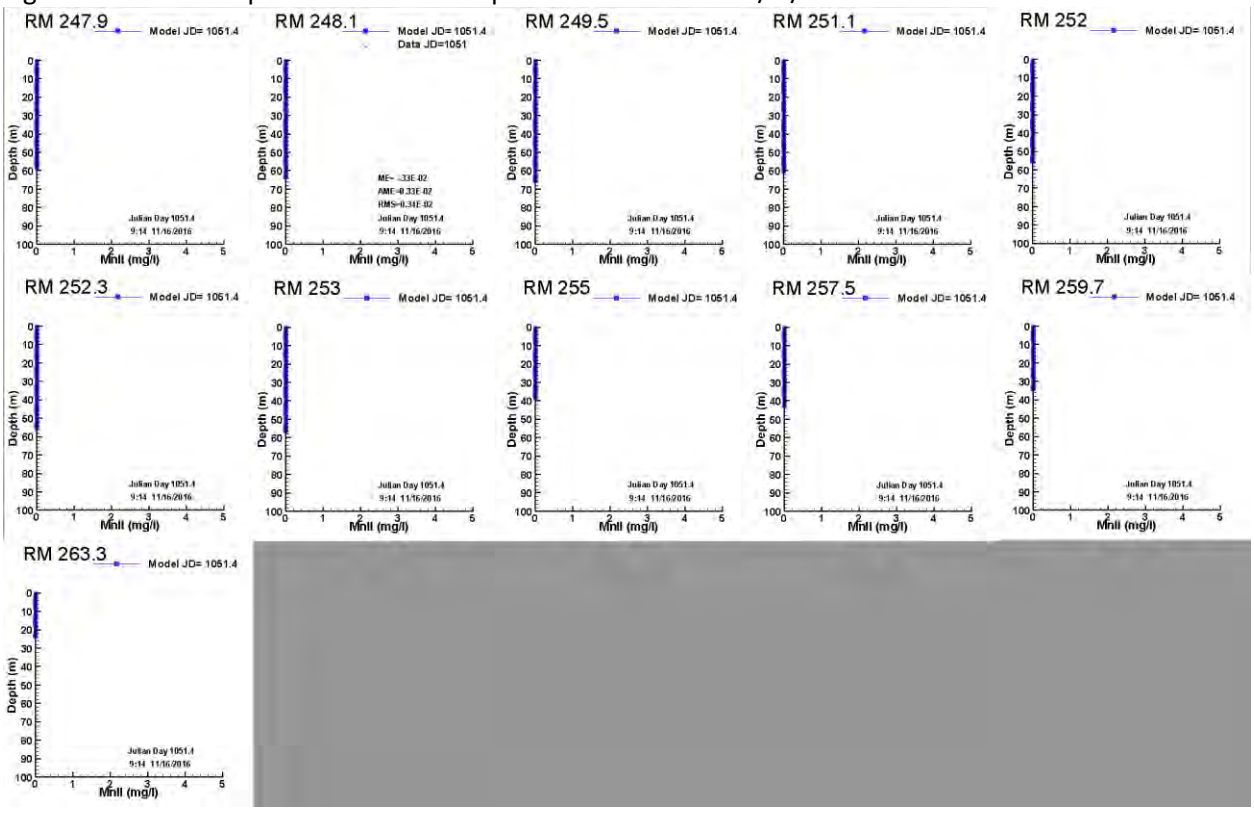


Figure 167. Vertical profiles of MNII compared with data for 11/16/2016.

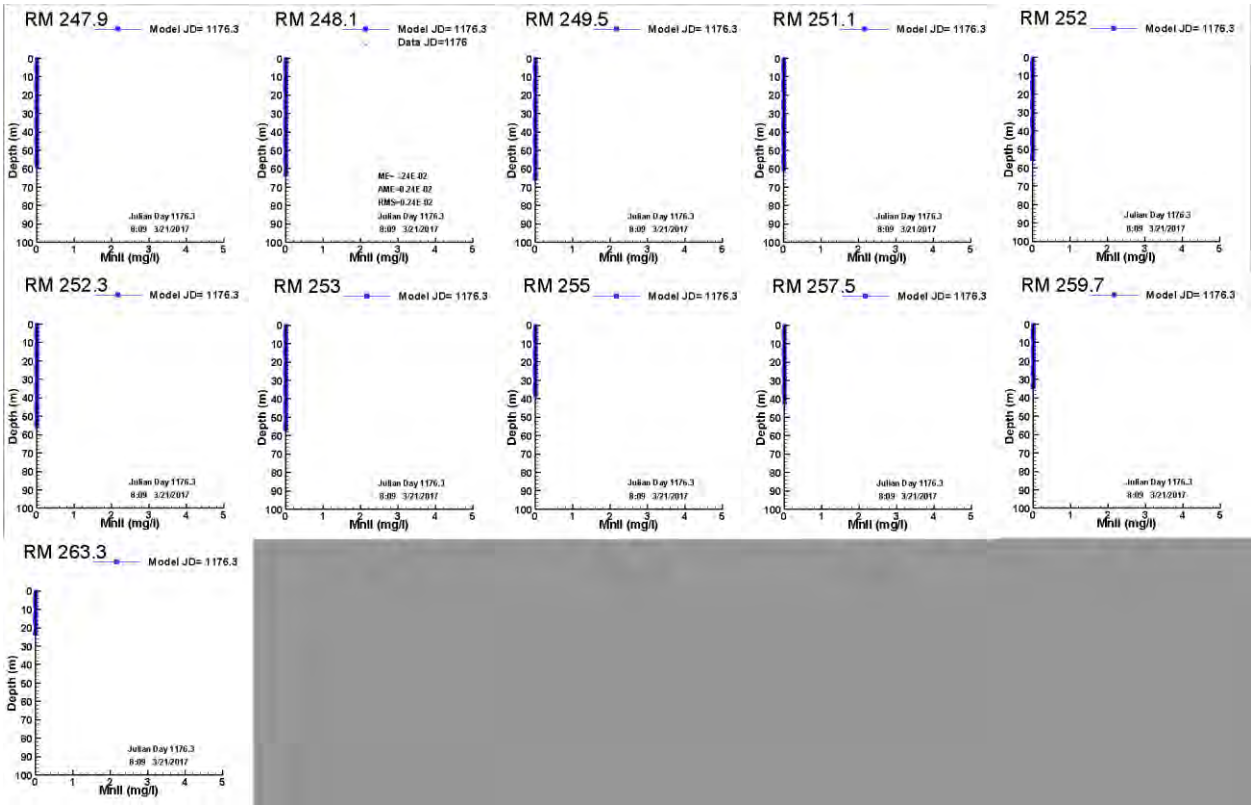


Figure 168. Vertical profiles of MNII compared with data for 3/21/2017.

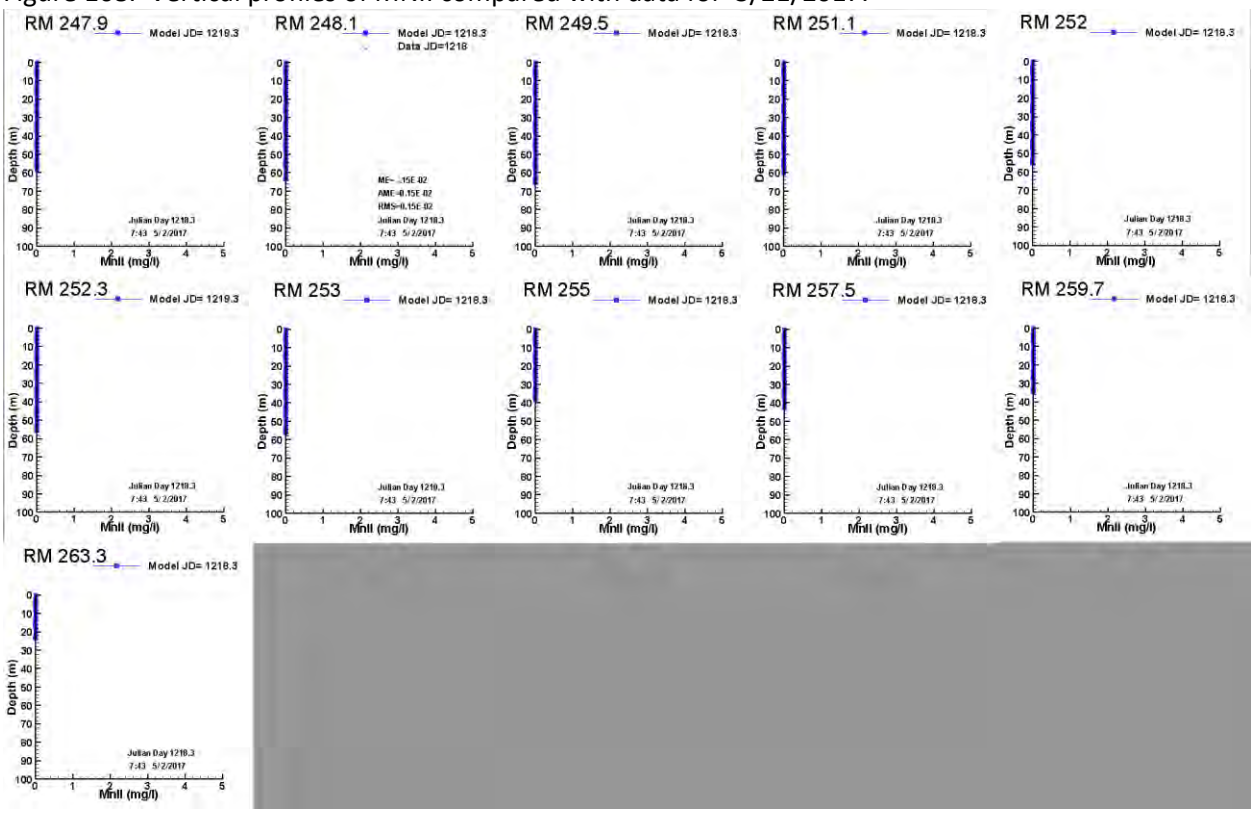


Figure 169. Vertical profiles of MNII compared with data for 5/ 2/2017.

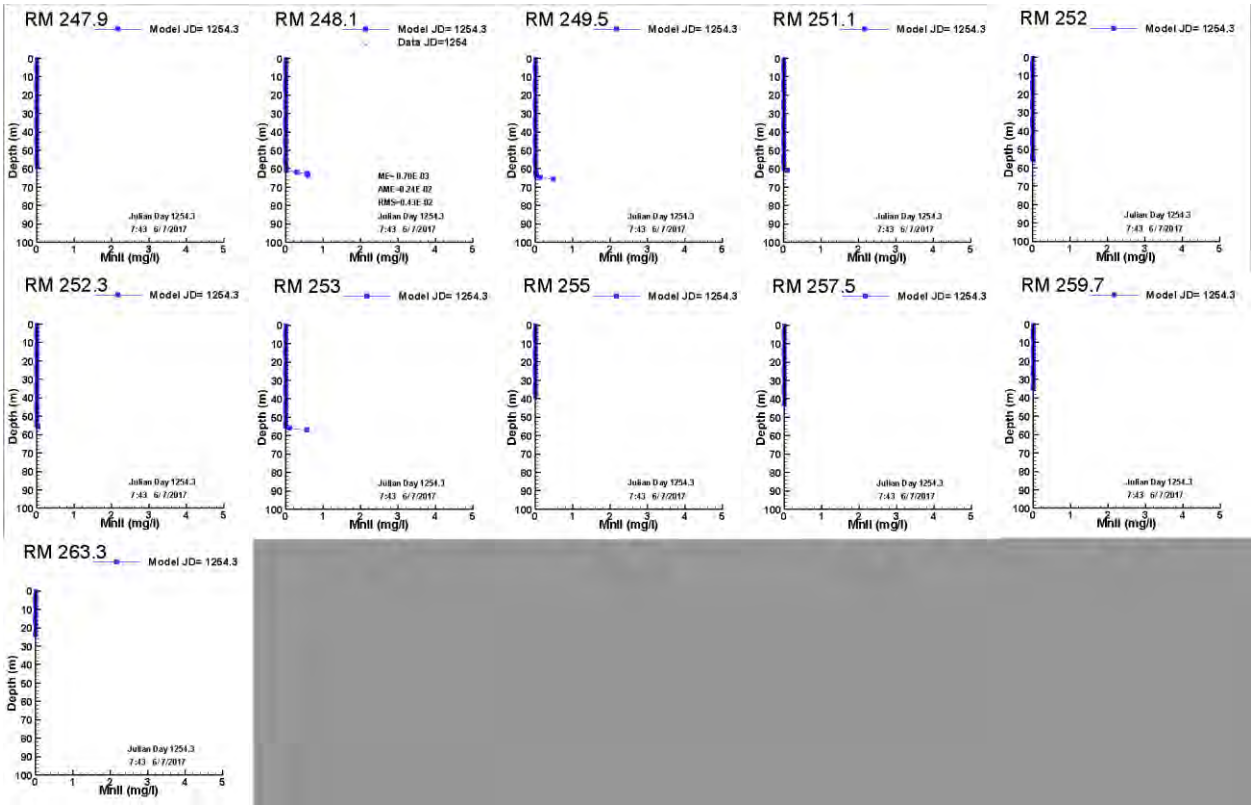


Figure 170. Vertical profiles of MNII compared with data for 6/ 7/2017.

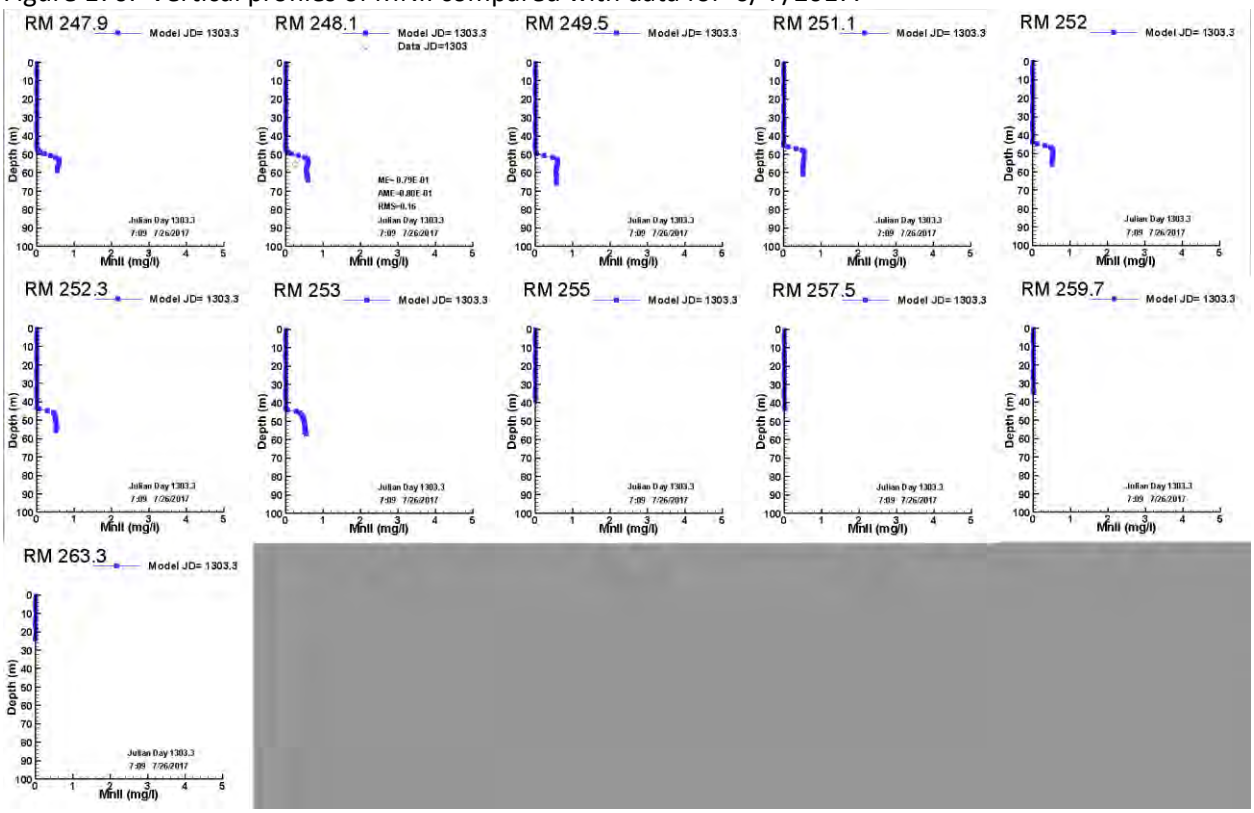


Figure 171. Vertical profiles of MNII compared with data for 7/26/2017.

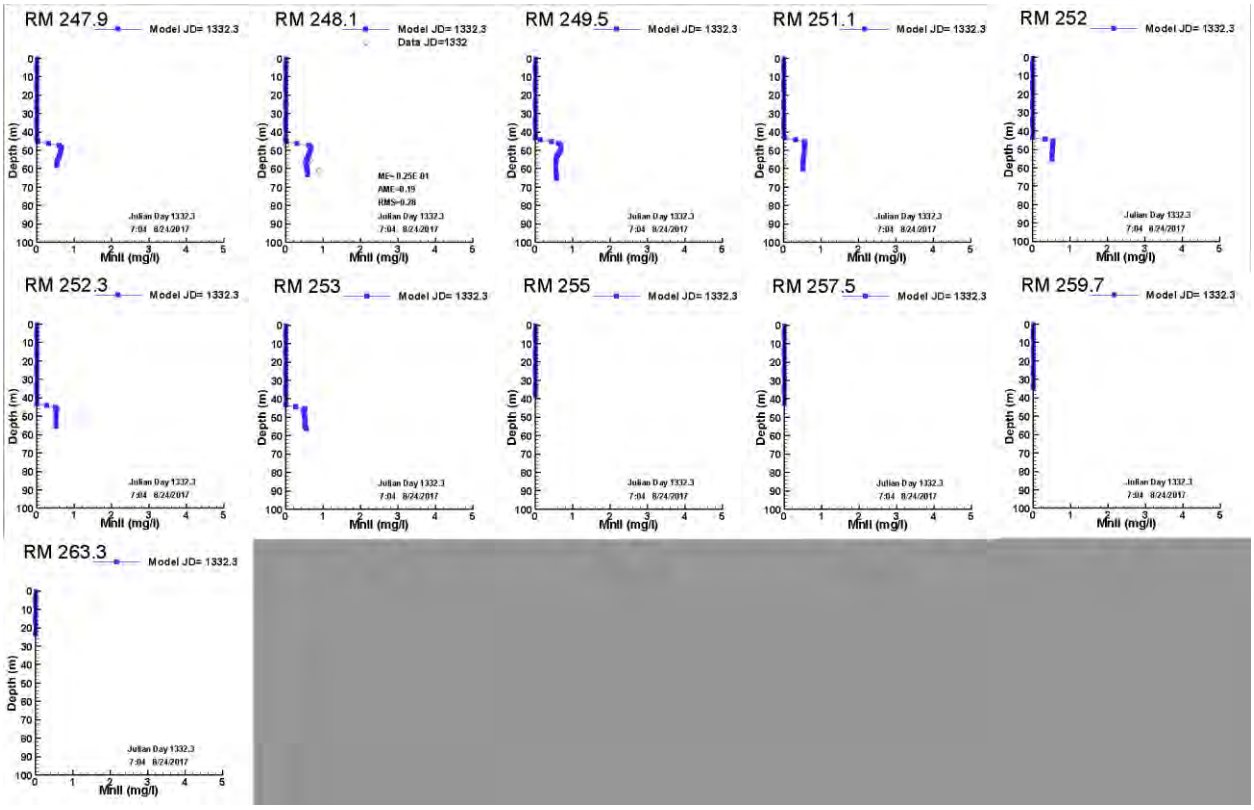


Figure 172. Vertical profiles of MNII compared with data for 8/24/2017.

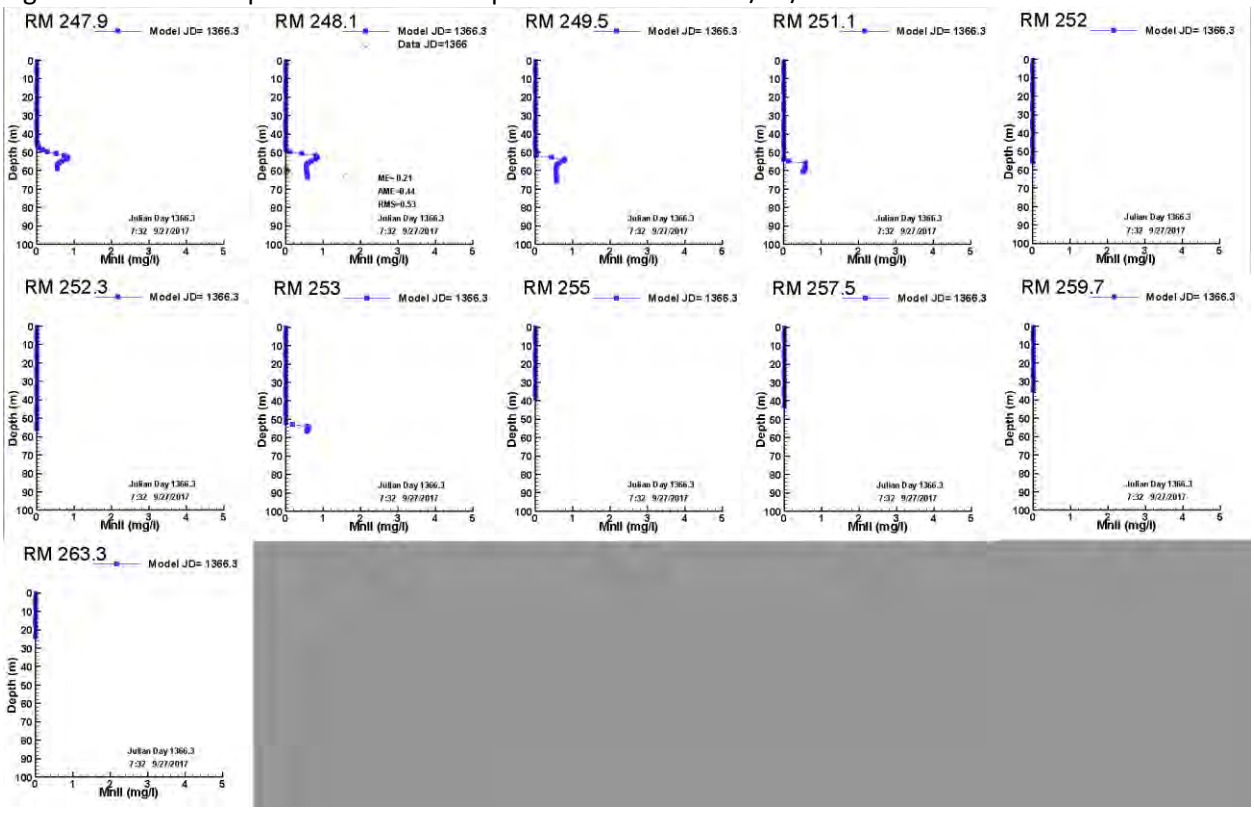


Figure 173. Vertical profiles of MNII compared with data for 9/27/2017.

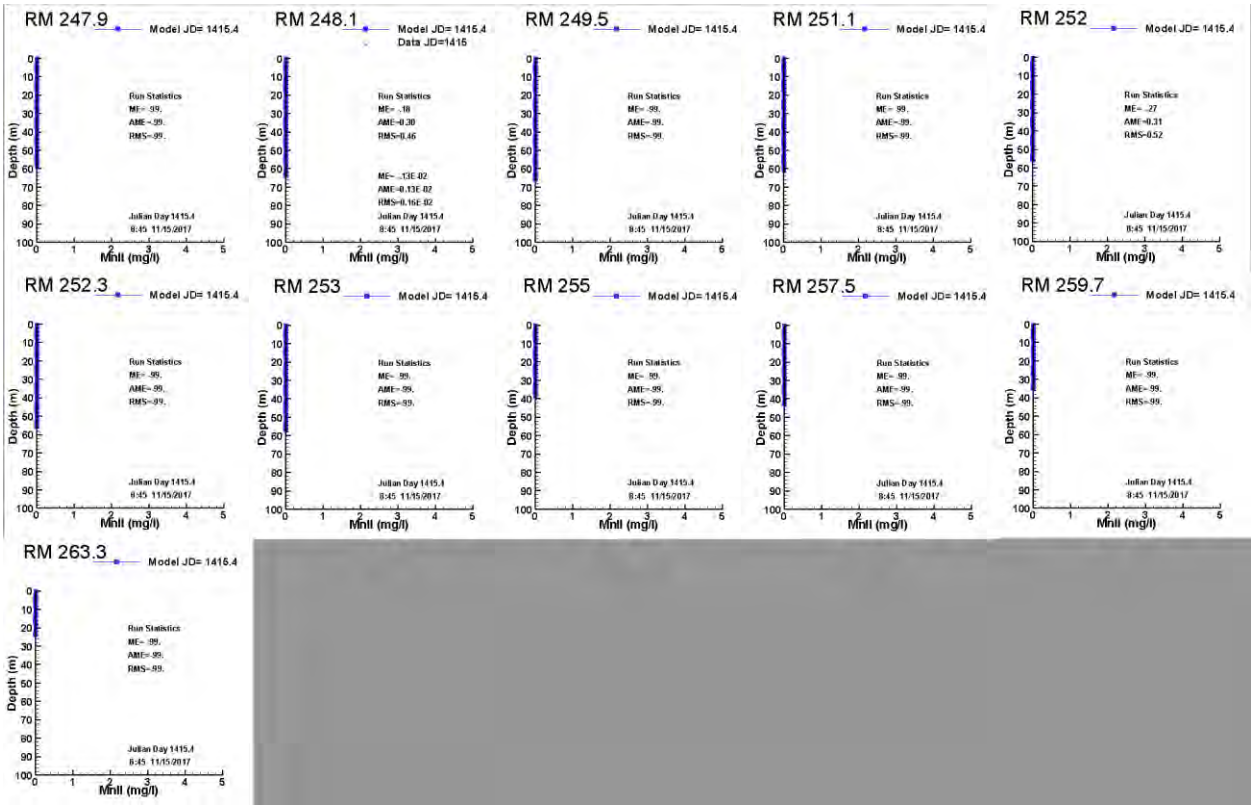


Figure 174. Vertical profiles of MNII compared with data for 11/15/2017.

MnO2

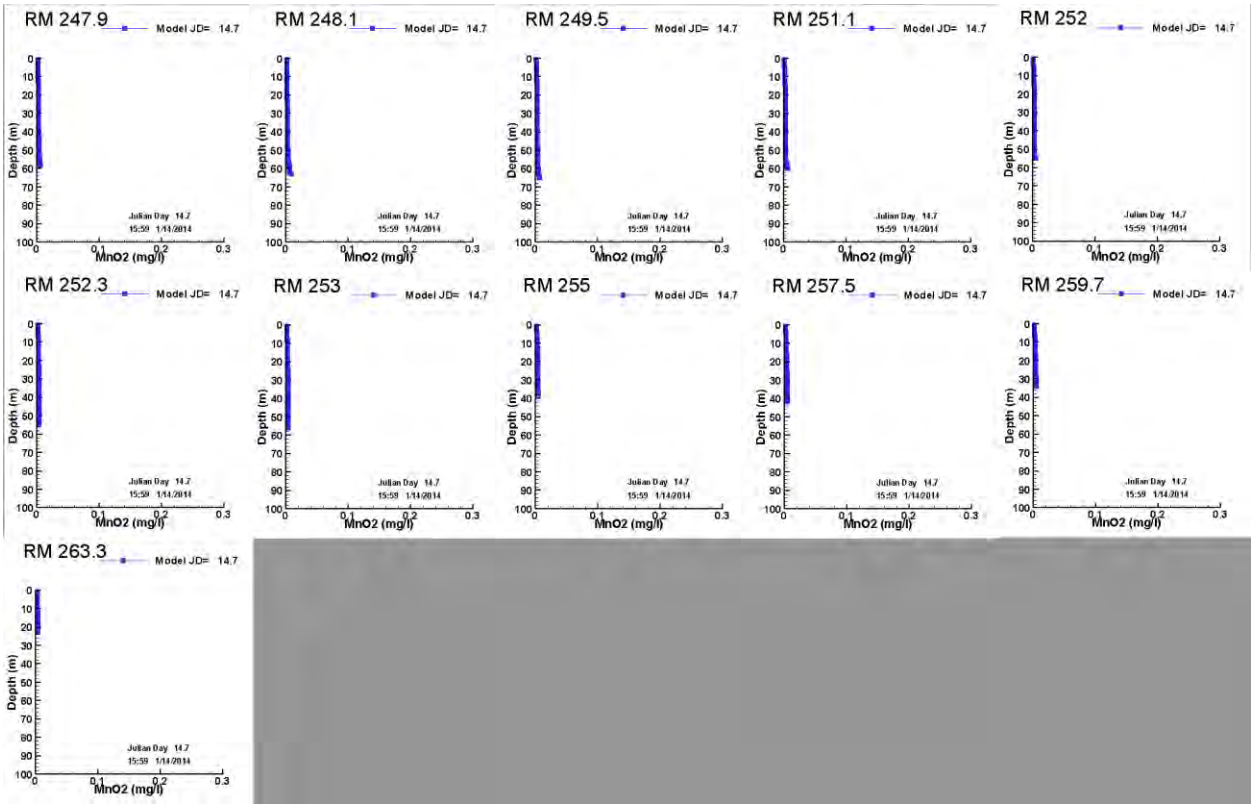


Figure 175. Vertical profiles of MnO2 compared with data for 1/14/2014.

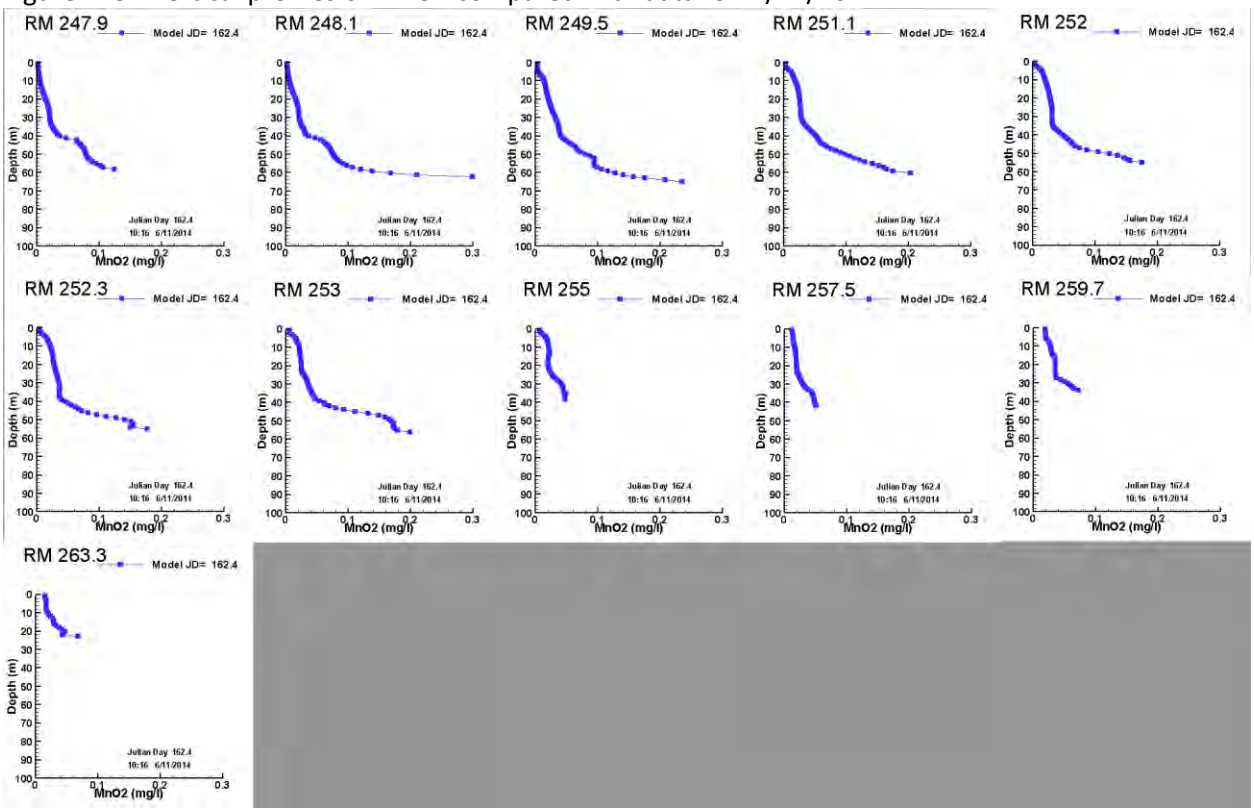


Figure 176. Vertical profiles of MnO2 compared with data for 6/11/2014.

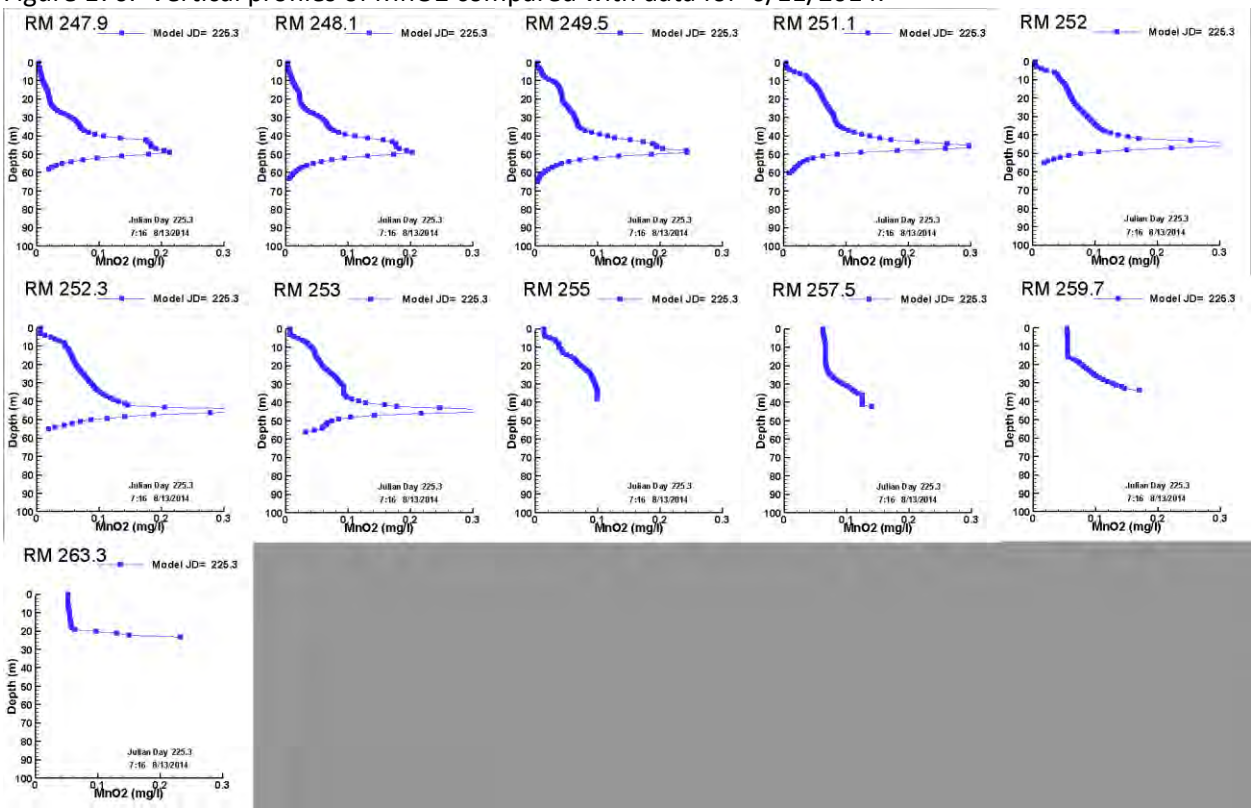


Figure 177. Vertical profiles of MnO2 compared with data for 8/13/2014.

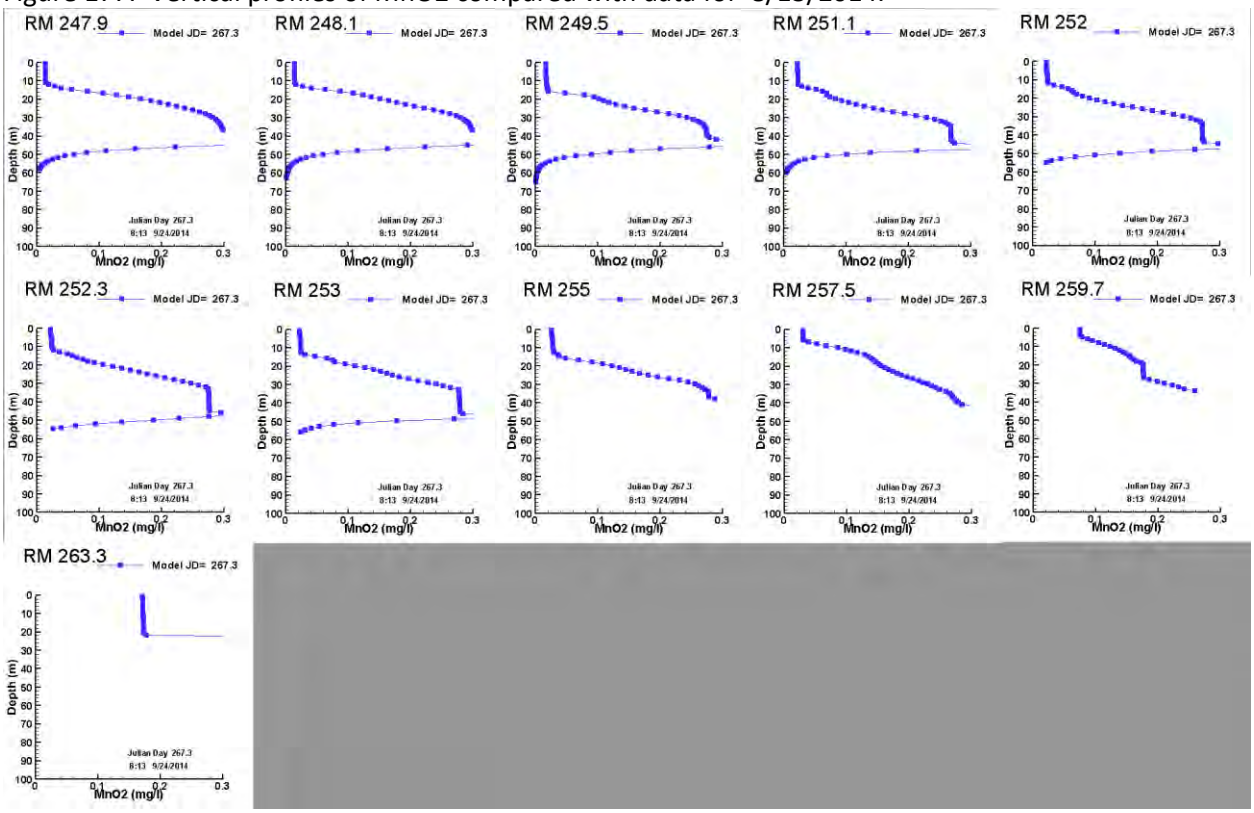


Figure 178. Vertical profiles of MnO2 compared with data for 9/24/2014.

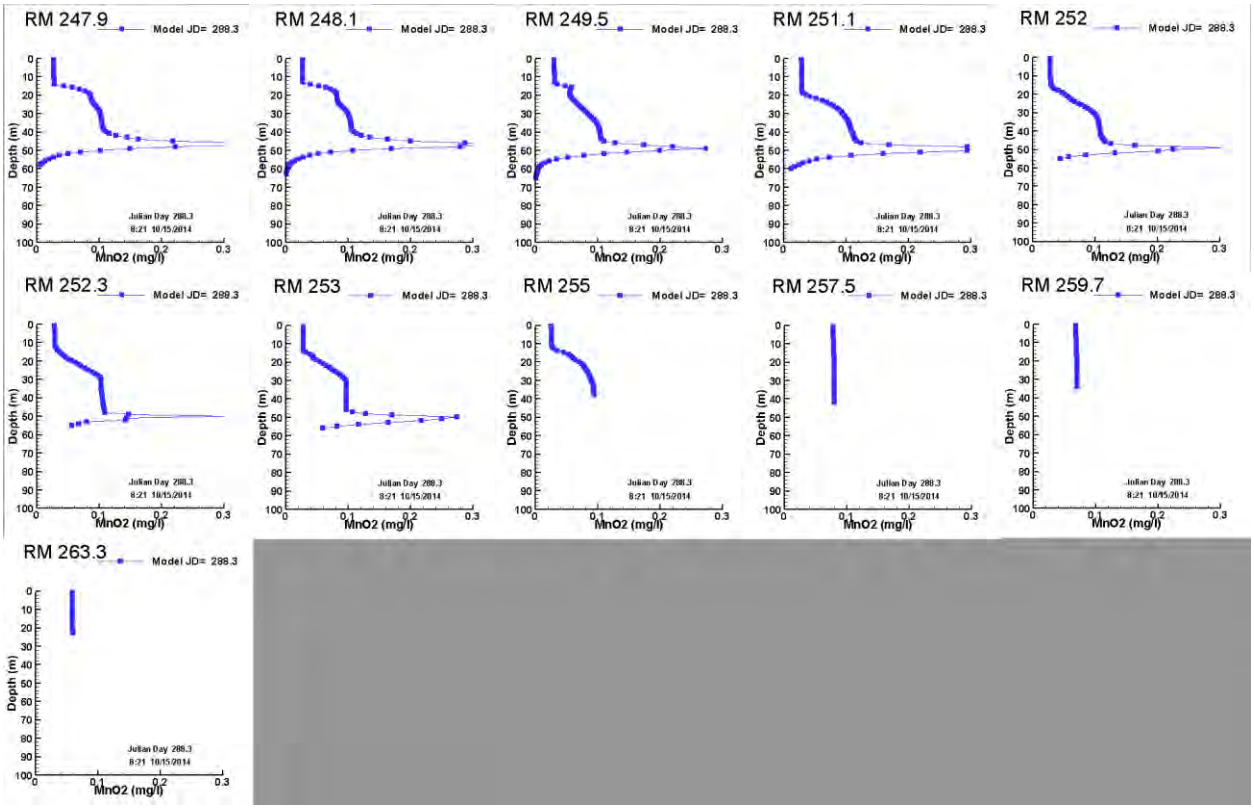


Figure 179. Vertical profiles of MnO2 compared with data for 10/15/2014.

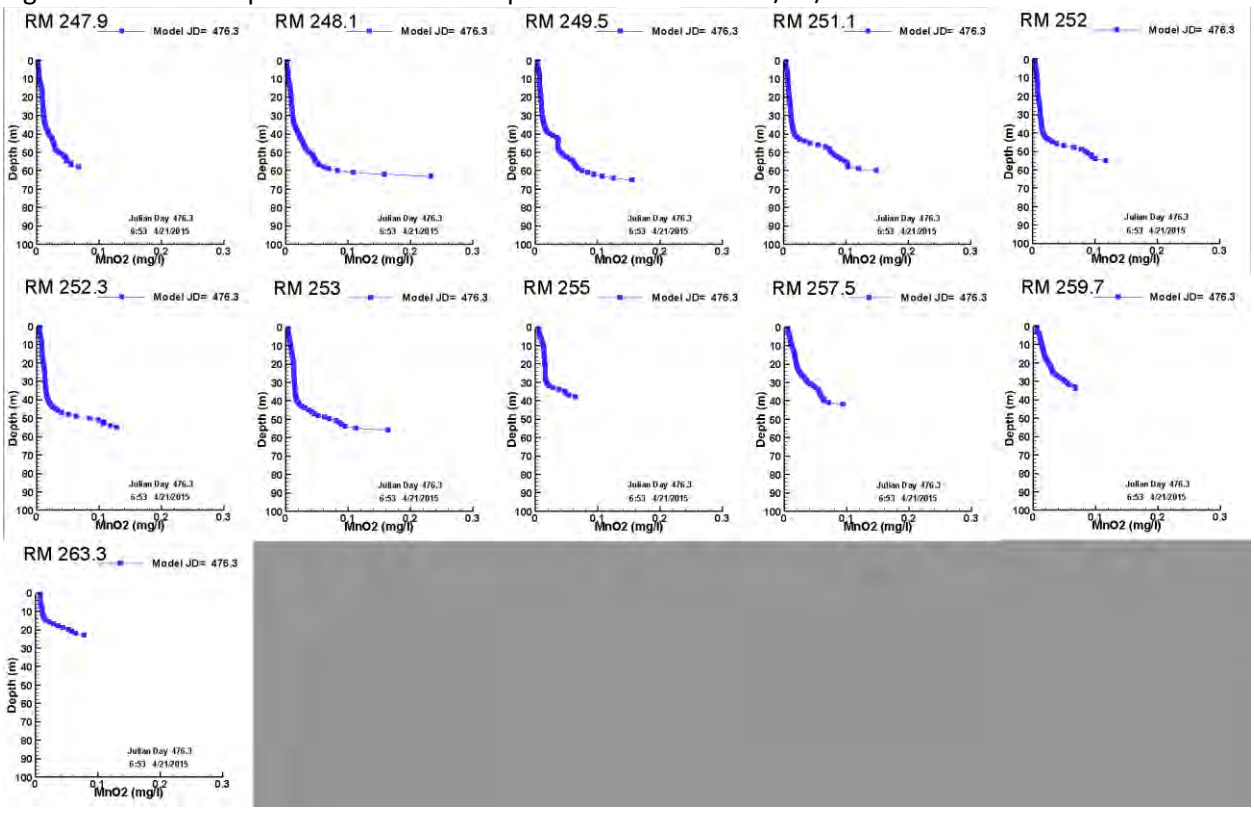


Figure 180. Vertical profiles of MnO2 compared with data for 4/21/2015.

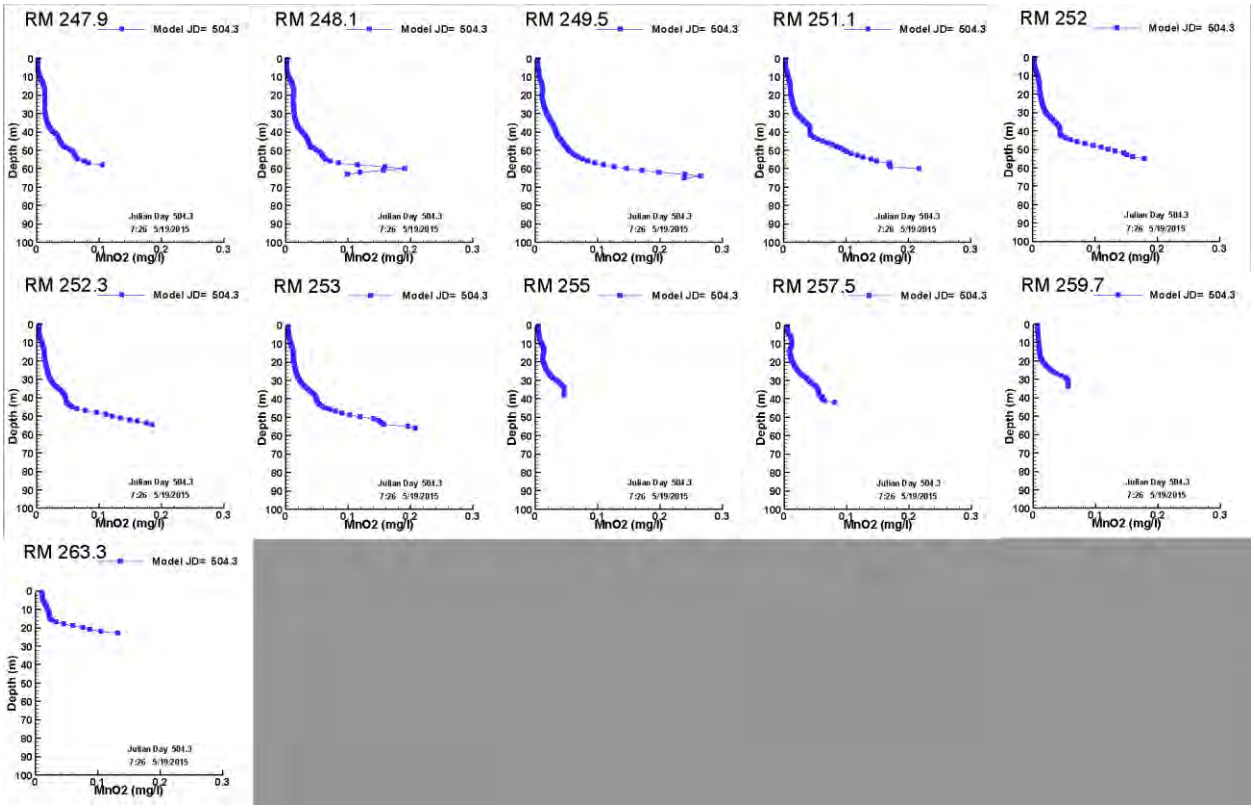


Figure 181. Vertical profiles of MnO2 compared with data for 5/19/2015.

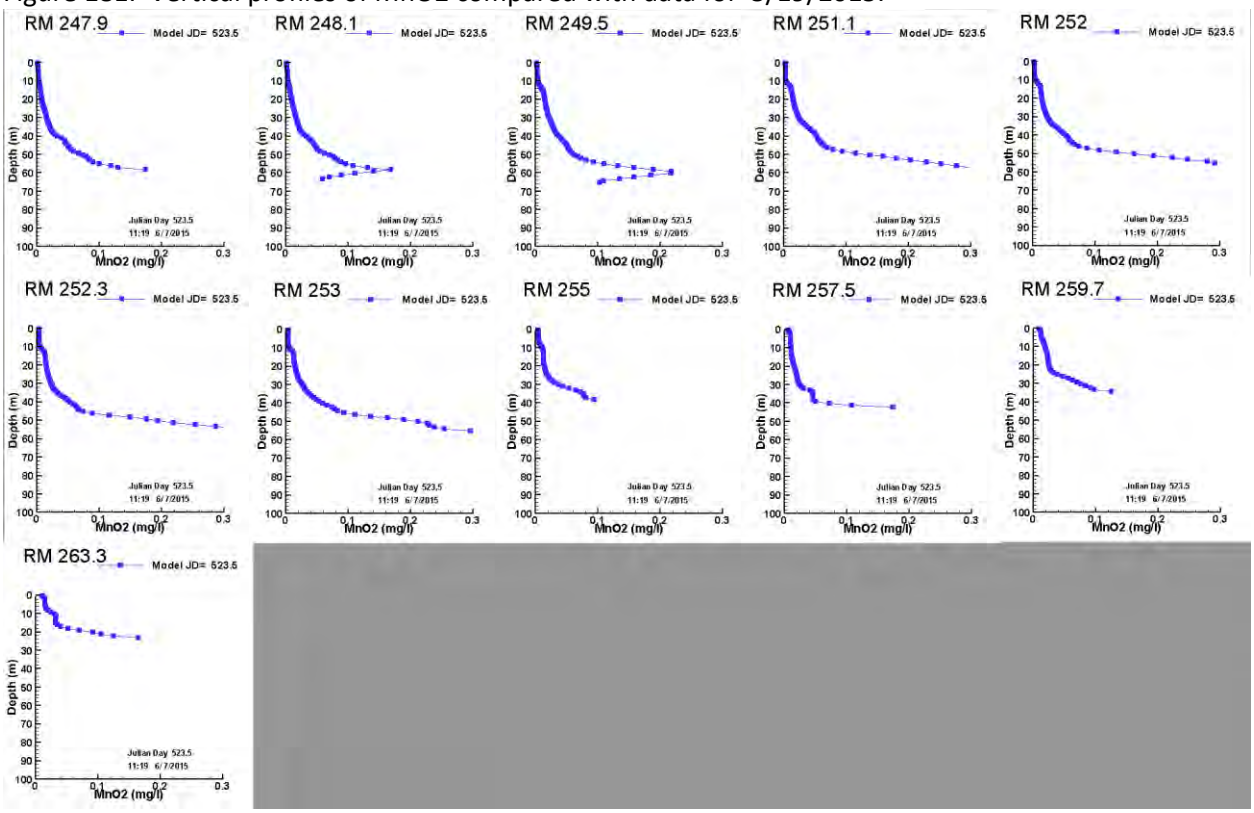


Figure 182. Vertical profiles of MnO2 compared with data for 6/ 7/2015.

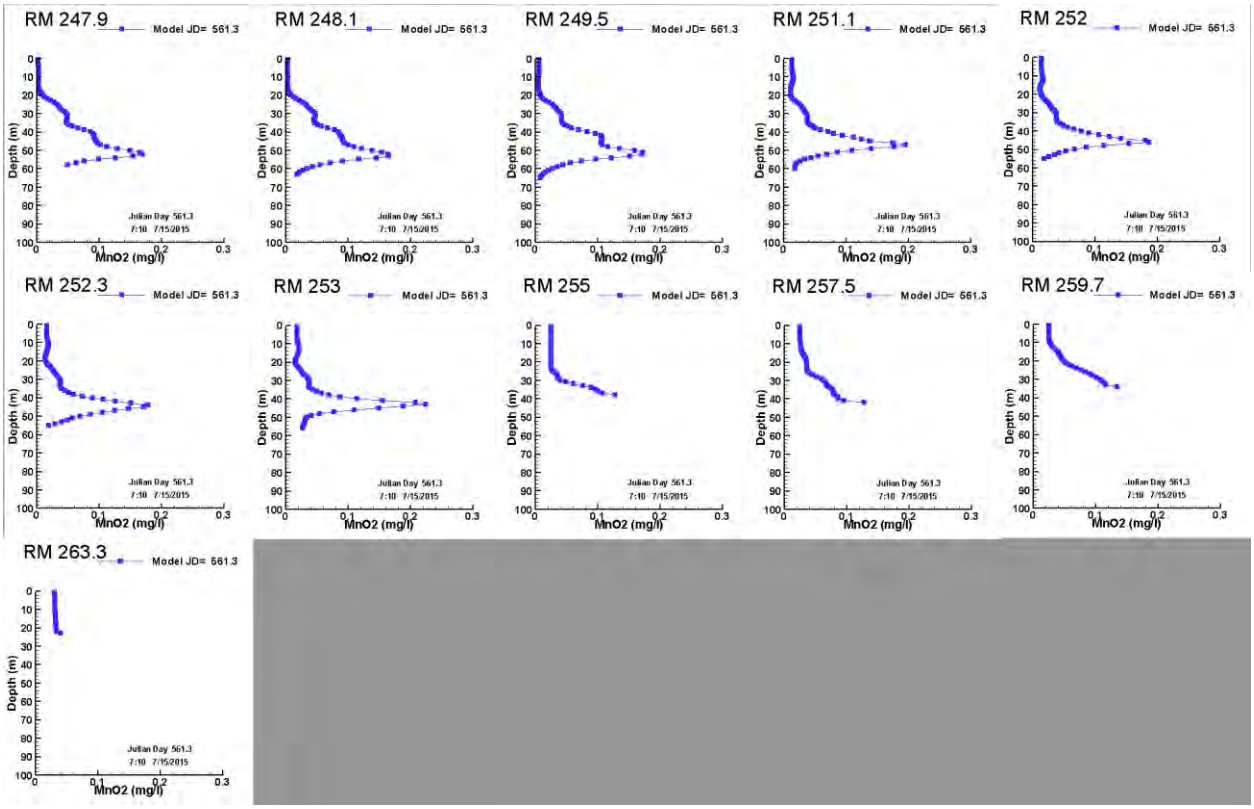


Figure 183. Vertical profiles of MnO2 compared with data for 7/15/2015.

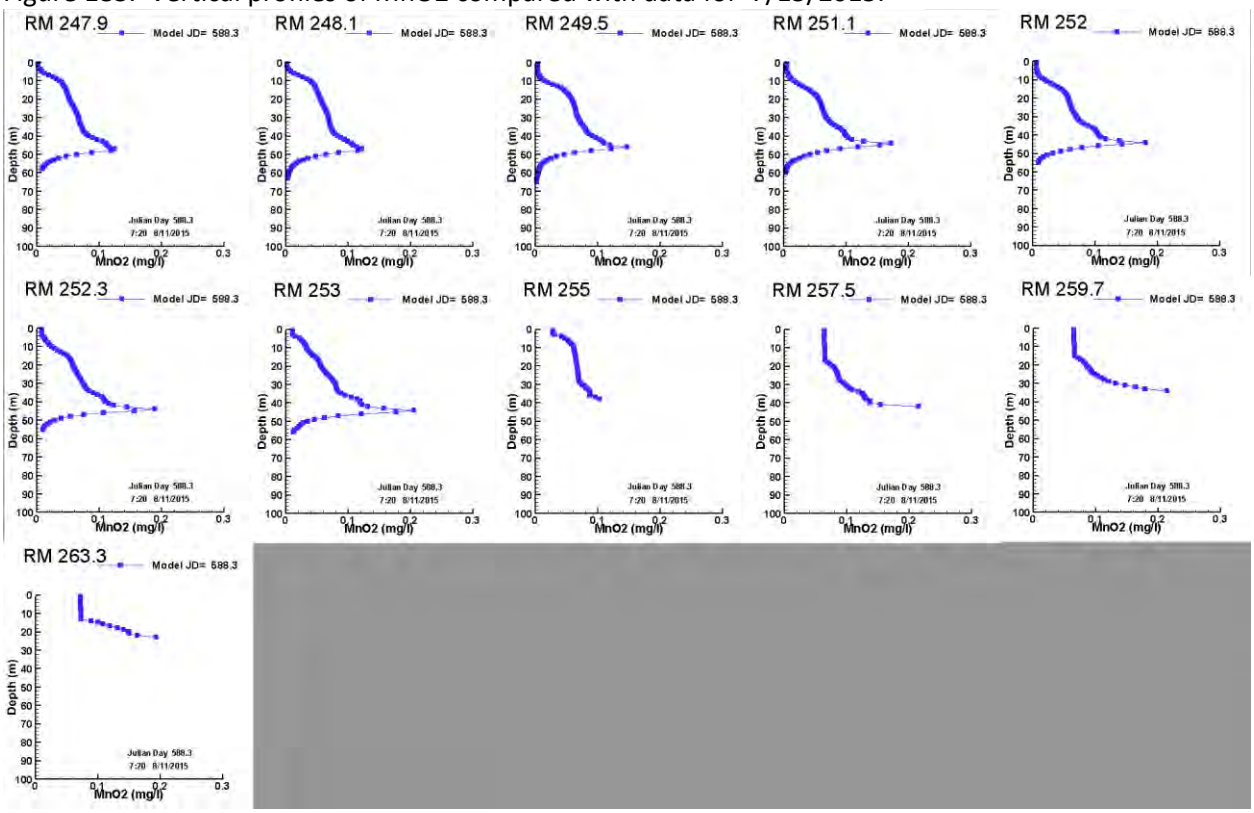


Figure 184. Vertical profiles of MnO2 compared with data for 8/11/2015.

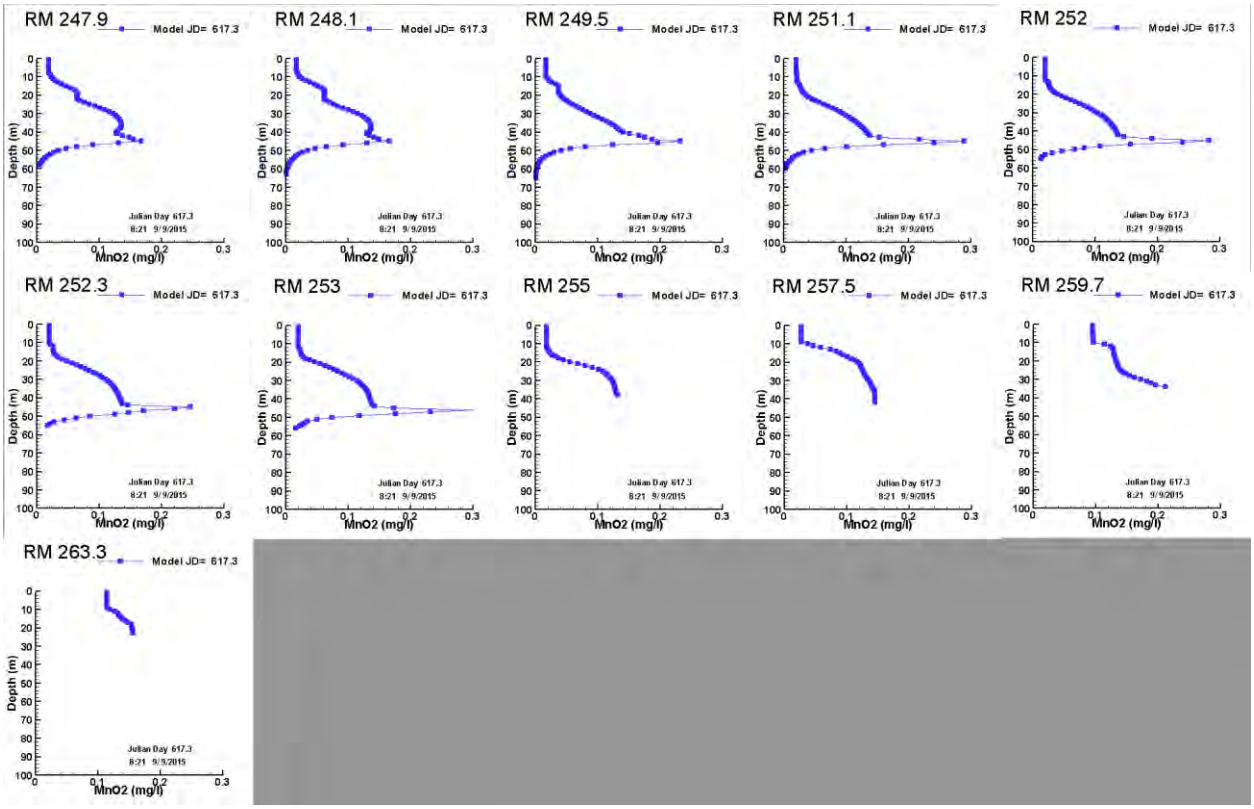


Figure 185. Vertical profiles of MnO2 compared with data for 9/ 9/2015.

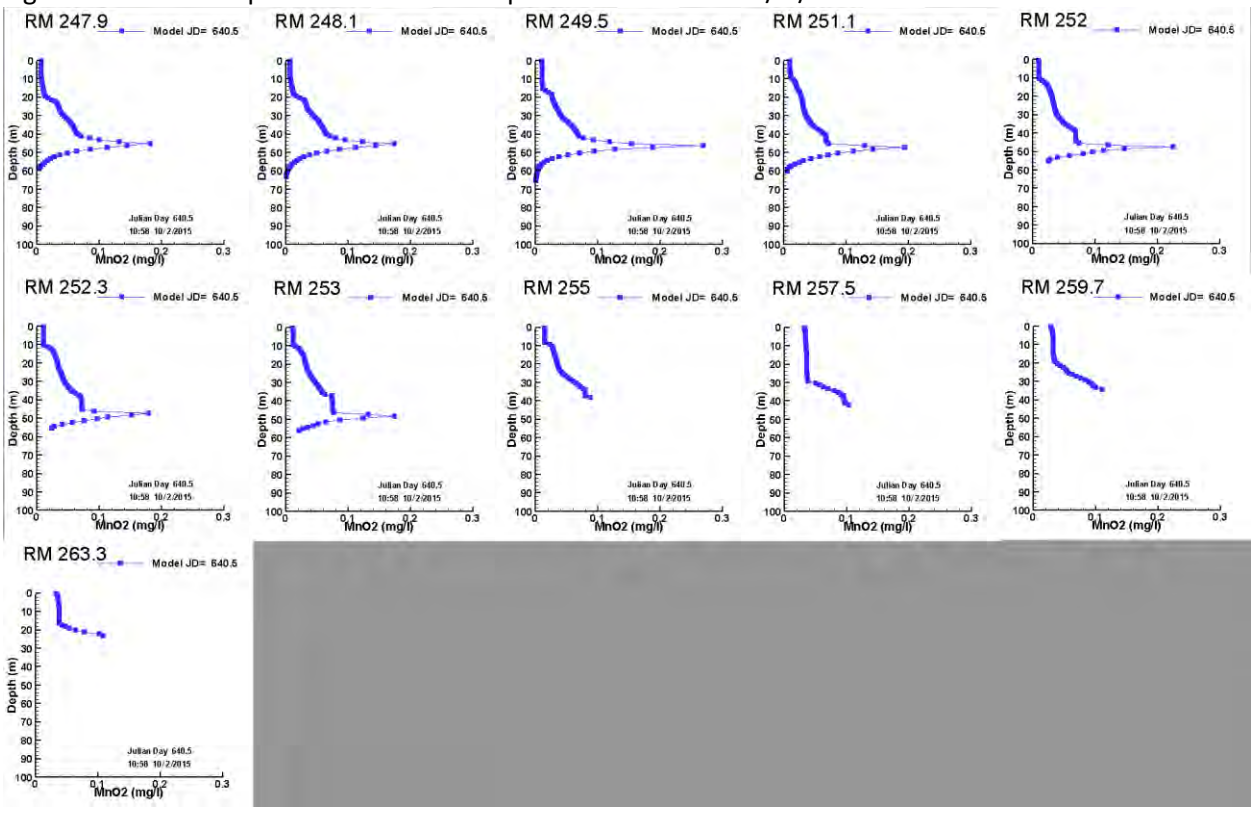


Figure 186. Vertical profiles of MnO2 compared with data for 10/ 2/2015.

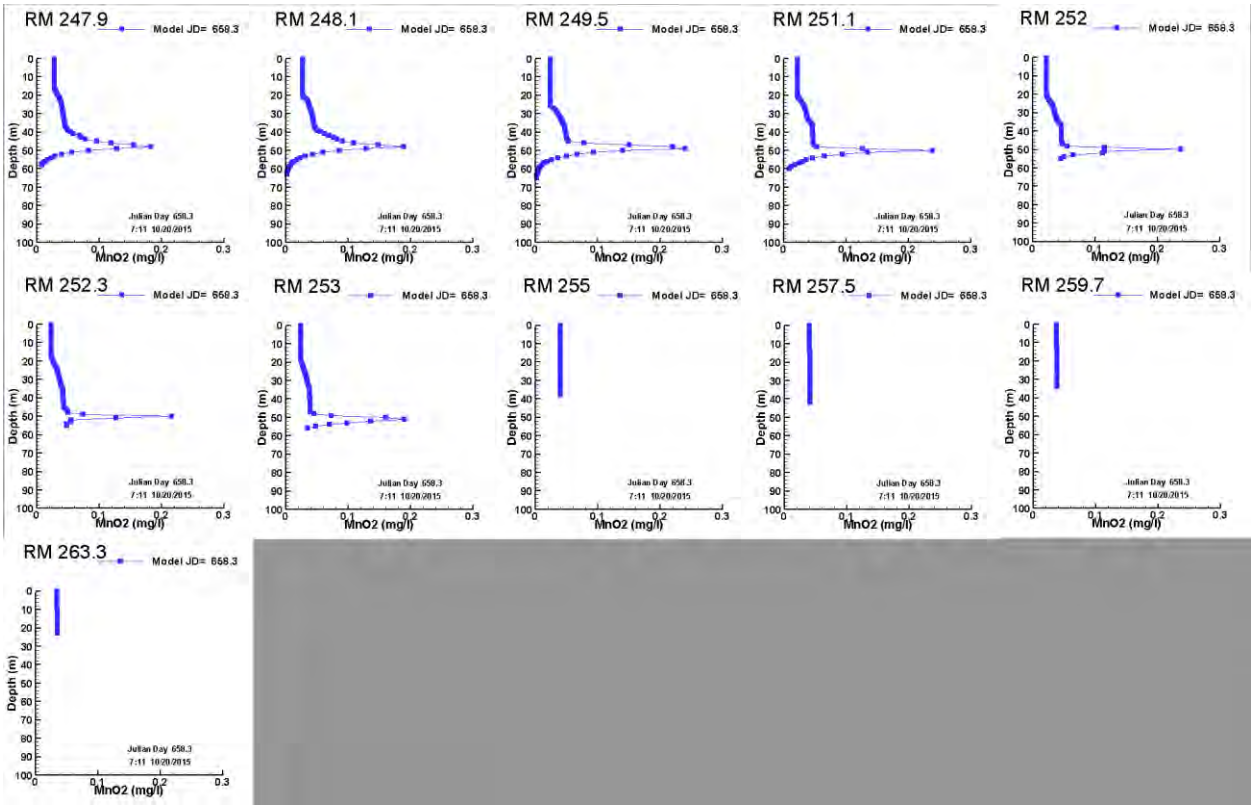


Figure 187. Vertical profiles of MnO2 compared with data for 10/20/2015.

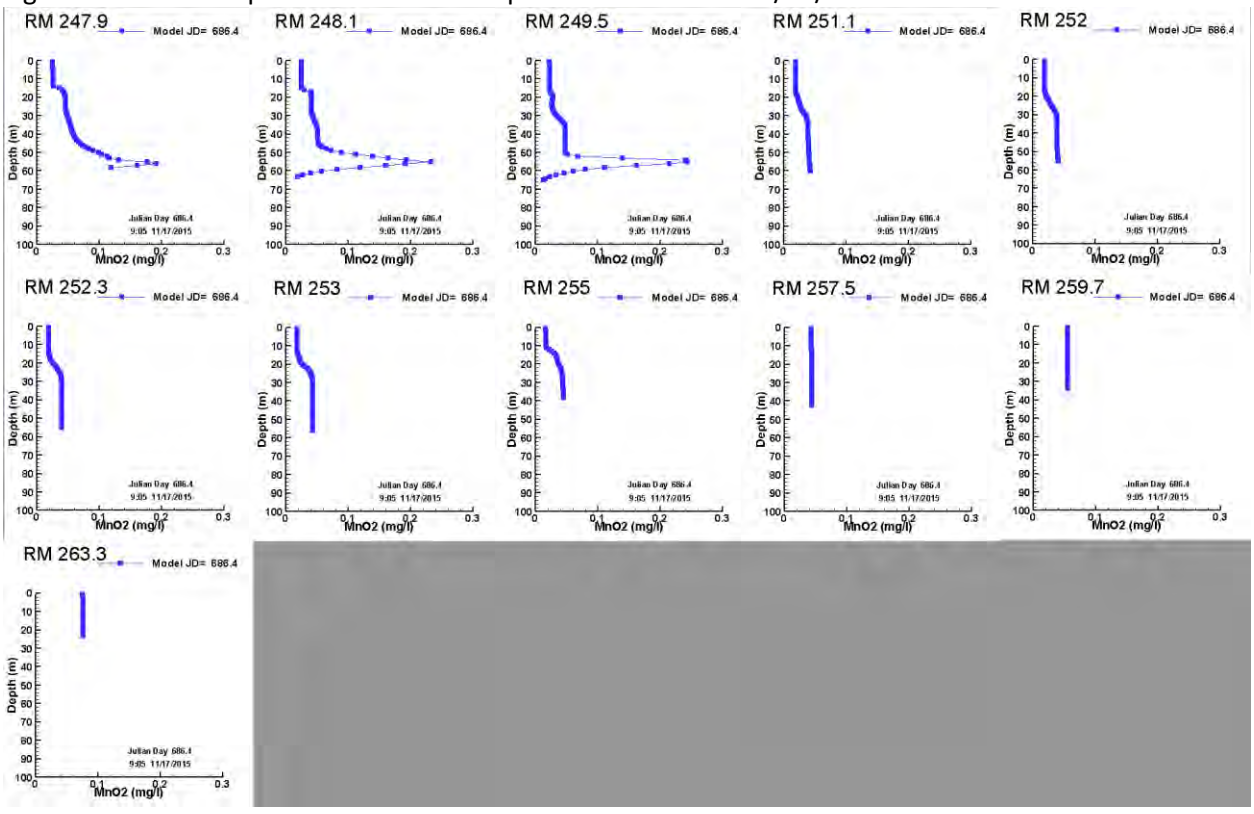


Figure 188. Vertical profiles of MnO2 compared with data for 11/17/2015.

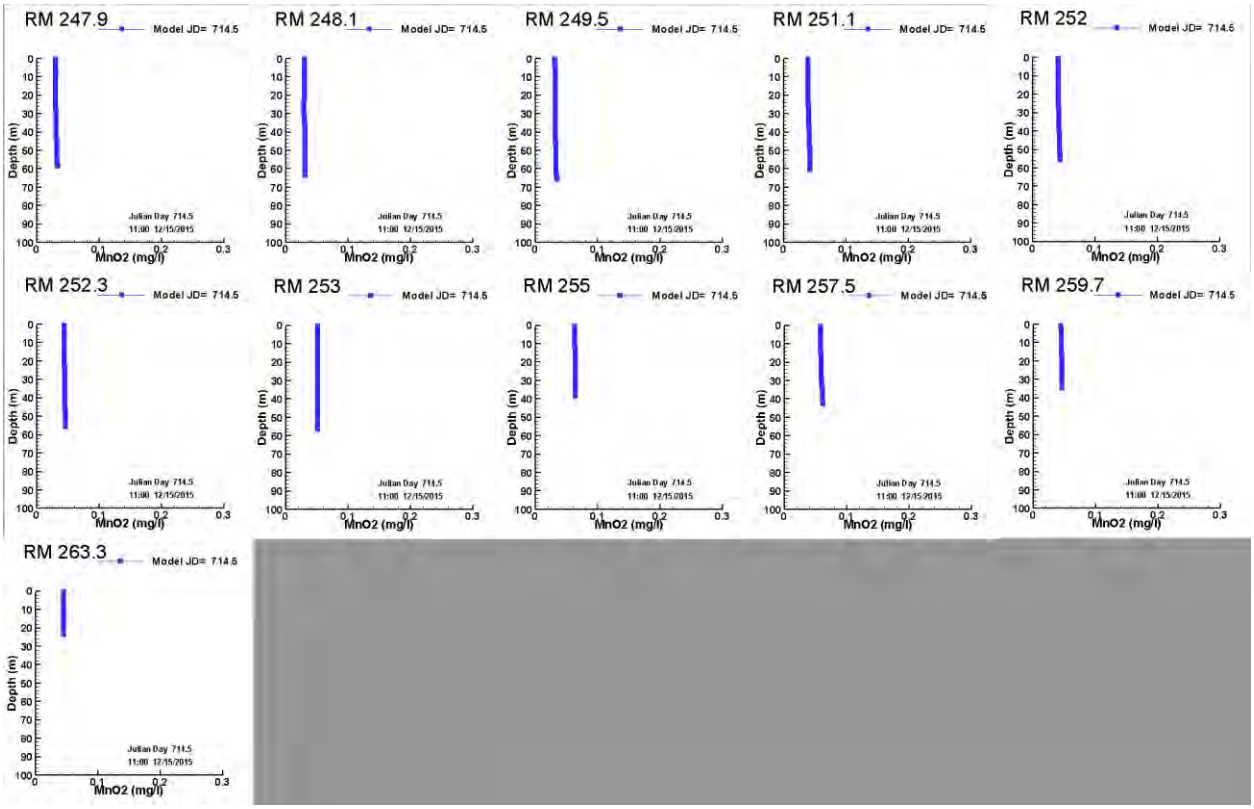


Figure 189. Vertical profiles of MnO2 compared with data for 12/15/2015.

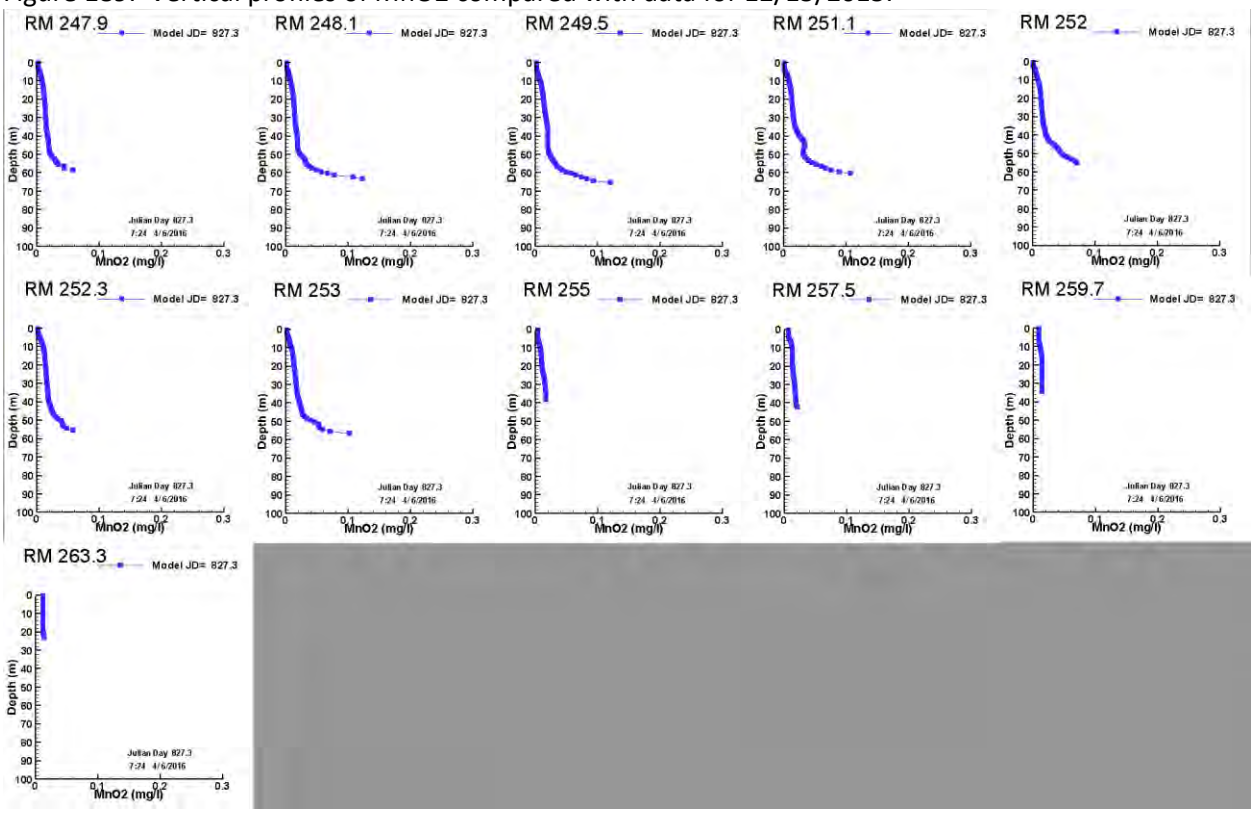


Figure 190. Vertical profiles of MnO2 compared with data for 4/ 6/2016.

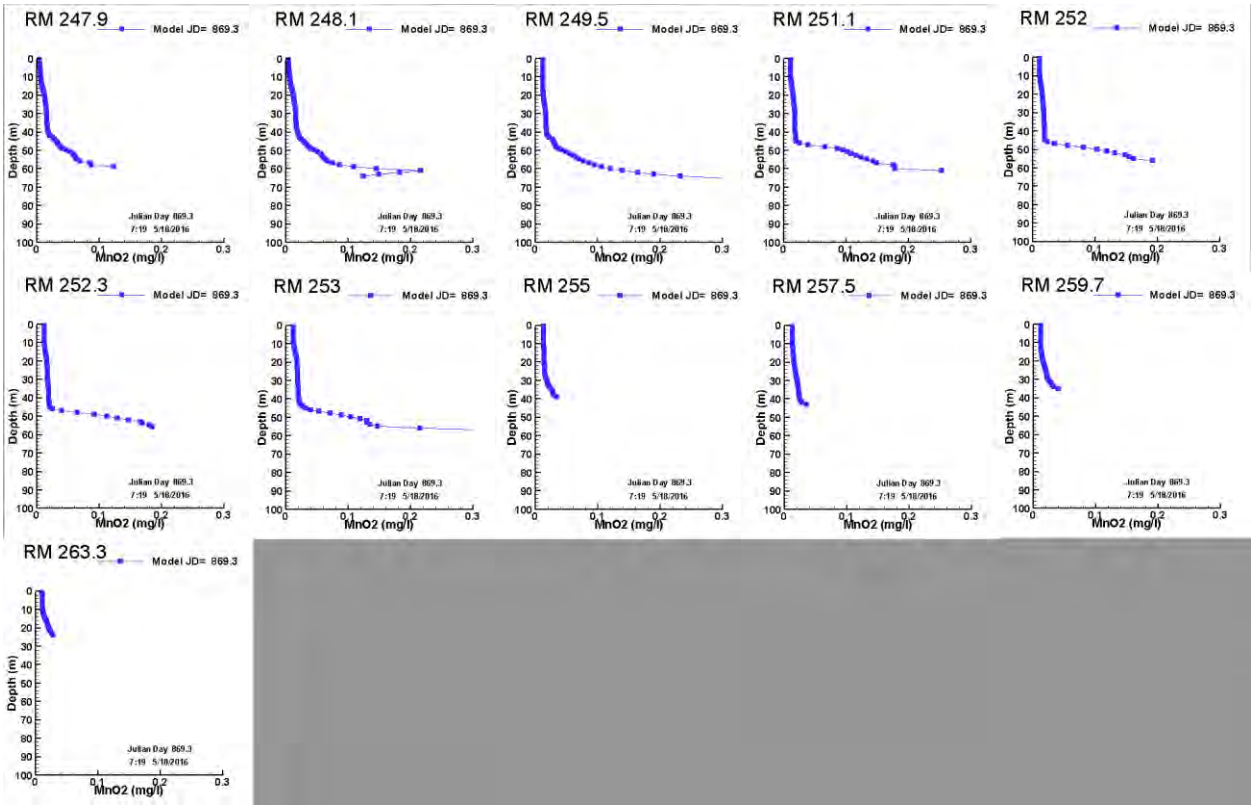


Figure 191. Vertical profiles of MnO2 compared with data for 5/18/2016.

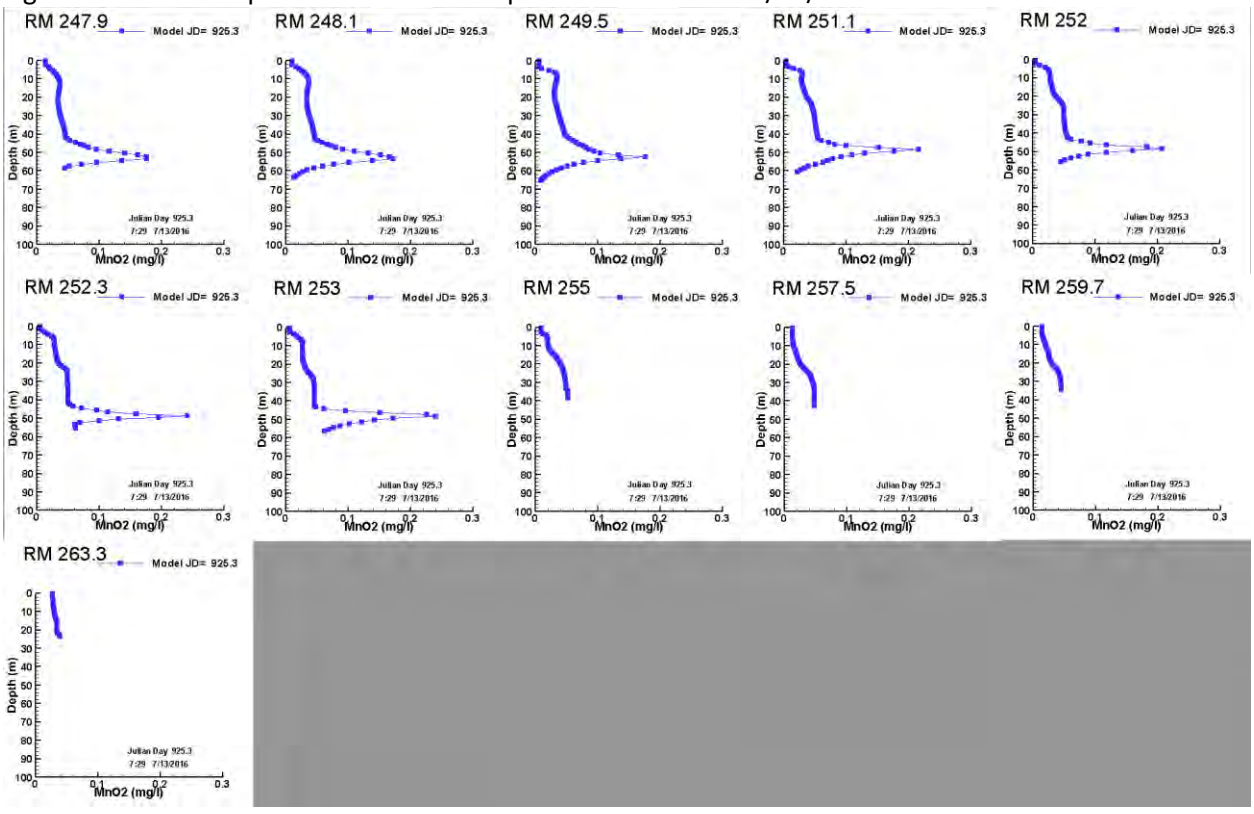


Figure 192. Vertical profiles of MnO2 compared with data for 7/13/2016.

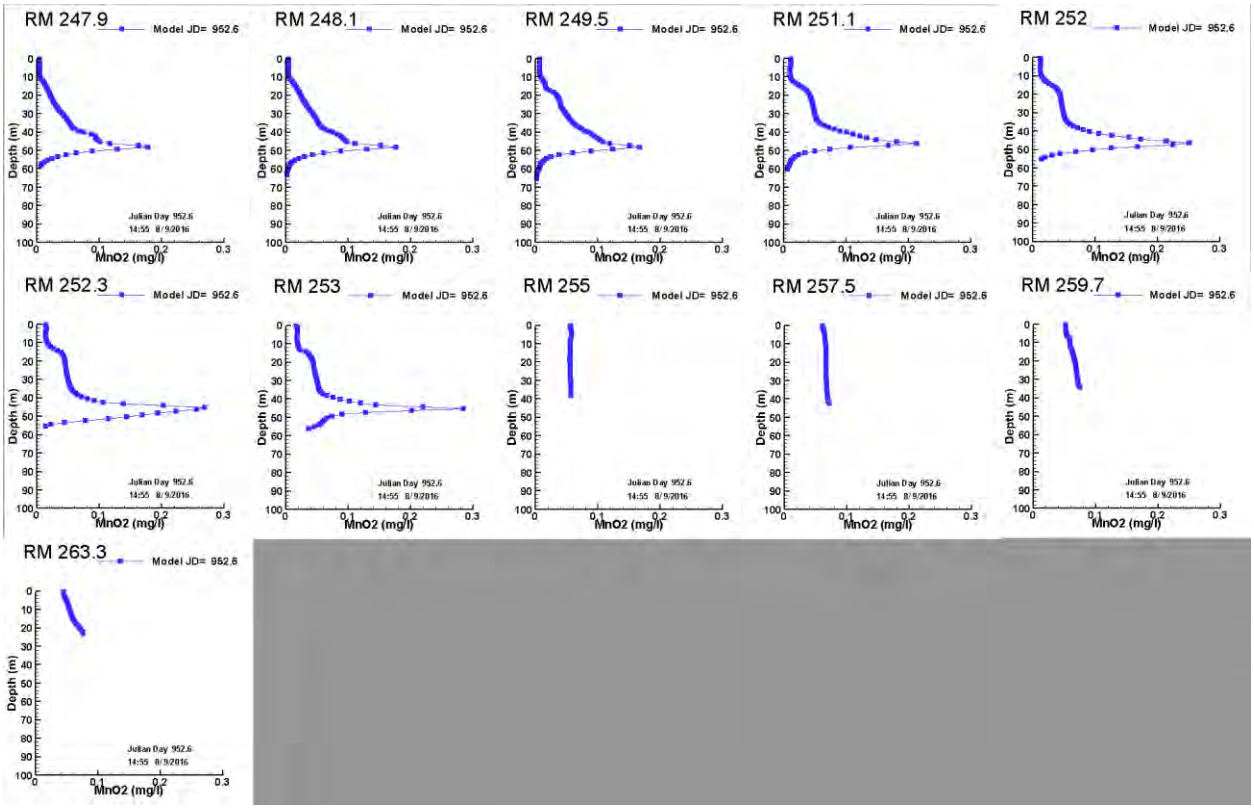


Figure 193. Vertical profiles of MnO2 compared with data for 8/ 9/2016.

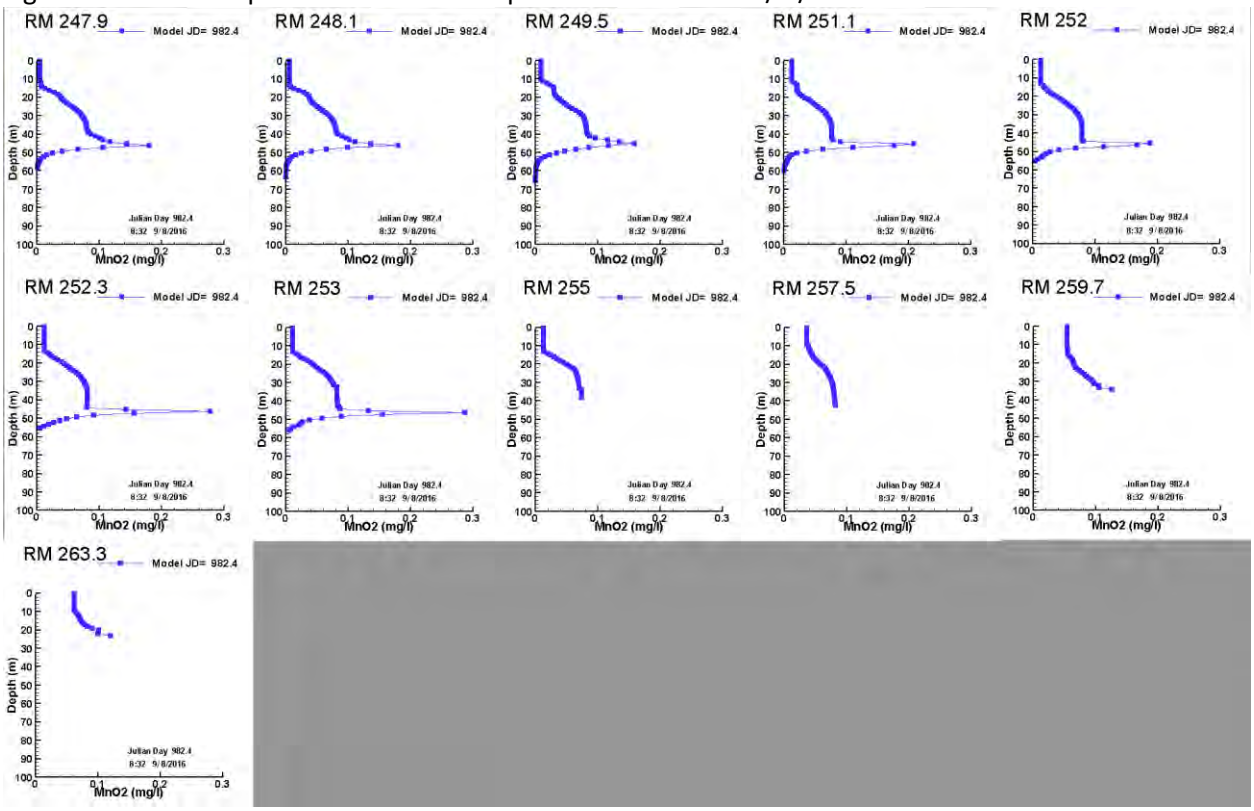


Figure 194. Vertical profiles of MnO2 compared with data for 9/ 8/2016.

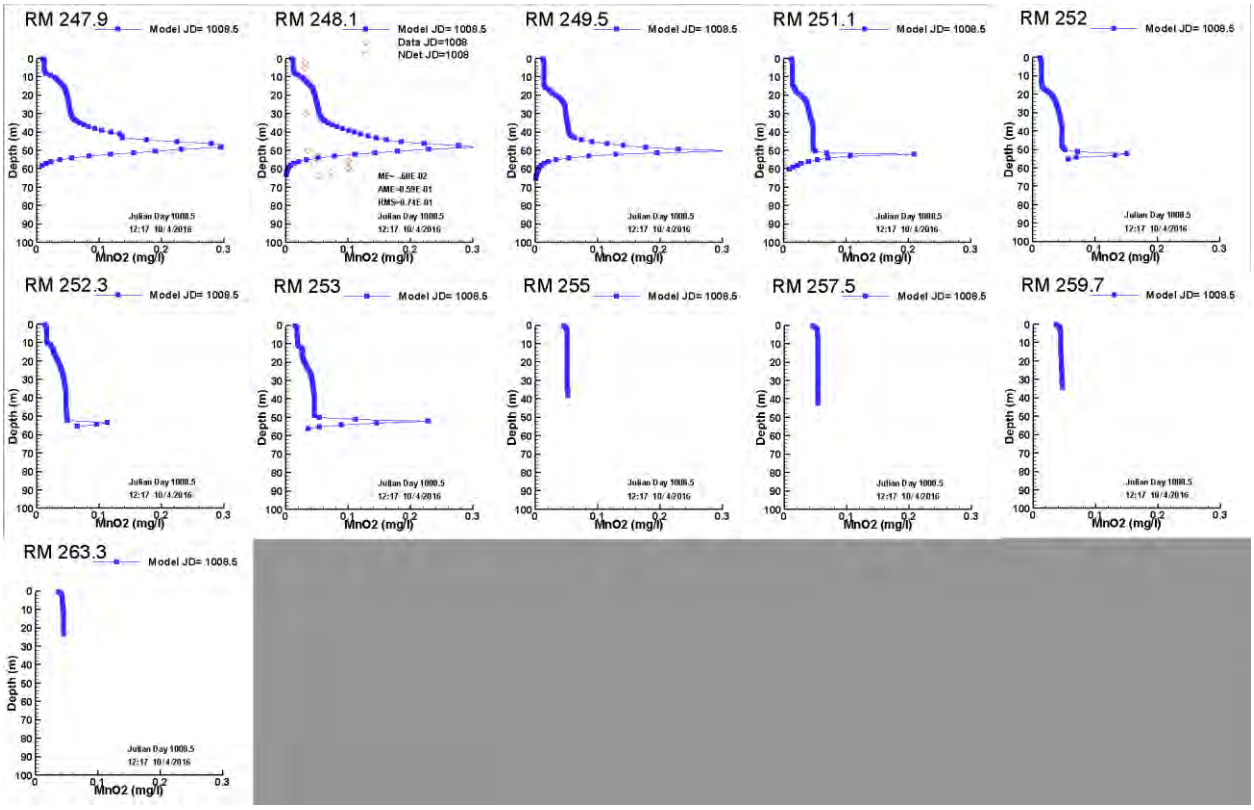


Figure 195. Vertical profiles of MnO2 compared with data for 10/ 4/2016.

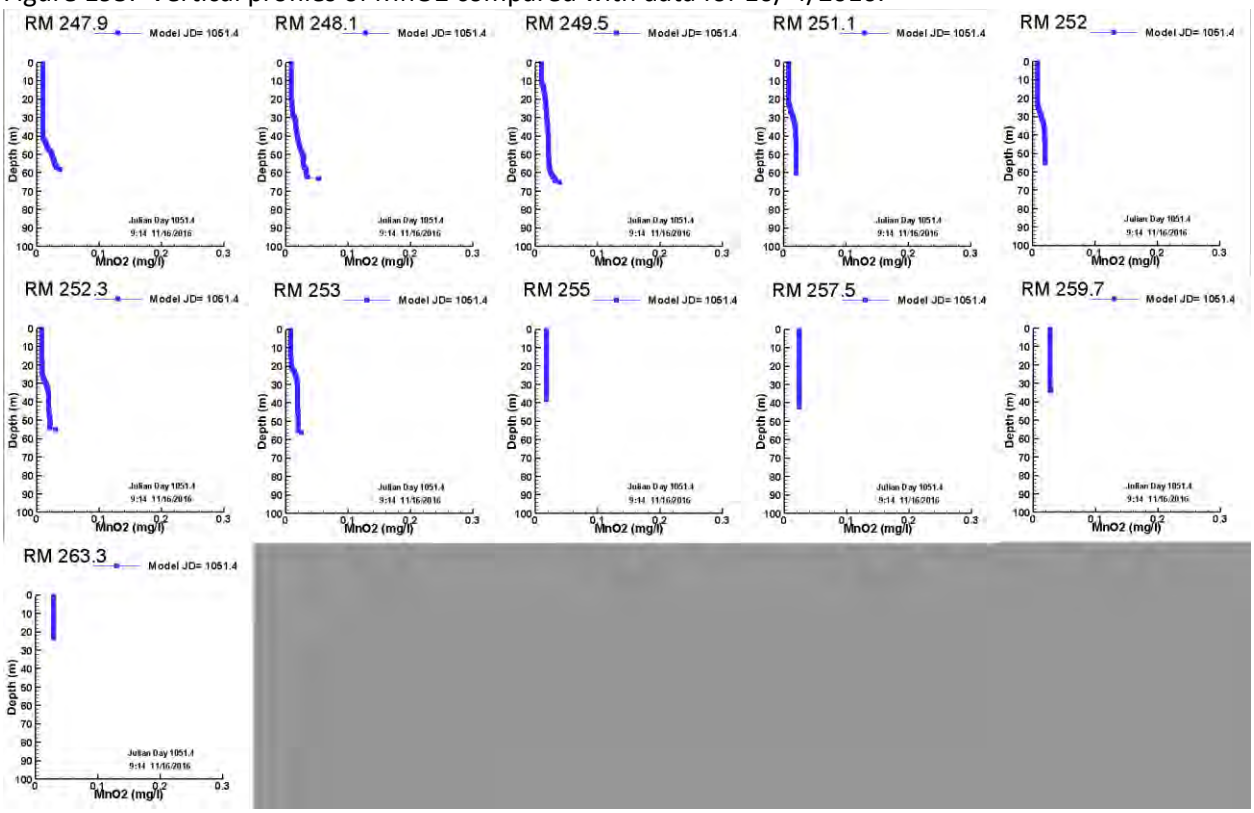


Figure 196. Vertical profiles of MnO2 compared with data for 11/16/2016.

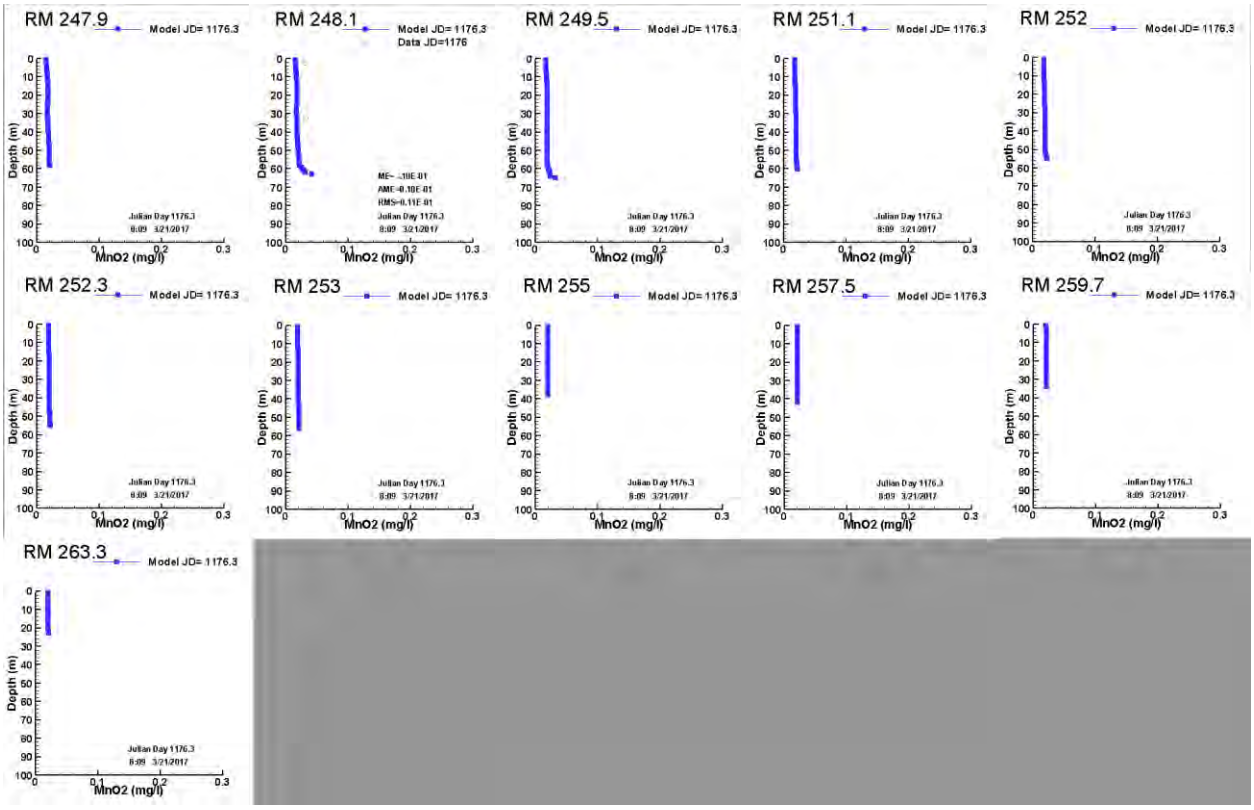


Figure 197. Vertical profiles of MnO2 compared with data for 3/21/2017.

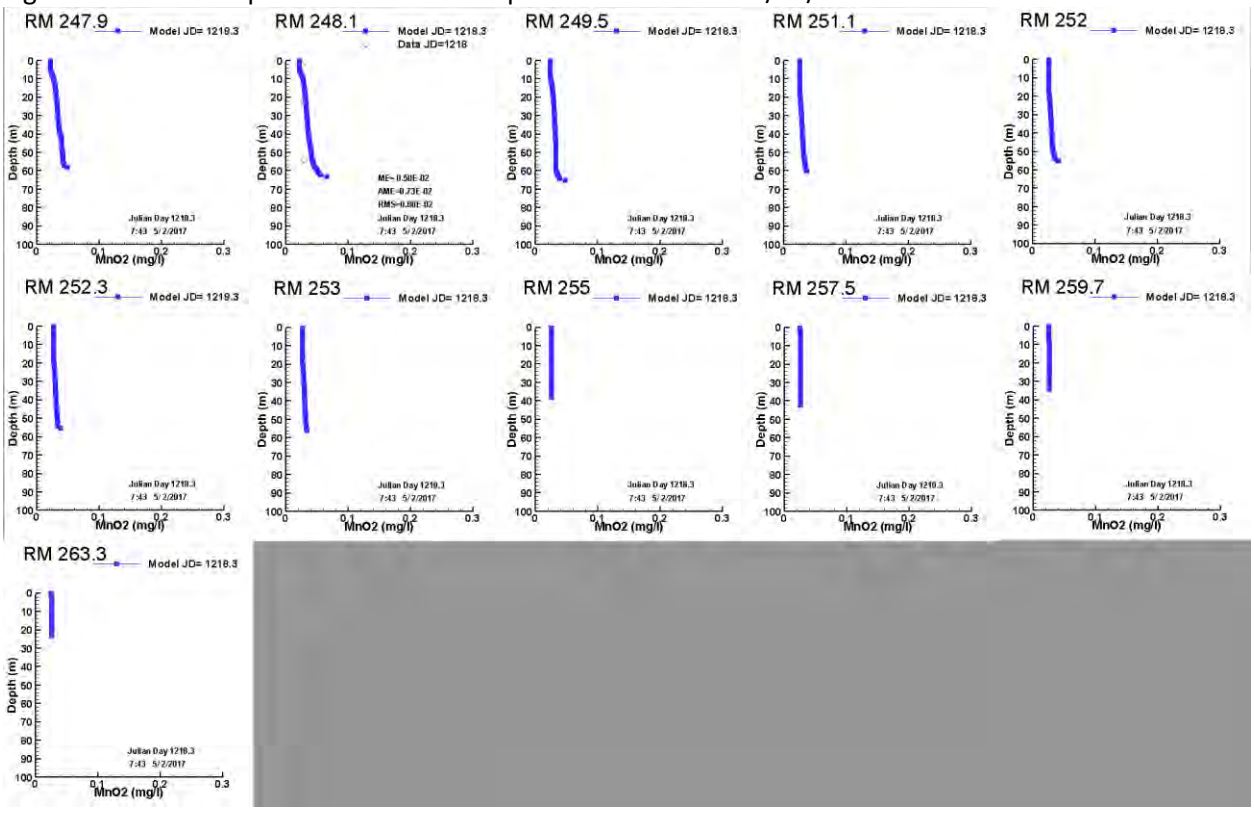


Figure 198. Vertical profiles of MnO2 compared with data for 5/ 2/2017.

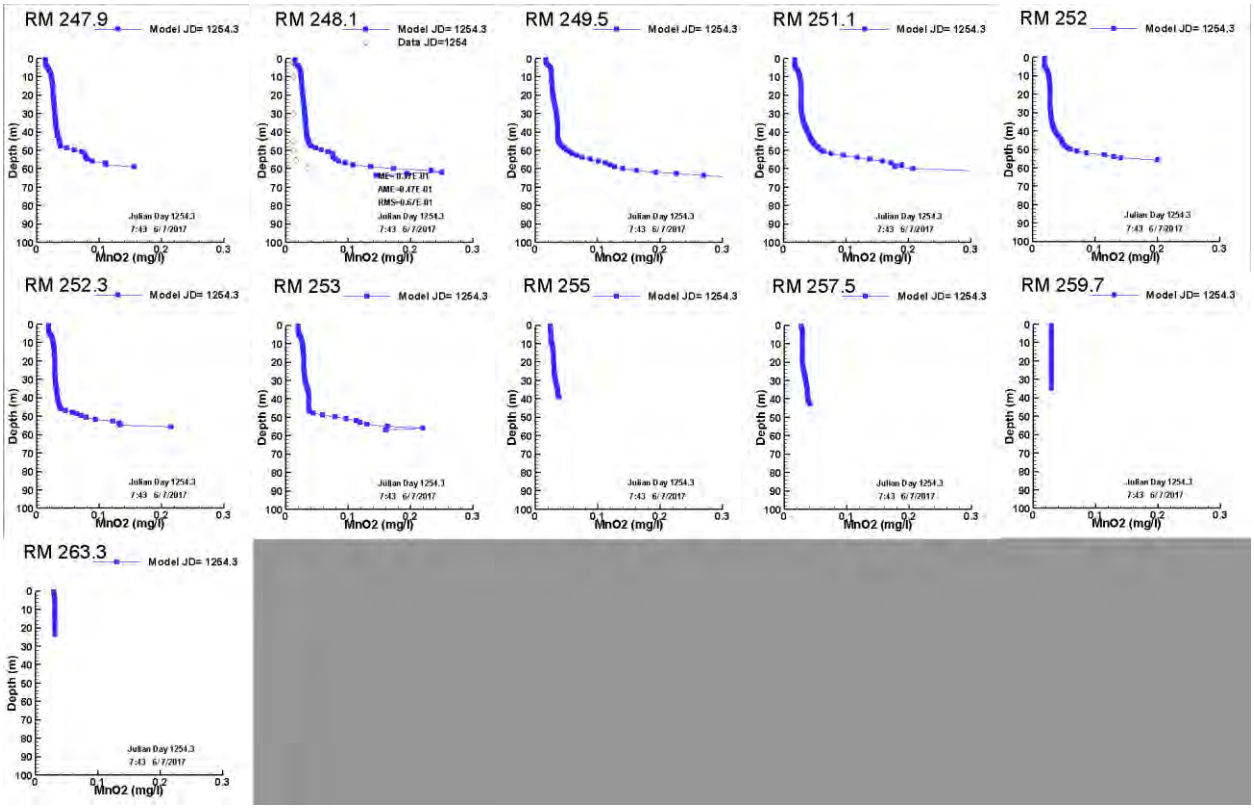


Figure 199. Vertical profiles of MnO2 compared with data for 6/ 7/2017.

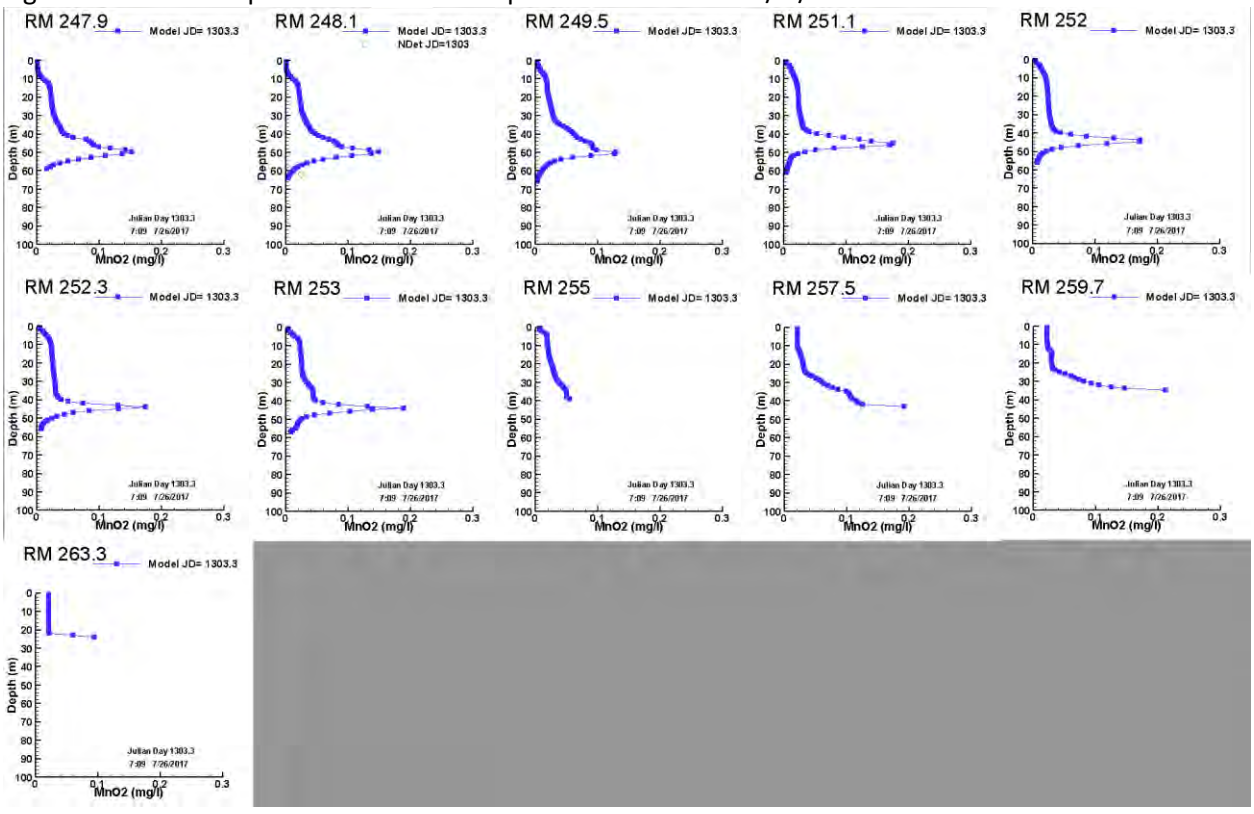


Figure 200. Vertical profiles of MnO2 compared with data for 7/26/2017.

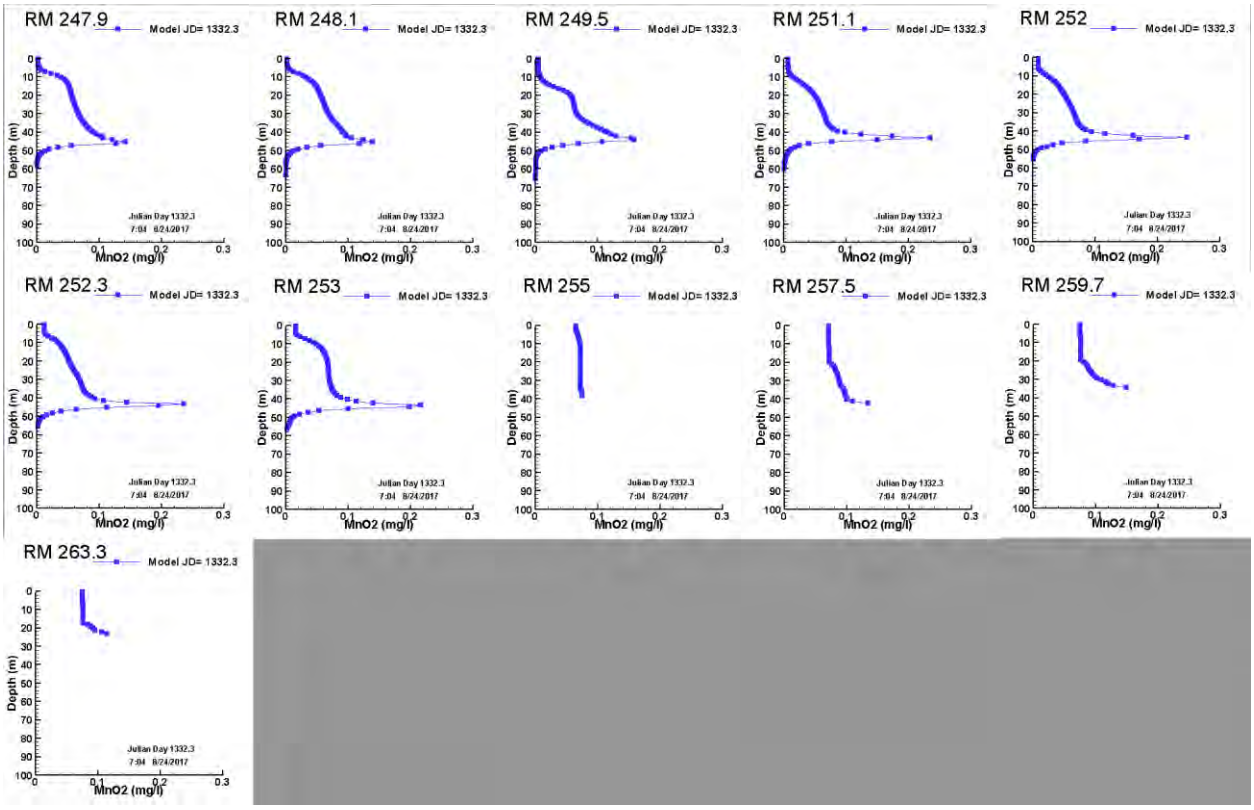


Figure 201. Vertical profiles of MnO2 compared with data for 8/24/2017.

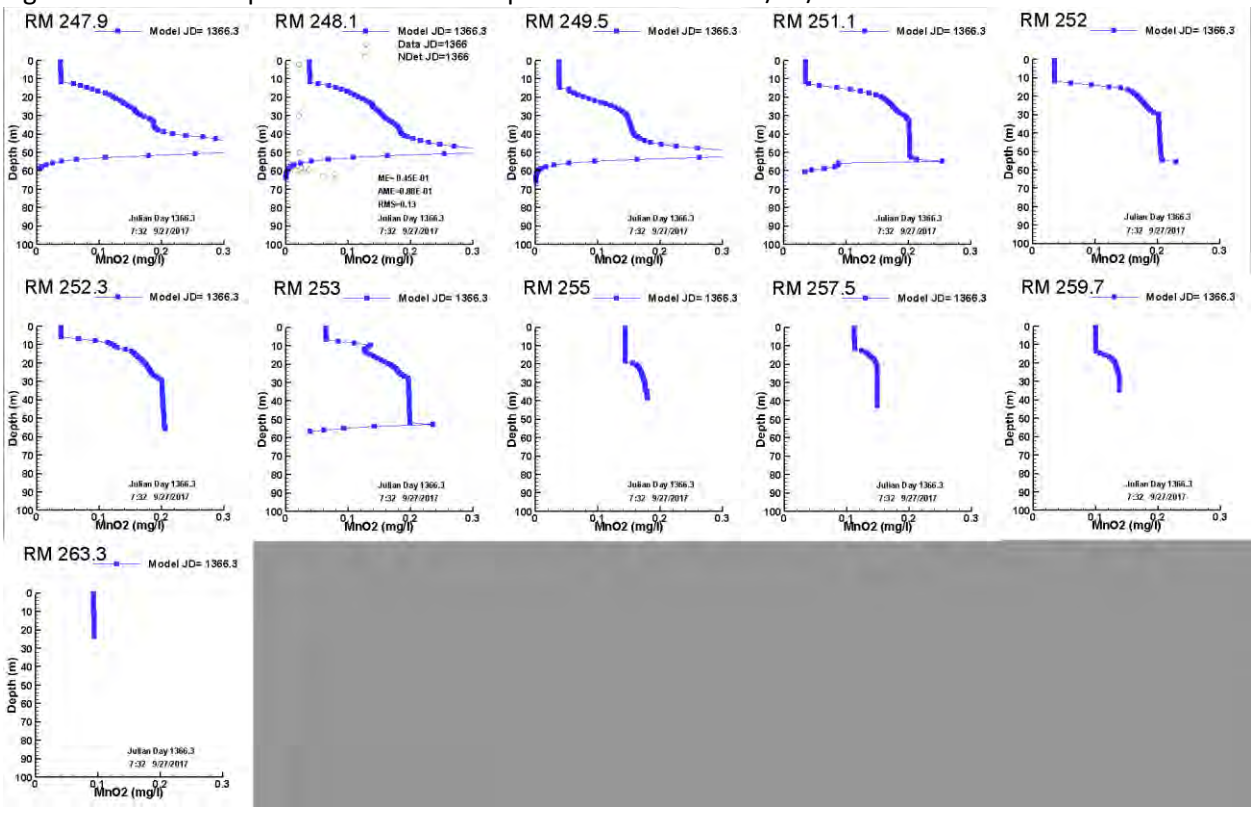


Figure 202. Vertical profiles of MnO2 compared with data for 9/27/2017.

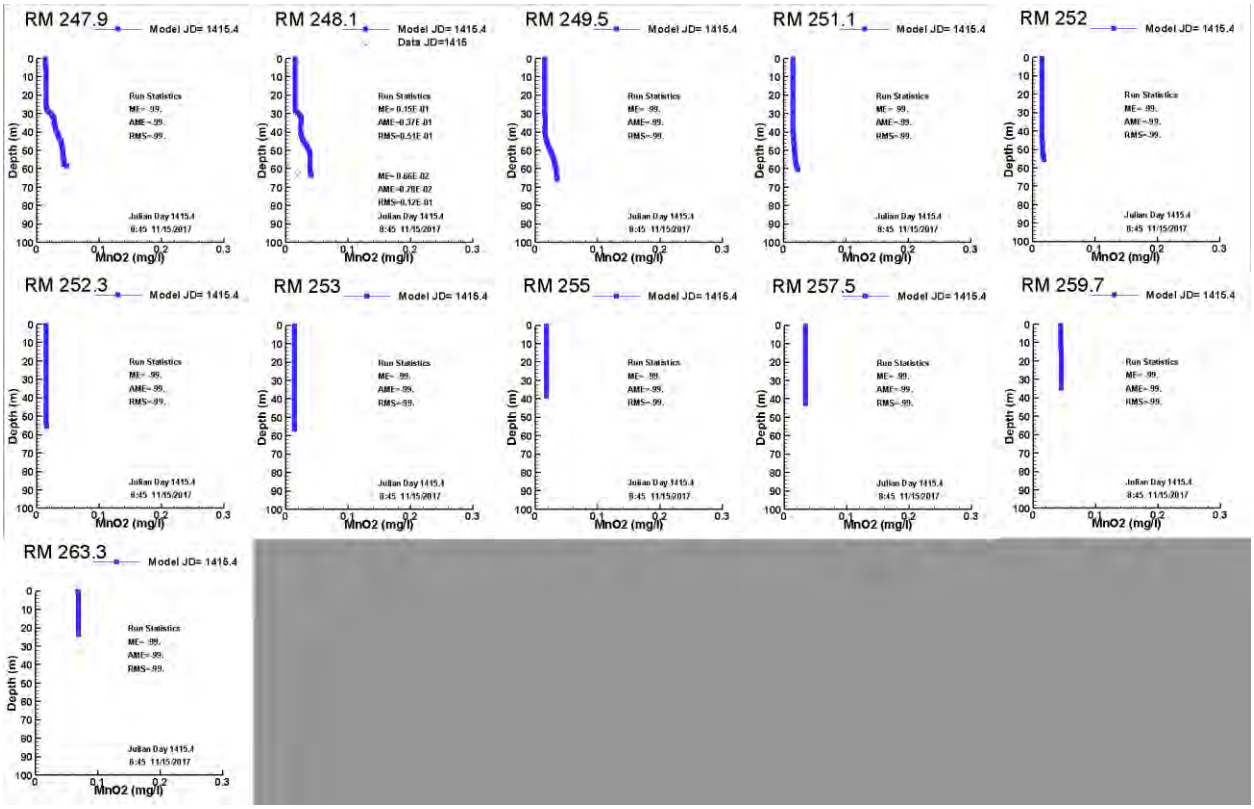


Figure 203. Vertical profiles of MnO2 compared with data for 11/15/2017.

Orthophosphate

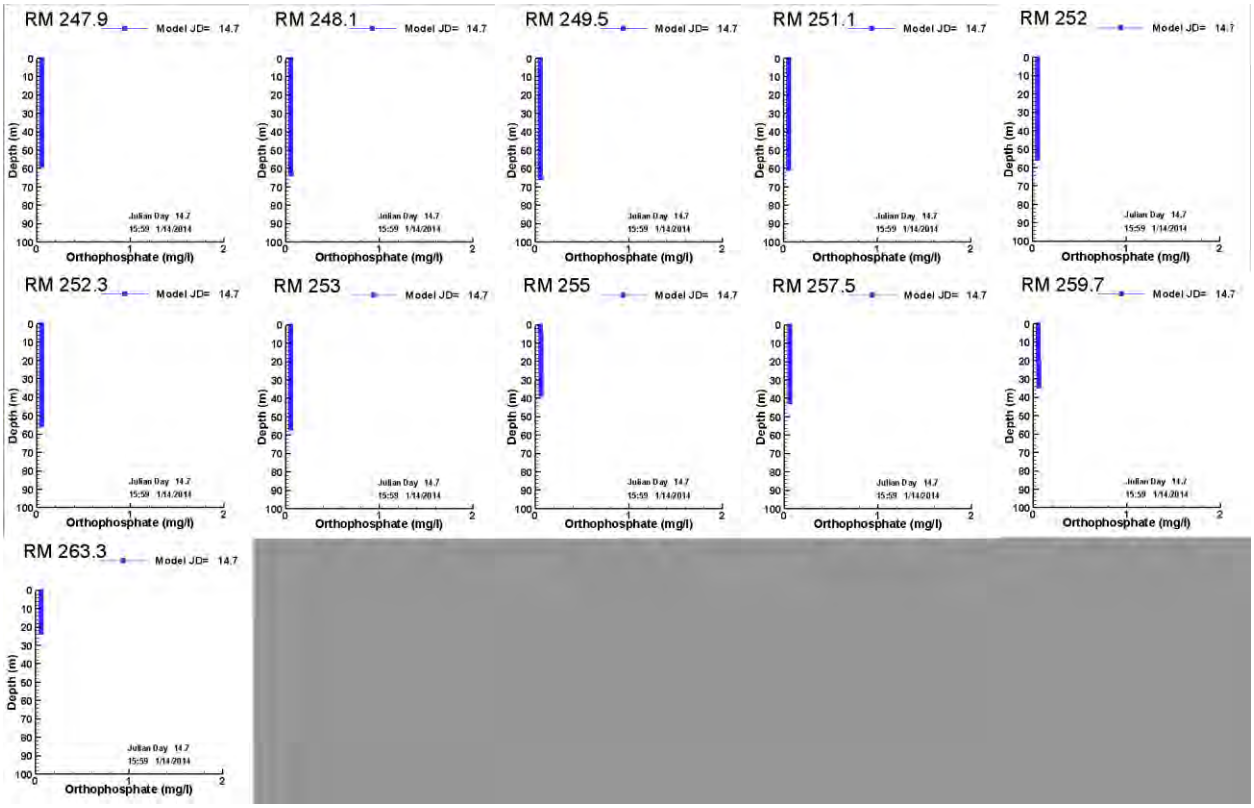


Figure 204. Vertical profiles of orthophosphate compared with data for 1/14/2014.

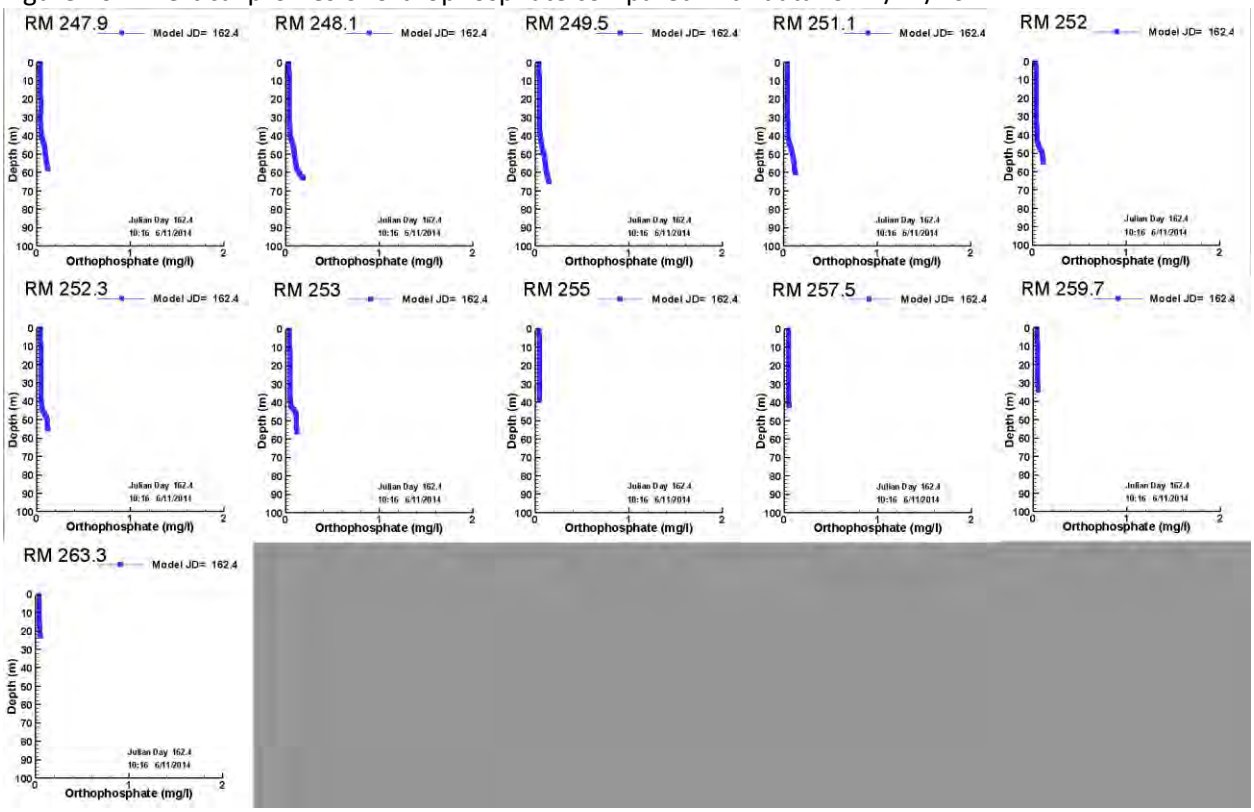


Figure 205. Vertical profiles of orthophosphate compared with data for 6/11/2014.

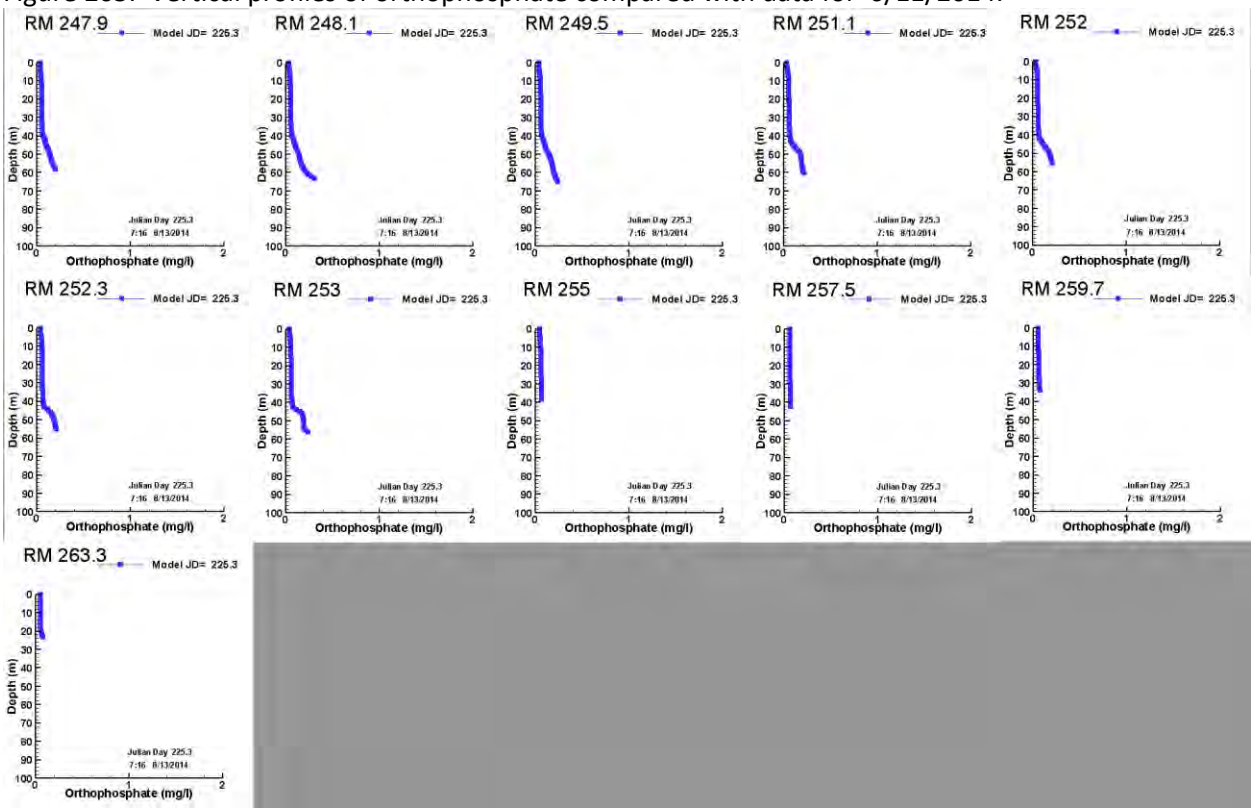


Figure 206. Vertical profiles of orthophosphate compared with data for 8/13/2014.

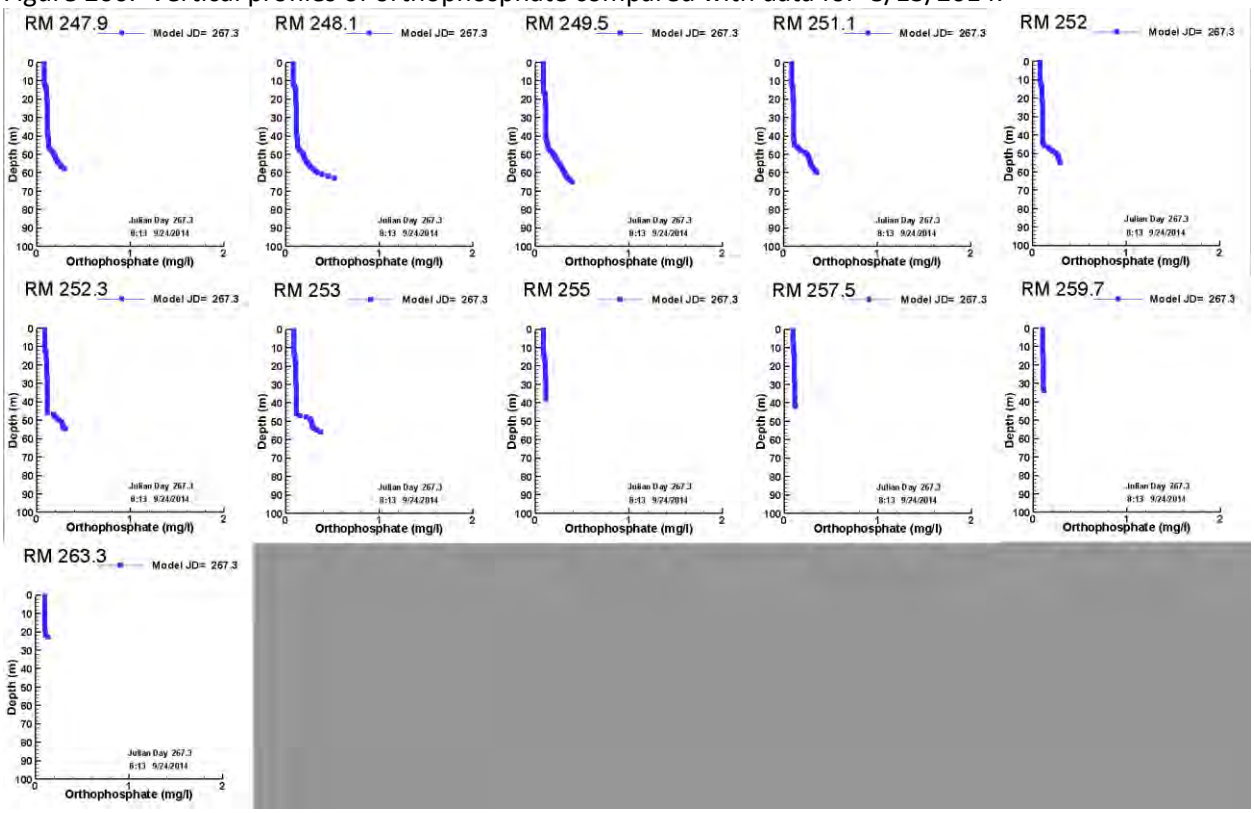


Figure 207. Vertical profiles of orthophosphate compared with data for 9/24/2014.

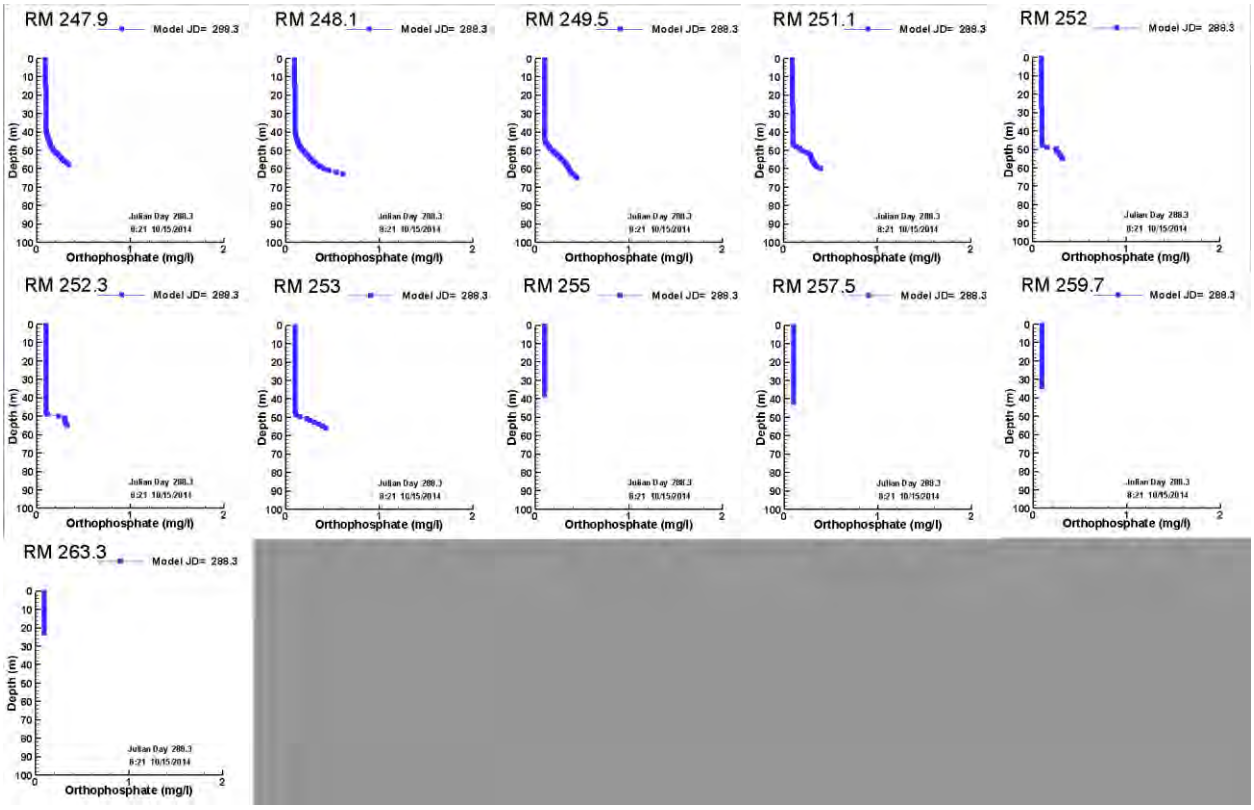


Figure 208. Vertical profiles of orthophosphate compared with data for 10/15/2014.

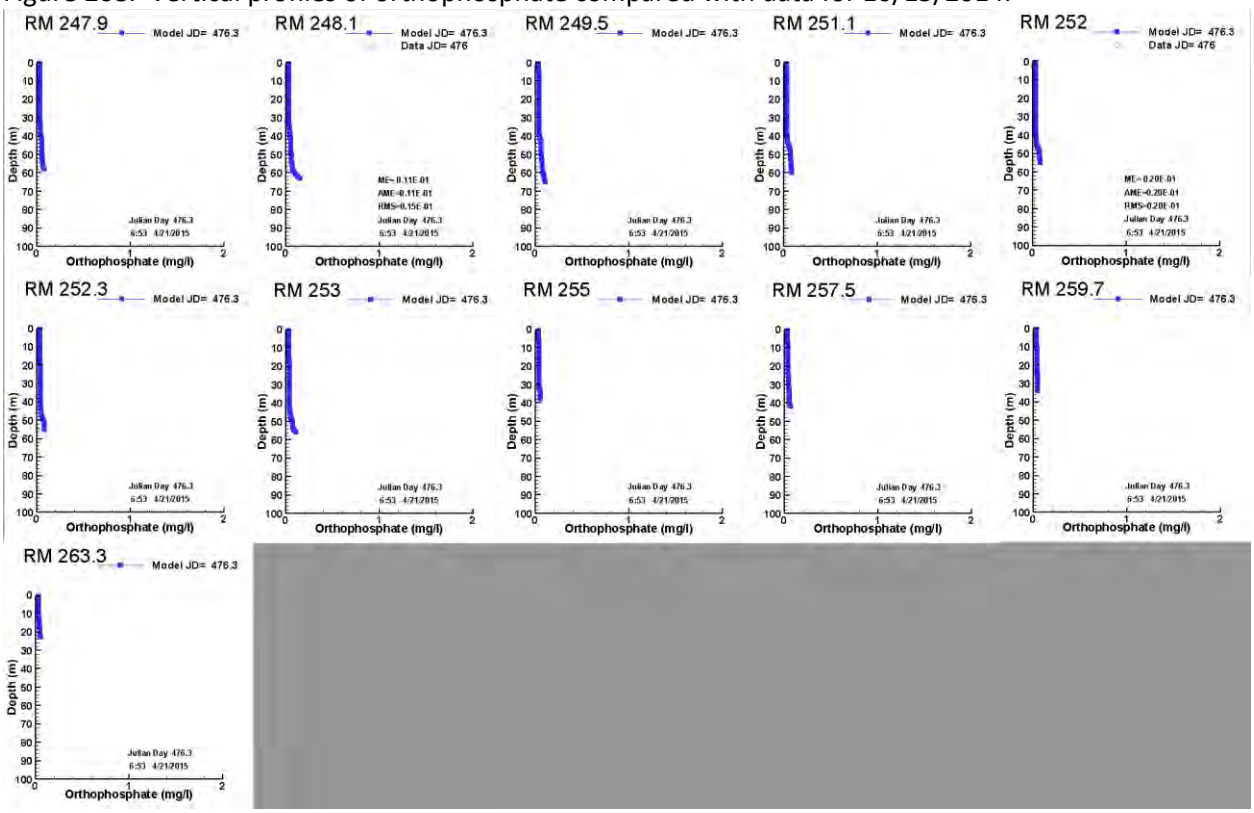


Figure 209. Vertical profiles of orthophosphate compared with data for 4/21/2015.

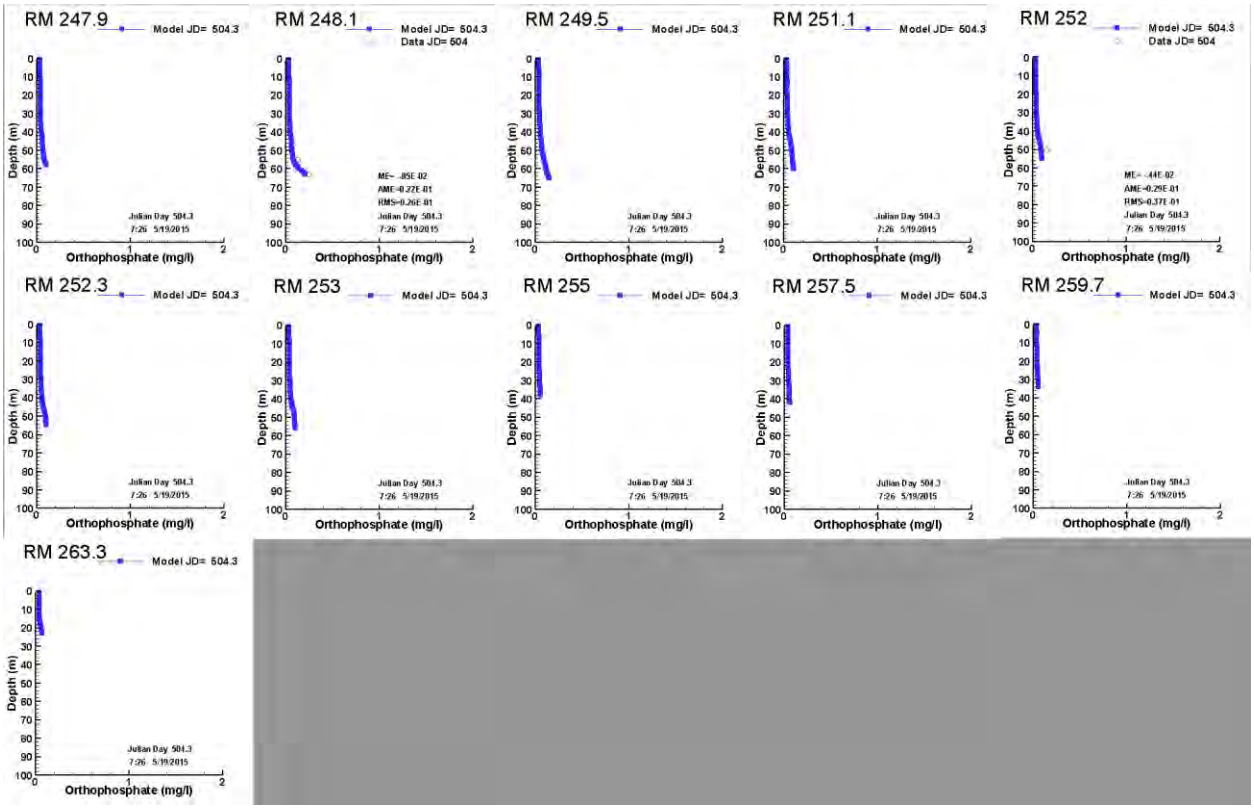


Figure 210. Vertical profiles of orthophosphate compared with data for 5/19/2015.

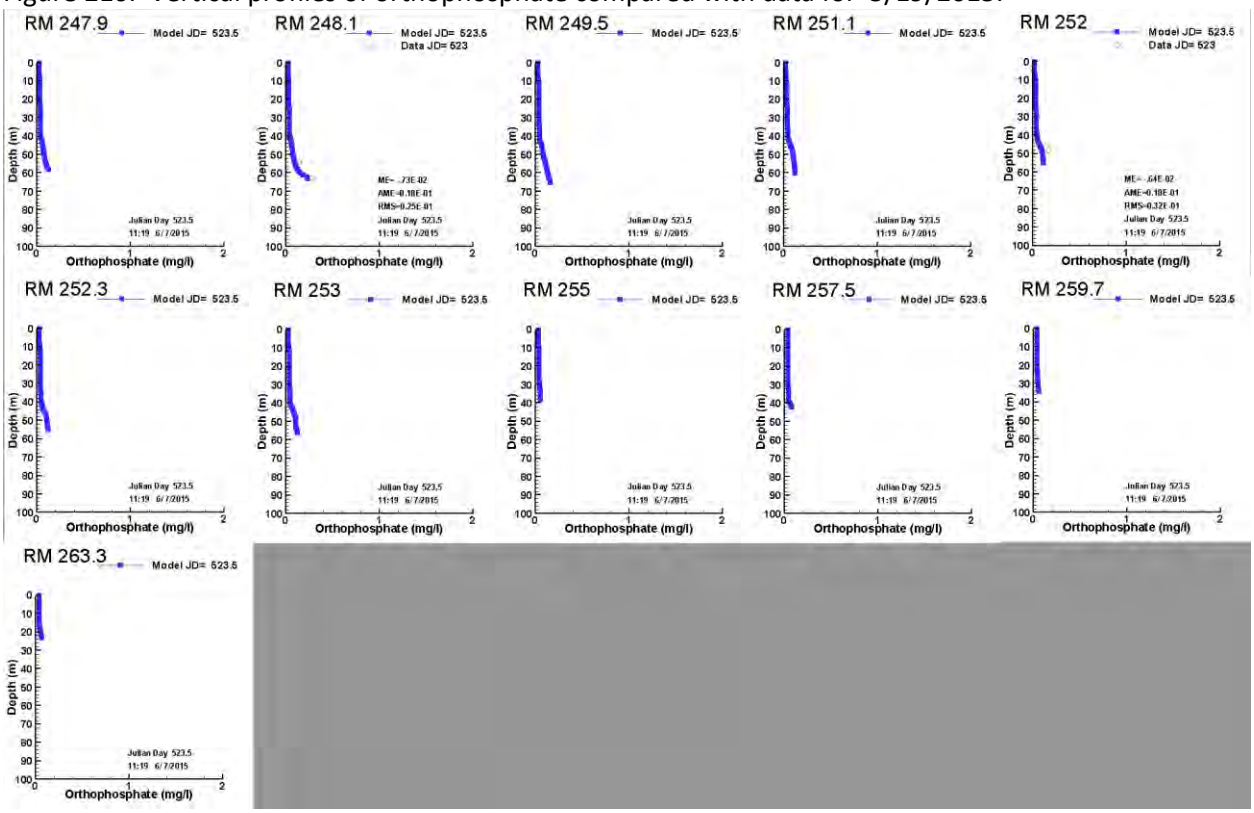


Figure 211. Vertical profiles of orthophosphate compared with data for 6/ 7/2015.

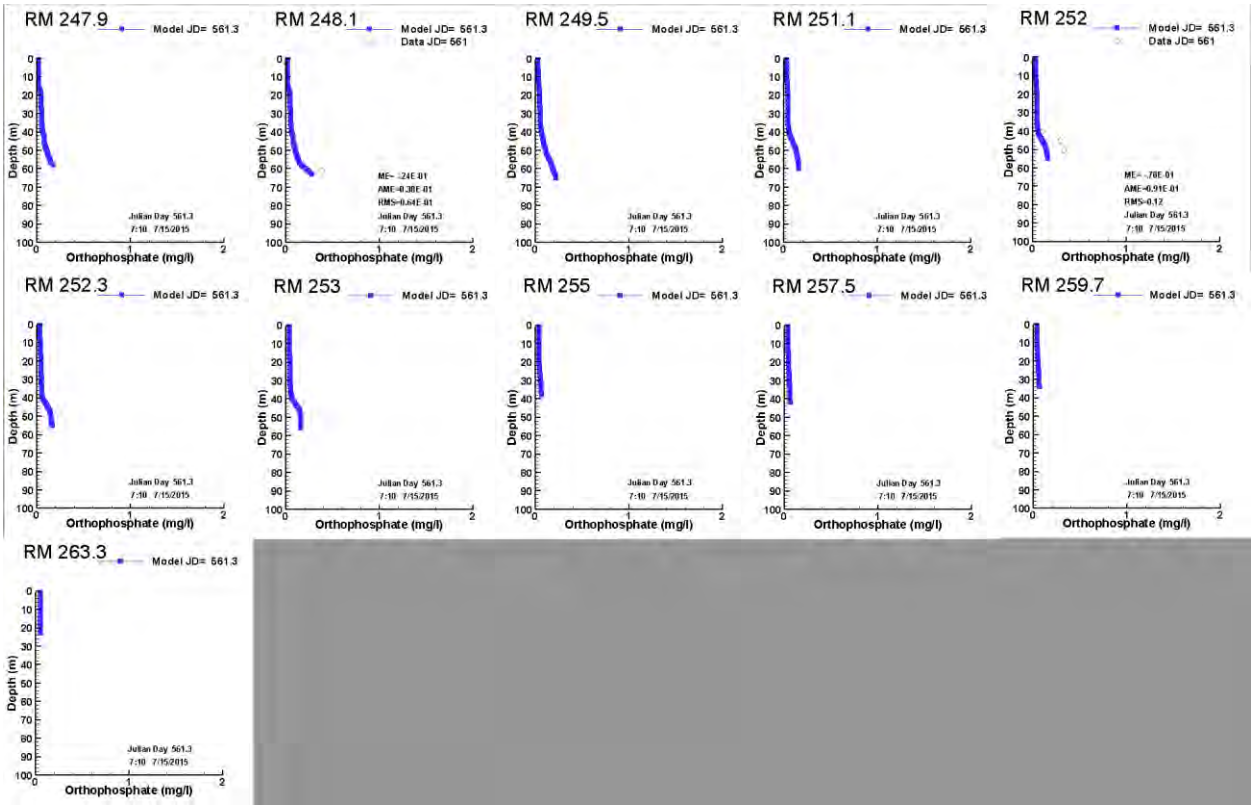


Figure 212. Vertical profiles of orthophosphate compared with data for 7/15/2015.

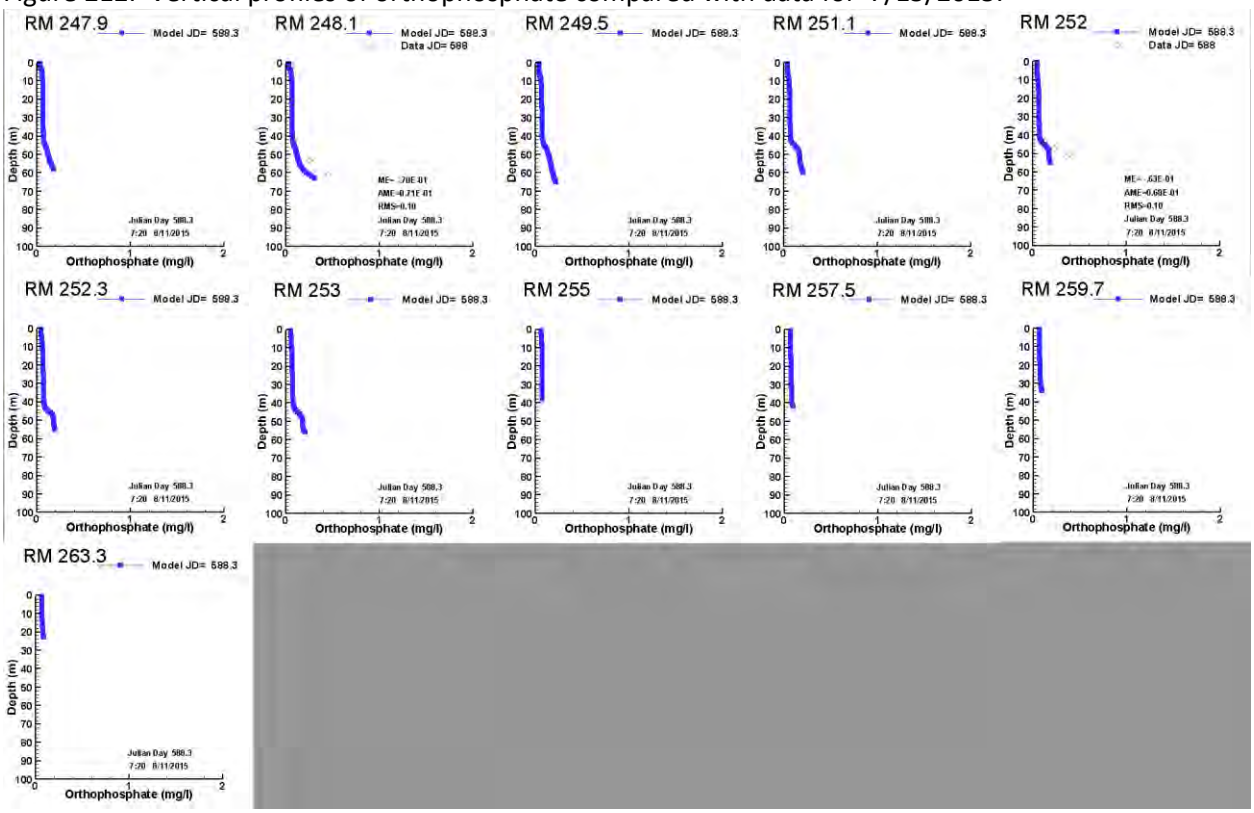


Figure 213. Vertical profiles of orthophosphate compared with data for 8/11/2015.

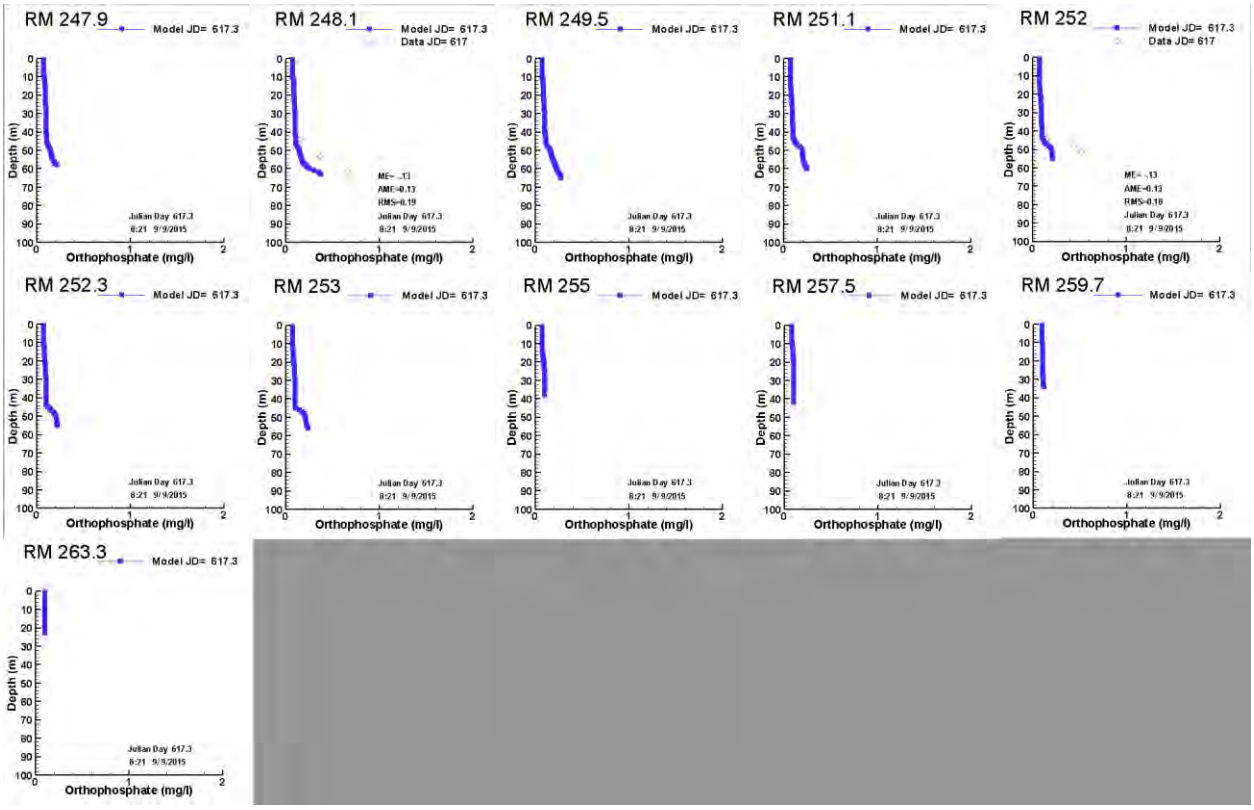


Figure 214. Vertical profiles of orthophosphate compared with data for 9/ 9/2015.

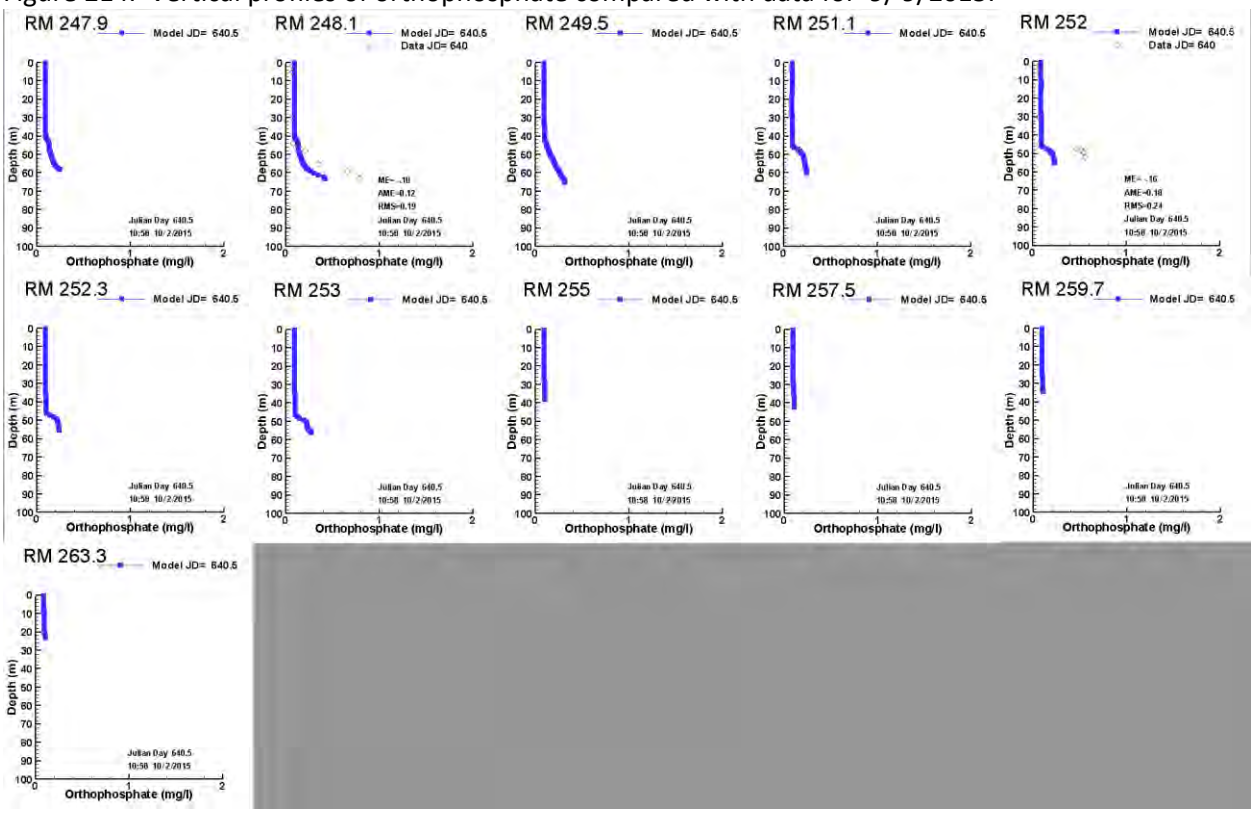


Figure 215. Vertical profiles of orthophosphate compared with data for 10/ 2/2015.

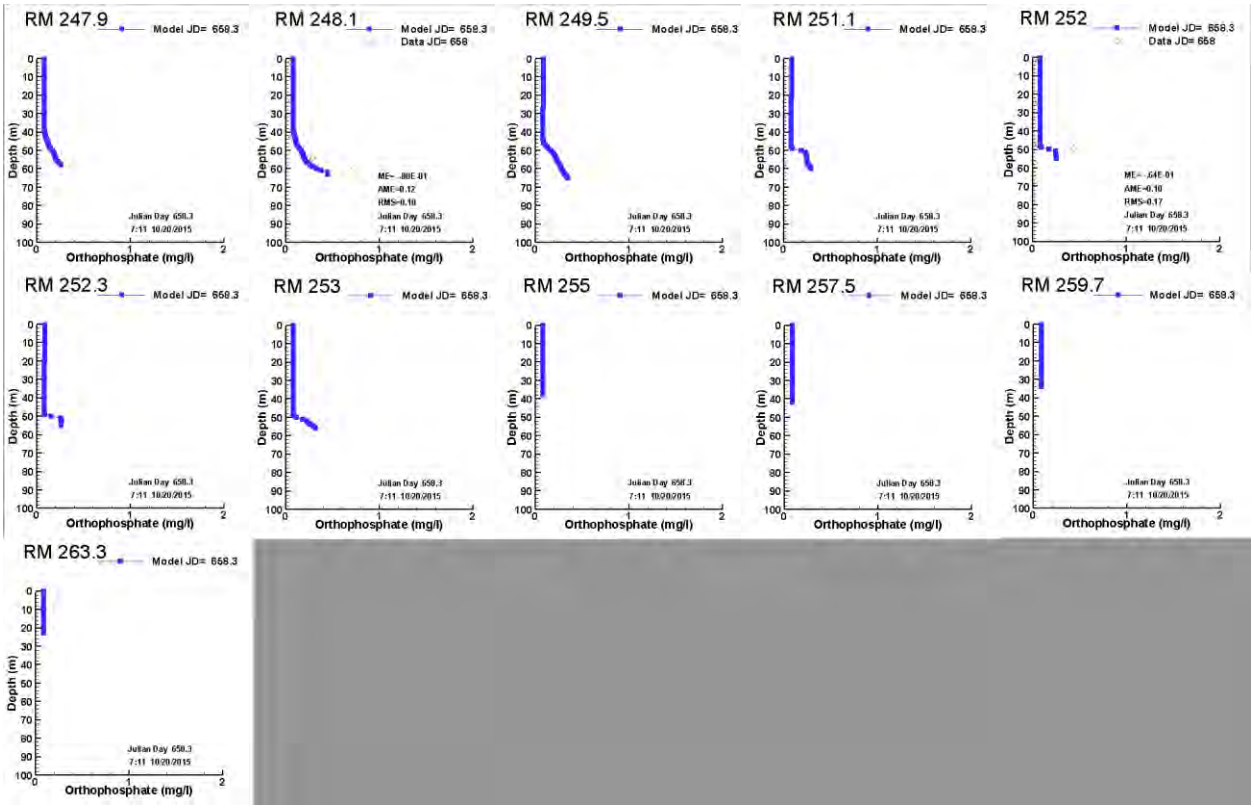


Figure 216. Vertical profiles of orthophosphate compared with data for 10/20/2015.

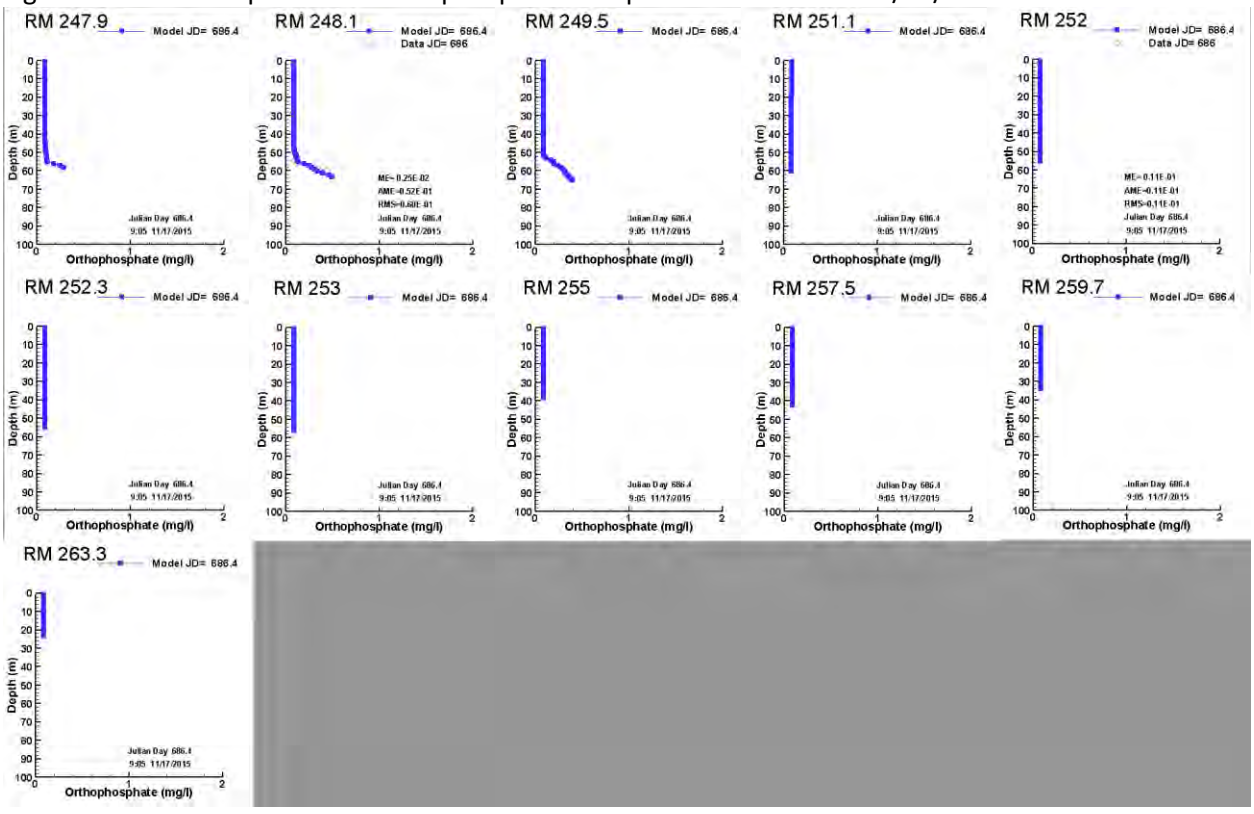


Figure 217. Vertical profiles of orthophosphate compared with data for 11/17/2015.

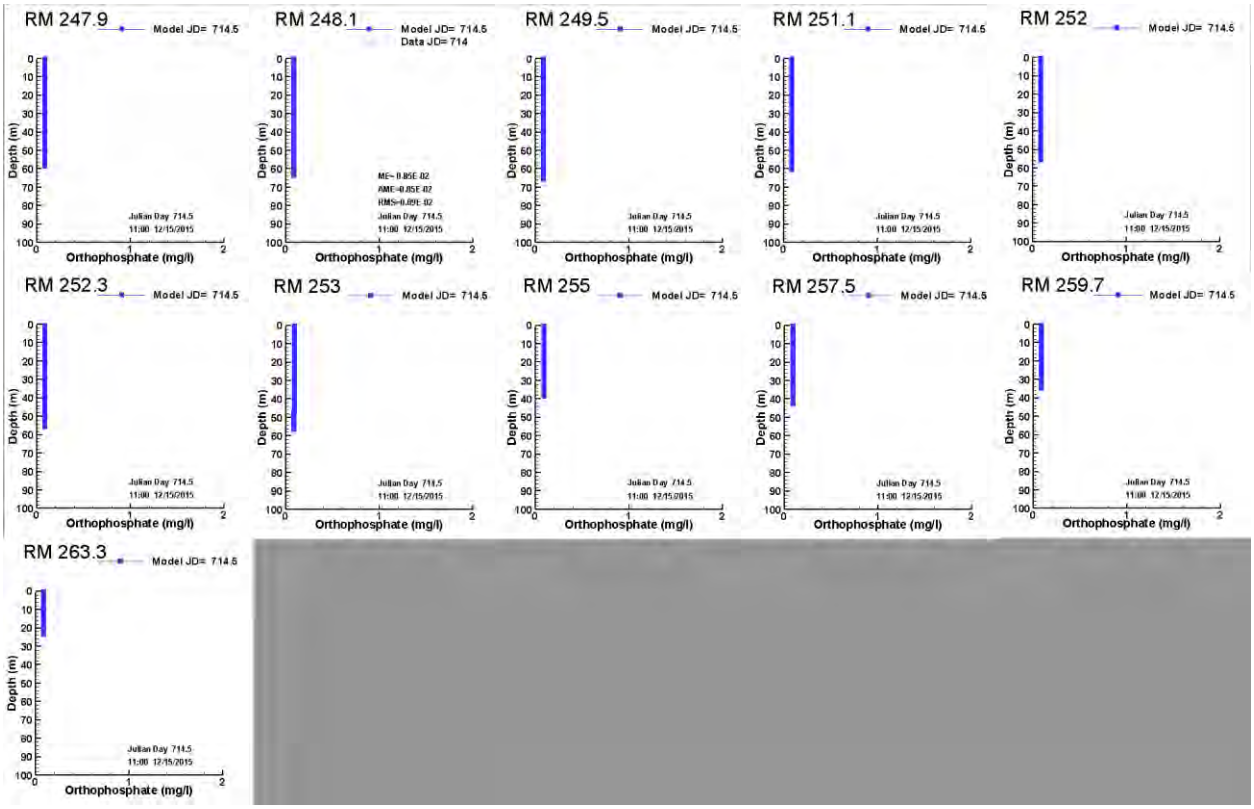


Figure 218. Vertical profiles of orthophosphate compared with data for 12/15/2015.

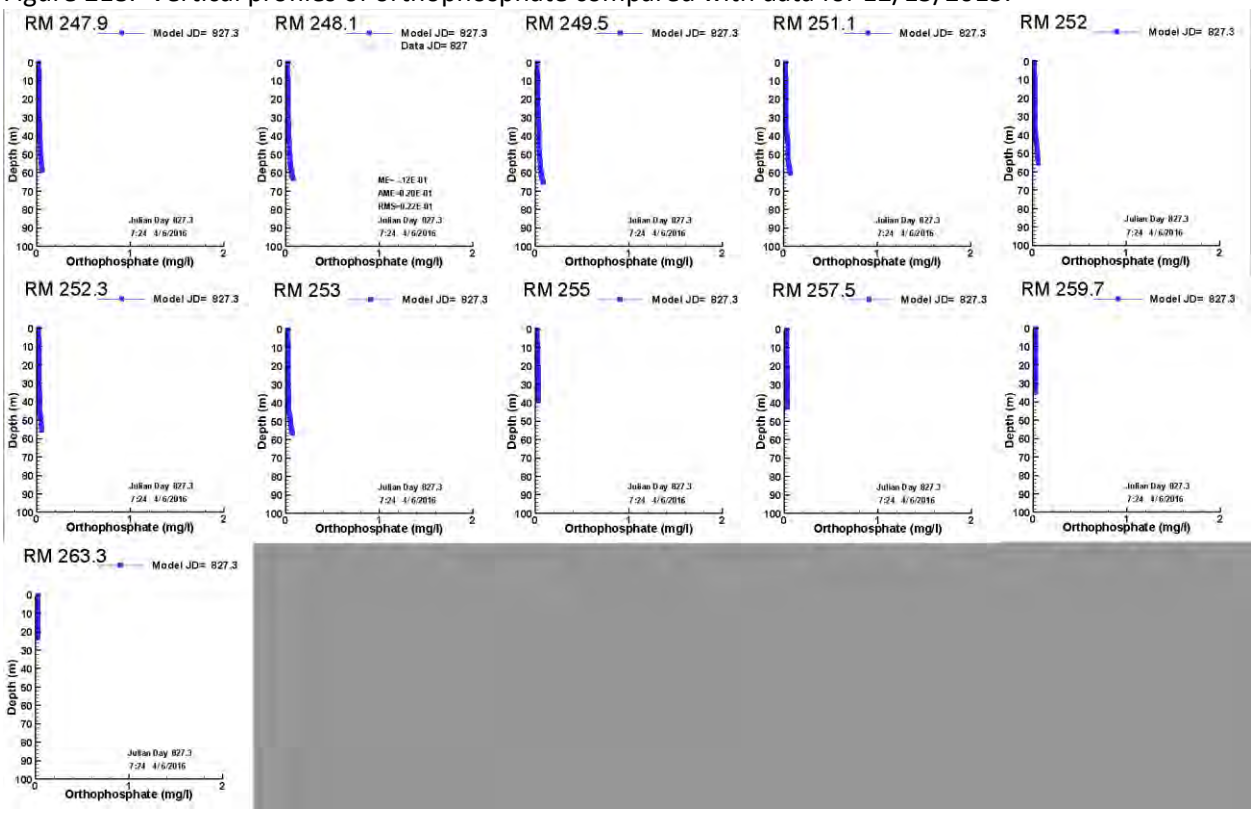


Figure 219. Vertical profiles of orthophosphate compared with data for 4/ 6/2016.

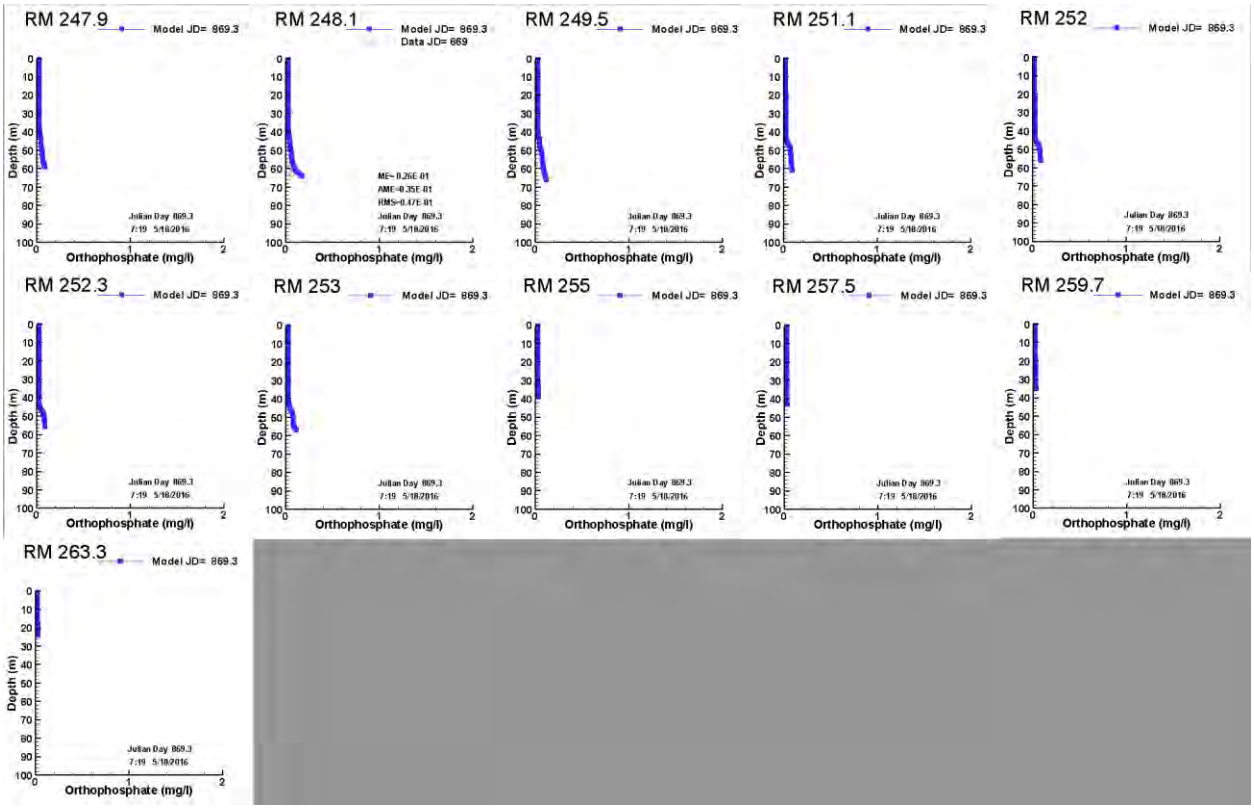


Figure 220. Vertical profiles of orthophosphate compared with data for 5/18/2016.

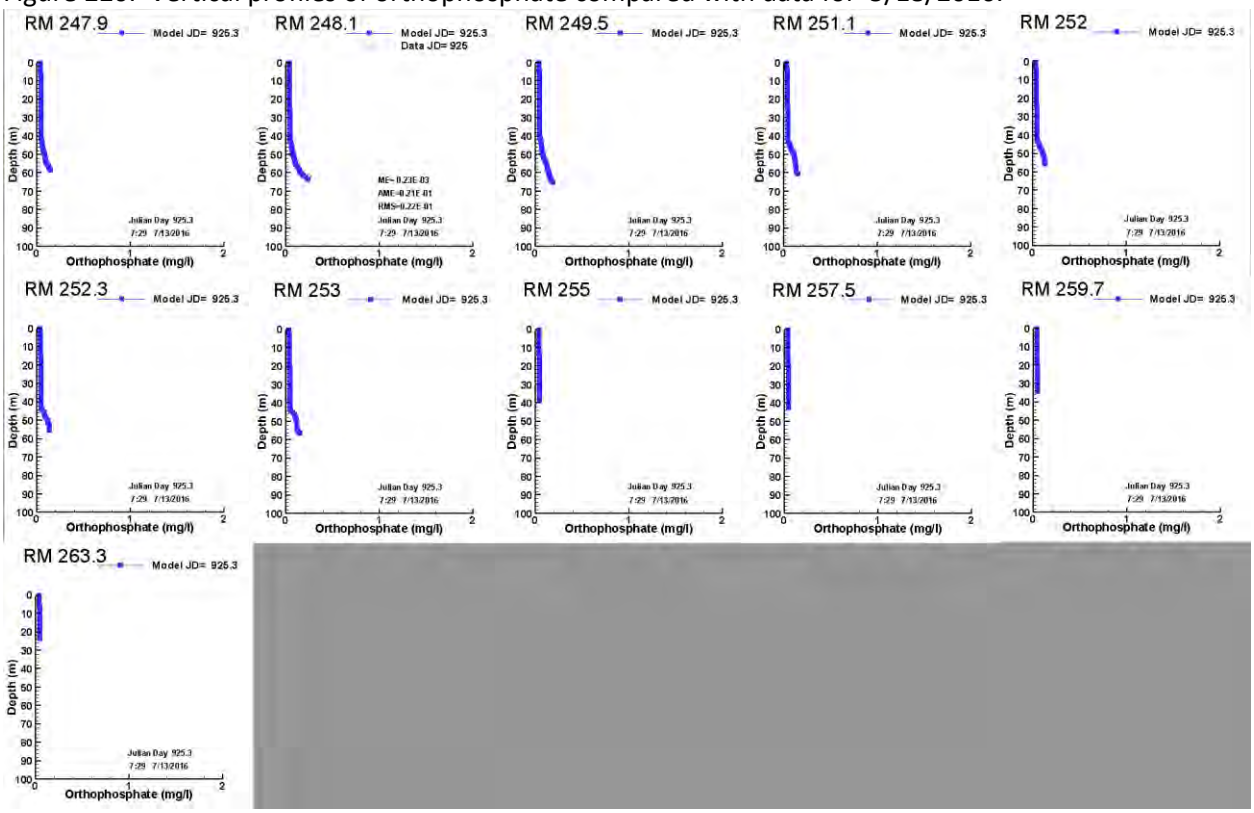


Figure 221. Vertical profiles of orthophosphate compared with data for 7/13/2016.

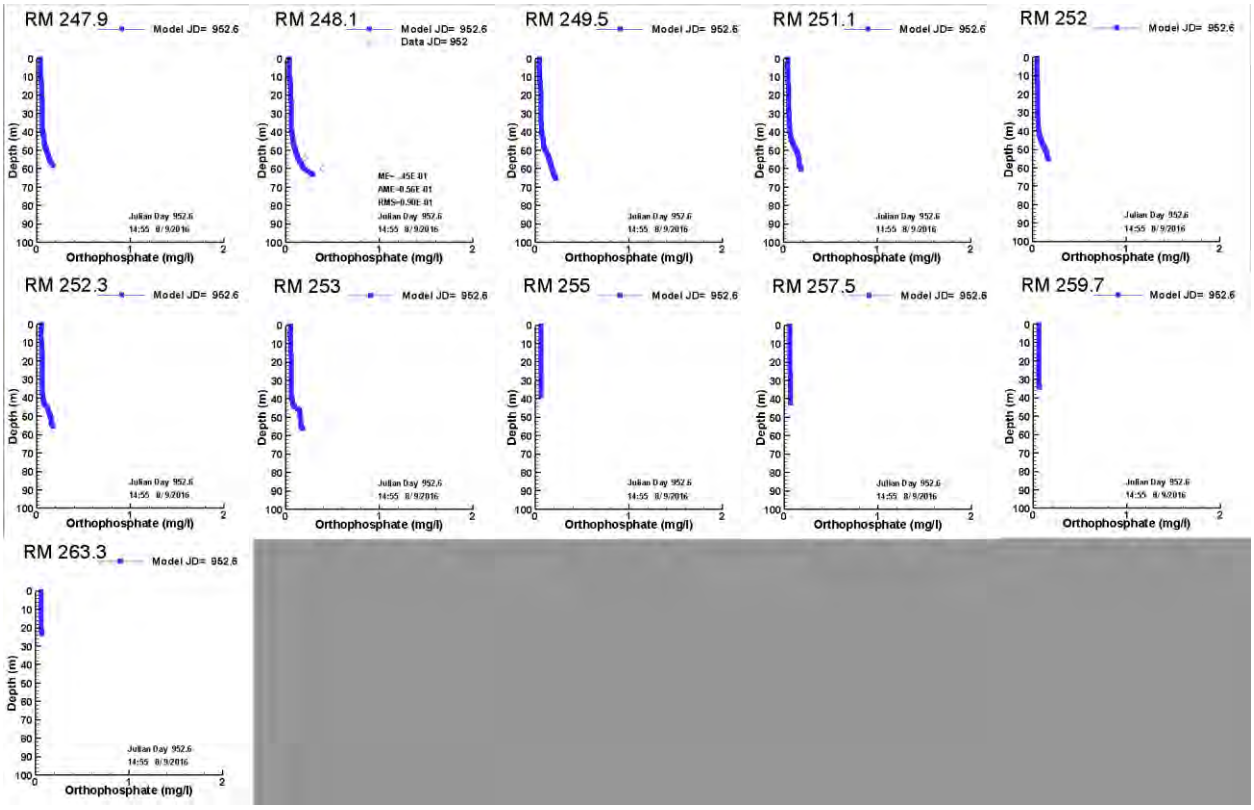


Figure 222. Vertical profiles of orthophosphate compared with data for 8/ 9/2016.

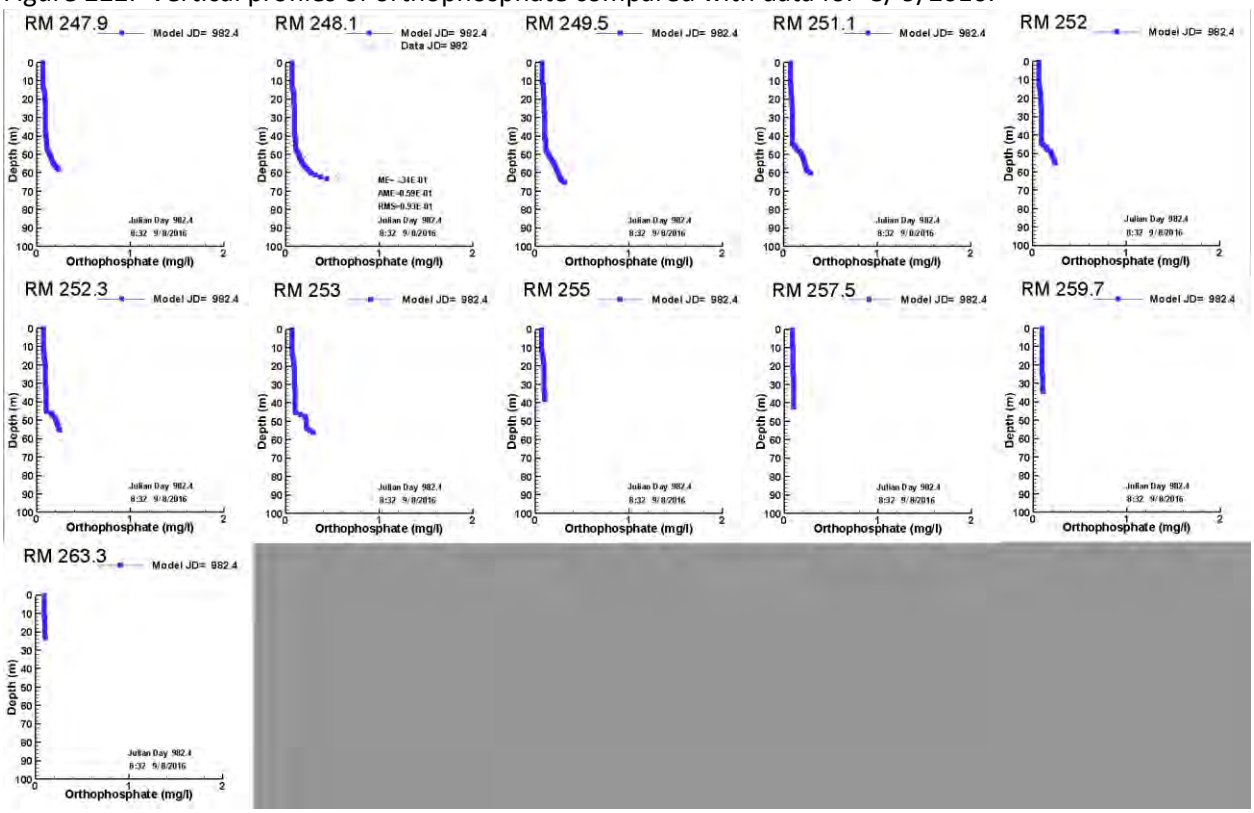


Figure 223. Vertical profiles of orthophosphate compared with data for 9/ 8/2016.

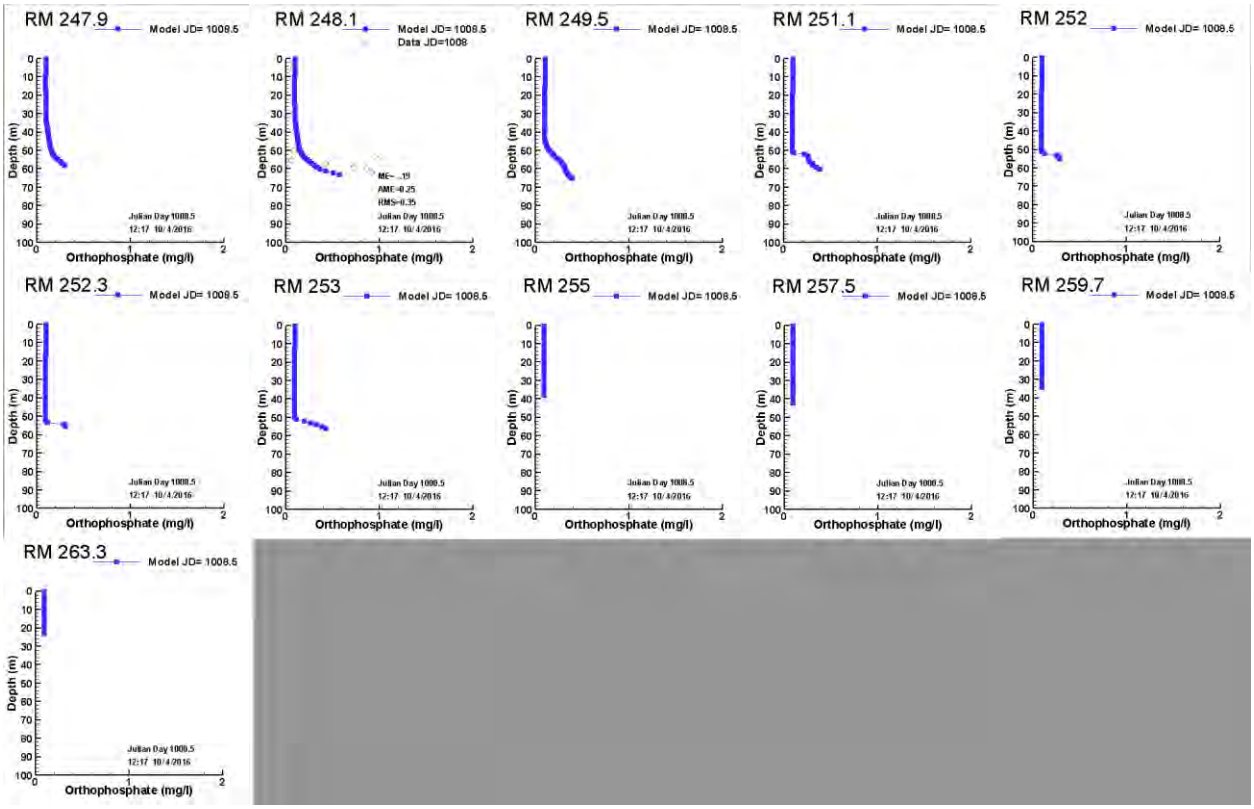


Figure 224. Vertical profiles of orthophosphate compared with data for 10/ 4/2016.

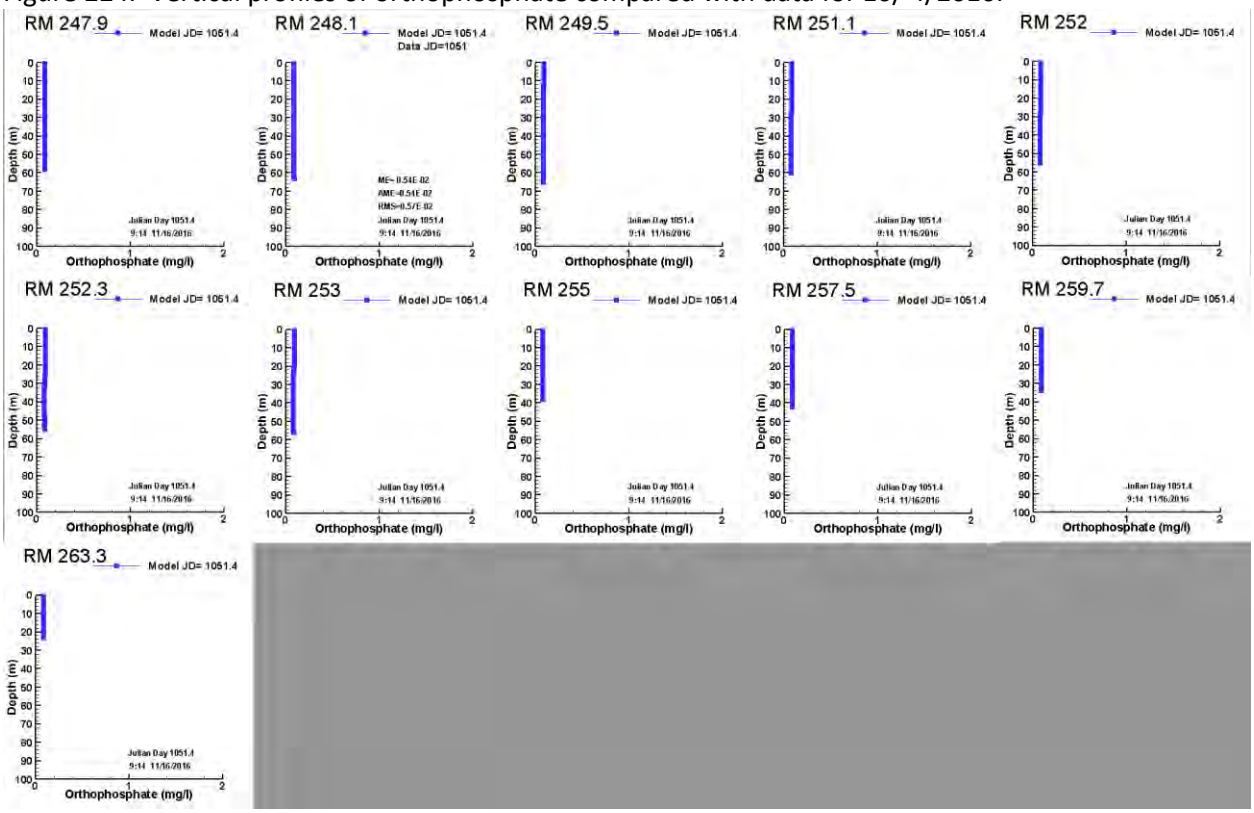


Figure 225. Vertical profiles of orthophosphate compared with data for 11/16/2016.

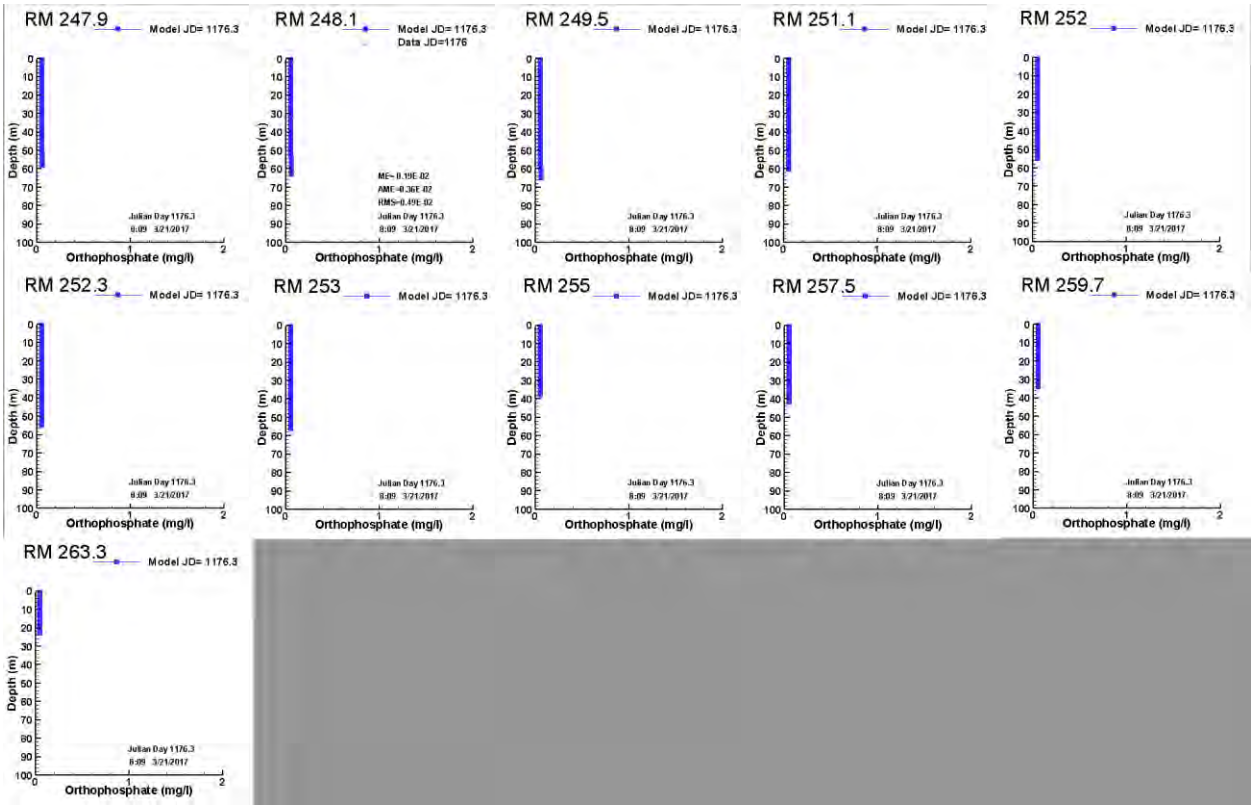


Figure 226. Vertical profiles of orthophosphate compared with data for 3/21/2017.

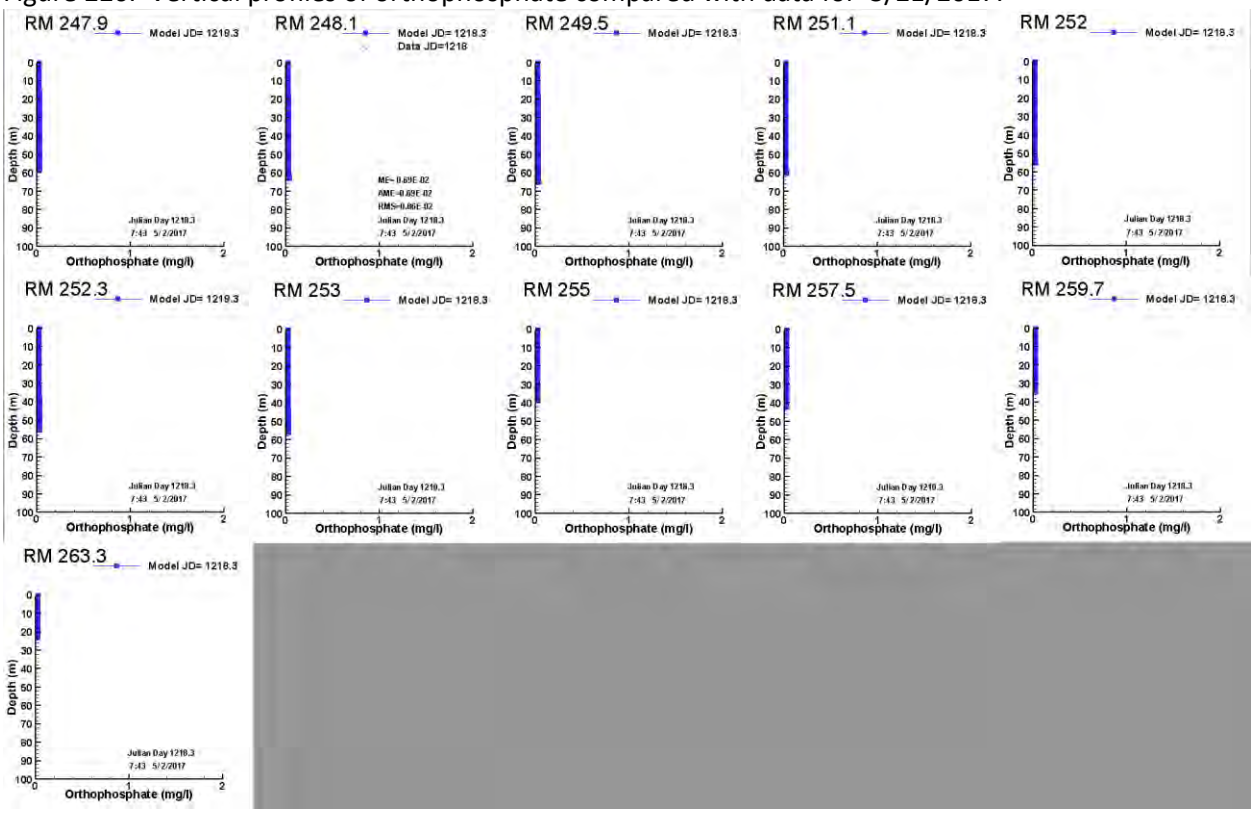


Figure 227. Vertical profiles of orthophosphate compared with data for 5/ 2/2017.

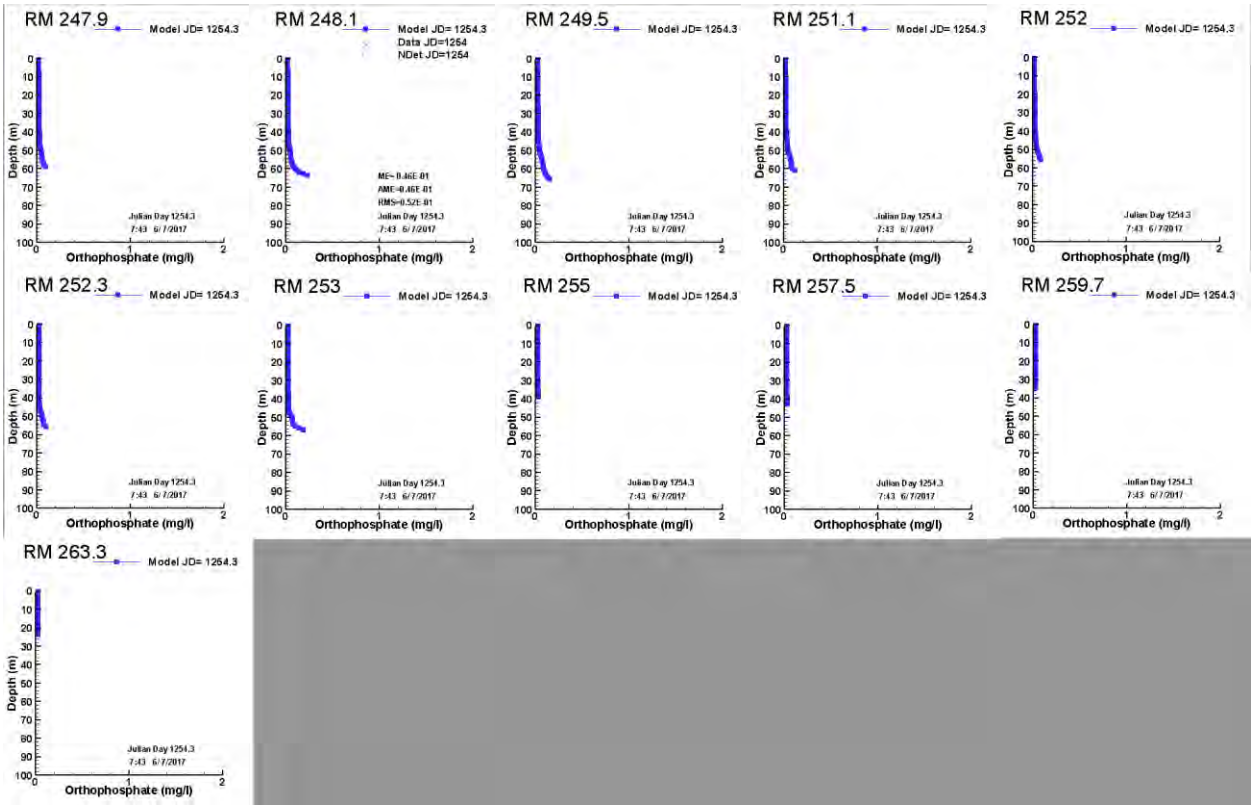


Figure 228. Vertical profiles of orthophosphate compared with data for 6/ 7/2017.

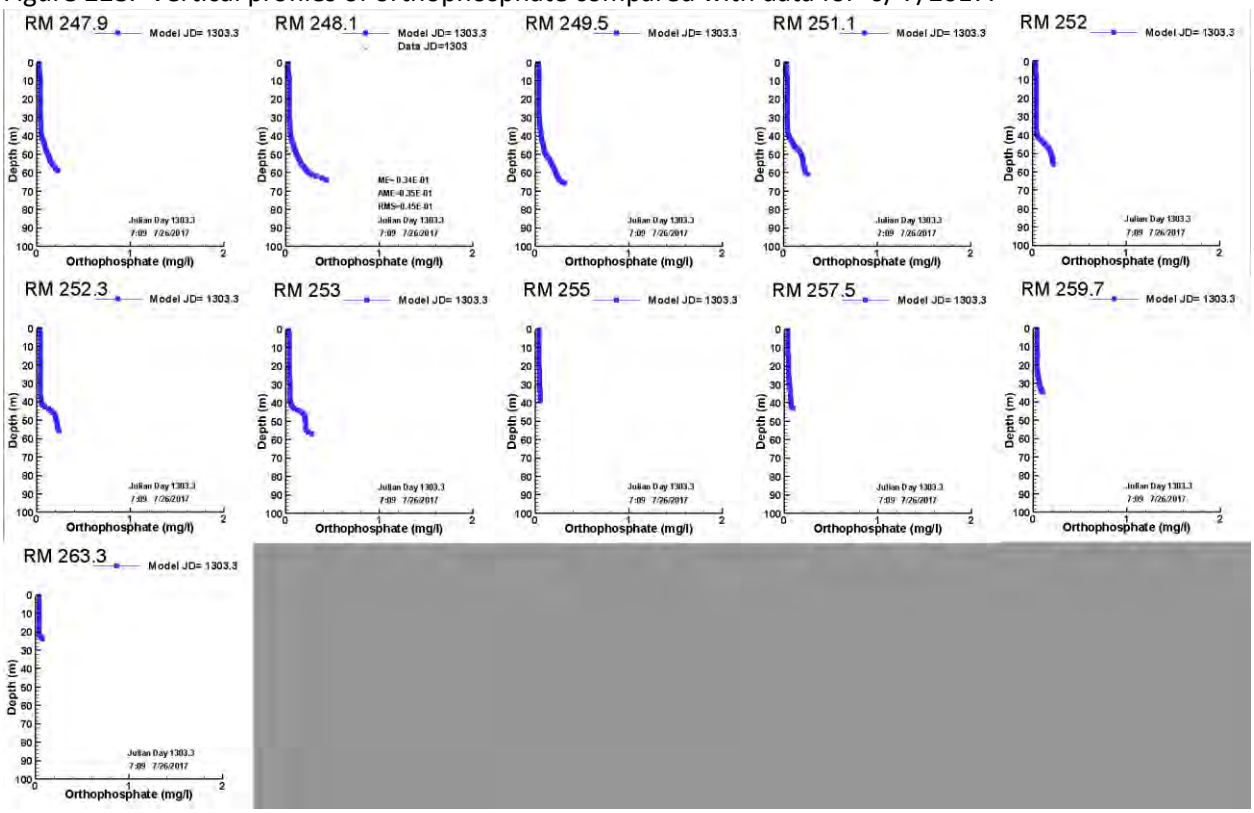


Figure 229. Vertical profiles of orthophosphate compared with data for 7/26/2017.

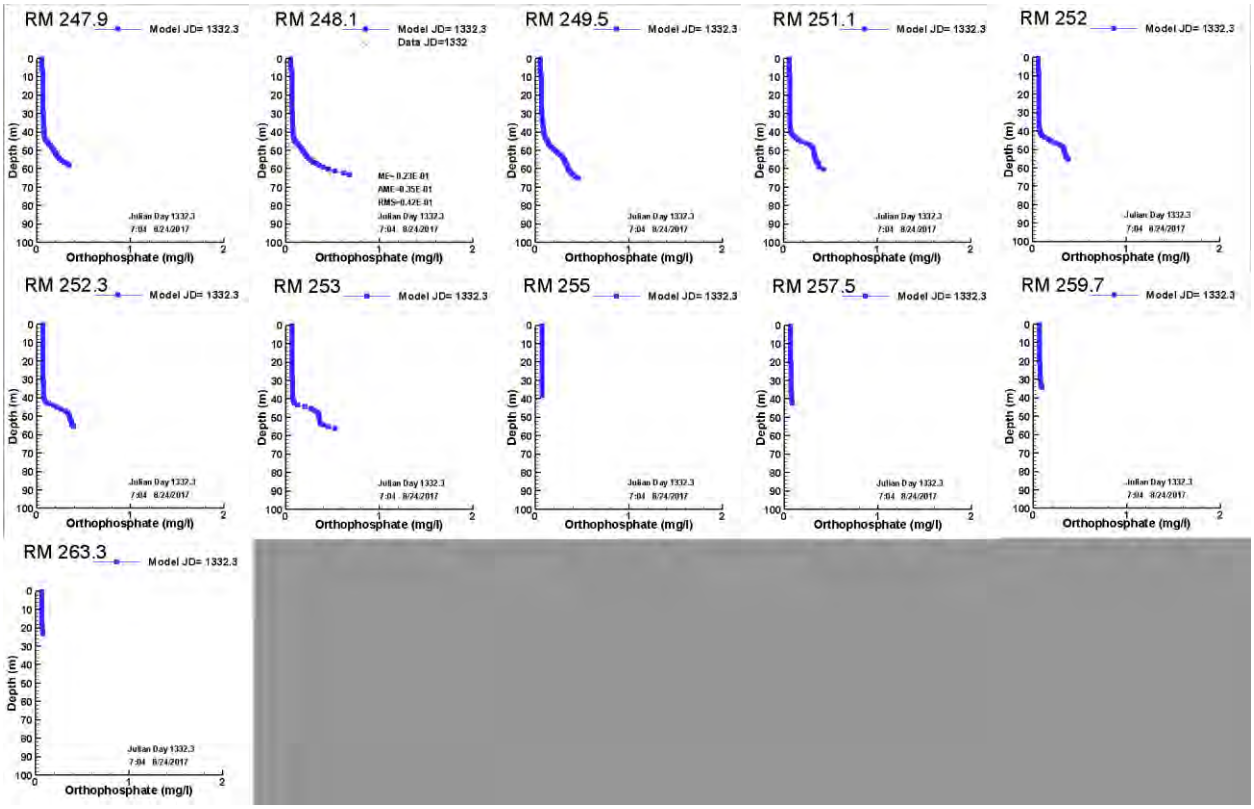


Figure 230. Vertical profiles of orthophosphate compared with data for 8/24/2017.

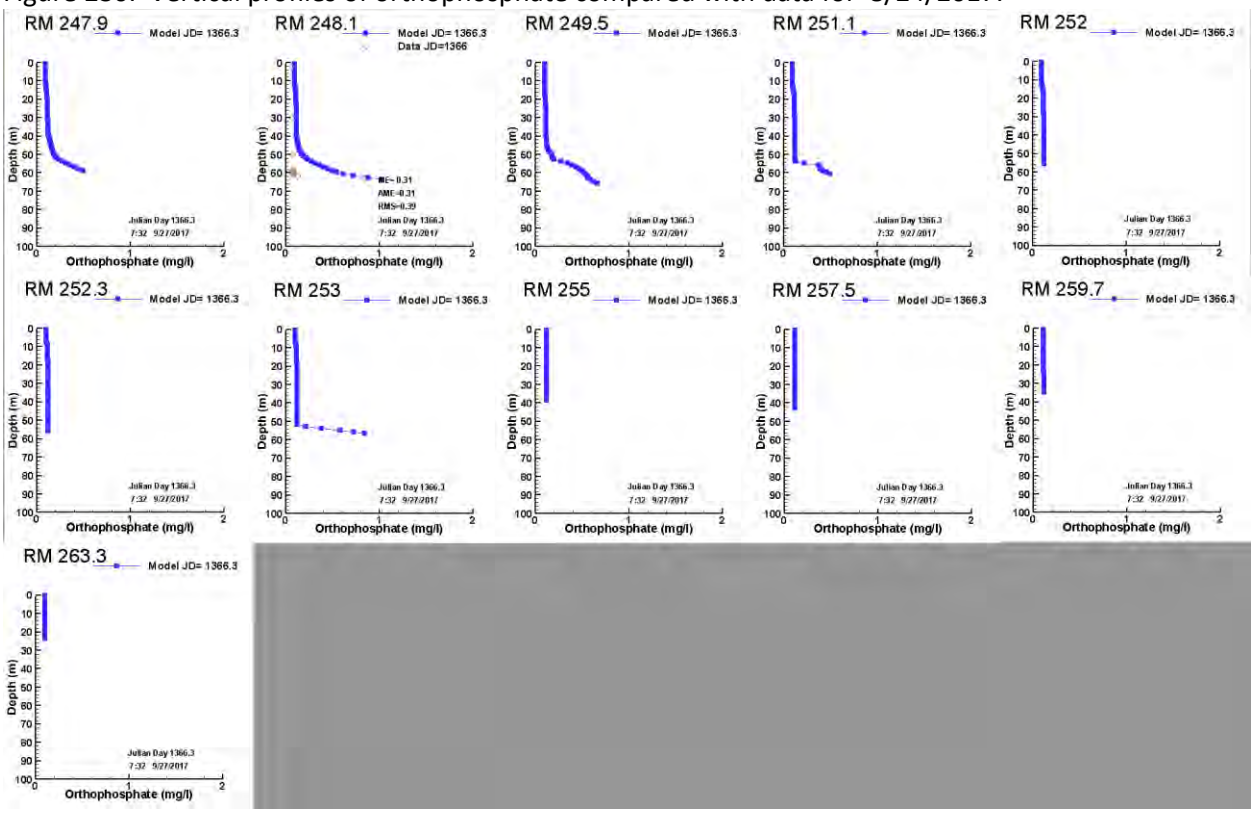


Figure 231. Vertical profiles of orthophosphate compared with data for 9/27/2017.

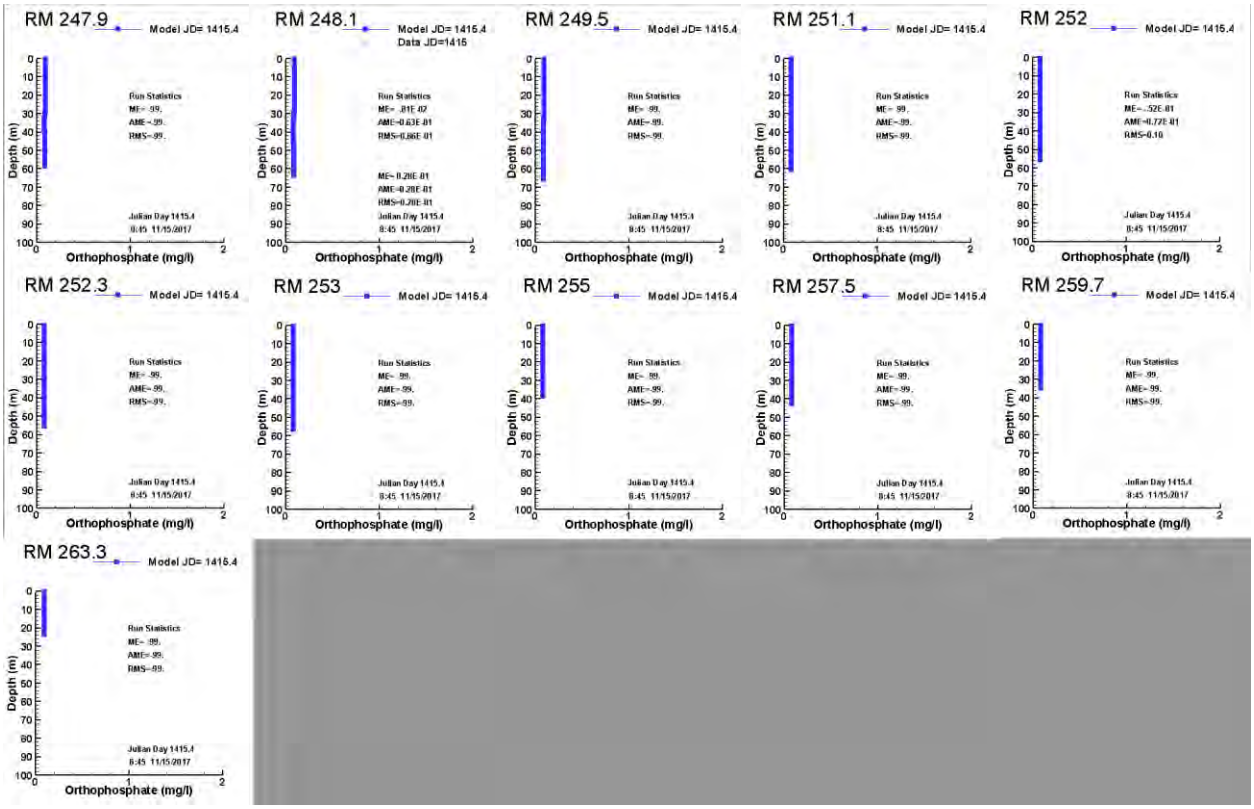


Figure 232. Vertical profiles of orthophosphate compared with data for 11/15/2017.

Nitrate Nitrogen

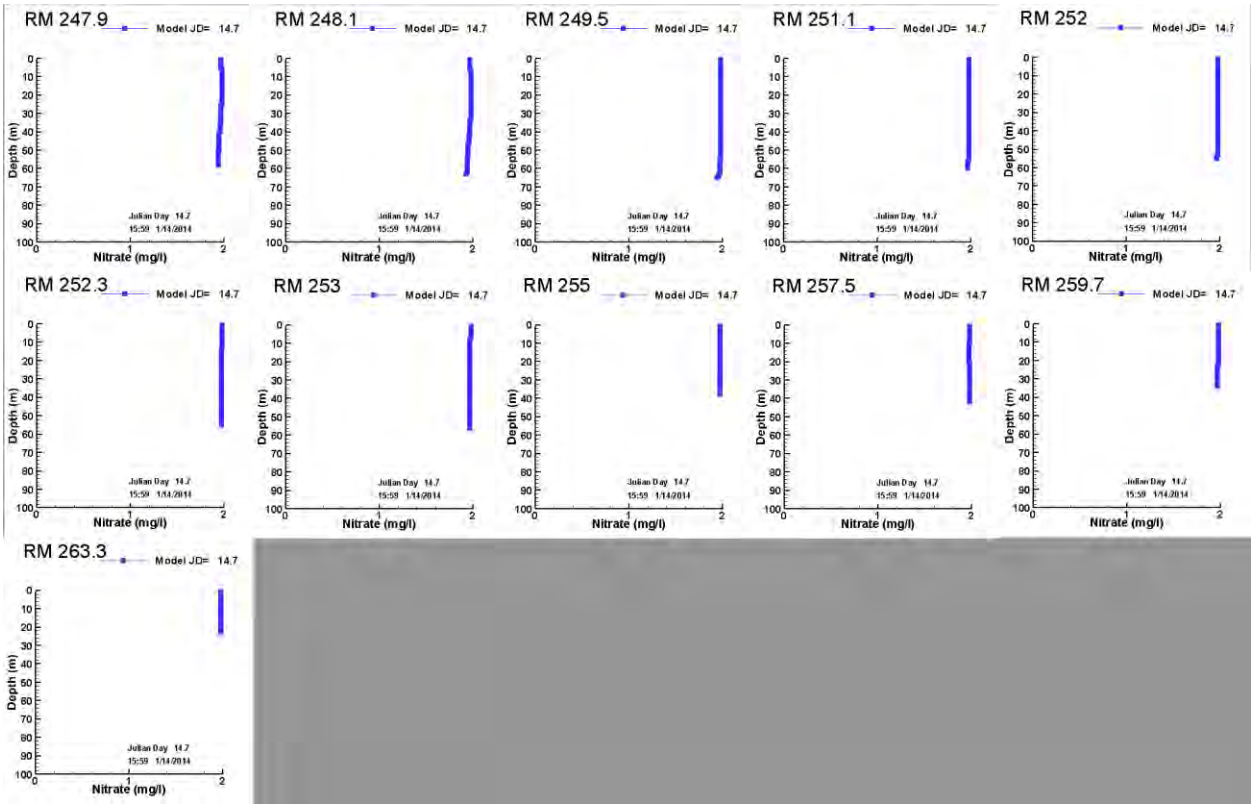


Figure 233. Vertical profiles of nitrate nitrogen compared with data for 1/14/2014.

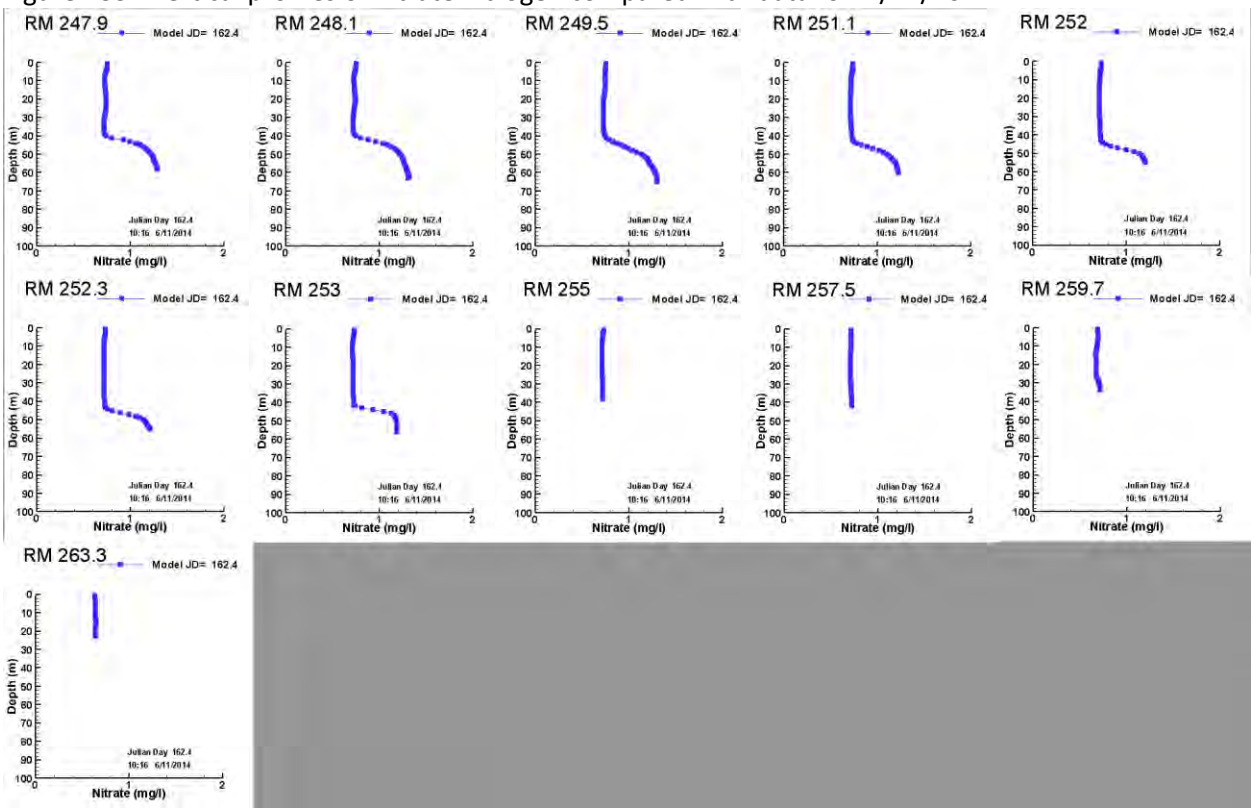


Figure 234. Vertical profiles of nitrate nitrogen compared with data for 6/11/2014.

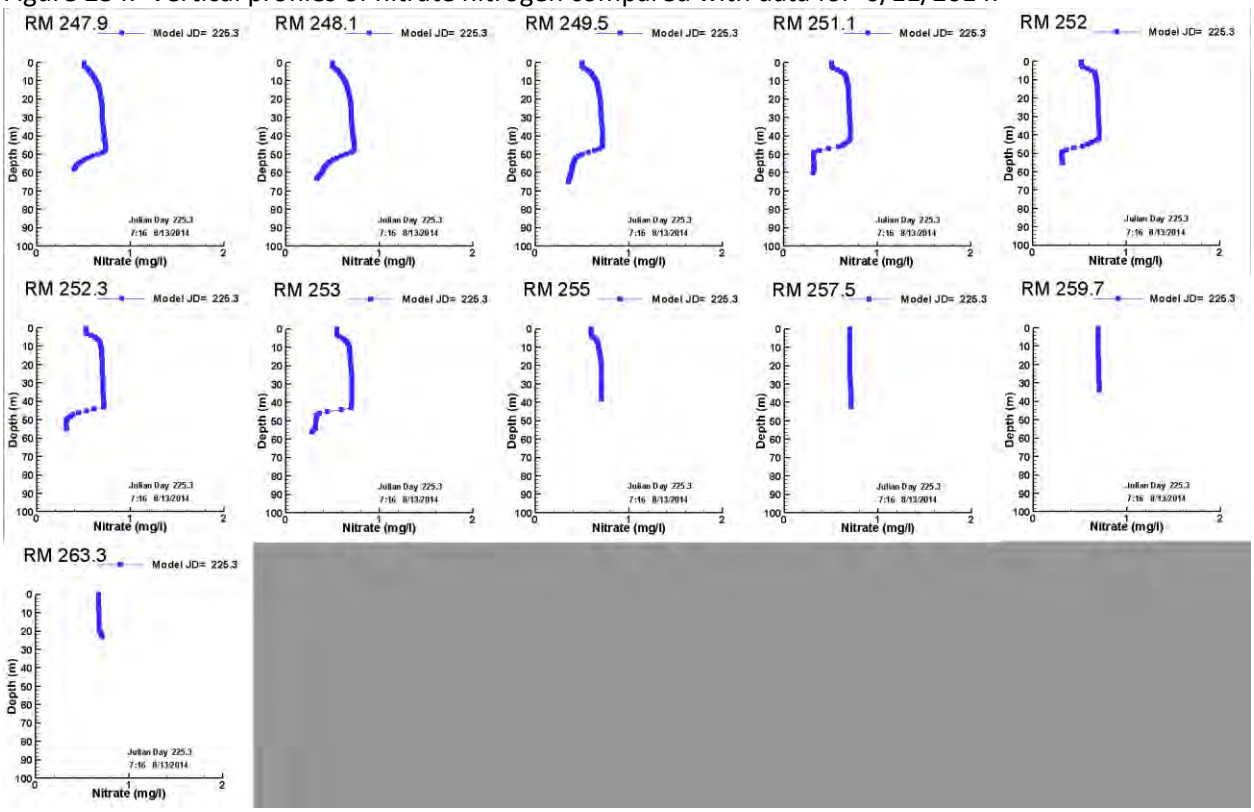


Figure 235. Vertical profiles of nitrate nitrogen compared with data for 8/13/2014.

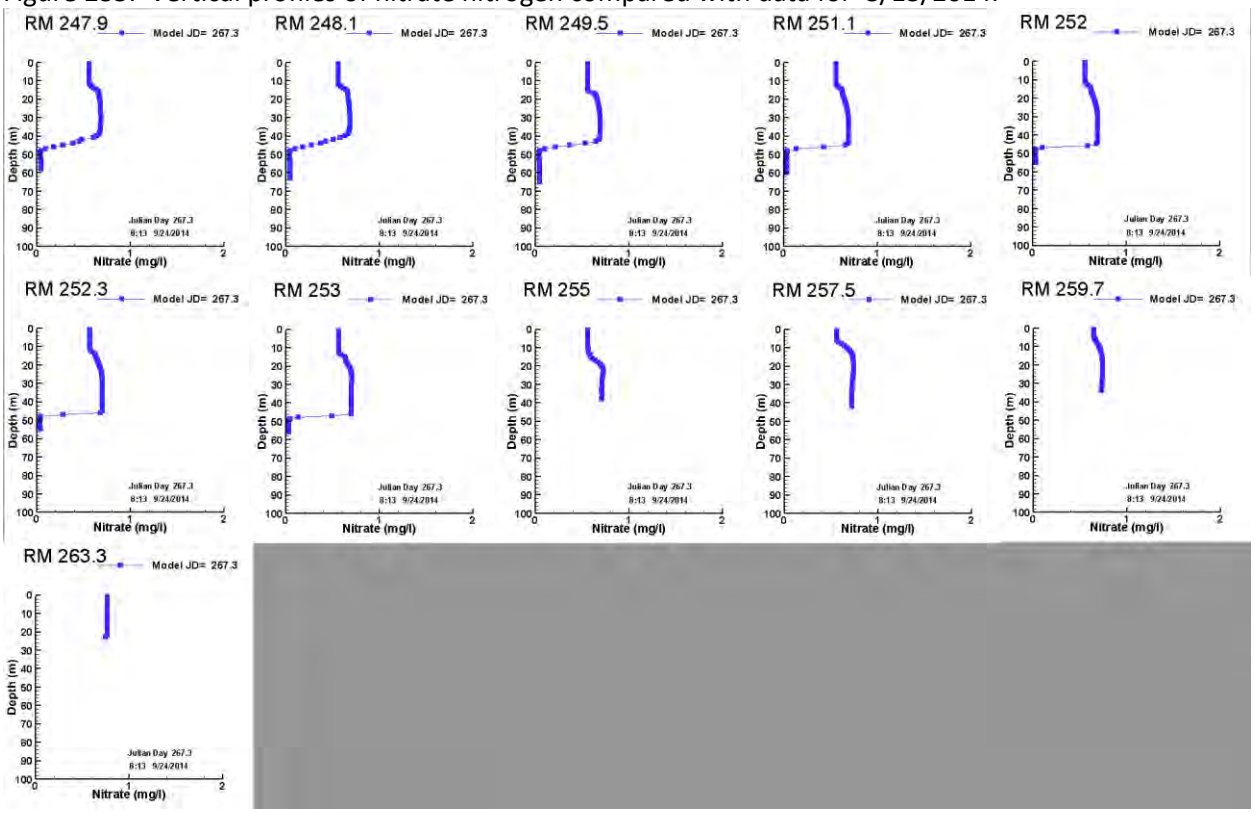


Figure 236. Vertical profiles of nitrate nitrogen compared with data for 9/24/2014.

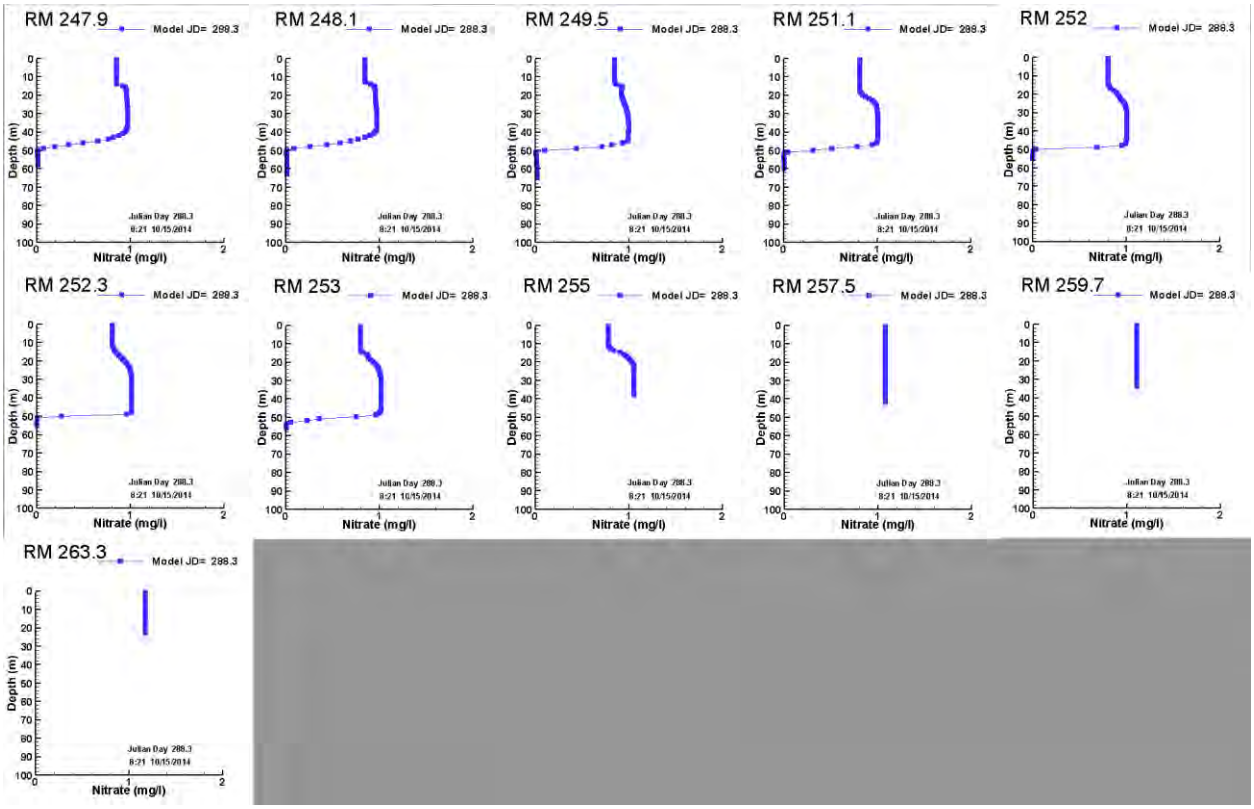


Figure 237. Vertical profiles of nitrate nitrogen compared with data for 10/15/2014.

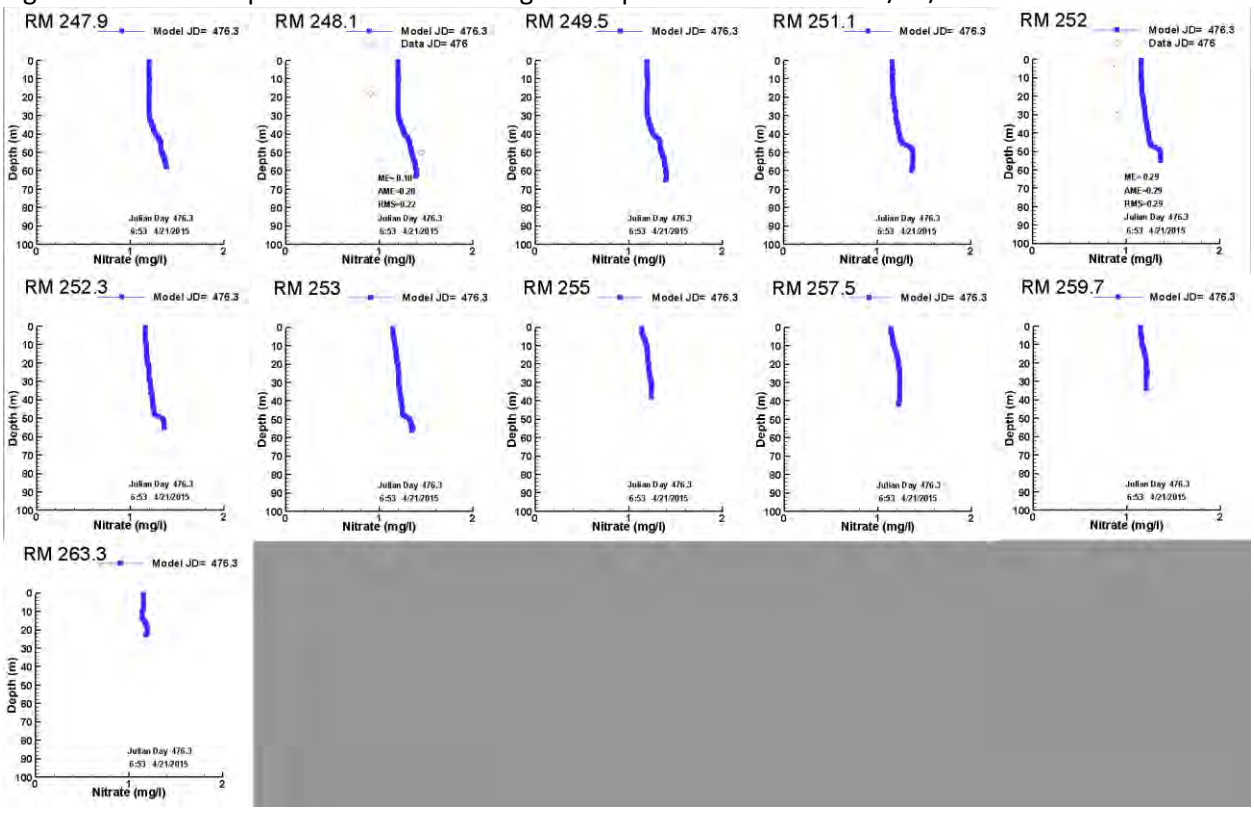


Figure 238. Vertical profiles of nitrate nitrogen compared with data for 4/21/2015.

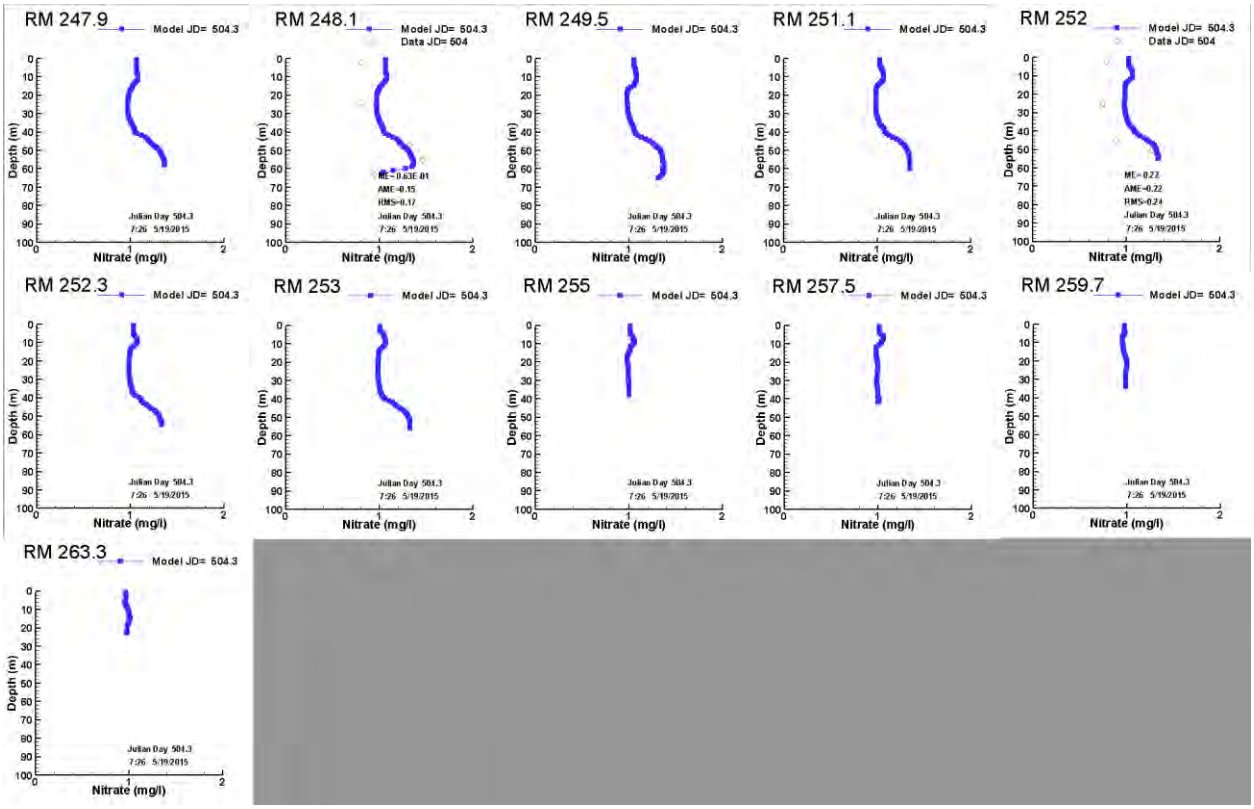


Figure 239. Vertical profiles of nitrate nitrogen compared with data for 5/19/2015.

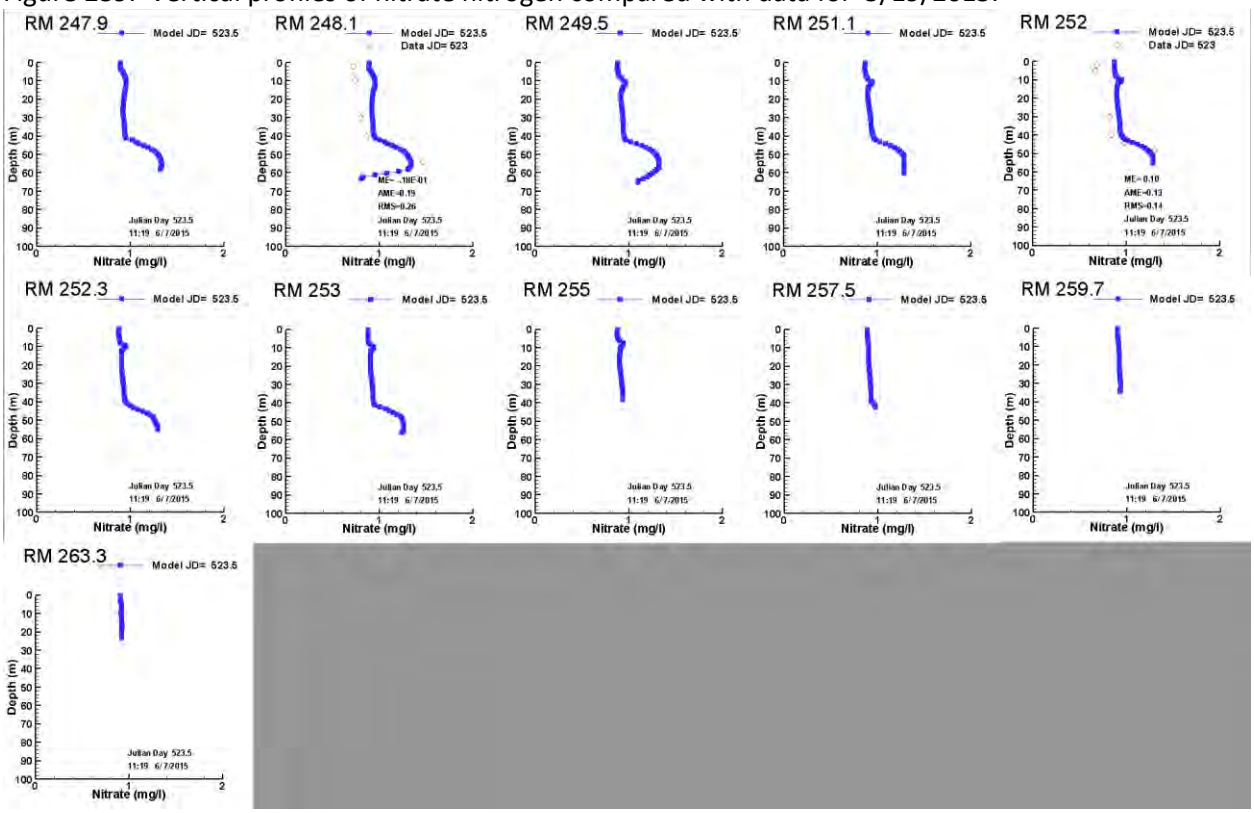


Figure 240. Vertical profiles of nitrate nitrogen compared with data for 6/ 7/2015.

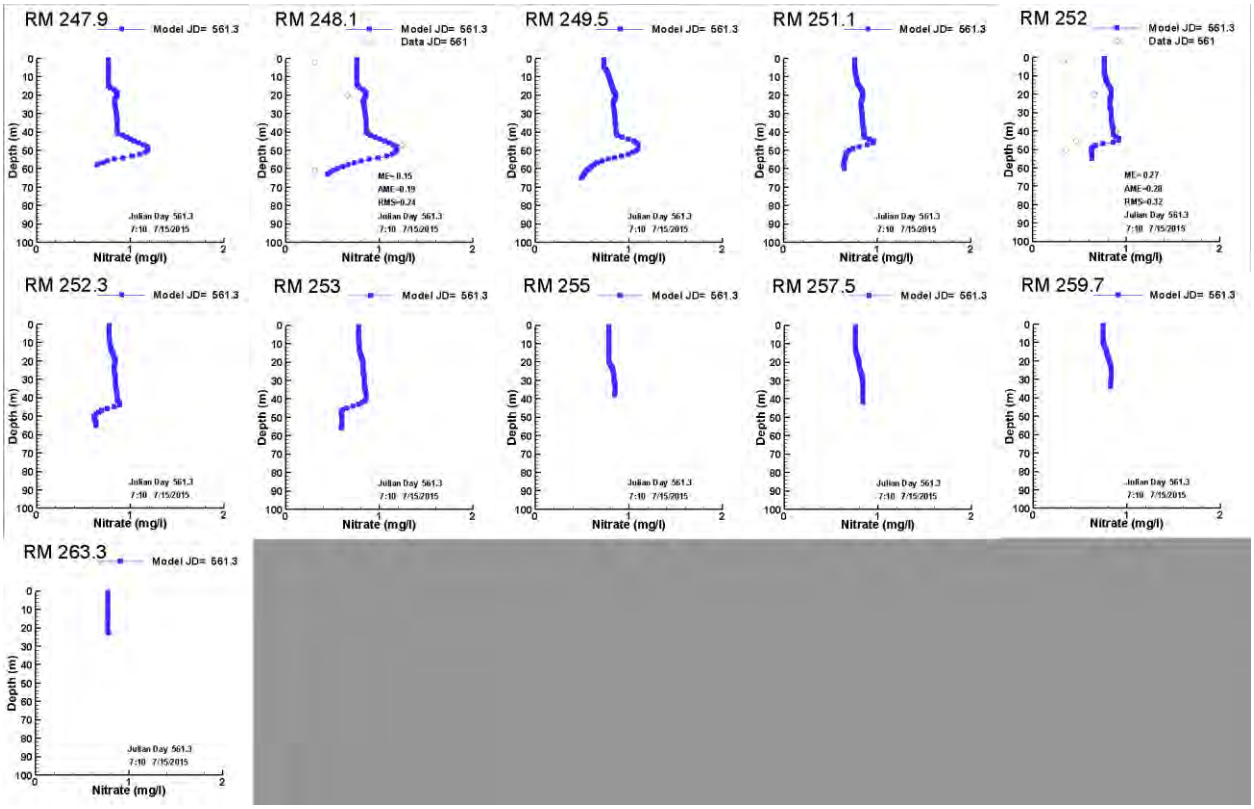


Figure 241. Vertical profiles of nitrate nitrogen compared with data for 7/15/2015.

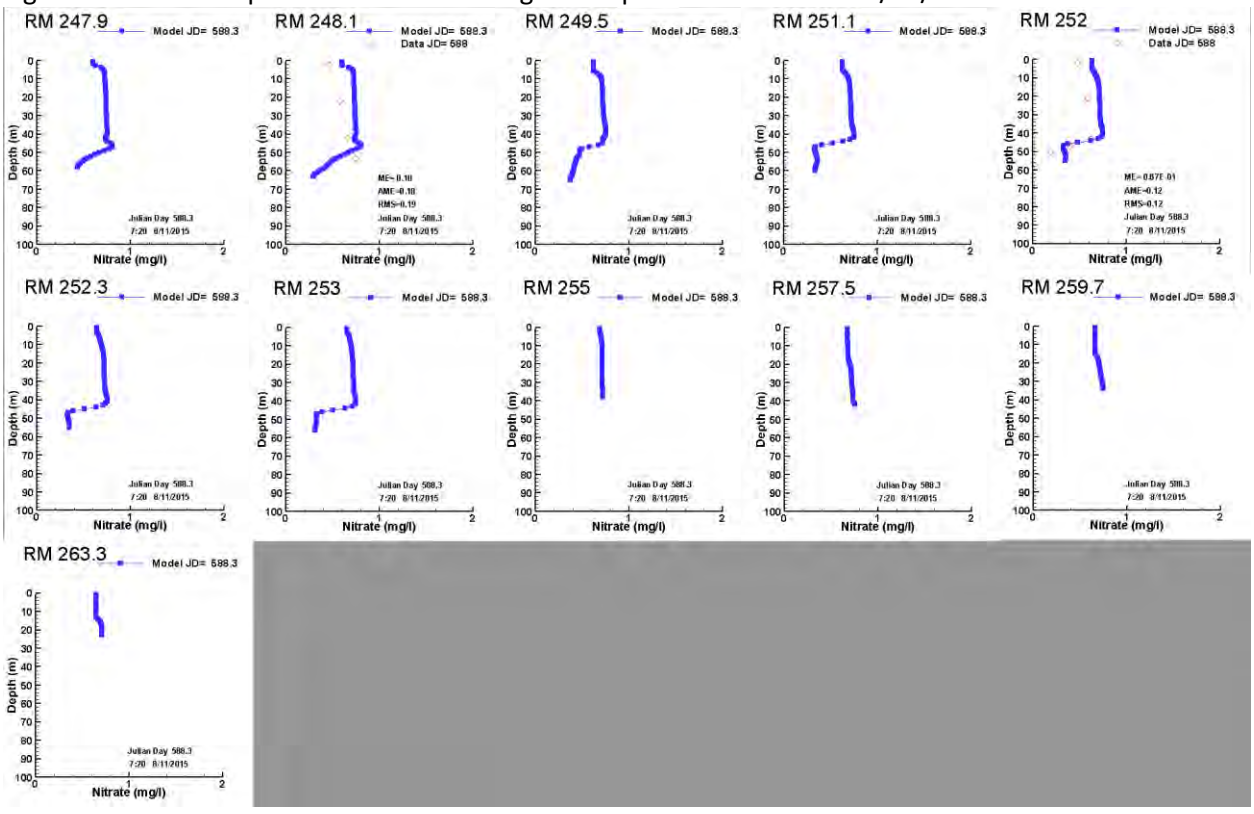


Figure 242. Vertical profiles of nitrate nitrogen compared with data for 8/11/2015.

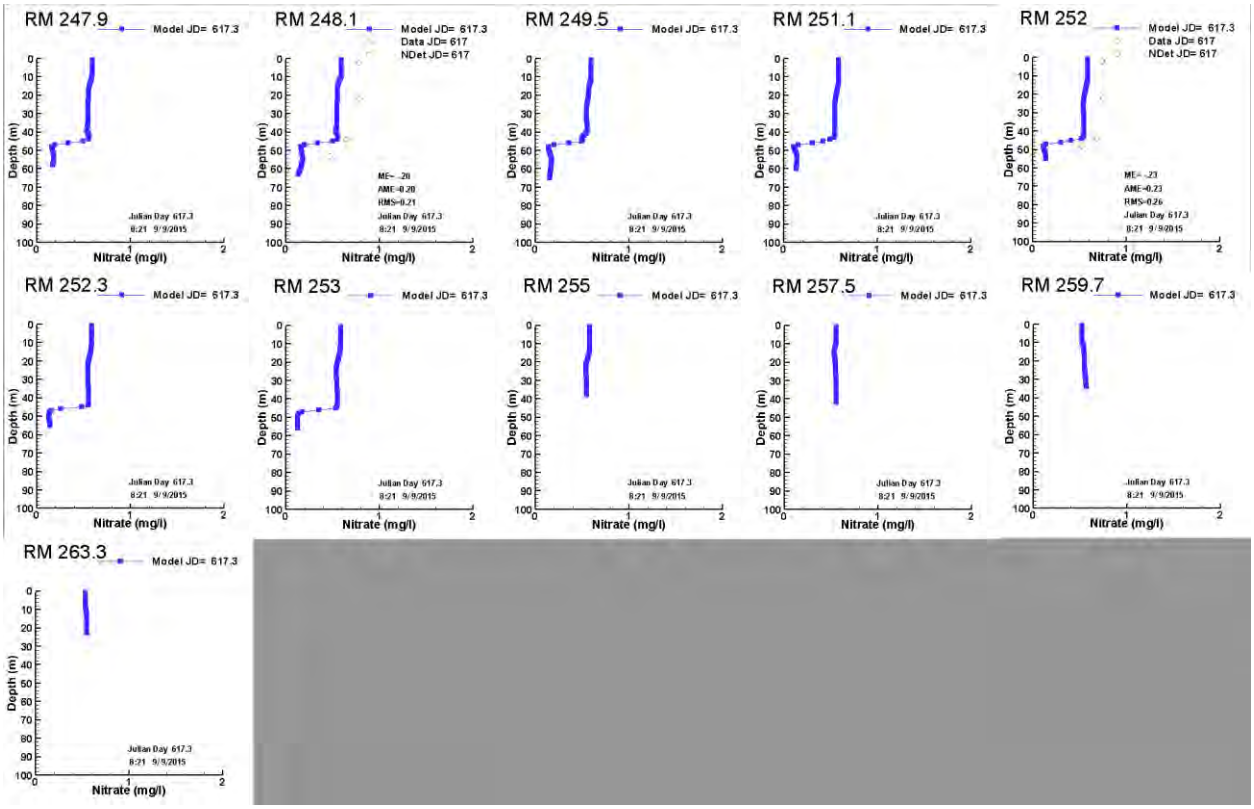


Figure 243. Vertical profiles of nitrate nitrogen compared with data for 9/ 9/2015.

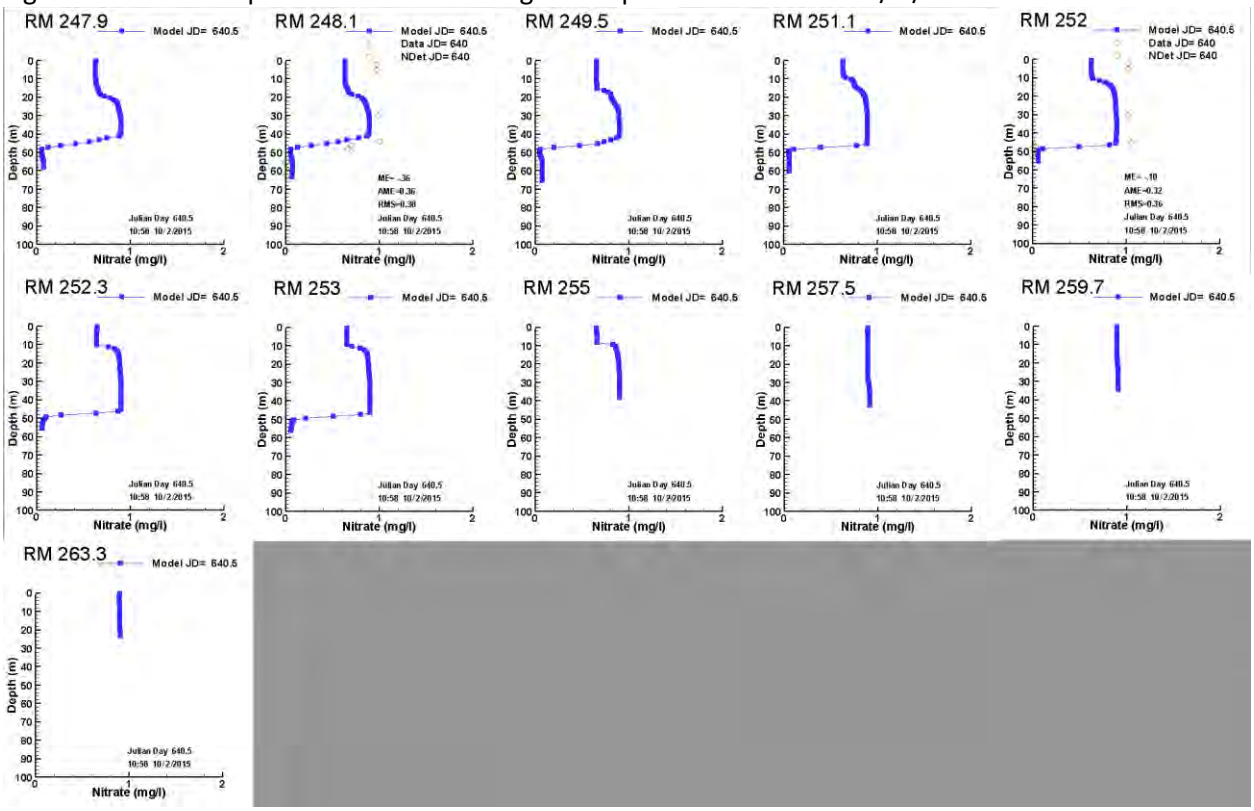


Figure 244. Vertical profiles of nitrate nitrogen compared with data for 10/ 2/2015.

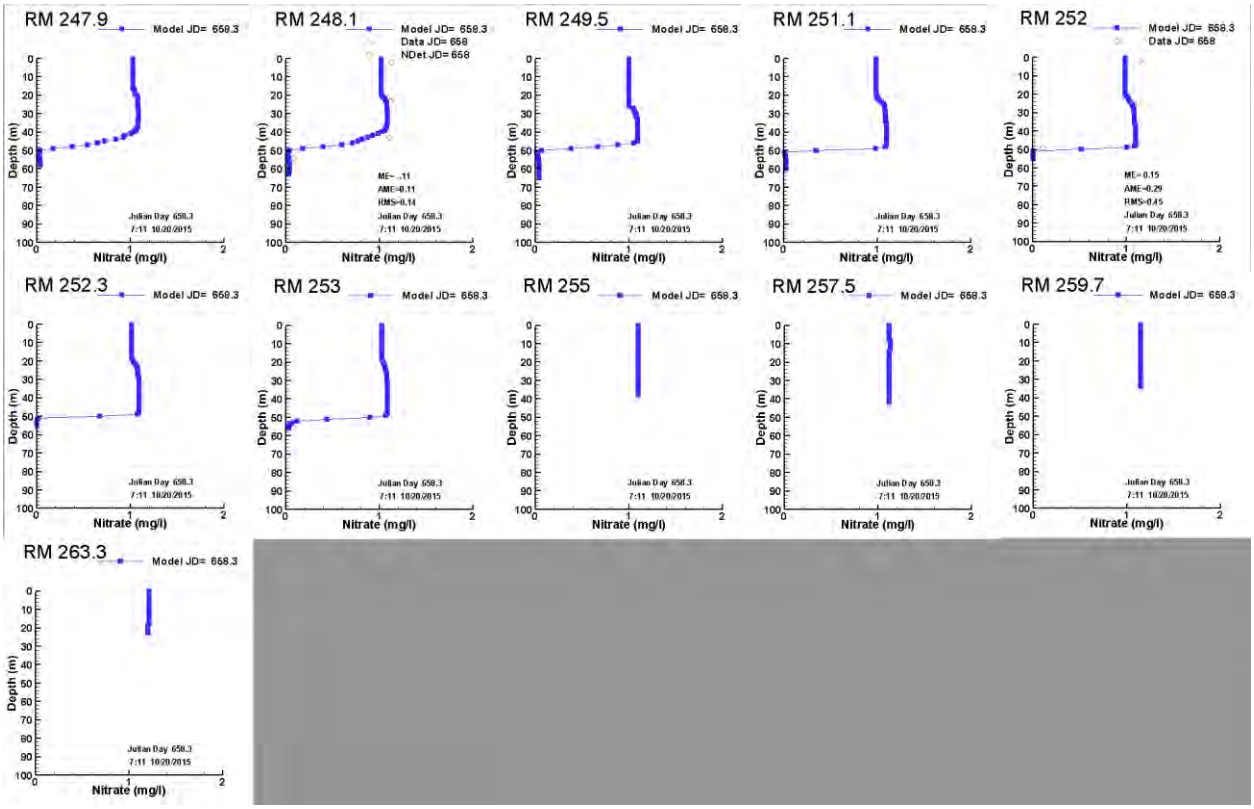


Figure 245. Vertical profiles of nitrate nitrogen compared with data for 10/20/2015.

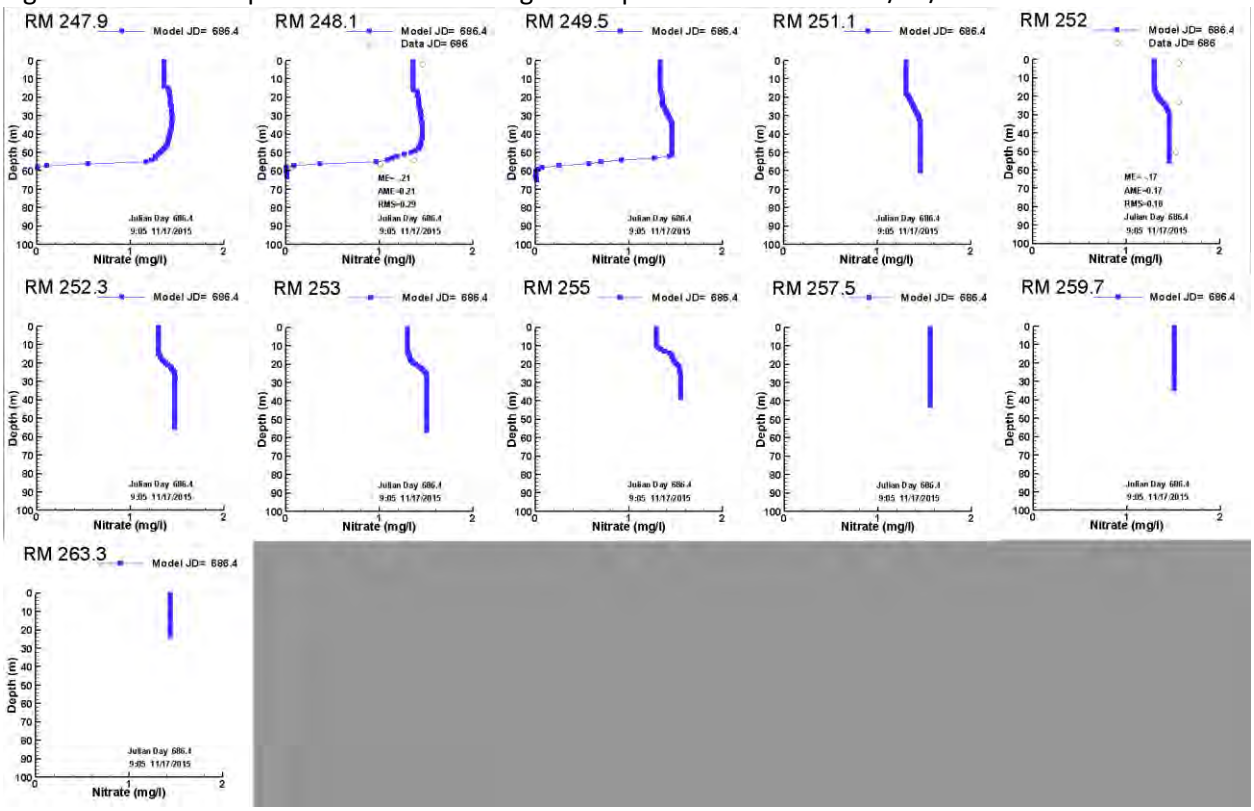


Figure 246. Vertical profiles of nitrate nitrogen compared with data for 11/17/2015.

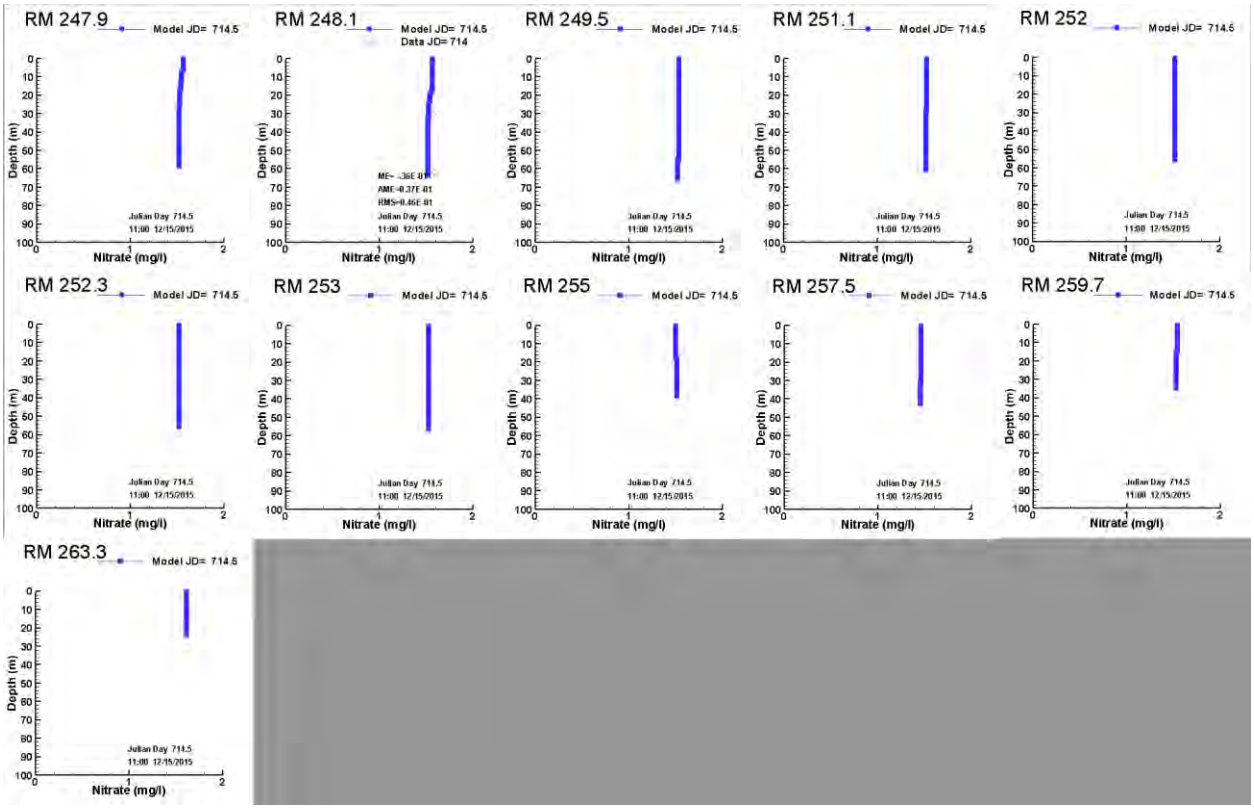


Figure 247. Vertical profiles of nitrate nitrogen compared with data for 12/15/2015.

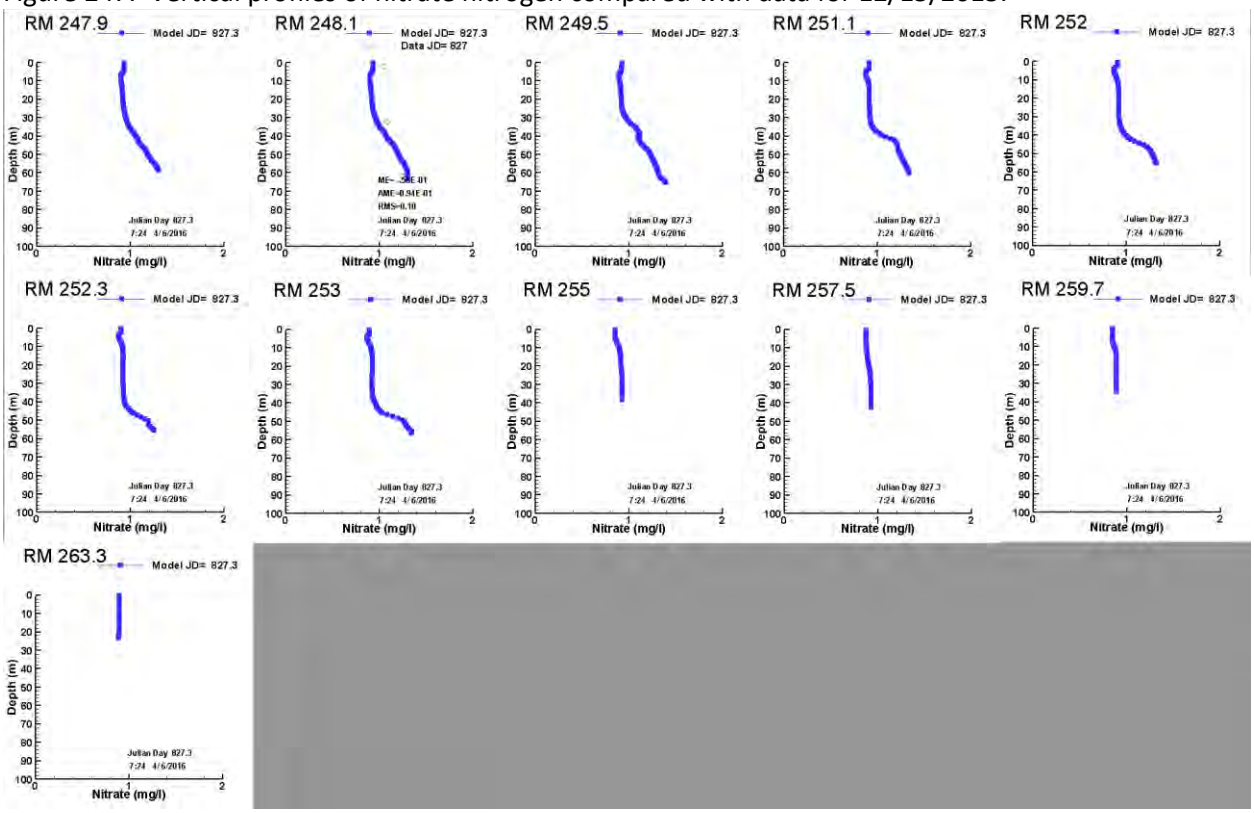


Figure 248. Vertical profiles of nitrate nitrogen compared with data for 4/ 6/2016.

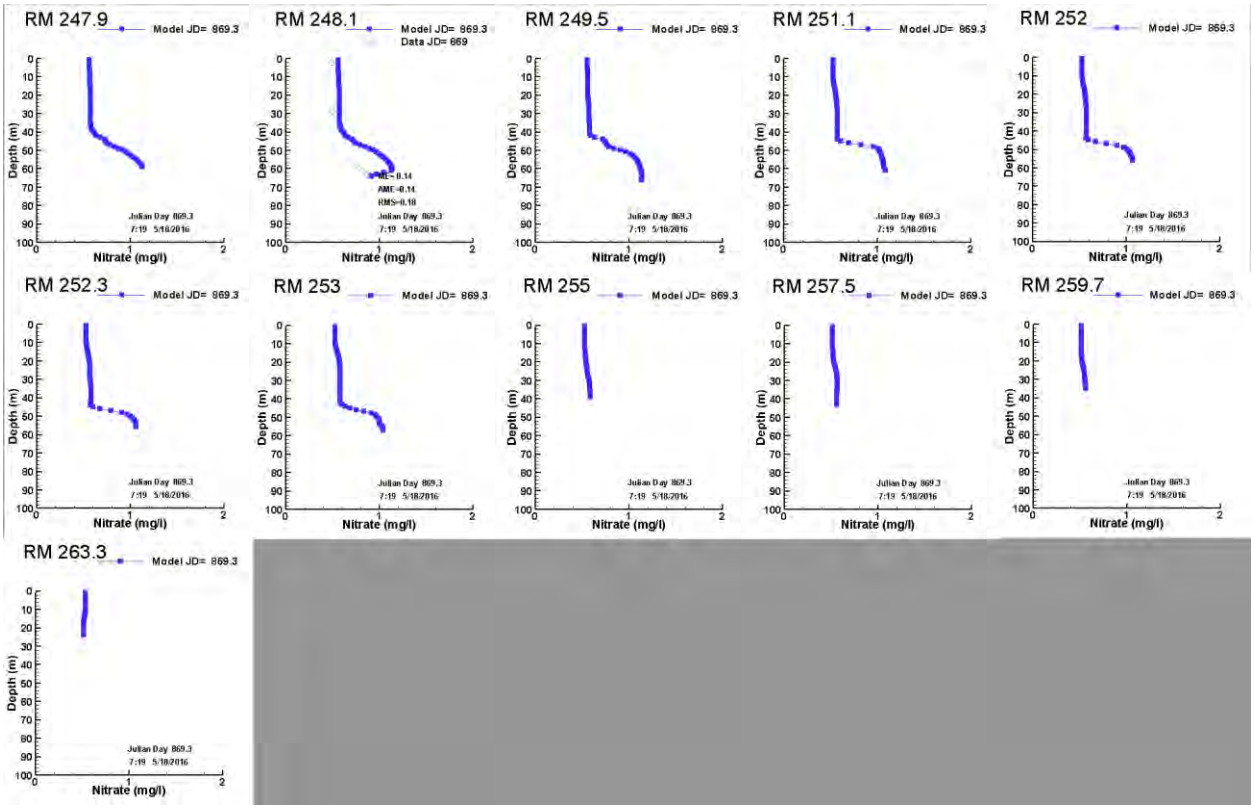


Figure 249. Vertical profiles of nitrate nitrogen compared with data for 5/18/2016.

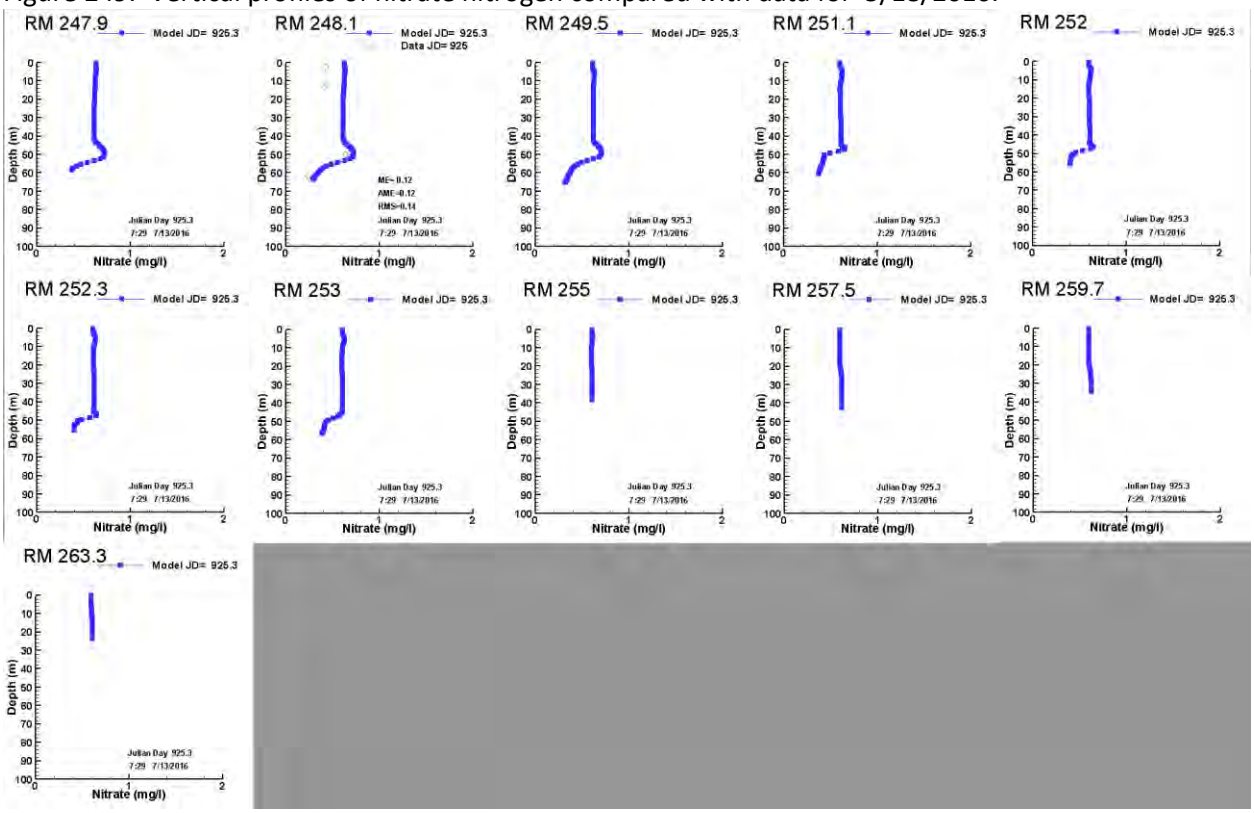


Figure 250. Vertical profiles of nitrate nitrogen compared with data for 7/13/2016.

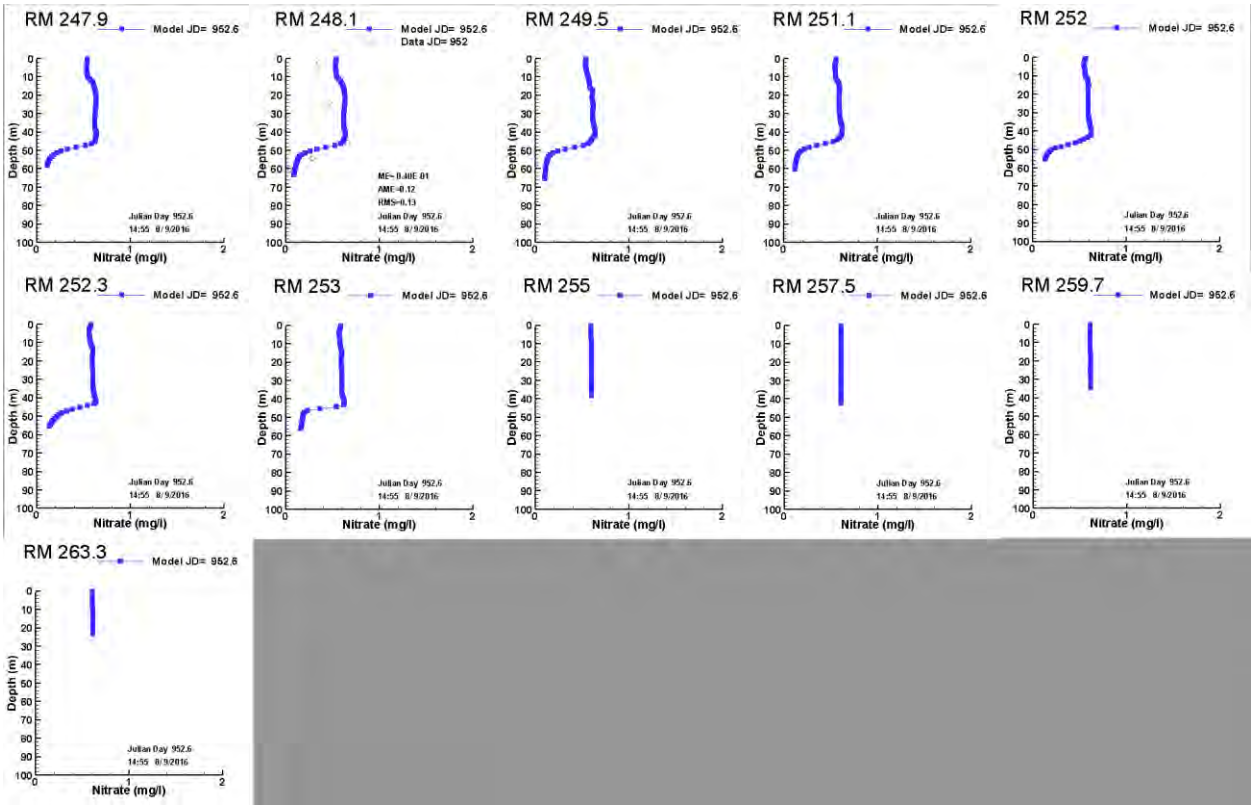


Figure 251. Vertical profiles of nitrate nitrogen compared with data for 8/ 9/2016.

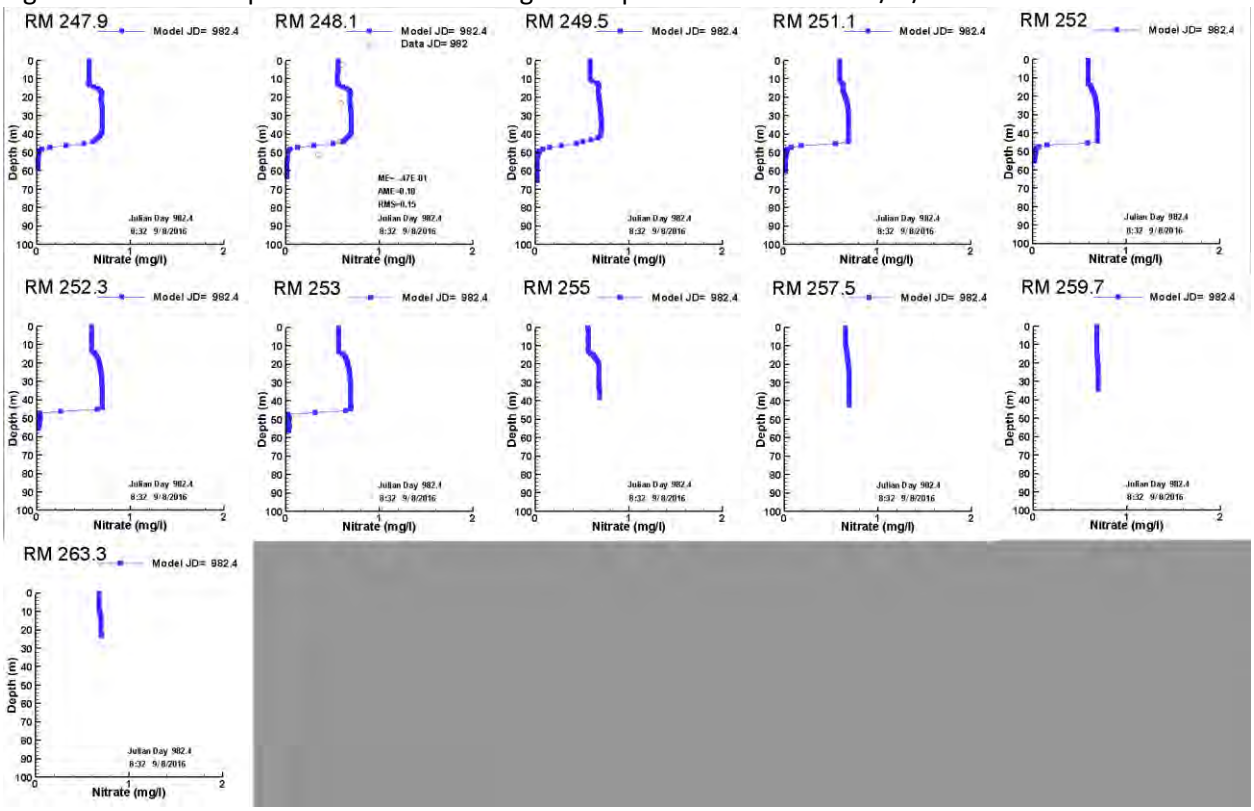


Figure 252. Vertical profiles of nitrate nitrogen compared with data for 9/ 8/2016.

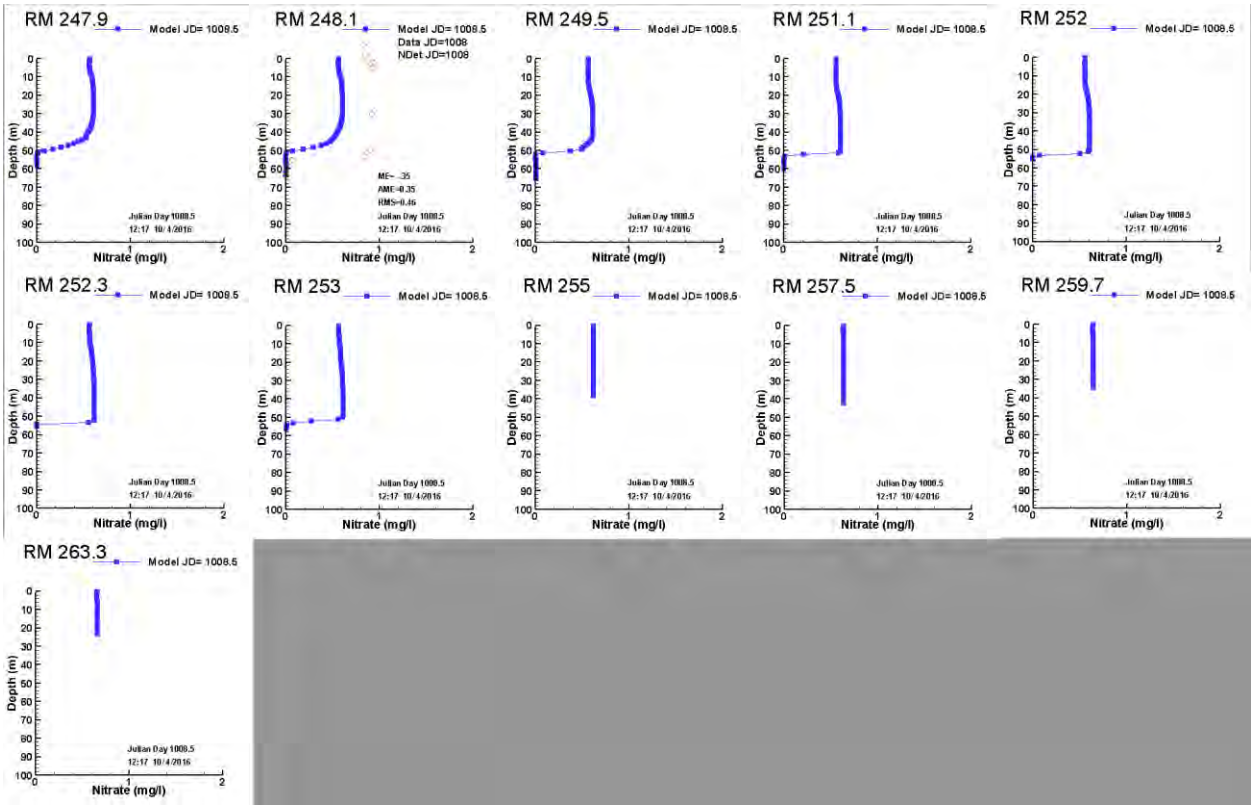


Figure 253. Vertical profiles of nitrate nitrogen compared with data for 10/ 4/2016.

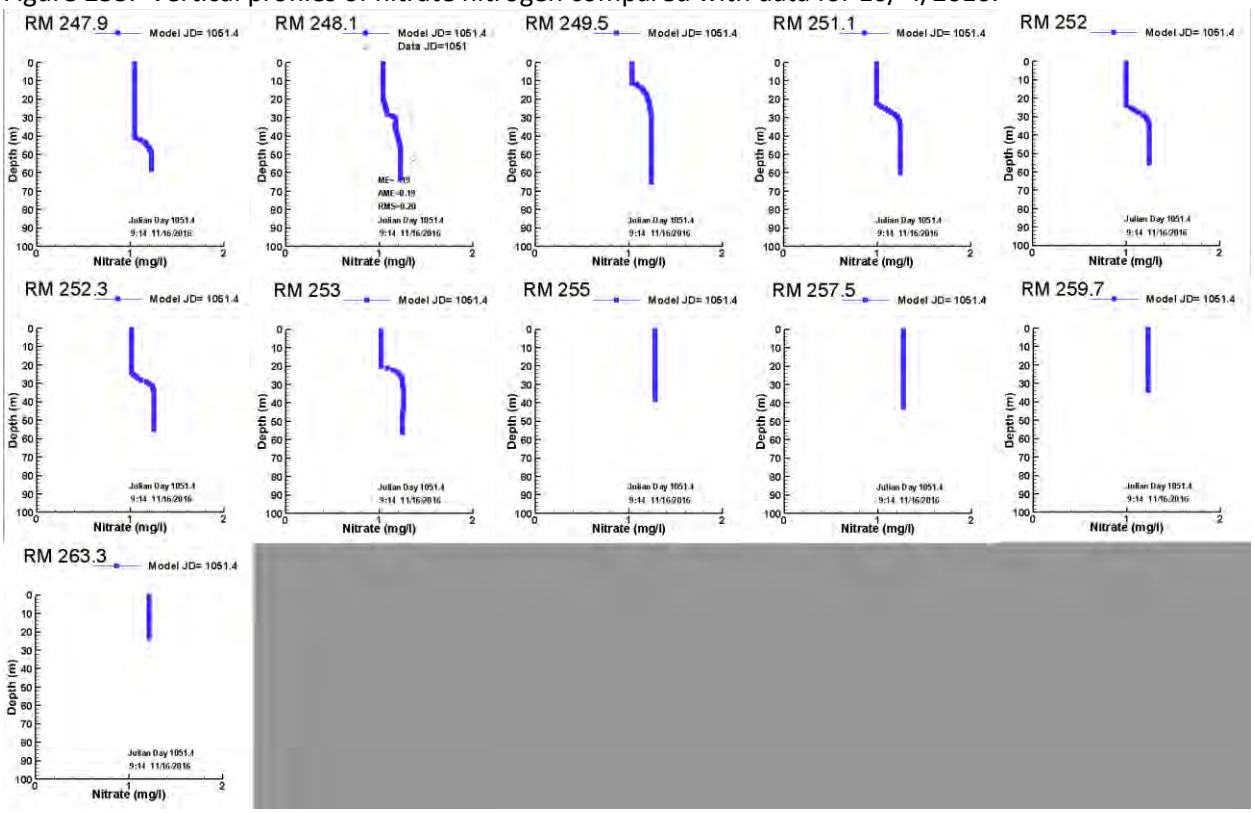


Figure 254. Vertical profiles of nitrate nitrogen compared with data for 11/16/2016.

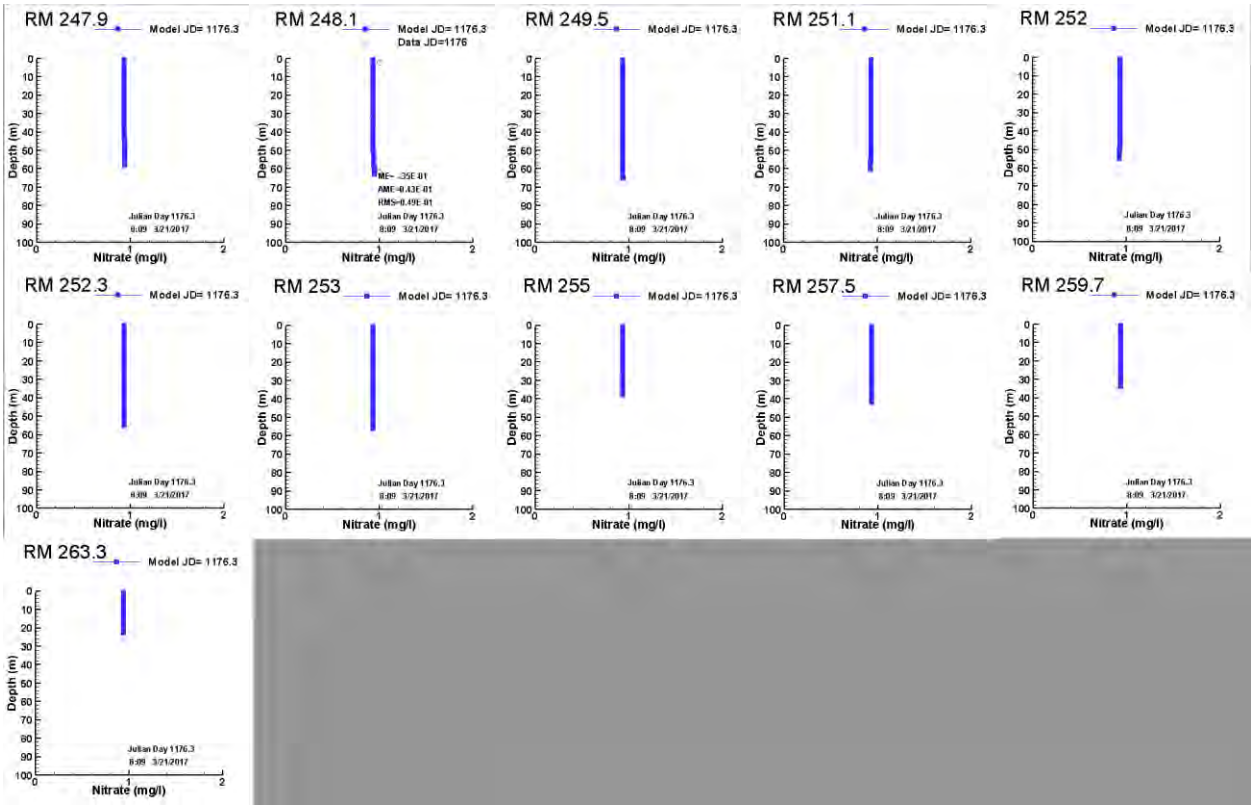


Figure 255. Vertical profiles of nitrate nitrogen compared with data for 3/21/2017.

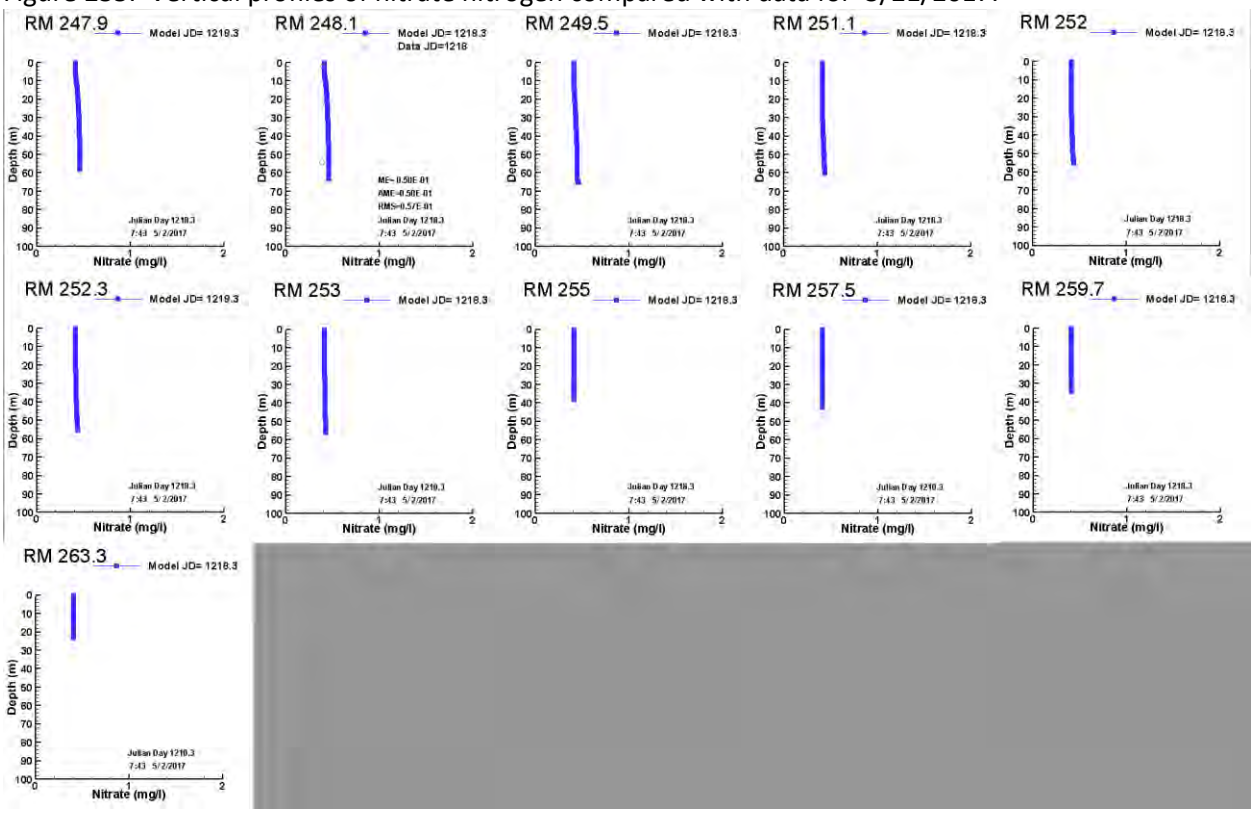


Figure 256. Vertical profiles of nitrate nitrogen compared with data for 5/ 2/2017.

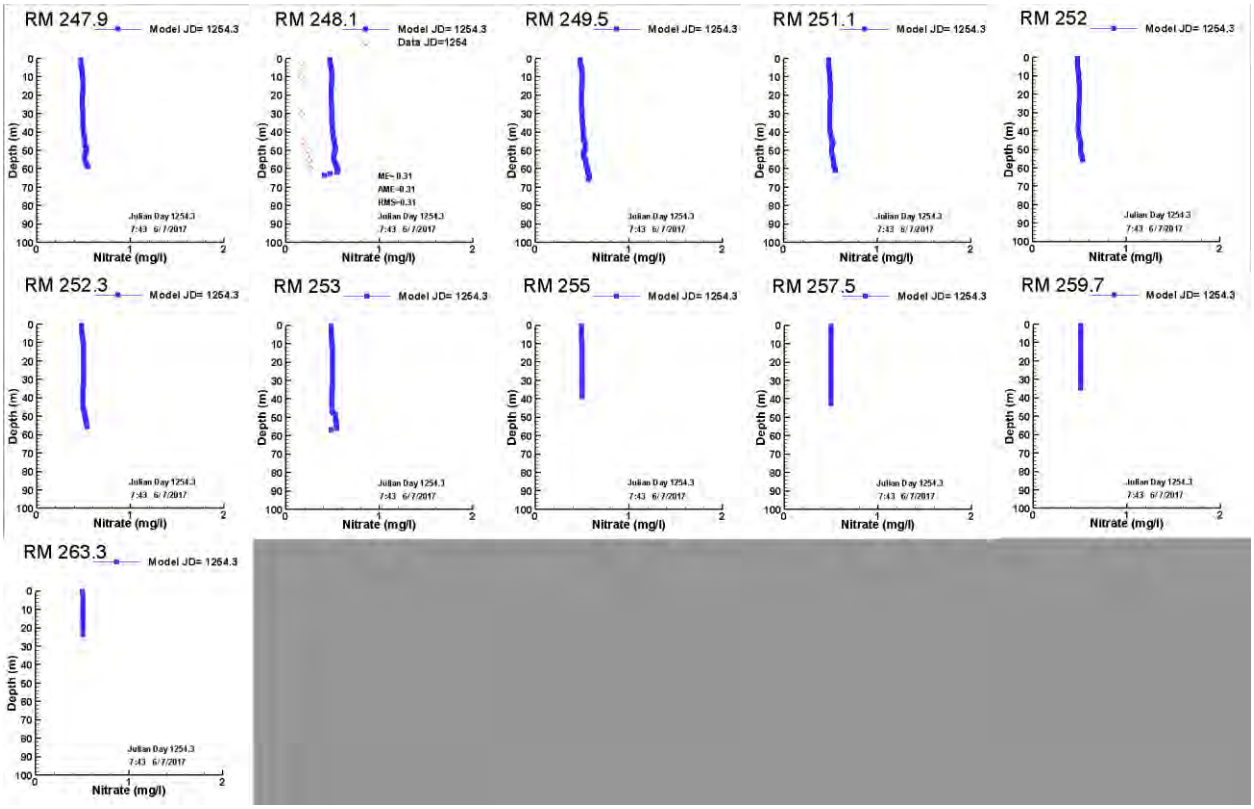


Figure 257. Vertical profiles of nitrate nitrogen compared with data for 6/ 7/2017.

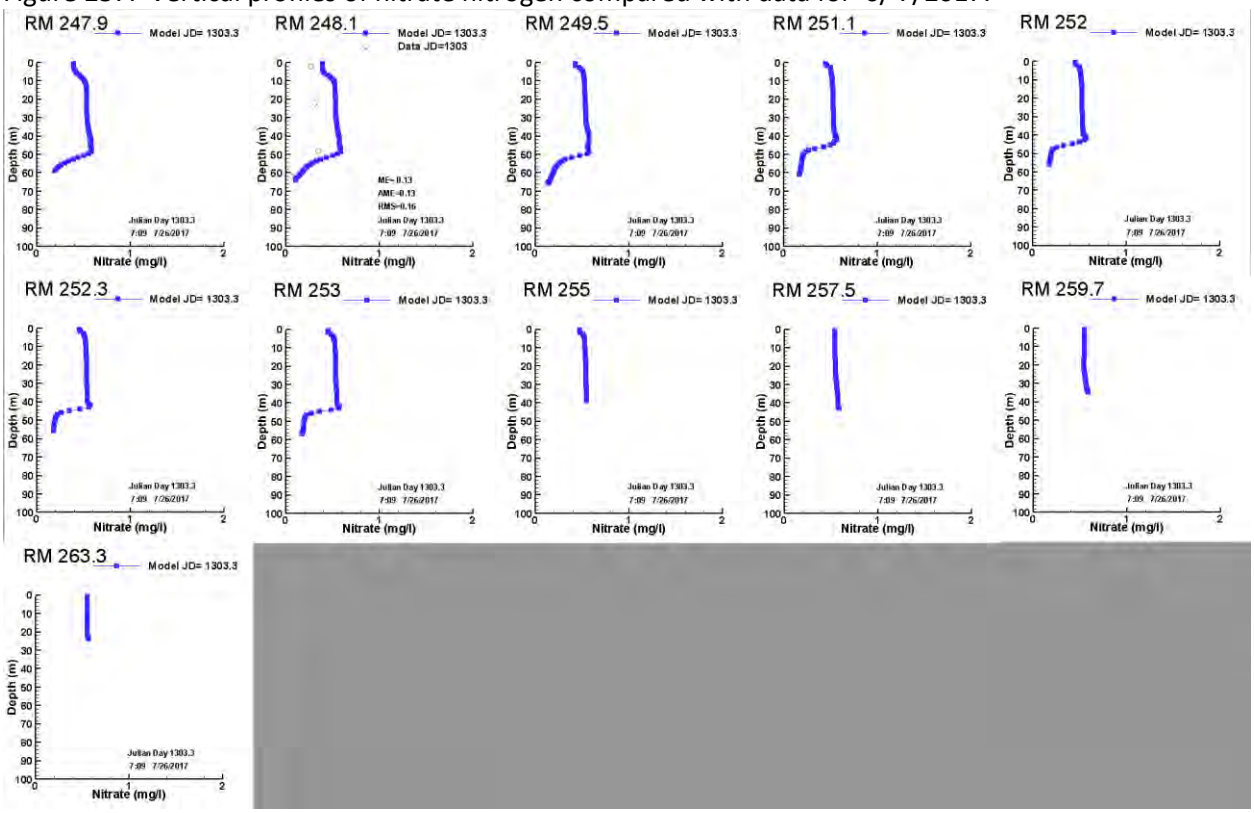


Figure 258. Vertical profiles of nitrate nitrogen compared with data for 7/26/2017.

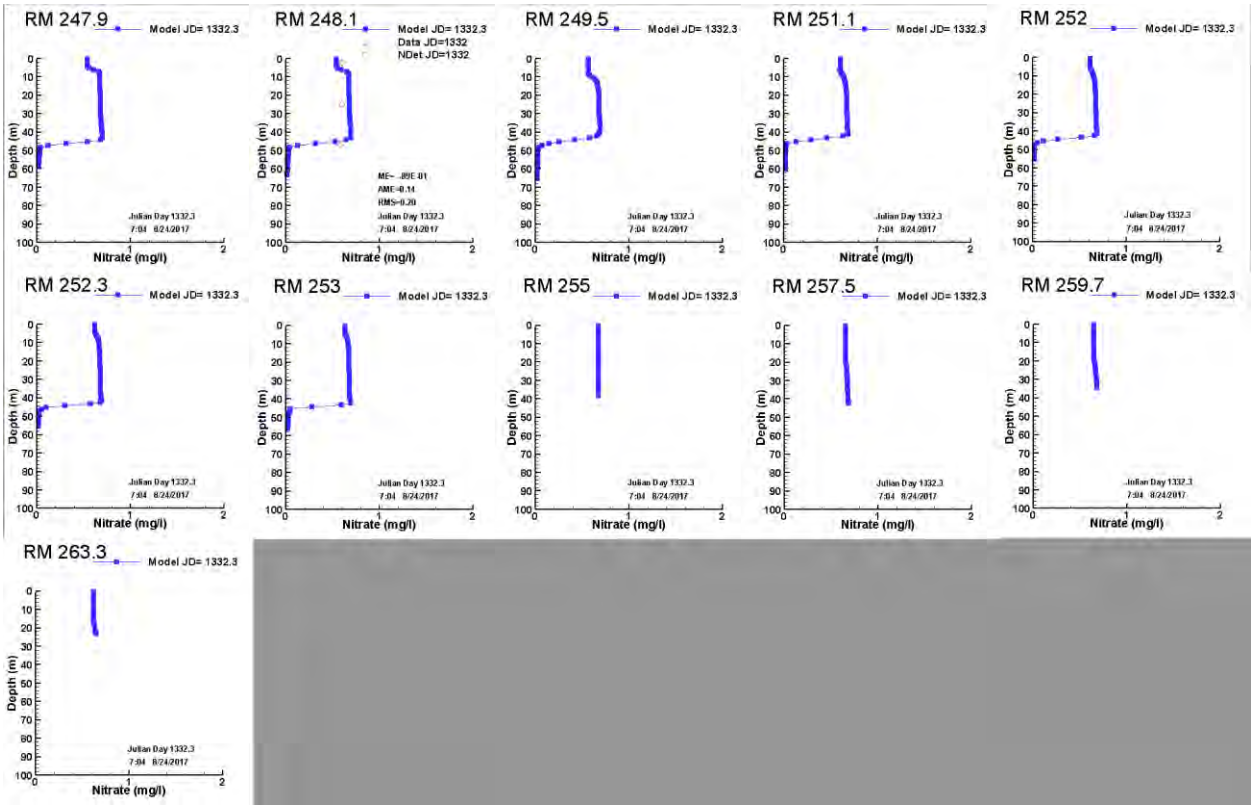


Figure 259. Vertical profiles of nitrate nitrogen compared with data for 8/24/2017.

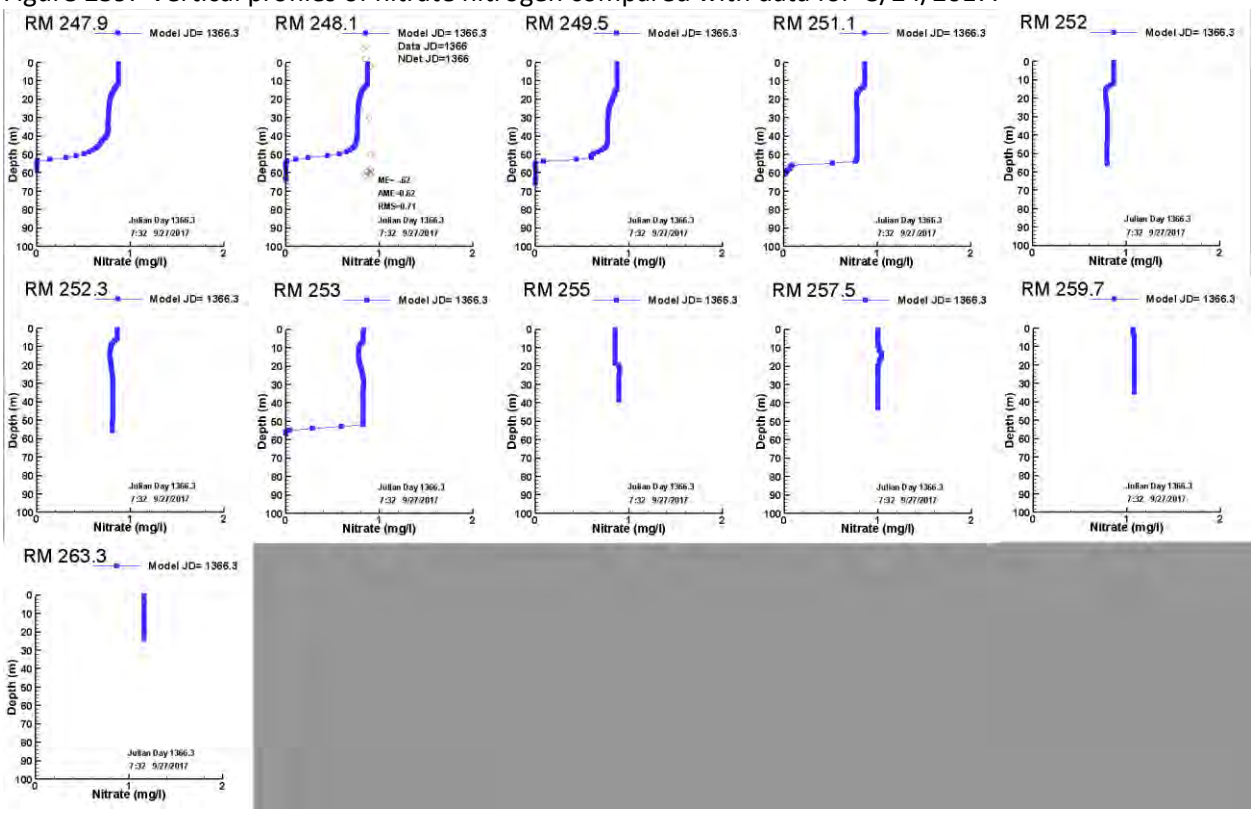


Figure 260. Vertical profiles of nitrate nitrogen compared with data for 9/27/2017.

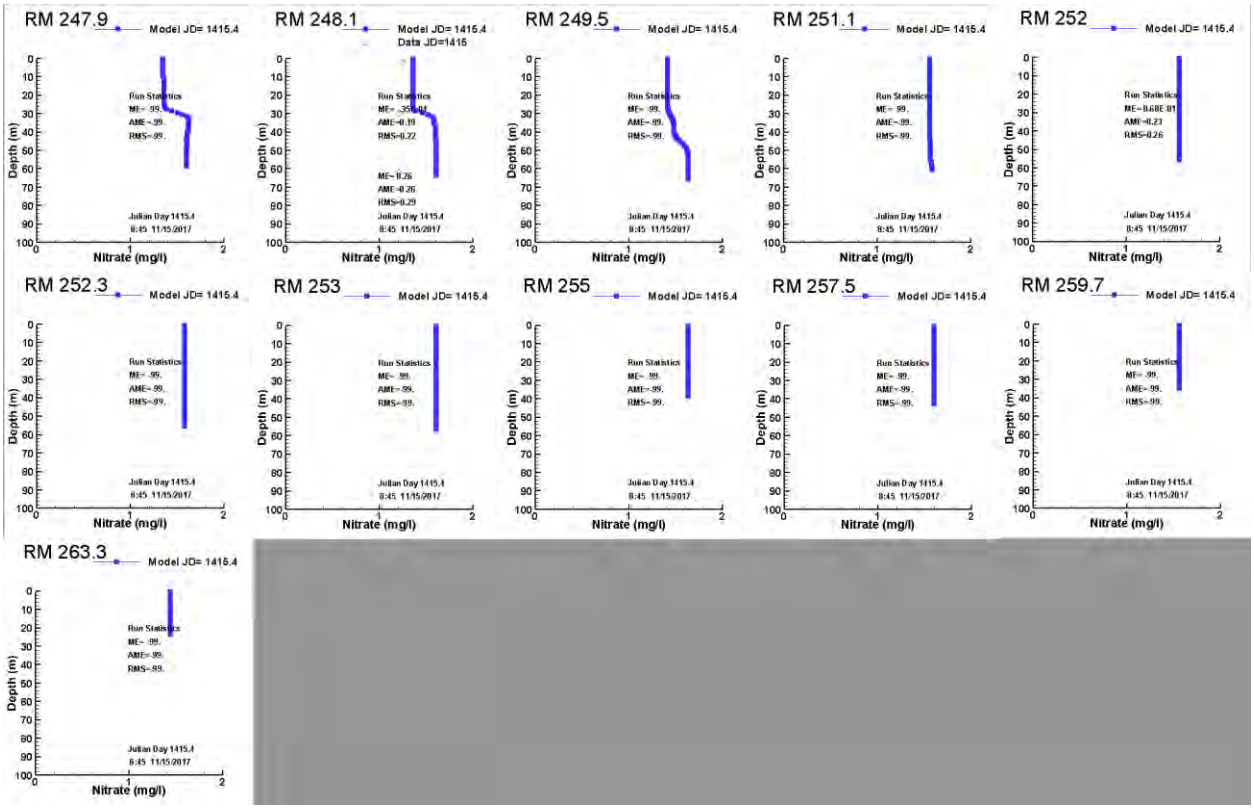


Figure 261. Vertical profiles of nitrate nitrogen compared with data for 11/15/2017.

Dissolved Oxygen

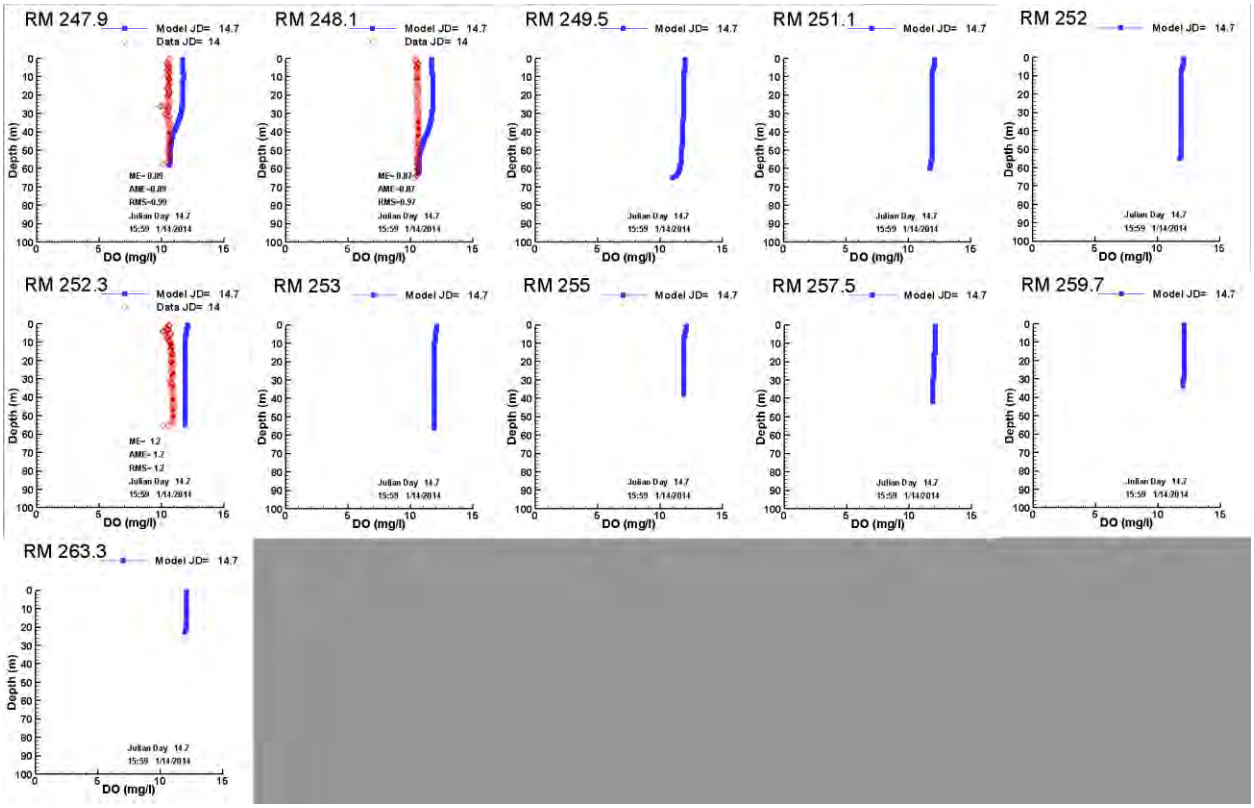


Figure 262. Vertical profiles of DO compared with data for 1/14/2014.

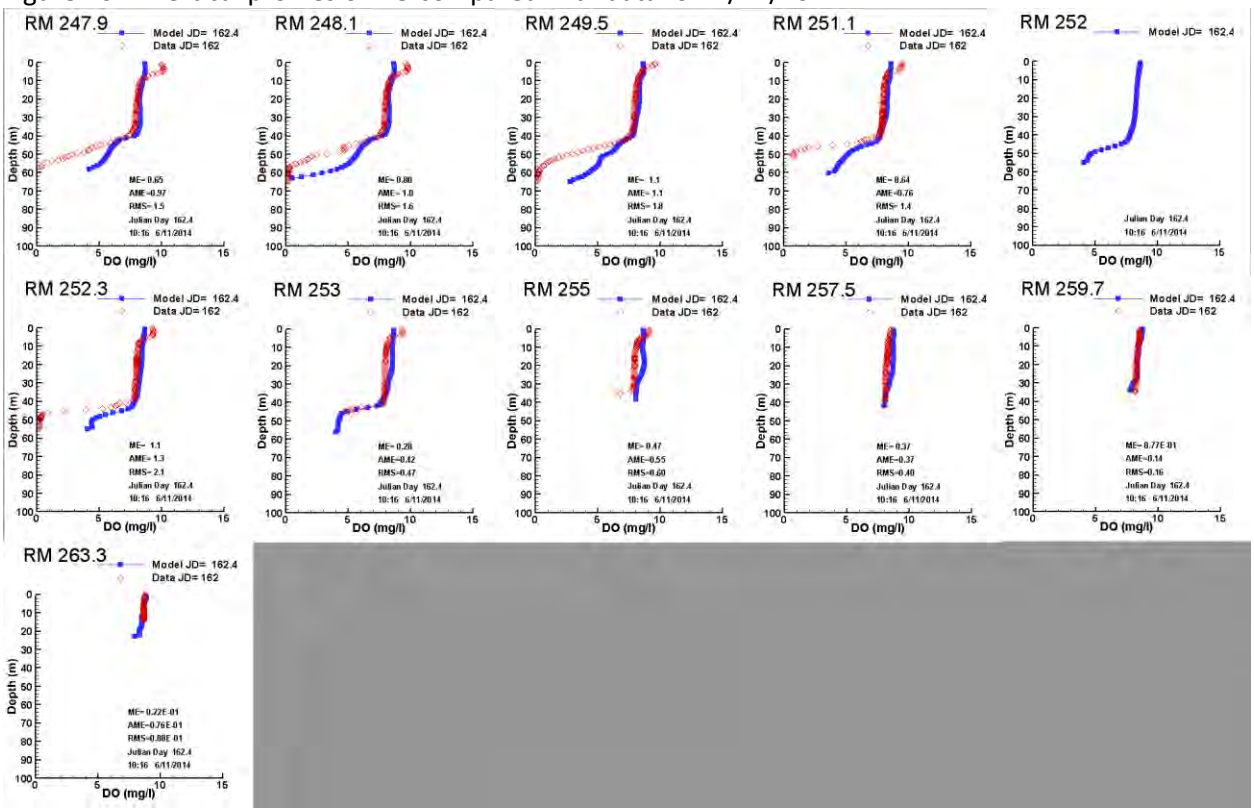


Figure 263. Vertical profiles of DO compared with data for 6/11/2014.

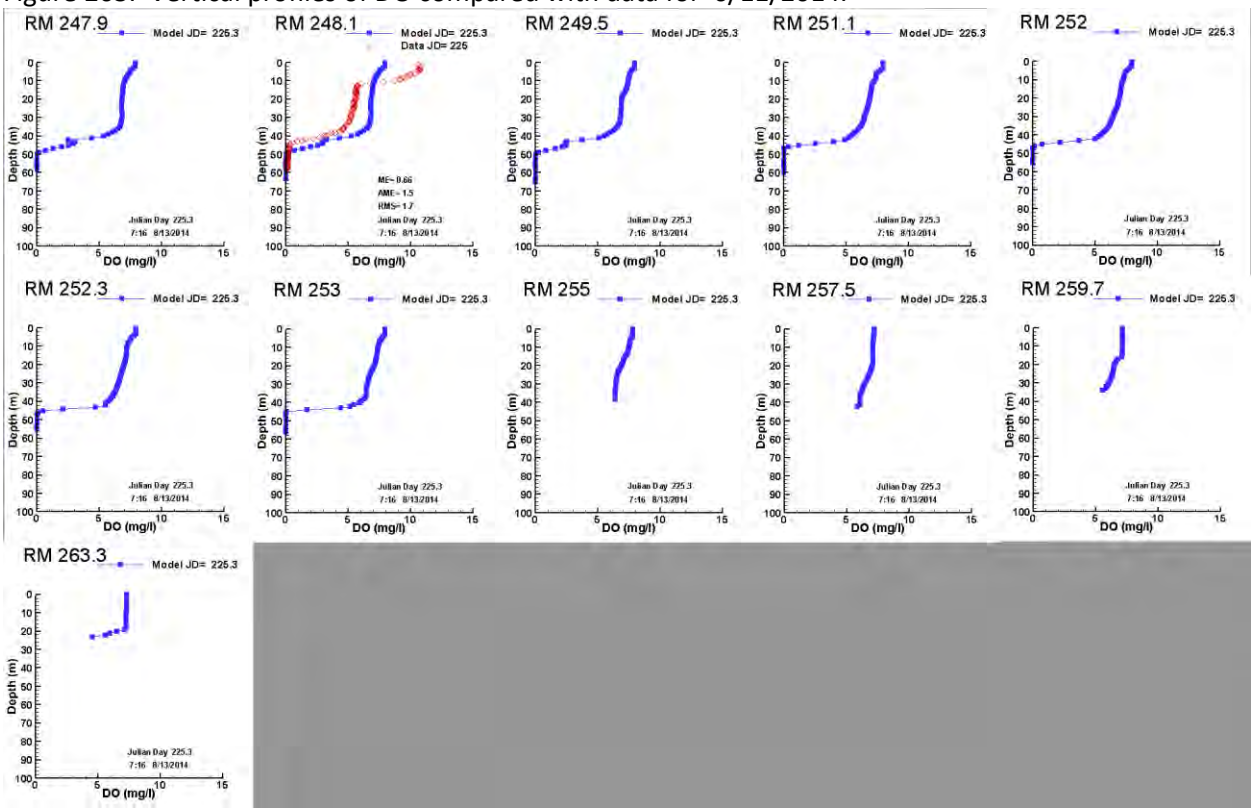


Figure 264. Vertical profiles of DO compared with data for 8/13/2014.

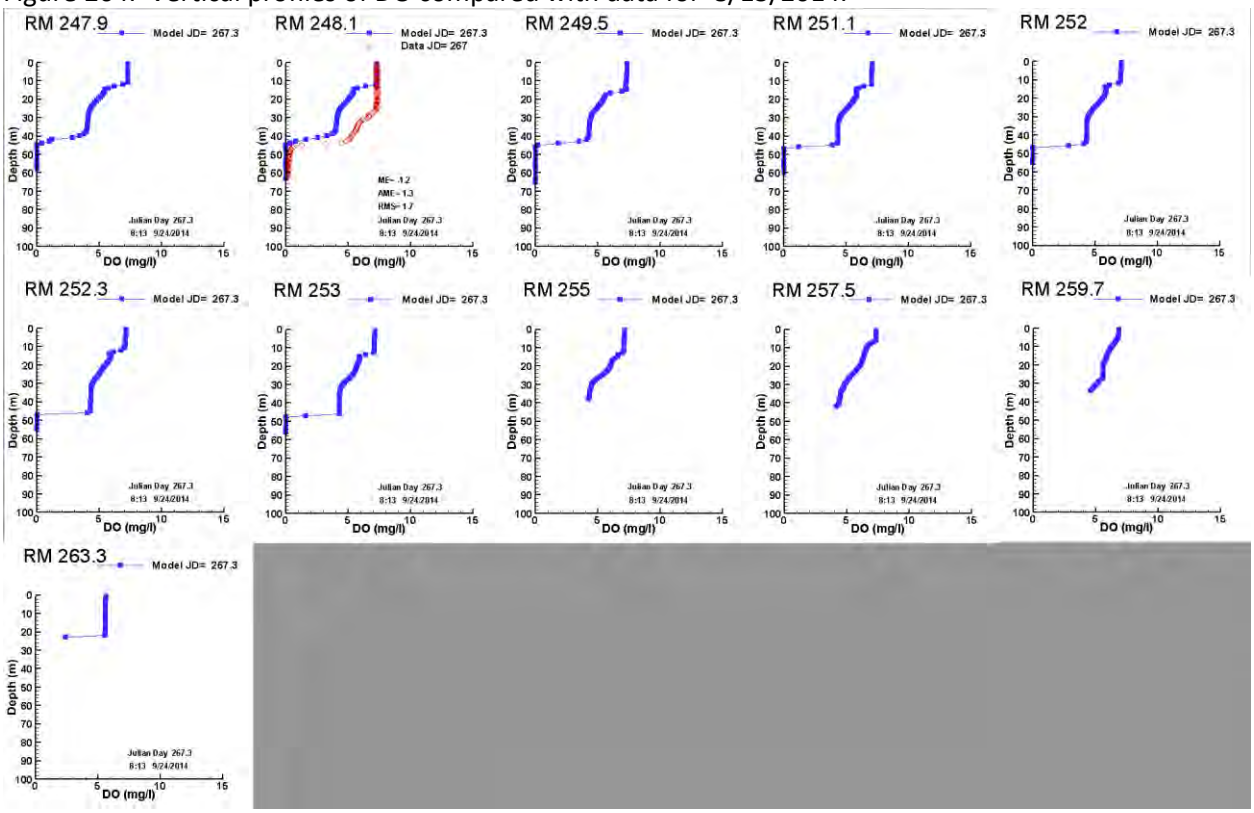


Figure 265. Vertical profiles of DO compared with data for 9/24/2014.

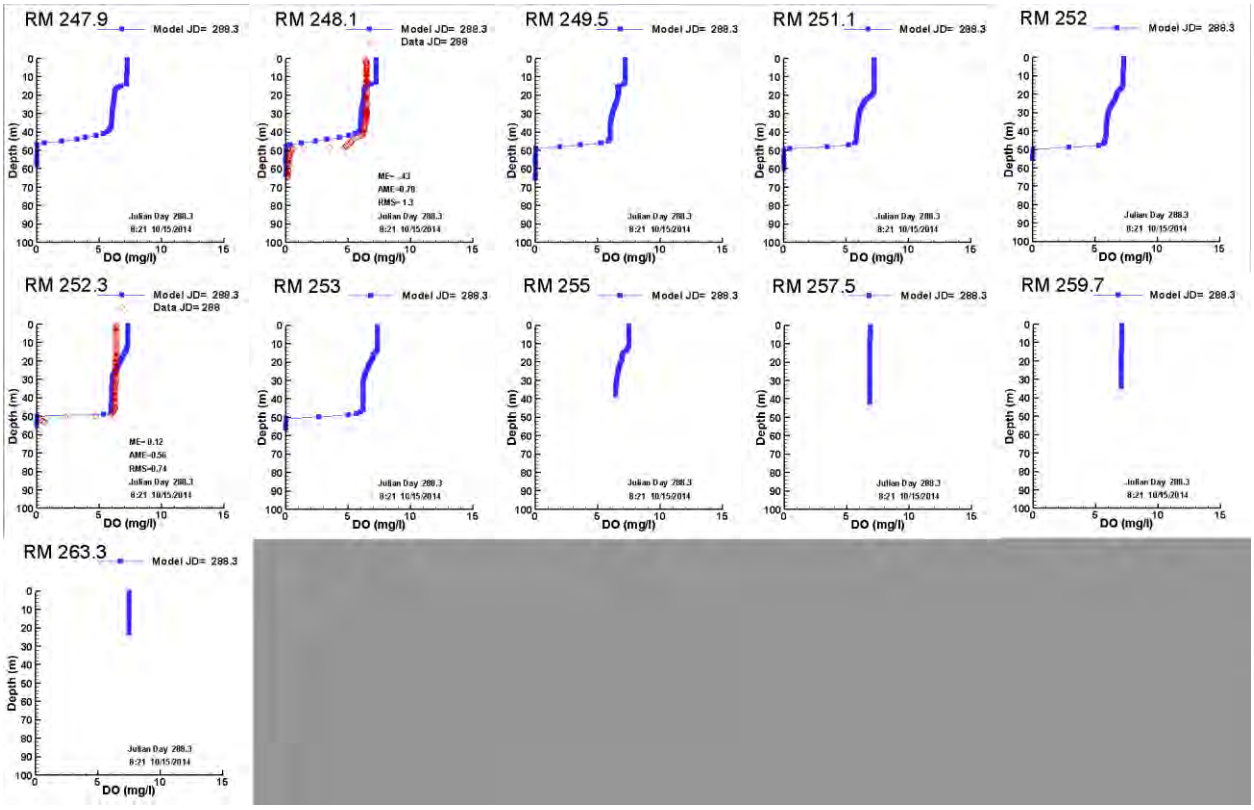


Figure 266. Vertical profiles of DO compared with data for 10/15/2014.

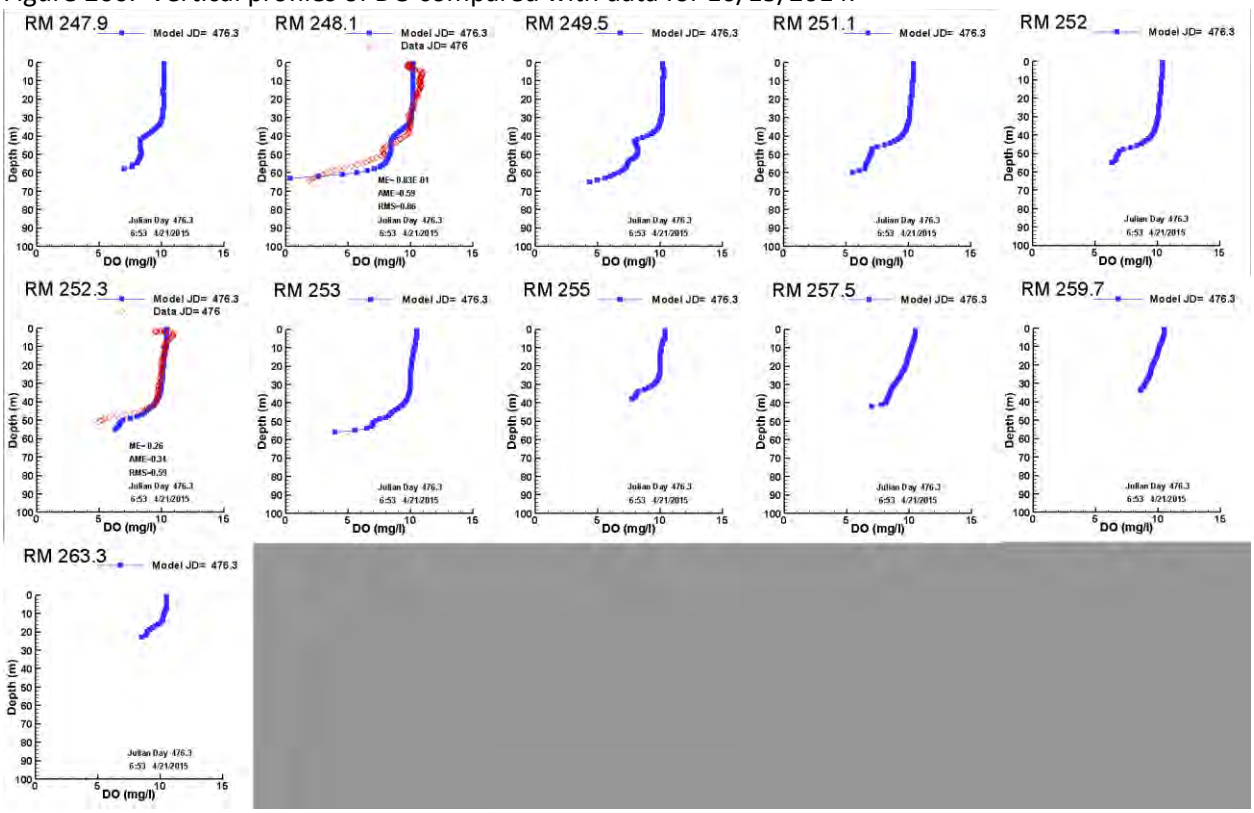


Figure 267. Vertical profiles of DO compared with data for 4/21/2015.

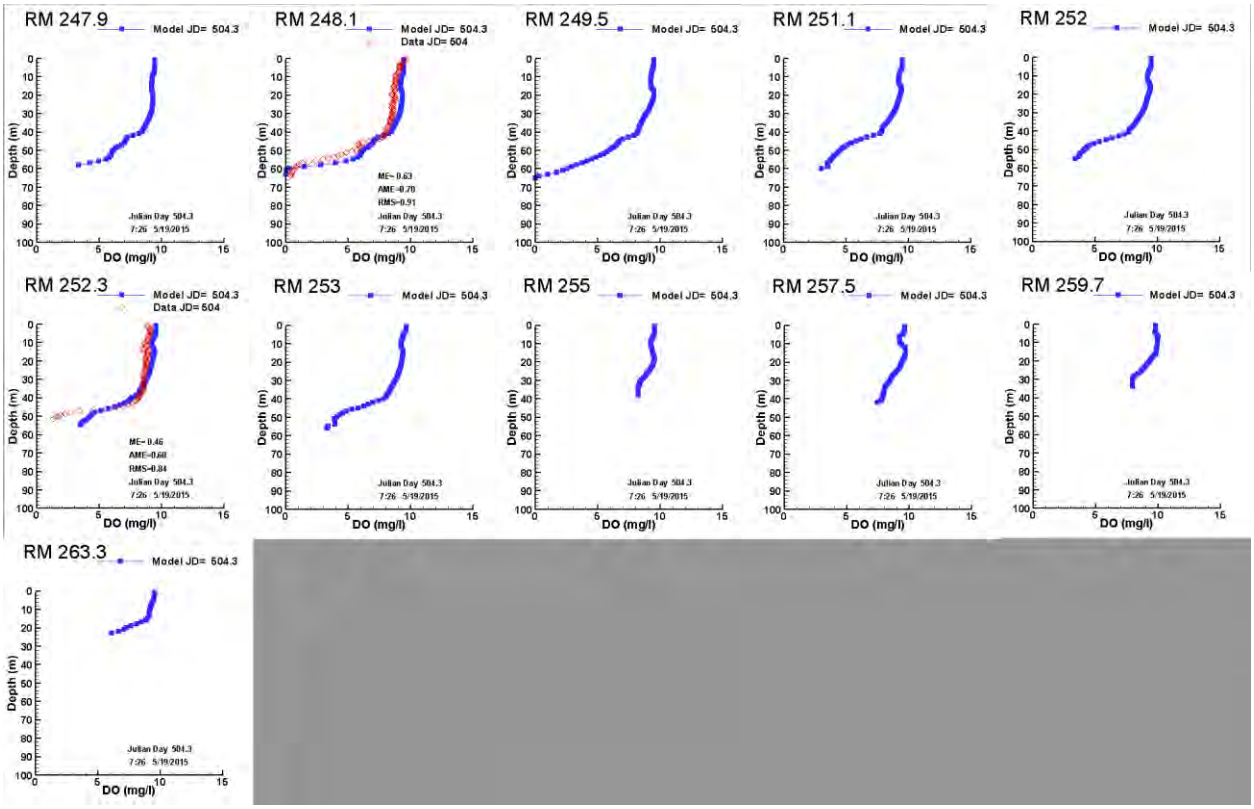


Figure 268. Vertical profiles of DO compared with data for 5/19/2015.

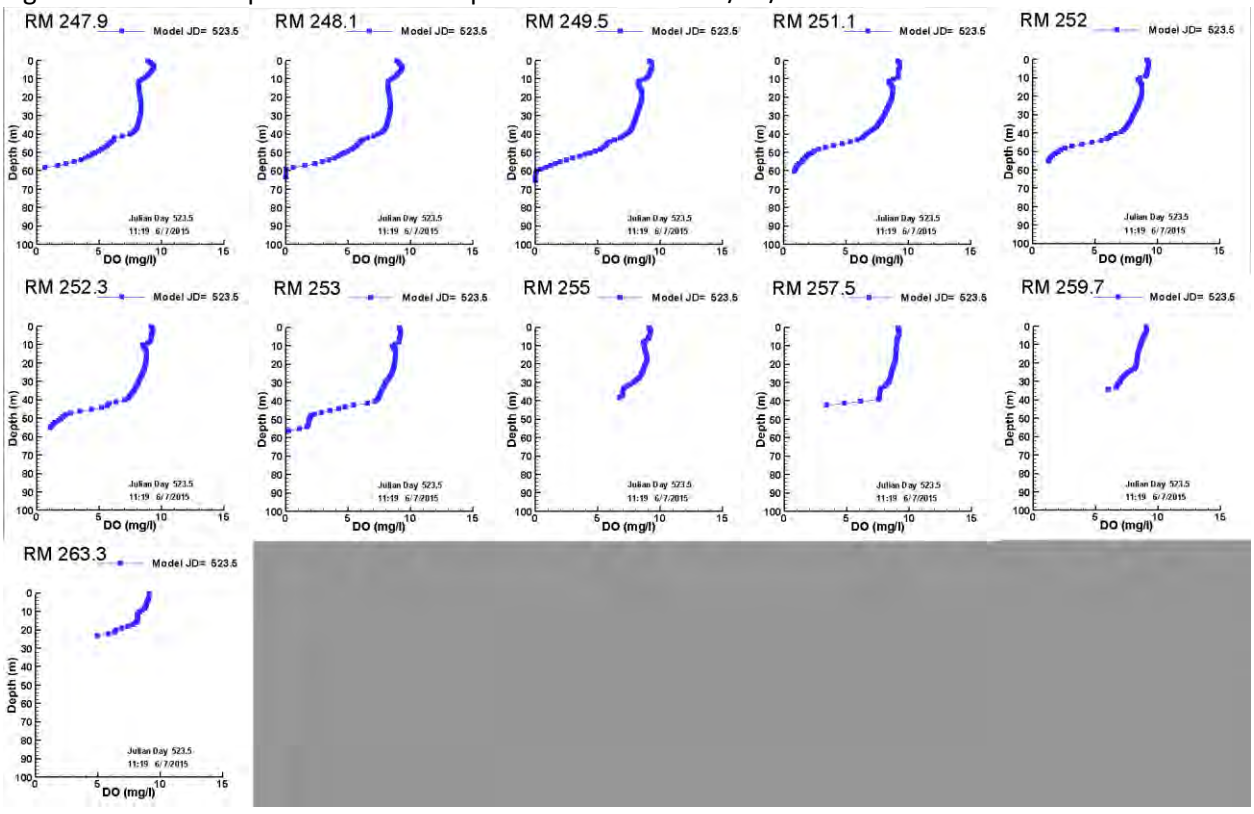


Figure 269. Vertical profiles of DO compared with data for 6/ 7/2015.

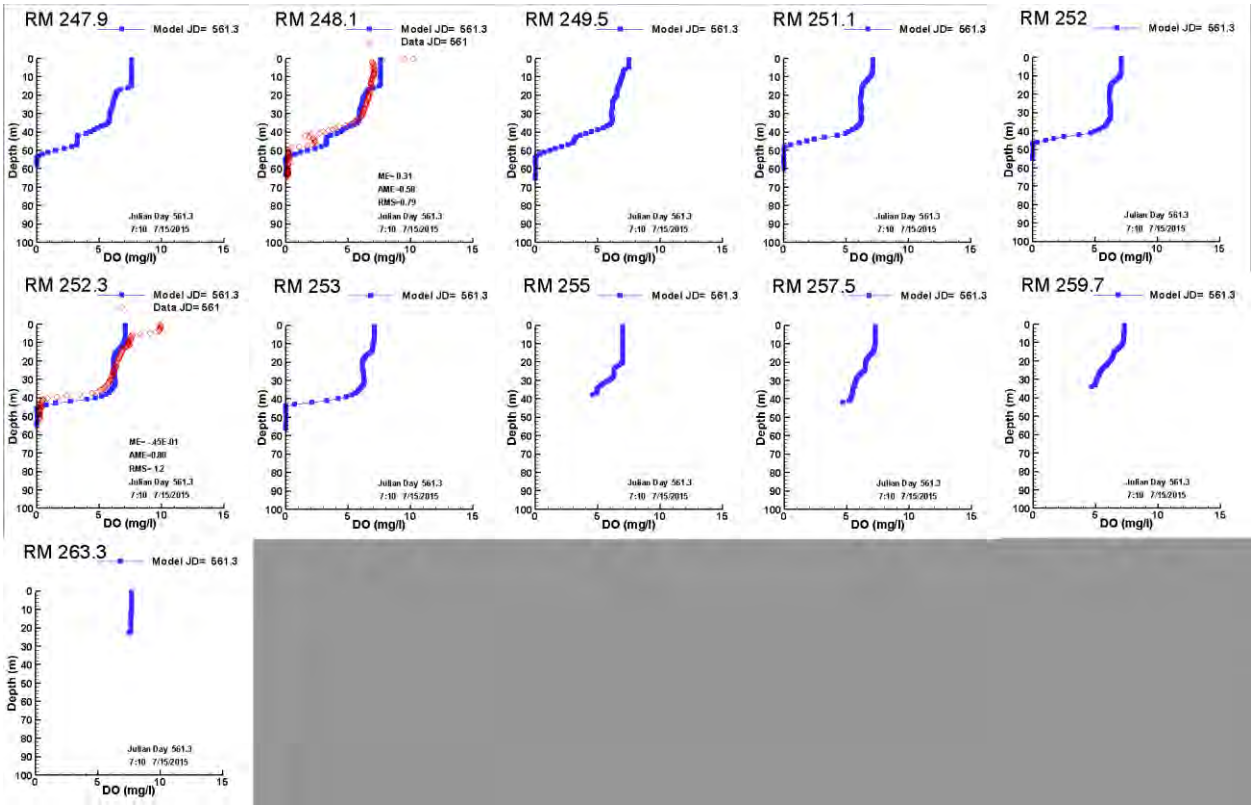


Figure 270. Vertical profiles of DO compared with data for 7/15/2015.

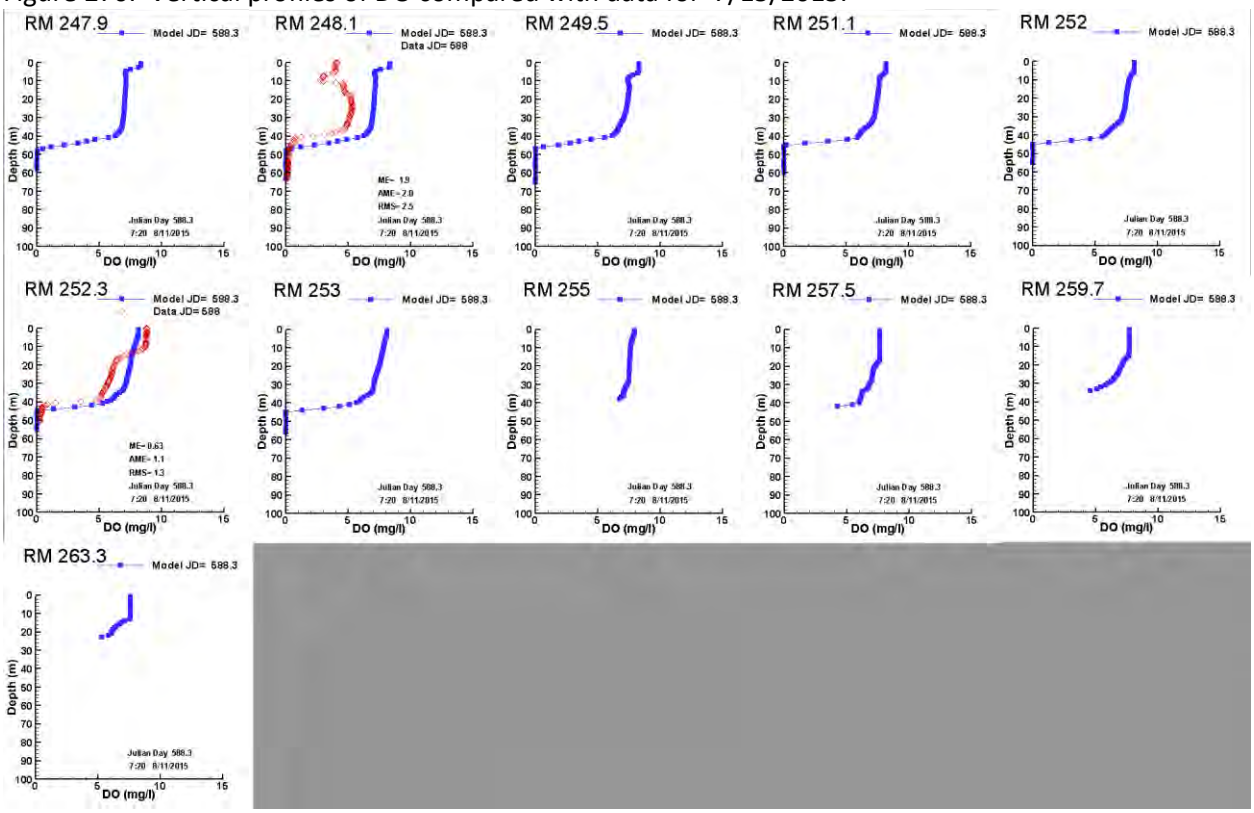


Figure 271. Vertical profiles of DO compared with data for 8/11/2015.

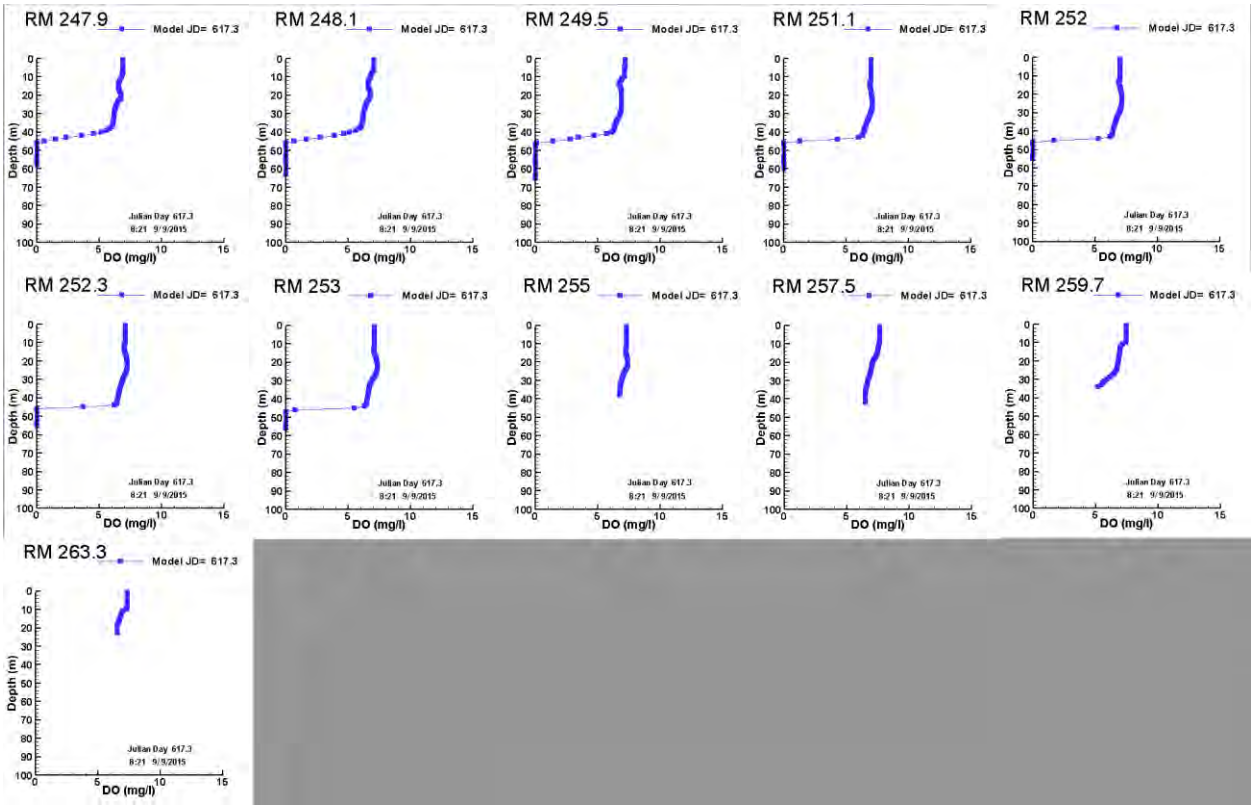


Figure 272. Vertical profiles of DO compared with data for 9/ 9/2015.

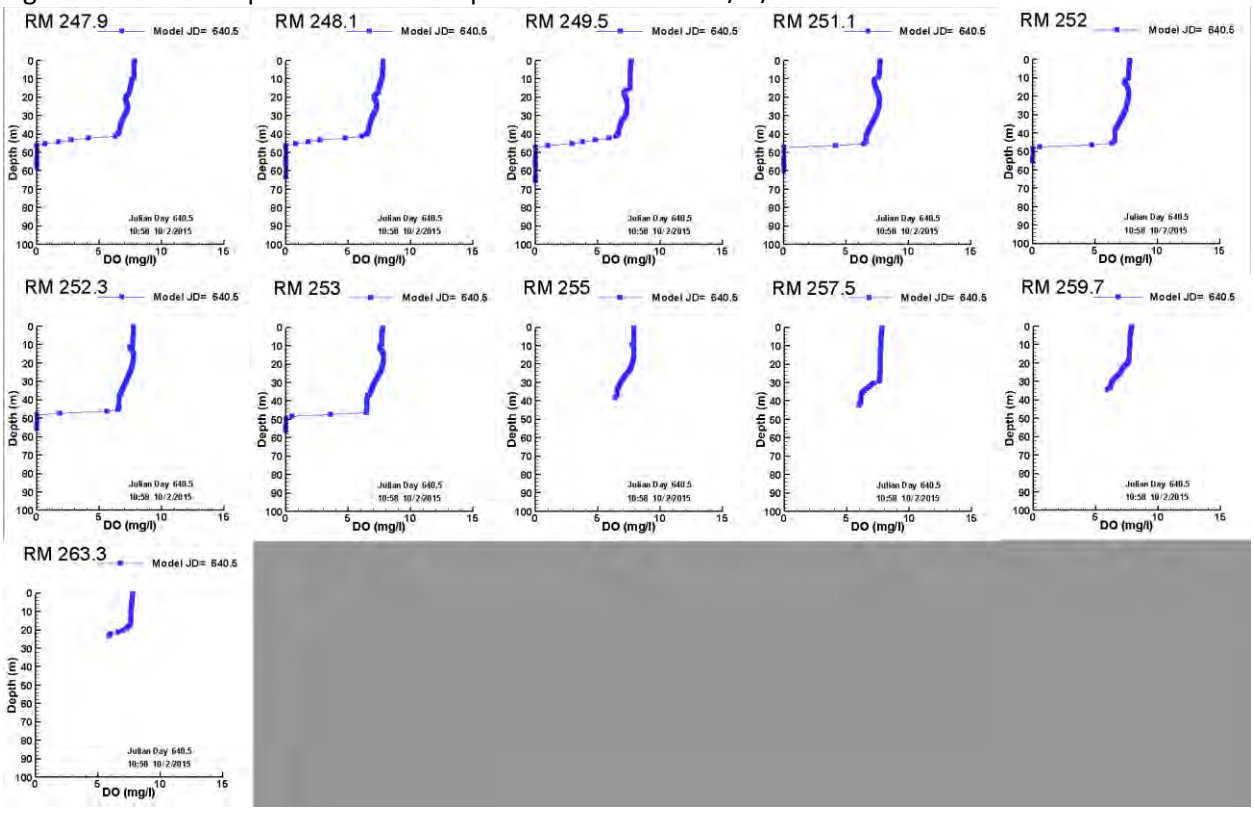


Figure 273. Vertical profiles of DO compared with data for 10/ 2/2015.

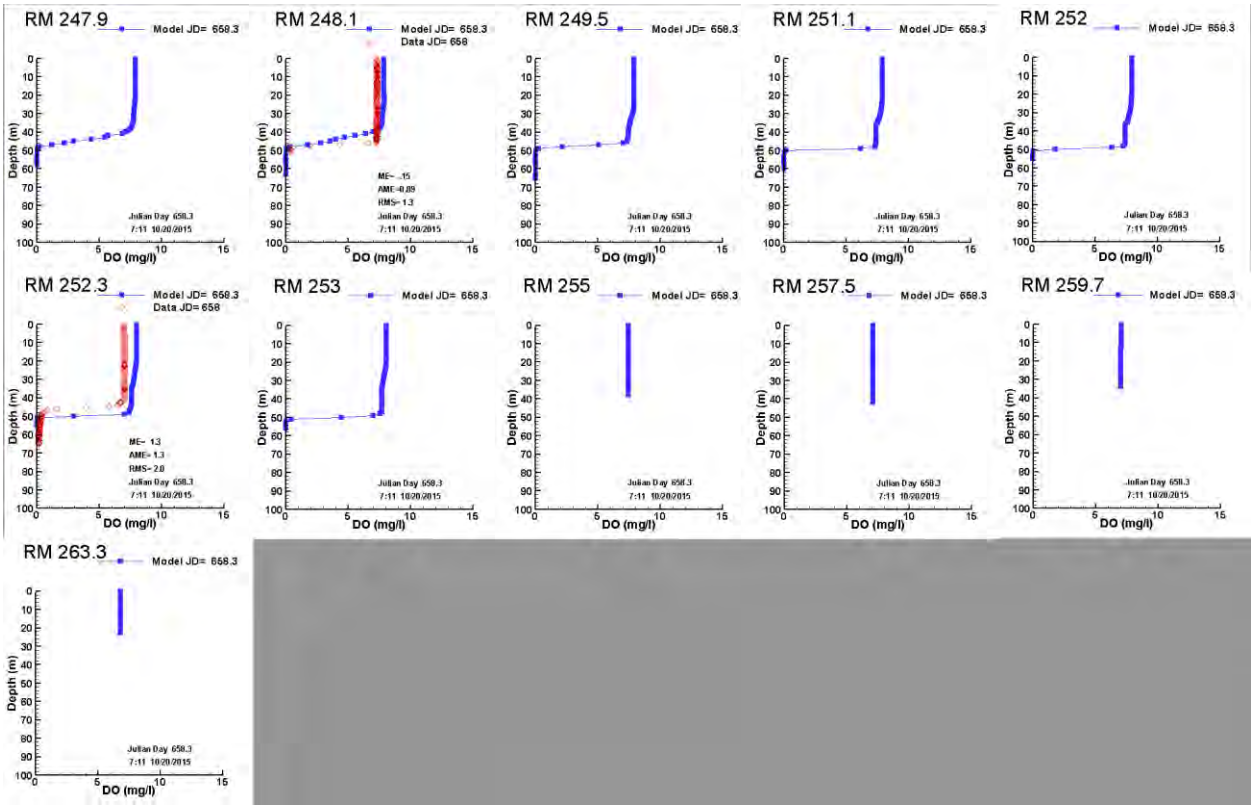


Figure 274. Vertical profiles of DO compared with data for 10/20/2015.

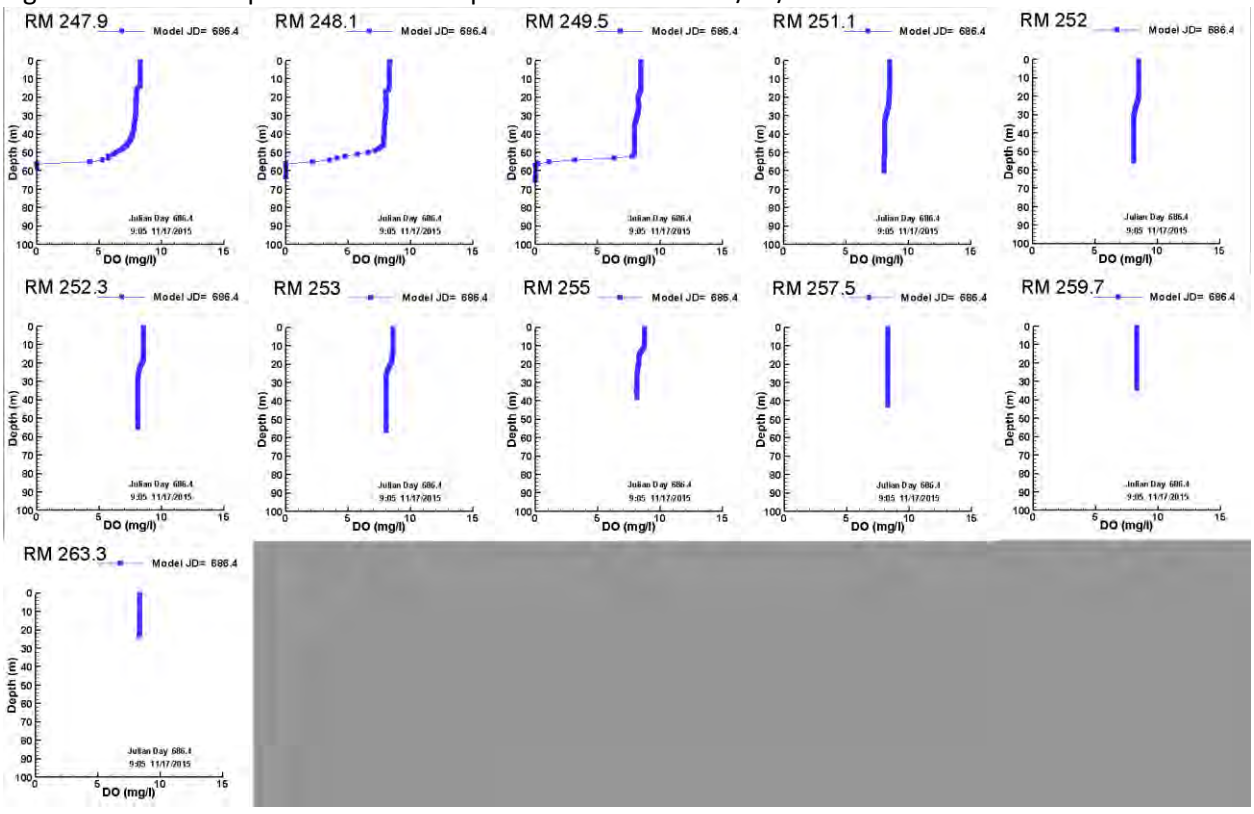


Figure 275. Vertical profiles of DO compared with data for 11/17/2015.

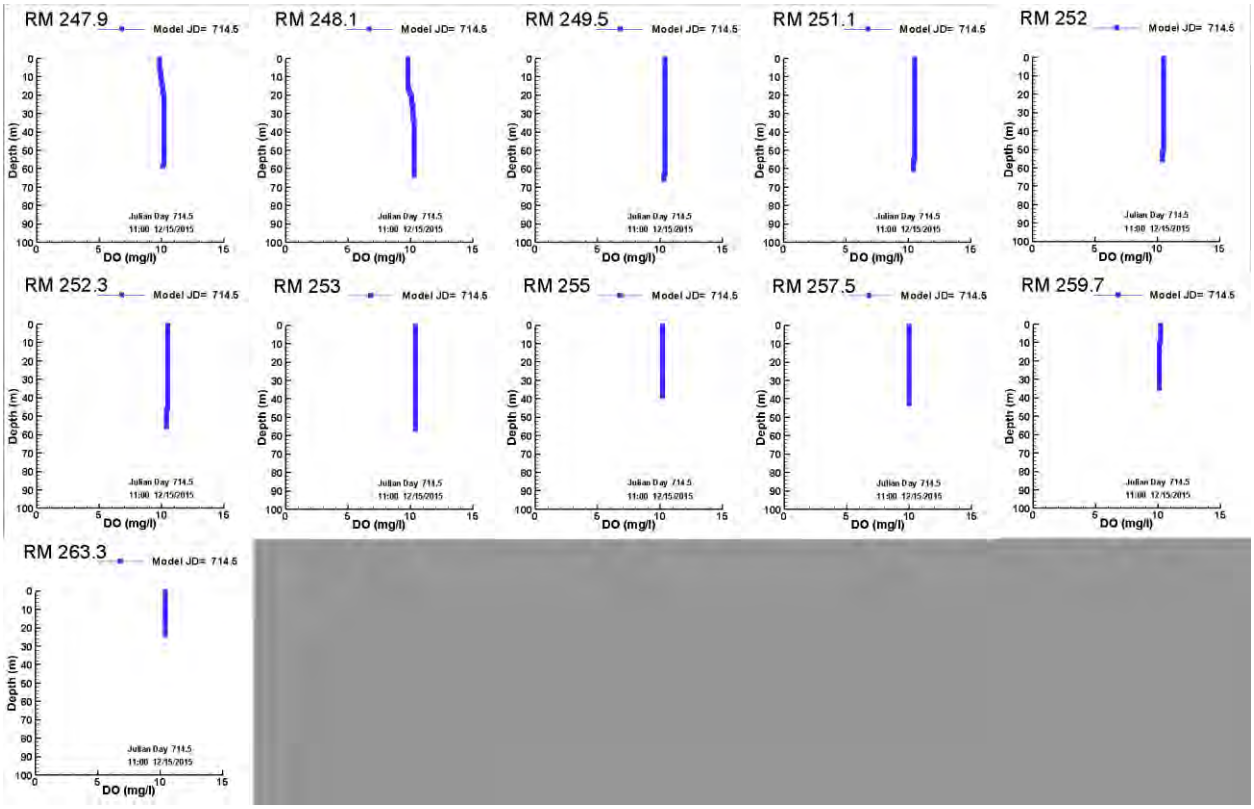


Figure 276. Vertical profiles of DO compared with data for 12/15/2015.

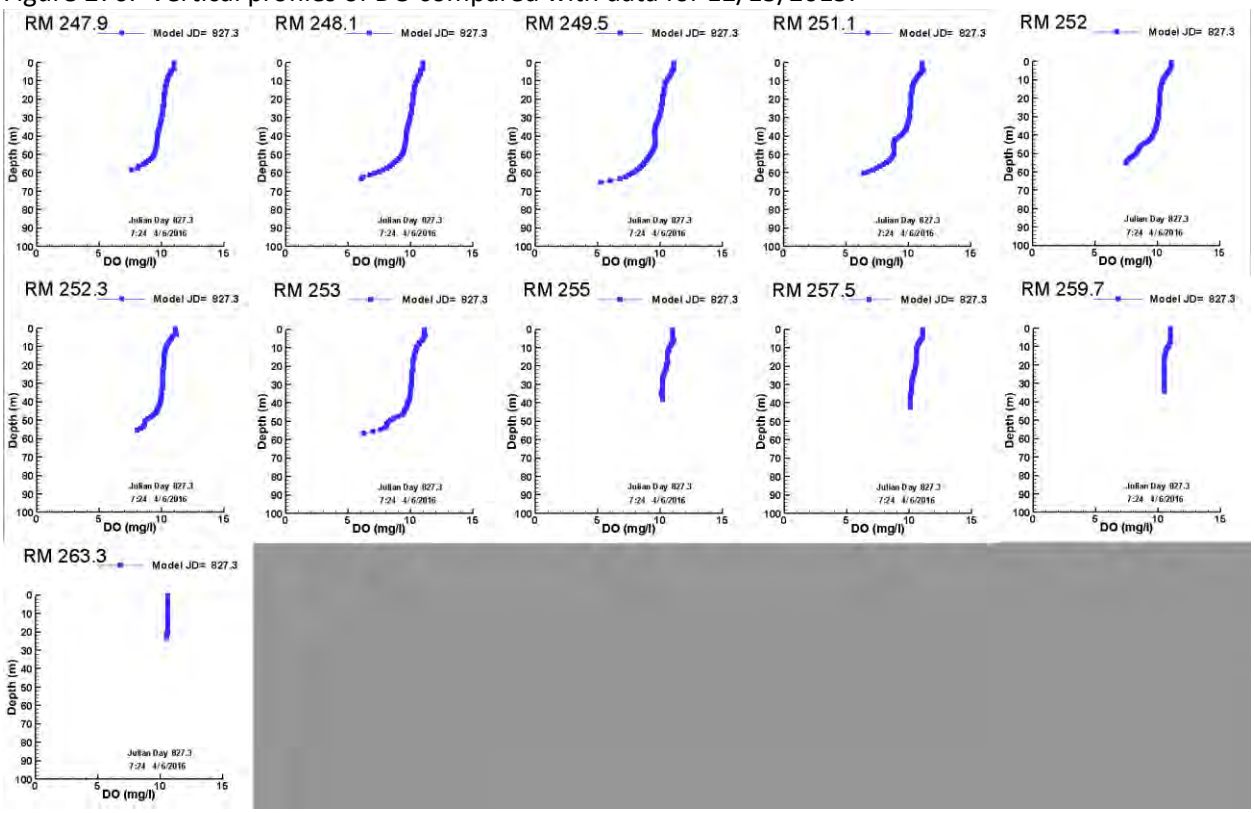


Figure 277. Vertical profiles of DO compared with data for 4/ 6/2016.

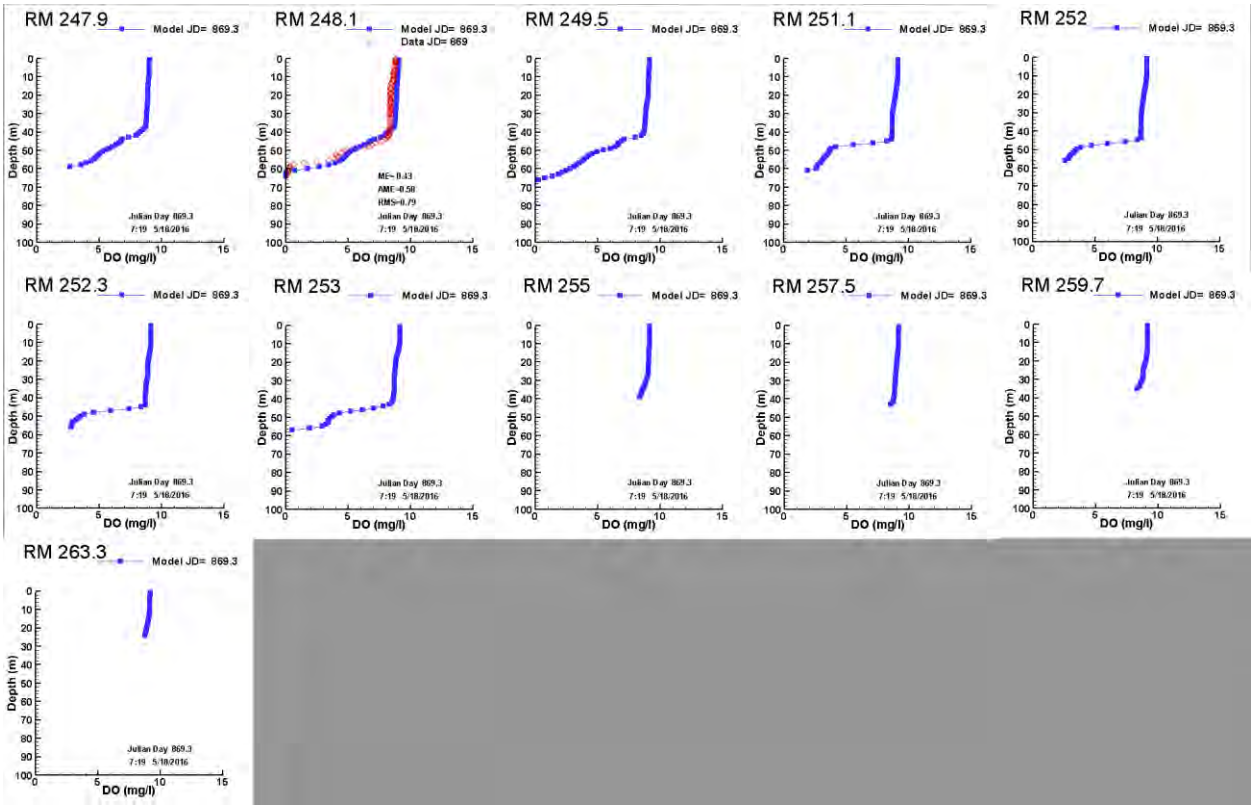


Figure 278. Vertical profiles of DO compared with data for 5/18/2016.

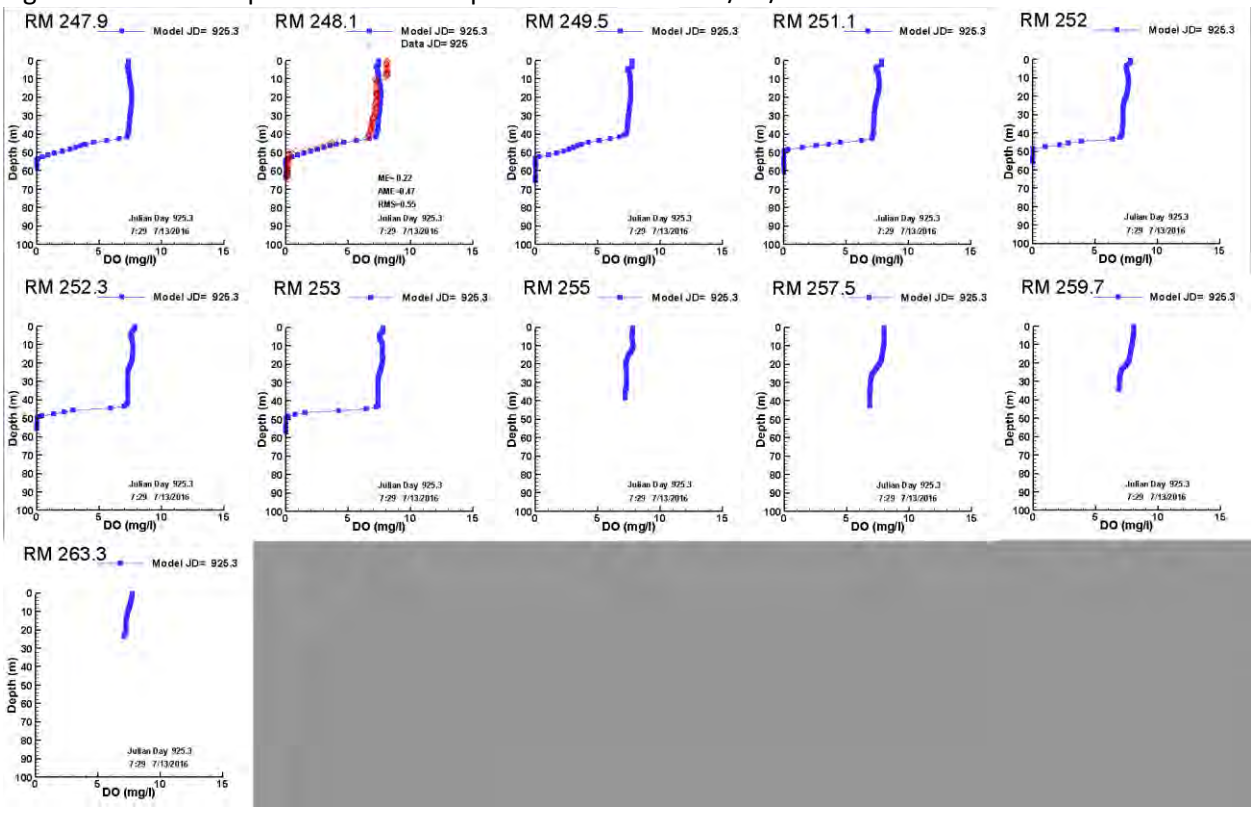


Figure 279. Vertical profiles of DO compared with data for 7/13/2016.

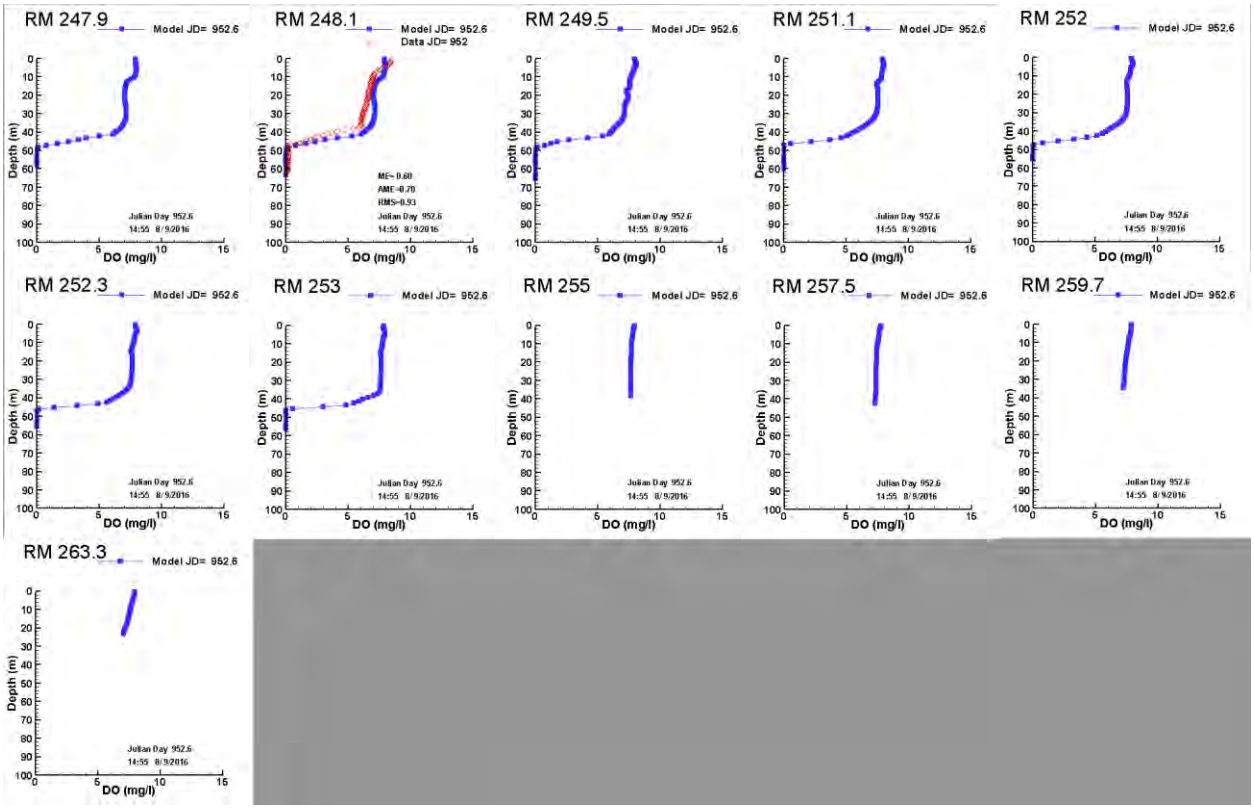


Figure 280. Vertical profiles of DO compared with data for 8/ 9/2016.

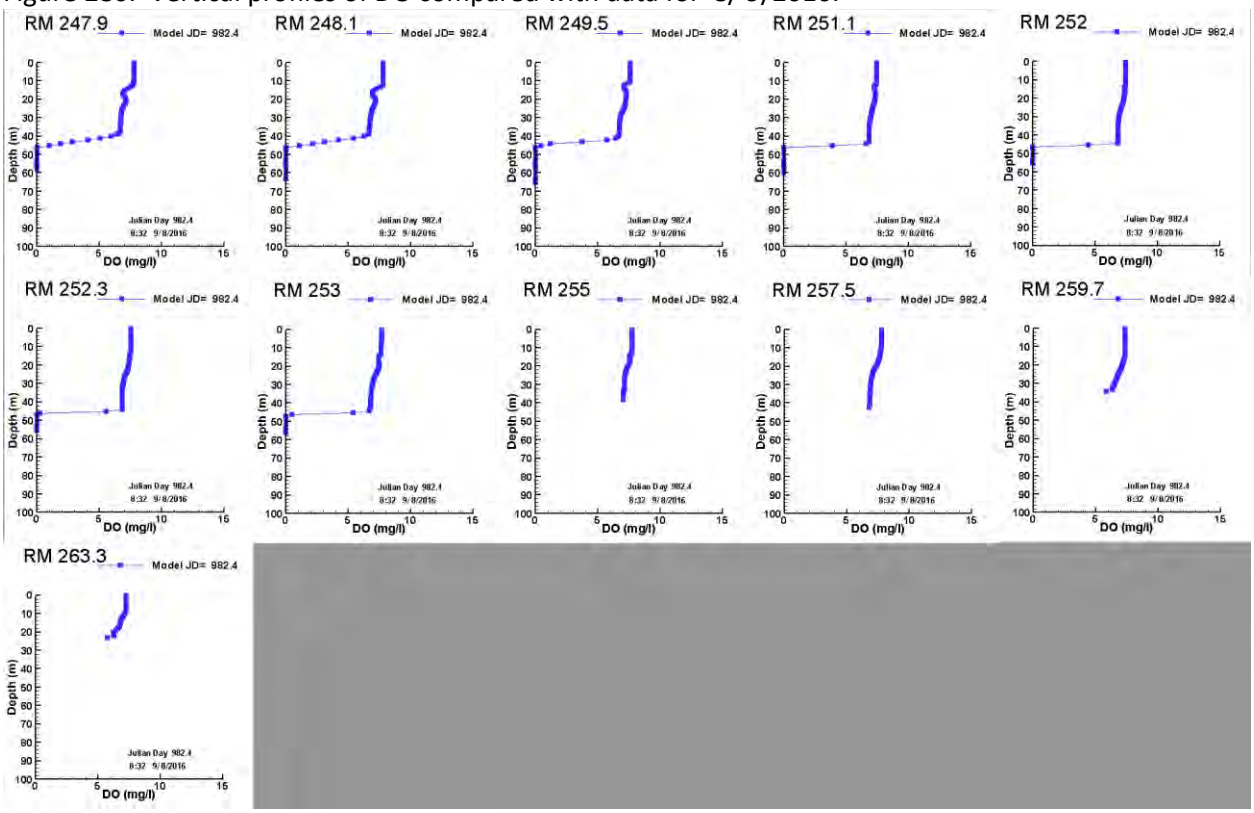


Figure 281. Vertical profiles of DO compared with data for 9/ 8/2016.

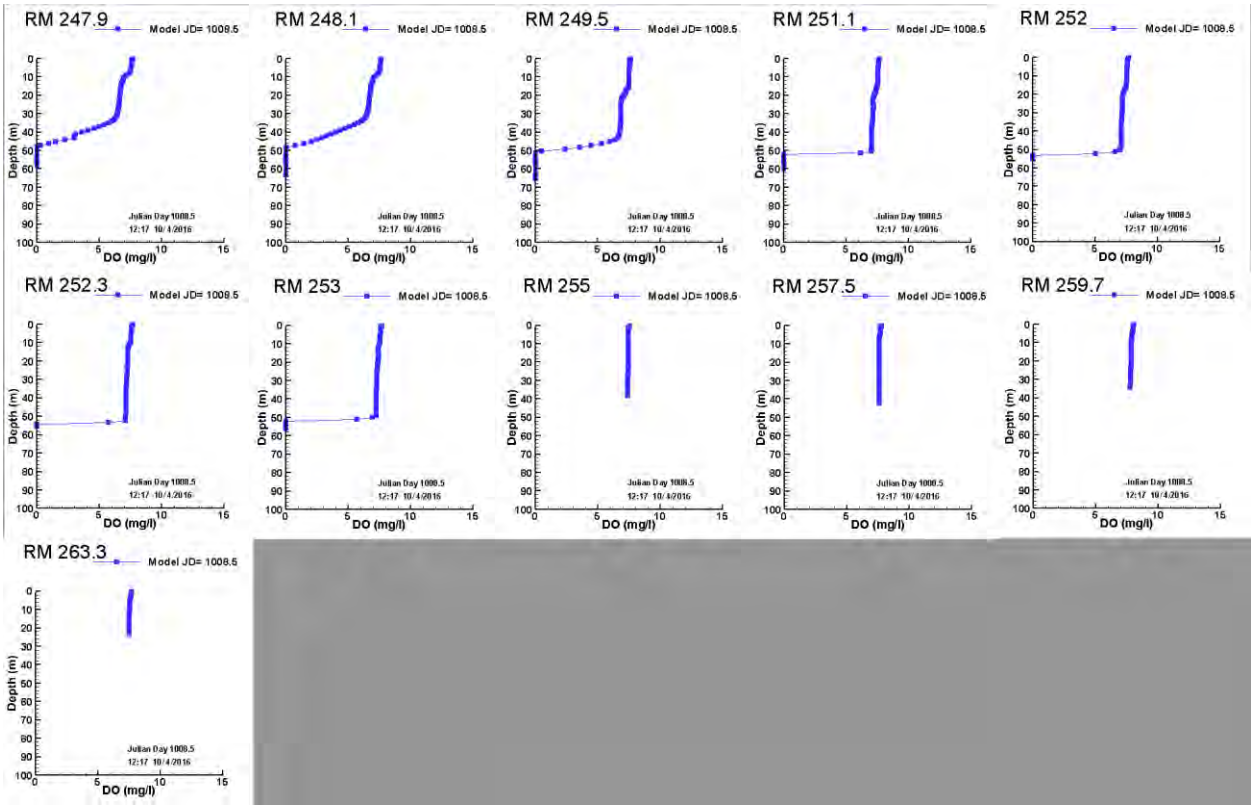


Figure 282. Vertical profiles of DO compared with data for 10/ 4/2016.

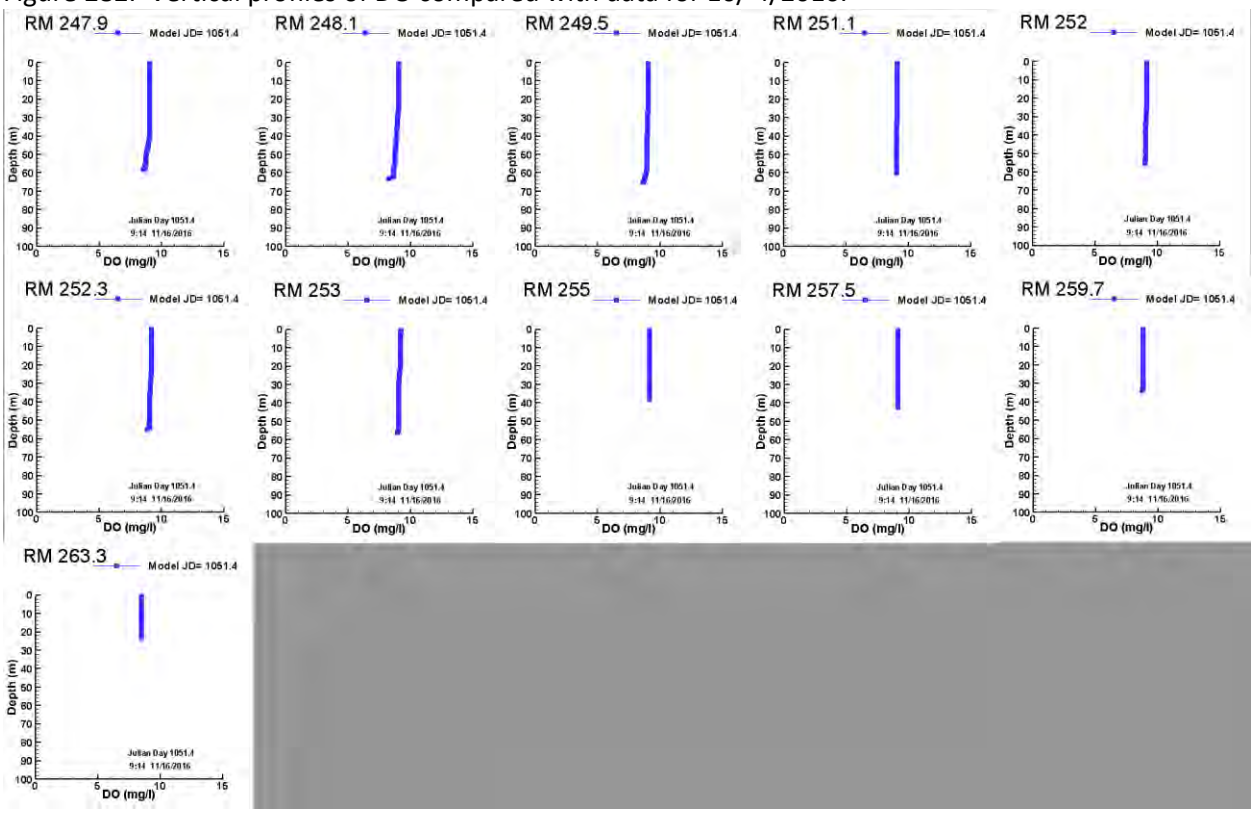


Figure 283. Vertical profiles of DO compared with data for 11/16/2016.

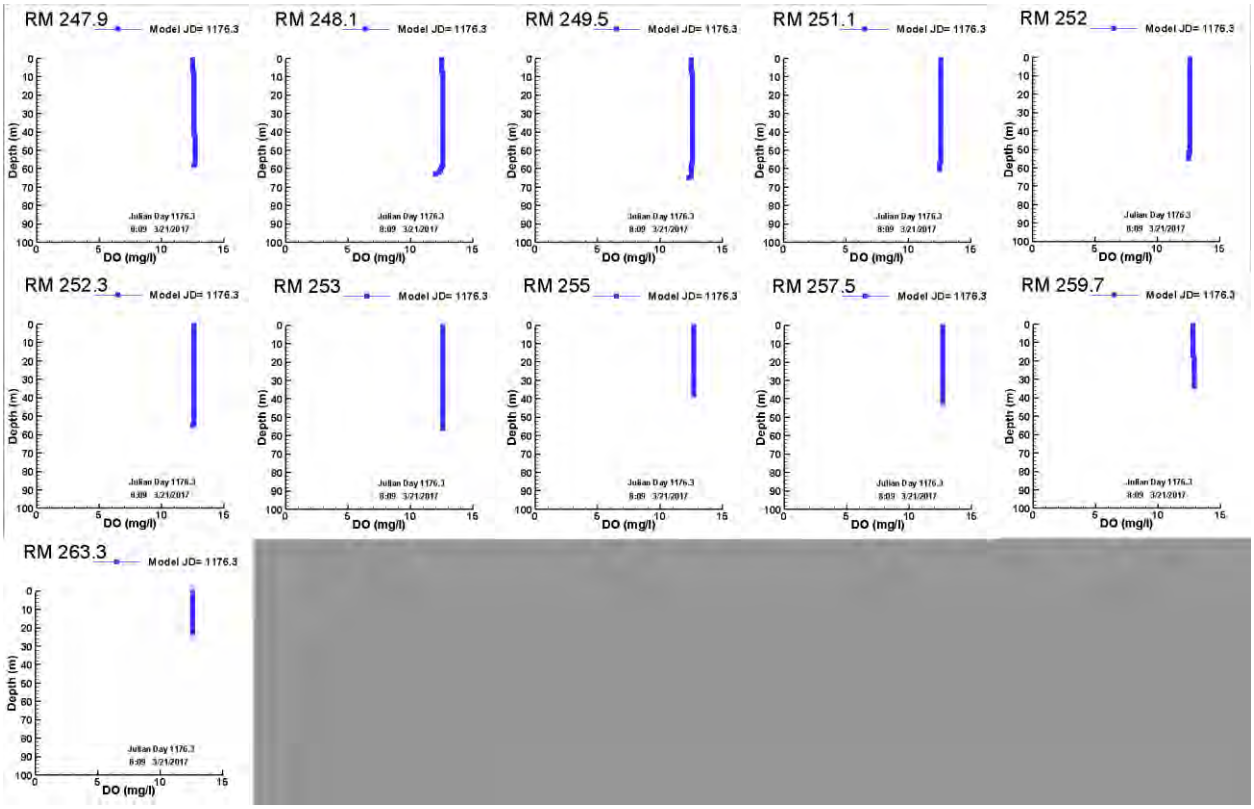


Figure 284. Vertical profiles of DO compared with data for 3/21/2017.

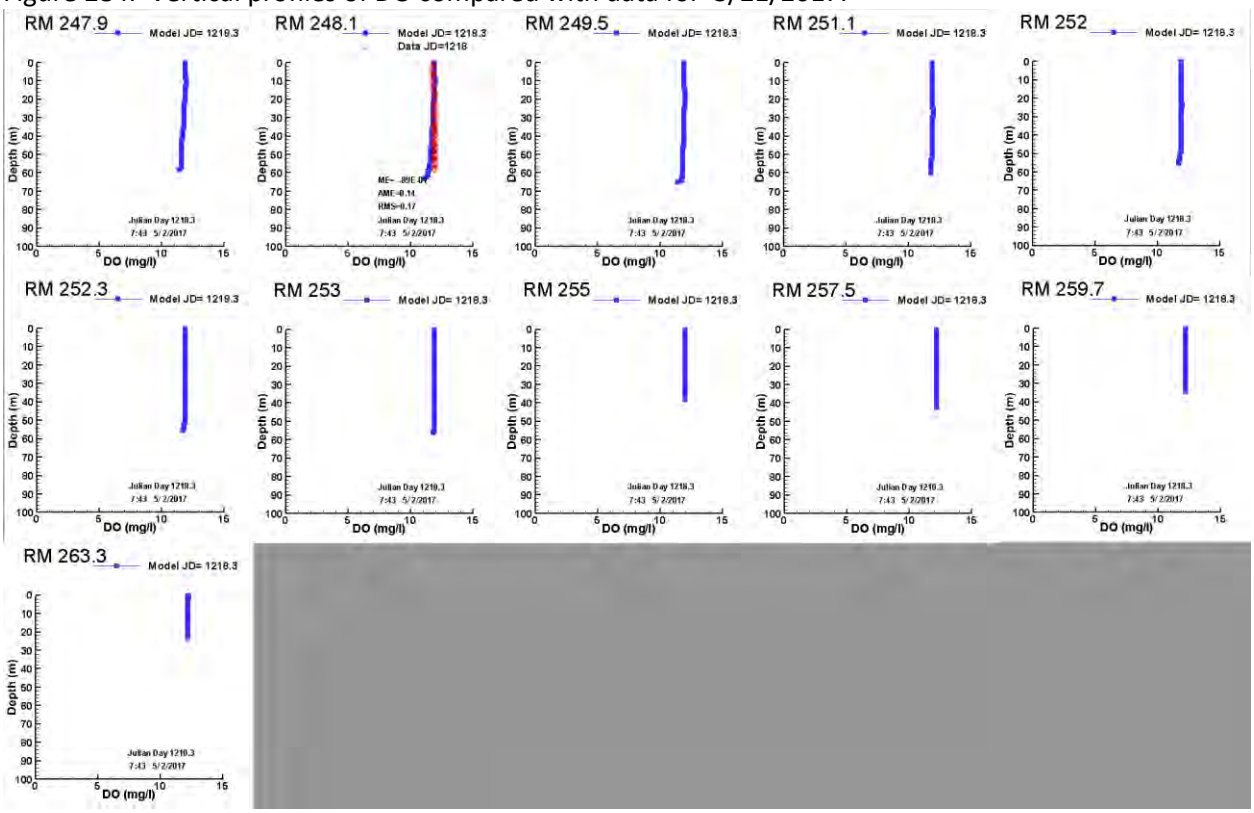


Figure 285. Vertical profiles of DO compared with data for 5/ 2/2017.

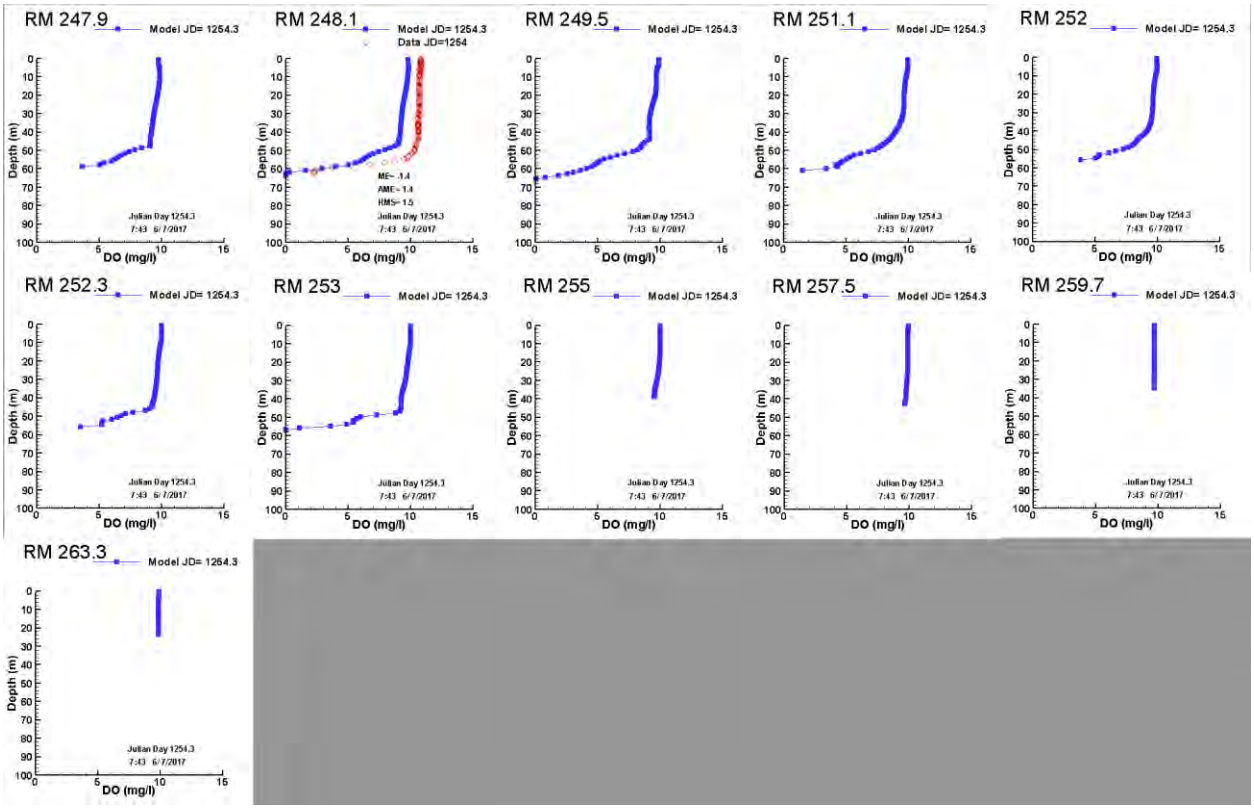


Figure 286. Vertical profiles of DO compared with data for 6/ 7/2017.

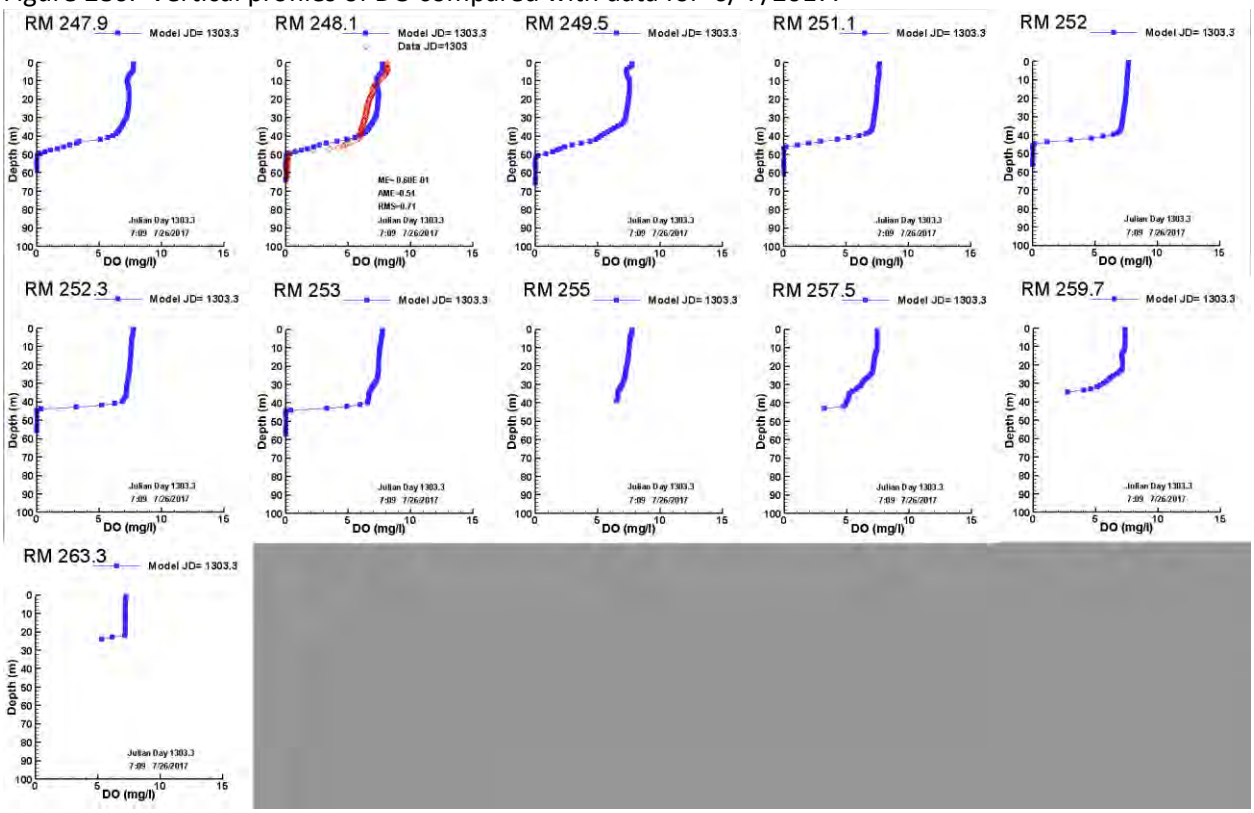


Figure 287. Vertical profiles of DO compared with data for 7/26/2017.

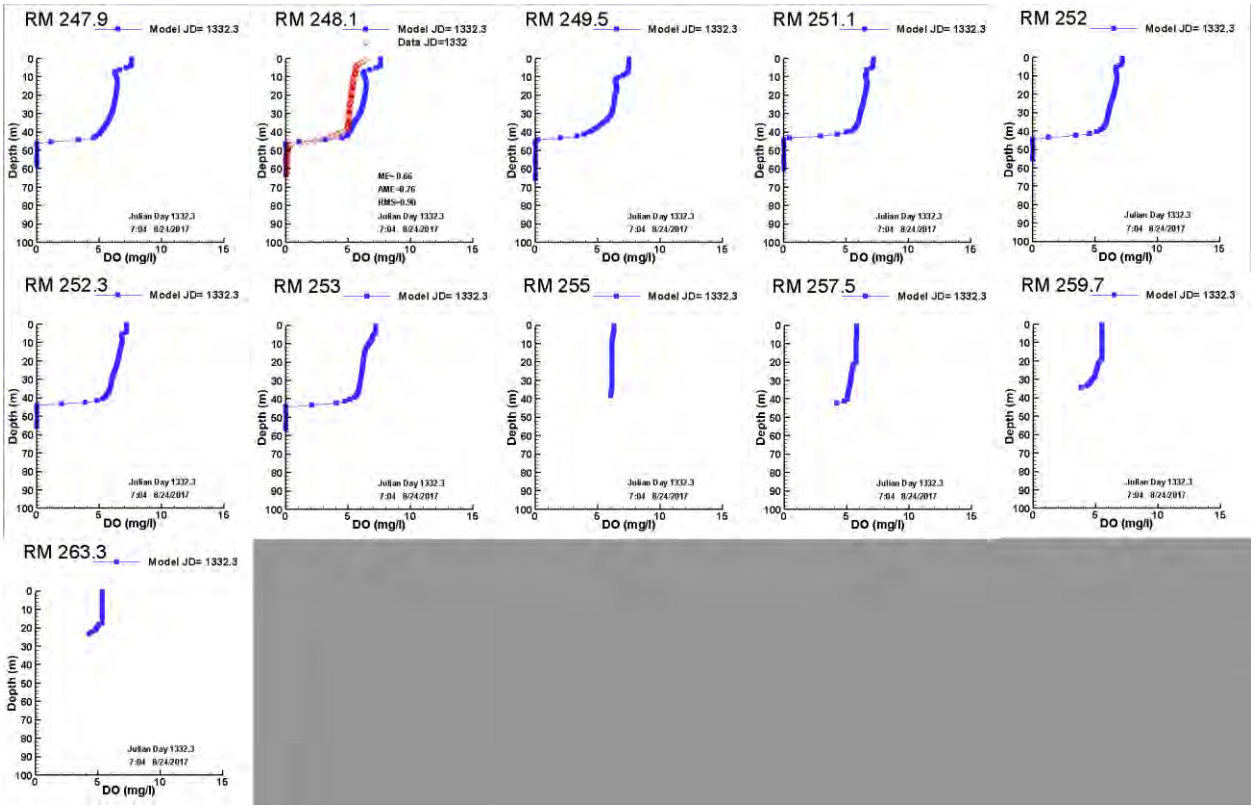


Figure 288. Vertical profiles of DO compared with data for 8/24/2017.

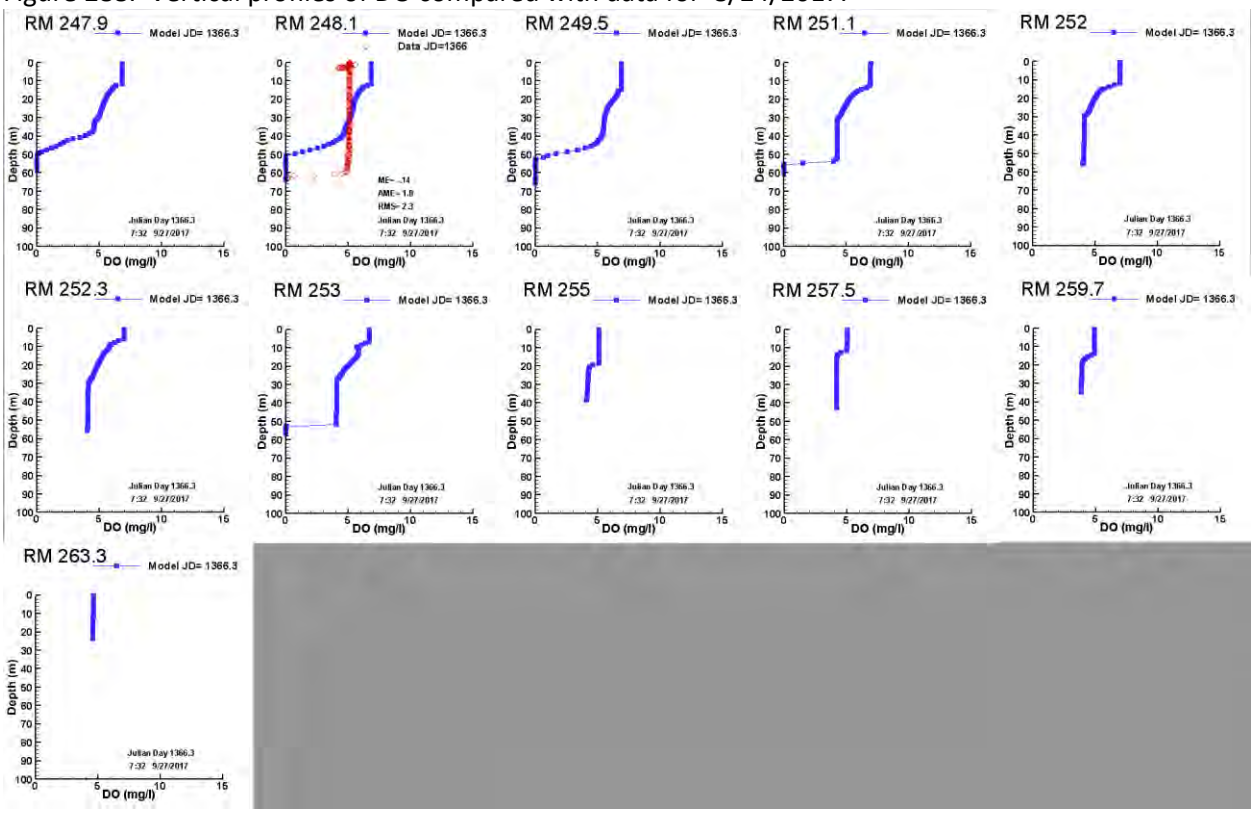


Figure 289. Vertical profiles of DO compared with data for 9/27/2017.

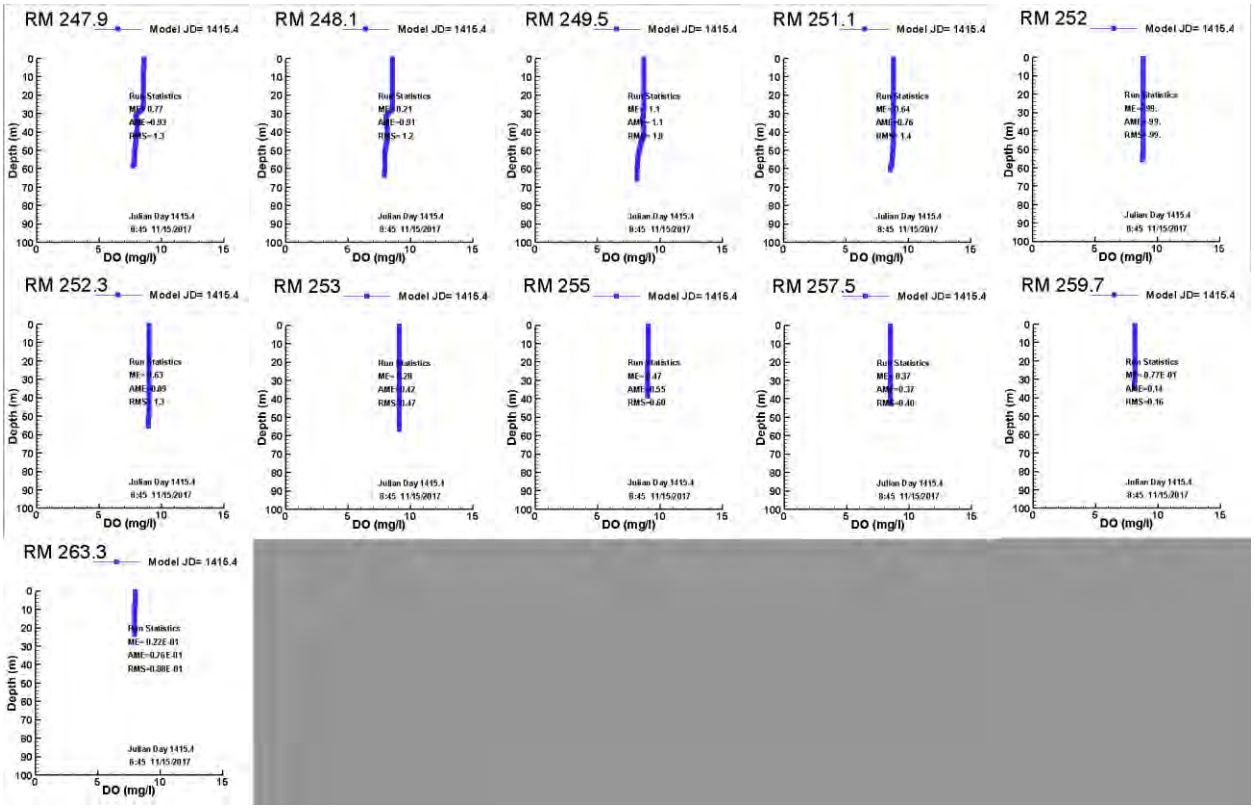


Figure 290. Vertical profiles of DO compared with data for 11/15/2017.

Total Inorganic Carbon

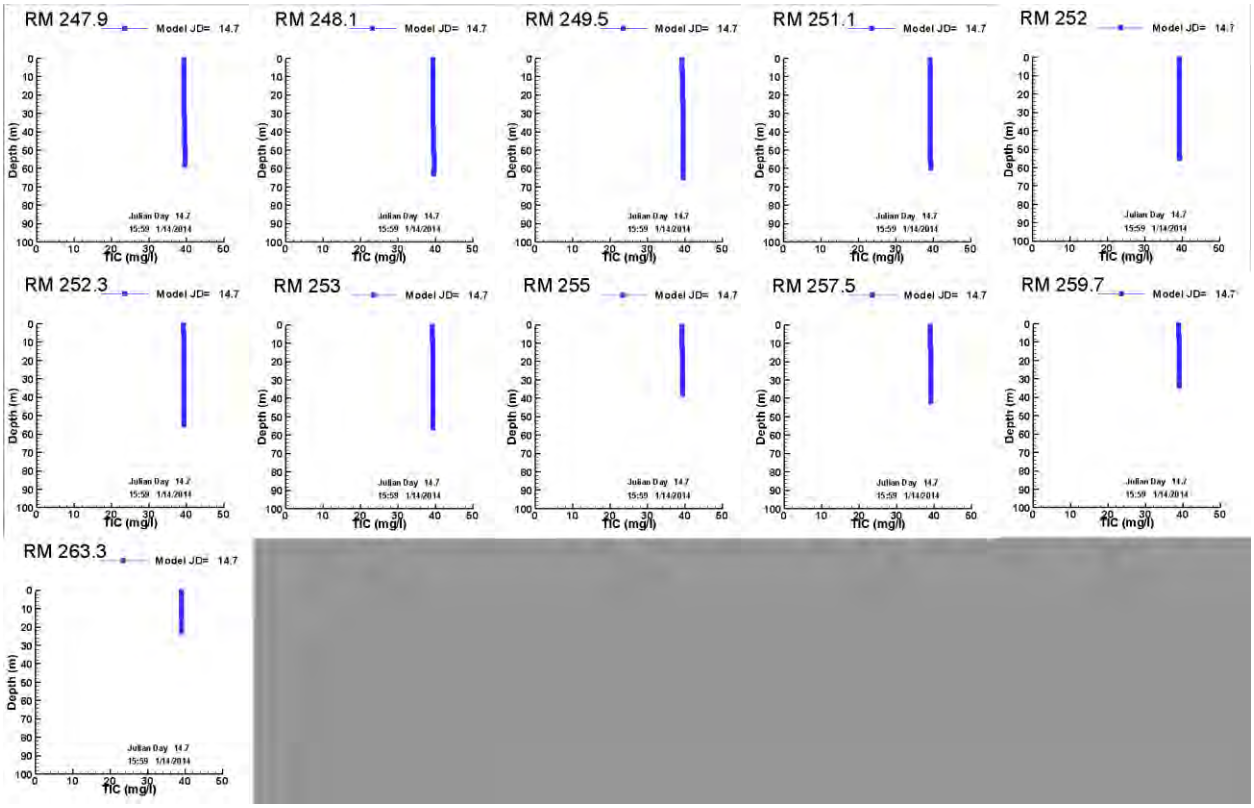


Figure 291. Vertical profiles of TIC compared with data for 1/14/2014.

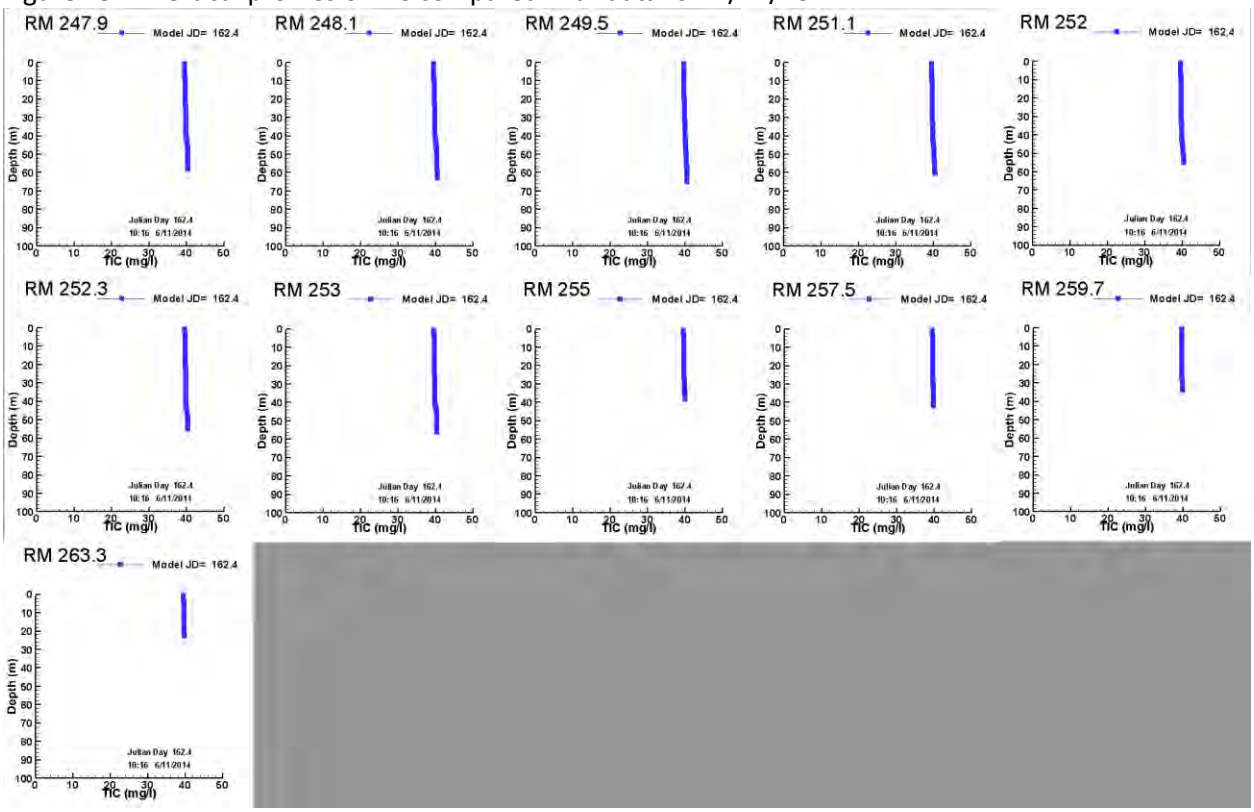


Figure 292. Vertical profiles of TIC compared with data for 6/11/2014.

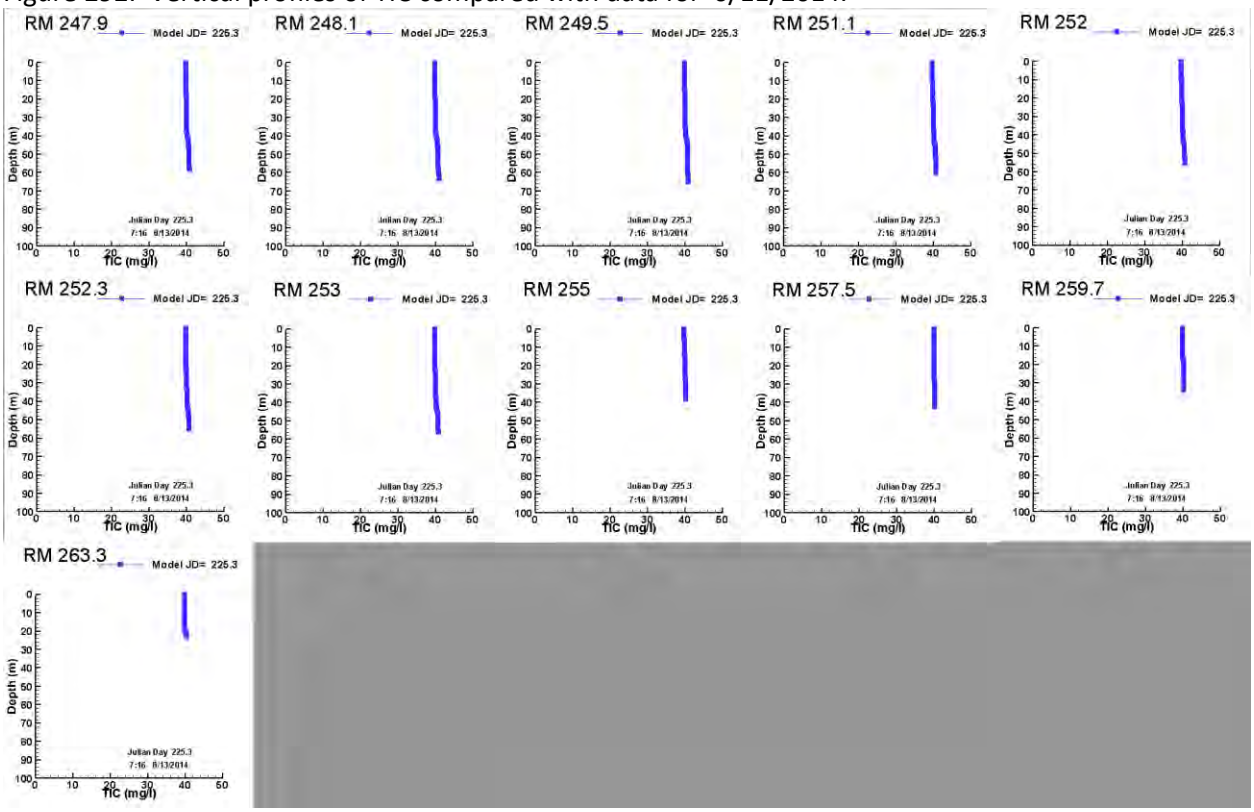


Figure 293. Vertical profiles of TIC compared with data for 8/13/2014.

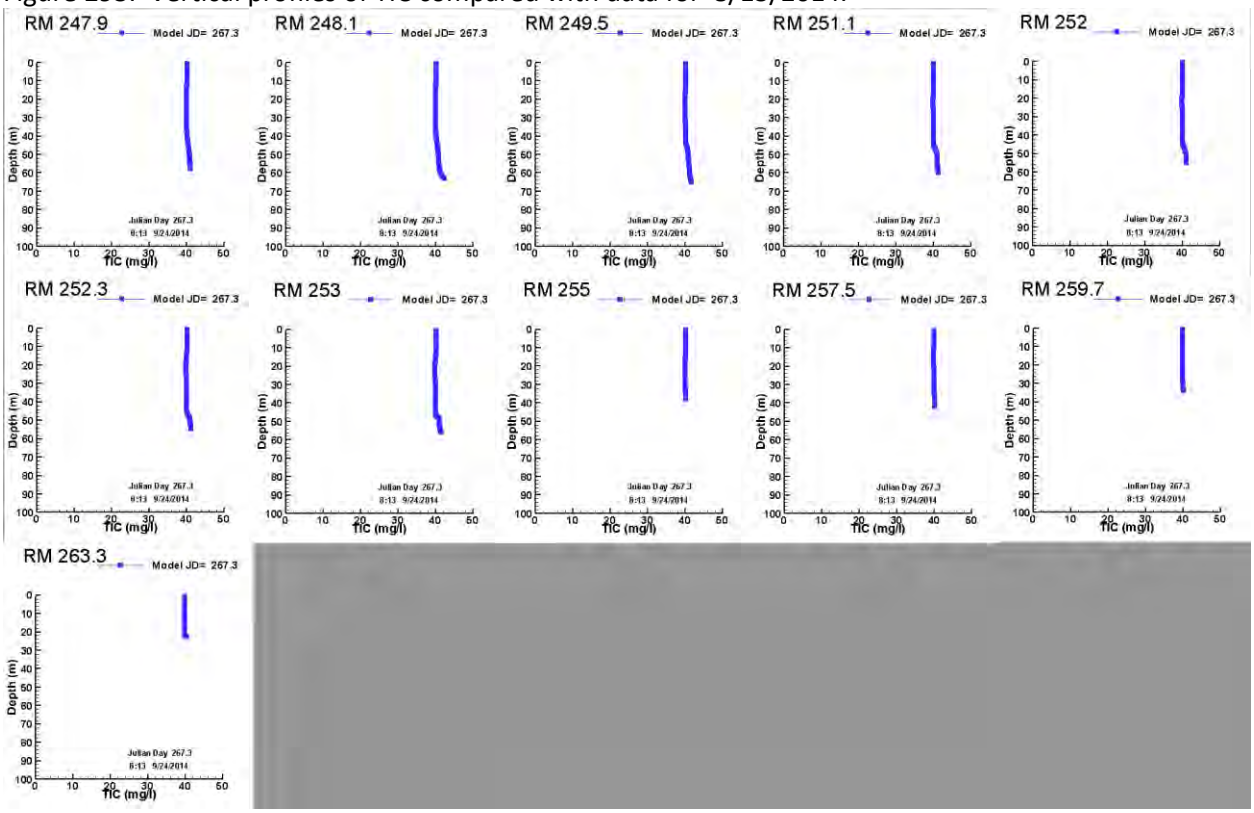


Figure 294. Vertical profiles of TIC compared with data for 9/24/2014.

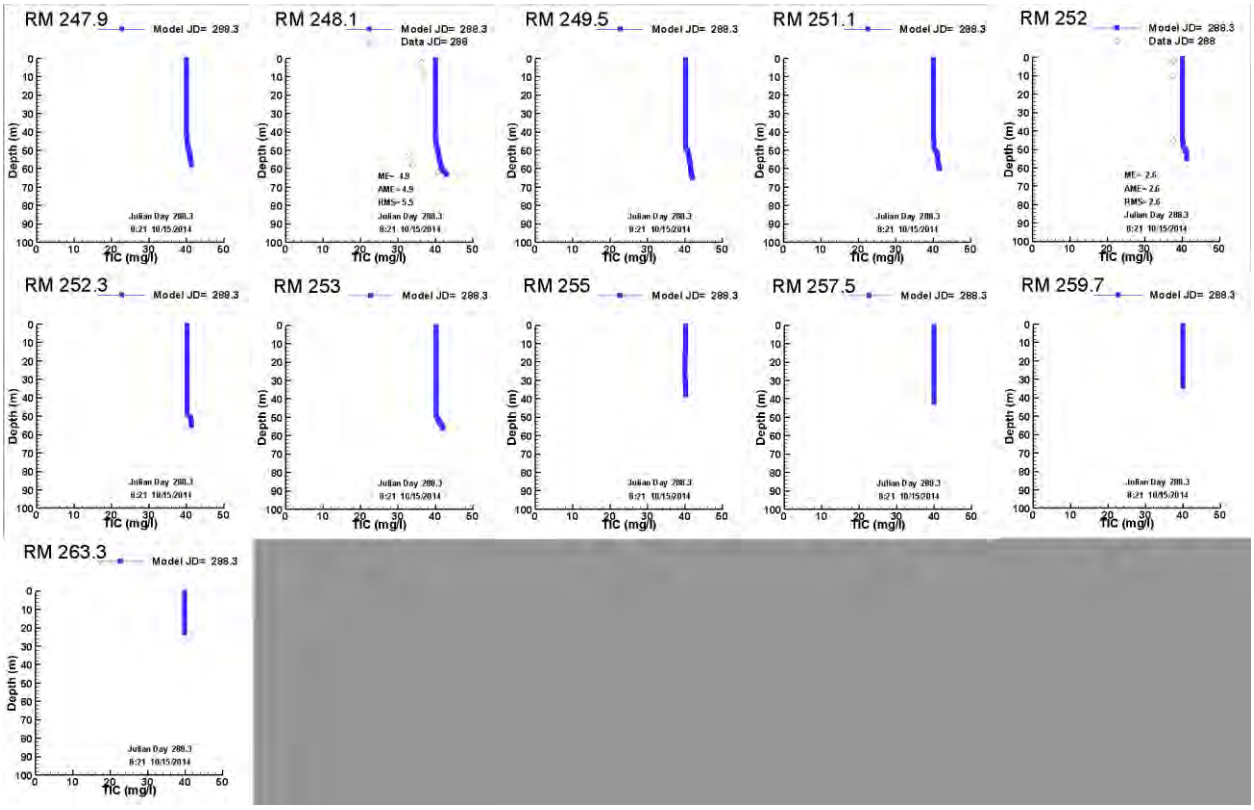


Figure 295. Vertical profiles of TIC compared with data for 10/15/2014.

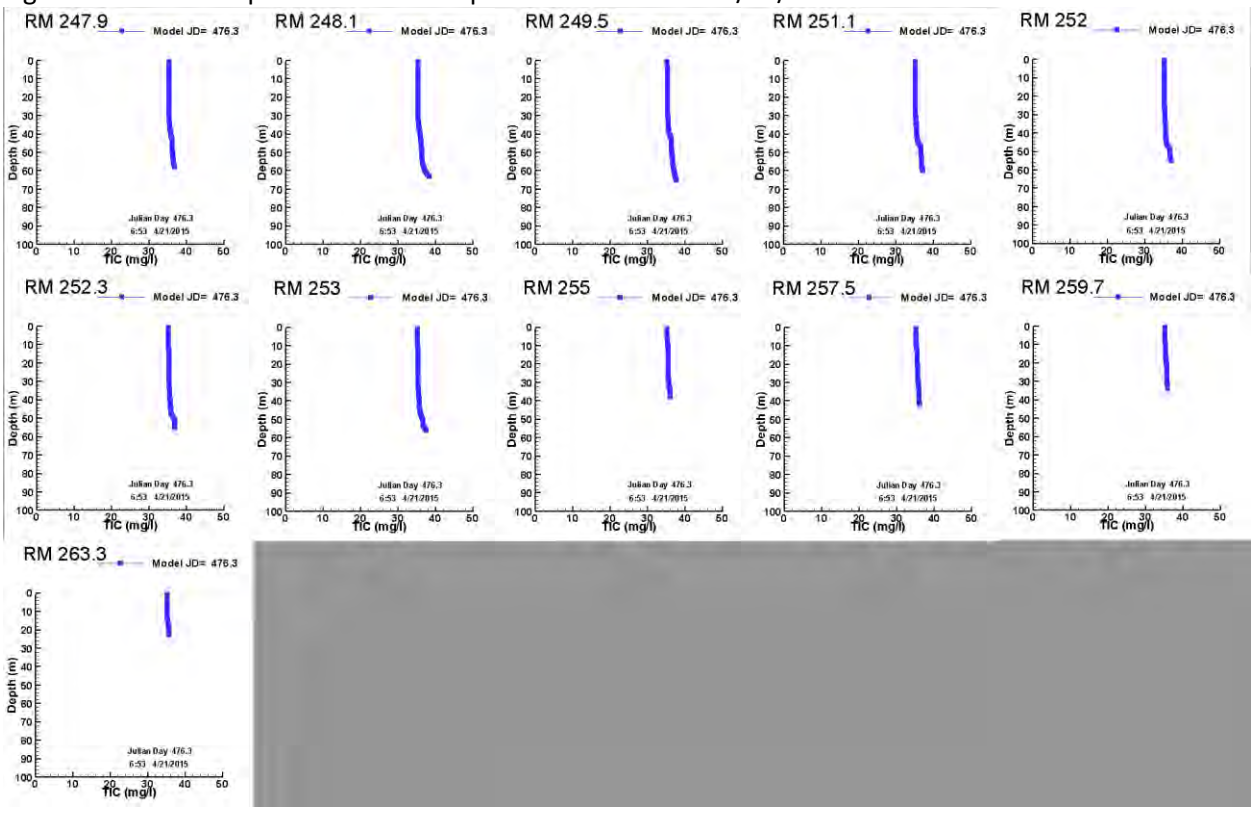


Figure 296. Vertical profiles of TIC compared with data for 4/21/2015.

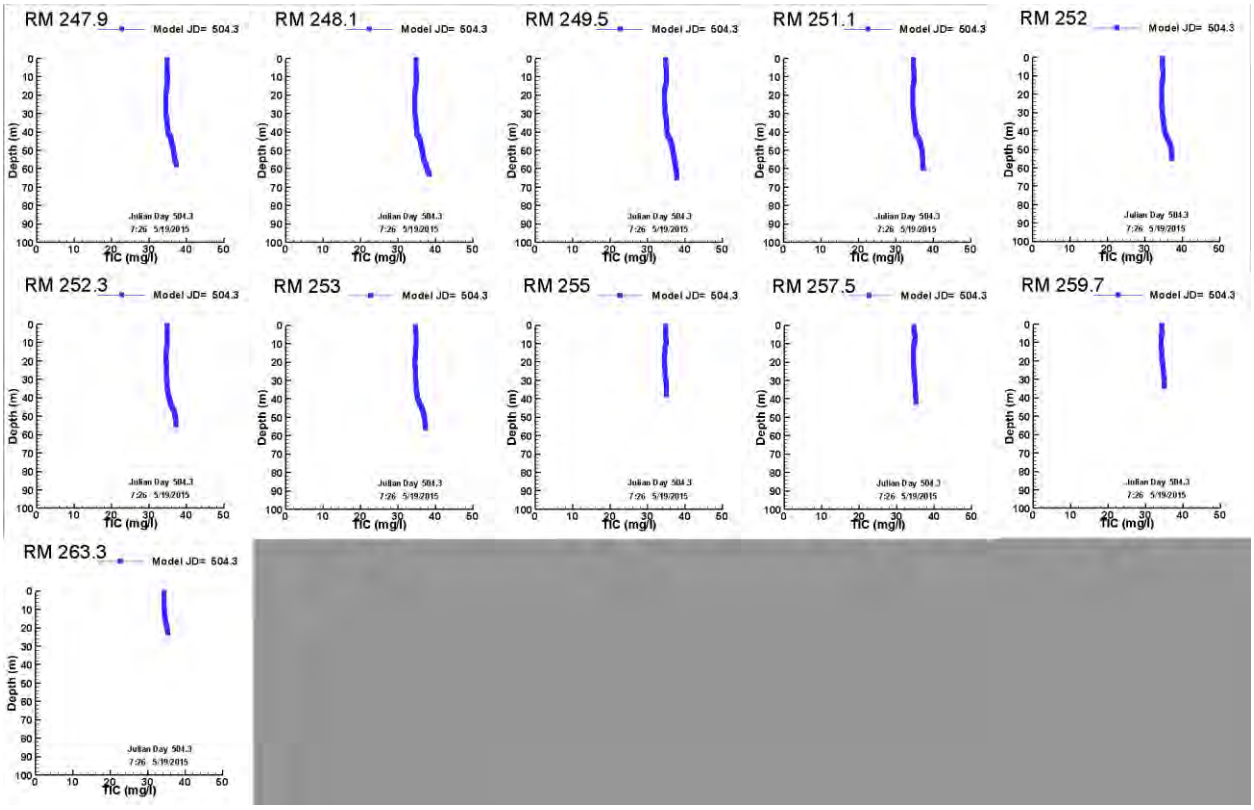


Figure 297. Vertical profiles of TIC compared with data for 5/19/2015.

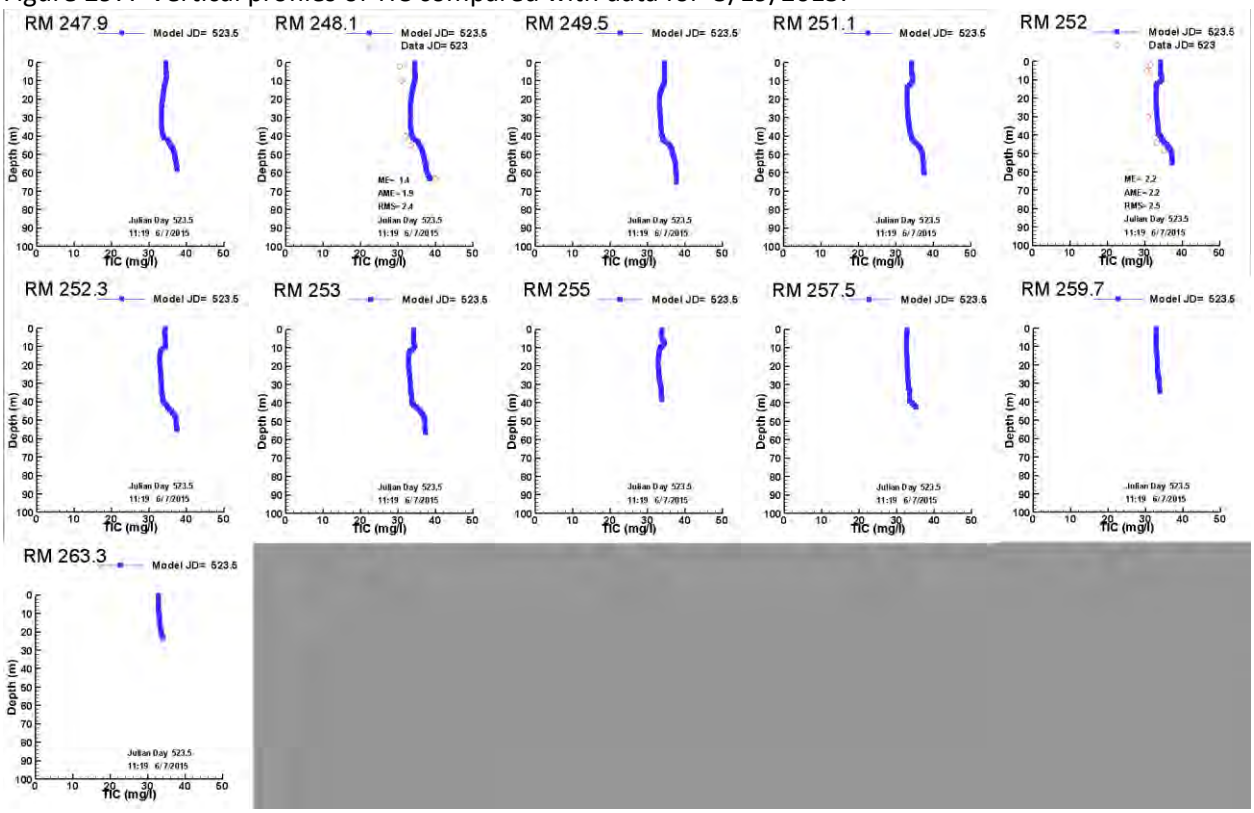


Figure 298. Vertical profiles of TIC compared with data for 6/ 7/2015.

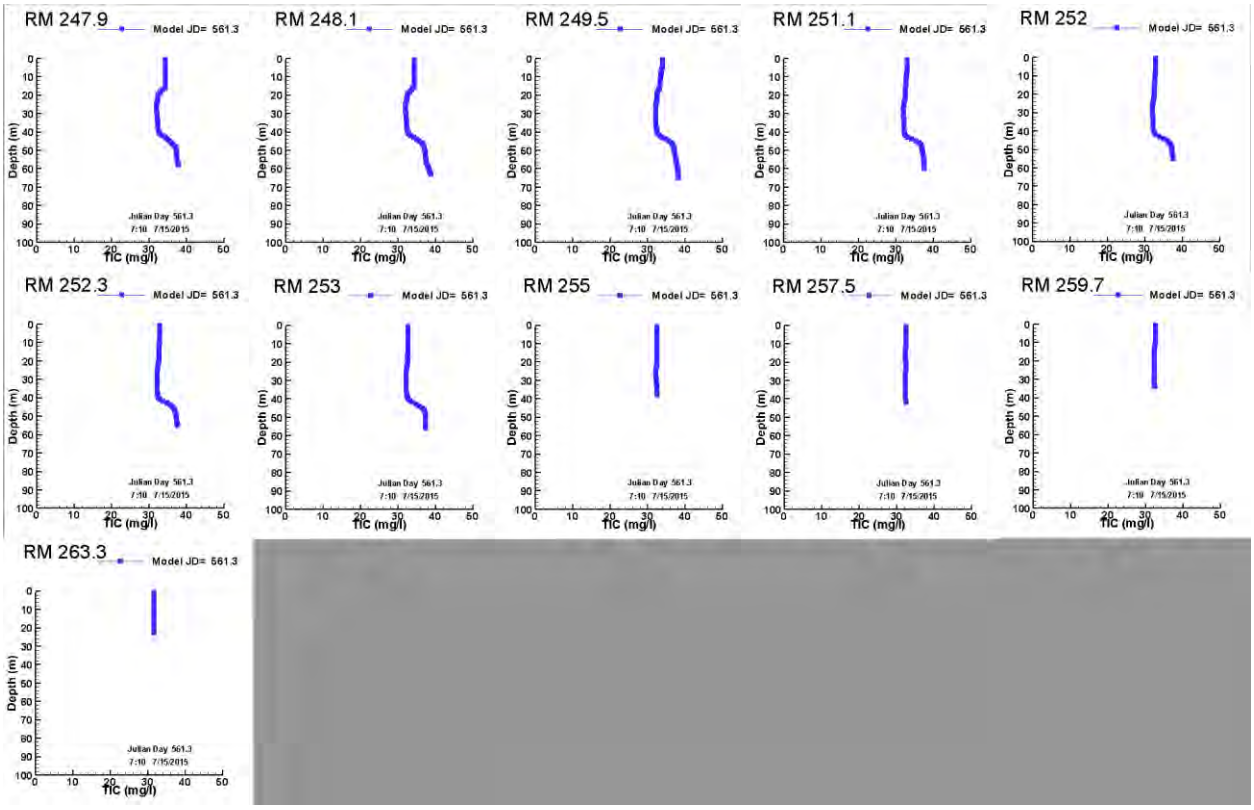


Figure 299. Vertical profiles of TIC compared with data for 7/15/2015.

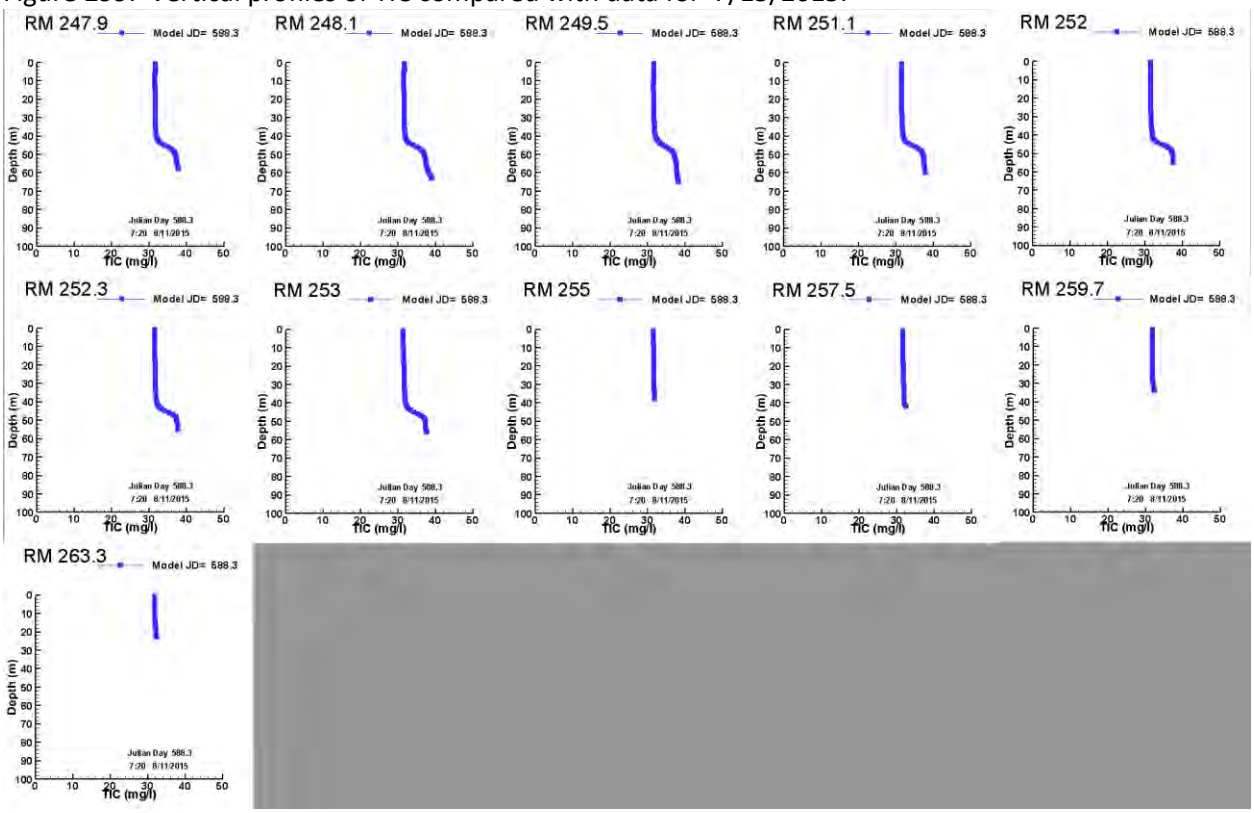


Figure 300. Vertical profiles of TIC compared with data for 8/11/2015.

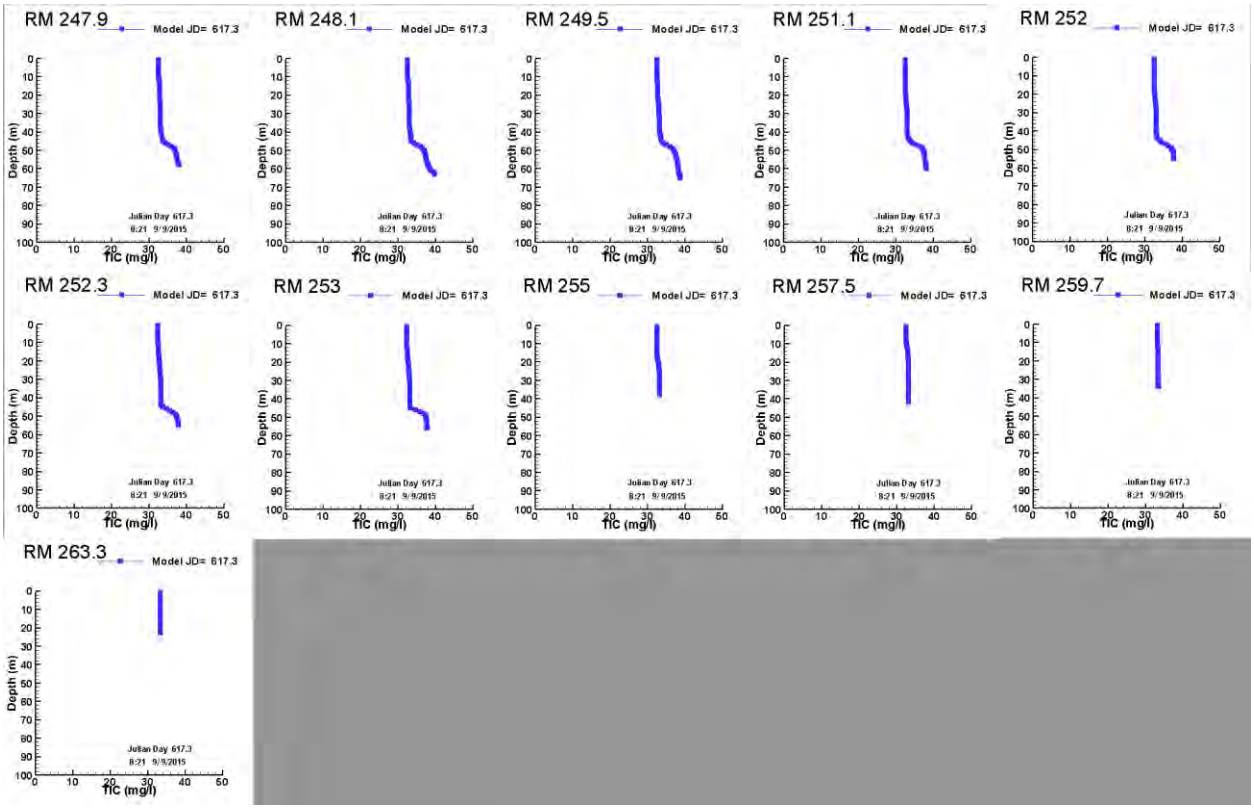


Figure 301. Vertical profiles of TIC compared with data for 9/ 9/2015.

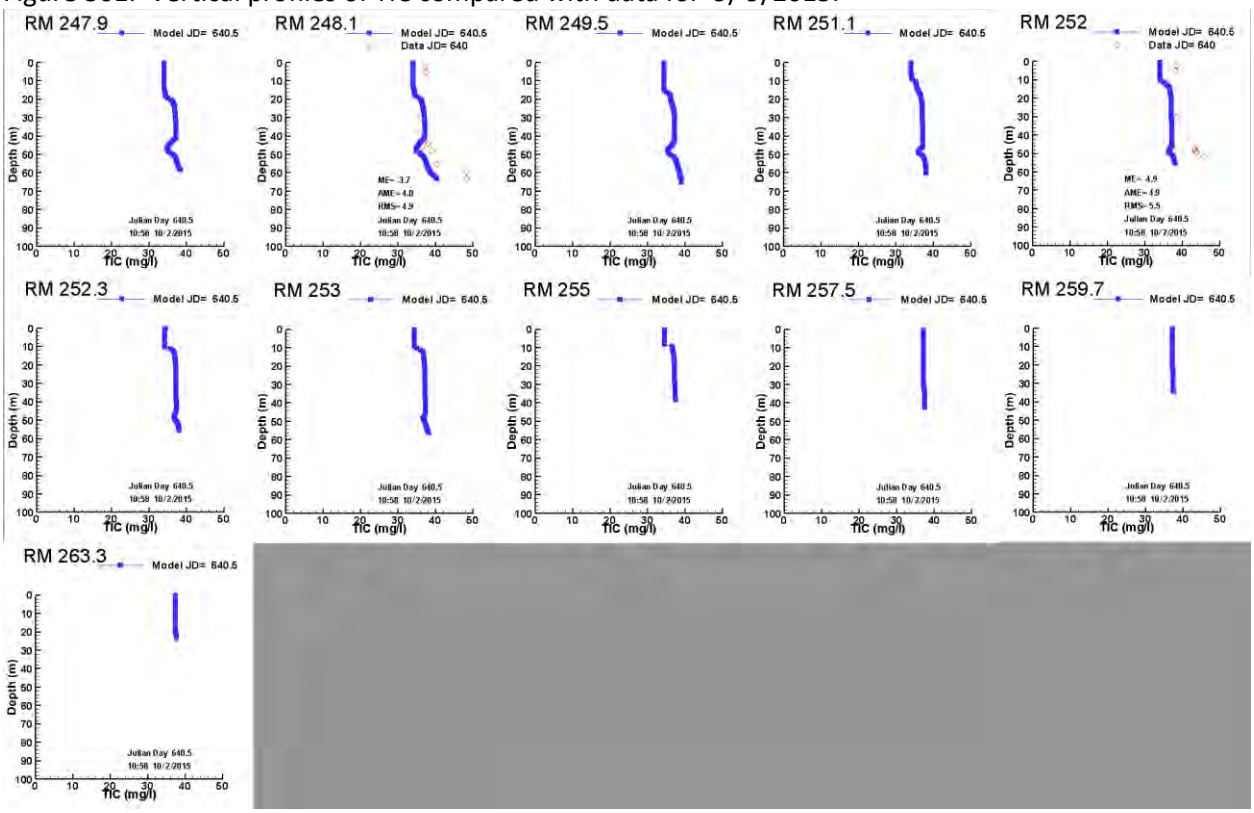


Figure 302. Vertical profiles of TIC compared with data for 10/ 2/2015.

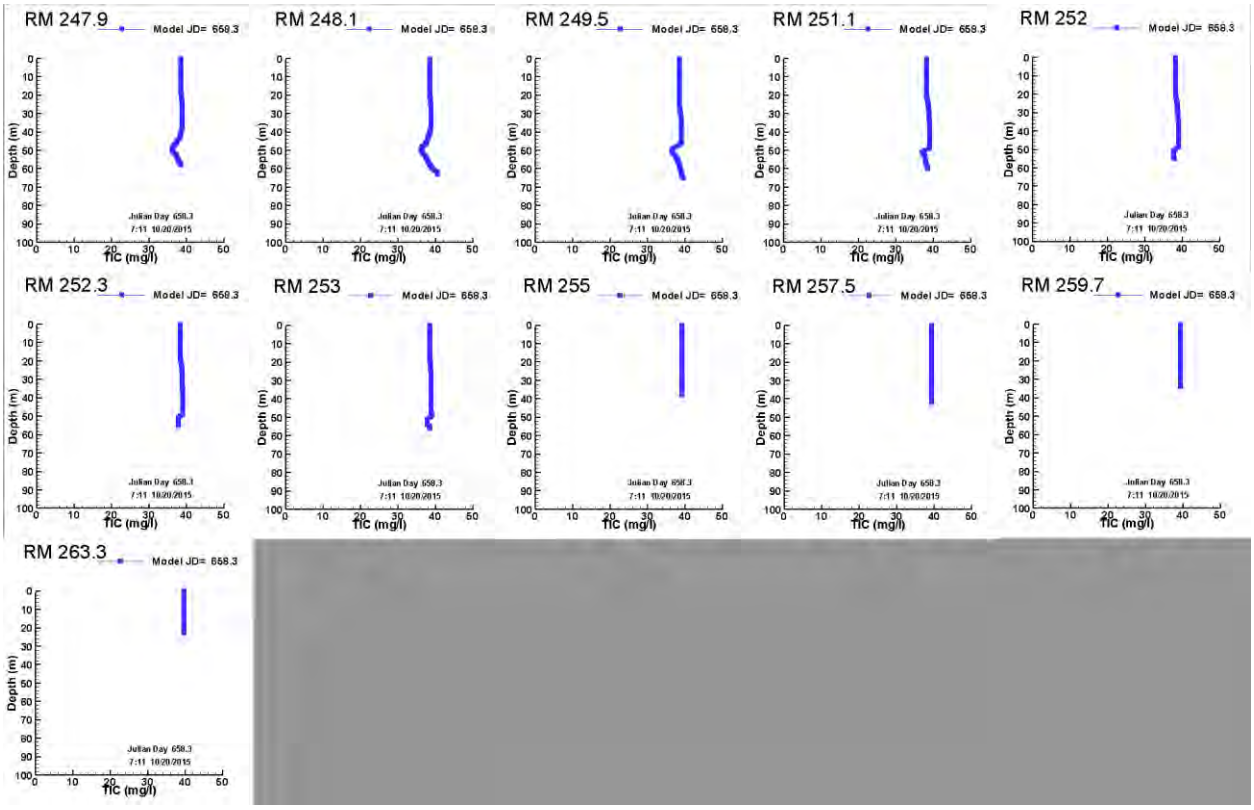


Figure 303. Vertical profiles of TIC compared with data for 10/20/2015.

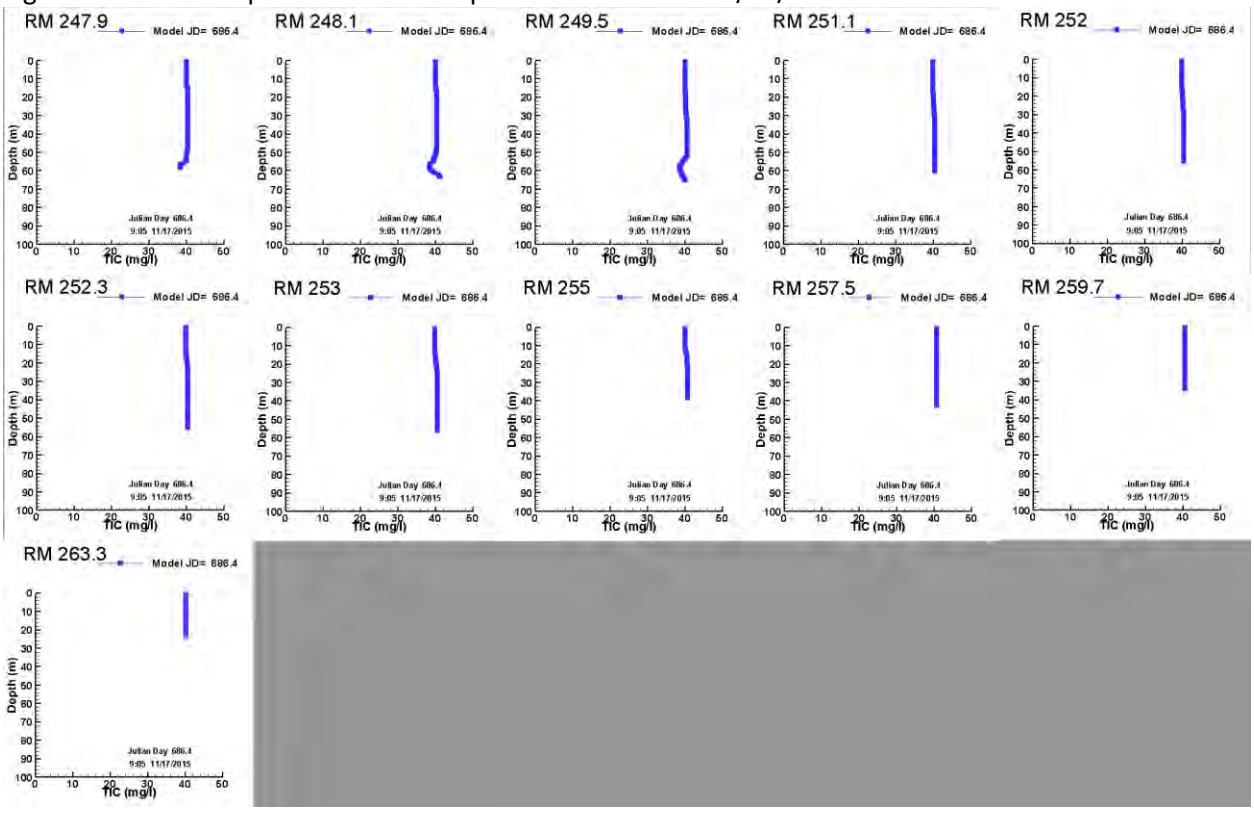


Figure 304. Vertical profiles of TIC compared with data for 11/17/2015.

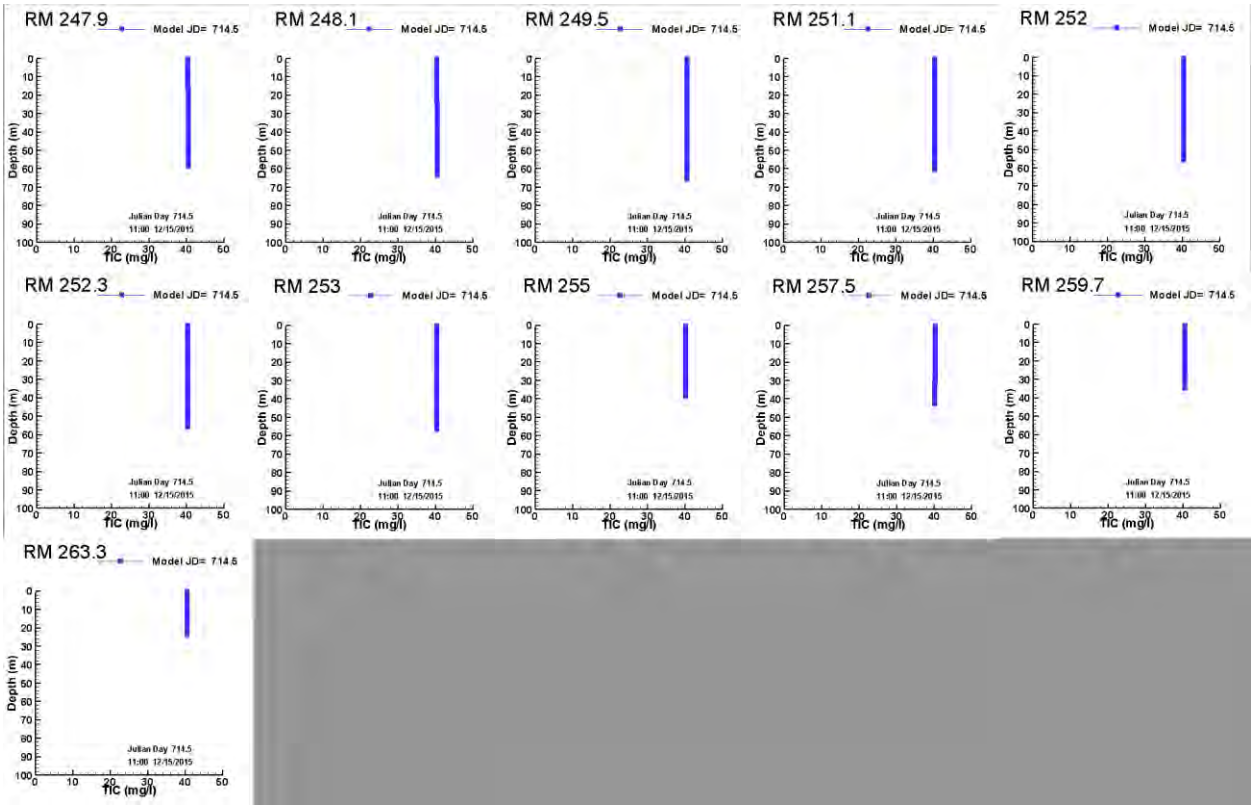


Figure 305. Vertical profiles of TIC compared with data for 12/15/2015.

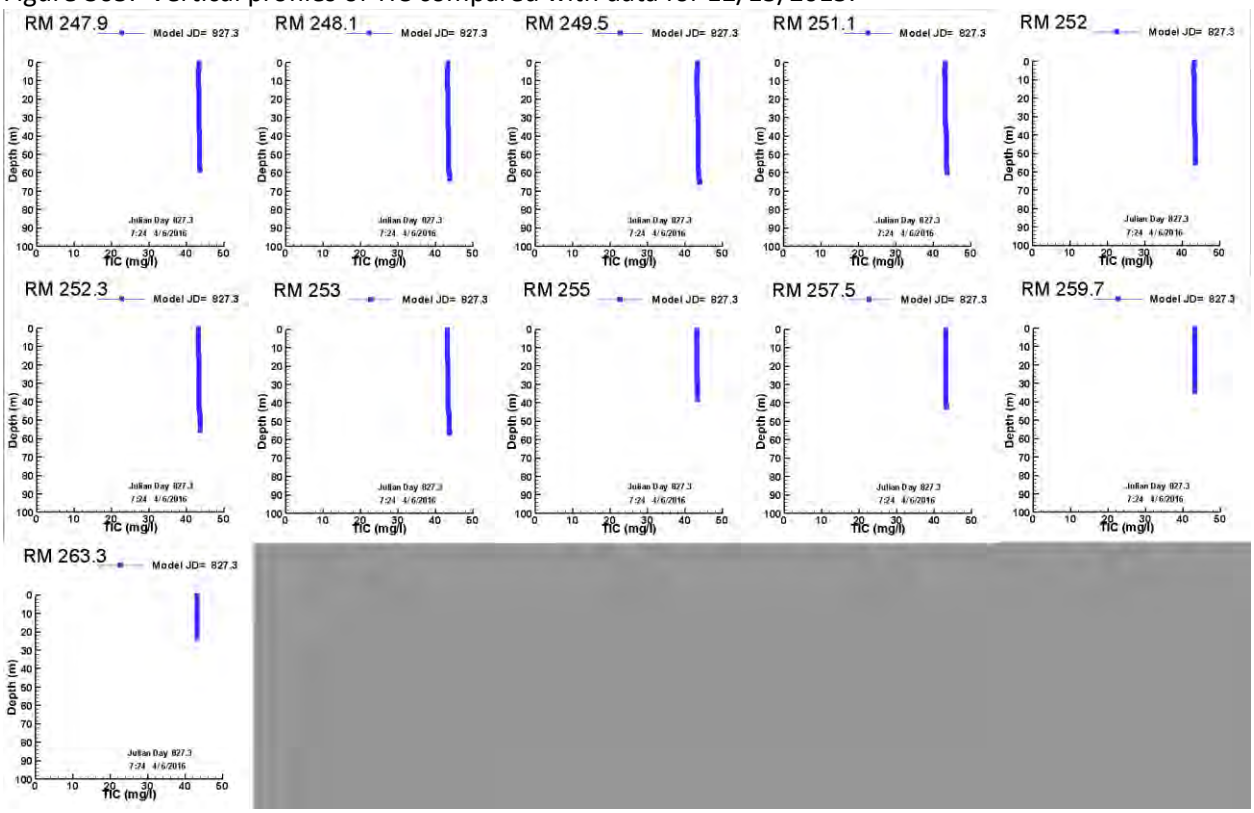


Figure 306. Vertical profiles of TIC compared with data for 4/ 6/2016.

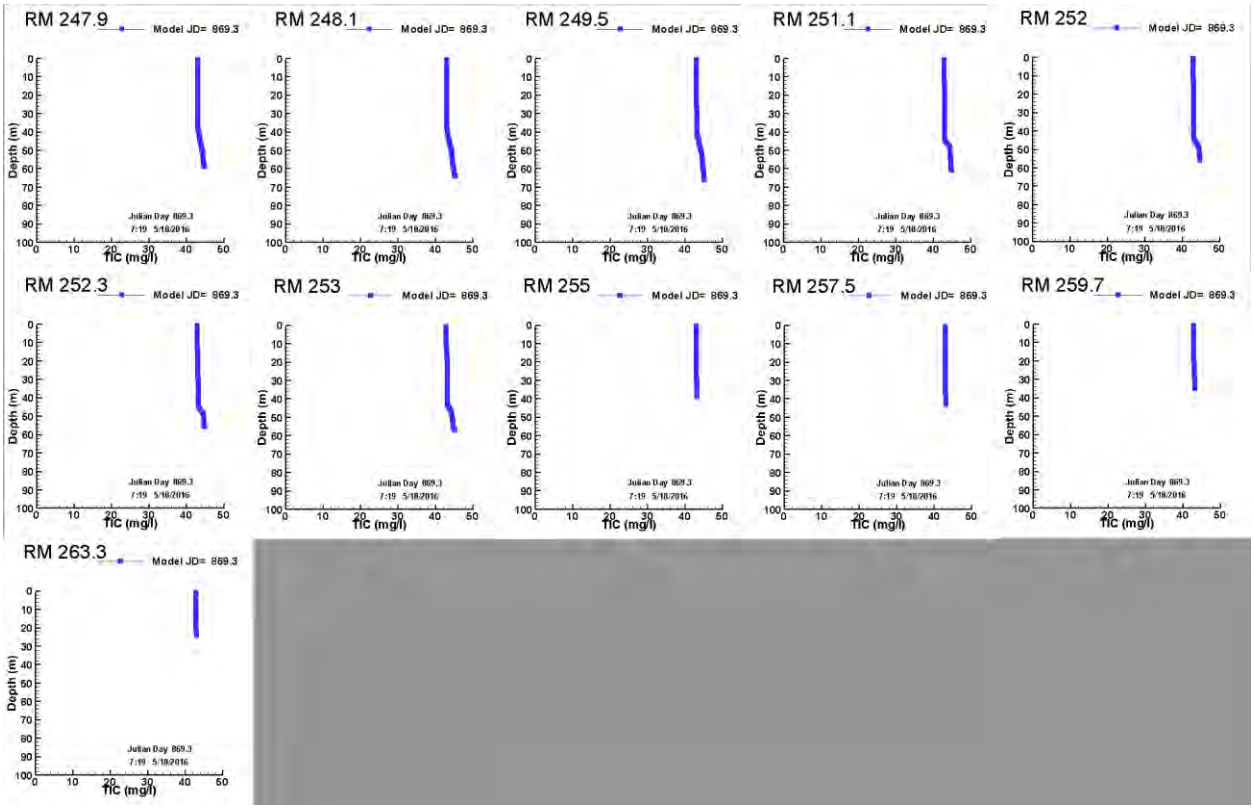


Figure 307. Vertical profiles of TIC compared with data for 5/18/2016.

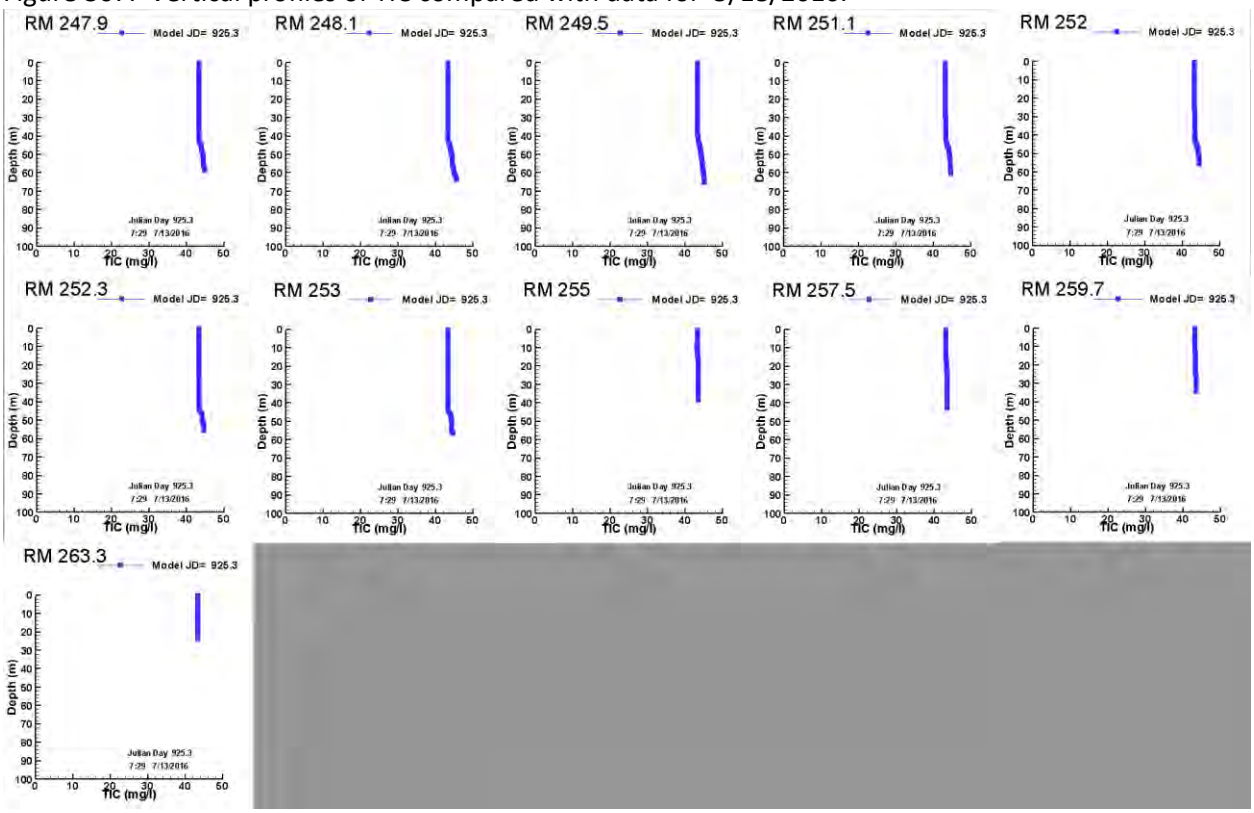


Figure 308. Vertical profiles of TIC compared with data for 7/13/2016.

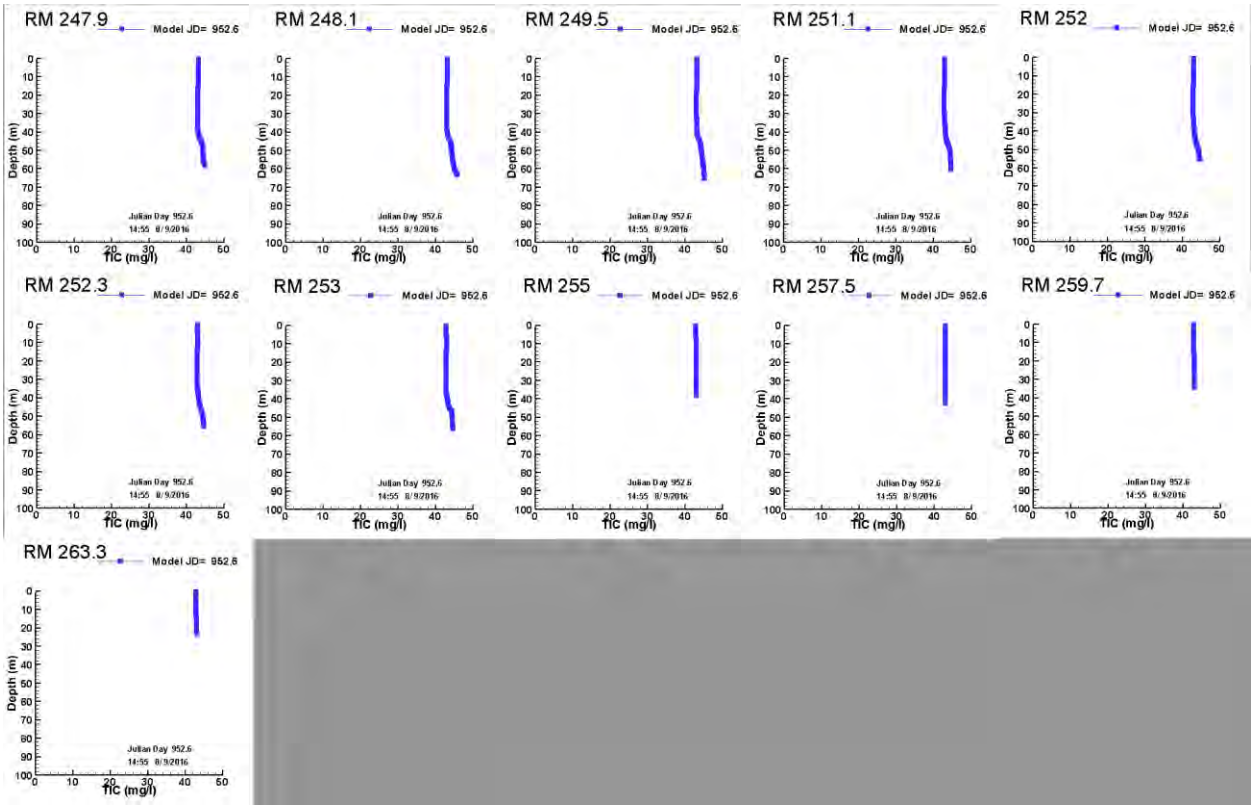


Figure 309. Vertical profiles of TIC compared with data for 8/ 9/2016.

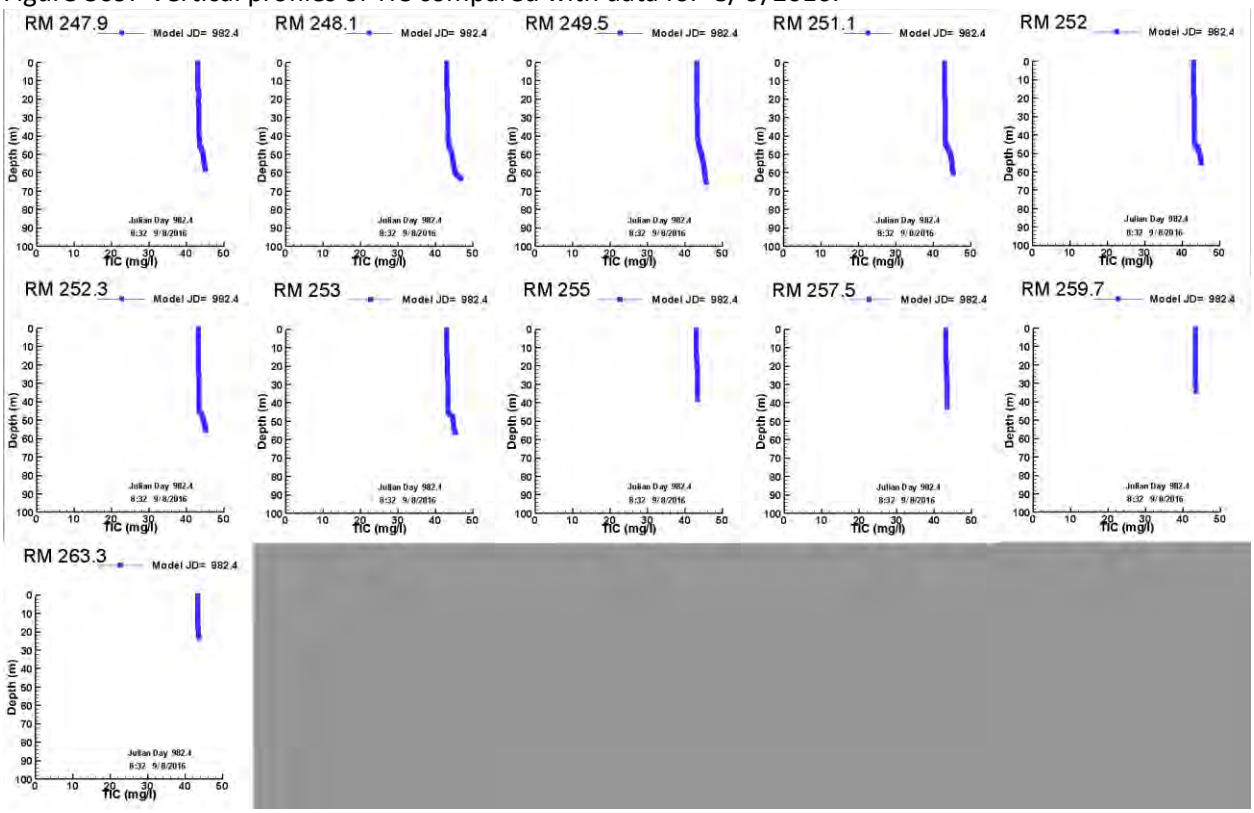


Figure 310. Vertical profiles of TIC compared with data for 9/ 8/2016.

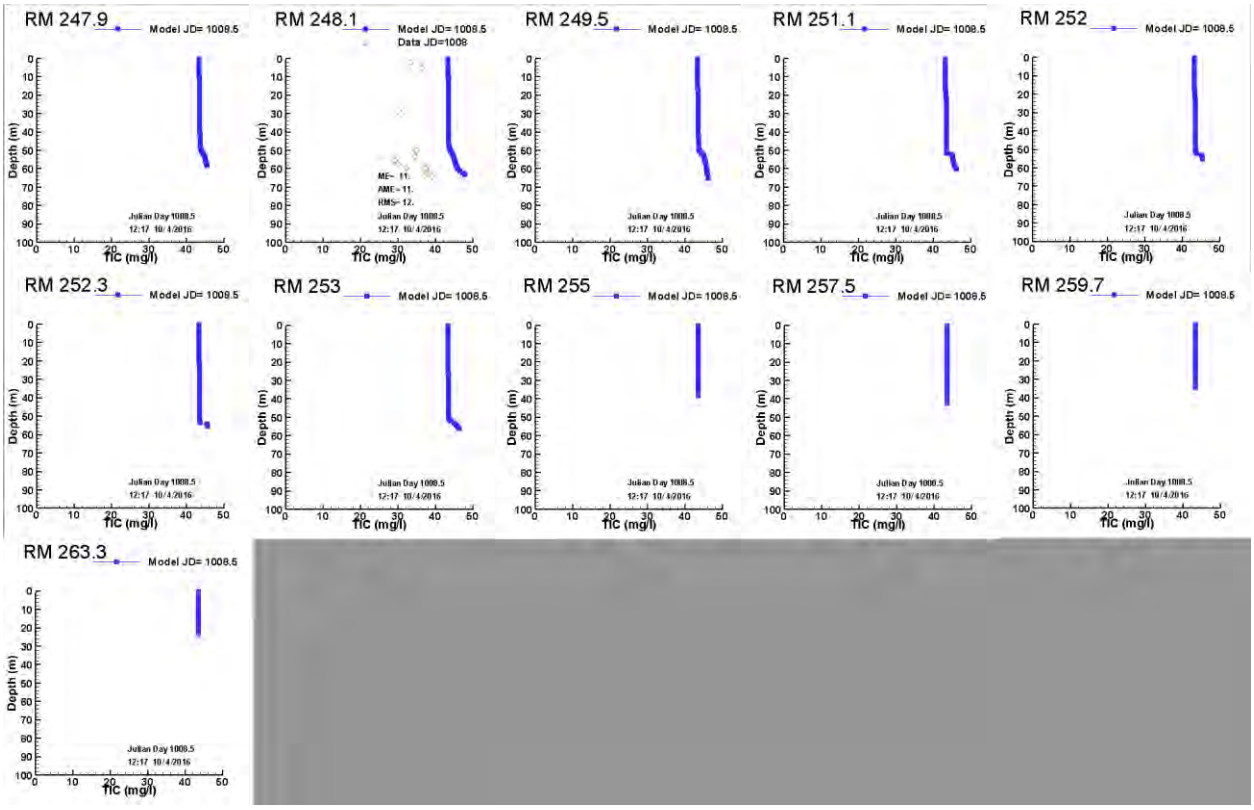


Figure 311. Vertical profiles of TIC compared with data for 10/ 4/2016.

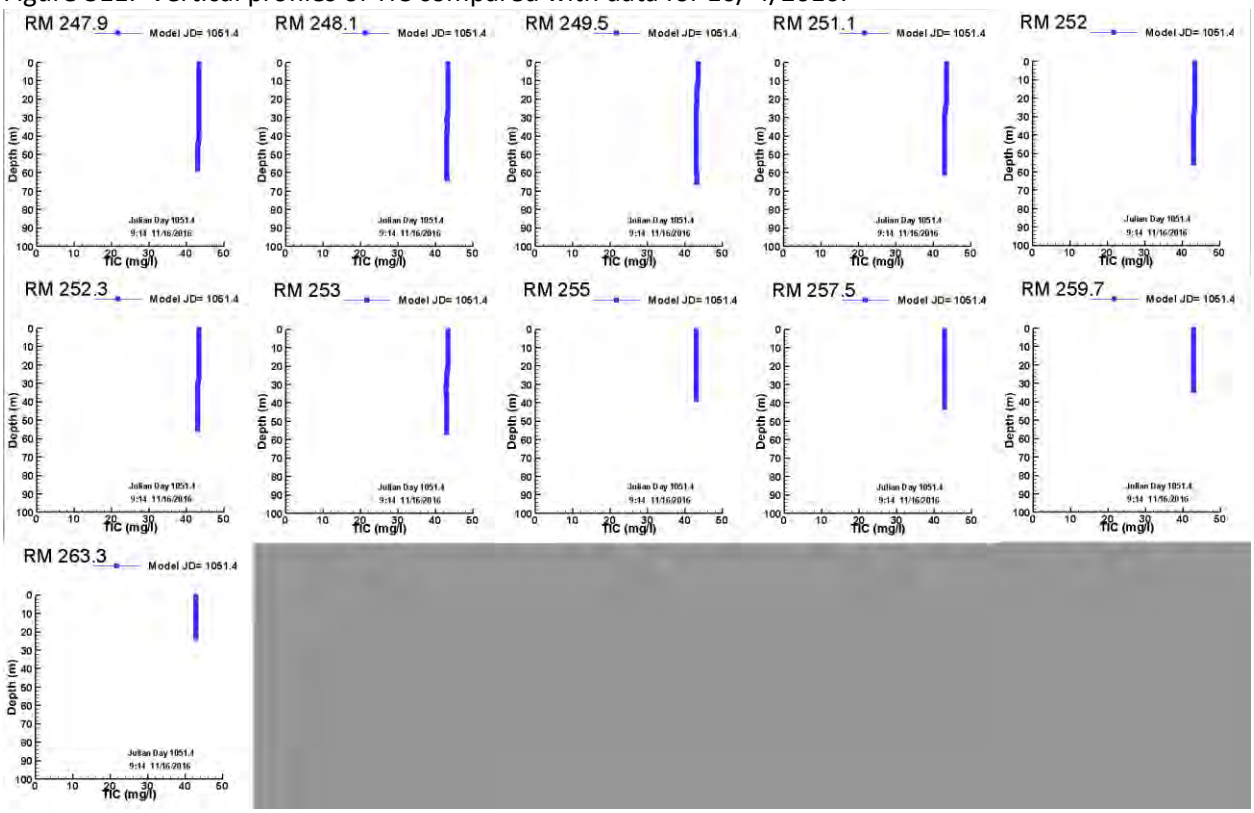


Figure 312. Vertical profiles of TIC compared with data for 11/16/2016.

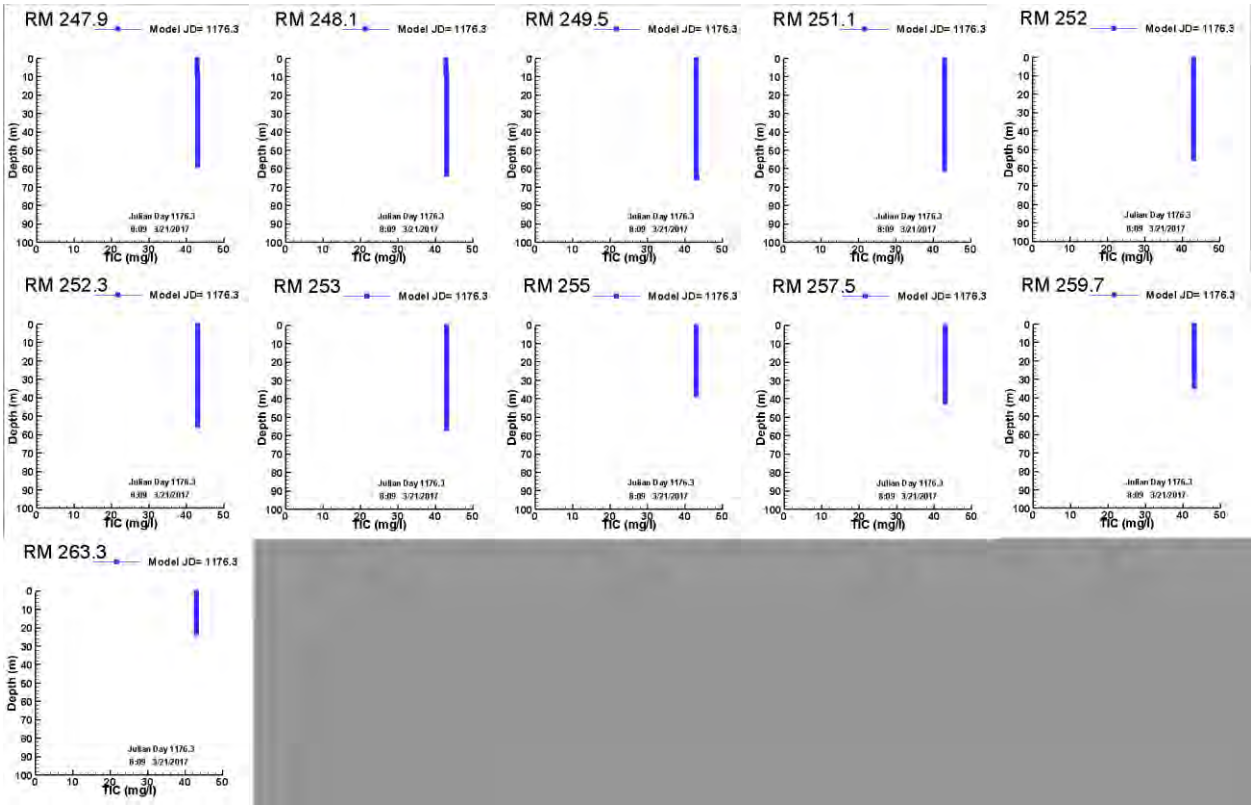


Figure 313. Vertical profiles of TIC compared with data for 3/21/2017.

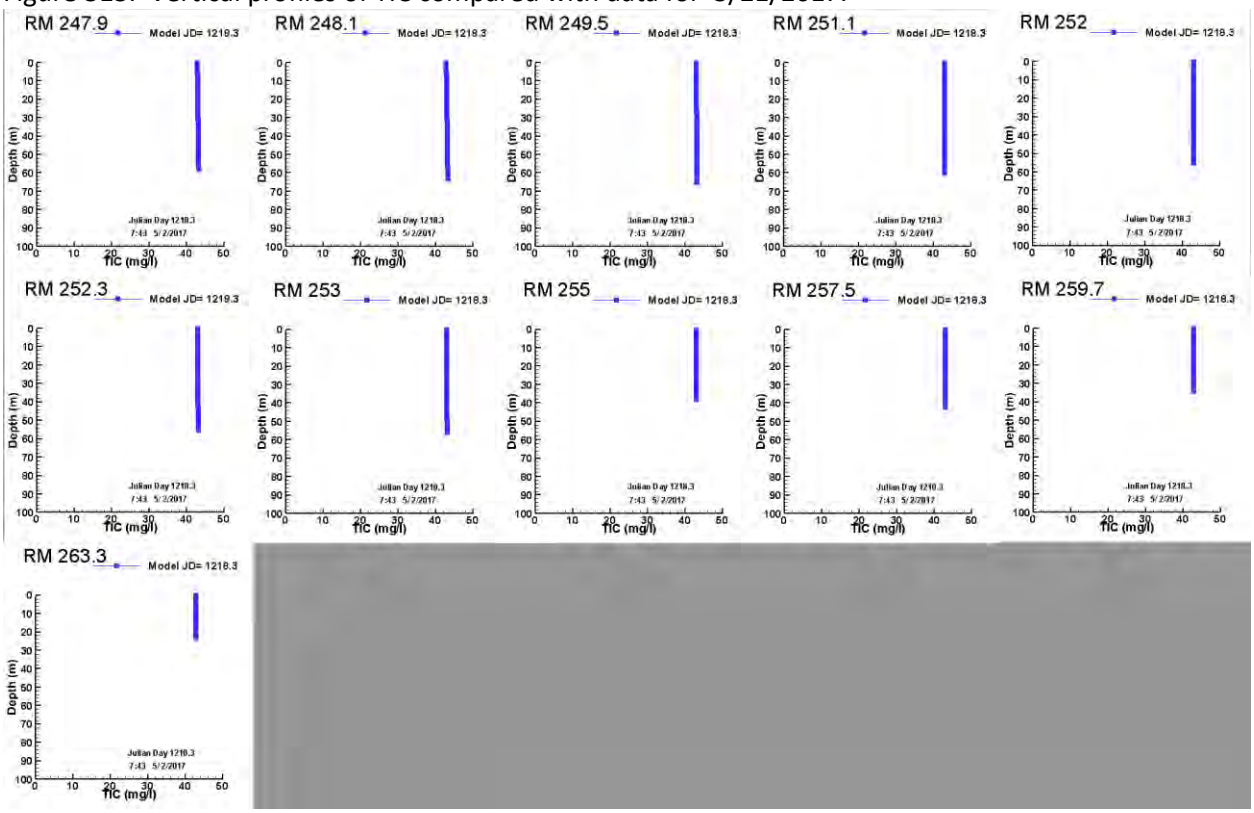


Figure 314. Vertical profiles of TIC compared with data for 5/ 2/2017.

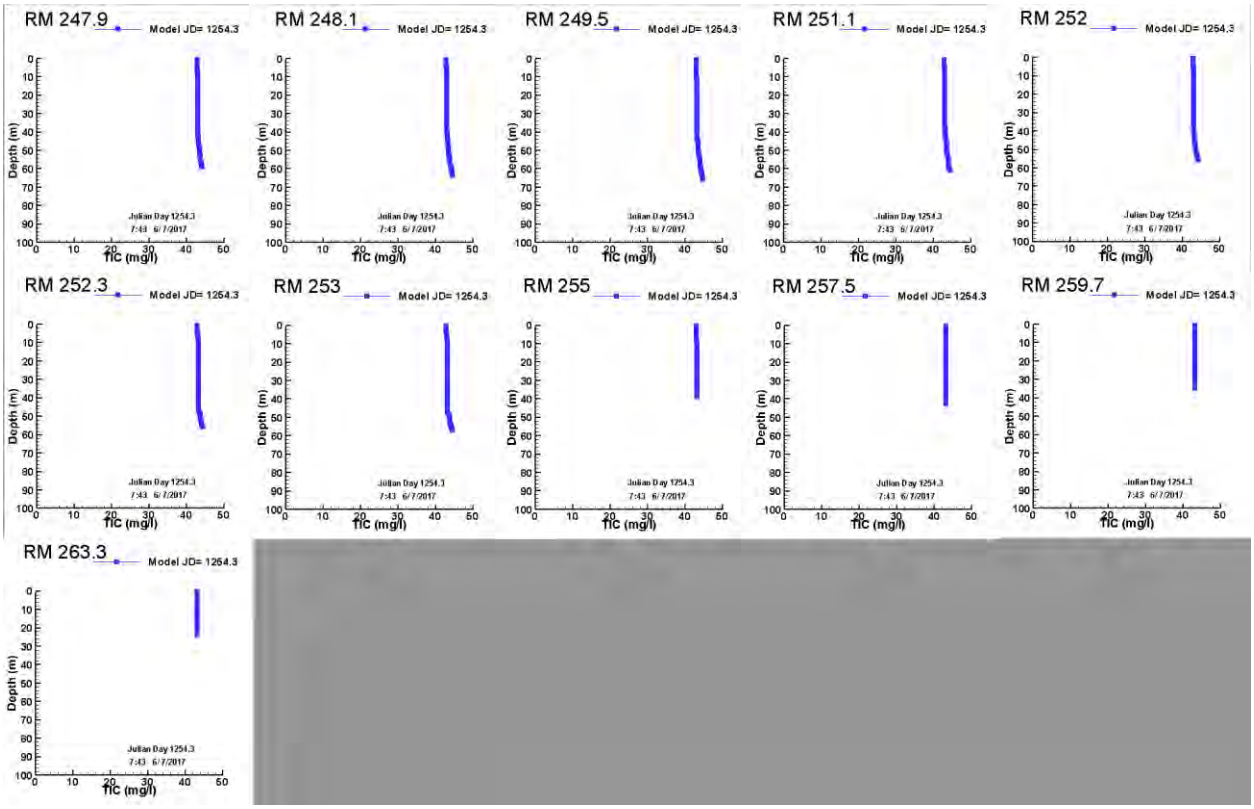


Figure 315. Vertical profiles of TIC compared with data for 6/ 7/2017.

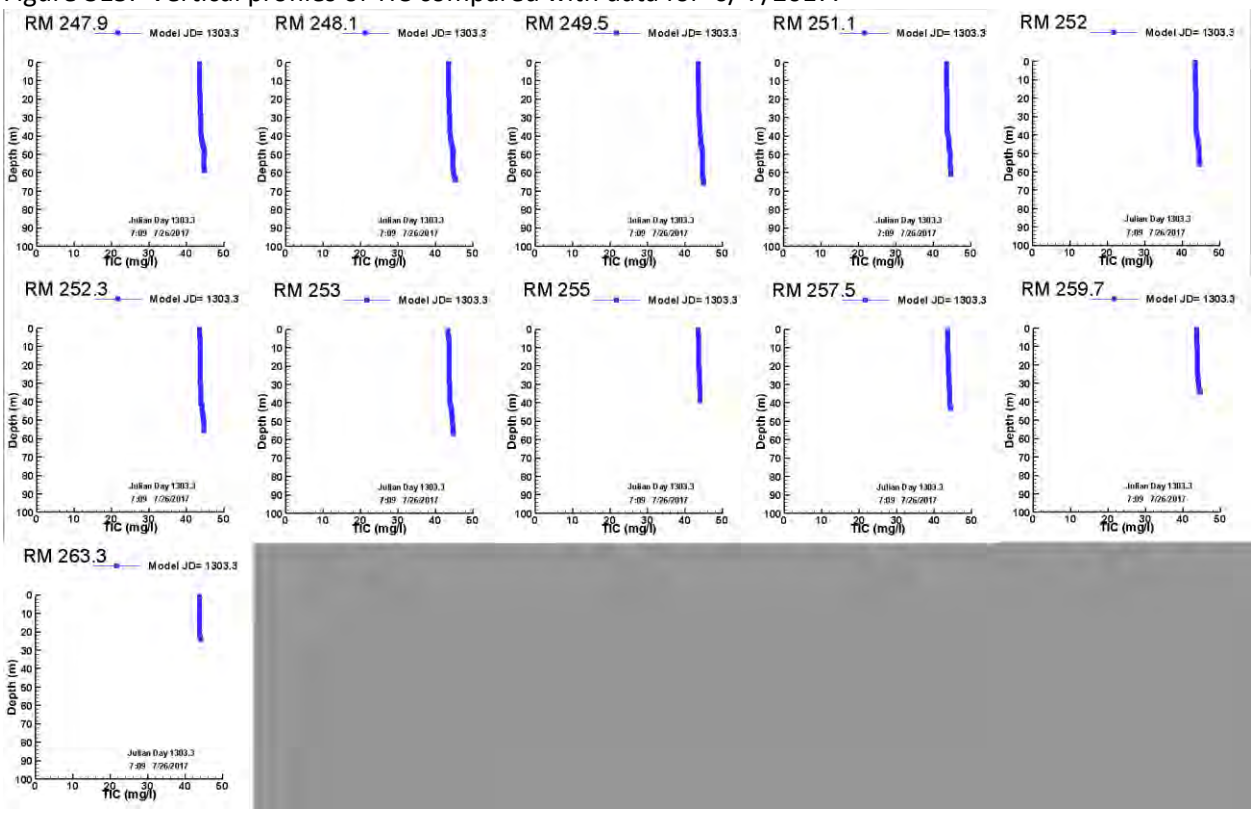


Figure 316. Vertical profiles of TIC compared with data for 7/26/2017.

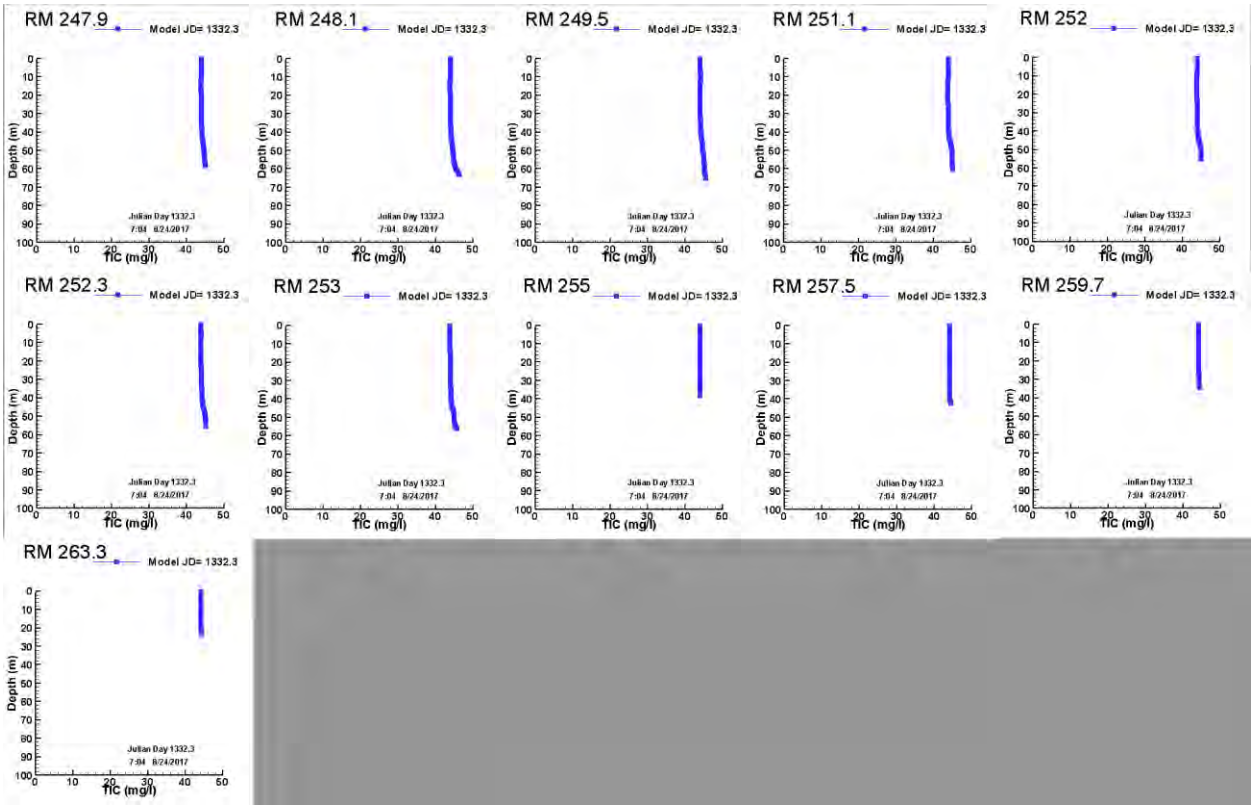


Figure 317. Vertical profiles of TIC compared with data for 8/24/2017.

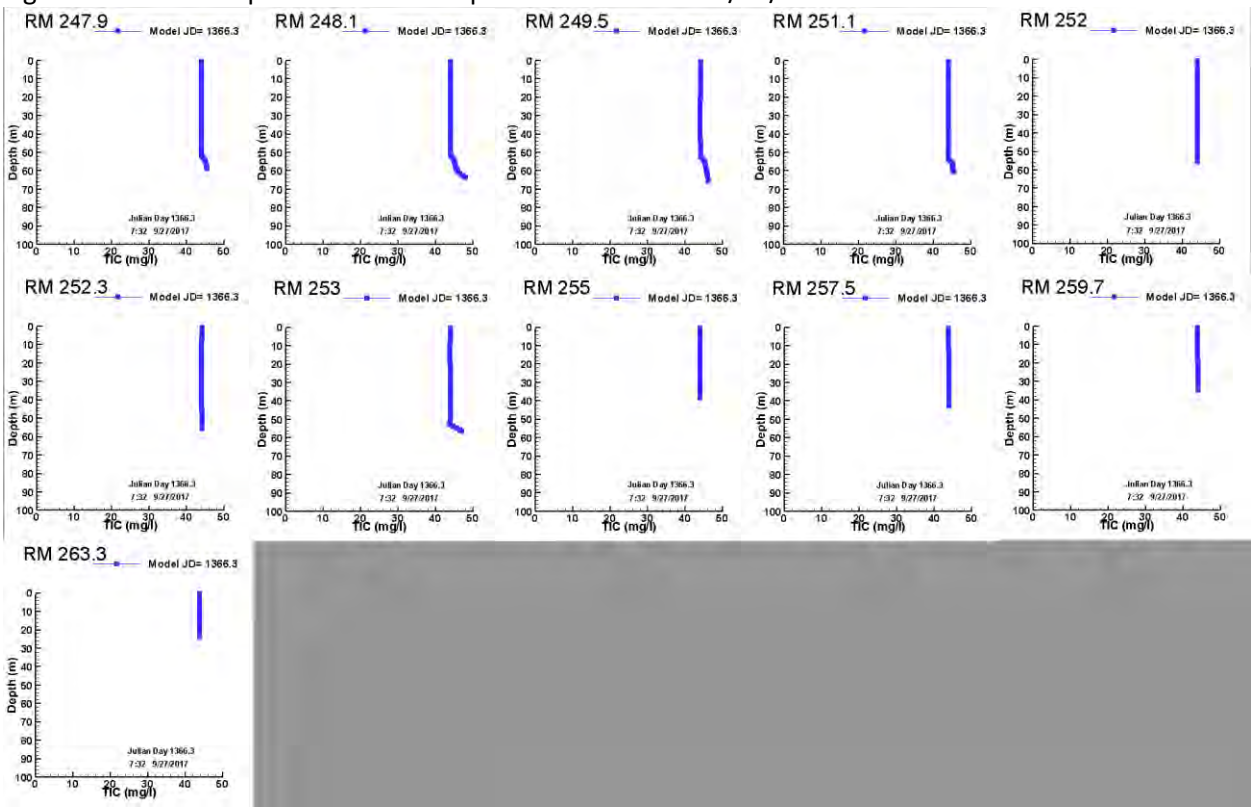


Figure 318. Vertical profiles of TIC compared with data for 9/27/2017.

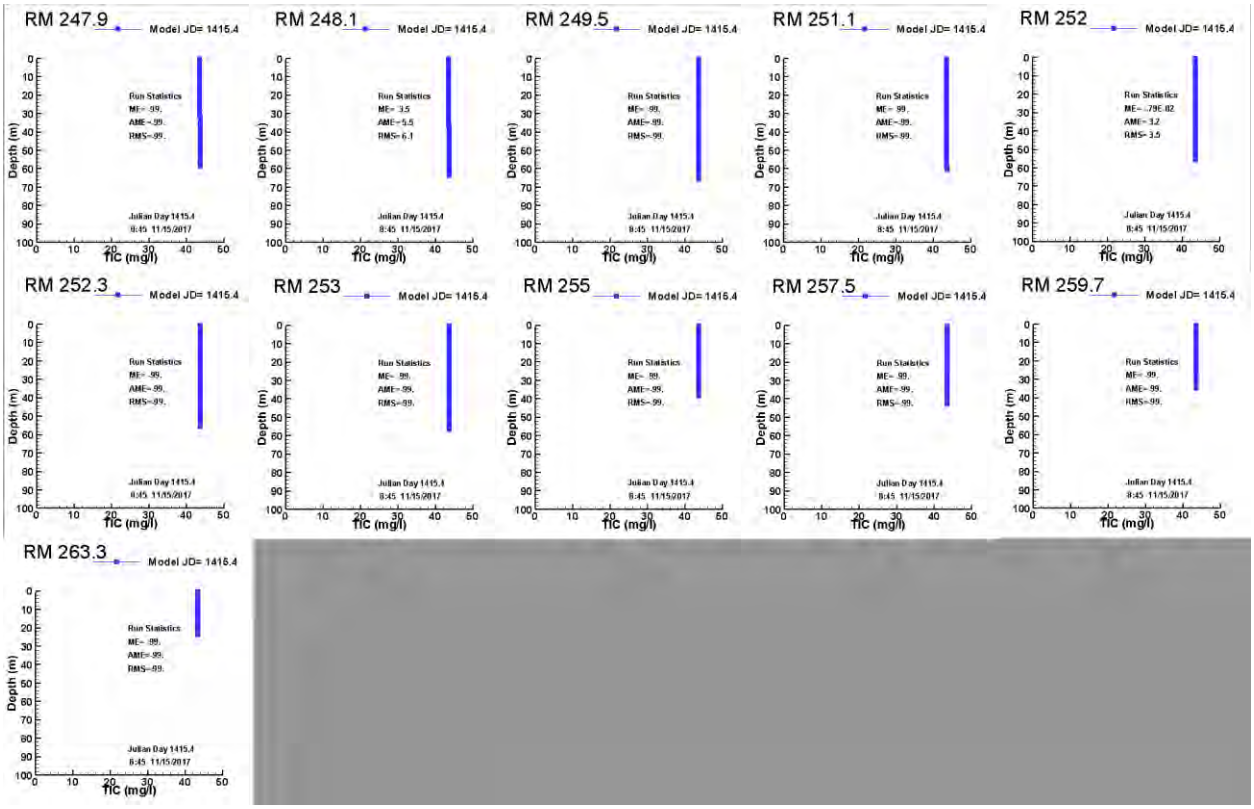


Figure 319. Vertical profiles of TIC compared with data for 11/15/2017.

Zooplankton

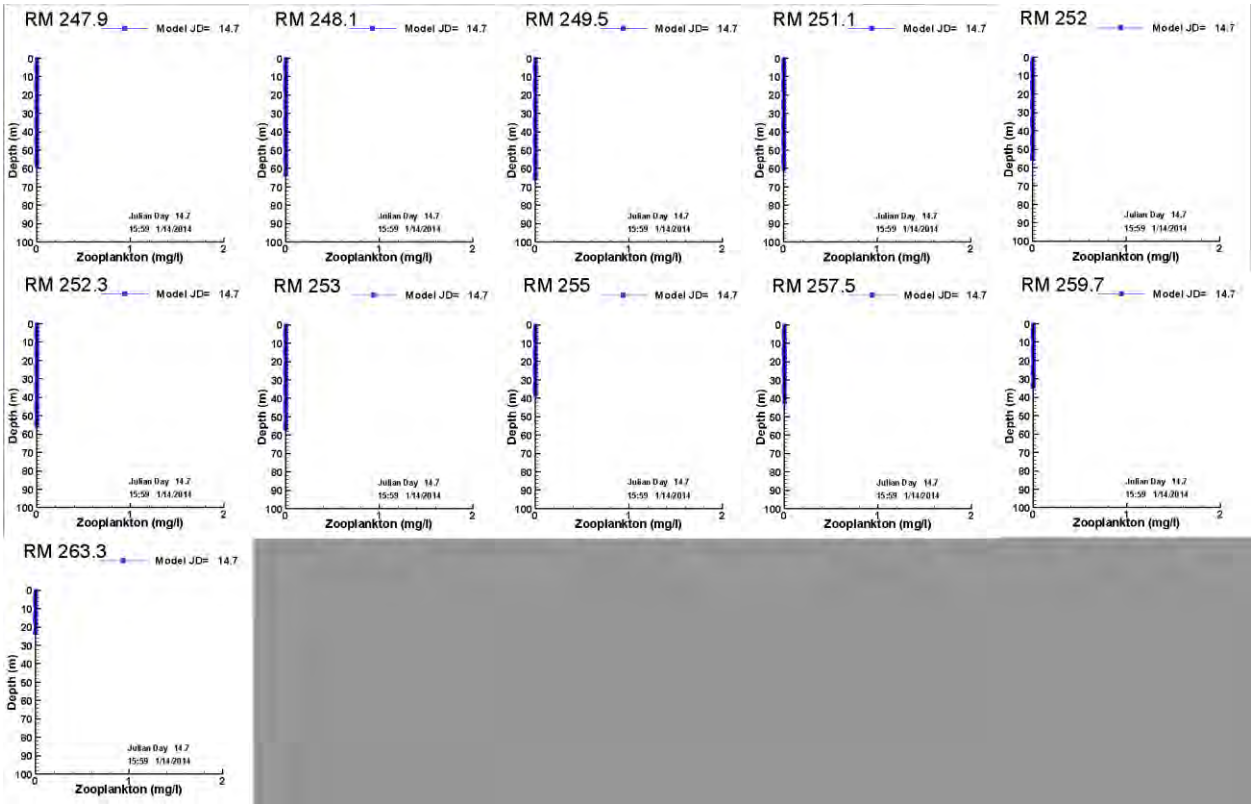


Figure 320. Vertical profiles of zooplankton compared with data for 1/14/2014.

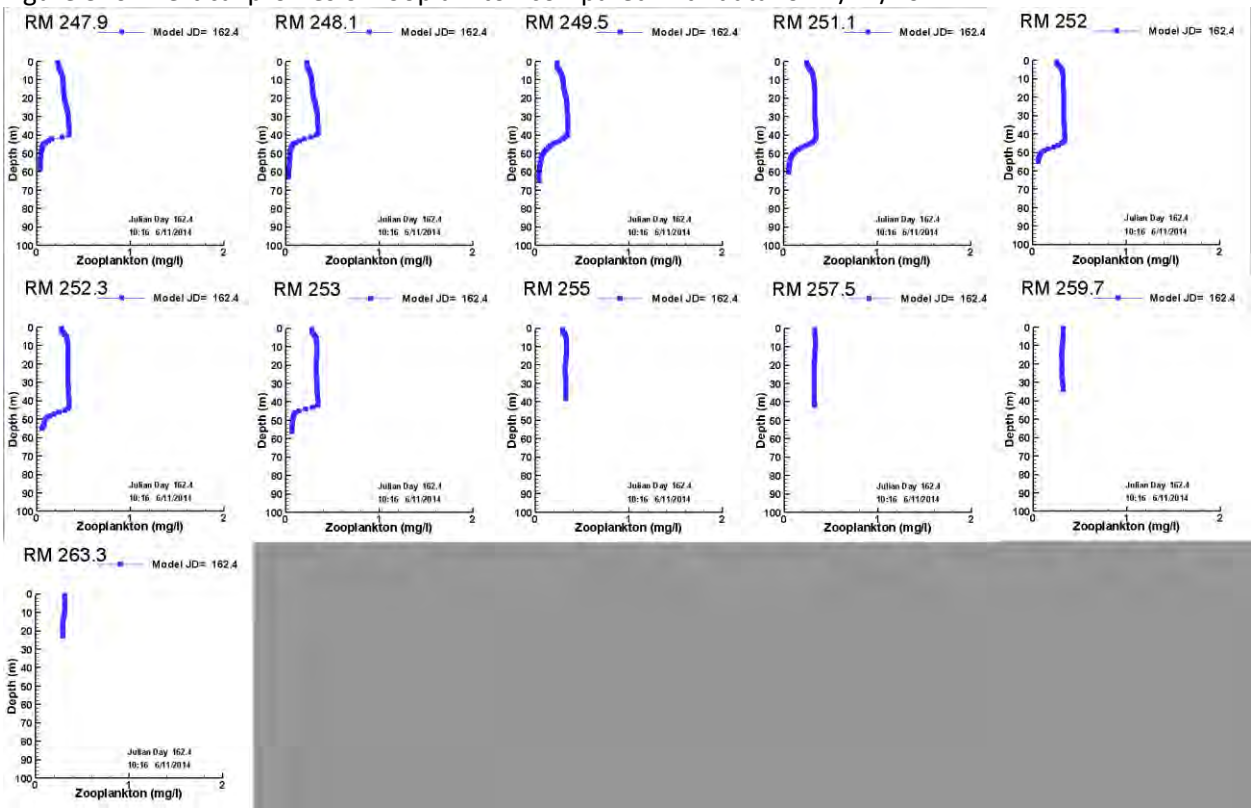


Figure 321. Vertical profiles of zooplankton compared with data for 6/11/2014.

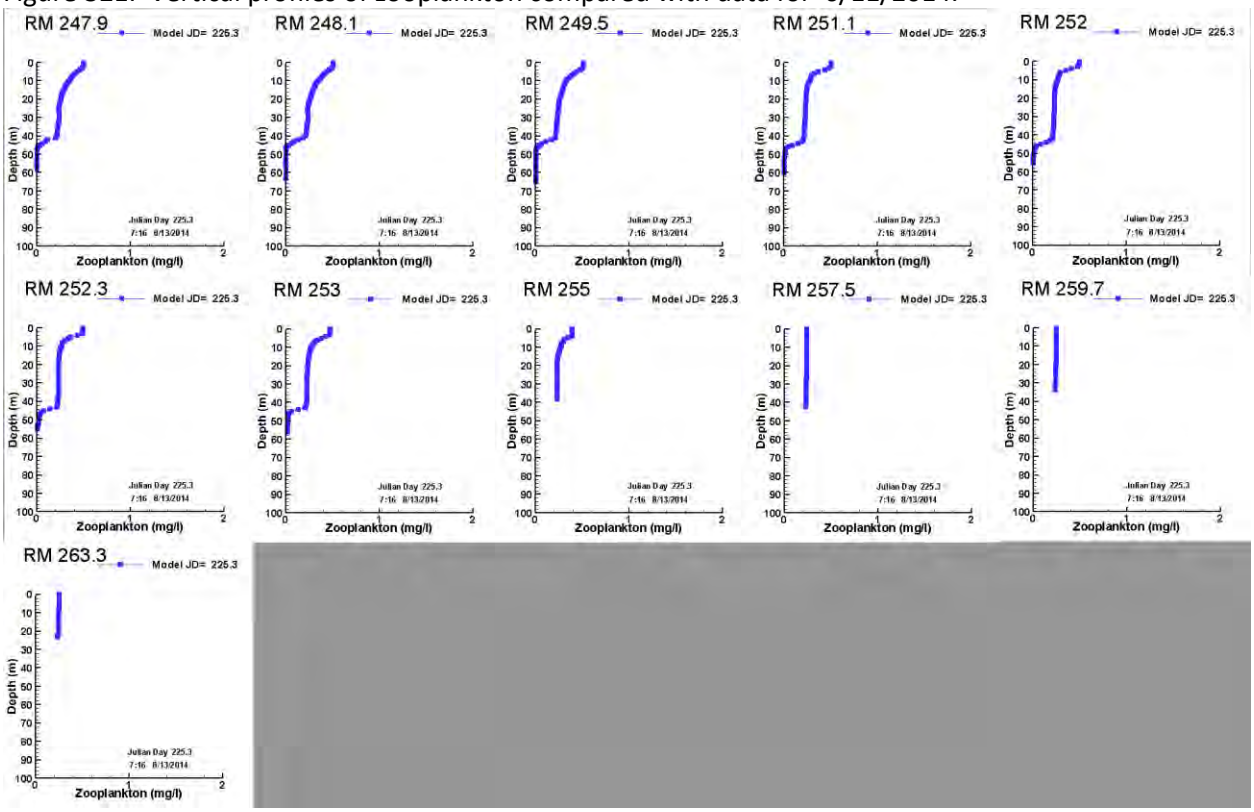


Figure 322. Vertical profiles of zooplankton compared with data for 8/13/2014.

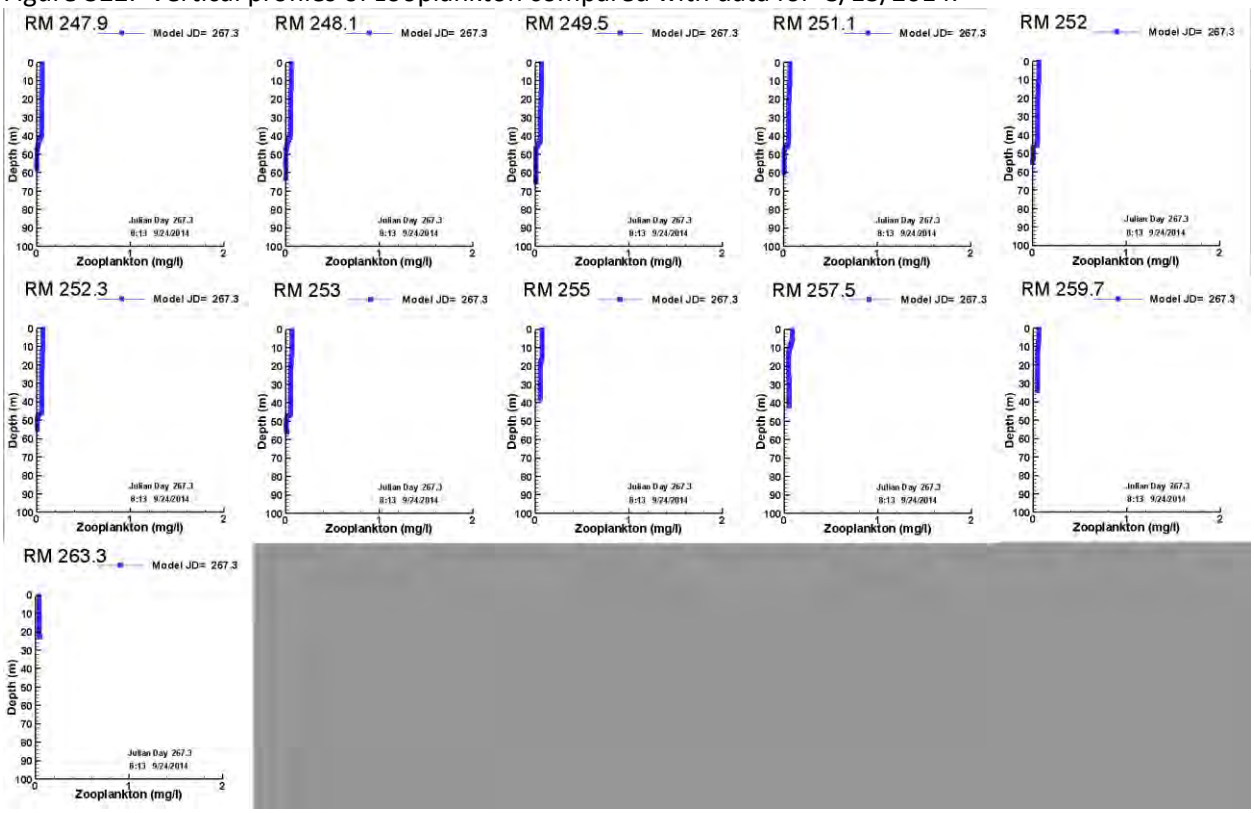


Figure 323. Vertical profiles of zooplankton compared with data for 9/24/2014.

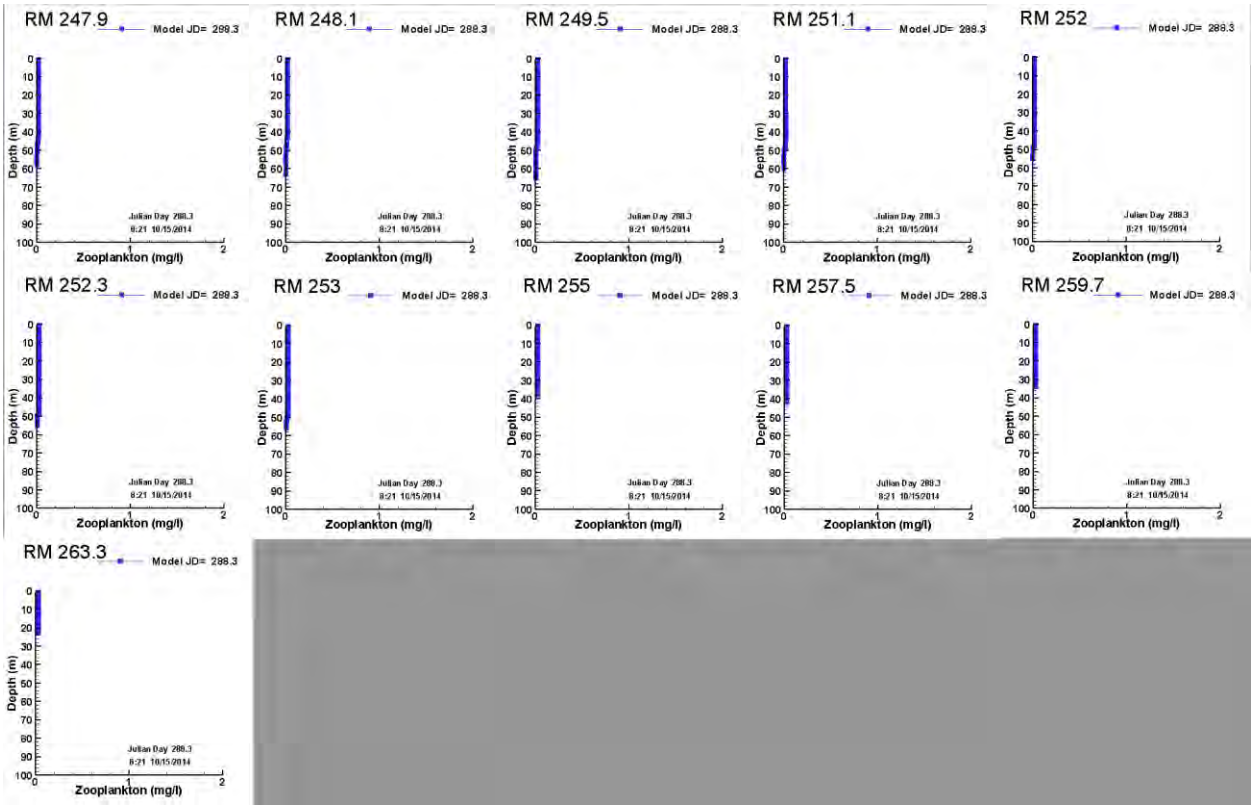


Figure 324. Vertical profiles of zooplankton compared with data for 10/15/2014.

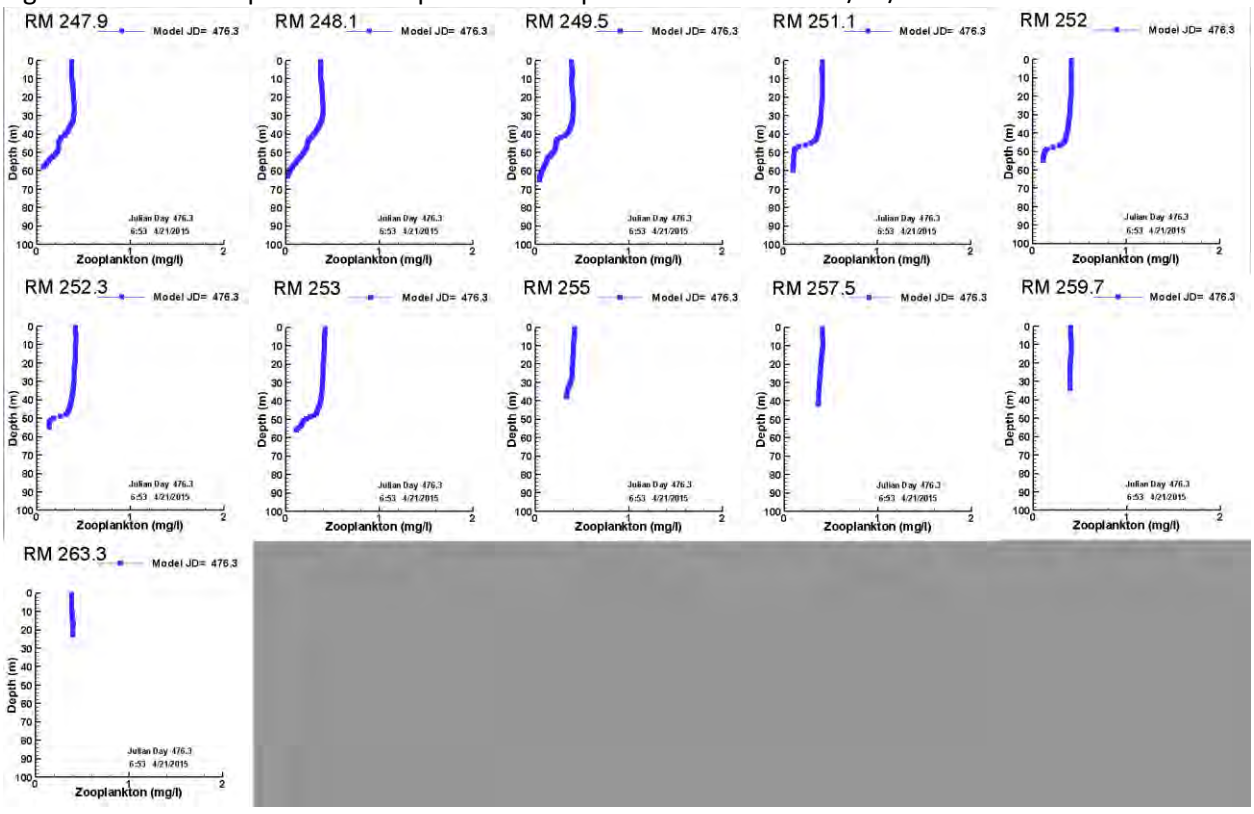


Figure 325. Vertical profiles of zooplankton compared with data for 4/21/2015.

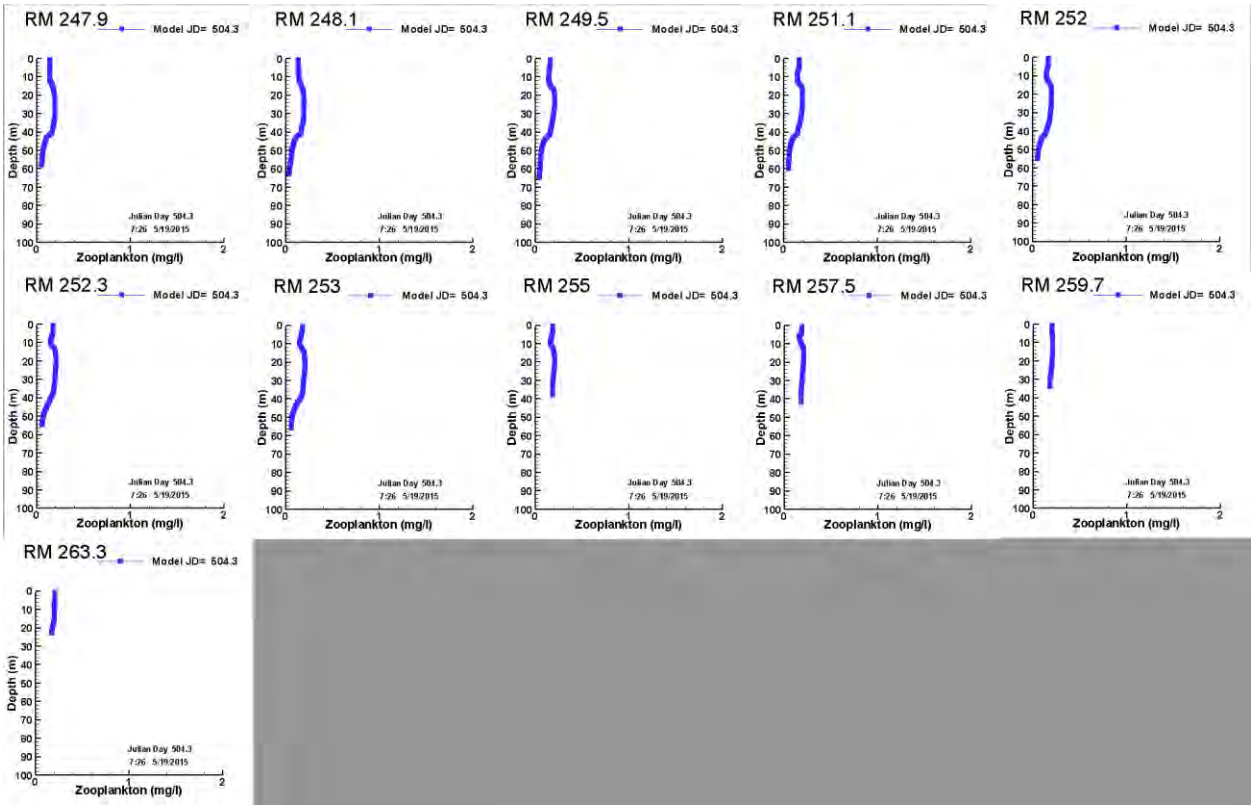


Figure 326. Vertical profiles of zooplankton compared with data for 5/19/2015.

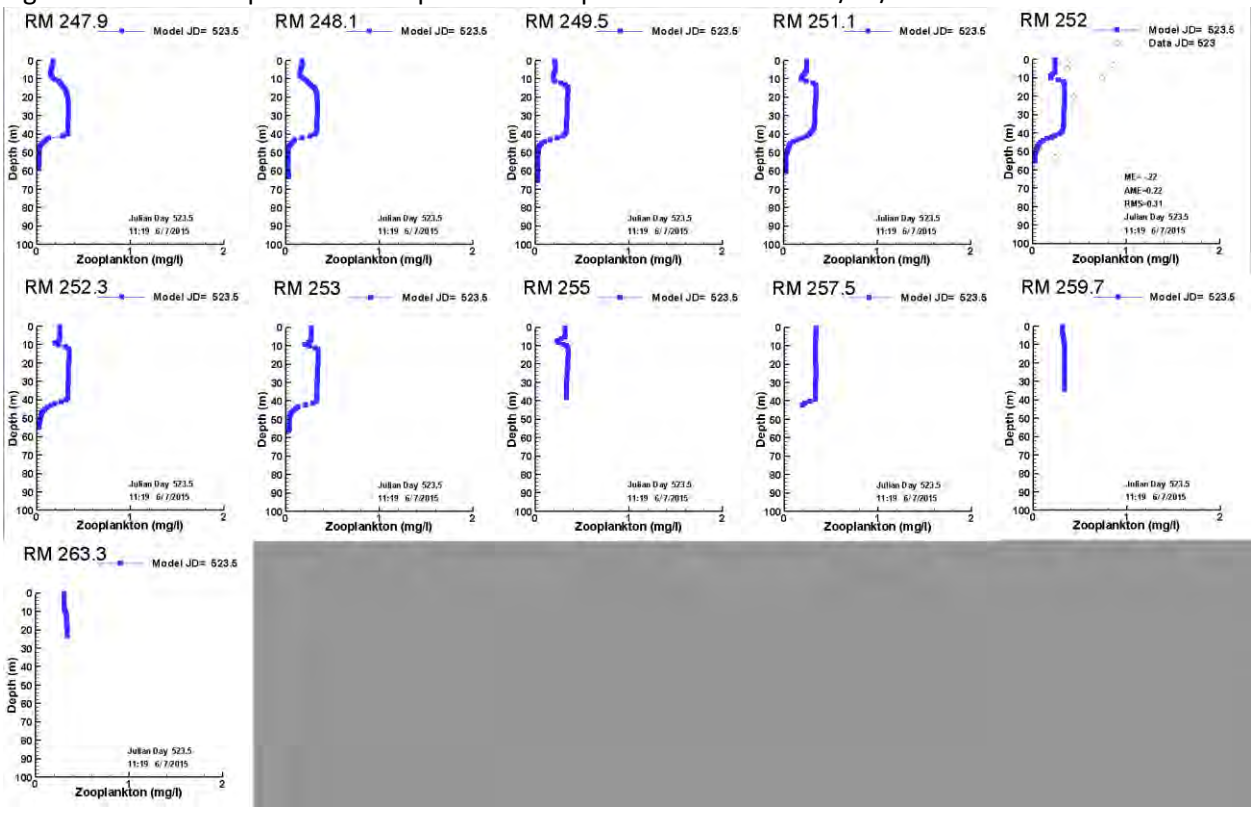


Figure 327. Vertical profiles of zooplankton compared with data for 6/ 7/2015.

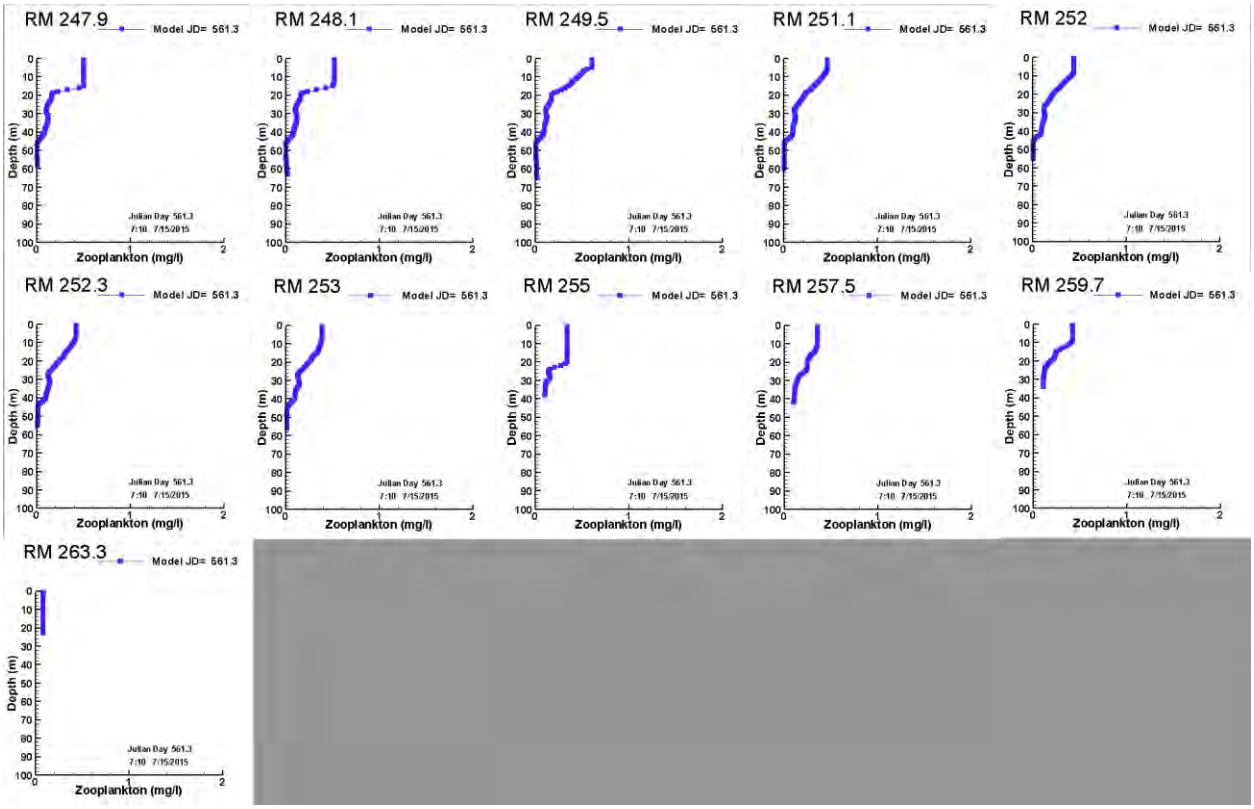


Figure 328. Vertical profiles of zooplankton compared with data for 7/15/2015.

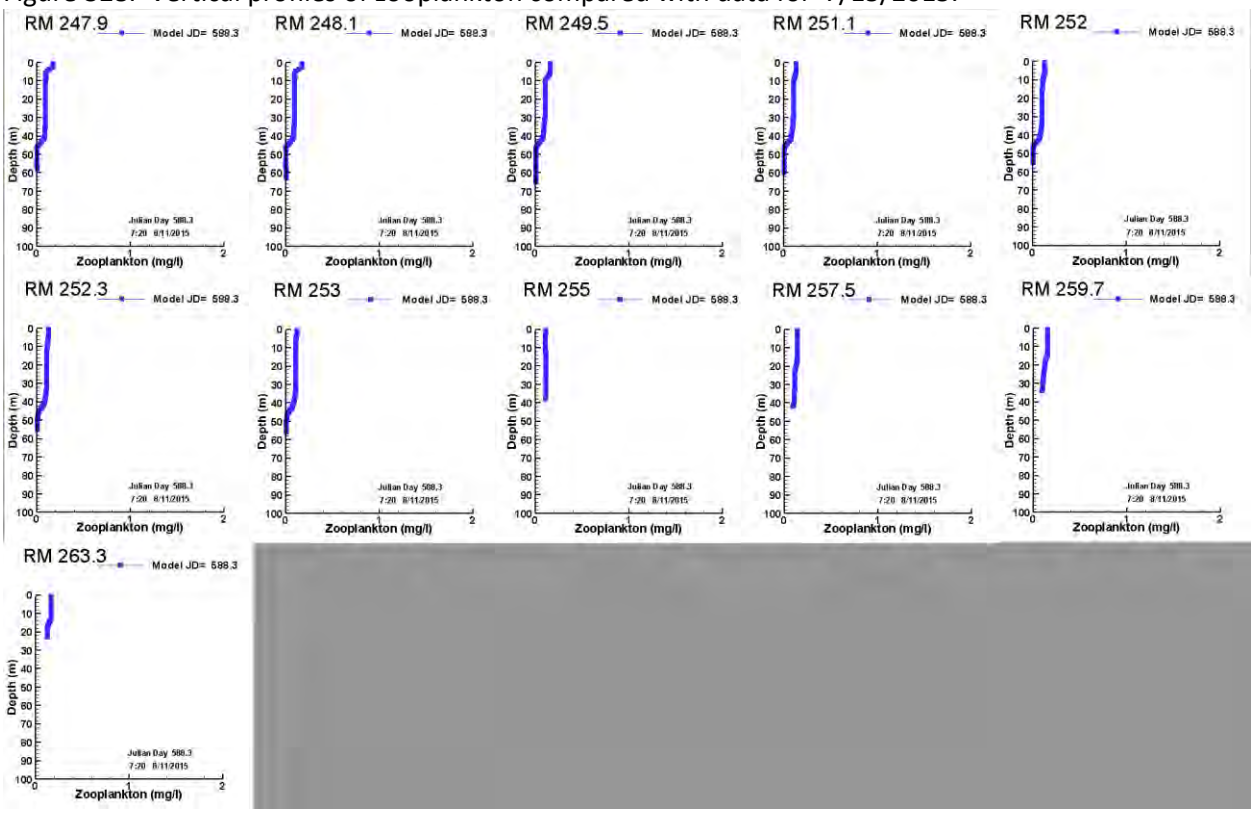


Figure 329. Vertical profiles of zooplankton compared with data for 8/11/2015.

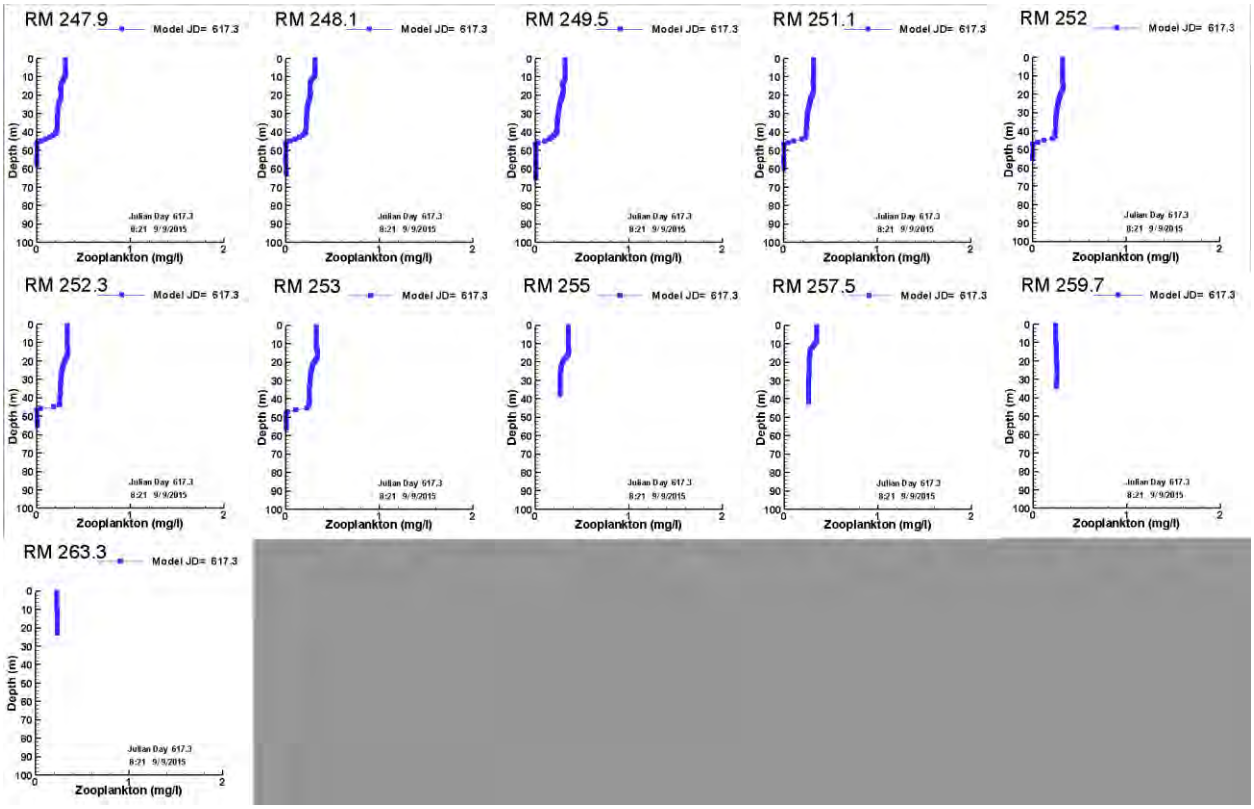


Figure 330. Vertical profiles of zooplankton compared with data for 9/ 9/2015.

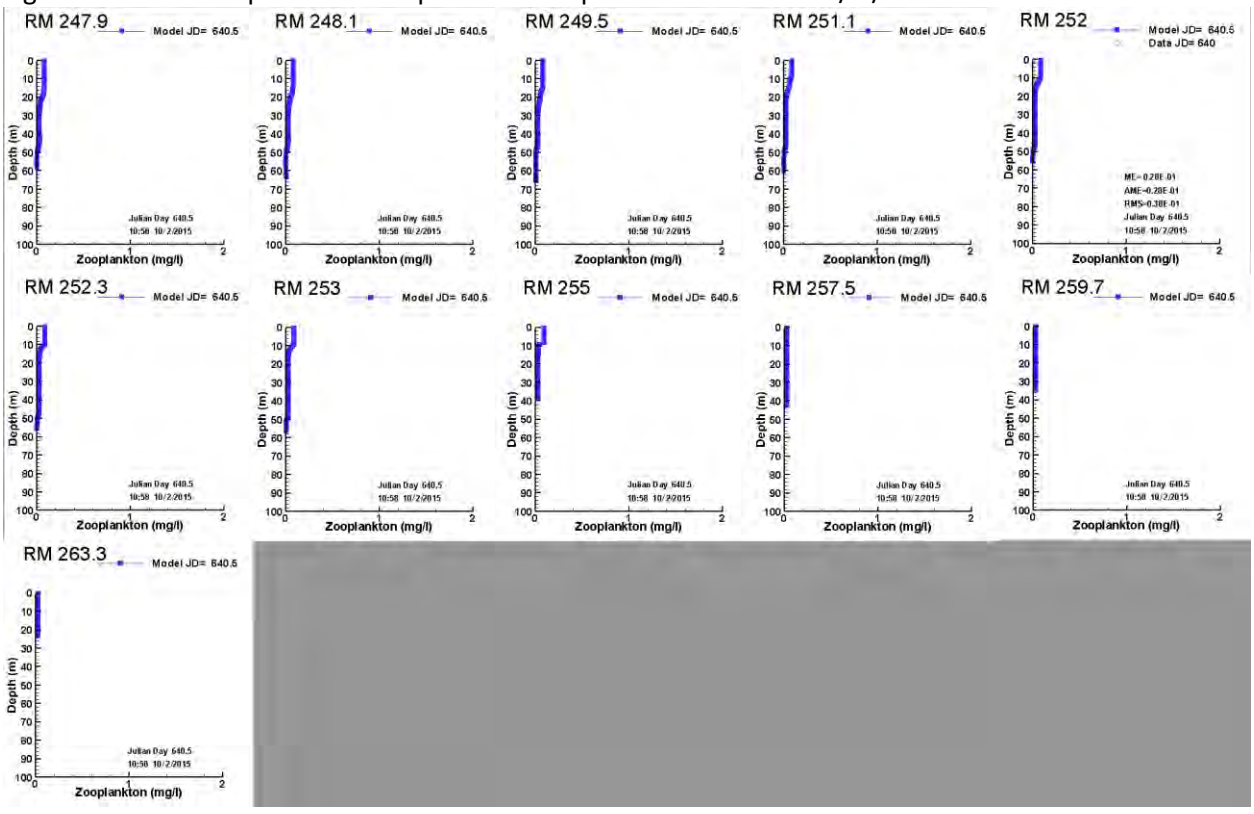


Figure 331. Vertical profiles of zooplankton compared with data for 10/ 2/2015.

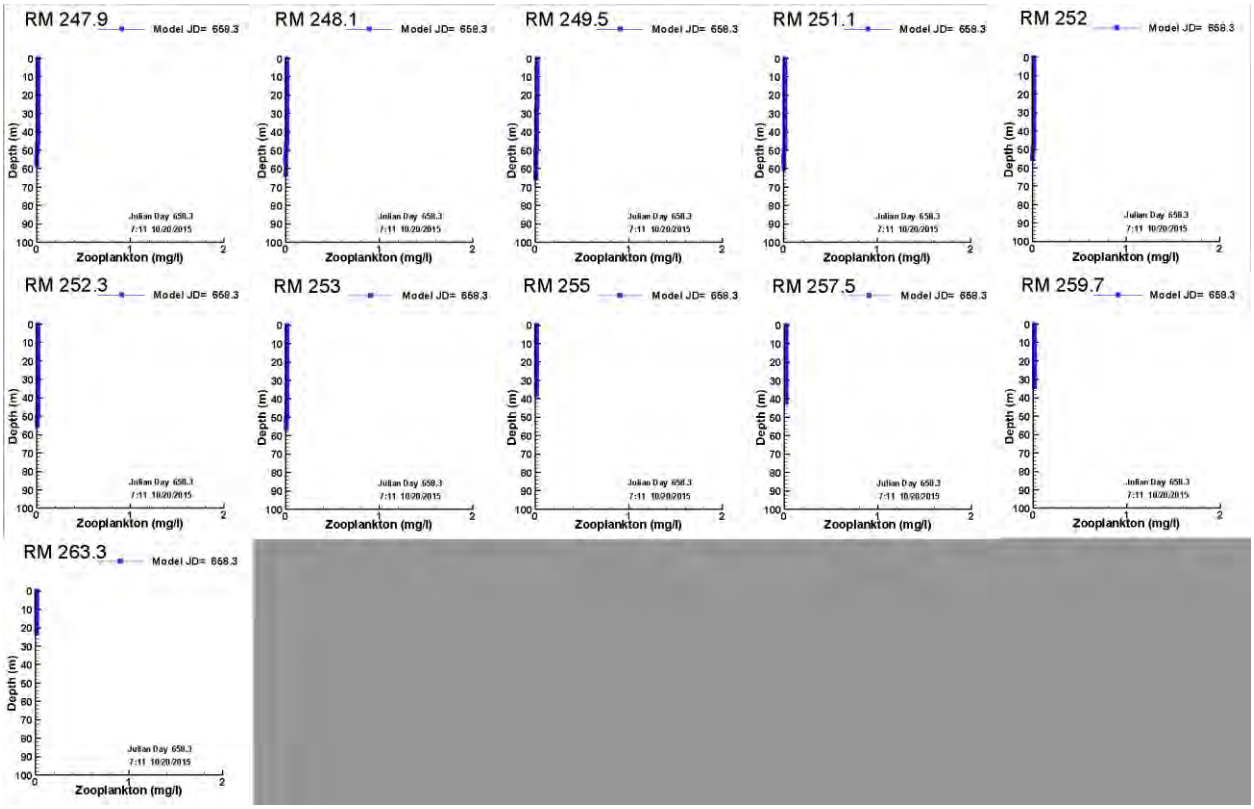


Figure 332. Vertical profiles of zooplankton compared with data for 10/20/2015.

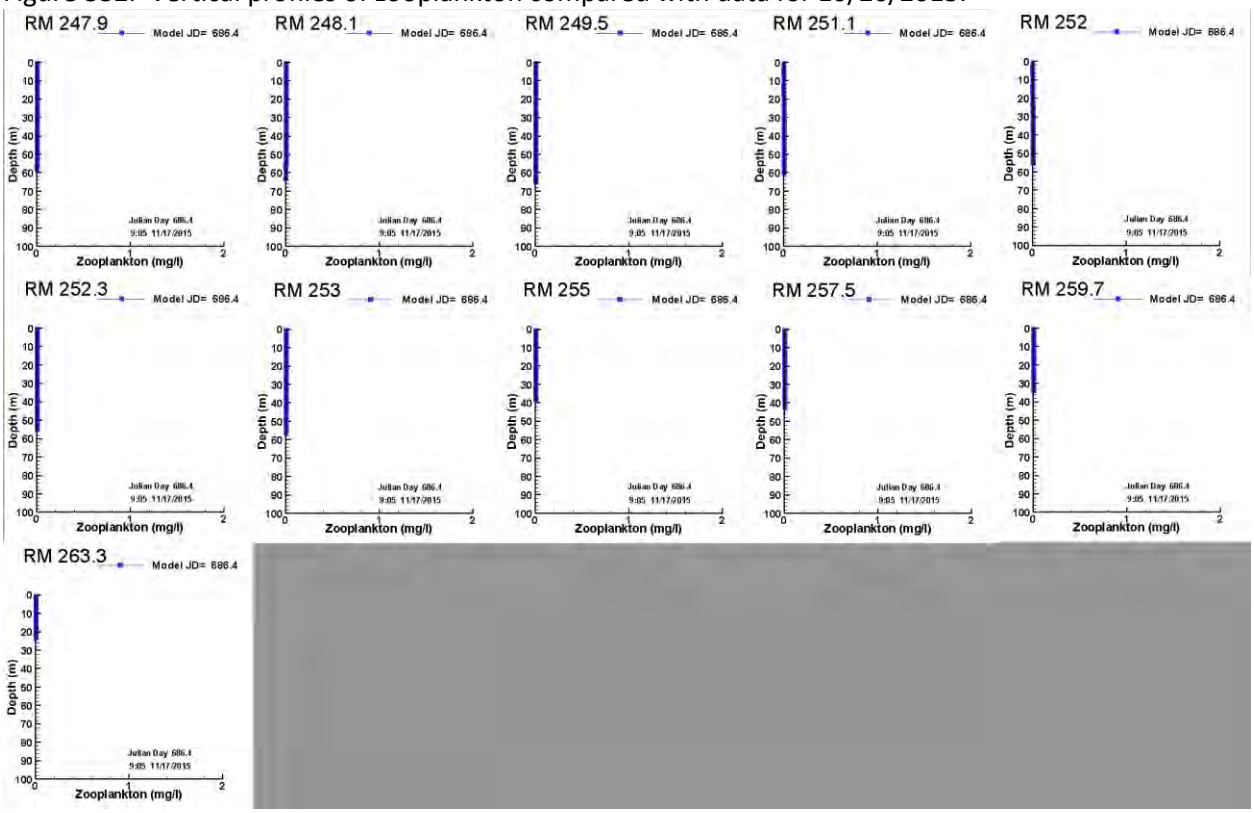


Figure 333. Vertical profiles of zooplankton compared with data for 11/17/2015.

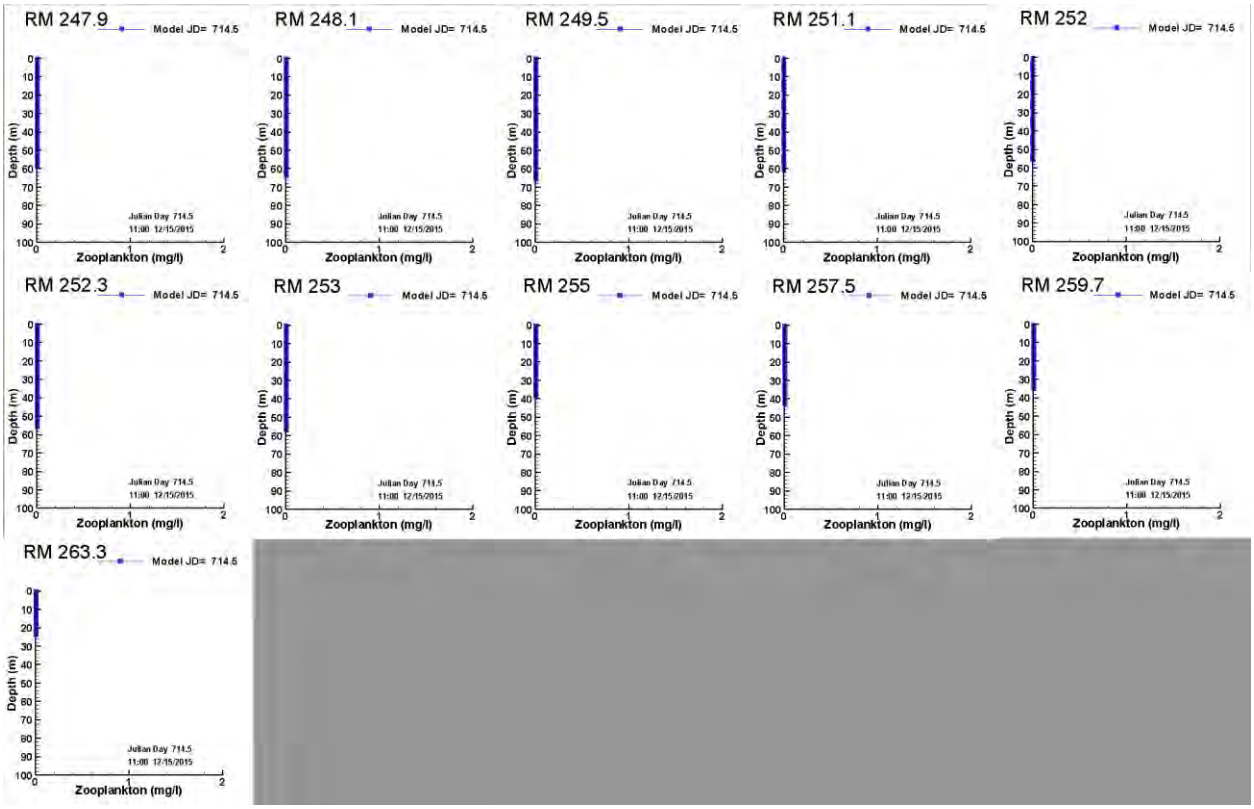


Figure 334. Vertical profiles of zooplankton compared with data for 12/15/2015.

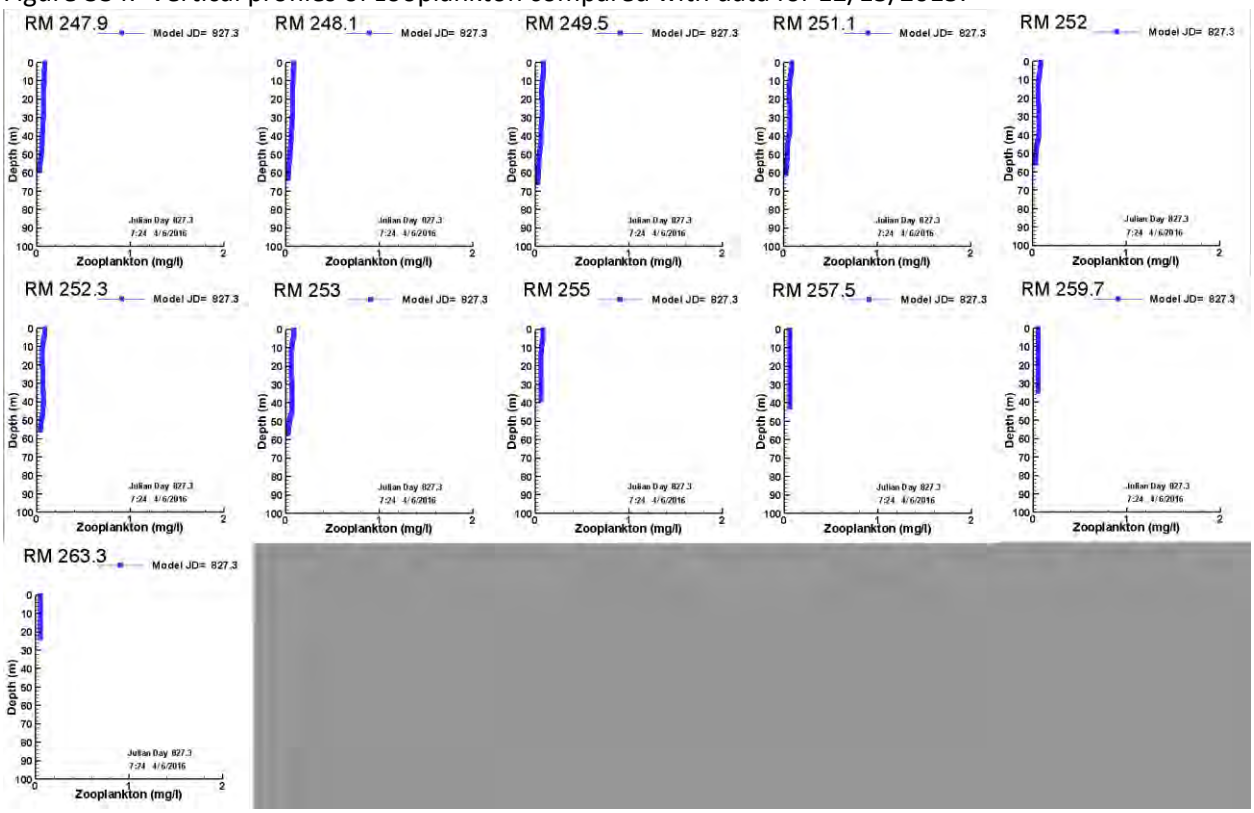


Figure 335. Vertical profiles of zooplankton compared with data for 4/ 6/2016.

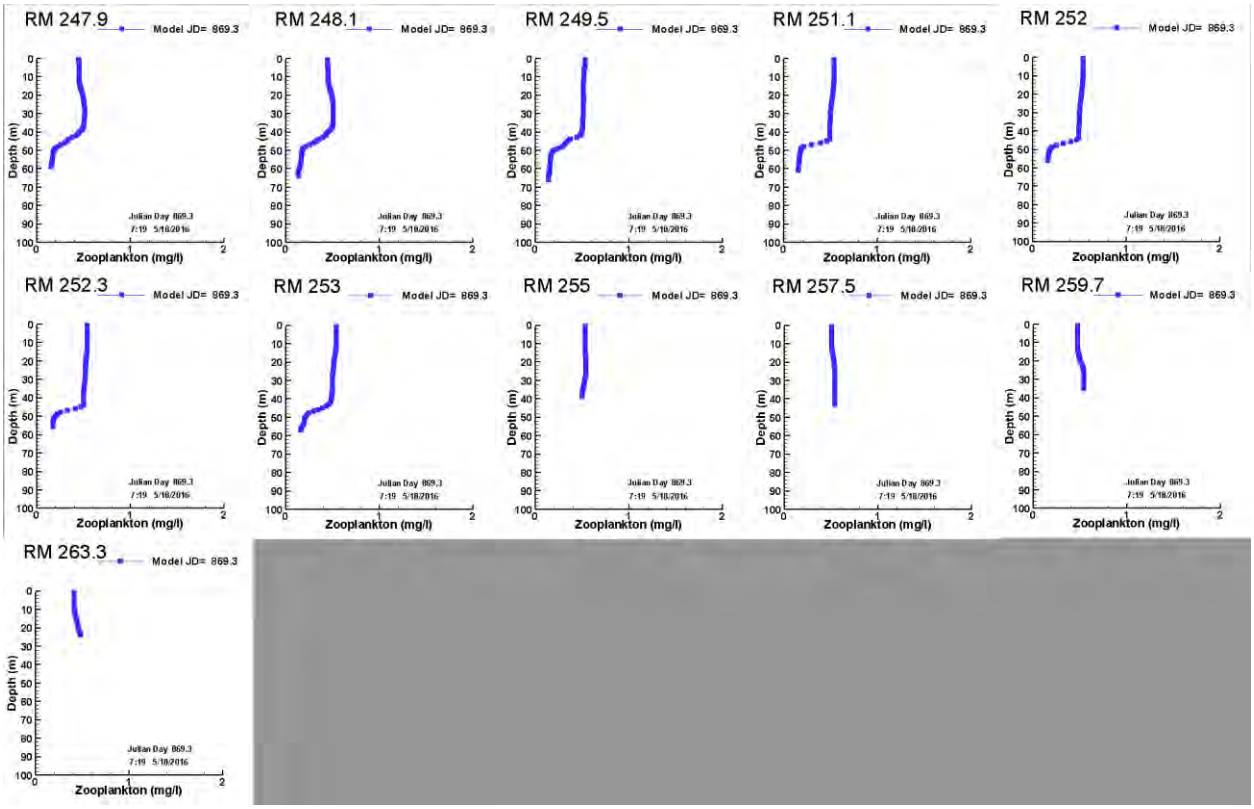


Figure 336. Vertical profiles of zooplankton compared with data for 5/18/2016.

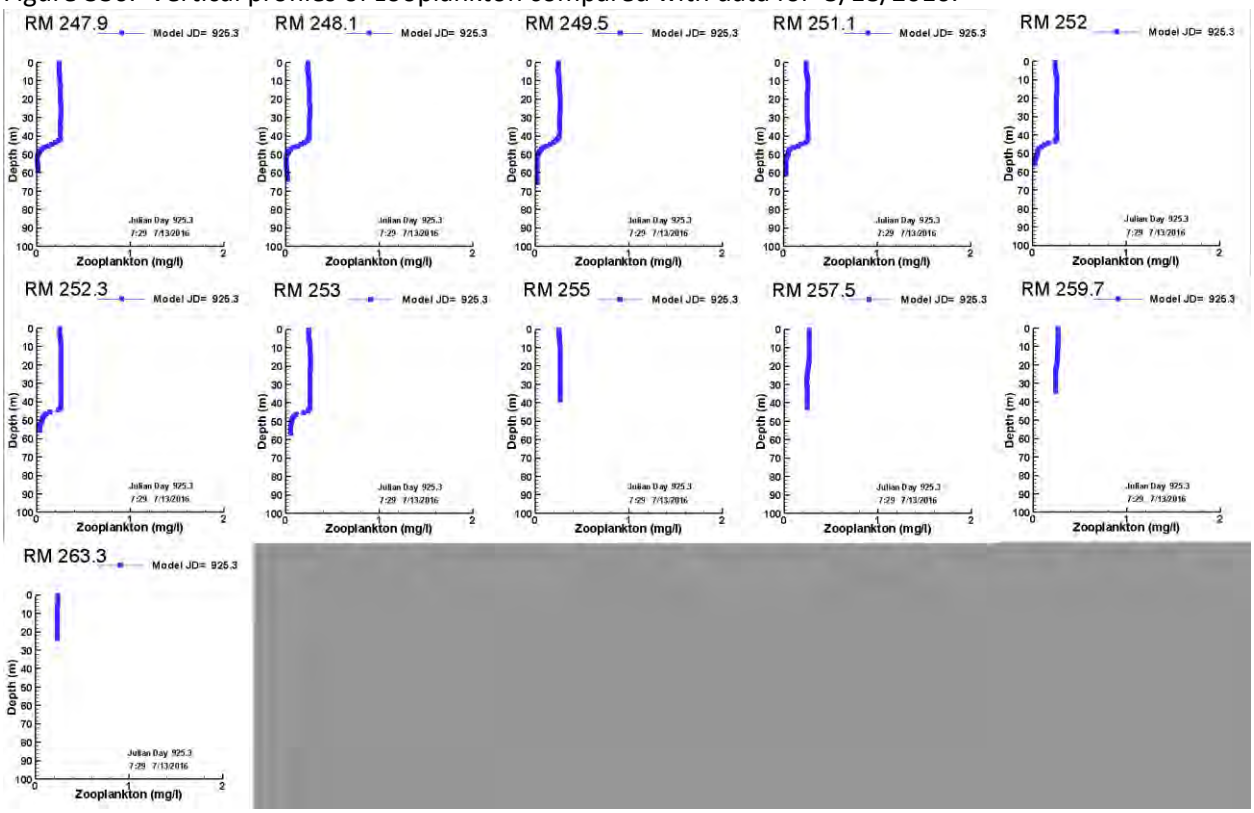


Figure 337. Vertical profiles of zooplankton compared with data for 7/13/2016.

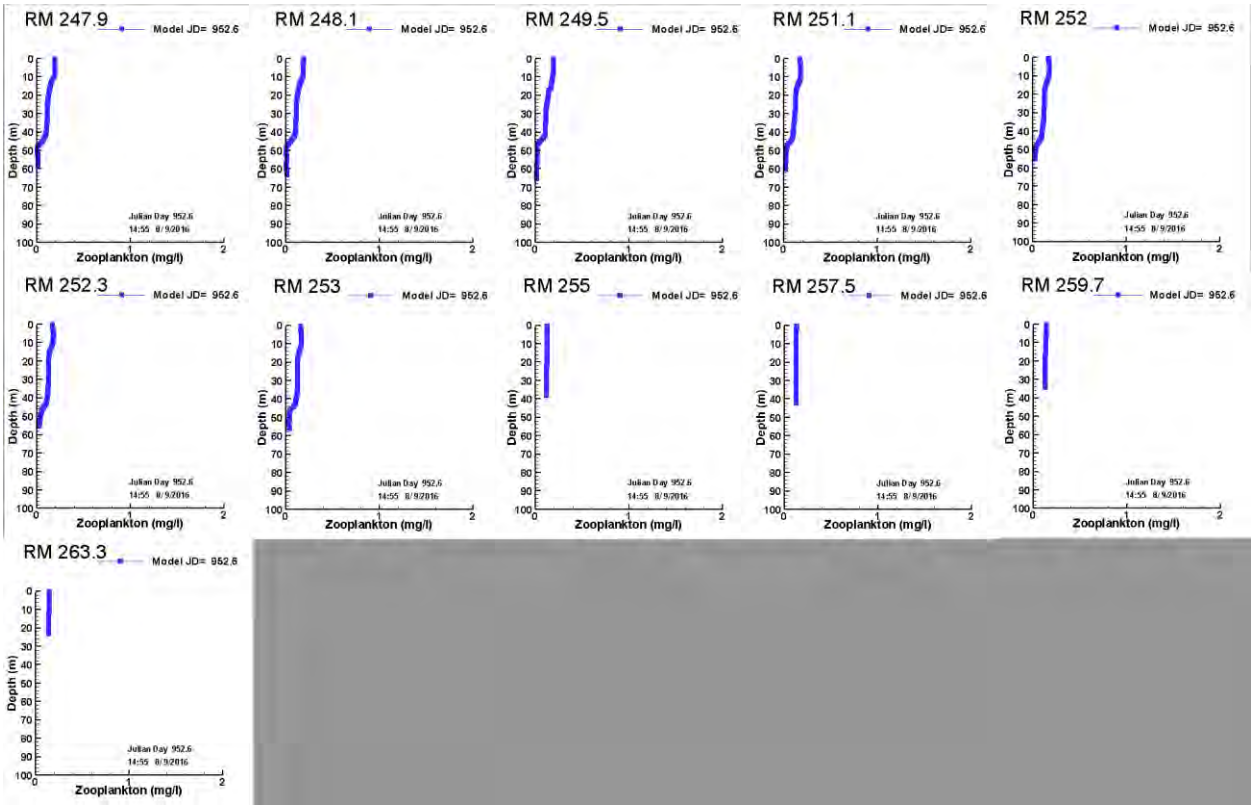


Figure 338. Vertical profiles of zooplankton compared with data for 8/ 9/2016.

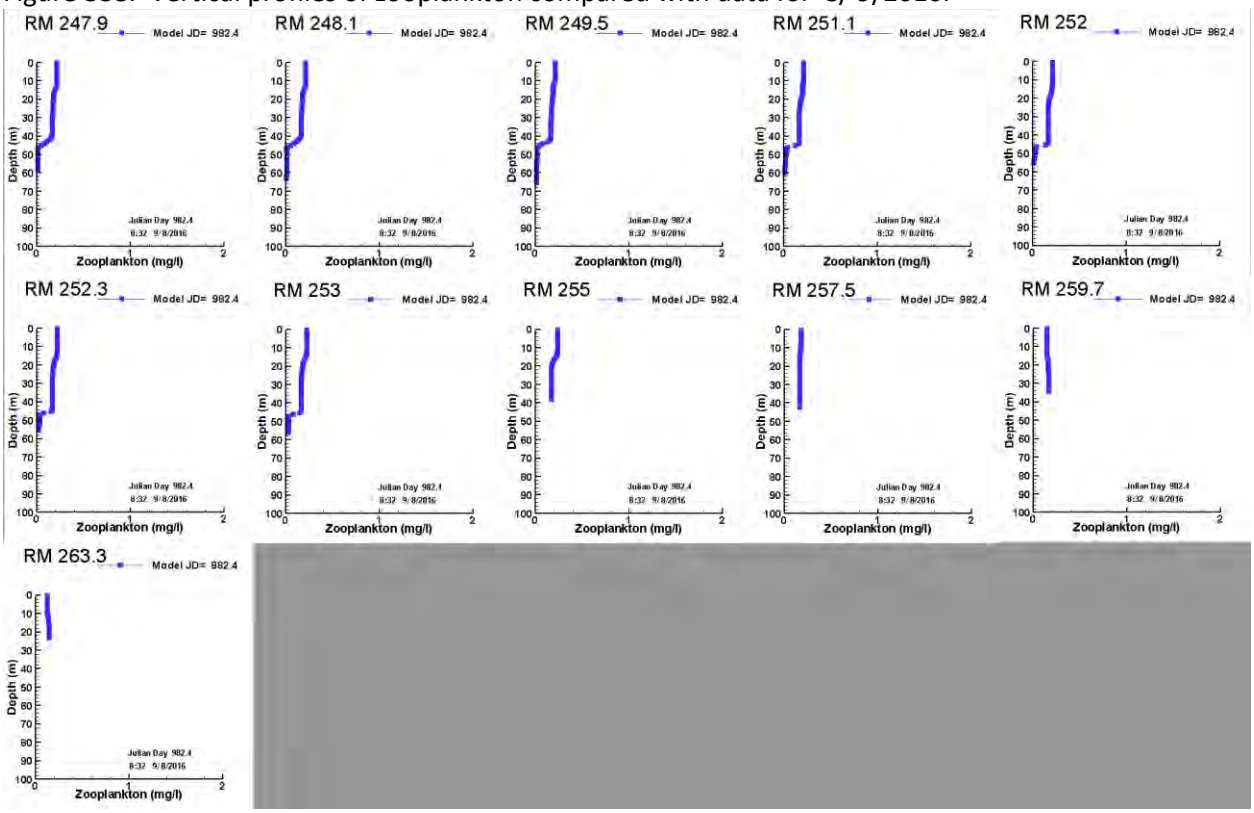


Figure 339. Vertical profiles of zooplankton compared with data for 9/ 8/2016.

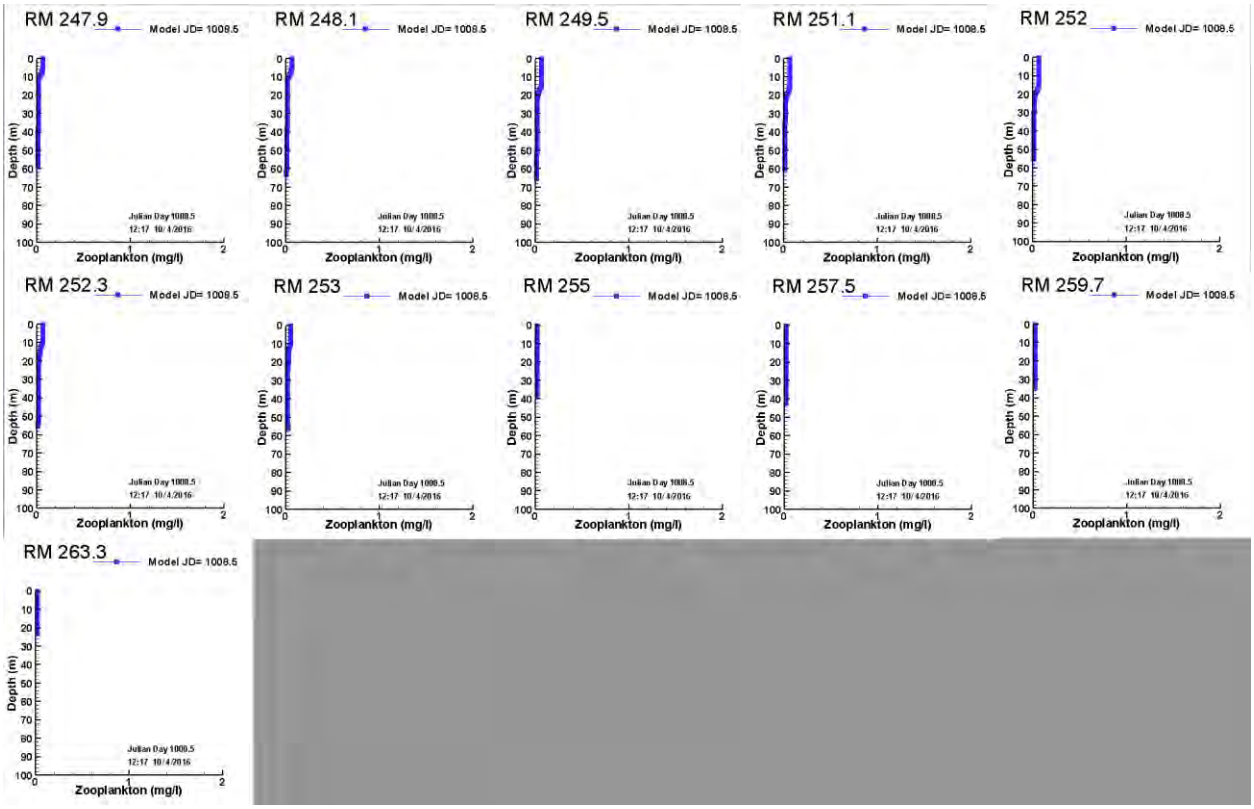


Figure 340. Vertical profiles of zooplankton compared with data for 10/ 4/2016.

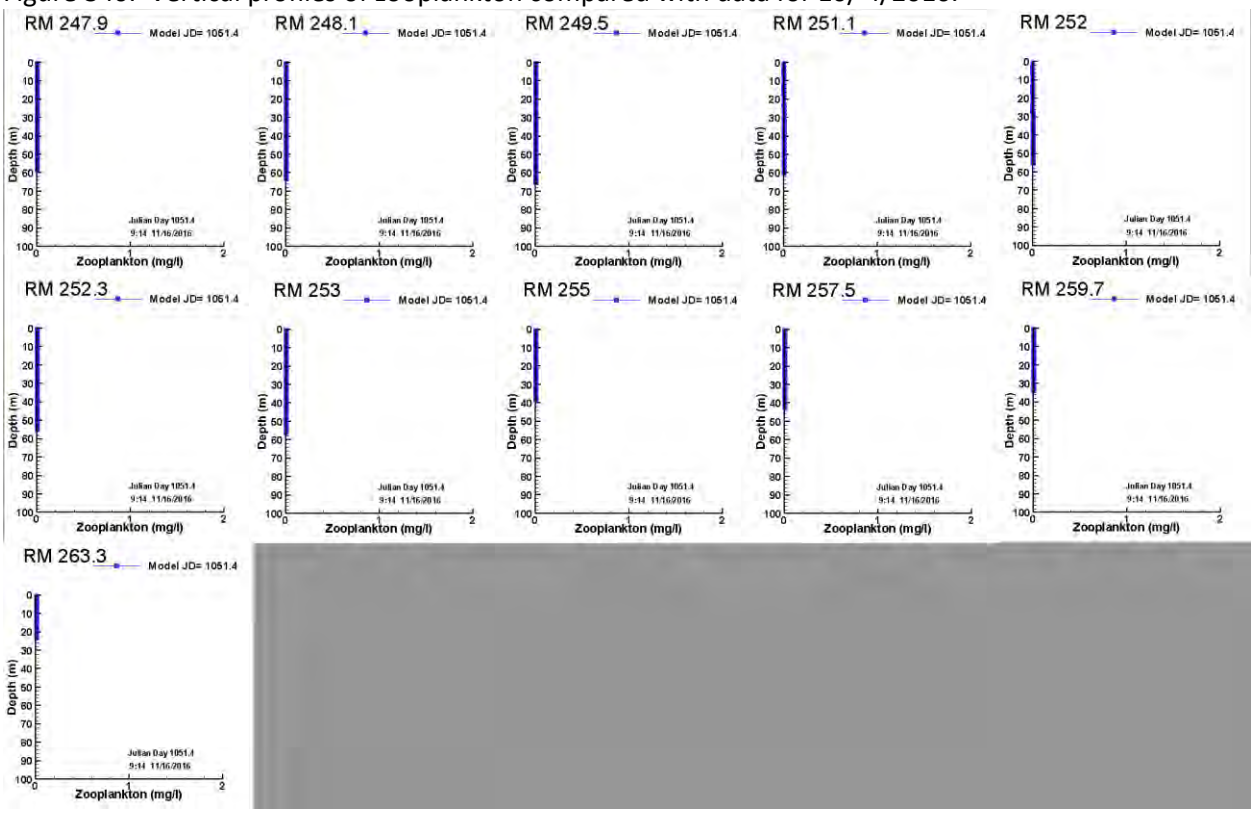


Figure 341. Vertical profiles of zooplankton compared with data for 11/16/2016.

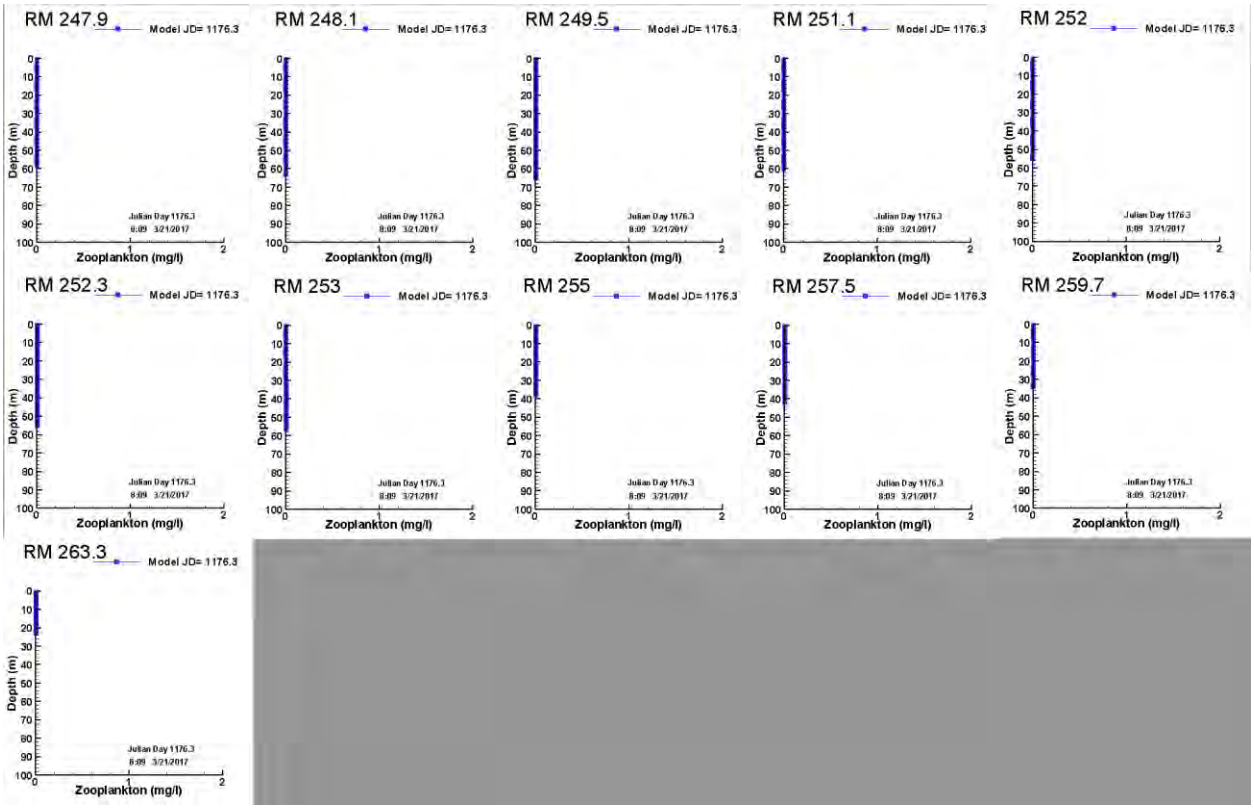


Figure 342. Vertical profiles of zooplankton compared with data for 3/21/2017.

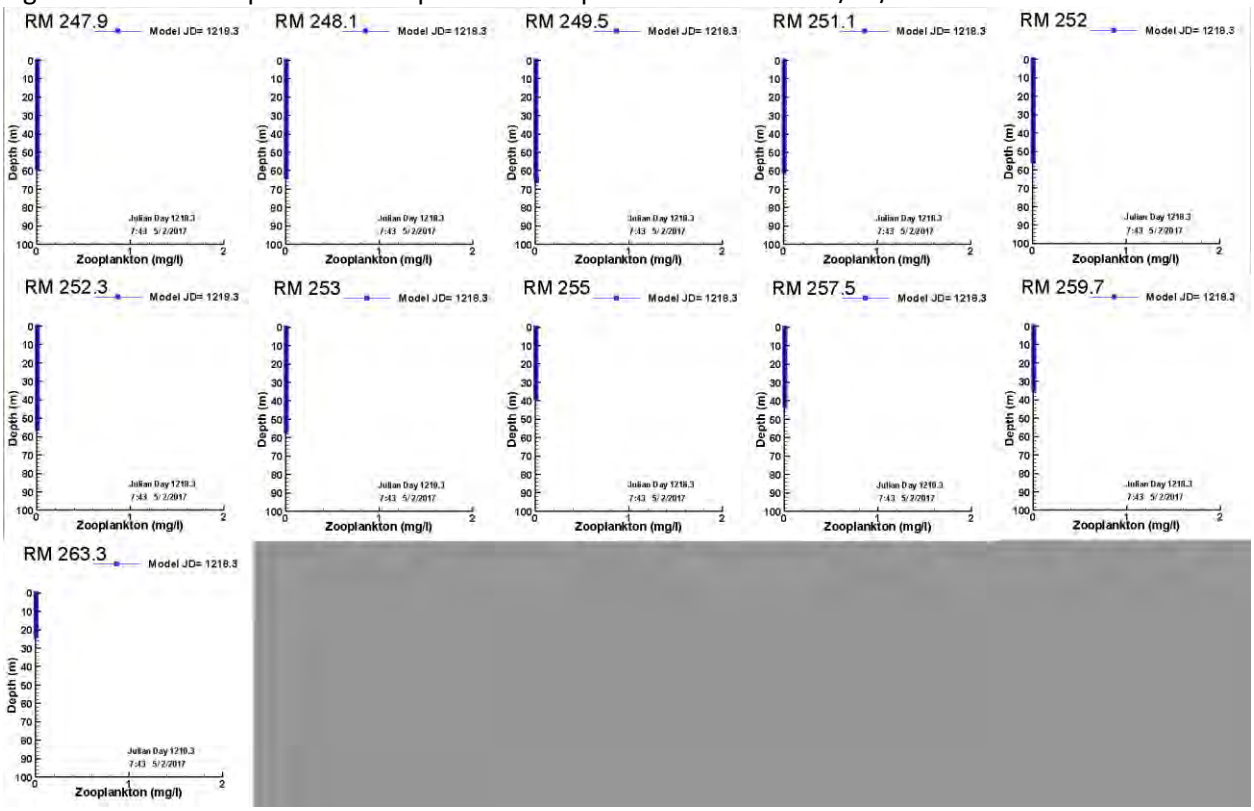


Figure 343. Vertical profiles of zooplankton compared with data for 5/ 2/2017.

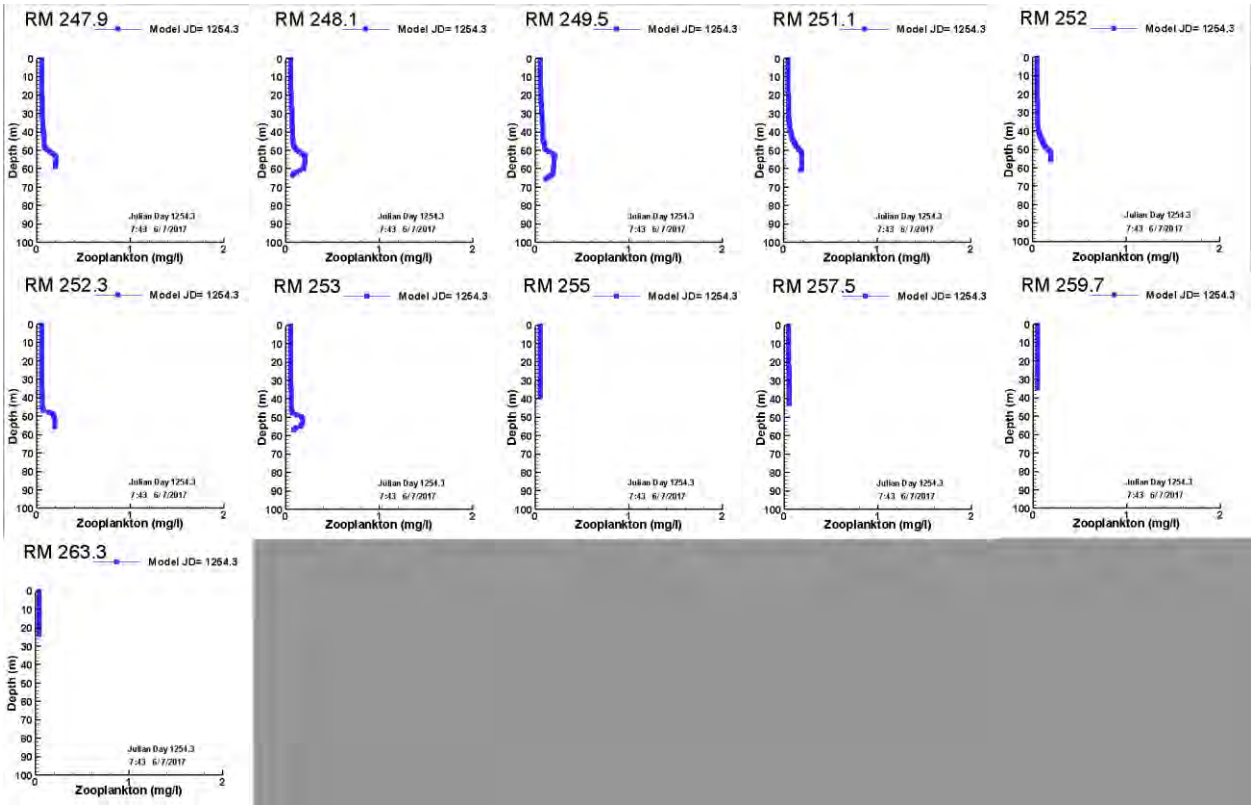


Figure 344. Vertical profiles of zooplankton compared with data for 6/ 7/2017.

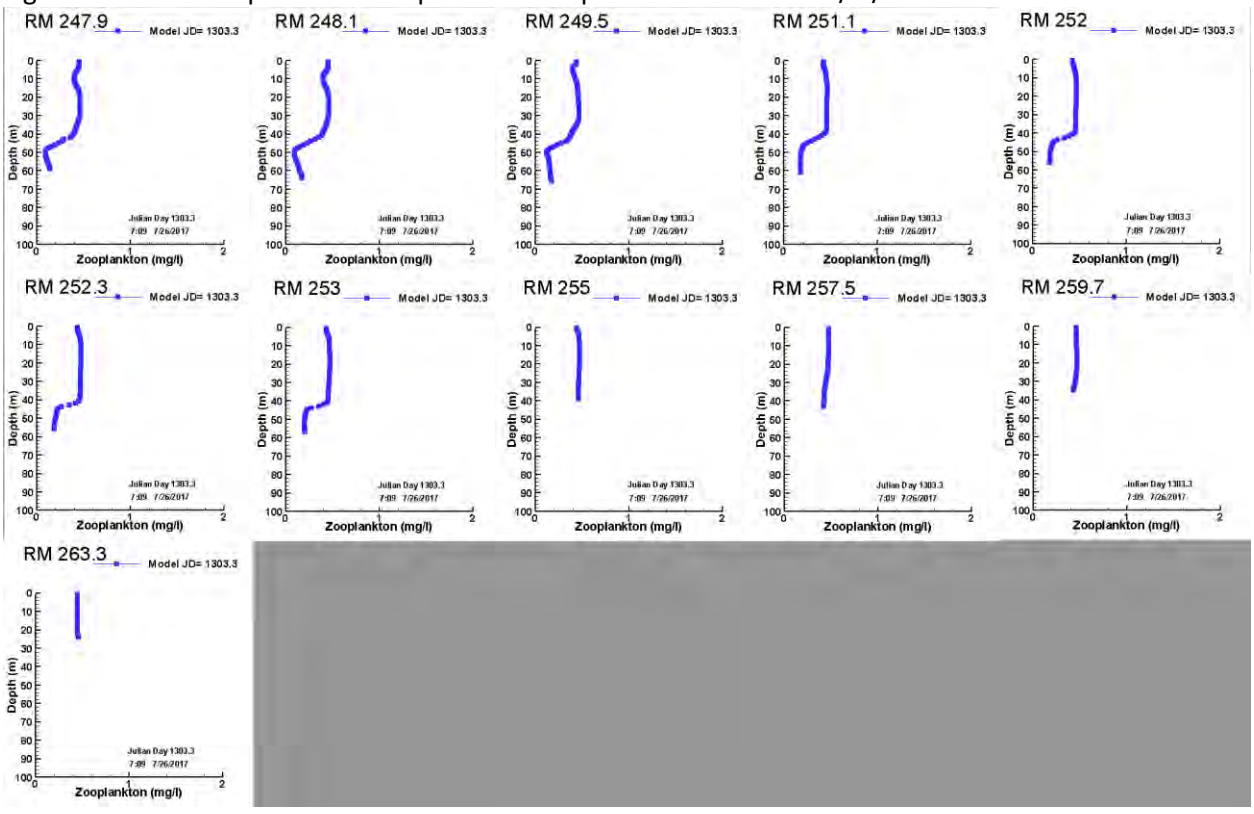


Figure 345. Vertical profiles of zooplankton compared with data for 7/26/2017.

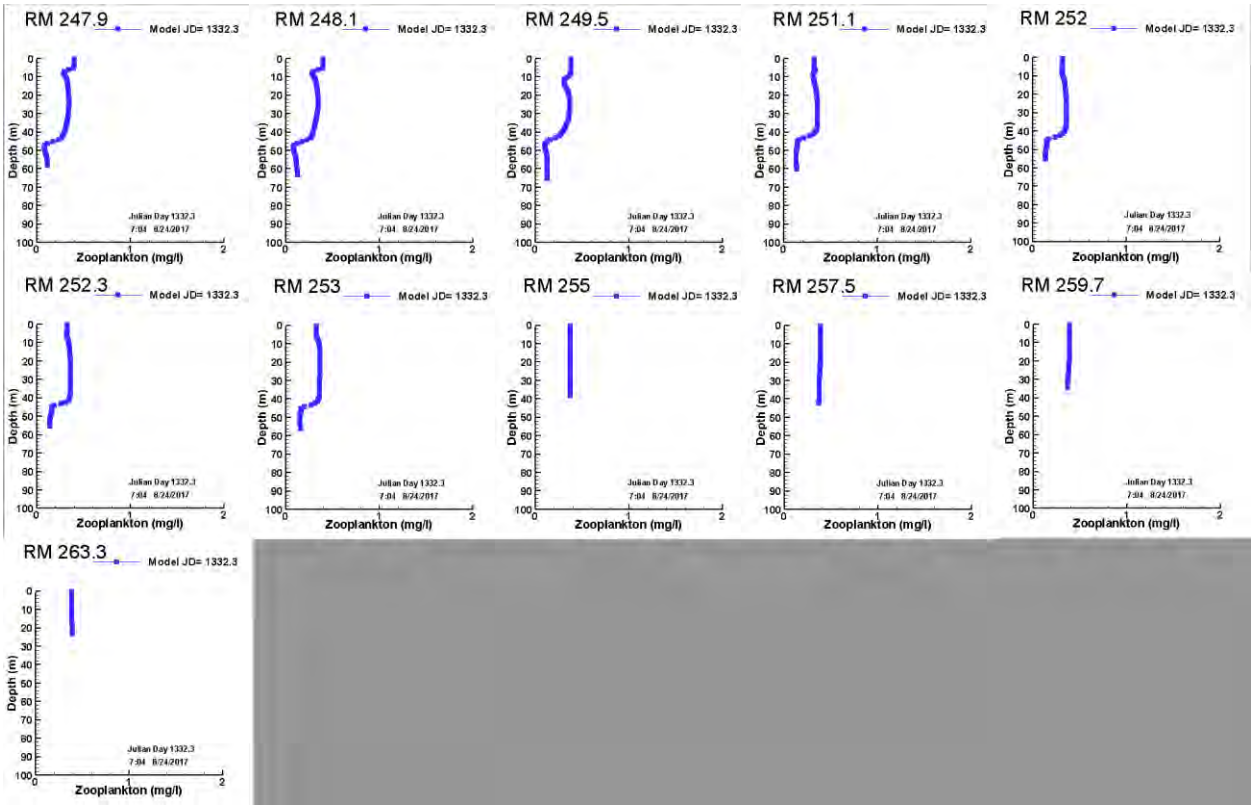


Figure 346. Vertical profiles of zooplankton compared with data for 8/24/2017.

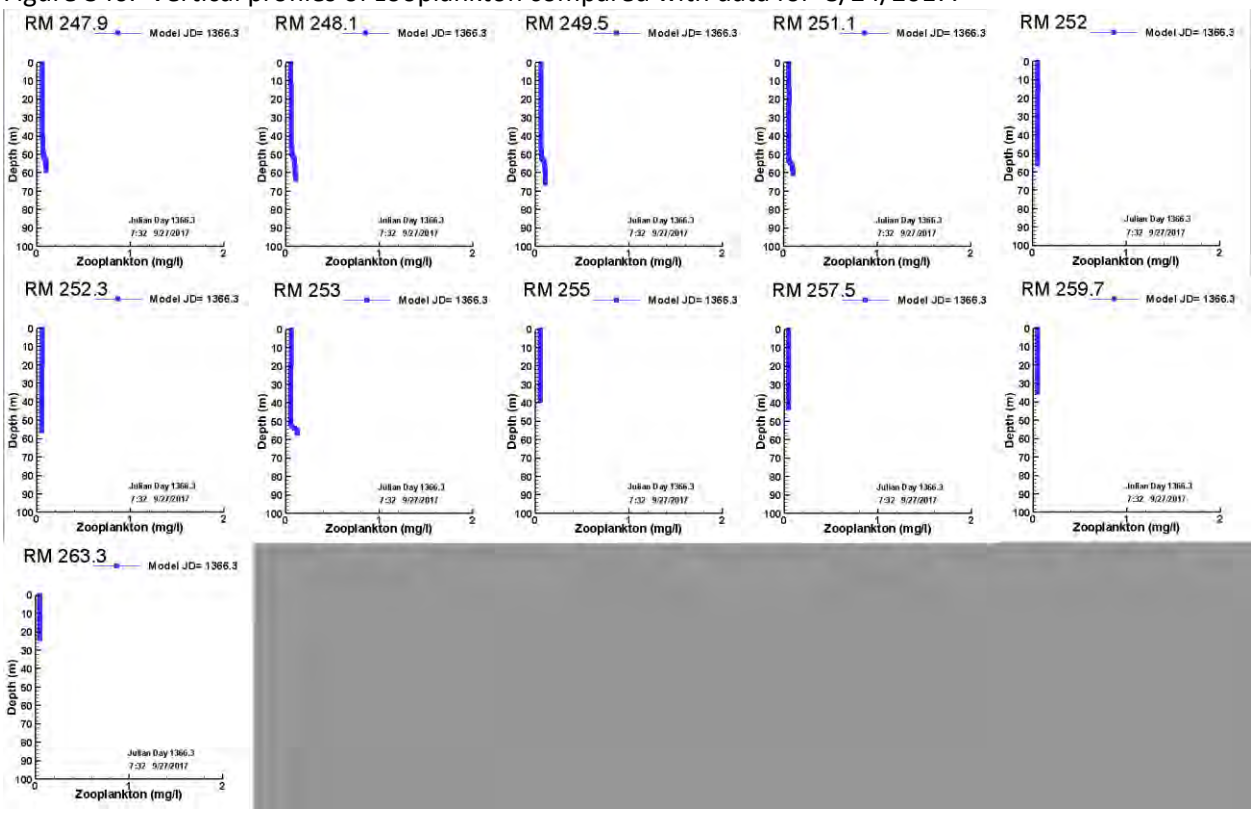


Figure 347. Vertical profiles of zooplankton compared with data for 9/27/2017.

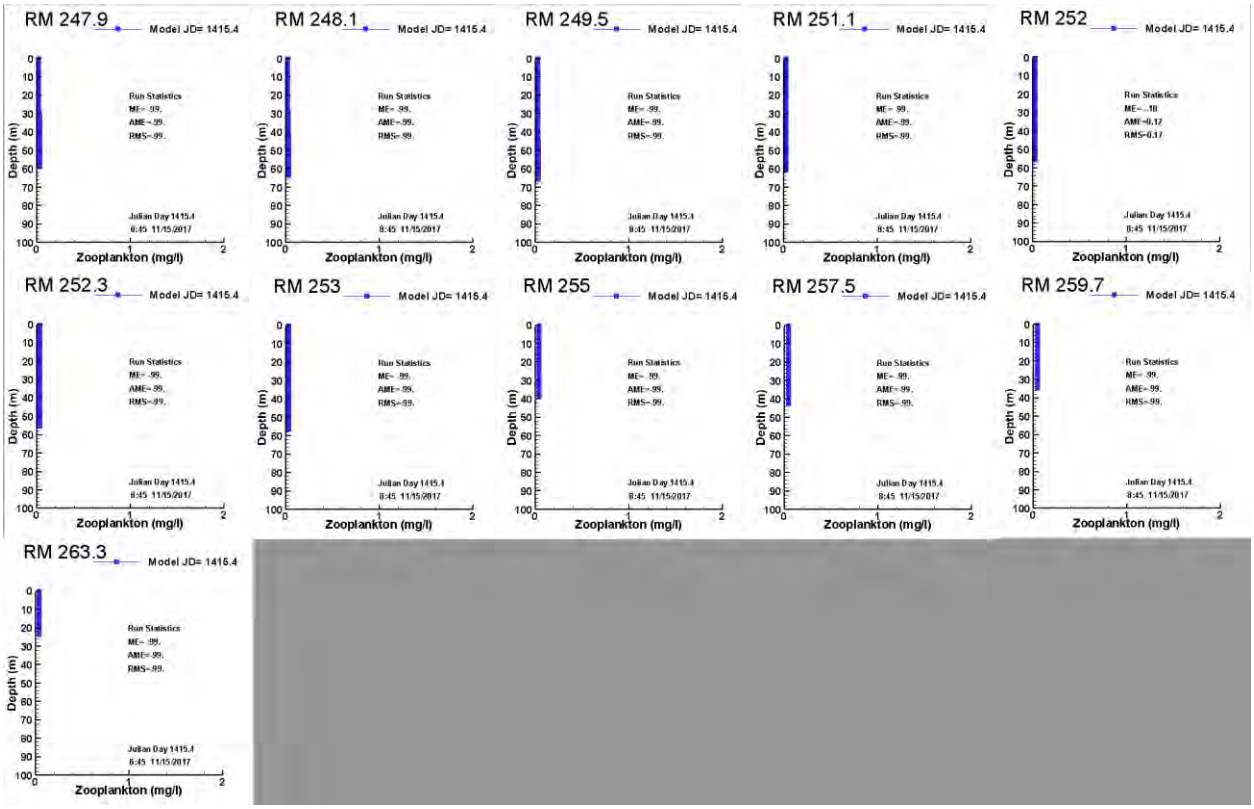


Figure 348. Vertical profiles of zooplankton compared with data for 11/15/2017.

Dissolved Organic Carbon

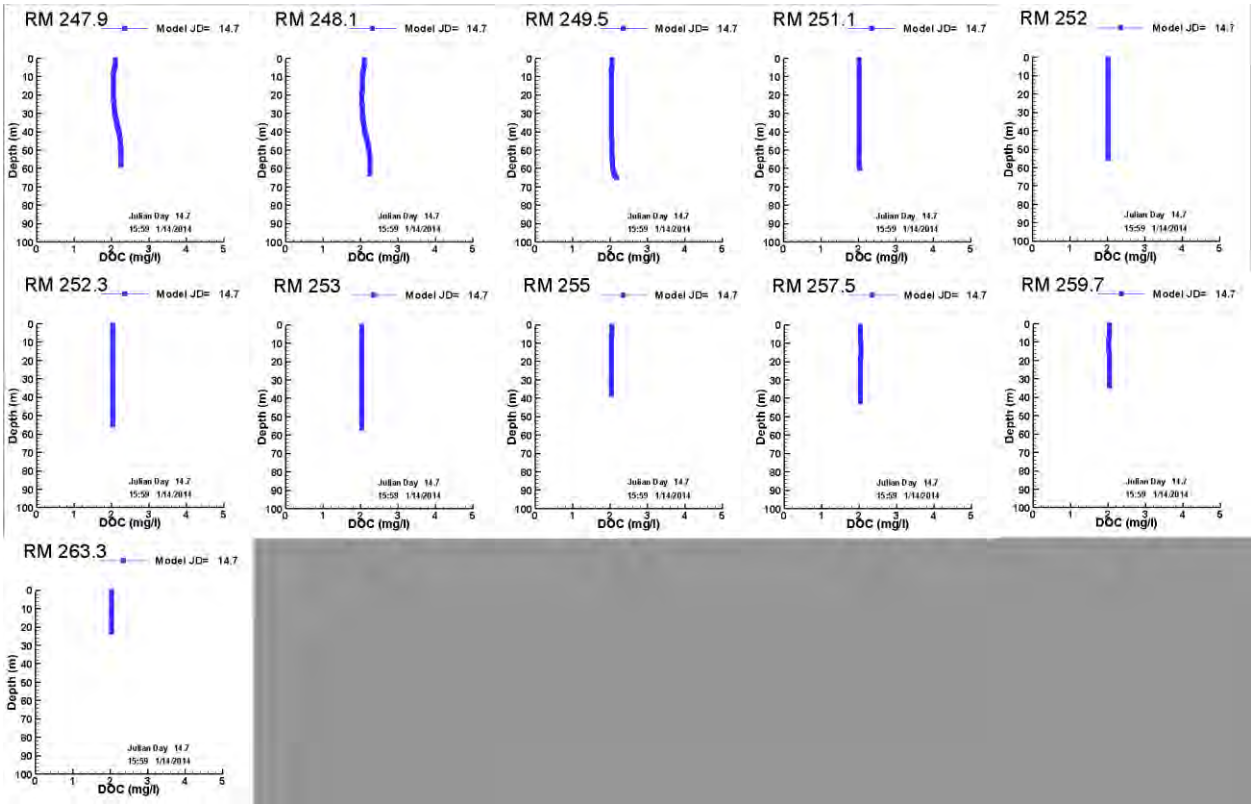


Figure 349. Vertical profiles of DOC compared with data for 1/14/2014.

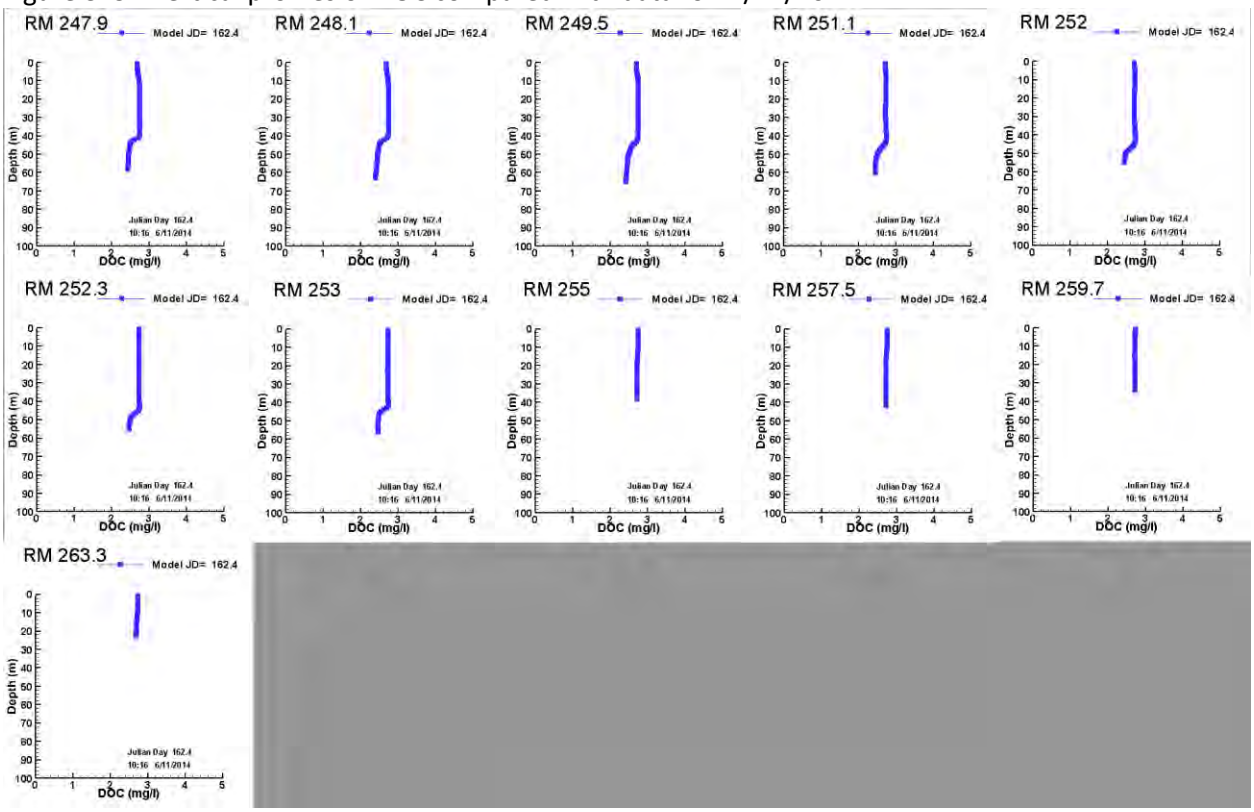


Figure 350. Vertical profiles of DOC compared with data for 6/11/2014.

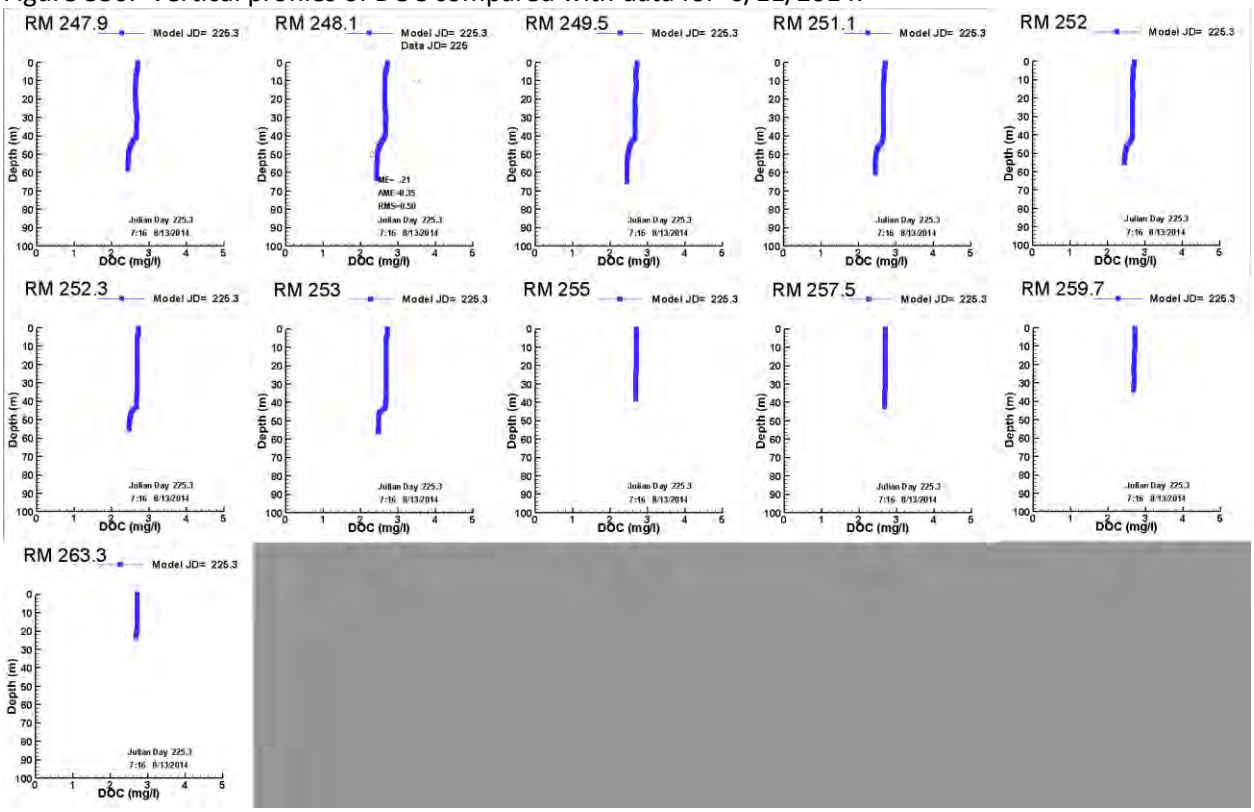


Figure 351. Vertical profiles of DOC compared with data for 8/13/2014.

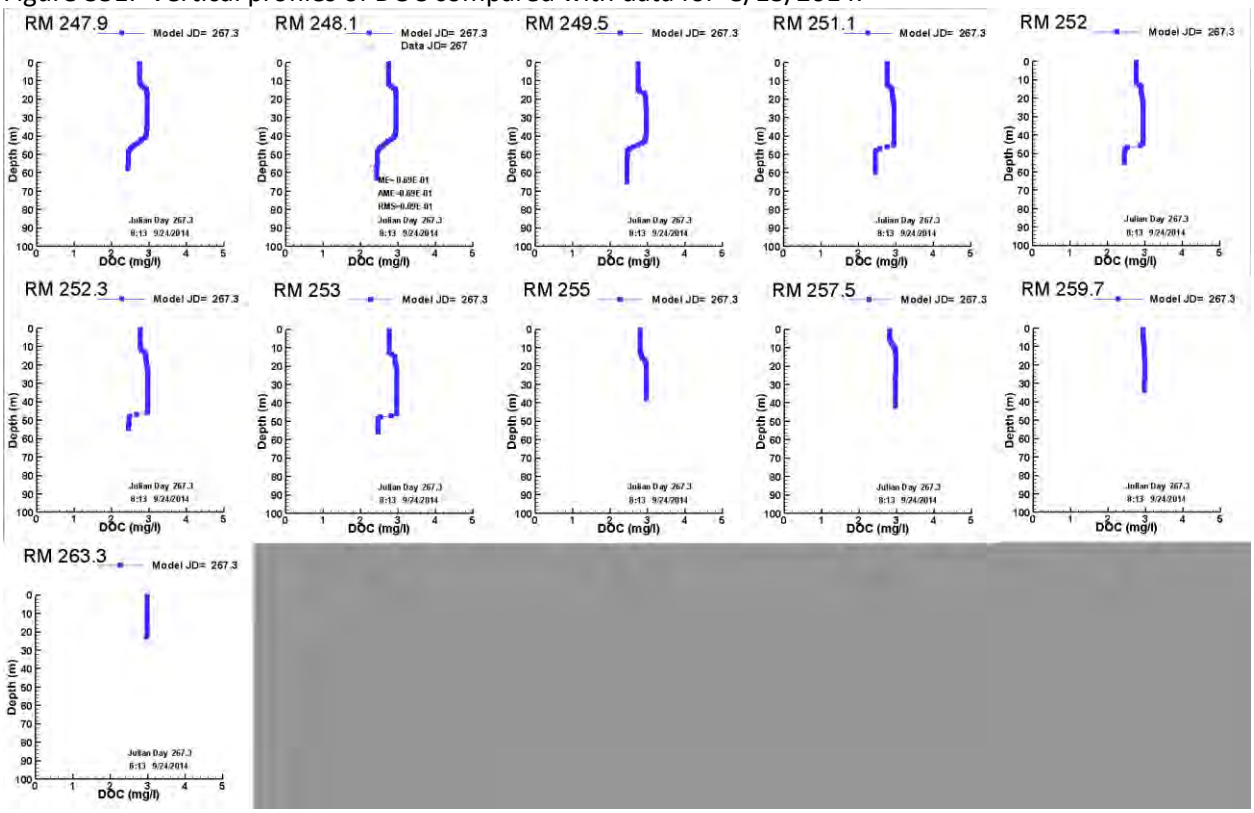


Figure 352. Vertical profiles of DOC compared with data for 9/24/2014.

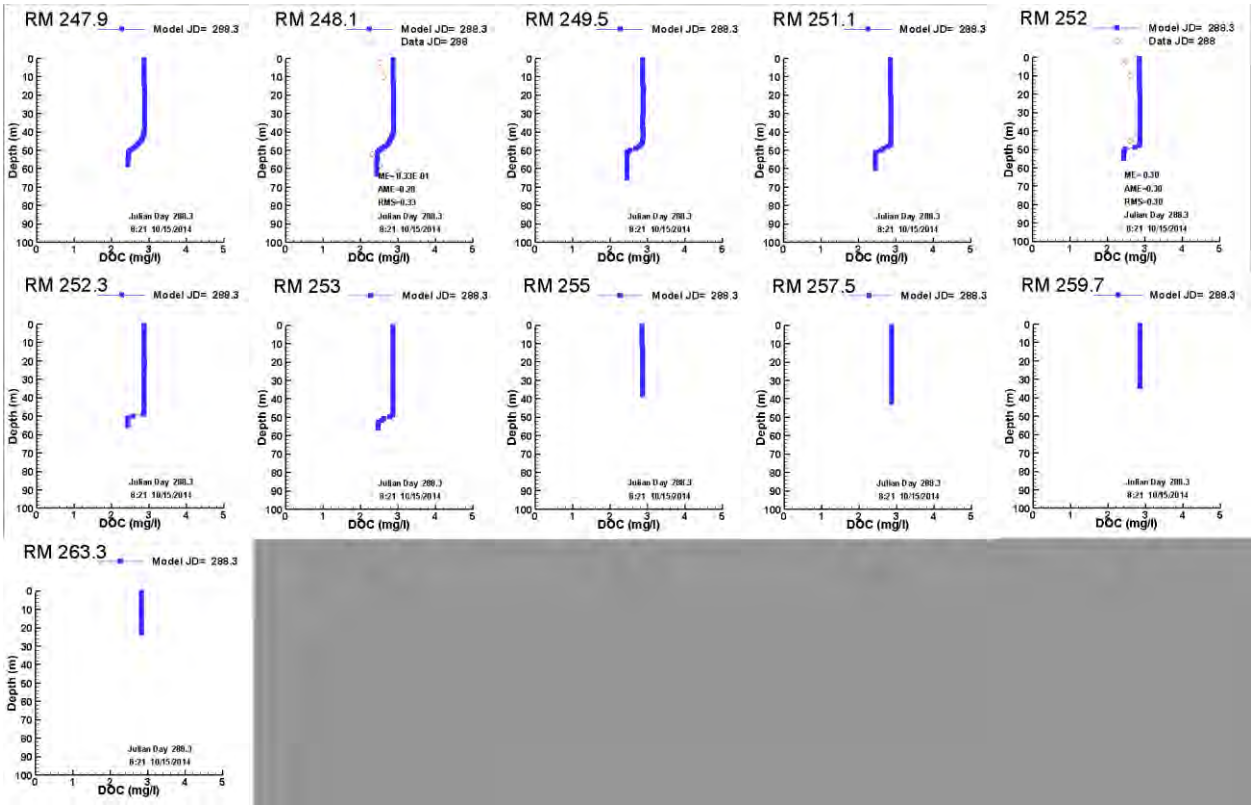


Figure 353. Vertical profiles of DOC compared with data for 10/15/2014.

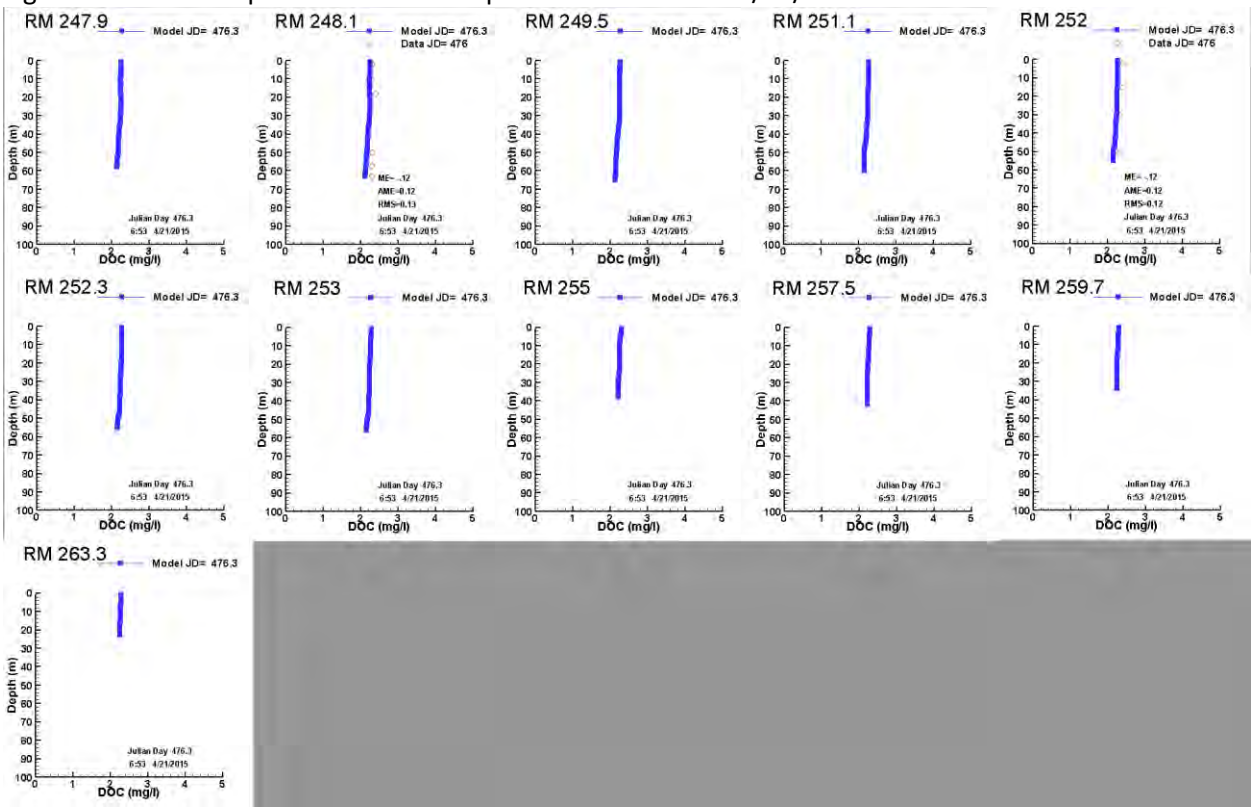


Figure 354. Vertical profiles of DOC compared with data for 4/21/2015.

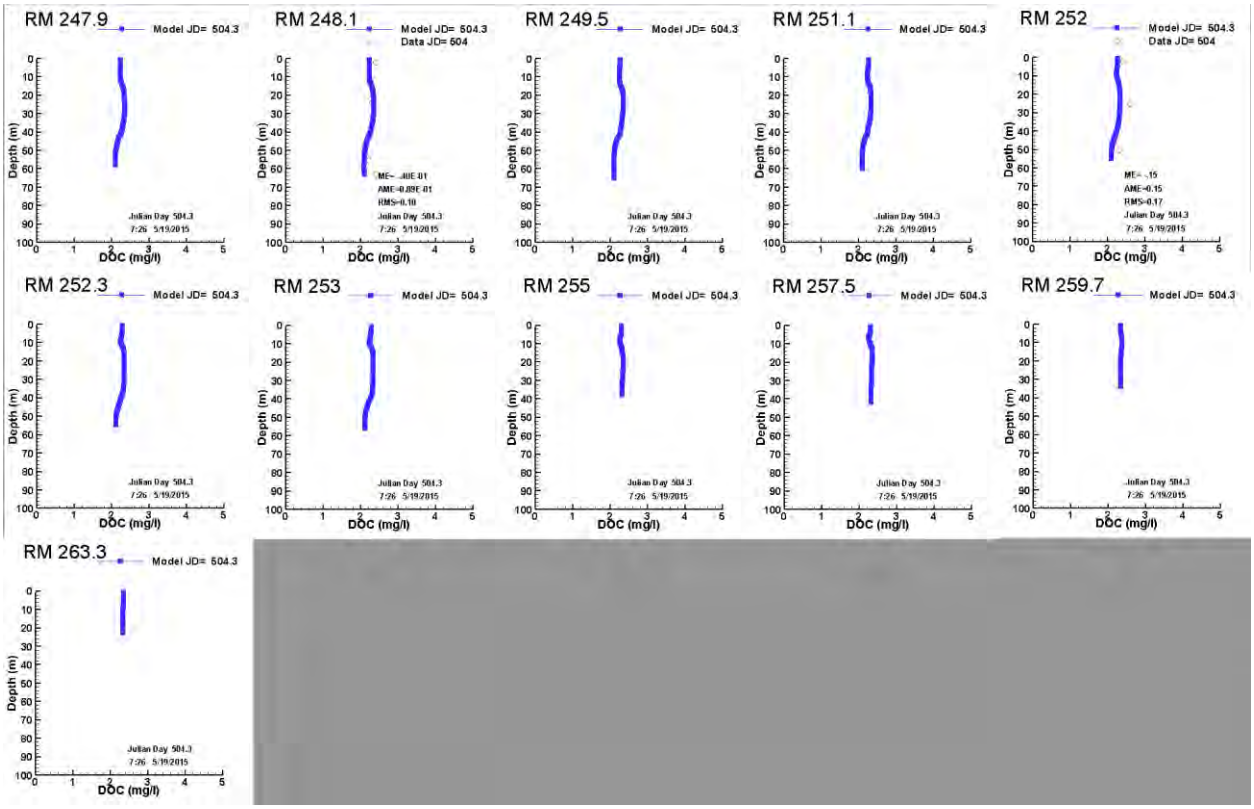


Figure 355. Vertical profiles of DOC compared with data for 5/19/2015.

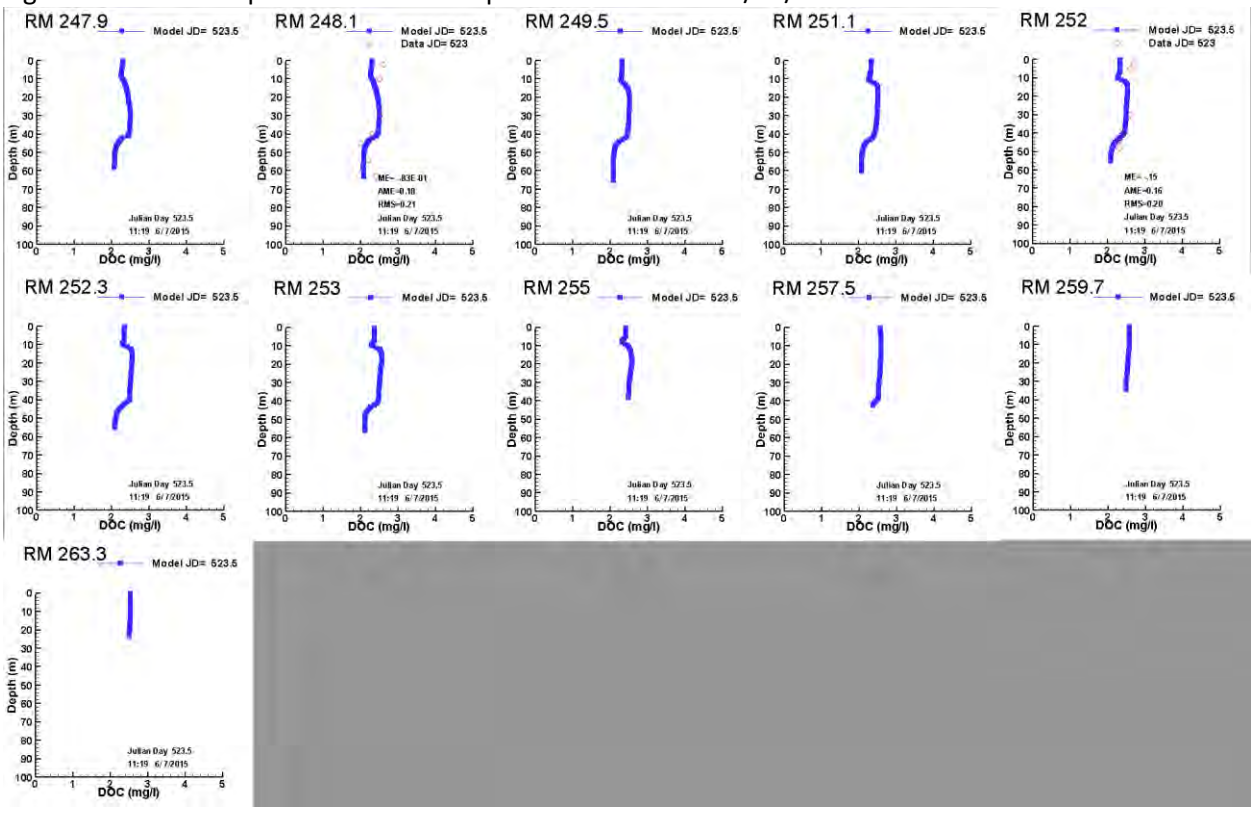


Figure 356. Vertical profiles of DOC compared with data for 6/ 7/2015.

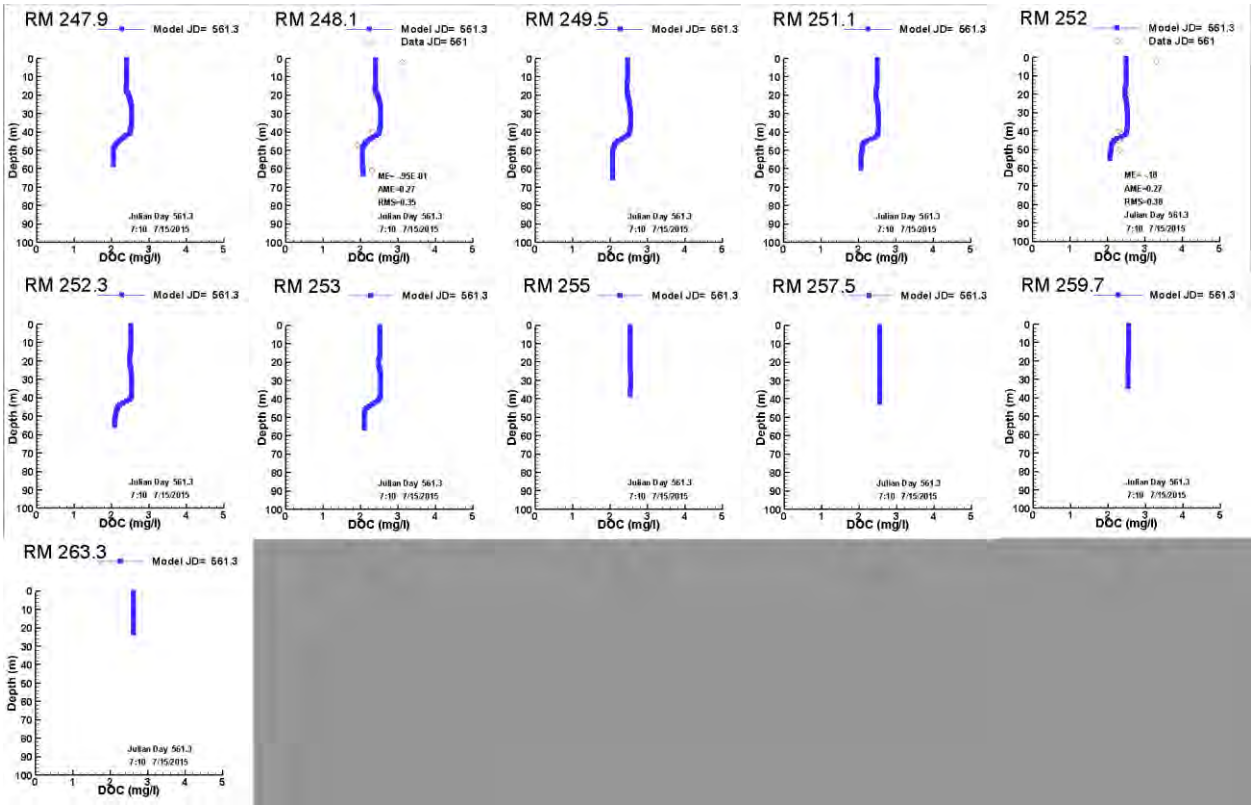


Figure 357. Vertical profiles of DOC compared with data for 7/15/2015.

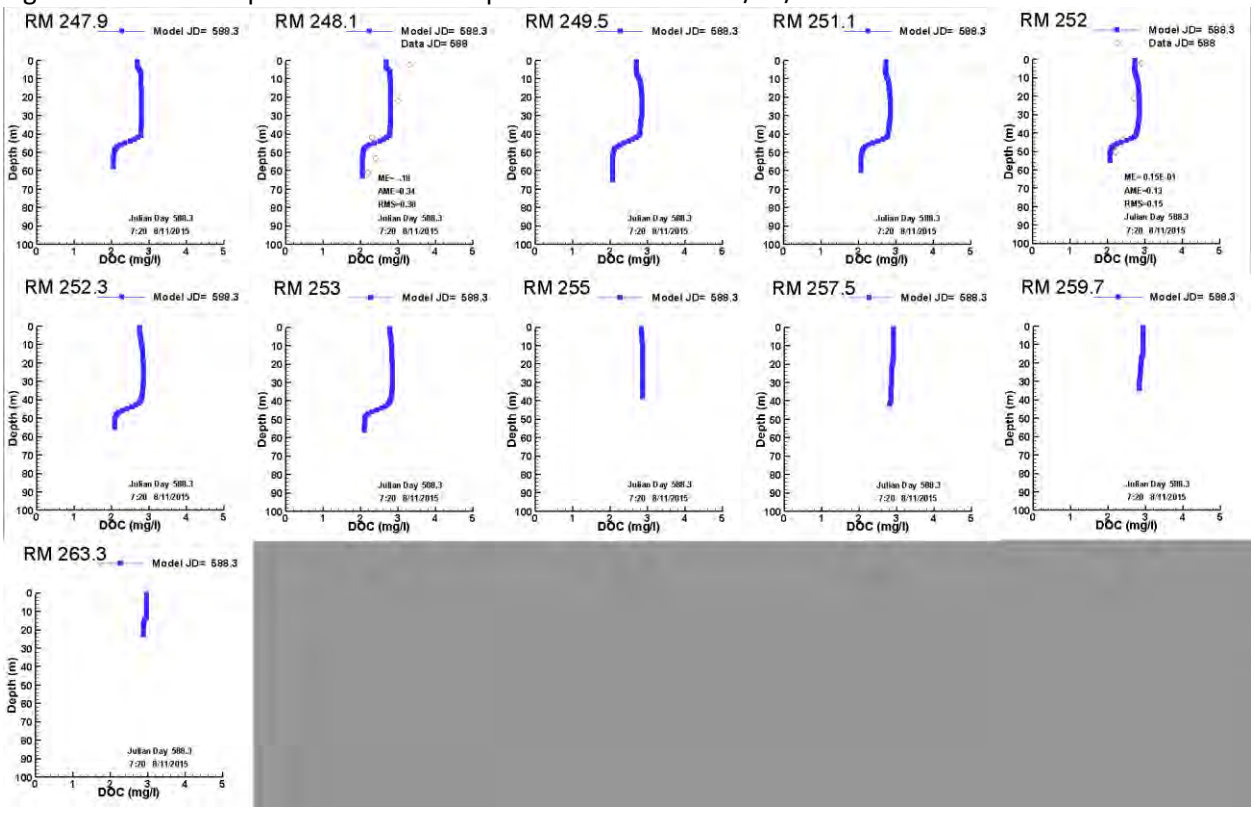


Figure 358. Vertical profiles of DOC compared with data for 8/11/2015.

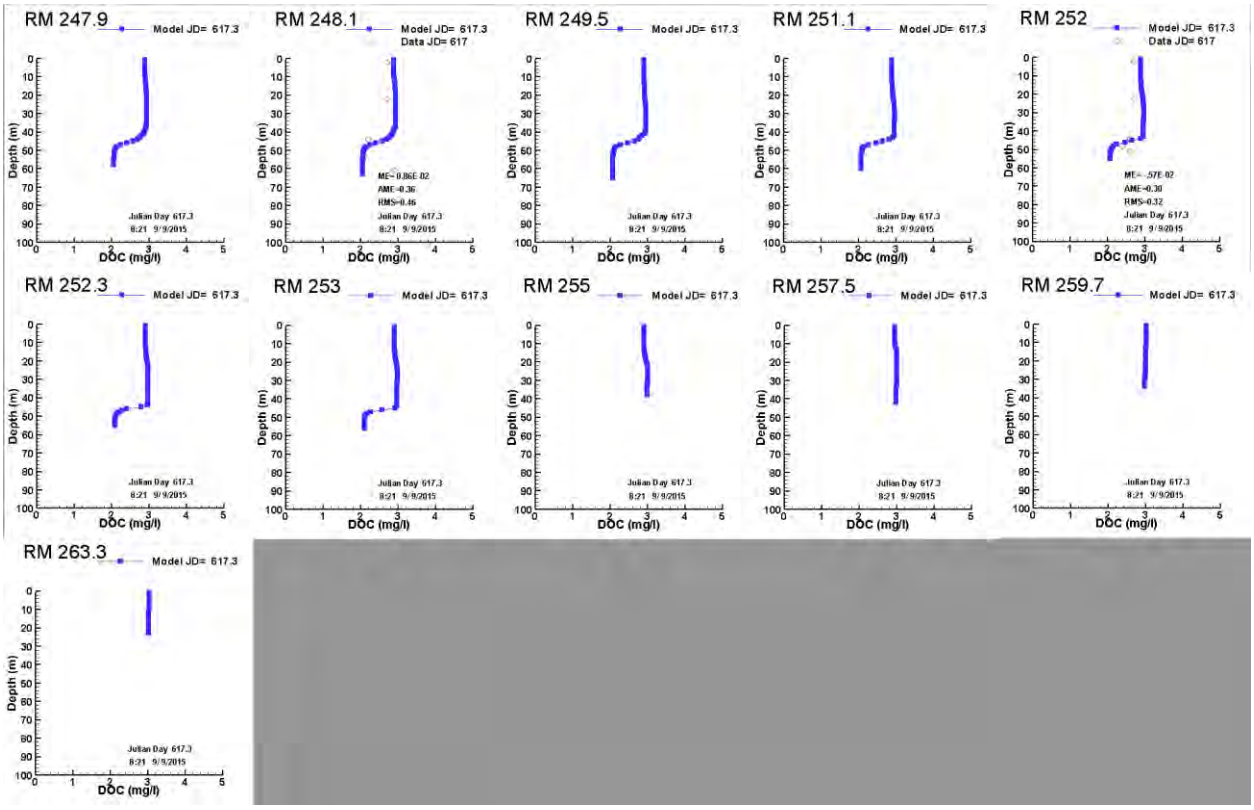


Figure 359. Vertical profiles of DOC compared with data for 9/ 9/2015.

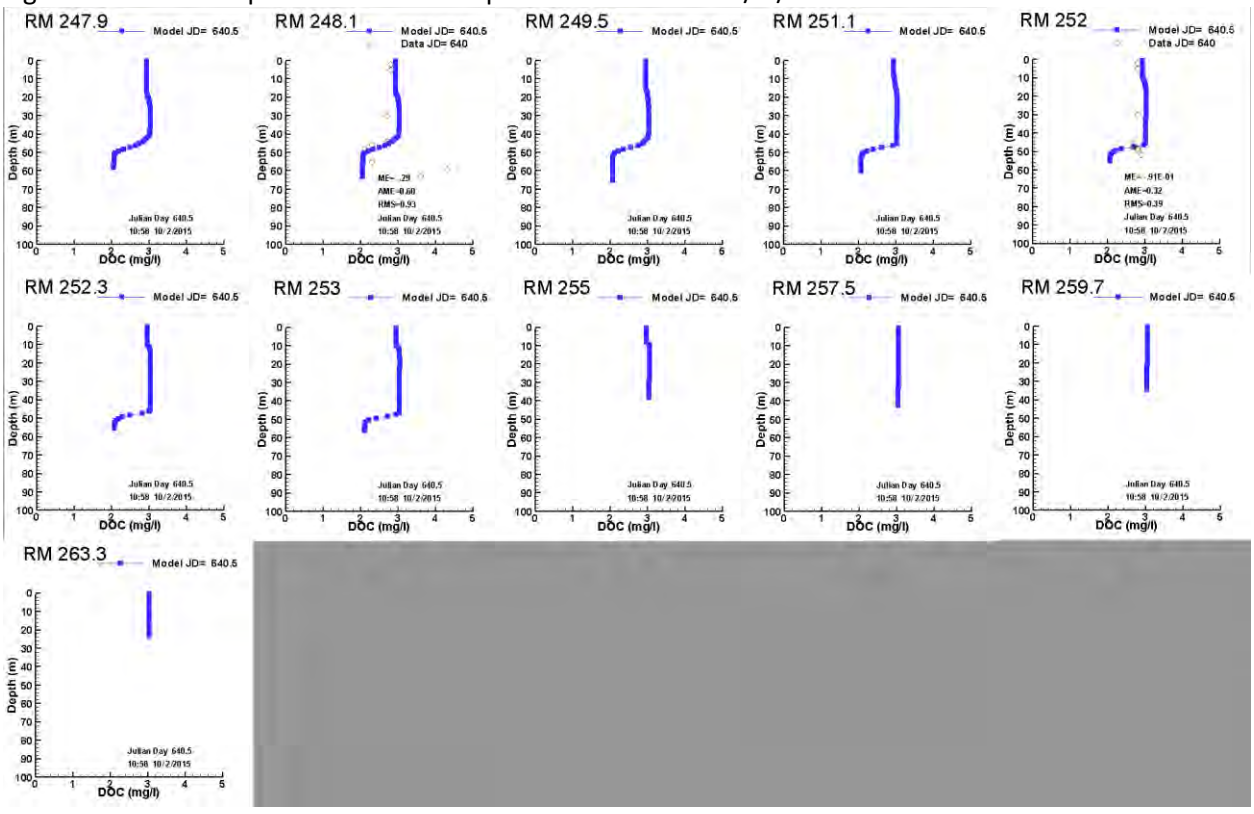


Figure 360. Vertical profiles of DOC compared with data for 10/ 2/2015.

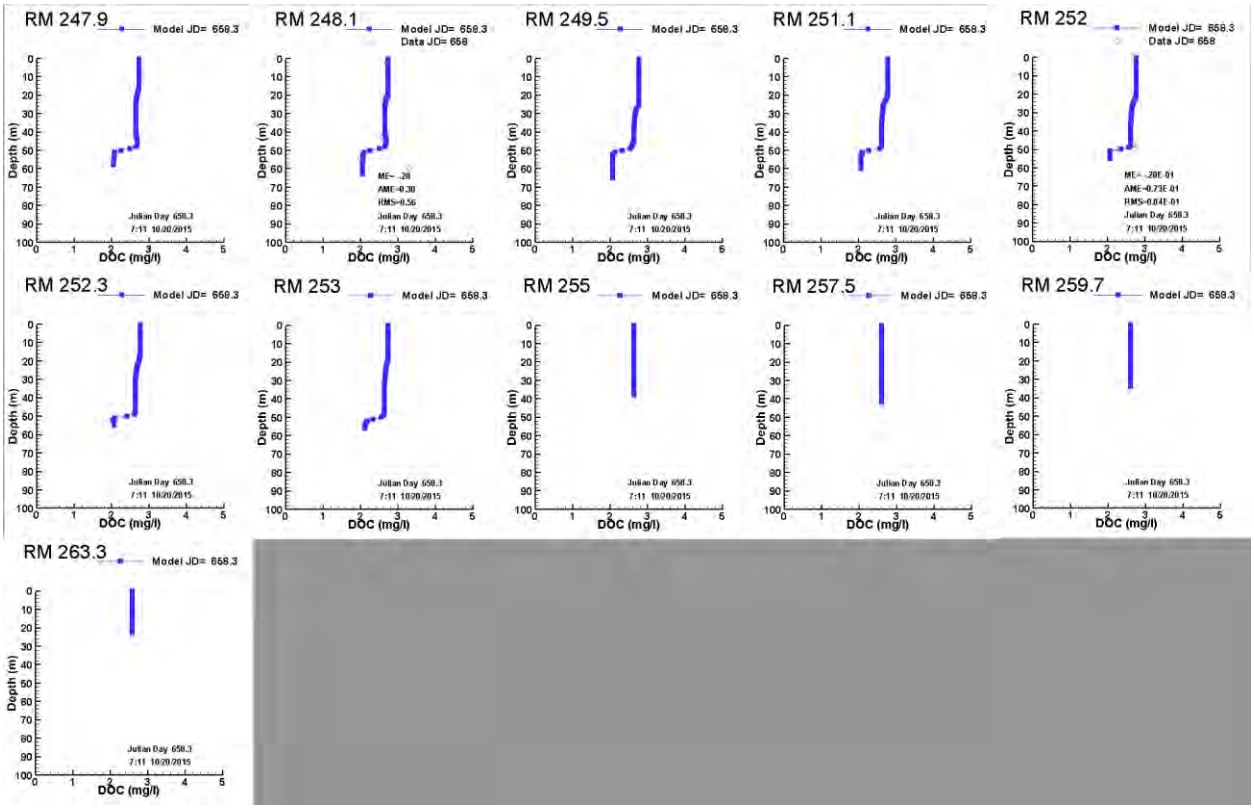


Figure 361. Vertical profiles of DOC compared with data for 10/20/2015.

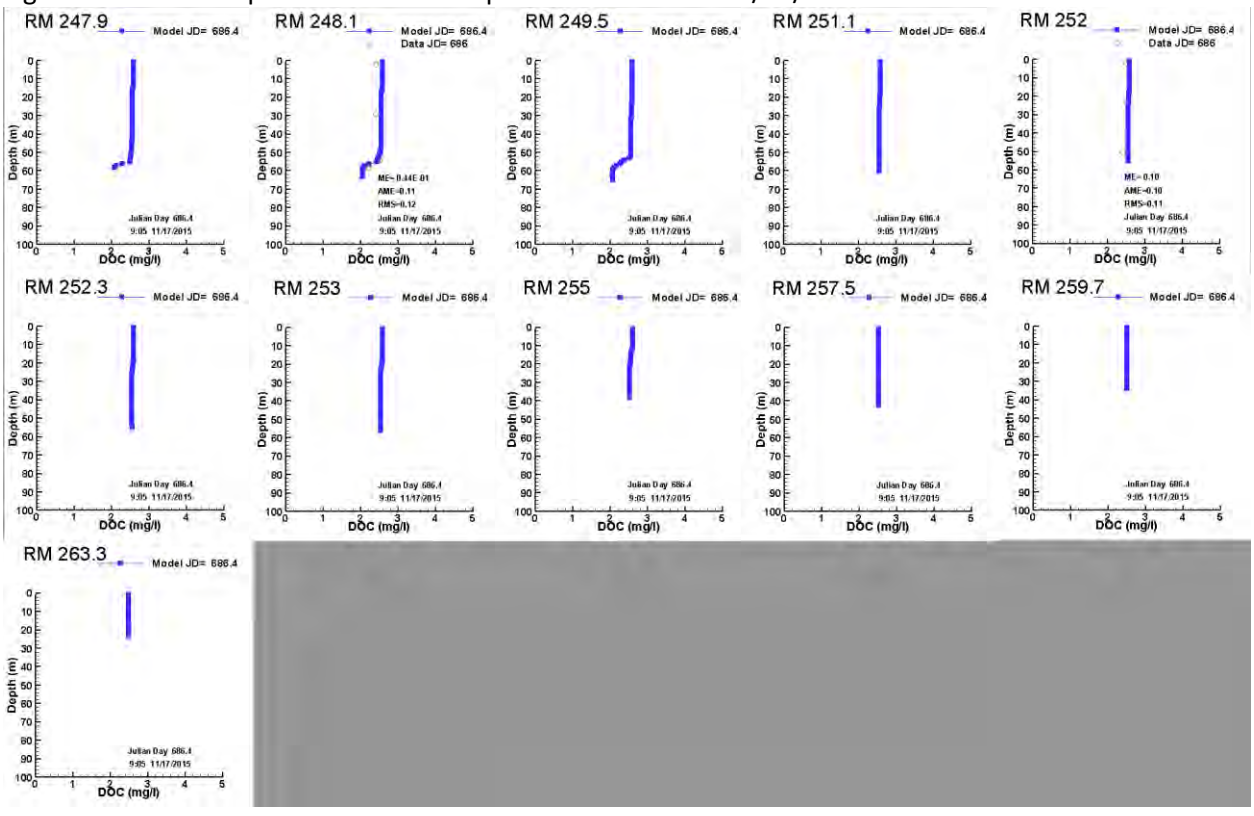


Figure 362. Vertical profiles of DOC compared with data for 11/17/2015.

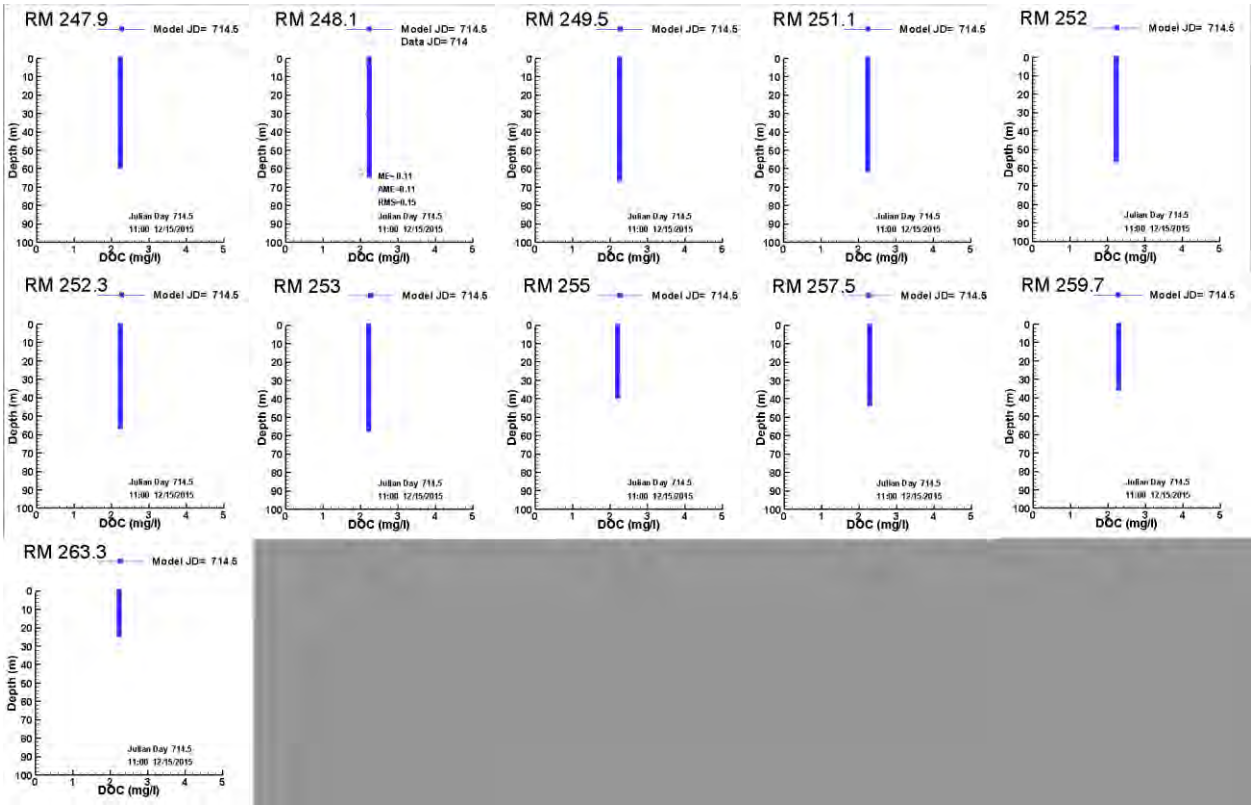


Figure 363. Vertical profiles of DOC compared with data for 12/15/2015.

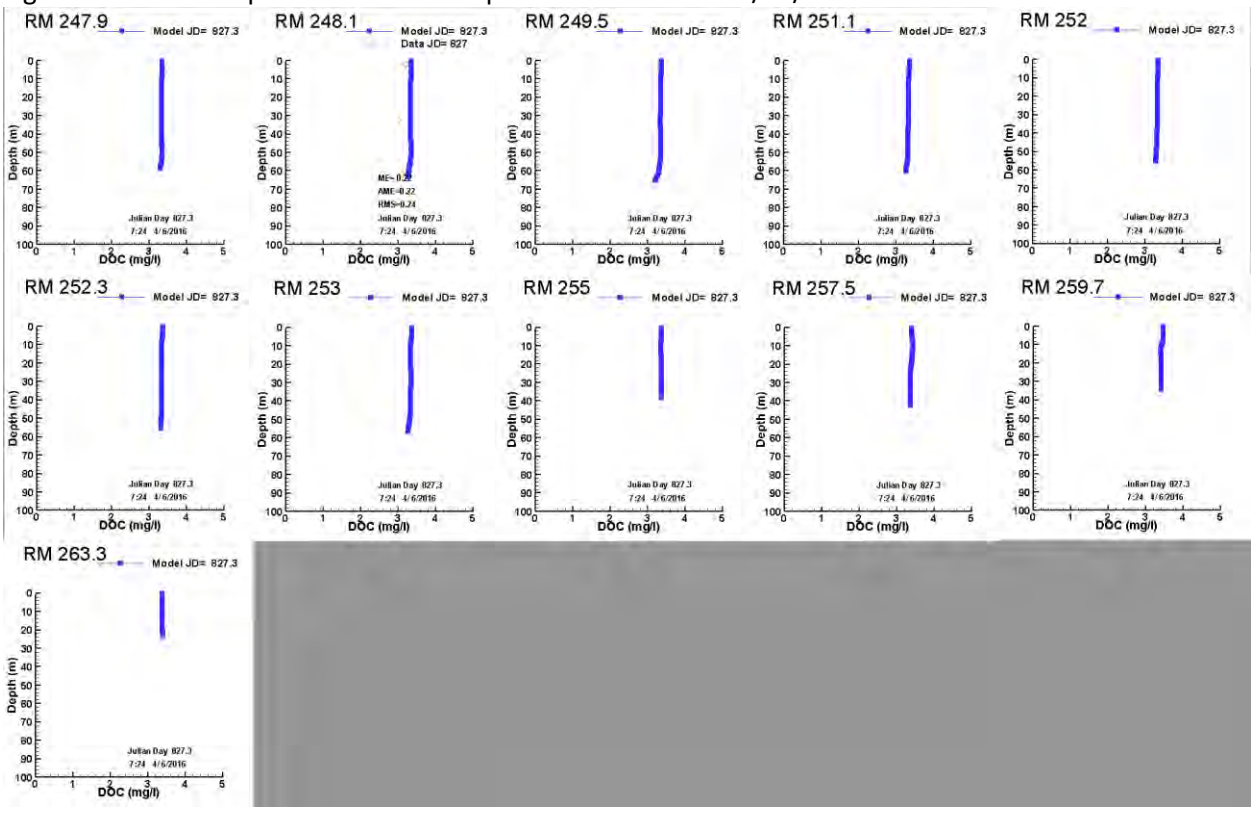


Figure 364. Vertical profiles of DOC compared with data for 4/ 6/2016.

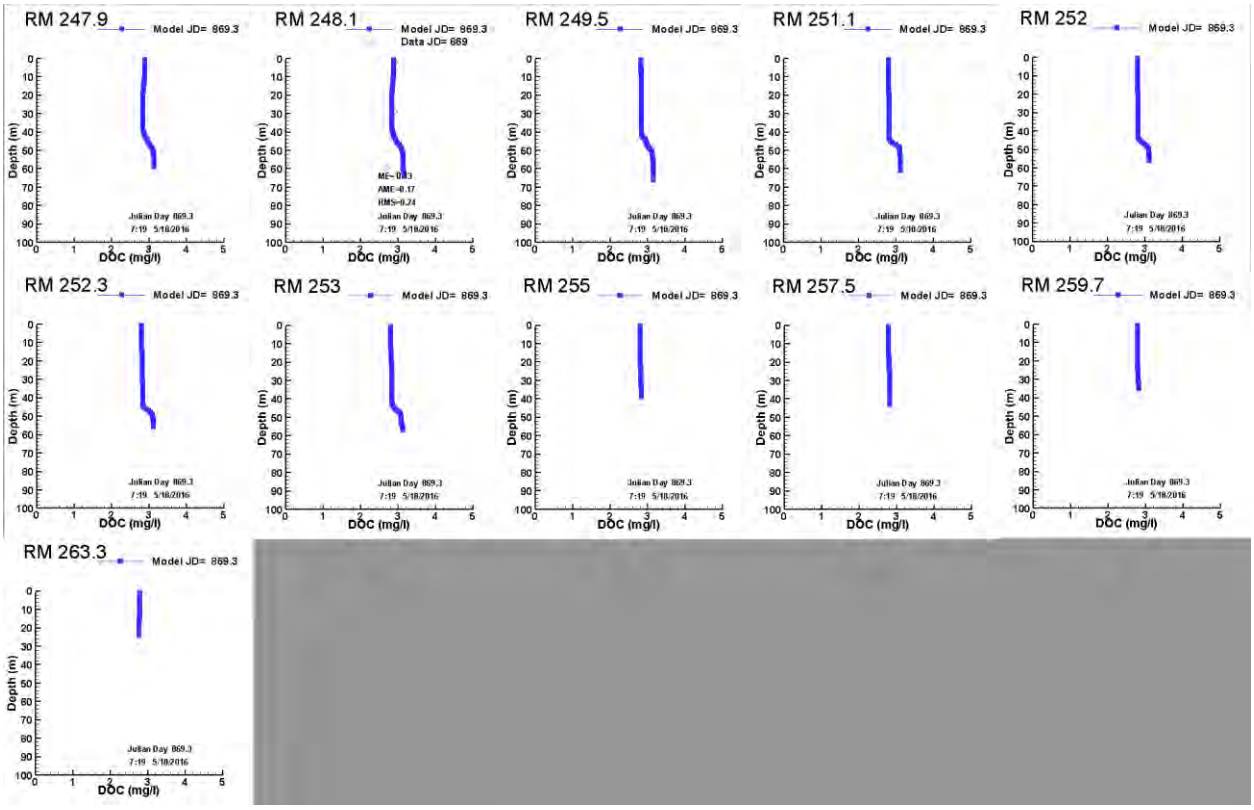


Figure 365. Vertical profiles of DOC compared with data for 5/18/2016.

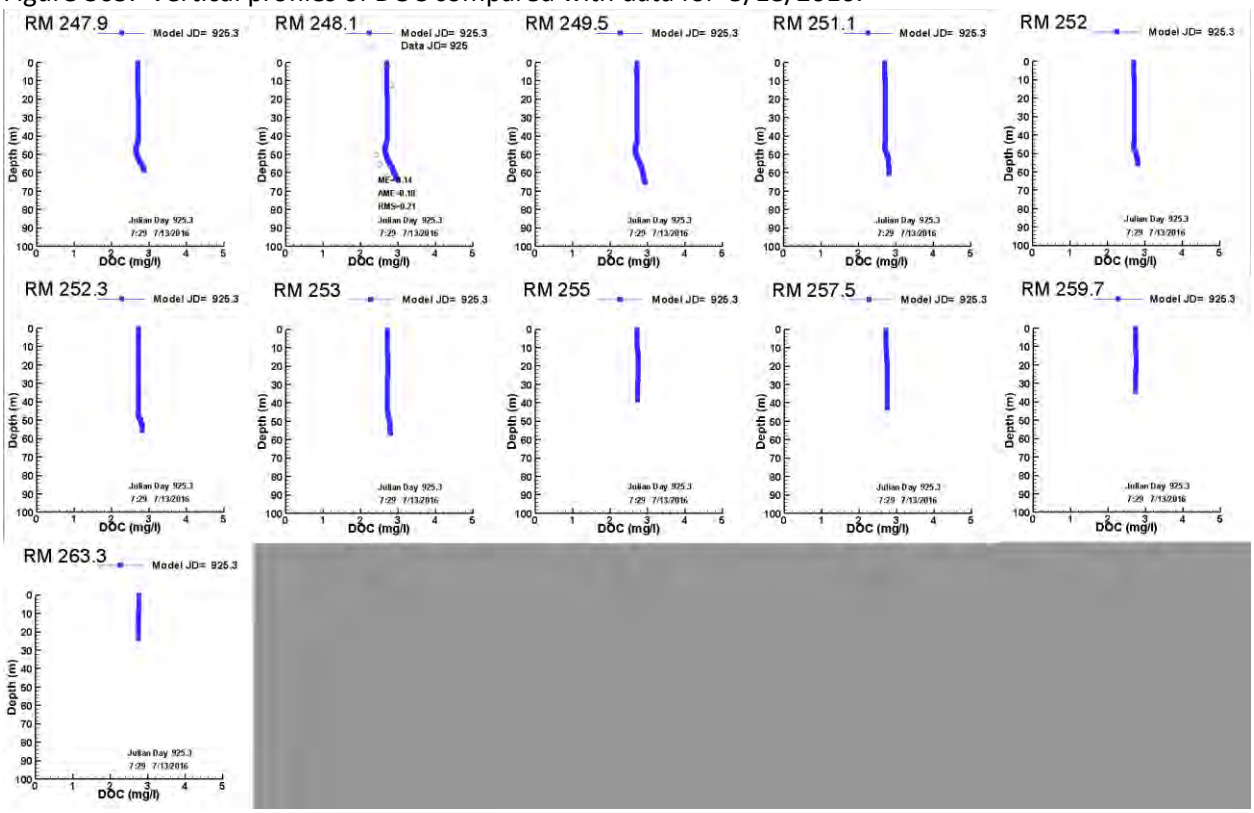


Figure 366. Vertical profiles of DOC compared with data for 7/13/2016.

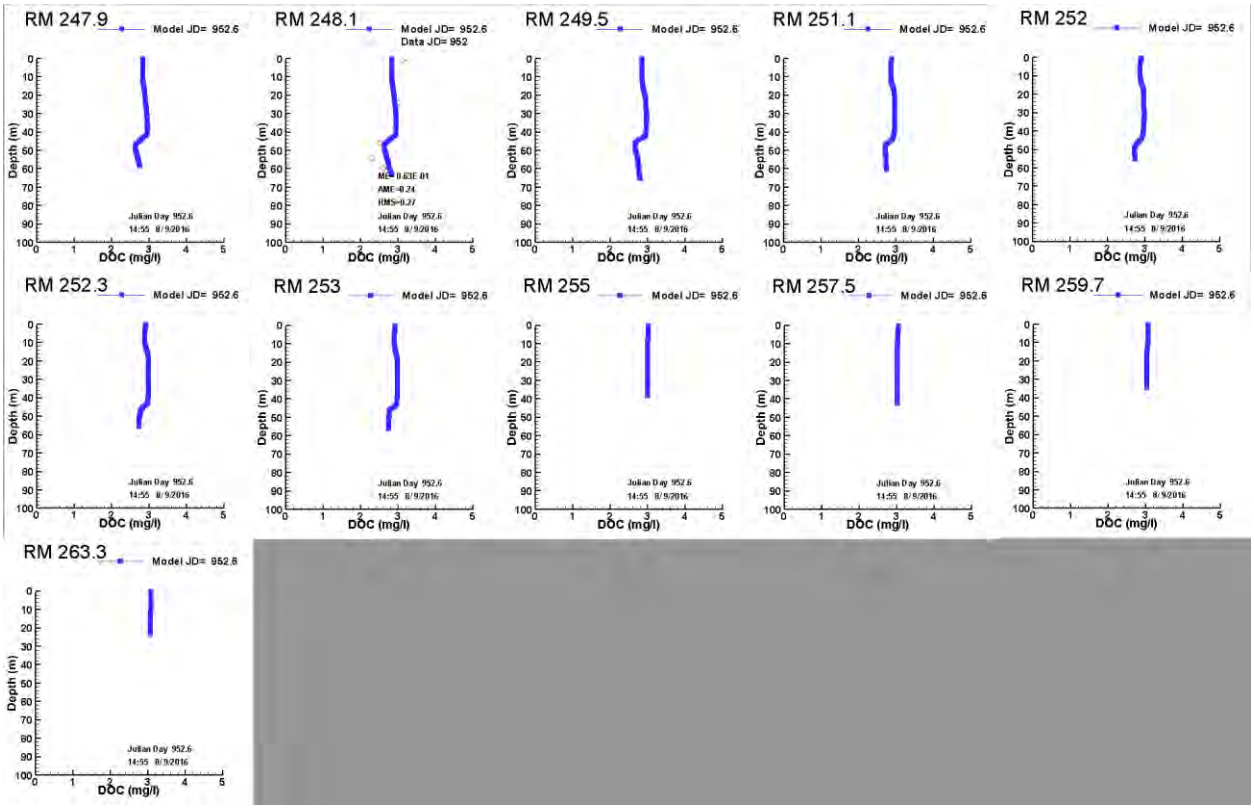


Figure 367. Vertical profiles of DOC compared with data for 8/ 9/2016.

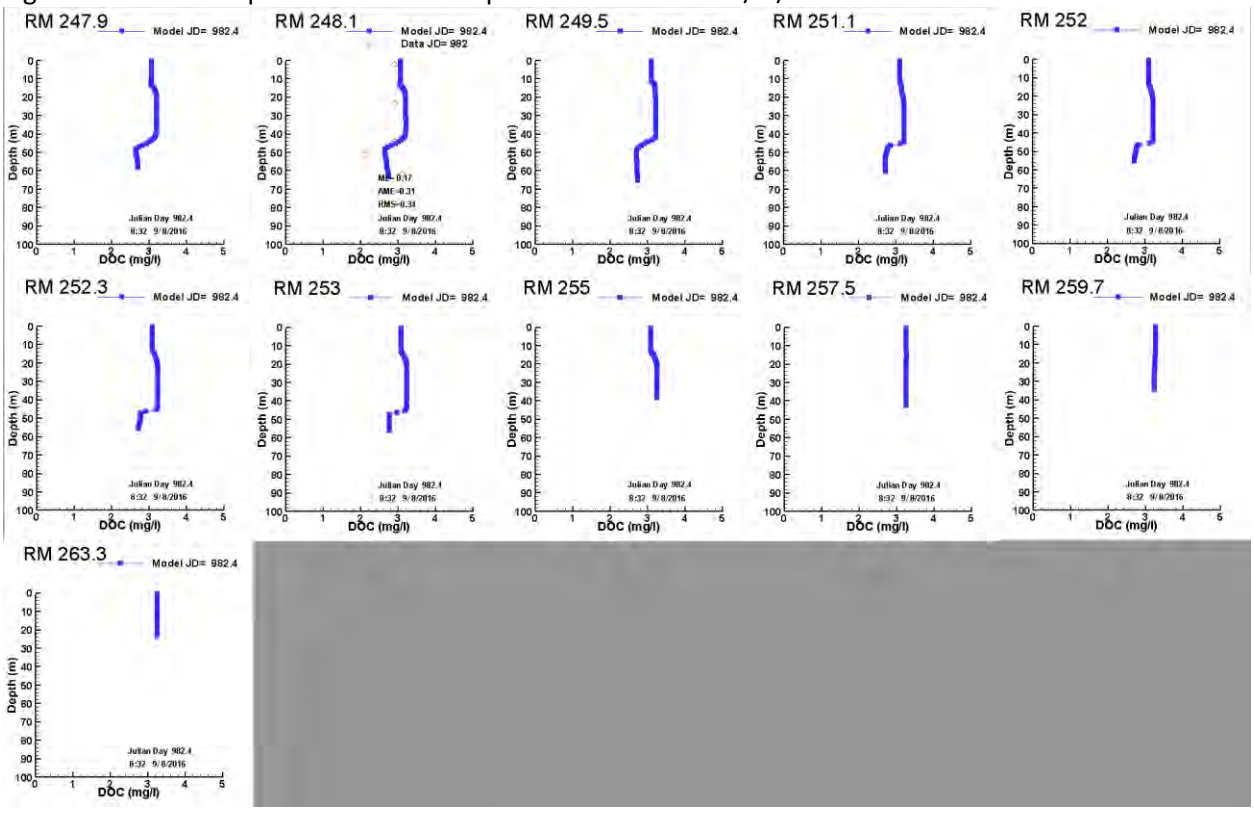


Figure 368. Vertical profiles of DOC compared with data for 9/ 8/2016.

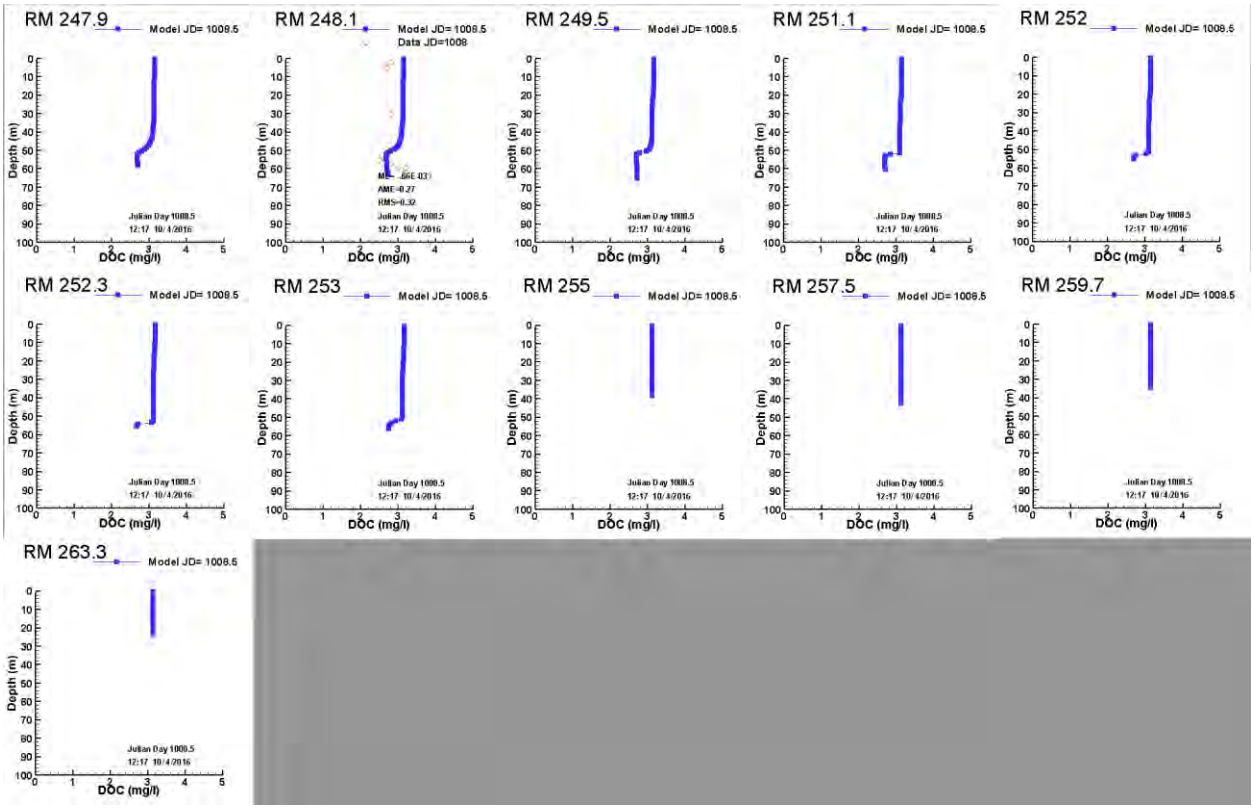


Figure 369. Vertical profiles of DOC compared with data for 10/ 4/2016.

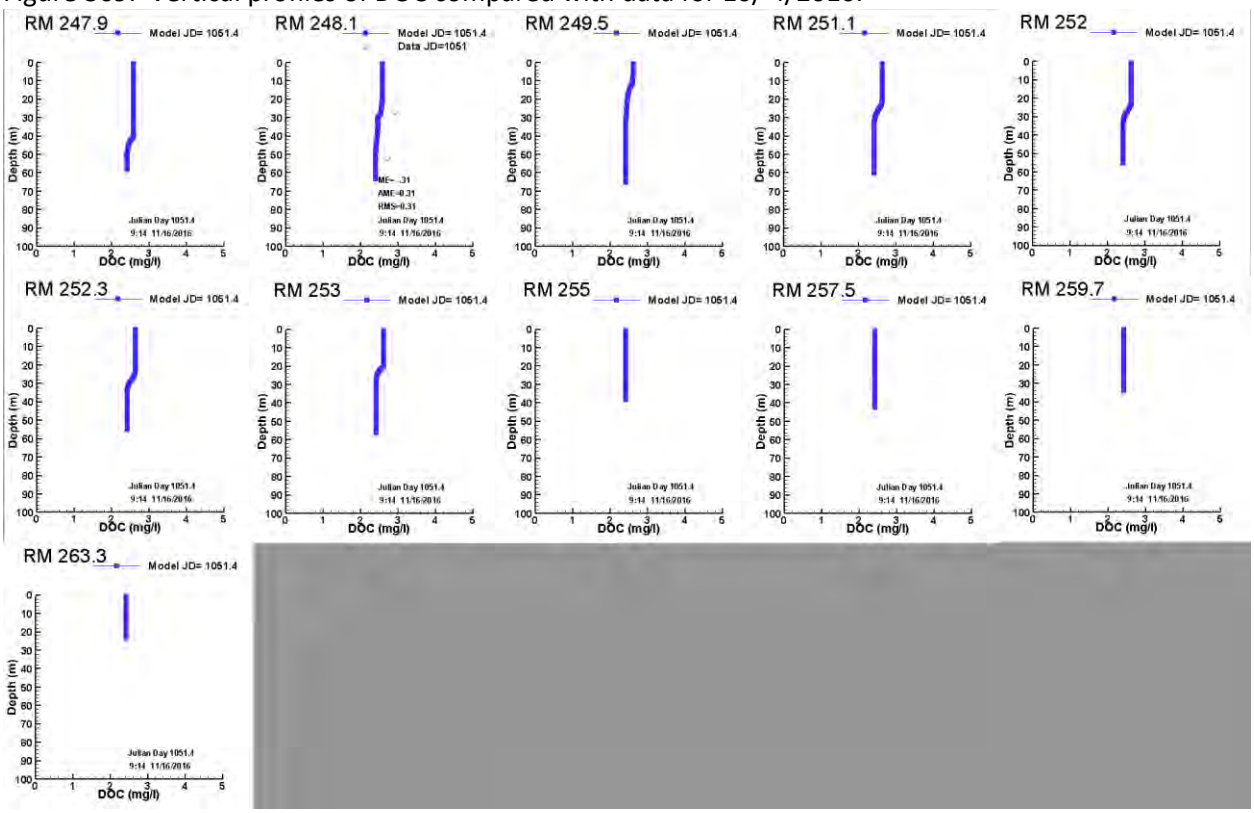


Figure 370. Vertical profiles of DOC compared with data for 11/16/2016.

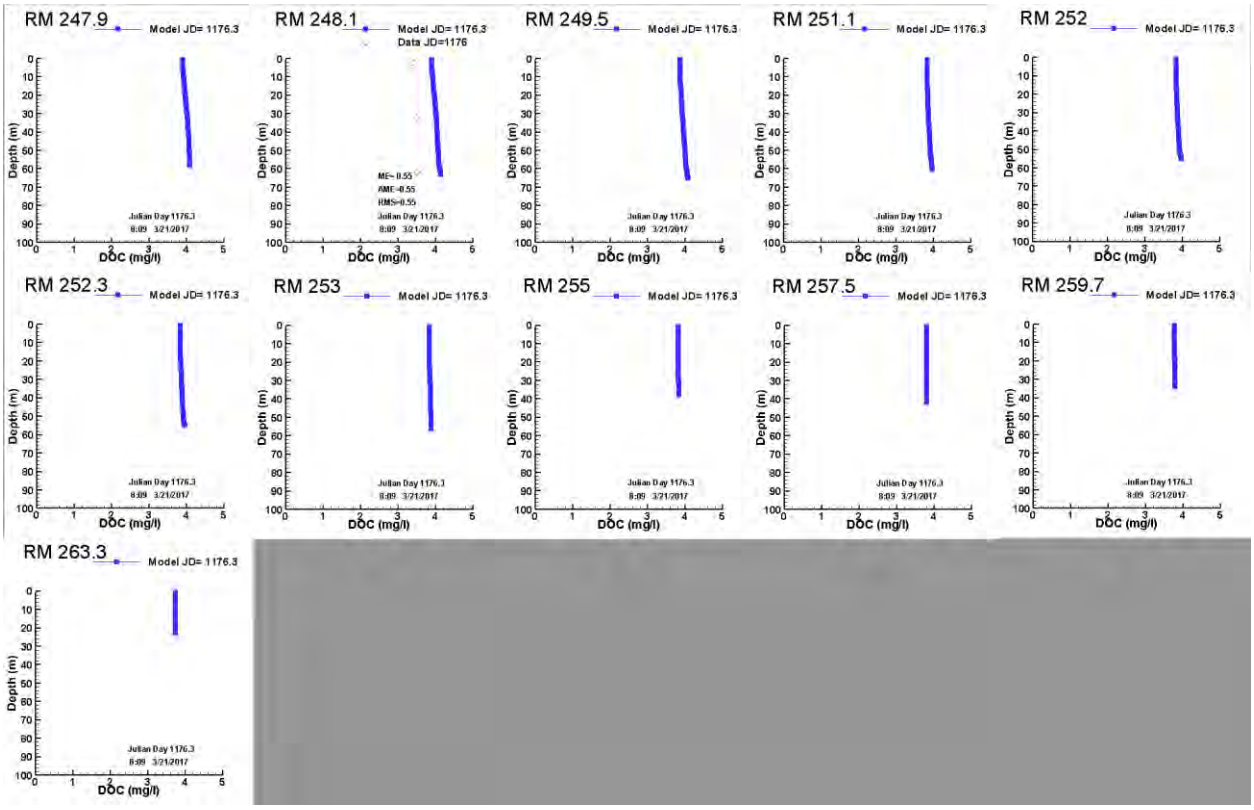


Figure 371. Vertical profiles of DOC compared with data for 3/21/2017.

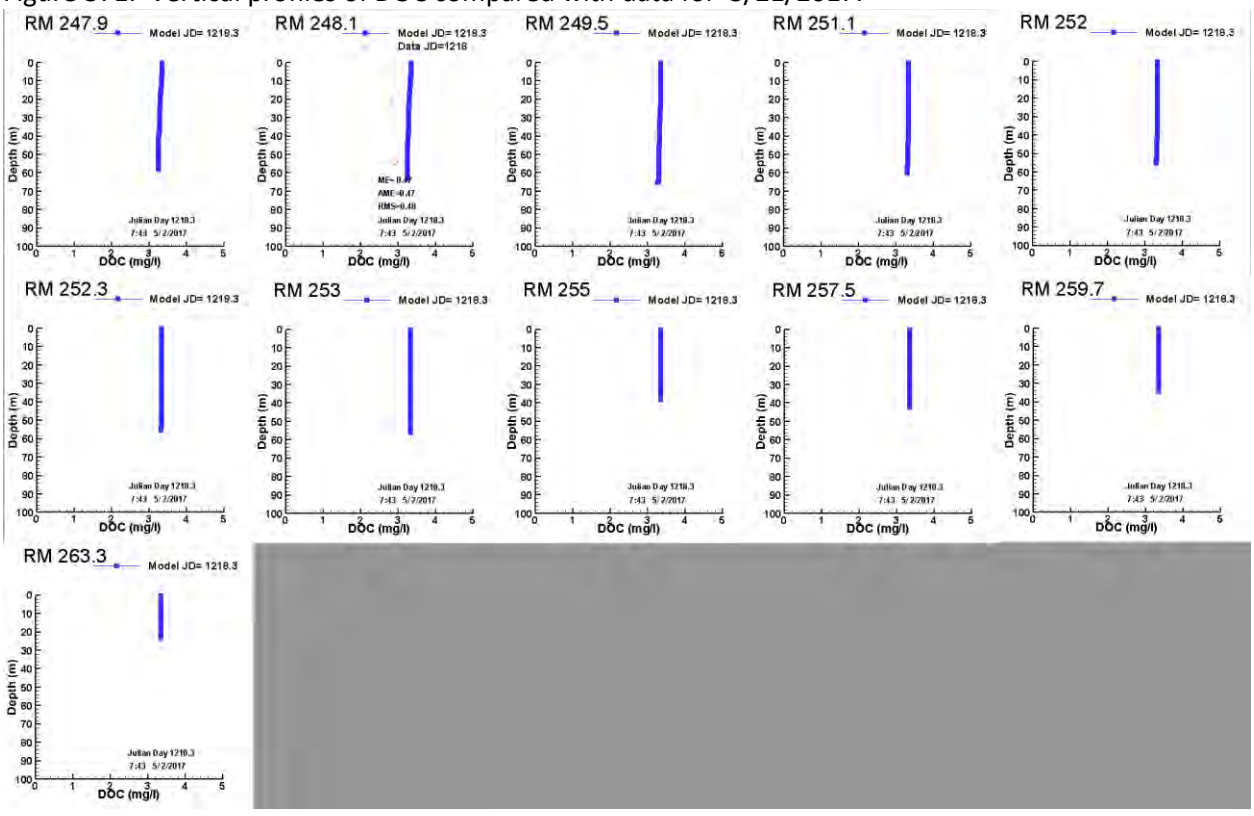


Figure 372. Vertical profiles of DOC compared with data for 5/ 2/2017.

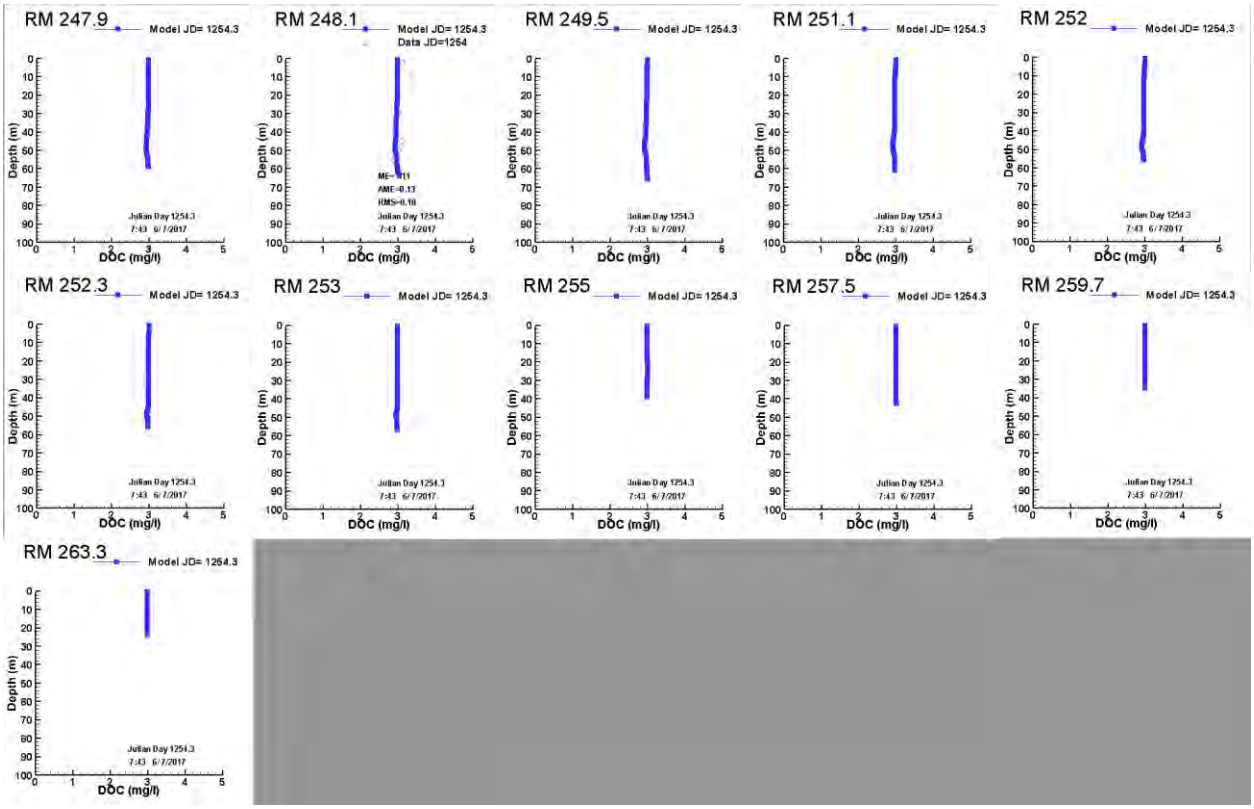


Figure 373. Vertical profiles of DOC compared with data for 6/ 7/2017.

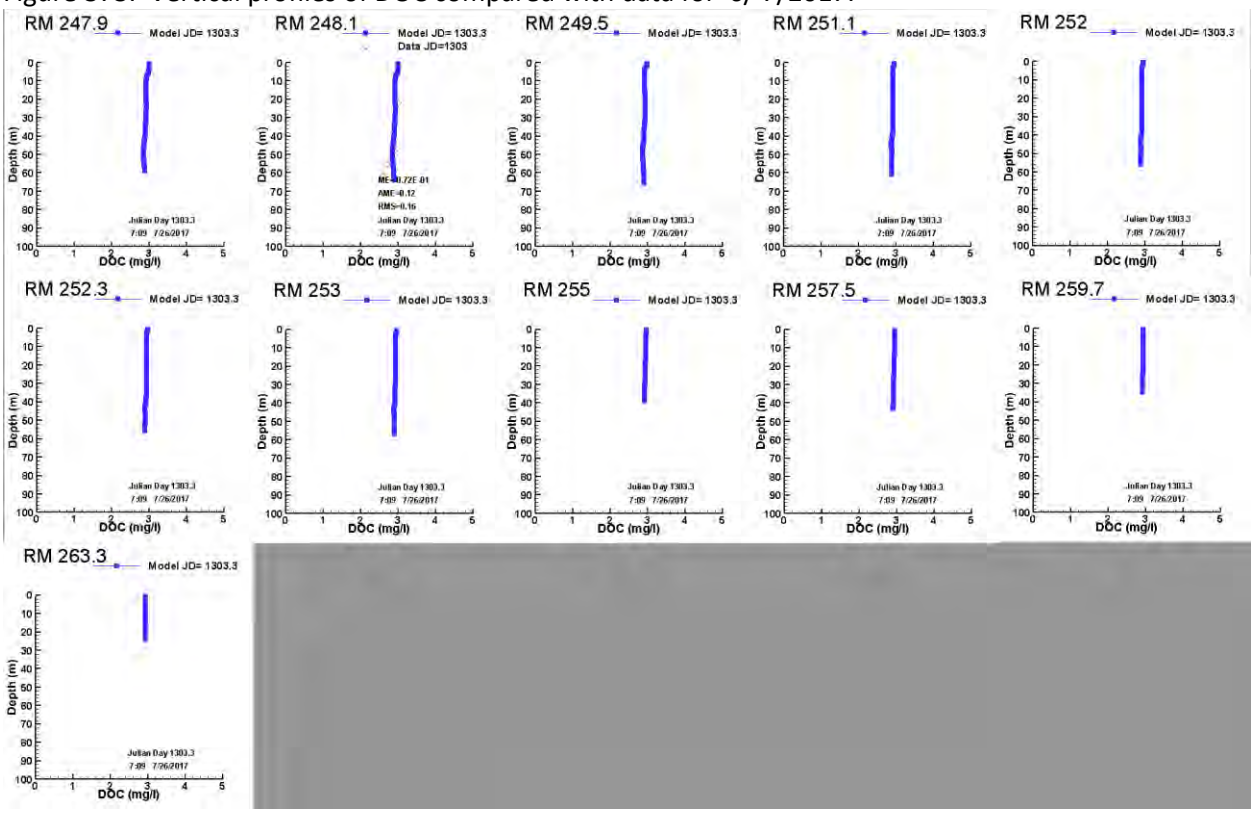


Figure 374. Vertical profiles of DOC compared with data for 7/26/2017.

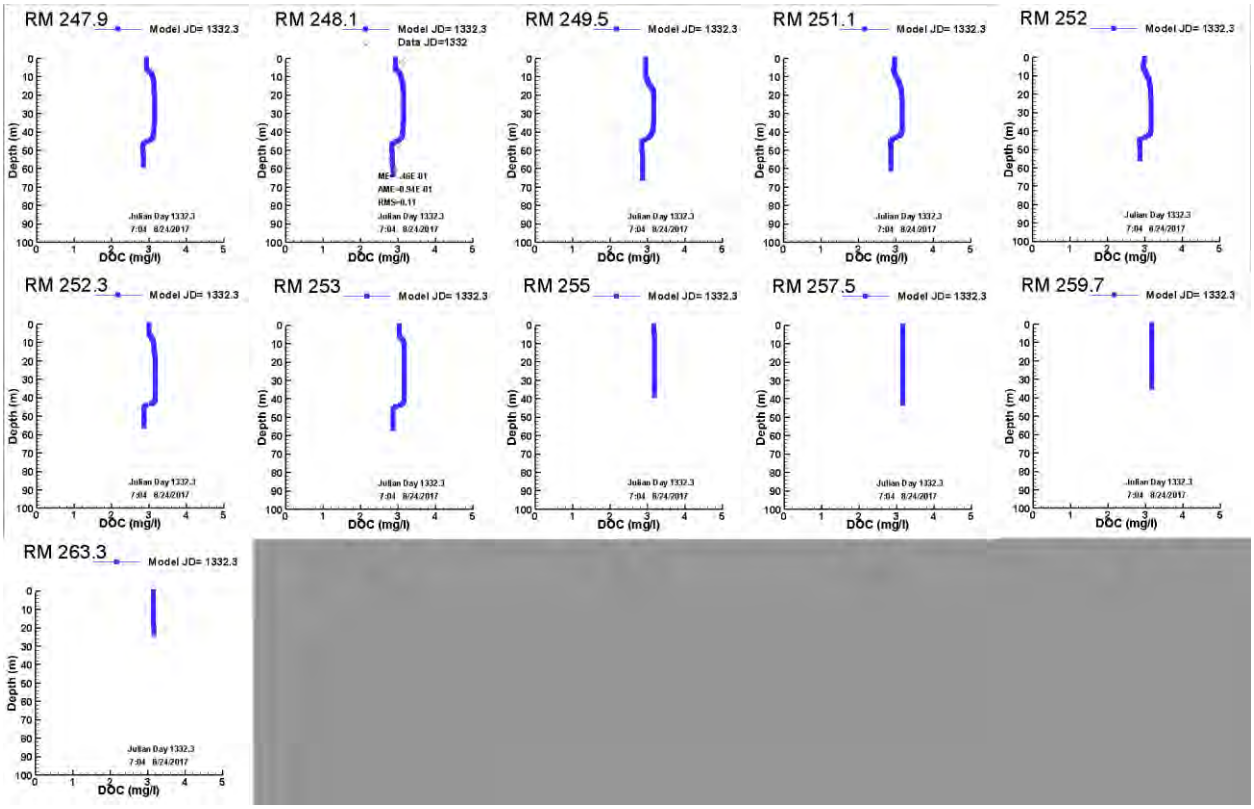


Figure 375. Vertical profiles of DOC compared with data for 8/24/2017.

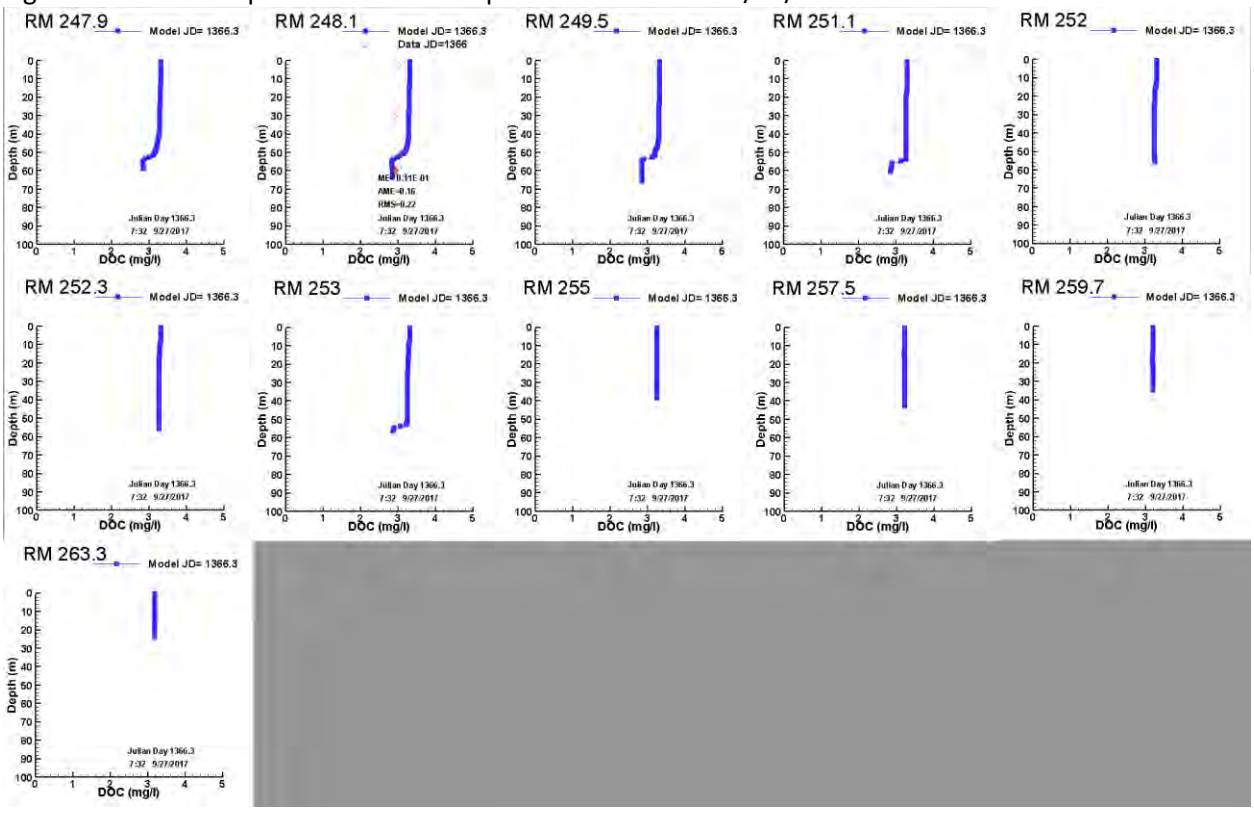


Figure 376. Vertical profiles of DOC compared with data for 9/27/2017.

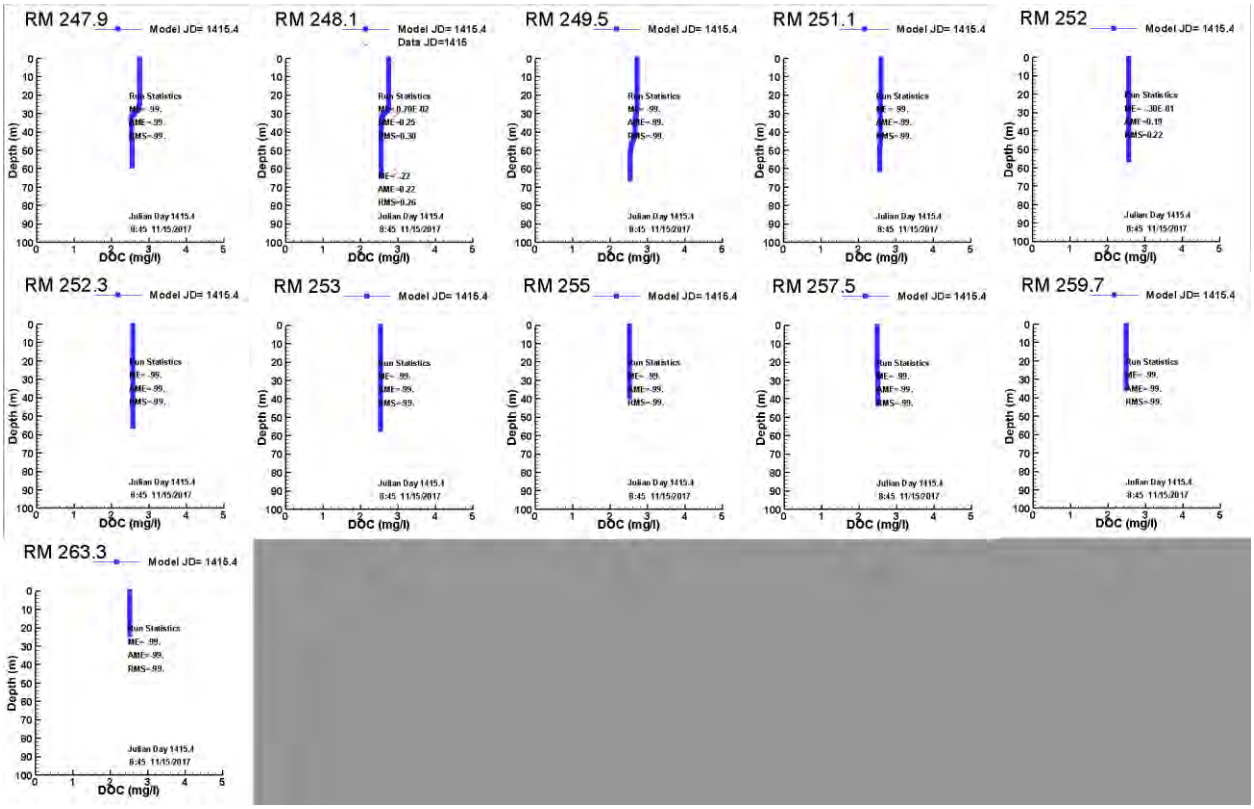


Figure 377. Vertical profiles of DOC compared with data for 11/15/2017.

Particulate Organic Carbon

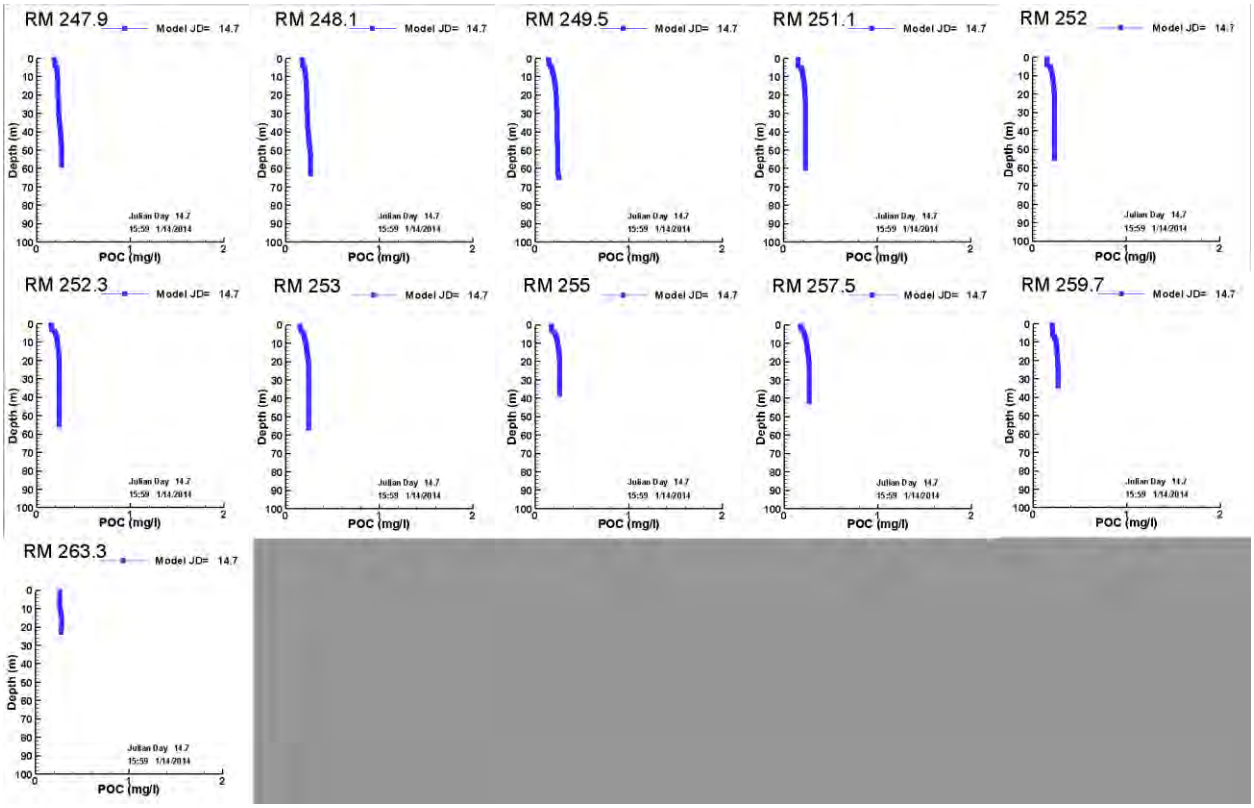


Figure 378. Vertical profiles of POC compared with data for 1/14/2014.

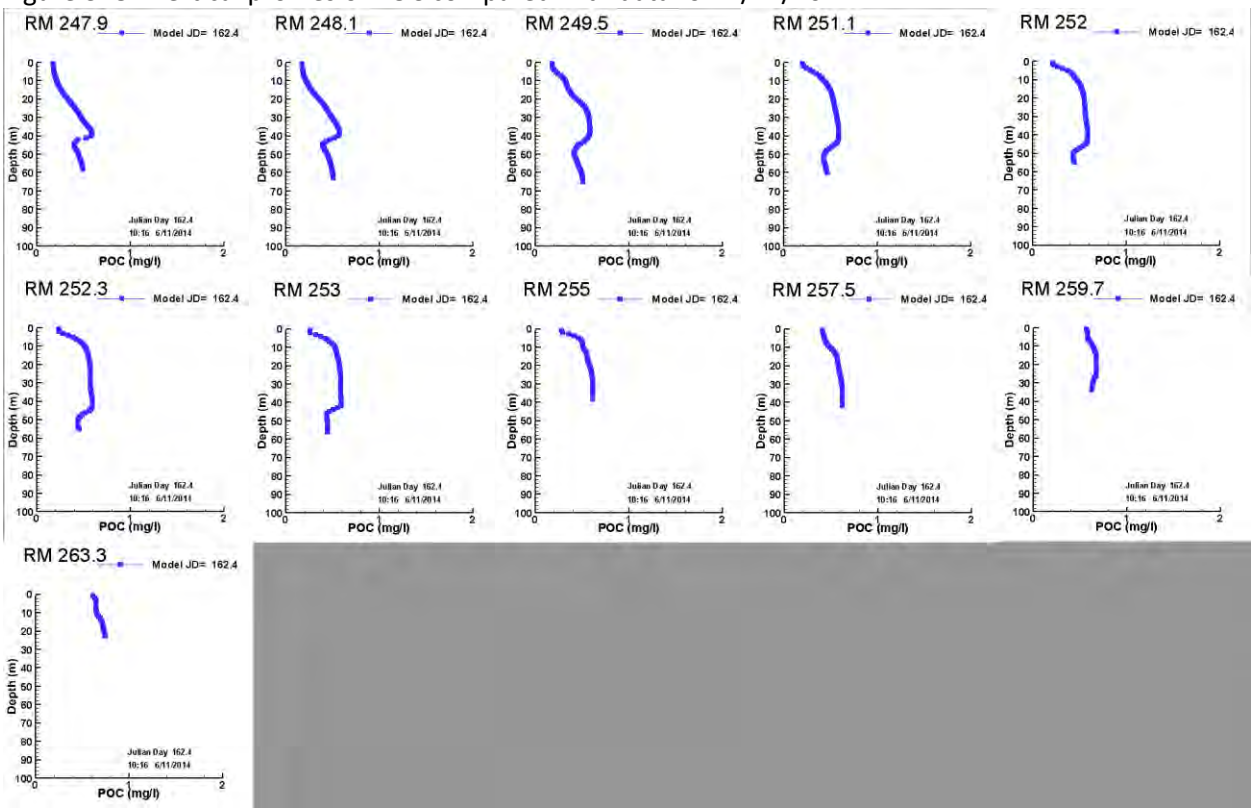


Figure 379. Vertical profiles of POC compared with data for 6/11/2014.

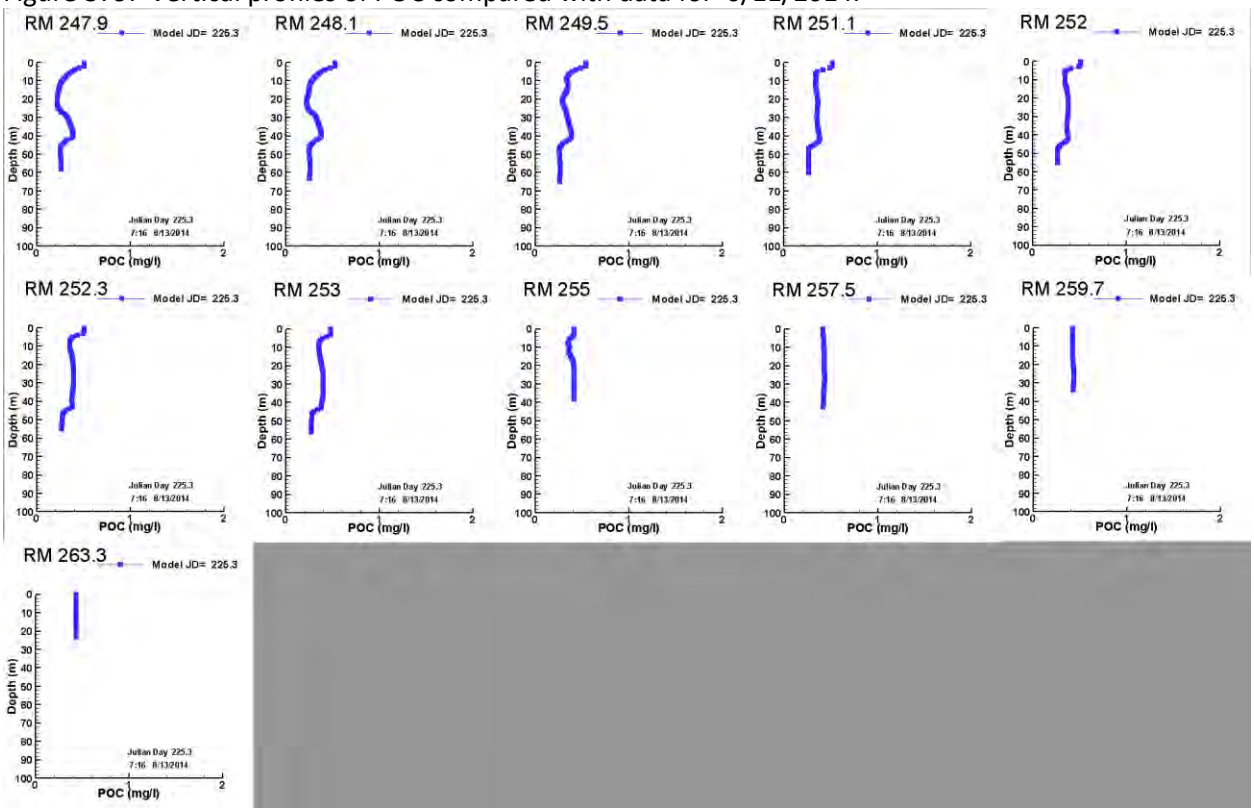


Figure 380. Vertical profiles of POC compared with data for 8/13/2014.

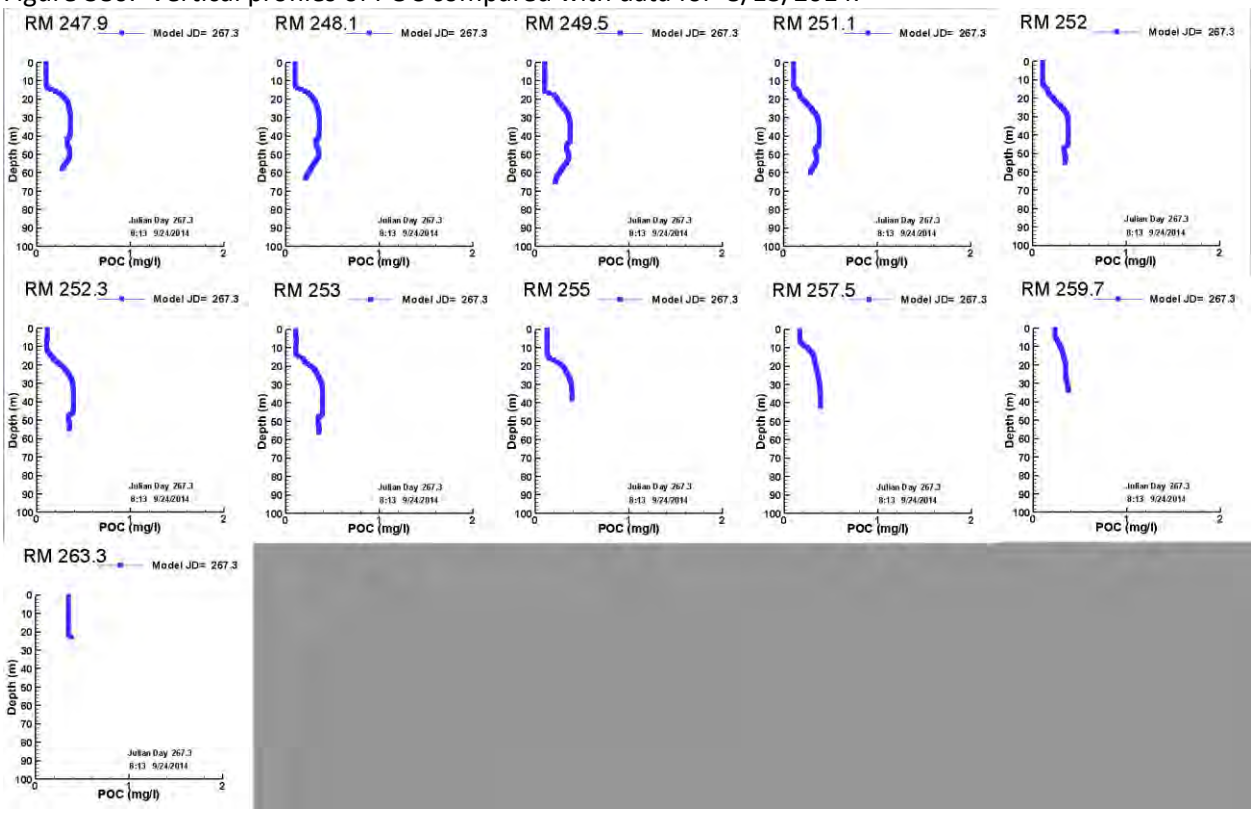


Figure 381. Vertical profiles of POC compared with data for 9/24/2014.

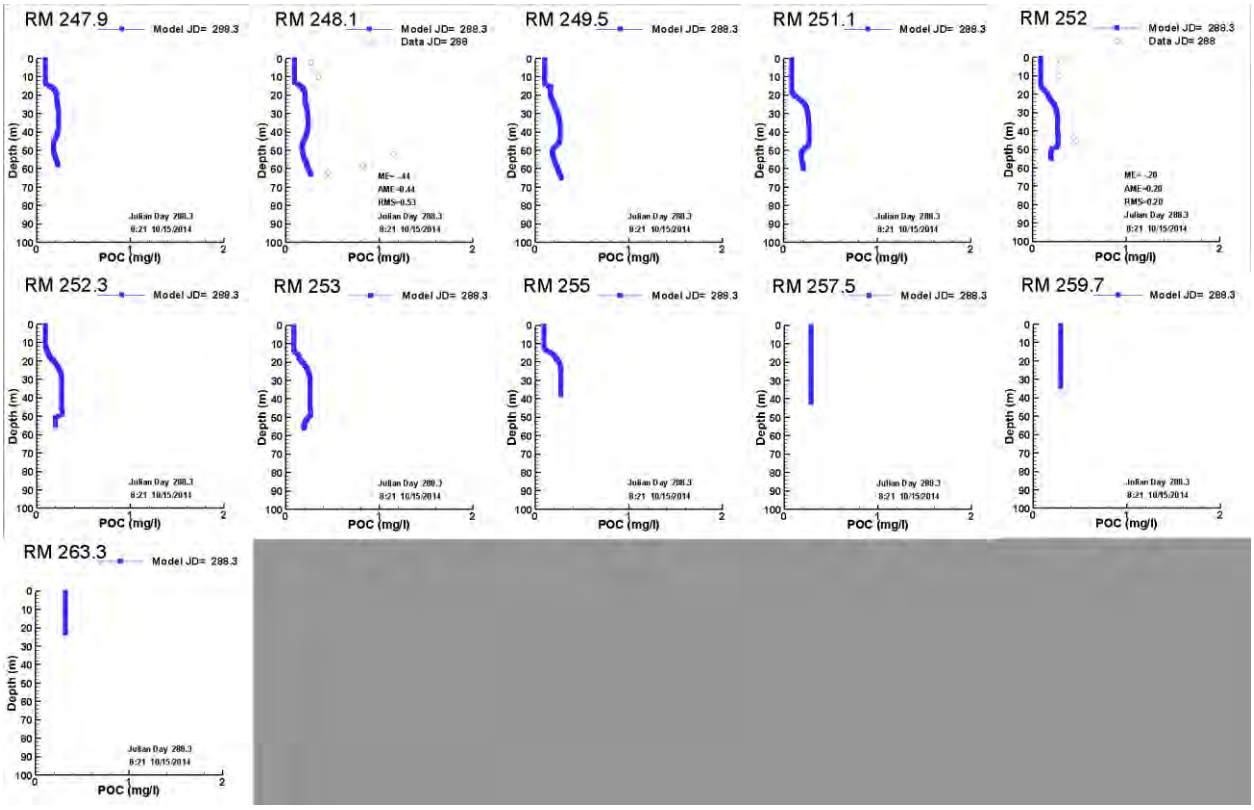


Figure 382. Vertical profiles of POC compared with data for 10/15/2014.

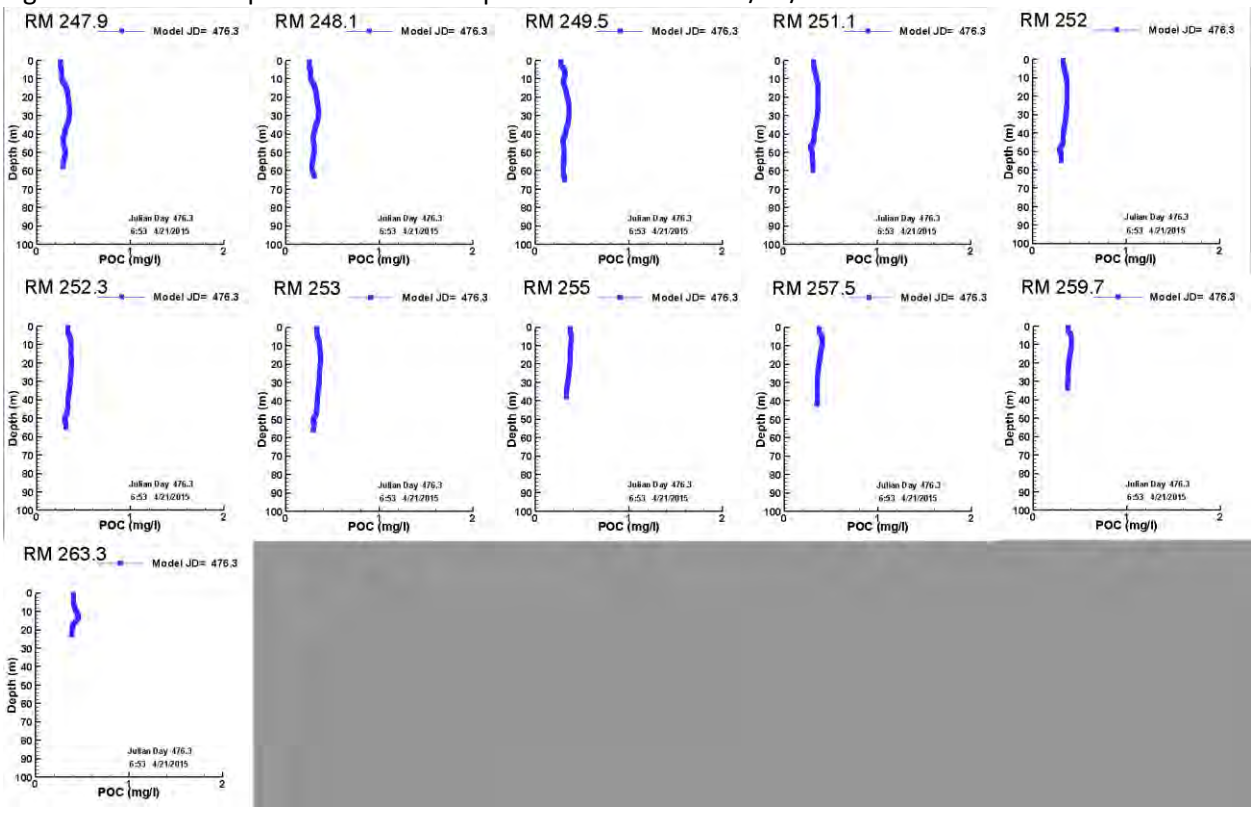


Figure 383. Vertical profiles of POC compared with data for 4/21/2015.

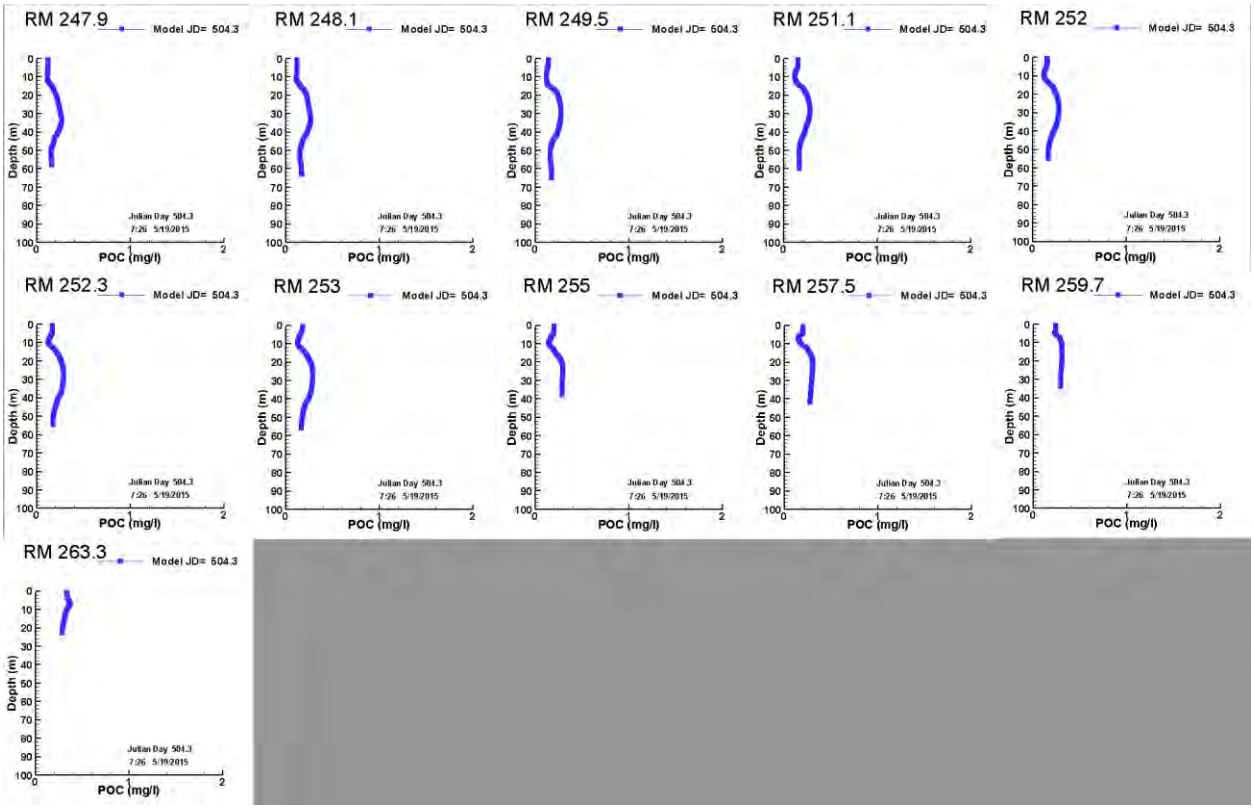


Figure 384. Vertical profiles of POC compared with data for 5/19/2015.

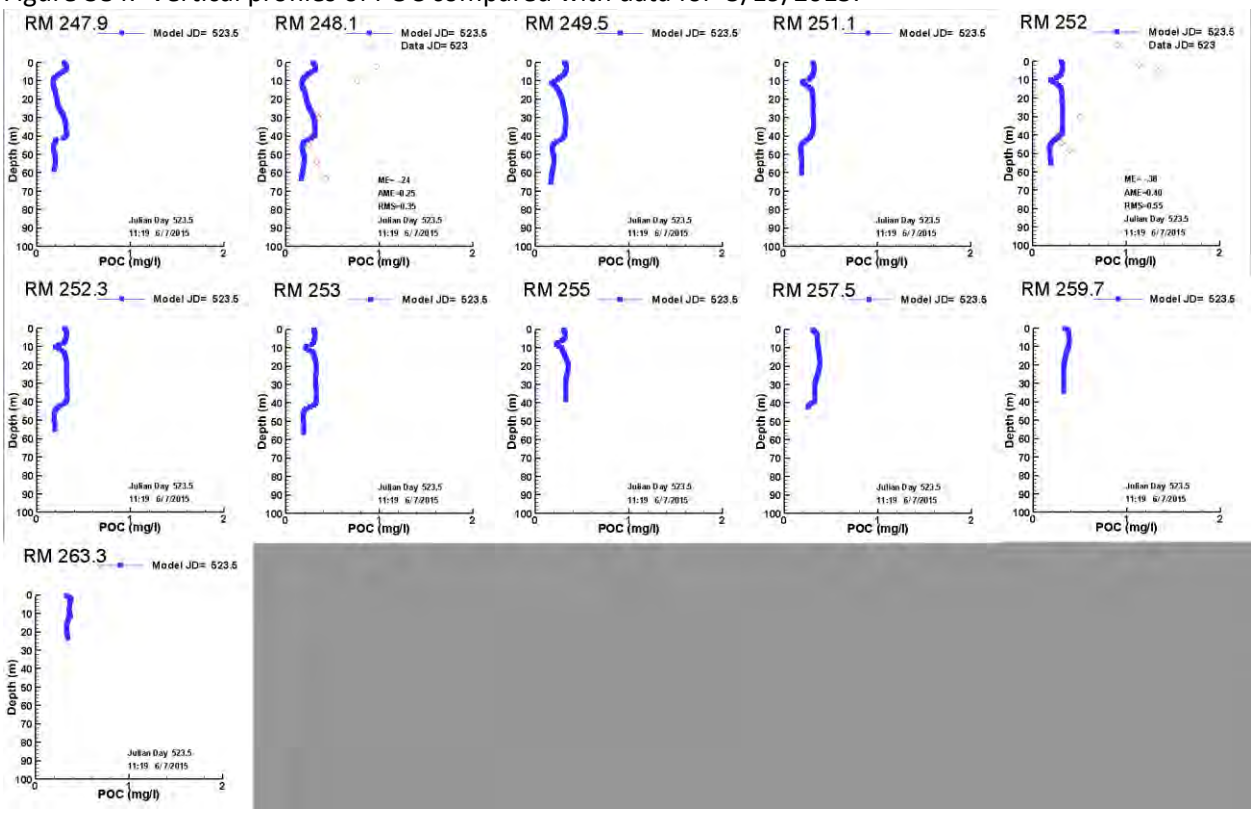


Figure 385. Vertical profiles of POC compared with data for 6/ 7/2015.

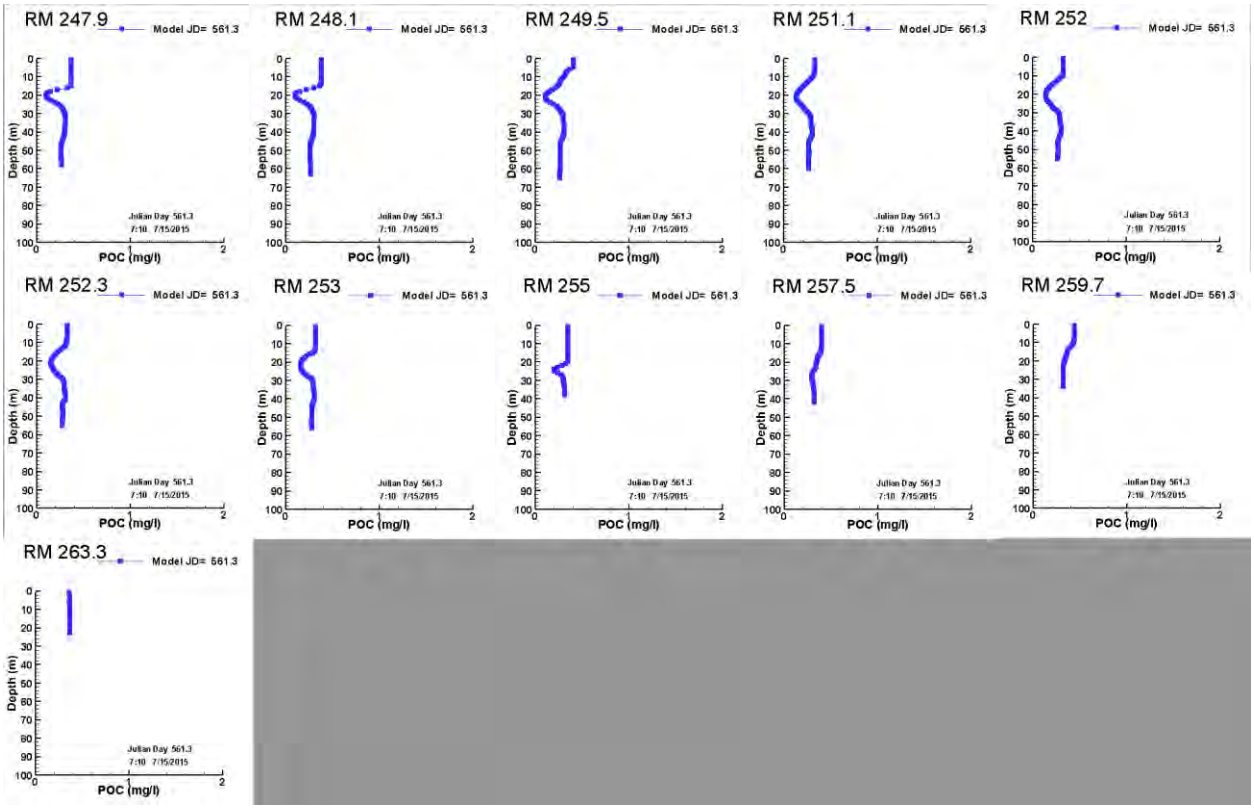


Figure 386. Vertical profiles of POC compared with data for 7/15/2015.

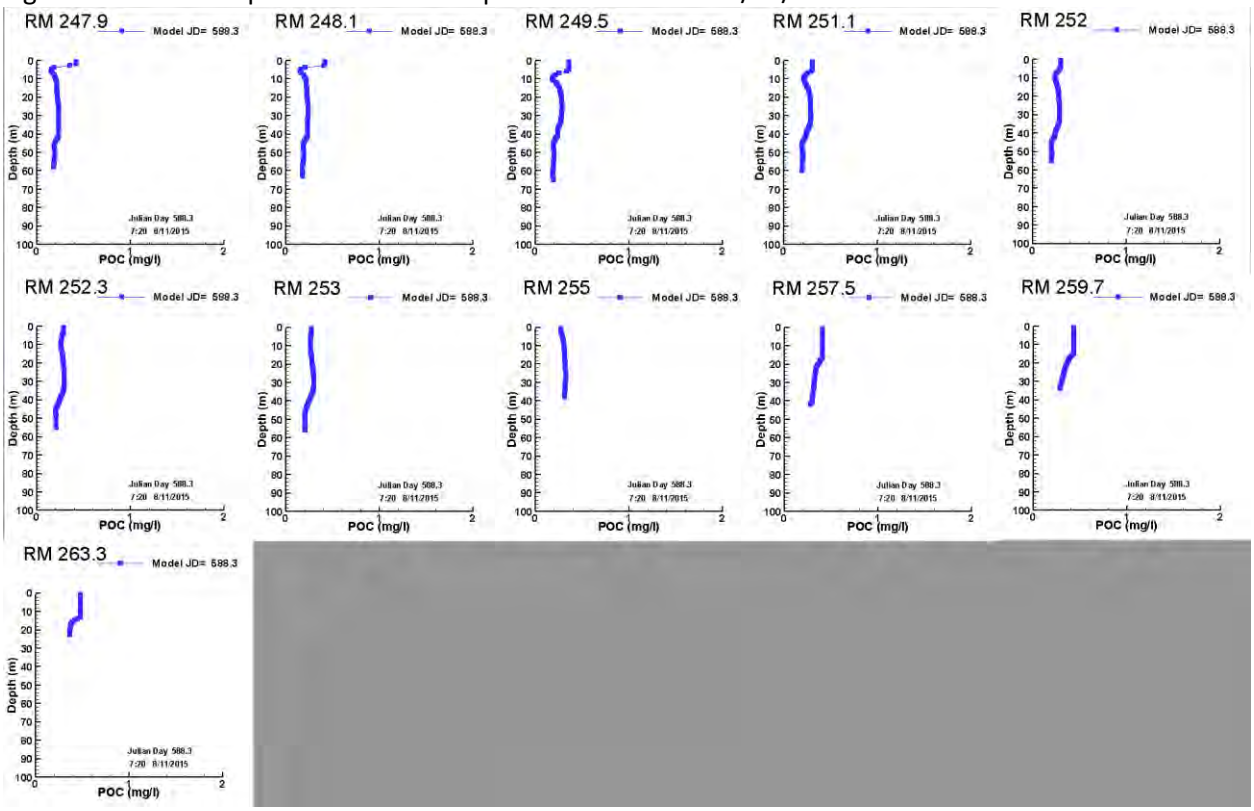


Figure 387. Vertical profiles of POC compared with data for 8/11/2015.

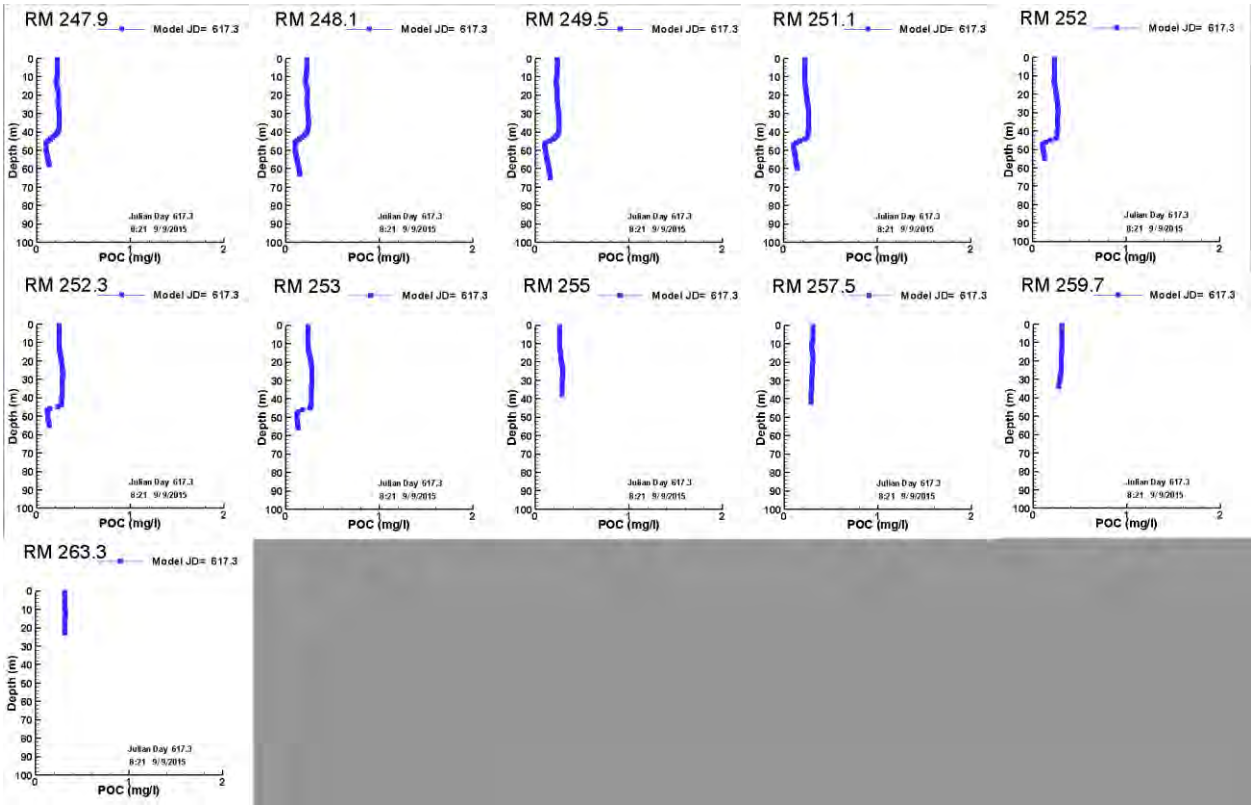


Figure 388. Vertical profiles of POC compared with data for 9/ 9/2015.

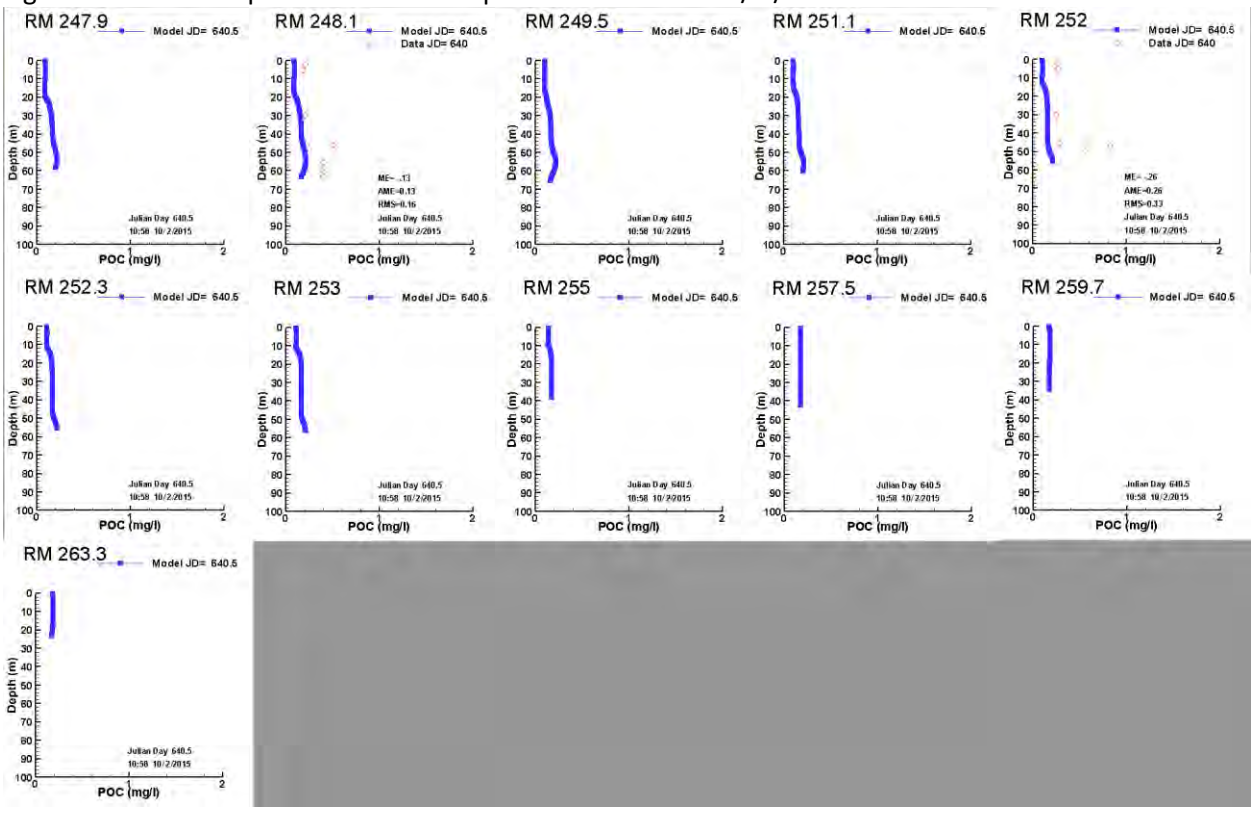


Figure 389. Vertical profiles of POC compared with data for 10/ 2/2015.

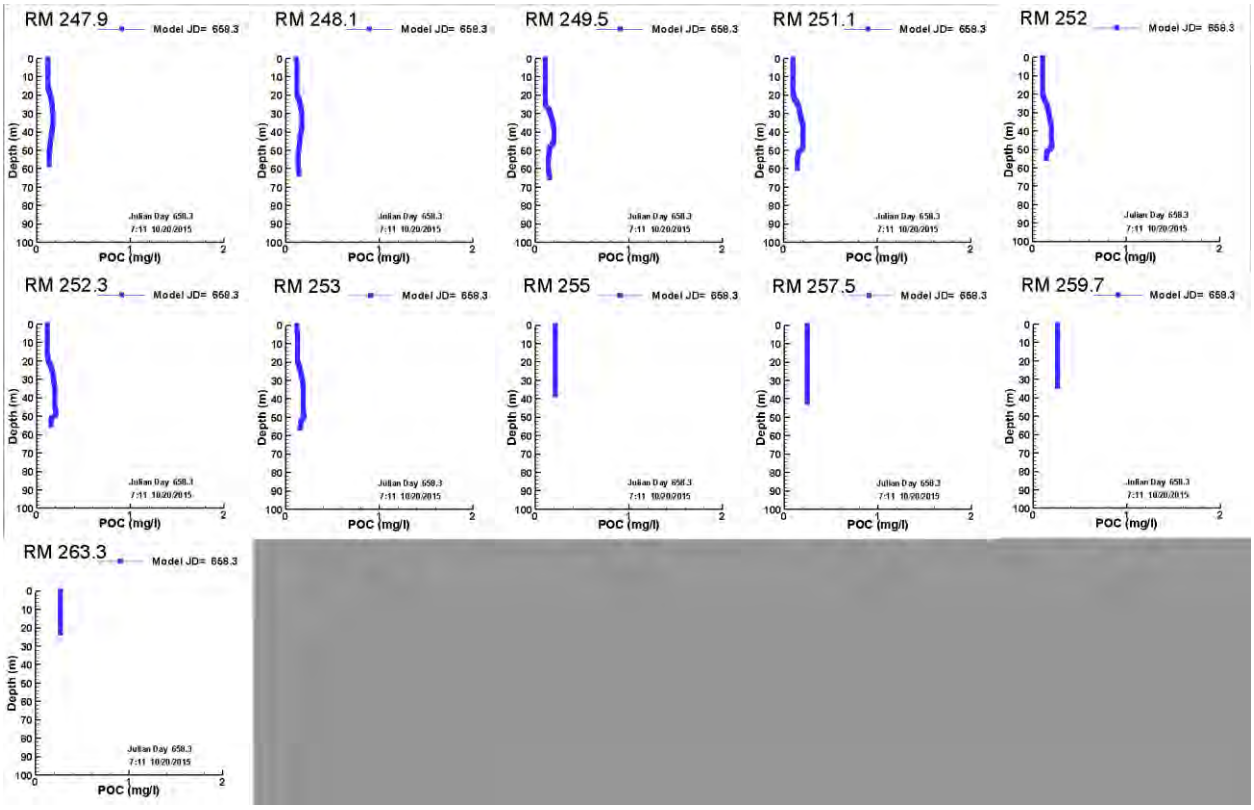


Figure 390. Vertical profiles of POC compared with data for 10/20/2015.

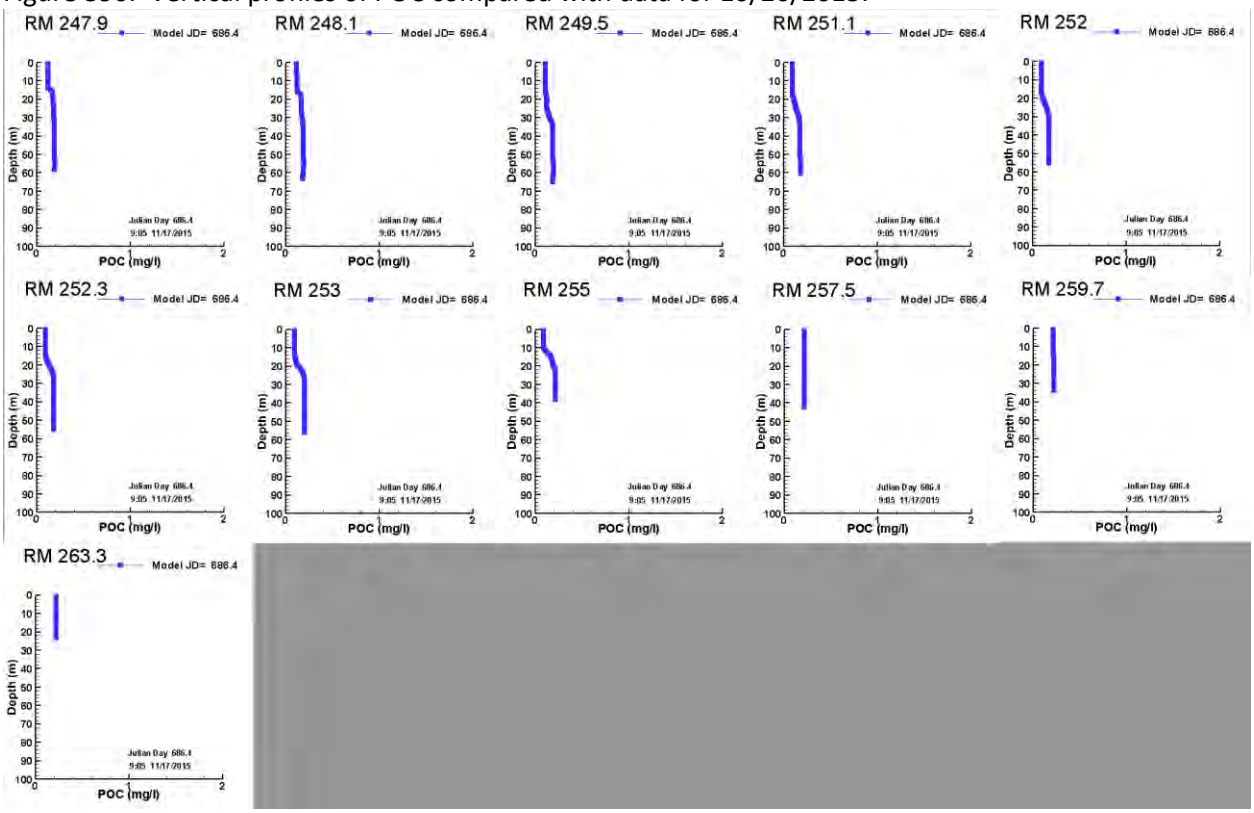


Figure 391. Vertical profiles of POC compared with data for 11/17/2015.

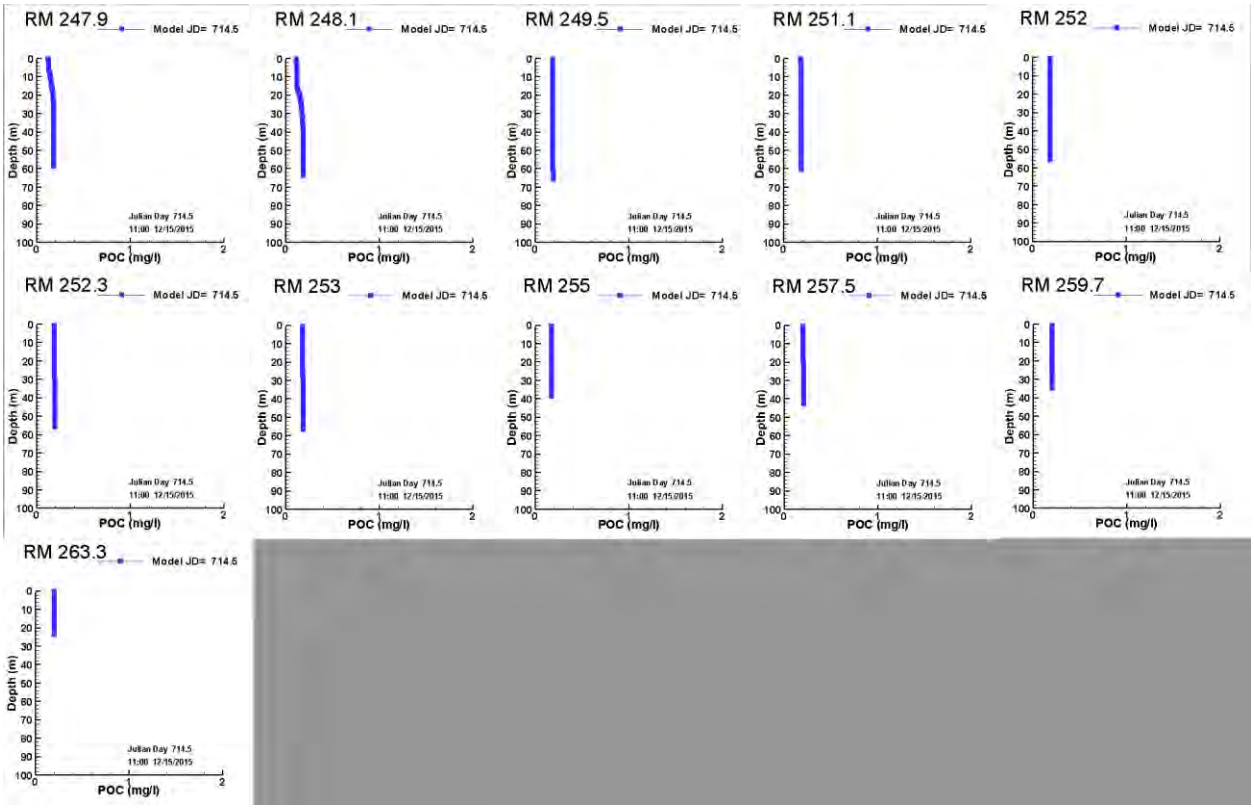


Figure 392. Vertical profiles of POC compared with data for 12/15/2015.

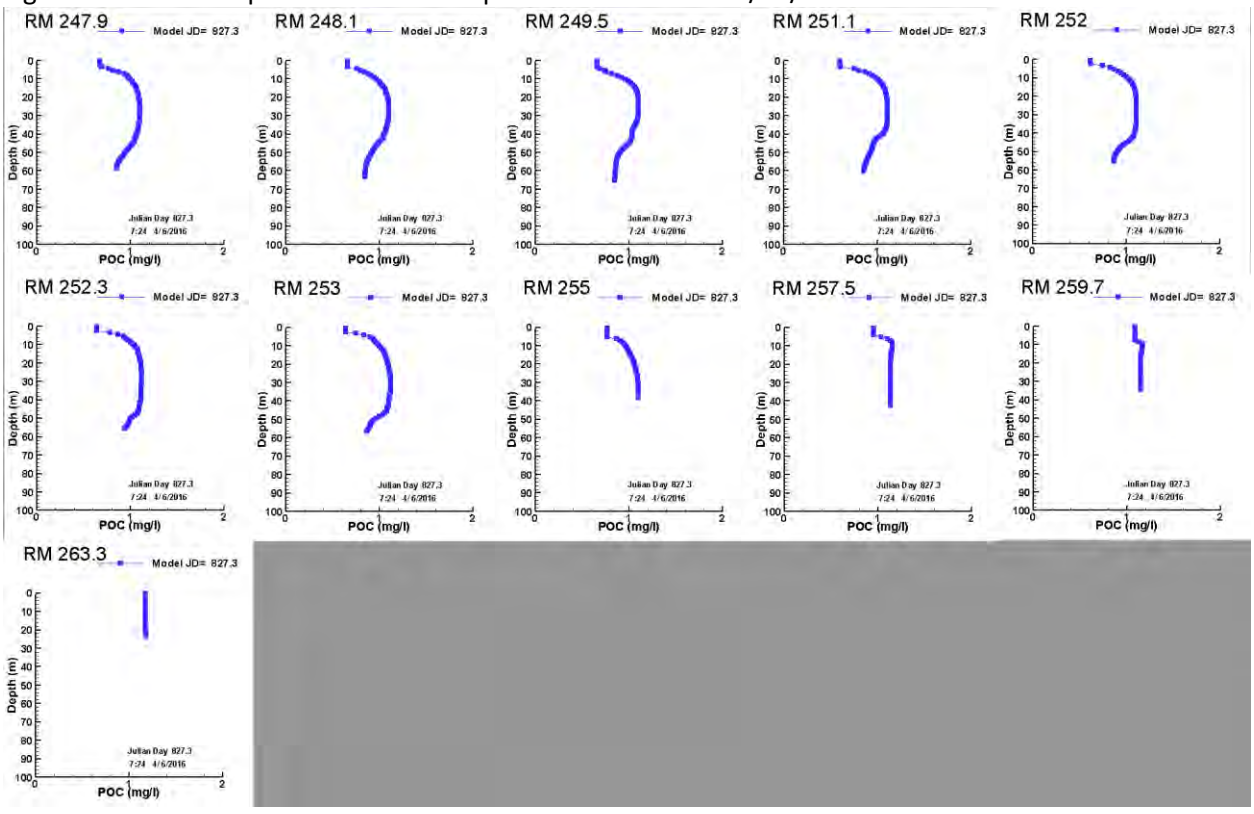


Figure 393. Vertical profiles of POC compared with data for 4/ 6/2016.

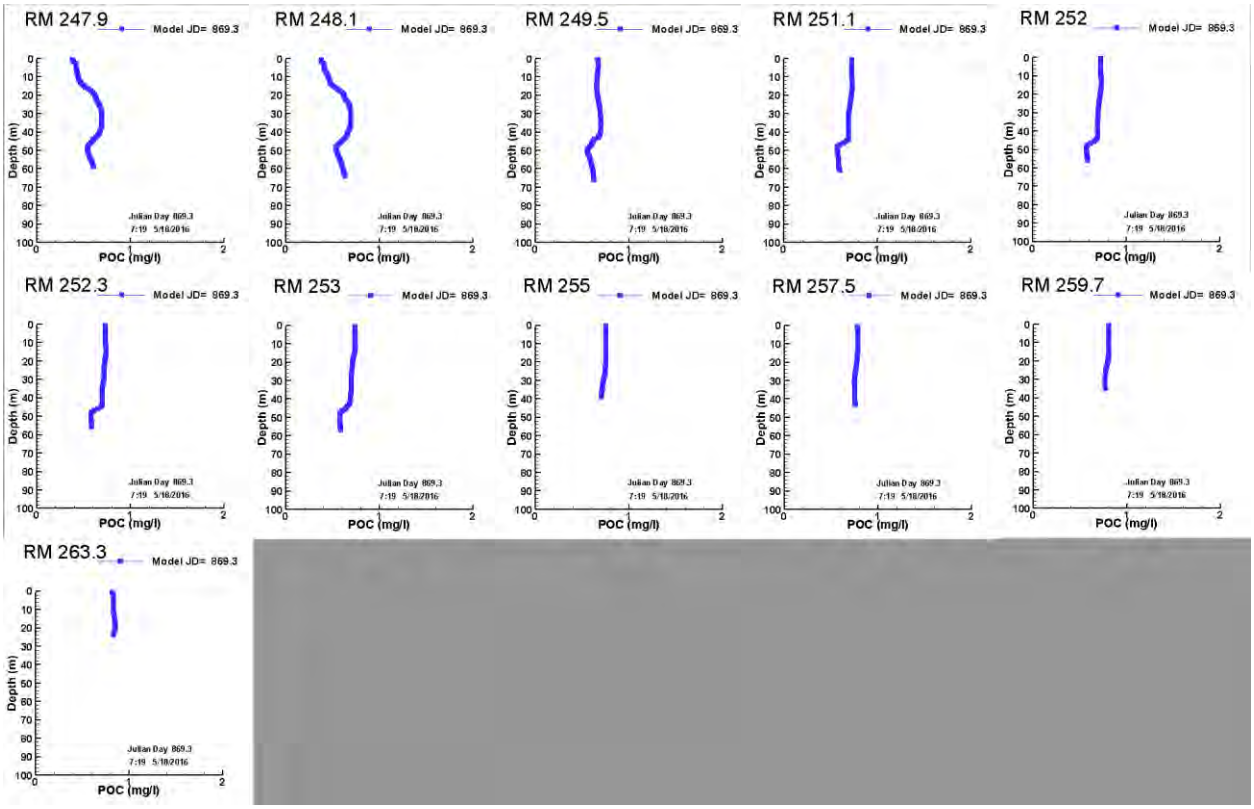


Figure 394. Vertical profiles of POC compared with data for 5/18/2016.

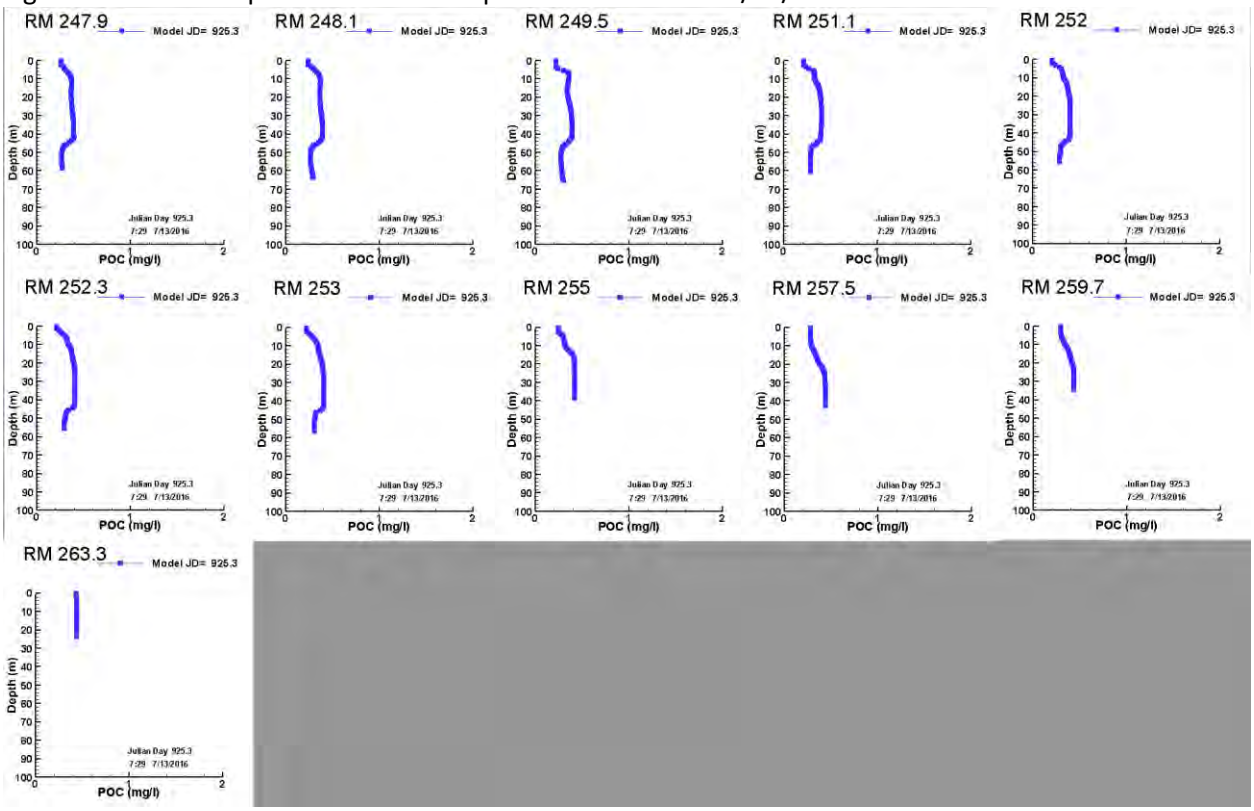


Figure 395. Vertical profiles of POC compared with data for 7/13/2016.

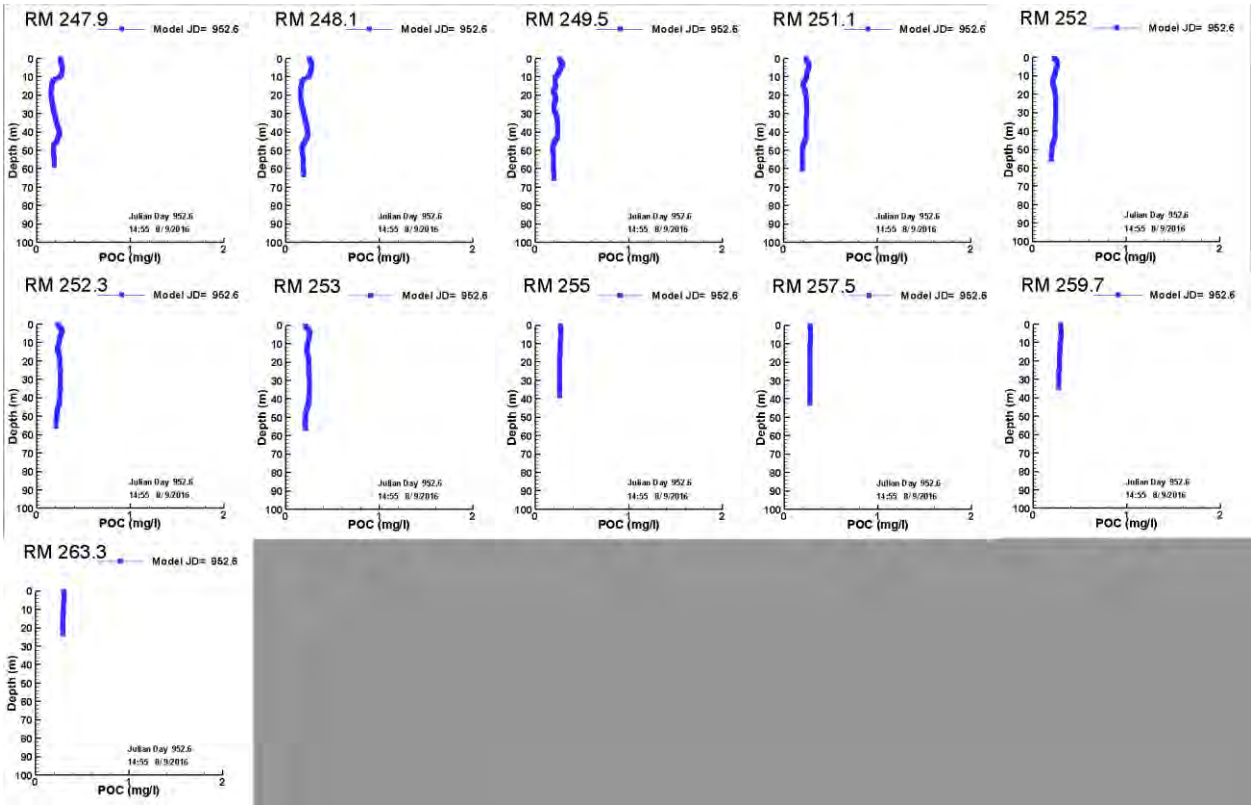


Figure 396. Vertical profiles of POC compared with data for 8/ 9/2016.

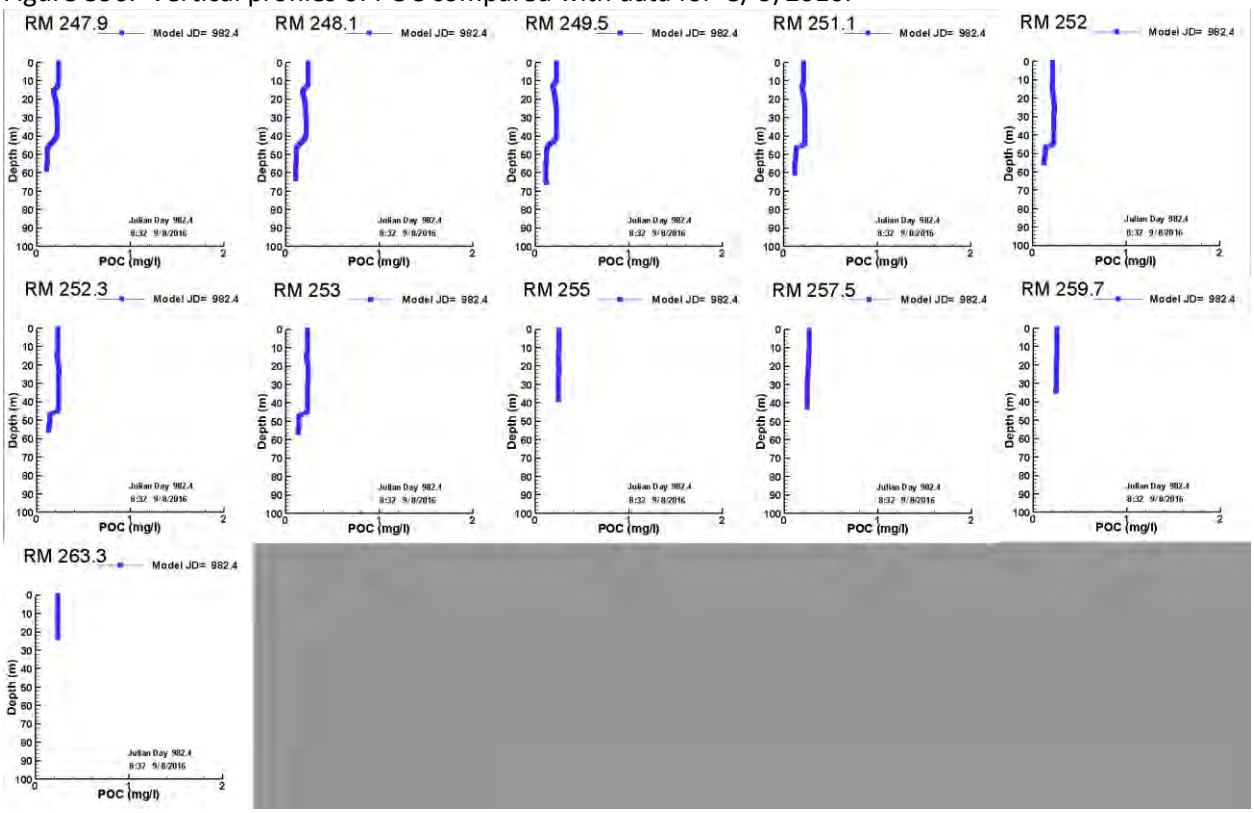


Figure 397. Vertical profiles of POC compared with data for 9/ 8/2016.

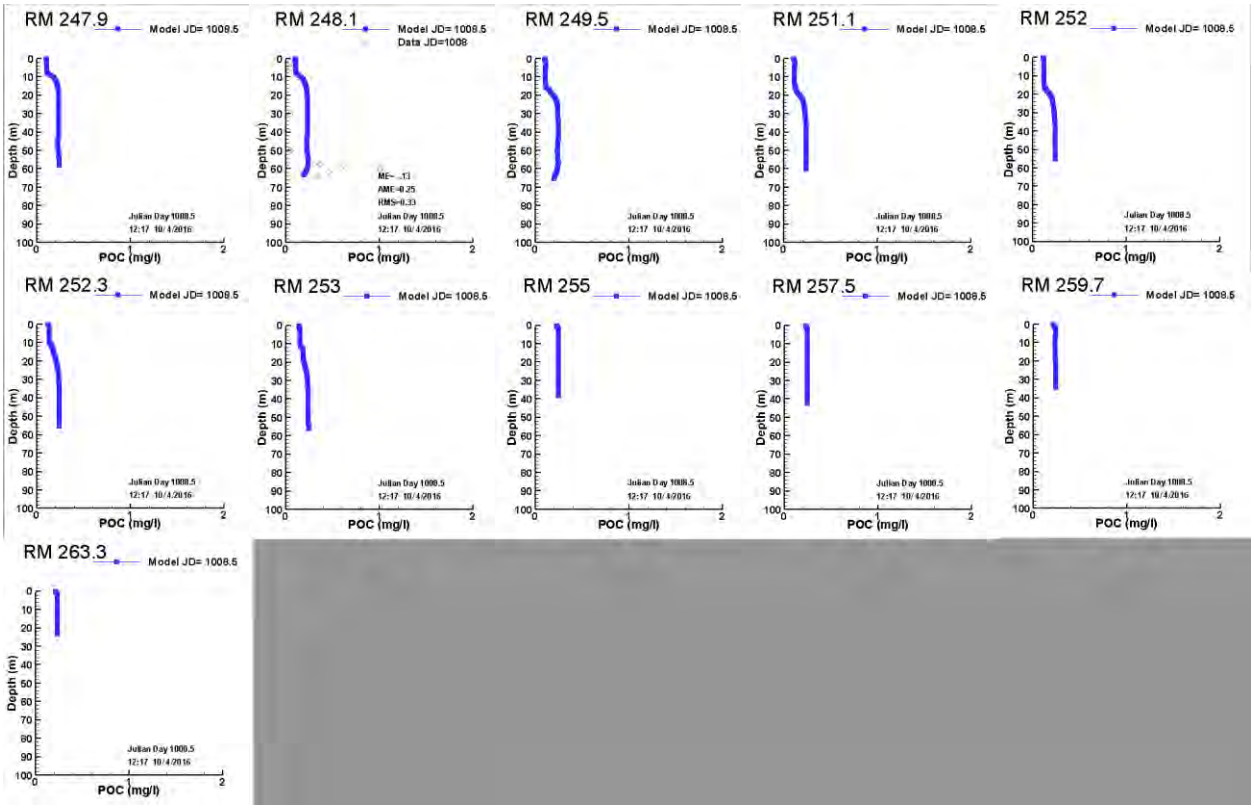


Figure 398. Vertical profiles of POC compared with data for 10/ 4/2016.

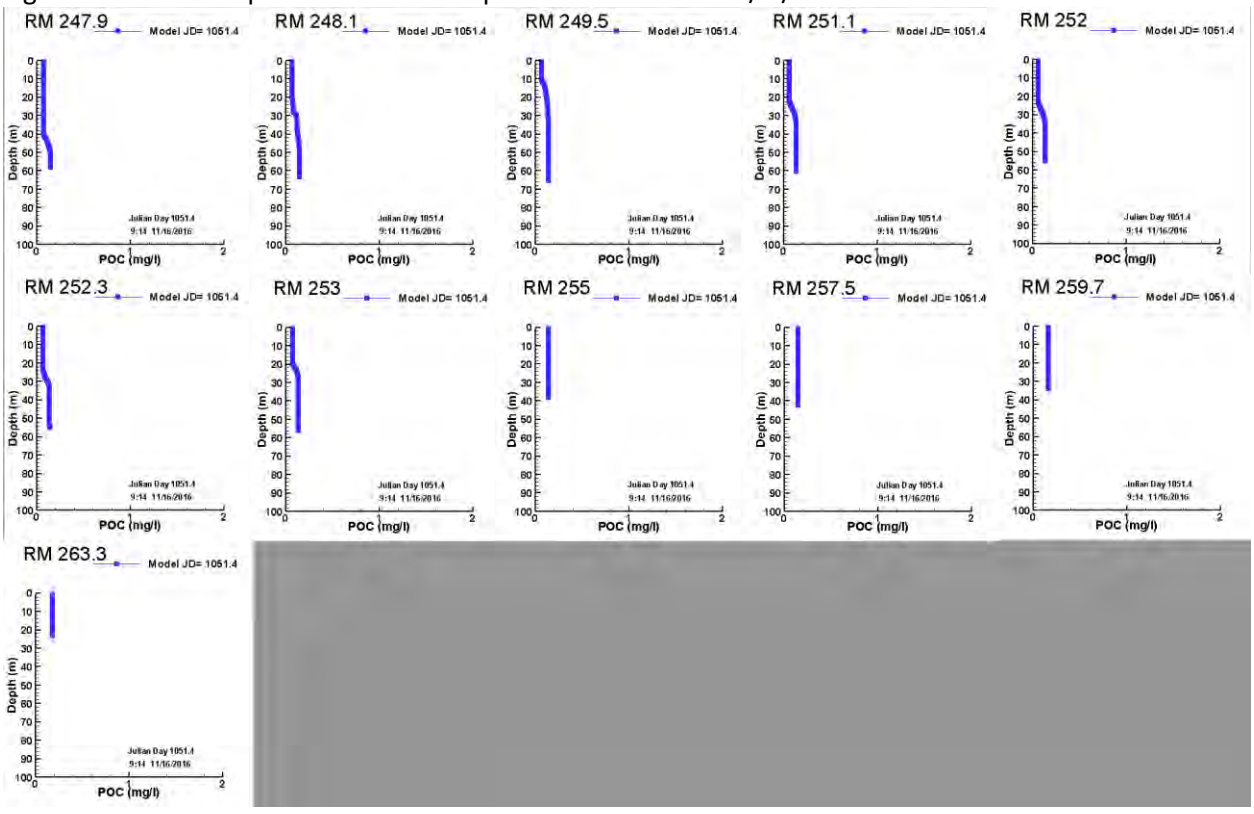


Figure 399. Vertical profiles of POC compared with data for 11/16/2016.

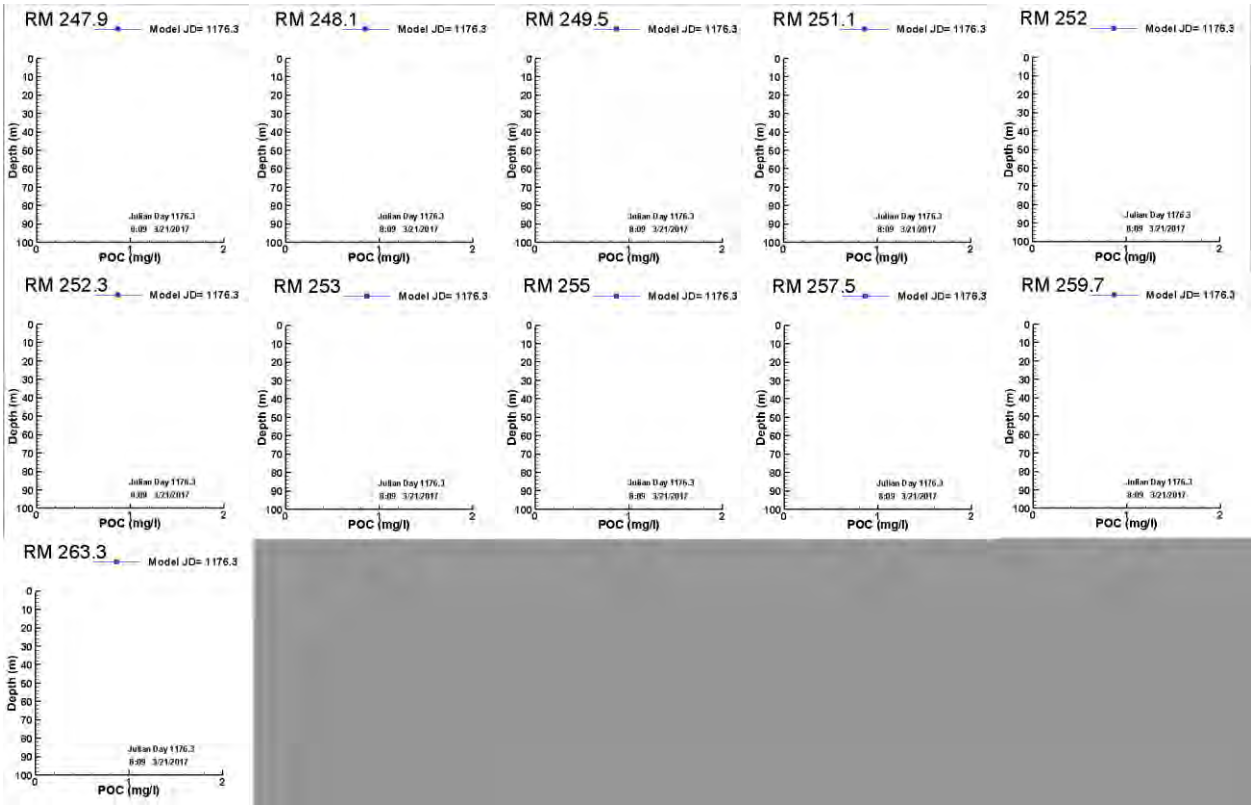


Figure 400. Vertical profiles of POC compared with data for 3/21/2017.

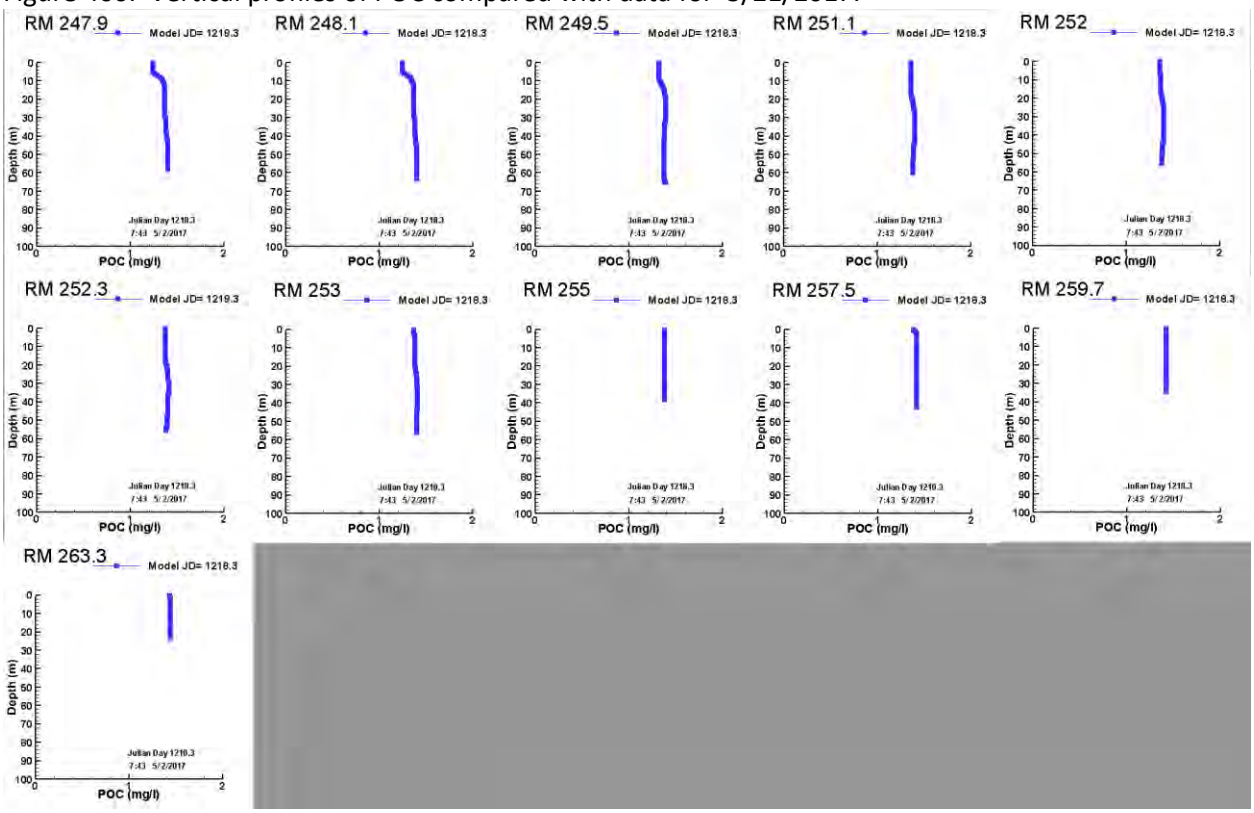


Figure 401. Vertical profiles of POC compared with data for 5/ 2/2017.

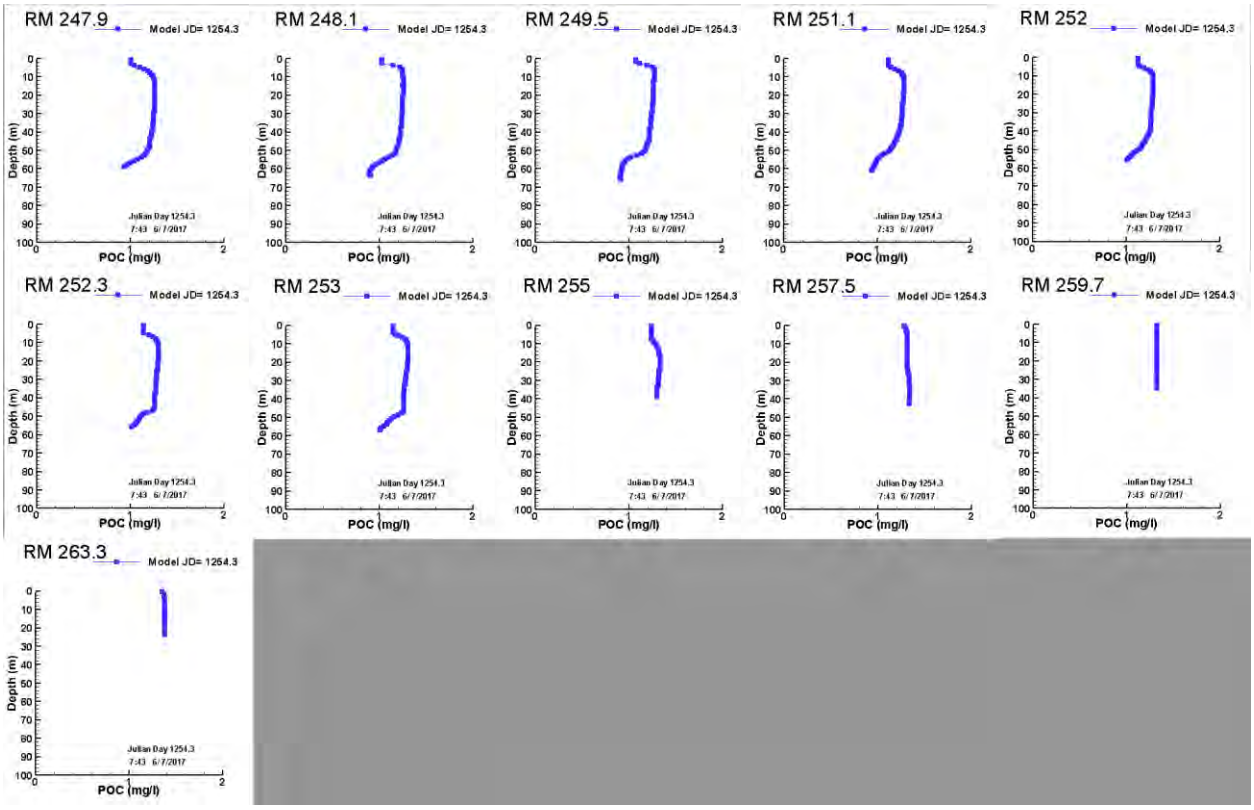


Figure 402. Vertical profiles of POC compared with data for 6/ 7/2017.

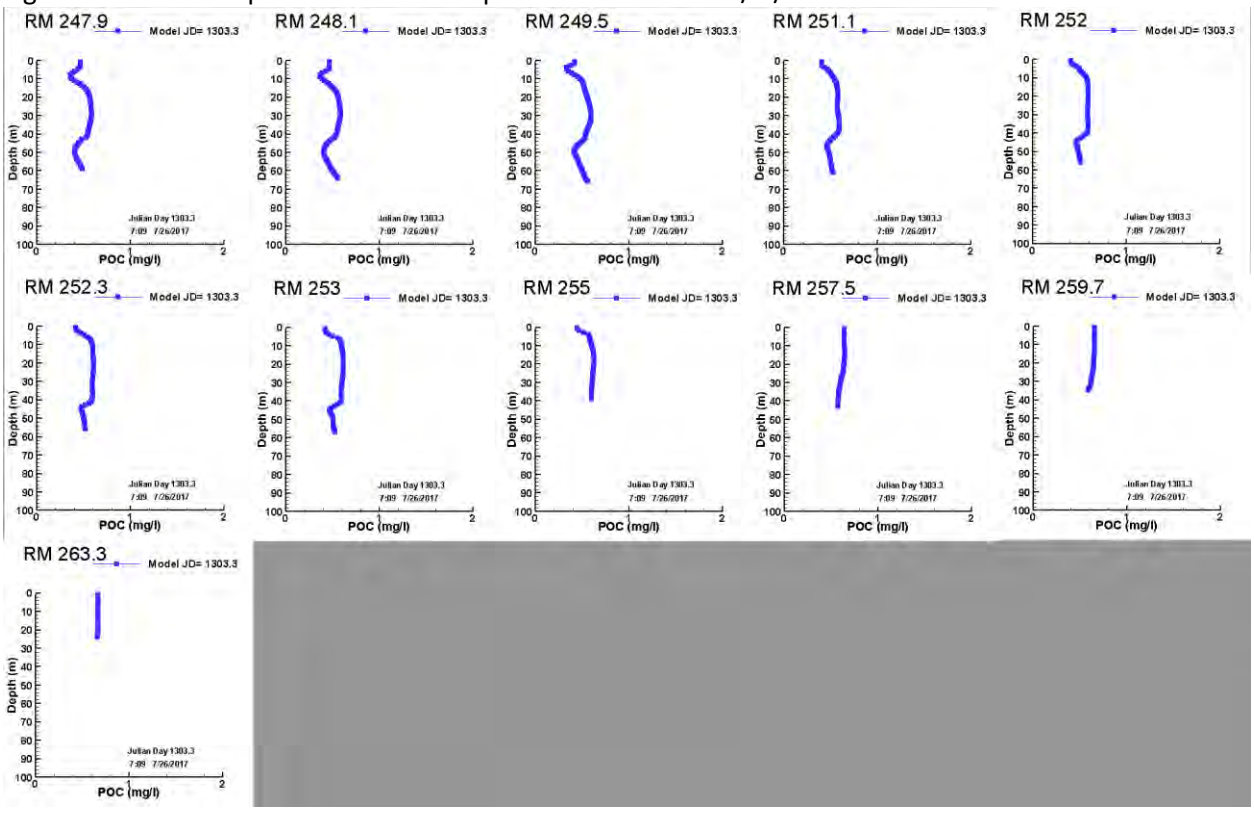


Figure 403. Vertical profiles of POC compared with data for 7/26/2017.

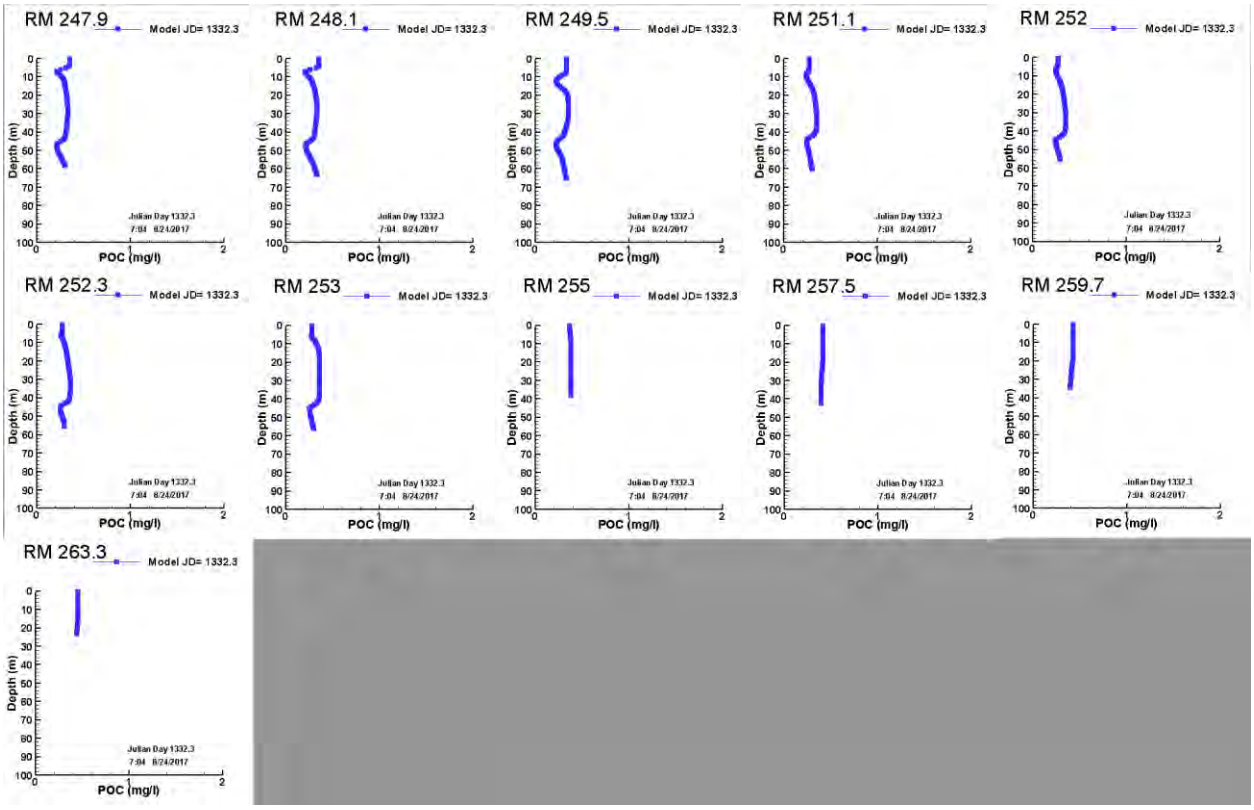


Figure 404. Vertical profiles of POC compared with data for 8/24/2017.

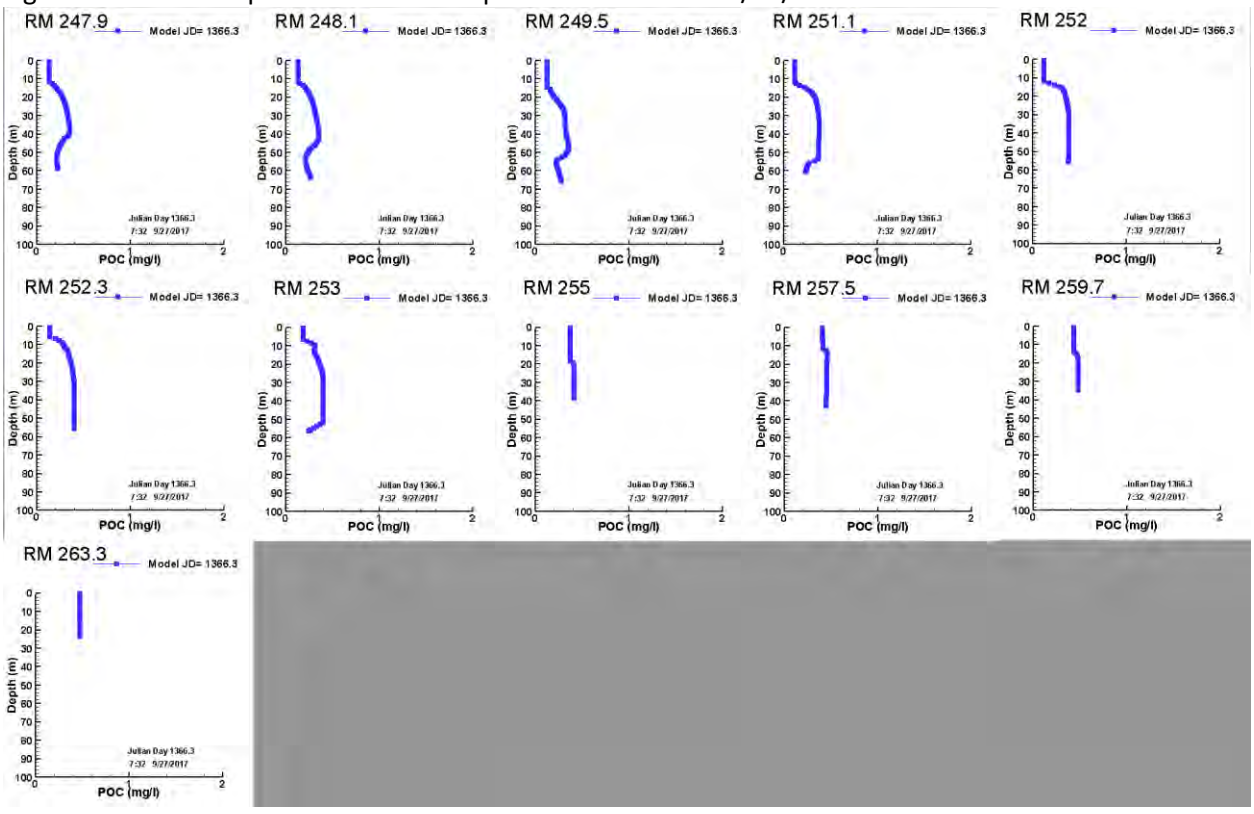


Figure 405. Vertical profiles of POC compared with data for 9/27/2017.

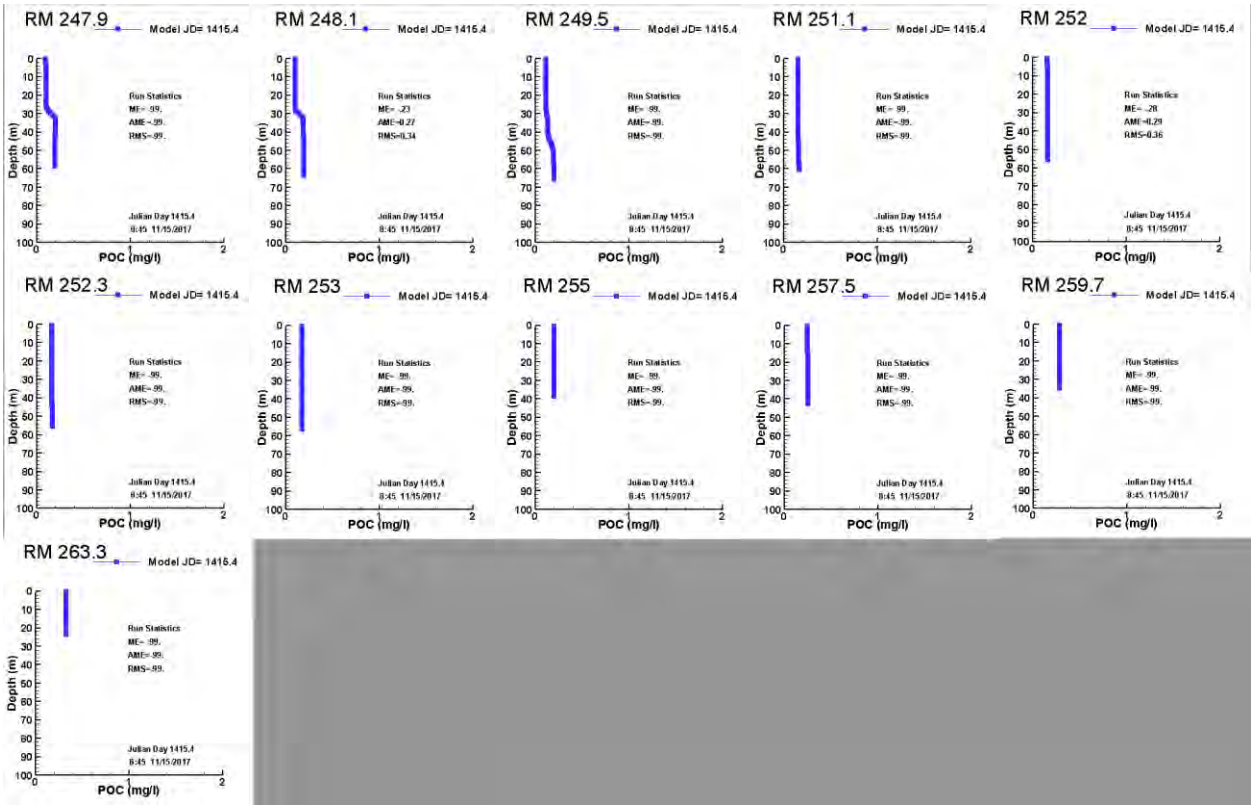


Figure 406. Vertical profiles of POC compared with data for 11/15/2017.

Particulate Organic Nitrogen

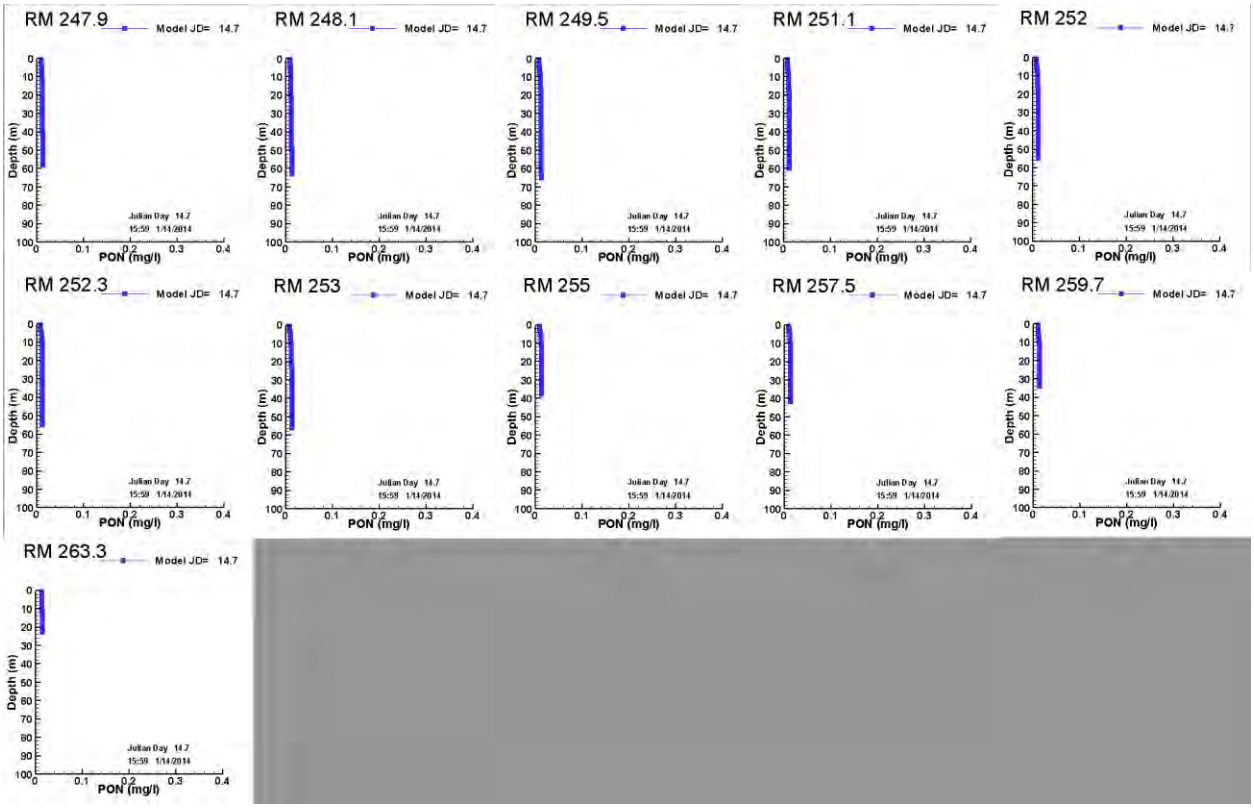


Figure 407. Vertical profiles of PON compared with data for 1/14/2014.

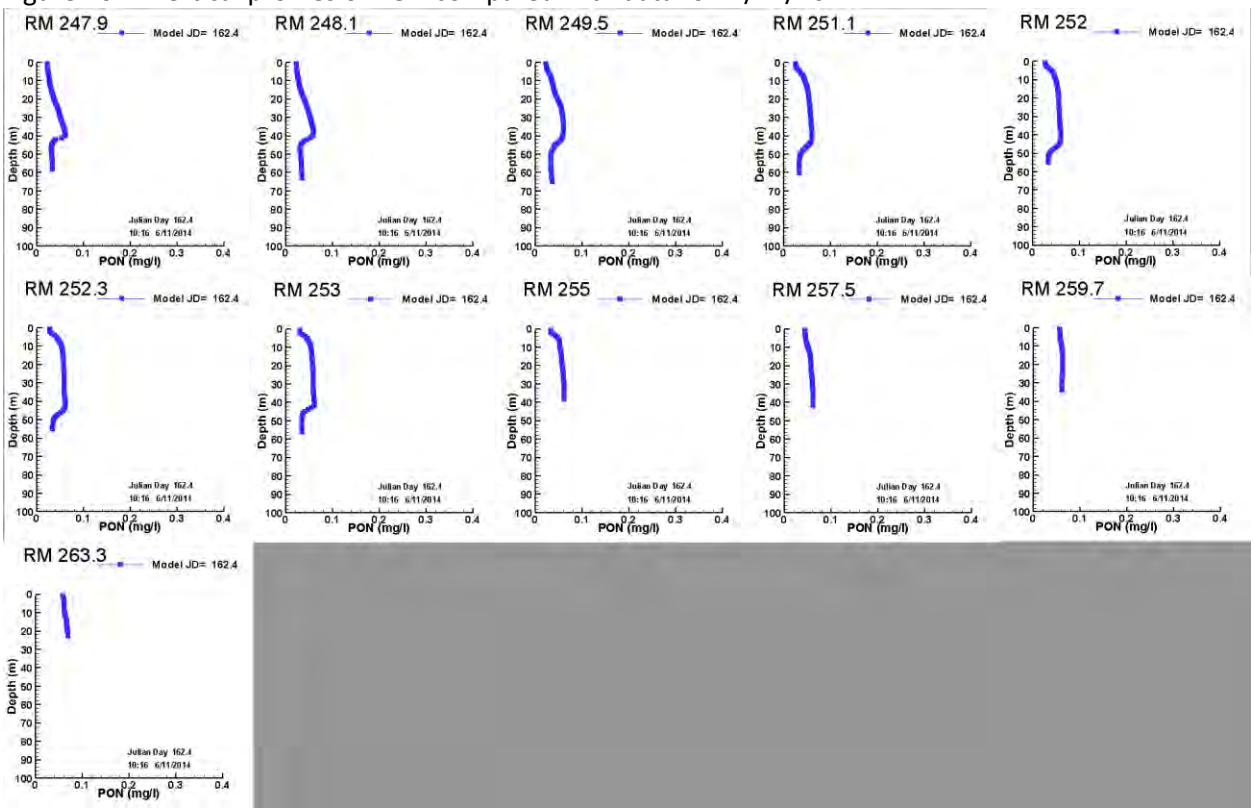


Figure 408. Vertical profiles of PON compared with data for 6/11/2014.

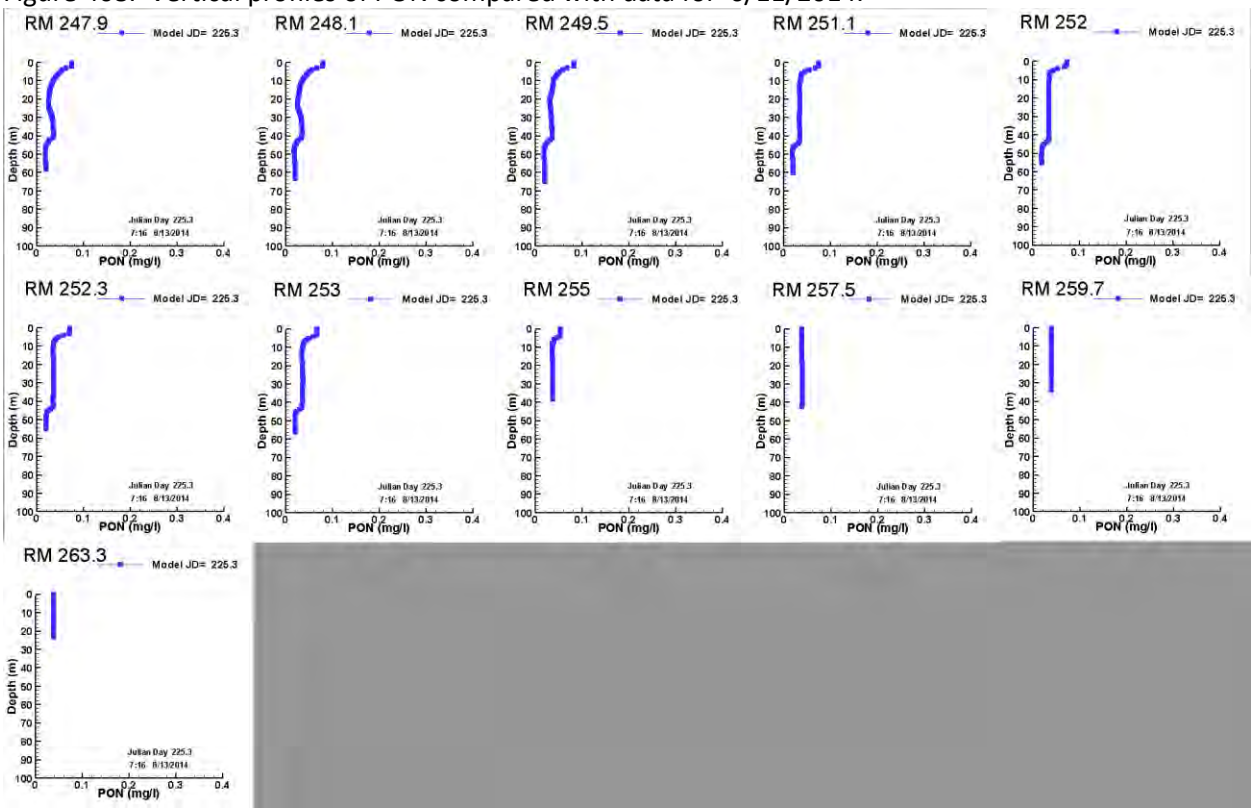


Figure 409. Vertical profiles of PON compared with data for 8/13/2014.

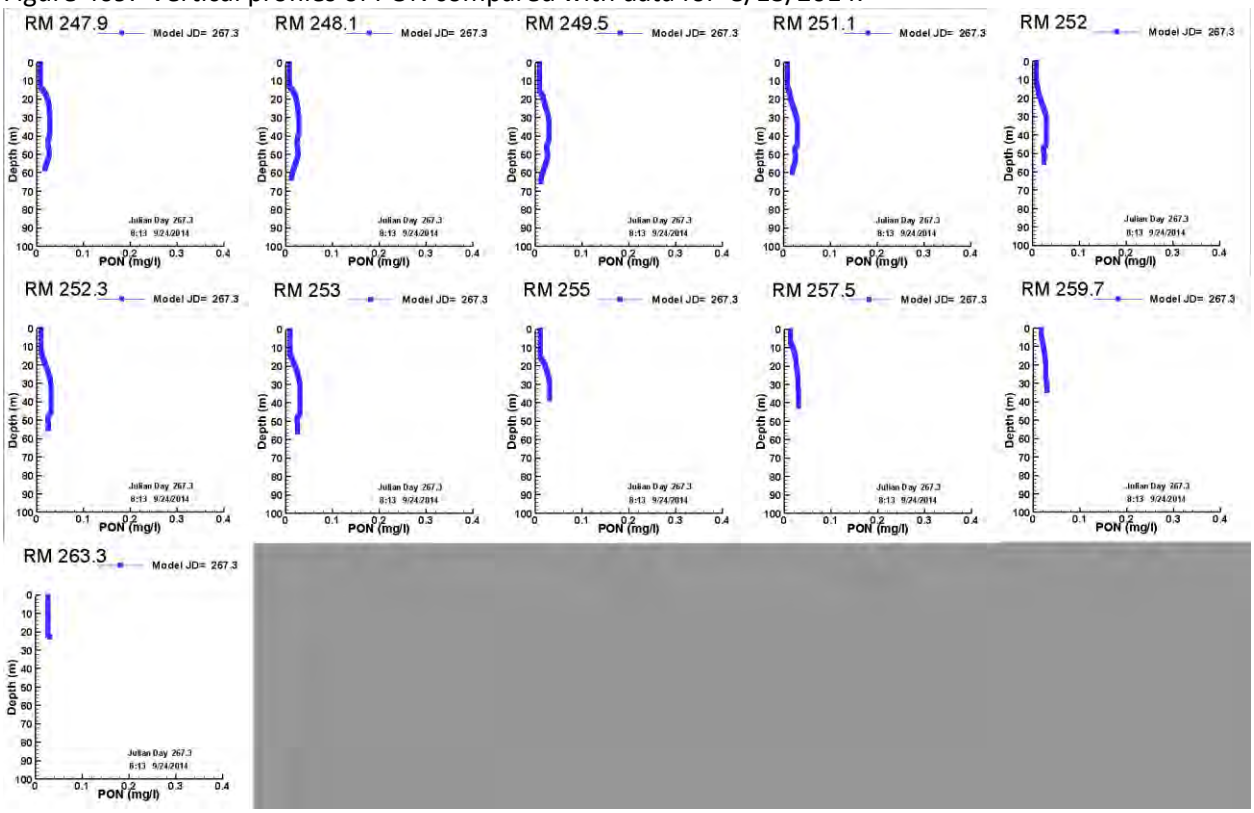


Figure 410. Vertical profiles of PON compared with data for 9/24/2014.

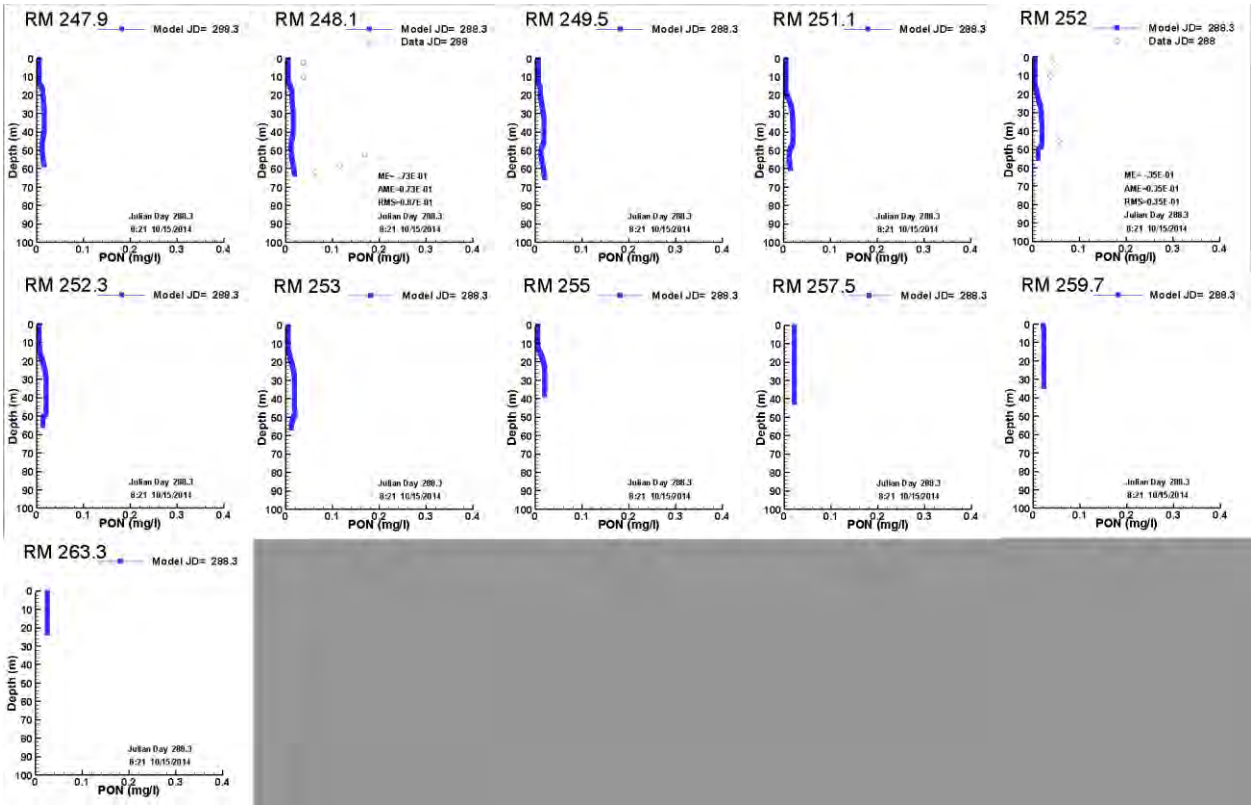


Figure 411. Vertical profiles of PON compared with data for 10/15/2014.

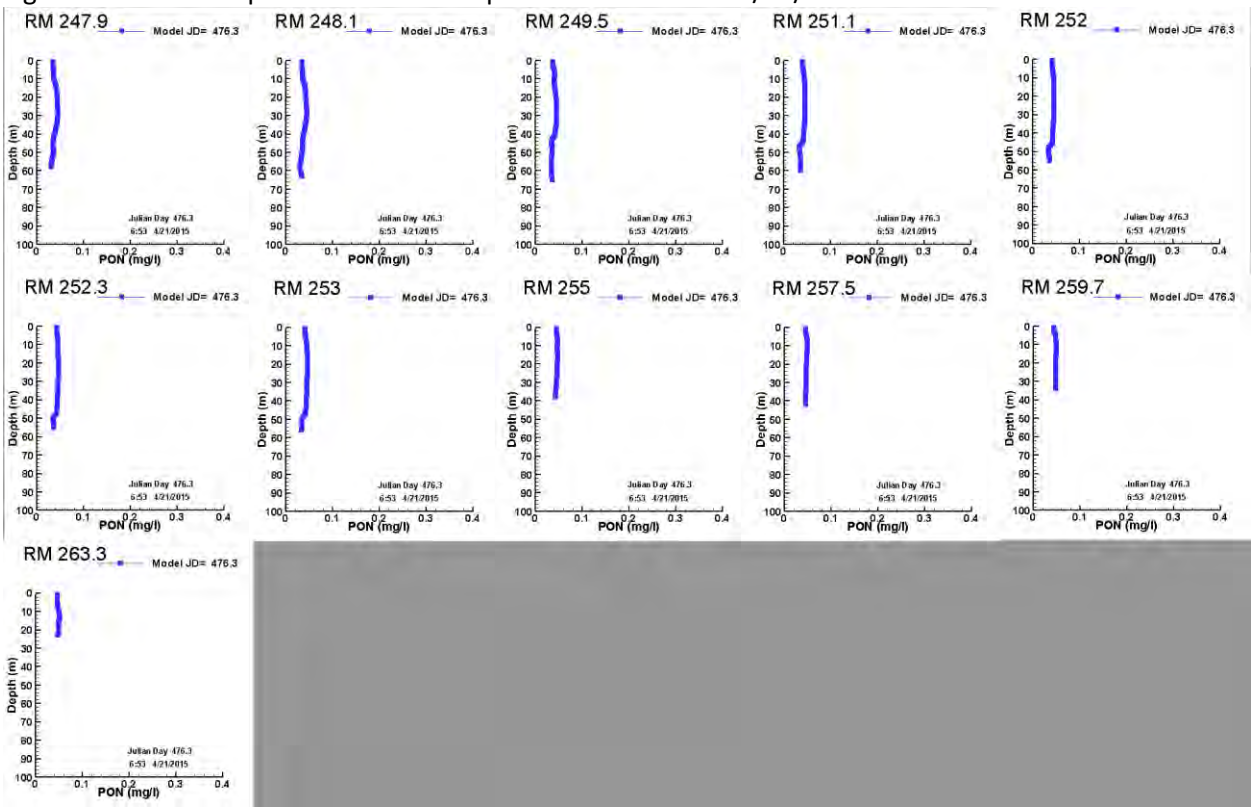


Figure 412. Vertical profiles of PON compared with data for 4/21/2015.

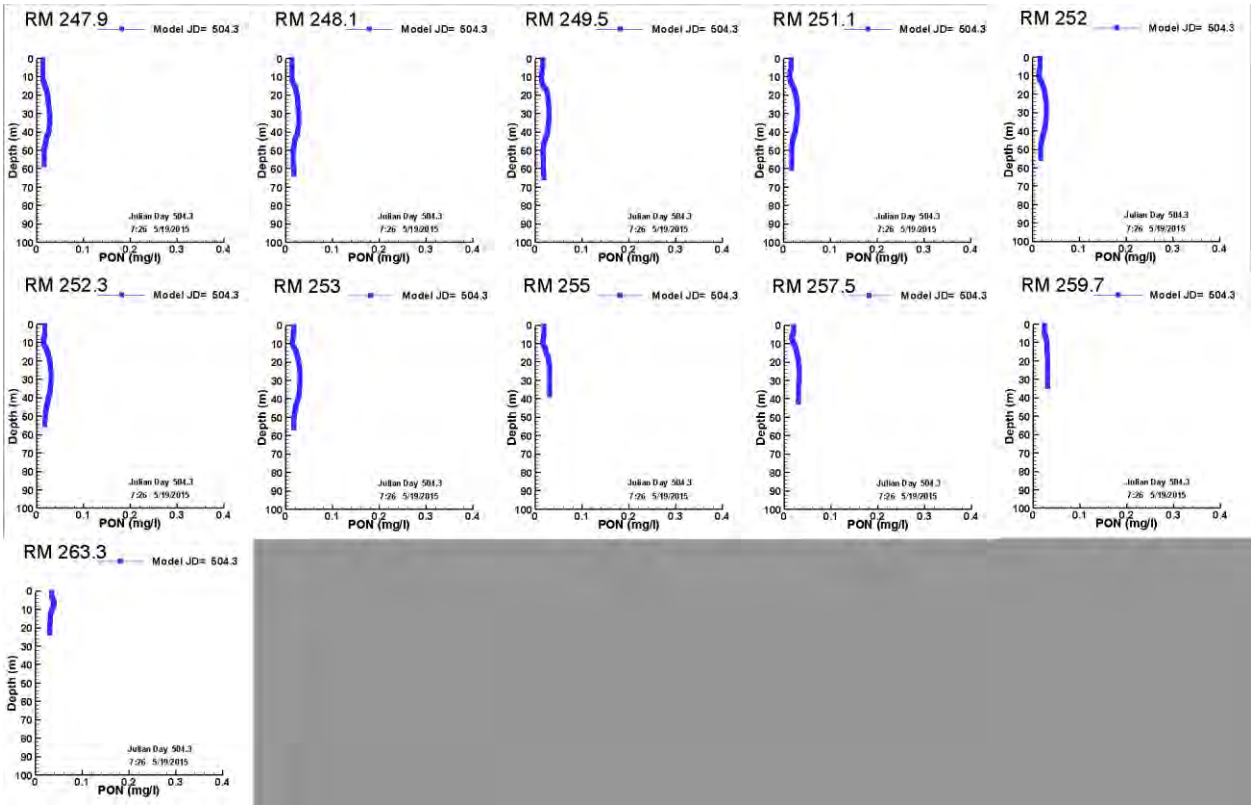


Figure 413. Vertical profiles of PON compared with data for 5/19/2015.

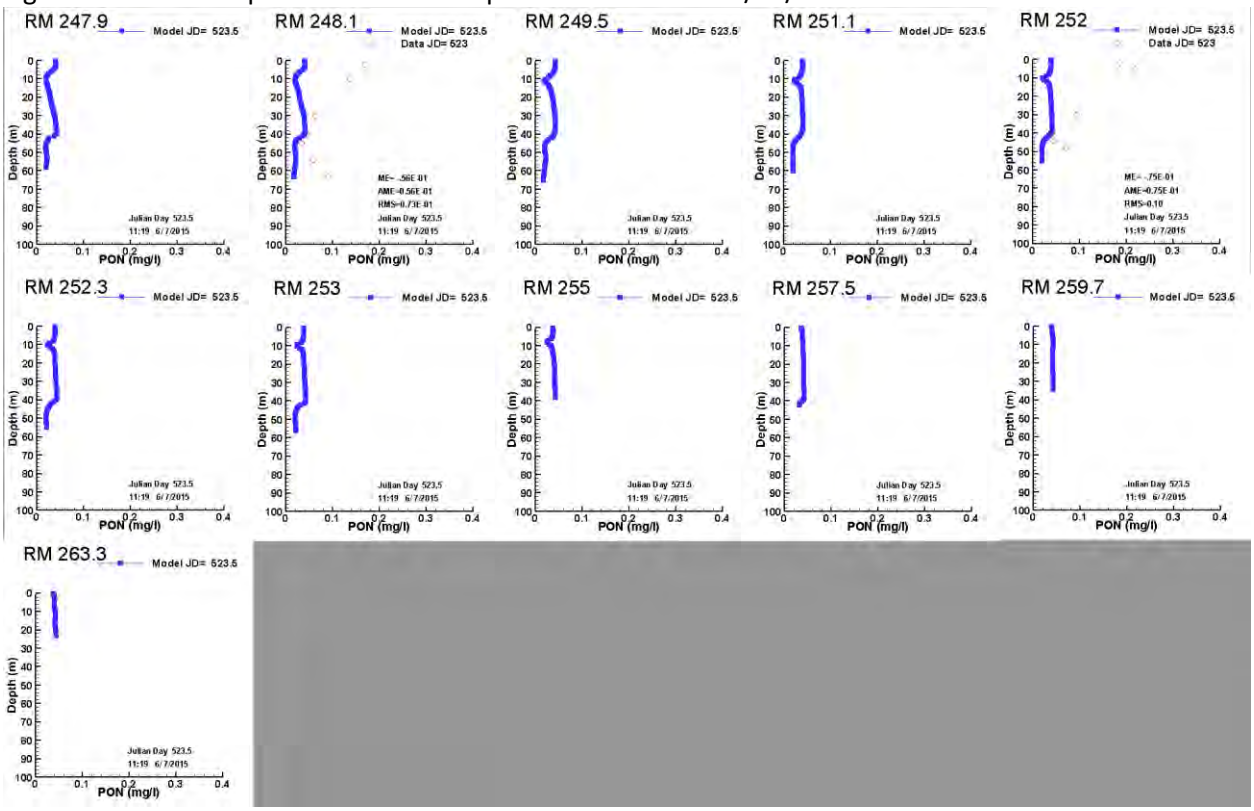


Figure 414. Vertical profiles of PON compared with data for 6/ 7/2015.

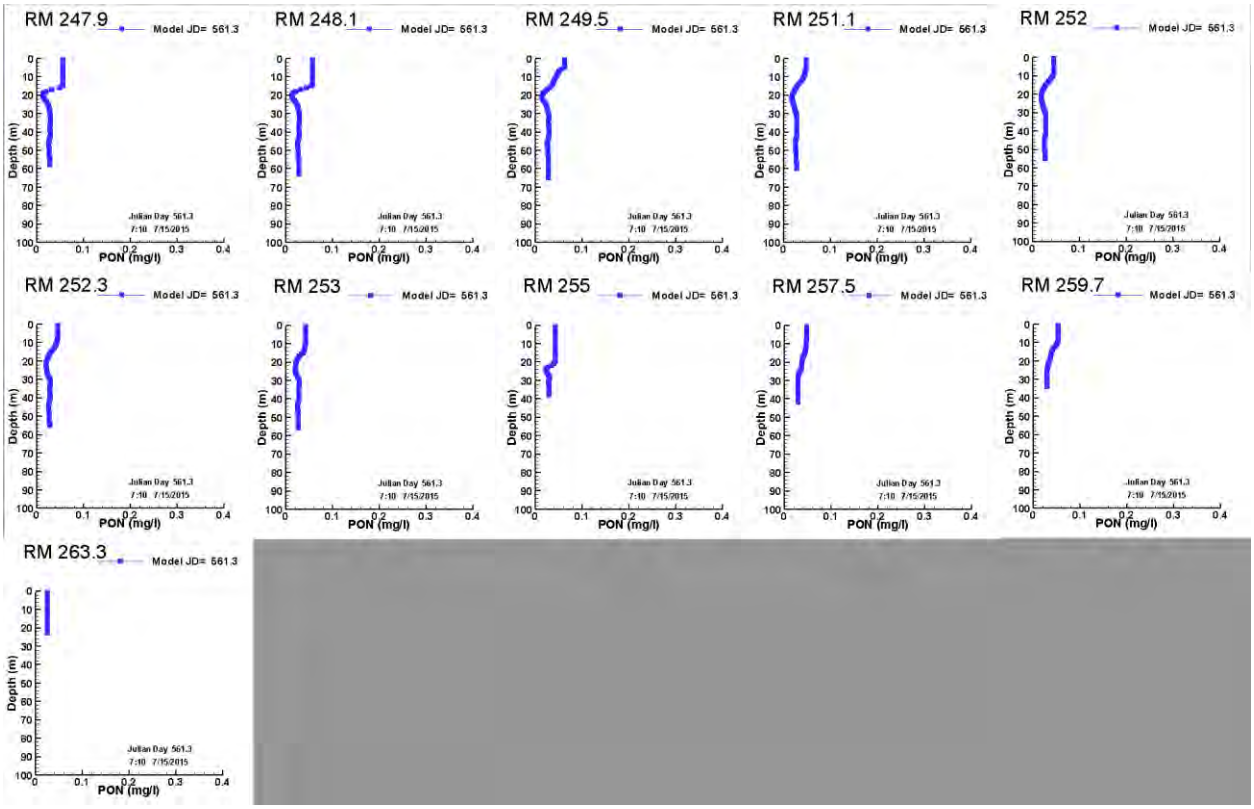


Figure 415. Vertical profiles of PON compared with data for 7/15/2015.

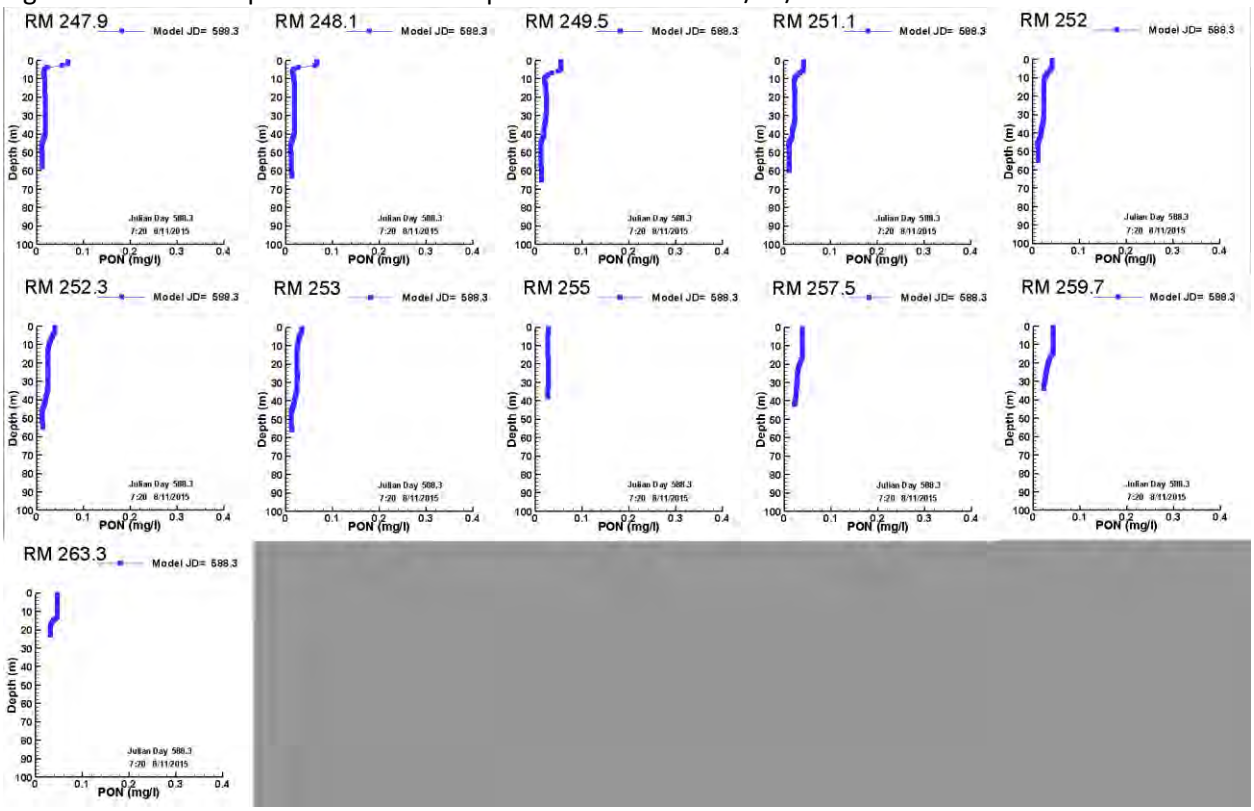


Figure 416. Vertical profiles of PON compared with data for 8/11/2015.

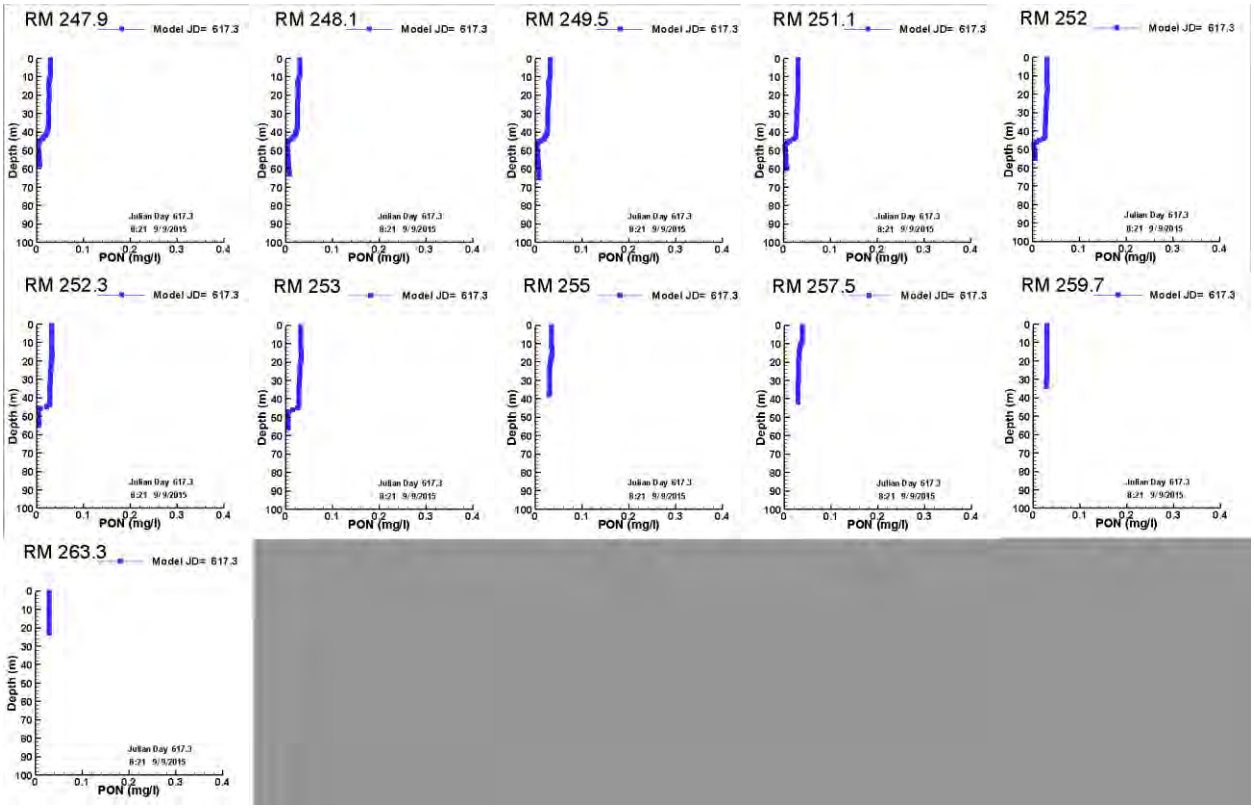


Figure 417. Vertical profiles of PON compared with data for 9/ 9/2015.

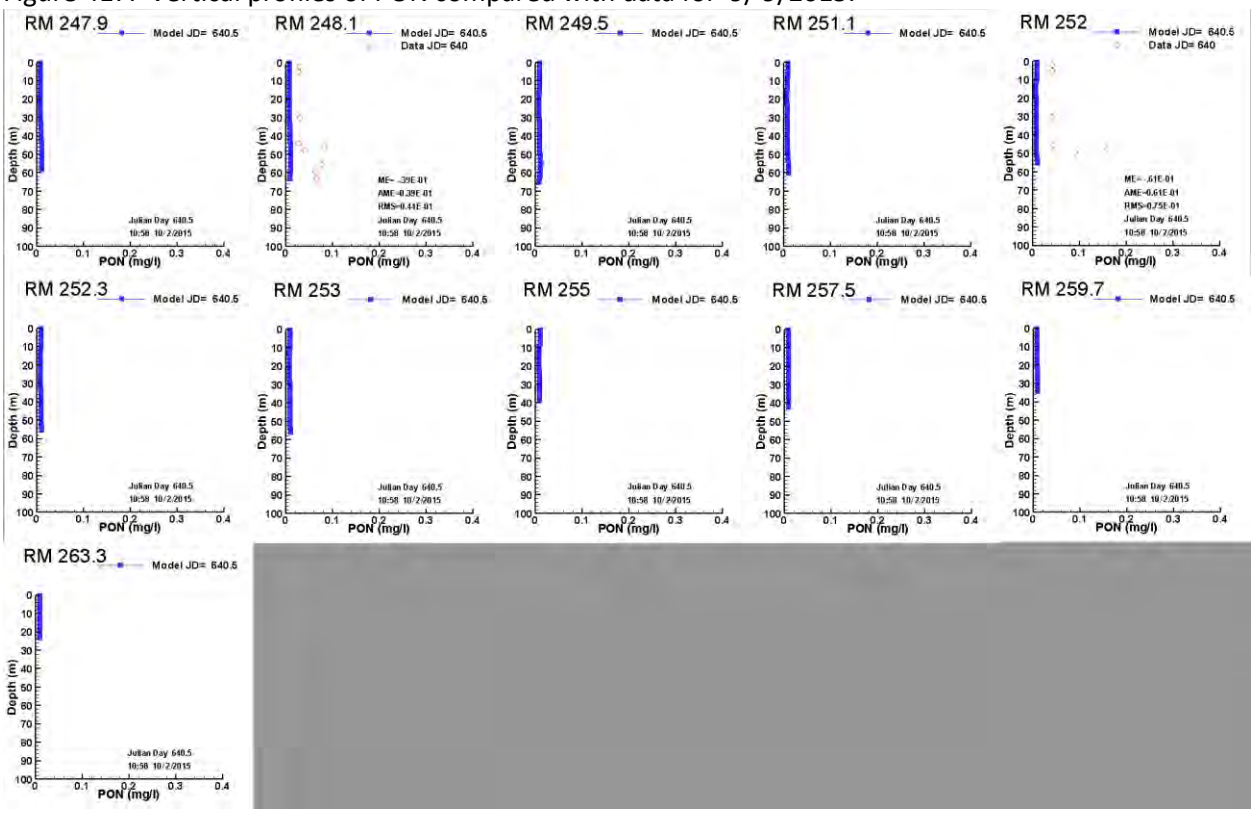


Figure 418. Vertical profiles of PON compared with data for 10/ 2/2015.

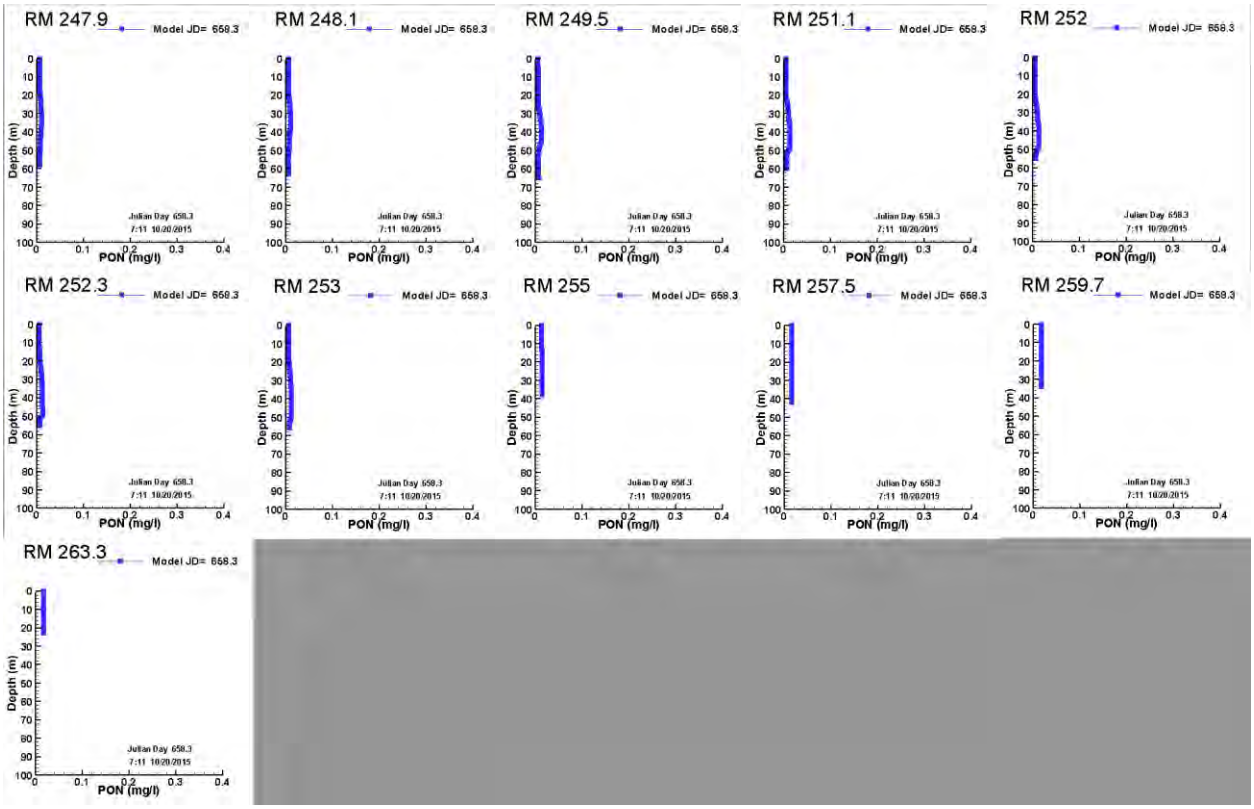


Figure 419. Vertical profiles of PON compared with data for 10/20/2015.

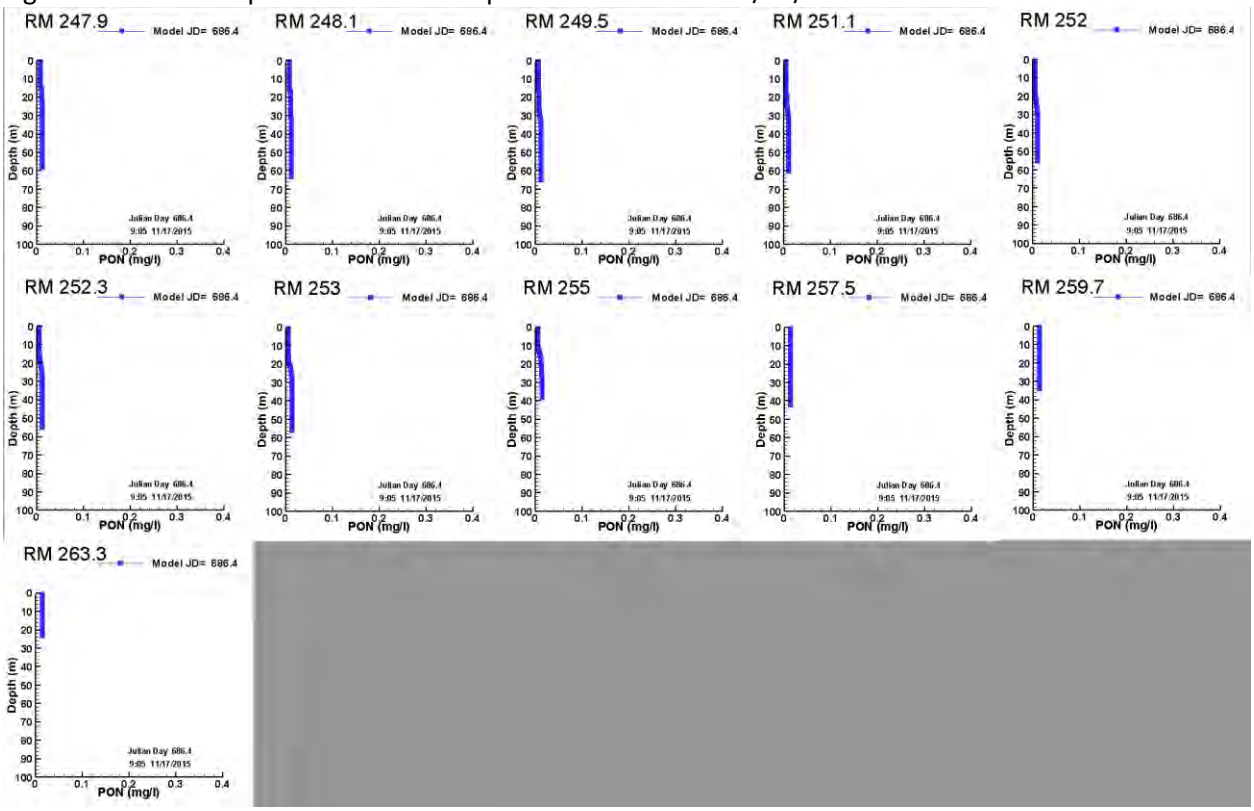


Figure 420. Vertical profiles of PON compared with data for 11/17/2015.

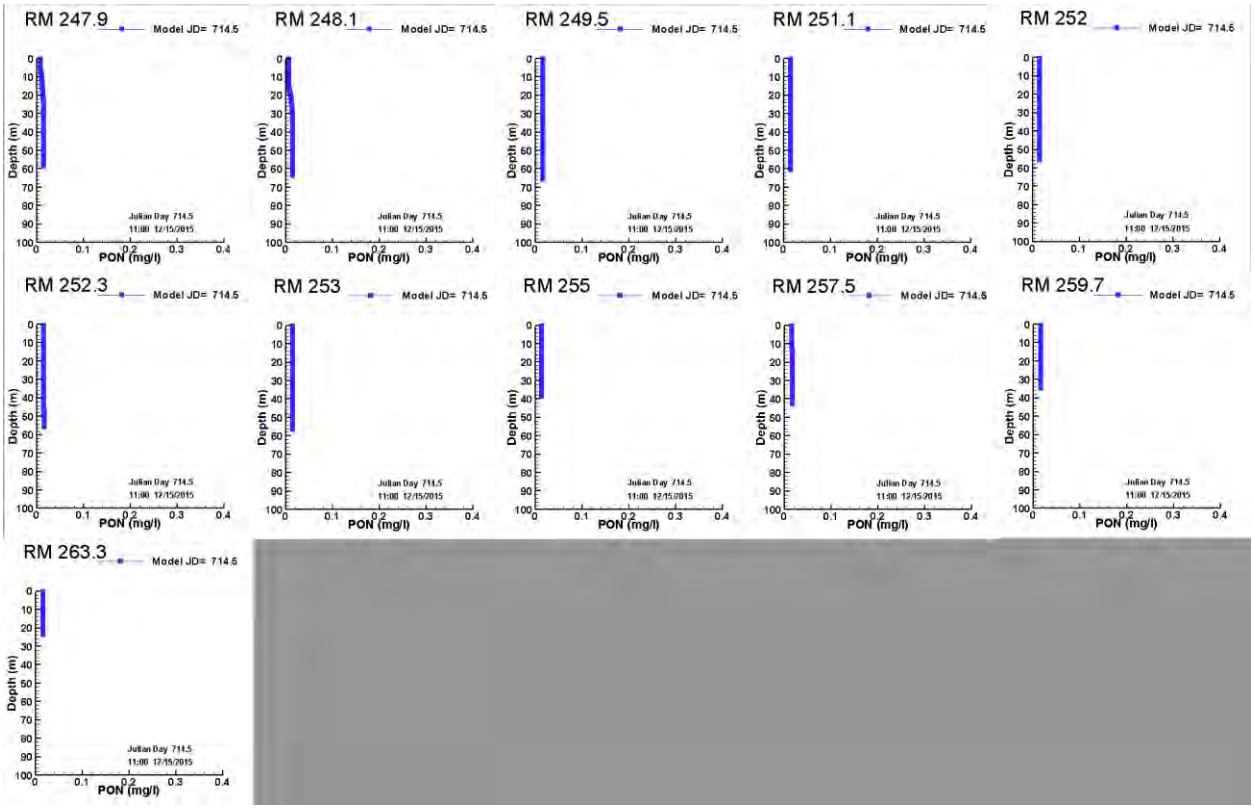


Figure 421. Vertical profiles of PON compared with data for 12/15/2015.

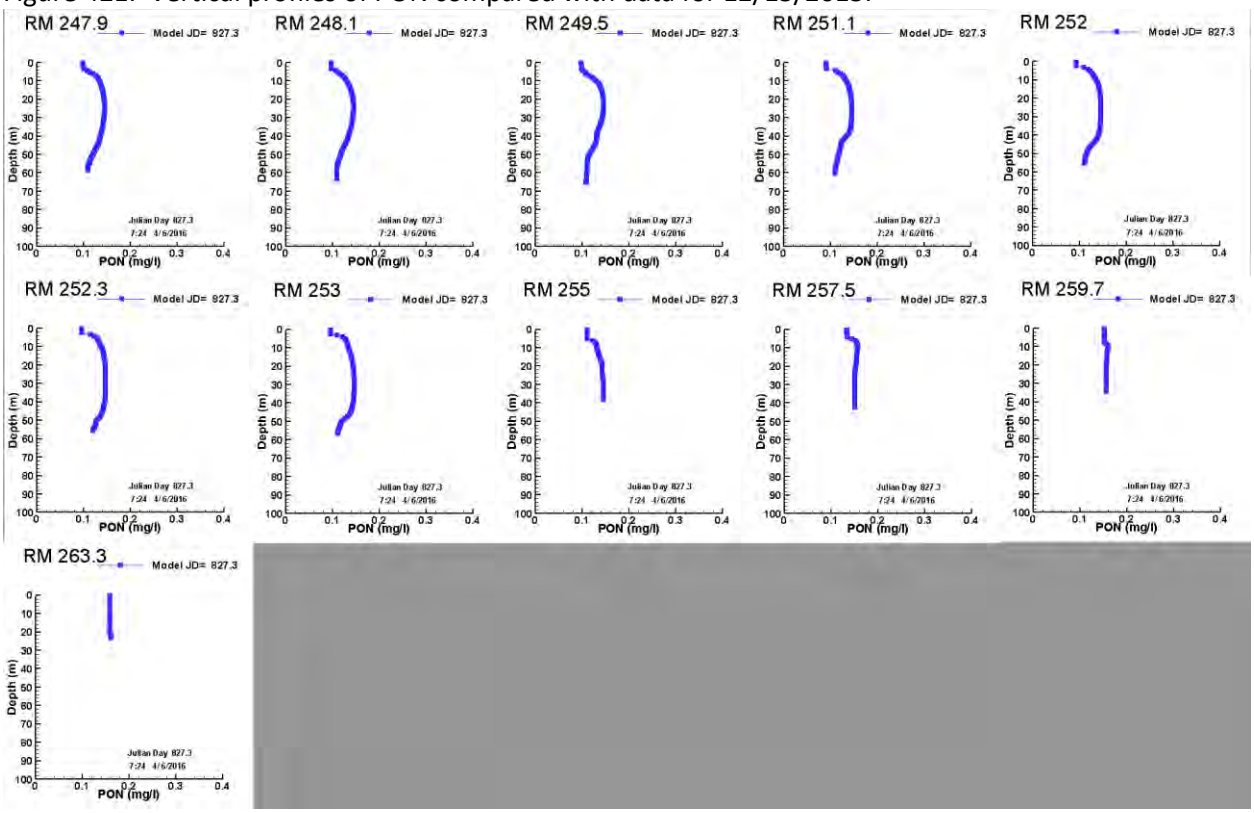


Figure 422. Vertical profiles of PON compared with data for 4/ 6/2016.

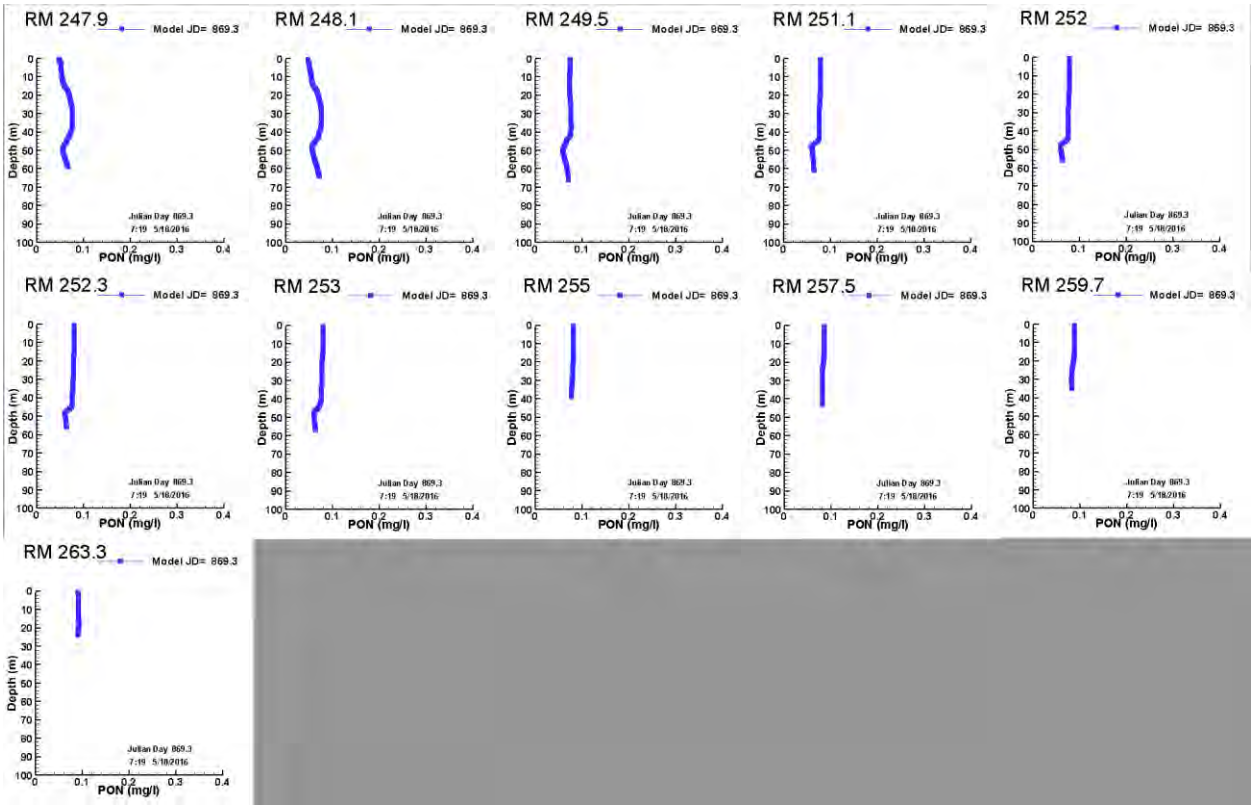


Figure 423. Vertical profiles of PON compared with data for 5/18/2016.

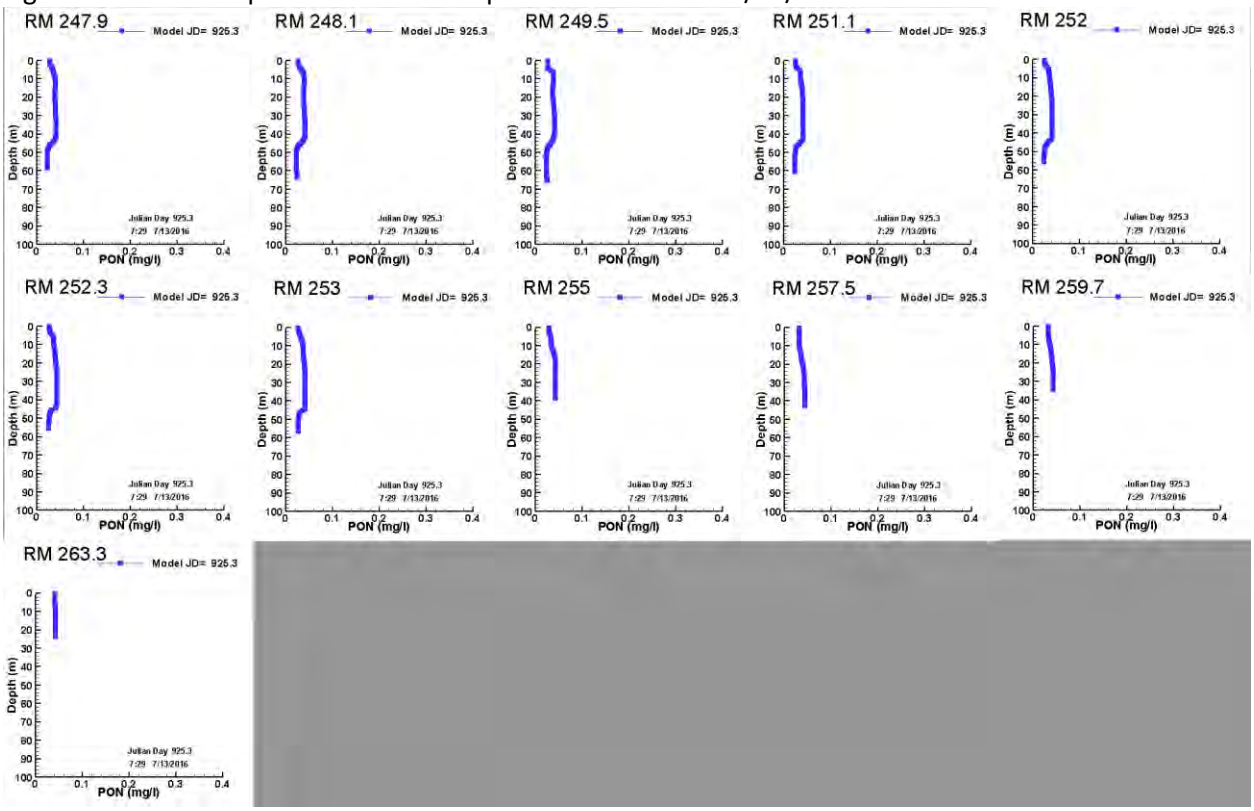


Figure 424. Vertical profiles of PON compared with data for 7/13/2016.

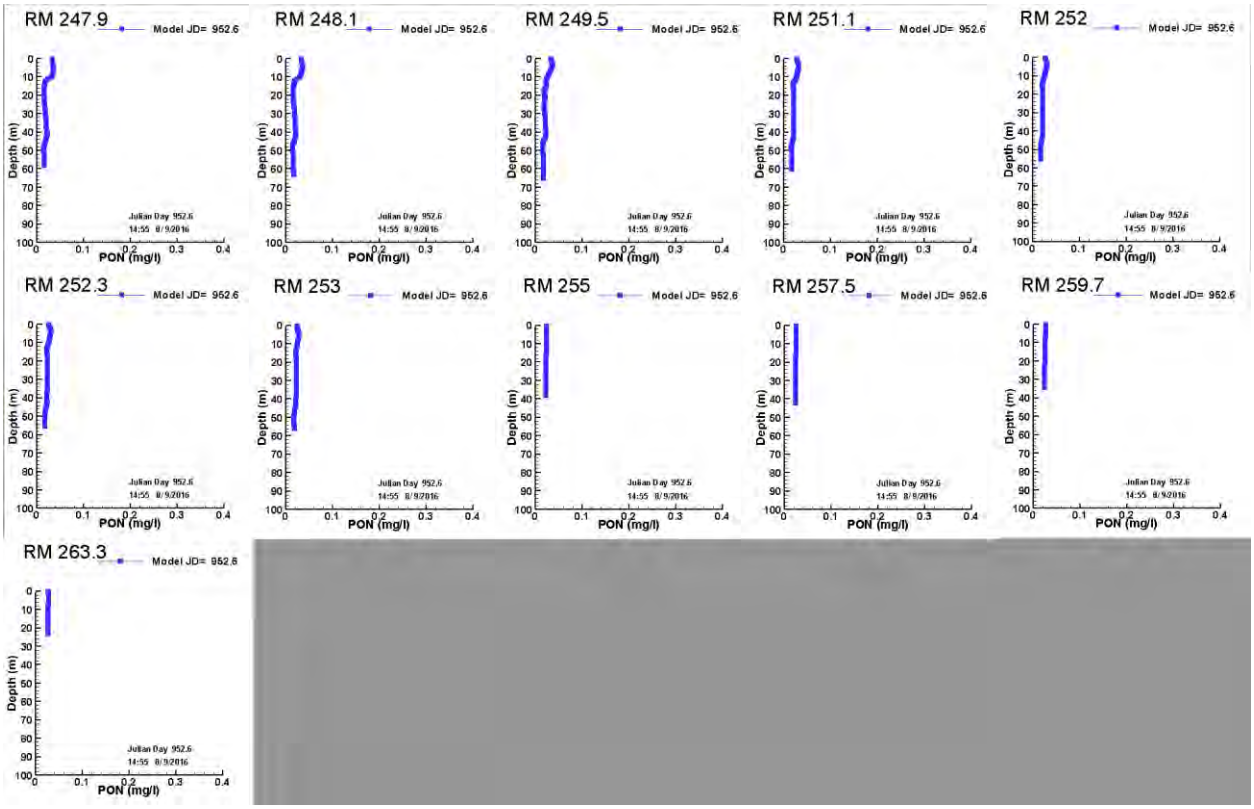


Figure 425. Vertical profiles of PON compared with data for 8/ 9/2016.

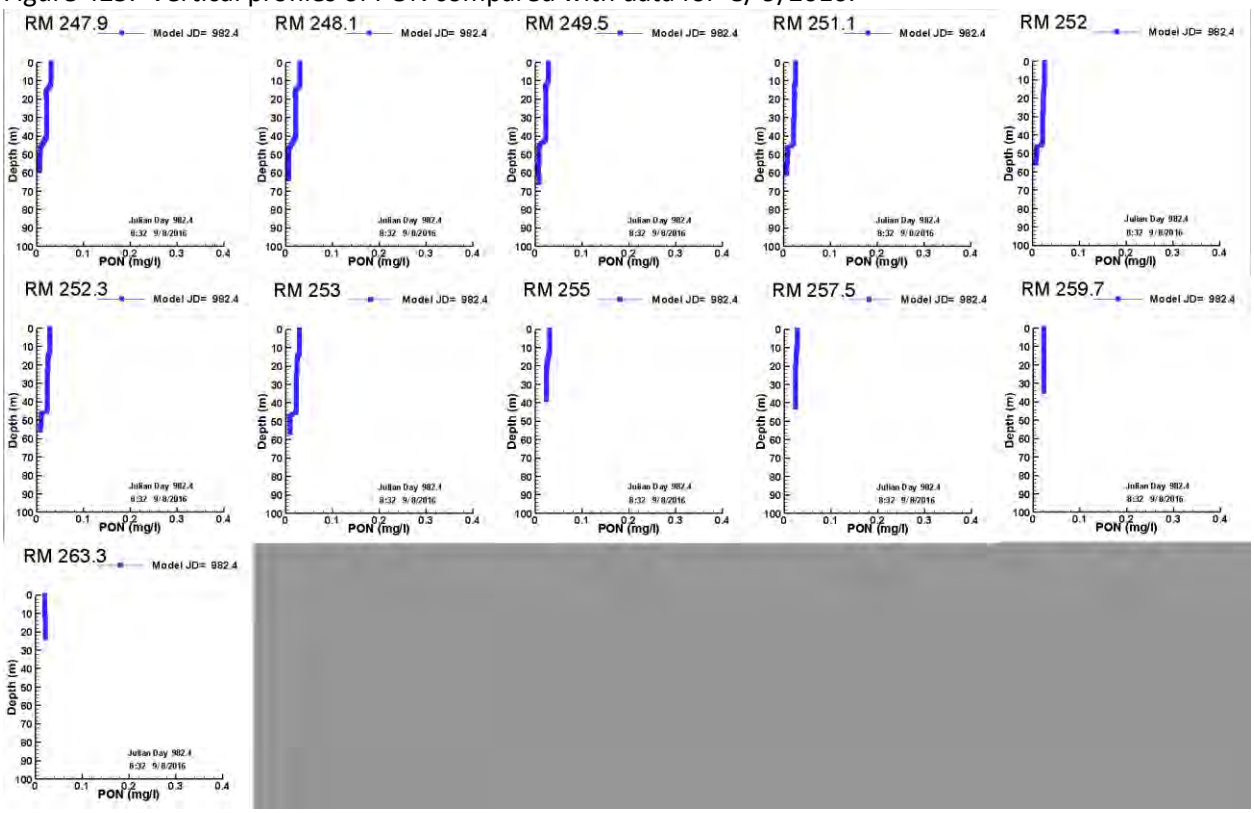


Figure 426. Vertical profiles of PON compared with data for 9/ 8/2016.

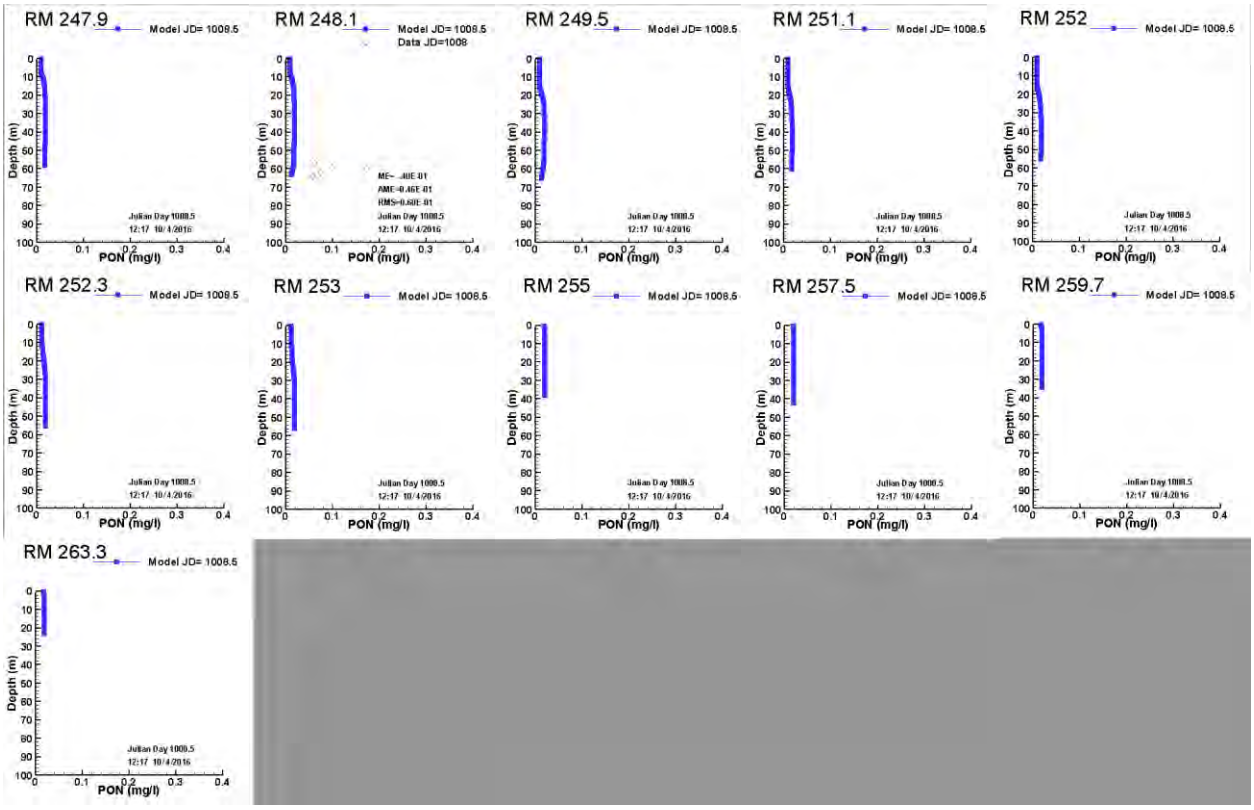


Figure 427. Vertical profiles of PON compared with data for 10/ 4/2016.

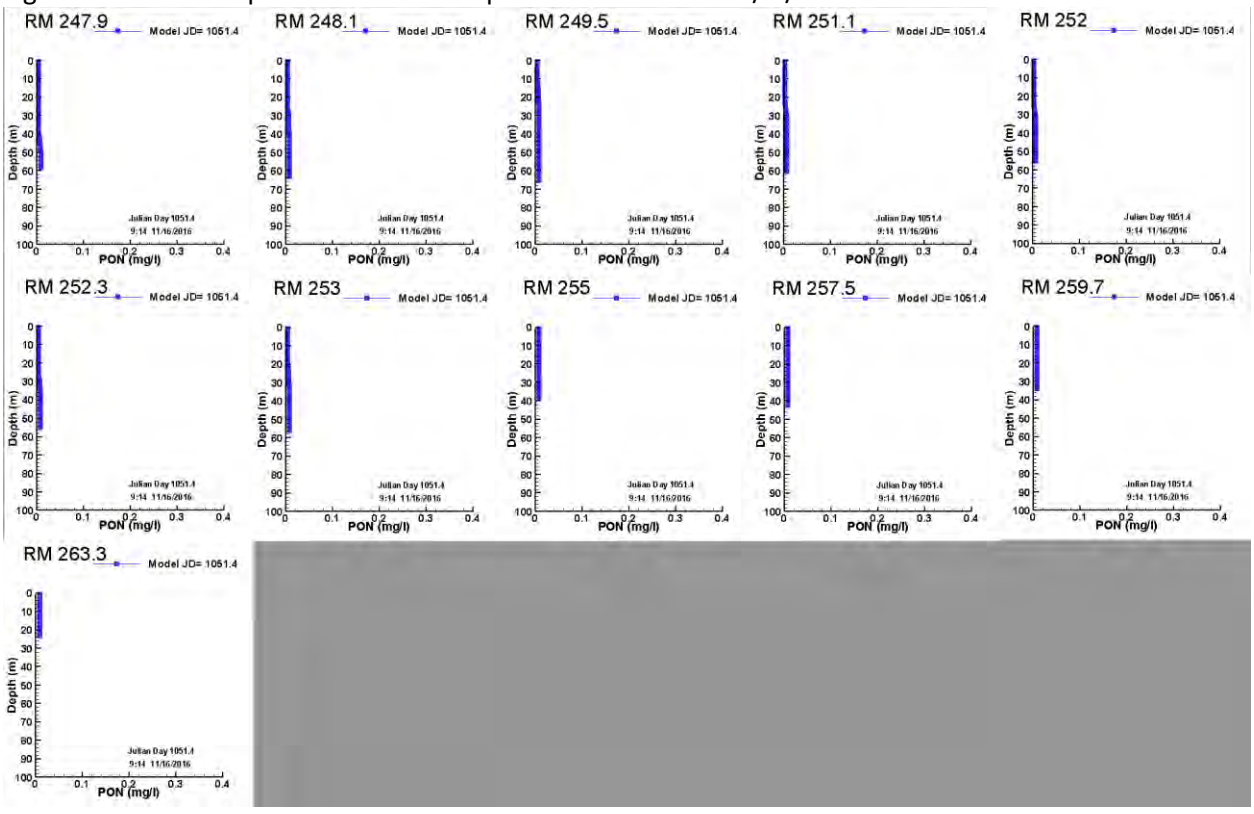


Figure 428. Vertical profiles of PON compared with data for 11/16/2016.

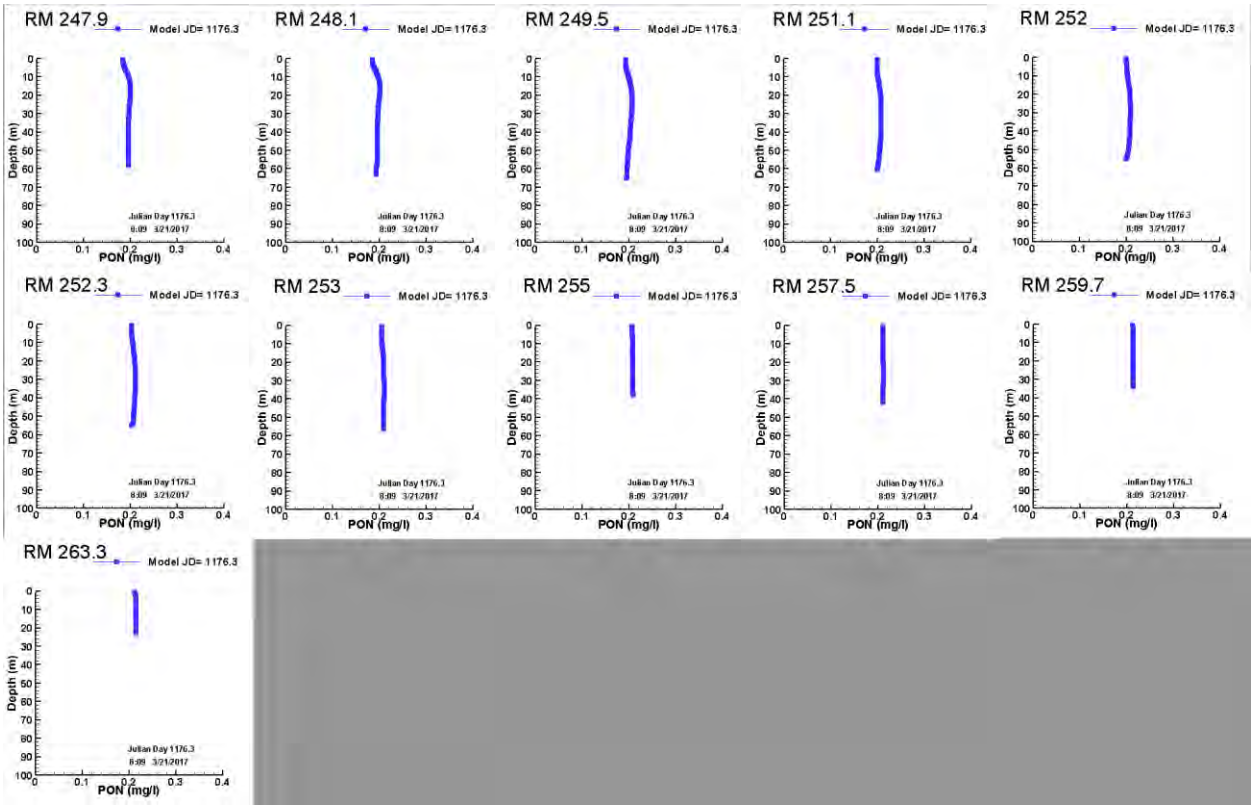


Figure 429. Vertical profiles of PON compared with data for 3/21/2017.

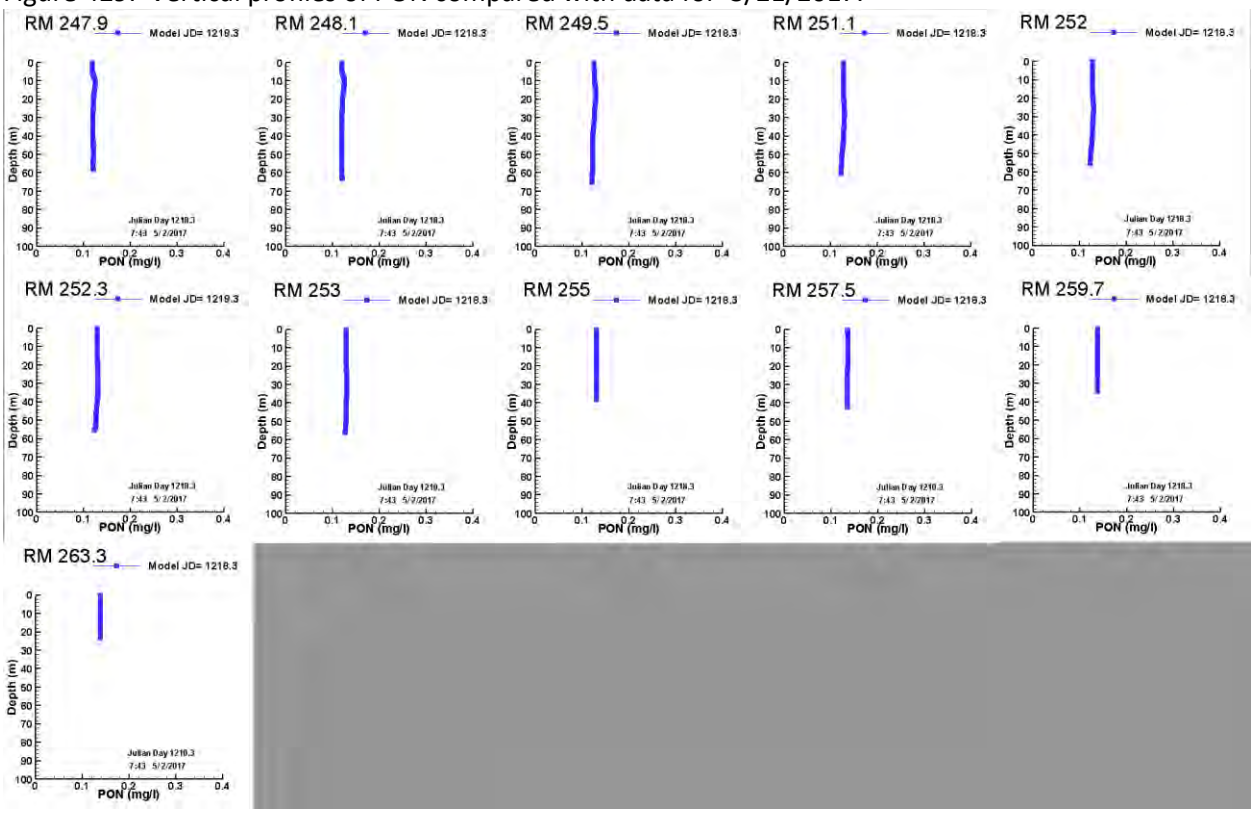


Figure 430. Vertical profiles of PON compared with data for 5/ 2/2017.

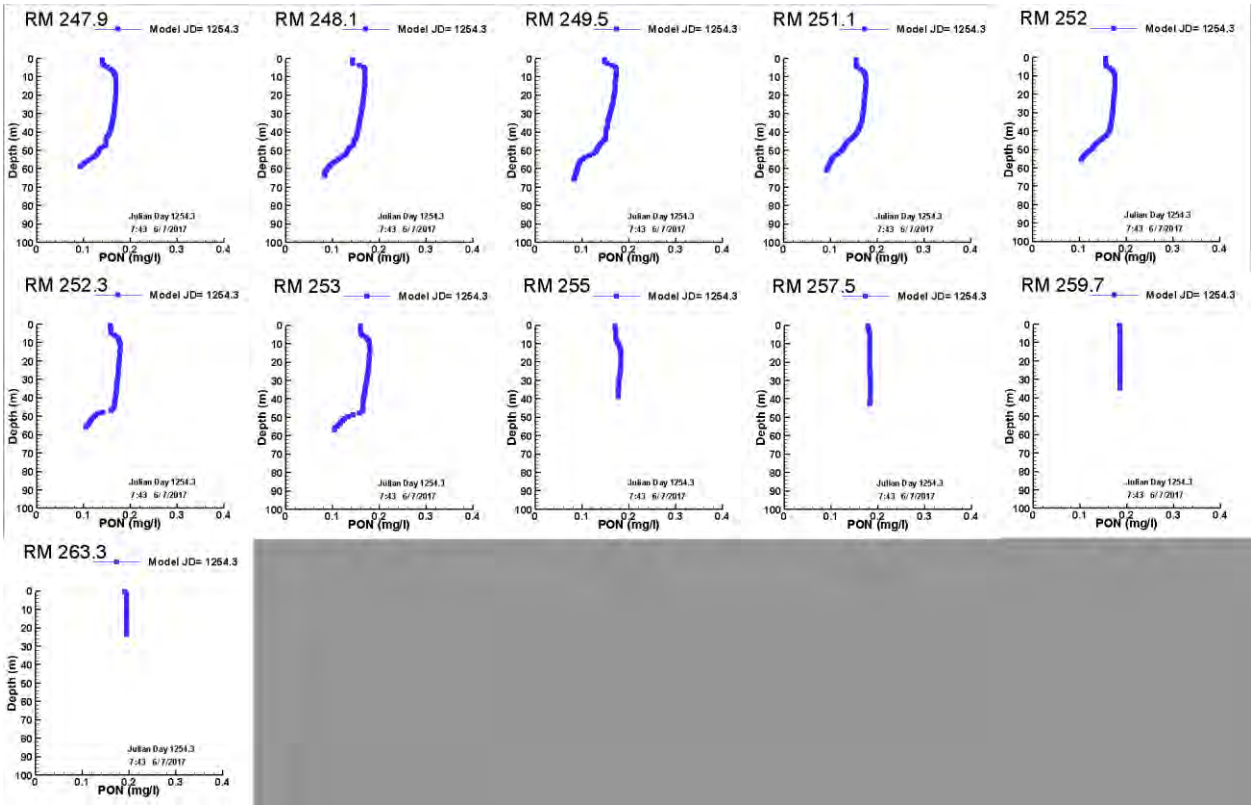


Figure 431. Vertical profiles of PON compared with data for 6/ 7/2017.

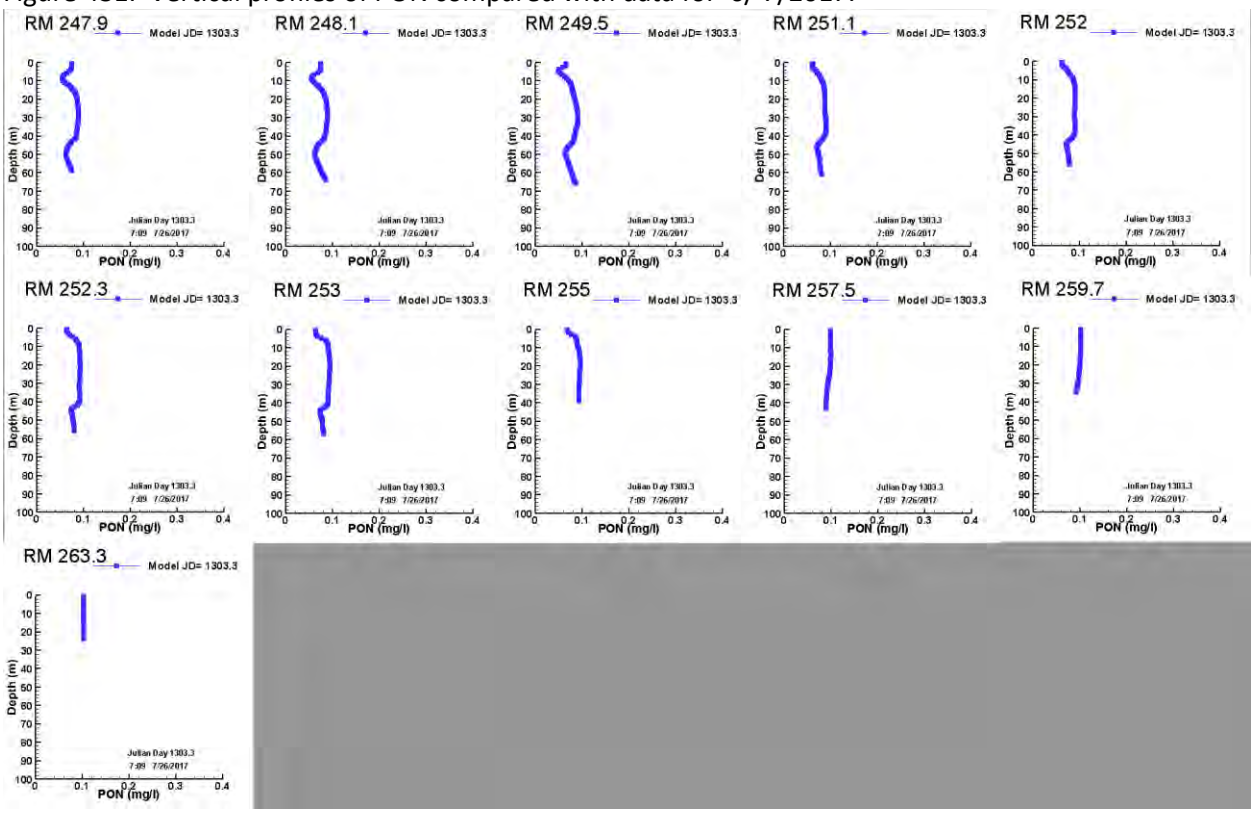


Figure 432. Vertical profiles of PON compared with data for 7/26/2017.

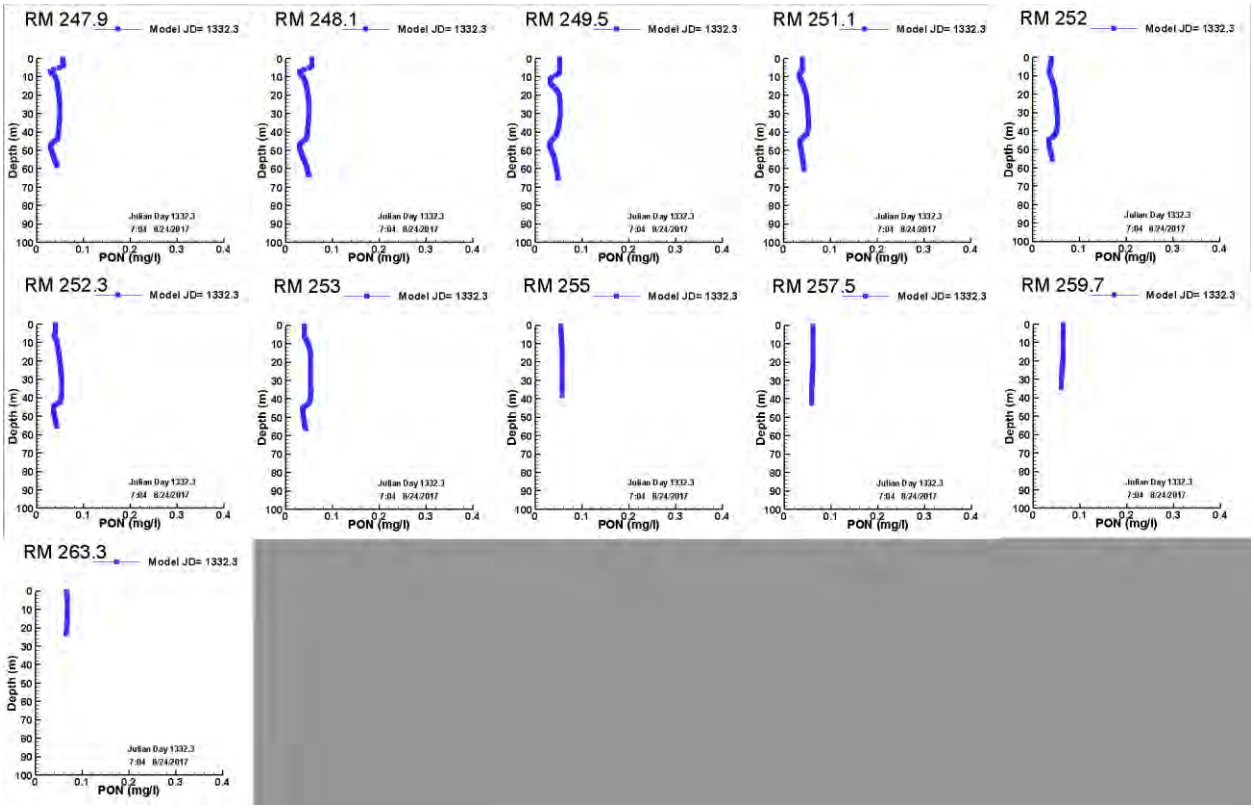


Figure 433. Vertical profiles of PON compared with data for 8/24/2017.

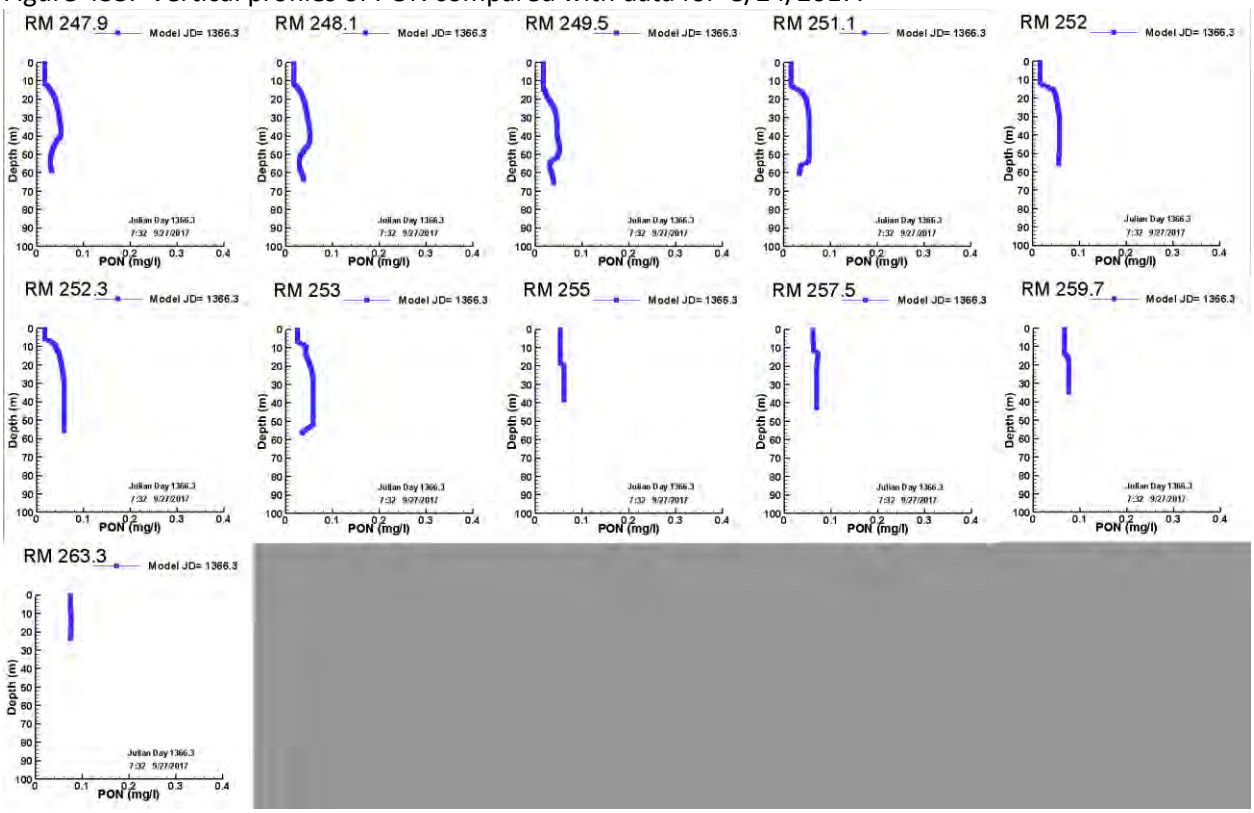


Figure 434. Vertical profiles of PON compared with data for 9/27/2017.

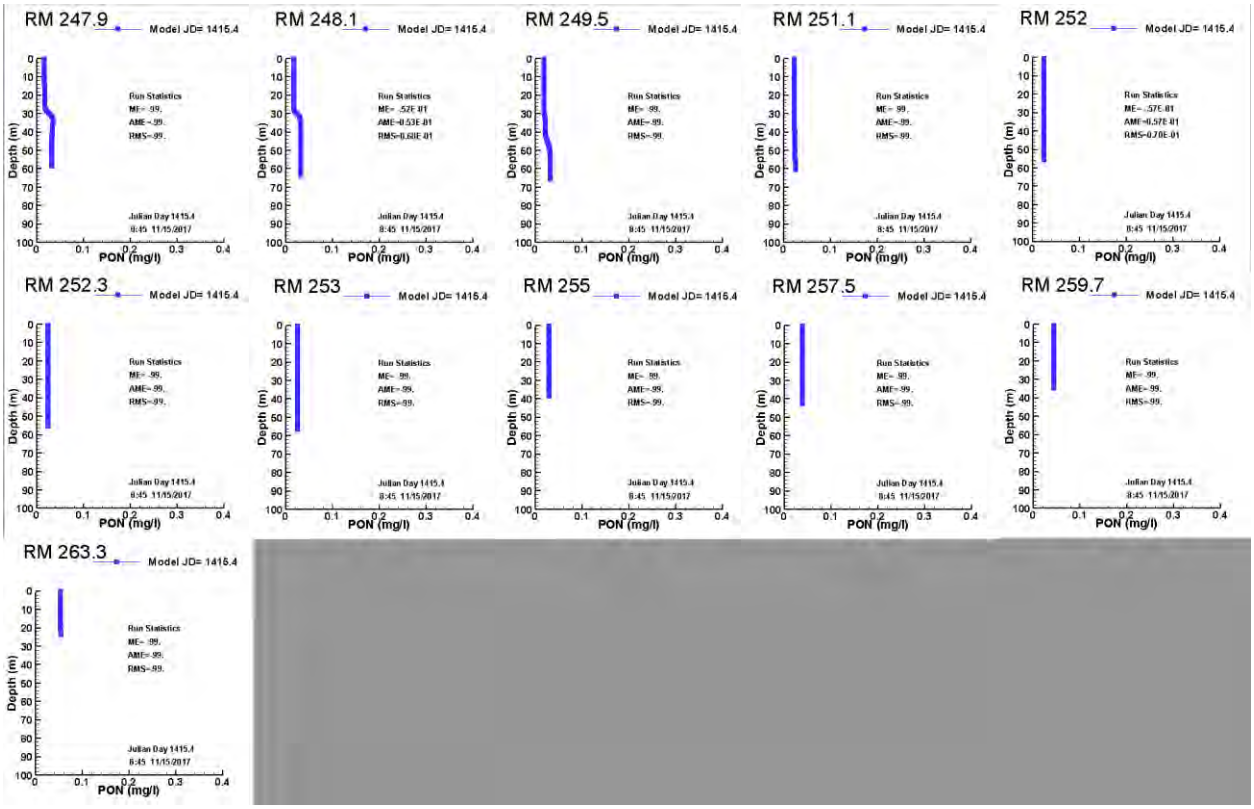


Figure 435. Vertical profiles of PON compared with data for 11/15/2017.

Total Suspended Solids

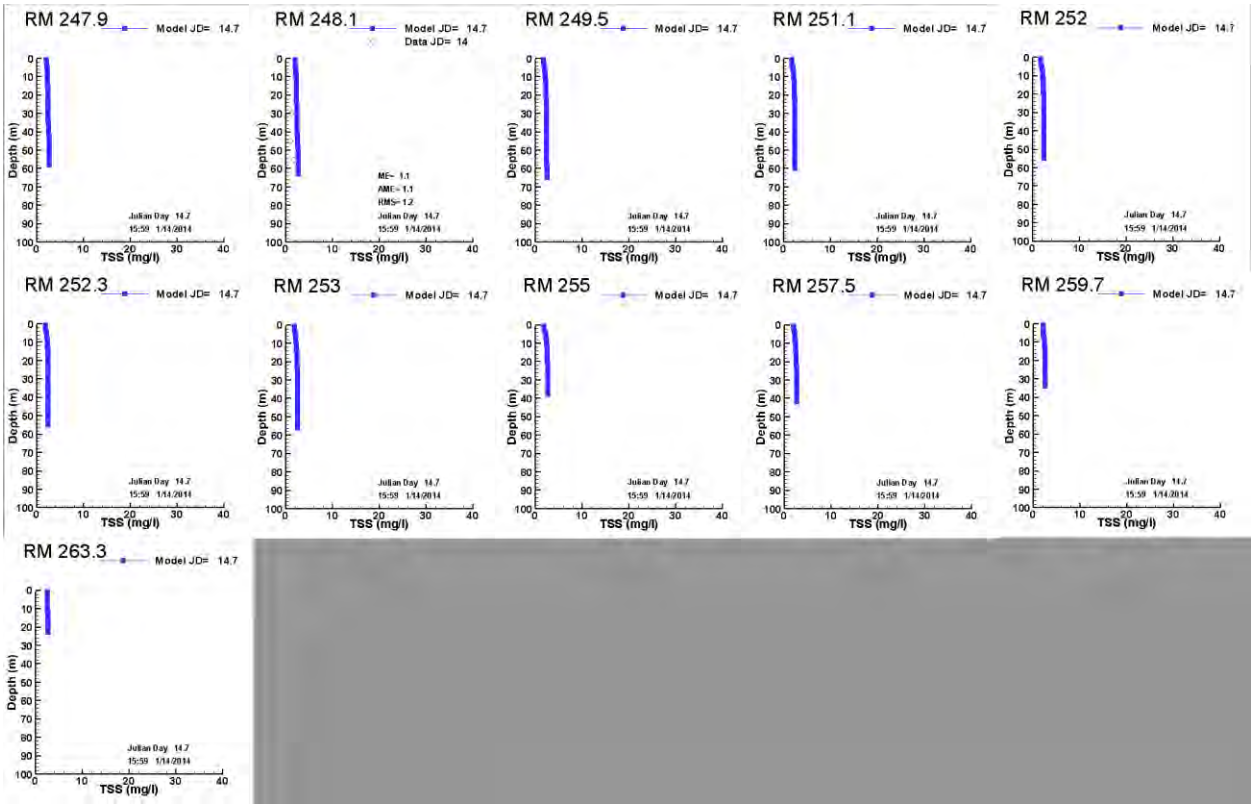


Figure 436. Vertical profiles of TSS compared with data for 1/14/2014.

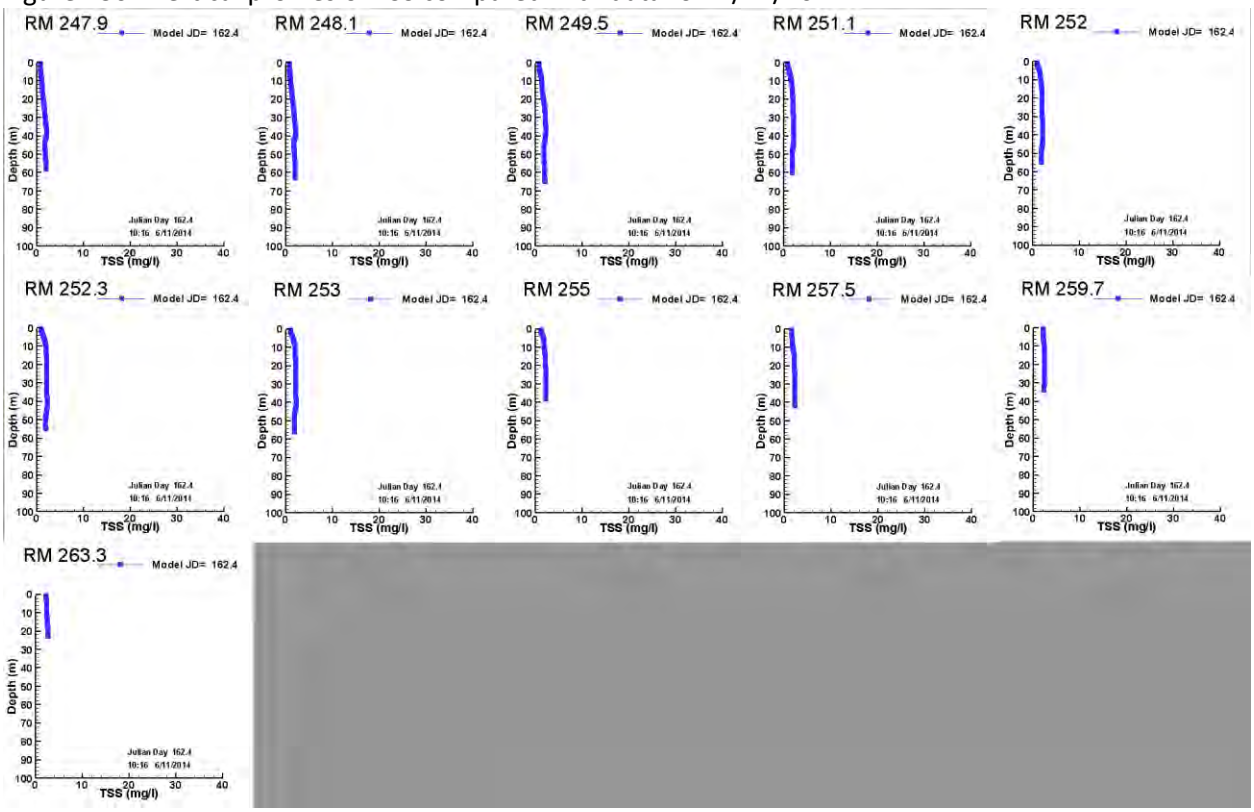


Figure 437. Vertical profiles of TSS compared with data for 6/11/2014.

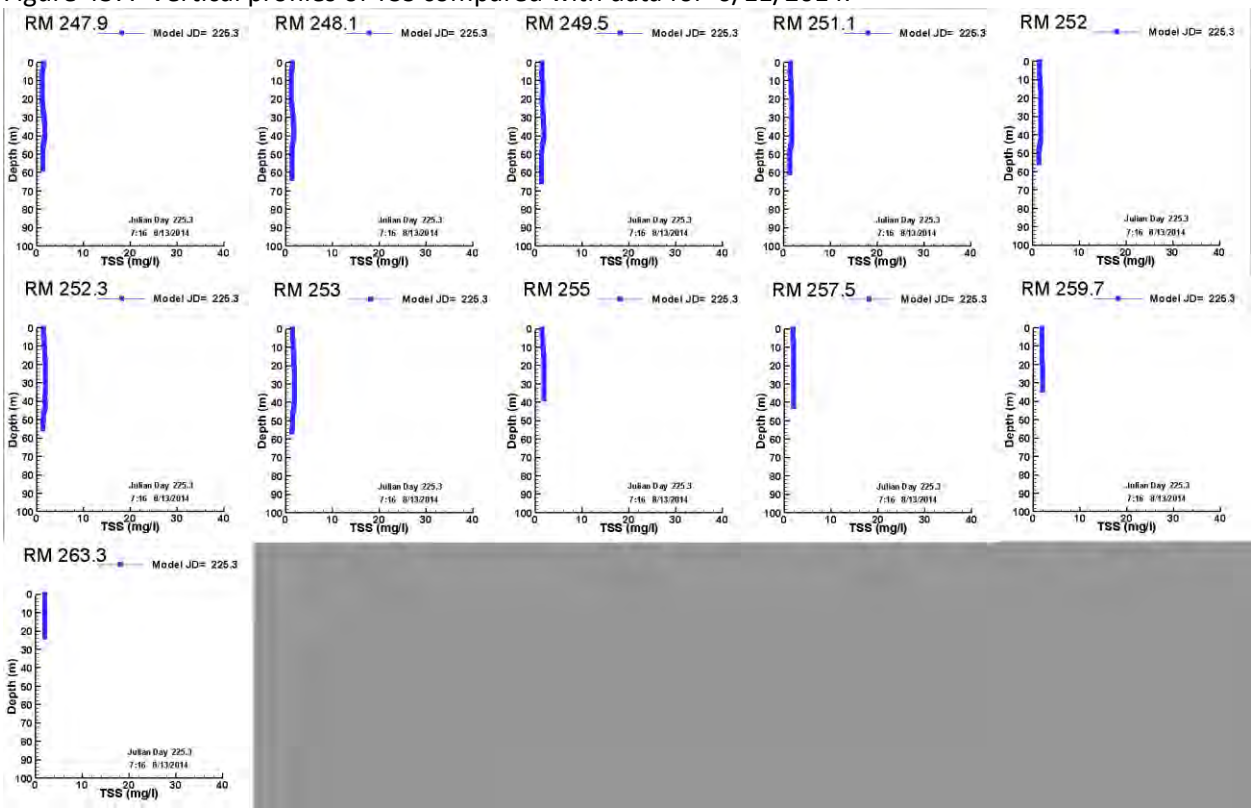


Figure 438. Vertical profiles of TSS compared with data for 8/13/2014.

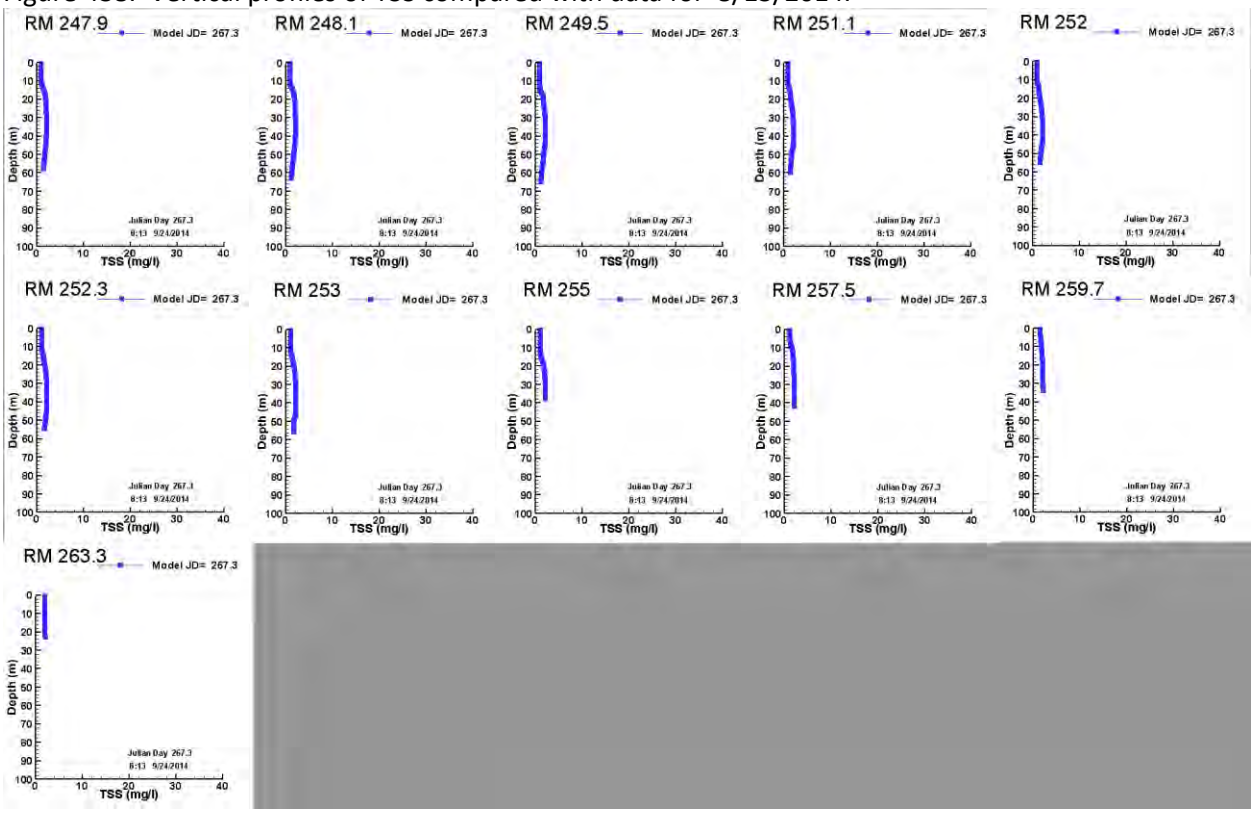


Figure 439. Vertical profiles of TSS compared with data for 9/24/2014.

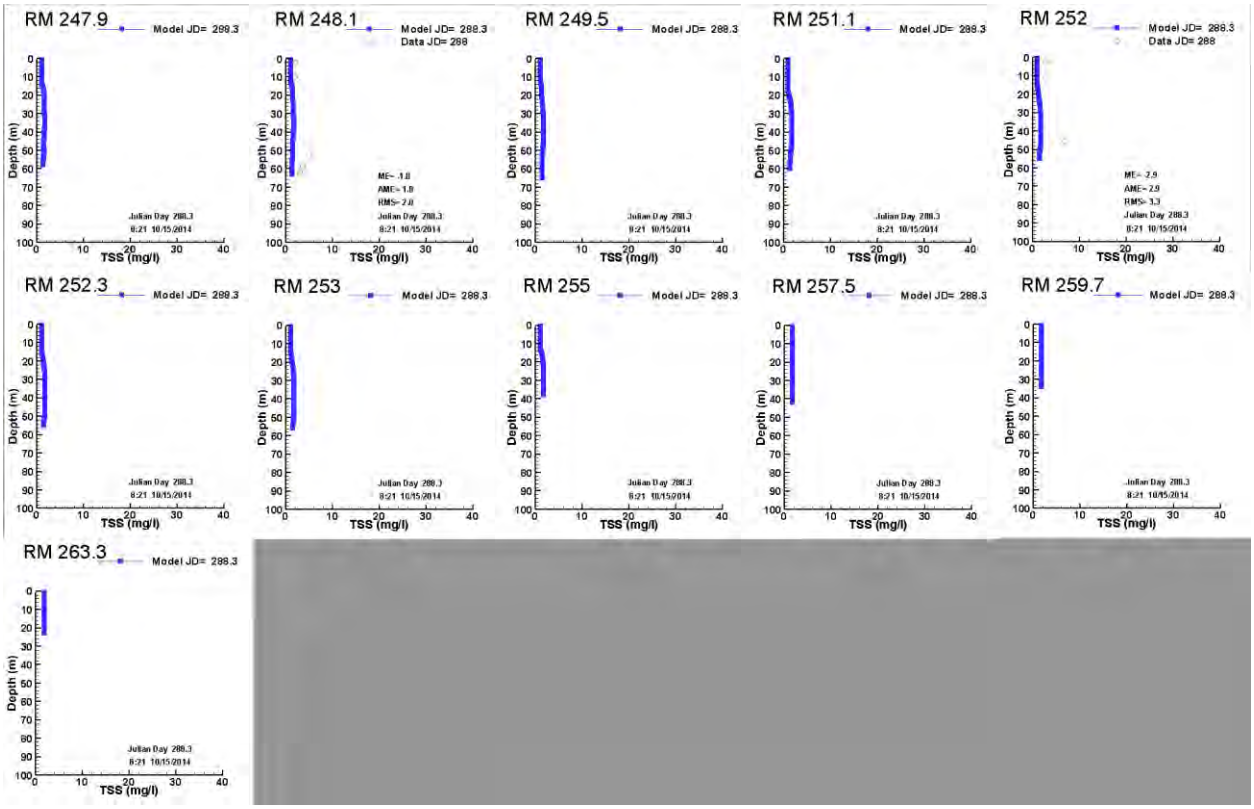


Figure 440. Vertical profiles of TSS compared with data for 10/15/2014.

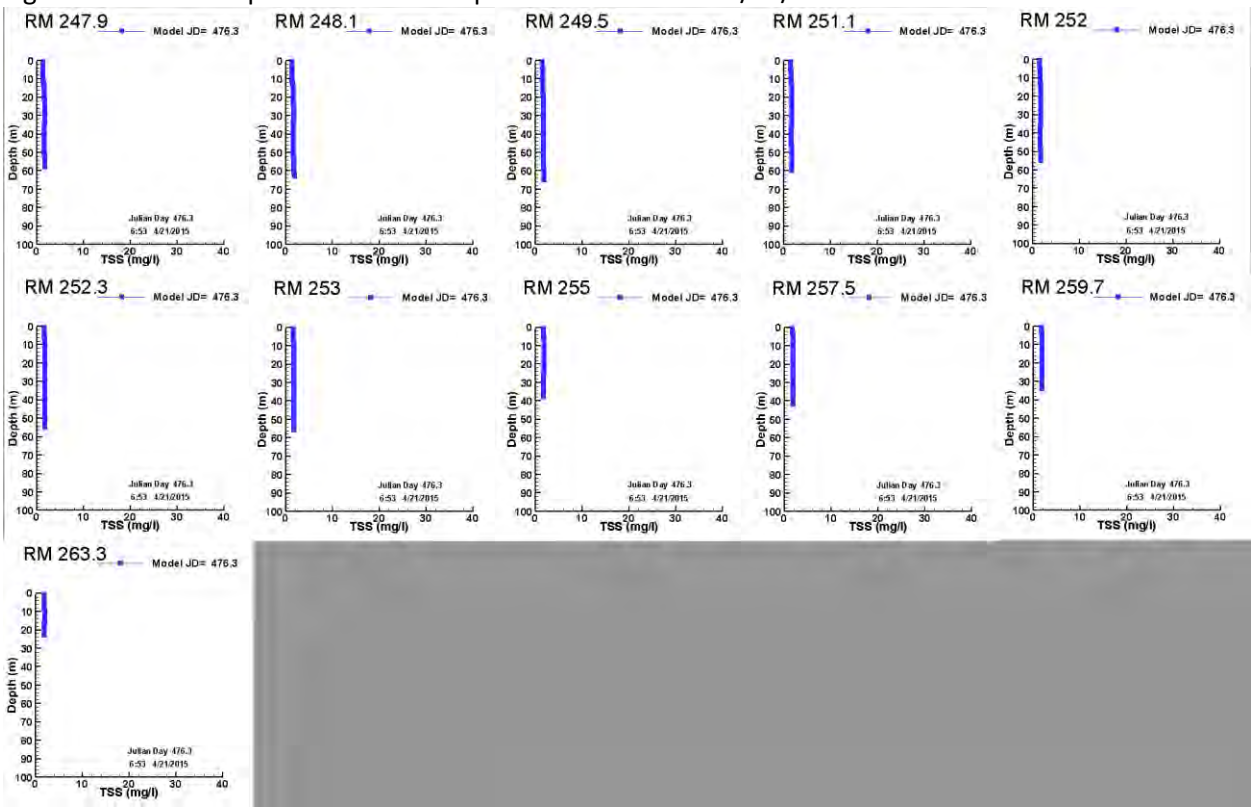


Figure 441. Vertical profiles of TSS compared with data for 4/21/2015.

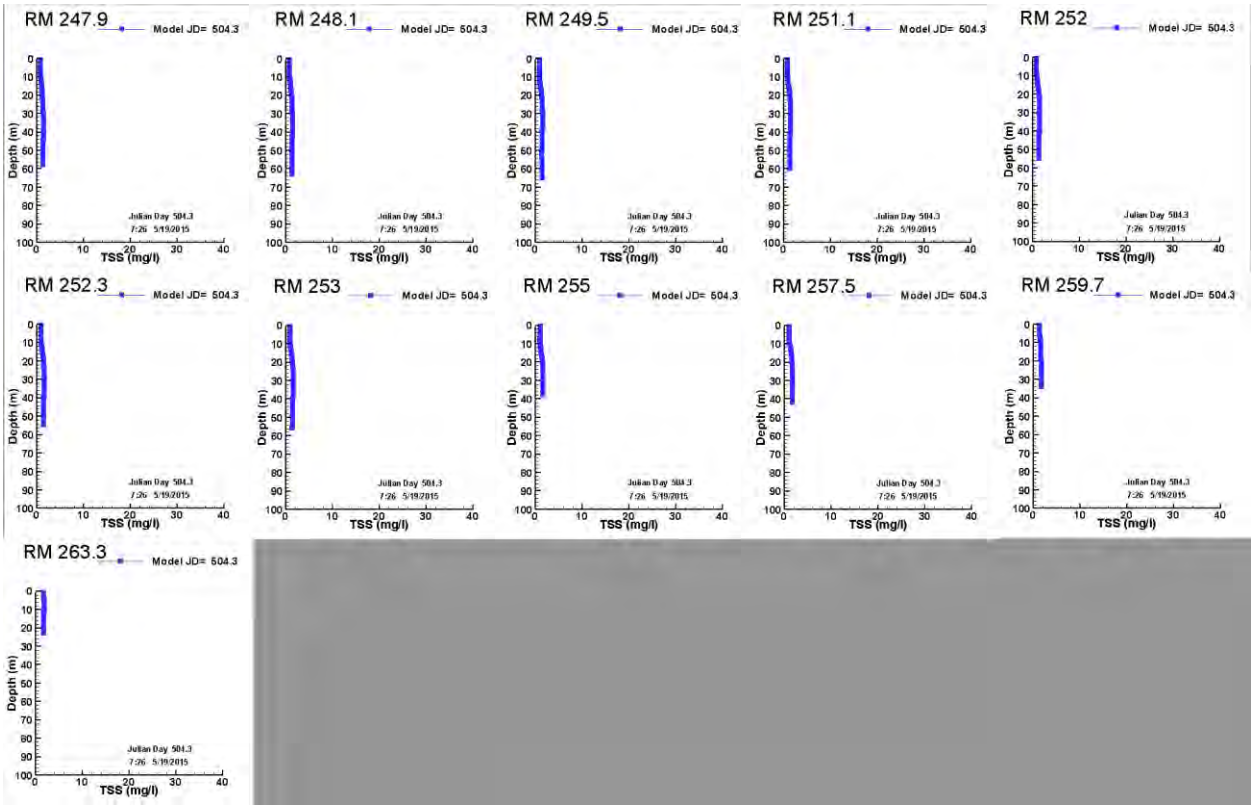


Figure 442. Vertical profiles of TSS compared with data for 5/19/2015.

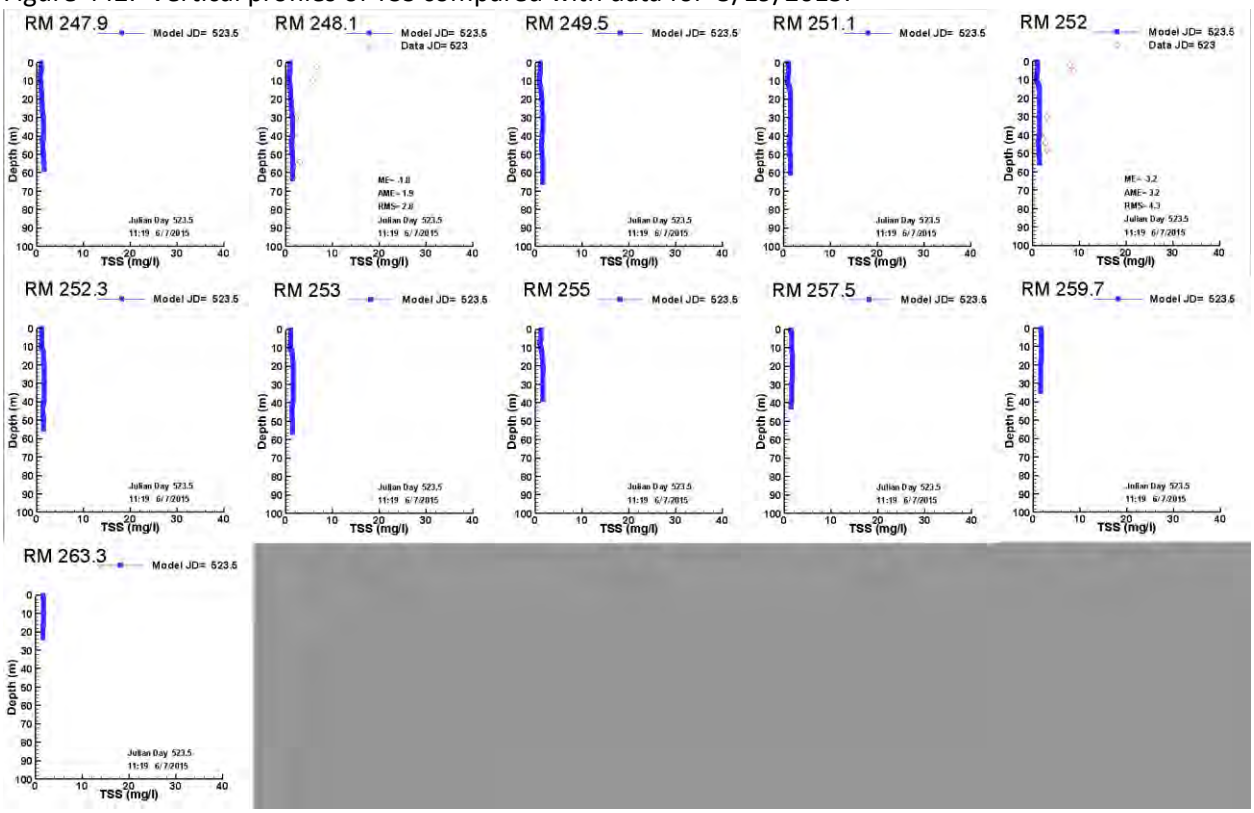


Figure 443. Vertical profiles of TSS compared with data for 6/ 7/2015.

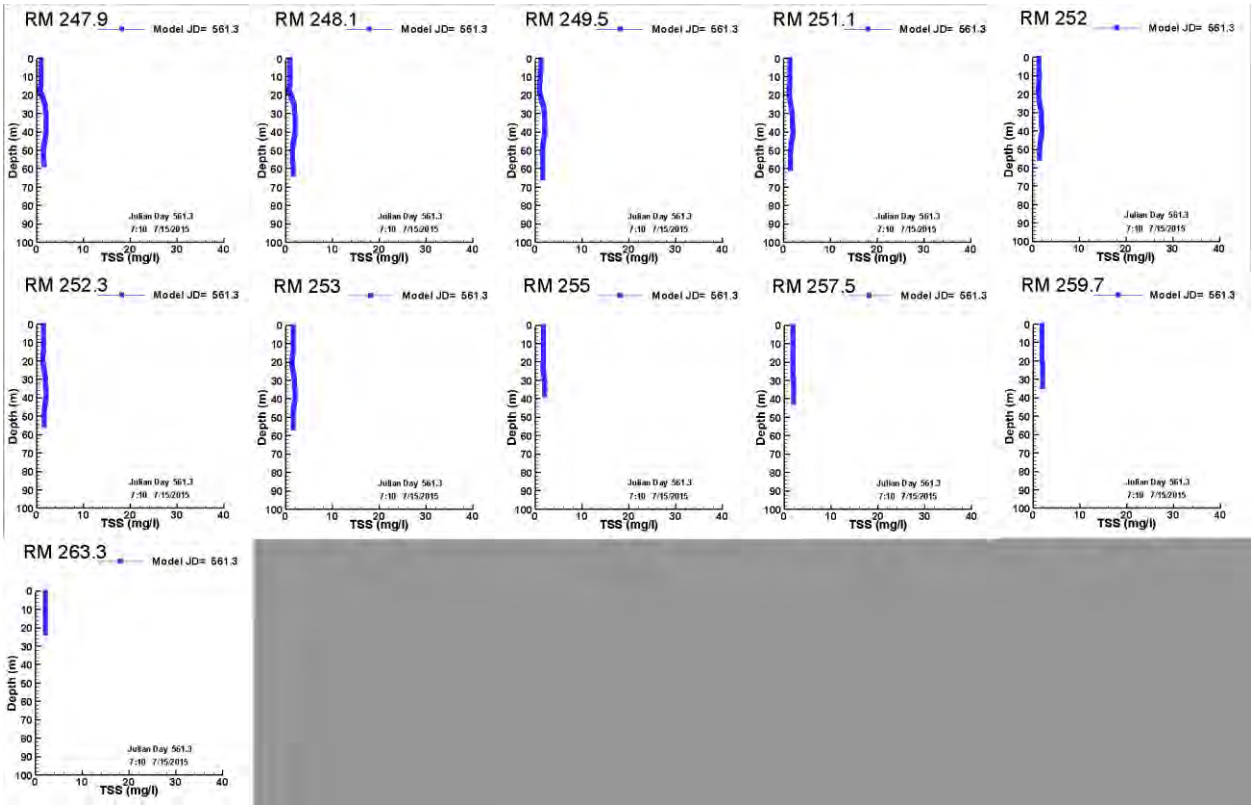


Figure 444. Vertical profiles of TSS compared with data for 7/15/2015.

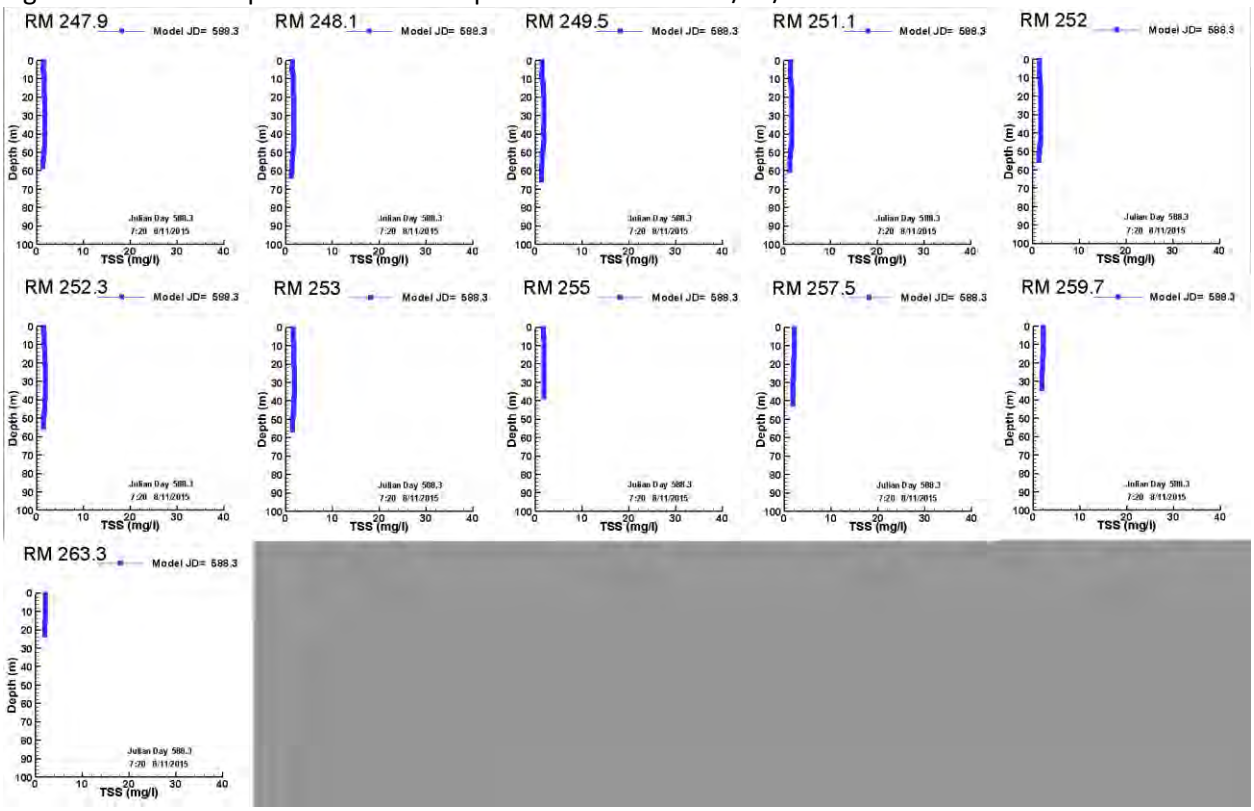


Figure 445. Vertical profiles of TSS compared with data for 8/11/2015.

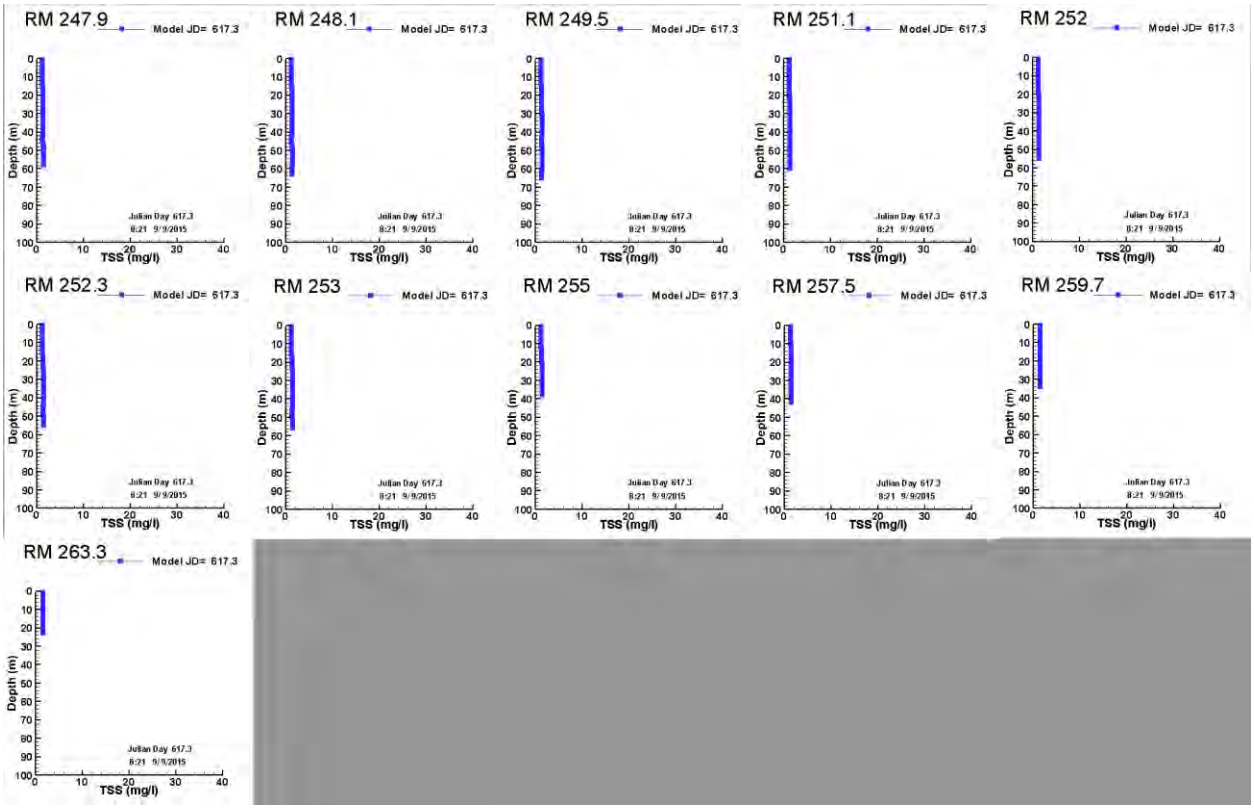


Figure 446. Vertical profiles of TSS compared with data for 9/ 9/2015.

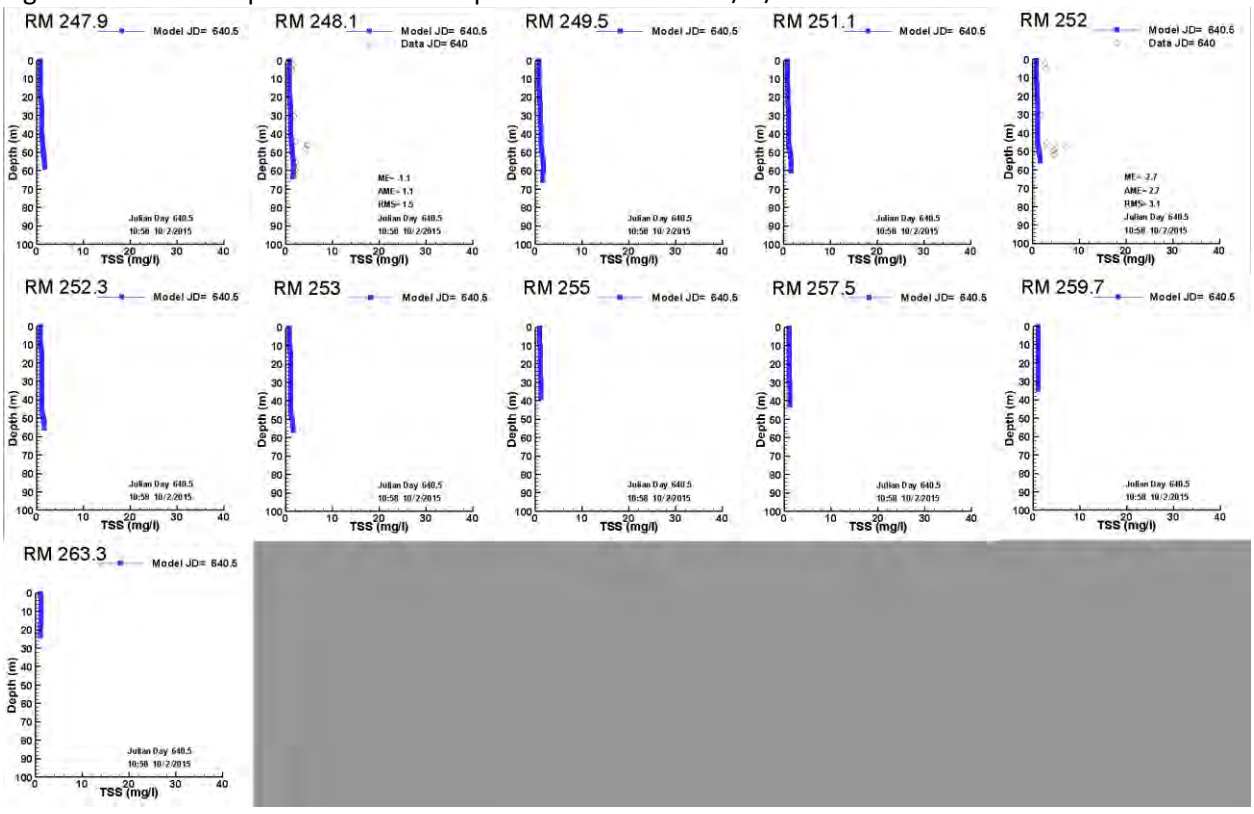


Figure 447. Vertical profiles of TSS compared with data for 10/ 2/2015.

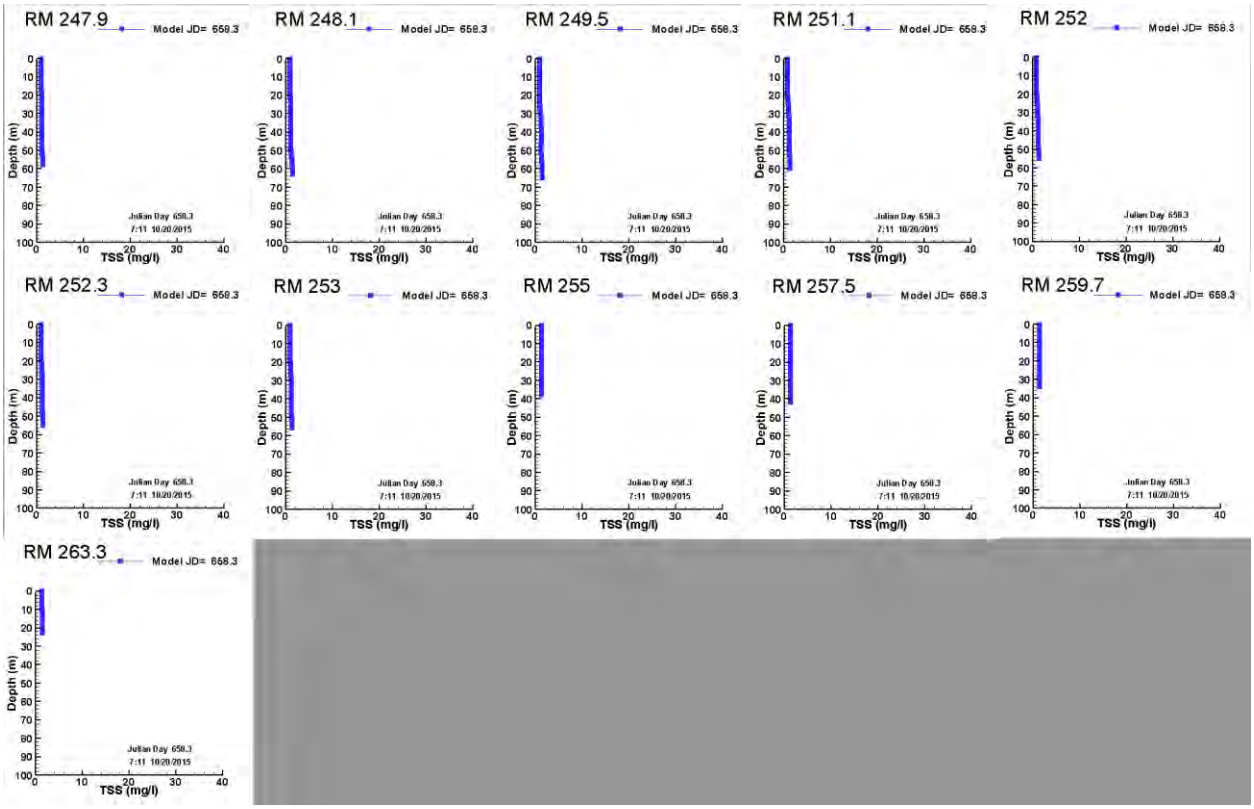


Figure 448. Vertical profiles of TSS compared with data for 10/20/2015.

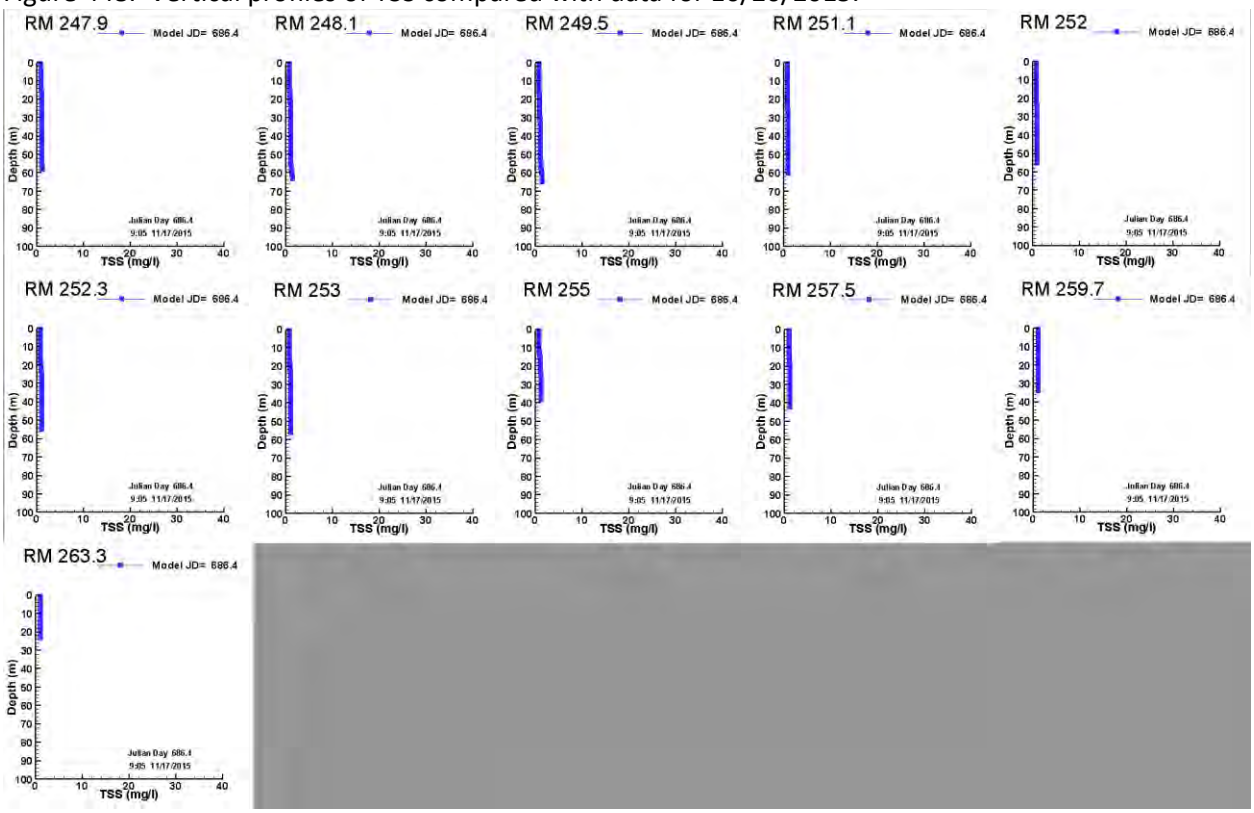


Figure 449. Vertical profiles of TSS compared with data for 11/17/2015.

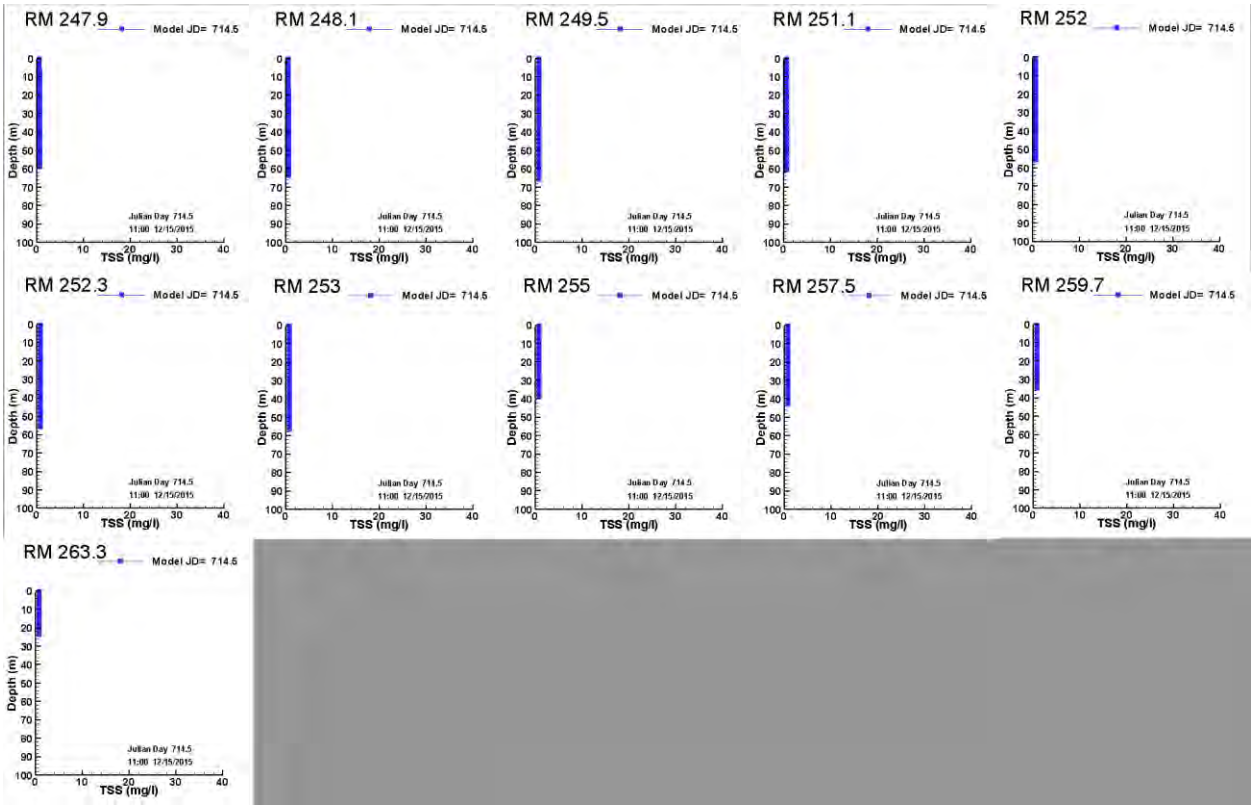


Figure 450. Vertical profiles of TSS compared with data for 12/15/2015.

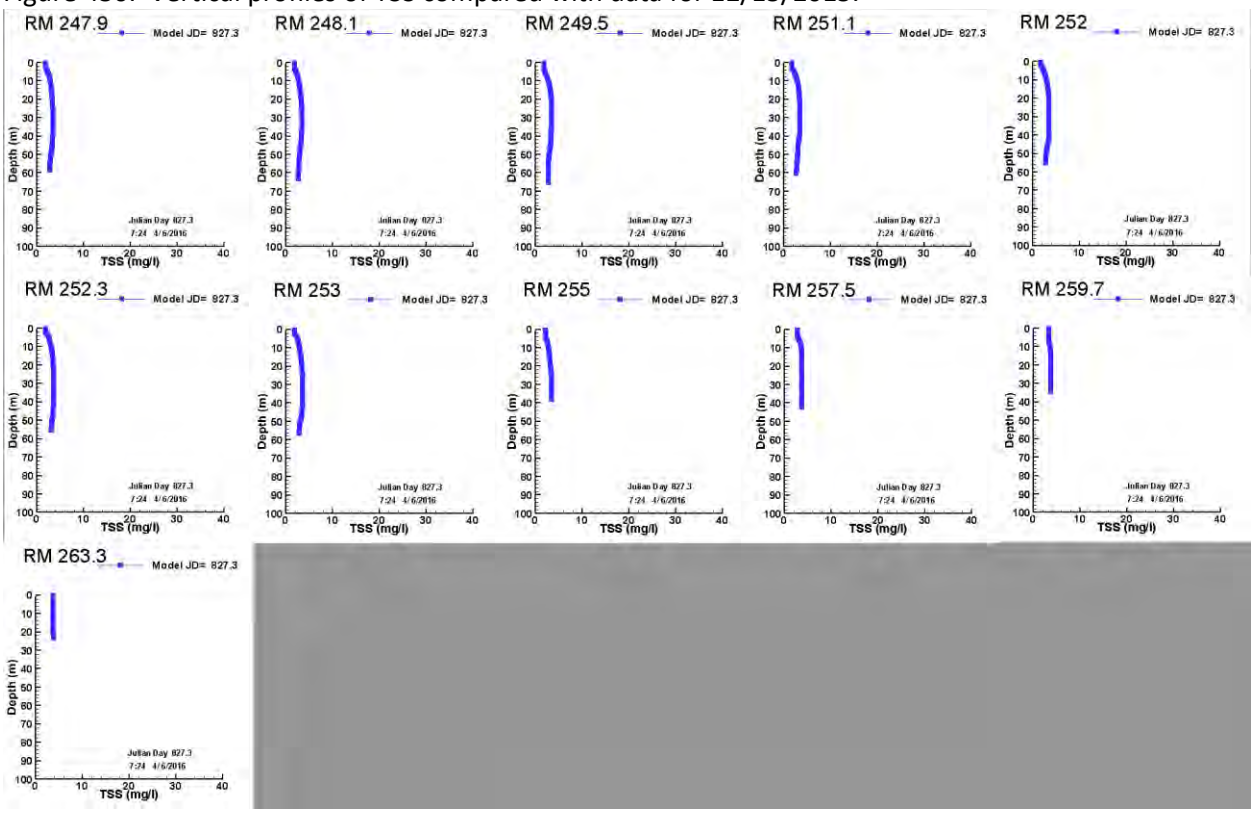


Figure 451. Vertical profiles of TSS compared with data for 4/ 6/2016.

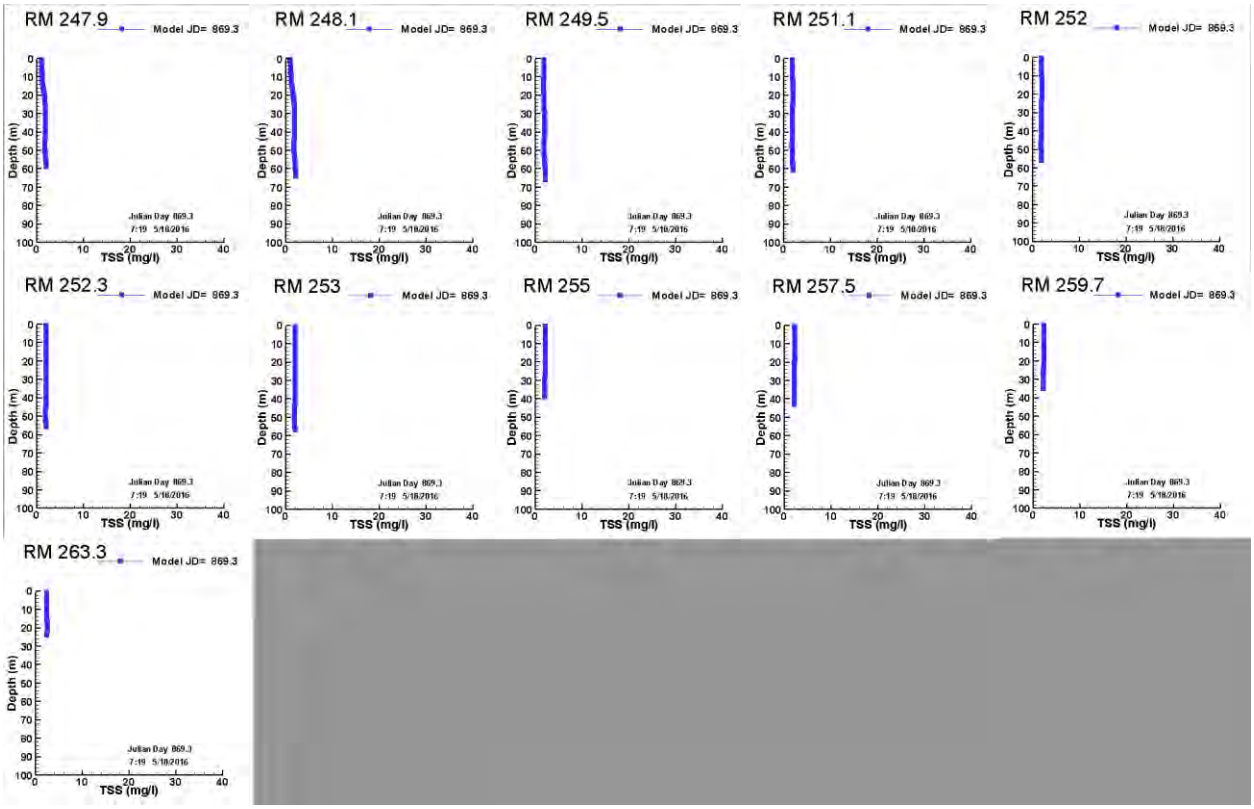


Figure 452. Vertical profiles of TSS compared with data for 5/18/2016.

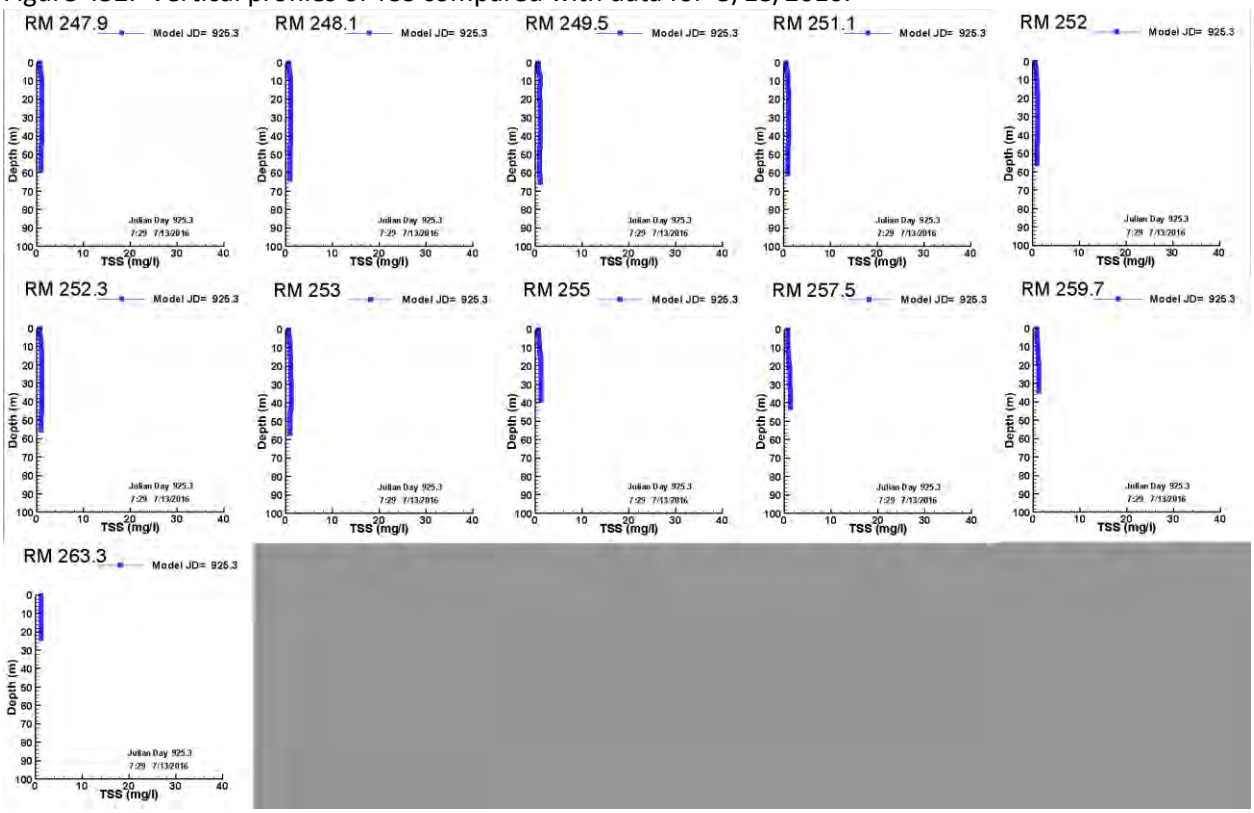


Figure 453. Vertical profiles of TSS compared with data for 7/13/2016.

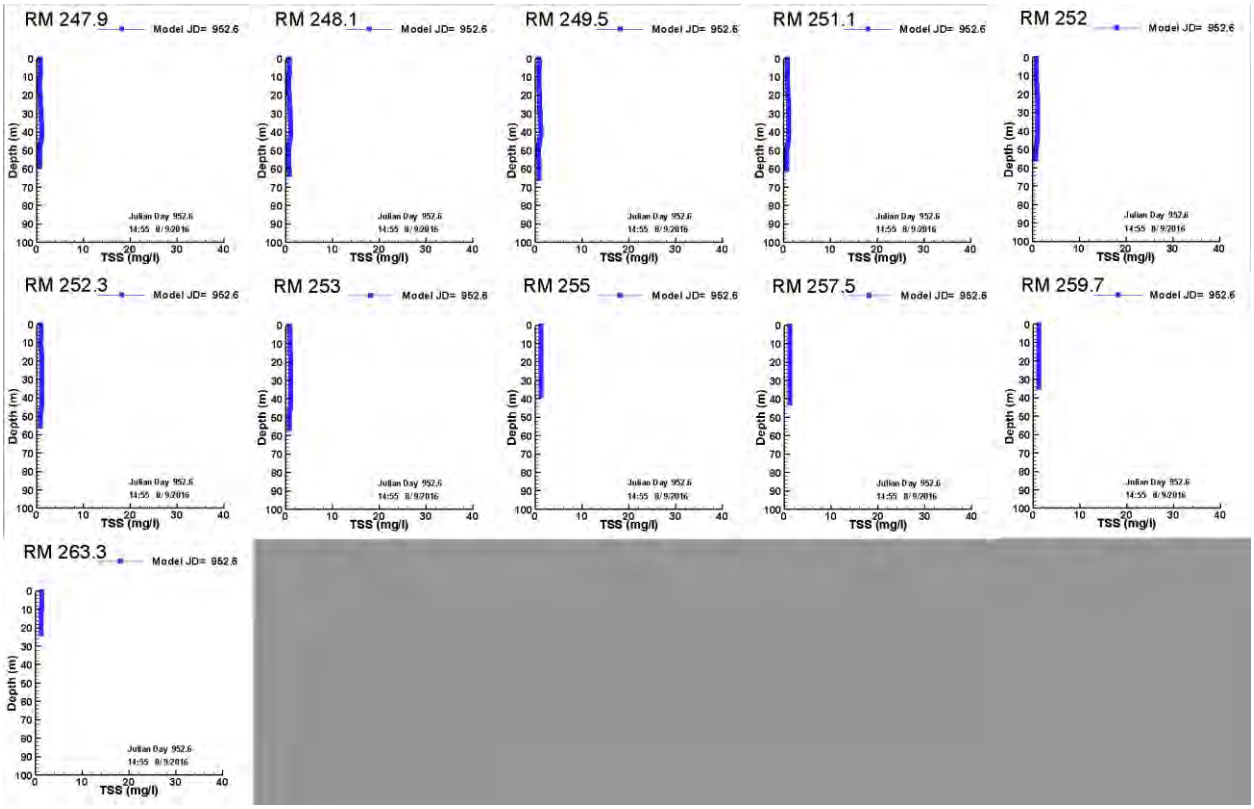


Figure 454. Vertical profiles of TSS compared with data for 8/ 9/2016.

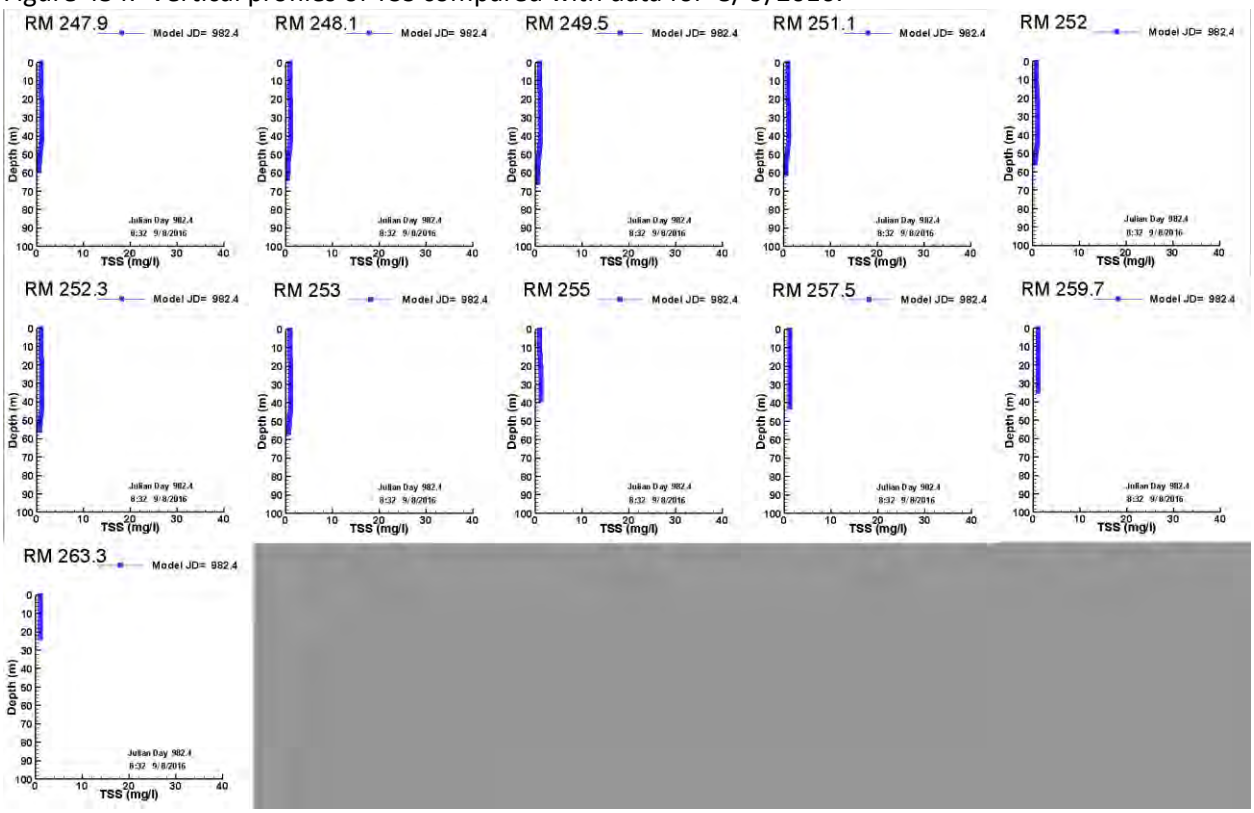


Figure 455. Vertical profiles of TSS compared with data for 9/ 8/2016.

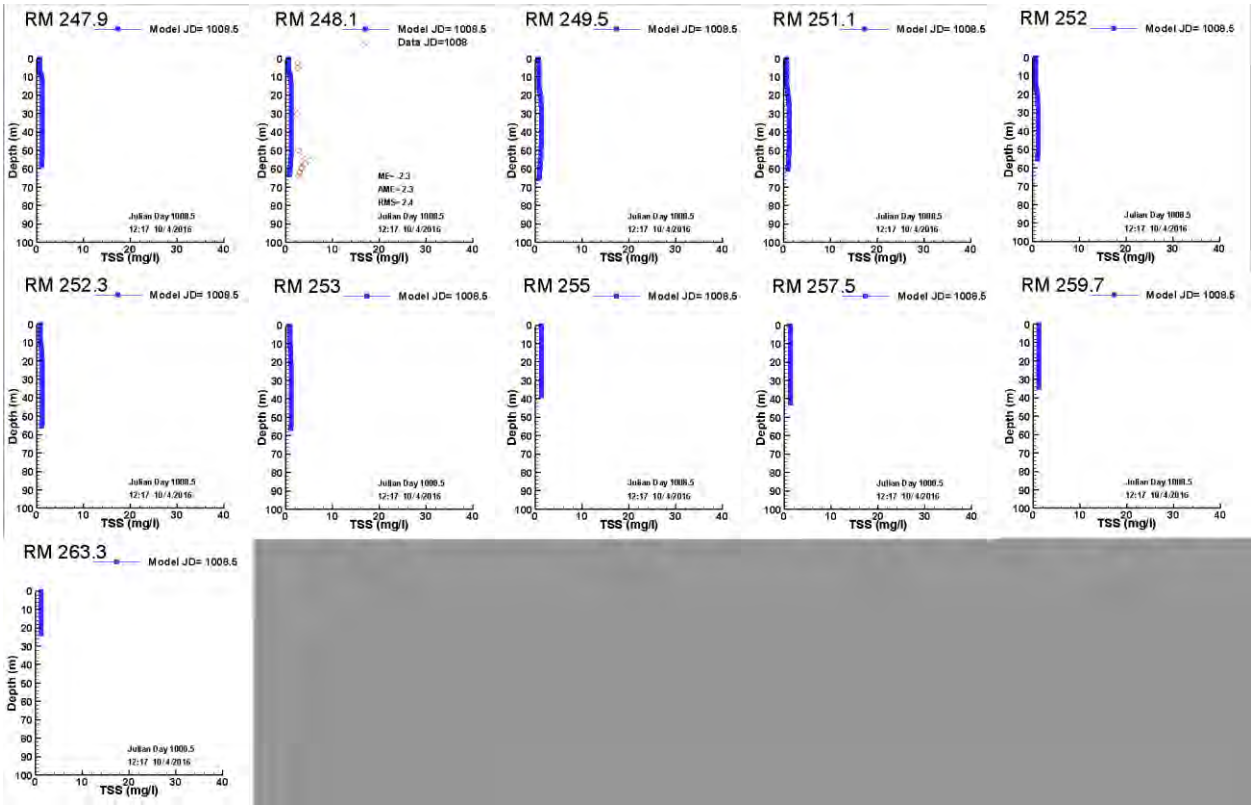


Figure 456. Vertical profiles of TSS compared with data for 10/ 4/2016.

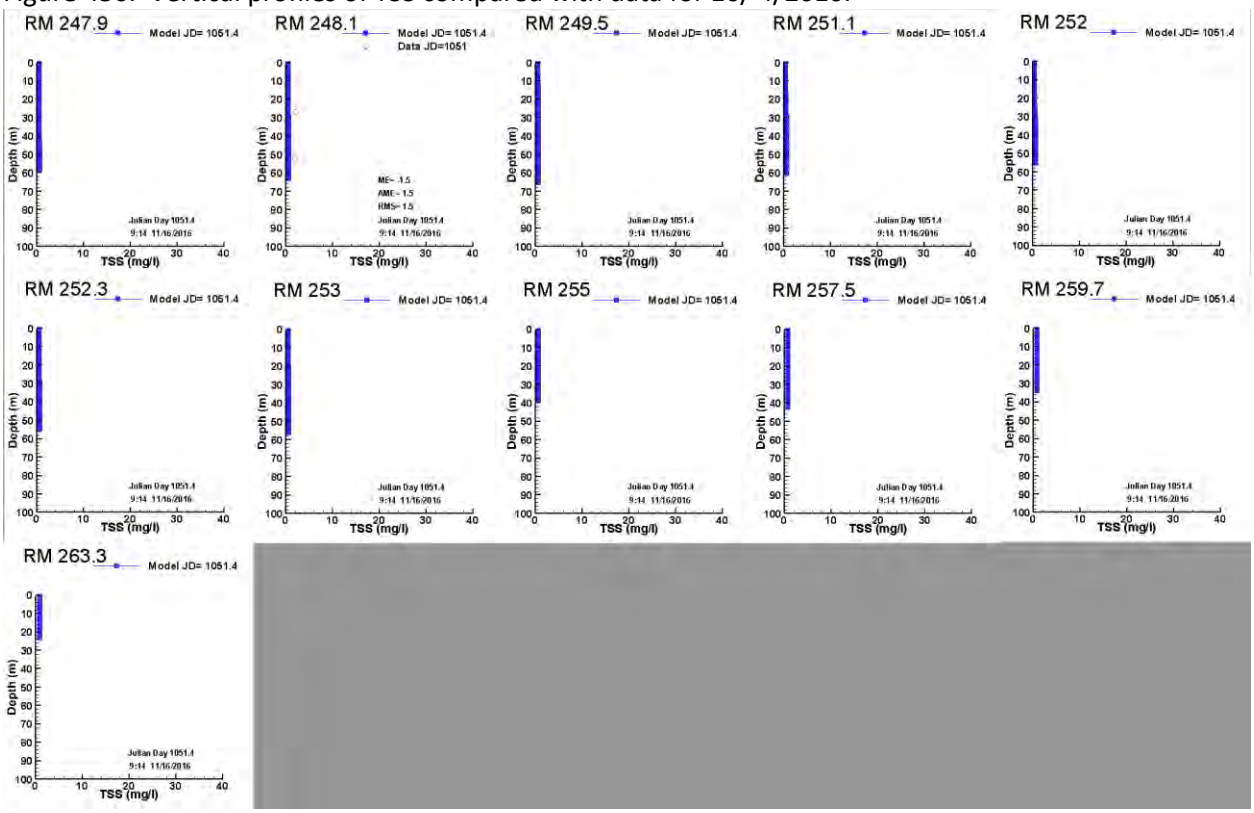


Figure 457. Vertical profiles of TSS compared with data for 11/16/2016.

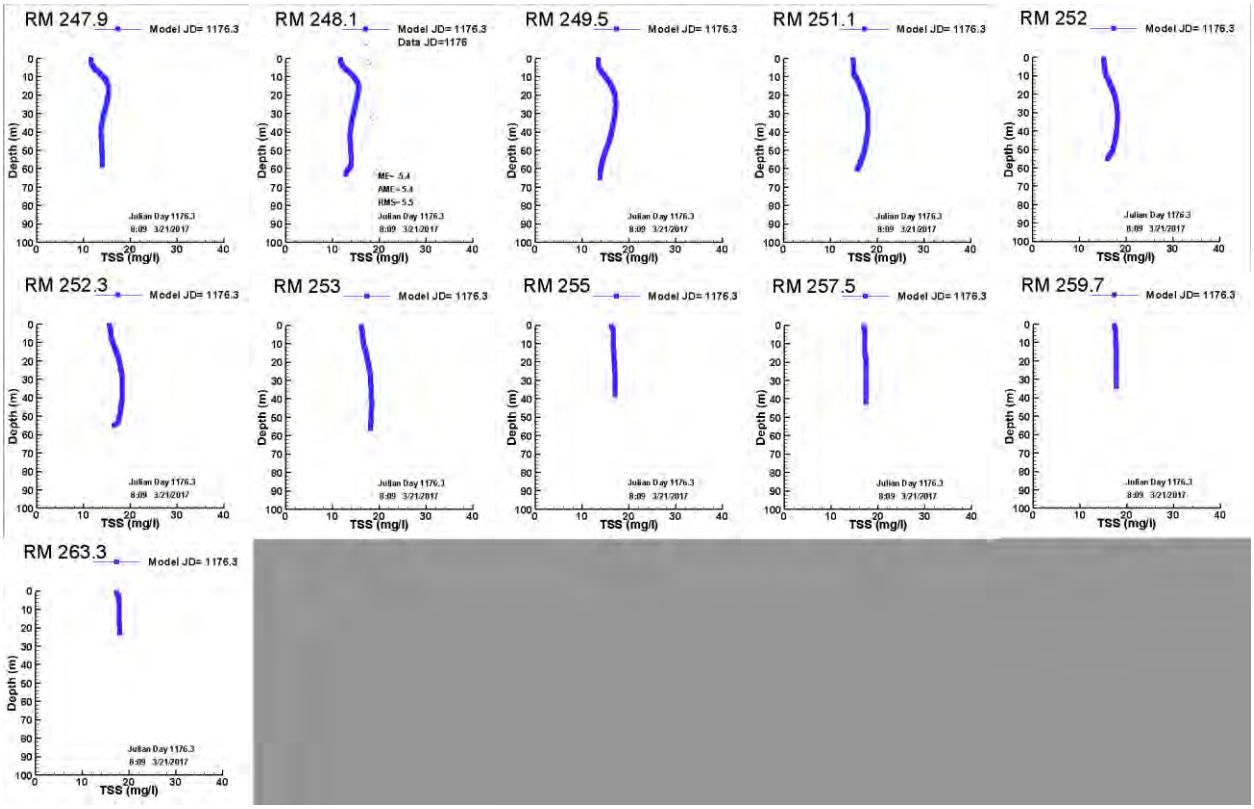


Figure 458. Vertical profiles of TSS compared with data for 3/21/2017.

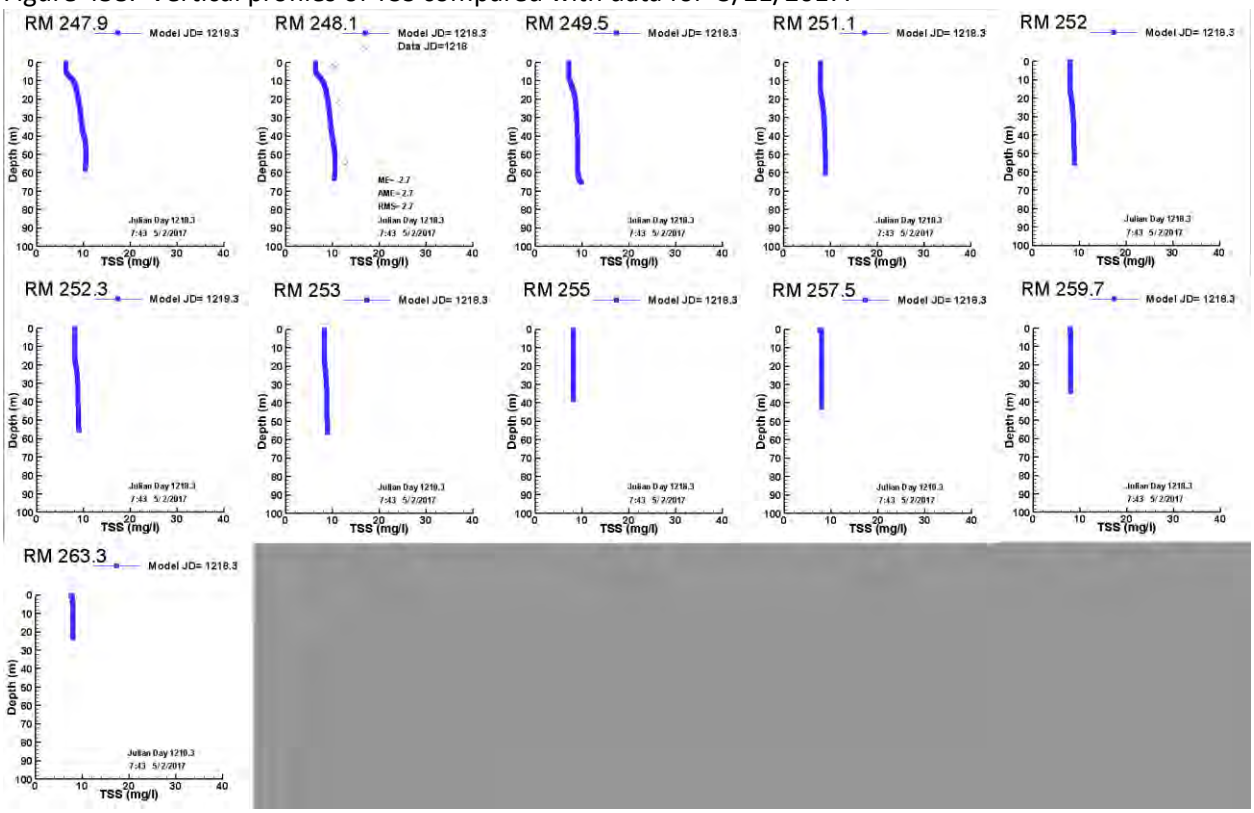


Figure 459. Vertical profiles of TSS compared with data for 5/ 2/2017.

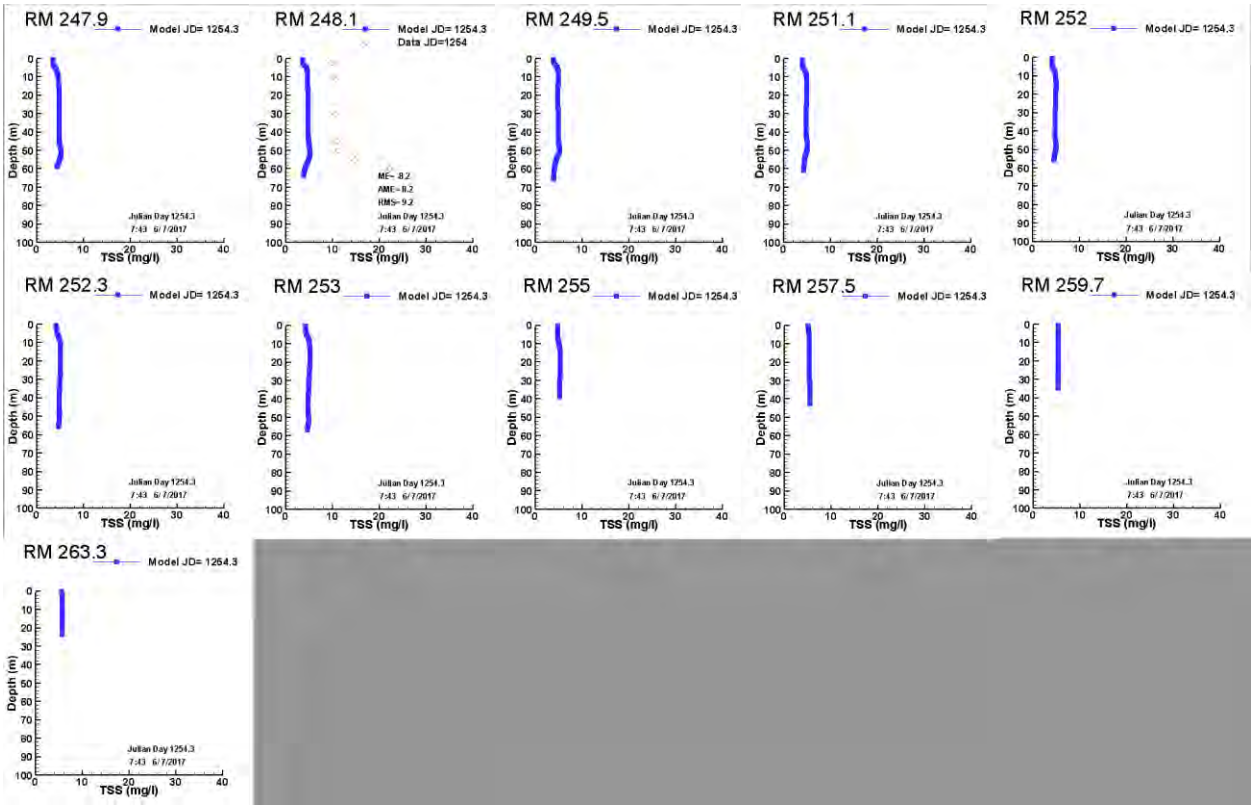


Figure 460. Vertical profiles of TSS compared with data for 6/ 7/2017.

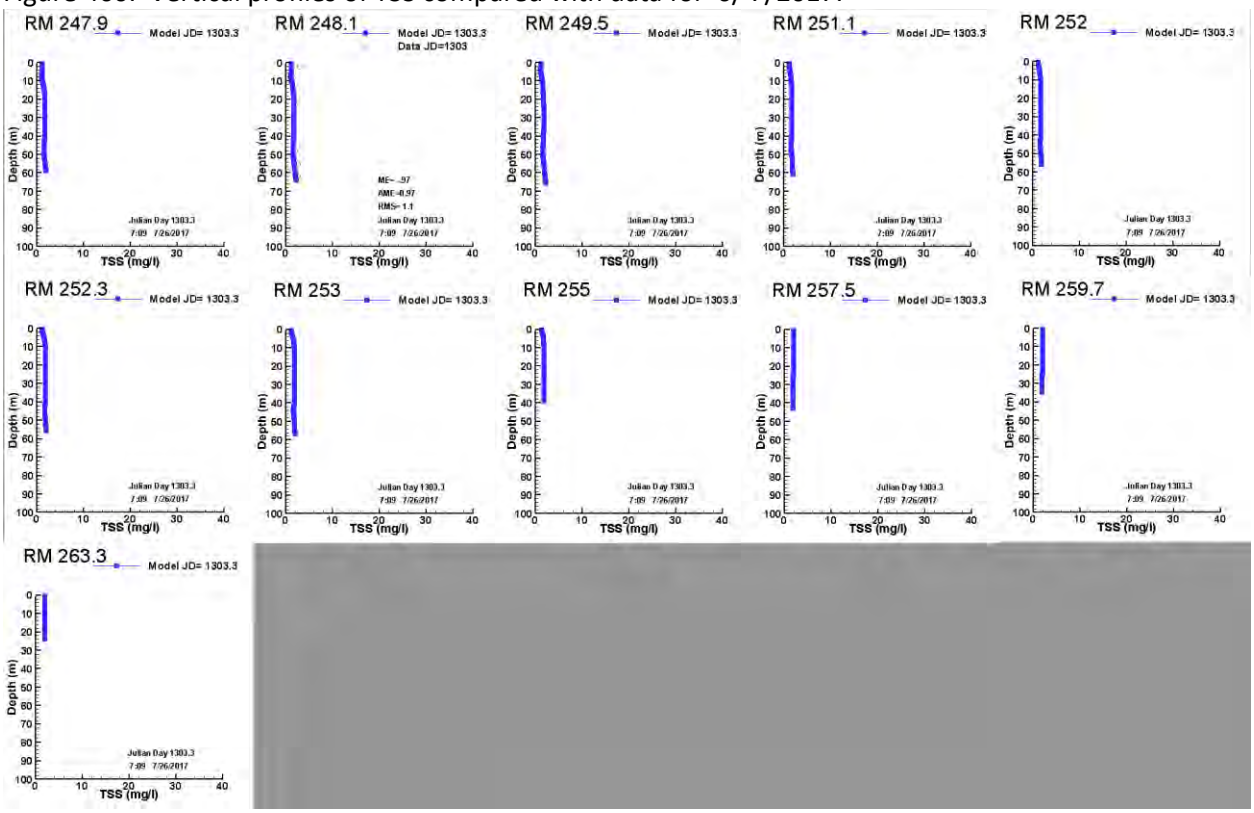


Figure 461. Vertical profiles of TSS compared with data for 7/26/2017.

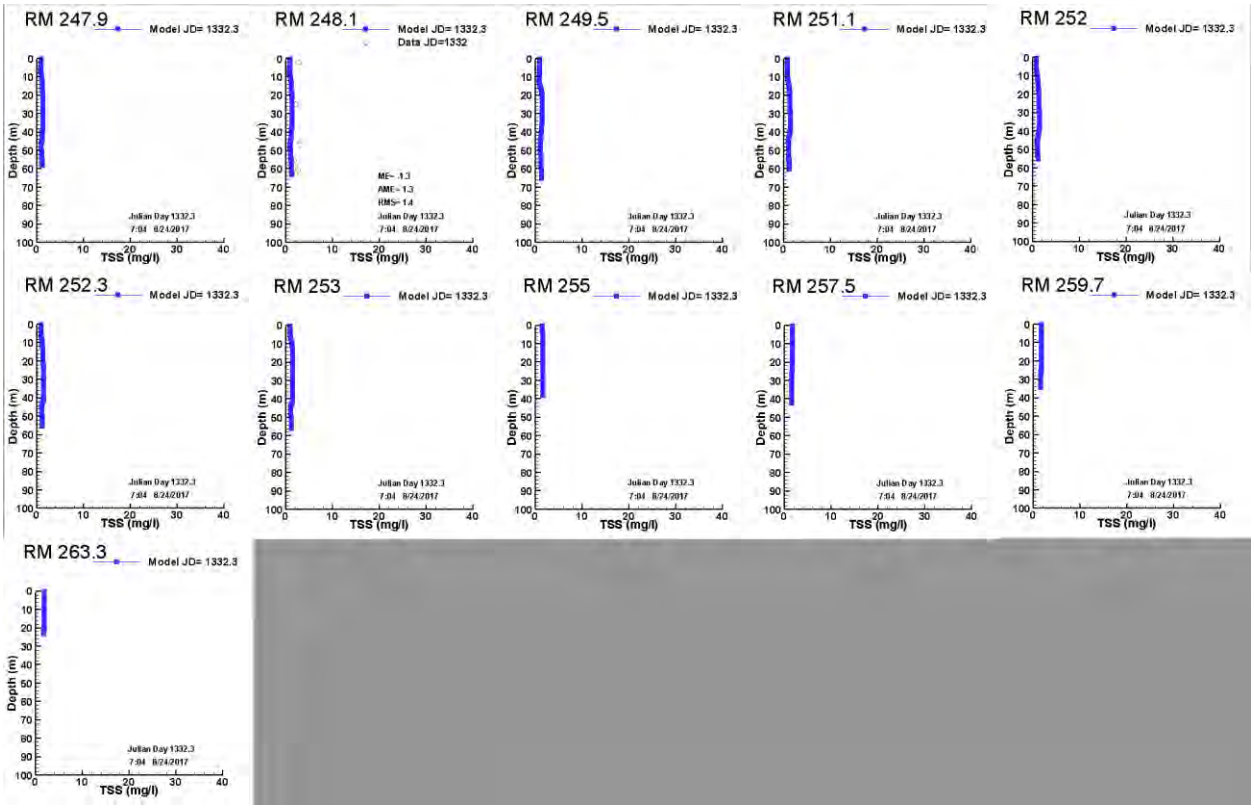


Figure 462. Vertical profiles of TSS compared with data for 8/24/2017.

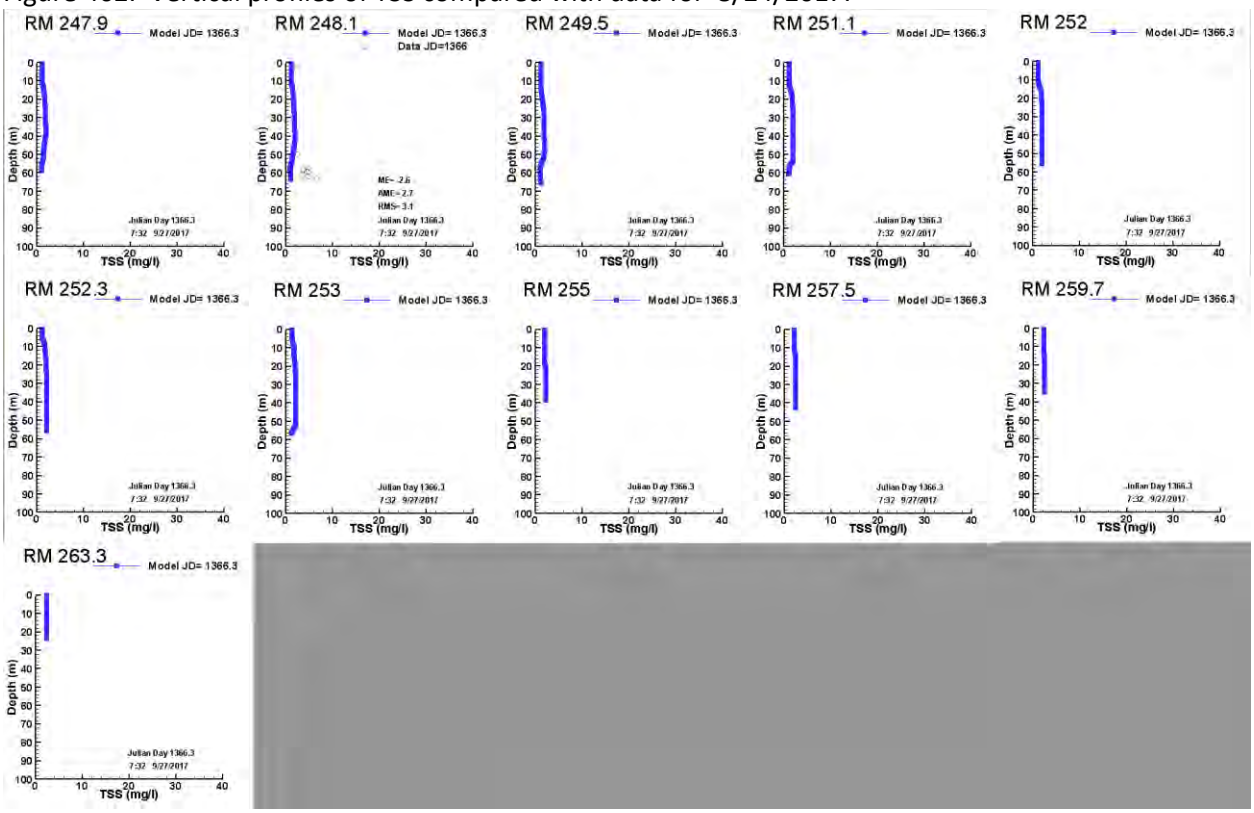


Figure 463. Vertical profiles of TSS compared with data for 9/27/2017.

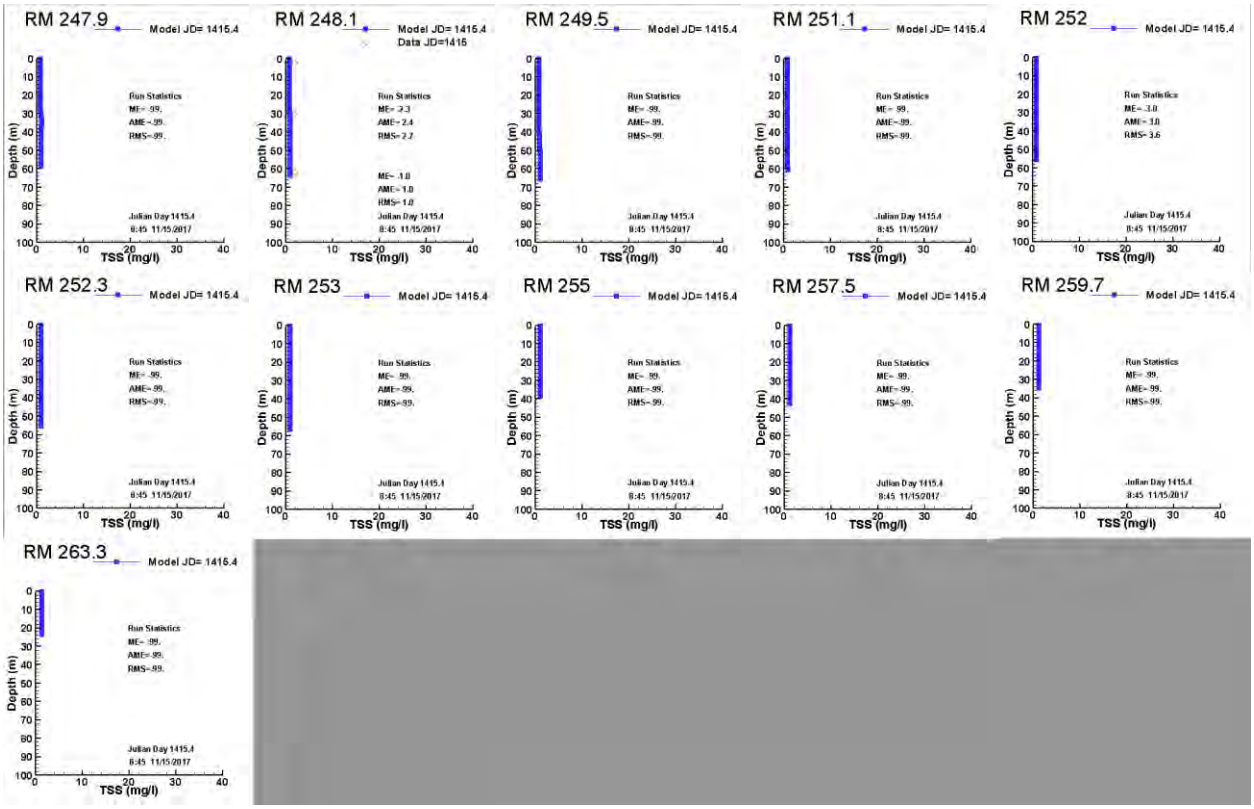


Figure 464. Vertical profiles of TSS compared with data for 11/15/2017.

pH

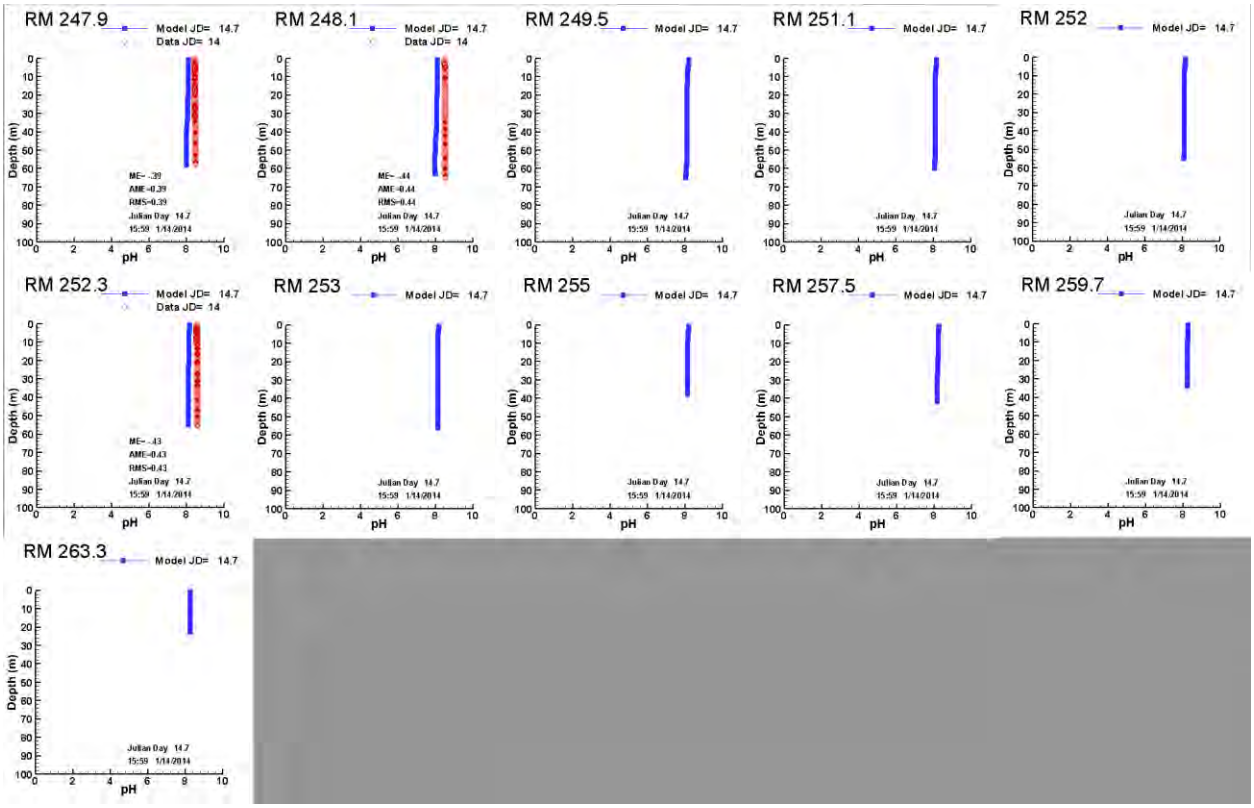


Figure 465. Vertical profiles of pH compared with data for 1/14/2014.

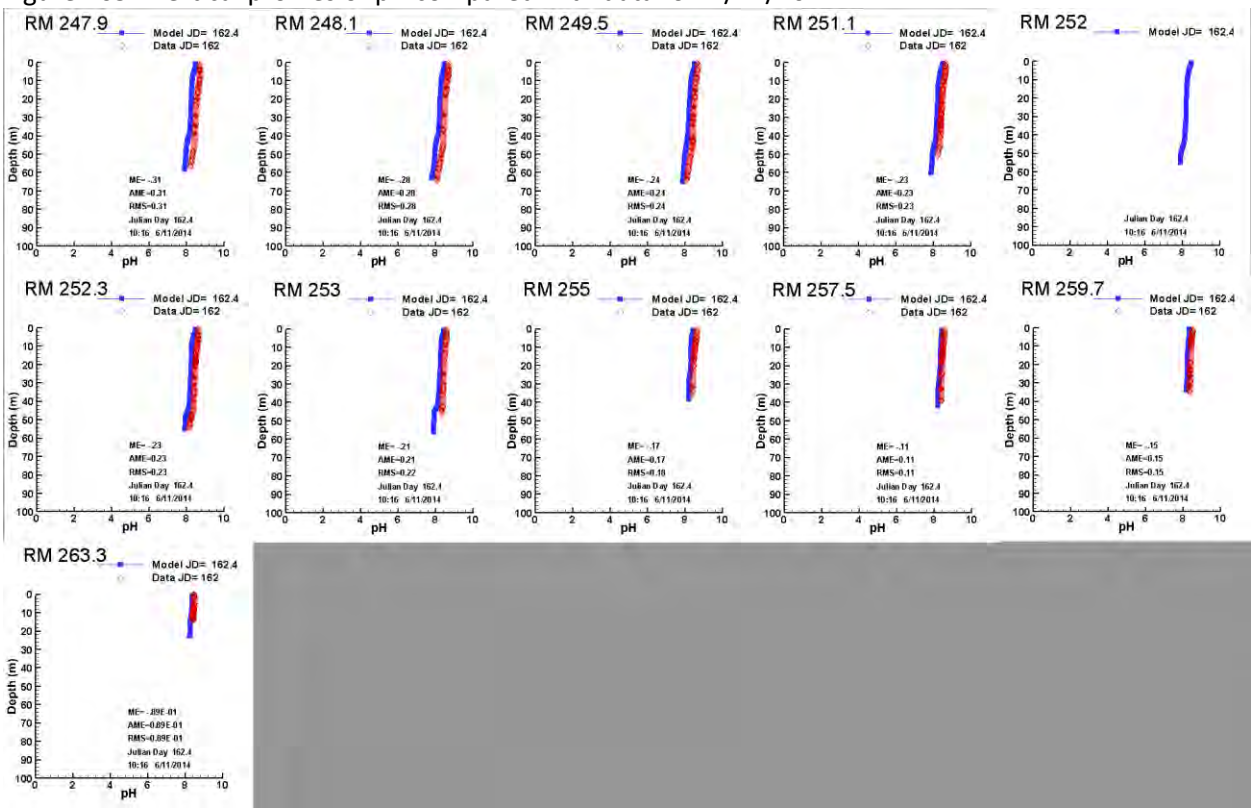


Figure 466. Vertical profiles of pH compared with data for 6/11/2014.

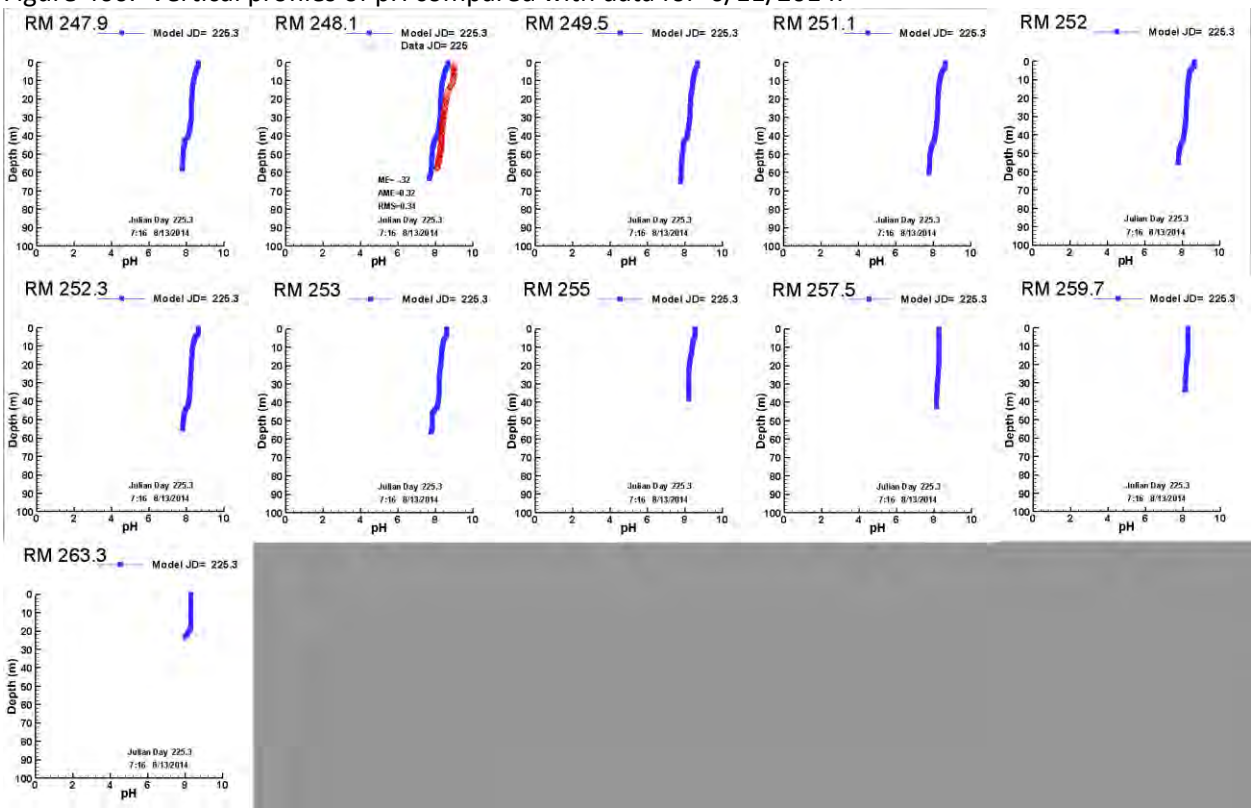


Figure 467. Vertical profiles of pH compared with data for 8/13/2014.

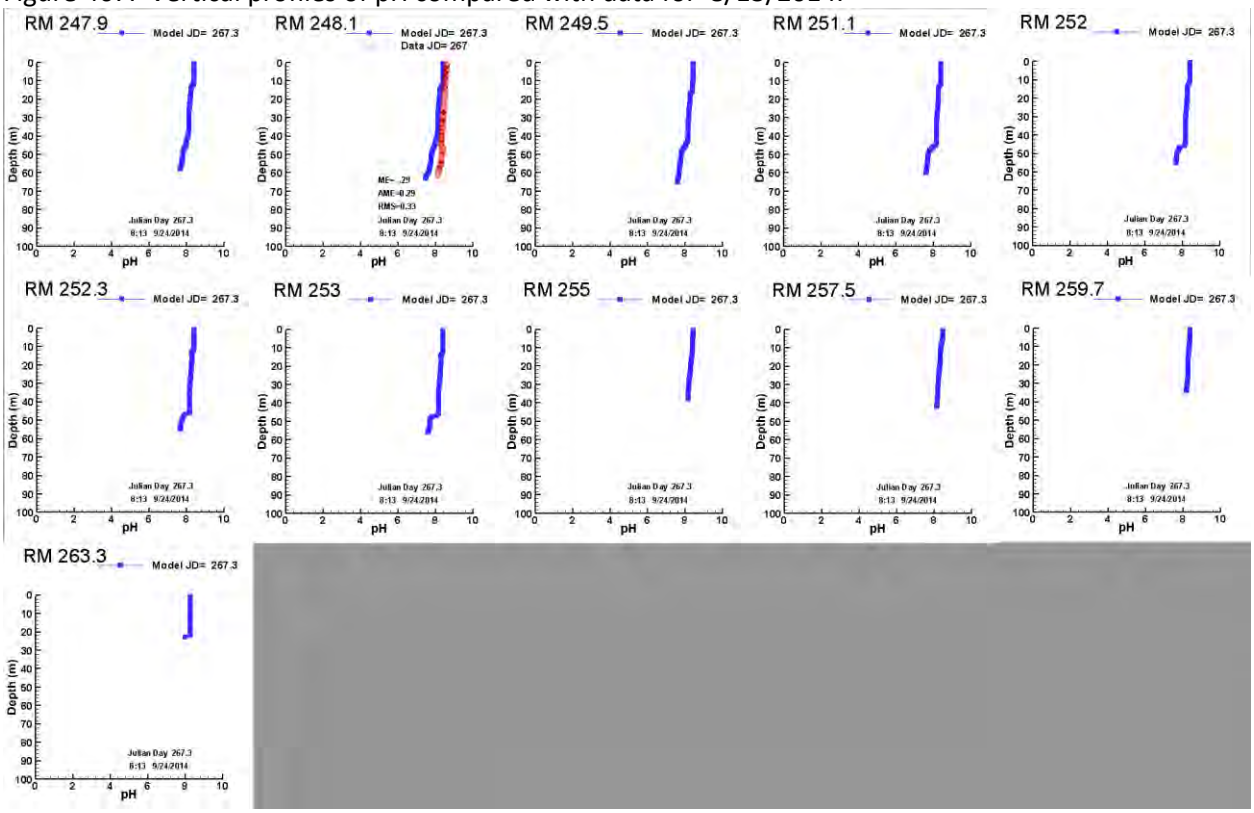


Figure 468. Vertical profiles of pH compared with data for 9/24/2014.

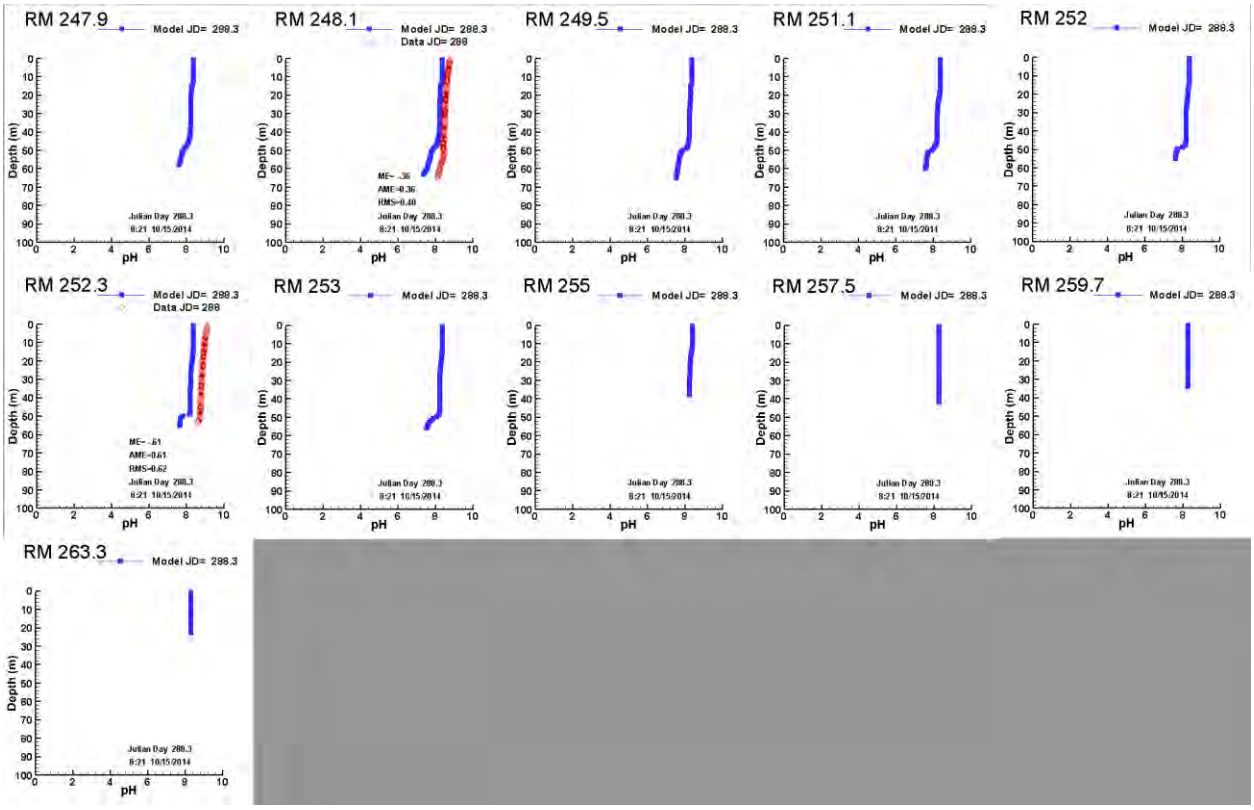


Figure 469. Vertical profiles of pH compared with data for 10/15/2014.

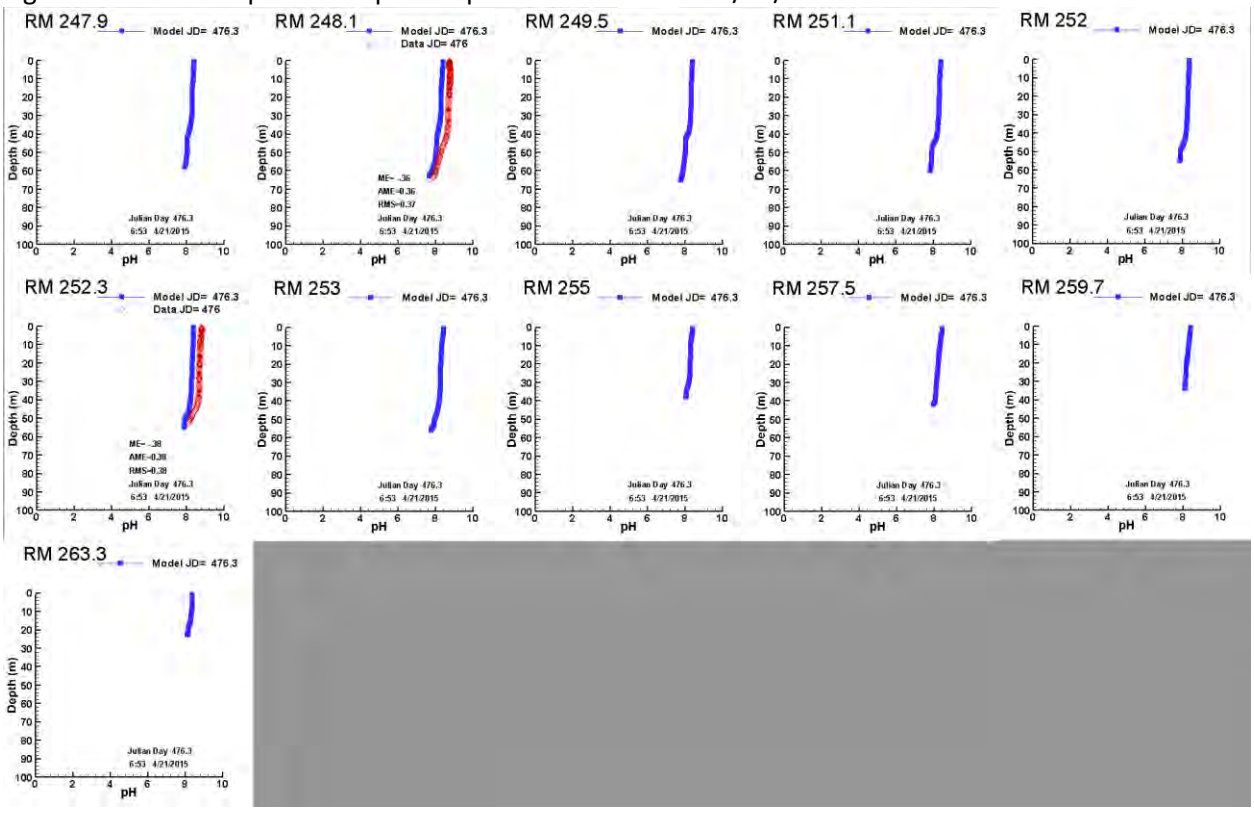


Figure 470. Vertical profiles of pH compared with data for 4/21/2015.

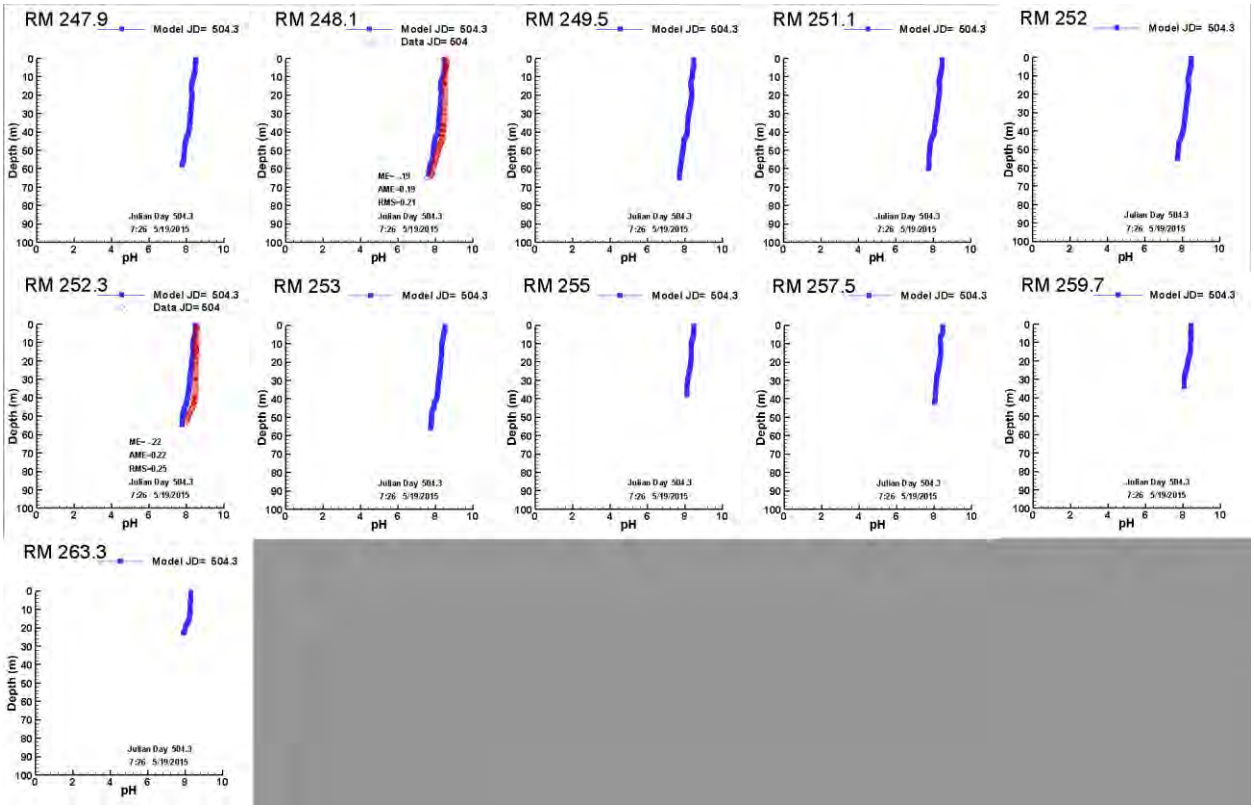


Figure 471. Vertical profiles of pH compared with data for 5/19/2015.

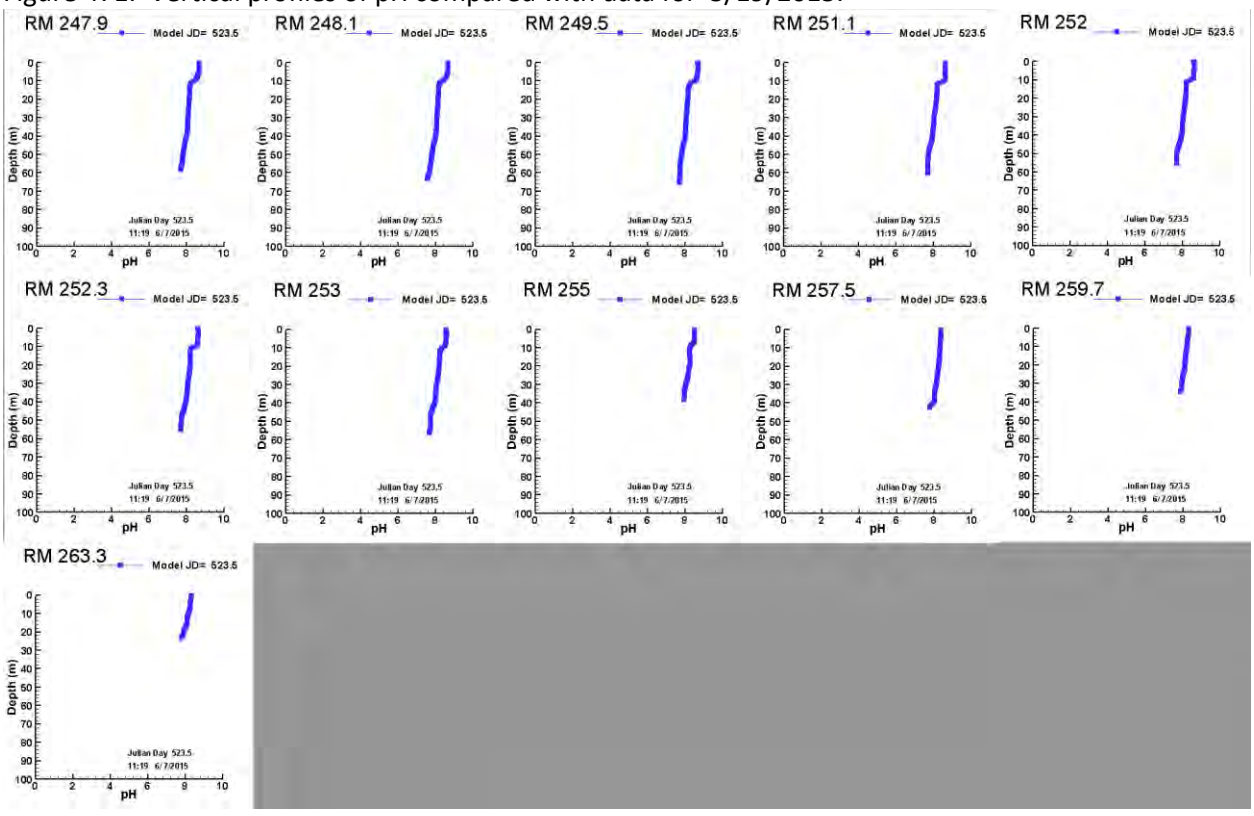


Figure 472. Vertical profiles of pH compared with data for 6/ 7/2015.

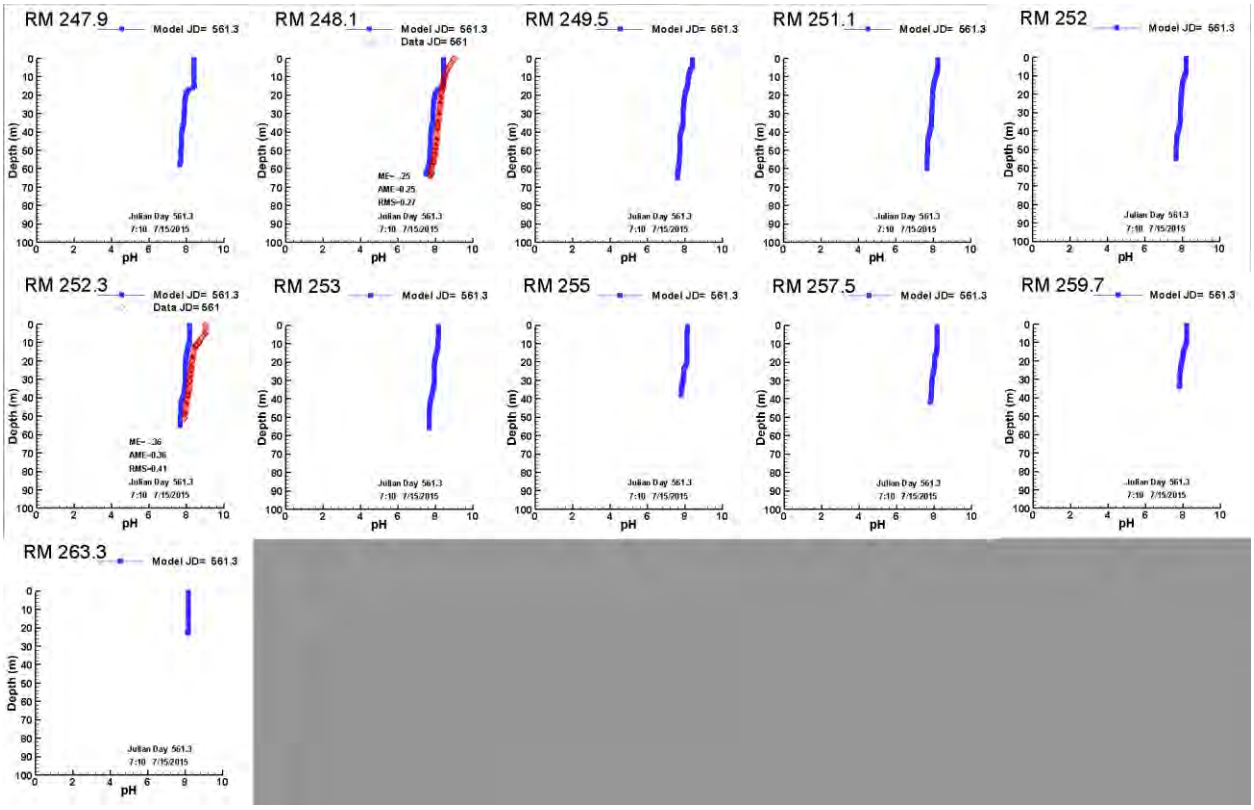


Figure 473. Vertical profiles of pH compared with data for 7/15/2015.

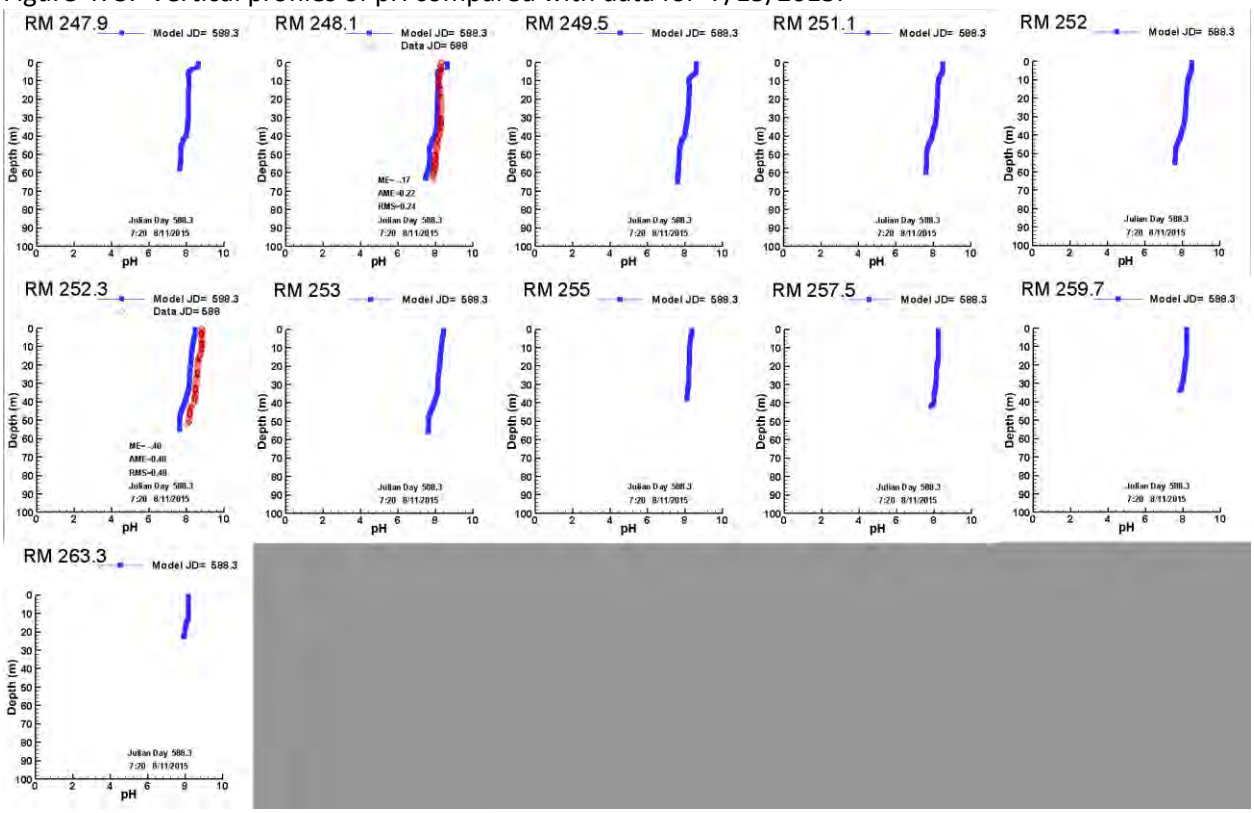


Figure 474. Vertical profiles of pH compared with data for 8/11/2015.

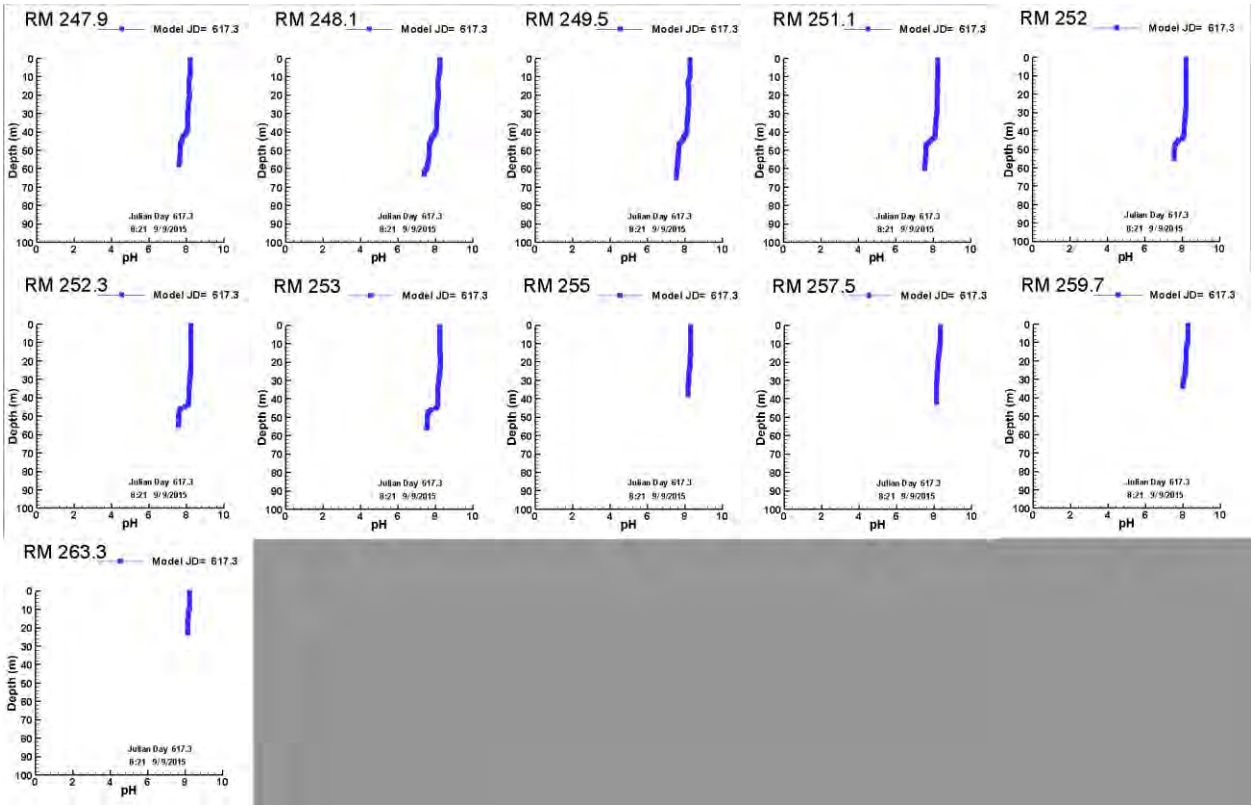


Figure 475. Vertical profiles of pH compared with data for 9/ 9/2015.

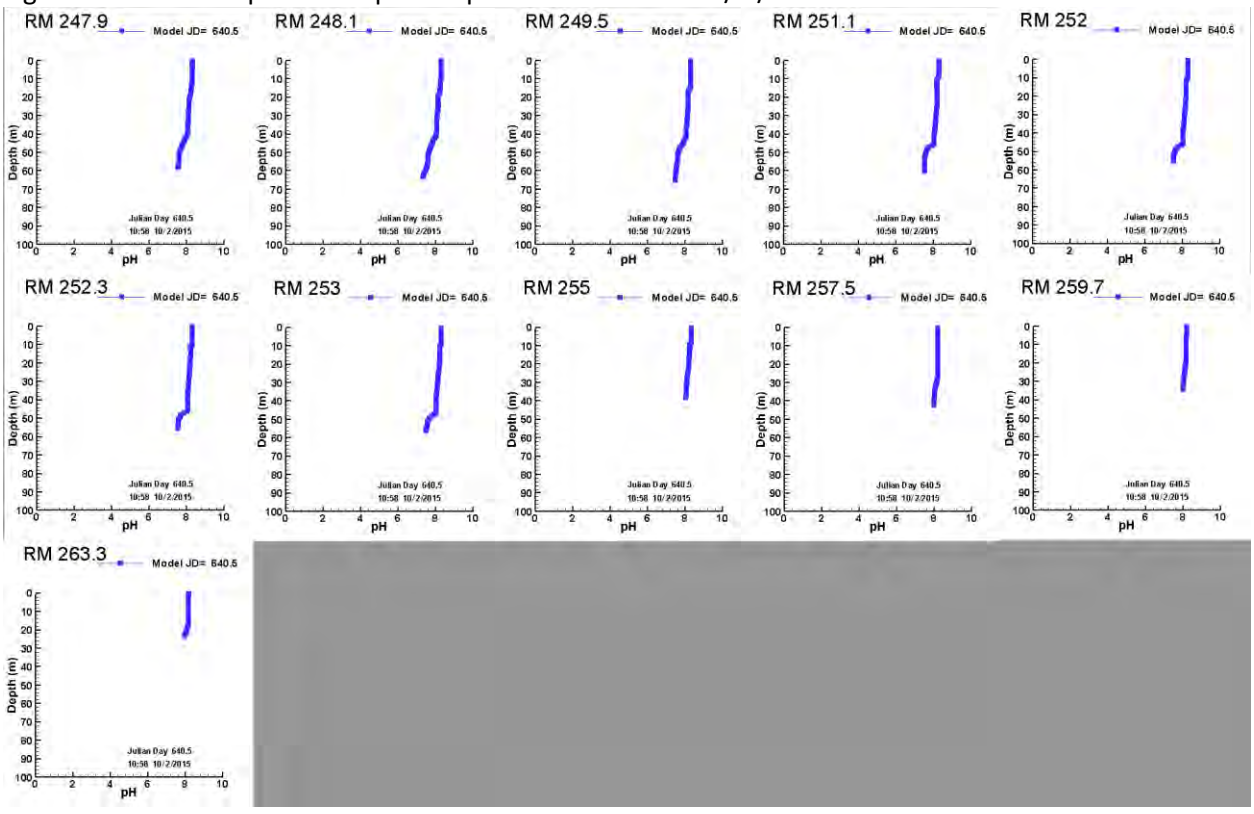


Figure 476. Vertical profiles of pH compared with data for 10/ 2/2015.

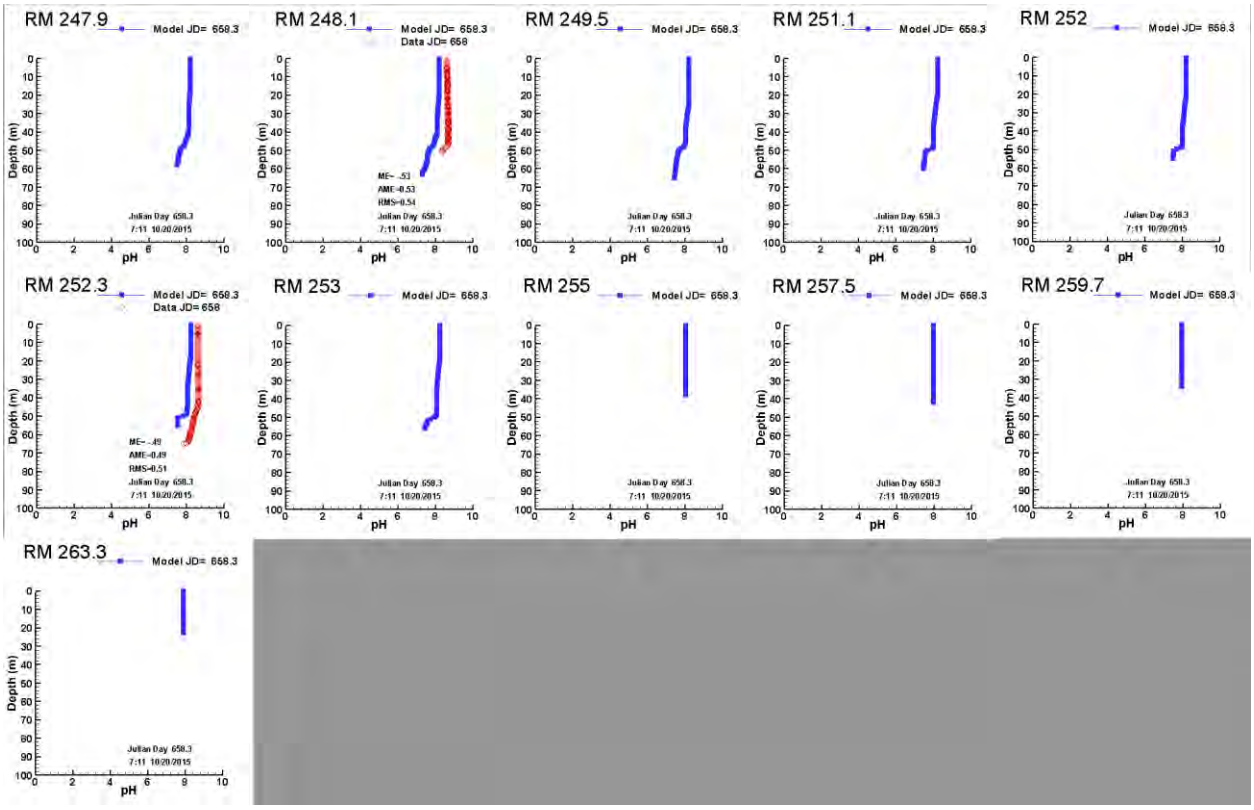


Figure 477. Vertical profiles of pH compared with data for 10/20/2015.

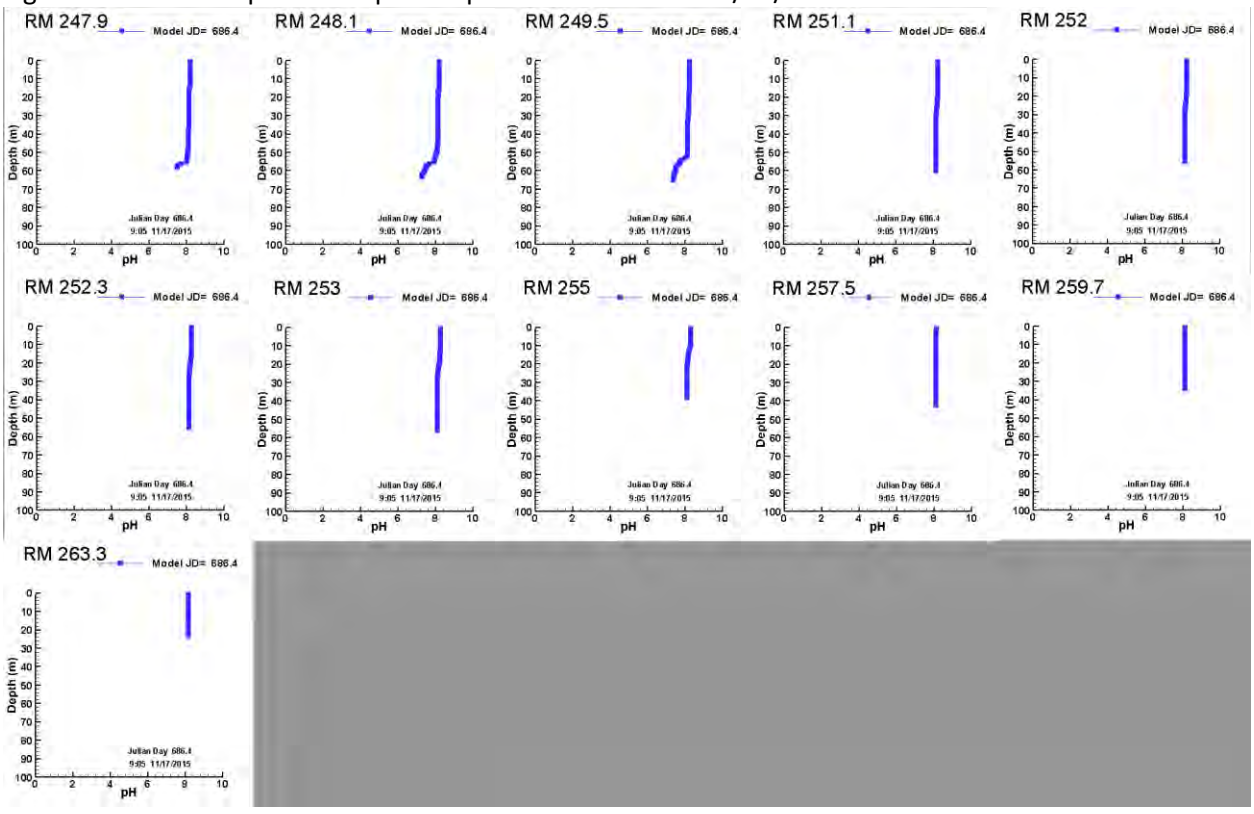


Figure 478. Vertical profiles of pH compared with data for 11/17/2015.

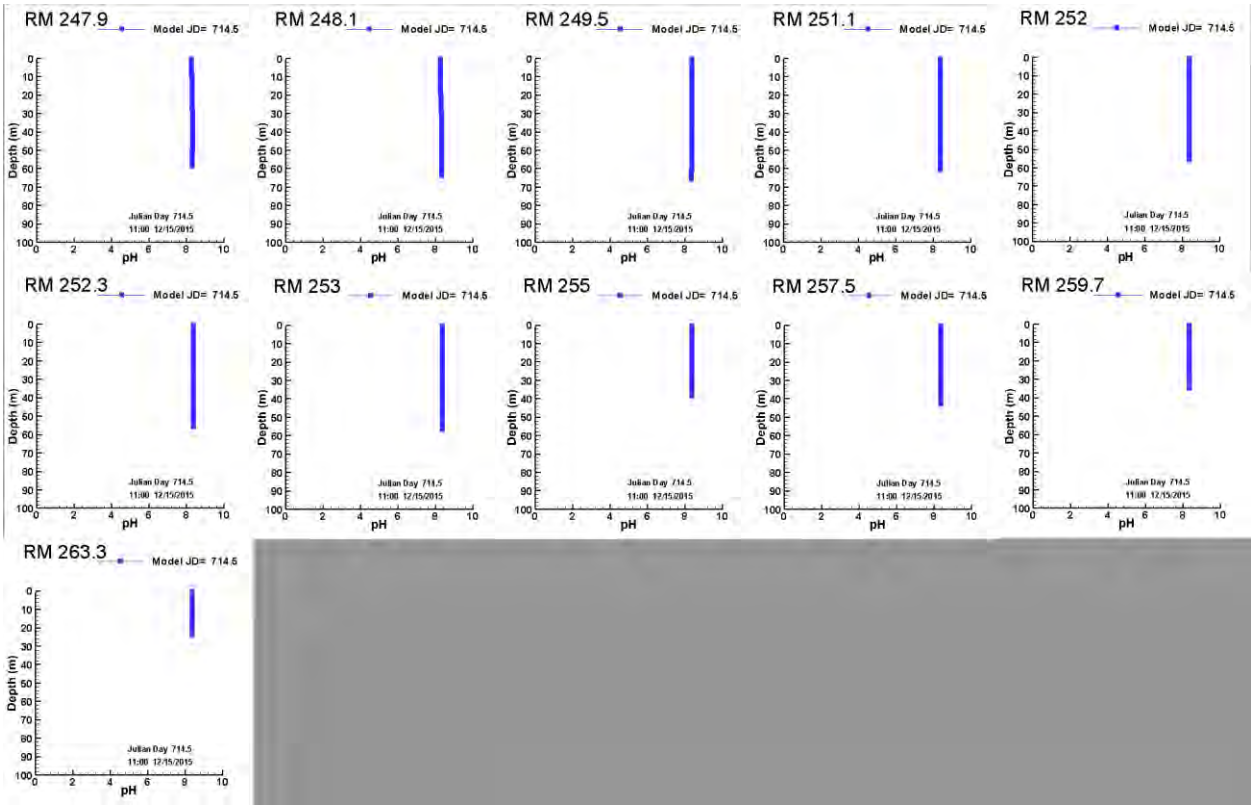


Figure 479. Vertical profiles of pH compared with data for 12/15/2015.

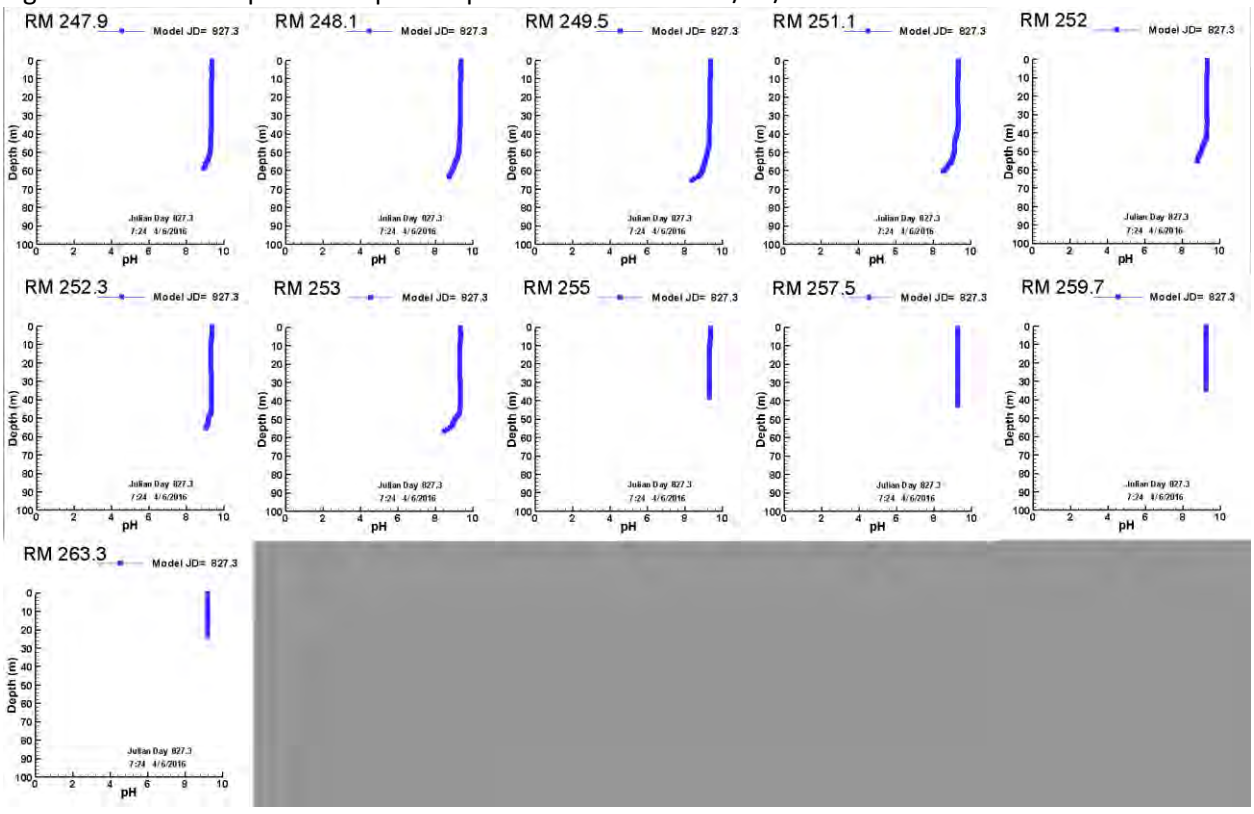


Figure 480. Vertical profiles of pH compared with data for 4/ 6/2016.

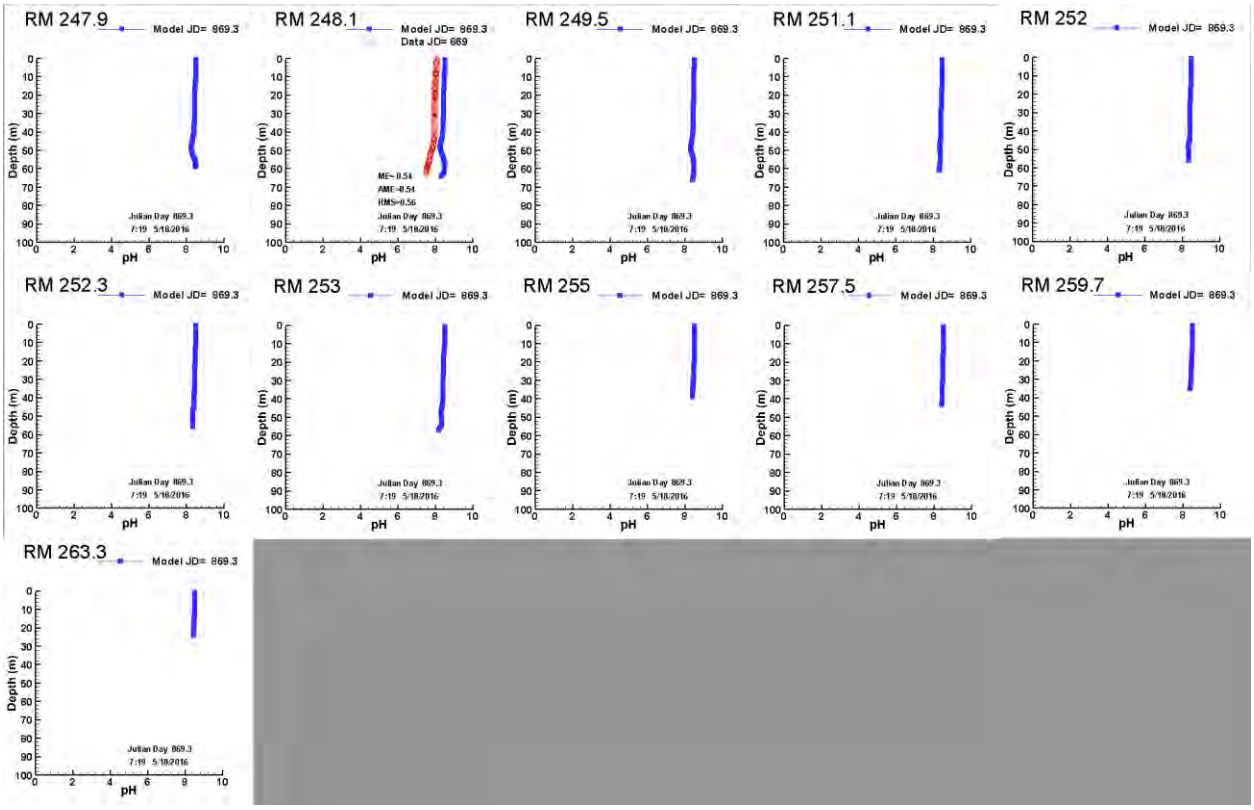


Figure 481. Vertical profiles of pH compared with data for 5/18/2016.

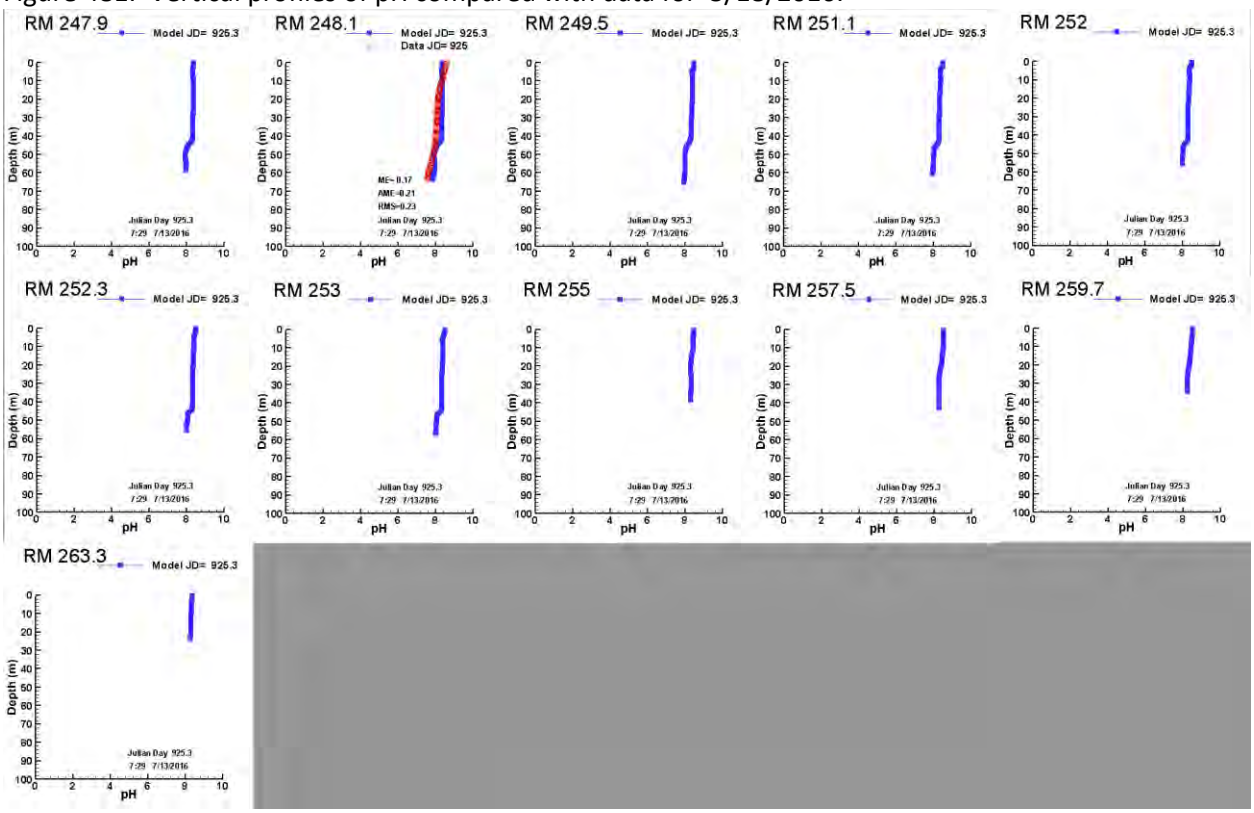


Figure 482. Vertical profiles of pH compared with data for 7/13/2016.

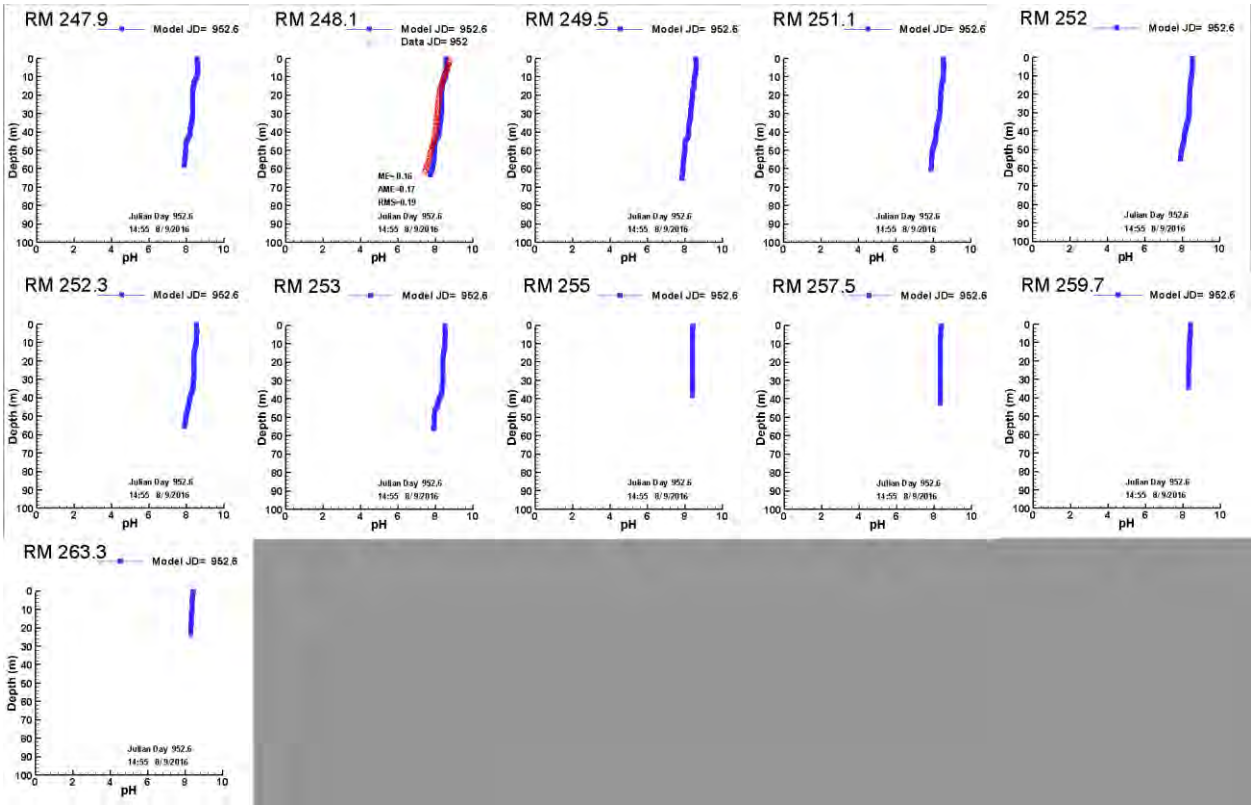


Figure 483. Vertical profiles of pH compared with data for 8/ 9/2016.

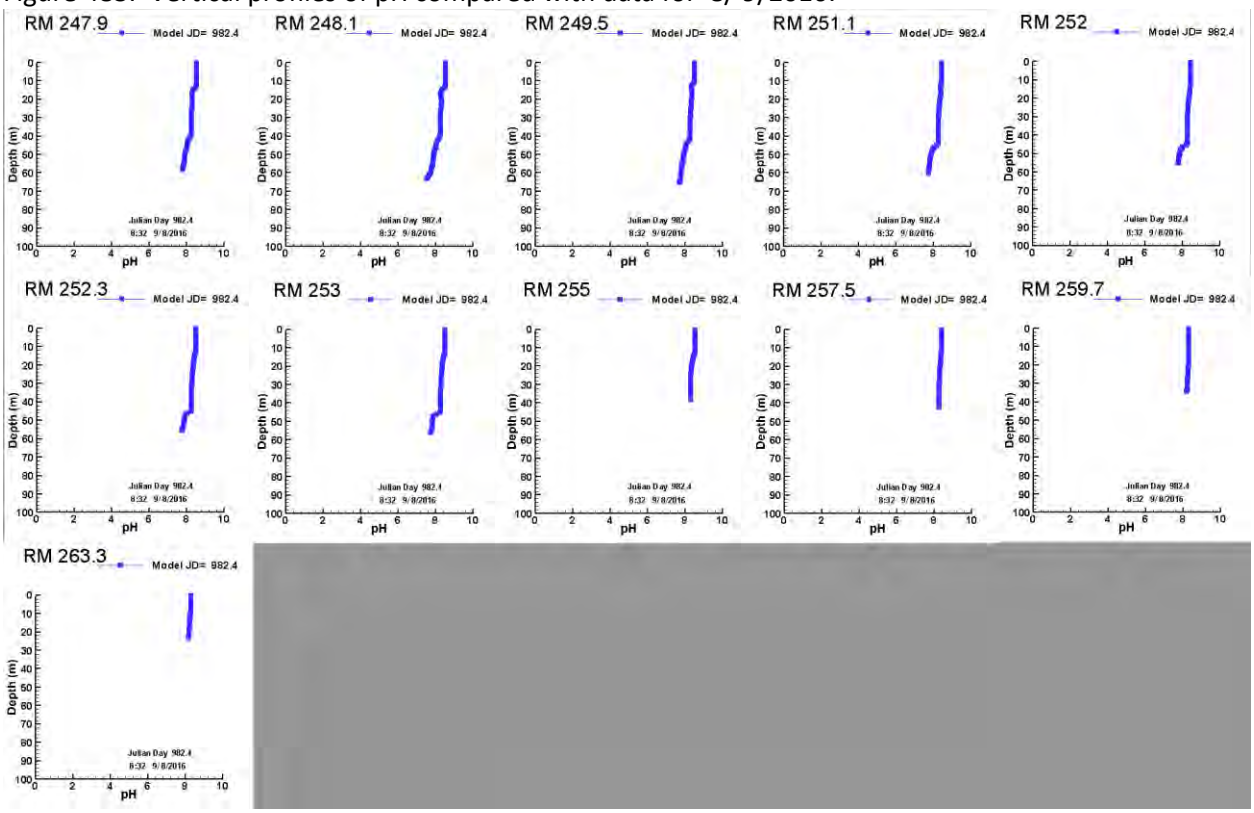


Figure 484. Vertical profiles of pH compared with data for 9/ 8/2016.

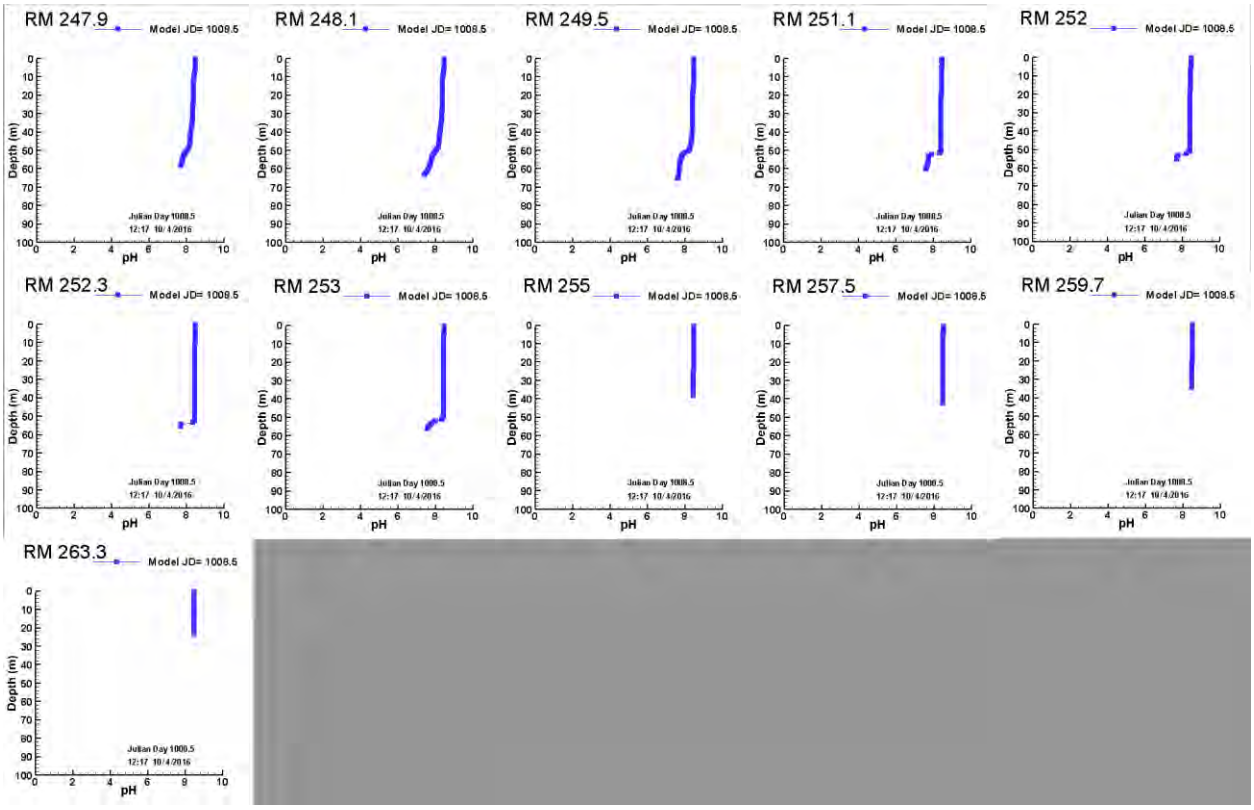


Figure 485. Vertical profiles of pH compared with data for 10/ 4/2016.

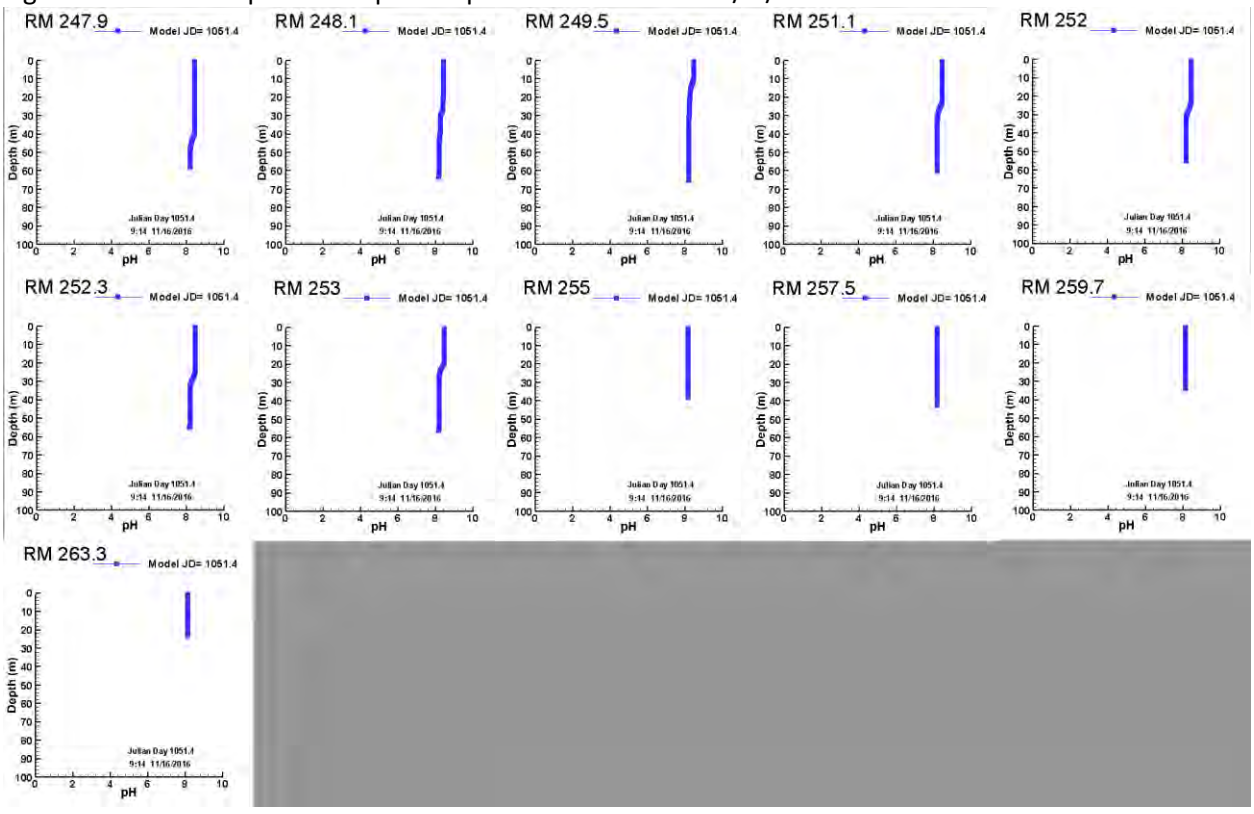


Figure 486. Vertical profiles of pH compared with data for 11/16/2016.

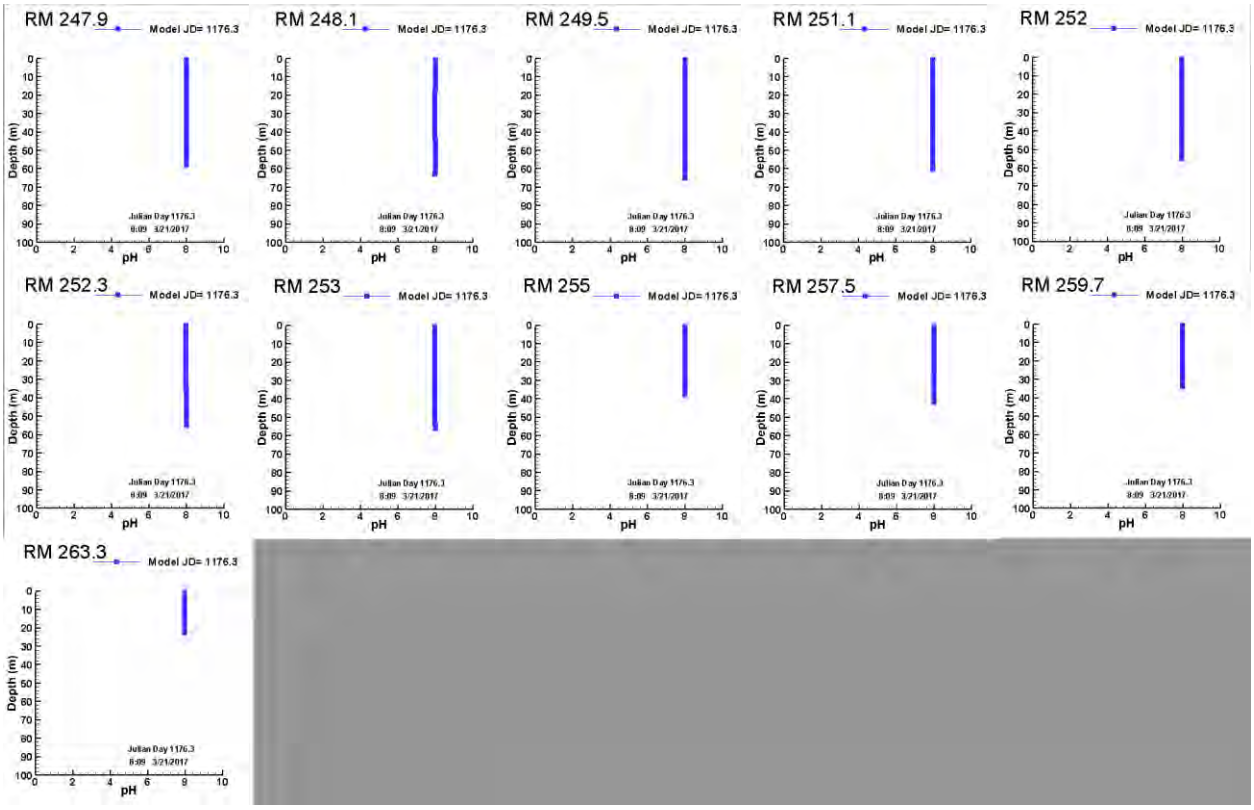


Figure 487. Vertical profiles of pH compared with data for 3/21/2017.

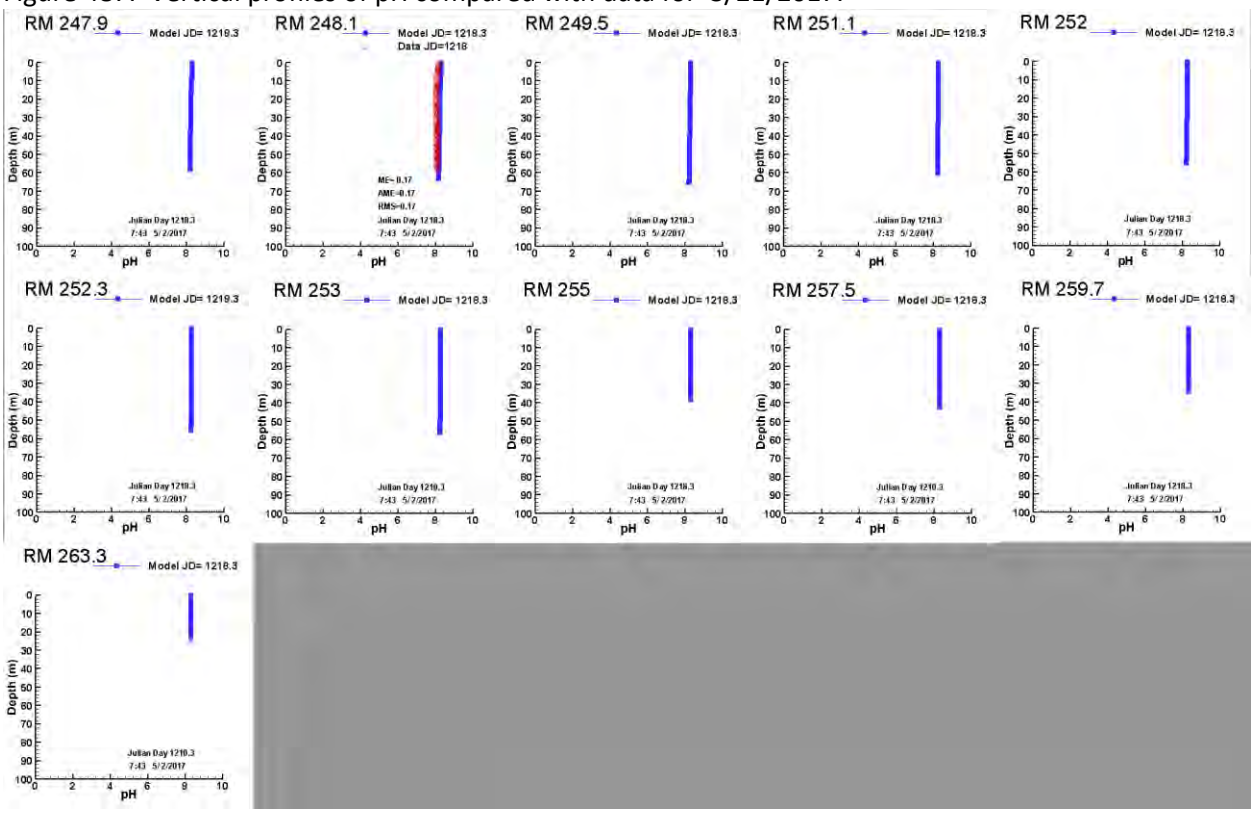


Figure 488. Vertical profiles of pH compared with data for 5/ 2/2017.

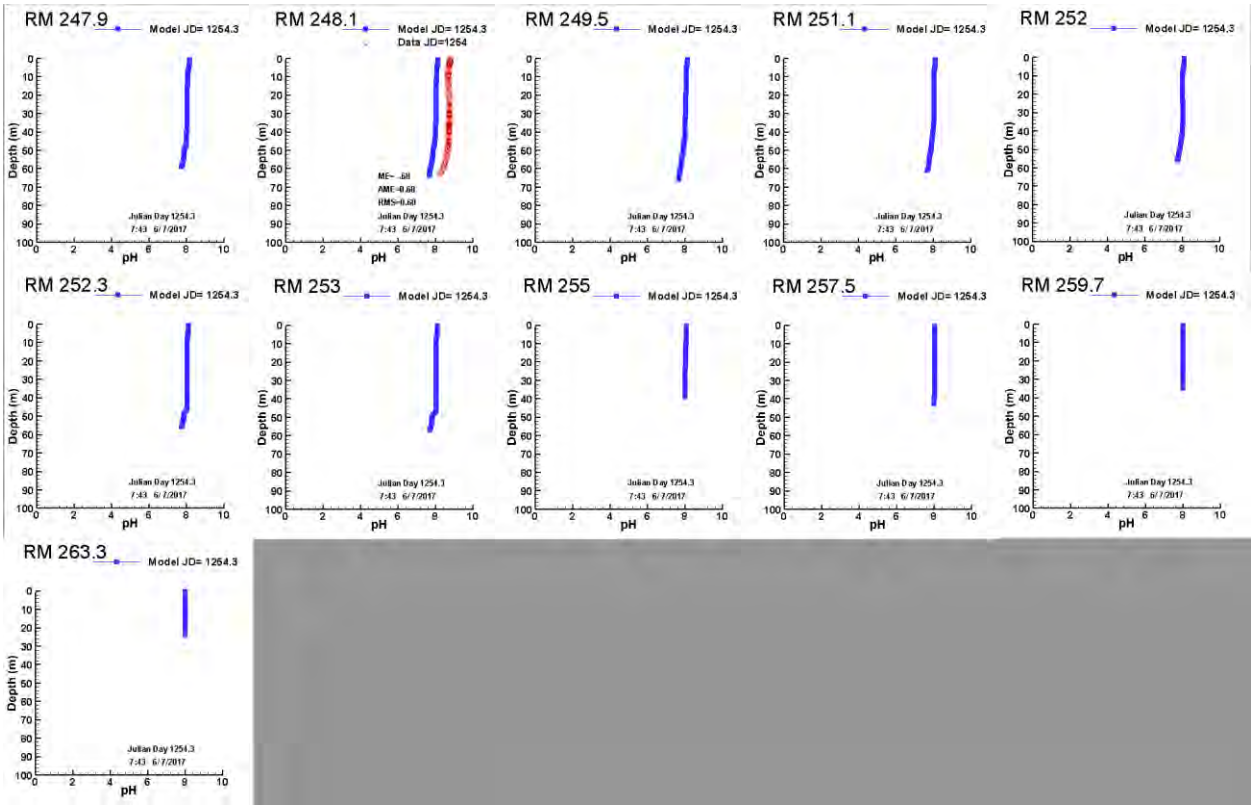


Figure 489. Vertical profiles of pH compared with data for 6/ 7/2017.

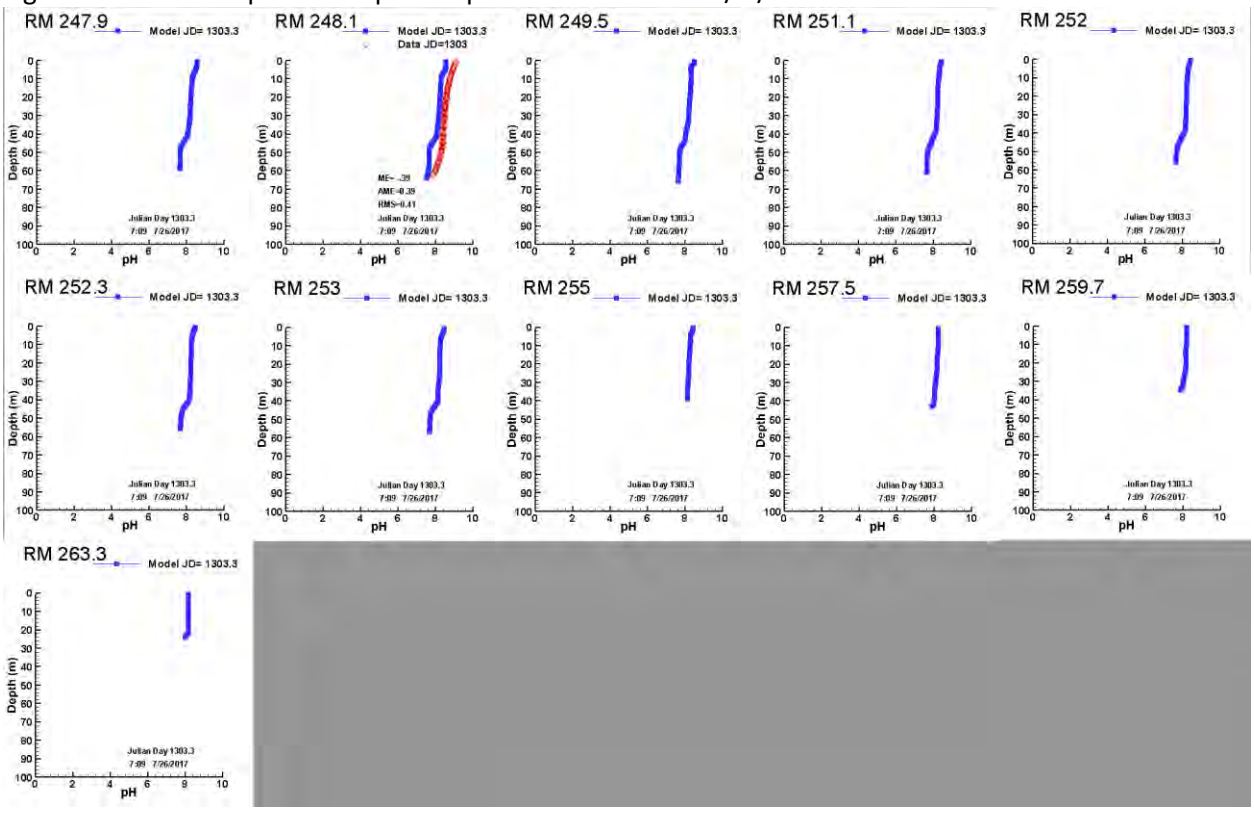


Figure 490. Vertical profiles of pH compared with data for 7/26/2017.

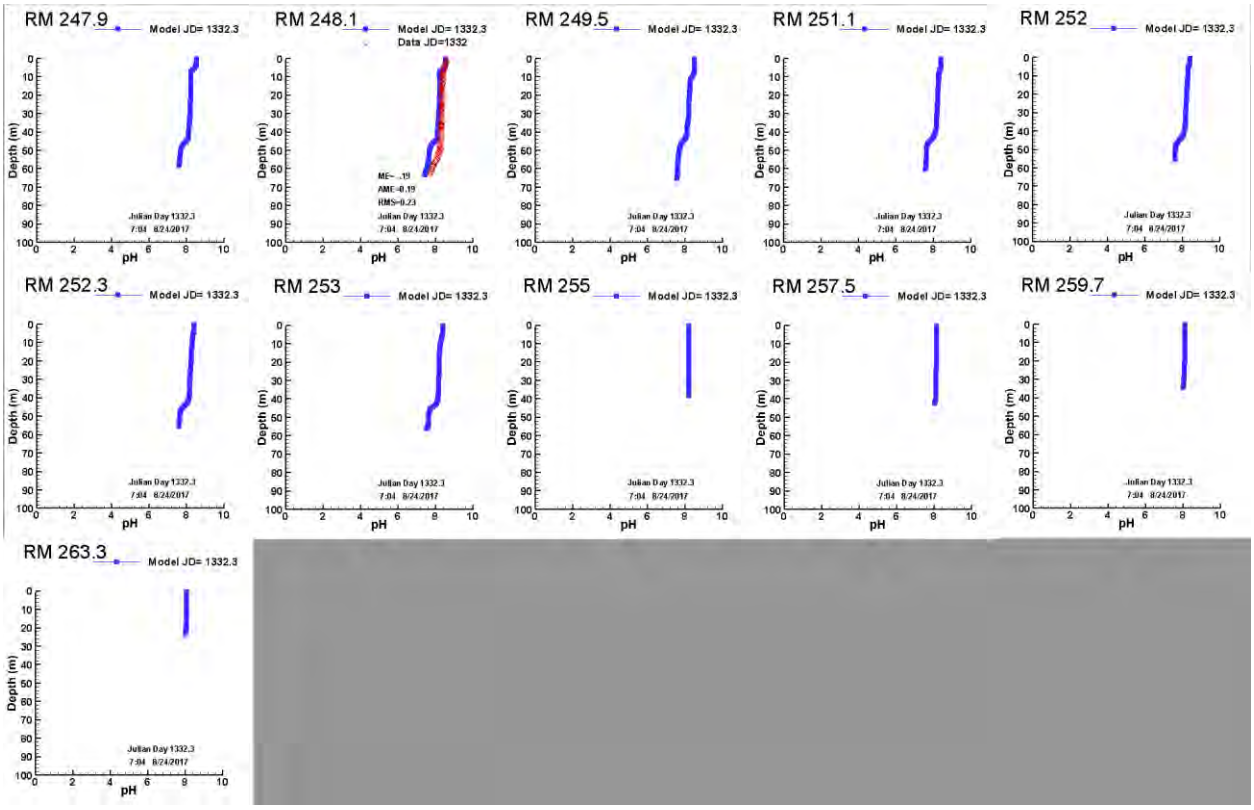


Figure 491. Vertical profiles of pH compared with data for 8/24/2017.

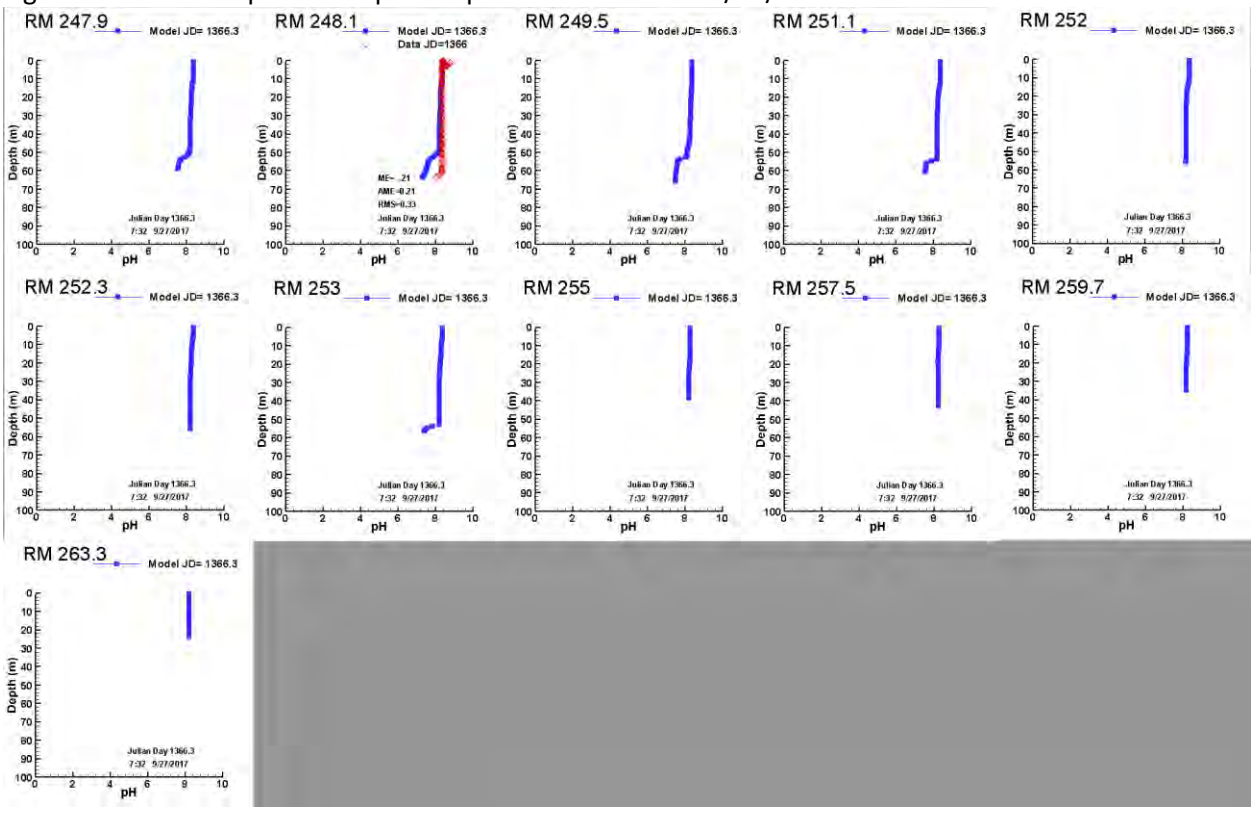


Figure 492. Vertical profiles of pH compared with data for 9/27/2017.

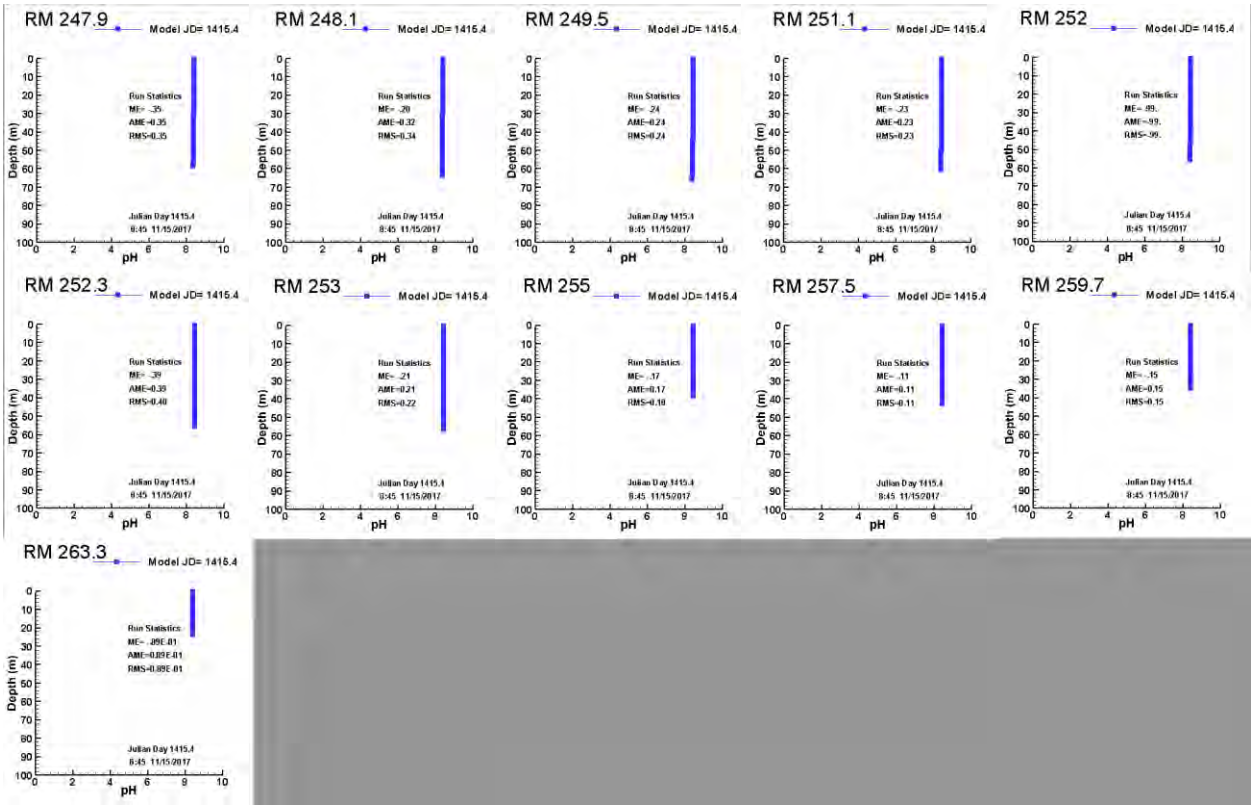


Figure 493. Vertical profiles of pH compared with data for 11/15/2017.

Temperature

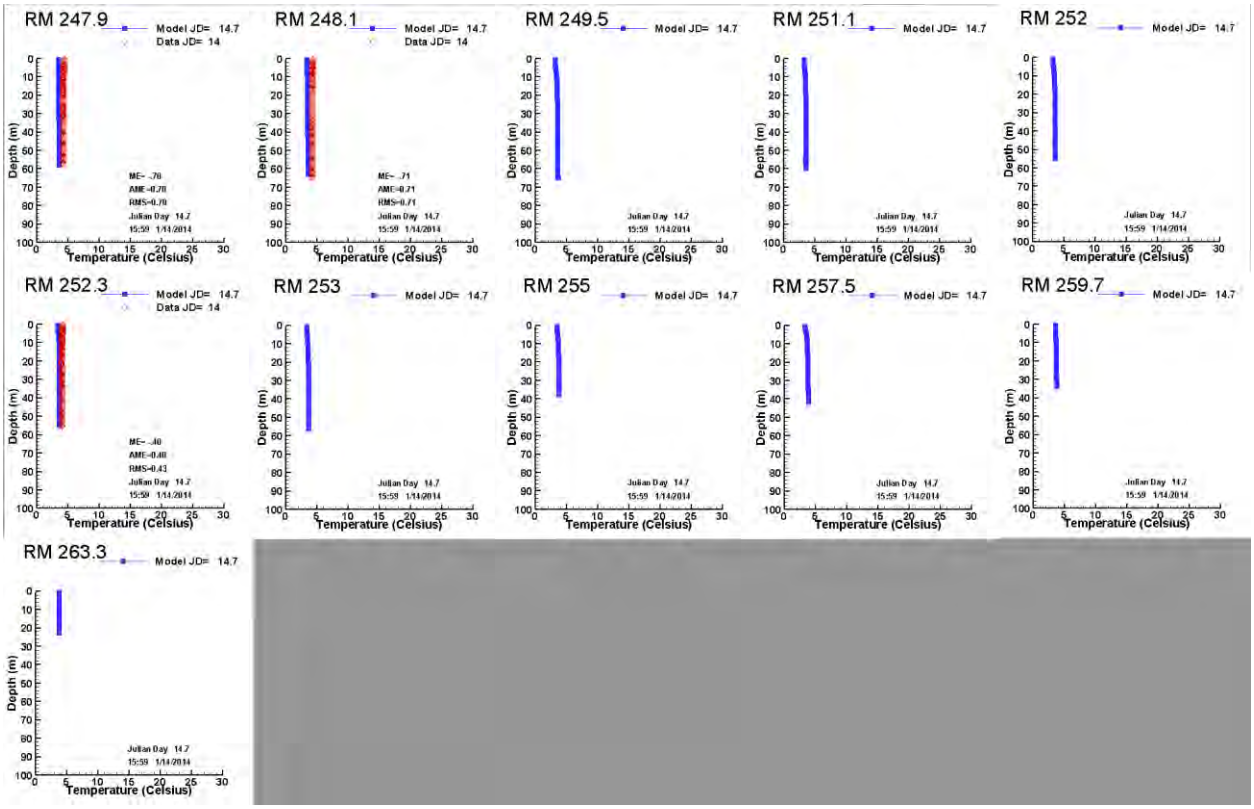


Figure 494. Vertical profiles of temperature compared with data for 1/14/2014.

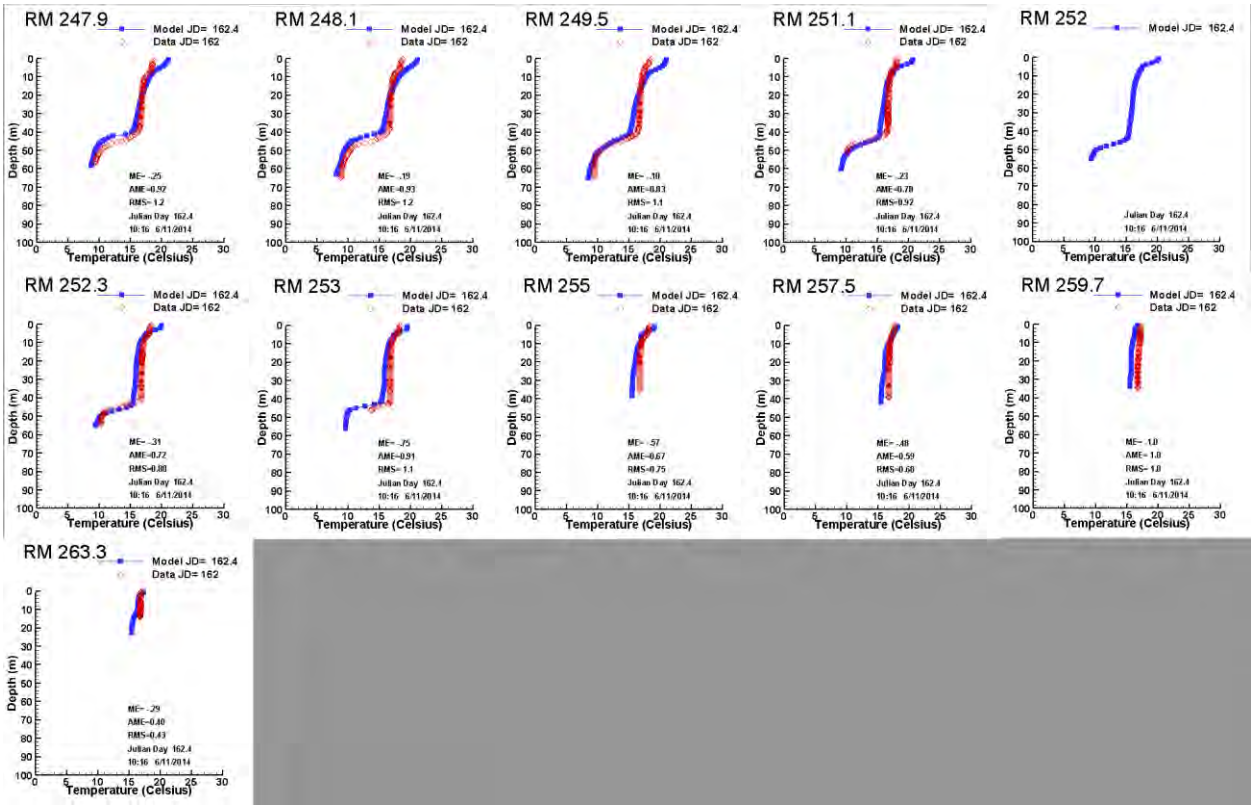


Figure 495. Vertical profiles of temperature compared with data for 6/11/2014.

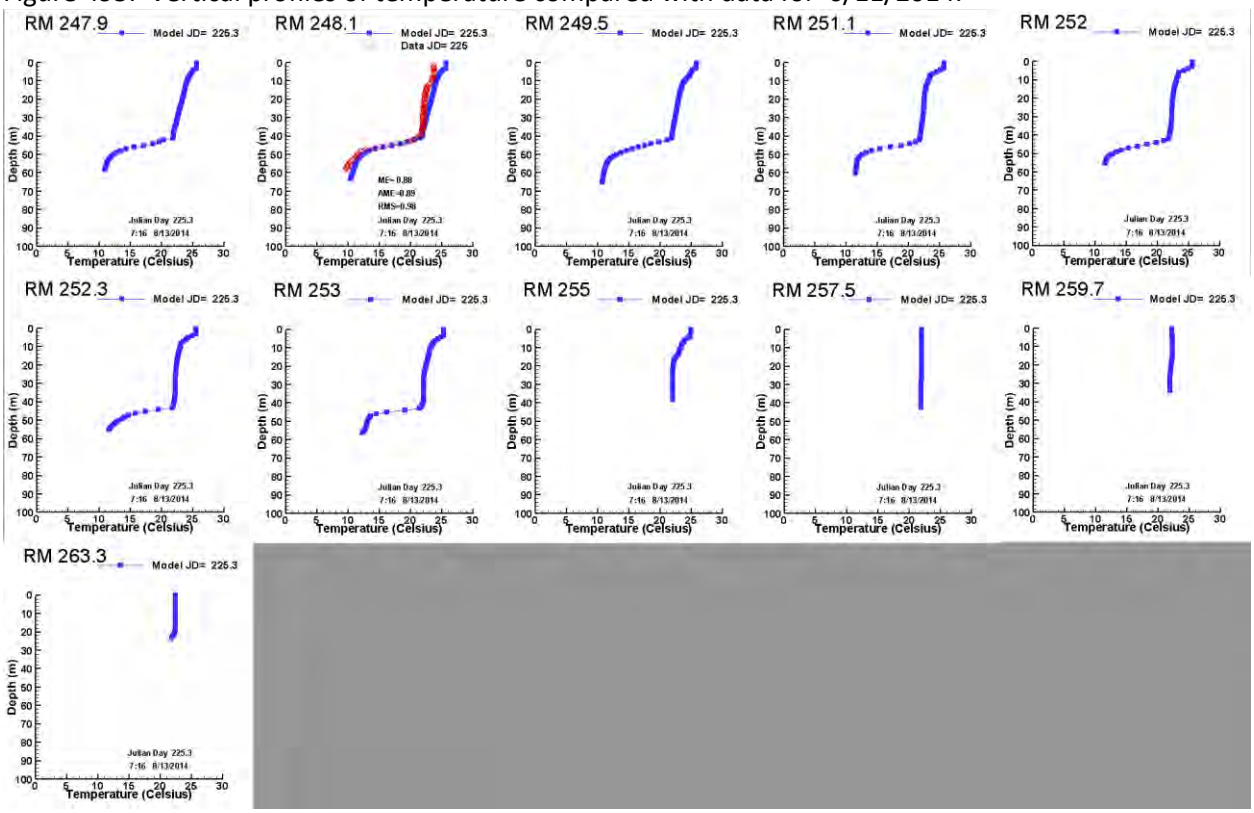


Figure 496. Vertical profiles of temperature compared with data for 8/13/2014.

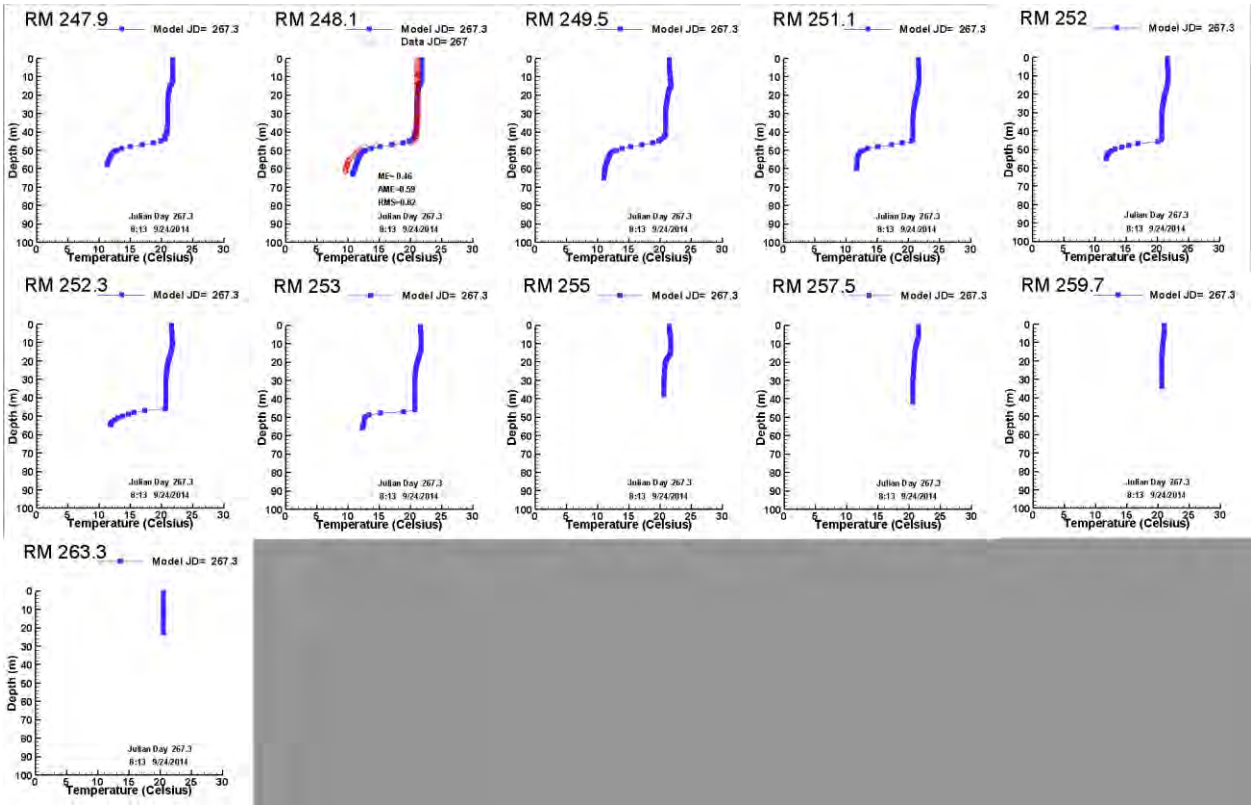


Figure 497. Vertical profiles of temperature compared with data for 9/24/2014.

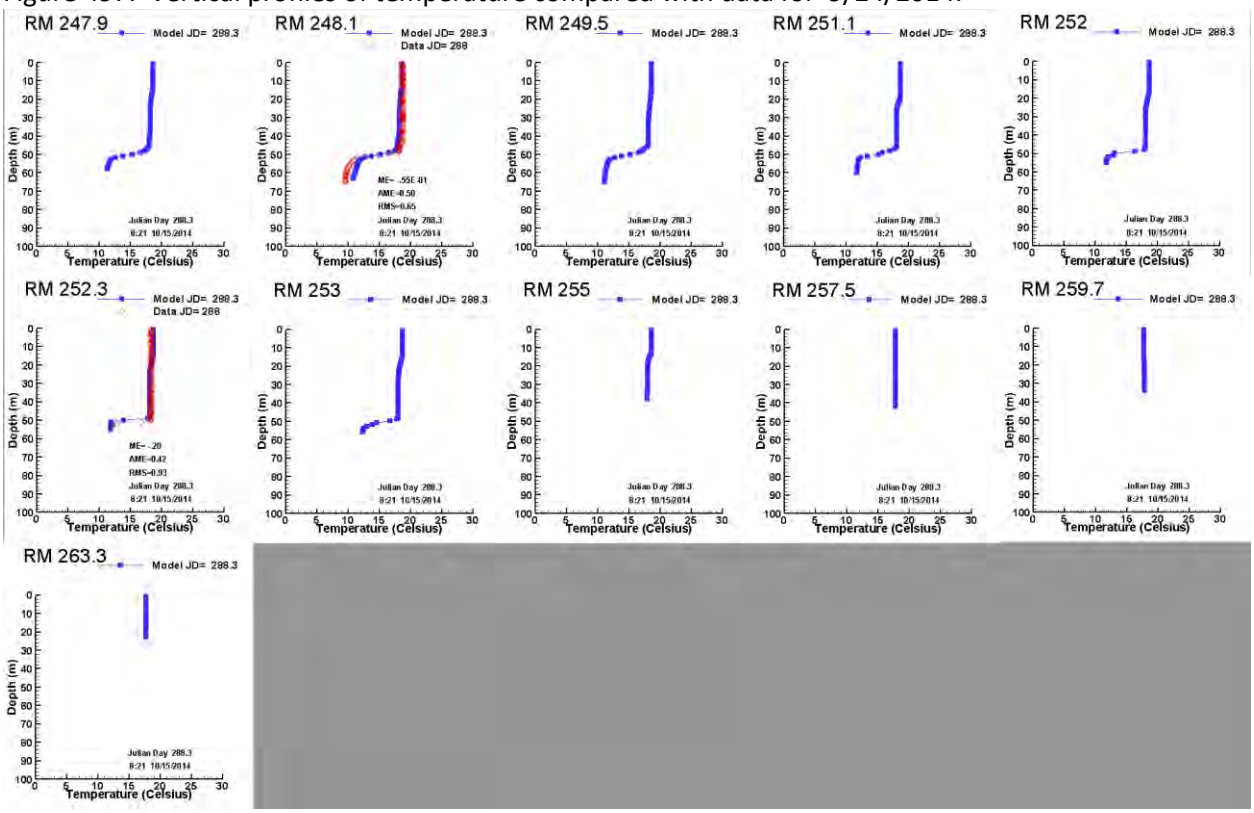


Figure 498. Vertical profiles of temperature compared with data for 10/15/2014.

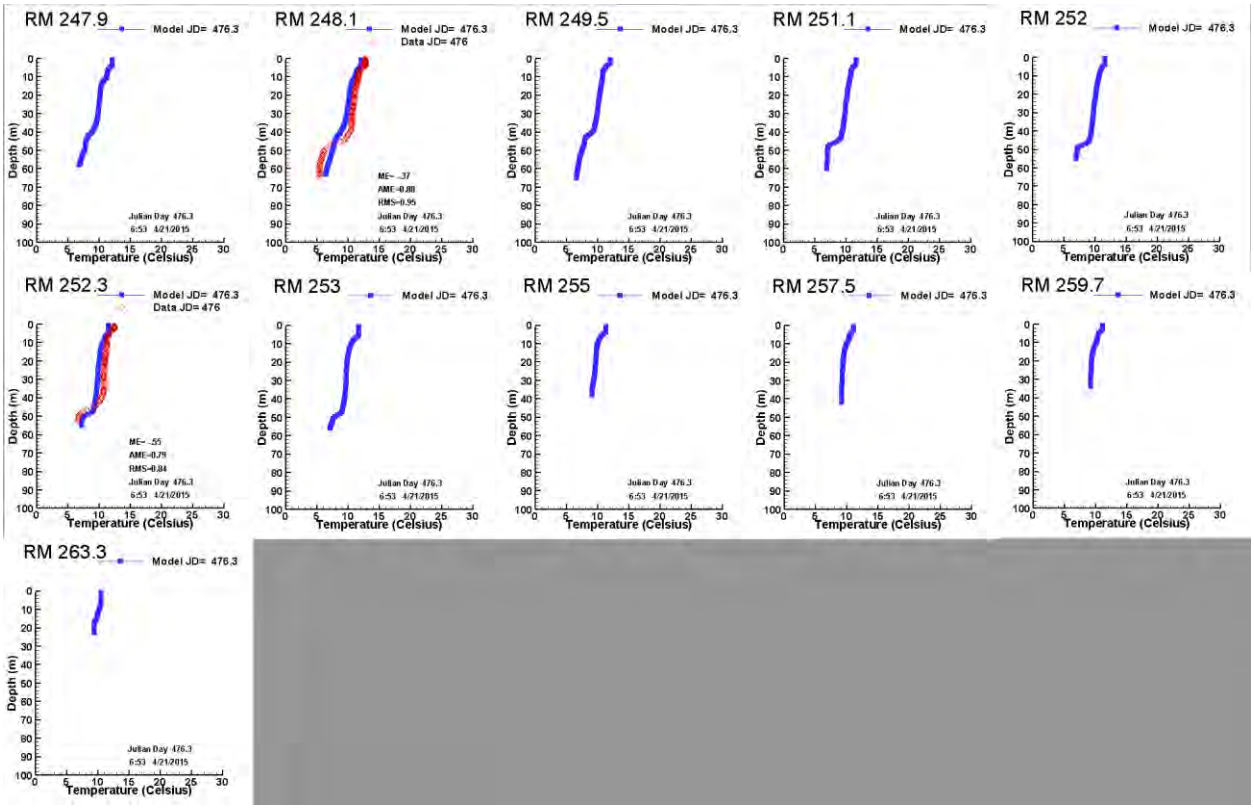


Figure 499. Vertical profiles of temperature compared with data for 4/21/2015.

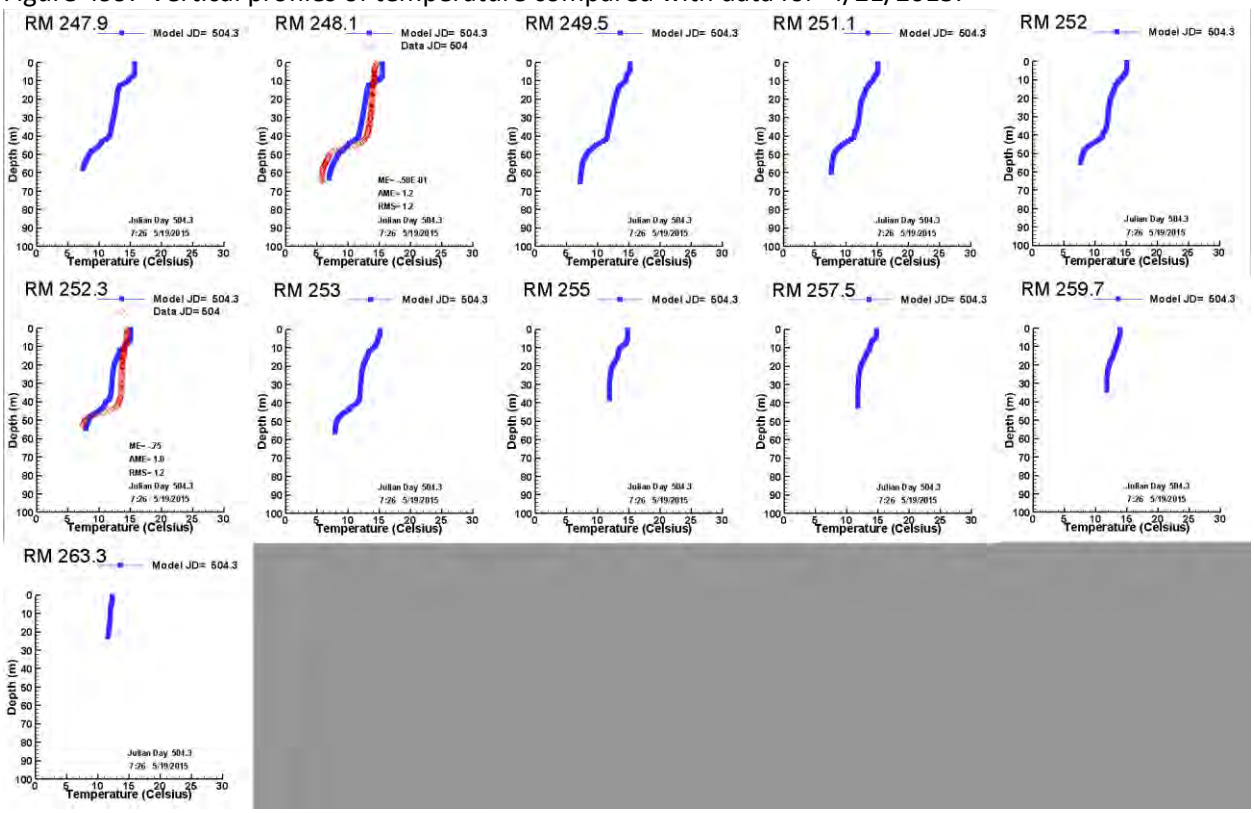


Figure 500. Vertical profiles of temperature compared with data for 5/19/2015.

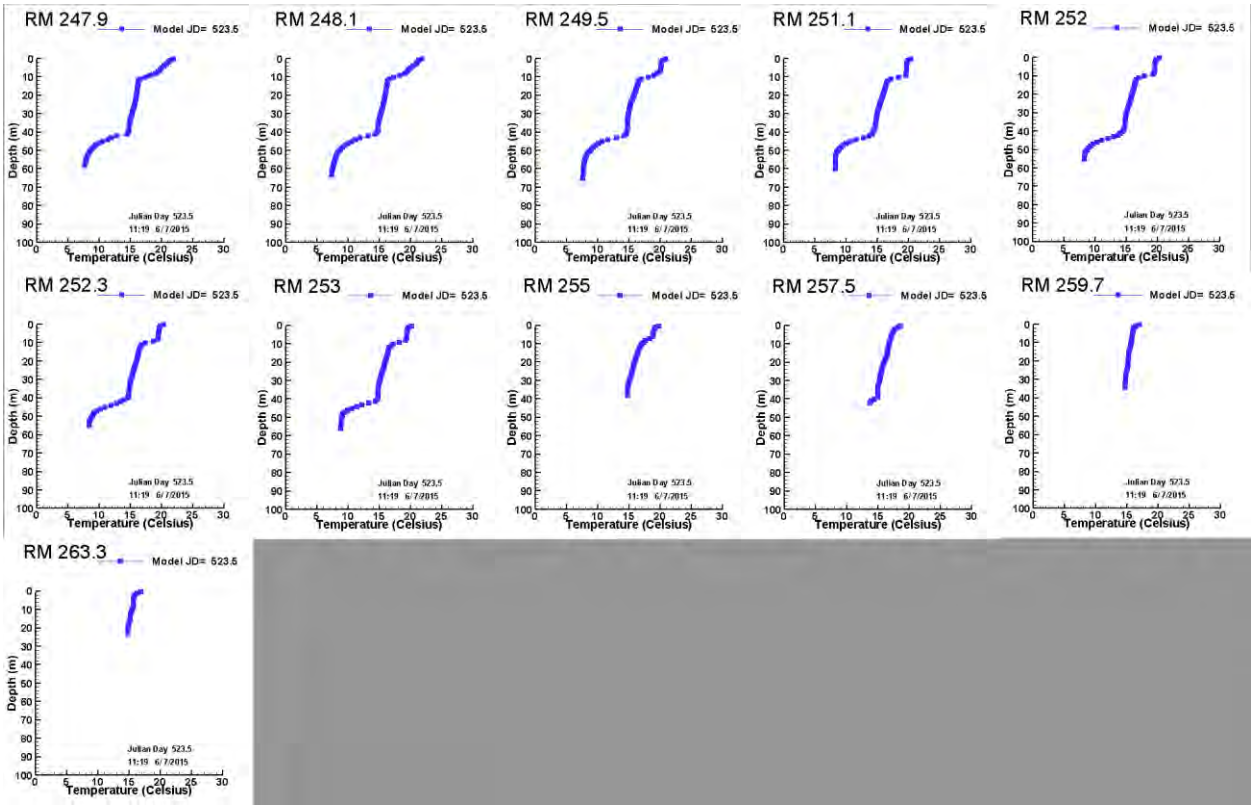


Figure 501. Vertical profiles of temperature compared with data for 6/ 7/2015.

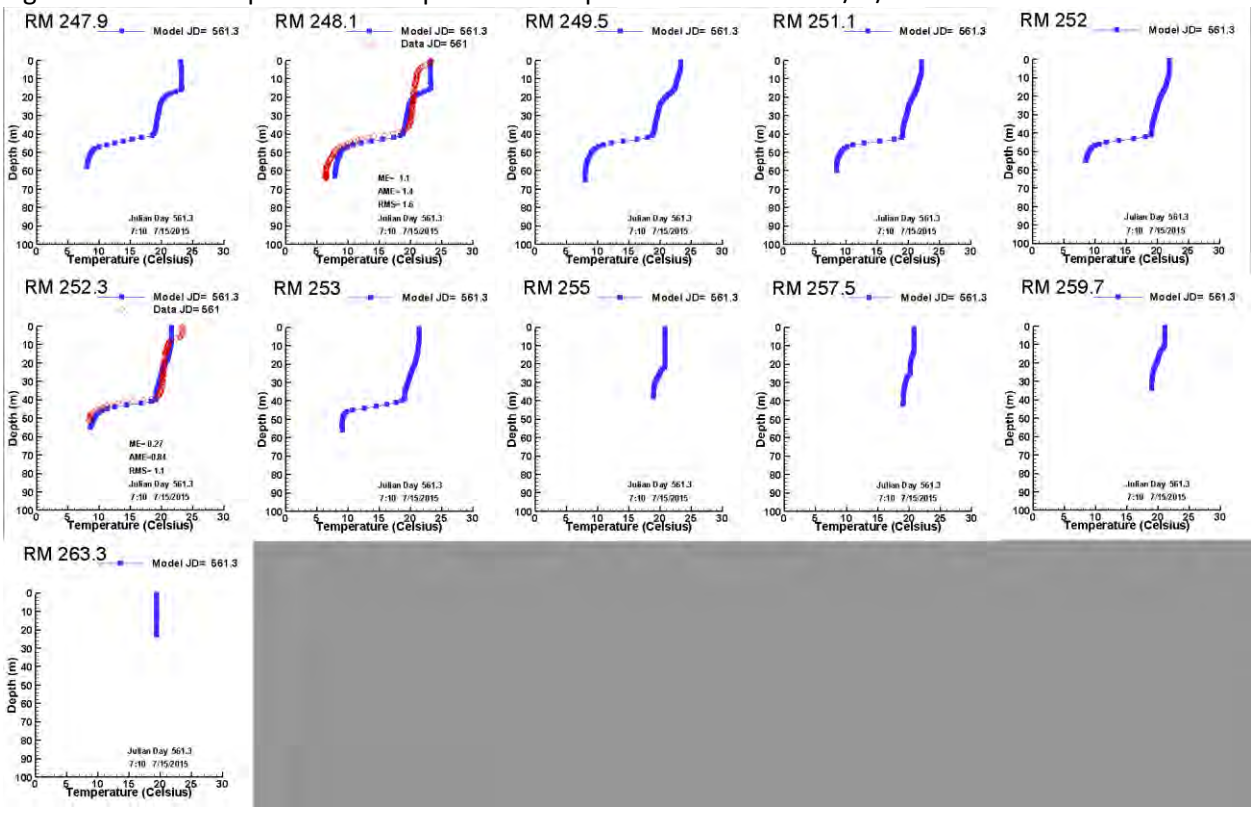


Figure 502. Vertical profiles of temperature compared with data for 7/15/2015.

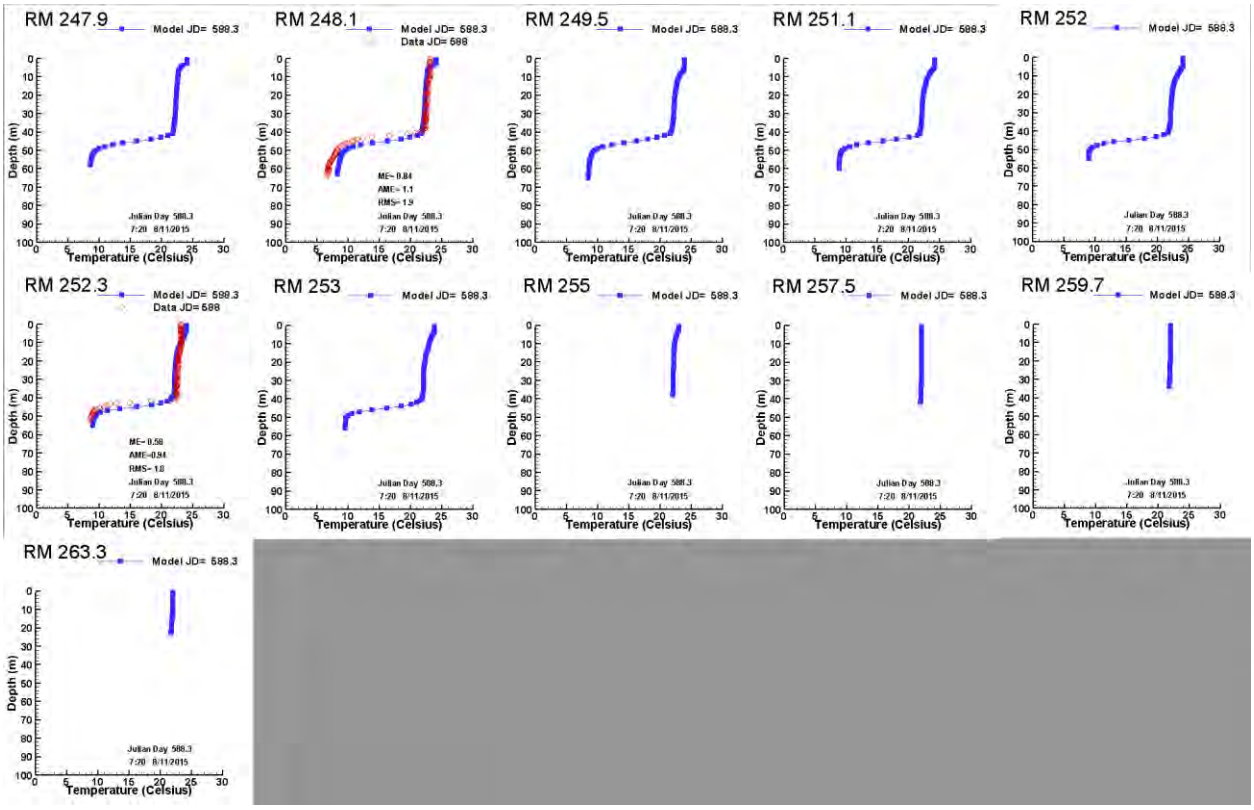


Figure 503. Vertical profiles of temperature compared with data for 8/11/2015.

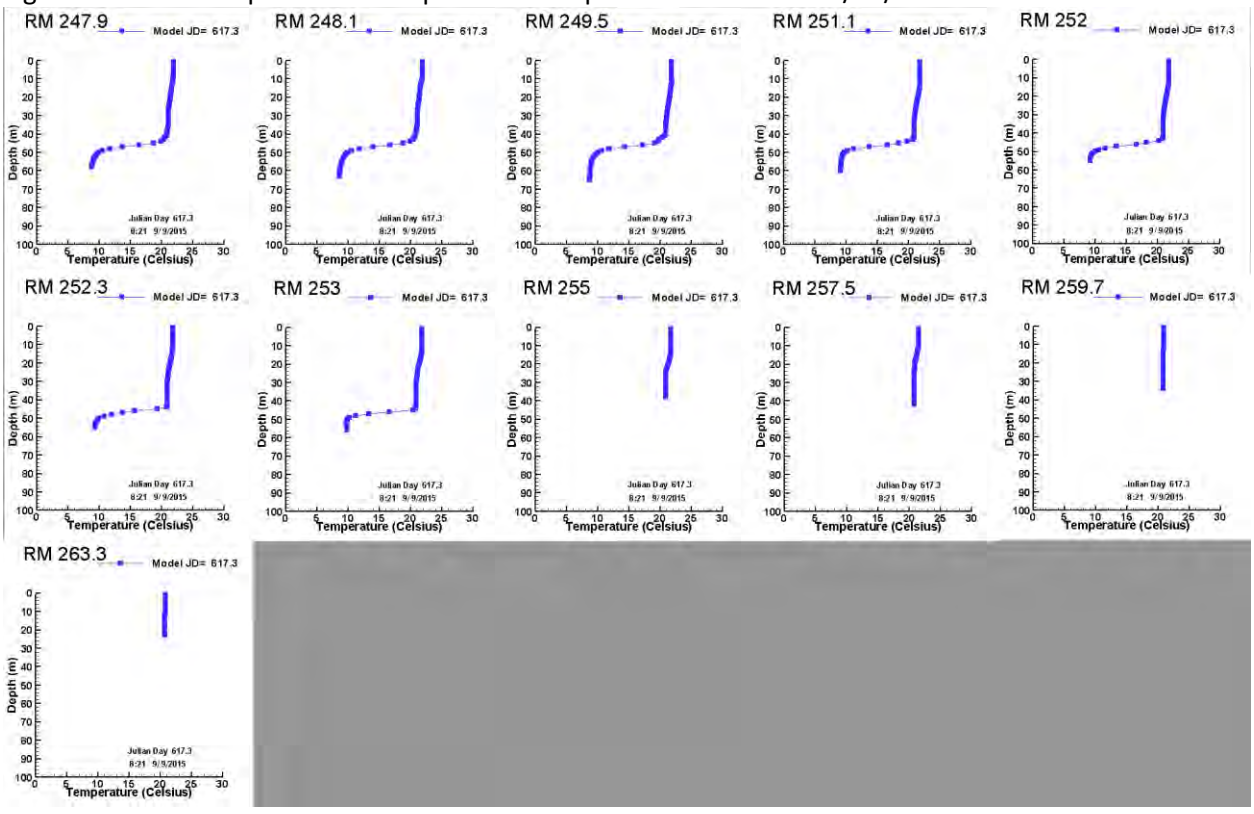


Figure 504. Vertical profiles of temperature compared with data for 9/ 9/2015.

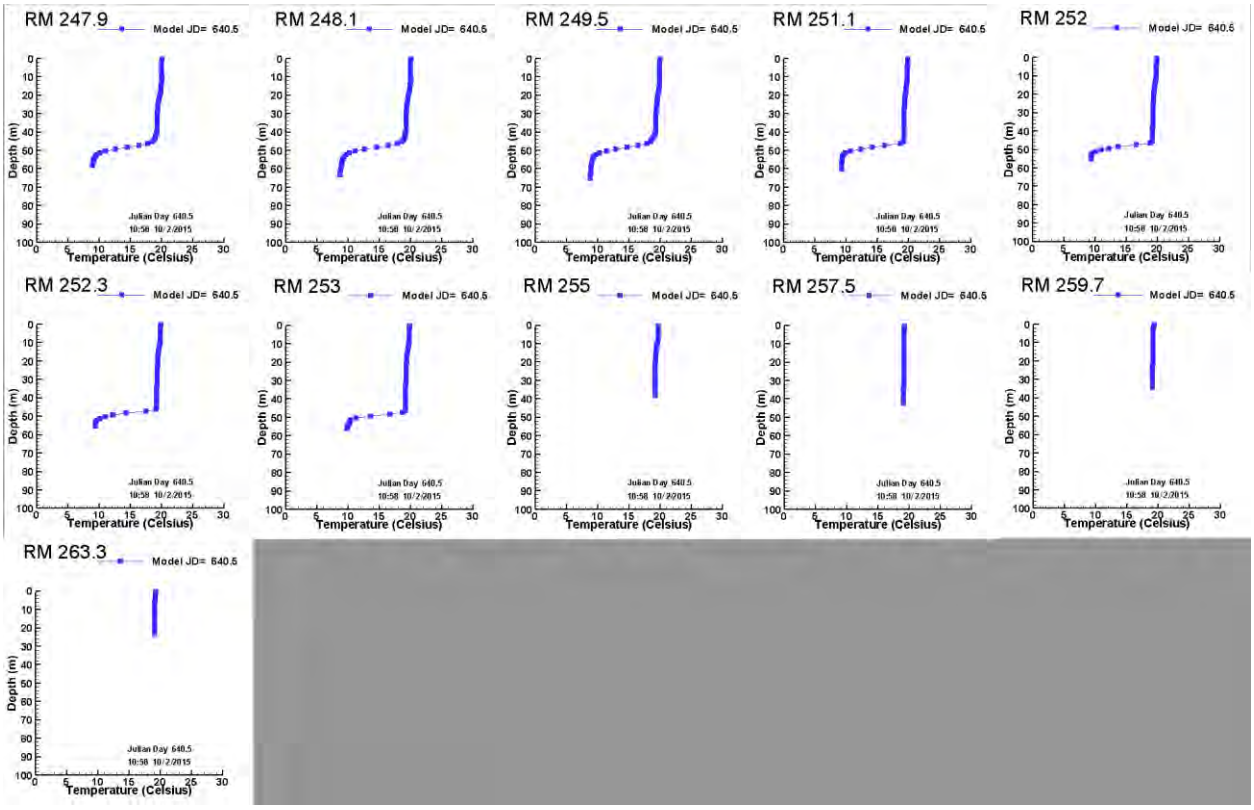


Figure 505. Vertical profiles of temperature compared with data for 10/ 2/2015.

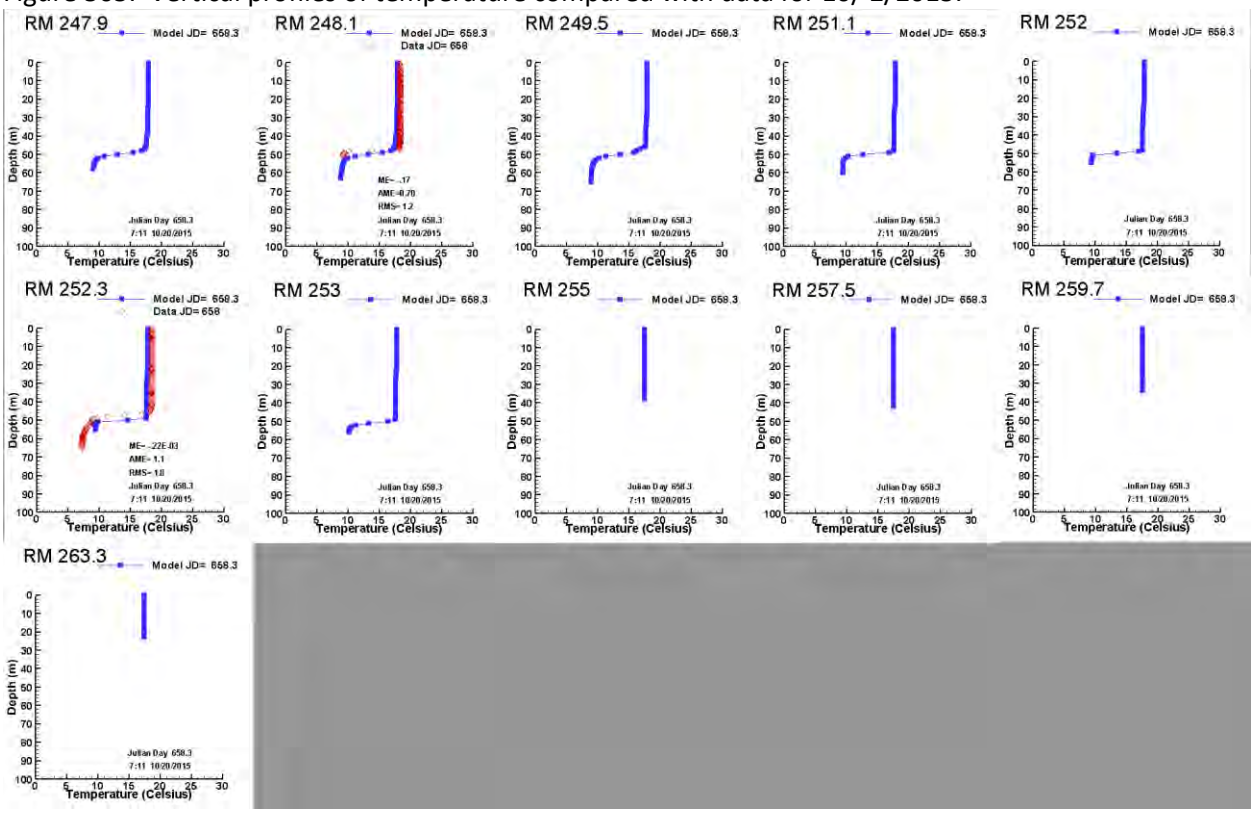


Figure 506. Vertical profiles of temperature compared with data for 10/20/2015.

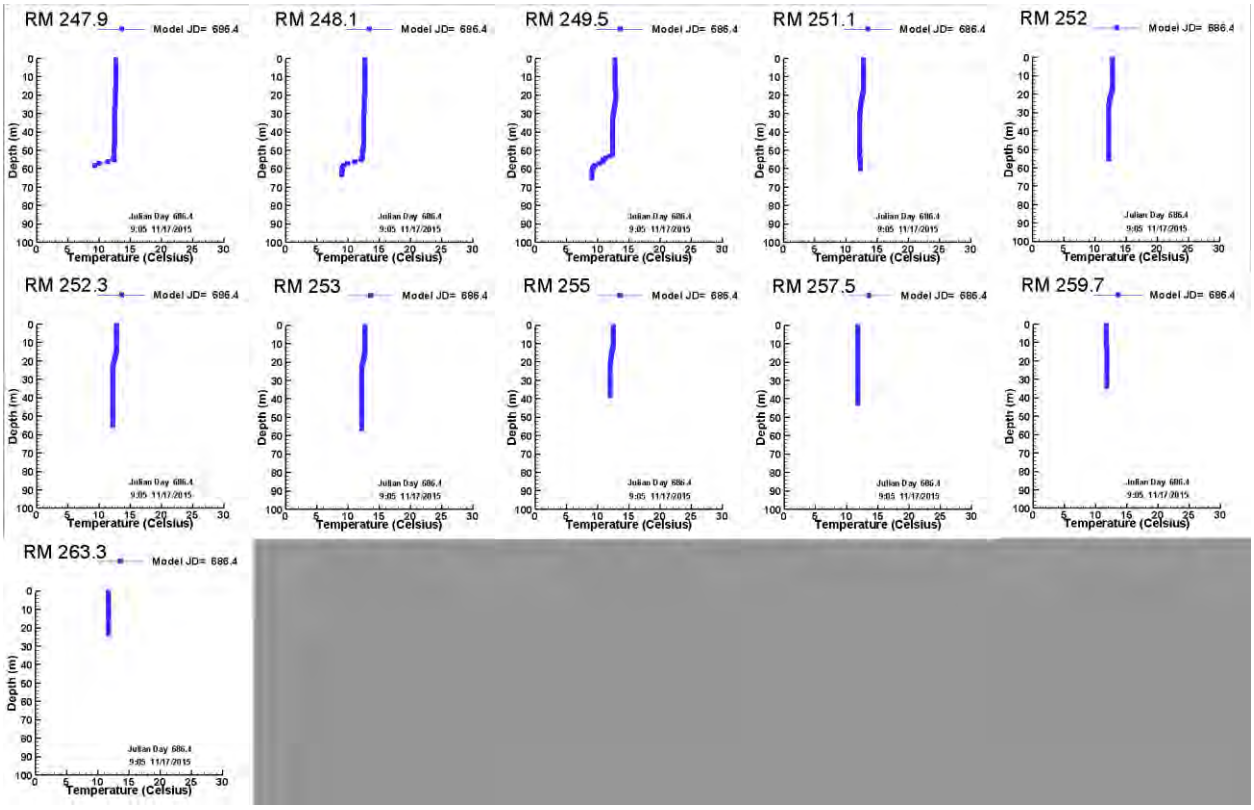


Figure 507. Vertical profiles of temperature compared with data for 11/17/2015.

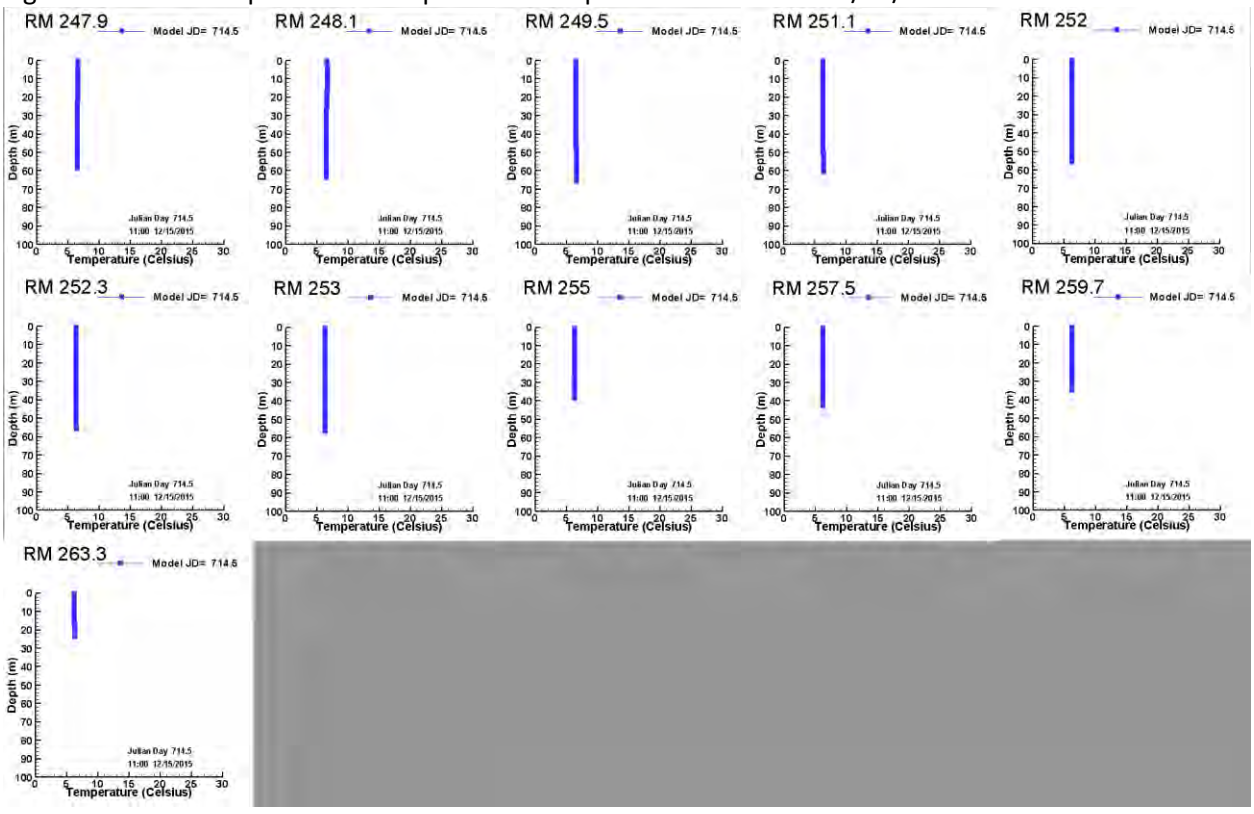


Figure 508. Vertical profiles of temperature compared with data for 12/15/2015.

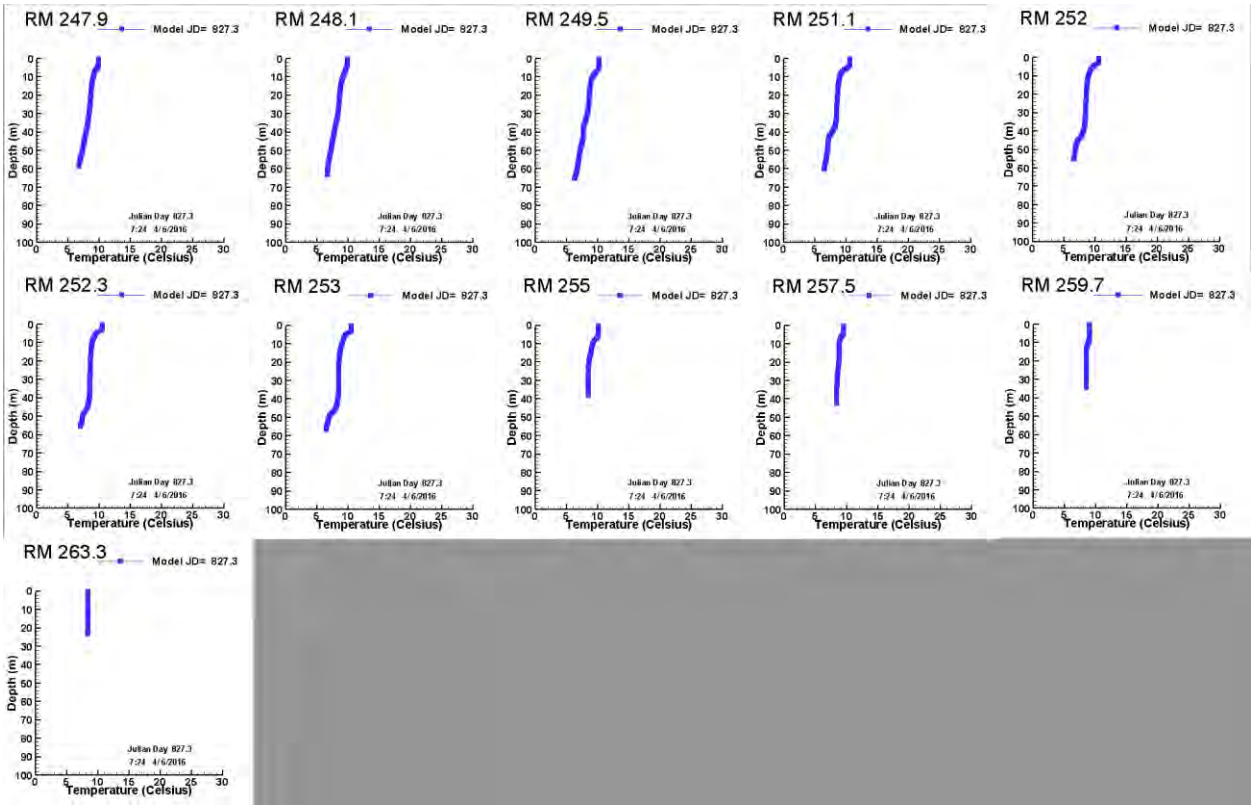


Figure 509. Vertical profiles of temperature compared with data for 4/ 6/2016.

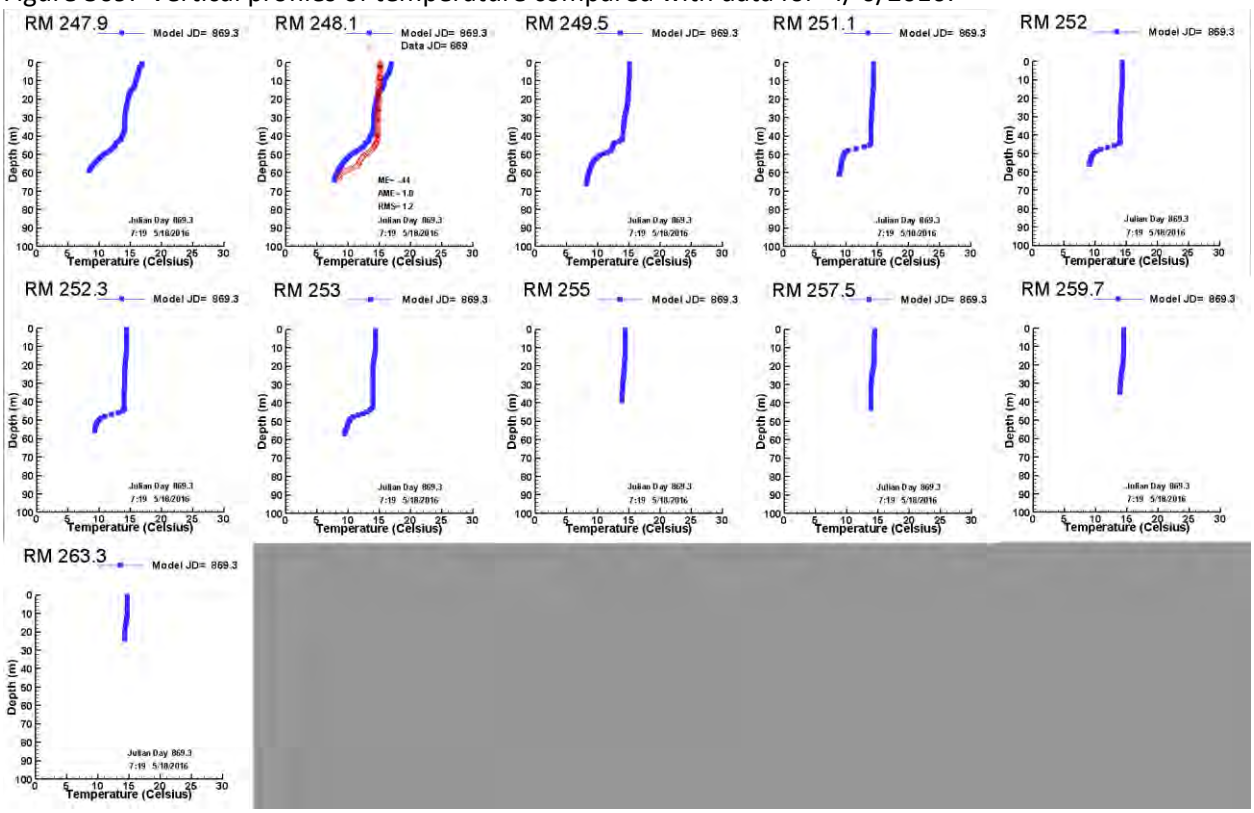


Figure 510. Vertical profiles of temperature compared with data for 5/18/2016.

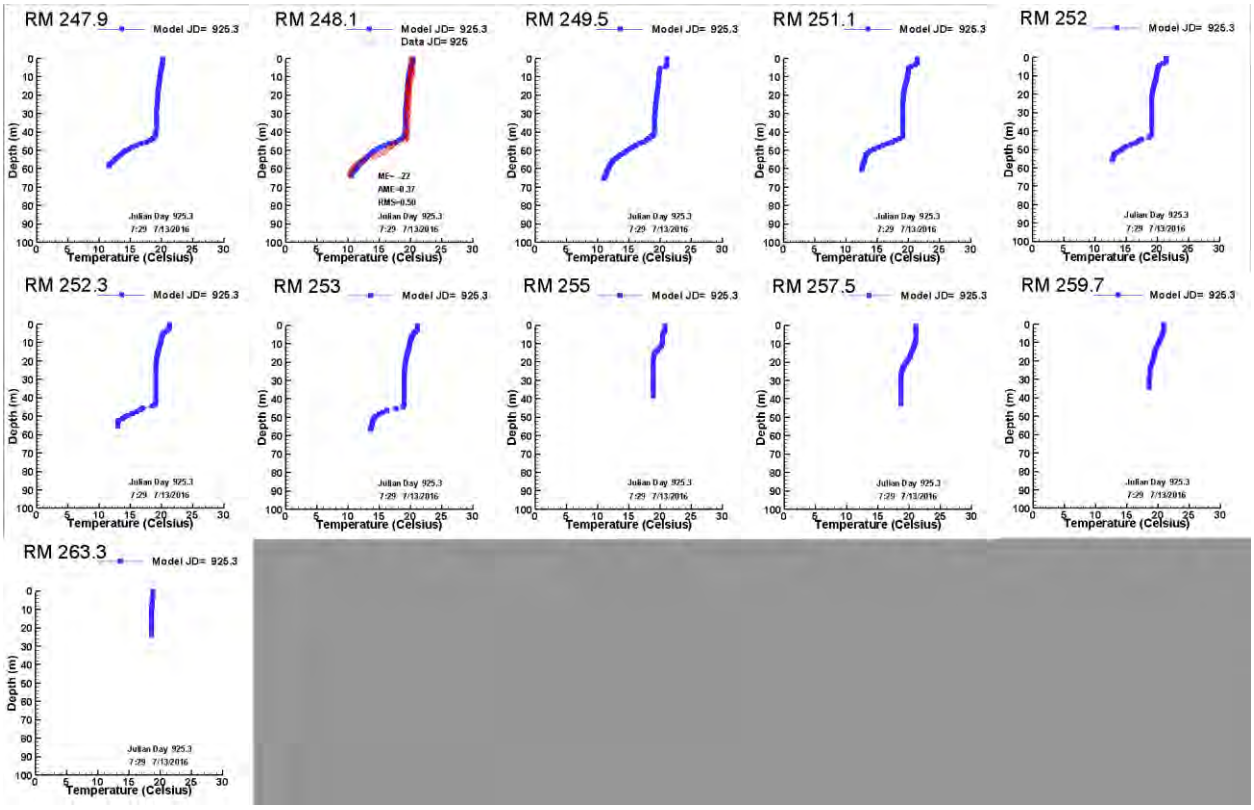


Figure 511. Vertical profiles of temperature compared with data for 7/13/2016.

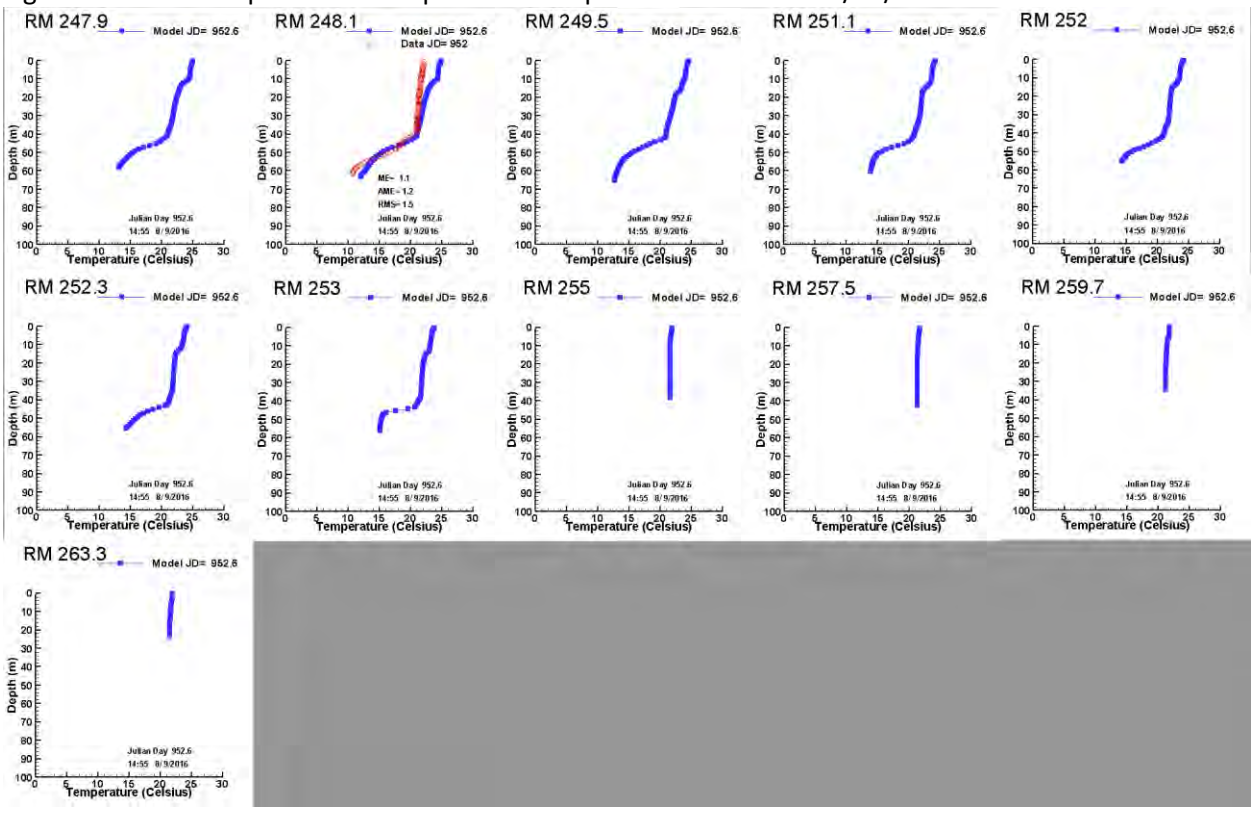


Figure 512. Vertical profiles of temperature compared with data for 8/ 9/2016.

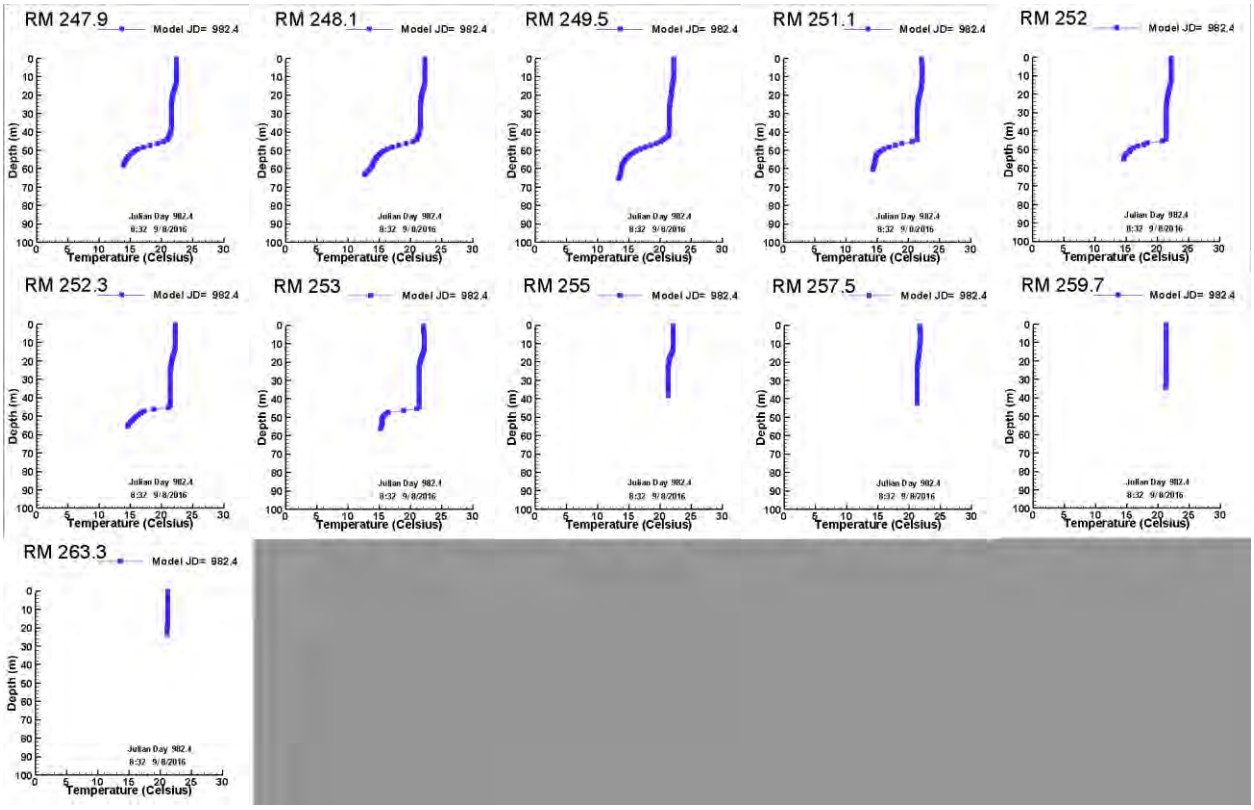


Figure 513. Vertical profiles of temperature compared with data for 9/ 8/2016.

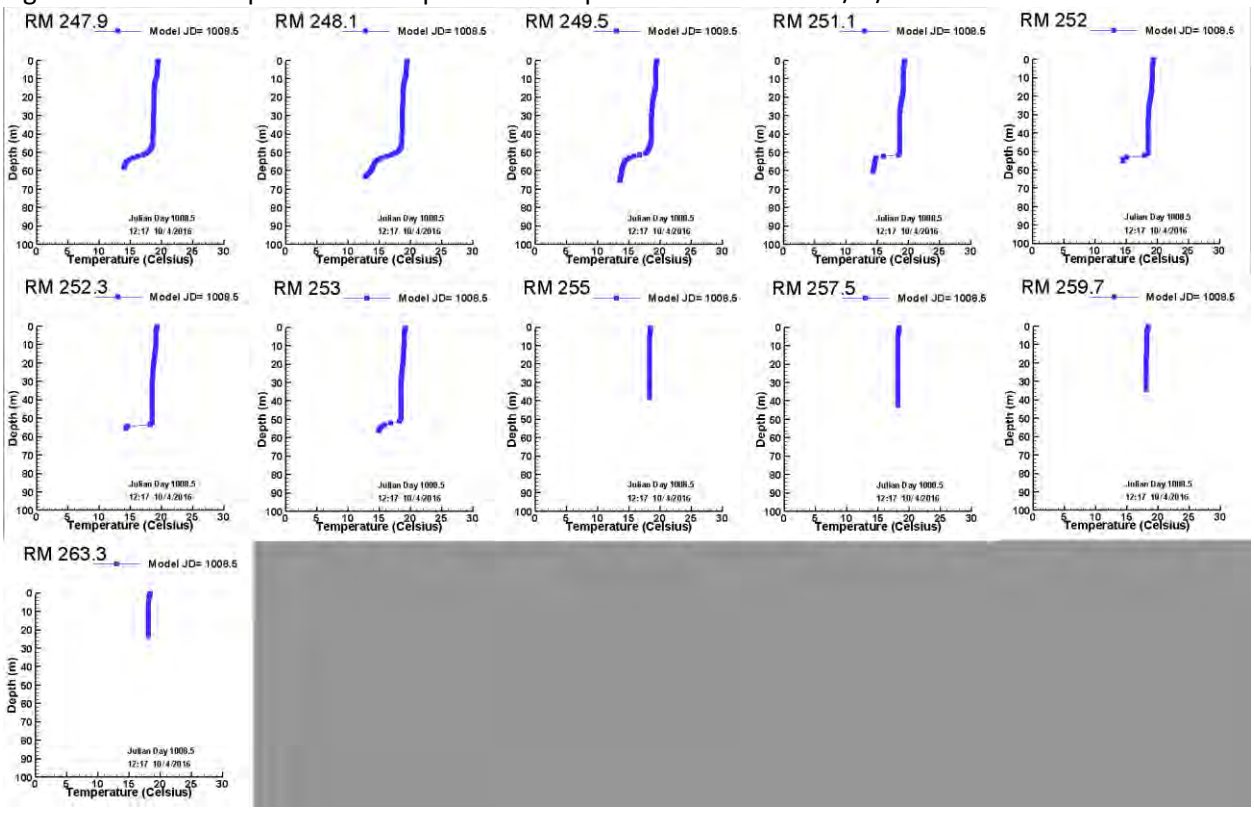


Figure 514. Vertical profiles of temperature compared with data for 10/ 4/2016.

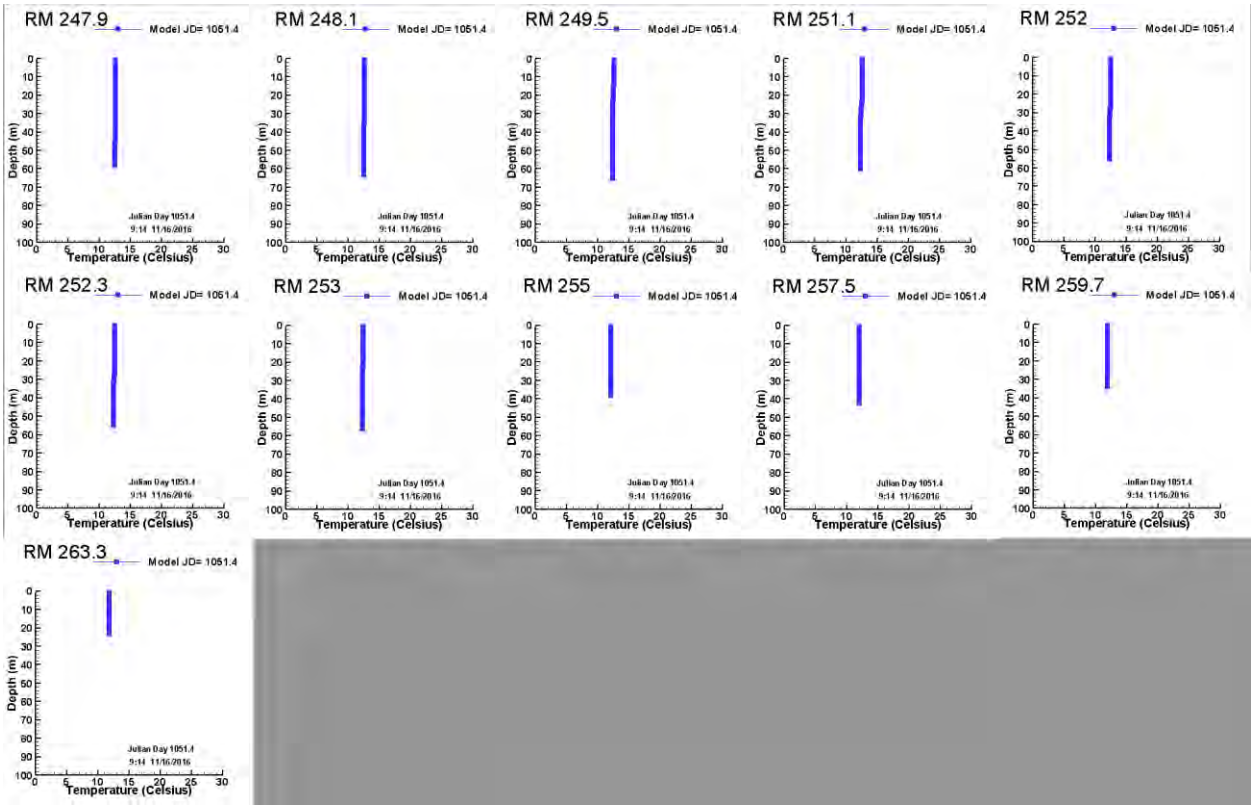


Figure 515. Vertical profiles of temperature compared with data for 11/16/2016.

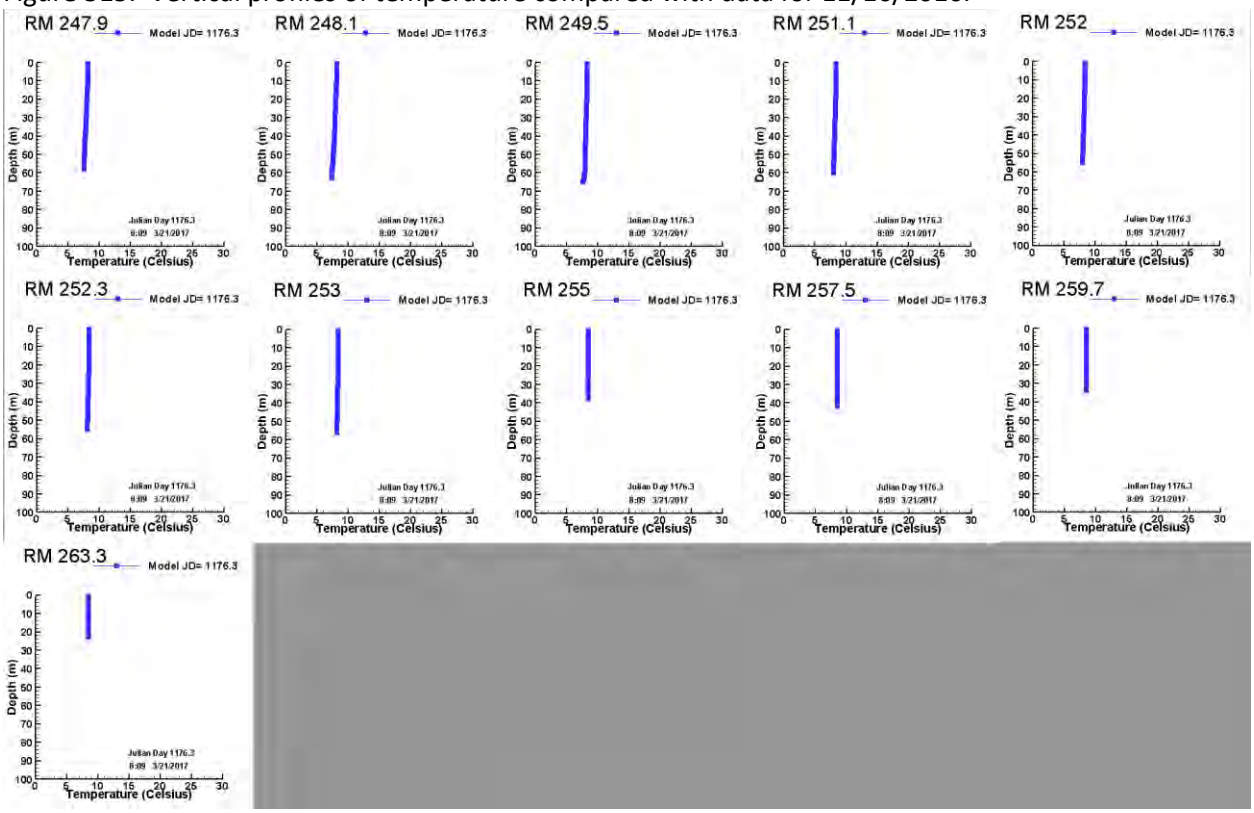


Figure 516. Vertical profiles of temperature compared with data for 3/21/2017.

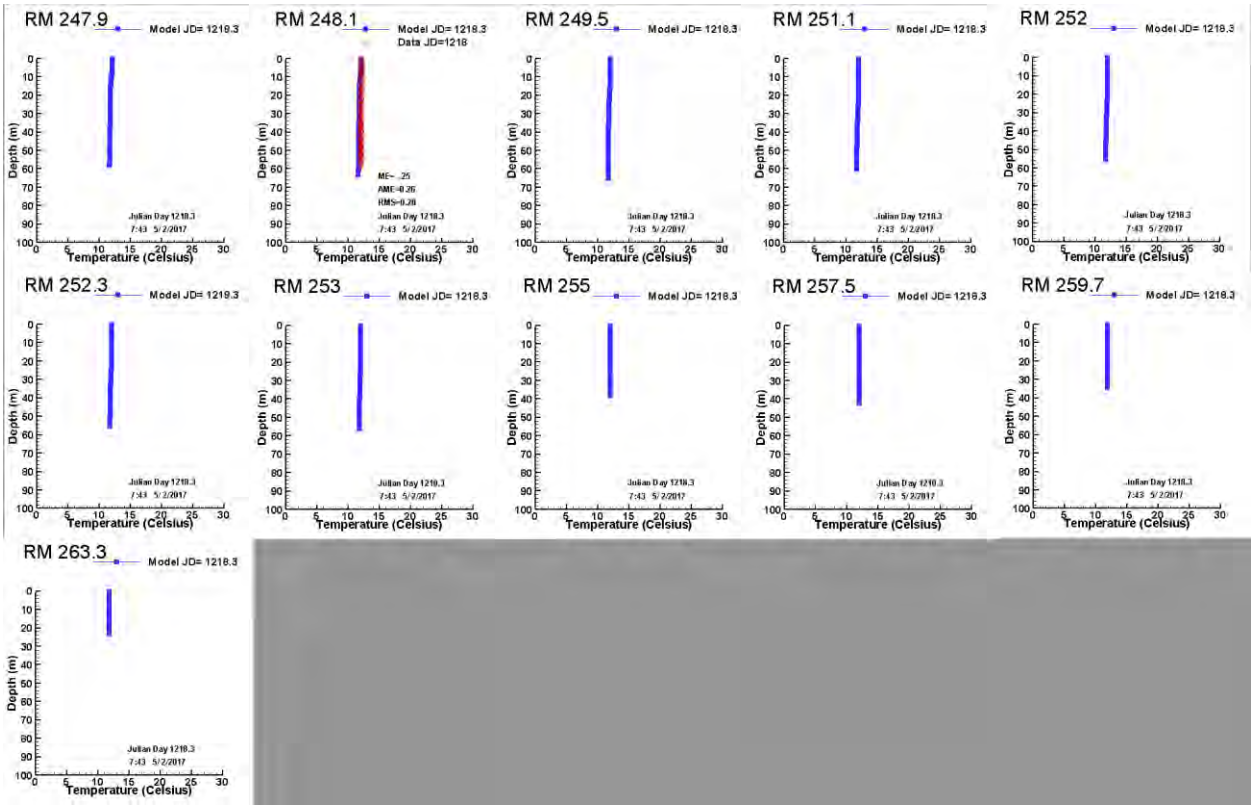


Figure 517. Vertical profiles of temperature compared with data for 5/ 2/2017.

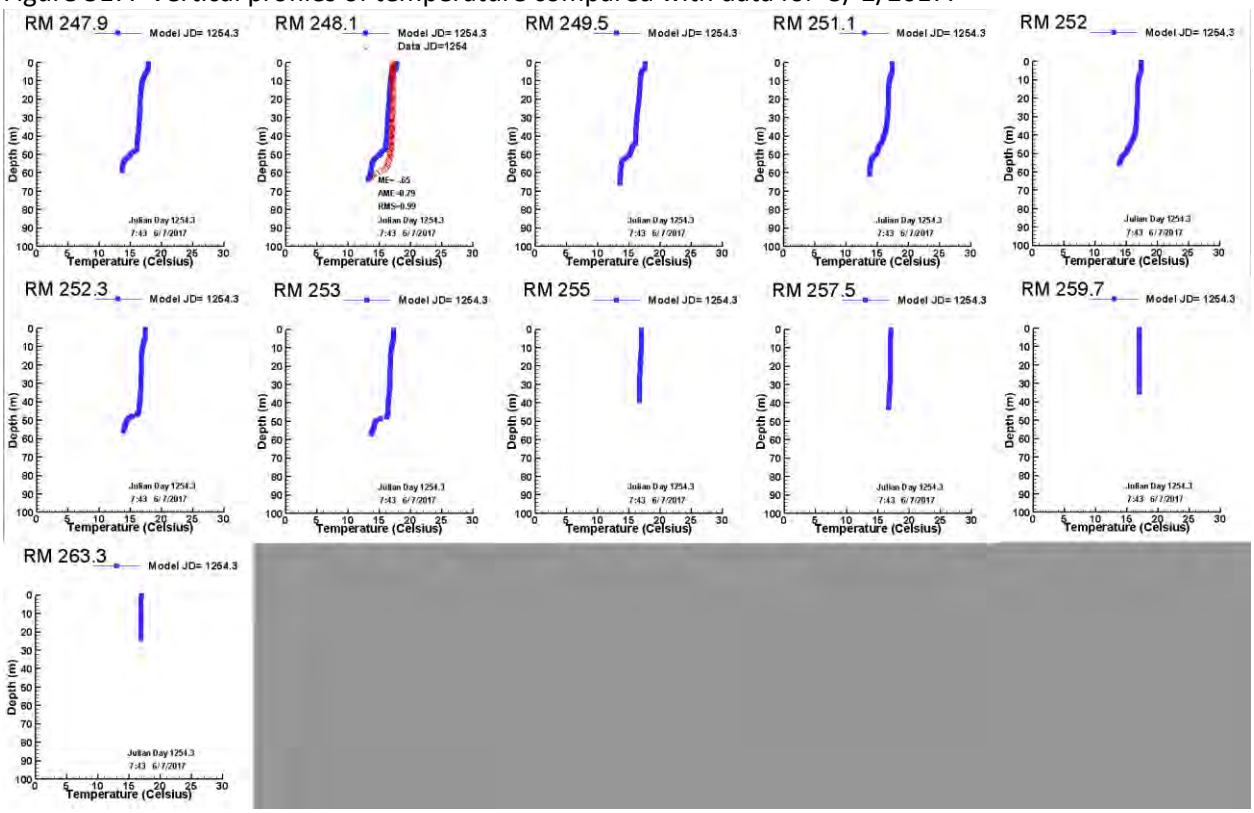


Figure 518. Vertical profiles of temperature compared with data for 6/ 7/2017.

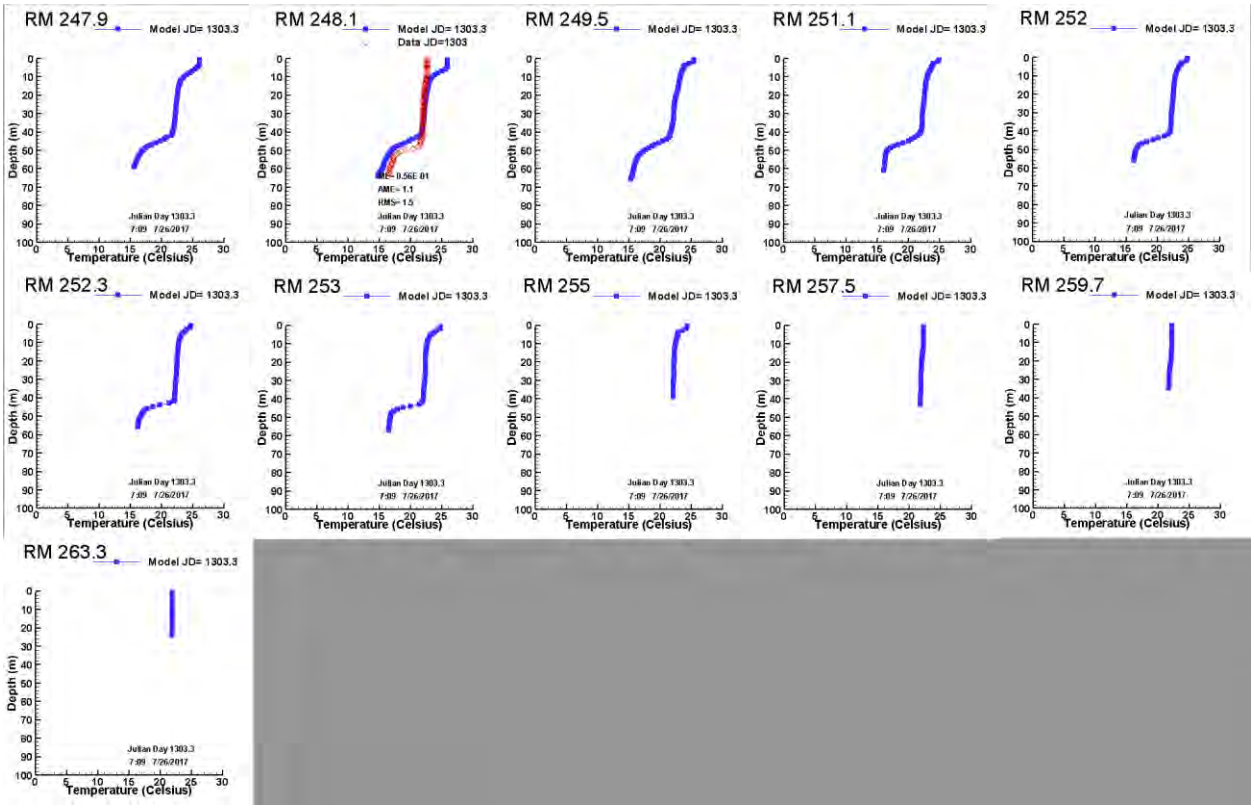


Figure 519. Vertical profiles of temperature compared with data for 7/26/2017.

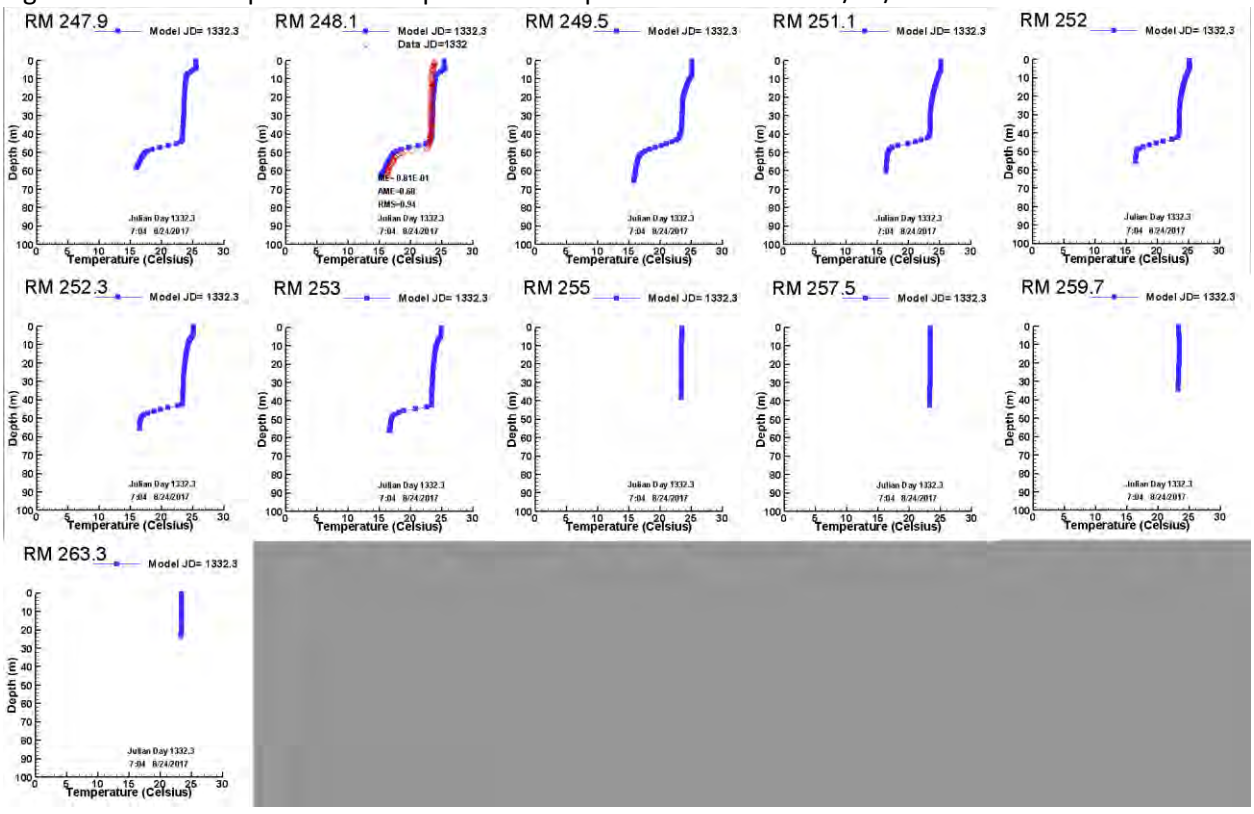


Figure 520. Vertical profiles of temperature compared with data for 8/24/2017.

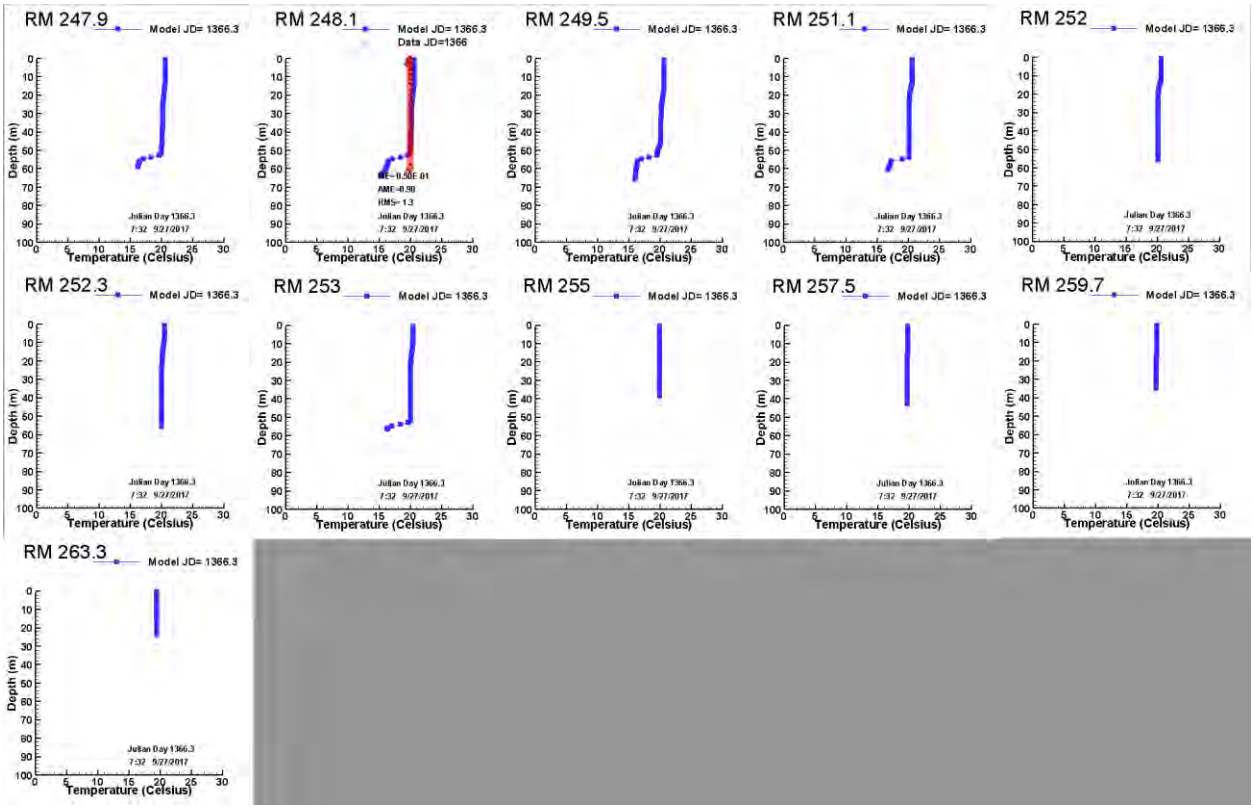


Figure 521. Vertical profiles of temperature compared with data for 9/27/2017.

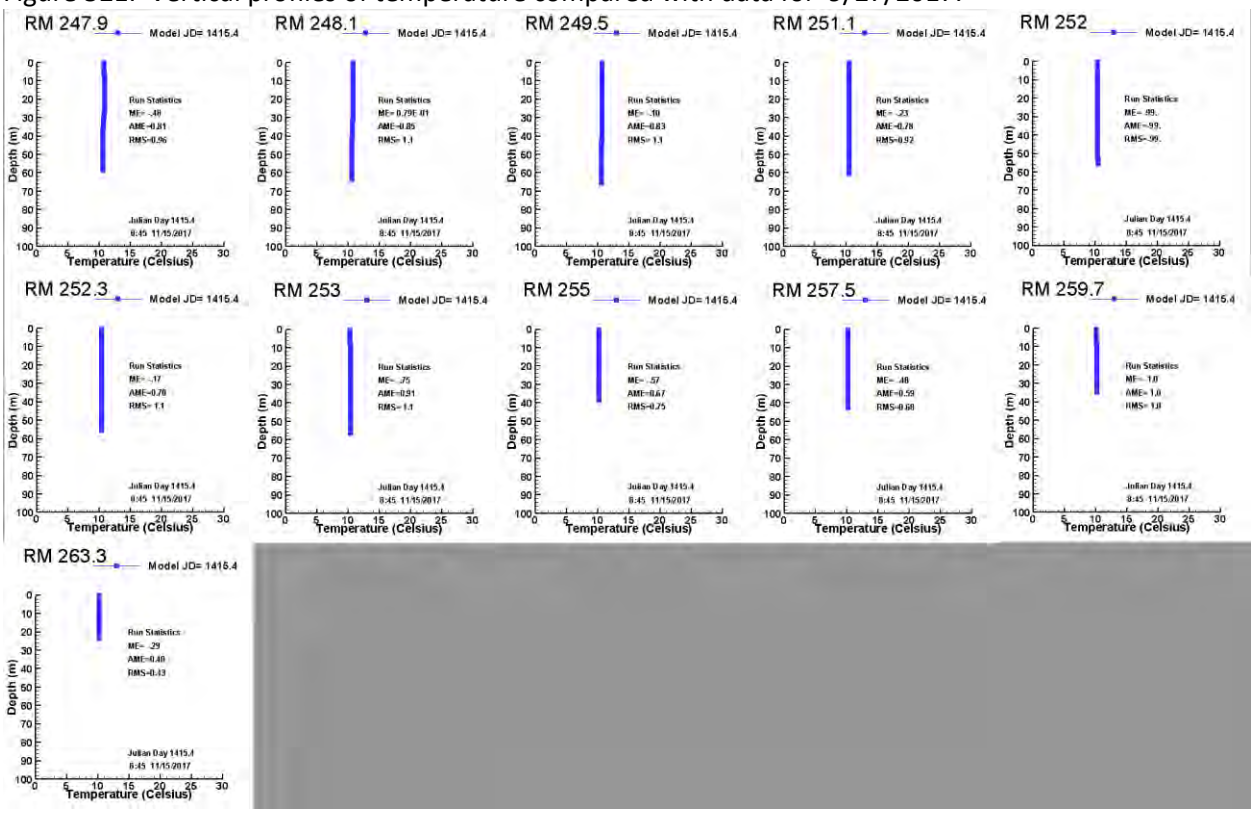


Figure 522. Vertical profiles of temperature compared with data for 11/15/2017.

Appendix A7 Brownlee Reservoir Continuous Temperature and DO Predictions

Temperature

Statistics

Table 1. Error statistics for continuous temperature data measured by the USGS.

RM	Depth	Segment	Count	ME_Error	AME_Error	RMS_error
286	1	198	50351	0.764	0.818	1.012
286	3	198	29797	0.827	0.848	0.998
286	6	198	50259	0.747	0.794	0.961
286	10	198	29794	0.626	0.676	0.822
286	15	198	50290	0.387	0.482	0.604
286	21	198	29793	0.229	0.446	0.567
286	30	198	29795	0.274	0.899	1.286
300	1	154	50634	0.953	0.968	1.130
300	3	154	29949	0.841	0.853	0.970
300	6	154	50570	0.728	0.739	0.837
300	10	154	29948	0.610	0.632	0.736
300	15	154	50569	0.484	0.531	0.647
300	21	154	29947	0.306	0.450	0.557
300	30	154	29948	0.005	0.921	1.420
318	1	97	30017	0.005	0.539	0.717
318	3	97	30017	0.037	0.483	0.638
318	6	97	30018	0.037	0.367	0.484
318	10	97	30018	-0.072	0.345	0.483
Total/Average			661714	0.478	0.667	0.833

* Note: ME: mean error; AME: absolute mean error; RMS: root mean square

RM 286

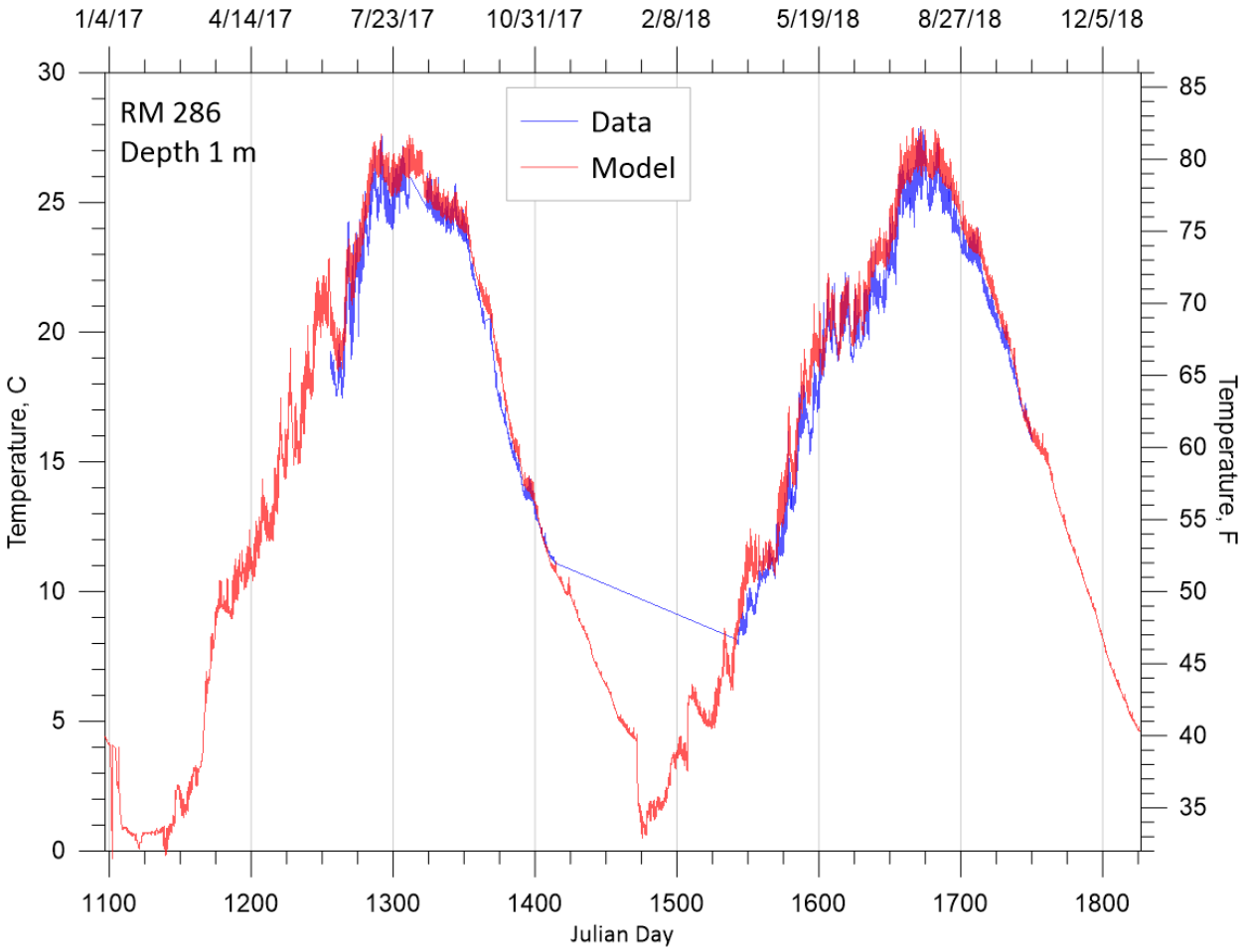


Figure 1. Model predicted temperatures compared with continuous data measured at RM 286 at a depth of 1 m.

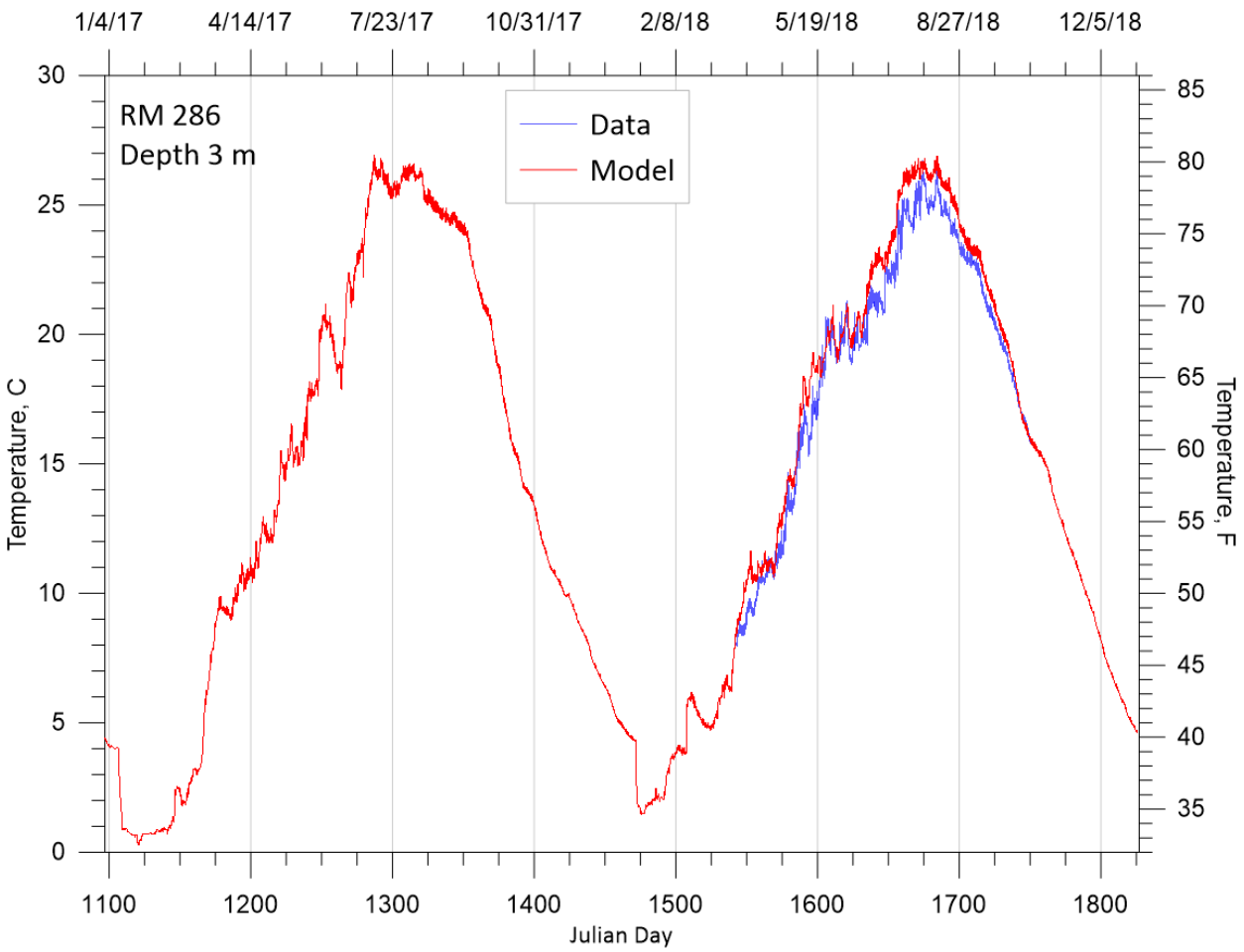


Figure 2. Model predicted temperatures compared with continuous data measured at RM 286 at a depth of 3 m.

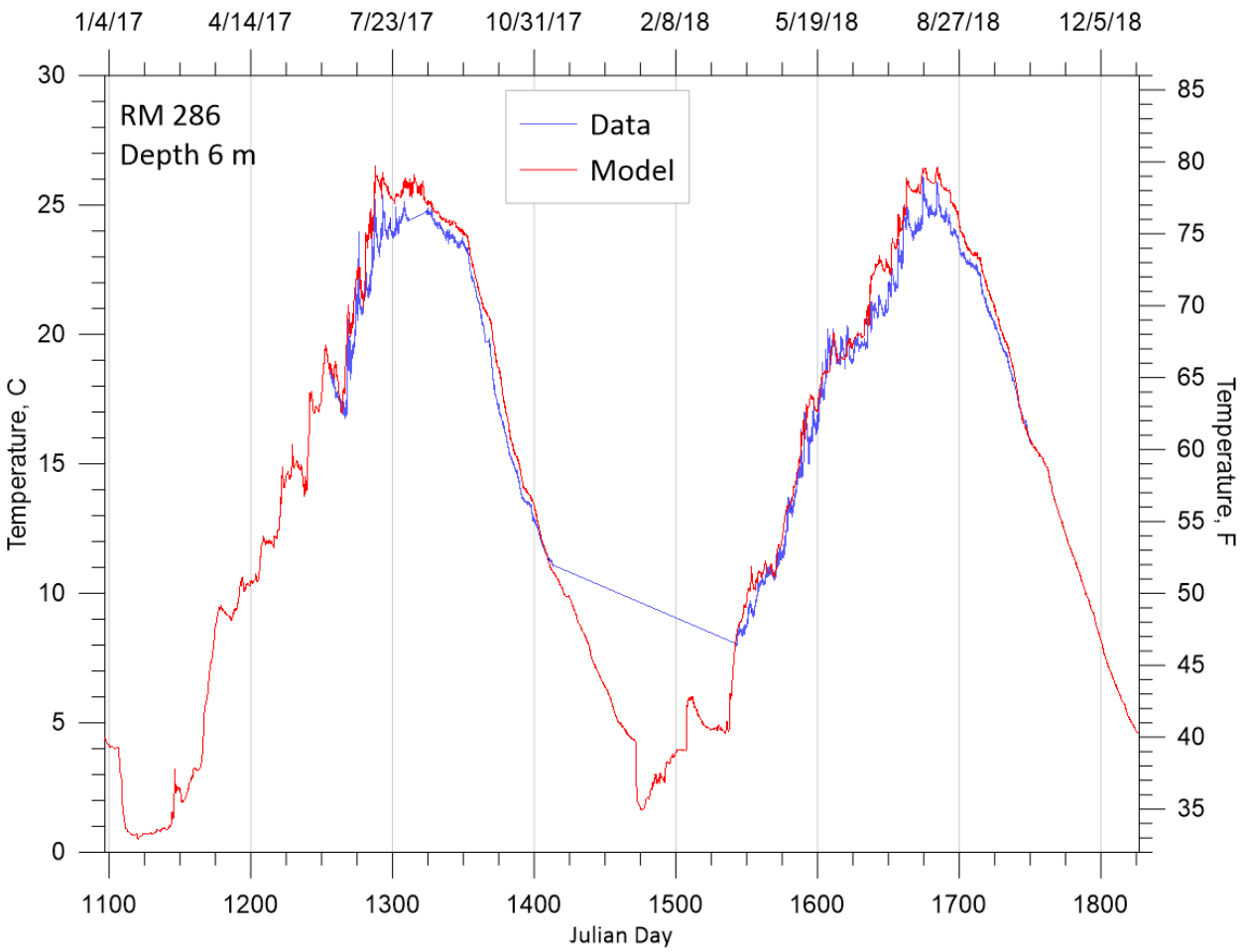


Figure 3. Model predicted temperatures compared with continuous data measured at RM 286 at a depth of 6 m.

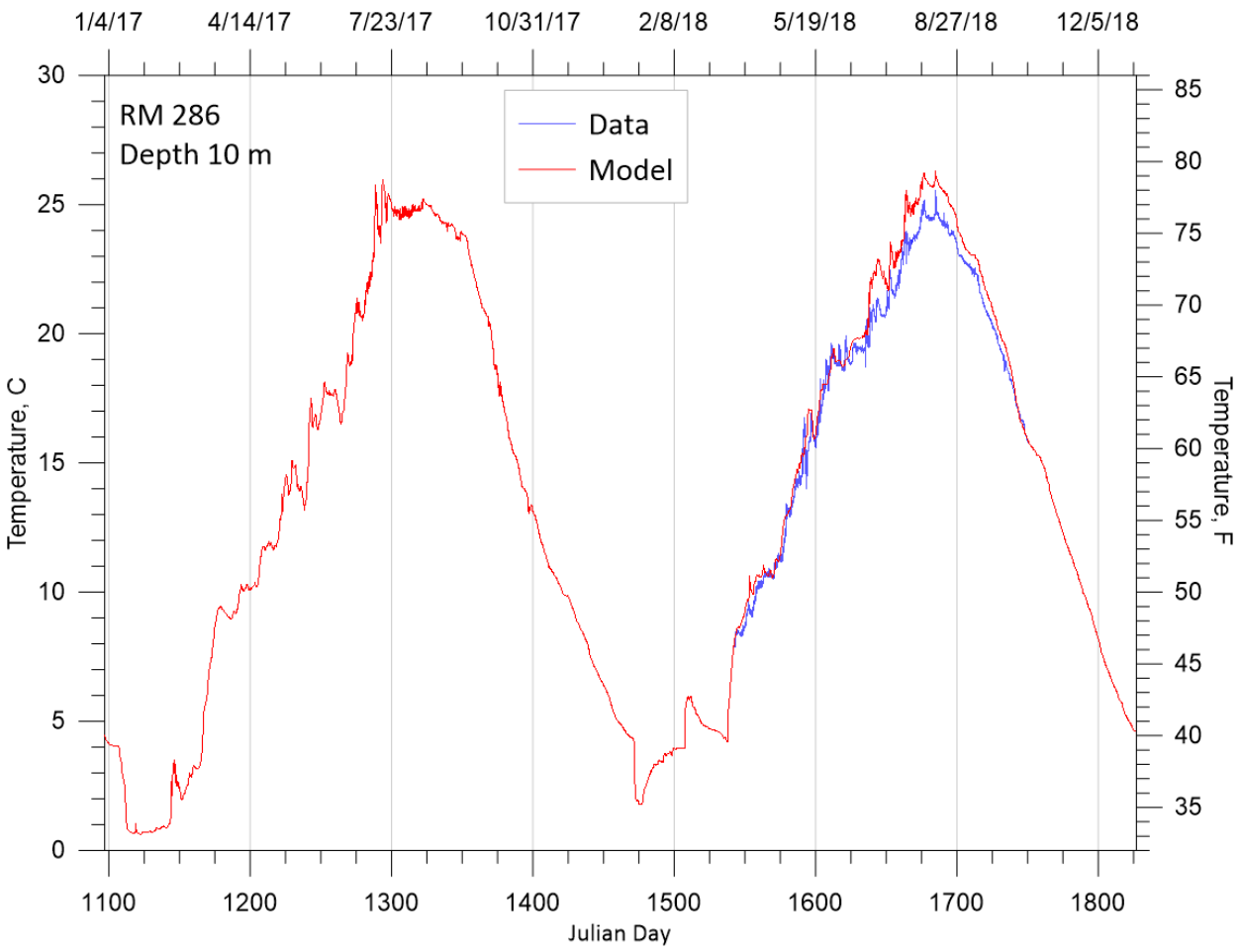


Figure 4. Model predicted temperatures compared with continuous data measured at RM 286 at a depth of 10 m.

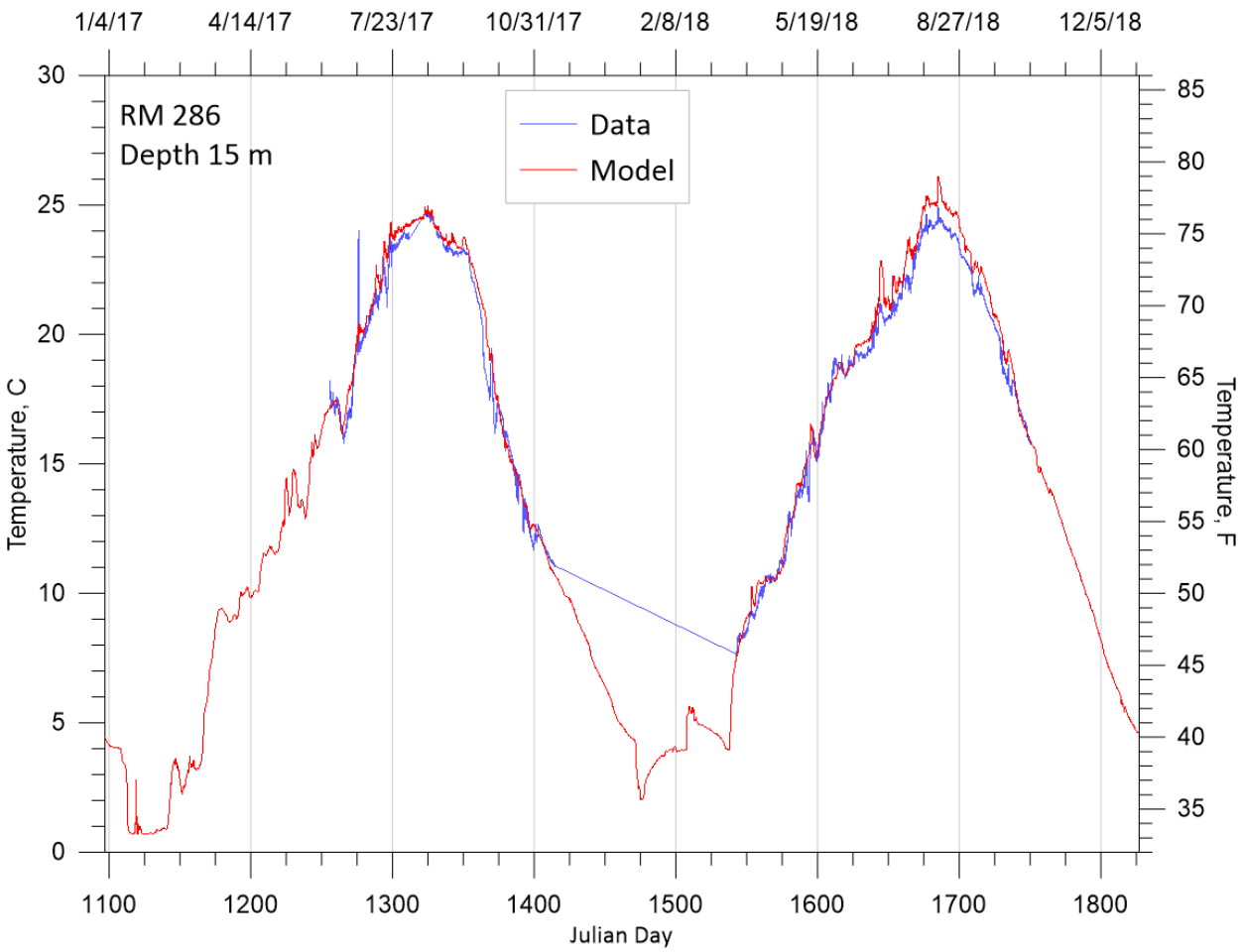


Figure 5. Model predicted temperatures compared with continuous data measured at RM 286 at a depth of 15 m.

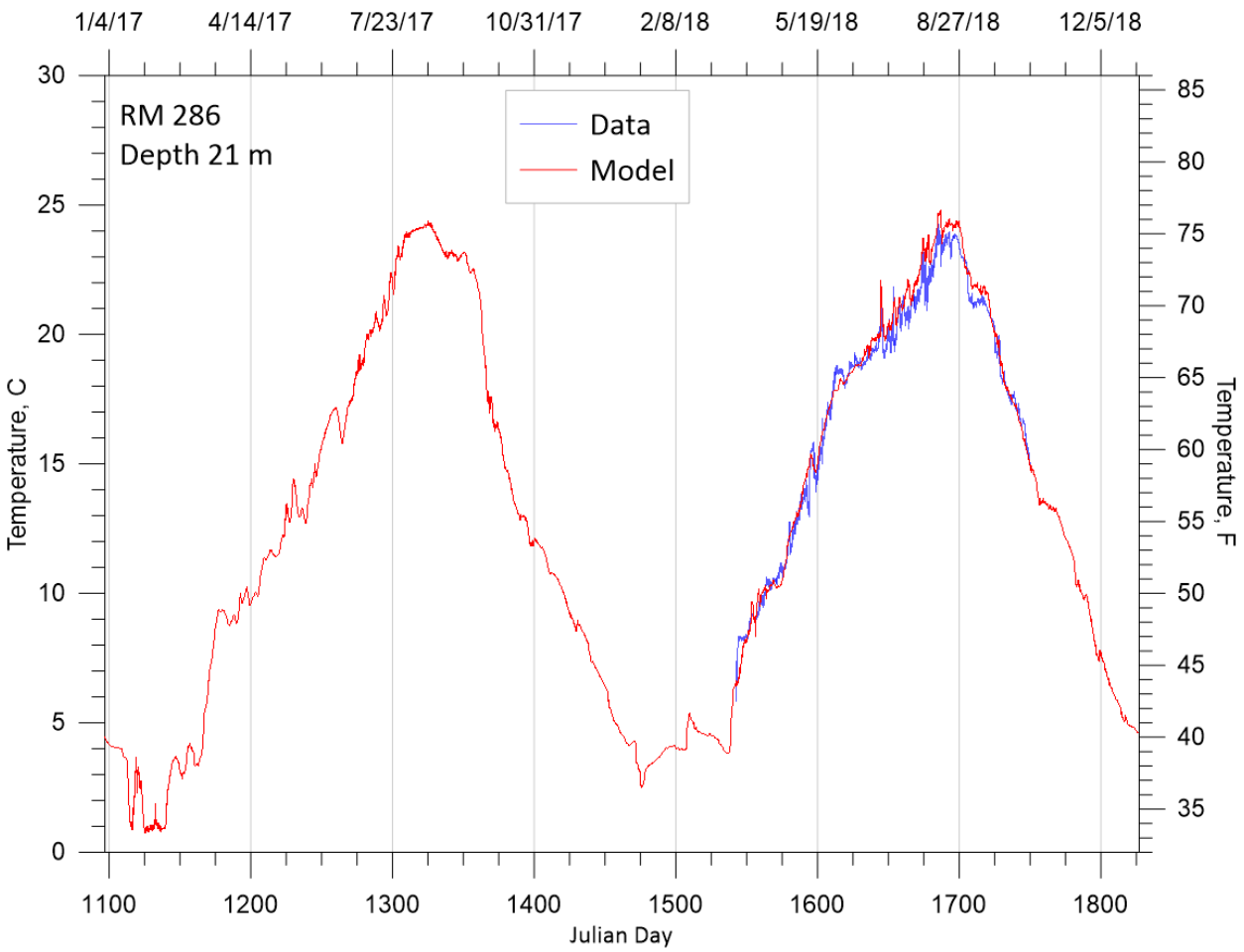


Figure 6. Model predicted temperatures compared with continuous data measured at RM 286 at a depth of 21 m.

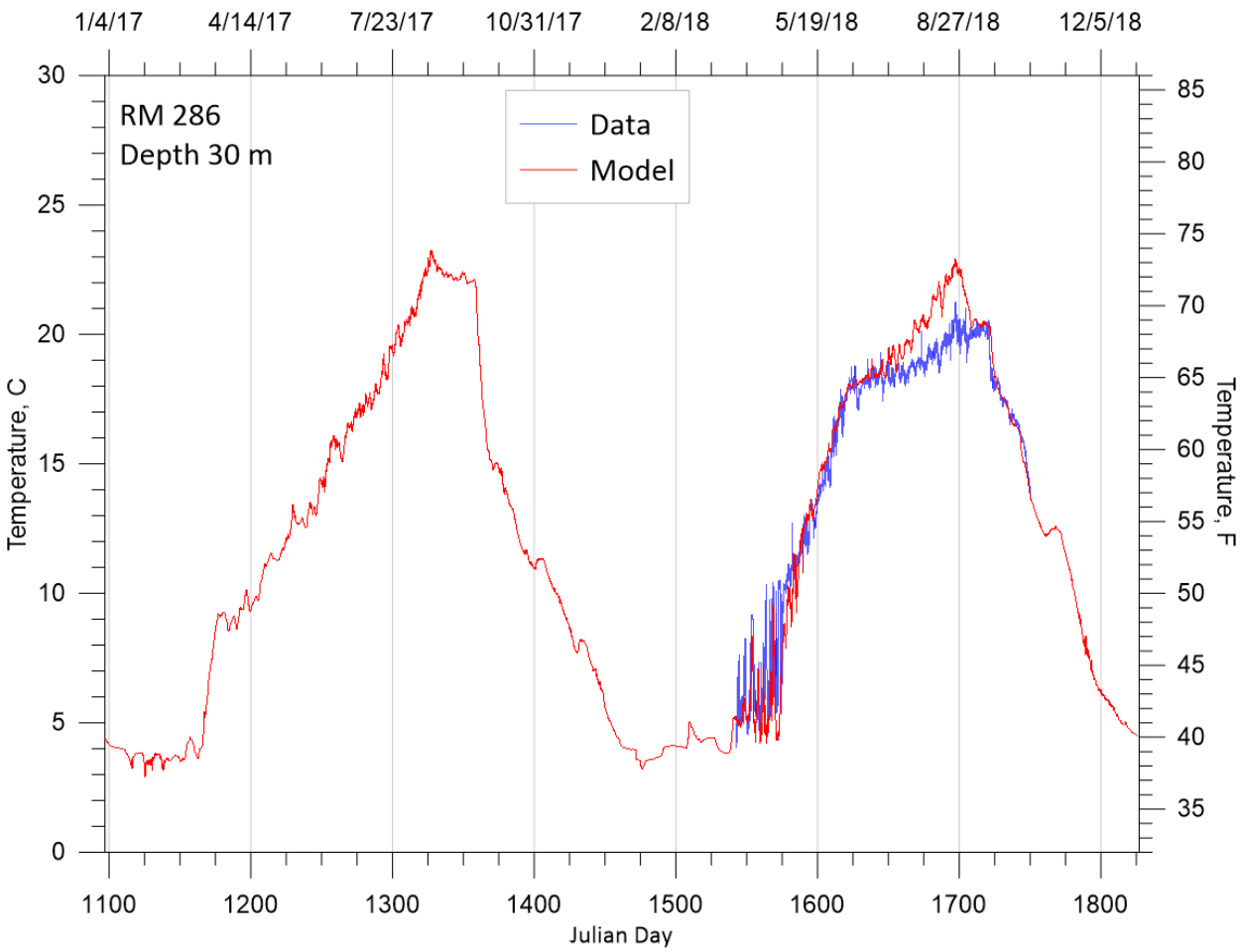


Figure 7. Model predicted temperatures compared with continuous data measured at RM 286 at a depth of 30 m.

RM 300

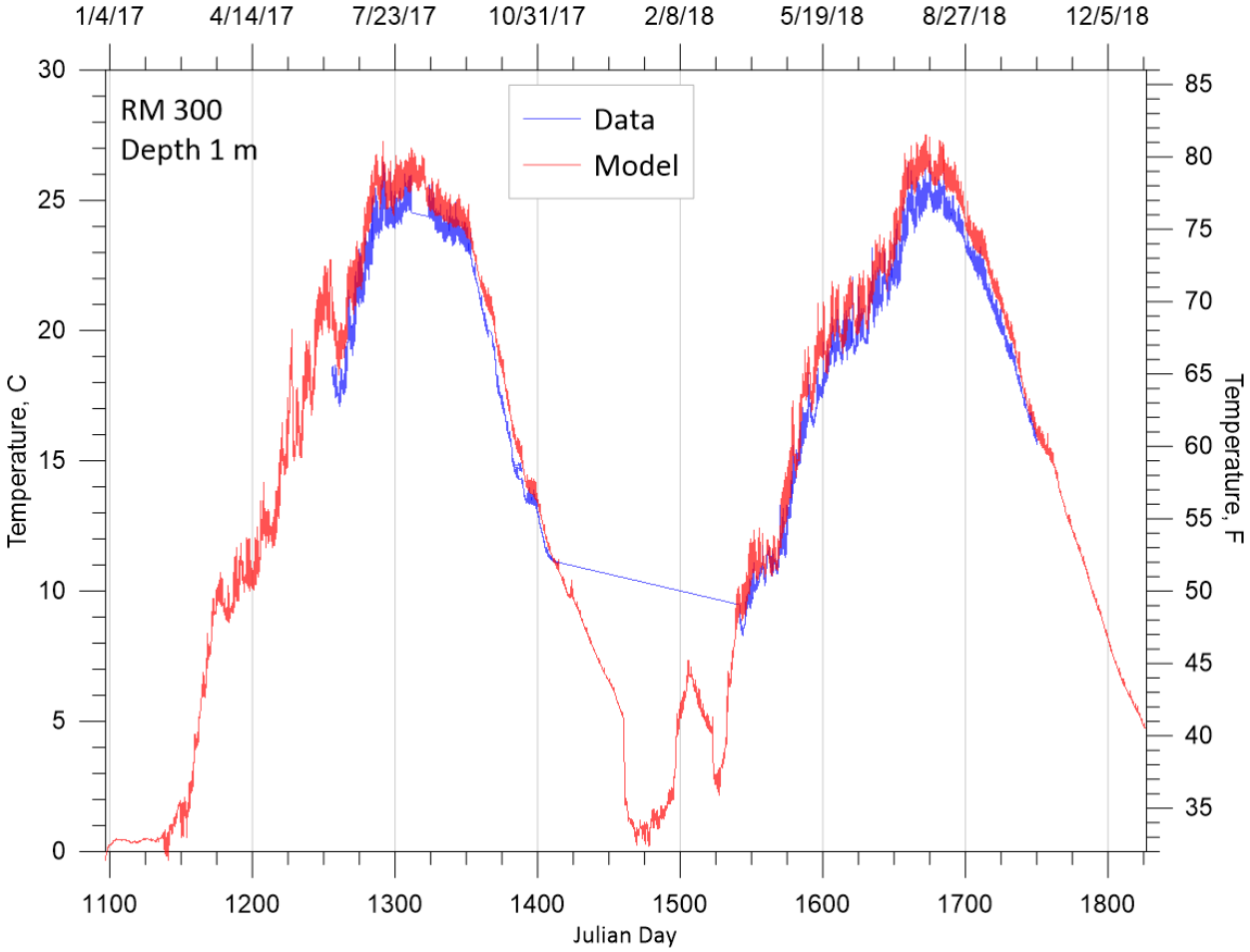


Figure 8. Model predicted temperatures compared with continuous data measured at RM 300 at a depth of 1 m.

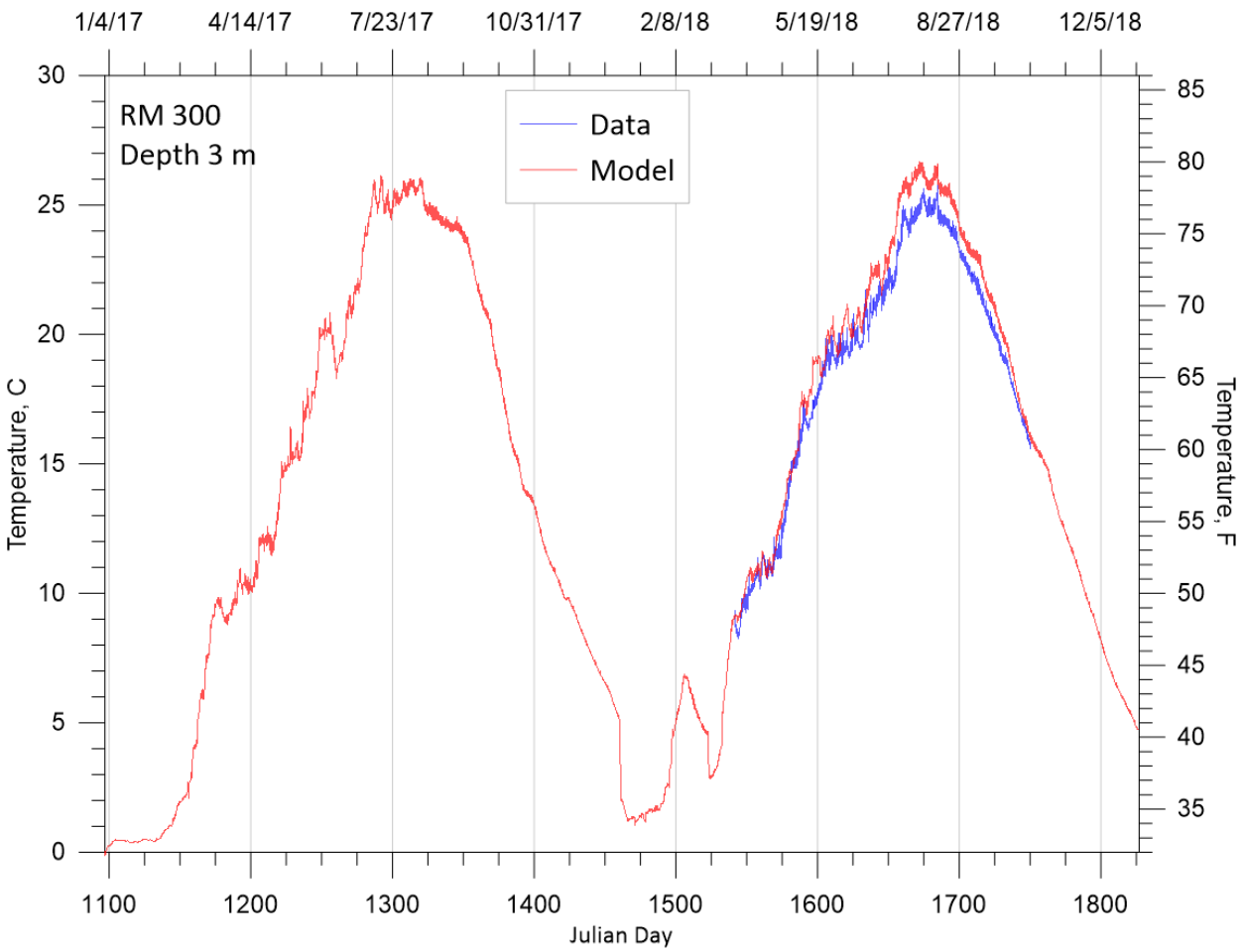


Figure 9. Model predicted temperatures compared with continuous data measured at RM 300 at a depth of 3 m.

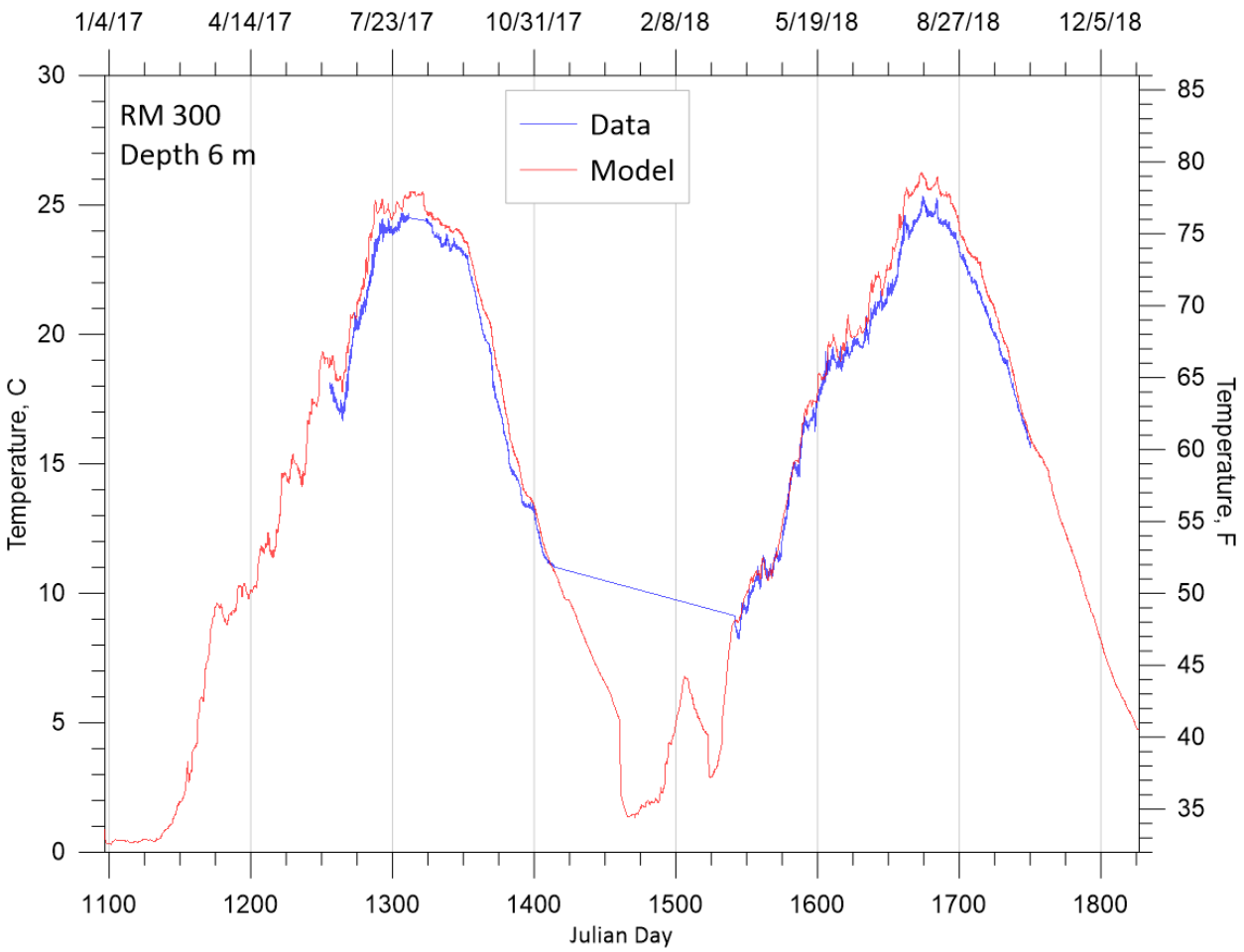


Figure 10. Model predicted temperatures compared with continuous data measured at RM 300 at a depth of 6 m.

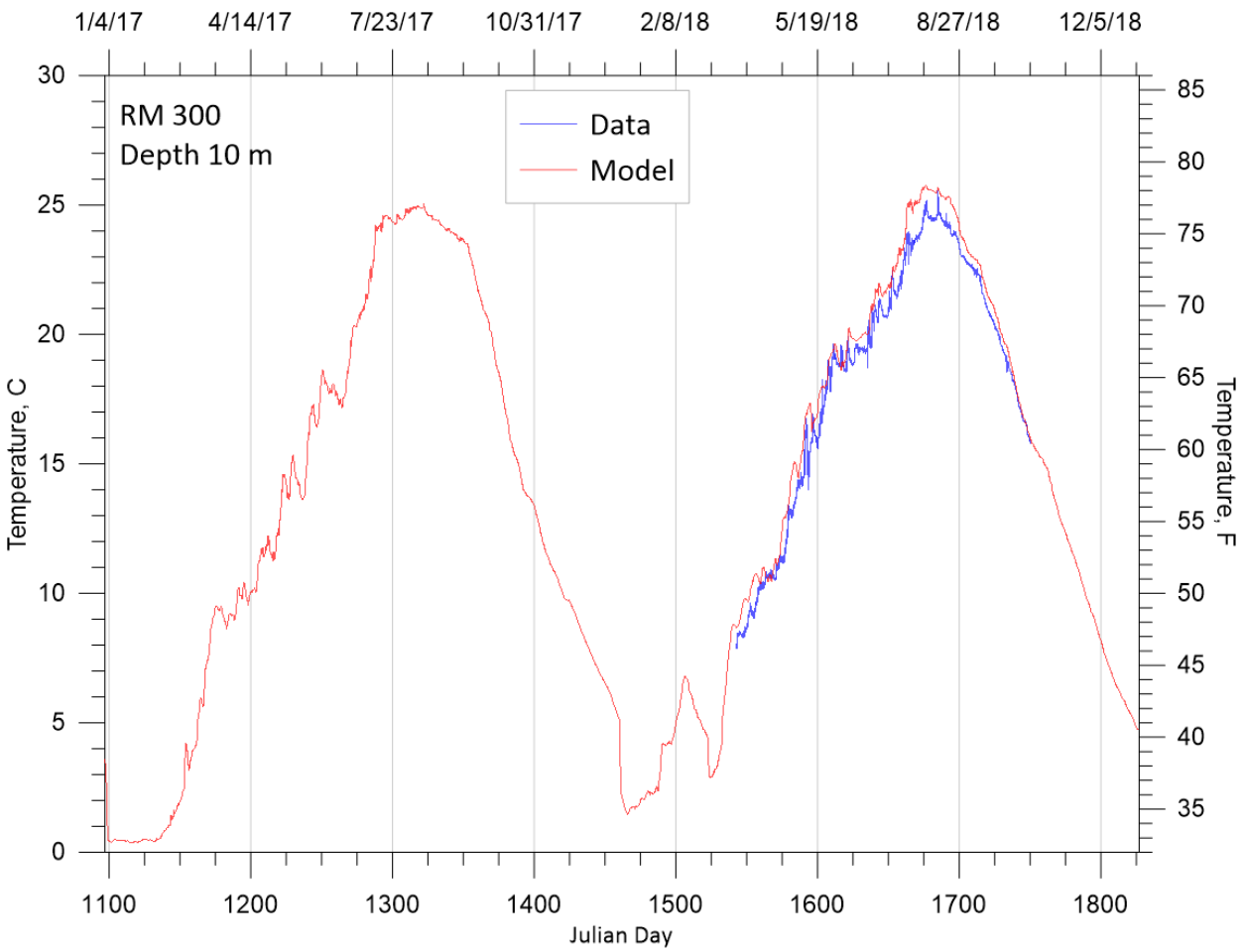


Figure 11. Model predicted temperatures compared with continuous data measured at RM 300 at a depth of 10 m.

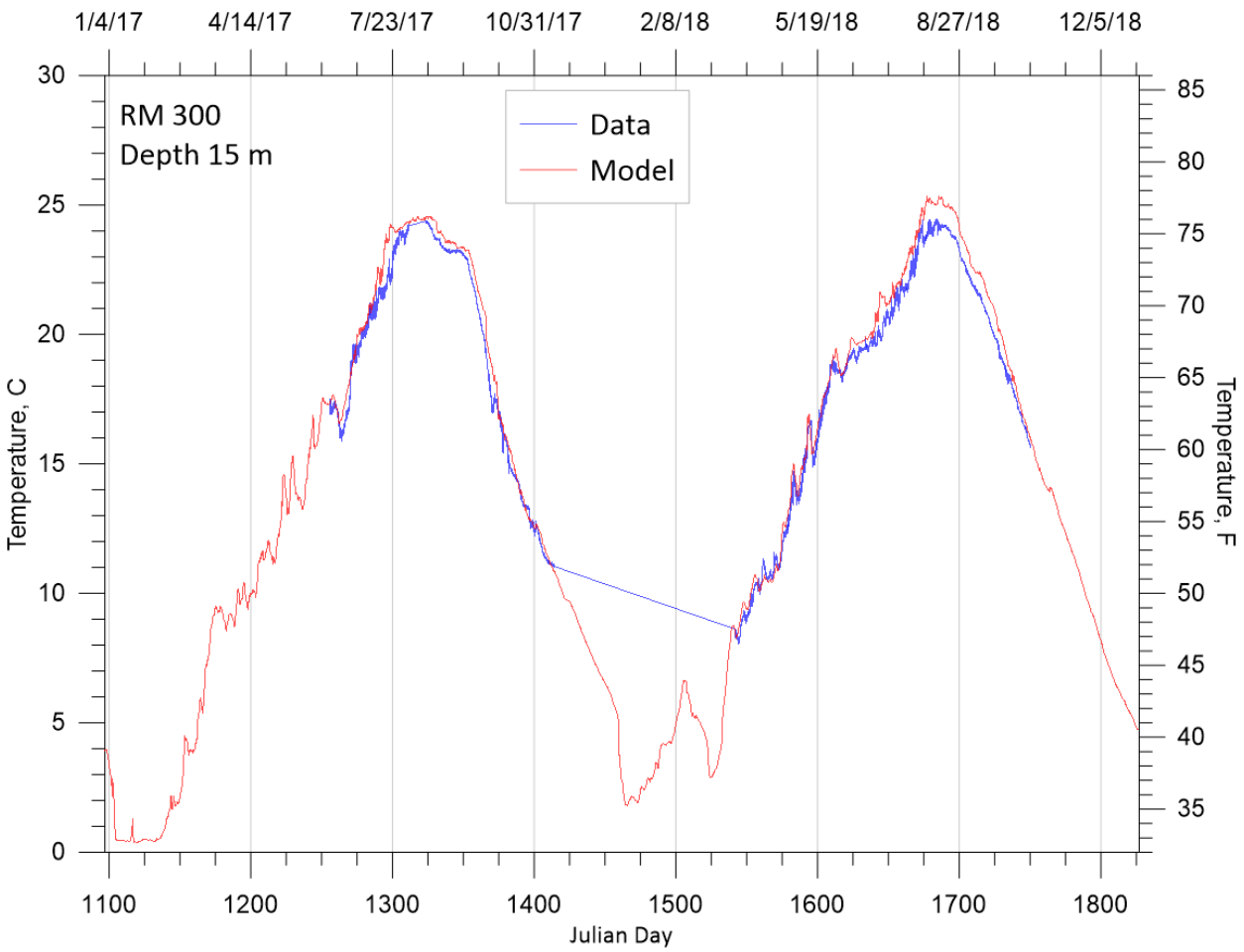


Figure 12. Model predicted temperatures compared with continuous data measured at RM 300 at a depth of 15 m.

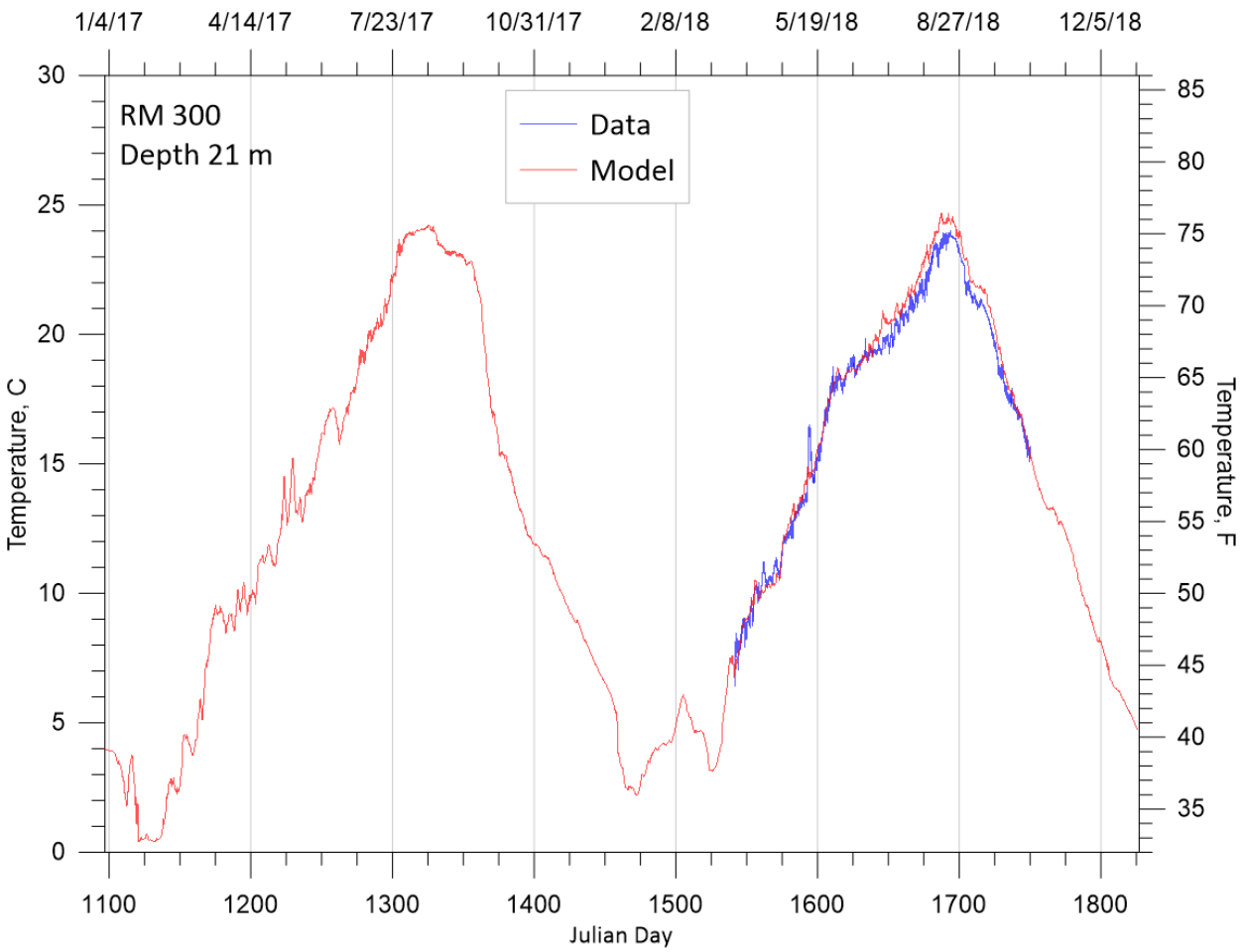


Figure 13. Model predicted temperatures compared with continuous data measured at RM 300 at a depth of 21 m.

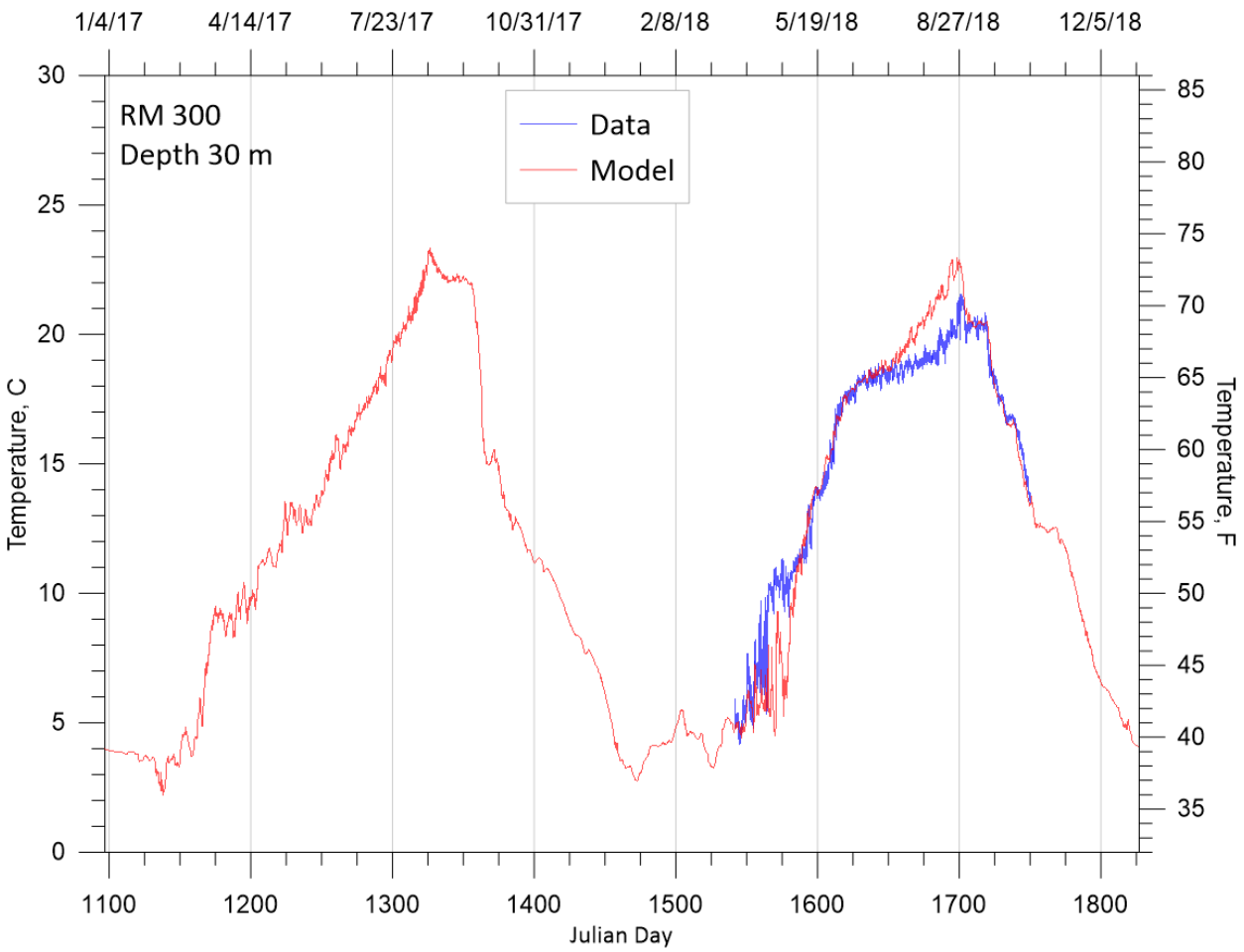


Figure 14. Model predicted temperatures compared with continuous data measured at RM 300 at a depth of 30 m.

RM 318

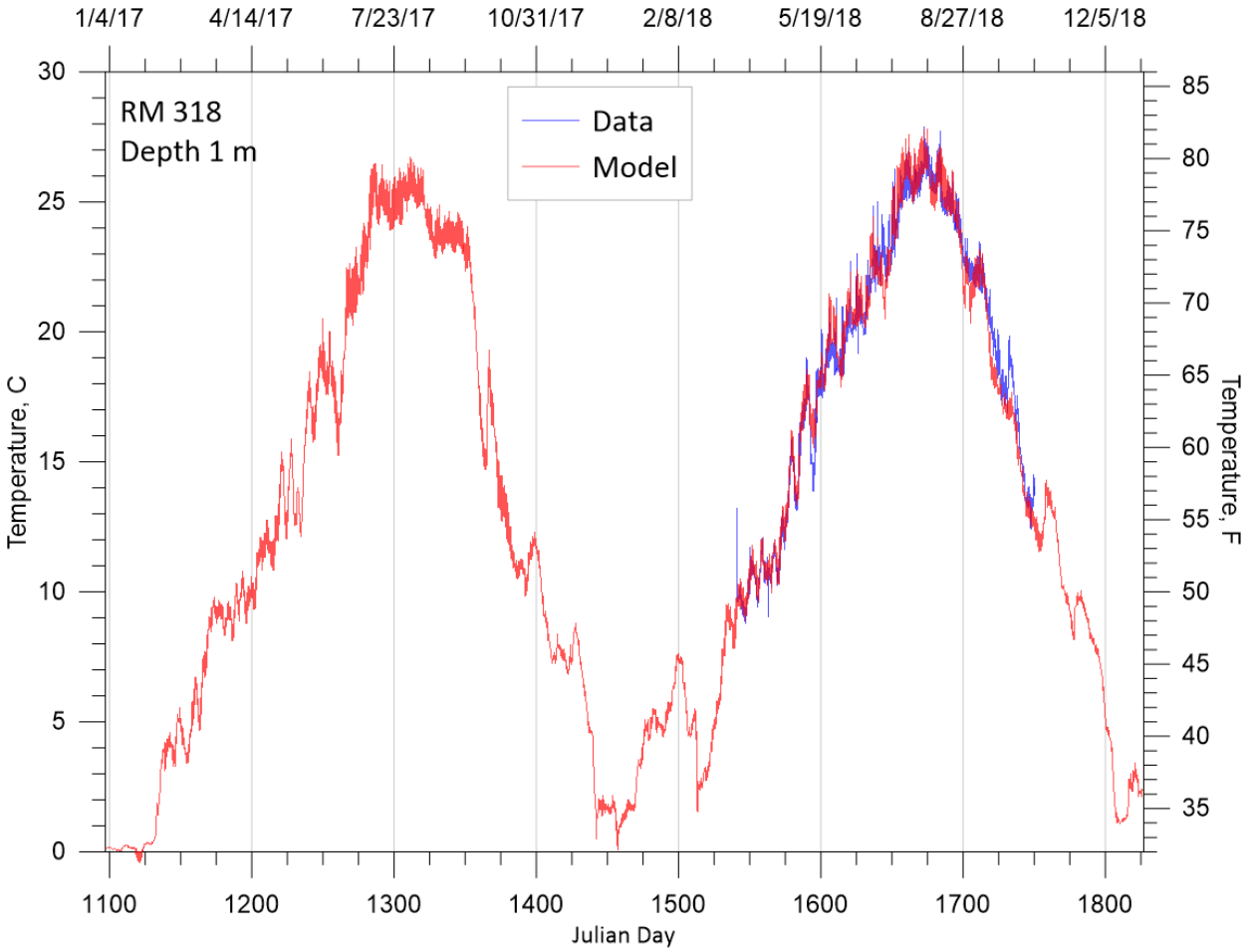


Figure 15. Model predicted temperatures compared with continuous data measured at RM 318 at a depth of 1 m.

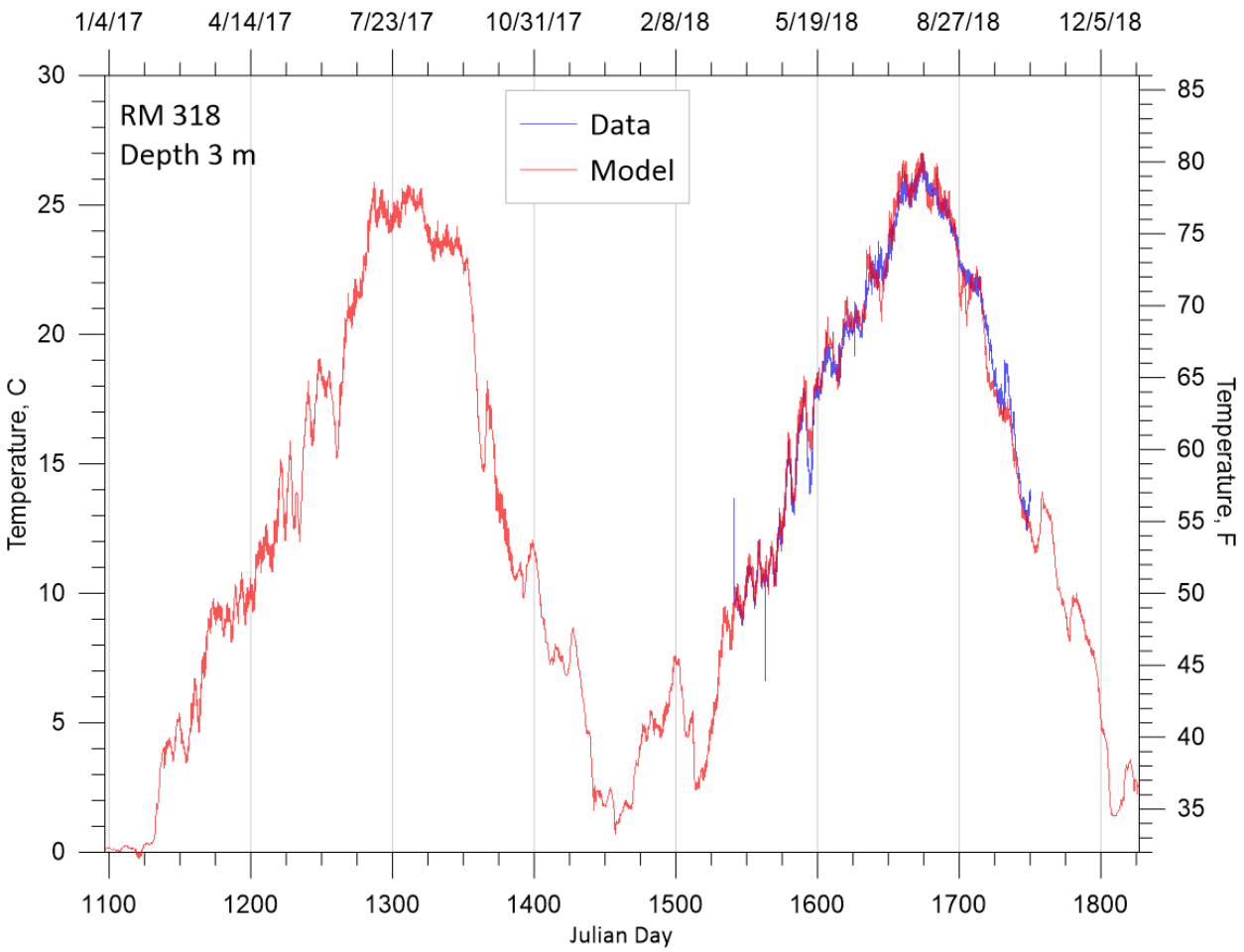


Figure 16. Model predicted temperatures compared with continuous data measured at RM 318 at a depth of 3 m.

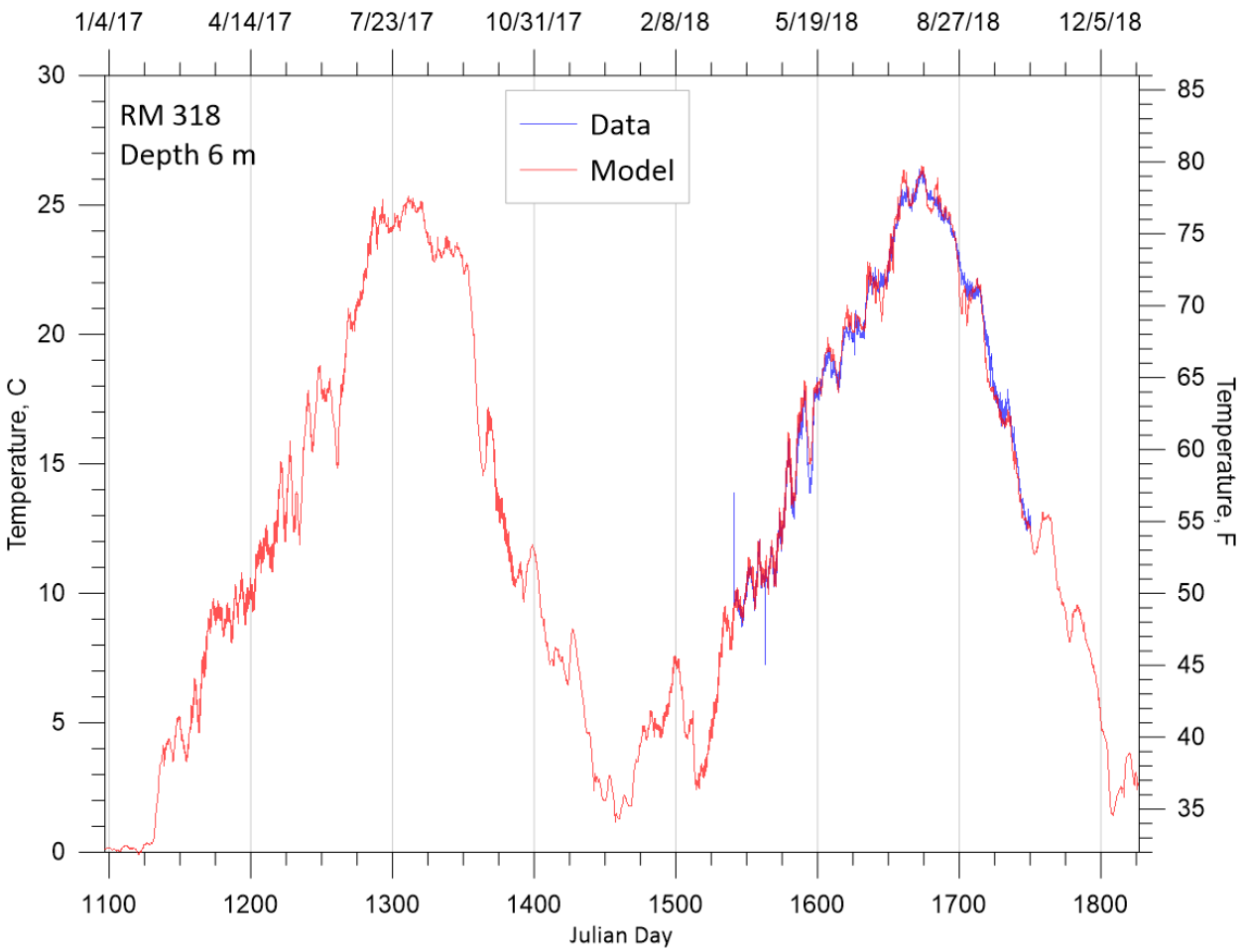


Figure 17. Model predicted temperatures compared with continuous data measured at RM 318 at a depth of 6 m.

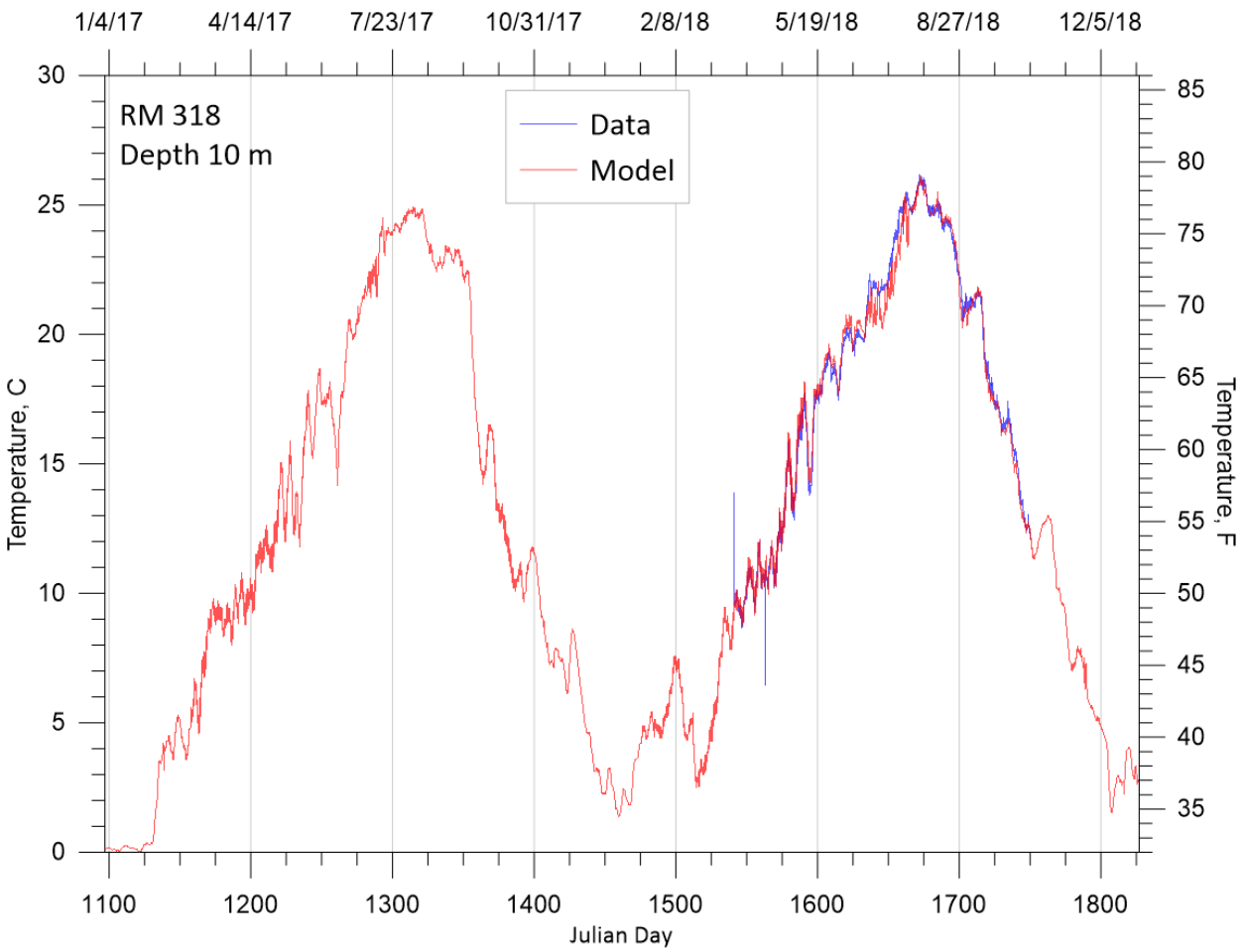


Figure 18. Model predicted temperatures compared with continuous data measured at RM 318 at a depth of 10 m.

Dissolved Oxygen

Statistics

Table 2. Error statistics for continuous DO data measured by the USGS.

RM	Depth	Segment	Count	ME_Error	AME_Error	RMS_error
286	1	198	50351	-1.791	2.301	3.226
286	3	198	29797	-0.210	1.204	1.495
286	6	198	50259	-0.005	1.127	1.444
286	10	198	29794	0.195	0.879	1.111
286	15	198	50290	-0.097	1.211	1.700
286	21	198	29793	0.150	1.153	1.715
286	30	198	29795	1.104	1.496	2.346
300	1	154	50634	-0.696	1.502	2.096
300	3	154	29949	0.212	0.955	1.242
300	6	154	50570	0.642	1.137	1.542
300	10	154	29948	0.657	0.808	0.993
300	15	154	50569	0.811	0.967	1.326
300	21	154	29947	1.006	1.090	1.357
300	30	154	29948	1.240	1.394	2.099
318	1	97	30017	-0.264	1.325	1.872
318	3	97	30017	0.526	1.112	1.514
318	6	97	30018	0.837	1.100	1.435
318	10	97	30018	0.350	0.814	1.118
Total/Average			661714	0.176	1.231	1.691

* Note: ME: mean error; AME: absolute mean error; RMS: root mean square

RM 286

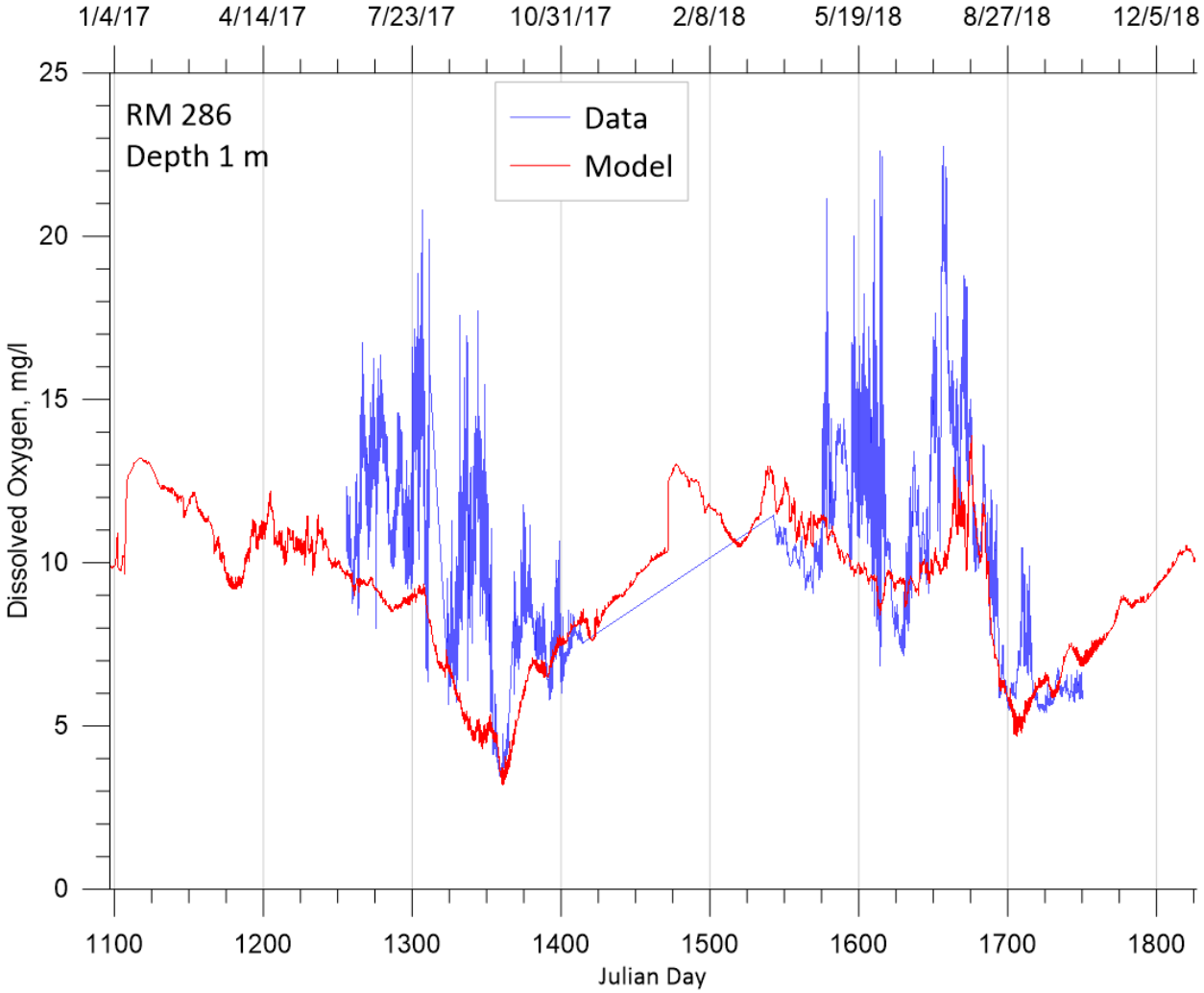


Figure 19. Model predicted DO concentrations compared with continuous data measured at RM 286 at a depth of 1 m.

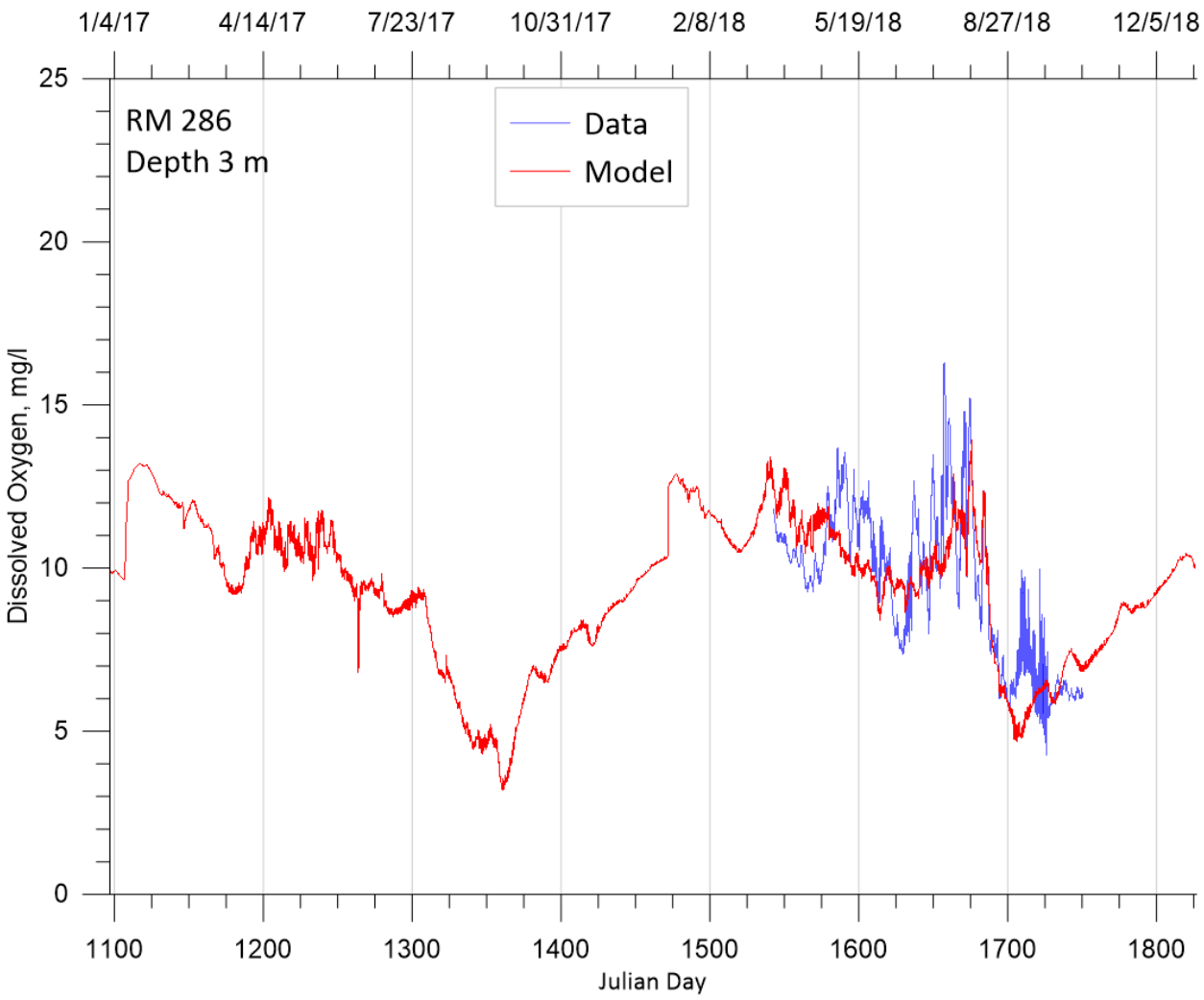


Figure 20. Model predicted DO concentrations compared with continuous data measured at RM 286 at a depth of 3 m.

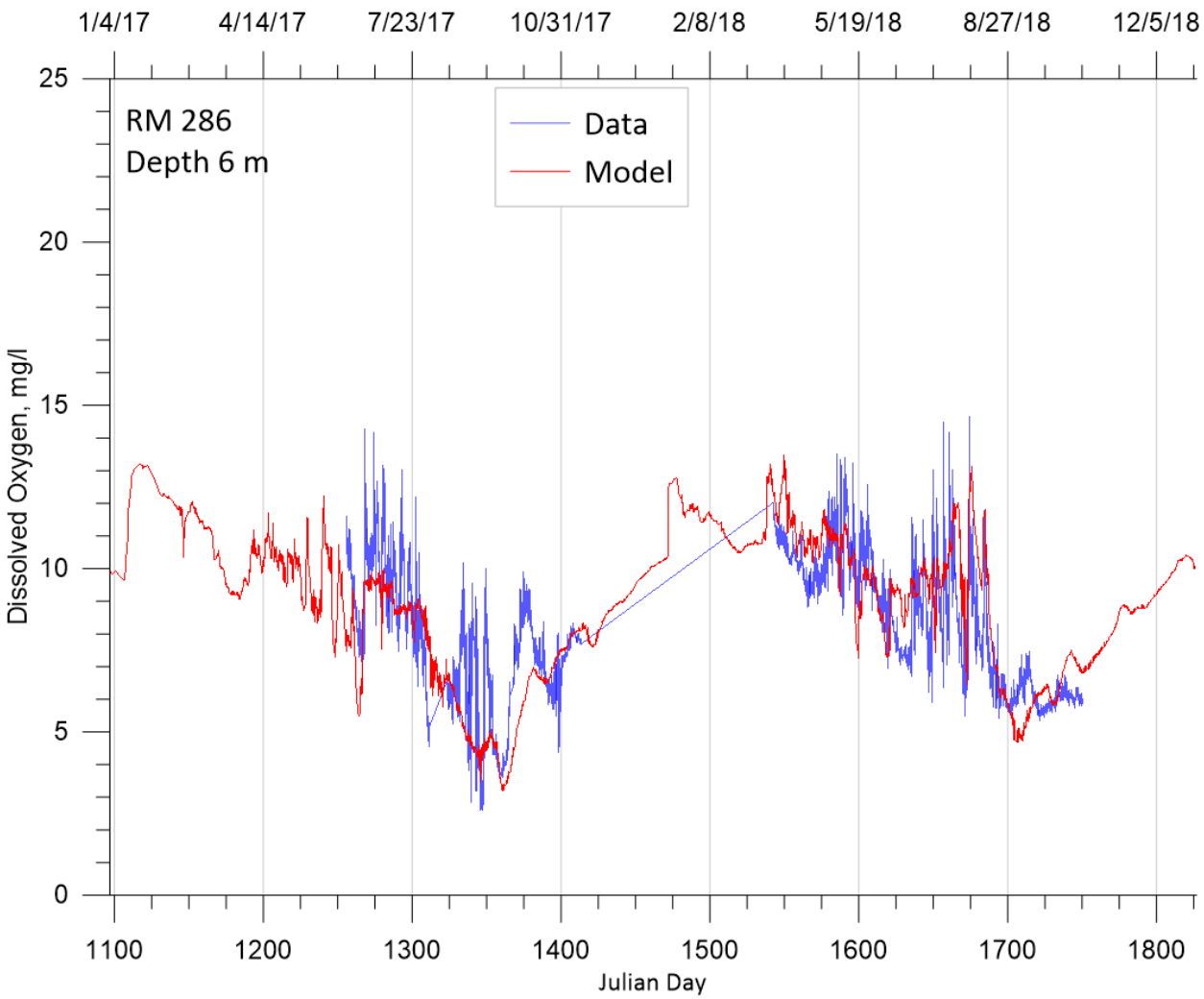


Figure 21. Model predicted DO concentrations compared with continuous data measured at RM 286 at a depth of 6 m.

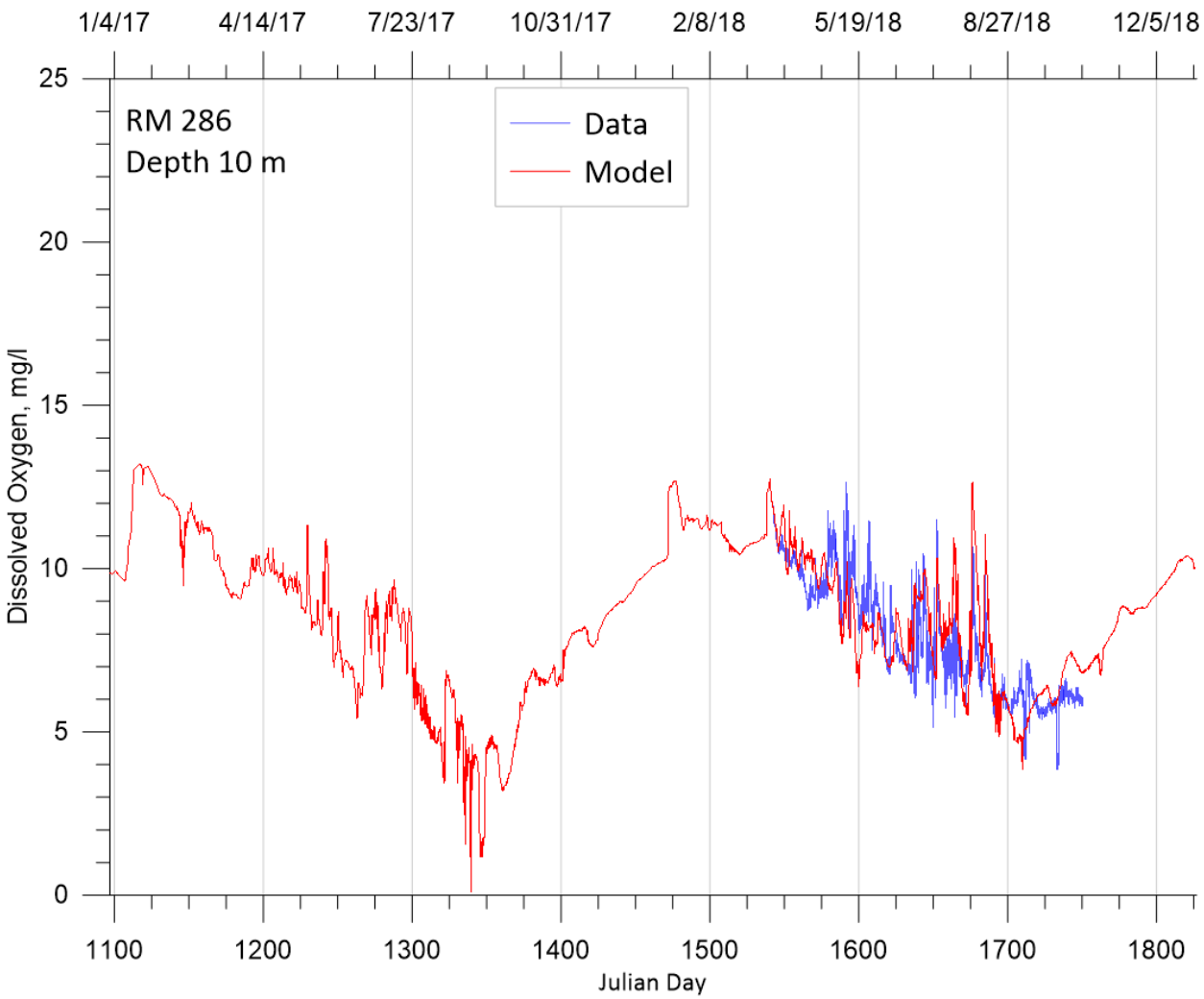


Figure 22. Model predicted DO concentrations compared with continuous data measured at RM 286 at a depth of 10 m.

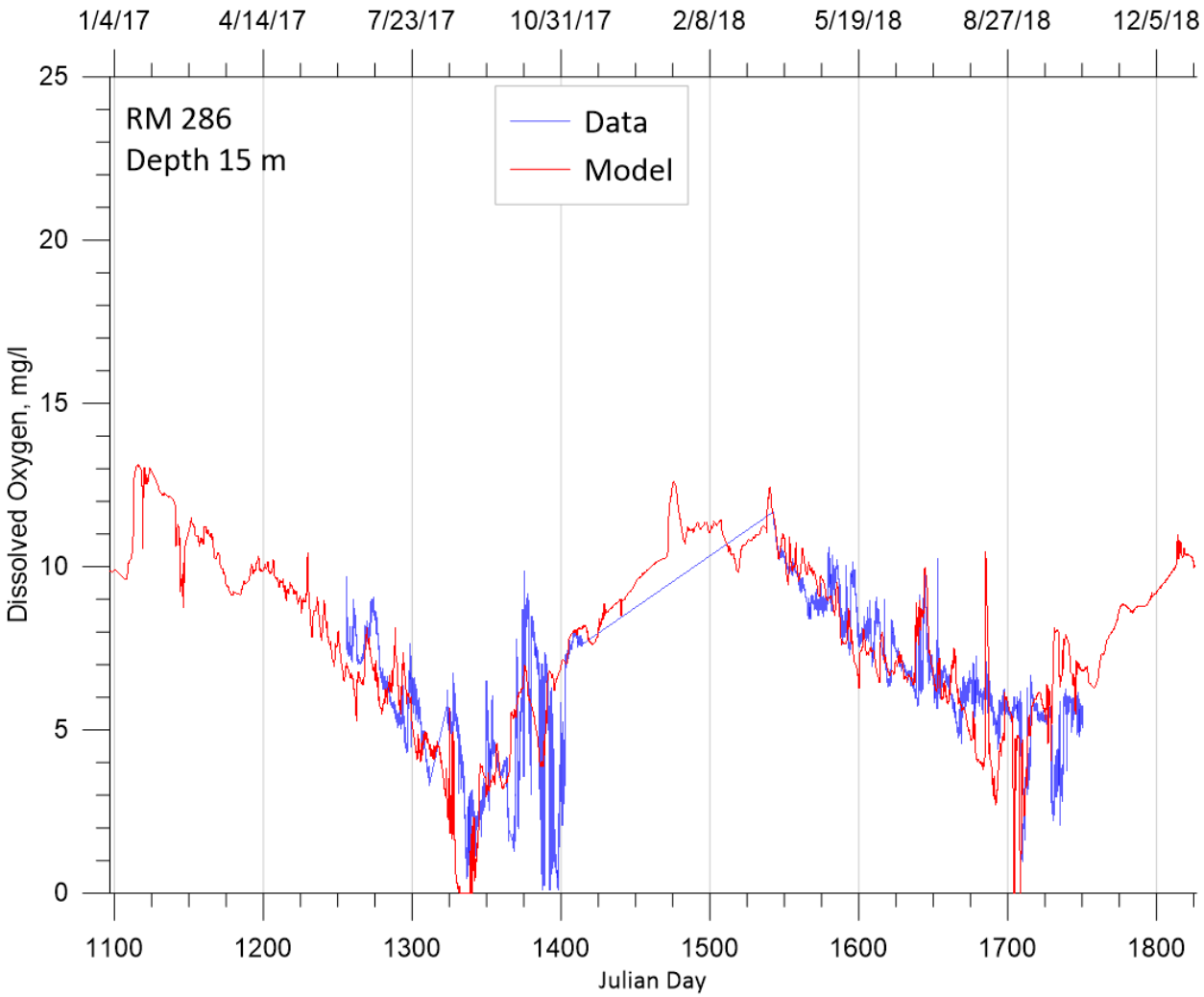


Figure 23. Model predicted DO concentrations compared with continuous data measured at RM 286 at a depth of 15 m.

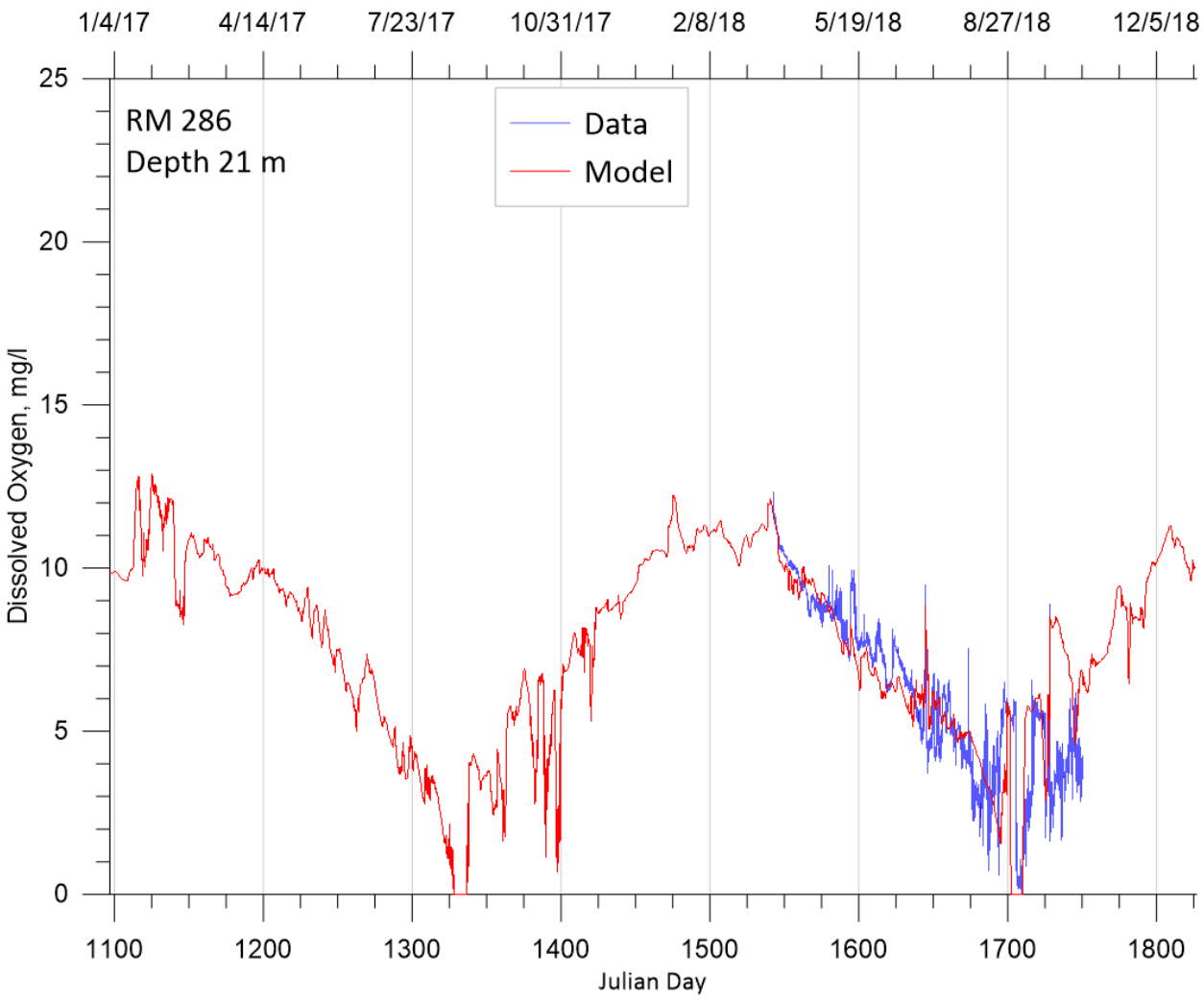


Figure 24. Model predicted DO concentrations compared with continuous data measured at RM 286 at a depth of 21 m.

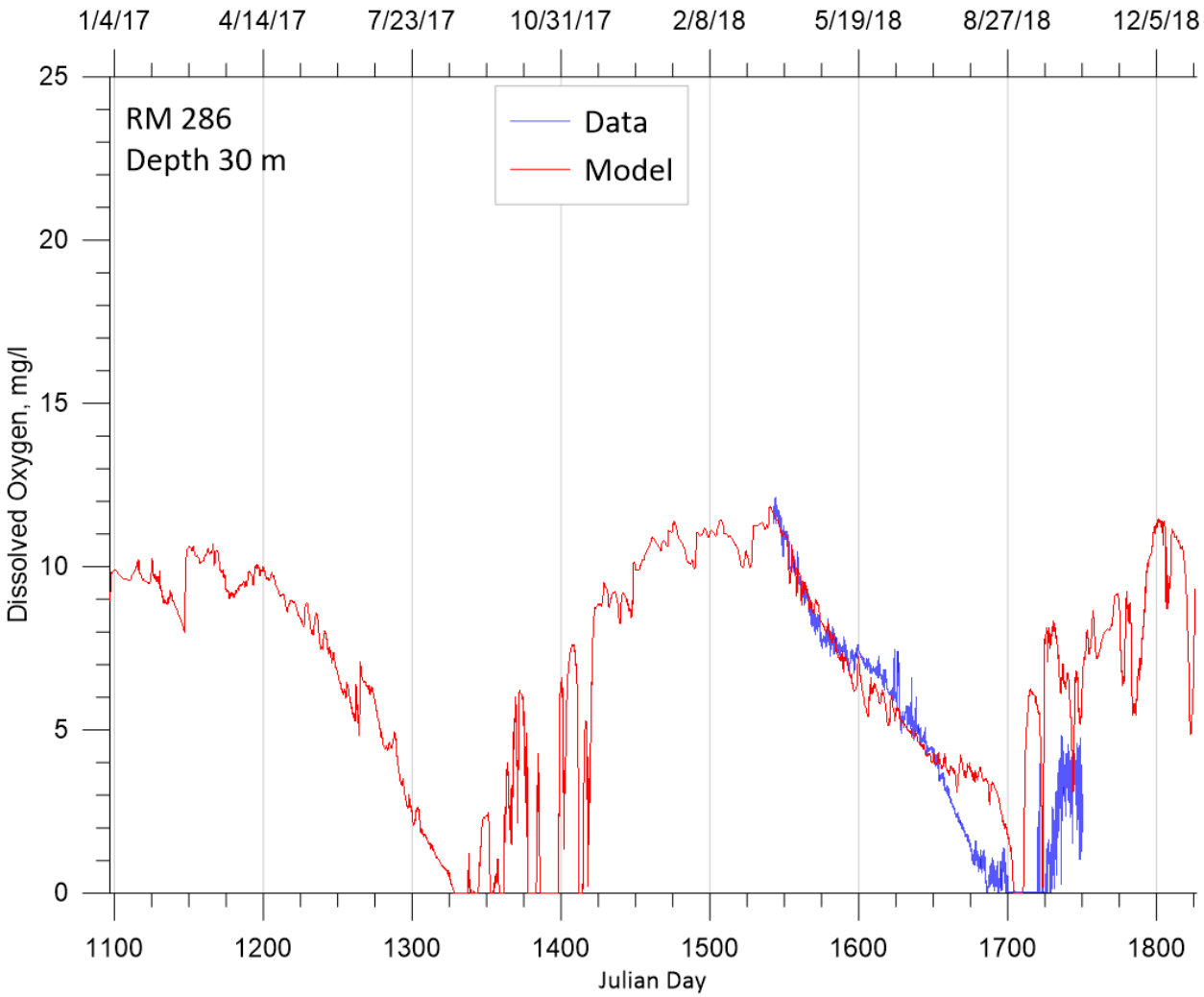


Figure 25. Model predicted DO concentrations compared with continuous data measured at RM 286 at a depth of 30 m.

RM 300

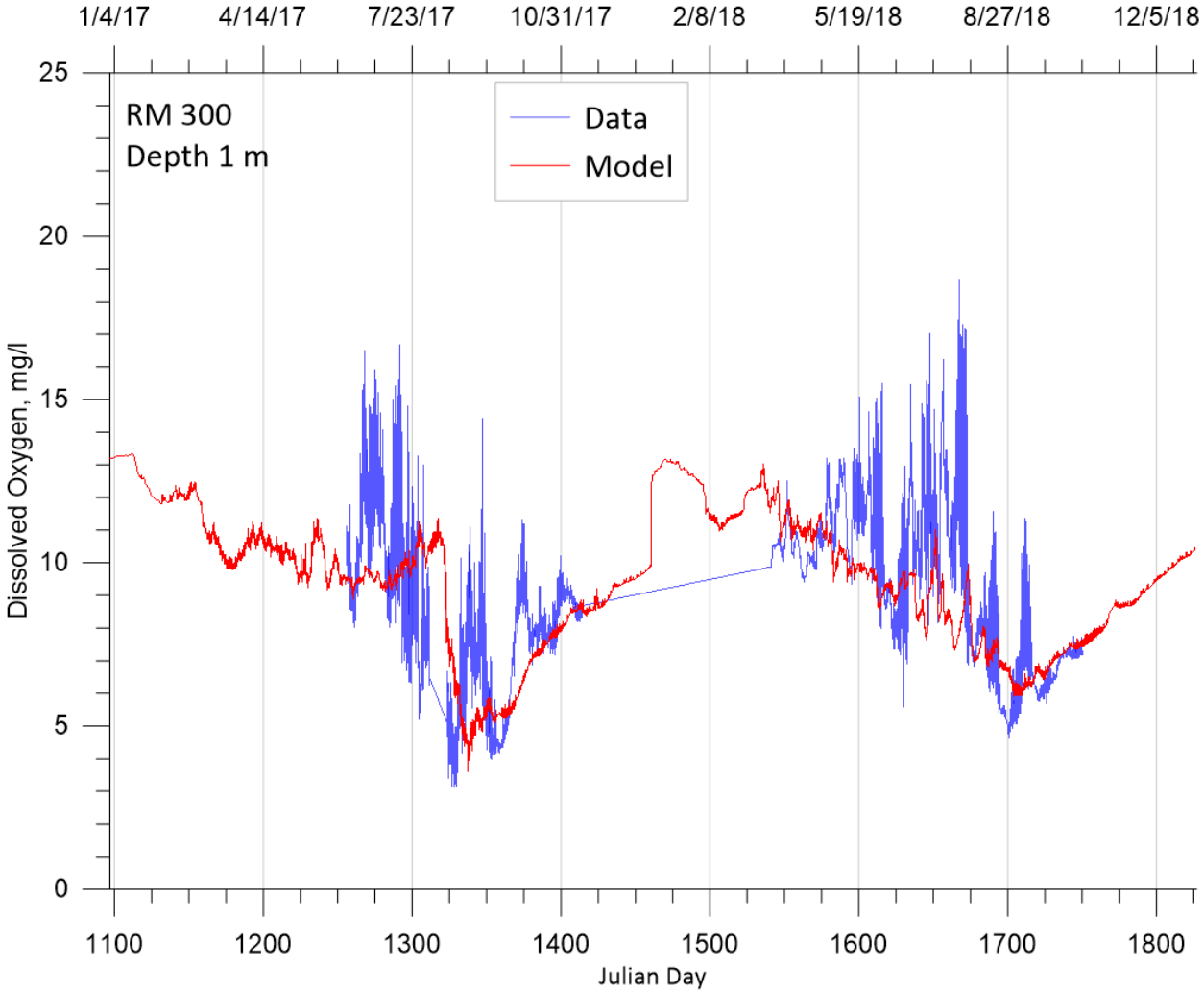


Figure 26. Model predicted DO concentrations compared with continuous data measured at RM 300 at a depth of 1 m.

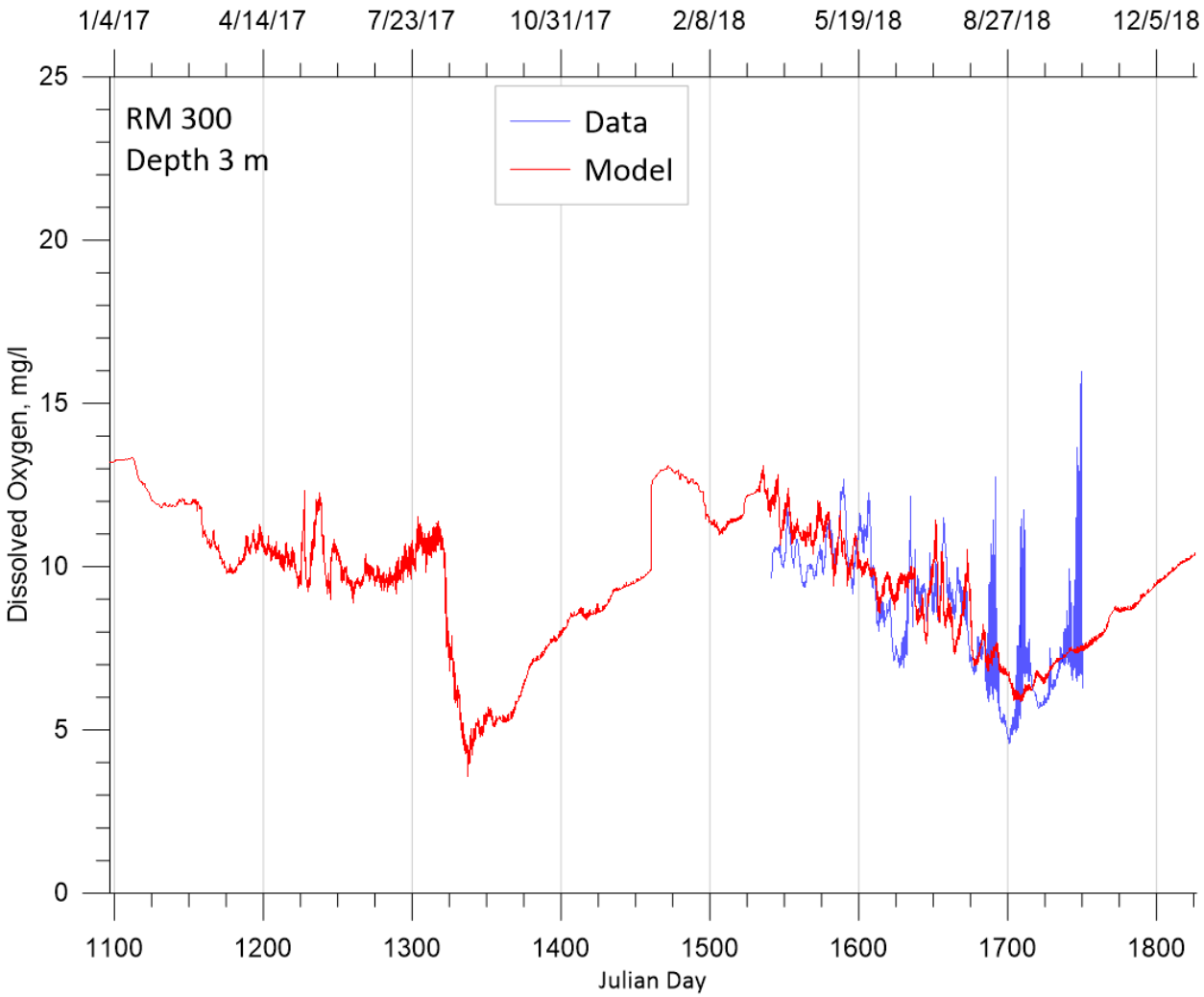


Figure 27. Model predicted DO concentrations compared with continuous data measured at RM 300 at a depth of 3 m.

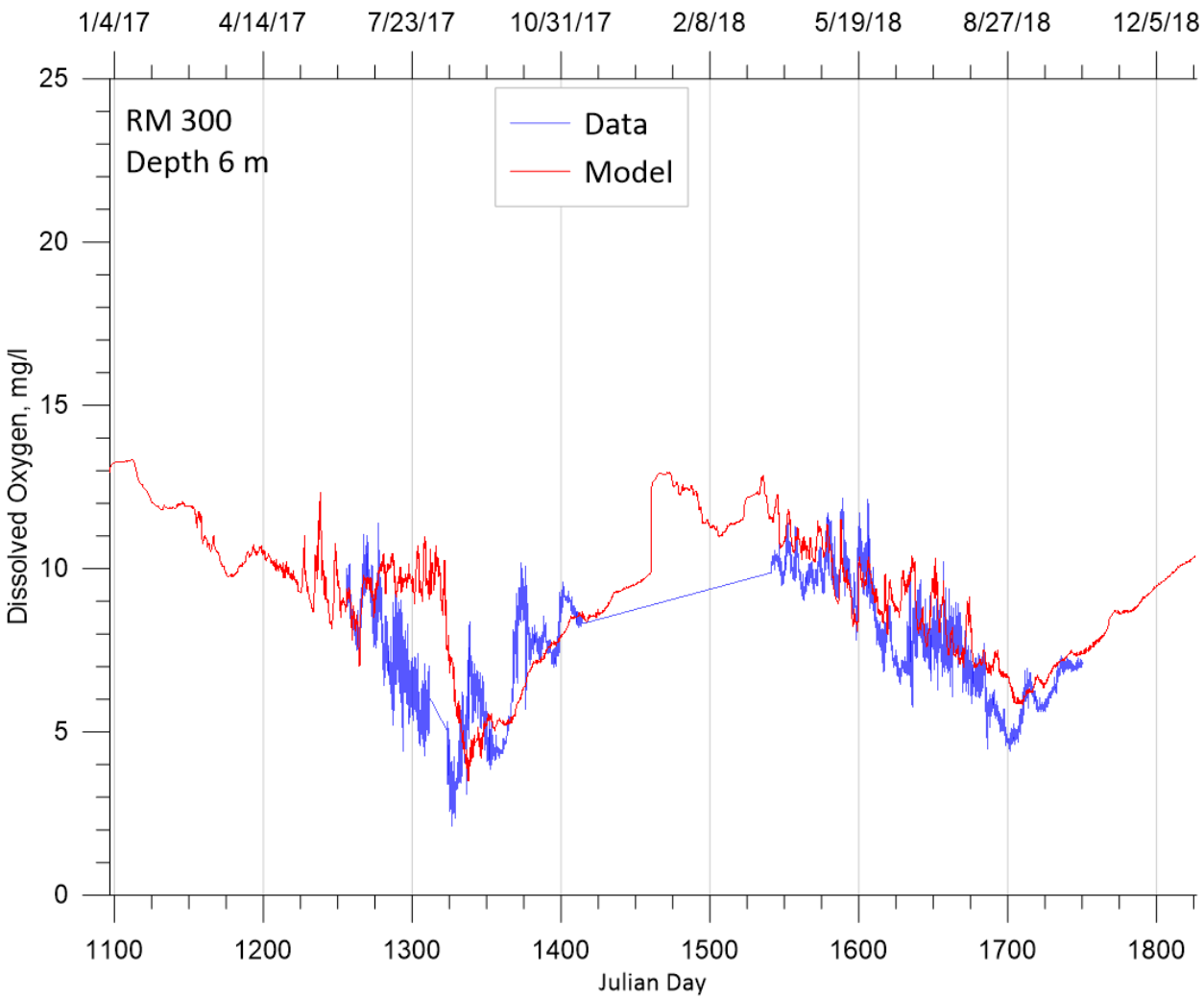


Figure 28. Model predicted DO concentrations compared with continuous data measured at RM 300 at a depth of 6 m.

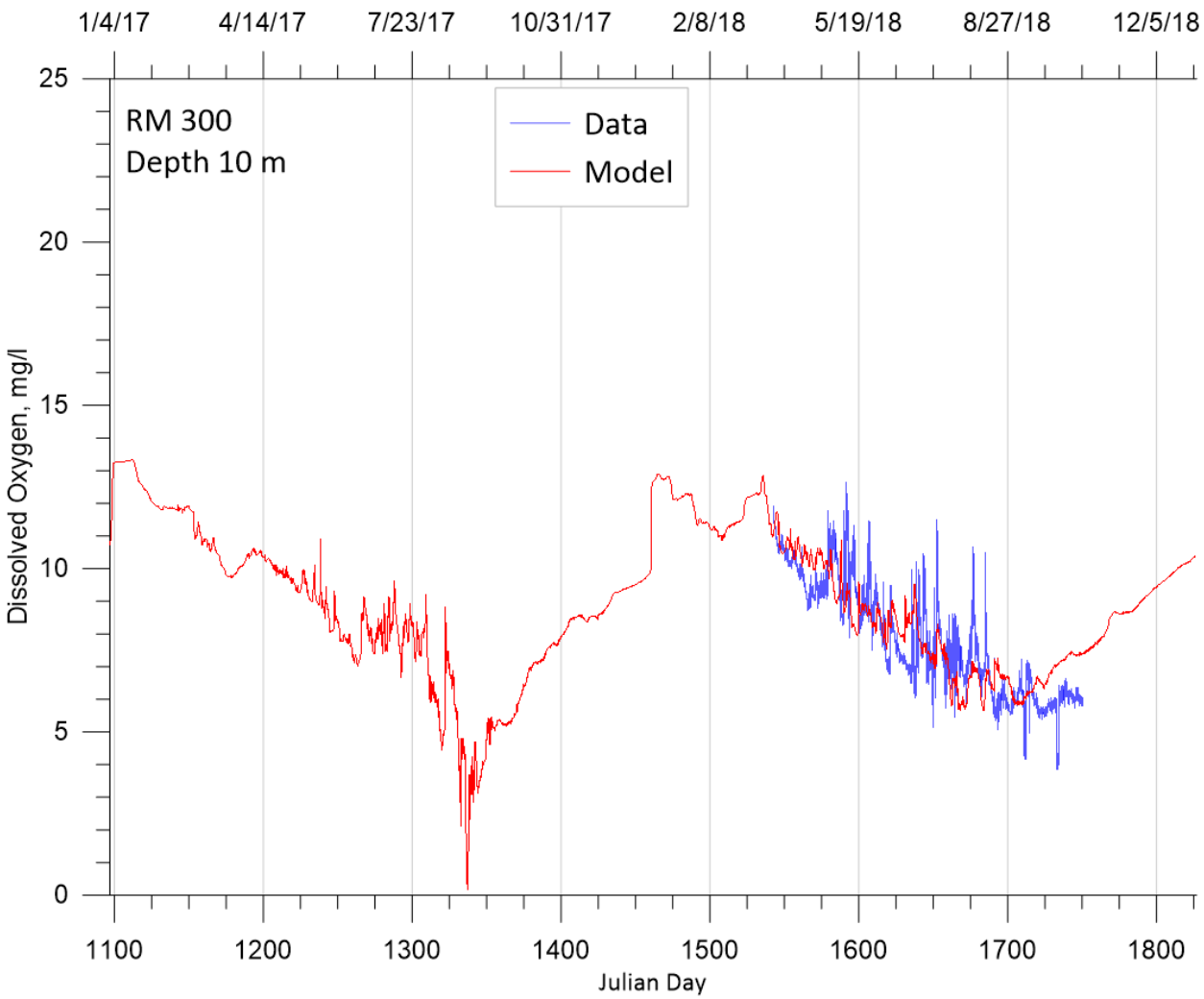


Figure 29. Model predicted DO concentrations compared with continuous data measured at RM 300 at a depth of 10 m.

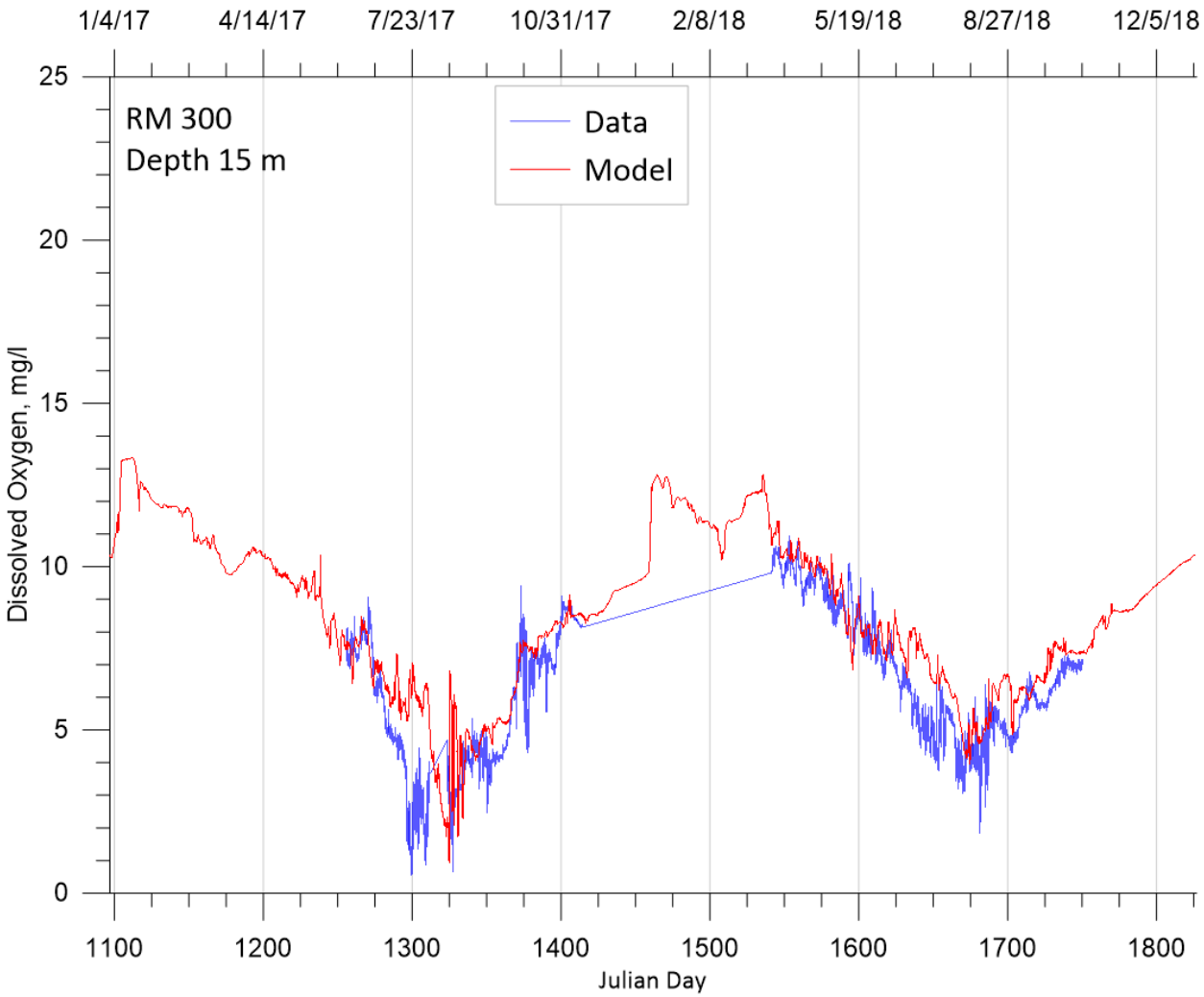


Figure 30. Model predicted DO concentrations compared with continuous data measured at RM 300 at a depth of 15 m.

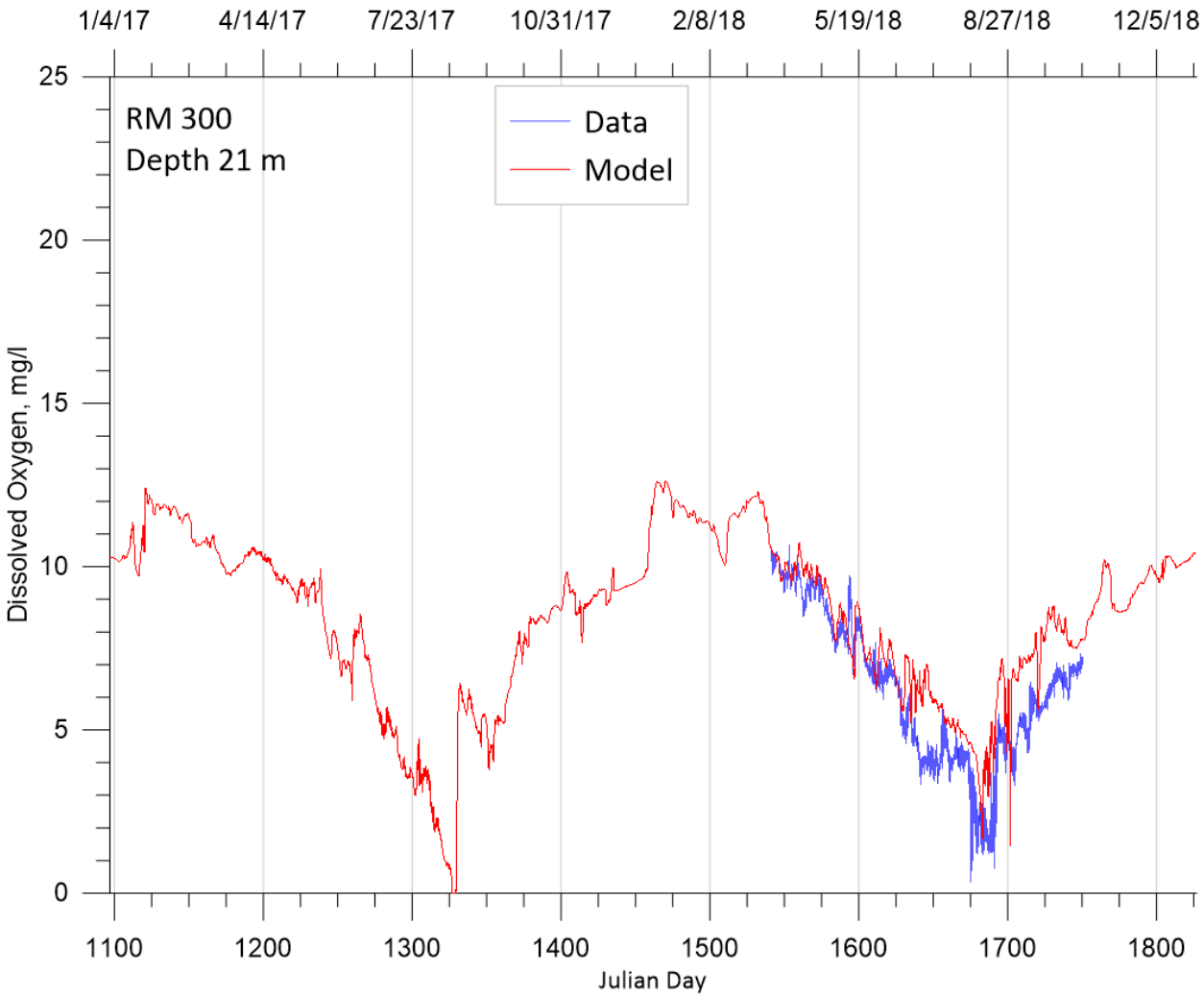


Figure 31. Model predicted DO concentrations compared with continuous data measured at RM 300 at a depth of 21 m.

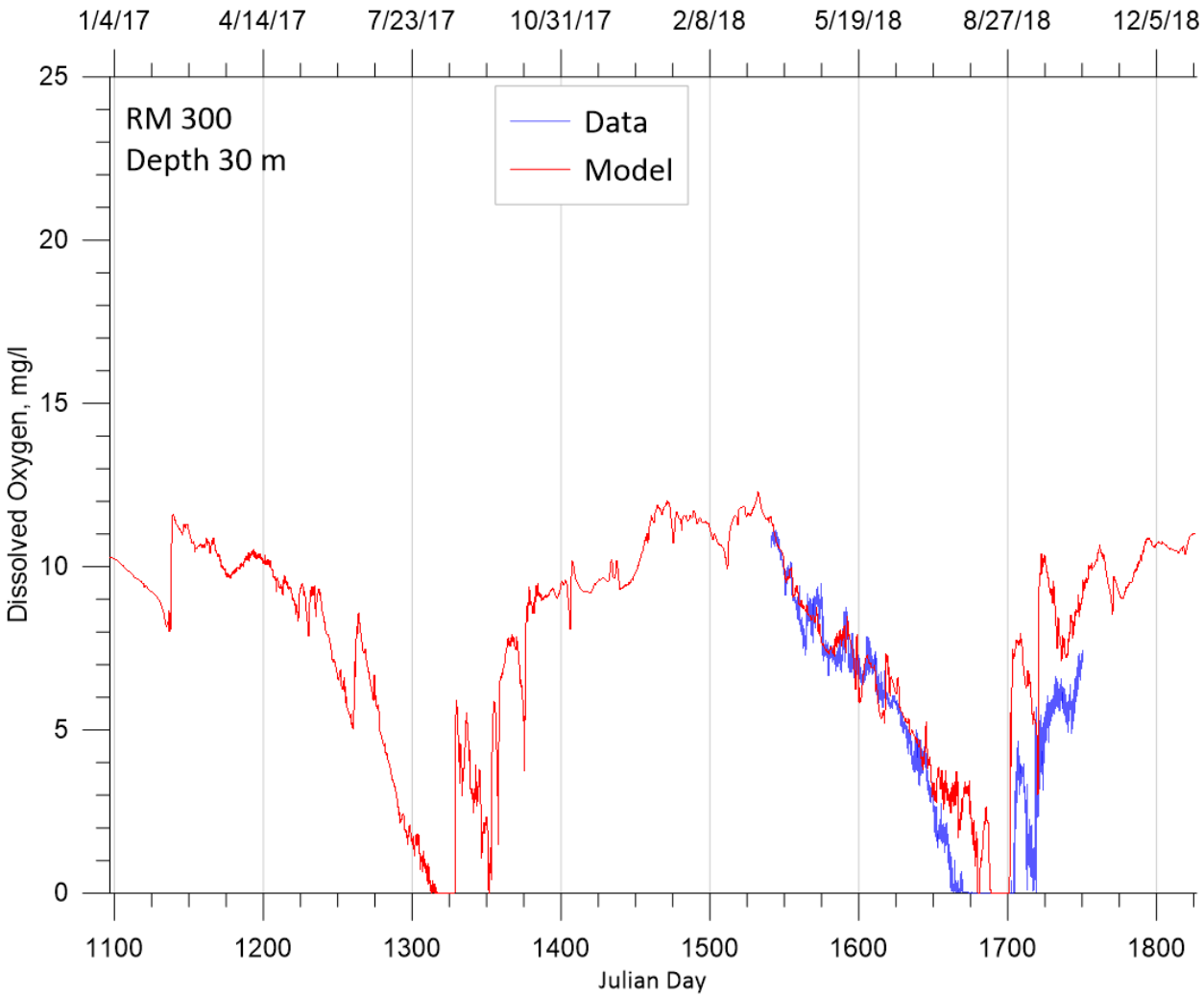


Figure 32. Model predicted DO concentrations compared with continuous data measured at RM 300 at a depth of 30 m.

RM 318

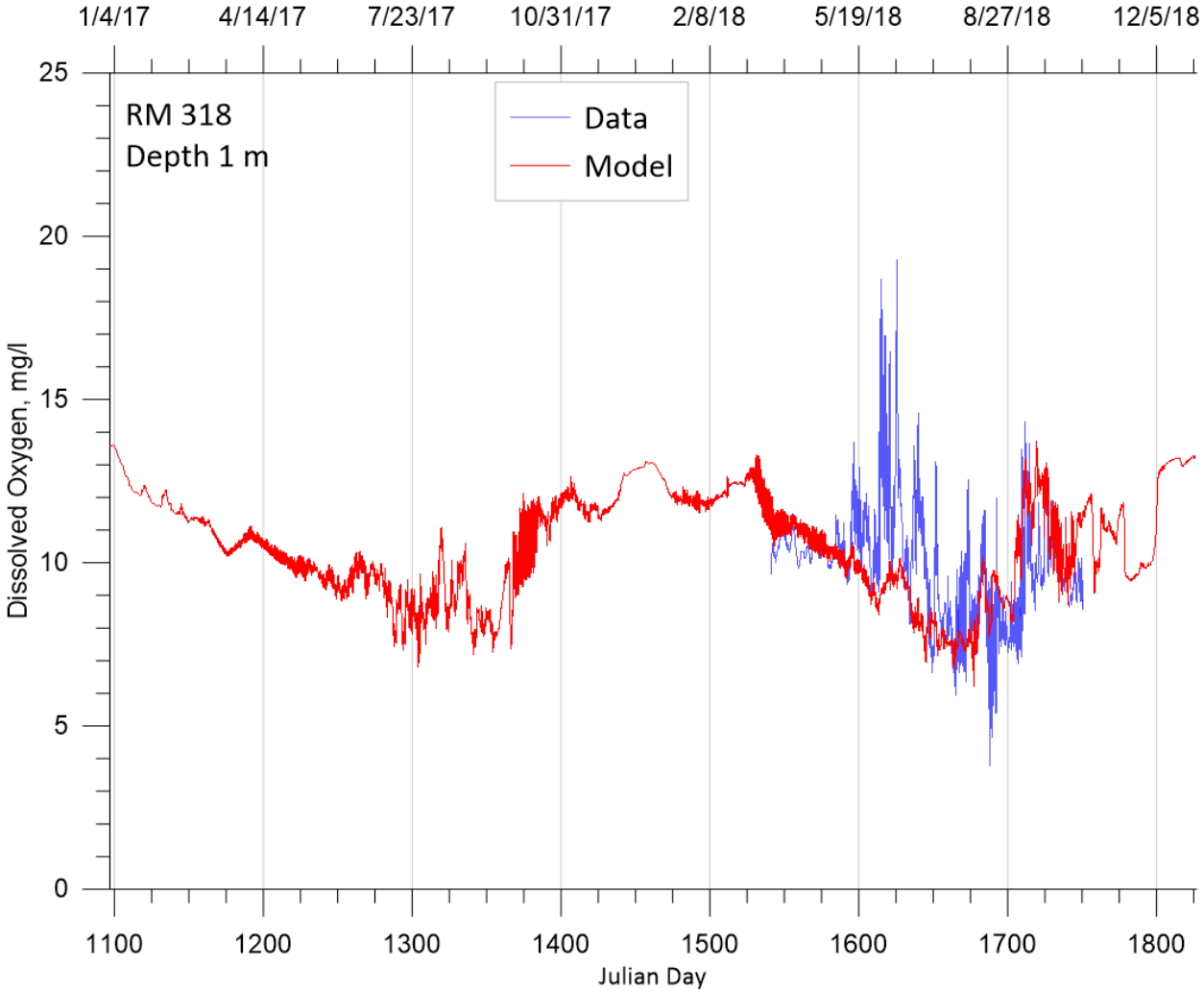


Figure 33. Model predicted DO concentrations compared with continuous data measured at RM 318 at a depth of 1 m.

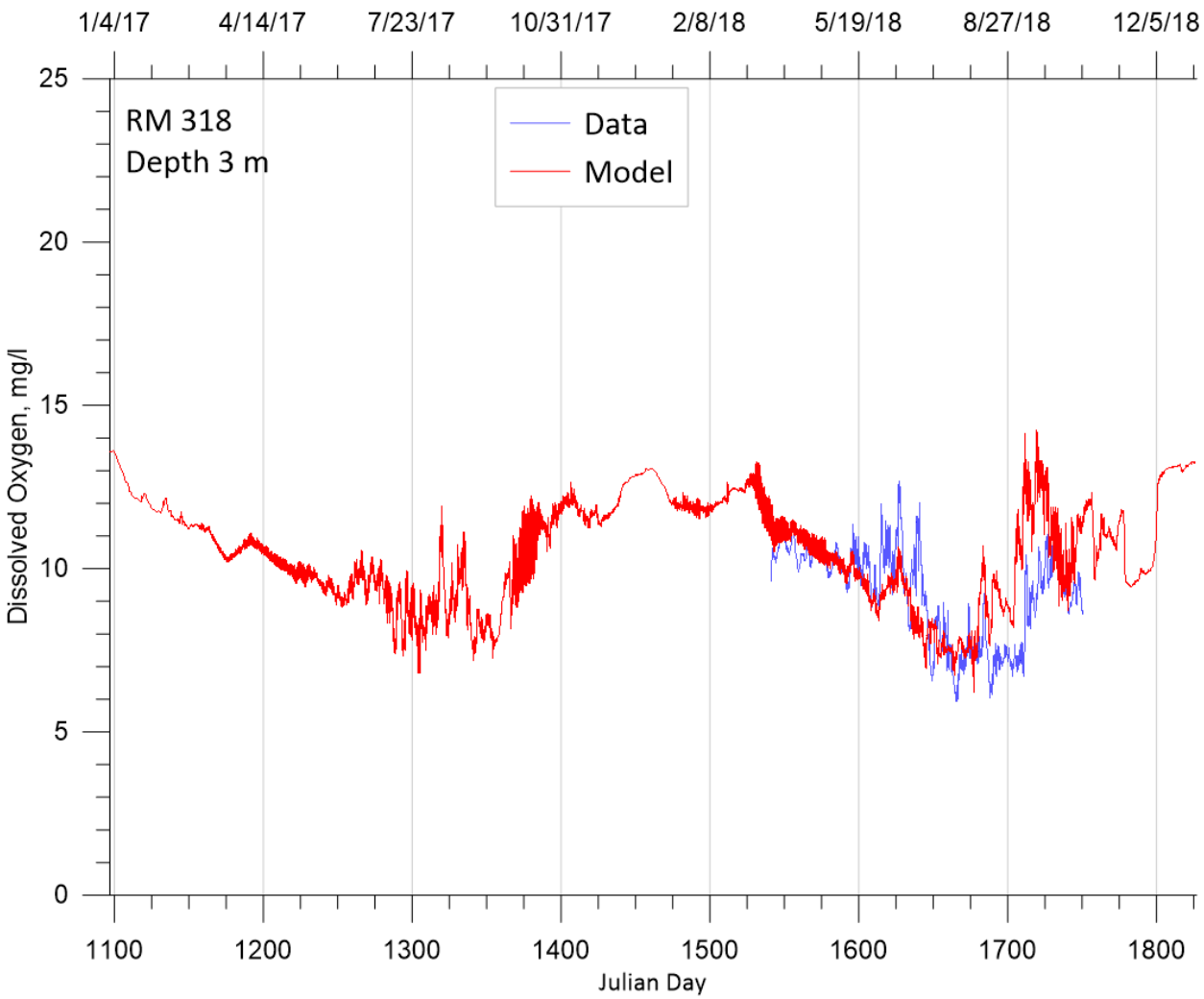


Figure 34. Model predicted DO concentrations compared with continuous data measured at RM 318 at a depth of 3 m.

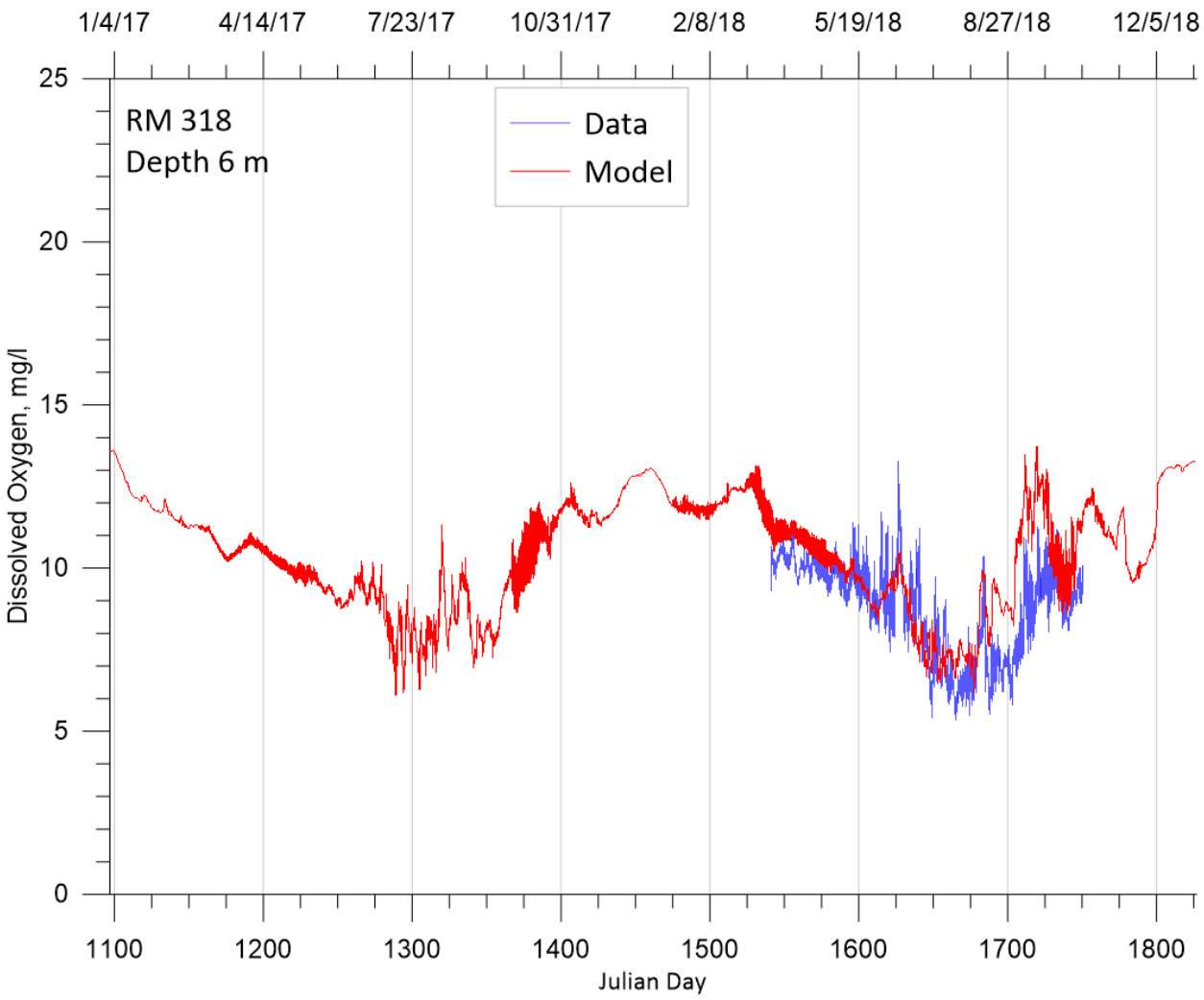


Figure 35. Model predicted DO concentrations compared with continuous data measured at RM 318 at a depth of 6 m.

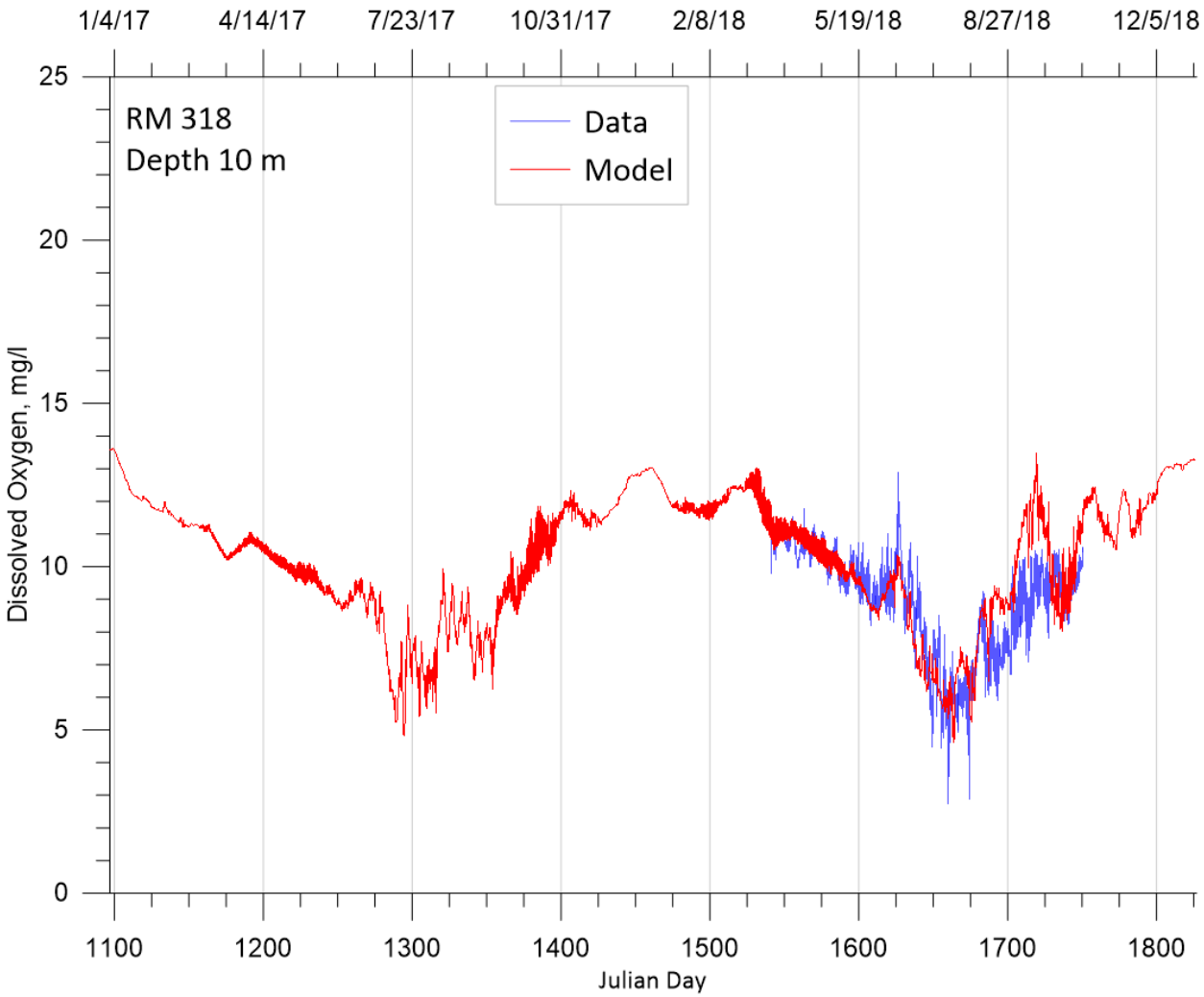


Figure 36. Model predicted DO concentrations compared with continuous data measured at RM 318 at a depth of 10 m.